Polyhedron Vol. 8, No. 1, pp. 1–6, 1989
Printed in Great Britain

0277–5387/89 $3.00+.00
© 1988 Pergamon Press plc

COMPARATIVE STUDIES OF THE COORDINATION MODE IN COMPLEXES OF COPPER WITH ASPARAGINE AND COPPER WITH ASPARTIC ACID IN SOLUTION AND SOLID STATE

LECHOSLAW LOMOZIK* and ANNA WOJCIECHOWSKA

Faculty of Chemistry, Adam Mickiewicz University, Grunwaldzka 6, 60-780 Poznan, Poland

(*Received* 18 *December* 1987; *accepted after revision* 13 *June* 1988)

Abstract—^{1}H NMR, ^{13}C NMR and IR studies have been employed to compare the mode of coordination of Cu complexes with DL-asparagine (Asn) and Cu with DL-aspartic acid (Asp) in solution and in isolated solid complexes: $Cu(Asn)_2$, $[Cu(Asn)(OH)(H_2O)_2]$, $K_2[Cu(Asp)_2]\cdot 2H_2O$, $Ba[Cu(Asp)_2]\cdot 2H_2O$ and $Ba[Cu(Asp)(OH)(H_2O)_2]_2$. It was found for DL-asparagine that only the carboxyl group participates in the coordination in complexes with Cu in solution at pH = 5, whereas carboxyl and amine groups participate in coordination at pH = 9. In the solid complex of Asn with Cu: Cu(Asn), the coordination was found to take place through the carboxyl, amine and amide groups, and in the complex $[Cu(Asn)(OH)(H_2O)_2]$ through carboxyl and amine groups. In the case of DL-aspartic acid it was found that carboxyl groups participate in the coordination of complexes with Cu in solution at pH = 5, whereas carboxyl and amine groups participate in the coordination at pH = 9. In the solid complexes of Asp with Cu: $K_2[Cu(Asp)_2]\cdot 2H_2O$ and $Ba[Cu(Asp)(OH)(H_2O)_2]_2$ coordination takes place through both the carboxyl and amine groups. Identical coordination in solution and in the solid state was found in hydroxo complexes of both investigated ligands with Cu.

Intensive studies of metal complexes in biological systems have been conducted in recent years.[1–3] The molecular weight of groups functioning as ligands in these systems is of the order of thousands, and the metal is only a minor constituent of them. Therefore, it is necessary to conduct investigations on much simpler models such as, for example, complexes of amino acids and peptides with metals. Such complexes are a source of information for better understanding of the laws governing biological systems. The reactions occurring in living organisms proceed mainly in solution, but data concerning the structure of the given complexes, in terms of the bond length and coordination mode, are frequently obtained in crystallographic studies of the crystals. Any conclusions drawn about the complexes in solution on the basis of results obtained for solids runs the risk of interpreting the data erroneously. It is incorrect to assume, prior to any experiments, that the coordination mode in the solids is identical with that in solution, especially as experiments of this type have proved that in many cases the model obtained for the solid complex is not identical to that existing in solution.[4–7] Copper plays a crucial role in systems of this type.[8]

In the present study we attempted to compare the results obtained in coordination mode studies of the complexes of copper with DL-asparagine and copper with DL-aspartic acid in aqueous solution and in isolated solid complexes. The results obtained are of particular significance for estimating the role of the metal and its coordination compounds in the processes occurring in living organisms.

EXPERIMENTAL

DL-asparagine (Asn) and DL-aspartic acid (Asp) by Reanal (Hungary), which were chromatographically pure, were used in the study. Copper perchlorate was obtained by dissolving cupric

*Author to whom correspondence should be addressed.

oxide in concentrated $HClO_4$, followed by crystallization. The following deuterated compounds were used in spectroscopic studies: D_2O (IBJ, Poland), DCl (PAN), NaOD (Veb-Berlin-Chemie). Samples for ^1H NMR, ^{13}C NMR and IR studies were prepared by dissolving copper perchlorate and DL-asparagine (DL-aspartic acid) in D_2O. The pH measurements were carried out on a pH-meter PHM-26 Radiometer and corrected according to the formula pD = pH + 0.40.[9] DL-asparagine and DL-aspartic acid concentrations in the samples were 0.20 and 0.50 M, respectively. The metal to ligand ratio was 1 : 50 in ^1H NMR and ^{13}C NMR studies, and 1 : 2 in IR investigations. ^1H NMR spectra were recorded on a BS-467 Tesla spectrometer with DSS as the internal standard, ^{13}C NMR spectra on a JEOL Fx 90 QFT spectrometer with dioxan as the internal standard. IR spectra were recorded on a Perkin–Elmer 180 spectrometer. All the IR spectra were performed for deuterated (the ligands were recrystallized three times from heavy water) and undeuterated ligands so that their results could be interpreted unambiguously. IR spectra of solid compounds were recorded within the range 4000–400 cm^{-1} as KBr discs, and within the range 700–200 cm^{-1} as CsBr discs.

Preparation of complexes

$Cu(Asn)_2$. This compound was prepared using a method similar to that described in ref. 10 (cupric acetate was substituted by cupric perchlorate). Analysis for $Cu(Asn)_2$: Found: N, 17.4; C, 29.5; H, 4.3. Calc.: N, 17.2; C, 19.4; H, 4.3.

$[Cu(Asn)(OH)(H_2O)_2]$. This was obtained by dissolving 0.03 mole of DL-asparagine and 0.005 mole of $Cu(ClO_4)_2$ in water. The solution was brought to pH = 9. The complex was precipitated with acetone, rinsed with absolute ethanol and dried in a desiccator over P_4O_{10} at room temperature. Navy blue crystals of the complex were obtained. Analysis for $[Cu(Asn)(OH)(H_2O)_2]$: Found: N, 11.1; C, 19.6; H, 4.8. Calc: N, 11.4; C, 20.0; H, 4.9.

$K_2[Cu(Asp)_2]\cdot 2H_2O$. This compound was prepared applying a method similar to that used for $Cu(Asn)_2$. (The method described in ref. 10 was modified by neutralizing the reaction mixture to pH = 7 by means of KOH.) Analysis for $K_2[Cu(Asp)_2]\cdot 2H_2O$: Found: N, 6.4; C, 21.4; H, 3.1. Calc: N, 6.4; C, 21.7; H, 3.2.

$Ba[Cu(Asp)_2]\cdot 2H_2O$. This compound was prepared employing a method described in ref. 11. Analysis for $Ba[Cu(Asp)_2]\cdot 2H_2O$: Found: N, 5.6; C, 19.5; H, 2.8. Calc: N, 5.6; C, 19.2; H, 2.8.

$Ba[Cu(Asp)(OH)(H_2O)_2]_2$. This was obtained by dissolving 0.015 mole of DL-aspartic acid and 0.003 mole of $CuSO_4$ in water. $Ba(OH)_2$ was added to the solution until pH = 13 was reached. CO_2 was passed through the mixture to precipitate the excess Ba^{2+}. After filtering off the precipitate, the complex was precipitated with dioxan. A light blue precipitate was obtained. The complex was air dried at 50°C. Analysis for $Ba[Cu(Asp)(OH)(H_2O)_2]_2$: Found: N, 4.4; C, 14.9; H, 3.8. Calc: N, 4.4; C, 15.1; H, 3.8.

RESULTS AND DISCUSSION

It follows from our earlier studies[12] as well as from the literature on Cu/Asp and Cu/Asn complexing equilibria (Table 1) that the following complexes arise in the systems: Cu(Asp), $Cu(Asp)_2^{2-}$, $Cu(HAsp)^+$, $Cu(Asp)(OH)^-$ and $Cu(Asn)^+$, $Cu(Asn)_2$, $Cu(Asn)(OH)^-$.

In order to determine the coordination mode in Cu complexes with DL-aspartic acid and DL-asparagine in solution, ^1H NMR, ^{13}C NMR and IR studies were carried out at pH = 5 and 9. At pH = 5 (as evidenced by our earlier observation[12]) predominant forms in the systems mentioned above

Table 1. Stability constants of the Cu^{II}–DL-aspartic acid and Cu^{II}–DL-asparagine complexes, entries are $\log \beta_{pqr}$ values for species $Cu_pH_qL_r$

	Cu_p	H_q	L_r	Our previous work[12]	Ref. 13,16	Ref. 14,17	Ref. 15,18
Asp+Cu	1	1	1	12.43	12.46		12.36
	1	2	2				23.54
	1	1	1				15.70
	1	0	1	9.14	8.85	8.57	8.70
	1	−1	1	3.54			
	1	0	2	16.16	15.83	15.35	15.70
Asn+Cu	1	0	1	7.69	7.79	7.78	
	1	−1	1	2.33			
	1	0	2	14.38	14.29	14.13	14.90

Table 2. Positions of ^{13}C NMR signals (ppm) of DL-aspartic acid (Asp), DL-asparagine (Asn) and their complexes with Cu^{II} (D_2O solutions)

		C(1)	C(2)	C(3)	C(4)	H(2)	H(3)
Asp	pH = 5	107.438	−14.466	−30.178	110.637	3.90	2.80
Asp+Cu	pH = 5	110.854	−14.355	−30.070	107.547	4.05	2.90
Asp	pH = 9	109.280	−13.978	−28.607	110.104	3.80	2.60
Asp+Cu	pH = 9	111.773	−12.165	−27.695	111.773	4.05	2.80
Asn	pH = 5	106.680	−15.224	−31.966	107.873	4.10	3.00
Asn+Cu	pH = 5	108.254	−16.055	−32.010	107.994	5.03	3.00
Asn	pH = 9	110.095	−13.328	−27.107	114.482	3.80	2.92
Asn+Cu	pH = 9	112.105	−16.271	−28.051	114.476	4.00	3.08

are the complexes of the ML and ML_2 type, whereas at pH = 9 the ML(OH) hydroxo complexes dominate. At pH = 5 in the ^1H NMR spectrum of DL-aspartic acid with Cu (Table 2), the signals of protons at C_2 and C_3 are shifted, and in the ^{13}C NMR spectrum (Table 2) shifts are exhibited by the atoms C_1, C_4 (the greatest shifts) and C_2, C_3 (almost identical shifts), see structure below.

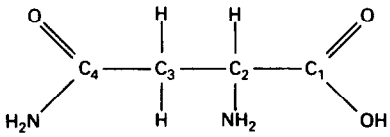

The above data indicate the coordination via both carboxyl groups of DL-aspartic acid at pH = 5, and 9 via both the carboxyl groups and amino group [in the ^1H NMR spectrum the shift of proton signals at C_2 and C_3 has been observed and also in the ^{13}C NMR spectrum the shift of signals coming from C_1, C_2, C_3, C_4 has been recorded (Table 2)]. The above conclusions were confirmed by IR studies (Table 3). In the IR spectrum of DL-aspartic acid with Cu, the signals from carboxyl groups are shifted towards lower frequencies, thus both carboxyl groups participate in the coordination.[19] The decay of the signal at 1627 cm^{-1} arriving from the $-C(\overset{+}{N}H_3)COO^-$ group in the spectrum of DL-aspartic acid with copper at pH = 9 (Table 3) also proves the coordination through nitrogen. In the ^1H NMR spectrum of DL-asparagine with copper at pH = 5, the proton signal at C_2 is shifted, though no shift of the proton signal is observed at C_3. Thus, it can be concluded that the carboxyl group participates in the coordinatiom with Cu, which is also supported by the data obtained from ^{13}C NMR spectra (Table 2), see structure below.

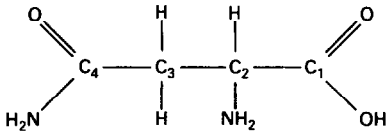

The absence of a proton signal shift at C_3 in the ^1H NMR spectrum at pH = 5 and relatively small shifts at C_2 and C_3 in the ^{13}C NMR spectrum let us conclude that the amide group, carbonyl oxygen as well as the amine group do not take part in the coordination. At pH = 9, DL-asparagine is coordinated with Cu through the carboxyl and amine groups. The value of the C_4 shift calculated from the ^{13}C NMR spectrum (Table 2) excludes the coordination by the amide group and the oxygen atom of the carbonyl group in this system. IR studies confirm the above conclusions (Table 4).

To obtain information about the coordination mode of DL-asparagine and DL-aspartic acid with Cu in the solid state, the following solid complexes

Table 3. IR spectra of Asp and Asp+Cu^{II} (cm^{-1}), (D_2O solution; CaF_2 cells)

System		$-COO^-$	$>C(\overset{+}{N}H_3)COO^-$
Asp	pH = 5	1583	1614
Asp+Cu	pH = 5	1556	1575
Asp	pH = 9	1592	1627
Asp+Cu	pH = 9	1585	

Table 4. IR spectra of Asn and Asn+Cu^{II} (cm^{-1}), (D_2O solution; CaF_2 cells)

System		$-COO^-$	$-C(=O)-NH_2$
Asn	pH = 5	1622	1640
Asn+Cu	pH = 5	1609	1640
Asn	pH = 9	1591	1632
Asn+Cu	pH = 9	1578	1632

were synthesized: $Cu(Asn)_2$, $[Cu(Asn)(OH)(H_2O)_2]$, $K_2[Cu(Asp)_2]\cdot 2H_2O$, $Ba[Cu(Asp)_2]\cdot 2H_2O$, as well as $Ba[Cu(Asp)(OH)(H_2O)_2]_2$ and their IR spectra were recorded. The recorded spectra were referred to the spectrum of the ligand alone. In the spectrum of the $Cu(Asn)_2$ complex (Table 5), the shift of the peak of the carboxyl group shows evidence of its participation in coordination with Cu. The amide group (peak shift), as well as the amine group ($—NH_2$ signal shift and disappearance of the $—NH_3$ peak in the spectrum of the complex) also participate in the coordination (Fig. 1). The carboxyl group coordinates with the metal through one oxygen of the carboxyl group (the carboxyl group signal shifts to higher frequencies). Additional peaks in the far-IR appearing in the spectrum of the complex prove coordination through oxygen and nitrogen (Fig. 2).

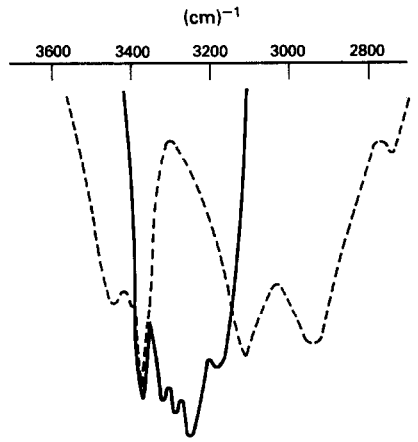

Fig. 1. IR spectra of: —— $Cu(Asn)_2$; --- $Asn\cdot H_2O$ (solid state in KBr, 3600–2800 cm^{-1}).

In the spectrum of the $[Cu(Asn)(OH)(H_2O)_2]$ complex (Table 5), the peak from the amide group remains at the unchanged position but it is broadened by the signal from H_2O (Fig. 3; compare with Fig. 1, where the amide and amine groups participate in coordination). The amine group of asparagine participates in the coordination (the peak from $—\overset{+}{N}H_3$ does not appear). The carboxyl group signal shifts, which indicates that the carboxyl group takes part in the complex formation and also the participation of both oxygens. The peak due to H_2O is located at higher frequencies than that ascribed to hydrated complexes, which indicates that water takes two positions in the metal's inner coordination sphere.[20,21]

The complex ions of DL-aspartic acid with copper were obtained as potassium and barium salts. In the IR spectrum of the complex $K_2[Cu(Asp)_2]\cdot 2H_2O$ in comparison with the spectrum of the ligand alone, a shift of the carboxyl group signal is observed. Thus, the coordination in this complex takes place through the oxygens of the carboxyl groups. The

Table 5. IR spectra of DL-asparagine and complexes of DL-asparagine with Cu^{II} (cm^{-1}). (Spectra recorded as KBr discs between 4000–400 cm^{-1}, and as CsI discs between 700–200 cm^{-1})

$Asn\cdot H_2O$ (solid)	$Cu(Asn)_2$ (solid)	$[Cu(Asn)(OH)(H_2O)_2]$ (solid)	Assignment
3441	3329	3441	—C(=O)—NH₂
3110	3252	3441	$—NH_2$
2952	3169		
1690	1690	1678	—C(=O)—
1575	1587	1585	—C(=O)—O⁻
		1585	H_2O
1527			$—\overset{+}{N}H_3$
		1025	Cu—OH
	563	566	Cu—N
	287	263	Cu—O

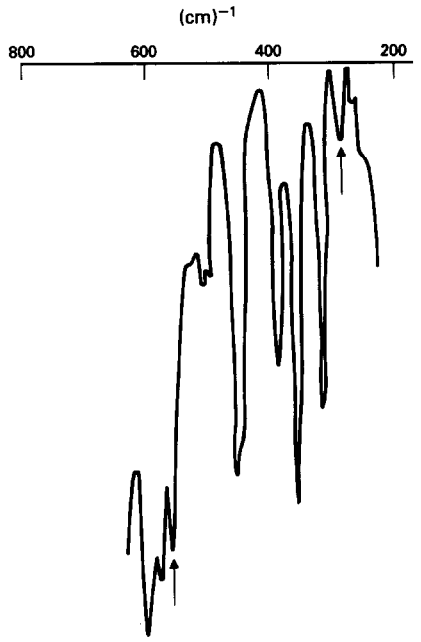

Fig. 2. IR spectrum of $Cu(Asn)_2$ (solid state in CsBr, far-IR).

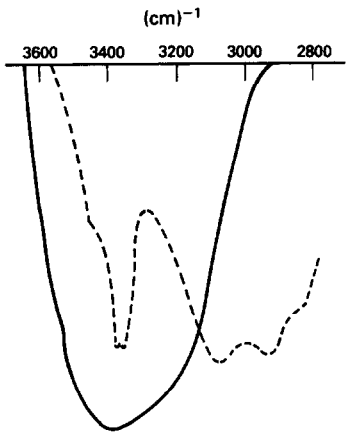

Fig. 3. IR spectra of: —— $[Cu(Asn)(OH)(H_2O)_2]$; --- $Asn \cdot H_2O$ (solid state in KBr, 3600–2800 cm^{-1}).

amine group also participates in the coordination, which was also confirmed by the studies in the far-IR (Table 6). An identical method of coordination was observed for the complex $Ba[Cu(Asp)_2] \cdot 2H_2O$ (Table 6). The coordination has been found to take place in the $Ba[Cu(Asp)(OH)(H_2O)_2]_2$ complex through the oxygens of the carboxyl groups and through the amine group. The participation of water in the coordination has also been found (Table 6).

In the IR spectra of $Cu(Asn)_2$, $K_2[Cu(Asp)_2] \cdot 2H_2O$ and $Ba[Cu(Asp)_2] \cdot 2H_2O$ complexes two new peaks have been recorded in the far IR, although they were not observed in the spectra of the ligands (Fig. 2, Tables 5 and 6). These peaks are due to the formation of metal–nitrogen and metal–oxygen bonds. On the basis of the above data and the symmetry rules[20–23] it can be concluded that the double complexes yielded occur in the *trans* configuration. For the synthesis of the complexes, DL-asparagine and DL-aspartic acid were used. The results obtained for complexes of both ligands with Cu are in agreement with the previous obser-

Table 6. IR spectra of DL-aspartic acid and complexes of DL-aspartic acid with Cu^{II} (cm^{-1}). (Spectra recorded as KBr discs between 4000–400 cm^{-1}, and as CsI discs between 700–200 cm^{-1})

Asp (solid)	$K_2[Cu(Asp)_2] \cdot H_2O$ (solid)	$Ba[Cu(Asp)_2] \cdot 2H_2O$ (solid)	$Ba[Cu(Asp)(OH)(H_2O)_2]_2$ (solid)	Assignment
3130	3400	3412	3242	$-NH_2$
3011	3400	3412	3138	
1680	1680	1680	1680	$>C=O$
	1602	1606	1567	H_2O
1587		covered by water signal		$-C(=O)-O^-$
1500				$-\overset{+}{N}H_3$
			975	Cu—OH
	569	543	593	Cu—N
	299	284	297	Cu—O

vation[20,24] according to which the complexes formed from the racemic amino acids adopt a *trans* structure.

In the analysis of the structure of the complexes of asparagine with copper in aqueous solution and solid state, fundamental differences have been observed, particularly for complexes occurring in solution at pH = 5. In the case of asparagine, the amide and amine groups do not participate in the coordination in solution at such pH conditions, whereas their participation in the coordination is observed in the solid complex $Cu(Asn)_2$. In solution, where solvent molecules compete with the ligand, at pH = 5 the $—NH_3$ group does not participate in the coordination and the free place in the metal's coordination sphere is taken by a water molecule. The same is true of the amide group. In the solid state both groups participate in the coordination. The $Cu(Asn)_2$ complex was the only solid complex obtained in our studies that was weakly water-soluble. This weak solubility may be due to the coordination through the amide group. This conclusion is also supported by the fact that the other type of the isolated complexes, $[Cu(Asn)(OH)(H_2O)_2]$, where the amide group does not participate in the coordination, is characterized by very good solubility in water.

In complexes of aspartic acid, differences have also been observed for complexes in solution (at pH = 5) and solid state. In the complexes in solution, coordination through the amine group has not been detected, whereas in solid complexes coordination takes place by participation of the amine. An identical coordination in solution and in the solid state has been determined for hydroxo complexes. For both asparagine and aspartic acid the carboxyl and amine groups participate in the coordination. In all of the isolated solid complexes the coordination number is six. Differences in the structure of coordination compounds in the solid state and in solution that have been found in the present study point to the necessity of taking this fact into consideration when results concerning solids are to be employed to determine the coordination mode of complex compounds in solution. Problems of this type are often encountered in studies on coordination compounds of metal ions with biomolecules when one tries to obtain correct information on the role of the metal in living organisms. Accurate conclusions can only be drawn after conducting experiments with a full awareness of the possible errors.

Acknowledgement—This work was financially supported by the Polish Academy of Sciences, project RPBP 01.6.

REFERENCES

1. R. W. Hay, *Bio-Inorganic Chemistry*. Ellis Horwood, Chichester (1984).
2. M. N. Huges, *The Inorganic Chemistry of Biological Processes*. J. Wiley, New York (1981).
3. G. L. Eichhorn and L. G. Marzilii (Eds), *Advances in Inorganic Biochemistry*, Vols 1, 3 and 4. Elsevier Biomedical, New York (1979, 1981, 1984, respectively).
4. R. D. Gillard and S. H. Laurie, *J. Chem. Soc. A* 1970, 59.
5. H. C. Freeman, *Adv. Protein Chem.* 1967, **22**, 258.
6. K. M. Wellman, T. G. Mecca, W. Mungall and C. R. Hare, *J. Am. Chem. Soc.* 1968, **90**, 805.
7. F. F. L. Ho, L. E. Erickson, S. R. Watkins and C. N. Reilley, *Inorg. Chem.* 1970, **9**, 1139.
8. H. Sigel (Ed.), *Metal Ions in Biological Systems*, Vols 1–14, M. Dekker, New York.
9. R. C. Glascoe and E. A. Long, *J. Phys. Chem.* 1960, **64**, 188.
10. F. S. Stephens, R. S. Vagg and P. A. Williams, *Acta Cryst.* 1975, **B31**, 841.
11. J. P. Greenstein and M. Winitz, *Chemistry of the Amino Acid*, p. 586. J. Wiley, New York (1961).
12. L. Lomozik, A. Wojciechowska and M. Jaskolski, *Monatsh. Chem.* 1983, **114**, 1185.
13. A. Gergely and E. Farkas, *J. Chem. Soc., Dalton Trans.* 1982, 381.
14. S. Chaberek Jr. and A. E. Martell, *J. Am. Chem. Soc.* 1952, **79**, 3036.
15. I. Liang and A. Olin, *Acta Chem. Scand.* 1984, **A38**, 247.
16. A. Gergely, J. Nagypal and E. Farkas, *J. Inorg. Nucl. Chem.* 1975, **37**, 551.
17. N. C. Li, E. Doody and J. M. White, *J. Am. Chem. Soc.* 1958, **80**, 5901.
18. A. Albert, *Biochem. J.* 1950, **47**, 531.
19. S. Kirchner, *J. Am. Chem. Soc.* 1956, **78**, 2372.
20. A. W. Herlinger, S. L. Wenhold and T. V. Long, *J. Am. Chem. Soc.* 1970, **92**, 6474.
21. A. W. Herlinger and T. W. Long, *J. Am. Chem. Soc.* 1970, **92**, 6481.
22. R. A. Condrate and K. Nakamoto, *J. Chem. Phys.* 1965, **42**, 2590.
23. T. J. Lane, J. A. Durkin and R. J. Hooper, *Spectrochim. Acta* 1963, **19**, 1195.
24. S. H. Laurie, *Aust. J. Chem.* 1967, **20**, 2609.

Polyhedron Vol. 8, No. 1, pp. 7–11, 1989
Printed in Great Britain

0277–5387/89 $3.00+.00
© 1988 Pergamon Press plc

ESR STUDY OF SOME COPPER(II) COORDINATION COMPOUNDS WITH SUBSTITUTED BIGUANIDINES—I

R. K. RAY

Department of Chemistry, Rama Krishna Mission Vivekananda Centenary College, Rahara-743186, 24-Parganas (North), West Bengal, India

(*Received* 21 *April* 1988; *accepted* 16 *June* 1988)

Abstract—Copper(II) complexes of substituted biguanides have been studied by ESR spectroscopy in water, in their polycrystalline form and in the corresponding nickel(II) complex matrix. In aqueous solution, nine nitrogen superfine lines on the higher field $3/2 \leftrightarrow 3/2$ copper hyperfine splitting component is indicative of four equivalent or nearly equivalent nitrogen atoms surrounding the copper(II) ion. α'^2 values indicate that like biguanide, 1-amidino-O-alkylureas, β-phthalocyanine and tetraphenylporphine, substituted biguanides and their protonated forms are equally strong-field ligands. The evaluation of the covalency parameters indicate that the unpaired electron of copper(II) spends about 36% of its time in the nitrogen donor sites of the ligands.

The structure of four-coordinated metal biguanide complexes has become a subject of varied interest. Based on chemical tests Ray and Saha[1] have suggested structure **I** (shown in Fig. 1) which was accepted by Kunchur and Mathew[2,3] after X-ray studies. From UV spectral data Sen[4] proposed another structure **II** (shown in Fig. 2) and from the NMR and X-ray diffraction pattern Creitz *et al.*[5] established structure **III** (shown in Fig. 3) for the bis(biguanide)nickel(II) chloride dihydrate.

The electron spin resonance (ESR) technique can be employed to detect the nature of the coordinating

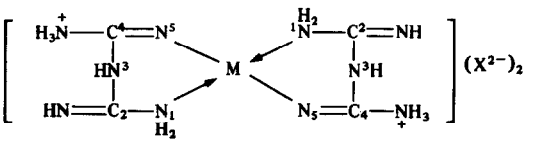

Fig. 1. Structures of bis(biguanide)metal(II) (M^{II} = Cu^{II}, Ni^{II}) halides (X = Cl, Br, I).

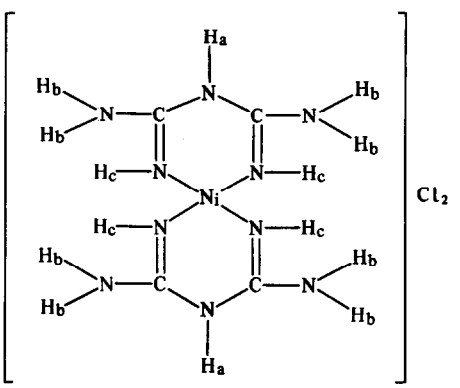

Fig. 3. Structure of bis(biguanide)nickel(II) chloride.

atoms in copper(II) complexes since the Spin Hamiltonian parameters obtained can be used to establish the metal–ligand bond nature. As few ESR studies of copper(II) biguanide complexes have appeared in the literature[6–8] and the bonding sites for the biguanide ligand are not unambiguous, we

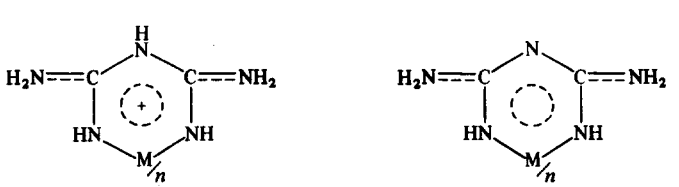

Fig. 2. (a) Biguanide complex. (b) Neutral metal biguanide complex.

undertook an investigation of the ESR and optical spectra of some copper(II) biguanide complexes in order to establish the extent of covalency in the metal–ligand interaction. While this work was in progress a brief ESR report of some copper(II) dibiguanide complexes was communicated.[9]

EXPERIMENTAL

Bis(substituted biguanide)copper(II) dichloride and bis(substituted biguanide)nickel(II) dichloride were prepared following published procedures.[1] Dehydration of $Cu(X\text{-}big)_2 \cdot nH_2O$ and $Ni(X\text{-}big)_2 \cdot nH_2O$ (X = CH_3-, C_2H_5-, etc., n = 1, 2, 3) was accomplished by heating the complexes *in vacuo* at about 70°C for 3 days. The stoichiometry of the complexes was confirmed by carbon, hydrogen, nitrogen and metal analyses.

Copper(II)-doped nickel $(X\text{-}big)_2$ was prepared by adding about 4% of $Cu(X\text{-}big)_2 \cdot 2.5H_2O$ to $Ni(X\text{-}big)_2 \cdot 3H_2O$ dispersed in 8 M aqueous sodium hydroxide. The mixture was well stirred, filtered, then washed with water and ethanol, air dried and finally dehydrated.

Electronic spectra (Nujol) were recorded by using a Cary 14 spectrophotometer at Wright State University, Dayton, OH, U.S.A., and ESR spectra were obtained on a Varian V4502-12X band spectrometer at the Instituto Chimico Policattedra, Universita di Cagliari, Italy.

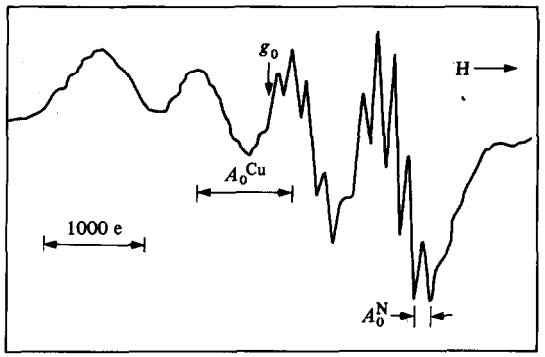

Fig. 4. Aqueous solution ESR spectrum of $[Cu(Me\text{-}bigH)_2]Cl_2$, frequency = 9.421 kMc.

RESULTS AND DISCUSSION

From the ESR spectrum, in aqueous media (Fig. 4), of bis(methyl biguanide)copper(II) chloride the average g-value (g_0), the isotropic hyperfine constant (A_0^{Cu}) and the isotropic ligand hyperfine structure constant (A_0^N) were determined. Other parameters $g_\parallel$, $g_\perp$, $A_\parallel^{Cu}$ and $A_\perp^{Cu}$ were measured from the anisotropic spectra of powdered magnetically dilute solids[10] (Fig. 5, Table 1). The ligand superfine structure components were observed but assignments of the components is not straightforward as the principal axes of the superfine tensor are not necessarily the same as those of the hyperfine tensor. The ESR spectra of all the complexes in solution show nine nitrogen super hyperfine com-

Table 1. g values and hyperfine structure constants for copper(I) complexes

Complex	Medium	g_0	g_{av}	$g_\parallel$	$g_\perp$	$A_\parallel^{Cu}$	$A_\perp^{Cu}$ ($\times 10^4$ cm^{-1})	A_0^{Cu}	A_0^N
$[Cu(Mc\text{-}big)_2]$	Ni^{II} complex	—	2.097	2.172	2.060	209	24	—	16.0
	Water	2.100	—	—	—	—	—	86.2	15.9
$[Cu(Me\text{-}bigH)_2]Cl_2$	Ni^{II} complex	—	2.098	2.185	2.056	208	20	83.1	16.1
	Water	2.099	—	—	—	—	—	85.9	15.8
$[Cu(Et\text{-}big)_2]$	Ni^{II} complex	—	2.100	2.179	2.059	209	22	—	16.0
	Water	2.098	—	—	—	—	—	87.1	15.8
$[Cu(Et\text{-}bigH)_2]Cl_2$	Ni^{II} complex	—	2.100	2.184	2.060	206	22	—	15.7
	Water	2.100	—	—	—	—	—	85.3	15.9
$[Cu(Me_2\text{-}big)_2]$	Ni^{II} complex	—	2.098	2.182	2.057	208	20	—	15.7
	Water	2.101	—	—	—	—	—	86.2	15.9
$[Cu(Me_2\text{-}bigH)_2]Cl_2$	Ni^{II} complex	—	2.094	2.168	2.058	209	24	—	15.9
	Water	2.098	—	—	—	—	—	85.8	15.8
$[Cu(Et_2\text{-}big)_2]$	Ni^{II} complex	—	2.098	2.174	2.061	203	19	85.7	15.3
	Water	2.099	—	—	—	—	—	85.6	15.1
$[Cu(Et_2\text{-}bigH)_2]Cl_2$	Ni^{II} complex	—	2.092	2.169	2.054	210	21	—	15.6
	Methanol	2.100	—	—	—	—	—	85.9	15.7

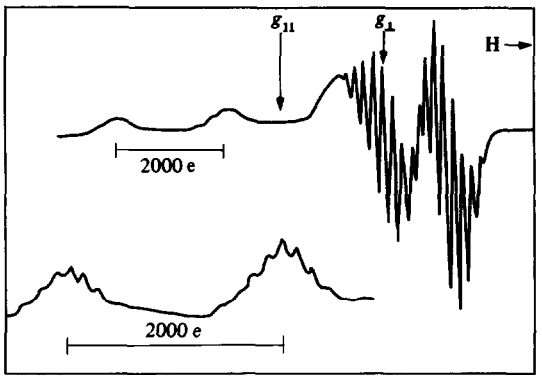

Fig. 5. ESR spectrum of $[Cu(Me\text{-}bigH)_2]Cl_2$ in $[Ni(Me\text{-}bigH)_2]Cl_2$: polycrystalline sample. In the lower left-hand side of the figure the low field $A_{\parallel}^{Cu}$ hyperfine components are shown enlarged by a factor of 10. Frequency = 9.518 kMc.

ponents indicating four equivalent or nearly equivalent nitrogen donor atoms surrounding the copper(II) ion with a $[CuN_4]$ chromophore. This is consistent with the single crystal X-ray studies.[2,3] These results are quite comparable to those of $[Cu(big)_2]$ and $[Cu(AMU)_2]$ (big-H = biguanide; AMUH = 1-amidino-O-methyl urea), both the ligands are strong field in character.[12,13] The electronic spectra of bis(ligand) copper(II) salts show typical absorption bands at 20,410 cm^{-1} in the solid state and at 19,230 cm^{-1} in aqueous medium which suggests a square planar $[CuN_4]$ chromophore.[14] Other square planar $[CuN_4]$ chromophores appear in bis(biguanide) copper(II) (19,230 cm^{-1} in water and 20,410 cm^{-1} in the solid state), bis(phenyl biguanide) copper(II) (18,200 cm^{-1} in water), (ethylene dibiguanide) copper(II) (19,230 cm^{-1} in water), bis(ethylene diamine) copper(II) (18,200 cm^{-1} in water), tetrakis(benzimidazole) copper(II) (19,000 cm^{-1}, solid phase).[15-18]

Taking into account the ESR spectral characteristics and the square-planar geometry as evidenced by the electronic spectra, one can consider that the copper(II) ion in these complexes is in a tetragonal field. The corresponding antibonding wave functions are[19-22]

$$\psi_{B1g} = \alpha d_{x^2-y^2} - \alpha'(-\sigma_x^{(1)} + \sigma_y^{(2)} + \sigma_x^{(3)} - \sigma_y^{(4)})/2$$

$$\psi_{B2g} = \beta_1 d_{xy} - \beta_1'(p_y^{(1)} + p_x^{(2)} - p_y^{(3)} + p_x^{(4)})/2$$

$$\psi_{A1g} = \alpha_1 d_{z^2} - \alpha'(\sigma_x^{(1)} + \sigma_y^{(2)} - \sigma_x^{(3)} - \sigma_y^{(4)})/2$$

$$\psi_{E1g} = \begin{cases} \beta d_{xz} - \beta'(p_z^{(1)} - p_z^{(3)})/2^{1/2} \\ \beta d_{yz} - \beta'(p_z^{(2)} - p_z^{(4)})/2^{1/2}. \end{cases}$$

Where α, β_1 and β are the coefficients which express the covalent character of the σ-bonding in-plane and out-of-plane π-bonding, respectively and the other symbols have their usual significance. These coefficients can be obtained from the relations which connect them with the spin Hamiltonian parameters for the axial symmetry.[23-25]

$$g_{\parallel} = 2.0023 - \frac{8\lambda_0\alpha\beta_1}{\Delta E_{xy}} \times \left\{\alpha\beta_1 - \alpha'\beta_1 S - \alpha'(1-\beta_1^2)^{1/2}\frac{T(n)}{2}\right\}$$

$$g_{\perp} = 2.0023 - \frac{2\lambda_0\alpha\beta}{\Delta E_{xz}} \times \left\{\alpha\beta - \alpha'\beta S - \alpha'(1-\beta^2)^{1/2}\frac{T(n)}{\sqrt{2}}\right\}.$$

Where α and α' were obtained using nitrogen superfine splittings. λ_0 ($= -828$ cm^{-1}) is the spin–orbit coupling constant for the free copper(II) ion and $T(n)$ was set equal to 0.333.[22] ΔE_{xy} and ΔE_{xz} are the electronic transition energies $^2B_{2g} \leftarrow {}^2B_{1g}$ and $^2E_g \leftarrow {}^2B_{1g}$, respectively.

The σ bonding parameter $(\alpha_N')^2$ was calculated from A_0^N and used to calculate α_N^2 using $\alpha^2 - 2\alpha.\alpha' S + \alpha'^2 = 1$, where S ($= 0.093$) is the integral overlap.[22] $\alpha_N'^2$ ($= 0.36$) indicates that the unpaired electron spends about 36% of its time in the nitrogen donor sites of biguanide ligands. In Table 2, the $\alpha_N'^2$ values (roughly the measure of the extent of electron delocalization) show that both biguanide and substituted biguanide anions and their protonatd forms are strong field ligands and they are placed slightly below the CN^- ion in the spectrochemical series.[12]

The in-plane σ-covalency parameter α_{Cu}^2 was calculated using a simplified expression:[22]

$$\alpha_{Cu}^2 = \frac{-A_{\parallel}}{0.036} + (g_{\parallel} - 2.002) + \frac{3}{7}(g_{\perp} - 2.002) + 0.04.$$

The α_{Cu}^2 values (0.80–0.85) account for the fraction of the unpaired electron density located on the copper(II) ion. The reported α_{Cu}^2 values of copper(II)–β-phthalocyanine and tetraphenylporphine complexes are 0.80 and 0.82.[26,27]

In D_{4h} symmetry the g values for the copper(II) ion with the $^2B_{1g}$ ground state can be expressed[28,29] as

$$g_{\perp} = 2.002 - 2k_{\perp}^2\lambda_0/\Delta E_{xz}$$

and

$$g_{\parallel} = 2.002 - 8k_{\parallel}^2\lambda_0/\Delta E_{xy}$$

from which orbital reduction factor k and G values were evaluated using the relation

$$G = \frac{g_{\parallel} - 2.002}{g_{\perp} - 2.002} = \frac{4k_{\parallel}^2\Delta E_{xy}}{k_{\perp}^2\Delta E_{xz}}.$$

The G values for the present complexes are found

Table 2. Orbital reduction factors and covalency parameters

Complex	Medium	G	$k_{\parallel}^2$	$k_{\perp}^2$	$\alpha_N^{2\prime}$	α_N^2	α_{Cu}^2	β_1^2	β^2	ΔE_{xy} ($\times 10^3$ cm^{-1})	ΔE_{xz}
[Cu(Me-big)$_2$]	Ni^{II} complex	2.93	0.52	0.82	0.36	0.72	0.81	0.72	1.14	20.41	23.40
[Cu(Me-bigH)$_2$]Cl$_2$	Ni^{II} complex	3.35	0.55	0.76	0.35	0.73	0.82	0.76	1.05	20.41	23.40
	Water				0.36	0.72		0.73	1.00	20.41	23.40
[Cu(Et-big)$_2$]	Ni^{II} complex	3.10	0.54	0.83	0.36	0.72	0.82	0.75	1.16	20.41	23.40
[Cu(Et-bigH)$_2$]Cl$_2$	Ni^{II} complex	3.14	0.56	0.82	0.36	0.72	0.81	0.77	1.14	20.41	23.40
[Cu(Me$_2$-big)$_2$]	Ni^{II} complex	3.27	0.56	0.78	0.37	0.72	0.82	0.77	1.08	20.41	23.40
[Cu(Me$_2$-bigH)$_2$]Cl$_2$	Ni^{II} complex	2.96	0.51	0.79	0.36	0.72	0.81	0.71	1.10	20.41	23.40
[Cu(Et$_2$-big)$_2$]	Ni^{II} complex	2.92	0.53	0.83	0.36	0.72	0.80	0.74	1.15	20.41	23.40
[Cu(Et$_2$-bigH)$_2$]Cl$_2$	Ni^{II} complex	3.21	0.51	0.73	0.37	0.72	0.85	0.71	1.014	20.41	23.40
[Cu(big)$_2$]	Ni^{II} complex	2.78			0.36	0.68		0.76	1.25	20.41	23.40
[Cu(β-phthalocyanino)]	Free ligand	3.69			0.35	0.69		0.79	0.99	20.41	23.40
[Cu(pyridine)$_4$](NO$_3$)$_2$	Pt^{II} complex				0.27	0.77		0.86	0.70	18.70	18.70
[Cu(AMU)$_2$]	Ni^{II} complex	3.26	0.50	0.71	0.35	0.69	0.81	0.70	1.05	20.41	23.53

to be less than 4 ($G = 2.92$–3.35) as expected for a non-ionic compound, which means the ligands under study are strong field in nature. The reported G values of tetraphenylporphine copper(II) and phthalocyanine copper(II) are 2.77 and 3.69, respectively.[26,27]

The in-plane and out-of-plane metal π-bonding coefficients β_1 and β are obtained from the expressions:[28,30]

$$\alpha^2\beta^2 \cong (g_{\perp} - 2.002)\Delta E_{xz}/1656\,\text{cm}^{-1}$$

$$\alpha^2\beta_1^2 \cong (g - 2.002)\Delta E_{xy}/6624\,\text{cm}^{-1}.$$

The uncertainty involved in the assignment of ΔE_{xz} and $g_{\perp}$ as obtained from polycrystalline samples[10,13] usually precludes a reliable estimate of the out-of-plane π-bonding parameter β^2. However, in cases where ΔE_{xz} are not known accurately, a 20% error in ΔE_{xz} values causes only about a 5% error in β.[22] Likewise, $\beta^2 = 1$ indicates total ionic character and $\beta^2 = 0.5$ a total covalent character of the in-plane π-bonding.[22] For the present complexes, $\beta^2 = 0.71$–0.77, indicating a pronounced covalent character.

Acknowledgements—The author is grateful to Prof. G. Ponticelli, Istituto Chimico Policattedra, Universita di Cagliari, Italy, for his help in recording the ESR spectra of some compounds and to Prof. G. B. Kauffman, Department of Chemistry, California State University, U.S.A., for facilities.

REFERENCES

1. P. Rây, *Chem. Rev.* 1961, **61**, 313.
2. N. R. Kunchur and M. Mathew, *J. Chem. Soc., Chem. Commun.* 1966, 86.
3. M. Mathew and N. R. Kunchur, *Acta Cryst.* 1970, **B26**, 2054.
4. D. Sen, *J. Chem. Soc. A* 1969, 2900.
5. T. C. Creitz, R. Gsell and D. L. Wamper, *J. Chem. Soc., Chem. Commun.* 1969, 1371.
6. J. R. Wasson and P. Zacharopoulos, *J. Inorg. Nucl. Chem.* 1969, **31**, 3881.
7. W. Schneider and P. Baccini, *Helv. Chem. Acta* 1969, **52**, 1955.
8. P. Spacu, C. Gheorghiu, O. Constantinescu and I. Pascaru, *Z. Physik Chem.* 1969, **65**, 249.
9. A. Syamal, *J. Indian Chem. Soc.* 1987, **64**, 719.
10. T. Vanngard and R. Aasa, *Proc. 1st Int. Conf. Paramag. Res.* (Edited by W. Low), Vol. 2, p. 509. Jerusalem, 1962. Academic Press, New York (1963).
11. G. F. Kokoszka and G. Gordon, *Techniques of Inorganic Chemistry* (Edited by H. B. Jonassen and A. Weissberger), p. 151. Interscience, New York (1968).
12. D. J. MacDonald, *Inorg. Chem.* 1967, **6**, 2269.
13. J. R. Wasson and C. Trapp, *J. Phys. Chem.* 1969, **73**, 3763.
14. A. Chakraborty and S. Basu, *J. Inorg. Nucl. Chem.* 1961, **17**, 55.
15. M. M. Ray and P. Rây, *J. Indian Chem. Soc.* 1959, **36**, 849.
16. K. Sone and S. Utsuno, *Bull. Chem. Soc. Japan* 1966, **39**, 1813.
17. R. L. Dutta, B. Sur and N. R. Sen Gupta, *J. Indian Chem. Soc.* 1960, **37**, 573.
18. M. Goodgame and L. I. B. Haines, *J. Chem. Soc. A* 1966, 174.
19. K. W. H. Stevens, *Proc. R. Soc. Lond.* 1953, **A219**, 542.
20. J. Owen, *Discuss Faraday Soc.* 1955, **19**, 127.
21. M. Tinkham, *Proc. R. Soc. Lond.* 1956, **A236**, 549.
22. D. Kivelson and R. Nieman, *J. Chem. Phys.* 1961, **35**, 149.
23. F. A. Cotton and J. J. Wise, *Inorg. Chem.* 1967, **6**, 915.

24. A. A. Abraham and M. H. L. Pryce, *Proc. R. Soc. Lond.* 1951, **A205**, 135.
25. E. Konig, *Physical Methods in Advanced Inorganic Chemistry* (Edited By H. A. O. Hill and P. Day), Chap. 7, p. 266. Wiley Interscience, New York (1968).
26. S. E. Harrison and J. M. Assour, *J. Chem. Phys.* 1964, **40**, 365.
27. J. Assour, *J. Chem. Phys.* 1965, **43**, 2477.
28. C. J. Ballhausen, *Introduction to Ligand Field Theory*. McGraw–Hill, New York (1962).
29. I. M. Proctor, B. J. Hathaway and P. Nicholls, *J. Chem. Soc. A* 1968, 1678.
30. D. E. Billing, B. J. Hathaway and P. Nicholls, *J. Chem. Soc. A* 1969, 316.

Polyhedron Vol. 8, No. 1, pp. 13–15, 1989
Printed in Great Britain

0277–5387/89 $3.00+.00
© 1988 Pergamon Press plc

METAL VAPOUR SYNTHESIS OF ZERO-VALENT NICKEL PHOSPHINE COMPLEXES AND THEIR CHARACTERIZATION BY ^{31}P NMR SPECTROSCOPY

KEITH J. FISHER and ELMER C. ALYEA*

Guelph-Waterloo Centre for Graduate Work in Chemistry, Guelph Campus, Department of Chemistry and Biochemistry, Guelph, Ontario, Canada N1G 2W1

(*Received* 3 *May* 1988; *accepted* 21 *June* 1988)

Abstract—A series of $Ni[P(p\text{-}X\text{—}C_6H_4)_3]_4$ complexes has been synthesized by the cocondensation of Ni atoms with various solvents at 77 K, followed by warm-up to room temperature in the presence of the excess *para*-substituted triphenylphosphine. The complexes show a linear correlation between the coordination chemical shift, $\Delta\delta(^{31}P)$, and both the pK_a of the phosphine ligands and the Hammett sigma function of the *para*-substituent. The ditertiary phosphine complexes $Ni(Ph_2P(CH_2)_nPPh_2)_2$ ($n = 1$–4), also prepared by metal vapour synthesis, display the expected ^{31}P chemical shift "chelate ring" effect for the $n = 2$ case.

Zero-valent nickel complexes of phosphines and phosphites have been extensively studied.[1,2] General syntheses utilize displacement of an organic ligand such as cyclopentadiene or cyclooctadiene from its nickel complex or reduction of a nickel(II) complex with $NaBH_4$, AlR_3, Zn dust or excess ligand; however, the metal vapour technique has been employed for a few $Ni(PR_3)_4$ complexes.[3] The importance of steric effects in determining the exchange equilibria among phosphorus ligands in these complexes as well as the ease of substitution of CO from $Ni(CO)_4$ led Tolman to the cone angle concept for describing the bulk of phosphorus donor ligands.[4–6] Tolman observed that electronic effects strongly influenced the rate constants for ligand dissociation from $Ni(PR_3)_4$.[5]

In initiating metal vapour synthesis (MVS) in our laboratory, we have explored the experimental conditions for the formation of zero-valent nickel–phosphine complexes. Particular interest was focussed on *para*-substituted triarylphosphines to allow a correlation of ^{31}P chemical shifts for the $Ni[P(p\text{-}X\text{—}C_6H_4)_3]_4$ complexes with parameters that reflect the electronic effects of the *para*-substituent.

*Author to whom correspondence should be addressed.

EXPERIMENTAL

A Torrovap MVS system was employed to cocondense nickel atoms with various solvents. Typically, *ca* 0.4 g of Ni were evaporated using the electron gun source and a pressure of less than 10^{-5} torr, with about 100 cm^3 of the solvent being codeposited on the inner wall of the 5 dm^3 rotating flask, which was immersed in a liquid dinitrogen bath. Following the cocondensation, normally requiring about 2 h, the reaction flask was allowed to warm until the matrix melted. The solvated metal solution was syphoned into a receiving flask held at 77 K. The flask was filled with dinitrogen and removed from the MVS system. All or portions of these solutions of solvated nickel atoms were reacted with excess phosphine ligands at various temperatures (see text) to produce the nickel(0) phosphine complexes.

All solvents were dried using standard procedures and degassed before use by freeze–pump–thaw cycles. Dinitrogen was dried and deoxygenated by passage over heated BTS catalyst. Samples for NMR spectral measurements were sealed in 10 mm tubes due to the dioxygen sensitivity of some of the complexes. ^{31}P NMR spectra were recorded at ambient temperature on a Bruker WH-400 spectrometer in the FT mode using 85% H_3PO_4 as external standard.

RESULTS AND DISCUSSION

As briefly mentioned in early MVS reports, $Ni(PR_3)_4$ complexes are readily prepared by cocondensing nickel atoms with various solvents at 77 K and adding excess phosphine ligands. Allowing for the loss of approximately 40% of the evaporated Ni atom that deposits on the electron focussing shield, conversion of solvated Ni atoms to $Ni(PR_3)_4$ is essentially quantitative if the phosphine ligands are added at or only slightly above 77 K. Suitable solvents used in our experiments included toluene, toluene/10% dimethoxyethane, acetone, methylcyclohexane and methylcyclohexane/20% dimethoxyethane. Of these solutions, only that of toluene/10% dimethoxyethane still showed the production of a small amount of $Ni(PR_3)_4$ when warmed to 253 K before addition of the phosphine ligand. Klabunde and coworkers[7] have shown earlier that toluene solutions of Ni atoms decompose to Ni metal if allowed to warm above 193 K. We observe that if Ni atoms are cocondensed with toluene containing norbornadiene the resultant brown, clear solution appears stable at room temperature, and reacts with dppe to give $Ni(dppe)_2$. The red solution obtained by codepositing Ni atoms with methylcyclohexane containing indene at 77 K is also stable at room temperature and does not react with PPh_3 or dppe. The nature of the solution species, probably $Ni(indene)_2$, is under further investigation. Similarly, we note that the dark brown solution obtained by evaporating Ni atoms into an acetone solution containing acetylacetone is stable at room temperature. Reaction of this solution occurs with both PPh_3 and dppe to give paramagnetic species of yet unknown structure; in the presence of dioxygen rather than phosphine, $Ni(acac)_2$ is isolated in 86% yield.

^{31}P NMR spectral data for the six $Ni[P(p\text{-}X\text{—}C_6H_5)_3]_4$ complexes prepared in this study by MVS are compiled in Table 1. Only $Ni[P(C_6H_5)_3]_4$ was studied previously, with Tolman[4] reporting that no detectable ^{31}P resonance was observed for a saturated solution of the complex in toluene, even with excess $P(C_6H_5)_3$ being added. This type of behaviour, with fast exchange and extensive dissociation according to the equation

$$NiL_4 \rightleftharpoons NiL_3 + L \qquad (1)$$

was later contrasted with that exhibited by other nickel(0) phosphine and phosphite complexes.[5] Our data, obtained in toluene solutions in the presence of excess phosphine, indicates that $Ni[P(C_6H_5)_3]_4$ shows an extreme in this type of behaviour. All of the other substituted phenylphosphine complexes give readily detected ^{31}P resonances even in the presence of only a slight excess of the phosphine.

A plot of the coordination chemical shift $\Delta\delta(\delta NiL_4 - \delta L)$ with the basicity of the phosphine, given by pK_a, is shown in Fig. 1 for the six com-

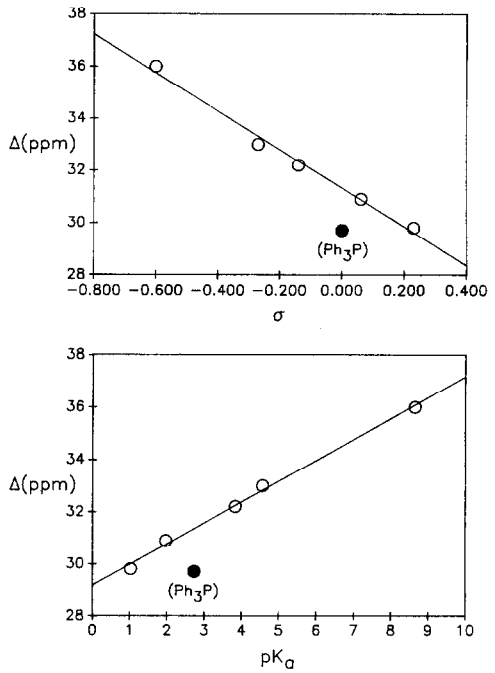

Fig. 1. Correlations of ^{31}P data with pK_a and σ_p for substituted triphenylphosphine nickel(0) complexes.

Table 1. ^{31}P NMR data of $Ni(PR_3)_4$ compounds (NiL_4)

L	pK_a	σ_p	$\delta^{31}P^a$	$\delta^{31}P(NiL_4)^a$	$\Delta\delta$
$(C_6H_5)_3P$	2.73	0.0	−4.2	25.5	29.7
$(p\text{-}ClC_6H_4)_3P$	1.03	0.23	−7.3	22.5	29.8
$(p\text{-}FC_6H_4)_3P$	1.97	0.06	−8.3	22.6	30.9
$(p\text{-}MeC_6H_4)_2P$	3.84	−0.14	−7.0	25.2	32.2
$(p\text{-}MeOC_6H_4)_3P$	4.57	−0.27	−8.7	24.3	33.0
$(p\text{-}Me_2NC_6H_4)_3P$	8.65	−0.60	−10.6	25.4	36.0

[a] Solvent, toluene.

Table 2. ^{31}P NMR data of NiL_2 compounds (L = diphosphine)

L	$\delta^{31}P$ (Free ligand)[a]	$\delta^{31}P$ (NiL_2)[a]	$\Delta\delta$
$(Ph_2P)_2CH_2$, dppm	−21.4	5.6	27.0
$(Ph_2P)_2C_2H_4$, dppe	−12.3	44.7	67.0
$(Ph_2P)_2C_3H_6$, dppp	−17.2	12.7	29.9
$(Ph_2P)_2C_4H_8$, dppb	−15.8	17.7	33.5
$Ni(PMePh_2)_4$[b]	−26.2	4.7	30.9

[a] Solvent, toluene.

[b] Literature values are −27.9, +2.9 and +30.8, respectively.[5]

plexes; also shown is a plot of $\Delta\delta$ with the Hammett sigma function of the *para*-substituent on the phenyl group. Since the triarylphosphines are sterically similar ($\theta = 145°$),[6] the two correlations were expected to demonstrate the differing electronic properties of the ligands. As expected, a good correlation was found between increased $\Delta\delta$, i.e. more deshielding of P, and the increased basicity of the triarylphosphine. The departure of the data for $Ni[P(C_6H_5)_3]_4$ from the correlation is attributed to the greater rate of exchange and degree of dissociation, which would lead to a smaller $\Delta\delta$ due to an averaging of ^{31}P signals. The apparent lower dissociation for the $[p\text{-X—}C_6H_5)_3P$ (X = Cl, F) complexes is noteworthy and may be indicative of enhanced d_π–d_π Ni—P back-donation due to the electronegative substituents. Regardless of this possibility, what is nevertheless clear from our ^{31}P NMR data is that the chemical shifts observed for this series of $Ni[P(p\text{-X—}C_6H_5)_3]_4$ complexes directly reflect the σ-bonding ability of the substituted triarylphosphine ligands.

^{31}P NMR spectral data for the four $Ni[Ph_2P(CH_2)_nPPh_2]_2$ (n = 1–4) complexes prepared in this MVS study are given in Table 2. The $\Delta\delta$ values are near 30 ppm for three of the complexes (n = 1, 3 and 4), i.e. similar to those found for the $Ni[P(p\text{-X—}C_6H_5)_3]_4$ complexes as well as the closer analogue, $Ni(PMePh_2)_4$. The $Ni(dppe)_2$ complex, however, shows the expected anomalous behaviour well documented for ditertiary phosphine complexes having five-membered chelate rings.[8] The ring contribution in this case, by comparison to the chemical shift value for $Ni(PMePh_2)_4$, the closest monodentate analogue, is 36 ppm.

Acknowledgements—K.J.F. thanks the University of Khartoum, Sudan for a research leave. E.C.A. thanks NSERC of Canada for an operating grant and support of the Southwestern Ontario NMR Centre. Purchase of the Torrovap system was made possible by a BILD grant from the Province of Ontario and an award from the President's Special Fund of the University of Guelph.

REFERENCES

1. L. Malatesta and S. Cenini, *Zero-valent Compounds of Metals*. Academic Press, New York (1974).
2. C. A. McAuliffe and W. Levason, *Phosphine, Arsine and Stibine Complexes of the Transition Elements*. Elsevier, New York (1979).
3. I. R. Blackborow and D. Young, *Metal Vapour Synthesis in Organometallic Chemistry*. Springer, Berlin (1979).
4. C. A. Tolman, *J. Am. Chem. Soc.* 1970, **92**, 2956.
5. C. A. Tolman, W. C. Seidle and L. W. Gosser, *J. Am. Chem. Soc.* 1974, **96**, 53.
6. C. A. Tolman, *Chem. Rev.* 1977, **77**, 313.
7. K. J. Klabunde, H. F. Efner, T. O. Murdock and R. Roppel, *J. Am. Chem. Soc.* 1976, **98**, 1021.
8. P. Garrou, *Chem. Rev.* 1981, **81**, 229.

Polyhedron Vol. 8, No. 1, pp. 17–20, 1989
Printed in Great Britain

0277–5387/89 $3.00+.00
© 1988 Pergamon Press plc

SYNTHESIS AND AIR STABILITY OF MIXED LIGAND LANTHANIDE ORGANOMETALLICS INVOLVING BOTH INDENYL AND CYCLOPENTADIENYL LIGANDS

ZHOU ZHENNAN,* WU ZHONGZHI, DU BAOHU and YE ZHONGWEN

Institute of Organic Chemistry, Anhui Normal University, Wuhu, China

(*Received* 3 *May* 1988; *accepted* 21 *June* 1988)

Abstract—By the reaction of Cp_2LnCl (Cp = C_5H_5; Ln = Sm, Dy, Ho, Er, Yb) with IndNa (Ind = C_9H_7), five new organolanthanides containing Cp and Ind groups have been synthesized. Comparing their air stability by exposure to air, we found these complexes were more stable in air than the corresponding Cp_3Ln, and their relative stability increased with a decrease of the metal ionic radii. All the complexes were characterized on the basis of their analytical and spectral data.

Tricyclopentadienyl and triindenyl organolanthanides have been presented previously in the literature,[1,2] but literature involving both cyclopentadienyl (Cp) and indenyl (Ind) mixed ligand organolanthanides have not been reported as yet. In this paper, we report the synthesis of five new mixed ligand organolanthanides by the following equation:

$$Cp_2LnCl + IndNa \xrightarrow[RT]{THF} Cp_2Ln(Ind)(THF) + NaCl$$

$$Ln = Sm^{I}, Dy^{II}, Ho^{III}, Er^{IV}, Yb^{V}.$$

These new complexes were characterized by elemental analysis (Table 1), IR (Table 2) and mass spectroscopy (Table 3), and their air stability was compared as follows.

RESULTS AND DISCUSSION

By the reaction of Cp_2LnCl (Ln = Sm, Dy, Ho, Er, Yb) with IndNa in THF at room temperature, five new organolanthanides have been synthesized. Elemental analysis data (Table 1) on all complexes were consistent with the formulation $Cp_2Ln(Ind)(THF)$. These complexes contained one solvated THF molecule which could not be removed under vacuum at room temperature. All the complexes were soluble in THF and ether but were only sparingly soluble in benzene, *n*-hexane and other hydrocarbon solvents.

Complexes I–V were characterized by IR and MS spectroscopy. All complexes in Table 2 exhibited a characteristic absorption of the aromatic C—H vibrations of C_5 and C_6 rings at 3000–3100 cm^{-1} and 700–850 cm^{-1}. In addition, an aliphatic C—H stretching vibration was observed between 2800 and 3000 cm^{-1}. This indicated the presence of a σ-metal-to-carbon bonding in all complexes.[3–5] In the mass spectra (see Table 3), the molecular ion peaks and main resulting ion fragment peaks were all shown. Based on the above results, we could clearly demonstrate that the five new mixed ligand organolanthanides were positively obtained. Since the metal–indenyl complexes[6–9] showed a remarkable similarity in structure to their cyclopentadienyl homologues, the structure of complexes I–V could not yet be elucidated from IR and MS.

Almost all the organolanthanides were sensitive to air and moisture. The coordinated unsaturation of the lanthanide complexes may be one of the important factors for their instability. Recently, the method of using bulky ligands to decrease the coordinated unsaturation of the organolanthanides has become favourable for the stabilization of lanthanide–carbon bonds.[10–12] The synthesis of the five new complexes reported in this paper could actually be regarded as substituting one Ind group for one Cp group of Cp_3Ln. Since the steric volume of the Ind group was bigger than the Cp group, the coordinated unsaturation of the new complexes decreased; the mixed ligand complexes should be

*Author to whom correspondence should be addressed.

Table 1. Analytical and other physical data for complexes I–V

Complex		Colour	M.p. (°C)[a]	Yield (%)	Elemental analysis[b] %Ln	%C	%H
$Cp_2Sm(Ind)(THF)$	(I)	Yellow–orange	115	80	32.2 (32.6)	59.1 (58.8)	5.4 (5.5)
$Cp_2Dy(Ind)(THF)$	(II)	Pale yellow	112	45	33.9 (34.3)	57.6 (57.5)	5.3 (5.2)
$Cp_2Ho(Ind)(THF)$	(III)	Yellow	126	50	34.2 (34.5)	57.3 (57.2)	5.2 (5.4)
$Cp_2Er(Ind)(THF)$	(IV)	Pink	125	55	34.5 (34.4)	57.0 (56.8)	5.2 (5.3)
$Cp_2Yb(Ind)(THF)$	(V)	Deep green	200[c]	30	35.3 (35.2)	56.3 (56.1)	5.1 (5.5)

[a] Melting points were determined in sealed argon-filled capillaries.
[b] Elemental analysis results were obtained on a Yanaco-MT-2 analyser. The elemental analysis data for Ln were obtained by a published method.[3] Found values are given in parentheses.
[c] Decomposition temperature.

more stable than their corresponding homogeneous ligand complexes (Cp_3Ln).

In order to compare the stability of Cp_3Ln and Cp_2LnInd, five known complexes of Cp_3Ln (THF) of an identical metal were also synthesized according to the literature method.[1] The two different kinds of complexes (mixed and homogeneous) were exposed to air (temperature = 20°C, relative humidity = 78%). When their colour changed or major characteristic absorption peaks in the IR disappeared, it was considered an indication of the decomposition of the complexes. The exposure time recorded for the complexes to decompose was specified as a criterion for their relative stability.

We found that the order of their relative stability was

(i) $Cp_2LnInd > Cp_3Ln$,
(ii) $Cp_2YbInd > Cp_2ErInd > Cp_2HoInd > Cp_2DyInd > Cp_2SmInd$.

From the above order, it was obvious that:

(i) by replacing one Cp group from Cp_3Ln with an Ind group, the new complexes would be more stable.

Table 2. IR spectral data[a] for complexes I–V (4000–200 cm^{-1})

Complex		Main absorptions (cm^{-1})
$Cp_2Sm(Ind)(THF)$	(I)	3085(w), 3062(m), 2923(m), 2853(m), 1605(m), 1485(m), 1453(m), 1393(m), 1320(m), 1220(w), 1045(m), 1011(s), 914(m), 840(m), 770(s), 740(s), 720(s), 255(w).
$Cp_2Dy(Ind)(THF)$	(II)	3090(w), 3068(m), 2921(m), 2853(m), 1602(m), 1485(m), 1445(s), 1395(m), 1320(m), 1218(w), 1054(w), 1011(s), 914(m), 840(m), 780(s), 767(s), 720(s), 249(w).
$Cp_2Ho(Ind)(THF)$	(III)	3080(w), 3065(m), 2923(m), 2852(m), 1605(m), 1480(m), 1445(s), 1395(m), 1320(m), 1217(w), 1054(w), 1010(s), 914(m), 838(m), 780(s), 765(s), 718(s), 242(w).
$Cp_2Er(Ind)(THF)$	(IV)	3085(w), 3060(m), 2920(m), 2853(m), 1602(m), 1485(m), 1446(s), 1393(m), 1321(s), 1217(m), 1053(w), 1011(s), 914(m), 840(m), 780(s), 767(s), 718(s), 240(w).
$Cp_2Yb(Ind)(THF)$	(V)	3080(w), 3065(m), 2925(m), 2853(m), 1605(m), 1480(m), 1445(s), 1390(m), 1300(m), 1210(w), 1055(w), 1011(s), 914(m), 845(m), 777(s), 765(s), 724(s), 250(w).

[a] The IR spectra were recorded on a Perkin–Elmer 983(G) spectrometer as Nujol or fluorocarbon oil mulls.

Table 3. Mass spectra data[a] for complexes I–V

Complex		Main peaks (m/e)[b]
M=Cp_2Sm(Ind)(THF)	(I)	397(M—THF), 332(M—Cp—THF), 282(M—Ind—THF), 267(M—2Cp—THF), 152(Sm), 115(Ind), 72(THF), 65(Cp)
M=Cp_2Dy(Ind)(THF)	(II)	409(M—THF), 344(M—Cp—THF), 294(M—Ind—THF), 279(M—2Cp—THF), 164(Dy), 115(Ind), 72(THF), 65(Cp)
M=Cp_2Ho(Ind)(THF)	(III)	410(M—THF), 345(M—Cp—THF), 295(M—Ind—THF), 280(M—2Cp—THF), 165(Ho), 115(Ind), 72(THF), 65(Cp)
M=Cp_2Er(Ind)(THF)	(IV)	411(M—THF), 346(M—Cp—THF), 296(M—Ind—THF), 281(M—2Cp—THF), 166(Er), 115(Ind), 72(THF), 65(Cp)
M=Cp_2Yb(Ind)(THF)	(V)	419(M—THF), 354(M—Cp—THF), 304(M—Ind—THF), 289(M—2Cp—THF), 174(Yb), 115(Ind), 72(THF), 65(Cp)

[a] MS spectra were recorded on VG ZAB-HS mass spectrometer.
[b] MS data are given for the isotopes ^{152}Sm, ^{164}Dy, ^{165}Ho, ^{166}Er, ^{174}Yb, the peak patterns correspond to theoretical values based on the natural abundance of isotopes.

(ii) The air stability of these new complexes increased with decrease of the metal ionic radii. These results agreed well with our previous report.[13]

Based on the above conclusions, the method of using steric bulky ligands to stabilize the coordinated unsaturation complexes was usually successful.

EXPERIMENTAL

All operations were performed in an atmosphere of prepurified argon using Schlenk techniques or in a glove-box. All solvents were refluxed and distilled over blue sodium benzophenone or finely divided $LiAlH_4$ under argon immediately prior to use. The reactants, Cp_2LnCl[14] and IndNa,[2] were prepared according to the literature methods. Indene was distilled in a commercial reagent and the 182°C distillate was collected.

General method of the synthesis of complexes I–V

A 60 cm^3 THF solution of 3 mmol of Cp_2LnCl was placed in a Schlenk flask and an equivalent amount of sodium indenide was added. The reaction mixture was allowed to stir at room temperature for 24 h. After the NaCl was removed from the reaction mixture by centrifugation, the resulting solution was concentrated *in vacuo* to about 20 cm^3. By addition of 50 cm^3 of *n*-hexane, a solid precipitated out which was recrystallized twice from THF/*n*-hexane and was dried *in vacuo* to obtain the product.

Yields, analyses and physical properties of all five complexes are listed in Table 1.

Acknowledgements—We wish to acknowledge Prof. Wang Xiuran and Mr Wang Shaov, who assisted with this research.

REFERENCES

1. G. Wilkinson and J. M. Birmingham, *J. Am. Chem. Soc.* 1956, **78**, 42.
2. M. Tsutsui and H. J. Gysling, *J. Am. Chem. Soc.* 1969, **91**, 3175.
3. C. T. Qian, C. Q. Ye, H. Z. Lu, Y. Q. Li and J. L. Zhou, *J. Organomet. Chem.* 1983, **247**, 161.
4. E. Samuel and M. Bigorgne, *J. Organomet. Chem.* 1969, **19**, 9.
5. H. P. Fritz, F. H. Kohler and K. E. Schwarzhans, *J. Organomet. Chem.* 1969, **19**, 4.
6. E. O. Fischer and D. Seus, *Z. Naturforsch. B.* 1954, **9**, 386.
7. E. O. Fischer and D. Seus, *Z. Naturforsch. B.* 1953, **8**, 694.
8. E. Samuel and R. Settm, *J. Organomet. Chem.* 1965, **4**, 156.
9. E. Samuel, *Bull. Soc. Chem. Fr.* 1966, **11**, 3548.
10. A. L. Wayda and W. J. Evans, *Inorg. Chem.* 1980, **19**, 2190.

11. T. D. Tilley and R. A. Anderson, *Inorg. Chem.* 1981, **20**, 3267.
12. M. Tsutsui, L. B. Chen, D. E. Bergbreiter and T. K. Miyamoto, *J. Am. Chem. Soc.* 1982, **104**, 855.
13. Z. W. Ye, Z. N. Zhou, Z. Y. Lou, X. R. Wang and F. R. Shen, *Sinica. Chim. Acta.* 1986, **44**, 707.
14. R. E. Maginn, S. Manastryrskyj and M. Dubeck, *J. Am. Chem. Soc.* 1963, **85**, 672.

Polyhedron Vol. 8, No. 1, pp. 21–24, 1989
Printed in Great Britain

0277–5387/89 $3.00+.00
© 1988 Pergamon Press plc

SOME LANTHANIDE CHLORIDE COMPLEXES OF PYRIDINALDAZINE AND PYRROLALDAZINE SCHIFF BASES*

MAHMOUD M. DAWOD, FAWWAZ I. KHALILI and AFIF M. SEYAM†

Department of Chemistry, University of Jordan, Amman, Jordan

(*Received* 3 *May* 1988; *accepted* 21 *June* 1988)

Abstract—Lanthanide chloride complexes with pyridinaldazine (PAA) and pyrrolaldazine (PyAA-H_2): $[Ln(L)Cl_2(H_2O)_n]Cl \cdot mH_2O$, where Ln = Ce, Nd, Sm, Yb; L = PAA, PyAA-H_2; $n = 2, 4$; $m = 0, 1, 2, 3.5$, have been prepared by the reaction of the corresponding lanthanide chloride with PAA or PyAA-H_2 ($YbCl_3 \cdot 6H_2O$ with PyAA-H_2 gave the 2:1 complex, $[Yb_2(PyAA)Cl_4(H_2O)_4] \cdot 2H_2O$) and characterized by spectral data, electrical conductance, magnetic susceptibility, thermal and elemental analysis.

A variety of Schiff base complexes with trivalent lanthanides have been reported over the last few years.[1] Pyridinaldazine (PAA) has been shown to produce metal complexes with a variety of different stoichiometries.[2,3] While there is some information about transition metal complexes with PAA and PMK (2-pyridylmethylketazine),[3,4] little is known about lanthanide complexes with the PMK ligand.[5] In this paper we wish to report the synthesis and characterization of some lanthanide chloride complexes of PAA and PyAA-H_2.

EXPERIMENTAL

Physical and analytical measurements

Proton magnetic resonance (^{1}H NMR) spectra were recorded on a Varian T-60A spectrometer in methanol-d_4. Chemical shifts are reported relative to internal $Si(CH_3)_4$. IR spectra were recorded on a Perkin–Elmer (577) spectrometer as KBr discs or Nujol mulls pressed between two NaCl discs or two polyethylene sheets. Conductivity measurements were carried out using a 10^{-3} M solution in methanol on a Philips PW 9509 digital conductivity meter at 25°C. Magnetic susceptibility measurements were carried out using Evans' method[6] with methanol as a solvent. Diamagnetic corrections for the ligands were calculated using Pascal's constants. UV–vis. spectra were recorded on a Beckman Du-7 spectrophotometer. Thermogravimetric analyses (TGA) were recorded on a Mettler TG 10A TA processor using a Mettler TG-50 thermobalance. Microanalyses were performed by Dr Franz Pascher from the Ellen Pascher Microanalysis laboratory, Bonn, F.R.G. Metal analyses were determined by titration with EDTA[7] after decomposition of the sample with HNO_3. The titration method was confirmed by analyses of the metals as the corresponding oxide. Chloride was determined gravimetrically as AgCl.[8]

Materials and methods

All synthetic procedures were performed under a dinitrogen atmosphere in Schlenk-type glassware using normal benchtop Schlenk techniques,[9] or in a dinitrogen filled glove-box. Acetone (previously distilled over $CaCO_3$), diethyl ether, tetrahydrofuran (previously distilled from Na/K benzophenone), methanol (previously distilled over Mg) were used. Commercially obtained pyridine-2-carboxyaldehyde (Fluka) was purified as in the literature,[10] pyrrole-2-carboxyaldehyde (BDH) was purified by stirring over active carbon in methanol; $CeCl_3 \cdot 6H_2O$, $NdCl_3 \cdot 6H_2O$, $SmCl_3 \cdot 6H_2O$ (Fluka), $YbCl_3 \cdot 6H_2O$ (K & K) were used without further purification. The ligands PAA and PyAA-H_2 were prepared according to Stratton's method.[2]

The complexes were prepared by the following general procedure using the appropriate stoichiometries for the ligand and the metal salt.

* This paper is part of the MSc thesis of M. M. Dawod.
†Author to whom correspondence should be addressed.

Table 1. Yields, analytical, magnetic and TGA data for the lanthanide complexes

Complex/Colour	Dec.P. (°C) (Yield %)	Calculated/Found (%) C	H	N	Cl	M	μ_{eff} (BM)	T[a] (°C)	TGA Weight lost (%)	Assignment
$[Ce(PAA)Cl_2(H_2O)_4]Cl$ (I)	240	27.3	3.4	10.6	20.1	26.5	2.55	86	1.85	—
pale yellow	(65)	27.2	3.1	10.3	19.8	26.8				
$[Nd(PAA)Cl_2(H_2O)_4]Cl \cdot 2H_2O$ (II)	200	25.3	3.9	9.8	18.7	25.4	3.75	100	5.12	$2H_2O$
greenish-yellow	(73)	25.9	3.1	9.8	18.8	25.7				
$[Sm(PAA)Cl_2(MeOH)(H_2O)_3]Cl \cdot 2H_2O$ (III)	175	26.5	4.1	9.5	18.1	25.5	1.68	108	5.99	$2H_2O$
pale yellow	(68)	26.8	4.1	9.6	18.2	25.8				
$[Yb(PAA)Cl_2(H_2O)_4]Cl \cdot 3.5H_2O$ (IV)	160	23.1	4.0	9.0	17.0	27.7	4.35	145	8.97	$3H_2O$
yellow	(70)	23.1	4.2	9.3	17.0	27.6				
$[Ce(PyAA\text{-}H_2)Cl_2(H_2O)_2]Cl \cdot H_2O$ (V)	210	24.7	3.3	11.5	21.9	28.8	2.71	85	3.70	H_2O
yellow	(70)	24.5	2.9	11.8	21.7	28.8				
$[Nd(PyAA\text{-}H_2)Cl_2(H_2O)_2]Cl \cdot H_2O$ (VI)	230	24.5	3.3	11.4	21.7	29.4	3.42	103	3.47	H_2O
light yellow	(70)	24.6	2.8	11.7	21.8	29.2				
$[Sm(PyAA\text{-}H_2)Cl_2(H_2O)_2]Cl$ (VII)	190	25.1	2.9	11.7	22.2	31.4	1.52	99	2.06	—
pale yellow	(60)	24.9	2.9	11.9	22.4	31.5				
$[Yb_2(PyAA)Cl_4(H_2O)_4] \cdot 2H_2O$ (VIII)	240	16.4	2.6	7.2	18.2	44.4	4.10	100	4.90	$2H_2O$
pale yellow	(65)	15.4	2.9	7.0	17.9	44.5				

[a] Starting temperature 45°C.

To a stirred solution of the metal salt (2.38 mmol) in a mixture of methanol–acetone (1 : 4), a solution of the ligand (2.38 mmol) in a mixture of methanol–diethyl ether (1 : 10) was added. The reaction mixture was stirred for 1 h in the case of PAA and overnight in the case of PyAA-H_2, to give the complex as a precipitate. The complex was filtered, recrystallized from a mixture of methanol–acetone–diethyl ether (1 : 3 : 5), washed with acetone and diethylether and dried *in vacuo* over P_4O_{10} at room temperature for three days.

RESULTS AND DISCUSSION

The new lanthanide complexes were synthesized by the reaction

$$LnCl_3 \cdot 6H_2O + L \longrightarrow [Ln(L)Cl_2(H_2O)_n]Cl \cdot mH_2O$$

where Ln = Ce, Nd, Sm, Yb; L = PAA, PyAA-H_2; n = 2,4; m = 0, 1, 2, 3.5. Work-up procedure involved filtration and crystallization; yields were generally high (60–73%). The complexes gave satisfactory analytical data (Table 1). The complexes are air-stable, hygroscopic, usually yellow coloured microcrystalline solids, soluble in methanol and ethanol, partially soluble in tetrahydrofuran and acetone, slightly soluble in diethyl ether but hydrolyzed in water. Elemental analysis show that the ratio of the metal-to-ligand in the complexes is 1 : 1 except in complex **VIII** where the ratio is 2 : 1.

Magnetic data (Table 1) indicate that these complexes have magnetic moments which are close to the theoretical values for the Ln^{3+} [11] and agree well with those for other lanthanide complexes.[12,13] They suggest that there is no metal–metal interaction or spin–spin coupling.

TGA data (Table 1) show that water of hydration is lost around 100°C and helps in assigning the number of water molecules of hydration in these complexes. Conductivity data (Table 2) show that these complexes behave as 1 : 1 electrolytes in methanol except for complex **VIII** which is a non-electrolyte.

^{1}H NMR (Table 2) of the complexes synthesized in this study show that the resonances are broad and shifted down field; this phenomenon is common in paramagnetic systems.[14] The presence of methanol in complex **III** was confirmed by ^{1}H NMR after hydrolyzing the complex in D_2O and a singlet at δ 3.3 ppm was observed which corresponds to methyl protons of methanol. Other complexes did not show any singlet corresponding to methyl protons of methanol after hydrolysis in D_2O.

UV–vis. data (Table 2) show that the electronic spectra of the complexes are dominated by ligand absorption bands with a hyperchromic effect. The domination of the ligand absorption bands could be related to the high absorption coefficient of the ligands as compared to the Ln^{3+} ions which masks any splitting of the band.[12]

IR spectroscopy is useful for probing the structure of Schiff base complexes.[3,4] IR data (Table 3) for the complexes **I**–**VII** show a distinct splitting of the C=N group stretching bands and of the ring breathing vibrational bands characteristic of the tridentate ligand. The ligand is coordinated through the nitrogens of the two rings and one nitrogen of the C=N groups. For complex **VIII**, the ring breathing region and the pyrrole N—H vibrational bands suggest that the ligand in this binuclear complex is coordinated in a tetradentate fashion as the

Table 2. Conductivity data, UV–vis. and ^{1}H NMR spectroscopy for the lanthanide complexes

Complex	Λ_m (ohm^{-1} cm^2 mol^{-1})	λ_{max} (nm) ($\varepsilon \times 10^{-4}$ dm^3 mol^{-1} cm^{-1})	^{1}H NMR (CD_3OD) δ (ppm)[a]
PAA	—	262(0.5761), 298(1.2618), 307(1.1754)	7.2–8.2(m), 8.9(s)
I	101	221(0.9047), 261(1.6888), 298(3.4681)	6.3–7.6(m), 8.7–9.6(br)
II	81	220(0.6399), 262(1.3128), 298(2.6965)	6.2–6.6(m), 7.0–7.7(br)
III	116	223(0.7750), 261(2.1873), 298(2.5171)	6.7–7.8(m), 8.8–8.9(br)
IV	109	223(0.7122), 265(1.3642), 298(2.2039)	5.3–6.7(m), 7.0–7.3(br)
PyAA-H_2	—	266(0.6827), 269(0.6781), 356(4.0766)	5.9–6.8(m), 8.2(s)
V	108	270(0.8790), 311(0.8230), 373(1.5024), 405(1.4421)	6.2–7.2(m), 7.6(s), 8.3(d), 11.6(br)
VI	101	270(1.1246), 356(2.8087), 363(2.8359)	5.7–6.7(m), 7.1(s), 7.8(d), 11.6(br)
VII	93	269(0.9118), 358(2.9785)	5.9–7.1(m), 7.4(s), 8.0(d), 11.2(br)
VIII	10	269(0.8869), 356(2.9046), 362(2.9335)	4.9–6.3(m), 6.7(s), 7.3(d)

[a] (s) singlet, (d) doublet, (m) multiplet, (br) broad.

Table 3. IR data (cm^{-1})[a]

Complex	ν(C═N)	Ring breathing	ν(N—H)	γ(N—H)	ν(N—N)	Others
PAA	1630(vs)	990(vs), 970(vs)			955(vs), 950(vs)	
I	1615(sh), 1600(vs)	1065(vs), 1020(vs)			985(w), 960(m)	420(s), 310(m), 210(w)
II	1615(s), 1600(s)	1065(s), 1020(vs)			980(sh), 960(s)	420(s), 310(m), 210(w)
III	1615(s), 1600(s)	1060(s,br), 1020(vs)			960(m,br)	415(s), 330(w), 240(m)
IV	1630(sh), 1615(s)	1060(w), 1020(s)			980(w)	415(s), 305(w), 230(w)
PyAA-H_2	1630(vs,br)	1055(sh), 1040(vs)	3230(s,br)	690(m)	970(w), 960(s)	
V	1655(vs), 1615(vs)	1055(vs), 1040(vs)	3390(m), 3320(m)	705(m)	965(s)	385(m), 315(s), 260(m), 250(m), 210(m)
VI	1655(vs), 1620(vs)	1055(vs), 1040(vs)	3390(m), 3320(m)	710(s)	965(s)	390(s), 330(vs), 260(m), 215(m)
VII	1655(vs), 1620(vs)	1055(vs), 1040(vs)	3400(m,br), 3300(m,br)	705(m)	965(vs)	400(s), 340(vs), 260(s), 215(m)
VIII	1645(vs), 1610(vs)	1050(w), 1035(vs)			960(s,br)	470(w), 360(m), 335(s), 260(vs), 230(m)

[a](s) = strong, (vs) = very strong, (m) = medium, (w) = weak, (br) = broad.

dianion, $PyAA^{2-}$. This is because of the smaller radius of Yb^{3+} in comparison to other lanthanides and the presence of a dinegative charge on $PyAA^{2-}$, that prefers a *trans, trans* configuration,[3] a dinuclear complex was formed. However, neutral PAA forms a mononuclear complex with Yb^{3+}.

Therefore, suggested formulae (Table 1), based on spectral data, electrical conductance, magnetic susceptibility, thermal and elemental analysis, show that, in complexes **I–IV**, **V–VII** and **VIII**, the coordination number is nine, seven and six, respectively, and this is expected for the lanthanides.[15]

Acknowledgement—The authors thank the University for financial help (M.M.D.).

REFERENCES

1. I. A. Kahwa, T. C.-Y. Hsieh, R. A. Laine and J. Selbin, *Inorg. Chim. Acta* 1986, **118**, 179 and refs. therein; G. Bombieri, F. Benetollo, A. Pollo, L. De Cola, D. L. Smailes and L. M. Vallarino, *Inorg. Chem.* 1986, **25**, 1127.
2. W. J. Stratton and D. H. Busch, *J. Am. Chem. Soc.* 1958, **80**, 1286.
3. C. J. O'Conner, R. J. Romananch, D. M. Robertson, E. E. Edudk and F. F. Fronczek, *Inorg. Chem.* 1983, **22**, 449; T. C. Woon, L. K. Thompson and Ph. Robichaud, *Inorg. Chim. Acta* 1984, **90**, 201.
4. W. J. Stratton and D. H. Busch, *J. Am. Chem. Soc.* 1960, **82**, 4834; W. J. Stratton, *Inorg. Chem.* 1970, **9**, 517; W. J. Stratton, M. F. Rettig and R. F. Drury, *Inorg. Chim. Acta* 1969, **3**, 97.
5. W. Radecka-Paryzek, *Inorg. Chim. Acta* 1981, **52**, 261.
6. D. F. Evans, *J. Chem. Soc.* 1959, 2003.
7. Frank J. Welcher, *The Analytical Uses of EDTA*. D. Van Nostrand, U.S.A. (1965).
8. A. I. Vogel, *Quantitative Inorganic Analysis*, 3rd Edn. Longmans, London (1961).
9. D. F. Shriver, *The Manipulation of Air-Sensitive Compounds*. McGraw-Hill, New York (1969).
10. A. I. Vogel, *Quantitative Organic Analysis*, 3rd Edn. Longmans, London (1961).
11. S. P. Sinha, *Complexes of the Rare Earths*. Pergamon Press, Oxford (1966).
12. M. Mohan, J. P. Tandon and N. S. Gupta, *J. Inorg. Nucl. Chem.* 1981, **43**, 1223.
13. G. P. Gupta and K. G. Sharma, *Russ. J. Inorg. Chem.* 1982, **27**, 49; M. Mishra, M. P. Singh and J. P. Singh, *J. Ind. Chem. Soc.* 1980, **57**, 249; D. G. Hendricker and R. J. Foster, *J. Inorg. Nucl. Chem.* 1972, **34**, 1949.
14. T. J. Marks, A. M. Seyam and J. R. Kolb, *J. Am. Chem. Soc.* 1973, **95**, 5529; P. J. Fagan, J. M. Manriquez, E. A. Maatta, A. M. Seyam and T. J. Marks, *J. Am. Chem. Soc.* 1981, **103**, 6650.
15. D. W. Harrison and J. G. Bunzli, *Inorg. Chim. Acta* 1985, **109**, 185.

Polyhedron Vol. 8, No. 1, pp. 25–28, 1989
Printed in Great Britain

0277–5387/89 $3.00+.00
© 1988 Pergamon Press plc

SYNTHESIS AND CHARACTERIZATION OF COMPLEXES OF NICKEL(II), PALLADIUM(II) AND PLATINUM(II) WITH THE NEW BIFUNCTIONAL AMINODIPHOSPHINE LIGAND $HN(CH_2CH_2CH_2PMe_2)_2$

P. G. EDWARDS* and R. G. JAOUHARI

Department of Chemistry, University College, P.O. Box 78, Cardiff CF1 1XL, U.K.

(*Received* 24 *August* 1987; *accepted after revision* 4 *July* 1988)

Abstract—The preparation of the new phosphine–amine ligand $HN(CH_2CH_2CH_2PMe_2)_2$ via radical addition of dimethylphosphine to diallylamine is described. Some simple coordination chemistry with Ni, Pd and Pt is also reported.

The investigation of functionalized phosphines and their use to construct and stabilize polynuclear transition metal compounds has undergone significant development in recent years.[1,2] The unusual combination of class A and class B donor atoms in these ligands leads to interesting structural types and reactivity of their complexes, which is potentially useful, e.g. in homogeneous catalysis.[3] Potentially terdentate linear amine phosphine compounds containing tertiary alkyl phosphine functions are rare and there are only a few previous examples of complexes of such ligands.[4] Similar ligands containing aryl phosphine donors are scarcely better studied.[5] We herein describe the straightforward and direct synthesis of the new terdentate ligand $[(CH_3)_2PCH_2CH_2CH_2]_2NH$, (PNP), from diallylamine and dimethyl phosphine and its coordination behaviour with group VIII transition metals. We report the preparation and characterization of complexes $(MCl_2PNP)_n$, where M is nickel(II), palladium(II) and platinum(II).

EXPERIMENTAL

The phosphine ligand was prepared and handled under vacuum or inert atmospheres. All solvents were degassed by nitrogen purge or freeze–thaw cycles immediately prior to use. Dimethylphosphine[6] and Zeise's dimer $[PtCl_2(C_2H_4)]_2$[7] were prepared according to literature methods, other reagents were purchased and used as obtained. NMR spectra were recorded on a Bruker WM360 instrument operating at 360.13 (^1H), 90.53 (^{13}C) and 145.80 MHz (^{31}P). IR spectra were obtained with a Perkin–Elmer 783 spectrometer, electronic spectra with a Pye Unicam Lamda 5 spectrophotometer and magnetic susceptibility measurements were on a Johnson Matthey Equipment Magnetic Susceptibility Balance. Microanalyses were obtained within this department.

Preparation of PNP

Into a nitrogen filled stainless steel autoclave (300 cm^3) was placed diallylamine (10 g, 0.103 M.), dimethylphosphine (15.7 g, 0.253 M.), α,α′-azobisisobutyronitrile (25 mg) and hexane (120 cm^3). The autoclave was sealed and held at 100°C for 20 h. The resultant solution was transferred to distillation apparatus where the solvent and unreacted volatile materials were removed under reduced pressure. The product was distilled to yield PNP, 10.5 g (48%) as a colourless liquid (b.p. 95–100°C, 0.5 mm).

Preparation of $NiCl_2$(PNP)

To a solution of $NiCl_2 \cdot 6H_2O$ (474 mg, 2 mmol) in ethanol (15 cm^3) was added PNP (442 mg, 2 mmol) with stirring. The resulting red–brown solution was stirred for a further 6 h. Ethanol was removed *in vacuo*, the residue was extracted into dichloromethane (20 cm^3), filtered and evaporated to dryness yielding a purple powder that was washed with hexane (20 cm^3) and diethylether (20 cm^3) and dried *in vacuo*. The yield was essentially quantitative.

*Author to whom correspondence should be addressed.

Preparation of [$PdCl_2$(PNP)]

To a solution of Na_2PdCl_4 (596 mg, 2 mmol) in ethanol (20 cm^3) was added PNP (442 mg, 2 mmol) with stirring. After 2 h, the yellow solution was evaporated to dryness and the yellow residue extracted into dichloromethane (20 cm^3), filtered and evaporated *in vacuo*. The yellow powder was washed with hexane (20 cm^3), diethylether (20 cm^3) and dried *in vacuo*. The yield was quantitative.

Preparation of [$PtCl_2$(PNP)]

To a solution of $[PtCl_2(CH_2{=}CH_2)]_2$ (294 mg, 0.5 mmol) in dichloromethane (25 cm^3) was added PNP (221 mg, 1 mmol) and the solution stirred for 12 h. The solvent was removed *in vacuo* and the residue extracted into ethanol (20 cm^3), filtered to remove traces of unreacted starting material and evaporated to dryness. The white powder was washed with hexane (20 cm^3) and dried *in vacuo*. The yield was essentially quantitative.

RESULTS AND DISCUSSION

Ligand synthesis

The synthesis of PNP relies on the ready addition of P—H functions across C=C double bonds. There are numerous reports of P—H addition to allylic phosphines[8] such that this is an established method for the preparation of oligophosphines. Similarly allylamine has been coupled with diphenylphosphine to yield $Ph_2P(CH_2)_3NH_2$.[9] We have extended this approach to the addition of two mole equivalents of dimethylphosphine to diallylamine catalysed by AIBN. The reaction requires a significant excess of $HPMe_2$ in order to maximize formation of the desired product. If less $HPMe_2$ is used, significant proportions of the lower boiling monophosphine $Me_2PCH_2CH_2N(H)C_3H_5$ (as determined by ^1H NMR) may be isolated. Polymerization does not appear to compete with product formation at any appreciable rate when the reaction is performed in hydrocarbon solvent, since very little residue is left upon distillation of the diphosphine. The yield of the reaction compares favourably with yields reported for similar reactions.[8,9] The diphosphineamine ligand is effectively characterized by elemental analysis, Table 1, and IR and NMR spectroscopies, Table 2.

Complex formation

When PNP is added to ethanolic solutions of $NiCl_2 \cdot 6H_2O$ and Na_2PdCl_4, a dichloromethane solution of $(Cl_2PtC_2H_4)_2$ complex formation occurs and powders may be isolated in each case. Since the compounds have not been obtained crystalline, purification is by washing only. However, elemental analyses correspond well to the formula MCl_2(PNP) (M = Ni, Pd, Pt). Analytical data for the complexes are summarized in Table 1.

The conductance data indicate that the complexes behave as non-electrolytes in dichloromethane. The poor solubilities of the complexes in suitable solvents precludes the determination of molecular weights by cryoscopy.

Of interest are comparisons of the X-ray powder photographs of these complexes. The patterns for the nickel and palladium complexes are virtually identical to each other but very different to that for the platinum complex. Thus, the nickel complex appears isostructural with the palladium complex, but not with the platinum complex. Since the purple

Table 1. Analytical data and properties of PNP and their complexes

Compound	Analysis: Found (%) (Calc. (%)) C	H	N	Cl	M	μ_{eff} (BM)	Λ_M[a] (ohm^{-1} mol^{-1} cm^2)	Electronic spectra[b] λ_{max} (nm) (ε/mol^{-1} dm^3 cm^{-1})
PNP	54.2	11.3	6.3					
	(54.4)	(11.1)	(6.5)					
$NiCl_2$PNP	33.9	7.2	3.9	20.1	16.5	2.94	2.25 (5.82)	450(383)
	(34.2)	(7.1)	(4.0)	(20.2)	(16.5)			231(3707)
$PdCl_2$PNP	30.1	6.3	3.7	17.4	26.9	0.80	3.20 (28.5)	255(5280)
	(30.1)	(6.2)	(3.5)	(17.8)	(26.7)			218(4250)
$PtCl_2$PNP	22.9	4.7	2.4			0.40	1.9	335(4436)
	(22.7)	(4.6)	(2.4)					230(10131)

[a] Values of mol conductivity for 10^{-3} M solutions in CH_2Cl_2, values in parentheses were obtained in CH_3NO_2.
[b] Measured in EtOH for Pd^{II} and Ni^{II} and in CH_2Cl_2 for Pt^{II}.

Table 2. ^1H, ^{13}C, ^{31}P, NMR[a] and IR[b] data of PNP and their complexes[a]

Compound	^1H	^{13}C	^{31}P	IR (cm^{-1})
PNP	0.96, d, $J = 2.41$ Hz 12H, CH_3P; 1.31–1.45, mult., 4H, CH_2P; 1.55–1.71, mult., 4H, CH_2; 2.66, t, 4H, CH_2N.	13.01, CH_3P 25.29, CH_2P 28.85, CH_2 49.96, CH_2N	−53.57	3300, 1360, 1280, 1150, 1040, 980, 900, 860, 660
$NiCl_2PNP$				3400, 1630, 1300, 1142, 950, 920, 750, 400, 360, 300, 280
$PdCl_2PNP$	1.77, S_{br}, 12H, CH_3P 2.04–2.86, m, 8H, CH_2CH_2P; 2.86–3.14, m, 4H, CH_2N;	13.82, S_{br}, CH_3P; 20.72, CH_2P; 23.45, CH_2 49.27, CH_2N;	−14.9, S_{br}; −0.75, S_{br};	1640, 1410, 1390, 1290 1155, 1050, 930, 750, 725, 350
$PtCl_2PNP$	1.98, S_{br}, 12H, CH_3P; 2.1–2.9, m, 8H, CH_2CH_2P; 2.95–3.40, m, 4H, CH_2N;	11.35, S_{br}, CH_3P 19.70, CH_2P 21.59, CH_2, 49.92, CH_2N	−19.3, $J_{Pt-P} = 2412$ Hz −26.78, $J_{Pt-P} = 3103$ Hz	3450, 1660, 1320, 1280, 1160 1100, 1080, 940, 850, 725, 700,620, 540, 350

[a] Chemical shifts (δ ppm) relative to Me_4Si for ^1H and ^{13}C spectra and to H_3PO_4 for ^{31}P NMR spectra, solvent: $CDCl_3$ for ^1H, ^{13}C and ^{31}P NMR spectra; br = broad.

[b] IR: neat for PNP, in Nujol for Pd^{II}, Ni^{II} and Pt^{II} complexes.

nickel(II) complex is paramagnetic and a non-electrolyte in solution, a square-planar configuration at the metal is precluded. A five-coordinate structure would be consistent with the data since similar magnetic and spectral (electronic) properties have been reported previously for NP_2X_2 (X = halide) donor sets.[10] Five coordination for palladium is also precedented, although in our case conductance measurements indicate the compound to be essentially a non-electrolyte in dichloromethane but a weak electrolyte in nitromethane. Again, this behaviour has previously been reported for similar complexes[10] and may be interpreted in terms of an equilibrium between five-coordinate **1** and a square-planar cation **2** as indicated in Scheme 1.

The bonding in the Pd and Pt compounds may be inferred from a combination of $^{31}P[^1H]$, $^{13}C[^1H]$, ^1H NMR and IR spectroscopies (Table 2). Coordination of phosphorus to Pd^{II} and Pt^{II} commonly results in a downfield shift of between 10–50 ppm in the $^{31}P[^1H]$ NMR. Both the spectra display two broad singlets due to coordinated phosphorus atoms and may be due to fluxional processes involving exchange of free for coordinated phosphorus and/or displacement of nitrogen by free phosphorus as indicated in Scheme 1. The platinum complex is presumably square-planar. The intermediate values of conductance in nitromethane again indicate a possible equilibrium between structures **3** or possibly **4** and the cation **2** as shown in Scheme 1. The two resonances in the ^{31}P NMR spectrum of this compound are presumably indicative of a slow exchange (on the NMR timescale) between two of the proposed structures, most likely **2** and **3** since no resonance due to an uncoordinated phosphine is observed.

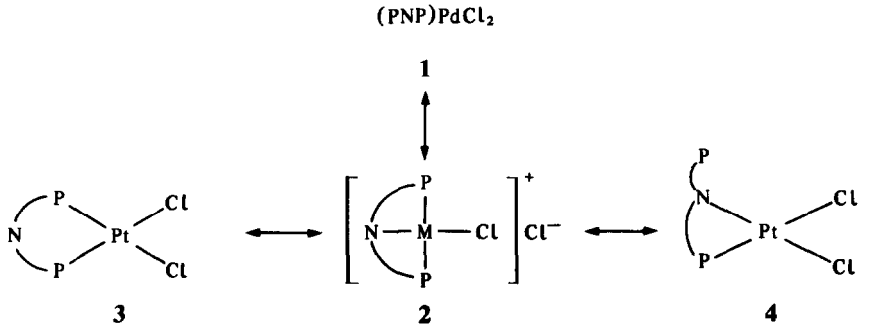

Scheme 1. Possible structures and solution behaviour for the palladium and platinum complexes. In **2**, M = Pd, Pt. $\frown$ = $-(CH_2)_3-$.

Acknowledgements—Support from the S.E.R.C. is gratefully acknowledged, as is Dr B. Delf of the Department of Physics, UCC for help in obtaining the X-ray powder diffraction pictures.

REFERENCES

1. P. Braunstein, D. Matt, Y. Dusausoy, J. Fischer, A. Mitscher and L. Ricard, *J. Am. Chem. Soc.* 1981, **103**, 5115.
2. R. J. Puddephatt, *Chem. Soc. Rev.* 1983, 99.
3. A. L. Balch, *Homogeneous Catalysis with Metal Phosphine Complexes* (Edited by L. H. Pignolet). Plenum Press, New York (1983).
4. M. D. Fryzuk, P. A. MacNeil and S. J. Rettig, *J. Am. Chem. Soc.* 1987, **109**, 2803; M. D. Fryzuk, P. A. MacNeil and S. J. Rettig, *Organometallics* 1986, **5**, 2469.
5. M. M. Taqui Khan, V. Vijay Sen Reddy and H. C. Bajaj, *Polyhedron* 1987, **6**, 921; M. D. Fryzuk, P. A. MacNeil and S. J. Rettig, *Organometallics* 1982, **1**, 918.
6. A. Trenkle and H. Vahrenkamp, *Inorg. Synth.* 1982, **21**, 180.
7. J. Chatt and M. L. Searle, *Inorg. Synth.* 1957, **5**, 210; G. W. Littlecott, F. J. McQuillin and K. G. Powell, *Inorg. Synth.* 1976, **16**, 113.
8. For example see E. Arpac and L. Dahlenburg, *Angew. Chem.* 1982, **94**, 929; M. Boake, S. Hietkamp, S. Morton and O. Stelzer, *Chem. Ber.* 1981, **114**, 3691.
9. K. Isslieb, A. Kipke and V. Hahnfeld, *Z. Anorg. Allg. Chem.* 1987, **444**, 5.
10. L. Sacconi and R. Morassi, *J. Chem. Soc. A* 1968, 2997.

Polyhedron Vol. 8, No. 1, pp. 29–38, 1989
Printed in Great Britain

0277–5387/89 $3.00+.00
© 1988 Pergamon Press plc

SYNTHESIS AND X-RAY CRYSTALLOGRAPHIC CHARACTERIZATION OF NEW DINUCLEAR BIS(PHENYLDIAZENIDO)MOLYBDENUM COMPLEXES $[\{Mo(C_6H_5N_2)_2X(\mu\text{-}OR)(C_6H_5NHNH_2)\}_2]$ (X = Cl, OR), $[\{Mo(C_6H_5N_2)_2(\mu\text{-}OR)(C_6H_5CONHO)\}_2]$ AND $[\{Mo(C_6H_5N_2)_2Cl(\mu\text{-}OEt)(EtOH)\}_2]$

VALÉRIE CHILOU, PIERRE GOUZERH, YVES JEANNIN,* GIUSEPPE OLIVARÈS and FRANCIS ROBERT

Laboratoire de Chimie des Métaux de Transition, CNRS-UA 419, Université Pierre et Marie Curie, 4 Place Jussieu, 75252 Paris cedex 05, France

and

T. C. HSIEH and JON ZUBIETA*

Department of Chemistry, State University of New York at Albany, Albany, NY 12222, U.S.A.

(*Received* 19 *April* 1988; *accepted* 4 *July* 1988)

Abstract—Polyoxomolybdates, monomeric chelated(O,O) oxomolybdenum(VI) and monomeric halogenooxomolybdenum(V) complexes reacted in alcohols with phenylhydrazine to yield dinuclear complexes of the following formulae noted (**1**), (**2**), (**3**), and (**4**): $[\{Mo(C_6H_5N_2)_2(\mu\text{-}OR)(C_6H_5CONHO)\}_2]$, $[\{Mo(C_6H_5N_2)_2(\mu\text{-}OR)(OR)(C_6H_5NHNH_2)\}_2]$, $[\{Mo(C_6H_5N_2)_2Cl(\mu\text{-}OR)(C_6H_5NHNH_2)\}_2]$ and $[\{Mo(C_6H_5N_2)_2Cl(\mu\text{-}OC_2H_5)(C_2H_5OH)\}_2]$; **a**: R = CH_3; **b**: R = C_2H_5; **c**: R = C_3H_7. **1b** crystallized in the triclinic space group $P\bar{1}$ $a = 9.728(3)$, $b = 11.154(1)$, $c = 12.720(2)$ Å, $\alpha = 97.92(1)°$, $\beta = 106.40(2)°$, $\gamma = 106.56(2)°$, $V = 1233$ Å^3, $Z = 1$. Refinement was based on 2549 reflections and converged at $R = 0.06$. **2a** crystallized in the monoclinic space group $P2_1/n$, $a = 11.404(2)$, $b = 11.998(1)$, $c = 16.778(4)$ Å, $\beta = 108.56(1)°$, $V = 2176$ Å^3, $Z = 2$. Refinement was based on 2481 reflections and converged at $R = 0.024$. Mixed crystals containing **2a** and **3a** in the same unit cell (70:30) are isomorphous with **2a**, $a = 11.443(3)$, $b = 11.826(4)$, $c = 16.785(4)$ Å, $\beta = 108.45(2)°$, $V = 2155$ Å^3, $Z = 2$. Refinement was based on 2623 reflections and converged at $R = 0.049$. **3c** crystallized in the triclinic space group $P\bar{1}$, $a = 9.534(3)$, $b = 12.057(2)$, $c = 12.751(3)$ Å, $\alpha = 98.90(1)°$, $\beta = 96.37(2)°$, $\gamma = 112.50(2)°$, $V = 1314$ Å^3, $Z = 1$. Refinement was based on 1615 reflections and converged at $R = 0.053$. **4** crystallized in the monoclinic space group $C2/m$, $a = 10.495(3)$, $b = 18.792(4)$, $c = 11.115(3)$ Å, $\beta = 101.91(1)°$, $V = 2145$ Å^3, $Z = 2$. Refinement was based on 1238 reflections and converged at $R = 0.055$. All these structures consist of discrete dinuclear units containing *cis*-bisdiazenido moieties $[Mo(C_6H_5N_2)_2]^{2+}$ bridged by two alkoxo groups. Molybdenum achieves six coordination either with a chelating bidentate ligand as in **1** or with two unidentate ligands as in **2**, **3** and **4**. A unique feature of **2** and **3** is the occurrence of phenylhydrazine and phenyldiazenido in the same coordination sphere.

*Authors to whom correspondence should be addressed.

In view of the perceived analogies of isopolymetalates to metal oxide surfaces, the coordination chemistry of these species with small organic molecules is of current interest.[1] A number of organooxygen[2] and organonitrogen[3] derivatives of high valent polyoxomolybdates are known for which we have a continued interest. Zubieta *et al.* have recently reported the reaction of isopolymolybdates with phenylhydrazine yielding tetranuclear, hexanuclear, or octanuclear species, depending on reaction conditions.[4] Jeannin and co-workers have reported the reactions of $[MoO_2(acac)_2]$ with phenylhydrazine and acetamidoxime yielding, respectively, a dinuclear bis(phenyldiazenido)molybdenum complex[5] and a nitrosylmolybdenum(II) complex.[6] We report here the reactions of phenylhydrazine with various Mo^{VI} and Mo^{V} oxo complexes yielding dinuclear bis(phenyldiazenido)molybdenum complexes of the following types: $[\{Mo(C_6H_5N_2)_2(\mu\text{-}OR)(C_6H_5CONHO)\}_2]$, (**1**); $[\{Mo(C_6H_5N_2)_2(\mu\text{-}OR)(OR)(C_6H_5NHNH_2)\}_2]$, (**2**); $[\{Mo(C_6H_5N_2)_2Cl(\mu\text{-}OR)(C_6H_5NHNH_2)\}_2]$, (**3**); $[\{Mo(C_6H_5N_2)_2Cl(\mu\text{-}OC_2H_5)(C_2H_5OH)\}_2]$, (**4**); **a**: R = CH_3; **b**: R = C_2H_5; **c**: R = C_3H_7. The synthesis and the X-ray structure of one of these complexes (**2a**) were recently reported by Zubieta *et al.*[7]

EXPERIMENTAL

Materials

Acetylacetone, benzohydroxamic acid and phenylhydrazine are commercially available. $(NBu_4)_2[Mo_6O_{19}]$,[8] α-$(NBu_4)_4[Mo_8O_{26}]$[9] and $[MoO_2(acac)_2]$[10] were prepared according to literature procedures. $(NEt_4)[MoOCl_4(H_2O)]$ and $(NH_4)_2[MoOBr_5]$ were prepared by reducing MoO_4^{2-} in concentrated hydrochloric or hydrobromic acid and adding $(NEt_4)Cl$ or NH_4Br.[11] $[MoO_2(C_6H_5CONHO)_2]\cdot CH_3OH$ was prepared from $[MoO_2(acac)_2]$ and PhCONHOH following a general procedure described by Murray and coworkers.[12]

Synthesis of $[\{Mo(C_6H_5N_2)_2(\mu\text{-}OEt)(C_6H_5CONHO)\}_2]$ (**1b**)

$[MoO_2(C_6H_5CONHO)_2]\cdot CH_3OH$ (0.40 g, 0.92 mmol) was dissolved in C_2H_5OH (10 cm^3) and $C_6H_5NHNH_2$ (0.5 cm^3, 5.1 mmol) was added. A deep purple colour developed immediately and dark violet microcrystals of $[\{Mo(C_6N_2)_2(\mu\text{-}OC_2H_5)(C_6H_5CONHO)\}_2]\cdot 2C_2H_5OH$ (**1b**) began to deposit within 1 h. They were filtered off after 12 h, washed with C_2H_5OH and air dried. Yield: 0.35 g (71%). Found; C, 51.4; H, 4.8; N, 13.3. Calc. for $C_{46}H_{54}N_{10}Mo_2O_8$: C, 51.8; H, 5.1; N. 13.1%. The crystallization was slower when the reactant concentrations were lowered but keeping the same $C_6H_5NHNH_2$/Mo ratio; crystals of a suitable size for X-ray work were obtained in this way. $[\{Mo(C_6H_5N_2)(\mu\text{-}OCH_3)(C_6H_5CONHO)\}_2]\cdot 2CH_3OH$ (**1a**) was prepared similarly to **1b** but with CH_3OH. Found: C, 49.8; H, 4.5; N, 14.1. Calc. for $C_{42}H_{46}N_{10}Mo_2O_8$: C, 49.9; H, 4.6; N, 13.9%.

Synthesis of $[\{Mo(C_6H_5N_2)_2(\mu\text{-}OCH_3)(OCH_3)(C_6H_5NHNH_2)\}_2]$ (**2a**)

The preparation of **2a** has been given by Hsieh and Zubieta.[7] Two other methods are reported hereunder.

Method 1. From $(NBu_4)_4[Mo_8O_{26}]$ *or* $(NBu_4)_2[Mo_6O_{19}]$. A large excess of $C_6H_5NHNH_2$ (20 cm^3, 0.20 mol) was added to $(NBu_4)_4[Mo_8O_{26}]$ (1.1 g, 0.5 mmol) in MeOH (50 cm^3). The resulting mixture was stirred at room temperature for 15 min during which time all the solid dissolved, and a purple–red colour developed. Well-shaped purple–black crystals of **2a** separated upon standing. The crystals were filtered off after 3 days, washed with CH_3OH and air-dried. Successive crops were collected over a period of 10 weeks. Yield: 1.2 g (62%, based on Mo). Found: C, 50.4; H, 5.1; N, 17.6; Mo, 19.6. Calc. for $C_{40}H_{48}N_{12}Mo_2O_4$: C, 50.4; H, 5.1; N, 17.6; Mo, 20.1%.

The reaction of $(NBu_4)_2[Mo_6O_{19}]$ (0.5 g, 0.36 mmol) with various amounts of $C_6H_5NHNH_2$ (from 0.15 cm^3 up to 10 cm^3) in CH_3OH (25 cm^3) was also studied at room temperature. A crystalline precipitate was formed within a few days. Its chemical analysis and IR spectroscopic study showed that pure $(NBu_4)_2[Mo_4O_8(OCH_3)_2(C_6H_5N_2)_4]$ was obtained for low $C_6H_5NHNH_2$/Mo ratios while essentially pure **2a** separated for high ratios. Mixtures of these two diazenido complexes were obtained for intermediate cases.

Method 2. From $[MoO_2(acac)_2]$. This synthesis was analogous to that used for $[\{Mo(C_6H_5N_2)_2(acac)(\mu\text{-}OCH_3)\}_2]$[5] but a larger $C_6H_5NHNH_2$/Mo ratio was used: 10 cm^3 of $C_6H_5NHNH_2$ and 0.65 g (2 mmol) of $[MoO_2(acac)_2]$ in 40 cm^3 of CH_3OH. The product collected after 2 days was spectroscopically identical with that obtained from method 1. Yield: 0.3 g, 31%.

Synthesis of $[\{Mo(C_6H_5N_2)_2(\mu\text{-}OC_2H_5)(OC_2H_5)(C_6H_5NHNH_2)\}_2]$ (**2b**)

An excess of $C_6H_5NHNH_2$ (5 cm^3, 51 mmol) was added to $(NH_4)_2[MoOBr_5]$ (1.1 g, 2 mmol) in

C_2H_5OH (100 cm^3) and the mixture was stirred at room temperature for 15 min. The colour changed from red–brown to purple–red and **2b**, purple–black crystals, slowly separated upon standing. Yield: 0.8 g, 79%. Found: C, 51.8; H, 5.6; N, 16.5. Calc. for $C_{44}H_{56}N_{12}Mo_2O_4$: C, 52.4; H, 5.6; N, 16.7%.

Synthesis of $[\{Mo(C_6H_5N_2)_2(\mu\text{-}OC_3H_7)(OC_3H_7)(C_6H_5NHNH_2)\}_2]$ **(2c)**

This synthesis was performed analogously to method 2 for **2a**. A large excess of $C_6H_5NHNH_2$ (20 cm^3) was added to $[MoO_2(acac)_2]$ (0.65 g, 2 mmol) in 1-propanol (25 cm^3) and the mixture was stirred for 10 min at room temperature. A dark purple crystalline solid began to deposit after several weeks; it was filtered off after 3 months and washed with 1-propanol and ether. Yield: 0.55 g, 52%. Found; C, 54.2; H, 6.1; N, 15.6. Calc. for $C_{48}H_{64}N_{12}Mo_2O_4$; C, 54.1; H, 6.1; N, 15.8%.

Synthesis of $[\{Mo(C_6H_5N_2)_2Cl(\mu\text{-}OR)(C_6H_5NHNH_2)\}_2]$ (**3a**: R = CH_3; **3b**: R = C_2H_5)

$C_6H_5NHNH_2$ (5 cm^3, 51 mmol) was added to $(NEt_4)[MoOCl_4(H_2O)]$ (1 g, 2.5 mmol) and the mixture was refluxed for 1 h. The resulting purple suspension was filtered and the filtrate was allowed to stand at room temperature yielding single crystals within 2 days. The IR spectra of the precipitate and of crystals were nearly identical and both samples were shown to be mixtures of **2a** and **3a**. Moreover it was shown by X-ray diffraction that **2a** and **3a** actually form mixed crystals, i.e. the unit cell contains both **2a** and **3a**. Analysis of a crystalline sample calculated for a mixture of 65% of $C_{40}H_{48}N_{12}Mo_2O_4$ and 35% of $C_{38}H_{42}N_{12}Cl_2Mo_2O_2$: C, 49.4; H, 4.8; N, 17.6; Cl, 2.6; Mo, 20.1. Found: C, 48.7; H, 4.8; N, 178.6; Cl, 2.6; Mo. 20.0%. This ratio was suggested by the chemical analysis and by the X-ray structure determination. Similar results were obtained if the whole reaction was carried out at room temperature.

Attempts to prepare **3b** similarly by the reaction of $C_6H_5NHNH_2$ with $(NEt_4)[MoOCl_4(H_2O)]$ in C_2H_5OH either at room temperature or under reflux yielded mixtures of **2b** and **3b**.

Synthesis of $[\{Mo(C_6H_5N_2)_2(\mu\text{-}OC_3H_7)(Cl)(C_6H_5NHNH_2)\}_2]\cdot 2C_3H_7OH$ **(3c)**

The synthesis was performed following a modification of the method used for **3a** and **3b**. $C_6H_5NHNH_2$ (4 cm^3) was added to $(NEt_4)[MoOCl_4(H_2O)]$ (0.5 g) suspended in 1-propanol (50 cm^3). The resulting mixture was stirred at room temperature for 5 h; the solution was purple and a grey–white precipitate separated. It was filtered off and was identified as $C_6H_5NHNH_2HCl$ by IR spectroscopy. Large dark purple needles were recovered from the mother solution after standing for 48 h at room temperature. Yield: 0.28 g, 39%. Found: C, 51.1; H, 5.4; N, 15.1; Cl, 5.9; Mo, 17.0. Calc. for $C_{48}H_{66}N_{12}Cl_2Mo_2O_4$: C, 50.7; H, 5.8; N, 14.8; Cl, 6.2; Mo, 16.9%.

Synthesis of $[\{Mo(C_6H_5N_2)_2Cl)(\mu\text{-}OEt)(EtOH)\}_2]$ **(4)**

$(NBu_4)_2[Mo_4O_8(C_6H_5N_2)_4]$[4a] (1.0 g, 0.66 mmol) was dissolved in CH_3CN/CH_2Cl_2 (10 cm^3/10 cm^3) and an excess of 12 N HCl (0.5 cm^3, 6.0 mmol) was added. Dark violet crystals of $[\{Mo(C_6H_5N_2)_2Cl(\mu\text{-}OEt)(EtOH)\}_2]$ **(4)** deposited after standing for 3 weeks at room temperature. Yield: 0.39 g (74%). Found: C, 48.1; H, 5.1; N, 13.8. Calc. for $C_{32}H_{42}N_8Cl_2Mo_2O_4$: C, 48.4; H, 5.3; N, 14.1%.

X-ray structures

Crystals were mounted on glass fibers with epoxy cement and were studied by precession and Weissenberg methods. Cell constants and data collection were measured at room temperature with Mo-K_α radiation (λ = 0.71069 Å) on an Enraf–Nonius CAD4 diffractometer equipped with a graphite monochromator. Unit cell dimensions were determined by a least-squares fit of the setting angles of 25 reflections. Data were corrected for Lorentz and polarization effects and an empirical absorption correction based upon Ψ-scan was applied. Structures were solved by Patterson and Fourier methods and refined by full-matrix least-squares using CRYSTALS program package.[13] Neutral atom form factors including anomalous dispersion were taken from *International Tables*.[14] Extinction was corrected. Crystallographic data are summarized in Table 1. Only specific points are quoted below for each case.

1b—Hydrogen atoms were included in refinement as fixed contributions. Carbon and oxygen atoms of the solvent molecule were constrained with the usual bond distances and with an overall isotropic thermal parameter; solvent hydrogen atoms were omitted.

2a—This structure was solved first by Hsieh and Zubieta[7] and independently by Jeannin and coworkers. Results are in agreement.

Mixed crystals of **2a** and **3a**—During refinement, it became apparent that the coordination site *trans* to $C_6H_5NHNH_2$ was disordered, being occupied either by a methoxo group or by a chlorine atom,

Table 1. Crystal data

	Compound **1b**	Compound **2a**	Compound **2a/3a**	Compound **3c**	Compound **4**
Formula	$C_{46}H_{54}N_{10}Mo_2O_8$	$C_{40}H_{48}N_{12}Mo_2O_4$	0.7 $C_{40}H_{48}N_{12}Mo_2O_4$: 0.3 $C_{38}H_{42}N_{12}Cl_2Mo_2O_2$	$C_{42}H_{50}N_{12}Cl_2Mo_2O_4$[c]	$C_{32}H_{42}N_8Cl_2Mo_2O_4$
Molecular weight	1066.87	952.78		1017.72	865.52
Crystal system	triclinic	monoclinic	monoclinic	triclinic	monoclinic
Space group	$P\bar{1}$	$P2_1/n$	$P2_1/n$	$P\bar{1}$	$C2/m$
a (Å)	9.728(3)	11.404(2)	11.443(3)	9.534(3)	10.495(3)
b (Å)	11.154(1)	11.998(1)	11.826(4)	12.057(2)	18.792(4)
c (Å)	12.720(2)	16.778(4)	16.785(4)	12.751(3)	11.115(3)
α (°)	97.92(1)	90.00	90.00	98.90(1)	90.00
β (°)	106.40(2)	108.56(1)	108.45(2)	96.37(2)	101.91(1)
γ (°)	106.56(2)	90.00	90.00	112.50(2)	90.00
V (Å^3)	1233	2176	2155	1314	2145
Z	1	2	2	1	2
$d_{calc.}$ (g cm^{-3})	1.44	1.45	1.47	1.29	1.34
$F(000)$	548	976	976	588	812
μ, Mo-K_α (cm^{-1})	5.65	6.24	6.64	6.27	7.32
Crystal dimensions (mm)	$0.42 \times 0.14 \times 0.09$	$0.24 \times 0.22 \times 0.18$		$0.30 \times 0.14 \times 0.10$	$0.43 \times 0.37 \times 0.29$
Diffractometer	CAD4	CAD4	CAD4	CAD4	R3m
Temperature (°C)	20	20	20	20	20
Radiation	Mo-K_α	Mo-K_α	Mo-K_α	Mo-K_α	Mo-K_α
Scan mode	θ–2θ	θ–2θ	θ–2θ	θ–2θ	θ–2θ
θ range (°)	1.5–25	1.5–25	1–25	1–23	2–23
Reflections collected	4317	3827	4187	3641	2569
Reflections used	2549	2481	2623	1615	1238
Criteria	$I > 3\sigma(I)$	$I > 3\sigma(I)$	$I > 3\sigma(I)$	$I > 3\sigma(I)$	$I > 3\sigma(I)$
Number parameters ref.	282	336	321	279	110
R[a]	0.0596	0.0245	0.0495	0.0533	0.0553
R_w[b]	0.0664	0.0252	0.0562	0.0587	0.0598
Weighting scheme	w = 1.0	w = 1.0	w = 1.0	w = 1.0	w = 1.0
rms (shift/esd)	0.08	0.15	0.09	0.01	0.02
Largest residue (e Å^{-3})	1.9	0.3	0.7	0.6	0.8

[a] $R = \Sigma(|F_o| - |F_c|)/\Sigma|F_o|$.
[b] $R_w = \{\Sigma w(F_o - F_c)^2/\Sigma wF_o^2\}^{1/2}$.
[c] Excluding solvent.

indicating mixed crystals; occupancy factors converged to 0.72 and 0.31, and were fixed at 0.7 and 0.3 in the final refinement. Hydrogen atoms were located on a difference Fourier map and all but five were refined with an overall isotropic thermal parameter. Only the hydrogen atoms of the terminal OCH_3 groups were omitted.

3c—The centrosymmetric dinuclear unit $[\{Mo(C_6H_5N_2)_2Cl(\mu\text{-}OC_3H_7)(C_6H_5NHNH_2)\}_2]$ was easily located and refined; however refinement revealed high thermal motion with temperature factors ranging from 5 Å^2 for molybdenum up to 22 Å^2 for the terminal carbon atom of the propanolato bridge which contains an unusually short C—C distance. This could arise from disorder or from departure from centrosymmetry. Attempts to refine in non-centrosymmetric $P1$ space group were not successful. The propanolato bridge was loosely constrained in further refinement. Hydrogen atoms were included as fixed contributions. Then at this stage, a difference Fourier series revealed weak diffuse residual peaks located around the inversion centre (1/2, 1/2, 1/2) suggesting the presence of solvent. The disorder was not solved. The best decrease of R was obtained with six carbon atoms introduced with 0.5 occupancy so that R dropped from 8.5 to 5.3. Despite these difficulties the structure of $[\{Mo(C_6H_5N_2)_2Cl(\mu\text{-}OC_3H_7)(C_6H_5NHNH_2)\}_2]$ seems reliable in view of its comparison with those of **2a**, **3a** and **4**.

4—The general conditions of data collection and the methodologies used in this structure were similar to those employed for structures **1b**–**3a**, except that data were collected on a Nicolet R3m diffractometer and the SHELXTL[13b] program package was used in the structure solution and refinement. The choice of the centric space group $C2/m$ yielded a centrosymmetric binuclear unit $[\{Mo(C_6H_5N_2)_2Cl(\mu\text{-}OC_2H_5)(C_2H_5OH\}_2]$ with the Mo, Cl, O(2), and C(3) atoms located on the mirror plane through $y = 0$. The oxygen atom O(1) and the methylene carbon C(1) of the bridging ethoxy group are located on the two-fold axis through $x = 0.5$, $z = 0.5$. As a consequence of this disposition of the binuclear unit, C(4) of the terminal ethoxy group is disordered about the mirror plane while C(2) of the bridging ethoxo group is disordered about the two-fold axis. Refinement in the acentric space group $C2$ produced no significant improvement in the residuals and resulted in temperature factors of 18–21 Å^2 for the terminal carbon atoms. The centric alternative $C2/m$ was assumed to be the correct choice.

Atomic positional and thermal parameters for **1b**, **2a**, mixed **2a**–**3a**, **3c** and **4**, and complete listings of bond angles and distances are available as supplementary material and from authors. Selected interatomic distances and bond angles showing a comparison between those five compounds are listed in Table 2.

Spectral measurements

IR spectra were determind as KBr or RbI pellets with a Perkin–Elmer 597 spectrophotometer. Absorption spectra were obtained with a Beckman 5240 spectrophotometer.

RESULTS AND DISCUSSION

Some general trends of the reaction of phenylhydrazine with Mo^{VI} oxo-compounds can be inferred from our synthetic work and from the work of other groups,[15,16] although reaction conditions are not strictly identical since phenylhydrazine hydrochloride was sometimes used by other groups and triethylamine was sometimes added to the reaction mixture:

—the main products of $C_6H_5NHNH_2$ reaction with polyoxomolybdates in alcohols are the tetranuclear species, $[Mo_4O_8(OR)_2(C_6H_5N_2)_4]^{2-}$,[4a] and dinuclear compounds, $[\{Mo(C_6H_5N_2)_2(\mu\text{-}OR)(OR)(C_6H_5NHNH_2)\}_2]$, depending on the $C_6H_5NHNH_2$/Mo ratio; aside from these compounds two complexes with different stoichiometries, $[Mo_8O_{26}(C_6H_5N_2)_6]^{4-}$[4d] and $[Mo_4O_{10}(OCH_3)_2(C_6H_5N_2)_2]^{2-}$[4c] have been characterized by Zubieta and co-workers;

—the reaction of $C_6H_5NHNH_2$ with $[MoO_2L_2]$ complexes yields dinuclear species $[\{Mo(C_6H_5N_2)_2(\mu\text{-}OR)L\}_2]$ or $[\{Mo(C_6H_5N_2)_2(\mu\text{-}OR)(C_6H_5NHNH_2)\}_2]$ when L is an (O,O)-chelate; this contrasts with the behaviour of (N,O)-, (N,S)-, and (S,S)-chelates which yield mononuclear $[Mo(C_6H_5N_2)_2L_2]$ complexes.[15,16] Compounds **1** are only slightly soluble in common solvents. Complexes **2** and **3** are more soluble, especially in chlorohydrocarbon solvents, but these solutions were found to be relatively unstable, even if dry solvents were used.

The IR spectra of complexes **1**, **2**, **3** and **4** show the characteristic pattern of singly-bent diazenido ligands in the range 1480–1650 cm^{-1}.[4a,15c,17,18] The visible absorption spectra of these complexes in solution are characterized by an intense band at *ca* 520 nm ($\varepsilon = 8 \times 10^{-4}$ mol^{-1} dm^3 cm^{-1} per Mo). These features are typical of the *cis*-$[Mo(C_6H_5N_2)_2]^{2+}$ unit.[4a]

The IR spectra of **2** and **3** show weak bands at 3220 and 3380 cm^{-1} assigned to ν(N—H). However, clear characterization of the hydrazine ligand by ^{1}H NMR in $CDCl_3$ was hampered by

Table 2. Selected interatomic distances (Å) and angles (°) with standard deviations in parentheses

		Compound **1b**	Compound **2a**	Compound **2a : 3a**	Compound **3c**	Compound **4**
Phenyldiazenido ligands						
No. 1	Mo—N(21)	1.817(8)	1.830(3)	1.822(6)	1.79(1)	1.830(6)
	N(21)—N(22)	1.24(1)	1.227(4)	1.225(8)	1.23(1)	1.235(9)
	Mo—N(21)—N(22)	171.6(7)	170.3(3)	171.0(5)	166.0(1)	173.8(5)
	N(21)—N(22)—C(23)	118.3(8)	117.3(3)	119.0(6)	119.0(1)	119.1(6)
No. 2	Mo—N(31)	1.841(8)	1.832(3)	1.817(7)	1.84(2)	
	N(31)—N(32)	1.26(1)	1.231(4)	1.227(8)	1.24(2)	
	Mo—N(31)—N(32)	175.7(7)	161.2(3)	163.2(6)	170.0(1)	
	N(31)—N(32)—C(33)	118.2(9)	121.4(3)	121.8(6)	118.0(2)	
Phenylhydrazine ligand						
	Mo—N(11)		2.267(3)	2.248(6)	2.22(1)	
	N(11)—N(12)		1.423(4)	1.413(9)	1.41(1)	
	Mo—N(11)—N(12)		115.5(2)	115.8(5)	118.3(8)	
	N(11)—N(12)—C(13)		119.2(3)	118.5(6)	119.0(1)	
Benzohydroxamato ligand						
	Mo—O(2)	2.114(6)				
	Mo—O(3)	2.050(5)				
	C(3)—O(2)	1.29(1)				
	C(3)—N(1)	1.33(1)				
	N(1)—O(3)	1.375(9)				
	O(2)—C(3)—N(1)	118.8(9)				
	C(3)—N(1)—O(3)	119.3(8)				
Bridging alkoxo ligands						
	Mo—O(1)	2.157(5)	2.112(2)	2.105(5)	2.094(8)	2.113(4)
	Mo—O(1′)	2.020(5)	2.127(2)	2.115(5)	2.108(9)	2.113(4)
Terminal methoxo ligand						
	Mo—O(2)		1.986(2)	2.04(1)		
Chloro ligand						
	Mo—Cl			2.36(1)	2.421(4)	2.441(3)
Ethanol ligand						
						2.143(7)

rather low solubility and by some instability of the solutions as mentioned above.

The IR spectrum of **3** shows a band at *ca* 290 cm^{-1} which is not present in the spectrum of **2** and is therefore assigned to stretching ν(Mo—Cl) consistently with published data.[19]

The molecular structures of the centrosymmetrical dinuclear complexes of **1b**, **2a**, **3a**, **3c** and **4** are shown in Figs 1, 2, 3, 4 and 5. All complexes contain the $[\{MO(C_6H_5N_2)_2(\mu\text{-}OR)\}_2]^{2+}$ unit which has already been found in a number of compounds.[4a,5] In this unit, the molybdenum atom is ligated to two bridging alkoxo and two phenyldiazenido groups; it achieves six coordination either by a chelating bidentate ligand as in **1**, or by two unidentate ligands as in **2**, **3** and **4**. In the first case, the geometry around molybdenum is forced by the chelate ring. In the second case, two different geometries are conceivable according to whether the unidentate ligands are mutually *cis* or *trans*. However, only the latter has been ever found. As a consequence of the *trans* influence of the phenyldiazenido, the bridge is dissymmetrical for **1** while it is nearly symmetrical for **2** and **3**.

The overall geometry of $[\{Mo(C_6H_5N_2)_2(\mu\text{-}OC_2H_5)(C_6H_5CONHO)\}_2]$ is similar to that of $[\{Mo(C_6H_5N_2)_2(\mu\text{-}OCH_3)(acac)\}_2]$ while those of complexes **2**, **3** and **4** are similar. In **4** the Mo—O(2) distance 2.113(4) Å is outside the range for terminal alkoxides;[20] it clearly indicates that the ligand is ethanol.

A unique feature of compounds **2** and **3** is the occurrence of phenylhydrazine and phenyldiazenido ligands in the same coordination sphere. There was no example of this kind of molybdenum complexes until the recent report

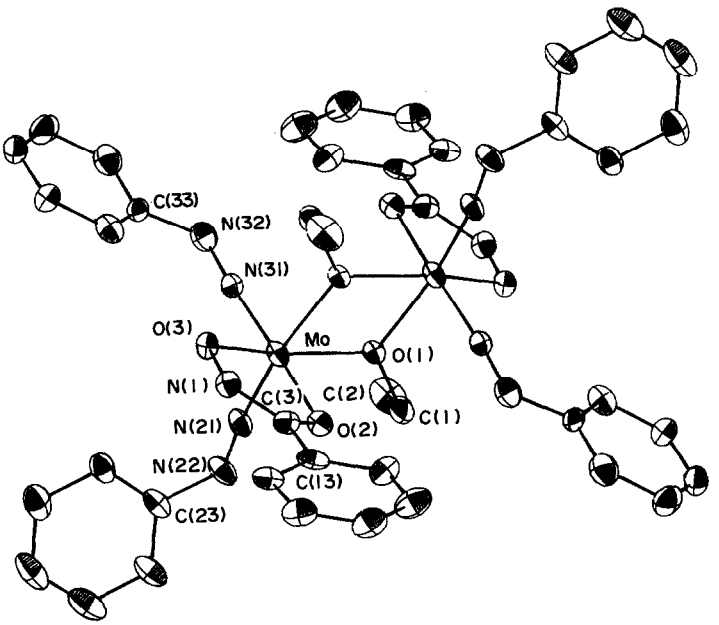

Fig. 1. Molecular structure and labelling scheme for $[Mo(C_6H_5N_2)_2(\mu\text{-}OC_2H_5)(C_6H_5CONHO)\}_2]$ (**1b**) with 20% thermal ellipsoids.

of Hsieh and Zubieta about the structure of **2a**.[7] This **2a** structure is the archetype of a new family of complexes with the general formula $[\{Mo(C_6H_5N_2)_2X(\mu\text{-}OR)(C_6H_5NHNH_2)\}_2]$ (X = OR, Cl; R = CH_3, C_2H_5, n-C_3H_7...) which are readily formed when polyoxometalates, monomeric oxomolybdenum(VI), or monomeric halogenomolybdenum(V) complexes are treated with an excess of phenylhydrazine in ROH. The vanadium complex $[VCl_2\{C_6H_5(CH_3)N_2\}\{C_6H_5(CH_3)NNH_2\}]^+$ is the only other case of a complex containing hydrazine residues in more than one protonated state which was obtained by reacting a metal compound with a substituted hydrazine.[21] Compounds **2** and **3** also appear to be the first molybdenum complexes where end-on hydrazine coordination is crystallographically supported; this coordination is likely to occur in complexes

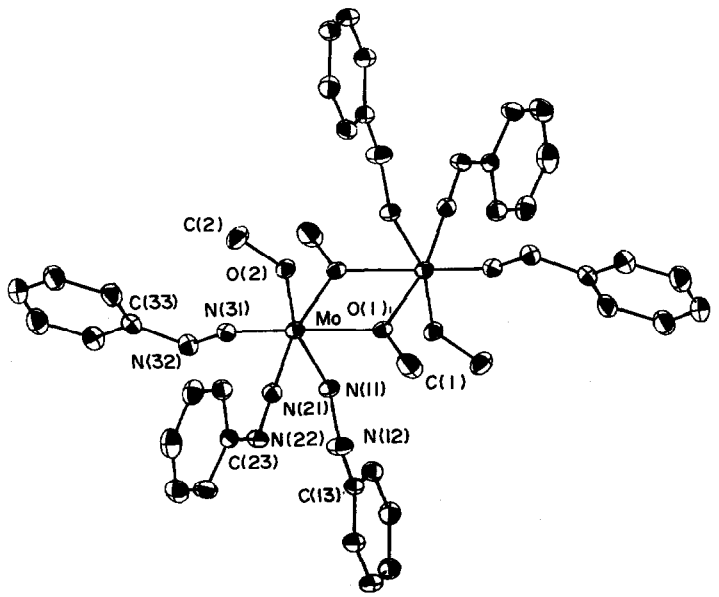

Fig. 2. ORTEP drawing of $[\{Mo(C_6H_5N_2)_2(\mu\text{-}OCH_3)(OCH_3)(C_6H_5NHNH_2)\}_2]$ (**2a**) with 20% thermal ellipsoids.

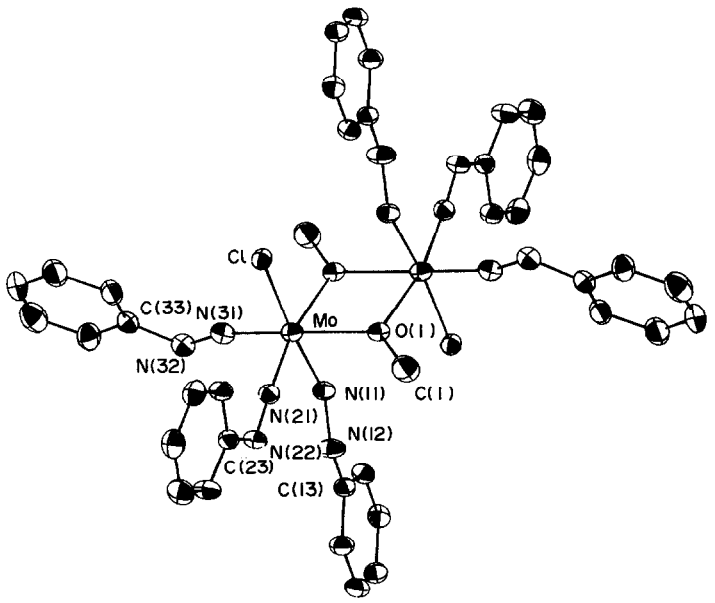

Fig. 3. ORTEP drawing of $[\{Mo(C_6H_5N_2)_2Cl(\mu\text{-}OCH_3)(C_6H_5NHNH_2)\}_2]$ occurring in mixed crystals (**2a**/**3a**) with 20% thermal ellipsoids.

such as $[Mo(CO)_5(C_6H_5NHNH_2)]$[22] and $[Mo(\eta^5\text{-}C_5H_5)I_2(NO)(C_6H_5NHNH_2)]$[23] studied by IR spectroscopy. The occurrence of neutral phenylhydrazine in **2** and **3** is consistent with electron count requirements; it is also supported by the appearance of NH_2 and NH hydrogen atoms in Fourier maps, their successful refinement, and the Mo—NH_2—NH—C_6H_5 geometry: the Mo—N and N—N distances 2.267(3) and 1.423(4) Å in **2a** are indicative of single bonds. The environment of the NH_2 nitrogen atom is roughly tetrahedral and the configuration about the N—N bond is *gauche*.

The geometry of the *cis*-$[Mo(C_6H_5N_2)_2]^{2+}$ unit ensures maximum π-interaction between the diazenido ligand π^*-orbitals and the molybdenum t_{2g} orbitals.[24] This is supported by the

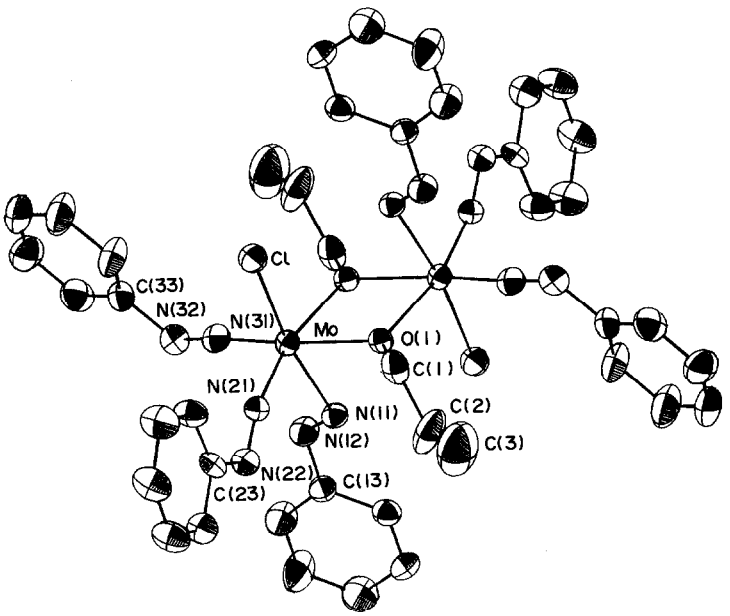

Fig. 4. ORTEP drawing of $[\{Mo(C_6H_5N_2)_2Cl(\mu\text{-}OC_3H_7)(C_6H_5NHNH_2)\}_2]$ (**3c**) with 15% thermal ellipsoids.

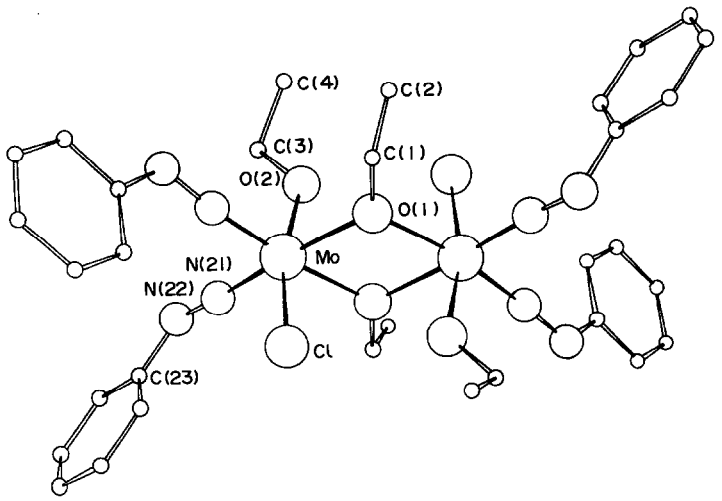

Fig. 5. Perspective drawing of $[\{Mo(C_6H_5N_2)_2Cl(\mu\text{-}OC_2H_5)(C_2H_5OH)\}_2]$ (**4**).

short Mo—N(diazenido) distances (1.82 Å average) and the wide angle of the Mo—N—N unit for the diazenido ligand (169° average).

Although there is obviously no π requirement for the phenylhydrazine ligand, its phenyl ring is not far from being coplanar with one diazenido ligand in both **2a** and **3c**; however the orientation of this phenyl ring in **3a** and **3c** with respect to the rest of the molecule is different while both $C_6H_5N_2$ groups are similarly orientated in both compounds.

Structural features of the benzohydroxamate ligand in **1b** are very similar to those of the hydroxamate ligand in $[MoO\{(CH_3)_2NO\}(C_6H_5CONHO)(C_6H_5CONO)]$[25] and in other hydroxamatomolybdenum complexes.[26] In **1b** crystals, an intermolecular hydrogen bond stretches between the NH group and the ethanol oxygen atom (N(1)···O(4) = 2.82(1) Å; N(1)—H(1)—O(4) = 153.3°).

Compounds **1**, **2**, **3** and **4** contain the $[Mo(C_6H_5N_2)_4(\mu\text{-}OR)_2]^{2+}$ unit which proves to be a robust core able to ligate various types of other ligands.

REFERENCES

1. M. T. Pope, *Heteropoly and Isopolyoxometalates*. Springer, New York (1983).
2. (a) R. D. Adams, W. G. Klemperer and R. S. Liu, *J. Chem. Soc., Chem. Commun.* 1979, 256; (b) V. W. Day, M. F. Frederick, W. G. Klemperer and R. S. Liu, *J. Am. Chem. Soc.* 1979, **101**, 491; (c) E. M. McCarron and R. L. Harlow, *J. Am. Chem. Soc.* 1983, **105**, 6179.
3. E. M. McCarron, J. F. Whitney and D. B. Chase, *Inorg. Chem.* 1984, **23**, 3275.
4. (a) T. C. Hsieh and J. A. Zubieta, *Polyhedron* 1986, **5**, 305; (b) T. C. Hsieh and J. A. Zubieta, *Polyhedron* 1986, **5**, 1655; (c) T. C. Hsieh and J. A. Zubieta, *J. Chem. Soc., Chem. Commun.* 1985, 1749; (d) S. N. Shaikh and J. A. Zubieta, *Inorg. Chim. Acta* 1986, **121**, L43.
5. D. Carrillo, P. Gouzerh and Y. Jeannin, *Nouv. J. Chim.* 1985, **9**, 749.
6. V. Chilou, P. Gouzerh, Y. Jeannin and F. Robert, *Inorg. Chim. Acta* 1987, **133**, 205.
7. T. C. Hsieh and J. A. Zubieta, *Inorg. Chim. Acta* 1987, **127**, L31.
8. M. Che, M. Fournier and J. P. Launay, *J. Chem. Phys.* 1979, **71**, 1954.
9. M. Filowitz, R. K. C. Ho, W. G. Klemperer and W. Shum, *Inorg. Chem.* 1979, **18**, 93.
10. G. J. J. Chen, J. W. McDonald and W. E. Newton, *Inorg. Chem.* 1976, **15**, 2612.
11. E. A. Allen, B. J. Brisdon, D. A. Edwards, G. W. A. Fowles and R. G. Williams, *J. Chem. Soc.* 1963, 4649.
12. M. D. FitzRoy, J. M. Frederiksen, K. S. Murray and M. R. Snow, *Inorg. Chem.* 1985, **24**, 3265.
13. (a) J. R. Carruthers and D. J. Watkin, CRYSTALS, *An Advanced Crystallographic Computer Program*. Oxford Crystallography Laboratory (1986); (b) G. M. Sheldrick, SHELXTL, *Program for Crystal Structure Determination*, revision (1982).
14. *International Tables for X-ray Crystallography*. Vol. 4. Kynoch Press, Birmingham, U.K. (1974).
15. (a) M. W. Bishop, J. Chatt and J. R. Dilworth, *J. Organomet. Chem.* 1974, **73**, C59; (b) G. Butler, J. Chatt and G. J. Leigh, *J. Chem. Soc., Chem. Commun.* 1978, 352; (c) M. W. Bishop, G. Butler, J. Chatt, J. R. Dilworth and G. J. Leigh, *J. Chem. Soc., Dalton Trans.* 1979, 1843.
16. A. Nakamura, M. Nakayama, K. Sugihashi and S. Otsuka, *Inorg. Chem.* 1979, **18**, 394.
17. C. Pickett, S. Kumar, P. A. Vella and J. Zubieta, *Inorg. Chem.* 1982, **21**, 908.
18. H. M. Ali and G. J. Leigh, *J. Chem. Soc., Dalton Trans.* 1986, 213.
19. (a) B. F. G. Johnson, *J. Chem. Soc. A* 1967, 475; (b) S. Sarkar and P. Subramanian, *Inorg. Chim. Acta* 1979, **35**, L357.

20. S. A. Koch and S. Lincoln, *Inorg. Chem.* 1982, **21**, 2904.
21. J. Bultitude, L. F. Larkworthy, D. C. Povey, G. W. Smith, J. R. Dilworth and G. J. Leigh, *J. Chem. Soc., Chem. Commun.* 1986, 1748.
22. H. D. Murdoch and R. Henzi, *J. Organomet. Chem.* 1966, **5**, 463.
23. W. G. Kita, J. A. McCleverty, B. E. Mann, D. Seddon, G. A. Sim and D. J. Woodhouse, *J. Chem. Soc., Chem. Commun.* 1974, 132.
24. D. L. DuBois and R. Hoffmann, *Nouv. J. Chim.* 1977, **1**, 479.
25. K. Wieghardt, W. Holzbach, E. Hofer and J. Weiss, *Inorg. Chem.* 1981, **20**, 343.
26. G. A. Brewer and E. Sinn, *Inorg. Chem.* 1981, **20**, 1823.

Polyhedron Vol. 8, No. 1, pp. 39–43, 1989
Printed in Great Britain

0277–5387/89 $3.00+.00
© 1988 Pergamon Press plc

γ-PHENOXYBUTANOIC ACIDS AND THEIR METAL(II) COMPLEXES. THE CRYSTAL STRUCTURES OF 4-(4-CHLOROPHENOXY)BUTANOIC ACID, 4-(2,4-DICHLOROPHENOXY)BUTANOIC ACID, DIAQUABIS [4-PHENOXYBUTANOATO]NICKEL(II), AND COBALT(II) AND DIAQUABIS[4-(4-CHLOROPHENOXY)BUTANOATO]NICKEL(II)

GRAHAM SMITH,* SHAHIDAH M. SHARIFF and ERIC J. O'REILLY

Department of Chemistry, Queensland Institute of Technology, Brisbane 4000, Australia

and

COLIN H. L. KENNARD

Department of Chemistry, University of Queensland, Brisbane 4067, Australia

(*Received* 18 *May* 1988; *accepted* 4 *July* 1988)

Abstract—The crystal structures of the complexes diaquabis[4-(phenoxy)butanoato] nickel(II) (**1**), diaquabis[4-(4-chlorophenoxy)butanoato]nickel(II) (**2**) and the acids 4-(4-chlorophenoxy)butanoic acid (**3**) and 4-(2,4-dichlorophenoxy)butanoic acid (**4**) have been determined using X-ray diffraction techniques. The yellow complexes **1** and **2** are isomorphous and isostructural and have distorted octahedral MO_6 stereochemistry with two slightly asymmetric bidentate carboxylate groups [Ni—O, 2.062, 2.181(2) Å, (**1**) and 2.068, 2.175(2) Å, (**2**)] and two waters [Ni—O, 2.021(1) Å, (**1**) and 2.016(2) Å, (**2**)]. The planar conformation of the acids **3** and **4** is retained in the complexes **1** and **2**.

Three known pale green six-coordinate nickel(II) complexes with phenoxyalkanoic acids[1–3] have stereotypical octahedral stereochemistry about the metal. The coordination comprises four waters and two oxygens from *trans*-related unidentate carboxylate groups. This is contrary to the early contention[4] that the nickel(II) carboxylates are invariably dimeric or polymeric. The yellow nickel(II) complexes are usually square-planar[5] but no examples with this stereochemistry are known among the nickel(II) carboxylates. Therefore, the structures of the yellow crystalline complexes which form readily with aqueous nickel(II) and (4-phenoxy)butanoic acid [PBAH] and 4-[4-chlorophenoxy)butanoic acid [PCBAH] [complexes (**1**) and (**2**)] were of particular interest. In addition, the comparative conformational features of the free acids and the coordinated ligands were of interest. The structures of 4-(4-chlorophenoxy) butanoic acid [PCBAH] (**3**) and the commercial herbicide 4-(2,4-dichlorophenoxy)butanoic acid, [2,4-DB][6] (**4**) are also reported.

*Author to whom correspondence should be addressed.

EXPERIMENTAL

Preparations

The phenoxybutanoic acids were synthesized from ethyl 4-bromobutanoate and the appropriate phenol, using the general procedure of Synerholm and Zimmerman.[7] Metal complexes were prepared by reacting 50% aqueous ethanolic solutions of the acids with nickel or cobalt carbonate as previously described.[8] Partial evaporation (room temperature) of the filtrates yielded yellow crystals of the nickel complexes with 4-(phenoxy)butanoic acid, $[(Ni(PBA)_2(H_2O)_2]$ (**1**), and 4-(4-chlorophenoxy) butanoic acid, $[Ni(PCBA)_2(H_2O)_2]$ (**2**). The red cobalt(II) complex with 4-(phenoxy)butanoic acid, $[Co(PBA)_2(H_2O)_2]$ (**1a**), was confirmed as isomorphous with **1** from single crystal X-ray

diffraction photographs, while elemental analysis and IR spectra of **1**, **1a** and **2**, (obtained as Nujol mulls on a Jasco IR-810 recording spectrometer) indicated that all three were structurally similar.

Crystals of 4-(4-chlorophenoxy)butanoic acid (**3**) and 4(2,4-dichlorophenoxy)butanoic acid (**4**) were obtained from a mixture of toluene and chloroform.

Crystal data, X-ray data and structure refinement

Table 1 lists information about unit cell parameters, data acquisition and structure refinement for compounds **1**, **2**, **3** and **4**. Data were collected either at room temperature (293 K) (**1** and **2**) or at low temperature (173 K) (**3** and **4**) on a Nicolet R3m four-circle diffractometer, using graphite monochromatized Mo-K_α radiation ($\lambda = 0.7107$ Å). Structures were solved by either the heavy-atom method (**1** and **2**) or direct methods (**3** and **4**) using the SHELX-76 set of programs.[9] Refinement was by blocked-matrix least-squares with all heavy atoms anisotropic. Hydrogens were located from difference-Fourier syntheses and were included in the respective refinements with both positional and isotropic thermal parameters refined. No corrections were made for absorption or extinction.

Neutral atom scattering factors were used.[10] Final atomic coordinates (including hydrogens), anisotropic thermal parameters, intraligand bond distances and angles, and observed and calculated

Table 1. Cell data and details of the structure solution for $[Ni(PBA)_2(H_2O)_2]$ (**1**); $[Ni(PCBA)_2(H_2O)_2]$ (**2**); (PCBAH) (**3**); (2,4-DB) (**4**)

	(1)	(2)	(3)	(4)
Formula	$C_{20}H_{26}NiO_8$	$C_{20}H_{24}Cl_2NiO_8$	$C_{10}H_{11}ClO_3$	$C_{10}H_{10}Cl_2O_3$
M_r	452.7	521.7	214.5	249.0
a (Å)	37.409(8)	43.250(7)[a]	6.987(1)	7.532(1)
b (Å)	5.469(1)	5.401(1)	7.444(1)	8.858(1)
c (Å)	10.679(2)	10.601(2)	11.164(2)	9.390(2)
α (°)	90	90	74.16(1)	80.66(1)
β (°)	105.5(1)	113.86(1)	88.00(1)	69.37(1)
γ (°)	90	90	64.31(1)	64.96(1)
V (Å^3)	2105.2(7)	2264.9(8)	501.1(1)	531.2(1)
D_c (g cm^{-3})	1.43	1.53	1.42	1.56
D_m (g cm^{-3})	1.40	1.50	[b]	[b]
Z	4	4	2	2
μ (cm^{-1})	9.7	11.4	3.6	5.9
λ (Å)	0.71069	0.71069	0.71069	0.71069
$F(000)$	952	1080	224	256
Space group	$C2/c$	$I2/c$[a]	$P\bar{1}$	$P\bar{1}$
Data Collection				
(a) Diffractometer	Nicolet R3m	Nicolet R3m	Nicolet R3m	Nicolet R3m
(b) Radiation	Mo-K_α	Mo-K_α	Mo-K_α	Mo-K_α
(c) Temperature (K)	293	293	173	173
(d) $2\theta_{max}$ (°)	50	50	50	50
(e) Total reflections	2226	2877	1917	1934
(f) Unique reflections	2187	1599	1545	1805
(g) Crystal size (mm)	$0.25\times0.13\times0.10$	$0.38\times0.16\times0.08$	$0.40\times0.30\times0.25$	$0.50\times0.28\times0.18$
Structure solution, refinement				
(a) Method used	Patterson	Patterson	Direct methods	Direct methods
(b) R	0.033	0.034	0.031	0.033
(c) R_w	0.034	0.035	0.035	0.038
(d) ω[c] A.	1.17	1.16	1.00	1.37
B.	8×10^{-4}	6×10^{-4}	5×10^{-4}	1×10^{-3}
(e) Data used	1527	1598	1545	1651
(f) Discrimination	$I > 2.5\sigma(I)$	$I > 2.5\sigma(I)$	$I > 2.5\sigma(I)$	$I > 2.5\sigma(I)$

[a] Standard space group $C2/c$: $a = 40.150(6)$, $b = 5.401(1)$, $c = 10.601(2)$ Å, $\beta = 99.89(1)°$ (isomorphous with **1**).
[b] Not determined.
[c] $\omega = A/(\sigma^2F_o + BF_o^2)^{1/2}$.

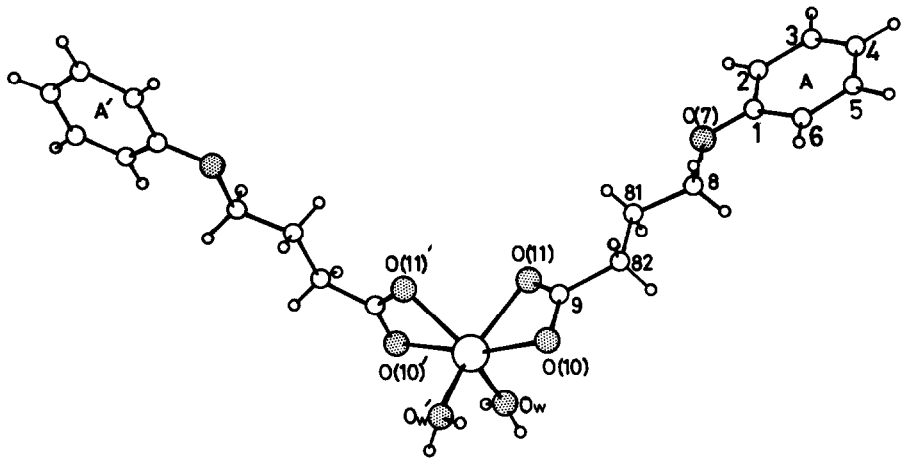

Fig. 1. Molecular conformation and atom naming scheme for $[Ni(PBA)_2(H_2O)_2]$ (1). Complex 2, $[Ni(PCBA)_2(H_2O)_2]$ is isomorphous.

Table 2. Bond distances (Å) and angles (°) about the coordination spheres for 1 and 2

	(1)	(2)
(a) Distances		
Ni—O(10)	2.181(2)	2.175(2)
Ni—O(11)	2.062(1)	2.068(2)
Ni—Ow	2.020(1)	2.016(2)
(b) Angles		
O(10)—Ni—O(11)	61.6(1)	61.5(1)
O(10)—Ni—O(10)′	87.4(1)	88.1(1)
O(10)—Ni—O(11)′	106.2(1)	107.4(1)
O(10)—Ni—Ow	151.9(1)	151.2(1)
O(10)—Ni—Ow′	94.2(1)	93.8(1)
O(11)—Ni—O(11)′	164.4(1)	165.7(1)
O(11)—Ni—Ow	91.3(1)	90.7(1)
O(11)—Ni—Ow′	99.1(1)	98.7(1)
Ow—Ni—Ow′	97.3(1)	98.1(1)
Ni—O(10)—C(9)	87.5(1)	87.5(2)
Ni—O(11)—C(9)	92.4(1)	92.4(2)

structure factors and IR spectra are available from the Editor or the authors.* Bond distances and angles about the coordination spheres for complexes 1 and 2 are given in Table 2.

DISCUSSION

Complexes 1, $[Ni(PBA)_2(H_2O)_2]$, and 2, $[Ni(PCBA)_2(H_2O)_2]$, are isomorphous and isostructural. The MO_6 stereochemistry in each is very distorted octahedral (Fig. 1) with molecular two-fold symmetry coincident with crystallographic symmetry. The coordination polyhedron comprises two waters [Ni—Ow, 2.021(2) Å, (1); 2.016(2) Å, (2)] and four oxygens from two slightly asymmetric bidentate carboxylate groups of the two γ-phenoxybutyrate ligands [Ni—O, 2.062, 2.181(2) Å, (1); 2.068, 2.175(2) Å, (2)]. This bidentate chelate complexing mode was previously unknown among the nickel(II) carboxylates. Examples having undistorted $[NiO_2(Ow)_4]$ octahedral stereochemistry, involving unidentate carboxyl groups are known; nickel(II) phenoxyacetate tetrahydrate,[1] nickel(II) acetate tetrahydrate[11,12] and nickel(II) formate dihydrate.[13] However, in the latter complex, the $[NiO_2(Ow)_2]$ unit is extended into a polymer structure via a second $[NiO_6]$ centre which involves six different carboxylate groups.

In contrast, zinc carboxylates, including phenoxyalkanoates and the analogous phenylthioalkanoates, having $MO_4(Ow)_2$ stereochemistry and crystallographic two-fold symmetry, are relatively well known.[8,14] These complexes, with only one exception (zinc acetate dihydrate[15]), all show considerable asymmetry in the bidentate carboxylate groups, ranging up to 2.03, 2.52 Å for zinc salicylate dihydrate.[16] These examples represent complexes of the *trans*-[M(bidentate)$_2$(unidentate)$_2$] type having small normalized bidentate "bite", which degenerate to skew-trapezoidal bipyramidal stereochemistry.[17] With complexes 1 and 2, the bidentate "bites" of the carboxyl groups are 2.17 Å (1) and 2.17 Å (2), which compare with 2.23 and 2.23 Å for the uncomplexed acids 4-(4-chlorophenoxy)butanoic acid (3) and 4-(2,4-dichlorophenoxy)butanoic acid (4), respectively. This is considerably shorter than the O···O distance found in normal carboxyl groups and results in a significant contraction in the O—C—O

*Atomic coordinates have also been deposited with the Cambridge Data Centre.

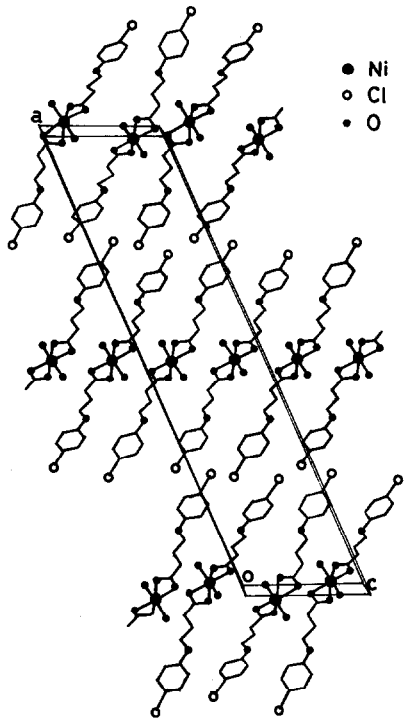

Fig. 2. Packing of complexes **1** and **2** in the unit cell.

bond angle of the group [118.5(2)° (**1**); 118.6(2)° (**2**), compared to 123.3(2)° (**3**) and 123.3(1)° (**4**)].

The monomeric complexes pack in the unit cell (Fig. 2) with only two intermolecular associations involving the coordinated water, Ow—O(10)′, [2.75 Å, (**1**) and 2.72 Å, (**2**)], and Ow—O(11)′ [2.77 Å, (**1**) and 2.78 Å, (**2**)]. Intramolecular stabilization results from longer associations between Ow(1) and O(11) [2.92 Å (**1**); 2.91 Å (**2**)]. The normally unassociated phenoxyalkanoate side-chains retain their preferred planar conformation (Table 3).

The isomorphism (single crystal X-ray preliminary photographs, chemical analysis and IR spectra), has been confirmed for the cobalt(II) complex, $[Co(PBA)_2(H_2O)_2]$ (**1a**). Although this phenomenon has not previously been observed for Ni and Co complexes with the phenoxyalkanoic acids, a number of cases of isomorphism involving other first transition series metal complexes have been described (Mn^{II}, Co^{II},[18] Co^{II}, Zn^{II}[19]). The inference is that like the Ni^{II} complexes (**1**) and (**2**), this Co^{II} complex is also very unusual since previous examples of these metal complexes with phenoxyalkanoic acids have been regular octahedral.

Acids and ligand conformation

The γ-phenoxyalkanoic acids (**3**) and (**4**) form centrosymmetric hydrogen bonded cyclic dimers [O···O, 2.62 Å (**3**) and 2.66 Å (**4**)], similar to most phenoxyalkanoic acids.[19] The oxybutanoic acid side-chains are essentially planar (Figs 3, 4), which is consistent with the observations for the phenoxyethanoic acids with no steric effects from 2,6-

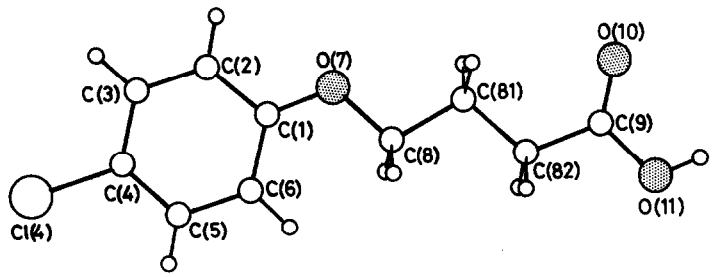

Fig. 3. Molecular conformation and atom naming scheme for (PCBAH) (**3**).

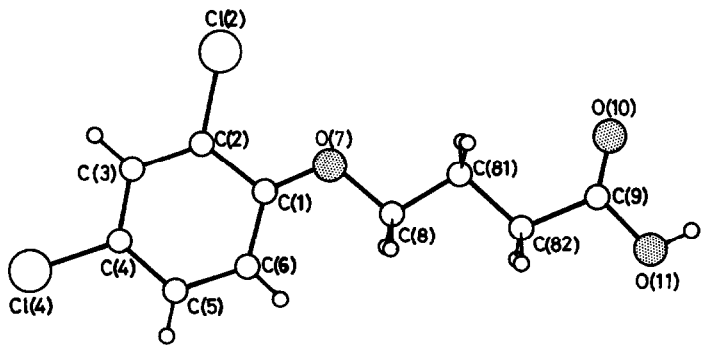

Fig. 4. Molecular conformation and atom naming scheme for (2,4-DB) (**4**).

Table 3. Comparative torsion angles (°) for the oxybutanoate side chains in **1** and **2** and the acids (PCBAH) and (2,4-DB)

	(1)	(2)	(PCBAH)	(2,4-DB)
C(2)—C(1)—O(7)—C(8)	+175.1(2)	+177.8(3)	+176.8(1)	+177.8(2)
C(1)—O(7)—C(8)—C(81)	−178.7(2)	−174.9(3)	−178.0(1)	−179.4(2)
O(7)—C(8)—C(81)—C(82)	−177.7(2)	−178.4(3)	−179.6(1)	+178.4(2)
C(8)—C(81)—C(82)—C(9)	+177.0(2)	+179.1(3)	−177.6(1)	−173.9(2)
C(81)—C(82)—C(9)—O(10)	−8.0(3)	−1.2(4)	−19.2(2)	10.2(3)

disubstitution in the ring system.[20] This conformation is retained on complexation in complexes **1** and **2**.

Acknowledgements—The authors acknowledge the support of F. Hoffmann la Roche Co., Basel, Switzerland, for the use of data collection and computing facilities during C.H.L.K.'s stay on special studies leave. The University of Queensland and the Queensland Institute of Technology are thanked for financial support.

REFERENCES

1. G. K. Prout, C. Walker and F. J. C. Rossotti, *J. Chem. Soc. A.* 1971, 556.
2. G. Smith, E. J. O'Reilly and C. H. L. Kennard, *Polyhedron* 1987, **6**, 871.
3. C. H. L. Kennard, G. Smith, E. J. O'Reilly and P. T. Manoharan, *Inorg. Chim. Acta.* 1984, **82**, 35.
4. C. Oldham, *Prog. Inorg. Chem.* 1986, **10**, 223.
5. F. A. Cotton and G. Wilkinson, *Advanced Inorganic Chemistry*, 3rd edn, p. 896. John Wiley, New York (1972).
6. E. Y. Spencer, *Guide to the Chemicals used in Crop Protection*, 6th edn, p. 153. Canada Department of Agriculture, Ottawa (1973).
7. M. E. Synerholm and P. W. Zimmerman, *Contrib. Boyce Thompson Inst.* 1945, **14**, 91.
8. G. Smith, E. J. O'Reilly, C. H. L. Kennard, K. Stadnicka and B. Oleksyn, *Inorg. Chim. Acta.* 1981, **111**, 120.
9. G. M. Sheldrick, SHELX-76 Program for Crystal Structure Determination. University of Cambridge (1976).
10. *International Tables for X-ray Crystallography* (Edited by J. A. Ibers and W. C. Hamilton), Vol. 4. Kynoch Press, Birmingham (1974).
11. R. E. Cramer, W. van Doorne and R. Dubois, *Inorg. Chem.* 1975, **14**, 2462.
12. J. N. van Niekerk and F. R. L. Schoening, *Acta Cryst.* 1953, **6**, 609; T. C. Downie, W. Harrison, E. S. Raper and M. A. Hepworth, *Acta Cryst. Sect. B* 1971, **27**, 706; E. N. Treushnikov, V. I. Kuskov, L. A. Aslanov and L. V. Soblova, *Kristallografiya* 1980, **25**, 287.
13. K. Krogmann and R. Mattes, *Z. Kristallogr.* 1963, **118**, 291.
14. T. C. W. Mak, W.-H. Yip, G. Smith, E. J. O'Reilly and C. H. L. Kennard, *Inorg. Chim. Acta* 1984, **84**, 57; W.-H. Chan, T. C. W. Mak, W.-H. Yip, G. Smith, E. J. O'Reilly and C. H. L. Kennard, *Polyhedron* 1987, **6**, 881.
15. J. N. van Niekerk, F. R. L. Schoening and J. H. Talbot, *Acta Cryst.* 1953, **6**, 720.
16. H. P. Klug, L. E. Alexander and G. G. Sumner, *Acta Cryst.* 1958, **11**, 41.
17. D. L. Kepert, *Progress in Inorganic Chemistry* (Edited by S. J. Lippard), Vol. 23, p. 1. J. Wiley, New York (1977).
18. G. Smith, E. J. O'Reilly and C. H. L. Kennard, *J. Chem. Soc., Dalton Trans.* 1980, 2462.
19. C. H. L. Kennard, E. J. O'Reilly, G. Smith and T. C. W. Mak, *Aust. J. Chem.* 1985, **38**, 1381.
20. C. H. L. Kennard, G. Smith and A. H. White, *Acta Cryst. Sect. B* 1982, **38**, 868.

Polyhedron Vol. 8, No. 1, pp. 45–49, 1989
Printed in Great Britain

0277–5387/89 $3.00+.00
© 1988 Pergamon Press plc

STUDIES ON THE STRUCTURE OF THE PARAMAGNETIC μ-OXO DIMER OF MOLYBDENUM(V) IN HYDROCHLORIC ACID SOLUTIONS BY EXAFS

KUNIHIKO YOKOI*

Department of Chemistry, Osaka Kyoiku University, Ikeda, Osaka 563, Japan

and

NOBUYUKI MATSUBAYASHI

National Chemical Laboratory for Industry, Yatabe, Ibaraki 305, Japan

and

TAKAFUMI MIYANAGA, IWAO WATANABE and SHIGERO IKEDA

Department of Chemistry, Faculty of Science, Osaka University, Toyonaka, Osaka 560, Japan

and

KATSUO MURATA

Naruto University of Teacher Education, Naruto, Tokushima 772, Japan

(*Received* 15 *February* 1988; *accepted after revision* 4 *July* 1988)

Abstract—X-ray absorption spectra for molybdenum(V) in hydrochloric acid solutions were measured and their XANES and EXAFS were analysed. The μ-oxo dimer of Mo^V was detected in 4.5–6.0 M HCl solutions. The Mo—Mo bond length in the dimer is 2.94–3.06 Å and the Mo—O—Mo angle is *ca* 104–111°.

For the Mo^V species in hydrochloric acid solution several investigations have been carried out by the means of magnetic susceptibility,[1] spectrophotometry,[2,3] ESR spectroscopy[4,5] and others.[6,7] These studies indicated that in highly acidic solutions (> 8 M HCl) the major dissolved species is a paramagnetic monomer of $MoOCl_5^{2-}$. When the acidity of the solution is decreased, dimerization occurs to produce a paramagnetic μ-oxo dimer of $Mo_2O_3Cl_8^{4-}$ (in 5–6 M HCl). A further decrease of the acidity results in a diamagnetic dimer having di-μ-oxo $Mo_2O_4^{2+}$ core. The $MoOCl_5^{2-}$ in solution shows spectral and magnetic properties essentially identical to those of the salts of M_2MoOCl_5 [M = NH_4^+, pyH^+, Cs^+, etc.],[8,9] indicating that the structure of $MoOCl_5^{2-}$ in solution remains almost the same as those in solids. For $Mo_2O_4^{2+}$, the spectral data indicate the structural similarity in solids and solutions.[3] The schematic illustrations of the structures for $MoOCl_5^{2-}$ and $Mo_2O_4^{2+}$ are shown in Fig. 1.

For $Mo_2O_3Cl_8^{4-}$, there have been few reports concerning its structure. Colton and Rose[12] reported the synthesis of $[(C_2H_5)_4N]_4[Mo_2O_3Cl_8]$. Its spectral data were usually associated with di-μ-oxo dimers of $Mo_2O_4^{2+}$ and not μ-oxo species.[7] It has also been reported that this synthesis was difficult to reproduce.[13] Therefore, there are some limitations to investigating the structure of the μ-oxo dimer of $Mo_2O_3Cl_8^{4-}$ in solution by comparing with the structure of $Mo_2O_3Cl_8^{4-}$ in solid crystals.

Extended X-ray absorption fine structure (EXAFS) has been useful to analyse various materials having no long-range order, such as amorphous compounds, metal complexes in enzymes and in solutions.[14] Cramer *et al.*[15] have already investigated the EXAFS for Mo^V in 3 M HCl solution and reported that the structure of the dissolved Mo^V species is similar to that of $Mo_2O_4^{2+}$ shown in Fig. 1. In the present work the

*Author to whom correspondence should be addressed.

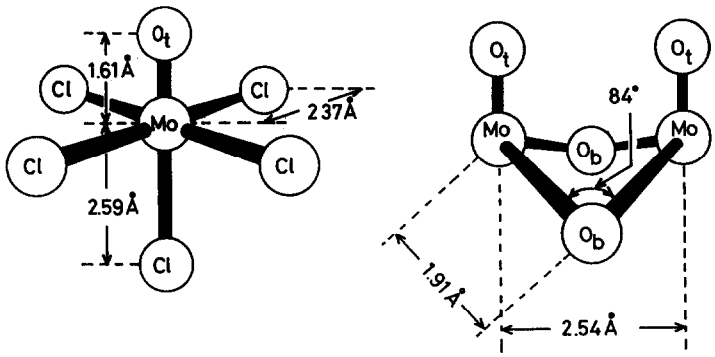

Fig. 1. Schematic illustrations of the structures for $MoOCl_5^{2-}$ and $Mo_2O_4^{2+}$, taken from refs 10 and 11.

structure of μ-oxo dimer of $Mo_2O_3Cl_8^{4-}$ is investigated by analysing its X-ray absorption near edge structure (XANES) and EXAFS and by comparing with those for other Mo^V samples.

EXPERIMENTAL

$BaMo_2O_4(C_2O_4)_2 \cdot 5H_2O$,[16] $Mo_2O_3[S_2CN(C_2H_5)_2]_4$,[17] $Mo_2O_3(S_2COC_2H_5)_4$,[17] $(NH_4)_2MoOCl_5$[18] and Mo^V in HCl solutions[19] were prepared according to the literature. Mo^V solutions were deaerated by bubbling pure nitrogen through them. The concentrations of Mo^V were adjusted to 0.12 M and were determined by spectrophotometry and cerium(IV) titration.[20] Other chemicals were of guaranteed reagent grade and were used without further purification.

X-ray absorption spectra were obtained with the EXAFS apparatus of the 2.5 GeV storage ring from Photon Factory at Tsukuba. Photon energy was calibrated by using a pre-edge peak of sodium molybdate, $Na_2MoO_4 \cdot 2H_2O$ at 20007.0 eV. Other conditions were the same as those reported previously.[21]

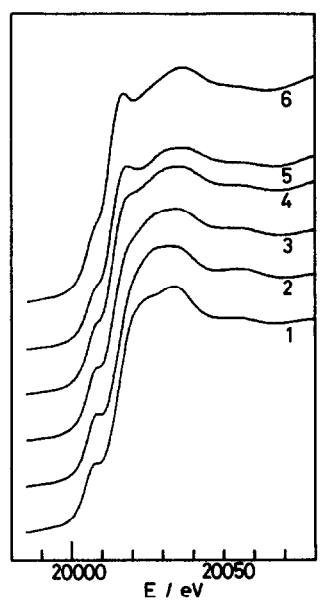

Fig. 2. Mo-K-edge XANES spectra for the Mo^V samples. (1) $BaMo_2O_4(C_2O_4)_2 \cdot 5H_2O$; (2), (3), (4) and (5) are for 0.12 M Mo^V in 3.0, 5.4, 6.0 and 8.0 M HCl, respectively; (6) $(NH_4)_2MoOCl_5$.

RESULTS AND DISCUSSION

K-edge XANES spectra of Mo^V taken for various samples are shown in Fig. 2. For $BaMo_2O_4(C_2O_4)_2 5H_2O$ (Ba-salt) a pre-edge peak is observed at 20008.7 eV. This pre-edge peak is assigned to a 1*s*–4*d* transition.[22] The pre-edge peak for Mo^V in HCl solution is observed clearly, when c_{HCl}, the concentration of HCl, is less than 5 M. However, in more acidic solutions the peak is obscured due to the red shift of the absorption edge. The coordination of the chloride ion may cause a shift of the edge, which is indicated by the result of EXAFS analysis described later in this paper. In HCl solutions molybdenum(V) complexes are involved in dimer(diamagnetic)–dimer (paramagnetic)–monomer(paramagnetic) equilibria and their core units are represented generally as follows:[7,23]

$$\underset{(\geqslant 8\text{ M HCl})}{2MoO^{3+}} \rightleftharpoons \underset{(5\text{–}6\text{ M HCl})}{\begin{matrix} Mo_2O_3^{4+} \\ + \\ 2H^+ \end{matrix}} \rightleftharpoons \underset{(3\text{ M HCl} \geqslant)}{\begin{matrix} Mo_2O_4^{2+} \\ + \\ 2H^+ \end{matrix}}$$

The intensities of the pre-edge peak in 1.2–5 M HCl solutions change little and correspond to the presence of one Mo=O bond (it is known that the intensity of the pre-edge peak correlates with the number of Mo=O bonds per molybdenum atom[21]). This result agrees with the fact that the dissolved species have one Mo=O bond per mol-

ybdenum atom. The threshold energy, E_0 (which was determined from the position of the half height of the absorption edge at around 20040 eV; in this method experimental errors for E_0 are within about $\pm$ 0.2 eV), for various Mo^{V} samples are listed in Table 1. The values of E_0 in HCl solutions of less than 3 M where major species contain the $Mo_2O_4^{2+}$ unit are close to that for Ba-salt. As c_{HCl} is increased the value of E_0 is decreased. In 5–6 M HCl solutions where the $Mo_2O_3^{4+}$ unit is present,[2] the value of E_0 varies from 20013.6 to 20012.3 eV. The solid samples of $Mo_2O_3[S_2CN(C_2H_5)_2]_4$ and $Mo_2O_3(S_2COC_2H_5)_4$, containing the $Mo_2O_3^{4+}$ unit, also have the value of 20012.4 and 20013.4 eV, respectively. In an 8 M HCl solution where the major species is considered to contain the unit of MoO^{3+}, the XANES spectrum and the value of E_0 are very close to those for $(NH_4)_2MoOCl_5$ (NH_4-salt).

EXAFS Fourier transforms (FT) for various Mo^{V} samples are shown in Fig. 3. In the FT, the corrections for the phase shift and the back-scattering amplitude were performed by using the parameters for the Mo—O bond given by Teo and Lee[24] (in this method experimental errors for bond distances are within about $\pm$ 0.02 Å). In the EXAFS FT for the Ba-salt, two distinct peaks are observed at 1.75 and 2.56 Å. The peak at 1.75 Å may correspond to both Mo—O_b (bridging oxygen atom) and Mo—O_t (terminal oxygen atom) (1.88 and 1.93 Å for Mo—O_b and 1.70 Å for Mo—O_t were reported[11]), in fact, also for Mo^{VI} compounds peaks for Mo—O_b and Mo—O_t are not observed separately by EXAFS.[21] The peak at 2.56 Å corresponds to Mo—Mo and this value agrees with that obtained by X-ray diffraction analysis.[11] In HCl solutions of less than 3 M the structures of the dissolved Mo^{V} species remain the same as that for $Mo_2O_4^{2+}$, for their EXAFS FT are almost the same as that for Ba-salt, as already reported by Cramer *et al.*[15] The increase in concentration of HCl brings about an appearance of a peak at about 2.3 Å (in > 4.5 M HCl), indicating the coordination of chloride ions to the molybdenum atom. In 5.4 M HCl, a distinct peak appears at 2.99 Å, and this is assigned to the Mo—Mo bond distance of the $Mo_2O_3^{4+}$ unit, as this peak is observed in the 4.5–6 M HCl solutions where the Mo^{V} species of $Mo_2O_3Cl_8^{4-}$ is considered to be present.[2] In an 8 M HCl solution peaks corresponding to Mo—Mo bonds disappear and peaks for Mo=O (1.67 Å) and Mo—Cl (2.36 Å) bonds are observed. These results are also observed for the NH_4-salt, indicating that $MoOCl_5^{2-}$ is present as the major species in 8 M HCl solution.

The numbers of coordinating oxygen, chlorine and molybdenum atoms, N_O, N_{Cl}, $N_{Mo(a)}$ (for the $Mo_2O_4^{2+}$ unit) and $N_{Mo(b)}$ (for $Mo_2O_3^{4+}$), respectively, for the Mo^{V} species in HCl solutions of various concentration are estimated by using the relation, $hR^2 = PN$, where h is the peak height in FT, R is the bond length and P is the proportional

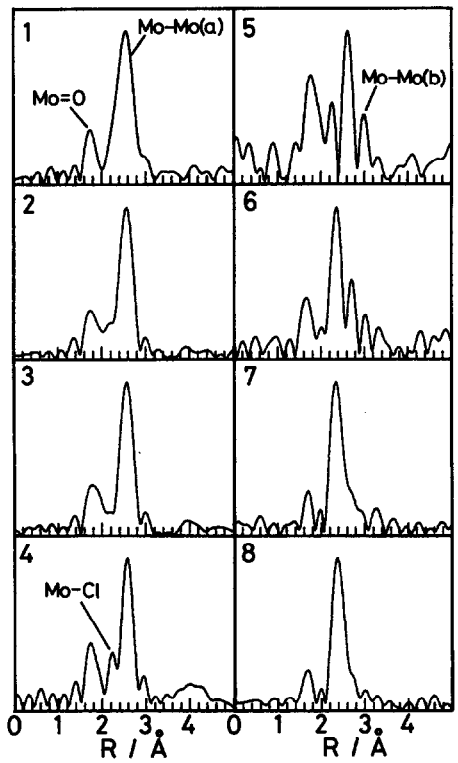

Fig. 3. EXAFS FT for various Mo^{V} samples. (1) $BaMo_2O_4(C_2H_4)_2 \cdot 5H_2O$; (2), (3), (4), (5), (6) and (7) are for 0.12 M Mo^{V} in 1.2, 3.0, 5.0, 5.4, 6.0 and 8.0 M HCl, respectively; (8) $(NH_4)_2MoOCl_5$. k: 5.5–17.5 $Å^{-1}$.

Table 1. E_0 values for various samples

	E_0 (eV)	c_{HCl} (M)	E_0 (eV)
solid **1**	20015.0	1.2	20014.5
2	20013.4	3.0	20014.4
3	20012.4	4.5	20014.1
4	20011.3	5.0	20013.6
		5.2	20013.4
		5.4	20013.2
		5.6	20012.9
		6.0	20012.3
		6.5	20011.8
		8.0	20011.6

1, **2**, **3** and **4** denote $BaMo_2O_4(C_2O_4)_2 \cdot 5H_2O$, $Mo_2O_3(S_2COC_2H_5)_4$, $Mo_2O_3[S_2CN(C_2H_5)_2]_4$ and $(NH_4)_2MoOCl_5$, respectively.

Table 2. Results of EXAFS FT

c_{HCl} (M)	R_0 (Å)	N_0	R_{Cl} (Å)	N_{Cl}	$R_{Mo(a)}$ (Å)	$N_{Mo(a)}$	$R_{Mo(b)}$ (Å)	$N_{Mo(b)}$
1.2	1.74	0.98	—	—	2.55	1.0	—	—
3.0	1.78	0.95	—	—	2.57	1.0	—	—
4.5	1.76	0.97	—	—	2.58	0.84	3.01	0.16
5.0	1.73	1.00	2.23	0.91	2.59	0.76	2.96	0.24
5.2	1.74	0.93	2.24	0.96	2.61	0.71	2.94	0.29
5.4	1.73	1.06	2.25	1.12	2.63	0.61	2.99	0.39
5.6	1.71	1.01	2.27	1.62	2.66	0.50	3.02	0.33
6.0	1.69	1.05	2.36	2.46	2.74	0.47	3.06	0.28
6.5	1.64	0.97	2.37	3.63	2.82	0.44	—	—
8.0	1.67	1.00	2.36	4.00	—	—	—	—

constant.[25] In this case the root–mean–square relative deviation (RMSRD) of R is assumed to be constant. This assumption leads to the experimental errors for N within about $\pm 7\%$. The reference samples used to determine the value of P were $MoOCl_5^{2-}$ (in 8 M HCl) for N_O and N_{Cl}, and $Mo_2O_4^{2+}$ (in 1.2 M HCl) for N_{Mo}. The values of R and N determined are listed in Table 2. In these analyses values for N are averaged ones for each molybdenum atom and therefore, not for each species. In HCl solutions of less than 3 M where the Mo^V dimer containing the $Mo_2O_4^{2+}$ unit is mainly present, the values of N_O are nearly one, i.e. it is equal to the number of Mo—O_t bonds, although the peaks at about 1.74–1.78 Å also have the character of the two Mo—O_b bonds. In 1.2–8 M HCl solutions the value of N_O remains nearly one and this result is in agreement with the structures of three major units that have one Mo—O_t bond per molybdenum atom. For the coordination of the chloride ion, the value of N_{Cl} increases when c_{HCl} is increased above 5 M HCl (in 4.5 M HCl a shoulder for Mo—Cl is observed at around 2.3 Å). For an 8 M HCl solution the value of N_{Cl} is four implying that four chlorine atoms which are *cis*-directed to the terminal oxygen are taken into consideration, that is, the value of N_{Cl} in Table 2 does not contain any information of the chlorine atom *trans*-directed to the terminal oxygen.

For the dimer ($Mo_2O_4^{2+}$)–dimer($Mo_2O_3^{4+}$)–monomer(MoO^{3+}) equilibria, concentrations of each species were determined from the values of $N_{Mo(a)}$ and $N_{Mo(b)}$, and fractions, [Mo^V in each species]/[total Mo^V] ([] denotes the concentration of the monomer), were calculated in HCl solutions of various concentration. The results are shown in Fig. 4. These results are in agreement with those obtained by spectrophotometric measurements.[2] That is, the peak at about 2.94–3.06 Å in 4.5–6 M HCl solutions can be assigned undoubtedly to the Mo—Mo bond in the $Mo_2O_3^{4+}$ unit. As shown in Fig. 4 the fraction for $Mo_2O_3^{4+}$ is less than *ca* 0.4 and this result is also in agreement with that reported previously.[2,4]

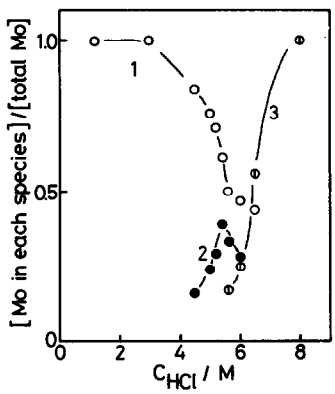

Fig. 4. Dependence of [Mo^V in each species]/[total Mo^V] on c_{CHl}. (1) $Mo_2O_4^{2+}$; (2) $Mo_2O_3^{4+}$; (3) MoO^{3+}.

The distance for Mo—Mo in the $Mo_2O_3^{4+}$ unit was determined to be 2.94–3.06 Å in 4.5–6 M HCl while its Mo—O_b distance cannot be determined precisely by the FT method as described above. However, assuming that the Mo—O_b distance is 1.86 Å, which is the averaged Mo—O_b value obtained from the literature for $Mo_2O_3(S_2COC_2H_5)_4$,[26] $Mo_2O_3[S_2CN(C_3H_7)_2]_4$[27] and $Mo_2O_3[S_2P(OC_2H_5)_2]_4$[28] (these species have linear μ-oxo bridges), it is concluded that the dimer containing the $Mo_2O_3^{4+}$ unit has a bent Mo—O—Mo bond with an angle of *ca* 104–111°. Blake *et al.*[26] deduced by molecular orbital considerations that if the $Mo_2O_3^{4+}$ unit has a linear μ-oxo bridge, the two Mo=O bonds in paramagnetic $Mo_2O_3^{4+}$ are present in different planes in order to avoid the three-centred *d–p–d* interaction. In this study, it is revealed that the paramagnetic dimer containing the $Mo_2O_3^{4+}$ unit in

HCl solution has a bent μ-oxo bridge, however, the two different Mo=O bonds may also be present in different planes in order to avoid a direct interaction between the Mo atoms in order to keep its paramagnetic character.

Acknowledgements—The authors thank Drs Tadashi Matsushita and Masaharu Nomura of the National Laboratory for High Energy Physics (K.E.K.) for their help with the X-ray absorption measurements.

REFERENCES

1. L. Sacconi and R. Cini, *J. Am. Chem. Soc.* 1954, **76**, 4239.
2. G. P. Haight Jr, *J. Inorg. Nucl. Chem.* 1962, **24**, 663.
3. M. Ardon and A. Pernick, *Inorg. Chem.* 1973, **12**, 2484.
4. C. R. Hare, I. Bernal and H. B. Gray, *Inorg. Chem.* 1962, **1**, 831.
5. I. N. Marov, Yu. N. Dubrov, G. A. Evtikova, V. K. Belyaeva, A. N. Ermakov and P. A. Korovaikov, *Russ. J. Inorg. Chem.* 1970, **15**, 1148.
6. S. Himeno and M. Hasegawa, *Inorg. Chim. Acta* 1984, **83**, L17.
7. E. I. Stiefel, *Progress in Inorganic Chemistry* (Edited by S. J. Lippard), Vol. 22, p. 45 and references therein. John Wiley, New York (1977).
8. R. G. James and W. Wardlaw, *J. Chem. Soc.* 1927, 2145.
9. E. A. Allen, B. J. Brisdon, D. A. Edwards, G. W. A. Fowles and R. G. Williams, *J. Chem. Soc.* 1963, 4649.
10. V. V. Tkavec, O. N. Krasocka and L. O. Atovmijan, *J. Struct. Chem.* 1976, **17**, 808.
11. F. A. Cotton and S. M. Morehouse, *Inorg. Chem.* 1965, **4**, 1377.
12. R. Colton and G. G. Rose, *Aust. J. Chem.* 1968, **21**, 883.
13. F. A. Cotton, D. L. Hunter, L. Ricard and R. Weiss, *J. Coord. Chem.* 1974, **3**, 259.
14. A. Biancone, L. Incoccia and S. Stipcich (Eds), *EXAFS and Near Edge Structure.* Springer, New York (1983).
15. S. P. Cramer, P. K. Eidem, M. T. Paffett, J. R. Winkler, Z. Dori and H. B. Gray, *J. Am. Chem. Soc.* 1983, **105**, 799.
16. R. G. James and W. Wardlaw, *J. Chem. Soc.* 1927, 2152.
17. F. W. Moore and M. L. Larson, *Inorg. Chem.* 1967, **6**, 998.
18. Y. Sasaki and A. G. Sykes, *J. Chem. Soc., Dalton Trans.* 1974, 1468.
19. N. H. Furman and W. M. Murry, *J. Am. Chem. Soc.* 1936, **58**, 1689.
20. G. A. Parker, *Analytical Chemistry of Molybdenum*, p. 34. Springer, New York (1983).
21. K. Yokoi, N. Matsubayashi, T. Miyanaga, I. Watanabe, K. Murata and S. Ikeda, *Chem. Lett.* 1987, 1453.
22. S. P. Cramer, K. O. Hodgson, W. O. Gillum and L. E. Mortenson, *J. Am. Chem. Soc.* 1978, **100**, 3398.
23. G. P. Haight and D. R. Boston, *J. Less-Common Met.* 1974, **36**, 95.
24. B. K. Teo and P. A. Lee, *J. Am. Chem. Soc.* 1979, **101**, 2815.
25. E. A. Stern, D. E. Sayers and F. W. Lytle, *Phys. Rev. B* 1975, **11**, 4836.
26. A. B. Blake, F. A. Cotton and J. S. Wood, *J. Am. Chem. Soc.* 1964, **86**, 3024.
27. L. Ricard, J. Estienne, P. Karagiannidis, P. Toledano, J. Fischer, A. Mitschler and R. Weiss, *J. Coord. Chem.* 1974, **3**, 277.
28. J. R. Knox and C. K. Prout, *Acta Cryst., Sect. B* 1968, **25**, 2281.

Polyhedron Vol. 8, No. 1, pp. 51–55, 1989
Printed in Great Britain

0277–5387/89 $3.00+.00
© 1988 Pergamon Press plc

KINETIC STUDIES OF THE OXIDATION OF DIAQUA-BIS(PICOLINATO)COBALTATE(II) BY PERIODATE

AHMED A. ABDEL-KHALEK

Chemistry Department, Faculty of Science, Cairo University, Beni-Suef City, Egypt

(*Received* 18 *February* 1988; *accepted after revision* 4 *July* 1988)

Abstract—A kinetic study of the oxidation of the bis complex of pyridinecarboxylic acid (picolinic acid) with cobalt(II), $[Co(pc)_2(H_2O)_2]$ (pc = picolinate), by periodate in an acetate medium has been performed. The kinetics obeyed the rate law $d[Co^{III}]/dt = (k'_2+k_3[CH_3COO^-])[Co^{II}(pc)_2(H_2O)_2][IO_4^-]$. An inner-sphere mechanism is proposed. An argument based on isokinetic correlations among activation parameters for the oxidation of a series of some cobalt(II) complexes, including the picolinato complex, is presented in support of a common mechanism for these reactions.

Periodate oxidations (IO_4^- products) are believed to proceed via an inner-sphere mechanism.[1–8] Its oxidation of organic substrates are specific when direct bonding of I^{VII} to e.g. OH, NH_2 etc. in the 1,2 positions with the formation of a cyclic intermediates.[1] An inner-sphere mechanism was proposed for iodide oxidation where an oxygen atom transfer with the formation of HOI as an intermediate was invoked.[2] Further support for this mechanism could be drawn from reactions of this oxidant with transition metal complexes. It was found that periodate readily oxidizes either labile complexes or inert complexes possessing at least one potential bridging ligand. In the oxidation of iron(II), stopped-flow traces clearly showed the formation and decomposition of an intermediate.[3] Intermediate cobalt(III) products, which are indicative of Co—O—IO_3 bond formation, were also identified spectrophotometrically in periodate oxidations of cobalt(II) complexes of edta[4] (ethylenediaminetetraacetate), hedta[5] (N-2-hydroxyethylethylenediaminetriacetate), edda[5] (ethylenediaminediacetate) and nta[6] (nitrilotriacetate). A common mechanism for the oxidation of these cobalt(II) complexes by periodate is proposed and supported by an excellent isokinetic relationship between ΔH^* and ΔS^* values for these reactions.[6] The initial cobalt(III) product was not observed in the case of oxidation of cdta (*trans*-1,2-diaminecyclohexanetetraacetate) by periodate because the rate of ring closure is faster than that of oxidation.[7] In the oxidation of chromium(III) by periodate, the hydroxo species is the reactive ion, with the hydroxide acting as the bridging ligand.[8]

In particular we have chosen the pyridinecarboxylic acids, supported by the fact that some properties of the respective complexes are influenced by the position and number of functional groups.

In the present study we report our findings on the oxidation of $[Co(pc)_2(H_2O)_2]$ by IO_4^-.

EXPERIMENTAL

Reagents

Reagent grade picolinic acid, sodium metaperiodate, cobalt nitrate hexahydrate, sodium acetate, sodium nitrate and glacial acetic acid were used without further purification. A stock solution of periodate was made up by weight and wrapped with Al foil to avoid photochemical decomposition.[9] A cobalt(II) nitrate solution was standardized with edta volumetrically. A stock solution of the sodium salt of picolinic acid was prepared by weighing the acid form and neutralizing with the appropriate amount of sodium hydroxide. The $[Co(pc)_2(H_2O)_2]$ was made up just before the kinetic run by mixing cobalt(II) and ligand solutions in the concentration ratio 1 : 2.3 to ensure complete formation. At lower ratios the oxidation is very difficult and a yellow precipitate always formed, which is similar to the precipitate obtained on mixing cobalt(II) and periodate. Solutions of sodium acetate and sodium

nitrate were made up by weight and those of acetic acid by dilution, and standardized against sodium hydroxide solution.

Oxidation products

The stoichiometry of the reaction can be represented by eq. (1).

$$2[Co^{II}(pc)_2]+IO_4^- \longrightarrow 2[Co^{III}(pc)_2]^+ + IO_3^- \quad (1)$$

where IO_4^- represents the total periodate. The ratio of [Co^{III} complex] produced to [IO_4^-] initially present was 2.00 ± 0.05.

The UV–vis. absorption spectra of the products from the oxidation of $[Co^{II}(pc)_2(H_2O)_2]$ by IO_4^-, in the absence and presence of acetate ions, were recorded on a Unicam SP8000 spectrophotometer. The maxima and molar absorption coefficients of the acetate-free cobalt(III) product at pH 4.0 were $\varepsilon_{max}^{535} = 174$ and $\varepsilon_{max}^{382} = 290$ $dm^3\ mol^{-1}\ cm^{-1}$.[10] In acetate medium these values were $\varepsilon_{max}^{533} = 204$ and $\varepsilon_{max}^{382} = 305\ dm^3\ mol^{-1}\ cm^{-1}$. The molar absorbance of the cobalt(III) product, in acetate buffer, varies with acetate ion concentration.

Kinetic measurements

A Unicam SP8000 spectrophotometer, equipped with a thermostatted cell holder, was used to monitor the reaction. The reactants in buffer solutions in the two compartments of an indented flask, were thermostatted for about 20 min. These were thoroughly mixed and quickly transferred to an absorption cell. The formation of the cobalt(III) complex was followed at 530 nm where the absorption is maximal at the pH of the reaction. Pseudo-first-order conditions were maintained in all runs by using a large excess of periodate concentrations (more than ten-fold) over that of $[Co^{II}(pc)_2(H_2O)_2]$. The pH of the reaction was measured on a Radiometer digital pH meter model PHM62. The ionic strength was maintained by using the appropriate amounts of sodium nitrate solution.

RESULTS

The UV–vis. absorption spectrum of the product from the oxidation of $[Co^{II}(pc)_2(H_2O)_2]$ by periodate gave only the final product $[Co^{III}(pc)_2(H_2O)_2^+]$. This is in contrast to what was found in oxidations of cobalt(II) complexes of edta,[4] hedta, edda,[5] and nta,[6] where intermediate cobalt(III) products were identified spectrophotometrically.

The kinetics of $[Co^{II}(pc)_2(H_2O)_2]$ oxidation by periodate were studied over the pH range 4.05–5.15, ionic strength 0.50 M and temperatures 20, 25, 30 and 35°C over a range of periodate and complex concentrations.

Plots of $\ln(A_\infty - A_t)$ vs time were linear up to $\geqslant 80\%$ of the reaction where A_∞ and A_t are absorbances at infinity and time t, respectively. Pseudo-first-order rate constants, obtained from the slopes of these plots using a linear least-squares program, are collected in Table 1. The constancy of k_{obs}, at a

Table 1. Kinetic parameters for the oxidation of $[Co^{II}(pc)_2(H_2O)_2]$ by IO_4^- at $I = 0.5$ M (CH_3CO_2Na) and 25°C

pH	$10^2[IO_4^-]$ (M)	$10^4[Co(II)(pc)_2(H_2O)_2]$ (M)	$10^3 k_{obs}$[a] (s^{-1})	$10k_2$[b] ($M^{-1}\ s^{-1}$)
4.05	0.5	5.0	0.75	1.50
4.05	1.0	5.0	1.37	1.37
4.05	1.5	5.0	2.15	1.43
4.05	2.0	2.0	2.90	1.45
4.05	2.0	5.0	2.84	1.42
4.05	2.0	7.0	2.80	1.40
4.05	2.5	5.0	3.84	1.54
4.05	3.0	5.0	4.41	1.47
4.05	3.5	5.0	5.05	1.44
4.05	4.0	5.0	5.58	1.40
4.05	5.0	5.0	7.31	1.46
4.33	3.0	5.0	4.72	1.57
4.48	3.0	5.0	5.21	1.74
4.76	3.0	5.0	4.96	1.65
4.83	3.0	5.0	4.31	1.44
5.15	3.0	5.0	4.16	1.39

[a] Standard deviations = 3%.
[b] $k_2 = k_{obs}/[IO_4^-]$.

Table 2. Dependence of k_2 on the acetate ion concentration at $I = 0.5$ M ($CH_3Co_2Na + NaNO_3$), pH = 4.33 and at different temperatures

$[CH_3CO_2^-]$ (M)	10^2k_2[a] ($M^{-1}s^{-1}$) 20.0°C	25.0°C	30.0°C	35.0°C
0.05	5.4	6.7	8.1	10.7
0.10	6.1	7.9	9.5	12.3
0.25	7.9	10.4	13.1	16.4
0.35	—	12.6	—	—
0.40	9.7	—	16.9	20.8
0.50	11.5	14.9	19.3	24.2

[a] Standard deviations = 2–4%.

fixed periodate concentration, pH, ionic strength and temperature over a range of complex concentration, is in agreement with a first-order dependence on $[Co^{II}(pc)_2(H_2O)_2]$.

The rate of the reaction was found to be directly proportional to the concentration of IO_4^-. The results in Table 1 show that k_{obs} varies linearly with $[IO_4^-]$ according to eq. (2).

$$k_{obs} = k_2[IO_4^-]. \quad (2)$$

The dependence of the reaction rate on pH was investigated over the range of pH 4.05–5.15. It was found that the change of k_{obs} with a change in pH value is not consistent over one unit of pH increase. It was decided to examine whether the apparent pH dependence arises from a mechanistic path or a medium effect. Kinetic runs were then carried out at constant pH and ionic strength using different acetate ion concentrations. The results in Table 2 and Fig. 1 show that k_2 depends on acetate ion

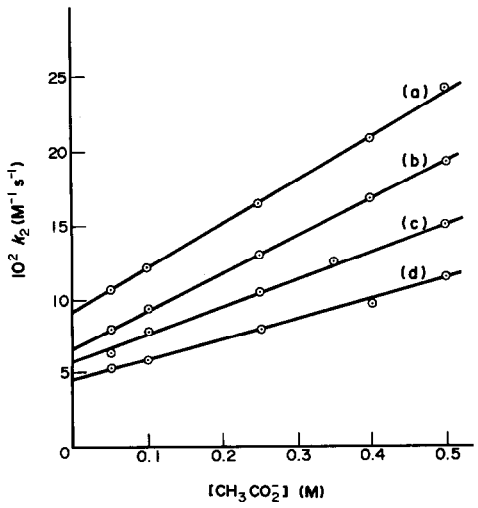

Fig. 1. Dependence of k_2 on $[CH_3CO_2^-]$ at (a) 35.0, (b) 30.0, (c) 25.0, (d) 20.0°C.

Table 3. Variation of acetate-dependent rate constant k'_2 and acetate-dependent rate constant k_3 with temperature

T (°C)	$10^2k'_2$ ($M^{-1}s^{-1}$)	$10k_3$ ($M^{-2}s^{-1}$)
20.0	4.7±0.6	1.3±0.3
25.0	5.9±0.5	1.8±0.7
30.0	6.9±0.4	2.5±0.6
35.0	9.2±0.7	2.9±0.8

concentration. This dependence can be described by eq. (3) at the temperature used.

$$k_2 = k'_2 + k_3[CH_2COO^-]. \quad (3)$$

From these results, the rate law for the oxidation of $[Co^{II}(pc)_2(H_2O)_2]$ by IO_4^- in acetate medium is given by eq. (4).

$$d[Co^{III}]/dt = (k'_2 + k_3[CH_3COO^-])[Co^{II}(pc)_2(H_2O)_2][IO_4^-]. \quad (4)$$

The values of k'_2 and k_3, collected in Table 3, at the temperature used, were obtained from the intercepts and the slopes, respectively, of Fig. 1. Enthalpies of activation associated with k'_2 and k_3, ΔH_2^* and ΔH_3^*, were calculated from a linear least-squares fit to the Eyring equation to be 30±2.5 and 40±2 kJ mol^{-1}, respectively. The corresponding entropies of activation ΔS_2^* and ΔS_3^* were calculated as −160±8 and −126±8 $JK^{-1}\,mol^{-1}$, respectively.

A plot of ΔH^* against ΔS^* for the oxidation of cobalt(II) complexes of hedta, edda, edta, and nta with periodate[6] is repeated, including values of ΔH^* and ΔS^* for the oxidation of $[Co^{II}(pc)_2(H_2O)_2]$, Table 4, as shown in Fig. 2. This plot reveals a

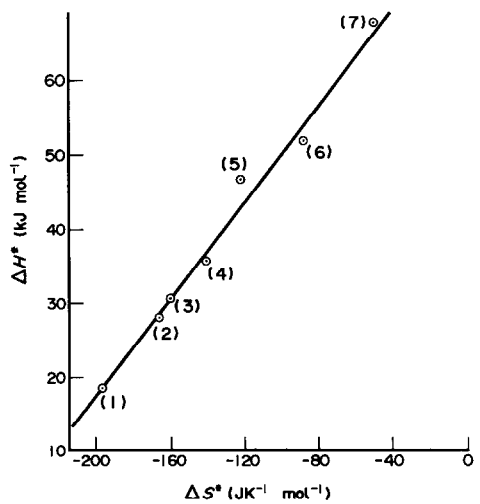

Fig. 2. Isokinetic plot for the oxidation of cobalt(II) complexes: (1) $[Co^{II}(edda)(H_2O)_2]$; (2) $[Co^{II}(hedta)(H_2O)]^-$; (3) $[Co^{II}(pc)_2(H_2O)_2]$; (4) $[Co^{II}(nta)(CH_3Co_2)(H_2O)]^{2-}$; (5) $[Co^{II}(pc)_2(CH_3CO_2)]^-$; (6) $[Co^{II}(edta)]^{2-}$; (7) $[Co^{II}(nta)(H_2O)_2]^-$ by periodate.

Table 4. Enthalpies and entropies of activation for the oxidation of some cobalt(II) complexes by periodate

Complex	$10k_2$[a] ($M^{-1}s^{-1}$)	ΔH^* (kJ mol^{-1})	ΔS^* ($JK^{-1}mol^{-1}$)	Ref.
$[Co^{II}(edda)(H_2O)_2]$	12.1±0.1	19±2	−196±3	5
$[Co^{II}(hedta)(H_2O)]^-$	16.4±0.4	28±2	−166±5	5
$[Co^{II}(pc)_2(H_2O)_2]$	59.1±0.5	31±2	−160±4	This work
$[Co^{II}(nta)(CH_3CO_2)(H_2O)]^{2-}$	18.2±0.7	35±2.5	−140±8	6
$[Co^{II}(pc)_2(CH_3CO_2)(H_2O)]^-$	18.4±0.5	40±2	−126±3	This work
$[Co^{II}(edta)]^{2-}$	24.0[b]	52±2	−88±8	4
$[Co^{II}(nta)(H_2O)_2]^-$	24.7±0.2	68±5	−48±17	6

[a] Values of k_2 at 25°C.
[b] Value obtained from Kk^{et} of eq. (1).

good isokinetic correlation among the activation parameters for these complexes.

DISCUSSION

Oxidation of $[Co^{II}(pc)_2(H_2O)_2]$ by periodate gave different cobalt(III) products in the absence and presence of the acetate ion. This indicates different cobalt(II) reactive species, the most likely species being $[Co^{II}(pc)_2(H_2O)_2]$ and $[Co^{II}(pc)_2(CH_3CO_2)(H_2O)]^-$. Coordination of the acetate ion to $[Co^{II}(pc)_2(H_2O)_2]$, prior to oxidation by IO_4^-, seems to be supported by the change in the spectrum of the cobalt(II) complex observed on addition of the acetate ion.

An inner-sphere mechanism is proposed for both the acetate-dependent and -independent pathways and may be represented by eqs (5)–(10)

$$[Co^{II}(pc)_2(H_2O)_2]+CH_3CO_2^- \underset{K_1}{\rightleftharpoons} [Co^{II}(pc)_2(CH_3CO_2)(H_2O)]^- + H_2O \quad (5)$$

$$[Co^{II}(pc)_2(H_2O)_2]+IO_4^- \underset{K_2}{\rightleftharpoons} [(pc)_2(H_2O)Co^{II}-OIO_3]^- \quad (6)$$

$$[Co^{II}(pc)_2(CH_3CO_2)(H_2O)]^- + IO_4^- \underset{K_3}{\rightleftharpoons} [(pc)_2(CH_3CO_2)Co^{II}-OIO_3]^{2-} \quad (7)$$

$$[(pc)_2(H_2O)Co^{II}-OIO_3]^- \xrightarrow[k_1]{H_2O} [Co^{III}(pc)_2(H_2O)_2]^+ + I^{VI} \quad (8)$$

$$[(pc)_2(CH_3CO_2)Co^{II}-OIO_3]^{2-} \xrightarrow[k_2]{H_2O} [Co^{III}(pc)_2(CH_3CO_2)(H_2O)]+I^{VI} \quad (9)$$

$$2I^{VI} \longrightarrow IO_4^- + IO_3^- . \quad (10)$$

The rate law derived from the above mechanism, assuming that K_1, K_2 and K_3 are small, is

$$\text{rate} = (k_1K_2+k_2K_1K_3[CH_3CO_2^-])[Co^{II}(pc)_2(H_2O)_2][IO_4^-]. \quad (11)$$

From a comparison of eqs (4) and (11) one obtains $k'_2 = k_1K_2$ and $k_3 = k_2K_1K_3$. The fact that acrilonitrile was polymerized seems to support the suggestion of the presence of a free radical I^{VI} in the reaction mechanisms.

The periodate ion is capable of acting as a ligand, as evidenced from its coordination to copper(III)[11] and nickel(IV).[12] Periodate oxidation of $[Co^{II}(pc)_2(H_2O)_2]$, like that of cdta,[7] did not show the formation of an initial cobalt(III) product. This may be due to the oxidation process being outer-sphere, and hence only $[Co^{III}(pc)_2(H_2O)_2]^+$ was produced. Alternatively, the oxidation process may be inner-sphere, but because the rate of conversion of the initial cobalt(III) product to the final product is faster than that of the oxidation process, the initial cobalt(III) product was not observed. The second alternative is consistent with an inner-sphere mechanism that is generally proposed for periodate oxidations.

The small changes in rate constants for the cobalt(II) complexes of hedta, edda, edta, nta and pc, see Table 4, may arise from parallel changes in ΔH^* and ΔS^* values. These changes lead to only small changes in ΔG^*, and for such a closely related series a common mechanism is supported.[13] This mechanism consists of periodate ion coordination to the cobalt(II) complex in a step preceding the rate-determining intramolecular electron transfer within the precursor complex.

REFERENCES

1. G. J. Buist, *Comprehensive Chemical Kinetics* (Edited by C. H. Bamford and C. F. H. Tipper), Vol. 6, p. 435. Elsevier, Amsterdam (1972).
2. A. Indelli, F. Ferranti and F. Secco, *J. Phys. Chem.* 1966, **70**, 631.
3. F. R. El-Eziri and Y. Sulfab, *Inorg. Chim. Acta* 1977, **24**, 15.
4. A. Y. Kassim and Y. Sulfab, *Inorg. Chim. Acta* 1977, **24**, 247.
5. A. A. Abdel-Khalek and Y. Sulfab, *J. Inorg. Nucl. Chem.* 1981, **43**, 3257.
6. M. A. Hussein, A. A. Abdel-Khalek and Y. Sulfab, *J. Chem. Soc., Dalton Trans.* 1983, 317.
7. A. A. Abdel-Khalek and Y. Sulfab, *Trans. Met. Chem.* 1982, **7**, 297.
8. A. Y. Kassim and Y. Sulfab, *Inorg. Chem.* 1981, **20**, 506.
9. M. C. R. Symons, *J. Chem. Soc.* 1955, 2794.
10. U. B. Ceipidor and V. Carunchio, *J. Inorg. Nucl. Chem.* 1975, **37**, 375.
11. I. Hadinec, L. Jensovsky, A. Linek and V. Synecek, *Naturwiss.* 1960, **47**, 377.
12. P. Ray, *Inorg. Synth.* 1957, **5**, 201.
13. R. G. Wilkins, *The Study of Kinetics and Mechanism of Reactions of Transition Metal Complexes*, p. 100. Allyn and Bacon, Boston (1974).

Polyhedron Vol. 8, No. 1, pp. 57–69, 1989
Printed in Great Britain

0277–5387/89 $3.00+.00
© 1988 Pergamon Press plc

SYNTHESIS AND SPECTROSCOPIC CHARACTERISTICS OF BIS-[DIMETHYL(PHENYL)SILYLMETHYL]PLATINUM(II) COMPLEXES WITH NITROGEN DONOR LIGANDS

BERNARDETA C. ANKIANIEC and G. BRENT YOUNG*

Inorganic Chemistry Laboratories, Imperial College of Science, Technology and Medicine, London SW7 2AY, U.K.

(*Received* 26 *May* 1988; *accepted* 6 *July* 1988)

Abstract—A series of bis-[dimethyl(phenyl)silylmethyl]platinum(II) complexes, $LPt(CH_2SiMe_2Ph)_2$ with bidentate, N-heteroaromatic ligands (L = 2,2′-bipyridyl; 4,4′-dimethyl-2,2′-bipyridyl; 4,4′-di-*t*-butyl-2,2′-bipyridyl; 2,2′-bipyrimidyl; 2,2′-bipyrazyl; 1,10-phenanthroline; 4,7-diphenyl-1,10-phenanthroline; 3,4,7,8-tetramethyl-1,10-phenanthroline and 2,9-dimethyl-4,7-diphenyl-1,10-phenanthroline) have been synthesized by the displacement of the diolefin from $(cod)Pt(CH_2SiMe_2Ph)_2$ or $(nbd)Pt(CH_2SiMe_2Ph)_2$, or by the displacement of the thioether from $[Pt(CH_2SiMe_2Ph)_2(\mu\text{-DMS})]_2$ (cod = cycloocta-1,5-diene; nbd = [2.2.1]bicyclohepta-2,5-diene; DMS = dimethyl sulphide). These new derivatives have been characterized by electronic, IR and NMR (^1H and ^{13}C) spectroscopy. Also reported is the synthesis and spectroscopic characterization of an isolable bis-pyridine analogue, *cis*-$(py)_2Pt(CH_2SiMe_2Ph)_2$.

Organo-transition metal compounds play crucial roles in various organic reactions mediated by transition metals. Understanding the behaviour of transition metal alkyl (or aryl) complexes is therefore fundamental to the elucidation of such metal-promoted processes.[1] A common thermolytic pathway favoured by many organometals is hydrogen transfer, most frequently from a β-carbon site, though α-hydrogen abstractions and metallations at more remote (γ- or δ-) sites have emerged recently. In addition to such intramolecular C—H activations, there have been several instances of intermolecular H-transfer from "inert" hydrocarbons.[2]

Following from our recent studies of neophyl† platinum(II) derivatives,[3] our aim is to explore in more detail the reactivity controls on aromatic C—H activation. Complexes containing the sila-neophyl† group have received scant attention.[4] Here, we describe the synthesis and spectroscopic characteristics of a series of bis(sila-neophyl) platinum(II) complexes, $LPt(CH_2SiMe_2Ph)_2$ [L = cycloocta-1,5-diene (cod); [2.2.1]bicyclohepta-2,5-diene (nbd); 2,2′-bipyridine (bipy); 4,4′-dimethyl-2,2′-bipyridine (Me_2bipy); 4,4′-di-*t*-butyl-2,2′-bipyridine (Bu^t_2bipy), 2,2′-bipyrimidine (bipym); 2,2′-bipyrazine (bipyz); 1,10-phenanthroline (phen); 4,7-diphenyl-1,10-phenanthroline (Ph_2phen); 3,4,7,8-tetramethyl-1,10-phenanthroline (Me_4phen); 2,9-dimethyl-4,7-diphenyl-1,10-phenanthroline (Me_2Ph_2phen)]. We also report the synthesis and characterization of a relatively inert bis(pyridine)platinum(II) complex—*cis*-$(py)_2Pt(CH_2SiMe_2Ph)_2$. Relatively few dialkylplatinum(II) derivatives containing pyridine as a ligand have been reported[5–7] although several diaryl complexes have emerged.[5,8]

*Author to whom correspondence should be addressed.

† Neophyl = 2-methyl-2-phenylpropyl; sila-neophyl = dimethyl(phenyl)silylmethyl.

EXPERIMENTAL

General and instrumental

Elemental analyses were carried out by Imperial College Microanalytical Laboratories. NMR spectra were recorded on Brüker WM250 (^1H, 250.13 MHz; ^{13}C, 62.9 MHz) and Jeol FX90Q (^1H, 89.55 MHz) spectrometers. IR data were collected on a Perkin–Elmer 683 instrument as 4% KBr dispersions and electronic spectra were recorded on a Shimadzu UV-160 spectrometer.

All reactions were carried out under argon, using

standard anaerobic techniques.[9] All apparatus was flame-dried before use. Solvents were distilled under nitrogen prior to use; diethyl ether and *n*-hexane from sodium/benzophenone, toluene from sodium.

Chloromethyldimethylphenylsilane (sila-neophyl chloride) and 2,2′-bipyrimidyl were used as supplied by Lancaster synthesis. Chloromethyldimethylchlorosilane supplied by Lancaster synthesis was stored under argon, but used without further purification. 2,2′-Bipyridyl, 4,4′-dimethyl-2,2′-bipyridyl, 1,10-phenanthroline, 4,7-diphenyl-1,10-phenanthroline, 3,4,7,8-tetramethyl-1,10-phenanthroline, 2,9-dimethyl-4,7-diphenyl-1,10-phenanthroline, cycloocta-1,5-diene, [2.2.1]bicyclohepta-2,5-diene and dimethyl sulphide were all used as supplied by Aldrich Chemical Company. Pyridine was supplied by Rose Chemicals and distilled under argon from sodium hydroxide prior to use. A sample of 4,4′-di-*t*-butyl-2,2′-bipyridyl was synthesized by a modified procedure.[10] The precursors (cod)$PtCl_2$,[11] (nbd)$PtCl_2$[5] and $(DMS)_2PtCl_2$[12] were prepared using published methods.

Preparation of chloromethyldimethylphenylsilane[13]

A solution of PhMgBr (167 mmol) in diethyl ether (200 cm^3) was slowly added dropwise to $ClCH_2SiMe_2Cl$ (22 cm^3, 167 mmol) in diethyl ether (50 cm^3). Upon stirring, the initially colourless solution gradually turned pale yellow and a white precipitate of magnesium halides was evolved. After addition of PhMgBr was complete, the mixture was refluxed for 24 h. The resulting stirred suspension was cooled to −15°C and hydrolysed by dropwise addition of degassed saturated ammonium chloride solution (100 cm^3). The pale yellow ethereal layer was separated and the aqueous phase washed with diethyl ether (3 × 20 cm^3). The ether extracts were combined, dried over magnesium sulphate and decolourized with activated charcoal to give an almost colourless solution. Removal of the diethyl ether *in vacuo* afforded a pale yellow oil of the crude product. Distillation under reduced pressure gave sila-neophyl chloride (22.6 g, 122 mmol, 77%, b.p. 114°C/10 mm Hg) as a colourless liquid. (^1H NMR $\delta \equiv 0.32$ ppm—CH_3, 2.85 ppm—CH_2, 7.14–7.47 ppm—C_6H_5.)

Preparation of bis(sila-neophyl)(cycloocta-1,5-diene)platinum(II)

To a stirred suspension of (cod)$PtCl_2$ (1.85 g, 4.94 mmol) in diethyl ether (30 cm^3) at −25°C a solution of $PhMe_2SiCH_2MgCl$[4a] (16 mmol) in diethyl ether (30 cm^3) was added dropwise. The mixture was allowed to reach room temperature and stirred for a further 16 h, during this time magnesium chloride was evolved, forming a white precipitate in a dark yellow solution. The stirred suspension was cooled to −25°C and hydrolysed dropwise with degassed saturated ammonium chloride solution (30 cm^3). On reaching ambient temperature the yellow ethereal layer was separated and the aqueous phase washed with diethyl ether (3 × 10 cm^3). The ether extracts were combined, dried over magnesium sulphate and decolourized with activated charcoal to give a colourless solution. Removal of the solvent *in vacuo* gave a white crystalline solid which was recrystallized from the minimum amount of hexane (10 cm^3) to afford large colourless prisms of the product. (Yield: 2.38 g, 80%.) IR: 3065w, 3045sh, 3020sh, 3010sh, 3000w, 2950m, 2920w, 2890w, 2870w, 2855w, 2840sh, 1590vw, 1518w, 1488w, 1475w, 1460w, 1428m, 1410sh, 1385vw, 1375vs, 1340w, 1315w, 1305w, 1262m, 1242s, 1190vw, 1000w, 995w, 980m, 950m, 895vw, 865m, 810vs,br, 780s, 765s, 750m,sh, 740s, 730s, 700s, 680sh, 632m, 550m, 475s, 390s, 370m.

Preparation of bis(sila-neophyl)([2.2.]bicyclohepta-2,5-diene)platinum(II)

A solution of $PhMe_2SiCH_2MgCl$ (14 mmol) in diethyl ether (40 cm^3) was added dropwise at −78°C to a stirred suspension of (nbd)$PtCl_2$ (1.6 g, 4.5 mmol) in diethyl ether (20 cm^3). The mixture was gradually warmed to room temperature and then stirred for a further 16 h. The stirred suspension was then cooled to −25°C and hydrolysed with saturated ammonium chloride solution (20 cm^3). The ethereal layer was separated and the aqueous phase washed with diethyl ether (5 × 10 cm^3). The ether extracts were combined, dried over $MgSO_4$ and decolourized with activated charcoal to give an almost colourless solution. Filtration, washing the $MgSO_4$ with diethyl ether (2 × 20 cm^3) and removal of the solvent *in vacuo* gave an off-white solid, which was recrystallized from the minimum amount of hexane (3 cm^3) to give white needles of the product. (Yield: 1.85 g, 70%.) (Nbd)$Pt(CH_2SiMe_2Ph)_2$ decomposes slowly at room temperature over a period of several days, hence all samples were stored at −20°C. IR: 3060w, 3048w, 3039sh, 3020vw, 3003w, 2988sh, 2966w, 2925sh, 2902sh, 2887w, 2842w, 1482w, 1431sh, 1422m, 1419sh, 1371w, 1359w, 1333vw, 1308m, 1258m, 1239m, 1189w, 1156vw, 1104s, 1064w, 1030w,br, 997vw, 988w, 977w, 961w, 949w, 932w, 920vw, 905vw, 832s, 808s,br, 790m, 753m, 748m, 744m, 736m, 724sh, 715m, 698s, 683m, 628m, 560w, 468m, 385m.

Preparation of tetrakis(sila-neophyl)-bis-(μ-dimethylsulphide)diplatinum(II)

A solution of sila-neophyllithium[4b] (3.9 mmol) in hexane (30 cm^3) was added, dropwise to a stirred suspension of $(DMS)_2PtCl_2$ (0.51 g, 1.3 mmol) in diethyl ether (30 cm^3) at −20°C. The mixture was gradually warmed to room temperature and stirred for a further 8 h. The stirred suspension was cooled to −20°C and hydrolysed with saturated ammonium chloride solution (30 cm^3). The ethereal layer was separated and the aqueous phase washed with diethyl ether (2 × 15 cm^3). The ether extracts were combined, dried over $MgSO_4$ and decolourized with charcoal. Removal of the solvents *in vacuo* gave a yellow–brown oily residue. Trituration with either hexane or toluene afforded the product as a white powder. (Yield: 0.4 g, 55%.) The solid decomposes at room temperature over a period of several hours and was stored at −20°C. IR: 3058w, 3040vw, 3016vw, 2944w, 2917w, 2877vw, 2860w, 2833w, 1484w, 1422m, 1419sh, 1408wm, 1259vw, 1250w, 1237m, 1106s, 1024wm, 997wm, 981s, 970w, 943w, 825s,br, 810sh, 803s,br, 768m, 763sh, 732s, 717m, 699s, 688sh, 650vw, 621w, 552w, 469m, 382wm, 366m.

Preparation of cis-*bis(sila-neophyl)-bis-(pyridine) platinum*(II)

(cod)Pt(CH_2SiMe_2Ph)$_2$ (0.2 g, 0.33 mmol) was dissolved in excess pyridine (15 cm^3, *ca* 186 mmol) and stirred at 60°C for 24 h to give a pale yellow solution. Excess pyridine was removed *in vacuo* to give a pale yellow semi-crystalline solid, which was dissolved in diethyl ether (2 cm^3) and *n*-hexane was added dropwise (0.5 cm^3). Cooling the solution to −20°C afforded small pale yellow plates of the product. (Yield: 0.19 g, 85%.) IR: 3073w, 3055w, 3028vw, 3018vw, 3000vw, 2978wm, 2942wm, 2927w, 2117w, 1601m, 1482m, 1448s, 1428m, 1361vw, 1352vw, 1264wm, 1238m,br, 1209w, 1192w, 1163w, 1109s, 1107sh, 1068m, 1047w, 1023w, 1014w, 1009w, 978sh, 976w, 957w, 838s, 813vs, 786m, 760s, 732vs, 700vs, 689sh, 640w, 632w, 580w, 475wm, 458w, 388m, 303w.

Preparation of bis(pyridine)-1-platina-3-silaindan

(py)$_2$Pt(CH_2SiMe_2Ph)$_2$ (0.1 g, 0.2 mmol) was dissolved in toluene (8 cm^3) and left at ambient temperature for 4 days. Removal of toluene *in vacuo* afforded a yellow–brown oily residue which was recrystallized from diethyl ether (1 cm^3) and hexane (0.5 cm^3) to give the product as a pale yellow crystalline solid. (Yield: 0.07 g, 91%.) IR: 3105w, 3074wm, 3065wm, 3048m, 2994w, 2950m, 2896wm, 2861wm, 2831wm, 1602s, 1568s, 1480m, 1463m, 1447vs, 1385w, 1244s,br, 1217m, 1155vw, 1109w, 1077s, 1069s, 1044m, 1026s, 977wm, 957w, 833vs,br, 759s, 743s, 695s, 664w, 637wm, 563wm,br, 502w, 438w, 406vw.

Preparation of bis(sila-neophyl)(2,2′-bipyridyl) platinum(II)

2,2′-Bipyridyl (0.5 g, 3.2 mmol) and (cod)Pt(CH_2SiMe_2Ph)$_2$ (0.2 g, 0.32 mmol) were dissolved in the minimum amount of toluene (15 cm^3) and the solution stirred at 60°C for 5 days. Excess ligand was removed by washing with saturated $FeSO_4$(aq) solution. The toluene extracts were dried over $MgSO_4$ and filtered. Concentration of the solution to *ca* 2 cm^3, dropwise addition of *n*-hexane (1 cm^3) to effect crystallization and cooling to −20°C afforded large orange needles of the product. (Yield: 0.22 g, 78%.) IR: 3060w, 3048vw, 3005vw, 2970w, 2798vw, 2863w, 2839w, 1601wm, 1487w, 1469m, 1444m, 1426m, 1385wm, 1310w, 1260w, 1238m, 1231sh, 1156w, 1108s, 1023w, 994w, 980vw, 958w, 950w, 943w, 833s, 812s, 769wm, 756s, 739m, 723m, 702s, 680wm, 630w, 568w, 472m, 426w, 370wm.

Preparation of bis(sila-neophyl)(4,4′-dimethyl-2,2′-bipyridyl)platinum(II)

(Nbd)Pt(CH_2SiMe_2Ph)$_2$ (0.2 g, 0.34 mmol) and Me_2bipy (0.063 g, 0.34 mmol) were dissolved in toluene (10 cm^3) and stirred at 60°C for 21 days to give an orange–red solution. Concentration of the resulting solution to *ca* 2 cm^3, followed by dropwise addition of *n*-hexane (1 cm^3) and cooling to −20°C gave orange needles of the product. (Yield: 0.2 g, 87%.) IR: 3093vw, 3062vw, 3043vw, 2015vw, 2972w, 2895sh, 2874w, 2860w, 2836w, 2574s, 1552m, 1487w, 1450w, 1427m, 1406s, 1377m, 1363sh, 1262w, 1238m, 1190vw, 1158vw, 1139vw, 1109s, 1080w,sh, 1020w, 1010w,br, 999w, 967vw, 950w, 940sh, 832s, 816s, 803s, 770m, 750s, 740s, 719s, 704s, 693wm, 687wm, 663wm, 630w, 576wm, 476m, 447w, 390vw, 371m.

*Preparation of bis(sila-neophyl)(4,4′-di-*tert*-butyl-2,2′-bipyridyl)platinum*(II)

[Pt(CH_2SiMe_2Ph)$_2$(μ-DMS)]$_2$ (0.16 g, 0.14 mmol) and Bu$^t_2$bipy (0.08 g, 0.3 mmol) were dissolved in toluene (10 cm^3) and left at ambient temperature for 4 days giving a deep orange–red solution. Excess Bu$^t_2$bipy was removed by washing with $FeSO_4$(aq). Concentration of the solution to *ca* 2

cm^3, followed by dropwise addition of *n*-hexane (0.1 cm^3) and cooling to −20°C yielded orange crystals of the product. (Yield: 0.21 g, 96%.) IR: 3077w, 3038w, 2959w, 2931sh, 2888m, 2863m, 2837m, 1610s, 1588sh, 1492w, 1495sh, 1478s, 1465sh,br, 1423m, 1418s, 1364m, 1333vw, 1312w, 1298w, 1280vw, 1259m, 1234s, 1200w, 1155vw, 1127sh, 1119sh, 1104s, 1018w, 1009wm, 997w, 902wm, 956w, 948w, 939w, 910vw, 898w, 882m, 847sh, 830vs, 810s, 769s, 757w, 734s, 717s, 698s, 678wm, 629w, 617vw, 600wm, 577w, 553w, 531vw, 490vw, 470m, 420vw, 370wm, 304w.

Preparation of bis(sila-neophyl)(2,2′-bipyrimidyl) platinum(II)

(cod)Pt(CH_2SiMe_2Ph)$_2$ (0.34 g, 0.56 mmol) and 2,2′-bipyrimidyl (0.20 g, 1.26 mmol) were dissolved in toluene (15 cm^3) and stirred at 60°C for 10 days to give a dark red solution. Excess bipym was removed by washing with $FeSO_4$(aq). Concentration to *ca* 2 cm^3, following by dropwise addition of *n*-hexane (2 cm^3) and cooling to −20°C afforded wine red hexagonal crystals of the product. (Yield: 0.28 g, 77%.) IR: 3093vw, 3062vw, 3043vw, 2915vw, 2972w, 2895sh, 2874w, 2860w, 2836w, 1574s, 1552m, 1487w, 1450w, 1427m, 1406s, 1377m, 1363sh, 1262w, 1238m, 1190vw, 1158vw, 1139vw, 1109s, 1080w,sh, 1020w, 1010w,br, 998w, 967vw, 950w, 940sh, 832s, 816s, 803s, 770m, 750s, 740s, 719m, 704s, 693wm, 687wm, 663wm, 630w, 576wm, 476m, 447w, 390vw, 371m.

Preparation of bis(sila-neophyl)(2,2′-bipyrazyl) platinum(II)

[Pt(CH_2SiMe_2Ph)$_2$(μ-DMS)]$_2$ (0.13 g, 0.12 mmol) and bipyz (0.04 g, 0.25 mmol) were dissolved in toluene (8 cm^3) and left at room temperature for 4 days to give a purple solution. Excess ligand was removed by washing with $FeSO_4$(aq). Concentration of the solution to *ca* 2 cm^3, addition of *n*-hexane (1 cm^3) dropwise and cooling to −20°C gave magenta rods of the product. (Yield: 0.13 g, 87%.) IR: 3059w, 3011w, 2956wm, 2940vw, 2892vw, 2847m, 2828m, 1582m, 1576sh, 1487w, 1480vw, 1463wm, 1422m, 1409s, 1392sh, 1306w, 1268m, 1258w, 1247w, 1237m, 1177m, 1166m, 1158sh, 1108s, 1069w, 1062w, 1059w, 1017vw, 996w, 985vw, 953vw, 942wm, 919vw, 827vw, 808s, 769s, 740s, 713s, 700m, 688sh, 680sh, 659wm, 627w, 571w, 472m, 368wm.

Preparation of tetrakis(sila-neophyl)(μ-2,2′-bipyrimidyl)diplatinum(II)

[Pt(CH_2SiMe_2Ph)$_2$(μ-DMS)]$_2$ (0.2 g, 0.18 mmol) and 2,2′-bipyrimidyl (0.03 g, 0.18 mmol) were dissolved in toluene (8 cm^3) and left at ambient temperature for 4 days. The initially colourless solution turned dark red after 5 min and dark green after 15 min. After 1 h fine needles began to precipitate. The solid was filtered and recrystallized from acetone (15 cm^3) to give dark green needles of the product. (Yield: 0.19 g, 97%.) IR: 3060w, 3040vw, 3016vw, 2990vw, 2945m, 2920sh, 2890sh, 2863wm, 2837w, 1422s, 1403s, 1256wm, 1237s, 1194w,br, 1106s, 1028w, 1011w, 996w, 956w,br, 829vs, 805vs,br, 787wm, 718m, 738m, 728s, 717m, 698s, 685sh, 624sh, 611vw, 631wm, 501w, 470m, 382m, 367w.

Preparation of bis(sila-neophyl)(1,10-phenanthroline)platinum(II)

(cod)Pt(CH_2SiMe_2Ph)$_2$ (0.25 g, 0.42 mmol) and 1,10-phenanthroline (0.15 g, 0.83 mmol) were dissolved in toluene (10 cm^3) and stirred at 60°C for 8 days forming an intense orange–red solution. Excess phen was removed by washing with a freshly prepared aqueous $FeSO_4$ solution (5 × 30 cm^3) until the washings were colourless. Concentration of the organic layer to *ca* 2 cm^3 and addition of *n*-hexane (2 cm^3) yielded large red plates of the product. (Yield: 0.23 g, 82%.) IR: 3065w, 3020vw, 3000sh, 2965w, 2950w, 2883w, 2850vw, 2840w, 1497vw, 1490vw, 1450vw, 1425m, 1415w, 1386w, 1320vw, 1300vw, 1265wm, 1240m, 1205vw, 1192w, 1110m, 1015wm, 960wm, 955sh, 910vw, 840s, 815s, 778m, 769wm, 740m, 722m, 705m, 680w, 577w, 478w, 375w.

Preparation of bis(sila-neophyl)(3,4,7,8-tetramethyl-1,10-phenanthroline)platinum(II)

(cod)Pt(CH_2SiMe_2Ph)$_2$ (0.35 g, 0.58 mmol) and 3,4,7,8-tetramethyl-1,10-phenanthroline (0.2 g, 0.85 mmol) were dissolved in toluene (20 cm^3) and stirred at 60°C for 14 days. The resulting orange solution was washed with $FeSO_4$(aq), concentrated to *ca* 2 cm^3 and *n*-hexane (1 cm^3) was added to give long orange needles of the product. (Yield: 0.32 g, 76%.) IR: 3072w, 3056w, 3025vw, 3002vw, 2961sh, 2957m, 2935sh, 2894w, 2878m, 2837m, 1520w, 1491w, 1443sh, 1428s, 1396sh, 1365w, 1340vw, 1322w, 1303w, 1268m, 1240s, 1112s, 1019m, 980vw, 967w, 952m, 917w, 870w, 839vs, 813vs, 772s, 743s, 726s, 703s, 691sh, 681m, 632w, 587sh, 572w, 540w, 480m, 374m, 333w, 308w.

Preparation of bis(sila-neophyl)(4,7-diphenyl-1,10-phenanthroline)platinum(II)

(cod)Pt(CH_2SiMe_2Ph)$_2$ (0.23 g, 0.38 mmol) and 4,7-diphenyl-1,10-phenanthroline (0.235 g, 0.71

mmol) were dissolved in toluene (20 cm^3) and stirred for 28 days at 60°C to give a dark orange–red solution. Excess ligand was removed by washing with $FeSO_4$(aq). Concentration of the solution to *ca* 3 cm^3 and addition of *n*-hexane (2 cm^3) gave vermillion red rods of the product. (Yield: 0.31g, 99%.) IR: 3060w, 3086vw, 3010vw, 2970w, 2894vw, 2875w, 2858w, 2838w, 1630w, 1595w, 1560w, 1515vw, 1494w, 1487w, 1446w, 1437w, 1423m, 1417wm, 1395w, 1384wm, 1320vw, 1298vw, 1262m, 1242m, 1237m, 1227w,sh, 1189vw, 1156w, 1100s, 1076sh, 1029wm, 1020wm, 1010wm, 998wm, 962wm, 952wm, 944w, 924vw, 910w, 848s, 831s, 812s, 770s, 765s, 740s, 720m, 703s, 633wm, 620sh, 582w, 571wm, 555wm, 500w, 475m, 372wm.

Preparation of bis(sila-neophyl)(2,9-dimethyl-4,7-diphenyl-1,10-phenanthroline)platinum(II)

$[Pt(CH_2SiMe_2Ph)_2(\mu\text{-DMS})]_2$ (0.15 g, 0.13 mmol) was dissolved in toluene (10 cm^3) and Me_2Ph_2phen (0.1 g, 0.27 mmol) was added. The mixture was left at room temperature for 3 h and then the solvent removed *in vacuo* to give an orange–red oily residue, which was extracted into *n*-hexane (3×15 cm^3). Evaporation of the solvent yielded a dark orange microcrystalline solid of the product. This may be further recrystallized from toluene (1 cm^3) and *n*-hexane (0.5 cm^3). Cooling to −20°C affords vermillion crystals of the product. (Yield: 0.18 g, 80%.) IR: 3062w, 3043w, 3003vw, 2962m, 2881wm,br, 1622wm, 1569wm, 1543w, 1513vw, 1483wm, 1438wm, 1425m, 1400w, 1385w, 1262s, 1104s,br, 1026s,br, 806vs,br, 771m,sh, 729m, 700s, 642w, 631wm, 577w, 537vw, 494w, 479wm, 468wm, 386m,br.

RESULTS AND DISCUSSION

(a) *Synthesis*

A variety of bis(sila-neophyl)platinum(II) compounds can be isolated in good yields using methods similar to those previously employed for analogous bis-alkyl and bis-aryl platinum(II) complexes.[3,14–18] Metathetical displacements of diene from $(cod)Pt(CH_2SiMe_2Ph)_2$ or $(nbd)Pt(CH_2SiMe_2Ph)_2$, or displacement of the thioether from $[Pt(CH_2SiMe_2Ph)_2(\mu\text{-DMS})]_2$ by nitrogen donor ligands produces $LPt(CH_2SiMe_2Ph)_2$. These substitutions are characteristically slow; sila-neophyl complexes are qualitatively more inert to diene displacement than their neophyl analogues.[3] Conversion is generally complete in 5–30 days at 60°C in toluene. Excess of the nitrogen donor ligand (2–15-fold) accelerates the reactions. Usually, the residual free ligand can be separated readily from the organometallic product by extraction into aqueous ferrous sulphate solution as $[Fe(L)_3]^{2+}$.

All of the complexes $LPt(CH_2SiMe_2Ph)_2$ are air-stable and, unlike pale yellow $(py)_2Pt(CH_2SiMe_2Ph)_2$, are brightly coloured crystalline solids. All have satisfactory elemental analyses (Table 1). ^1H and ^{13}C NMR, IR and electronic spectroscopy are discussed below. Most of these complexes rapidly decompose in toluene solutions exposed to air. In addition, they react with chlorocarbon solvents. Chloroform and dichloromethane were avoided as recrystallization solvents.

Table 1. Analytical data for bis(sila-neophyl)platinum(II) complexes

Compound	Colour	Found (Calculated) C%	H%	N%
$(cod)Pt(CH_2SiMe_2Ph)_2$	Colourless	51.7(51.9)	6.3(6.4)	
$(nbd)Pt(CH_2SiMe_2Ph)_2$	White	51.1(51.3)	5.9(5.8)	
$[Pt(CH_2SiMe_2Ph)_2(\mu\text{-DMS})]_2$	White	42.9(43.2)	5.7(5.8)	
$(py)_2Pt(CH_2SiMe_2Ph)_2$	Pale yellow	51.8(51.6)	5.6(5.6)	4.3(4.3)
$(py)_2Pt(CH_2SiMe_2C_6H_4)$	Pale yellow	45.1(45.5)	4.6(4.4)	5.7(5.6)
$(bipy)Pt(CH_2SiMe_2Ph)_2$	Orange	51.7(51.7)	5.3(5.3)	4.3(4.3)
$(Me_2bipy)Pt(CH_2SiMe_2Ph)_2$	Orange	53.1(53.1)	5.5(5.6)	4.1(4.1)
$(Bu^t_2bipy)Pt(CH_2SiMe_2Ph)_2$	Orange	57.1(56.7)	6.7(6.6)	3.6(3.7)
$(bipym)Pt(CH_2SiMe_2Ph)_2$	Maroon	48.2(47.9)	4.9(4.9)	8.6(8.6)
$(bipyz)Pt(CH_2SiMe_2Ph)_2$	Magenta	48.0(47.9)	4.9(4.9)	8.9(8.6)
$[Pt_2(CH_2SiMe_2Ph)_4(\mu\text{-bipym})]$	Dark green	46.1(46.1)	5.1(5.1)	4.8(4.9)
$(phen)Pt(CH_2SiMe_2Ph)_2$	Red	53.5(53.5)	5.0(5.1)	4.1(4.2)
$(Ph_2phen)Pt(CH_2SiMe_2Ph)_2$	Vermillion	61.2(61.1)	5.0(5.1)	3.4(3.4)
$(Me_4phen)Pt(CH_2SiMe_2Ph)_2$	Orange	55.9(55.9)	5.8(5.8)	3.7(3.8)
$(Me_2Ph_2phen)Pt(CH_2SiMe_2Ph)_2$	Vermillion	62.5(62.6)	5.9(5.7)	3.3(3.2)

(b) *Spectroscopic studies of bis(sila-neophyl) platinum*(II) *complexes*

(i) *Conventions.* The numbering system follows that for the neophyl and platinaindan analogues (Fig. 1).[3] The phenyl carbon attached (or potentially attached) to the platinum is labelled C_2, while the alkyl-substituted carbon is designated C_1. Also shown in Fig. 1 are numerical conventions for the nitrogen donor ligands.

Throughout the discussion, peaks which show a coupling to ^{195}Pt ($I = 1/2$, 34% abundant) are denoted by $\delta(J)$; where δ is the chemical shift (ppm) and J is the observed coupling constant (Hz) to ^{195}Pt. Such multiplets are termed "triplets" ("t") to distinguish them from binomial 1:2:1 triplets.

(ii) ^1H *NMR* (*Table* 2). ^1H NMR spectroscopy provides very useful characteristics. A doubled doublet at low field (δ 7.6–7.9 ppm) is particularly diagnostic of the coordinated sila-neophyl skeleton. The platinum-bound methylene hydrogens generate 1:4:1 "triplets" and $^2J_{Pt-H}$ for these protons is in the range 88–101 Hz. The ^{195}Pt-"satellites" of these signals are noticeably broader in complexes with nitrogen donor ligands in comparison with (cod)Pt(CH_2SiMe_2Ph)$_2$ (Fig. 2). This phenomenon appears more pronounced for phenanthroline ligands than for those of the bipyridyl family. It is attributed to enhanced relaxation of the ^{195}Pt nuclei by quadrupolar ^{14}N.[8,22] A related effect has been observed in the ^1H NMR spectrum of H_3CHgI, in which $^2J_{Hg-H}$ is not observed due to rapid relaxation of ^{199}Hg by ^{127}I.[19] General broadening of ^1H NMR signals has been noted occasionally as

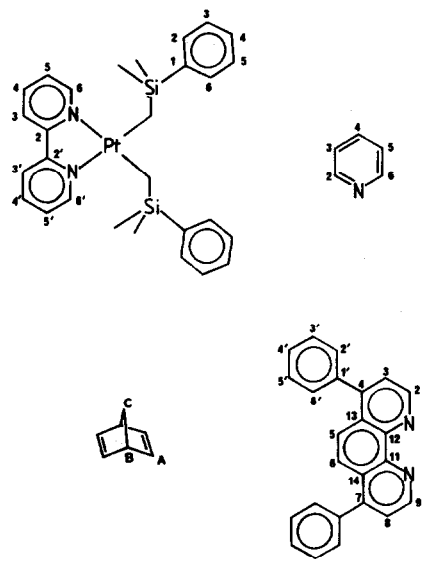

Fig. 1. Conventions employed for bis(sila-neophyl) platinum(II) complexes.

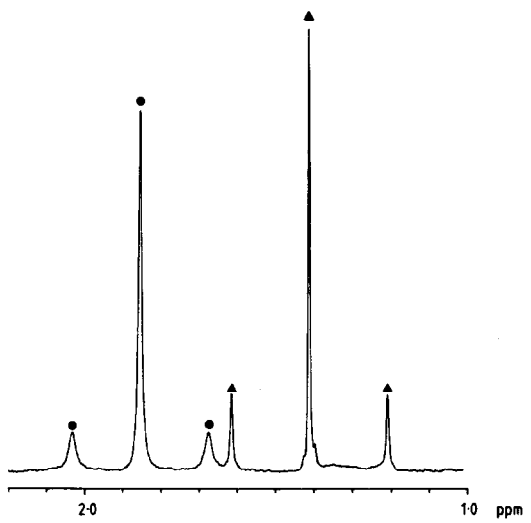

Fig. 2. Satellite broadening in the Pt–methylene resonance of (Ph$_2$phen)Pt(CH_2SiMe_2Ph)$_2$. ● = [Ph$_2$phen)Pt (CH_2SiMe_2Ph)$_2$; ▲ = (nbd)Pt(CH_2SiMe_2Ph)$_2$.

a characteristic of N-coordination[20] but although some effect can be detected for the central resonance, it is not as pronounced as that in the Pt-satellites. Resonances assigned to the neutral ligands are largely as expected and the values of $^3J_{Pt-H}$ for the protons adjacent to the nitrogen atoms are about 20 Hz.

Compared with bis(neophyl)platinum(II) complexes,[3] hydrogens in both the Si-bound methyl groups and the Pt-bound methylene groups resonate, as expected, at higher fields due to the proximal silicon. Among the aromatic hydrogens the doubled doublet of H_2 is generally downfield of that in the corresponding bis-neophyl complex. In addition, the values of $^2J_{Pt-H}$ are marginally higher than those of bis(neophyl) compounds (Fig. 3), in accord with a greater *s*-character in the Pt—C—H skeleton (*vide infra*).

(iii) ^{13}C *NMR* (*Table* 3). All the bis(sila-neophyl) compounds have been characterized by their $^{13}C\{^1H\}$ NMR spectra. Most are very complicated by the number and variety of aromatic carbons present.

The compounds LPt(CH_2SiMe_2Ph)$_2$ all show marked coordination shifts for both Si—CH_3 and aryl carbon atoms relative to Me_3SiPh (Tables 4 and 5). In accord with the general trends observed previously for $PhMe_2Si(X)$,[21] magnitudes of coordination shifts ($\Delta\delta$) are in the order $C_1 > C_4 > C_2 > C_3$; the chemical shifts of *meta*-carbon atoms in monosubstituted benzenes are least affected by changing the substituents. In all cases C_1 and C_2 are shifted downfield relative to Me_3SiPh, and C_3 and C_4 upfield. A downfield shift

Complex	δ ^{1}H (ppm): Hydrocarbyl ligands (J_{Pt-H}) (Hz) [Assignment]			δ^1 H (ppm): Neutral donor ligands (J_{Pt-H}) (Hz) [Assignments] ($J_{H_X-H_Y}$) (Hz)
	CH_2	CH_3	Aromatic ($J_{H_7-H_3}$) (Hz)	
(cod)Pt(CH_2SiMe_2Ph)$_2$	1.15 (92.2)	0.43	7.13–7.21, m, [H_3, H_4, H_5]; 7.60, dd, [H_2, H_6] (6.4)	1.46–1.59, m, [CH_2]; 4.14, "t", (42.7) [CH]
(nbd)Pt(CH_2SiMe_2Ph)$_2$[b]	1.09 (98.2)	0.26	7.21–7.33, m, [H_3, H_4, H_5]; 7.59, dd, [H_2, H_6] (8.0)	1.28–1.29, m, [H_C]; 3.54–3.58, m, [H_B]; 4.41, "t", (41.3) [H_A]
[Pt(CH_2SiMe_2Ph)$_2$(μ-DMS)]$_2$[c]	0.66 (101.1)	0.55	7.27–7.35, m, [H_3, H_4, H_5]; 7.85, dd, [H_2, H_6] (7.5)	1.62, "t", (20.0) [S—CH_3]
(py)$_2$Pt(CH_2SiMe_2Ph)$_2$	0.87 (88.4)	0.42	6.96–7.06, m, [H_3, H_4, H_5]; 7.63, dd, [H_2, H_6] (6.2)	6.13, m, [H_3, H_5] (2–3 = 6.4); 6.66, m, [H_4] (3–4 = 7.6); 8.06, dd, (20.7); 8.06, dd, [H_2, H_6] (2–4 = 1.5 Hz)
(py)$_2$Pt($CH_2SiMe_2C_6H_4$)	0.86 (100.4) [$J_{H_A-H_B}$ = 5.1 Hz]	0.07	7.01–7.19, m, [H_4, H_5]; 7.46, dd, [H_6] ($J_{H_4-H_6}$ = 2.0 Hz; $J_{H_5-H_6}$ = 7.5 Hz); 7.68, dd, (67.0) [H_3] ($J_{H_3-H_4}$ = 7.9 Hz; $J_{H_3-H_5}$ = 1.3 Hz)	6.20, m, [H_3, H_5] (3–4 = 7.6; 2–3 = 6.4); 6.39, m, [$H_{3'}$, H_5] (3′–4′ = 7.6; 2′–3′ = 6.4); 6.65, m, [H_4]; 6.77, m, [$H_{4'}$]; 8.31, dd, (25.7) [H_2, H_6] (2–4 = 1.6); 8.47, dd, (20.0) [$H_{2'}$, $H_{6'}$] (2–4 =
(bipy)Pt(CH_2SiMe_2Ph)$_2$	1.41 (89.5)	0.57	6.97–7.15, m, [H_3, H_4, H_5]; 7.81, dd, [H_2, H_6] (7.7)	6.26, m, [H_5] (5–6 = 5.6); 6.95, dd, [H_4], (3–4 = 7.5); 6.71, dd, [H_3] (3–5 = 1.2), 8.68, dd (22.8) [H_6] (6–4 = 1.4)
(Me_2bipy)Pt(CH_2SiMe_2Ph)$_2$	1.37 (89.0)	0.59	7.04–7.16, m, [H_3, H_4, H_5]; 7.86, dd, [H_2, H_6] (7.7)	1.53, s, [CH_3]; 6.11, dd, [H_5] (5–6 = 5.6; 3–5 = 0.8); 6.74, s, [H_3]; 8.58, dd, (22.2) [H_6]
(Bu^t_2bipy)Pt(CH_2SiMe_2Ph)$_2$	1.44 (88.9)	0.65	6.97–7.09, m, [H_3, H_4, H_5]; 7.85, dd, [H_2, H_6] (7.5)	0.92, s, [CH_3]; 6.36, dd, [H_5] (3–5 = 1.9; 5–6 = 5.9); 7.39, d, [H_3]; 7.60, dd, (24.0) [H_6] (3–6 = 0.6)
(bipym)Pt(CH_2SiMe_2Ph)$_2$	1.37 (90.9)	0.57	6.90–7.05, m, [H_3, H_4, H_5]; 7.68, dd, [H_2, H_6] (7.0)	5.86, dd, [H_5] (5–6 = 5.5); 8.17, dd, [H_4] (4–5 = 4.6); 8.36, dd, (20.7) [H_6] (4–6 = 2.2)
(bipyz)Pt(CH_2SiMe_2Ph)$_2$	1.64 (90.8)	0.51	6.97–7.04, m, [H_3, H_4, H_5]; 7.64, dd, [H_2, H_6] (6.1)	7.63, s, [H_5]; 8.00, s, [H_3]; 8.28, dd, (21.3) [H_6] (5–6 = 3.1; 3–6 = 1.0)
[Pt_2(CH_2SiMe_2Ph)$_4$(μ-bipym)]	1.44 (92.9)	0.50	6.95–7.03, m, [H_3, H_4, H_5]; 7.62, dd, [H_2, H_6] (6.6)	5.52, m, [H_5] (5–6 = 5.4); 8.30, d, (*ca* 22) [H_4, H_6]
(phen)Pt(CH_2SiMe_2Ph)$_2$	1.60 (90.3)	0.62	6.99–7.05, m, [H_3, H_4, H_5]; 7.82, dd, [H_2, H_6] (6.5)	6.51, m, [H_3, H_8] (2–3 = 5.2); 6.87, s, [H_5, H_6]; 7.36, dd, [H_4, H_7]; 8.89, dd, (22.1) [H_2, H_9] (2–4 = 1.3)
(Ph_2phen)Pt(CH_2SiMe_2Ph)$_2$	1.70 (89.7)	0.70	6.99–7.06, m, [H_3, H_4, H_5]; 7.89, dd, [H_2, H_6] (7.4)	6.62, d, [H_3, H_8] (3–2 = 5.4); 7.08–7.19, m, [C_6H_5]; 7.32, s, [H_5, H_6]; 9.02, d, (22.4) [H_2, H_9]
(Me_4phen)Pt(CH_2SiMe_2Ph)$_2$	1.54 (89.7)	0.67	6.94–7.04, m, [H_3, H_4, H_5]; 7.86, dd, [H_2, H_6] (8.0)	1.72, s, [4,7-CH_3]; 1.74, s, [3,8-CH_3]; 7.80, s, [H_5, H_6]; 8.71, "t", (23.1) [H_2—H_9]
(Me_2Ph_2phen)Pt(CH_2SiMe_2Ph)$_2$	1.62 (97.6)	0.50	6.90–7.11, m, [H_3, H_4, H_5]; 7.84, dd, [H_2, H_6] (7.6)	2.64, s, [CH_3]; 6.72, s, [H_3, H_8]; 7.12–7.23, m, [C_6H_5]; 7.30, s, [H_5, H_6]

[a] In d^8-toluene unless stated otherwise. [b] In d-chloroform. [c] In d^6-benzene.

Table 3. ^{13}C NMR characteristics of bis(sila-neophyl)platinum(II) complexes[a]

Complex	δ ^{13}C (ppm): Hydrocarbyl ligands (J_{Pt-C}) (Hz) [Assignment]			δ ^{13}C (ppm): Ancillary ligands (J_{Pt-C}) (Hz) [Assignment]
	Pt—CH_2	Si—CH_3	Aromatic	
(cod)Pt(CH_2SiMe_2Ph)$_2$	12.34(710.0)	2.14(31.8)	127.77 [C_3, C_5];[b] [C_4]; 134.12 [C_2, C_6]; 144.50, (26.4) [C_1]	29.78, [CH_2]; 97.89, (64.7) [CH]
(nbd)Pt(CH_2SiMe_2Ph)$_2$[c]	14.28(752.5)	1.56(33.4)	127.40 [C_3, C_5]; 128.02 [C_4]; 133.62 [C_2, C_6]; 144.52, (25.4) [C_1]	48.77, (40.6) [C_B]; 72.54, (53.5) [C_C]; 85.45, (54.3) [C_A]
[Pt(CH_2SiMe_2Ph)$_2$(μ-DMS)]$_2$[c]	14.22(785.5)	1.77(37.7)	127.32 [C_3, C_5]; 127.96 [C_4]; 134.05 [C_2, C_6]; 144.23, (20.8) [C_1]	29.73, (39.1) [S—CH_3]
(py)$_2$Pt(CH_2SiMe_2Ph)$_2$[d]	−13.16(739.8)	1.55(27.4)	127.21 [C_3, C_5]; 127.64 [C_4]; 133.88 [C_2, C_6]; 146.29, (29.7) [C_1]	124.92 [C_3, C_5]; 134.71 [C_4]; 150.50, (33.7) [C_2, C_6]
(bipy)Pt(CH_2SiMe_2Ph)$_2$	−8.26(745.4)	1.79(35.0)	127.35 [C_3, C_5]; 128.29 [C_4]; 134.62 [C_2, C_6]; 145.82, (29.7) [C_1]	121.53, (11.2) [C_5]; 125.98, (20.4) [C_3]; 134.62 [C_4]; 147.35, (32.4) [C_6]; 155.85, (10.3) [C_2]
(Me_2bipy)Pt(CH_2SiMe_2Ph)$_2$	−9.16(743.7)	1.89(34.3)	127.38 [C_3, C_5];[b] [C_4]; 134.61 [C_2, C_6]; 146.17, (31.4) [C_1]	21.07 [CH_3]; 122.44, (11.0) [C_5]; 126.85, (21.3) [C_3]; 146.40 [C_4]; 146.94, (32.8) [C_6]; 155.94, (10.3) [C_2]
(Bu^t_2bipy)Pt(CH_2SiMe_2Ph)$_2$	−8.69(742.3)	1.93(35.9)	127.32 [C_3, C_5];[b] [C_4]; 134.73 [C_2, C_6]; 146.11, (28.3) [C_1]	29.78 [CH_3]; 35.07 [C-CH_3]; 118.09 [C_5]; 123.47, (20.0) [C_3]; 147.28, (32.4) [C_6]; 156.29 [C_2]; 159.26 [C_4]
(bipym)Pt(CH_2SiMe_2Ph)$_2$	−7.81(759.3)	1.53(39.0)	127.32 [C_4]; 127.86 [C_3, C_5]; 134.68 [C_2, C_6]; 145.09, (27.7) [C_1]	122.75, (16.4) [C_5]; 152.42, (27.6) [C_6]; 155.00 [C_4]; 162.36 [C_2]
(bipyz)Pt(CH_2SiMe_2Ph)$_2$	−5.21(750.5)	1.50(37.4)	127.40 [C_3, C_5];[b] [C_4]; 134.55 [C_2, C_6]; 144.74, (23.2) [C_1]	140.14, (29.5) [C_6]; 143.68, (12.5) [C_5]; 148.76 [C_2]; 149.05, (16.1) [C_3]
[Pt_2(CH_2SiMe_2Ph)$_4$(μ-bipym)][c]	−8.63(767.1)	1.40(37.3)	127.90 [C_3, C_5]; 128.68 [C_4]; 135.02 [C_2, C_6]; 145.23, (25.7) [C_1]	127.51, (15.7) [C_5]; 151.64; (26.0) [C_4, C_6]; 166.28 [C_2]
(phen)Pt(CH_2SiMe_2Ph)$_2$	−9.03(749.5)	1.84(36.1)	127.30 [C_3, C_5]; 128.14 [C_4]; 134.64 [C_2, C_6]; 145.91, (29.2) [C_1]	125.05, (20.8) [C_3, C_8]; 126.39 [C_5, C_6]; 130.15, (11.3) [C_{13}, C_{14}]; 133.94 [C_4, C_7]; 147.15, (32.6) [C_2, C_9]; 147.99 [C_{11}, C_{12}]
(Ph_2phen)Pt(CH_2SiMe_2Ph)$_2$	−8.36(744.2)	1.93(36.4)	127.33 [C_3, C_5]; 128.29 [C_4]; 134.73 [C_2, C_6]; 146.06, (28.8) [C_1]	124.56 [$C_{4'}$]; 125.71, (20.8) [C_3, C_8]; 127.06 [C_5, C_6]; 128.91 [$C_{3'}$, $C_{5'}$]; 129.16 ($C_{2'}$, $C_{6'}$]; 129.46 [C_{13}, C_{14}]; 137.80 [C_4, C_7]; 146.76, (33.4) [C_2, C_9]; 147.01 [$C_{1'}$]; 148.53 [C_{11}, C_{12}]

Table 3—*continued*

Complex	δ ^{13}C (ppm): Hydrocarbyl ligands (J_{Pt-C}) (Hz) [Assignment]			δ ^{13}C (ppm): Ancillary ligands (J_{Pt-C}) (Hz) [Assignment]
	Pt—CH_2	Si—CH_3	Aromatic	
$(Me_4phen)Pt(CH_2SiMe_2Ph)_2$	−9.295(744.4)	1.99(37.9)	127.21 [C_3, C_5]; 127.33 [C_4]; 134.64 [C_2, C_6]; 146.32, (26.1) [C_1]	14.25 [4,7-CH_3]; 17.10 [3,8-CH_3]; 122.32 [C_5, C_6]; 128.78 [C_{13}, C_{14}]; 133.18, (22.2) [C_3, C_8]; 140.56 [C_4, C_7]; 146.79 [C_{11}, C_{12}]; 148.46, (32.9) [C_2, C_9]
$(Me_2Ph_2phen)Pt(CH_2SiMe_2Ph)_2$[d]	−17.30(749.2)	2.11(31.8)	125.70 [C_4]; 127.34 [C_3, C_5]; 134.34 [C_2]; 146.00, (30.6) [C_1]	27.87, (18.8) [2,9-CH_3]; 123.13 [$C_{4'}$]; 125.56, (23.2) [C_3, C_8]; 125.91 [C_5, C_6]; 128.71 [$C_{3'}$, $C_{5'}$]; 129.23 [$C_{2'}$, $C_{6'}$]; 133.76, (34.3) [C_2, C_9]; 137.57 [C_4, C_7]; 146.45 [$C_{1'}$]; 149.32, (30.4) [C_{11}, C_{12}]; 159.35, (23.6) [C_{13}, C_{14}]
$(py)_2\overline{Pt(CH_2SiMe_2C_6H_4)}$	−8.56(771.0)	4.29(33.3) 5.66(45.8)	121.92, (12.9) [C_4]; 126.80 [C_6]; 133.94 [C_5]; 139.36, (33.5) [C_3]; 142.04, (28.3) [C_1]; 143.29, (841.2) [C_2]	124.75, (20.6) [C_3, C_5]; 124.91, (14.5) [$C_{3'}$, $C_{5'}$]; 135.20 [$C_{4'}$]; 135.67 [C_4]; 150.97, (14.2) [$C_{2'}$, $C_{6'}$]; 151.57, (16.5) [C_2, C_6]

[a] In d^6-benzene unless stated otherwise.
[b] Obscured by solvent.
[c] In d^1-chloroform.
[d] In d^8-toluene.
[e] In d^6-acetone.

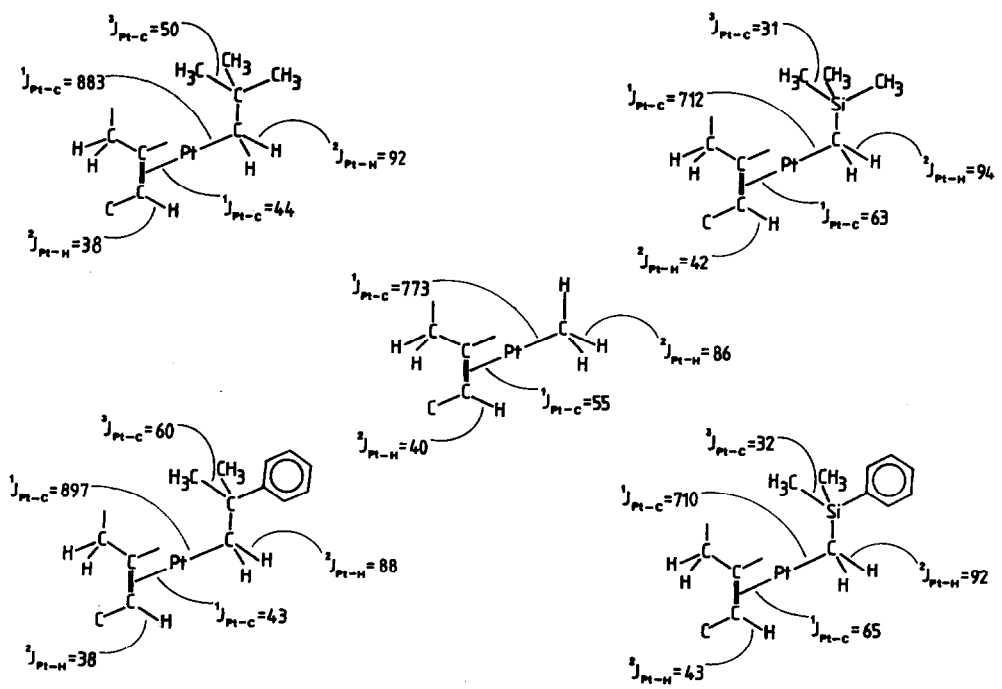

Fig. 3. Comparative NMR characteristics for (cod)PtR_2.

Table 4. ^{13}C NMR of Me_3SiPh in different solvents

Solvent	δ ^{13}C (ppm): Hydrocarbyl ligand				
	Si—CH_3	C_1	C_2	C_3	C_4
benzene-d^6	−1.02	140.33	133.62	128.06	129.10
toluene-d^8	−1.12	140.09	133.44	127.88	128.92
acetone-d^6	−0.96	140.76	133.99	128.55	129.59
chloroform-d^1	−1.13	140.35	133.27	127.72	128.76

Table 5. ^{13}C NMR coordination shifts of bis(sila-neophyl)platinum(II) complexes

Complex	$\Delta\delta$ ^{13}C (ppm): Hydrocarbyl ligand[a,b]				
	Si—CH_3	C_1	C_2	C_3	C_4
(cod)Pt(CH_2SiMe_2Ph)$_2$	+3.16	+4.17	+0.50	−0.29	[c]
(nbd)Pt(CH_2SiMe_2Ph)$_2$	+2.69	+4.17	+0.35	−0.32	−0.74
[Pt(CH_2SiMe_2Ph)$_2$(μ-DMS)]$_2$	+2.90	+3.88	+0.78	−0.40	−0.80
(py)$_2$Pt(CH_2SiMe_2Ph)$_2$	+2.67	+6.20	+0.44	−0.67	−1.28
(bipy)Pt(CH_2SiMe_2Ph)$_2$	+2.81	+5.49	+1.00	−0.71	−0.81
(Me_2bipy)Pt(CH_2SiMe_2Ph)$_2$	+2.91	+5.84	+0.99	−0.68	[c]
(Bu^t_2bipy)Pt(CH_2SiMe_2Ph)$_2$	+2.95	+5.78	+1.11	−0.74	[c]
(bipym)Pt(CH_2SiMe_2Ph)$_2$	+2.55	+4.76	+1.06	−0.20	−1.78
(bipyz)Pt(CH_2SiMe_2Ph)$_2$	+2.52	+4.41	+0.93	−0.66	[c]
[Pt$_2$(CH_2SiMe_2Ph)$_4$(μ-bipym)]	+2.36	+4.47	+1.03	−0.65	−0.91
(phen)Pt(CH_2SiMe_2Ph)$_2$	+2.86	+5.58	+1.02	−0.76	−0.96
(Ph_2phen)Pt(CH_2SiMe_2Ph)$_2$	+2.95	+5.73	+1.11	−0.73	−0.81
(Me_4phen)Pt(CH_2SiMe_2Ph)$_2$	+3.01	+5.99	+1.02	−0.85	−1.77
(Me_2Ph_2phen)Pt(CH_2SiMe_2Ph)$_2$	+3.23	+5.91	+0.90	−0.54	−3.22

[a] Positive sign indicates downfield shift.
[b] Negative sign indicates upfield shift.
[c] Obscured by solvent.

for C_2 indicates that LPt(R) is electron withdrawing (relative to H). The silicon-bound methyl carbons also display downfield coordination shifts, again reflecting that LPt(R)CH_2^- is more electron withdrawing than a methyl group. In general though, the coordination shifts do not display a marked variation with changing L, suggesting that the inductive properties of the metal fragment is rather insensitive to L. Relatedly, $^3J_{Pt—C}$ for the sila-neophyl group changes little as L varies.

The magnitude of $^1J_{Pt—C}$ for the sila-neophyl derivatives is characteristically *ca* 200 Hz smaller than that for the neophyl analogue.[3,18] We have observed this trend elsewhere[22] in related systems and have attributed it to the reduced ability of silylmethyl groups to concentrate carbon 2*s*-character into the Pt—C bond, in accord with the propositions of isovalent hybridisation,[23] assuming, reasonably, that Fermi contact contributions to *J* predominate.[24]

Comparison of (cod)Pt(CH_2SiMe_2Ph)$_2$ with (cod)Pt(CH_2CMe_2Ph)$_2$ (Fig. 3) suggests that there is a correspondingly variable response from Pt in the extent to which it commits the 6*s* orbital to the two mutually *trans* bonds to carbon. While $^1J_{Pt—C}$ for the alkyl group increases from 710 to 897 Hz from the silicon to the carbon analogue, $^1J_{Pt—C}$ for the η^2-alkene decreases correspondingly from 43 to 65 Hz. In the neophyl complex, platinum is diverting less 6*s* character towards its η^2-M—C bond and more to its η^1-M—C interaction, presumably in response to the greater 2*s* contribution to Pt—C bonding by the metal-bound carbon of neophyl. Neophyl, by the usual criteria, exercises a stronger bond-weakening *trans*-influence than sila-neophyl.[25] We are evaluating bond strength variations in these complexes by other (thermochemical, diffractometric) techniques.

Notably $^1J_{Pt—C}$ for (cod)PtMe_2[26] has the intermediate value of 773 Hz (H has electronegativity intermediate between C and Si). $^2J_{Pt—H}$ varies in the same sense as $^1J_{Pt—C}$ in accord with these prop-

ositions. $^1J_{C-H}$ is expected also to be greater for the neophyl methylene group but has not been measured for any of these complexes.

(iv) *IR spectroscopy*. IR data for this series of compounds is listed in the Experimental. Absorption characteristics of bis(sila-neophyl) complexes arise mainly from the phenyl and silicon–carbon vibrations. Those at *ca* 1600 cm^{-1} and 1470–1430 cm^{-1} are aryl C—C vibrations. The strong peaks at 760–750 cm^{-1} and 710–700 cm^{-1} are out-of-plane C—H bending modes typical of five adjacent phenyl hydrogens. The peak at 1240–1230 cm^{-1} is a symmetric CH_3 deformation and the two strong bands at 860–830 cm^{-1} and 815–810 cm^{-1} are assigned to Si—C stretching modes. The strong band at 1110–1105 cm^{-1} is a characteristic X-sensitive band. In addition, the band near 580 cm^{-1} may be attributed to a Pt—C stretching mode.

(v) *Electronic spectroscopy* (*Table* 6). The electronic spectra of $LPt(CH_2SiMe_2Ph)_2$ (where L = neutral nitrogen donor ligand) are particularly characterized by two absorptions attributed to metal–ligand charge-transfer (MLCT) $d\pi \rightarrow \pi^*$ transitions and have been employed as a measure of relative electronic effects of such ligands.[15,17] The more energetic of the two is often obscured by the more intense ligand $\pi \rightarrow \pi^*$ transitions in the near-UV. The lower energy absorption can always be observed and hence has been a gauge of the energy differences between the ($d\pi$) HOMO of the metal and the (π^*) LUMO of the ligand. The energy of λ_1 increases in the order: μ-bipym < bipyz < bipym < Ph_2phen < Me_2Ph_2phen < phen ≃ bipy < Me_2bipy ≃ Bu^t_2bipy < Me_4phen.

The lower MLCT energies for the bipyz and bipym complexes relative to the bipy analogue is consistent with the generally observed reduction in complexes of N-bonded heteroatomatic ligands with electronegative ring atoms or substituents.[27] The LUMO for bipym is proposedly lower in energy than for bipy, resulting in a smaller separation from the $d\pi$ orbitals of platinum. Similarly, the higher energy of this absorption for Me_2bipy and Bu^t_2bipy complexes (relative to bipy) is explained by the electron-releasing substituent raising the energy of the LUMO. The phenanthroline ligands, with their increased conjugation, might be expected to exhibit lower energy absorption relative to bipy. Ph_2phen (in which conjugation can be further augmented by suitable orientation of the phenyl substituents) does give rise to a relatively minor reduction in energy of the π^* orbitals but phen and bipy exhibit similar absorption energies. For the dinuclear complex, $[Pt_2(CH_2SiMe_2Ph)_4(\mu\text{-bipym})]$, the absorption occurs at considerably longer wavelengths than for the mononuclear analogue. This phenomenon, which has been noted previously,[17] is believed to be due to the presence of a relatively high energy, largely non-bonding HOMO, spanning both metals in the binuclear complex.

The energy of the MLCT bands exhibited solvatochromism as observed for related comlexes.[13] On changing from acetone to dichloromethane, fairly small bathochromic shifts were observed for the bipy and the various phenanthroline complexes, while the bipym (both mono and bis-bidentate) and bipyz complexes displayed significant energetic lowering of the absorption (15–18 nm). In toluene, on the other hand, all the complexes displayed significant shifts. The energy of the λ_1 absorption, in general, was lowered by 15–25 nm with the exception of $(bipyz)Pt(CH_2SiMe_2Ph)_2$, where a smaller shift (7 nm) was observed. It has been suggested that direct interaction with the metal centre is responsible for the solvatochromic shifts of MLCT bands in closely related bis-dialkylplatinum(II) complexes.[28]

Comparing the electronic spectra of cor-

Table 6. Electronic spectra of bis(sila-neophyl)platinum(II) complexes

Complex	λ_{max} (nm) Actone	CH_2Cl_2	Toluene
$(bipy)Pt(CH_2SiMe_2Ph)_2$	475.5	478.0	504.0
$(Me_2bipy)Pt(CH_2SiMe_2Ph)_2$	467.5	468.0	497.5
$(Bu^t_2bipy)Pt(CH_2SiMe_2Ph)_2$	465.5	468.5	497.0
$(bipyz)Pt(CH_2SiMe_2Ph)_2$	525.0	541.0	548.0
$(bipym)Pt(CH_2SiMe_2Ph)_2$	487.5	505.5	528.5
$[Pt_2(CH_2SiMe_2Ph)_4(\mu\text{-bipym})]$	591.5	616.5	624.0
$(phen)Pt(CH_2SiMe_2Ph)_2$	475.0	475.0	500.5
$(Ph_2phen)Pt(CH_2SiMe_2Ph)_2$	485.0	489.5	506.0
$(Me_4phen)Pt(CH_2SiMe_2Ph)_2$	429.0	432.5	468.5
$(Me_2Ph_2phen)Pt(CH_2SiMe_2Ph)_2$	479.0	482.0	504.0

responding bis(neophyl) complexes revealed no significant differences in the relative electronic effects of the ligands, suggesting that the ligands confer similar electronic environments in both types of complexes. Thus, the different reactivity of sila-neophyl and neophyl derivatives probably do not originate with the electronic influence of the ancillary ligand.

(c) *Thermolytic behaviour of bis(sila-neophyl) platinum*(II) *complexes*

Qualitatively, bis(sila-neophyl) complexes are more substitution inert than the related dineophyl analogues, higher temperatures are required for the displacement of the diolefin by the nitrogen donor ligand. Preliminary investigations indicate that sila-neophyl complexes with bidentate N-donor ligands are also more thermolytically inert than the corresponding neophyl complexes, as no detectable metallacyclization occurs in toluene solutions up to 140°C. Toluene solutions of $(py)_2Pt(CH_2SiMe_2Ph)_2$ at ambient temperature (or above) do rearrange to the corresponding platinasilaindan. We are currently investigating the thermal behaviour of these and related bis-hydrocarbyl platinum(II) complexes.

Acknowledgements—We thank Dick Sheppard and Sue Johnson for high field NMR measurements and Steve Black for a sample of 4,4′-di-*tert*-butylbipyridyl. The award of a studentship by the SERC (to B.C.A.) is gratefully acknowledged. We are also indebted to Johnson Matthey for continuous support via generous loans of platinum and to the SERC, Royal Society and the University of London Central Research Fund for equipment grants in support of our work.

REFERENCES

1. See for example: (a) Y. Aoyama, T. Yoshida, K-I. Sakurai and H. Ogoshi, *Organometallics* 1986, **5**, 168; (b) W. D. Jones and F. J. Feher, *J. Am. Chem. Soc.* 1985, **107**, 620; (c) I. P. Rothwell, *Polyhedron* 1985, **4**, 177; (d) P. O. Stoutland and R. G. Bergman, *J. Am. Chem. Soc.* 1985, **107**, 4581; (e) G. W. Parshall, *Acc. Chem. Res.* 1975, **8**, 113; (f) W. D. Jones and F. J. Feher, *J. Am. Chem. Soc.* 1982, **104**, 4241; (g) S. Komiya, Y. Morimoto, A. Yamamoto and T. Yamamoto, *Organometallics* 1982, **1**, 1528; (h) A. C. Skapski, V. F. Sutcliffe and G. B. Young, *J. Chem. Soc., Chem. Commun.* 1985, 609; (i) S. D. Chappell and D. J. Cole-Hamilton, *J. Chem. Soc., Dalton Trans.* 1983, 1051; (j) S. D. Chappell and D. J. Cole-Hamilton, *J. Chem. Soc., Chem. Commun.* 1980, 238; (k) A. E. Shilov, *Activation of Saturated Hydrocarbons by Transition Metal Complexes*, Chap. 5. Reidel, Dordrecht (1984); (l) J. W. Bruno and T. J. Marks, *J. Am. Chem. Soc.* 1982, **104**, 7357.
2. See for example: (a) C. S. Cundy, B. M. Kingston and M. F. Lappert, *Adv. Organomet. Chem.* 1973, **11**, 253 and refs therein; (b) P. J. Davidson, M. F. Lappert and R. Pearce, *Chem. Rev.* 1976, **76**, 219; (c) R. R. Schrock and G. W. Parshall, *Chem. Rev.* 1976, **76**, 243; (d) P. J. Davidson, M. F. Lappert and R. Pearce, *Acc. Chem. Res.* 1974, **7**, 209; (e) M. R. Collier, M. F. Lappert and M. M. Truelock, *J. Organomet. Chem.* 1970, **25**, C36; (f) P. Foley, R. DiCosimo and G. M. Whitesides, *J. Am. Chem. Soc.* 1980, **102**, 6713; (g) J. A. Ibers, R. DiCosimo and G. M. Whitesides, *Organometallics* 1982, **1**, 13; (h) R. DiCosimo, S. S. Moore, A. F. Sowiński and G. M. Whitesides, *J. Am. Chem. Soc.* 1982, **104**, 124; (i) C. M. Fendrick and T. J. Marks, *J. Am. Chem. Soc.* 1986, **108**, 425; (j) G. M. Smith, J. D. Carpenter and T. J. Marks, *J. Am. Chem. Soc.* 1986, **108**, 6805.
3. D. C. Griffiths and G. B. Young, *Organometallics*, in press.
4. (a) M. R. Collier, M. F. Lappert and R. Pearce, *J. Chem. Soc., Dalton Trans.* 1973, 445; (b) J. W. Bruno, G. M. Smith, T. J. Marks, C. K. Fair, A. J. Schultz and J. M. Williams, *J. Am. Chem. Soc.* 1986, **108**, 40.
5. C. R. Kistner, J. H. Hutchinson, J. R. Doyle and J. C. Storlie, *Inorg. Chem.* 1963, **2**, 1255.
6. T. G. Appleton, J. R. Hall, D. W. Neale and M. A. Williams, *J. Organomet. Chem.* 1984, **176**, C73.
7. B. Wozniak, J. D. Ruddick and G. Wilkinson, *J. Chem. Soc., Dalton Trans.* 1971, 3116.
8. S. E. Himmel and G. B. Young, *Organometallics*, in press.
9. (a) D. F. Shriver, *The Manipulation of Air-Sensitive Compounds*. McGraw-Hill, New York (1969); (b) H. C. Brown, G. W. Kramer, A. B. Levy and M. M. Midland, *Organic Synthesis via Boranes*. John Wiley, New York (1975).
10. S. I. Black and G. B. Young, *Polyhedron*, in press.
11. J. X. McDermott, J. F. White and G. M. Whitesides, *J. Am. Chem. Soc.* 1976, **98**, 6521.
12. E. G. Cox, H. Saenger and W. Wardlaw, *J. Chem. Soc.* 1934, 182.
13. (a) C. Eaborn and A. Pidcock, *J. Chem. Soc.* 1954, 4268; (b) C. Eaborn and A. Pidcock, *J. Chem. Soc.* 1959, 3753.
14. G. B. Young and G. M. Whitesides, *J. Am. Chem. Soc.* 1978, **100**, 5808.
15. N. Chaudhury and R. J. Puddephatt, *J. Organomet. Chem.* 1975, **84**, 105.
16. M. Bochmann, G. Wilkinson and G. B. Young, *J. Chem. Soc., Dalton Trans.* 1980, 1879.
17. V. F. Sutcliffe and G. B. Young, *Polyhedron* 1984, **3**, 87.
18. D. C. Griffiths, PhD Thesis, University of London (1985).
19. D. N. Ford, P. R. Wells and P. C. Lauterbur, *J. Chem. Soc., Chem. Commun.* 1967, 616.

20. B. E. Mann, B. L. Shaw and A. J. Stringer, *J. Organomet. Chem.* 1974, **73**, 129.
21. (a) N. D. Chuy, V. Chvalovský, J. Schraml, M. Mägi and E. Lippmaa, *Coll. Czech. Chem. Commun.* 1975, **40**, 875; (b) J. Schrami, V. Chvalovský, M. Mägi, E. Lippmaa, R. Calas, J. Donoguès and P. Bourgeois, *J. Organomet. Chem.* 1976, **120**, 41.
22. (a) S. K. Thomson and G. B. Young, *Polyhedron*, 1988, **7**, 1953; (b) R. D. Kelly and G. B. Young, *Polyhedron*, in press.
23. H. A. Bent, *Chem. Rev.* 1961, **61**, 275.
24. A. Pidcock, *Adv. Chem. Ser.* 1982, **196**, 1.
25. T. G. Appleton, H. C. Clark and L. E. Manzer, *Coord. Chem. Rev.* 1973, **10**, 335.
26. B. E. Mann and B. F. Taylor, ^{13}C-*NMR Data for Organometallic Compounds*. Academic Press, London (1981).
27. R. R. Rumininski and J. D. Petersen, *Inorg. Chem.* 1982, **21**, 3706.
28. V. F. Sutcliffe, PhD Thesis, University of London (1985).

Polyhedron Vol. 8, No. 1, pp. 71–76, 1989
Printed in Great Britain

0277–5387/89 $3.00+.00
© 1988 Pergamon Press plc

THE ADSORPTION OF TUNGSTEN(VI) ON ACTIVATED CARBON FROM 1.0 M Na(H)Cl SOLUTION

J. J. CRUYWAGEN* and A. T. PIENAAR

Department of Chemistry, University of Stellenbosch, Stellenbosch, 7600 South Africa

(*Received* 2 *June* 1988; *accepted* 6 *July* 1988)

Abstract—The adsorption of tungsten(VI) onto activated carbon has been investigated as a function of pH_c in the range 2.0–6.5 at constant ionic strength (1 M NaCl) and temperature (25°C). The tungsten concentration was varied from 5×10^{-4} to 2×10^{-2} M. Adsorption is very strong at $pH_c < 4.5$ and depending on equilibrium conditions, loadings of ~ 2.8 mM W^{VI} per g activated carbon can be obtained. Computer treatment of distribution data led to an adsorption model, similar to that proposed (J. J. Cruywagen and H. F. de Wet, *Polyhedron* 1988, **7**, 547) for molybdenum(VI), comprising mainly dimeric species and small amounts of monomeric species. The chemisorption is explained in terms of complexation of tungsten(VI) with basic oxygen atoms at the surface of the activated carbon. Adsorption constants of tungsten and molybdenum correlate well with complex formation constants of tungsten and molybdenum with oxalate and citrate.

It is known that tungsten(VI)[1] and molybdenum(VI)[2–4] are strongly adsorbed by activated carbon from acid solution. Very recently it has been shown that the adsorption behaviour of molybdenum can be explained quantitatively in terms of the adsorption of mononuclear and dimeric species of which the latter predominates.[4] Very little has been published about the adsorption of tungstate onto activated carbon. Work aimed at the separation of tungsten has been carried out under non-equilibrium conditions and the data have been interpreted qualitatively in terms of the adsorption of polyanions.[1] In view of the results obtained for molybdenum[4] an equilibrium study of the adsorption of tungsten is of special interest. A comparison of the adsorption models for the two systems could provide some further insight into the mechanism of adsorption of molybdate and tungstate onto activated carbon. The strong adsorption of molybdenum(VI) species has been rationalized in terms of chemical bonding with basic oxygen atoms available at the surface of the activated carbon. If similar coordination of tungsten(VI) by oxo groups in the structure of the activated carbon takes place, the relative tendencies of tungsten and molybdenum to adsorb should parallel those of complex formation with ligands such as oxalate and citrate; stability constants for these complexes are available. With these considerations in mind the present investigation of the adsorption of tungsten onto activated carbon (as a function of both tungsten concentration and pH) has been carried out under conditions similar to those of the previous molybdenum study.[4]

*Author to whom correspondence should be addressed.

EXPERIMENTAL

Materials and solutions

Analytical grade chemicals and water obtained from a Milli-Q system were used for the preparation of all solutions. Sodium tungstate and sodium chloride solutions were prepared from the recrystallized salts and standardized gravimetrically as described previously.[5] Hydrochloric acid was standardized indirectly against potassium hydrogen phthalate by titration with sodium hydroxide. Granular peat based activated carbon (Chemviron, type BPL) of particle size 0.5–2.0 mm was used in the adsorption experiments. The carbon was soaked for a week in a concentrated acid solution (10 M HCl; 1 M HF) to remove soluble ash components, iron and other metal ions.[6] It was washed, first with 1 M HCl and then repeatedly with distilled water to remove the acid. The carbon was dried at 110°C.

pH_c Measurements

The free hydrogen ion concentration, h, was determined by measuring the potential (to $\pm$ 0.2 mV) with a T & C Model 1002 Research pH meter. A Ross combination electrode (supplied by Orion Research) with a 3 M KCl internal filling solution was used. The relationship between the measured potential E (in mV) and the hydrogen ion concentration at 25°C is given by the equation

$$E = E^0 + 59.16\,pH_c \qquad (1)$$

where $pH_c = -\log h$. E^0 was determined by titration of a 1.0 M NaCl solution with 0.10 M HCl, which was 0.90 M with respect to NaCl.

Adsorption measurements

A known mass of carbon (usually $\sim$ 0.25 g) was equilibrated with 50 cm^3 of sodium tungstate solution in a well stoppered polythene tube by slow mechanical shaking for seven days in a water bath at 25°C. In the case of molybdenum adsorption on activated carbon it has been shown that a period of seven days was sufficient for adsorption equilibrium to be established. Preliminary adsorption experiments carried out with a 1.0 mM tungstate solution at $pH_c \sim 2$ likewise showed that the tungstate concentration in the liquid phase remains practically constant after an equilibration period of six to seven days. Time dependent reactions that occur in dilute tungstate solutions, acidified to a degree of protonation $Z > 1.2$, became very slow after about a week[7] and did not seem to have any effect on the establishment of adsorption equilibrium for the experiments pertaining to the two lowest concentrations (cf. Discussion below). The tungstate solutions were 1.0 M with respect to sodium chloride and for each series of experiments at a given tungsten(VI) concentration, the hydrochloric acid concentration was varied to obtain pH_c values in the range 2–6 after equilibration. The initial tungstate concentrations for the various adsorption experiments were 0.5, 1.0, 5.0, 10.0 and 20.0 mM. For comparison purposes an adsorption experiment was also carried out with a 1.0 mM molybdate solution under the same conditions. Due to the very strong adsorption of tungsten (and molybdenum) on activated carbon, the amount adsorbed could be obtained with sufficient accuracy from the difference between the initial and equilibrium concentration in the aqueous phase.

The tungsten concentration in the aqueous phase was determined colorimetrically using a Varian Cary 210 spectrophotometer. The excellent Tiron method for the colorimetric determination of molybdenum[8] has been slightly adapted for the determination of tungsten. Maximum absorbance of the tungsten(VI) tiron complex occurs at $\sim$ 320 nm, but the wavelength of 340 nm was chosen because of the very sharp increase in absorption of tiron itself at wavelengths < 340 nm. A small increase in absorption ($\sim$ 3%) takes place during the first 4 h after the reagents have been mixed and then remains constant for several hours. The molar absorption coefficient, ε, at 340 nm then has the value 9400 $cm^{-1}\,M^{-1}$.

RESULTS AND DISCUSSION

The results of adsorption experiments at various tungsten(VI) concentrations are shown in Fig. 1 as plots of the logarithm of adsorption (mmol W^{VI} per g activated carbon) against equilibrium pH_c. It is seen that the adsorption increases with an increase in initial tungstate concentration. At a given pH_c in the range 2–4 the adsorption is proportional to the initial tungstate concentration up to $\sim$ 5.0 mM. Adsorption is very strong and at $pH_c = 2.3$, for example, about 97% of the tungstate in the aqueous phase is adsorbed. Although the percentage adsorption decreases with further increase in tungstate concentration it is still rather high at 20.0 mM, namely $\sim$ 70% at $pH_c = 2.3$. Also represented in Fig. 1 are results for the adsorption of molyb-

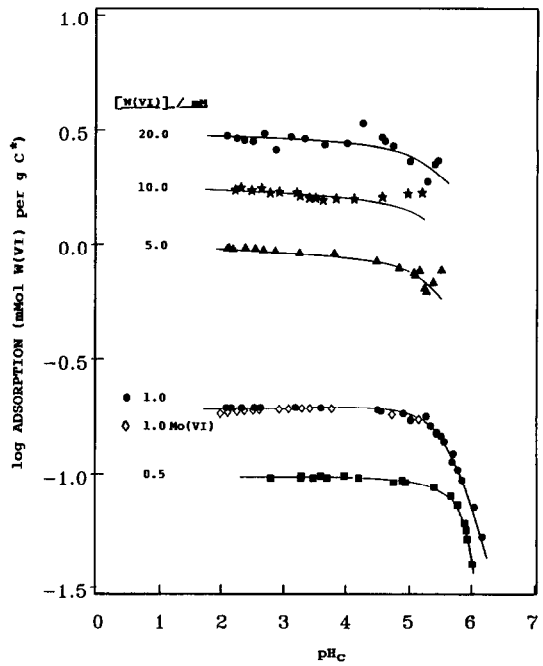

Fig. 1. Adsorption of tungsten(VI) [and molybdenum(VI)] by activated carbon from a 1.0 M Na(H)Cl solution, as a function of pH_c, at various tungsten concentrations.

denum(VI) at a concentration of 1.0 mM, from which it can be seen that the adsorption behaviour of the two metals is very similar at this concentration. At a much higher concentration, adsorption of tungsten is somewhat weaker than that reported for molybdenum.[4] At $pH_c = 2.5$ and initial concentration of 20.0 mM, for instance, the amount of tungsten adsorbed is 2.85 mmol g^{-1} compared to 3.00 mmol g^{-1} in the case of molybdenum. This result is consistent with the interpretation (put forward for the molybdenum system) that adsorption of polyanions is insignificant. At high concentration the percentage of polyanions in the aqueous phase increases and since the polyanions of tungsten(VI) are more stable than those of molybdenum(VI), adsorption of tungsten will be weaker. For the heptanuclear polyanions, $W_7O_{24}^{6-}$ and $Mo_7O_{24}^{6-}$ for example, the values for $\log\beta_{7,8}$ are 65.2 and 52.8, respectively.[5,9]

The variation in the distribution of tungsten between the activated carbon and aqueous solution, as a function of pH_c, for the experiments at the two lowest concentrations are shown in Fig. 2. It is seen that maximum distribution occurs at $pH_c \sim 3.4$ for the experiment with a tungsten concentration of 0.5 mM and decreases sharply with an increase in pH_c. For the experiment at 1.0 mM concentration the maximum appears at a slightly lower pH_c and the distribution at the maximum is somewhat higher.

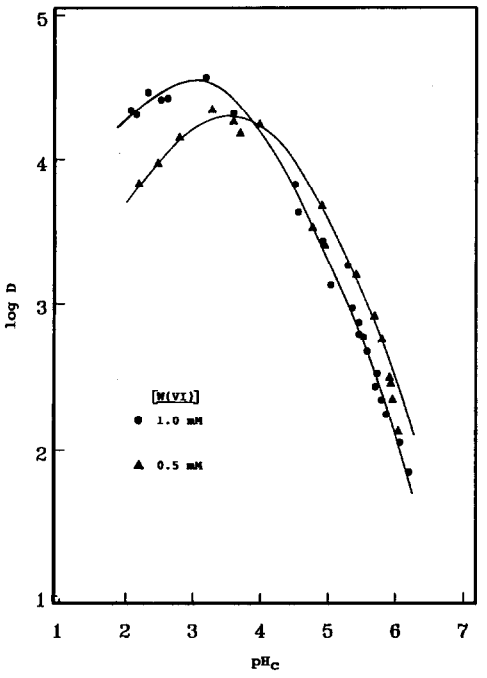

Fig. 2. Distribution of tungsten(VI) between activated carbon and a 1.0 M Na(H)Cl solution as a function of pH_c at initial concentrations of 0.5 and 1.0 mM. The curves are calculated from the constants given in Table 1.

These distribution curves resemble those for the adsorption of molybdenum.[4] It therefore seemed worthwhile to attempt a quantitative interpretation of the distribution curves in terms of the adsorption model derived for molybdenum.

The tungsten system, however, is much more complicated and quantitative treatment of the data is difficult because of the lack of information about equilibria for $Z > 1.2$. Because of slow reactions the polyanions are poorly characterized and some are described only in terms of symbols such as ψ, X and Y.[10,11] For this reason only the lowest concentrations could be used for the calculations and by making some simplifying approximations a satisfactory interpretation of the data could be obtained. Also, the distribution curves for the higher concentrations showed too many irregularities to justify quantitative treatment.

Equilibria and calculations

For the molybdenum adsorption system it has been shown that molybdate is bound to the carbon mainly in the dimeric form and that relatively small amounts of the monomeric species $[HMoO_4]^-$ and $Mo(OH)_6$ also adsorb.[4] Assuming similar behaviour for tungsten, the overall adsorption equilibria (in 1 M NaCl medium) are represented by the equations

$$2WO_4^{2-} + 3H^+ + C^* \rightleftharpoons HW_2O_7^-(ads) \quad (2)$$

$$WO_4^{2-} + H^+ + C^* \rightleftharpoons HWO_4^-(ads) \quad (3)$$

$$WO_4^{2-} + 2H^+ + C^* \rightleftharpoons W(OH)_6(ads) \quad (4)$$

where C* represents the activated carbon. The concentrations of the adsorbed species are expressed in terms of mmol tungsten(VI) adsorbed per g of activated carbon. For very small amounts adsorbed it is a good approximation to assume a constant activity for the activated carbon. The overall adsorption constants are than given by

$$K_{2,3} = [HW_2O_7^-(ads)]/[WO_4^{2-}]^2[H^+]^3 \quad (5)$$

$$K_{1,1} = [HWO_4^-(ads)]/[WO_4^{2-}][H^+] \quad (6)$$

$$K_{1,2} = [W(OH)_6(ads)]/[WO_4^{2-}][H^+]^2. \quad (7)$$

The distribution of tungsten between the solid and liquid phases is given by

$$D = \{2[HW_2O_7^-(ads)] + [HWO_4^-(ads)] + [W(OH)_6(ads)]\}/B \quad (8)$$

where B is the total tungsten concentration in solution after equilibration and by substitution using eqs (5)–(7) gives the expression

$$D = (2K_{2,3}b^2h^3 + K_{1,1}bh + K_{1,2}bh^2)/B \quad (9)$$

where,

$$b = [WO_4^{2-}].$$

The equilibria for the various possible protonation and condensation reactions of tungstate can be presented by the general equation

$$pWO_4^{2-} + qH^+ \rightleftharpoons (WO_4^{2-})_p(H^+)_q. \quad (10)$$

Formation constants for the species are denoted by $\beta_{p,q}$, for example $\beta_{7,8}$ for the polyanion $[W_7O_{24}]^{6-}$. For brevity, species will occasionally be described by the stoichiometric coefficients p and q, i.e. (7,8) for $[W_7O_{24}]^{6-}$. The total tungsten concentration, B, in the solution is given by

$$B = b + \sum p\beta_{pq}b^p h^q. \quad (11)$$

For $Z < 1.2$, equilibria are established rapidly and formation constants for the following polyanions have been reported for the ionic medium 1.0 M NaCl:[5] $[W_6O_{20}(OH)_2]^{6-}$, $[W_7O_{24}]^{6-}$, $[HW_7O]_{24}^{5-}$, $[H_2W_{12}O_{42}]^{10-}$. At very low tungsten concentrations, such as those pertaining to the aqueous phase after equilibration, the monomeric species $[HWO_4]^-$ and $W(OH)_6$ must be taken into account. Equilibrium constants reported for these species under somewhat different conditions, i.e. ionic strength 0.1 and temperature 20°C were used.[10] To make provision for slow equilibria at $Z > 1.2$, formation constants were used that had been obtained from potentiometric measurements of acidified tungstate solutions aged for seven days.[7] A reaction model that gave a satisfactory description of the potentiometric data for the aged solutions comprised the four polyanions mentioned above and two additional species, namely $[H_2W_7O_{24}]^{4-}$ and $[W_8O_{26}]^{4-}$ for which the values of the equilibrium constants were $\log\beta_{7,10} = 76.30$ and $\log\beta_{8,12} = 90.20$.

Computer treatment of data

The variation in distribution with change in pH_c, expressed in terms of the various tungstate species, is given by the following equation

$$D = \sum pK_{pq}b^p h^q/(b + \sum p\beta_{pq}b^p h^q). \quad (12)$$

The experimental points on the distribution curve (log values) were fitted to eq. (12) using the non-linear least-squares program *BMDPAR*.[12] The free $[WO_4]^{2-}$ concentration, b, at each point was calculated from the total tungsten concentration in a subroutine by iteration according to Newton's method.[13]

The calculations were started using the data of the experiment at the lowest concentration (0.5 mM) for which the proportions of polyanions in the solution are the smallest. In the first computer run, adsorption of mononuclear species was neglected and despite the uncertainties about the identity of some polyanions, and also of some of the formation constants introduced into eq. (12), a reasonable fit of the theoretical curve on the experimental points was obtained. The fit could be improved by adding the two mononuclear species as additional adsorbing species. The same result was obtained for calculations using data for the experiment at a tungsten concentration of 1.0 mM. Computations carried out on the assumption that either only mononuclear species or some polyions e.g. a hexa- or heptanuclear species adsorb, resulted in a totally unacceptable fit. From these results it may be concluded that for the pH_c range and concentrations investigated, tungsten is adsorbed mainly in the dimeric form. Significant adsorption of the monomeric species, $[HWO_4]^-$ and $W(OH)_6$, occurs only at $pH_c > 5.5$ and $pH_c < 3.0$, respectively (Fig. 3).

In the case of the molybdenum adsorption system some formation constants could be calculated which agreed well with values obtained by other methods. Several more runs were therefore done in an attempt to extract some useful information about tungsten(VI) equilibria from the distribution data at concentrations of 0.5 and 1.0 mM. Because of the very strong adsorption and extremely low concentrations of tungsten in the aqueous phase the accuracy of the data does not justify extensive model testing. It was found, however, that the fit could be improved by introducing a dimeric cation similar to that characterized in the case of molybdenum.[14] A dimeric tungsten anion analogous to $[HMo_2O_7]^-$ on the other hand was not accepted; the formation constant refined to an insignificant small value. Next, constants of species occurring in relatively high concentrations in the aqueous phase ($\sim 50\%$) were treated as unknowns, i.e. $\beta_{1,2}$, $\beta_{7,9}$ and $\beta_{8,12}$. Because of convergence problems not all these constants could be treated simultaneously as unknown parameters together with the three adsorption constants. By fixing the values of either two, three or four constants in turn, new values for all constants were calculated with concommitant improvement of the fit; the (8,12) species, however, was rejected.

The results of the computer treatment of the distribution data are summarized in Table 1. The values listed for the constants are those that resulted in the best fit for each of the distribution curves. (Constants for other species were fixed on literature values.) The agreement between the values for $\log K_{2,3}$, $\log\beta_{1,2}$ and $\log\beta_{2,5}$ for the two experiments

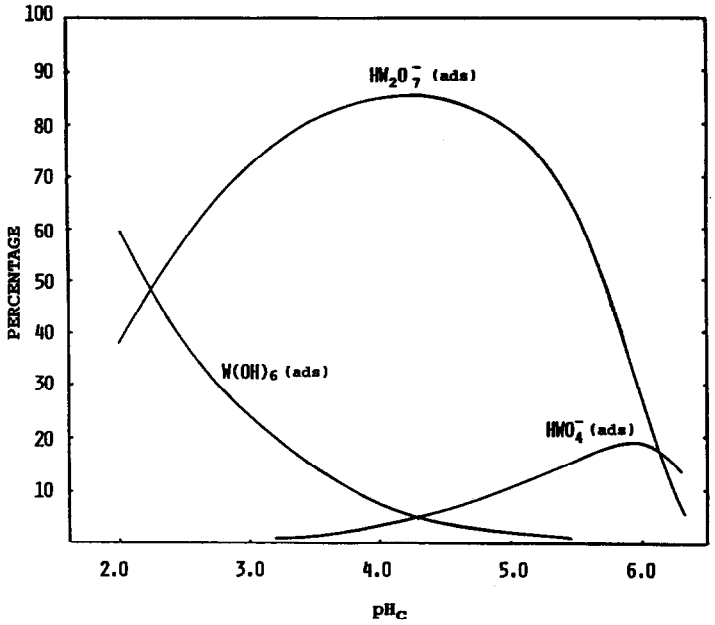

Fig. 3. Concentration of adsorbed species, expressed as a percentage of the total amount of tungsten(VI) adsorbed, as a function of pH_c. The curves are calculated for an initial concentration of 1.0 mM using average values of the adsorption constants.

Table 1. Values obtained for adsorption (K_{pq}) and formation (β_{pq}) constants from the computer treatment of the distribution data at initial tungsten(VI) concentrations of 0.5 and 1.0 mM. Error limits are estimated values

	0.5 mM	1.0 mM
$\log K_{1,1}$	8.2±0.5	7.9±0.5
$\log K_{1,2}$	11.8±0.5	12.6±0.5
$\log K_{2,3}$	22.9±0.3	22.8±0.3
$\log \beta_{1,2}$	8.3±0.2	8.2±0.2
$\log \beta_{2,5}$	23.1±1.0	22.8±1.0
$\log \beta_{7,10}$	77.0±1.0	76.0±1.0

is good. In addition to the satisfactory fit of the theoretical curves on the experimental points the agreement between the values for $K_{2,3}$ is very strong evidence for the dimeric nature of the predominant adsorbed species. Because of the much weaker adsorption of the monomeric species the values of $K_{1,1}$ and $K_{1,2}$ could not be determined with great accuracy. The differences between the values for these constants therefore reflect experimental inaccuracies, but it might also be an indication of some deficiencies in the assumed reaction model of the aqueous phase. Good agreement, however, was obtained between the present values for $\log \beta_{1,2}$ (8.2 and 8.3) and that reported previously (8.1).[10] Also reasonable is the agreement between the values now calculated for $\log \beta_{7,10}$ (76.0 and 77.0) and that obtained from potentiometric measurements[7] of aged (seven days) tungstate solutions ($\log \beta_{7,10} = 75.8$). Although the existence of a (7,10) polyanion, $[H_2W_7O_{24}]^{4-}$, has not been postulated before in the literature, its inclusion serves well to obtain an adequate description of the aqueous phase equilibria. The existence of such an ion does not seem unreasonable in view of the experimental evidence recently obtained for the heptanuclear tungsten(VI) polyions (7,8) and (7,9).[5,15,16] The value of $\log \beta_{7,10} = 76 \pm 1$ is acceptable if compared with $\log \beta_{7,8} = 65.19$ and $\log \beta_{7,9} = 69.96$.[5]

This is the first time that evidence for a (2,5) tungsten(VI) species has been obtained and a value for its formation constant was determined. Again it is difficult to assess the probability of the existence of this species from the present data. Its inclusion, however, does improve the fit and a similar dimeric molybdenum(VI) cation has been characterized.[14] The value of $\log \beta_{2,5} = 23$ for the tungsten species is significantly higher than the values obtained for the molybdenum cation, $\log \beta_{2,5} = 18.4$ and 19 pertaining to a 3 M $NaClO_4$ medium.[14,17] This difference is consistent with the greater stability of condensed tungsten species; compare for example the values of the formation constants of $[W_7O_{24}]^{6-}$ and $[Mo_7O_{24}]^{6-}$ in a 1.0 M NaCl medium, namely $\log \beta_{7,8} = 65.2$ and 52.8, respectively.[5,4]

The adsorption model

A satisfactory description of the tungsten(VI) adsorption data at low concentrations in the pH_c

range 2–6 is afforded in terms of a model comprising a dimeric and two monomeric species. This model also worked quite well for the adsorption of molybdenum, for which it had been tested for concentrations up to 10 mM.[4] It is interesting to compare the adsorption constants of the different tungsten and molybdenum species. Stronger adsorption of tungsten(VI) onto activated carbon is indicated by greater adsorption constants for each of the tungsten species, namely $\log K_{1,1} \sim 8.0$ and 6.4, $\log K_{1,2} \sim 12.2$ and 10.5, $\log K_{2,3} \sim 22.9$ and 19.8.

The explanation advanced for the strong adsorption of molybdenum(VI) on activated carbon in terms of chemical bonding to basic surface oxygen atoms,[4] analogous to complex formation of oxalate,[18] citrate,[19] lactate,[20] etc. seems to be equally well suited for tungsten(VI). A strong driving force for the chemisorption reaction would be the gain in bond energy when the coordination spheres of molybdenum(VI) and tungsten(VI) are expanded from four to six. Relatively large negative ΔH values have been measured for the complexation reactions of molybdate[18,19] and tungstate[21] with oxalate and citrate; in such complexes molybdenum(VI) and tungsten(VI) are usually octahedrally coordinated.[22–24]

When the formation constants for dinuclear complexes of tungstate[21] and molybdate[18] with oxalate are compared it is seen that the tungsten complex is more stable, which corresponds with the stronger adsorption of tungsten compared to that of molybdenum (cf. $K_{2,3}$ values above):

	$\log \beta$
$2WO_4^{2-} + 5H^+ + 2C_2O_4^{2-} \rightleftharpoons [W_2O_5(C_2O_4)_2(OH)H_2O]^{3-}$	32.8
$2MoO_4 + 5H^+ + 2C_2O_4^{2-} \rightleftharpoons [Mo_2O_5(C_2O_4)_2(OH)H_2O]^{3-}$	31.8.

Also, if the formation constants for the citrate complexes of molybdenum[19] and tungsten[21] are compared it is found that the values are greater for tungsten than for molybdenum:

	$\log \beta$	
	Mo^{VI}	W^{VI}
$MO_4^{2-} + Cit^{3-} + H^+ \rightleftharpoons [MO_3Cit]^{4-} + H_2O$	8.25	10.14
$MO_4^{2-} + Cit^{3-} + 2H^+ \rightleftharpoons [MO_3HCit]^{3-} + H_2O$	15.08	17.08
$MO_4^{2-} + Cit^{3-} + 3H^+ \rightleftharpoons [MO_3H_2Cit]^{2-} + H_2O$	19.7	21.6.

Also noteworthy are the comparable differences between the molybdenum and tungsten constants for complexation and adsorption, respectively. This consistency between the adsorption and complexation constants for the two metals supports the interpretation of the adsorption behaviour in terms of surface complex formation.

Acknowledgements—Financial support by MINTEK and the University of Stellenbosch is gratefully acknowledged.

REFERENCES

1. K. Ohashi, K. Murakami and K. Yamamoto, *Bunseki Kagaku* 1983, **32**, 313.
2. A. Sai, A. Onuki, K. Ohashi, K. Motojima and K. Yamamoto, *Bunseki Kagaku* 1981, **30**, 804.
3. E. A. Sigworth, *Proc. Ontario Ind. Waste Conf.* 1963, **10**, 177.
4. J. J. Cruywagen and H. F. de Wet, *Polyhedron* 1988, **7**, 547 and refs cited.
5. J. J. Cruywagen and I. F. J. van der Merwe, *J. Chem. Soc., Dalton Trans.* 1987, 1701.
6. K. A. Kraus and F. Nelson, *12th Bien. Conf. Carbon*, Pittsburg (1975).
7. I. F. J. van der Merwe, MSc Thesis, University of Stellenbosch (1984).
8. F. Will and J. H. Yoe, *Anal. Chim. Acta* 1953, **8**, 546.
9. K. H. Tytko, G. Baethe and J. J. Cruywagen, *Inorg. Chem.* 1985, **24**, 3132.
10. G. Schwarzenbach, G. Geier and J. Littler, *Helv. Chim. Acta* 1962, **45**, 2601.
11. M. T. Pope, *Heteropoly and Isopoly Oxometalates*. Springer, Berlin (1983).
12. W. J. Dixon (Ed.), *BMDP Statistical Software*. University of California Press, Berkeley, California (1981).
13. D. M. Hirst, *Mathematics for Chemists*. MacMillan, London (1976).
14. J. J. Cruywagen, J. B. B. Heyns and E. F. C. H. Rohwer, *J. Inorg. Nucl. Chem.* 1978, **40**, 53.
15. J. Fuchs and E. P. Flindt, *Z. Naturforsch B* 1979, **34**, 412.
16. R. I. Maksimovskaya and K. G. Burtseva, *Polyhedron* 1985, **4**, 1559.
17. Y. Sasaki and L. G. Sillén, *Acta Chem. Scand.* 1964, **18**, 1014.
18. J. J. Cruywagen, J. B. B. Heyns and R. F. van de Water, *J. Chem. Soc., Dalton Trans.* 1987, 1701.
19. J. J. Cruywagen and R. F. van de Water, *Polyhedron* 1986, **5**, 521.
20. M. M. Caldeira and V. M. S. Gil, *Polyhedron* 1986, **5**, 381.
21. L. Kruger, MSc Thesis, University of Stellenbosch (1988).
22. E. I. Stiefel, *Prog. Inorg. Chem.* 1977, **22**, 1.
23. M. M. Caldeira, M. L. Ramos and V. M. S. Gil, *Can. J. Chem.* 1987, **65**, 827.
24. L. R. Nassimbeni, M. L. Niven, J. J. Cruywagen and J. B. B. Heyns, *J. Cryst. Spec. Res.* 1987, **17**, 99.

Polyhedron Vol. 8, No. 1, pp. 77–81, 1989
Printed in Great Britain

0277–5387/89 $3.00+.00
© 1988 Pergamon Press plc

COMPLEXATION AND INTRAMOLECULAR ALKYLATION OF BIPYRIDYL LIGANDS BY $Zr(OAr)_2R_2$ ($R = CH_3$, CH_2Ph) COMPOUNDS

LISA M. KOBRIGER, ANNE K. McMULLEN, PHILLIP E. FANWICK and IAN P. ROTHWELL†

Department of Chemistry, Purdue University, West Lafayette, IN 47907, U.S.A.

(*Received* 20 *April* 1988; *accepted* 13 *July* 1988)

Abstract—Addition of the α-di-imine ligands 2,2′-bipyridine (bipy), 4,4′-dimethyl-2,2′-bipyridine (4,4′-Me_2bipy) or 1,10-phenanthroline (phen) to the bis-alkyls $Zr(OAr\text{-}2,6Bu^t_2)_2(R)_2$ ($OAr\text{-}2,6Bu^t_2$ = 2,6-di-*tert*-butylphenoxide; $R = CH_3$, CH_2Ph) results in the formation of two types of product. In the case of the dimethyl substrate a simple adduct such as $Zr(OAr\text{-}2,6Bu^t_2)_2(Me)_2(bipy)$ is generated. However, with dibenzyl the products obtained are the result of an intramolecular alkylation of the α-di-imine ligands. Spectroscopic data confirm the asymmetric nature of the ensuing alkylated heterocycles. A single crystal X-ray diffraction study on $Zr(OAr\text{-}2,6Bu^t_2)_2(Me)_2$(4,4′-bipy) confirmed the stoichiometry and showed a very crowded coordination sphere about the six-coordinate metal centre with the two *trans* methyl groups being severely bent towards the bipyridine chelate rings.

The ability of neutral donor ligands such as ethers, tertiary phosphines, amines and nitrogen heterocyclic compounds to coordinate to and stabilize the homoleptic alkyls of the high valent early *d*-block, lanthanide and actinide metals has been well recognized for some time.[1–3] However, recent developments have shown that pyridine based ligation can sometimes undergo further reactions subsequent to coordination to the metal. Hence, Erker has shown that treatment of (η^4-butadiene)$ThCp^*_2$ with pyridine led to the formation of an η^3-allyl thorium compound resulting from attack at the α-carbon of the pyridine ring.[4] Recent work on the chemistry of early *d*-block metal η^2-acyls has also shown that pyridine heterocycles are candidates for undergoing carbon–carbon bond forming reactions subsequent to coordination. Hence, treatment of the di-alkyls $(ArO)_2MR_2$ (OAr = 2,6-di-*tert*-butylphenoxide; M = Zr, Hf; $R = CH_3$, CH_2Ph) with CO in the presence of pyridine leads to the high yield formation of α,α-disubstituted pyridine–dimethoxide ligation.[5] A pathway involving stepwise attack of intermediate η^2-acyl groups on the pyridine ring is envisioned. Work by Tilley *et al.* has shown similar reactivity for η^2-sila–acyl ligands. Preliminary mechanistic data is consistent with a pathway involving nucleophilic attack of the metal–acyl group at the α-carbon of the pyridine ring followed by a facile 1,2-hydrogen shift to generate the observed α-substituted pyridinemethoxide linkage.[5,6] The alkylation of pyridine and bipyridine substrates by alkyl–lithium reagents is a well documented process and is used extensively in the synthesis of 2-alkylpyridines and *ortho*-alkylated bipyridines and phenanthrolines.[7]

In this paper we wish to report the intramolecular alkylation of bipyridyl ligands by zirconium alkyls of the type $Zr(OAr\text{-}2,6Bu^t_2)_2(R)_2$. Structural studies on a six-coordinate adduct of stoichiometry $Zr(OAr\text{-}2,6Bu^t_2)_2(Me)_2$(bipy) strongly suggests that steric crowding is important in inducing the alkylation.

RESULTS AND DISCUSSION

The two, pale yellow di-alkyls, $Zr(OAr\text{-}2,6Bu^t)_2M_2$[8] and $Zr(OAr\text{-}2,6Bu^t)_2(CH_2Ph)_2$[9] form deep yellow–orange solutions in benzene or toluene on addition of 2,2′-bipyridine (bipy). In the cases of the dimethyl, reaction with one equivalent

†Author to whom correspondence should be addressed. Camille and Henry Dreyfuss Teacher–Scholar, 1985–1990. Fellow of Alfred P. Sloan Foundation, 1986–1990.

leads to orange products of stoichiometry $Zr(OAr\text{-}2,6Bu^t_2)_2(Me)_2(bipy)$ (**1a**) or $Zr(OAr\text{-}2,6Bu^t_2)_2(Me)_2(4,4'\text{-}Me_2bipy)$ (**1b**), which can be recrystallized from toluene on cooling as large orange blocks. The ^1H NMR of **1** is found to be broad at ambient temperatures and concentration dependent. We interpret this observation as being due to a rapid equilibrium of the type shown:

$$Zr(OAr\text{-}2,6Bu^t_2)_2(Me)_2 + bipy \rightleftharpoons Zr(OAr\text{-}2,6Bu^t_2)_2(Me)_2(bipy). \quad (\mathbf{1b})$$

Apart from these changes, solutions of **1a** or **1b** in hydrocarbon solvents are stable for weeks at room temperature.

In contrast, addition of one equivalent of bipy or $4,4'\text{-}Me_2bipy$ to the dibenzyl $Zr(OAr\text{-}2,6Bu^t_2)_2(CH_2Ph)_2$ results in initially orange solutions which lighten to a pale yellow over a period of an hour. During this time dramatic changes in the ^1H NMR spectrum take place. Although it is possible to isolate pure materials of stoichiometry "$Zr(OAr\text{-}2,6Bu^t_2)_2(CH_2Ph)_2(bipy)$" from the reaction, the spectroscopic data is consistent with a more complex formulation in which intramolecular transfer of a benzyl group to one of the bipy or phenanthroline α-carbon atoms has occured (Scheme 1). A similar alkylation product can also be obtained using 1,10-phenanthroline. In this case the initially orange solution of the intermediate adduct is replaced by an intense red solution containing product **2c** (Scheme 1).

The ^1H and ^{13}C NMR spectra of the three alkylation products, **2**, contain certain similar features. Particularly informative are the series of multiplets that appear in the region δ 3.0–6.5 ppm in the ^1H NMR spectra. These well-resolved, sharp signals are highly characteristic of pyridyl rings which have undergone 1,2-addition reactions,[7,10] in this case of a $Zr—CH_2Ph$ function. Comparison of the spectra of the bipy, 4,4'-bipy and phen derivatives of **2** allows an unequivocal assignment of these resonances. The characteristic doublet due to the *ortho*-proton of the non-alkylated pyridyl rings is also present in the δ 8.0–8.5 ppm region. The other aromatic proton resonances in the δ 6.5–7.5 ppm region are too difficult to resolve for accurate assignment. The diastereotopic methylene protons of the two benzyl groups, one of which has been transferred to the pyridyl ring are also observed as AB patterns in the δ 2.5–3.5 ppm region at low temperatures. The remaining proton resonances, those of the *tert*-butyl groups of the aryloxide ligands appear at ambient temperatures as three, broad resonances of intensity 2:1:1. The asymmetry induced in the bipyridyl ligands on alkylation at one of their faces means that non-equivalent aryloxide groups should ensue in any static structure that one can envisage. This is consistent with the observed spectra, except that it also appears that restricted rotation about one of the aryloxide, Zr—O—Ar bonds is taking place, presumably for steric reasons, resulting in non-equivalent *tert*-butyl groups. Similar restricted rotation of 2,6-di-*tert*-butylphenoxide ligands has been previously well documented.[11] However, although the low temperature limiting spectra are consistent with the expected structure of these molecules, the high temperature ^1H NMR spectra contain some puzzling features. At all temperatures from -60 to $+80°C$ the resonance due to the protons attached to the

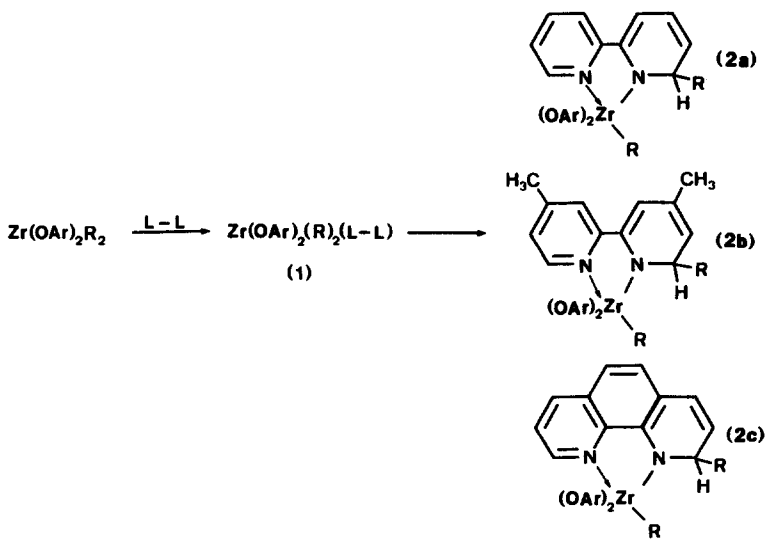

Scheme 1.

alkylated pyridyl system remain sharp and well resolved. However, as the temperature is raised the AB patterns of the two benzyl groups broaden and collapse into two singlets at the expected weighted average of the low temperature AB patterns. No exchange of benzyl groups appears to be occurring on the NMR time scale. Although the equilibration of the diastereotopic benzyl protons at higher temperatures is indicative of some fluxional process taking place, it is very difficult to see how this can be occurring for the benzyl group attached to the pyridyl ring. At all temperatures this group should remain diastereotopic as long as carbon–carbon bond breaking processes are ruled out. Similarly the aryloxide *tert*-butyl groups broaden, coalesce and appear as a broad singlet at 80°C in the ^{1}H NMR spectrum. At the present time we have no totally satisfactory explanation for these observations. The alkylated bipyridyl ligands might very well be expected to undergo rapid dissociation and recoordination of the undisrupted pyridine ring. A process such as this would explain the exchange of non-equivalent aryloxide ligands but again could not account for the high temperature singlets for the benzyl ligands. In the ^{13}C NMR spectrum the two α-carbon single atoms of the non-equivalent benzyl groups are observed as resonances at $\approx \delta$ 50 and $\approx$ 70 ppm.

Unfortunately it was not found possible to obtain single crystals of the alkylation products, **2**, suitable for crystallographic study. However, suitable crystals of the dimethyl adduct **1b** were obtained and subjected to a structural analysis. The solid state structure of **1b** is shown in Fig. 1, while Table 1 contains some pertinent bond distances and angles. The molecule can be seen to contain a six-coordinate zirconium atom with a coordinate geometry considerably distorted from octahedral. The Zr—OAr, Zr—CH_3 and Zr—N(pyridyl) distances appear well into the normal range reported for related groups bound to Zr^{IV},[8,12] The distortions of the coordination sphere from octahedral are certainly significant in view of the observed alkyl transfer seen to take place in the benzyl complexes. The angle between the bulky *cis*-aryloxide groups is opened up to 107.9(1)°. Meanwhile the methyl groups, which in an idealized geometry would be mutually *trans* are both bent towards the 4,4′-Me_2bipy ligand to give a CH_3—Zr—CH_3 angle of only 144.2(2)°. The heterocyclic chelate generates only a modest 67.3(1)° bite at the metal. The structure can be envisaged in terms of the 4,4′-Me_2bipy ligand trying to squeeze between the two methyl groups in a tetrahedral $Zr(OAr\text{-}2,6Bu^t_2)_2(CH_3)_2$ molecule, with the bulky aryloxide ligands sterically resisting the opening up of the CH_3—Zr—CH_3 angle. In the structurally characterized bis-benzyl, $Zr(OAr\text{-}2,6Bu^t_2)_2(CH_2Ph)_2$, O—Zr—O and C—Zr—C angles of 116.2(2) and 110.0(3)°, respectively, were observed.[9] The severe

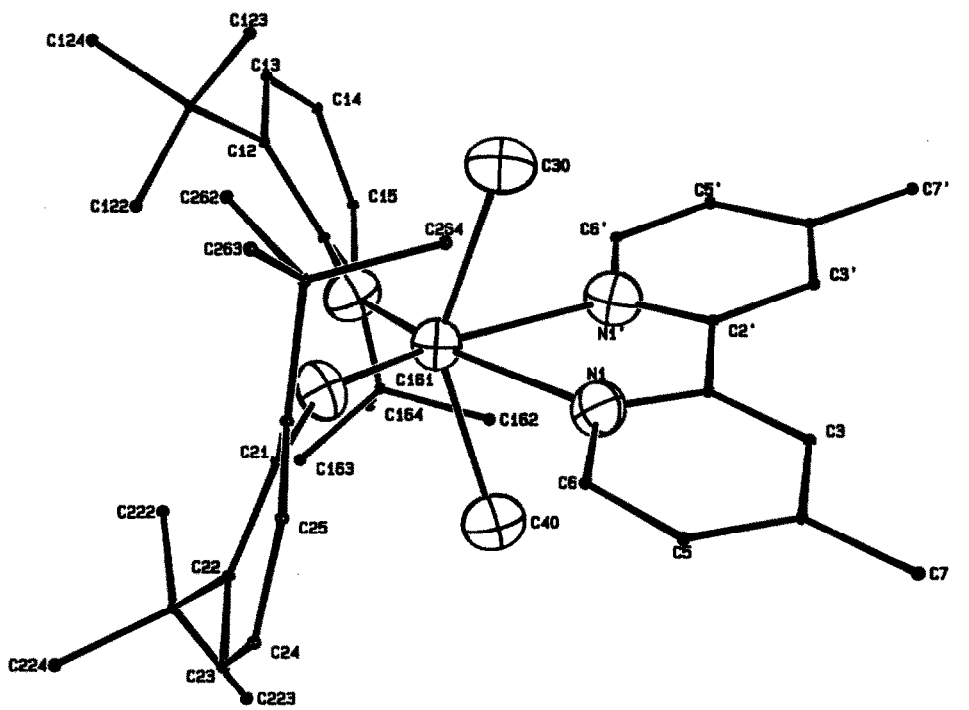

Fig. 1. ORTEP view of **1b** emphasizing the central coordination sphere.

Table 1. Selected bond distances (Å) and angles (°) for (**1b**)

Zr—O(10)	1.983(3)	Zr—O(20)	1.990(3)
Zr—N(1)	2.381(4)	Zr—N(1′)	2.390(4)
Zr—C(30)	2.317(5)	Zr—C(40)	2.321(5)
O(10)—Zr—O(20)	107.9(1)	N(1)—Zr—N(1′)	67.3(1)
O(10)—Zr—N(1)	160.4(1)	N(1)—Zr—C(30)	80.0(2)
O(10)—Zr—N(1′)	94.2(1)	N(1)—Zr—C(40)	70.5(2)
O(10)—Zr—C(30)	100.2(2)	N(1′)—Zr—C(30)	80.4(2)
O(10)—Zr—C(40)	101.1(2)	N(1′)—Zr—C(40)	144.2(2)
O(20)—Zr—N(1)	91.2(1)	Zr—O(10)—C(11)	161.1(3)
O(20)—Zr—N(1′)	157.5(1)	Zr—O(20)—C(21)	154.2(3)
O(20)—Zr—C(30)	101.1(2)		
O(20)—Zr—C(40)	99.3(2)		

crowding present in this molecule is also evident in the distortions clearly seen in the aryl rings of the OAr-2,6Bu$^t_2$ groups (Fig. 1). The inability of the alkyl groups to "back away" from the incoming bipyridyl ligands presumably is the reason that alkyl transfer occurs. The lack of observed alkylation by the dimethyl over its benzyl counterpart may be a consequence of the even greater steric crowding present in the intermediate [Zr(OAr-2,6Bu$^t_2$)$_2$(CH$_2$Ph)$_2$(bipy)]. However, thermodynamic considerations such as the fact that L$_n$M—CH$_2$Ph bonds are typically weaker than L$_n$M—CH$_3$ bonds may be an important consideration.[13]

EXPERIMENTAL

The bis-alkyls Zr(OAr-Bu$^t_2$)$_2$(CH$_3$)$_2$[8] and Zr(OAr-Bu$^t_2$)$_2$(CH$_2$Ph)$_2$[9] were synthesized as previously reported. The heterocyclic compounds 2,2′-bipyridine (bipy), 4,4′-dimethyl-2,2′-bipyridine (4,4′-Me$_2$bipy) and 1,10 phenanthroline (phen) were obtained commercially and dried by melting under a dynamic vacuum of 10^{-2}–10^{-3} torr for 20–30 min. ^{1}H and ^{13}C NMR spectra were obtained using a Varian Associates XL-200 spectrometer while microanalyses were performed in-house at Purdue.

Zr(OAr-2,6Bu$^t_2$)$_2$(CH$_3$)$_2$(bipy) (**1a**)

Although ^{1}H NMR spectra of 1 : 1 mixtures of Zr(OAr-2,6Bu$^t_2$)$_2$(CH$_3$)$_2$ and bipy in benzene-d$_6$ showed the presence of a new compound, recrystallization from such solutions sometimes yielded mixtures of starting materials as well as **1a**. The best results for obtaining pure crystalline **1a** was found to be cooling a mixture of the dimethyl and bipyridine (2 equiv) in toluene whereupon large orange blocks of product were obtained. Found: C, 68.2; H, 8.2; N, 4.0. Calc. for ZrC$_{40}$H$_{56}$N$_2$O$_2$: C, 68.8; H, 8.2; N, 4.1%. ^{1}H NMR (C$_6$D$_6$, 30°C): δ 1.62 (s, OAr-*Bu$^t_2$*); 1.87 (s, Zr—CH$_3$); 8.61 (d, 2,2′-H).

Zr(OAr-2,6Bu$^t_2$)$_2$(CH$_3$)$_2$(4,4′-Me$_2$bipy) (**1b**)

An essentially identical procedure to that used for **1a** above yielded **1b** as very large orange blocks. Found: C, 70.1; H, 8.4; N, 3.7. Calc. for ZrC$_{42}$H$_{60}$N$_2$O$_2$: C, 70.4; H, 8.4; N, 3.9%. ^{1}H NMR (C$_6$D$_6$, 30°C): δ 1.59 (s, OAr-*Bu$^t_2$*); 1.86 (s, Zr—*CH$_3$*); 2.15 (s, 4,4′-*Me$_2$*bipy); 8.50 (d, 2,2′-H).

Zr(OAr-2,6Bu$^t_2$)$_2$(CH$_2$Ph)(bipy-CH$_2$Ph) (**2a**)

The addition of bipy (1 equiv) to a solution of Zr(OAr-2,6Bu$^t_2$)$_2$(CH$_2$Ph)$_2$ in toluene results in the formation of a dark orange solution after 4 h. Addition of hexane to the solution results in the precipitation of the product as small yellow microcrystals. Found: C, 74.0; H, 7.7; N, 3.4. Calc. for ZrC$_{52}$H$_{64}$N$_2$O$_2$: C, 74.3; H, 7.7; N, 3.3%. ^{1}H NMR (−30°C, C$_6$D$_5$CD$_3$): δ 1.03 (s), 1.34 (s), 1.76 (s, ratio of 1 : 1 : 2, OAr-Bu$^t_2$); 2.58, 2.68 (AB pattern, *CH$_2$*Ph); 2.94, 3.39 (AB pattern, *CH$_2$*Ph); 3.45 (broad triplet, 4′-H); 4.16 (dd, 3′-H); 5.24 (d, 5′-H); 6.01 (t, 2′-H); 8.22 (d, 2-H); 6.5–7.3 (m, other aromatics). ^{13}C NMR (C$_6$D$_6$, 30°C): δ 46.9 (bipy-*C*H$_2$Ph); 72.2 (Zr—CH$_2$Ph); 32.9, 32.5, 31.98 (OAr-2,6Bu$^t_2$).

Zr(OAr-2,6Bu$^t_2$)$_2$(CH$_2$Ph)(4,4′-Me$_2$bipy-CH$_2$Ph) (**2b**)

An identical procedure to that used to prepare **2a** only now using 4,4′-Me$_2$bipy yielded **2b** as small yellow–orange plates. Found: C, 74.4; H, 8.3; N, 3.3. Calc. for ZrC$_{54}$H$_{70}$N$_2$O$_2$: C, 74.7; H, 7.9; N, 3.2%. ^{1}H NMR (−30°C, C$_6$D$_5$CD$_3$): δ 1.07 (s), 1.38 (s), 1.76 (s, ratio of 1 : 1 : 2, OAr-2,6Bu$^t_2$); 2.58, 2.62 (AB pattern, *CH$_2$*Ph); 3.00, 3.40 (AB pattern, *CH$_2$*Ph); 1.21 (s), 1.78 (s, 4,4′-*Me$_2$*); 4.09 (dd, 3′-

H); 5.25 (d, 5′-H); 5.95 (d, 2′-H); 6.5–7.5 (m, other aromatics).

$Zr(OAr\text{-}2,6Bu^t_2)_2(CH_2Ph)(Phen\text{-}CH_2Ph)$ (2c)

Obtained as deep red microcrystals by an essentially identical procedure using phen instead of bipy. Found: C, 76.5; H, 7.5; N, 4.2. Calc. for $ZrC_{54}H_{64}N_2O_2$: C, 75.0; H, 7.5; N, 3.2%. ^1H NMR (−30°C, $C_6D_5CD_3$): δ 0.90 (s), 1.39 (s), 1.80 (s, 1:1:2 ratio, OAr-2,6Bu^t_2); 2.84, 2.92 (AB pattern, CH_2Ph); 3.10, 3.35 (AB pattern, CH_2Ph); 6.32 (dd, 2′-H); 4.29 (dd, 4′-H); 3.91 (m, 3′-H); 8.51 (d, 2-H); 6.5–7.7 (m, other aromatics). ^{13}C NMR (C_6D_6, 30°C): δ 49.5 (phen-CH_2Ph); 74.1 (Zr—CH_2Ph).

Crystallographic studies

Crystal data and data collection parameters are contained in Table 2. The procedures used in the data collections are those typically used by the Purdue Crystallographic Center and have been reviewed.[14] All non-hydrogen atoms were refined anisotropically while the positions for hydrogen atoms were calculated assuming idealized geometry and a bond distance of 0.95 Å. For methyl groups, one hydrogen was located in a difference Fourier map, its position idealized and the remaining positions calculated. The three intensity standards were measured after every 5000 s of beam time and showed no decay. An extinction correction was not applied.

Table 2. Crystal data and data collection parameters

Formula	$ZrO_2N_2C_{45}H_{63}$
f_w	755.24
Space gp	$P2_1/c$
a (Å)	10.980(1)
b (Å)	19.571(1)
c (Å)	20.483(2)
β (°)	104.269(8)
V (Å^3)	4266.(1)
Z	4
d_{calc} (g cm^{-3})	1.176
Crystal dimensions (mm)	0.65 × 0.59 × 0.54
Temperature (°C)	22
Radiation (wavelength)	Mo-K_α (0.71073 Å)
Monochromater	Graphite
Linear abs. coef. (cm^{-1})	2.87
Absorption correction applied	None
Diffractometer	Enraf–Nonius CAD4
Scan method	ω–2θ
h, k, l limits	−11–11 0–21 0–22
2θ range (°)	4.00–45.00
Scan width (°)	0.73 + 0.35 tan (θ)
Take-off angle (°)	2.80
Programs used	Enraf–Nonius SDP
F_{000}	1612.0
ρ-factor used in weighting	0.070
Data collected	5754
Unique data	5754
Data with $I > 3.0S(I)$	3593
Number of variables	436
Largest shift/esd in final cycle	0.01
R	0.044
R_w	0.058
Goodness-of-fit	1.208

Acknowledgements—We thank the National Science Foundation (Grant CHE-8612063 to I.P.R.) for financial support of this research. We also thank the NSF Chemical Instrumentation Program (Grant CHE-8615556) for support of the X-ray diffraction facility at Purdue. I.P.R. also gratefully acknowledges the Camille and Henry Dreyfus Foundation for the award of a Teacher–Scholar Grant and the Alfred P. Sloan Foundation for a fellowship.

REFERENCES

1. *Comprehensive Organometallics Chemistry* (Edited by G. Wilkinson, F. G. A. Stone and E. Abel). Pergamon Press, Oxford (1982).
2. P. G. Edwards, R. A. Andersen and A. Zalkin, *J. Am. Chem. Soc.* 1981, **103**, 7792; P. G. Edwards, R. A. Anderson and A. Zalkin, *Organometallics* 1984, **3**, 293.
3. W. J. Evans, *Adv. Organomet. Chem.* 1985, **24**, 131.
4. G. Erker, T. Muhlenbernd, R. Benn and A. Rufinskra, *Organometallics* 1986, **5**, 402.
5. P. E. Fanwick, L. Kobriger, A. K. McMullen and I. P. Rothwell, *J. Am. Chem. Soc.* 1986, **108**, 8095.
6. T. D. Tilley, personal communication.
7. G. R. Newkome and W. W. Paudler, *Contemporary Heterocyclic Chemistry: Synthesis, Reactions and Applications*. John Wiley, New York (1982).
8. L. R. Chamberlain, L. D. Durfee, P. E. Fanwick, L. Kobriger, S. L. Latesky, A. K. McMullen, I. P. Rothwell, K. Folting, J. C. Huffman, W. E. Streib and R. Wang, *J. Am. Chem. Soc.* 1987, **109**, 390.
9. S. L. Latesky, A. K. McMullen, I. P. Rothwell and J. C. Huffman, *Organometallics* 1985, **4**, 902.
10. R. M. Silverstein, G. C. Baxter and T. C. Morrill, *Spectrophotometric Identification of Organic Compounds*, 4th edn. John Wiley, New York (1980).
11. S. L. Latesky, A. K. McMullen, J. Keddington, I. P. Rothwell and J. C. Huffman, *Inorg. Chem.* 1985, **24**, 995.
12. L. R. Chamberlain, L. D. Durfee, P. E. Fanwick, L. M. Kobriger, S. L. Latesky, A. K. McMullen, B. D. Steffey, I. P. Rothwell, K. Folting and J. C. Huffman, *J. Am. Chem. Soc.* 1987, **109**, 6068.
13. G. Henrici-Olivé and S. Olivé, *Coordination and Catalysis*. Verlag Chemie, New York (1977).
14. P. E. Fanwick, A. E. Ogilvey and I. P. Rothwell, *Organometallics* 1987, **6**, 73.

Polyhedron Vol. 8, No. 1, pp. 83–86, 1989
Printed in Great Britain

0277–5387/89 $3.00+.00
© 1988 Pergamon Press plc

LIGAND REACTIVITY IN 2,2′-BIPYRIDINE COMPLEXES; CHARGE EFFECTS UPON REACTIONS WITH BASE

EDWIN C. CONSTABLE

University Chemical Laboratory, Lensfield Road, Cambridge CB2 1EW, U.K.

(*Received* 21 *March* 1988; *accepted* 13 *July* 1988)

Abstract—^{1}H and ^{13}C NMR studies indicate that the 2,2′-bipyridine ligands in $[Rh(bipy)_3]^{3+}$ (bipy = 2,2′-bipyridine) salts are in a different electronic environment to those in $[Ru(bipy)_3]^{2+}$ salts. The rhodium(III) cation undergoes a rapid and specific deuteration reaction upon treatment with solutions of $Na[OCD_3]$ in CD_3SOCD_3/CD_3OD. Exchange occurs rapidly at H_6 and more slowly at H_3. These observations are interpreted in terms of a separability of σ- and π-bonding contributions to the metal–ligand interaction.

It is well established that ligand reactivity may be modified upon coordination to a metal ion.[1–5] Particular interest has centred on the reactions of pyridine and oligopyridine complexes which are among the commonest components of both homogeneous and heterogeneous systems for solar energy photoconversion. The reactivity of oligopyridine complexes has been the subject of some controversy.[6–11] It has been noted that the σ- and π-components of the metal–ligand interaction are separable and opposed in complexes with π-acceptor ligands.[12–17] A number of years ago, we reported a novel deuterium exchange reaction associated with coordinated 2,2′-bipyridine ligands in solutions of $[Ru(bipy)_3]^{2+}$ salts.[18] Other workers have confirmed these results[19–21] and extended the observations to $[Os(bipy)_3]^{2+}$ salts.[21] More recently it has been demonstrated that $[Ru(terpy)_2]^{2+}$ salts undergo analogous reactions, and that the relative rates of reaction at the central and terminal pyridyl rings preclude a pathway involving cyclometallated intermediates.[22] We have now extended these observations to complexes of 2,2′-bipyridine and 2,2′:6′,2″-terpyridine with other metals, and report herein our studies of $[Rh(bipy)_3]^{3+}$ salts.

EXPERIMENTAL

^{1}H and ^{13}C NMR spectra were recorded on Bruker WM250 or AM400 spectrometers. Electronic spectra were recorded on a Pye–Unicam 8800 spectrophotometer.

Relaxation measurements were made using the inversion recovery technique. Measurements were made using degassed 20 mM solutions of the ruthenium or rhodium complexes in CD_3SOCD_3. In each case, ten different τ values ranging from 0.05 to 7 s were used for the experimental data sets. Deuteration studies were made using 10 mM solutions of $[Rh(bipy)_3][PF_6]_3$ in 1:1 CD_3SOCD_3/CD_3OD. Solutions of $Na[OCD_3]$ in CD_3OD were prepared by the reaction of weighted amounts of sodium metal with CD_3OD.

Rhodium trichloride trihydrate was used as supplied (Johnson Matthey); 2,2′-bipyridine (Aldrich) was recrystallized under nitrogen before use.

Tris(2,2′-*bipyridine*)*rhodium*(III) *hexafluorophosphate*

A solution of $[Rh(bipy)_3]Cl_3$ in aqueous ethanol was prepared as described by Lehn,[23] and treated with a 2 M excess of aqueous $[NH_4][PF_6]$. The yellow precipitate ws collected by filtration and recrystallized from ethanol–acetone to give yellow plates of $[Rh(bipy)_3][PF_6]_3$.

RESULTS AND DISCUSSION

The ^{1}H NMR chemical shifts and associated T_1 relaxation times for 20 mM solutions of $[M(bipy)_3]^{n+}$ (M = Ru, $n = 2$; M = Rh, $n = 3$) in CD_3SOCD_3 are presented in Table 1. We have previously reported the use of relaxation measurements in the assignment of the NMR spectra of coordinated 2,2′-bipyridine ligands.[24] The spectrum of the rhodium complex was fully assigned on the basis of a COSY experiment.

Table 1. ^{1}H NMR chemical shift values (δ) and relaxation times (T_1, s) for CD_3SOCD_3 solutions of $[M(bipy)_3][PF_6]_n$ (20 mM, M = Ru, $n = 2$; M = Rh, $n = 3$)

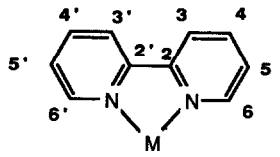

	Ru		Rh		
	δ	T_1 (s)	δ	T_1 (s)	$\Delta\delta^a$
H_3	8.40	0.41	9.04	0.45	0.64
H_4	8.17	0.72	8.57	0.79	0.40
H_5	7.53	0.66	7.79	0.72	0.26
H_6	7.73	0.88	7.85	0.90	0.12

$^a\Delta\delta = \delta(Rh) - \delta(Ru)$.

The spectrum of the rhodium(III) complex closely resembles that of the corresponding ruthenium(II) compound. The most noticeable feature is the downfield shift of H_3 with respect to the free ligand, and the origins of this effect in the conformational changes resulting from the adoption of a *cis* conformation of the ligand upon coordination have been discussed.[5,24-27] A comparison of the chemical shifts of the rhodium(III) complex with those of the ruthenium(II) complex reveals the expected downfield shift for all the resonances in the tripositive cation. The $\Delta\delta$ values are also listed in Table 1 and are of some interest.

The crystal and molecular structures of the cations $[Rh(bipy)_3]^{3+}$ and $[Ru(bipy)_3]^{2+}$ reveal the two ions to possess extremely similar structures;[28,29] the M—N distances and all other molecular parameters in the two are the same within experimental error. Any differences in ground state and reactivity properties will thus be due to the difference in charge between the two ions. The similarity in the T_1 relaxation times is further evidence that the structures and solute–solvent interactions of the two complexes are similar. A simple electrostatic model for the metal–ligand interaction would predict the greatest deshielding to occur close to the metal, i.e. at H_6. The relationship between the ^{1}H NMR chemical shift and electron density at a directly bonded carbon atom has been established for aromatic molecules, and is expected to hold for molecules as closely related as the rhodium(III) and ruthenium(II) cations.[30] The $\Delta\delta$ values decrease in the order $H_3 > H_4 > H_5 > H_6$, with a remarkably small shift in $\Delta\delta$ of 0.12 associated with H_6. The net deshielding is a function of the *total* electron density at each site, which includes contributions from both σ- (electron withdrawing) and π- (electron releasing) components. These results are in general accord with those previously reported for $[M(NH_3)_5py]^{n+}$ (M = Ru, $n = 2$; M = Rh, $n = 3$)[21,32] and with the predictions of the electroneutrality principle;[33] indeed, the efficiency of the back-donation at quenching the charge build-up at the six-position is remarkable. These results provide a quantitative measure of the efficiency of d(or p)–π^* back-donation in isoelectronic d^6 ions. As expected, the higher positive charge on the rhodium(III) centre results in a greater polarization of the ligand, and also results in a contraction of the $4d$ and $5p$ orbitals involved in the back-donation. Thus the rhodium ion is *less* able to compensate for the *larger* positive charge build-up in the ligand. The net effect is as we observe; the reduced back-donation from the rhodium only acts effectively to prevent charge build up at the site of highest positive charge closest to the metal (i.e. at the six position). These results are consistent with quantum chemical studies at various levels of sophistication which have been reported for these systems.[14-17]

The ^{13}C NMR spectra of the complexes exhibit similar changes, and values of δ and $\Delta\delta$ are listed in Table 2. Once again, these are consistent with effective back-donation reducing the charge build-up at C_6. The pattern of $\Delta\delta$ values is similar to that observed in the $[M(NH_3)_5py]^{n+}$ complexes mentioned earlier.[31,32] Specifically, C_2 and C_6 undergo upfield shifts on passing from the ruthenium(II) to the rhodium(III) complexes; this is exactly the opposite to that expected in the absence of back-donation.

Treatment of a CD_3SOCD_3 solution of $[Rh(bipy)_3]$

Table 2. ^{13}C NMR chemical shift values (δ) for CD_3SOCD_3 solutions of $[M(bipy)_3][PF_6]_n$ (20 mM, M = Ru, $n = 2$; M = Rh, $n = 3$)

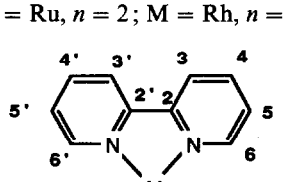

	Ru	Rh	
	δ	δ	$\Delta\delta^a$
C_2	156.6	154.5	−2.1
C_3	124.5	126.8	+2.3
C_4	137.9	143.1	+5.2
C_5	127.8	130.4	+2.6
C_6	151.2	150.9	−0.3

$^a\Delta\delta = \delta(Rh) - \delta(Ru)$.

$[PF_6]_3$ with $Na[OCD_3]$ in CD_3OD resulted in the immediate formation of a deep brown solution. The ^1H NMR spectrum of this solution exhibited 12 separate resonances, four of which could be assigned to free 2,2′-bipyridine. Upon the addition of CF_3COOD, the solution changed colour to yellow and the resonances due to the free ligand broadened (presumably due to fast protonation–deprotonation equilibria) and a spectrum containing eight sharp resonances was obtained.

Treatment of solutions of $[Rh(bipy)_3][PF_6]_3$ in 1 : 1 CH_3SOCH_3/CH_3OH with $Na[OCH_3]$ resulted in no change in the electronic spectrum. However, rapid changes in the ^1H NMR spectrum of a solution of the complex in 1 : 1 CD_3SOCD_3/CD_3OD occurred upon the addition of $Na[OCD_3]$ at 40° (Fig. 1). Upon the addition of $Na[OCD_3]$ the intensity of the δ 7.85 doublet (H_6) diminishes. Associated with this process, the triplet at δ 7.79 collapses to a doublet. Under the reaction conditions described, the exchange of H_6 is complete within 25 min, after which period a noticeable reduction in the signal for H_3 occurs, with a concommittant collapse of H_4 from a triplet to a doublet. The exchange of H_3 and H_6 is virtually complete after 1 h; after prolonged reaction times further exchange occurs at H_5 and the signal for H_4 is observed as a singlet at δ 8.57.

The behaviour reported above is in marked contrast to that previously reported for the corresponding osmium(II) and ruthenium(II) complexes, in which the fastest exchange is observed at H_3.[18–22] Whilst these observations are in accord with our initial predictions of a large inductive charge build-up at C_6, they are not consistent with the ^1H NMR shift data which indicates effective back-donation at this site.

A number of mechanisms for the proton–deuteron exchange reaction have been proposed, including cyclometallation at C_3, addition–elimination at C_4 and an acid–base reaction giving a metal-stabilized pyridyl anion. The involvement of cyclometallated intermediates has been eliminated previously,[22] and the present observation of exchange at H_6 effectively confirms this. If we assume a common mechanism for the exchange at H_3 and H_6 we may effectively preclude addition–elimination reactions, since the π-centred mesomeric effects at C_4 (for exchange of $H_{3,5}$) and C_5 (for exchange of H_6) are different and opposite. This leaves a simple acid–base reaction involving methoxide acting as a base rather than a nucleophile.

Under the conditions of the reaction (40°C, excess $Na[OCD_3]$), deprotonation is expected to lead to the thermodynamic anion (although the *kinetic* product will be the C_3 anion, since the parent acid bears the greatest positive charge at this site). Thus, H_6 is the most acidic proton in the ion, although C_6 is the site that shows least change in total electron density. However, C_6 is the position which shows the greatest change in σ electron density as a result of polarization by the metal ion. In the anion, we may regard the negative charge as being localized in an in-plane sp^2 orbital, which is most sensitive to the charge distribution within the σ-bonded framework, and only affected by the net charge to a lesser



Fig. 1. ^1H NMR spectra of $[Rh(bipy)_3][PF_6]_3$ (30 mM, 1 : 1 CD_3SOCD_3/CD_3OD) in the presence of $Na[OCD_3]$ (400 mM) at 40°C.

extent. In other words, the higher positive charge on the rhodium(III) stabilizes the pyridyl anion regardless of any other π-bonding changes which are occurring.

In conclusion, this study has given a considerable amount of information regarding metal–ligand interactions in pyridine complexes. The proton–deuterium exchange reaction in 2,2′-bipyridine complexes proceeds by an acid–base mechanism rather than by nucleophilic attack upon the coordinated ligand. The use of total charge densities in predicting the reactivities of coordinated ligands can only be expected to give reasonable results in the case of π-innocent systems. The balance of σ- and π-components in the metal–ligand interaction may be used to effectively tune the reactivity of coordinated ligands at various sites.

Acknowledgements—I should like to thank the Royal Society for a grant towards the purchase of a spectrophotometer and Johnson Matthey plc for the loan of rhodium trichloride and ruthenium trichloride. I also with to thank Drs Malcolm Gerloch and Antony Stone for helpful discussions.

REFERENCES

1. M. M. Jones, *Ligand Reactivity and Catalysis*. Academic Press, New York (1968).
2. D. H. Busch, in *Reactions of Coordinated Ligands and Homogeneous Catalysis* (Edited by D. H. Busch), ACS No. 37 (1963).
3. J. P. Collman, in *Transition Metal Chemistry* (Edited by R. L.Carlin), Vol. 2. E. Arnold, London (1966).
4. E. C. Constable, *Ligand Reactivity*. Ellis Horwood, Chichester (1988).
5. E. C. Constable, *Inorg. Chim. Acta* 1988, **145**, 49.
6. R. D. Gillard, *Coord. Chem. Rev.* 1975, **16**, 67.
7. E. C. Constable, *Polyhedron* 1983, **2**, 551.
8. N. Serpone, G. Ponterini, M. A. Jamieson, F. Bolletta and M. Maestri, *Coord. Chem. Rev.* 1983, **50**, 209.
9. R. D. Gillard, *Coord. Chem. Rev.* 1983, **50**, 303.
10. E. C. Constable, *Polyhedron* 1984, **3**, 1037.
11. G. Nord, *Comm. Inorg. Chem.* 1985, **4**, 193.
12. P. A. Lay, *Inorg. Chem.* 1984, **23**, 4775.
13. E. C. Constable, *Inorg. Chim. Acta* 1986, **117**, L33.
14. R. D. Gillard and D. W. Clack, *Transition Met. Chem. (Weinheim, Ger.)* 1985, **10**, 419.
15. E. C. Constable and T. A. Leese, *Inorg. Chim. Acta* 1988, in press.
16. E. C. Constable and C. E. Housecroft, *Transition Met. Chem. (Weinheim, Ger.)* 1988, **13**, 19.
17. D. W. Clack, L. A. P. Kane-Maguire, D. W. Knight and P. A. Williams, *Transition Met. Chem. (Weinheim, Ger.)* 1980, **5**, 376.
18. E. C. Constable and K. R. Seddon, *J. Chem. Soc., Chem. Commun.* 1982, 34.
19. S. F. McClanahan and J. R. Kincaid, *J. Am. Chem. Soc.* 1986, **108**, 3840.
20. S. F. McClanahan, T. Hayes and J. Kincaid, *J. Am. Chem. Soc.* 1983, **105**, 4486.
21. O. Wernberg, *J. Chem. Soc., Dalton Trans.* 1986, 1993.
22. E. C. Constable, *J. Chem. Soc., Dalton Trans.* 1985, 2687.
23. M. Kirch, J-M. Lehn and J-P. Sauvage, *Helv. Chim. Acta* 1979, **62**, 1345.
24. E. C. Constable and J. Lewis, *Inorg. Chim. Acta* 1983, **70**, 251.
25. F. E. Lytle, L. M. Petrowsky and L. R. Carlson, *Anal. Chim. Acta* 1971, **57**, 239.
26. H. Elsbernd and J. K. Beattie, *J. Inorg. Nucl. Chem.* 1972, **34**, 771.
27. A. Flamini and A. M. Giuliani, *Inorg. Chim. Acta* 1986, **112**, L7.
28. B. Hubesch, B. Mahieu and J. Meunier-Piret, *Bull. Soc. Chim. Belg.* 1985, **94**, 685.
29. D. P. Rillema, D. S. Jones and H. A. Levy, *J. Chem. Soc., Chem. Commun.* 1979, 849.
30. J. C. Shug and J. C. Deck, *J. Chem. Phys.* 1972, **37**, 2618.
31. D. K. Lavallee, M. D. Baughman and M. P. Phillips, *J. Am. Chem. Soc.* 1977, **99**, 718.
32. D. K. Lavellee and E. B. Fleischer, *J. Am. Chem. Soc.* 1972, **94**, 2583.
33. L. Pauling, *The Nature of the Chemical Bond and the Structure of Molecules and Crystals*, 3rd edn. Cornell University Press, Cornell (1960).

Polyhedron Vol. 8, No. 1, pp. 87–90, 1989
Printed in Great Britain

0277–5387/89 $3.00+.00
© 1988 Pergamon Press plc

THE PREPARATION AND CHARACTERIZATION OF THIOUREA COMPLEXES OF VANADIUM(IV): THE CRYSTAL STRUCTURE OF DICHLOROBIS-(1,3-DIMETHYLIMIDAZOLIDINE-2-THIONE)-OXOVANADIUM(IV)

STUART BRISTOW* and SEAN C. M. McAVILLEY

Department of Chemistry, University of Exeter, Exeter EX4 4QD, U.K.

and

WILLIAM CLEGG*

Department of Inorganic Chemistry, The University, Newcastle-upon-Tyne, NE1 7RU, U.K.

and

DAVID COLLISON

Department of Chemistry, University of Manchester, Manchester M13 9PL, U.K.

(*Received* 23 *May* 1988; *accepted* 20 *July* 1988)

Abstract—The new compound $[VOCl_2(MeCN)_2(H_2O)]$ has been prepared and characterized by elemental analysis, and IR and ESR spectroscopies. This compound is a versatile starting material for a wide range of complexes, in particular for those of the general formula $[VOCl_2L_2]$. As an illustration of the chemistry of $[VOCl_2(MeCN)_2(H_2O)]$, several complexes have been prepared where L = Ph_3PO, tetramethylurea, imidazolidine-2-thione and 1,3-dimethylimidazolidine-2-thione, and these have been characterized by elemental analysis; UV–vis, IR, and ESR spectroscopies; and for L = 1,3-dimethylimidazolidine-2-thione (dmit), by X-ray crystallography. $[VOCl_2(dmit)_2]$ crystallizes in the orthorhombic space group *Pnn*2, with $a = 9.9684(6)$, $b = 10.4631(9)$ and $c = 8.5624(6)$ Å, and $Z = 2$. The molecule has square-pyramidal coordination geometry, with the thiourea ligands *trans* to each other. This is the first example of a crystal structure of a vanadium(IV)–thiourea complex.

The synthesis of coordination complexes containing the $VOCl_2$ moiety can be hampered by the lack of suitable starting materials.[1] Herein, we report the simple preparation of such a starting material which is soluble in polar media, namely $[VOCl_2(MeCN)_2(H_2O)]$. As an illustration of its chemistry, two thiourea complexes of the type $[VOCl_2L_2]$ have been prepared from it and characterized by UV-vis, IR and ESR spectroscopies, and by elemental analysis. In addition, the X-ray crystal structure of one complex of this type, where L = 1,3-dimethylimidazolidine-2-thione (dmit), has also been determined. Whereas urea complexes of vanadium(IV) are well known and have been thoroughly studied,[2] the corresponding thiourea complexes have not been well characterized previously. Consequently, the present report of the structural characterization of $[VOCl_2(dmit)_2]$ is the first example of a vanadium(IV)–thiourea crystal structure.

*Authors to whom correspondence should be addressed.

EXPERIMENTAL

Materials and instrumentation

A 50% w/v aqueous solution of $VOCl_2$ was obtained from BDH; reagent grade MeCN was dried by distillation from P_4O_{10}; reagent grade $SOCl_2$ was used as received from Fisons; imidazolidine-2-thione was obtained from Aldrich; 1,3-dimethylimidazolidine-2-thione was prepared by the method of Maier.[3]

Analyses were carried out by the University of Manchester Microanalytical Laboratory. IR spectra in the region 600–4000 cm^{-1} were recorded for samples mulled in liquid paraffin and held between NaCl plates on a Perkin–Elmer Model 297 spectrophotometer. UV-vis spectra were recorded for samples dissolved in MeCN and contained in matched silica cells of 1 cm pathlength on a Perkin–Elmer Model 402 spectrophotometer. ESR spectra were obtained on fluid solutions of the compounds in CH_2Cl_2 at room temperature at X-band frequencies with a Varian 112 spectrometer.

Preparation of $[VOCl_2(MeCN)_2(H_2O)]$

An aqueous solution of $VOCl_2$ (50% w/v, 15 cm^3) was evaporated to a dark green paste and triturated with 5 cm^3 of $SOCl_2$, yielding a pale blue solid. Excess $SOCl_2$ was removed by decantation and evaporation under reduced pressure, and the residue dissolved in 25 cm^3 of MeCN. This blue solution was then evaporated to dryness, and the resulting dark blue paste triturated a second time with 5 cm^3 of $SOCl_2$, to give a dark brown solid. Excess $SOCl_2$ was again removed by decantation and evaporation under reduced pressure. To the residue, 50 cm^3 of MeCN was added, whereupon a green solution was formed from which a bright blue precipitate of $[VOCl_2(MeCN)_2(H_2O)]$ appeared on standing. This solid was isolated by filtration, washed with MeCN, and dried *in vacuo*. The product was stored in a Schlenk tube under dry dinitrogen. Found: C, 19.0; H, 3.4; N, 10.9; Cl, 30.7; V, 21.4. $C_4H_8Cl_2N_2O_2V$ requires C, 20.2; H, 3.4; N, 11.8; Cl, 29.8; V, 21.4%.

Preparation of $[VOCl_2$(1,3-*dimethylimidazolidine-2-thione*$)_2]$

The preparations of the thiourea complexes were identical, and one representative example is given. $[VOCl_2(MeCN)_2(H_2O)]$ (0.78 g, 3.3 mmol) was dissolved in MeCN (15 cm^3), and to this solution 1,3-dimethylimidazolidine-2-thione (0.83 g, 6.4 mmol) in MeCN (10 cm^3) was added with stirring. The solution immediately turned bright green. After stirring the reaction mixture for 15 min, the solution was evaporated to dryness, yielding a pale green, microcrystalline powder.

Crystals suitable for examination by X-ray diffraction were obtained by recrystallizing the crude product from dry MeCN in air, protected by a $CaCl_2$ guard tube. Found: C, 29.0; H, 5.1; N, 13.4; Cl, 18.0; V, 13.0. Calc. for $C_{10}H_{20}Cl_2N_4O_2S_2V$: C, 30.2; H, 5.06; N, 14.1; Cl, 17.8; V, 12.8%.

Crystal structure determination

Crystal data. $C_{10}H_{20}Cl_2N_4OS_2V$, $M = 398.27$. Orthorhombic, $a = 9.9684(6)$, $b = 10.4631(9)$, $c = 8.5624(6)$ Å, $V = 893.06$ Å^3 (refined from 32 reflections with $20° \leqslant 2\theta \leqslant 40°$), Cu-$K_\alpha$ radiation, ($\lambda = 1.54184$ Å), space group *Pnn*2 (No. 34), $Z = 2$, $D_x = 1.488$ g cm^{-3}. Crystal colour: green. Crystal size: $0.19 \times 0.26 \times 0.43$ mm. $F(000) = 410$, $\mu = 9.71$ mm^{-1}.

Data collection and reduction.[4] The crystal was mounted in a capillary tube. Siemens AED2 diffractometer, ω–θ scan mode, temperature = 295 K. A total of 4095 reflections were measured with $3° \leqslant 2\theta \leqslant 130°$, yielding 790 unique, non-extinguished reflections, of which the 733 reflections having $F > 4\sigma_c$ (σ_c based on counting statistics) were deemed observed and used for structure solution and refinement. The intensities of three reflections were monitored during data collection and a correction for the *ca* 4% decay observed was applied. Data were also corrected for Lorentz and polarization effects, including effects of the monochromator, and a semi-empirical absorption correction was applied. Transmission factors ranged from 0.024 to 0.083.

Structure solution and refinement.[5] Direct methods. Refined by least-squares with all non-hydrogen atoms anisotropic, minimizing $\Sigma w(|F_o|-|F_c|)^2$, where $w^{-1} = \sigma^2(F) = \sigma_c^2(F)+6-49G+117G^2-3S-S^2-20GS$ and $G = F_0/F_{max}$ and $S = \sin\theta/\sin\theta_{max}$.[6] Hydrogen atoms were included subject to the following constraints: C—H = 0.96 Å, H—C—H = 109.5°, $U(H) = 1.2U_{eq}(C)$. Final discrepancy indices were $R = 0.0452$ and $R' = 0.0445$. The final difference-synthesis showed no peaks greater than 0.31 nor less than −0.28 e Å^{-3}. Selected bond lengths and interbond angles are given in Table 1.

RESULTS AND DISCUSSION

The partial dehydration of aqueous solutions of $VOCl_2$ with $SOCl_2$ followed by treatment with aceto-

Table 1. Selected bond lengths (Å) and interbond angles (°) for $[VOCl_2(dmit)_2]$

V—O	1.607(8)	V—Cl	2.331(1)
V—S	2.424(1)	S—C(1)	1.728(4)
C(1)—N	1.311(4)	N—C(2)	1.470(5)
N—C(3)	1.450(4)	C(3)—C(3b)	1.504(7)
O—V—Cl	104.3(1)	O—V—S	103.7(1)
Cl—V—S	91.3(1)	Cl—V—Cl(a)	151.4(1)
S—V—Cl(a)	82.0(1)	S—V—S(a)	152.5(1)
V—S—C(1)	105.2(1)		

Symmetry operators: (a) $1-x, -y, z$; (b) $x, y, -z$.

nitrile gives a good yield of the hygroscopic blue complex $[VOCl_2(MeCN)_2(H_2O)]$. Previous workers[1,7] have prepared the fully dehydrated complex $[VOCl_2(MeCN)_2]$, but that preparation requires the isolation of a very reactive intermediate product, $VOCl_2$, which is then treated with acetonitrile. The present synthesis is faster, can be carried out in one reaction vessel and yields a material which can be used to prepare a wide range of $VOCl_2$ adducts. For example, we have used $[VOCl_2(MeCN)_2(H_2O)]$ to prepare the previously known complexes $[VOCl_2(tmu)_2]$[8] (tmu = tetramethylurea) and $[VOCl_2(Ph_3PO)_2]$[9] in addition to the thiourea complexes mentioned below. Despite the presence of one mole equivalent of H_2O per mole in $[VOCl_2(MeCN)_2(H_2O)]$, it may still be used (in dry solvents) to prepare hydrolytically sensitive materials, such as the thiourea complexes prepared in this study. Thus, it has greater synthetic utility than might be expected at first sight.

The identity of $[VOCl_2(MeCN)_2(H_2O)]$ was confirmed by elemental analysis and IR and ESR spectroscopies. In the IR spectrum of the material, five principal bands were observed and assigned as follows: 3300 (br, OH stretch); 2320, 2300 (CN stretches); 1620 (OH bend); 990 cm^{-1} (V=O stretch).

$[VOCl_2(MeCN)_2(H_2O)]$ reacts with thiourea and its cyclic derivatives such as imidazolidine-2-thione (ethylenethiourea) to give complexes of the type $(VOCl_2L_2]$, where L is the thiourea. We were successful in crystallizing one of these adducts, where L = 1,3-dimethylimidazolidine-2-thione, to give crystals suitable for an X-ray crystal structure determination. $[VOCl_2(dmit)_2]$ has square-pyramidal coordination geometry about vanadium (Fig. 1). In the crystal, the molecule occupies a position of 2/*m* crystallographic symmetry, with the two-fold axis passing through the V=O bond, and the chlorine and sulphur atoms lying in the mirror plane. This situation gives rise to disorder in the crystal structure, since the V=O bond may point in either a positive or negative direction with respect to the normal to the mirror plane. Similar types of disorder have been found before.[10]

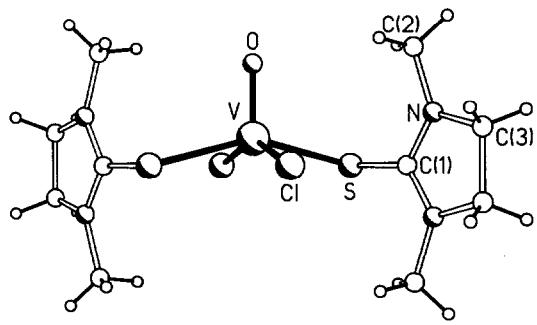

Fig. 1. Molecular structure of $[VOCl_2(dmit)_2]$.

The dimensions of the $VOCl_2$ fragment (Table 1) are unremarkable when compared to other adducts of this type.[8,9] However, the V—S distance of 2.424(1) Å is rather long in comparison to some other mean V—S bond lengths such as V—S(thiolate) = 2.378 Å,[11] V—S(dithiolene) = 2.337 Å[12] and V—S(dithiocarbamate) = 2.402 Å.[13] This may be due in part to the different charges on the sulphur-containing ligands, but it could also relate to the observation by ESR spectroscopy, (*vide infra*) that at least two species are formed when $[VOCl_2L_2]$, L = imidazolidine-2-thione or 1,3-dimethylimidazolidine-2-thione, is dissolved in CH_2Cl_2. The long V—S bond may indicate that it is relatively weak, allowing the thiourea ligands to dissociate in solution. There are two significant changes in the dimensions of the thiourea ligand itself on coordination. Firstly, the C=S bond length increases from 1.673(5) Å in the free ligand[14] to 1.728(4) Å in the complex and secondly, the C—N bond length decreases from 1.342(5) and 1.334(5) Å in the free ligand to 1.311(4) Å in the complex.

The IR spectra of the complexes in the region 4000–600 cm^{-1} contained bands due to the thiourea ligands and bands due to the V=O stretching mode. V—S and V—Cl vibrational modes appear below 600 cm^{-1}. The V=O stretching wavenumbers for

Table 2. IR and UV–vis data for the thiourea complexes prepared in this study

Compound	$\nu_{V=O}$ (cm^{-1})	λ_{max} (nm)	ε(dm^3 mol^{-1} cm^{-1})
$[VOCl_2(imdt)_2]$	998	720	46
$[VOCl_2(dmit)_2]$	1002	730	43

the complexes studied are given in Table 2. The UV-vis spectra of the solutions formed by dissolving the thiourea complexes in MeCN are unremarkable, being dominated in the visible region by a broad band in the red region. The UV-vis peak maxima positions and extinction coefficients are given in Table 2.

ESR spectra of the complexes measured at X-band frequencies in solution in CH_2Cl_2 indicated the presence of two ESR-active species, with average g and A values as shown in Table 3. These species probably arise from dissociation of thiourea ligands from the complex in solution, since addition of an excess of the appropriate thiourea ligand causes a change in the relative intensities of the signals from the two species. There is precedent for the dissociation of neutral sulphur donor ligands from early transition metal complexes: for example, Ph_3PS was found to dissociate from the $MoOCl_3$ moiety in complexes of the type $[MoOCl_3L]$.[18] Comparing the relatively large $\bar{g}$ values and relatively small $\bar{A}$ values found in the ESR spectra of these thiourea complexes with the similar values found for other sulphur donor ligand complexes, and with the different values found for typical oxygen donor ligand complexes (Table 3), it is clear that the data are consistent with the retention of at least some sulphur donor ligation in solution, despite the evidence for ligand dissociation.

REFERENCES

1. J. Cave, P. R. Dixon and K. R. Seddon, *Inorg. Chim. Acta* 1978, **30**, L349.
2. (a) D. Collison, B. Gahan, C. D. Garner and F. E. Mabbs, *J. Chem. Soc., Dalton Trans.* 1980, 667; (b) B. Gahan and F. E. Mabbs, *J. Chem. Soc., Dalton Trans.* 1983, 1695.
3. L. Maier, *Helv. Chim. Acta* 1970, **53**, 1417.
4. W. Clegg, *Acta Cryst.* 1981, **A37**, 22.
5. G. M. Sheldrick, *SHELXTL*, an integrated system for solving, refining and displaying crystal structures from diffraction data. Revision 5. University of Göttingen, F.R.G. (1985).
6. W. Hong and B. E. Robertson, *Structure and Statistics in Crystallography* (Edited by A. J. C. Wilson), p. 125. Adenine Press, New York (1985).
7. J. G. H. du Preez and F. G. Sadie, *Inorg. Chim. Acta* 1967, **1**, 202.
8. J. Coetzer, *Acta Cryst.* 1970, **B26**, 872.
9. M. R. Caira and B. J. Gellatly, *Acta Cryst.* 1980, **B36**, 1198.
10. D. Collison, F. E. Mabbs, J. Temperley, G. Christou and J. C. Huffman, *J. Chem. Soc., Dalton Trans.* 1988, 309.
11. J. K. Money, J. C. Huffman and G. Christou, *Inorg. Chem.* 1985, **24**, 3297.
12. R. Eisenberg and H. B. Gray, *Inorg. Chem.* 1967, **6**, 1844.
13. K. Henrick, C. L. Raston and A. H. White, *J. Chem. Soc., Dalton Trans.* 1976, 26.
14. C. Chieh and S. K. Cheung, *Can. J. Chem.* 1983, **61**, 211.
15. J. K. Money, K. Folting, J. C. Huffman, D. Collison, J. Temperley, F. E. Mabbs and G. Christou, *Inorg. Chem.* 1986, **25**, 4583.
16. J. Temperley, PhD Thesis. University of Manchester, U.K. (1987).
17. B. Gahan and F. E. Mabbs, *J. Chem. Soc., Dalton Trans.* 1983, 1713.
18. P. M. Boorman, C. D. Garner and F. E. Mabbs, *J. Chem. Soc., Dalton Trans.* 1975, 1299.

Table 3. Comparison of the ESR data for the thiourea complexes prepared in this study with values obtained for other S-donor ligand complexes and two O-donor ligand complexes

Compound	$\bar{g}$	$\bar{A}$(10^{-4} cm^{-1})	Reference
$[VOCl_2(imdt)_2]$	1.985±0.003	−91.7±0.5	This work
$[VOCl_2(dmit)_2]$	1.985±0.003	−91.7±0.5	This work
$[VO(mnt)_2]^{2-}$	1.982	−74.7	10
$[VO(edt)_2]^{2-}$	1.977	−71.1	15
$[VOCl_2(tmtu)_2]$	1.973	−89.5	16
$[VOCl_2(tmu)_2]$	1.966	−103.8	2(b)
$[VOCl_2(Ph_3PO)_2]$	1.959	−102.4	17

imdt = imidazolidine-2-thione; dmit = 1,3-dimethylimidazolidine-2-thione; mnt^{2-} = 1,2-dicyanoethene-1,2-dithiolate; edt^{2-} = ethane-1,2-dithiolate; tmtu = tetramethylthiourea; tmu = tetramethylurea.

Polyhedron Vol. 8, No. 1, pp. 91–96, 1989
Printed in Great Britain

0277–5387/89 $3.00+.00
© 1988 Pergamon Press plc

THE COORDINATION CHEMISTRY OF SILYL–SULPHURDIIMIDES

RAY JONES, DAVID J. WILLIAMS, PAUL T. WOOD and J. DEREK WOOLLINS*

Department of Chemistry, Imperial College of Science and Technology, South Kensington, London SW7 2AY, U.K.

(*Received* 6 *June* 1988; *accepted* 20 *July* 1988)

Abstract—Reaction of $RNSNSiMe_3$ (R = Me_3Si, 'Bu, *p*-$O_2NC_6H_4S$-) with $PtCl_2$(dppe) gives, in the case of R = *p*-$O_2NC_6H_4S$-, [Pt($NSNSC_6H_4NO_2$)$_2$(dppe)]. Reaction of $(Me_3Si)_2N_2S$ (**1**) or Bu'$NSNSiMe_3$ (**4**) with $Pt(C_2H_4)(PPh_3)_2$ gives Pt$(NSNR)_2(PPh_3)_2$ (R = Me_3Si or 'Bu). The X-ray structure of *p*-$O_2NC_6H_4SNSNSiMe_3$ reveals an essentially coplanar arrangement of the aryl and SNSN fragments. The bond lengths in the S_2N_2 chain are more closely related to those in $S_2N_2^{2-}$ ligands than those in $S_2N_2H^-$ ligands. The X-ray crystal structure of [Pt($NSNSC_6H_4NO_2$)(dppe)] (**5**) confirms the expected *cis* square-planar coordination of the platinum by the chelate phosphine and two *p*-$O_2NC_6H_4SNSN^-$ ligands. Of the atoms in the S—N ligand only the terminal nitrogen atoms lie in the platinum coordination plane. The rest of these ligands are essentially planar with their backbones *trans*-axial and approximately normal with respect to the PtN_2P_2 plane.

There have been several reports[1] on the coordination properties of sulphurdiimides, RNSNR, but it was only quite recently that the use of a silyl sulphurdiimide, $(Me_3Si)_2N_2S$ (**1**), in the preparation of the σ-bonded diimido complex *cis*-Pt$(NSNSiMe_3)_2(PPh_3)_2$ (**2**) was described.[2] Here we report full details of the preparation of **2** together with the results of our investigations into the reactivity of substituted silyl diimides $RNSNSiMe_3$ [R = *p*-$O_2NC_6H_4S$- (**3**), 'Bu, (**4**)]. As part of these studies we have characterized *p*-$O_2NC_6H_4SNSNSiMe_3$ (**3**) and the platinum complex Pt$(NSNSC_6H_4NO_2)_2(PPh_3)_2$ (**5**) by X-ray crystallography. The geometry of the S_2N_2 group in **3** is compared with that of the related $S_2N_2H^-$ and $S_2N_2^{2-}$ ligands.[3–5]

EXPERIMENTAL

All procedures were carried out under an inert atmosphere (Ar or N_2) unless stated otherwise. Solvents were dried before use; CH_2Cl_2 was distilled from CaH_2; diethyl ether, tetrahydrofuran (THF), toluene and *n*-hexane were distilled from sodium–benzophenone. ^{31}P-{^1H} NMR spectra were obtained using a JEOL FX90Q spectrometer operating at 36.21 MHz and are referred to external 85% H_3PO_4. IR spectra were recorded using a PE 683 as pressed KBr discs or Nujol mulls. Elemental analyses were performed by the microanalytical service at Imperial College.

The compounds, *cis*-[$PtCl_2(PR_3)_2$], were obtained from $PtCl_2$COD whilst $MCl_2(CH_3CN)_2$ (M = Pd, Pt) and $Pt(C_2H_4)(PPh_3)_2$ were prepared by standard methods.[6–8] Bis(trimethylsilyl)sulphurdiimide and *p*-$O_2NC_6H_4SNSNSiMe_3$ were prepared by adaptation of the literature methods.[9,10] *t*-$BuNSNSiMe_3$ was obtained[11] from the reaction of *t*-BuNSO with $(Me_3Si)_2NLi$.

p-$O_2NC_6H_4SNSNSiMe_3$ (3)

Bis(trimethylsilyl)sulphurdiimide (2.66 g, 0.013 mol) was dissolved in dichloromethane (75 cm^3) and cooled in an ice bath. To this stirred solution was added over 30 min, *p*-$O_2NC_6H_4SCl$ (2.46 g, 0.013 mol) in dichloromethane (60 cm^3). During this time the solution changed colour from pale yellow to red–orange. The solvent was removed *in vacuo* and the resulting solid was extracted with hexane (80 cm^3) which upon cooling to −20°C gave the product as pale orange–yellow needles. Yield

*Author to whom correspondence should be addressed.

1.1 g, 29%. Found: C, 37.8; H, 4.4; N, 14.5. Calc.: C, 37.6; H, 4.6; N, 14.6%. Crystals suitable for X-ray analysis were obtained by slow crystallization from a hexane solution.

$Pt(NSNSiMe_3)_2(PPh_3)_2$

$(Me_3Si)_2N_2S$ (0.3 cm^3, 0.28 g, 1.3 mmol) was added to a solution of $Pt(C_2H_4)(PPh_3)_2$ (1.0 g, 1.3 mmol) in benzene (25 cm^3). The reaction was stirred at room temperature for 2 h and then all volatile material was removed under reduced pressure to give a yellow solid which was triturated with hexane, redissolved in benzene (20 cm^3) and filtered through Celite. The volume of benzene was reduced to *ca* 10 cm^3 and 20 cm^3 of *n*-hexane were added. The product crystallized as pale yellow plates. Yield 0.32 g, 50%. $^{31}P-\{^1H\}$: $\delta = 11.76$, $^1J(Pt—P) = 3098$ Hz. IR: $\nu(NSN)_a$ 1167, $\nu(NSN)_s$ 1022w, $\delta(NSN)$ 835br cm^{-1}. Found: C, 50.4; H, 4.6; N, 5.3. Calc.: C, 51.2; H, 4.9; N, 5.7%.

$Pt(NSN^tBu)_2(PPh_3)_2$

Me_3SiNSN^tBu (0.1 g, 0.13 mmol) and $Pt(C_2H_4)(PPh_3)_2$ (0.51 g, 0.056 mmol) were stirred together in toluene (5 cm^3) for 2 h. The solvent was removed *in vacuo* and the product extracted into *n*-hexane (2×20 cm^3). The hexane was reduced to *ca* 5 cm^3 and cooled (−20°C) to give the product. Yield 11 mg, 9%. $^{31}P-\{^1H\}$: $\delta = 11.76$, $^1J = 3101$ Hz. Found: C, 53.0; H, 5.2; N, 5.4. Calc.: C, 52.9; H, 5.0; N, 5.7%.

$Pt(NSNSC_6H_4NO_2)_2(dppe)$

$PtCl_2(dppe)$ (0.024 g, 0.03 mmol) and p-$O_2NC_6H_4SNSNSiMe_3$ (0.077 g, 0.16 mmol) were stirred together in chloroform for 1 month. After this time the solvent was removed *in vacuo* and the remaining solid extracted with benzene (10 cm^3). Addition of hexane (10 cm^3) gave the product as a red precipitate. Crystals suitable for X-ray analysis were obtained by slow diffusion of hexane into a benzene solution. Yield 25 mg, 70%. Found: C, 44.7; H, 3.7; N, 7.1. Calc. for $[Pt(NSNSC_6H_4NO_2)_2(dppe)\cdot C_6H_6]$: C, 44.7; H, 3.9; N, 7.1%. $^{31}P-\{^1H\}$ ($CDCl_3$): $\delta = 33.43$ ppm, $^1J(Pt—P) = 3130$ Hz.

$Pd(HNSNSC_6H_4NO_2)Cl_2$

A solution of p-$O_2NC_6H_4SNSNSiMe_3$ (0.3 g, 1 mmol) in benzene (5 cm^3) was added to a solution of $PdCl_2(PhCN)_2$ (0.4 g, 1 mmol) in benzene (80 cm^3). On mixing, the solution became cloudy and after stirring for 1 week an orange–brown precipitate was formed together with a lightening of the solution from red to orange. The solid was filtered off, washed with hexane (3×10 cm^3) and dried *in vacuo*. Yield 0.3 g, 75%. Found: C, 16.7; H, 1.5; N, 10.4. Calc.: C, 18.4; H, 1.3; N, 10.7%.

Crystal data

$C_9H_{13}N_3O_2S_2Si$ (**3**). $M = 287.4$, triclinic, $a = 5.839(4)$, $b = 11.574(6)$, $c = 11.598(10)$ Å, $\alpha = 111.84(5)$, $\beta = 110.08(6)$, $\gamma = 100.00(5)°$, $U = 691$ Å^3, space group $P\bar{1}$, $Z = 2$, $D_c = 1.39$ g cm^{-3}. Yellow air-stable irregular polyhedron, crystal dimensions $0.1 \times 0.1 \times 0.1$ mm. $\mu(Cu\text{-}K_\alpha) = 43$ cm^{-1}, $\lambda = 1.54178$ Å, $F(000) = 300$.

$C_{38}H_{32}N_6O_4P_2PtS_4$ (**5**). $M = 1022.0$, monoclinic, $a = 16.760(4)$, $b = 17.581(6)$, $c = 27.517(9)$ Å, $\beta = 90.73(2)°$, $U = 8107$ Å^3, space group $P2_1/c$, $Z = 8$ (two crystallographically independent molecules), $D_c = 1.68$ g cm^{-3}. Red–orange air-stable irregular polyhedron, crystal dimensions $0.15 \times 0.1 \times 0.2$ mm. $\mu(Cu\text{-}K_\alpha) = 96.0$ cm^{-1}, $\lambda = 1.54178$ Å, $F(000) = 4047$.

Data collection and processing for **3** *and* **5**

Nicolet R3m diffractometer, ω-scan method, ($2\theta \leqslant 116°$ for **3** and 100° for **5**), graphite monochromated Cu-K_α radiation, 1843 and 8322 independent measured reflections of which 1273 and 6655 were considered observed [$|F_o| > 3\sigma(|F_o|)$] for **3** and **5**, corrected for Lorentz and polarization factors. For both **3** and **5** empirical absorption corrections based on 360 azimuthal scans were applied.

Structure analysis and refinement for **3**

The structure was solved by direct methods and the non-hydrogen atoms refined anisotropically. The methyl groups were refined as rigid bodies, the positions of all the other hydrogen atoms were idealized (C—H = 0.96 Å), assigned isotropic thermal parameters, [$U(H) = 1.2U_{eq}(C)$] and allowed to ride on their parent carbons. Refinement was by block-cascade full-matrix least-squares to give $R = 0.069$, $R_w = 0.068$ ($w^{-1} = \sigma^2(F) + 0.00093F^2$) ($R = \Sigma[|(F_o - F_c)|]/\Sigma|F_o|$). The maximum residual electron density in the final ΔF map was 0.37 e Å^{-3}. The mean and maximum shifts/error in the final refinement cycle were 0.012 and 0.057, respectively. Computations were carried out on an Eclipse S140 computer using the *SHELXTL* program system.[12]

Structure analysis and refinement for **5**

The structure was solved by the heavy-atom method and all non-hydrogen atoms refined aniso-

tropically. Refinement (for two separate data collections on different crystals) showed the structure to be subject to severe anisotropic thermal motion in all of the aryl rings in both independent molecules. This disorder/anisotropic thermal motion could not be resolved into alternate partial occupancy orientations so refinement was terminated at $R = 0.115$.

RESULTS AND DISCUSSION

Sulphur diimides are known to coordinate in a variety of ways.[1] With organic substituents such as 'Bu or Ph the complexes are bonded through one or both nitrogen atoms except in those cases where fragmentation to RNS complexes occurs. We have investigated the reactivity of $(Me_3Si)_2N_2S$ and $RNSNSiMe_3$ [R = 'Bu, *p*-$O_2NC_6H_4S$ (**3**)] with simple metal phosphine halides and with $Pt(C_2H_4)(PPh_3)_3$ since the Si—N bond is relatively weak particularly in comparison to the Si—Cl bond. It was hoped that this would provide a rational synthetic route to diimido complexes. The formation of **3** from **1** [eq. (1)] is a typical example of the reactivity of this molecule.

$$(Me_3Si)_2N_2S + p\text{-}O_2NC_6H_4SCl \rightarrow p\text{-}O_2NC_6H_4SNSNSiMe_3 + Me_2SiCl. \quad (1)$$

Elimination of Me_3SiCl provides the driving force for the reaction although it should be noted that a significant side product is the insoluble bis compound RSNSNSR and **3** is only obtained in *ca* 30% yield.

The X-ray structure of **3** (Fig. 1, Table 1) reveals a planar S_2N_2 chain [maximum deviation from the mean plane 0.007 Å for S(1)] which is rotated slightly with respect to the aromatic ring (C(2)—C(1)—S(2)—N(2) torsion angle 5°). The bond distances and angles within the S_2N_2 chain closely resemble those in the metallacycle $Pt(S_2N_2)(PMe_3)_2$,[13] but are markedly dissimilar from those in $[Pt(S_2N_2H)(PMe_2Ph)_2]BF_4$[4] (Table 2).

Of particular interest is the packing arrangement adopted by **3** in the crystal (Fig. 2). The molecules form infinite parallel stacks along the crystallographic *a* direction with their planes inclined. The interplanar separation between the S_2N_2 groups is 3.75 Å; the closest contact is C(1)—S(1)′ 3.65 Å. Within each stack, the S(1)—N(2) bond of one molecule lies over the aryl ring of the next.

Reaction of **1**, **3** or **4** with *cis*-$[PtCl_2(PR_3)_2]$ ($PR_3 = PPh_3$, PEt_3, PMe_2Ph and 1/2dppe) does not proceed as hoped except in the case of treatment of $PtCl_2$(dppe) with **3**, which gives $Pt(NSNSC_6H_4NO_2)$(dppe) (**5**). The latter product was characterized by IR, NMR and X-ray crystallography, however, it is not obtained via a smooth, simple reaction. The reaction takes 1 month at room temperature in chloroform and is insensitive to more vigorous conditions (e.g. reflux in toluene). ^{31}P NMR spectra were taken at time intervals during the course of the reaction. Thus after 1 week, the spectrum consists of *ca* 25% unreacted starting material, 25% of **5** and a third compound **6** with $\delta = 35.1$ ($^1J = 3014$ Hz), $\delta = 38.0$ ($^1J = 3798$ Hz) and $^2J(^{31}P—^{31}P) = 9$ Hz. For comparison, **5** has $\delta = 33.4$ and $^1J = 3130$ Hz and **2** has $\delta = 11.76$ ppm and $^1J = 3098$ Hz. It has been proposed[16] that

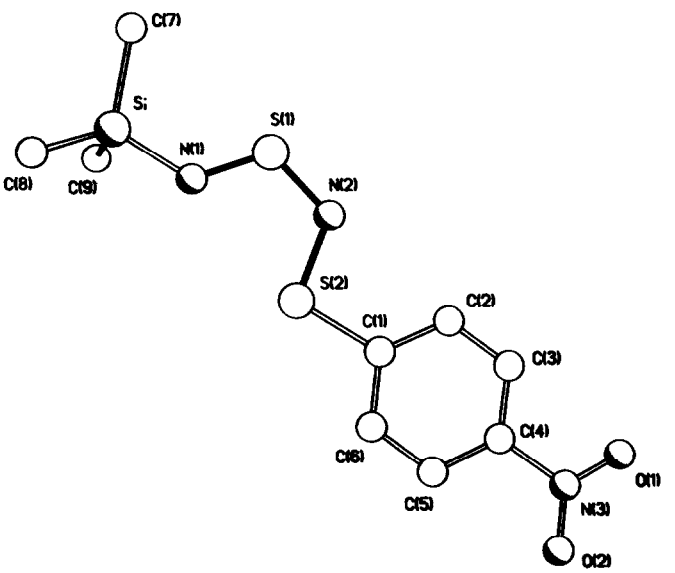

Fig. 1. The X-ray crystal structure of *p*-$O_2NC_6H_4$ $SNSNSiMe_3$ (**3**).

Table 1. Selected bond distances (Å) and angles (°) in **3**

S(1)—N(1)	1.503(5)	S(1)—N(2)	1.558(7)
S(2)—N(2)	1.653(7)	S(2)—C(1)	1.761(7)
Si(1)—N(1)	1.749(6)	Si(1)—C(7)	1.851(8)
Si(1)—C(8)	1.817(7)	Si(1)—C(9)	1.849(10)
O(1)—N(3)	1.213(9)	O(2)—N(3)	1.199(13)
N(3)—C(4)	1.493(11)		
N(1)—S(1)—N(2)	114.1(4)	N(2)—S(2)—C(1)	100.5(3)
N(1)—Si(1)—C(7)	110.2(3)	N(1)—Si(1)—C(8)	107.9(4)
C(7)—Si(1)—C(8)	110.8(4)	N(1)—Si(1)—C(9)	105.5(4)
C(7)—Si(1)—C(9)	111.2(5)	C(8)—Si(1)—C(9)	111.0(4)
S(1)—N(1)—Si(1)	128.8(4)	S(1)—N(2)—S(2)	116.1(3)
O(1)—N(3)—O(2)	125.6(8)	O(1)—N(3)—C(4)	117.0(9)
O(2)—N(3)—C(4)	117.4(6)	S(2)—C(1)—C(2)	124.5(6)
S(2)—C(1)—C(6)	115.3(4)		

Table 2. Comparative SN bond distances (Å) and angles (°) in **3**, $S_2N_2^{2-}$ and $S_2N_2H^-$ complexes. Because of their poor precision comparative distances for **5** have not been included

Compound	N(1)—S(1)	S(1)—N(2)	N(2)—S(2)	N(1)—S(1)—N(2)	S(1)—N(2)—S(2)
3	1.503(5)	1.558(7)	1.656(7)	114.1(4)	116.1(3)
$Pt(S_2N_2)(PMe_3)_2$[4]	1.492(13)	1.576(16)	1.668(17)	117.7(8)	115.0(8)
$Pt(S_2N_2)(PPh_3)_2$[13]	1.546(16)	1.567(19)	1.682(16)	116.0(9)	116.1(11)
$[Pt(S_2N_2H)(PEt_3)_2][Me_3SnCl_2]$[14]	1.572(12)	1.554(10)	1.667(10)	109.4(5)	119.8(7)
$[Pt(S_2N_2H)(PMe_2Ph)_2]Cl$[15]	1.582(8)	1.561(8)	1.647(8)	108.2(4)	120.5(5)

in $Pt(PPh_3)_2(PhNSNPh)$ (**7**) the diimide coordinates assymmetrically in an edge-on fashion through one N=S bond. In the ^{31}P NMR of **7** the ^{31}P—^{195}Pt coupling constants are 3368 and 4320 Hz and $\delta = 17.4$ ppm (both ^{31}P resonances). Since both **5** and **6** involve a different phosphine to **2** and **7** direct comparison of δ values is not possible but the coupling constants are quite dissimilar. The most plausible structure for intermediate **6** is $PtCl(dppe)(NSNSC_6H_4NO_2)$.

The X-ray structure of **5** (which has been briefly reported elsewhere[17]) although of limited precision because of disorder/thermal anisotropy problems reveals (Fig. 3) square-planar coordination of the platinum by the chelate phosphine and two anionic *p*-$O_2NC_6H_4SNSN^-$ ligands. Each of the independent molecules has approximate non-crystallographic C_2 symmetry about an axis bisecting the N—Pt—N and P—Pt—P angles. The *p*-$O_2NC_6H_4SNSN^-$ ligands are essentially planar with a *syn,syn* conformation about the N_2S group as might be expected from recent calculations.[18] In contrast to **2** the backbones of the *cis* diimido ligands are *trans*-axial relative to the coordination plane of the platinum with resulting pseudo-octahedral coordination of the Pt^{II} atom by the distal S_2N_2 sulphur atoms. The apical Pt···S contacts for both independent molecules are 3.19, 3.44, 3.25 and 3.37 Å. The mean inclination of the Pt···S vectors to the PtP_2N_2 plane is *ca* 60°.

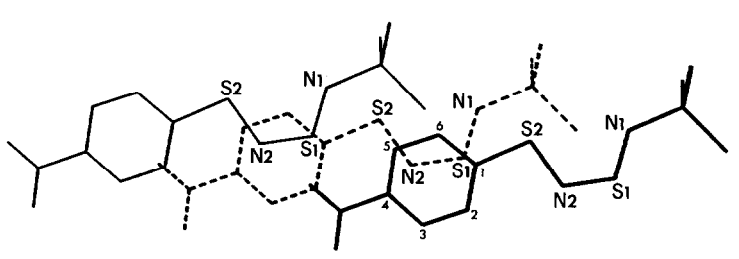

Fig. 2. Viewed parallel to the S_2N_2 plane showing the continuous stepped stacking of lattice translated molecules of (**3**) in the crystal. Uppermost molecule is shown heavy, middle dashed and lower light.

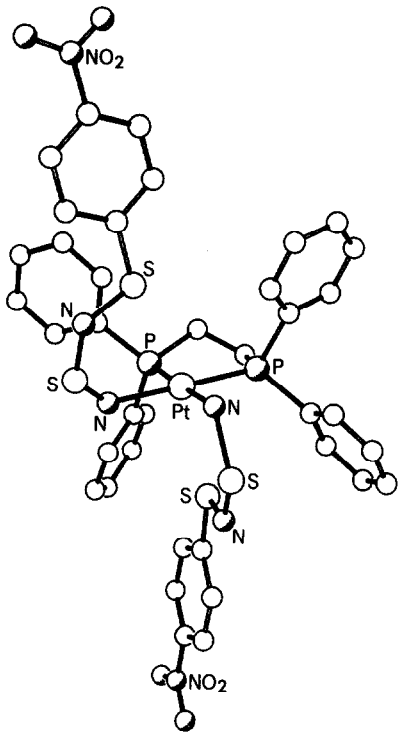

Fig. 3. The X-ray crystal structure of $Pt(NSNSC_6H_4NO_2)_2(PPh_3)_2$ (**5**).

The similarity of the ^1J values for **2** and **5** is as expected if the R group in $RNSN^-$ is only of marginal importance but we do not believe this to be the case. It should be noted[13,14] that in $[Pt(S_2N_2H)(dppe)][PF_6]$ the phosphorus *trans* to nitrogen has $\delta = 38.6$ ppm and $^1J = 3162$ Hz whilst in $Pt(S_2N_2)(dppe)$ the signal is at $\delta = 41.1$ and has $^1J = 2784$ Hz. We would have expected that the $S_2N_2^{2-}$ complex would have been more directly comparable with the p-$O_2NC_6H_4SNSN^-$ complex as was the case with $Pt(S_2N_2)(PPh_3)_2$ and **2**. It thus seems likely that changing from $R = Me_3Si$ to p-$O_2NC_6H_4S$ and from PPh_3 to dppe has mutually opposed effects on the magnitude of ^1J resulting in **2** and **5** fortuitously having remarkably similar parameters. This observation serves to underline the difficulties in making use of ^{31}P NMR data in an empirical fashion!

$Pt(C_2H_4)(PPh_3)_2$ reacts smoothly with the bis-silyldiimide to give $Pt(NSNSiMe_3)_2(PPh_3)_2$. With Me_3SiNSN^tBu the reaction appears clean by NMR but the product $[Pt(NSN^tBu)_2(PPh_3)_2$ (**8**)] is extremely soluble and could only be isolated in low yield. **3** gives a mixture of products which, to date, we have been unable to separate. The structure of **2** has been established by X-ray crystallography. It consists of a square-planar Pt^{II} with *cis* σ-bonded $NSNSiMe_3$ ligands.[15] Comparison of the ^{31}P NMR of **2** and **3** reveals almost identical chemical shifts and coupling constants as expected.

Reaction of $PdCl_2(PhCN)_2$ with **3** gives a complex with a microanalysis corresponding to $PdCl_2(HNSNSC_6H_4NO_2)$ (**9**). The IR spectrum of **9** is significantly different from both the starting material and the simple σ-bonded complexes (Table 3). Apart from the variation in frequency of the ν(NSN) vibrations the most obvious feature is the presence of bands due to NH. We speculate that **9** contains an edge-on coordinated $HNSNSC_6NO_2$ ligand.

Acknowledgement—We are grateful to Johnson Matthey Chemicals for loans of precious metals.

REFERENCES

1. P. F. Kelly and J. D. Woollins, *Polyhedron* 1986, **5**, 607.
2. N. P. C. Walker, M. B. Hursthouse, C. P. Warrens

Table 3. Selected vibrational bands in **3** and its complexes

3		**5**	**9**		
IR	Raman	IR	IR	Raman	
			3190m		ν(NH)
			1408m		δ(NH)
1194m,br	1197w	1090m	1059s	1063m	$\nu(NSN)_{as}$
1000w	998m	960w	968w	985m	$\nu(NSN)_s$
				966m	
850br,vs	857w	824w			δ(NSN)
655m	—				ν(NS)
			620s		δ(NH)
—	541w				
			355w		ν(PdN)
			330m		ν(PdCl)

and J. D. Woollins, *J. Chem. Soc., Chem. Commun.* 1985, 227.
3. R. Jones, P. F. Kelly, D. J. Williams and J. D. Woollins, *Polyhedron* 1985, **4**, 1947.
4. R. Jones, P. F. Kelly, C. P. Warrens, D. J. Williams and J. D. Woollins, *J. Chem. Soc., Chem. Commun.* 1986, 711.
5. R. Jones, P. F. Kelly, D. J. Williams and J. D. Woollins, *J. Chem. Soc., Chem. Commun.* 1985, 1325.
6. J. C. Bailar and H. Itanani, *Inorg. Chem.* 1965, **4**, 1618.
7. F. R. Hartley, *The Chemistry of Platinum and Palladium*. Applied Science, New York (1973).
8. C. D. Cook and G. S. Jauhal, *J. Am. Chem. Soc.* 1968, **90**, 1464.
9. C. P. Warrens and J. D. Woollins, *Inorg. Synth.*, in press.
10. J. Kuyper and G. B. Street, *J. Am. Chem. Soc.* 1977, **99**, 7848.
11. R. Appel and M. Montenarh, *Z. Naturforsch.* 1975, **30B**, 847.
12. G. M. Sheldrick, *SHELXTL*, An integrated system for solving, refining and displaying crystal structures from diffraction data. University of Göttingen, F.R.G. (1978); Revision 4.1 (1983).
13. P. A. Bates, M. B. Hursthouse, P. F. Kelly and J. D. Woollins, *J. Chem. Soc., Dalton Trans.* 1986, 2367.
14. R. Jones, C. P. Warrens, D. J. Williams and J. D. Woollins, *J. Chem. Soc., Dalton Trans.* 1987, 907.
15. R. Jones, P. F. Kelly, D. J. Williams and J. D. Woollins, *J. Chem. Soc., Dalton Trans.*, submitted.
16. R. Meij, D. J. Stufkens, K. Vrieze, E. Roosndaal and H. Schenk, *J. Organomet. Chem.* 1978, **155**, 323.
17. P. F. Kelly, I. P. Parkin and J. D. Woollins, *Phosphorus Sulphur*, accepted.
18. H. R. Rzepa and J. D. Woollins, *J. Chem. Soc., Dalton Trans.*, in press.

Polyhedron Vol. 8, No. 1, pp. 97–102, 1989
Printed in Great Britain

0277–5387/89 $3.00+.00
© 1988 Pergamon Press plc

SYNTHESIS AND CHARACTERIZATION OF CYANATE–COPPER(II) COMPLEXES WITH 2,2′:6′,2″-TERPYRIDINE. CRYSTAL STRUCTURE OF THE DIMERIC COMPOUND $[Cu(terpy)(NCO)_2]_2 \cdot 2H_2O$

TEOFILO ROJO,* ANDONI GARCIA and JOSE L. MESA

Departamento de Química Inorgánica, Facultad de Ciencias, Universidad del País Vasco, Apartado 644, 48080 Bilbao, Spain

and

MARIA I. ARRIORTUA and JOSE L. PIZARRO

Departamento de Mineralogia-Petrologia, Facultad de Ciencias, Universidad del Pais Vasco, Apartado 644, 48080 Bilbao, Spain

and

AMPARO FUERTES

Instituto de Ciencia de Materiales (C.S.I.C.), Marti i Franqués, s/n. 08028 Barcelona, Spain

(*Received* 7 *June* 1988; *accepted* 20 *July* 1988)

Abstract—The cyanate–copper(II) complexes $[Cu(terpy)(NCO)_2] \cdot nH_2O$ ($n = 0$, 1) have been synthesized and characterized by spectroscopic techniques and analytical data. The crystal structure of the hydrated complex has been determined by X-ray diffraction methods. The compound crystallizes in the space group $P\bar{1}$ with $a = 8.684(3)$, $b = 9.485(6)$, $c = 10.774(7)$ Å, $\alpha = 83.58(5)$, $\beta = 87.21(4)$, $\gamma = 68.44(3)°$, $U = 851(2)$ Å^3; $Z = 2$, $D_m = 1.63(4)$, $D_x = 1.62$ g cm^{-3}, μ(Mo-K_α) = 14.3 cm^{-1}, $F(000) = 402$, $T = 293$ K. The structure was refined to $R = 0.055$ ($R_w = 0.055$). The centrosymmetric dimeric structure consists of two $[Cu(terpy)(NCO)_2] \cdot H_2O$ units, which are linked through hydrogen bonds between the cyanate groups and the water molecules. The coordination sphere of the copper(II) ion is approximately regular square pyramid. The half-field absorption in the $\Delta M_s = 2$ region of the powdered X-band ESR spectra has been observed for the dimeric compound.

2,2′:6′,2″-terpyridine (terpy) is a tridentate rigid "quasi planar" ligand that forms complexes with divalent 3*d* transition ions.[1] The coordination chemistry of terpy includes two kinds of complexes: the bis-terpyridine complexes corresponding to ratio of metal to terpy 1:2, which are always discrete molecules[2–5] and the mono-terpyridine complexes (ratio 1:1) which can give rise to mononuclear[6–14] and polynuclear species.[15–17]

In previous papers, we have reported the synthesis and characterization of a wide set of five-coordinate compounds of the formulation $[Cu(terpy)X_2]$ (X = coordinating anion: halide or pseudohalide).[18–20] These complexes are discrete molecules, with the copper(II) ion bonded to three N-atoms of the tridentate ligand and the two X^- ions, or by one X^- and one H_2O molecule as in the nitrite complex.[7] Some mononuclear species exhibit an unusual symmetry in which the coordination polyhedron of the copper(II) ion shows a C_{2v} symmetry.[19,20]

On the other hand, the ability and adaptability of the cyanate ligand as a bridging one is well estab-

*Author to whom correspondence should be addressed.

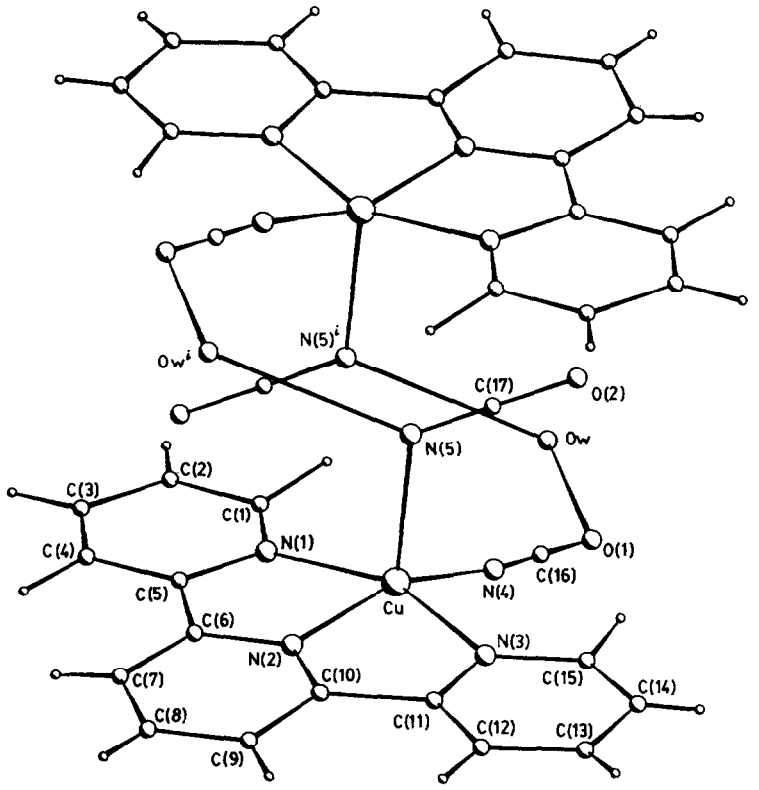

Fig. 1. Molecular structure of the $[Cu(terpy)(NCO)_2]_2 \cdot 2H_2O$ complex showing the atom numbering.

lished.[21–25] In order to know the behaviour of this ligand in the complexes of the type $[Cu(terpy)X_2]$, we decided to carry out a study of the $[Cu(terpy)(NCO)_2] \cdot nH_2O$ ($n = 0, 1$) compounds.

RESULTS AND DISCUSSION

Figure 1 shows a perspective view of the dimeric complex $[Cu(terpy)(NCO)_2]_2 \cdot 2H_2O$, with the detailed labelling of the atoms, and Fig. 2 shows a stereoscopic view of the unit cell. Significant bond distances and angles are given in Table 1.

The centrosymmetric dimeric structure consists of two $[Cu(terpy)(NCO)_2] \cdot H_2O$ units, which are linked through hydrogen bonds between the cyanate groups and the water molecules. The coordination sphere of the copper(II) ion is better described as a distorted square pyramid. The basal positions are occupied by the three nitrogens of the terpyridine ligand (Cu—N(1), N(2), N(3); 2.046(6), 1.957(6), 2.043(7) Å, respectively) and one N-cyanate group (Cu—N(4), 1.904(7) Å). The apical site is occupied by the other N-cyanate ligand (Cu—N(5) = 2.188(7) Å). The average value of

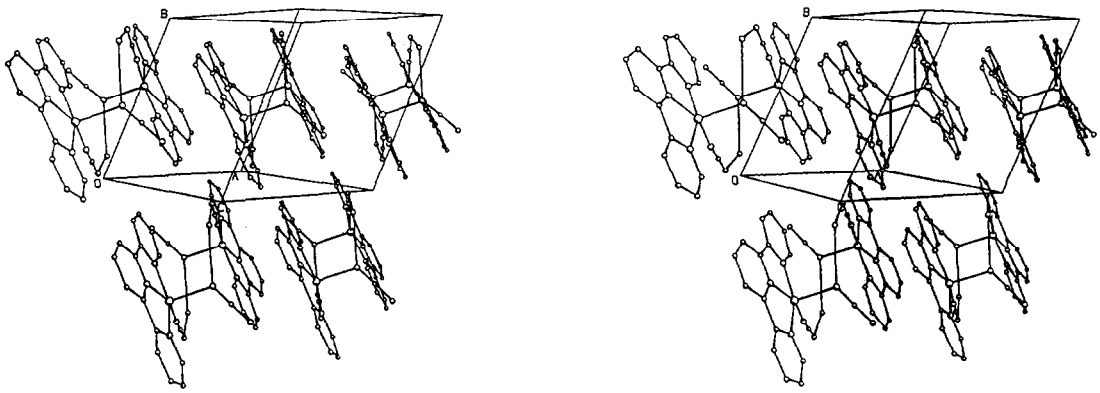

Fig. 2. Stereoview of the contents of the unit cell for $[Cu(terpy)(NCO)_2]_2 \cdot 2H_2O$.

Table 1. Some selected bond distances (Å), angles (°) and esds (in parentheses) of the $[Cu(terpy)(NCO)_2]_2 \cdot 2H_2O$ complex

Cu—N(1)	2.046(6)	Cu—N(2)	1.957(6)
Cu—N(3)	2.043(7)	Cu—N(4)	1.904(7)
Cu—N(5)	2.188(7)	N(1)—C(1)	1.336(10)
N(1)—C(5)	1.365(9)	C(5)—C(6)	1.453(11)
C(6)—N(2)	1.353(9)	N(2)—C(10)	1.308(10)
C(10)—C(11)	1.484(11)	C(11)—N(3)	1.365(11)
C(11)—C(12)	1.371(12)	N(4)—C(16)	1.142(10)
C(16)—O(1)	1.211(10)	N(5)—C(17)	1.170(11)
C(17)—O(2)	1.213(11)	Cu—Cu^{i}	6.759(1)
Ow···O(1)	2.910(55)	Ow···N(5)^{i}	2.868(65)

N(5)—Cu—N(1)	98.1(3)
N(5)—Cu—N(2)	99.9(3)
N(5)—Cu—N(3)	94.2(3)
N(5)—Cu—N(4)	100.9(3)
N(1)—Cu—N(3)	156.8(2)
N(2)—Cu—N(4)	159.1(3)
N(1)—Cu—N(2)	80.2(3)
N(1)—Cu—N(4)	98.6(3)
N(2)—Cu—N(3)	78.4(3)
N(3)—Cu—N(4)	98.2(3)
N(4)—C(16)—O(1)	178.9(9)
N(5)—C(17)—O(2)	179.4(10)
Cu—N(4)—C(16)	169.7(8)
Cu—N(5)—C(17)	118.1(6)

i = $1-x, 1-y, 1-z$.

the angles N_{apical}—Cu—N_{basal} is 98(3)°, while the *trans*-basal angles, N(1)—Cu—N(3) and N(2)—Cu—N(4) are 156.8(2) and 159.1(3)°, respectively. The basal atoms are coplanar within ±0.067 Å and the copper(II) ion is displaced 0.29 Å from the mean plane. The terpy ligand is planar within ±0.04 Å. Because of the rigidity of the terpyridine rings the angles N(2)—Cu—N(1) and N(2)—Cu—N(3) deviate from 90° by about 11° and the Cu—N(2) bond length is smaller than Cu—N(1),N(3) by ≈ 0.1 Å.

The simultaneous presence of "end-on" and "end-to-end" bonds in the cyanate groups of the $[Cu(terpy)(NCO)_2]_2 \cdot 2H_2O$ compound is one remarkable structural feature. Both NCO groups are practically linear [angles N(4)—C(16)—O(1) and N(5)—C(17)—O(2), average value 179(1)°]. The copper(II) ion is nearly in the plane defined by the N(4), C(16) and O(1) atoms of the equatorial cyanate (the Cu—N(4)—C(16)—O(1) torsion angle is 6.9°) and, is clearly out of the plane defined by the N(5), C(17) and O(2) atoms of the apical cyanate (the Cu—N(5)—C(17)—O(2) torsion angle is 85.9°). This fact explains the shortening of the Cu—N(4) bond length, which is 0.284 Å shorter than that obtained for the Cu—N(5) bond. This suggests that there is more π-donor character in the Cu—N(4) bond, which is in agreement with the shorter N(4)—C(16) bond length (1.142(10) Å) than N(5)—C(17) (1.170(11) Å). The CO distance is practically similar in both cyanate groups (average value, 1.21(1) Å).

In the dimeric compound, each water molecule forms intramolecular hydrogen bonds with both the O(1) atom of the basal-cyanate group (Ow···O(1), 2.910(55) Å) and the N(5)^{i} atom of the apical-cyanate ligand belonging to the other half of the dimer (Ow···N(5)^{i}, 2.868(65) Å). The intradimeric copper–copper distance is 6.759(1) Å.

The distortion of the coordination polyhedron from trigonal bipyramid ($\Delta = 0$) towards a regular square pyramid ($\Delta = 1$) was calculated by quantification of the Muetterties and Guggenberger description.[26,27] The value thus obtained for the title compound ($\Delta = 0.80$) indicates a topology near to regular square pyramid. A similar result is observed using Kepert's model based on an interligand repulsion approach.[28]

The interest of the IR spectra of the $[Cu(terpy)(NCO)_2] \cdot nH_2O$ ($n = 0, 1$) complexes lies mainly in the bands due to the NCO groups. For the hydrated compound, the first feature is the well defined splitting of the bands due to the ν_{as} vibration at 2250, 2230 and 2180, 2170 cm^{-1}, which is in good agreement with the presence of two different cyanate ions bonded to the water molecules. The symmetric stretching vibration ν_s is at 1340 cm^{-1}, in the range of N-bonded cyanates. The splitting observed in the bending mode, δ, 600, 610 and 630 cm^{-1} appears in complexes containing bridging-bonded NCO groups.[21–25] For the water molecule, the stretching, bending and rotation vibrations appear at 3580, 3400; 1660 and 480 cm^{-1}, respectively. The IR spectrum of the anhydrous compound $[Cu(terpy)(NCO)_2]$ exhibits bands corresponding to ν_{as} at 2230, 2220 cm^{-1}; ν_s at 1355 cm^{-1} and δ at 625, 615 cm^{-1}, which suggest the presence of terminally N-bonded cyanate groups in this complex.[21–25]

Some IR and structural data for cyanate–terpyridine complexes are given in Table 2. In good agreement with other cyanate complexes given in the literature,[21–25] it can be seen that: (i) the stretching vibration ν_{as} appears in the range 2250–2200 cm^{-1} when the MNC angle approaches 180°, and the CN distance is short, indicative of a C≡N triple bond; (ii) for the compounds where the MNC angle approaches 120° and the CN distance tends towards what would be expected for a C=N double bond, the ν_{as} vibration is in the range 2220–2100 cm^{-1}; (iii) the splitting of the bending vibration (δ) in the complexes containing terminally bonded NCO

Table 2. Some IR and structural data for the cyanate–terpyridine complexes

Compound	ν_{as} (cm^{-1})	ν_s (cm^{-1})	δ (cm^{-1})	MNC (°)	NC (Å)	CO (Å)	NCO (°)	Reference
(1) [Co(terpy)(NCO)$_2$]	2220	1355	625,615	160.9(8)	1.126(9)	1.197(9)	178.3(11)	9
(2) [Ni(terpy)(NCO)(OH$_2$)](PF$_6$)	2170,2120	1370	677,615	133.8(7)	1.19(1)	1.18(1)	179.8(9)	17
(3) [Cu(terpy)(NCO)$_2$]$_2$·2H$_2$O	2250,2230	1340	630,610	169.7(8)	1.142(10)	1.211(10)	178.9(9)	
	2180,2170		600	118.1(6)	1.170(11)	1.213(11)	179.4(10)	This work
(4) [Cu(terpy)(NCO)$_2$]	2230,2200	1355	625,615	—	—	—	—	This work
(5) [Cu(terpy)(NCO)(OH$_2$)](NO$_3$)	2225	[a]	615	163(1)	1.131(13)	1.205(14)	177(1)	33

In compound 1, the N-cyanate groups are related by the binary axis. Compounds 2 and 5 show bridged [M—N(CO)—M] and terminal [M—NCO] cyanate ligands, respectively.

[a] This band is obscured by the nitrate group.

(only 10 cm^{-1} or less) is shorter than that observed in the compounds with bridged NCO ligands.

The X-band ESR spectra of polycrystalline samples of the [Cu(terpy)(NCO)$_2$]$_2$·2H$_2$O compound show axial-type signals which remain unchanged from room temperature down to 125 K. Figure 3(a) shows the ESR spectrum at 125 K.

The values $g_{\parallel} = 2.249 > g_{\perp} = 2.096 > g_0 = 2.0023$ point towards a mainly copper(II) $d_{x^2-y^2}$ orbital ground state.[6] This result agrees with the regular square pyramidal geometry of the [CuN$_5$] coordination polyhedron. Likewise, in the ESR spectrum the appearance of a weak absorption corresponding to the $\Delta M_s = 2$ forbidden transition can be noted at "half-field" values ($\approx$ 1600 G). This signal implies a magnetic interaction between the copper(II) ions of the dimeric compound. From the ESR spectrum, the distance "r" between the two copper(II) ions interacting in the dimeric compound has been calculated. The expression, relative intensity = (intensity of $\Delta M_s = 2$/total intensity of $\Delta M_s = 1$) = Ar^{-6} $(9.1/\nu^2)$ (where ν is the spectrometer operating frequency in G Hz, and $A = 21 \pm 2$ is a calculated parameter) was used.[29] The value obtained, $r = 6.5$ Å, fits nicely to the crystallographically determined (Cu—Cu^i = 6.759(1) Å).

The ESR spectra of the anhydrous compound [Cu(terpy)(NCO)$_2$] show a *o*-rhombic resolution for the "g"-tensor, which is not modified at 125 K, $g_1 = 2.270$, $g_2 = 2.132$, $g_3 = 2.036$ [Fig. 3(b)]. This result indicates a deviation of the geometry of the coordination polyhedron from the regular square pyramid towards the trigonal bipyramid. The absorption corresponding to the $\Delta M_s = 2$ transition is not observed.

In the visible region, the reflectance electronic spectrum of the [Cu(terpy)(NCO)$_2$]$_2$·2H$_2$O complex exhibits one broad unresolved band centred around 14000 cm^{-1}. We tentatively assigned this band to the non-resolved transition $B_1 \rightarrow B_2$, E in C_{4v} symmetry.[6] The covalence factor (K) has been calculated from the ESR and reflectance measurements.[6] The value obtained ($K = 0.76$) is slightly greater than that calculated for the chlorinated compound [Cu(terpy)Cl$_2$]·nH$_2$O ($n = 0$, 1), with a similar regular square pyramidal geometry.[6] This fact is possibly due to the higher π-donor character of the Cu—NCO bonds in the cyanate complex.

EXPERIMENTAL

Synthesis

Solutions of terpy (0.121 g, 0.52 mmol) in ethanol (10 cm^3) and Cu(NO$_3$)$_2$·3H$_2$O (0.123 g, 0.52 mmol)

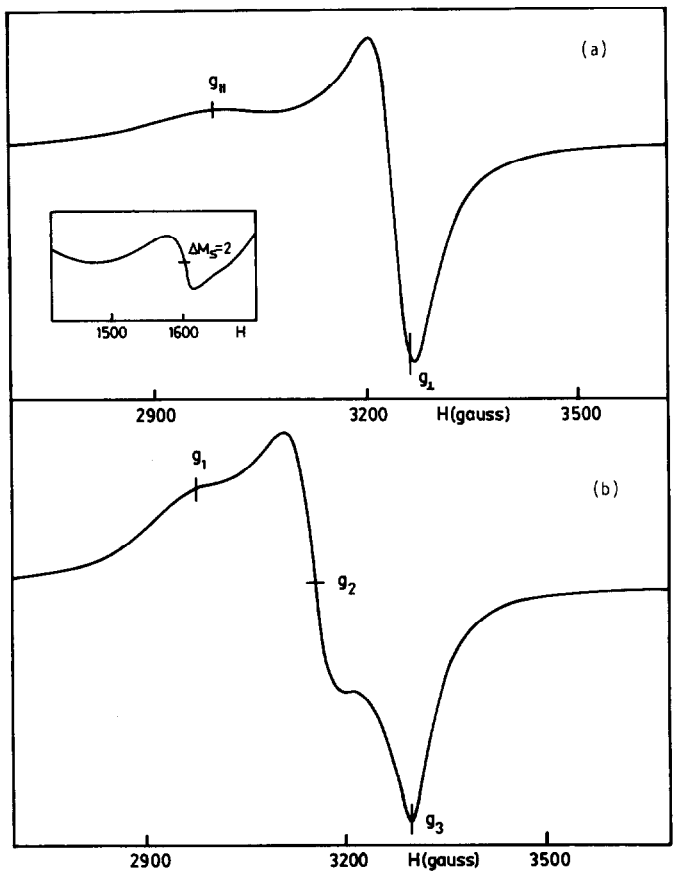

Fig. 3. X-band ESR spectra (125 K) of powdered samples of the (a) $[Cu(terpy)(NCO)_2]_2 \cdot 2H_2O$ and (b) $[Cu(terpy)(NCO)_2]$ complexes.

in water (10 cm^3) were mixed with stirring. A green microcrystalline solid was obtained immediately by addition of the KNCO pseudohalide (0.117 g, 1.44 mmol) dissolved in water (5 cm^3). The solid was filtered and washed with water and diethyl ether. Crystallization from a saturated water–acetone (1 : 2) mixture of the product gave green crystals. Found: C, 50.9; H, 3.2; N, 17.2. $[Cu(C_{15}H_{11}N_3)(NCO)_2] \cdot H_2O$ requires: C, 51.1; H, 3.3; N, 17.5%. The thermogravimetric analysis indicates the presence of one water molecule per copper(II) ion. The anhydrous compound was obtained by dehydration of the $[Cu(terpy)(NCO)_2] \cdot H_2O$ at 55°C. Found: C, 53.5; H, 2.8; N, 18.3. $[Cu(C_{15}H_{11}N_3)(NCO)_2]$ requires: C, 53.6; H, 2.9; N, 18.4%.

Crystal structure determination

A single crystal of dimension $0.3 \times 0.15 \times 0.015$ mm was used for data collection. Formula weight 398.5, triclinic, $P\bar{1}$; $a = 8.684(3)$, $b = 9.485(6)$, $c = 10.774(7)$ Å, $\alpha = 83.58(5)$, $\beta = 87.21(4)$, $\gamma = 68.44(3)°$ and $U = 851(2)$ $Å^3$; $Z = 2$, $D_m = 1.63(4)$, $D_x = 1.62$ g cm^{-3}, μ(Mo-K_α) = 14.3 cm^{-1}, $F(000) = 402$, $T = 293$ K. The density was measured by flotation in a bromoform–acetone mixture.

Intensity data were collected at room temperature on an Enraf–Nonius CAD 4 automatic four-circle diffractometer using the $\omega/2\theta$ scan technique with Mo-K_α ($\lambda = 0.7107$ Å, graphite monochromated) radiation. Cell dimensions were taken from least-squares refinements of 25 reflections ($2 \leqslant 2\theta \leqslant 19°$). A total of 3054 independent reflections ($\theta < 25°$, $-10 \leqslant h \leqslant 10$, $-11 \leqslant k \leqslant 11$, $0 \leqslant l \leqslant 12$) were collected with three orientation standard reflections measured every 50 reflections and one intensity standard reflection every 3600 s. The variation in the intensity of this standard reflection was within 1.6%. A total of 1605 reflections were considered observed with $I \geqslant 2.5\sigma(I)$ and included in the refinement. The intensity data were corrected for Lorentz polarization factors. Absorption effects were neglected.

Direct methods, *MULTAN84*,[30] were used to locate 20 of 26 non-H atoms. The remaining non-H atoms were found by Fourier syntheses. All H

atomic sites, minor H of the water molecule, were located by subsequent difference Fourier maps but not refined. The structure was refined by full-matrix least-squares techniques with *SHELX 76*.[31] The function minimized was $\Sigma\omega[|F_o|-|F_c|]^2$ where the weights ω were taken as $\omega = [\sigma^2|F_o|+K|F_o|^2]^{-1}$, where $K = 0.001500$. The atomic scattering factors were taken from ref. 32. The final agreement factors R and R_ω reached, respectively, 0.055 and 0.055 for all observed reflections. Maximum and minimum electron densities in the final difference map were 0.53, -0.38 e Å^{-3}.

Physical measurements

Water was determined thermogravimetrically using a Perkin–Elmer TGS-1 thermobalance. The IR spectra (KBr pellets) were recorded on a Perkin–Elmer 1430 spectrophotometer. The diffuse reflectance electronic spectrum on solid powder was registered using a Perkin–Elmer Lambda-9 US/VIS/NIR spectrophotometer. A Brucker ER 200tt spectrometer equipped with a standard low-temperature device, operating at X-band calibrated by a NMR probe for the magnetic field and a HP 5342 A frequency counter for the microwave frequency, was used to record the ESR powder spectra of the complexes at different temperatures.

Acknowledgements—This work was supported in part by grant 2930/83 from the CAICYT, which we gratefully acknowledge. J.L.M. thanks the Spanish Ministerio de Educación y Ciencia for a FPI fellowship.

REFERENCES

1. E. C. Constable, *Adv. Inorg. Chem. Radiochem.* 1986, **30**, 69.
2. E. N. Maslen, C. L. Raston and A. H. White, *J. Chem. Soc., Dalton Trans.* 1974, 1803.
3. C. L. Raston and A. H. White, *J. Chem. Soc., Dalton Trans.* 1976, 7.
4. R. Allman, W. Henke and D. Reinen, *Inorg. Chem.* 1978, **17**, 378.
5. M. I. Arriorta, T. Rojo, J. M. Amigó, G. Germain and J. P. Declercq, *Acta Cryst.* 1982, **B38**, 1323.
6. W. Henke, S. Kramer and D. Reinen, *Inorg. Chem.* 1983, **22**, 2858.
7. R. Allmann, S. Kremer and D. Kucharczy, *Inorg. Chim. Acta* 1984, **85**, L19.
8. J. Elmsley, A. Muhammad, P. A. Bates and M. B. Hursthouse, *Inorg. Chim. Acta* 1988, **143**, 25.
9. D. L. Kepert, E. Kucharski and A. H. White, *J. Chem. Soc., Dalton Trans.* 1980, 1932.
10. (a) D. E. C. Corbridge and E. G. Cox, *J. Chem. Soc.* 1956, 594; (b) F. W. B. Einstein and B. R. Penfold, *Acta Cryst.* 1966, **20**, 924.
11. M. Vlasse, T. Rojo and D. Beltrán, *Acta Cryst.* 1983, **C39**, 560.
12. R. Cortés, M. I. Arriortua, T. Rojo, X. Soláns, C. Miravitlles and D. Beltrán, *Acta Cryst.* 1985, **C41**, 1733.
13. R. Cortés, M. I. Arriortua, T. Rojo, X. Soláns and D. Beltrán, *Polyhedron* 1986, **5**, 1990.
14. R. Cortés, M. I. Arriortua, T. Rojo, J. L. Mesa, X. Soláns and D. Beltrán, *Acta Cryst.* 1988, **C44**, 986.
15. T. Rojo, M. Arriortua, J. Darriet, G. Villeneuve, D. Beltrán and J. Ruiz, *J. Chem. Soc., Dalton Trans.* 1987, 285.
16. T. Rojo, M. I. Arriortua, J. L. Mesa, R. Cortés, G. Villeneuve and D. Beltrán, *Inorg. Chim. Acta* 1987, **134**, 59.
17. R. Cortés, M. I. Arriortua, T. Rojo, D. Beltrán and T. Debaerdemaeker, *Transition Metal Chem.* 1986, **11**, 238.
18. T. Rojo, M. Vlasse and D. Beltrán-Porter, *Acta Cryst.* 1983, **C39**, 194.
19. M. I. Arriortua, J. L. Mesa, T. Rojo, T. Debaerdemaeker, H. Stratemeier, D. Reinen and D. Beltrán, *Inorg. Chem.* 1988, **27**, 2976.
20 T. Rojo, A. Garcia, J. L. Mesa, J. Via and M. I. Arriortua, *Inorg. Chim. Acta Lett.* 1988, **149**, 159.
21. A. H. Norbury, *Adv. Inorg. Chem. Radiochem.* 1975, **17**, 232.
22. A. H. Golub, H. Kohler and V. V. Slopenko, *Chemistry of Pseudohalides*, p. 239. Elsevier, Amsterdam (1986).
23. J. Kohout, M. Hvastijova and J. Gazo, *Chem. Rev.* 1987, **27**, 141.
24. J. Nelson and S. M. Nelson, *J. Chem. Soc. A* 1969, 1597.
25. D. M. Duggan and D. N. Hendrickson, *Inorg. Chem.* 1974, **13**, 2056.
26. E. L. Muetterties and L. J. Guggenberger, *J. Am. Chem. Soc.* 1974, **96**, 1748.
27. J. L. Mesa, M. I. Arriortua, L. Lezama, J. L. Pizarro, T. Rojo and D. Beltrán, *Polyhedron* 1988, **7**, 1383.
28. (a) M. C. Favas and D. L. Kepert, *Prog. Inorg. Chem.* 1980, **27**, 325; (b) D. L. Kepert, E. S. Kucharski and A. H. White, *J. Chem. Soc., Dalton Trans.* 1980, 1932; (c) D. L. Kepert, *Inorg. Chem. Concept.* 1982, **6**, 1.
29. (a) S. S. Eaton and G. R. Eaton, *J. Am. Chem. Soc.* 1982, **104**, 5002; (b) S. S. Eaton, K. M. More, B. H. Sawant and G. R. Eaton, *J. Am. Chem. Soc.* 1983, **105**, 6560.
30. P. Main, G. Germain and M. M. Woolfson, *MULTAN 84*. A system of computer programs for the automatic solution of crystal structures from X-ray diffraction data. University of York, U.K. and Louvain, Belgium (1988).
31. G. M. Sheldrick, *SHELX 76*. Program for crystal structure determination. University of Cambridge, U.K. (1976).
32. *International Tables for X-ray Crystallography*, Vol. 4. Kynoch Press, Birmingham (1974).
33. T. Rojo, M. I. Arriortua, J. Via and J. L. Mesa, to be published.

Polyhedron Vol. 8, No. 1, pp. 103–107, 1989
Printed in Great Britain

0277–5387/89 $3.00+.00
© 1988 Pergamon Press plc

COMPLEXES OF RUTHENIUM(II) WITH THE MONO-OXIMES OF 1,2-NAPHTHOQUINONE: X-RAY CRYSTAL STRUCTURE OF BIS(1,2-NAPHTHOQUINONE 1-OXIMATO)DIPYRIDINE RUTHENIUM(II)

JOHN CHARALAMBOUS,* WILLIAM C. STOTEN and KIM HENRICK

Department of Applied Chemistry and Life Sciences, The Polytechnic of North London, Holloway, London N7 8DB, U.K.

(*Received* 12 *April* 1988; *accepted* 25 *July* 1988)

Abstract—The ruthenium(II) complexes $Ru(nqo)_2$ [nqoH = 1,2-naphthoquinone 1-oxime (1-nqoH) or 1,2-naphthoquinone 2-oxime (2-nqoH)] were prepared by the interaction of the quinone oxime with hydrated ruthenium(III) chloride. Reaction of the chloride with the sodium salts of the oximes in ethanol or acetic acid afforded complexes of the type $Na[Ru(nqo)_3]$ and $Ru(nqo)_2(nqoH)$, respectively. The complex $Ru(nqo)_2$ reacted with pyridine or triphenylphosphine to give 1:2 adducts but showed no tendency to react with hydrochloric acid. The adduct $Ru(1\text{-}nqo)_2(py)_2 \cdot 1.5py$ was characterized by X-ray crystallography.

RESULTS AND DISCUSSION

Complex formation between ruthenium salts and 1,2-naphthoquinone 1-oxime (1-nqoH) and 1,2-naphthoquinone 2-oxime (2-nqoH) (the abbreviation nqoH will be used to denote both 1-nqoH and 2-nqoH) in aqueous media has been known for some time and it has been successfully used for the spectrophotometric determination of ruthenium.[1–3] Although the species arising from these systems have not been isolated, characterized, or otherwise studied to any significant extent, they have been generally formulated as ruthenium(III) complexes.[4,5] As a continuation of our studies of complexes derived from 1,2-quinone mono-oximes,[6–9] we now report on the reactions of hydrated ruthenium trichloride with the mono-oximes of 1,2-naphthoquinone or their sodium salts and the characterization and study of the ruthenium(II) complexes arising from them. We also report on the crystal and molecular structure of the complex bis(1,2-naphthoquinone 1-oximato)di(pyridine)ruthenium(II). Several ruthenium(II) oximic complexes have previously been obtained from the reaction of the oxime with dichlorotris(triphenylphosphine)ruthenium(II).[10]

The complexes $Ru(1\text{-}nqo)_2$ and $Ru(2\text{-}nqo)_2$ were obtained from the reaction of ruthenium(III) chloride with the sodium salt of the respective 1,2-naphthoquinone mono-oxime in aqueous tetrahydrofuran. Reaction in ethanol using 3 mol equiv. of the sodium salts afforded complexes of the type $Na[Ru(nqo)_3]$, whereas in acetic acid complexes of the type $Ru(nqo)_2(nqoH)$ resulted. The formulation of the products of the above reactions as ruthenium(II) complexes is indicated by their diamagnetic character. The formation of ruthenium(II) complexes in the reactions involving ruthenium(III) chloride and the naphthoquinone oximes or their sodium salts reflects the high ligand-field effect and π-acceptor properties of quinone oximato ligands. Ruthenium(II) complexes have also been obtained from the reactions of ruthenium(III) chloride with triphenylphosphine,[11] dipyridine,[12] 1,10-phenanthroline[13] and sodium thiocarbamates[14] which are ligands also noted for their strong ligand-field effect and π-acceptor properties. In contrast, reactions of the ruthenium(II) chloride with the weaker ligand field species acetylacetone,[15] edta[16] and ethylene diamine[17] lead to ruthenium(III) complexes unless a strong reductant is present: e.g. zinc. Reduction of the metal is also observed in reactions involving iron(III) mono-oximes of 1,2-naphthoquinone.[18] However, in these cases iron(III)

*Author to whom correspondence should be addressed.

complexes $Fe(nqo)_3$ accompany the iron(II) products.

The complexes $Ru(nqo)_2$ did not react with hydrochloric acid whereas the complexes $Ru(nqo)_2(nqoH)$ did exhibit some degree of decomposition to give $Ru(nqo)_2$ and the protonated ligand. The inertness of the complexes $Ru(nqo)_2$ towards hydrochloric acid parallels that of the corresponding rhodium(III) chelates,[9] and contrasts the facile acidolysis of first row transition metal complexes of the quinoneoximic ligands.[19]

Pyridine and triphenylphosphine reacted with the complexes $Ru(nqo)_2$ to give the adducts $Ru(nqo)_2(LB)_2$ (LB = py or Ph_3P). Significantly, the reaction with triphenylphosphine did not lead to deoxygenation of the naphthoquinoneoximic ligand or reduction of the metal. This behaviour contrasts with that of first row transition metal complexes of quinone-mono-oximes which generally undergo deoxygenation of the ligand and/or reduction of the metal on treatment with triphenylphosphine.[6,20] However, similar resistance towards the phosphine is shown by the complexes $Rh(nqo)_3$,[9] and can be accounted for by the Ru^{II} and Rh^{III} low-spin d^6 configuration.

All the complexes $Ru(nqo)_2$, $Ru(nqo)_2$, $Ru(nqo)_2(nqoH)$ and $Na[Ru(nqo)_3]$ are diamagnetic suggesting a low-spin d^6 configuration. Their IR spectra show strong absorptions at 1540–1610 cm^{-1}, characteristic of chelated quinoneoximato ligands. The complexes of the type $Ru(nqo)_2(nqoH)$ also exhibit bands at *ca* 2800 cm^{-1} in accord with the presence of a protonated nqoH ligand. The UV–vis spectra of all the complexes show intense charge-transfer absorptions at 530–580 and 615–645 nm which tail into the visible region. In general the spectra show very close similarity to those reported earlier for ruthenium quinone oximic complexes erroneously formulated as ruthenium(III) species.[2–5] Thermal gravimetric analysis (Table 1) on the pyridine adducts showed that pyridine is lost quantitatively at *ca* 260°C to give $Ru(nqo)_2$ which decomposes at *ca* 300°C.

Crystal and molecular structure of $Ru(1\text{-}nqo)_2(py)_2$

Crystal data. $C_{30}H_{22}RuN_4O_4 \cdot 1.5(C_5H_5N)$. The crystals were obtained by slow crystallization from pyridine–acetone. Triclinic, $P\bar{1}$, $a = 16.321(4)$, $b = 11.519(4)$, $c = 9.354(5)$ Å, $\beta = 102.22(3)°$, $U = 1646.90$ Å, $D_c = 1.22$ g cm^{-3}, $Z = 2$. A crystal of size $0.81 \times 0.18 \times 0.18$ mm was used in the data collection. Data were collected in the θ-range 3–25° with a scan width of 0.8°, on a Philips PW1100 four-circle diffractometer using graphite monochromated Mo-K_α radiation. The structure was solved and refined using 4030 unique reflections [$I > 3\sigma(I)$] out of 4114. The coordinates of the metal atom were deduced from a Patterson synthesis, and the remaining non-hydrogen atoms were located from subsequent difference-Fourier syntheses. The hydrogen atoms were located in a difference-Fourier synthesis calculated using data with $\sin\theta < 0.35$ and were included in the structure factor calculations but were not further refined. Ru, N and the carbonyl O atoms were assigned anisotropic thermal parameters in the final cycles of full-matrix refinement which converged at $R = 0.0505$, with weights of $w = 1/\sigma 2F_o$. The bond lengths and the angles are listed in Tables 2 and 3, and the atomic numbering is explained in Fig. 1.

As with other 1,2-quinone oximato complexes of *d*-block metals the chelate ring in bis(1,2-naphthoquinone 1-oximato)di(pyridine)ruthenium(II) is five-membered. The bond lengths in the chelate ring

Table 2. Bond lengths (Å) for $Ru(1\text{-}nqo)_2(py)_2$

Ru—O(12)	2.100(3)	Ru—N(11)	1.963(5)
Ru—O(22)	2.060(4)	Ru—N(21)	1.965(4)
Ru—N(31)	2.085(4)	Ru—N(41)	2.120(4)
O(12)—C(12)	1.278(6)	C(11)—N(11)	1.381(6)
N(11)—O(11)	1.270(5)	O(22)—C(22)	1.293(6)
C(21)—N(21)	1.393(7)	N(21)—O(21)	1.259(5)
N(31)—C(31)	1.355(7)	N(31)—C(35)	1.343(7)
N(41)—C(41)	1.321(7)	N(41)—C(45)	1.329(7)

Table 1. Thermal gravimetric analysis

Compound	Weight of sample (mg)	T (°C)	Weight loss[a] (mg) Found	Calc.	Decomposition temperature (°C) of $Ru(nqo)_2$
$Ru(1\text{-}nqo)_2(py)_2$	99	270	25	24	310
$Ru(2\text{-}nqo)_2(py)_2$	101	245	25	24	296

[a] Loss of pyridine.

Table 3. Bond angles (°) for $Ru(1\text{-nqo})_2(py)_2$

N(11)—Ru—O(12)	79.7(2)	O(22)—Ru—O(12)	95.0(1)
O(22)—Ru—N(11)	90.1(2)	N(21)—Ru—O(12)	173.3(2)
N(21)—Ru—N(11)	95.0(2)	N(21)—Ru—O(22)	80.9(2)
N(31)—Ru—O(12)	85.9(2)	N(31)—Ru—N(11)	91.4(2)
N(31)—Ru—O(22)	178.3(2)	N(31)—Ru—N(21)	98.4(2)
N(41)—Ru—O(12)	93.9(2)	N(41)—Ru—N(11)	173.3(2)
N(41)—Ru—O(22)	88.5(2)	N(41)—Ru—N(21)	91.2(2)
N(41)—Ru—N(31)	90.0(2)	C(12)—O(12)—Ru	110.7(3)
C(11)—N(11)—Ru	117.1(3)	O(11)—N(11)—Ru	123.6(4)
C(22)—O(22)—Ru	110.7(3)	C(21)—N(21)—Ru	115.1(5)
O(21)—N(21)—Ru	125.2(4)	C(35)—N(31)—Ru	119.8(4)
C(31)—N(31)—Ru	122.8(4)	C(41)—N(41)—Ru	119.9(4)
C(45)—N(41)—Ru	122.6(4)	C(11)—C(12)—O(12)	121.4(5)
C(13)—C(12)—O(12)	121.4(5)	N(11)—C(11)—C(12)	110.9(5)
C(10)—C(11)—N(11)	127.0(5)	O(11)—N(11)—C(11)	119.3(5)
C(14)—C(13)—C(12)	120.6(6)	C(21)—C(22)—O(22)	121.3(5)
C(23)—C(22)—O(22)	119.6(5)	N(21)—C(21)—C(22)	111.8(5)
C(20)—C(21)—N(21)	126.2(5)	O(21)—N(21)—C(21)	119.7(4)
C(35)—N(31)—C(31)	117.4(5)	C(32)—C(31)—N(31)	122.4(6)
C(34)—C(35)—N(31)	122.8(6)	C(45)—N(41)—C(41)	117.4(6)
C(42)—C(41)—N(41)	123.6(7)	C(44)—C(45)—N(41)	122.7(7)

agree well with results for other 1,2-naphthoquinone oximato complexes and the short C(3)—C(4) bond lengths provide additional evidence for the quinone oximic character.[20–22] The NO groups of the two chelating ligands are in a *cis* arrangement whereas in other related complexes, e.g. $Cu(1\text{-nqo})_2(Me_2CO)_2$,[21] the arrangement is *trans*.

EXPERIMENTAL

IR and UV–vis spectra were recorded with Pye–Unicam SP 2000 and 1200 spectrophotometers,

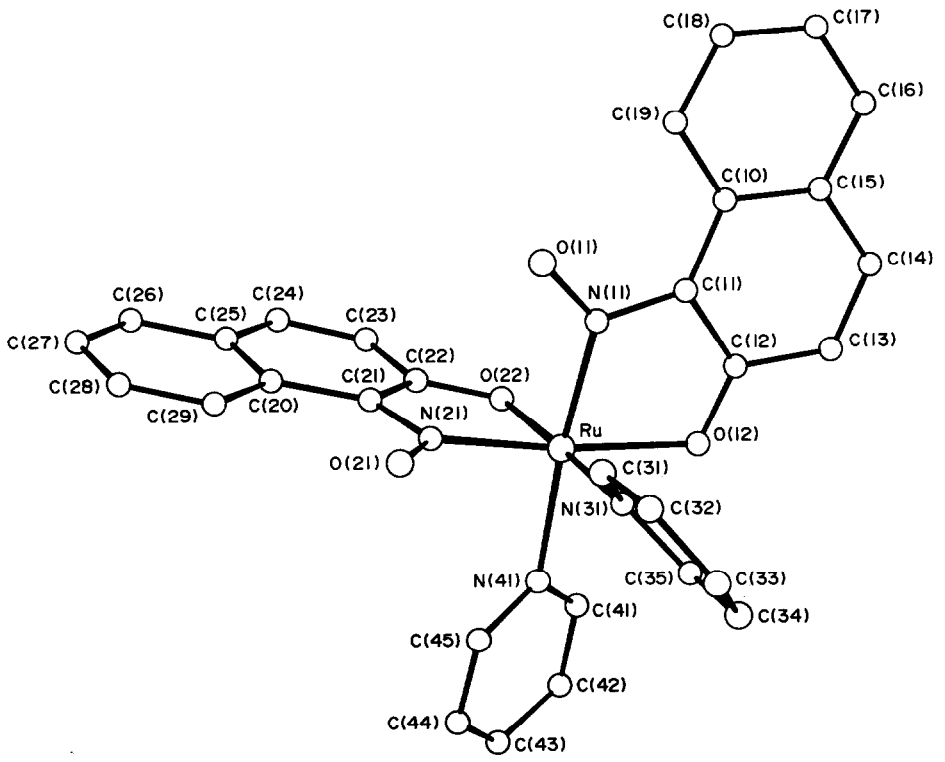

Fig. 1. Structure of $Ru(1\text{-nqo})_2(py)_2$.

respectively. Magnetic measurements were made at room temperature using a Gouy balance equipped with a permanent magnet of 3600 Oe. Thermal gravimetric measurements were made using a Stanton HT-SM thermobalance, programmed for a linear rise between 20–400°C at a rate of 4.5°C min^{-1}. A downward flow of nitrogen (5 dm^3 h^{-1}) was maintained. Hydrated ruthenium(III) chloride, $RuCl_3 \cdot 2H_2O$, was provided by Johnson Matthey.

Reaction of hydrated ruthenium(III) *trichloride with the sodium salts of the mono-oximes of* 1,2-*naphthoquinone in aqueous THF*

A solution of hydrated ruthenium(III) chloride (1.21 g, 5 mmol) in water (50 cm^3) was added to a stirred suspension of sodium 1,2-naphthoquinone 1-oximate (1.96 g, 10 mmol) in a 1:1 water–THF mixture (100 cm^3) with stirring. After 4 h the mixture was filtered to give purple–brown bis(1,2-naphthoquinone 1-oximato)ruthenium(II) (2.18 g, 98%). (Found: C,53.6; H, 2.7; N, 6.1; Ru, 22.4. $C_{20}H_{12}N_2O_4Ru$ requires: C, 53.6; H, 2.7; N, 6.3; Ru, 22.7%.)

Similarly, sodium 1,2-naphthoquinone 2-oximate gave brown bis(1,2-naphthoquinone 2-oximato)ruthenium(II) (2.10 g, 92%). (Found: C, 53.8; H, 2.4; N, 6.0; Ru, 22.6. $C_{20}H_{12}N_2O_4Ru$ requires: C, 53.6; H, 2.7; N, 6.3; Ru, 22.7%.)

Reaction of hydrated ruthenium(III) *chloride with sodium* 1,2-*naphthoquinone mono-oximates in ethanol*

A solution of hydrated ruthenium(III) chloride (2.08 g, 8.5 mmol) in ethanol (100 cm^3) was added to a solution of sodium 1,2-naphthoquinone oximate (5.8 g, 27 mmol) in ethanol (150 cm^3) and heated under reflux for 24 h. After cooling, filtration gave purple sodium tris(1,2-naphthoquinone 1-oximato)ruthenate (II) (4.89 g, 89%). Found: C, 55.8; H, 3.0; N, 6.4; Na, 3.5; Ru, 16.1. $C_{30}H_{18}N_3NaO_6Ru$ requires: C, 56.2; H, 2.8; N, 6.6; Na, 3.6; Ru, 16.1%.)

Similarly, sodium 1,2-naphthoquinone 2-oximate gave blue sodium tris(1,2-naphthoquinone 2-oximato)ruthenate(II) (2.14 g, 81%). (Found: C, 56.1; H, 2.7; N, 6.5; Na, 3.5; Ru, 15.7. $C_{30}H_{18}N_3NaO_6Ru$ requires: C, 56.2; H, 2.8; N, 6.6; Na, 3.6; Ru, 16.1%.)

Reaction of hydrated ruthenium(III) *chloride with sodium* 1,2-*naphthoquinone mono-oximates in acetic acid*

A solution of hydrated ruthenium(III) chloride (2.08 g, 8.5 mmol) in dilute acetic acid (30%, 50 cm^3) was added to a solution of sodium 1,2-naphthoquinone 1-oximate (5.85 g, 27.5 mmol) in glacial acetic acid (250 cm^3) and the mixture was heated under reflux for 24 h. Filtration gave blue–violet bis(1,2-naphthoquinone 1-oximato)(1,2-naphthoquinone 1-oxime)ruthenium(II). (Found: C, 57.9; H, 3.0; N, 6.7; Ru, 16.2. $C_{30}H_{19}N_3O_6Ru$ requires: C, 58.3; H, 3.1; N, 6.8; Ru, 16.2%.)

Similarly, sodium 1,2-naphthoquinone 2-oximate gave blue bis(1,2-naphthoquinone 2-oximato)(1,2-naphthoquinone 2-oxime)ruthenium(II) (79%). (Found: C, 57.9; H, 2.9; N, 6.9; Ru, 16.5. $C_{30}H_{19}N_3O_6Ru$ requires: C, 58.3; H, 3.1; N, 6.8; Ru, 16.2%.)

Reaction of $Ru(1\text{-}nqo)_2(1\text{-}nqoH)$ *and* $Ru(2\text{-}nqo)_2(2\text{-}nqoH)$ *with dilute hydrochloric acid*

Bis(1,2-naphthoquinone 1-oximato)(1,2-naphthoquinone 1-oxime)ruthenium(II) (0.62 g, 1 mmol) was heated in dilute hydrochloric acid (10%, 100 cm^3) for 6 h. Filtration of the mixture yielded bis(1,2-naphthoquinone 1-oximato)ruthenium(II) (0.45 g, 99%) (identified by TLC and IR) and 1,2-naphthoquinone 1-oxime (0.16 g, 99%) (identified by TLC and IR).

Similarly, bis(1,2-naphthoquinone 2-oximato)(1,2-naphthoquinone 2-oxime)ruthenium(II) gave (1,2-naphthoquinone 2-oximato)ruthenium(II) (97%) (identified by TLC and IR) and 1,2-naphthoquinone 2-oxime (91%) (identified by TLC and IR).

Attempted reactions of $Ru(1\text{-}nqo)_2$ *or* $Ru(2\text{-}nqo)_2$ *with concentrated hydrochloric acid*

$Ru(1\text{-}nqo)_2$ or $Ru(2\text{-}nqo)_2$ (*ca* 0.50 g) was recovered in *ca* 99% yield after being heated with concentrated hydrochloric acid (20 cm^3) for 7 days.

Reaction of $Ru(1\text{-}nqo)_2$ *and* $Ru(2\text{-}nqo)_2$ *with pyridine*

Bis(1,2-naphthoquinone 1-oximato)ruthenium (II) (0.45 g, 1 mol) was stirred in pyridine (50 cm^3) at 20°C for 4 h. Removal of the solvent at 60°C/35 mm Hg gave bis(1,2-naphthoquinone 1-oximato)di(pyridine)ruthenium(II) (0.61 g, 99%). (Found: C, 59.6; H, 3.4; N, 9.4; Ru, 17.1. $C_{30}H_{22}N_4O_4Ru$ requires: C, 59.7; H, 3.6; N, 9.3; Ru, 16.7%.)

Similarly, bis(1,2-naphthoquinone 2-oximato)ruthenium(II) gave violet bis(1,2-naphthoquinone 2-oximato)di(pyridine)ruthenium(II) (97%). (Found: C, 60.1; H, 3.6; N, 9.1; Ru, 16.8. $C_{30}H_{22}N_4O_4Ru$ requires: C, 59.7; 3.6; N, 9.3; Ru, 17.1%.)

Reaction of $Ru(1\text{-nqo})_2$ *and* $Ru(2\text{-nqo})_2$ *with triphenylphosphine*

Bis(1,2-naphthoquinone 1-oximato)ruthenium (II) (0.5 g, 1.1 mmol) and triphenylphosphine (1.1 g, 4 mmol) were heated under reflux in THF (50 cm^3) for 7 days. Filtration of the mixture afforded bis(1,2-naphthoquinone 1-oximato)bis (triphenylphosphine)ruthenium(II) (0.72 g, 69%). (Found: C, 70.4; H, 3.9; N, 2.7; P, 6.2; Ru, 10.5. $C_{56}H_{42}N_2O_4P_2Ru$ requires: C, 69.3; H, 4.3; N, 2.9; P, 6.5; RU, 10.5%.)

Similarly, bis(1,2-naphthoquinone 2-oximato) ruthenium(II) gave bis(1,2-naphthoquinone 2-oximato)bis(triphenylphosphine)ruthenium(II) (85%). (Found: C, 70.0; H, 4.1; N, 2.8; P, 5.9; Ru, 10.8. $C_{56}H_{42}N_2O_4P_2Ru$ requires: C, 69.3; H, 4.3; N, 2.9; P, 6.5; Ru, 10.5%.)

Acknowledgements—We thank Dr D. T. Thompson, Dr A. A. Berzins and Johnson Matthey Technology Centre, for their advice and interest in this work.

REFERENCES

1. S. C. Ogburn Jr, *J. Am. Chem. Soc.* 1926, **48**, 2493.
2. G. Kesser, R. J. Meyer and R. P. Larsen, *Anal. Chem.* 1966, **38**, 221.
3. D. L. Manning and O. Menis, *Anal. Chem.* 1962, **34**, 94.
4. C. Konecny, *Anal. Chim. Acta.* 1963, **29**, 423.
5. C. Konecny, *Anal. Chim. Acta* 1964, **31**, 352.
6. J. Charalambous, M. J. Kensett and J. M. Jenkins, *J. Chem. Res.* 1982, **5**, 306.
7. J. Charalambous, G. Soobramanien, A. Betts and J. Bailey, *Inorg. Chim. Acta* 1982, **60**, 157.
8. J. Charalambous, L. I. B. Haines, J. S. Morgan, D. S. Peat, M. J. M. Cambell and J. Bailey, *Polyhedron* 1987, **6**, 1027.
9. J. Charalambous, K. Henrick, Y. Musa, R. G. Rees and R. N. Whiteley, *Polyhedron* 1987, **6**, 1509.
10. A. R. Middleton, J. R. Thornback and G. Wilkinson, *J. Chem. Soc., Dalton Trans* 1980, 1740.
11. F. H. Jardine, *Prog. Inorg. Chem.* 1984, **31**, 265.
12. F. H. Burstall, *J. Chem. Soc.* 1936, 173.
13. F. P. Dwyer and E. C. Gyarfas, *Proc. R. Soc. N.S. Wales* 1949, **83**, 170.
14. G. N. Schrauzer and W. Heinrick, *Angew. Chem.* 1964, **3**, 381.
15. G. A. Barbieri, *Atti. Acad. Linc.* 1914, **23**, 336.
16. W. P. Griffith, *The Chemistry of the Rarer Platinum Metals*, p. 158. Interscience, London (1967).
17. A. D. Allen and C. V. Senoff, *Can. J. Chem.* 1965, **43**, 888.
18. J. Charalambous, J. S. Morgan and M. J. Whelehan, unpublished results.
19. G. Cronheim, *J. Org. Chem.* 1947, **12**, 7.
20. R. G. Buckley, J. Charalambous, M. J. Kensett, M. McPartlin, D. Mukerjee, E. G. Brain and J. M. Jenkins, *J. Chem. Soc., Perkin Trans. I* 1983, 693.
21. H. Saarinen and J. Korvenranta, *Acta Chem. Scand.* 1975, **29A**, 409.
22. P. W. Carreck, J. Charalambous, M. J. Kensett, M. McPartlin and R. Sims, *Inorg. Nucl. Chem. Lett.* 1974, **10**, 749.

Polyhedron Vol. 8, No. 1, pp. 109–112, 1989
Printed in Great Britain

0277–5387/89 $3.00+.00
© 1988 Pergamon Press plc

PEROXO COMPLEXES OF Zr^{IV}, Th^{IV}, W^{VI} AND U^{VI} IONS STABILIZED BY MULTIDENTATE ORGANIC LIGANDS

M. T. H. TARAFDER* and A. A. M. ANWARUL ISLAM

Department of Chemistry, University of Rajshahi, Rajshahi, Bangladesh

(*Received* 29 *June* 1988; *accepted* 25 *July* 1988)

Abstract—Several new peroxo complexes of zirconium, thorium, tungsten and uranium containing organic ligands, ethylenediaminetetraacetic acid and succinic acid, have been prepared. The complexes have the compositions $[M(O_2)(H_2edta)]$, $[M'(O)(O_2)(H_2edta)]$ and $[M''(O_2)(scac)\cdot 2L]$ (H_2edta = dianion of ethylenediaminetetraacetic acid; scac = dianion of succinic acid; M = Zr^{IV} and Th^{IV}; M′ = W^{VI} and U^{VI}; M″ = Zr^{IV} and Th^{IV}; L = $OPPh_3$ or $OAsPh_3$), respectively. The present complexes were found to be very stable and inert towards oxidation. The size of the metals as well as the electronic nature of the auxiliary ligands (L) influence the mode of coordination of the peroxo moiety. The frequency of the ν_1 mode of the $M(O_2)$ grouping decreases with an increase in the atomic numbers of metals in a particular group and in donor strength of the ancillary ligands used.

The study of the chemistry of peroxo complexes has advanced rapidly in the last decade due to developments in the application of such complexes as oxidants in synthetic organic chemistry.[1–9] The reactivity of metal peroxides depends on the nature of other auxiliary ligands used. Peroxo complexes containing monodentate and bidentate auxiliary ligands were found to undergo oxygen transfer reactions to various substrates,[1–9] however, those containing tridentate ligands have been found to be very stable and inert towards oxidation reactions.[6,7,10] We are interested to extend such a study with new peroxo complexes of different elements of Group 4A and 6A containing ethylenediaminetetraacetic acid and succinic acid as quadridentate and bidentate ligands, respectively. The synthesis and properties of peroxo complexes of titanium(IV),[11] niobium(V) and tantalum(V)[12] containing $edta^{2-}$ have been reported. However, reports on the peroxo complexes of zirconium, thorium, tungsten and uranium containing $edta^{2-}$ and $scac^{2-}$ as ancillary ligands are lacking. We present here the synthesis of these complexes and their possible attempted oxygen transfer reactions. An attempt has also been made to study the effect of the size of the metal ions and the electronic nature of auxiliary ligands ($OPPh_3$ and $OAsPh_3$) on ν_1(O—O) modes of the complexes in their IR spectra.

*Author to whom correspondence should be addressed.

EXPERIMENTAL

Physical measurements

IR spectra (as KBr discs) were recorded with a Pye–Unicam SP3-300 IR spectrophotometer. Conductivities of 10^{-3} M solutions of the complexes in dimethyl sulphoxide (DMSO) were measured at 25°C using a WPA CM35 conductivity meter and dip-type cell with platinized electrodes.

Reagents

All chemicals used were reagent grade and were used as supplied by Merck.

Analyses

Zirconium,[7] thorium,[6] tungsten[9] and uranium[5] were determined gravimetrically. Carbon and hydrogen analyses were done by Mikroanalytisches Labor Pascher, Germany.

Preparation of complexes

General method for the preparation of the complexes $[M(O_2)(H_2edta)]$ (M = Zr^{IV} *and* Th^{IV} *and* $[U(O)(O_2)(H_2edta)]$ (**1**, **2** *and* **4**). $M(NO_3)_4\cdot 6H_2O$ (M = Zr^{IV} or Th^{IV}) or $UO_2(NO_3)_2\cdot 6H_2O$ (0.005 mol) was dissolved in water (20 cm^3) to which a solu-

tion of $Na_2edta \cdot 2H_2O$ (disodium sodium salt of edta) (0.005 mol) in the same solvent (25 cm^3) and 30% H_2O_2 (20 cm^3) were added successively. The precipitate was filtered and washed with water and ether, and dried *in vacuo* over P_4O_{10}.

Preparation of $[W(O)(O_2)(H_2edta)]$ (**3**). A suspension of WO_3 (0.015 mol) in 30% H_2O_2 (70 cm^3) was stirred overnight at 45–50°C. This was filtered and to the clear filtrate was added a solution of Na_2edta (0.015 mol) in water (50 cm^3). The mixture was stirred while cooling at the same time in an ice-salt bath. A yellow precipitate appeared, which was washed successively with water and ether, and dried *in vacuo* over P_4O_{10}.

General method for the preparation of the complexes $[M(O_2)(scac) \cdot 2L]$ ($M = Zr^{IV}$ *or* Th^{IV}; scac = *dianion of succinic acid*; $L = OPPh_3$ *or* $OAsPh_3$) (**5–7**). A solution of $M(NO_3)_4 \cdot 6H_2O$ (0.004 mol) in water (20 cm^3) was added to a solution of succinic acid (0.004 mol) in methanol (20 cm^3). A solution of L (0.008 mol) in methanol (25 cm^3) was then added to the above mixture followed by the addition of 30% H_2O_2 (20 cm^3). The product was filtered, washed successively with water and ether, and stored.

Attempted reactions of **1** *and* **2** *with allyl alcohol and of* **4** *and* **5** *with triphenylphosphine and triphenylarsine, respectively*

Refluxing of **1** with allyl alcohol in a 1 : 1 molar ratio in tetrahydrofuran (THF) medium for 48 h failed to produce any reaction. **1** was recovered unchanged.

Refluxing of **2** with allyl alcohol in the presence of a large excess of 30% H_2O_2 in dioxane medium for 48 h at 90°C also failed to produce any reaction. **2** was recovered unchanged.

Refluxing of **4** and **5** with equimolar quantities of triphenylphosphine and triphenylarsine, respectively in THF for 48 h also failed to produce any reaction. **4** and **5** were recovered unchanged.

RESULTS AND DISCUSSION

The analytical data of the complexes are given in Table 1. The molar conductance values indicated that all of the complexes were non-electrolytes in DMSO indicating that the anions are covalently bonded in all the cases. These data are consistent with six-fold coordination of Zr^{IV} and Th^{IV} complexes, while the W^{IV} and U^{VI} complexes are seven-coordinated.

IR spectral data are shown in Table 2. The H_2edta^{2-} behaves as a quadridentate dinegative ligand coordinating at the two amino nitrogens and the two carboxylate anions. IR spectra of **1–4** indicate the presence of two kinds of carboxo groups. Complexes **1–4** show ν(C=O) bands at around 1600 cm^{-1}—lower than the free ligand value, indicating carboxylate binding in the complexes. However, these complexes also show bands at $\sim$ 1665 cm^{-1} as expected for the free carbonyl group in Na_2edta molecule (Table 2). In addition, a broad band at 3400–3520 cm^{-1} does persist in the spectra of **1–4** dried *in vacuo*, indicating the presence of —OH groups in the coordinated $edta^{2-}$ ion also. Further, the presence of M—N bonds in **1–4** are evident from the appearance of ν(M—N)[5–9] modes at 265–320 cm^{-1} in the far-IR spectra of the complexes. Complexes **5–7** display ν(C=O) bands at 1635–1650 cm^{-1}, significantly lower than the free ligand (Table 2) value which indicates coordination by the carboxylate anions. The ν(O—H) observed for the free $scacH_2$ molecule disappears upon coordination in **5–7** revealing that succinic acid is a bidentate dinegative ligand coordinating through both carboxylate anions. Further support for M—O′ (O′ = oxygen in organic ligand) bonding in **1–7** is apparent from the ν(M—O′) modes at 380–425 cm^{-1} (Table 2) in the far-IR spectra of the complexes.[5–9] The complexes **3** and **4** display ν(M=O) modes at 955 and 910 cm^{-1}, respectively.[4–9]

The metal peroxo grouping gives rise to three IR-active vibrational modes. These are predominantly

Table 1. Analytical data and other physical properties of the peroxo complexes

Compound	Colour	% Metal		% Carbon		% Hydrocarbon	
		Calc.	Found	Calc.	Found	Calc.	Found
$[Zr(O_2)(H_2edta)]$ (**1**)	Colourless	22.1	22.0	29.0	29.0	3.4	3.3
$[Th(O_2)(H_2edta)]$ (**2**)	Colourless	41.9	41.6	21.7	21.5	2.5	2.5
$[W(O)(O_2)(H_2edta)]$ (**3**)	Yellow	35.2	35.0	23.0	22.9	2.7	2.5
$[U(O)(O_2)(H_2edta)]$ (**4**)	Yellow	41.3	41.1	20.8	20.7	2.4	2.4
$[Zr(O_2)(scac) \cdot 2OPPh_3]$ (**5**)	Colourless	11.5	11.3	60.4	60.1	4.3	4.2
$[Th(O_2)(scac) \cdot 2OPPh_3]$ (**6**)	Colourless	24.8	24.7	51.3	51.2	3.6	3.6
$[Th(O_2)(scac) \cdot 2OAsPh_3]$ (**7**)	Colourless	22.7	22.5	46.9	46.6	3.3	3.3

Table 2. IR spectral data for the complex[a] band maxima (cm^{-1})

Compound	ν(OH)	ν(C=O)	ν(M=O)	ν_1(O—O)	ν_3(M<O,O>)	ν_2(M<O,O>)	ν(M—O′)	ν(M—N)
Na_2(edta)	3400–3520br	1665sh 1620vs						
1	3400–3520br	1665sh 1600s		840s	650s	600m	410w	320m
2	3400–3520br	1665s 1600s		828s	650s	600m	390w	300m
3	3400–3550br	1665sh 1600s	955vs	860vs	632a	600m	380m	290m
4	3400–3520br	1660s 1600s	910s	800vs	630s	590sh	430m	265w
$scacH_2$	3400–3600br	1700vs						
5		1650s	ν(E=O) 1120vs	852s	695m	600m	425m	
6		1635vs	1122vs	830s	695s	635w	420m	
7		1650vs	860s	800s	690m	600m	420w	

[a] Relative band intensities are denoted by vs, s, m, w, sh and br, meaning very strong, strong, medium, weak, shoulder and broad, respectively. E stands for P and As.

O—O stretching (ν_1), the symmetric M—O stretch (ν_2) and the antisymmetric M—O stretch (ν_3). The characteristic ν_1(O—O) modes of **1**–**7** appear at 800–860 cm^{-1}. There is a decrease in ν_1 upon passing from zirconium complexes (**1** and **5**) to the thorium complexes (**2**, **6** and **7**). Again, in the case of the peroxo complexes of the elements from group 6A, there is a decrease in ν_1 upon passing from the tungsten complex (**3**) to the corresponding uranium complex (**4**). The present data, thus clearly reveal that for the $M(O_2)$ grouping, the ν_1 modes decrease with an increase in the atomic numbers of metals in a particular group. In the present examples, the ν_3 and ν_2 modes appear at 630–695 and 570–635 cm^{-1}, respectively. Complexes **6** and **7** show a decrease in ν(P=O) of 72 and 70 cm^{-1}, respectively, compared to the free ligand value (1192 cm^{-1}),[13] suggesting coordination by the oxygen of $OPPh_3$. Complex **7** shows a decrease in ν(As=O) of 20 cm^{-1} from the free ligand value (880 cm^{-1}),[14] indicating coordination by the oxygen of $OAsPh_3$. For **6** and **7**, the ν_1 mode appears at lower frequency in the arsenic compound (**7**, 800 cm^{-1}) compared to that in the phosphorus analogue (**6**, 830 cm^{-1}). It is argued that ν_1(O—O) in the peroxo complexes is decreased by replacing a given ligand by one which is a stronger donor.[4,5] We have previously reported that the oxygen in the arsine oxide is more negative, and values of 2.45×10^{-10} and 1.78×10^{-10} esu were obtained for arsine oxide and phosphine oxide, respectively.[8] This points to a greater polarity in the case of arsine oxides and hence ≡As—O is a stronger donor than ≡P—O. This causes a weaker coulombic interaction in the Th^{4+}—O_2^{2-} moiety for compounds containing $OAsPh_3$. This argument seems to account for the lower ν_1 value observed for **7** than for **6**.

Reactivity

The present peroxo complexes were found to be very stable and were not explosive. To explore the reactivity of the present peroxo complexes toward olefins and other substrates, **1** and **2** were allowed to react with allyl alcohol. These compounds failed to oxidize allyl alcohol even when refluxing at 90°C was continued for 48 h. Compounds **4** and **5** were also inert towards phosphine and arsine. These negative results outline the enhanced stability of the metal peroxo moiety in the presence of quadridentate and bidentate dinegative chelating ligands which precludes oxygen transfer reactions. The present findings also demonstrate that the chelate action derived from bidentate, dinegative ligands equals that of the quadridentate ligand used. We also observed similar behaviour for various peroxo complexes containing tridentate ligands.[5–7,10]

Acknowledgements—We are indebted to the Department of Chemistry, Rajshahi University, Bangladesh, for the financial support and for the provision of laboratory facilities. We thank Prof. M. A. Raqib, former Vice-Chancellor of Rajshahi University for funding the costs of microanalyses in Germany.

REFERENCES

1. H. Mimoun, I. S. de Roch and L. Sajus, *Tetrahedron* 1976, **26**, 37.
2. H. Mimoun, *J. Mol. Catal.* 1980, **7**, 1.
3. S. E. Jacobson, R. Tang and F. Mares, *Inorg. Chem.* 1978, **17**, 3055.
4. A. D. Westland, F. Hague and J. M. Bouchard, *Inorg. Chem.* 1980, **19**, 225.
5. A. D. Westland and M. T. H. Tarafder, *Inorg. Chem.* 1981, **20**, 3992.
6. A. D. Westland and M. T. H. Tarafder, *Inorg. Chem.* 1982, **21**, 3228.
7. M. T. H. Tarafder and M. A. L. Miah, *Inorg. Chem.* 1986, **25**, 2265.
8. M. T. H. Tarafder and A. Ahmed, *Ind. J. Chem.* 1986, **25A**, 729.
9. M. T. H. Tarafder and A. R. Khan, *Polyhedron* 1987, **6**, 275.
10. M. T. H. Tarafder, *Ind. J. Chem.* 1987, **26A**, 874.
11. F. J. Kristine, R. E. Shepherd and S. Siddiqui, *Inorg. Chem.* 1981, **20**, 2571.
12. N. Vuletic and E. Prcic, *Z. Anorg. Allg. Chem.* 1979, **450**, 67.
13. D. Brown, J. Hill and C. E. F. Rickard, *J. Chem. Soc. A* 1970, 499.
14. J. Burnstein, M. Halman, S. Pinchas and D. Samuel, *J. Chem. Soc.* 1964, 821.

Polyhedron Vol. 8, No. 1, pp. 113–115, 1989
Printed in Great Britain

0277–5387/89 $3.00+.00
© 1988 Pergamon Press plc

COMMUNICATION

OXIDATION OF NICKEL(II) BIS(SALICYLALDIMINE) COMPLEXES: SOLVENT CONTROL OF THE ULTIMATE REDOX SITE

KENNETH A. GOLDSBY,* JEAN K. BLAHO and LISA A. HOFERKAMP

Department of Chemistry, The Florida State University, Tallahassee, FL 32306-3006, U.S.A.

(*Received* 1 *July* 1988; *accepted* 15 *August* 1988)

Abstract—The oxidation of nickel(II) bis(salicylaldimine) complexes has been examined by cyclic voltammetry. The complexes are reversibly oxidized in strong donor solvents, but in weak donor solvents, they are oxidatively polymerized at the electrode surface. A ligand–radical coupling mechanism involving the phenolic portion of the salicylaldimine chelate is proposed, and the solvent dependence is explained in terms of the solvent's ability to stabilize the nickel(III) oxidation state relative to ligand-localized oxidation.

Transition metal bis(salicylaldimine) complexes have received much attention as synthetic dioxygen carriers[1] and as catalysts for the oxidation of organic molecules.[2] Although the oxidation of transition metal bis(salicylaldimine) complexes has been extensively investigated,[3,4] oxidation of the salicylaldimine chelate itself has not been addressed. Herein we report that nickel(II) bis(salicylaldimine) complexes of the type shown in structure I† are oxidatively polymerized in poor donor solvents which

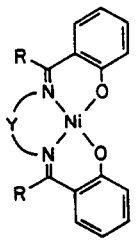

Ia: R = H; Y = CH_2CH_2

Ib: R = H; Y = o-C_6H_4

Ic: R = Me; Y = CH_2CH_2

cannot stabilize the nickel(III) oxidation state relative to ligand-localized oxidation. The oxidative polymerization of these complexes demonstrates a previously unrecognized mode of ligand-localized redox chemistry for the salicylaldimine chelate.

The nickel(II) bis(salicylaldimine) complexes used in these studies were synthesized by standard literature procedures.[5] As previously reported by Kapturkiewicz and Behr for [Ni(H-sal$_2$en)],[4] the nickel(II) bis(salicylaldimine) complexes gave reversible voltammograms in good donor solvents such as pyridine (DN = 33.1),‡ dimethylsulphoxide (DN = 29.8), and N,N-dimethylformamide (DN = 26.6). The electrochemical behaviour observed in weak donor solvents, however, was considerably more complex. For example, initial scan voltammograms of the nickel(II) complexes in acetonitrile (DN = 14.1) showed two distinct oxidations in the potential range 0.8–1.2 V *vs* SSCE, followed by a single reduction of lesser current intensity. Subsequent scans between 0.5 and 1.4 V resulted in rapid current enhancement of the cathodic wave and the appearance of a new anodic wave which grew rapidly at the expense of the initial oxidations (Fig. 1). The increase in current observed with each new scan is indicative of oxidative polymerization of the redox active species to give surface-modified electrodes.[6] With continued scanning, an *insoluble* orange film formed on the electrode surface, which is also consistent with polymer formation. Oxidative polymerization of the nickel(II) salicylaldimine complexes also occurred

*Author to whom correspondence should be addressed.

† The abbreviated names, [Ni(R-sal$_2$Y)], are derived from structure I where Y is en (ethylenediamine, CH_2CH_2) or phen (*o*-phenylenediamine, *o*-C_6H_4).

‡ DN refers to the Gutmann Donor Number[8] for that solvent.

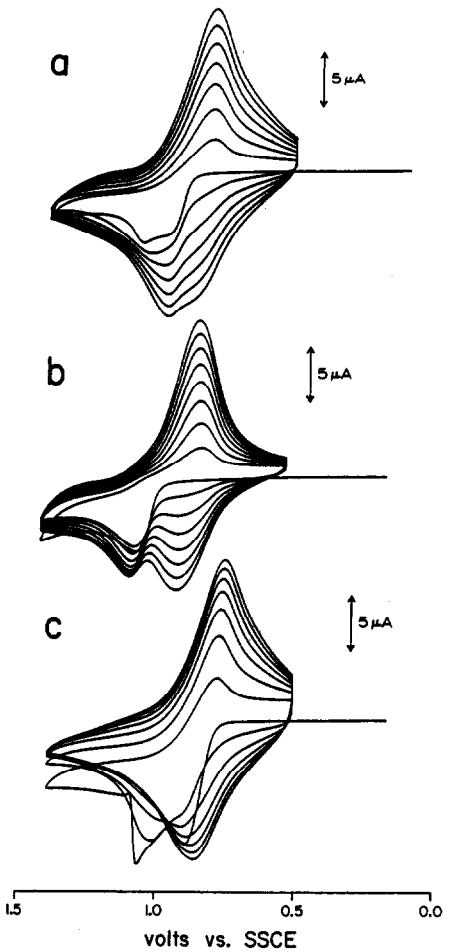

Fig. 1. Cyclic voltammograms showing oxidative polymerization of the nickel(II) bis(salicylaldimine) complexes at a platinum disc electrode in 0.1 M n-Bu_4NPF_6/CH_3CN: (a) 3×10^{-4} M [Ni(H-sal$_2$en)]; (b) 3×10^{-4} M [Ni(H-sal$_2$phen)]; (c) 1×10^{-3} M [Ni(Me-sal$_2$en)]. Scan rate = 100 mV s^{-1}.

in acetone (DN = 17.0) and methylene chloride (DN $\simeq$ 0) electrolyte solutions. The presence of nickel in these films was confirmed by energy-dispersive spectroscopy of the electrode surfaces.[7] Furthermore, visible spectra of films obtained on indium(tin) oxide coated glass electrodes showed broad spectral features characteristic of the nickel(II) bis(salicylaldimine) complexes.

The solvent dependence observed for the oxidative polymerization of the nickel(II) bis(salicylaldimine) complexes can be understood in terms of the solvent's role in governing the ultimate site of oxidation. In strong donor solvents, the oxidation of square planar nickel(II) complexes to nickel(III) occurs with a concomitant increase in coordination number as the higher oxidation state is stabilized by axial ligation. The degree to which axial ligation can stabilize the higher oxidation state of the metal is determined by the donating ability of the solvent.[8] For [Ni(H-sal$_2$en)], this relationship is reflected in the solvent dependence of the [Ni(H-sal$_2$en)]$^{+/0}$ couple.[4] For ligand systems where ligand-localized oxidations are also accessible, it has been shown that the ultimate site of oxidation is determined largely by the solvent's ability to stabilize nickel(III) through axial ligation.[9] In this respect, it is important to note that the bis(salicylaldimine) ligands, H_2(R-sal$_2$Y), are irreversibly oxidized at potentials about 200 mV higher than the corresponding [Ni(R-sal$_2$Y)] complexes. Consequently, the following mechanism can be proposed for the solvent dependent oxidative polymerization of the nickel(II) bis(salicylaldimine) complexes: in good donor solvents, Ni^{II} is oxidized to Ni^{III}. In more weakly donating solvents, however, the nickel(III) oxidation state is not stabilized relative to ligand oxidation, and oxidative polymerization occurs via a ligand–radical coupling mechanism. Electrochemical studies of unsymmetrical nickel(II) Schiff base complexes suggest that the initial site of oxidation is metal-localized, followed by rapid internal electron transfer to give ligand-oxidized species.[10]

The oxidative carbon–carbon coupling of phenols is known to occur by a radical coupling mechanism;[11] therefore, it seems reasonable that oxidative polymerization of nickel(II) bis(salicylaldimine) complexes occurs by an analogous mechanism involving the phenolic portion of the salicylaldimine chelate. As a test for this coupling mechanism, the complexes shown in structure **II–IV** were synthesized* and examined by cyclic voltammetry. It is well known that alkyl substitution at the *ortho* and *para* positions inhibits the oxidative coupling of phenols at these sites.[11] Consistent with the radical coupling mechanism proposed here, the cyclic voltammogram of **II** shows two distinct oxidations, but no evidence for polymerization at the electrode. Furthermore, polymerization occurs for **III** but not for **IV**, which is reasonable given the steric hindrance expected for *ortho–ortho* coupling of the nickel(II) bis(salicylaldimine) complexes and the greater radical electron density at the *para* carbon.[11]

In summary, the oxidative electrochemical behaviour of nickel(II) bis(salicylaldimine) complexes is governed by the solvent's ability to stabilize nickel(III) relative to ligand-localized oxidation. In

*These complexes were prepared by standard procedures[5] and characterized by ^{13}C NMR spectroscopy and chemical ionization mass spectroscopy. The precursor methyl-substituted salicylaldehydes were synthesized by a literature method.[12]

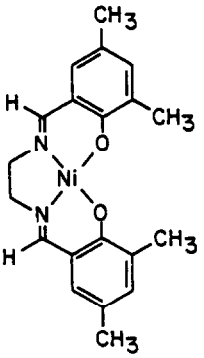

II

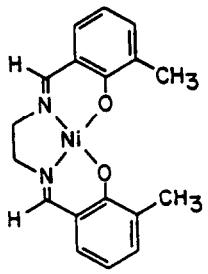

III

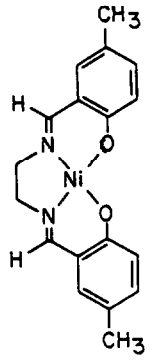

IV

weak donor solvents, the nickel(II) bis(salicylaldimine) complexes are oxidatively polymerized via a ligand–radical coupling mechanism, suggesting that the possibility of ligand redox reactions must be included when considering the potential oxidative decomposition pathways for other metal salicylaldimine complexes. The properties of the surface modified electrodes prepared in this manner will be the subject of a future manuscript.

Acknowledgements—We gratefully acknowledge the Donors of the Petroleum Research Fund, administered by the American Chemical Society, and the Florida State University Foundation for support of this research.

REFERENCES

1. (a) D. Chen and A. E. Martell, *Inorg. Chem.* 1987, **26**, 1026; (b) K. S. Leslie, R. S. Drago, A. B. Griffis, D. E. Hamilton and C. J. O'Connor, *Inorg. Chem.* 1987, **26**, 1951; (c) E. C. Niederhoffer, J. H. Timmons and A. E. Martell, *Chem. Rev.* 1984, **84**, 137.
2. (a) B. B. Corden, R. S. Drago and R. P. Perito, *J. Am. Chem. Soc.* 1985, **107**, 2903; (b) E. G. Samsel, K. Srinivasan and J. K. Kochi, *J. Am. Chem. Soc.* 1985, **107**, 7606; (c) A. Nishinaga, H. Iwasaki, T. Shimizu, Y. Toyoda and T. Matsuura, *J. Org. Chem.* 1986, **51**, 2257; (d) N. Kitajima, K. Whang, Y. Morooka, A. Uchida and Y. Sasada, *J. Chem. Soc., Chem. Commun.* 1986, 1504.
3. See, for example: P. Zanello and A. Cinquantini, *Transition Met. Chem.* 1985, **10**, 370 and refs therein.
4. A. Kapturkiewicz and B. Behr, *Inorg. Chem. Acta* 1983, **69**, 247.
5. R. H. Holm, G. W. Everett and A. Chakravorty, *Prog. Inorg. Chem.* 1966, **7**, 83.
6. (a) R. W. Murray, *Electroanal. Chem.* 1984, **13**, 141; (b) R. W. Murray, *Acc. Chem. Res.* 1980, **13**, 135.
7. H. Yakowitz and J. I. Goldstein, in *Practical Scanning Electron Microscopy* (Edited by J. I. Goldstein and H. Yakowitz), Chap. 11. Plenum Press, New York (1975).
8. V. Gutmann, *The Donor–Acceptor Approach to Molecular Interactions*. Plenum Press, New York (1980).
9. M. Y. Chavan, T. J. Meade, D. H. Busch and T. Kuwana, *Inorg. Chem.* 1986, **25**, 314.
10. K. A. Goldsby, *J. Coord. Chem.* 1988, in press.
11. H. Musso, in *Oxidative Coupling of Phenols* (Edited by W. I. Taylor and A. R. Battersby), Chap. 1. Marcel Dekker, New York (1967).
12. G. Casiraghi, G. Casnati, M. Cornia, A. Pochini, G. Puglia, G. Sartori and R. Ungaro, *J. Chem. Soc., Perkin I* 1978, 318.

Polyhedron Vol. 8, No. 1, pp. 117–119, 1989
Printed in Great Britain

0277–5387/89 $3.00+.00
© 1988 Pergamon Press plc

COMMUNICATION

HETEROLEPTIC POLYPYRAZOLYLBORATE DERIVATIVES OF THE LANTHANIDE IONS. THE SYNTHESIS OF TROPOLONATE COMPLEXES AND THE X-RAY CRYSTAL STRUCTURE OF $[Yb\{HB(C_3N_2H_3)_3\}_2\{OC_7H_5O\}]$

MICHAEL A. J. MOSS and CHRISTOPHER J. JONES*

Department of Chemistry, University of Birmingham, PO Box 363, Birmingham, B15 2TT, U.K.

(*Received* 3 *May* 1988; *accepted* 15 *August* 1988)

Abstract—The air- and moisture-stable complexes $[Ln\{HB(C_3N_2H_3)_3\}_2\{O_2C_7H_5\}]$ (Ln = La, Ce, Pr, Nd, Sm, Eu, Tb, Yb, Lu, Y), have been prepared and characterized. The molecular structure of the ytterbium complex reveals a distorted square antiprismatic coordination geometry around the eight-coordinate Yb^{3+} ion. The tropolonate ligand occupies a position which links the two approximately square faces of the coordination polyhedron.

The tripodal ligand hydrotrispyrazol-1-ylborate,[1] L^-, forms homoleptic complexes of formula $[LnL_3]$ (Ln represents a lanthanide element or yttrium) with trivalent lanthanides.[2] The complexes of the smaller lanthanide ions were found to be soluble in organic solvents but those with Ln = La–Gd were not. A structural study of the ytterbium complex[3] has shown that two of the ligands are tridentate while the third is bidentate giving an overall coordination number of eight. The observed coordination geometry was unusual with bicapped trigonal prismatic (BCTP), a dodecahedral (Dod) or square antiprismatic geometry (SAP) usually being preferred.

In a study of heteroleptic complexes containing the $\{LnL_2\}^+$ moiety, we have prepared compounds of the formula $[LnL_2(acac)]$ (acacH = pentane-2,5-dione) which contain a uninegative bidentate co-ligand. Powder X-ray diffraction studies have shown that the complexes $[LnL_2(acac)]$ could, like $[LnL_3]$, by divided into two structural classes. Thus, the group from Ln = La–Dy were structurally distinct from the Ln = Ho–Lu group. The compounds with $X = acac^-$ and Ln = Ce or Yb were structurally characterized by single crystal X-ray diffraction techniques.[4] These studies revealed a substantial distortion of the BCTP geometry in the complex structure on going from Ce^{3+} to the smaller Yb^{3+} ion. Having established the sensitivity of the coordination geometry on metal ion size in the series $[LnL_2(acac)]$, we were interested to investigate the effect of co-ligand chelate ring size on the structure and properties of these systems. We have now prepared a series of complexes using the tropolonate ligand (trop) which can form a five-membered chelate ring in $[LnL_2X]$ as opposed to the six-membered ring formed with X = acac.

The reaction of Ln^{3+} salts with L^- and tropolone (tropH), in water at pH > 7 proceeded smoothly to precipitate $[LnL_2(trop)]$ (Ln = La, Ce, Pr, Nd, Sm, Eu, Tb, Yb, Lu, Y), in high yield.† All the derivatives were air- and moisture-stable and those with Ln = Nd, Sm, Eu, Tb, Yb and Lu were freely soluble in CH_2Cl_2 whilst those of the larger ions, Ln = La, Ce and Pr, were not. Thus in the case of the tropolonate complexes an intermediate situation prevails in that not all the complexes are sol-

* Author to whom correspondence should be addressed.

† All the new compounds have been fully characterized by ^1H NMR, IR and MS. All give satisfactory elemental analyses for C, H and N.

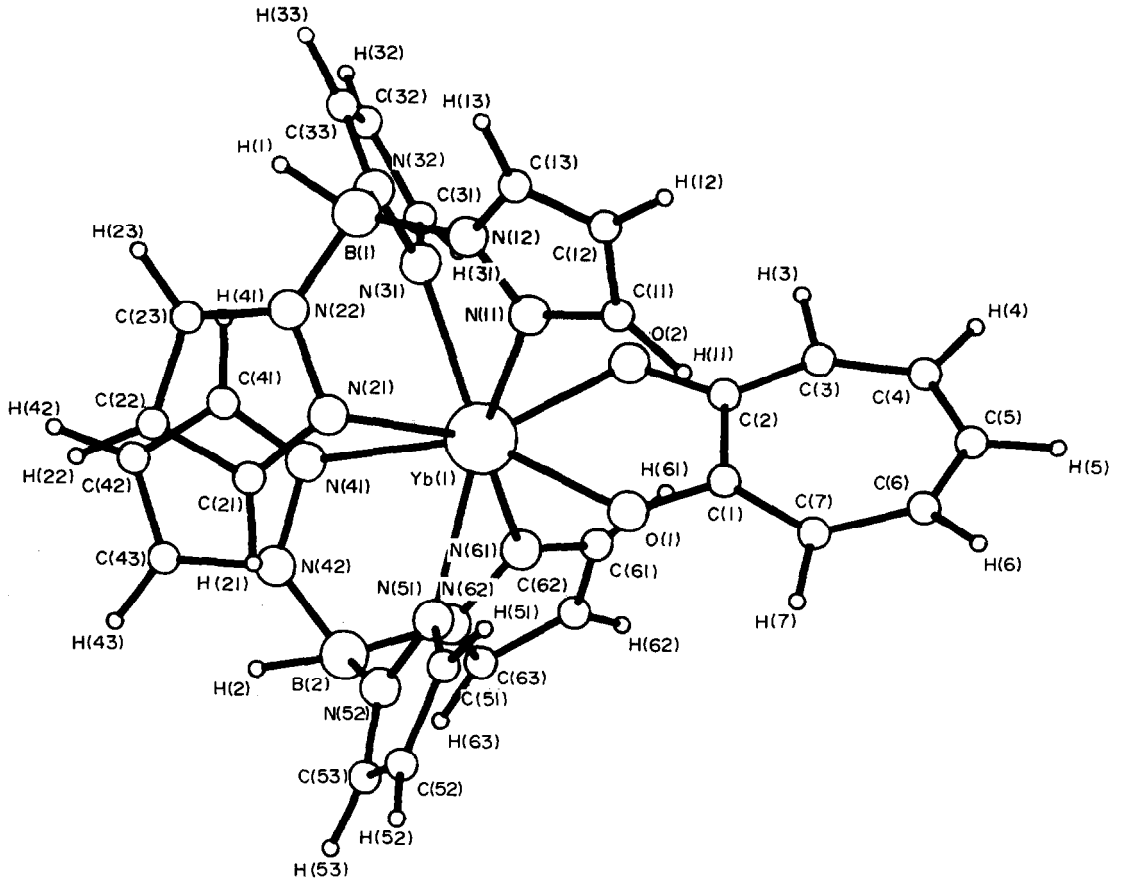

Fig. 1. The molecular structure of $[Yb\{HB(C_3N_2H_3)_3\}_2(C_7H_5O_2)]$ showing the numbering of atoms other than C and H. Selected bond distances and angles: Yb—O(1) 2.222(9), Yb—O(2) 2.267(8), Yb—N(11) 2.501(10), Yb—N(21) 2.482(11), Yb—N(31) 2.425(12), Yb—N(41) 2.548(10), Yb—N(51) 2.439(11), Yb—N(61) 2.474(11); O(1)—Yb—O(2) 69.2(3), N(11)—Yb—N(21) 69.1(3), N(21)—Yb—N(31) 80.5(4), N(31)—Yb—N(11) 74.7(4), N(41)—Yb—N(51) 79.2(4), N(51)—Yb—N(61) 74.3(4), N(61)—Yb—N(41) 73.5(4).

uble in CH_2Cl_2, unlike the $[LnL_2(acac)]$ series (Ln = La–Lu) which are all soluble. However, solubility is maintained over a wider range of cation radius than for the tris complexes, $[LnL_3]$. Like their $[LnL_2(acac)]$ counterparts, the soluble $[LnL_2(trop)]$ complexes were found to be non-rigid on the NMR timescale, only three pyrazolyl proton environments being observed in $CDCl_3$ solution.

In order to structurally characterize a representative of this new series of heteroleptic complexes a single crystal X-ray diffraction study of $[YbL_2(trop)]$ has been carried out.*

$YbL_2(trop)$ is an eight-coordinate monomer as shown in Fig. 1. The coordination geometry is best described as square antiprismatic, although it is on the geometric reaction pathway from SAP to BCTP. Interestingly, the bidentate ligand in $[YbL_3]$ and $[CeL_2(acac)]$ spans one edge of a square, whereas in this structure the tropolonate ligand spans between the two squares. This is, to our knowledge, the first structural characterization of the tropolonate ligand bound to a lanthanide ion.

* *Crystal data.* $C_{25}H_{25}B_2N_{12}O_2Yb$, $M = 720.2$. Orthorhombic, $a = 9.280(2)$, $b = 17.840(8)$, $c = 19.393(2)$ Å, $U = 3211$ Å^3, $Z = 4$, $D_c = 1.48$ g cm^{-3}, space group $P2_12_12_1$ (No. 19), Mo-K_α radiation ($\lambda = 0.7107$ Å, $\mu = 28$ cm^{-1}). Data were collected on a CAD4 diffractometer at the Crystallography Unit, Universities of Aston and Birmingham. 5961 reflections were measured ($2 < 2\theta < 55°$), giving 2813 unique reflections with $I > 2.5\sigma I$ after merging ($R = 0.0434$). The structure was solved using conventional heavy-atom methods on the merged data. In the final stages of full-matrix least-squares refinement, unmerged data were used.

The final model, shown in Fig. 1, refined to $R = 0.0613$ and R_w $\{[\Sigma w(|F_o|-|F_c|)^2]^{1/2}\} = 0.0652$. The refinement of the other enantiomer converged to a model with $R = 0.069$ and $R_w = 0.074$. Atomic coordinates, bond lengths and angles, and thermal parameters have been deposited at the Cambridge Crystallographic Data Centre.

The results described here show that only a small structural change occurs when acac is replaced by trop in $[YbL_2X]$. However, the replacement of acac by trop does have a significant effect on the solubility properties of the heteroleptic $[LnL_2X]$ (X = acac or trop) complexes of the early lanthanides. The replacement of trop by bidentate L similarly has a marked effect on the solubility properties of complexes with the lanthanide ions in the middle of the series. The effect of further reducing the chelate ring size of the co-ligand X in these systems is currently being investigated using carboxylate co-ligands.

Acknowledgements—We are grateful to Dr A. J. Edwards and Prof. W. J. Evans for helpful discussions, to the SERC and B.P. Chemicals International for support to (M.A.J.M.) and to NATO for the provision of travel grant 175/84.

REFERENCES

1. S. Trofimenko, *Prog. Inorg. Chem.* 1986, **34**, 115.
2. K. W. Bagnall, A. C. Tempest, J. Takats and A. P. Masino, *Inorg. Nucl. Chem. Lett.* 1976, **12**, 555.
3. M. V. R. Stainer and J. Takats, *Inorg. Chem.* 1982, **21**, 4050.
4. M. A. J. Moss, C. J. Jones and A. J. Edwards, *Polyhedron* 1987, 7, 79.

Polyhedron Vol. 8, No. 1, pp. 121–122, 1989
Printed in Great Britain

0277–5387/89 $3.00+.00
© 1988 Pergamon Press plc

COMMUNICATION

HYDROGENATION OF ALDEHYDES WITH AN IRIDIUM(I)–PERCHLORATO COMPLEX

CHONG SHIK CHIN,* SUNG CHUL PARK and JUN HO SHIN

Department of Chemistry, Sogang University, CPO Box 1142, Seoul 121-741, Korea

(*Received* 29 *June* 1988; *accepted* 15 *August* 1988)

Abstract—The iridium(I)–perchlorato complex, $Ir(ClO_4)(CO)(PPh_3)_2$ catalyses the hydrogenation of aldehydes to alcohols at 25°C under atmospheric pressure of hydrogen.

While various metal complexes have been reported to show catalytic activities for the hydrogenation of aldehydes and ketones to alcohols,[1–4] catalytic hydrogenation of a carbonyl group with iridium complexes is less well known[5] and no report has been made on the hydrogenation with iridium complexes at room temperature under atmospheric pressure of H_2. In this paper we wish to report the catalytic hydrogenation of aldehydes to the corresponding alcohols in the presence of $Ir(ClO_4)(CO)(PPh_3)_2$ (**1**)[6] at 25°C under atmospheric pressure of H_2.

*Author to whom correspondence should be addressed.

Although no hydrogenation products were detected in the reaction of *trans*-$C_6H_5CH{=}CHCHO$ (**2**) with H_2 in the presence of **1** in neat **2**,[7] $C_6H_5CH_2CH_2CHO$ (**3**) was observed by increasing the concentration of **1** and employing an appropriate amount of solvent at 25°C under atmospheric pressure of H_2; and **3** is further hydrogenated to $C_6H_5CH_2CH_2CH_2OH$ (**4**) when the pressure of H_2 is increased (see Table 1). This observation led us to examine the hydrogenation of aldehydes to alcohols in the presence of **1** (Table 1).

Hydrogenation of more substituted aldehydes is slower than that of less substituted aldehydes and practically no hydrogenation products were

Table 1. Hydrogenation of aldehydes (3.0 mmol) with $Ir(ClO_4)(CO)(PPh_3)_2$ (0.1 mmol) in $CDCl_3$ (2.0 cm^3) at 25°C under hydrogen (P_{H_2} = 1 atm) for 5 h

Substrate	Product	Yield (%)	Remarks
CH_3CHO	CH_3CH_2OH	82	
CH_3CH_2CHO	$CH_3CH_2CH_2OH$	70	
$CH_3(CH_2)_3CHO$	$CH_3(CH_2)_3CH_2OH$	58	
$CH_3CH{=}CHCHO$	$CH_3(CH_2)_2CH_2OH$	22	
	$CH_3(CH_2)_2CHO$	48	
$CH_2{=}C(CH_3)CHO$	$CH_3CH(CH_3)CHO$	63	
$(CH_3)_2CHCHO$			No reaction
C_6H_5CHO	$C_6H_5CH_2OH$	15	
$C_6H_5CH_2CH_2CHO$	$C_6H_5CH_2CH_2CH_2OH$	10	
$C_6H_5CH{=}CHCHO$[a]	$C_6H_5CH_2CH_2CHO$	47	
	$C_6H_5CH_2CH_2CH_2OH$	100	P_{H_2} = 3 atm
	[$C_6H_5CH_2CH_2CHO$	28	P_{H_2} = 3 atm for 3 h
	$C_6H_5CH_2CH_2CH_2OH$]	78	
$(CH_3)_2CO$	$(CH_3)_2CHOH$	1	

[a] Hydrogenation of $C_6H_5CH{=}CHCHO$ was not observed when the concentration of $Ir(ClO_4)(CO)(PPh_3)_2$ was considerably low in neat aldehydes.[7] Also see text.

observed in the reactions of ketones (see Table 1); this fact is readily understood by the steric effect of the substituents on the interaction between the metal and the carbonyl group.

It is already known that complex **1** reacts with **2** and *trans*-$CH_3CH{=}CHCHO$ (**5**) to give $[IrL(CO)(PPh_3)_2]ClO_4$ (L = **2**, **5**) where **2** and **5** are coordinated through the oxygen atom but not through the π-system of the olefinic group, and the reaction of $[IrL(CO)(PPh_3)_2]ClO_4$ with H_2 in the presence of excess **2** or **5** produces only $Ir(H)_2(ClO_4)(CO)(PPh_3)_2$ (**6**).[7] In this study, it has been found that the reaction of **6** with aldehydes under nitrogen produces alcohols, e.g. 0.5 mmol of **6** with 2.5 mmol of C_6H_5CHO in 2.0 cm^3 of $CDCl_3$ under nitrogen at 70°C for 5 h produced 0.2 mmol of $C_6H_5CH_2OH$. Accordingly, a dihydrido(aldehyde)iridium(III) complex (**7**) is suggested as the intermediate for the hydrogenation [see eq. (1)]. A dihydrido metal complex, $LnM(H)_2(O{=}CR_2)$, analogous to **7** was previously suggested as the intermediate in the hydrogenation of carbonyl compounds to alcohols.[8] It should be noted that no iridium complexes of saturated aldehydes have been isolated from the reactions of **1** and saturated aldehydes.

$$Ir(H)_2(ClO_4)(CO)(PPh_3)_2 \xrightarrow{RCHO} \underset{(6)}{} \quad [Ir(H)_2(OCHR)(CO)(PPh_3)_2]ClO_4 \xrightarrow[-RCH_2OH]{H_2} (6). \qquad (1)$$
(7)

Acknowledgements—The authors wish to thank the Korea Science and Engineering Foundation and the Ministry of Education, the Republic of Korea for their support of this study.

REFERENCES

1. D. E. Linn and J. Halpern, *J. Am. Chem. Soc.* 1987, **109**, 2969.
2. Y. Hayashi, S. Komiya, T. Yamamoto and A. Yamamoto, *Chem. Lett.* 1984, 1363.
3. K. Tani, K. Suwa, E. Tanigawa, T. Yoshida, T. Okano and S. Otsuka, *Chem. Lett.* 1982, 261.
4. R. A. Sanchez-Delgado, A. Andriollo, O. L. De Ochoa, T. Suarez and N. Valencia, *J. Organomet. Chem.* 1981, **209**, 77.
5. (a) E. Farnetti, M. Pesce, J. Kaspar, R. Spogliarich and M. Graziani, *J. Mol. Catal.* 1987, **43**, 35; E. Farnetti, M. Pesce, J. Kaspar, R. Spogliarich and M. Graziani, *J. Chem. Soc., Chem. Commun.* 1986, 746; (b) P. Kvintovics, J. Bakos and B. Heil, *J. Mol. Catal.* 1985, **32**, 114; (c) R. Spogliarich, G. Zassinovich, J. Kaspar and M. Graziani, *J. Mol. Catal.* 1982, **16**, 359; (d) G. Zassinovich, C. D. Bianco and G. Mestroni, *J. Organomet. Chem.* 1981, **222**, 323; (e) A. Camus, G. Mestroni and G. Zassinovich, *J. Mol. Catal.* 1979, **6**, 231; (f) W. Stroheimer and H. Steigerwald, *J. Organomet. Chem.* 1977, **129**, C43; (g) R. S. Coffey, *J. Chem. Soc., Chem. Commun.* 1967, 923.
6. J. Peone Jr and L. Vaska, *Angew. Chem. Int. Ed.* 1971, **10**, 511.
7. K. J. Yang and C. S. Chin, *Inorg. Chem.* 1987, **26**, 2732.
8. A. Yamamoto, *Organotransition Metal Chemistry*, p. 369. John Wiley, New York (1986).

Polyhedron Vol. 8, No. 1, pp. 123–125, 1989
Printed in Great Britain

0277-5387/89 $3.00 + .00
© 1988 Pergamon Press plc

COMMUNICATION

OXIDATIVE ADDITION OF 1,4-DIISOPROPYL-1,4-DIAZABUTADIENE TO HEXAKISISOPROPOXYDIMOLYBDENUM (M≡M). $Mo_2(OPr^i)_6(Pr^iNCHCHNPr^i)$ AND $Mo_2(OPr^i)_5(Pr^iNCHCHNPr^i)_2$

MALCOLM H. CHISHOLM,* KIRSTEN FOLTING, JOHN C. HUFFMAN and J. J. KOH

Department of Chemistry and Molecular Structure Center, Indiana University, Bloomington, IN 47405, U.S.A.

(*Received* 22 *August* 1988; *accepted* 22 *August* 1988)

Abstract—Addition of $Pr^iNCHCHNPr^i$ (1 equiv) to hydrocarbon solutions of $Mo_2(OPr^i)_6$ (M≡M) leads to formation of the black crystalline compound $Mo_2(OPr^i)_6(Pr^iNCHCHPr^i)$ (I), which has been shown to contain a reduced diimine ligand (2−) and an oxidized $(Mo{=}Mo)^{8+}$ centre, Mo—Mo = 2.539(2) Å, supported by a pair of bridging OPr^i ligands. The local coordination geometry about each Mo atom corresponds to a distorted tbp and the $Pr^iNCH{=}CHNPr^i$ ligand is chelated to one metal atom through axial and equatorial bonds.

Double bonds between metal atoms are relatively rare in the chemistry of multiple bonds between metal atoms.[1,2] Attempts to synthesize $(M{=}M)^{8+}$ containing compounds by oxidative addition reactions involving $M_2(OR)_6$ compounds have almost invariably led to $(M{-}M)^{10+}$ compounds, e.g. in their reactions with halogens,[3] alkyl- or benzylhalides,[4] *ortho*-quinones[5] and α-diketones.[6] Indeed, only the addition of Pr^iOOPr^i to $Mo_2(OPr^i)_6$ (M≡M) led to the clean conversion of a M—M triple bond to a double bond, eq. (1).[3]

$$Mo_2(OPr^i)_6(M{\equiv}M) + Pr^iOOPr^i \rightarrow Mo_2(OPr^i)_8(M{=}M). \quad (1)$$

We describe here our discovery of the second reaction in which a M—M triple bond is transformed to a double bond, namely, the reaction shown in eq. (2).

$$Mo_2(OPr^i)_6(M{\equiv}M) + Pr^iNCHCHNPr^i \xrightarrow[\text{hexane}]{22^\circ C} Mo_2(OPr^i)_6(Pr^iNCH{=}CHNPr^i). \quad (2)$$

We were intrigued by the notion that Diels–Alder type cyclo-addition reactions might be operative for M—M triple bonds and 1,3-butadienes. When we found that for M = Mo and R = Pr^i there was no apparent reaction with 1,3-butadiene we turned our attention to the reaction between 1,4-diaza-1,3-butadiene recognizing that the formation of Mo—N bonds might be thermodynamically more favourable. 1,4-Diaza-1,3-butadiene ligands (α-diimines), RN=CH—CH=NR, have been shown to exhibit a diverse coordination chemistry.[7]

The addition of $Pr^iNCHCHNPr^i$ (1 equiv) to hydrocarbon solutions of $Mo_2(OPr^i)_6(M{\equiv}M)^8$ leads to an immediate reaction.† Black crystals, $Mo_2(OPr^i)_6(Pr^iNCHCHNPr^i)$ (I) were obtained by cooling the concentrated mother liquor to −15°C. Crystal data for I at −160°C: $a = 9.696(6)$, $b = 19.517(14)$, $c = 19.202(12)$ Å, $\beta = 114.51(2)^\circ$, $Z = 4$, $d_{calc} = 1.375$ g cm^{-3} and space group $P2_1/c$. A total of 5092 reflections were collected using Mo-K_α, $6^\circ \leqslant 2\theta \leqslant 45^\circ$, of which 4362 were unique. The structure was solved by using the 3562 reflections that had $F > 3.0\sigma(F)$ and a combination of direct methods (MULTAN) and Fourier methods leading to the residuals: $R(F) = 0.0359$ and $R_w(F) = 0.0367$. All the hydrogen atoms were located in a difference Fourier, computed after initial

*Author to whom correspondence should be addressed.

†Dry and oxygen free solvents and atmospheres (N_2) were used throughout.

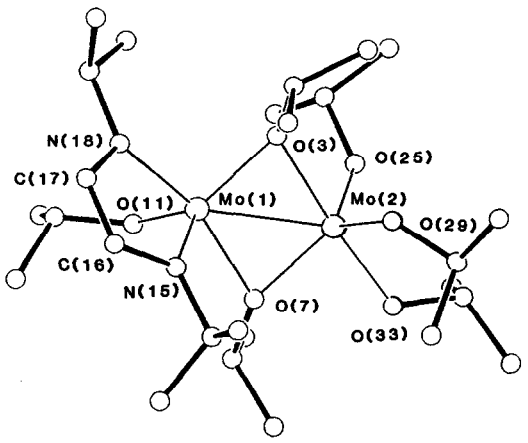

Fig. 1. Ball-and-stick drawing of the $Mo_2(OPr^i)_6(Pr^iNCHCHNPr^i)$ molecule giving the atom numbering scheme used in Table 1.

Table 1. Selected bond distances (Å) and bond angles (°) for the $Mo_2(OPr^i)_6(Pr^iNCHCHNPr^i)$ molecule

A	B	Distance
Mo(1)	Mo(2)	2.5386(18)
Mo(1)	O(3)	1.981(4)
Mo(1)	O(7)	2.097(4)
Mo(1)	O(11)	1.919(3)
Mo(1)	N(15)	1.959(4)
Mo(1)	N(18)	2.078(4)
Mo(2)	O(3)	2.147(4)
Mo(2)	O(7)	1.959(4)
Mo(2)	O(25)	1.887(4)
Mo(2)	O(29)	1.894(4)
Mo(2)	O(33)	1.975(4)
N(15)	C(16)	1.393(7)
N(18)	C(17)	1.355(7)
C(16)	C(17)	1.350(8)

A	B	C	Angle
O(3)	Mo(1)	O(7)	103.89(14)
O(3)	Mo(1)	O(11)	128.86(15)
O(3)	Mo(1)	N(15)	114.22(17)
O(3)	Mo(1)	N(18)	91.31(16)
O(7)	Mo(1)	O(11)	83.25(15)
O(7)	Mo(1)	N(15)	88.12(17)
O(7)	Mo(1)	N(18)	163.37(15)
O(11)	Mo(1)	N(15)	116.61(17)
O(11)	Mo(1)	N(18)	92.51(17)
N(15)	Mo(1)	N(18)	79.40(18)
O(3)	Mo(2)	O(7)	102.86(14)
O(3)	Mo(2)	O(25)	85.94(15)
O(3)	Mo(2)	O(29)	83.84(14)
O(3)	Mo(2)	O(33)	175.25(13)
O(7)	Mo(2)	O(25)	119.67(15)
O(7)	Mo(2)	O(29)	121.83(15)
O(7)	Mo(2)	O(33)	81.86(15)
O(25)	Mo(2)	O(29)	118.42(16)
O(25)	Mo(2)	O(33)	91.29(15)
O(29)	Mo(2)	O(33)	94.12(15)

refinement of the heavy atoms. The refinement was completed using anisotropic thermal parameters on non-hydrogen atoms. A ball-and-stick drawing of the molecule is given in Fig. 1 and selected bond distances and angles in Table 1.*

Compound **I** has a Mo—Mo distance of 2.539(2) Å, closely similar to that seen in $Mo_2(OPr^i)_8$, 2.523(1) Å.[9] The Mo—N distances, 1.959(4) and 2.078(4) Å are much shorter than the N-to-Mo distances in $Mo_2(OPr^i)_6(py)_2$, Mo—N = 2.32(1) Å (av)[10] and are similar to those seen in $Mo(NMe_2)_4$, 1.93(1) Å (av),[11] and $W(NMe_2)_6$, 2.03(1) Å.[12,13] The C(16)—C(17) distance, 1.350(8) Å, is short comparable to the C—C double bond distance in ethylene, 1.34(1) Å.[14] Collectively, the structural data are indicative of a $(Mo{=}Mo)^{8+}$ unit supported by a pair of bridging OPr^i ligands and a reduced, 2−, $Pr^iN{-}CH{=}CH{-}NPr^i$ ligand. The local coordination about each metal atom approximates that of a trigonal bipyramid and the two halves of the molecule share a common axial–equatorial edge. The $Pr^iNCHCHNPr^i$ ligand behaves as a chelate to one metal atom. Presumably this is preferred to spanning the Mo—Mo bond because the formation of a five-membered ring is favoured relative to a six-membered ring.

Compound **I**, like $Mo_2(OPr^i)_8$, is fluxional in solution and reactive. It behaves as a coordinatively unsaturated molecule and even reacts further with $Pr^iNCHCHNPr^i$ to give, by elimination of Pr^iO, a paramagnetic compound $Mo_2(OPr^i)_5(Pr^iNCHCHNPR^i)_2$ (**II**). Based on preliminary structural data compound **II** contains two reduced, 2−, $Pr^iNCH{=}CHNPr^i$, ligands and a central Mo_2^{9+} moiety (Mo—Mo = 2.71 Å) supported by three bridging OPr^i ligands.[15]

The present finding suggests that, by suitable choice of R and R′, reactions between $M_2(OR)_6(M{\equiv}M)$ and R′NCHCHNR′ may afford access to a series of M—M double bonded compounds, $M_2(OR)_6(R'NCH{-}CHNR')$, for both molybdenum and tungsten. Further studies are in progress.

*Atomic coordinates have been deposited with the Director, Cambridge Crystallographic Centre.

Acknowledgement—We thank the National Science Foundation for support.

REFERENCES

1. F. A. Cotton and R. A. Walton, in *Multiple Bonds Between Metal Atoms*. Wiley, New York (1982).
2. L. S. Messerle, *Chem. Rev.* 1988, in press.
3. M. H. Chisholm, J. C. Huffman and C. C. Kirkpatrick, *Inorg. Chem.* 1981, **20**, 871.
4. M. H. Chisholm, J. C. Huffman, A. L. Ratermann and C. A. Smith, *Inorg. Chem.* 1984, **23**, 1596.
5. T. P. Blatchford, M. H. Chisholm and J. C. Huffman, *Inorg. Chem.* 1988, **27**, 2059.
6. M. H. Chisholm, J. C. Huffman and A. L. Ratermann, *Inorg. Chem.* 1983, **22**, 4100.
7. G. Van Koten and K. Vrieze, *Adv. Organomet. Chem.* 1982, **21**, 151.
8. M. H. Chisholm, F. A. Cotton, C. A. Murillo and W. W. Reichert, *Inorg. Chem.* 1977, **16**, 1801.
9. M. H. Chisholm, F. A. Cotton, M. W. Extine and W. W. Reichert, *Inorg. Chem.* 1978, **17**, 2944.
10. M. H. Chisholm, *Polyhedron* 1983, **2**, 681.
11. M. H. Chisholm, F. A. Cotton and M. W. Extine, *Inorg. Chem.* 1978, **11**, 356.
12. D. C. Bradley, M. H. Chisholm, C. E. Heath and M. B. Hursthouse, *Chem. Commun.* 1969, 1261.
13. M. H. Chisholm, F. A. Cotton, M. W. Extine and B. R. Stults, *J. Am. Chem. Soc.* 1976, **98**, 4477.
14. K. Kuchitsu, *MTP Int. Rev. Sci., Phys. Chem. Ser. I* 1972, **11**, 221.
15. M. H. Chisholm, K. Folting, J. C. Huffman and J. J. Koh, results to be published.

Polyhedron Vol. 8, No. 1, pp. 127–128, 1989
Printed in Great Britain

0277–5387/89 $3.00+.00
© 1988 Pergamon Press plc

COMMUNICATION

A DIIRON–DITUNGSTEN CLUSTER SUPPORTED BY CARBONYL AND ALKOXIDE LIGANDS: $Fe_2W_2(OPr^i)_6(CO)_5(py)$

MALCOLM H. CHISHOLM,* JOHN C. HUFFMAN and J. J. KOH

Department of Chemistry and Molecular Structure Center, Indiana University, Bloomington, IN 47405, U.S.A.

(*Received* 22 *August* 1988; *accepted* 22 *August* 1988)

Abstract—From the reaction between $W_2(OPr^i)_6(py)_2(M{\equiv}M)$ and $Fe_2(\mu\text{-}S_2)(CO)_6$ in hexane at room temperature the first heteronuclear mixed alkoxide–carbonyl cluster $Fe_2W_2(\mu_3\text{-}S)_2(OPr^i)_6(CO)_5(py)$ has been obtained and structurally characterized. The central planar distorted rhomboidal Fe_2W_2 unit is capped by $\mu_3\text{-}S^{2-}$ ligands. There are two Fe—W bonds, in addition to Fe—Fe and W—W bonds.

It is now well established that polynuclear metal carbonyl complexes $M_x(CO)_y$ may be attached to metal oxide supports with retention of the essential framework of the M_x cluster and in certain cases catalytic activity of the supported cluster has been studied.[1] In these types of systems the support–cluster interaction is relatively innocent and the advantages that may result are derived from either mechanical considerations (the ease of handling of the catalyst, substrate/separations) or because the life of the catalyst may be enhanced due to the reduction in intermolecular reactions between clusters. There are, however, other types of interactions that can be envisaged between a metal oxide support and a carbonyl cluster that are non-innocent in nature. Two plausible and potentially common modes of reaction involve (i) redox reactions and (ii) the formation of M—M′ bonds between the metal atoms of the carbonyl cluster and those of the support.

Our work with metal alkoxides, whose structures often mimic those found for metal oxides,[2] led us to examine the reactivity between certain molybdenum and tungsten alkoxide clusters and carbonyl clusters of the later transition elements. We describe here our first results in this area, namely the synthesis and the structural characterization of the product formed in the reaction between $W_2(OPr^i)_6(py)_2(M{\equiv}M)$[3] and $Fe_2(\mu\text{-}S_2)(CO)_6$.[4] Our choice of reactants was made on the basis of (i) the well established chemistry of each of the dinuclear compounds, (ii) the obvious potential for a redox-active interaction, (iii) the substitutional lability of $W_2(OPr^i)_6(py)_2$, which dissociates pyridine in solution, and (iv) the fact that dinuclear compounds provide the simplest of clusters upon which to test the hypothesis.

Alkane solutions of $W_2(OPr^i)_6(py)_2$ and $Fe_2(\mu\text{-}S_2)(CO)_6$ (1 : 1 stoichiometry) reacted at room temperature to yield dark solutions from which a black crystalline product was obtained by concentration of the solution and cooling to *ca* −15°C. The crystals were collected by filtration and dried *in vacuo* to yield 35% based on 1 : 1 stoichiometry. The ^1H NMR spectrum revealed the presence of six different OPr^i ligands, together with resonances due to pyridine. The IR spectrum suggested the presence of only terminal CO ligands and the existence of a molecule having little if any symmetry. It was readily apparent that an assignment of molecular structure was not going to be possible based on spectroscopic data and a suitable crystal was selected for an X-ray diffraction study.†

A ball-and-stick drawing of the $Fe_2W_2(OPr^i)_6$

*Author to whom correspondence should be addressed.

†Cell dimensions at −158°C: $a = 19.069(6)$, $b = 9.460(2)$, $c = 24.458(7)$ Å, $\beta = 120.87(1)°$, $Z = 4$, $d_{calc} = 1.959$ g cm^{-3} and space group *Aa*. Of 2732 reflections collected (Mo-K_α, $6° \leqslant 2\theta \leqslant 45°$), 2491 reflections were unique and the 2324 having $F > 3.0\sigma(F)$ were used in the refinement. All non-hydrogen atoms were refined anisotropically. Hydrogen atoms were not located but were included in the final model as idealized fixed atom contributors with d(C—H) = 0.95 Å. Final residuals are $R(F) = 0.041$ and $R_w(F_o) = 0.042$. Listings of programs and general operating procedures have been published.[5] Atomic positional parameters have been deposited with the Director, Cambridge Crystallographic Centre.

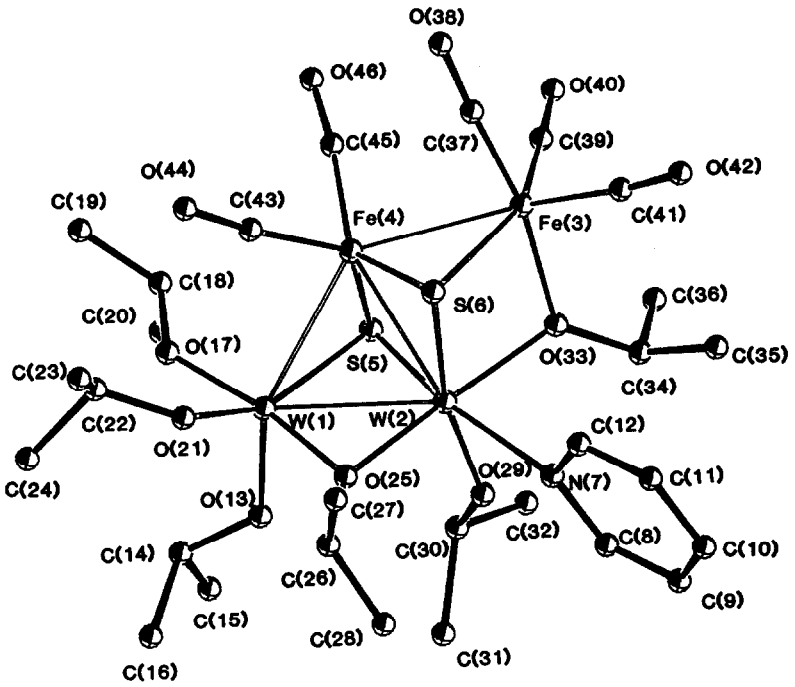

Fig. 1. A ball-and-stick drawing of the $Fe_2W_2(\mu_3\text{-}S)_2(OPr^i)_6(CO)_5(py)$ molecule showing the atom numbering scheme.

$(CO)_5(py)$ molecule is shown in Fig. 1. There is a central planar rhomboidal Fe_2W_2 core with adjacent Fe_2 and W_2 atoms. A μ_3-sulphido ligand caps each W_2Fe and Fe_2W triangle above and below the Fe_2W_2 plane. The formation of $Fe_2W_2(OPr^i)_6(CO)_5(py)$ occurs according to the stoichiometry shown in eq. (1) with the liberation of one equivalent of pyridine and carbon monoxide.

$$W_2(OPr^i)_6(py)_2 + Fe_2(\mu\text{-}S_2)(CO)_6 \rightarrow Fe_2W_2(OPr^i)_6(CO)_5(py) + py + CO. \quad (1)$$

The $(W{\equiv}W)^{6+}$ centre in $W_2(OPr^i)_6(py)_2$ acts as a reducing agent towards the μ-S_2^{2-} ligand in the generation of two S^{2-} ligands which together with loss of CO generate unsaturation at the iron atoms. The latter is compensated for by the formation of (i) an alkoxide bridge to Fe(3) and (ii) M—M bonds between: W(1)—Fe(4) = 2.699(3) and W(2)—Fe(4) = 2.648(4) Å. The W(2) to Fe(3) distance which is spanned by the μ-OPr^i ligand is 3.148(3) Å, a non-bonding distance.

The W—W distance, 2.714(1) Å and the Fe—Fe distance, 2.648(4) Å, are indicative of M—M single bonds.

The product of reaction (1) may be viewed as arising from the following hypothetical reaction pathway. (1) The $(W{\equiv}W)^{6+}$ centre reduces the S_2^{2-} ligand to give $(W{=}W)^{8+}$ and two S^{2-} groups. (2) Loss of CO, formally from Fe(3), generates a carbene-like metal centre that adds across the $(W{=}W)^{8+}$ group to generate a $(W{-}W)^{10+}$ moiety bridged by both sulphur and iron atoms. This results in a pseudo-octahedral geometry about each W atom and the 18-electron rule is satisfied for both Fe atoms as a result of W—Fe, Fe—Fe and Fe–ligand bonding which includes the use of an alkoxide bridge from a neighbouring W centre.

The present finding suggests that reactions between early transition metal alkoxides and later transition metal carbonyl clusters may provide access to a new class of heteronuclear clusters with multi-functional sites for reactivity. Further studies are in progress.

Acknowledgement—We thank the National Science Foundation for support.

REFERENCES

1. J. Evans and B. P. Gracey, *J. Chem. Soc., Chem. Commun.* 1983, 247; S. L. Cook and J. Evans, *J. Chem. Soc., Chem. Commun.* 1983, 713; S. L. Cook, J. Evans and G. N. Greaves, *J. Chem. Soc., Chem. Commun.* 1983, 1287.
2. M. H. Chisholm, *J. Solid State Chem.* 1985, **57**, 120.
3. M. H. Chisholm, *Angew. Chem. Intl. Ed. Engl.* 1986, **25**, 21.
4. D. Seyferth, R. S. Henderson and L-C. Song, *Organometallics* 1982, **1**, 125.
5. M. H. Chisholm, K. Folting, J. C. Huffman and C. C. Kirkpatrick, *Inorg. Chem.* 1984, **23**, 1021.

Polyhedron Vol. 8, No. 1, pp. 129–131, 1989
Printed in Great Britain

0277–5387/89 $3.00+.00
© 1988 Pergamon Press plc

COMMUNICATION

DOUBLE BONDS BETWEEN MOLYBDENUM ATOMS SUPPORTED BY DIMETHYLAMIDO LIGANDS: $Mo_2(NMe_2)_4(OR)_4$ COMPOUNDS, WHERE R = 4-METHYLCYCLOHEXYL AND DIISOPROPYLMETHYL

MALCOLM H. CHISHOLM,* CHARLES E. HAMMOND and JOHN C. HUFFMAN

Department of Chemistry and Molecular Structure Center, Indiana University, Bloomington, IN 47405, U.S.A.

(*Received* 22 *August* 1988; *accepted* 22 *August* 1988)

Abstract—Hydrocarbon solutions of $Mo(NMe_2)_4$ and the alcohols, ROH (2 equiv) (where R = 4-methylcyclohexyl and diisopropyl) react to give compounds of empirical formula $Mo(NMe_2)_2(OR)_2$ which are dimeric both in solution and in the solid-state. The derivative for R = 4-methylcyclohexyl has a crystallographically imposed centre of inversion and a central planar $Mo_2(\mu\text{-}N)_2$ moiety: Mo—Mo = 2.5431(5) Å. The local geometry about each Mo atom corresponds to a distorted trigonal bipyramid and the two halves of the molecule are joined along a common equatorial–axial edge.

Though molybdenum shows a remarkable propensity to form multiple bonds (Mo—Mo), well characterized compounds where $n = 2$ are very rare.[1] We report here our discovery of a new class of Mo≡Mo bonded compounds of formula $Mo_2(NMe_2)_4(OR)_4$ and our structural characterization of one example, namely that where R = 4-methylcyclohexyl.

Molybdenum in its +4 oxidation state forms a series of monomeric compounds of formula MoL_4, where L = NMe_2,[2,3] $P(C_6H_{11}^{cy})_2$,[4] SBu^t[5] and OBu^t.[6] The compounds where L = NMe_2,[3] $P(C_6H_{11}^{cy})_2$[4] and SBu^t[5] are diamagnetic and have been structurally characterized, whereas the *tert*-butoxide, which is not structurally characterized is paramagnetic. The diamagnetism of the MoL_4 compounds (L = NMe_2, $P(C_6H_{11}^{cy})_2$ and SBu^t) can be understood in terms of ligand-to-metal π-bonding. All attempts to attain a suitably crystalline sample of a monomeric $Mo(OR)_4$ compound for an X-ray study have thus far proved unsuccessful. However, during attempts to prepare a monomeric compound of formula $Mo(NMe_2)_{4-x}(OR)_x$ suitable for an X-ray study, we discovered the formation of compounds of empirical formula $Mo(NMe_2)_2(OR)_2$ that were diamagnetic. We show here they are diamagnetic because of Mo—Mo double bond formation.

Hydrocarbon solutions of the highly air-sensitive compound $Mo(NMe_2)_4$ react with ROH (2 equiv), where R = 4-methylcyclohexyl and diisopropylmethyl ($CHPr^i_2$), to give dark solutions from which dark purple–brown crystals can be obtained in *ca* 30–40% yield.

The compound where R = 4-methylcyclohexyl was examined in an X-ray study.[7] (Crystal data at −142°C: $a = 10.083(1)$, $b = 11.623(1)$, $c = 9.637(1)$ Å, $\alpha = 111.10(1)°$, $\beta = 100.53(1)°$, $\gamma = 74.62(1)°$, $Z = 1$, $d_{calc} = 1.349\ g\ cm^{-3}$ and space group $P\bar{1}$. Final residuals are $R(F) = 0.0255$ and $R_w(F) = 0.0279$.]† A ball-and-stick drawing of the centrosymmatic molecule is shown in Fig. 1.

There is a central planar $Mo_2(\mu\text{-}N)_2$ unit with Mo—Mo = 2.5431(5) Å similar to the few other characterized d^2–d^2 $(Mo{=}Mo)^{8+}$-containing compounds.[8] The coordination about each Mo atom

*Author to whom correspondence should be addressed.

†Atomic positional parameters have been deposited with the Director, Cambridge Crystallographic Centre.

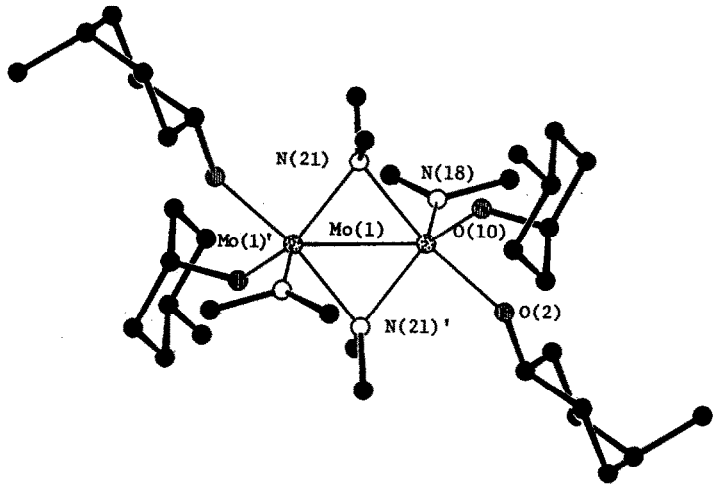

Fig. 1. A ball-and-stick drawing of the centrosymmetric molecule $Mo_2(NMe_2)_4(OC_6H_{10}^{cy}\text{-}4\text{-}Me)_4$ showing the atomic numbering scheme. Selected bond distances (Å) and angles (°) are as follows: Mo—Mo = 2.5431(5), Mo(1)—O(2) = 1.990(2), Mo(1)—O(10) = 1.966(2), Mo(1)—N(18) = 1.919(2), Mo(1)—N(21)′ = 2.096(2), Mo(1)—N(21) = 2.168(2); O(2)—Mo(1)—O(10) = 82.36(7), O(2)—Mo(1)—N(18) = 98.52(8), O(2)—Mo(1)—N(21) = 160.40(8), O(2)—Mo(1)—N(21)′ = 86.70(8), O(10)—Mo(1)—N(18) = 117.67(9), O(10)—Mo(1)—N(21) = 78.27(7), O(10)—Mo(1)—N(21)′ = 141.78(8), N(18)—Mo(1)—N(21) = 93.11(9), N(21)—Mo(1)—N(21)′ = 106.79(7), Mo(1)—N(21)—Mo(1)′ = 73.21(7).

corresponds to a distorted trigonal bipyramid and the two halves of the molecule are joined along a common equatorial–axial edge.

The structure is similar to that seen for $Mo_2(OPr^i)_8$[9] and it is of particular interest to see that in the present structure there is a preference for the NMe_2 groups to bridge rather than the alkoxide ligands. This may result from steric factors that allow the NC_2 blades to occupy the bridging positions with a minimum degree of internal congestion. The terminal NMe_2 ligands occupy equatorial sites with Mo—N distances of 1.92(1) Å comparable to those in monomeric $Mo(NMe_2)_4$, which implies a significant degree of Mo—N double bond character. Also worthy of mention is that the axial bonds (terminal Mo—O and bridging M—N) are longer than their equatorial counterparts—a feature previously seen in $Mo_2(OPr^i)_8$.[9] The structure is similarly related to that of $[Zr(NMe_2)_4]_2$ recently reported in this journal.[10] The Zr-to-Zr distance of 3.704(1) Å in the d^0–d^0 $M_2(\mu\text{-}NMe_2)_2$-containing compound compared to the d^2–d^2 distance, 2.54 Å, in the present compound emphasizes the significance of metal–metal bonding. Indeed, one might well wonder why $Mo(NMe_2)_4$ does not adopt a dinuclear structure $Mo_2(NMe_2)_8$ having a Mo—Mo double bond. Apparently there must be a subtle interplay between maximizing M–N π-bonding and maximizing M—M bonding that favours, in the case of $Mo(NMe_2)_4$, the monomer.

Variable temperature ^1H NMR studies on the $Mo_2(NMe_2)_4(OR)_4$ compounds (R = 4-methylcyclohexyl and diisopropylmethyl) indicate that a dimeric structure is maintained in solution. Specifically there are distinct signals associated with the terminal and bridging NMe_2 ligands even at room temperature. At low temperatures there is evidence for the presence of two isomers which can reasonably be formulated as *syn* and *anti* isomers as shown in Fig. 2. Presumably at higher temperatures a turnstyle operation involving the terminal ligands exchanges the axial–equatorial bonds and leads to *syn* ⇄ *anti* isomerization. Further studies are in progress.

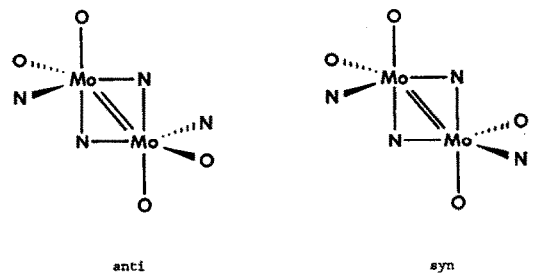

Fig. 2. *Syn* and *anti* isomers of the $Mo_2(NMe_2)_4(OR)_4$ compounds.

Acknowledgement—We thank the National Science Foundation for support.

REFERENCES

1. F. A. Cotton and R. A. Walton, in *Multiple Bonds Between Metal Atoms*. Wiley, New York (1982).
2. D. C. Bradley and M. H. Chisholm, *J. Chem. Soc. A* 1971, 2741.
3. M. H. Chisholm, F. A. Cotton and M. W. Extine, *Inorg. Chem.* 1978, **17**, 2944.
4. R. T. Baker, P. J. Krusic, T. H. Tulip, J. C. Calabrese and S. S. Wreford, *J. Am. Chem. Soc.* 1983, **105**, 6763.
5. S. Otsuka, M. Kamata, K. Hirotsu and T. Higuchi, *J. Am. Chem. Soc.* 1981, **103**, 3011. A related arylthiolato compound $Mo(SC_6H_2\text{-}2,4,6\text{-}Pr^i_3)_4$ has also been structurally characterized and found to be paramagnetic: E. Roland, E. C. Walborsky, J. C. Dewan and R. R. Schrock, *J. Am. Chem. Soc.* 1985, **107**, 5795.
6. M. H. Chisholm, P. Thornton and W. W. Reichert, *J. Am. Chem. Soc.* 1978, **17**, 767.
7. General operating procedures and listings of programs have been reported: M. H. Chisholm, K. Folting, J. C. Huffman and C. C. Kirkpatrick, *Inorg. Chem.* 1984, **23**, 102.
8. M. H. Chisholm, *Polyhedron* 1983, **2**, 681.
9. M. H. Chisholm, F. A. Cotton, M. W. Extine and W. W. Reichert, *Inorg. Chem.* 1978, **17**, 2944.
10. M. H. Chisholm, C. E. Hammond and J. C. Huffman, *Polyhedron* 1988, **7**, 2515.

Polyhedron Vol. 8, No. 1, p. 133, 1989
Pergamon Press plc. Printed in Great Britain

BOOK REVIEW

Gmelin Handbook of Inorganic Chemistry, Pb—organolead Compounds, part 1. Tetramethyllead. Published by Gmelin Institute for Inorganic Chemistry of the Max Planck Society for the Advancement of Science. 8th Edn. Springer, Berlin, 1987. ISBN 3-540-93560-6, XII + 194 pp. DM 896.

Few compounds receive the accolade of having a book devoted to them, but this volume of Gmelin is exclusively about tetramethyllead. Few chemists, even organometallic chemists will have handled it directly, but all will have made indirect use of it because its importance lies in its use as an antiknock agent for internal combustion engines.

Here is indeed all that you ever wanted to know about tetramethyllead; the literature is covered up to the end of 1986.

A compilation of reports and monographs on tetramethyllead, starting in the 1920s and listed chronologically, occupies the first 55 pages. This includes analytical methods, toxicology, applications and environmental aspects.

The preparation of the compound is then covered in 40 pages (which include 638 references). The principal methods are the reaction of a Grignard reagent, or of methyllithium or other methylmetallic compounds with lead(II) chloride, or the reaction of a lead–sodium alloy with methyl chloride, or the electrolysis of methylmagnesium chloride using a sacrificial lead anode.

Methods of analysis, spectroscopy and physical properties are thoroughly covered. there is a thorough treatment (35 pages) of chemical reactions, and sections on physiological properties and toxicity, on uses, and on tetramethyllead in the environment.

The presentation and printing is of Gmelin's usual impeccable standard.

Department of Chemistry
University College London
20 Gordon Street
London WC1 H 0AJ, U.K.

A. G. DAVIES

Polyhedron Vol. 8, No. 2, pp. 135–141, 1989
Printed in Great Britain

0277–5387/89 $3.00+.00
© 1988 Pergamon Press plc

TRANSITION METAL COMPLEXES WITH THE THIOSEMICARBAZIDE-BASED LIGANDS—III. SYNTHESIS, PHYSICO-CHEMICAL PROPERTIES AND VOLTAMMETRIC CHARACTERIZATION OF SOME Fe^{III} COMPLEXES WITH TER- AND QUADRIDENTATE S-METHYLISOTHIOSEMICARBAZIDE DERIVATIVES

VUKADIN M. LEOVAC,† LJILJANA S. JOVANOVIĆ, LUKA J. BJELICA and VALERIJA I. ČEŠLJEVIĆ

Institute of Chemistry, Faculty of Sciences, V.Vlahovića 2, 21000 Novi Sad, Yugoslavia

(*Received* 23 *December* 1987; *accepted* 6 *July* 1988)

Abstract—Several high-spin Fe^{III} complexes of the type $Fe(HL)Cl_2$ and Fe(L)Cl (HL = monoanion of terdentate NNO ligand and L = dianion of quadridentate ONNO ligand, respectively), based on the condensation products of S-methylisothiosemicarbazide and different aromatic 2-hydroxy-aldehydes, have been prepared and characterized by elemental analysis, conductivity and magnetic measurements, IR and electronic spectra, as well as by cyclic voltammetry. For all solid complexes a pentacoordinated structure is proposed, while in DMF solutions hexacoordination is suggested. Differences in some physico-chemical properties, arising from structural changes in the coordinated ligand, are discussed.

In our previous paper[1] we described the synthesis and some physico-chemical and voltammetric characteristics of different types of mono- and bis-(ligand) chelate complexes with the terdentate salicylaldehyde semi-, thiosemi- and S-methyl-lisothiosemicarbazones. Here, we present the analogous data for two novel mono(ligand) Fe^{III} complexes with 5-nitrosalicylaldehyde S-methyl-isothiosemicarbazone (H_2L^1) and 2-hydroxy-1-naphthaldehyde S-methylisothiosemicarbazone (H_2L^2) of general formula $Fe(HL)Cl_2$ (HL = monoanionic form of the terdentate ligand), as well as for several complexes of the type Fe(L)Cl, where L = the dianionic form of quadridentate ligands S-methyl-1,4-bis(arilydene)isothiosemicarbazide, viz.

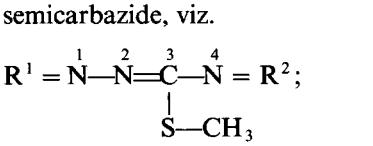

R^1 = salicylidene (H_2L^3)
= 5-chlorosalicylidene (H_2L^4)
= 3,5-dichlorosalicylidene (H_2L^5)
= 3,5-dibromosalicylidene (H_2L^6)
= 5-nitrosalicylidene (H_2L^7)
= 2-hydroxy-1-naphthalidene (H_2L^8)

†Author to whom correspondence should be addressed.

R^1 = salicylidene,
R^2 = 2-hydroxy-1-naphthalidene (H_2L^9).

EXPERIMENTAL

Chemicals and methods

For all syntheses only the Merck $FeCl_3$ or $FeCl_3 \cdot 6H_2O$ reagent grade were used. Other chemicals for syntheses were also of p.a. quality but of a different make.

The voltammetric, conductometric and spectrophotometric measurements were carried out in freshly distilled N,N-dimethylformamide (DMF). The salts used as supporting electrolytes (tetrabutylammonium perchlorate (TBAP) and lithium chloride) were used after recrystallization. The C, H, N analysis procedure and magnetic susceptibility measurements have been described earlier.[2]

The air-dried samples were used for all measurements except voltammetry and spectrophotometry; in the latter case the samples were dried at 110°C.

The apparatus and procedure for conductivity measurements, IR spectrometry, UV–vis. spectrophotometry and voltammetry have been described earlier.[1] In voltammetric experiments a glassy carbon disc served as the working electrode and an aqueous SCE as the reference electrode, and

all potentials were reported against the latter electrode.

Synthesis of ligands

The S-methylisothiosemicarbazones were obtained by the reaction of stoichiometric amounts of a hot aqueous solution of S-methylisothiosemicarbazidehydrogen iodide[3] and an alcoholic solution of the corresponding aldehyde. After neutralization of the mixture with aqueous $Na_2CO_3 \cdot 10H_2O$ solution, the light yellow crystals of the ligands obtained were filtered off and washed with water (to a negative reaction on I^-) and finally with EtOH. Yield: 70–90%.

Synthesis of complexes

$Fe(HL^1)Cl_2$. The mixture of 0.56 g (2 mmol) of H_2L^1 and 0.40 g (2.5 mmol) of $FeCl_3$ (anhydrous) was heated for 5 min with 10 cm^3 of absolute EtOH. The black crystals, formed in the brown solution during 1 h, were filtered off and washed with EtOH and Et_2O. Yield: 0.40 g.

$Fe(HL^2)Cl_2 \cdot 0.5EtOH$. To 30 cm^3 of the hot ethanolic solution of H_2L^2 (0.50 g, 2 mmol) was added 10 cm^3 of ethanolic solution of $FeCl_3 \cdot 6H_2O$ (0.67 g, 2.5 mmol). The obtained mixture was heated for about 5 min to dissolve the ligand completely. The needle-like crystals which formed in the green solution after 10 h of crystallization were filtered off and washed with EtOH and Et_2O. Yield: 0.50 g.

Fe(L)Cl (L = L^3, L^7, L^8, L^9). The mixture of $Fe(HL)Cl_2$ (HL = HL* = monoanion of salicylaldehyde S-methylisothiosemicarbazone or HL^1 or HL^2) (2 mmol) and of the corresponding aldehyde (2.5 mmol) in MeOH (20 cm^3) was heated under reflux for 1–1.5 h. After 5 h, the brown crystals obtained were filtered off and washed with MeOH and Et_2O. Yield: 40–50%.

Fe(L)Cl (L = L^4, L^5, L^6). A mixture of 2 mmol of S-methylisothiosemicarbazone of the corresponding aldehyde, 2.5 mmol of the same aldehyde and 2.5 mmol of $FeCl_3$ (anhydrous) in 10 cm^3 of absolute EtOH was refluxed for 2–3 h. After several hours the precipitated crystals were filtered off and washed with EtOH and Et_2O. Yield: 30–35%.

RESULTS AND DISCUSSION

Syntheses and general characteristics of complexes

The synthesis of $Fe(HL^*)Cl_2$ was accomplished by the reaction of warm ethanolic solutions of Fe^{III} chloride and the ligand.[4] In the same way we prepared the new Fe^{III} complexes with H_2L^1 and H_2L^2, described here. The three complexes served as the basis for the synthesis of the corresponding complexes with quadridentate ligands (H_2L^3, H_2L^7–H_2L^9).

The condensation reaction involving the NH_2 group of the terdentate S-methylisothiosemicarbazone and the C=O aldehyde group of the corresponding aldehyde, carried out in warm methanolic solutions of these complexes, yielded the complex with a quadridentate ONNO ligand (Scheme 1).

Because the other dichloro-(S-methylisothiosemicarbazonato)-ferrum^{III} complexes are hard to crystallize, the corresponding Fe(ONNO)Cl complexes were synthesized by a direct template reaction, i.e. by the reaction of S-methylisothiosemicarbazone and the corresponding aldehyde in the presence of the Fe^{III} ion as template. It was observed that the best results are achieved using anhydrous $FeCl_3$ and absolute ethanol as solvent.

It should be mentioned that this template reaction was first discovered in the synthesis of Ni^{II}, Cu^{II} and VO^{II} complexes, which was carried out in a water–ethanol medium, in the presence of a base (NaOH, KOH or NH_3).[5] The attempts to synthesize some analogous Fe^{III} complexes under the same reaction conditions were unsuccessful. However, using non-aqueous solvents in the presence of different organic bases (pyridine, N,N-dimethylformamide, benzimidazole), Gerbeleu and coworkers.[6] were able to prepare the complexes with H_2L^3, H_2L^4, H_2L^6 and H_2L^7. The crystallization time required was one to several days and the yields were 23–85%. However, we have shown that the Fe^{III} complexes of this type may be obtained in

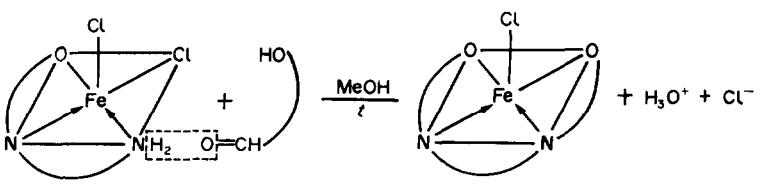

Scheme 1.

Table 1. Some physical characteristics and analytical data for Fe^{III} complexes

Complex	Colour	M.P. (°C)	μ_{eff}^{a} (BM)	λ_M^{b} (Ω^{-1} cm^2 mol^{-1})	Found (Calc.) (%) C	H	N
$Fe(HL^1)Cl_2$	black	> 350	5.83	26.6	28.7 (28.4)	2.6 (2.4)	14.2 (14.7)
$Fe(HL^2)Cl_2 \cdot 0.5EtOH$	black	230[c]	5.89	15.3	41.9 (41.2)	3.8 (3.7)	10.7 (10.3)
$Fe(L^3)Cl$	light brown	305	5.94	7.3	47.7 (47.7)	3.4 (3.2)	10.3 (10.4)
$Fe(L^4)Cl$	dark brown	> 350	5.82	7.3	40.8 (40.8)	2.5 (2.4)	8.8 (8.9)
$Fe(L^5)Cl \cdot 0.5EtOH$	dark brown	310	6.06	5.6	36.5 (36.2)	2.2 (2.2)	7.3 (7.5)
$Fe(L^6)Cl$	dark brown	> 350	5.79	10.3	27.1 (26.8)	1.4 (1.3)	5.7 (5.8)
$Fe(L^7)Cl \cdot 0.5MeOH$	light brown	> 350	5.91	7.3	38.3 (38.9)	2.6 (2.6)	13.6 (13.8)
$Fe(L^8)Cl$	dark brown	343[c]	5.79	7.6	57.0 (57.3)	3.6 (3.4)	8.1 (8.1)
$Fe(L^9)Cl$	dark brown	> 350	5.76	7.6	52.6 (53.1)	3.5 (3.3)	9.5 (9.3)

[a] Measured at 298 K.
[b] In DMF, 1 mmol dm^{-3} solutions at 25°C.
[c] Decomposed.

satisfactory yield in a much shorter time and in the absence of organic bases. This may be achieved either by direct syntheses using $FeCl_3$ (anhydrous), S-methylisothiosemicarbazone of an aldehyde and the corresponding aldehyde in absolute EtOH, or by the reaction of $Fe(HL)Cl_2$ and the corresponding aldehyde in commercial MeOH.†

All the complexes isolated are black or dark brown crystalline substances (Table 1) which are stable up to 300°C. The exception is $Fe(HL^2)Cl_2$ which melts at 255°C.

The complexes are soluble in DMF and Me_2CO but less soluble in MeOH and EtOH. Complexes of the Fe(L)Cl type are also sparingly soluble in Et_2O and $CHCl_3$, whereas the $Fe(HL)Cl_2$ complexes are insoluble in these solvents. None of the complexes are soluble in water.

The effective magnetic moments (Table 1) are characteristic for the high-spin Fe^{III} complexes. This means that the ligands involved belong to the low-strength ligand field group. However, it has been reported[7] that a similar ligand, 3-hydroxy-2-naphthaldehyde thiosemicarbazone, forms a low-spin Fe^{III} complex.

Geometric configuration of complexes

The molecular structures of some representatives of both types of complexes have been already reported. Thus, the X-ray analysis of $Fe(HL)Cl_2$ (HL = monoanion of the terdentate NNO 2-hydroxyacetophenone S-methylisothiosemicarbazone) showed that it has a trigonal bipyramidal configuration involving the chelate ligand and both chloride ions.[8] On the basis of spectral and magnetic measurements, a square pyramidal structure was ascribed to $Fe(HL)Cl_2$ (HL = the monoanion of the terdentate ONS, 3-hydroxy-2-naphthaldehyde thiosemicarbazone).[7] Finally, X-ray analysis showed that $Fe(L^3)Cl$ forms a square pyramid with the chloride atom at the apex.[9]

On taking into account the IR data and the analogy between the above complexes and those described here, it can be concluded that the latter also have a pentacoordination structure. Thus, the IR spectra of all S-methylisothiosemicarbazones contain, in the region 3500–3000 cm^{-1}, three bands viz. a strong high-frequency band at 3450 ± 20, a weak narrow band at 3290 ± 30 and a broad low-

† Various reaction conditions are the cause of differences in composition of the present and previously reported complexes. Therefore, in ref. 6 the complexes $Fe(L^4)Cl$, $Fe(L^6)Cl$ and $Fe(L^7)Cl \cdot 0.5MeOH$ were isolated as crystallosolvates with 0.5DMF, 0.5THF and 1EtOH · 1DMF, respectively.

frequency band of medium intensity at 3100 ± 40 cm^{-1}, corresponding to $\nu_a(NH)$, $\nu_s(NH)$ and $\nu(OH)$, respectively. Furthermore, the $\nu(OH)$ band disappears, which indicates coordination of the deprotonized OH group of the phenolic hydroxyl. On the other hand, the spectrum of $Fe(HL^1)Cl_2$ contains only one broader band (the maximum at 3320 cm^{-1}) which can be ascribed to the $\nu(NH)$ vibrations (in the non-complexed ligand: $\nu_a(NH) = 3440$, $\nu_s(NH) = 3280$ cm^{-1}). The maxima of the $\nu(NH)$ bands in the spectrum of $Fe(HL^2)Cl_2$ are not clearly defined, which may suggest the presence of relatively strong hydrogen bonds. In any case, the position of the $\delta(NH_2)$ band in the spectra of the non-coordinated ligand (1625 cm^{-1}) and its shift of 25 cm^{-1} towards lower energies upon coordination, indicates the involvement of the nitrogen atom of the NH_2 group in the above two complexes. (It should be mentioned that a terdentate NNO character of the H_2L^1 ligand was confirmed by X-ray analysis of its complex with Cu^{II}.[10]) In the IR spectra of the Fe(L)Cl complexes there are no characteristic $\nu(NH)$ bands, which suggests that the condensation reaction of S-methylisothiosemicarbazone and the corresponding ligand took place. Finally, a very strong band from the azomethine group, $\nu(-CH=N-)$, appearing in the spectrum of S-methylisothiosemicarbazone at about 1630 cm^{-1}, is also shifted after coordination towards lower energies by *ca* 35 cm^{-1}.

The molar conductivities (Table 1) of the DMF solutions of both mono- and dichloro complexes are significantly lower than those expected for the 1:1 type of electrolyte in this solvent (65–90 Ω^{-1} mol^{-1} cm^2).[11] Therefore, it is clear that the chloride ions are also involved in coordination. It should be noticed that the conductivity of the solution does not change even after 24 h, which can be referred to the relative strength of the Fe—Cl bond. Another support of the coordination of chloride is the presence of a band of variable intensity at 350 cm^{-1} belonging, most probably, to the $\nu(Fe—Cl)$.[12]

On the basis of all the above, a pentacoordinated structure can be ascribed to all of the complexes isolated. However, none of the two possible coordination polyhedra can be preferentially ascribed to the $Fe(HL)Cl_2$ complexes. On the other hand, all the data indicate that the Fe(L)Cl complexes may have a tetragonal pyramidal structure, with the chelate ligand at the bases and the chlorine atom at the apex. In DMF solution, however, an octahedral structure, which is most common for Fe^{III} complexes, may be formed on account of coordination of a solvent molecule in the other axial position.

Electronic spectra

The electronic spectra of all complexes with quadridentate ligands are generally quite similar (Table 2). One common feature is the absence of absorption bands in the visible region which would correspond to *d–d* transitions. Another characteristic is the appearance of two main bands in the region 20,400–33,300 cm^{-1}. The lower broad band in the 21,700–23,250 cm^{-1} region, which after the addition of an excess of Cl^- (LiCl) shifted by about 500–1000 cm^{-1} towards higher wavelengths, corresponds to the $d–\pi^*$ interactions in the complex. The one or two ill-defined bands around 26,300 cm^{-1} appear at the foot of the main band whose maximum occurs in the range 29,400–33,300 cm^{-1}. On the basis of its position and the corresponding value of ε (30,000–40,000), this band can be ascribed

Table 2. Electronic spectral data for Fe^{III} complexes in DMF

Complex	λ^a_{max} (ε^b)
$Fe(HL^1)Cl_2$	27,780(2.42), 34,250(2.16)
$Fe(HL^2)Cl_2 \cdot 0.5EtOH$	27,550(1.52 sh[c]), 28,490(1.58), 31,750(2.11)
$Fe(L^3)Cl$	22,880(1.04 b.p.[d]), 26,590(1.40 sh), 32,680(2.97)
$Fe(L^4)Cl$	22,170(1.15 b.p.), 24,450(1.13 sh), 26,880(1.35 sh), 32,470(3.10)
$Fe(L^5)Cl \cdot 0.5EtOH$	22,070(1.00 b.p.), 26,380(1.37 sh), 32,050(2.93)
$Fe(L^6)Cl$	22,030(0.98 b.p.), 26,040(1.43 sh), 32,050(3.05)
$Fe(L^7)Cl \cdot 0.5$ MeOH	23,310(1.69 b.p.), 28,330(3.77 b.p.), 30,770(3.92), 32,790(3.67 sh)
$Fe(L^8)Cl$	21,460(1.58 b.p.), 25,060(1.95 sh), 29,150(2.57)
$Fe(L^9)Cl$	21,980(1.43 b.p.), 26,450(1.85 sh), 30,670(2.60)

[a] In cm^{-1}.
[b] In dm^3 mol^{-1} $cm^{-1} \times 10^{-4}$.
[c] Shoulder.
[d] Broad peak.

to the π–π^* interactions of the ligand. An exception is the spectrum of Fe(L^7)Cl which, instead of one, exhibits three strong ill-separated bands. Since the addition of Cl^- (LiCl) causes significant changes (two unequal well separated maxima at 27,470 and 31,540 cm^{-1} are obtained), it can be supposed that the introduction of another Cl^- on coordination induces some changes in the electronic configuration of the ligand containing the *p*-NO_2 group. On the other hand, this region of the spectra for other complexes is not affected by the addition of chloride, which indicates the absence of any significant electronic interaction between the coordinated Cl^- and the organic ligand.

The DMF solutions of the complexes with terdentate ligands absorb very strongly only in the narrow region of 27,000–34,500 cm^{-1}. So, the *d–d* interactions are also excluded. However, because the ligand itself absorbs very strongly in this region, it is not quite clear whether the bands at about 27,700 cm^{-1} belong exclusively to the d–π^* transitions or whether there is an overlap with the π–π^* bands. The bands at $\lambda > 30{,}700$ cm^{-1} belong most probably to the intraligand electronic transitions (π–π^*). Addition of Cl^-(LiCl) produces changes in the whole absorption range, which is a consequence of structural alterations of the complex species in the solution.

Voltammetric studies

Complexes with terdentate ligands. Since the appearance of cyclic voltammograms of these complexes is greatly influenced by the supporting electrolyte, the discussion will be given accordingly.

Perchlorate medium (TBAP): in the presence of an inert supporting electrolyte such as TBAP, several Fe^{III} complex species of different composition may be present in solution. As a result, the cyclic voltammograms contain several ill-separated one-electron peaks representing the reduction of the complex. At about 0.0 V the complex $[FeCl_x(DMF)_y]^{(3-x)+}$ ($x \leqslant 4$, $x+y=6$) is reduced, whereas the peaks at more negative potentials (up to -1.1 V) can be ascribed to the reduction of $[Fe(HL)Cl_x(DMF)_y]^{(2-x)+}$ ($x+y=3$), and $[Fe(HL)_2]^+$. All the reduction peaks have their oxidation counterparts. If, however, the potential limit is set sufficiently negative, a multielectron irreversible reduction of the ligand itself is observed in the region of -2.0 to -2.5 V. In the case of the complex containing the 5-NO_2–salicylaldehyde moiety, the additional reduction peaks observed in the range -1.2 to -1.8 V may be explained by the presence of an electrophilic substituent in the benzene ring.

These complexes can be oxidized in two or three steps in the potential region $+0.5$ to $+1.6$ V. The processes are followed by irreversible chemical reactions of the complex decomposition.

Chloride medium (LiCl): in contrast to the above, the cyclic voltammograms of the complexes in the presence of LiCl exhibit three well-defined one-electron reduction peaks (I–III) and the corresponding oxidation counterparts (I′–III′) (Fig. 1). The voltammetric behaviour of these complexes is quite similar to that of salicylaldehyde S-methylisothiosemicarbazone, whose cyclic voltammogram is given in the inset. Therefore, the same dimeric formula $[Fe(HL)_2][FeCl_4]$[1] can be ascribed to these complexes. Furthermore, one HL^- in the $[Fe(HL)_2]^+$ can be replaced by three Cl^- ions, so that the species reacting at the potentials of peaks I and II are $[FeCl_4]^-$ and $[Fe(HL)Cl_3]^-$, respectively; peak III represents the reduction of $[FeL_2]^-$, formed by a specific chemical reaction after the reduction at peak II.[13]

General voltammetric characteristics of these complexes are presented in Table 3. As evident from its potentials, the I/I′ couple represents a quasi-reversible process with no chemical complications. The controlled-potential electrolysis at peak I gives 1 mole of electrons per mole of reactant taken as the dimer. Another mole of electrons is consumed in the reduction at peaks II and III, half of it at each potential. This result confirms the specific nature of the chemical reaction by which $[Fe(HL)Cl_3]^-$ is transformed into $[FeL_2]^-$.[13] The $\Delta E/\Delta \log v$ slope of -30 to -50 mV, observed at low sweep rates,

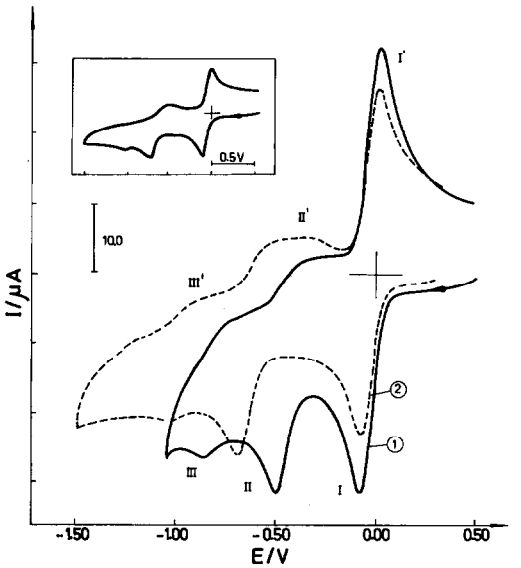

Fig. 1. Cyclic voltammograms for Fe(HL^1)Cl_2 (**1**) and Fe(HL^2)Cl_2 (**2**) (inset: Fe(HL*)Cl_2); 0.1 mol dm^{-3} LiCl GC electrode, 0.20 V s^{-1}.

Table 3. Cyclic voltammetry data for $Fe(HL)Cl_2$ complexes in 0.1 mol dm^{-3} LiCl on a glassy carbon electrode

Ligand	v^a	$E^b_{p(I)}$	$E_{p(I')}$	$E_{p(II)}$	$E_{p(II')}$	$E_{p(III)}$	$\frac{I^c_{p(I)}}{cv^{1/2}}$	$\frac{I_{p(II)}}{cv^{1/2}}$	$\frac{i_{p(III)}}{cv^{1/2}}$
H_2L*	0.02	−0.06	0.00	−0.67	i.d.[d]	−1.03	67.8	37.0	8.0
	0.20	−0.07	0.00	−0.73	−0.50	−1.04	62.3	38.5	4.0
H_2L^1	0.02	−0.06	0.00	−0.45	−0.34	−0.84	67.8	30.1	9.5
	0.20	−0.07	0.00	−0.50	−0.33	−0.86	64.0	36.8	8.9
H_2L^2	0.02	−0.06	0.00	−0.64	i.d.	−1.00	59.1	38.5	11.0
	0.20	−0.07	0.01	−0.68	~ −0.55	−1.02	59.5	38.7	8.7

[a] In V s^{-1}.
[b] In V vs SCE. Letters in parentheses denote the corresponding peak.
[c] In μA $mmol^{-1}$ dm^3 $V^{-1/2}$ $s^{1/2}$, the concentration calculated for the dimer.
[d] Ill-defined peak.

is also support of the presence of an irreversible chemical reaction. It should be noticed that the difference in current function of peak I and the sum of current functions of peaks II and III may be mainly the consequence of different diffusion coefficients of the reacting species.

The potentials of peaks II and III do not practically depend on the nature of the ligand containing an unsubstituted aldehyde. On the other hand, the introduction of an electrophilic substituent (p-NO_2) into the benzene ring makes the electron transfer much easier (the potentials of both peaks are more positive by about 200 mV).

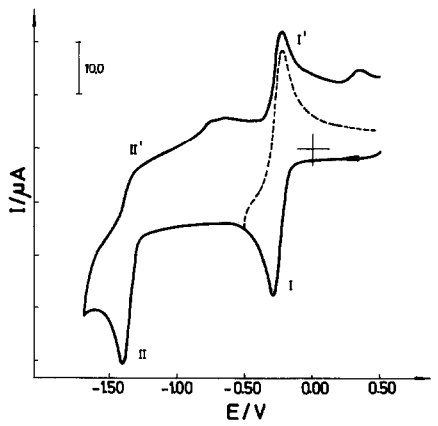

Fig. 2. Cyclic voltammograms for $Fe(L^3)Cl$; 0.1 mol dm^{-3} LiCl. GC electrode, 0.20 V s^{-1}.

Complexes with quadridentate ligands. Unlike those described above, these complexes generally exhibit the same voltammetric behaviour in both the electrolytes used.[14] [Fe(L)Cl(DMF)], the main complex species in the presence of TBAP, is transformed into $[Fe(L)Cl_2]^-$ when Cl^- is present in excess in the solution. As a result, the corresponding peak potentials are about 50 mV more negative.

Chloride medium (LiCl): all the complexes are reduced in two one-electron processes (peaks I and II; peaks I′ and II′ being the oxidation counterparts) as shown in Fig. 2.

The process (I/I′) has the characteristics of a quasi-reversible electron transfer, accompanied by a slow irreversible chemical reaction of first order (the $\Delta E/\Delta \log v$ is about −20 to −30 mV at $v < 0.10$ V s^{-1}). The ratio $I_{p(I')}/I_{p(I)} \approx 1$ at $v \geqslant 0.02$ V s^{-1} is obtained for all complexes with the exception of $Fe(L^5)Cl$ and $Fe(L^7)Cl$. In the voltammograms of these complexes, and especially that of $Fe(L^7)Cl$, an increase in the sweep rate produces a slight decrease of $I_{p(I)}$, an increase of the half-peak width, and an increase of the slope $\Delta E/\Delta \log v$ to −60 mV. At the same time, peak I′ exhibits no complications. Since this behaviour is not observed in the presence of TBAP, the kinetic complications may be ascribed to the Cl^- introduced into the other axial position in the complex. Obviously, a stable electronic configuration, after the electronation of a species containing two strong electrophilic groups (—NO_2) at the *para* position with respect to the phenolic oxygen, i.e. the Fe^{III} central atom, and in the presence of Cl^- at both axial positions, can be obtained only after reorganization of the molecule. Hence, at low sweep rates, the kinetic complications are apparently not reflected on the recorded curve.

The reduction at peak II is a quasi-reversible process followed by a fast irreversible chemical reaction of second-order. Peak II′ normally appears at $v > 1$ V s^{-1} and increases with increasing v until the ratio $I_{p(II')}/I_{p(II)}$ approaches unity. At the same time the peak shifts in the positive direction with $\Delta E/\Delta \log v \approx 10$ mV. The irreversible chemical reaction following the reduction of the complex is probably the complex decomposition giving rise to

Table 4. Cyclic voltammetry data for Fe(L)Cl complexes in 0.1 mol dm^{-3} LiCl on a glassy carbon electrode ($v = 0.20$ V s^{-1})

Ligand	$E^a_{p(I)}$	$E_{p(I')}$	$E_{p(II)}$	$\frac{I^b_{p(I)}}{cv^{1/2}}$	$\frac{I_{p(II)}}{cv^{1/2}}$	$\frac{I_{p(I')}}{I_{p(I)}}$
H_2L^3	−0.28	−0.21	−1.40	52.9	51.6	1.05
H_2L^4	−0.25	−0.17	−1.28	45.4	46.7	1.02
H_2L^5	−0.19	−0.10	−1.16	36.0	42.5	1.09
H_2L^6	−0.17	−0.09	−1.15	39.9	40.6	1.09
H_2L^7	−0.20	−0.06	−1.10[c]	35.8	~41[c]	1.15
H_2L^8	−0.23	−0.16	−1.46	47.1	46.6	0.95
H_2L^9	−0.26	−0.19	−1.43	50.4	52.2	1.02

[a] In V vs SCE. Letters in parentheses denote the corresponding peak.
[b] In μA $mmol^{-1}$ dm^3 $V^{-1/2}$ $s^{1/2}$.
[c] This peak overlapped with the ligand reduction peak.

several peaks at more positive potentials than peak II′. After the two-electron electrolysis (either directly at peak II, or stepwise at peak I and II), the complex cannot be reoxidized because of a strong blocking of the GC electrode by complex decomposition products.

Some voltammetric characteristics of the complexes are presented in Table 4. The differences in peak potentials for different complexes indicate that the introduction of an electrophilic substituent into the benzene ring facilitates transfer of the first, and especially of the second electron, thus suggesting that the reduction of the complex is predominantly of the ligand type.

Acknowledgement—The authors thank the Scientific Fund of SAP Vojvodina for financial support of the present work.

REFERENCES

1. V. M. Leovec, L. Bjelica and Lj. Jovanović, *Polyhedron* 1985, **4**, 233.
2. V. M. Leovac, V. Divjaković, D. Petrović, Gy. Argai and A. Kálmán, *Polyhedron* 1983, **2**, 1307.
3. M. Freund and T. Paradies, *Ber. Deut. Chem. Ges.* 1901, **34**, 3113.
4. N. V. Gerbeleu, K. I. Turte, V. D. Canić, V. M. Leovac and V. B. Arion, *Koord. Khim.* 1980, **6**, 446.
5. N. V. Gerbeleu, *Reaktsii na Matritsakh.* Shtiintsa, Kishinev (1980).
6. S. G. Shova, M. A. Yampol'skaya, B. G. Zemskov, N. V. Gerbeleu, K. I. Turte and I. N. Ivleva, *Zhur. Neorg. Khim.* 1985, **30**, 2309.
7. Y. K. Bhoon, *Polyhedron* 1983, **2**, 365.
8. M. A. Yampol'skaya, S. G. Shova, Yu. A. Simonov, N. V. Gerbeleu, K. I. Turte and V. E. Zavodnik, *Zhur. Neorg. Khim.* 1985, **30**, 1221.
9. M. A. Yampol'skaya, S. G. Shova, N. V. Gerbeleu, V. K. Bel'skii and Yu. A. Simonov, *Zhur. Neorg. Khim.* 1982, **27**, 2551.
10. V. Divjaković and A. Petrović, *5th Italian–Yugoslav Cryst. Cong.* C43. Padova, Italy (1986).
11. W. J. Geary, *Coord. Chem. Rev.* 1971, **7**, 81.
12. K. Nakamoto, *Infrared and Raman Spectra of Inorganic and Coordination Compounds* (4th edn). Wiley-Interscience, New York (1986).
13. L. Bjelica and Lj. Jovanović, *J. Electroanal. Chem.* 1986, **213**, 85.
14. L. Bjelica, Lj. Jovanović and N. Ević, *10th Yugoslav Symp. Electrochem.*, pp. 303–305. Bečići (1987).

Polyhedron Vol. 8, No. 2, pp. 143–147, 1989
Printed in Great Britain

0277–5387/89 $3.00+.00
© 1988 Pergamon Press plc

ORGANOAMIDOMETALLICS—III.* 2,6-DIMETHYLPYRIDINE AND 1,4-DIOXAN AS WEAKLY COORDINATING POLAR SOLVENTS FOR DECARBOXYLATION SYNTHESES OF N,N-DIMETHYL-N′-(POLYFLUOROPHENYL)ETHANE-1,2-DIAMINATO(1−)PLATINUM(II) COMPLEXES

D. P. BUXTON and G. B. DEACON†

Chemistry Department, Monash University, Clayton, Victoria, 3168, Australia

and

D. ST. C. BLACK

School of Chemistry, University of New South Wales, Kensington, New South Wales 2033, Australia

(*Received* 7 *June* 1988; *accepted* 6 *July* 1988)

Abstract—The complexes, $Pt[N(p\text{-}HC_6F_4)CH_2CH_2NMe_2]X(L)$ (X = Cl, L = Ph_3P; X = I, L = pyrazine) have been prepared by reaction of PtX_2(dmen) (dmen = N,N-dimethylethane-1,2-diamine) with $TlO_2CC_6F_4H$-*p*, C_6F_5H and L in hot 2,6-dimethylpyridine (dmpy), and are considered to have L *trans* to —NMe_2. The pyrazine complex was also obtained in very low yield from an analogous synthesis in 1,4-dioxan. Reaction of $PtBr_2$(dmen) with $TlO_2CC_6F_4H$-*p* and C_6F_5H in 2,6-dimethylpyridine without an added ligand gave a low yield of $Pt[N(p\text{-}HC_6F_4)CH_2CH_2NMe_2](O_2CC_6F_4H\text{-}p)$(dmpy).

The decarboxylation reaction of $PtCl_2$(en) (en = ethane-1,2-diamine) with thallous pentafluorobenzoate in pyridine unexpectedly yields the diorganoamidoplatinum(II) complex, $Pt[N(p\text{-}HC_6F_4)CH_2]_2(py)_2$,[2,3] rather than $Pt(C_6F_5)_2$(en) [cf. the decarboxylation synthesis of $Pt(C_6F_5)_2$(2,2′-bipyridyl)[4]]. Analogous complexes, $Pt[NRCH_2]_2(py)_2$ (e.g. R = C_6F_5, *p*-BrC_6F_4, 2,3,5-$F_3C_6H_2$) have been prepared by reaction of $PtCl_2$(en) with thallous 2,3,5,6-tetrafluorobenzoate and an appropriate fluorocarbon, RF.[3] These syntheses can be extended to give N,N-dimethyl-N′-polyfluorophenylethane-1,2-diaminato(1−)platinum(II) complexes $Pt[NRCH_2CH_2NMe_2]X(py)$ (X = Cl, Br or I; e.g. R = *p*-HC_6F_4, C_6F_5 or *p*-ClC_6F_4) by reacting PtX_2(dmen) (dmen = N,N-dimethylethane-1,2-diamine) with thallous pentafluorobenzoate (for R = *p*-HC_6F_4) or with thallous 2,3,5,6-tetrafluorobenzoate and the appropriate fluorocarbon RF in pyridine.[1,5] Besides providing a new route to organoamidometallics, the reactions yield ethane-1,2-diaminatoplatinum(II) complexes which are moisture stable in contrast with the behaviour of simpler complexes, e.g. $Pt(NHCH_2CH_2NH_2)_2$.[6] Up to this stage, a limitation of the CO_2 elimination syntheses is that the neutral ligand, L, in the organoamidometallic products $Pt[NRCH_2]_2L_2$ and $Pt[NRCH_2CH_2NMe_2]X(L)$ is restricted to solvents suitable as decarboxylation media, viz. pyridine and some substituted pyridines.[1–3,5] In an attempt to overcome this, we have examined decarboxylation reactions in 2,6-dimethylpyridine (which has steric inhibition of coordination) and 1,4-dioxan (oxy donors give less stable Pt complexes) in the presence of added ligands.

RESULTS AND DISCUSSION

Reaction of PtX_2(dmen) with thallous 2,3,5,6-tetrafluorobenzoate and pentafluorobenzene in the presence of triphenylphosphine (X = Cl) or pyrazine (pyz) (X = I) in 2,6-dimethylpyridine (dmpy)

* For part II, see ref. 1.

†Author to whom correspondence should be addressed.

resulted in substantial decarboxylation and the formation of the organoamidoplatinum(II) complexes, **1a** and **1b** in low yield.

$$PtX_2(dmen) + TlO_2CC_6F_4H\text{-}p + C_6F_5H + 2L \text{ (or } L + dmpy) \rightarrow TlX + p\text{-}H_2C_6F_4 + CO_2 + LHF \text{ (or dmpyHF)} + Pt[N(p\text{-}HC_6F_4)CH_2CH_2NMe_2]X(L) \quad (1)$$

1a X = Cl; L = Ph_3P

1b X = I; L = pyz.

Extensive purification of the products was needed (see Experimental) and this was a major cause of the low yields (see also ref. 3). An attempt to carry out reaction (1) (L = pyz, X = I) in 1,4-dioxan resulted in much less decarboxylation than in 2,6-dimethylpyridine and gave a very low yield of **1b**. The complex [Pt(dmen)pyz($O_2CC_6F_4H$-*p*)]I was obtained in substantial yield (although in only very low yield after purification), reflecting the incomplete decarboxylation. Thus, use of sterically hindered or weakly donating ligands enables the synthesis of $Pt[N(R)CH_2CH_2NMe_2]X(L)$ complexes where L ≠ decarboxylation solvent.

The decarboxylation reaction of $PtBr_2$(dmen) with thallous 2,3,5,6-tetrafluorobenzoate and pentafluorobenzene in 2,6-dimethylpyridine without an added ligand gave less carbon dioxide than reaction (1) and a very low yield of an impure organoamidoplatinum complex, **2**.

$$PtBr_2(dmen) + 2TlO_2CC_6F_4H\text{-}p + C_6F_5H + 2dmpy \rightarrow 2TlBr + CO_2 + p\text{-}H_2C_6F_4 + dmpyHF + Pt[N(p\text{-}HC_6F_4)CH_2CH_2NMe_2] \quad (2)$$

(2) $(O_2CC_6F_4H\text{-}p)(dmpy)$. (2)

The formation of **2** rather than $Pt[N(p\text{-}HC_6F_4)CH_2CH_2NMe_2]Br(dmpy)$ (**1c**) is surprising in view of the use of a 1 : 1 mole ratio of platinum complex : thallium salt and the outcome of (1) and similar reactions (see Introduction) in pyridine and other substituted pyridines.[1,5] Since decarboxylation is incomplete (41%), substantial unreacted thallous 2,3,5,6-tetrafluorobenzoate is available to convert **1c** into **2**.

The constitution of **1a** and **1b** as organoamidoplatinum(II) complexes follows from the observation of parent ions in their mass spectra (Experimental), the absence of ν(NH) IR absorption or N*H* proton resonances and ^{19}F NMR resonances similar to those of other 2,3,5,6-tetrafluorophenylethane-1,2-diaminato(1— or 2—)platinum(II) complexes, e.g. $Pt[N(p\text{-}HC_6F_4)CH_2CH_2NMe_2]X(py)$ [X = Cl (**1d**) or I (**1e**)][1] or $Pt[N(p\text{-}HC_6F_4)CH_2]_2(py)_2$.[3] Both **1a** and **1b** have intense IR absorption characteristic (see examples in refs 1,3,4,7) of ν(CF) of a *p*-HC_6F_4 group. There are two possible isomers (**A** or **B**) for $Pt[N(R)CH_2CH_2NMe_2]X(L)$ complexes.

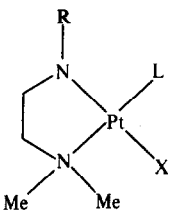

A

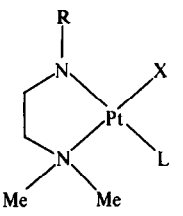

B

Crystal structures of **1d** and $Pt[N(C_6F_5)CH_2CH_2NMe_2]I_{0.63}Cl_{0.37}(py)$[1] and unit cell data for $Pt[N(C_6F_5)CH_2CH_2NMe_2]I(py)$[1] (**1f**) show that these complexes have structure **A**. Other reported $Pt[N(R)CH_2CH_2NMe_2]X(L)$ complexes have spectroscopic data, particularly ^3J(PtH) coupling constants, similar to those of crystallographically characterized compounds and are also considered to have structure **A**.[1] Complex **1b** has $^3J[PtH(NMe_2)]$ and ^3J[PtH(pyz)] coupling constants and a ν(PtI) frequency (Experimental) similar to those of **1e** (30, 38 Hz, and 171 cm^{-1}, respectively) and **1f** (31, 38 Hz, and 164 cm^{-1}, respectively), hence structure **A** (R = *p*-HC_6F_4, X = I, L = pyz) is likely. Recently, a second isomer (hence structure **B**) of $Pt[N(p\text{-}HC_6F_4)CH_2CH_2NMe_2]Cl(py)$ has been isolated and has $^3J[PtH(NMe_2)]$ of 38 Hz and ^3J[PtH(py)] of 26 Hz.[8] For **1a**, the $^3J[PtH(NMe_2)]$ coupling constant (20 Hz) is much smaller than those (av. 31 Hz) of **1b** and **1d–f**,[1] indicating[9,10] that the ligand *trans* to NMe_2 has a stronger *trans* influence than pyridine or pyrazine and hence[9] is triphenylphosphine rather than chlorine. Furthermore, ^4J(HP) coupling is observed for the N*Me*$_2$ and C*H*$_2$NMe$_2$ resonances and not the C*H*$_2$N(*p*-HC_6F_4) resonance. Since coupling of hydrogen to *trans* phosphorus donor atoms is usually larger than to *cis* donor atoms,[11] structure **A** (R = *p*-HC_6F_4, L = Ph_3P, X = Cl) rather than **B** is indicated. In addition, ν(Pt—Cl) of **1a** is in good agreement with that (313 cm^{-1})[1] of **1d**, and ^3J[PtH(C*H*$_2$NR)] is near the average value (32 Hz) observed for reported complexes with structure **A**.

Identification of **2**, which was not obtained pure, is based on observation of a parent ion in the mass spectrum, and detection, assisted by substituent chemical shift data,[1,3,12] of the dmpy, *p*-$HC_6F_4CO_2$, and N(*p*-HC_6F_4)$CH_2CH_2NMe_2$ ligands by ^1H and ^{19}F NMR spectroscopy (Experimental). A pair of IR bands at 950 and 940 cm^{-1} is attributable to ν(CF)

of the two p-HC_6F_4 groups, whilst the separation (311 cm^{-1}) between the $\nu(CO_2)$ frequencies (Experimental) is much greater than that (205 cm^{-1})[13] of sodium 2,3,5,6-tetrafluorobenzoate, indicative[14] of unidentate carboxylate coordination. Of the PtH coupling constants useful in structural diagnosis, only ^3J[PtH(CH_2NMe_2)] of 31 Hz could be resolved. This is slightly larger than the average (27 Hz) for several compounds with structure **A**,[1] but it is still probably more consistent with 2,6-dimethylpyridine rather than carboxyl (weak *trans* influence[9]) *trans* to CH_2NMe_2. For the complex Pt(dmen)(pyz)(p-$HC_6F_4CO_2$)I (obtained from the preparation of **1b** in dioxan), PtH coupling establishes coordination of the neutral ligands and the separation (245 cm^{-1}) between the $\nu(CO_2)$ frequencies suggests unidentate carboxylate coordination. Thus, iodide is probably ionic, although there are examples of ionic polyfluorobenzoates with separations somewhat greater than those of the corresponding sodium salts.[4,15] The ^3J[PtH(NMe_2)] and ^3J[PtH(pyz)] coupling constants (Experimental) are consistent with pyrazine *trans* to NMe_2.

The ease of the decarboxylation reactions (1) and (2) increases with added ligands (L) in the sequence L = none < pyz < Ph_3P. On the basis of the proposed reaction path for other decarboxylation syntheses of organoamidoplatinum(II) complexes,[1-3] reactions (1) and (2) probably involves initial formation of [Pt(dmen)L_2]X($O_2CC_6F_4H$-p) (L = dmpy, pyz or Ph_3P) (**3**), decarboxylation with hydrogen abstraction from the NH_2 group giving [Pt($NHCH_2CH_2NMe_2$)L_2]X (**4**), nucleophilic attack of the amido nitrogen of **4** on C_6F_5H giving [Pt[N(p-HC_6F_4)$CH_2CH_2NMe_2$]L_2]X, and, for reaction (1), displacement of L *trans* to the amido nitrogen by halide ions giving **1a** and **1b**. The extent of formation of **3** in a pre-rate determining equilibrium depends on the nucleophilicity of L (dmpy- < pyz < Ph_3P towards Pt).[16] Isolation of [Pt(dmen)(pyz)($O_2CC_6F_4H$-p)]I from the synthesis of **1b** in dioxan indicates incomplete formation of **3** (L = pyz, X = I), inhibiting the rate of decarboxylation.

EXPERIMENTAL

General

Microanalyses were carried out by the Australian Microanalytical Service, Melbourne. Carbon dioxide was determined gravimetrically as barium carbonate. Decarboxylation was monitored using a small volume barium hydroxide trap additional to the main trap, and reactions were terminated when carbon dioxide evolution slowed significantly. Spectroscopic methods are given in Part I.[3] Listed IR bands of Nujol and hexachlorobutadiene mulls are restricted to those of medium or greater intensity for the region 4000–650 cm^{-1}, except for platinum–halogen stretching frequencies. Proton chemical shifts are in ppm downfield from internal Me_4Si, and ^{19}F chemical shifts in ppm upfield of internal $CFCl_3$. The solvent was $(CD_3)_2CO$ unless indicated otherwise. Listed mass spectra are restricted to ions above m/z 300, the base peak being m/z 58, $C_3H_8N^+$, in all cases. For platinum-containing ions, only the most intense peak [containing ^{195}Pt or ^{231}(PtCl)] is given for each cluster which showed the correct isotope pattern. Visible spectra are for ethanol solutions in the range 350–700 nm.

Solvents and reagents

2,6-Dimethylpyridine (EGA) was refluxed over and distilled from potassium hydroxide pellets, refluxed over aluminium trichloride (14 g/150 cm^3) for 3 h and then distilled, and finally refluxed over $BF_3 \cdot OEt_2$ (4 cm^3/120 cm^3) followed by distillation and storage under nitrogen. Other solvents were purified as described previously.[1,3] Polyfluoroaromatics were from Bristol Organics, pyrazine from EGA, and triphenylphosphine from BDH. Preparations of thallous 2,3,5,6-tetrafluorobenzoate[17] and dihalogeno(N,N-dimethylethane-1,2-diamine)platinum(II) complexes[1] have been given. Nitrogen was purified by passage through a BASF R3/11 catalyst and molecular sieves.

Decarboxylation reactions in 2,6-dimethylpyridine or 1,4-dioxan

2,6-Dimethylpyridine (or dioxan) was added by syringe to the solid reagents in a Schlenk flask which had been purged with nitrogen. Pentafluorobenzene was then added. The reaction mixture was heated under nitrogen which was passed into a barium hydroxide trap. After reaction, the reaction mixture was evaporated to dryness under vacuum (10^{-3} mm), and the residue was washed with petrol (usually b.p. 60–85°C) to remove traces of solvent and extracted with acetone or ether. The solution was filtered to remove thallous halide and evaporated to dryness. Subsequent purification is given below.

Attempted synthesis of bromo(2,6-dimethylpyridine)[N,N - dimethyl - N′ - (2,3,5,6 - tetrafluorophenyl)ethane - 1,2 - diaminato(1−)]platinum(II). Dibromo(N,N-dimethylethane-1,2-diamine)platinum(II) (0.80 mmol), thallous 2,3,5,6-tetrafluorobenzoate (0.80 mmol) and pentafluorobenzene (45 mmol) in 2,6-dime-

thylpyridine (10 cm^3) were heated at 100–115°C for 1 h giving carbon dioxide (41%). The solid from acetone extraction was washed with petrol (b.p. 60–85°C) and extracted with ether. Addition of petrol and evaporation gave a few yellow crystals of 2,6-dimethylpyridine[N,N - dimethyl - N′ - (2,3,5,6 - tetrafluorophenyl)ethane - 1,2 - diaminato(1−)] (2,3,5,6 - tetrafluorobenzoato)platinum(II) (**2**) (3%). ^{19}F NMR: −139.7, m, 2F, F3,5 ($HC_6F_4CO_2$); −144.1, m, 2F, F2,6 ($HC_6F_4CO_2$): −144.7, m, 2F, F3,5 (HC_6F_4N); −150.6, m, 2F, F2,6 (HC_6F_4N). ^1H NMR: 2.62, t, ^3J(HH) 5 Hz, with satellites ^3J(PtH) 31 Hz, 2H, CH_2NMe_2; 3.00, s, 8H, Me_2N and $CH_2N(C_6F_4H)$; 3.29, s, 6H, Me (dmpy); 6.39, tt, ^3J(HF) 11 Hz, ^4J(HF) 7 Hz, 1H, HC_6F_4N; 7.10, d, ^3J(HH) 8 Hz, 2H, H3,5 (dmpy); 7.37, tt, ^3J(HF) 10 Hz, ^4J(HF) 7 Hz, 1H, $HC_6F_4CO_2$; 7.56, t, ^3J(HH) 8Hz, 1H, H4 (dmpy). Some weak impurity resonances were also present. IR: 1655s and 1640s [$\nu_{as}(CO_2)$], 1610s, 1584m, 1494vs, 1460s, 1336vs [$\nu_s(CO_2)$], 1178s, 1168s, 1133s, 1075m, 1063m, 950s, 940s, 896m, 850m, 800m, 773s and 718s cm^{-1}. Mass spectrum: *m/z* 730 [5%, M^+]; 623 [1, $(M—dmpy)^+$]; 536 [1, $(M—HC_6F_4CO_2H)^+$]; 534 [1, $Pt(C_{10}H_8F_4N_2)dmpy^+$]; 495 [2, $Pt(HC_6F_4CO_2)dmpy^+$]; 478 [2, $Pt(C_7H_2F_4N)dmpy^+$]; 427 [3, $Pt(C_{10}H_8F_4N_2)^+$]; 359 [1, $Pt(HC_6F_4NH_x)^+$]; 344 [1, $Pt(HC_6F_4)^+$], 301 [3, $Pt(C_7H_8N)^+$]. The ether insoluble residue contained a substantial amount of the products, and the ^{19}F NMR spectrum showed five different *p*-HC_6F_4 groups to be present.

b - *Chloro* - c(N),d(N′) - [N,N - *dimethyl* - N′ - (2,3,5,6 - *tetrafluorophenyl)ethane* - 1,2 - *diaminato* (1−)]-a-*triphenylphosphineplatinum*(II) (**1a**).

Dichloro(N,N - dimethylethane - 1,2 - diamine)platinum(II) (1.0 mmol), thallous 2,3,5,6-tetrafluorobenzoate (1.0 mmol), pentafluorobenzene (18.0 mmol) and triphenylphosphine (2.0 mmol) in 2,6-dimethylpyridine (10 cm^3) were heated at 115°C for 20 min giving carbon dioxide (95%). The solid from ether extraction was recrystallized from ether–petrol (b.p. < 40°C) and twice from toluene–petrol at −28°C giving yellow crystals (15%), m.p. 207–208°C (Found: C, 46.5; H, 3.6; F, 10.5; N, 3.8. $C_{28}H_{26}ClF_4N_2PPt$ requires C, 46.2; H, 3.6; F, 10.4; N, 3.9%.) ^{19}F NMR: −144.6, m, 2F, F3,5; −150.5, m, 2F, F2,6. ^1H NMR: 2.39, m, ^3J(HH) 5 Hz, ^4J(HP) 2 Hz, 2H, CH_2NMe_2; 3.01, d, ^4J(HP) 3 Hz, with satellites ^3J(PtH) 20 Hz, 6H, NMe_2; 3.34, t, ^3J(HH) 5 Hz, with satellites ^3J(PtH) 35 Hz, 2H, $CH_2N(C_6F_4H)$; 6.11, tt, ^3J(HF) 11 Hz, ^4J(HF) 7 Hz, 1H, HC_6F_4; 7.29–7.43, m, 9H, H3,4,5 (Ph_3P); 7.62–7.69, m, 6H, H2,6 (Ph_3P). Visible spectrum: 424 nm (ε = 570). IR: 3050m, 2945m, 2928m, 1627m, 1585m, 1489vs, 1468m, 1451s, 1435s, 1421m, 1264m, 1169m, 1160m, 1101s, 1094vs, 1021m, 998s, 939m, 926s, 886m, 817m, 780m, 744s, 706s, 697vs, 691vs, 312s [ν(PtCl)] cm^{-1}. Mass spectrum: *m/z* 728 [4%, M^+]; 514 [1, $Pt(C_{21}H_{22}NP)^+$]; 456 [1, $Pt(C_{18}H_{14}P)^+$]; 378 [1, $Pt(C_{12}H_8P)^+$].

c(N),d(N′)-[N,N-*Dimethyl*-N′-(2,3,5,6-*tetrafluorophenyl)ethane* - 1,2 - *diaminato*(1−)] - b - *iodo* - a - *pyrazineplatinum*(II) (**1b**).

(i) *In* 2,6-*dimethylpyridine*: diiodo(N,N-dimethylethane-1,2-diamine)platinum(II) (1.0 mmol), thallous 2,3,5,6-tetrafluorobenzoate (1.0 mmol), pyrazine (5.0 mmol) and pentafluorobenzene (18.0 mmol) in 2,6-dimethylpyridine (10 cm^3) were heated at 105–110°C for 1 h giving carbon dioxide (72%). The solid from acetone extraction was washed with ethanol (5 cm^3) to remove dark impurities. Ether extraction, filtration, evaporation to dryness, and recrystallization from ether/petrol (b.p. 60–85°C) gave an orange solid, which was dissolved in pyridine (2 cm^3) and precipitated by the addition of water.* After vigorous shaking, the precipitate was collected and recrystallized from ether–petrol (b.p. < 40°C) at 0°C, yield 10%, m.p. 176°C (Found: C, 26.1; H, 2.3; F, 12.0; N, 9.2. $C_{14}H_{15}F_4IN_4Pt$ requires C, 26.4; H, 2.4; F, 11.9; N, 8.8%.) ^{19}F NMR ($CDCl_3$): −142.9, m, 2F, F3,5; −150.6, m, 2F, F2,6. ^1H NMR ($CDCl_3$): 2.51, t, ^3J(HH) 5 Hz, 2H, CH_2NMe_2; 3.20, s with satellites ^3J(PtH) 32 Hz, 6H, NMe_2; 3.26, m, 2H, $CH_2N(C_6F_4H)$; 6.25, tt, ^3J(HF) 10 Hz, ^4J(HF) 7 Hz, 1H, HC_6F_4; 8.27, dd, ^3J(HH) 3 Hz, 2H, H3,5 (pyz); 8.58, d, ^3J(HH) 3 Hz with satellites ^3J(PtH) 41 Hz, 2H, H2,6 (pyz). Visible spectrum: 416 nm ($\varepsilon = 1.8 \times 10^3$). IR: 1634m, 1576m, 1493vs, 1461vs, 1450vs, 1419s, 1278m, 1152m, 1128m, 1053m, 935vs, 888m, 810m, 171w [ν(PtI)] cm^{-1}. Mass spectrum: *m/z* 637 [0.7%, M^+]; 557 [0.3, $(M—pyz)^+$]; 430 [0.3, $(M—pyz—I)^+$]; 427 [0.2, $Pt(C_{10}H_8F_4N_2)^+$].

(ii) *In* 1,4-*dioxan*: similar amounts of the first three reagents from (i) and pentafluorobenzene (45 mmol) in dioxan (10 cm^3) were heated at 100°C for 1.5 h giving carbon dioxide (37%). The product from acetone extraction was similarly extracted with ether and the resulting solid recrystallized from a minimum of ether at 0°C giving **1b** (3%), m.p. 170°C (dec.) (Found: C, 26.7; H, 2.4; F, 12.1; N, 8.8%) with spectroscopic properties in agreement with those from synthesis (i). The dark ether-insoluble residue was washed with tetrahydrofuran (20

* Dissolution in pyridine converts any $(pyz)_2PtI_2$ or $(dmpy)_2PtI_2$ into water-soluble $[py_4Pt]I_2$.

cm^3) and recrystallized from acetone–petrol (65–80°C) with activated charcoal to give white (N,N-dimethylethanc-1,2-diamine)pyrazine(2,3,5,6-tetrafluorobenzoato)platinum(II) iodide (4% cf. *ca* 50% prior to recrystallization), m.p. > 230°C (dec.) (Found: C, 26.8; H, 2.2; N, 7.6. $C_{15}H_{17}F_4IN_4O_2Pt$ requires C, 26.4; H, 2.5; N, 8.2%.) ^{19}F NMR: −140.6, m, 2F, F3,5; −144.6, m, 2F, F2,6. ^1H NMR: 3.00, br s (PtH satellites incompletely resolved), 4H, CH_2; 3.19, s, with satellites ^3J(PtH) 32 Hz, 6H, NMe_2; 7.22, tt, ^3J(HF) 10 Hz, ^4J(HF) 7 Hz, 1H, HC_6F_4; 7.34, br s, 2H, NH_2; 8.69, m, 2H, H3,5 (pyz); 9.16, m with satellites ^3J(PtH) 37 Hz, 2H, H2,6 (pyz). IR: 3068m, 1608 and 1602vs [$\nu_{as}(CO_2)$], 1490vs, 1419m, 1360s [$\nu_s(CO_2)$], 1335m, 1237m, 1171m, 1017m, 942s, 841m, 819m, 783m, 756s, 713m cm^{-1}. No platinum containing ions were observed in the mass spectrum. The presence of iodine was established by qualitative tests.

Acknowledgements—This work was carried out during the tenure of a grant from the Anti-Cancer Council of Victoria. This support, that of the Australian Research Grants Scheme, and a loan of platinum from Johnson Matthey, are gratefully acknowledged.

REFERENCES

1. D. P. Buxton, G. B. Deacon, B. M. Gatehouse, I. L. Grayson and D. St. C. Black, *Aust. J. Chem.* 1988, **41**, 943.
2. G. B. Deacon, B. M. Gatehouse and I. L. Grayson, *Polyhedron* 1984, **3**, 753.
3. D. P. Buxton, G. B. Deacon, B. M. Gatehouse, I. L. Grayson, R. J. Thomson and D. St. C. Black, *Aust. J. Chem.* 1986, **39**, 2013.
4. G. B. Deacon and I. L. Grayson, *Transition Met. Chem.* 1982, **7**, 97.
5. D. P. Buxton, G. B. Deacon, B. M. Gatehouse, I. L. Grayson and P. J. Wright, *Acta Cryst.* 1985, **C41**, 1049.
6. G. W. Watt, R. E. McCarley and J. W. Dawes, *J. Am. Chem. Soc.* 1957, **79**, 5163.
7. R. J. Phillips and G. B. Deacon, *Aust. J. Chem.* 1979, **32**, 2381; G. B. Deacon and D. G. Vince, *Aust. J. Chem.* 1975, **28**, 1931; H. B. Albrecht and G. B. Deacon, *Aust. J. Chem.* 1972, **25**, 57.
8. G. B. Deacon, A. M. James and S. J. Knowles, unpublished data.
9. T. G. Appleton, H. C. Clark and L. E. Manzer, *Coord. Chem. Rev.* 1973, **10**, 335.
10. M. H. Chisholm, H. C. Clark, L. E. Manzer and J. B. Stothers, *J. Am. Chem. Soc.* 1972, **94**, 5087.
11. J. P. Collman, F. D. Vastine and W. R. Roper, *J. Am. Chem. Soc.* 1968, **90**, 2282.
12. M. I. Bruce, *J. Chem. Soc. A* 1968, 1459.
13. G. B. Deacon and R. J. Phillips, *Aust. J. Chem.* 1978, **31**, 1709.
14. G. B. Deacon and R. J. Phillips, *Coord. Chem. Rev.* 1980, **35**, 227.
15. P. G. Cookson and G. B. Deacon, *Aust. J. Chem.* 1972, **25**, 2095.
16. F. A. Cotton and G. Wilkinson, *Advanced Inorganic Chemistry*, 4th edn, p. 1199. John Wiley, New York (1980).
17. G. B. Deacon, S. J. Faulks and J. M. Miller, *Transition Met. Chem.* 1980, **5**, 305.

Polyhedron Vol. 8, No. 2, pp. 149–155, 1989
Printed in Great Britain

0277–5387/89 $3.00+.00
© 1988 Pergamon Press plc

FORMATION OF GOETHITE FROM FERRIHYDRITE AT PHYSIOLOGICAL pH UNDER THE INFLUENCE OF CYSTEINE

R. M. CORNELL* and W. SCHNEIDER

Laboratorium für anorganische Chemie, ETH-Zentrum, CH-8092 Zürich, Switzerland

(*Received* 11 *March* 1988; *accepted* 13 *July* 1988)

Abstract—The presence of L-cysteine at L-cysteine: Fe ratios $\geqslant 0.2$ causes ferrihydrite ($5Fe_2O_3 \cdot 9H_2O$) to transform rapidly to goethite [α-FeO(OH)] in the pH range 7.5–9 and at temperatures between 25–70°C. L-Cysteine is the first example of an organic ligand that directly promotes the formation of goethite; all organic ligands studied previously, suppressed the transformation of ferrihydrite to goethite.

L-Cysteine is a reducing ligand which exhibits associative interactions with interfacial iron sites of ferrihydrite. It appears to act by converting these sites to more labile sites thus facilitating the transformation to goethite, possibly in conjuction with enhanced dissolution of ferrihydrite.

The presence of phosphate or silicate species stabilized ferrihydrite and reduced the goethite promoting effect of cysteine.

The implications of these results for biomineralization of iron oxides is considered. It is suggested that the crystals of goethite found in the teeth of limpets (*Patella vulgata*) may have formed via activated reorganization of ferrihydrite, rather than by oxidatively induced hydrolysis of a ferrous precursor.

Ferrihydrite is a poorly ordered ferric oxyhydroxide which with time transforms into the thermodynamically more stable crystalline compounds, goethite [α-FeO(OH)] and haematite (α-Fe_2O_3). These oxides form by separate pathways.[1,2] Formation of goethite involves dissolution of ferrihydrite followed by reprecipitation of goethite in solution, whereas haematite arises via a solid state transformation within the particles of ferrihydrite. As these mechanisms are competitive, reaction conditions that promote haematite are unfavourable for goethite formation and *vice versa*. At pH 7–8 the solubility of ferrihydrite is at a minimum and supersaturation with respect to goethite is very low. In this pH range precipitation of goethite is slow enough for haematite to be the predominant transformation product.

Foreign ions can determine which reaction pathway predominates and investigations of the various effects of different ions have provided interesting details of the transformation mechanisms. The influence of organic ligands such as carboxylic and hydroxy carboxylic acids[3,4] and also simple sugars[5] has been studied intensively. One reason for this interest is that these ligands possess the same functional groups as those found in the organic matrix in which bioinorganic goethite is precipitated and thus might shed some light on the mechanisms by which biomineralization is achieved. All organic ligands studied to date suppressed formation of goethite from ferrihydrite and in some cases, actively promoted haematite formation.[6] These results appeared to suggest that biomineralization of goethite could not involve a ferrihydrite precursor.

Recently, we extended our investigations to another organic ligand, L-cysteine. This ligand is of interest because it is a powerful reducing agent and so might be expected to promote dissolution of ferrihydrite at physiological pH.

We report here the complete and rapid transformation of ferrihydrite to goethite at pH 7.5–8.5 in the presence of L-cysteine. This is the first example of an organic ligand that promotes the formation of goethite from ferrihydrite. Two specific aims of this investigation were (1) to determine the

*Author to whom correspondence should be addressed.

effect of various levels of cysteine on the kinetics and the products of the reaction and (2) to consider whether cysteine could overcome the stabilizing effect on ferrihydrite of ions such as silicate and phosphate. A further aim was to consider the significance of these results for the biomineralization of goethite.

EXPERIMENTAL

Ferrihydrite was precipitated from ferric nitrate solution with 1 M KOH and the pH adjusted to between 7.5–8.5 with bicarbonate buffer solution. Enough L-cysteine to give a final concentration of between 10^{-3}–10^{-1} M (L : Fe = 0.1–10) was then added to the freshly precipitated ferrihydrite; most experiments were carried out using 2×10^{-3} M cysteine. As cysteine is readily oxidized, a fresh stock solution was prepared just before each experiment. The suspensions (1 g ferrihydrite/dm^3) were held in closed polypropylene bottles and aged in the dark (to avoid photochemical decomposition of cysteine) for up to 48 h. Several suspensions were aged at 25 or 40°C, but the majority were held at 70°C to facilitate comparison with earlier studies. No attempt to exclude air was made as the main aim of this work was to investigate the effect of cysteine on the transformation under standard conditions. Additional experiments were performed in which L-cysteine was replaced by D-penicillamine, cysteamine or glycine. In a further series of experiments, phosphate or silicate, as well as cysteine were added to the system. All chemicals were analytical grade (Fluka).

The kinetics of the reaction were followed by taking subsamples during the reaction and dissolving unconverted ferrihydrite using a 30 min extraction with 0.4 M HCl. The acid–oxalate extraction method of Schwertmann[7] could not be used in the present work because the combination of cysteine and oxalate led to complete reductive dissolution of all the solid phases (including goethite) in the system. Preliminary experiments showed that the acid treatment adopted provided a satisfactory separation of the crystalline and amorphous iron hydroxides. The extent of the transformation was expressed as the ratio, Fe_A/Fe_T, where Fe_A is the acid soluble material (i.e. unconverted ferrihydrite) and Fe_T is the total iron in the system. Analysis for Fe was carried out using atomic absorption spectroscopy (AAS).

The crystalline product of the transformation was washed and dried at 50°C. X-ray powder diffraction (XRD) patterns were obtained using a Guinier–Enraf camera (Mk IV) with Fe-K_{α_1} radiation. Where the reaction product consisted of a mixture of goethite and haematite, the proportion of each was estimated by comparison with a series of standards made by mixing known amounts of synthetic goethite and haematite. The 110 and 111 XRD lines of goethite and the 102 peak of haematite were used for comparison.

Transmission electron micrographs were obtained using a Hitachi H-600 electron microscope operating at 100 kV. For TEM examination the samples were dispersed in twice distilled water with ultrasonic treatment and a drop of suspension evaporated to dryness on a carbon coated bronze grid. Elemental analysis for C, N, H and S was carried out by the microanalytical department.

The interaction between cysteine and iron oxides was followed using pulse polarography (Polaroid E 506 metrohm polarograph). Suspensions of cysteine and either ferrihydrite or goethite (0.1 g/100 cm^3, pH 8) were equilibrated for 1 min, 2 or 24 h at 25°C, centrifuged and the level of cysteine in the supernatant liquid found by polarography. Standard solutions of cysteine (pH 8) were also prepared for calibration purposes: the cysteine peak was observed at −0.51 V. Goethite (BET surface area 70 m^2 g^{-1}) was prepared by ageing ferrihydrite at pH 12.5 and 70°C for 48 h.

RESULTS AND DISCUSSION

Reaction products

These depended on the ratio of cysteine to iron in the system (Table 1). In the absence of cysteine (control system), ferrihydrite transformed entirely to haematite in the pH range 7–9. Addition of 10^{-3} M cysteine (L : Fe = 0.1) led to a product which XRD showed to consist only of haematite. TEM, however, indicated the presence of some tiny crystals of goethite (1–2%). Seeding the system with 6% goethite raised the amount of goethite in the product to around 30%, whereas seeding the control system did not promote goethite formation.

Doubling the concentration of cysteine in the

Table 1. Effect of cysteine concentration on the transformation products of ferrihydrite, pH 8, 70°C, 24 h

L : Fe	Product
0	Haematite
0.1	Haematite + trace goethite
0.2	Goethite
0.4	Goethite
1.0	Goethite
10.0	Cystine + 10 Å phase

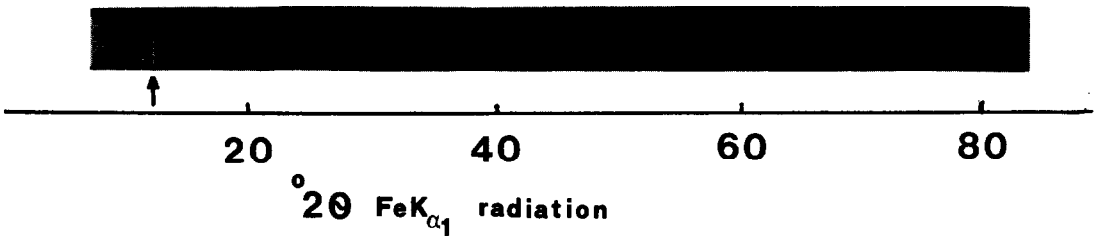

Fig. 1. X-ray powder diffraction pattern of the 10 Å intermediate formed at cysteine: Fe = 10.0. The arrow indicates the 10 Å XRD line.

system (L : Fe = 0.2) caused ferrihydrite to transform entirely to goethite in a few hours at both 70 and 40°C. At room temperature the transformation took 48 h. With higher levels of cysteine (up to 10^{-2} M), goethite was again the only solid end product. The organic end product (cystine) remained in the supernatant liquid.

A large excess of cysteine (L : Fe = 10) led to the formation, within 24 h, of a mixture of cysteine and a dark iron compound. The latter compound was washed, dried and X-rayed. It gave a well-defined, reproducible XRD pattern with a characteristic line at 10 Å (Fig. 1). This XRD pattern did not correspond to that of any previously recorded iron oxide or hydroxide. However, elemental analysis of the compound showed that it was not an iron–cysteine compound such as Fe^{II}cysteine$(H_2O)_{1.5}$ or $Na_2Fe^{II}(cysteine)_2H_2O$ reported by other workers.[8] Less than 2% C, N or S was present: probably some organic material was adsorbed on the surface of the precipitate. This compound (henceforth referred to as the 10 Å phase) may be a mixed valence Fe hydroxide. Its identification is not a major issue as the emphasis in the present investigation is on the formation of goethite at much lower cysteine: Fe ratios (0.2) at which this compound does not form.

Progress of the transformation

Upon addition of 2×10^{-3} M cysteine the ferrihydrite darkened, probably as a result of formation of a mixed valence Fe^{II}–Fe^{III} surface. XRD analysis of subsamples taken at intervals during the transformation showed that for a system with L : Fe = 0.2, the only crystalline phase present was goethite. TEM examination of subsamples showed a mixture of goethite crystals and an amorphous phase. Goethite formed as acicular crystals around 3000 Å in length. These crystals had poorly developed terminal faces, probably as a result of interference in growth by adsorbed ligand.

The stage during the transformation at which cysteine was added determined the proportion of goethite in the reaction product (Table 2). Addition of 2×10^{-3} M cysteine at increasingly later stages after precipitation led to an increase in haematite formation at the expense of goethite. Addition of cysteine to ferrihydrite that had been aged (pH 8) at 70°C for 4 h produced no goethite. The ferrihydrite was still X-ray amorphous and completely oxalate soluble. Nevertheless, the structural rearrangement foreshadowing haematite nucleation must have been underway already, producing a more structured, more stable material. Addition of a high enough level of cysteine to this structured material led to formation of some goethite (Table 2).

Table 2. Effect on the reaction product of stage of addition of cysteine to ferrihydrite, pH 8, 70°C

[Cysteine] (M)	Time of ageing before cysteine addition (h)	Product
2×10^{-3}	0	Goethite
	1	Goethite
	2	Haematite + 10% goethite
	4	Haematite
4×10^{-3}	2	Goethite + 10% haematite
	4	Goethite + 50% haematite

Kinetics

The transformation of ferrihydrite into crystalline goethite was complete at 70°C and with $0.2 \leqslant L : Fe \leqslant 1.0$ within 10 h. Typical plots of the extent of transformation vs time are shown in Fig. 2. These kinetic curves consisted of an initial induction period followed by a faster transformation stage and are similar to those observed for transformations carried out at pH 12 in the absence of cysteine.[9]

With 10^{-3} M cysteine in the system the transformation was retarded to some extent. The lowest

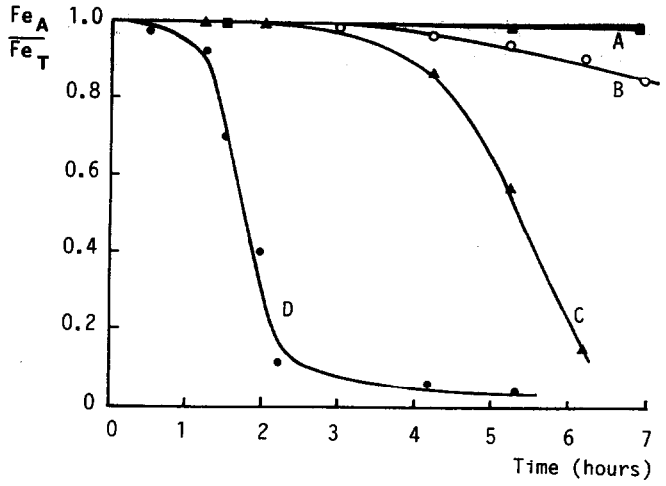

Fig. 2. Fe_A/Fe_T as a measure of the degree of transformation of ferrihydrite into goethite vs time: (A) control, (B) with 10^{-3} M cysteine, (C) with 10^{-2} M cysteine and (D) with 2×10^{-3} M cysteine; pH 8, 70°C. Fe_A = acid extractable iron, Fe_T = total iron in the system.

level of cysteine needed to effect complete transformation into goethite (2×10^{-3} M) markedly accelerated the overall transformation by reducing the induction period from 4–5 h to 30 min. The induction period is the time needed to increase the supersaturation with respect to goethite above the critical level needed for formation of nuclei.[9] Once this had been achieved, the transformation proceeded at a rate of 10^{-2} min^{-1}. This is an order of magnitude higher than the rate constant for the transformation (in the absence of cysteine) at pH 12, indicating that cysteine has accelerated the overall reaction. As the level of cysteine increased from 2×10^{-3} to 10^{-2} M, the induction period gradually increased and the rate of the subsequent transformation decreased (Fig. 2).

At 40°C (physiological temperature) and with 2×10^{-3} M cysteine, the transformation was complete within 7 h. Experiments at 25, 40 and 70°C showed that the transformation had an activation energy of 30.1 KJ mol^{-1}.

Interaction of cysteine with iron oxides

After contact with ferrihydrite at pH 8 and 25°C for 1 min, a solution of cysteine showed polarographic peaks at −0.51, −0.63 and −0.94 V. The two latter peaks are due to the presence of cystine[10] and were missing from solutions of cysteine to which ferrihydrite had not been added. The ability of soluble ferric species to catalyse oxidation of cysteine is well documented[11] and the present results show that solid ferric hydroxides have the same ability.

Oxidation of cysteine was initially very rapid, but decreased as the level of cysteine in the system fell. With 2×10^{-3} M cysteine present, initially around 90% thiol was oxidized almost at once, but after a further 2 h, some cysteine was still present in solution.

Ottow[12] showed that low redox potentials (−350 mV) alone had only a very slight reductive effect on stable Fe–oxides: to achieve a significant reduction, *adsorption* of the reducing ligand was necessary. Clearly the first step in the interaction must involve adsorption of cysteine on ferrihydrite. Adsorption is followed by reduction of surface ferric sites and desorption into solution of a cysteine free radical. The free radicals combine in solution to produce the disulphide (cystine). A similar mechanism is considered to operate during mobilization of iron from ferritin by thiols.[13] In the present work, cysteine was always oxidized to a large extent at once, regardless of the level originally added (always $\geqslant 10^{-3}$ M). However, with low cysteine: Fe ratios (0.1) ferrihydrite appeared to be more or less unaffected: only as the L: Fe ratio increased was ferrihydrite as well as cysteine altered.

Oxidation of cysteine was slower for goethite than for ferrihydrite. With 2×10^{-3} M cysteine equilibrated with goethite, there was a 50% drop in the level in solution after 2 h. The lower reactivity of goethite is the result of its more structured surface, not the lower surface area. With sufficient goethite to provide a surface area equivalent to that of ferrihydrite, the extent of oxidation at any stage was still far less than with ferrihydrite. This is expected on thermodynamic grounds.

Comparison with probe ligands

Cysteine has three functional groups, namely $RCOO^-$ ($pK_1 = 1.9$), RS^- ($pK_2 = 8.3$) and RNH_2 ($pK_3 = 10.8$). A comparison of the effect of cysteine on the formation of goethite with that of probe ligands with different combinations of functional groups (Table 3) indicated that cysteine owes its goethite promoting ability to adsorption on ferrihydrite through the sulphedral group.

Penicillamine which differs from cysteine mainly in that two hydrogen atoms adjacent to the sulphedral group are replaced by two methyl groups, has a much lower goethite inducing effect. Apparently, steric hindrance by the methyl groups reduces the extent to which coordination to the surface iron through the sulphedral groups takes place.

Only haematite formed in the presence of 10^{-2} M glycine, whereas with the same level of cysteamine ($NH_2CH_2CH_2SH$), the reaction product was 100% goethite (Table 3). Besides confirming the crucial role of the sulphedral group, these observations indicate that the role of the carboxylate groups is simply to assist surface coordination.

Interaction of cysteine with stabilized ferrihydrite

A phosphate or silicate stabilized ferrihydrite (L : Fe = 0.1) remained unchanged for weeks in the presence of between 2×10^{-3} and 10^{-2} M cysteine, regardless of whether cysteine was added before or after the addition of stabilizing ligand to ferrihydrite. With L : Fe = 0.1, all phosphate or silicate in the system is adsorbed to give a monolayer of adsorbed species on the ferrihydrite surface.[14] Cysteine does not displace these inorganic ligands even when present in a 10-fold excess. On the other hand, phosphate or silicate could displace adsorbed cysteine.

These observations provide support for the assumption that adsorption of cysteine on ferrihydrite preceeds any oxidation–reduction reactions.

Interactions of cysteine with ferrihydrite leading to goethite

Unlike all other ligands investigated previously, cysteine directly promotes the transformation of ferrihydrite to goethite. Cysteine induced the formation of goethite at pH 7.5–8.5 by converting the interfacial iron sites of ferrihydrite (by the binding of sulphedral groups and concurrent electron transfer) to more labile sites (local complexes) than those in the normal ferrihydrite structure.

In the system in which goethite forms most rapidly (L : Fe = 0.2), the ratio of cysteine to iron is not high enough to ensure complete reductive dissolution of ferrihydrite. Only a fraction of the ferric ions are reduced : this is sufficient, however, to convert parts of ferrihydrite into dark, mixed valence Fe^{II}–Fe^{III} hydroxide domains which are probably related to the green rusts. No crystalline material apart from goethite was detected by TEM or XRD indicating that the mixed valence precursor is very poorly ordered as expected according to the concept of activated sites mentioned above. This activation leads to far more rapid formation of goethite in solution. The system is saturated with oxygen and hence ferrous ions produced by interaction of ferrihydrite with cysteine would be reoxidized readily.

Table 3. Effect of different ligands on the transformation products of ferrihydrite, pH 8, 70°C, 24 h

	Ligand	[L] (M)	Product
Cysteine	$HSCH_2CHNH_2COOH$	10^{-2}	Goethite
		2×10^{-3}	Goethite
Penicillamine	$HS{-}\underset{\displaystyle CH_3}{\overset{\displaystyle CH_2}{\overset{|}{\underset{|}{C}}}}{-}NH_2COOH$	10^{-2}	Goethite + 10% haematite
Cysteamine	$NH_2CH_2CH_2SH$	2×10^{-3}	Goethite
		10^{-2}	Goethite
Glycine	NH_2CH_2COOH	10^{-2}	Haematite

The transformation can be summarized as:

$$\text{ferrihydrite} + RSH \rightarrow Fe^{II}_x Fe^{III}_y \text{hydroxide} + \tfrac{1}{2}RSSH + \tfrac{1}{2}H^+ \rightarrow \text{goethite}.$$

Although with L : Fe = 0.1 some cysteine is oxidized, insufficient Fe^{II} is produced to solubilize ferrihydrite to any extent and haematite formation is far more competitive than that of goethite. As seeding with goethite promotes goethite formation, however, the presence of cysteine must have led to a slight increase of solubility over that of pure ferrihydrite (where seeding with goethite has no effect).

Fischer[15] showed that at pH 6–7, Fe^{II} can promote formation of goethite by reductively dissolving ferrihydrite. At least 10 ppm Fe^{II} was required. We have found that low levels (2×10^{-3}–4×10^{-3} M) of Fe^{II} lead to goethite formation, but far more slowly than do equivalent concentrations of cysteine. We conclude that in our systems the ferrous ions produced do not reductively dissolve ferrihydrite: instead interaction with cysteine, which includes partial reduction, leads to formation of a new type of more labile iron site or mixed valence compound.

The most important feature of this investigation is the ability of cysteine to promote the transformation of ferrihydrite to goethite. Details of all the reactions involving cysteine and iron, particularly those in solution, have not been established. The results of other authors permit some suggestions as to possible reactions to be made. With L : Fe $\geqslant$ 1.0, qualitative analysis indicated that ferrous species were immediately released into solution. The supernatant liquid, however, had a red–violet tinge which is consistent with oxidation of a bis ferrous cysteine complex by molecular oxygen. This tinge fades with time, owing to autoreductive decomposition of the ferric cysteine complex to cystine and ferrous cysteinate.[16] The violet–red colour could be regenerated by shaking the solution with air and the cycle continued until all the thiol was reduced to the disulphide. This cycle was confined to the early stage (first hour) of the transformation reaction.

Despite the production of ferrous ions, no magnetite (Fe_3O_4) formed in these systems. With 4×10^{-3} M ferrous ions in the system and in the *absence* of cysteine, magnetite formed together with goethite. Earlier studies have shown that addition of other divalent ions such as Mn[17] and Cu[18] to ferrihydrite at M^{II} : Fe^{III} ratios greater than 0.2, led to the formation of a spinel phase: the essential step is interaction of the divalent ion with the ferrihydrite surface. With high levels of cysteine in the system this pathway is bypassed because ferrihydrite is rapidly converted into another compound. Magnetite cannot form in systems with lower levels of cysteine because the ratio of Fe^{II} produced to Fe^{III} in the system does not attain the threshold ratio of 0.2.

Implications for the biomineralization of goethite

Well-formed acicular crystals of goethite develop in the mature teeth of the limpet (*P. vulgata*) in a few days.[19] The mechanism by which goethite forms in these teeth at neutral pH has not been established. It seems probable that the organic matrix of chitin and protein in which the goethite grows and also the presence of inorganic ions such as phosphate and silicate should direct the transformation.

Mann *et al.*[19] considered that as formation of goethite from ferrihydrite requires temperatures of 60–70°C and pH $\geqslant$ 11 to proceed at a significant rate, formation of goethite in limpets' teeth probably involved oxidation of ferrous solutions, rather than transformation of ferrihydrite. Earlier results[4,5] which showed that organic ligands suppress formation of goethite from ferrihydrite appeared to support this hypothesis.

We now suggest an alternative mechanism for biomineralization of goethite. Our present results show that low levels of a reducing organic ligand can induce rapid formation of goethite at neutral pH and 40°C. This mechanism may also operate in limpet teeth. Mann *et al.* showed that besides goethite, the teeth contain large deposits of amorphous ferric hydroxide.[19] There is more amorphous material in immature than in mature teeth suggesting that a transformation may have occurred. In these teeth goethite crystals were mainly located in the cusp, whereas amorphous material associated with high levels of Si and P was concentrated at the base of the tooth. The distribution of these phases is in line with our results which showed that high levels of Si or P stabilized ferrihydrite against interaction with cysteine. Before examination of the mineralized component of these teeth, Mann *et al.*[19] removed the organic material, hence the presence of sulphur groups has not been reported. Identification of the proteins present in the organic material would be of interest and could help to confirm whether a reductive transformation of ferrihydrite could occur in the teeth.

A further point of interest is why goethite forms in the teeth of limpets and magnetite develops in chiton (*Polyplacophora*) teeth.[20] In both types of teeth amorphous ferric hydroxide has been detected. Our studies using synthetic systems show that reduction of ferrihydrite by an organic ligand

produced goethite, whereas interaction with a divalent cation leads to magnetite or a spinel. If the amorphous material in these teeth is the precursor of the crystalline phase, these observations suggest that the composition of the crystalline phase depends simply on the nature of the foreign species in the local environment.

Acknowledgements—We are indebted to Professor R. Giovanoli (Bern) for the X-ray diffraction measurements and electron microscopy and for useful discussions. Financial support was provided by ETH–Kredite für Unterricht und Forschung (Inter-institutional projects 1987).

REFERENCES

1. W. Feitknecht and W. Michaelis, *Helv. Chim. Acta* 1962, **26**, 212.
2. U. Schwertmann and W. R. Fischer, *Z. Anorg. Allg. Chem.* 1966, **346**, 137.
3. U. Schwertmann, *Geoderma* 1969, **3**, 207.
4. R. M. Cornell and U. Schwertmann, *Clays Clay Miner.* 1979, **27**, 402.
5. R. M. Cornell, *Clays Clay Miner.* 1985, **33**, 219.
6. R. M. Cornell, *Z. Pflernähr. Düng. Bodenk.* 1987, **150**, 304.
7. U. Schwertmann, *Z. Pflernähr. Düng. Bodenk.* 1964, **105**, 194.
8. R. Panossian, G. Terzian and M. Gioliano, *Spectros. Lett.* 1979, **12**, 715.
9. R. M. Cornell and R. Giovanoli, *Clays Clay Miner.* 1985, **33**, 424.
10. C. A. Mairesse-Ducarmoir, G. J. Patriarche and J. L. Vandenbalck, *Anal. Chim. Acta* 1974, **71**, 165.
11. C. A. McAuliffe and S. G. Murray, *Inorg. Chim. Acta Rev.* 1972, **6**, 103.
12. I. G. C. Ottow, *Z. Pflernähr. Düng. Bodenk.* 1982, **145**, 191.
13. F. Funk, J. P. Lender, R. Crichton and W. Schneider, *Eur. J. Biochem.* 1985, **152**, 167.
14. R. M. Cornell, R. Giovanoli and P. W. Schindler, *Clays Clay Miner.* 1987, **35**, 21.
15. W. R. Fischer, *Pseudogley and Gley*: Genesis and Use of Hydromorphic Soils (Edited by E. Schlichtling and U. Schwertmann), Vol. 37. Proc. Int. Soil Sci. Trans., Stuttgart (1973).
16. N. Tanaka, I. M. Kolthoff and W. Stricks, *J. Am. Chem. Soc.* 1955, 77, 1966.
17. R. M. Cornell and R. Giovanoli, *Clays Clay Miner.* 1987, **35**, 11.
18. R. M. Cornell and R. Giovanoli, *Polyhedron* 1988, **7**, 385.
19. S. Mann, C. C. Perry, J. Webb, B. Luke and R. J. P. Williams, *Proc. R. Soc. London. B.* 1986, **227**, 179.
20. H. A. Lowenstamm, *Science* 1981, **171**, 487.

Polyhedron Vol. 8, No. 2, pp. 157–160, 1989
Printed in Great Britain

0277–5387/89 $3.00+.00
© 1988 Pergamon Press plc

MAGNETISM AND SPECTROSCOPY OF COMPOUNDS $Cu\{C(CN)_3\}_2(tmpz)_2$ AND $Cu\{N(CN)_2\}_2(tmpz)_2$ WHERE tmpz = 3,4,5-TRIMETHYLPYRAZOLE

JERZY MROZIŃSKI

Institute of Chemistry, Wrocław University, 50 383 Wrocław, Poland

and

JIŘÍ KOHOUT* and MÁRIA HVASTIJOVÁ

Department of Inorganic Chemistry, Slovak Technical University, 812 37 Bratislava, Czechoslovakia

(*Received* 11 *February* 1988; *accepted* 13 *July* 1988)

Abstract—The title compounds were studied by measuring their magnetic susceptibilities up to 4.2 K and by use of their IR, ligand field and ESR spectra. Distorted octahedral structures are ascertained for both compounds, the $C(CN)_3$ or $N(CN)_2$ groups having a bidentate bridging function. Spin exchange coupling takes place in both compounds, being both antiferromagnetic and ferromagnetic in nature, the latter appears to prevail at low temperatures.

The preparation of the compounds CuX_2L_2, where $X = N(CN)_2$, $C(CN)_3$ and L = pyrazole or its derivative, has recently been published.[1,2] The low temperature magnetic measurements combined with IR, ligand field and ESR spectra showed that in $Cu\{N(CN)_2\}_2(pz)_2$ infinite arrays of Cu^{II} atoms joined by bridging dicyanamide ligands propagate a weak but noticeable magnetic exchange interaction.[1] In other CuX_2L_2 complexes according to their spectral properties bridging X ligands are also present.[2] To investigate the influence of these bridges on the magnitude and kind of exchange interaction occurring, we measured the temperature dependence of the magnetic susceptibilities of $Cu\{C(CN)_3\}_2(tmpz)_2$ and $Cu\{N(CN)_2\}_2(tmpz)_2$ (tmpz = 3,4,5-trimethylpyrazole) which had been ascertained to possess sub-normal room-temperature magnetic moments.[2] Moreover, spectroscopic methods were also employed with a view to complete the picture.

EXPERIMENTAL

The compounds under investigation were prepared as described elsewhere.[2] IR spectra (4000–400 cm^{-1}) were recorded on a Perkin–Elmer 180 spectrophotometer using KBr pellets. FIR (400–50 cm^{-1}),[3] electronic[4] and ESR spectra,[5] as well as magnetic susceptibilities in the range 4.2–290 K,[5] were measured as given in the cited papers.

RESULTS AND DISCUSSION

IR spectra

The pseudohalide vibrations in the IR spectra were assigned by comparison with the spectra of trimethylpyrazole[6] and $C(CN)_3^-$ or $N(CN)_2^-$;[7] the data are listed in Table 1.

For $Cu\{C(CN)_3\}_2(tmpz)_2$ the $\nu(C{\equiv}N)$ values in the regions of about 2245 and 2195 cm^{-1} indicate,[7,8] unambiguously, a bidentate function of the tricyanmethanide ligands, Cu—NC·C·(CN)·CN—Cu. In the case of $Cu\{N(CN)_2\}_2(tmpz)_2$ the issue is less clear on account of the $\nu(C{\equiv}N)$ number and spread. After comparing the $\nu(C{\equiv}N)$ values with those for many other $M\{N(CN)_2\}_2L_2$ complexes (M = Cu, Ni, Co; L = a pyrazole or pyridine type ligand) with pseudooctahedral configurations,[1,2,4] where the $\nu(C{\equiv}N)$ values range between *ca* 2265–2240 and 2190–2140 cm^{-1},

*Author to whom correspondence should be addressed.

Table 1. Selected IR data (cm^{-1}) for both compounds

$Cu\{C(CN)_3\}_2(tmpz)_2$		$Cu\{N(CN)_2\}_2(tmpz)_2$		Assignment
3259ms[a]		3359ms[a]	3297ms[a]	ν(N—H)
		2314s[b]	2286s	$\nu_s+\nu_{as}$(C—N)
2250m	2222m	2258s	2234s	ν(C≡N)
2196vs	2191sh	2182vs	2149vs	
1245w				ν(C—C)
		1386s[c]	1362s[c]	ν_{as}(C—N)
		919w		ν_s(C—N)
567s				γ(C—C≡N)
		522s	508ms	δ(NCN)
302s	284s[a,c]	292s[d]	247s	ν(Cu—N)
265s				
94m[a,c]		94sh[a,c]		ν(Cu—N_{ax})

[a] Some splitting occurs.
[b] The assignment is not clear.
[c] The band may also be connected with a tmpz vibration.
[d] Broad band with a complex splitting.

the bidentate bridge dicyanamide ligands may be taken as being quite acceptable.

In the far-IR region, strong bands between *ca* 305–245 cm^{-1} are tentatively assigned to the Cu—N stretching vibrations. These frequencies corroborate the symmetric bridging of the pseudo-halide groups through their cyanide nitrogens.[4,9] The absorptions that occur for both complexes at *ca* 95 cm^{-1} belong most likely to the stretches of the long Cu—N bonds in axial direction,[3] although they may also be due to a vibration of the free tmpz.[6]

Ligand field and ESR spectra

The position of the ligand field band maxima and the low wavenumber shoulders (Table 2) are in agreement with a distorted octahedral arrangement of donors around the Cu^{II} atoms,[10] having in the case of $Cu\{N(CN)_2\}_2(tmpz)_2$ a weaker tetragonal distortion.[11]

The compound, $Cu\{C(CN)_3\}_2(tmpz)_2$, at room temperature and $Cu\{N(CN)_2\}_2\cdot(tmpz)_2$ at 77 K (Fig. 1) show tetragonal ESR spectra with g values (Table 2) indicating a $d_{x^2-y^2}$ ground state.[10] The room temperature ESR spectrum of $Cu\{N(CN)_2\}_2(tmpz)_2$ consists of an asymmetric single line. According to the G parameters slightly below four, the g values are practically unaffected by the exchange coupling present[10] (see below).

Magnetism

Selected variable-temperature magnetic data for both compounds are listed in Table 3. The temperature dependences of the reciprocal magnetic susceptibilities obey the Curie–Weiss law (Fig. 2); however, the Weiss constants calculated for the low and high temperature regions are different from each other, and also from the overall Weiss constants (Table 4).

The magnetic moment of $Cu\{C(CN)_3\}_2(tmpz)_2$

Table 2. Ligand field and ESR spectral data for both compounds

Compound	$\tilde{\nu}_{max}$ (μm^{-1})[a]		$g_\perp$	$g_\parallel$	g_{av}[b]	G[c]
$Cu\{C(CN)_3\}_2(tmpz)_2$	≈ 1.24sh	1.58	2.09	2.34	2.18	3.78
$Cu\{N(CN)_2\}_2(tmpz)_2$	≈ 1.15sh	1.45			2.10[d]	
			2.07[e]	2.27[e]	2.14	3.86

[a] sh = shoulder.
[b] Calculated according to the relation $g_{av} = [\frac{1}{3}(g_\parallel^2+2g_\perp^2)]^{1/2}$.
[c] Given as the ratio $(g_\parallel-2)/(g_\perp-2)$.
[d] Value of g at the inflection point of the derivation curve.
[e] From the 77 K spectrum.

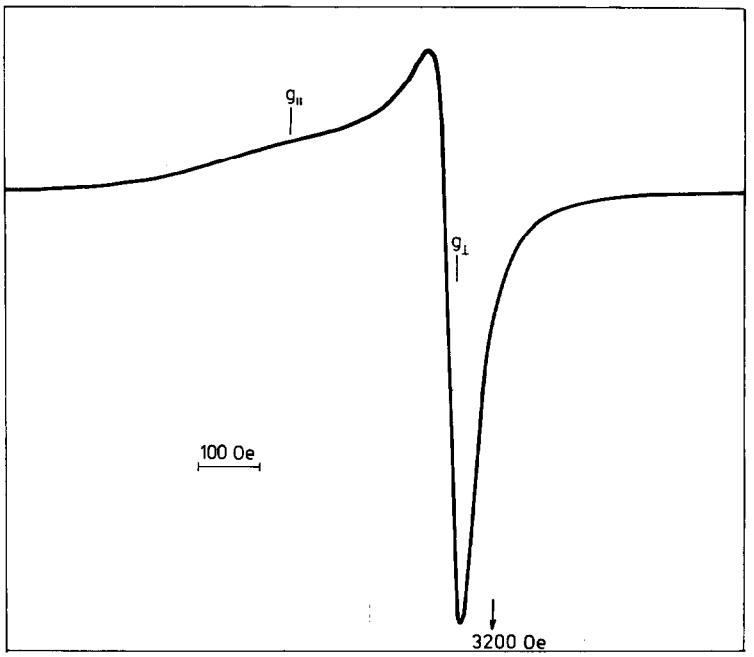

Fig. 1. ESR spectrum of $Cu\{N(CN)_2\}_2(tmpz)_2$ at 77 K.

Table 3. Magnetic susceptibility data for both compounds[a]

	$Cu\{C(CN)_3\}_2(tmpz)_2$		$Cu\{N(CN)_2\}_2(tmpz)_2$	
T (K)	$\chi_M^{cor} \times 10^5$ ($cm^3\ mol^{-1}$)	μ_{eff} (BM)	$\chi_M^{corr} \times 10^5$ ($cm^3\ mol^{-1}$)	μ_{eff} (BM)
290	104	1.55	117	1.65
255	119	1.56	134	1.66
200	150	1.55	168	1.64
140	215	1.55	245	1.66
80	377	1.55	462	1.72
35	868	1.56	1080	1.74
20	1500	1.55	1940	1.74
16	1910	1.56	2360	1.74
12	2600	1.58	3140	1.74
8	3920	1.58	4930	1.78
7	4480	1.58	5680	1.78
6	5220	1.58	6980	1.83
5	6960	1.66	8620	1.86
4.2	8030	1.64	11,300	1.95

[a] Some values selected from among 66 experimental points are presented.

exhibits a sub-spin value which remains constant, 1.56 ± 0.02 BM, within the range 16–290 K; at lower temperatures the μ_{eff} values moderately increase. For $Cu\{N(CN)_2\}_2(tmpz)_2$, the μ_{eff} value above 100 K is also somewhat sub-spin and constant: 1.65 ± 0.01 BM. Below this temperature, the magnetic moments increase considerably and reach 1.95 BM at 4.2 K. The χ_M^{corr} T values increase from 0.344 to 0.374 $cm^3\ mol^{-1}$ K in the temperature range

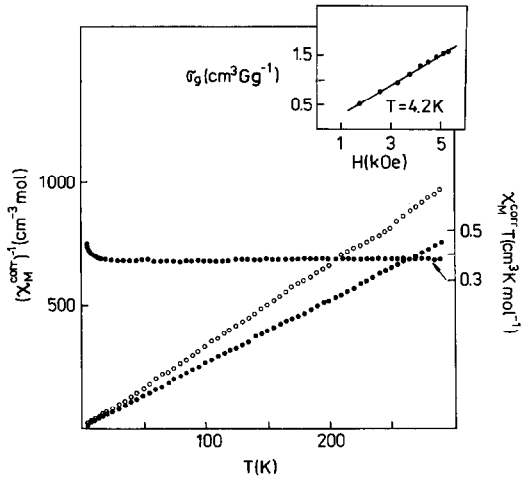

Fig. 2. Plots of $(\chi_M^{corr})^{-1}$ vs T for $Cu\{C(CN)_3\}_2(tmpz)_2$ (○) and $Cu\{N(CN)_2\}_2(tmpz)_2$ (●), χ_M^{corr} T vs T and σ_g vs H for $Cu\{N(CN)_2\}_2(tmpz)_2$.

measured (Fig. 2). The dependence of the specific magnetization, σ_g, against field strength, H, at 4.2 K is a straight line, so that the ferromagnetic admixture effect can be excluded.

The attempt to explain the experimental function $\chi_M^{corr} = f(T)$ for $Cu\{C(CN)_3\}_2(tmpz)_2$ by approximation to the two-dimensional model of a square-planar antiferromagnet[12] was made,

$$\chi_M = \frac{N_A g^2 \mu_B^2}{4kT}\left(1+\frac{2}{x}+\frac{2}{x^2}+\frac{1.333}{x^3}+\frac{0.250}{x^4}+\frac{0.4833}{x^5}+\frac{0.003797}{x^6}\right)^{-1}$$

Table 4. Parameters from the Curie–Weiss law for both compounds

	$Cu\{C(CN)_3\}_2(tmpz)_2$		$Cu\{N(CN)_2\}_2(tmpz)_2$	
Temperature range (K)	C (cm^3 K mol^{-1})	θ (K)	C (cm^3 K mol^{-1})	θ (K)
4.2–RT[a]	0.301	0.36	0.333	3.3
4.2–20	0.292	0.57	0.367	0.57
25–RT	0.301	0.40	0.330	5.1
50–RT	0.302	−0.19	0.329	5.5

[a] RT = room temperature.

where $x = kT/|J|$. The g_{av} value obtained from the ESR spectrum was used as a constant in the process of fitting data. The exchange parameter, $|J|$, is 0.57 cm^{-1}, which is also very small and with respect to the relatively high ERR value (for definition see ref. 5) of 5.73×10^4, no particular significance can be assigned to it. For $Cu\{N(CN)_2\}_2(tmpz)_2$ with even more complicated magnetic behaviour, the experimental susceptibility data were not fitted to any model of magnetic interaction.

It is very probable that both compounds by mutual assistance of pseudohalide bridges and sterically influential tmpz molecules possess complex three-dimensional structures, in which we are dealing with weak antiferromagnetic and ferromagnetic couplings. The common effect of both is the averaging and relative constancy of the magnetic moments. At lower temperatures, the changes of μ_{eff} suggest the ferromagnetic coupling is predominant, especially in $Cu\{N(CN)_2\}_2(tmpz)_2$. Structural crystallographic data are necessary for detailed understanding of these unusual magnetic properties but only polycrystalline powder materials are available at present.

CONCLUSIONS

The results entered in the paper prove that both compounds under study have complex polymeric structures with pseudohalide bridges mediating magnetic interaction between the Cu^{II} atoms. This interaction is both antiferromagnetic and ferromagnetic in nature, and results in averaging the magnetic moments which are, except with low temperatures, almost invariable. At low temperatures the magnetic moments increase thus indicating a strengthening ferromagnetic interaction.

REFERENCES

1. J. Mroziński, J. Kohout, M. Hvastijová and H. Köhler, *Transition Met. Chem.* 1986, **11**, 481.
2. M. Hvastijová, J. Kohout, H. Köhler and G. Ondrejovič, *Z. Anorg. Allg. Chem.*, in press.
3. J. Kohout, M. Hvastijová and J. Mroziński, *J. Mol. Struct.* 1984, **116**, 211.
4. M. Hvastijová, J. Kohout, H. Wusterhausen and H. Köhler, *Z. Anorg. Allg. Chem.* 1984, **510**, 37.
5. J. Kohout, J. Mroziński and M. Hvastijová, *Polyhedron* 1985, **4**, 1975.
6. M. Hvastijová and J. Kohout, unpublished results.
7. A. M. Golub, H. Köhler and V. V. Skopenko (Eds), *Chemistry of Pseudohalides*. Elsevier, Amsterdam (1987).
8. H. Köhler, R. Skirl and V. V. Skopenko, *Z. Anorg. Allg. Chem.* 1977, **428**, 115.
9. H. Köhler, A. Kolbe and G. Lux, *Z. Anorg. Allg. Chem.* 1977, **428**, 103.
10. B. J. Hathaway and D. E. Billing, *Coord. Chem. Rev.* 1970, **5**, 143; B. J. Hathaway, *J. Chem. Soc., Dalton Trans.* 1972, 1196.
11. A. A. G. Tomlinson, B. J. Hathaway, D. E. Billing and P. Nicholls, *J. Chem. Soc. A* 1969, 65.
12. G. S. Rushbrooke and P. J. Wood, *Molec. Phys.* 1958, **1**, 257; C. A. Baker Jr, H. E. Gilbert, J. Eve and G. S. Rushbrooke, *Phys. Lett. A* 1967, **25**, 207; M. E. Lines, *J. Phys. Chem. Solids* 1970, **31**, 101; J. Darriet, M. S. Haddad, E. N. Duesler and D. N. Hendrickson, *Inorg. Chem.* 1979, **18**, 2679.

Polyhedron Vol. 8, No. 2, pp. 161–165, 1989
Printed in Great Britain

0277–5387/89 $3.00+.00
© 1988 Pergamon Press plc

CLEAVAGE OF THE TETRAMERIC PALLADIUM(II) COMPLEX $[Pd_4(PPr^n_3)_4(NO_2)_4(ONO)_4]$ WITH NUCLEOPHILES. X-RAY CRYSTAL STRUCTURES OF THE PRODUCTS *TRANS*-$[Pd(PPr^n_3)(NO_2)_2Cl][As(C_6H_5)_4]$ AND $[Pd_2(PPr^n_3)_2Cl_2(NO_2)_2]$

G. BRUNO,* S. CAMPAGNA, M. CUSUMANO, A. GIANNETTO and V. RICEVUTO

Dipartimento di Chimica Inorganica e Struttura Molecolare, Salita Sperone 31, Vil.S.Agata, 98016 Messina, Italy

(*Received* 20 *May* 1988; *accepted* 20 *July* 1988)

Abstract—The tetrameric complex $[Pd_4(PPr^n_3)_4(NO_2)_4(ONO)_4]$ readily reacts with the nucleophiles NO_2^- and Cl^- to give a variety of palladium(II) square-planar complexes of PPr^n_3. A scheme for these reactions is proposed. The crystal structures of *trans*-$[Pd(PPr^n_3)(NO_2)_2Cl][As(C_6H_5)_4]$, obtained by reaction of the tetramer with $[As(C_6H_5)_4]NO_2$, and of $[Pd_2(PPr^n_3)_2(NO_2)_2Cl_2]$, obtained by reaction of the tetramer with the bridged complex $[Pd_2(PPr^n_3)_2Cl_4]$ have been determined by single crystal X-ray diffraction: (**1**) $[Pd(PPr^n_3)(NO_2)_2Cl][As(C_6H_5)_4]$, $M_r = 777.45$, orthorhombic, $P2_12_12_1$, $a = 17.723(2)$, $b = 14.890(1)$, $c = 13.178(1)$ Å, $V = 3477.7(5)$ Å^3, $Z = 4$, $D_x = 1.48$ Mg m^{-3}, λ(Mo-K_α) = 0.71069 Å, $\mu = 0.78$ cm^{-1}, $F(000) = 1584$, $T = 293$ K, $R = 0.053$ for 1710 independent reflections with $I > 3\sigma(I)$. (**2**) $[Pd_2(PPr^n_3)_2Cl_2(NO_2)_2]$, $M_r = 696.2$, monoclinic, $P2_1/n$, $a = 13.665(2)$, $b = 7.855(1)$, $c = 13.704(2)$ Å, $\beta = 101.4(1)$, $V = 1441.8(4)$ Å^3, $Z = 4$, $D_x = 1.60$ Mg m^{-3}, λ(Mo-K_α) = 0.71069 Å, $\mu = 0.74$ cm^{-1}, $F(000) = 704$, $T = 293$ K, $R = 0.030$ for 1993 independent reflections with $I > 3\sigma(I)$.

We have recently shown[1] that by reaction of the bridged complex $[Pd_2(PPr^n_3)_2Cl_4]$ with $NaNO_2$ in methanol the tetrameric compound $[Pd_4(PPr^n_3)_4(NO_2)_4(ONO)_4]$ is obtained. In this species an approximate square of Pd atoms is joined together by nitro–nitrito bridges; a nitro group and a tri-*n*-propylphosphine complete the coordination. This complex is very labile and is promptly cleaved, in different solvents, by nucleophiles to give various square-planar complexes of PPr^n_3. In this paper we describe the reaction of $[Pd_4(PPr^n_3)_4(NO_2)_4(ONO)_4]$ with the nucleophiles Cl^- and NO_2^- and report the crystal structure of one of the products of the reaction with the latter nucleophile, *trans*-$[Pd(PPr^n_3)(NO_2)_2Cl][As(C_6H_5)_4]$, and of the complex $[Pd_2(PPr^n_3)_2(NO_2)_2Cl_2]$ obtained by reaction of the tetramer with $[Pd_2(PPr^n_3)_2Cl_4]$.

EXPERIMENTAL

The preparation of $[Pd_4(PPr^n_3)_4(NO_2)_4(ONO)_4]$ has already been reported.[1] $[Pd(PPr^n_3)(NO_2)_3]$ $[As(C_6H_5)_4]$ was obtained by reacting $[Pd_4(PPr^n_3)_4(NO_2)_4(ONO)_4]$ in methanol, in the presence of $[As(C_6H_5)_4][NO_3]$ in a ratio of 1 : 10, with a large excess of $NaNO_2$. The solution was stirred for 1 h and the solvent evaporated off. The residue, after washing several times with water, was crystallized from methanol–diethyl ether.

$[Pd_2(PPr^n_3)_2Cl_4]$. The tetrameric compound $[Pd_4(PPr^n_3)_4(NO_2)_4(ONO)_4]$, dissolved in methanol, was treated with a large excess of LiCl. The resulting solution was left under magnetic stirring for 24 h and the solvent was evaporated off. The solid residue was washed with water and crystallized from cold ethanol.

The complexes *trans*-$[Pd(PPr^n_3)(NO_2)_2Cl][As(C_6H_5)_4]$, $[Pd(PPr^n_3)(NO_2)Cl_2][As(C_6H_5)_4]$ and $[Pd(PPr^n_3)Cl_3][As(C_6H_5)_4]$ were prepared by reacting $[Pd_4(PPr^n_3)_4(NO_2)_4(ONO)_4]$ with $[As(C_6H_5)_4][NO_2]$, in the appropriate ratio in methanol. The resulting solution was stirred for 1 h and the solvent evaporated off. The residue was dissolved in CH_2Cl_2 and the product was precipitated as a crystalline solid by the addition of diethyl ether.

$[Pd_2(PPr^n_3)_2(NO_2)_2Cl_2]$ was obtained as a crystalline solid by reacting the tetramer with $[Pd_2$

*Author to whom correspondence should be addressed.

$(PPr^n_3)_2Cl_4]$, in methanol, in a ratio of 1:2. LiCl, NaCl and $NaNO_2$, as well as all the solvents used, were of reagent grade.

UV–vis spectra were recorded using a Perkin–Elmer Lambda 5 spectrophotometer. IR spectra in the range 250–4000 cm^{-1} were recorded as Nujol mulls on a Perkin–Elmer 783 spectrometer. Conductivity measurements were carried out with a Radiometer CDM3 conductivity bridge.

Diffraction data, for **1** and **2**, were collected on a Siemens–Stoe Four Circle diffractometer using graphite-monochromated Mo-K_α radiation ($\lambda = 0.71069$ Å). Accurate unit cell dimensions and crystal orientation matrices were obtained from least-squares refinement of 2θ, ω, χ and ψ values of 20 strong reflections in the range $14 < 2\theta < 24°$. Three standard reflections were monitored periodically during the course of the data collection as a check of the crystal stability, and these varied by less than 3% for both compounds. Of 3800 and 3950 independent reflections measured by the ω–2θ scan technique, in the range $3 < 2\theta < 50$, 1710 and 1993 ($R_{int} = 0.022$, 0.018) having net intensity $I > 3\sigma(I)$ were used in the solution and refinement of the structure. Corrections for Lorentz and polarization effects were made, but not those for absorption ($\mu = 16.3$ and 15.5 cm^{-1}). Both the structures were solved by using standard Patterson methods. The Fourier difference synthesis phased with the heavy-atom positions allowed the location of the non-hydrogen atoms in **1** and **2**. Full-matrix least-squares refinement of the models was carried out by minimizing the function $\Sigma w(|F_o|-|F_c|)^2$. The weighting scheme used in the last refinement cycles were $w = 0.7186/[\sigma^2(F_o)+0.005366F_o^2]$ for **1** and $w = 0.6979/[\sigma^2(F_o)+0.001878F_o^2]$ for **2**, which showed reasonable consistency in a test of $w\Delta^2$ for data sectioned with respect to both F_o and $\sin\theta/\lambda$. Anisotropic temperature factors were introduced for all non-hydrogen atoms; in compound **1** the phenyl rings of the triphenylarsine cation were refined as rigid groups and restricted to their normal geometry (D_{6h} symmetry; $d_{C-C} = 1.395$ Å) by using the group refinement procedure. Each ring was assigned an individual isotropic thermal parameter. Hydrogen atoms were added at calculated positions and included in the structure factor calculations with a common thermal parameter ($U = 0.06$ Å^2). Both models reached convergence with $R = [\Sigma|F_o|-|F_o|]/\Sigma|F_o| = 0.053$ and 0.030 $wR[\Sigma w(|F_o|-|F_c|)^2/\Sigma w|F_o|^2]^{1/2} = 0.056$ and 0.036 for **1** and **2**, respectively. Scattering factors for non-hydrogen atoms were taken from ref. 2 and for hydrogen atoms from ref. 3. Anomalous dispersion corrections for Pd, Cl and P atoms were taken from ref. 4.

Reversing the sign of the imaginary anomalous scattering component for **1**, which has the non-centrosymmetric space group $P2_12_12_1$, increased R from 0.053 to 0.071. This difference is highly significant, and therefore the model has the correct absolute configuration.

All calculations were performed with the *SHELX 76*[5] and *PARST*[6] set of programs on the IBM 4341 computer at the "Centro di Calcolo dell' università di Messina". Atomic coordinates, anisotropic temperature factors and calculated and observed structure factors are available as supplementary material. Atomic coordinates have also been deposited with the Cambridge Crystallographic Data Centre.

RESULTS AND DISCUSSION

On addition of excess nitrite or chloride to a methanol or dichloromethane solution of $[Pd_4(PPr^n_3)_4(NO_2)_4(ONO)_4]$, an immediate reaction occurs as shown by the large spectral variation, in the UV region, associated with the process. However, when using NaCl or LiCl as the nucleophile only the starting complex is recovered if the solvent is evaporated off. The reaction product in the case of NO_2^-, $[Pd(PPr^n_3)(NO_2)_3]^-$, can be obtained in the solid state as a pure compound, providing the nucleophile/complex ratio is $\geqslant 4$, in the presence of a bulky counter ion such as $[As(C_6H_5)]^+$. When the nucleophile is Cl^-, various substances are obtained as a function of the chloride concentration. Thus, when the chloride/complex ratio is 4 only $[Pd(PPr^n_3)(NO_2)_2Cl]^-$ forms in solution; with a large excess of chloride (over 100-fold with respect to the complex) either $[Pd(PPr^n_3)Cl_3]^-$ or the chloro-bridged complex $[Pd_2(PPr^n_3)_2Cl_4]$ are the reaction products. The former, as well as $[Pd(PPr^n_3)(NO_2)_2Cl]^-$, precipitates in the presence of $[AS(C_6H_5)_4]^+$; the latter substance is obtained, using LiCl or NaCl as the nucleophile, when the solvent is evaporated off. Intermediate Cl^- concentrations lead to a mixture of variously substituted complexes of PPr^n_3 including a substance which precipitates in the presence of $[As(C_6H_5)_4]NO_3$ and can be formulated, on the basis of elemental analysis, as $[Pd(PPr^n_3)(NO_2)Cl_2][As(C_6H_5)_4]$. In this compound, the two chlorides most likely occupy mutual *cis* positions; the IR spectrum (Nujol mull) shows in fact two stretching frequencies at 265 and 329 cm^{-1} assignable to the Pd—Cl *trans* and *cis*, respectively, to phosphine.[7] In addition, reaction of a 1:1 ratio of this complex and PPr^n_3 does not lead to *trans*-$[Pd(PPr^n_3)_2Cl_2]$ as expected if NO_2 were *trans* to

phosphine but to $[Pd(PPr^n_3)_2ClNO_2][As(C_6H_5)_4]$. The IR spectrum of this product shows a stretching frequency Pd—Cl at 285 cm^{-1} characteristic of Cl *trans* to phosphine[7] and only one Pd—P stretching frequency at 425 cm^{-1} as expected for phosphines *trans* to each other.

The IR spectrum of $[Pd(PPr^n_3)(NO_2)_2Cl][As(C_6H_5)_4]$ exhibits a band at 285 cm^{-1} attributable to Pd—Cl with the chloride *trans* to phosphine. This type of structure has been conclusively confirmed by X-ray analysis of the substance. The structure of $[Pd_2(PPr^n_3)_2(NO_2)_2Cl_2]$ has also been established by single crystal determination. On the basis of the nature of the reaction products a possible reaction scheme is predicted in Scheme 1.

The existence of an equilibrium between the tetramer and a solvo-species is supported by the conductivity data. A methanol solution of the tetramer (1×10^{-4} M) exhibits a molar conductance of about 9 $\Omega^{-1}\,cm^2\,M^{-1}$ which is unexpected for a neutral complex.[8]

By reacting the tetramer with the bridged complex $[Pd_2(PPr^n_3)_2Cl_4]$, $[Pd_2(PPr^n_3)_2(NO_2)_2Cl_2]$ is obtained:

$$[Pd_4(PPr^n_3)_4(NO_2)_4(ONO)_4] + 2[Pd_2(PPr^n_3)_2Cl_4] \rightarrow 4[Pd_2(PPr^n_3)_2(NO_2)_2Cl_2]. \quad (2)$$

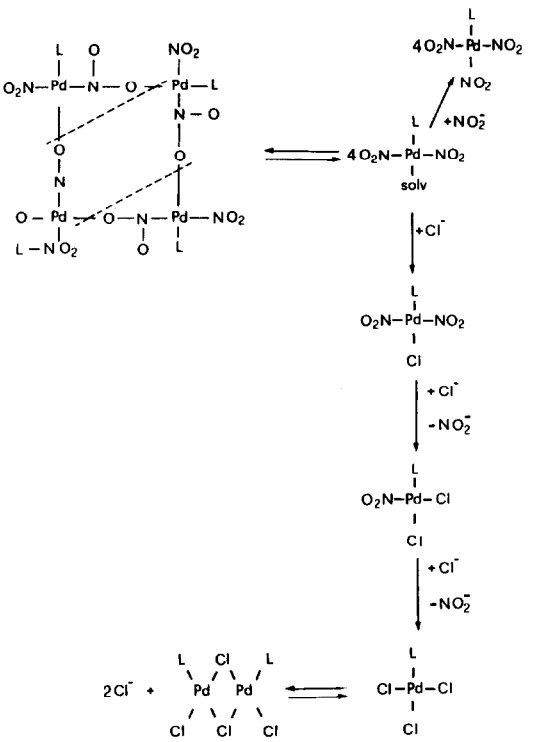

Scheme 1.

The structure of $[Pd_2(PPr^n_3)_2(NO_2)_2Cl_2]$ has also been established by single crystal determination.

Molecular structure of $[Pd_2(PPr^n_3)(NO_2)_2Cl][As(C_6H_5)_4]$ **(1)**

The crystal structure of **1**, depicted in Fig. 1 with the atomic labelling, consists of a discrete

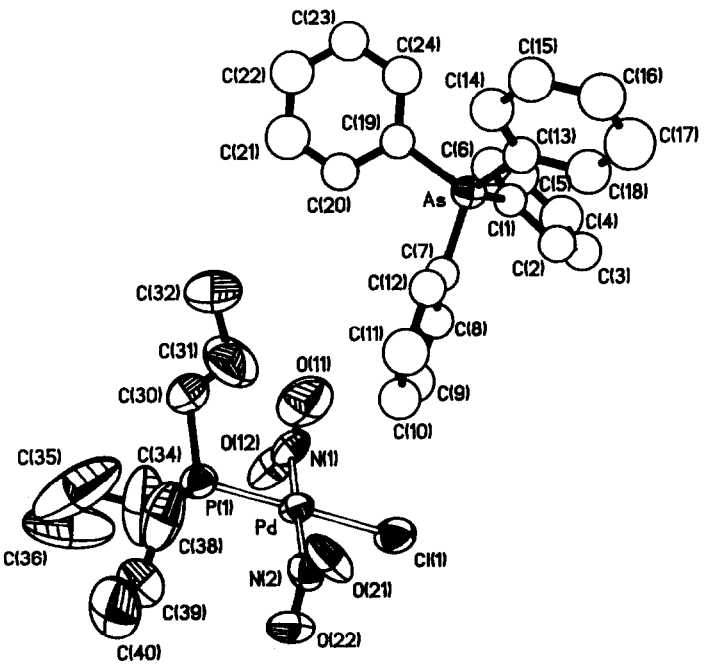

Fig. 1. Molecular structure of *trans*-$[Pd(PPr^n_3)(NO_2)_2Cl][As(C_6H_5)_4]$.

anion, in which the metal atom is fully coordinated, and separated from the cation $[As(C_6H_5)_4]^+$ by normal van der Waals interactions. Bond distances and angles are reported in Table 1. The local anion geometry is, as expected, square-planar slightly distorted as the atom-to-plane deviations are all lower than 0.02 Å. The two nitrogen atoms of the nitro groups *trans* to each other form an angle [N(1)—Pd(1)—N(2)] of 178.1(6)°. Both the Pd(1)—N(1) and Pd(1)—N(2) bond distances are comparable (2.037(19) and 2.007(18) Å) with the corresponding values in $[Pd(PPr^n_3)(NO_2)_3][As(C_6H_5)_4]$[9] and other nitro complexes.[10,11] The geometry of the nitrite groups is characterized by N—O distances (mean 1.16(3) Å) and the O—N—O angle of 122.6(2)°. In addition, the planes of the nitrite groups are nearly perpendicular to the coordination plane, being rotated by 88.7(9) and 91.9(8)° with respect to it. The Pd(1)—P(1) bond distance of 2.243(6) Å is comparable with the corresponding value of 2.262(6) Å in $[Pd(PPr^n_3)(NO_2)_3][As(C_6H_5)_4]$[9] and 2.248(4) Å in $[Pd_4(PPr^n_3)_4(NO_2)_4(ONO)_4]$[1] and is much lower than the value of 2.327(3) Å in $[Pd_2(PPr^n_3)_2(NCS)(SCN)_2(\mu\text{-CN})]$[11] where the two phosphines are mutually *trans*. The Pd(1)—Cl bond distance of 2.347(5) Å is slightly lower than the value of 2.359(1) Å found for Pd—Cl *trans* to $As(C_6H_5)_3$ in *cis*-$[Pd(SNNMe_2)(As(C_6H_5)_3)Cl_2]$[12] and is significantly longer than the value of 2.300 Å mediated over a series of Pd—Cl bonds[13] where two chlorine atoms are *trans* to each other.

Table 1. Selected bond lengths (Å) and bond angles (°) for *trans*-$[Pd(PPr^n_3)(NO_2)_2Cl][As(C_6H_5)_4]$

Bond distances (Å)			
Pd(1)—Cl(1)	2.347(6)	Pd(1)—N(1)	2.037(19)
Pd(1)—N(2)	2.007(18)	Pd(1)—P(1)	2.243(6)
N(1)—O(11)	1.085(36)	N(1)—O(12)	1.156(28)
N(2)—O(21)	1.185(24)	N(2)—O(22)	1.220(23)
P(1)—C(30)	1.865(27)	P(1)—C(34)	1.978(36)
P(1)—C(38)	1.813(28)		
Angles (°)			
N(2)—Pd(1)—P(1)	92.3(4)	N(1)—Pd(1)—P(1)	89.6(5)
N(1)—Pd(1)—N(2)	178.1(6)	Cl(1)—Pd(1)—P(1)	178.6(2)
Cl(1)—Pd(1)—N(2)	88.6(5)	Cl(1)—Pd(1)—N(1)	89.5(5)
Pd(1)—N(1)—O(12)	116.1(20)	Pd(1)—N(1)—O(11)	119.8(20)
O(11)—N(1)—O(12)	124.1(23)	Pd(1)—N(2)—O(22)	117.7(13)
Pd(1)—N(2)—O(21)	120.9(14)	O(21)—N(2)—O(22)	121.2(18)
Pd(1)—P(1)—C(38)	118.4(9)	Pd(1)—P(1)—C(34)	107.7(10)
Pd(1)—P(1)—C(30)	112.5(9)		

Table 2. Selected bond lengths (Å) and bond angles (°) for $[Pd_2(PPr^n_3)_2Cl_2(NO_2)_2]$

Bond distances (Å)			
Pd—P	2.232(1)	Pd—Cl	2.316(2)
Pd—Cl′	2.417(1)	Pd—N	1.979(4)
P—C(1)	1.812(5)	P—C(4)	1.809(6)
P—C(7)	1.797(5)	N—O(1)	1.198(7)
N—O(2)	1.162(8)		
Angles (°)			
Cl—Pd—N	176.8(1)	Cl—Pd—Cl′	87.5(1)
P—Pd—N	92.9(1)	P—Pd—Cl′	177.6(1)
P—Pd—Cl	90.3(1)	Pd—P—C(7)	111.1(2)
Pd—P—C(4)	111.1(2)	Pd—P—C(1)	114.5(1)
C(4)—P—C(7)	103.7(2)	C(1)—P—C(7)	107.5(2)
C(1)—P—C(4)	108.3(3)	Pd—Cl—Pd′	92.5(1)
Pd—N—O(2)	118.5(4)	Pd—N—C(1)	118.0(4)
O(1)—N—O(2)	123.1(5)		

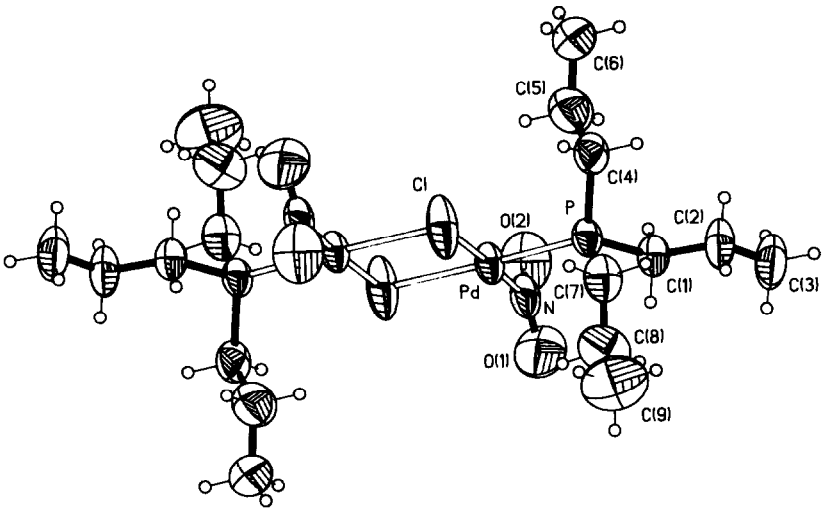

Fig. 2. Molecular structure of $[Pd_2(PPr^n_3)_2Cl_2(NO_2)_2]$.

As—C bond distances (mean value 1.865 Å) and other structural features of $[As(C_6H_5)_4]^+$ and of PPr^n_3 are as usual and require no special comment.

Molecular structure of $[Pd_2(PPr^n_3)_2Cl_2(NO_2)_2]$ (**2**)

The crystal structure of **2** with atomic labelling is depicted in Fig. 2. Bond distances and angles are reported in Table 2. The crystal of compound **2** consists of packing of discrete dimeric molecules $[Pd_2(PPr^n_3)_2Cl_2(NO_2)_2]$ separated by normal van der Waals contacts. Each metal atom is surrounded by a P atom from the PPr^n_3 ligand, an N-bonded nitrite group and two unsymmetrical *cis* chlorine atoms in a planar configuration. The two Pd—Cl bond distances are 2.316(1) and 2.417(1) Å; the latter value refers to a Pd—Cl *trans* to PPr^n_3. The Pd—P bond distance of 2.232(1) Å is at the lower limit found for this type of bond. The two palladium atoms are connected together at a distance of 3.420 Å. The dihedral angle between the two coordination planes is only 1.30(7)°. The P(1)—Pd—Cl(1) and P(1)—Pd—Cl(1′) bond angles are 90.25(4) and 177.58(4)°, respectively. The Pd—N bond distance is 1.979(4) Å slightly shorter than the corresponding values for **1**. Furthermore, the nitro group plane is rotated by 86.0(3)° with respect to the coordination plane. This orientation seems to be the usual one in the absence of steric overcrowding. In the PPr^n_3 ligand the P—C bond distances are as expected and range from 1.797(5) to 1.812(5) Å. The other bond lengths and angles within this ligand, as well as the relatively large thermal motion of the propyl chain, are as usual.

REFERENCES

1. G. Bombieri, G. Bruno, M. Cusumano and G. Guglielmo, *Acta Cryst.* 1984, **C40**, 409.
2. D. T. Cromer and J. B. Mann, *Acta Cryst.* 1968, **A24**, 321.
3. R. F. Stewart, *J. Chem. Phys.* 1970, **53**, 3175.
4. *International Tables for X-ray Crystallography*, Vol. IV. Kynoch Press, Birmingham (1974).
5. G. M. Sheldrick, *System of Computing Programs*. University of Cambridge, U.K. (1976).
6. M. Nardelli, *Comput. Chem.* 1983, **7**, 95.
7. R. J. Goodfellow, P. L. Goggin and D. A. Duddel, *J. Chem. Soc. A* 1968, 504.
8. W. D. Geary, *Coord. Chem. Rev.* 1971, **7**, 81.
9. G. Bruno, S. Campagna, M. Cusumano, A. Giannetto and V. Ricevuto, unpublished work.
10. L. M. Tack, J. L. Hubbard, G. R. Kriek, J. Dubrawski and J. H. Enemark, *Cryst. Struct. Commun.* 1981, **10**, 385.
11. G. Bombieri, G. Bruno, M. Cusumano, G. Guglielmo and V. Ricevuto, *Polyhedron* 1985, **4**, 1365.
12. G. Tresoldi, G. Bruno, P. Piraino, G. Faraone and G. Bombieri, *J. Organomet. Chem.* 1984, **265**, 311.
13. A. Albinati, C. Arz and P. S. Pregosin, *Inorg. Chem.* 1987, **26**, 508, and refs therein.

Polyhedron Vol. 8, No. 2, pp. 167–173, 1989
Printed in Great Britain

0277–5387/89 $3.00+.00
© 1988 Pergamon Press plc

2-QUINALDINATE CARBONYL COMPLEXES OF RHODIUM(I) WITH SUBSTITUTED TRIARYLPHOSPHINE LIGANDS

J. V. HERAS,* M. CANO, M. A. LOBO and E. PINILLA

Departamento de Química Inorgánica, Facultad de Ciencias Químicas, Universidad Complutense, 28040-Madrid, Spain

(*Received* 16 *October* 1987; *accepted* 25 *July* 1988)

Abstract—A number of square-planar rhodium(I) complexes [Rh(N⁀O)LL′] [L,L′ = CO; L = CO, L′ = P(X—C_6H_4)$_3$ (X = 4-CH_3O, 4-CH_3, 3-CH_3, 2-CH_3, 4-F, 4-Cl)], containing 2-quinaldinate (C_9NH_6—COO^-) as monoanionic N⁀O bidentate have been synthesized by means of the reaction [Rh(quin)(NBD)]+CO → [Rh(quin)(CO)$_2$]+NBD [NBD = norbornadiene (bicyclo-2,2,1-hepta-2,5-diene)], or alternatively by reaction of [Rh(acac)(CO)$_2$] with 2-quinaldinic acid. Only one of the carbonyl groups in the [Rh(quin)(CO)$_2$] could be substituted by triarylphosphine ligands and complexes of the type [Rh(quin)(CO) P(X—C_6H_4)$_3$]] were obtained in all cases. The square-planar monocarbonyl complexes were isolated in one or two isomeric forms depending on the π-acceptor properties of the phosphine ligand present. Using excess of triarylphosphine the new pentacoordinated compounds [Rh(quin)(CO)[P(X—C_6H_4)$_3$]$_2$] were obtained and two isomeric forms were separated in most cases.

It is well known that the dicarbonylic complexes of the type [Rh(N⁀O)(CO)$_2$] [(N⁀O) = anionic chelate, N⁀O donor ligand] react with neutral ligands (L) such as PPh_3 or $AsPh_3$ to give the monocarbonyl derivatives [Rh(N⁀O)(CO)(L)].[1–6] In these reactions,

$$[Rh(N\frown O)(CO)_2] + L \rightarrow [Rh(N\frown O)(CO)(L)] + CO,$$

two isomers are possible, but only one has been isolated in all the cases investigated.

The crystallographic results for one series of the above monocarbonyl complexes indicated that the nitrogen atom of the chelate ring has a larger *trans*-influence than that of the oxygen atom.[7–10]

On the other hand, in complexes of the type [Rh(quin)(CO)$_2$] and [Rh(β-diketonate)(CO)$_2$] it has been observed that two carbonyl groups are substituted by triphenylphosphite to form the corresponding bis-triphenylphosphite complexes.[11–13] This fact is explained by Leipoldt and co-workers[13] by the formation of two very strong Rh—P bonds as a result of the largest π-acceptor properties of the triphenylphosphite.[14]

Although in the above examples, the two carbonyl groups can be substituted, in recent work Leipoldt suggested that the [Rh(quin)(CO)$_2$] complex only yields the monosubstituted complex in their reactions with triphenylphosphine.[13] It is reasonable to think that the formation of mono- or disubstituted species is clearly dependent on the nature of the P-donor ligands.[13,15]

Based on these considerations, we set out to investigate the reactivity of the [Rh(quin)(CO)$_2$] dicarbonyl complex[1] with triarylphosphine ligands of different π-acceptor capacity, P(X—C_6H_4)$_3$ (X = 4-CH_3O, 4-CH_3, 3-CH_3, 2-CH_3, 4-F, 4-Cl). A stoichiometric molar ratio of phosphine/complex or an excess of these ligands has been employed in all cases.

RESULTS AND DISCUSSION

[Rh(quin)(NBD)] *and* [Rh(quin)(CO)$_2$] *complexes*

Reaction of the dimeric rhodium(I) complex, [RhCl(NBD)]$_2$, in benzene with an equimolar amount of 2-quinaldinic acid (Hquin) in the presence of sodium carbonate, gave rise to a break of the chlorine bridges in the dimeric compound, and an orange solid was isolated from the reaction

*Author to whom correspondence should be addressed.

medium. The new compound has been characterized on the basis of the analytical and spectroscopic data as [Rh(quin)(NBD)] (**I**).

The bubbling of carbon monoxide through a dichloromethane solution of this complex caused the displacement of the coordinated diolefin yielding the dicarbonyl derivative [Rh(quin)$(CO)_2$] (**II**) according to eq. (1):

$$[Rh(quin)(NBD)] + 2CO \rightarrow [Rh(quin)(CO)_2] + NBD. \quad (1)$$

Both compounds (**I**) and (**II**) are air-stable and non-electrolytes in acetone solutions (10^{-3} M), and they were obtained in high yields. The analytical data were consistent with the formulation proposed (Table 1).

The red–orange dicarbonylic derivative, which has been previously described,[1,13] can be also isolated by reaction of the [Rh(acac)$(CO)_2$] complex with an excess of Hquin.

The IR spectrum (Table 2) in the solid state of the [Rh(quin)(NBD)] complex shows one very strong ν_{as}(COO) band at 1640 cm^{-1}. This band appears in the same range of frequencies as that observed for the [Rh(pyc)(NBD)] complex, for which a bidentate N,O coordination is proposed.[6] Additionally, the bands which appear at 1310 and 717 cm^{-1} are assigned to the presence of the NBD ligand.[16]

The IR spectrum of the dicarbonyl derivative is in accord with that described by Ugo *et al.* for the same compound.[1]

The ^{1}H NMR spectrum of [Rh(quin)(NBD)] shows two multiplet peaks centred at δ = 1.35 and 4.4 ppm, which are attributed, respectively, to $>CH_2$ and $>CH+>CH$ protons of the NBD ligand; two multiplet peaks at δ = 8.4 (H^1) and 8–7.4 (H^2–H^6) ppm are attributed to the 2-quinaldinate ligand.

Table 1. Analytical data, physical properties and yields for the four-coordinated complexes

Complex	Colour	Analyses [Found (Calc.)(%)] C	H	N	M.p. (°C)	Yield (%)
[Rh(quin)(NBD)]	Orange	55.3 (55.7)	3.8 (3.8)	3.7 (3.8)	214[a]	75
[Rh(quin)$(CO)_2$]	Red–orange	42.5 (43.4)	1.9 (2.1)	4.1 (4.2)	218	98
[Rh(quin)(CO)[P(4-CH_3O—$C_6H_4)_3$]]	Yellow	58.4 (58.7)	4.2 (4.1)	1.9 (2.1)	112	72
[Rh(quin)(CO)[P(4-CH_3—$C_6H_4)_3$]]	Yellow	62.9 (63.3)	4.6 (4.4)	2.5 (2.3)	225	85
[Rh(quin)(CO)[P(4-F—$C_6H_4)_3$]]	Orange–yellow	55.9 (56.2)	2.9 (2.9)	2.3 (2.3)	178[a]	75
[Rh(quin)(CO)[P(4-Cl—$C_6H_4)_3$]]	Orange–yellow	51.6 (52.1)	2.9 (2.7)	2.2 (2.1)	135	75
[Rh(quin)(CO)[P(3-CH_3—$C_6H_4)_3$]]	Yellow	63.2 (63.3)	4.6 (4.4)	2.1 (2.3)	242	80
[Rh(quin)(CO)[P(2-CH_3—$C_6H_4)_3$]]	Yellow	62.9 (63.3)	4.4 (4.4)	2.3 (2.3)	250[a]	80

[a] Decomposition temperature.

Table 2. IR and ^{31}P NMR spectral data for the four-coordinated complexes

Complex	IR (KBr, cm^{-1}) ν(C≡O)	ν_{as}(COO)	ν_{sym}(COO)	$\Delta\nu$(COO)	^{31}P NMR ($CDCl_3$ solution) δ (ppm)	J (Hz)
[Rh(quin)(NBD)]	—	1640vs	1330vs	310		
[Rh(quin)$(CO)_2$]	2100vs 2000vs	1658vs	1325vs	360		
[Rh(quin)(CO)[P(4-CH_3O—$C_6H_4)_3$]]	1959vs	1658vs	1325vs	333	38.61d	168.14
[Rh(quin)(CO)[P(4-CH_3—$C_6H_4)_3$]]	1961vs	1660vs	1324vs	336	40.89d	168.46
[Rh(quin)(CO)[P(4-F—$C_6H_4)_3$]]	1972vs 1960vs	1660vs	1325vs	335	41.20d 41.14d	171.64 171.63
[Rh(quin)(CO)[P(4-Cl—$C_6H_4)_3$]]	1970vs 1960vs	1660vs	1324vs	336	42.37d 42.19d	172.02 172.43
[Rh(quin)(CO)[P(3-CH_3—$C_6H_4)_3$]]	1960vs	1662vs	1328vs	334		
[Rh(quin)(CO)[P(2-CH_3—$C_6H_4)_3$]]	1955vs	1661vs	1325vs	336		

$[Rh(quin)(CO)[P(X—C_6H_4)_3]]$ (X = 4-CH_3O, 4-CH_3, 3-CH_3, 2-CH_3, 4-F, 4-Cl)

Addition of triarylphosphine ligands to a dichloromethane solution of $[Rh(quin)(CO)_2]$ in a 1:1 molar ratio gave monocarbonyl compounds of the type $[Rh(quin)(CO)[P(X—C_6H_4)_3]]$.

The new complexes are air-stable at room temperature, soluble in CH_2Cl_2 or $CHCl_3$ and moderately soluble in other polar solvents. The analytical data, Table 1, were consistent with the formulations proposed.

The IR spectra (Table 2) of the solid compounds show one band in the 1662–1658 cm^{-1} region assigned to $\nu_{as}(COO)$ of the carboxylic group. This band is not significantly shifted with respect to the initial compounds and it is characteristic of a bidentate N,O coordination of ligands of the type pyridincarboxylate.[17–19]

On the other hand, a very strong absorption band in the 1972–1955 cm^{-1} region has been assigned to the $\nu(C{\equiv}O)$ of the carbonyl group. This band appears to be split when the phosphine ligands are $P(4\text{-}F—C_6H_4)_3$ and $P(4\text{-}Cl—C_6H_4)_3$, and it can be attributed either to solid state effects or to the presence of two isomeric forms.

In the cases in which one $\nu(C{\equiv}O)$ vibration is observed, it can be reasonably assumed that the only isomer is obtained with the phosphine *trans* to the heterocyclic nitrogen, due to the strong *trans* effect of this atom. This is in agreement with the results of structure determinations on [Rh(oxine)(CO)(PPh_3)], [Rh(oxine)(COD)], [Rh(Sal—NR)(PR_3)] and [Rh(pyc)(CO)(PPh_3)].[7–10] All the compounds show characteristic IR absorptions of the coordinated phosphine ligand.[20]

A correlation between $\nu(C{\equiv}O)$ and the basicity of the triarylphosphine ligands can be observed, and an increase in the basicity of the triarylphosphine causes a shift in the $\nu(C{\equiv}O)$ towards lower frequencies.

The ^{31}P NMR spectra of the complexes containing *p*-substituted triarylphosphine ligands have been registered (Table 2). Different behaviour is also observed depending on the phosphine ligands. Thus, in the cases in which X = 4-CH_3O or 4-CH_3, only one doublet appears at δ = 38.61 ppm, J = 168.14 Hz and δ = 40.89 ppm, J = 168.46 Hz, respectively. However, when X = 4-F, 4-Cl, two doublets with the same J(Rh—P) (Table 2) were observed. It is reasonable to attribute this to the presence of two isomeric forms. On the other hand, it is remarkable that the two doublets have the same intensity when X = 4-F and a very different intensity (1:6) when X = 4-Cl.

The above $\nu(C{\equiv}O)$ and J(Rh—P) data support the formation of square-planar rhodium(I) compounds.[5]

It is noteworthy that the isomers are observed only in the cases in which the substituted triarylphosphine ligands show the strongest π-acceptor properties. In these cases, the *σ–trans* effect of the nitrogen relative to the oxygen of the 2-quinaldinate ligand does not seem significantly different. This fact has also been reported by Leipoldt and co-workers in the [Rh(quin)$[P(O—C_6H_5)_3]_2$] complex.[13] Thus, the two isomers observed in our compounds are attributed to the substitution in the $[Rh(quin)(CO)_2]$ of the carbonyl group *trans* to the nitrogen or oxygen atom, respectively. Unfortunately, we have not been able to separate these isomers.

$[Rh(quin)(CO)[P(X—C_6H_4)_3]_2]$ (X = 4-CH_3O, 4-CH_3, 3-CH_3, 4-F, 4-Cl)

New compounds of the type [Rh(quin)(CO)$[P(X—C_6H_4)_3]_2$] have been isolated when the complexes $[Rh(quin)(CO)[P(X—C_6H_4)_3]]$ or [Rh(quin)$(CO)_2$] were allowed to react with the triarylphosphine ligands in a 1:1 or 1:2 molar ratio, respectively. However, different behaviour was observed with $P(2\text{-}CH_3—C_6H_4)_3$ and in these reactions only the square-planar $[Rh(quin)(CO)[P(2\text{-}CH_3—C_6H_4)_3]]$ species was obtained. It is possible that the steric characteristics of this ligand may prevent an increase in the coordination.

All the $[Rh(quin)(CO)[P(X—C_6H_4)_3]_2]$ complexes investigated in this work, with exception of the $[Rh(quin)(CO)[P(4\text{-}CH_3O—C_6H_4)_3]_2]$ derivative, were obtained in two isomeric forms, "a" and "b", in the solid state (Table 3). The solids isolated are diamagnetic, of moderate to good stability, soluble in solvents such as CH_2Cl_2 or $CHCl_3$ and moderately soluble in acetone, EtOH, MeOH etc.

Table 3 lists some identifying properties of the solid isomers. It was found, in solution, that all the solid "a" and "b" present a more or less quick evolution towards the square-planar compounds, and in all the cases after 24 h these species can be precipitated from their solutions.

The IR spectra of the solid "a" and "b" isomers in the carbonyl stretching region show in all cases one single strong $\nu(C{\equiv}O)$ absorption without splitting or shoulders (Table 3). These bands are shifted to lower frequencies with respect to the tetracoordinated starting compounds (Table 2). This fact is consistent with an increase in the electronic density of the rhodium atom caused by the coordination of a new phosphine ligand. It is remarkable that this shift is more enhanced in the "a" than the "b" sets. The sequence of their values is again in

Table 3. Colour, analytical and IR spectral data for the [Rh(quin)(CO)[P(X—C_6H_4)$_3$]$_2$] complexes

	Complex	Colour	Analyses [Found(Calc.)](%) C	H	N	IR (cm^{-1}) KBr discs ν(C≡O)	ν_{as}(COO)	ν_{sym}(COO)	$\Delta\nu$(COO)	ν(Rh—O=C)	CH_2Cl_2 solution[a] ν(C≡O)	ν_{as}(COO)
	[Rh(quin)(CO)[P(4-CH_3O—C_6H_4)$_3$]$_2$]	Yellow	62.7(63.2)	4.6(4.8)	1.4(1.4)	1911vs	1634vs	1353s	281	347w	1967sh, 1931s (1966vs)[b]	1654sh, 1629s (1653vs)[b]
	[Rh(quin)(CO)[P(4-CH_3—C_6H_4)$_3$]$_2$]	Yellow	68.2(69.0)	5.5(5.3)	1.5(1.5)	1930vs	1633vs	1360s	273	350w	1968sh, 1933s (1967vs)[b]	1655sh, 1628s (1655vs)[b]
'a'	[Rh(quin)(CO)[P(3-CH_3—C_6H_4)$_3$]$_2$]	Yellow	68.2(69.0)	5.1(5.3)	1.7(1.5)	1918vs	1631vs	1351s	280	352w	1966sh, 1936s (1967vs)[b]	1658sh, 1630s (1657vs)[b]
	[Rh(quin)(CO)[P(4-F—C_6H_4)$_3$]$_2$]	Yellow	59.8(60.3)	3.4(3.2)	1.6(1.5)	1920vs	1633vs	1355s	278	346w	1971sh, 1940s (1972s)[b]	1659sh, 1630s (1659s)[b]
	[Rh(quin)(CO)[P(4-Cl—C_6H_4)$_3$]$_2$]	Yellow	53.7(54.6)	3.1(2.9)	1.3(1.3)	1926vs	1640vs	1351s	289	349w	1973sh, 1943s (1974vs)[b]	1661sh, 1631s (1659vs)[b]
	[Rh(quin)(CO)[P(4-CH_3—C_6H_4)$_3$]$_2$]	Orange	68.1(69.0)	5.2(5.3)	1.5(1.5)	1950vs	1610vs	1362s	248	350w	1969sh, 1935s	1657sh, 1629s
'b'	[Rh(quin)(CO)[P(3-CH_3—C_6H_4)$_3$]$_2$]	Orange	67.9(69.0)	5.1(5.3)	1.6(1.5)	1950vs	1612vs	1366s	246	352w	1968sh, 1937s	1658sh, 1630s
	[Rh(quin)(CO)[P(4-F—C_6H_4)$_3$]$_2$]	Orange	59.7(60.3)	3.4(3.2)	1.5(1.5)	1958vs	1612vs	1361s	251	346w	1970sh, 1940s	1658sh, 1630s
	[Rh(quin)(CO)[P(4-Cl—C_6H_4)$_3$]$_2$]	Orange	53.8(54.6)	3.0(2.9)	1.3(1.3)	1962vs	1618vs	1365s	253	349w	1972sh, 1942s	1660sh, 1630s

[a] Freshly prepared solutions.

[b] Values in parentheses refer to spectra of [Rh(quin)(CO)[P(X—C_6H_4)$_3$]] parent compounds.

agreement with the basicity of the phosphine ligand.

A significant trend was also observed for the —COO stretching modes of the carboxylate group of the 2-quinaldinate ligand. In all cases the decrease in ν_{as}(COO) and the increase in ν_{sym}(COO) with respect to the parent compounds may be significant of a new interaction occuring through the oxygen of the —C=O group which was uncoordinated in the square-planar parent compounds. These modifications are also different in the "a" and "b" series and the highest values of $\Delta\nu(COO) = \nu_{as} - \nu_{sym}$ are found in the compounds of type "a".

The position of the antisymmetric stretching carbonyl band at *ca* 1610 cm^{-1} for the "b" isomers is very similar to that observed in other pyridine carboxylate complexes[17,19] for which a bidentate or bridge O,O coordination is suggested in the solid state.

On the other hand, in most of the examples of 2-pyridincarboxylate complexes a coordination involving terminal and/or bridging carboxylate groups and the pyridine nitrogen atom was observed. However, when terminal carboxylate groups are present the ν_{as}(COO) appears at values higher than 1660 cm^{-1}.

For the above considerations a monodentate coordination through only one oxygen is ruled out for our compounds, and it is suggested that the 2-quinaldinate ligand is coordinated through one oxygen of the carboxylate group and possibly through the heterocyclic nitrogen. Additional interactions, which are higher for "b" than for "a" isomers, through the other carboxylic oxygen are also

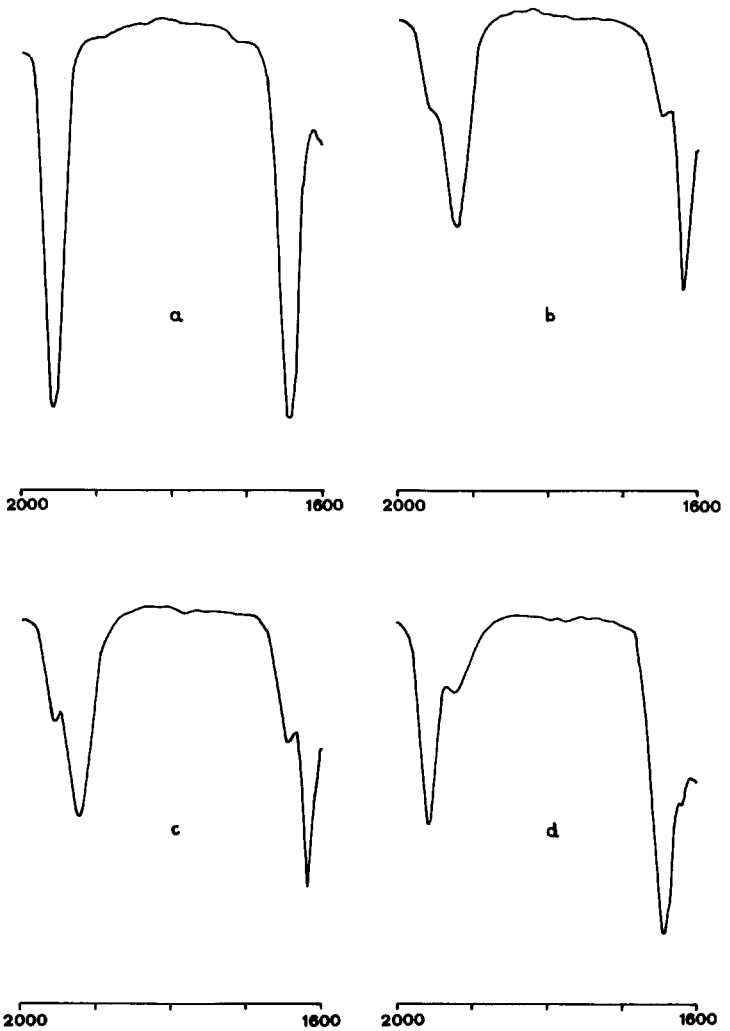

Fig. 1. IR spectra (2000–1600 cm^{-1}) in CH_2Cl_2 solution of (a): [Rh(quin)(CO)[P(4-CH_3O—C_6H_4)$_3$]$_2$]; (b): [Rh(quin)(CO)[P(4-CH_3O—C_6H_4)$_3$]$_2$] in fresh solution; (c): [Rh(quin)(CO)[P(4-CH_3O—C_6H_4)$_3$]$_2$] after 3 h; (d): [Rh(quin)(CO)[P(4-CH_3O—C_6H_4)$_3$]$_2$] after 20 h.

possible and they are consistent with the values of the ν_{as}(COO) frequencies. This is also supported by the appearance of new bands at 346–352 cm^{-1} (Table 3) tentatively assigned to ν(M—O) vibrations.[19,21,22]

In contrast, the IR spectra in CH_2Cl_2 solutions were the same for the "a" and "b" isomers of each phosphine ligand. In all cases the pattern of the bands in carbonyl stretching region showed one strong sharp absorption with a shoulder [Table 3, Fig. 1(b)]. The shoulders were identical in position to the ν(C≡O) bands in the parent tetracoordinated monocarbonyl compounds (Table 3) and their intensities increased with time [Fig. 1(c) and (d)].

Similar behaviour was observed in the stretching carboxylate ν(COO) region. In all cases when the IR were registered a few minutes after the solutions were prepared, two bands at *ca* 1660 and 1630 cm^{-1} were observed. The first band was in the same position as that of the ν_{as}(COO) of the square-planar compounds [Rh(quin)(CO)[P(X—C_6H_4)$_3$]] (Table 3). An increase in the intensity of the former together with a decrease in the latter bands was observed with time [Fig. 1(c) and (d)], and after 24 h only the characteristic bands of the starting tetracoordinated complexes were present [Fig. 1(a)].

The above considerations indicate that the compounds [Rh(quin)(CO)[P(X—C_6H_4)$_3$]$_2$] present two isomeric forms "a" and "b" in the solid state but in CH_2Cl_2 solution only one is detected and this is transformed towards the tetracoordinated starting materials.

It is probable that the new compounds present in the solid state have a five-coordinate geometry, but there are many possible isomeric forms for it and unfortunately characterization by X-ray diffraction has not been possible because attempts to crystallize the compounds caused conversion to the square-planar tetracoordinated [Rh(quin)(CO)[P(X—C_6H_4)$_3$]].

The ^{31}P NMR spectra for the "a" and "b" isomers [Rh(quin)(CO)[P(4-F—C_6H_4)$_3$]$_2$] recorded in $CDCl_3$ solutions for 10 min, present only one broad peak at δ = 43.73 ppm, which is not split by coupling with the ^{103}Rh atom. This fact can also be explained if an interchange process has been occurring. The signal is slightly shifted with time but in none of the cases was Rh—P coupling observed. After 20 min, the spectra show a broad signal at δ = 26.84 ppm which is approximately in the average position of the square-planar species and the free phosphines ligand. After 5 h, this signal was not modified.

We think that in solution the [Rh(quin)(CO)[P(X—C_6H_4)$_3$]$_2$] species are transformed into the square-planar complexes according to eq. (2):

$$[Rh(quin)(CO)[P(X—C_6H_4)_3]_2] \rightleftharpoons [Rh(quin)(CO)[P(X—C_6H_4)_3]] + P(X—C_6H_4)_3 \quad (2)$$

and that a fast interchange process may exist between the free and coordinated phosphine ligands.[15]

EXPERIMENTAL

C, H, N analyses were carried out by Elemental Micro-Analyses Ltd Laboratories, Amberley, Beaworth, Devon, U.K. IR spectra in the 4000–200 cm^{-1} region were recorded on Perkin–Elmer 325 and 1300 spectrophotometers using KBr discs and dichloromethane solutions. The ^{1}H NMR spectrum was recorded on a Perkin–Elmer R-12 apparatus at 90 MHz. The ^{31}P NMR spectra were recorded on a Varian FT-80A apparatus at 200 MHz. Conductance measurements were performed in acetone solutions (approx 10^{-3} M) with a Philips PR9500 conductimeter.

[Rh(quin)(NBD)]

A stoichiometric amount of 2-quinaldinic acid (Hquin) was added to a benzene suspension of the [RhCl(NBD)]$_2$ complex. After the addition of an excess of Na_2CO_3 and stirring for 12 h at room temperature the reaction mixture was filtered. The orange solid was dissolved in dichloromethane, the Na_2CO_3 was filtered off and the complex precipitated by addition of cold Et_2O; it was recrystallized from CH_2Cl_2–Et_2O, washed with Et_2O and vacuum-dried (Yield 75%).

[Rh(quin)(CO)$_2$]

Method (*a*). Carbon monoxide was bubbled through a solution of the [Rh(quin)(NBD)] complex in CH_2Cl_2 at room temperature for 1 h. The colour of the solution changed from yellow to orange. The red–orange complex was precipitated by the addition of Et_2O, recrystallized from CH_2Cl_2–Et_2O and vacuum-dried.

Method (*b*). An excess of 2-quinaldinic acid was added to an acetone solution of [Rh(acac)(CO)$_2$]. Immediately, the colour of the solution changed from yellow to red–orange. After 1 h stirring the addition of water gave rise to the quantitative precipitation of the red–orange dicarbonyl compound, which was filtered off, washed with water and vacuum-dried (Yield 98%).

[Rh(quin)(CO)[P(X—C_6H_4)$_3$]] (X = 4-CH_3O, 4-CH_3, 3-CH_3, 2-CH_3, 4-F, 4-Cl)

The addition of P(X—C_6H_4)$_3$ to a solution of [Rh(quin)(CO)$_2$] in CH_2Cl_2, in a 1 : 1 stoichiometric ratio, caused evolution of CO and the colour changed from orange to yellow. The solution was stirred for about 18 h, and then cold *n*-hexane was added and the faint yellow precipitate that appeared was separated by filtration. After concentration of the solution under reduced pressure the solid compounds were obtained; they were filtered off, recrystallized from CH_2Cl_2–*n*-hexane and vacuum-dried.

[Rh(quin)(CO)[P(X—C_6H_4)$_3$]$_2$] (X = 4-CH_3O, 4-CH_3, 3-CH_3, 4-F, 4-Cl)

A solution of [Rh(quin)(CO)$_2$] (100 mg, 0.3 mmol) in 20 cm^3 of dichloromethane was added to 0.6 mmol of the phosphine ligand (X = 4-CH_3O, 212 mg; X = 4-CH_3, 3-CH_3, 183 mg; X = 4-F, 190 mg; X = 4-Cl, 220 mg).

When the phosphine ligand was P(4-F—C_6H_4)$_3$ the solution was stirred for 30 min, then 5 cm^3 of *n*-hexane were added and a light orange precipitate ("b"-isomer) was obtained. This was filtered off, washed with *n*-hexane and vacuum dried. The solution was concentrated and a light yellow solid ("a"-isomer) was obtained and separated by the same procedure.

For the phosphine ligand, P(3-CH_3—C_6H_4)$_3$, a fast reaction occurred. After the addition of hexane (40 cm^3), filtration and concentration of the solution, a light yellow solid was obtained, which was filtered off, washed with *n*-hexane and vacuum-dried ("a"-isomer). Hexane was added to an acetone solution of the "a"-isomer and an orange solid ("b"-isomer) was separated by an analogous procedure to the above.

When the phosphine ligands employed were P(4-CH_3—C_6H_4)$_3$ and P(4-Cl—C_6H_4)$_3$, the reactions in dichloromethane–*n*-hexane (40 cm^3) yielded the simultaneous precipitation of the "a" and "b" isomers. In the first case (X = 4-CH_3), a reaction temperature of 0°C was necessary and the reaction occurred instantaneously. The separation of the two forms was possible by treatment of the mixture with benzene–*n*-hexane (1 : 3) or *n*-hexane–dichloromethane (6 : 1), to give an orange ("b"-isomer) or yellow ("a"-isomer) precipitate, respectively. These were filtered off and vacuum-dried. In the second case (X = 4-Cl), the reaction time was 20 min; the isomer mixture was treated with *n*-hexane–dichloromethane (6 : 1) or acetone–*n*-hexane (1 : 3), and the "b" or "a" isomers were respectively isolated by concentration of the solutions, which we than filtered off and vacuum-dried.

In the reaction with P(4-CH_3O—C_6H_4)$_3$ only the "a"-isomer was obtained and this reaction occurred instantaneously. The addition of *n*-hexane gave rise to precipitation of a yellow solid, which was isolated as in the above cases.

REFERENCES

1. R. Ugo, G. La Monica, S. Cenini and F. Bonati, *J. Organomet. Chem.* 1968, **11**, 159.
2. L. G. Kuzmina, Yu. S. Varshavskii, N. G. Bokii, Yu. T. Struchkov and T. G. Cherkasova, *Zh. Strukt. Khim.* 1971, **12**, 653; L. G. Kuzmina, Yu. S. Varshavskii, N. G. Bokii, Yu. T. Struchkov and T. G. Cherkasova, *J. Struct. Chem.* 1971, **12**, 593.
3. Yu. S. Varshavskii, T. G. Cherkasova and N. A. Buzina, *Zh. Neorg. Khim.* 1972, **17**, 2208; Yu. S. Varshavskii, T. G. Cherkasova and N. A. Buzina, *Russ. J. Inorg. Chem.* 1972, **17**, 1150.
4. Yu. S. Varshavskii, T. G. Cherkasova, N. A. Buzina and V. A. Kormer; *J. Organomet. Chem.* 1974, **77**, 107.
5. R. Usón, L. A. Oro, M. Sanaú, P. Lahuerta and K. Hildenbrand, *J. Inorg. Nucl. Chem.* 1981, **43**, 419.
6. J. V. Heras, E. Pinilla and M. Martínez, *Polyhedron* 1983, **2**, 1009.
7. J. G. Leipoldt, S. S. Basson and C. R. Dennis, *Inorg. Chim. Acta* 1981, **50**, 121.
8. J. G. Leipoldt and E. C. Grobler, *Inorg. Chim. Acta* 1983, **72**, 17.
9. J. G. Leipoldt, S. S. Basson, E. C. Grobler and A. Roodt, *Inorg. Chim. Acta* 1985, **99**, 13.
10. J. G. Leipoldt, G. J. Lamprecht and D. E. Graham, *Inorg. Chim. Acta* 1985, **101**, 123.
11. A. M. Trzeciak and J. J. Ziólowski, *Inorg. Chim. Acta* 1982, **64**, L267.
12. G. J. Lamprecht, J. G. Leipoldt and G. J. van Zyl, *Inorg. Chim. Acta* 1985, **97**, 31.
13. G. J. Lamprecht, J. H. Beetge, J. G. Leipoldt and D. R. De Waal, *Inorg. Chim. Acta* 1986, **113**, 157.
14. J. E. Huheey, *Inorganic Chemistry Principles of Structure and Reactivity*. Harper and Row, New York (1972).
15. A. M. Trzeciak and Jófer J. Ziólowski, *Inorg. Chim. Acta* 1985, **96**, 15.
16. I. A. Zakharova, Ya V. Salyn, I. A. Garbouzova, V. T. Aleksanyan and M. A. Prianichnikova, *J. Organomet. Chem.* 1975, **102**, 227.
17. A. J. Crowe, R. Hill and P. J. Smith, *J. Organomet. Chem.* 1981, **204**, 47.
18. T. E. Dorsett and R. A. Walton, *J. Chem. Soc., Dalton Trans.* 1976, 347.
19. S. K. Sengupta, S. K. Sahni and R. N. Kapoor, *Polyhedron* 1983, **2**, 317.
20. G. B. Deacon and J. H. S. Green, *Spectrochim. Acta* 1968, **24A**, 845.
21. D. M. Adams, *Metal Ligand and Related Vibrations*, E. Arnold, London (1967).
22. J. R. Ferraro, *Low-frequency Vibrations of Inorganic and Coordination Compounds*. Plenum Press, New York (1971).

Polyhedron Vol. 8, No. 2, pp. 175–178, 1989
Printed in Great Britain

0277–5387/89 $3.00+.00
© 1988 Pergamon Press plc

COMPLEXATION OF IRON(II) WITH 3-HYDROXYIMINOPENTANE-2,4-DIONE (Hinaa)

ANTHONY R. BUTLER,* ADRIANNE M. CALSY and CHRISTOPHER GLIDEWELL

Department of Chemistry, The University, St. Andrews, Fife KY16 9ST, Scotland, U.K.

(*Received* 16 *March* 1988; *accepted* 15 *August* 1988)

Abstract—Iron(II) reacts with Hinaa (3-hydroxyiminopentane-2,4-dione) in the pH range 6.80–7.58 to give a complex ion of composition $[Fe(inaa)_3]^-$. NMR evidence suggests that it is the *fac* isomer. A kinetic study, using stopped-flow spectrophotometry, demonstrated that the rate of formation of the complex depends upon $[inaa^-]^3$. Therefore, the rate-determining step must be cyclization of the *third* $inaa^-$ ligand.

It has been known[1] for a number of years that 3-hydroxyiminopentane-2,4-dione [(1), otherwise named isonitrosoacetylacetone and abbreviated to Hinaa] forms highly coloured complexes with some transition metals. More recently,[2,3] this has been exploited as a means of extracting metal ions from aqueous solution. Also the reaction of **1** with iron(II) to give a blue complex has been used as a method of assay[4] for iron(II) in the presence of iron(III), with which **1** has no reaction.

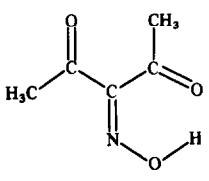

(1)

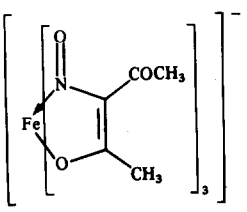

(2)

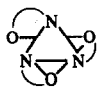

(3)

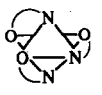

(4)

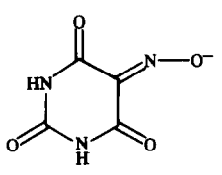

(5)

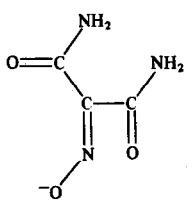

(6)

*Author to whom correspondence should be addressed.

RESULTS AND DISCUSSION

There is some disagreement in the literature concerning the structure of the blue complex. It has been described[2–4] as the neutral species $Fe^{II}(inaa)_2$, consistent with its solubility in organic solvents. However, Ablov and Zubarev[5] formulated this product as $Na[Fe^{II}(inaa)_3]$, containing octahedral low-spin iron(II), on the basis of elemental analysis (for Fe and N), the observed diamagnetism, and its behaviour as a 1:1 electrolyte in methanol solution. Our elemental analysis confirms the identity of our product with that of Ablov and Zubarev, while the observation of sharp NMR spectra confirms the diamagnetism of the iron, which must therefore be present as low spin iron(II). The structure of the $[Fe(inaa)_3]^-$ ion can be deduced with a measure of certainty by comparison of its spectroscopic data with those of related complexes. Cobalt(III) forms a complex with Hinaa which is the octahedral neutral species $Co^{III}(inaa)_3$. IR spectra (Table 1) and ^1H NMR spectra have established[6] that here $inaa^-$ is a bidentate ligand, bound to the metal through the oxime nitrogen and the oxygen of one carbonyl group. Two neutral complexes have been isolated,[7,8] from the reaction of palladium(II) with Hinaa, of identical composition, $Pd(inaa)_2$. Again IR and ^1H NMR spectroscopy have established that they are *cis* and *trans* isomers in which chelation of $inaa^-$ is the same as that in $Co(inaa)_3$. Table 1 shows the principal IR frequencies and ^1H chemical shifts of the iron(II) $inaa^-$ complex, together with those of $Co(inaa)_3$ and $Pd(inaa)_2$ for comparison. The close similarities suggest that the binding in $[Fe(inaa)_3]^-$ is the same as that in $Co(inaa)_3$ and $Pd(inaa)_2$, i.e. as in **2**. However, ion

Table 1. Spectroscopic data for metal–inaa complexes

	Cobalt(III)[6]	Palladium(II)[7,8] *trans*	Palladium(II)[7,8] *cis*	Iron(II)
IR frequencies (cm^{-1})				
ν(C=O), free	1684	1662	1660	1665
ν(C=C), perturbed, and/or ν(C=N)	1530	1520	1520	1525
^{1}H NMR, $\delta(CH_3)$ (ppm)	2.7, 3.2[a]	2.3, 2.6[b]	2.3, 2.6[b]	2.1, 2.5[c]

[a] CCl_4 solution.
[b] $CDCl_3$ solution.
[c] DMSO solution.

2 can exist in two isomeric forms, *fac* and *mer* **3** and **4**. The two methyl groups of each ligand are in different environments (see **2**) and will give rise to two signals in the ^{1}H NMR spectrum. In the form $[Fe(inaa)_3]^-$ it is only the *fac* isomer which has the three ligands equivalent. The ^{1}H NMR spectrum of $[Fe(inaa)_3]^-$ in DMSO has signals (2.10 and 2.50 ppm) corresponding to only two methyl groups with no evidence of splitting, consistent with the complex existing as the *fac* isomer. This is the preferred form for the related ligands violurate (**5**) and isonitrosomalamide (**6**) in the salts ammonium tris(violurato)ferrate(II)[9] and potassium tris (isonitrosomalamido)ferrate(II),[10] established by X-ray crystallography.

The conversion of $[Fe(H_2O)_6]^{2+}$ into $[Fe(inaa)_3]^-$ must occur by stepwise replacement of water as a ligand and we investigated the kinetics of reaction in order to ascertain the rate-determining step. The appearance of the absorbance at 600 nm due to $[Fe(inaa)_3]^-$ on mixing an aqueous solution of an Fe^{II} salt with an alkaline solution of Hinaa occurred on the stopped-flow time scale. The kinetics of reaction were examined under pseudo first-order conditions with $inaa^-$ in excess over Fe^{2+}. Because of the possibility that changes in pH could affect the reaction rate the reaction mixture was buffered using Hinaa as its own buffer. For this a solution of Hinaa was partially neutralized with NaOH to give a buffer based on the conjugate acid–base pair Hinaa–$inaa^-$. From the measured pH of this buffer and the known[11] pK_a of Hinaa, we calculated the $inaa^-$ concentration in each solution. This was further varied by dilution of the buffer with 0.50 M KCl solution; this changed [$inaa^-$] but not the pH. The buffer was placed in one arm of a stopped-flow spectrophotometer, while the other contained 5×10^{-4} M iron(II) sulphate. On mixing, the absorbance at 600 nm, due to $[Fe(inaa)_3]^-$, appeared in a first-order manner and from this the pseudo first-order rate constant (k_{obs}) was calculated. The results are displayed in Table 2. A plot k_{obs} is curved but monotonic; at identical values of [$inaa^-$] the pH has essentially no effect on the value of k_{obs} and so we conclude that it is [$inaa^-$] rather than the pH, which controls the rate of complexation. Curvature in the plot of k_{obs} against [$inaa^-$] suggests a dependence at a power greater than unity and, in fact, a plot of k_{obs} against [$inaa^-$]^3 is linear with no intercept (Fig. 1). This is consistent with the slow step being substitution of water by the *third* $inaa^-$ ligand, with the previous two substitutions being equilibrium processes (Scheme 1).

Table 2. Kinetic data[a] for the reaction of $inaa^-$ and iron(II)[b] at 25°C

10^2[$inaa^-$] (M)	pH	k_{obs} (s^{-1})
2.50	7.40	29
2.25	7.14	27
2.00	7.40	16
1.80	7.58	13
1.75	7.14	12
1.50	7.40	6.7
1.50	7.14	5.4
1.20	7.40	5.3
1.12	7.14	4.5
1.00	7.40	2.1
1.00	6.80	1.9

[a] I = 0.25 M.
[b] $[Fe^{2+}] = 2.5 \times 10^{-4}$ M.

The irreversible step (k_3 in Scheme 1) is not, of course, a single process. It can be broken down into three steps: (a) formation of complex **9**, (b) ligation by one end of the bidentate ligand $inaa^-$ with loss of one water molecule to give **10**, and (c) a second ligation with displacement of the final water molecule (Scheme 2). Step (a) is unlikely to be anything but fast. Also, it does not seem likely that (b), loss of the fifth water ligand to form complex **10**, will be slow as comparable reactions typically have rates

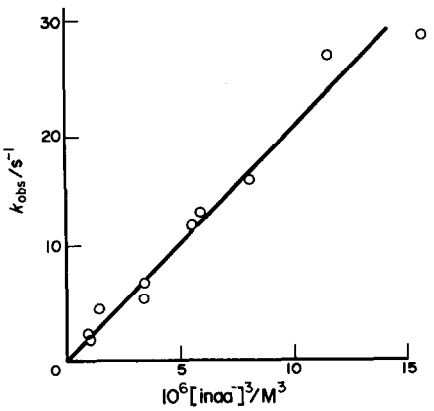

Fig. 1.

$$[Fe(H_2O)_6]^{2+} + inaa^- \overset{K_1}{\rightleftharpoons} [Fe(H_2O)_4(inaa)]^+ \quad (7)$$

$$(7) + inaa^- \overset{K_2}{\rightleftharpoons} [Fe(H_2O)_2(inaa)_2] \quad (8)$$

$$(8) + inaa^- \xrightarrow{k_3} [Fe(inaa)_3]^- \quad (2)$$

$$[(7)] = K_1[[Fe(H_2O)_6]^{2+}][inaa^-]$$

$$[(8)] = K_1K_2[[Fe(H_2O)_6]^{2+}][inaa^-]^2$$

$$d[(2)]/dt = k_3[(8)][inaa^-]$$

$$= k_{obs}[[Fe(H_2O)_6]^{2+}]$$

$$k_{obs} = k_3K_1K_2[inaa^-]^3$$

Scheme 1.

of the same order of magnitude as solvent exchange for labile species. Complexes in which some water ligands have been replaced are also generally subject to inductive labilization. Thus, we deduce that loss of the sixth water ligand and ring closure of $inaa^-$, k_c, is the rate-determining step. A similar scheme has been proposed[12] for the formation of $Fe(L)_3^{2+}$, where L is 1,10-phenanthroline or 2,2′-bipyridyl, from Fe^{2+} and the ligand in acid solution.

A notable feature in the formation of $[Fe(inaa)_3]^-$ is the change of spin state of iron during reaction; $Fe(H_2O)_6^{2+}$ is a d^6 high spin complex, and therefore kinetically labile, but as a diamagnetic species[5] $[Fe(inaa)_3]^-$ is a low spin, kinetically inert complex. By analogy[13] with the examples of $[Fe(phen)_2(H_2O)_2]^{2+}$ and $[Fe(phen)_3]^{2+}$, it is probable that the change to a low spin, diamagnetic complex occurs after complexation by the third $inaa^-$ ligand.

Although $inaa^-$ forms complexes with cobalt and palladium as well as iron(II) it was not possible to detect complex formation with ruthenium, nickel, copper, manganese or vanadium. Likewise, no reaction between iron(II) and 4-hydroxyimino-2,2,6,6-tetramethylheptane-3,5-dione in alkaline solution was detected, probably for steric reasons.

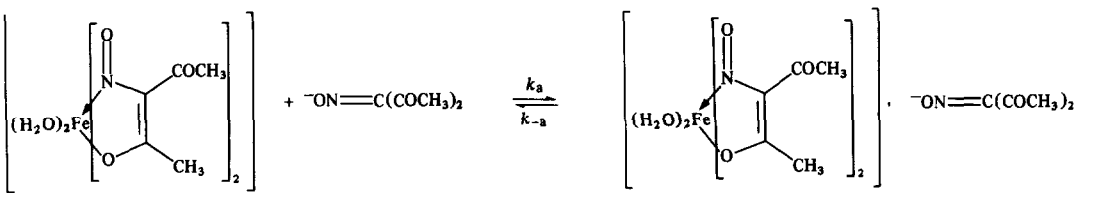

(8) (9)

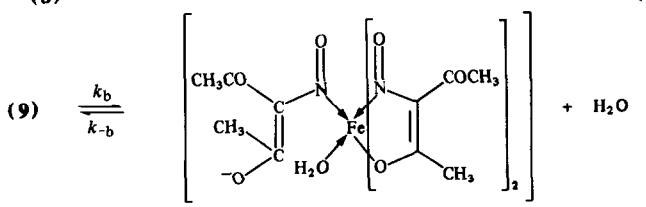

(10)

(10) $\xrightarrow{k_c}$ (2) + H_2O

Scheme 2.

EXPERIMENTAL

Hinaa (**1**)[14] and 4-hydroxyimino-2,2,6,6-tetramethyl-3,5-dione[15] were made by literature methods. Sodium acetate (30 mmol) was added to a solution of $FeCl_2$ (10 mmol) and Hinaa (30 mmol) in water (20 cm^3). After heating at 45–50°C under an atmosphere of nitrogen for 30 min the resulting dark blue crystals were filtered off and washed several times with cold water. Found: C, 38.2; H, 3.8; N, 8.9. $Na[Fe(inaa)_3]$, $C_{15}H_{18}FeN_3NaO_9$ requires: C, 38.9; H, 3.9; N, 9.1%.

For the kinetic studies a Hi-Tech stopped-flow spectrophotometer was used. A solution containing Hinaa–$inaa^-$ was placed in one syringe and a solution of iron(II) in the other. The ionic strength was set at 0.25 M by the addition of KCl.

REFERENCES

1. T. W. J. Taylor and E. K. Ewbank, *J. Chem. Soc.* 1926, 218.
2. A. Mrozowski and T. Lipiec, *Acta Pol. Pharm.* 1971, **28**, 291.
3. J. Bernal Nievas and J. Aznarez Alduan, *Rev. Acad. Cienc. Exactus Kis-Quim. Natur. Zaragoza* 1971, **26**, 381.
4. U. B. Talwar and B. C. Haldar, *J. Ind. Chem. Soc.* 1972, **49**, 785.
5. A. V. Ablov and V. N. Zubarev, *Rus. J. Inorg. Chem.* 1968, **13**, 1563.
6. N. J. Patel and B. C. Haldar, *J. Inorg. Nucl. Chem.* 1967, **29**, 1037.
7. U. B. Talwar and B. C. Haldar, *J. Inorg. Nucl. Chem.* 1970, **32**, 213.
8. D. A. White, *J. Chem. Soc. A* 1971, 233.
9. C. L. Raston and A. H. White, *J. Chem. Soc., Dalton Trans.* 1976, 1915.
10. C. L. Raston, A. H. White and R. M. Golding, *J. Chem. Soc., Dalton Trans.* 1977, 329.
11. J. D. Aubort, R. F. Hudson and R. C. Woodcock, *Tetrahedron Lett.* 1973, **24**, 2229.
12. H. Holyer, C. D. Hubbard, S. F. A. Kettle and R. G. Wilkins, *Inorg. Chem.* 1965, **4**, 929.
13. H. Irving and D. H. Mellor, *J. Chem. Soc.* 1962, 5222.
14. L. Wolff, *Anal.* 1902, **325**, 129.
15. C. W. Shoppee and D. Stevenson, *J. Chem. Soc., Perkin I* 1972, 3015.

Polyhedron Vol. 8, No. 2, pp. 179–187, 1989
Printed in Great Britain

0277–5387/89 $3.00+.00
© 1988 Pergamon Press plc

SYNTHESIS OF HETEROBIMETALLIC THIO– AND SELENO–ACYL COMPLEXES

ANTHONY F. HILL, BASHIR A. NASIR and F. GORDON A. STONE*

Department of Inorganic Chemistry, The University of Bristol, Bristol BS8 1TS, U.K.

(*Received* 25 *July* 1988; *accepted* 15 *August* 1988)

Abstract—The μ-alkylidyne dimetal complexes $[MFe(\mu\text{-}CC_6H_3Me_2\text{-}2,6)(CO)_5(\eta\text{-}C_5H_5)]$ (M = Cr, Mo, or W) react with elemental sulphur or selenium yielding the heterobimetallic compounds $[MFe(\mu\text{-}\eta^2\text{-}ECC_6H_3Me_2\text{-}2,6)(CO)_5(\eta\text{-}C_5H_5)]$ (E = S, Se). The complexes $[MFe(\mu\text{-}\eta^2\text{-}ECC_6H_3Me_2\text{-}2,6)(\mu\text{-dppm})(\mu\text{-CO})(CO)_2(\eta\text{-}C_5H_5)]$ (E = S, M = Cr or Mo; E = Se, M = W; dppm = bis(diphenylphosphino)methane) are obtained by treating the species $[MFe(\mu\text{-}\eta^2\text{-}ECC_6H_3Me_2\text{-}2,6)(CO)_5(\eta\text{-}C_5H_5)]$ with dppm. The reaction between $[MoFe_2(\mu_3\text{-}CC_6H_4Me\text{-}4)(\mu\text{-CO})(CO)_8(\eta\text{-}C_5H_5)]$ and selenium affords the μ_3-selenide complex $[MoFe_2(\mu\text{-}CC_6H_4Me\text{-}4)(\mu_3\text{-Se})(CO)_7(\eta\text{-}C_5H_5)]$.

Reactions between transition metal–alkylidene compounds and chalcogens often lead, via carbon–chalcogen bond formation, to complexes in which chalcoaldehyde or chalcoketone groups ligate a single metal centre,[1] or bridge metal–metal bonds.[2] This methodology has allowed the stabilization of the labile species $CH_2{=}E$ (E = S, Se or Te) within the coordination sphere of a metal ion.[1c,3]

The corresponding chemistry of alkylidyne–metal complexes has been less extensively studied as yet, however, parallels are emerging. Thus the osmium complex $[OsCl(\equiv CC_6H_4Me\text{-}4)(CO)(PPh_3)_2]$ reacts with chalcogens to give the compounds $[OsCl(\eta^2\text{-}ECC_6H_4Me\text{-}4)(CO)(PPh_3)_2]$ (E = S, Se or Te).[4] In contrast, the molybdenum and tungsten alkylidyne complexes $[M(\equiv CR)L_2(\eta\text{-}C_5H_5)]$ (M = Mo, R = CH_2Bu^t L = CO or $P(OMe)_3$; M = W, R = C_6H_4Me-4, L = CO) and $[W(\equiv CMe)(CO)_3\{H_2B(pz)_2\}]$ ($H_2B(pz)_2$ = dihydrobis(pyrazol-1-yl)borate) react with sulphur or selenium to give, respectively, the compounds $[Mo(\eta^2\text{-}E_2CCH_2Bu^t)L_2(\eta\text{-}C_5H_5)]$ (L = CO, E = S or Se; L = $P(OMe)_3$, E = S), $[W(\eta^2\text{-}E_2CC_6H_4Me\text{-}4)(CO)_2(\eta\text{-}C_5H_5)]$ (E = S or Se)[5a] and $[W(\eta^2\text{-}S_2CMe)(CO)_3\{H_2B(pz)_2\}]$.[5b] In these syntheses there was no direct evidence for the intermediacy of mononuclear molybdenum or tungsten compounds containing η^2-ECR (E = S or Se, R = CH_2Bu^t, Me or C_6H_4Me-4) fragments. Thioacyl ligands exist, however, in the products $[MFe(\mu\text{-}\eta^2\text{-}SCC_6H_4Me\text{-}4)(CO)_5L]$ (M = Mo, L = η-C_5H_5 or $HB(pz)_3$ {hydrotris(pyrazol-1-yl)borate}; M = W, L = η-C_5Me_5) (**1**) of reactions between sulphur and the dimetal compounds $[MFe(\mu\text{-}CC_6H_4Me\text{-}4)(CO)_{n+2}L]$ (M = Mo, n = 4, L = η-C_5H_5;[6a] n = 3, L = $HB(pz)_3$;[6b] M = W, n = 3, L = η-C_5Me_5),[6c] and in the complex $[WFe_2(\mu_3\text{-}\eta^2\text{-}SCMe)(CO)_8(\eta\text{-}C_5H_5)]$ (**2**), obtained by treating $[WFe_2(\mu_3\text{-}CMe)(\mu\text{-CO})(CO)_8(\eta\text{-}C_5H_5)]$ with sulphur.[7]

It was observed[7] that the latter reaction also affords the compound $[WFe_2(\mu\text{-CMe})(\mu_3\text{-S})(CO)_7(\eta\text{-}C_5H_5)]$ (**3a**), and that this μ_3-sulphido complex is formed when (**2**) is refluxed in THF (tetrahydrofuran). Interestingly, the reaction between selenium and $[WFe_2(\mu_3\text{-CMe})(\mu\text{-CO})(CO)_8(\eta\text{-}C_5H_5)]$ requires more vigorous conditions than that involving sulphur, and consequently the μ_3-selenido complex (**3b**) is the only isolable product. It seems likely, therefore, because of the ready conversion of (**2**) into (**3a**), that compound (**3b**) also forms via an intermediate μ_3-SeCMe complex akin to (**2**). Similarly, the compounds $[WFe_2(\mu_3\text{-}CC_6H_4Me\text{-}4)(\mu\text{-CO})(CO)_8(\eta\text{-}C_5H_5)]$ and $[WFe_2(\mu_3\text{-}CC_6H_4Me\text{-}4)(\mu\text{-dppm})(\mu\text{-CO})(CO)_6(\eta\text{-}C_5H_5)]$ (dppm = $Ph_2PCH_2PPh_2$) react with sulphur or selenium to give the complexes (**3c**), (**3d**), (**4a**) and (**4b**), respectively.[7] It is probable that these products are also formed via species similar to (**2**) containing μ_3-η^2-ECC_6H_4Me-4 (E = S or Se) ligands. Thus the overall reaction is one in which bond formation occurs between the alkylidyne group and the chalcogen, but this is followed by

*Author to whom correspondence should be addressed.

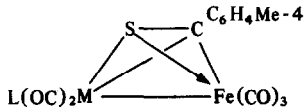

	M	L
(1a)	Mo	η-C_5H_5
(1b)	Mo	$HB(pz)_3$
(1c)	W	η-C_5Me_5

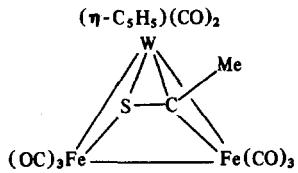

(2)

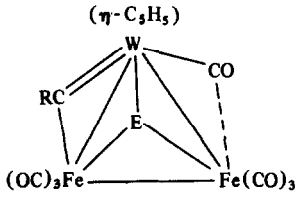

	M	R	E
(3a)	W	Me	S
(3b)	W	Me	Se
(3c)	W	C_6H_4Me-4	S
(3d)	W	C_6H_4Me-4	Se
(3e)	Mo	C_6H_4Me-4	Se

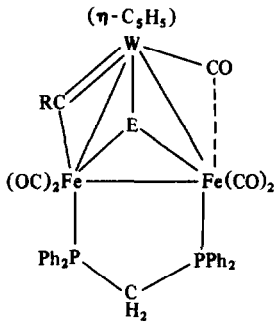

	R	E
(4a)	C_6H_4Me-4	S
(4b)	C_6H_4Me-4	Se

breakage of this bond with transfer of the alkylidyne ligand to an edge bridging site on the metal triangle.

In this paper we report the synthesis of several complexes in which μ-η^2-$ECC_6H_3Me_2$-2,6 groups span bonds between iron and chromium, molybdenum or tungsten. The new compounds were obtained from reactions between sulphur or selenium and the unsaturated 32 valence electron species $[MFe(\mu\text{-}CC_6H_3Me_2\text{-}2,6)(CO)_5(\eta\text{-}C_5H_5)]$ (M = Cr, Mo or W).[8]

RESULTS AND DISCUSSION

The reaction between $[WFe(\mu\text{-}CC_6H_3Me_2\text{-}2,6)(CO)_5(\eta\text{-}C_5H_5)]$ and sulphur in diethyl ether at room temperature affords in high yield the red complex $[WFe(\mu\text{-}\eta^2\text{-}SCC_6H_3Me_2\text{-}2,6)(CO)_5(\eta\text{-}C_5H_5)]$ (**5a**), characterized by the data given in Tables 1 and 2. Similar reactions between sulphur and the compounds $[MFe(\mu\text{-}CC_6H_3Me_2\text{-}2,6)(CO)_5(\eta\text{-}C_5H_5)]$ (M = Mo or Cr) yield the analogous molybdenum– and chromium–iron complexes (**5b**) and (**5c**), respectively. The products (**5a**)–(**5c**) are similar to the previously obtained dimetal species (**1**).[6] Moreover, the structure of (**1a**) was established by X-ray diffraction.[6a] It is noteworthy that the IR spectra of (**5a**) and (**5b**) in the carbonyl stretching region are very similar to those of (**1a**) and (**1c**). Thus for (**1c**),[6c] bands occur at 2039, 1975, 1964 and 1900 cm^{-1}, to be compared with those in the spectrum of (**5a**) (Table 1) at 2046, 1985, 1968 and 1902 cm^{-1}.

The ^1H and ^{13}C-$\{^1H\}$ NMR spectra of the compounds (**5a**)–(**5c**) show the expected signals (Table 2) for the formulations proposed. Thus whereas in the ^{13}C-$\{^1H\}$ NMR spectra of the precursors $[MFe(\mu\text{-}CC_6H_3Me_2\text{-}2,6)(CO)_5(\eta\text{-}C_5H_5)]$ resonances for the μ-$CC_6H_3Me_2$-2,6 nuclei occur at δ 391.8 (W), 407.4 (Mo) and 438.5 ppm (Cr), these diagnostic signals for an alkylidyne–carbon nucleus are absent in the spectra of (**5a**)–(**5c**). However, in the spectra of (**5a**) and (**5c**) signals at δ 127.6 and 112.6 ppm, respectively, are assigned to the μ-$SCC_6H_3Me_2$-2,6 nuclei. No peak due to the bridgehead carbon was observed in the spectrum of (**5b**), probably due to an insufficiently concentrated solution for this weak signal to be observed. In the ^{13}C-$\{^1H\}$ NMR spectra of the related species (**1a**) and (**1c**) the resonances due to the ligating carbon of the thioacyl groups occur at δ 113.4[6a] and 95.6 ppm,[6c] respectively. The corresponding peak in the spectrum of the homonuclear dimetal complex $[Fe_2(\mu\text{-}\eta^2\text{-}SCC_{10}H_{15})(NO)(CO)_4(PPh_3)]$ occurs at 144.6 ppm.[9] Evidently these signals cover a wide range of chemical shifts.

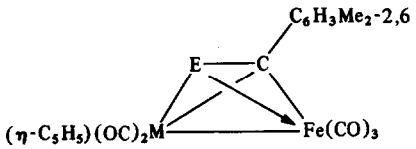

	M	E
(5a)	W	S
(5b)	Mo	S
(5c)	Cr	S
(5d)	W	Se
(5e)	Mo	Se
(5f)	Cr	Se

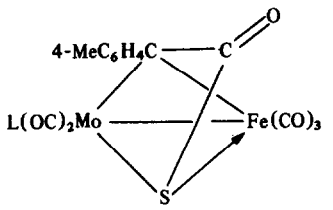

	L
6a)	η-C5H5
(6b)	HB(pz)3

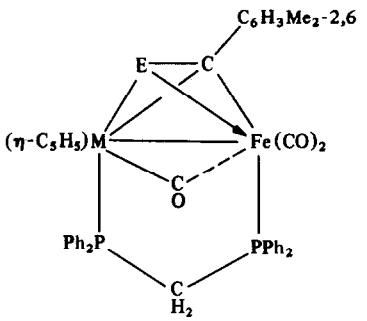

	M	E
(7a)	Mo	S
(7b)	Cr	S
(7c)	W	Se

In the CO region of their $^{13}C-\{^{1}H\}$ NMR spectra the compounds (**5a**)–(**5c**) show three peaks; two signals being due to the CO groups ligating the W, Mo or Cr atoms, and one being due to the $Fe(CO)_3$ fragment. The CO ligands of the latter evidently undergo rapid intramolecular site exchange on the NMR time-scale, a common property for this group.

An interesting feature of the reactions which afford (**5a**)–(**5c**) is the absence of any product containing the μ-$C(C_6H_3Me_2$-2,6)C(O)S fragment. The reaction between $[MoFe(\mu\text{-}CC_6H_4Me\text{-}4)(CO)_6(\eta\text{-}C_5H_5)]$ and sulphur yields, in addition to (**1a**), the complex $[MoFe\{\mu\text{-}C(C_6H_4Me\text{-}4)C(O)S\}(CO)_5(\eta\text{-}C_5H_5)]$ (**6a**).[6a] Moreover, there is some evidence for the formation of the related species (**6b**), simultaneously with (**1b**), in the reaction between $[MoFe(\mu\text{-}CC_6H_4Me\text{-}4)(CO)_5\{HB(pz)_3\}]$ and sulphur.[6b] The products (**6**) are assumed to form via attack of sulphur on an intermediate in which a μ-$C(C_6H_4Me$-4)C(O) ligand bridges the molybdenum–iron bonds. Dimetal compounds with μ-ketenyl groups have been implicated, or even in some instances isolated, in several reactions of carbonyl complexes containing bridging alkylidyne groups.[10]

As mentioned earlier, reactions between elemental selenium and the compounds $[WFe_2(\mu_3\text{-}CR)(\mu\text{-}CO)(CO)_8(\eta\text{-}C_5H_5)]$ (R = Me or C_6H_4Me-4) afford, respectively, the capping μ_3-selenido complexes (**3b**) and (**3d**), and no direct evidence of the existence of products containing μ-SeCR groups was obtained.[7] In contrast, the dimetal compounds $[MFe(\mu\text{-}CC_6H_3Me_2$-2,6)$(CO)_5(\eta\text{-}C_5H_5)]$ (M = W, Mo or Cr) react slowly with selenium in diethyl ether at room temperature to give the complexes $[MFe(\mu\text{-}\eta^2\text{-}SeCC_6H_3Me_2$-2,6)$(CO)_5(\eta\text{-}C_5H_5)]$ [M = W (**5d**), Mo (**5e**) and Cr (**5f**)], respectively. Data characterizing these products are given in Tables 1 and 2, from which it is evident that (**5d**)–(**5f**) are the selenium analogues of (**5a**)–(**5c**).

In the synthesis of (**5d**)–(**5f**) use of a low power ultrasound bath significantly decreased the time required for completion of the reaction, with no decrease in the yield. Moreover, because the preparation of the precursors $[MFe(\mu\text{-}CC_6H_3Me_2$-2,6)$(CO)_5(\eta\text{-}C_5H_5)]$ from the alkylidyne complexes $[M(\equiv CC_6H_3Me_2$-2,6)$(CO)_2(\eta\text{-}C_5H_5)]$ (M = W, Mo or Cr) proceeds in high yield,[8] it was possible to prepare (**5d**)–(**5f**) directly in a one-pot reaction from the mononuclear metal alkylidyne compounds. In this procedure, a second equivalent of

$[Fe_2(CO)_9]$ was employed to facilitate the removal of CO as $[Fe(CO)_5]$.

A feature common to the ^1H and $^{13}C-\{^1H\}$ NMR spectra of (**5a**)–(**5f**) is the presence of peaks indicating the chemical inequivalence of the two methyl groups of the $C_6H_3Me_2$-2,6 fragment. These molecules have no element of symmetry and, accordingly, diastereotopic Me group environments exist, even if rapid rotation about the μ-EC—C($C_6H_3Me_2$-2,6) bond occurs. This is distinct from the situation with the precursors $[MFe(\mu\text{-}CC_6H_3Me_2\text{-}2,6)(CO)_5(\eta\text{-}C_5H_5)]$ which possess time-averaged mirror symmetry about the M(μ-C)Fe planes, and hence the Me_2-2,6 group gives rise to one resonance in both the ^1H and $^{13}C-\{^1H\}$ NMR spectra.[8]

Treatment of (**5b**) with dppm in toluene at reflux temperatures (*ca* 110°C) affords, after *ca* 48 h, the dimetal compound $[MoFe(\mu\text{-}\eta^2\text{-}SCC_6H_3Me_2\text{-}2,6)(\mu\text{-dppm})(\mu\text{-CO})(CO)_2(\eta\text{-}C_5H_5)]$ (**7a**) in high yield. Alternatively, complex (**7a**) may be obtained by treating $[MoFe(\mu\text{-}CC_6H_3Me_2\text{-}2,6)(\mu\text{-dppm})(\mu\text{-CO})(CO)_2(\eta\text{-}C_5H_5)]$ (**8**) in toluene with sulphur; it being necessary to reflux the mixture for reaction to occur. Although only moderate yields of (**7a**) are obtained by this route, it is noteworthy that several other compounds containing dimetallacyclopropene ring structures, such as (**8**), react with sulphur with metal–metal bond cleavage to give the aforementioned mononuclear molybdenum or tungsten complexes $[M(S_2CR)(CO)_2(\eta\text{-}C_5H_5)]$ (M = Mo or W, R = C_6H_4Me-4). These dimetal species include $[MoMn(\mu\text{-CR})(CO)_4(\eta\text{-}C_5H_5)(\eta\text{-}C_5H_4Me)]$, $[Mo_3(\mu\text{-CR})_2(CO)_6(\eta\text{-}C_5H_5)_2]$[11] and $[WZr(\mu\text{-CR})(\mu\text{-}\sigma:\eta^2\text{-CO})(CO)(\eta\text{-}C_5H_5)_3]$.[12] Evidently the presence of the μ-dppm ligand in (**8**) prevents metal–metal bond rupture.

The compounds $[MFe(\mu\text{-}\eta^2\text{-}ECC_6H_3Me_2\text{-}2,6)(\mu\text{-dppm})(\mu\text{-CO})(CO)_2(\eta\text{-}C_5H_5)]$ [M = Cr, E = S (**7b**); M = W, E = Se (**7c**)] were prepared by treating (**5c**) with sulphur, and (**5d**) with selenium, respectively, in refluxing toluene. The data characterizing (**7a**)–(**7c**) (Tables 1–3) indicate that all three compounds are structurally similar. The IR spectrum in the carbonyl region for each compound reveals three bands, the absorption near 1800 cm^{-1} indicating the presence of a semi-bridging CO group. This feature is reflected in the $^{13}C-\{^1H\}$ NMR spectra (Table 2), since the relatively deshielded resonances at δ 251.3 (**7a**), 264.6 (**7b**) and 238.7 ppm (**7c**) may be assigned to this group. Moreover, these signals occur as doublets due to coupling with one ^{31}P nucleus. Peaks due to the μ-$ECC_6H_3Me_2$-2,6 nuclei could not be assigned in the spectra; these resonances are probably hidden under the many signals for the Ph and C_6H_3 moieties. The $^{31}P-\{^1H\}$ spectra (Table 3) each showed the expected two resonances, occurring as doublets [*J*(PP) *ca* 90 Hz]. The PFe signal occurs in the range δ 47.2–51.4 ppm, but the chemical shifts for the PM (M = Cr, Mo or W) resonances are more variable (δ 19.2–80.5 ppm), being increasingly deshielded in the order W < Mo < Cr. Not surprisingly the data for (**7a**) and (**8**) are very similar.

Interestingly, the compounds (**5d**)–(**5f**) are recovered unchanged after refluxing toluene solutions for several hours, and there was thus no evidence for C—Se bond cleavage leading to products with μ-Se and μ-$CC_6H_3Me_2$-2,6 groups. Two electron μ-selenido ligands are known in bimetallic chemistry,[13–15] as well as four electron μ_3-selenido groups in trimetallic systems.[7,16] The stability of the tetrahedrane M · Se · C · Fe cores in the compounds (**5d**)–(**5f**) may be due to the special properties of the bulky $C_6H_3Me_2$-2,6 substituent, since we have observed several examples of unusual structural phenomena associated with this group.[8,17] However, the thermal stability of (**5d**)–(**5f**) may be due to other factors discussed below.

As mentioned earlier, the trimetal compounds $[WFe_2(\mu_3\text{-}CC_6H_4Me\text{-}4)(\mu\text{-CO})(CO)_8(\eta\text{-}C_5H_5)]$ and $[WFe_2(\mu_3\text{-}CC_6H_4Me\text{-}4)(\mu\text{-dppm})(\mu\text{-CO})(CO)_6(\eta\text{-}C_5H_5)]$ react with selenium to yield the compounds (**3d**) and (**4b**), respectively, via a pathway believed to involve the intermediacy of species containing μ_3-η^2-$SeCC_6H_4Me$-4 groups.[7] Unfortunately, the corresponding tungsten–diiron compounds with capping μ_3-$CC_6H_3Me_2$-2,6 fragments do not form,[8] and so whether or not with selenium they afford products with μ_3-η^2-$SeCC_6H_3Me_2$-2,6 ligands, or whether complexes with μ_3-Se and μ-$CC_6H_3Me_2$-2,6 groups, are produced, cannot be determined. To complete the earlier studies[7] we have investigated the reaction between selenium and $[MoFe_2(\mu_3\text{-}CC_6H_4Me\text{-}4)(\mu\text{-CO})(CO)_8(\eta\text{-}C_5H_5)]$. In diethyl ether at room temperature, these reagents afford the μ_3-selenido complex $[MoFe_2(\mu\text{-}CC_6H_4Me\text{-}4)(\mu_3\text{-Se})(CO)_7(\eta\text{-}C_5H_5)]$ (**3e**). The spectroscopic data for (**3e**) (Tables 1 and 2) are very similar to those of (**3d**). Thus (**3e**) shows in its IR spectrum CO bands at 2057, 2015, 1995, 1977, 1954 and 1854 cm^{-1}, to be compared with those in the spectrum of (**3d**) at 2053, 2011, 1989, 1973, 1951 and 1862 cm^{-1}. A resonance at δ 344.5 ppm in the $^{13}C-\{^1H\}$ NMR spectrum of (**3e**) is diagnostic for the presence of a μ-CC_6H_4Me-4 nucleus bridging two metal centres. The corresponding peak in the spectrum of (**3d**) occurs at δ 318.5 ppm.[7]

The formation of (**3e**) under such mild conditions, compared with those required for the synthesis of (**3d**), necessitating heating the reagents in THF, is surprising. If, as seems likely, (**3d**) and (**3e**) form via intermediates structurally similar to

Table 1. Analytical[a] and physical data for the complexes

	Compound[b]	Colour	Yield (%)	ν(CO)[c] (cm^{-1})	Analysis(%) C	H
(5a)	[WFe(μ-η^2-SCR)(CO)$_5$(η-C_5H_5)]	Red	80	2046vs, 1985vs, 1968s, 1902w(br)	38.1(38.4)[d]	2.4(2.4)
(5b)	[MoFe(μ-η^2-SCR)(CO)$_5$(η-C_5H_5)]	Red	80	2048vs, 1990vs, 1969s, 1900w(br)	45.2(45.1)[e]	2.8(2.8)
(5c)	[CrFe(μ-η^2-SCR)(CO)$_5$(η-C_5H_5)]	Yellow–brown	78	2051vs, 1988vs, 1973s, 1877w(br)	49.0(49.4)[f]	3.2(3.0)
(5d)	[WFe(μ-η^2-SeCR)(CO)$_5$(η-C_5H_5)]	Orange	74	2044vs, 1984vs, 1968s, 1898w(br)	34.3(35.5)	2.4(2.2)
(5e)	[MoFe(μ-η^2-SeCR)(CO)$_5$(η-C_5H_5)]	Red	76	2048vs, 1990vs, 1969s, 1900w(br)	40.9(41.3)	2.6(2.5)
(5f)	[CrFe(μ-η^2-SeCR)(CO)$_5$(η-C_5H_5)][g]	Brown	75	2050vs, 1988vs, 1979sh, 1868w(br)		
(7a)	[MoFe(μ-η^2-SCR)(μ-dppm)(μ-CO)(CO)$_2$(η-C_5H_5)]	Orange	94	1967vs, 1907s, 1801m(br)	60.4(59.6)[h]	4.6(4.3)
(7b)	[CrFe(μ-η^2-SCR)(μ-dppm)(μ-CO)(CO)$_2$(η-C_5H_5)]	Green	95	1970vs, 1910s, 1790m(br)	63.2(63.8)	4.8(4.6)
(7c)	[WFe(μ-η^2-SeCR)(μ-dppm)(μ-CO)(CO)$_2$(η-C_5H_5)]	Orange	95	1962vs, 1902s, 1797m(br)	52.6(52.0)	4.0(3.7)
(8)	[MoFe(μ-CR)(μ-dppm)(μ-CO)(CO)$_2$(η-C_5H_5)]	Green	73	1968vs, 1912s, 1777m(br)	62.2(62.8)	5.1(4.5)
(3e)	[MoFe$_2$(μ-CC$_6$H$_4$Me-4)(μ_3-Se)(CO)$_7$(η-C_5H_5)]	Brown	40	2057s, 2015vs, 1995m, 1977m, 1954sh, 1854w	37.2(36.9)	2.0(1.9)

[a] Calculated values are given in parentheses.
[b] R = $C_6H_3Me_2$-2,6.
[c] In CH_2Cl_2.
[d] S, 5.3(5.4%).
[e] S, 6.3(6.4%).
[f] S, 7.8(7.9%).
[g] Analytically pure sample not obtained.
[h] S, 3.6(3.8%).

Table 2. ^{1}H and ^{13}C NMR data[a] for the complexes

Compound	$^{1}H(\delta)$	$^{13}C(\delta)$[b]
(5a)	2.38, 2.46 (s × 2, 3 H × 2, Me_2-2,6), 5.20 (s, 5 H, C_5H_5), 6.96 (m, 3 H, C_6H_3)	216.6, 214.3 (WCO), 210.6 (FeCO), 144.6 [$C^1(C_6H_3)$], 138.0, 133.5, 129.5, 129.0 (C_6H_3), 127.6 (CS), 125.4 (C_6H_3), 90.1 (C_5H_5), 25.4, 22.9 (Me_2-2,6)
(5b)	2.39, 2.50 (s × 2, 3 H × 2, Me_2-2,6), 5.10 (s, 5 H, C_5H_5), 6.95–7.00 (m, 3 H, C_6H_3)	231.8,[c] 226.7 (MoCO), 210.4 (FeCO), 145.1 [$C^1(C_6H_3)$], 138.2, 133.1, 129.7, 129.1, 125.8 (C_6H_3), 92.8 (C_5H_5), 25.4, 22.5 (Me_2-2,6)
(5c)	2.22, 2.36 (s × 2, 3 H × 2, Me_2-2,6), 4.59 (s, 5 H, C_5H_5), 6.97–7.02 (m, 3 H, C_6H_3)	244.3, 237.4 (CrCO), 209.5 (FeCO), 145.9 [$C^1(C_6H_3)$], 139.0, 132.9, 129.8, 129.0, 126.3 (C_6H_3), 112.6 (CS), 92.0 (C_5H_5), 25.6, 22.1 (Me_2-2,6)
(5d)	2.39, 2.46 (s × 2, 3 H × 2, Me_2-2,6), 5.19 (s, 5 H, C_5H_5), 6.98–6.92 (m, 3 H, C_6H_3)	215.7, 214.9 (WCO), 210.6 (FeCO), 148.9 [$C^1(C_6H_3)$], 136.6, 132.5, 129.7, 129.1, 125.1 (C_6H_3), 112.9 (CSe), 89.9 (C_5H_5), 26.4, 23.5 (Me_2-2,6)
(5e)	2.40, 2.50 (s × 2, 3 H × 2, Me_2-2,6), 5.10 (s, 5 H, C_5H_5), 6.95–7.02 (m, 3 H, C_6H_3)	231.4, 227.5 (MoCO), 210.4 (FeCO), 149.4 [$C^1(C_6H_3)$], 136.8, 132.1 (C_6H_3), 126.5 (CSe), 129.8, 129.2, 125.5 (C_6H_3), 92.6 (C_5H_5), 25.4, 22.9 (Me_2-2,6)
(5f)	2.23, 2.34 (s × 2, 3 H × 2, Me_2-2,6), 4.61 (s, 5 H, C_5H_5), 6.96–7.02 (m, 3 H, C_6H_3)	[c]243.5, 238.0 (CrCO), 209.0 (FeCO), 142.3 [$C^1(C_6H_3)$], 140.6, 131.2, 129.4, 129.1, 126.2 (C_6H_3), 91.3 (C_5H_5), 25.8, 22.0 (Me_2-2,6)
(7a)	[d]2.48, 2.66 (s × 2, 3 H × 2, Me_2-2,6), 3.44, 3.89 (m × 2, 2H, PCH_2P), 4.58 (s, 5 H, C_5H_5), 6.8–7.8 (m, 23 H, C_6H_3 and Ph)	[c]251.3 [d, MoCO, *J*(PC) 13], 218.6, 217.3 (FeCO), 149.6 [$C^1(C_6H_3)$], 139–124 (C_6H_3 and Ph), 92.3 (C_5H_5), 36.7 [d of d, PCH_2P, *J*(PC) 28, 15], 25.8, 22.2 (Me_2-2,6)
(7b)	[d]2.53, 2.71 (s × 2, 3 H × 2, Me_2-2,6), 3.41, 3.69 (m × 2, 2 H, PCH_2P), 4.18 [s(br), 5 H, C_5H_5], 6.8–7.8 (m, 23 H, C_6H_3 and Ph)	[c,d]264.6 [s(br), CrCO], 217.8 [s(br), FeCO], 150.7 [$C^1(C_6H_3)$], 141–124 (C_6H_3 and Ph), 91.3 (C_5H_5), 35.0 [d of d, PCH_2P, *J*(PC) 15], 26.1, 22.1 (Me_2-2,6)
(7c)	[d]2.48, 2.59 (s × 2, 3 H × 2, Me_2-2,6), 3.70 (m, 2 H, PCH_2P), 4.68 (s, 5 H, C_5H_5), 6.8–7.8 (m, 23 H, C_6H_3 and Ph)	[c,d]238.7 [d, WCO, *J*(PC) 8], 217.8, 217.4 (FeCO), 153.2 [$C^1(C_6H_3)$], 141–120 (C_6H_3 and Ph), 89.6 (C_5H_5), 41.1 [d of d, PCH_2P, *J*(PC) 16, 17], 26.9, 23.1 (Me_2-2,6)
(8)	[d]1.91, 1.96 (s × 2, 3 H × 2, Me_2-2,6), 4.61 (m, 1 H, PCH_2P), 4.86 (s, 5 H, C_5H_5), 5.12 (m, 1 H, PCH_2P), 6.6–7.9 (m, 23 H, C_6H_3 and Ph)	[d]385.2 (μ-C), 241.2 [d, MoCO, *J*(PC) 17], 219.6 (s, FeCO), 217.5 [d, FeCO, *J*(PC) 11], 116.1 [$C^1(C_6H_3)$], 143–124 (C_6H_3 and Ph), 95.2 (C_5H_5), 39.0 [d of d, PCH_2P, *J*(PC) 26, 18], 22.9, 22.4 (Me_2-2,6)
(3e)	2.34 (s, 3 H, Me-4), 5.64 (s, 5 H, C_5H_5), 7.17 [s(br), 4 H, C_6H_4]	344.5 (μ-C), 249.9 (μ-CO), 211.7, 209.4 (FeCO), 152.1 [$C^1(C_6H_4)$], 139.9, 129.2, 126.8 (C_6H_4), 95.6 (C_5H_5), 21.6 (Me-4)

[a] Chemical shifts (δ) in ppm, coupling constants in Hz. Measurements at ambient temperatures, in $CDCl_3$ unless otherwise indicated.
[b] ^{1}H decoupled, chemical shifts are positive to high frequency of $SiMe_4$.
[c] Signal for bridgehead μ-C nucleus not observed.
[d] In CD_2Cl_2.

Table 3. ^{31}P NMR data[a]

Compound	$^{31}P(\delta)$
(**7a**)	51.4 [d, FeP, J(PP) 96], 44.3 [d, MoP, J(PP) 96]
(**7b**)	80.5 [d(br), CrP, J(PP) 85], 47.2 [d(br), FeP, J(PP) 85]
(**7c**)	48.9 [d, FeP, J(PP) 90], 19.2 [d, WP, J(PP) 90, J(WP) 76]
(**8**)	53.3 [d, FeP, J(PP) 93], 39.9 [d, MoP, J(PP) 93]

[a] ^1H decoupled, chemical shifts (δ) in ppm to high frequency of 85% H_3PO_4 (external), coupling constants in Hz. Measurements at room temperature, in CD_2Cl_2. No corrections made for roof effects.

(**2**), but containing μ_3-η^2-$SeCC_6H_4Me$-4 groups, it may be that Se—C (or S—C) bonds cleave more readily when E—CR fragments occupy triply bridging sites on a metal triangle, rather than when they are part of a tetrahedrane structure as in the compounds (**5**).

EXPERIMENTAL

All experiments were carried out under nitrogen using Schlenk tube techniques. Solvents were rigorously dried before use. Light petroleum refers to that fraction of b.p. 40–60°C. IR spectra were measured with Nicolet MX10 and MX5 FT spectrometers, and NMR spectra were recorded with JNM FX 90Q, GX 270 and GX 400 instruments. The compounds [M(≡$CC_6H_3Me_2$-2,6)$(CO)_2(\eta$-$C_5H_5)$] (M = W, Mo or Cr) were prepared as described previously,[8] as was the complex [$MoFe_2(\mu_3$-CC_6H_4Me-4)$(\mu$-CO)$(CO)_8(\eta$-$C_5H_5)$].[18] The chalcogens used were in the form of resublimed sulphur and grey selenium. The compound [$MoFe(\mu$-$CC_6H_3Me_2$-2,6)$(\mu$-dppm)$(\mu$-CO)$(CO)_2(\eta$-$C_5H_5)$] (**8**) was synthesized by the method used to obtain the tungsten analogue.[8] The compound [$MoFe(\mu$-$CC_6H_3Me_2$-2,6)$(CO)_5(\eta$-$C_5H_5)$] (1.50 g, 3.16 mmol) and dppm (1.21 g, 3.16 mmol) were stirred in Et_2O (100 cm^3) for 20 min. Solvent was removed *in vacuo* and the residue dissolved in CH_2Cl_2 (3 cm^3) and light petroleum (12 cm^3) and chromatographed on a water-cooled column (3 × 30 cm) packed with alumina. Eluting with the same solvent mixture removed a small amount of starting material which was discarded. The second and major green fraction which was eluted was concentrated under reduced pressure to *ca* 5 cm^3 and cooled to *ca* −78°C (dry ice) to afford the product (**8**) as dark green *microcrystals* (1.86 g), characterized by the data given in Tables 1–3.

Preparation of the complexes [$MFe(\mu$-η^2-$ECC_6H_3Me_2$-2,6)$(CO)_5(\eta$-$C_5H_5)$] (M = W, Mo *or* Cr; E = S *or* Se)

The preparations of the compounds (**5**) were similar and hence only details of two syntheses are given.

(i) A Et_2O (50 cm^3) solution of [$WFe(\mu$-$CC_6H_3Me_2$-2,6)$(CO)_5(\eta$-$C_5H_5)$] (0.50 g, 0.88 mmol) and sulphur (0.05 g, 1.60 mg atom) was stirred for 4 h, and then volatile material was removed *in vacuo*. The residue was dissolved in a mixture of CH_2Cl_2 (6 cm^3) and light petroleum (4 cm^3) and chromatographed on a water-cooled Kieselgel column (*ca* 3 × 30 cm), eluting with the same solvent mixture. The major red eluate was collected, and the solvent was reduced in volume *in vacuo* to *ca* 6 cm^3. Cooling to *ca* −78°C afforded red *microcrystals* of [$WFe(\mu$-η^2-$SCC_6H_3Me_2$-2,6)$(CO)_5(\eta$-$C_5H_5)$] (**5a**) (0.86 g).

The compounds [$MFe(\mu$-η^2-$SCC_6H_3Me_2$-2,6)$(CO)_5(\eta$-$C_5H_5)$] [M = Mo (**5b**, 0.41 g) or Cr (**5c**, 0.44 g)] were similarly prepared from [$MFe(\mu$-$CC_6H_3Me_2$-2,6)$(CO)_5(\eta$-$C_5H_5)$] (M = Mo or Cr), respectively.

(ii) A suspension of [W(≡$CC_6H_3Me_2$-2,6)$(CO)_2(\eta$-$C_5H_5)$] (0.50 g, 1.85 mmol) and [$Fe_2(CO)_9$] (1.42 g, 3.9 mmol) in Et_2O (75 cm^3) was stirred for 15 h. The solvent and resultant [$Fe(CO)_5$] (**CAUTION**) were removed *in vacuo*. The residue was treated with selenium (0.20 g, 2.50 mg atom) and Et_2O (75 cm^3), and the mixture was stirred for 15 h. Solvent was removed *in vacuo*, and the residue extracted with a mixture of CH_2Cl_2 (6 cm^3) and light petroleum (14 cm^3). The extracts were chromatographed on a water-cooled Kieselgel column (*ca* 3 × 30 cm), eluting with the same solvent mixture. Initial eluates containing iron carbonyl were discarded, and the major orange fraction was collected. Solvent was reduced in volume *in vacuo* to *ca* 4 cm^3, and the solution was cooled to −78°C to yield orange *microcrystals* of [$WFe(\mu$-η^2-$SeCC_6H_3Me_2$-2,6)$(CO)_5(\eta$-$C_5H_5)$] (**5d**) (0.42 g).

Similar treatment of [M(≡$CC_6H_3Me_2$-2,6)$(CO)_2(\eta$-$C_5H_5)$] (M = Mo or Cr) gave the compounds [MFe(μ-η^2-$SeCC_6H_3Me_2$-2,6)$(CO)_5(\eta$-$C_5H_5)$] [M = Mo (**5e**, 0.46 g) or Cr (**5f**, 0.52 g)], respectively.

Preparation of the complexes [MFe(μ-η^2-$ECC_6H_3Me_2$-2,6)(μ-dppm)(μ-CO)$(CO)_2(\eta$-$C_5H_5)$] (M = Mo *or* Cr, E = S; M = W, E = Se)

(i) A representative synthesis was as follows. A toluene (20 cm^3) solution of (**5b**) (0.10 g, 0.20 mmol) and dppm (0.08 g, 0.20 mmol), contained in a Schlenk tube fitted with a high-pressure stopcock, was heated at 110°C in an oven for 48 h. After cooling to room temperature, solvent was removed *in vacuo*. The residue was dissolved in a mixture of Et_2O (10 cm^3) and light petroleum (10 cm^3), and the solution was chromotographed on a water-cooled Kieselgel column. Elution with the same solvent mixture removed an orange–red eluate, which was concentrated *in vacuo* to *ca* 3 cm^3. Cooling to −78°C afforded orange *microcrystals* of [MoFe(μ-η^2-$SCC_6H_3Me_2$-2,6)(μ-dppm)(μ-CO)$(CO)_2(\eta$-$C_5H_5)$] (**7a**) (0.16 g).

Similar treatment of (**5c**) with sulphur, and (**5d**) with selenium, afforded the compounds [CrFe(μ-η^2-$SCC_6H_3Me_2$-2,6)(μ-dppm)(μ-CO)$(CO)_2(\eta$-$C_5H_5)$] (**7b**) (0.14 g) and [WFe(μ-η^2-$SeCC_6H_3Me_2$-2,6)(μ-dppm)(μ-CO)$(CO)_2(\eta$-$C_5H_5)$] (**7c**) (0.15 g), respectively.

(ii) A THF (50 cm^3) solution of (**8**) (0.14 g, 0.17 mmol) and sulphur (0.05 g, 1.6 mg atom), contained in a Schlenk tube fitted with a high-pressure stopcock, was heated at 70°C in an oven for 5 days. After cooling to room temperature, solvent was removed *in vacuo*, and the residue was dissolved in a mixture of Et_2O (4 cm^3) and light petroleum (16 cm^3) and chromatographed on a water-cooled Kieselgel column (*ca* 2 × 50 cm). The column was eluted with a mixture of Et_2O and light petroleum (1:1). The initial brown–yellow eluate was discarded. Further elution with Et_2O–light petroleum (8:1) removed an orange fraction. Solvent was removed from the latter *in vacuo*, and the residue was crystallized from hexane (5 cm^3) at −78°C to afford orange *microcrystals* of [MoFe(μ-η^2-$SCC_6H_3Me_2$-2,6)(μ-dppm)(μ-CO)$(CO)_2(\eta$-$C_5H_5)$] (**7a**) (0.11 g).

Synthesis of the compound [$MoFe_2$(μ-CC_6H_4Me-4)(μ_3-Se)$(CO)_7(\eta$-$C_5H_5)$]

A Et_2O (50 cm^3) solution of [Mo(≡CC_6H_4Me-4)$(CO)_2(\eta$-$C_5H_5)$] (0.32 g, 1.00 mmol) and [$Fe_2(CO)_9$] (0.78 g, 2.20 mmol) was stirred at room temperature for 15 h. All volatile material was removed *in vacuo* (**CAUTION** [$Fe(CO)_5$]) leaving [$MoFe_2$(μ_3-CC_6H_4Me-4)(μ-CO)$(CO)_8(\eta$-$C_5H_5)$][18] as the residue. The latter was dissolved in Et_2O (50 cm^3) and treated with selenium (0.20 g, 2.50 mg atom), the mixture being stirred for 72 h. Solvent was removed *in vacuo*, and the residue was extracted twice with a mixture of CH_2Cl_2 (6 cm^3) and light petroleum (14 cm^3). The combined extracts were chromatographed on a water-cooled alumina column (*ca* 3 × 30 cm). Elution with the same solvent mixture gave a dark brown fraction from which solvent was removed *in vacuo*. The residue was crystallized from hexane (5 cm^3) at −78°C to give brown *microcrystals* of [$MoFe_2$(μ-CC_6H_4Me-4)(μ_3-Se)$(CO)_7(\eta$-$C_5H_5)$] (**3e**) (0.26 g).

Acknowledgements—We thank the SERC for support, and the University of the Punjab (Lahore) and the University Grants Commission of Pakistan for a Fellowship (to B.A.N.).

REFERENCES

1. (a) E. O. Fischer and S. Riedmüller, *Chem. Ber.* 1974, **107**, 3326; (b) H. Fischer and S. Zeuner, *Z. Naturf.* 1985, **40B**, 954; H. Fischer, S. Zeuner and J. Riede, *Angew. Chem. Int. Ed. Engl.* 1984, **23**, 726; (c) A. F. Hill, W. R. Roper, J. M. Waters and A. H. Wright, *J. Am. Chem. Soc.* 1983, **105**, 1365.
2. W. A. Herrmann, R. Serrano, K. Bleichschmitt, H. Pfisterer and M. L. Ziegler, *Angew. Chem. Int. Ed. Engl.* 1983, **22**, 314.
3. W. E. Buhro, A. T. Patton, C. E. Strouse, J. A. Gladysz, F. D. McCormick and M. C. Etter, *J. Am. Chem. Soc.* 1983, **105**, 1056.
4. G. R. Clark, K. Marsden, W. R. Roper and L. J. Wright, *J. Am. Chem. Soc.* 1980, **102**, 6570; G. R. Clark, N. R. Edwards, R. A. Pauptit, W. R. Roper, J. M. Waters and A. H. Wright, *J. Organomet. Chem.* 1983, **244**, C57.
5. (a) D. S. Gill, M. Green, K. Marsden, I. Moore, A. G. Orpen, F. G. A. Stone, I. D. Williams and P. Woodward, *J. Chem. Soc., Dalton Trans.* 1984, 1343; (b) M. D. Bermúdez, F. P. E. Brown and F. G. A. Stone, *J. Chem. Soc., Dalton Trans.* 1988, 1139.
6. (a) P. G. Byrne, M. E. Garcia, J. C. Jeffery, P. Sherwood and F. G. A. Stone, *J. Chem. Soc., Dalton Trans.* 1987, 1215; (b) M. D. Bermúdez, E. Delgado, G. P. Elliott, N. H. Tran-Huy, F. Mayor-Real, F. G. A. Stone and M. J. Winter, *J. Chem. Soc. Dalton Trans.* 1987, 1235; (c) E. Delgado, J. Hein, J. C. Jeffery, A. L. Ratermann, F. G. A. Stone and L. J. Farrugia, *J. Chem. Soc. Dalton Trans.* 1987, 1191.
7. E. Delgado, A. T. Emo, J. C. Jeffery, N. D. Simmons and F. G. A. Stone, *J. Chem. Soc., Dalton Trans.* 1985, 1323.
8. S. J. Dossett, A. F. Hill, J. C. Jeffery, F. Marken, P. Sherwood and F. G. A. Stone, *J. Chem. Soc., Dalton Trans.* 1988, 2453.

9. W. Ziegler, H. Umland and U. Behrens, *J. Organomet. Chem.* 1988, **344**, 235.
10. J. C. Jeffery, C. Marsden and F. G. A. Stone, *J. Chem. Soc., Dalton Trans.* 1985, 1315; L. J. Farrugia, J. C. Jeffery, C. Marsden, P. Sherwood and F. G. A. Stone, *J. Chem. Soc., Dalton Trans.* 1987, 51; M. E. Garcia, N. H. Tran-Huy, J. C. Jeffery, P. Sherwood and F. G. A. Stone, *J. Chem. Soc., Dalton Trans.* 1987, 2201; J. Hein, J. C. Jeffery, P. Sherwood and F. G. A. Stone, *J. Chem. Soc., Dalton Trans.* 1987, 2211; I. J. Hart, A. E. Jardin, J. C. Jeffery and F. G. A. Stone, *J. Organomet. Chem.* 1988, **341**, 391; J. C. Jeffery, M. A. Ruiz and F. G. A. Stone, *J. Organomet. Chem.* 1988, **355**, 231.
11. A. F. Hill, F. Marken, B. A. Nasir and F. G. A. Stone, *J. Chem. Soc., Dalton Trans.* 1989, in press; A. F. Hill, B. A. Nasir and F. G. A. Stone, unpublished results.
12. A. F. Hill, H. D. Hönig and F. G. A. Stone, *J. Chem. Soc., Dalton Trans.* 1988, 3031.
13. W. A. Herrmann, J. Rohrmann and Ch. Hecht, *J. Organomet. Chem.* 1985, **290**, 175.
14. M. A. Jennings and A. Wojcicki, *J. Organomet. Chem.* 1968, **14**, 231.
15. B. Gautheron, G. H. Tainturier and S. Pouly, *J. Organomet. Chem.* 1984, **268**, C56.
16. W. Hieber and J. Gruber, *Z. Anorg. Allg. Chem.* 1958, **296**, 90.
17. F. E. Baumann, J. A. K. Howard, R. J. Musgrove, P. Sherwood and F. G. A. Stone, *J. Chem. Soc., Dalton Trans.* 1988, 1879; D. D. Devore, J. A. K. Howard, J. C. Jeffery, M. U. Pilotti and F. G. A. Stone, *J. Chem. Soc., Dalton Trans.* 1989, in press; A. F. Hill, J. A. K. Howard, B. A. Nasir, T. S. Spaniol and F. G. A. Stone, unpublished results.
18. M. E. Garcia, J. C. Jeffery, P. Sherwood and F. G. A. Stone, *J. Chem. Soc., Dalton Trans.* 1987, 1209.

Polyhedron Vol. 8, No. 2, pp. 189–195, 1989
Printed in Great Britain

0277–5387/89 $3.00+.00
© 1988 Pergamon Press plc

POTENTIOMETRIC STUDIES ON THE MIXED LIGAND COMPLEXES IN SOLUTION: M^{II}–TETRACYCLINE–GLYCINE SYSTEMS

MAHMOUD A. GHANDOUR, H. A. AZAB,* AHMED HASSAN and A. M. ALI

Department of Chemistry, Faculty of Science, Asiut University, Asiut, Egypt

(*Received* 11 *July* 1988; *accepted* 15 *August* 1988)

Abstract—The interaction of Be, Mg, Ca, Sr and Ba ions with tetracycline was followed by pH-metry and stability constants were determined for the chelates containing 1 : 1 ratio of ligand to metal ion at $t = 25°C$ and $\mu = 0.1$ mol dm^{-3} ($NaNO_3$), for the above mentioned metals except Be where 1 : 1 and 2 : 1 complexes were detected. The protonation constants of tetracycline were also determined under the same conditions. The stability constants of the 1 : 1 complexes formed decrease in the order Be > Mg > Ca > Sr > Ba. Potentiometric equilibrium measurements have been made under the same conditions for the interaction of tetracycline and Be, Mg, Ca, Sr, Ba, Cu and Zn with the biologically important secondary ligand (glycine) in a (1 : 1 : 1) ratio. The $\Delta \log K$ values

$$[\Delta \log K = \log k^{M(TC)}_{M(TC)(gly)} - \log K^{M}_{M(gly)}]$$

were interpreted on the basis of statistical considerations and the nature of species formed in solution.

Among the most important broad-spectrum antibiotics are the members of the tetracycline family. The phenomenon of complex formation between tetracycline analogues and various cations is well documented.[1–12] Metal ion complex formations are among the prominent interactions in nature,[13–15] and the glycine residue is an important and versatile binding site of protein while tetracycline is equally important as an antibiotic. For an improved understanding of the driving forces leading to mixed-ligand complexes in biological systems, ternary complexes of the type M^{II}–TC–glycine, where M = Ca, Mg, Cu or Zn, have been investigated to determine the stability constants of the complexes formed. Although Be, Sr and Ba interactions with tetracycline and/or glycine are of little interest, since these metal ions are not normally present in the human body, these systems were studied for comparison.

EXPERIMENTAL

Calvin–Bjerrum's technique as adopted by Irving and Rossotti[16] was used to determine the protonation constants of the ligands (tetracycline and glycine) and formation constants of the metal complexes at 25°C in aqueous solutions.

pH Measurements were carried out on a Corning 601A precision research ionalyzer digital pH meter. During the titrations, oxygen-free nitrogen was bubbled through the solution. The electrode system was calibrated in terms of hydrogen-ion concentrations instead of activities. Thus, all constants determined in this work are concentration constants. The solutions of Mg, Ca, Sr, Ba, Cu and Zn (AR, BDH) as nitrates were prepared and titrated complexometrically by EDTA. AR beryllium sulphate solution was prepared and standardized as recommended. Tetracycline was obtained as the hydrochloride and used without purification as fresh solutions in bidistilled water.

In the binary systems studied, the following solutions were titrated potentiometrically against standard carbonate-free sodium hydroxide (0.1 mol dm^{-3}) solution:

(a) 0.01 mol dm^{-3} HCl,

(b) **(a)** + 0.01 mol dm^{-3} tetracycline hydrochloride,

(c) **(b)** + 2.5×10^{-3} mol dm^{-3} metal nitrate solution.

*Author to whom correspondence should be addressed.

In ternary systems studied, numerous titrations of different M^{II}/tetracycline and/or glycine mixtures in 1:1:1 molar ratio (1×10^{-3} mol dm^{-3}, for each) were performed. The solutions titrated can be represented according to the following scheme:

HCl (**a**);
HCl + tetracycline (**b**);
HCl + tetracycline + M^{II} (**c**);
HCl + glycine (**d**);
HCl + glycine + M^{II} (**e**);
HCl + tetracycline + glycine + M^{II} (**f**).

The total volume was adjusted to 50 cm^3 by adding double-distilled water in each case. The titrations were performed at 25°C and $\mu = 0.1$ mol dm^{-3} ($NaNO_3$).

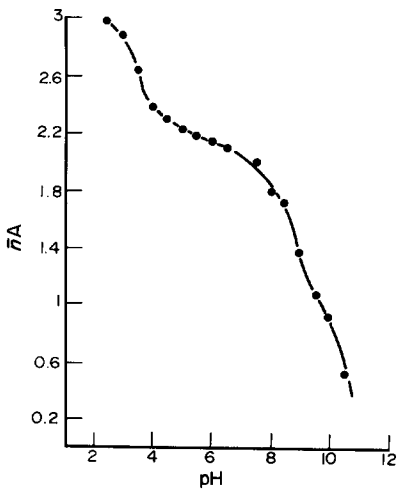

Fig. 2. Proton–tetracycline formation curve.

RESULTS AND DISCUSSION

Representative titration curves are shown in Fig. 1. The values of $\bar{n}_A$ as determined by the method of Irving and Rossotti[16] were compiled from the titration data using solutions (**a**) and (**b**). Calculations of proton ligand association constants were carried out by plotting a graph of $\bar{n}_A$ against pH (Fig. 2). The values of log K_1^H, log K_2^H and log K_3^H (the first, second and third proton association constants of tetracycline, respectively) are the pH values corresponding to $\bar{n}_A = 0.5$, 1.5 and 2.5, respectively. The values of log K_1^H, log K_2^H and log K_3^H (Table 1) agree quite well with those previously reported.[4]

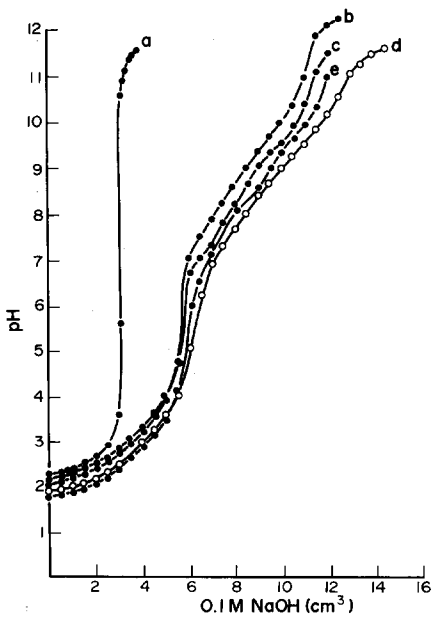

Fig. 1. Titration curves of (a) 0.01 M HCl + 0.1 M $NaNO_3$, (b) mixture (a) + 0.01 M tetracycline hydrochloride, (c) mixture (b) + 2.5×10^{-3} M Ba^{2+}, (d) mixture (b) + 2.5×10^{-3} M Be^{2+} and (e) mixture (b) + 2.5×10^{-3} Mg^{2+} with 0.1 M NaOH; total volume 50 cm^3.

The titration curves of the metal–ligand solutions (**c**) are well separated from the ligand solution (**b**) (Fig. 1.) Thus, replacement of H^+ ions is due to complexation. From these titration curves, $\bar{n}$ (average number of ligand molecules attached per metal ion) and pL (free ligand exponent) values were calculated.[16] The $\bar{n}$ values were plotted against the corresponding pL values to get the formation curves of the metal complexation equilibria. The formation curves are shown in Fig. 3. From these formation curves, the values of stability constants listed in Table 1 were determined using the half-integral method.[16] Only 1:1 ligand/metal complexes were formed between Mg, Ca, Sr and Ba ions and tetracycline. Be reacts with tetracycline to give 1:1 and 2:1 ligand/metal complexes. In particular Be may well display different titration and formation curves (cf. Figs 1 and 3) support to the formation of hydroxo complexes.

For alkaline earth metal ions studied, the stability constants of the 1:1 complexes formed with tetracycline decrease in the order of "ionic potential" (or polarizing power), which is defined as formal charge/ionic radius. Thus, the corresponding stability constants decrease in the order: Be > Mg > Ca > Sr > Ba.

Figures 4, 5 and 6 represent typical titration curves for the different M^{II}–TC–glycine systems studied. It is observed that the M^{II}–TC titration curve (c) diverges from TC curve (b) at different pH values (pH ~ 3.2 for Mg, pH ~ 2.6 for Cu and pH ~ 4.5 for Zn) denoting the formation of M^{II}–TC binary complexes. For the titration curves of the ternary systems studied, one observes that the (c, f) however overlap with each other at lower pH values in case of Mg and Cu, while that for Zn is

Table 1. Proton ligand association constants of tetracycline and stability constants of binary and ternary complexes formed in this study at 25°C, $\mu = 0.1$ mol dm^{-3} ($NaNO_3$)

Cation	$\log K_1^H$	$\log K_2^H$	$\log K_3^H$	M(TC) $\log K_1$	M(TC) $\log k_2$	M(gly) $\log K_1$	$\log K^{M(TC)}_{M(TC)(gly)}$	$\log B^{M}_{M(TC)(gly)}$	$\Delta \log K$
H^+	10.46	8.50	3.36	—	—	—	—	—	—
Be				9.50	3.9	6.80	3.80	13.30	−3.00
Mg				8.40	—	3.30	4.20	12.60	+0.90
Ca				7.90	—	4.60	4.10	12.00	−0.50
Sr				7.10	—	3.20	3.80	10.90	+0.60
Ba				4.00	—	3.50	3.80	7.80	+0.30
Cu				8.60	—	7.00	4.60	13.20	−2.40
Zn				4.30	—	5.90	9.00	13.30	+3.10

well separated. This indicates the formation of Zn–TC–glycine at lower pH values which may be considered as evidence for the formation of a protonated tetracycline mixed ligand complex.

The stability constants of the ternary metal ion complexes containing tetracycline and glycine were calculated for eq. (1) from the data obtained from potentiometric pH titrations:

$$M(TC) + gly \rightleftharpoons M(TC)(gly), \quad (1)$$

$$K^{M(TC)}_{M(TC)(gly)} = \frac{[M(TC)(gly)]}{[M(TC)][gly]}$$

[$I = 0.1$ mol dm^{-3} ($NaNO_3$); 25°C]. Similarly, the constants of the binary complexes (eqs 2 and 3) were also determined

$$M + TC \rightleftharpoons M(TC), \quad (2)$$

$$K^{M}_{M(TC)} = \frac{[M(TC)]}{[M][TC]}$$

$$M + gly \rightleftharpoons M(gly), \quad (3)$$

$$K^{M}_{M(gly)} = \frac{[M(gly)]}{[M][gly]}$$

It is assumed, for convenience, that complexation of the secondary ligand (glycine) starts after the complete formation of the M^{II}/tetracycline 1:1

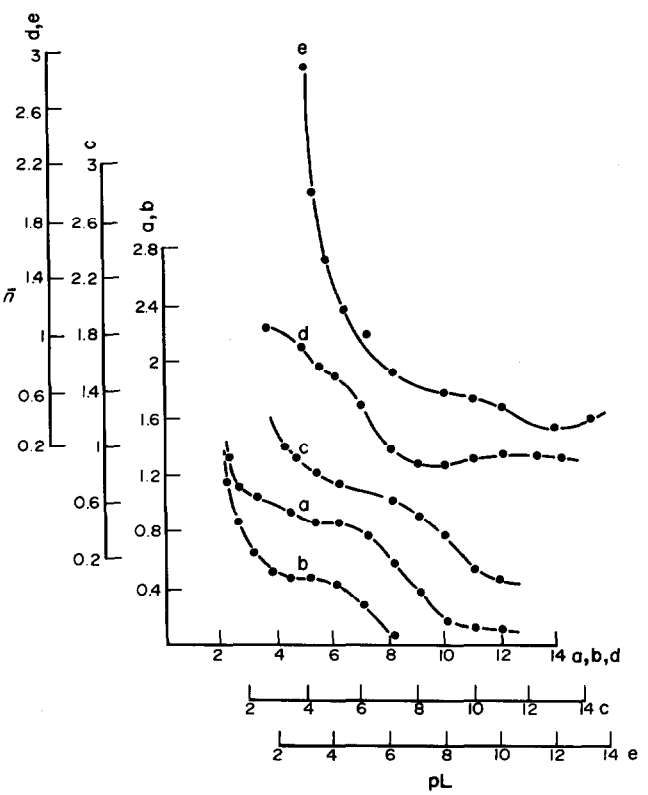

Fig. 3. Alkaline earth metal ion–tetracycline formation curves, (a) Mg^{2+}–TC, (b) Ba^{2+}–TC, (c) Ca^{2+}–TC, (d) Sr^{2+}–TC and (e) Be^{2+}–TC.

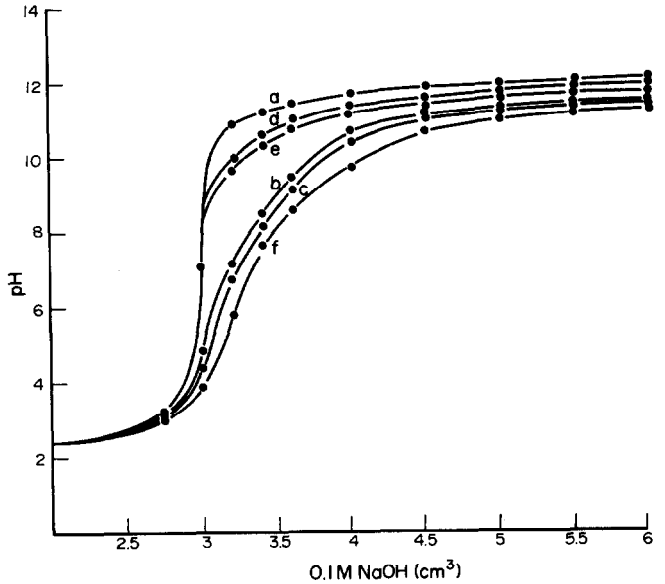

Fig. 4. Titration curves for the Mg^{II}–TC–glycine system.

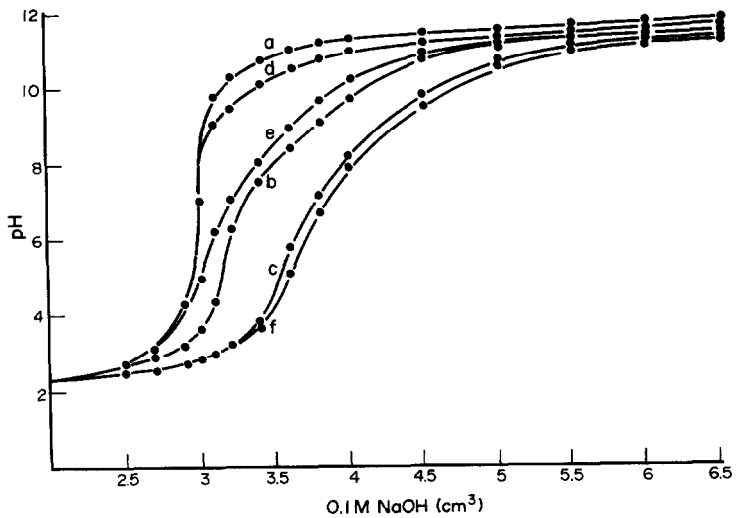

Fig. 5. Titration curves for the Cu^{II}–TC–glycine system.

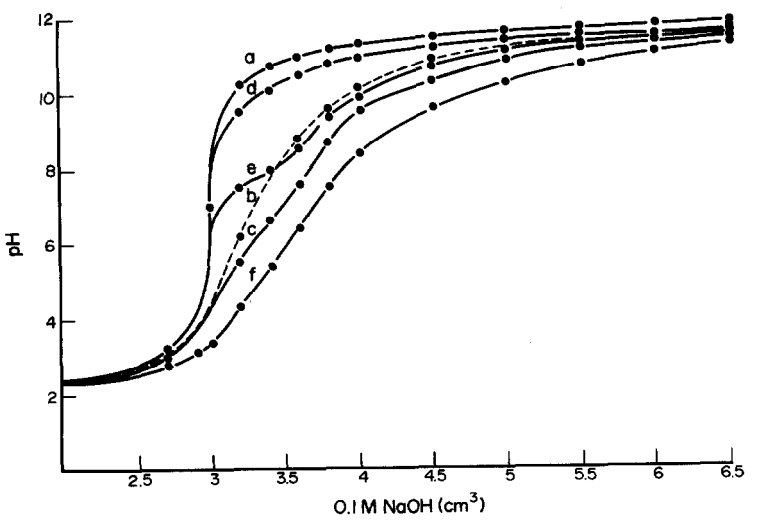

Fig. 6. Titration curves for the Zn^{II}–TC–glycine system.

complex. Thus, the overall stability constant $\beta^{M}_{M(TC)(gly)}$ may be represented by eq. (4):

$$M + TC + gly \rightleftharpoons M(TC)(gly), \qquad (4)$$

$$\beta^{M}_{M(TC)(gly)} = \frac{[M(TC)(gly)]}{[M][TC][gly]} = K^{M(TC)}_{M(TC)(gly)} \times K^{M}_{M(TC)}.$$

At the experimental pH values used in the calculation in this work the interfering effects of hydroxo complexes are negligible. Thus, the secondary ligand, glycine, combines with the binary 1 : 1 metal/tetracycline complex in a similar manner to its interaction with aquated metal ions in solutions. The horizontal distance between curves (c) and (f) can be measured and used for the calculation of $\bar{n}_{mix}$ (average number of secondary ligand molecules associated with one [M(TC)] ion). The equation used for the calculation of $\bar{n}_{mix}$ will be the same as in the original paper[16]

$$\bar{n}_{mix} = \frac{(V_f - V_c)[N^0 + E^0 + T^0_L(y - \bar{n}_H)]}{(V_0 + V_c)\bar{n}_H T^0_M}. \qquad (5)$$

In eq. (5), T^0_M is the concentration of [M(TC)] which is equal to the concentration of M^{II} used; y = number of dissociable protons of glycine ($y = 1$); values of $\bar{n}_H$, for the secondary ligand at different pH values, were calculated from the amino acid formation curve. All other symbols have their usual meanings. From the values of $\bar{n}_{mix}$ so obtained, free secondary ligand exponent, pL'_{mix} was calculated using the equation,

$$pL'_{mix} = \log\left(\frac{\sum_{n=0}^{j} \beta^H_n \left(\frac{1}{10^B}\right)^n}{T^0_L - \bar{n}_{mix} T^0_M} \times \frac{V_0 + V_f}{V_0}\right), \qquad (6)$$

where

β = second formation constant value of glycine,
B = the pH-meter reading.

The second formation constant of glycine was determined from the titration curves (a, d) using the Rosotti and Irving formula.[16] The obtained value (9.70) is in a good agreement with literature value.[17] The stability constants determined in this work for Mg, Cu or Zn complexes of glycine, agree well with literature values.[18,19] The disagreement found for the values of Ba, Ca or Sr complexes of glycine, may be attributed to the different ionic strengths and methods used for determination.[18,20] The stability constants of the Cu and Zn complexes of tetracycline agree with the values found in literature.[2]

Formation curves corresponding to the various mixed ligand M^{II}–TC–glycine systems were obtained by ploting $\bar{n}_{mix}$ vs pL'_{mix}. Representative results are shown in Fig. 7. The corresponding formation constants $\log K^{M(TC)}_{M(TC)(gly)}$ obtained by the average value method are reported in Table 1. $\Delta\log K$, defined by eq. (7), is a measure of the stability of the ternary complexes with respect to

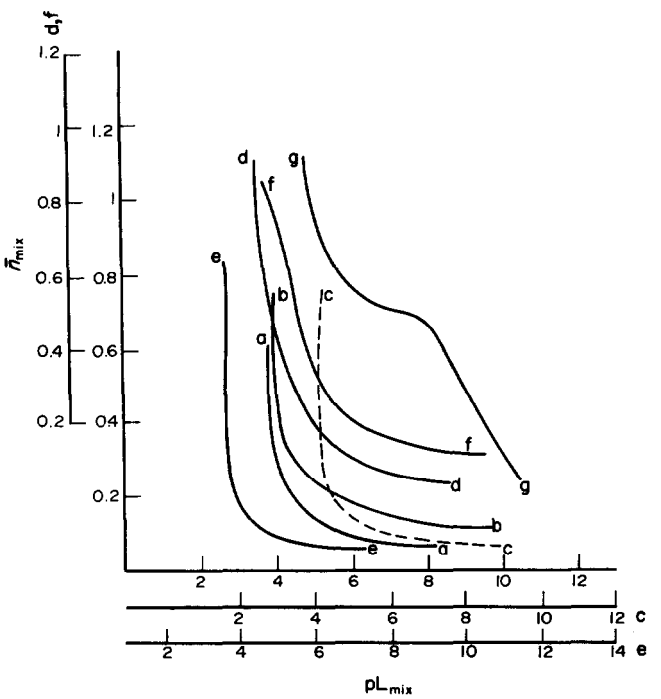

Fig. 7. M^{II}–TC–glycine formation curves (a) Be^{II}, (b) Mg^{II}, (c) Ca^{II}, (d) Sr^{II}, (e) Ba^{II}, (f) Cu^{II}, (g) Zn^{II}.

the binary complexes,

$$\Delta\log K = \log K^{M(TC)}_{M(TC)(gly)} - \log K^{M}_{M(gly)}. \quad (7)$$

In the case of M^{II}–TC–glycine systems, where M^{II} = Mg, Ca, Sr or Ba, $\Delta\log K$ is found to be slightly positive or negative (Table 1) in accordance with statistical expectations.[21] In the ternary complex systems, the two oxygen atoms of the phenolic B-diketone moiety of the tetracycline molecule form σ-bonds with the metals. In addition to this there exists a tendency for a $M \rightarrow O$ π-interaction due to back donation of electrons from the metal π-orbital to the vacant delocalized π-orbital over the phenolic B-diketone moiety of the tetracycline molecule. As a result of this back donation the concentration of electrons around the metal ion in M^{II}–TC does not increase significantly and the electronegativity of the metal ion in this species remains almost the same as in the aquated metal ion. This justifies the small values of $\Delta\log K$. The strong covalent bond formed between Be and the tetracycline molecule may disfavour the formation of the ternary complex Be–TC–glycine. The $\Delta\log K$ value for this system is negative in accordance with the statistical considerations[14] where the statistical, steric and electrostatic factors result in a lower stability constant for the 1:1:1 metal/ligand complexes as compared with those for the binary systems.

The higher stability constant of Zn–TC–glycine ternary complex compared with the binary system may be attributed to the difference in the nature of the species formed in solution. The Zn–TC–glycine system involves a protonated binary species MHTC in acidic medium whereas the Cu ions form a ternary complex through the interaction with the neutral binary species MTC with the secondary ligand. The Zn–TC–glycine system is more stable due to extra hydrogen bonding of the proton with oxygen atom of the secondary ligand molecules.

Tetracycline hydrochloride LH_3^+ Cl^-, has three sites and the protons may be dissociated from these sites in proportions which vary with the degree of neutralization. These sites are shown in Fig. 8 as the amide system (A), the phenolic B-diketone moieties (B) and (B′), and the dimethyl-ammonium cation (c): The first dissociation constant pK_1^H is generally attributed to site (A).[22,23] Stephens *et al.*[22] have assigned the second and the third dissociation constants, pK_2^H and pK_3^H, to site (C) and the combined (B) and (B′) system, respectively, while Lesson *et al.*[23] reverse these assignments in the case of protonated tetracycline, considering a complete dissociation scheme for all. Sachan[5] suggested that pK_2^H is due to system (B). Doluisio and Martin[1] concluded that the chelation occurs through the co-ordination of the nitrogen atom of the dimethylamino group at C_4 and the oxygen atom of the hydroxyl group either at C_3, or at C_{12_a}. On the basis of absorption spectra, Conover[24] concluded that the normal site for metal binding by tetracycline is the enolized B-diketone group at C_{11} and C_{12}, i.e. group (B′) in Fig. 8. According to Baker and Brown,[25] on the basis of reflectance spectra, the dimethylamino group does not take part in the co-ordination, and the chelation is through oxygen atoms, probably in system (A). Sachan[5] concluded that the co-ordination sites of the TC are the oxygen atoms of system (B).

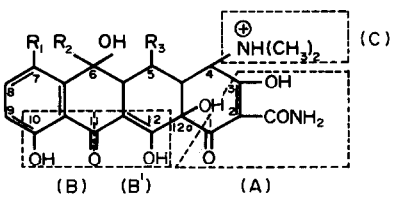

Fig. 8.

Thus, there is lack of agreement as to the assignment of the site of co-ordination. The following considerations may be suggested.

(a) Albert[26] pointed out that only the functional group having a dissociation constant of approximately 7.0 undergoes ionization when chelation takes place.

(b) The presence of an OH group at C_3 suggests that the complexation of metal ions with TC should be independent of pK_1^H, and consequently the complexing species should not be LH_2.[6]

(c) Covalent forces, rather than electrovalent forces, are dominating in the phenol–B-diketone system and in the dimethyl ammonium group between O and H atoms at C_{10} and between N and H atoms at C_4, respectively.[4] From these we may assume that the complexation of alkaline earth metal ions as well as Cu and Zn with tetracycline takes place through the pK_2^H value of the antibiotic, and that the complexing species were LH^- for these systems. Formation of Zn–TC–glycine complex which starts at lower pH values may take place through the pK_1^H value of tetracycline and the complexing species may be LH_3^+. Considering that metal complexation may be involved in the antibacterial activity[27–29] and that the phenolic group in tetracycline[30] is responsible for part of its antibacterial activity, then that may be considered as a further support for our conclusion.

REFERENCES

1. J. T. Doluisio and A. N. Martin, *J. Med. Chem.* 1963, **6**, 16.
2. A. Albert and C. W. Rees, *Nature* 1956, **177**, 433.
3. T. Chin and J. L. Lach, *Am. J. Hosp. Pharm.* 1975, **32**, 625.
4. N. P. Sachan, K. M. Suyan, C. P. S. Chandel and C. M. Gupta, *J. Ind. Chem. Soc.* 1983, **60**, 741.
5. N. P. Sachan and C. M. Gupta, *Talanta* 1980, **27**, 457.
6. N. P. Sachan, C. P. S. Chandel and C. M. Gupta, *J. Ind. Chem. Soc.* 1983, **60**, 1040.
7. D. S. Veselinovic, S. Dragan and M. D. Jelikic, *Glas. Hum. Drus. Beograd*, 1983, **48**, 739.
8. D. C. Grove and W. A. Randall, *Assay Methods for Antibiotics: a Laboratory Manual.* Medical Encyclopedia Inc., New York (1955).
9. J. Levine, E. A. Garlock and H. Fischbach, *J. Am. Pharm. Ass. Sci. Edn* 1949, **38**, 473.
10. F. Monastero, J. A. Means, T. C. Grenfell and F. H. Hedger, *J. Am. Pharm. Ass. Sci. Edn* 1951, **40**, 241.
11. L. G. Chatten and S. I. Krause, *J. Pharm. Sci.* 1971, **60**, 107.
12. B. Janik and D. Hohat, *Acta Polon. Pharm.* 1972, **29**, 168.
13. G. L. Eichhorn, Ed., *Inorganic Biochemistry*, Vols 1 and 2. Elsevier, New York (1973).
14. H. Sigel, Ed., *Metal Ions in Biological Systems*, Vol. 2. Dekker, New York (1973).
15. J. M. Wood, *Naturwissenschaften* 1975, **62**, 357.
16. H. Irving and H. Rossotti, *J. Chem. Soc.* 1953, 3397; 1954, 2904.
17. A. Gergely, I. Nagypal and J. Mojzes, *Acta Chim. Acad. Sci. Hung.* 1967, **51**, 381.
18. C. B. Monk, *Trans. Faraday Soc.* 1951, **47**, 285; 292; 297; 1233.
19. A. Gergely and I. Nagypal, *Acta Univ. Debrecen* 1965, 113.
20. C. A. Colman-Porter and C. B. Monk, *J. Chem. Soc.* 1952, 4363.
21. H. Sigel, *Coordination Chemistry*, Vol. 20 (Edited by Banerjea D.). Pergamon Press, Oxford (1980).
22. C. R. Stephens, K. Murai, K. J. Brunings and R. B. Woodward, *J. Am. Chem. Soc.* 1956, **78**, 4155.
23. L. J. Lessen, J. E. Krueger and R. A. Nash, *Tetrahedron Lett.* 1963, **8**, 1155.
24. L. M. Conver, Special publication, No. 5, P. 48. The Chemical Society, London (1956).
25. W. A. Baker Jr and P. M. Brown, *J. Am. Chem. Soc.* 1966, **88**, 1314.
26. A. Albert, *Nature* 1955, **172**, 201.
27. D. Sampolimsky and Z. Samra, *J. Bact.* 1972, **110**, 468.
28. A. K. Saz and R. B. Slie, *J. Am. Chem. Soc.* 1953, **75**, 4626.
29. J. J. R. F. Silva and M. H. M. Dias, *Rev. Port. Quim.* 1973, **15**, 1.
30. B. Sakagucki and K. Sakashita, *Chemotherapy (Tokyo)* 1956, **4**, 41.

Polyhedron Vol. 8, No. 2, pp. 197–202, 1989
Printed in Great Britain

0277–5387/89 $3.00+.00
© 1988 Pergamon Press plc

SPECTROPHOTOMETRIC STUDY OF THE COMPLEXATION EQUILIBRIA AND THE DETERMINATION OF PALLADIUM(II) WITH 4-(5′-METHYL-3′-ISOXAZOLYLAZO)-RESORCINOL

J. P. PÉREZ TRUJILLO,* Z. SOSA and J. J. ARIAS*

Department of Analytical Chemistry, University of La Laguna, 38204 La Laguna, Spain

(*Received* 15 *July* 1988; *accepted* 15 *August* 1988)

Abstract—The complexation equilibria between Pd^{II} and 4-(5′-methyl-3′-isoxazolylazo)-resorcinol (MIAR) have been studied and the existence of the species PdH_2R^{2+}, $PdHR^+$, PdR and $PdOHR^-$ have been established; the acid dissociation constants for the first three are $pK_{121a} = 2.65 \pm 0.16$, $pK_{111a} = 7.09 \pm 0.15$ and $pK_{101a} = 9.57 \pm 0.20$. The ternary complex Pd^{II}–MIAR–hexamine has also been studied. A new method for the determination of 0.4–4.0 ppm Pd ($\varepsilon = 1.8 \times 10^4$ l mol^{-1} cm^{-1}) has been developed and applied to samples of hydrogenation catalysts.

Hetero-azo phenols based on pyridine and thiazole have been widely used as reagents for palladium[1–3] although in most cases little attention has been given to the study of the corresponding equilibria in solution. However, the system Pd^{II}–4-(2-pyridylazo)-resorcinol (PAR) has been investigated in some detail.

Thus, Busev and Ivanov[4] detected the formation of two complexes, a green one extractable into ethyl-acetate and formed in 0.35–5 M sulphuric acid medium, and a red one formed at pH 7. Flaschka and Hicks[5] showed that the green complex can only be extracted in the presence of chloride ions. Saxena *et al.*[6] indicated that as least three complex species are formed: at pH 2.0 an unstable green 1 : 1 species, and at pH 3.7–5.0 and 5.6–12.2, two red complexes with a stoichiometry of 1 : 1 and 3 : 2, respectively, these complexes change their colour and/or composition as a function of the pH. Yotsuyanagi *et al.*[7] studied the acid–base equilibria among the different complexes and establishing the existence in solution of four 1 : 1 species: a green one $[Pd(H_2R)H_2O]^{2+}$ at pH < 4, a cationic red species $[Pd(HR)H_2O]^+$ and a neutral red species $[Pd(R)H_2O]$ in the pH region 4–7, and an anionic red species $[Pd(R)OH]^-$ at pH > 8, attributing the spectral changes to proton dissociation from the *o*- and *p*-hydroxyl groups and the molecule of water bonded to the forth coordination site of the square planar structure of the Pd^{II} complexes.

On the other hand, Vostova and Sommer[8] investigated the complexation equilibria of Pd^{II} with various hetero-azo derivatives, one of which was TAR.

In the present work, a study of the complexation equilibria in the system Pd^{II}–MIAR by spectrophotometric methods is presented with a view to contribute to the knowledge of the chemistry of palladium with hetero-azo compounds.

EXPERIMENTAL

4-(5′-Methyl-3′-isoxazolylazo)-resorcinol (MIAR), 10^{-3}M solution in absolute ethanol.[9] Standard 10^{-2} M solution of palladium perchlorate, prepared from the chloride by perchloric acid treatment, and standardized by AAS. The ionic strength, *I*, of the solution was kept constant at 0.1 M ($NaClO_4$). Hexamine–perchloric acid buffer solution, pH 6.5.

Analytical reagent grade chemicals and demineralized water were used throughout with no further purification.

The pH measurements were made with a radiometer PHM64 digital pH-meter with glass–calomel combination electrode. Absorption measurements were made with a Hitachi Perkin–Elmer 200 recording spectrophotometer provided with 1-cm matched quartz cells. A selecta vibromatic mechanical shaker was used. Measurements were made at 25 ± 0.1°C. Calculations were made on a Digital VAS/VMX 11/780 (V.4.0) computer.

*Authors to whom correspondence should be addressed.

Extraction—spectrophotometric determination of palladium

To the solution under study, containing 4–40 μg of palladium, 4 cm^3 of 10^{-3} M MIAR and 1 cm^3 of pH 6.5 hexamine–$HClO_4$ buffer solution were added and made up to 10 cm^3 with demineralized water. This solution was shaken with 10 cm^3 of chloroform for 45 min, centrifuged, and the absorbance of the organic layer at 490 nm was measured against a reagent blank.

Determination of palladium in hydrogenation catalysts

A 0.50 g sample of the catalyst was dissolved by treatment with perchloric acid, nitric acid, aqua regia or EDTA, according to the catalyst support, heating if necessary. The solution was diluted and made up to volume with 1 M perchloric acid in a 100 cm^3 standard flask. An aliquot was analysed for palladium according to the procedure described previously.

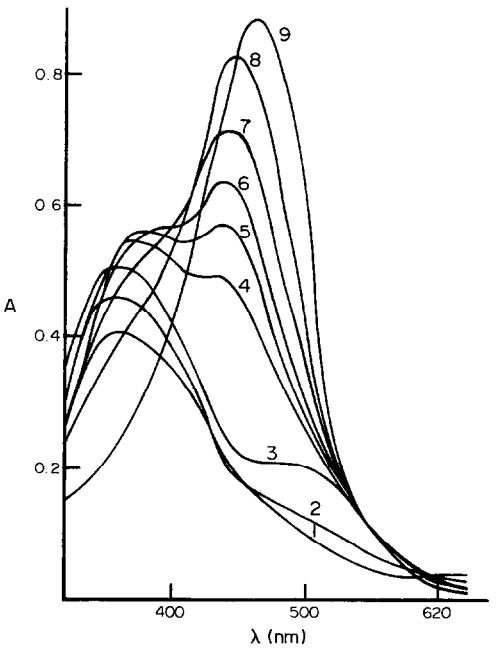

Fig. 2. Absorption spectra of the system Pd^{II}–MIAR; $C_R = 2C_M = 4 \times 10^{-5}$ M; $I = 0.1$ M ($NaClO_4$); 20%(v/v) ethanol–water. pH (1) 0.90; (2) 2.11; (3) 4.21; (4) 6.16; (5) 7.18; (6) 9.00; (7) 10.36; (8) 11.00; (9) 12.00.

RESULTS AND DISCUSSION

Complexation equilibria in the Pd^{II}–MIAR system

Pd^{II} and MIAR react to give different colours according to the C_{Pd}/C_R ratio and the pH of the medium. Thus, in equimolar solutions (Fig. 1) a green colour is formed at pH < 3, and has an absorption maximum at 427 nm; at pH > 3, the colour is red, with an absorption band at 465–495 nm, which continuously increases in height as the acidity of the medium is decreased. In solutions containing excess of MIAR (Fig. 2) the colour is yellow, with a maximum at 365 nm and an absorption band centred at 495 nm at pH < 4.5; at pH 6–9 two new maxima appear, at 380 and 440 nm that coalesce as the pH increases, to give way at pH 11 to a well-defined maximum at 460 nm.

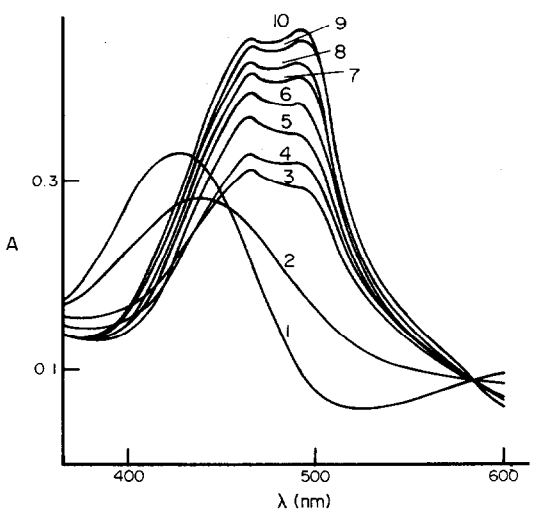

Fig. 1. Absorption spectra of the system Pd^{II}–MIAR; $C_R = C_M = 2 \times 10^{-5}$ M; $I = 0.1$ M ($NaClO_4$); 20%(v/v) ethanol–water, pH (1) 0.93; (2) 2.58; (3) 3.58; (4) 4.50; (5) 5.70; (6) 7.25; (7) 8.54; (8) 9.52; (9) 10.52; (10) 11.08.

The absorbance (A)–pH curves obtained at 427, 440, 450 and 495 nm for different C_{Pd}/C_R ratios (Fig. 3) confirm the existence of different species in solution, depending on the pH and the C_{Pd}/C_R ratio.

Determination of the stoichiometry by the continuous variations and mole ratio methods, applied at pH 1.0, 4.2, 7.2 and 9.5 and at 427, 440 and 495 nm, indicate the presence of 1:1 and 1:2 Pd/R complexes.

Accordingly it can be assumed that the variation of the absorbance observed in the pH region 1–4 for $C_{Pd}/C_R = 1$ corresponds to the acid–base equilibrium between the green and red Pd/R 1:1 species, and the progressive increase in absorbance at pH > 6 may be due to deprotonation and/or hydrolysis of the red species. The change in absorbance at pH 1.5–3.5 when excess of reagent is present ($C_{Pd}/C_R = 1:2$) is observed only at 495 nm (curve 4) and is analogous to that observed for $C_{Pd}/C_R = 1$, but is of lesser magnitude; the change is even smaller $C_{Pd}/C_R = 0.1$. This can be interpreted as

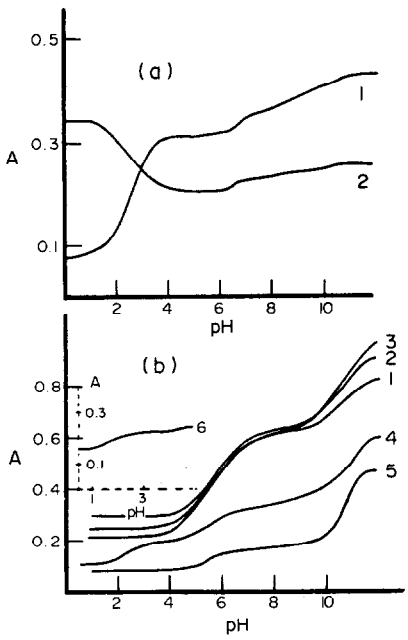

Fig. 3. Absorption–pH curves for the system Pd^{II}–MIAR (a) $C_R = C_M = 2 \times 10^{-5}$ M; $I = 0.1$ M ($NaClO_4$); 20%(v/v) ethanol–water. λ = (1) 495 nm; (2) 427 nm. (b) $C_R = 2C_M = 4 \times 10^{-5}$ M; $I = 0.1$ M ($NaClO_4$); 20%(v/v) ethanol–water. λ = (1) 427 nm; (2) 440 nm; (3) 450 nm; (4) 495 nm; (5) reagent, $\lambda = 440$ nm; (6) $C_R = 10C_M$, $\lambda = 495$ nm.

due to the presence of complexes with 1 : 1 and 1 : 2 Pd/R stoichiometry, when the reagent is in excess, while for the $C_{Pd}/C_R = 1$ only complexes of 1 : 1 Pd/R stoichiometry exist.

The simultaneous presence of species with different stoichiometry in solutions with excess of reagent makes the study of the corresponding equilibria practically impossible either by graphical or numerical calculation methods. Therefore, only the study of the A–pH curves obtained for the equimolar ratio and in excess of palladium has been undertaken in this work.

Assuming that the transition between the green and red 1 : 1 species is caused by an acid–base equilibrium, the method of Sommer *et al.*[10] for graphical analysis of the A–pH curves was used, to calculate the transition constant, from which $pK_a = 2.70 \pm 0.13$ is calculated and it is deduced that one proton is released during the transition from the green to the red species. The non-existence of well-defined zones in the rest of the A–pH curve makes its graphical analysis impossible.

The A–pH curve for the equimolar solution was next analysed by applying the LETAGROP–SPEFO program[11,12] for which the curve was divided into two steps: the first at pH 1–4.5, corresponding to the green–red transition, and the second at pH 5–12. The results in Table 1, indicate that for the first step the best fit with the experimental data is obtained when a single proton is interchanged, and for the second step when two protons are successively interchanged. The data obtained in the joint analysis of the entire experimental A–pH curve are also included in Table 1.

All the above leads to the conclusion that in the pH region 1–12, in equimolar solutions, the system Pd–MIAR presents three acid–base equilibria and four complex species related to each other by the following equilibria:

Table 1. Values of U,[a] $\sigma(A)$[b] and pK_a for the different species calculated by the LETAGROP–SPEFO method

Species	U	$\sigma(A)$	pK_a	ε (l mol^{-1} cm^{-1})	
			$1 < pH < 4.5$	$\lambda = 427$	490
PdH_2R	0.261×10^{-3}	0.004		16,500±150	4100±90
PdHR				10,300±160	16,000±9
			$5 < pH < 12$		
PdHR				10,200±100	15,500±85
PdR	0.198×10^{-3}	0.002		12,000±50	19,300±80
PdOHR				12,700±4	21,200±40
			$1 < pH < 12$		
PdH_2R				16,900±50	3500±50
PdHR	0.354×10^{-3}	0.002		10,300±35	15,600±35
PdR				11,800±46	18,700±46
PdOHR				12,700±40	21,100±40

[a] Sum of squares of residuals.
[b] Standard deviation.

$$[Pd(H_2R)]^{2+} \underset{\text{green}}{\overset{K_{121a}}{\rightleftharpoons}} [Pd(HR)]^{+}_{\text{red}}$$

$$\overset{K_{111a}}{\rightleftharpoons} [Pd(R)]_{\text{red}} \overset{K_{101a}}{\rightleftharpoons} [Pd(OH)R]^{-}_{\text{red}},$$

in accordance with Yotsuyanagi.[7]

Equilibria in the system Pd^{II}*–MIAR–hexamine*

In equimolar solutions of MIAR and Pd^{II} with excess of hexamine (2%) present, the formation at pH < 3 of a green complex (λ_{max} = 430 nm) is observed. At pH 3–9 the colour changes to red, with an absorption band at 465–495 nm, which decreases slightly in intensity at pH > 9. In excess of reagent, C_{Pd}/C_R = 1:2 (2% hexamine), a green colour is observed at pH 1, with an absorption band at 360–430 nm, and the colour changes to red as the acidity of the medium is decreased; at pH 4 there is a maximum at 365 nm and a band at 465–495 nm which coincides with that of the complex formed in equimolar solution; at pH > 9 a new maximum appears at 460 nm, which at pH > 12 coincides with that of the binary complex in the absence of hexamine.

The absorbances are independent of ionic strength when this is $> 10^{-2}$ M, and decrease according to nature of the anion of the electrolyte employed for this purpose in the sequence $ClO_4^- > NO_3^- > Cl^- > Br^-$.

The *A*–pH curves (Fig. 4) show a transition in the pH region 1.5–4.5, analogous to observed in the absence of hexamine (Fig. 3) and the fact that the spectra when reagent excess is present do not indicate the formation of new species points to the transition of the green ternary complex to the red one with loss of the *o*-OH proton of the reagent and to the presence of hexamine molecules co-ordinated to Pd(II), hindering the formation of 1:2 Pd/R complexes. At Ph > 10 and equimolar reactant ratio, a slight decrease in absorbance is observed, attributable to the dissociation of the proton of the *p*-OH group. The formation of hydroxylated species is hindered by the hexamine molecule bonded to the fourth co-ordination site in the square planar Pd^{II} complex. In contrast, when reagent excess is present a sharp increase in absorbance appears which does not correspond to the absorbance sum for the ternary complex and the excess of reagent. Since, moreover, at these pH values the spectra coincide with those of the binary complex, it is thought that deprotonation of the *p*-OH group of the ternary compound, ionization of the excess of reagent and transition between the ternary complex and the 1:2 Pd/R binary complex, occur simultaneously.

The stoichiometry, determined by the usual methods, at pH 4.2 and 7.2 and at 470 and 490 nm (2% hexamine), indicates a 1:1 Pd/R ratio. However, the number of molecules of hexamine forming part of the complex could not be established, it being found only that a 50-fold excess of hexamine with respect to the palladium present is necessary for the absorbance readings to reach a plateau. However, the co-ordinating possibilities of Pd^{II} point to the possible formation of a 1:1:1 Pd/R hexamine complex.

In accordance with the above it can also be assumed that the variation in absorbance that is produced in the first step of the *A*–pH curves is caused by an acid–base equilibrium between the green and red ternary complexes, of the type:

$$Pd(H_2R)(\text{hexamine}) \underset{\text{green}}{\overset{K_t}{\rightleftharpoons}}$$

$$Pd(H_yR)(\text{hexamine}) + qH^+, \quad (y = 2-q).$$
$$\text{red}$$

Analysis of these *A*–pH curves by the method of Sommer *et al.* gave a mean value of $pK_t = 2.75 \pm 0.02$. The application of the LETAGROP–SPEFO program to the experimental data affords the best fit for the system formed by the species $Pd(H_2R)$(hexamine) and Pd(HR)(hexamine) with release of a proton, and $pK_t = 2.70 \pm 0.03$ ($U = 0.270 \times 10^{-3}$; $\sigma = 0.003$). A comparison with the data included in Table 1 shows the good agreement of the data obtained here for K_t with the value for the binary complex, which seems to indicate that the molecule of hexamine

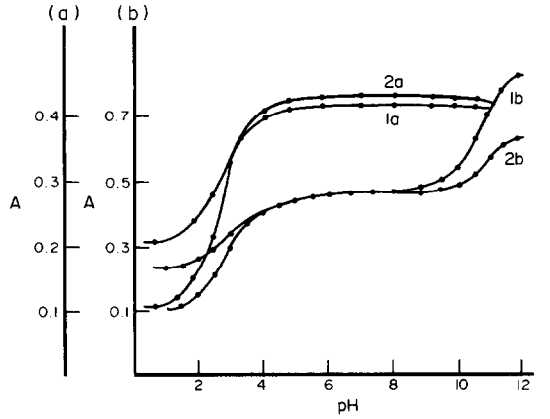

Fig. 4. Absorption–pH curves for the system Pd^{II}–MIAR–hexamine. I = 0.1 M ($NaClO_4$); 20%(v/v) ethanol–water; |hexamine| = 2%. (a) $C_R = C_M = 2 \times 10^{-5}$ M; (b) $C_R = 2C_M = 4 \times 10^{-5}$ M; λ = (1) 470 nm; (2) 490 nm.

co-ordinated to palladium in the ternary complex influences the first transition equilibrium.

Because the variation in the absorbance in the second step of the A–pH curve for Pd/R = 1 was very small, neither graphical nor numerical analysis was applied to it.

Extraction of the red Pd–*MIAR–hexamine complex into chloroform*

With a view to increasing the sensitivity and/or selectivity of the determination of palladium with MIAR, it seemed worthwhile to combine formation of the complexes with their extraction into organic solvents.

Preliminary tests has indicated that both free reagent and ternary complex were extractable with different organic solvents, chloroform giving better and more stable absorbance readings after 45 min of mechanical shaking. Neither the 1 : 1 nor the 1 : 2 Pd/R complexes are extracted, but form precipitates at the interphase. In any case, the ternary complex must be formed in the aqueous phase and then extracted into chloroform, since if a solution of MIAR in chloroform is used as the extractant the kinetics of the process is so slow that the method would not be of any practical interest.

The wavelength of the absorption maximum and the value of the absorbance of the spectra in organic phase are dependent on the anion of the inert electrolyte. The absorbance decreases in the sequence $ClO_4^- > NO_3^- > Cl^- > Br^-$. Using 0.1 M $NaClO_4$ as inert electrolyte the Pd–MIAR–hexamine complex shows an absorption maximum at 490 nm and is extracted in the pH range 4–9 (Fig. 5) coinciding with the region of predominance of the species $[Pd(HR)(hexamine)]^+$ in the aqueous phase. The presence of ethanol (4–20%) in the aqueous medium is necessary in order to facilitate the extraction.

The stoichiometry of the extracted species determined by the usual methods, at pH 6.5 and 490 nm,

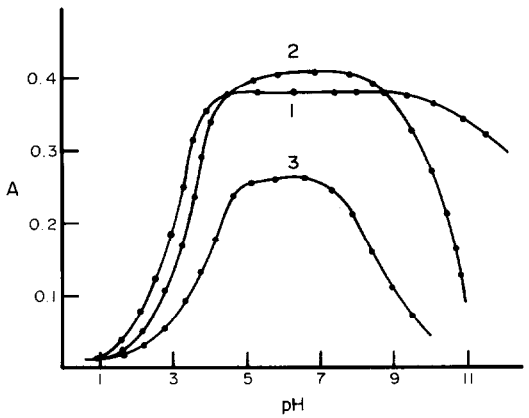

Fig. 5. Extraction curve for the system Pd^{II}–MIAR–hexamine as a function of the pH of the homogeneous phase. $I = 0.1$ M ($NaClO_4$); 10%(v/v) ethanol–water; $\lambda = 490$ nm; (1) $C_R = C_M = 2 \times 10^{-5}$ M, |hexamine| = 2%; (2) $C_R = 5C_M = 1 \times 10^{-4}$ M, |hexamine| = 2%; (3) $C_R = C_M =$ |hexamine| $= 2 \times 10^{-5}$ M.

indicates a 1 : 1 Pd/R ratio. However, the number of molecules of hexamine forming part of the complex could not be established, it being found only that a 20-fold excess of hexamine with respect to the palladium present is necessary for the absorbance reading to reach a plateau.

In accordance with the above information it can be assumed that the extracted species is the ionic couple:

$$[Pd(HR)(hexamine)]^+ClO_4^-.$$

Spectrophotometric determination of palladium

Table 2 presents a summary of the characteristics of the spectrophotometric methods developed, based on (a) the formation of the yellow complex $[Pd(HR)_2]$ in homogeneous medium; (b) the formation of the ternary complex $[Pd(HR)(hexamine)]^+$ in homogeneous medium and (c) the extraction of the latter into chloroform. As can

Table 2. Characteristics of the different methods developed for the determination of palladium

Species	pH	λ_{max} (nm)	ε (l mol^{-1} cm^{-1})	Beer (ppm)	Ringbom (ppm)
$Pd(H_2R)$	1	485	8500	0.42–6.3	2.13–5.3
$[Pd(HR)U]^a$	7.2	490	20,700	0.20–4.2	0.85–4.2
$[Pd(HR)U]^b$	6.5	490	18,300	0.40–4.0	0.85–3.8

U: Hexamine.

[a] Homogeneous phase.

[b] Extraction into chloroform.

be observed the extractive–spectrophotometric method not only maintains the sensitivity of the method based on the formation of the ternary complex in homogeneous solution, which turn is twice as sensitive as the method based on the formation of the binary yellow complex.

The statistical study, for the extractive-spectrophotometric method, carried out on ten samples, each containing 2.13 ppm of Pd^{II}, gave 2.123 ppm as the mean value, 0.016 ppm as the standard deviation and 0.5% as the relative error ($P = 0.05$).

The effect of several ions on the determination of 2.13 ppm palladium, was studied by application of the recommended procedure. The criterion for interference was a deviation of more than 2% between the palladium concentration found and that taken. The ions F^-, Cl^-, Br^-, SCN^-, Cd^{2+}, Ca^{2+}, Mg^{2+}, La^{3+} and Zn^{2+} can be present up to 100:1 $C_x:C_{Pd}$ ratio, Ba^{2+} and Al^{3+} up to 25:1; Ru^{3+}, Pt^{2+} and Au^{3+} up to 1:1 and Cu^{2+}, Co^{2+} and Ni^{2+} interfere even in the 1:1 ratio, but can be present in 50:1 ratio when the spectrophotometric method at pH 1 is used.

The method developed was applied to the determination of palladium in samples of hydrogenation catalysts: Pd–asbestos (4.26% Pd), Pd–carbon activo (4.56% Pd), Pd–$CaCO_3$ (5.14% Pd), Pd–Al_2O_3 (4.60% Pd) and Pd–$BaSO_4$ (3.88% Pd) with recoveries of 4.23, 4.34, 5.03, 4.75 and 3.99%, respectively, as mean values of three determinations.

Acknowledgement—The authors acknowledge the financial support of this work by the Canary Islands Autonomous Government grant No. 49/22.04.85.

REFERENCES

1. H. R. Hovind, *Analyst* 1975, **100**, 769.
2. R. G. Anderson and R. M. Nickless, *Analyst* 1967, **92**, 207.
3. S. Shibata, *Chelates in Analytical Chemistry*, Vol. 4 (Edited by H. A. Flaschka and A. J. Barnard), p. 1. Dekker, New York (1972).
4. A. I. Busev and V. M. Ivanov, *Zh. Anal. Khim.* 1964, **19**, 232.
5. H. Flaschka and J. Hicks, *Microchem. J.* 1966, **1**, 517.
6. K. Saxena, B. V. Agarwala and A. K. Dey, *Mikrochim. Acta* 1969, 694.
7. T. Yotsuyanagi, H. Hoshino and K. Aomura, *Anal. Chim. Acta* 1974, **71**, 349.
8. J. Vostova and L. Sommer, *Collect. Czech. Chem. Commun.* 1976, **41**, 1137.
9. J. P. Pérez Trujillo, Z. Sosa, J. J. Arias and F. García Montelongo, *Quim. Anal.* 1987, **7**, 55.
10. L. Sommer, *Scripta Fac. Sci. Nat. Univ. Purk. Brno* 1964, **1**, 1.
11. L. G. Sillen, *Acta Chem. Scand.* 1962, **16**, 159.
12. L. G. Sillen and B. Warnqvist, *Arkiv Kemi* 1969, **31**, 377.

Polyhedron Vol. 8, No. 2, pp. 203–209, 1989
Printed in Great Britain

0277–5387/89 $3.00+.00
© 1988 Pergamon Press plc

η^3-ALLYL COMPLEXES OF MOLYBDENUM—IV.* PREPARATION AND CRYSTAL STRUCTURES OF SOME SUBSTITUTED-CYCLOPENTADIENYL MOLYBDENUM ALLYL DERIVATIVES

O. ANDELL,† R. GODDARD, S. HOLLE, P. W. JOLLY,‡ C. KRÜGER and Y. H. TSAY

Max-Planck-Institut für Kohlenforschung, D-4330 Mülheim a. d. Ruhr, F.R.G.

(*Received* 13 *July* 1988; *accepted* 25 *August* 1988)

Abstract—A series of substituted-cyclopentadienyl molybdenum allyl derivatives has been prepared by reacting $(\eta^3\text{-}C_3H_5)_3MoCl$ with substituted-cyclopentadienyl and -indenyl alkali metal salts. In general, the isolated products are of the type $Cp'Mo(\eta^3\text{-}C_3H_5)_2$ and in three cases this has been confirmed by crystal structure determinations. Spectroscopic evidence suggests that at low temperatures compounds have the composition $Cp'Mo(\eta^3\text{-}C_3H_5)_2(\eta^1\text{-}C_3H_5)$ are also formed. The reaction with potassium fluorenyl is anomalous: the NMR spectra and a crystal structure determination show that the product (η^3-fluorenyl)Mo $(\eta^3\text{-}C_3H_5)_3$, contains four η^3-allyl groups bonded unsymmetrically to the metal atom.

The dormancy in the chemistry of tetra(η^3-allyl) molybdenum was interrupted after *ca* twenty years with the isolation of $(\eta^3\text{-}C_3H_5)_3MoCl$ (**1**) from the reaction with gaseous HCl in pentane at $-70°C$ [eq. (1)] and this compound has been used to prepare a series of η^3-allyl molybdenum complexes.[1–3]

One of the more interesting reactions studied has been that with sodium cyclopentadienide from which the paramagnetic complex $CpMo(\eta^3\text{-}C_3H_5)_2$ (**2**) could be isolated and its structure and electron deformation density determined by X-ray methods.[4]

$$(\eta^3\text{-}C_3H_5)_4Mo \xrightarrow[-C_3H_6]{HCl} \underset{\mathbf{1}}{(\eta^3\text{-}C_3H_5)_3MoCl} \xrightarrow[-NaCl/[C_3H_5]]{NaCp} \underset{\mathbf{2}}{CpMo(\eta^3\text{-}C_3H_5)_2} \quad (1)$$

Although these results have considerably extended the chemistry of the allyl molybdenum system, the compounds have proved rather unreactive, (**2**), in particular, (in contrast to the related chromium compound)[5] shows no remarkable reactivity in either stoichiometric or catalytic reactions. There are two obvious approaches for improving the situation—the introduction of substituents either into the cyclopentadienyl ring or the allyl group. Here we report the synthesis of a series of substituted-cyclopentadienyl and -indenyl molybdenum allyl complexes and a subsequent publication will be devoted to their reactions.

RESULTS AND DISCUSSION

The substituted-cyclopentadienyl and -indenyl molybdenum allyl compounds shown in Table 1 have been prepared in 60–80% yield by reacting $(\eta^3\text{-}C_3H_5)_3MoCl$ (**1**) with the appropriate alkali metal salt in THF at *ca* $-30°C$. With a few exceptions (see below), the products are of the type $Cp'Mo(\eta^3\text{-}C_3H_5)_2$ e.g. [eq. (2)].

* Part III—Benn *et al.*[1]

† Present address: Department of Organic Chemistry, The Royal Institute of Technology, S-100 44 Stockholm, Sweden.

‡Author to whom correspondence should be addressed.

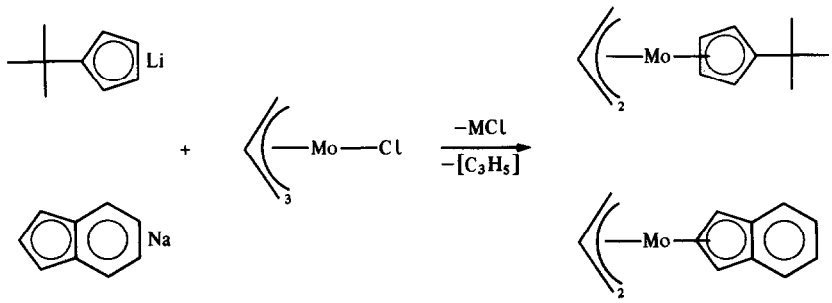

(2)

The compounds are in general orange–red solids and are thermally stable at room temperature. The anticipated and observed paramagnetism (one unpaired electron, Table 1) prevented the use of NMR-spectroscopy to obtain useful structural information and since it was not clear how the indenyl system would bond to the metal (η^3-, η^5- or even η^6- situations are conceivable), we have undertaken crystal structure determinations of the compounds containing the 2-methylindenyl, 2-methoxyindenyl and 5,6-dimethoxyindenyl groups: in all cases the indenyl derivative is bonded in an η^5- manner (see discussion below).

The product of the analogous reactions between $(\eta^3\text{-}C_3H_5)_3WCl$ and CpNa is $CpW(\eta^3\text{-}C_3H_5)_2C_3H_5$ and contains both η^1- and η^3-allyl groups and, moreover, this compound shows no tendency to react further with loss of an allyl group.[6] This apparent difference in the behaviour of the molybdenum and tungsten systems (which we attribute to a difference in the strength of the M—C bonds involved) encouraged us to study the reactions involving molybdenum at even lower temperatures and indeed spectroscopic evidence suggests that initially a species is generated which contains an η^1-allyl group. For example, by carrying out the

Table 1. Distances (Å) and angles (°)

Distances	I	II	III		IV
Mo—D1	2.06	2.04	2.04	2.05	2.342(2)
Mo—D2	1.98	2.00	2.00	1.87	2.07
Mo—D3	2.00	1.99	2.01	2.01	2.07
Mo—D4	—	—	—	—	2.09
C14—C15	1.412(6)	1.346(8)	1.20(4)	1.35(4)	1.404(5)
C15—C16	1.412(5)	1.38(1)	1.29(4)	1.60(4)	1.385(4)
C17—C18	1.404(5)	1.40(1)	1.15(4)	1.28(4)	1.381(5)
C18—C19	1.411(5)	1.39(1)	1.45(5)	1.39(4)	1.390(5)
C20—C21	—	—	—	—	1.396(4)
C21—C22	—	—	—	—	1.384(4)
C1—C2	1.434(4)	1.439(5)	1.44(2)	1.52(2)	1.465(4)
C1—C5	1.440(4)	1.436(6)	1.40(2)	1.42(2)	1.407(3)
C2—C3	1.420(4)	1.403(6)	1.39(2)	1.33(2)	1.433(3)
C3—C4	1.422(4)	1.416(6)	1.34(2)	1.51(2)	1.458(3)
C4—C5	1.435(4)	1.428(5)	1.42(2)	1.40(2)	1.476(3)
Angles					
D1—Mo—D2	129.6	126.9	128.3	132.5	107.6
D1—Mo—D3	129.7	131.4	130.3	127.5	107.8
D2—Mo—D3	100.8	101.7	100.5	97.4	95.2
D1—Mo—D4	—	—	—	—	103.4
D2—Mo—D4	—	—	—	—	137.6
D3—Mo—D4	—	—	—	—	102.2
C14—C15—C16	119.0(3)	120.5(8)	146(3)	127(3)	122.3(3)
C17—C18—C19	118.4(3)	121.4(7)	136(3)	121(2)	123.3(3)
C20—C21—C22	—	—	—	—	123.3(2)

D1: midpoint C1—C5 (in **IV** = C4); D2: midpoint C14—C16; D3: midpoint C17—C19; D4: midpoint C20—C21.

reaction with indenyl–lithium in ether at −78° and washing the product repeatedly with pentane at −78°C, it is possible to obtain a small amount of a relatively insoluble red–violet material whose IR spectrum (KBr, −78°C) suggests the presence of an η^1-allyl group ($\nu_{C:C}$1640, 910 cm^{-1}) while the ^{1}H-NMR spectrum (D_8-THF, −78°C) although not completely interpretable is that of a diamagnetic species and shows absorptions compatible with the presence of a vinyl group ($\delta_{HC:}$ *ca* 5.9–5.8 m,br, 4.3 d, 4.1 dd; for comparison, the vinyl protons in (t-$C_4H_9C_5H_4$)W(η^3-C_3H_5)$_2C_3H_5$ are found at 5.68 m, 4.33 d and 4.23 dd ppm[6]). Similar absorptions are observed in the low temperature IR spectra of the products of the reaction with t-$C_4H_9C_5H_4Li$ ($\nu_{C:C}$1635, 908 cm^{-1}) and CpLi ($\nu_{C:C}$1640, 912 cm^{-1}) and are absent from the spectra of the related Cp$Mo(\eta^3$-$C_3H_5)_2$ and (indenyl)$Mo(\eta^3$-$C_3H_5)_2$ species.

In the case of the reaction with 5,6-dimethoxyindenyl lithium, the IR spectrum and elemental analysis indicate that the major component containing an η^1-allyl group ($\nu_{C:C}$1622, 905 cm^{-1}) is stable at room temperature and here repeated washing has also enabled a sample to be isolated whose ^{1}H-NMR spectrum suggests the presence of a vinyl group ($\delta_{HC:}$ 5.9–5.8 m,br, 4.26 d, 4.13 d) although the broadness of the signals suggests contamination by paramagnetic material (the structure of what is presumably the minor component, viz. (η^5-5,6-dimethoxyindenyl)$Mo(\eta^3$-$C_3H_5)_2$, is presented below). The elemental analysis of the product of the reaction with 2-phenylindenyl lithium suggests that this compound should also be formulated as (2-phenylindenyl)$Mo(C_3H_5)_3$ in agreement with the observed diamagnetism. Unfortunately, we were unable to prepare sufficient of this compound for an NMR-spectoscopic study or to obtain suitable crystals for an X-ray diffraction study so that we cannot decide whether this compound should be formulated as (η^3-2-phenylindenyl)$Mo(\eta^3$-$C_3H_5)_3$ (see the fluorenyl compound discussed below) or (η^5-2-phenylindenyl)$Mo(\eta^3$-$C_3H_5)_2C_3H_5$. The analytical data for the product of the reaction with 1-$CyCH_2$indenyl lithium lies between that expected for tris-allyl and bis-allyl systems, so that presumably a mixture of the two species is formed.

To summarize, with the exception of the 2-phenylindenyl and 5,6-dimethoxyindenyl derivatives mentioned above, the main product of the reaction between (η^3-$C_3H_5)_3MoCl$ and the substituted-cyclopentadienyl or -indenyl derivatives at *ca* −30° are the paramagnetic compounds of the type Cp′$Mp(\eta^3$-$C_3H_5)_2$ while at −78° these are contaminated with Cp′$Mo(\eta^3$-$C_3H_5)_2C_3H_5$ systems.

The reaction with fluorenyl potassium takes a different course: a purple, diamagnetic compound is formed which has the composition (fluorenyl)$Mo(\eta^3$-$C_3H_5)_3$. The crystal structure determination (see below) and the NMR spectral data (see Experimental) indicate that the fluorenyl group is acting as an η^3-organic ligand and that the molecule, in addition, contains three η^3-C_3H_5-groups [eq. (3)].

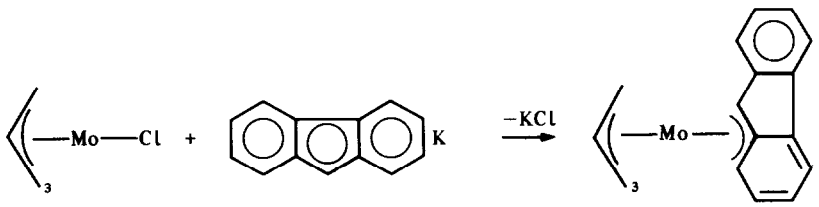

(3)

All fifteen H-atoms of these three groups are magnetically inequivalent indicating that they are asymmetrically bonded to the metal atom. Particularly remarkable in the ^{1}H-NMR spectrum is the difference in the chemical shifts of the *meso*-H-atoms: two have "normal" values of *ca* 4 ppm whereas one experiences a high field shift to 0.22 ppm. We assign this signal to the *meso*-H-atom which lies above the fluorenyl plane (H-21, see crystal structure). The allylic H-atoms of the fluorenyl group give rise to a singlet at 6.14 ppm (9′) and a doublet at 4.35 ppm (1′) while the remaining fluorenyl H-atoms are assigned to four doublets and three triplets lying between 8.35 and 7.05 ppm.

CRYSTAL STRUCTURE DETERMINATIONS

The molecular structure of three substituted-indenyl molybdenum derivatives viz. (η^5-2-methylindenyl)$Mo(\eta^3$-$C_3H_5)_2$ **(I)**, (η^5-2-methoxyindenyl) $Mo(\eta^3$-$C_3H_5)_2$ **(II)** and (η^5-5,6-dimethoxyindenyl)$Mo(\eta^3$-$C_3H_5)_2$ **(III)**, as well as of (fluorenyl)$Mo(\eta^3$-$C_3H_5)_3$ **(IV)** have been determined by single crystal X-ray diffraction methods and are shown in Figs 1 and 2. Selected bond distances and bond angles and interplanar angles are summarized in Tables 1 and 2.

The molybdenum atom in the three substituted-indenyl derivatives is bonded to the five membered ring in an η^5-manner. In the case of the 5,6-dimethoxyindenyl derivative, the unit cell contains two

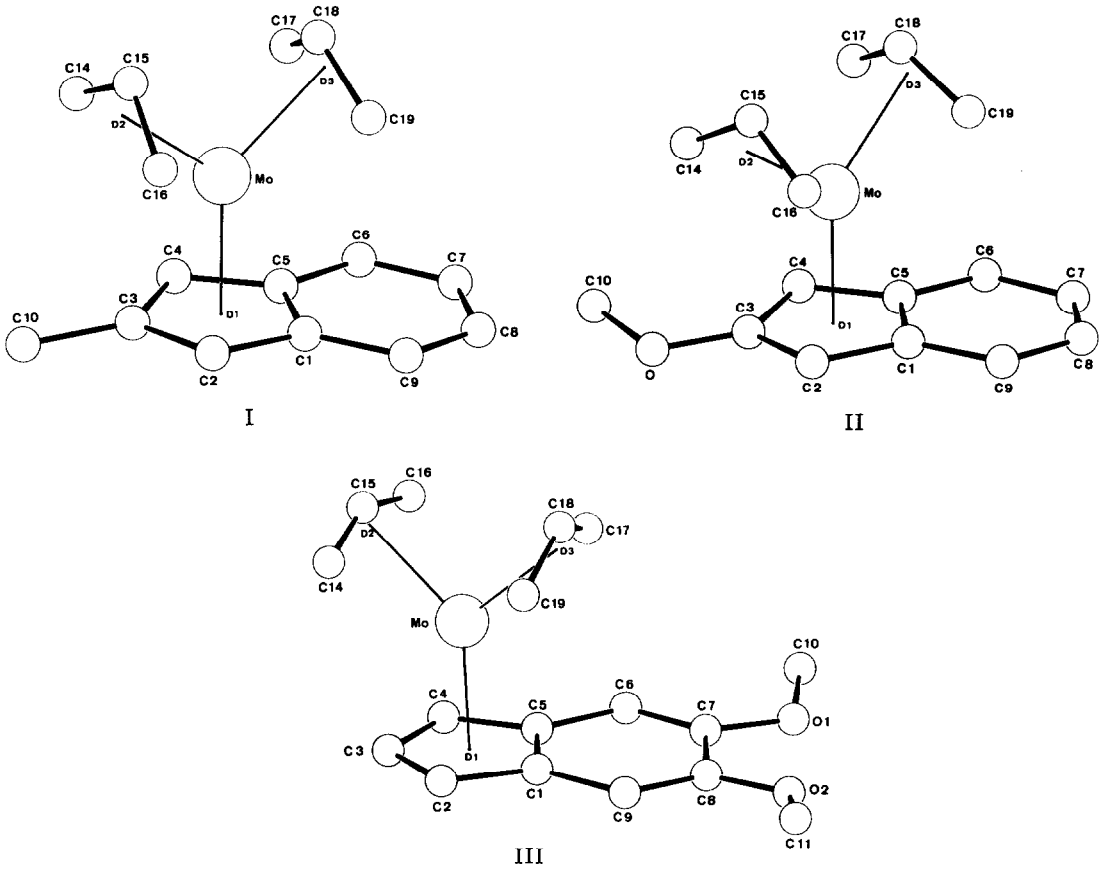

Fig. 1. The molecular structures of $[(\eta^5\text{-2-methylindenyl})Mo(\eta^3\text{-}C_3H_5)_2]$ (**I**), $[(\eta^5\text{-2-methoxyindenyl})Mo(\eta^3\text{-}C_3H_5)_2]$ (**II**) and $[(\eta^5\text{-5,6-dimethoxyindenyl})Mo(\eta^3\text{-}C_3H_5)_2]$ (**III**).

independent molecules but the poor quality of the data (Table 2) precludes any further discussion. The structure of the 2-methylindenyl and 2-methoxyindenyl derivatives are similar to that observed for $(\eta^5\text{-}C_5H_5)Mo(\eta^3\text{-}C_3H_5)_2$[2] with the metal lying in a trigonal planar environment. The allyl groups are arranged in a non-parallel, *cis*-configuration with the *meso*-C-atoms directed away from the metal.

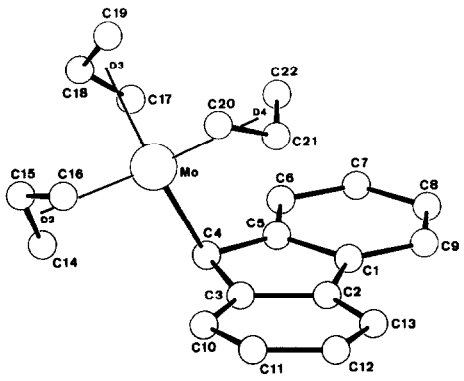

Fig. 2. The molecular structure of $[(\text{fluorenyl})Mo(\eta^3\text{-}C_3H_5)_3]$ (**IV**).

Table 2. Angles between planes

	I	II	III		IV
allyl(a)/C*p*	72.2	75.5	79.6	94.9	58.8
allyl(b)/C*p*	76.1	76.4	91.5	79.3	52.2
allyl(c)/C*p*	—	—	—	—	32.0
allyl(a)/allyl(b)	25.7	28.2	14.1	18.9	36.0
allyl(a)/allyl(c)	—	—	—	—	44.9
allyl(b)/allyl(c)	—	—	—	—	62.0

allyl(a): C14,C15,C16; allyl(b): C17,C18,C19; allyl(c): C20,C21,C22; Cp: C1—C5.

The angles between the allyl planes (25.7° for **I**, 28.2° for **II**) are similar to that observed for $(\eta^5\text{-}C_5H_5)Mo(\eta^3\text{-}C_3H_5)_2$ (25.6°).

The four organic ligands in $(\text{fluorenyl})Mo(\eta^3\text{-}C_3H_5)_3$ are arranged in an essentially tetrahedral manner around the central metal atom. The fluorenyl group is bonded asymmetrically to molybdenum [Mo—C(4) 2.342(2), Mo—C(3) 2.611(2) and Mo—C(10) 2.856(3)] indicating considerable rehybridization towards an η^1-allyl situation.

EXPERIMENTAL

All experiments were carried out under argon using anhydrous and oxygen-free solvents. $(\eta^3\text{-}C_3H_5)_3MoCl$ was prepared according to Benn *et al.*[3] The following compounds were prepared by published procedures: MeC_5H_4Na,[7] $i\text{-}C_3H_7C_5H_4Na$,[7] $t\text{-}C_4H_9C_5H_4Na$,[8] Me_5C_5Tl,[9] indenylNa,[10] 2-Me-indenylLi,[11] 2-MeO-indenylLi,[12] 2-Ph-indenylLi,[13] 5,6-dimethoxyindenylLi[14] and fluorenylK.[15] ^1H NMR spectra were recorded on a Brucker WH 400 instrument and mass spectra using a Varian CH 5 with ^{98}Mo as the standard. Microanalyses were carried out by Dornis and Kolbe, Microanalytical Laboratory, Mülheim a. d. Ruhr.

$[(\eta^5\text{-}t\text{-}C_4H_9C_5H_4)Mo(\eta^3\text{-}C_3H_5)_2]$

A solution of *t*-butylcyclopentadienyl lithium (1.23 g, 9.6 mmol) in monoglyme (80 cm^3) was added to a stirred suspension of $(\eta^3\text{-}C_3H_5)_2MoCl$ (2.15 g, 8.5 mmol) in THF (50 cm^3) at $-35°$ over a period of 30 min and stirred at this temperature for a further 18 h. The solvent was evaporated at room temperature and the orange–brown residue extracted with pentane. The pentane-extract was filtered through Avicel, evaporated and the solid residue recrystallized from hexane at $-35°C$ to give the compound as red–orange crystals. Yield 1.89 g (75% theory). The analytical data is summarized in Table 3.

$[(\eta^5\text{-}MeC_5H_4)Mo(\eta^3\text{-}C_3H_5)_2]$

Prepared as above from methylcyclopentadienyl lithium in THF at $-30°C$ and purified by vacuum sublimation (70°C/10^{-4} mmHg).

$[(\eta^5\text{-}i\text{-}C_3H_7C_5H_4)Mo(\eta^3\text{-}C_3H_5)_2]$

Prepared as above from *i*-propylcyclopentadienyl sodium in THF at $-35°C$.

$[(\eta^5\text{-}Me_5C_5)Mo(\eta^3\text{-}C_3H_5)_2]$

Prepared as above from pentamethylcyclopentadienyl thallium in THF at -78 to $-10°C$.

$[(\eta^5\text{-}indenyl)Mo(\eta^3\text{-}C_3H_5)_2]$

Prepared as above from indenyl lithium or sodium in THF or ether at $-35°C$.

$[(\eta^5\text{-}2\text{-}methylindenyl)Mo(\eta^3\text{-}C_3H_5)_2]$

Prepared as above from 2-methylindenyl lithium in THF at -78 to $-30°C$.

Table 3. Analytical data for the Cp′Mo(η^3-C_3H_5)$_2$ compounds and related systems

Cp′	Yield (%)	Colour (m.p. °C)	μ_{eff} (BM)	MS (70 eV)	%Mo (calc.)	%C (calc.)	%H (calc.)
C_5H_5[a]		orange(120–122dec.)					
MeC_5H_4	20.4	orange(120–122dec.)	—	259(M^+)	37.1(37.3)	56.2(56.0)	6.6(6.7)
$i\text{-}C_3H_7C_5H_4$	64	orange(47–49)	—	288(M^++1)	33.4(33.4)	59.0(58.9)	7.4(7.4)
$t\text{-}C_4H_9C_5H_4$	75	red–orange(89–90)	1.6/1.5	301(M^+)	31.9(32.1)	60.2(60.2)	7.9(7.7)
Me_5C_5	60	orange(86–88)	—	—	30.7(30.7)	—	—
Indenyl	49	wine-red(103–104)	1.7	295(M^+)	32.7(32.7)	61.2(61.4)	5.9(5.8)
2-Meindenyl	58	orange–red(121–122)	1.6/1.6	305(M^+-4H)	31.0(31.2)	62.6(62.5)	6.2(6.2)
1-$CyCH_2$indenyl	59	orange–red	—	—	23.5(24.7)[b]	69.1(67.9)	7.4(7.5)
2-MeOindenyl	54	red(136–138)	1.7/1.6	362($M^+ + C_3H_5$)	29.2(29.7)	60.6(59.4)	6.1(5.9)
2-Phindenyl	7	red(153–163)	diamagn.	371($M^+ - C_3H_5$)	23.3(23.4)[c]	70.2(70.2)	6.4(6.4)
5,6-$(MeO)_2$indenyl	83(crude)	wine-red(145–148)	1.7	351($M^+ - C_3H_5$)	24.3(24.3)[c]	61.7(60.9)	6.7(6.6)
Fluorenyl	40	purple(175–180)	diamagn.	345($M^+ - C_3H_5$)	25.2(25.0)[c]	68.8(68.7)	6.4(6.3)

[a] See Jolly *et al.*[2]
[b] Calc. for $(C_{10}H_6CH_2Cy)Mo(C_3H_5)_3$ %Mo 22.33, %C 69.77, %H 7.90.
[c] (η^5-organyl)Mo(η^3-C_3H_5)$_3$ compound.

[(η^5-2-*methoxyindenyl*)Mo(η^3-C_3H_5)$_2$]

Prepared as above from 2-methoxyindenyl lithium in THF at −78 to −15°C.

[(η^5-2-*phenylindenyl*)Mo(C_3H_5)$_3$]

Prepared as above from 2-phenylindenyl lithium in THF at −78°C.

[(η^5-1-$CyCH_2$*indenyl*)Mo(C_3H_5)$_n$] (n = 2, 3)

Prepared as above from 1-$CyCH_2$indenyl lithium in THF at −30°C.

[(η^5-5,6-*dimethoxyindenyl*)Mo(C_3H_5)$_3$]

Prepared as above from 5,6-dimethoxyindenyl lithium in THF at −78 to −25°C.

[(η^3-1,9,10-*fluorenyl*)Mo(η^3-C_3H_5)$_3$]

Fluorenyl potassium (3.0 g, 14.6 mmol) was added to a stirred suspension of (η^3-C_3H_5)$_3$MoCl (3.6 g, 14.3 mmol) in THF (300 cm^3) at −78°C over a period of 2 h and stirred for a further 18 h. The solvent was evaporated and the dark purple residue extracted with pentane at 5°C, the pentane-extract was filtered through Avicel at 5°C, the solvent evaporated at −35°C and the residue recrystallized twice from hexane to give the compound as small purple crystals. Yield 2.2 g (40% theory).

^{1}H NMR (D_8-THF, 243 K, 400 MHz): δ 4.50 (m, 2), 3.45 (dd, 1a/3s), 2.74 (dd, 1s), 0.65 (dd, 3a), J (1a, 1s) ~ 0, J (2, 3a) 11.0, J (2, 1s) 8.3, J (2, 1a) 12.8, J (2, 3s) 8.3; 2.82 (dd, 6s), 2.53 (dd, 4a), 0.33 (dd, 4s), 0.22 (m, 5), −0.30 (dd, 6a), J (4s, 6s) 2.1, J (5, 6a) 12.7, J (5, 4s) 8.8, J (5, 4a) 13.0, J (5, 6s) 8.8; 4.04 (m, 8), 3.80 (dd, 7s), 2.50 (dd, 7a), 1.58 (dd, 9s), −0.52 (dd, 9a), J (7s, 9s) 2.0, J (8, 9a) 10.3, J (8, 9s) 8.1, J (8, 7a) 13.0, J (8, 7s) 8.3; 8.35 (d, 4′), 8.03 (d, 5′), 7.71 (d, 8′), 7.50 (t, 3′), 7.37 (t, 7′), 7.24 (t, 6′), 7.05 (t, 2′), 6.14 (s, 9′), 4.35 (d, 1′), J (1′, 2′) 7.0, J (2′, 3′) 7.8, J (3′, 4′) 7.4, J (5′, 6′) 7.5, J (6′, 7′) 7.2, J (7′, 8′) 7.6—numbering scheme shown below.

^{13}C NMR (D_8-THF): 104.4/104.1/99.4 (2/5/8, J 160/160/158), 51.1/53.3/60.7/65.8/65.9/80.3 (1/3/4/6/7/9. J 158,160/158,160/160,164/154/154/156). 55.1 (9′, J 164), 104.7 (1′, J 160), 125.0 (10′), 122.2 (4′, J 158), 123.5 (3′, J 159), 124.0 (2′, J 160), 136.2 (11′), 141.9 (12′), 120.0 (5′, J 158), 127.8 (6′, J 158), 128.6 (7′, J 160), 126.0 (8′, J 160), 152.7 (13′)—numbering scheme shown below.

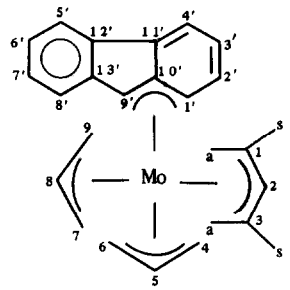

Table 4. Crystal data

	I $C_{16}H_{19}Mo$	II $C_{16}H_{19}OMo$	III $C_{17}H_{21}O_2Mo$	IV $C_{22}H_{24}Mo$
a (Å)	6.114(1)	17.771(6)	11.568(1)	15.500(2)
b	7.532(1)	9.719(2)	7.945(1)	
c	15.304(1)	8.178(3)	17.868(2)	
α (°)	99.74(1)	90	90	111.46(1)
β	93.22(1)	90	104.02(1)	
γ	105.07(1)	90	90	
V (Å^3)	667	1412	1593	2634
d (g cm^{-3})	1.53	1.52	1.47	1.45
μ(Mo) (cm^{-1})	9.36	8.92	8.02	7.26
Z	2	4	4	6
Space group	$P\bar{1}$	$Pna2_1$	$P2_1$	$R\bar{3}$
Independent reflections	2999	4066	4904	4824
Observed reflections	2770	3280	3331	3590
Number of variables	230	163	300	304
R	0.026	0.028	0.063	0.023
R_w	0.035	0.032	0.074	0.023

Crystal structure determination

A detailed description of the experimental procedure has been reported previously.[16] Crystal data for I–IV are summarized in Table 4.

Acknowledgments—O.S.A. thanks the Swedish Board for Technical Development for the award of a stipendium. R.G., C.K. and Y.H.T. were responsible for the crystal structure determinations. We thank Dr A. Rufińska and B. Gabor for interpreting the NMR-spectra of (η^3-$C_3H_5)_3$(η^3-fluorenyl)Mo and Dr K. Seevogel and B. Waßmuth for interpreting the low temperature IR spectra.

REFERENCES

1. R. Benn, S. Holle, P. W. Jolly, R. Mynott and C. Romão, *Angew. Chem.* 1986, **98**, 555.
2. P. W. Jolly, C. Krüger, C. C. Romão and M. J. Romão, *Organometallics* 1984, **3**, 936.
3. R. Benn, S. Holle, P. W. Jolly, C. Krüger, C. C. Romão, M. J. Romão, A. Rufińska and G. Schroth, *Polyhedron* 1986, **5**, 461.
4. K. Angermund, K. H. Claus, R. Goddard and C. Krüger, *Angew. Chem.* 1985, **97**, 241.
5. K. Angermund, A. Döhring, P. W. Jolly, C. Krüger and C. C. Romão, *Organometallics* 1986, **5**, 1268.
6. T. Brock, C. Dias and P. W. Jolly, manuscript in preparation.
7. H. von Brachel and U. Bahr, *Methoden der Organischen Chemie* 5/1c, p. 659, Houben-Weyl (1970).
8. K. Hafner, U.S. Pat. 2,953,607; *Chem. Abstr.* 1961, **55**, 7320e.
9. R. S. Threlkel and J. E. Bercaw, *J. Organometal. Chem.* 1977, **136**, 1.
10. R. Weißgeber, *Chem. Ber.* 1909, **42**, 569.
11. C. F. Koelsch and P. R. Johnson, *J. Am. Chem. Soc.* 1943, **65**, 567.
12. B. Eliasson and U. Edlund, *J. Chem. Soc., Perkin Trans. II*, 1981, 403.
13. F. G. Bordwell and G. E. Drucker, *J. Org. Chem.* 1980, **45**, 3325.
14. R. Lukes and J. Ernest, *Chem. Lists* 1952, **46**, 361; *Chem. Abstr.* 1953, **47**, 6922c.
15. H. F. Ebel, *Methoden der Organischen Chemie* 3/1, p. 276, Houben-Weyl (1970).
16. R. Goddard, P. Faria dos Santos Filho and U. Schuchardt, *Acta Cryst.* 1987, **C43**, 1300.

Polyhedron Vol. 8, No. 2, pp. 211–214, 1989
Printed in Great Britain

0277–5387/89 $3.00+.00
© 1988 Pergamon Press plc

ADDUCTS OF COORDINATION COMPOUNDS—XIV.* THE NATURE OF POULENC'S SILVER BROMIDE, "$[Rh(py)_4Br_2Ag]Br_2$"

R. D. GILLARD,† SIMON H. MITCHELL and DYFRIG J. THOMAS

Department of Chemistry, University of Wales, P.O. Box 912, Cardiff CF1 3TB, Wales, U.K.

(*Received* 29 *July* 1988; *accepted* 25 *August* 1988)

Abstract—The 1 : 1 adducts of silver bromide with the complex salts *trans*-$[M(py)_4X_2]Br$ (py = pyridine; M = Rh, X = Br—Poulenc's compound; M = Rh or Ir, X = Cl—newly synthesized compounds) are salts, *trans*-$[M(py)_4X_2](AgBr_2)$, of the dibromo-argentate(I) ion (ν_3 at *ca* 240 cm^{-1}), rare in solid species.

Large cations like tetraphenylarsonium and phosphonium (Ph_4E^+; Ph = C_6H_5; E = P or As) containing flat aromatic substituents on a central atom are commonly used to precipitate anions. Pyridine based cations often precipitate unusual anions. For example, [diquat] bromide treated with bromine yields[2] $[diquat](Br_3)_2$ and the paraquat salt of the InI_3^{2-} ion is stable.[3] In a similar way, cations *trans*-$[RhL_4X_2]^+$ (L = an N-heterocycle like pyridine, X = chloride or bromide) form salts with common anions (like halide or nitrate) which themselves readily give rise to adducts with a surprising range of substances. Many of the adducts have interesting or unusual components.

Among those which have been studied are several (chiefly of the dibromo–pyridine cation above, abbreviated to B here) initially discovered[4] by Poulenc. These include: $[B](NO_3)HNO_3$, a hydrogen dinitrate; $[B](NO_3)AgNO_3$, a dinitrato-argentate(I)—these two types form the subject of the previous paper[1] in this series; $[B](H_5O_2)Br_2$,[5] and [B]BrAgBr, formulated by Poulenc as *trans*-$[Rh(py)_4Br(BrAg)]Br_2$, a possible structure again supported recently.[6] Our present note reformulates the last as the dibromoargentate(I), only the second example of such a solid salt. We have also made the analogous chlororhodium and chloroiridium(III) compounds, by precipitation. For completeness, the many other adducts, solvates and the like, including salts of trihalide ions, may be mentioned.

The interactions via chloride or bromide ions, of silver(I) with rhodium(III) or iridium(III) are of particular interest, because of the much-used but ill-understood "rhodium effect" and "iridium effect" on the speed of photographic emulsions (usually achieved technically[7] by adding simple or complex halides of these platinum metals to the precipitating emulsion of silver halide).

RESULTS AND DISCUSSION

Poulenc obtained[4] his adduct *trans*-$[Rh(py)_4Br_2](AgBr_2)$ in rather low yield while trying to remove bromide coordinated to rhodium(III) by precipitation. We find that the same product may be obtained in high yield by a much simpler scheme (1):

$$trans\text{-}[Rh(py)_4Br_2]Br + (AgBr_2)^- \longrightarrow trans\text{-}[Rh(py)_4Br_2](AgBr_2). \quad (1)$$

This reaction of *trans*-$[Rh(py)_4Br_2]Br \cdot 6H_2O$ with AgBr dissolved in saturated aqueous potassium bromide by either of the two methods was successful.

(1) An aqueous or 25% (v/v) aqueous ethanol solution of the complex was added to and rapidly mixed with the aqueous KBr–AgBr solution. *Trans*-$[Rh(py)_4Br_2]AgBr_2$ immediately precipitates as an orange–yellow powder.

(2) *Trans*-$[Rh(py)_4Br_2]Br$ ground with the aqueous KBr–AgBr solution changes rapidly to a fine powder of the product.

The analogous (and isomorphous) salts of iridium(III) and of dichlororhodium(III) were made by the first method. All three compounds decompose

* For part XIII, see ref. 1.

†Author to whom correspondence should be addressed.

in water because of the insolubility of silver bromide.

$$[M(py)_4X_2](AgBr_2) \longrightarrow AgBr\downarrow + [M(py)_4X_2]^+_{(aq.)} + Br^-_{(aq.)}.$$

The IR spectrum of *trans*-$[Rh(py)_4Br_2](AgBr_2)$ is very similar to that of its parent *trans*-$[Rh(py)_4Br_2]Br \cdot 6H_2O$. There is one new band at 240 cm^{-1}. This probably arises from the Ag—Br_2 asymmetric stretch $\nu_3(\Sigma_u^+)$. There is a general paucity of data[6,8] on Ag—Br modes. The careful study[8b] of $[N(CH_3)_4][AgX_2]$ dissolved in tri(*n*-butyl)phosphine oxide by Waters and Basak placed the IR active $\nu_3(\Sigma_u^+)$ mode of $AgBr_2^-$ at 253 cm^{-1}. Bottger and Geddes[8c] isolated solid salts of the stoichiometry $[E(CH_3)_4](AgBr_2)$ (E = N or P), but their vibrational spectra strongly suggested that the anions were made up by linked AgX_4 tetrahedra, and certainly did not contain linear two-coordinate silver ions.

IR spectra are recorded in Table 1.

Similarly, for the new iridium compound, *trans*-$[Ir(py)_4Cl_2](AgBr_2)$, the spectra confirm the presence of pyridine (1650, 776, 709 cm^{-1}) and the presence of a pyridine–Ir bond (339 cm^{-1}). The only notable difference between the parent and adduct is again the absorption (which we assign as ν_3) at 238 cm^{-1} of the adduct.

The solubility of silver halides in aqueous silver salts and aqueous halides is well known and understood. The relevant stability constants[6,11] indicate that the chief species in excess of *aqueous* halide X^- are AgX_2^- (while compounds like $(NH_4)_2AgBr_3$ may be made, for example in methylethyl ketone, they are insensitive to light). A simple method[12] of making large crystals of silver chloride depends on the slow reversal of (2).

$$HCl + AgCl \rightleftharpoons \text{“}H[AgCl_2]\text{”}. \qquad (2)$$

So the anion AgX_2^- (X = halide) has long been recognized[13] as a solution species, but in the solid state there are few examples.[14] Poulenc's compound has been proposed[15] as a further example, without structural work. It is the last of those remarkable adducts which were originally reported[4] by Poulenc to be dealt with in this series (cf. *trans*-$[Rh(py)_4Br_2](H_5O_2)Br_2$,[5] *trans*-$[Rh(py)_4Br_2][H(ONO_2)_2]$[1,16] and *trans*-$[Rh(py)_4Br_2][Ag(ONO_2)_2]$).[1]

In the first established example[14] of a linear silver dibromide anion, $[Au(dtc)_2]AgBr_2$, the silver atom is linearly coordinated by bromine and lies on a special position in the lattice. There is[17] an analogous but not isomorphous gold compound, containing linear $AuBr_2^-$.

Besides $AgBr_2^-$, there are a small number of monomeric linear cationic AgX_2^+ or anionic AgX_2^- complexes (X = NH_3,[18,19] py[20] and NCO[21]), so this structure for $AgBr_2^-$ is not too unexpected. However it is much rarer than would be thought in view of its common occurrence in solution.

Instead of the two coordinated linear dihaloargentate(I) structures expected from solution studies, distorted tetrahedral coordination of silver by hal-

Table 1. Selected IR bands (in cm^{-1}) of *trans*-$[M(py)_4X_2]Y$

Mode	M = Rh, X = Br, Y = $AgBr_2$	M = Ir, X = Cl,[a] Y = $Cl \cdot 6H_2O$	M = Ir, X = Cl,[b] Y = $AgBr_2$
py	—	1650	1650
py	—	776	776
py	—	709	709
py(ν_{27})	466_w	—	—
Rh_{py}	340_w	—	—
Rh_{py}	311_w	—	—
IrCl	—	338	338
Ag—Br[c]	239m[d]	—	238

[a] For crystal structure see ref. 9.

[b] Our methods produced powders. In view of the aqueous insolubility of the compounds, it may be necessary to employ a different solvent system to prepare crystals. AgX_2^- is stable[10] in DMSO, which might be suitable.

[c] The chloride analogue *trans*-$[Rh(py)_4Cl_2](AgCl_2)$ could not be prepared by our present methods, so a different solvent system might also be needed.

[d] $\nu_3(\Sigma_u^+)$ of linear $[AgBr_2]^-$.

ide is common in the solid state. The tetrahedra may be paired, sharing edges ($[Ag_2I_6^{4-}]$),[22] or linked together to form chains, either single AgX_2^- (X = Br or I)[23] and AgI_3^{2-},[24] or double $Ag_2I_3^-$ [25,26] and $Ag_3I_4^-$ [27] (but this last one also has a silver atom occupying an octahedral hole between each pair of double tetrahedra). One other arrangement is found: a polymer of edge-sharing trigonal bipyramids (AgX_2^-, X = Cl[28] or Br[29]).

None of the known silver halide–silver nitrate double salts contains a simple linear X—Ag—X sequence. Usually the silver and halide form a polymeric structure, and there are several distinct types of silver atoms. In the few cases where an almost linear sequence *is* found, there is always nitrate also coordinated to the silver.[30–32]

In view of the frequent similarity (diagonal relationship) between S^{2-} and Br^-, the existence[33] of the linear ion AgS_2^{3-} containing two coordinated silver (isoelectronic with $AgCl_2^-$) in the salt Na_3AgS_2 is interesting. Nevertheless, salts of linear $AgBr_2^-$ are extremely rare, and it is interesting that Poulenc's salt precipitates this monomeric anion.

EXPERIMENTAL

IR spectra were measured in Nujol mulls, and X-ray photographs used Cu-K_α radiation and 6 h exposure.

trans-$[Ir(py)_4Cl_2]Cl \cdot 6H_2O$

A known synthesis[9] was used, substituting commercial iridium trichloride for K_3IrCl_6. $IrCl_3$ (0.507 g) dissolved in water (18 cm^3), with pyridine (6.5 cm^3) and ethanol (3 cm^3) was heated (steam bath) for 20 min. The solution was made acid (conc. HCl) and cooled in ice. The yellow crystals which formed were collected and crystallized from water. Yield 56%. An aqueous solution (4.52×10^{-5} M) showed peaks at 255.8 and 195.7 nm. The former had a molar extinction coefficient, ε, of 20,974, close to Jørgensen's value[34] (which confirms the presence of 4 mol of pyridine per iridium).

trans-$[Ir(py)_4Cl_2](AgBr_2)$

To 30 cm^3 of saturated aqueous KBr, $AgNO_3$ solution was added until the first sign of a permanent precipitation: saturated KBr was added dropwise until the precipitate just disappeared. This was now a saturated KBr/AgBr solution containing silver(I) chiefly as $[AgBr_2]^-$ (see text). *trans*-$[Ir(py)_4Cl_2]Cl$ (0.256 g) was dissolved in water (30 cm^3) by gentle warming. The KBr/AgBr solution was mixed with this solution and left in the dark for 1 h. The precipitate was washed thoroughly with saturated KBr solution, to remove any traces of solid AgBr; it was then washed with water. The precipitate was dried in a desiccator over conc. H_2SO_4. Yield = 0.253 g (72%).

The adduct (0.0729 g, 8.61×10^{-5} mol) was boiled in water for 20 min in the dark. The silver bromide formed was collected and washed with water, ethanol and finally ether, then weighed (0.01588 g, 8.41×10^{-5} mol).

trans-$[Rh(py)_4Cl_2](AgBr_2)$

Saturated KBr/AgBr was added to a solution of *trans*-$[Rh(py)_4Cl_2]Cl$ (0.3141 g/30 cm^3). A yellow precipitate immediately formed. This was collected and washed throughly with saturated KBr solution, then with water. The powder was dried in a desiccator over conc. H_2SO_4. Yield = 0.3314 g (73.6%). An X-ray powder diffraction photograph was taken (Cu-K_α radiation for 6 h).

Poulenc's compound: trans-$[Rh(py)_4Br_2](AgBr_2)$

Poulenc's original method[4] and the precipitation were used. The products from both reactions were washed with saturated aqueous KBr to remove AgBr, then with water and finally ethanol. The yield by method (2) is 93.8%. Found: C, 28.7; H, 2.3; N, 6.3. Calc. for $C_{20}H_{20}AgBr_4N_4Rh$: C, 28.4; H, 2.4; N, 6.6%.

Acknowledgements—We thank Dr B. W. Delf for help with X-ray powder photography.

REFERENCES

1. R. D. Gillard and S. H. Mitchell, *Polyhedron* 1987, **6**, 1885.
2. (a) R. M. Thomas, F. R. Gerus and J. L. Sands, German patent 1,953,230 (1970); *Chem. Abstr.* 1970, **73**, 14708; (b) Great Lakes Chem. Corp., French patent 2,173,830 (1973); *Chem. Abstr.* 1974, **80**, 108566.
3. G. Contreras and D. G. Tuck, *J. Chem. Soc., Dalton Trans.* 1973, 922.
4. P. Poulenc, *Annls Chim.* 1935, **4**, 567.
5. D. Dollimore, R. D. Gillard and E. D. McKenzie, *J. Chem. Soc.* 1965, 4479.
6. R. J. Lancashire, in *Comprehensive Coordination Chemistry* (Edited by G. Wilkinson, R. D. Gillard and J. A. McCleverty), Vol. 5, pp. 775 and 822–823. Pergamon Press, Oxford (1987).
7. (a) J. M. Harbison and M. E. Spencer, in *The Theory of the Photographic Process* (Edited by T. H. James), 4th edn, pp. 149 and 157. Macmillan, New York (1977); (b) Metal Dopants, abstracts 338–344 in *Papers of the International Congress of Photographic*

Science (Edited by H. H. Adam), pp. 176–187. Royal Photographic Society of Great Britain, Cambridge (1982); (c) D. D. Chapman and E. R. Schmittou, in *Comprehensive Coordination Chemistry* (Edited by E. Wilkinson, R. D. Gillard and J. A. McCleverty), Vol. 6, p. 95. Pergamon Press, Oxford (1987).
8. (a) G. L. Bottger and A. L. Geddes, *Spectrochim. Acta* 1967, **23A**, 1551; (b) D. N. Waters and B. Basak, *J. Chem. Soc. A* 1971, 2733; (c) G. L. Bottger and A. L. Geddes, *Spectrochim. Acta* 1967, **23A**, 1551.
9. R. D. Gillard, S. H. Mitchell, P. A. Williams and R. S. Vagg, *J. Coord. Chem.* 1984, **13**, 325.
10. B. Bry and B. Tremillon, *J. Chem. Res.* (*S*) 1979, 156; B. Bry and B. Tremillon, *J. Chem. Res.* (*M*) 1979, 1884.
11. (a) G. I. P. Levenson, in *The Theory of the Photographic Process* (Edited by T. H. James), 4th edn, p. 437. Macmillan, New York (1977); (b) J. Pouradier, A. Pailliolet and C. R. Berry, in *The Theory of the Photographic Process* (Edited by T. M. James), 4th edn, p. 7. Macmillan, New York (1977).
12. J. C. Bailar, *Inorg. Synth.* 1980, **20**, 18.
13. L. G. Sillen, The Chemical Society, special publication No. 17 (1971); L. G. Sillen, The Chemical Society, special publication No. 25 (1964).
14. J. A. Cras, J. H. Noordik, P. T. Beurskens and A. M. Verhoeven, *J. Cryst. Mol. Struc.* 1971, **1**, 155.
15. A. W. Addison and R. D. Gillard, *J. Chem. Soc., Dalton Trans.* 1973, 2009.
16. (a) R. D. Gillard and R. Ugo, *J. Chem. Soc.* 1966, 549; (b) R. D. Gillard and R. Ugo, *Abstract B4, Chem. Soc. Autumn Meet.* Nottingham (September 1965).
17. P. T. Beurskens, H. J. A. Blaauw, J. A. Cras and J. J. Steggerda, *Inorg. Chem.* 1968, **7**, 805.
18. H. M. Maurer and A. Weiss, *Z. Kristallogr.* 1977, **146**, 227.
19. T. Yamaguchi and O. Lindqvist, *Acta Chem. Scand.* 1983, **A37**, 685.
20. S. Menchetti, G. Rossi and V. Tazzoli, *Rc. Ist. Lomb. Sci. Lett. A.* 1970, **104**, 309.
21. K. Aarlot and K. Ase, *Acta Chem. Scand.* 1974, **A28**, 137.
22. H. J. Keller, B. Keppler and H. Pritzkow, *Acta Cryst.* 1982, **B38**, 1603.
23. R. Stomberg, *Acta Chem. Scand.* 1969, **23**, 3498.
24. C. Brink and C. H. MacGillavry, *Acta Cryst.* 1949, **2**, 158.
25. H.-J. Meyer, *Acta Cryst.* 1963, **16**, 788.
26. C. Brink, N. F. Binnendijk and J. van de Linde, *Acta Cryst.* 1954, **7**, 176.
27. C. J. Gilmore, P. A. Tucker and P. Woodward, *J. Chem. Soc. A* 1971, 1337.
28. H. C. Gaebell, G. Meyer and R. Hoppe, *Z. Anorg. Allg. Chem.* 1983, **497**, 199.
29. H. C. Gaebell and G. Meyer, *Z. Anorg. Allg. Chem.* 1984, **513**, 15.
30. K. Persson, *Acta Cryst.* 1979, **B35**, 1432.
31. K. Persson and B. Holmberg, *Acta Cryst.* 1977, **B33**, 3768.
32. R. Birnstock and D. Britton, *Z. Kristallogr.* 1970, **132**, 87.
33. K. O. Klepp and W. Bronger, *J. Less-common Metals* 1985, **106**, 95.
34. C. K. Jørgensen, *Absorption Spectra and Chemical Bonding*. Academic Press, London (1962).

Polyhedron Vol. 8, No. 2, pp. 215–218, 1989
Printed in Great Britain

0277–5387/89 $3.00+.00
© 1988 Pergamon Press plc

COMMUNICATION

REACTION OF SOLID SODIUM HYDRIDE WITH SOLID AMMONIUM THIOCYANATE IN HMPA–TOLUENE:* AN ESR SPECTROSCOPIC INVESTIGATION AND CRYSTAL STRUCTURES OF THE TWO PRODUCTS OF THE REACTION, $[(NaNCS \cdot HMPA)_2]_\infty$ AND $(NaNCS \cdot 2HMPA)_2$

DONALD BARR, MICHAEL J. DOYLE, SIMON R. DRAKE, PAUL R. RAITHBY, RONALD SNAITH† and DOMINIC S. WRIGHT

University Chemical Laboratory, Lensfield Road, Cambridge CB2 1EW, U.K.

(*Received* 11 *August* 1988; *accepted* 24 *August* 1988)

Abstract—Reaction of solid NH_4SCN with solid NaH and HMPA (1 : 1 : 2 molar ratios) in toluene produces two complexes, $(NaNCS \cdot HMPA)_n$ (**1**), which has an S···Na-linked polymeric structure ($n = 2\infty$) with a repeat dimeric unit of form $SCN \cdot Na(\mu_2\text{-}HMPA)_2Na \cdot NCS$, and $(NaNCS \cdot 2HMPA)_n$ (**2**), which is a discrete symmetrical dimer ($n = 2$) with two μ_2-HMPA ligands and with terminal HMPA and NCS^- ligands (one of each per Na centre) arranged *trans*; the reaction appears to proceed via an electron-transfer mechanism, radical species having been detected by ESR spectroscopy.

A previous communication[1] noted the reaction of solid NH_4SCN with Bu^{n}Li and 2HMPA [O:P(NMe$_2$)$_3$] in toluene, and presented ESR spectroscopic evidence that formation, via numerous colour changes, of the product, $(HMPA)_2Li \cdot (\mu_2\text{-}HMPA)_2 \cdot Li(NCS)_2$, involved the intermediacy of radicals. An earlier report[2] had shown that NH_4 Hal solids (Hal = Cl, Br, I) also react with Bu^{n}Li in the presence of various Lewis bases, L (e.g. HMPA, TMEDA, PMDETA), to give complexes of the type $(LiHal \cdot xL)_n$. Here we show that such syntheses of alkali metal complexes are not limited to lithium, nor is the source of the metal restricted to a solution of an organometallic. Thus, solid NH_4SCN reacts rapidly with solid NaH and 2 equiv of HMPA, in toluene, giving two products, $NaNCS \cdot HMPA$ (**1**) and $NaNCS \cdot 2HMPA$ (**2**); a similar reaction, but with Na metal replacing NaH, gives **2** alone. In the crystal, **1** is polymeric, with dimeric $(SCN)Na \cdot (\mu_2\text{-}HMPA)_2 \cdot Na(NCS)$ units linked by NaNCS···Na interactions, while **2** is a discrete dimer, also having a central $Na(\mu_2\text{-}HMPA)_2Na$ ring but with a terminal NCS^- and a (further) terminal HMPA ligand attached, in a *trans* manner, to each Na. An ESR spectroscopic study has shown that radicals are involved in these reactions.

Addition of HMPA (3.58 g, 20 mmol) to a mixture of NH_4SCN (0.76 g, 10 mmol) and NaH (0.24 g, 10 mmol) solids in toluene (12 cm^3) at room temperature gave an immediate blue coloration. Vigorous gas evolution occurred forthwith, the colour changing to turquoise, then green, then (after *ca* 30 min) pale yellow; at this final stage, no solids remained. The solution was warmed and further toluene (10 cm^3) added before filtration. Cooling to 25°C afforded cubic crystals of $NaNCS \cdot HMPA$ (**1**). After further filtration, addition of hexane (18 cm^3) to the filtrate, followed by refrigeration, gave finely faceted crystals of $NaNCS \cdot 2HMPA$, **2**.‡§

* The synthetic routes described are the subjects of a preliminary patent (British Patent Application No. 8724662) filed by the Associated Octel Co. Ltd, U.K.

† Author to whom correspondence should be addressed.

‡ Yield of **1**, 29% relative to NH_4SCN taken; m.p. 149°C. Yield of **2**, 57%; m.p. 67–68°C. Satisfactory analyses (±0.2% of calculated values for C, H, N, Na, P) were obtained for **1** and **2**.

§ The direct syntheses of **1** and **2** have been reported, by dissolution of NaSCN in methanol or acetone, followed by addition of HMPA, then evaporation. Crystals isolated had melting points of 150–151 and 76–77°C, respectively.[3]

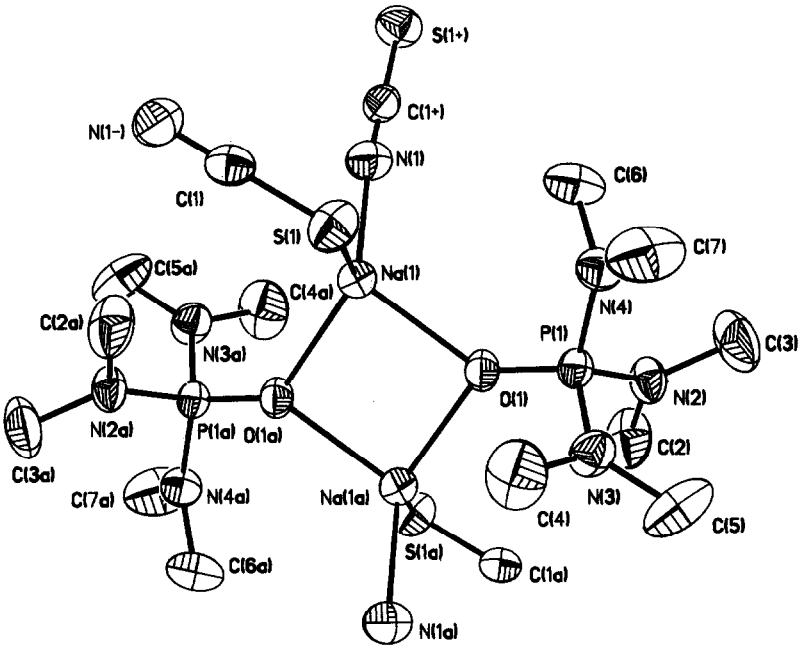

Fig. 1. The molecular structure of **1** showing the atom numbering scheme. Hydrogens have been omitted for clarity and the thermal ellipsoids represent the 30% probability level.

This latter product (but not **1**) was also obtained (in 75% yield) by reacting Na metal with NH_4SCN(s) and 2HMPA in toluene: this mix also initially gave a blue, then blue–green colour, but the reaction was much slower, a pale yellow solution resulting after stirring at 25°C for 1.5 days.

The crystal structures of both products have been determined.* The 1 : 1 complex, **1** (Fig. 1) is polymeric and has, as its central repeat unit, a $Na(\mu_2$-HMPA$)_2Na$ dimeric ring with alternating Na—O distances of 2.295(3) and 2.322(3) Å (cf. data in ref. 1). Each Na^+ is attached also, within the dimer, to a linear NCS^- ligand [Na—N, 2.328(4) Å; $Na\widehat{N}C$, 173.7(3)°; $\widehat{NCS}$, 179.6(4)°], and the S-ends of such ligands link four such dimers together in infinite 2D layers [Na···S, 2.895(2) Å; Na···$\widehat{SC}$, 101.6(2)°]. Such a bifunctional mode for thiocyanate has only been observed once before for alkali metal derivatives, in the 1D polymeric structure of $(LiSCN \cdot TMEDA)_\infty$.[4] The crystal structure of **2** contains, in contrast, *discrete* dimers (Fig. 2), again with bridging HMPA ligands [average Na—O, 2.336(3) Å], but now with each Na completing its four-coordination, in a *trans* manner, with a linear NCS^- ligand [Na—N, 2.348(6) Å; $Na\widehat{N}C$, 160.0(3)°; $\widehat{NCS}$, 179.4(5)°] and with an oxygen-attached HMPA ligand [Na—O, 2.239(4) Å]; clearly then, the additional HMPA molecules (one per Na) in **2** have served to replace the Na···SCN interdimer contacts apparent in **1**. Complexes **1** and **2** are the first structurally characterized NaSCN complexes in which L is not a macrocyclic ligand;[5] these (crowns etc.) lead to monomers, with or without Na···NCS contacts, so that **2** is the first oligomer (a dimer) of this kind, and **1** the first polymer (itself accrued through dimers).

The colours seen during the reaction of NH_4SCN(s) and 2HMPA with NaH(s) in toluene, giving **1** and **2**, have been investigated. As background, binary mixtures of NH_4SCN(s)+2HMPA, NH_4SCN(s)+NaH(s), and NaH(s)+2HMPA in toluene were examined: no colours were observed,

*Crystal data for **1**: $C_{14}H_{36}N_8Na_2O_2P_2S_2$, $M = 520.55$, monoclinic, space group $P2_1/c$ (No. 14), $a = 10.794(2)$, $b = 8.500(2)$, $c = 15.776(3)$ Å, $\beta = 106.65(2)°$, $V = 1386.7(5)$ Å^3, $D_c = 1.246$ g cm^{-3}, $Z = 2$, $F(000) = 552$, λ(Cu-K_α) = 1.5418 Å, μ(Cu-K_α) = 33.51 cm^{-1}; 2195 measured intensities ($2\theta_{max} = 116°$), 1567 unique with $F > 3\sigma(F)$. Structure solved by direct methods and refined by blocked-cascade least-squares to $R = 0.051$ and $R_w = 0.054$.

Crystal data for **2**: $C_{26}H_{72}N_{14}Na_2O_4P_4S_2$, $M = 878.96$, triclinic, space group $P\bar{1}$ (No. 2), $a = 10.044(1)$, $b = 11.715(2)$, $c = 12.002(2)$ Å, $\alpha = 105.63(1)$, $\beta = 96.49(1)$, $\gamma = 113.08(1)°$, $V = 1212.4(3)$ Å^3, $D_c = 1.203$ g cm^{-3}, $Z = 1$, $F(000) = 472$, λ(Cu-K_α) = 1.5418 Å, μ(Cu-K_α) = 27.60 cm^{-1}; 3616 measured reflections ($2\theta_{max} = 116°$), 2750 unique with $F > 3\sigma(F)$. Structure solved by direct methods and refined by blocked-cascade least-squares to $R = 0.060$ and $R_w = 0.067$.

Atomic coordinates, bond lengths and angles, and thermal parameters have been deposited at the Cambridge Crystallographic Data Centre.

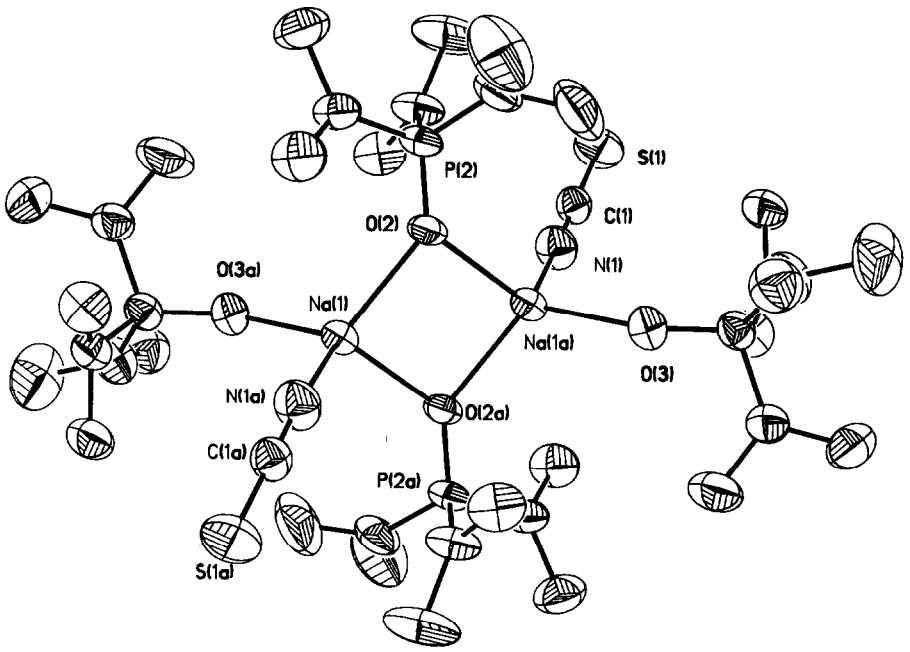

Fig. 2. The molecular structure of **2** showing the atom numbering scheme. Hydrogens have been omitted for clarity and the thermal ellipsoids represent the 30% probability level.

neither were there any apparent reactions or discernible dissolutions of solids. Thus, all *three* reactants [NH_4SCN(s), NaH(s), 2HMPA] in toluene are needed to afford reaction/a blue colour. ESR spectra were obtained on this blue-coloured reaction mixture over the temperature range −269 to −100°C and some typical spectra are shown in Fig. 3.

At −269°C, three signals seem apparent [Fig. 3(a)]. However, microwave power saturation measurements reveal that the highest field resonance in fact consists of two signals [Fig. 3(b)];[6] thus, there are two types of radicals present, giving rise to four signals. The first three of these (from low to high field) have g tensors which occur at precisely the same fields ($g_1 = 2.026$, $g_2 = 2.009$, $g_3 = 1.980$ and $g_{av} = 2.005$) as the signals obtained from the NH_4SCN(s)–Bu^{n}Li–2HMPA reaction system in toluene,[1] which were attributed to a thiocyanate-based radical, e.g. $(SCN)_2^-$. As observed previously, the line widths and line shapes of the three g tensors are temperature dependent over the temperature range −269 to −100°C, and diminish slowly with progressive warming. Also as in that lithium system, all three reactants [NH_4SCN(s), NaH(s), 2HMPA] must be present here, otherwise these three signals (and the blue colour) are not observed: the implication is that HMPA-assisted electron-transfer from Na(H) to SCN^- occurs. The fourth, low intensity signal, $g = 1.975$, is also found in the ESR spectra of any binary system containing NaH(s) [i.e. for NaH(s)+NH_4SCN(s) or

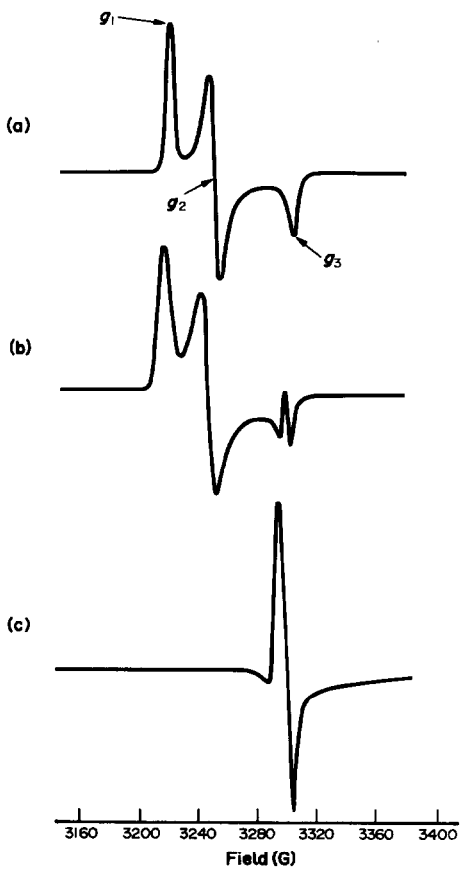

Fig. 3. ESR spectra recorded at −269°C on (a) a frozen toluene solution of the NH_4SCN(s)–NaH(s)–2HMPA reaction mixture, at a power of 5 mW; (b) the same system at 50 mW; (c) solid NaH at 10 mW.

NaH(s)+2HMPA, both in toluene, but not for NH_4SCN(s)+2HMPA], and indeed in those of NaH(s) in toluene and of NaH(s) alone [Fig. 3(c)]; it can thus be ascribed to an impurity, as yet unidentified, in the commercially supplied NaH.

Acknowledgements—We thank the SERC (D.B., P.R.R., R.S.), the Associated Octel Co. Ltd (R.S., D.S.W.), ICI (M.J.D.), and St. John's College, Cambridge (S.R.D.) for financial support.

REFERENCES

1. D. Barr, M. J. Doyle, S. R. Drake, P. R. Raithby, R. Snaith and D. S. Wright, *J. Chem. Soc., Chem. Commun.* 1988, in press.
2. D. Barr, R. Snaith, D. S. Wright, R. E. Mulvey and K. Wade, *J. Am. Chem. Soc.* 1987, **109**, 7891.
3. D. C. Luehrs and J. P. Kohut, *J. Inorg. Nucl. Chem.* 1974, **36**, 1459.
4. D. Barr, M. J. Doyle, R. E. Mulvey, P. R. Raithby, R. Snaith and D. S. Wright, *J. Chem. Soc., Chem. Commun.* 1988, 145.
5. Search of the Cambridge Crystallographic Data Base (Director: Dr O. Kennard), University of Cambridge.
6. C. P. Poole, *Electron Spin Resonance*, 2nd edn. Wiley, New York (1983).

Polyhedron Vol. 8, No. 3, pp. 219–274, 1989
Printed in Great Britain

0277–5387/89 $3.00+.00
Pergamon Press plc

POLYHEDRON REPORT NUMBER 25

HOMONUCLEAR AND HETERONUCLEAR OXO-BRIDGED COMPOUNDS OF THE TRANSITION ELEMENTS

BRUCE O. WEST
Department of Chemistry, Monash University, Clayton, Victoria, Australia, 3168

CONTENTS

1. HOMONUCLEAR STRUCTURAL OVERVIEW 219
1.1 Structure and bonding considerations 220
1.2 "Supported" oxo bridging 223
1.3 The (μ_3-O) trigonal structure 225
1.4 Polymetal clusters with (μ-O) and (μ_3-O) bridging 227
1.5 Oxo bridging in groups 9–12 228
1.6 Oxo bridging in organometallic compounds 229
1.7 (μ_5-O) compounds 229

2. FORMATION OF HOMONUCLEAR OXO-BRIDGED COMPOUNDS 230
2.1 Reduction processes 230
2.2 Oxidation processes 231
2.3 Olation and oxolation reactions 236

3. PHYSICAL PROPERTIES OF OXO-BRIDGED COMPOUNDS 237
3.1 Magnetic susceptibilities 237
3.2 Vibrational spectra 240
3.3 ^{17}O NMR 240
3.4 Optical electronic spectra 242

4. HETERONUCLEAR OXO-BRIDGED COMPOUNDS 242
4.1 Bridging by oxo groups as Lewis bases 242
4.2 (μ-O) formation by ester elimination 246
4.3 Inner sphere electron transfer formation of (μ-O) links 248
4.4 Heterotrinuclear (μ_3-O) complexes 259

5. HETERONUCLEAR ORGANOMETALLIC OXO-BRIDGED COMPOUNDS 263

6. HETEROBINUCLEAR PEROXO SPECIES 267

ACKNOWLEDGEMENTS 267

ABBREVIATIONS 267

REFERENCES 268

1. HOMONUCLEAR STRUCTURAL OVERVIEW

The oxo group, formally considered as O^{2-}, is an extremely versatile ligand. It is capable of binding as a terminal group to a metal (M=O) (4 electron donor) or bridging 2, 3, 4 or 5 metal atoms. In the latter situations it acts as a 4, 6 or 8 electron donor, respectively. Bridging oxygens are designated as (μ-O) (for dinuclear bridging), (μ_3-O), (μ_4-O) or (μ_5-O). A variety of oxo bridging modes (Fig. 1) have been identified for such bridging between transition metal ions including several where

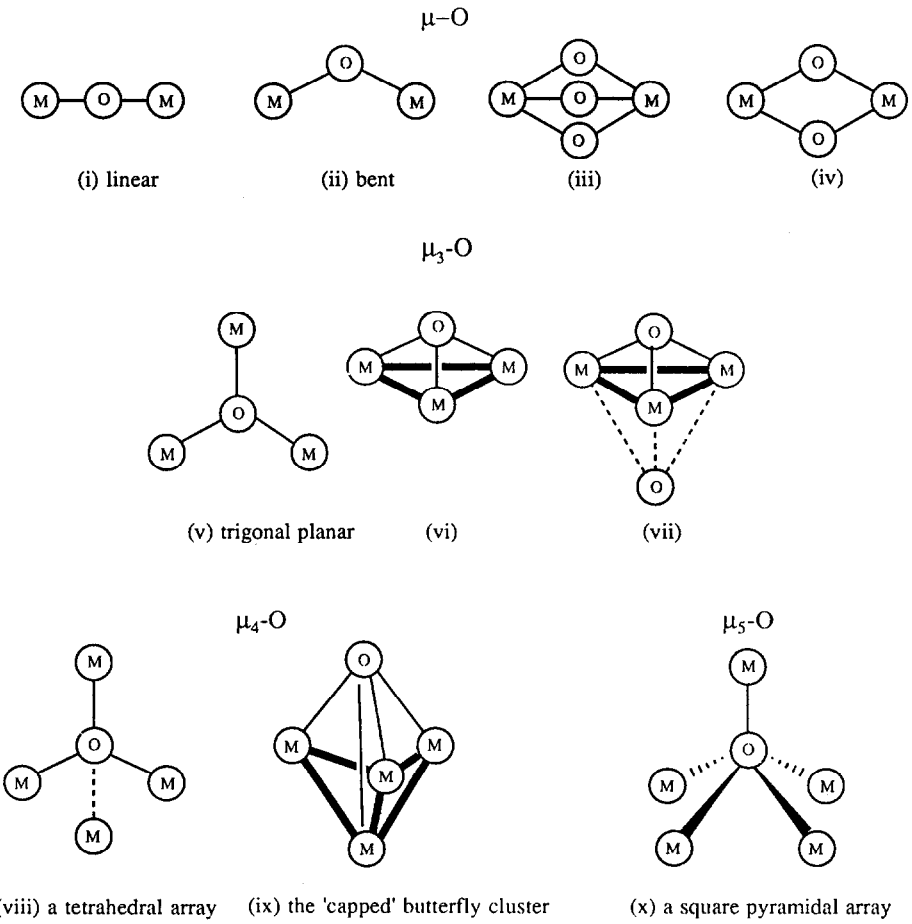

Fig. 1. Oxo bridging mode.

oxygen behaves as a "capping" ligand and lies above a metal–metal bonded cluster of metal atoms. Depending on the metal, further oxygen atoms may be bound as terminal groups.

Homonuclear oxo-bridged species are predominantly formed by metals in groups 4–8, i.e. the triads from Ti, Zr, Hf to Fe, Ru, Os, examples being known for each of the 15 elements involved.

Earlier general reviews on oxo compounds by Griffith[1] and Jezowska-Trzebiatowska[2] listed many of the early structure determinations which established bonding modes (i)–(v), while Murray[3] (Fe^{III}) and Stiefel[4] (Mo^{V}) gave accounts of the oxo bridging compounds of these two elements. Holm[5] has recently presented a further substantially updated, selective catalogue of oxo-bridged compounds of types (i)–(iv) as an accompaniment to his detailed review of metal-centred oxygen atom transfer. This review will be primarily concerned with complexes containing a single oxygen linked to two or more metals and only brief mention will be made of compounds having more than one oxygen atom linking two metals [structural types (iii) and (iv)].

1.1 *Structure and bonding considerations*

A collection of representative structural data for mono-oxo-bridged complexes is given in Table 1. The metals range in electron configuration from d^0 to d^5. No complexes having unsupported M—O—M bridges have been characterized for metals having d^n configurations greater than d^5. Linear (180°) or "almost" linear (173–180°) M—O—M linkages predominate amongst (μ-O) complexes. Exceptions are found for d^0 (Ti^{IV}) and especially d^5 (Fe^{III}, Ru^{III}). Iron(III) oxo-bridged complexes are known with FeOFe angles in the range 139–180° with the majority having angles $<180°$. Oxo complexes of Mo^{V} and Re^{V} also contain non-bridging terminally bound oxo groups whose distances from the metal are notably shorter than the bridging M—O distances in line with

their formulation as M=O bonds. The bridging distances are generally some way between these values for M=O links and "pure" single bond M—O links where these have been identified indicating some degree of double bond character in the bridging bonds.

A molecular orbital treatment was first applied to the RuORu system in $[Ru_2^{IV}OCl_{10}]^{4-}$ in a now classical paper by Dunitz and Orgel[38] which considered the Ru—O linkages to be made up of σ-

Table 1. MO bond distances and MOM bond angles in homobinuclear μ-oxo compounds

d^n	Compound	M=O_T (Å)	M—(μ-O) (Å)	M—O—M (°)	Reference
d^0	$[(Cp)_2Ti^{IV}Cl]_2O$		1.837(2)	173.8	6a
	$[Ti^{IV}(CH_2C_6H_5)_3]_2O$		1.798(0)	180	6b
	$[Ti^{IV}(acac)_2Cl]_2O$		1.8(2)	167.5(11)	7
	$[Ti^{IV}(TACH)]_2O$		1.838(3)	152.0(2)	8
	$[V^{V}O(Q)_2]_2O$	1.587(6)	1.779(2)	173.4(4)	9
d^1	$[Mo^{V}O(TPP)]_2O$	1.707(3)	1.936(3)	180	10
	$[Mo^{V}O(Et_2(dtp)_2)_2]_2O$	1.65(1)	1.86(1)	180	11a
	$[Mo^{V}O(Et_2dtc)_2]_2O$[a]	1.691(14)	1.859(1)	180.0	11b
		1.686(13)	1.875(14)	172.2(9)	
d^2	$[V^{III}(THF)_3Cl_2]_2O$		1.769(5)	180	13
	$[Re^{V}O(Et_2dtc)_2]_2O$	1.722(7)	1.910	175.5(3)	14
	$\{[Re^{V}O(CN)_4]_2O\}[Pt(NH_3)_4]_2$	1.698(7)	1.9149(4)	180	15
d^3	$K_4\{[Re^{IV}Cl_5]_2O\}$		1.86(1)	180	16
	$\{[Cr^{III}(NH_3)_5]_2O\}Cl_4$		1.821(3)	180	17
	$\{[Cr^{III}(TPyEA)NCS]_2O\}[BPh_4]_2$		1.82(1)	176.5(6)	18a
	$\{[Cr^{III}(tmpa)NCS]_2O\}[NCS]_2$		1.8001(4)	180	18b
	$[Mn^{IV}(TPP)N_3]_2O$		1.743(4)	180	20
			1.794(4)		
d^4	$[Mn^{III}(Pc)py]_2O$		1.71(4)	178	21
	$\{[Fe^{IV}(Hp)]_2O\}_x$		av. 2.01	170.5(7)	22a
				158.2(7)	
	$[Ru^{IV}(TPP)(OR)]_2O$ (R = p-$CH_3C_6H_4$)		1.789(11)	177.8(7)	23
	$[Ru^{IV}(OEP)(OH)]_2O$		1.847(13)	180	24a
	$[Ru^{IV}(OEP)Cl]_2O$		1.793(2)	180	24b
	$K_4\{[Ru^{IV}Cl_5]_2O\}$		1.80(2)	180	26
	$[Os^{IV}(\mu\text{-dppm})Cl_3]_2O$		1.792(1)	180	25
d^5	$[Fe^{III}(DBAT)]_2O$		1.792(1)	142.75(9)	27
	$[Fe^{III}(Hp)]_2O \cdot H_2O$		1.782(6) – H_2O	180	22b
			1.739(7)		
	$[Fe^{III}(acen)]_2O$		1.775(13)	150.7(13)	29
	$[Fe^{III}(salen)]_2O$		1.77(1)	144(1)	30a
	$[Fe^{III}(salen)]_2O \cdot py_2$		1.82(2)	139(1)	30b
	$[Fe^{III}(salen)]_2O \cdot CH_2Cl_2$		1.79(1)	142(1)	30c
	$[Fe^{III}(tsalen)]_2O \cdot py$		1.78(1)	159(3)	30d
	$[enH_2]\{[Fe^{III}(EDTA)]_2O\}$		1.79(1)	165(1)	31
	$[Fe^{III}(TPP)]_2O$		1.753(1)	174.5(1)	32
	$Fe_2^{III}(FFP) \cdot O$		1.787(18)	161.1(4)	33
	$[Fe^{III}(Pc)(1\text{-MeIm})]_2O$		1.75	174	34
	$[PyH]_2\{[Fe^{III}Cl_3]_2O\}$		1.755(3)	155.6(7)	35
	$[N_5Fe—O—FeCl_3]^+$		1.751(4)(Cl)	149.8(3)	36
			1.782(4)(N_5)		
	$\{[Fe^{III}(phen)_2H_2O]_2O\}(NO_3)_4$		1.785(7)	155.1(4)	28a
	$\{[Ru^{III}(bpy)_2H_2O]_2O\}(ClO_4)_4$		1.869(1)	165.4(3)	37a
	$\{[Ru^{III}(bpy)_2NO]_2O\}(ClO_4)_2$		1.876(6)	157.2(3)	37b
			1.890(7)		

[a] Two crystallographically distinct $Mo_2O_3(Et_2dtc)_4$ units are found in the crystal of symmetry C_i and C_2.

and π-bonding components. This basic method has been extended and subsequently applied to other $[M_2OCl_{10}]^{4-}$ [2,39] ions, $[Cr^{III}(NH_3)_5]_2O$[40] and, bridged metalloporphyrins[41] where the bridging atoms may be O, N or C. The π-bonding, antibonding and non-bonding orbitals concerned may be represented as $(e_u^b)[(b_{2g})(b_{1u})(e_g)](e_u^*)$ where the exact ordering of b_{2g}, b_{1u} and e_g levels may vary with changes in the metal and the nature of the ligands attached to it. The linearity and diamagnetism of $[Ru_2^{IV}OCl_{10}]^{4-}$ are accounted for by the accommodation of eight ruthenium and four oxygen electrons in the configuration $(e_u^b)^4[(b_{2g})^2(b_{1u})^2(e_g)^4](e_u^*)$ while the room temperature paramagnetism of the linear, mixed valence complex $[Re_2^{IV/V}OCl_{10}]^{3-}$ ($3.75\mu_B$ at 293 K) is in agreement with the configuration[39] $(e_u)^4[(e_g)^3(b_{2g})^1(b_{1u})^1](e_u^*)^0$ with very close spacing of the e_g, b_{2g} and b_{1u} orbitals. A similar relative ordering of the levels [40] but with a greater energy separation between e_g and two closely grouped b_{2g}, b_{1u} levels can qualitatively account for the low magnetic moment [42] observed for the $d^3 \cdot d^3$ complex $\{[Cr(NH_3)_5]_2O\}^{4+}$ ($1.8\mu_B$ at 293 K and virtual decrease to zero at 125 K), viz. $(e_u)^4[(e_g)^4(b_{2g})^1(b_{1u})^1](e_u^*)^0$.

Jezowska-Trzebiatowska[26] appears to have first suggested limitation to the formation of stable linear M—O—M compounds to metals having d^n electron configurations in the range $n = 0$–5 in line with the MO picture of bonding in the M—O—M unit. This requires a maximum of 12 electrons to fill all π-bonding and non-bonding orbitals, i.e. up to d^4 metal configurations, while for d^5 metal ions, electrons must enter the π-antibonding level (e_u^*) with consequent destabilization of the linear π-bond structure, forcing a bent configuration on the resulting molecule. This is in line with the range of MOM angles found for Fe_2O systems. Higher numbers of d electrons (d^6, d^7, d^8, d^9) would only be accommodated in higher level antibonding orbitals with increased destabilization of the oxo bridge, again in line with the virtual absence of such compounds amongst the metals of groups 9–12.

Tatsumi and Hoffman[41] have greatly extended this approach to compare the bonding requirements of model $[Fe(N_4)]_2X$ systems where X = O, N or C. They have reiterated the critically important role played by M—O π-bonding in stabilizing MOM linkages and showed how the bond angle in FeOFe compounds, where π-antibonding levels would have to be occupied in the linear MO concept, can vary over a wide range in order to maximize what π-bonding component can be generated and to minimize occupancy of M—O π^*-antibonding levels. They concluded that the angle found for a given $[Fe(L)]_2O$ complex would be decided largely by the extent of intermolecular interaction between the ligands attached to Fe. Thus, in $[Fe(TPP)]_2O$ (**1**) where the bulky, "flat", inflexible porphyrins will interact quite considerably with each other, the bond approaches linearity at 174°, whereas the quadridentate open-chain ligand $salen^{2-}$ in $[Fe(salen)]_2O$ (**2**) can reduce intermolecular contacts by having the bulky bridging groups arranged in a *trans* fashion about the FeOFe links allowing the FeOFe angle to be considerably reduced to *ca* 140°. Clearly, the presence of other unbounded solvent molecules in the crystal can alter the angle due to packing effects for this molecule. Ruthenium(III) oxo compounds also containing d^5 ions show similarly bent bonds (Table 1).

With systems having d^1 or d^2 metals (Mo^V, Re^V) there should be no bar to linearity in MOM links and this situation is commonly found (Table 1). However, these metals may also have additional

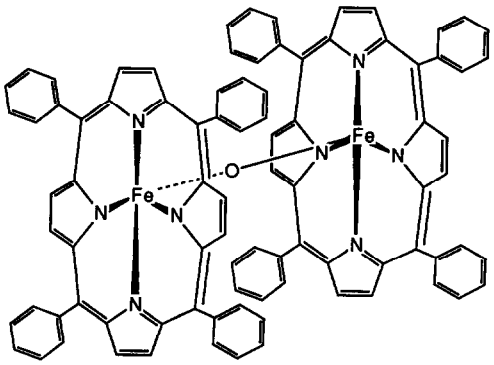

[(TPP)Fe]$_2$O (1).

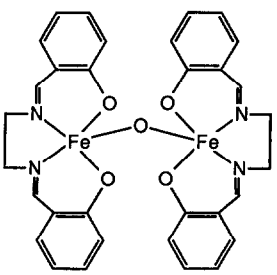

[Fe(salen)]$_2$O (2).

terminal oxo groups attached and the possibility of several different structural forms then arises.† The linear structure (3) has been found for each Re_2O_3 compound so far examined, while both *cis–cis* and *cis–trans* forms have been determined for Mo_2O_3 derivatives.[4] The linear form of $[Mo^VO(TPP)]_2O$[10] is the only example of this arrangement structurally proved for Mo in (6). The

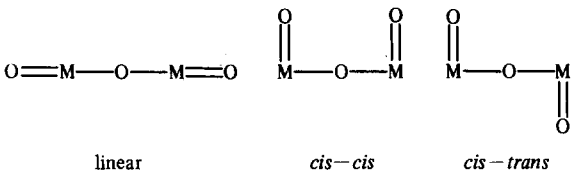

(3) (4) (5)

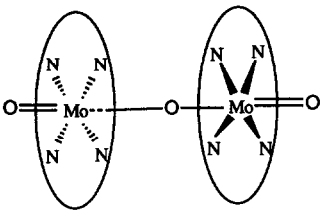

$[Mo^V(O)(TPP)]_2O$ (6).

Mo^V oxo-porphyrin complex is also found to be paramagnetic[44] at room temperature whereas the other oxo-bridged complexes of Mo^V are diamagnetic.[4] A *cis*-dioxo array in Mo^{VI} derivatives is also commonly found rather than a *trans* arrangement because such structures allow oxygen to participate in the most favourable π-interactions with the metal. It has been argued[41] that the structure resulting for a given complex will result from a balance between the minimal M d_π–O p_π antibonding interaction which favours a linear OMOMO array, and maximum π-bonding favouring a *cis* (or *cis–trans*) arrangement. The extent of π-bonding between O and M increases as the number of *d* electrons decreases since a larger number of empty *d* orbitals becomes available for interaction with O p_π electrons. Indeed, the remarkable compound $Nb_2O_3(TPP)_2$,[10,41] a d^0 system, has all three O atoms bridging between both Nb atoms [Fig. 1(iii)] and utilizing a maximum number of *d* orbitals for π-bonding.[45] The linearity of $Mo_2O_3(P)_2$[41] would appear to result from the inflexible planar structure of the porphyrin which, with a *cis*-oxo array, would constrain the single *d* electron of each Mo to orbitals involving increased M—O π^*-antibonding character. Other types of ligand so far examined are apparently flexible enough to allow minimization of this type of interaction. Metals having the d^2 configuration, Re^V and Tc^V, are predicted to have linear O=M—O—M=O arrangements since the increased number of *d* electrons will reduce the M—O π-interaction still further and increase the antibonding component in a *cis* arrangement.

1.2. *"Supported" oxo bridging*

Iron forms oxo-bridged complexes with great facility and a wide variety of ligands. Such compounds are involved in a variety of processes in biological systems either with porphyrin groups coordinated to the metal, i.e. haem compounds,[46] or with non-haem type coordination. In particular, the non-haem oxygen-carrying haemerythrin proteins found in certain invertebrates appear to contain Fe—O—Fe units to which a molecule of oxygen can be coordinated reversibly.[47]

Lippard[48] (7) and Wieghardt[49] (8) have separately developed model compounds for the hae-

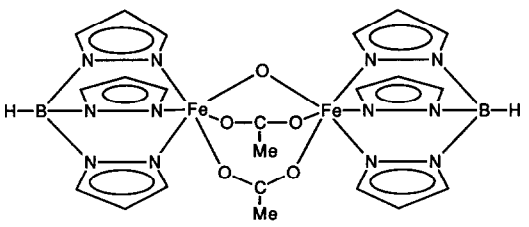

$[(HBPz)Fe^{III}(\mu\text{-}CH_3COO)]_2O$ (7).

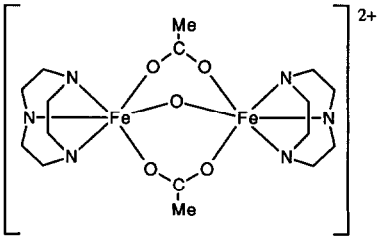

$\{[(TACN)Fe^{III}(\mu\text{-}CH_3COO)]_2O\}^{2+}$ (8).

† A fourth structural form with the M=O linkages mutually at right-angles (the "skew" form) can exist, but no examples of such a configuration are known.

Table 2. Structural data for $Mn_2(\mu\text{-O})$ compounds

Compound	$M_1(\mu\text{-O})$ (Å)	$M_2(\mu\text{-O})$ (Å)	$M_1—O_1—M_2$ (°)	Reference
$[(bpy)_2Mn^{III}(\mu\text{-O})_2Mn^{IV}(bpy)_2](ClO_4)_3$	1.855(6)	1.784(5)	96.6(1)	56
$[(phen)_2Mn^{III}(\mu\text{-O})_2Mn^{IV}(phen)_2](PF_6)_3 \cdot CH_3CN$	1.814(6)	1.814(6)	96.0(1)	57
$[(phen)_2Mn^{IV}(\mu\text{-O})_2Mn^{IV}(phen)_2](ClO_4)_4 \cdot CH_3CN$	1.802(4)	1.798(1)	99.5(2)	57
$[(picen)Mn^{III}(\mu\text{-O})_2Mn^{IV}(picen)](ClO_4)_3 \cdot 3H_2O$	1.833(4)	1.793(4)	—	58
$[(\mu\text{-tren})Mn^{III}(\mu\text{-O})_2Mn^{IV}(\mu\text{-tren})](CF_3SO_3)_3 \cdot CH_3CN$	1.773(4)	1.849(4)	95.3	59
$[(MACN)_2Mn^{III}Mn^{IV}(\mu\text{-O})(\mu\text{-}CH_3COO)_2](ClO_4)_3$	1.826(6)	1.814(6)	125.1(3)	52b

merythrin core which contain Fe—O—Fe units "supported" by carboxylato bridges and having a tridentate ligand capable of coordinating in the "*fac*" mode to each metal ion. Similar supported oxo-bridged groupings, $[M_2O(CH_3COO)_2]^{2+}$, have been prepared for Ti^{IV},[50] V^{III},[51] Mn^{III} [52] and Os^{IV}.[53] The acetate bridged oxo complexes are extremely stable species. They are related to the well known "basic acetate" complexes of Fe^{III} and other trivalent metals discussed below (Table 3) representing, as it were, a single bridged segment of the trinuclear species.

Manganese oxo complexes have also received increasing attention in recent years because of the key role played by that element in the photosynthetic water oxidation–oxygen evolution cycle.[54] There is believed to be a requirement for two or four Mn atoms for each photosystem II centre and this group or aggregate can cycle through a range of oxidation states. EXAFS and ESR data have indicated that O and N are nearest neighbours to manganese in the metalloprotein unit.[55] A series of mono- and dioxo-bridged Mn complexes have been prepared for modelling purposes. The majority are dimanganese dioxo-bridged compounds, most of which can be obtained in several of the possible valence state combinations $Mn^{III}(O)_2Mn^{III}$, $Mn^{III}(O)_2Mn^{IV}$, $Mn^{IV}(O)_2Mn^{IV}$.

Wieghardt *et al.*[52b] have shown that a dinuclear Mn^{II} hydroxy–aceto-bridged complex $\{[LMn^{II}(\mu\text{-}CH_3COO)]_2(\mu\text{-OH})\}^+$ can be oxidized first to an oxo-bridged dimanganese(III) ion $\{[LMn^{III}(\mu\text{-}CH_3COO)]_2(\mu\text{-O})\}^{2+}$ then to the mixed oxidation state ion $\{[LMn^{III}(\mu\text{-}CH_3COO)](\mu\text{-O})[LMn^{IV}(\mu\text{-}CH_3COO)]\}^{3+}$ and finally the Mn^{IV} dinuclear complex. The Mn—(μ-O) distances in the III/IV complex are equal within the experimental accuracy of the X-ray diffraction study but disorder among the ClO_4^- ions of the complex examined may have limited the ability to distinguish between the two oxidation states. The Mn^{III}/Mn^{IV} ions were shown to be coupled antiferromagnetically with the spin-exchange constant $J = -80\ cm^{-1}$ whereas the Mn^{III}/Mn^{III} compound displayed ferromagnetic coupling[52a] with $J = +18\ cm^{-1}$. A comproportionation constant of 7×10^8 was obtained from redox potential measurements for the reaction between the Mn^{III}/Mn^{III} and Mn^{IV}/Mn^{IV} complexes which forms the mixed valence complex Mn^{III}/Mn^{IV}.[52b] Structural data are presented in Table 2. Differences between Mn^{III}—(μ-O) and Mn^{IV}—(μ-O) distances have been observed in the bpy-[56] and tren-containing complexes indicating localization of the valence centres. The tren complex has arms of the ligands bridging between the metal ions and a di-(μ-O) bridge[59] (**9**).

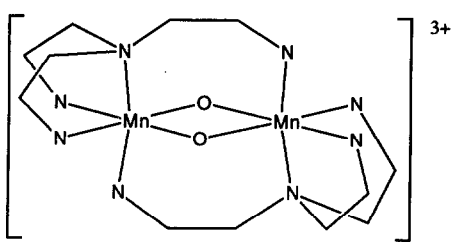

$[Mn^{III}Mn^{IV}(tren)_2(\mu\text{-O})_2]^{3+}$ (**9**).

Table 3. Structural data for (μ_3-O) bonded trinuclear carboxylates

Compound	Space group	M—(μ_3-O) (Å)	M—O[a] (Å)	M···M (Å)	Reference
(a) M^{III} *complexes*					
$[Cr_3(\mu_3\text{-}O)(CH_3COO)_6(H_2O)_3]Cl \cdot 6H_2O$	$P2_12_12$	1.89	1.97	3.28	62
$[Fe_3(\mu_3\text{-}O)(CH_3COO)_6(H_2O)_3]ClO_4$	$P2_1/C$	1.91	2.02	3.29	63
$[Fe_3(\mu_3\text{-}O)((CH_3)_3CCOO)_6(CH_3OH)_3]Cl$	$P6_3$	1.905(5)[b]	2.04	3.274(5)	64
$K_2(Mn(H_2O)_2\{[Mn_3(\mu_3\text{-}O)(HCOO)_9]\}_2$	$P\bar{1}$	1.90(2)	2.15	3.29(1)	65
$[V_3(\mu_3\text{-}O)(CH_2ClCOO)_6(H_2O)_3]CF_3SO_3$	$P\bar{1}$	1.92(1)	2.012	3.329(7)	66
$[V_3(\mu_3\text{-}O)(CH_2ClCOO)_6(H_2O)_3]ClO_4$	$P2_1/C$	1.93(1)	2.01	3.337(7)	67
$[V_3(\mu_3\text{-}O)(CH_3COO)_6(CH_3COOH)_2THF][VCl_4(CH_3COOH)_2]$	$C2/C$	1.910(6)	2.03	3.307(2)	68
$[V_3(\mu_3\text{-}O)(CH_3COO)_6(THF)_3]_2[V_2O_2Cl_6]$	$C2/M$	1.914(2)	2.00	3.316(4)	66
$[Co_3(\mu_3\text{-}O)(CH_3COO)_5(OH)py_2][pyCoBr_3]$	$P2_1C$	1.803(7)	—	3.182(2) 3.178(2) 2.578(2)	69
$[Rh_3(\mu_3\text{-}O)(CH_3COO)_6(H_2O)_3]ClO_4 \cdot (H_2O)_2$	$P2_1/C$	1.923(12)	2.01	3.33	70
(b) *Mixed valence complexes* $M_2^{III}M^{II}$					
$[Fe_3(\mu_3\text{-}O)(CH_3COO)_6(4\text{-}Mepy)_3] \cdot C_6H_6$	$R32$	1.907(1)	2.069		71
$[Fe_3(\mu_3\text{-}O)(CH_3COO)_6(4\text{-}Etpy) \cdot 4\text{-}Etpy$	$C2/c$	163 K 2.010(4) 1.856(7) 1.856(1)	2.05	163 K 3.321(2)	72a, b
		298 K 1.953(5) 1.879(2) 1.879(2)		298 K 3.307(1)	
$[V_3(\mu_3\text{-}O)(CH_3COO)_6py_3]$	$R32$	1.927(3)	2.04	3.337(5)	66
$[V_3(\mu_3\text{-}O)(CF_3COO)_6(THF)_3]$	$P2_1/m$	1.942(25)	2.05	3.364(10)	66
$[Cr_3(\mu_3\text{-}O)(CF_2HCOO)_6py_3] \cdot (C_2H_5)_2O$	$R32$	1.938(1)	2.03	3.356(2)	73
$[Cr_3(\mu_3\text{-}O)(CF_2HCOO)_6(4\text{-}CNpy)_3] \cdot C_6H_5CH_3$	$R\bar{3}C$	1.926(1)	2.03	3.336(1)	73
$[Mn_3(\mu_3\text{-}O)(CH_3COO)_6py_3]$	$R32$	1.941(1)	2.07	3.363(1)	74
$[Mn_3(\mu_3\text{-}O)(CH_3COO)_6(3\text{-}Clpy)_3]$	$P2_1/a$	1.863(4) 2.034(4)			75
$[Mn_3(\mu_3\text{-}O)(CH_3COO)_6py_3] \cdot py$	$R32$	1.936(2)	2.07 2.14	3.353(1)	76
$[Mn_3(\mu_3\text{-}O)(C_6H_5COO)_6(py)_2H_2O]O \cdot 5CH_3CN$	$P2_1$	1.817(14) 2.154(13) 1.822(14)	2.13	3.218(4) 3.418(5) 3.396(5)	76
$[Ru_3(\mu_3\text{-}O)(CH_3COO)_6(PPh_3)_3]$	$P\bar{1}$	1.92(2)	2.06	3.320(3)	77

[a] M—O–carboxylate, averaged distances.
[b] μ_3-O is 0.24 Å from the Fe_3 plane.

No established experiment using any of the model complexes described has successfully oxidized water in homogeneous solution, but a report has been made[60] of O_2 evolution from H_2O when the complex $[(bpy)_2Mn^{III}(\mu\text{-}O)_2Mn^{IV}(bpy)_2](ClO_4)_3$ is suspended in water in the presence of the powerful oxidant Ce^{IV}. The heterogeneous physical conditions were thought to mimic the actual photosynthetic site more clearly than a homogeneous system.

1.3 *The* (μ_3-O) *trigonal structure*

The planar trinuclear oxo structure [Fig. 1 (v)] of D_{3h} symmetry is structurally well established[61] as the central unit in a series of carboxylato-bridged ions of general formula $[M_3(\mu_3\text{-}O)(RCOO)_6L_3]^+$, M = Cr, Fe, V, Co, Mn, Rh; R = CH_3 (the "basic" acetates) and a wide range of other carboxylates; L = H_2O, pyridine or substituted pyridines, tetrahydrofuran (**10**) (Table 3). Ruthenium[78,79] and Ir[80]

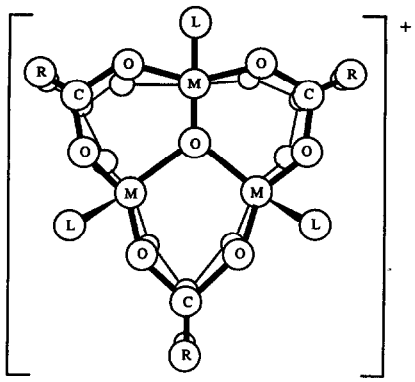

$[M_3(\mu_3\text{-}O)(\mu\text{-}RCOO)_6L_3]^+$ (**10**).

complexes have also been prepared but not structurally characterized. This structure is also found for mixed valence neutral compounds having the formal oxidation state distribution of $[M^{III}_2M^{II}(\mu_3\text{-}O)(CH_3COO)_6L_3]$ M = Fe, Cr, V, Mn, Ru, at least in most "room temperature" structure determinations, indicating either that full electron delocalization has occurred, rapid electron transfer between metal sites is taking place or the $M^{III}_2M^{II}$ triangular arrays are disordered in the crystal so as to produce a randomized distribution of metal centres with different oxidation states. This matter is addressed as part of the discussion of related heterotrinuclear oxo compounds in Section 4.4.

There is practical interest in such trinuclear oxo complexes since several are known to be catalysts for various processes. Thus, $[Ru_3(\mu_3\text{-}O)(CH_3COO)_6(H_2O)_3][CH_3COO]$[81] catalyses olefin hydrogenation in DMF solution in the presence of H_2, through formation of $[HRu_3(O)(CH_3COO)_5(DMF)_3]^+$, or isomerization of terminal olefins in the absence of H_2. Only one Ru atom appears to be involved. $[Fe^{III}_2Fe^{II}(\mu_3\text{-}O)(CH_3COO)_6py_3]$, and several heteronuclear analogues (Fe_2CO, Fe_2Mn, Fe_2Ni) catalyse[82] the reduction of aromatic nitro compounds by a mercaptoethanol; $[Co_3(\mu_3\text{-}O)(CH_3COO)_5(OH)py_3]^+$ and $[Co_3(\mu_3\text{-}O)(CH_3COO)_6py_3]^+$ are catalyst[69] precursors for the autoxidation of aromatic hydrocarbons.

A distinct group of complexes derived from Mo, W and Nb has a similar molecular formula to those of the "basic acetates" of the trivalent metal ions, viz. $[M_3(\mu_3\text{-}O)(\mu_3\text{-}X)(RCOO)_6L_3]^{2+}$, but a different structure. The work of Bino and Cotton[88] has elucidated the unique structural feature of these compounds which is based on a metal–metal bonded equilateral triangle of metal atoms with an oxygen placed above the triangle, bonding to all three metal atoms (**11**). A second oxygen or an alkylidyne group, CCH_3, can occupy the analogous μ_3-bridging position on the opposite side of the triangle. Two carboxylato groups bridge each pair of metal atoms and a final trio of ligands such as water, THF or even further monodentate carboxylate groups are coordinated to the metals. A generalized treatment of the bonding in these molecules has been given.[101] Comparative structural data are given in Table 4. A variation in structural type is found in complexes having single alkoxide groups bridging each pair of metal atoms in the equilateral triangle with two monodentate alkoxide groupings coordinated to each metal (**12**).[98–100] An extension of the MO treatment used for the carboxylato compounds has provided a basis for the redox behaviour shown by such molecules.[102]

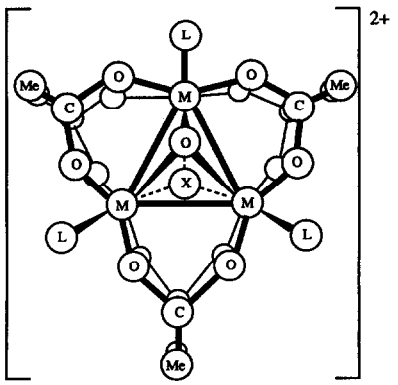

$[M_3(\mu_3\text{-}O)(\mu_3\text{-}X)(\mu\text{-}CH_3COO)_6L_3]^{2+}$ (**11**).

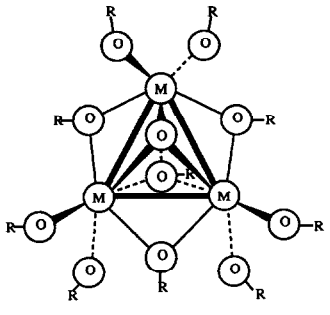

$[M_3(\mu_3\text{-}O)(\mu_3\text{-}OR)(\mu\text{-}OR)_3(OR)_6]$ (**12**).

Table 4. Metal–metal bonded trinuclear compounds containing (μ_3-O) caps

Compound	M—(μ_3-O) (Å)	M—M (Å)	M—O—M (°)	Reference
(a) $[M_3(\mu_3\text{-O})(\mu_3\text{-X})(RCOO)_6L_3]$				
$[Mo_3(\mu_3\text{-O})_2(CH_3COO)_6(H_2O)_3][CF_3SO_3]_2$	1.994(5)	2.759(1)	87.6(3)	89
$[Mo_3(\mu_3\text{-O})_2(CH_3COO)_6(H_2O)(OH)_2]$	2.012(7)	2.796(1)	88.4(2)	90
	1.999(5)	2.796(1)		
	2.773(1)			
$[Mo_3(\mu_3\text{-O})_2(C_2H_5COO)_6(H_2O)_3][CF_3SO_3]_2$	1.984(4)	2.752(2)	87.6(4)	91
$[Mo_3(\mu_3\text{-O})(\mu_3\text{-}CCH_3)(CH_3COO)_6(H_2O)_3][BF_4]$	1.983(4)	2.752(1)	87.6(2)	92
$[W_3(\mu_3\text{-O})_2(CH_3COO)_6(H_2O)_3][CF_3SO_3]_2$	2.011(5)	2.746(1)	86.1(1)	93a
$[W_3(\mu_3\text{-O})_2((CH_3)_3C\cdot COO)_6((CH_3)_3C\cdot COO)_2(H_2O)]$	1.98(2)	2.76(1)	88.3(7)	93b
$[W_3(\mu_3\text{-O})(CH_3COO)_6(H_2O)_3][ZnBr_4]$	1.96(2)	2.710(4)	87.7(6)	94
$[W_3(\mu_3\text{-O})_2(CH_3COO)_9]Cs$	1.99(1)	2.769(2)	88.2(5)	93b
$[W_3(\mu_3\text{-O})(\mu_3\text{-}CCH_3)(CH_3COO)_6(H_2O)_3]Br_2$	1.99(2)	2.801(1)	85(1)	95
$[Nb_3(\mu_3\text{-O})_2((CH_3)_3CCOO)_6(THF)_3][BPh_4]$	2.035(6)	2.842(3)	88.5(3)	96
$[Nb_3(\mu_3\text{-O})_2(SO_4)_6(H_2O)_3]K_4(H_5O_2)$	2.051(9)	2.875(1)	88.9(3)	97
	2.889(1)		89.8(3)	
	2.892(1)			

(b) $M_3(\mu_3\text{-O})(\mu_3\text{-OR})(\mu_2\text{-OR})_3(OR)_6$

	M—(μ_3-OR) (Å)	M—(μ_3-O) (Å)	M—M	Reference
M = Mo, R = $CH_2C(CH_3)_3$	2.21(3)	2.03(3)	2.529(9)	98
R = $CH(CH_3)_2$	av. 2.17	av. 2.061	av. 2.534	99
M = W, R = $CH(CH_3)_2$			2.540(6)	100

1.4 *Polymetal clusters with* (μ-O) *and* (μ_3-O) *bridging*

Polynuclear Fe^{III} oxo-bridged species with $Fe_2(\mu\text{-O})$ or $Fe_3(\mu_3\text{-O})$ bridging units are known with four, six, eight or 11 Fe atoms in the cluster unit, the Fe—O—Fe linkages generally being supported by other bridging units such as hydroxide, alkoxide, carboxylate or polyamine. The present status of this biologically important field has been reviewed by Lippard,[83] one of its major contributors. The $[Fe_{11}O_6(OH_6)(PhCOO)_{15}]^-$ anion has magnetic, spectroscopic and structural properties similar to those of the poly-iron core of ferritin, the iron storage protein. There is speculation as to whether Fe_{11} oxo-bridged units are basic to the structure of the protein.[84]

Similarly high nuclearity Mn oxo complexes have been formed when "basic manganese acetates", containing Mn^{III} or $Mn_2^{III}Mn^{II}$, $Mn_3(\mu_3\text{-O})$ units react with various bridging ligands. Examples of such compounds are $[Mn_4(\mu_3\text{-O})_2(RCOO)_7(bpy)_2]^+$ [85] (**13**) from the reaction of $[Mn_3(\mu_3\text{-O})(RCOO)_6L_3]^{0/+}$ with bipyridine (L = py, H_2O; R = CH_3, Ph), $[Mn_4(\mu_3\text{-O})(\mu_3\text{-Cl})(HIm)(CH_3COO)_3Cl_5]$[86] and $[Mn_9(\mu_3\text{-O})_2(PhCOO)_8(sal)_4(salH)_2(py)_4]$[87] (salH represents salicyclic acid). This latter complex essentially consists of two $Mn_4(\mu_3\text{-O})_2$ units of comparable pyramidal structure to others already described, and containing Mn^{III} ions, coordinated to a central Mn^{II} via bridging salicylate ions (**13**).

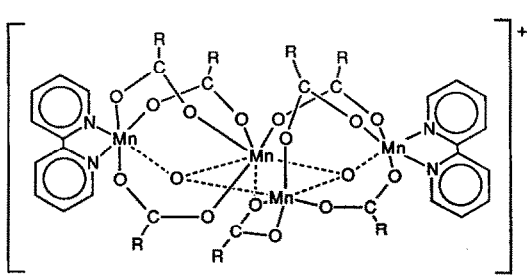

$[Mn_4(\mu_3\text{-O})_2(\mu\text{-RCOO})_7(bpy)_2]^+$ (**13**).

The Mn_4O_2 complexes can undergo oxidation processes to yield a variety of states reminiscent of the naturally occurring photosystem II aggregates of four Mn ions.[85]

The magnetic properties of the Mn_4 species indicate extensive antiferromagnetic coupling[85,86,87] between Mn ions in these complexes, most probably in pairs which in turn couple more weakly with each other. Ferromagnetic coupling between such pairs is given as an explanation of the temperature dependence of magnetic susceptibility of the (μ_3-Cl) bridged complex.[86]

1.5 *Oxo bridging in groups* 9–12

Although a number of oxo or oxo-bridged compounds of the remaining transition elements (groups 9–12, triads Co, Rh, Ir to Zn, Cd, Hg) have been proposed, structures authenticated by X-ray studies are rare. This situation is in line with the prediction of instability in M_2O systems when M has more than five *d* electrons to be allocated to the non-bonding and antibonding molecular orbitals of such systems.[26] Thus, for Co, the complex[69] $[Co_3(\mu_3\text{-}O)(CH_3COO)_5(OH)py_3]^+$ has been shown to have the trinuclear "basic acetate" structure (**10**) and is the only Co complex demonstrated to contain Co—O—Co linkages by a structural study. This contrasts with the ability of dioxygen to coordinate, often reversibly, to a wide range of Co^{II} complexes forming essentially Co^{III}–superoxo ($Co^{III} \cdot O_2$) or bridged peroxo($[Co^{III}]_2O_2$) complexes.[103]

The compound $Co_4O((CH_3)_3CCOO)_6$ has been proposed on spectroscopic grounds[104a] to have an oxygen ion bridging four Co^{II} ions, a type of structure authenticated by X-ray structural studies for Be^{II} and Zn^{II} "basic acetate" complexes of the general formula $M_4(\mu_4\text{-}O)(CH_3COO)_6$.[104b] This consists of a tetrahedral array of metal ions bonded by an O^{2-} ion at the centre of the tetrahedron with the metal ions linked by carboxylate bridges along the six edges of the tetrahedron.

Complexes of other elements in these latter groups, of low oxidation state (Ni^0, Pt^0, Ir^I, Rh^I), also react with dioxygen, usually giving peroxo type species by oxidative addition.[103b]

The reactions of Cu^I compounds with oxygen are in many cases believed to form oxo-bridged species but structural evidence is largely lacking at present. The unusual (μ_4-O) Cu^{II} species $[Cu_4(\mu_4\text{-}O)(OPPh_3)_4Cl_6]$ has been defined, however, by an X-ray study[104c] (**14**). The copper-containing oxygen

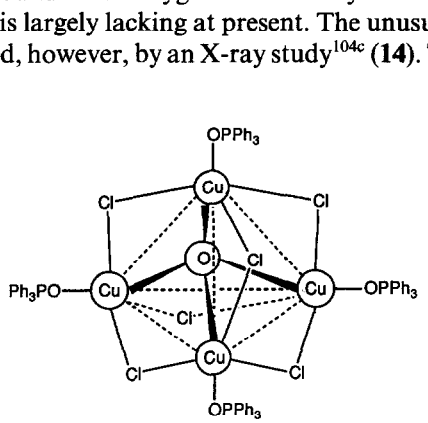

$[Cu_4(\mu_4\text{-}O)(OPPh_3)_4(\mu\text{-}Cl)_6]$ (**14**).

carrier haemocyanin which is found in certain molluscs and arthropods may contain a μ-oxo $Cu_2^{II}O$ linkage, and efforts to prepare compounds to model this system have been made.[105]

Examples of complexes considered to contain such linkages and formed by the reaction of Cu^I complexes with molecular oxygen include $[Cu^{II}(phen)Cl]_2O$[106a] and $\{[Cu^{II}(PBA)]_2O\}(PF_6)_2$[106b] (PBA = bis[2(2-pyridyl)ethyl]benzylamine) while $[Cu^{II}HB(3,5\text{-}Me_2Pz)_3]_2O$[107a] ($HB(3,5\text{-}Me_2Pz)_3^-$ is the 3,5-dimethylpyrazolylborate anion) has been formed by the reaction of iodosyl benzene with $[Cu^IHB(3,5\text{-}Me_2Pz)_3PPh_3]$. This complex is reported to react further with H_2O_2 to give a peroxo-bridged dimer.[107b]

None of these types of complexes have yet been authenticated by an X-ray structure study and their constitutions have been proposed on the basis of microanalyses together with a variety of other evidence, including reaction with PPh_3[106a,107a] to form $OPPh_3$ and reduction to the Cu^I starting complex, low magnetic moments[106b,107] or ESR spectra[106a] indicating magnetic coupling between Cu^{II} ions and molecular ion observation in a field desorption mass spectrum.[107]

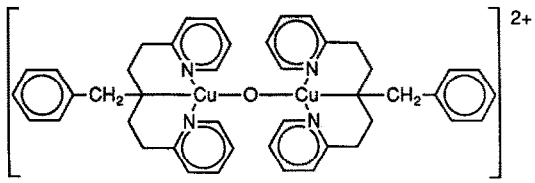

$\{[Cu^{II}(PBA)]_2O\}^{2+}$ (**15**).

$\{[Cu(PBA)]_2O\}(PF_6)_2$ (**15**) reacts with H_2O[106b] to give the dihydroxy-bridged compound $\{[Cu(PBA)OH]_2\}(PF_6)_2$ which has been structurally characterized. This hydroxy dimer also has a low magnetic moment indicating magnetic coupling between two metal centres.

Direct reaction in methanol of $Cu^{II}Cl_2$ and the triaza-macrocycle N,N′,N″-trimethyl-1,4-triazacyclononane (MACN) is also postulated to form an oxo-bridged complex[108] with a further bridging water molecule. The structural study of this complex was prevented by oxygen disorder in the bridge. It shows antiferromagnetic behaviour over a temperature range.

1.6 *Oxo bridging in organometallic compounds*

Increasing interest has been shown in recent years in the preparation of metal cluster oxo compounds which have organometallic groups attached to the metals, particularly carbonyl and cyclopentadienyl groupings. Oxygen has been shown to be capable of bridging two or three metals in such low valent compounds. An example of a (μ_3-O) complex being the $[Fe_3(CO)_9(\mu_3\text{-}O)]^{2-}$ anion which has the oxygen-capped structure (vi) in Fig. 1. It also promotes the formation of metal oxo-bridged cluster systems, e.g. $[CpTi]_6(\mu_3\text{-}O)_8$ (**16**). An extensive review of such compounds has been made.[109] The term "organometallic oxides" has been used to describe these compounds,[109b] the phrase being particularly apt with regard to the mixed metal systems derived from the reactions of polyoxometallates with organometallic cations, e.g. $[CpTi(Mo_5O_{18})]^{3-}$,[110] $\{[Cp_2U]_2(\mu\text{-}K_2O\text{-}TiW_5O_{19})_2\}^{4-}$.[111] Their synthesis and study is directed towards providing a better understanding of the mechanisms of catalysis of organic reactions on metal oxides and may lead to the production of new catalytic materials.

Polyoxometallate anions may also be bound to complex cations forming heteronuclear oxo-bridged species, e.g. $[Fe_2(MACN)_2Mo_3O_{12}]$[112] (**17**). This potentially very large group of heteronuclear oxo complexes will not be reviewed in this report because of space limitations.

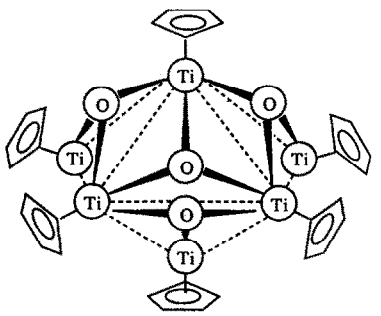

$(CpTi)_6(\mu_3\text{-}O)_8$ (**16**).

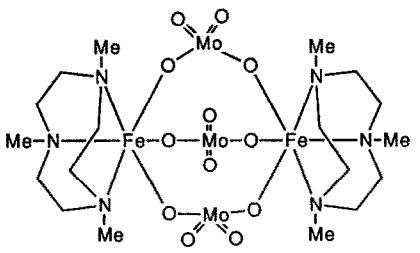

$[Fe_2^{III}(MACN)_2Mo_3O_{12}]$ (**17**).

1.7 (μ_5-O) *compounds*

Although (μ_5-O) compounds of transition metals have not yet been reported, there are two other polymetallic systems containing lanthanide or main group metals which have been shown by X-ray diffraction studies to contain a single oxygen coordinated to five metal ions in a square-pyramidal array. These are the alkoxy-bridged complexes $(\eta^5\text{-}C_5H_5\text{-}Y)_5(\mu\text{-}OCH_3)_4(\mu_3\text{-}OCH_3)_4(\mu_5\text{-}O)$[113a] and $In_5(\mu\text{-}O^iPr)_4(\mu_3\text{-}O^iPr)_4(O^iPr)_5(\mu_5\text{-}O)$ (**18**).[113b] The Y and Yb analogues of the latter complex have

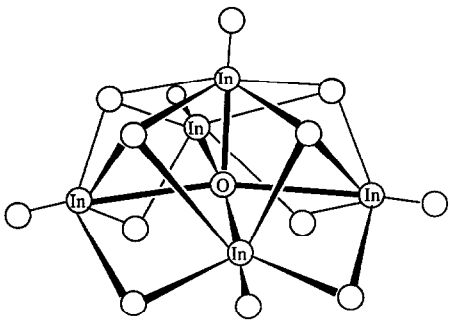

$In_5(\mu\text{-}O^iPr)_4(\mu_3\text{-}O^iPr)_4(O^iPr)_5(\mu_5\text{-}O)$ **(18)**.

also been prepared.[113b] These remarkable compounds represent further potentially very useful examples of soluble "polymetallic oxides". The bonding arrangements in the $(C_5H_5\text{-}Y)(\mu_5\text{-}O)$ complex have been compared with those in polyboranes.

It may now be anticipated that analogous $(\mu_5\text{-}O)$ bound transition metal complexes will be identified in due course along with a wider range of main group species.

2. FORMATION OF HOMONUCLEAR OXO-BRIDGED COMPOUNDS

The widespread occurrence of homonuclear μ-oxo compounds would suggest that heteronuclear analogues would also be known in considerable numbers. However, relatively few compounds having an authenticated M—O—M′ linkage have been known until the last few years, no doubt because routes for the directed synthesis of such linkages have not been sought until recently. It is pertinent, therefore, to briefly review the methods used for preparing homonuclear species. Although precise mechanisms of formation are scarcely known for any of the methods used, they may be conveniently grouped under the headings Reduction, Oxidation and Olation–Oxolation, the last term indicating formation of an oxo group by deprotonation of a hydro group.

2.1 *Reduction processes*

The well studied decahalo compounds $[M_2OX_{10}]^{4-}$ (M = Ru^{IV}, Os^{IV}, Re^{IV}, W^{IV}) containing linear MOM have been prepared[1,2] by reduction of an oxide, e.g. $Ru^{VIII}O_4$, or oxometallate anion, e.g. $W^{VI}O_4^{3-}$ in halic acid solutions. $(lig)_2OMo^{V}OMo^{V}(lig)_2$ complexes with various bidentate ligands are also prepared by reduction of $Mo^{VI}(O)_2(lig)_2$[115] complexes with reagents such as dithionite, PPh_3, etc., although direct reaction with $MoCl_5$ can also give the oxo complexes. The reaction of PPh_3 in excess with $Mo^{VI}(O)_2(dtc)_2$ complexes forms mono-oxo Mo^{IV} complexes, $MoO(dtc)_2$.[116]

$$(dtc)_2Mo^{VI}(O)_2 + PPh_3 \longrightarrow (dtc)_2Mo^{IV}O + OPPh_3. \quad (1)$$

Many Mo^{V} oxo-bridged complexes have been found to undergo disproportionation in solution to Mo^{VI} and Mo^{IV} species.[115b,117–119] This reaction has usually been recognized by the failure of the UV–vis spectrum of an oxo-bridged complex to obey Beer's law. Redox reactions between the Mo^{VI} and Mo^{IV} compounds[117b] have also been shown to form oxo-bridged Mo^{V} compounds, presumably via an inner sphere electron transfer mechanism involving an initial $OMo^{VI}{=}O \rightarrow Mo^{IV}O$ transition state.

$$(dtc)_2Mo^{VI}(O)_2 + OMo^{IV}(dtc)_2 \longrightarrow [(dtc)_2Mo^{V}O]_2O. \quad (2)$$

Such a reaction is presumably involved in the formation of oxo-bridged Mo^{V} complexes when reducing agents react with $Mo^{VI}(O)_2$ complexes.

Measurements of the kinetic (Table 5) and thermodynamic (Table 6) parameters for a number of these reactions have been made. It has been shown by Berg and Holm[120] that the formation of an oxo-bridged complex by such a reaction can be prevented when the ligand attached to Mo is sufficiently bulky to inhibit the approach of two Mo centres to a distance appropriate for oxo bridge formation, even though electron transfer may take place **(19)**.

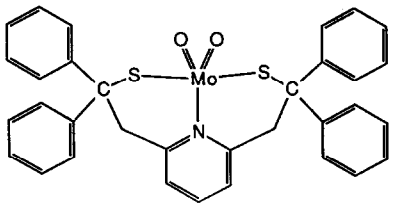

$Mo^{IV}(O)_2$(DMEpy) (**19**).

Table 5. Rate and equilibrium data for the disproportionation reactions:

$$L_2(O)Mo^{V}OMo^{V}(O)L_2 \underset{k_{-1}}{\overset{k_1}{\rightleftharpoons}} L_2Mo^{VI}(O)_2 + L_2Mo^{IV}O$$

L	k_1 (s^{-1})	k_{-1} ($M^{-1}\,s^{-1}$)	$K(\times 10^3)$ ($M\,dm^{-3}$)	T (°C)	Solvent	Reference
$^nPr_2NC(S, S)^-$			*ca* 4	41	o-$C_6H_4Cl_2$	117a
$Et_2NC(S, S)^-$	4.9	2350	2.1	25	CH_2Cl_2	117b
	2.93±0.29	1470±20	2±0.2	25	1,2-$C_2H_4Cl_2$	118
$Et_2NC(S, Se)^-$	3.78±0.11	900±1.0	4.2±0.5	25	1,2-$C_2H_4Cl_2$	118
$Et_2NC(Se, Se)^-$	10.8±0.1	830±10	13.0±0.2	25	1,2-$C_2H_4Cl_2$	118
$^iPrSC(S, S)^-$	12.2	3.2×10^4	0.38	25.3	1,2-$C_2H_4Cl_2$	119

Table 6. Thermodynamic quantities for the disproportionation of $Mo_2O_3L_4$ complexes

L	ΔH (kJ mol^{-1})	ΔS (J $mol^{-1}\,K^{-1}$)	ΔG (298 K) (kJ mol^{-1})	Reference
$Et_2NC(S, S)^-$	50.5	116	15.9	118
$Et_2NC(S, Se)^-$	63.1	166	13.7	118
$Et_2NC(Se, Se)^-$	24.9	47	10.8	118
$^iPrSC(S, S)^-$	53.7	−132	93.0	119

$(L)_2Mo(O)OMo(O)(L)_2$ complexes (L = anions of 8-quinolinol or acetylacetone)[116,121] have been prepared by the reduction of the corresponding Mo^{VI} species, but disproportionation of these complexes has not been detected. Indeed, the $Mo^{IV}O$ complexes containing these ligands have not so far been prepared even by oxygen abstraction using PPh_2Et.[116] $[Mo^{V}O(acac)_2]_2O$ does not appear to be reduced by common reagents although the 8-quinolinol product does. A $Mo^{IV}O$ complex could not be isolated, however.[121]

2.2 *Oxidation processes*

(a) *Dioxygen.* Oxo-bridged $(ML)_2O$ compounds of the transition metals Fe, Cr, Mn and Ru have been prepared with porphyrin (Fe^{III},[122] Cr^{III},[123] Ru^{IV}[23,124]) or phthalocyanine ligands (Fe^{III},[125] Mn^{III}[21,126]) by reaction of the M^{II}(lig) complex with molecular oxygen in solution. Many other Fe^{II}[3,29] and a few Cr^{II}[18] complexes have been found to react similarly with oxygen but many reactions of Cr^{II}[127] and Mn^{II}[128] complexes with oxygen have resulted in impure oxo–hydroxy species being formed. Since the heat of reaction with air or pure oxygen is often sufficient to cause visible decomposition of the complexes in a number of cases, oxidation with very low concentrations of oxygen in solution may aid in the isolation of new compounds.

The oxidative reaction of Fe(P) porphyrins with oxygen has been studied extensively because of its relevance to the reversible oxygen-carrying functions of haem proteins where μ-oxo formation is prevented.[129]

The following overall sequence has been proposed.

$$(P)Fe^{II} + O_2 \rightleftharpoons (P)Fe^{III}(O_2) \xrightleftharpoons{(P)Fe^{II}} (P)Fe^{III}—O—O—Fe^{III}(P) \quad (3)$$

$$(P)Fe^{III}—O—O—Fe^{III}(P) \longrightarrow 2(P)Fe^{IV}O \quad (4)$$

$$(P)Fe^{IV}O + Fe^{II}(P) \longrightarrow (P)Fe^{III}—O—Fe^{III}(P). \quad (5)$$

Most of the intermediate species have been identified only by spectral or other means, their high reactivity making isolation difficult or impossible. Thus, La Mar *et al.*[131] have presented ^1H NMR evidence for the formation of the peroxo-bridged species (P)FeO—OFe(P) and $(P)Fe^{IV}O(B)$ complexes at low temperatures (< 193 K). Formation of "ferryl" $Fe^{IV}O$ complexes is facilitated by the presence of a heterocyclic base (B). It has further been shown that $(P)Fe^{III}—O—Fe^{III}(P)$ is formed when $Fe^{II}(P)$ is reacted with such an $Fe^{IV}O$ species at low temperatures.[130,132] Holm[5] has provided an extensive summary of the work on identification of $Fe^{IV}O$ species.

The critical step involving fission of the O—O linkage has had little direct experimental support until recently when Groves and Watanabe[133] presented kinetic and spectral studies on the decomposition of the peroxo linkage in an acylperoxy Fe^{III} porphyrin leading to formation of an $Fe^{IV}O$ porphyrin cation radical.

In the overall reaction leading to oxo-bridged species two additional pathways have been suggested for the decomposition of the proposed peroxy dinuclear system viz.

$$(P)Fe^{III}—O—O—Fe^{III}(P) \longrightarrow (P)Fe^{III}—O—Fe^{III}(P) + O_2 \quad (6)$$

$$(P)Fe^{III}—O—O—Fe^{III}(P) + 2Fe^{II}(P) \longrightarrow (P)Fe^{III}—O—Fe^{III}(P). \quad (7)$$

Evidence for each route[131] was obtained at temperatures above $-30°C$, indicating that the overall reaction may well proceed by a variety of paths.

The reaction of Cr^{II} porphyrin complexes with molecular oxygen leads to the formation of $[Cr^{III}(P)]_2O$ compounds when the supply of oxygen is limited.[134] In the presence of excess oxygen stable $Cr^{IV}O(P)$ complexes are formed in striking contrast to the highly reactive $Fe^{IV}O(P)$ species. The overall reaction sequence for the formation of $Cr^{IV}O(P)$ is considered to be the same as that proposed for Fe^{II} reactions.[123]

$$(P)Cr^{II} + O_2 \rightleftharpoons (P)Cr^{III}(O_2) \xrightleftharpoons{(P)Cr^{II}} (P)Cr^{III}—O—OCr^{III}(P) \quad (8)$$

$$(P)Cr^{III}—O—O—Cr^{III}(P) \longrightarrow 2(P)Cr^{IV}O \quad (9)$$

$$(P)Cr^{IV}O + Cr^{II}(P) \rightleftharpoons (P)Cr^{III}—O—Cr^{III}(P). \quad (10)$$

The existence of the equilibrium in reaction (10) has been demonstrated by spectroscopic means[134] and $[Cr(P)]_2O$ complexes prepared by direct reaction of $Cr^{IV}O(P)$ and $Cr^{II}(P)$ compounds.[123]

Spectroscopic evidence for the existence of the superoxide precursor $Cr^{III}(P) \cdot O_2$ has been obtained from the reaction of solid $Cr^{II}(TPP)(py)_2$ with dry oxygen.[135] The oxygen compound, when dissolved in toluene, is converted to $Cr^{IV}O(TPP)$.[123]

A careful magnetic and spectroscopic study of the reaction between oxygen and solid $Cr^{II}(Pc)$[136] indicated the likely formation of a dimeric $[Cr(Pc)]_2O_2$ compound thought to contain Cr^{IV} entities rather than being a peroxo-bridged Cr^{III} compound. Earlier attempts to react $Cr^{II}(Pc)$ with oxygen in solution had led to the formation of mixtures of hydroxy-containing $Cr^{III}(Pc)$ products[136] rather than a clearly defined oxo-bridged compound.

Mn^{II} porphyrins show reversible reactions with molecular oxygen at low temperatures but do not yield oxo-bridged or other identified oxo compounds at higher temperatures.[137,138] The presence of Lewis bases can prevent any reaction occurring between $Mn^{II}(P)$ and oxygen because of preferential coordination of the base molecules to Mn^{II}.[137] Manganese(II) phthalocyanine, however, reacts readily in the presence of pyridine to form an oxo-bridged compound having further molecules of pyridine coordinated to each Mn^{III} ion.[21] The early complications experienced in defining the nature of the product[139] formed when oxygen reacted with $Mn^{II}(Pc)$ appear to relate to the adventitious presence of water in many reactions which led to the formation of Mn—OH species and impure samples of the oxo-bridged complex.

Many Co^{II} complexes including porphyrin derivatives react reversibly with dioxygen to form

(P)Co^{III}–superoxo species[103] as well as the dinuclear peroxo compounds

$$Co^{II}(L)+O_2 \rightleftharpoons Co^{III}(L)\cdot O_2 \overset{Co^{II}(L)}{\rightleftharpoons} (L)Co^{III}—O—O—Co^{III}(L). \quad (11)$$

There have been no reported instances where a μ-oxo compound has been detected as the by-product of such reactions.

The action of oxygen on the ions $[Ru^{II}(lig)_2Cl\cdot S]^{+}$[247](lig = bipyridyl, 1,10-phenanthroline) or $[Ru^{II}(NH_3)_5\cdot S]^{2+}$[248] (S = acetone) results in the formation of the oxo-bridged Ru^{III} species[37a] $\{[Ru^{III}(lig)_2Cl]_2O\}^{2+}$ and $\{[Ru^{III}(NH_3)_5]_2O\}^{4+}$. Boiling solutions of the bpy and phen chloro complexes in the presence of Ag^+ ions converts them to the aqua complexes $\{[Ru^{III}(lig)_2H_2O]_2O\}^{4+}$. Water in turn can be replaced by NO_2^-[247] or pyridine[249] giving $\{[Ru^{III}(lig)_2L]_2O\}^{2+}$ (L = NO_2^-, pyridine). The unsymmetrically substituted complex $\{[Ru^{III}(lig)_2py]O[Ru^{III}(lig)_2H_2O]\}^{4+}$ has also been obtained.[249] Structural studies on $\{[Ru^{III}(bpy)_2H_2O]_2O\}(ClO_4)_4$[37a] and $\{[Ru^{III}(bpy)_2NO_2]_2O\}(ClO_4)_2$[37b] have revealed bent RuORu bonds (Table 1) (**20**). The group of Ru^{III} complexes

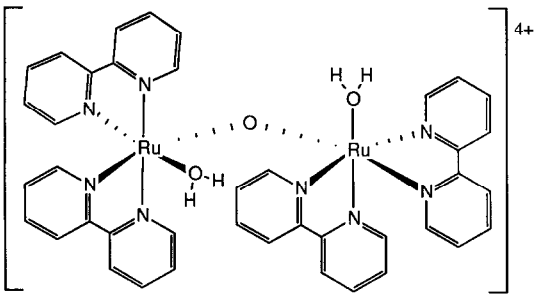

$\{[Ru(bpy)_2H_2O]_2O\}^{4+}$ (**20**).

have low magnetic moments[247,248] in the range 1.7–18 μ_B per Ru atom. The variation of susceptibility with temperature of $\{[Ru^{III}(bpy)_2NO_2]_2O\}(PF_6)_2$ indicates[247] strong magnetic coupling between the Ru ions via the bridging O^{2-} ions. The data is adequately accounted for by use of the Bleaney–Bowers expression having the coupling constant $2J = -173$ cm^{-1} and $g = 2.48$. The phen analogue has $2J = -119$ cm^{-1} and $g = 2.29$. ESR signals have not been observed for the compounds.

The complexes show UV–vis spectra having quite different features to those shown by normal monomeric Ru^{III} bpy and phen complexes which display weak bands related to *d–d* transitions. In particular, the oxo-bridged compounds each show an intense absorption band in the region of 630–670 nm with $\varepsilon = ca\ 20\times10^3$, a feature found for a number of MOM bonded compounds having delocalized electronic bonding systems. Such a view of the bonding in these complexes is also considered to account for the magnetic coupling.

A particular feature of the complexes is their ability to undergo oxidation[37a,248] in a number of stages to give a range of higher oxidation state compounds including a number with mixed oxidation states, e.g. $Ru^{III}ORu^{IV}$, $Ru^{IV}ORu^{V}$ and $Ru^{V}ORu^{V}$. The $Ru^{IV}ORu^{IV}$ species is generally not observed, however, and appears to undergo ready disproportionation to $Ru^{III}Ru^{IV}$ and $Ru^{V}Ru^{V}$ ions. The redox chemistry of the complexes is notably dependent on pH and the higher oxidation state systems have been characterized as containing terminal oxo groups attached to Ru, derived by loss of protons from water molecules, e.g. $\{[Ru^{V}(bpy)_2O]_2O\}^{4+}$.

The ions $\{[Ru^{III}(bpy)_2H_2O]_2O\}^{4+}$ and $\{[Ru^{III}(bpy)_2py]O[Ru^{III}(bpy)_2H_2O]\}^{4+}$ are found to act as catalysts in the oxidation of water to oxygen when Ce^{IV} ions are added to aqueous solutions containing these ions.[37a,250] The exact oxidation states of the species involved in the final oxygen evolution step are not established with certainty but must involve Ru^{IV}/Ru^{V} systems. The possibility has been considered that O_2 could arise by combination of the terminal oxygen atoms believed to be attached to Ru in the Ru^{V} type compounds. However, such a mechanism is thought unlikely because of the estimated distance apart of the oxygens, based on the coordinated water positions established by X-ray studies.[37a] ESCA measurements have supported a delocalized electronic con-

figuration for the compounds since the mixed valent complexes $\{[Ru^{III}(bpy)_2Cl]O[Ru^{IV}(bpy)_2Cl]\}(PF_6)_3$[247] and $\{[Ru^{III}(NH_3)_5]O[Ru^{IV}(NH_3)_5]\}(ClO_4)_5$[248] show equivalent Ru centres.

A mixed valent Os analogue of these complexes has been prepared, $\{[Os^{III}(bpy)_2H_2O]O[Os^{IV}(bpy)_2OH]\}^{4+}$.[251] The spectral properties are similar to those of the Ru complexes in that an intense band is found at *ca* 600 nm, its position being pH dependent. The number of accessible redox couples is considerably greater for this system than for Ru, extending from Os^{II}—O—Os^{II} to Os^{V}—O—Os^{V}.

(b) *Oxo-transfer reagents.* Oxo-bridged compounds have resulted from the reaction of oxo-transfer reagents such as iodosyl benzene (PhIO) with metal porphyrins. The reactions most probably involve a comproportionation reaction. Thus, $Mn^{III}(TPP)\cdot N_3$ reacts with PhIO to yield the Mn^{IV} compound $N_3\cdot(TPP)Mn^{IV}OMn^{IV}(TPP)\cdot N_3$[20] (**21**). The initial reaction is expected to form

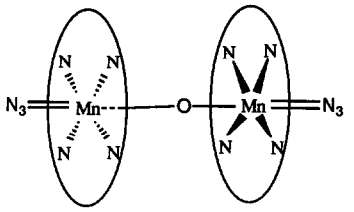

$[Mn^{IV}(TPP)N_3]_2O$ (**21**).

$Mn^{V}O(TPP)\cdot N_3$ which could then react via an inner sphere bridged transition state with further $[Mn^{III}(TPP)]^+$ to give the Mn^{IV} product.

$$N_3\cdot(TPP)Mn^{III}\overset{e}{\frown}O{=}Mn^{V}(TPP)\cdot N_3 \longrightarrow N_3\cdot(TPP)Mn^{IV}{-}O{-}OMn^{IV}(TPP)\cdot N_3. \quad (12)$$

$Cr^{III}(TPP)Cl$ forms the highly reactive $[Cr^{V}O(TPP)]^+$ on reaction with PhIO,[140] but the eventual product is $Cr^{IV}O(TPP)$ rather than the readily oxidized $[Cr^{III}OCr^{III}]$ intermediate.

Various nitrogen oxides or RNO species have also been found valuable reagents in transferring oxygen to organometallic substrates. The molecularity of the oxo-bridged organometallic clusters which form can vary with the choice of the amine oxide. Thus[141]

$$\begin{array}{l} C_5H_5NO\ \ [CpV(\mu_3\text{-}O)]_4 + [CpV]_6(\mu_3\text{-}O)_8 + (Cp)_5(O)V_6(\mu_3\text{-}O)_8 \\ \quad + \\ (Cp)_2V \nearrow\searrow \\ \quad + \\ (CH_3)_3NO\ \ \{(Cp)_5V_6(\mu_3\text{-}O)_8\}_2\{(\mu\text{-}O)_2(CpV)(N(CH_3)_3)_2\} + [CpV]_6(\mu_3\text{-}O)_8. \end{array} \quad (13)$$

The oxo-bridged aqua ion $\{[Cr^{III}(H_2O)_5]_2O\}^{4+}$ has been reported to form in low yield (*ca* 4%) when $[Cr((H_2O)_6]^{2+}$ ions react with 1,4-benzoquinone.[252a] $[Cr(H_2O)_6]^{3+}$ and several Cr–hydroquinone complexes are also formed in major amounts in the reaction. The ions are separable by ion exchange. The "oxo" ion has an absorption spectrum showing three sharp, intense peaks in the near-UV region very reminiscent of the bands shown by $\{[Cr(NH_3)_5]_2O\}^{4+}$, a complex whose linear CrOCr bridge has been characterized by a crystallographic study.[17] Electronic transitions within the linear π-bonded CrOCr segment have been identified as the source of this spectral feature. The ion $\{[Cr(H_2O)_5]_2O\}^{4+}$ undergoes rapid hydrolysis[252b] in acid solution to yield the hexaqua ion $[Cr(H_2O)_6]^{3+}$; the kinetics of the reaction have been interpreted as showing that two alternate pathways can be used, one of which (the major) is acid dependent. The rate is also catalysed by a large number of cations including alkali metal ions and $[Cr(H_2O)_6]^{3+}$, and by perchlorate ions. It has been suggested that the acid dependent path involves an initial protonation of the oxo group with the resultant hydroxo-bridged species remaining linear and only slowly converting to the expected "bent" CrOHCr form which is rapidly hydrolysed to $[Cr(H_2O)_6]^{3+}$. The half-life of acid hydrolysis is 70 min in 1.0 M $HClO_4$ at 25°C. The ammine complex $\{[Cr(NH_3)_5]_2O\}^{4+}$ is not susceptible to rapid hydrolysis at room temperature and studies have been carried out at 55°C to obtain reasonable rates.[253]

The reaction of molecular oxygen with $[Cr(H_2O)_6]^{2+}$ has been reported[254a] to form a dihydroxo bridged species $\{[Cr(H_2O)_4OH]_2\}^{4+}$, a distinction between this ion and the oxo compound having

the same charge $\{[Cr(H_2O)_5]_2O\}^{4+}$ having been drawn on the basis of $H_2{}^{18}O$ exchange studies.[254b] The crystal structure of the tosylate of this ion has also been reported by Marty and co-workers[255] establishing CrOHCr angles of 101°. This group has also established the existence of polychromium ions linked by hydroxy groups rather than oxo bridges.[256] The studies on $\{[Cr(NH_3)_5]_2O\}^{4+}$ and $[(NH_2)_5Cr(OH)Cr(NH_3)_4H_2O]^{5+}$ have established (a) the linearity of the CrOCr bridge[17] and the bent nature of the Cr(OH)Cr linkage ($168 \pm 5°$)[17] and (b) the existence of strong magnetic coupling in the oxo complex leading to a notable lowering of the magnetic moment per Cr, compared to little or no coupling in the hydroxy-bridged complex which shows a moment only slightly smaller than the spin-only value for a d^3 ion ($\mu_{eff} = 3.44\mu_B$).

The analogous monohydroxo-bridged complex ion[257] $\{[Cr(H_2O)_5]_2OH\}^{5+}$ which is formed from the dihydroxy compound in strong acid solution has a moment of $3.45\mu_B$. The dihydroxo complex has $\mu_{eff} = 3.74\mu_B$.

Acid hydrolysis of the monohydroxy-bridged species has been reported to be slow ($t_{1/2}$ *ca* 6 days in 2 M acid), indicating a relatively stable species, and this fact is difficult to reconcile with the hydrolytic instability of the oxo compound reported by Holwerda and co-workers.

An example of an oxo–hydroxo bridged species has been provided by Springborg and Toftlund[258] who reported that the dihydroxy-bridged ion $\{[Cr(en)_2OH]_2\}^{4+}$ is converted to an oxo-bridged species in strong alkali [see eq. (14)].

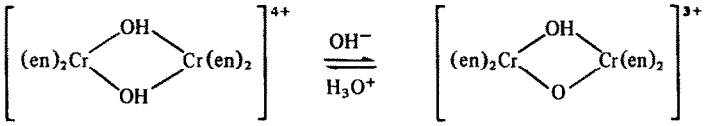

(14)

The oxo-hydroxo complex was isolated as a perchlorate salt. The diol compound has a pK_a of 12 at 0°C.

Conversion of the aqua Cr^{III} hydroxo complexes to oxo-bridged species is not feasible by use of OH^- since condensation to higher nuclearity $[Cr(OH)]_n$ species occurs as the pH is raised.

Holwerda and co-workers[18b] have recently shown that NCS^- converts a dihydroxy-bridged Cr^{III} complex to a mono-oxo-bridged complex in boiling water (**22**).

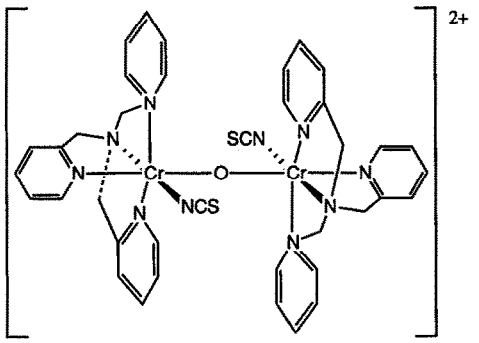

$\{[Cr^{III}(tmpa)NCS]_2O\}^{2+}$ (**22**).

(c) *Formation of metal–metal bonded* M_3O *species*. The formation of M_3 triangular metal–metal bonded arrays for M = Mo, W with O capping on either one or both sides and carboxylate anions bridging each pair of metal atoms (Table 4), results from the reactions of Mo(W) hexacarbonyls with mixtures of the free acid and anhydride.[142] The μ_3-bridging group X may be O, or an alkylidyne (CCH_3), the latter presumed to be formed by reduction of an acetate group.[92b] The complexes must generally be separated from other accompanying products by ion-exchange chromatography. Niobium analogues of these compounds are prepared from the metal–metal bonded complex $Nb_2Cl_6(Me_2S)_3$. The source of the oxygen atom has generally not been determined but may arise from the air since the reactions were seldom performed under oxygen-free conditions.

One reaction has been devised for the directed synthesis of oxo-bridged, "triangulo" compounds having alkoxy groups bridging the metal pairs. This involves a comproportionation[98,99] reaction between triply bonded $Mo(OR)_6$ species and oxo Mo^{VI} compounds.

$$(RO)_3Mo{\equiv}Mo(OR)_3 + Mo(O)(OR)_4 \longrightarrow Mo_3(\mu_3\text{-}O)(OR)_{10} \quad (15)$$

2.3 *Olation and oxolation reactions*

Iron(III) oxo complexes in particular can be formed by reactions which appear to proceed via Fe—OH intermediates[3] participating in an olation or more specifically an "oxolation" reaction

$$Fe{-}OH + HO{-}Fe \longrightarrow Fe{-}O{-}Fe + H_2O. \quad (16)$$

Synthetic procedures either use aqueous solutions of Fe^{III} aqua ions in which Fe—OH entities are prevalent even at pHs below seven or non-aqueous solutions of complexes containing groups such as Fe—Cl which can be replaced by the addition of OH^-. Direct structural evidence for the Fe^{III}—OH group in coordination complexes is not extensive but several examples where OH groups bridge Fe^{III} ions have been reported.[143] $Fe^{II}(P)$ complexes containing *meso*-tetramesitylporphyrin or *meso*-tetrakis(2,4,6-trimethoxy)phenylporphyrin give $Fe^{III}(P)OH$ compounds[144a,b] on reaction with oxygen, instead of the more usual oxo-bridged products. The hydroxy compounds also result from the reaction of OH^- ions with $Fe^{III}(P)Cl$. They are high spin Fe^{III} compounds and can be readily distinguished from oxo-bridged species by this property, together with their ^1H NMR and ESR spectra, which are both typical of $Fe^{III}(P)X$ compounds. Their IR spectra are also typical of hydroxy containing species with broad absorptions *ca* 3400 cm^{-1} and no evidence for the 850 cm^{-1} peak which is normally observed as an antisymmetric vibration of the FeOFe linkage. The bulky substituents may be considered to prevent a sufficiently close approach of "Fe—OH or Fe—O" species which could result in Fe—O—Fe bridge formation. Reduction of this steric restraint by use of Fe porphyrins containing *meso*-tetrakis(3,4,5-trimethoxyphenyl)porphyrin or the tetrapentafluorophenyl derivative allows mixtures of Fe(P)OH and $[Fe(P)]_2O$ complexes to be observed in solution.[144b] Tetramesitylporphyrin has been found to stabilize the formation of $(P)Fe^{IV}O$[144c] by preventing the sufficiently close approach of an $Fe^{II}(P)$ molecule to allow the redox reaction $Fe^{IV}O + Fe^{II} \rightarrow Fe^{III}OFe^{III}$ to occur (**23**).

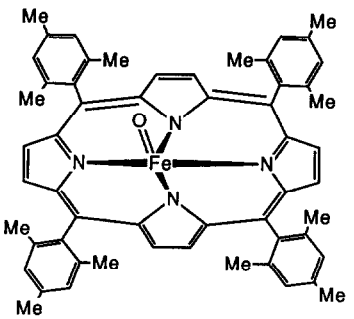

$Fe^{IV}(O)(TMesP)$ (**23**).

The trinuclear compounds $[M_3(\mu_3\text{-}O)(\mu\text{-}RCOO)_6(H_2O)_3]^+$ ($M = Fe^{III}$, Cr^{III}, Mn^{III}, V^{III}, Rh^{III}, Ru^{III}, Ir^{III}, Os^{III})[78,79,80] have also been prepared by reacting M^{III} salts with excess carboxylate ions in aqueous solution. Acetate has been the most common anion employed but a range of other carboxylates is entirely possible. The formal mixed valent compounds $Fe_2^{III}Fe^{II}$, $Cr_2^{III}Cr^{II}$, $Mn_2^{III}Mn^{II}$, etc. (Table 3) are also prepared by mixing appropriate amounts of metal salts of the different oxidation states. The mechanism by which the final M_3O unit is formed has not been the subject of a detailed study but a plausible route would involve the initial formation of M—O—M species, supported by carboxylate bridges, to which a further M^{III} unit can add, rather like protonation of an oxo group. Such reactions have been considered by Lippard[83] as contributing to the formation of poly $Fe^{III}O$ clusters.

The mixed valence $[Ru_3(O)(CH_3COO)_6(PPh_3)_3]$[77] and the cationic Co^{III} complex[80] are prepared by similar aqueous procedures but using "Ru^{II} acetate" and Co^{II} acetate, so that oxidation processes must also be involved here.

3. PHYSICAL PROPERTIES OF OXO-BRIDGED COMPOUNDS

A number of measurements other than a direct X-ray structure determination have some value in indicating whether an oxo-bridged structure may exist in a new complex isolated for the first time.

3.1 *Magnetic susceptibilities*

Magnetic moments, lower than the "spin-only" values appropriate to the constituent metal ions, are generally observed for oxo-bridged complexes. Many such complexes are diamagnetic. The variation of magnetic susceptibility with temperature of these paramagnetic complexes, also in the main, is found to show antiferromagnetic behaviour. The spin coupling effect is demonstrated by a representative selection of compounds collected in Table 7 showing the experimental magnetic

Table 7. M—O—M stretching frequencies and magnetic moments of oxo-bridged complexes

	Compound	$\nu_{as\ MOM}$ (cm^{-})	$\nu_{M=O}$ (cm^{-1})	μ_{eff}^{a} (μ_B/metal ion)	μ_S	Reference
					1.73	
d^1	$[Mo^{V}O(TPP)]_2O$	615, 656	905	1.4		10
	$[Mo^{V}O(^{n}Pr_2dtc)_2]_2O$	770	975, 930	diamagnetic		153
	$[Mo^{V}O(Et_2dtc)_2]_2O$	750	930	diamagnetic		153
	$[Mo^{V}O(S_2P(OEt_2))_2]_2O$	782	967	diamagnetic		153
	$[Mo^{V}O(salen)]_2O$	762	930, 903	0.98		12
					2.83	
d^2	$[Re^{V}O(Et_2dtc)_2]_2O$	671	957	diamagnetic		19, 207b
	$[Re^{V}O(Ph_2dtc)_2]_2O$	670	955	diamagnetic		19
	$[Re^{V}O(py)_2Cl_2]O$	671	970	diamagnetic		208, 207b
					3.87	
d^3	$\{[Cr^{III}(NH_3)_5]_2O\}^{4+}$	873		1.29		42
	$\{[Cr^{III}(TPyEA)(NCS)]_2O\}^{2+}$	830		1.63		18a
	$\{[Cr^{III}(tmpa)NCS]_2O\}^{2+}$	850				18b
	$[Cr^{III}(salen)]_2O$	870, 858		2.22		12
	$[Cr^{III}(TPP)]_2O$	860		1.43		123
	$[Mn^{IV}(TPP)N_3]_2O$	794		2.0		20
					4.90	
d^4	$[Mn^{III}(Pc)py]_2O$	[b]		diamagnetic		126b
	$[Ru^{IV}(TPP)(OR)]_2O$	[b]		diamagnetic		23
					5.92	
d^5	$[Fe^{III}(DBAT)]_2O$	890, 882		1.96		27
	$[Fe^{III}(Hp)]_2O \cdot H_2O$	878		2.09 (294 K) 1.48 (83.5 K)		22b
	$[Fe^{III}(acen)]_2O$	840		1.80		29
	$[Fe^{III}(salen)]_2O$	[b]		1.87		30e
	$[(N_5)Fe^{III}OFe^{III}Cl_3]^{+}$	850, 835		1.59		36
	$[Fe^{III}(TPP)]_2O$	890.2, 873.8 (^{16}O) (^{18}O) 831.3		1.74		189, 3 189
	$\{[Fe^{III}(phen)_2H_2O]_2O\}^{4+}$	827		1.83		28b

[a] Measurements all reported at or near to 293 K.
[b] Not defined.

moments measured at or close to 293 K (considered as "room temperature") together with the "spin-only" values of their magnetic moments per metal ion, i.e. assuming absence of magnetic coupling. As described earlier, a description of the bonding in the MOM unit using a molecular orbital approach and considering σ- and π-bonding between metal *d* and oxygen *p* orbitals has provided an appropriate way of defining ground state electronic configurations for a number of linear MOM systems, particularly where diamagnetism is encountered. A more widely applicable approach when studying magnetic properties *per se* has been to treat the magnetic susceptibility as arising from an exchange interaction between a series of metal ions without the need to define a mechanism for the exchange process. The procedure requires definition of a spin Hamiltonian, in the simplest form being

$$\mathscr{H} = -2\Sigma J_{ij} S_i S_j,$$

with J_{ij} being an exchange integral between metal centres i and j having a negative value for antiferromagnetic interaction between the centres and positive for ferromagnetic interaction. An expression for the molar susceptibility for the system can then be defined using the Van Vleck equation. The theoretical treatment has been termed the Heisenberg–Dirac–Van Vleck or HDVV method. The general theoretical approach has been described.[3,61,145] It has been found to provide a good fit for experimental data for many Fe_2O systems[3,145] and the Cr_2O complex $\{[Cr(NH_3)_5]_2O\}^{4+}$.[42] The mechanism for exchange is best considered as a "super-exchange" process involving participation of the metal *d* orbital interaction with the *p* orbitals of oxygen.

Iron(III) compounds remain the most accurately studied complexes of any oxo complexes showing exchange coupling.[3] Holm and co-workers[146] have examined the influence of FeOFe angle on extent of coupling by comparing the two complexes $[Fe(salen)]_2O$ and $[Fe(3\text{-}^tBusaltmen)]_2O$ (**24**)

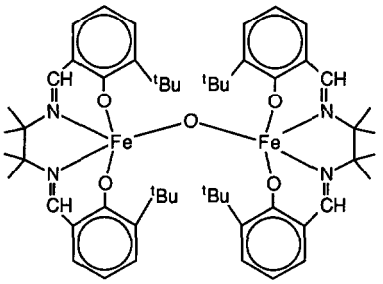

$[Fe(3\text{-}^tBusaltmen)]_2O$ (**24**).

which contain very similar ligands although the bulky substituents of the latter compound can prevent too much bending of the FeOFe linkage. The extent of coupling as measured by the *J* values increases as the bond angle increases, although the differences are small (Table 8). This is in line with the bonding picture for such compounds which shows a reduced Fe—O π-interaction as the bond departs from linearity.[41] The $[Fe(3\text{-}^tBusaltmen)]_2X$ (X = O, S) compounds have very similar bond angles and this allows the conclusion to be drawn that coupling through S is greater than through O.

The nature of the ligand attached to the metal will also influence the extent of coupling and an attempt has been made to gauge the influence of peripheral substituents on the magnetic coupling in a series of substituted tetraphenylporphyrin $[Fe(P)]_2O$ compounds[147] (Table 8). The variation in substituent was from electron withdrawing $CF_3C_6H_4$ and C_6F_5 groups to the electron donating $CH_3O \cdot C_6H_4$. It was argued that the extent of FeOFe coupling should increase as the core size of the porphyrin ring increases because this would allow greater attraction for axial ligands by the metal. The core size of the porphyrin ring would be predicted to increase as the electron donating capacity of substituents on the *meso*-phenyl rings increased. Detailed crystallographic data is not yet available to be considered along with the magnetic evidence but the increase in *J* values followed an increase in the electron releasing property of the substitution, i.e. *J* increases in the order $4\text{-}CF_3C_6H_4 < C_6H_5 < 4\text{-}MeOC_6H_4$.

Table 8. Values of the magnetic coupling constant J for Fe^{III} oxo-bridged species

Complex	$-J$ (cm^{-1})	M—O—M (°)	Reference
	Data from ref. 146		
$[Fe(salen)]_2O$	183	144.6(6)	30a
$[Fe(3\text{-}^tBusaltmen)]_2O$	200	173.4(2)	146
$[Fe(salen)]_2S$	178	121.8(1)	148
$[Fe(3\text{-}^tBusaltmen)]_2S$	218	167.0(2)	146
	Data from ref. 147		
$[Fe(T(4\text{-}MeOP)P)]_2O$[a]	146.8 (solid)		
	150[b]		
$[Fe(TPP)]_2O$	135.7 (solid)		
	145.0[b]		
$[Fe(T(4\text{-}CF_3P)P)]_2O$	136.4		
$[Fe(TPFPP)]_2O$	146.9 (solid)		

[a] The various (TXP) abbreviations represent the dianions of *meso*-substituted tetraaryl porphyrins, the aryl groups being phenyl (TPP), 4-methoxyphenyl (T(4-MeOP)P), 4-trifluoromethylphenyl (T(4-CF_3P)P), pentafluorophenyl (TPFPP).

[b] Derived from ^{13}C NMR measurements.

The pentafluorophenyl complex shows a similar J value to that of the 4-$CH_3OC_6H_4$ complex based on solid state magnetic data. Values of J obtained from ^{13}C paramagnetic shift data, however, while in good agreement with solid state data for the other compounds studied, gave an appropriately lower coupling constant for the C_6F_5 complex. The difference between the two sets of data for this compound may relate to some major stereochemical difference between the pentafluorophenyl derivatives and the remaining complexes.

Trinuclear (μ_3-O) complexes such as the triangular $[M_3O(CH_2COO)_6(L)_3]^+$ species (M = Fe^{III}, Cr^{III}, Mn^{III}) also show magnetic coupling between the metal centres. The crystallographically confirmed D_{3h} symmetry for the arrangement of three Fe^{III} or Cr^{III} ions in these complexes leads to a spin Hamiltonian[145] having a single coupling constant to describe the interaction of the ions

$$\mathscr{H} = -2J(\hat{S}_1 \cdot \hat{S}_2 + \hat{S}_2 \cdot \hat{S}_3 + \hat{S}_1 \cdot \hat{S}_3).$$

Expressions derived for the variation of magnetic susceptibilities with temperature from 300 to below 100 K for both Fe_3O and Cr_3O acetato complexes have not been completely successful in simulating the experimental data, the deviations being greatest at the lowest temperatures.

Improvements in the fit of such expressions have been produced by a variety of approaches[149] including assuming (a) an isosceles triangular array of the metal ions rather than equilateral[145] for which the spin Hamiltonian may be represented as

$$\mathscr{H} = -2J(\hat{S}_1 \cdot \hat{S}_2 + \hat{S}_2 \cdot \hat{S}_3) - 2J'(\hat{S}_3 \cdot \hat{S}_1);$$

(b) the existence of two different forms of the compound at low temperatures; (c) inter-trimer exchange coupling; and (d) dynamic distortion of the structure of the complex,[149] i.e. allowing each M^{3+} ion to vary its distance from the other two ions rapidly, a process termed "fast fluxionality". The idea that different forms of the complex may exist in the same crystal gains support from heat capacity measurements which have disclosed that a phase transition occurs[150] in $[Cr_3(\mu_3\text{-}O)(CH_3COO)_6H_2O]Cl \cdot 6H_2O$ at low temperatures due to reorganization of the solvate water molecules. While time resolved optical spectroscopic studies have shown that there are two different Cr_3O complexes[151] present in crystals of that complex which can take part in excitation energy transfer processes.

Table 9. Raman and IR spectral data (cm^{-1})

Compound	$\nu_{as(MOM)}$ (IR) (cm^{-1})	$\delta_{(MOM)}$ (IR) (cm^{-1})	$\nu_{s(MOM)}$ (Raman) (cm^{-1})	Reference
$K_4[Ru_2OCl_{10}]$	887	469	256.2	114, 39
$Cs_4[Ru_2OBr_{10}]$			243	152
$K_4[Re_2OCl_{10}]$	857.2	401	220.3	39
$Cs_3[Re_2OCl_{10}]$	892	410.7	228.2	114, 39
$Cs_4[OS_2OCl_{10}]$	852	454	224.3	39, 152
$[W_2OCl_{10}]^{4-}$			222.5[a]	114
$[W_2OBr_{10}]^{4-}$			236[a]	114

[a] Solution spectra.

The magnetic properties of the Mn^{III} (μ_3-O)acetato-bridged compound (L = py) have been studied[76] using the same basic theoretical approach[145] assuming three equivalent Mn^{III} ions arrayed in an equilateral triangular array around oxygen. The antiferromagnetic interaction is considerably weaker for $Mn_3^{III}O$ than $Fe_3^{III}O$ and comparable to that in the $Cr_3^{III}O$ system. ($-J = 10.2$ cm^{-1} (Mn_3O); 11 cm^{-1} (Cr_3O, L = H_2O);[214] 30 cm^{-1} (Fe_3O, L = H_2O)[214]) and this has been related[76] to the greater occupancy of d_{z^2} orbital directed towards the bridging O^{2-} ion in Fe^{III} d^5 systems than for Cr^{III}, d^4 or Mn^{III}, d^3. Since the overall exchange process is considered to be a super-exchange interaction via oxygen, a larger interaction is possible with occupancy of the d_{z^2} metal orbitals.

Interaction via the carboxylato bridges or by direct M···M interaction is not considered to contribute to the process[145] of magnetic coupling in any of these M^{III} compounds.

3.2 *Vibrational spectra*

Vibrations of a linear MOM unit of D_{4h} symmetry give rise to a Raman active symmetric vibration frequency and asymmetric stretching and bending vibrations in the IR spectral region. A bent MOM array of C_{2v} symmetry will give rise to asymmetric, symmetric and bending vibrations active both in the IR and Raman regions. Recent accurate Raman measurements on the linear $[M_2OCl_{10}]^{4-}$ ions have identified frequencies for each type of vibration (Table 9) for a number of these complexes. The ν_{as} and ν_s values lie in the frequency ranges suggested earlier for such types of vibrations (ν_{as} 750–900 cm^{-1}; ν_s 200–500 cm^{-1}) but the bending modes are found at much higher frequencies (400–450 cm^{-1}) than had earlier been suggested.[2b]

In many of the presently known homonuclear complexes the presence of organic ligands provides a multitude of additional bands and this has made clear-cut identification of the various frequencies more difficult and rather subjective. ^{18}O labelling has been applied in only a few cases with effect. More often than not broad sections of the spectrum of the labelled compound show increased or decreased intensities rather than single, identifiable bands.

Metals which also have terminal oxygen atoms attached, e.g. $Mo^{V}O$, $V^{V}O$ provide a source of further M—O vibrations and allocations of such vibrations have been made for Mo=O vibrations[153] on the basis of comparison of ^{18}O labelling studies on $MoO_2(LL)_2$, $MoO(LL)_2$, $Mo_2O_3(LL)_4$ and $Mo_2O_4(LL)_2$ compounds (LL represents dithiocarbamates and other S_2 chelating ligands). Related data for the $[M_3O(RCOO)_6L_3]^+$ cations (M = CR, Fe, Mn, Ru, Rh) have been reported.[154] Some data are shown in Table 10.[18]O-Substituted $[Fe_3(^{18}O)(CH_3COO)_6py_3]^+$ has been examined to enable assignments to be made of both in-plane ($\nu_{as\,Fe_3O}$) and out-of-plane (δ_{s,Fe_3O}) vibrations of the oxo unit.[155]

3.3 ^{17}O *NMR*

Direct observation of a bridging oxygen atom or distinguishing it from a terminal oxygen in the same molecule by some means has an obvious importance in initial studies of a potentially oxo-bridged

Table 10. Vibrational spectra of $[M_3(\mu_3\text{-}O)(\mu\text{-}RCOO)_6L_3][X]$ complexes[155]

M	R	L	X	ν_{as,M_3O} (IR–Raman) (cm^{-1})	δ_{s,M_3O} (IR) (cm^{-1})	ν_{s,M_3O} (Raman) (cm^{-1})	ν_{M-N} (cm^{-1})
Cr	H	H_2O	Cl	655	352		
	H	H_2O	HCO_2	646	352	179	
	H	py	ClO_4	650	362		240
	H	4-pic	ClO_4	650	351		
	CH_3	H_2O	ClO_4	660	283	150	
		py	Cl	650	315		250
		4-pic	ClO_4	655	312		240
Fe	CH_3	H_2O	NO_3	595	305	176	
			ClO_4	609(sh)	230	148	
		py	NO_3	604(sh)	234		249
		4-pic	ClO_4	605(sh)	235		243
Ru	CH_3	H_2O	ClO_4	440	282		
		py	ClO_4	466	297		222
		4-pic	ClO_4	445	297		210
Rh	CH_3	H_2O	ClO_4	450	302		
		py	ClO_4	455	322		240
		4-pic	ClO_4	455	322		228
Mn	CH_3	py	ClO_4	590	289		230

complex. In principle, ^{17}O NMR measurements provide such a means, chemical shifts being expected to differ for each type of oxygen. Despite the complications of detecting the nucleus due to its large nuclear spin ($I = 5/2$) and electronic quadropole moment, the use of the technique has been extended since the advent of Fourier transform techniques applied to NMR spectroscopy.[156] The need to produce ^{17}O labelled species for examination requiring use of the expensive isotope has also been removed, or at least reduced, with the advent of higher frequency spectrometers. The technique has been used extensively by Klemperer in studies on the diamagnetic polyoxometallates and mixed-metal compounds containing such anions.[157] It does not give an advantage, however, to studies on paramagnetic complexes. Chemical shift values for some oxo-bridged complexes are given in Table 11.

Table 11. ^{17}O NMR resonance spectra of oxo-bridged complexes. Chemical shift values for selected compounds

Compound	Solvent	δ ppm[a] (line widths Hz) M—O—M	M=O	Reference
$[Mo_6O_{10}]^{2-}$	DMF	559(50)	927(130)	157b
	CH_3CN	563(10)	933(20)	157b
$MoO_2(Et_2dtc)_2$	CH_2Cl_2		975(362)	156
$MoO_2(acac)_2$	DMF		1025(400)	156
$Mo_2O_3(Et_2dtc)_4$	CH_2Cl_2	588(550)	935(330)	156
$MoO(Et_2dtc)_2$	CH_2Cl_2		820(24)	156
$Mo_2O_3(Et_2dtp)_4$	CH_2Cl_2	612(660)	978(390)	156
$MoO(Et_2dtp)_2$	CH_2Cl_2		842(75)	156
$[W_6O_{19}]^{2-}$	DMF	413(70)	772(100)	157b
$[Nb_6O_{19}]^{8-}$	H_2O(pH, 14)	392(90)	607(90)	157b
$[VMo_5O_{19}]^{3-}$	CH_3CN	665(250) (VOMo) 531(30) (MoOMo)	1200(390)(V) 885(60)(Mo)	157b

[a] Measurements are downfield from external $H_2{}^{17}O$.

3.4 *Optical electronic spectra*

The UV–vis spectra of oxo-bridged complexes do not, in general, show outstanding features that indicate the presence of an oxo bridge. However, some cases exist, particularly for linear MOM species, where distinct spectral features have been recognized and related to transitions in the electronic framework encompassing the MOM linkage. Thus, the distinct dark purple colours of $[Mo^{V}O]_2O$ dithiocarbamate compounds have been associated with intense absorptions in the region of 500–520 nm.[4] Such absorptions appear to be characteristic of the Mo—O—Mo linkage and have been suggested to arise from transitions involving an antibonding level of the three centre Mo—O—Mo linkage.[158]

Absorptions around 500 nm, associated with dark colours, appear to correlate generally with M—O—M linear configurations since such absorption bands have been observed for a number of complexes of different metals and attached ligands. Thus the V^{V} complex containing 8-quinolinolato ligands (Q^-), $[Q_2V^{V}O]_2O$, is also reported to have a very dark colour and its solution shows a similar absorption around 550 nm.[159] $\{[Re^{V}O(CN)_4]_2O\}^{4-}$ also has an intense purple colour[152] with an absorption at 540 nm.

The series of iso-structural halide compounds $[M_2OX_{10}]^{n-}$ ($M = Ru^{IV}$, Os^{IV}, Re^{IV}, W^{IV}; X = Cl, Br; $n = 4$) and the mixed valence species $[Re_2OCl_{10}]^{3-}$ having linear MOM arrangements, also display strong charge-transfer bands around 500 nm giving rise to the dark colours of the compounds. The bands have been assigned to $e_u^* \leftarrow e_g$ transitions of the π-electron systems of these MOM linkages.[152] For these ions the transition is in resonance with the symmetric stretching vibration for the MOM unit.

The $[M_3(\mu_3O)(CH_3COO)_6L_3]^+$ complexes of Fe^{III} and Cr^{III} have absorption spectra with general features resembling those of the metal ions in fields approaching octahedral symmetry.[160] Absorption bands are observed, however, which show enhanced intensities that can be linked with the exchange interactions in such molecules which result in their reduced magnetic moments.

4. HETERONUCLEAR OXO-BRIDGED COMPOUNDS

Interest in obtaining heterobinuclear oxygen-bridged compounds to model biologically important systems containing two metal components or the surfaces of heteronuclear oxide catalysts has resulted in the preparation of a variety of such materials in recent years. Since the spread of elements and the types of complexes involved is still relatively small, it is convenient to arrange the discussion by the method of synthesis used for each class of μ-oxo compounds.

4.1 *Bridging by oxo groups as Lewis bases*

An oxo group bound to a metal is normally represented as M=O leaving two lone pairs of electrons associated with oxygen. Holm[5] has recognized that stable M=O groupings are restricted to metals having oxidation states of IV or greater and electron configurations in the range d^0–d^4, i.e. for transition elements in groups 4–8.

Depending on the electron density available on the oxygen atom in (L)M=O compounds, a donor–acceptor reaction could take place with an appropriate electron deficient partner to produce an oxo-bridged product

$$(L)M{=}O + M'(L') \longrightarrow (L)M{=}O \longrightarrow M'(L'). \qquad (17)$$

The two bond distances M—O and M′—O would be expected to differ considerably (M=O < M′ ← O) and the oxidation states of M and M′ would be unaltered.

The extent to which the M=O oxygen can act as a Lewis base will be influenced by the extent of further π-bonding to the metal involving an oxygen electron pair to form an M≡O structure, as envisaged by Ballhausen and Gray[161] in their molecular orbital treatment of bonding in VO^{2+}. They concluded that the remaining oxygen lone pair would occupy an sp_σ type hybrid orbital of largely s character which would thus show little capacity to bond to other Lewis acids.

Nevertheless, a number of heterobinuclear compounds have been obtained, with d^0 M=O systems apparently behaving as Lewis bases (Table 12).

Table 12. The oxo group as a Lewis base

Donor	$\nu_{M=O}$ (cm^{-1})	Acceptor	Complex	ν_{M-O-M} (cm^{-1})	Reference
$Re^{VII}O_3Cl$		$AlCl_3$	$Cl \cdot O_2Re{=}O{-}AlCl_3$	949	162a
		$NbCl_5$	$Cl \cdot O_2Re{=}O{-}NbCl_5$	900	162a
		$SbCl_5$	$Cl \cdot O_2Re{=}O{-}SbCl_5$	890	162a
$Os^{VIII}O_4$		$SbCl_5$	$O_2Os{=}(O{-}Sb{-}Cl_5)_2$	600	162b
$M^{VI}OX(R)_3$	978	$AlCl_3$	$(R)_3ClW{=}O{-}AlCl_3$	952	163b
M = Mo, W	(W = O)	BBr_3	$(R)_3BrW{=}O{-}BBr_3$	978	163b
X = Cl, Br		$GaCl_3$	$(R)_3BrW{=}O{-}GaCl_3$	—	163b
$R = CH_2C(CH_3)_3$		$SnCl_4$	$(R)_3BrW{=}O{-}SnCl_4$	860	163b
		$MgBr_2$	$(R)_3BrW{=}O{-}MgBr_2$	898	163b
		$ZnCl_2$	$(R)_3BrW{=}O{-}ZnCl_2$	915	163b
$(DBAT)Ti^{IV}O$	930	$Ti^{IV}(salen)Cl_2$	$[(L)Ti{=}O{-}Ti(salen)][BPh_4]_2$	775	164
$[(L)Ti{=}O]$		$Fe^{II}(salen)$	$[(L)Ti{=}O{-}Fe(salen)]$	842	164
		$Fe^{III}(salen)Cl$	$[(L)Ti{=}O{-}Fe(salen)]_2[BPh_4]_2$	866	164
		$[Cr^{III}(salen)(H_2O)_2]PF_6$	$[(L)Ti{=}O{-}Cr(salen)][PF_6]$	900	164
		$Cr^{III}(TPP)Cl$	$[(L)Ti{=}O{-}Cr(TPP)Cl]$	906	164
		$Mn^{II}(salen)$	$[(L)Ti{=}O{-}Mn(salen)]$	884	164
		$V^{III}(salen)Cl$	$[(L)Ti{=}O{-}V(salen)Cl]$	896	164
		$Sn(CH_3)_3Cl$	$[(L)Ti{=}O{-}Sn(CH_3)_3Cl]$	913	164
		$Mo(CO)_6$	$[(L)Ti{=}O{-}Mo(CO)_5]$	898	164
$V^{IV}O^{2+}_{aq}$	1000	$[Ru^{II}(NH_3)_5H_2O]^{2+}$	$[(H_2O)_{aq}V{=}O{-}Ru(NH_3)_5]^{4+}$	975	165
$[V^{IV}O(EDTA)]^{2-}$			$[(EDTA)V{=}O{-}Ru(NH_3)_5]$		166
$[V^{IV}O(HEDTA)]^{-}$			$[(HEDTA)V{=}O{-}Ru(NH_3)_5]^{+}$		166
$[V^{IV}O(EDDA)]$			$[(EDDA)V{=}O{-}Ru(NH_3)_5]^{2+}$		166

Direct reaction between the oxyhalide ReO_3Cl or OsO_4 and Lewis acid halides such as $AlCl_3$, $SbCl_5$ or $NbCl_5$ in CCl_4 solution results in the isolation of compounds denoted as μ-oxo compounds[162] (**25**). No structural data is available to confirm these structures but shifts in IR spectral bands due to Re—O stretching frequencies were interpreted as a consequence of Re—O—M bond formation. In the absence of X-ray data the possibility of halide bridging Re—Cl—Al, however, cannot be completely ruled out.

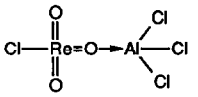

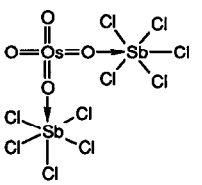

$ClO_2Re{=}O{-}AlCl_3$, $O_2Os(OSbCl_5)_2$ (**25**).

Similar types of complexes have been reported to form between $M(VI)O \cdot X(neopentyl)_3$ (M = Mo, W; X = Cl, Br, OR) and a range of Lewis acids (Table 12), Mo^{IV}—O—M coordination being again indicated by shifts in the M=O stretching frequencies.[163] A number of these compounds are excellent catalysts for olefin metathesis whereas the parent oxo complexes are not.[167] The production of a greater electron deficiency at the metal following coordination of an appropriate Lewis acid is suggested to facilitate reductive ($W^{VI} \rightarrow W^{IV}$) α-elimination processes to form carbenes for reaction with olefins.

A more elaborate study of the stable, dark green product isolated from the reaction between $[Ru(NH_3)_5H_2O]^{2+}$ and VO^{2+} ions in water[165] in the absence of air has been made. It is considered

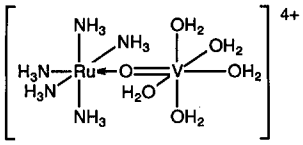

$[(NH_3)_5Ru{-}O{=}V(H_2O)_5]^{4+}$ (**26**).

to be the bridged species $[(NH_3)_5Ru^{II}OV^{IV}(H_2O)_5]^{4+}$ (**26**). A further complex isolated in the presence of SO_4^{2-} ions, was assigned the formula $[(NH_3)_5RuOV(H_2O)_4SO_4]SO_4$. The former complex ion shows a characteristic intense absorption at 378 nm ($\varepsilon = 1.3 \times 10^4$ M^{-1} cm^{-1}) with a weaker band at 625 nm ($\varepsilon \sim 2 \times 10^3$ M^{-1} cm^{-1}) which accounts for the colour of the complex. Similar spectral bands are observed for other $[Ru(NH_3)_5L]^{2+}$ species where L is a π-bonding ligand such as CO. $[Ru(NH_3)_5H_2O]^{2+}$ shows only weak absorptions in its UV–vis spectrum, transitions being Laporte forbidden in such a spin paired d^6 system. The complex does not dissociate when nitrogen is passed through the solution indicating that the strength of the VO → Ru bond is sufficient to resist competition from molecular nitrogen which is known to bind readily to Ru^{II} as $[Ru(NH_3)_5N_2]^{2+}$. This observation allowed a lower limit of 10^7 to be set for the stability constant of the RuOV complex. An IR stretching frequency at 975 cm^{-1} has been assigned to the V=O stretching frequency which in $[VO(H_2O)_n]^{2+}$ has a value[168] of 1000 cm^{-1}. The Ru portion of the complex is oxidized to $[Ru(NH_3)_5OH]^{2+}$ when a solution in water is exposed to oxygen.

The complex might be considered as $Ru^{II}OV^{IV}$ or $Ru^{III}OV^{III}$ depending on whether or not a redox reaction had occurred. The ESR spectrum of the solid compound gave $g = 1.98$, very close to the value for d^1 V^{IV} in $[VO]SO_4$ but with a line width approximately twice that of the vanadyl salt. A more detailed treatment of the ESR spectrum has not subsequently been attempted but this is necessary to resolve the question of localization of the electron.

The same μ-oxo compound can also be formed by reaction between $[Ru^{III}(NH_3)_5Cl]^{2+}$ and V_{aq}^{3+}, but kinetic studies disclosed that a preliminary redox stage occurs involving primarily V^{3+} ions (as $[VO]^+$ or $[V(OH)_2]$) thus:

$$[Ru(NH_3)_5Cl]^{2+} + [VO(H_2O)_x]^+ \longrightarrow [Ru(NH_3)_5H_2O]^{2+} + [VO(H_2O)_x]^{2+} + 2H^+ + Cl^- . \tag{18}$$

The bridge-forming reaction can then take place

$$[Ru(NH_3)_5H_2O]^{2+} + [VO(H_2O)_x]^{2+} \longrightarrow [(NH_3)_5Ru^{II}OV^{IV}(H_2O)_5]^{4+} . \tag{19}$$

Comparison of rate constants and activation parameters for $[Ru^{II}(NH_3)_5H_2O]^{2+}$ reacting by a second-order process with $[VO(H_2O)_x]^{2+}$ and other ligands such as N_2 or pyridine which show similar kinetic characteristics, led to the conclusion that the bridging reaction is essentially an SNI ligand substitution process with H_2O being displaced by VO^{2+} considered as an incoming ligand.

A MO bonding scheme has been proposed[165] for the RuOV system which treats VO^{2+} as similar to dinitrogen. The single unpaired electron expected for the $Ru^{II}OV^{IV}$ formulation is allotted to a non-bonding orbital on vanadium.

The high stability to dissociation of the RuOV system is thus ascribed to Ru···O···V π-bonding with d_{xz} and d_{yz} orbitals of Ru having the correct energies and symmetries to overlap with E-type empty orbitals of VO^{2+}, just as with N_2.

Similar types of $[(NH_3)_5RuOV(L)]^{(4-n)+}$ complexes are formed in solution when $[(NH_3)_5Ru(H_2O)]^{2+}$ reacts with VO^{2+} complexes of EDTA ($n = 4$), HEDTA ($n = 3$) and EDDA ($n = 2$).[166] The compounds each show the distinctive green colour observed for the $RuOV_{aq}$ complex due to charge-transfer bands close to 605 nm (ε = *ca* 1.2×10^4) assigned to $d_{xy}(B_2)Ru \rightarrow \pi^*(E)VO^{2+}$ transitions. They also each possess a further intense band *ca* 390 nm (ε = *ca* 1.2×10^4) similar to the aqua complex, arising from $\pi_b(E)Ru^{2+} \rightarrow \pi_a^*(E)VO^{2+}$ transitions. ESR spectra indicate the presence of V^{IV} in each case. Formation of the complexes is strongly pH dependent in contrast to the formation of the aqua compound, and particular pH ranges have been prescribed for each

complex. All are fully formed, however, at pHs > 4.5. A further distinction from the vanadium aqua complex $[(NH_3)_5RuOV_{aq}]^{4+}$ lies in the fact that each RuOV–polydentate chelate complex will undergo an overall intramolecular electron transfer reaction at low pH leading to the formation of Ru^{III} and V^{III} products. The oxo-bridged complexes, however, can be regenerated from such solutions under pH-jump conditions.[166] The kinetic parameters indicating that this reaction proceeds by an inner sphere reaction, contrast with the Ru^{III} and V^{III}_{aq} reaction which gives the $Ru^{II}OV^{IV}$ complex by an outer sphere redox process.[165] A mechanism involving a hydroxy-bridged intermediate Ru^{III}—OH—V^{III}(L) is suggested.

In the first study that has produced X-ray structural data for donor–acceptor oxo bridging, Yang and Goedken[164] isolated compounds from the reaction of the macrocyclic titanyl complex $Ti^{IV}O$(DBAT) (**27**) with a variety of transition metal compounds in which Ti=O → M linkages

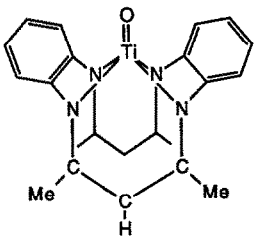

$Ti^{IV}O$(DBAT) (**27**).

were proposed. The empirical formulae of the compounds are given in Table 12, together with IR data purporting to represent asymmetric stretching frequencies for Ti—O—M bonds.

In each of these compounds the TiO group is behaving as a ligand coordinating to the second metal. No oxidation state change has occurred. TiO(TPP) apparently does not react to form such a range of complexes, indicating a smaller Lewis basicity for the oxygen in the metalloporphyrin.[164]

An X-ray structural study of the [(DBAT)TiOFe(salen)]$^+$ cation (**28**) isolated as the $[B(Ph)_4]^-$

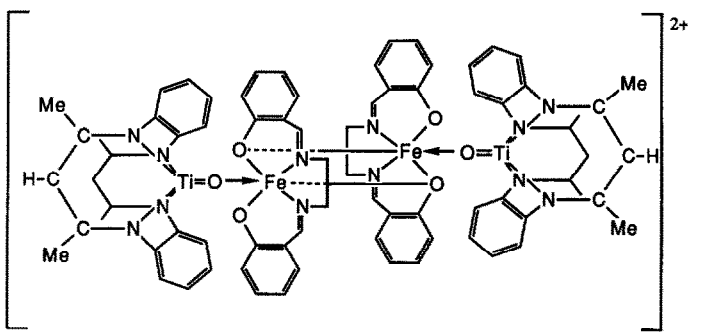

[(DBAT)Ti^{IV}=O—Fe^{III}(salen)]$_2$[BPh_4]$_2$ (**28**).

salt showed it to contain the expected Ti—O—Fe linkage. In addition, the heterobinuclear ion was dimerized by bridging between Fe atoms and salicylaldimine oxygen atoms on two neighbouring [Fe(salen)]$^+$ units. This structural arrangement has also been found for [Fe(salen)Cl]$_2$.[169]

The Ti—O—Fe link is bent (161.6 Å) as are other Ti—O—Ti and Fe—O—Fe systems (Table 1). The Ti—O bond distance (1.701(6) Å) is shorter than is found in homobinuclear Ti—O—Ti systems, in line with considerable residual Ti=O character in the link. The Fe^{III}—O linkage (1.935(6) Å) however, is longer than in [Fe(salen)]$_2$O and other Fe_2O compounds, again in line with the nature of the bonding mode proposed for the complex.

4.2. (μ-O) *Formation by ester elimination*

Silyl acetates have been shown to react[170] with metal alkoxides (M = Ti, Zr, Ta, Fe, V) with elimination of esters and formation of metal alkylsiloxides.

$$M(OR)_m + xR'_3SiO_2CCH_3 \longrightarrow (RO)_{m-x}M{-}(O{-}SiR'_3)_x + xROOCCH_3. \quad (20)$$

Similarly, titanium alkoxides react with titanium carboxylates to eliminate esters forming TiOTi linkages and the application of this reaction has been patented.[171] A related reaction between aluminium alkoxides and zinc acetate has been used by Osgan and Teyssié[172] to produce a complex considered to contain AlOZnOAl linkages. The reaction has been extended to other metal acetates of Cr^{II}, Mn^{II}, Fe^{II}, Co^{II} and Mo^{II}.[173,174]

$$2(RO)_3Al + M(OOCCH_3)_2 \longrightarrow (RO)_2Al{-}O{-}M{-}O{-}Al(OR)_2 + 2ROOCCH_3. \quad (21)$$

The general method reported involves heating a stoichiometric mixture of $Al(OR)_3$ and M^{II} acetate (2:1) in an inert solvent such as decalin at temperatures above 200°C. An alternative process[175] involves controlled hydrolysis of mixed Al—M alkoxides $[(RO)_3Al]_2M(OR)_2$, the so-called Meerwein complexes. This reaction would formally release an alcohol.

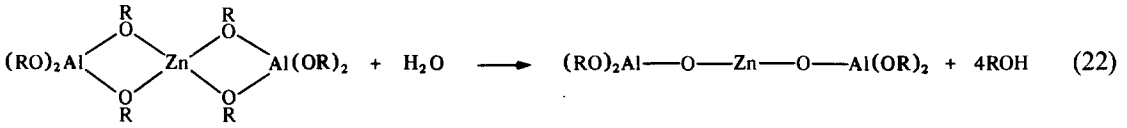

(22)

The "high temperature" synthetic route is said[172] to have other side reactions occurring and complete analytical purity of the products was seldom achieved. Certain of the complexes, notably the $(AlO)_2Zn$ species,[172,176] were found to be soluble catalysts for the polymerization of epoxides,[172] oxiranes[176] and cyclic esters[177] and the preparation and use of a number of these materials have been the subject of patent coverage.[178] The "Osgan–Teyssié" catalysts, however, are reported to be very sensitive to the presence of polar impurities in a reaction mixture and this has retarded their commercial use.[179]

Alkyl–alkoxy aluminium derivatives have been employed[179] to produce $[R_2AlO]_2Zn$ type species which show greater resistance to decomposition. A relatively limited amount of detailed synthetic information, spectroscopic or other data has been reported for the compounds and no structural determination has been made. The existence of Al—O—M bonding is inferred from the stoichiometry of the elimination of esters in the initial formation reactions. The compounds are said to be very soluble in most organic solvents, particularly hydrocarbons, and show degrees of association, measured cryoscopically, varying with the solvent and bulk of the alkoxide group[173,174] (Table 13). The presence of ^{i}Pr and ^{t}Bu groups leads to lower degrees of association, as does use of benzene as solvent. Surprisingly, a number of complexes are reported not to vary their level of association with concentration.[173] This was considered to indicate the existence of thermodynamically stable polynuclear species. The most widely applicable catalysts contain Al and Zn and have been allotted the molecular formula $\{[(RO)_2AlO]_2Zn\}_4$ in benzene solution. The complex of formula $[(^iPrO)_2AlO]_2Mo$ is not associated in benzene.[173] Its proton decoupled ^{13}C NMR spectrum measured in deuterated toluene, however, shows resonances at $\delta = 26.0$ and 28.4 corresponding to two different CH_3 groups, and at $\delta = 63.6$ and 69.2 due to the CH groups. These results have been taken to indicate the presence of bridging alkoxide groups as well as terminal ones, and indicate that association must occur in this solvent though not in benzene. The mass spectra for the compounds show ions corresponding to $M(OAl)_2$ fragments with varying numbers of alkoxide groups attached.

A Mo complex prepared by "thermal condensation" in decalin between equimolar quantities of $[Mo^{II}(CH_3COO)_2]_2$ and $Al(O^iPr)_3$[180] has been subjected to X-ray structural study[181] and found to resemble the parent Mo^{II} acetate. Its formal molecularity may be represented as $(\mu\text{-}OOCCH_3)_2$

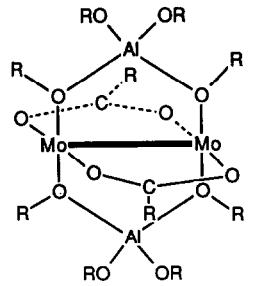

$[Mo(\mu\text{-}CH_3COO)(\mu\text{-}O^iPr)_2Al(O^iPr)_2]_2$ (**29**).

$Mo_2[(\mu\text{-}O^iPr)_2Al(O^iPr)_2]_2$ (**29**). The Mo atoms are metal–metal bonded and bridged by two acetato groups and the oxygen atoms of four alkoxide groups in pairs. There is no single oxo Mo—O—Al linkage. The complex is described as orange in colour whereas the supposed Mo—O—Al products are said to be deep red or green.[173] The orange compound absorbs oxygen irreversibly from the air until a molar ratio Mo/O_2 of 1 is reached. The product generates acetone slowly over a period of some hours.[180]

The green Fe^{II} complexes, $[(RO)_2AlO]_2Fe$, prepared by heating Fe^{II} acetate and $Al(OR)_3$ at 500°C in decalin under argon (R = ^{n}Bu, ^{i}Pr, ^{i}Bu), are reported[182] to react reversibly with molecular oxygen in heptane solution to form the red complexes $\{[(RO)_2AlO]_2Fe\}_2O_2$. The starting compounds are octameric in heptane while the final complexes are monomers. Their empirical formulae were determined by volumetric oxygen uptake and cryoscopic molecular weight measurements. Oxygen can be removed by refluxing in *o*-dichlorobenzene. The oxygen-containing complexes have iron as

Table 13. Oxo bridging by ester elimination—formation of $(RO)_2Al—O—M^{II}—O—Al(OR)_2$ complexes[173]

M[a]	R	Colour	$\bar{\eta}$[b] (solvent)
Fe^{II}	$^iC_3H_7$	Green	1 (A)
			2.1 (B)
	$^nC_4H_9$	Green	2–8[c] (B)
	sec-C_4H_9	Green	1.1 (A)
	$^tC_4H_9$	Green	1.1 (A)
			4 (B)
Co^{II}	$^iC_3H_7$	Violet–red	2 (A)
			3 (B)
	$^nC_4H_9$	Blue	4.1 (A)
			6.2 (B)
Mo^{II}	$^iC_3H_7$	Deep red	1.1 (A)
	$^nC_4H_9$	Deep green	3.0 (B)
Cr^{II}	$^iC_3H_7$	Blue	1.1 (A)
	$^nC_4H_9$	Blue	2.0 (B)
Zn^{II}	$^nC_4H_9$	Yellow	4–8[c] (A)
	sec-C_4H_9	Yellow	4–8[c] (A)

A = benzene; B = cyclohexane.

[a] Other complexes referred to in ref. 173 are said to be based on Ni^{II}, Fe^{III}, Cr^{III} or Ti^{IV} linked to $OAl(OR)_2$ or $OSnR_3$ groups; but no details of their properties are given.

[b] $\bar{\eta}$ = degree of association measured cryoscopically.

[c] Mean degree of association varies with concentration.

Fe^{III}, determined by an EDTA titration, the oxygen presumably being considered to be the peroxo group O_2^{2-}. ESR measurements detecting the presence of Fe^{III} at 298 K ($g = 2.3$) were also made in order to prove that the oxygen reaction is fully reversible. The overall reaction is represented as

$$\frac{2}{n}\{[(RO)_2AlO]_2Fe^{II}\}_n + O_2 \underset{450\ K}{\overset{298\ K}{\rightleftharpoons}} \begin{array}{c}(RO)_2AlOFe^{III}OAl(OR)_2\\ |\\ O\\ |\\ O\\ |\\ (RO)_2AlOFe^{III}OAl(OR)_2\end{array} \tag{23}$$

The ESR signal of the solid "peroxo" complex changed little in intensity over the temperature range 77–320 K and the authors suggest this indicates ferromagnetic behaviour.

The reaction is extremely interesting since reversible oxygen carriage by Fe^{II} species other than "blocked" porphyrins is relatively rare. Further studies have not been reported on these complexes but they would repay re-investigation, with attention being given to their magnetic behaviour. Neither magnetic nor visible spectra data have been reported for the Fe, Co or Cr compounds as initially synthesized and nothing can be said with certainty about their oxidation states or stereochemistries.

The high temperature conditions said to be necessary to prepare the complexes and the occurrence of other unspecified side reactions do not appear conducive to obtaining pure compounds. However, the reaction forming a M—O—M′ linkage appears attractive as a synthetic route and would repay further study, particularly if the elimination of an ester can be accomplished between single entities.

$$(Lig)M—OR + (Lig')M'—OOCR' \quad (Lig)M—O—M'(Lig') + R\cdot OOCCR'. \tag{24}$$

4.3 *Inner sphere electron transfer formation of* (μ-O) *links*

Just as homobinuclear μ-oxo compounds can be formed by redox reactions of the comproportionation type, so too should heterobinuclear μ-oxo species. The conditions necessary to form such compounds call for an oxo group, coordinated to one metal ($A^x{=}O$), to be capable of forming an "inner sphere" oxo-bridged complex with a second metal (B^y) across which an electron can transfer.

$$(L)A^xO + B^y(L') \longrightarrow (L)A^x{=}O{-}{-}{-}B^y(L') \longrightarrow (L)A^{x-1}—O—B^{y+1}(L'). \tag{25}$$
$$\qquad\qquad\qquad

It contains two haem-Fe and two Cu centres and its function appears to require an initial reaction of dioxygen with an Fe–Cu pair.[183] The pair of haem and Cu sites has been found to show strong antiferromagnetic coupling when the enzyme is fully oxidized or in its "resting state" and this led to the suggestion that an Fe—X—Cu bridge can be established where X is an oxo group.[184] Homobinuclear μ-oxo complexes are generally found to show such magnetic coupling and this property could also be expected for a heterobinuclear Fe—Cu bridged intermediate. The magnitude of exchange coupling has been estimated to be large ($-J > 200\ cm^{-1}$) with an $S = 2$ ground state.[186] However, other small molecules or ions such as the imidazolato[185a] or mercapto[185b] have been suggested as bridging units.

Initial attempts[187] to mimic the structural requirements which cause the strong coupling in the oxidase were made by appending "strapping" groups from the porphyrin ring system which coordinates Fe^{III}, while Cu^{II} was held in the "strap". Any oxygen in a bridging mode was anticipated to arise, "serendipitously". Antiferromagnetic coupling, however, was small and in no case was it possible to determine clearly whether O^{2-} or another ligand accepted the bridging site.[187] A further attempt by Chang *et al.*[188] involved a porphyrin for coordinating Fe, to which was attached a thiazole sulphide "strap" linked via pyrrole rings intended to provide a more flexible coordination site for a Cu^{II} ion. Flexibility in coordination stereochemistry was considered important for Cu^{II} so that appropriate orbitals could align with those of Fe to allow magnetic coupling.[187,188] The product had an analytical composition corresponding to $FeCu(P)(O)(H_2O)(CH_3COO)L$. The compound appeared stable to solution in CH_2Cl_2 and recovery by evaporation. An IR spectral band at 880 cm^{-1} was assigned to be a M—O—M′ asymmetric stretching vibration. The magnetic susceptibility versus temperature data down to *ca* 4 K could be fitted to a simplified Van Vleck equation assuming interaction between a high spin Fe^{III} ($S = 5/2$) ion and a Cu^{II} ($S = 1/2$). The two states ($S = 2, 3$) resulting from this coupling are separated by $-3J = 132 \pm 5\ cm^{-1}$, a relatively small value compared with the coupling measured in the oxidase.

Wilson and co-workers[189] attempted a more fundamental redox reaction to form an Fe^{III}—O—Cu^{II} bridge by reacting $Fe^{IV}O(TPP)$ [formed at $-78°C$ in pyridine by reaction of oxygen with $Fe^{II}(TPP)$] with a pentadentate Cu^{I} complex—known to bind molecular oxygen reversibly in solution although not form an oxo-bridged Cu^{II} species. The reaction was expected to be

$$Fe^{IV}O(TPP) + Cu^{I}(Lig)^{+} \longrightarrow [(TPP)Fe^{III}—O—Cu^{II}(Lig)]^{+}. \quad (27)$$

The product (**30**) was isolated as a $[BF_4]^-$ salt. Preparation of the ^{18}O labelled complex by using

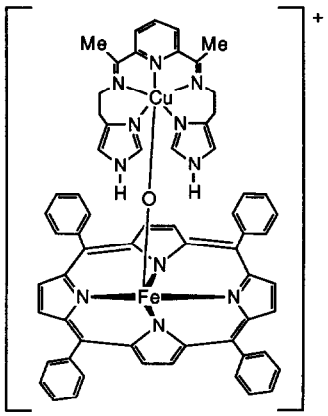

$[(TPP)Fe^{III}(\mu\text{-}O)Cu^{II}(Lig)]^{+}$ (**30**).

$Fe^{IV}{}^{18}O(TPP)$ showed that IR bands previously observed at 890.2 and 872.8 cm^{-1} in the [Fe^{III}—^{16}O—Cu^{II}] product and assigned to the asymmetric stretching mode were missing in the ^{18}O labelled complex, and a new peak at 880.5 cm^{-1} had appeared. The complementary band expected was possibly not distinguishable because of other ligand absorptions in the region where it would be expected to appear, although increased absorbance was noted in the area around 847.7 cm^{-1}. These results supported the existence of an Fe—O—Cu structure for the complex.

The magnetic susceptibility of the complex showed a decrease from $\mu_{eff} = 4.23$ at 298 K to 3.95 at 10 K. The complex was ESR silent at 10 K. The Mössbauer spectrum consisted of a doublet having $\delta(Fe^{\circ}) = 0.23$ mm s^{-1} and $\Delta E_Q = 2.06$ mm s^{-1} at 136 K. The authors considered these results to indicate strong antiferromagnetic coupling, however, but the $S = 1$ ground state resulting differed from the $S = 2$ state of the natural cytochrome *c* oxidase.

Other Fe–porphyrin–Cu complexes incorporating imidazolate[190] or sulphur[191] bridging have failed to produce complexes showing the strong antiferromagnetic coupling of the natural product and, although further examples of well authenticated Fe—O—Cu type systems have not been reported, oxo bridging as the coupling mode in the enzyme still appears plausible.

$Cr^{IV}O(P)$ *as an oxidant.* The direct synthesis of a series of heterobinuclear μ-oxo complexes having Cr^{III} as one component in the bridge has been accomplished using $Cr^{IV}O$ porphyrin complexes as oxidants and a variety of Fe^{II},[192] Mn^{II},[193] $Mo^{IV}O$[194,195] or $V^{IV}O$[196] complexes as reductants.

$Cr^{III}OFe^{III}$ *compounds.* Reaction occurs rapidly at room temperature in toluene or THF solution between $Cr^{IV}O(P)$ and various Fe^{II} complexes in the absence of moisture and oxygen. The range of donor atom sets in the Fe complexes studied has been N_4, O_2N_2, S_2N_2, O_2N_3, $(S_2)_2$ (Table 14).

Table 14. Magnetic moments per molecule of M—O—M′ compounds with electron configurations M d^m, M′ d^n

Compound ($d^m \cdot d^n$)	μ_s (calc.)	Magnetic moments (μ_B) μ_{eff}(300 K)	μ_{eff}(4.2 K)	Reference
$d^3 \cdot d^5$	7.07			
(TPP)CrOFe(TPP)		3.12	1.90	192b
(TTP)CrOFe(TPP)		3.05	1.99	192b
(TFP)CrOFe(TPP)		3.17	2.01	192b
(TPP)CrOFe(TMP)		3.34	2.33	192b
(TMP)CrOFe(TPP)		3.26		192b
(TXP)CrOFe(TPP)		3.13		192b
(TPP)CrOFe(TCP)		3.35		192b
(TPP)CrOFe(salen)		3.3		193
(TPP)CrOFe(salphen)		3.4		193
(TPP)CrOFe(tsalen)		3.8		193
(TPP)CrOFe(salah)		3.4		193
(TPP)CrOFe(salmah)		3.2	2.5	193, 203
(1-MeIm)(TPP)CrOFe(salmah)		3.2	2.6	193, 203
(TPP)CrOFe(Et_2dtc)$_2$		4.3	2.3	193, 203
(TPP)CrOFe(Pyrdtc)$_2$		4.4	2.5	193, 203
$d^3 \cdot d^4$	6.24			
(TPP)CrOMn(salah)		5.3	3.9	193
(TPP)CrOMn(salmah)		5.3		193
$d^3 \cdot d^1$	4.24			
(TPP)CrOMo(O)(Et_2dtc)$_2$		3.8	3.4	195, 203
(TPP)CrOMo(O)(Pyrdtc)$_2$		4.2		195
(TPP)CrOMo(N-*p*-tol)(Pyrdtc)$_2$		3.8	2.7	195, 203
$d^3 \cdot d^0$	3.87			
(TPP)CrOV(O)(Q)$_2$		3.8	3.7	196
(TPP)CrOV(O)(acac)$_2$		3.6		196
$d^5 \cdot d^1$	6.16			
(salen)FeOMo(O)(Et_2dtc)$_2$		5.3		193
(salmah)FeOMo(O)(Et_2dtc)$_2$		5.3		193
$d^4 \cdot d^1$	5.2			
(Et_2dtc)$_2$MnOMo(O)(Et_2dtc)$_2$		5.2		193

$$Cr^{IV}O(P) + Fe^{II}(Lig) \longrightarrow (P)Cr^{III}—O—Fe^{III}(Lig). \quad (28)$$

Only one X-ray diffraction study and that of limited accuracy has been made so far[192b] on any of these compounds, because of difficulties in obtaining adequate crystals. This study of the mixed porphyrin complex (py)(TPP)CrOFe(TMP), which also had a pyridine molecule coordinated to Cr, was of lower accuracy than necessary to define bond distances with high accuracy ($R = 0.149$) because of the presence of unresolved extraneous solvent. However, the essential structural features of the molecule have been indicated (**31**), the Cr and Fe centres being identifiable by the nature of

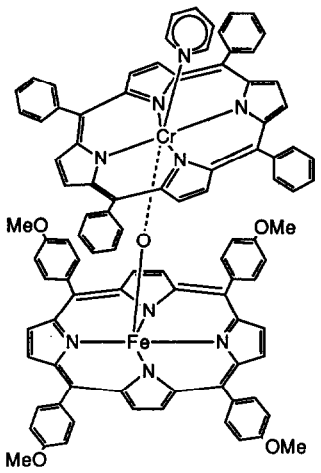

(py)(TPP)Cr^{III}(μ-O)Fe^{III}(TMP) (**31**).

the *meso*-aryl substances attached to them. The CrOFe linkage is essentially linear (178(2)°) while the two rings are rotated by 32(1)° with respect to each other in order to accommodate the sets of aryl rings.

The three CrOCr compounds that have been structurally characterized each have linear Cr_2O units (Table 1) while $[(TPP)Fe]_2O$ also has an almost linear Fe_2O arrangement. The flexible nature of FeOFe linkage systems and their angular dependence primarily upon interligand repulsions coupled with the predicted preferred linear arrangement of $d^3 \cdot d^3$ Cr_2O systems (see Section 1) suggests that in these mixed complexes the CrOFe array will normally be close to linear even when Fe^{III} is not coordinated by a porphyrin or similarly bulky ligand.

The complexes are generally stable in solution in toluene or $CHCl_3$ in the absence of moisture or air. In the presence of oxygen $Cr^{IV}O(P)$ can be detected spectroscopically together with the appropriate $(Lig)Fe^{III}OFe^{III}(Lig)$, indicating that some disproportionation must occur

$$(P)Cr^{III}OFe^{III}(Lig) \longrightarrow Cr^{IV}O(P) + Fe^{II}(Lig) \quad (29)$$

allowing further reaction with oxygen to take place.

$$4Fe^{II}(Lig) + O_2 \longrightarrow 2(Lig)FeOFe(Lig). \quad (30)$$

Water also slowly attacks the compounds leading to formation of the species defined as "$Cr^{III}(P)$" hydroxo complexes, whilst Fe_2O complexes can generally be isolated from such mixtures.[123]

The phthalocyanine complex (TPP)CrOFe(Pc) also gives CrO(P) and $[(Pc)Fe]_2O$ when exposed to air in toluene.[192b] However, a different behaviour is observed when the heteronuclear oxo complex is allowed to react with oxygen in pyridine solution. $Fe(Pc)(py)_2$ and the pyridine adduct of $[(TPP)Cr]_2O$ were initially detected by their visible spectra and the CrOCr compound slowly converted to $(py)Cr^{IV}O(TPP)$ with time.

Ercolani *et al.*[197] have shown that $[Fe(Pc)]_2O$ is converted to $Fe(Pc)(py)_2$ in the presence of excess pyridine and $[(P)Cr]_2O$ may be formed from a comparable reaction with (TPP)CrOFe(Pc), giving both $Cr^{II}(TPP)py_2$ and $Fe^{II}(Pc)(py)_2$. $Cr^{II}(TPP)$ is known to react with oxygen more slowly in pyridine than toluene,[123] thus allowing the intermediate CrOCr complex to be detected.

A number of complexes can be isolated[192b,193] containing a mole of water when recrystallized in the presence of moist air, although solutions left exposed for some hours will show decomposition. IR spectral evidence was not always found for the presence of the molecule, although microanalytical data appeared to indicate its presence. In view of the crystallographic identification of pyridine coordinated to Cr in (py)(TPP)CrOFe(TMP) and the spectroscopic evidence for various donors coordinating to other CrOFe species (see below), the formulae of a number of the compounds have been reported as having water coordinated to the Cr ion.

Visible spectra: the complexes with porphyrin ligands coordinated to both Cr and Fe[192] show only one major Soret absorption band in the 422–427 nm region with log ε values ranging from 4.96 to 5.36 in benzene. Two less intense bands occur near 560 and 600 nm. This pattern is found even though dissimilar porphyrins are coordinated to each metal.

A point of inflection near 400 nm occurs in each spectrum. Chromium(II) and Fe^{II} homonuclear oxo complexes have Soret bands at 412 and 407 nm, respectively, while Cr^{III}(P)Cl shows its major absorption at 447 nm and Fe^{III}(P)Cl at 417 nm. The single Soret bands observed in the heterobinuclear oxo complexes presumably represent envelopes for transitions involving both Cr(P) and Fe(P′) species. The single (P)CrOFe(Pc) complex reported shows bands that could be associated with each segment of the molecule, a Soret type band at 431 nm and a "phthalocyanine" major peak at 699 nm. Complexes with the Fe–salicylaldimines and –dithiocarbamate[193] ligands have spectra dominated by the Cr^{III} porphyrin segments (Cr(TPP) in the complexes reported) showing a Soret band at *ca* 437 nm with the corresponding two further peaks at *ca* 560 and 600 nm. The Soret bands are more symmetrical than those for the mixed Fe/Cr prophyrin derivatives.

The UV–vis spectra of all these complexes vary in the presence of Lewis bases, indicating further coordination can occur.[192–194] The structural identification of (py)(TPP)CrOFe(TMP) which was obtained from a toluene–pyridine solution with excess pyridine present, points to coordination of bases being more favourable at Cr^{III} than Fe^{III} in those heteronuclear oxo complexes. Indeed, neither $[Fe(TPP)]_2O$[198] nor $[Fe(salen)]_2O$[30b] appear able to coordinate Lewis bases.

Measurements of equilibrium exchange constants have been made by a standard spectroscopic technique[195] for the reaction of several nitrogenous Lewis bases with the complex (THF)(TPP) CrOFe(salmah) in THF solution (Table 15) (**32**). The Fe complex being six-coordinate, any

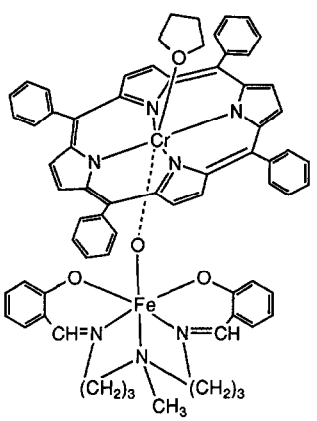

(THF)(TPP)Cr^{III}(μ-O)Fe^{III}(salmah) (**32**).

base coordination process is expected to occur at the Cr^{III} centre.

$$\text{(THF)(TPP)CrOFe(salmah)} + \text{B} \rightleftharpoons \text{(B)(TPP)CrOFe(salmah)} + \text{THF}. \qquad (31)$$

Highly hindered Lewis bases such as 2- and 2,6-substituted pyridines fail to show evidence for coordination even when in very large excess (B/Cr, 10^4), while the ability of other bases to coordinate increases with basic strength of the amine just as has been observed for reactions of such bases with Cr(TPP)Cl.[199] The heterocyclic base 1-methylimidazole was also found to bind more strongly than

Table 15. The binding of Lewis bases to (TPP)CrOFe (salmah) at 25°C[196]

Base	Log K ($\pm$0.1)
	Solvent: THF
py	2.3
4-pic	2.6
3,5-lut	2.7
1Me-Im	4.5
sec-$BuMH_2$	3.4
pip	3.2
H_2O	1.8
	Solvent: toluene
THF	2.2
py	4.8

py = pyridine; 4-pic = 4-picoline; 3,5-lut = 3,5-lutidine; 1Me-Im = 1-methyl-imidazole; pip = piperidine; THF = tetrahydrofuran.

would be indicated by its pK_a value. Significant ligand → metal π-bonding has been suggested to account for this anomaly.[199]

The complex (H_2O)(TPP)CrOFe(salmah) was used in the studies and comparisons of its spectra in pure toluene and in toluene–THF mixtures indicated that at the concentrations used (10^{-5}–10^{-6} M), water had either completely dissociated (in toluene) or been displaced by THF. The addition of further high concentrations of water to such THF solutions allowed a determination of the log K value for the H_2O–THF exchange (Table 15).

However, a second slow reaction occurs in aq. THF which could be followed by observing the growth of a new intense band at 448 nm due to the formation of the imperfectly characterized Cr(TPP) "hydroxy species".[123]

Measurements in toluene for the reaction

$$\text{(TPP)CrOFe(salmah)} + \text{B} \rightleftharpoons \text{B(TPP)CrOFe(salmah)} \qquad (32)$$

showed that the affinities of Cr^{III} for the THF and pyridine are similar to those of the metal in Cr(TPP)Cl. The log K value for the addition of 1-methylimidazole in toluene was too large to be measured by the spectroscopic technique employed, but it could be estimated as log $K = 6.6$ from the sum of the 1-MeIm–THF exchange constant (log $K = 4.4$) and the THF binding constant in toluene (2.2). Attempts to obtain a measure of the binding of water to (TPP)CrOFe(salmah) in toluene were hampered by the hydrolysis reaction. An approximate value can be estimated from the log K values for the H_2O–THF exchange reaction and the THF binding constant viz. log $K_{H_2O} = 4.0$.

The spectral changes upon addition of pyridine to THF solutions of (THF)(TPP) CrOFe(Pyrdtc)$_2$ and (THF)(TPP)CrOMn(salah) are consistent with coordination only to Cr^{III}. The values of log K only differ slightly from that for pyridine coordinating to (TPP)CrOFe(salmah).

IR spectra: bands attributable to CrOFe stretching frequencies have been reported for (P)CrOFe(P′) complexes in the region of 845 cm^{-1} and assigned to an asymmetric CrOFe stretching vibration (Table 14). The identification of the band at 842.5 cm^{-1} in (TPP)CrOFe(TPP) was supported by ^{18}O labelling experiments.[192b] A variety of ligand bands in the 800–900 cm^{-1} region have made it impossible to detect comparable frequencies in the Fe(Pc) and other Fe(Lig) systems.

^1H *NMR spectra*:[192b] the various types of protons associated with each of the porphyrins coordinated to either Cr or Fe can be detected in the ^1H NMR spectra of the paramagnetic (P)CrOFe(P′) complexes. The relatively sharply defined resonances for each type of proton in the Fe–porphyrin moiety occur at positions very close to those recorded for the homonuclear complexes (P′)

FeOFe(P′)[200] though with some minor variations in the breadth of peaks. Similarly, other broad resonance peaks allocated to composites of *meso*-phenyl protons can be observed at positions very close to those for porphyrin protons in Cr(P)Cl complexes. Resonances due to pyrrole β-hydrogens cannot be detected in these latter molecules but they are believed to contribute a broad resonance appearing at *ca* 40 ppm in the oxo complex. The similarities in the chemical shifts between the Fe_2O and CrOFe species imply that the effective electron spin at the Fe atoms in both types of complexes is the result of similar strong magnetic coupling. The paramagnetic shifts for uncoupled ($S = 5/2$) Fe^{III} porphyrin complexes such as Fe(P)Cl species are much larger because of dipolar and contact contributions.

Mössbauer spectra: zero field Mössbauer spectra of the CrOFe complexes (except for (TPP) $CrOFe(Et_2dtc)_2$) show single quadrupole split doublets at each temperature examined. Isomer shift and quadrupole splitting parameters are presented in Table 16 together with data for some homobinuclear Fe_2O compounds and other Fe^{II} and Fe^{III} complexes for comparison.

The data are consistent with the Fe^{III} centres being high-spin ($S = 5/2$). The spectra of the compounds like other Fe_2O species do not show the magnetic broadening at 77 K observed for mononuclear Fe^{III} ($S = 5/2$) complexes. This has been ascribed[192b] to rapid spin relaxation within the $S' = 1$ state of the CrOFe compounds, leading to a predicted broadening at higher temperatures where some excited states may be occupied. Iron(III) oxo complexes with tetradentate ligands attached and an overall five-coordinate array about Fe^{III} generally have quadrupole splitting values less than 1 mm s^{-1}. The larger value found for the salmah complex[201e] where Fe has six-fold coordination suggests a larger electronic field gradient for the compound. Similar values of ΔE have been observed for other six-coordinate ($S = 5/2$) Fe^{III} oxo complexes $[enH_2][\{Fe(HEDTA)\}_2O]$[201c] and $[Fe(salen)(Im)_2]PF_6$.[201d] Detailed Mössbauer or magnetic measurements are not available for $[Fe(salmah)]_2O$. By contrast, the complex having a five-coordinate, presumably square pyramidal array about Fe^{III}, (TPP)CrOFe(salen), shows similar values of δ and ΔE to those in $[Fe(salen)_2]_2O$.

Table 16. Mössbauer spectral parameters for CrOFe complexes and related Fe derivatives

Complexes	T(K)	δ[a] (mm s^{-1})	ΔE (mm s^{-1})	Reference
(TPP)CrOFe(TPP)	4.2	0.49	0.82	192
	77	0.51	0.85	
	295	0.39	0.84	
(TPP)CrOFe(TMP)	77	0.50	1.11	192
(TPP)CrOFe(TPP)	77	0.50	1.11	192
(TPP)CrOFe(salmah)	4.2	0.56	1.83	195
(TPP)CrOFe(salen)	77	0.44	0.84	195
(TPP)CrOFe(Pyrdtc)$_2$	77	0.47	2.04	195
(TPP)CrOFe(Et$_2$dtc)$_2$	77	0.48 (44%)	1.86	195
		0.49 (42%)	0.66	
	4	0.48 (64%)	1.87	
		0.45 (36%)	0.75	
(TPP)FeOFe(TPP)	77	0.40	0.66	201a
	4.2	0.28	0.02	
(salen)FeOFe(salen)	77	0.46	0.78	201b
$enH_2[(Fe(HEDTA))_2O]\cdot 6H_2O$	77	0.48	1.75	201c
	295	0.37	1.69	
$[Fe(salen)(Im)_2][PF_6]$	300	0.44	1.41	201d
$[Fe(salah)(2Me\text{-}Im)_2][BPh_4]$	78	0.28	2.72	201e
	298	0.32	1.00	
$[Fe(Et_2dtc)_2]X$	77	0.48	2.5–2.9	201f
$[Fe(Et_2dtc)_2]X\cdot THF$	300	0.34	0.72	201g
$Fe(Et_2dtc)_3$	77	0.46	0.55	201h
$Fe(Et_2dtc)_2$	77	0.87	4.19	201i

[a] Measured relative to α-Fe at room temperature.

The complexes containing dithiocarbamate groups show different features to the other heterobinuclear complexes. The pyrrolidyl complex shows a large quadrupole splitting, the value being close to the range typically observed by five-coordinate $Fe(dtc)_2X$ (X = halide) compounds.[201b] Iron has a spin quartet ground state in such complexes. Homobinuclear oxo-bridged Fe–dithiocarbamates have not so far been described. The diethyldithiocarbamate compound obtained exhibits two quadrupole doublets indicating two inequivalent iron sites. The relative intensities of the quadrupole pairs varied with temperature (T) and with different preparations of the complex despite the samples showing excellent microanalytical data. The inner pair reduces in intensity by comparison with the outer as T is lowered. The isomer shifts of the doublets are in the region generally associated with Fe^{III} dithiocarbamate derivatives.[201h] The large ΔE observed for the main (outer) quadrupole pair is similar to that for the pyrrolidyl species and other five-coordinate $Fe(dtc)_2X$[201b] compounds, while the smaller quadrupole splitting of the inner doublet corresponds to a value in the range normally found for neutral six-coordinate $Fe(dtc)_3$ compounds.[201b] However, the variation of the relative intensities of the Mössbauer peaks with temperature and the constancy of microanalytical data indicates the phenomenon is not due to $Fe(dtc)_3$ impurity. "Spin-crossover" effects can be eliminated as a cause for two species since complexes showing magnetic spin equilibria show only one Mössbauer doublet,[201h] the "cross-over rate" being shorter than the lifetime of the ^{57}Fe excited state. A peak due to the presence of a small amount of THF in the mass spectrum of $(TPP)CrOFe(Et_2dtc)_2$ suggests that the explanation is due to the occurrence of small amounts of the THF adduct $(TPP)CrOFe(Et_2dtc)_2THF$ which causes Fe to achieve six-coordination. Some $Fe(Et_2dtc)_2X \cdot THF$, incorporated in the main product $Fe(Et_2dtc)_2X$ when the parent complex is recrystallized from THF, has also been found to give rise to two doublets in the Mössbauer spectrum of the latter complex.[201g] The inner doublet has a small quadrupole splitting similar to those found with six-coordinate Fe–dtc compounds. Because of the large molecular weight of the heteronuclear complex, amounts of THF considerably less than 1 mole per mole of complex would not readily be detected by microanalysis.

Magnetic susceptibilities: at room temperature, $Cr^{III}OFe^{III}$ heterobinuclear μ-oxo complexes show magnetic moments considerably reduced below the values expected for molecules containing uncoupled $S = 3/2$ 5/2 centres (Table 14). The variation of magnetic moment and susceptibility with temperature has been studied for a number of compounds from 300 to 4 K at which temperature μ_{eff} has decreased to values of the order of 2.8 BM. This behaviour is consistent with the presence of moderately strong antiferromagnetic coupling in all the complexes studied.

A simple Heisenberg–Van Vleck isotropic coupling model leading to the expression

$$\chi'_m = \frac{N\beta^2 g^2}{kT} \frac{2\exp(-9x)+10\exp(-7x)+28\exp(-4x)+60}{3\exp(-9x)+5\exp(-7x)+7\exp(-4x)+9}$$

with $\chi = J/kT$, was found to adequately reproduce the experimental data above 25 K for the porphyrin complexes (P)CrOFe(P').[192b] It leads to an $S' = 1$ ground state for the complexes with $J = ca. -150\ cm^{-1}$ (Table 17). A sharp decrease in μ_{eff} below 25 K, however, was observed for each of the complexes studied whether with Fe(P), Fe(salmah)[203] or $Fe(Et_2dtc)_2$[203] moieties, which could not be accommodated by this treatment. Such sharp decreases in μ_{eff} at low temperatures have also been observed in other heteronuclear systems with a variety of bridging ligands including

Table 17. Magnetic coupling parameters for (P)CrOFe(L) compounds

Complex	$-J$ (cm^{-1})	D_{Fe} (cm^{-1})	D_{Cr} (cm^{-1})	g_{Fe}	g_{Cr}	R (%)	Reference
(TPP)CrOFe(TPP)	150	4.9	−1	2.01	1.95	1.21	192b
(TTP)CrOFe(TPP)	146	4.0	−1	1.98	1.98	0.65	192b
(TFP)CrOFe(TPP)	143	4.4	−1	2.01	2.01	0.70	192b
(TPP)CrOFe(TMP)	137	3.8	−1	2.05	1.90	1.05	192b
(H_2O)(TPP)CrOFe(salmah)	116	1.62	−1	1.95	2.00	1.10	202
(1-Me-Im)(TPP)CrOFe(salmah)	118	1.57	−1	2.00	2.00	1.07	202

M(X, Y)M′ dibridged species contained in compartmental ligands.[202] The effect has been explained either by assuming superposition of weak interdimeric antiferromagnetic coupling or zero field splitting, or both effects acting simultaneously.

The experimental data for CrOFe compounds containing Cr^{III}(P) moieties linked to various Fe(L) systems have been found to be fitted by the Hamiltonian

$$\mathscr{H} = -2J\hat{S}_1\hat{S}_2 + D_1(\hat{S}_{1z}^2 - 1/3S_1^2) + D_2(\hat{S}_{2z}^2 - 1/3S_2^2) + g_1\beta\hat{H}\hat{S}_1 + g_2\beta\hat{H}\hat{S}_2$$

which includes single zero field splitting terms for each metal (Fe^{III} being taken as having $S = 5/2$ and Cr^{III}, $S = 3/2$). The parameters obtained for the compounds are shown in Table 17. The magnitude of the coupling constant J is notably larger for the (P)CrOFe(P′) complexes than the (P)CrOFe(salmah) complexes, the only non-porphyrin derivatives so far studied.[203] The two axial ligands coordinated to Cr^{III} and completing six-fold coordination for that element in the (P)CrOFe(salmah) compounds appear to have little influence on J values.

$Cr^{III}OM$ *compounds* (M = Mn^{III}, $V^{V}O$, $Mo^{VI}O$)

The pentadentate complex Mn^{II}(salah) is reported to react with oxygen to give first, peroxo-bridged complexes (salah)MnO—OMn(salah), which can then react further in an unknown manner with excess oxygen.[204]

$Cr^{IV}O$(TPP) reacts with both Mn^{II}(salah) and Mn^{II}(salmah) to give products characterized as μ-oxo species,[193] analogous to the Fe compounds (Table 14). The visible spectra of the compounds are again dominated by the porphyrin contribution. A clear IR spectral identification of a CrOMn asymmetric stretching frequency could not be made.

The room temperature magnetic moments of the proposed $CrOMn^{III}$ complexes are reduced from the spin-only values expected for an $S = 3/2$, $S = 2$ system (Table 14). The considerable decrease of the Mn(salah) complex value with temperature is indicative of antiferromagnetic coupling between the metal centres. Attempts to fit a simple Heisenberg–Van Vleck coupling model for an $S = 3/2$, $S = 2$ dimer to the data have only been successful if the g value is assumed less than 1.9.[195] However, theoretical considerations suggest g should be in the range 1.9–2.0.

The V^{IV} quinolinol complex $V^{IV}O(Q)_2py$, which has been shown to give the homobinuclear oxo-bridged complex $[(Q)_2V^{V}O]_2O$ upon reaction with oxygen,[205,9] has been found to react with $Cr^{IV}O$(TPP), giving a complex characterized as the oxo-bridged species (py)(TPP)Cr^{III} $OV^{V}(O)(Q)_2$[195] (**33**). Since the V atom has a coordination number of six, the pyridine molecule will be attached to Cr.

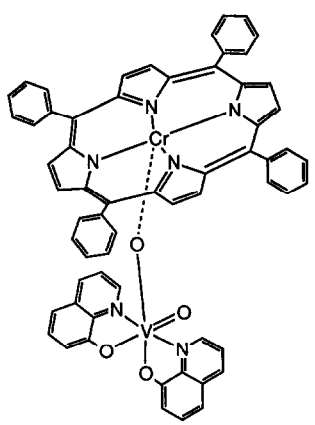

(TPP)$Cr^{III}(\mu$-O)V^{V}(O)$(Q)_2$ (**33**).

CrO(TPP) also reacts with $V^{IV}O(acac)_2$ to yield a similar oxo-bridged complex formulated as (TPP)$Cr^{III}OV^{V}$(O)$(acac)_2$[196] although the parent V^{IV} complex is inactive towards molecular oxygen. The ESR spectra of both the presumed oxo-bridged complexes in frozen CH_3CN–DMF solutions under N_2 display weak, broad bands at *ca* $g = 4.4$ arising from the d^3 Cr^{III} metal centre. There is

complete absence of a strong signal at *ca* $g = 2.0$ which would indicate a V^{IV}, d^1 centre. This confirms that a redox reaction has occurred and supports the allocation of μ-oxo structure. The magnetic moments of the complexes at 293 K are both *ca* 3.83 BM as expected for a spin-free Cr^{III}–V^{V} d^3–d^0 system. The quinolinato complex showed Curie–Weiss behaviour over the entire range 300–4.2 K.

The complexes display medium intensity IR bands at *ca* 940 cm^{-1} which are assigned to the stretching frequencies of terminal V—O_t groups.[110,205] Strong bands at *ca* 850 cm^{-1} in each complex are assigned to asymmetric CrOV vibrations. ^{18}O Labelling of the bridging O, by use of $Cr^{18}O(TPP)$ to prepare $(TPP)Cr^{18}OV(O)(acac)_2$, resulted in a greatly reduced intensity of the band at 850 cm^{-1}, but porphyrin ligand absorptions in the 800–700 cm^{-1} region prevented clear recognition of the $Cr^{18}OV$ frequency.[195] Increased absorption was observed, however, in the region near 800 cm^{-1}.

Just as $Mo^{IV}O(dtc)_2$ derivatives have been shown to react with $Mo^{VI}(O)_2(dtc)_2$ to form homonuclear oxo-bridged complexes,[117b] $Mo^{IV}O(Et_2dtc)_2$ and $Mo^{IV}O(Pyrdtc)_2$ correspondingly react with $Cr^{IV}O(TPP)$ to form complexes believed to contain $Cr^{III}OMo^{V}$ linkages.[194,195] Thus

$$Cr^{IV}O(TPP) + Mo^{IV}O(Et_2dtc)_2 \longrightarrow (TPP)Cr^{III}OMo^{V}O(Et_2dtc)_2. \quad (33)$$

This same complex can also be formed by a Cr^{II}–Mo^{VI} reaction[195]

$$Cr^{II}(TPP) + Mo^{VI}(O)_2(Et_2dtc)_2 \longrightarrow (TPP)Cr^{III}OMo^{V}(Et_2dtc)_2. \quad (34)$$

The compounds are purple in colour, dissolving to give red–green solutions in most polar organic solvents. The imido complex $Mo^{IV}(N—p\text{-tol})(Pyrdtc)_2$[206] also reacts to give a compound assigned a μ-oxo configuration (TPP)Cr—O—Mo(N—*p*-tol)(Pyrdtc)$_2$. A homobinuclear μ-oxo complex, $[(dtc)_2Mo(N—p\text{-tol})]_2O$, has been formed[206] by reaction of $Mo^{VI}(O)(N—p\text{-tol})(Et_2dtc)_2$ with the Mo^{IV} imido derivative and an oxo bridge, rather than imido bridge formulation assigned on the grounds that the final complex did not show an IR band in the region expected for terminal Mo=O viz. 980–920 cm^{-1}; strong bands in this region being associated with a *cis* arrangement of terminal and bridging oxygens.[153]

The two CrOMo compounds derived from $Mo^{IV}O(dtc)_2$ complexes each show a weak, broad IR band at *ca* 925 cm^{-1} but this band is absent in the complex derived from the organoimido complex. ^{18}O Labelling experiments were not able to verify this assignment conclusively.[195] Preparation of 40% ^{18}O labelled $(TPP)CrOMo(^{18}O)(Et_2dtc)_2$ gave a sample whose IR spectrum only showed broadening of the weak band at 925 cm^{-1}. A similar broadening of a porphyrin band at 890 cm^{-1} was also observed which is in the region expected for Mo—^{18}O terminal vibrations. "Weak" rather than "strong" absorptions have been observed for terminal M=O stretching frequencies in $[MoO(TPP)]_2O$,[207a] $[Re^{V}O(Et_2dtc)_2]_2O$[207b] and $Re_2O_3py_4Cl_4$[208] where the M_2O_3 units are in a linear, *trans* array, O=M—O—M=O.

Whether the CrOMo(O) species have such a linear arrangement (CrOMo=O) cannot be answered in the absence of a structural study, but steric resistance from the porphyrin ring might encourage such organization as in the $[MoO(TPP)]_2O$ complex.

The magnetic moments for these complexes at 293 K are only slightly less than expected for a Cr^{III} ($S = 3/2$), Mo^{V} ($S = 1/2$) complex (Table 14). The decrease in the magnetic moments of these species at low temperatures suggests weak antiferromagnetic coupling is taking place. This is in contrast to the strong coupling in homobinuclear d^1 $[(dtc)_2MoO]_2O$ complexes which are diamagnetic. The linearly arranged oxygens in $[MoO(P)]_2$ (P = TPP, OEP) are considered to contribute to the paramagnetism ($\mu_{eff} = 1.48$ BM per Mo) found in these complexes. The dithiocarbamate complexes have *cis* arrangements of the terminal and bridge oxygens which allows overlap of the appropriate ground state orbitals on the Mo atom to produce the strong coupling observed, whereas the linear arrangement of terminal and bridge oxygens prevents this overlap.[41]

The relatively weak coupling observed in the heterobinuclear compounds and the weak IR CrOMo stretching frequency identified may also indicate a linear CrOMo=O array in these compounds.

$Mo^{V}OFe^{III}$ and $Mo^{V}OMn^{III}$ compounds. Several Fe^{II} complexes have been found capable of reducing $Mo^{VI}(O)_2(Et_2dtc)_2$ in THF to form μ-oxo complexes[193] $(Et_2dtc)_2Mo^{V}(O)Fe^{III}(Lig)$ (Table 14). The characteristic doublet at 910 and 877 cm^{-1} in the IR spectrum arising from the MoO_2 combination in the starting complex is no longer observed in the products. A band at 933 cm^{-1} was assigned to the terminal Mo=O bond which should remain in the bridged compound, but no clearly defined absorption could be identified for an MoOFe vibration. The magnetic moments for the

complexes at 293 K are notably lower than the spin-only value appropriate for a Mo^{V} ($S = 1/2$), Fe^{III} ($S = 5/2$) system and indicate magnetic coupling exists in this complex.

Evidence that the complexes dissociate in solution was found in the observation that both $Mo(O)_2(Et_2dtc)_2$ and Fe(salmah) were slowly precipitated when hexane was added to a solution of $(Et_2dtc)_2Mo(O)OFe$(salmah) in acetone. Furthermore, on attempting recrystallization of $(Et_2dtc)_2Mo(O)OFe$(salen) from acetone the compound Fe^{III}(salen)(Et_2dtc) was isolated,[195] indicating some considerable degree of lability associated with the Mo segment.

Reactions attempted between $Mo(O)_2(Et_2dtc)_2$ and Mn^{II}(salmah) or $Mn^{II}(Et_2dtc)_2$ have given rise to products analysing as $(Et_2dtc)_2Mo(O)Mn(Lig)$ species.[193] The doublet in the IR spectrum, due to the MoO_2 unit, was no longer present in the products and a clearly defined peak due to the terminal Mo=O linkage could not be detected. The magnetic moments of analytically pure samples were comparable to the spin-only values for systems containing Mn^{III} ($S = 2$), Mo^{V} ($S = 1/2$) centres, indicating little coupling was involved. The complexes also dissociated in solution with slow evaporation of a solution of the $Mn(Et_2dtc)_2$ product yielding $Mn^{III}(Et_2dtc)_3$. It has been reported[209] that $Mn^{II}(Et_2dtc)_2$ forms $Mn^{III}(Et_2dtc)_3$ when solutions are exposed to air. These types of complexes need further investigation to determine whether antiferromagnetic behaviour can be observed with different ligands.

In an attempt to produce MoOFe or MoOCr complexes which might show greatly increased resistance to dissociation, redox reactions were attempted using $Mo^{VI}(O)_2(L)_2$ (L = acac, 8-quinolinato) since the Mo^{V} oxo-bridged homobinuclear complexes containing these ligands show little or no detectable dissociation.[116] However, no reaction could be observed with Fe^{II}(L) (L = salah, $(Et_2dtc)_2$) or Cr^{II}(TPP).[195] Such differences in oxidative behaviour between Mo^{VI} dithiocarbamates and the corresponding acetylacetone or 8-quinolinol compounds have been reported for reactions involving oxidations of hydrazines, tertiary phosphines and alcohols.[210]

The formation of heterobinuclear oxo complexes of Mo and Fe has been claimed[211] from the reaction of a compound described only as "Fe^{III} molybdate" with several dithiocarbamates including Et_2dtc^{-} and 8-quinolinol in a mixture of 7 M HCl and acetic acid. The formulae of the complexes which were reported to precipitate from solution were represented as $FeMoO_2(Lig)_4H_2O$. The complex of similar formula having Lig = Et_2dtc, prepared by the redox method, would be totally decomposed in the presence of an HCl–CH_3COOH mixture, or indeed excess H_2O alone.[195] The magnetic moment of the Et_2dtc^{-} complex was reported to be 2.95 BM at room temperature and similarly low values were observed for the other dithiocarbamates examined. The 8-quinolinol complex, however, was said to show a high moment of 6.93 BM, larger even than the spin-only value of 6.16 BM, calculated for a Mo^{V} ($S = 1/2$), Fe^{III} ($S = 5/2$) system. The presence of an FeOMo linkage was suggested on the basis of an IR absorption band at 640 cm^{-1} unrelated to other data.

Whatever the nature of these compounds, it is unlikely that they contain a simple FeOMo linkage as postulated to result from the redox route. If the compounds are pure, they may relate to mixed-metal polyoxometallate complexes.

A $V^{IV}OTi^{IV}$ *compound.* A rather unusual reaction involving oxidation of only one metal reagent has been reported by Floriani and co-workers[212] who found that $V^{IV}O$(acen) reacted with $TiCl_3(THF)_3$ at $-70°C$ to produce the bridged compound $(Cl)(acen)V^{IV}OTi^{IV}(Cl)_3(THF)_2$ (**34**). At the temperature of refluxing THF, reductive deoxygenation occurs to yield $(Cl)V^{III}$(acen).

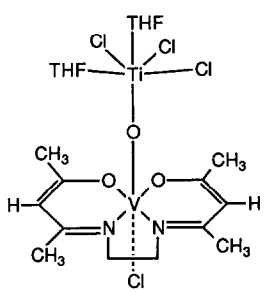

$[Cl(acen)V^{IV}(\mu\text{-}O)Ti^{IV}Cl_3(THF)_2]$ (**34**).

A plausible route for the formation of the oxo-bridged complex as an intermediate in the overall deoxygenation process has been proposed which involves an initial donor–acceptor complex formation followed by intermolecular Cl transfer.

The bridging VO distance (1.937(6) Å) is notably longer than in other VOV complexes (Table 1) while the TiO distance is shorter, at 1.691(6) Å, than in other homobinuclear TiOTi systems. The VOTi angle 169.1(3)°, is said[212] to indicate virtual *sp* hybridization, which could account for the short TiO linkage on the basis of some multiple character in the bond. An IR band at 835 cm^{-1} was suggested as arising from vibration in such a TiO band.

4.4 *Heterotrinuclear* (μ_3-O) *complexes*

$[M_2M'(\mu_3\text{-O})(CH_3COO)_6L_3]$ *compounds*. Mixed-metal hydroxy acetates of Fe^{III} with various divalent transition metal ions were reported[213] before the constitution of the "basic acetate" complexes $[M_3(\mu_3\text{-O})(CH_3COO)_6L_3]^{n+}$ was recognized and were allotted somewhat misleading polynuclear compositions. The true nature of such complexes as analogues of the (μ_3-O) bridged compounds was realised by Blake and co-workers.[214]

Mixed-metal analogues of the trinuclear oxo complexes $[M_3(\mu_3\text{-O})(RCOO)_6L_3]^{n+}$ have now been prepared for the combinations $Fe_2^{III}M^{II}$,[214a,215] ($n = 0$; M^{II} = Mg, Mn, Co, Ni, Zn); $Cr_2^{III}M^{II}$,[215,214b] ($n = 0$; M^{II} = Mg, Fe, Co, Ni); $Cr^{III}Fe^{III}M^{II}$,[214b] ($n = 0$; M^{II} = Mn, Co, Ni, Fe); with R = CH_3 and L = H_2O, py. Fe_2^{III} Cr^{III} and $Cr_2^{III}Fe^{III}$ complexes with acetato[215,216] or O—O bonded glycine[217–219] molecules are known as well as a $Ru_2^{III}Rh^{III}$[220] acetato complex ($n = 1$ and L = H_2O or py) for these M_3^{III} mixed-metal systems.

The complexes have been synthesized by reacting appropriate molar ratios of metal salts (perchlorate, nitrate, halide) in aqueous solution in the presence of a large excess of a carboxylate salt. Many of the oxo compounds are insoluble in the medium and precipitate as the aqua complexes (L = H_2O), a number of complexes also containing water of crystallization. The coordinated water is replaced by pyridine on recrystallization of the aqua compound from that solvent. $Cr_2^{III}M^{II}$ complexes have generally been formed by using Cr^{II} acetate as a reagent, although Cr^{III} Fe^{III} compounds have been prepared by interaction of Cr^{III} and Fe^{III} salts. The heterotrinuclear complexes $Fe^{III}Cr^{III}M^{II}$[214b] have been prepared by addition of Cr^{II} acetate to the corresponding $Fe_2^{III}M^{II}$ preformed complex. The $Ru_2^{III}Rh^{III}$[220] complex was separated from Ru_3^{III} and Rh_3^{III} species by ion-exchange chromatography from the reaction mixture produced by interaction of substitution-inert Rh^{III} and Ru^{III} halides in hot aqueous or methanolic acetic acid containing a source of acetate ions. The $Rh_2^{III}Ru^{III}$ complex was not detected.

The related series of mixed valence, homotrinuclear complexes may be appropriately considered together with these heteronuclear compounds, since their properties might be expected to relate to hetero species of similar valence distribution. Complexes having the formal oxidation state distribution $[M_2^{III}M^{II}(\mu_3\text{-O})(CH_3COO)_6L_3]$ (L = H_2O, pyridine or a substituted pyridine) have been structurally characterized for the combinations $Fe_2^{III}Fe^{II}$, $Cr_2^{III}Cr^{II}$, $Mn_2^{III}Mn^{II}$, $V_2^{III}V^{II}$, $Ru_2^{III}Ru^{II}$ (Table 3). The complexes usually have solvent associated, e.g. benzene, or additional molecules of L in the lattice.

X-ray structural studies of $[Fe^{III}Cr_2^{III}(\mu_3\text{-O})(CH_3COO)_6(H_2O)_3]X$ species (X = $[FeCl_4]^-$,[216] NO_3^- [221]) while confirming the similarity of the structure to those of the Fe_3^{III} and Cr_3^{III} compounds, were unable to distinguish between the individual metal ions and a statistical distribution of ions in the crystal was indicated.

Indeed, some doubt was cast[216] on whether the earlier compound[221] studied was a truly mixed-metal complex on the grounds that the reported red colour of the complex examined was appropriate to the homotrinuclear Fe_3O compound. The sample examined in the later study[216] was almost black in colour and was separately shown to contain Fe and Cr ions in the same molecular unit by an electrochemical procedure. The M—O bond distances were comparable with those found for the Cr_3O complex. The $Fe_2^{III}Cr^{III}$ glycinate[217] complex, however, shows an ordered arrangement in the crystal. Refinement of the crystallographic data, assuming the metal sites were each filled by Fe^{III} ions, resulted in a considerably higher temperature factor for one atom, presumably indicating the Cr site. The cations within the unit cell are arranged so that the Cr—(μ_3O) bonds are aligned indicating the existence of magnetic ordering. The non-bonded M···M distances are very similar

Table 18. Vibrational spectra (cm^{-1}) of mixed valent and heterotrinuclear complexes $[Fe_2M'(\mu_3\text{-}O)(\mu\text{-}CH_3COO)_6L_3]$[223]

M′	L	$\nu_{as(M_2M'O)}$	$\nu_{as(M_2M'O)}$	$\delta_{s(M_2M'O)}$
Fe^{II}	py	[a]	570	274
Mn^{II}	py	712	535	274
Co^{II}	py	712	545	278
Ni^{II}	py	722	565	283
Ni^{II} [b]	py	[a]	550	274
Fe^{II}	H_2O	710	555	282
Mn^{II}	H_2O	775	555	280
Co^{II}	H_2O	775	565	284
Mn^{II}	H_2O	730	580	288

[a] Band obscured.
[b] ^{18}O labelled.[224]

to those in the Cr_3 and Fe_3 systems with only slight variations being detected between the Cr—O and Fe—O distances.

The M^{III}—O and M^{II}—(μ_3-O) bond distances should differ in a molecule containing the formal oxidation states $M_2^{III}M^{II}$ "trapped" in a $[M_3(\mu_3\text{-}O)(CH_3COO)_6L_3]$ structure. The three metal ions would surround the central O^{2-} ion, lying at the vertices of an isosceles triangle. The site symmetry at the oxygen would then be C_{2v} rather than D_{3h} as in the M_3^{III} systems. Structural studies on a variety of such mixed valence complexes have failed to discern any difference between the three metal ions except in the case of $[Mn_2^{III}Mn^{II}(\mu_3\text{-}O)(CH_3COO)_6(3\text{-}Cl\text{-}py)_3]$ where the three Mn ions form an isosceles triangular array indicating the position of an Mn^{II} ion (Table 3). In other cases, the apparent equivalence of the metal sites, judged by the structural evidence, indicates either a rapid electron transfer between the metal ions, possibly via the central oxygen, or a bonding array of M_3O in which the metal and oxygen electrons are delocalized and are accommodated in molecular orbitals embracing the entire cluster. Such a delocalization has been described for the $Ru_2^{III}Ru^{II}$ complex to account for its diamagnetism.[77] A third possibility is that there is a statistical distribution of $M_2^{III}M^{II}$ units thoughout the crystal, making each metal position appear equivalent. Mössbauer spectral studies on the $Fe_2^{III}Fe^{II}$ species, $[Fe_2^{III}Fe^{II}(\mu_3\text{-}O)(CH_3COO)_6L_3]S$ (L = pyridine, 4-Et-py, S = L);[72] (L = 4-Me-py, S = benzene),[71] have shown that both Fe^{III} and Fe^{II} sites can be detected at low temperatures (to 11 K), quadrupole split doublets being observed in the intensity ratios 2:1, Fe^{III}/Fe^{II}. As the temperature is increased, changes in the relative intensities and positions of the doublets occur until, at *ca* 300 K, only a single averaged spectrum is observed. X-ray diffraction studies show equivalence of the Fe sites at room temperature. A sufficiently rapid electron transfer process is considered to be occurring at room temperature that oxidation state differences between the Fe ions cannot be detected by processes having the longer time scales of X-ray diffraction or Mössbauer spectroscopy.[222]

The temperature at which electron transfer becomes sufficiently rapid to "equilibrate" the metal ions in the solid state has been shown to depend on the nature of the non-coordinated solvent molecules co-crystallized with individual complexes, and not solely on the overcoming by thermal motion of the thermal barrier to electron transfer.[71]

No single crystal X-ray structural studies have yet been reported for any of the $Fe_2^{III}M^{II}$ or $Cr_2^{III}M^{II}$ complexes, but a number[215] have been shown by X-ray examination to form rhombohedral crystals with one molecule per unit cell and to be isomorphous with $[Mn_2^{III}Mn^{II}(\mu_3\text{-}O)(CH_3COO)_6py_3]$.[74] This complex shows equivalent Mn centres and thus indicates that the heterotrinuclear complexes are disordered with the divalent metal ion randomly occupying one of the three equivalent metal sites.

A unique octanuclear mixed metal complex, $[V^{III}Zn^{II}(\mu_4\text{-}O)(C_6H_5COO)_3(THF)]_4$, has been structurally identified by Cotton *et al.*[246] It was prepared under argon by reaction of the double salt $[V_2Cl_3(THF)_6]_2[Zn_2Cl_6]$ with benzoate ions in THF. The complex may be viewed as containing a tetrahedral grouping of V atoms with a Zn ion capping each face of the tetrahedral array, with a

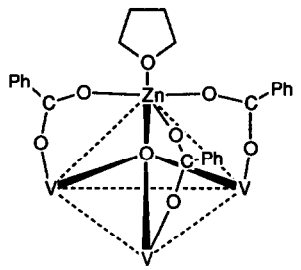

$[V^{III}Zn^{II}(\mu_4\text{-O})(\mu\text{-}C_6H_5COO)_3(THF)]_4$, view of a ZnV_3O unit (**35**).

μ_4-O atom inside each V_3Zn pyramid about 2.0 Å from each metal ion (**35**). The benzoate carboxylato groups bridge each of the 12 V–Zn pairs and the THF molecules coordinated to each Zn complete the five-fold trigonal bipyramidal coordination around these ions. The V ions are effectively octahedrally coordinated. The V ions are more closely packed (V ··· V) at 2.965(4) Å than in the V_3O carboxylato complexes (3.3 Å, Table 3), probably because of the bonding by the oxo bridges.

The $M_4(\mu_4\text{-O})$ unit is also known in the "basic" acetato structures[104b] of $[M_4(\mu_4\text{-O})(CH_3COO)_6]$, (M = Be^{II}, Zn^{II}).

The source of oxygen in the V_4Zn_4 compound is unknown. Molecular oxygen was supposedly excluded from the reaction mixture and H_2O is thought unlikely since the complex decomposes further on exposure to air or moisture. Abstraction from a carboxylate group has been suggested.

Vibrational spectra: Cannon and co-workers[223] have examined the M_3—O vibration modes by IR spectroscopy to try to establish the "true" molecular symmetry of $Fe_2^{III}Fe^{II}$ systems. The procedure was to compare the spectra of mixed-metal valence compounds with corresponding mixed-metal complexes, necessarily of C_{2v} symmetry. In C_{2v} symmetry, the asymmetric vibration associated with the $Fe_2M^{II}(\mu_3\text{-O})$ unit would be split into two components, A_1 and B_2. Such bands have been assigned[223] for a range of $[Fe_2M^{II}(\mu_3\text{-O})(CH_3COO)L_3]$ complexes (Table 18). The assignments for the Fe_2Ni compound were defined with the aid of ^{18}O substitution for the $(\mu_3\text{-O})$.[224] The frequencies were found to increase in the order Mn < Co < Ni, i.e. of increasing crystal field stabilization and dissociative stability. These assignments have allowed the allocation of the related bands in $[Fe_2^{III}Fe^{II}(\mu_3\text{-O})(CH_3COO)_6L_3]$ compounds at room temperature, supporting the existence of discrete Fe^{III} and Fe^{II} centres, detectable on the time scale appropriate to molecular vibrations.[223]

Magnetic susceptibilities: the magnetic susceptibilities of a series of the mixed-metal oxo-acetate complexes $Cr_2^{III}M^{II}$, $Fe_2^{III}M^{II}$ (M = Ni, Mn, Mg) have been studied between 295–4.2 K.[215] The data have been fitted to the isotropic Hamiltonian

$$\mathcal{H} = -2\Sigma_{ij}J_{ij}S_iS_j + \mu_B\Sigma_i g_i S_i H$$

Table 19. Magnetic data for heterotrinuclear complexes[214] $[M_2M'(\mu_3\text{-O})(\mu\text{-}CH_3COO)_6L_3]^{+/0}$

M_2	M′	L	$-J_{12}$ (cm^{-1})	$-J_3{}^a$ (cm^{-1})
Cr^{III}	Cr^{III}	H_2O	11(1)	
Cr^{III}	Co^{II}	py	27(2)	
Cr^{III}	Ni^{II}	py	26(2)	47(2)
Fe^{III}	Fe^{III}	H_2O	30(3)	
Fe^{III}	Mg^{II}	py	62(3)	
Fe^{III}	Mn^{II}	py	64(3)	21(1)
Fe^{III}	Ni^{II}	py	73(3)	33(2)
Fe^{III}	Ni^{II}	H_2O	71(3)	31(3)

[a] $-J_{13} = -J_{23} \equiv -J_3$.

defining the interaction of the three magnetic ions in the cluster with each other and the applied field H. With $S_1 = S_2$, $g_1 = g_2$ and $J_{13} = J_{23}$ (written as J_3) it is given the form

$$\mathscr{H} - 2J_{12}S_1S_2 - 2J_3S_{12}S_3 + \mu_B[g_1S + (g_3 - g_1)S_3] \cdot H$$

where $S_{12} = S_1 + S_2$ and $S = S_{12} + S_3$.

The values of the coupling constants are shown in Table 19 for the combinations whose experimental data were fit. It is noteworthy that the J_{Fe-Fe} and J_{Cr-Cr} values in the heterotrinuclear series are approximately twice their values in the homotrinuclear compounds and almost independent of the nature of M^{II}, an indication that coupling proceeds via the oxygen atom as the main superexchange pathway. The in-plane p orbitals of the oxygen are seen as particularly effective in facilitating exchange.

The $Cr_2^{III}Fe^{II}$ complex data could not be adequately fitted to the Hamiltonian, possibly because of spin–orbit coupling in the Fe^{II} ground state.[215]

The complete sequence of mixed $Cr^{III}_{3-x}Fe^{III}_x(\mu_3\text{-O})$ bridged trinuclear carboxylato complexes has been prepared[219] with the N-protonated glycinato ion bridging via its carboxyl group, as defined by structural studies[217] on $[Fe_2Cr(\mu_3\text{-O})(H^+NH_2CH_2COO)_6(H_2O)_3](ClO_4)_7$. The magnetic susceptibilities of the four complexes Cr_3, Fe_3, Cr_2Fe and Fe_2Cr have been studied down to 80 K together with that of the mixed valence derivative $[Fe_2^{III}Fe^{II}(\mu_3\text{-O})(H^+NH_2CH_2COO)_6(H_2O)_3]Cl_6$. Attempts were made to fit the data to a susceptibility expression which would allow that the three metal ions in each compound occupied the vertices of an isosceles triangle and not an equilateral array. This involved the use of a factor representing the ratio of two integrals such that $J_{12} = J_{23} = \alpha J_{13}$. Both the values of α and J were varied in order to obtain the best fit with the experiment. For Cr_3 and Cr_2Fe complexes, best fits were obtained with $\alpha = 1$ indicating close approximation to an equilateral triangular configuration for the metal ions, whereas best fits for the Fe_3 complex data were obtained when the α-value was 0.7 indicating that something less than an equilateral triangle fitted the structure. The Fe_2Cr complex appeared somewhat insensitive to the arrangement of the metal atoms. The $Fe_2^{III}Fe^{II}$ compound showed the most extreme influence of shape and the best fit was obtained when the complex was considered as a binuclear Fe_2^{III} species with virtually no contribution from the Fe^{II} ion being necessarily included. This could suggest a considerable degree of spin localization exists in this complex in contrast to most other $Fe_2^{III}Fe^{II}$ species so far examined.

Electronic spectra: the replacement of one trivalent ion in $[M_3(\mu_3\text{-O})(CH_3COO)_6L_3]^+$ by a divalent M^{II} ion reduces the ligand field around each remaining M^{III} ion, and shifts to lower frequencies are observed for *d–d* transitions associated with the Cr^{III} and Fe^{III} ions.[214b,215] This reduction in ligand field and its effect on absorption spectra contrasts with the increased M^{III}—M^{III} magnetic exchange observed,[215] which is suggested to be related to increased M^{III}—O—M^{III} π-bonding. The spectral transitions due to individual M^{II} ions have been allocated for a number of the systems.[215] The $Cr^{III}Fe^{III}M^{II}$ complexes are purple in colour, contrasting with the less intense green of most $Cr_2^{III}M^{II}$ and $Fe_2^{III}M^{II}$ complexes prepared. The colour appears to be associated with a band at *ca* 19,000 cm^{-1}.[215] Comparison with the spectra of Cr_3^{III} and Fe_3^{III}, and the mixed systems $Cr_2^{III}Fe^{III}$ and $Cr^{III}Fe_2^{III}$ show that intense bands are found at 18,600 and 25,500 cm^{-1} for the $Cr_2^{III}Fe^{III}$ complex (which has a purple–red colour) which do not correspond to bands in the spectra of Cr_3^{III} or Fe_3^{III}. The $Cr^{III}Fe_2^{III}$ complex is red–brown in colour and shows less well defined absorptions, having a spectrum somewhat akin to a super position of Cr_2Fe and Fe_3 spectra, although the intensities of bands are greater than for a simple mixture of species. The Cr_3 and Fe_3 complexes are green and olive-green, respectively.

A reason for this colour difference between the mixed-metal and homotrinuclear systems is suggested to involve simultaneous (Cr^{III}, Fe^{III}) double excitations.[214]

Other spectral studies on $M_2^{III}M'^{III}$ *complexes*: the $[Ru_2Rh(\mu_3\text{-O})(CH_3COO)_6L_3]^+$ (L = H_2O or pyridine) complexes[220] show ^{13}C and ^1H NMR resonances for the methyl groups of the acetate bridging groups in the ratio of 1 : 2 integrated intensities, providing unambiguous evidence that the isosceles triangular Ru_2RhO configuration occurs. X-ray photoelectron spectra of the complexes show small but detectable differences in the Ru $3d_{5/2}$ binding energies between the Ru_3 and Ru_2 complexes.

Metal–metal bonded $M_3(\mu_3\text{-O})$ *and* $M_3(\mu_3\text{-O})_2$ *compounds.* Mixed-metal acetato bridged compounds containing metal–metal bonded triangular arrays of Mo_2W and MoW_2, with (μ_3-O) groups "capping" the triangular arrays, have been prepared[225] by an adaptation of the reduction process used in making the homotrinuclear compounds. This involved reduction of mixtures of sodium tungstate and molybdate with Zn in acetic anhydride. A mixture of the W_3, Mo_2W and W_2Mo cations $[M_3(\mu\text{-O})_2(CH_3COO)_6(H_2O)_3]^{2+}$ was formed and separated by cation exchange chromatography. The time of the separation procedure was reported to last one month! Chemical identification of the clusters was carried out by ^1H NMR spectroscopy in D_2O. The homotrinuclear Mo_3 and W_3 compounds show one sharp CH_3 singlet, while the M_2M' species each show two CH_3 resonances with the intensity ratio of 2 : 1. Although a full structure determination has not been completed, lattice parameters for the mixed MoW complexes are very similar to those of the Mo_3 complex, indicating statistical disorder for the Mo_2W and W_2Mo units in the crystal. X-ray photoelectron spectra of the four complexes Mo_3, W_3, Mo_2W and W_2Mo have been used to determine binding energies for Mo 3*d*, W 4*d* and W 4*f* electrons.[226] The various values show successive decreases in energy in the sequence Mo_3, Mo_2W, MoW_2W_3, although the separations between the various electron levels (e.g. Mo $3d_{3/2}$, Mo $3d_{5/2}$) are essentially constant and larger than for the Ru_2Rh, non-metal–metal bonded compound.[220] The changes have been related to a charge shift along the metal–metal bonds, reflecting greater electronegativity of the Mo^{IV} state over the corresponding W state. The structural evidence indicates that the M—M bond lengths do not change greatly along the whole series from Mo_3, Mo_2W, W_2Mo to W_3. ^{183}W and ^{95}Mo NMR spectra have also been recorded for the complexes.[227]

The redox reaction devised by Chisholm and co-workers[100] has been applied to the directed synthesis of Mo_2W mixed-metal species.

$$(RO)_3Mo^{III}{\equiv}Mo^{III}(OR)_3 + OW^{VI}(OR)_4 \longrightarrow Mo_2^{IV}W^{IV}(\mu_3\text{-O})(OR)_{10}. \quad (35)$$

The compound $Mo_2W(\mu_3\text{-O})(O^iPr)_{10}$ is isomorphous with the Mo_3 complex and has a disordered arrangement of Mo and W atoms. The reaction involving $W_2(OR)_6$ and $OMo(OR)_4$ did not yield the W_2Mo complex cleanly, $W_3(\mu_3\text{-O})(OR)_{10}$ being obtained in the largest yield. A plausible explanation[100] for this involves the oxo-transfer reaction

$$Mo(O)(O^iPr)_4 + W_2(O^iPr)_6 \longrightarrow MoW(O^iPr)_6 + WO(O^iPr)_4 \quad (36)$$

being favoured, followed by reaction of $WO(O^iPr)_4$ with $W_2(O^iPr)_6$. The interesting reaction may have a much wider scope than production of oxo-bridged complexes since a variety of $MX(OR)_4$ species may well be used. Mixed-metal complexes with an alkylidene cap have been prepared by reaction of $Mo_2(OR)_6$ with $(RO)_3W{\equiv}CMe$,[228] but attempts to prepare mixed Nb, Ta and Mo, W compounds with (μ_3-OR) capping groups have not been successful.[100]

5. HETERONUCLEAR ORGANOMETALLIC OXO-BRIDGED COMPOUNDS

There is only a relatively small number of heteronuclear oxo-bridged organometallic compounds yet known, no doubt related to the lack of synthetic procedures for preparing them. Several compounds have been reported amongst mixed-metal carbonyl derivatives where oxygen has been inserted into the cluster fortuitously, it would appear, in each case. Thus, an attempt to add the coordinatively unsaturated organometallic species $Fe(CO)_4$, produced *in situ* by photolysis of $Fe_2(CO)_9$, to the Mo≡Mo triple bond in $Mo_2(C_5Me_5)_2(CO)_4$, gave the μ_3-O bonded cluster $(C_5Me_5)_2Mo_2Fe(\mu_3\text{-O})(CO)_7$[229] (**36**). The source of oxygen was shown to be dioxygen and an im-

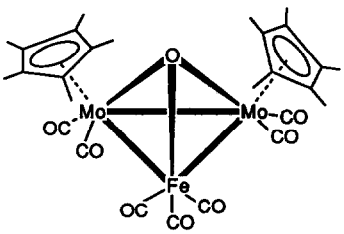

$(C_5Me_5)_2Mo_2Fe(\mu_3\text{-O})(CO)_7$ (**36**).

proved synthetic method which involved pretreatment of the mixture of reactants with dioxygen before irradiation commenced was devised.

$(CpCrSC(CH_3)_3)_2S$ has been found to react with $Co_2(CO)_8$ in benzene in the presence of pivalic acid to give the paramagnetic material $Cp_3Cr_3(\mu_3\text{-}S)_3(\mu_3\text{-}O)Co(CO)_3 \cdot Me_3CCOOH$[230] (**37**). Again,

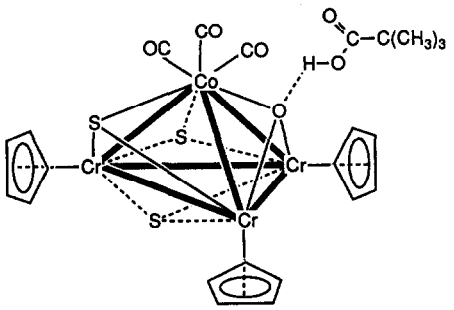

$(Cp)_3Cr_3(\mu_3\text{-}S)_3(\mu_3\text{-}O)Co(CO)_3(Me_3C \cdot COOH)$ (**37**).

the source of oxygen is unclear. The structure consists of an isosceles triangle of Cr atoms bonded to a sulphur atom. The bridging oxygen atom links two Cr and the Co atoms and is attached to the shorter Cr—Cr bond. The $Co(CO)_3$ group is weakly bound to the oxygen and two further sulphur atoms which, in turn, are triply bridging to two Cr atoms and the Co.

One compound has been reported in which oxygen bridges four metals viz. $[(PPh_3)_2N][Fe_3Mn(CO)_{12}(\mu_4\text{-}O)]$—a "butterfly oxo cluster"[231] (**38**). The complex is formed by reaction of the

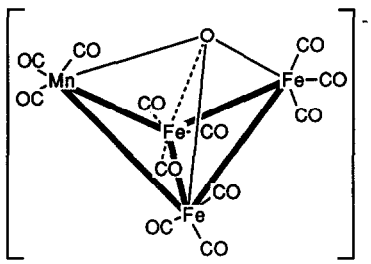

$[Fe_3Mn(CO)_{12}(\mu_4\text{-}O)]^-$ (**38**).

$(\mu_3\text{-}O)$-capped ion[232] $[Fe_3(\mu_3\text{-}O)(CO)_9]^{2-}$ containing a triangle of metal–metal bonded Fe atoms with $[Mn(CO)_3(CH_3CN)_3][PF_6]$ in acetone. The $Mn(CO)_3$ unit may be thought of as adding to an $Fe_2(\mu_3\text{-}O)$ face of the Fe_3O group. The count of 62 cluster valence electrons achieved by assuming oxygen provides six electrons makes this molecule comparable with the molecular orbital descriptions of similarly shaped butterfly carbides. The M—O distances are short, averaging 1.89(2) Å. The complex decomposes under CO in acetone over several hours, giving CO_2 and Fe compounds of lower nuclearity. This type of reaction may account for the relative rarity of oxo-bridged metal carbonyls compared to carbido and nitrido species.

A number of heteropolynuclear carbonyl cluster compounds containing bridging oxo ligands are known where the oxygen bridge has been formed by the breakdown of an oxygen-containing group in a precursor molecule. Thus, heating the tetranuclear acylcarbonyl $(Cp)WOs_3(CO)_{11}$ $(\mu_3\text{-}\eta^2\text{-}C(O)CH_2C_6H_4CH_3)$, which contains a lengthened and hence "activated" CO bond, causes the C—O bond to break with formation of the μ-oxo alkylidyne complex $(Cp)WOs_3(CO)_9(\mu\text{-}O)$ $(\mu_3\text{-}C \cdot CH_2C_6H_4CH_3)$[233] (**39**). The shorter length of the W—O (1.812(7) Å) bond compared to the

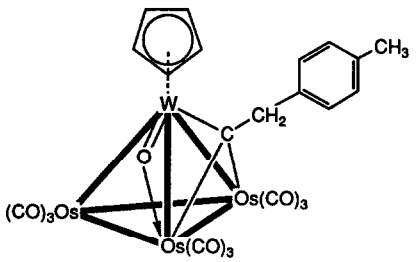

$(Cp)WOs_3(CO)_9(\mu\text{-}O)(\mu_3\text{-}C \cdot CH_2C_6H_4CH_3)$ (**39**).

Os—O bond (2.169(8) Å) and even to W—O in the parent compound (2.150(10) Å) strongly suggests the donor–acceptor mode W=O → Os for this oxo bridge. The nearly coplanar arrangement of WOs_3 atoms in the parent has changed to a pseudo-tetrahedral array in the oxo-bridged product. The W—O—Os angle (80°) is still, however, similar to that in the parent. Pyrolysis of the complex in toluene or reaction with H_2 does not affect the oxo group.

A second example[234] of a W—O—Os bridge has resulted from reaction of Me_3NO with the acetylene complex $CpWOs_3(CO)_{10}(\mu_3\text{-}\eta^2\text{-}C_2H_2)H$ yielding $CpWOs_3(CO)_8(\mu\text{-}O)(\mu_3\text{-}\eta^2\text{-}C_2H_2)H$. The bonding mode is again W=O → Os as evidenced by the metal–oxygen distances (W—O 1.76(8) Å and Os—O 2.200(8) Å). The oxo group is almost coplanar with the WOs_2 plane. Similar oxo-bridged WOs_3 units have been found in $CpWOs_3(CO)_9(\mu\text{-}O)(\mu\text{-}CHCH_2C_6H_4Me)(\mu\text{-}H)$ and $CpWOs_3(CO)_9(\mu_2\text{-}C{=}CHC_6H_4Me)(\mu\text{-}H)$. Such edge-bridging oxygens are implicated in the dissociation of CO molecules in the Fischer–Tropsch reaction but had been assumed previously to be bound symmetrically to a pair of metal atoms.

Aerial oxidation of the heterotrimetallic complex $(Cp_2)_2ReW_2(\mu\text{-}Br)(\mu\text{-}CR)(\mu\text{-}CO)(CO)_3$ (R = *p*-tolyl) gives an oxo-bridged species,[235] $(Cp_2)_2ReW_2(\mu\text{-}Br)(\mu\text{-}O)(\mu\text{-}CR)(\mu_3\text{-}CR)(CO)_3$ (**40**), in which

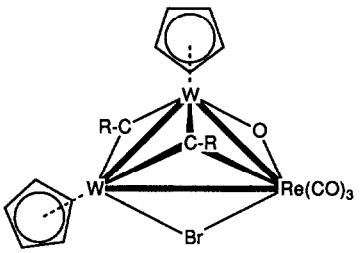

$(Cp)_2ReW_2(\mu\text{-}Br)(\mu\text{-}O)(\mu\text{-}CR)(\mu_3\text{-}CR)(CO)_3$ (**40**).

oxygen replaces a bridging CO ligand between W and Re and the capping tolylmethylidyne group becomes bound more asymmetrically to the ReW_2 triangle than in the parent. This is because of a considerable increase in the Re—C bond distance (μ-C—Re 2.248(12)–2.515(20) Å). The ReOW angle is necessarily small (93.7(6)°).

Oxo bridging results from the extrusion of an alkene from the oxo-alkyl bridge in the W—Zr heterobinulcear complex formed as follows,[236]

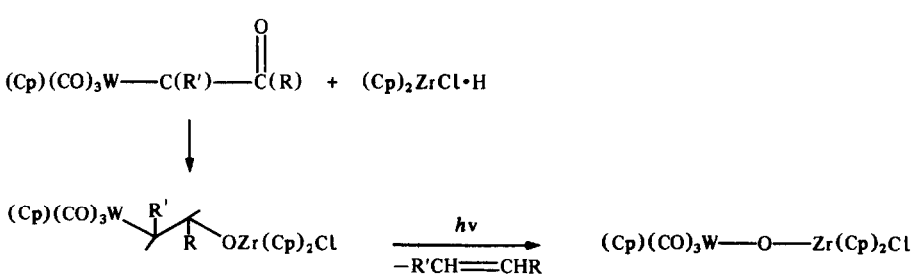

(37)

The ZrOW linkage is virtually linear (175.7°) but asymmetric with the WO bond (2.065 Å) longer than ZrO (1.871 Å).

The IR spectrum contains a broad absorption at 789 cm^{-1} which is shifted to 750 cm^{-1} on ^{18}O substitution at the bridge. The ^{17}O NMR spectrum shows a single resonance at $\delta = 194$, well beyond the range of homobinuclear species containing oxo bridging. This suggests a reduced degree of π-bonding between oxygen and one of the two metals, presumably W. The bridge is left intact when the complex reacts with PMe_3 or acetylenes, substitution taking place at W, or with LiMe, when the (Zr)—Cl atom is replaced. Acetyl chloride, however, converts the oxo-bridged compound to the acetate $(Cp)(CO)_3W(O_2CCH_3)$ and Cp_2ZrCl_2.

A redox reaction occurs between Vaska's compound $Ir(PPh_3)_2CO \cdot Cl$ and OsO_4 in the presence of heterocyclic bases at −78°C to give an Ir^{III}—O—Os^{VI} species[237] which also possesses a uniquely bridging CO_2 molecule formed *in situ* by an oxygen from OsO_4 reacting with the CO molecule (**41**).

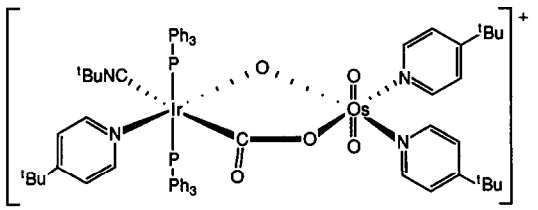

$[(4\text{-}^t\text{Bupy})(^t\text{BuNC})(PPh_3)_2Ir(\mu\text{-}CO_2)(\mu\text{-}O)Os(O)_2(4\text{-}^t\text{Bupy})_2]^+$ (**41**).

Methylation at the exocyclic oxygen of the bridging CO_2 unit can occur and the structure of the resulting molecule has been obtained. The Os—O—Ir angle is 120.6(4)°.

Molecules in which "anionic" oxo-organometallic species are bound to Mg^{2+} have been prepared by the reaction of Mg mono- and bifunctional alkyls with Mo^{VI} or W^{VI} oxo-halides $(MOCl_4)$[238–240] or $[Me_3NH][ReO_4]$.[241,242] A series of THF solvated compounds having Mg—O—M^V bonding, have been characterized by X-ray structural studies viz. $(THF)_4Mg(OWMe_4)_2$[240] (**42**), $(THF)_4Mg(OReMe_4)_2$,[241] $(THF)_4Mg\{OW[(2\text{-}CH_2C_6H_4)_2]_2\}_2$[239] and $(THF)_4Mg\{OW[C_6H_4(CH_2)_2]_2\}_2$.[238]

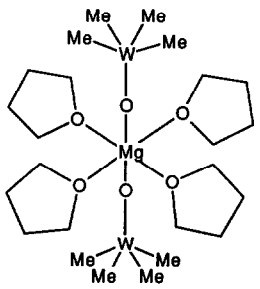

$Mg(THF)_4(OW^VMe_4)_2$ (**42**).

The M—O bond distances are comparable to M^V—O in μ-oxo homonuclear species. The Mo and W compounds are paramagnetic[240] as befits d^1 compounds and have ESR spectra at 98 K in toluene appropriate for square-pyramidal compounds having $S = 1/2$; whereas the d^2 Re^V species are diamagnetic. Long range magnetic dipole–dipole interaction between the two W atoms causes splitting of the peaks. LiMe also reacts to form $LiOMR_4$ compounds.[240] Methyl ^1H resonances are not observed at room temperature for the $LiOReMe_4$ compound, but at lower temperature a broad peak appears which condenses to a sharp singlet at δ 3.12 ppm at −60°C. The reason for this unusual behaviour is uncertain but is suggested[240] to perhaps be related to an unusually short spin–lattice relaxation time through coupling with the quadrupolar isotopes ^{185}Re and ^{187}Re having $I = 5/2$.

6. HETEROBINUCLEAR PEROXO SPECIES

In the light of the extensive chemistry of peroxo-bridged metal compounds (particularly that of Co^{III}) it might be expected that a range of heteronuclear peroxo M—O_2—M′ complexes would be accessible. Only one such compound appears to have been reported by Arzoumanian *et al.*[243] Thus, $K_5[(CN)_5Co^{III}O_2Mo^{VI}(O)(Cl)(CN)_5]$ is formed by passing oxygen through an aqueous solution containing Co^{II}, Mo^{V} and KCN. The Mo=O linkage gave an IR band at 918 cm^{-1} while the peroxide ligand was associated with a band at 893 cm^{-1} and was analysed by titration with Ce^{IV}. The complex readily exchanged Cl for H_2O and in solution under an oxygen atmosphere the complex $[Mo(O)(O_2)(CN)_4]^{2-}$ was produced.[244] The peroxo group in this latter complex was shown by ^{18}O labelling experiments to be derived from the gaseous oxygen in the reaction vessel and was not transferred from the initial dimetallic compound.[244] This indicated dissociation into a Co^{III} superoxo species followed by reaction with gaseous oxygen[245] to give $[(O_2)Mo(O)(CN)_4]^{2-}$ and a cyano free radical. This was inferred to have been formed by the subsequent detection of the tetracyanoethylene radical anion from its ESR spectrum in the reaction mixture. It was presumably formed by reaction of CN˙ with the solvent CH_2Cl_2.[245]

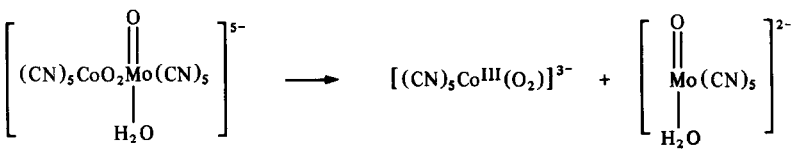

(38)

The initial thought[244b] that this particular reaction might have implications for catalytic systems is not realistic, in terms of O_2 transfer, but the study of the reactions of Co^{III}–superoxo species with the other oxidizable metal substrates may well result in other CoO_2M bridged systems being isolated.

Acknowledgements—The author is indebted to Mrs Anne Heffernan and Dr Peter Nichols for their assistance in completing this Report. Unpublished work by the author in this Report has been supported by the Australian Research Grants Committee.

ABBREVIATIONS

acac	acetylacetonate(-1)
acen	N,N′-ethylenebis(acetylacetoneiminate)(-2)
bpy	α,α′-bipyridyl
Cp	η^5-cyclopentadienyl
DBAT	7,16-dihydro-6,8,15,17,tetramethyl-dibenzo[b,i]-[1,4,8,11]-tetraazacyclotetradecanate(-2)
DMEPy	2,6-bis(2,2-diphenyl-2-thioethyl)pyridinate(-2)
dppm	bis(disphenylphosphino)methane
Et_2dtc	diethyldithiocarbamate(-1)
Et_2dtp	diethyldithiophosphate(-1)
EDTA	ethylenediaminetetraacetate(-4)
EDDA	ethylenediaminediacetate(-2)
FFP	the tetraanion formed by the "face-to-face" linking of two tetraphenylporphyrin molecules via a urea bridge between two *meso*-phenyl groups at the two-positions
HEDTA	N-(hydroxyethyl)ethylenediamine-N,N′,N′-triacetate(-3)
Hp	hemiporphyrazinate(-2)
1-MeIm	1-methylimidazole
N_5	N,N,N′-tris[(2-benzimidazolyl)methyl]-N′-(2-hydroxyethyl)-1,2-diaminoethane
MACN	N,N′,N″-1,4,7-trimethyltriazacyclononane
OEP	octaethylporphyrinate(-2)
Pc	phthalocyaninate(-2)
phen	1,10-phenanthroline
picen	N,N′-bis(2-pyridylmethyl)ethane-1,2-diamine
Pyrdtc	Pyrrolidyldithiocarbamate(-1)

Q	8-oxoquinolinate(-1)
salen	N,N′-ethane-1,2-diylbis(salicylideneiminate)(-2)
salah	N,N′-4-azaheptane-1,7-diylbis(salicylideneiminate)(-2)
salmah	N,N′-4-methyl-4-azaheptane-1,7-diylbis(salicylideneiminate)(-2)
salphen	N,N,′-benzene-1,2-diylbis(salicylideneiminate)(-2)
TACH	the tri-imido ion of 1,5,9,13-tetraazacyclohexadecane
TACN	1,4,7-triazacyclononane
tmpa	tris(2-pyridylmethyl)amine
TPyEA	tris(2-pyrazol-1-ylethyl)amine
tren	tris(2-aminoethyl)amine
tsalen	N,N′-ethane-1,2-diylbis(thiosalicylideneiminate)(-2)
T—P	5,10,15,20-tetraaryl substituted porphyrinates thus:
TCP	tetra-4-chlorophenyl
TFP	tetra-4-fluorophenyl
TMP	tetra-4-methoxyphenyl
TMesP	tetra-2,4,6-mesityl
TPP	tetraphenyl
TTP	tetra-4-tolyl
TXP	tetra-3-5-xylyl

REFERENCES

1. W. P. Griffith, *Coord. Chem. Rev.* 1970, **5**, 459.
2. (a) B. Jezowska-Trzebiatowska, *Coord. Chem. Rev.* 1968, **3**, 255; (b) B. Jezowska-Trzebiatowska, *Pure Appl. Chem.* 1971, **27**, 89.
3. K. S. Murray, *Coord. Chem. Rev.* 1974, **12**, 1.
4. E. I. Stiefel, *Prog. Inorg. Chem.* 1977, **22**, 1.
5. R. H. Holm, *Chem. Rev.* 1987, **87**, 1401.
6. (a) Y. LePage, J. D. M. McCowan, B. K. Hunter and R. D. Heyding, *J. Organomet. Chem.* 1980, **193**, 201; (b) H. Stoeckli-Evans, *Helv. Chim. Acta* 1974, **57**, 684.
7. K. Watenpaugh and C. N. Caughlan, *Inorg. Chem.* 1967, **6**, 963.
8. M. M. Olmstead, P. P. Power and M. Viggiano, *J. Am. Chem. Soc.* 1983, **105**, 2927.
9. S. Yamada, C. Katayama, M. Tanaka and T. Tanaka, *Inorg. Chem.* 1984, **23**, 253.
10. J. F. Johnson and W. R. Scheidt, *Inorg. Chem.* 1978, **17**, 1280.
11. (a) J. R. Knox and C. K. Prout, *Acta Cryst.* 1969, **B25**, 2281; (b) O. Garner, N. C. Howlader, F. E. Mabbs, A. T. McPhail and K. D. Onan, *J. Chem. Soc., Dalton Trans.* 1979, 962.
12. R. Lancashire and T. D. Smith, *J. Chem. Soc., Dalton Trans.* 1982, 693.
13. P. Chandresekhar and P. H. Bird, *Inorg. Chem.* 1984, **23**, 3677.
14. S. R. Fletcher and A. C. Skapski, *J. Chem. Soc., Dalton Trans.* 1972, 1073.
15. R. Shandles, E. O. Schlomper and R. K. Murmann, *Inorg. Chem.* 1971, **10**, 2785.
16. T. Lis, T. Glowiak and B. Jezowska-Trzebiatowska, *Bull. Acad. Pol. Sci. Ser. Sci. Chim.* 1975, **23**, 739.
17. M. Yevitz and J. A. Stanko, *J. Am. Chem. Soc.* 1971, **93**, 1512.
18. (a) M. Di Vaira and F. Mani, *Inorg. Chem.* 1984, **23**, 409; (b) B. G. Gafford, R. A. Holwerda, H. J. Schugar and J. A. Potenza, *Inorg. Chem.* 1988, **27**, 1126.
19. J. F. Rowbottom and G. Wilkinson, *J. Chem. Soc., Dalton Trans.* 1972, 826.
20. (a) B. C. Schardt, F. J. Hollander and C. L. Hill, *J. Chem. Soc., Chem. Commun.* 1981, 765; (b) B. C. Schardt, F. J. Hollander and C. L. Hill, *J. Am. Chem. Soc.* 1982, **104**, 3964.
21. L. H. Vogt, A. Zalkin and D. H. Templeton, *Inorg. Chem.* 1967, **6**, 1725.
22. (a) W. Hiller, J. Strähle, A. Datz, M. Hanak, W. E. Hatfield, L. W. ter Haar and P. Gütlich, *J. Am. Chem. Soc.* 1984, **106**, 329; (b) I. Collamati, G. Dessy and V. Fares, *Inorg. Chim. Acta* 1986, **111**, 149.
23. J. P. Collman, C. E. Barnes, P. J. Brothers, T. J. Collins, T. Ozawa, J. C. Gallucci and J. A. Ibers, *J. Am. Chem. Soc.* 1984, **106**, 5151.
24. (a) H. Masuda, T. Taga, K. Osaki, H. Sugimoto, M. Mori and H. Ogashi, *J. Am. Chem. Soc.* 1981, **103**, 2199. (b) H. Masuda, T. Taga, K. Osaki, H. Sugimoto, M. Mori and H. Ogashi, *Bull. Chem. Soc. Jpn* 1982, **55**, 3887.
25. A. K. Chakravarty, F. A. Cotton and W. Schwotzer, *Inorg. Chem.* 1984, **23**, 99.
26. (a) A. M. Mathieson, D. P. Mellor and N. C. Stephenson, *Acta Cryst.* 1952, **5**, 185; (b) J.-P. Deloume, R. Faure and G. Thomas-David, *Acta Cryst.* 1979, **B35**, 558.
27. V. L. Goedken and M. C. Weiss, *Inorg. Chem.* 1979, **18**, 819.
28. (a) J. E. Plowman, T. M. Loehr, C. K. Schauer and O. P. Anderson, *Inorg. Chem.* 1984, **23**, 3553; (b) A. V. Khedekar, J. Lewis, F. E. Mabbs and H. Weigold, *J. Chem. Soc. A* 1967, 1561.

29. F. Corazza, C. Floriani and M. Zehnder, *J. Chem. Soc., Dalton Trans.* 1987, 709.
30. (a) J. E. Davies and B. M. Gatehouse, *Acta Cryst.* 1973, **B29**, 1934; (b) M. Gerloch, E. D. McKenzie and A. D. C. Towl, *J. Chem. Soc. A* 1969, 2850; (c) P. Coggon, A. T. McPhail, F. E. Mabbs and V. N. McLachlan, *J. Chem. Soc. A* 1971, 1014; (d) P. J. Marini, K. S. Murray and B. O. West, *J. Chem. Soc., Dalton Trans.* 1983, 143; (e) J. Lewis, F. E. Mabbs and A. R. Richards, *J. Chem. Soc. A* 1967, 1014.
31. S. J. Lippard, H. L. Schugar and C. Walling, *Inorg. Chem.* 1967, **6**, 1825.
32. A. B. Hoffman, D. M. Collins, V. W. Day, E. B. Fleischer, T. S. Srivastava and J. L. Hoard, *J. Am. Chem. Soc.* 1972, **94**, 3620.
33. J. T. Landrum, D. Grimmitt, K. J. Haller, W. R. Scheidt and C. A. Reed, *J. Am. Chem. Soc.* 1981, **103**, 2640.
34. C. Ercolani and V. Goedken, private communication.
35. M. G. B. Drew, V. McKee and S. M. Nelson, *J. Chem. Soc., Dalton Trans.* 1978, 80.
36. P. Gomez-Romero, G. C. DeFotis and G. B. Jameson, *J. Am. Chem. Soc.* 1986, **108**, 851.
37. (a) J. A. Gilbert, D. S. Eggleston, W. R. Murphy, D. A. Geselowitz, S. W. Gerston, D. J. Hodgson and T. J. Meyer, *J. Am. Chem. Soc.* 1985, **107**, 3855; (b) D. W. Phelps, E. M. Khan and D. J. Hodgson, *Inorg. Chem.* 1975, **14**, 2486.
38. J. D. Dunitz and L. E. Orgel, *J. Chem. Soc.* 1953, 2594.
39. J. R. Campbell and R. J. H. Clark, *Mol. Phys.* 1978, **36**, 1133.
40. H.-H. Schmidtke, *Theor. Chim. Acta* 1971, **20**, 92.
41. K. Tatsumi and R. Hoffmann, *J. Am. Chem. Soc.* 1981, **103**, 3328.
42. E. Pedersen, *Acta Chem. Scand.* 1972, **26**, 333.
43. J. W. Buchler and K. Rohbock, *Inorg. Nucl. Chem. Lett.* 1972, **8**, 1073.
44. R. G. Hayes and W. R. Scheidt, *Inorg. Chem.* 1978, **17**, 1082.
45. C. Lecomte, J. Protas, R. Giulard, B. Fliniaux and P. Fournari, *J. Chem. Soc., Dalton Trans.* 1979, 1306.
46. D. Dolphin (Ed.), *The Porphyrins*, Vol. VII. Academic Press, New York (1979).
47. (a) P. C. Wilkins and R. G. Wilkins, *Coord. Chem. Rev.* 1987, **7**, 195; (b) I. M. Klotz and D. M. Kurtz, *Acc. Chem. Res.* 1984, **17**, 16.
48. (a) W. H. Armstrong and S. J. Lippard, *J. Am. Chem. Soc.* 1983, **105**, 4837; (b) W. H. Armstrong, A. Spool, G. C. Papaefthymiou, R. B. Frankel and S. J. Lippard, *J. Am. Chem. Soc.* 1984, **106**, 3653.
49. (a) K. Wieghardt, K. Pohl and W. Gebert, *Angew. Chem. Int. Ed. Engl.* 1983, **22**, 727; (b) K. Wieghardt, K. Pohl and D. Ventur, *Angew. Chem. Int. Ed. Engl.* 1985, **24**, 392.
50. N. W. Alcock, P. N. Bartlett, D. Gordon, T. F. Illson and M. G. H. Wallbridge, *J. Chem. Soc., Chem. Commun.* 1986, 614.
51. K. Wieghardt, M. Köppen, B. Nuber and J. Weiss, *J. Chem. Soc., Chem. Commun.* 1986, 1530.
52. (a) K. Wieghardt, U. Bossek, D. Ventur and J. Weiss, *J. Chem. Soc., Chem. Commun.* 1985, 347; (b) K. Wieghardt, U. Bossek, J. Weiss, J. Bonvoisin, P. Beauvillain, J.-J. Girerd, B. Nuber and J. Heinze, *Angew. Chem. Int. Ed. Engl.* 1986, **25**, 1030; (c) J. E. Sheats, R. S. Czernuszewicz, G. C. Dismukes, A. L. Rheingold, V. Petrouleas, J. Stubbe, W. H. Armstrong, R. H. Beer and S. J. Lippard, *J. Am. Chem. Soc.* 1987, **109**, 1435.
53. J. E. Armstrong, W. R. Robinson and R. A. Walton, *Inorg. Chem.* 1983, **22**, 1301.
54. (a) J. Livorness and T. D. Smith, *Struct. Bond. (Berlin)* 1982, **48**, 2; (b) J. Amesz, *Biochim. Biophys. Acta* 1983, **726**, 1; (c) G. Dismukes, *Photochem. Photobiol.* 1986, **43**, 99.
55. G. C. Dismukes, K. Ferris and P. Watnick, *Photobiochem. Photobiophys.* 1982, **3**, 243.
56. P. M. Plaksin, R. C. Stoufer, M. Mathew and G. J. Palenik, *J. Am. Chem. Soc.* 1972, **94**, 2121.
57. M. Stebler, A. Ludi and H.-B. Bürgi, *Inorg. Chem.* 1986, **25**, 4743.
58. M. A. Collins, D. J. Hodgson, K. Michelsen and D. K. Towle, *J. Chem. Soc., Chem. Commun.* 1987, 1659.
59. K. S. Hagen, W. H. Armstrong and H. Hope, *Inorg. Chem.* 1988, **27**, 967.
60. R. Ramaraj, A. Kira and M. Kaneko, *Angew. Chem. Int. Ed. Engl.* 1986, **25**, 825.
61. J. Catterick and P. Thornton, *Adv. Inorg. Chem. Radiochem.* 1977, **20**, 291.
62. S. C. Chang and G. A. Jeffrey, *Acta Cryst.* 1970, **B26**, 673.
63. K. Anzenhofer and J. J. de Boeer, *Rec. Trav. Chim.* 1969, **88**, 286.
64. A. B. Blake and L. R. Fraser, *J. Chem. Soc., Dalton Trans.* 1975, 193.
65. T. Lis and B. Jezowska-Trzebiatowska, *Acta Cryst.* 1977, **B33**, 2112.
66. F. A. Cotton, M. W. Extine, L. R. Falvello, D. B. Lewis, G. E. Lewis, C. A. Murillo, W. Schwotzer, M. Tomas and J. M. Troup, *Inorg. Chem.* 1986, **25**, 3505.
67. T. Glowiak, M. Kubiak and B. Jezowska-Trzebiatowska, *Bull. Acad. Pol. Sci. Ser. Sci. Chim.* 1977, **25**, 359.
68. F. A. Cotton, G. E. Lewis and G. N. Mott, *Inorg. Chem.* 1982, **21**, 3316.
69. C. E. Sumner and G. R. Steinmetz, *J. Am. Chem. Soc.* 1985, **107**, 6124.
70. T. Glowiak, M. Kubiak and T. Szymanska-Buzar, *Acta Cryst.* 1977, **B33**, 1732.

71. S. E. Woehler, R. J. Wittebort, S. M. Oh, D. N. Hendrickson, D. Inniss and C. E. Strouse, *J. Am. Chem. Soc.* 1986, **108**, 2938.
72. (a) S. M. Oh, D. N. Hendrickson, K. L. Hassett and R. E. Davis, *J. Am. Chem. Soc.* 1985, **107**, 8009; (b) S. M. Oh, D. N. Hendrickson, K. L. Hassett and R. E. Davis, *J. Am. Chem. Soc.* 1984, **106**, 7984.
73. F. A. Cotton and W. Wang, *Inorg. Chem.* 1982, **21**, 2675.
74. A. R. E. Baikie, M. B. Hursthouse, D. B. New and P. Thornton, *J. Chem. Soc., Chem. Commun.* 1978, 62.
75. A. R. E. Baikie, M. B. Hursthouse, L. New, P. Thornton and R. G. White, *J. Chem. Soc., Chem. Commun.* 1980, 684.
76. J. B. Vincent, H. R. Chang, K. Folting, J. C. Huffman, G. Christou and D. N. Hendrickson, *J. Am. Chem. Soc.* 1987, **109**, 5703.
77. F. A. Cotton and J. G. Norman, *Inorg. Chim. Acta* 1972, **6**, 411.
78. (a) A. Spencer and G. Wilkinson, *J. Chem. Soc., Dalton Trans.* 1972, 1570; (b) A. Spencer and G. Wilkinson, *J. Chem. Soc., Dalton Trans.* 1974, 786.
79. J. A. Baumann, D. J. Salmon, S. T. Wilson, T. J. Meyer and W. E. Hatfield, *Inorg. Chem.* 1978, **17**, 3342.
80. S. Uemura, A. Spencer and G. Wilkinson, *J. Chem. Soc., Dalton Trans.* 1973, 2565.
81. S. A. Fouda and G. L. Rempel, *Inorg. Chem.* 1979, **18**, 1.
82. S. Murata, M. Muira and M. Nomura, *Chem. Lett.* 1988, 361.
83. S. J. Lippard, *Angew. Chem. Int. Ed. Engl.* 1988, **27**, 344.
84. S. M. Gorun, G. C. Papaefthymiou, R. B. Frankel and S. J. Lippard, *J. Am. Chem. Soc.* 1987, **109**, 3337.
85. (a) J. B. Vincent, C. Christmas, J. C. Huffman, G. Christou, H.-R. Chang and D. N. Hendrickson, *J. Chem. Soc., Chem. Commun.* 1987, 236; (b) C. Christmas, J. B. Vincent, J. C. Huffman. G. Christou, H.-R. Chang and D. N. Hendrickson, *J. Chem. Soc., Chem. Commun.* 1987, 1303.
86. J. S. Bashkin, H.-R. Chang, W. E. Streib, J. C. Huffman, D. N. Hendrickson and G. Christou, *J. Am. Chem. Soc.* 1987, **109**, 6502.
87. C. Christmas, J. B. Vincent, J. C. Huffman, G. Christou, H.-R. Chang and D. N. Hendrickson, *Angew. Chem. Int. Ed. Engl.* 1987, **26**, 915.
88. (a) F. A. Cotton, *Polyhedron* 1986, **5**, 3; (b) A. Müller, R. Jostes and F. A. Cotton, *Angew. Chem. Int. Ed. Engl.* 1980, **19**, 875.
89. F. A. Cotton, Z. Dori, D. O. Marler and W. Schwotzer, *Inorg. Chem.* 1983, **22**, 3104.
90. A. Birnbaum, F. A. Cotton, Z. Dori, D. O. Marler, G. M. Reisner, W. Schwotzer and M. Shaia, *Inorg. Chem.* 1983, **22**, 2723.
91. M. Ardon, A. Bino, F. A. Cotton, Z. Dori, M. Kaftory and G. Reisner, *Inorg. Chem.* 1982, **21**, 1912.
92. (a) A. Bino, F. A. Cotton, Z. Dori, L. R. Falvello and G. M. Reisner, *Inorg. Chem.* 1982, **21**, 3750; (b) A. Bino, F. A. Cotton, Z. Dori and B. W. S. Kolthammer, *J. Am. Chem. Soc.* 1981, **103**, 5779.
93. (a) A. Bino, K.-F. Hesse and H. Küppers, *Acta Cryst.* 1980, **B36**, 723; (b) A. Bino, F. A. Cotton, Z. Dori, S. Koch, H. Küppers, M. Millar and J. C. Sekutowski, *Inorg. Chem.* 1978, **17**, 3245.
94. M. Ardon, F. A. Cotton, Z. Dori, A. Fang, M. Kapon, G. M. Reisner and M. Shaia, *J. Am. Chem. Soc.* 1982, **104**, 5394.
95. F. A. Cotton, Z. Dori, M. Kapon, D. O. Marler, G. M. Reisner, W. Schwotzer and M. Shaia, *Inorg. Chem.* 1985, **24**, 4381.
96. F. A. Cotton, S. A. Duraj and W. J. Roth, *J. Am. Chem. Soc.* 1984, **106**, 3527.
97. (a) A. Bino, *J. Am. Chem. Soc.* 1980, **102**, 7991; (b) A. Bino, *Inorg. Chem.* 1982, **21**, 1917.
98. M. H. Chisholm, K. Folting, J. C. Huffman and C. C. Kirkpatrick, *J. Am. Chem. Soc.* 1981, **103**, 5967.
99. M. H. Chisholm, K. Folting, J. C. Huffman and C. C. Kirkpatrick, *Inorg. Chem.* 1984, **23**, 1021.
100. M. H. Chisholm, K. Folting, J. C. Huffman and E. M. Kober, *Inorg. Chem.* 1985, **24**, 241.
101. B. F. Bursten, F. A. Cotton, M. B. Hall and R. C. Najjar, *Inorg. Chem.* 1982, **21**, 302.
102. M. H. Chisholm, F. A. Cotton, A. Fang and E. M. Kober, *Inorg. Chem.* 1984, **23**, 749.
103. (a) R. D. Jones, D. A. Summerville and F. Basolo, *Chem. Rev.* 1979, **79**, 139; (b) M. H. Gubelman and A. F. Williams, *Struct. Bond. (Berlin)* 1983, **55**, 1; (c) E. C. Niederhoffer, J. H. Timmons and A. E. Martell, *Chem. Rev.* 1984, **84**, 137.
104. (a) A. B. Blake, *J. Chem. Soc., Chem. Commun.* 1966, 569; (b) H. Koyama and Y. Saito, *Bull. Chem. Soc. Jpn.* 1954, **27**, 112; (c) J. A. Bertrand, *Inorg. Chem.* 1967, **6**, 495.
105. K. D. Karlin and Y. Gultneh, *Prog. Inorg. Chem.* 1987, **35**, 219.
106. (a) C. Lapinte, H. Riviere and A. Roselli, *J. Chem. Soc., Chem. Commun.* 1981, 1109; (b) K. D. Karlin, Y. Gultneh, J. C. Hayes and J. Zubieta, *Inorg. Chem.* 1984, **23**, 519.
107. (a) N. Kitajima, T. Koda and Y. Moro-oka, *Chem. Lett.* 1988, 347; (b) N. Kitajima, T. Koda, T. Kitagawa and Y. Moro-oka, *J. Chem. Soc., Chem. Commun.* 1988, 151.
108. P. Chaudhuri, D. Ventur, K. Wieghardt, E.-M. Peters, K. Peters and A. Simon, *Angew. Chem. Int. Ed. Engl.* 1985, **24**, 57.
109. (a) F. Bottomley and L. Sutin, *Adv. Organomet. Chem.* 1988, **28**, 339; (b) W. A. Herrmann, E. Herdtweck, M. Flöel, J. Kulpe, U. Küsthardt and J. Okuda, *Polyhedron* 1987, **6**, 1165.

110. (a) V. W. Day, M. F. Fredrich, M. R. Thompson, W. G. Klemperer, R.-S. Liu and W. Shun, *J. Am. Chem. Soc.* 1981, **103**, 3597; (b) T. M. Che, V. W. Day, L. C. Francesconi, M. T. Fredrich and W. G. Klemperer, *Inorg. Chem.* 1985, **24**, 4055.
111. V. W. Day, C. W. Earley, W. G. Klemperer and D. J. Maltbie, *J. Chem. Soc.* 1985, **107**, 8261.
112. C. Phalguri, K. Wieghardt, B. Nuber and J. Weiss, *J. Chem. Soc., Chem. Commun.* 1987, 1198.
113. (a) W. J. Evans and M. S. Sollberger, *J. Am. Chem. Soc.* 1986, **108**, 6095; (b) D. C. Bradley, H. Chudzynska, D. M. Frigo, M. B. Hursthouse and M. A. Mazid, *J. Chem. Soc., Chem. Commun.*, 1988, 1258.
114. J. R. Campbell and R. J. H. Clark, *J. Chem. Soc., Faraday II* 1980, **76**, 1103.
115. (a) R. N. Jowitt and P. C. H. Mitchell, *J. Chem. Soc. A* 1970, 1702; (b) W. E. Newton, J. L. Corbin, D. C. Bravard, J. E. Searles and J. W. McDonald, *Inorg. Chem.* 1974, **13**, 1100.
116. G. J. J. Chen, J. W. MacDonald and W. E. Newton, *Inorg. Chem.* 1976, **15**, 2612.
117. (a) R. Barral, C. Bocard, I. Seree de Roch and L. Sajus, *Tetrahedron Lett.* 1972, **17**, 1693; (b) W. E. Newton, G. D. Watt and J. W. McDonald, Chemical uses of Mo, *Proc. Int. Conf.* 1979, **3**, 259.
118. T. Matsuda, K. Tanaka and T. Tanaka, *Inorg. Chem.* 1979, **18**, 454.
119. S.-I. Miyake, K. Tanaka and T. Tanaka, *J. Chem. Soc., Dalton Trans.* 1981, 292.
120. J. M. Berg and R. H. Holm, *J. Am. Chem. Soc.* 1985, **107**, 917.
121. R. N. Jowitt and P. C. H. Mitchell, *J. Chem. Soc. A* 1969, 2632.
122. J. O. Alben, W. H. Fuchsmau, C. A. Beaudredy and W. S. Caughey, *Biochemistry* 1968, **7**, 624.
123. D. J. Liston and B. O. West, *Inorg. Chem.* 1985, **24**, 1568.
124. J. P. Collman, C. E. Barnes, T. J. Collins and P. J. Brothers, *J. Am. Chem. Soc.* 1981, **103**, 7030.
125. (a) C. Ercolani, M. Gardini, F. Monacelli, G. Pennesi and G. Rossi, *Inorg. Chem.* 1983, **22**, 2584; (b) C. Ercolani, G. Rossi and F. Monacelli, *Inorg. Chim. Acta* 1980, **44**, L215.
126. (a) J. A. Elvidge and A. B. P. Lever, *Proc. Chem. Soc.* 1959, 195; (b) A. B. P. Lever, J. P. Wilshire and S. K. Quan, *Inorg. Chem.* 1981, **20**, 761.
127. D. H. Gerlach and R. H. Holm, *Inorg. Chem.* 1970, **9**, 588.
128. W. M. Coleman and L. T. Taylor, *Coord. Chem. Rev.* 1980, **32**, 1.
129. J. Buchler, *Angew. Chem. Int. Ed. Engl.* 1978, **17**, 407.
130. D.-H. Chin, G. N. La Mar and A. L. Balch, *J. Am. Chem. Soc.* 1980, **102**, 4344.
131. L. Latos-Grazynski, R.-J. Cheng, G. N. La Mar and A. L. Balch, *J. Am. Chem. Soc.* 1982, **104**, 5992.
132. D.-H. Chin, A. L. Balch and G. N. La Mar, *J. Am. Chem. Soc.* 1980, **102**, 1446.
133. J. T. Groves and Y. Watanabe, *J. Am. Chem. Soc.* 1986, **108**, 7834.
134. J. R. Budge, B. M. K. Gatehouse, M. C. Nesbit and B. O. West, *J. Chem. Soc., Chem. Commun.* 1981, 370.
135. (a) S. K. Cheung, C. J. Grimes, J. Wong and C. A. Reed, *J. Am. Chem. Soc.* 1976, **98**, 5028; (b) C. A. Reed and S. K. Cheung, *Proc. Natl. Acad. Sci. U.S.A.* 1977, **74**, 1780.
136. K. H. Nill, F. Wasgestian and A. Pfeil, *Inorg. Chem.* 1979, **18**, 564.
137. C. J. Weschler, B. M. Hoffman and F. Basolo, *J. Am. Chem. Soc.* 1975, **97**, 5278.
138. B. Gonzalez, J. Kouba, S. Lee, C. A. Reed, J. Kirner and W. R. Scheidt, *J. Am. Chem. Soc.* 1975, **97**, 3247.
139. G. W. Rayner Canham and A. B. P. Lever, *Inorg. Nucl. Chem. Lett.* 1973, **9**, 513.
140. (a) J. T. Groves and W. S. Kruper, *J. Am. Chem. Soc.* 1979, **101**, 7613; (b) J. T. Groves and R. C. Haushalter, *J. Chem. Soc., Chem. Commun.* 1981, 1165; (c) J. T. Groves, W. J. Kruper, R. C. Haushalter and W. M. Butler, *Inorg. Chem.* 1982, **21**, 1363.
141. (a) F. Bottomley, D. F. Drummond, D. E. Paez and P. S. White, *J. Chem. Soc., Chem. Commun.* 1986, 1752; (b) F. Bottomley, D. E. Paez and P. S. White, *J. Am. Chem. Soc.* 1985, **107**, 7226.
142. A. Bino, F. A. Cotton and Z. Dori, *J. Am. Chem. Soc.* 1981, **103**, 243.
143. (a) J. A. Thich, C. Chih Ou, B. Powers, B. Vasiliou, D. Mastrapaolo, J. A. Potenza and H. J. Schugar, *J. Am. Chem. Soc.* 1976, **98**, 1425; (b) L. Borer, L. Thalken, C. Ceccarelli, M. Glick, J. H. Zhang and W. M. Reiff, *Inorg. Chem.* 1983, **22**, 1719.
144. (a) A. L. Balch, Y.-W. Chan, R.-J. Cheng, G. N. La Mar, L. Latos-Grazynski and M. W. Renner, *J. Am. Chem. Soc.* 1984, **106**, 7779; (b) R.-J. Cheng, L. Latos-Grazynski and A. L. Balch, *Inorg. Chem.* 1982, **21**, 2412; (c) J. T. Groves, R. C. Haushalter, M. Nakamura, T. E. Nemo and B. J. Evans, *J. Am. Chem. Soc.* 1981, **103**, 2884.
145. (a) F. E. Mabbs and D. J. Machin, *Magnetism and Transition Metal Complexes*, Chap. 7. Chapman and Hall, London (1973); (b) R. L. Martin in *New Pathways in Inorganic Chemistry* (Edited by E. A. V. Ebsworth, A. G. Maddock and A. G. Sharpe), Chap. 9, p. 175. Cambridge University Press, Cambridge (1968).
146. R. N. Mukherjee, T. D. P. Stack and R. H. Holm, *J. Am. Chem. Soc.* 1988, **110**, 1850.
147. J. H. Helms, I. W. ter Haar, W. E. Hatfield, D. L. Harris, K. Jayaraj, G. E. Toney, A. Gold, T. D. Mewborn and J. R. Pemberton, *Inorg. Chem.* 1986, **25**, 2334.

148. J. R. Dorfman, J.-J. Girerd, E. D. Simhon, T. D. P. Stack and R. H. Holm, *Inorg. Chem.* 1984, **23**, 4407.
149. D. H. Jones, J. R. Sams and R. C. Thompson, *J. Chem. Phys.* 1984, **81**, 440 and refs therein.
150. M. Sorai, M. Tachiki, H. Suga and S. Seki, *J. Phys. Soc. Jpn* 1971, **30**, 750.
151. (a) K. J. Schenk and H. U. Gudel, *Inorg. Chem.* 1982, **21**, 2253; (b) L. Dubicki, J. Ferguson and B. Williamson, *Inorg. Chem.* 1983, **22**, 3200.
152. J. San Filippo Jr, P. J. Fagan and F. J. Di Salvo, *Inorg. Chem.* 1977, **16**, 1016.
153. W. E. Newton and J. W. McDonald, *J. Less-Common Met.* 1977, **54**, 51.
154. M. K. Johnson, D. B. Powell and R. D. Cannon, *Spectrochim. Acta* 1981, **37A**, 995.
155. L. Montri and R. D. Cannon, *Spectrochim. Acta* 1985, **41A**, 643.
156. K. F. Miller and R. A. D. Wentworth, *Inorg. Chem.* 1979, **18**, 984; K. F. Miller and R. A. D. Wentworth, *Inorg. Chem.* 1980, **19**, 1818.
157. (a) W. G. Klemperer, *Angew. Chem. Int. Ed. Engl.* 1978, **17**, 246; (b) M. Filowitz, R. K. C. Ho, W. G. Klemperer and W. Shum, *Inorg. Chem.* 1979, **18**, 93.
158. F. W. Moore and M. L. Larson, *Inorg. Chem.* 1967, **6**, 998.
159. A. Yuchi, H. Muranaka, S. Yamada and M. Tanaka, *Bull. Chem. Soc. Jpn* 1980, **53**, 1560.
160. L. Dubicki and P. Day, *Inorg. Chem.* 1972, **11**, 1868.
161. C. J. Ballhausen and H. B. Gray, *Inorg. Chem.* 1962, **1**, 111.
162. (a) R. Loessberg and K. Dehnicke, *Z. Naturfor. Anorg. Chem. Org. Chem.* 1979, **34B**, 1040; (b) R. Loessberg and K. Dehnicke, *Z. Naturfor. Anorg. Chem. Org. Chem.* 1980, **35B**, 1587.
163. J. Kress, M. Wesolek, J.-P. Le Ny and J. A. Osborn, *J. Chem. Soc., Chem. Commun.* 1981, 1039.
164. C.-H. Yang and V. L. Goedken, *Inorg. Chim. Acta* 1986, **117**, L19.
165. H. de Smedt, A. Persoons and L. De Mayer, *Inorg. Chem.* 1974, **13**, 90.
166. F. J. Kristine and R. E. Shepherd, *Inorg. Chem.* 1978, **17**, 3145.
167. J. R. M. Kress, M. J. M. Russell, M. G. Wesolek and J. A. Osborn, *J. Chem. Soc., Chem. Commun.* 1980, 431.
168. J. C. Evans, *Inorg. Chem.* 1963, **2**, 372.
169. M. Gerloch and F. E. Mabbs, *J. Chem. Soc. A* 1967, 1900.
170. D. C. Bradley and I. M. Thomas, *J. Chem. Soc.* 1959, 3404.
171. C. M. Langkammerer, U.S. Patent 2,621,193 (1952).
172. (a) M. Osgan and P. Teyssié, *Polym. Letts* 1967, **5**, 789; (b) M. Osgan, P. Teyssie and J.-P. Wauquier, *Am. Chem. Soc. Div. Petroleum Chem. Prepr.* 1968, **13**, A89.
173. T. Ouhadi, J. P. Bioul, C. Stevens, R. Warin, L. Hocks and P. Teyssié, *Inorg. Chim. Acta* 1976, **19**, 203.
174. L. Hocks, J. P. Bioul, P. Durbut, A. Hamitou, J. L. Marbehant, T. Ouhadi, Ch. Stevens and P. Teyssié, *J. Mol. Catal.* 1977/78, **3**, 135.
175. M. Organ, J. J. Pasero and P. Teyssié, *Polym. Letts* 1970, **88**, 319.
176. P. Teyssié, J. P. Bioul, P. Condé, J. Druet, J. Heuschen, R. Jérôme, T. Ouhadi and R. Warin, *Am. Chem. Soc., Symp. Ser.* 1985, **286**, 97.
177. T. Ouhadi, A. Hamitou, R. Jérôme and P. Teyssié, *Macromol.* 1976, **9**, 927.
178. M. Osgan, J. P. Silly and P. Teyssié, U.S. Patent 3,432,445 (1969); M. Osgan, R. Charpentier and P. Teyssié, U.S. Patent 3,607,785 (1971).
179. E. J. Vandenberg, *J. Polym. Sci.* 1986, **24A**, 1423.
180. L. Hocks, P. Durbut and P. Teyssié, *J. Mol. Catal.* 1980, **7**, 75.
181. J. Lamotte, O. Dideberg, L. Dupont and P. Durbut, *Cryst. Struct. Commun.* 1981, **10**, 59.
182. T. Ouhadi, A. J. Hubert, P. Teyssié and E. G. Derouane, *J. Am. Chem. Soc.* 1973, **95**, 6481.
183. W. S. Caughey, W. J. Wallace, J. A. Volpe and S. Yoshikawa, *The Enzymes* (Edited by P. D. Boyer), 3rd Edn. Vol. XIII, p. 299. Academic Press, New York (1976).
184. C. R. Reed and J. T. Landrum, *FEBS Letts* 1979, **106**, 265.
185. (a) G. Palmer, G. T. Babcock and L. E. Vickery, *Proc. Natl. Acad. Sci. U.S.A.* 1976, **73**, 2206; (b) L. Powers, B. Chance, Y. Ching and P. Angiolillo, *Biophys. J.* 1981, **34**, 465.
186. M. F. Tweedle, L. J. Wilson, L. Garcia-Iniguez, G. T. Babcock and G. Palmer, *J. Biol. Chem.* 1978, **253**, 8065.
187. M. J. Gunter, L. N. Mander, K. S. Murray and P. E. Clark, *J. Am. Chem. Soc.* 1981, **103**, 6784 and refs therein.
188. C. K. Chang, M. S. Koo and B. Ward, *J. Chem. Soc., Chem. Commun.* 1982, 716.
189. R. J. Saxton, L. W. Olson and L. J. Wilson, *J. Chem. Soc., Chem. Commun.* 1982, 984.
190. L. J. Wilson and R. J. Saxton, *J. Chem. Soc., Chem. Commun.* 1984, 359.
191. B. R. Serr, C. E. L. Headford, C. M. Elliott and O. P. Anderson, *J. Chem. Soc., Chem. Commun.* 1988, 92.
192. (a) D. J. Liston, K. S. Murray and B. O. West, *J. Chem. Soc., Chem. Commun.* 1982, 1109; (b) D. J. Liston, B. J. Kennedy, K. S. Murray and B. O. West, *Inorg. Chem.* 1985, **24**, 1561.
193. R. L. Elliott, P. J. Nichols and B. O. West, *Aust. J. Chem.* 1986, **39**, 975.

194. R. L. Elliott, P. J. Nichols and B. O. West, *J. Chem. Soc., Chem. Commun.* 1986, 840.
195. R. L. Elliott, PhD thesis, Monash University Victoria, Australia (1987).
196. R. L. Eliott and B. O. West, *Aust. J. Chem.* 1988, **41**, 1417.
197. C. Ercolani, G. Gardini, G. Pennesi and G. Rossi, *J. Chem. Soc., Chem. Commun.* 1983, 549.
198. W. S. Caughey, C. H. Barlow, D. H. O'Keefe and M. C. O'Toole, *Ann. N.Y. Acad. Sci.* 1973, **206**, 296.
199. (a) D. A. Summerville, R. D. Jones, B. M. Hoffman and F. Basolo, *J. Am. Chem. Soc.* 1977, **99**, 8195; (b) T. Ozwawa and A. Hanaki, *Inorg. Chim. Acta* 1985, **102**, 169.
200. (a) M. Nicholas, R. Mustacich and D. Jayne, *J. Am. Chem. Soc.* 1972, **94**, 4518; (b) G. N. La Mar, G. R. Eaton, R. H. Holm and F. A. Walker, *J. Am. Chem. Soc.* 1973, **95**, 63; (c) P. D. W. Boyd and K. S. Murray, *J. Chem. Soc. A* 1971, 2711.
201. (a) I. A. Cohen, *J. Am. Chem. Soc.* 1969, **91**, 1980; (b) A. N. Buckley, I. R. Herbert, B. D. Rumbold, G. V. H. Wilson and K. S. Murray, *J. Phys. Chem. Solids* 1970, **31**, 1423; (c) H. J. Schugar, G. R. Rossman, C. G. Barraclough and H. B. Gray, *J. Am. Chem. Soc.* 1972, **94**, 2683; (d) B. J. Kennedy, A. C. McGrath, K. S. Murray, B. W. Skelton and A. H. White, *Inorg. Chem.* 1987, **26**, 483; (e) N. Matsumoto, S. Ohta, C. Yoshimura, A. Obyoshi, S. Kohata, H. Okawa and Y. Maeda, *J. Chem. Soc., Dalton Trans.* 1985, 2575; (f) L. M. Epstein and D. K. Straub, *Inorg. Chem.* 1969, **8**, 560; (g) A. Malliaris and D. Niarchos, *Inorg. Chem.* 1976, **15**, 1340; (h) L. M. Epstein and D. K. Straub, *Inorg. Chem.* 1969, **8**, 784; A. G. El A'mma and R. S. Drago, *Inorg. Chem.* 1977, **16**, 2975; (i) B. W. Fitzsimmons, S. E. Al-Mukhtar, L. F. Larkworthy and R. R. Patel, *J. Chem. Soc., Dalton Trans.* 1975, 1969.
202. (a) Y. Journaux, O. Kahn, J. Zarembowitch, J. Galy and J. Jand, *J. Am. Chem. Soc.* 1983, **105**, 7585; (b) M. Julve, M. Verdognier, M.-F. Charlot, O. Kahn and R. Claude, *Inorg. Chim. Acta* 1984, **82**, 5; (c) M. J. Gunter, L. N. Mander and K. S. Murray, *J. Chem. Soc., Chem. Commun.* 1981, 799.
203. E. Bakshi, R. L. Elliott, K. S. Murray and B. O. West, unpublished data.
204. (a) W. M. Coleman and L. T. Taylor, *Inorg. Chem.* 1977, **16**, 1114; (b) W. M. Coleman and L. T. Taylor, *Inorg. Chim. Acta* 1978, **30**, L291.
205. M. Pasquali, A. Landi and C. Floriani, *Inorg. Chem.* 1979, **18**, 2397.
206. D. D. Devore and E. A. Maatta, *Inorg. Chem.* 1985, **24**, 2846.
207. (a) H. J. Ledon, M. C. Bonnet, Y. Brigandat and F. Veresion, *Inorg. Chem.* 1980, **19**, 3488; (b) A. T. Casey, D. J. Mackay, R. L. Martin and A. H. White, *Aust. J. Chem.* 1972, **25**, 477.
208. F. A. Cotton, W. R. Robinson and R. A. Walton, *Inorg. Chem.* 1967, **6**, 223.
209. D. M. Hill, L. E. Larkworthy and M. W. O'Donoghue, *J. Chem. Soc., Dalton Trans.* 1975, 1726.
210. A. Nakamura, M. Nakayama, K. Sugihashi and S. Otsuka, *Inorg. Chem.* 1979, **18**, 394.
211. J. D. A. Raj, K. S. Nagaraja and M. R. Udupa, *Transition Met. Chem.* 1986, **11**, 176.
212. M. Mazzanti, C. Floriani, A. Chiesi-Vela and C. Guastini, *Inorg. Chem.* 1986, **25**, 4158.
213. R. Weinland and H. Holtmeier, *Z. Anorg. Allg. Chem.* 1928, **173**, 49.
214. (a) A. B. Blake, A. Yavari and H. Kubicki, *J. Chem. Soc., Chem. Commun.* 1981, 796; (b) A. B. Blake and A. Yavari, *J. Chem. Soc., Chem. Commun.* 1982, 1247.
215. A. B. Blake, A. Yavari, W. E. Hatfield and C. Sethulekshmi, *J. Chem. Soc., Dalton Trans.* 1985, 2509.
216. W. Clegg, O. M. Lam and B. P. Straughan, *Inorg. Chim. Acta* 1984, **90**, L75.
217. W. Clegg, O. M. Lam and B. P. Straughan, *Angew. Chem. Int. Ed. Engl.* 1984, **23**, 434.
218. B. P. Straughan and O. M. Lam, *Inorg. Chim. Acta* 1985, **98**, 7.
219. B. P. Straughan, O. M. Lam and A. Earnshaw, *J. Chem. Soc., Dalton Trans.* 1987, 97.
220. Y. Sasaki, A. Tokiwa and T. Ito, *J. Am. Chem. Soc.* 1987, **109**, 6341.
221. T. Glowiak, M. Kubiak, T. Szymanska-Buzar and B. Jezowska-Trzebiatowska, *Acta Cryt.* 1977, **B33**, 3106.
222. R. D. Cannon, L. Montri, D. B. Brown, K. M. Marshall and C. M. Elliott, *J. Am. Chem. Soc.* 1984, **106**, 2591.
223. L. Messuk, U. A. Jayasooriya and R. D. Cannon, *J. Am. Chem. Soc.* 1987, **109**, 2009.
224. L. Messuk, U. A. Jayasooriya and R. D. Cannon, *Spectrochim. Acta* 1987, **43A**, 687.
225. B. Wang, Y. Sasaki, A. Nagasawa and T. Ito, *J. Am. Chem. Soc.* 1986, **108**, 6059.
226. B. Wang, Y. Sasaki, S. Ikari, K. Kimura and T. Ito, *Chem. Lett.* 1987, 1955.
227. A. Nagasawa, Y. Sasaki, B. Wang, S. Ikari and T. Ito, *Chem. Lett.* 1987, 1271.
228. M. H. Chisholm, K. Folting, J. A. Heppart, D. M. Hoffman and J. C. Huffman, *J. Am. Chem. Soc.* 1985, **107**, 1234.
229. C. P. Gibson, J.-S. Huang and L. F. Dahl, *Organometallics* 1986, **5**, 1676.
230. I. L. Fremenko, A. A. Pasynskii, G. Sh. Gasanov, B. Orazsakhatov, Y. T. Struchkov and V. E. Schklover, *J. Organomet. Chem.* 1984, **275**, 71.
231. C. K. Schauer and D. F. Schriver, *Angew. Chem. Int. Ed. Engl.* 1987, **26**, 255.
232. A. Ceriotti, L. Resconi, F. Demartin, G. Langoni, M. Manassero and M. Sansoni, *J. Organomet. Chem.* 1983, **249**, C35.

233. J. R. Shapley, J. T. Park, M. R. Churchill, J. W. Ziller and L. R. Beanan, *J. Am. Chem. Soc.* 1984, **106**, 1144.
234. M. R. Churchill, C. Bueno, J. T. Park and J. R. Shapley, *Inorg. Chem.* 1984, **23**, 1017.
235. G. A. Carriedo, J. C. Jeffery and F. G. A. Stone, *J. Chem. Soc., Dalton Trans.* 1984, 1597.
236. E. N. Jacobsen, M. K. Trost and R. G. Bergman, *J. Am. Chem. Soc.* 1986, **108**, 8092.
237. J. D. Audett, T. J. Collins, B. D. Santarsiero and G. H. Spies, *J. Am. Chem. Soc.* 1982, **104**, 7352.
238. M. F. Lappert, C. L. Raston, G. L. Rowbottom, B. W. Skelton and A. H. White, *J. Chem. Soc., Dalton Trans.* 1984, 883.
239. L. M. Engelhardt, R. I. Papasergio, C. L. Raston, G. Salem and A. H. White, *J. Chem. Soc., Dalton Trans.* 1986, 789.
240. P. Stavropoulos, G. Wilkinson, M. Motevalli and M. B. Hursthouse, *Polyhedron* 1987, **6**, 1081.
241. P. Stavropoulos, P. G. Edwards, G. Wilkinson, M. Motevalli, K. M. A. Malik and M. B. Hursthouse, *J. Chem. Soc., Dalton Trans.* 1985, 2167.
242. P. Stavropoulos, P. G. Edwards, T. Behling, G. Wilkinson, M. Motevalli and M. B. Hursthouse, *J. Chem. Soc., Dalton Trans.* 1987, 169.
243. H. Arzoumanian, R. A. Lopez, A. D. Kowalak and J. Metzger, *J. Am. Chem. Soc.* 1977, **99**, 5175.
244. (a) H. Arzoumanian, R. Lai, R. L. Alvarez, J. F. Petrignani, J. Metzger and J. Fuhrhop, *J. Am. Chem. Soc.* 1980, **102**, 845; (b) H. Arzoumanian, R. Lai, R. Lopez Alvarez, J. Metzger and J. F. Petrignani, *J. Mol. Catal.* 1980, **7**, 43.
245. H. Arzoumanian, R. Lai, J. Metzger, J. F. Petrignani and P. Tordo, *Inorg. Chem.* 1983, **22**, 2097.
246. F. A. Cotton, S. A. Duraj and W. J. Roth, *Inorg. Chem.* 1984, **23**, 4042.
247. T. R. Weaver, T. J. Meyer, S. A. Adeyemi, G. M. Brown, R. P. Eckberg, W. E. Hatfield, E. C. Johnson, R. W. Murray and D. Untereker, *J. Am. Chem. Soc.* 1975, **97**, 3039.
248. J. A. Baumann and T. J. Meyer, *Inorg. Chem.* 1980, **19**, 345.
249. P. Doppelt and T. J. Meyer, *Inorg. Chem.* 1987, **26**, 2027.
250. S. W. Gersten, G. J. Samuels and T. J. Meyer, *J. Am. Chem. Soc.* 1982, **104**, 4029.
251. J. A. Gilbert, D. Gesslowitz and T. J. Meyer, *J. Am. Chem. Soc.* 1986, **108**, 1493.
252. (a) R. A. Holwerda and J. S. Petersen, *Inorg. Chem.* 1980, **19**, 1775; (b) R. F. Johnston and R. A. Holwerda, *Inorg. Chem.* 1983, **22**, 2942; R. F. Johnston and R. A. Holwerda, *Inorg. Chem.* 1985, **24**, 3176.
253. D. W. Hoppenjans and J. B. Hunt, *Inorg. Chem.* 1969, **18**, 505.
254. (a) M. Ardon and R. A. Plane, *J. Am. Chem. Soc.* 1959, **81**, 3197; (b) R. W. Kolaczkowski and R. A. Plane, *Inorg. Chem.* 1964, **3**, 322.
255. L. Spiccia, H. Stoeckli-Evans, W. Marty and R. Giovanoli, *Inorg. Chem.* 1987, **26**, 474.
256. (a) H. Stunzi and W. Marty, *Inorg. Chem.* 1983, **22**, 2145; (b) H. Stunzi, F. P. Rotzinger and W. Marty, *Inorg. Chem.* 1984, **23**, 2160; H. Stunzi, F. P. Rotzinger and W. Marty, *Inorg. Chem.* 1986, **25**, 489.
257. M. Thompson and R. E. Cormick, *Inorg. Chem.* 1981, **20**, 2279.
258. J. Springborg and H. Toftlund, *J. Chem. Soc., Chem. Commun.* 1975, 422; J. Springborg and H. Toftlund, *Acta Chem. Scand.* 1976, **30A**, 171.

Polyhedron Vol. 8, No. 3, pp. 275–284, 1989
Printed in Great Britain

0277-5387/89 $3.00 + .00
©1989 Pergamon Press plc

KINETICS AND MECHANISM OF AQUATION REACTIONS OF DIHALO-, DIACETONITRILE- AND BROMOACETONITRILE-(3,3′,3″-TRIAMINOTRIPROPYLAMINE)COBALT(III) PERCHLORATE

SALAH S. MASSOUD* and RONALD M. MILBURN

Department of Chemistry, Boston University, Boston, MA 02215, U.S.A.

(*Received* 1 *May* 1988; *accepted* 21 *June* 1988)

Abstract—The octahedral cobalt(III) complexes with the tripodal quadridentate amine, 3,3′,3″-triaminotripropylamine [trpn = $N(CH_2CH_2CH_2NH_3)_3$], $[Co(trpn)Cl_2]ClO_4$, $[Co(trpn)Br_2]ClO_4$, $[Co(trpn)F_2]ClO_4 \cdot 3/2H_2O$, $[Co(trpn)(CH_3CN)_2](ClO_4)_3$ and $[Co(trpn)(CH_3CN)Br]BrClO_4$ have been synthesized. The acid hydrolysis of $[Co(trpn)Cl_2]^+$ and the rate of bromide substitution in $[Co(trpn)(CH_3CN)Br]^{2+}$, clearly demonstrate the extreme lability of these complexes. The aquation of $[Co(trpn)F_2]^+$ ion was examined in both neutral and acidic medium. In neutral aqueous medium, the primary aquation determined at 25°C and $\mu = 0.5$ M, gave $k_1 = 1.28 \times 10^{-3}$ s^{-1}, $\Delta H_1^\ddagger = 12.8$ kcal mol^{-1} and $\Delta S_1^\ddagger = -28.9$ cal K^{-1} mol^{-1}, while for the secondary aquation step (25°C and $\mu = 1.0$ M) the acid-independent pathway gave $k_2 = 1.4 \times 10^{-4}$ s^{-1}, $\Delta H_2^\ddagger = 21.3$ kcal mol^{-1} and $\Delta S_2^\ddagger = -4.7$ cal K^{-1} mol^{-1}. The acid hydrolysis of $[Co(trpn)(CH_3CN)_2]^{3+}$ was studied over the pH range 1–4 and the temperature range 8–20°C. The hydrolysis proceeds in two consecutive steps:

$$[Co(trpn)(CH_3CN)_2]^{3+} \xrightarrow{k_1} [Co(trpn)(CH_3CN)(H_2O)]^{3+} \xrightarrow{k_2} [Co(trpn)(H_2O)_2]^{3+}.$$

Analysis of the kinetic data gave $k_1 = 1.2 \times 10^{-2}$ s^{-1} (20°C), $\Delta H_1^\ddagger = 16.0$ kcal mol^{-1} and $\Delta S_1^\ddagger = -12.7$ cal K^{-1} mol^{-1}, and $k_2 = 2.38 \times 10^{-3}$ s^{-1} (20°C), $\Delta H_2^\ddagger = 14.9$ kcal mol^{-1} and $\Delta S_2^\ddagger = -19.4$ cal K^{-1} mol^{-1}. The results of the kinetics of these substitution reactions are discussed in relation to data for the other tetraamine cobalt(III) complexes.

The complexes of cobalt(III) with the tripod quadridentate ligand 3,3′,3″-triaminotripropylamine [trpn = $N(CH_2CH_2CH_2NH_2)_3$] dramatically enhance the rate of hydrolysis of ATP[1-3] (ATP = adenosine-5′-triphosphate) in comparison to the unpromoted hydrolysis. They appear to be very valuable for "model system" studies of the metal ion effect on non-enzymatic reactions, which are related to similar biologically important processes.

Complexes of the tripod tetraamine, 2,2′,2″-triaminotriethylamine [tren = $N(CH_2CH_2NH_2)_3$] have been extensively studied, and the subject has been reviewed.[4] Use of this ligand led to the preparation of either five-coordinate[5] or *cis*-octahedral complexes.[6] The addition of another CH_2 group into each ethylene bridging chain of tren produces the more flexible trpn ligand, which allows the formation of tetrahedral, trigonal bipyramidal or octahedral complexes.[7-9] Also, in many species of octahedral tetraamine complexes, the *cis*/*trans* isomerization complicates the study. This problem is avoided by using the trpn ligand, for which the fifth and sixth coordination sites are fixed and forced to be in the *cis* position.

It has been suggested that replacement of five-membered ethylenediamine (en) with six-membered trimethylenediamine (tn) rings causes marked labilization in some cobalt(III) complexes.[10] Thus the combined effects of marked labilization associated with the six-membered ring systems and the absence of *cis* ⇌ *trans* isomerization in Co(III)–trpn systems offer a unique opportunity to gather significant

*Author to whom correspondence should be addressed: Department of Chemistry, Faculty of Science, Alexandria University, Alexandria, Egypt.

information about metal-ion catalysed reactions.[1-3]

Since no kinetic data were available for the cobalt(III)–trpn systems and in order to gain more insight into the mechanism of the substitution reactions in these complexes, we have decided to study the acid hydrolysis of the complex ions $[Co(trpn)F_2]^+$, $[Co(trpn)Cl_2]^+$, $[Co(trpn)Br_2]^+$, $[Co(trpn)(CH_3CN)_2]^{3+}$ and $[Co(trpn)(CH_3CN)Br]^{2+}$.

EXPERIMENTAL

Synthesis of the complexes

The complexes $[Co(trpn)Cl_2]ClO_4$, $[Co(trpn)Br_2]ClO_4$, $[Co(trpn)F_2]ClO_4 \cdot 3/2H_2O$, $[Co(trpn)(CH_3CN)_2](ClO_4)_3$ and $[Co(trpn)(CH_3CN)Br]BrClO_4$ were prepared as previously described in our recent report.[11]

Electronic spectra and rate data were recorded using a Cary 210 spectrophotometer. pH measurements were made with an Orion Research pH meter model 601 A fitted with a combination electrode.

Kinetic measurements

All rate measurements were made spectrophotometrically at an appropriate wavelength, where a large difference between the molar absorptivities for the reactants and products exists. In each kinetic run, an equilibrated solution (H_2O, aqueous $HClO_4$ solution or equal volumes of 0.20 M $HClO_4$ and CH_3CN) was added to a thermostated volumetric flask containing a weighed sample of the complex together with $NaClO_4$ (for adjusting the ionic strength). The addition was made quickly and with vigorous swirling. Then, the solution was transferrred into a thermostated 1 cm quartz cell, where the rate of hydrolysis was monitored spectrophotometrically with time.

Acid hydrolysis of the $[Co(trpn)X_2]^+$ *ion* (X = F, Cl, Br). The acid hydrolysis of $[Co(trpn)Cl_2]^+$ ion (5 mM) in 0.1 M $HClO_4$ at 25°C and $\mu = 0.5$ M was measured by following the absorbance change vs time at 530 nm. The primary aquation of $[Co(trpn)F_2]^+$ ion (3 mM) in neutral aqueous medium was followed at 368 nm. The secondary aquation was measured in 0.09–1.1 M $HClO_4$ and the reaction was examined at 368 nm, as well as at 338 nm.

Acid hydrolysis of the $[Co(trpn)(CH_3CN)_2]^{3+}$ *ion.* In a typical experiment a weighed sample of the complex, $[Co(trpn)(CH_3CN)_2](ClO_4)_3$ (7.85 mg) in a thermostated volumetric flask, was treated with an aqueous solution (pH 1.0–4.0) equilibrated at the same temperature to give a solution of concentration 2.5 mM of the complex. Hydrolysis was monitored at 510 nm.

Acid hydrolysis of the $[Co(trpn)(CH_3CN)Br]^{2+}$ *ion.* A weighed sample of $[Co(trpn)(CH_3CN)Br]ClO_4$ complex was dissolved in aqueous acetonitrile solution (equal volumes of 0.20 M $HClO_4$ and CH_3CN) to give a 2.5 mM solution of the complex. The rate of the reaction was followed over the temperature range 4–35°C, by measuring the absorbance change at 500 nm.

Ion exchange procedures

These were carried out with Bio-Rad cation exchange resin (A.R., AG 50 W-X8, 100–200 mesh, in the H^+ form). A jacketed column (12 × 1.2 cm) was used and cold water was circulated through the jacket. The neutral solutions of $[Co(trpn)F_2]^+$ were allowed to undergo the primary aquation for ~ 45 min (~ $5t_{1/2}$ at 25°C) and were then charged onto the column. The column was washed with deionized–distilled water until the washings appeared neutral. The collected washings were than titrated with standardized $Th(NO_3)_4 \cdot 4H_2O$ using sodium alizarin as an indicator.[12] It is important to note that runs with NaF (Gold label from Aldrich) confirmed that F^- could be recovered quantitatively from the ion exchange column.

RESULTS AND DISCUSSION

Structural aspects

A series of cobalt(III)-trpn complexes has been prepared and isolated.[11] The isolated complexes under investigation are presented in Scheme 1. The visible spectral data of these complexes summarized in Table 1, are consistent with the *cis*-octahedral geometry.[11,13]

In an attempt to find a suitable solvent in which the aquation of $[Co(trpn)X_2]^+$ (X = F, Cl, Br) could be studied, it was observed that DMF, THF and CH_3CN reacted with the complex. The product of the reaction $[Co(trpn)Br_2]ClO_4$ with acetonitrile has been separated out and characterized; $[Co(trpn)(CH_3CN)Br]BrClO_4$. Such a complex is sparingly soluble in acetonitrile and it does not react further to produce the corresponding diacetonitrile, even with prolonged reflux. On the other hand, the reaction of $[Co(trpn)(H_2O)_2](ClO_4)_3$ with acetonitrile afforded the $[Co(trpn)(CH_3CN)_2](ClO_4)_3$ complex.

Acid hydrolysis kinetics

$[Co(trpn)X_2]^+$ (X = Cl *or* Br). In acid medium the complex ions $[Co(trpn)Cl_2]^+$ and $[Co(trpn)Br_2]^+$

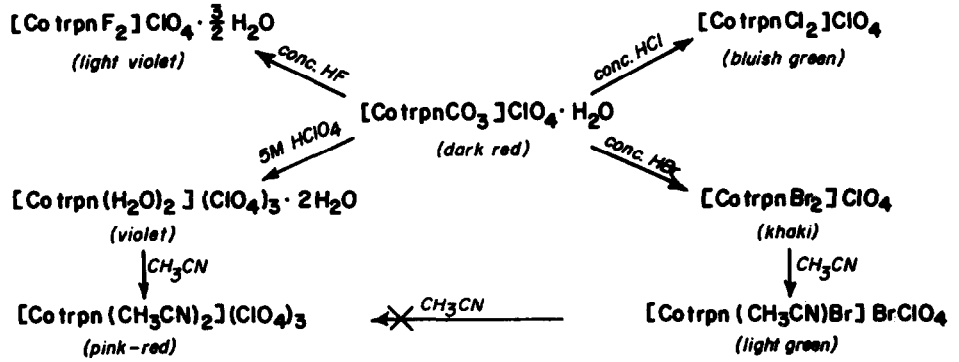

Scheme 1.

Table 1. Absorption maxima and minima in the 300–700 nm range for some cobalt(III)–trpn complexes

Complex ion	Solvent	λ_{max} (ε)[a]	λ_{min} (ε)	λ_{max} (ε)	λ_{min} (ε)
$[Co(trpn)Cl_2]^{+}$ [b]	37% HCl	578(55.0)	485(125)		
$[Co(trpn)Br_2]^{+}$	24% HBr	~ 589(71)	~ 522(55)		
$[Co(trpn)(H_2O)_2]^{3+}$	0.1 M $HClO_4$	530(57)	445(14.3)	368(90.8)	341(68.5)
$[Co(trpn)(CH_3CN)_2]^{3+}$ [b]	CH_3CN	498(97.6)	418(27.6)		
$[Co(trpn)(CH_3CN)Br]^{2+}$ [c]	CH_3CN	580			
$[Co(trpn)(CH_3CN)(H_2O)]^{3+}$ [d]	pH 4	510(66.3)	425(25)		

[a] λ in nm and ε in M^{-1} cm^{-1}.
[b] Data taken from ref. 11.
[c] Saturated solution.
[d] Calculated based on kinetic data.

were found to hydrolyse very rapidly. The complete conversion of these ions to the diaqua, $[Co(trpn)(H_2O)_2]^{3+}$, occurred within a few minutes. Attempts to find a suitable non-aqueous solvent, in which the aquation could be studied, failed and therefore, we were unable to investigate the primary aquation step in these complexes. However, an attempt was made to obtain an estimate for the rate of the second aquation for $[Co(trpn)Cl_2]^{+}$ ion, by dissolving $[Co(trpn)Cl_2]ClO_4$ in aqueous 0.1 M $HClO_4$ at 25°C, and following the absorbance change at 530 nm. In this way, we were able to observe a part of the conversion of $[Co(trpn)(H_2O)Cl]^{2+}$ to $[Co(trpn)(H_2O)_2]^{3+}$. The estimated half-life for this change is ~ 125 s, which corresponds to a rate constant $k_2 \simeq 5.5 \times 10^{-3}$ s^{-1}. On the other hand, the conversion of the dibromo species to the diaqua was too fast to be followed.

However, it is interesting to compare the result of the acid hydrolysis of the $[Co(trpn)Cl_2]^{+}$ ion with other similar tetraamine species $[CoN_4Cl_2]^{+}$ (N_4 = non-replacable monodentate or polydentate amine). The results collected in Table 2 for the secondary aquation in these systems, clearly demonstrate the extreme lability of the trpn system relative to the other tetraamines. Briefly, the rate of the second chloride substitution decreases in the order: trpn > tn_2 > tren ⩾ en_2.

Table 2. The secondary acid hydrolysis rate constant of the $[CoN_4Cl_2]^{+}$ ion at 25°C

N_4	k_2 (s^{-1})	Relative rate	Reference
cis-en_2	1.6×10^{-6}	1	14
trans-tn_2	2.14×10^{-4}	135	10
tren	2.38×10^{-6}	1.5	15
trpn	~ 5.5×10^{-3}	~ 3400	This work

Aquation of $[Co(trpn)F_2]^{+}$. In neutral aqueous medium, the hydrolysis of the $[Co(trpn)F_2]^{+}$ ion led to spectral changes with a very small shift of the lowest energy *d–d* band maxima to lower wavelengths. The spectral scans displayed an isosbestic point at 580 nm, which was maintained throughout the reaction. The final spectral trace gave λ_{max} at 368 nm with ε = 62 M^{-1} cm^{-1}, which is different from that observed for the diaqua species (Table 1). The stoichiometry of the reaction can be repre-

sented by eq. (1):

$$[Co(trpn)F_2]^+ + H_2O \xrightarrow{k_1} [Co(trpn)(H_2O)F]^{2+} + F^- \quad (1)$$

Evidences for this reaction stoichiometry include the following: (i) the isosbestic point at 580 nm remained during the course of the reaction, (ii) the final spectral scans showed no appreciable change over a period of 90 min, (iii) pseudo-first-order kinetics were observed for at least 3 half-lives, (iv) titration of the released fluoride ion with standardized thorium(IV) nitrate gave an average of 1.04 ± 0.06 mol of F^- released/mol of complex (see Experimental).

First-order rate constants were calculated from the slopes of the linear plots of $\ln(A_\infty - A_t)$ vs time. The rate data are listed in Table 3. The activation parameters ($\Delta H^\ddagger$ and $\Delta S^\ddagger$) were evaluated by linear least-squares analysis of Eyring graphs ($\ln k_1/T$ vs $1/T$; k_1 is the primary hydrolysis rate constant and T is the absolute temperature). These values are $\Delta H_1^\ddagger = 12.8 (\pm 0.5)$ kcal mol^{-1} and $\Delta S_1^\ddagger = -28.9 (\pm 1.5)$ cal K^{-1} mol^{-1}.

The hydrolysis of $[Co(trpn)F_2]^+$ ion was also conducted in acid medium over the concentration range 0.1–1.1 M of $HClO_4$. The spectral scans displayed a new isosbestic point at 425 nm with the disappearance of the former one observed at 580 nm. Furthermore, the final spectral trace was consistent with the formation of the well characterized $[Co(trpn)(H_2O)_2]^{3+}$ ion.[11] The first spectral scan recorded after 3 min (time taken to dissolve the complex) gave molar absorptivities in the range 63–67 M^{-1} cm^{-1} at 368 nm. It was apparent, that in acidic medium the rate of the primary aquation of the $[Co(trpn)F_2]^+$ ion had occurred very quickly, probably during the time of dissolution, i.e. the spectral scans refer to the secondary aquation step, which was found to be acid-catalysed.

The pseudo-first-order rate constants for the secondary aquation of $[Co(trpn)F_2]^+$ ion, measured at various $[H_3O^+]$ concentrations and at different temperatures are presented in Table 4. The observed pseudo-first-order rate constants (k_{obs}) calculated at 368 and 338 nm were in agreement to within 6%, confirming the assumption that no other side reactions are complicating the study.

Table 3. Values of k_1 for the primary hydrolysis of $[Co(trpn)F_2]^+$ in neutral aqueous medium ($\mu = 0.5$ M)

Temperature (°C)	$10^3 k_1$ (s^{-1})
25.0	1.28
30.0	2.05
35.0	2.85
40.0	3.82

Table 4. Values of pseudo-first-order rate constants for the secondary aquation of the $[Co(trpn)F_2]^+$ ion, measured at various perchloric acid concentrations and at different temperatures, with $\mu = 1.0$ M[a]

$[H_3O^+]$ (M)	$10^4 k_{obs}$ (s^{-1})			
	25.0°C	30.0°C	35.0°C	40.0°C
0.0940	2.07		8.02	14.42
0.376	6.00	10.43	17.88	27.23
0.564	7.57	14.08	23.60	38.23
0.708	8.62	16.87	29.65	46.52
1.0619[b]	13.78			

[a] Ionic strength maintained with $NaClO_4$.
[b] $\mu = 1.1$ M in this case.

The plots of k_{obs} vs $[H_3O^+]$, shown in Fig. 1, gave straight lines with a positive intercept at $[H_3O^+] = 0$. The non-zero intercept indicates the presence of a reaction pathway, which is independent of the hydrogen ion concentration. The other pathway depends on the hydrogen ion concentration, and presumably involves a rapid reversible acid–base pre-equilibrium, where the protonated form of the complex is more labile than the unprotonated form. This can be represented by the following mechanism:

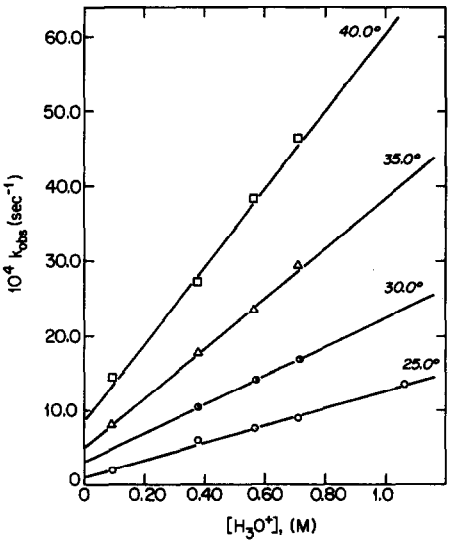

Fig. 1. The dependence of the pseudo-first-order rate constant on the hydrogen ion concentration for the secondary acid hydrolysis of $[Co(trpn)F_2]^+$ (3 mM) at different temperatures: (○) 25.0°C, (◑) 30.0°C; (△) 35.0°C; (□) 40.0°C.

$$[Co(trpn)(H_2O)F]^{2+} + H_3O^+ \underset{}{\overset{K_{eq,fast}}{\rightleftharpoons}} [Co(trpn)(H_2O)FH]^{3+} + H_2O \quad (2)$$

$$[Co(trpn)(H_2O)F]^{2+} + H_2O \xrightarrow{k_2} [Co(trpn)(H_2O)_2]^{3+} + F^- \quad (3)$$

$$[Co(trpn)(H_2O)FH]^{3+} + H_2O \xrightarrow{k'_2} [Co(trpn)(H_2O)_2]^{3+} + HF \quad (4)$$

where K_{eq} is the equilibrium constant for the protonation reaction 2, and k_2 and k'_2 are the rate constants for reactions 3 and 4, respectively. Under pseudo-first-order conditions of constant hydrogen ion concentration, combination of eqs (2)–(4) leads to the rate law given by eq. (5).

$$-\frac{dC_t}{dt} = k_{obs}C_t = \frac{k_2 + k'_2K_{eq}[H_3O^+]}{1 + K_{eq}[H_3O^+]}C_t \quad (5)$$

where C_t represents the total concentration of the monofluoro complex in both protonated and unprotonated forms. When $K_{eq}[H_3O^+] \ll 1$, eq. (5) is reduced to:

$$k_{obs} = k_2 + k'_2K_{eq}[H_3O^+]. \quad (6)$$

This latter expression fits the data, as is shown by the straight lines obtained from a plot of k_{obs} vs $[H_3O^+]$ (Fig. 1). The least-squares slopes and intercepts, corresponding to the values of k'_2K_{eq} and k_2, respectively, are given in Table 5.

The activation parameters corresponding to k_2 and k'_2K_{eq} were obtained from linear Eyring plots over the range 25.0–40.0°C. For the acid-independent path (k_2), the activation parameters are $\Delta H_2^{\ddagger} = 21.3(\pm 0.7)$ kcal mol^{-1} and $\Delta S_2^{\ddagger} = 4.7(\pm 2)$ cal K^{-1} mol^{-1}, while for the acid-catalysed path (k'_2K_{eq}), the parameters are $\Delta H^{\ddagger} = 19.2(\pm 0.4)$ kcal mol^{-1} and $\Delta S^{\ddagger} = -7.7(\pm 1.2)$ cal K^{-1} mol^{-1}.

The observed rate constant for the second aquation of $[Co(trpn)F_2]^+$, at a given hydrogen ion concentration at 25°C and $\mu = 1.0$ M, can be calculated by the expression:

$$k_{obs}(s^{-1}) = 1.40 \times 10^{-4} + (1.07 \times 10^{-3})[H_3O^+]. \quad (7)$$

Table 5. Values of k_2 and k'_2K_{eq} at various temperatures for the secondary aquation of $[Co(trpn)F_2]^+$ ($\mu = 1.0$ M)

Temperature (°C)	$10^4 k_2$ (s^{-1})	$10^3 k'_2K_{eq}$ (s^{-1} M^{-1})
25.0	1.40	1.07
30.0	3.14	1.94
35.0	4.70	3.47
40.0	8.80	5.24

Although for the acid-independent pathways the ratio of $k_1/k_2 \simeq 10$, the reaction in neutral aqueous medium did not show the second hydrolysis step. This might be attributed to the presence of an equilibrium between the monoaqua and the diaqua species; i.e.:

$$[Co(trpn)(H_2O)F]^{2+} + H_2O \rightleftharpoons [Co(trpn)(H_2O)_2]^{3+} + F^-.$$

A related result has been obtained for the hydrolysis of $[Cr(tren)F_2]^+$ where, in both basic and acidic solutions, the release of a second fluoride was not observed.[16] It might be expected that the removal of ligands which retain some basicity, even when coordinated, would be acid catalysed, as in the case of most metallic complexes containing the oxalate,[17] cyanide[18] and fluoride ion.[19–23] Comparing the rate constants for the primary acid-independent hydrolysis for the series *cis*-$[CoN_4F_2]^+$, reveals that k_1 (s^{-1}) decreases in the order trpn (1.3×10^{-3}) $\gg$ tren[23] (9.0×10^{-6}) > en$_2$[19] (3.0×10^{-6}). The large labilization induced by the trpn ligand compared to the tren ligand may be attributed to the much lower $\Delta H^{\ddagger}$ value [$\Delta H^{\ddagger}_{trpn} - \Delta H^{\ddagger}_{tren} = -9.5$ kcal mol^{-1}]. The entropy of activation favours the tren system [$-T(\Delta S^{\ddagger}_{trpn} - \Delta S^{\ddagger}_{tren}) = +6.7$ kcal mol^{-1}], but this is not sufficient to offset the large difference in $\Delta H^{\ddagger}$.

Acid hydrolysis of $[Co(trpn)(CH_3CN)_2]^{3+}$. The kinetics of aquation of $[Co(trpn)(CH_3CN)_2]^{3+}$ ion was studied in the pH range 1–4 and over the temperature range 8–20°C. The spectral changes for the acid hydrolysis is shown in Fig. 2. A careful inspection of these curves suggests that three species are involved in the reaction, namely $[Co(trpn)(CH_3CN)_2]^{3+}$ (A), $[Co(trpn)(CH_3CN)(H_2O)]^{3+}$ (B) and $[Co(trpn)(H_2O)_2]^{3+}$ (C). The former and latter complexes have been isolated and characterized.[11] For the kinetic measurements the wavelength chosen was 510 nm. During the first part of the reaction, two isosbestic points at 531 and 417 mm, were observed and the lower energy *d–d* band (λ_{max}) shifted gradually from 498 nm to 510(± 2) nm. Then, during the second part of the reaction, this band moved to 530(± 2) nm. Also, the isosbestic points moved to 537 and ~410 nm, respectively, and the final spectrum corresponds to the diaqua species. Thus, the overall reaction can be represented by eq. (8).

$$[Co(trpn)(CH_3CN)_2]^{3+} \xrightarrow{H_2O} [Co(trpn)(H_2O)_2]^{3+} + 2CH_3CN. \quad (8)$$

For two consecutive irreversible first-order reactions:[24]

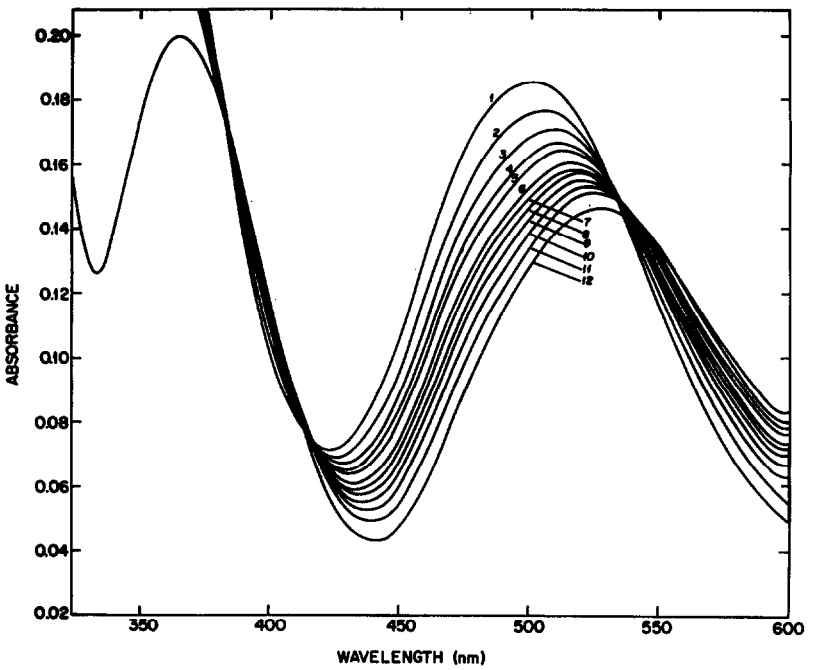

Fig. 2. Spectral changes during the aquation of $[Co(trpn)(CH_3CN)_2]^{3+}$ (2.5 mM) in aqueous medium (pH = 4.0), at 11.5°C as a function of time [curve no., time (min)]: 1, 2.0; 2, 3.5; 3, 5.0; 4, 6.5; 5, 8.0; 6, 10.0; 7, 11.5; 8, 14.0; 9, 17.0; 10, 22.0; 11, 33; 12, 50.

$$A \xrightarrow{k_1} B \xrightarrow{k_2} C \tag{9}$$

it can be shown that the concentration of the species A, B and C at any time t, are given by:

$$[A] = [A]_0 e^{-k_1 t} \tag{10}$$

$$[B] = \frac{[A]_0 k_1}{k_2 - k_1}(e^{-k_1 t} - e^{-k_2 t}) \tag{11}$$

$$[C] = [A]_0\left\{1 + \frac{1}{k_1 - k_2}(k_2 e^{-k_1 t} - k_1 e^{-k_2 t})\right\}. \tag{12}$$

The absorbance A_t at any time t, for a 1 cm cell, is given by eq. (13)

$$A_t = \varepsilon_a[A] + \varepsilon_b[B] + \varepsilon_c[C]. \tag{13}$$

Also it is not difficult to show that:[25]

$$A_t - A_\infty = a_1 e^{-k_1 t} + a_2 e^{-k_2 t} \tag{14}$$

where $A_\infty = \varepsilon_c[A]_0$, the absorbance at infinite time. $[A]_0$ is the initial complex concentration, a_1 and a_2 are composed of rate constants k_1 and k_2, and the molar absorptivities ε_a, ε_b and ε_c for the species A, B and C, respectively.

Figure 3 shows a typical plot of ln $(A_t - A_\infty)$ vs t for the acid hydrolysis of the $[Co(trpn)(CH_3CN)_2]^{3+}$ ion. From the straight-line portion of this curve, the first-order rate constant for the slow reactions (k_2) was obtained. When the logarithm of the difference between the extrapolated straight-line portion and the experimental curve was plotted vs time (Fig. 3), the rate constant of the more rapid reaction (k_1) was obtained. The rate constants k_1 and k_2 are collected in Table 6.

The activation parameters were evaluated from the linear plots of $\ln k_1/T$ and $\ln k_2/T$ vs $1/T$. For the fast step $\Delta H_1^\ddagger = 16.0(\pm 2.0)$ kcal mol^{-1} and $\Delta S_1^\ddagger = -12.7(\pm 6.0)$ cal K^{-1} mol^{-1}, while for the slow step $\Delta H_2^\ddagger = 14.9(\pm 2.0)$ kcal mol^{-1} and $\Delta S_2^\ddagger = -19.4(\pm 6.0)$ cal K^{-1} mol^{-1}. Over the temperature range examined, the rate of the first aquation is only about four times greater than that of the second aquation. Also, the aquation of $[Co(trpn)(CH_3CN)_2]^{3+}$ is independent of pH over the range 1.0–4.0 (Table 6).

Table 6. The rate constants for the aquation of $[Co(trpn)(CH_3CN)_2]^{3+}$ in acidic medium and at different temperatures

Temperature (°C)	pH	$10^3 k_1$ (s^{-1})	$10^3 k_2$ (s^{-1})
8.3	4.0	3.31	0.88
11.5	4.0	5.17	1.16
16.0	4.0	7.59	1.91
20.0	4.0	11.3	2.59
20.0	2.5	12.8	2.36
20.0	1.0	11.9	2.38

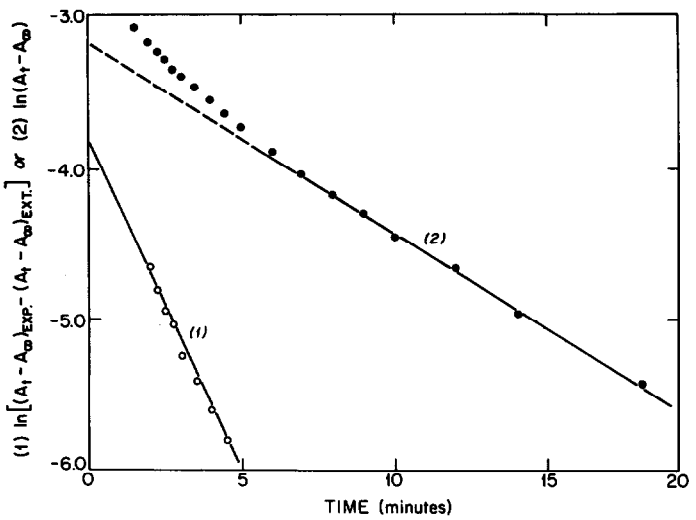

Fig. 3. Plot of the experimental data for the aquation of $[Co(trpn)(CH_3CN)_2]^{3+}$ in acidic aqueous medium (pH = 4.0) at 16.0°C, λ = 510 nm.

The pK_1 for the acid dissociation constant of the coordinated water in $[Co(trpn)(H_2O)_2]^{3+}$ is 4.8 (25°C and $\mu = 0.1$ M).[26] This value led us to expect that the corresponding pK of $[Co(trpn)(CH_3CN)(H_2O)]^{3+}$ would not be less than 5.0. Therefore, the species formed during the acid hydrolysis of the $[Co(trpn)(CH_3CN)_2]^{3+}$ ion would not be complicated by the presence of hydroxo–acetonitrile species as shown from the data in Table 6. Similar behaviour has been found during the aquation of the *cis*-$[Cr(C_2O_4)_2(DMSO)_2]^-$ ion[27] and the $[Co(NH_3)_5(CH_3CN)]^{3+}$ ion.[28]

However, it might be noted that metal complexes of organic nitriles of the formula $[ML_5(RCN)]^{3+}$ ($M = Co^{III}$, Cr^{III}, Rh^{III}; $L = NH_3$, H_2O; $RCN = CH_3CN$, C_6H_5CN) are known for a number of kinetically inert metal ions[29–31] and show kinetic stability towards simple aquation, the complexes hydrolyse to the corresponding carboxamide in neutral and alkaline solutions.[32,33] Therefore, the rapid aquation of the $[Co(trpn)(CH_3CN)_2]^{3+}$ ion is surprising in view of the normal kinetic inertness of the above mentioned nitrile complexes.

The spectrum of the intermediate, $[Co(trpn)(CH_3CN)(H_2O)]^{3+}$, was calculated using the kinetic data (k_1 and k_2), the molar absorptivities (ε_a and ε_c) and eqs (10)–(13). The calculations were made at an optimum time in order to have a high concentration of the intermediate. An approach of this type was first made in studying the hydrolysis of the $[Cr(en)_3]^{3+}$ ion[34] and in other systems.[27,35] The result of this calculation is depicted in Fig. 4, together with the visible spectra of $[Co(trpn)(CH_3CN)_2]^{3+}$ and $[Co(trpn)(H_2O)_2]^{3+}$ ions. It is interesting to note that the position of the lower energy *d–d* band (λ_{max}) is shifted to longer

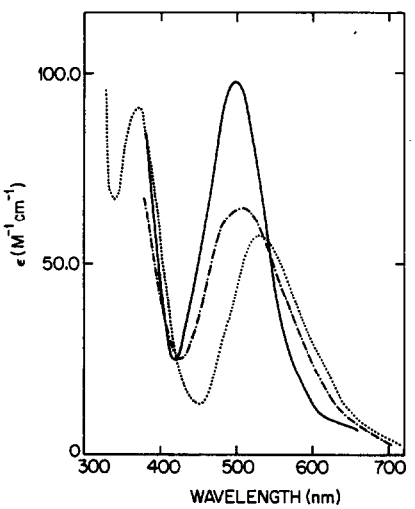

Fig. 4. Absorption spectra of (——) $[Co(trpn)(CH_3CN)_2]^{3+}$ in acetonitrile, (····) $[Co(trpn)(H_2O)_2]^{3+}$ in aqueous 0.1 M $NaClO_4$ (pH ~ 4) and (–·–·–) $[Co(trpn)(CH_3CN)(H_2O)]^{3+}$ (calculated) in aqueous medium (pH 4.0).

wavelength with reducing ligand field. i.e. diacetonitrile → monoaquaacetonitrile → diaqua species. The calculations reveal that the $[Co(trpn)(CH_3CN)(H_2O)]^{3+}$ ion has λ_{max} at 510 nm with $\varepsilon = 66.3$ $M^{-1}\,cm^{-1}$.

Aquation of the $[Co(trpn)(CH_3CN)Br]^{2+}$ *ion.* Due to the extreme lability of the $[Co(trpn)Br_2]^+$ ion towards acid hydrolysis, it was very difficult to extract quantitative information about its rate of aquation. The lack of suitable solvent for $[Co(trpn)Br_2]ClO_4$ ruled out the use of stopped-flow technique. Therefore, we considered the hydrolysis of $[Co(trpn)(CH_3CN)Br]^{2+}$, which in

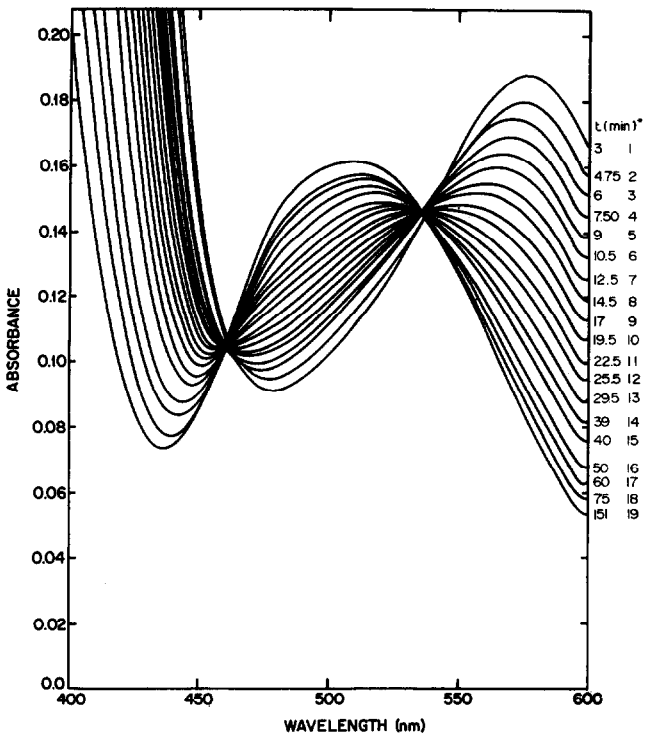

Fig. 5. Spectral changes of $[Co(trpn)(CH_3CN)Br]^{2+}$ (2.5 mM) in 50% (by volume) aqueous 0.2 M $HClO_4$ and CH_3CN solution at 13.7°C as a function of time.

principle should not differ too much from the hydrolysis of the $[Co(trpn)(H_2O)Br]^{2+}$ ion.

When the hydrolysis of $[Co(trpn)(CH_3CN)Br]^{2+}$ was carried out in acidic aqueous medium, the kinetics were complicated due to the small difference in the reactivity of $[Co(trpn)(CH_3CN)Br]^{2+}$ and $[Co(trpn)(CH_3CN)(H_2O)]^{3+}$ towards aquation, i.e. the rate of bromide replacement by water in $[Co(trpn)(CH_3CN)Br]^{2+}$ was very close to the rate of replacement of acetonitrile in the primary product of the hydrolysis; $[Co(trpn)(CH_3CN)(H_2O)]^{3+}$. To overcome these difficulties, the hydrolysis of $[Co(trpn)(CH_3CN)Br]^{2+}$ was conducted in aqueous acetonitrile solution, where the second step in the reaction is suppressed.

The kinetics for $[Co(trpn)(CH_3CN)Br]^{2+}$ were studied in a mixed solvent containing equal volumes of 0.20 M $HClO_4$ and CH_3CN. The spectral scans as a function of time, shown in Fig. 5, indicate that more than one step is involved in the reaction. These curves clearly show the pronounced deviation from the isosbestic point at 536 nm, particularly at the beginning of the reaction. Moreover, the final spectral trace for the reaction gave an absorption band λ_{max} at 510(±2) nm. The intensity of this band varies with the H_2O : CH_3CN volume ratio, implying the presence of an equilibrium mixture in the products. At low temperatures (4–14°C), the plots of $\ln(A_\infty - A_t)$ vs time show a deviation from linearity. The first-order rate constants k_a and k_b for the fast and slow reaction, respectively, were evaluated as described before for the aquation of $[Co(trpn)(CH_3CN)_2]^{3+}$. These values are tabulated in Table 7. Thus, the reaction of $[Co(trpn)(CH_3CN)Br]^{2+}$ in aqueous acetonitrile solution can be represented by:

$$[Co(trpn)(CH_3CN)Br]^{2+} + H_2O \xrightarrow{k_a} [Co(trpn)(CH_3CN)(H_2O)]^{3+} + Br^- \quad (15)$$

$$[Co(trpn)(CH_3CN)(H_2O)]^{3+} + H_2O \underset{k_{-2}}{\overset{k_2}{\rightleftharpoons}} [Co(trpn)(H_2O)_2]^{3+} + CH_3CN. \quad (16)$$

The rate constant k_b depends on k_2 and k_{-2}, and the equilibrium position between the aquaacetonitrile and the diaqua species [eq. (16)].

Eyring plots yielded $\Delta H^\ddagger = 18.1(\pm 0.6)$ kcal mol^{-1} and $\Delta S^\ddagger = -6.6(\pm 2.0)$ cal K^{-1} mol^{-1} for the fast reaction and $\Delta H^\ddagger = 17.0(\pm 0.55)$ kcal mol^{-1} and $\Delta S^\ddagger = -13.2(\pm 1.5)$ cal K^{-1} mol^{-1} for the slow reaction. These data reveal that the rate of the first step is only ~ four times greater than the rate in the second step. This difference in rate appears to arise from the small difference in the entropy of activation between the two steps.

Table 7. Pseudo-first-order rate constants (k_a and k_b) for the reaction of $[Co(trpn)(CH_3CN)Br]^{2+}$ in 50% aqueous (0.20 M $HClO_4$)–acetonitrile solutions

Temperature (°C)	$10^3 k_a$ (s^{-1})	$10^3 k_b$ (s^{-1})
4.30	1.21	0.32
7.80	1.52	0.46
11.60	2.92	
13.70	3.42	0.81
20.5		1.84
25.0		3.04
28.0		3.55
32.0		5.51

The rate of replacement of the Br^- ion in $[Co(trpn)(CH_3CN)Br]^{2+}$ with H_2O ($k \simeq 1.17 \times 10^{-2}$ s^{-1} at 25°C) is probably not much different than the rate of the second aquation of $[Co(trpn)Br_2]^+$. This rate is about twice that for replacement of Cl^- ion in $[Co(trpn)(H_2O)Cl]^{2+}$. The same observation has also been found for the aquation[10] of $[Cotn_2(H_2O)Br]^{2+}$ relative to $[Cotn_2(H_2O)Cl]^{2+}$. Furthermore, the rate of aquation of $[Co(trpn)(CH_3CN)Br]^{2+}$ reflects the extreme lability of these complexes due to the trpn ligand. For example, the relative rate of replacement of the bromide ion by water in the tetraamine–cobalt(III) complexes $[Co(tren)(H_2O)Br]^{2+}$:[36] $[Cotn_2(H_2O)Br]^{2+}$:[10] $[Co(trpn)(CH_3CN)Br]^{2+}$ is 1:165:3560.

In conclusion, some comments must be considered: (i) the reactivity of the tetraamine–cobalt (III) complexes can be enhanced or retarded by modifying the nature of the amine ligand(s); (ii) the replacement of the five-membered rings ($N_4 = en_2$ or tren), and even the six-membered rings ($N_4 = tn_2$) with the tripod trpn ligand causes marked labilization in tetraaminecobalt(III) complexes; (iii) the reactivity towards substitution reactions in the dihalotetraamine–cobalt(III) complexes decreases in the order trpn > tn_2 > tren > en_2.

The high lability of the $Co(trpn)^{3+}$ species is believed to be associated, at least in part, with the flexibility of the six-membered ring system (in contrast to the much less flexible five-membered amine rings $Co(en)_2^{3+}$ and $Co(tren)^{3+}$). Such flexibility is likely to contribute to the ease of forming the transition state by a mechanism which is primarily dissociative in nature.[10] Furthermore, the complexes of $Co(trpn)^{3+}$ represent a compromise between a system with fixed *cis* geometry and a fully labile species. These features might be of great importance in some biological processes such as the dephosphorylation of ATP.[1-3]

REFERENCES

1. F. Tafesse and R. M. Milburn, *Inorg. Chem. Acta*, 1987, **135**, 119.
2. F. Tafesse, S. S. Massoud and R. M. Milburn, *Inorg. Chem.* 1985, **24**, 2591.
3. G. Rawji, M. Hediger and R. M. Milburn, *Inorg. Chim. Acta* 1983, **79**, 247.
4. S. G. Zipp, A. P. Zipp and S. K. Madan, *Coord. Chem. Rev.* 1974, **14**, 29.
5. G. S. Benner and D. W. Meek, *Inorg. Chem.* 1967, **6**, 1399.
6. W. K. Kuo, W. V. Miller and S. K. Madan, *J. Inorg. Nucl. Chem.* 1973, **35**, 957.
7. A. Dei, P. Paoletti and A. Vacca, *Inorg. Chem.* 1968, **7**, 865.
8. A. Vacca and P. Paoletti, *J. Chem. Soc.* 1968, 2378.
9. J. L. Shafer and K. N. Raymond, *Inorg. Chem.* 1971, **10**, 1799.
10. I. R. Jonasson, R. S. Murray, D. R. Stranks and J. K. Yandell, *Proc. 12th Int. Conf. Coord. Chem.*, p. 32. Sydney, Australia (1966).
11. S. S. Massoud and R. M. Milburn, submitted for publication.
12. A. I. Vogel, *Quantitative Inorganic Analysis*, 2nd edn. Longmans, Green and Co., London (1951).
13. F. Basolo, C. J. Ballhausen and J. Bjerrum, *Acta Chem. Scand.* 1955, **9**, 810.
14. S. C. Chan, *J. Chem. Soc.* 1963, 5137.
15. W. V. Miller and S. K. Madan, *Inorg. Chem.* 1971, **10**, 1250.
16. M. J. Saliby, P. S. Sheridan and S. K. Madan, *Inorg. Chem.* 1980, **19**, 1291.
17. E. Deutsch and H. Taube, *Inorg. Chem.* 1968, **77**, 1532.
18. D. K. Wakefield and W. B. Schapp, *Inorg. Chem.* 1969, **8**, 512.
19. F. Basolo, W. R. Matoush and R. G. Pearson, *J. Am. Chem. Soc.* 1956, **78**, 4883.
20. S. C. Chan, *J. Chem. Soc.* 1964, 2375.
21. K. R. A. Fehrmann and C. S. Garner, *J. Am. Chem. Soc.* 1961, **83**, 1276.
22. T. W. Swaddle and E. L. King, *Inorg. Chem.* 1965, **4**, 532.
23. K. W. Kuo and S. K. Madan, *Inorg. Chem.* 1971, **10**, 229.
24. J. W. Moore and R. G. Pearson, *Kinetics and Mechanisms*, 3rd edn, p. 290. John Wiley, New York (1981).
25. D. A. Buckingham, J. D. Francis and A. M. Sargeson, *Inorg. Chem.* 1974, **11**, 2630.
26. S. S. Massoud and R. M. Milburn, unpublished results.
27. K. R. Ashely and R. E. Hamm, *Inorg. Chem.* 1965, **5**, 1645.
28. D. Jordan, W. C. Kupferschmidt and R. B. Jordan, *Inorg. Chem.* 1984, **23**, 1986.
29. R. B. Jordan, A. M. Sargeson and H. Taube, *Inorg. Chem.* 1966, **5**, 1091.
30. A. W. Zanella and P. C. Ford, *Inorg. Chem.* 1975, **14**, 700.

31. D. A. Buckingham, F. R. Keene and A. M. Sargeson, *J. Am. Chem. Soc.* 1973, **95**, 5649.
32. D. Pinnell, G. B. Wright and R. B. Jordan, *J. Am. Chem. Soc.* 1972, **95**, 6104.
33. I. I. Creaser, M. J. Harrowfield, F. R. Keene and A. M. Sargeson, *J. Am. Chem. Soc.* 1981, **103**, 3559.
34. E. Jørgensen and J. Bjerrum, *Acta Chem. Scand.* 1959, **13**, 2075.
35. J. A. Weyh and R. E. Hamm, *Inorg. Chem.* 1969, **8**, 2298.
36. W. V. Miller and S. K. Madan, *Inorg. Chem.* 1970, **9**, 2362.

Polyhedron Vol. 8, No. 3, pp. 285–291, 1989
Printed in Great Britain

0277–5387/89 $3.00+.00
© 1989 Pergamon Press plc

SYNTHESIS AND CHARACTERIZATION OF SOME NEW ORGANOMETALLIC COMPLEXES OF NICKEL(II) CONTAINING TRIMETHYLPHOSPHINE

ERNESTO CARMONA,* MARGARITA PANEQUE and MANUEL L. POVEDA

Departamento de Química Inorgánica e Instituto de Ciencias de Materiales, Universidad de Sevilla-CSIC, 41071-Sevilla, Spain

(*Received* 31 *May* 1988; *accepted* 6 *July* 1988)

Abstract—$[Ni(cod)_2]_2$ (cod = 1,5-cyclooctadiene) oxidatively adds $C_6H_5CH_2Cl$ in the presence of 1 or 2 equiv of PMe_3 affording $[Ni(\eta^3\text{-}CH_2C_6H_5)Cl(PMe_3)]$ or *trans*-$[Ni(\eta^1\text{-}CH_2C_6H_5)Cl(PMe_3)_2]$, respectively. Variable temperature NMR studies carried out with a mixture of these two complexes indicate that both are involved in a fast equilibrium which interchanges the two types of benzylic ligands. The above mentioned compounds decompose in the presence of excess PMe_3 with the formation of $[NiCl_2(PMe_3)_3]$, $[Ni(PMe_3)_4]$ and the reductive elimination product $(C_6H_5CH_2)_2$. In addition, the synthesis and spectral characterization of the new complexes *trans*-$[Ni(C_6H_5)X(PMe_3)_2]$ (X = Cl, Br), *trans*-$[Ni(2,4,6\text{-}C_6H_2Me_3)X(PMe_3)_2]$ (X = Cl, Br) and $[(\eta^5\text{-}C_5H_5)Ni(2,4,6\text{-}C_6H_2Me_3)(PMe_3)]$, are also described.

It is well known that the benzyl ligand, $C_6H_5CH_2$, can adopt a variety of coordination modes (which include the alkyl-type coordination, **A**, as well as the pseudoallylic η^3-bonding, **B**) and that the adoption of a particular coordination mode is strongly

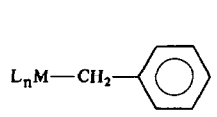

A

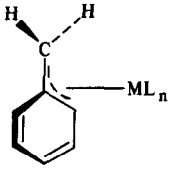

B

influenced by the nature of the ML_n fragment to which the benzyl group is bonded. While η^1-interactions are commonly found among transition metal–benzyl complexes,[1] relatively few η^3-structures are known[2] and for nickel only a few examples have been reported to date, among them the η^3-*o*-methylbenzyl derivative, $[Ni(\eta^3\text{-}CH_2C_6H_4\text{-}o\text{-}Me)Cl(PMe_3)]$, recently prepared in our laboratory.[3]

As an extension of this and previous work concerning the chemistry of nickel alkyl and acyl complexes,[4] we now report the formation of η^1- and η^3-benzyl complexes of the compositions $[Ni(\eta^1\text{-}CH_2C_6H_5)Cl(PMe_3)_2]$ (**1a**) and $[Ni(\eta^3\text{-}CH_2C_6H_5)Cl(PMe_3)]$ (**2**), that of the aryl derivatives $[NiX(Ar)(PMe_3)_2]$, [Ar = C_6H_5, X = Cl (**3a**); X = Br (**4a**); Ar = 2,4,6-$C_6H_2Me_3$ (mesityl), X = Cl (**5**); X = Br (**6**)] and $[Ni(\eta^5\text{-}C_5H_5)(2,4,6\text{-}C_6H_2Me_3)PMe_3]$ (**7**) and their reactions with CO to afford the acyl compounds $[NiX(\eta^1\text{-}COR)(PMe_3)_2]$, [R = $CH_2C_6H_5$, X = Cl (**1b**); R = C_6H_5, X = Cl (**3b**); X = Br (**4b**)]. Variable temperature NMR studies on the benzyl complexes, **1a** and **2**, have been carried out, and are also reported.

RESULTS AND DISCUSSION

Synthesis and spectroscopic characterization of the benzyl complexes trans-$[Ni(\eta^1\text{-}CH_2C_6H_5)Cl(PMe_3)_2]$ (**1a**) *and* $[Ni(\eta^3\text{-}CH_2C_6H_5)Cl(PMe_3)]$ (**2**)

The room temperature reaction of the dichloride, $[NiCl_2(PMe_3)_2]$, with *ca* 2 equiv of $Mg(CH_2C_6H_5)Cl$, produces a brown suspension from which a brown crystalline material can be obtained after work-up. Spectroscopic studies reveal the presence of a mixture of the benzyl derivatives *trans*-$[Ni(\eta^1\text{-}CH_2C_6H_5)Cl(PMe_3)_2]$ (**1a**) and $[Ni(\eta^3\text{-}CH_2C_6H_5)Cl(PMe_3)]$ (**2**). In addition to these products, formation of a very dark, sparingly soluble

*Author to whom correspondence should be addressed.

crystalline species is sometimes observed. The latter displays an IR absorption at 3580 cm^{-1}, which indicates the presence of hydroxo ligands, and this, together with the similarity in colour, solubility and other properties with those found for the recently prepared *o*-methylbenzyl compound $[Ni_3(CH_2C_6H_4\text{-}o\text{-}Me)_4(PMe_3)_2(\mu_3\text{-}OH)_2]$,[3] whose structure was determined by X-ray crystallography, suggest an analogous formulation as $[Ni_3(\eta^1\text{-}CH_2C_6H_5)_4(PMe_3)_2(\mu_3\text{-}OH)_2]$. No satisfactory analytical data can however be obtained for this complex which, as with the related *o*-methylbenzyl derivative, decomposes upon attempted recrystallization, even under an inert atmosphere. For these reasons its investigation has not been pursued any further.

Compounds **1a** and **2** are best prepared by the oxidative addition of $C_6H_5CH_2Cl$ to $[Ni(cod)_2]$ in the presence of the required amount of PMe_3, as shown in eqs (1) and (2).

$$[Ni(cod)_2]+C_6H_5CH_2Cl+2PMe_3 \longrightarrow [Ni(\eta^1\text{-}CH_2C_6H_5)Cl(PMe_3)_2]+2cod \quad (1)$$

$$[Ni(cod)_2]+C_6H_5CH_2Cl+PMe_3 \longrightarrow [Ni(\eta^3\text{-}CH_2C_6H_5)Cl(PMe_3)]+2cod. \quad (2)$$

They have been found to be related by an intermolecular process which involves PMe_3 association and dissociation [eq. (3)], and indeed, on a macroscopic scale, compound **2** can be obtained by addition of 1 equiv of PMe_3 to solutions of **2**, while the latter is formed by PMe_3 abstraction from **1a** using $[Ni(cod)_2]$.

$$[Ni(\eta^1\text{-}CH_2C_6H_5)Cl(PMe_3)_2] \underset{+PMe_3}{\overset{-PMe_3}{\rightleftharpoons}} [Ni(\eta^3\text{-}CH_2C_6H_5)Cl(PMe_3)]. \quad (3)$$

Both compounds have been characterized by IR and ^1H, ^{13}C and ^{31}P NMR spectroscopy. The ^1H NMR spectrum of **1a** shows two singlets at δ 0.98 (18H) and 1.71 (2H) ppm corresponding to the PMe_3 and the methylene benzylic protons, respectively. The lack of observation of coupling is clearly due to an exchange process involving PMe_3 dissociation. A similar situation has been found in other nickel alkyl complexes of related composition, and has been explained in terms of a fast exchange between traces of free PMe_3 and complexed PMe_3, possibly through the intermediacy of a five-coordinate species.[4] Such a process, however, could not be operative in the present system, since addition of free PMe_3 to solutions of **1a** does not increase the rate of PMe_3 exchange, but it rather induces decomposition, with formation of $[NiCl_2(PMe_3)_3]$, $[Ni(PMe_3)_4]$ and $C_{14}H_{14}$ (1,2-diphenylethane) as shown in eq. (4).

$$2[Ni(\eta^1\text{-}CH_2C_6H_5)Cl(PMe_3)_2]+3PMe_3 \longrightarrow [NiCl_2(PMe_3)_3]+[Ni(PMe_3)_4]+C_{14}H_{14}. \quad (4)$$

Hence, it seems more likely that the process responsible for the observed NMR features implies phosphine dissociation and re-association through the intermediacy of the pseudoallylic complex **2**, and this is not only in accord with the above comments regarding the reversible transformation **1a** $\rightleftharpoons$ **2** but also with the observation of only one set of proton resonances for mixtures of **1a** and **2**, with chemical shifts being an average of those corresponding to compounds **1a** and **2** (see below). As expected, **1a** exhibits a single $^{31}P\{^1H\}$ NMR signal, while in the $^{13}C\{^1H\}$ NMR spectrum a singlet is observed for each of the carbon atoms of the benzyl ligand as well as for those of the PMe_3 groups (Table 1).

A related situation is found in the η^3-benzyl complex, **2**. The fluxionality of this species is clearly indicated by the appearance of broad, unresolved signals in the NMR spectra. Thus, the $^{31}P\{^1H\}$ NMR exhibits a broad singlet at -7.9 ppm, while the ^1H NMR spectrum displays a broad singlet at 1.0 ppm for the methylene benzylic protons. In the room temperature $^{13}C\{^1H\}$ NMR spectrum, a doublet is observed at δ 15.0 ppm for the PMe_3 ($^1J_{CP}$ = 30.2 Hz), a broad singlet at 22.0 ppm for the methylene carbon atom and three resonances (intensity ratio *ca* 2 : 2 : 1) between 117–134 ppm for the *ortho*, *meta* and *para* benzyl carbon atoms. No signal can be found for the *ipso* carbon atom of the benzyl ligand. In order to gain further information on the fluxionality of these species and on their interconversion process, variable temperature NMR studies have been carried out with complex **2** and with approximately equimolar mixtures of **1a** and **2**.

Upon cooling a toluene-d_8 solution of **2** at $-60°C$, a doublet at 0.9 ppm is observed for the PMe_3 protons ($^2J_{HP}$ = 9.8 Hz) and a second doublet at 1.1 ppm ($^3J_{HP}$ = 21.3 Hz) for the two benzyl protons, which remain equivalent under these conditions. Only broad, partially resolved signals are found for the aromatic protons. These features are maintained at temperatures down to $-90°C$, the spectrum becoming less resolved due possibly to viscosity effects. Similarly, the methylene carbon atom gives rise to a doublet at 23.7 ppm ($^2J_{CP}$ = 11.3 Hz) due to coupling to the phosphorus nucleus, while four resonances at 133.5 (2C), 128.2 (1C) and 117.7 (2C) are observed in the aromatic region, along with a singlet at 114.6 ppm which is due to the quaternary carbon atom. The equivalence of the two benzyl methylene protons and that of the two *ortho* and the two *meta* carbon atoms can be

explained in terms of a fast suprafacial rearrangement,[5] as shown in eq. (5).

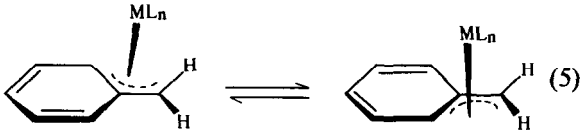

(5)

This process, however, would not account for the loss of coupling, observed at temperatures above $-10°C$, between the methylene carbon or hydrogen atoms and the ^{31}P nucleus of the phosphine ligand. A second fluxional process, which is very slow in the NMR time scale at temperatures of $-10°C$ and below, must therefore operate at temperatures above $-10°C$, and this is proposed to be the intermolecular process depicted in eq. (3), that, as already indicated, interrelates complexes **1a** and **2** through a PMe_3 dissociation and association process. Its occurrence can be conclusively demonstrated by variable temperature NMR studies. Thus, the $^{31}P\{^1H\}$ NMR of a *ca* 1 : 1 mixture of **1a** and **2** exhibits, at room temperature, a very broad signal, which splits into two singlets at -7.9 (**1a**) and -16.4 (**2**) on cooling at $-40°C$. Similarly, the room temperature $^{13}C\{^1H\}$ NMR spectrum displays three broad resonances for the *ortho*, *meta* and *para* carbon atoms of species **1a** and **2**, present in the frozen equilibrium of eq. (3). This temperature-dependent behaviour clearly demonstrates the existence of the equilibrium between the η^1-benzyl complexes **1a** and the pseudoallylic species **2**.

In conclusion, two different types of fluxional processes are observed for complex **2**. A suprafacial jump, similar to that observed in other benzyl complexes,[5,6] which is very fast even at $-90°C$, and an intermolecular phosphine exchange with traces of PMe_3 present in solution. From the above data and by similarity with the structure found for the *o*-methylbenzyl analogue by X-ray studies,[3] structure **C** can be proposed for this compound.



C

Aryl derivatives of composition $[NiAr(X)(PMe_3)_2]$ *and* $[(\eta^5\text{-}C_5H_5)Ni(Ar)(PMe_3)]$. *Preparation and spectral properties*

The addition of *ca* 1 equiv of the Grignard reagent $Mg(C_6H_5)Br$ to a suspension of $[NiCl_2(PMe_3)_2]$ in diethyl ether, produces extensive decomposition and formation of the desired aryl derivative only in very low yields. The chloride complex $[Ni(C_6H_5)Cl(PMe_3)_2]$ (**3a**), and its bromide analogue, $[Ni(C_6H_5)Br(PMe_3)_2]$ (**4a**), can be obtained in good yields by the oxidative addition of C_6H_5X (X = Cl, Br), to $[Ni(cod)_2]$, in the presence of 2 equiv of PMe_3. While the reaction with bromobenzene takes place readily under ambient conditions, that of chlorobenzene requires heating at 60°C, for 24 h, for completion.

NMR studies for the complexes $[Ni(C_6H_5)X(PMe_3)_2]$ indicate a square-planar structure with *trans* phosphine ligands. Thus, the ^1H NMR spectrum for complex **4a** shows a virtually coupled triplet at 0.9 ppm, characteristic of bisphosphine compounds with strong coupling between the phosphorus nuclei ($^2J_{HP_{app}} = 3.6$ Hz). In addition, the phosphine ligands give rise to a singlet in the $^{31}P\{^1H\}$ NMR spectrum and to a triplet at 13.6 ppm in the $^{13}C\{^1H\}$ NMR. Other pertinent NMR data for these aryl derivatives are included in Table 1 and require no further comment.

Upon addition of 1 equiv of the Grignard reagent derived from the mesityl ligand, $Mg(2,4,6\text{-}C_6H_2Me_3)Br$, to a suspension of $[NiCl_2(PMe_3)_2]$, a fairly clean and fast reaction takes place which provides good yields (*ca* 60%) of the mesityl derivative $[Ni(2,4,6\text{-}C_6H_2Me_3)Br(PMe_3)_2]$ (**6**). Formation of this bromo derivative is obviously due to a metathetical replacement of the chloride ligand in complex $[Ni(2,4,6\text{-}C_6H_2Me_3)Cl(PMe_3)_2]$ (**5**) by the bromide present in solution. Similar M—X to M—X′ exchanges (X′ = heavier halogen) are frequently observed during alkylation reactions.[7,8] For instance, alkylation of $[M(\eta^5\text{-}C_5H_5)_2Cl_2]$ (M = Ti, Zr, Hf) with $Mg(CH_2SiMe_3)Br$, gives the bromoalkyl product $[M(\eta^5\text{-}C_5H_5)_2Br(CH_2SiMe_3)]$, without contamination of the chloro complex, and the driving force for this exchange has been associated with the "hard" nature of the Mg^{2+} ion. The chloride derivative $[Ni(2,4,6\text{-}C_6H_2Me_3)Cl(PMe_3)_2]$ (**5**) can be obtained by reaction of the dichloride, $[NiCl_2(PMe_3)_2]$, with 1 equiv of the diaryl magnesium reagent, $Mg(2,4,6\text{-}C_6H_2Me_3)_2$. Compounds **5** and **6** are highly crystalline materials, soluble in common organic solvents and fairly air stable, even in solution. Spectroscopic data for these compounds (Table 1) are also in accord with their formulation as *trans*-$[Ni(2,4,6\text{-}C_6H_2Me_3)X(PMe_3)_2]$.

Interaction of **5** or **6** with an excess of NaCp (1.5 equiv), produces the cyclopentadienyl derivative $[Ni(\eta^5\text{-}C_5H_5)(2,4,6\text{-}C_6H_2Me_3)(PMe_3)]$ (**7**) in high yields [eq. (6)].

$$[Ni(2,4,6\text{-}C_6H_2Me_3)X(PMe_3)_2] + NaCp \longrightarrow [CpNi(2,4,6\text{-}C_6H_2Me_3)(PMe_3)] + NaX + PMe_3 \quad (6)$$

Table 1. Selected NMR data for the new complexes

Compound	^1H[a]				$^{31}P\{^1H\}$	$^{13}C\{^1H\}$[b]			
		R					R		
	PMe_3	CH_3	CH_2	Aromatic		PMe_3	CH_3	CH_2	Aromatic
$Ni(\eta^1\text{-}CH_2C_6H_5)Cl(PMe_3)_2$ (**1a**)[c]	0.98s	—	1.71s	7.0–7.7m	−16.45s	12.9s	—	7.2s	146.2s (C) 123.9 s (CH) 127.8s (CH) 129.3s (CH)
$Ni(\eta^3\text{-}CH_2C_6H_5)Cl(PMe_3)$ (**2**)[c]	0.87pst (6.4)	—	1.03brs	6.5–7.5m	−7.73brs	15.0d (30.2)	—	22.0bs	117.4s (2CH) 127.8s (CH) 133.4s (2CH)
$Ni(C_6H_5)Cl(PMe_3)_2$ (**3a**)[d,e]	0.80brs	—	—	6.7–7.4m	−14.5s	12.4brs	—	—	121.5s (CH) 126.7s (2CH) 136.0s (2CH)
$Ni(C_6H_5)Br(PMe_3)_2$ (**4a**)[c]	0.87pst (3.6)	—	—	6.6–7.4m	+12.7s	13.6pst (13.6)	—	—	121.6s (CH) 126.9s (2CH) 135.9s (2CH) 156.4t (*C*—Ni) (34.5)
$Ni(2,4,6\text{-}C_6H_2Me_3)Cl(PMe_3)_2$ (**5**)[f]	0.87pst (3.6)	2.20s 2.70s (2Me)	—	6.58s	−13.6s	13.4t (13.8)	20.6s 25.6s (2Me)	—	125.9t (2CH) (3.4) 131.2s (*C*Me) 140.6s (2*C*Me)
$Ni(2,4,6\text{-}C_6H_2Me_3)Br(PMe_3)_2$ (**6**)[f]	1.08pst (3.5)	2.12s 2.70s (2Me)	—	6.49s	−13.6s	14.8t (14.2)	20.6s 25.4s (2Me)	—	126.3s (2CH) 131.8s (*C*Me) 140.6s (2*C*Me) 149.7t (*C*—Ni) (34.5)

$(C_5H_5)Ni(2,4,6\text{-}C_6H_2Me_3)(PMe_3)$ (**7**)[d,g]	0.62s (9.3)	2.27s 2.70s (2Me)	—	6.79brs	−2.6s	18.3d (29.5)	20.6s	—	125.8s (2CH) 130.9s (*C*Me) 138.5d (C—Ni) (36.1) 145.7s (2*C*Me)
$Ni(COCH_2C_6H_5)Cl(PMe_3)_2$ (**1b**)[c]	0.78s	—	3.81s	7.0–7.6m	−16.0s	13.1s	—	58.4s	126.4s (CH) 128.4s (CH) 129.7s (CH) 134.7s (C)
$Ni(COC_6H_5)Cl(PMe_3)_2$ (**3b**)[c,h]	1.11pst (3.7)	—	—	7.44m 8.30m	−14.1s	12.9pst (14.1)	—	—	127.5s (2CH) 128.5s (2CH) 131.7s (CH) 140.9s (C)
$Ni(COC_6H_5)Br(PMe_3)_2$ (**4b**)[c,i]	1.10pst (3.3)	—	—	7.43m 8.28m	−16.5s	13.6pst (14.1)	—	—	127.3s (2CH) 128.5s (2CH) 131.6s (CH) 140.9s (C)

Coupling constants in Hz. pst = pseudotriplet.
[a] In parentheses *J*(HP).
[b] In parentheses *J*(CP).
[c] In CD_2Cl_2.
[d] In C_6D_6.
[e] Fluxional at r.t.
[f] In $CDCl_3$.
[g] δC_5H_5 5.17s; C_5H_5 90.3s.
[h] δNi—CO 253.0t (26.5).
[i] δNi—CO 253.4t (23.7).

As expected, the Cp protons give rise to a singlet at 5.17 ppm, indicating pentahapto coordination to the nickel atom. ^{13}C and ^{31}P NMR studies are also in agreement with the proposed formulation. Compound **7** is very thermally stable and can be sublimed under vacuum (0.1 mm), at 100°C, without decomposition.

Carbonylation reactions

Interaction of carbon monoxide (20°C, 1 atm) with compounds **1a**, **3a** and **4a**, produces the corresponding insertion products, **1b**, **3b** and **4b**, as exemplified in eq. (7) for the benzyl derivative **1b**.

$$[Ni(\eta^1\text{-}CH_2C_6H_5)Cl(PMe_3)_2] + CO \longrightarrow [Ni(\eta^1\text{-}COCH_2C_6H_5)Cl(PMe_3)_2] \quad (7)$$

All these carbonyl species are orange crystalline solids, which show no tendency towards CO dissociation under ambient conditions. The presence of an acyl ligand is indicated by the appearance of a medium intensity IR band in the region 1600–1630 cm^{-1}, due to the CO stretching of the coordinated acyl group. The similarity of their NMR spectra with those of the parent compounds **1a**, **3a** and **4a**, clearly suggests conservation of the *trans* geometry. At variance with the behaviour found for these compounds, carbonylation of the mesityl derivatives **6** and **7**, cannot be achieved even under rather forcing conditions (4–5 atm of CO, 50–60°C). This is likely due to steric hindrance of the *o*-methyl groups of the mesityl ligand,[9] which may prevent association of CO to yield the aryl–carbonyl intermediate species proposed for the carbonylation reaction.

EXPERIMENTAL

Microanalyses were by Pascher Microanalytical Laboratory, Bonn and the Microanalytical Service of the University of Sevilla. The spectroscopic instruments used were Perkin–Elmer models 577 and 684 for IR spectra and Varian XL-200 for ^1H, ^{13}C and ^{31}P NMR spectra. All preparations and other operations were carried out under oxygen-free nitrogen, following conventional Schlenk techniques. Solvents were dried and degassed before use. The light petroleum used had b.p. 40–60°C. PMe_3,[10] $NiCl_2(PMe_3)_2$[11] and $Ni(cod)_2$[12] were prepared according to literature methods.

$[Ni(\eta^1\text{-}CH_2C_6H_5)Cl(PMe_3)_2]$ (**1a**) *and* $[Ni(\eta^3\text{-}CH_2C_6H_5)Cl(PMe_3)]$ (**2**)

Since the conventional Grignard route does not provide reproducible and efficient procedures for the independent preparation of compounds **1a** and **2** (see Results and Discussion), only the oxidative addition of $C_6H_5CH_2Cl$ to $[Ni(cod)_2]$ procedure is reported.

To a stirred suspension of $[Ni(cod)_2]$ (0.274 g, *ca* 1 mmol) in 30 cm^3 of diethyl ether, cooled to −70°C, an excess of $C_6H_5CH_2Cl$ (0.15 cm^3, 1.3 mmol) and 0.2 cm^3 of PMe_3 (2 mmol) were added. The reaction mixture was warmed and stirred at room temperature for 20 h, when a yellow–brown solution was obtained. The solvent was removed under vacuum, the residue extracted with 20 cm^3 of diethyl ether and filtered to give a clear solution from which yellow–brown crystals of the desired product were collected after partial removal of the solvent and cooling overnight. Yield 0.2 g, *ca* 60%.

A similar reaction, using 1 equiv of PMe_3, provided the pseudoallyl complex **2** in *ca* 50% yield. Complex **2** is obtained as red crystals from diethyl ether. Found: C, 45.9; H, 6.2. Calc. for $C_{10}H_{16}PClNi$: C, 45.9; H, 6.1%.

Interconversion reactions of **1a** *and* **2**

(a) To a suspension of $[Ni(\eta^3\text{-}CH_2C_6H_5)Cl(PMe_3)]$ (**2**) (0.26 g, *ca* 1 mmol) in Et_2O (20 cm^3), PMe_3 was added (0.1 cm^3, 1 mmol). The mixture was stirred for 30 min, during which time the red starting material dissolved forming a brown solution. The solvent was evaporated to dryness and the residue crystallized from Et_2O to afford yellow crystals of **1a** in 60% yield.

(b) To a mixture of $[Ni(\eta^1\text{-}CH_2C_6H_5)Cl(PMe_3)_2]$ (**1a**) (0.1 g, *ca* 0.3 mmol) and $[Ni(cod)_2]$ (0.05 g, *ca* 0.15 mmol), Et_2O (10 ml) was added. The solution, initially brown–yellow, darkened to red. After stirring for 10 min, the solution was cooled to produce compound **2** in 20% yield.

Reaction of $[Ni(\eta^1\text{-}CH_2C_6H_5)Cl(PMe_3)_2]$ (**1a**) *with an excess of* PMe_3

A solution of **1a** (0.33 g, *ca* 1 mmol) in Et_2O (20 cm^3) was treated with 0.5 cm^3 of PMe_3. The mixture was stirred at room temperature for 3 h and cooled at −30°C. Crystalline dark blue $[NiCl_2(PMe_3)_3]$ (0.15 g, 0.4 mmol) was filtered off and the remaining pale solution was evaporated to dryness. ^1H, $^{31}P\{^1H\}$ and $^{13}C\{^1H\}$ studies, carried out with a C_6D_6 solution of the residue, reveal the presence of $[Ni(PMe_3)_4]$ and $C_{14}H_{14}$ (1,2-diphenylethane, identified by comparison of its IR, ^1H and ^{13}C NMR spectra with those of an authentic sample) as the major species in solution.

$[Ni(C_6H_5)X(PMe_3)_2]$ [X = Cl (**3a**); Br (**3b**)]

These compounds are prepared as described above for the benzyl derivative **1a**, using C_6H_5X (X = Cl, Br). The reaction of $[Ni(cod)_2]$ with C_6H_5Br was complete within about 4 h, while that with C_6H_5Cl required stirring in tetrahydrofuran, at 50–60°C for 20–24 h. Yields were about 50–65%, and the compounds could be crystallized from diethyl ether. $[Ni(C_6H_5)Cl(PMe_3)_2]$. Found: C, 44.8; H, 7.2. Calc. for $C_{12}H_{23}P_2ClNi$: C, 44.6; H, 7.1%. $[Ni(C_6H_5)Br(PMe_3)_2]$. Found: C, 39.1; H, 6.3. Calc. for $C_{12}H_{23}P_2BrNi$: C, 39.2; H, 6.3%.

$[Ni(2,4,6\text{-}C_6H_2Me_3)X(PMe_3)_2]$, [X = Cl (**5**); Br (**6**)] *and* $[Ni(2,4,6\text{-}C_6H_2Me_3)(C_5H_5)PMe_3]$ (**7**)

2.7 cm^3 of a 0.55 N solution of $Mg(2,4,6\text{-}Me_3C_6H_2)_2$ in tetrahydrofuran (*ca* 1.5 eq) were added to a cold (−60°C) suspension of $[NiCl_2(PMe_3)_2]$ (0.42 g, 1.5 mmol) in Et_2O (30 cm^3). The solution was allowed to reach room temperature and stirred for 5 h. The solvent was then stripped off under reduced pressure and the residue extracted with 25 cm^3 of Et_2O and centrifuged. Upon cooling at −30°C overnight the product was obtained as brown–yellow crystals (0.33 g, 60% yield).

The bromide derivative, **6**, was prepared similarly, but using $Mg(2,4,6\text{-}C_6H_2Me_3)Br$ as the alkylating reagent. The reaction mixture, composed of 2 mmol of $[NiCl_2(PMe_3)_2]$ and 2 mmol of the Grignard reagent was stirred at −60°C for 30 min and at room temperature for an additional 20 min (Yield 0.51 g, 62%). Found: C, 44.0; H, 7.2. Calc. for $C_{15}H_{29}P_2BrNi$: C, 43.9; H, 7.1%.

The reaction of **5** or **6** with an excess of NaCp (1.5 equiv) at 20°C for 12 h, produces complex **7** in 80% yield as red–brown needles. Found: C, 64.0; H, 8.6. Calc. for $C_{17}H_{25}PNi$: C, 64.0; H, 7.8%.

$[Ni(COR)X(PMe_3)_2]$, [R = $C_6H_5CH_2$, X = Cl (**1b**); R = C_6H_5, X = Cl (**3b**); X = Br (**4b**)]

Carbon monoxide was bubbled at room temperature through a solution of the alkyl or aryl precursors, **1a**, **3a** or **4a**, in diethyl ether (*ca* 0.5 mmol; 25 cm^3) for about 5 min, after which time an orange crystalline precipitate of the carbonylation product was obtained. The solvent was removed under reduced pressure and the resulting solid recrystallized from diethyl ether at 0°C, to provide orange crystals of the desired products in *ca* 90% yield. $[Ni(COCH_2C_6H_5)Cl(PMe_3)_2]$. IR (Nujol mull) 1600 cm^{-1} (CO). $[Ni(COC_6H_5)Cl(PMe_3)_2]$. Found: C, 44.7; H, 6.8. Calc. for $C_{13}H_{23}P_2ClONi$: C, 44.4; H, 6.6%. IR (Nujol mull) 1610 cm^{-1} (CO). $[Ni(COC_6H_5)Br(PMe_3)_2]$. Found: C, 39.8; H, 5.9. Calc. for $C_{13}H_{23}P_2BrONi$: C, 39.4; H, 5.8%. IR (Nujol mull) 1625 cm^{-1} (CO).

Acknowledgements—We are grateful to the Comisión Asesora de Investigación Científica y Técnica for support of this work. M.P. thanks the Ministerio de Educación y Ciencia for support of a research grant.

REFERENCES

1. (a) S. D. Chappel and D. J. Cole-Hamilton, *J. Chem. Soc., Dalton Trans.* 1983, 1051; (b) V. K. Jacob, K. H. Thiele, Ch. Keilberg and R. Niebuhr, *Z. Anorg. Allg. Chem.* 1975, **415**, 109.
2. (a) F. A. Cotton and M. D. La Prade, *J. Am. Chem. Soc.* 1968, **90**, 5418; (b) S. D. Chappel, D. J. Cole-Hamilton, A. M. R. Galas, M. B. Hursthouse and N. P. C. Walker, *Polyhedron* 1985, **4**, 121; (c) S. L. Latesky, A. K. McMullen, G. P. Niccolai, J. P. Rothwell and J. C. Huffman, *Organometallics* 1985, **4**, 902.
3. E. Carmona, J. M. Marin, M. Paneque and M. L. Poveda, *Organometallics* 1987, **6**, 1757.
4. (a) E. Carmona, F. González, M. L. Poveda, J. L. Atwood and R. D. Rogers, *J. Chem. Soc., Dalton Trans.* 1980, 2108; (b) E. Carmona, M. Paneque, M. L. Poveda, R. D. Rogers and J. L. Atwood, *Polyhedron* 1984, **3**, 317.
5. See: Y. Becker and J. K. Stille, *J. Am. Chem. Soc.* 1978, **100**, 845 and refs therein.
6. F. A. Cotton and T. J. Marks, *J. Am. Chem. Soc.* 1969, **91**, 1339.
7. E. Carmona, M. A. Muñoz and R. D. Rogers, *Inorg. Chem.* 1988, **27**, 1598.
8. J. Jeffery, M. F. Lappert, N. T. Luong-Thi, M. Webb, J. L. Atwood and W. E. Hunter, *J. Chem. Soc., Dalton Trans.* 1981, 1593.
9. F. A. Cotton and G. Wilkinson, *Advanced Inorganic Chemistry*, p. 1123. John Wiley, New York (1980).
10. W. Wolfsberger and H. Schmidbaur, *Synth. React. Inorg. Metal-Org. Chem.* 1974, **4**, 149.
11. O. Dahl, *Acta Chem. Scand.* 1969, **23**, 2342.
12. F. Guerrieri and G. Salermo, *J. Organomet. Chem.* 1976, **114**, 339.

Polyhedron Vol. 8, No. 3, pp. 293–300, 1989
Printed in Great Britain

0277–5387/89 $3.00+.00
© 1989 Pergamon Press plc

SYNTHESIS AND NMR STUDIES OF DIFLUOROPHOSPHINE-SUBSTITUTED UREAS

WIELAND KRÜGER and REINHARD SCHMUTZLER*

Institut für Anorganische und Analytische Chemie der Technischen Universität, Hagenring 30, D-3300 Braunschweig, F.R.G.

and

HANS-MARTIN SCHIEBEL

Institut für Organische Chemie der Technischen Universität, Hagenring 30, D-3300 Braunschweig, F.R.G.

and

VICTOR WRAY

Gesellschaft für Biotechnologische Forschung mbH, Mascheroder Weg 1, D-3300 Braunschweig, F.R.G.

(*Received* 13 *June* 1988; *accepted* 11 *July* 1988)

Abstract—Difluorophosphine-substituted ureas have been prepared by the reaction of PF_2Cl with N,N′-bis(trimethylsilyl)ureas. Three of these PF_2-substituted ureas have been employed to synthesize chelate complexes from $Ni(CO)_4$ and $Mo(CO)_6$. The ^1H, ^{13}C, ^{19}F and ^{31}P NMR characterization of both the PF_2-substituted ligands and their $Ni(CO)_2$- and Mo^0-chelate complexes is described. A complete set of coupling constants was determined from the iterative analysis of the low temperature ^{19}F and ^{31}P spectra of N,N′-bis(difluorophosphino)-N,N′-dimethylurea.

Phosphorus-containing derivatives of urea have attracted industrial interest since the 1970's.[1] Some compounds were shown to be potential flame retardants while others were found to display biological activity. Their use as herbicides has been described.[1] Urea derivatives containing difluorophosphine groups have not, however, been described previously.

Through the modification of a synthetic principle mentioned in the literature[2] we have been able to synthesize the compound PF_2Cl efficiently and in appreciable quantity,[3,4] enabling the use of this compound as a precursor to PF_2-substituted ureas.[3] The synthesis of some N—PF_2 substituted ureas, and some of their complexes with Ni^0 and Mo^0, and the characterization of these by NMR spectroscopy are the subject of this paper.

Synthesis of difluorophosphine-substituted derivatives of urea

The synthesis method employed throughout was the reaction of N,N′-bis(trimethylsilyl)ureas with PF_2Cl, which was found to proceed smoothly at −30 to −25°C, in accord with eq. (1),

$$\underset{\textbf{1a–d}}{(R^1)(Me_3Si)NC(:O)N(SiMe_3)(R^2)} + \underset{\textbf{2}}{2PF_2Cl} \rightarrow \underset{\textbf{3a–d}}{(R^1)(F_2P)NC(:O)N(PF_2)(R^2)} + 2Me_3SiCl \quad (1)$$

1a, 3a: $R^1 = R^2 = H$
1b, 3b: $R^1 = R^2 = Me$
1c, 3c: $R^1 = Me$; $R^2 = Et$
1d, 3d: $R^1 = Me$; $R^2 = c\text{-}C_6H_{11}$.

*Author to whom correspondence should be addressed.

Dedicated to Sir Geoffrey Wilkinson, on the occasion of his retirement from Imperial College, London, in recognition of his seminal contributions to organometallic and coordination chemistry.

The reactions were conducted in heavy-walled glass tubes, in the absence of solvent. Product **3a** was obtained as an unstable solid, after volatile products had been pumped off, while products **3b–3d** were liquids which could be purified by vacuum distillation. The characterization of compounds **3a–3d** was by elemental analysis, mass spectrometry and NMR spectroscopy (*vide infra*).

The ligand properties of the novel PF_2-substituted ureas have been evaluated, in some cases. Derivatives involving $(H)(PF_2)NC(=O)N(PF_2)(H)$ (**3a**) and $(Me)(PF_2)NC(=O)N(PF_2)(Me)$ (**3b**) with Ni^0 and Mo^0, have been synthesized through displacement reactions with **3a** and **3b** of the carbonyls $Ni(CO)_4$ and $Mo(CO)_6$, in accord with eqs (2) and (3)

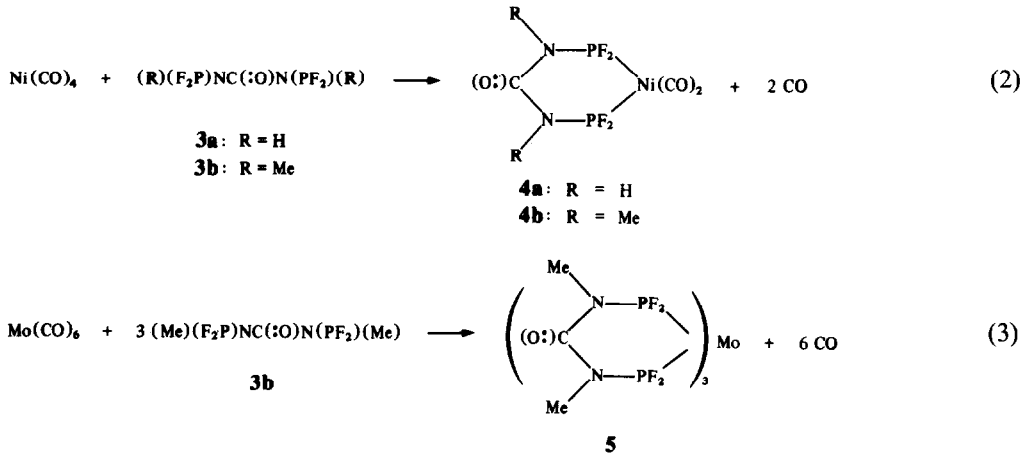

(2)

(3)

While the substitution reaction in $Ni(CO)_4$ was conducted in the temperature range $-20°C$ to room temperature, the reaction of $Mo(CO)_6$ was effected at room temperature, with UV irradiation. The complexes **4a**, **4b** and **5** were characterized by elemental analysis (with exceptions), mass spectrometry and NMR spectroscopy (*vide infra*). Two reports by Nixon and his co-workers have appeared, concerning the use of **3b** as a ligand in complexes with Rh and Ir,[5] and in a mixed-metal complex, involving Mo and Rh.[6]

Mass spectra of compounds **3a–3d**, **4a**, **4b** *and* **5**

Mass spectra have been recorded for all the PF_2-substituted ureas, **3a–3d**, and for their metal complexes **4a**, **4b** and **5**. Although of low relative abundance, a molecular ion peak has been observed in all cases, confirming the molecular weight and identity of the compounds. In the case of the uncoordinated compounds **3a–3d**, and for the tris-chelate of Mo^0, the fragment $m/z = 69$ $(PF_2)^7$ was characteristically observed as the most abundant degradation product. Other fragments, originating from the urea backbone were equally characteristic (see Table 1). In addition to their nominal masses the molecular ions of the metal complexes, **4a**, **4b** and **5**, are characterized by their specific isotopic patterns.

NMR spectroscopic investigations

The NMR data in Table 2 are all consistent with the proposed structures. The ^{19}F shifts are in the expected range and the formation of the nickel dicarbonyl complexes, **4a** and **4b**, from compounds **3a** and **3b** causes the anticipated decrease in nuclear screening. Thus the change of 28.7 and 29.4 ppm for **3a** on going to **4a**, and **3b** on going to **4b** is similar to data reported in the literature for Me_2NPF_2 (22.0 ppm) and $C_5H_{10}NPF_2$ (22.1 ppm).[8]

The poor solubility of **3a** and **4a** in most organic liquids prevented a variable temperature NMR investigation. This was possible, however, with **3b**, **3c** and **4b**. The ambient temperature ($\sim 30°C$) ^{19}F and ^{31}P NMR spectra of **3b** were analysed as the A and X parts, respectively, of an $(A_2X)_2$ spin system.[9] Even at this temperature, however, various lines in the spectrum have line widths different to the others (see Fig. 1) and the spectral parameters are solvent dependent (Table 3). Thus the exceptionally large value of $^4J_{PP}$ is particularly sensitive to the effect of the solvent and temperature (Table 4). The temperature behaviour of both the ^{19}F and ^{31}P NMR spectra are shown in Fig. 1. At the lowest temperature ($-112°C$) both spectra are consistent with the system being of the $(ABX)_2$ type. Iteration gave the parameters in Table 2. The equivalence of the phosphorus atoms in the analysis excludes hindered rotation about the C—N bond as the cause of the form of these spectra. The largest fluorine–fluorine coupling constant (21.05 Hz) is due to geminal

Table 1. Characteristic peaks in the mass spectra of compounds **3a–3d**, **4a**, **4b** and **5**. The tentative assignments are based on low resolution data

Compound	Fragments	m/z	Relative abundance (%)	Compound	Fragments	m/z	Relative abundance (%)
3a	M^+	196	5	**4a**	M^+	310[a]	5
	$M—NHPF_2^+$	112	10		$M—CO^+$	282	9
	$F_2PNH_2^+$	85	61		$M—2CO^+$	254	9
	PF_2^+	69	100		$CONHPF_2^+$	112	25
					NH_2CO^+	44	100
3b	M^+	224	5	**4b**	M^+	338[a]	< 1
	$M—PF_2^+$	155	37		$M—CO^+$	310	1
	$M—MeNPF_2^+$	126	60		$M—2CO^+$	282	4
	$MeNPF_2^+$	98	16		$MeNCO^+$	57	84
	PF_2^+	69	100		$C_2H_3N^+$	41	100
3c	M^+	238	8	**5**	M^+	770[b]	3
	$M—PF_2^+$	169	34		$M—L^+$	546	3
	$M—Me(F_2P)N^+$	140	14		$M—L—MeNCO^+$	489	5
	$M—Et(F_2P)N^+$	126	58		$M—L—Me(PF_2)NCO^+$	420	5
	$M—MeF_2PNCO^+$	112	34		PF_2^+	69	88
	$M—EtF_2PNCO^+$	98	53		$CHNO^+$	43	100
	PF_2^+	69	100		(L = $[Me(PF_2)N]_2CO$)		
3d	M^+	292	5				
	$M—PF_2^+$	223	33				
	$M—MeNPF_2^+$	194	6				
	$C_6H_{11}NPF_2^+$	166	7				
	$MeNPF_2CO^+$	126	32				
	$C_6H_{11}^+$	83	27				
	PF_2^+	69	100				

[a] Based on ^{58}Ni.
[b] Based on ^{98}Mo.

coupling and not to long range through-space coupling.

Although the temperature behaviour of this complex system has not been simulated using band-shape analysis[10] the coalescence temperature of approximately −82°C in the fluorine NMR spectrum suggests an energy barrier in the region 6–10 kcal mol^{-1}.* This value is characteristic of the barrier to internal rotation about the P—N bond.[11] Thus the molecule in its lowest energy conformation corresponds to either conformers a or b, or some rotationally averaged mixture of them; the unsymmetrical structure, c, may be ruled out.

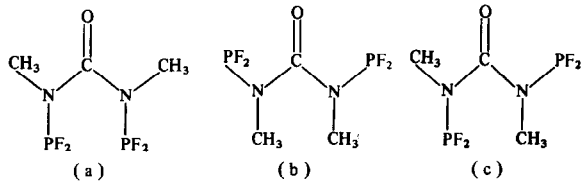

* Although a simple two-site exchange gives a barrier of 8 kcal mol^{-1} such a simplification probably leads to considerable error in the calculated barrier.

The magnitude of the barrier to internal rotation about the C—N bond cannot be evaluated as a second coalescence phenomenon was not observed. The large $^4J_{PP}$ suggests a planar system with the coupling information being transmitted through the bonds, as a through-space transmission would also necessitate long-range fluorine–fluorine interactions[12] of which there appears to be very little evidence ($^6J_{FF}$ are all ~ 0 Hz).

The ^{13}C NMR spectra of **3c** and **3d** unambiguously confirm the proposed structures. The ^{19}F and ^{31}P NMR spectra of **3a** were broad at ambient temperature. Cooling to −30°C gave a sharpening of the lines but no apparent coalescence phenomenon. At this temperature the non-symmetrical spectra were indicative of hindered rotation about the N—P bond. Although the spectra could not be simulated, attempts at simulation showed that the form of the spectrum could only be produced by assuming an ABCDXY spin system with non-equivalence of all the fluorine and phosphorus nuclei. Similarly an analysis of the complex ^{19}F spectrum of **3d** was not attempted.

Table 2. NMR spectral parameters for compounds **3a–3d**, **4a**, **4b** andf **5** at ambient temperature (~ 30°C)

Compound		Solvent	δ ^{19}F (ppm)	δ ^{31}P (ppm)	δ ^{1}H (ppm)	δ ^{13}C (ppm)	J(PF) (Hz)
$[H(F_2P)N]_2C(O)$	**3a**	CD_3CN	−70.4	[a]	—	[a]	$\lvert {}^1J_{PF} + {}^5J_{PF} \rvert$ 1241.4
$[CH_3(F_2P)N]_2C(O)$	**3b**	CD_3CN	−76.0	+136.8	+2.5	[c]	${}^1J_{PF} \mp 1278.4$ ${}^5J_{PF} \pm 27.1$
$CH_3(F_2P)N$ $C(:O)$ $C_2H_5(F_2P)N$	**3c**	CD_3CN	−75.4[b]	+137.3[b]	[c]	156.3 (CO) 37.4 (CH_2) 14.9 (CH_3) C_2H_5 27.7 (CH_3)	
$CH_3(F_2P)N$ $C(:O)$ c-$C_6H_{11}(F_2P)N$	**3d**	C_6D_6	−73.9[b]	[c]	+1.7(CH_2) +3.0(CH_3) +3.7(CH)	155.6 (CO) 57.2 C1 32.2 C2,6 c-C_6H_{11} 27.0 C3,5 25.8 C4 27.0 CH_3	
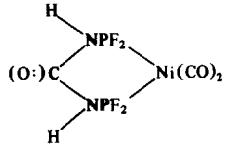	**4a**	C_6D_6	−41.7	[a]	—	[a]	$\lvert {}^1J_{PF} + {}^3J_{PF} \rvert$ 1152.6
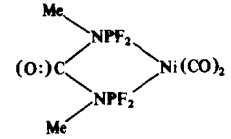	**4b**	C_6D_6	−46.6	+152.8	+3.1	[c]	${}^1J_{PF} \mp 1246.3$ ${}^3J_{PF} \pm 97.5$
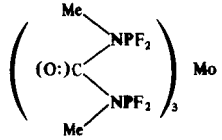	**5**	C_6D_6	−22.8	+175.9	+2.9	[c]	${}^1J_{PF}$ 1174

[a] Not sufficiently soluble to obtain spectrum.
[b] Centre of spectrum.
[c] Not recorded.

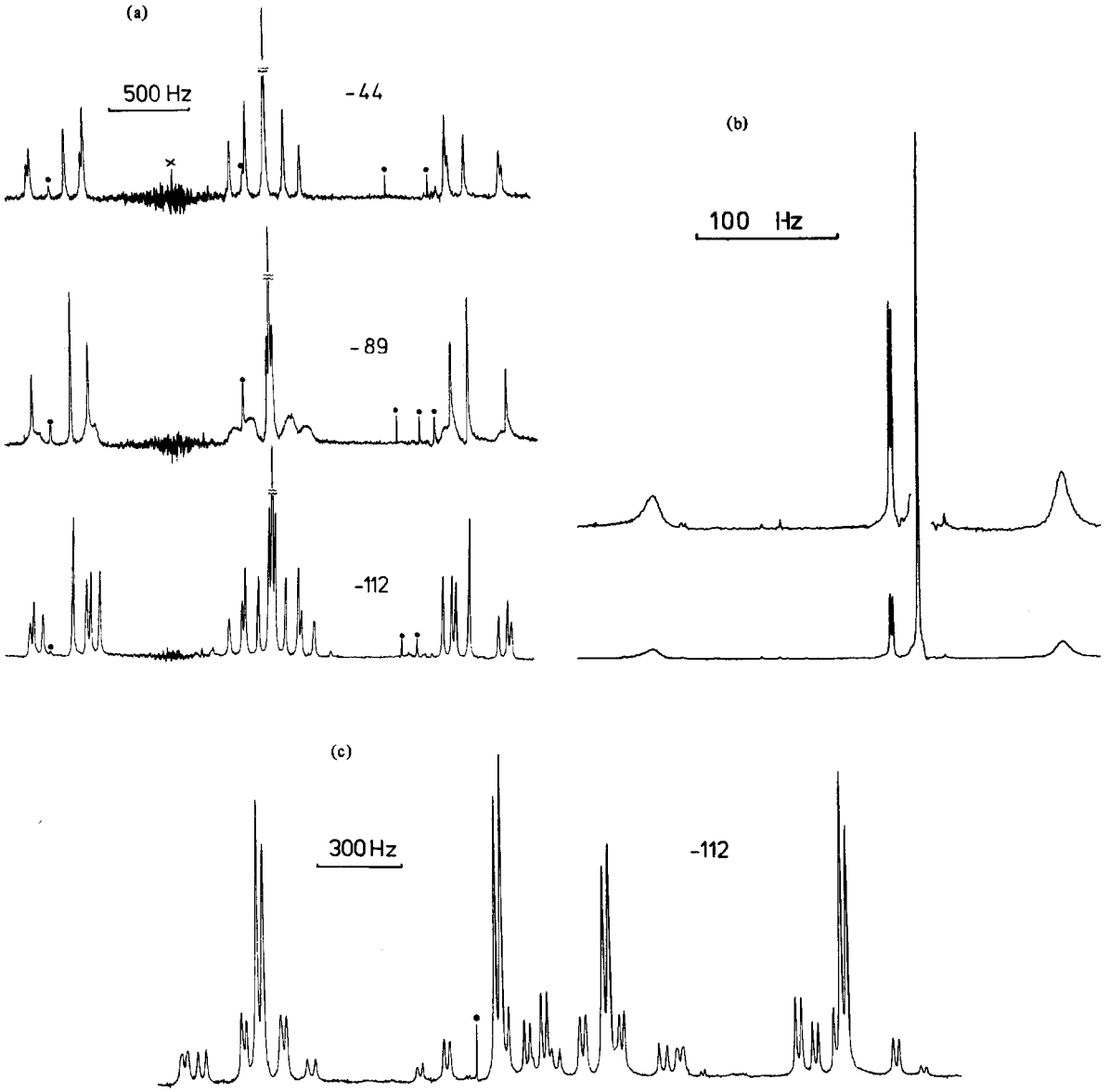

Fig. 1. Variable temperature NMR spectra of (Me)(F_2P)NC(:O)N(PF_2)(Me) (**3b**) (· denotes impurities; × instrumental artifacts). (a) Full ^{31}P NMR spectra at −44, −89 and −112°C; (b) low frequency half of symmetrical ^{19}F {^{1}H} NMR spectrum at 30°C; (c) full ^{19}F NMR spectrum at −112°C.

As expected, the ^{19}F and ^{31}P NMR spectra of **4b** were temperature independent over a limited temperature range. Analysis of the spectra was straightforward. The equivalence of the phosphorus shifts and the presence of two $^4J_{FF}$ values indicate the presence of the ring system. For **4a** only the intense lines of the fluorine spectrum were observed. However, the value $|^1J_{PF}+{}^3J_{PF}|$ of 1152.6 Hz is indicative of ring formation, being similar to that for **4b** (1148.8 Hz) but quite different from that of the non-complexed analogues (**3a**, 1241.4 and **3b**, 1244.8 Hz).

EXPERIMENTAL

All experiments were conducted with careful exclusion of air and moisture. Solvents were dried by standard procedures.[13]

NMR spectra. The NMR data were recorded on JEOL C-60 HL (^{1}H, ^{19}F, ^{31}P), Varian XL-100 (^{19}F, ^{31}P, ^{13}C) and Varian CFT-20 (^{13}C) NMR spectrometers. The variable temperature spectra used in the spectral analyses of **3b**, **3c** and **4b** were recorded in the FT-mode on the Varian XL-100 spectrometer, which was controlled with a Varian

Table 3. NMR parameters from the spectral analysis of **3b** and **4b** using LAOCOON III

Compound	Solvent	Temperature	Couplings (±0.1) (16) (45)	(26) (35)	(15) (46)	(25) (36)	(12) (34)	(56)	(13) (24)	(23)	(14)	rms error
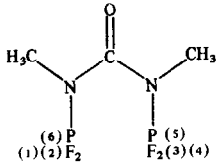 **3b**	CD_3CN											
	Et_2O	30	∓1278.4		±27.1			287.9				0.2
		30	∓1273.2		±28.4			342.1				0.2
	Et_2O	−112	∓1228.4	∓1311.7	∓15.05	±68.91	21.05	350.6	−0.1	0.5	−0.3	0.8[a]
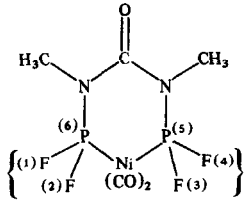 **4b**	C_6D_6	30	−1246.3		±97.5			196.6	15.4	19.3		0.2

[a] $(\delta_{2,3}-\delta_{1,4})$ 852.0 Hz.

Table 4. Temperature dependence of $^4J_{PP}$ in **3b**

Temperature (°C)	$^4J_{PP}$ (Hz)	Solvent
119	256	None
100	269	None
83	283	None
59	297	None
41	315	None
0	318	10% in CH_2Cl_2
−25	328	10% in CH_2Cl_2
−50	337	10% in CH_2Cl_2
−75	351	10% in CH_2Cl_2

620-L computer equipped with a moving head disc together with complementary software. The spectra were analysed with the aid of a program based upon LAOCOON III and all computations were carried out in single precision on a PDP-10 computer.

Chemical shifts were measured relative to internal tetramethylsilane for ^1H and ^{13}C, fluorotrichloromethane for ^{19}F and external 85% *ortho*-phosphoric acid for ^{31}P. All shifts follow the IUPAC convention and are given on the δ scale with positive values being used to denote a shift to high frequency of the reference.

IR spectra. These were recorded on a Beckman IR-20 instrument (capillary films between KBr discs).

Mass spectra. These were recorded on either an AEI MS 30 or a Varian-MAT CH4 instrument (direct inlet system, 70 eV).

Starting materials. The following compounds were prepared by the procedures indicated: PF_2Cl (**2**),[7] $[(H)(Me_3Si)NC(:O)N(SiMe_3)(H)]$ (**1a**),[14] $[(Me)(Me_3Si)NC(:O)N(SiMe_3)(Me)]$ (**1b**),[15] $[(Me)(Me_3Si)NC(:O)N(SiMe_3)(Et)]$ (**1c**).[16] $[(Me)(Me_3Si)NC(:O)N(SiMe_3)(c\text{-}C_6H_{11})]$ (**1d**) is a new compound which was synthesized from cyclohexylisocyanate and hexamethyldisilazane, following the method of Klebe *et al.*[15]

A mixture of hexamethyldisilazane (40 g, 0.228 M) and cyclohexylisocyanate (28.5 g, 0.228 mol) was stirred for 3 days at room temperature. Unreacted starting materials were pumped off at 30°C (0.01 mm). The higher-boiling residue was fractionally distilled at 83–87°C (0.01 mm). The yield of **1d** was 25 g (36%). $C_{14}H_{32}N_2OSi_2$ (300.58) Found: C, 56.1; H, 11.2; N, 10.3; Si, 18.42. Calc.: C, 55.9; H, 10.7; N, 9.3; Si, 18.7%. ^1H and ^{13}C NMR spectra were recorded in $CDCl_3$ on a Bruker AM 400 spectrometer and were compatible with the proposed structure.

Reaction of N,N′-bis(trimethylsilyl)-N,N′-bis(hydrogen or organo)ureas with difluorophosphorus(III) chloride, PF_2Cl—general procedure

The experiments were conducted in 250 cm^3 heavy-walled glass tubes, fitted with a TEFLON® stopcock and a side arm, bearing an NS 14.5 ground joint. These tubes were heated to 130°C and allowed to cool slowly to room temperature while a stream of dry nitrogen was passed through them. Subsequently, the N,N′-bis(trimethylsilyl)urea was placed into the tube in a countercurrent of nitrogen. The stopcock was closed, and the tube was attached to a vacuum line, via the stopcock. The contents of the tube were cooled to −196°C, evacuated and the appropriate amount of PF_2Cl (**2**) (weighed separately in a trap) was condensed in. The reaction mixture was allowed to reach the reaction temperature which was maintained, using a cryostat. Subsequently, the reaction mixture was again cooled to liquid nitrogen temperature and the tube was evacuated via the vacuum line. The reaction mixtures were separated into their components by fractional condensation. If the desired compound did not exhibit a vapour pressure measurable at −63°C all volatile by-products could be removed by distillation from a chloroform–dry ice bath at −63°C. As a rule, $SiMe_3Cl$ and the product remained as a residue. If the latter was sufficiently stable it was fractionally distilled at reduced pressure.

In the case where the product had a vapour pressure at −63°C, fractional condensation was used. $SiMe_3Cl$ was collected in a −63°C trap, $SiMe_3F$ in a −96°C trap, PF_2Cl in a −160°C trap, and PF_3 in a −196°C trap. The cold baths employed are specified with the individual experiments.

N,N′-Bis(difluorophosphine)urea, $[H(F_2P)N]_2C(:O)$ (**3a**). N,N′-Bis(trimethylsilyl)urea (**1a**) (7.0 g, 34.2 mmol) and **2** (9.6 g, 91.9 mmol) were allowed to react for 4 h at −25°C. The product, **3a**, is readily decomposed in air. In solvents, e.g. CH_2Cl_2 and CD_3CN, decomposition with formation of PF_3 is apparent after *ca* 15 min. Yield: quantitative; m.p. 169–173°C (dec.). On account of its instability **3a** was not analysed.

N,N′-Bis(difluorophosphino)-N,N′-dimethylurea, $[Me(F_2P)N]_2C(:O)$ (**3b**). N,N′-Bis(trimethylsilyl)-N,N′-dimethylurea (**1b**) (8.0 g, 34.4 mmol) and **2** (10.4 g, 99.6 mmol) were allowed to react at −28°C for 3 h. Yield: 6.95 g (90%); b.p. 52°C (9.5 mm). $C_3H_6F_4N_2OP_2$ (224.03) Found: C, 16.3; H, 2.7; F, 33.6. Calc.: C, 16.1; H, 2.7; F, 33.9%.

N,N′-Bis(difluorophosphino)-N-methyl-N′-ethylurea, $[Me(F_2P)NC(:O)N(PF_2)Et$ (**3c**). **3c** was obtained from $Me(Me_3Si)NC(:O)N(SiMe_3)Et$ (**1c**)

(4.64 g, 18.69 mmol) and **2** (4.45 g, 46.63 mmol) as a colourless liquid. Yield: 2.28 g (51%); b.p. 29°C (1.8 mm). $C_4H_8F_4N_2OP_2$ (238.06) Found: C, 20.8; H, 3.5; F, 31.0. Calc.: C, 20.2; H, 3.4; F, 31.9%.

N,N'-Bis(difluorophosphino)-N-methyl-N'-cyclohexylurea, $Me(F_2P)NC(:O)N(PF_2)C_6H_{11}$ (**3d**). **3d** was obtained as a liquid from $Me(Me_3Si)NC(:O)N(SiMe_3)C_6H_{11}$ (7.8 g, 25.9 mmol) and **2** (8.1 g, 77.6 mmol) after reaction for 4 h at −28°C. Yield: 4.69 g (62%); b.p. 58°C (0.06 mm). $C_8H_{14}F_4N_2OP_2$ (292.15) Found: C, 33.4; H, 4.96; F, 25.2. Calc.: C, 32.9; H, 4.83; F, 26.0%.

[*N,N'* - *Bis(difluorophosphino)urea]dicarbonylnickel*(0), $[H(F_2P)NC(:O)N(PF_2)H]Ni(CO)_2$ (**4a**). The reaction was conducted in a r.b. flask charged, in a nitrogen atmosphere, with nickel carbonyl (1.0 g, 5.86 mmol, in 15 cm^3 of pentane). 30 cm^3 of a mixture of pentane–tetrahydrofuran was then added, followed by the dropwise addition of **3a** (1.0 g, 5.1 mmol, in 15 cm^3 of tetrahydrofuran). The reaction mixture was stirred magnetically for 7 h at room temperature. All volatile products were pumped off at *ca* 1 mm, and the product was left as an oil. Yield: 1.1 g (70%). The mass spectrum showed a molecular ion peak at *m/z* 310 based on ^{58}Ni ($C_3H_2F_4N_2NiO_3P_2$, mol. wt 309.883). IR absorptions in the carbonyl region (ether): 2077, 2042, 1750 cm^{-1}.

[*N,N'* - *Bis(difluorophosphino)* - *N,N'-dimethylurea*] *dicarbonylnickel*(0), $[Me(F_2P)NC(:O)N(PF_2)Me]Ni(CO)_2$ (**4b**). A mixture of $Ni(CO)_4$ (1.41 g, 8.26 mmol) in 10 cm^3 petroleum ether (40/60) and **3b** (1.97 g, 8.79 mmol) was prepared at −20°C. After the mixture had been stirred at room temperature for 24 h volatile products were removed by pumping at *ca* 1 mm. **4b** was left as an oil. Yield: 1.35 g (45%). The mass spectrum showed a molecular ion peak at *m/z* 338 based on ^{58}Ni ($C_5H_6F_4N_2NiO_3P_2$, mol. wt 337.914). IR absorptions in the carbonyl region (petroleum ether) 2085, 2043, 1695 cm^{-1}.

Tris[N,N'-bis(difluorophosphino)-N,N'-dimethylurea]molybdenum(0), $[Me(F_2P)NC(:O)N(PF_2)Me]_3Mo$ (**5**). A mixture of **3b** (2.28 g, 10.18 mmol) and $Mo(CO)_6$ (0.72 g, 2.73 mM) in 150 cm^3 ether was subjected for 30 h to UV irradiation. After the volatile materials had been removed **5** was left as a crystalline solid, which was readily soluble in ether and dichloromethane. Yield: 1.99 g (91%). The mass spectrum showed a molecular ion peak at *m/z* 770, based on ^{98}Mo ($C_9H_{18}F_{12}MoN_6O_3P_6$, mol. wt 769.873).

Acknowledgements—W.K. acknowledges support by Deutsche Forschungsgemeinschaft, Verband der Chemischen Industrie, and by Land Niedersachsen. BASF AG, BAYER AG and HOECHST AG have generously supplied chemicals used in this research. The assistance of Fonds der Chemischen Industrie is gratefully acknowledged. Petra Look is thanked for experimental assistance.

REFERENCES

1. See, for example, G. H. Birum, (to Monsanto Co.), U.S. Patent, 3,965,127 (22 June 1976) and U.S. Patent, 4,003,965 (18 January 1977).
2. Zh. M. Ivanova, *Zhur. Obshch. Khim.* 1965, **35**, 164.
3. W. Krüger, PhD Thesis. Technische Universität, Braunschweig (1978).
4. W. Krüger, M. Sell and R. Schmutzler, *Z. Naturforsch.* 1983, **38b**, 1074.
5. P. B. Hitchcock, S. Morton and J. F. Nixon, *J. Chem. Soc., Dalton Trans.* 1985, 1295.
6. M. F. Meidine, C. J. Meir, S. Morton and J. F. Nixon, *J. Organometal. Chem.* 1985, **297**, 255.
7. W. Albers, W. Krüger and R. Schmutzler, *Synth. React. Inorg. Metal-Org. Chem.* 1985, **15**, 187.
8. (a) G. S. Reddy and R. Schmutzler, *Inorg. Chem.* 1967, **6**, 823; (b) G. S. Reddy and R. Schmutzler, *Z. Naturforsch.* 1970, **25b**, 1199.
9. R. J. Abraham, *The Analysis of High Resolution NMR Spectra*, p. 226. Elsevier, Amsterdam (1971).
10. G. Binsch, in *Dynamic Nuclear Magnetic Resonance Spectroscopy* (Edited by L. M. Jackman and F. A. Cotton), p. 45. Academic Press, London (1975).
11. S. C. Peake, M. J. C. Hewson, O. Schlak, R. Schmutzler, R. K. Harris and M. I. M. Wazeer, *Phosphorus Sulfur* 1978, **4**, 67.
12. J. Hilton and L. H. Sutcliffe, *Prog. NMR Spectrosc.* 1975, **10**, 27.
13. D. D. Perrin, W. K. F. Armarego and D. R. Perrin, *Purification of Laboratory Chemicals*. Pergamon Press, Oxford (1966).
14. U. Wannagat, H. Bürger, C. Krüger and J. Pump, *Z. Anorg. Allg. Chem.* 1963, **321**, 208.
15. (a) J. F. Klebe, J. B. Bush Jr and J. E. Lyons, *J. Am. Chem. Soc.* 1964, **86**, 4400.
16. O. Schlak, R. Schmutzler, R. K. Harris, E. M. McVicker and M. I. M. Wazeer, *Phosphorus Sulfur* 1981, **10**, 87.

Polyhedron Vol. 8, No. 3, pp. 301–304, 1989
Printed in Great Britain

0277–5387/89 $3.00 + .00
© 1989 Pergamon Press plc

SYNTHESIS AND X-RAY CRYSTAL STRUCTURE OF PYRIDINE-2-AMIDOXIME, $C_6H_7N_3O$, AND AQUA-BIS-(PYRIDINE-2-AMIDOXIME)COPPER(II) CHLORIDE, $[Cu(C_6H_7N_3O)(H_2O)]Cl_2$

GEORGE A. PEARSE,* PAUL R. RAITHBY and JACK LEWIS

University Chemical Laboratory, Lensfield Road, Cambridge CB2 1EW, U.K.

(*Received* 22 *July* 1986; *accepted after revision* 25 *July* 1988)

Abstract—The crystals of pyridine-2-amidoxime, $C_6H_7N_3O$, are monoclinic, space group $C2/c$ with $a = 21.672(1)$, $b = 4.615(1)$, $c = 13.398(1)$ Å, $\beta = 106.58(1)°$ and $Z = 8$. The reaction of the ligand with copper(II) chloride dihydrate yields a dark green precipitate of formula $[Cu(C_6H_7N_3O)_2(H_2O)]Cl_2$ which crystallized in the monoclinic space group $C2/c$ with $a = 16.856(1)$, $b = 7.076(1)$, $c = 14.843(1)$ Å, $\beta = 106.40(1)°$ and $Z = 4$. The X-ray structure of the complex shows the five-coordinate nature of the metal atom which is bound through the heterocyclic and oxime nitrogen atoms of two *trans*-oriented bidentate ligands plus a water molecule to give a square-based pyramidal chelate.

Although the synthesis of pyridine-2-amidoxime (Py2AO) was reported about 30-years ago,[1] the literature contains no structural determination of either this bidentate ligand or its transition metal complexes. Py2AO (Fig. 1) possesses the α,α'-diimine moiety, —N=C—C=N—, similar to that present in 1,10-phenanthroline and 2,2′-bipyridyl, but without the steric rigidity of these two compounds, and forms solid complexes with transition metal ions.[2] Because of its unsymmetrical configuration, the possibility exists for *cis*- and *trans*-isomers in chelates having a 1:2 copper/ligand stoichiometry (Fig. 2). This investigation was carried out with the specific purpose of determining the structure of both the ligand and its copper(II) chloride complex. The results have been compared to a similar 1:2 compound of copper(II) with pyridine-2-aldoxime.[3]

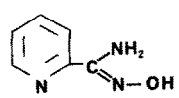

Fig. 1. Block diagram of the structure of pyridine-2-amidoxime.

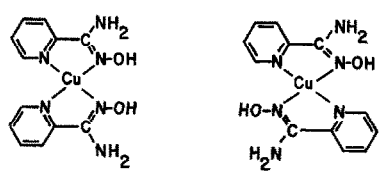

Fig. 2. Block diagram of the structure of *cis*- and *trans*-bis(Py2AO)Cu^{II}.

EXPERIMENTAL

2-Cyanopyridine was purchased from Aldrich Chemical Co. and used without further purification. All other chemicals were reagent grade. Density measurements were made by the floatation method using a mixture of diethyl ether and carbon tetrachloride for Py2AO and a mixture of benzene and 1,2-dibromoethane for the copper complex.

Pyridine-2-amidoxime, $C_6H_7N_3O$, was synthesized from 2-cyanopyridine as previously reported.[4] Recrystallization by slow evaporation of an aqueous solution gave large, well-formed, colourless crystals suitable for diffraction studies. Found: C, 52.4; H, 5.50; N, 30.5. Calc. for $[C_6H_7N_3O]$: C, 52.5; H, 5.1; N, 30.6%.

*Author to whom correspondence should be addressed. Visiting Professor on leave from Le Moyne College, Syracuse, NY 13214, U.S.A., 1985–1986.

Aqua-bis-(pyridine-2-amidoxime)copper(II) chloride $[Cu(C_6H_7N_3O)_2(H_2O)]Cl_2$

To a solution of 1.70 g (10 mmol) of copper(II) chloride dihydrate in 40 cm^3 of distilled water was added 2.74 g (20 mmol) of pyridine-2-amidoxime in the minimum required amount of 95% ethanol. The solution turned dark green and crystals separated almost immediately (yield 82%, 3.50 g). Recrystallization by slow evaporation of a dilute aqueous solution gave large, well-formed, dark green crystals suitable for diffraction studies. Found: C, 33.9; H, 3.6; N, 19.6. Calc. for $[Cu(C_6H_7N_3O)_2(H_2O)]Cl_2$: C, 33.8; H, 3.8; N, 19.7%.

X-ray crystallography

General procedures have been described elsewhere.[5] Information about data collection for pyridine-2-amidoxime and aqua-bis-(pyridine-2-amidoxime)copper(II) chloride is given in Table 1. Atomic coordinates, thermal parameters and lists of F_o and F_c values have been deposited with the Editor. Atomic coordinates have also been deposited with the Cambridge Crystallographic Data Centre.

RESULTS AND DISCUSSION

Figure 3 is a perspective view of pyridine-2-amidoxime showing the atom numbering. In the crystalline state the ligand exists as the *syn* isomer. Previous work,[4] using IR data, showed that the ligand is also in the *syn* configuration in solution. Because of the free rotation about the C(1)—C(6) bond, the ligand can assume the α,α'-diimine structure involving the N(1)—C(1)—C(6)—N(3) portion of the molecule. A comparison with pyridine-2-aldoxime leads to the conclusion that both ligands should react in a similar fashion utilizing the heterocyclic and oxime nitrogen atoms.

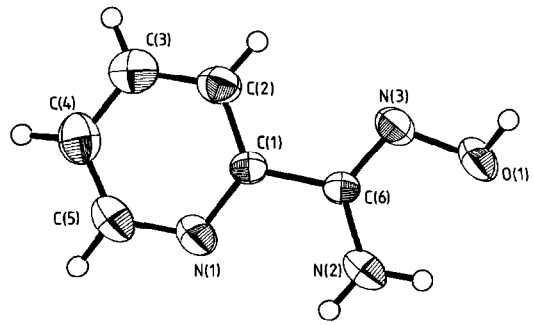

Fig. 3. Crystal structure of $C_6H_7N_3O$ showing the atomic numbering scheme.

The bis-(pyridine-2-amidoxime)copper(II) complex is shown in Fig. 4. The two ligands are arranged in a *trans* mode about the metal atom. An axially coordinated water molecule completes the pentadentate, square-based pyramidal structure.

Table 1. Summary of crystal data

	I	II
Formula	$C_6H_7N_3O$	$[Cu(C_6H_7N_3O)_2(H_2O)]Cl_2$
Formula weight	137.14	426.73
Crystal system	Monoclinic	Monoclinic
Space group	*C*2/*c*	*C*2/*c*
a (Å)	21.672(1)	16.856(1)
b (Å)	4.615(1)	7.076(1)
c (Å)	13.398(1)	14.843(1)
β (°)	106.58(1)	106.40(1)
V (Å^3)	1284	1698
Z	8	4
$d_{calc.}$ (g cm^{-3})	1.419	1.669
$d_{meas.}$ (g cm^{-3})	1.415	1.663
Crystal size (mm)	0.07 × 0.49 × 0.44	0.29 × 0.34 × 0.50
Data collection instrument	Stoe	Stoe
Radiation (Å)	Mo-K_α (0.71069)	Mo-K_α (0.71069)
Data collection range (2θ)(°)	$5 \leqslant 2\theta \leqslant 45$	$5 \leqslant 2\theta \leqslant 50$
Scan method	ω–2θ	ω–2θ
Transmission factors (max, min)	0.9949, 0.9733	0.6807, 0.4263
F(000)	576	864
R	0.0372	0.0347
R_w	0.0411	0.0366
Number of reflections measured	3380	1898
Number of observed reflections [$F > 4\sigma(F)$]	724	1352

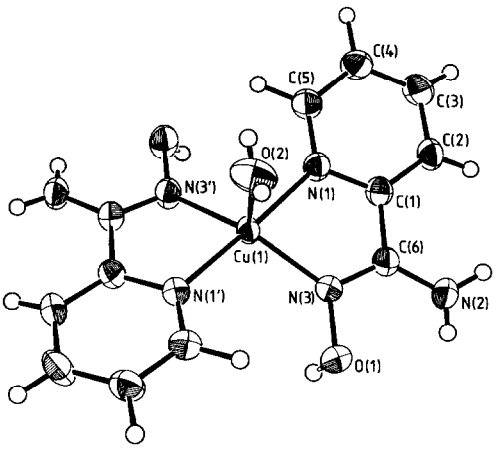

Fig. 4. Crystal structure of $[Cu(C_6H_7N_3O)_2(H_2O)]Cl_2$ showing the atomic numbering scheme.

Although the crystal structure of 1:2 copper(II) chloride/pyridine-2-aldoxime has not been reported, analytical and IR data strongly suggest that the ligands are in a *cis* arrangement.[3] Loss of one oxime hydrogen results in the solid coordination compound being *cis*-monohydrogen-bis-(pyridine-2-aldoxime)copper(II) chloride whereas this research resulted in the synthesis of *trans*-di-hydrogen-bis-(pyridine-2-amidoxime) copper(II) chloride. All attempts to prepare the *cis*-isomer with copper(II) chloride and pyridine-2-amidoxime were unsuccessful. Molecular models of the *cis*-pyridine-2-amidoxime/copper(II) chloride isomer do not preclude its formation based upon steric factors.

The bond lengths and angles for the ligand and the copper(II) complex are listed in Tables 2 and 3,

Table 2. Bond lengths and bond angles for $C_6H_7N_3O$

Bond length (Å)			
N(1)—C(1)	1.336(3)	C(5)—N(1)	1.336(3)
C(1)—C(2)	1.389(3)	C(1)—C(6)	1.484(3)
C(2)—C(3)	1.367(4)	C(6)—N(2)	1.348(3)
C(3)—C(4)	1.367(4)	C(6)—N(3)	1.291(3)
C(4)—C(5)	1.371(4)	N(3)—O(1)	1.419(2)
Bond angle (°)			
N(1)—C(1)—C(2)	122.7(2)	N(1)—C(1)—C(6)	115.4(2)
C(1)—C(2)—C(3)	118.7(2)	C(2)—C(1)—C(6)	121.9(2)
C(2)—C(3)—C(4)	119.4(3)	C(1)—C(6)—N(2)	118.2(2)
C(3)—C(4)—C(5)	118.3(3)	C(1)—C(6)—N(3)	118.3(2)
C(4)—C(5)—N(1)	124.1(2)	C(6)—N(3)—O(1)	109.1(2)
C(5)—N(1)—C(1)	116.7(2)	N(3)—C(6)—N(2)	123.4(2)

Table 3. Bond lengths and angles for $[Cu(C_6H_7N_3O)_2(H_2O)]Cl_2$

Bond length (Å)			
Cu—N(1)	2.010(2)	C(4)—C(5)	1.379(4)
Cu—N(3)	1.969(2)	C(5)—N(1)	1.335(3)
Cu—O(2)	2.238(4)	C(1)—C(6)	1.484(4)
N(1)—C(1)	1.352(4)	C(6)—N(2)	1.320(4)
C(1)—C(2)	1.377(4)	C(6)—N(3)	1.292(4)
C(2)—C(3)	1.390(5)	N(3)—O(1)	1.414(3)
C(3)—C(4)	1.381(5)		
Bond angle (°)			
Cu—N(1)—C(5)	126.1(2)	C(3)—C(4)—C(5)	119.2(3)
Cu—N(3)—C(6)	118.2(2)	C(4)—C(5)—N(1)	118.9(2)
Cu—N(1)—C(1)	114.5(2)	C(5)—N(1)—C(1)	119.0(2)
Cu—N(3)—O(1)	128.8(2)	N(1)—C(1)—C(6)	113.6(2)
N(1)—Cu—N(3)	79.7(1)	C(2)—C(1)—C(6)	124.6(3)
N(1)—Cu—O(2)	86.6(1)	C(1)—C(6)—N(2)	121.3(3)
N(3)—Cu—O(2)	103.2(1)	C(1)—C(6)—N(3)	113.8(2)
N(1)—C(1)—C(2)	121.8(3)	C(6)—N(3)—O(1)	112.6(2)
C(1)—C(2)—C(3)	119.0(3)	N(3)—C(6)—N(2)	124.8(3)
C(2)—C(3)—C(4)	118.9(3)		

Table 4. Comparison of selected bond lengths and angles of the amidoxime group

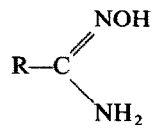

Compound	C=N (Å)	N—O (Å)	C=N—O (°)	N=C—N (°)	Reference
N-benzyl-*syn*-benzamidoxime	1.272	1.438	110.7	123.9	6
2,2′-Iminobis-(acetamidoxime)	1.278	1.426	109.0	125.6	7
(Methylene dioxy-3,4)-phenyl-2-hydroxy-2-acetamidoxime	1.284	1.435	110.0	125.1	8
Formamidoxime	1.288	1.415	109.7	126.7	9
2-Methyl-N,N-dimethyl-benzamidoxime	1.287	1.424	112.1	117.7	10
Pyridine-2-amidoxime	1.291	1.419	109.1	123.4	This work

respectively. A comparison of these data shows that the ligand undergoes little distortion on complexation with copper(II), resulting in a very stable coordination compound. Selected bond lengths and angles for several other amidoxime ligands are listed in Table 4. The C=N and N—O bond lengths of the oxime group for the five listed compounds are quite compatible with those of pyridine-2-amidoxime. The bond angles for the C=N—O of the oxime group and the N=C—N of the oxime–amine group show little variation with the exception of those for 2-methyl-N,N-dimethylbenzamidoxime. This can be attributed to steric factors caused by the two methyl groups on the amine nitrogen which are not present in the other amidoximes.

From this work it has been ascertained that the amidoxime group in the free ligand exists in the amino–oxime form, —C:NOH(NH_2), rather than the tautomeric imino–hydroxylamine form, —C:NH(NHOH). The copper(II) complex utilizes the oxime nitrogen of the amidoxime group rather than the amine nitrogen to form a five-membered ring with the heterocyclic nitrogen.

Using atomic coordinates and isotropic thermal parameters, available as supplementary data, atomic deviations from various planes were calculated. When considering the C(1)—C(6)—N(2)—N(3) plane for the free ligand, there is little deviation from planarity with respect to the oxime and amine nitrogens. The same plane for the copper(II) complex exhibits an atomic deviation increase of approximately 0.11 Å between the oxime and amine nitrogens. This is to be expected from the square-pyramidal configuration of the complex which causes a slight rotation of the C(1)—C(6) bond upon complexation. Rotation of this bond causes the observed reduction in planarity of the N(2)—N(3) nitrogens. This research has shown that pyridine-2-amidoxime forms a *trans*-dihydrogen-bis-(pyridine-2-amidoxime) chelate with copper(II) chloride whereas pyridine-2-aldoxime forms a monohydrogen-*cis*-bis compound under the same preparative conditions.

Acknowledgements—G.A.P. gratefully acknowledges a Visiting Professorship from the Department of Inorganic Chemistry at the University of Cambridge. Partial support of this research was provided by the Le Moyne College Research Committee.

REFERENCES

1. E. Bernasek, *J. Org. Chem.* 1957, **22**, 1263.
2. G. S. Sanyal, A. B. Modak and A. K. Mundi, *Ind. J. Chem.* 1983, **22A**, 387.
3. C. H. Liu and C. F. Liu, *J. Am. Chem. Soc.* 1961, **83**, 4169.
4. G. A. Pearse Jr, *Acta Chem. Scand.* 1979, **B33**, 742.
5. C. W. G. Ansell, J. Lewis, P. R. Raithby and T. D. O'Donoghue, *J. Chem. Soc., Dalton Trans.* 1983, 177.
6. A. Gieren and B. Dederer, *Acta Cryst.* 1977, **B33**, 3296.
7. X. Solans, C. Mirravitlles, J. P. Leclercq and G. Germain, *Acta Cryst.* 1980, **B36**, 3121.
8. H. Gozlan and C. Riche, *Acta Cryst.* **B32**, 1662.
9. D. Hall, *Acta Cryst.* 1965, **18**, 955.
10. H. Gozlan, R. Michelot, C. Riche and R. Rips, *Tetrahedron* 1977, **33**, 2535.

Polyhedron Vol. 8, No. 3, pp. 305–310, 1989
Printed in Great Britain

0277–5387/89 $3.00+.00
© 1989 Pergamon Press plc

SYNTHESIS AND X-RAY CRYSTAL STRUCTURE OF TWO COMPLEXES OF NICKEL(II) NITRATE WITH PYRIDINE-2-AMIDOXIME ($C_6H_7N_3O$): $[Ni(C_6H_7N_3O)_2(NO_3)_2]$ AND $[Ni(C_6H_7N_3O)_3](NO_3)_2 \cdot H_2O$

GEORGE A. PEARSE,* PAUL R. RAITHBY, CAROLINE M. HAY and JACK LEWIS

University Chemical Laboratory, Lensfield Road, Cambridge, CB2 1EW, U.K.

(*Received* 22 *July* 1986; *accepted after revision* 25 *July* 1988)

Abstract—The reaction between stoichiometric amounts of nickel(II) nitrate hexahydrate and pyridine-2-amidoxime in ethanol produces crystalline $[Ni(C_6H_7N_3O)_2(NO_3)_2]$, but in water yields $[Ni(C_6H_7N_3O)_3](NO_3)_2 \cdot H_2O$. Both complexes have been characterized by X-ray crystallography. The crystals of $[Ni(C_6H_7N_3O)_2(NO_3)_2]$ are triclinic, space group $P\bar{1}$ (no. 2), with $a = 8.544(1)$, $b = 9.300(1)$, $c = 12.790(1)$ Å, $\alpha = 85.14(1)$, $\beta = 77.81(1)$, $\gamma = 63.26(1)°$ and $Z = 2$. The crystals of $[Ni(C_6H_7N_3O)_3](NO_3)_2 \cdot H_2O$ are monoclinic, space group $P2_1/n$, with $a = 10.453(1)$, $b = 13.261(2)$, $c = 19.059(4)$ Å, $\beta = 98.19(1)°$ and $Z = 4$. Both complexes have a slightly distorted octahedral structure with the nitrate groups being coordinated ligands in the 1:2 complex and counter-ions in the 1:3 complex. The organic ligands coordinate through the heterocyclic and oxime nitrogens in both compounds.

As a bidentate ligand, pyridine-2-amidoxime incorporates the structural features of pyridine-2-aldoxime and 2-pyridylamine in a single molecule. The 1:2 and 1:3 nickel(II) nitrate complexes of the latter two ligands have been investigated.[1,2] In each case there can be no ambiguity with respect to the five-membered ring formed by the coordination of nickel(II) with the two available nitrogen atoms per ligand. Because pyridine-2-amidoxime contains both an oxime and an amine nitrogen on a carbon substituted at the pyridine ring α-position, coordination with nickel(II) could involve either of these two nitrogen atoms and the heterocyclic nitrogen. To determine the mode of chelation, both the bis- and tris-chelates of nickel(II) nitrate were prepared and the crystal structures were determined.

EXPERIMENTAL

2-Cyanopyridine was purchased from Aldrich Chemical Co. and used without further purification in the synthesis of pyridine-2-amidoxime as previously reported.[3] All other chemicals were reagent grade. Density measurements were made by the floatation method using a mixture of benzene and 1,2-dibromoethane.

Preparation of $[Ni(C_6H_7N_3O)_2(NO_3)_2]$

To a solution of 2.90 g (10 mmol) of nickel(II) nitrate hexahydrate in 75 cm^3 of absolute alcohol was added 2.74 g (20 mmol) of pyridine-2-amidoxime in the minimum required amount of the same solvent. The resulting mixture was heated to boiling, filtered and cooled to room temperature. Blue crystals formed which were separated by decantation, washed with cold ethanol and ether, and dried *in vacuo*. Found: C, 31.4; H, 3.1; N, 24.4. Calc. for $NiC_{12}H_{14}N_8O_8$: C, 31.5; H, 3.1; N, 24.5%.

Preparation of $[Ni(C_6H_7N_3O)_3](NO_3)_2 \cdot H_2O$

To a solution of 4.02 g (30 mmol) of pyridine-2-amidoxime in the minimum required amount of 95% ethanol was added 2.90 g (10 mmol) of nick-

*Author to whom correspondence should be addressed. Visiting Professor on leave from Le Moyne College, Syracuse, NY 13214, U.S.A., 1985–1986.

el(II) nitrate hexahydrate in 50 cm^3 of distilled water. The resulting mixture was heated to 80–90°C, filtered and allowed to evaporate to one third its original volume at room temperature, during which time red–brown crystals precipitated. The crystals were removed by filtration, washed with ethanol and ether, and air-dried. Found: C, 35.1; H, 3.7; N, 25.1. Calc. for $NiC_{18}H_{23}N_{11}O_{10}$: C, 35.3; H, 3.8; N, 25.2%.

X-ray crystallography

General procedures have been described elsewhere.[4] Information about data collection for the two nickel(II)–pyridine-2-amidoxime complexes is given in Table 1. Atomic coordinates, thermal parameters and lists of F_o and F_c values have been deposited with the Editor. Atomic coordinates have also been deposited with the Cambridge Crystallographic Data Centre.

RESULTS AND DISCUSSION

When an ethanolic solution of nickel(II) nitrate hexahydrate is treated with pyridine-2-amidoxime, a dark blue solution results if the ratio of ligand to nickel does not exceed 2 : 1. From this solution a blue complex of the formula $Ni(Py2AO)_2(NO_3)_2$ crystallizes in which Py2AO is the unionized ligand (Fig. 1). If three moles of ligand are added to one mole of nickel(II) in aqueous solution the initial colour is blue, which changes to wine-red and the tris-pyridine-2-amidoxime nickel(II) complex is obtained as red–brown crystals (Fig. 2).

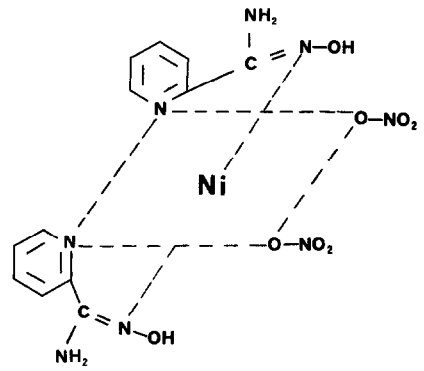

Fig. 1. Block diagram structure of the bis-nitrato-bis(Py2AO) Ni^{II}, $[Ni(C_6H_7N_3O)_2(NO)_3)_2]$.

Figure 3 is a perspective view of bis-nitrato-bis-(Py2AO)nickel(II). In the crystalline state this octahedral complex has two coordinated nitrate groups in the equatorial plane which are *cis* to each other.

Table 1. Summary of crystal data

	I	II
Formula	$[Ni(C_6H_7N_3O)_2(NO_3)_2]$	$[Ni(C_6H_7N_3O)_3](NO_3)_2 \cdot H_2O$
Formula weight	456.98	612.14
Crystal system	Triclinic	Monoclinic
Space group	$P\bar{1}$ (no. 2)	$P2_1/n$
a (Å)	8.544(1)	10.435(1)
b (Å)	9.300(1)	13.261(2)
c (Å)	12.790(1)	19.059(4)
α (°)	85.14(1)	90.00
β (°)	77.81(1)	98.19(1)
γ (°)	63.26(1)	90.00
V (Å^3)	887	2610
Z	2	4
$d_{calc.}$ (g cm^{-3})	1.711	1.558
$d_{meas.}$ (g cm^{-3})	1.688	1.549
Crystal size (mm)	$0.51 \times 0.42 \times 0.23$	$0.48 \times 0.10 \times 0.17$
Data collection instrument	Stoe	Stoe
Radiation (Å)	Mo-K_α(071069)	Mo-K_α(071069)
Data collection range (2θ)(°)	$5 \leqslant 2\theta \leqslant 50$	$5 \leqslant 2\theta \leqslant 45$
Scan method	ω–θ	ω–θ
Transmission factors (max, min)	0.9080, 0.6420	0.9145, 0.8438
F(000)	468	1224
R	0.0335	0.0592
R_w	0.0404	0.0564
Number of reflections measured	3337	3824
Number of observed reflection [$F > 4\sigma(F)$]	2911	2455

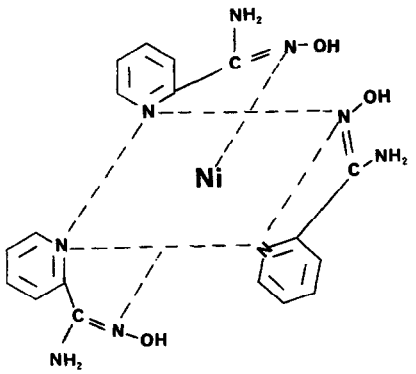

Fig. 2. Block diagram structure of the tris-(Py2AO)Ni^{II} nitrate, $[Ni(C_6H_7N_3O)_3](NO_3)_2$.

It is suggested that in the preparation of the 1 : 3 complex in aqueous solution, the initial blue colour is due to the $[Ni(Py2AO)_2(H_2O)_2]^{2+}$ ion as has been reported for the reaction of nickel(II) with 2,2-bipyridyl[5] and 1,10-phenanthroline.[6] As the ligand is added, the two *cis*-equatorial molecules are replaced by the third ligand, resulting in the structure shown in Fig. 4. Attempts to prepare $[Ni(Py2AO)_2(H_2O)_2](NO_3)_2$ were unsuccessful even though dissolution of $[Ni(Py2AO)_2(NO_3)_2]$ in water gives a unidivalent electrolyte. Addition of a third equivalent of the ligand to the 1 : 2 complex in aqueous solution results in the formation of the 1 : 3 complex. Therefore, it seems reasonable to assume that the aqueous blue solution of the 1 : 2 complex results from the replacement of the coordinated nitrate groups by water molecules.

The data in Tables 2 and 3 show that the Ni—N (pyridine) bond distances for both the 1 : 2 and 1 : 3 complexes are longer than the Ni—N(oxime) bonds. This is consistent with observations reported for the two isomeric nickel(II) complexes with 2,2′-iminodiacetamidoxime.[7,8] Studies in this laboratory show the bis-(Py2AO) copper(II) complex to exhibit this same bond length pattern.[9]

In the 1 : 2 nickel(II)–Py2AO complex, the two nitrate groups and the two heterocyclic nitrogens are approximately planar having a *cis–cis* arrangement. The axial positions are occupied by the oxime nitrogens. Figure 2 shows that the three organic ligands in the 1 : 3 complex have their heterocyclic nitrogens co-planar with one oxime nitrogen and the nickel(II) atom as determined by the X-ray study. This results in the two remaining oxime nitrogen atoms being *trans* to each other. All attempts to prepare additional isomers of the 1 : 2 and 1 : 3 complexes gave crystals of the structures shown in Figs 1 and 2.

This work has ascertained that pyridine-2-amidoxime utilizes the oxime nitrogen rather than the amine nitrogen of the amidoxime group to form five-membered chelate rings with the heterocyclic nitrogen and nickel(II). Preference for coordination in this manner results in an α,α′-diimine bidentate ligand similar to 2,2′-bipyridyl and 1,10-phenanthroline. Although the 1 : 2 complex could exist in a square-planar configuration, this research has shown both compounds to be octahedral in the solid state. It is interesting to note that in both of the compounds, the amine and oxime nitrogen

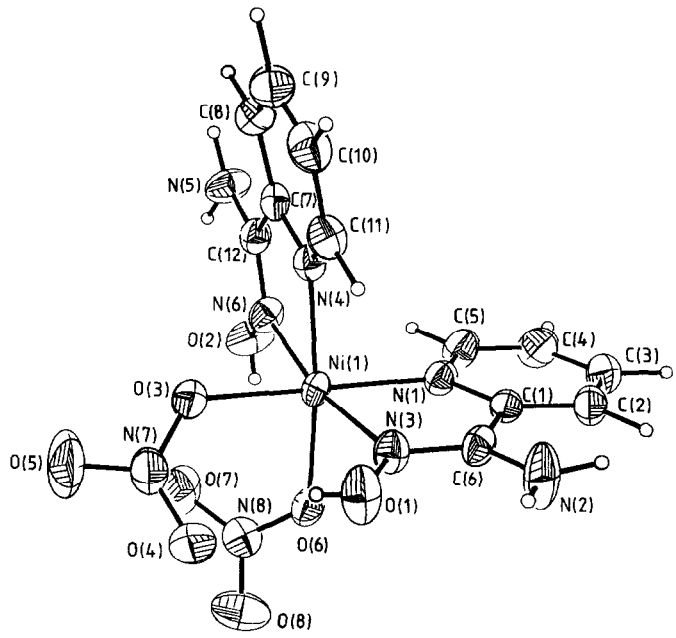

Fig. 3. Crystal structure of $[Ni(C_6H_7N_3O)_2(NO_3)_2]$ showing the atomic numbering scheme.

Table 2. Bond lengths and bond angles for $[Ni(C_6H_7N_3O)_2(NO_3)_2]$

Bond lengths (Å)			
Ni(1)—N(1)	2.084(2)	N(4)—C(7)	1.347(3)
Ni(1)—N(3)	2.048(2)	C(7)—C(8)	1.374(4)
Ni(1)—N(4)	2.090(2)	C(8)—C(9)	1.388(4)
Ni(1)—N(6)	2.048(2)	C(9)—C(10)	1.360(4)
Ni(1)—O(3)	2.123(2)	C(10)—C(11)	1.378(4)
Ni(1)—O(6)	2.083(2)	C(11)—C(12)	1.340(3)
N(1)—C(1)	1.340(3)	C(7)—C(12)	1.485(3)
C(1)—C(2)	1.381(4)	C(12)—N(5)	1.347(3)
C(2)—C(3)	1.396(3)	C(12)—N(6)	1.273(3)
C(3)—C(4)	1.372(4)	N(6)—O(2)	1.411(3)
C(4)—C(5)	1.365(5)	O(3)—N(7)	1.257(3)
C(5)—N(1)	1.346(3)	O(4)—N(7)	1.242(3)
C(1)—C(6)	1.483(3)	O(5)—N(7)	1.222(4)
C(6)—N(2)	1.327(3)	O(6)—N(8)	1.255(3)
C(6)—N(3)	1.283(4)	O(7)—N(8)	1.249(3)
N(3)—O(1)	1.411(3)	O(8)—N(8)	1.225(3)
Bond angle (°)			
N(1)—Ni(1)—N(3)	76.4(1)	N(1)—Ni(1)—O(6)	88.5(1)
N(1)—Ni(1)—O(3)	171.2(1)	N(1)—Ni(1)—N(4)	96.3(1)
N(1)—Ni(1)—N(6)	94.8(1)	N(3)—Ni(1)—O(6)	89.0(1)
N(3)—Ni(1)—O(3)	96.0(1)	N(3)—Ni(1)—N(4)	96.8(1)
N(3)—Ni(1)—N(6)	168.7(1)	O(6)—Ni(1)—O(3)	96.0(1)
O(6)—Ni(1)—N(4)	173.2(1)	O(6)—Ni(1)—N(6)	98.0(1)
O(3)—Ni(1)—N(4)	79.9(1)	O(3)—Ni(1)—N(6)	92.1(1)
N(4)—Ni(1)—N(6)	76.9(1)	Ni(1)—N(1)—C(1)	115.5(2)
Ni(1)—N(4)—C(7)	115.0(2)	N(1)—C(1)—C(2)	122.6(2)
N(4)—C(7)—C(8)	122.5(2)	C(1)—C(2)—C(3)	118.2(2)
C(7)—C(8)—C(9)	118.3(2)	C(2)—C(3)—C(4)	119.3(3)
C(8)—C(9)—C(10)	120.0(3)	C(3)—C(4)—C(5)	118.9(2)
C(9)—C(10)—C(11)	118.4(2)	C(4)—C(5)—N(1)	123.1(2)
C(10)—C(11)—N(4)	123.0(2)	N(1)—C(1)—C(6)	114.3(2)
N(4)—C(7)—C(12)	114.1(2)	C(2)—C(1)—C(6)	123.1(2)
C(8)—C(7)—C(12)	123.3(2)	C(1)—C(6)—N(2)	120.5(3)
C(7)—C(12)—N(5)	120.8(2)	C(1)—C(6)—N(3)	113.8(2)
C(7)—C(12)—N(6)	114.8(2)	C(6)—N(3)—O(1)	112.4(2)
C(12)—N(6)—O(2)	111.7(2)	N(2)—C(6)—N(3)	125.6(2)
N(5)—C(12)—N(6)	124.3(2)	C(5)—N(1)—Ni(1)	126.6(2)
C(11)—N(4)—Ni(1)	126.6(2)	C(5)—N(1)—C(1)	117.9(2)
C(11)—N(4)—C(7)	117.8(2)	Ni(1)—N(6)—C(12)	119.0(2)
Ni(1)—N(3)—O(1)	127.7(2)	Ni(1)—N(3)—C(6)	119.1(2)
Ni(1)—N(6)—O(2)	129.0(2)		

Table 3. Bond lengths and bond angles for $[Ni(C_6H_7N_3O)_3](NO_3)_2 \cdot H_2O$

Bond length (Å)			
Ni(1)—N(1)	2.079(5)	C(8)—C(9)	1.388(10)
Ni(1)—N(3)	2.057(4)	C(9)—C(10)	1.370(9)
Ni(1)—N(4)	2.080(5)	C(10)—C(11)	1.384(10)
Ni(1)—N(6)	2.062(4)	C(11)—N(4)	1.339(8)
Ni(1)—N(7)	2.109(5)	C(7)—N(12)	1.479(8)
Ni(1)—N(9)	2.061(5)	C(12)—N(5)	1.344(8)
N(1)—C(1)	1.350(7)	C(12)—N(6)	1.303(8)
C(1)—C(2)	1.380(9)	N(6)—O(2)	1.401(6)
C(2)—C(3)	1.384(10)	N(7)—C(13)	1.339(8)
C(3)—C(4)	1.361(9)	C(13)—C(14)	1.391(9)
C(4)—C(5)	1.385(10)	C(14)—C(15)	1.366(10)
C(5)—N(1)	1.326(8)	C(15)—C(16)	1.368(10)
C(1)—C(6)	1.483(9)	C(16)—C(17)	1.385(10)
C(6)—N(2)	1.361(8)	C(17)—N(7)	1.330(8)
C(6)—N(3)	1.287(8)	C(13)—C(18)	1.475(9)
N(3)—O(1)	1.411(6)	C(18)—N(8)	1.329(9)
N(4)—C(7)	1.351(7)	C(18)—N(9)	1.280(8)
C(7)—C(8)	1.377(9)	N(9)—O(3)	1.426(6)
Bond angle (°)			
N(1)—Ni(1)—N(3)	76.9(2)	Ni(1)—N(4)—C(7)	114.9(4)
N(1)—Ni(1)—N(7)	94.6(2)	N(4)—C(7)—C(8)	122.5(5)
N(1)—Ni(1)—N(9)	169.3(2)	C(7)—C(8)—C(9)	118.8(6)
N(1)—Ni(1)—N(6)	99.4(2)	C(8)—C(9)—C(10)	119.1(6)
N(1)—Ni(1)—N(4)	92.5(2)	C(9)—C(10)—C(11)	119.1(6)
N(3)—Ni(1)—N(7)	92.7(2)	N(4)—C(7)—C(12)	113.9(5)
N(3)—Ni(1)—N(9)	96.8(2)	C(8)—C(7)—C(12)	123.7(5)
N(3)—Ni(1)—N(6)	171.0(2)	C(7)—C(12)—N(5)	120.9(6)
N(3)—Ni(1)—N(4)	94.0(2)	C(7)—C(12)—N(6)	115.4(5)
N(7)—Ni(1)—N(9)	76.9(2)	C(12)—N(6)—O(2)	112.0(4)
N(7)—Ni(1)—N(6)	95.8(2)	N(5)—C(12)—N(6)	123.7(6)
N(7)—Ni(1)—N(4)	171.1(2)	C(11)—N(4)—Ni(1)	127.1(4)
N(9)—Ni(1)—N(6)	88.1(2)	C(11)—N(4)—C(7)	118.0(5)
N(9)—Ni(1)—N(4)	96.6(2)	Ni(1)—N(6)—C(12)	115.6(4)
N(6)—Ni(1)—N(4)	77.8(2)	Ni(1)—N(6)—O(2)	126.9(3)
Ni(1)—N(1)—C(1)	115.0(4)	Ni(1)—N(7)—C(13)	113.6(4)
N(1)—C(1)—C(2)	122.4(6)	N(7)—C(13)—C(14)	121.7(5)
C(1)—C(2)—C(3)	118.0(6)	C(13)—C(14)—C(15)	118.8(6)
C(2)—C(3)—C(4)	120.6(7)	C(14)—C(15)—C(16)	119.7(7)
C(3)—C(4)—C(5)	117.5(7)	C(15)—C(16)—C(17)	118.6(6)
C(4)—C(5)—N(1)	123.8(6)	C(16)—C(17)—N(7)	119.7(7)
N(1)—C(1)—C(6)	114.6(5)	N(7)—C(13)—C(18)	118.6(6)
C(2)—C(1)—C(6)	123.0(5)	C(14)—C(13)—C(18)	123.3(6)
C(1)—C(6)—N(2)	114.6(5)	C(13)—C(18)—N(8)	121.8(6)
C(1)—C(6)—N(3)	113.7(5)	C(13)—C(18)—N(9)	114.2(5)
C(6)—N(3)—O(1)	112.3(4)	C(18)—N(9)—O(3)	111.3(5)
N(2)—C(6)—N(3)	123.4(6)	N(8)—C(18)—N(9)	124.0(6)
C(5)—N(1)—Ni(1)	127.1(5)	C(17)—N(7)—Ni(1)	127.4(4)
C(5)—N(1)—C(1)	117.7(5)	C(17)—N(7)—C(13)	118.8(5)
Ni(1)—N(3)—C(6)	118.2(4)	Ni(1)—N(9)—C(18)	116.6(4)
Ni(1)—N(3)—O(1)	128.0(3)	Ni(1)—N(9)—O(3)	125.3(3)
C(10)—C(11)—N(5)	122.6(6)		

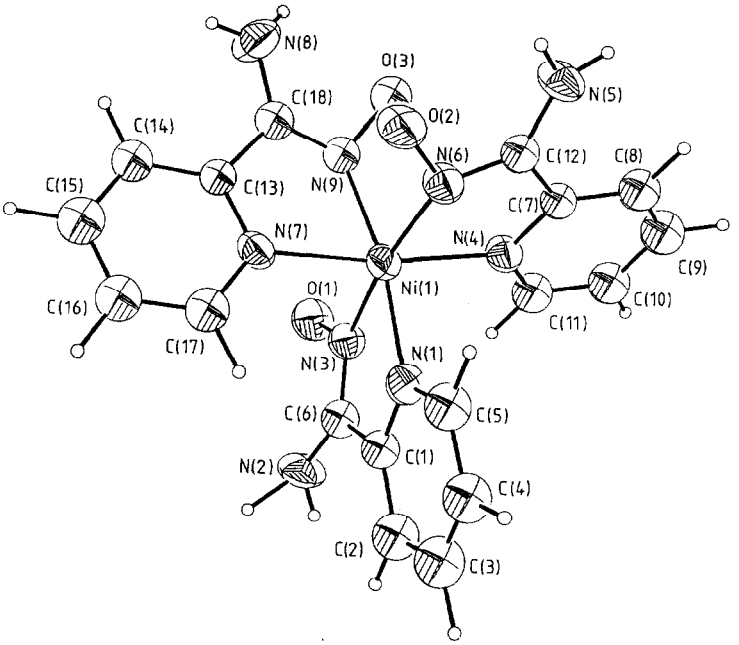

Fig. 4. Crystal structure of $[Ni(C_6H_7N_3O)_3](NO_3)_2 \cdot H_2O$ showing the atomic numbering scheme.

atoms in each five-membered chelate ring show either very little or no deviation from planes inclusive of these atoms.

Acknowledgements—G.A.P. gratefully acknowledges a Visiting Professorship from the Department of Inorganic Chemistry at the University of Cambridge. Partial support of this research was provided by the Le Moyne College Research Committee.

REFERENCES

1. G. J. Sutton, *Aust. J. Chem.* 1960, **13**, 74.
2. R. A. Krause and D. H. Busch, *J. Am. Chem. Soc.* 1960, **82**, 4830.
3. G. A. Pearse, *Chem. Sci.* 1979, **13**, 110.
4. C. W. G. Ansell, J. Lewis, P. R. Raithby and T. D. O'Donoghue, *J. Chem. Soc., Dalton Trans.* 1983, 177.
5. F. Basolo and F. P. Dwyer, *J. Am. Chem. Soc.* 1954, **76**, 1454.
6. P. Pfeiffer, V. Dominik, A. Fritzen and B. Werdelmann, *Z. Anorg. Chem.* 1949, **260**, 84.
7. L. P. Eddy, S. K. McEwen and S. R. Wilson, *Acta Cryst.* 1985, **C41**, 1029.
8. D. L. Cullen and E. C. Longafelter, *Inorg. Chem.* 1970, **9**, 1865.
9. G. A. Pearse, P. R. Raithby and J. Lewis, *Polyhedron* 1988, **7**, 301.

Polyhedron Vol. 8, No. 3, pp. 311–315, 1989
Printed in Great Britain

0277–5387/89 $3.00+.00
© 1989 Pergamon Press plc

SYNTHESIS AND CHARACTERIZATION OF $[Cp_2Ti(CH_3CN)_3]^{2+}[AsF_6^-]_2$ — ^{19}F NMR SPECTROSCOPY OF TITANOCENE HEXAFLUOROARSENATES*

TH. KLAPÖTKE

Institut für Anorganische und Analytische Chemie, Technische Universität Berlin, D-1000 Berlin 12, F.R.G.

(*Received* 5 *July* 1988; *accepted* 25 *July* 1988)

Abstract—$Cp_2Ti(AsF_6)_2$ (**1**) ($Cp = \eta^5$-C_5H_5) reacts with an excess of CH_3CN yielding quantitatively the new cationic titanocene complex $[Cp_2Ti(CH_3CN)_3]^{2+}[AsF_6^-]_2$ (**2**). **2** was characterized by elemental analysis, IR, ^1H NMR and ^{19}F NMR spectroscopy. Surprisingly, no reaction of **1** with CF_3CN could be observed. The ^{19}F NMR spectra of **1** at various temperatures are reported and discussed, too. The reaction behaviour of Cp_2TiCl_2 (**3**) towards ClF was investigated, and $CpTiCl_3$ (**4**) and traces of $CpTiCl_2F$ (**5**) were shown to be the products of this reaction. Surprisingly, no evidence for the formation of Cp_2TiClF could be found. These results are discussed and can be understood easily on the basis of simple thermodynamic estimations.

The reaction of **3** with nitriles in the presence of suitable Lewis acids MCl_n, yields ionic complexes with one or two nitrile ligands bonded to the Ti. The complexes $[Cp_2Ti(C_8H_4N_2)_2][SbCl_6]_2$ ($C_8H_4N_2$ = phthalonitrile), $[Cp_2Ti(Cl)(C_3H_2N_2)]_2[FeCl_4]$ ($C_3H_2N_2$ = malonitrile), and $[Cp_2Ti(Cl)(CH_3CN)][FeCl_4]$ have been isolated.[1–3] The N coordinated chelate complexes $[Cp_2Ti(bipy)][CF_3SO_3]_2$ and $[Cp_2Ti(phen)][CF_3SO_3]_2$ are also known.[4] Very recently we reported the synthesis of the first stable Lewis base free $Cp_2Ti(MF_6)_2$ (M = pnicogen) complexes where the MF_6 unit is directly coordinated to the Cp_2Ti fragment.[5,6] Whereas the mono-cyclopentadienyl species, $CpTi(MF_6)_3$, are unstable and till now were identified only at low temperature in solution,[7] $Cp_2Ti(MF_6)_2$ (M = As, Sb) are stable in the solid state and the structure of **1** was elucidated by single crystal X-ray diffraction.[6] The IR spectra and X-ray structure clearly show the covalent $Cp_2Ti(\cdots F\cdots AsF_5)_2$ bond interaction in **1** with a bridging fluorine and reduced MF_6 symmetry.

As the ^1H NMR spectroscopy was not sufficient to elucidate the Cp_2Ti—MF_6 bond situation in solution,[5,6] we investigated this particular problem by temperature-dependent ^{19}F NMR spectroscopy. In addition to this it seemed to be of interest to discover whether stable **1** would react with neutral nitrile ligands, yielding cationic titanocene derivatives according to eq. (1). Ternary adducts of $Ni(EF_6)_2$ (E = Sb, Bi) like $[Ni(CH_3CN)_6][EF_6]_2$ have been reported quite recently.[8]

$$\mathbf{1} + nR\text{—}CN \longrightarrow [Cp_2Ti(RCN)_n]^{2+}[AsF_6^-]_2. \quad (1)$$

As **1** can be prepared either by reaction of **3** with $AgAsF_6$ or by reaction of Cp_2TiF_2 with AsF_5,[6] we were interested to achieve a simple synthesis of Cp_2TiF_2. This is of interest because of the high price for the commercially available $AgAsF_6$, which usually is prepared by fluorination of a mixture of elemental Ag or AgF and an excess of As_2O_5 with BrF.[9] One possible way seemed to be the reaction of **3** with ClF according to eq. (2) which was estimated to be thermodynamically favoured (see below).

$$\mathbf{3} + 2ClF \longrightarrow Cp_2TiF_2 + 2Cl_2. \quad (2)$$

The results of our investigations according to the goals outlined above are described in this paper.

* Organotransition metal chemistry of highly fluorinated ligand systems (Organo-Übergangsmetall-Chemie hochfluorierter Ligand-Systeme): 4th communication (for 3rd communication see ref. 7).

EXPERIMENTAL

All techniques have been described in ref. 6. Cp_2TiCl_2 (**3**)[10] and $Cp_2Ti(AsF_6)_2$ (**1**)[6] were prepared as described in the works cited. Sulphur dioxide, ClF, AsF_5, CH_3CN and CF_3CN were purified by distillation. SO_2 and CH_3CN were dried over CaH_2. Silver fluoride (Alfa, 10125) was used without further purification. All reactions took place in an atmosphere due to the vapour pressure of SO_2, CH_3CN or CF_3CN, respectively.

Preparation of silver hexafluoroarsenate(V) [$AgAsF_6$]

In a 50 cm^3 thick-walled glass reaction vessel incorporating a "Young" valve (POR-10), 8 g of AsF (63.06 mmol) were suspended in 20 cm^3 of CO_2 (1). After cooling this mixture to −196°C, 13 g of AsF_5 (76.51 mmol) were condensed onto the frozen SO_2. The reaction mixture was allowed to warm to room temperature and was stirred at RT in the dark for 12 h. After the solvent had been evaporated, the remaining white residue was dried *in vacuo* at RT for 4 h. Yield: 18.69 g (99.87%). IR: ν (cm^{-1}) (Nujol mull) 700 vs (ν_3), 385 s (ν_4); (cf. ref. 11).

Preparation of bis(η^5-cyclopentadienyl)tris(acetonitrile)bis(hexafluoroarsenato)titanium(IV) [$Cp_2Ti(CH_3CN)_3][AsF_6]_2$ (*complex* **2**)

0.0691 g (0.1243 mmol) of **1** were dissolved in 5 cm^3 of CH_3CN and stirred at RT for 1 h. The solvent was condensed into a second vessel ($\Delta T \approx 10$°C, 5–10 h) and the remaining microcrystalline deep red residue was dried *in vacuo* at RT for 24 h. Yield: 0.0841 g, 0.1238 mmol (99.60%). Found: C, 27.9; H, 2.7; N, 6.1. Calc. for $C_{16}H_{19}As_2F_{12}N_3Ti$ (679.05) C, 28.3; H, 2.8; N, 6.2%. ^{1}H NMR (SO_2) δ (ppm) (int.) 7.28 (10.00) s, 2.69 (8.85) s, relative to TMS. ^{19}F NMR (CD_3CN) δ (ppm) (int.) −49.7 (1), −59.6 (1), −69.8 (1), −79.4 (1), relative to $CFCl_3$. $\Delta\nu = 929 \pm 25$ Hz. IR: ν (cm^{-1}) (Nujol mull) 3128 m (ν-CH, Cp), 2320 m ($\nu_3+\nu_4$, CH_3CN), 2293 s (ν-CN, ν_2-CH_3CN), 1128 w, 1028 sh and 1018 m (δ-CH, Cp), 957 w, 858 s (γ-CH, Cp), 698 vs (ν-AsF, ν_3-AsF_6), 398 s (δ-AsF, ν_4-AsF_6).

Attempted synthesis of $[Cp_2Ti(CF_3CN)_n]^{2+}[AsF_6^-]_2$ ($n = 2, 3$)

1.00 g (10.52 mmol) of CF_3CN (g) was condensed at −196°C onto 0.2561 g (0.4607 mmol) of **1** and this was allowed to warm up to room temperature. As **1** is insoluble in CF_3CN (under high pressure) a suspension was formed. After 2 h at RT the reaction mixture was recooled to −78°C and the volatiles were pumped off at this temperature *in vacuo*. The remaining solid (0.2558 g) was identical with **1** (^{1}H NMR and IR data).

Reaction of **3** *with* ClF

Onto a frozen solution of 0.270 g (1.08 mmol) of **3** in 5 cm^3 of SO_2, 0.118 g (2.17 mmol) of ClF were condensed at −196°C. After warming up and stirring for 12 h at RT, the solvent and the volatiles were pumped off *in vacuo* also at RT. Yield: 0.220 g (93%, calc. for $CpTiCl_3$). ^{1}H NMR ($CDCl_3$) δ (ppm) 7.07 s, relative to TMS. MS (50°C, 70 eV): *m/z* (int.), 218 (100) $CpTiCl_3^+$, 202 (11) $CpTiCl_2F^+$, 183 (76) $CpTiCl_2^+$, 148 (34) $CpTiCl^+$, 118 (36) $TiCl_2^+$, 109 (19) $CpTiCl_3^{2+}$, 83 (53) $TiCl^+$.

^{19}F *NMR of* **1**

^{19}F NMR (SO_2) δ (ppm) $T = 20$°C: −57.02 s, $b_{1/2} = 200$ Hz, $T = -70$°C: −61.53 s, $b_{1/2} = 350$ Hz; relative to $CFCl_3$.

RESULTS AND DISCUSSION

Preparative aspects

The reaction of **1** with an excess of CH_3CN (solvent) led in 100% yield to the preparations of **2** according to eq. (3).

$$\mathbf{1} + 3CH_3CN \xrightarrow{CH_3CN} \mathbf{2}. \qquad (3)$$

The identity of **2** was proved by elemental analysis, IR, ^{1}H and ^{19}F NMR spectroscopy (see Experimental and below).

Whereas some related cationic titanocene derivatives with one and two via N coordinated neutral ligands are known (see above and refs 1–4), **2** contains three CH_3CN molecules, thus realizing the coordination number five. The 12-electron fragment Cp_2Ti^{2+} obtains the noble gas configuration by coordinating three two-electron donor ligands. In the MO scheme of Cp_2Ti^{2+} two of the three unoccupied orbitals lowest in energy are bonding ($2a_1$ and b_2), while one is non-bonding ($1a_1$).[12] This is in agreement with the experimental result that one of the three CH_3CN ligands can be removed by pumping off **2** at a higher temperature for several days according to eq. (4).

$$\mathbf{2} \xrightarrow[40\text{–}50°C]{\text{dyn. vac.}} [Cp_2Ti(CH_3CN)_2]^{2+}[AsF_6^-]_2. \qquad (4)$$

The loss of one equivalent of CH_3CN was proved by weight change.

Surprisingly, **1** does not react with an excess of CF_3CN, yielding a cationic complex by analogy to the observed reaction with CH_3CN. **1** also crystallizes from SO_2 (l) as the covalent species and does not contain coordinated SO_2. Assuming that the crystal lattice energies of **2** and the CF_3CN analogue are more or less identical, the gaining of energy due to coordination of CF_3CN to Cp_2Ti^{2+} is less than the sum of the energy terms due to entropy and $Ti\cdots AsF_6$-bond interaction, which are working against the salt formation.

The preparation of Cp_2TiF_2 from **3** and ClF according to eq. (2) was not successful, surprisingly $CpTiCl_3$ was the reaction product [eq. (5)] and was identifed by ^1H NMR and mass spectroscopy.

$$3 + ClF \xrightarrow{SO_2} CpTiCl_3 + \text{"CpF"}. \quad (5)$$

According to eq. (6) the preparation of $AgAsF_6$ in 100% yield was shown to be very convenient. In this reaction all of the expensive AsF_5 is converted into $AgAsF_6$. Silver fluoride can be prepared from Ag_2O by using HF.[13] Equation (7) also describes a common method to prepare $AgAsF_6$.

$$AgF + AsF_5 \xrightarrow{SO_2} AgAsF_6 \quad (6)$$

$$2Ag + 3AsF_5 \longrightarrow 2AgAsF_6 + AsF_3. \quad (7)$$

Vibrational spectroscopy

In the IR spectrum (see Fig. 1) of **1** the strong, broad absorption at 530 cm^{-1} was assigned to the Ti—F symmetric and asymmetric stretching mode.[5,6] The disappearance of this band indicates that also in the solid state there is no direct bonding interaction between the $[Cp_2Ti(CH_3CN)_3]^{2+}$ cation and the $[AsF_6^-]$ anions.

Free acetonitrile (liquid) shows the C—N stretching mode (ν_2) at 2254 cm^{-1}.[14] In **2** this band is shifted to 2293 cm^{-1}. This result may indicate that **2** has strong σ-donor ($CH_3CN \rightarrow Ti$) but weak π-acceptor (back) bonding (cf. CN^-: 5σ, weakly antibonding; $2p\pi^*$ antibonding[15]).

NMR spectroscopy

The integration of the proton NMR spectrum of **2** in SO_2 solution clearly shows the composition of the complex as $[Cp_2Ti(CH_3CN)_3]^{2+}$ (see Fig. 2). The chemical shift in the ^1H NMR spectrum of **2** in SO_2 is similar to that observed for **1** in SO_2 solution.[6] However, CH_3CN in solution is also still coordinated as the only methyl singlet appears at 2.67 ppm, whereas free acetonitrile in SO_2 has a chemical shift of 2.05 ppm (own results).

The ^{19}F NMR spectra of **1** in SO_2 and **2** in SO_2 and CD_3CN show this effect, also. For instance, the

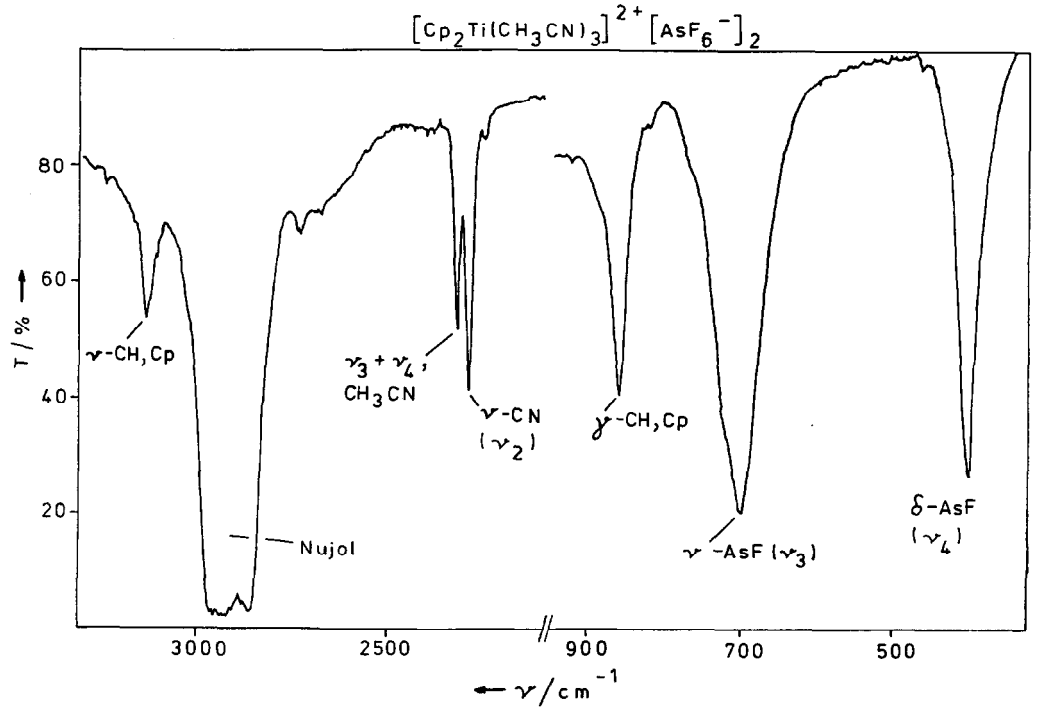

Fig. 1. IR spectrum of **2** in the regions 200–1000 cm^{-1} and 2000–3300 cm^{-1}.

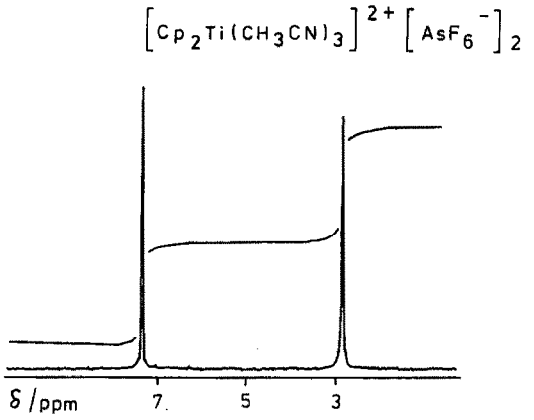

Fig. 2. ^{1}H NMR spectrum of **2** in SO_2, 20°C.

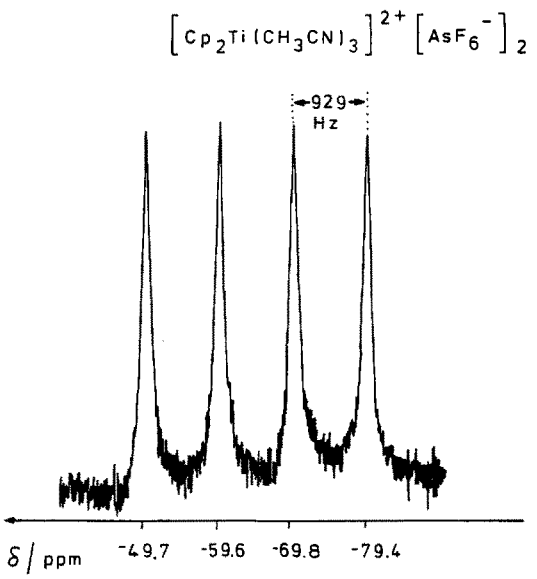

Fig. 3. ^{19}F NMR spectrum of **2** in CD_3CN, −40°C.

^{19}F NMR spectrum of **2** in CD_3CN, even at low temperatures (−40°C), consists of a nicely dissolved four-line pattern due to the As—F couplings (I, $^{75}_{33}As = 3/2$) in the octahedral AsF_6^- anion (see Fig. 3).

On the other hand, **1** dissolved in SO_2 shows at RT in the ^{19}F NMR spectrum only one peak which does not split into the expected pattern even at low temperatures (−70°C). This indicates free highly symmetric AsF_6^- ions in the first case (**2**), whereas this group is coordinated to the Ti centre in the second case (**1**), showing rapid exchange (pseudo-rotation) even at low temperatures (otherwise no singlet in the proton NMR spectrum could be expected).

Thermodynamic aspects

By the reaction of **3** with ClF neither Cp_2TiClF nor Cp_2TiF_2, but only $CpTiCl_3$ (with traces of $CpTiCl_2F$) was identified as the product. Nevertheless the reaction according to eq. (8) should be exothermic, $\Delta H_8 = -144$ kJ mol^{-1}, as was estimated in Scheme 1.

$$\mathbf{3} + ClF \longrightarrow Cp_2TiClF + Cl_2. \qquad (8)$$

However, a reaction according to eq. (9) was estimated to be even more thermodynamically favourable (see Scheme 2), $\Delta H_9 = -358$ kJ mol^{-1}.

$$\mathbf{3} + ClF \longrightarrow CpTiCl_3 + \text{"CpF"}. \qquad (9)$$

Therefore one can easily understand why a process, shown by eq. (9) and not as indicated by eq. (8), occurs. Moreover, the sums of the bond energies of Ti—Cl (429 kJ mol^{-1})[16,17] and C—F (485 kJ mol^{-1})[19] on one side and Ti—F (585 kJ mol^{-1})[19] and C—Cl (327 kJ mol^{-1})[19] on the other side, explain that $CpTiCl_3$ is formed as the main product and only a small amount of $CpTiCl_2F$ was found.

It seems likely that some of the bond strength estimation data may either bear some experimental error or may be slightly inaccurate, as only ΔH but no ΔS values were estimated. However, this simple

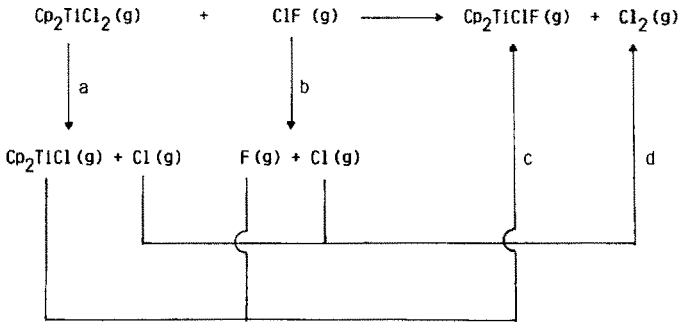

Scheme 1. Thermodynamic cycle to estimate the heat of reaction 8. (a) Ti—Cl bond energy in **3**: 429 kJ mol^{-1};[17] (b) Cl—F bond energy in ClF: 255 kJ mol^{-1};[18] (c) Ti—F bond energy in TiF_4: 585 kJ mol^{-1};[19] (d) Cl—Cl bond energy in Cl_2: 243 kJ mol^{-1}.[18]

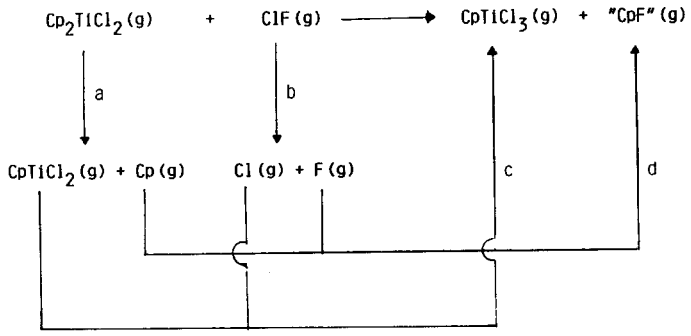

Scheme 2. Thermodynamic cycle to estimate the heat of reaction 9. (a) Ti—Cp bond energy in **3**: 301 kJ mol^{-1};[17] (b) Cl—F bond energy in ClF: 255 kJ mol^{-1};[18] (c) Ti—Cl bond energy in **3**: 429 kJ mol^{-1};[17] (d) C—F bond energy: 485 kJ mol^{-1}.[19]

thermodynamic analysis clearly shows that a synthesis of Cp_2TiF_2 from **3** and ClF according to eq. (2) seems to be very unlikely or even impossible.

CONCLUSIONS

Quite recently we described the first synthesis and characterization of stable titanocene derivatives containing MF_6^- groups (M = pnicogen) directly coordinated to the Cp_2Ti centre.[5,6] In the present work the preparation of the ionic $[Cp_2Ti(CH_3CN)_3]^{2+}[AsF_6^-]_2$ (**2**) is reported, in which three nitrile ligands are bonded to the Cp_2Ti^{2+} fragment. This also clearly shows the importance of the "covalent" hexafluoroarsenates mentioned above as useful reagents in the synthesis of cationic metallocene complexes. These compounds (neutral and cationic) are of interest not only on account of their structure in solution and in crystals, but also in respect of their transition metal fluorine bond situation and the rapid exchange processes of the coordinated hexafluoropnictogenate ligands. In addition, the highly hydrophilic (and water soluble) cationic species may well open up a new form of chemotherapeutics, as compounds containing the Cp_2Ti group often show antiproliferative activity, but their application is limited by their low solubility in polar solvents.[20]

Acknowledgements—Our thanks are due to M. Schriver for NMR spectra, A. Stöckel for mass spectra and to Prof. Jack Passmore for many helpful discussions.

REFERENCES

1. K. Berhalter and U. Thewalt, *J. Organomet. Chem.* 1987, **332**, 123.
2. M. G. Meirim and E. W. Neuse, *Transition Met. Chem.* 1984, **9**, 337.
3. U. Thewalt, K. Berhalter and E. W. Neuse, *Transition Met. Chem.* 1985, **10**, 393.
4. U. Thewalt and K. Berhalter, *J. Organomet. Chem.* 1986, **302**, 193.
5. Th. Klapötke, *Polyhedron* 1988, **7**, 1221.
6. Th. Klapötke and U. Thewalt, *J. Organomet. Chem.*, in press.
7. Th. Klapötke, *Inorg. Chim. Acta* 1988, **150**, 165.
8. R. Bougon, P. Charpin, K. O. Christe, J. Isabey, M. Lance, M. Nierlich, J. Vigner and W. W. Wilson, *Inorg. Chem.* 1988, **27**, 1389.
9. J. C. Bailar, H. J. Emeléus, R. Nyholm and A. F. Trotman-Dickenson, In *Comprehensive Inorganic Chemistry*, Vol. 2, p. 672. Pergamon Press, Oxford (1973).
10. G. Wilkinson and J. M. Birmingham, *J. Am. Chem. Soc.* 1954, **76**, 4281.
11. K. Nakamoto, In *Infrared and Raman Spectra of Inorganic and Coordination Compounds*, 4th edn, p. 150. Wiley-Interscience, New York (1986).
12. J. W. Lauher and R. Hoffmann, *J. Am. Chem. Soc.* 1976, **98**, 1729.
13. N. N. Greenwood and A. Earnshaw, In *Chemistry of the Elements*, p. 1374. Pergamon Press, Oxford (1984).
14. P. Venkateswarlu, *J. Chem. Phys.* 1951, **19**, 293.
15. K. Nakamoto, In *Infrared and Raman Spectra of Inorganic and Coordination Compounds*, 4th edn, p. 272. Wiley-Interscience, New York (1986).
16. F. A. Cotton and G. Wilkinson, In *Anorganische Chemie*, 4th edn, p. 96. Verlag Chemie, Weinheim (1982).
17. V. I. Tel'noi, I. B. Rabinovich, V. D. Tikhonov, V. N. Latyaeva, L. I. Vyshinskaya and G. A. Razuvaev, *Dokl. Phys. Chem. Proc. Acad. Sci. USSR* 1967, **172/177**, 467.
18. D. A. Johnson, In *Some Thermodynamic Aspects of Inorganic Chemistry*, 2nd edn, p. 201. Cambridge University Press, Cambridge (1982).
19. J. E. Huheey, In *Inorganic Chemistry*, 3rd edn, appendix. Harper International, Cambridge (1983).
20. P. Köpf-Maier, *Naturwiss.* 1987, **74**, 374, and refs therein.

Polyhedron Vol. 8, No. 3, pp. 317–323, 1989
Printed in Great Britain

0277–5387/89 $3.00 + .00
© 1989 Pergamon Press plc

SYNTHESIS AND CHARACTERIZATION OF COPPER, MANGANESE AND ZINC COMPLEXES OF THE BIDENTATE DIISOCYANO LIGANDS 2,5-DIMETHYL 2,5-DIISOCYANOHEXANE (TMB) AND 1,2-DIISOCYANOETHANE(DHB)

MICHÈLE DARTIGUENAVE,† YVES DARTIGUENAVE, ANDRÉ GUITARD and ALAIN MARI

Laboratoire de Chimie de Coordination du CNRS, associé à l'Université P. Sabatier, 205 route de Narbonne, 31077 Toulouse-Cedex, France

and

ANDRÉ L. BEAUCHAMP

Département de Chimie, Université de Montréal, C.P. 6128, Succ.A, Montréal, QC, Canada H3C 3J7

(*Received* 7 *June* 1988; *accepted* 27 *July* 1988)

Abstract—By reaction of 2,5-dimethyl 2,5-diisocyanohexane (TMB) and 1,2-diisocyanoethane (DHB) with CuX_2 ($X = CF_3SO_3^-$, ClO_4^-, BF_4^-), three types of complexes were isolated and characterized by magnetic susceptibility and EPR spectroscopy. In the violet CuL_2X_2 compounds, Cu^{II} atoms are in a square-planar environment and not magnetically interacting. For the mixed-valence green complexes $Cu_2L_3X_3$, the Cu^{II} and Cu^{I} metal centres both have a tetrahedral coordination, and the presence of independent Cu^{II} and Cu^{I} atoms in a 1:1 ratio was deduced from a magnetization experiment. Diamagnetic Cu^{I} complexes CuL_2X were also isolated. TMB complexes were prepared with Mn^{II} and Zn^{II}. In the former case, high-spin $Mn(TMB)(CF_3SO_3)_2 \cdot 2H_2O$ and low-spin $Mn(TMB)_3(PF_6)_2$ complexes were obtained, whereas Zn^{II} gave $Zn_2(TMB)_3(CF_3SO_3)_2 \cdot 2H_2O$. The ν(CN) frequency in the infrared spectra increases with the charge on the complex, and for complexes of the same charge, decreases when the diisocyanide-to-metal ratio increases. Although solubility was improved by using $CF_3SO_3^-$ as counter ion, it remained low and the complexes are likely to be polymeric, with the diisocyanide ligands in extended conformations playing a bridging role.

The metal complexes with diisocyanide ligands that most attracted attention were probably those of rhodium(I) and iridium(I), since these dinuclear molecules exhibit interesting properties for energy storage[1,2] or catalysis.[3] Dimeric palladium and platinum compounds,[4] and heterobimetallic Mn–Rh systems[5] have also been examined. Recently, a series of polymeric silver(I) complexes were described and structurally characterized.[6] With first-row transition metals, however, only a few complexes are known, because side reactions such as isocyanide polymerization, hydrolysis and decomposition, are catalysed by these metals.[7,8] The tetrameric nickel(II) compound $[Ni_4(OCH_3)_4(O_2CCH_3)_2(TMB)_4](BPh_4)_2$[9] appears to be the only one characterized by X-ray diffraction. Various $[\{Fe_2(Cp)_2(CO)_3\}_2(CN{-}(CH_2)_n{-}NC)]$ compounds[7] have been reported. Compounds of the types $[ML_3]PF_6$ and $M(CO)_nL$ with isocyanide-substituted diphenoxyethane ligands are also known.[10]

In the present study, TMB (**I**, "tetramethyl-bridge": 2,5-dimethyl 2,5-diisocyanohexane, $CNC(CH_3)_2CH_2CH_2C(CH_3)_2NC$) and DHB (**II**,

† Author to whom correspondence should be addressed.

"dihydrogen bridge": 1,2-diisocyanoethane $CNCH_2CH_2CN$) were reacted with first-row metal salts MX_2 ($M = Cu^{2+}$, Mn^{2+}, Zn^{2+}; $X = CF_3SO_3^-$, ClO_4^-, BF_4^- and PF_6^-). These three metals were selected because they adopt different coordination geometries and show different abilities to participate in redox processes. In order to minimize the formation of infinite polynuclear sequences via bridging by the counter ion, we used non-coordinating anions, mainly the $CF_3SO_3^-$ ion that commonly improves complex solubility.

EXPERIMENTAL

All reactions were carried out under N_2. The solvents were Puriss, Grade Fluka. The 2,5-dimethyl 2,5-diisocyanohexane (TMB) and 1,2-diisocyanoethane (DHB) ligands were prepared following literature methods.[11–13] Blue $Cu(CF_3SO_3)_2 \cdot 4H_2O$ was obtained by reaction of 2 equivalents of trifluoromethanesulphonic acid with basic copper carbonate ($CuCO_3 \cdot Cu(OH)_2$) in water. Very hygroscopic anhydrous $Cu(CF_3SO_3)_2$ was isolated when the reaction was conducted in methanol. $Zn(CF_3SO_3)_2 \cdot H_2O$ was obtained from a 2:1 ratio of CF_3SO_3H and basic carbonate ($2ZnCO_3 \cdot 3Zn(OH)_2$) in methanol. The same method was used to prepare $Mn(CF_3SO_3)_2 \cdot H_2O$ from methanol, starting with Mn^{II} carbonate. $Cu(BF_4)_2$ and $Cu(ClO_4)_2$ were generated *in situ* by reaction of $CuCl_2$ with the Ag^+ salt of the corresponding anion. $Mn(PF_6)_2$ was similarly obtained from $MnCl_2$ and $AgPF_6$.

Elemental analyses were performed by the Service Central de Microanalyse du CNRS, Lyon, France.

$Cu(TMB)_2(CF_3SO_3)_2$ (1)

TMB (4 mmol, 0.7 g) dissolved in methanol (20 cm^3) was quickly added to a stirred methanol solution (20 cm^3) of $Cu(CF_3SO_3)_2$ (2 mmol, 0.9 g), whereupon the solution turned blue. A violet precipitate was obtained at $-80°C$, which was collected by filtration, washed with cold ether, and dried *in vacuo*. Found: C, 38.1; H, 4.8; N, 7.9. Calc. for $C_{22}H_{32}F_6N_4O_6S_2Cu$: C, 38.3; H, 4.7; N, 8.1%.

$Cu(TMB)_2(ClO_4)_2$ (2)

Obtained from $Cu(ClO_4)_2$ by the same procedure. Found: C, 40.3; H, 5.3; N, 9.2. Calc. for $C_{20}H_{32}Cl_2N_4O_8Cu$: C, 40.6; H, 5.5; N, 9.5%.

$Cu(DHB)_2(CF_3SO_3)_2 \cdot H_2O$ (3)

By a similar procedure, 5.5 mmol (0.43 g) of DHB in ether (15 cm^3) were added at $-20°C$ to a stirred acetone solution (20 cm^3) of $Cu(CF_3SO_3)_2 \cdot 4H_2O$ (2.75 mmol, 1 g). Precipitation of a violet powder occurred immediately, which was filtered, washed with cold ether, and dried *in vacuo*. Found: C, 24.4; H, 2.2; N, 10.3; S, 10.8; F, 21.5; Cu, 12.5. Calc. for $C_{10}H_{10}F_6N_4O_7S_2Cu$: C, 22.2; H, 1.9; N, 10.4; S, 11.9; F, 21.1; Cu, 11.8%.

$Cu(DHB)_2(BF_4)_2$ (4)

Obtained from $Cu(BF_4)_2$ following the same procedure. Found: C, 24.1; H, 2.0; N, 14.0. Calc. for $C_8H_8N_4B_2F_8Cu$: C, 24.2; H, 2.0; N, 14.1%.

$Cu_2(TMB)_4(CF_3SO_3)_3 \cdot 5H_2O$ (5)

To 4.5 mmol (0.74 g) of TMB in ether (40 cm^3 were added 5 mmol (1.8 g) of $Cu(CF_3SO_3)_2 \cdot 4H_2O$ in ether (40 cm^3). A violet complex precipitated immediately. Ether was evaporated under vacuum and 30 cm^3 of acetone added. While the solution was refluxed for 30 min, it turned green. The volume was then reduced until a light green hygroscopic powder precipitated, which was filtered, washed with ether–dichloromethane and dried *in vacuo*. Found: C, 38.4; H, 5.7; N, 7.9. Calc. for $C_{43}H_{64}N_8F_9O_9S_3Cu_2$: C, 39.1; H, 5.6; N, 8.5%. We were unable to get completely satisfactory analytical results because **5** is very hygroscopic.

$Cu_2(DHB)_4(CF_3SO_3)_3 \cdot (CH_3)_2CO$ (6)

To 5 mmol (0.40 g) of DHB in 10 cm^3 of acetone were added 8 mmol (0.9 g) of $Cu(CF_3SO_3)_2 \cdot 4H_2O$ in 20 cm^3 of acetone. A blue-violet precipitate appeared immediately, which turned light green by heating the mixture at 50°C for 1 h. The green powder was filtered, washed with ether and dried *in vacuo*. Found: C, 27.5; H, 2.7; N, 11.4; F, 17.4; S, 9.2; Cu, 13.8. Calc. for $C_{22}H_{22}N_8F_9S_3O_{10}Cu_2$: C, 27.7; H, 2.3; N, 11.8; F, 17.9; S, 10.1; Cu, 13.3%.

$Cu_2(DHB)_4(BF_4)_3$ (7)

Obtained from $Cu(BF_4)_2$ following the same procedure. Found: C, 27.1; H, 2.1; N, 15.5. Calc. for $C_{16}H_{16}N_8F_{12}B_3Cu_2$: C, 27.1; H, 2.3; N, 15.8%.

$Cu(TMB)_2(CF_3SO_3)$ (8)

TMB (8 mmol, 1.4 g) in methanol (150 cm^3) was added slowly to 200 cm^3 of a 10^{-2} M solution of

$Cu(CF_3SO_3)_2$ in methanol at room temperature. The mixture was stirred for 2 h, then concentrated to 20 cm^3. At $-30°$, a white powder precipitated, which was filtered, washed with cold ether and dried *in vacuo*. Found: C, 46.9; H, 6.0; N, 10.1. Calc. for $C_{21}H_{32}N_4F_3SO_3Cu$: C, 46.6; H, 6.0; N, 10.3%.

$Cu(DHB)_2(CF_3SO_3)$ (9)

$Cu(DHB)_2(CF_3SO_3)_2 \cdot H_2O$ (**3**, 2 mmol, 1.1 g) suspended in methanol (200 cm^3) was stirred for 2 h under reflux. The solution became colourless and a white precipitate formed, which was filtered, washed with cold ether, and dried under reduced pressure. Found: C, 29.3; H, 2.4; N, 15.2. Calc. for $C_9H_8N_4F_3O_3SCu$: C, 29.0; H, 2.2; N, 15.0%.

$Mn(TMB)(CF_3SO_3)_2 \cdot 2H_2O$ (10)

To 5 mmol of $Mn(CF_3SO_3)_2 \cdot H_2O$ in acetone (20 cm^3) were added 5 mmol (0.82 g) of TMB in ether (50 cm^3). The solution was stirred for 2 h at room temperature. A white precipitate formed, which was filtered, washed with ether and dried *in vacuo*. Found: C, 26.1; H, 3.3; N, 5.5; F, 20.7; S, 12.6; Mn, 10.0. Calc. for $C_{12}H_{20}N_2F_6S_2O_8Mn$: C, 26.0; H, 3.6; N, 5.2; F, 20.6; S, 11.6; Mn, 9.9%.

$Mn(TMB)_3(PF_6)_2$ (11)

To 2.5 mmol of $Mn(PF_6)_2$ in methanol (50 cm^3) were added 7.5 mmol of TMB (1.23 g) in ether (50 cm^3). The solution was concentrated and at $-30°C$ a light yellow powder precipitated, which was filtered, washed with ether and dried *in vacuo*. Found: C, 41.8; H, 5.7; N, 9.7; F, 27.1; P, 7.3; Mn, 6.6. Calc. for $C_{30}H_{48}N_6P_2F_{12}Mn$: C, 43.0; H, 5.8; N, 10.0; F, 27.2; P, 7.4; Mn, 6.6%.

$Zn_2(TMB)_3(CF_3SO_3)_4 \cdot 2H_2O$ (12)

TMB (5 mmol, 0.82 g) dissolved in ether (60 cm^3) was added to 2.5 mmol of $Zn(CF_3SO_3)_2 \cdot H_2O$ in acetone (20 cm^3). The solution turned light yellow, and after concentration a light yellow powder precipitated, which was filtered, washed with ether and dried *in vacuo*. Found: C, 33.5; H, 4.0; N, 6.6; S, 10.3; F, 16.5; Zn, 10.4. Calc. for $C_{34}H_{52}N_6F_{12}S_4O_{14}Zn_2$: C, 32.5; H, 4.2; N, 6.7; S, 10.2; F, 18.1; Zn, 10.4%.

Physical measurements

IR spectra were recorded as Nujol mulls on a Perkin–Elmer 577 spectrophotometer. UV–vis. spectra were obtained on a Cary 14 spectrophotometer equipped with a diffuse reflectance attachment. EPR spectra were measured on a Bruker ER 200 TT spectrometer operating at X-band frequency between 100 and 300 K.

Magnetic susceptibilities were determined by the Faraday method, using a Cahn microbalance coupled with a Drusch electromagnet. Measurements were performed between 20 and 320 K. $HgCo(NCS)_4$ was used as standard ($X_g = 16.44 \times 10^{-6}$ cgs emu). The experimental values were corrected for the diamagnetism of the ligands.[14]

Magnetization was measured by translating the sample in a pick-up coil system. The induced voltage was first amplified by a high-performance amplifier and then integrated, a bipolar voltage-to-frequency converter and a reversible counter providing the true integral of the input voltage. Flux resolution was better than one maxwell, corresponding to a magnetization resolution of *ca* 10^{-5} emu. The measurements were commonly reproducible within 10^{-4} emu.

RESULTS AND DISCUSSION

Copper complexes

The reactions of DHB and TMB with CuX_2 salts containing the poorly coordinating X groups, $CF_3SO_3^-$, BF_4^- and ClO_4^-, were found to be solvent- and temperature-dependent. Three types of complexes were obtained in good yield (> 80%). The violet Cu^{II} complexes, $Cu(TMB)_2X_2$ (**1**, **2**) and $Cu(DHB)_2X_2$ (**3**, **4**), precipitated upon cooling, when two moles of diisocyanides were allowed to react with one mole of CuX_2. Heating dilute (10^{-2} M) solutions of $Cu(TMB)_2(CF_3SO_3)_2$ or $Cu(DHB)_2(CF_3SO_3)_2$ in methanol (2 h) led to the white Cu^I complexes, $Cu(TMB)_2(CF_3SO_3)$ (**8**) or $Cu(DHB)_2(CF_3SO_3)$ (**9**).

Mixed-valence Cu^I–Cu^{II} complexes $Cu_2(TMB)_4(CF_2SO_3)_3$ and $Cu_2(DHB)_4(CF_3SO_3)_3$ were reproducibly obtained as green powders when the corresponding $CuL_2(CF_3SO_3)_2$ compounds were heated at 50°C in acetone or in an acetone–ether mixture. The resulting compounds, which first crystallized as acetone solvates, were very hygroscopic, which explains the difficulties in getting reproducible microanalyses. However, reliable results were obtained for the corresponding $Cu_2(DHB)_4(BF_4)_3$ material, which gave the same EPR data as the $CF_3SO_3^-$ salt, and a similar IR spectrum, except for anion bands.

The Cu^{II} compounds are insoluble in all common organic solvents, whereas the Cu^I and the mixed-valence Cu^{II}–Cu^I species are sparingly soluble in methanol or acetonitrile.

Table 1. IR and magnetic data[a]

Compound	ν(C≡N)	μ_{eff}	EPR[b] $g_\perp$	$g_\parallel$	$\langle\bar{g}\rangle$	$A_\parallel$
TMB	2120					
DHB	2150					
$Cu(TMB)_2(CF_3SO_3)_2$ (**1**)	2230	1.83	2.037	2.138	2.070	205
$Cu(TMB)_2(ClO_4)_2$ (**2**)	2240	1.91	2.050	2.149	2.083	200
$Cu(DHB)_2(CF_3SO_3)_2 \cdot H_2O$ (**3**)	2260	1.71	2.058	2.164	2.093	160
$Cu(DHB)_2(BF_4)_2$ (**4**)	2260	1.73	—	—	2.073	
$Cu_2(TMB)_4(CF_3SO_3)_3 \cdot 5H_2O$ (**5**)	2170	1.35	2.095	2.337	2.175	140
$Cu_2(DHB)_4(CF_3SO_3)_3 \cdot (CH_3)_2CO$ (**6**)	2200	1.15	2.090	2.360	2.180	133
$Cu_2(DHB)_4(BF_4)_3$ (**7**)	2200	1.33	2.094	2.356	2.181	130
$Cu(TMB)_2(CF_3SO_3)$ (**8**)	2160					
$Cu(DHB)_2(CF_3SO_3)$ (**9**)	2190					
$Mn(TMB)(CF_3SO_3)_2 \cdot 2H_2O$ (**10**)	2210	5.95	—	—	2.062	
					(2.008)	(95)
$Mn(TMB)_3(PF_6)_2$ (**11**)	2180	2.70	—	—	2.013	
					(2.008)	(98)
$Zn_2(TMB)_3(CF_3SO_3)_4 \cdot 2H_2O$ (**12**)	2260					

[a] 293 K.

[b] In the solid state, except for parenthesized values for Mn compounds, which were obtained from methanol solutions.

As already noted for metals in not very low oxidation states,[8,10,15] the ν(CN) frequency increases upon complexation (Table 1). As no bands are detected in the 1600–1700 cm^{-1} region, the isocyanide group cannot be present in a polymerized form or coordinated in a bridging bidentate way.[7,8] There are no residual absorptions for free isocyanide groups. The frequency decreases in the order Cu^{II} > mixed-valence Cu^{II}–Cu^{I} > Cu^{I}. Since the isocyanide-to-metal ratio is constant throughout the series, this trend can be related to the charge decreasing from Cu^{II} to Cu^{I}, which is also paralleled by increased back-bonding from filled copper *d* orbitals into the NC π^* system.[10]

Magnetic moments and EPR parameters of complexes **1–7** are reported in Table 1. Complexes **1–4** are paramagnetic Cu^{II} d^9 complexes without a Cu–Cu magnetic interaction. Their magnetic moments are within the normal range (1.7–2.2 BM)[16,17] for Cu^{II}. Square-planar coordination is indicated by the EPR parameters (A = 160–205 G) and consistent with the electronic spectra (band, *ca* 19100 cm^{-1} in the diffuse reflectance spectra).[18–20]

In contrast, complexes **5–7** have low magnetic moments, between 1.15 and 1.35 BM, at room temperature. They follow a Curie–Weiss law between 80 and 300 K (for **5**, $X(T-5.92) = 0.220$, and for **6**, $X(T-7.72) = 0.128$), showing that the copper centres are not magnetically coupled. The presence of Cu^{I} atoms must be assumed to explain the low magnetic moments. Thus, the compounds are presumably mixed-valence complexes of type I, that is, without magnetic interaction between the Cu atoms. This is confirmed by the magnetization curve measured for complex **5** at 1.05 K.†[21] The experimental data are represented in Fig. 1 together with the theoretical magnetization curves. If only Cu^{II} is assumed to be present, the magnetization value at saturation of 0.545 (b) gives rise to j and s values of 0.25. Obviously only about half of the copper is Cu^{II}, the remaining copper centre being diamagnetic Cu^{I}. Indeed, considering only Cu^{II} would give rise to the calculated magnetization curve (a) with M = 1.085 MB at saturation. This hypothesis is confirmed by the excellent fit between the experimental data and the theoretical curve calculated for a Cu^{II} population of 0.508 and a Cu^{I} population of 0.492 i.e. a 1 : 1 Cu^{II}/Cu^{I} ratio. The EPR data for compounds **3–5** are in agreement with this result

† The general equation for magnetization M in the case of an uncoupled $J = 1/2$ spin system reduces to $M = 0.5\,N\beta g \tan h(\beta gH/2kT)$, where g is the Lande factor and the remaining symbols have their usual meanings. At saturation, $M = g \cdot J$. The experimental EPR data give a g value of 2.175, allowing to calculate a J value of 0.25. For a magnetically dilute Cu^{II} species, $L = 0$, consequently, $J = S = 0.25$. The magnetic moment of the Cu^{II} species is related to J by the equation $\mu = g[J(J+1)]^{1/2}$. The experimental values of $g = 2.175$ and $J = 0.5$ give $\mu = 1.875$ BM, consistent with the expected values $1.7 < \mu < 2.2$ BM.

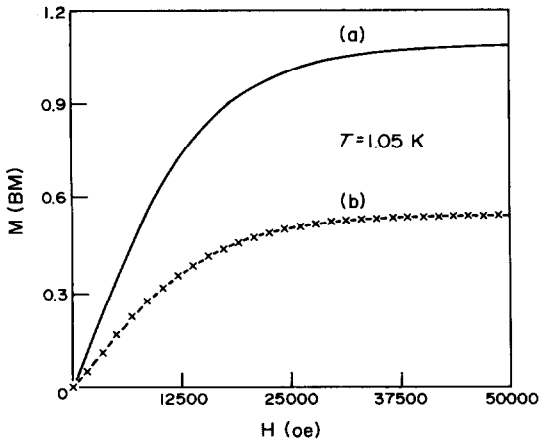

Fig. 1. Magnetization curves for $Cu_2(TMB)_4(CF_3SO_3)_3$ (**5**). (x = experimental points). Continuous curves calculated assuming (a) that all copper is present as Cu^{II}, and (b) that the complex is mixed-valence with Cu^{II} and Cu^{I} populations of 0.502 and 0.498, respectively.

since they correspond to magnetically dilute Cu^{II} atoms in tetrahedral environment (A = 130–140 G). This coordination geometry is also supported by the electronic spectra (band at 14,100 cm^{-1} for **5** and 12,000 cm^{-1} for **6**).[20,22,23]

Complexes **8** and **9** are diamagnetic copper(I) species. They are slightly soluble in polar solvents, but only microcrystalline powders were obtained. Copper(I) probably lies in a tetrahedral environment, since this geometry, common for d^{10} Cu^{I} complexes,[20] has been observed for the unidentate methylisocyanide complex $[Cu(CNMe)_4]BF_4$.[24]

The poor solubility of these complexes points to polymeric structures, and this must be achieved by bridging via the diisocyanide ligands. Indeed, besides the fact that the "non-coordinating" anions used here would not be efficient in bridging copper atoms into stable infinite chains, a simple count of the overall number of —NC groups per copper shows that they saturate the metal coordination sphere. In agreement with this conclusion are the spectroscopic data which show no evidence for free isocyanide groups. However, beyond the immediate metal surroundings, there is no basis to propose detailed polymerization patterns for these compounds.

Manganese complexes

Only TMB yielded well characterized compounds with MnX_2 salts. The colourless $Mn(TMB)(CF_3SO_3)_2 \cdot 2H_2O$ (**10**) precipitated from a 1 : 1 mixture of $Mn(CF_3SO_3)_2 \cdot H_2O$ and TMB, whereas the light yellow solid $Mn(TMB)_3(PF_6)_2$ (**11**) was obtained from a mixture of $Mn(PF_6)_2$ with excess ligand. Both materials are soluble in polar solvents, e.g. alcohols and acetonitrile.

The ν(CN) band occurs at 2210 cm^{-1} in **10** and at 2180 cm^{-1} in **11**. It is displaced to a higher frequency by coordination, as observed with $[Mn(CN)_6]^{2-}$ complexes,[25] and it decreases with increasing TMB/Mn molar ratio. The EPR data listed in Table 1 were determined on the solids and on methanol solutions. They are consistent with d^5 Mn^{II} species,[26] but interestingly, the compounds are in different spin states. Compound **10** is a high-spin Mn^{II} complex ($^6A_{1g}$ ground state) with a magnetic moment μ_{eff} of 5.95 BM at 298 K, nearly equal to the spin-only value.[16,17] Increasing the number of strong-field ligands around Mn results in a low-spin paramagnetic Mn^{II} species $Mn(TMB)_3(PF_6)_2$ ($^2T_{2g}$ ground state) with a magnetic moment μ_{eff} of 2.70 BM at 298 K. $[Mn(CN)_6]^{4-}$ and $[Mn(CNR)_6]^{2+}$ are also known to be low-spin systems.[25,27,28] No Mn^{II}–Mn^{II} magnetic interactions are detected from the EPR spectra, or the magnetic susceptibility data for **11**, which follows a Curie–Weiss law between 80 and 300 K ($X(T-6.39) = 0.869$).

In $Mn(TMB)_3(PF_6)_2$, the number of —NC groups per metal and the absence of uncoordinated —NC groups deduced from the IR spectra suggest a Mn^{II} centre surrounded by an octahedron of —NC ligands as in the $[Mn(CN)_6]^{4-}$ ion[29] and presumably in the various $[Mn(CNR)_6]^{2+}$ species.[25,28] Bridging by this large number of ligands probably defines a complex three-dimensional pattern in **11**. In complex **10**, the coordination sphere, including only two —NC groups per Mn, must be completed by water and/or $CF_3SO_3^-$ oxygens. Dissolution in methanol undoubtedly involves breaking of the polymeric structure into small units, but no details on this point are provided by the available data.

Zinc complex

The light yellow $Zn_2(TMB)_3(CF_3SO_3)_4 \cdot 2H_2O$ compound was obtained in good yield when TMB was added to $Zn(CF_3SO_3)_2 \cdot H_2O$ in a 2 : 1 ratio. Only one ν(CN) band is apparent at 2260 cm^{-1}, in the same range as for the Cu^{II} complexes. In Ag^{I} compounds of the same stoichiometry, the ν(CN) frequency was found to be 2180 cm^{-1}. The greater frequency observed here is consistent with the higher charge of Zn^{II}. The $[Ag_2(TMB)_3]X_2$ complexes ($X = ClO_4^-, PF_6^-$) form one-dimensional ladder-like polymers, with TMB molecules cross-linking infinite —Ag—TMB—Ag—TMB— chains.[6] With three soft —NC groups coordinated per metal, zinc is likely to retain a low coordination number and adopt the tetrahedral geometry common for this metal.[30] A structure similar to those

of silver salts in which the coordination sphere would be completed by water or anions can be proposed.

CONCLUSION

To achieve coordination with an —NC group, the metal normally defines a linear —N—C—M arrangement. Whether the two donor groups in a given diisocyanide can be suitably oriented to chelate a single atom, bridge a pair of adjacent metal atoms, or link distant metals along an infinite polymeric pattern is controlled to a large extent by the architecture of the carbon chain between the donor groups. There is evidence that at least a C_7 hydrocarbon chain is needed for a diisocyanide to form a chelate.[31]

We recently discussed in detail the conformations of TMB present in the various polymeric units observed for silver complexes.[6] Clearly, chelation would require severe distortions in the hydrocarbon chain, and both low-energy conformations of TMB position the —N—C units in orientations favouring polymers.

In the DHB molecule, the —N—C groups are so oriented that even in the eclipsed cisoid conformation I, the terminal sections are divergent and make chelation virtually impossible. Any rotation about the CH_2—CH_2 bond would make chelation still less favourable. Thus, the ligand lower-energy conformations II and III clearly favour polymeric arrangements rather than small molecular units. Two metal atoms lying 2.0 Å away from C along the lone pair direction in I would be 4.6 Å apart, and further apart in II and III. Therefore, as observed, no magnetic interactions can take place between the metal centres.

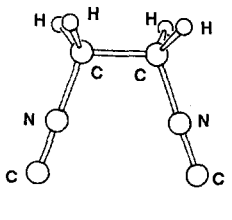

I

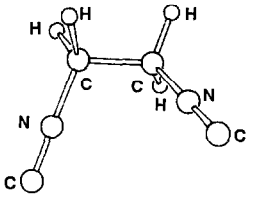

II

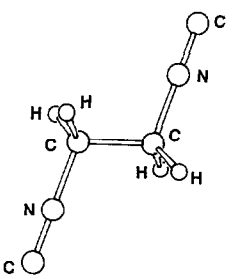

III

Despite the fact that the resulting polymers could not be completely defined in terms of uni, di- or tridimensional arrangements, the present work shows that under suitable conditions, side reactions can be avoided and diisocyanide complexes can be prepared with first-row metals.

Acknowledgement—This work was made possible by travel grants in the framework of the Programme d'Echanges Universitaires Franco-Québécois.

REFERENCES

1. K. R. Mann, N. S. Lewis, V. M. Miskowski, D. K. Erwin, G. S. Hammond and H. B. Gray, *J. Am. Chem. Soc.* 1977, **99**, 5525; V. M. Miskowski, G. L. Nobinger, D. S. Kliger, G. S. Hammond, N. S. Lewis, K. R. Mann and H. B. Gray, *J. Am. Chem. Soc.* 1978, **100**, 485; S. J. Milder, R. A. Goldbeck, D. S. Kliger and H. B. Gray, *J. Am. Chem. Soc.* 1980, **102**, 6761; I. S. Sigal, K. R. Mann and H. B. Gray, *J. Am. Chem. Soc.* 1980, **102**, 7252; V. Miskowski and H. B. Gray, *Inorg. Chem.* 1987, **26**, 1108; A. W. Maverick, T. P. Smith, E. F. Maverick and H. B. Gray, *Inorg. Chem.* 1987, **26**, 4336.
2. P. D. Enlow and C. Woods, *Inorg. Chem.* 1985, **24**, 1273; M. R. Rhodes and K. R. Mann, *Inorg. Chem.* 1984, **23**, 2053; D. R. Womach, P. D. Enlow and C. Woods, *Inorg. Chem.* 1983, **22**, 2653.
3. A. Efraty, I. Feinstein, F. Frolow and L. Wackerle, *J. Am. Chem. Soc.* 1980, **102**, 6341; A. Efraty, I. Feinstein, L. Wackerle and F. Frolow, *Angew. Chem. Int. Ed. Engl.* 1980, **19**, 633; A. Efraty, I. Feinstein, F. Frolow and A. Goldman, *J. Chem. Soc., Chem. Commun.* 1980, 864.
4. C. M. Che, F. H. Herbstein, W. P. Schaefer, R. E. Marsh and H. B. Gray, *Inorg. Chem.* 1984, **23**, 2572.
5. D. A. Bohling, T. P. Gill and K. R. Mann, *Inorg. Chem.* 1981, **20**, 194.
6. A. Guitard, A. Mari, A. L. Beauchamp, Y. Dartiguenave and M. Dartiguenave, *Inorg. Chem.* 1983, **22**, 1603; M. Dartiguenave, Y. Dartiguenave, A. Mari, A. Guitard, M. J. Olivier and A. L. Beauchamp, *Can. J. Chem.*, in press.
7. J. A. S. Howell and A. J. Rowan, *J. Chem. Soc., Dalton Trans.* 1981, 297.
8. L. Malatesta and F. Bonati, *Isocyanide Complexes of Metals*. Wiley, London (1969).
9. W. L. Gladfelter, M. W. Lynch, W. P. Schaefer, D. N. Hendrickson and H. B. Gray, *Inorg. Chem.* 1981, **20**, 2390.
10. R. J. Angelici, M. H. Quick and G. A. Kraus, *Inorg.*

Chim. Acta 1980, **44**, L137; R. J. Angelici, M. H. Quick, G. A. Kraus and D. T. Plummer, *Inorg. Chem.* 1982, **21**, 2178; D. T. Plummer and R. J. Angelici, *Inorg. Chem.* 1983, **22**, 4063.
11. W. P. Weber, G. W. Gokel and I. K. Ugi, *Angew. Chem. Int. Ed. Engl.* 1972, **11**, 530.
12. W. P. Weber, G. W. Gokel and R. P. Widera, *Org. Synth.* 1976, **55**, 96.
13. A. W. Hofmann, *Annu. Chem.* 1867, **144**, 114.
14. G. Foëx, *Table de constantes et données numériques—Diamagnétisme et paramagnétisme.* Masson, Paris (1957).
15. F. A. Cotton and F. Zingales, *J. Am. Chem. Soc.* 1961, **83**, 351.
16. R. S. Drago, *Physical Methods in Chemistry*, Chap. 11, p. 425. Saunders, London (1977).
17. A. Earnshaw, *Introduction to Magnetochemistry.* Academic Press, London (1968).
18. R. D. Willett, O. L. Liles Jr and C. Michelson, *Inorg. Chem.* 1967, **6**, 1885.
19. F. Valach, J. Kohout, M. Dunaj-Jurco, M. Hvastikova and J. Gazo, *J. Chem. Soc., Dalton Trans.* 1979, 1867.
20. B. J. Hathaway in *Comprehensive Coordination Chemistry* (Edited by G. Wilkinson, R. D. Gillard and J. A. McCleverty) Vol. 5, Chap. 53. Pergamon Press, Oxford (1987).
21. D. H. Martin, *Magnetism in Solids*, p. 188. Iliffe Books, London (1967).
22. H. Yokoi and A. W. Addison, *Inorg. Chem.* 1977, **16**, 1341.
23. R. C. Rosenberg, C. A. Root, P. K. Bernstein and H. B. Gray, *J. Am. Chem. Soc.* 1975, **97**, 2092.
24. A. L. Spek, *Cryst. Struct. Commun.* 1982, **11**, 413.
25. D. S. Matteson and R. A. Bailey, *J. Am. Chem. Soc.* 1969, **91**, 1975.
26. A. Abragam and B. Bleaney, *Résonance Paramagnétique des Ions de Transition.* Presses Universitaires de France (1971).
27. B. Chiswell, E. D. McKenzie and L. F. Lindoy, in *Comprehensive Coordination Chemistry* (Edited by G. Wilkinson, R. D. Gillard and J. A. McCleverty) Vol. 4, Chap. 41. Pergamon Press, Oxford (1987).
28. P. M. Treichel, *Comprehensive Organometallic Chemistry* (Edited by G. Wilkinson, F. G. A. Stone and E. W. Abel) Vol. 4, Chap. 29. Pergamon Press, Oxford (1982).
29. A. Tullberg and N. G. Vannerberg, *Acta Chem. Scand.* 1974, **28A**, 551.
30. N. N. Greenwood and E. Earnshaw, *Chemistry of the Elements*, p. 1402. Pergamon Press, Oxford (1984).
31. K. Kawakami, M. Okajima and T. Tanaka, *Bull. Chem. Soc. Jpn* 1978, **51**, 2327.

Polyhedron Vol. 8, No. 3, pp. 325–332, 1989
Printed in Great Britain

0277–5387/89 $3.00+.00
© 1989 Pergamon Press plc

COPPER(I) COMPLEX FORMATION IN CHLORIDE MELTS. RAMAN SPECTROSCOPIC AND CRYOSCOPIC STUDY

E. CHRISTENSEN and R. W. BERG

Chemistry Department A, The Technical University of Denmark, DK-2800 Lyngby, Denmark

and

J. H. VON BARNER*

The Institute of Mineral Industry, The Technical University of Denmark, DK-2800 Lyngby, Denmark

(*Received* 8 *July* 1988; *accepted* 27 *July* 1988)

Abstract—Raman spectra of equimolar MCl–CuCl melts (M = Na, K, Rb and Cs) at 500°C consist of one single band with a frequency increasing from 255 to 268 cm^{-1} when going from Na to Cs. For KCl–CuCl melts no change in band position was observed either with changes in temperature (200–600°C) or with compositional changes ($0.250 < X_{CuCl} < 0.667$). CuCl–$AlCl_3$ melts ($0.33 < X_{CuCl} < 0.67$, $t = 300$ and 400°C) show a copper chlorine vibration at 220 cm^{-1}. The Al–Cl stretching and bending vibrations are shifted towards lower frequencies, relative to the vibrations of $AlCl_4^-$ in alkali chloride–aluminium chloride melts. Also the intensity ratio between 308 and 342 cm^{-1} bands (the strongest for $Al_2Cl_7^-$ and $AlCl_4^-$, respectively) is lower compared to MCl–$AlCl_3$ melts of similar $AlCl_3$ mole fraction. This suggests the formation of [$CuAlCl_4$] species with bent Cu—Cl—Al bridging and a distortion in the tetrahedral configuration of the chloride around aluminium. For CuCl dissolved in basic MCl–$AlCl_3$ (M = K, Cs) melts, both Raman spectra and freezing point depression data indicate formation of linear $CuCl_2^-$ complexes. Two liquid phases (essentially CuCl and $KAlCl_4$) were formed when CuCl was added to neutral KCl–$AlCl_3$ melts. In acidic MCl–$AlCl_3$–CuCl melts, a 220 cm^{-1} band was observed arising from a copper chloride vibration as in the CuCl–$AlCl_3$ melts. The density of the equimolar KCl–CuCl melt is 2.436 and 2.389 g cm^{-3} at 421 and 556°C, respectively.

Chloride melts containing copper have received considerable attention because of their application as catalysts, e.g. for the Deacon reaction and for the oxidative chlorination of hydrocarbons in connection with vinyl chloride production. Since the chemistry of such catalysts is rather poorly understood we decided to perform a Raman spectroscopic investigation on different copper(I) containing chloride melts in an attempt to better understand their properties.

The coordination chemistry of copper(I) has only been subject to a small number of investigations. According to the crystal structure studies performed, several types of coordination geometries are found: typically, copper(I) is tetrahedrally coordinated as in K_2CuCl_3, $CsCu_2Cl_3$, $CuAlCl_4$, and in the low and high temperature modifications of CuCl.[1–5] Two colinear bonds, i.e. $CuCl_2^-$, are known to exist in some copper(I) salts with large organic cations.[6–8]

This dichlorocuprate(I) ion is also present in organic solutions of copper(I) chloride with excess chloride added (as LiCl or HCl).[9,10] The Raman spectrum of this ion consists of one single band near 300 cm^{-1} assigned to the symmetrical stretching mode of the linear ion.[6,9,10] In melts at around 500°C, the Raman spectra[11] have bands at two

*Author to whom correspondence should be addressed.

different positions: at 275 cm^{-1} in CsCl–CuCl melts of 50–50 mol % composition and at 250 cm^{-1} in pure CuCl, basic CsCl–CuCl and LiCl–CuCl melts of all compositions. The bands have previously been explained[11] as being due to copper(I) chloride species with an average coordination number of two (275 cm^{-1}) and four (250 cm^{-1}).

Apart from Raman spectroscopy, several other methods have been applied to study MCl–CuCl melts.[12–17] The activities of CuCl determined by vapour pressure[12] and EMF measurements,[13,14] show large deviations from ideality for KCl–CuCl melts. Similar but smaller deviations are observed for the enthalpy of mixing for MCl–CuCl (M = Li, Na) and these increase markedly[15,16] for M = K, Rb and Cs. In the MCl–CuCl phase diagrams no evidence of compound formation is obvious in the case of M = Li, Na,[18,19] whereas compound formation is observed for M = K, Rb and Cs.[20–22] Finally, conductivity measurements[17] on KCl–CuCl melts in the temperature range 440–630°C show a minimum in equivalent conductivity at a copper(I) chloride mole fraction of nearly 0.33.

Few studies have been made on melts containing copper(I) chloride and aluminium chloride.[23,24] The phase diagram of the KCl–$AlCl_3$ system near equimolar composition has recently been studied with high precision.[25] The freezing point of a pure neutral $KAlCl_4$ melt was found to be 257.3 ± 0.1°C and the cryoscopic constant was 27 ± 2°C kg mol^{-1}. The phase diagram of the binary system CuCl–$AlCl_3$ showed that a congruently melting 1 : 1 compound is formed.[23] The NQR spectrum of this compound showed[26] only one ^{35}Cl-line and a recent investigation[3] of the crystal structure indicated the formation of a polymeric structure in which both Al^{III} and Cu^{I} atoms are surrounded by four chlorine atoms. $CuAlCl_4$ molecules exist in the vapour phase in the temperature range 189–390°C.[27] The results of an electrochemical study[24] on copper(I) chloride dissolved in NaCl–$AlCl_3$ melts at 175°C were explained in terms of the equilibrium $Cu^+ + 2Cl^- \rightleftharpoons CuCl_2^-$, with an equilibrium constant of 6.5×10^4 dm^6 mol^{-2}.

EXPERIMENTAL

Aluminium chloride, alkali chlorides and anhydrous copper(II) chloride were prepared by methods similar to the ones described in previous works.[28,29] Copper(I) chloride was synthesized directly in the melts by reaction between anhydrous copper(II) chloride[30] and excess copper metal (99.99% pure, obtained from N.K.T., Denmark). The reaction was carried out at 600°C in the case of the MCl–CuCl melts, and at 400°C for the melts which contained aluminium chloride. During reduction the colour of the melt changed from dark brown to yellow for the binary alkali chloride–copper(I) chloride melts and to faintly yellow for the aluminium chloride containing melts. The reaction was usually complete in two days, after which time no band due to copper(II) chloride complexes[31] could be observed in the visible spectra of the melts.

The apparatus and method for measuring the Raman spectra were almost identical to the ones previously described.[32] The optical cells were made of fused quartz tubing and sealed under vacuum. Most of them were equipped with a filter, which was used to remove excessive copper metal after the reduction was complete. The Raman spectra were recorded using a JEOL-JRS-400D spectrometer coupled to a cooled photomultiplier and a photon counting system. The 514.5 nm line of a CR argon ion laser with a typical intensity of 300 mW was used to excite the melts. The scan rates and spectral resolutions were 25–50 cm^{-1} min^{-1} and 2–5 cm^{-1}, respectively.

The densities were measured by a method developed in our laboratory.[33] For these experiments, in order to get reliable results, it was necessary to premix potassium chloride, copper(II) chloride and copper metal and filter off the excess metal. The cryoscopic measurements were performed using a technique similar to the one previously described.[34] The copper(I) was added as the $KCuCl_2$ mixed salt.

Other technical details and the nomenclature used in this work are the same as in previous publications.[31,32] The formality C' is defined as the initial molar amounts of the added salt dissolved in 1 dm^3 of the melt. The composition of the melts are given in mole fractions (X_{CuCl}, X_{KCl}, X_{AlCl_3}, etc.), but for the case in which two phases are present the notation $MCl/AlCl_3/CuCl$ is used indicating the molar ratios which were weighed. MCl–$AlCl_3$–CuCl melts are called acidic if $X_{AlCl_3} > X_{MCl}$ and basic if the opposite is the case.

The density necessary to calculate C'_{CuCl} in the MCl–$AlCl_3$–CuCl melts was obtained assuming ideal mixing of MCl–$AlCl_3$ with CuCl except for basic KCl–$AlCl_3$–CuCl melts for which ideal mixing between KCl–$AlCl_3$ and $KCuCl_2$ was supposed. The dependence of the density on composition and temperature is known for all of the binary MCl–$AlCl_3$ solvent mixtures: NaCl–$AlCl_3$,[35] KCl–$AlCl_3$[36] and CsCl–$AlCl_3$.[37] The data from the work of Klemm were used for the densities of CuCl.[38] Apparently no density work exists for the $KCuCl_2$ melt; therefore, we measured the density for this composition at two temperatures: 556 and 421°C. The densities were found to be 2.389 and 2.436 g

cm^{-3}, respectively. For values at other temperatures linear interpolation was assumed to give reasonably accurate results for the purpose of this work.

Raman spectra of MCl–CuCl *melts*

Figure 1 shows the spectra of MCl–CuCl melts (M = Na, K, Rb and Cs) with a mole fraction of 0.500, all recorded at 500°C. As can be seen from this figure all of the melts give rise to only a single band in the measured wavelength region. The position of each band is given in Fig. 1.

As it can be seen, the Raman frequency for the equimolar MCl–CuCl melts goes up steadily from 255 cm^{-1} for M = Na and to 268 cm^{-1} for M = Cs. For the latter band Gilbert *et al.*[11] obtained a value of 273 cm^{-1} at a lower temperature (450°C) and for M = Li a value of 250 cm^{-1} was found. Our spectra of KCl–CuCl melts with mole fractions of CuCl equal to 0.667, 0.333 and 0.250 were indistinguishable from the spectrum of the equimolar composition. To investigate whether the temperature had any effect, Raman spectra of KCl–CuCl melts with $X_{CuCl} = 0.667$ were measured between 200 and 600°C. In this temperature range the change in the Raman spectra were negligible.

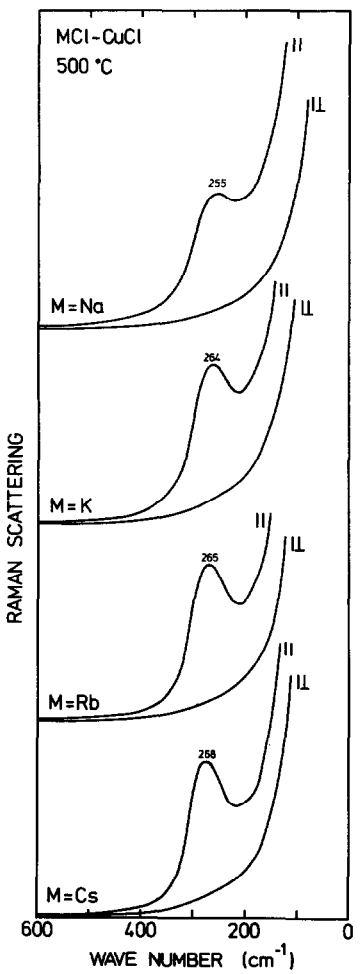

Fig. 1. Polarized (||) and depolarized (|⊥) Raman spectra of MCl–CuCl melts (M = Na, K, Rb, Cs) at 500°C, $X_{CuCl} = 0.500$. Slit width ~ 3 cm^{-1}.

From these results one can conclude that the coordination of chloride to copper(I) in the investigated range of KCl–CuCl melts does not change significantly neither with temperature nor with composition. In contrast to this, Gilbert *et al.*[11] have claimed that the KCl–CuCl melts behaved similarly to the CsCl–CuCl melts (i.e. gave two Raman bands at high alkali chloride contents). The band observed in the MCl–CuCl melts must be due to some kind of coordination between Cu and Cl, because the band is much more distinct than the usual broad Raman-wing bands characteristic of spectra from completely dissociated monatomic liquids like molten NaCl and KCl.[39] A possible explanation of the origin of Raman bands of equimolar MCl–CuCl melts is that copper(I) is tetrahedrally surrounded by chloride ions in LiCl–CuCl, as proposed by Gilbert *et al.*[11] and that a gradual change of the coordination from tetrahedral towards linear coordination of Cu^{I} occurs for increasing atomic number of the alkali metal counter cation. Support for this view can be found in the enthalpy of mixing data[15,16] in which only small interactions were observed in the cases of LiCl–CuCl and NaCl–CuCl melts, in contrast to KCl–CuCl, RbCl–CuCl and CsCl–CuCl melts where considerable deviations from ideality occurred. Furthermore, the large negative deviations in the vapour pressure[12] and EMF data[13,14] and the minimum in the equivalent conductivity of KCl–CuCl melts[17] also indicate structural changes in these melts compared to the pure CuCl melt.

Raman spectra of $CuCl–AlCl_3$ *melts*

Figure 2 shows Raman spectra of $CuCl–AlCl_3$ melts at various compositions; band positions are also indicated in this figure. The spectra of melts with a CuCl mole fraction of 0.33 and 0.50 were recorded at 300°C, whereas in the case of $X_{CuCl} = 0.667$, it was necessary to raise the temperature to 400°C because of the higher melting point at this composition.

It can be seen from Fig. 2 that all of the spectra have a strong polarized band at around 342 cm^{-1}. This band is assigned to the ν_1 (A_1) vibration of $AlCl_4^-$.

In addition to this band, a band appears at 308 cm^{-1} for $X_{CuCl} = 0.500$ and 0.333. The intensity of

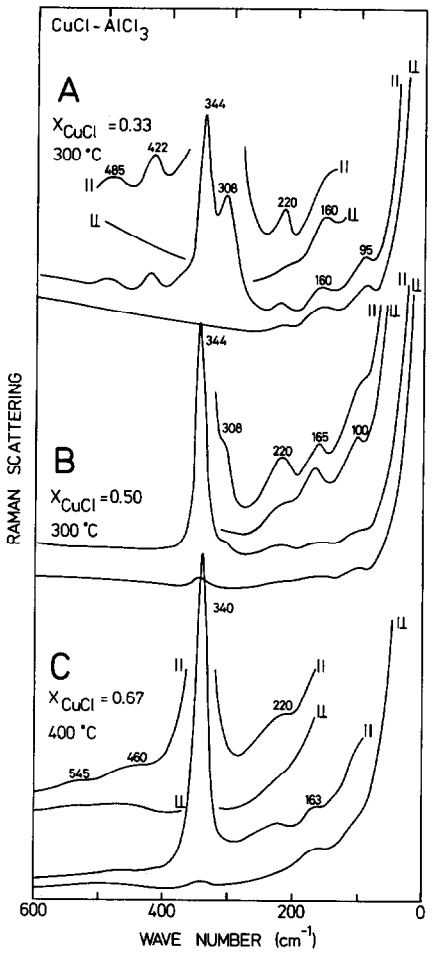

Fig. 2. Polarized (∥) and depolarized (∥⊥) Raman spectra of CuCl–$AlCl_3$ melts. Mole fractions and temperatures are indicated in the figure. For the amplified parts of the spectra the sensitivity was raised by a factor of 2.5 ($X_{CuCl} = 0.33$) and 5.0 ($X_{CuCl} = 0.50$ and 0.67).

this band relative to the 342 cm^{-1} band increases with the $AlCl_3$ contents of the melts. Also the frequency of 308 cm^{-1} is very near to that of the strongest band of the $Al_2Cl_7^-$ complex known from acidic MCl–$AlCl_3$ melts (M = alkali metal).[40,41] Therefore there is good reason to believe that $Al_2Cl_7^-$ is present in equimolar as well as in acidic CuCl–$AlCl_3$ melts. Other bands at around 100, 162, 422, 460, 485 and 545 cm^{-1} are also assigned to aluminium–chloro vibrations.

The band at 220 cm^{-1} observed in all of the melts is probably due to a copper chloride vibration, although Al_2Cl_6 also has a vibration near this frequency. It is, however, unlikely that this species should exist in the melts with a CuCl mole fraction of 0.50 or larger. This view can be justified since with increasing $AlCl_3$ contents $Al_2Cl_7^-$ should be formed prior to Al_2Cl_6, and from the intensity of the 308 cm^{-1} band observed in the Raman spectra with an $AlCl_3$ mole fraction of up to 0.500 one can see that $Al_2Cl_7^-$ is only present in small amounts in these melts. On the other hand, the presence of Al_2Cl_6 cannot be excluded in the melt with a CuCl mole fraction of 0.33.

In Table 1, the main Raman frequencies of the CuCl–$AlCl_3$ melts observed in our work are listed and compared to other binary chloro–aluminate melts. From this table it can be seen that the position of the ν_1 vibration for $AlCl_4^-$ in the CuCl–$AlCl_3$ melts at 344 cm^{-1} is lower than for the equimolar MCl–$AlCl_3$ melts (M = Na, K), in which it is well known that $AlCl_4^-$ forms a regular tetrahedron.[40,41] The bands at 100 and 165 cm^{-1} also occur at lower frequencies than the ν_2 and ν_4 vibrations of $AlCl_4^-$ in MCl–$AlCl_3$ melts. It is remarkable that these frequencies are close to those observed for the $Al_2Cl_7^-$ complex in the alkali tetrachloroaluminate melts.[40,41]

These band displacements indicate a distortion of the $AlCl_4^-$ tetrahedron in the CuCl–$AlCl_3$ melts. It should be further noticed that similar displacements are observed in the $SnCl_2$–$AlCl_3$ system.[42]

The intensity ratio of the 308 cm^{-1} band relative to the 342 cm^{-1} band for $X_{AlCl_3} = 0.67$ is much lower than the ratio of the corresponding bands (311 cm^{-1}/350 cm^{-1}) observed in MCl–$AlCl_3$ melts

Table 1. Main Raman frequencies ($\Delta\nu$ in cm^{-1}) of MCl_x–$AlCl_3$ melts of various compositions[a]

MCl_x	X_{MCl_x}	T (°C)	$AlCl_4^-(\nu_1)$	$AlCl_4^-(\nu_2)$	$AlCl_4^-(\nu_3)$	$AlCl_4^-(\nu_4)$	$Al_2Cl_7^-$	M---Cl	Reference
CuCl	0.667	400	340	~ 100	485, 422	163	—	220	This work
CuCl	0.500	300	344	100	—	165	308	220	This work
CuCl	0.333	300	342	95	545, 460	160	308	222	This work
NaCl	0.500	225	351	121	490	186	—	—	41
NaCl	0.333	225	—	—	—	—	313	—	41
KCl	0.500	300	350	122	487	182	—	—	40
$SnCl_2$	0.350	235	341	~ 100	—	166	310	225	42

[a] $x = 1$ or 2 depending on the valency of metal (M).

(M = Li, Na, K and Cs) at the same $AlCl_3$ mole fraction and temperature.[40,41,43] This is probably an indication of bonding between Cu^I and $AlCl_4$ tetrahedra resulting in a displacement of the equilibrium

$$2AlCl_4^- \rightleftharpoons Al_2Cl_7^- + Cl^- \qquad (1)$$

to the left.

The rather low position (220 cm^{-1}) of the copper(I) chloride vibration in the CuCl–$AlCl_3$ melt suggests that copper is not linearly coordinated by chloride. A possible explanation is that the copper atom is connected to aluminium by bent chloride bridges forming a [$CuAlCl_4$] complex as shown in Structure 1. This is supported by the position of

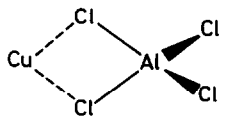

Structure 1.

the previously mentioned displaced ν_1, ν_2 and ν_4 vibrations and by the splitting of the ν_3 vibration (at around 487 cm^{-1}) of $AlCl_4^-$ (Table 1). A similar model has recently been proposed by Gilbert *et al.*[42] for the coordination of Sn^{II} in $SnCl_2$–$AlCl_3$ for $X_{AlCl_3} > 0.66$. Also in this case, a low frequency band appears at ~ 220 cm^{-1} superimposed on the bands arising from aluminium–chloro vibrations. It is of course possible that $CuAlCl_4$ complexes are not monomeric, but form $(CuAlCl_4)_n$.

CuCl–MCl–$AlCl_3$ *melts* (M = K, Cs)

General. Figure 3 shows Raman spectra of 3.7 F CuCl (i.e. formal concentration = 3.7) dissolved in KCl–$AlCl_3$ melts with varying acidity. The bands around 120, 180, 350 and 490 cm^{-1} are the well known[40,41,43] vibrations of $AlCl_4^-$. For CuCl dissolved in acidic solvents [Fig. 3(A)], additional bands are observed at 222 cm^{-1} (polarized) and at ~310 cm^{-1}. The ~ 310 cm^{-1} band is probably due to the strongest vibration of $Al_2Cl_7^-$ whilst the 222 cm^{-1} band must arise from a copper chloride vibration (Al_2Cl_6 cannot be present at this composition). Spectra B and B′ arise from the bottom and top phase of the same sample. Only one band at 250 cm^{-1} is observed in spectrum B, whereas spectrum B′ shows the four bands characteristic of $AlCl_4^-$ and the ~ 310 cm^{-1} band from $Al_2Cl_7^-$. Spectra C and D are very similar to each other. In addition to the $AlCl_4^-$ bands, only one band in the 270–290 cm^{-1} region is observed.

Raman spectra of CuCl dissolved in CsCl–$AlCl_3$

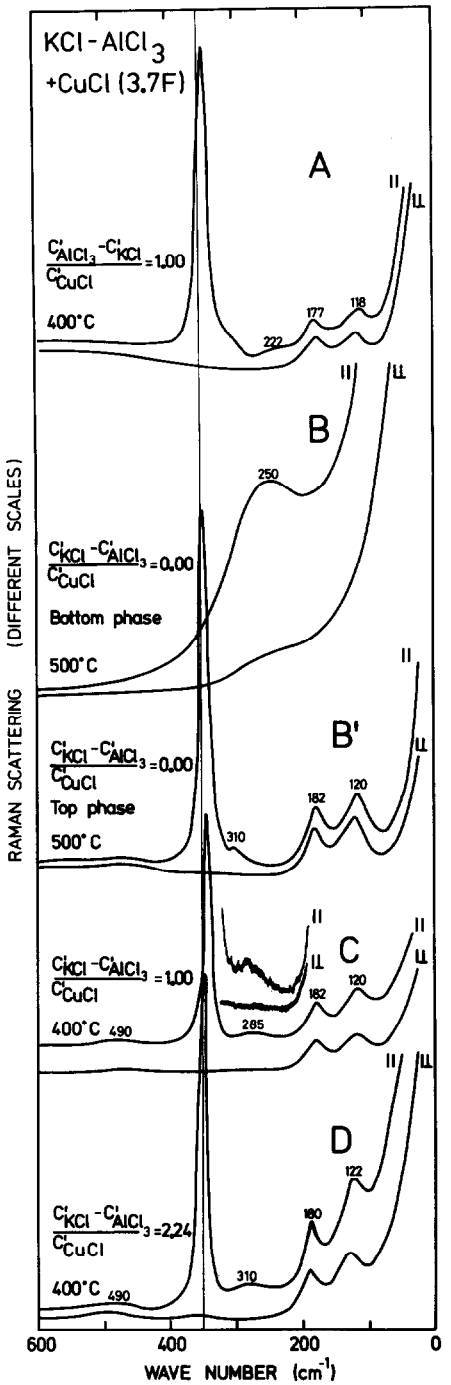

Fig. 3. Polarized (‖) and depolarized (‖⊥) Raman spectra of CuCl–KCl–$AlCl_3$ melts. The formal concentration of CuCl was 3.7 for all samples and the mole fractions of KCl and $AlCl_3$ were: (A) 0.2383_1, 0.3819_7; (B′) (bottom and top phase of the same sample), 0.3855_9, 0.3855_9; (C) 0.5000_0, 0.2880_4; (D) 0.6171_3, 0.1941_7. The temperatures are given on the figure together with the ratio of the excess formality of $AlCl_3$ or KCl to the formality of CuCl.

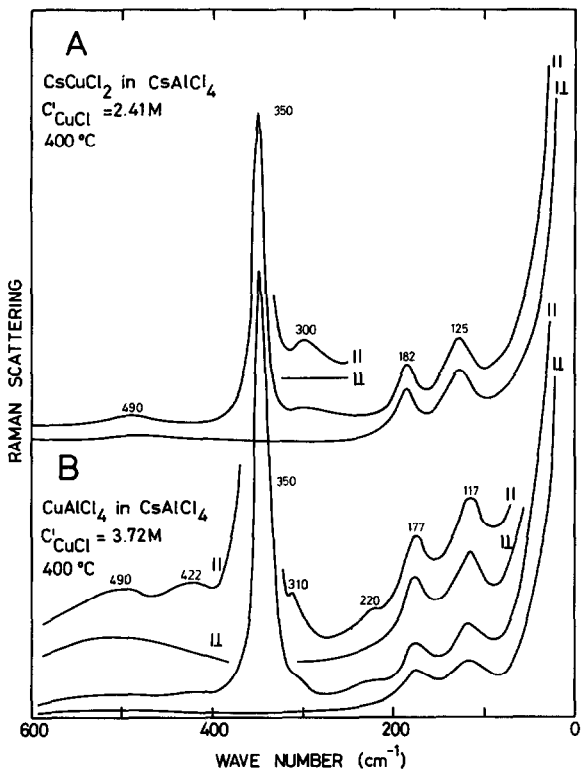

Fig. 4. Polarized (‖) and depolarized (‖⊥) Raman spectra of CuCl–CsCl–$AlCl_3$ melts. The formality of CuCl and the temperatures are given in the figure. The mole fractions of CsCl and $AlCl_3$ were: (A) 0.5004, 0.3436; (B) 0.2501, 0.4999. For the amplified parts of the spectra the sensitivity was raised by a factor of 2.5 for spectrum (A) and for spectrum (B) by a factor of 2.0 ($\nu < 350\ cm^{-1}$) and 5.0 ($\nu > 350\ cm^{-1}$).

melts of different compositions were recorded at 400°C (Fig. 4). The CsCl–$AlCl_3$ solvent in Fig. 4(A) is basic, allowing for the possible formation of $CsCuCl_2$. In this spectrum, a band at 300 cm^{-1} is observed together with the usual bands from $AlCl_4^-$. In Fig. 4(B), the solvent is acidic. Four bands are still observed due to $AlCl_4^-$, although two bands are slightly shifted towards lower frequencies (125 → 117 cm^{-1} and 182 → 177 cm^{-1}). In addition to the 310 cm^{-1} band of $Al_2Cl_7^-$, two bands at 220 and 422 cm^{-1} are also seen.

CuCl *in basic solvent.* A series of Raman spectra of $KAlCl_4$ solvent melts with $KCuCl_2$ added at formal concentrations between 1.91 and 3.72 showed the same bands as in Fig. 3(C). With increasing additions of $KCuCl_2$ the 285 cm^{-1} band increased relative to the 350 cm^{-1} band. This indicates that the 285 cm^{-1} band is due to a copper chloride vibration.

For the CuCl–CsCl–$AlCl_3$ melts, the 300 cm^{-1} band [in Fig. 4(A)] has the typical Raman position of linear $CuCl_2^-$ ions (known from organic solutions and solid compounds).

Cryoscopy: The formation of copper chloride complexes was further studied by cryoscopy. Figure 5 shows freezing point depression data for a neutral melt of $KAlCl_4$ during the addition of increasing amounts of $KCuCl_2$. Measured temperatures, compositions of the melts and the number of particles formed are listed in Table 2. These cryoscopic data unequivocally show that one particle, foreign to the solvent consisting of K^+ and $AlCl_4^-$, is formed per one added virgin $KCuCl_2$ particle.

The interpretation of this result is that the hypothetical reactions

$$KCuCl_2 \rightarrow K^+ + Cu^+ + 2Cl^- \quad (2)$$

$$KCuCl_2 \rightarrow K^+ + Cl^- + CuCl \quad (3)$$

can be excluded, since they produce three and two particles per $KCuCl_2$ (K^+ is common to the solvent). On the other hand, the reaction

$$KCuCl_2 \rightarrow K^+ + CuCl_2^- \quad (4)$$

is in accordance with the cryoscopic data, as are the series of homologuous reactions

$$\eta KCuCl_2 \rightarrow \eta K^+ + (\eta - 1)Cl^- + Cu_\eta Cl_{\eta+1}^- \quad (5)$$

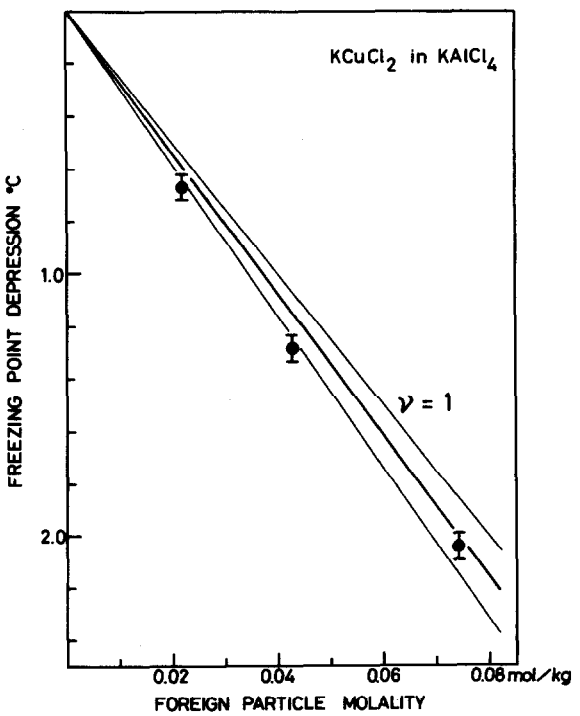

Fig. 5. Freezing point depression of $KCuCl_2$ in molten $KAlCl_4$. The lines show what one particle gives in theory, based on $\lambda = 27 \pm 2$°C kg mol^{-1}.

Table 2. Determination of the cryoscopic effect of $KCuCl_2$ on $KAlCl_4$[a]

Added sum of $KCuCl_2$ (mmol)	Molality, m_{KCuCl_2} (mol kg^{-1})	Observed freezing point, T_f (°C)	Depression, θ (°C)	Particle number, ν[b]
0	0	256.18	0	—
0.6097	0.02194	255.51	0.67	1.13
1.1893	0.04279	254.90	1.28	1.11
2.0571	0.07401	254.14	2.04	1.02

[a] The initial sample consisted of 27.7945 g of $KAlCl_4$, having an $AlCl_3$ mole fraction of 0.4990, calculated from weights.

[b] The particle number ν is defined as $\nu = \theta/\lambda m$, where λ is the cryoscopic constant of the solvent (here 27 ± 2°C kg mol^{-1}) and m is the molality in moles per kg of the solvent.

involving hypothetical ions like $Cu_2Cl_3^-$, $Cu_3Cl_4^-$, ..., $Cu_\eta Cl_{\eta+1}^-$. Such ions are not likely in melts (compare the crystal structure of KCu_2Cl_3).[1]

The common conclusion from the Raman spectra and the cryoscopic data is that copper(I) forms $CuCl_2^-$ in basic to neutral KCl–$AlCl_3$ and CsCl–$AlCl_3$ melts.

CuCl *in neutral solvents.* As mentioned previously, two liquid phases are observed when CuCl is added to neutral KCl–$AlCl_3$ melts (3.7 F CuCl in a melt of the composition $KCl/AlCl_3 = 1:1$) at 500°C. The top phase is colourless and the bottom phase is orange. On cooling the samples, the latter solidifies as the first one (at approximately 420°C). The Raman spectra of the two phases [Fig. 3(B) and (B′)] can be interpreted in the following way: the one band at 250 cm^{-1} observed in the bottom phase [Fig. 3(b)] corresponds in frequency and shape to the band observed by Gilbert *et al.*[11] for pure molten CuCl. Since the melting point and colour are also close to that of CuCl, it seems safe to conclude that the bottom phase mainly consists of CuCl. The Raman spectrum of the top phase [Fig. 3(B′)] only shows bands that can be assigned to $AlCl_4^-$ and $Al_2Cl_7^-$.

CuCl *in acidic solvents.* The Raman spectra of CuCl–KCl–$AlCl_3$ [Fig. 3(A)] and CuCl–CsCl–$AlCl_3$ [Fig. 4(B)] melts both show a polarized band at approximately 220 cm^{-1} in addition to the bands from the aluminum chloride vibrations. The band at 220 cm^{-1} is probably similar to the copper(I) chloride vibration observed in the CuCl–$AlCl_3$ melts, suggesting a non-linear coordination of Cu^I to chloride. In the case of CuCl–CsCl–$AlCl_3$, a band is observed at $\sim$ 422 cm^{-1}. This band can either be due to the $Al_2Cl_7^-$ vibration at 431 cm^{-1} in CsCl–$AlCl_3$ melts or to a splitting of the 493 cm^{-1} ν_3 vibration of $AlCl_4^-$. The latter explanation implies an association between Cu^+ and $AlCl_4^-$ as found for the CuCl–$AlCl_3$ melts.

Acknowledgements—Thanks are due to the Danish Council for Scientific and Industrial Research and to the Technical Chemistry Foundation for financial support (to J.H.v.B. and E.C.). E. Rytter (NTH, Trondheim) is thanked for valuable comments.

REFERENCES

1. C. Brink and C. H. MacGillavry, *Acta Cryst.* 1949, **2**, 158.
2. C. Brink, N. F. Binnendijk and J. van de Linde, *Acta Cryst.* 1954, **7**, 176.
3. K. Hildebrandt, P. G. Jones, E. Schwartsmann and G. Scheldrik, *Z. Naturforsch.* 1982, **376**, 1129.
4. H. E. Swanson, R. K. Fugat and G. M. Ugrinic, Nat. Bur. Std. Report No. 2691 (1953).
5. M. R. Lorenz and J. S. Prener, *Acta Cryst.* 1956, **9**, 538.
6. G. A. Bowmaker, L. D. Brockliss and R. Whiting, *Aust. J. Chem.* 1973, **26**, 29.
7. M. G. Newton, H. D. Gaughmann and R. G. Taylor, *J. Chem. Soc. (D)* 1970, 1227.
8. M. Asplund, S. Jagner and M. Nilsson, *Acta Chem. Scand.* 1983, **37A**, 57.
9. J. A. Creighton and E. R. Lippincott, *J. Chem. Soc.* 1963, 5134.
10. D. N. Waters and B. Basak, *J. Chem. Soc. (A)* 1971, 2733.
11. B. Gilbert, K. W. Fung, G. Manatov and G. M. Begun, *J. Inorg. Nucl. Chem.* 1975, **37**, 921.
12. M. M. Arski, *Z. Anorg. Allg. Chem.* 1971, **386**, 345.
13. P. Mirabel and J. Guion, *C.R. Acad. Sci. Paris* 1969, **269**, 516.
14. Z. Giazitzoglou, *Electrochim. Acta* 1983, **28**, 491.

15. P. Dantzer, *J. Phys. Chem.* 1981, **85**, 724.
16. P. Dantzer and O. J. Kleppa, *Inorg. Chem.* 1973, **12**, 2699.
17. K. Sakai and S. Hayashi, *J. Chem. Soc. Jpn* 1954, **75**, 186.
18. C. Sandonnini, *Gazz. Chim. Ital.* 1914, **44**, 297.
19. C. Sandonnini, *Gazz. Chim. Ital.* 1914, **44**, 302.
20. C. M. Fontana, E. Gorin, G. A. Kidder and C. S. Meridith, *Ind. Engng Chem.* 1952, **44**, 363.
21. R. Kanno, Y. Takeda, Y. Masuyama, O. Yamamoto and T. Takahashi, *Solid State Ionics* 1983, **11**, 221.
22. E. M. Levin, C. R. Robbins and H. F. McMurdie, *Phase Diagrams for Ceramists*, p. 4740. The American Ceramic Society, Columbus, U.S.A. (1964).
23. J. Kendall, E. D. Crittenden and H. K. Miller, *J. Am. Chem. Soc.* 1923, **45**, 977.
24. L. G. Boxall, H. L. Jones and R. A. Osteryoung, *J. Electrochem. Soc.* 1974, **121**, 212.
25. R. W. Berg, H. A. Hjuler and N. J. Bjerrum, *Inorg. Chem.* 1985, **24**, 4506.
26. W. Fichtner and A. Weiss, *Z. Naturforsch.* 1980, **356**, 170.
27. W. C. Laughlin and N. W. Gregory, *J. Phys. Chem.* 1976, **80**, 127.
28. R. Fehrmann, J. H. von Barner, N. J. Bjerrum and O. F. Nielsen, *Inorg. Chem.* 1981, **20**, 1972.
29. H. A. Hjuler, A. Mahan, J. H. von Barner and N. J. Bjerrum, *Inorg. Chem.* 1982, **21**, 402.
30. H. A. Andreasen, A. Mahan and N. J. Bjerrum, *J. Chem. Engng Data* 1981, **26**, 195.
31. J. H. von Barner, P. B. Brekke and N. J. Bjerrum, *Inorg. Chem.* 1985, **24**, 2162.
32. R. W. Berg, S. von Winbush and N. J. Bjerrum, *Inorg. Chem.* 1980, **19**, 2688.
33. H. A. Andreasen, N. J. Bjerrum and C. E. Foverskov, *Rev. Sci. Instrum.* 1977, **48**, 1340.
34. R. W. Berg, H. A. Hjuler and N. J. Bjerrum, *Inorg. Chem.* 1984, **23**, 557.
35. R. W. Berg, H. A. Hjuler and N. J. Bjerrum, *J. Chem. Engng Data* 1983, **28**, 251.
36. H. A. Andreasen, N. J. Bjerrum and N. H. Hansen, *J. Chem. Engng Data* 1980, **25**, 236.
37. R. W. Berg, T. L. Lauridsen, T. Østvold, H. A. Hjuler, J. H. von Barner and N. J. Bjerrum, *Acta Chem. Scand.* 1986, **A40**, 646.
38. W. Z. Klemm, *Anorg. Chem.* 1926, **152**, 235.
39. E. W. J. Mitchell and C. Raptis, *J. Phys. C. Solid State Phys.* 1983, **16**, 2973.
40. E. Rytter, H. A. Øye, S. J. Cyvin, B. N. Cyvin and P. J. Klæboe, *J. Inorg. Nucl. Chem.* 1973, **35**, 1185.
41. F. Torsi, G. Mamantov and G. M. Begun, *Inorg. Nucl. Chem. Lett.* 1970, **6**, 553.
42. B. P. Gilbert, F. Taulelle and B. Tremillon, *J. Raman Spect.* 1988, **19**, 1.
43. R. W. Berg and T. Østvold, *Acta Chem. Scand.* 1986, **A40**, 445.

Polyhedron Vol. 8, No. 3, pp. 333–340, 1989
Printed in Great Britain

0277–5387/89 $3.00+.00
Pergamon Press plc

STABILITY CONSTANTS AND STRUCTURES OF HOMOLOGOUS DINUCLEAR MOLYBDATE AND TUNGSTATE COMPLEXES OF ALDOSES BY POTENTIOMETRY AND ^{13}C AND ^{95}Mo NMR

J. F. VERCHERE*

Laboratoire de Chimie Macromoléculaire, U.A. 500 du CNRS, Université de Rouen, Faculté des Sciences, B.P. 118, 76134 Mont-Saint-Aignan Cedex, France

and

S. CHAPELLE

Laboratoire de RMN de l'Université de Rouen, Faculté des Sciences, B.P. 118, 76134 Mont-Saint-Aignan Cedex, France

(*Received* 18 *July* 1988; *accepted* 15 *August* 1988)

Abstract—A potentiometric study showed that aldoses of the *lyxo*-series: D-lyxose, D-mannose and L-rhamnose, form dinuclear anionic complexes with tungstate or molybdate ions in acidic solutions. ^{95}Mo NMR confirmed this result by revealing the presence of two non-equivalent metal atoms in the molybdate complexes. The corresponding formation constants were determined. The D-lyxose complexes had the higher stabilities, and the W^{VI} complexes were more stable than their Mo^{VI} homologues. The ^{13}C NMR spectra were reassigned by means of a 2-D experiment and showed that all three carbohydrates were complexed in pyranose form. The chelating hydroxyl groups were strongly deshielded and displayed increased direct coupling constants $^1J_{CH}$. It can be concluded that the prevailing species in aqueous acidic solution cannot be furanose complexes similar to that characterized in solid state from molybdate–D-lyxose mixtures.

Bilik's discovery[1] of an aldose epimerization reaction catalysed by Mo^{VI} in aqueous acidic solution has renewed the interest in the chemistry of molybdate complexes of sugars, which were not as well known as the related polyol complexes.[2] Although several studies by Weigel *et al.*[3–5] had established the formation of homologous molybdate or tungstate complexes of sugars in the 2:1 ratio, two polarimetric studies[6,7] concluded the existence of 1:1 molybdate–sugar species. However, a subsequent determination[8] of the structure of a crystalline molybdate–lyxose complex revealed a 2:1 stoichiometry, the ligand being complexed in furanose form. In solution, the structures of Mo^{VI}–sugar complexes have been investigated[9,10] by ^1H and ^{13}C NMR. It was suggested that the sugars were in pyranose form and that three hydroxyl groups chelated a metal atom. The ^{13}C spectra of W^{VI}–alditol complexes have been recently reported.[11]

Mechanistic studies[12–14] of the epimerization reaction have considered the above complexes as possible models for the reactive intermediate species. In this respect, further discussion would require the knowledge of the relative stabilities of such compounds. However, literature only afforded data[2,15] for the Mo^{VI} or W^{VI} complexes of two alditols, D-mannitol and D-glucitol. "Pseudo-stability constants" of tungstate carbohydrate complexes have been defined[16] from an electrophoretic study.

We have shown in a preliminary communication[17] that the affinities of polyhydroxy ligands towards tungstate and borate ions could be partially correlated. This paper presents a full report of the first determination of the thermodynamical stabilities of Mo^{VI} and W^{VI} complexes of aldoses. The ^{13}C NMR spectra of the most stable

*Author to whom correspondence should be addressed.

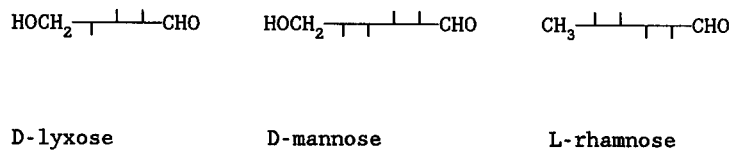

L-rhamnose is 6-deoxy-L-mannose.

Scheme 1.

complexes, formed with sugars of the *lyxo*-series (Scheme 1), were reinvestigated in order to precise their structures in aqueous solution. The ^{95}Mo spectra of Mo^{VI}–carbohydrate complexes were also obtained for the first time.

Potentiometric determination of formation constants

Since dinuclear complexes of Mo^{VI} and W^{VI} are generally formed with ligands of the carbohydrate family, the definition of "classical" stability constants appears impossible. As a matter of fact, uncomplexed dinuclear species of these elements do not exist in aqueous solution. Molybdate MoO_4^{2-} and tungstate WO_4^{2-} ions condensate in acidic medium to give heptameric isopolyanions $M_7O_{24}^{6-}$ (M stands for either Mo or W) and numerous other species. Detailed accounts on the composition of acidic solutions of molybdate[18,19] or tungstate[20] have been recently published. Therefore, it has become common practice to define the *formation constant* of a complex represented by (x, y, z) as the equilibrium constant of reaction (1):

$$xMO_4^{2-} + yL + zH^+ \rightleftharpoons (x, y, z)^{(2x-z)-} + nH_2O. \quad (1)$$

Souchay realized first[21] that since equilibrium (1) involved protons, pH measurements could be used to determine the stoichiometric coefficients x, y and z. This method was later developed for the determination of formation constants. Petterson[2] has reviewed and rationalized the large number of investigations on the D-mannitol–molybdate system, and Mikesova and Bartusek[15] have described an application to polyol complexes of Mo^{VI} and W^{VI}. The same principle was used to study the stabilities of carbohydrate complexes, but the procedure was adapted in order to obtain simultaneously their stoichiometries, which had been debated in the literature.

Principle

Let us admit that a unique complex of unknown composition (x, y, z) is formed by reaction (1). The charge of the complex is omitted for clarity. Its formation constant K_{xyz} is defined by relation (2):

$$K_{xyz} = (x, y, z)/(MO_4^{2-})^x(L)^y(H^+)^z. \quad (2)$$

Assuming K_{xyz} value is high, and using an excess of ligand, the addition of protons to a MO_4^{2-}–L mixture will form the complex in an almost quantitative amount. Hence, as observed earlier,[4,22,23] the titrations by a strong acid of molybdate and tungstate in the presence of various polyols and sugars define an equivalence point when exactly one proton per metal ion has been consumed, indicating that $x = z$.

From such titrations, a $pH_{1/2}$ value can be determined at the half-equivalence point. The equilibrium concentrations at this point are easily calculated from mass–balance relations:

$$(MO_4^{2-}) = c_M/2; \quad (x, y, z) = c_M/2x;$$
$$(L) = c_L - y(x, y, z),$$

in which c_M and c_L are the initial concentrations of MO_4^{2-} and L. Since ligand is in excess, generally $(L) \approx c_L$ and relation (2) becomes (3):

$$K_{xyz} = 2^{x-1}/x \cdot c_M^{x-1} \cdot c_L^y \cdot (H^+)_{1/2}^z, \quad (3)$$

which can be written in logarithmic form,

$$\log K_{xyz} = \log(2^{x-1}/x) - (x-1)\log c_M - y \log c_L + z\, pH_{1/2}. \quad (4)$$

EXPERIMENTAL

Materials

Mo^{VI} and W^{VI} stock solutions (0.1 mol l^{-1}) were prepared from disodium salts (Prolabo) and kept in polyethylene bottles. The carbohydrates of the purest analytical grade (Fluka or Aldrich) were used as obtained. The ionic strength of the solutions was kept constant ($I = 0.1$ mol l^{-1}) by the addition of KCl of analytical grade, and the titrations were made with standard HCl solutions (Prolabo Normadose).

Determination of formation constants

pH measurements were made using a Metrohm E 632 pH meter fitted with a combined Metrohm glass electrode. The temperature was maintained at 25°C by means of a water-jacketed cell and a thermostat.

In a typical experiment, a sodium molybdate or tungstate solution ($c_M = 5 \times 10^{-3}$ mol l^{-1}, $v = 100$ cm^3, KCl 0.1 mol l^{-1}) was first half-titrated with 2.50 cm^3 of HCl 0.1 mol l^{-1}. The sugar was then immediately added in solid form (0.5–1 g) to minimize dilution, and the pH was monitored for 15 min until stabilization. The operation was repeated four or five times to give the variations of $pH_{1/2}$ vs $\log c_L$. Then the titration was continued until the overall addition of 10 cm^3 of acid. A first equivalence point was observed at 5.00 ± 0.05 cm^3. In some cases, a second equivalence was found for 7.50 cm^3 of acid. The corresponding pK_a was determined at the half-equivalence point, corresponding to 6.25 cm^3 of acid and did not depend on c_M or c_L.

Some experiments were made using different c_M concentrations, typically 10^{-3} or 5×10^{-2} mol l^{-1}, in order to determine the variations of $pH_{1/2}$ vs $\log c_M$.

Attention was paid to the following points:

(a) The tungstate ions were not allowed to stay in acidic medium in the absence of ligand, because slow and irreversible condensation to inert dodecatungstates would occur.[24a]

(b) The glass electrodes were left in the solutions for the shortest possible time, in order to avoid their degradation by the molybdate or tungstate ions.[24b] Their quality was frequently checked with standard buffer solutions.

(c) We also verified that the use of large amounts of carbohydrates (> 0.1 mol l^{-1}) did not modify the values of the formation constants, as could have been expected from changing the aqueous solvent to water–sugar mixtures. This supposed effect could never be observed and was assumed to be smaller than the experimental errors.

NMR experiments

All 1-D and 2-D NMR spectra were recorded on a Bruker AM 400 spectrometer equipped with a 5 mm multinuclear probe.

Solution samples were prepared by dissolving weighted amounts of the reagents in 0.5 cm^3 of D_2O. The sugar concentration c_L was 1 mol l^{-1} and the metal/ligand ratio was 2.5. The solution was made acidic with concentrated aq. HCl (0.02 cm^3).

The ^{95}Mo spectra were measured at 26.076 MHz using sweep widths of 15,000 Hz and acquisition times of 30 ms. The chemical shifts were determined by the substitution method[25] using a 2 M Na_2MoO_4 solution in D_2O as reference. To reduce the effects of probe ringing on the baseline, left shifts were applied on the free induction decay prior to Fourier transform.

The following parameters were used for the ^{13}C spectra at 100.13 MHz: a sweep width of 8500 Hz, an acquisition time of 1 s and a digital resolution of 0.5 Hz/pt. The relaxation delay was 1 s and the pulse width corresponded to a 90° tip angle. The proton coupled spectra were obtained with nuclear overhauser enhancement by gating off the decoupler during data acquisition. The chemical shifts were referenced to TMS using an external C_6D_6 signal at 128 ppm.

RESULTS

Formation of (2,1,2) *complexes*

As the titration curves show that $x = z$, the x and y values can be obtained from the variations of $pH_{1/2}$ with $\log c_M$ and $\log c_L$, using another expression of relation (4), in which A is a constant term:

$$pH_{1/2} = A + (x - 1/x) \log c_M + (y/x) \log c_L.$$

In all the studied systems, plotting $pH_{1/2}$ vs $\log c_M$ or $\log c_L$ gave straight lines of slope = 0.50 within experimental error. We could conclude then that the stoichiometric coefficients were $x = 2$, $y = 1$ and $z = 2$, defining $(2,1,2)^{2-}$ formulae for the complexes.

The formation constants K_{212} were calculated using relation (5), obtained from relation (4) and the above stoichiometric coefficients:

$$\log K_{212} = 2pH_{1/2} - \log c_M - \log c_L. \qquad (5)$$

Examples of calculations for the three ligands, showing the variations of $pH_{1/2}$ vs $\log c_L$ at fixed c_M, are given in Table 1.

Formation of (2,1,3) *complexes*

A second protonation step occurred in the titrations of all molybdate complexes and was revealed by a second equivalence point when 3/2 protons had been consumed per metal atom. In agreement with other authors,[2,15] it was attributed to the formation of $(2,1,3)^-$ species:

$$(2,1,2)^{2-} + H^+ \rightleftharpoons (2,1,3)^-.$$

In the case of tungstate complexes, such a reaction was also observed in the case of L-rhamnose.

Table 1. Tungstate and molybdate complexes of aldoses of the *lyxo*-series. Variations of $pH_{1/2}$ (see text) with the ligand concentration c_L. Examples of calculations of formation constants. K_{212} is the formation constant of the (2,1,2) complex from $2MO_4^{2-}$, L and $2H^+$. $t = 25°C$; $I(KCl) = 0.1$ mol l^{-1}

m[a] (g)	c_L (mol l^{-1})	$\log c_L$	Tungstate complex $pH_{1/2}$	Tungstate complex $\log K_{212}$[b]	Molybdate complex $pH_{1/2}$	Molybdate complex $\log K_{212}$[b]
			D-Lyxose			
1.0	0.065	−1.19	7.30	18.10	5.75	15.00
1.5	0.0975	−1.01	7.39	18.10	5.84	15.00
2.0	0.130	−0.89	7.45	18.10	5.90	15.00
2.5	0.163	−0.79	7.49	18.08	5.93	14.96
3.0	0.195	−0.71	7.53	18.08	5.97	14.96
			D-Mannose			
1.0	0.054	−1.27	6.96	17.50	5.47	14.52
2.0	0.108	−0.97	7.11	17.50	5.61	14.50
3.0	0.162	−0.79	7.20	17.50	5.69	14.48
4.0	0.216	−0.67	7.26	17.50	5.75	14.48
5.0	0.270	−0.57	7.30	17.48	5.79	14.46
			L-Rhamnose			
1.0	0.054	−1.27	6.74	17.06	5.17	13.92
2.0	0.107	−0.97	6.88	17.04	5.31	13.90
3.0	0.160	−0.79	6.97	17.04	5.39	13.88
4.0	0.214	−0.67	7.03	17.04	5.45	13.87
5.0	0.267	−0.57	7.08	17.04	5.50	13.88

[a] m: Mass of D-lyxose, M = 150.15 g mol^{-1}, in 102.5 cm^3; mass of D-mannose, M = 180.16 g mol^{-1}, in 102.5 cm^3; mass of L-rhamnose hydrate, M = 182.18 g mol^{-1}, in 102.5 cm^3.

[b] Calculated using eq. (5); c_{Mo} or $c_w = 4.88 \times 10^{-3}$ mol l^{-1}.

On the other hand, no further protonation could be observed with D-lyxose and D-mannose.

The corresponding pK_a were determined as usual:

$$K_a = [(2,1,2)^{2-}](H^+)/[(2,1,3)^-].$$

The formation equilibrium of these species were written:

$$2MO_4^{2-} + L + 3H^+ \rightleftharpoons (2,1,3)^- + nH_2O.$$

Their formation constants K_{213} could be calculated as a combination of K_a and of K_{212}: $\log K_{213} = \log K_{212} + pK_a$.

The different formation constants are presented in Table 2.

NMR spectroscopy

The uncomplexed sugars in aqueous solution exist as a mixture of the α- and β-pyranose anomers.

Table 2. Formation constants ($t = 25°C$; $I(KCl) = 0.1$ mol l^{-1}) of molybdate and tungstate complexes of sugars of the *lyxo*-series. $\log K_{xyz}$ refers to the formation of the (x, y, z) species from xMO_4^{2-}, yL and zH^+. K_a is the acidity constant of the (2,1,3) complex

Carbohydrate	D-Lyxose		D-Mannose		L-Rhamnose	
Metal ion M	Mo^{VI}	W^{VI}	Mo^{VI}	W^{VI}	Mo^{VI}	W^{VI}
$\log K_{212}$	14.98	18.08	14.50	17.50	13.89	17.04
pK_a	3.70	—	3.60	—	3.70	3.50
$\log K_{213}$	18.68	—	18.10	—	17.59	20.54

Accuracy: $\log K_{212} \pm 0.06$; $\log K_{213} \pm 0.11$.

Their complexes were formed by adding MoO_4^{2-} or WO_4^{2-} ions and acidifying by HCl. To increase complex formation, a small excess of metal was used (metal/ligand ratio = 2.5).

^{13}C NMR allowed the identification of the complexes in the presence of unbound ligand. Only one complex of D-lyxose was revealed (five new signals) with either Mo or W, and the chemical shifts did not depend on the nature of the metal. On the contrary, D-mannose formed several complexes in unequal ratio (from the comparison of signal intensities). The prevailing one showed a spectrum very similar to those of D-lyxose. The other species are currently under study.

In the case of L-rhamnose, only one tungstate complex could be observed, with the same pattern as those of the homologues described above. In contrast, molybdate formed two complexes in equal ratio, one of them was similar to the unique tungstate species.

The ^1H NMR spectra were determined and agreed closely with those reported[9] by Alfoldi *et al.*, who found that the $^3J_{HH}$ coupling constants had values characteristic of a pyranoid ring. It allowed us to perform a 2-D heteronuclear ^{13}C–^1H correlation experiment which gave the complete assignment of the ^{13}C spectrum of the D-lyxose complex. A comparison with Alfoldi *et al.*'s earlier assignments[10] showed that the C-2 and C-3 signals had been incorrectly attributed. Using the remarkable analogies between the ^{13}C spectra of these three sugars which belong to the same configurational series, the spectra of the complexes of D-mannose and L-rhamnose were readily assigned (Tables 3 and 4).

A ^{95}Mo NMR spectrum was determined for each sugar (Fig. 1) and displayed two characteristic signals for the complexed Mo^{VI} at $\delta = 30 \pm 4$ ppm and $\delta = 42 \pm 1$ ppm by reference to external MoO_4^{2-}. The presence of other complexes in low proportion broadened both signals for the complexes of D-mannose and L-rhamnose and could even give a supplementary signal in the case of L-rhamnose. The treatment of the signals by a Gaussian function before Fourier Transform improved the resolution and permitted us to determine the linewidths: < 90 Hz for D-lyxose, and between 150–180 Hz for D-mannose and L-rhamnose. Such differences between the sugars agree with the expected increase of the linewidths with the molecular radii. The sharpness of the signals nevertheless indicated that Mo^{VI} was situated in a relatively symmetrical environment. Moreover, both signals were always of identical intensities, showing that they must be assigned to two non-equivalent Mo atoms present in the dinuclear complexes.

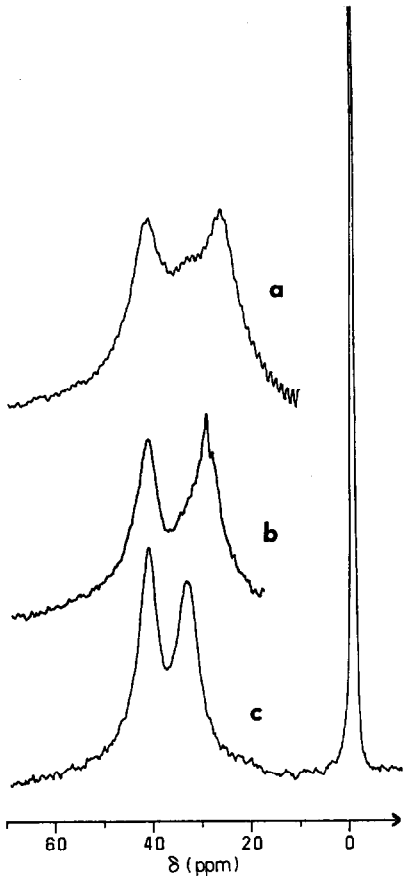

Fig. 1. 26.076 MHz ^{95}Mo NMR spectra of solutions of sodium molybdate (2.5 mol l^{-1}) and aldoses (1 mol l^{-1}) of the *lyxo*-series at pH ≈ 5. t = 20°C. (a) L-rhamnose; (b) D-mannose; (c) D-lyxose. The signal at $\delta = 0$ ppm is due to uncomplexed MoO_4^{2-} ions.

DISCUSSION

Structures of the complexes

The results of the potentiometric study prove without doubt that the complexes involve dinuclear species of Mo^{VI} and W^{VI} combined with one molecule of sugar. Although the measurements were made using a large excess of ligand, we did not detect the presence of 1 : 1 complexes, as had been claimed[6,7] in earlier reports. It is confirmed by the ^{95}Mo NMR study which clearly revealed the presence of two non-equivalent Mo atoms in the complexes of the three studied ligands.

The striking similarity of all the ^{13}C NMR spectra indicates that the three ligands have closely related structures in their Mo and W complexes. This method allows the identification of the carbons bearing the bonding hydroxyls, which appear strongly deshielded[10,11] and show increased values of their direct coupling constant $^1J_{CH}$.

Acyclic structures of the ligands were excluded, since no ^{13}C signals for terminal CHO groups were observed in the 150–200 ppm region.

Table 3. ^{13}C chemical shifts and direct coupling constants $^{1}J_{CH}$ of D-lyxose, D-mannose and of their molybdate and tungstate complexes

Ligand	Carbon position 1	2	3	4	5	6
D-*Lyxose*						
δ (ppm) in L(α-py)	95.6	71.3	71.9	69.0	64.5	
$^{1}J_{CH}$ (Hz)	168	146	146	144	147	
δ (ppm) in L(β-py)	95.6	71.3	73.8	68.0	65.3	
$^{1}J_{CH}$ (Hz)	162	146	146	144	147	
Molybdate complex						
δ (ppm)	112.8	84.1	87.7	81.2	68.5	
$^{1}J_{CH}$ (Hz)	177	158	155	151	145	
$\Delta\delta$ (ppm)/β-py	17.2	12.8	13.9	13.2	3.2	
ΔJ (Hz)/β-py	15	12	9	7	−2	
Tungstate complex						
δ (ppm)	112.9	84.6	88.3	81.6	68.8	
$^{1}J_{CH}$ (Hz)	174	156	154	154	144	
$\Delta\delta$ (ppm)/β-py	17.3	13.3	14.5	13.6	3.5	
ΔJ (Hz)/β-py	12	10	8	10	−3	
D-*Mannose*						
δ (ppm) in L(α-py)	95.4	72.0	71.5	68.1	73.7	62.3
$^{1}J_{CH}$ (Hz)	171[a]	148	143	143	146	144
δ (ppm) in L(β-py)	95.0	72.6	74.3	68.0	77.4	62.4
$^{1}J_{CH}$ (Hz)	161[a]	148	143	143	142	144
Molybdate complex						
δ (ppm)	112.7	84.6	88.8	80.2	79.8	65.3
$^{1}J_{CH}$ (Hz)	178	156	155	152	145	145
$\Delta\delta$ (ppm)/β-py	17.7	12.0	14.5	12.2	2.4	2.9
ΔJ (Hz)/β-py	17	8	12	9	3	1
Tungstate complex						
δ (ppm)	112.7	84.0	88.0	79.7	79.7	65.2
$^{1}J_{CH}$ (Hz)	180	157	157	153	148	142
$\Delta\delta$ (ppm)/β-py	17.7	11.4	13.7	11.7	2.3	2.8
ΔJ (Hz)/β-py	19	9	14	10	6	−2

[a] Lit. values[26] for C-1 of L-mannose: 170.4 Hz(α-py), 160.7 Hz(β-py).
Aldose assignments from ref. 27.
Ligand assignments from a 2-D experiment on D-lyxose (see text).
Accuracy: $^{1}J_{CH}$ values ± 2 Hz; δ values ± 0.1 ppm.

Table 4. ^{13}C chemical shifts and direct coupling constants $^{1}J_{CH}$ of L-rhamnose and of its molybdate and tungstate complexes

Ligand	Carbon position 1	2	3	4	5	6
L-Rhamnose						
δ (ppm) in L(α-py)	95.0	71.9	71.2	73.3	69.4	18.4
$^{1}J_{CH}$ (Hz)	169	147	142	145	143	127
δ (ppm) in L(β-py)	94.8	72.8	74.0	73.2	73.4	18.4
$^{1}J_{CH}$ (Hz)	161	147	142	147	145	127
Molybdate complex						
δ (ppm)	112.3	84.6	89.0	83.9	75.6	23.5
$^{1}J_{CH}$ (Hz)	178	156	153	151	146	126
$\Delta\delta$ (ppm)/β-py	17.5	11.8	15.0	10.7	2.2	5.1
ΔJ (Hz)/β-py	17	9	11	4	1	−1
Tungstate complex						
δ (ppm)	112.5	84.0	88.3	83.3	75.8	23.4
$^{1}J_{CH}$ (Hz)	182	156	156	149	146	125
$\Delta\delta$ (ppm)/β-py	17.7	11.2	14.3	10.1	2.4	5.0
ΔJ (Hz)/β-py	21	9	14	2	1	−2

Aldose assignments from ref. 27.
Ligand assignments from a 2-D experiment on D-lyxose (see text).
Accuracy: $^{1}J_{CH}$ values ± 2 Hz; δ values ± 0.1 ppm.

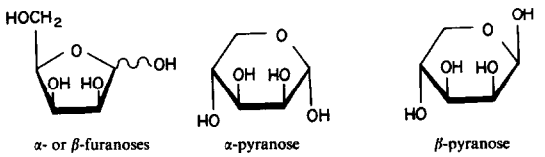

α- or β-furanoses α-pyranose β-pyranose

Fig. 2. Haworth's formulae of the cyclic forms of D-lyxose.

In the case of D-lyxose, the pyranose or furanose nature of the cyclic form adopted by the ligand was deduced by remarking that the signal of the C-5 methylene carbon was little affected by complexation (Table 3). It contrasted with the behaviour of all other methine carbons, which were deshielded and displayed increased direct coupling constants. Thus the metal ion was bound to the four vicinal hydroxyls borne by C-1 to C-4, and not to the C-5 one. Since the carbon which bears no hydroxyl is C-5 in pyranose form and C-4 in furanose form (Fig. 2), it is obvious that D-lyxose is not complexed in furanose form.

It is difficult to decide whether the α- or β-pyranose form is involved in the complexes because the spectra of both uncomplexed pyranoses are very similar, which leads to almost equal chemical shift variations in both hypotheses. We favour the β-form on the basis of structural considerations, since the C-1 and C-2 hydroxyls are in *trans*-orientation in the α-form (Fig. 2). In this hypothesis, complexation has a deshielding effect of ≈ 10–15 ppm on the carbons C-2 to C-4 which bear bound hydroxyl groups. A larger effect, 17–18 ppm, is observed on C-1 which bear the anomeric OH group. The difference observed between C-1 and C-2, compared to the almost equal effect on C-3 and C-4 (which are in *trans*-orientation) suggests that C-1 and C-2 are orientated *cis*. This is another argument in favour of a β-pyranose structure of the ligands.

A final conclusion is that the dinuclear metallic core is chelated in an assymetric fashion by four OH groups of the ligand. This result disagrees with earlier interpretations[9,10] in which the ligand was assumed to be tridentate. A tentative assignment of the ^{95}Mo NMR signals was made by remarking that the 42 ppm signal did not depend on the sugar nature. Since the three sugars have identical configurations at C-1 to C-4, but differ at C-5, this signal was likely due to an Mo atom coordinated to C-1 and neighbouring hydroxyl groups. The more shielded signal at ≈ 30 ppm shifted by changing the sugar and should then be attributed to the Mo atom bound to C-4 and neighbouring hydroxyl groups.

Stabilities of the complexes

It was surprising to find that the tungstate complexes were nearly three orders of magnitude more stable than their molybdate homologues (Table 2), whereas both elements generally form complexes of similar stabilities.[28,29] The same finding was nevertheless reported[15] in the case of alditol complexes, indicating that the phenomenon could be specific for polyhydroxy ligands. However, we think that it does not necessarily implicate a particular affinity of tungstate towards this type of ligand, but can be a consequence of the dinuclear nature of the complexes. It is well known[20] that tungstate forms polyanions more easily then molybdate, and since the formation constants include a term due to the dimerization of the MO_4^{2-} ions, it is likely that the values calculated for W^{VI} might be higher than those relative to Mo^{VI}.

Accordingly, the differences between the $\log K_{212}$ values determined for W^{VI} and Mo^{VI} appear to be almost independent of the nature of the sugar, which is a strong indication that they may be due to intrinsic properties of the inorganic elements.

Considering now the ligands, the fact that D-lyxose and D-mannose form complexes of higher stabilities than those of all other known aldoses[17] and that they possess similar pyranose structures must be related to their belonging to the same configurational series, if carbons C-1 to C-4 are considered. It is another proof that complexation does not involve the CH_2OH groups of the ligands.

Since the stability order of tungstate complexes of pentoses has been shown[17] to be: D-lyxose > D-ribose > D-arabinose > D-xylose, and that the same order seems to hold for molybdate[9] complexes, it appears that a C-2, C-3 diol group of *erythro*-configuration is a much more favourable site for complexation than a *threo*-diol group. A related observation was made[17] in the alditol series, in which erythritol formed more stable W^{VI} complexes than DL-threitol.

On the other hand, the presence of the supplementary C-6 hydroxyl group in D-mannose does not seem to be favourable to complexation, since the D-lyxose complexes are the most stable. Yet, the even lower stabilities of the L-rhamnose complexes suggest that two opposite effects operate: an unfavourable steric hindrance of the C-5 substituent and a favourable influence of a hydroxyl group borne by C-6.

In conclusion, our results support dinuclear structures like those proposed long ago[5] by Angus, Bourne and Weigel for alditol complexes, which were recently confirmed.[11] Nevertheless, since the pyranose cycles are more rigid than the acyclic alditols, an adequate configuration of the four chelating hydroxyls (*lyxo* or *ribo*) is compulsory to accommodate the metallic core. Another possible model is given by the well-characterized bis(oxalate)–

dimolybdate complex[30] which can be written:

$[(C_2O_4)(H_2O)MoO_2—O—MoO_2(C_2O_4)(H_2O)]^{2-}$.

Because each Mo atom is chelated by a separate oxalate ligand, there is no steric strain in the compound and the Mo—O—Mo bridge was found[30] to be linear. However, in the carbohydrate complexes, the four chelating OH groups must be borne by the same molecule. Thus, in order to shorten the Mo—Mo distance, the metal ion may adopt a bent Mo—O—Mo bridged structure, and also form additional oxygen bridges. As a matter of fact, the dimolybdate–lyxose complex[8] characterized in the solid state was found to possess three Mo—O—Mo bridges, and a similar structure was later reported[31] for (bis)*ortho*quinone–dimolybdate complexes. It is clear however that since the aldoses studied in this paper were demonstrated to adopt the pyranose form in their complexes, furanose compounds analogous to that described by Taylor and Waters[8] could not be the prevailing species in aqueous acidic solution.

REFERENCES

1. (a) V. Bilik, *Chem. Zvesti* 1972, **26**, 183, 187, 372; (b) V. Bilik, W. Voelter and E. Bayer, *Angew. Chem. Int. Ed. Eng.* 1971, **10**, 909.
2. L. Petterson, *Acta Chem. Scand.* 1972, **26**, 4067 and references therein.
3. E. J. Bourne, D. H. Hutson and H. Weigel, *J. Chem. Soc.* 1960, 4252.
4. H. J. F. Angus and H. Weigel, *J. Chem. Soc.* 1964, 3994.
5. H. J. F. Angus, E. J. Bourne and H. Weigel, *J. Chem. Soc.* 1965, 21.
6. J. T. Spence and S. Kiang, *J. Org. Chem.* 1963, **28**, 244.
7. L. Velluz and M. Legrand, *C. R. Acad. Sci. Paris* 1966, **263**, 1429.
8. G. E. Taylor and J. M. Waters, *Tetrahedron Lett.* 1981, **22**, 1277.
9. J. Alfoldi, L. Petrus and V. Bilik, *Collect. Czech. Chem. Commun.* 1978, **43**, 1476.
10. J. Alfoldi, V. Bilik and L. Petrus, *Collect. Czech. Chem. Commun.* 1980, **45**, 123.
11. E. Llopis, J. A. Ramirez and A. Cervilla, *Polyhedron* 1986, **5**, 2069.
12. V. Bilik, L. Petrus and J. Zemek, *Chem. Zvesti* 1978, **32**, 242.
13. M. L. Hayes, N. L. Pennings, A. S. Serianni and R. Barker, *J. Am. Chem. Soc.* 1982, **104**, 6764.
14. B. Klaic, Z. Raza, M. Sankovic and V. Sunjic, *Helv. Chim. Acta* 1987, **70**, 59.
15. M. Mikesova and M. Bartusek, *Collect. Czech. Chem. Commun.* 1978, **43**, 1867.
16. H. J. F. Angus, J. Briggs, N. A. Sufi and H. Weigel, *Carbohydr. Res.* 1978, **66**, 25.
17. J. F. Verchère and J. P. Sauvage, *Bull. Soc. Chim. Fr.* 1988, 263.
18. J. J. Cruywagen and J. B. B. Heyns, *Inorg. Chem.* 1987, **26**, 2569.
19. K. H. Tytko, G. Baethe and J. J. Cruywagen, *Inorg. Chem.* 1985, **24**, 3132.
20. J. J. Cruywagen and I. F. J. van der Merwe, *J. Chem. Soc., Dalton Trans.* 1987, 1701.
21. P. Souchay, *Bull. Soc. Chim. Fr.* 1949, 122.
22. R. A. Chalmers and A. G. Sinclair, *J. Inorg. Nucl. Chem.* 1967, **29**, 2065.
23. A. G. Sinclair, *Talanta* 1969, **16**, 459.
24. G. Goldstein, C. M. Wolff and J. P. Schwing, *Bull. Soc. Chim. Fr.* 1971, (a) 1195; (b) 1201.
25. G. Brévard and P. Granger, *Handbook of High Resolution Multinuclear NMR*, p. 40. Wiley, New York (1981).
26. T. E. Walker, R. E. London, T. W. Whaley, R. Barker and N. A. Matwiyoff, *J. Am. Chem. Soc.* 1976, **98**, 5807.
27. K. Bock and C. Pedersen, *Adv. Carbohydr. Chem. Biochem.* 1983, **41**, 27.
28. S. Natansohn, J. I. Krugler, J. E. Lester, M. S. Chagnon and R. S. Finocchiaro, *J. Phys. Chem.* 1980, **84**, 2972.
29. R. J. Kula and D. L. Rabenstein, *Analyt. Chem.* 1966, **38**, 1934.
30. F. A. Cotton, S. M. Morehouse and J. S. Wood, *Inorg. Chem.* 1964, **3**, 1603.
31. C. G. Pierpont and R. M. Buchanan, *J. Am. Chem. Soc.* 1975, **97**, 6450.

Polyhedron Vol. 8, No. 3, pp. 341–349, 1989
Printed in Great Britain

0277–5387/89 $3.00+.00
© 1989 Pergamon Press plc

SYNTHESIS AND INTRAMOLECULAR COUPLING OF TANTALUM η^2-IMINOACYL (η^2-RNCR′) AND η^2-IMINE (η^2-RNCR′$_2$) FUNCTIONAL GROUPS

LINDA R. CHAMBERLAIN, BRYAN D. STEFFEY and IAN P. ROTHWELL*

Department of Chemistry, Purdue University, West Lafayette, IN 47907, U.S.A.

and

JOHN C. HUFFMAN

Molecular Structure Center, Indiana University, Bloomington, IN 47405, U.S.A.

(*Received* 29 *March* 1988; *accepted* 17 *August* 1988)

Abstract—The migratory insertion of organic isocyanides into the metal–carbon bonds of a series of tri-alkyls, $Ta(OAr)_2R_3$ (OAr = 2,6-dimethylphenoxide; R = CH_3, CH_2Ph), has been examined. Addition of 2,6-dimethylphenyl- or 2,6-di-isopropylphenylisocyanide (Ar′NC $\geqslant$ 2 equivalents) results in the essentially quantitative formation of the bis-insertion products, $Ta(OAr)_2(\eta^2\text{-}Ar'NCR)_2R$ (**1**). Spectroscopic as well as structural data are consistent with both iminoacyls being η^2-bound to the metal centre. In contrast, addition of *tert*-butylisocyanide to the tris-aryl $Ta(OAr)_2Ph_3$ proceeds to produce a mixed η^2-imine, η^2-iminoacyl compound $Ta(OAr)_2(\eta^2\text{-}Bu^tNCPh_2)(\eta^2\text{-}Bu^tNCPh)$ (**2**). This compound is presumably formed by a second phenyl group migration taking place in an intermediate of type (**1**). All of these compounds exhibit thermal instability to varying degrees. The methyl compound $Ta(OAr)_2(\eta^2\text{-}Ar'NCMe)_2(Me)$ rearranges over days at 25°C to produce a mixed amido, imido complex $Ta(OAr)_2(Ar'NCMe{=}CMe_2)(NAr')$ (**3a**). This is believed to be formed by intramolecular coupling and fragmentation in an intermediate, $Ta(OAr)_2(\eta^2\text{-}Ar'NCMe_2)(\eta^2\text{-}Ar'NCMe)$ of type (**2**). Support for this hypothesis comes from thermolysis of (**2**) to produce $Ta(OAr)_2(Bu^tNCPh{=}CPh_2)(NBu^t)$ (**3b**) which has been structurally characterized. The benzyl derivatives $Ta(OAr)_2(\eta^2\text{-}Ar'NCCH_2Ph)_2(CH_2Ph)$ also thermally produce mixed imido, amido compounds, only this time more dramatic fragmentation occurs to produce $Ta(OAr)_2(Ar'NCH_2CH_2Ph)(NAr')$ (**4**) and an organic fragment, $PhCH_2C{\equiv}CPh$. Structural studies confirmed this formulation. Mechanistic aspects of the reactivity of these η^2-iminoacyl and η^2-imine functionalities are discussed. Crystal data for $TaC_{48}H_{61}N_2O_2$ (**3b**) at −158°C are $a = 21.806(5)$, $b = 19.568(6)$, $c = 10.078(2)$ Å, $\beta = 90.63(1)°$, $Z = 4$, $d_{calc} = 1.358$ g cm^{-3}, in space group $P2_1/n$. Of the 5642 unique intensities collected with Mo-K_α, the 4790 with $F > 2.33\sigma(F)$ were used in the least-squares refinement to yield $R = 0.0419$, $R_w = 0.0439$. Crystal data for $TaC_{44}H_{51}N_2O_2$ (**4**) at −155°C are $a = 12.423(5)$, $b = 20.772(10)$, $c = 14.840(6)$ Å, $\beta = 93.27(2)°$, $Z = 4$, $d_{calc} = 1.426$ g cm^{-3} in space group $P2_1/n$. Of the 5004 unique intensities collected with Mo-K_α, the 3209 with $F_o > 3.00\ \sigma(F)$ were used in the least-squares refinement to yield $R = 0.0574$, $R_w = 0.0498$.

The migratory insertion of carbon monoxide into transition metal alkyl bonds is an important reaction which has deservedly received considerable resarch interest.[1–3] In the case of the high valent early *d*-block, lanthanide and actinide metals, the resulting acyl group is found exclusively to adopt an η^2-bound mode and exhibit a diverse range of reactivity.[4–8] A particularly characteristic reaction involves either the inter- or intramolecular coupling of these groups to produce *cis* and *trans* ene–diolate

*Author to whom correspondence should be addressed.

linkages.[7,8] The intramolecular version of this carbon–carbon double bond forming reaction has received mechanistic/theoretical treatment.[9] In the case of the isoelectronic η^2-iminoacyl group formed by the migratory insertion of organic isocyanides into metal–alkyl bonds,[10] we have demonstrated related reactivity.[10–12] Hence, intramolecular coupling to produce ene–diamide ligands has been observed, as well as the cross-coupling of acyls and iminoacyls to produce enamidolates.[11,12] Reactivity studies have indicated that acyl groups undergo these carbon–carbon bond forming reactions much faster than their nitrogen analogues.[13]

However, another important carbon–carbon bond forming reaction of η^2-acyls involves their further reduction by metal–alkyl bonds. Hence, there are numerous reports of ketone formation (either liberated or metal-bound) during carbonylation of early metal alkyls.[14,15] This pathway is a crucial step in the metal mediated reduction of CO, and in the case of metal–hydrides this type of reactivity (both inter- and intramolecular) has been extensively studied.[4–6,16] In the case of η^2-iminoacyls, the formation of imines has recently been documented[17] as well as further reduction to produce amido ligands.[18] During our studies of the reactivity of aryloxide supported metal–η^2-iminoacyl groups we have also observed facile η^2-imine formation under certain conditions.[17] In this paper we wish to report the formation and characterization of a series of tantalum η^2-imine complexes and their ensuing reactivity.

RESULTS AND DISCUSSION

Synthesis of η^2-imine and η^2-iminoacyl compounds

The reaction of the tris-alkyl compounds $Ta(OAr)_2R_3$ (OAr = 2,6-dimethylphenoxide, R = CH_3, CH_2Ph, Ph) with two or more equivalents of 2,6-dimethyl- or 2,6-di-isopropylphenylisocyanide results in the formation of the corresponding bis(η^2-iminoacyl) compounds (**1**) (Scheme 1). Attempts to insert a further equivalent of isocyanide proved fruitless. The solid state structure of (**1a**) has been reported previously.[10] The iminoacyl groups are seen to be both η^2-bound to the tantalum atom, and arranged so as to occupy four equatorial sites in a pentagonal bipyramidal coordination sphere. The carbon atoms of the iminoacyls are mutually *cis* with a C—Ta—C angle of 111.8(2)°. The spectroscopic data for all of the bis(η^2-iminoacyl) compounds (**1**) is entirely consistent with their adopting the same geometry in solution.[10] Especially characteristic is the chemical shift for the iminoacyl carbons at δ 245–260 ppm in the ^{13}C NMR spectrum. The observed arrangements of the two iminoacyl groups in compounds of type (**1**) is exactly the conformation one might initially expect prior to intramolecular coupling to produce an ene–diamido ligand. However, although all of these bis(η^2-iminoacyls) exhibit thermal reactivity to various degrees (*vide infra*) we have as yet to detect any ene–diamide derivative formed by their thermolysis. This contrasts with the clean (albeit high temperature) intramolecular coupling observed for $Ta(OAr)_3(\eta^2\text{-}ArNCCH_2Ph)_2$ to produce $Ta(OAr)_3[ArNC(CH_2Ph){=}C(CH_2Ph)NAr]$.[11,12] Theoretical studies of this coupling reaction at Group 4 metals as well as on the related intramolecular coupling of η^2-acyl groups at Cp^*_2M (M = Th, U) centres indicate that a concerted, in-plane formation of the carbon–carbon double bond is a symmetry disallowed, high energy pathway.[9,13,19] In the case of the bis(η^2-iminoacyl) compounds that contain only aryloxide ligation, it appears that there are no alternate reaction pathways besides ene-diamide formation. However, for mixed alkyl, η^2-iminoacyls, thermal reactivity proceeds via a more facile reaction sequence (*vide infra*).

$$Ta(OAr)_2R_3 + 2R'NC \longrightarrow Ta(OAr)_2(\eta^2\text{-}R'NCR)_2(R)$$

	R	R′
(**1a**)	CH_3	Ar
(**1b**)	CH_2Ph	Ar
(**1c**)	Ph	Ar
(**1d**)	CH_3	Ar′
(**1e**)	CH_2Ph	Ar′

Ar = 2,6-dimethylphenyl;
Ar′ = 2,6-di-isopropylphenyl

Scheme 1.

The addition of *tert*-butylisocyanide to the triphenyl compound $Ta(OAr)_2Ph_3$ results in the rapid formation of a different type of derivative (**2**) (Scheme 2) in high yield. Spectroscopic data for (**2**) are consistent with it containing both an η^2-iminoacyl group as well as an η^2-imine function. This latter function results from a double alkyl migration to an organic isocyanide molecule, presumably via an intermediate η^2-iminoacyl of type (**1**).[17] However, attempts to spectroscopically (^1H NMR) detect an intermediate of type (**1**) in this reaction failed. The mild, pyridine induced formation of an η^2-imine compound from a mixed alkyl, η^2-iminoacyl compound has previously been demonstrated at Ti^{IV} aryloxide metal centres.[17] The two different types of metal-bound tertiary carbon atoms are clearly evident in the ^{13}C NMR spectrum of (**2**), appearing at δ 247.8 (η^2-Bu^t*N*CPh) and δ 78.8 ppm (η^2-Bu^{t}B*N*CPh_2). This latter value is in close proximity to those reported for other η^2-imine ligands

$$Ta(OAr)_2Ph_3 + 2Bu^tNC \longrightarrow Ta(OAr)_2(\eta^2\text{-}Bu^tNCPh_2)(\eta^2\text{-}Bu^tNCPh)$$
(2)

Scheme 2.

attached to Ta^{V}[20] and related d^0-metal centres.[21] A significant separation of the two types of N*Bu*^{t} groups is also observed in the ^{1}H NMR spectra, δ 0.78 and 1.50 ppm.

Thermal reactivity

Both types of compounds (**1**) and (**2**) exhibit thermal instability to varying degrees. In the case of the methyl derivative (**1a**), the compound will convert over days at 25°C in hydrocarbon solvents into a new tantalum compound (**3a**). The reaction can be readily monitored by ^{1}H NMR and spectra indicate that the conversion of (**1a**) to (**3a**) is essentially quantitative with no detectable intermediates. The spectroscopic data on (**3a**) is consistent with its formulation as a mixed imido, amido compound $Ta(OAr)_2(=NAr)(ArNCMe{=}CMe_2)$ as shown (Scheme 3). Specifically the ^{1}H NMR spectrum clearly shows the three non-equivalent methyl groups of the vinyl–amido function ($ArNCMe{=}CMe_2$) as well as the non-equivalent N-xylyl methyl resonances. We believe that (**3a**) is formed via initial formation of a very reactive η^2-imine, η^2-iminoacyl intermediate of type (**2**). This idea has excellent support by the product obtained on thermolysis of the isolated η^2-imine derivative (**2**). Mild thermolysis in toluene or benzene solution leads to an analogous product (**3b**), containing a triphenyl substituted vinyl linkage (Scheme 4). A plausible pathway for the reaction involves initial coupling of the η^2-imine and η^2-iminoacyl groups followed by fragmentation as shown (Scheme 5). The formulation of (**3b**) was confirmed by a single crystal X-ray diffraction study (Fig. 1). Table 1 contains some selected bond distances and angles for (**3b**). The molecular structure of (**3b**) (Fig. 1) can be seen to consist of an approximately tetrahedral arrangement of two oxygen and two nitrogen atoms around the tantalum metal centre. The aryloxide coordination, with relatively short Ta—O distances and large Ta—O—Ar angles, is unexceptional for this group bound to d^0-metal centres.[2] The Ta—NBu^t distance of 1.766(13) Å is comparable to those found for other tantalum(V) organoimido compounds as is the expected, almost linear, Ta—N—Bu^t angle of 170°.[23–25] The coordination properties of the vinyl, alkyl amido group,

$$Ta(OAr)_2(\eta^2\text{-}ArNCMe)_2(Me) \longrightarrow Ta(OAr)_2(=NAr)(ArNCMe{=}CMe_2)$$
(1a) $\searrow$ $\nearrow$ **(3a)**
$$[Ta(OAr)_2(\eta^2\text{-}ArNCMe_2)(\eta^2\text{-}ArNCMe)]$$

Ar = 2,6-dimethylphenyl

Scheme 3.

$$Ta(OAr)_2(\eta^2\text{-}Bu^tNCPh_2)(\eta^2\text{-}Bu^tNCPh) \longrightarrow Ta(OAr)_2(=NBu^t)(Bu^tNCPh{=}CPh_2)$$
(2) **(3b)**

Scheme 4.

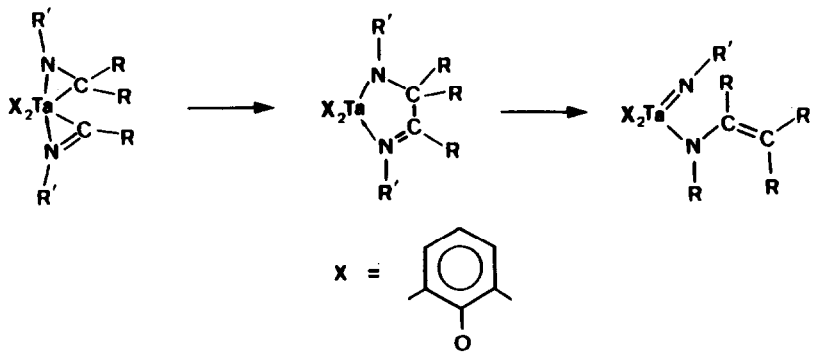

Scheme 5.

Table 1. Selected bond distances (Å) and angles (°) for (**3b**)

Ta(1)—O(2)	1.915(10)	Ta(1)—N(20)	1.766(13)
Ta(1)—O(11)	1.931(10)	Ta(1)—N(27)	1.996(11)
O(2)—Ta(1)—O(11)	110.0(4)	Ta(1)—O(2)—C(3)	155.5(9)
O(2)—Ta(1)—N(20)	109.1(5)	Ta(1)—O(11)—C(12)	152.8(10)
O(2)—Ta(1)—N(27)	110.0(5)	Ta(1)—N(20)—C(21)	169.1(12)
O(11)—Ta(1)—N(20)	107.3(5)	Ta(1)—N(27)—C(26)	104.2(8)
O(11)—Ta(1)—N(27)	114.9(4)	Ta(1)—N(27)—C(28)	133.1(9)
N(20)—Ta(1)—N(27)	105.3(5)	C(26)—N(27)—C(28)	121.2(11)

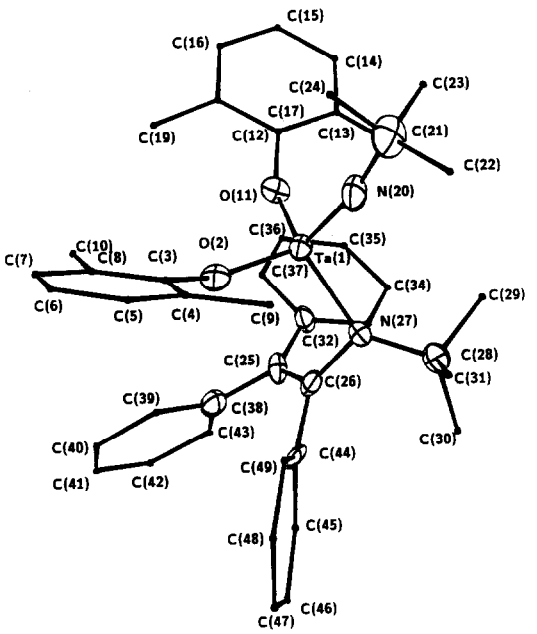

Fig. 1. ORTEP view of $Ta(OAr)_2(=NBu^t)(Bu^tNCPh{=}CPh_2)$ (**3b**) emphasizing the central coordination sphere.

$Bu^tNCPh{=}CPh_2$ is worthy of some comment. The Ta—N(27) distance of 1.996(11) Å is longer than the distance to the imido group by ~0.23 Å. This difference correlates well with the contraction of (0.2–0.3 Å) typically found on going from tantalum(V) bound alkyl to alkylidene functional groups.[26] The amido group coordination is distorted slightly as evidenced by the asymmetric Ta—N—C angles of 104.2(8) and 133.1(9)°. The opening up of the angle to the Bu^t group probably reflects the influence of steric pressures. A similar distortion is seen in another asymmetric amido ligand below. The C—C distance in the vinyl substituent attached to nitrogen is consistent with the presence of a double bond. However, the olefinic environment is twisted leading to a torsion angle of ≃20° between the NC(26)Ph and PhC(25)Ph planes. This twisting is presumably due to the steric pressure of the three phenyl substituents.

In contrast to this behaviour of the methyl and phenyl compounds, the benzyl derivatives (**1b**) and (**1e**) appear to be thermally more robust. However, on extended thermolysis in hydrocarbon solvents, they undergo conversion to a mixture of products, one organic, the other a new type of tantalum compound (**4a**) and (**4b**). Analysis of the organic product by ^1H NMR, GC–MS and IR spectroscopy identified the material as benzyl, phenyl acetylene, $PhCH_2C{\equiv}CPh$. The organometallic products (**4**) were identified as mixed imido, amido derivatives (Scheme 6), only this time the amido group contains a phenethyl (NCH_2CH_2Ph) side chain. This linkage is clearly visible in the ^1H NMR, appearing as a distinctive pair of multiplets separated by over 1 ppm (Experimental). A solid state structural study of (**4b**) confirmed this formulation (Fig. 2) and Table 2 contains some selected bond distances and angles. The molecular structure of (**4b**) can be seen

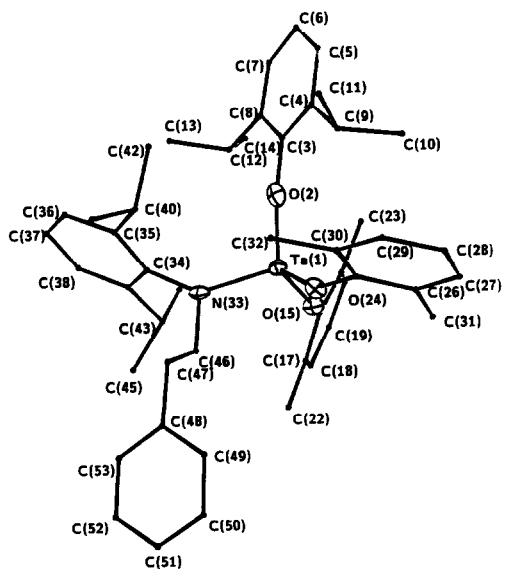

Fig. 2. ORTEP view of $Ta(OAr)_2(=NAr')(Ar'NCH_2CH_2Ph)$ emphasizing the central coordination sphere.

$$Ta(OAr)_2Ta(\eta^2\text{-}R'NCCH_2Ph)_2(CH_2Ph) \longrightarrow Ta(OAr)_2(=NR')(R'NCH_2CH_2Ph) + PhCH_2C{\equiv}CPh$$

(**1b**), R′ = Ar; (**1e**), R′ = Ar′ (**4a**), R′ = Ar; (**4b**), R′ = Ar′

Ar = 2,6-dimethylphenyl; Ar′ = 2,6-di-isopropylphenyl

Scheme 6.

Table 2. Selected bond distances (Å) and angles (°) for (**4b**)

Ta(1)—O(5)	1.923(5)	Ta(1)—N(2)	1.776(8)
Ta(1)—O(24)	1.916(5)	Ta(1)—N(33)	1.951(7)
O(15)—Ta(1)—O(24)	108.5(2)	Ta(1)—O(15)—C(16)	149.6(5)
O(15)—Ta(1)—N(2)	114.0(3)	Ta(1)—O(24)—C(25)	149.6(5)
O(15)—Ta(1)—N(33)	107.8(3)	Ta(1)—N(2)—C(3)	172.0(6)
O(24)—Ta(1)—N(2)	111.6(3)	Ta(1)—N(33)—C(34)	135.3(5)
O(24)—Ta(1)—N(33)	108.3(3)	Ta(1)—N(33)—C(46)	110.5(5)
N(2)—Ta(1)—N(33)	106.5(3)	C(34)—N(33)—C(46)	113.6(6)

to be closely related to that of (**3b**) discussed above. The Ta—O and Ta—N distances are essentially identical between the two structures. Again a distortion of the amido ligand takes place, increasing the Ta—N-xylyl angle to 135.3(5)° compared to 110.5(5)° for the less bulky Ta—N—CH_2CH_2Ph side. The formation of (**4**) and benzyl, phenyl acetylene from (**1b**) could be rationalized using a number of different, equally contorted pathways. However, we feel that the initial step of the reaction involves thermal formation of a mixed η^2-imine, η^2-iminoacyl intermediate of type (**2**). Why this does not then undergo intramolecular coupling and fragmentation to produce vinyl amido compounds similar to those formed with methyl and phenyl derivatives is unclear. A steric rationalization seems unjustified in view of the fact that benzyl groups lie sterically between CH_3 and C_6H_5. A pathway which we favour is a sequential metallation of the α-benzyl carbon of the η^2-imine linkage, with the transfer of the hydrogen atoms to the η^2-iminoacyl to generate the $ArNCH_2CH_2Ph$ group (Scheme 7). The η^2-imine group is converted by this process to an azametallocyclobutene ring, which on elimination of the observed acetylene leaves behind the Ta=NAr, imido linkage.

These reactions, involving overall cleavage of organic isocyanides to form organoimido functions, have precedence in the reaction of WMe_6 with Bu′NC reported by Wilkinson *et al.*[21] as well as in a number of reactions involving the carbonylation of early transition metal poly-alkyl compounds.[27,28] In the latter cases, overall cleavage of CO is observed to generate oxo ligands at Ta^V and Zr^{IV} as well as trialkylvinyloxy groups. It, therefore, seems reasonable that similar pathways are operational for the reaction of both RNC and CO with these alkyl substrates. However, as with the formation of enediolates and enediamides, the organic isocyanide reactions proceed considerably slower than for their oxygen counterparts.

EXPERIMENTAL

All operations were carried out under a dry nitrogen atmosphere either in a Vacuum Atmospheres dri-lab, or by standard Schlenck techniques. Hydrocarbon solvents were dried by distillation from

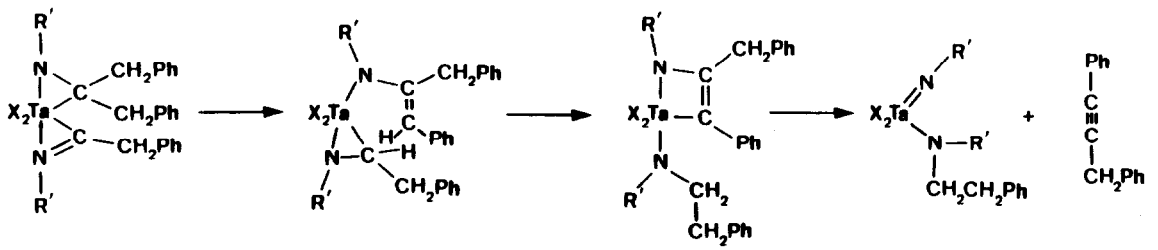

Scheme 7.

sodium benzophenone under a nitrogen atmosphere. The preparation and spectroscopic properties of the compounds $Ta(OAr)_3Cl_2$,[29] $Ta(OAr)_2R_3$ (R = CH_3, CH_2Ph),[30] and $Ta(OAr)_2(\eta^2\text{-}R'NCR)_2R$ (R′ = 2,6-dimethylphenyl; 2,6-diisopropylphenyl; R = CH_3, CH_2Ph) have been previously reported.[10] ^1H and ^{13}C NMR spectra were obtained using a Varian Associates XL-200 spectrometer, while microanalytical data were obtained either at Purdue or from Galbraith.

Preparation of $Ta(OAr)_2Ph_3$

To an orange solution of $Ta(OAr)_3Cl_2$ (1.0 g, 1.63 mmol) in benzene (50 cm^3) was added slowly LiC_6H_5 (0.55 g, 6.5 mmol) with constant vigorous stirring at room temperature. The colour of the mixture lightened during the addition, progressing through pale yellow to almost colourless. After being allowed to stir for 3 h the suspension was filtered to remove LiCl and a little insoluble dark material. The clear filtrate was evaporated *in vacuo* to give the crude product as a grey–white solid which was washed with hexane. Recrystallization from toluene–hexane gave the pure product as pale yellow blocks. Yield = 40%. Found: C, 68.1; H, 5.6. $TaC_{44}H_{33}O_2$ requires: C, 68.2; H, 4.3%. ^1H NMR (C_6D_6, 30°C): δ 1.85 (s, OAr—2,6Me_2); 8.03 (m, *ortho* Ta—C_6H_5); 6.8–7.5 (m, other aromatics). ^{13}C NMR (C_6D_6, 30°C): δ 18.6 (OAr—2,6Me_2), 200.2 (Ta—C_6H_5, *ipso* carbon).

$Ta(OAr_2)(\eta^2\text{-}Ar'NCPh)_2(Ph)$ (**1c**)

To a solution of $Ta(OAr)_2Ph_3$ (0.44 g, 0.67 mmol) in benzene (25 cm^3) xylylisocyanide (0.18 g, 1.4 mmol) was added slowly. The resulting clear solution was stirred for 1 h before the solvent was removed *in vacuo*. The resulting slightly tacky solid was washed with hexane and then taken up in the minimum amount of toluene. Slow cooling gave the product as colourless crystals. Yield = 70%. Found: C, 68.3; H, 6.1; N, 3.2. $TaC_{52}H_{51}N_2O_2$ requires: C, 68.1; H, 5.6; N, 3.1%. ^1H NMR (C_6D_6, 30°C): δ 2.06 (s, NAr—2,6Me_2), 2.42 (s, OAr—2,6Me_2); 8.35 (d, NCC_6H_5); 9.00 (d, Ta—C_6H_5), 6.9–7.4 (m, other aromatics). ^{13}C NMR (C_6D_6, 30°C): δ 182.9 (Ta—C_6H_5, *ipso* carbon), 231.5 (η^2-N*C*).

$Ta(OAr)_2(\eta^2\text{-}Bu^tNCPh_2)(\eta^2\text{-}Bu^tNCPh)$ (**2**)

To a solution of $Ta(OAr)_2(Ph)_3$ (1.0 g, 1.53 mmol) in benzene (25 cm^3) was added Bu^tNC (0.28 g, 3.30 mmol). The mixture was allowed to stand for 1 h before the solvent was removed *in vacuo* to yield a red solid. The product proved difficult to purify, being very soluble in all hydrocarbon solvents. Yield = 78%. Found: C, 63.9; H, 6.7; N, 2.9. $TaC_{42}H_{51}N_2O_2$ requires: C, 63.1; H, 6.4; N, 3.5%. ^1H NMR (C_6D_6, 30°C): δ 2.21 (s, OAr—2,6Me_2), 0.78 (s), 1.50 (s, NBu^t), 6.9–7.9 (m, aromatics). ^{13}C NMR (C_6D_6, 30°C): δ 247.8 (η^2-Bu^tNCPh), 78.8 (η^2-Bu^tNCPh_2), 18.2 (OAr—2,6Me_2), 29.9, 33.3 (NCMe_3).

$Ta(OAr)_2(=NAr)(ArNCMe{=}CMe_2)$ (**3a**)

A toluene solution of $Ta(OAr)_2(\eta^2\text{-}Ar'NCMe)_2(Me)$ (**1a**) was allowed to stand at room temperature for 10 days. The initially pale yellow solution slowly turned purple. Monitoring the reaction by ^1H NMR showed the smooth conversion of (**1a**) to (**3a**). The resulting solution was concentrated and hexane added to yield the product as dark crystals. The purple colour associated with this product is a mystery. On heating for a short time at $\approx$100°C in toluene the solution turned to a clear yellow with no changes whatsoever in the ^1H NMR spectrum. The purple colour is believed by us to be due to trace amounts of a highly coloured impurity possibly formed by polymerization of trace amounts of ArNC. Yield = (typically) 70–80%. Found: C, 60.9; H, 6.5; N, 3.8. $TaC_{37}H_{45}O_2N_2$ requires: C, 60.8; H, 6.2; N, 3.8%. ^1H NMR (C_6D_6, 30°C): δ 3.45 (s, NCMe=CMe_2), 1.46, 1.61 (s, NCMe=CMe_2), 2.14, 2.21 (s, NAr—2,6Me_2), 2.30 (s, OAr—2,6Me_2), 6.8–7.2 (m, aromatics).

$Ta(OAr)_2(=NBu^t)(Bu^tNCPh{=}CPh_2)$ (**3b**)

A solution of the mixed imine, iminoacyl (**2**) in toluene was heated at 105°C in a sealed tube for 30 min. The initially red–orange solution turned yellow during this time. Removal of solvent and recrystallization form toluene–hexane gave pale crystals of the product. Yield = 45%. Found: C, 64.4; H, 6.3; N, 3.4. $TaC_{42}H_{51}N_2O_2$ requires: C, 63.3; H, 6.4; N, 3.5%. ^1H NMR (C_6D_6, 30°C): δ 1.08 (s), 1.58 (s, NBu^t), 2.32 (s, OAr—2,6Me_2), 6.8–7.8 (m, aromatics). ^{13}C NMR (C_6D_6, 30°C): δ 18.1 (OAr—2,6Me_2), 33.2, 34.0 (NCMe_3), 60.2, 67.4 (N*C*Me$_3$).

$Ta(OAr)_2(=NAr)(ArNCH_2CH_2Ph)$ (**4a**)

A solution of $Ta(OAr)_2(\eta^2\text{-}ArNCH_2Ph)_2(CH_2Ph)$ in toluene was heated at 110°C for 1 h. Removal of solvent gave a yellow oil whose ^1H NMR showed a mixture of (**4a**) and PhC≡CCH_2Ph (^1H NMR in C_6D_6, δ 3.15, singlet due to CCH_2Ph).

Taking the mixture up in hexane and cooling gave the organometallic product (**4a**) as pale yellow crystals on cooling. Yield = 38%. Found: C, 62.1; H, 5.8; N, 3.6. $TaC_{40}H_{45}N_2O_2$ requires: C, 62.7; H, 5.9; N, 3.6%. ^1H NMR (C_6D_6, 30°C): δ 2.43 (s, OAr—2,6Me_2), 2.40 (s), 2.62 (s, NAr—2,6Me_2), 4.71 (m, N$CH_2$$CH_2$Ph), 3.37 (m, NCH$_2$$CH_2$Ph), 6.5–7.5 (m, aromatics).

$Ta(OAr)_2(=NAr')(Ar'NCH_2CH_2Ph)$ (**4b**)

Prepared essentially in an identical fashion to (**4a**) only using $Ta(OAr)_2(\eta^2$-Ar—$NCH_2Ph)_2(CH_2Ph)$ (**1e**) as the thermolysis substrate. Yield = 28%. Found: C, 66.0; H, 6.8; N, 2.9. $TaC_{48}H_{61}N_2O_2$ requires: C, 65.6; H, 7.0; N, 3.2%. ^1H NMR (C_6D_6, 30°C): δ 2.33 (s, OAr—2,6Me_2), 0.99 (d), 1.13 (d, NAr'—2,6CHMe_2), 4.47 (m, NCH_2 CH_2Ph), 3.23 (m, NCH$_2$$CH_2$Ph), 6.8–7.3 (m, aromatics).

CRYSTALLOGRAPHIC STUDIES

Data pertinent to the crystallographic studies are contained in Table 3.

$Ta(OAr)_2(=NBu')(Bu'NCPh=CPh_2)$ (**3b**)

A suitable crystal was located and transferred to the goniostat using standard inert atmosphere handling techniques employed by the Indiana University Molecular Structure Center[31] and cooled to −155°C for characterization and data collection.

A systematic search of a limited hemisphere of reciprocal space located a set of diffraction maxima with symmetry and systematic absences corresponding to the unique monoclinic space group $P2_1/n$. Subsequent solution and refinement of the structure confirmed this choice.

Data were collected in the usual manner using a continuous θ–2θ scan with fixed backgrounds. Data

Table 3. Crystal structure determination data

	(**3b**)	(**4b**)
Formula	$TaC_{44}H_{51}O_2N_2$	$TaC_{48}H_{61}N_2O_2$
Formula weight	820.85	878.97
Space group	$P2_1/n$	$P2_1/n$
a (Å)	12.423(5)	21.806(5)
b (Å)	20.772(10)	19.568(6)
c (Å)	14.840(6)	10.078(2)
α (°)	90	90
β (°)	93.27(2)	90.63(1)
γ (°)	90	90
Z	4	4
V (Å^3)	3823.4	4300.0
Density (calc) (g cm^{-3})	1.426	1.358
Crystal size (mm)	[a]	0.12 × 0.12 × 0.16
Crystal colour	Yellow	Yellow
Radiation	Mo-K_α (λ = 0.7, 1069 cm^{-1})	Mo-K_α
Linear abs. coeff. (cm^{-1})	28.764	25.622
Temperature (°C)	−155	−158
Detector aperature	3 mm wide × 4 mm high	3 mm wide × 4 mm high
Takeoff angle	2.0	2.0
Scan speed (° min^{-1})	4.0	4.0
Scan width (°)	2.0 + dispersion	2.0 + dispersion
Background counts (s)	6	8
2θ range (°)	6–45	6–45
Unique data	5004	5642
Unique data with $F_o > 3.00\sigma(F)$	3209	4709
$R(F)$	0.0574	0.0419
$R_w(F)$	0.0498	0.0439
Goodness-of-fit	0.774	0.897
Largest Δ/σ	0.05	0.05

[a] Crystal dimensions were: Face = 1 0 −1 d = 0.0450 mm. Face = −1 0 1 d = 0.0450 mm. Face = 0 1 0 d = 0.0260 mm. Face = 0 −1 0 d = 0.0260 mm. Face = −2 1 −2 d = 0.0400 mm. Face = 2 −1 2 d = 0.0400 mm.

were reduced to a unique set of intensities and associated sigmas in the usual manner. The structure was solved by a combination of Patterson and Fourier techniques. The positions of all hydrogen atoms were clearly visible in a difference Fourier phased on the non-hydrogen atoms, and the coordinates and isotropic thermal parameters for hydrogens were varied in the final cycles of refinement.

Data were corrected for absorption for the final cycles of least squares. A final difference Fourier was essentially featureless, with the largest peak being 0.63e A^{-3}.

$Ta(OAr)_2(=NAr')(Ar'NCH_2CH_2Ph)$ (**4b**)

A suitable crystal was located and transferred to the goniostat and cooled to $-158°C$ for characterization and data collection. A systematic search of a limited hemisphere of reciprocal space located a set of diffraction maxima with monoclinic symmetry and systematic absences corresponding to the unique space group $P2_1/n$ (alternate setting of $P2_1/c$). Subsequent solution and refinement of the structure confirmed this choice. The structure was solved by a combination of direct methods (MULTAN78) and Fourier techniques, and refined by full-matrix least-squares. Hydrogen atoms were visible in a Fourier phased on the non-hydrogen parameters and were included in the final cycles. Non-hydrogen atoms were assigned anisotropic thermal parameters while hydrogens were allowed to vary isotropically.

A final difference Fourier was essentially featureless, with the largest peak being 0.50e A^{-3}. No absorption correction was performed, with psi scans for two peaks near chi = 90^0 being nearly flat.

Acknowledgements—We thank the National Science Foundation (Grant CHE-8612063 to I.P.R.) as well as the Department of Energy (Pittsburgh Energy Technology Centre Grant) for support of the research. I.P.R. also gratefully acknowledges the Camille and Henry Dreyfus Foundation for the award of a Teacher–Scholar Grant and the Alfred P. Sloan Foundation for a Fellowship.

REFERENCES

1. F. Calderazzo, *Angew. Chem. Int. Ed. Engl.* 1977, **16**, 299; E. J. Kuhlmann and J. J. Alexander, *Coord. Chem. Rev.* 1980, **33**, 195.
2. A. Wojcicki, *Adv. Organomet. Chem.* 1973, **11**, 87; T. C. Flood, in *Topics in Stereochemistry* (Edited by G. L. Geoffrey), Vol. 12, p. 83. Wiley, New York (1981); J. J. Alexander, in *The Chemistry of the Metal–Carbon Bond* (Edited by F. R. Hartley), Vol. 2. Wiley, New York (1985); J. A. Gladys, *J. Adv. Organomet. Chem.* 1982, **20**, 1 and refs therein.
3. P. C. Ford (Ed.), Catalytic activation of carbon monoxide, *Am. Chem. Soc., Symp. Ser.* 1981, 152; E. Singleton, *Adv. Organomet. Chem.* 1983, **22**, 267; P. L. Bock, D. J. Boschetto, J. R. Rasmussen, J. P. Demers and G. M. Whitesides, *J. Am. Chem. Soc.* 1974, **96**, 2814; M. J. Wax and R. G. Bergman, *J. Am. Chem. Soc.* 1981, **103**, 7028.
4. G. Erker, *Accts Chem. Res.* 1984, **17**, 103.
5. P. T. Wolazanski and J. E. Bercaw, *Accts Chem. Res.* 1980, **13**, 121.
6. J. Teuben, in *Fundamental and Technological Aspects of Organo-f-Element Chemistry* (Edited by T. J. Marks and I. L. Fragala). Dordrecht, Holland (1986); K. G. Moloy and T. J. Marks, *J. Am. Chem. Soc.* 1984, **106**, 7051.
7. J. M. Manriquez, D. R. McAlister, R. D. Sanner and J. E. Bercaw, *J. Am. Chem. Soc.* 1978, **100**, 2716; J. M. Manriquez, D. R. McAlister, R. D. Sanner and J. E. Bercaw, *J. Am. Chem. Soc.* 1976, **98**, 6733.
8. J. A. McCleverty and G. Wilkinson, *J. Chem. Soc.* 1963, 4096; P. J. Fagan, K. E. Moloy and T. J. Marks, *J. Am. Chem. Soc.* 1981, **103**, 6959; W. J. Evans, J. W. Grate and R. J. Doedens, *J. Am. Chem. Soc.* 1985, **107**, 1671; D. A. Katahira, K. G. Moloy and T. J. Marks, *Organometallics* 1982, **1**, 1723.
9. K. Tatsumi, A. Nakamura, P. Hofmann, R. Hoffmann, K. G. Moloy and T. J. Marks *J. Am. Chem. Soc.* 1986, **108**, 4467.
10. L. R. Chamberlain, L. D. Durfee, P. E. Fanwick, L. Kobriger, S. L. Latesky, A. K. McMullen, I. P. Rothwell, K. Folting, J. C. Huffman, W. E. Streib and R. Wang, *J. Am. Chem. Soc.* 1987, **109**, 390 and refs therein.
11. L. R. Chamberlain, L. D. Durfee, P. E. Fanwick, L. M. Kobriger, S. L. Latesky, A. K. McMullen, B. D. Steffey, I. P. Rothwell, K. Folting and J. C. Huffman, *J. Am. Chem. Soc.* 1987, **109**, 6068; L. R. Chamberlain, I. P. Rothwell and J. C. Huffman, *J. Chem. Soc., Chem. Commun.* 1986, 1203.
12. A. K. McMullen, I. P. Rothwell and J. C. Huffman, *J. Am. Chem. Soc.* 1985, **107**, 1072; P. E. Fanwick, L. Kobriger, A. K. McMullen and I. P. Rothwell, *J. Am. Chem. Soc.* 1986, **108**, 8095.
13. L. D. Durfee, A. K. McMullen and I. P. Rothwell, *J. Am. Chem. Soc.*, in press.
14. E. Negishi and T. Takahashi, *Synthesis* 1988, **1**, 1 and refs therein; G. S. Girolami, V. V. Mainz, R. A. Andersen, S. H. Vollmer and V. W. Day, *J. Am. Chem. Soc.* 1981, **103**, 3953; B. Hessen, J. Teuben, T. H. Lemmen, J. C. Huffman and K. G. Caulton, *Organometallics* 1985, **4**, 946; G. Fachinetti and C. Floriani, *J. Chem. Soc., Chem. Commun.* 1972, 654; H. Masai, K. Sonogashira and N. Hagihara, *Bull. Chem. Soc. Jpn* 1968, **41**, 750.
15. G. Erker, U. Dorf, P. Czisch and J. L. Petersen, *Organometallics* 1986, **5**, 668; F. Rosenfeldt and G. Erker, *Tetrahedron Lett.* 1980, **21**, 1637; S. Stella and C. Floriani, *J. Chem. Soc., Chem. Commun.* 1986, 1053; R. M. Waymouth, K. R. Clauser and

R. H. Grubbs, *J. Am. Chem. Soc.* 1986, **108**, 6385.
16. J. A. Marsella, J. C. Huffmann, K. Folting and K. G. Caulton, *Inorg. Chim. Acta* 1985, **96**, 161.
17. L. D. Durfee, P. E. Fanwick, I. P. Rothwell, K. Folting and J. C. Huffman, *J. Am. Chem. Soc.* 1987, **109**, 4720.
18. W. Fromberg and G. Erker, *J. Organomet. Chem.* 1985, **280**, 355.
19. K. Tatsumi, personal communication.
20. P. T. Wolczanski and J. E. Bercaw, *J. Am. Chem. Soc.* 1979, **101**, 6450.
21. K. W. Chiu, R. A. Jones, G. Wilkinson, A. M. R. Galas and M. B. Hursthouse, *J. Am. Chem. Soc.* 1980, **102**, 7978; J. W. Chiu, R. A. Ruones, G. Wilkinson, A. Galas and M. B. Hursthouse, *J. Chem. Soc., Dalton Trans.* 1981, 2088.
22. M. H. Chisholm and I. P. Rothwell, in *Comprehensive Coordination Chemistry* (Edited by G. Wilkinson, R. Gillard and J. A. McCleverty), Vol. 2, Chap. 15-3. Pergamon Press, Oxford (1987).
23. M. H. Chisholm and I. P. Rothwell, in *Comprehensive Coordination Chemistry*, (Edited by G. Wilkinson, R. Gillard and J. A. McCleverty), Vol. 2, Chap. 13-4. Pergamon Press, Oxford (1987).
24. R. W. Chesnut, P. E. Fanwick and I. P. Rothwell, *Inorg. Chem.* 1988, **27**, 752.
25. W. A. Nugent and B. L. Haymore, *Coord. Chem. Rev.* 1980, **31**, 123.
26. R. R. Schrock, in *Reactions of Coordinated Ligands* (Edited by P. S. Bratemann). Plenum Press, New York (1987).
27. C. D. Wood and R. R. Schrock, *J. Am. Chem. Soc.* 1979, **101**, 5421.
28. R. P. Planalp and R. A. Andersen, *J. Am. Chem. Soc.* 1983, **105**, 7774.
29. L. R. Chamberlain, I. P. Rothwell and J. C. Huffman, *Inorg. Chem.* 1984, **23**, 2575.
30. L. R. Chamberlain, I. P. Rothwell, K. Folting and J. C. Huffman, *J. Chem. Soc., Dalton Trans.* 1987, 155.
31. M. H. Chisholm, K. Folting, J. C. Huffman and C. C. Kirkpatrick, *Inorg. Chem.* 1984, **23**, 1021.

Polyhedron Vol. 8, No. 3, pp. 351–355, 1989
Printed in Great Britain

0277–5387/89 $3.00+.00
© 1989 Pergamon Press plc

TUNGSTEN(II) ALKYNE COMPLEXES CONTAINING MONODENTATE NEUTRAL OXYGEN AND SULPHUR DONOR LIGANDS

PAUL K. BAKER* and ELAINE M. ARMSTRONG

Department of Chemistry, University College of North Wales, Bangor, Gwynedd LL57 2UW, Wales, U.K.

(*Received* 11 *August* 1988; *accepted* 25 *August* 1988)

Abstract—The compounds $[WI_2(CO)(NCMe)(\eta^2\text{-}RC_2R)_2]$ (R = Me or Ph) react with one equivalent of L (L = $OC(NH_2)_2$ or $SC(NH_2)Me$) at room temperature (for R = Me, L = $OC(NH_2)_2$ in acetone–methanol; R = Me, L = $SC(NH_2)Me$ in methanol; R = Ph, L = $OC(NH_2)_2$, $SC(NH_2)Me$ in acetone) to give good yields of the acetonitrile substituted products $[WI_2(CO)L(\eta^2\text{-}RC_2R)_2]$. ^{13}C NMR spectroscopy indicates that the alkyne ligands in these complexes are donating a total of six electrons to the metal. Reaction of $[WI_2(CO)(NCMe)(\eta^2\text{-}PhC_2Ph)_2]$ with one equivalent of L [L = $SC(NH_2)_2$ (tu) and $SC(NMe_2)_2$ (tmtu)] in acetone at various temperatures gave a mixture of products. However, reaction of $[WI_2(CO)(NCMe)(\eta^2\text{-}MeC_2Me)_2]$ with two equivalents of L (L = tu or tmtu) in acetone at room temperature gave the monobut-2-yne products $[WI_2(CO)L_2(\eta^2\text{-}MeC_2Me)]$, whereas reaction of $[WI_2(CO)(NCMe)(\eta^2\text{-}PhC_2Ph)_2]$ with two equivalents of tu in dichloromethane–methanol gave the non-carbonyl containing bisdiphenylacetylene complex $[WI_2(tu)_2(\eta^2\text{-}PhC_2Ph)_2]$. Reaction of $[WI_2(CO)(NCMe)(\eta^2\text{-}PhC_2Ph)_2]$ with two equivalents of tmtu in acetone eventually gave the unusual iodide-bridged dimer $[W(\mu\text{-}I)I(CO)(tmtu)(\eta^2\text{-}PhC_2Ph)]_2 \cdot$ tmtu. ^{13}C NMR spectroscopy suggests that the alkyne ligands in $[WI_2(tu)_2(\eta^2\text{-}PhC_2Ph)_2]$ are donating six electrons to the metal and each alkyne in the dimer $[W(\mu\text{-}I)I(CO)(tmtu)(\eta^2\text{-}PhC_2Ph)]_2$ is donating four electrons to the tungsten.

Although there are a wide variety of alkyne complexes known containing anionic sulphur donor ligands of molybdenum(II) and tungsten(II), in particular complexes of the type $[M(CO)(\eta^2\text{-}RC_2R')(S_2CNR_2'')_2]$ and $[M(\eta^2\text{-}RC_2R')_2(S_2CNR_2'')_2]$ (M = Mo or W; R, R' = H, alkyl, aryl etc.; R'' = Me, Et, ^{i}Pr etc.),[1] to date there have been no alkyne complexes of molybdenum(II) and tungsten(II) containing monodentate neutral oxygen or sulphur donor ligands.

Since the discovery of $[WI_2(CO)_2L(\eta^2\text{-}PhC_2H)]$ (L = PMe_3 or $AsMe_3$) by Umland and Vahrenkamp[2] and $[WBr_2(CO)(\eta^2\text{-}CF_3C_2CF_3)_2]$ by Davidson *et al.*[3] in 1982 there has been considerable interest in haloalkyne complexes of molybdenum(II) and tungsten(II).[4] In recent years we have been investigating the chemistry of the highly versatile bisalkyne complexes $[WI_2(CO)(NCMe)(\eta^2\text{-}RC_2R)_2]$ (R = Me or Ph).[5] In this paper we wish to describe the reactions of these complexes with some monodentate neutral oxygen and sulphur donor ligands.

*Author to whom correspondence should be addressed.

EXPERIMENTAL

The complexes $[WI_2(CO)(NCMe)(\eta^2\text{-}RC_2R)_2]$ (R = Me or Ph) were prepared according to the published method.[5] All chemicals were purchased from commercial sources. ^1H and ^{13}C NMR spectra were recorded either on a Jeol FX60 or a Bruker WH-400MHz NMR spectrometer (all spectra were calibrated against tetramethylsilane). IR spectra were recorded on a Perkin–Elmer 197 IR spectrophotometer as $CHCl_3$ films between NaCl plates unless otherwise stated. The molecular weight of $[W(\mu\text{-}I)I(CO)(tmtu)(\eta^2\text{-}PhC_2Ph)]_2 \cdot$ tmtu was determined using Rast's method,[6] using camphor as the solvent. Elemental analyses for carbon, hydrogen and nitrogen were recorded on a Carlo Erba Elemental Analyser MOD 1106 (using helium as a carrier gas).

$[WI_2(CO)\{OC(NH_2)_2\}(\eta^2\text{-}MeC_2Me)_2]$ (1)

To $[WI_2(CO)(NCMe)(\eta^2\text{-}MeC_2Me)_2]$ (0.500 g, 0.813 mmol) dissolved in a 40:60 (v/v) acetone–methanol mixture (20 cm^3), with continuous stirring under a stream of dry nitrogen, was added $OC(NH_2)_2$ (0.049 g, 0.816 mmol). After 17 h, filtration and removal of solvent *in vacuo* afforded the pale green complex, $[WI_2(CO)\{OC(NH_2)_2\}(\eta^2\text{-}MeC_2Me)_2]$, which was recrystallized from dichloromethane–acetone (Yield: 0.30 g, 58%).

In a similar reaction of $[WI_2(CO)(NCMe)(\eta^2\text{-}PhC_2Ph)_2]$ with 1 equivalent of $OC(NH_2)_2$ in acetone at room temperature gave $[WI_2(CO)\{OC(NH_2)_2\}(\eta^2\text{-}PhC_2Ph)_2]$ (2) (see Table 1 for yield and analytical data).

$[WI_2(CO)\{SC(NH_2)Me\}(\eta^2\text{-}MeC_2Me)_2]$ (3)

To $[WI_2(CO)(NCMe)(\eta^2\text{-}MeC_2Me)_2]$ (0.500 g, 0.813 mmol) dissolved in methanol (15 cm^3), with continuous stirring under a stream of dry nitrogen, was added $SC(NH_2)Me$ (0.061 g, 0.812 mmol). After 15 h, filtration and removal of solvent afforded the yellow crystalline complex, $[WI_2(CO)\{SC(NH_2)Me\}(\eta^2\text{-}MeC_2Me)_2]$, which was recrystallized from dichloromethane (Yield: 0.46 g, 87%).

In a similar reaction, $[WI_2(CO)(NCMe)(\eta^2\text{-}PhC_2Ph)_2]$ with 1 equivalent of $SC(NH_2)Me$ in acetone at room temperature gave $[WI_2(CO)\{SC(NH_2)Me\}(\eta^2\text{-}PhC_2Ph)_2]$ (4) (see Table 1 for yield and analytical data).

$[WI_2(CO)\{SC(NH_2)_2\}_2(\eta^2\text{-}MeC_2Me)]$ (5)

To $[WI_2(CO)(NCMe)(\eta^2\text{-}MeC_2Me)_2]$ (0.500 g, 0.813 mmol) dissolved in acetone (15 cm^3), with continuous stirring under a stream of dry nitrogen, was added $SC(NH_2)_2$ (0.186 g, 2.445 mmol). After 15 h, filtration and removal of solvent *in vacuo* afforded a purple crystalline complex, $[WI_2(CO)\{SC(NH_2)_2\}_2(\eta^2\text{-}MeC_2Me)]$, which was columned on silica at 0°C in 2-butanone, and recrystallized twice from acetone (Yield: 0.29 g, 53%).

$[WI_2\{SC(NH_2)_2\}_2(\eta^2\text{-}PhC_2Ph)_2]$ (6)

To a solution of $[WI_2(CO)(NCMe)(\eta^2\text{-}PhC_2Ph)_2]$ (0.300 g, 0.348 mmol) dissolved in a mixture of dichloromethane (15 cm^3) and methanol (3 cm^3), with continuous stirring under a stream of dry nitrogen, was added $SC(NH_2)_2$ (0.053 g, 0.693 mmol). After stirring at 30°C for 24 h, filtration and removal of solvent *in vacuo* afforded a pale yellow powder, $[WI_2\{SC(NH_2)_2\}_2(\eta^2\text{-}PhC_2Ph)_2]$, which was recrystallized from dichloromethane (Yield: 0.23 g, 69%).

$[WI_2(CO)\{SC(NMe_2)_2\}_2(\eta^2\text{-}MeC_2Me)]$ (7)

To a solution of $[WI_2(CO)(NCMe)(\eta^2\text{-}MeC_2Me)_2]$ (0.500 g, 0.813 mmol) dissolved in acetone (15 cm^3) with continuous stirring under a stream of dry nitrogen was added $SC(NMe_2)_2$ (0.322 g, 2.435 mmol). After 15 h, filtration and removal of solvent *in vacuo* left purple $[WI_2(CO)$

Table 1. Physical and analytical[a] data for the complexes $[WI_2(CO)L(\eta^2\text{-}RC_2R)_2]$, $[WI_2(CO)L_2(\eta^2\text{-}MeC_2Me)]$, $[WI_2\{SC(NH_2)_2\}_2(\eta^2\text{-}PhC_2Ph)_2]$ and $[W(\mu\text{-}I)I(CO)\{SC(NMe_2)_2\}(\eta^2\text{-}PhC_2Ph)]_2 \cdot \{SC(NMe_2)_2\}$

Complex	Colour	Yield (%)	C	H	N
(1) $[WI_2(CO)\{OC(NH_2)_2\}(\eta^2\text{-}MeC_2Me)_2]$	Pale green	58	18.6 (19.0)	3.0 (2.5)	4.8 (4.4)
(2) $[WI_2(CO)\{OC(NH_2)_2\}(\eta^2\text{-}PhC_2Ph)_2]$	Pale yellow	67	41.4 (40.8)	2.7 (2.7)	3.3 (3.2)
(3) $[WI_2(CO)\{SC(NH_2)Me\}(\eta^2\text{-}MeC_2Me)_2]$	Pale yellow	87	20.2 (20.4)	2.5 (2.6)	1.8 (2.2)
(4) $[WI_2(CO)\{SC(NH_2)Me\}(\eta^2\text{-}PhC_2Ph)_2]$	Pale yellow	19	41.3 (41.5)	3.3 (2.8)	1.2 (1.6)
(5) $[WI_2(CO)\{SC(NH_2)_2\}_2(\eta^2\text{-}MeC_2Me)]$	Purple	53	13.1 (12.5)	2.5 (2.1)	8.2 (8.3)
(6) $[WI_2\{SC(NH_2)_2\}_2(\eta^2\text{-}PhC_2Ph)_2]$	Pale yellow	69	37.7 (38.1)	3.3 (3.0)	5.3 (5.9)
(7) $[WI_2(CO)\{SC(NMe_2)_2\}_2(\eta^2\text{-}MeC_2Me)]$	Purple	57	23.5 (23.0)	4.4 (3.9)	6.8 (7.1)
(8) $[W(\mu\text{-}I)I(CO)\{SC(NMe_2)_2\}(\eta^2\text{-}PhC_2Ph)]_2 \cdot \{SC(NMe_2)_2\}$	Dark green	82	32.0 (32.1)	3.8 (3.4)	5.4 (5.0)

[a] Calculated values in parentheses.

$\{SC(NMe_2)_2\}_2(\eta^2\text{-}MeC_2Me)]$ which was columned on silica at 0°C in 2-butanone. Removal of the solvent *in vacuo* and recrystallization from acetone afforded (**7**) (Yield: 0.36 g, 57%).

$[W(\mu\text{-}I)I(CO)\{SC(NMe_2)_2\}(\eta^2\text{-}PhC_2Ph)]_2\{SC(NMe_2)_2\}$ (**8**)

To $[WI_2(CO)(NCMe)(\eta^2\text{-}PhC_2Ph)_2]$ (0.500 g, 0.579 mmol) dissolved in acetone (15 cm^3), with continuous stirring under a stream of dry nitrogen, was added $SC(NMe_2)_2$ (0.153 g, 1.157 mmol). After stirring for 15 h the deep green precipitate was allowed to settle and the solvent decanted off. The product was washed with 4×10 cm^3 portions of acetone followed by 3×5 cm^3 portions of CH_2Cl_2. The complex was dried *in vacuo* (Yield: 0.40 g, 82%). Molecular weight for $C_{45}H_{56}N_6I_4O_2S_3W_2$: Found: 1637. Calc: 1684.

RESULTS AND DISCUSSION

The complexes $[WI_2(CO)(NCMe)(\eta^2\text{-}RC_2R)_2]$ (R = Me or Ph) react with one equivalent of L (L = $OC(NH_2)_2$ or $SC(NH_2)Me$) at room temperature (for R = Me, L = $OC(NH_2)_2$ in acetone–methanol; R = Me, L = $SC(NH_2)Me$ in methanol, R = Ph, L = $OC(NH_2)_2$, $SC(NH_2)Me$ in acetone) to give good yields of the new substituted products $[WI_2(CO)L(\eta^2\text{-}RC_2R)_2]$ (**1–4**). Reaction of $[WI_2(CO)(NCMe)(\eta^2\text{-}MeC_2Me)_2]$ with an excess of L [L = $SC(NH_2)_2$ (tu) or $SC(NMe_2)_2$ (tmtu)] in acetone at room temperature afford the monoalkyne complexes $[WI_2(CO)L_2(\eta^2\text{-}MeC_2Me)]$ (**5** and **7**). However, the bisdiphenylacetylene complex $[WI_2(CO)(NCMe)(\eta^2\text{-}PhC_2Ph)_2]$ reacts with 2 equivalents of tu at 30°C in dichloromethane–methanol to give the non-carbonyl containing bisalkyne complex $[WI_2(tu)_2(\eta^2\text{-}PhC_2Ph)_2]$ (**6**). By contrast, reaction of the compound $[WI_2(CO)(NCMe)(\eta^2\text{-}PhC_2Ph)_2]$ with 2 equivalents of tmtu in acetone at room temperature eventually gives the novel iodide-bridged dimer $[W(\mu\text{-}I)I(CO)(tmtu)(\eta^2\text{-}PhC_2Ph)]_2(tmtu)$ (**8**). All the new complexes have been fully characterized by elemental analysis (C, H and N) (Table 1), IR (Table 2), ^1H and in some cases ^{13}C NMR spectroscopy (Tables 3 and 4). The tmtu solvate $[W(\mu\text{-}I)I(CO)(tmtu)(\eta^2\text{-}PhC_2Ph)]_2 \cdot tmtu$ (**8**) was confirmed by repeated elemental analyses, ^1H and ^{13}C NMR spectroscopy. The dimeric nature of (**8**) was confirmed by molecular weight measurements using Rast's method[6] (see Experimental). The new complexes (**1–8**) described in this paper are extremely air-sensitive and thermally unstable. They can be stored at 0°C under nitrogen for several hours.

Table 2. IR data[a] for the complexes $[WI_2(CO)L(\eta^2\text{-}RC_2R)_2]$, $[WI_2(CO)L_2(\eta^2\text{-}MeC_2Me)]$, $[WI_2\{SC(NH_2)_2\}_2(\eta^2\text{-}PhC_2Ph)_2]$ and $[W(\mu\text{-}I)I(CO)\{SC(NMe_2)_2\}(\eta^2\text{-}PhC_2Ph)]_2 \cdot \{SC(NMe_2)_2\}$

Complex	$\nu(C{\equiv}O)$ (cm^{-1})	$\nu(C{\equiv}C)$ (cm^{-1})
(**1**)	2050 (s)	1660 (vw)
(**2**)	2080 (s)	1655 (vw)
(**3**)	2052 (s)	1700 (vw)
(**4**)	2080 (s)	1680 (vw)
(**5**)	1915 (s)	Not observed
(**6**)	—	1740 (w)
(**7**)	1895 (s)	1630 (vw)
(**8**)	1913 (s), 1905 (s)	1665 (vw)

[a] Spectra recorded as acetone films between NaCl plates.

s: strong; vw: very weak; w: weak.

The reactions of $[WI_2(CO)(NCMe)(\eta^2\text{-}RC_2R)_2]$ with 1 equivalent of L (L = $OC(NH_2)_2$ or $SC(NH_2)Me$) probably proceed via an associative mechanism, since the alkyne ligands can rearrange their mode of bonding from supplying a total of six electrons to the tungsten in $[WI_2(CO)(NCMe)(\eta^2\text{-}RC_2R)_2]$ to both alkynes donating two electrons each in the intermediate $[WI_2(CO)(NCMe)L(\eta^2\text{-}RC_2R)_2]$. Loss of acetonitrile from this intermediate would give the observed products.

The complexes $[WI_2(CO)(NCMe)(\eta^2\text{-}RC_2R)_2]$ have very similar spectral properties and colours to

Table 3. ^1H NMR data for the complexes $[WI_2(CO)L(\eta^2\text{-}RC_2R)_2]$, $[WI_2(CO)L_2(\eta^2\text{-}MeC_2Me)]$, $[WI_2\{SC(NH_2)_2\}_2(\eta^2\text{-}PhC_2Ph)_2]$ and $[W(\mu\text{-}I)I(CO)\{SC(NMe_2)_2\}(\eta^2\text{-}PhC_2Ph)]_2 \cdot \{SC(NMe_2)_2\}$

Complex	^1H (δ) (ppm)
(**1**)	3.13, 2.88 (d, *J* 14.8 Hz, 12H, *Me*C_2); 1.68, 1.53 (bm, 4H, N*H*$_2$)
(**2**)	7.45 (bm, 20H, *Ph*C_2); 2.59–1.81 (bm, 4H, N*H*$_2$)
(**3**)[a]	2.95 (s, 3H, Me); 2.88, 2.71 (d, *J* 10.1 Hz, 12H, *Me*C_2); 1.67 (bs, 2H, N*H*$_2$)
(**4**)[a]	7.56–7.43 (bm, 20H, *Ph*C_2); 3.41, 3.39 (q, *J* 7.0 Hz, 2H, N*H*$_2$), 2.53 (bs, 3H, Me)
(**5**)	7.98 (bs, 8H, N*H*$_2$); 3.02 (s, 6H, *Me*C_2)
(**6**)	7.38 (bm, 10H, *Ph*C_2 and 8H, N*H*$_2$)
(**7**)	3.24 and 3.02 (m, 12H, *Me*N and 6H, *Me*C_2)
(**8**)[a]	7.56–7.35 (bm, 20H, *Ph*C_2); 3.34 and 3.07 (bs, 36H, *Me*N)

[a] Spectra recorded on a Bruker WH400 MHz spectrometer.

All spectra recorded in $(CD_3)_2CO$ (+25°C).

b: broad; d: doublet; m: multiplet; s: singlet.

Table 4. ^{13}C NMR spectra of selected complexes

Complex	^{13}C (δ) (ppm)
(2)	198.55 (s, *C*≡O); 171.34 and 160.06 (s, *C*≡*C*); 158. 89 (s, *C*≡O)
(3)[a]	209.81 (s, *C*≡O); 169.99 and 149.19 (s, *C*≡*C*); 132.06 (s, C═S); 28.53 (s, *Me*C_2); 19.56 (s, *Me*)
(6)	206.88 (s, *C*═S); 157.08 and 140.47 (s, *C*≡*C*); 131.51–126.44 (m, *Ph*C_2)
(8)[a]	209.88 (s, *C*≡C); 201.15 (s, C≡O); 195.59 (s, *C*═S coord.) 163.01 (s, *C*═S, free); 132.27–123.98 (m, *Ph*C_2); 43.17 (s, *Me*)

[a] Spectra recorded on a Bruker WH 400 MHz spectrometer.

All spectra recorded in $(CD_3)_2CO$ (+25°C).

s: singlet; m: multiplet.

$[WI_2(CO)L(\eta^2\text{-}RC_2R)_2]$ (**1–4**). The X-ray crystal structures of $[WI_2(CO)(NCMe)(\eta^2\text{-}RC_2R)_2]$ (R = Me or Ph) have been determined,[5] hence the proposed structure of the complexes (**1–4**) is shown in Fig. 1.

The ^1H NMR spectra of (**1–4**) agreed with static structures shown in Fig. 1. The ^{13}C NMR spectra of (**2**) and (**3**) have alkyne (C≡C) contact carbon resonances at δ = 171.34 and 160.06 ppm for (**2**) and δ = 169.99 and 149.19 ppm for (**3**). Templeton and Ward[7] have correlated the values of ^{13}C alkyne contact carbon chemical shifts with the average number of electrons donated to the metal. The values given above for (**2**) and (**3**) indicate that the alkynes are donating three electrons each to the tungsten in these complexes. It is likely, however that one alkyne is donating four electrons and the other two electrons in these complexes with rapid exchange between these resonance hybrids (faster than the NMR time scale).

It is interesting to note that reaction of $[WI_2(CO)(NCMe)(\eta^2\text{-}RC_2R)_2]$ (R = Me or Ph) with one equivalent of L [L = $SC(NH_2)_2$ (tu) or $SC(NMe_2)_2$ (tmtu)] in acetone at various temperatures always gives a mixture of products. Several unsuccessful attempts were made to separate these mixtures by column chromatography.

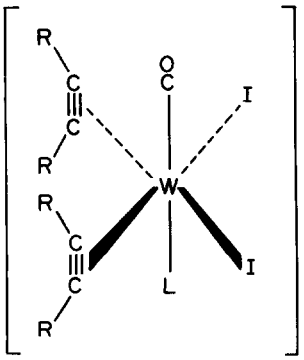

Fig. 1. Proposed structure for $[WI_2(CO)L(\eta^2\text{-}RC_2R)_2]$.

Reaction of $[WI_2(CO)(NCMe)(\eta^2\text{-}MeC_2Me)_2]$ with an excess of L (L = tu or tmtu) in acetone at room temperature gave the monoalkyne complexes $[WI_2(CO)L_2(\eta^2\text{-}MeC_2Me)]$. These complexes are analogous to the complexes $[MX_2(CO)L_2(\eta^2\text{-}RC_2R')]$ (M = Mo or W; X = Cl or Br; L = PEt_3, PPh_3 or py; $L_2 = Ph_2P(CH_2)_2PPh_2$) reported by Templeton and co-workers[4a,d] and $[WBr_2(CO)L_2(\eta^2\text{-}RC_2R')]$ (L = $CNBu^t$, $P(OMe)_3$ or PPh_3) by Davidson and Vasapollo[4b,c]. In order for these complexes to obey the effective atomic number rule, the but-2-yne ligands must donate four electrons to the metal which is suggested by the highly coloured nature of these compounds. However, due to the instability of these complexes in solution for long periods, no ^{13}C NMR spectra were obtained which should have confirmed this. However, it was found that the single resonance at δ = 3.02 ppm for the but-2-yne for (**5**) did not coalesce even down to −80°C in CD_2Cl_2.

By contrast reaction of $[WI_2(CO)(NCMe)(\eta^2\text{-}PhC_2Ph)_2]$ with 2 equivalents of tu in dichloromethane–methanol at 30°C affords the non-carbonyl containing product, $[WI_2(tu)_2(\eta^2\text{-}PhC_2Ph)_2]$ (**6**). This can be explained since diphenylacetylene is a poorer σ-donor and better π-acceptor ligand than but-2-yne and hence, substituting the acetonitrile by tu (which is a better π-acceptor ligand than acetonitrile) facilitates the loss of carbon monoxide rather than the alkyne ligand in this complex. The ^{13}C NMR spectrum indicated that both alkyne ligands in (**6**) are donating a total of six electrons to the tungsten (see Table 4).

Two equivalents of the more electron rich tmtu ligand react with $[WI_2(CO)(NCMe)(\eta^2\text{-}PhC_2Ph)_2]$ to eventually give the novel iodide-bridged dimer $[W(\mu\text{-}I)I(CO)(tmtu)(\eta^2\text{-}PhC_2Ph)]_2 \cdot tmtu$ (**8**). Following this reaction by IR spectroscopy indicated an initial green solution is formed after 3 min which has a carbonyl band at ν(CO) = 1908 cm^{-1} which is likely to be due to the monoalkyne complex $[WI_2(CO)(tmtu)_2(\eta^2\text{-}PhC_2Ph)]$. The disappearance of the band at 1908 cm^{-1} is concomitant with the formation of two new bands at ν(CO) = 1913 and 1905 cm^{-1} which are due to the dimer (**8**). Complex (**8**) is analogous to some of the other dimeric complexes we have previously reported $[M(\mu\text{-}I)I(CO)(NCMe)(\eta^2\text{-}RC_2R')]_2$ (M = Mo or W; R = R′ = Ph; R = Ph; R′ = Me)[8] formed from reaction of $[MI_2(CO)_3(NCMe)_2]$ with 1 equivalent of RC_2R'. As expected the ^{13}C NMR spectrum of

(**8**) shows a resonance at $\delta = 209.88$ ppm due to the alkyne contact carbons, which suggests[7] the alkyne ligands are donating four electrons each to the tungsten atoms in this complex.

Finally, it should be noted that 2 equivalents of $OC(NH_2)_2$ and $SC(NH_2)Me$ react in acetone with $[WI_2(CO)(NCMe)(\eta^2\text{-}RC_2R)_2]$ to give a mixture of products. Hence, subtle differences in the electronic and steric effects of the four ligands $OC(NH_2)_2$, $SC(NH_2)Me$, $SC(NH_2)_2$ and $SC(NMe_2)_2$ give a variety of different products when reacted with $[WI_2(CO)(NCMe)(\eta^2\text{-}RC_2R)_2]$.

Acknowledgements—We wish to thank Dr O. W. Howarth for obtaining several ^1H and ^{13}C NMR spectra at the University of Warwick and we thank the SERC for support.

REFERENCES

1. (a) J. W. McDonald, W. E. Newton, C. T. C. Creedy and J. L. Corbin, *J. Organomet. Chem.* 1975. **92**, C25; (b) R. S. Herrick and J. L. Templeton, *Organometallics* 1982, **1**, 842; (c) B. C. Ward and J. L. Templeton, *J. Am. Chem. Soc.* 1980, **102**, 1532; (d) J. L. Templeton, R. S. Herrick and J. R. Morrow, *Organometallics* 1984, **3**, 535; (e) M. A. Bennett and I. W. Boyd, *J. Organomet. Chem.* 1985, **290**, 165; (f) J. R. Morrow, T. L. Tonker and J. L. Templeton, *J. Am. Chem. Soc.* 1985, **107**, 5004.
2. P. Umland and H. Vahrenkamp, *Chem. Ber.* 1982, **115**, 3580.
3. J. L. Davidson, G. Vasapollo, M. Manojlovic-Muir and K. W. Muir, *J. Chem. Soc., Chem. Commun.* 1982, 1025.
4. (a) P. B. Winston, S. J. N. Burgmayer and J. L. Templeton, *Organometallics* 1983, **2**, 167; (b) J. L. Davidson and G. Vasapollo, *Polyhedron* 1983, **2**, 305; (c) J. L. Davidson and G. Vasapollo, *J. Chem. Soc., Dalton Trans.* 1985, 2239; (d) P. B. Winston, S. J. N. Burgmayer, T. L. Tonker and J. L. Templeton, *Organometallics* 1986, **5**, 1707; (e) A. Mayr, K. S. Lee, M. A. Kjelsberg and D. Van Engen, *J. Am. Chem. Soc.* 1986, **108**, 6079; (f) C. M. Giandomenico, C. T. Lam and S. J. Lippard, *J. Am. Chem. Soc.* 1982, **104**, 1263.
5. E. M. Armstrong, P. K. Baker and M. G. B. Drew, *Organometallics* 1988, **7**, 319.
6. F. G. Mann and B. C. Saunders, *Practical Organic Chemistry*, pp. 342–344. Longmans Green, London (1954).
7. J. L. Templeton and B. C. Ward, *J. Am. Chem. Soc.* 1980, **102**, 3288.
8. P. K. Baker and E. M. Keys, *Polyhedron* 1986, **5**, 1233.

Polyhedron Vol. 8, No. 3, pp. 357–360, 1989
Printed in Great Britain

0277–5387/89 $3.00+.00
© 1989 Pergamon Press plc

SYNTHESIS AND PROPERTIES OF BERYLLIUM IODATES—III. SYNTHESIS, IR SPECTRA AND X-RAY DIFFRACTION ANALYSIS OF $Be(IO_3)_2 \cdot 2HIO_3 \cdot 6H_2O$

M. MANEVA* and M. GEORGIEV

Department of Inorganic Chemistry, Higher Institute of Chemical Technology, 1156 Sofia, Bulgaria

(*Received* 17 *March* 1988; *accepted after revision* 25 *August* 1988)

Abstract—The compound $Be(IO_3)_2 \cdot 2HIO_3 \cdot 6H_2O$ has been synthesized and identified by quantitative analysis, IR spectra and X-ray diffraction analysis. On the basis of the absorption bands in the IR spectra of the compound and its partially deuterated analogue the basic structural units making up the compound were shown to be $Be(H_2O)_4(IO_3)_2 \cdot 2HIO_3 \cdot 2H_2O$, as well as the existence of two kinds of non-equivalent water molecules.

Information on beryllium iodates is rather scanty and consists mainly of data about the synthesis and some properties of $Be(IO_3)_2 4H_2O$,[1–3] of $[Be_3(OH)_3(H_2O)_6](IO_3)_3 2HIO_3$[4] and of $[Be_3(OH)_3(H_2O_6](IO_3)_3 \cdot H_2O$.[5] The aim of the present investigation was to synthesize a new beryllium iodate from strongly acid solutions of HIO_3, the compounds obtained being identified by the methods of quantitative analysis, IR spectroscopy and X-ray diffraction analysis.

EXPERIMENTAL

The initial compounds used were $BeCO_3$ and HIO_3 (p.a. grade). Synthesis was performed under the following conditions: 0.76 g $BeCO_3$ were added to 100 cm^3 0.5 M solution of HIO_3 with continuous stirring, at constant temperature 343 K. The transparent solution obtained was concentrated to one-fourth of its initial volume, followed by cooling and by the addition of 75 cm^3 absolute C_2H_5OH to it. A colourless gel-like mass was obtained, which was treated several times with C_2H_5OH in the course of 48 hours. The crystalline precipitate obtained was filtered off, air-dried, and kept under ordinary conditions.

A compound of the same composition was also obtained upon dissolution of $Be(IO_3)_2 \cdot 4H_2O$ in concentrated solution of HIO_3 in 1:2 molar ratio followed by isothermal evaporation of the solution at 298 K.

The deuterated sample was prepared by two-fold dissolution of the compound in heavy water and precipitation with C_2H_5OH, with due observance of the conditions determined in the synthesis.

The compound synthesized in the described manner was subjected to quantitative gravimetric analysis for Be^{2+},[6] iodometrically for IO_3^- and I_2,[7] for OH^- by the Chernov[8] method and for hydrate water by Fisher's method. The analysis for OH^- was carried out in order to determine whether the beryllium aqua-complex contained in it had been hydrolysed. The quantitative measurements were carried out on samples obtained during different syntheses and upon different periods of storage. The data revealed complete reproducibility.

The IR spectra of the investigated compound and of its deuterated analogue were taken in the region of 4000–2800 cm^{-1} in a suspension of Hostaflon and of 2800–400 cm^{-1} in KBr tablets on a UR-10 Zeiss apparatus. The data from the X-ray diffraction analysis were obtained on a HZG 4C Zeiss apparatus and by Cu-K_α radiation.

RESULTS AND DISCUSSION

The data from the quantitative analysis of the composition of the compound are the following: Be = 1.10%; I = 61.96%; H_2O = 13.6%; OH^- = 0%. These data coincide most satisfactorily when compared with the theoretical ones for a compound with the composition $Be(IO_3)_2 \cdot 2HIO_3 \cdot 6H_2O$, namely: Be = 1.09%; I = 62.06%; H_2O = 13.8%; OH^- = 0%.

*Author to whom correspondence should be addressed.

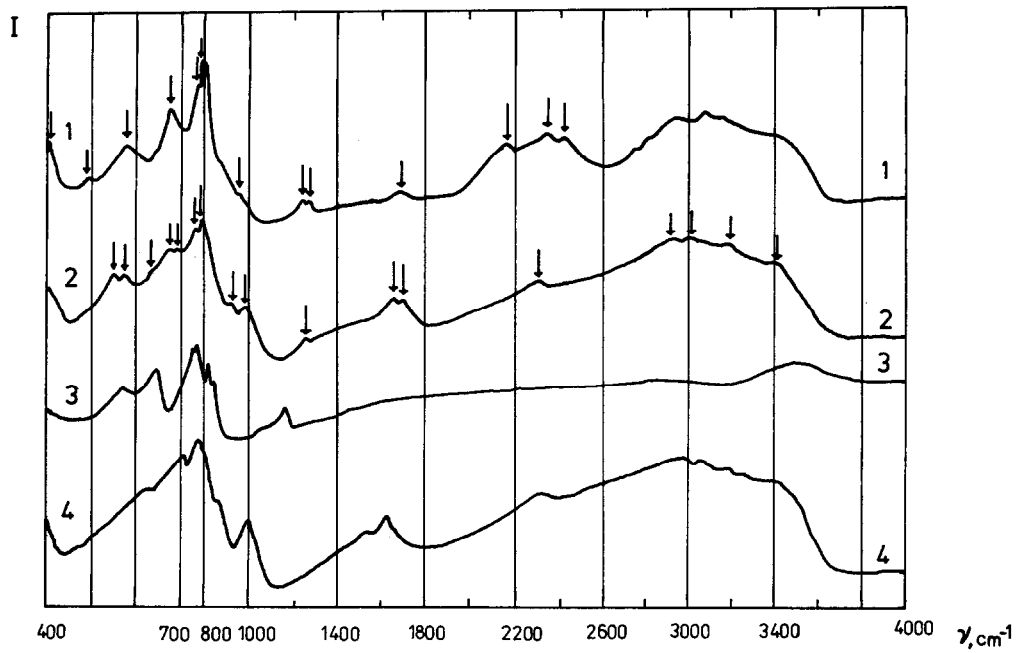

Fig. 1. IR spectra of: (1) partially deuterated product; (2) $Be(IO_3)_2 \cdot 2HIO_3 \cdot 6H_2O$; (3) HIO_3; (4) $Be(IO_3)_2 \cdot 4H_2O$.

The IR spectra of the compound and of its partially deuterated analogue are presented in Table 1 and Fig. 1. The interplanar distances recorded from the diffractograms of $Be(IO_3)_2 \cdot 2HIO_3 \cdot 6H_2O$, compared to those of $Be(IO_3)_2 \cdot 4H_2O$, HIO_3, are presented in Fig. 2.

Table 1

Vibrations observed H-form	D-form	ν_H/ν_D	Character of the vibration
3420 ss	—		
3240 ss	2420 ss	1.34	ν(OH)
3050 ss	2290 ss	1.33	
2920 ss	2180 ss	1.33	
2360 w	1765 w	1.33	$\delta(H_2O)+\nu_L$
1680 m	1270 m	1.33	$\delta(H_2O)$
1650 m	1235 m	1.34	
1240 w	1230	–	δ(IOH)
980 m	950	1.03	δ(Be—OH_2)
860 w			$\nu_3(BeO_4)$
785 s	780 s		
750 s	750 s		ν_3(I—O)
685 sw	680 s		
670 sw	495 sw		ν_L
640 w			ν(I—O(H))
575 w	575 m		γ(I—OH)
545 sw	405 w	1.34	$\nu_\omega(H_2O)$

The presence of the $[Be(H_2O)_4]^{2+}$ complex in the structure of the investigated compound is to be anticipated, because the conditions of the synthesis do not allow for its hydrolysis. This complex is identified by its characteristic absorptions (Table 1, Fig. 1), the one at 860 cm^{-1} being due to the ν_3-valency vibration of the BeO_4 tetrahedron,[9-11] while the absorption at 980 cm^{-1} is due to the bending vibration δ(Be—OH_2). In the spectrum of the partially deuterated analogue the latter is observed at 950 cm^{-1} ($\nu_H/\nu_D = 1.03$). The existence of hydrate water coordinated around the beryllium is proved also by the presence of a weak librational vibration observed at 670 cm^{-1}. Its identification is confirmed by the observed weak absorption at 2360 cm^{-1}, which corresponds to the composite vibration $\delta(H_2O)+\nu_L$.[12]

A proof of the presence of entire redissociated molecules of iodic acid in the structure of the compound is absorption at 575 cm^{-1}, corresponding to the non-planar bending vibration γ(I—OH) (Table 1). The latter is to be observed also in the spectrum of iodic acid. The latter accounts also for the absorption at 640 cm^{-1} of ν(I—O(H)) and for that of the planar bending vibration δ(IOH) at 1240 cm^{-1}. This value is, however, considerably higher than that in the spectrum of the free iodic acid—1165 cm^{-1} (Fig. 1a)—which can be explained by the increased IOH angle in the structure of $Be(IO_3)_2 \cdot 2HIO_3 \cdot 6H_2O$.

The pattern in the region of the stretching vibrations IO_3^- is more complex than in the case of

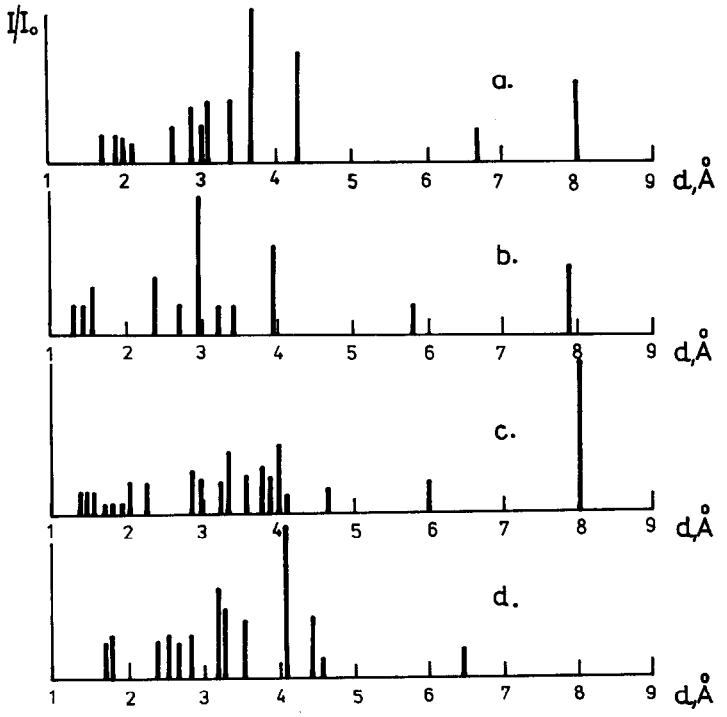

Fig. 2. Interplanar distance of: (a) $Al(IO_3)_2 \cdot 2HIO_3 \cdot 6H_2O$; (b) $Be(IO_3)_2 \cdot 2HIO_3 \cdot 6H_2O$; (c) $Be(IO_3)_2 \cdot 4H_2O$; (d) HIO_3.

HIO_3 (Fig. 1c). A three-fold splitting of the stretching vibration ν_3 is to be observed, with maxima at 785, 750 and 685 cm^{-1}. This is to be expected, having in mind the complex pattern of interaction of the other IO_3^- groups—on the one hand linked directly with the aqua-complex, while on the other hand associated with the HIO_3 molecules on the basis of very strong hydrogen bonds. The latter may be accountable for the strongly shifted absorption band of one of the ν(OH) vibrations at 2920 cm^{-1}. Parallel with that, the HIO_3 molecules participate also in the hydrogen bonds with the water molecules not coordinated around beryllium, namely $HIO_3^- \cdots H_2O$. The stretching vibrations of their OH groups are manifested in the region of 3420–3050 cm^{-1}. The maxima observed in this absorption band for the ordinary and for the deuterated compounds show isotopic shifting within the limits of 1.32–1.34 and are easy to record. Its position in the spectrum is shifted considerably toward the lower frequencies, this being an indication of considerable covalency of the coordinative bond and of the presence of strong hydrogen bonds in the structure of the compound.

The planar bending vibration of the water molecules ($\delta(H_2O)$) is split, with $\Delta\delta = 30$ cm^{-1}. This fact is a proof of the presence of two kinds of crystallochemically inequivalent water molecules in the structure, and confirms the assumption about the presence of coordinated water molecules and of such as are participating only in hydrogen bonds with proton-acceptor groups.

It follows from the information obtained about the compound that its molecule is made up of tetrahedral beryllium aqua-complexes and of highly deformed iodate groups associated by means of very strong hydrogen bonds with the entire HIO_3 molecules. The latter, on the other hand, are also in a state of interaction with the water molecules not coordinated around beryllium, likewise on the basis of hydrogen bonds.

Consequently, the following molecular formula may be assumed for the compound:

$$\begin{bmatrix} H_2O & & H_2O \\ & \searrow\ \swarrow & \\ & Be & \\ & \nearrow\ \nwarrow & \\ H_2O & & H_2O \end{bmatrix} IO_3 \cdots HIO_3 \cdots H_2O$$

$$IO_3 \cdots HIO_3 \cdots H_2O.$$

The investigated compound has been characterized by its X-ray diffractogram (Fig. 2). The data obtained show that the interplanar distances recorded differ from those of the initial components.

REFERENCES

1. Gmelin, System Num. 8 (1933); H. Atterberg, *Soc. Chem.* 1973, **19**, 449.
2. V. Biber, I. Neiman and A. Bragina, *Zh. Obst. Khim.* 1941, **11**, 861.

3. M. Maneva and M. Georgiev, *Therm. Acta* 1985, **92**, 627.
4. M. Maneva and M. Georgiev, *God. Chem. Techn. Inst.-Sofia* 1983, **29**, 29.
5. M. Georgiev and M. Maneva, *God. Chem. Techn. Inst.-Sofia*, in press.
6. W. Giilibrand, T. Lendel and G. Brait, *Prakticheskoe Rukovodstvo po Neorganicheskomu Analizu*, p. 586. Chemie, Moscow (1966).
7. I. Kolthof, W. Stenger and D. Magsuyamo, *Obemniy Analiz*, Vol. III, pp. 518, 577. GHTI-CHI, Moscow (1961).
8. V. Tchernov, *O Prirode Potchvenoy Kislotnosti*, p. 41. Moscow, AN USSR (1947).
9. V. Sipachev and A. Grigoriev, *Zh. Strukt. Khim.* 1969, **10**, 820.
10. A. Grigoriev, V. Sipachev and A. Novoselova, *Dokl. Adad. Nauk SSSR* 1965, **160**, 383.
11. A. Grigoriev, A. Sipachev and E. Pogofilova, *Zh. Strukt. Khim.* 1970, **11**, 485.
12. K. Nakamoto, *Infrared Spectra of Inorganic and Coordination Compounds* (2nd Edn), p. 89. John Wiley, New York (1969).

Polyhedron Vol. 8, No. 3, pp. 361–365, 1989
Printed in Great Britain

0277–5387/89 $3.00+.00
© 1989 Pergamon Press plc

STUDY BY SERS OF THE ELECTROREDUCTION OF THE PENTACYANONITROSYLFERRATE(II) ANION

J. R. BERTOLINO, C. O. DELLA VÉDOVA* and O. SALA†

Instituto de Química, Universidade de São Paulo, C.P. 20780, São Paulo, Brazil

(*Received* 26 *February* 1988; *accepted* 25 *August* 1988)

Abstract—The surface enhanced Raman scattering (SERS) of the nitroprusside anion adsorbed on a silver electrode were obtained and compared with the normal Raman spectra of the chemically reduced species $[Fe(CN)_5NO]^{3-}$ and $[Fe(CN)_4NO]^{2-}$. The results are in agreement with the reversibility of the system at the two first waves coupled with the equilibrium

$$[Fe(CN)_5NO]^{3-} \rightleftharpoons [Fe(CN)_4NO]^{2-} + CN^-,$$

as indicated by the characteristic vibrational bands of surface complexes $[Ag(CN)_{x+1}]^{x-}$ generated from this equilibrium. The attempts to obtain the spectra at the third reduction wave were not successful.

SERS effect has been a useful technique to study complexes adsorbed on silver and copper electrodes[1–3] and oxidation–reduction reactions.[4–7] The electroreduction of the nitroprusside ion had been studied in both aqueous solution[8,9] and non-aqueous aprotic media.[10–12] Voorst and Hemmerich[8] have shown that upon the reduction of nitroprusside in the pH range 7–10, the brown complex $[Fe(CN)_5NO]^{3-}$ is obtained, and at pH 4 the reduction yields the blue $[Fe(CN)_5NOH]^{2-}$ complex. Schmidt *et al.*[11–13] and Cheney *et al.*[9] have shown, respectively for aprotic and aqueous media, that the one-electron reduction of the nitroprusside produces mainly $[Fe(CN)_5NO]^{3-}$ and $[Fe(CN)_4NO]^{2-}$, which are O_2 sensitive, generating the $[Fe(CN)_5NO]^{2-}$, $[Fe(CN)_4NO(OH)]^{2-}$ and polymeric species. Nast and Schmidt[12] have characterized the compounds obtained by the reduction of nitroprusside with alkaline metals in liquid ammonia and assigned their most important IR bands. Masek *et al.*[14,15] have studied the reactions involving the nitroprusside reduction products obtained during the three polarographic waves, in acidic and basic media.

In the present work the electroreduction of the nitroprusside ion adsorbed on a silver electrode was investigated by SER spectroscopy in the CN stretching and skeletal vibration regions. The results were compared with the normal Raman spectra of the products of one- and two-electron reduction of the nitroprusside, with the IR spectra reported in the literature[12] and with the studies of electroreduction on mercury electrode.[14,15]

EXPERIMENTAL

The $Na_2[Fe(CN)_5NO]\cdot 2H_2O$ was kindly donated by Dr H. E. Toma. Electrolyte solutions, 0.1 M KCl or KBr and 0.003 M nitroprusside ion, were prepared with double-distilled water and dissolved air, removed by N_2 bubbling. The working electrode, a 0.1 cm^2 silver rod supported by acrylic resin, was polished with 600 mesh wet sandpaper prior to use. The auxiliary and reference electrodes were platinum and saturated calomel (SCE), respectively. The spectrometer, potentiostat and experimental set-up were described elsewhere.[16,17]

The procedure to obtain the SERS was as follows: (i) after several oxidation–reduction cycles to activate the electrode surface, the sample was added to the cell at a potential close to the electrode oxidation potential (−0.1 V, KCl 0.1 M); (ii) a new cycle was performed at a rate of 20 mV s^{-1} and the spectra recorded at steps of 0.1 V, from −0.5 to

*Permanent address: Departamento de Química, Facultad de Ciencias Exactas, Universidad Nacional de La Plata, La Plata, Argentina.

†Author to whom correspondence should be addressed.

Table 1. Raman frequencies (cm^{-1}) for nitroprusside

Skeletal region				CN *stretching region* SERS				
Aqueous solution	SERS[a]	Chemically reduced species	Aqueous solution	−1.2 V	−1.0 V	−0.8 V	−0.6 V	Chemically reduced species
410	220	435	2157	2010	2000	—	—	2060
475	375	560		2050	2040	2050	2060	2090
660	430	660		—	—	2095sh	2095sh	2115
	500			2105	2100	2100	2100	
	560							

[a] For all potentials from −1.2 to −0.6 V.

−1.2 V and also in the reverse way, from −1.2 to −0.5 V.

The spectral resolution was 7 cm^{-1} and the laser power (514.5 and 647.1 nm) adjusted to *ca* 20 mW.

The chemically reduced species used to obtain the normal Raman spectra, for comparison, were obtained from reduction of nitroprusside with $NaBH_4$.[8,9]

RESULTS AND DISCUSSION

In Fig. 1a, b the SERS of nitroprusside adsorbed on a silver electrode are shown at several electrode potentials, respectively for the skeletal and CN stretching vibration regions. The vibrational frequencies (cm^{-1}) for these regions are listed in Table 1. The spectra in Fig. 1 were obtained from −1.2 to −0.5 V; identical results were obtained changing the potential from −0.5 to −1.2 V.

According to Masek *et al.*[14,15] at potentials more negative than −0.4 V, reduced species are expected to be present in the bulk solution. Since the SERS differ from the spectra of the nitroprusside, both in solution and solid state (particularly in the CN stretching region), it is reasonable to suppose they are due to that reduced species.

Masek and Máslová[15] have shown that the reduction of nitroprusside on mercury electrode occurs in three steps: the two first reduction waves are represented as follows,

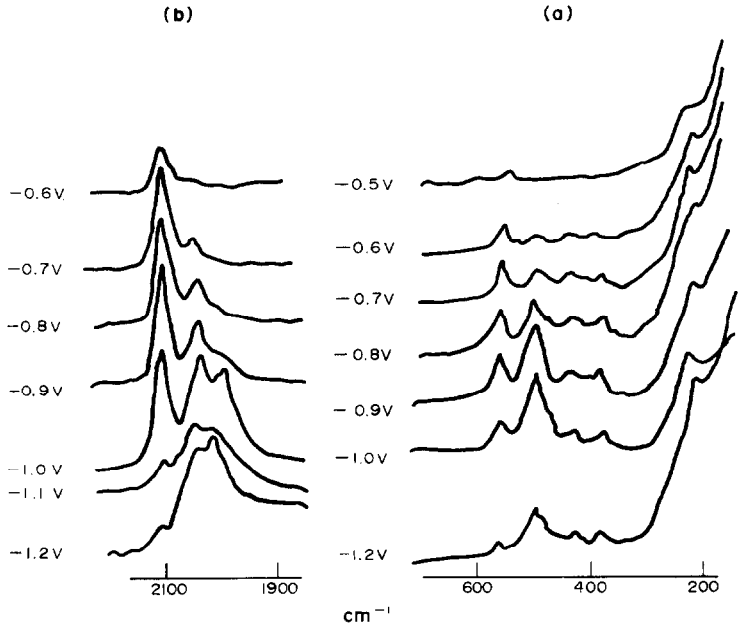

Fig. 1. SERS spectra of the electroreduced species on a silver electrode at the indicated potentials in 0.1 M KCl, $\lambda_{exc.}$ = 514.5 nm. (a) skeletal region and (b) CN region.

$$[Fe(CN)_5NO]^{2-} \overset{(i)}{\rightleftharpoons} [Fe(CN)_5NO]^{3-}$$
$$\downarrow\uparrow$$
$$[Fe(CN)_4NO]^{3-} \overset{(ii)}{\rightleftharpoons} [Fe(CN)_4NO]^{2-} + CN^-,$$

(i) the one-electron reduction at $E_{1/2} = -0.36$ V, yielding a primary product $[Fe(CN)_5NO]^{3-}$ in equilibrium with $[Fe(CN)_4NO]^{2-}$ and CN^-; (ii) the reduction, at $E_{1/2} = -0.56$ V, from $[Fe(CN)_4NO]^{2-}$ to $[Fe(CN)_4NO]^{3-}$ that reacts with $[Fe(CN)_5NO]^{2-}$ giving back the first electroreduction equilibrium. The third reduction wave, $E_{1/2} = -1.32$ V, yields $[Fe(CN)_5NH_2OH]^{3-}$. These authors mention the possibility, at pH > 6.5, of the formation of the two linkage isomers of nitroprusside, i.e. $[Fe(CN)_4(NC)(NO)]^{3-}$ and $[Fe(CN)_4(NC)(NO)]^{4-}$, after the second one-electron reduction. In acidic medium,[18] the first electroreduction gives the same products obtained in basic medium. However, the second reduction wave involving the protonated species $[Fe(CN)_5NOH]^{2-}$, gives the $[Fe(CN)_5NOH]^{3-}$ which, by a third reduction yields $[Fe(CN)_5NH_2OH]^{3-}$ at *ca* −1.3 V. Since the electroreduction of the nitroprusside has been studied on mercury electrodes, in order to be compared with our results on silver electrodes, the voltammograms using this electrode and a mercury electrode were obtained, giving the values −0.6 V, −0.9 V and *ca* −1.3 V on silver and −0.4 V, −0.6 V and −1.3 V on mercury, for such species.

It is worthwhile to discuss the behaviour of the bands at 500 and 560 cm^{-1}, in the skeletal region, and 2010 and 2060 cm^{-1}, in the CN stretching region. Figure 2 represents the intensity ratios I_{500}/I_{560} and I_{2010}/I_{2060} as functions of the applied potential. From Figs 1 and 2 it can be seen that the intensity of the bands at 500 and 2010 cm^{-1} increases when the potential is more negative than the second reduction wave (−0.9 V). The intensity of the bands at 560 and 2060 cm^{-1} shows only small dependence on the potential, in the range −0.6 to −1.2 V.

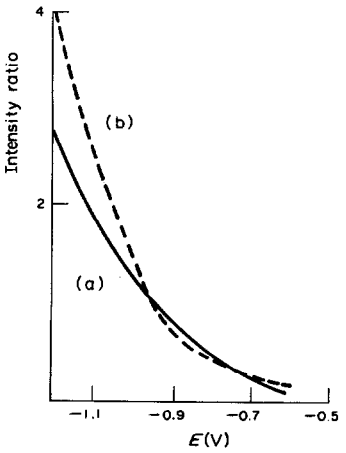

Fig. 2. Raman Intensity ratio vs potential: (a) I_{2010}/I_{2060} and (b) I_{500}/I_{560}, in 0.1 M KCl and $\lambda_{exc.} = 514.5$ nm.

In order to characterize the electroreduced species, the spectra of nitroprusside chemically reduced with one or two equivalents of $NaBH_4$, at pH 7.1, were obtained. In Fig. 3 the spectra of nitroprusside, normal Raman and SERS (−0.8 V), and that of the reduced species are compared. The spectra for the species reduced by one or two equivalents of $NaBH_4$ are practically identical. In the skeletal region, the SER spectrum shows more similarity with the spectrum of the reduced species, except for the absence of the band at 660 cm^{-1}, which has a contribution of the NO moiety.[19] In the CN stretching region, the band at 2157 cm^{-1} of the nitroprusside originates the bands at 2060, 2090 and 2115 cm^{-1} in the reduced species and at 2010, 2060, 2095(sh) and 2105 cm^{-1} in the SERS. There is a correspondence between the bands at *ca* 2060 and 2090 cm^{-1}. The band at 2105 cm^{-1} may correspond to the 2115 cm^{-1} or to a surface complex $[Ag(CN)_{x+1}]^{x-}$, which will be discussed later.

The bands at 500 and 2010 cm^{-1}, as previously mentioned, are enhanced at potentials more negative than the second one-electron reduction (−0.9 V) and can be assigned to the reduced species $[Fe(CN)_4NO]^{3-}$, at pH > 7. The assignment of the 2010 cm^{-1} is in agreement with Nast and Schmidt,[12] who observed bands at *ca* 2040 cm^{-1} in the IR spectra of this reduced species. According to these authors, when the Fe^{n+} ion is in an oxidation state lower than II the CN stretching shifts to lower frequencies. They assume that $[Fe(CN)_4NO]^{3-}$ has a configuration Fe^0–NO^+, obtained from the reduction of $[Fe(CN)_4NO]^{2-}$ (configuration $Fe^{I-}NO^+$). The Raman spectrum of nitroprusside, chemically reduced at pH 4, shows a band at 2115 cm^{-1}, also observed in the IR spectrum of $[Fe(CN)_4NO]^{2-}$.[12] The assignment of the band at 500 cm^{-1} is more difficult. However, due to its similar behaviour with the band at 2010 cm^{-1}, it can be assigned to the species $[Fe(CN)_4NO]^{3-}$. Nevertheless, the possibility of assigning it to $[Fe(CN)_5NO]^{3-}$ can not be discarded.

Efforts to observe the NO stretching vibration in the SERS were not successful, the same occurring with the attempts to obtain the SERS at pH 4 in buffered medium. The spectra in pH 7.0 buffered solution are identical to those at pH > 7. In non-buffered solutions an increase in the pH was observed after the electroreduction, probably due to the formation of CN^- ions.

In Fig. 1, strong bands at 220 and 2105 cm^{-1} are

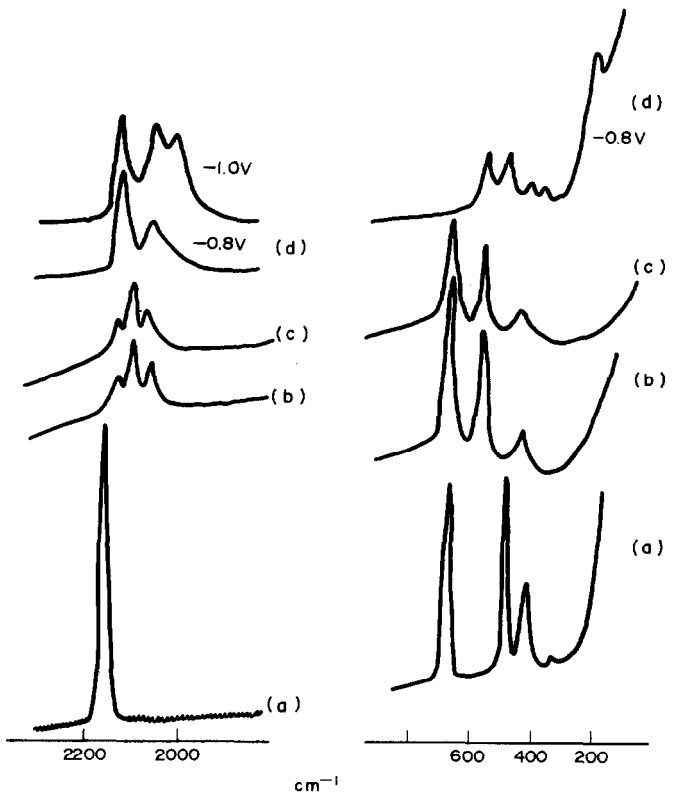

Fig. 3. Raman spectra : (a) nitroprusside, aqueous solution ; (b) product of the one-electron reduction of nitroprusside, $[Fe(CN)_5NO]^{3-}$; (c) product of the two-electron reduction of nitroprusside, $[Fe(CN)_4NO]^{3-}$, and (d) SERS at the indicated potentials, 0.1 M KCl, $\lambda_{exc.} = 514.5$ nm.

observed. The band at 220 cm^{-1} is not observed either in the nitroprusside or in the $[Fe(CN)_5NO]^{3-}$ normal Raman spectra. Since after the first reduction there is the equilibrium $[Fe(CN)_5NO]^{3-} \rightleftharpoons [Fe(CN)_4NO]^{2-} + CN^-$, those bands may be assigned to surface complexes $[Ag(CN)_{x+1}]^{x-}$ as described by several authors[20-23] for SERS of CN^- adsorbed on a silver electrode. This assignment is confirmed by the presence of the 220 cm^{-1} band in the SERS spectra in a 0.1 M KBr support electrolyte. In addition, the potential behaviour of the band at 2105 cm^{-1} corroborates this hypothesis.

At potentials more positive than -0.2 V the spectra in the presence of CN^- show a shift from 2110 to 2146 cm^{-1}, consistent with the decrease in the proportion of the surface complexes $[Ag(CN)_4]^{3-}$ and $[Ag(CN)_3]^{2-}$ relative to $[Ag(CN)_2]^-$.[20,21] In this work, we could not observe this behaviour since for potentials more positive than -0.4 V, the $[Fe(CN)_5NO]^{3-}$ is oxidized to $[Fe(CN)_5NO]^{2-}$, displacing the equilibria set up after the two electroreductions towards the nitroprusside. This embodying of the CN^- ions into the complexes $[Fe(CN)_4NO]^{3-}$ and $[Fe(CN)_4NO]^{2-}$ explains the absence of the surface complexes $[Ag(CN)_{x+1}]^{x-}$ spectra.

Summarizing, the SERS of the nitroprusside complex is consistent with the reversibility of the two reduction waves of the nitroprusside suggested by Masek and Maslova.[15] The spectra were assigned to the species $[Fe(CN)_5NO]^{3-}$ and $[Fe(CN)_4NO]^{3-}$, by comparison with the normal Raman of the chemically reduced species and also by the behaviour of the Raman intensity vs applied potential. The bands at 220 and 2105 cm^{-1} are assigned to the surface complex $[Ag(CN)_{x+1}]^{x-}$ originated from the release of the CN^- ions. The non-observation of SERS spectra at potentials more negative than -1.3 V (third reduction wave) is probably due to the lability of the complex $[Fe(CN)_5NH_2OH]^{3-}$.

Acknowledgements—This work was supported by FINEP and CNPq. C.O.D.V. and J.R.B. are indebted to CONICET/CNPq and CAPES(UFSC), respectively, for the grant of a fellowship. The authors acknowledge Dr H. E. Toma for helpful discussions.

REFERENCES

1. M. J. Weaver, S. Farquharson and M. A. Taddayoni, *J. Chem. Phys.* 1985, **82**, 4867.

2. J. A. Chambers and R. P. Buck, *J. Electroanalyt. Chem.* 1984, **163**, 297.
3. A. M. Stacy and R. P. Van Duyne, *Chem. Phys. Lett.* 1983, **102**, 365.
4. S. Farquharson, K. L. Guyer, R. A. Magnuson and M. J. Weaver, *J. Am. Chem. Soc.* 1984, **106**, 5123.
5. B. Simic-Glavaski, S. Zecevic and E. Yeager, *J. Electroanalyt. Chem.* 1983, **150**, 469.
6. S. Farquharson, P. A. Lay and M. J. Weaver, *Spectrochim. Acta* 1984, **40A**, 907.
7. J. R. Bertolino, M. L. A. Temperini and O. Sala, to be published.
8. J. D. W. Van Voorst and P. Hemmerich, *J. Chem. Phys.* 1966, **45**, 3914.
9. R. P. Cheney, M. G. Simic, M. Z. Hoffmann, I. A. Taub and K. D. Asmus, *Inorg. Chem.* 1977, **16**, 2187.
10. W. L. Bowden, P. Bonnan, D. B. Brown and W. E. Geiger, *Inorg. Chem.* 1977, **16**, 41.
11. J. Schmidt, H. Kuhr, W. L. Dorn and J. Kopt, *Inorg. Nucl. Chem. Lett.* 1974, **10**, 55.
12. R. Nast and J. Schmidt, *Z. Anorg. Allg. Chem.* 1976, **421**, 15.
13. J. Schmidt and W. Dorn, *Inorg. Chim. Acta* 1976, **16**, 223.
14. J. Fiedler and J. Masek, *Inorg. Chim. Acta* 1984, **81**, 117.
15. J. Masek and E. Maslova, *Collect. Czech. Chem. Commun.* 1974, **39**, 2141.
16. M. L. A. Temperini, H. C. Chagas and O. Sala, *Chem. Phys. Lett.* 1981, **79**, 75.
17. M. L. A. Temperini, W. J. Barreto and O. Sala, *Chem. Phys. Lett.* 1983, **99**, 148.
18. J. Masek and J. Dempir, *Collect. Czech. Chem. Commun.* 1969, **34**, 727.
19. J. B. Bates and R. K. Khanna, *Inorg. Chem.* 1970, **9**, 1376.
20. J. Billmann and A. Otto, *Surf. Sci.* 1984, **138**, 1.
21. T. T. Chen, K. U. Von Raben, D. V. Murphy, B. L. Laube and R. K. Chang, *Surf. Sci.* 1984, **143**, 369.
22. M. E. Pemble, M. Fleischmann and I. R. Hill, *J. Electroanalyt. Chem.* 1982, **136**, 361.
23. R. Kotz and E. Yeager, *J. Electroanalyt. Chem.* 1981, **123**, 335.

Polyhedron Vol. 8, No. 3, pp. 367–369, 1989
Printed in Great Britain

0277–5387/89 $3.00+.00
© 1989 Pergamon Press plc

THE X-RAY CRYSTAL STRUCTURE OF TRIS (2,2′-BIPYRIDINE)OSMIUM(II) HEXAFLUOROPHOSPHATE

EDWIN C. CONSTABLE,* PAUL R. RAITHBY and DIANA N. SMIT

University Chemical Laboratory, Lensfield Road, Cambridge CB2 1EW, U.K.

(*Received* 28 *July* 1988; *accepted* 8 *September* 1988)

Abstract—The X-ray crystal structure of the complex (bipy = 2,2′-bipyridine) is reported. The complex is isostructural with the corresponding ruthenium(II) complex $[Ru(bipy)_3][PF_6]_2$ with Os—N, 2.056(8) Å.

Complexes of the d^6 platinum group metal ions with diimine ligands (2,2′-bipyridine, 1,10-phenanthroline and 2,2′:6′,2″-terpyridine) have been known for many years, and have been of considerable recent interest because of their attractive photochemical and photophysical properties.[1] In particular, these complexes have been intensively investigated as components of both homogeneous and heterogeneous systems for photoconversion.[1] Furthermore, the solution properties of the ions indicate specific interactions between solvent molecules and the cations, which may be of relevance to their rôles as photocatalysts.[2] In order to understand the ground and excited state electronic properties of the complexes, and to probe possible solvent–solute interactions, it is necessary to have a good knowledge of their structures. In this paper, we report the crystal and molecular structure of the complex $[Os(bipy)_3][PF_6]_2$.

EXPERIMENTAL

2,2′-Bipyridine (Aldrich) and "osmium trichloride" (Johnson Matthey) were used as supplied; $[Os(bipy)_2Cl_2]Cl$ was prepared by the literature method.[3] Electronic spectra were recorded using a Pye-Unicam 8800 spectrophotometer; IR spectra were recorded using Perkin–Elmer 1710 FT or 983 spectrometers with the compound in compressed KBr pellets or in suspension in Nujol. NMR spectra were recorded on Brüker WM250 or AM400 spectrometers.

*Author to whom correspondence should be addressed.

Preparation of $[Os(bipy)_3][PF_6]_2$

2,2′-Bipyridine (0.312 g, 2 mmol) and $[Os(bipy)_2Cl_2]Cl$ (0.608 g, 1 mmol) were heated to reflux in $MeOCH_2CH_2OH$ (25 cm^3) for 24 h, after which period the dark coloured solution was filtered and diluted with MeOH (25 cm^3). A solution of $[NH_4][PF_6]$ (2.0 g) in MeOH (10 cm^3) was added, and the resultant dark green precipitate collected by filtration to yield $[Os(bipy)_3][PF_6]_2$ (0.600 g, 63%) (Found: C, 37.7; H, 2.6; N, 8.7. Calc. for $C_{30}H_{24}N_6OsP_2F_{12}$: C, 38.0; H, 2.5; N, 8.9%).

Crystal structural determination of $[Os(bipy)_3][PF_6]_2$

Dark green blocks of the complex were obtained by the recrystallization of $[Os(bipy)_3][PF_6]_2$ from hot methanol. A suitable dark green crystal was mounted on a glass fibre with epoxy resin.

Crystal data. $C_{30}H_{24}N_6OsP_2F_{12}$, dark green blocks, $M = 948.6$, trigonal, $a = 10.772(1)$, $c = 16.342(1)$ Å, $U = 2962$ Å^3 (by least-squares refinement of diffractometer angles for 54 automatically centred reflections, $20 < 2\theta < 25°$, $\lambda = 0.71609$ Å), space group $P3c1$ (No. 165), $Z = 2$, $D_c = 2.49$ g cm^{-3}, $F(000) = 926$. Crystal dimensions $0.076 \times 0.106 \times 0.513$ mm, Mo-K_α radiation ($\lambda = 0.7107$ Å), μ(Mo-K_α) = 128.76 cm^{-1}.

Data collection and processing. Stoe–Siemens four-circle diffractometer, 24-step ω-θ mode with scan width 0.04° per step, scan time 0.5–2.0 s per step, graphite monochromated Mo-K_α radiation; 6333 profile fitted intensities measured ($5.0 \leqslant 2\theta \leqslant 45.0°$), 969 unique [merging $R = 0.0104$

after empirical absorption correction based on an ellipsoidal fit of 256 azimuthal data (maximum, minimum transmission factors, 0.252, 0.207)] giving 814 with $F > 4\sigma(F)$. Three standard reflections showed no decrease in intensity during data collection.

Structure analysis and refinement. The structure was solved by direct methods followed by Fourier difference techniques. The Os and P atoms occupy special positions. Blocked full-matrix least-squares refinement with Os, P, N and C atoms anisotropic. Hydrogen atoms were not located directly, but were placed in idealized positions and allowed to ride on the relevant carbon with C—H fixed at 0.96 Å, and refined with a common isotropic temperature factor, $U = 0.078(19)$ Å^2. The PF_6^- counter ion was disordered, two sets of positions being located for the F atoms; these were refined with partial occupancies and a common isotropic factor, $U = 0.099(3)$ Å^2. The weighting scheme $w = 0.8179/[\sigma^2(F)+0.002|F|^2]$ gave satisfactory agreement analyses. Final converged R and R_w values were $R = 0.057$ and $R_w = 0.058$. A final electron density map showed no significant regions of electron density. Complex neutral atom scattering factors were taken from ref. 4. Calculations were performed using SHELX 76 on the IBM 370/165 computer at the University of Cambridge.[5]

RESULTS AND DISCUSSION

The green complex salt $[Os(bipy)_3][PF_6]_2$ is readily prepared by the reaction of $[Os(bipy)_2Cl_2]Cl$ with an excess of 2,2′-bipyridine in 2-methoxyethanol. In this reaction, the 2-methoxyethanol acts as both a solvent and a reductant. Recrystallization of the complex from methanol yields X-ray quality crystals. Microanalysis and ^{1}H NMR studies indicated that the complex contained no lattice solvent. The ^{1}H NMR and electronic spectra of solutions in methanol, and in 0.05 and 0.1 M methanolic CH_3ONa were identical, suggesting that significant nucleophilic attack by methoxide was not occurring.

The structure of the $[Os(bipy)_3]^{2+}$ cation, together with the numbering scheme adopted, is shown in Fig. 1. Selected bond lengths and bond angles are presented in Table 1. The cation exists as a discrete $[Os(bipy)_3]^{2+}$ ion, with crystallographically imposed trigonal symmetry. All the Os—N distances are equivalent, with Os—N, 2.056(8) Å. The bite angle of each 2,2′-bipyri-

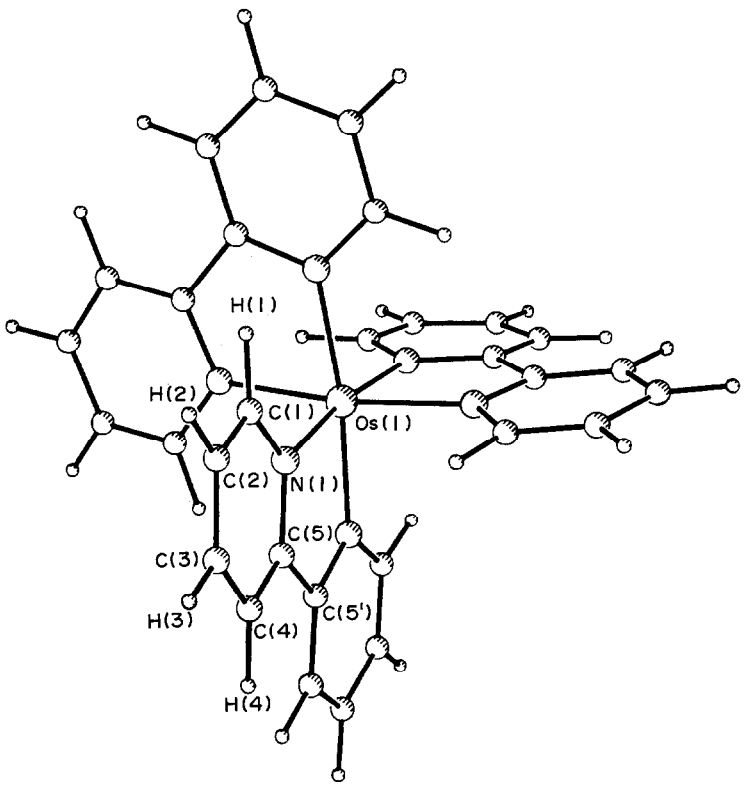

Fig. 1. The molecular structure of the $[Os(bipy)_3]^{2+}$ cation showing the numbering scheme adopted.

Table 1. Selected bond lengths (Å) and interbond angles (°) for $[Os(bipy)_3][PF_6]_2$ with ESDs in parentheses

Lengths (Å)			
Os(1)—N(1)	2.056(8)	P(1)—F(1)	1.538(19)
P(1)—F(2)	1.586(18)	P(1)—F(3)	1.592(33)
P(1)—F(4)	1.645(40)	C(1)—C(2)	1.355(15)
C(1)—N(1)	1.353(13)	C(2)—C(3)	1.376(19)
C(3)—C(4)	1.374(16)	C(4)—C(5)	1.380(12)
C(5)—N(1)	1.358(11)	C(5)—C(5)′	1.495(16)
Angles (°)			
F(4)—P(1)—F(3)	86.2(18)	F(2)—P(1)—F(1)	86.1(9)
F(2)—P(1)—F(2)	85.5(10)	F(2)—P(1)—F(2)	85.5(10)
F(3)—P(1)—F(3)	105.7(17)	F(3)—P(1)—F(3)	105.7(17)
F(4)—P(1)—F(4)	81.0(22)	F(4)—P(1)—F(4)	81.0(22)
N(1)—C(1)—C(2)	121.0(11)	C(3)—C(2)—C(1)	120.9(11)
C(4)—C(3)—C(2)	119.2(11)	C(5)—C(4)—C(3)	118.0(11)
N(1)—C(5)—C(4)	122.6(8)	C(1)—N(1)—Os(1)	124.5(7)
C(5)—N(1)—Os(1)	117.4(6)	C(5)—N(1)—C(1)	118.1(9)
N(1a)—Os(1)—N(1)	96.3(3)	N(1c)—Os(1)—N(1a)	96.3(3)
N(1c)—Os(1)—N(1b)	77.8(4)	N(1b)—Os(1)—N(1)	90.1(4)

dine ligand at the osmium is 77.8(4)°. There are no significant intermolecular contacts between the $[Os(bipy)_3]^{2+}$ cations and the $[PF_6]^-$ anions, and there is no evidence for the presence of lattice solvent molecules. All bond angles and bond lengths within the 2,2′-bipyridine ligands are unremarkable, and closely resemble those observed in other 2,2′-bipyridine complexes.[6]

The most remarkable feature of this structure is its similarity to those of $[Ru(bipy)_3][PF_6]_2$, with which it is isostructural, and other structurally characterized d^6 $[M(bipy)_3]^{n+}$ complexes. The M—N distances in $[Ru(bipy)_3]^{2+}$ (2.055 Å),[7,8] $[Ir(bipy)_3]^{3+}$ (1.999–2.033 Å),[9] and $[Rh(bipy)_3]^{3+}$ (2.031–2.039 Å)[10] do not differ significantly (within 3 ESDs) from those determined here for $[Os(bipy)_3]^{2+}$. Similarly, the bite angles in $[Ru(bipy)_3]^{2+}$ (78.7°),[7,8] $[Ir(bipy)_3]^{3+}$ (78.4–79.1°),[9] and $[Rh(bipy)_3]^{3+}$ (80.1–80.6°)[10] closely resemble those observed in $[Os(bipy)_3][PF_6]_2$.

The similarity of the structures of $[Os(bipy)_3][PF_6]_2$ and $[Ru(bipy)_3][PF_6]_2$ confirm that the differences in photophysical behaviour may be attributed solely to electronic differences in the metal–ligand interactions rather than to any steric or structural differences.

REFERENCES

1. A. Juris, V. Balzani, F. Barigelletti, S. Campagna, P. Belser and A. von Zelewsky, *Coord. Chem. Rev.* 1988, **84**, 85; D. J. Cole-Hamilton and D. W. Bruce in *Comprehensive Coordination Chemistry* (Edited by G. Wilkinson, R. D. Gillard and J. A. McCleverty), Vol. 7, p. 487. Pergamon Press, Oxford (1986).
2. E. C. Constable, *Polyhedron* 1983, **2**, 551; R. D. Gillard, *Coord. Chem. Rev.* 1975, **16**, 16; R. D. Gillard, *Coord. Chem. Rev.* 1983, **50**, 303; N. Serpone, G. Ponterini, M. A. Jamieson, F. Bolletta and M. Maestri, *Coord. Chem. Rev.* 1983, **50**, 209; G. Nord, *Comments Inorg. Chem.* 1985, **4**, 193.
3. P. A. Lay, A. M. Sargeson and H. Taube, *Inorg. Synth.* 1986, **24**, 293.
4. *International Tables for X-Ray Crystallography*, Vol. 4. Kynoch Press, Birmingham (1974).
5. G. M. Sheldrick, SHELX 76, crystal structure solving package, Cambridge (1976).
6. E. C. Constable, *Adv. Inorg. Chem. Radiochem.*, in press.
7. T. Tada, *J. Sci. Hiroshima Univ.* 1982, **46**, 73.
8. D. P. Rillema, D. S. Jones and H. A. Levy, *J. Chem. Soc., Chem. Commun.* 1979, 849.
9. A. C. Hazell and A. C. Hazell, *Acta Cryst.* 1984, **C40**, 806.
10. B. Hubesch, B. Mahieu and J. Meunier-Piret, *Bull. Soc. Chim. Belg.* 1985, **94**, 685.

Polyhedron Vol. 8, No. 3, pp. 371–373, 1989
Printed in Great Britain

0277–5387/89 $3.00+.00
© 1989 Pergamon Press plc

THIOCYANATE AND AZIDE COMPLEXES CONTAINING A MOLYBDENUM(II) MONONITROSYL CENTRE

NAJAT ALOBAIDI,* CHRISTOPHER J. JONES† and JON A. McCLEVERTY

Department of Chemistry, University of Birmingham, PO Box 363, Birmingham B15 2TT, U.K.

(*Received* 15 *June* 1988; *accepted* 28 *September* 1988)

Abstract—The formally 16 electron complexes $[Mo(NO)LX_2]$ (L = $\{HB(3,5\text{-}Me_2C_3N_2H)_3\}$ and X = N_3 or NCS) have been synthesized. Both undergo one electron reduction (at −0.13 V (SCE) when X = N_3 and at −1.64 V when X = NCS).

The sterically demanding tripodal ligand hydrotris(3,5-dimethylpyrazolyl)borate (L) may be used to restrict both molybdenum(II), in the form of $\{Mo(NO)\}^{3+}$, and molybdenum(V), in the form of $\{MoO\}^{3+}$ to octahedral six-coordination. Enemark has exploited this principal in preparing models of the molybdenum cofactor in enzymes such as *sulphite oxidase*. Thus a range of derivatives [Mo(O)LXY] (X and Y are halide, alkoxide, phenoxide thiophenoxide) were prepared and their electrochemical properties determined.[1] All the complexes were found to undergo reversible or quasi-reversible one-electron reduction processes at potentials which varied depending upon the nature of X and Y. The azide and thiocyanate complexes, $[Mo(O)L(N_3)_2]$ and $[Mo(O)L(NCS)_2]$, were also prepared and the latter was found to undergo particularly facile reduction. Thus while bis-alkoxide complexes were reduced at *ca* −1.1 V (Ag/AgCl) and the bis-thiophenoxide at −0.28 V, the bis-azide was reduced at −0.31 V and the bis-thiocyanate at +0.12 V.

A related series of molybdenum(II) mononitrosyl derivatives, [Mo(NO)LXY] (X and Y are halide, alkoxide, phenoxide, thiophenoxide) has been prepared in our laboratories.[2] Electrochemical studies have shown that these too undergo reversible or quasi-reversible one-electron reduction processes at potentials which depend upon the nature of X and Y.[3,4] In view of the parallels between the syntheses of [Mo(O)LXY] and [Mo(NO)LXY], we were interested in extending the series of known nitrosyl complexes to include [Mo(NO)LXY] (X = Y = N_3 or NCS).

EXPERIMENTAL

All reagents were used as supplied, $[Mo(NO)\{HB(3,5\text{-}Me_2C_3N_2H)_3\}I_2]$ was prepared according to a previously described method.[5] Silica gel 60 (70–230 mesh) was used as the stationary phase for column chromatography unless otherwise stated. All reactions were carried out under nitrogen but purification procedures were carried out in air. Elemental analyses were carried out by the Microanalytical Laboratory, University of Birmingham.

IR spectra were recorded using a PE 297 spectrometer, ^1H NMR spectra were obtained using a Jeol GX 270 (270 MHz) instrument. Cyclic voltammetric and other electrochemical measurements were made using a Hitek PPR 1 waveform generator and DT 2101 potentiostat or a PAR 174A polarograph. Solutions were *ca* 10^{-3} mol dm^{-3} in the complex and 0.2 mol dm^{-3} in $[Bu^n_4N]BF_4$ as the base electrolyte. A platinum bead test electrode was used with an SCE reference electrode and ferrocene as internal standard. Under these conditions the formal electrode potential, E_f, for the Fc/Fc^+ couple was found to be at 0.43 V, with the cathodic and anodic peak potential separation, $\Delta E_p = 60$ mV. The number of electrons associated with electrode processes was estimated by comparison with $[Mo(NO)LCl_2]$.

$[Mo(NO)L(NCS)_2]$

A mixture of $[Mo(NO)LI_2]$ (0.5 g, 0.75 mmol), NaNCS (0.158 g, 2 mmol) and dibenzo-18-crown-6

* New address: Department of Physics, College of Education, AlMustansiriyah University, Baghdad, Iraq.
† Author to whom correspondence should be addressed.

(0.266 g, 0.74 mmol) was stirred in CH_2Cl_2 (50 cm^3) for 18 h, during which time the solution became red–brown in colour. The reaction mixture was filtered and the solvent removed from the filtrate by evaporation under reduced pressure. The residue was purified by column chromatography using CH_2Cl_2–hexane (70/30 v/v) as the eluent. The major red fraction to elute was collected, the solvent removed under reduced pressure and the residue recrystallized from a CH_2Cl_2–hexane mixture to give a dark red microcrystalline product (70 mg, 18%). Found: C, 37.9; H, 4.4; N, 23.2. Calc. for $C_{15}H_{22}N_{13}BMoO$: C, 37.9; H, 4.1; N, 23.4%.

[Mo(NO)L(N_3)$_2$]

A mixture of [Mo(NO)LI_2] (2.0 g, 3 mmol), NaN_3 (0.424 g, 6.5 mmol) and dibenzo-18-crown-6 (1.064 g, 3 mmol) was stirred in CH_2Cl_2 (150 cm^3) for 16 h, during which time the solution became green in colour. The reaction mixture was filtered and the solvent removed from the filtrate by evaporation under reduced pressure at room temperature. The residue was then immediately subjected to column chromatography using CH_2Cl_2 as the initial eluent but with a gradually increasing concentration of THF added to elute a major light green fraction. This was collected, the solvent removed under reduced pressure at room temperature and the residue recrystallized from a CH_2Cl_2–hexane mixture to give a green microcrystalline product (0.288 g, 19%). This material was found to be unstable and decomposed on warming or on standing in solution for prolonged periods. The thermal instability of this compound has precluded satisfactory elemental analyses, low values for N always being obtained. This may be attributed to the loss of N_2 from the compound by decomposition reactions occurring before combustion commenced.

RESULTS AND DISCUSSION

The complex [Mo(NO)L(NCS)$_2$] was formed in the direct reaction between [Mo(NO)LI_2] and sodium thiocyanate in dichloromethane, although only in low yield. Dibenzo-18-crown-6 was added as a phase transfer catalyst to promote dissolution of the sodium salt, and the components of the reaction mixture were separated by column chromatography to give the bis-thiocyanate complex as a dark red solid. The reaction between [Mo(NO)LI_2] and sodium azide in dichloromethane in the presence of dibenzo-18-crown-6 similarly afforded the bis-azide complex. However, in this case purification proved more difficult. Careful chromatography was necessary to separate the light green product from a mixture of paramagnetic brown and dark green materials which were also formed during the reaction. The purification of the bis-azide derivative was further complicated by its thermal instability and subsequent recrystallizations were performed at room temperature without warming, to avoid the decomposition reactions which occurred on heating this material. Attempts to prepare the monosubstituted derivatives, [Mo(NO)LIX] (X = N_3, NCS), using 1:1 reactant stoichiometries have thus far failed and only the bis derivatives have been isolated. Attempts to prepare [Mo(NO)L(NCO)$_2$] were also unsuccessful. Although a reaction between [Mo(NO)LI_2] and sodium cyanate occurred, the product proved too unstable to be isolated in a pure form.

The new compounds were characterized by spectroscopic methods and, in the case of [Mo(NO)L(NCS)$_2$], by elemental analysis. The IR spectrum of [Mo(NO)L(NCS)$_2$] contained ν_{NO} at 1675 cm^{-1}, ν_{BH} at 2550 cm^{-1} and $\nu_{NC(S)}$ at 2030 and 1965 cm^{-1}. The low values found for $\nu_{NC(S)}$ are indicative of N-bound thiocyanate, S-bound thiocyanate usually giving rise to $\nu_{(S)CN}$ in the region of 2100 cm^{-1}.[6] The appearance of a band attributable to $\nu_{(N)CS}$ at 805 cm^{-1} is also in accord with the presence of N-bound thiocyanate since S-bound thiocyanate gives rise to $\nu_{(N)CS}$ in the region 780–690 cm^{-1}.[6] The ^1H NMR spectrum of this complex contained signals in the area ratios 3:3:6:6 at δ_{TMS} = 2.30, 2.32, 2.43 and 2.49 ppm, attributable to the pyrazolyl methyl protons in L. The pyrazolyl 4-H protons appeared as signals of area ratio 1:2 at δ_{TMS} = 5.70 and 6.07 ppm. This spectrum is consistent with the presence of a plane of symmetry in the molecule as required by its formulation as a bis-thiocyanate derivative. The mass spectrum contained a molecular ion envelope based at m/z = 541 (^{98}Mo, ^{11}B) along with an ion at m/z = 511 attributable to $[M—(NO)]^+$.

The IR spectrum of [Mo(NO)L(N_3)$_2$] contained ν_{NO} at 1675 cm^{-1}, ν_{BH} at 2550 cm^{-1}, and ν_{N_3} at 2065 and 2040 cm^{-1}. These latter values maybe compared with that of 2068 cm^{-1} reported[1] for [Mo(O)L(N_3)$_2$]. The ^1H NMR spectrum of this complex contained signals in the area ratios 3:3:6:6 at δ_{TMS} = 2.32, 2.35, 2.37 and 2.51 ppm attributable to the pyrazolyl methyl protons in L. The pyrazolyl 4-H protons appeared as signals of area ratio 1:2 at δ_{TMS} = 5.80 and 5.94 ppm. Again this spectrum is consistent with the presence of a plane of symmetry in the molecule as required by its formulation as a bis-azide derivative.

The electrochemical properties of the new complexes were examined in MeCN solution by cyclic

Table 1. Selected reduction potentials for [Mo(E)LXY] (E = NO or O)

X	Y	$E_{fN}(E = NO)^a$ (V)	$E_{fO}(E = O)^b$ (V)	ΔE_f ($E_{fN} - E_{fO}$ V)
Cl	Cl	+0.09	−0.25	+0.34
Cl	OPh	−0.42	−0.59	+0.17
Cl	SPh	−0.37	−0.33	−0.04
OPh	OPh	−0.74	−0.88	+0.14
SPh	SPh	−0.64	−0.28	−0.36
N_3	N_3	−0.31	+0.12	−0.43
NCS	NCS	−1.64	−0.31	−1.33
toluene-3,4-dithiol		−0.35	−0.28	−0.07

[a] Platinum bead electrode, MeCN, 0.2 mol dm^{-3} Bu_4NBF_4, SCE.[3]
[b] Platinum bead electrode, MeCN, 0.2 mol dm^{-3} Bu_4NBF_4, Ag/AgCl.[1]

voltammetry. Both showed only poorly defined oxidation processes and a single one-electron reduction process. In the case of [Mo(NO)L(NCS)$_2$] this occurred at $E_f = -1.68$ V with $\Delta E_p = 90$ mV and was subject to some kinetic control. However, the function $i_p^c v^{-1/2}$ (i_p^c = cathodic peak current) was independent of the scan rate, v. In the case of [Mo(NO)L(N$_3$)$_2$] a reversible reduction occurred at $E_f = -0.13$ V with $\Delta E_p = 60$ mV and again $i_p^c v^{-1/2}$ was independent of the scan rate.

The syntheses of [Mo(NO)L(NCS)$_2$] and [Mo(NO)L(N$_3$)$_2$] further extend the known range of related pairs of complexes [Mo(O)LXY] and [Mo(NO)LXY]. Thus a parallel between the chemistries of the $\{Mo(=O)L\}^{2+}$ and $\{Mo(NO)L\}^{2+}$ moieties may be seen in terms of the type of co-ligands X and Y which can form isolable complexes with these molybdenum centres. However, this parallel does not extend to the electrochemical properties of the two series of complexes. There appears to be no general correlation between the variations in the reduction potentials of [Mo(NO)LXY] and of [Mo(O)LXY] as a function of X and Y as shown in Table 1. In particular, the complex [Mo(NO)L(N$_3$)$_2$] has an anodic reduction potential comparable with that of [Mo(NO)LCl$_2$], while the reduction potential for [Mo(NO)L(NCS)$_2$] is more comparable with those found for bis-amide complexes [Mo(NO)L(NHR)$_2$].[3] The molybdenum(V) azide complex, [Mo(O)L(N$_3$)$_2$], also has a reduction potential similar to that of its dichloro analogue, but the potential for the reduction of [Mo(O)L(NCS)$_2$] is surprisingly anodic whereas that for [Mo(NO)L(NCS)$_2$] is very cathodic. There is no consistent difference between the reduction potentials of the two series of complexes as shown by the ΔE_f values. Furthermore, a linear regression analysis of the relationship between E_{fN} and E_{fO} gave a correlation coefficient of 0.2099, indicating that there is no significant correlation between the reduction potentials for the two series of complexes. There is, of course, no particular reason to expect a good correlation since the oxo-complexes are formally d^1 systems containing a π-donor oxo ligand, whereas the nitrosyl derivatives are formally d^4 and contain a π-acceptor ligand. In this context it is noteworthy that the replacement of OPh by SPh produces a more pronounced anodic shift in the reduction potentials of the oxo complexes than of the nitrosyl complexes.

Acknowledgements—We are grateful to Messrs T. Green, A. S. E. Brown, P. Hodder and T. Rebbeck for experimental assistance and to Mustansiriyah University of Iraq for support (to N.AlO.).

REFERENCES

1. W. E. Cleland Jr., K. M. Barnhart, K. Yamanouchi, D. Collison, F. E. Mabbs, R. B. Ortega and J. H. Enemark, *Inorg. Chem.* 1987, **26**, 1017.
2. J. A. McCleverty, *Chem. Soc. Rev.* 1983, **12**, 331.
3. N. AlObaidi, M. Chaudhury, D. Clague, J. C. Pearson, C. J. Jones, J. A. McCleverty and S. S. Salam, *J. Chem. Soc., Dalton Trans.* 1987, 1733.
4. N. AlObaidi, S. M. Charsley, W. Hussain, C. J. Jones, J. A. McCleverty, B. D. Neaves and S. J. Reynolds, *Transition Met. Chem.* 1987, **12**, 143.
5. S. J. Reynolds, C. F. Smith, C. J. Jones, J. A. McCleverty, D. C. Bower and D. Templeton, *Inorg. Synth.* 1985, **23**, 4.
6. K. Nakamoto, *Infrared and Raman Spectra of Inorganic and Coordination Compounds*, 3rd edn. Wiley Interscience, New York (1978).

Polyhedron Vol. 8, No. 3, pp. 375–377, 1989
Printed in Great Britain

0277–5387/89 $3.00+.00
© 1989 Pergamon Press plc

COMMUNICATION

PREPARATION AND CRYSTAL STRUCTURE OF $[(1,5\text{-}C_8H_{12})Rh(\mu\text{-}\eta^2\text{-}ReO_4)]_n$

JOHN R. SHAPLEY,* BRUCE R. WHITTLESEY and SCOTT R. WILSON

School of Chemical Sciences and Materials Research Laboratory, University of Illinois, Urbana, IL 61801, U.S.A.

(*Received* 10 *August* 1988; *accepted* 30 *September* 1988)

Abstract—The reaction of $[(COD)Rh(\mu\text{-}Cl)]_2$ (COD = $1,5\text{-}C_8H_{12}$) with 2 equivalents of $AgReO_4$ in dry tetrahydrofuran (THF) at room temperature leads to orange, crystalline $[(COD)Rh(\mu\text{-}\eta^2\text{-}ReO_4)]_n$. The structure consists of infinite chains in which square-planar rhodium and tetrahedral rhenium centres are linked by oxygen bridges to form a $(—ReO_2—O—Rh(COD)—O—)_n$ polymer. The two unique Rh—O—Re angles are 176(1) and 157(1)°.

The organometallic chemistry of metal centres coordinated to oxyanion ligands is receiving much current attention.[1] There has also been strong interest in studying platinum metal complexes on oxide supports in order to examine the nature of the metal–oxygen interaction and its possible affect on heterogeneously catalysed reactions.[2] In the course of our studies of low-valent platinum metal complexes in oxide environments,[3] we have synthesized the compound $[(COD)Rh(\mu\text{-}\eta^2\text{-}ReO_4)]_n$ **(1)** (COD = $1,5\text{-}C_8H_{12}$). To our knowledge, compound **1** is the first structurally characterized example of a complex in which the perrhenate group acts as a bidentate bridging ligand.

The reaction of $[(COD)Rh(\mu\text{-}Cl)]_2$ with 2 equivalents of $AgReO_4$ in dry THF under nitrogen at room temperature produces $[(COD)Rh(\mu\text{-}\eta^2\text{-}ReO_4)]_n$, which, after filtering and concentrating the solution, is isolated as orange crystals. Complex **1** is soluble only in coordinating organic solvents. In the solid state it reacts readily with traces of moisture in the air, as shown by the loss of resolution for the IR bands attributed to coordinated ReO_4^- at 943(vs), 935(sh), 909(sh) and 899(vs) cm^{-1}.[4] The polymeric nature of **1** is suggested by its field desorption mass spectrum, which exhibits peaks corresponding to the formula units $[(COD)Rh]_3[ReO_4]_2$, $[(COD)Rh]_2[ReO_4]_2$ and $[(COD)Rh]_2[ReO_4]$, as well as $[(COD)Rh][ReO_4]$.

The solid state structure of **1** consists of infinite chains in which the metal atoms are connected by oxygen bridges to form a $(—ReO_2—O—Rh(COD)—O—)_n$ polymer. The basic structural unit is shown in Fig. 1 and the molecular dimensions are collected in Table 1.† Each polymer chain is propagated as a spiral along a crystallographic two-fold screw axis and consequently is chiral; this metal–oxygen chain structure is similar to that found in pyroxene silicates.[5] Each of the rhodium atoms is coordinated to two bridging oxygens and the midpoints of the two olefinic bonds of the cyclooctadiene ligand in a square-planar fashion. The rhenium atoms are tetrahedrally coordinated to two bridging and two terminal oxygens. One of the two unique Re—O—Rh angles in the complex is nearly linear, and the other is significantly bent. This is consistent with a largely σ-bonding interaction of one oxygen atom with the Rh(1) centre and a largely

*Author to whom correspondence should be addressed.

†Crystal data for $[(COD)Rh(\mu\text{-}\eta^2\text{-}ReO_4)]_n$ at 26°C: orthorhombic $P2_12_12_1$ (D_2^4, No. 19), $a = 9.374(4)$, $b = 11.981(6)$, $c = 9.141(4)$ Å, $V = 1026.6(8)$ Å^3, $Z = 4$, $d_{calc} = 2.984$ g cm^{-3}, $\mu = 135.13$ cm^{-1}, $\lambda(Mo\text{-}K_\alpha) = 0.71073$ Å. Intensity data: Syntex $P2_1$ diffractometer, ω–2θ scan mode, 1560 reflections measured, $3.0° < 2\theta < 55°$. The heavy atom positions were located by Patterson methods, and the structure was refined (full-matrix least-squares) to $R = 0.044$ and $R_w = 0.050$ for 1033 unique reflections having $I > 2.58\sigma(I)$.

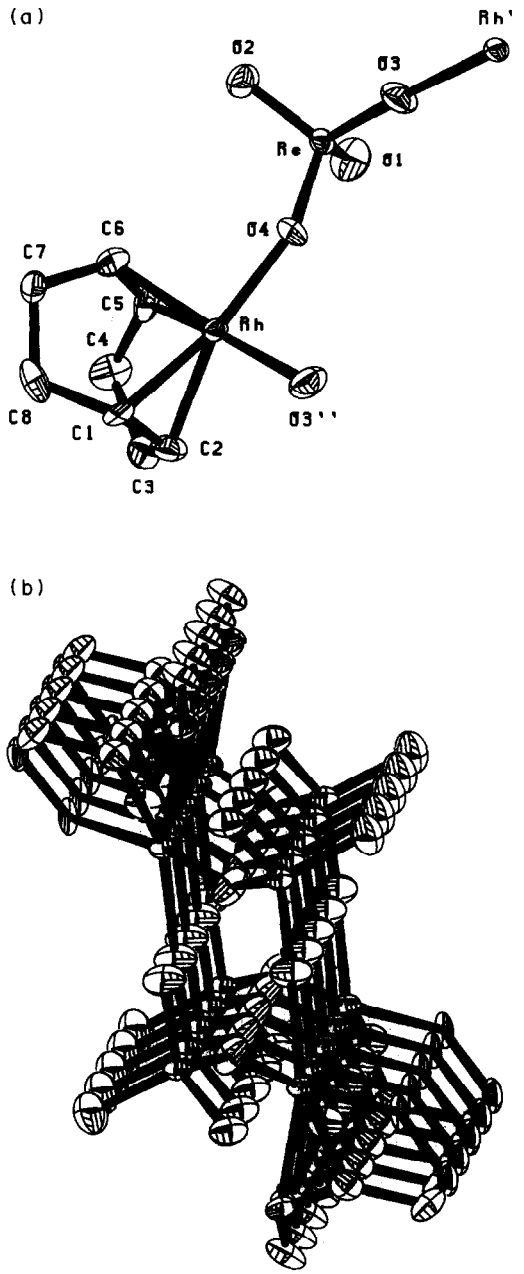

Fig. 1. (a) ORTEP diagram of the repeating unit in $[(COD)Rh(\mu\text{-}\eta^2\text{-}ReO_4)]_n$ (**1**), showing the atom numbering scheme. (b) A section of the polymer, showing the spiral structure.

Table 1. Molecular dimensions for **1**

Distances (Å)	
Re—O(1)	1.70(2)
Re—O(2)	1.69(2)
Re—O(3)	1.72(2)
Re—O(4)	1.74(2)
Rh—O(3)	2.09(2)
Rh—O(4)	2.07(2)
Rh—[C(1)—C(2)][a]	2.00(2)
Rh—[C(5)—C(6)][a]	1.99(3)
Angles (°)	
O(1)—Re—O(2)	107.4(10)
O(1)—Re—O(3)	111.8(9)
O(1)—Re—O(4)	108.8(10)
O(2)—Re—O(3)	111.0(9)
O(2)—Re—O(4)	108.4(8)
O(3)—Re—O(4)	109.3(9)
Re—O(3)—Rh	176.0(1)
Re—O(4)—Rh	157.0(1)
O(3)—Rh—O(4)	87.4(7)
O(3)—Rh—[C(1)—C(2)]	91.5(8)
O(3)—Rh—[C(5)—C(6)]	179.1(9)
O(4)—Rh—[C(1)—C(2)]	176.0(8)
O(4)—Rh—[C(5)—C(6)]	93.0(9)
[C(1)—C(2)]—Rh—[c(5)—C(6)]	88.2(10)

[a] [C(1)—C(2)] and [C(5)—C(6)] are the midpoints of the C(1) to C(2) and C(5) to C(6) bonds.

π-bonding interaction from the other. However, the two Rh—O distances are virtually equal, and the Re—O_{bridge} and Re—$O_{terminal}$ distances are likewise only marginally different. The 1,5-cyclooctadiene ligand does not exhibit any unusual features.

A variety of transition metal complexes containing the ReO_4^- moiety are known.[6–12] In nearly all of the complexes that have previously been characterized structurally by X-ray diffraction, the perrhenate group coordinates as a unidentate ligand to one metal. However, in the compound $[(^tBuN)_2(Me_3SiO)Re]_2(\mu\text{-}O)(\mu\text{-}OSiMe_3)(\mu\text{-}\eta^1\text{-}OReO_3)$,[6] one of the perrhenate oxygen atoms bridges two other rhenium atoms in a manner similar to an alkoxide group. The structure of compound **1** is related to the mode of coordination found in $[\{(NBD)Rh\}_5\{Nb_2W_4O_{19}\}_2]^{3-}$,[13] in which each diene–rhodium unit is connected to two different metal centres via separate oxygen bridges, one of which is nearly linear (167°) and the other strongly bent (121°). It is not completely clear why this is the preferred structure for **1**, although it may be significant that this geometry is the most suitable for forming "linear" Rh—O—Re bridges while maintaining favourable O—M—O angles at the rhodium and rhenium centres. Further studies are necessary to determine if this is a general tendency.

Acknowledgement—This work was supported by a grant from the National Science Foundation to the Materials Research Laboratory of the University of Illinois (DMR 86-12860).

REFERENCES

1. (a) F. Bottomley and L. Sutin, *Adv. Organomet. Chem.* 1988, **28**, 339; (b) W. E. Buhro and M. H.

Chisholm, *Adv. Organomet. Chem.* 1987, **27**, 311; (c) W. A. Herrmann, E. Herdtweck, M. Flöel, J. Kulpe, U. Küsthardt and J. Okuda, *Polyhedron* 1987, **6**, 1165.
2. H. F. J. van't Blik, J. B. A. D. van Zon, T. Huizinga, J. C. Vis, D. C. Koningsberger and R. Prins, *J. Am. Chem. Soc.* 1985, **107**, 3139.
3. R. L. Keiter, D. S. Strickland, S. R. Wilson and J. R. Shapley, *J. Am. Chem. Soc.* 1986, **108**, 3846.
4. L. Bencivenni, H. M. Nagarathna, D. W. Wilhite and K. A. Gingerich, *Inorg. Chem.* 1984, **23**, 1279.
5. N. H. Ray, *Inorganic Polymers*, pp. 110–113. Academic Press, New York (1978).
6. W. A. Nugent and R. L. Harlow, *J. Chem. Soc., Chem. Commun.* 1979, 1105.
7. W. A. Herrmann, R. Serrano, U. Küsthardt, M. L. Ziegler, E. Guggolz and T. Zahn, *Angew. Chem. Int. Ed. Engl.* 1984, **23**, 515.
8. G. Ciani, A. Sironi, T. Beringhelli, G. D'Alfonso and M. Freni, *Inorg. Chim. Acta* 1986, **113**, 61.
9. I. B. Liss and E. O. Schlemper, *Inorg. Chem.* 1975, **14**, 3035.
10. J. W. Johnson, J. F. Brody, G. B. Ansell and S. Zentz, *Acta Cryst.* 1984, **C40**, 2024.
11. J. Heidrich, D. Loderer and W. Beck, *J. Organomet. Chem.* 1986, **312**, 329.
12. N. Zhang and P. A. Shapley, *Inorg. Chem.* 1988, **27**, 976.
13. C. J. Besecker, W. G. Klemperer and V. W. Day, *J. Am. Chem. Soc.* 1982, **104**, 6158.

Polyhedron Vol. 8, No. 3, pp. 379–380, 1989
Printed in Great Britain

0277–5387/89 $3.00+.00
© 1989 Pergamon Press plc

COMMUNICATION

A NOVEL SYNTHESIS AND PROPERTIES OF N-BIS(TRIFLUOROMETHYL)NITROXY-IMINOPHOSPHINE, $(CF_3)_2NON{=}PH$

H. G. ANG* and F. K. LEE

Chemistry Department, National University of Singapore, Kent Ridge Road, Singapore 0511, Republic of Singapore

(*Received* 26 *August* 1988; *accepted* 30 *September* 1988)

Abstract—$(CF_3)_2NON{=}PH$, synthesized by a novel method involving the reactions of $(CF_3)_2NONO$ and PH_3, underwent cleavage of the NO—NP bond by HI to give $IN{=}PH$ and substitution reactions with the $(CF_3)_2NO$ radical to afford $RN{=}PR$, where $R = ON(CF_3)_2$. While $IN{=}PH$ gave the relatively stable addition product, INHPHI, with HI, the addition product RNHPRI, derived from $RN{=}PR$, proved to be unstable even at low temperatures.

In recent years, growing research interest has emerged on the chemistry of unsaturated compounds of the main-group elements with low coordination numbers.[1] Among them are the two-coordinate phosphorus(III) compounds of the type $RN{=}PR'$.[2] However until now, relatively few such compounds have been synthesized: $Bu^tN{=}PBu^t$ and $Me_3SiN{=}PN(SiMe_3)_2$.[3,4] Their stability has been attributed to the presence of bulky substituents.[5] We now report a novel method of preparing a new fluorine-containing iminophosphine, namely N - bis(trifluoromethyl)nitroxy - iminophosphine, $(CF_3)_2NON{=}PH$. Investigations of its properties have led to the discovery of a few other similar iminophosphine derivatives.

The reactions of *o*-nitrosobis(trifluoromethyl) hydroxylamine and phosphine in a 1:1 molar ratio, at room temperature in an evacuated glass ampoule, afforded N-bis(trifluoromethyl)nitroxy-iminophosphine, $(CF_3)_2NON{=}PH$, in 60% yield:

$$(CF_3)_2NONO + PH_3 \rightarrow (CF_3)_2NON{=}PH + H_2O. \quad \textbf{(A)}$$

An orange solid which is hygroscopic was also formed in the reaction ampoule. The iminophosphine (A) was isolated at −96°C in a trap as a white solid by trap-to-trap fractionation under high vacuum. Its IR spectrum gave the following peaks: 2272 cm^{-1}, ν(P—H); 821 cm^{-1}, δ(P—H); 1324, 1244, 1050 cm^{-1}, ν(C—F); 721 cm^{-1}, δ(C—F). The peak at 1662 cm^{-1} can be attributed to the P=N stretching vibration. The EI MS (70 eV) of (A) did not exhibit the parent ion but gave characteristic fragmentation ions at m/e 195 $[C_2F_5NON{=}PH]^{+\cdot}$, 176 $[C_2F_4NON{=}PH]^{+\cdot}$, 168 $[C_2F_6NO]^{+\cdot}$, 149 $[C_2F_5NO]^{+\cdot}$, 83 $[CF_3N]^{+\cdot}$ and 69 $[CF_3]^{+\cdot}$. Molecular weight determination by Regnault's method gave 215 g mol^{-1} ($C_2F_6ON_2P$ requires 214 g mol^{-1}).

Anhydrous hydrogen iodide did not undergo addition reactions with (A). Instead, it preferentially cleaved the NO—NP bond to give N-iodoiminophosphine, $IN{=}PH$ in 54% yield, together with a quantitative amount of bis(trifluoromethyl)hydroxylamine, as shown by the following equation:

$$(CF_3)_2NON{=}PH + HI \rightarrow (CF_3)_2NOH + IN{=}PH. \quad \textbf{(B)}$$

In addition, an intractable hygroscopic yellow solid was also formed in the reaction ampoule.

N-Iodoiminophosphine was trapped at −126°C as a white solid on vacuum fractionation. Its IR spectrum showed the P—H stretching vibration at

*Author to whom correspondence should be addressed.

Dedicated to Professor H. J. Emeleus, FRS in honour of his 85th birthday.

2245 cm^{-1} and P—H deformation at 846 cm^{-1}. The N=P stretching vibration was located at 1646 cm^{-1}. Its EI MS gave the parent ion at *m/e* 173 and a fragmentation ion at 142 $[INH]^{+\cdot}$. Molecular weight determination by Regnault's method gave 172 g mol^{-1} (INPH requires 172 g mol^{-1}). Analysis of iodine gave 72.98% (INPH requires 73.41%).

To date, N-iodoiminophosphine is the smallest stable four-atom iminophosphine that has been discovered. The presence of the N=P double bond was chemically confirmed by the addition product (**C**) which was formed with anhydrous hydrogen iodide at room temperature, according to the following equation:

$$IN{=}PH + HI \rightarrow INHPHI,$$
(**C**)

whereby the hydrogen migrated to the nitrogen atom and the iodine to the more electropositive phosphorus atom. Compound (**C**), trapped at −96°C as a pale yellow solid on vacuum fractionation, is a colourless gas at room temperature. Its IR spectrum gave peaks due to the NH group at 3220 cm^{-1} and the PH group at 2209 and 807 cm^{-1}. The peak at 1646 cm^{-1} due to the N=P stretching vibration disappeared. It is unstable on standing at room temperature, decomposing to give iodine, non-condensable gases and a pale yellow intractable solid which contains iodine and phosphorus. The EI MS of (**C**) gave the parent ion at *m/e* 301, and fragmentation ion at 299 $[INPI]^{+\cdot}$. Analysis of iodine gave 83.49% (H_2I_2NP requires 84.38%).

The presence of the P—H bond in (**A**) was demonstrated by the reaction with bis(trifluoromethyl)nitroxyl, which is a powerful hydrogen abstractor and a radical scavenger. The reactions afforded bis(trifluoromethyl)nitroxy-substituted iminophosphine (**D**) in 80% yield, together with a quantitative amount of bis(trifluoromethyl) hydroxylamine;

$$(CF_3)_2NON{=}PH + 2(CF_3)_2NO \rightarrow (CF_3)_2NON{=}PON(CF_3)_2 + (CF_3)_2NOH.$$
(**D**)

The iminophosphine (**D**) was isolated at −60°C in a trap as a colourless liquid on vacuum fractionation. Its IR spectrum gave peaks due to the $(CF_3)_2NO$ group at 1324, 1300, 1243, 1270, 1001 and 723 cm^{-1}, and the N=P stretching vibration at 1663 cm^{-1}. The EI MS of (**D**) did not give the parent ion but gave characteristic fragmentation ions at *m/e* 343 $[C_2F_6NON{=}PONC_2F_4]^{+\cdot}$, 199 $[PONC_2F_6]^{+\cdot}$, 168 $[(CF_3)_2NO]^{+\cdot}$ and 69 $[CF_3]^{+\cdot}$. Molecular weight determination by Regnault's method gave 382 g mol^{-1} (compound (**D**) requires 381 g mol^{-1}). The reactions between the bis (trifluoromethyl)nitroxyl radical and (**B**) did not follow the same course as those with (**A**). Instead, an intractable hygroscopic brown, polymeric solid and some bis(trifluoromethyl)hydroxylamine were produced. The brown solid contained iodine, phosphorus and the $(CF_3)_2NO$ group. The reactions most probably underwent concomitant polymerization and attack of the PH hydrogen by the nitroxyl radical.

Reactions of (**D**) with hydrogen iodide at −90°C gave 1 mole of bis(trifluoromethyl)nitroxyl, iodine, an intractable orange solid and non-condensable gases which were most probably nitrogen and hydrogen. Hydrogen abstraction did not occur as no bis(trifluoromethyl)hydroxylamine was detected. The orange solid contained the $(CF_3)_2NO$ group, as indicated by its IR spectrum, and phosphorus. The products from these reactions can be rationalized in terms of the formation of the addition product (**E**), which then underwent decomposition via the radical intermediates (**F**) and (**G**), as illustrated by the following reaction scheme:

$$(CF_3)_2NON{=}PON(CF_3)_2 + HI \rightarrow$$

$$(CF_3)_2NON(H)-PON(CF_3)_2(I)$$
(**E**)
$$\downarrow$$
$$(CF_3)_2NONH + (CF_3)_2NOPI$$
(**F**) (**G**)

$$2(CF_3)_2NONH \rightarrow 2(CF_3)_2NO + H_2 + N_2$$

$$(CF_3)_2NOPI \rightarrow 1/2I_2 + 1/n[(CF_3)_2NOP]_n.$$

Acknowledgements—We thank the National University of Singapore for a Research Grant and one of us (L.F.K.) is grateful to the University for a Research Scholarship.

REFERENCES

1. A. H. Cowley, *Accts Chem. Res.* 1984, **17**, 386; J. Satge, *Adv. Organomet. Chem.* 1982, **21**, 291; N. Wiberg, *J. Organomet. Chem.* 1984, **273**, 141; M. W. Schmidt and M. S. Gordon, *Inorg. Chem.* 1986, **25**, 248. R. West, *Angew. Chem. Int. Ed Engl.* 1987, **26**, 120.
2. W. E. Abel and S. A. Mucklejohn, *Phosphorus Sulfur* 1981, **9**, 235; E. Fluck, *Top. Phosphorus Chem.* 1980, **10**, 193.
3. E. Niecke and W. Flick, *Angew. Chem. Int. Ed Engl.* 1973, **7**, 585.
4. E. Niecke, R. Ruger and W. W. Schoeller, *Angew. Chem. Int. Ed Engl.* 1981, **20**, 1034.
5. J. Esendie, C. Couret, J. Satge, M. Andrianarison and J.-D. Andriamizaka, *J. Am. Chem. Soc.* 1985, **107**, 3378.

Polyhedron Vol. 8, No. 3, p. 381, 1989
Pergamon Press plc. Printed in Great Britain

CORRIGENDA

Redox reactions involving hexacarbonylvanadium(0) and compounds containing element–halide, element–hydrogen and element–carbon bonds. Synthesis, and crystal and molecular structure of $Ph_3PbV(CO)_6$. F. Calderazzo, G. Pampaloni, G. Pelizzi and F. Vitali (*Polyhedron* Vol. 7, No. 19/20, pp. 2039–2048, 1988).

The authors wish to insert the references as listed below:

p. 2040, line seven of the Experimental should read: "C_5H_5R), R = H,[14] CH_2Ph[15a] were prepared"

p. 2040, line one of the right-hand column should read: "identified from its IR spectrum and elemental analysis.[15b,c]

p. 2043, lines 23 and 24 of the right-hand column should read: "has been known since 1964,[24a] $Ph_3PbV(CO)_6$ was recently prepared by a different route:[24b] it adds to the restricted family of hepta-"

p. 2047, references 15 and 24 should read:

15. (a) G. E. Herberich and E. Bauer, *J. Organomet. Chem.* 1969, **16,** 301; (b) M. Gomberg, *Chem. Ber.* 1900, **33,** 3150; (c) H. Lankamp, V. Th. Nauta and C. MacLean, *Tetrahedron Lett.* 1968, 249.

24. (a) A. S. Kasenally, R. S. Nyholm, R. J. O'Brien and M. H. B. Stiddard, *Nature* 1964, **204,** 871; (b) R. Talay and D. Rehder, *J. Organomet. Chem.* 1984, **262,** 25.

Polyhedron Vol. 8, No. 4, pp. 383–405, 1989
Printed in Great Britain

0277–5387/89 $3.00+.00
© 1989 Pergamon Press plc

POLYHEDRON REPORT NUMBER 26

KINETIC DEUTERIUM ISOTOPE EFFECTS IN TRANSITION METAL HYDRIDE CLUSTERS

EDWARD ROSENBERG

Department of Chemistry, California State University, Northridge, CA 91330, U.S.A.

CONTENTS

1. INTRODUCTION 383

2. THE SMALL PRIMARY ISOTOPE EFFECT (kH/kD = 1.4–2.0) 386
   2.1 Direct exchange of two μ-hydrides 386
   2.2 Axial–radial exchange of carbonyl groups 388
   2.3 Face migrations of hydrocarbon ligands 390
   2.4 Chemical reactions involving hydride migrations 393

3. THE LARGE PRIMARY ISOTOPE EFFECT (kH/kD = 7–50) 398
   3.1 Ligand to metal hydrogen transfers in protonations of clusters 398
   3.2 Metal to ligand hydrogen transfers 401

4. CONCLUSIONS AND FUTURE WORK 403

ACKNOWLEDGEMENTS 404

REFERENCES 404

APPENDIX 405

1. INTRODUCTION

Primary deuterium kinetic isotope effects have been used by organic chemists for many years to elucidate the rate-determining steps and the nature of the transition states in a wide range of organic reactions. However, the mechanistic interpretation of the magnitude of observed kH/kD ratios has always been somewhat problematic. The "maximum" primary isotope effect can be estimated from the observed differences in zero point energies (i.e. differences in the X—D versus X—H stretching frequencies) using the Bigeleisen equation [eq. (1)]

$$k\mathrm{H}/k\mathrm{D} \sim \exp\left[\frac{hc}{2kT}(\nu_{\mathrm{H}}-\nu_{\mathrm{D}})\right] \tag{1}$$

for a reaction which is thought to have a linear symmetrical transition state and in which substitution of deuterium for hydrogen has no effect on the energy of the transition state. These constraints are rarely realized. Non-linear transition states are thought to attenuate the size of the isotope effect. Reactions with late transition states (i.e. the rate of bond breaking exceeds the rate of bond making for the hydrogen transfer) would be expected to lower the energy of the transition state and also attenuate the size of the isotope effect. Recently it has been proposed that reactions with linear transition states should show temperature dependent kH/kD ratios while those with non-linear transition states should show temperature independent kH/kD ratios.[1]

In addition, there is a separate class of isotope effects in which the observed kH/kD ratio is larger than that predicted from eq. (1).[1,2] These large kH/kD values are thought to be associated with 'barrier tunnelling'. Reactions in which the ground state geometry of the reactant resembles that of the product very closely would be expected to have a very narrow barrier. If the barrier width approaches the wavelength of the hydrogen atom, proton or hydride involved in the reaction, the particle can tunnel through the barrier rather than go over it. Substitution of deuterium for hydrogen would effectively turn off the tunnelling component of the reaction leading to unexpectedly high kH/kD ratios. The observation of a high kH/kD ratio is not, however, a sufficient criterion for ascribing barrier tunnelling to a reaction. The observed difference in activation energy on going from the protium to the deuterium system must be greater than that calculated from differences in zero point energy (i.e. $\Delta E_{a_H^D} \gg \Delta E_{o_H^D}$).[1] In order to meet this criterion, details of the differences in zero point energy must be available and it must be possible to obtain kH/kD values over a range of temperatures. These requirements are not often met by many kinetic studies and thus there are few well documented examples of barrier tunnelling for different reaction types. The best documented cases of barrier tunnelling exist for reactions involving proton transfer.[1-3]

In the organometallic chemistry of mononuclear and dinuclear species, kinetic deuterium isotope effects have been used extensively to elucidate the mechanisms of H—H and C—H activation processes and in processes involving M—H bond cleavage. No attempt will be made here to be comprehensive, but rather to present examples which illustrate the range of systems studied with regard to reaction type, metal centre and the magnitude of observed isotope effects.

Perhaps the most straightforward example of a kinetic deuterium isotope effect in transition metal chemistry comes from the work of Norton *et al.* who studied the proton self-exchange between cyclopentadienyl metallates [eq. (2)].[4]

$$(\eta\text{-}C_5H_5)M(CO)_3H + (\eta\text{-}C_5H_5)M'(CO)_3^- \rightleftharpoons (\eta\text{-}C_5H_5)M(CO)_3^- + (\eta\text{-}C_5H_5)M'(CO)_3H \qquad (2)$$

$$M = M' = Cr, Mo, W.$$

The observed kH/kD ratios of 3.7 for eq. (2) are in excellent agreement with the value of 3.39 calculated from eq. (1).[4] These results clearly suggest a linear symmetrical transition state taking place directly between metal atoms and demonstrate that there is nothing intrinsically anomalous about the magnitude of kinetic deuterium isotope effects involving the M—H bond.

The largest kinetic deuterium isotope effects involving transition metal centres appear to be associated with C—H activation processes at electrophilic metal centres. For example, Bercaw and co-workers have noted a kH/kD = 9.7 at 34°C for the formation of an azametallocyclopropane [eq. (3)].[5]

$$Cp^*Ta\{N(CH_3)_2\}(CH_3)_3 \longrightarrow Cp^*\overline{Ta\{N(CH_3)CH_2\}}(CH_3)_2 + CH_4 \qquad (3)$$

$$Cp^* = \eta\text{-}C_5(CH_3)_5.$$

Given that the kH/kD calculated from eq. (1) for cleavage of an aliphatic C—H bond is 7 at room temperature, this value implies a significant tunnelling component for this intramolecular hydrogen transfer. Similarly kH/kD values of 4.8 (114°C) and 5.2 (180°C) have been reported for the elimination of toluene from a zirconium centre [eqs (4) and (5)][6]

$$Zr(OAr')_2(CH_2C_6H_5)_2 \xrightarrow[\Delta]{} \overline{Zr(OAr')(OC_6H_3Bu^tC(CH_3)_2CH_2)}(CH_2C_6H_5) + CH_3C_6H_5 \qquad (4)$$

$$Ta(OAr')_2(CH_3)_3 \xrightarrow[\Delta]{} \overline{Ta(OAr')(OC_6H_3Bu^tC(CH_3)_2CH_2)}(CH_3)_2 + CH_4 \qquad (5)$$

$$(OAr') = 2,6\text{-di-}t\text{-butylphenoxide.}$$

The reverse reaction (i.e. cleavage of a metallocycle by a hydrocarbon at an electrophilic metal centre) also shows a relatively large isotope effect. Thus cleavage of a metallocyclobutane at a thorium(IV) centre by methane [eq. (6)] gives kH/kD = 6 ± 2.[7]

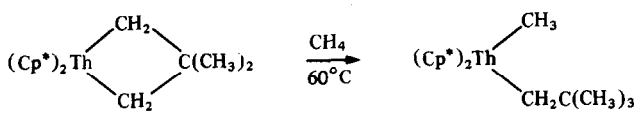

(6)

Activation of the aromatic C—H bond in benzene by an electrophilic metal centre gives a $kH/kD = 5.5$ [eq. (7)][8]

$$(Cp^*)_2LuCH_3 + C_6H_6 \longrightarrow (Cp^*)_2LuC_6H_5 + CH_4. \tag{7}$$

This isotope effect is operative for the bimolecular term of a two-term rate law (i.e. rate $= [k_1 + k_2(C_6H_6)][\text{complex}]$). The first-order term shows no isotope effect with C_6D_6 and is thought to arise from the reversible formation of a ring metallated intermediate.[8]

Much smaller isotope effects are observed for C—H activation at low valent late transition metal centres. Thus the photochemically generated intermediate $(Cp^*)IrP(CH_3)_3$, shows a $kH/kD = 1.38$ for the activation of cyclohexane [eq. (8)].[9]

$$(Cp^*)IrP(CH_3)_3H_2 \xrightarrow[-H_2]{h\nu} (Cp^*)IrP(CH_3)_3 \xrightarrow{C_6H_{12}} (Cp^*)Ir(PCH_3)_3(C_6H_{11})H. \tag{8}$$

Activation of the C—H bond in benzene at an electron rich osmium centre gave a $kH/kD = 2.2$ [eq. (9)].[10]

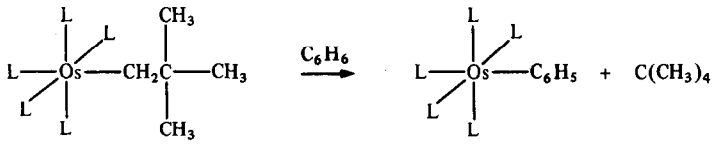

(9)

L = $P(CH_3)_3$

The large differences between kH/kD ratios at electrophilic metal centres and at electron rich metal centres delineated here, can be rationalized on the basis of early (for electrophilic metal centres) versus late (for electron rich metal centres) transition states for cleavage of the C—H bond. On the other hand, all the examples presented here for electrophilic metal centres involve direct transfer of hydrogen between carbon atoms, a reaction which could involve a large tunnelling component. The electron rich metal centres generally proceed via hydride intermediates which necessarily involve significant changes in geometry at the metal centre and might be expected to have little or no tunnelling component. These ideas need to be investigated further by carrying out variable temperature studies on the kH/kD ratios.

Reductive eliminations of C—H bonds from late electron rich transition metal centres also give relatively small kH/kD values. Thus, reductive elimination from a dihydride-alkene rhodium complex gives a $kH/kD = 1.15$ for the formation of a rhodium alkyl in the rate-determining step for olefin reductions [eq. (10)].[11]

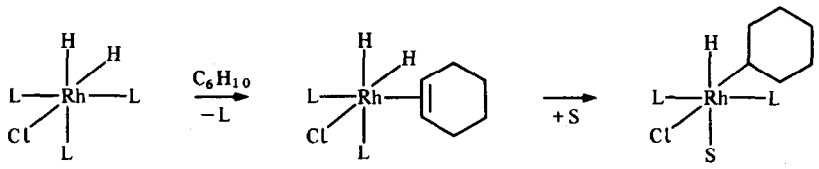

(10)

L = PR_3 S = Solvent

Also, the binuclear reductive elimination mechanism elucidated by Norton *et al.* for osmium(II) hydrido alkyls shows a $kH/kD = 1.5$ [eq. (11)].[12]

$$2Os(CO)_4(H)CH_3 \xrightarrow[\Delta]{} CH_4 + H(CO)_4OsOs(CO)_4(CH_3). \tag{11}$$

It can be concluded from these examples that both C—H oxidative addition to and reductive elimination from mono- and binuclear electron rich metal centres will involve relatively small deuterium kinetic isotope effects (i.e. $kH/kD = 1$–2).

The oxidative addition of H_2 to electron rich metal centres also shows relatively small isotope effects ($kH/kD = 1$–2). Oxidative addition of $H_2(D_2)$ to the photochemically generated intermediate $Rh(Cl)\{P(C_6H_5)_3\}_2$ shows a $kH/kD = 1.4$ [eq. (12)].[13]

$$RhCl(CO)\{P(C_6H_5)_3\}_2 \xrightarrow[-CO]{h\nu} RhCl\{P(C_6H_5)_3\}_2 + H_2 \longrightarrow H_2RhCl\{P(C_6H_5)_3\}_2. \quad (12)$$

This value is in excellent agreement with the calculated value of 1.48 based on a theoretical model of the transition metal–dihydrogen bond involving donation from the H_2 σ-bond to empty orbitals on the metal (i.e. side-on coordination) and back donation from filled metal orbitals to the H_2 σ^*-orbital. The value of 1.4 is consistent with an early three-centred transition state involving little H—H bond breaking.[14]

Reductive elimination of H_2 from $H_2Os(CO)_4$ which has also been shown to proceed by a binuclear mechanism [as for eq. (11)] exhibits a kHH/kHD = 1.4 and a kHH/kDD = 2.9 [eq. (13)].[15]

$$2H_2Os(CO)_4 \longrightarrow H_2 + H_2Os_2(CO)_8. \quad (13)$$

Although these isotope effects are small they do indicate that reductive elimination of H_2 is one of two rate-determining steps in the reaction, the other being CO loss which preceeds formation of a proposed binuclear intermediate.

The reversible activation of H_2 has been observed by ^{1}H NMR techniques in the mononuclear dihydrogen complex $Os(\eta^2\text{-}H_2)H(CH_3CH_2)_2PCH_2CH_2P(CH_2CH_3)_2]^+$.[16] Here the terminal hydride exchanges with the side-on bound H_2 molecule and variable temperature studies on the $Os(\eta^2\text{-}HD)D$ system reveal kH/kD = 1.4, also in excellent agreement with the theoretical model for H_2 activation at transition metal centres.

Thermodynamic or 'inverse' isotope effects are quite common in organometallic chemistry and are observed in reactions where there is a reversible hydrogen transfer from a heavy metal atom to a light atom (O, N, C). They arise from the fact that ν(M—H) − ν(M—D) ≪ ν(C—H) − ν(C—D). The effect is generally manifested as a more rapid approach to equilibrium by the deuterated metal species. For example, in the addition of $HFe_2(CO)_8^-$ to α,β-unsaturated ketones a rapid pre-equilibrium between a diiron–alkene complex and the resulting diiron alkyl is established before the rate-determining step.[17] When $DFe_2(CO)_8^-$ is employed this equilibrium shifts towards the diiron alkyl since it has a C—D bond as opposed to an Fe—D bond. This gives a kD/kH = 3.5 which is in good agreement the value is 3.3, calculated from the expected differences in zero point energy using typical values for the Fe—H(D) and C—H(D) stretching frequencies.[17]

There are several examples in the literature of thermodynamic isotope effects in metal cluster chemistry.[18,19] In the equilibrium between the isomeric $(\mu\text{-}H)_2(\mu\text{-}CH_2)Os_3(CO)_{10}$ and $(\mu\text{-}H)(\mu\text{-}CH_3)Os_3(CO)_{10}$, site selection of deuterium for carbon over metal sites was observed for the dideuterated analogues of both isomers and was found to be ~ 1.5 : 1 by ^{1}H NMR methods and ~ 2.0 from neutron diffraction data at 35°C.[18] Calculated values based on differences in zero point energy gave a value of 2.2.[18] The observation of a significant thermodynamic isotope promises to be a valuable tool for identifying reversible M—H to C—H hydrogen transfers in multi-step reactions in mono- and polynuclear organometallic systems.

In the course of our studies on the mechanisms of reactions of small organic molecules with trinuclear transition metal clusters we have uncovered what appear to be two distinct categories of primary deuterium kinetic isotope effects, each of which is associated with a separate cluster process. We have observed a small isotope effect (kH/kD = 1.4–2.0) in cases where bridge opening or edge-to-edge migration of a μ-hydride is a rate-determining step in a ligand migration or in a cluster ligand reaction. A second category of large isotope effects (kH/kD = 28–50) seems to be associated with reactions involving transfer of hydrogen from a coordinated ligand to the metal core, or the reverse process. This categorization promises to provide an additional tool for finding the rate-determining step(s) in complex multi-step cluster reactions. We report here a summary of our experimental results to date including both published data and some preliminary results, along with results of other workers in the field who have documented similar observations.

2. THE SMALL PRIMARY ISOTOPE EFFECT (kH/kD = 1.4–2.0)

2.1 *Direct exchange of two μ-hydrides*

It was first pointed out by Johnson and co-workers[20] that when $(\mu\text{-}H)_2Os_3(CO)_9(\mu_3\text{-}\eta^2\text{-}C{=}CH_2)$ (**1**) is deuterated by exchange with CF_3COOD to give $(H)(D)Os_3(CO)_9(\mu_3\text{-}\eta^2\text{-}C{=}CH_2)$ (**1**-d_1) the rate of exchange of the inequivalent hydrides appeared to be slower in the deuterated species **1**-d_1.

Later, we measured the size of this kinetic isotope effect on hydride exchange by line-shape analyses of the ^{1}H NMR averaging of the two inequivalent hydrides in the complexes $(\mu\text{-H})_2(\mu_3\text{-}\eta^2\text{-HC}{=}\text{C}^t\text{Bu})\text{Ru}_3(\text{CO})_9^{2+}$ (**2**) and $(\mu\text{-H})(\mu\text{-D})(\mu_3\text{-}\eta^2\text{-DC}{=}\text{C}^t\text{Bu})\text{Ru}_3(\text{CO})_9^{2+}$ [(**2**-d_2) eq. (14), Fig. 1].[21]

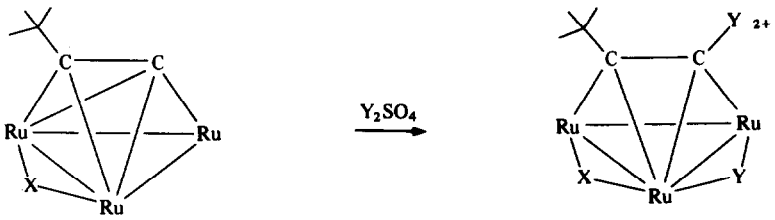

(14)

(**2**) X = H Y = H
(**2**-d_2) X = H Y = D
(**2**-d_3) X = D Y = D

A value of kHH/kHD = 1.4±0.1 was obtained at 55°C. We also measured the rate of deuteride exchange in $(\mu\text{-D})_2(\mu_3\text{-}\eta^2\text{-DC}{=}\text{C}^t\text{Bu})\text{Ru}_3(\text{CO})_9^{2+}$ (**2**-d_3) (obtained according to eq. (1) using $(\mu\text{-D}(\mu_3\text{-}\eta^2\text{-C}^t_2\text{Bu})\text{Ru}_3(\text{CO})_9)$ by ^{2}H NMR and obtained a value of kHH/kDD = 1.8 (Fig. 1). This value must be taken as approximate since it was obtained from simulations which did not include quadrupolar effects in the line-shape analysis. However, the fact that kHH/kDD > kHH/kHD does exclude the possibility that the rate constant for migration of one hydride in $(\mu\text{-H})_2\text{Ru}_3(\text{CO})_9(\mu_3\text{-}$

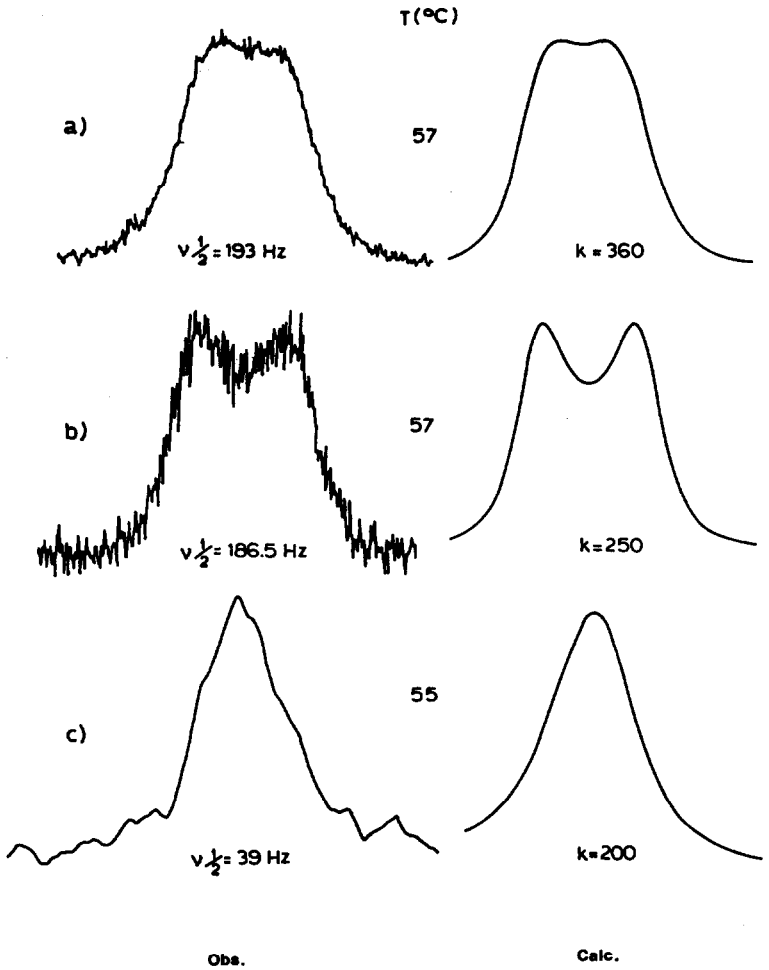

Fig. 1. (a) ^{1}H NMR of the hydride region of **2** in H_2SO_4 at 200 MHz; (b) ^{1}H NMR of **2**-d_2 in D_2SO_4 at 200 MHz; (c) ^{2}H NMR of **2**-d_3 in D_2SO_4 at 75 MHz.

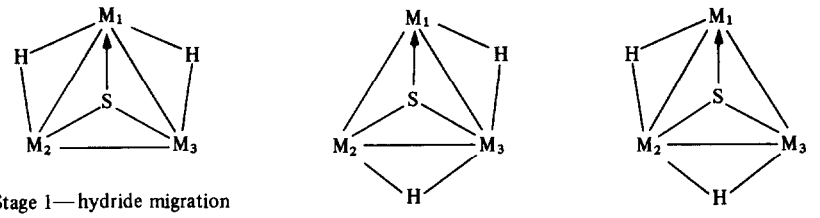

Stage 1—hydride migration

Stage 2—axial radial exchange

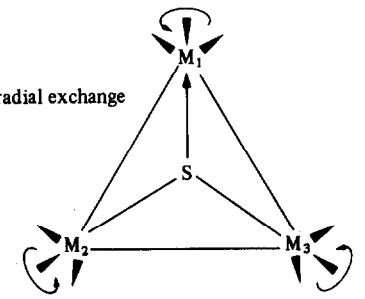

Scheme 1.

η^2-HC=C^{t}Bu)$^{2+}$ is much faster than the rate for the other unless the observed isotope effects are secondary, which they are not (*vide infra*). From the results obtained so far it does not seem likely that the isotope effect ratios obtained from direct hydride exchange in polyhydride species will be useful in distinguishing between consecutive and concerted hydride exchange because of their small size. More dynamic studies need to be carried out using ^{2}H NMR on polydeuterated clusters and mononuclear species before the full range of the isotope effect and its mechanistic implications can be appreciated.

In cases such as $(\mu\text{-H})_2M_3(CO)_9(\mu_3\text{-S})$ [M = Ru(**3**), Os(**4**)] where the two hydrides are magnetically equivalent, it is not possible to follow hydride exchange by ^{1}H NMR. These complexes exhibit a two stage carbonyl exchange process. The first stage of the exchange involves averaging of the three equatorial environments and the two axial environments, while the second stage of the exchange involves averaging of the axial with the radial carbonyls.[22] These results can be explained by invoking hydrogen migrations for the first stage of the exchange and localized axial–radial exchange for the second stage of the process (Scheme 1). In the case of **4**, actual motion of hydrogens has been demonstrated by the observed collapse of two sets of *trans*-^{1}H—^{183}Os two-bond coupling satellites to one in the same temperature range observed for the first stage of the exchange.[23] Studies of the VT–^{13}C NMR of phosphine derivatives of **4** show there is no intermetallic scrambling.[23] We have studied the VT–^{13}C NMR of $(\mu\text{-D})_2M_3(CO)_9(\mu_3\text{-S})$ [M = Ru (**3**-d_2), Os (**4**-d_2)] and found kH/kD ~ 1.5–1.7 for the first stage of the exchange from line-shape analysis of the VT–^{13}C NMR spectra, thus showing that the mechanism of exchange is the same for the osmium and ruthenium analogues (Fig. 2).[24] These results indicate that hydrogen migration is indeed responsible for the observed averaging of the three metal atom environments in the first stage of the exchange. It is also important to note here that the size of the isotope effect is insensitive to the mass of metal atom since kH/kD is almost identical for both the ruthenium and osmium analogues, as expected from the reduced masses ($\mu = (m_M \times m_H/m_M + m_H) \sim 1$). We are currently investigating the isotope effect on the higher energy exchange process in this class of molecules. So far, these studies illustrate the usefulness of kinetic deuterium isotope effects on hydride migrations in uncovering 'hidden processes' in the ligand dynamics of transition metal clusters.

2.2 *Axial–radial exchange of carbonyl groups*

The most useful application of the small primary isotope has been in establishing the connectivity of hydride migrations to other ligands on trinuclear clusters. Perhaps the clearest demonstration of

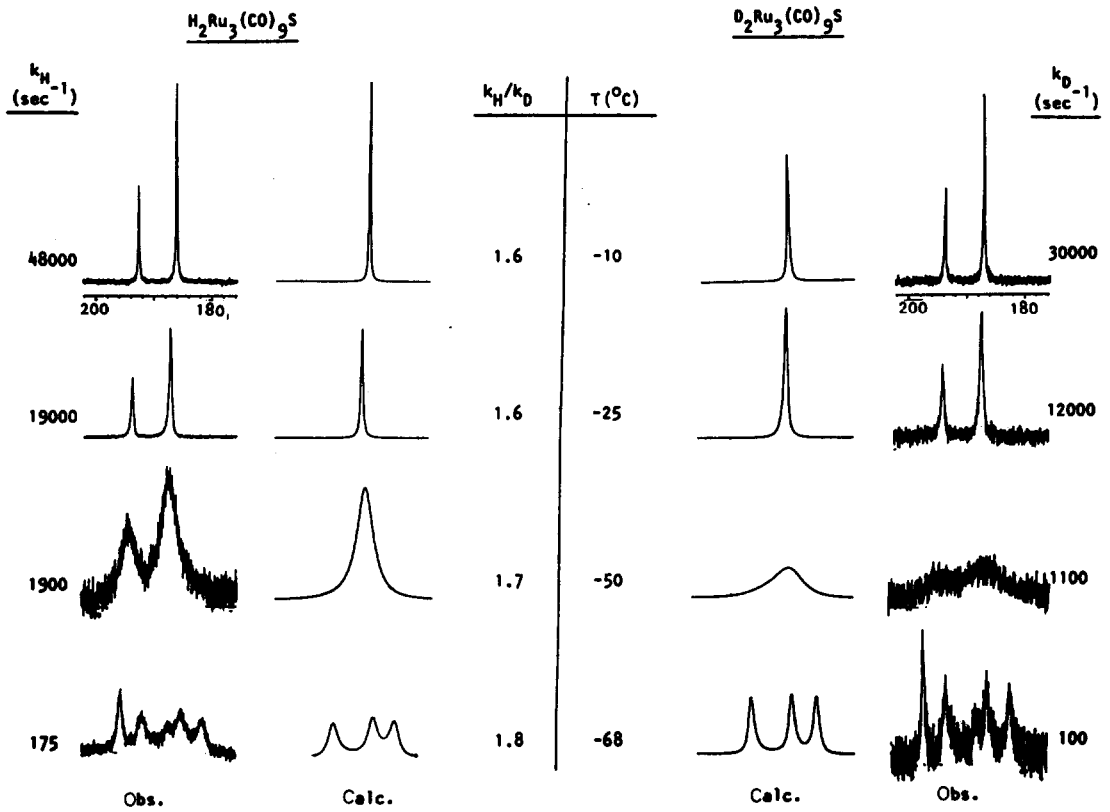

Fig. 2. VT–^{13}C NMR of (μ-H)$_2$Ru$_3$(CO)$_9$(μ_3-S) (**3**) and (μ-D)$_2$Ru$_3$(CO)$_9$(μ_3-S) (**3**-d$_2$) showing observed and calculated spectra for the first stage of exchange at 68 MHz.

this effect comes from VT–^{13}C NMR studies of (μ-H)HOs$_3$(CO)$_{10}$P(C$_6$H$_5$)$_3$ (**5**).[21,25] The bridge and terminal hydrogens in this series of complexes exchange according to Fig. 3. The turnstile motion of the two hydrides and CO(A) and CO(B) requires that CO(A) and CO(B) exchange sites. This process shows a temperature independent deuterium kinetic isotope effect for **5** of kHH/kDD = 1.5 (Fig. 3). This effect is also seen with (μ-H)(H)Os$_3$(CO)$_{10}$CN^{t}Bu (**6**) where the

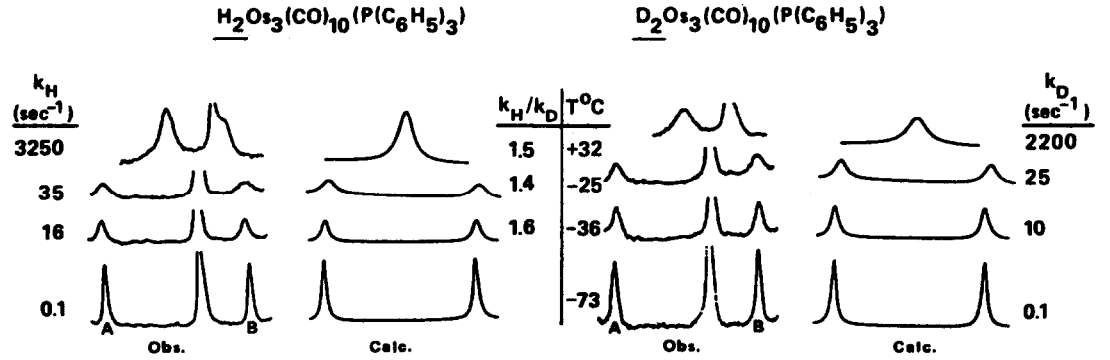

Fig. 3. Observed and calculated VT–^{13}C NMR in the carbonyl region of H(μ-H)Os$_3$(CO)$_{10}$P(C$_6$H$_5$)$_3$ (**5**) and D(μ-D)Os$_3$(CO)$_{10}$P(C$_6$H$_5$)$_3$ (**5**-d$_2$) at 20.1 MHz.

isocyanide occupies an axial position. Here the bridge–terminal interchange of the hydrides can be followed by ^{1}H NMR since these isocyanide complexes exist as mixtures of *cis* and *trans* isomers (with respect to the axial–terminal hydride and the isocyanide) which are interconverted by bridge–terminal exchange.[21]

Significantly, the higher energy localized exchange of the two carbonyl environments at the hydride bridge of the Os_3 triangle in $(\mu\text{-H})_2Os_3(CO)_{10}$ (**7**) shows no deuterium kinetic isotope effect (kHH/kDD = 1.0).[21,25] The hydrides have been shown to be rigid in $H_2Os_3(CO)_{10}$ at room temperature[25] and the absence of an isotope effect at least suggests that they are rigid near the fast exchange limit of the carbonyl environments at the hydride bridged edge of **7**. Taken together with the results for the $(\mu\text{-H})HOs_3(CO)_{10}L$ complexes, these results definitely show that the small isotope effect observed on axial–radial exchange of carbonyl groups cannot be secondary in nature.

With the above results in hand it is now possible to detect whether the motion of a hydride is connected with motion of other ligands even when it is not possible to directly observe hydride site exchange. For example, in the complex $(\mu\text{-H})Ru_3(CO)_9(\mu_3\text{-}\eta^2\text{-}C_2^tBu)$ (**8**) axial–radial exchange of the carbonyl groups at the hydride bridged edge of the triangle takes place at a significantly slower rate ($\Delta G^\ddagger = 62.7 \pm 1$ kJ mol^{-1}) than axial–radial exchange at the unique ruthenium atom ($\Delta G^\ddagger = 46 \pm 1$ kJ mol^{-1}).[26] The axial–radial exchange at the hydride bridged edge of the triangle shows an isotope effect (kH/kD $\sim$ 2) when the VT–^{13}C NMR spectra of the deuterated analogue $(\mu\text{-D})Ru_3(CO)_9(\mu_3\text{-}\eta^2\text{-}C_2^tBu)$ (**8**-d_1) was examined.[21] The value of this isotope effect must be taken as approximate since overlap of resonances precluded an accurate line-shape analysis. However, motion of the hydride is indicated or no kinetic deuterium isotope effect would be observed. The type of hydride motion however, is not indicated by these results. Alternate opening of the hydride bridge to a terminal hydride at each bridged ruthenium atom and movement of the hydride to a face bridging mode are the two likely possibilities. The hydride in this molecule has been located by neutron diffraction and is observed below the plane of the Ru_3 triangle on the opposite face to which the acetylido moiety is bound.[26] This position suggests that the hydride would have to move somehow in order to allow the pinwheeling motion by which axial–radial exchange occurs in this face capped cluster.[27] This conclusion is born out by the fact that the barrier to axial–radial exchange at the formerly bridged edge in the corresponding anion, $Ru_3(CO)_9(\mu_3\text{-}\eta^2\text{-}C_2^tBu)^-$, is considerably lower ($\Delta G^\ddagger = 41.8 \pm 2$ kJ mol^{-1}) than in **8**.[28]

2.3 *Face migrations of hydrocarbon ligands*

In the case of **8**, discussed in the previous section, and also in the case of the $\mu^3\text{-}\eta^3$-allyl clusters, $(\mu\text{-H})Ru_3(CO)_9(\mu_3\text{-}\eta^3\text{-}RC{=}{=}{=}C(R'){=}{=}{=}CR)$, our VT–^{13}C NMR studies indicate that the organic ligand is rigid relative to the carbonyl ligands which undergo localized axial–radial exchange and intermetallic carbonyl exchange.[26,28] In other structural configurations such as $(\mu\text{-H})_2Os_3(CO)_9(\mu_3\text{-}\eta^2\text{-}RC{\equiv}CR)$ and $(\mu\text{-H})M_3(CO)_9(\mu_3\text{-}\eta^2\text{-}RC{=}C{=}CR_2)$ (M = Ru, Os) both hydrogen and hydrocarbon ligand motions are indicated from VT–NMR studies, but the relationship between these two processes could not be clearly delineated.[29,30]

The class of molecules $(\mu\text{-H})_2Os_3(CO)_9(\mu_3\text{-}\eta^2\text{-}RC{\equiv}CR)$ exhibits a three stage exchange process for the carbonyl ligands. The first stage of the exchange involves collapse of the nine resonances observed at the low temperature (-100°C) limit to five resonances (at -70°C) and is readily explained by edge hopping of one hydride but not site exchange of the two hydrides (Fig. 4).[30] The second stage of the exchange collapses the five resonances to two in 1 : 2 relative intensity (at -20°C) and is thought to arise from localized scrambling of the carbonyl groups. The third stage of the exchange (above -20°C) averages all carbonyl environments and exchanges the two hydrides. This last stage of the exchange could involve alkyne motion and/or intermetallic carbonyl exchange.

Taking advantage of the diastereotopic methylene protons in $(\mu\text{-H})_2Os_3(CO)_9(\mu_3\text{-}\eta^2\text{-}CH_3CH_2C{\equiv}CCH_2CH_3)$ (**9**) we have shown that the alkyne is rigid in the temperature range of -100 to -20°C since the diastereotopic methylene resonances remain as a sharp AB pattern up to -20°C.[31] Above this temperature, alkyne motion and exchange of the two hydrides begin which averages all carbonyl environments. The calculated activation energy for hydride exchange ($\Delta G^\ddagger$ (300 K) $= 54 \pm 1$ kJ mol^{-1}) is slightly lower than that calculated for alkyne migration ($\Delta G^\ddagger = 60.0 \pm 1$ kJ mol^{-1}). An examination of the VT–^{1}H NMR of $(\mu\text{-D})_2Os_3(CO)_9(\mu_3\text{-}\eta^2\text{-}CH_3CH_2C{\equiv}CCH_2CH_3)$ (**9**-d_2) revealed an isotope effect of kHH/kDD = 1.50–1.75, in the temperature range -20 to $+34$°C,

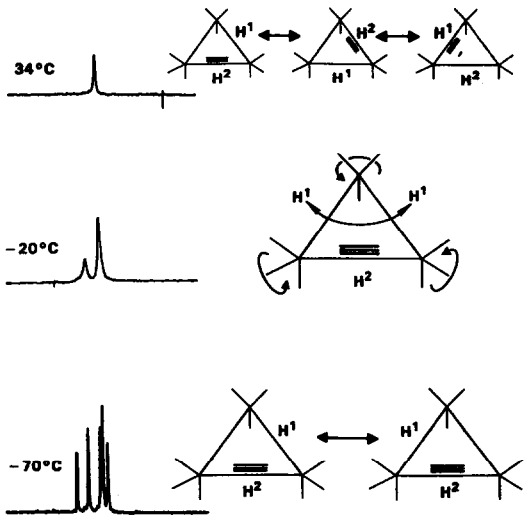

Fig. 4. VT–^{13}C NMR of the carbonyl region of $(\mu\text{-H})_2Os_3(CO)_9(\mu_3\text{-}\eta^2\text{-RC}{\equiv}\text{CR})$ [R = CH_2CH_3 (**9**)] with the proposed exchange process for each stage of the exchange.

on the rate of migration of the alkyne group (Fig. 5).[31] The observed variation in the kHH/kDD ratio with temperature is approximately within the experimental error in the line-shape analysis ($\pm$10%). The average value of kHH/kDD = 1.65 is very close to a value of 1.5 observed for the axial–radial exchange of carbonyl groups, although formally different motions of the hydride are involved. In the $(\mu\text{-H})HOs_3(CO)_9L$ systems, opening of one hydride (or closing of the terminal

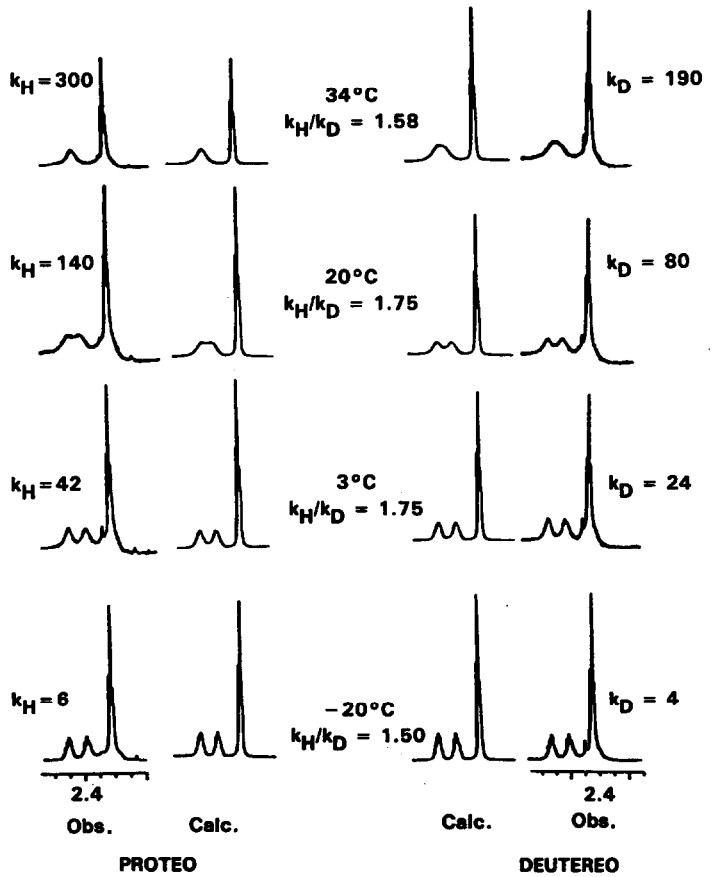

Fig. 5. VT–^{1}H NMR of **9** and **9**-d_2 showing the simulated and observed spectrum for the alkyne protons.

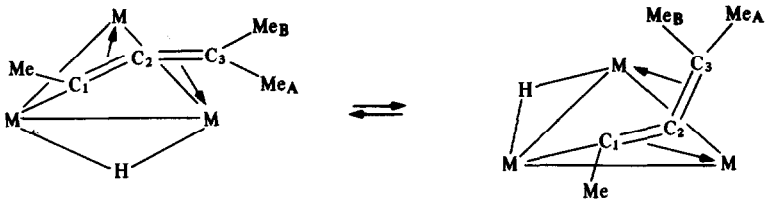

M = Ru, Os

Scheme 2.

hydride to a doubly bridged species) is the motion required, while in **9** edge hopping of the hydride is the required motion. Our results so far suggest that any type of motion of the hydride which is required for site exchange of another ligand (i.e. carbonyl or alkyne) will show an isotope effect where kH/kD ~ 1.5. It should also be noted here that the low temperature edge-to-edge migration of one hydride in **9** which results in the five line spectra seen at −70°C (Fig. 4) also shows an observable isotope effect, but it was not possible to evaluate kHH/kDD for this process due to severe overlap of resonances in the intermediate exchange regime.[31]

In the allenic complexes (μ-H)M_3(CO)$_9$(μ_3-η^3-RC═C═C(R)R) (M = Ru, Os; R = CH_3) we have observed an oscillating motion of the organic ligand which is apparently coupled with edge-to-edge migration of the hydride (Scheme 2). However, it was not possible to say whether the activation energy for the two processes is actually the same since the proton is in equivalent magnetic environments in both chemical configurations. We have addressed this point by synthesizing the unsymmetrical derivative (μ-H)Os_3(CO)$_9$(μ_3-η^3-CH_3C═C═C(CH_3)CH(CH_3)$_2$) (**10**) which exists as two isomers in solution (Scheme 3). Line-shape analysis of the VT-^{1}H NMR of the hydride and the

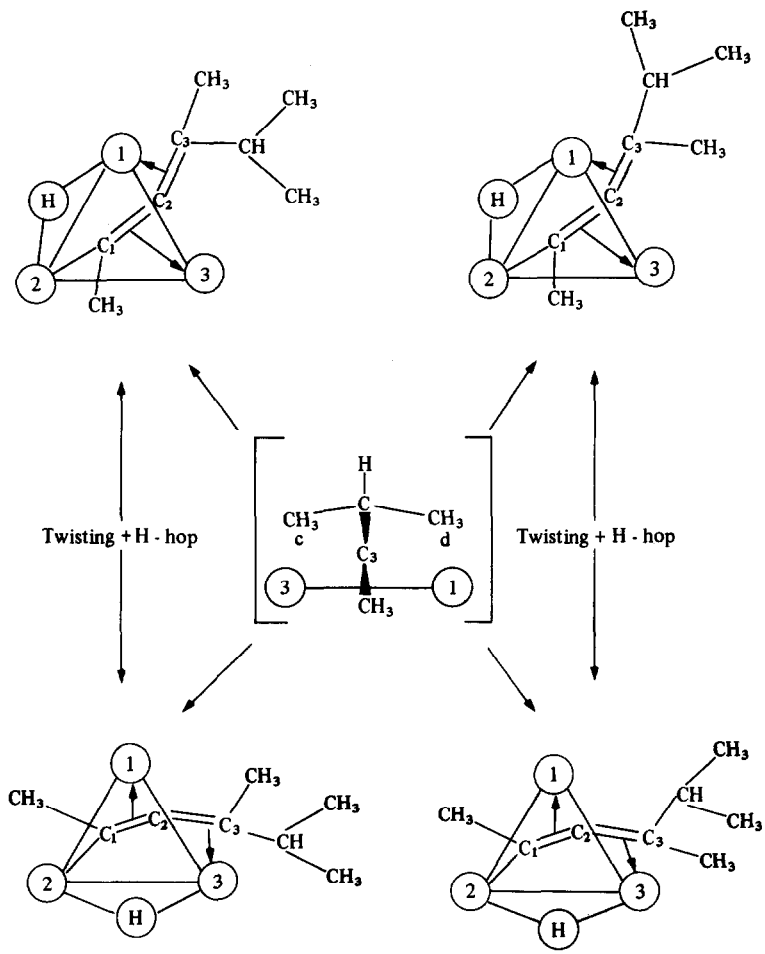

Scheme 3.

hydrocarbon regions gave identical activation energies ($\Delta G^{\ddagger}$ (300 K) = 70.8 ± 1 kJ mol^{-1}) for the averaging of the hydride and the methyl group environments in each isomer. A sample of **10** deuterated in the hydride position showed an isotope effect of kH/kD = 1.5 on the rate of averaging of the methyl groups in each isomer.[31]

Both of the examples discussed above show that when a hydrocarbon ligand migration requires hydride motion to exchange two equivalent geometries the motion of the hydride is the rate-determining step. This appears to be true even when the activation energy is slightly lower for hydrogen migration than for hydrocarbon motion.

2.4 *Chemical reactions involving hydride migrations*

It has been recognized for some time that the time scale of polytopal rearrangements in polynuclear clusters merges with the reaction time scale. However, examples where the rate of a specific dynamic process influences the rate of a cluster reaction have not been forthcoming. Recognizing the small isotope effect on hydride migrations discussed in the previous sections, we[32,33] and others [34] have recently uncovered several examples where substituting deuterium for hydrogen on a μ-hydride cluster changes the rate and/or the product distribution in a cluster reaction. In the three cases reported so far the kH/kD values reported are in the range 1.5–1.7. In light of the results discussed in sections 2.1–2.3 these kH/kD values suggest that opening or migration of μ-hydride is involved in the rate-determining step of these reactions.

The first observation of a kinetic deuterium isotope effect in μ-hydride cluster chemistry was made in a study of the protonation of (μ-H)Ru$_3$(CO)$_8$(μ_3-η^2-C$'_2$Bu)(P(C$_6$H$_5$)$_5$) (**11**).[32] This complex undergoes a two step protonation in H_2SO_4 to give two kinetic products **12a** and **12b** [eq. (15)] in a 1.5 : 1 ratio.

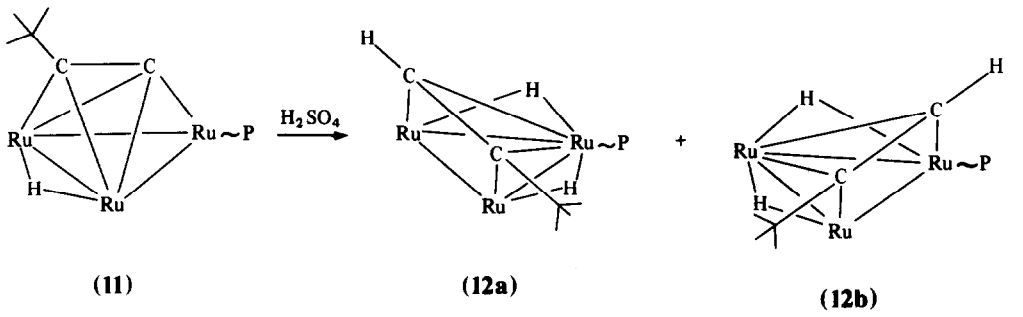

(15)

(11) **(12a)** **(12b)**

Isomer **12b** slowly isomerizes to **12a** which can be isolated from the reaction mixture as its hexafluorophosphate salt. When D_2SO_4 is reacted with **11** only **12a** is detected by ^{1}H NMR [i.e. < 8% isomer b, eq. (16)].

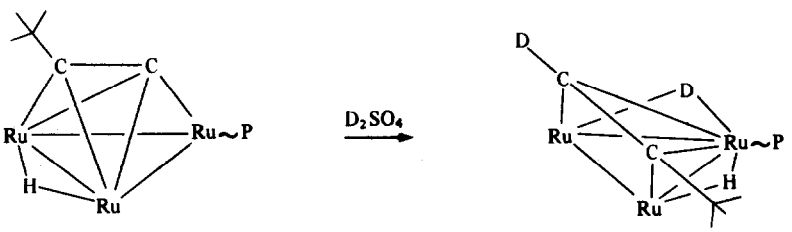

(16)

(11) **(12a)**

A sample of **11**, 65% deuterated in the hydride position, gave a 3 : 4 ratio of **12a**/**12b** when it was reacted with H_2SO_4, thus inverting the kinetic product distribution. Isomer **12b** slowly converts to isomer **12a** at the same rate as in the fully protic case.

These results can be understood in terms of the mechanism shown in Scheme 4. Initial protonation of **11** occurs on the metal core in H_2SO_4 as well as in acid solutions of CD_2Cl_2 and in neat

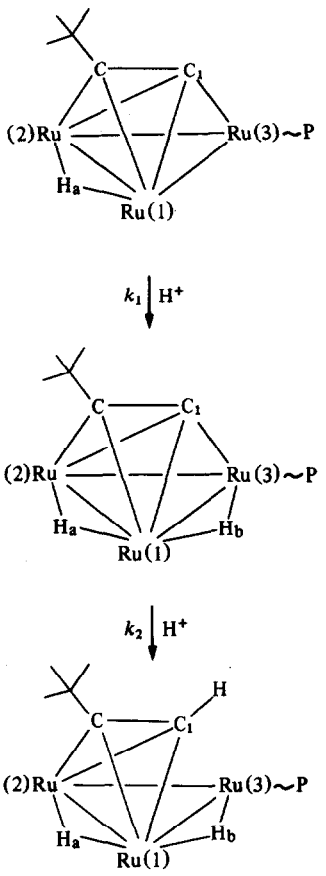

(13)

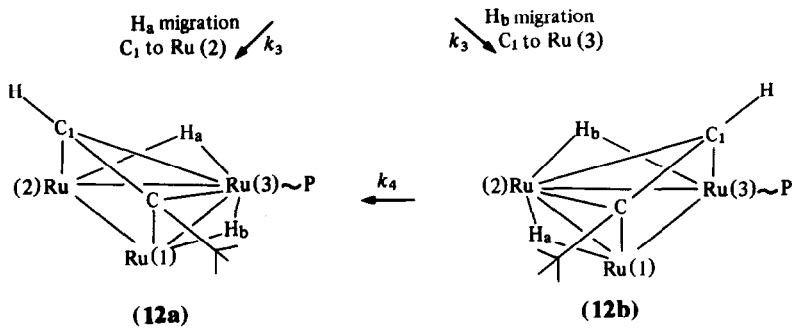

(12a) **(12b)**

Scheme 4.

CF_3COOH (Scheme 4). If the second protonation takes place at the carbon atom, and is faster than hydride migration, intermediate **13** is produced. We propose that rearrangement of the organic ligand from a $5e^-$ to a $4e^-$ ligand requires a twisting motion of the ligand and migration of either H_a or H_b to give isomers **12a** or **12b**. In D_2SO_4 intermediate **13**-d_b is formed from which H_a migration and σ-bond formation to Ru(1) and Ru(2) is favoured [eq. (17)].

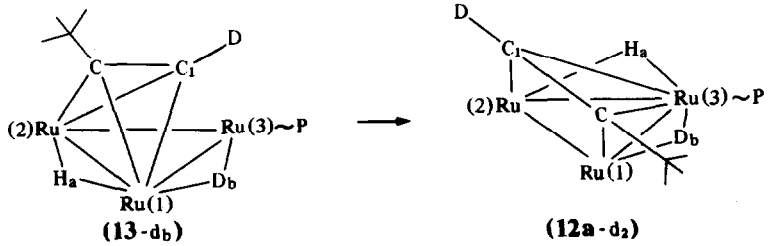

(13-d_b) **(12a-d_2)** (17)

σ-bond formation of Ru(2) and Ru(3) with *no* H_a or D migration is ruled out since this would yield some of the **b** isomer as a kinetic product and this is not observed. The use of 65% deuterated **11** gives **13**-d_a from which H_b migration and σ-bond formation to Ru(1) and Ru(3) is favoured [eq. (18)].

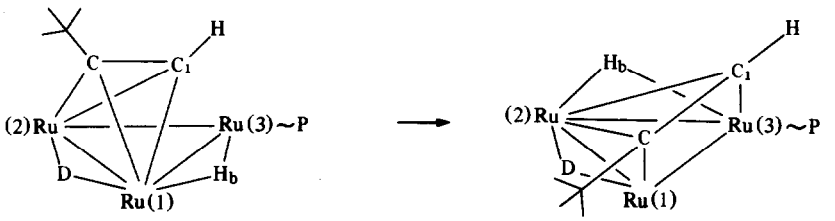

(13-d_a) (12b) (18)

This interpretation of the observed deuterium isotope effect only requires that isomers **12a** and **12b** [eq. (15)] differ in their disposition of the hydride ligand with respect to the phosphine ligand, as they clearly do. An accompanying twisting motion of the organic ligand is also required to give **12a**, a structure which is symmetrical with respect to the phosphine ligand and unsymmetrical with respect to the organic ligand. We cannot rigorously exclude the possibility of intramolecular phosphine ligand migration but there is no precedent for this process in the literature, while there is precedent for migrations of organic ligands being associated with hydride migrations on trimetallic clusters, of the general type proposed here.[30,31]

It is not possible to extract an exact number for the deuterium isotope effect from these experiments since we do not know absolute rates of formation of **12a** or **12b**. The observed rate of rearrangement of **12a** to **12b** does not show a deuterium isotope effect after correction for the initial differences in isomer ratio. This is reasonable in that intramolecular hydride exchange randomizes deuterium on the metal core in the formation of **12a** when D_2SO_4 in reacted with **11**. The deuterium isotope effect is only observed for the more rapid hydride plus organic ligand migration. Since we have calculated the rate constant for hydride migration to be 10^2 s^{-1},[21] the second protonation step must have a rate constant larger than this value. We feel this is not unreasonable in the strong acid medium of H_2SO_4. The mechanism discussed above now has a basis in the observed isotope effects on hydride migrations and their direct connection to the motion of a μ_3-η^2-alkyne over the face of a trinuclear cluster (sections 2.1 and 2.3).

A recent study by Shore and co-workers[34] on intermolecular carbonyl exchange in $(\mu\text{-X})Ru_3(CO)_{11}^-$ [X = H(**14**) or D(**14**-d)] showed that the rate of ^{13}CO–^{12}CO exchange was 1.5 faster in the protic case for the associative part of the overall rate law:

$$\text{rate of } {}^{13}CO\text{–}{}^{12}CO \text{ exchange} = k_1[\text{cluster}] + k_2[\text{cluster}][CO].$$

This result was rationalized by invoking an opening of the μ-H-hydride bridge to a terminal hydride upon CO association [eq. (19)].

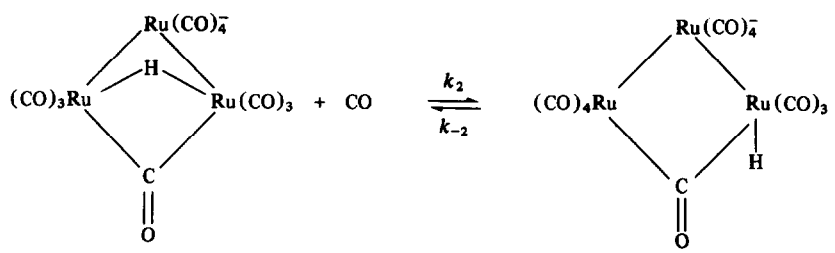

(14) (19)

The value of $k_2H/k_2D = 1.5$ fits very well with the observed isotope effect on hydride bridge opening in $H(\mu\text{-H})Os_3(CO)_{10}L$ systems (section 2.2). At very low CO pressures dissociative carbonyl exchange, for which hydride bridge opening is not required, is the dominant process for which a

kH/kD ~ 1 is observed. Similar results and the same kH/kD ratio were observed for the osmium analogue of **14**.

A second example where substitution of deuterium for hydrogen on a cluster results in a change in the kinetic product distribution is the reaction of $(\mu\text{-H})_2Os_3(CO)_{10}$ with terminal alkynes.[33] This reaction yields three major triosmium decacarbonyl products [eq. (20)]:

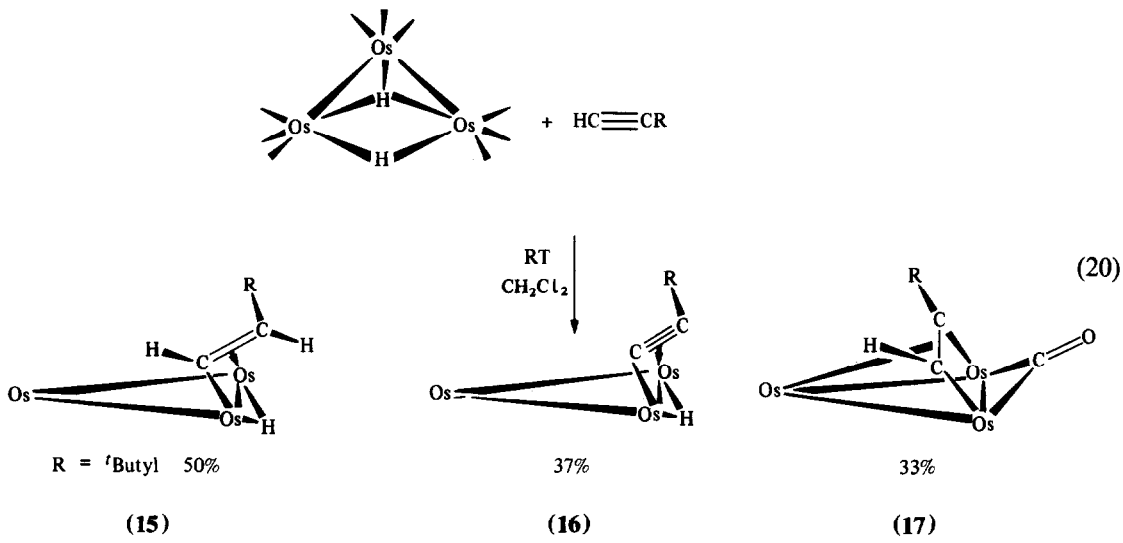

(20)

a μ-σ-π-vinyl complex (**15**), μ-σ-π-acetylido product (**16**) and a μ_3-η^2-alkyne complex (**17**). The product distribution in this reaction is highly sensitive to the steric bulk of the alkyl group of the terminal alkyne.[34] Thus, the relative amounts of **16** and **17** increase at the expense of **15** with increasing size of the alkyl group. In the case of acetylene, **15** is the only product, while for *t*-butyl acetylene the relative amounts shown in eq. (20) are obtained.

We have conducted a series of crossover experiments using deuterated cluster and alkyne (Table 1).[33] The experiments revealed a significant deuterium isotope effect on the product distribution. The

Table 1. Results of crossover experiments[a,b] for the reaction of $X_2Os_3(CO)_{10}+XC_2^tBu$ (X = H or D)

Case	Reactants, H vs D site: X in $X_2Os_3(CO)_{10}$	X in XC_2^tBu	Product percentages: **15**	**16**	**17**
1	H	H	50	37	13
2	H	D	45 (33% D in hydride)	39 (100% D in hydride)	16 (100% D)
3	D	H	32 (67% D in hydride)	51 (100% H in hydride)	17 (100% H)
4	D	D	23	56	21

[a] Reaction conditions: CH_2Cl_2, 25°C, 24 h, 3:1 mole ratio of alkyne to trinuclear cluster.

[b] Per cent conversion to **15**, **16** and **17** was 90% in all cases.

overall effect is the same as that obtained by increasing the steric bulk of the alkyl group on the alkyne, with **16** and **17** increasing in relative amounts at the expense of **15**. In addition, there is statistical scrambling of deuterium into the hydride position of **15** while there is no deuterium scrambling into the hydride position of **16** and the terminal alkyne hydrogen in **17** (Table 1).

The first step in this reaction is undoubtedly the coordination of the alkyne to the cluster. Because of the steric bulk of the alkyne, coordination is almost certainly in a radial position [eq. (21)].

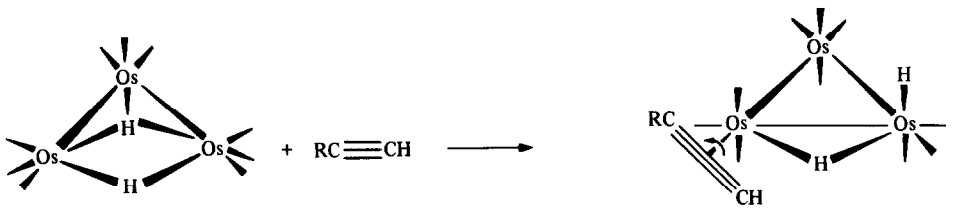

(21)

From this intermediate (which forms in undetectable amounts[33]), addition of an Os—H bond to the alkyne can occur with the hydrogen adding to either the terminal or internal carbon of the alkyne. Addition of the hydrogen to the terminal carbon could give an intermediate which undergoes reductive elimination of alkene and reaction with a second alkyne molecule to give **16** and **17**, while addition to the internal carbon would give **15** directly. Thus, the steric effect on the reaction can be understood in terms of the orientation of addition to the alkyne bond. However, it is more difficult to rationalize the observed isotope effects in terms of the orientation of addition to the alkyne bond alone. If the reductive elimination of alkene is a reversible process and the back reaction (alkene + cluster) is competitive with reaction of an unsaturated cluster intermediate with free alkyne, an inverse or thoermodynamic isotope effect could be operative. The observed shift in product distribution to **16** and **17** results from a shift in the equilibrium involving the alkyne adduct towards the unsaturated cluster intermediate and free alkene where more carbon–deuterium bonds are present. This explanation of the observed isotope effect on product distribution hinges on the reversibility of the reductive elimination of alkene for which there is no direct precedent in triosmium chemistry. We also feel that reaction with free alkyne would be much faster than the back reaction with alkene.

An alternative explanation for the observed kinetic isotope effect on product distribution, which also explains the observed steric effect, centres on the rate at which radial to axial migration of the coordinated alkyne occurs. Since **15** has the organic ligand coordinated on the face of the cluster, edge-to-face migration must take place during its formation from the radially coordinated alkyne adduct [eq. (21)]. Both the steric bulk of the alkyne and the presence of deuterium in the μ-hydride position (section 2.2) would slow down axial–radial interchange. Longer residence times in the radial position could allow a reversible hydride addition at the terminal end of the alkyne to occur to give an unstable edge bridged σ–π vinyl complex which could undergo reductive elimination of alkene or revert to the radially coordinated alkyne adduct (Scheme 5). A σ–π interchange of the edge bridging vinyl group which accomplishes a *cis–trans* interconversion would account for the observed scrambling of deuterium in compound **15** which is ultimately formed. The reversible formation of other edge bridged intermediates such as the μ-vinylidene complexes, $H(\mu\text{-}H)Os(CO)_{10}(\mu C{=}C(H)R)$ could also account for the observed scrambling. Irrespective of the nature of the edge bridged intermediate this interpretation of the deuterium isotope effect on the product distribution in eq. (20) has precedent in the known isotope effect for the axial–radial exchange and simultaneously explains the observed deuterium scrambling in **15** (Table 1) and the steric effect on the reaction.

The isotope effect ratio for this reaction is 1.6 (Table 1), which is very close to the value observed for axial–radial exchange in $H_2Os_3(CO)_{10}L$ (section 2.2). It is difficult to predict the size of a thermodynamic isotope effect for eq. (20), but a range of 2.0–3.5 would be predicted based on previous observations of this effect[18] and the calculated differences in zero point energies between $H_2Os_3CO_{10}L$ and $D_2Os_3(CO)_{10}L$ systems as calculated from the bridging and terminal hydride IR stretching frequencies.[35] The two alternative interpretations of the isotope effect observed for this

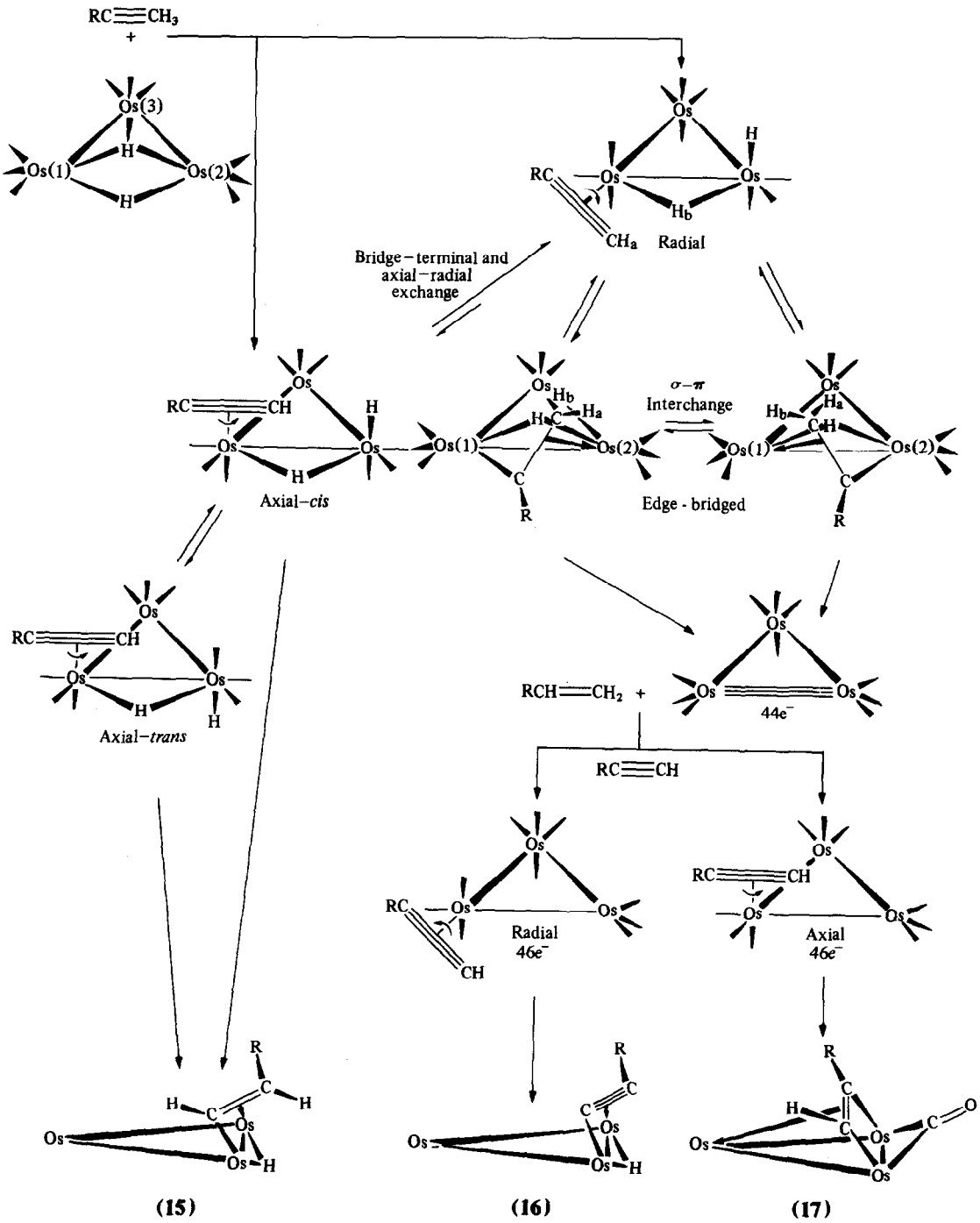

Scheme 5.

reaction [eq. (20)] illustrate the difficulties that can be encountered in interpreting small isotope effects in multi-step cluster reactions.

3. THE LARGE PRIMARY ISOTOPE EFFECT ($kH/kD = 7$–50)

3.1 *Ligand to metal hydrogen transfers in protonations of clusters*

Mays *et al.* have previously observed very large isotope effects in the protonation of neutral and anionic clusters with mineral acids (see Table 2).[36] In organic chemistry large isotope effects (i.e.

Table 2. Kinetic isotope effects in the protonation of transition metal clusters[a]

Compound	kH/kD
$FeCo_3(CO)_{12}^-$	16.8±1.0
$RuCo_3(CO)_{12}^-$	15.4±1.0
$OsCo_3(CO)_{12}^-$	16.2±1.0
$Os_3(CO)_{12}$	11±2
$[(\pi\text{-}C_5H_5)Fe(CO)_2]_2$	7±1

[a] Taken from J. Knight and M. J. Mays, *J. Chem. Soc. A* 1970, 711.

isotope effects larger than calculated values based on differences in zero point energy) are thought to arise from reactions in which the barrier width is small and where the wavelength of the proton is similar to the width of the barrier. These types of barriers are usually associated with reactions in which there is very little distortion of the reactant ground state geometry on going from reactant to product.[1,3] The most common example of this type of reaction in organic chemistry is intramolecular proton transfer. The presence or absence of large kH/kD ratios has been used to characterize the transition states of these proton transfers.[3] In considering the large protonation isotope effects observed by Mays *et al.* we thought that their origin might be due to an initial protonation of oxygen followed by an intramolecular proton transfer down to the metal core [eq. (22)].

$$M_n(CO)_m^{n-} + H^+ \longrightarrow M_n(CO)_{m-1}(COH)^{(n-1)-} \longrightarrow HM_n(CO)_m^{(n-1)-} \quad (n = 0, 1). \qquad (22)$$

This seemed to us a very likely possibility in light of the recent work of Shriver[37] and Kiester[38] on the protonation of $(\mu\text{-H})M_3(CO)_{11}^-$ (M = Fe, Ru) (see structure **18**).

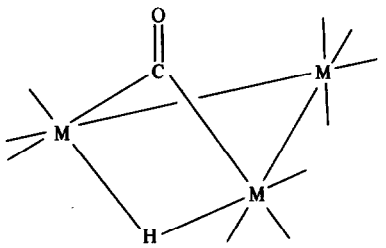

18 M = Fe, Ru, Os

In both the iron and ruthenium cases, initial protonation is at oxygen. In the ruthenium case, however, subsequent rearrangement to the dihydrido species $(\mu\text{-H})(H)Ru_3(CO)_{11}$ (**19**) can be observed [eq. (23)]. We have made a further investigation on the low temperature protonation of the $(\mu\text{-H})M_3(CO)_{11}^-$ (M = Fe, Ru) anions as well as the first investigation of the low temperature protonation of $(\mu\text{-H})Os_3(CO)_{11}^-$.[39] Indeed, we observed very large deuterium kinetic isotope effects on the transformation presented in eq. (22) for the low temperature protonation of the ruthenium and osmium anions.

$$\underset{\textbf{14}}{(\mu\text{-H})Ru_3(\mu\text{-CO})(CO)_{10}^-} + H^+ \xrightarrow{-80°C} \underset{\textbf{19}}{(\mu\text{-H})Ru_3(\mu\text{-COH})(CO)_{10}} \xrightarrow{-80°C} \underset{\textbf{20}}{(\mu\text{-H})(H)Ru_3(CO)_{11}} \qquad (23)$$

The protonation of $(\mu\text{-H})Fe_3(CO)_{11}^-$ with HSO_3F at −80°C gives only $(\mu\text{-H})(\mu\text{-COH})Fe_3(CO)_{10}$. This O-protonated species shows no tendency to rearrange to a dihydrido species at low temperature but decomposes with the evolution of H_2 as the temperature is increased to ambient.[37] The overall rate of protonation is the same when DSO_3F is used at −80°C, and no scrambling is observed

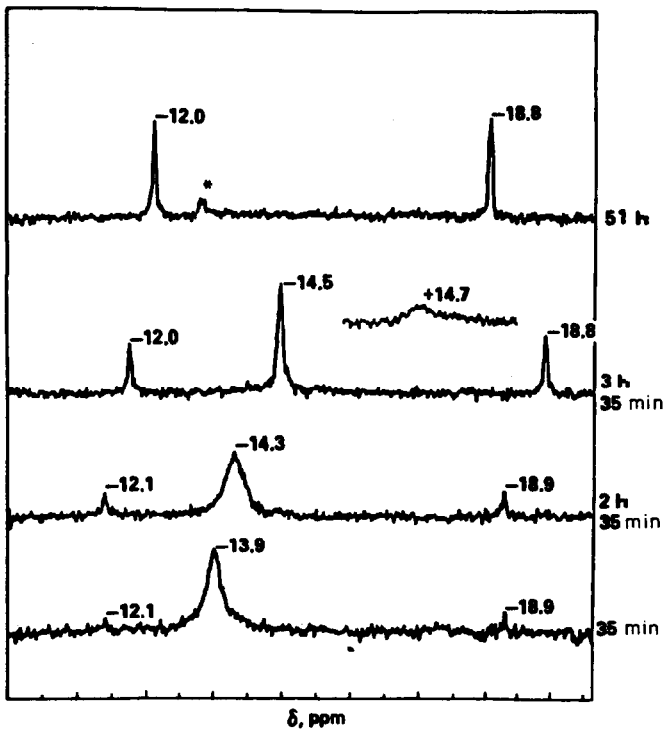

Fig. 6. Time dependent ^1H NMR spectra after addition of one equivalent of HSO_3F to a CD_2Cl_2 solution of **14** at −80°C. (*) Original **14** hydride signal observed at −13.0 ppm indicating a slight deficiency of the acid.

between the deuterium on the oxygen and the bridging hydride in the $(\mu\text{-H})(\mu\text{-COD})Fe_3(CO)_{10}$ produced.[39] These results clearly showed that there is no deuterium kinetic isotope effect in the proton transfer step from the acid to the oxygen of the bridging carbonyl [eq. (23)] and that there is no exchange between the hydride and the hydrogen on the oxygen.

In the case of **14** we found conditions (−80°C, 1 equiv HSO_3F in CD_2Cl_2) where only the O-protonated species $(\mu\text{-H})(\mu\text{-COH})Ru_3(CO)_{10}$ (**19**) is initially formed and where gradual conversion to the dihydrido species **20** is complete in approximately 50 h (Fig. 6). Under identical conditions, on protonation of **14** with DSO_3F, no conversion of **19** to **20** is observed (Fig. 7). At −40°C with HSO_3F, conversion of **19** to **20** is complete in about 1 h. When **14** is deuterated with DSO_3F at −80°C then warmed to −40°C, conversion to $(HD)Ru_3(CO)_{11}$ is only partially complete after 47 h. Clean conversion of $(\mu\text{-H})(\mu\text{-COD})Ru_3(CO)_{10}$ to $(HD)Ru_3(CO)_{11}$ is complicated by the formation of another unidentified hydride containing species at −40 to −60°C. It is therefore not possible to accurately access the magnitude of kH/kD for this ligand to metal hydrogen transfer, except to set a lower limit for the effect of ~ 50 at −40°C. Based on differences in zero point energy the maximum value for kH/kD (i.e. for a symmetrical–linear transition state) for cleavage of an O—H versus an O—D bond is ~ 50 at −80°C and ~ 25 at −40°C.* Given that it is highly unlikely that the transition state for this ligand to metal hydrogen transfer is either symmetrical or linear it is reasonable to propose that there is a significant tunnelling component for transfer of a hydrogen from a protonated carbonyl group to the metal core. In order to prove this one must show that $\Delta E_{a_D^H} \gg \Delta E_{0_D^H}$ (where E_a is the activation energy and E_0 is the zero point energy), which is not possible in the case of the conversion of **19** to **20**. These results do strongly suggest that the large isotope effects observed by Mays (Table 2) at room temperature arise from the initial protonation at the oxygens of the metal carbonyls followed by proton transfer to the metal core. That this type of transformation should involve a large tunnelling component seems reasonable since only minor

* Using a value of 3600 cm^{-1} for the O—H^- bond and 2525 cm^{-1} for the O—D bond.

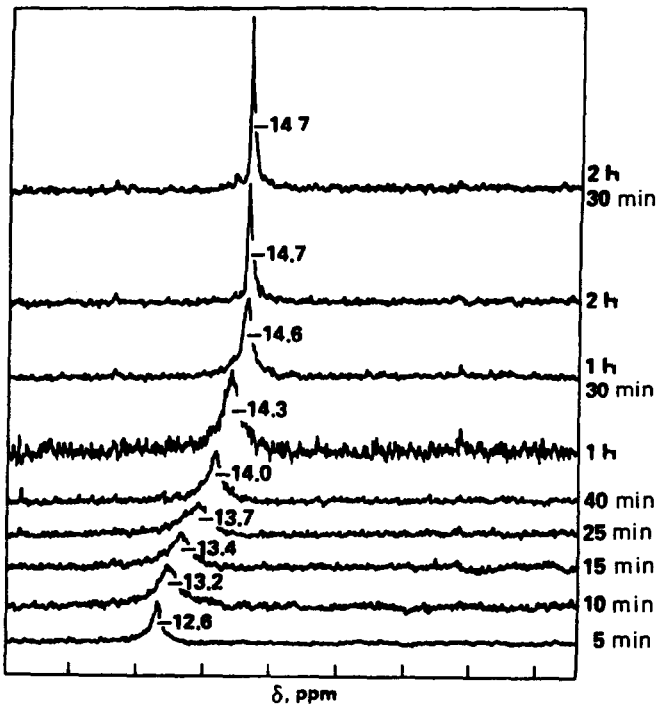

Fig. 7. Time dependent ^1H NMR spectra after addition of one equivalent of DSO_3F to a CD_2Cl_2 solution of **14** at −80°C. Original **14** hydride signal was observed at −13.0 ppm.

changes in cluster geometry are required on going from an O-protonated to M or M—M-protonated species. We are currently examining the low temperature protonations of the complexes investigated by Mays and co-workers at room temperature.[36]

Regardless of the actual magnitude of this large isotope effect or whether or not barrier tunnelling is actually involved, its sheer size will make it useful for identifying the kinetic site of protonation in polynuclear carbonyl clusters. For example, low temperature protonation of $(\mu\text{-H})Os_3(CO)_{11}^-$ with HSO_3F gives $H(\mu\text{-H})Os_3(CO)_{11}$ directly as the only detectable product.[39] Under the same conditions protonation with DSO_3F gives only $(\mu\text{-H})(\mu\text{-COD})Os_3(CO)_{10}$ up to 4 h after neutralization.[39] This species has never been observed before and was identified in solution on the basis of its low temperature ^{13}C NMR spectrum, for which the pattern of carbonyl resonances observed is identical with that of its iron analogue.[37] These studies reveal that the kinetic site of protonation in all three $(\mu\text{-H})M_3(CO)_{11}^-$ (M = Fe, Ru, Os) anions is the oxygen of the bridging carbonyl, despite the large increase in the stability of the metal–hydrogen bond of $H(\mu\text{-H})M_3(CO)_{11}$ as one goes down the iron triad.[36]

3.2 *Metal to ligand hydrogen transfers*

The large deuterium kinetic isotope effects for ligand to metal hydrogen transfers discussed in the previous section suggest that a similar effect should be observed in reactions where the reverse process (i.e. hydrogen transfer from metal to ligand) is the rate-determining step. This is particularly true for reactions with a large tunnelling component where proton barrier tunnelling would be quenched by deuterium substitution at the metal or the ligand atom.

The thermal reactivity of the series of complexes $H(\mu\text{-H})Os_3(CO)_{10}(CNR)$ (**21**) (R = CH_3, C_6H_5, $C(CH_3)_3$) has been studied by Adams and Golembeski.[40] Varying amounts of the two metal to ligand hydrogen transfer products, $(\mu\text{-H})Os_3(CO)_{10}(\mu\text{-}\eta^1\text{-C=N(H)R})$ (**22**) and $(\mu\text{-H})Os_3(CO)_{10}(\mu\text{-}\eta^2\text{-HC=NR})$ (**23**) are obtained in addition to smaller amounts of the two isomers of $(\mu\text{-H})_2Os_3(CO)_9(CNR)$ (**24**) and $Os_3(CO)_{11}(CNR)$ [eq. (24)].

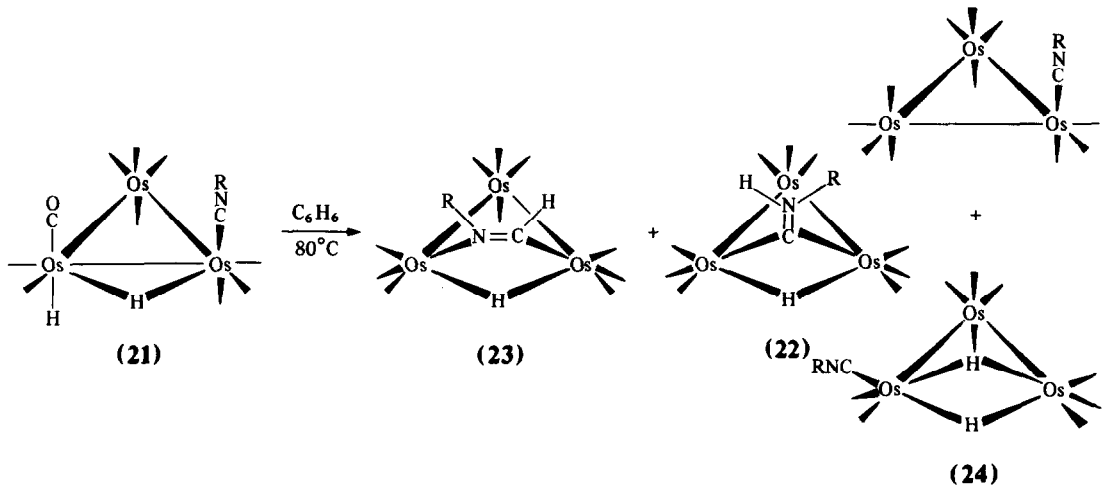

(24)

Transfer of hydrogen to nitrogen to give **22** is favoured in coordinating solvents, and is catalysed by base. Transfer of hydrogen to carbon to give **23** requires a carbonyl dissociation–association and can be formed from **24** in the presence of CO.[40,41] The amounts of **22** and **23** obtained are also dependent on R and these two products do not interconvert.[40]

We have found that for **21** ($R = CH_3$) clean conversion to **22** takes place at room temperature even in dry benzene-d_6 with a first-order rate constant, $k_H = 8.5 \pm 0.3 \times 10^{-4}$ min^{-1} at 30°C.[41] The same conversion using (D)(μ-D)$Os_3(CO)_{10}(CNCH_3)$ (**21**-d_2) gives a rate constant $kD = 3.1 \pm 0.3 \times 10^{-5}$ min^{-1} ($kH/kD = 26.9$). The calculated "maximum" isotope effect for this reaction is 3.5 based on the observed difference in stretching frequencies between the terminal M—H and M—D bond (2.7 based on the difference between the bridging M—H versus M—D bond).[35] These results strongly suggest a significant tunnelling component for this apparently polar osmium to nitrogen hydrogen transfer. Variable temperature studies to verify this point are underway. It is important to point out here that addition of base to benzene solutions of **21**-d_2 quenches the observed isotope effect as well as accelerating the rate of the metal to nitrogen hydrogen transfer (Table 3). Thus intermolecular proton transfer is a separate reaction pathway.

Thermolysis of **21** ($R = C_6H_5$) in benzene-d_6 gives only **23** ($kH = 1.23 \pm 0.2 \times 10^{-2}$ min^{-1} at 60°C). Thermolysis of the deuterated analogues under identical conditions showed a small inverse effect ($kD = 2.01 \pm 0.2 \times 10^{-2}$ min^{-1}, $kH/kD = 0.5$). This indicates that the metal to carbon hydrogen transfer is a reversible process.[40] Taken together with the fact that formation of **23** is repressed by a carbon monoxide atmosphere these results suggest that the metal to carbon hydrogen transfer is a reversible reductive elimination which takes place via an $H_2Os_3(CO)_9(RCN)$ intermediate [eq. (25)].

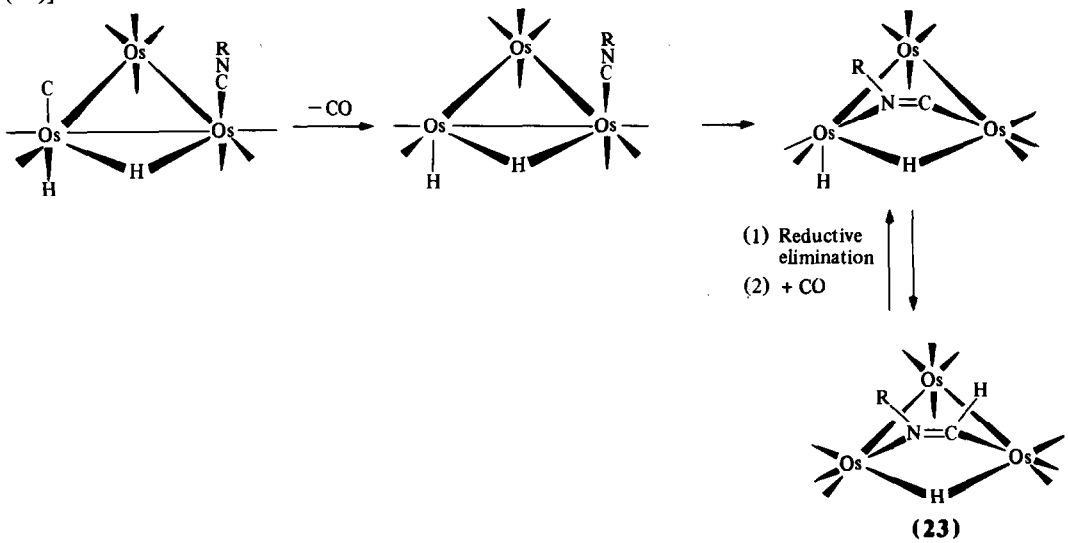

(25)

Table 3. Kinetic data for base catalysed conversion of $X_2Os_3(CO)_{10}(CH_3NC)$ to $XOs_3(CO)_{10}(\mu_3\text{-}\eta^1C{=}N(H)CH_3)$ at 25°C (X = H or D)

Base: $NH_2CH_2CH_2CH_3$				$N(CH_2CH_2CH_3)_3$			
$[B:]\times10^{-3}$	kH	kD	kH/kD	$[B]\times10^{-4}$	kH	kD	kH/kD
3.0	0.14	0.11	1.2	4.8	0.073	0.60	1.2
1.2	0.082	0.040	2.1	0.76	0.0055	0.0021	2.6
0.19	0.0083	0.0013	6.3				

Table 4. Relative % yields for the thermolysis of $X_2Os_3(CO)_{10}(CNR)$ (X = H or D; R = *para*-tolyl)

X	$H(HC{=}NR)Os_3(CO)_{10}$ (22)	$H(HN(R){=}C)Os_3(CO)_{10}$ (23)	$H_2Os_3(CO)_9(CNR)$ (24)
H	60	30	10
Under vacuum			
D	80	5	15
Under vacuum			
H	0	100	0
Under CO			
D	60	35	5
Under CO			

These conclusions are further corroborated by our recent investigation of the thermolysis of **21** (R = *p*-$CH_3C_6H_5$) where **22**, **23** and **24** are all obtained in detectable amounts (Table 4).[41] As can be seen from the data in Table 4 deuterium substitution on the cluster increases the amount of **23** while decreasing the amount of **22**. In fact, by performing the reaction under a carbon monoxide atmosphere **22** is the only product, while with deuterium under vacuum **23** is almost the exclusive product. These results illustrate the usefulness of deuterium kinetic isotope effects in evaluating the rate-determining step in multi-product reactions involving metal to ligand hydrogen transfers in transition metal hydride clusters. Furthermore, they show that metal to ligand hydrogen transfers can take place by very different mechanisms.

4. CONCLUSIONS AND FUTURE WORK

The two types of kinetic deuterium isotope effects presented here illustrate two ways in which cluster reaction pathways can involve a hydride ligand in a rate-determining step. The small primary isotope effect can be operative where edge-to-edge migration or bridge opening of a μ-hydride is a requirement for or a connected process with: (1) migration of a μ_3-capping ligand over the face of a cluster; (2) axial–radial (edge-to-face) interconversion; (3) opening of a coordination site on one metal atom of a cluster. Saturated clusters appear to behave like cog and wheel mechanisms and it is not surprising to find these connections in their intramolecular rearrangements. It is surprising, however, that the small primary isotope is so similar in magnitude for different dynamical processes. Theoretical studies which try to model the energies of μ-hydride bridge opening and the associated changes in metal–metal bond length are needed to gauge the expected magnitude of this effect. Unfortunately accurate potential surfaces for second and third row clusters like those presented here are difficult to come by. At this time it is not known whether this small isotope effect is strictly confined to μ-hydrides. It may well be that terminal hydride migration between two stereochemically distinct environments in a mononuclear species would also show this type of isotope effect. In fact, we recently observed an isotope effect (kH/kD = 1.6) on the *cis–trans* interconversion in $[(\eta\text{-}C_6H_5)Cr(CO)_2(P(CH_3)_2C_6H_5)H]^+$.[42] The small size of this effect is consistent with an early transition state in which there is little M—H bond breaking.[14] For the intramolecular hydrogen migrations

studied herein this seems quite reasonable since the hydride never completely dissociates from the metal cluster.

The examples of the large primary deuterium kinetic isotope effects presented here all appear to be associated with intramolecular proton transfers from metal to ligand or the reverse process. However, there is no reason to assume that deuterium kinetic isotope effects of similar magnitude could not be observed in reactions where a hydrogen atom or hydride transfer are involved in the rate-determining step. The primary criteria for a reaction to have a large tunnelling component are that the ground state geometry of the reactant and product are very similar and that the reaction should be close to thermoneutral.[1-3] The results obtained so far suggest that isotope effects in metal clusters are considerably larger than those observed for similar reactions in mononuclear species. However, the examples discussed here all involve transformations which occur at one edge of a trinuclear cluster and should therefore be observed in similar transformations in binuclear systems. It is more difficult, but not impossible, to imagine cases where proton transfer to or from a ligand in a mononuclear system would not involve considerable distortion of the ground state reactant geometry on going to the product. We are currently examining a series of mononuclear and binuclear systems where hydrogen transfer takes place from a metal atom to a coordinated ligand in order to elucidate these points further.

Acknowledgements—I gratefully acknowledge the support of the National Science Foundation (CHE-8711549) and the donors to the Petroleum Research Foundation administered by the American Chemical Society (19781-B3-C) for support of this research. A special thanks goes to M. Green, P. Keyes and J. Javaheri for help with preparation of the manuscript.

REFERENCES

1. H. Kwart, *Acc. Chem. Res.* 1982, **15**, 401.
2. (a) F. Westheimer, *Chem. Rev.* 1961, 265; (b) R. P. Bell, *Chem. Soc. Rev.* 1974, **3**, 513; (c) L. Melander and W. H. Saunders, *Reaction Rates of Isotopic Molecules*. Wiley, New York (1980).
3. D. J. McLennan, *Aus. J. Chem.* 1979, **32**, 1883.
4. J. R. Norton, J. M. Sullivan and R. T. Edidin, *J. Am. Chem. Soc.* 1987, **109**, 3945.
5. J. M. Mayer, C. J. Curtes and J. E. Bercaw, *J. Am. Chem. Soc.* 1983, **105**, 2651.
6. I. P. Rothwell, *Acc. Chem. Res.* 1988, **21**, 153.
7. C. M. Fendrick and T. J. Marks, *J. Am. Chem. Soc.* 1986, **108**, 425.
8. P. L. Watson, *J. Am. Chem. Soc.* 1983, **105**, 6491.
9. A. H. Janowicz and R. G. Bergman, *J. Am. Chem. Soc.* 1983, **105**, 3929.
10. P. J. Desrosiers, R. S. Shinomoto and T. C. Flood, *J. Am. Chem. Soc.* 1986, **108**, 1346.
11. J. P. Collman, L. S. Hegedus, J. R. Norton and R. G. Finke, *Principles and Applications of Organotransition Metal Chemistry*, p. 534. University Science Books, Mill Valley, CA (1987).
12. J. R. Norton and S. J. Okrasinski, *J. Am. Chem. Soc.* 1977, **99**, 295.
13. D. Wink and P. C. Ford, *J. Am. Chem. Soc.* 1985, **107**, 1794.
14. P. Zhou, A. A. Vitale, J. San Filippo and W. H. Saunders, *J. Am. Chem. Soc.* 1985, **107**, 8049.
15. J. Evans and J. R. Norton, *J. Am. Chem. Soc.* 1974, **96**, 7577.
16. M. Bautista, K. A. Earl, R. H. Morris and A. Sella, *J. Am. Chem. Soc.* 1987, **109**, 3780.
17. J. P. Collman, R. G. Finke, P. L. Matlock, R. Wahren and J. I. Brauman, *J. Am. Chem. Soc.* 1976, **98**, 4685.
18. R. B. Calvert, J. R. Shapley, A. J. Schultz, J. M. Williams, S. L. Suib and G. D. Stucky, *J. Am. Chem. Soc.* 1978, **100**, 6240.
19. A. J. Deeming and M. Underhill, *J. Chem. Soc., Chem. Commun.* 1973, 277.
20. W. G. Jackson, B. F. G. Johnson and J. Lewis, *J. Organometal. Chem.* 1975, **90**, C13.
21. E. Anslyn, C. Barner, E. Rosenberg, S. Aime, L. Milone and D. Osella, *Organometallics* 1984, **3**, 1796.
22. A. Forster, B. F. G. Johnson, J. Lewis and T. W. Matheson, *J. Organometal. Chem.* 1976, **104**, 225.
23. A. J. Deeming, S. Aime and R. Gobetto, private communication.
24. E. Rosenberg, R. Gobetto, S. Hajela and S. Aime, to be published.
25. E. Rosenberg, S. Aime, D. Osella and L. Milone, *J. Organometal. Chem.* 1981, **213**, 207.
26. (a) D. M. Skinner, E. Rosenberg, C. Jangala, S. Aime, E. Sappa and L. Milone, *Inorg. Chem.* 1980, **19**, 1571; (b) S. Aime, O. Gombino, L. Milone, E. Sappa and E. Rosenberg, *Inorg. Chim. Acta* 1975, **15**, 53; (c) M. Catti, G. Gervasio and S. A. Mason, *J. Chem. Soc., Dalton Trans.* 1977, 2260.
27. E. Rosenberg, C. Barner, S. Aime and L. Milone, *Inorg. Chem.* 1985, **24**, 231.

28. C. Barner, K. I. Hardcastle, E. Rosenberg, J. Siegel, A. Tiripicchio and A. M. Manotti-Lanfredi, *Inorg. Chem.* 1981, **20**, 4306.
29. R. Gobetto, S. Aime, L. Milone, D. Osella and E. Rosenberg, *Organometallics* 1982, **1**, 640.
30. J. Evans, B. F. G. Johnson, J. Lewis and T. W. Matheson, *J. Organometal. Chem.* 1975, **97**, C16.
31. M. Zhang, Masters thesis, California State University, Northridge (1987).
32. E. Rosenberg, G. Saatjian, C. B. Thorsen, L. Milone, S. Aime and D. Osella, *Inorg. Chem.* 1981, **20**, 1592.
33. E. Anslyn, E. Rosenberg, L. Milone, S. Aime, D. Osella and R. Gobetto, *Gaz. Chim. Ital.* 1988, **118**, 299.
34. M. W. Payne, D. L. Leussing and S. G. Shore, *J. Am. Chem. Soc.* 1987, **109**, 617.
35. J. B. Kiester and J. R. Shapley, *Inorg. Chem.* 1982, **21**, 3304.
36. (a) M. J. Mays and R. N. F. Simpson, *J. Chem. Soc. A* 1968, 1444; (b) J. Knight and M. J. Mays, *J. Chem. Soc. A* 1970, 711.
37. H. A. Hodali, D. F. Shriver and C. A. Ammelung, *J. Am. Chem. Soc.* 1978, **100**, 5239.
38. J. B. Kiester, *J. Organometal. Chem.* 1980, **190**, C36.
39. E. Rosenberg and D. Pribich, *Organometallics* 1988, 7, 1741.
40. R. D. Adams and N. M. Golembeski, *J. Am. Chem. Soc.* 1979, **101**, 2579.
41. E. Rosenberg, E. Anslyn, M. Green and G. Nicola, to be published.
42. (a) S. Hajela and E. Rosenberg, to be published; (b) T. C. Flood, A. Sirhangi and E. Rosenberg, *J. Am. Chem. Soc.* 1977, **99**, 4334.

APPENDIX

List of compounds

Number	Formula
1	$(\mu\text{-H})_2Os_3(CO)_9(\mu_3\text{-}\eta^2\text{-C}{=}CH_2)$
1-d$_1$	$(\mu\text{-H})(\mu\text{-D})Os_3(CO)_9(\mu_3\text{-}\eta^2\text{-C}{=}CH_2)$
2	$(\mu\text{-H})_2Ru_3(CO)_9(\mu_3\text{-}\eta^2\text{-CH}{=}C^tBu)^{2+}$
2-d$_2$	$(\mu\text{-H})(\mu\text{-D})Ru_3(CO)_9(\mu_3\text{-}\eta^2\text{-CD}{=}C^tBu)^{2+}$
2-d$_3$	$(\mu\text{-D})_2Ru_3(CO)_9(\mu_3\text{-}\eta^2\text{-CD}{=}C^tBu)^{2+}$
3	$(\mu\text{-H})_2Ru_3(CO)_9(\mu_3\text{-S})$
4	$(\mu\text{-H})_2Os_3(CO)_9(\mu_3\text{-S})$
3-d$_2$	$(\mu\text{-D}_2)Ru_3(CO)_9(\mu_3\text{-S})$
4-d$_2$	$(\mu\text{-D}_2)Ru_3(CO)_9(\mu_3\text{-S})$
5	$H(\mu\text{-H})Os_3(CO)_{10}P(C_6H_5)_3$
5-d$_2$	$D(\mu\text{-D})Os_3(CO)_{10}P(C_6H_5)_3$
6	$H(\mu\text{-H})Os_3(CO)_{10}(CN^tBu)$
7	$(\mu\text{-H})_2Os_3(CO)_{10}$
8	$(\mu\text{-H})Ru_3(CO)_9(\mu_3\text{-}\eta^2\text{-C}'_2Bu)$
8-d$_1$	$(\mu\text{-D})Ru_3(CO)_9(\mu_3\text{-}\eta^2\text{-C}'_2Bu)$
9	$(\mu\text{-H})_2Os_3(CO)_9(\mu_3\text{-}\eta^2\text{-}CH_3CH_2C{\equiv}CCH_2CH_3)$
9-d$_2$	$(\mu\text{-D})_2Os_3(CO)_9(\mu_3\text{-}\eta^2\text{-}CH_3CH_2C{\equiv}CCH_2CH_3)$
10	$(\mu\text{-H})Os_3(CO)_9(\mu_3\text{-}\eta^2\text{-}CH_3C{=}C{=}C(CH_3)CH(CH_3)_2)$
11	$(\mu\text{-H})Ru_3(CO)_8(\mu_3\text{-}\eta^2\text{-C}'_2Bu)P(C_6H_5)_3$
12a	$(\mu\text{-H})_2Ru_3(CO)_8(\mu_3\text{-}\eta^2\text{-CH}{=}C^tBu)P(C_6H_5)_3^{2+}$
12b	$(\mu\text{-H})_2Ru_3(CO)_8(\mu_3\text{-}\eta^2\text{-CH}{=}C^tBu)P(C_6H_5)_3^{2+}$
14	$(\mu\text{-H})(\mu\text{-CO})Ru_3(CO)_{10}^-$
14-d$_1$	$(\mu\text{-D})(\mu\text{-CO})Ru_3(CO)_{10}^-$
15	$(\mu\text{-H})Os_3(CO)_{10}(\mu\text{-}\eta^2\text{-CH}{=}CHR)$
16	$(\mu\text{-H})Os_3(CO)_{10}(\mu\text{-}\eta^2\text{-C}{\equiv}CR)$
17	$(\mu\text{-CO})Os_3(CO)_9(HC{\equiv}CR)$
18	$(\mu\text{-H})(\mu\text{-CO})M_3(CO)_{10}$
19	$(\mu\text{-H})(\mu\text{-COH})Ru_3(CO)_{10}$
20	$(H)(\mu\text{-H})Ru_3(CO)_{11}$
21	$H(\mu\text{-H})Os_3(CO)_{10}CNR$
21-d$_2$	$H(\mu\text{-D})Os_3(CO)_{10}CNR$
22	$(\mu\text{-H})Os_3(CO)_{10}(\mu\text{-}\eta^1\text{-C}{=}N(H)R)$
23	$(\mu\text{-H})Os_3(CO)_{10}(\mu\text{-}\eta^2\text{-HC}{=}NR)$
24	$(\mu\text{-H})_2Os_3(CO)_9(CNR)$

Polyhedron Vol. 8, No. 4, pp. 407–413, 1989
Printed in Great Britain

0277–5387/89 $3.00+.00
Pergamon Press plc

POLYHEDRON REPORT NUMBER 27

BI-PHASIC AND PHASE TRANSFER CATALYSIS

TIMOTHY G. SOUTHERN*

Coal and Hydrocarbon Processing, The Alberta Research Council, 250 Karl Clark Road, (P.O. Box 8330, Postal Station F) Edmonton, Alberta, Canada T6H 5X2

CONTENTS

1. INTRODUCTION 407

2. DEFINITION OF TERMS 408

3. CATALYTIC PROCESSES 408
3.1 Hydrogenation 408
3.2 Sulphur removal 410
3.3 Nitrogen removal 410
3.4 Oxygen removal 411
3.5 Isomerization 411

4. CONCLUSIONS 411

ACKNOWLEDGEMENTS 411

REFERENCES 411

1. INTRODUCTION

The advantages of homogeneous catalysts with respect to reactivity and selectivity are well documented.[1] However, the sensitivity of the catalyst or its precursor to air or moisture, and the problems associated with the separation of the products from the catalyst have frequently presented a major economic barrier to commercial applications. Although research is still very active in the field of "heterogenized" homogeneous catalysis, with the aim of producing supported systems possessing the selectivity and reactivity advantages of homogeneous catalysts, coupled with the ease of separating products offered by heterogeneous systems, there has been little or no commercial success.

An alternative solution to the separation problem was proposed in the early 1970s,[2–4] when it was realized that a liquid–liquid bi-phasic system could be used and that the catalyst and its substrate need not necessarily be in the same liquid phase. Parshall[2] demonstrated the concept using molten $[R_4N][SnCl_3]$ or $[R_4N][GeCl_3]$, in combination with platinum chloride, as catalyst precursors for the hydrogenation of olefins. However, it was not until the exploitation of water soluble transition metal complexes based on sodium diphenylphosphinobenzene-*m*-sulphonate (**1**, DPPS)[5–11] that bi-phasic catalysis really became practical. The uses of bi-phasic hydrogenation have been reviewed by Joo and Toth,[11] and more recently, Sinou[12] has reviewed both the synthesis of water-soluble phosphines and their applications in catalysis. The industrial interest in the use of bi-phasic systems for hydroformylation and related processes can be seen from the patent literature.[13–18]

A second and related technique is that of transition metal phase transfer catalysis. This technique

* Present address: Johnson Matthey Technology Centre, Blount's Court, Sonning Common, Reading RG4 9NH, U.K.

based on an aqueous–organic system, containing both a phase transfer agent and a transition metal complex, has already been reviewed by Alper.[19–21] Possible applications of this technique for several processes related to heavy oil upgrading have already been demonstrated.

The industrial uses of this process are expanding rapidly. In North America alone it is estimated[22] that between 50,000,000 and 100,000,000 lb of chemicals are produced annually by phase transfer processes and that the demand for phase transfer agents has increased from an estimated 40,000 lb in 1980 to over 1,000,000 lb in 1985. This review is particularly concerned with the use of phase transfer and bi-phasic systems for the upgrading of crude hydrocarbon fractions.

2. DEFINITION OF TERMS

The term bi-phasic catalysis has been used to describe both two phase liquid–liquid as well as liquid–solid, gas–liquid and gas–solid reactions. In this review the term is used uniquely to describe a catalytic process using a mixture of two immiscible liquids but which does NOT require the presence of a phase transfer agent.

In general, but not necessarily, the catalyst has a high solubility in one phase, but only very limited solubility in the second phase in which the products (and substrates) are very soluble. The separation of products becomes, in such cases, a matter of separating the two immiscible phases.

Phase transfer catalysis normally refers to an aqueous–organic system in which a phase transfer agent possessing both hydrophobic and hydrophilic functions is necessary in order for the catalytic process to take place.

In the majority of phase transfer processes reported to date, the transition metal complex and the organic substrate are located in the organic phase. Therefore, although this technique involves a two phase liquid–liquid system, it does not necessarily overcome the problems associated with the separation of products and reactants from the soluble catalyst. Throughout this review a number of ligand and counter-ion systems will be encountered.

3. CATALYTIC PROCESSES

3.1 *Hydrogenation*

(a) *Bi-phasic hydrogenation.* Although some work has been reported on bi-phasic catalytic hydrogenation of water soluble unsaturated substrates using an organic soluble transition metal complex,[5,79,80] it was very soon realized that for the system to be of widespread practical use, the catalyst would have to be water soluble and the substrate should remain in the organic phase. It is therefore not surprising that the major developments in bi-phasic catalysis have paralleled developments in the preparation and chemistry of organophosphine ligands which would render their metal complexes soluble in highly polar solvents yet retain catalytic properties similar to those of organic soluble complexes. The first such phosphine synthesized was reported in 1958[23] but it was not until the mid 1970s[5–11] that bi-phasic catalytic applications of this ligand were reported. In the intervening period, the preparation and reactivity towards transition metals of other functionalized phosphine compounds were reported.[24] The catalytic activity of the resulting complexes was significantly lower than the complexes of the corresponding unfunctionalized phosphine.

The bi-phasic catalytic hydrogenation of a number of unsaturated species has been reported for both rhodium[5,6,13–18,25,26] or ruthenium[6–11,26] derivatives of sodium diphenylphosphinobenzene-*m*-sulphonate (**1**) and for rhodium derivatives of amphos ($[(Ph_2P)_2CH_2CH_2NMe_3]^+$).[27–31]

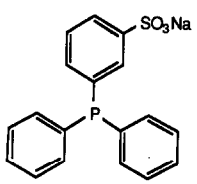

1

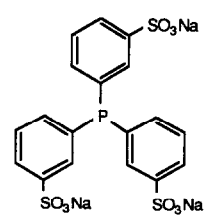

2

Several attempts are being made to apply bi-phasic catalytic hydrogenation to optically active systems using chiral diphosphine derivatives.[32–45] Although the objectives differ, the results obtained and the catalytic activity of the complexes studied is worthy of note. The use of the trisodium salt of tris(*m*-sulphonatophenyl)phosphine (**2**) as a ligand in various group VIII metal complexes has been reported[46] and the catalytic activity of the resulting complexes is being investigated. The use of solutions containing this ligand and $RhCl_3 \cdot 3H_2O$ as hydrogenation catalysts has been reported by Patin and co-workers.[47,48]

Other than the work carried out by Beck and co-workers[10] on the mechanism for the bi-phasic catalytic hydrogenation of various unsaturated substrates using $[RuCl_2(DPPS)_2]$ or $[HRuCl(DPPS)_3]$ and the kinetics for the hydrogenation of various unsaturated carboxylic acids[25] using $[RhCl(DPPS)_3]$, very little information concerning the mechanistic aspects of these reactions has been reported, Wilkinson[6] suggests that the mechanisms for $[RhCl(DPPS)_3]$ resemble those reported for $[RhCl(PPh_3)_3]$.[49] In their paper on the hydrogenation of cyclohexene at 1 atm using $[RhCl(DPPS)_3]$, Dror and Manassen[5] report that a co-solvent is necessary, and that the reaction occurs in the bulk of the aqueous phase. In contrast Wilkinson, using the same complex and substrate at 3 atm H_2 pressure, reports[6] that no co-solvent is necessary and that the reaction apparently occurs at the interface between the two phases.

For the catalytic hydrogenation of cyclohexene using $[RhCl(DPPS)_3]$[5,6] the co-solvent plays a major role. The rate is very solvent dependent, and this can be attributed, to an increase in both the hydrogen and the substrate solubility in the co-solvent aqueous phase.

For these bi-phasic systems, the recovery and re-use of the catalyst is of major economic importance. Wilkinson[6] remarks that, for $[RhCl(DPPS)_3]$ systems, the organic phase is colourless after a catalytic run. Dror and Manassen[5] report that the aqueous solutions of this complex do retain their catalytic activity and can be re-used. The rhodium content of the organic phase for the system based on amphos ($[(Ph_2P)CH_2CH_2NMe_3]^+$) as the ligand have been determined and less than 0.1% of the rhodium remains in the organic phase.[27–31]

Baird and Wilkinson[6,27–31] have reported on the stability of the various complexes with respect to air. The species based on DPPS have been reported to be very air-sensitive when the group VIII metal is rhodium and the system has been exposed to H_2. In contrast, the complexes based on the amphos ($[(Ph_2P)CH_2CH_2NMe_3]^+$) system are much more stable to oxidation by air and can even be used in a partial air atmosphere.[27–31] The lack of stability of the diphenylphosphinobenzene-*m*-sulphonate systems in the presence of various ketonic co-solvents has been reported by Dror and Manassen.[5] Recent work by Patin and co-workers[47,48] using tris(phenylsulphonato)phosphine as ligands for a rhodium complex, formed *in situ* from $RhCl_3$ hydrate, have indicated that the phosphine is oxidized during the catalytic reaction, and that the active species in this system may be colloidal rhodium.[81]

Preliminary studies[50] of the tolerance of $[RhCl(DPPS)_3]$ to sulphur compounds are very encouraging, with no loss of reactivity towards the substrate (1-hexene or cyclohexene) being detected. Further work examining the tolerance of this and other water soluble systems, to the sulphur species likely to be found in heavy oils, are being examined.

(b) *Phase transfer hydrogenation.* A number of articles have described the use of water soluble $K_3[Co(CN)_5H]$ for the catalytic hydrogenation of various unsaturated compounds[51–55] under both bi-phasic and phase transfer conditions. This system and the related diamine substituted system[56] cleanly hydrogenate dienes to alkenes. Although these systems are catalytically active in the absence of the phase transfer agent, their activity is very limited. The presence of the phase transfer agent greatly improves the stability of the catalyst to both base attack and to poisoning by the substrate, and also increases the reaction rate. Alper and Heverling[57] have shown that cobalt carbonyl under acidic phase transfer conditions and in the presence of molecular hydrogen can hydrogenate various alkenes. This system, however, was apparently unreactive towards the hydrogenation of anthracene but is stable in the presence of sulphur compounds.[58,59]

The complex $[\{(hxd)Rh(\mu\text{-}Cl)\}_2]$ is an active catalyst precursor for the hydrogenation of arenes under phase transfer conditions and of α,β-unsaturated carbonyl compounds under bi-phasic conditions. In each of the reports on the use of this rhodium species,[60,61] it is not clear whether or not the catalyst is in solution, and, at least for the bi-phasic system, there is evidence to suggest that the catalyst may be a very active form of colloidal rhodium.

Blum and co-workers have demonstrated the reactivity of rhodium chloride in the presence of

Aliquat 336 (tricaprylmethylammonium chloride), under phase transfer conditions, for the hydrogenation of a variety of alkynes, alkenes and arenes[62] as well as α,β-unsaturated species.[63] When a $RhCl_3$–Aliquat solution is exposed to H_2 in the absence of substrate, an unreactive precipitate of rhodium metal is formed. However, if the organic substrate is added before exposing the system to H_2, then both the aqueous and organic phases remain free from solid or colloidal material. This result has been interpreted in terms of the formation of a rhodium hydride intermediate which is stabilized by the unsaturated organic substrate. Although the rhodium is in the organic phase it can be recovered in the aqueous phase by the use of sodium chlorate,[64] the organic phase does, however, retain its catalytic activity and can be re-used providing it is not exposed to oxygen. This system is apparently active in the presence of mercaptans. These rhodium based phase transfer systems use an organic soluble transition metal species which must be recycled if these routes are to be of significant use.

3.2 *Sulphur removal*

(a) *Bi-phasic.* Cobalt carbonyl has been shown to be an effective catalyst precursor for the desulphurization of mercaptans under bi-phasic conditions.[58,59,65] In 1985, Alper *et al.*[66] reported their work on the desulphurization of mercaptans under both bi-phasic and phase transfer conditions. The reaction is reported to be non-catalytic with respect to the metal carbonyl, although catalytic amounts converted the mercaptans into thioethers in reasonable yields. In each of these systems the metal complex is added in the organic phase, in which it will presumably remain. If these systems are to be exploited some method of catalyst recovery must be developed (or such small amounts of metals used that recovery becomes unnecessary).

(b) *Phase transfer systems.* (i) Basic phase transfer conditions: The first reported catalytic applications of phase transfer techniques to the treatment of organosulphur compounds were by Blum[62] and Alper.[66] Stoichiometric elimination of sulphur from aryl mercaptans occurred at 60°C, in 5 M sodium hydroxide using $[Fe_3(CO)_{12}]$ and tetrabutyl ammonium hydrogen sulphate. This work, and the related work using $[Mn(CO)_5Br]$ and elemental sulphur[67] have formed the basis for a study, for AOSTRA, on the use of a catalytic phase transfer systems for the desulphurization of crude oil and bitumens. Of a wide range of catalyst precursors tested, the most effective in basic media is $[Mn(CO)_5Br]$. More recent work[69,70] suggests that this system is complex and that the results obtained are very dependent on the particular hydrocarbon feed used. There are some limitations to the use of $[Mn(CO)_5Br]$; PhSH and Ph_2S react with the $[BzEt_3N]^+$ cation to yield BzSPh and other compounds. No H_2S was evolved on acidification of the aqueous phase.

These results suggest that the primary attack is not at sulphur, and that various redistribution reactions occur. Further evidence to support this hypothesis comes from the differences between the size exclusion chromatograms of products and feed on a sample of Athabasca bitumen. These preliminary results suggest a loss in the middle molecular weights to form both higher and lower molecular weight fractions.

(ii) Acidic phase transfer conditions: The use of both bi-phasic and phase transfer conditions with aqueous tetrafluoroboric acid for the stoichiometric sulphur removal from mercaptans by $[Fe_3(CO)_{12}]$ was reported by Alper and Sibtain.[71] This reaction was not catalytic under either CO or N_2 atmospheres. More recently this work has been extended to the catalytic elimination of sulphur from an Athabasca bitumen. The most effective catalyst appears to be $[Mo(CO)_6]$, although these reactions are considerably slower than those with $[Mn(CO)_5Br]$ under basic conditions. These systems are extremely active for the polymerization of *n*-alkanes, and such polymerization reactions would be very detrimental to any heavy oil upgrading process where the cleavage of high molecular weight fragments into lower molecular weight species is necessary.

3.3 *Nitrogen removal*

To date there have been no reports of the reduction of nitrogen containing hetero-atom species to the corresponding hydrocarbon and ammonia. Alper has, however, reported the conversion of nitro compounds to amines under phase transfer conditions using $[RuCl_2(PPh_3)_3]$[72] in the presence of synthesis gas. Similar results were obtained using bimetallic rhodium–cobalt[73] or rhodium carbonyls[74] in the presence of carbon monoxide. A detailed study of the processes in the bimetallic

system, revealed that the role of the cobalt species is to re-activate the rhodium species, which is poisoned by the quarternary ammonium salt.

The formation of Et_2NPh, EtNHPh and PhMe from solutions containing $[Mn(CO)_5Br]$ and $[BzEt_3N]^+$ has been noted.[70] This reaction appears to be catalytic with the initial major product being Et_2NPh, which undergoes further reactions.

3.4 *Oxygen removal*

References to oxygen removal using either phase transfer or bi-phasic systems have not been reported, although Zahalka and Alper[75] reported the use of $[\{(hxd)Rh(\mu\text{-}Cl)\}_2]$ in the presence of β-cyclodextrin and H_2 to reduce aromatic carbonyl compounds to the corresponding hydrocarbons at room temperature and atmospheric pressure. The primary reaction under these conditions is carbonyl reduction, but some ring hydrogenation is also observed. Aliphatic carbonyl compounds are unreactive under these conditions.

3.5 *Isomerization*

(a) *Bi-phasic.* Although the use of bi-phasic catalytic systems for the hydrogenation of hydrocarbons has not been studied specifically, several authors have commented on side reaction in which terminal alkenes are isomerized to internal alkenes. Both Baird[30] and Wilkinson[6] report that up to 25% of their products from the intended hydrogenation of 1-hexene, using rhodium complexes of either amphos ($[(Ph_2P)CH_2CH_2NMe_3]^+$) or sodium diphenylphosphinobenzene-*m*-sulphonate as ligands, was 2-hexene. Similarly the use of water soluble rhodium complexes[18] or ruthenium complexes for the hydroformylation of terminal alkenes can also lead to the formation of relatively large amounts of internal olefins.

(b) *Phase transfer processes.* The use of rhodium or ruthenium based phase transfer systems for the isomerization of various allyl alcohol derivatives has been reported.[64,76–78] Blum[64] has demonstrated that terminal alkene substituted aromatics can be isomerized using rhodium chloride in the presence of Aliquat 336 (tricaprylmethylammonium chloride) with reasonable rates. These authors report that although the catalyst is in the organic phase it can be extracted back into the aqueous phase by the use of sodium chlorate.

4. CONCLUSIONS

There is ample evidence to demonstrate the potential utility of either bi-phasic or phase transfer processes for hydrogenation, sulphur (and to a more limited extent, nitrogen) removal. If, however, these systems are to be used towards the upgrading of heavy oil or bitumen, more experimental work is necessary to determine the fate of the transition metal species in the presence of the heteroatom compounds, especially the sulphur species.

The results obtained so far support the idea that it is feasible to undertake the upgrading of heavy oils or bitumens under extremely mild conditions.*

Acknowledgements—I should like to thank Professor H. Alper and Drs T. Cyr and A. R. Sanger for helpful discussions, and ARC-AOSTRA for financial support. This manuscript is ARC contribution No. 1577.

REFERENCES

1. G. W. Parshall, *Homogeneous Catalysis: The Applications and Chemistry of Catalysis by Soluble Transition Metal Complexes.* Wiley, New York (1980).
2. G. W. Parshall, *J. Am. Chem. Soc.* 1972, **94**, 8716.
3. J. C. Bailar Jr, *Catal. Rev.* 1974, **10**, 17.
4. Z. M. Michalska and D. E. Webster, *Platinum Met. Rev.* 1974, **18**, 65.
5. Y. Dror and J. Manassen, *J. Mol. Catal.* 1977, **2**, 219.

* A report containing an extended version of this paper, together with extensive tabular data may be obtained from the author.

6. A. F. Borowski, D. J. Cole-Hamilton and G. Wilkinson, *Nouv. J. Chem.* 1978, **2**, 137.
7. F. Joo and M. T. Beck, *React. Kinet. Catal. Lett.* 1975, **2**, 257.
8. F. Joo, Z. Toth and M. T. Beck, *Inorg. Chim. Acta* 1977, **25**, L61.
9. F. Joo, Z. Toth and M. T. Beck, *Proc. XIX. ICCC Prague*, Vol. II, 62D (1978).
10. Z. Toth, F. Joo and M. T. Beck, *Inorg. Chim. Acta* 1980, **42**, 153.
11. F. Joo and Z. Toth, *J. Mol. Catal.* 1980, **8**, 369.
12. D. Sinou, *Bull. Soc. Chim. Fr.* 1987, 480.
13. Fr. Demande, 75 19407 (20 June 1975) to Rhone Poulenc Industries, France.
14. Ger. Pat., 26 27 354 (20 June 1975) to E. Kuntz (Rhone Poulenc Industries, France).
15. Ger. Pat., 27 00 904 (13 January 1976) to E. Kuntz (Rhone Poulenc Industries, France).
16. Ger. Pat., 27 33 516 (27 July 1976) to E. Kuntz (Rhone Poulenc Industries, France).
17. Eur. Pat. Appl., 0 044 771 to Rhone Poulenc Industries, France.
18. U.K. Pat. Appl., GB 2 085 874 to Johnson Matthey plc.
19. H. Alper, *Adv. Organometal. Chem.* 1981, **19**, 183.
20. H. Alper, *Fund. Res. Homogeneous Catal.* 1984, **4**, 79.
21. H. Alper, *Am. Chem. Soc., Symp. Ser.* 1987, **326**, 8.
22. C. M. Stark, *Am. Chem. Soc., Symp. Ser.* 1987, **326**, 1.
23. S. Ahrland, J. Chatt, N. R. Davies and A. A. Williams, *J. Chem. Soc.* 1958, 276.
24. J. Chatt, G. J. Leigh and R. M. Slade, *J. Chem. Soc., Dalton Trans.* 1973, 2021.
25. F. Joo, L. Somsak and M. T. Beck, *J. Mol. Catal.* 1984, **24**, 71.
26. F. Joo and M. T. Beck, *J. Mol. Catal.* 1984, **24**, 135.
27. R. T. Smith and M. T. Baird, *Transition Met. Chem.* 1981, **6**, 197.
28. R. T. Smith, R. K. Ungar and M. C. Baird, *Transition Met. Chem.* 1982, **7**, 288.
29. R. T. Smith and M. C. Baird, *Inorg. Chim. Acta* 1982, **62**, 135.
30. R. T. Smith, R. K. Ungar, L. J. Sanderson and M. C. Baird, *Organometallics* 1983, **2**, 1138.
31. R. T. Smith, R. K. Ungar, L. J. Sanderson and M. C. Baird, *Ann. New York Acad. Sci.* 1983, **415**, 253.
32. M. E. Wilson and G. M. Whitesides, *J. Am. Chem. Soc.* 1978, **100**, 306.
33. M. E. Wilson, R. G. Nuzzo and G. M. Whitesides, *J. Am. Chem. Soc.* 1978, **100**, 2269.
34. R. G. Nuzzo, D. Feitler and G. M. Whitesides, *J. Am. Chem. Soc.* 1979, **101**, 3683.
35. R. G. Nuzzo, S. L. Haynie, M. E. Wilson and G. M. Whitesides, *J. Org. Chem.* 1981, **46**, 2861.
36. S. S. Moore and G. M. Whitesides, *J. Org. Chem.* 1982, **47**, 1489.
37. U. Nagel and E. Kinzel, *Chem. Ber.* 1986, **119**, 1731.
38. R. Benhamza, Y. Amrani and D. Sinou, *J. Organomet. Chem.* 1985, **288**, C37.
39. D. Sinou and Y. Amrani, *J. Mol. Catal.* 1986, **36**, 319.
40. Y. Amrani and D. Sinou, *J. Mol. Catal.* 1984, **24**, 231.
41. F. Alario, Y. Amrani, Y. Colleuille, T. P. Dang, J. Lenck, D. Morel and D. Sinou, *J. Chem. Soc., Chem. Commun.* 1986, 202.
42. Y. Amrani, D. Lafont and D. Sinou, *J. Mol. Catal.* 1985, **32**, 333.
43. D. Sinou and Y. Amrani, *J. Mol. Catal.* 1986, **36**, 319.
44. F. Joo and E. Trocsanyi, *J. Organomet. Chem.* 1982, **231**, 63.
45. T. Hayashi, T. Mise, S. Mitachi, K. Yamamoto and M. Kumada, *Tetrahedron Lett.* 1976, 1133.
46. B. Fontal, J. Orlewski, C. C. Santini and J. M. Basset, *Inorg. Chem.* 1986, **25**, 4320.
47. C. Larpent, R. Dabard and H. Patin, *Tetrahedron Lett.* 1987, **28**, 2507.
48. C. Larpent, R. Dabard and H. Patin, *Comp. Rend. Acad. Sci. Ser. II* 1987, **304**, 1055.
49. J. A. Osborn, F. H. Jardin, J. F. Young and G. Wilkinson, *J. Chem. Soc. A* 1966, 1711.
50. M. C. Baird and T. G. Southern, unpublished results.
51. D. L. Reger and M. M. Habib, *Am. Chem. Soc., Adv. Chem. Ser.* 1979, **173**, 43.
52. D. L. Reger and M. M. Habib, *J. Mol. Catal.* 1978, **4**, 315.
53. D. L. Reger, M. M. Habib and D. J. Fauth, *Tetrahedron Lett.* 1979, 115.
54. D. L. Reger and M. M. Habib, *J. Mol. Catal.* 1980, **7**, 365.
55. D. L. Reger, M. M. Habib and D. J. Fauth, *J. Org. Chem.* 1980, **45**, 3860.
56. D. L. Reger and A. Gabrielli, *J. Mol. Catal.* 1981, **12**, 173.
57. H. Alper and J. Heverling, *J. Chem. Soc., Chem. Commun.* 1983, 365.
58. S. C. Shim, S. Antebi and H. Alper, *Tetrahedron Lett.* 1985, **26**, 1935.
59. V. Galamb, S. C. Shim, F. Sibtain and H. Alper, *Isr. J. Chem.* 1985, **26**, 216.
60. K. R. Januszkiewicz and H. Alper, *Organometallics* 1983, **2**, 1055.
61. K. R. Januszkiewicz and H. Alper, *Can. J. Chem.* 1984, **62**, 1031.
62. J. Blum, J. Amer, A. Zoran and Y. Sasson, *Tetrahedron Lett.* 1983, **24**, 4139.
63. J. Azran, O. Buchman, I. Amer and J. Blum, *J. Mol. Catal.* 1986, **34**, 229.
64. Y. Sasson, A. Zoran and J. Blum, *J. Mol. Catal.* 1981, **11**, 293.
65. H. Alper and D. J. H. Smith, Int. Pat. Appl. PCT/GB85/00221.

66. H. Alper, F. Sibtain and J. Heveling, *Tetrahedron Lett.* 1983, **24**, 5329.
67. H. Alper, F. Sibtain, F. W. B. Einstein and A. C. Willis, *Organometallics* 1985, **4**, 604.
68. H. Alper, F. Sibtain and S. Calet, private communication.
69. H. Alper, private communication.
70. T. G. Southern, unpublished results.
71. H. Alper and F. Sibtain, *J. Organomet. Chem.* 1985, **285**, 225.
72. K. Januszkiewicz and H. Alper, *J. Mol. Catal.* 1983, **19**, 139.
73. K. E. Hashem, J. F. Petrignani and H. Alper, *J. Mol. Catal.* 1984, **26**, 285.
74. F. Joo and H. Alper, *Can. J. Chem.* 1985, **63**, 1157.
75. H. A. Zahalka and H. Alper, *Organometallics* 1986, **5**, 1909.
76. Y. Sasson, A. Zoran and J. Blum, *J. Mol. Catal.* 1979, **6**, 289.
77. H. Alper and K. Hachem, *J. Org. Chem.* 1980, **45**, 2269.
78. H. Alper and K. Hachem, *Transition Met. Chem.* 1981, **6**, 219.
79. British Pat., 2070 023A to Johnson Matthey plc.
80. United States Pat., 4,469,849 to Johnson Matthey plc.
81. C. Larpent and H. Patin, *J. Mol. Catal.* 1988, **44**, 191.

Polyhedron Vol. 8, No. 4, pp. 415–418, 1989
Printed in Great Britain

0277–5387/89 $3.00+.00
© 1989 Pergamon Press plc

KINETICS OF SOLVOLYSIS OF DIHALO-(3,3′,3″-TRIAMINOTRIPROPYLAMINE)COBALT(III) PERCHLORATE

SALAH S. MASSOUD* and RONALD M. MILBURN

Department of Chemistry, Boston University, Boston, MA 02215, U.S.A.

(*Received* 11 *May* 1988; *accepted* 21 *June* 1988)

Abstract—The kinetics of the primary solvolysis reaction of $[Co(trpn)X_2]^+$ ions (trpn = 3,3′,3″-triaminotripropylamine = $N(CH_2CH_2CH_2NH_2)_3$; X = F, Cl, Br) in acetonitrile were studied. At 25°C, the rate constants for the release of one halide are 7.8×10^{-4}, 1.66×10^{-3} and 1.87×10^{-2} s^{-1} for X = F, Cl and Br, respectively. The corresponding activation parameters $\Delta H^{\ddagger}$ (kcal mol^{-1}) and $\Delta S^{\ddagger}$ (cal K^{-1} mol^{-1}) are as follows: 24.7(±0.6), 10.8(±1.8); 13.6(±0.6), −25.8(±1.8); 5.05(±0.8), −49.5(±2.4) for the same series. The rate constants were found to be independent of the initial complex concentration. The solvolysis product $[Co(trpn)(CH_3CN)Br]BrClO_4$, of the reaction of the complex $[Co(trpn)Br_2]ClO_4$ with acetonitrile, was isolated and characterized. No evidence was found for the second solvolysis step. The results are discussed in terms of the dissociative I_d mechanism.

The acid hydrolysis kinetics of octahedral $[Co(trpn)X_2]^+$ (trpn = 3,3′,3″-triaminotripropylamine = $N(CH_2CH_2CH_2NH_2)_3$; X = F, Cl, Br) and $[Co(trpn)(CH_3CN)_2]^{3+}$ ions have been studied and compared with those of the other tetraamine cobalt(III) complexes.[1] The kinetic data showed that the rates of acid hydrolysis for $[CoN_4X_2]^+$ species (N_4 = non-replacable monodentate– or polydentate–amine) decreases in the order trpn > tn_2 > tren > en_2 [en = $NH_2(CH_2)_2NH_2$; tn = $NH_2(CH_2)_3NH_2$; tren = $N(CH_2CH_2NH_2)_3$]. We have also pointed out that Co(III)–trpn represents a compromise between a system of fixed geometry, due to the tripodal nature of the ligand the fifth and the sixth coordination sites are forced to be *cis*, and a fully labile species.[1] These properties might be of great importance in some biological processes, particularly in the dephosphorylation reactions of ATP^{2-4} (ATP = adenosine 5′-triphosphate).

The extreme lability of $[Co(trpn)X_2]^+$ complexes was attributed to the flexibility of the six-membered ring systems in the Co^{III}–trpn moiety, such flexibility is likely to contribute to the ease of forming the transition state in a mechanism which is primarily dissociative in nature.[1,5]

In this paper we have expanded our study on $[Co(trpn)X_2]^+$ complexes to the non-aqueous medium, which might expose light, and should be useful in understanding the behaviour of these complexes in substitution reactions. Many studies of solvolysis reactions of cobalt(III)– and chromium(III)–tetraamine have been undertaken, but most of these reactions were complicated by *cis*/*trans* isomerization.[6–11] However, the solvolysis reactions of $[M(tren)Cl_2]^+$ ($M = Cr^{III}$ or Co^{III}) have been examined in different aprotic solvents and were not complicated by *cis*/*trans* equilibria.[12] Therefore, it is anticipated that the trpn ligand would be of similar stereochemical interest as tren, and this paper reports the results of the investigation of the rate of solvolysis of the complex ions $[Co(trpn)X_2]^+$ (X = F, Cl, Br) in acetonitrile.

EXPERIMENTAL

The complexes $[Co(trpn)F_2]ClO_4 \cdot 3/2$, $[Co(trpn)Cl_2]ClO_4$ and $[Co(trpn)Br_2]ClO_4$ were synthesized as described in our recent report.[13] The kinetic measurements were made spectrophotometrically (Cary 210 UV–vis. spectrophotometer) at an appropriate wavelength,

*Author to whom correspondence should be addressed. Present address: Department of Chemistry, Faculty of Science, Alexandria University, Alexandria, Egypt.

where a substantial absorption difference occurs between the reactants and products. This wavelength was 430 nm for the difluoro, 450 nm for the dichloro and 500 nm for the dibromo species. A weighed sample of the complex, held in a 5 cm^3 volumetric flask was rapidly treated with dry acetonitrile (acetonitrile was dried over 4 Å Linde molecular sieves and then distilled), which has been equilibrated at the same temperature. The flask was swirled vigorously (2–3 min), the volume was completed to the mark by adding acetonitrile to give a solution of 3–6 mM of the complex, and a part of the contents was then transferred to the thermostatted spectrophotometric 1 cm cell. The temperature was controlled to within ± 0.1°C by circulating water through the compartment surrounding the cells.

The rate constants were calculated by linear least-squares of the first-order plots $\ln(A_t - A_\infty)$ vs time, where A_∞ is the final absorbance and was taken when no further changes were detected and A_t is the absorbance at time t. These plots were linear for at least three half-lives. Duplicate runs agreed to within 5%.

RESULTS AND DISCUSSION

The crystallization of $[Co(trpn)(H_2O)_2](ClO_4)_3 \cdot 2H_2O$ in acetonitrile afforded the well characterized diacetonitrile complex.[13] The reaction of $[Co(trpn)Br_2]ClO_4$ with acetonitrile led to the isolation of $[Co(trpn)(CH_3CN)Br]BrClO_4$. The IR spectra of the acetonitrile complexes showed $\bar{\nu}_{CN}$ at 2300 cm^{-1} suggesting the coordination of CH_3CN to the central cobalt.[13] However, when the bromoacetonitrile complex was refluxed for a long time in dry CH_3CN, the diacetonitrile complex was not isolated. Also, when the solvolysis of the $[Co(trpn)X_2]^+$ species (X = F, Cl or Br) was carried out in dry acetonitrile, the product solution gave constant spectra, even when it was heated in the stoppered spectrophotometric cell at 40–50°C for 30 min. No changes in the spectrum were observed either after heating or after standing for a prolonged period of time. Such observations clearly indicate the absence of occurrence of any further slower reaction in these systems after the completion of the primary solvolysis step. Thus, the kinetics of the primary solvolysis step of the complex ions $[Co(trpn)X_2]^+$ (X = F, Cl or Br) in CH_3CN were not complicated either by further reactions or by isomerization,[13] and the species formed is $[Co(trpn)(CH_3CN)X]^{2+}$, where the halide must be *cis* to the coordinated CH_3CN molecule. The absorption spectral data of the halo-acetonitrile and the diacetonitrile complexes are given in Table 1. The visible spectra of these species in acetonitrile is consistent with the octahedral *cis* geometry[13] and clearly show that the lower energy *d–d* band maxima is shifted to longer wavelengths with decreasing ligand field strength, i.e. in the order $CH_3CN > F > Cl > Br$.

Theoretically, two possible isomers are possible for the solvolysis product; $[Co(trpn)(CH_3CN)X]^{2+}$ depending on whether the coordinated halide is *cis* or *trans* to the tertiary nitrogen in the Co–trpn moiety. These two positions are chemically non-equivalent;[14] replacement of the *trans*-halide in the $[Co(trpn)X_2]^+$ ion would produce the α-haloacetonitrile isomer, while replacement of the *cis*-halide would lead to the β-isomer. The possible isomers of the $[Co(trpn)(CH_3CN)X]^{2+}$ ion are shown in Fig. 1.

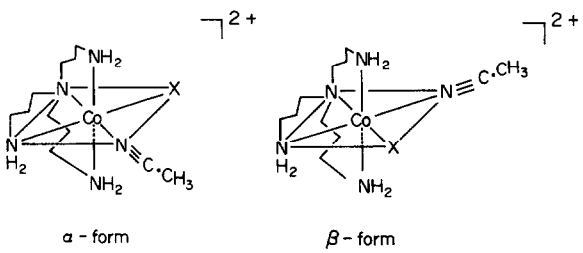

Fig. 1. Possible isomers of the $[Co(trpn)(CH_3CN)X]^{2+}$ cation.

Table 1. Absorption bands of cobalt(III)–trpn–acetonitrile complexes in acetonitrile

Complex ion	$\lambda_{max}(\varepsilon)^a$	$\lambda_{min}(\varepsilon)$	$\lambda_{max}(\varepsilon)$	$\lambda_{min}(\varepsilon)$
$[Co(trpn)(CH_3CN)F]^{2+}$	529(69.6)	446(52.5)	362(95.9)	345(92.7)
$[Co(trpn)(CH_3CN)Cl]^{2+}$	575(57.6)	484(21.3)		
$[Co(trpn)(CH_3CN)Br]^{2+}$ [b,c]	~ 580			
$[Co(trpn)(CH_3CN)_2]^{3+}$ [c]	498(97.6)	418(27.6)		

[a] λ in nm and ε in $M^{-1}\,cm^{-1}$.
[b] Saturated solution.
[c] Data taken from ref. 1.

Of the two possible halo ligands that can be lost in the first solvolysis step, the one *trans* to the tertiary amine group in the trpn is thought to be the most labile. The assignment was made based on the X-ray study of the *mer*-[Co(dien)$(NO_2)_2$Cl] complex [dien = $NH(CH_2CH_2NH_2)_2$], where the *trans* position to the NH group in the polyamine was found to be the most labile.[15]

Thus, the solvolysis of the $[Co(trpn)X_2]^+$ ions in acetonitrile proceeds according to the stoichiometric equation (1).

$$[Co(trpn)X_2]^+ + CH_3CN \xrightarrow{k_1} [Co(trpn)(CH_3CN)X]^{2+} + X^- \quad (1)$$

The rate law for the reaction is given by

$$-\frac{d[Co(trpn)X_2]^+}{dt} = k_1[Co(trpn)X_2]^+$$

The rate constants k_1, calculated from the linear plots of $\ln(A_\infty - A_t)$ vs t are summarized in Table 2. It should also be noted that the rate is essentially unaffected by the initial complex concentration. Inspection of the data in Table 2 reveals that, at a given temperature, the rate of solvolysis decreases in the order Br > Cl > F. The same pattern of reactivity was also observed for substitution reactions in alkyl halides for an S_N1 mechanism.[16] Therefore, it seems that the solvolysis reactions of $[Co(trpn)X_2]^+$ complexes proceeded via a dissociative I_d mechanism. The same mechanism has also been suggested for the solvolysis reactions of *cis*-$[Coen_2X_2]^+$ (X = Cl or Br) in DMF,[7,8] and for $[M(tren)Cl_2]^+$ [M = Co^{III} or Cr^{III}] in different aprotic solvents.[12]

The activation parameters ($\Delta H_1^\ddagger$ and $\Delta S_1^\ddagger$) were evaluated from the linear Eyring plots of $\ln k_1/T$ vs $1/T$, and are collected in Table 3. The relationship between $\Delta H_1^\ddagger$ and $\Delta S_1^\ddagger$ for the series studied is illustrated in Fig. 2. The parallel changes in $\Delta H_1^\ddagger$ and $\Delta S_1^\ddagger$ lead only to small changes in $\Delta G^\ddagger$, and for such a closely related series a common mechanism is implied.[17] The slope of the linear plot of $\Delta H_1^\ddagger$ vs $\Delta S_1^\ddagger$ gives the isokinetic temperature, which is equal to 315 K. Below this temperature the reactions are

Table 2. Rate constants (k_1, s^{-1}) for the primary solvolysis of $[Co(trpn)X_2]^+$ ions in acetonitrile at different temperatures

T (°C)	$10^3 k_1$	T (°C)	$10^3 k_1$	T (°C)	$10^3 k_1$
X = F		X = Cl		X = Br	
25.0	0.78	25.0	1.66	6.6	10.0
35.0	2.97	29.7	2.37	9.5	11.4
39.8	6.98	34.3	3.38	13.9	12.7
44.2	9.55	38.0	4.50	17.8	15.3

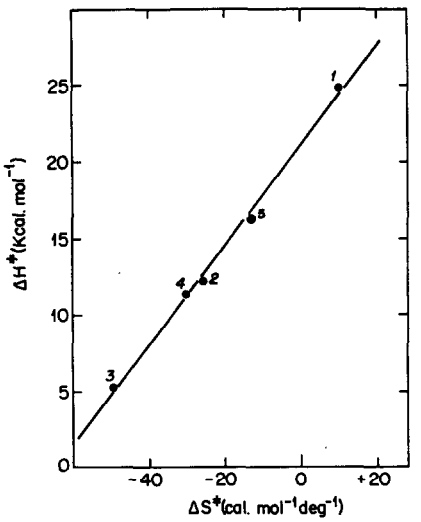

Fig. 2. Plot of $\Delta H_1^\ddagger$ vs $\Delta S_1^\ddagger$ for the primary substitution reactions of $[Co(trpn)X_2]^+$ and $[Co(trpn)(CH_3CN)_2]^{3+}$ ions: $[Co(trpn)X_2]^+ + CH_3CN \xrightarrow{k_1} [Co(trpn)(CH_3CN)X]^{2+} + X^-$. (1) X = F; (2) X = Cl; (3) X = Br; (4) $[Co(trpn)F_2]^+ + H_2O \xrightarrow{k_1} [Co(trpn)(H_2O)F]^{2+} + F^-$ (acid-independent); (5) $[Co(trpn)(CH_3CN)_2]^{3+} + H_2O \xrightarrow{k_1} [Co(trpn)(CH_3CN)(H_2O)]^{3+} + CH_3CN$ (acid hydrolysis).

Table 3. The rate constants at 25°C and the activation parameters for the primary substitution reactions: $[Co(trpn)X_2]^{+/3+} + Y \xrightarrow{k_1} [Co(trpn)XY]^{2+/3+} + X^{-/0}$

X	Y	$10^3 k_1$ (s^{-1})	$\Delta H_1^\ddagger$ (kcal mol^{-1})	$\Delta S_1^\ddagger$ (cal K^{-1} mol^{-1})
F	CH_3CN	0.78	24.7(±0.6)	10.8(±1.8)
Cl	CH_3CN	1.66	13.6(±0.6)	−25.8(±1.8)
Br	CH_3CN	18.7	5.05(±0.8)	−49.5(±2.4)
F[a]	H_2O	1.28	12.8(±0.5)	−28.9(±1.5)
CH_3CN[a]	H_2O	19.1	16.0(±2.0)	−12.7(±6.0)

[a] Data taken from ref. 1.

controlled by $\Delta H_1^{\ddagger}$ values and above this temperature by $\Delta S_1^{\ddagger}$ values.[17]

Inspection of the data in Table 3 reveals that $\Delta S_1^{\ddagger}$ values are both positive and negative, probably due to the variable nature of the complex–solvent interactions. For the complex ions $[Co(trpn)X_2]^+$, the rate of halide substitution by CH_3CN decreases in the order Br > Cl > F and $\Delta H_1^{\ddagger}$ decreases in the opposite direction. This correlation reflects the ease of Co—X bond breaking in the transition state for a dissociative type of reaction. Further, the rate of fluoride substitution in water is greater than in acetonitrile (Table 3). Since it is now accepted that a solvent with a larger dielectric constant should be better in facilitating the separation of charges in the transition state for a dissociative type reaction.[18]

In conclusion, it should be repeated that the results of substitution reactions of $[Co(trpn)X_2]^+$ can be explained on the basis of a dissociative I_d mechanism.

REFERENCES

1. S. S. Massoud and R. M. Milburn, *Polyhedron* 1988, **7**, 275.
2. F. Tafesse, S. S. Massoud and R. M. Milburn, *Inorg. Chem.* 1985, **24**, 2591.
3. F. Tafesse and R. M. Milburn, *Inorg. Chim. Acta* 1987, **135**, 119.
4. G. Rawji, M. Hediger and R. M. Milburn, *Inorg. Chim. Acta* 1983, **79**, 247.
5. I. R. Jonasson, R. S. Murray, D. R. Stranks and J. K. Yandell, *Proc. 12th Int. Conf. Coord. Chem.* p. 32. Sydney, Australia (1969).
6. W. G. Jackson, P. D. Vowles and W. W. Fee, *Inorg. Chim. Acta* 1977, **22**, 111.
7. W. G. Jackson and W. W. Fee, *Inorg. Chem.* 1975, **14**, 1154.
8. D. A. Palmer and D. W. Watts, *Aust. J. Chem.* 1967, **20**, 53.
9. W. R. Fitzgerald and D. W. Watts, *Aust. J. Chem.* 1966, **19**, 935.
10. M. L. Tobe and D. W. Watts, *J. Chem. Soc.* 1964, 2991.
11. C. H. Lanford, *Inorg. Chem.* 1964, **3**, 228.
12. M. J. Saliby, D. West and S. K. Madan, *Inorg. Chem.* 1981, **20**, 723.
13. S. S. Massoud and R. M. Milburn, submitted for publication.
14. E. Martins and P. S. Sheridan, *Inorg. Chem.* 1978, **17**, 2822.
15. A. V. Ablov and E. V. Popa, *Russ. J. Inorg. Chem.* 1963, **8**, 161.
16. C. K. Ingold, *Structures and Mechanisms in Organic Chemistry*, p. 339. Bell, London (1953).
17. R. G. Wilkins, *The Study of Kinetics and Mechanisms of Reactions of Transition Metal Complexes*, p. 100. Allyn and Bacon, Boston (1974).
18. S. Asperger, M. Orhanovic, M. Pribanic and V. Reic, *J. Chem. Soc. A* 1966, 589.

Polyhedron Vol. 8, No. 4, pp. 419–426, 1989
Printed in Great Britain

0277–5387/89 $3.00+.00
Pergamon Press plc

HYDRAZINE AUTOXIDATION IN SOLUTION: CATALYSIS BY PENTACYANOFERRATE(II)

IRENE A. FUNAI and MIGUEL A. BLESA*

Departamento Química de Reactores, Comisión Nacional de Energía Atómica, Avenida del Libertador 8250, 1429 Buenos Aires, Argentina

and

JOSÉ A. OLABE*

Departamento de Química Inorgánica, Analítica y Química Física, Facultad de Ciencias Exactas y Naturales, Universided de Buenos Aires, Argentina

(*Received* 14 *October* 1987; *accepted after revision* 6 *July* 1988)

Abstract—Hydrazine is oxidized by dissolved oxygen in aqueous solutions containing $[Fe(CN)_5]^{3-}$, in slightly acidic or alkaline conditions. The reaction involves the oxidation of $[Fe^{II}(CN)_5(N_2H_4)]^{3-}$ to $[Fe^{III}(CN)_5(N_2H_4)]^{2-}$ as the first step, and kinetic features suggest that this is followed by dimerization to $[(NC)_5Fe^{III}—(N_2H_4)—Fe^{II}(CN)_5]^{5-}$; $Fe^{III}—Fe^{III}$ and $Fe^{II}—Fe^{II}$ dimers are then originated by fast electron-transfer. The first of these evolves to $[(NC)_5Fe^{II}—(N_2H_2)—Fe^{II}(CN)_5]^{6-}$; this diimide complex shows a strong MLCT band at 515 nm and is very stable in alkaline solutions (pH 8) free of O_2 or H_2O_2. In the presence of these, or in more acidic media it evolves further to $[Fe(CN)_5(H_2O)]^{3-} + N_2$.

The mechanism of hydrazine oxidation in aqueous solution depends on the nature of the oxidizing agent, particularly on its ability to act as a one- or two-electron reagent. Much work has been carried out to unravel the nature of the hydronitrogen species formed in the course of evolution from N_2H_4 to N_2. The intimate features of the reactions with the different transition metal complexes used as oxidants are however, to a large extent, still an open question: the prevalence of inner- vs outer-sphere routes, the nature and reactivity of radical intermediates, decomposition products, etc.[1]

The autoxidation of hydrazine is a slow process in aqueous solution, due to kinetic barriers; however, it has been known for a long time that traces of metal ions (Cu, Fe) catalyse the oxidation of hydrazine by dissolved oxygen. Similar questions, as mentioned above, can be posed about the mechanism of these important processes.[2] It is likely that coordination of hydrazine to the metallic centre occurs previous to the electron-transfer step, but the identification of coordinated reactants, intermediates or products is not easy in labile species such as the aquo-ions of the first transition series.

A more favourable situation is set up with the $[Fe(CN)_5(N_2H_4)]^{3-}$ complex; the rates of dissociation and the stability constants of this ion, and of the related ion $[Fe^{III}(CN)_5(N_2H_5)]^{2-}$, have been determined in aqueous deoxygenated solutions. When air is present, however, orange–red colours develop and decomposition of the complex ensues, with the evolution of gaseous products. Oxidative dehydrogenation of amines coordinated to transition metal ions has been reported.[4–6] As shown in this paper, hydrazine is autoxidized in the presence of the $[Fe(CN)_5]^{3-}$ moiety.

EXPERIMENTAL

Reagents

$Na_2[Fe(CN)_5(N_2H_5)]\cdot 2H_2O$ was prepared as described before,[7] and characterized by its UV–vis. and IR spectra.

$[Fe^{III}(CN)_5(H_2O)]^{2-}$ was prepared in solution following, in general, the procedure of James *et al.*[8]

*Authors to whom correspondence should be addressed.

0.46 g of $Na_3[Fe^{II}(CN)_5(NH_3)]\cdot 3H_2O$, was oxidized with aqueous Br_2 (4 cm^3). Excess Br_2 was removed by streaming N_2 for 10 min; 16 cm^3 of NaOH (0.125 N) was added and the solution was left standing in the dark for 1 h to complete the formation of $[Fe^{III}(CN)_5(OH)]^{3-}$. This species was purified by gel permeation chromatography; the eluted fraction containing the desired species was identified spectrophotometrically. Addition of adequate buffers (acetic acid/acetate for pH 4; phosphate for pH 6.26) yields $[Fe^{III}(CN)_5(H_2O)]^{2-}$, as shown by its spectrum.

All other reagents were analytical grade and were used without any further purification. Solutions were prepared with doubly distilled water.

Spectral measurements

Visible and UV spectra and absorbance–time profiles were recorded on a Shimadzu UV 210 A spectrophotometer fitted with a thermostated cell holder. When needed, the cells were tightly stoppered and sealed with paraffin wax to avoid air entering. Near-IR measurements were performed in a Cary 2300 spectrophotometer. Raman spectra were recorded in a Spex spectrophotometer, provided with a 1403 double monochromator; the 514.5 nm line of a Spectra-Physics 165 argon ion laser was used for excitation (power: 50–100 mW). The solution flowed through a capillary to avoid decomposition.

Kinetic measurements

These were performed spectrophotometrically at adequate wavelengths (400, 440 and 515 nm). For slow reactions successive spectra were recorded in the whole visible range.

Experiments were carried out under very diverse conditions of complex, hydrazine, oxygen and H^+ concentrations. Typical experimental conditions are listed in Table 1. The pH was adjusted with acetic acid/acetate (pH ~ 4), phosphate (pH 6–8) and borax (pH ~ 9). In the case of a large hydrazine excess (*ca* 10^{-2} mol dm^{-3}) the time evolution of this reagent in aerated solutions was followed by titrating periodically, samples with KIO_3.[9]

In the experiments performed to study the early stages of reaction, a small amount of complex was dissolved directly in the appropriate solution and placed in the spectrophotometric cell. The experiments designed to study the following reactions were carried out with weighed amounts of solid and involved isolation of the cell from the atmosphere.

Gel permeation chromatography experiments

Solutions of $[Fe^{II}(CN)_5(N_2H_4)]^{3-}$ were partially oxidized by reaction with restricted amounts of oxygen in a closed vessel to yield red solutions, and subsequently treated with ascorbic acid to reduce the Fe^{III} species; the red complex formed during the first stage does not fade on addition of ascorbic acid. The mixture was seeded in a Shephadex G-25 column and the spectra of the eluted fractions were recorded.

Table 1. Experimental conditions in kinetic measurements

$[Fe^{II}(CN)_5(N_2H_4)]^{3-}$ initial concentration (mol dm^{-3})	Oxygenation conditions	pH	Observations
2×10^{-4}	[a]	Varies, in the range pH 4.1–9.3	$[N_2H_4] = 10^{-2}$ mol dm^{-3}
2.5×10^{-4}	[b]	Varies, in the range pH 4.2–9.3	—
5×10^{-3}	[c]	Varies, in the range pH 6.1–7.2	—
Varies, in the range 5×10^{-4}–10^{-2}	[b] or [c]	6	—
—	[b]	6	$[Fe^{III}(CN)_5(H_2O)]^{2-}/[N_2H_4] = 1$
Varies	—	Varies	Addition of pyridine
4×10^{-3}	See text	8.33	Ascorbic acid 5×10^{-2} mol dm^{-3}

[a] Hydrazine catalysed autoxidation experiments. Air saturated solutions in free contact with air over long periods of time free O_2 availability.

[b] Excess oxygen.

[c] Excess Fe^{II}.

RESULTS

Catalytic autoxidation of hydrazine in the presence of $[Fe^{II}(CN)_5L]^{n-}$ *ions*

Labile $[Fe^{II}(CN)_5L]^{n-}$ ions (L = H_2O, NH_3, N_2H_4) enhance the rate of hydrazine autoxidation, in a process that is highly pH-dependent. At pH 4 there is no enhancement of the rate of hydrazine consumption compared to blank solutions, whilst at pH 6.2 and 9.3, the effect of $[Fe^{II}(CN)_5L]^{n-}$ ions is great. Thus, at 25°C the concentration of a hydrazine solution which was originally 0.01 mol dm^{-3}, decreases after 20 h to 9.6×10^{-3} in the absence of metal complexes, and to 9.3×10^{-3}, 5.2×10^{-3} and 7.2×10^{-3} in the presence of $[Fe^{II}(CN)_5(N_2H_4)]^{3-}$ (2×10^{-4} mol dm^{-3}) at pH 4.10, 6.24 and 9.29, respectively.

These observations clearly indicate that hydrazine autoxidation proceeds via $[Fe^{II}(CN)_5(N_2H_4)]^{3-}$ ions; the $[Fe^{II}(CN)_5]^{3-}$ moiety is able to process hydrazine in large amounts compared to the stoichiometric ratio of the complex, suggesting the involvement of Fe^{II}–Fe^{III}–Fe^{II} cycles:

$$[Fe^{II}(CN)_5(H_2O)]^{3-} + N_2H_4 \longrightarrow [Fe^{II}(CN)_5(N_2H_4)]^{3-} + H_2O$$

$$[Fe^{II}(CN)_5(N_2H_4)]^{3-} \xrightarrow{+O_2,\ -N_2} [Fe^{III}(CN)_5(N_2H_4)]^{2-} \xrightarrow{+O_2} \quad (1)$$

At pH ~ 4 blue-greenish colloidal precipitates begin to form after 30 min. From approximately 22 to 50 h, the spectra of the supernatant solutions show only a weak band at 440 nm, which decreases in intensity with time. The precipitates are known to be of the Prussian Blue type, arising as products of the thermal and/or photochemical decomposition of Fe^{II} and Fe^{III} species through cyanide release.[10] At pH 6, precipitates are observed after several hours; these are however white.

The subsequent discussion will refer to experiments containing no excess free hydrazine, i.e. the mechanism of the reaction of $[Fe(CN)_5(N_2H_4)]^{3-}$ with oxygen shall be explored, with solid $Na_2[Fe(CN)_5(N_2H_5)]\cdot2H_2O$ being used as the source of the complex anion.

The reaction of $[Fe(CN)_5(N_2H_4)]^{3-}$ *with oxygen*

(1) Fe^{II} *oxidation to* Fe^{III} *without decomposition of hydrazine.* At pH 4, the spectra of the products in the early stages indicate that $[Fe^{III}(CN)_5(H_2O)]^{2-}$ is present (390, 340 nm);[8] this fact, together with the previously stated results on the lack of consumption of hydrazine, suggest that the reaction is similar to that observed in the aquation–autoxidation reactions of the $[Fe(CN)_5(NH_3)]^{3-}$ ion;[11] the evolution of our system appears to be even faster, due to the lower half-life for the aquation of $[Fe(CN)_5(N_2H_5)]^{2-}$, *ca* 10 s.[3]

$$[Fe^{II}(CN)_5(N_2H_5)]^{2-} + H_2O \longrightarrow [Fe^{II}(CN)_5(H_2O)]^{3-} + N_2H_5^+ \quad (2)$$

$$[Fe^{II}(CN)_5(H_2O)]^{3-} + 0.5O_2 + H^+ \longrightarrow [Fe^{III}(CN)_5(H_2O)]^{2-} + 0.5H_2O_2. \quad (3)$$

The mechanism is not simple, however. Step (3) has been shown to be catalysed by aqueous ferrous species;[11] furthermore, in our system a peak at *ca* 1300 nm develops together with the build-up of the 390–340 nm absorptions, strongly suggesting the presence of mixed-valence $Fe^{II,III}$ species,[12] most probably $[(CN)_5Fe^{II}—NC—Fe^{III}(CN)_4(OH)_2]^{5-}$. As stated earlier, the system rapidly evolves with the formation of precipitates of the Prussian Blue type.*

(2) *Oxidation of hydrazine through* Fe^{II}—Fe^{III}—Fe^{II} *cycles*

(2.1) *UV–vis. spectral evidence*: at pH 6–7, observed spectral changes include the following sequential processes, see Fig. 1.

(a) A fast shift from 400 to 440 nm, accompanied by a substantial increase in absorbance. This process is complete in a few minutes not only at pH 6–7, but also at the higher studied pH values; the resulting species is characterized by λ_m = 440 nm, $\varepsilon = 2\times10^3$ dm^3 mol^{-1} cm^{-1}. Evidence points to the formation of a species containing Fe^{III}: thus, the initial spectrum and further evolution is similar to that observed in mixtures of N_2H_4 and $[Fe^{III}(CN)_5(H_2O)]^{2-}$; both the energy and intensity of the band are reasonable for a LMCT transition in a $[Fe^{III}(CN)_5]^{2-}$ moiety.[13]

In view of the evidence to be discussed below, we postulate this species to be a dimer, $[(CN)_5Fe^{III}(N_2H_4)Fe^{III}(CN)_5]^{4-}$, [**1**, III–III].† Quantitative

* The time scale, as well as the spectral data, are also compatible with the operation of a mechanism involving firstly an outer sphere oxidation of the original ion, and secondly a rapid electron scrambling with aquated ferrous complexes.

† In what follows, hydronitrogen bridged dimers are identified as complexes [**i**, *m*–*n*], **i** characterizing the bridging ligand (**i** = **1**, N_2H_4; **i** = **2**, N_2H_2) and *m* and *n* being Roman numerals that indicate the oxidation state of each Fe centre.

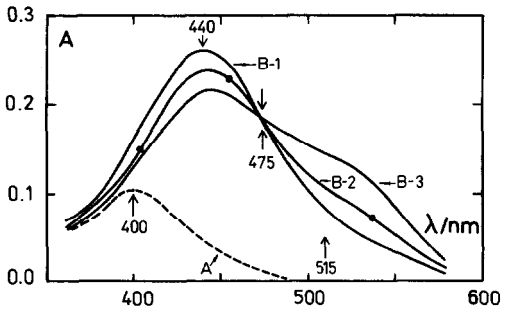

Fig. 1. (A) Spectrum of a solution containing 2×10^{-4} mol dm^{-3} $[Fe(CN)_5N_2H_4]^{3-}$, 0.1 mol dm^{-3} hydrazine and 10^{-3} mol dm^{-3} ascorbic acid (pH 6.10). (B) Sequential spectra of 2.3×10^{-4} mol dm^{-3} $[Fe(CN)_5N_2H_4]^{3-}$: (1) 4 min, (2) 7 min and (3) 12 min (pH 6.00). O_2 initial concentration = 2.3×10^{-4} mol dm^{-3}.

transformation of $[Fe(CN)_5(N_2H_4)]^{3-}$ to [**1**, III–III], resolved from further reactions, is achieved only for a low initial $[Fe(CN)_5(N_2H_4)]^{3-}$ concentration and in excess oxygen. Under other conditions, the expected maximum absorbance is not attained, indicating a consumption of either $[Fe^{II}(CN)_5(N_2H_4)]^{3-}$ or [**1**, III–III] (or both) through other processes during the same time scale.

At pH > 8, the fast process is better resolved in time and shows complex features, such as an initial increase in the absorbance at 440 nm followed by a decrease and a second increase, probably reflecting the complexities of the evolution from the monomeric iron(II) complex to the dimeric iron(III) complex [**1**, III–III].

(b) The second stage corresponds to the decay of the 440 nm band and the formation of a red species, band maximum at 515 nm. At pH 6.1, this process is reasonably well resolved in time from subsequent events, although the kinetics indicate some overlapping (see below). Simple first-order behaviour is observed in solutions where the ratio $[Fe^{II}]/[O_2]_0$ is high, indicating that the simplest situation can be envisaged as a transformation of the Fe^{III} species absorbing at 440 nm into the red species, without participation of oxygen; if this is present however, its influence is two-fold: both the rates of appearance and fading of the 515 nm band increase; the maximum absorbance attained is also very sensitive to excess oxygen, and decreases substantially in oxygen-rich solutions. From the data in oxygen-defective solutions, the molar absorptivity of the red species is $\sim 3 \times 10^3$ dm^3 mol^{-1} cm^{-1}. Spectral characteristics indicate a diimide complex featuring N_2H_2 bound to an Fe^{II} centre(s), the electronic transition being of the MLCT type, from Fe^{II} to ligand antibonding orbitals.[14] A similar transition has been reported for the $[Fe(CN)_4(NH{=}CH{-}CH{=}NH)]^{2-}$ ion formed by oxidation of $[Fe(CN)_4(en)]^{2-}$[15] and for $[Fe(CN)_5N(C_6H_4)C(H){=}NH]^{3-}$ formed from $[Fe(CN)_5N(C_6H_4)CH_2NH_2]^{3-}$.[4] Intense red colours have also been found in $[Ru(NH_3)_6]^{2+}$–N_2H_4–O_2 systems and attributed to the $[Ru(NH_3)_5(NH{=}NH)]^{2+}$ ion.[16]

The rate of formation and the stability of the red species is very sensitive to pH, see Fig. 2, and to the presence of excess Fe^{II} complexes or oxygen.

(c) The last stage is the decay of the 515 nm band. As stated, this process is very sensitive to other species in solution. At high pH and large Fe^{II} excess, the fading process becomes vanishingly slow (see Fig. 2, curve D).

The above observations suggest that Scheme 1 applies at pH 6–8.

(2.2) *Resonance Raman evidence*: direct evidence on the nature of the red species, confirming its identification as a diimide complex is given by the appearance of a peak at 1440 cm^{-1} in the resonance Raman spectrum of the red solution; this is shifted to lower wave numbers compared to the N=N stretching in solid transdiimide (ν_3 = 1529 cm^{-1}),[17] as expected from the back-bonding influence of Fe^{II}.[3] Furthermore, a peak at a similar wave number has been reported for diimide Cu^{I} complexes.[18]

(2.3) *Near IR evidence*: in the solutions obtained in the early stages of the reaction at pH 6.1, there is no absorption in the 1300 nm region; the situation contrasts with the spectral behaviour of oxygenated solutions of aquated $[Fe(CN)_5(NH_3)]^{3-}$ in the same concentration range (*ca* 10^{-3} mol dm^{-3}).[19] Thus, hydrazine hinders the formation of cyanide bridged dimers; it should be noted that the negative IR

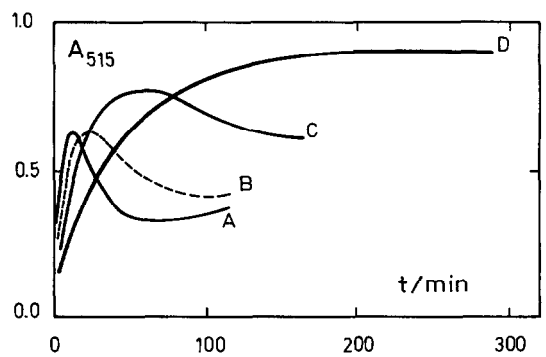

Fig. 2. Absorbance at 515 nm as a function of time; $[Fe(CN)_5N_2H_4]^{3-} = 5 \times 10^{-3}$ mol dm^{-3}; pH: (A) 6.06, (B) 6.33, (C) 6.74 and (D) 7.22. The rather fast decay observed at pH 6.1–6.3 is due to an excess of the reactant ion. At lower concentrations the decay is much slower (if due precaution is taken to avoid air entering).

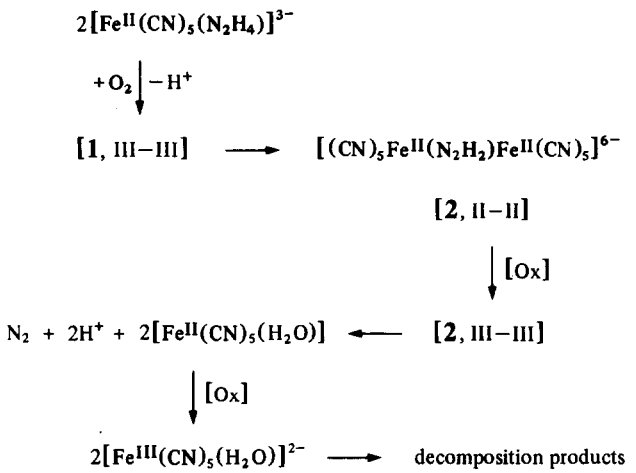

Scheme 1.

evidence does not rule out the occurrence of [1, II–III] dimers formed through reaction (4), because of the saturated nature of hydrazine.

$$[Fe^{III}(CN)_5(N_2H_4)]^{2-} + [Fe^{II}(CN)_5(H_2O)]^{3-} \rightleftharpoons [1, II\text{–}III] + H_2O. \quad (4)$$

(2.4) *Gel permeation chromatographic behaviour.* Gel permeation chromatographic separation of the parent complex and the red species was carried out in mixtures formed through partial oxidation followed by quenching with ascorbic acid. Such mixtures are indefinitely stable in the absence of light. Upon passage through the Sephadex column, the red species is eluted approximately 10 min earlier than $[Fe^{II}(CN)_5(N_2H_4)]^{3-}$. This behaviour demonstrates that the red species is of larger size, substantiating its identification as a dimer.

Cyanide-bridged dimers formed in the absence of hydrazine behave in a similar fashion.[20]*

DISCUSSION

Kinetic evidence

In most cases, quantitative kinetic data cannot be obtained because of the complexity of many concurring parallel and sequential steps. Some features are however of interest.

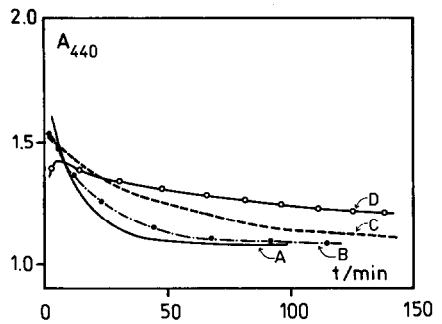

Fig. 3. Absorbance at 440 nm as a function of time, of a solution containing 5×10^{-3} mol dm^{-3} $[Fe(CN)_5N_2H_4]^{3-}$ and 2.3×10^{-4} mol dm^{-3} $[O_2]$ at various pH values: (A) 6.06, (B) 6.33, (C) 6.74 and (D) 7.22.

(a) The rate of the initial process (400 → 440 nm) decreases with pH (range 6–9); in all cases the reaction is complete within 1 min. The process at pH ⩾ 6, provides a sigmoidal A/t profile that suggests some type of autocatalysis, e.g. the involvement of labile Fe^{II} species.

(b) The decay of the 440 nm band cannot be fitted in general to first-order kinetics (see Fig. 3) except at pH 6 and high enough iron concentration (5×10^{-3} mol dm^{-3}) (Fig. 4). Under these conditions $k = 1.3 \times 10^{-3}$ s^{-1}. Figure 3 shows that a change in pH from 6.06 to 7.22 slows the apparent decay at 440 nm; the behaviour is no longer first-order, probably because of overlapping with the following stages. Even at pH 6, for $[Fe]_{total} < 5 \times 10^{-3}$ mol dm^{-3}, absorbance decay departs from first-order behaviour.

The rate of transformation of the N_2H_4 complex into the corresponding N_2H_2 complex increases as the pH decreases. This pH effect can be explained as a consequence of shifts in the dimerization equilibrium:

* Even though Emschwiller suggests that the dimers obtained in ref. 20 are of the type

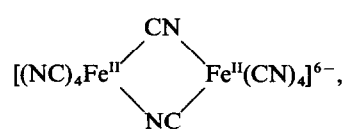

mixed valence cyanide single-bridged species are more likely in aerated media (see refs 12 and 19).

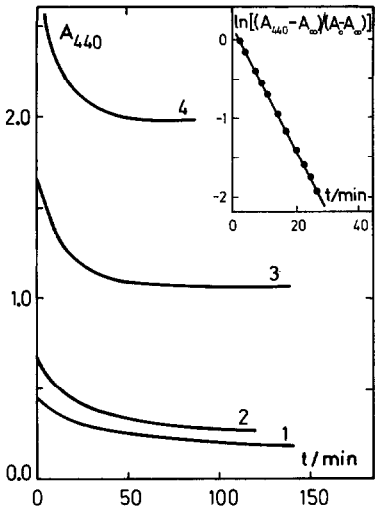

Fig. 4. Absorbance at 440 nm as a function of time at pH 6.06, $[O_2]_0 = 2.3 \times 10^{-4}$ mol dm^{-3}, and various initial $[Fe(CN)_5N_2H_4]^{3-}$ concentrations: (1) 5×10^{-4}, (2) 10^{-3}, (3) 5×10^{-3} and (4) 10^{-2} mol dm^{-3}. Inset: first-order plot corresponding to plot (3).

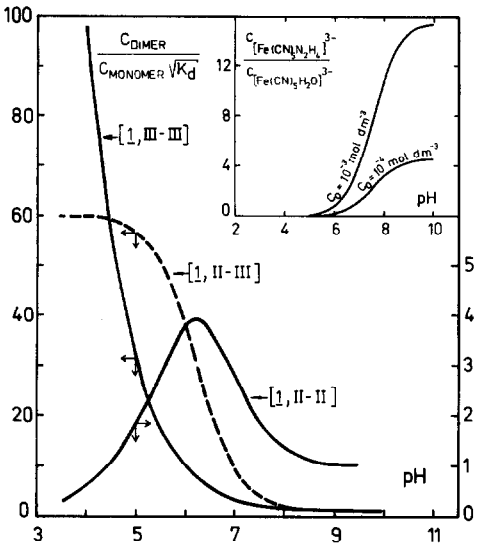

Fig. 5. pH influence on the ([Dimer]/[Monomer]) $\times (K_d)^{-1/2}$ relation for [Dimer] = [(1, II–II)], [(1, III–III)], or [(1, II–III)]. K_d is the corresponding dimerization equilibrium constant, i.e. eq. (4) for (1, III–III) and analogous equilibria for the other two cases. Inset: dependency of $([Fe(CN)_5N_2H_4]^{3-}/[Fe(CN)_5H_2O]^{3-})$ concentration relation with pH for total complex concentration (C_0) 10^{-4} and 10^{-3} mol dm^{-3}.

$$[\mathbf{1}, \text{III–III}] + N_2H_4 \rightleftharpoons 2[Fe^{III}(CN)_5(N_2H_4)]^{2-} \quad (5)$$

coupled with:

$$N_2H_4 + H^+ \rightleftharpoons N_2H_5^+ \quad (6)$$

which is important in the pH range 6–9. Thus, higher pH values would be conducive to dimer destruction through eq. (5); on the other hand, at lower pH, aquation of Fe^{II}—$(N_2H_5)^+$ hinders hydrazine oxidation (note also that hydrazine, either free or complexed, is monopronated in this pH range, deprotonation being therefore a prerequisite for dimer formation). Even though the ratio [(1, III–III)]/[Fe^{III}—(N_2H_4)] continues to increase, [(1, III–III)] and [Fe^{III}—(N_2H_4)] both become very low. The pH dependency of the ratio [(1, III–III)]/[Monomer] is shown in Fig. 5; combined with the aquation equilibrium depicted in the inset of Fig. 5, this equilibrium suffices to rationalize the pH influence.

(c) The rate of decay of the red diimide complex is sensitive to several species: oxygen, Fe^{III} complexes, excess $[Fe^{II}(CN)_5(N_2H_4)]^{3-}$ and pyridine; it is also very sensitive to pH, see Fig. 5. Thus, not only oxidants [O_2, Fe^{III}], may destroy coordinated diimide. The influence of excess pyridine can be explained through substitution equilibria of N_2H_2 in the dimer [2, II–II]:

$$[\mathbf{2}, \text{II–II}] + H_2O \underset{k_{-7}}{\overset{k_7}{\rightleftharpoons}} [(NC)_5Fe^{II}(N_2H_2)]^{3-} + [Fe^{II}(CN)_5(H_2O)]^{3-} \quad (7)$$

$$[(NC)_5Fe^{II}(N_2H_2)]^{3-} + H_2O \xrightarrow{k_8} \begin{cases} [Fe^{II}(CN)_5(H_2O)]^{3-} + N_2H_2 \\ \xrightarrow{\text{fast}} N_2 \end{cases} \quad (8)$$

Free diimide decomposes rapidly in aqueous solution, and the overall rate should then be controlled by the ratio $k_8/k_{-7}[Fe^{II}(CN)_5(H_2O)]^{3-}$. In the absence of scavengers, very small amounts of $[Fe^{II}(CN)_5(H_2O)]^{3-}$ suffice to prevent the destruction of the red species [at least through pathways (7) and (8)]. At pH 6, when the red solutions are treated with excess pyridine, this scavenges the $[Fe^{II}(CN)_5(H_2O)]^{3-}$ produced in eq. (7), and the resulting observation is a decay of the red colour. This suggests that the $[Fe^{II}(CN)_5(N_2H_2)]^{3-}$ monomer, in the absence of $[Fe^{II}(CN)_5(H_2O)]^{3-}$ to restore the dimer, decomposes rapidly through eq. (8).

The instability of the diimide complex in less alkaline media can be accounted for by the prevalence of different further reactions of H_2O_2;[6] in acidic media Fe^{II} centres are oxidized to Fe^{III}:[21]

$$\{Fe^{II}(CN)_5\}^{3-} + H_2O_2 \overset{H^+}{\rightleftharpoons} \{Fe^{III}(CN)_5\}^{2-}. \quad (9)$$

In eq. (9), $\{Fe^{III}(CN)_5\}^{2-}$ represent metal moieties featuring various possible sixth ligands (H_2O, N_2H_4). The $\{Fe^{III}(CN)_5\}^{2-}$ moieties created in eq. (9) later oxidize bound diimide, most probably through outer sphere electron exchange to yield Fe^{III}—(N_2H_2)—Fe^{III} complexes that further decompose, thus the red colour fades in acidic media. This interpretation is supported by the following observation: if an alkaline solution containing the fairly stable diimide complex is acidified with a solution containing ascorbic acid as an antioxidant, the red colour remains unchanged for large periods indicating that H^+ *per se* does not attack the diimide complex. Pathway (9) becomes more important when excess complex is present.

In alkaline media, reaction (9) becomes very slow and only a direct oxidation[3] of N_2H_4 is possible (during longer time spans):

$$[\mathbf{1}, \text{II–II}] + H_2O_2 \xrightarrow{OH^-} [\mathbf{2}, \text{II–II}]. \quad (10)$$

Evidence from related systems

The mechanistic conclusions outlined above are in line with known facts from related systems. In our case, in more alkaline media, $[Fe(CN)_5(N_2H_4)]^{3-}$ becomes more stable towards aquation,[3] and eq. (11) alone should represent the initial stages of reaction.

$$2[Fe^{II}(CN)_5(N_2H_4)]^{3-} + O_2 + H^+ \longrightarrow 2[Fe^{III}(CN)_5(N_2H_4)]^{2-} + HO_2^-. \quad (11)$$

Although it is not possible to learn much about the mechanism of reaction (11) from our data, the time scale is comparable with that of outer sphere autoxidation reactions of $[Ru(NH_3)_5L]^{n+}$ complexes.[22] The sigmoidal character of the plot of absorbance at 440 nm vs time suggests a possible catalytic path involving labile Fe^{II} centres.[11]

Next, evidence useful to assess the likelihood of dimerization shall be considered: the rate constant for the substitution of water in $[Fe^{II}(CN)_5(H_2O)]^{3-}$ by a double negatively charged ligand [dimerization reaction (4)] is of the order of 3 $dm^3\ mol^{-1}\ s^{-1}$ (I = 1 mol dm^{-3}, $NaClO_4$);[23] thus, under our conditions reaction (4) could occur readily, in a time scale governed by the rate of formation of $[Fe^{II}(CN)_5(H_2O)]^{3-}$. At pH 6, this is formed essentially according to eq. (2) with a pseudo-first-order rate constant $k = 2.0 \times 10^{-2}\ s^{-1}$;[3] aquation should proceed until an equilibrium ratio $[Fe^{II}(CN)_5(H_2O)]^{3-}/([Fe^{II}(CN)_5(N_2H_4)]^{3-} + [Fe^{II}(CN)_5(N_2H_5)]^{2-})$ in the range 0.40–1.76 is achieved (for total complex concentration in the range 10^{-4}–10^{-3} mol dm^{-3}).

Dimerization of two labile Fe^{II} complexes is also possible by a process similar to (4), eq. (12), although the higher negative charge on the incoming $[Fe^{II}(CN)_5N_2H_4]^{3-}$ substituent would make the process slower.[24]

$$[Fe^{II}(CN)_5(N_2H_4)]^{3-} + [Fe^{II}(CN)_5(H_2O)]^{3-} \rightleftharpoons [\mathbf{1}, \text{II–II}] + H_2O. \quad (12)$$

Fast electron exchange between monomers and dimers should give rise to the dimers [**1**, II–II] and [**1**, III–III] from [**1**, II–III].[24] These three dimers and the related Fe^{II} and Fe^{III} monomers may be considered as equilibrated for any process taking place in longer time spans.

From dimerization equilibrium data for related systems,[24] it is possible to estimate $K_d \cong 7 \times 10^{-4}$ for reaction (13). This amounts to 5% of the iron being present as dimer [**1**, II–II] in our experiments at pH > 10 (no N_2H_4 protonation).

$$2[Fe^{II}(CN)_5(N_2H_4)]^{3-} \overset{K_d}{\rightleftharpoons} [\mathbf{1}, \text{II–II}] + N_2H_4. \quad (13)$$

Substantially higher values are calculated for Fe^{III}—Fe^{II} dimers. A higher stability of the hydrazine bridged dimer as compared to [Fe^{II}—(NC)—Fe^{III}] dimers is also suggested as a possible explanation for the absence of IV bands at 1300 nm.

A high affinity of Fe—(NH=NH) for $[Fe(CN)_5(H_2O)]^{3-}$ is expected: pyrazine bridged dimers are well known;[25] the stability constant K'_D:

$$[(NC)_5Fe^{II}\text{—}(NH{=}NH)]^{3-} + [Fe^{II}(CN)_5(H_2O)]^{3-} \overset{K'_D}{\rightleftharpoons} [\mathbf{2}, \text{II–II}] + H_2O \quad (14)$$

is expected to be 10^4–10^6 mol dm^{-3}, depending on the ionic strength. Whence, the ratio [**2**, II–II]/$[(NC)_5Fe^{II}\text{—}(NH{=}NH)]^{3-}$ in solutions containing

excess $[Fe^{II}(CN)_5(N_2H_4)]^{3-}$ is calculated to be always high.

When compared with the mechanism of dehydrogenation of diamines bis-coordinated to the $[Fe^{III}(CN)_4]^-$ moiety,[6] the different influence of pH on the rate of formation and stability of the red species is related to the possibility of coordinating two Fe^{III} centres to the bridging ligand in the present system, and the need of two (as opposed to four in ref. 4) oxidant equivalents per mole of ligand.

Dimerization equilibria, being labile, largely change the reactivity pattern of the system. The formation of a red species with —C=N— bonds in the ligand has also been observed with $[Fe(CN)_5(picolilamine)]^{3-}$; in this case oxidation by persulphate leads to coordinated 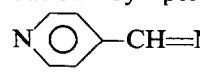 , yielding red complexes;[5] dimers are also involved in this system.

Acknowledgements—To Prof. E. L. Varetti (Programa QUINOR) for the resonance Raman measurements. Partial support by CICPBA and CONICET is gratefully acknowledged. M.A.B. and J.A.O. are members of the Research Carrier (CONICET).

REFERENCES

1. F. Bottomley, *Quart. Rev.* 1970, 617.
2. L. F. Audrieth and B. A. Ogg, *The Chemistry of Hydrazine*. John Wiley, New York (1951).
3. J. A. Olabe and L. A. Gentil, *Transition Metal Chem.* 1983, **8**, 65.
4. P. Williams, PhD Thesis, University of La Plata (1986).
5. A. M. da Costa Ferreira and H. E. Toma, *J. Chem. Soc., Dalton Trans.* 1983, 2051.
6. M. Goto, M. Takeshita, N. Kauda, T. Sakai and V. L. Goedken, *Inorg. Chem.* 1985, **24**, 582 and refs therein.
7. N. E. Katz, J. A. Olabe and P. J. Aymonino, *J. Inorg. Nucl. Chem.* 1977, **39**, 908.
8. A. D. James, R. S. Murray and W. C. E. Higginson, *J. Chem. Soc., Dalton Trans.* 1974, 1273.
9. A. I. Vogel (Ed.), *Química Analítica Cuantitativa*, Vol. 1. Kapeluz, Buenos Aires (1977).
10. (a) A. Chadwick and A. G. Sharpe, *The Chemistry of Cyano Complexes of the Transition Metals*. Academic Press, New York (1976); (b) J. A. Olabe and H. O. Zerga, *Inorg. Chem.* 1983, **22**, 4156.
11. H. E. Toma, *Inorg. Chim. Acta* 1975, **15**, 205.
12. R. Glauser, U. Hauser, F. Herreu, A. Ludi, P. Roder, E. Schmidt, H. Siegenthaler and F. Wenk, *J. Am. Chem. Soc.* 1973, **95**, 8457.
13. (a) R. Gale and A. J. McCaffery, *J. Chem. Soc., Dalton Trans.* 1973, 1344; (b) D. F. Gutterman and H. B. Gray, *Inorg. Chem.* 1972, **11**, 1727.
14. H. A. Itano and E. A. Robinson, *J. Am. Chem. Soc.* 1961, **83**, 3339.
15. V. L. Goedken, *J. Chem. Soc., Chem. Commun.* 1972, 207.
16. F. Bottomley, *Can. J. Chem.* 1970, **48**, 351.
17. J. W. Nibler and V. E. Bondybey, *J. Chem. Phys.* 1974, **60**, 1307.
18. D. Petredis, A. Burke and A. L. Balch, *J. Am. Chem. Soc.* 1970, **92**, 428.
19. F. Cukiernik and J. A. Olabe, work in progress.
20. G. Emschwiller, *CR Acad. Sci. (France)* 1964, **259**, 4281.
21. M. L. Bowers, D. Kovacs and R. E. Shepherd, *J. Am. Chem. Soc.* 1977, **99**, 6555.
22. D. M. Stanbury, O. Haas and H. Taube, *Inorg. Chem.* 1980, **19**, 518.
23. Z. Bradic, M. Pribanic and S. Asperger, *J. Chem. Soc., Dalton Trans.* 1975, 353.
24. A. D. James and R. S. Murray, *J. Chem. Soc., Dalton Trans.* 1977, 326.
25. F. Felix and A. Ludi, *Inorg. Chem.* 1978, **17**, 1782.

Polyhedron Vol. 8, No. 4, pp. 427–431, 1989
Printed in Great Britain

0277-5387/89 $3.00+.00
© 1989 Pergamon Press plc

SYNTHESIS AND STUDY OF SOME NOVEL Co^{II}, Ni^{II} AND Cu^{II} COMPLEXES WITH SILICON ISOTHIOCYANATES AS LIGANDS

A. S. SYNGOLLITOU-KOURAKOU,* I. A. TOSSIDIS and A. CHRISTOFIDES

Department of General and Inorganic Chemistry, Aristotelian University of Thessaloniki, Thessaloniki, Greece

(*Received* 23 *February* 1988; *accepted* 6 *July* 1988)

Abstract—New complexes of Co^{II}, Ni^{II} and Cu^{II} with silicon isothiocyanates of the type $R_xSi(NCS)_{4-x}$ (where $x = 0, 1, 2, 3$) have been synthesized and characterized using elemental analyses, magnetic susceptibility measurements and spectral (electronic and infrared) data. The Co^{II} and Ni^{II} complexes have a polymeric tetrahedral structure, whereas a tetragonal structure has been assigned to the Cu^{II} complexes. Various ligand field and nephelauxetic parameters have been evaluated and thermoanalytical data for the complexes of $CH_3Si(NCS)_3$ are also reported.

So far, little has been reported concerning the nucleophilic reactivity of silicon isothiocyanates.[1–5] In the course of this work it was found that a- and b-unsaturated organosilanes are useful reagents as mild and stable nucleophiles, acting formally as the corresponding organometallics.[6,7] In fact, the trimethylsilicon isothiocyanate showed nucleophilic behaviour at the nitrogen and sulphur ends, respectively.[5] The same compound has been also reported[8] as an HNCS-donor in several heterocyclic syntheses. Moreover, the structure and the donor activity of the silicon isothiocyanate products have been described.[9] More recently, $(CH_3)_2Si(NCS)_2$ and $(CH_3)_3SiNCS$ have been employed as ligands for preparing complexes with either soft or hard acids.[10]

In an effort to understand the coordination ability of $Si(NCS)_4$, $CH_3Si(NCS)_3$, $(CH_3)_2Si(NCS)_2$ and $(CH_3)_3SiNCS$ ligands, we have prepared some complexes with transition metal ions such as Co^{II}, Ni^{II} and Cu^{II}.

The results concerning the synthesis and characterization of twelve novel complexes are reported in this paper. The thermal properties of the $CH_3Si(NCS)_3$ complexes with Co^{II}, Ni^{II} and Cu^{II} are also reported and discussed.

*Author to whom correspondence should be addressed.

EXPERIMENTAL

(a) *Physical measurements*

IR spectra were recorded in the region 4000–250 cm^{-1} on a Perkin–Elmer 467 spectrophotometer using KBr discs. Electronic absorption spectra were obtained on a Perkin–Elmer Hitachi 200 spectrophotometer in the solid state with Nujol mulls. The carbon, hydrogen and nitrogen analyses were performed on a Perkin–Elmer 240 elemental Analyser. The metal determinations were carried out by published methods.[11] Magnetic susceptibility measurements in the solid state were carried out by the Faraday technique using $Hg[Co(SCN)_4]$ as the calibrant, at room temperature. The thermoanalytical curves were obtained on a Mettler TA 2000 system in a dynamic atmosphere of nitrogen; sample sizes of 20–40 mg were used at a heating rate of a 6° min^{-1}. The chart speed was maintained at 5 mm min^{-1}.

(b) *Preparation of the complexes*

The ligands were prepared by procedures outlined elsewhere.[12,13] All the complexes were synthesized in a similar way and the following example is representative.

The ligand $Si(NCS)_4$ (0.22 mmol) dissolved in

Table 1. Analytical data and relevant IR frequencies (cm^{-1}) for the new silicon isothiocyanate complexes of Co^{II}, Ni^{II} and Cu^{II}

	Compound	%C	%H	%M	%N	ν(C—N)	ν_{as}(Si—C)	ν_{sym}(SiC)	ν(C—S)	δ(NCS)		ν(M—S)
I	$[Si(NCS)_4 \cdot 4CoCl_2]$	6.0		29.6	7.0	2140s	740m	690m	720s	460s	430m	305s
		(6.1)		(30.0)	(7.2)							
II	$[Si(NCS)_4 \cdot 4NiCl_2]$	5.8		29.3	6.8	2130s	760m	700s	700m	470s	420m	310s
		(6.1)		(30.1)	(7.1)							
III	$[Si(NCS)_4 \cdot 4CuCl_2]$	6.7		37.5	7.6	2140s	750m	680m	690s	460s	420s	325s
		(7.1)		(38.3)	(8.3)							
IV	$[CH_3Si(NCS)_3 \cdot 3CoCl_2]$	7.2	0.5	28.3	6.7	2140m	770m	620m	690s	450s	430m	330m
		(7.9)	(0.5)	(29.1)	(6.9)							
V	$[CH_3Si(NCS)_3 \cdot 3NiCl_2]$	7.3	0.4	28.5	6.6	2140m	775m	640m	720s	460m	440m	310m
		(7.9)	(0.5)	(29.0)	(6.9)							
VI	$[CH_3Si(NCS)_3 \cdot 3CuCl_2]$	7.0	0.5	29.9	7.0	2130s	770m	660s	700m	445m	420m	305m
		(7.7)	(0.5)	(30.7)	(6.7)							
VII	$[(CH_3)_2Si(NCS)_2 \cdot 2CoCl_2]$	10.6	1.0	26.5	6.2	2125s	775m	680s	710m	460s	420s	330m
		(11.0)	(1.4)	(27.1)	(6.4)							
VIII	$[(CH_3)_2Si(NCS)_2 \cdot 2NiCl_2]$	10.6	0.9	26.7	6.2	2120s	750s	670s	700s	460m	420s	340m
		(11.0)	(1.3)	(27.0)	(6.7)							
IX	$[(CH_3)_2Si(NCS)_2 \cdot 2CuCl_2]$	9.4	1.0	28.0	6.0	2140s	760s	620m	690s	460s	420s	335m
		(10.0)	(1.3)	(28.6)	(6.3)							
X	$[(CH_3)_3Si(NCS) \cdot CoCl_2]$	17.8	3.3	21.8	5.0	2140s	740m	660w	720m	470m	430s	340m
		(18.4)	(3.4)	(22.6)	(5.3)							
XI	$[(CH_3)_3Si(NCS) \cdot NiCl_2]$	17.9	3.2	21.9	4.9	2135m	760m	680m	700m	465s	425m	310s
		(18.4)	(3.4)	(22.5)	(5.3)							
XII	$[(CH_3)_3Si(NCS) \cdot CuCl_2]$	17.6	3.3	23.3	5.0	2130s	750m	670m	710m	470m	420s	320s
		(18.0)	(3.4)	(23.9)	(5.2)							

Table 2. Solid state magnetic moments and electronic spectra of the new complexes of the silicon isothiocyanates

	Compound	Bands observed	Assignments	10 *Dq* (cm^{-1})	*B* (cm^{-1})	β	μ_{eff} (BM)
I	$[Si(NCS)_4 \cdot 4CoCl_2]$	15700	$^4T_1(P) \leftarrow {}^4A_2(F)$	3160	794	0.821	4.47
		5680	$^4T_1(F) \leftarrow {}^4A_2(F)$				
		45040	$\pi^* \leftarrow \pi$				
		38460	$\pi^* \leftarrow n$				
II	$[Si(NCS)_4 \cdot 4NiCl_2]$	15000	$^3T_1(P) \leftarrow {}^3T_1(F)$	3444	862	0.837	3.40
		6200	$^3A_2(F) \leftarrow {}^3T_1(F)$				
		45450	$\pi^* \leftarrow \pi$				
		40000	$\pi^* \leftarrow n$				
III	$[Si(NCS)_4 \cdot 4CuCl_2]$	15200	$^2T_{2g} \leftarrow {}^2E_g$				
		23300sh					
		45000	$\pi^* \leftarrow \pi$				
		39200	$\pi^* \leftarrow n$				
IV	$[CH_3Si(NCS)_3 \cdot 3CoCl_2]$	16000	$^4T_1(P) \leftarrow {}^4A_2(F)$	3194	811	0.838	4.46
		5750	$^4T_1(F) \leftarrow {}^4A_2(F)$				
		45040	$\pi^* \leftarrow \pi$				
		38470	$\pi^* \leftarrow n$				
V	$[CH_3Si(NCS)_3 \cdot 3NiCl_2]$	14900	$^3T_1(P) \leftarrow {}^3T_1(F)$	3388	857	0.832	3.48
		6100	$^3A_2(F) \leftarrow {}^3T_1(F)$				
		45400	$\pi^* \leftarrow \pi$				
		39000	$\pi^* \leftarrow n$				
VI	$[CH_3Si(NCS)_3 \cdot 3CuCl_2]$	15000	$^2T_{2g} \leftarrow {}^2E_g$				
		23100sh					
		45100	$\pi^* \leftarrow \pi$				
		39000	$\pi^* \leftarrow n$				
VII	$[(CH_3)_2Si(NCS)_2 \cdot 2CoCl_2]$	16100	$^4T_1(P) \leftarrow {}^4A_2(F)$	3183	818	0.845	4.46
		5730	$^4T_1(F) \leftarrow {}^4A_2(F)$				
		45000	$\pi^* \leftarrow \pi$				
		39000	$\pi^* \leftarrow n$				
VIII	$[(CH_3)_2Si(NCS)_2 \cdot 2NiCl_2]$	14870	$^3T_1(P) \leftarrow {}^3T_1(F)$				
		5990	$^3A_2(F) \leftarrow {}^3T_1(F)$	3327	858	0.833	3.47
		45400	$\pi^* \leftarrow \pi$				
		39300	$\pi^* \leftarrow n$				
IX	$[(CH_3)_2Si(NCS)_2 \cdot 2CuCl_2]$	15600	$^2T_{2g} \leftarrow {}^2E_g$				
		45000	$\pi^* \leftarrow \pi$				
		39000	$\pi^* \leftarrow n$				
		23200sh					
X	$[(CH_3)_3Si(NCS) \cdot CoCl_2]$	15800	$^4T_1(P) \leftarrow {}^4A_2(F)$	3170	800	0.827	4.46
		5700	$^4T_1(F) \leftarrow {}^4A_2(F)$				
		45080	$\pi^* \leftarrow \pi$				
		39000	$\pi^* \leftarrow n$				
XI	$[(CH_3)_3Si(NCS) \cdot NiCl_2]$	14700	$^3T_1(P) \leftarrow {}^3T_1(F)$	3333	846	0.822	3.47
		6000	$^3A_2(F) \leftarrow {}^3T_1(F)$				
		45100	$\pi^* \leftarrow \pi$				
		40000	$\pi^* \leftarrow n$				
XII	$[(CH_3)_3Si(NCS) \cdot CuCl_2]$	15300	$^2T_{2g} \leftarrow {}^2E_g$				
		23500sh					
		45000	$\pi^* \leftarrow \pi$				
		39500	$\pi^* \leftarrow n$				

B (free ion) Co = 967 cm^{-1}. *B* (free ion) Ni = 1030 cm^{-1}.

CCl_4 (20 cm^3) was added slowly under continuous stirring and cooling, to a solution of the metal chloride (0.2 mmol) in CCl_4 (50 cm^3). The mixture was then refluxed for 3 h affording a coloured precipitate, which was filtered off, washed with dry ethanol and ether and dried *in vacuo*.

RESULTS AND DISCUSSION

The reaction of $Si(NCS)_4$, $CH_3Si(NCS)_3$, $(CH_3)_2Si(NCS)_2$ and $(CH_3)_3SiNCS$ with chlorides of Co^{II}, Ni^{II} and Cu^{II} gave solid coloured compounds of the following types: $[Si(NCS)_4 \cdot 4MX_2]$, $[CH_3Si(NCS)_3 \cdot 3MX_2]$, $[(CH_3)_2Si(NCS)_2 \cdot 2MX_2]$ and $[(CH_3)_3Si(NCS) \cdot MX_2]$ regardless of the amount of ligand.

The complexes are insoluble in water and in most common organic solvents, the latter suggesting polymeric structures. The majority of the compounds, which were obtained in 50–70% yields, are not air stable. The characterization of the novel compounds was established by elemental analysis, spectroscopic methods (IR, UV–vis.) and magnetic measurements. The thermoanalytical analysis data for complexes **IV**, **V**, **VI** are also discussed. The analytical results with the IR data and their assignments are presented in Table 1.

All the studied compounds show [14–19] the three diagnostic regions, C—N stretching, C—S stretching and NCS bending modes of the —NCS group at 2150–2050 cm^{-1}, 720–690 cm^{-1} and 470–420 cm^{-1}, respectively. The position of the ν(C—N) band is shifted to higher frequencies in comparison to those of the free ligand.[12,13] However, the ν(C—S) band is shifted to lower wavenumbers compared to those of the free ligands, whereas the band due to δ(NCS) lies at 470–420 cm^{-1} and is shifted to higher wave numbers than those of the free ligands. The sharp peak obtained above 2000 cm^{-1} is assigned to ν(C—N) and the frequencies of the bands (C—S) and (NCS) which are considered as criteria for establishing[15,16,18] that the ligands are S-bonded. However, a weaker coordination through the nitrogen atom in the case of polymeric structures is not excluded.

The electronic spectral data and the solid state magnetic moments of the studied complexes are given in Table 2. All the electronic spectra show a maximum of medium intensity at 45.0–46.0 kK and an intensive band at 38.4–40.0 attributable[20] to $\pi \rightarrow \pi^*$ and $n \rightarrow \pi^*$ transitions located on the ligand. The spectra of the Co^{II} complexes exhibit bands in 5.7–6.0 and 15.7–16.1 kK regions which can be assigned to $^4T_1(F) \leftarrow {}^4A_2(F)$ and $^4T_1(P) \leftarrow {}^4A_2(F)$ transitions, respectively. The Ni^{II} complexes show bands at 6.0–6.2 and 14.7–15.0 kK attributable to $^3A_2(F) \leftarrow {}^3T_1(F)$ and $^3T_1(P) \leftarrow {}^3T_1(F)$ transitions, respectively. The electronic spectra, the Dq, B and β values,[21] the colours and the magnetic moments at room temperature, for the Co^{II} and Ni^{II} complexes suggest that they have an essentially tetrahedral structure and the NCS groups are S-bonded since the N-bonded thiocyanate lies above Cl^- in the spectrochemical series.[22]

In the Cu^{II} complexes the absence of a magnetic moment is rather indicative of the presence of dinuclear Cu^{II} species with a diamagnetic ground state.

The thermogravimetric study for the **IV**, **V** and **VI** complexes shows that these compounds have two decomposition stages. The TG thermogram of the complex **IV** displays two steps at 160 and 280°C, both endothermic, which correspond to the loss of $\{CH_3Si(NC)_3Cl\}$ first (Found: 25.8. Calc.: 26.6%) and then $\{CoS_3Cl_6\}$ (Found: 54.7. Calc.: 53.4%), leaving a residue of 2Co (Found: 19.4. Calc.: 20.0%).

The DTA thermogram of complex **V** has endothermic peaks at 170 and 360°C, and the mass losses correspond to the loss of $\{CH_3Si(NC)_3Cl_4\}$ (Found: 43.4. Calc.: 43.2%) and $\{Ni_2S_3Cl_2\}$ (Found: 46.9. Calc.: 46.7%), leaving a residue of Ni (Found: 9.6. Calc.: 10.1%). The DTA thermogram of compound **VI** shows endothermic peaks at 160 and 330°C which correspond to the loss of $\{CH_3Si(NC)_3Cl_3\}$ (Found: 36.6. Calc.: 37.6%), $\{Cu_2S_3Cl_3\}$ (Found: 53.0. Calc.: 52.6%) and a residue of Cu (Found: 10.2. Calc.: 9.8%).

Generally, the TG and DTA curves of the studied complexes show that first a mixture of organosilicon species is removed, which contains no sulphur and may be considered as a decomposition product of the ligand involved. In the same step the metal also forms a compound with sulphur and chlorine which in the second one decomposes leaving the metal as a residue above 450°C. The presence of decomposition products containing sulphur and metal may imply that the M—S bond is more thermally stable than the C—S bond.

REFERENCES

1. D. Seyferth and N. Kahlen, *J. Am. Chem. Soc.* 1960, **82**, 1080.
2. T. Sasaki, A. Usuki and M. Ohno, *Tetrahedron Lett.* 1978, **49**, 4925.
3. P. F. Hudrlick, *New Application of Organometallic Reagents in Organic Synthesis* (Edited by D. Seyferth), p. 127. Elsevier, New York (1976).
4. T. Sasaki, A. Usuki and M. Ohno, *J. Org. Chem.* 1980, **45**, 3559.
5. T. Sasaki, A. Usuki and M. Ohno, *J. Org. Chem.* 1981, **46**, 5445.

6. T. H. Chan and T. Fleming, *Synthesis* 1979, 761.
7. T. Fleming, in *Comprehensive Organic Chemistry* (Edited by D. N. Jone), Pt 13, Vol. 3. Pergamon Press, Oxford (1979).
8. R. Neidlein and Wolf. D. Ober, *Monatsh. Chem.* 1976, **107**, 1241; *Chem. Abstr.* 1977, **86**, 89772z.
9. Yu. V. Kolodyazhnyi, I. V. Zhakova, S. B. Bulgarevish, A. P. Sadimenko and A. D. Garnovskii, *Zh. Obshch. Khim.* 1983, **53**, 2266, *Chem. Abstr.* 1984, **100**, 103442h.
10. I. V. Zhakova, A. D. Garnovskii, Yu. V. Kolodyazhnyi and L. Yu. Ukhin, *Koord. Khim.* 1983, **9**, 1143; *Chem. Abstr.* 1983, **99**, 132729y.
11. A. I. Vogel, *Quantitative Inorganic Analysis*, 3rd edn, pp. 443, 445, Longmans, Green and Co, London (1961)
12. D. B. Sowerby, *J. Inorg. Nucl. Chem.* 1961, **22**, 205.
13. H. H. Anderson, *J. Am. Chem. Soc.* 1947, **69**, 3049.
14. P. Mitchell and R. Williams, *J. Chem. Soc.* 1960, 1912.
15. A. Sebatini and I. Bertini, *Inorg. Chem.* 1965, **4**, 959, 1665; A. Sebatini and I. Bertini, *Inorg. Chem.* 1966, **5**, 1025.
16. M. Chamberlain and J. C. Bailar Jr, *J. Am. Chem. Soc.* 1959, **81**, 6412.
17. A. Turco and C. Pecile, *Nature* 1961, **191**, 66.
18. J. Lewis, R. S. Nyholm and P. Smith, *J. Chem. Soc.* 1961, 4590.
19. J. Burmeister, *Coord. Chem. Rev.* 1966, **1**, 205; J. Burmeister, *Coord. Chem. Rev.* 1968, **3**, 225.
20. T. Veszprémi, J. Nagy and I. Barta, *Acta Chim. Acad. Sci. Hung.* 1978, **96**, 217.
21. A. Liehr and C. Ballhausen, *Ann. Phys.* 1959, **6**, 134.
22. Ch. K. Jørgensen, *Absorption Spectra and Chemical Bonding in Complexes*, p. 109. Pergamon Press, Oxford (1962).

Polyhedron Vol. 8, No. 4, pp. 433–445, 1989
Printed in Great Britain

0277–5387/89 $3.00+.00
© 1989 Pergamon Press plc

SYNTHESIS AND SPECTROSCOPIC CHARACTERISTICS OF BIS(ETHENYLDIMETHYLSILYLMETHYL)PLATINUM(II) COMPLEXES CONTAINING TERTIARY PHOSPHINE LIGANDS

ROBERT D. KELLY and G. BRENT YOUNG*

Inorganic Chemistry Laboratories, Imperial College of Science, Technology and Medicine, London SW7 2AY, U.K.

(*Received* 26 *May* 1988; *accepted* 6 *July* 1988)

Abstract—Various complexes $L_2Pt(CH_2SiMe_2CH:CH_2)_2$ have been synthesized by diene displacement from $(cod)Pt(CH_2SiMe_2CH:CH_2)_2$ [$L = PMe_3$, PEt_3, $PMePh_2$, PPh_3; L_2 = dppm, dppe, dppp, dppb, dppf].† With monodentate phosphines, monophosphine complexes $LPt(CH_2SiMe_2CH:CH_2)(CH_2SiMe_2CH:CH_2)$ may be formed, in which tetracoordination of platinum is completed by η^2-binding of one ethenylsilyl ligand. With tricyclohexylphosphine, this is isolated as the sole product, while with less bulky phosphines inseparable mixtures develop of monophosphine, bis-phosphine and diene complexes. All of these species have been characterized by ^1H, ^{13}C and ^{31}P NMR and IR techniques.

Thermolytic rearrangements of organotransition metals frequently involve hydrogen migrations from alkyl and sometimes aryl or alkenyl ligands. Hydrogen transfer from β- and α-carbons were established fairly early as important reaction paths.[1] More recently, migrations from more remote carbon atoms have emerged[2] in addition to a variety of cyclometallations on ligands with ligating atoms other than carbon.[3] It is recognized that study of these relatively controllable, intramolecular C—H bond activations may yield an important understanding of the phenomenon as a whole and may lead to the evolution of metal systems which mediate the direct functionalization of inert hydrocarbons. Concurrently, a few organometallic species have been discovered which activate C—H bonds in an intermolecular fashion in homogeneous solution.[4]

In prevous studies we have examined δ-hydrogen migrations from both aromatic and aliphatic sites which generate five-membered rings.[5,6] Our interest in comparing the reactivity of corresponding olefinic C—H bonds has led us to synthesize complexes of types $L_2Pt(CH_2SiMe_2CH:CH_2)_2$ and $[LPt(R)(CH_2SiMe_2CH:CH_2)$, which have, in principle, a five-membered cyclometallation potential. Here, we report on their preparations and some notable spectroscopic characteristics. These ligands are more correctly termed "ethenyldimethylsilylmethyl" but for the sake of brevity we shall refer instead to "sila-neohexenyl" groups.

EXPERIMENTAL

General and instrumental

Elemental analyses were carried out by Imperial College Microanalytical Laboratories. NMR spectra were recorded on Bruker WM250 (^1H, 250.13 MHz; ^{13}C, 62.9 MHz), Bruker WM400 (^1H, 400.13 MHz) and JEOL FX90Q (^1H, 89.55 MHz; ^{13}C, 22.51 MHz; ^{31}P, 36.21 MHz) spectrometers. The instruments were temperature-calibrated for kinetic measurements using a methanol reference standard.[7] IR data were collected as 4% KBr dispersions on a Perkin–Elmer 683 or 1720 Fourier Transform instrument.

All reactions were carried out under nitrogen or argon unless otherwise noted, using standard anaerobic techniques.[8] Solvents were distilled under

*Author to whom correspondence should be addressed.

† Abbreviations: cod = 1,5-cyclooctadiene; dppm = bis (diphenylphosphino)methane; dppe = 1,2-bis(diphenyl phosphino)ethane; dppp = 1,3-bis(diphenylphosphino) propane; dppb = 1,4-bis(diphenylphosphino)butane; dppf = 1,1′-bis(diphenylphosphino)ferrocene.

nitrogen prior to use; diethyl ether and hexane from sodium/benzophenone, toluene from sodium.

Chloromethyldimethyl(vinyl)silane was used as supplied by Lancaster Synthesis. Trimethylphosphine, triethylphosphine, diphenylmethylphosphine, tricyclohexylphosphine, dppm, dppe, dppp and dppb were used as supplied by Strem Chemicals. Triphenylphosphine, cod, dppf, d_8-toluene and d_6-benzene were used as supplied by Aldrich Chemical Company.

(1) *Preparations of* cis-L_2PtR_2 [R = $CH_2SiMe_2CH:CH_2$]

Bis-sila-neohexenyl(cycloocta-1,4-diene)platinum(II). $Mg(CH_2SiMe_2CH:CH_2)Cl$ was prepared by addition of $ClCH_2SiMe_2CH:CH_2$ (8.0 g, 59.2 mmol) in diethyl ether (30 cm^3) to a stirred suspension of Mg shot (6.1 g, 0.25 mol) in diethyl ether (30 cm^3) at room temperature. After 12 h stirring at ambient temperature, the solution was filtered off and analysed (0.9 mol dm^{-3}, 91% yield). A portion of the Grignard solution (8.2 cm^3, 11.46 mmol) was added dropwise to a stirred suspension of (cod)$PtCl_2$[9] (1.42 g, 3.82 mmol) in diethyl ether (60 cm^3) at −20°C. The mixture was allowed to reach room temperature and stirred for a further 4 h. The resulting stirred suspension was cooled to −15°C and hydrolysed by dropwise addition of degassed, saturated ammonium chloride solution (40 cm^3). The ethereal layer was separated and the aqueous phase washed with diethyl ether (20 cm^3) and the combined ether extracts dried over anhydrous magnesium sulphate and decolourized with activated charcoal. Removal of the solvent *in vacuo* gave a white oil (1.2 g, 71%) with a satisfactory analysis (Table 1). (IR: 3050m, 3005m, 2960–2850s, 1590w, 1520w, 1480w, 1435m, 1400s, 1340m, 1315w, 1245vs, 1185w, 1165w, 1015s, 945vs, 835vs, 815vs, 765vs, 725s, 680s, 605w, 520m, 460w.)

cis - *bis*(*sila - neohexenyl*) - *bis* - (*trimethylphosphine*) *platinum*(II). To a solution of (cod)$Pt(CH_2SiMe_2CH:CH_2)_2$ (0.20 g, 0.40 mmol) in benzene (3 cm^3) at room temperature was added by microsyringe PMe_3 (81.4×10^{-3} cm^3, 0.80 mmol). The flask was left overnight at ambient temperature. Solvent removal *in vacuo* gave the analytically pure white oil. Yield: 100%. (IR: 3035m, 2945s, 2905s, 1585w, 1420m, 1400m, 1300m, 1285m, 1235s, 1010m, 960s, 890s, 830s, 810s, 760m, 720s, 675m, 520w.)

Prepared according to the same method were:

cis - *bis*(*sila - neohexenyl*) - *bis* - (*triethylphosphine*) *platinum*(II). Product: colourless oil. Yield: 100%. (IR: 3045m, 2980–2890vs, 1590w, 1455s, 1400s, 1380m, 1240s, 1035vs, 1010s, 940s, 830vs, 810vs, 760vs, 715vs, 680s, 630w, 520w.)

Table 1. Analytical data

Compound	Element % (Calc.) C	Found H
(cod)PtR_2	43.0	7.1
	(43.1)	(6.8)
$(PMe_3)_2PtR_2$	36.1	7.7
	(35.2)	(7.4)
$(PEt_3)_2PtR_2$	41.9	8.5
	(41.9)	(8.3)
$(PPh_2Me)_2PtR_2$	54.7	6.1
	(54.5)	(6.1)
$(PPh_3)_2PtR_2$	60.2	5.7
	(60.2)	(5.7)
(dppm)PtR_2	54.5	5.8
	(54.0)	(5.7)
(dppe)PtR_2	55.4	6.0
	(54.6)	(5.8)
(dppp)PtR_2	55.6	6.2
	(55.1)	(6.0)
(dppb)PtR_2	55.8	6.2
	(55.7)	(6.1)
(dppf)PtR_2	55.9	5.4
	(55.7)	(5.3)
$(PCy_3)\overline{PtR(R)}$	50.1	8.3
	(50.0)	(8.2)

cis - *bis*(*sila - neohexenyl*) - *bis* - (*diphenylmethylphosphine*)*platinum*(II). Product: colourless crystals from hexane. Yield: 54%. (IR: 3045s, 2980s, 2930vs, 2880vs, 1595m, 1580w, 1480m, 1430vs, 1415s, 1395s, 1305m, 1235vs, 1085vs, 1010s, 1000s, 950s, 935s, 895s, 880vs, 815vs, 765s, 745vs, 725vs, 690vs, 525s, 510vs, 485s, 435s, 420s, 360w.)

cis - *bis*(*sila - neohexenyl*) - *bis* - (*triphenylphosphine*) *platinum*(II). Product: colourless crystals from hexane. Yield: 55%. (IR: 3050m, 2960m, 2935m, 2875m, 1590w, 1575w, 1485m, 1435s, 1400m, 1260s, 1240s, 1185m, 1095vs, 1030s, 1015s, 960m, 940m, 815vs, 760–725s, 690vs, 540vs, 520vs, 515vs, 490s, 435m, 420m.)

cis - *bis*(*sila - neohexenyl*)[*bis*(*diphenylphosphino*) *methane*]*platinum*(II). Product: white crystals from hexane. Yield: 56%. (IR: 3052m, 2966s, 2895m, 2849s, 1590m, 1579w, 1489m, 1442vs, 1399m, 1367m, 1309w, 1269w, 1242vs, 1187m, 1105vs, 1089s, 1003s, 980m, 940vs, 831vs, 815vs,

772vs, 756–678vs, 549vs, 506vs, 486vs, 443s, 441s, 361m.)

cis - *bis*(*sila - neohexenyl*)[*bis*(1,2 - *diphenylphosphino*) *ethane*]*platinum*(II). Product: white crystals from hexane. Yield: 49%. (IR: 3052m, 2959s, 2903m, 2872s, 1590w, 1575w, 1489m, 1438vs, 1406s, 1312w, 1238s, 1105vs, 1074m, 1003s, 941vs, 831vs, 815vs, 760–670vs, 537vs, 490vs, 447s, 357m.)

cis - *bis*(*sila - neohexenyl*)[*bis*(1,3 - *diphenylphosphino*) *propane*]*platinum*(II). Product: white crystals from hexane. Yield: 60%. (IR: 3051m, 2939s, 2881m, 2864m, 1587w, 1572w, 1484m, 1449s, 1400m, 1235s, 1155m, 1099s, 1009m, 969m, 944s, 816(d)vs, 750s, 741s, 725s, 696vs, 654s, 512vs, 494s, 486s, 445w.)

cis-*bis*(*sila-neohexenyl*)[*bis*(1,4-*diphenylphosphino*) *butane*]*platinum*(II). Product: white crystals from hexane. Yield: 66%. (IR: 3052m, 2951s, 2888s, 1590m, 1575w, 1489m, 1442vs, 1403s, 1312m, 1242s, 1183m, 1101s, 1003s, 952s, 913s, 835vs, 819vs, 768vs, 745vs, 702vs, 529vs, 502vs, 443s, 361m.)

cis - *bis*(*sila - neohexenyl*)[*bis*(1,1 - *diphenylphosphino*) *ferrocene*]*platinum*(II). Product: yellow needles from hexane. Yield: 44%. (IR: 3052w, 2950m, 2904m, 1590w, 1579w, 1481m, 1438s, 1406m, 1312w, 1265m, 1242s, 1168s, 1101vs, 1034s, 1019s, 941m, 819vs, 768s, 749vs, 729s, 702vs, 647m, 553s, 522s, 498vs, 475s, 443s, 353w.)

(2) *Preparations of* $L\overline{Pt(CH_2SiMe_2CH:CH_2)}R$

cis-(*sila-neohexenyl*)(η^2-*cycloplatinasila-neohexenyl*) (*tricyclohexylphosphine*)*platinum*(II). Both (cod) $Pt(CH_2SiMe_2CH:CH_2)_2$ (0.20 g, 0.40 mmol) and Cy_3P (0.12 g, 0.40 mmol) were dissolved in benzene (4 cm^3) and left at ambient temperature for 17 days. Removal of the solvent *in vacuo* gave a white solid which was analytically pure (0.13 g, 47%). (IR: 3052m, 2943vs, 2857vs, 1590w, 1563w, 1508m, 1450s, 1403m, 1367w, 1344m, 1301m, 1265s, 1238s, 1203m, 1179s, 1104s, 1031s, 937s, 882s, 850s, 819vs, 768s, 745s, 686m, 674m, 608m, 525s, 498m, 455w, 396m, 369w.)

cis - (*sila - neohexenyl*)(η^2 - *cycloplatinasila - neohexenyl*)(*trimethylphosphine*)*platinum*(II). (cod)Pt $(CH_2SiMe_2CH:CH_2)_2$ (0.20 g, 0.40 mmol) was dissolved in toluene (3 cm^3) and PMe_3 (40.7×10^{-3} cm^3, 0.40 mmol) added by microsyringe. The solution was left in the dark at ambient temperature for 33 days. Removal of the solvent *in vacuo* gave a pale yellow oil which contained the product (25%, Table 2), but could not be purified further.

Similar observations applied to:

cis-(*sila-neohexenyl*)(η^2-*cycloplatinasila-neohexenyl*) (*triethylphosphine*)*platinum*(II). Yield: 41% (Table 2).

cis-(*sila-neohexenyl*)(η^2-*cycloplatinasila-neohexenyl*) (*diphenylmethylphosphine*)*platinum*(II). Yield: 54% (Table 2).

cis-(*sila-neohexenyl*)(η^2-*cycloplatinasila-neohexenyl*) (*triphenylphosphine*)*platinum*(II). Yield: 77% (Table 2).

cis - (*sila - neohexenyl*)(η^2 - *cycloplatinasila - neohexenyl*)(*tri - t - butylphosphine*)*platinum*(II). (cod) $Pt(CH_2SiMe_2CH:CH_2)_2$ (0.011 g, 0.022 mmol) was dissolved in d_8-toluene (0.5 cm^3) and PBu^t_3 (5×10^{-3} cm^3, 0.022 mmol) added by micro-

Table 2. ^{31}P NMR characteristics, mixture composition and cone angle for $L\overline{PtR(R)}$ complexes[a,b]

Compound	δ ^{31}P (ppm)[c]	$^1J_{P-Pt}$	Mixture composition (%) $(PR_3)\overline{PtR(R)}$: $(PR_3)_2PtR_2$: $(cod)PtR_2$			θ (°) for PR_3[d]
$(PMe_3)\overline{PtR(R)}$	−21.9	2014	25	51	24	118
$(PEt_3)\overline{PtR(R)}$	+7.2	2034	41	3	56	132
$(PPh_2Me)\overline{PtR(R)}$	+6.2	2034	54	26	20	136
$(PPh_3)\overline{PtR(R)}$	+23.8	2040	77	13	11	145
$(PCy_3)\overline{PtR(R)}$	+18.9	2020	100	0	0	170

[a] Recorded in benzene-d_6 with broad band ^1H-decoupling.
[b] Coupling constants J in Hz.
[c] With reference to external 85% H_3PO_4/D_2O.
[d] Cone angles (θ) from ref. 10.

syringe. After 6 days at room temperature the starting materials were unchanged.

cis-(*sila-neohexenyl*)(η^2-*cycloplatinasila-neohexenyl*)(*tri-o-tolylphosphine*)*platinum*(II). Both (cod)Pt($CH_2SiMe_2CH{:}CH_2$)$_2$ (0.20 g, 0.40 mmol) and P(4-C_6H_4Me)$_3$ (0.12 g, 0.40 mmol) were dissolved in benzene (2 cm^3) and left at ambient temperature for 30 days. Removal of the solvent *in vacuo* gave the unreacted starting materials.

RESULTS AND DISCUSSION

(a) *Synthesis*

(1) cis-L_2PtR_2. These complexes have been isolated using methods similar to those previously reported.[5] Treatment of (cod)$PtCl_2$ in ether with three equivalents of RMgCl produces the diolefin complex (cod)PtR_2. Displacement of the diene by stoichiometric amounts of tertiary phosphines produces *cis*-L_2PtR_2 (L = PMe_3, PEt_3, PPh_2Me, PPh_3; L_2 = dppm, dppe, dppp, dppb, dppf) in good yields. These substitutions are generally complete in 1–14 days at ambient temperature.

The compounds are mostly air-inert, white, crystalline solids except for those with cod, PMe_3 and PEt_3, which are colourless liquids. All have been characterized by elemental analysis (Table 1). Their NMR (^1H, ^{13}C and ^{31}P) and IR spectroscopic characteristics are discussed later.

(2) $L\overline{Pt(R)(CH_2SiMe_2CH{:}CH_2)}$. There is clear potential for the unsaturated function of the sila-neohexenyl ligand to coordinate to platinum.[10] This feature is likely to influence their reactivity relative to, say, their sila-neophenyl* analogues. We were interested to characterize isolable examples of η^2-ene derivatives.

The tricyclohexylphosphine complex of this type has been isolated as an air-stable, white solid by reaction of one equivalent of phosphine with (cod)PtR_2 at ambient temperature for 17 days. The identity and structure of this species has been established by elemental analysis, and by ^1H, ^{13}C and ^{31}P NMR studies.

Attempts to produce analogues with a range of monodentate phosphines have, in all other cases, produced inseparable mixtures of (cod)PtR_2, L_2PtR_2 and $L\overline{Pt(R)(R)}$ (L = PMe_3, PEt_3, PPh_2Me, PPh_3), even with reaction times of up to 33 days (Table 2). The thermal lability of (cod)PtR_2 (at 60°C) and of $L\overline{Pt(R)(R)}$ (L = PMe_3, PEt_3) (at 45°C) precluded heating the mixtures. ^{31}P NMR spectroscopy on freshly mixed reaction solutions showed that the added phosphine first forms L_2PtR_2 by displacement of diene. This is followed by an intramolecular displacement of one phosphine by alkene to form $L\overline{Pt(R)(R)}$.

A major influence on these equilibria is evidently the steric bulk of the phosphine (Table 2). For PCy_3 ($\theta = 170°$)[11] the bis-phosphine complex cannot be prepared. Reactions of (cod)PtR_2 with P(2-C_6H_4Me)$_3$ ($\theta = 194°$)[10] and $P(Bu^t)_3$ ($\theta = 182°$)[11] afforded no phosphine complexes. These ligands are apparently too bulky to allow even mono-coordination.

Although we have been unable as yet to isolate many of these compounds, their NMR characteristics (^1H, ^{13}C, ^{31}P) have been collected (*vide infra*). At temperatures up to thermal decomposition onset, there is no evidence for intramolecular fluxionality in which the coordinated and uncoordinated alkenes exchange roles.

(b) *Spectroscopic studies*

(1) *cis*-L_2PtR_2. (i) ^1H NMR (*Table* 3): a notable feature of these spectra is the multiplet observed for the hydrogens on the ligating carbon, an apparent quartet with platinum "satellites". The second-order resonance is most correctly attributed, in the PMe_3 complex, for example, to an $A_2A'_2RR'X_9X'_9$ spin system [A = ^1H (Pt–methylene), R = ^{31}P, X = ^1H (P–methyl)].[12] The satellite set correspondingly comprise an $A_2A'_2MRR'X_9X'_9$ system (M = ^{195}Pt, 34% abundant).

The general pattern is similar to that observed in related $L_2Pt(neophyl)_2$† complexes (L = PEt_3, dppe),[5] although the ^2J(H—Pt) values are 5–15 Hz larger for sila-neohexenyl derivatives.

The vinylic hydrogens produce the expected pattern of three doubled doublets; in each case $J_{trans} > J_{cis} > J_{gem}$ (Table 3).

The hydrogens on coordinated phosphine show typical, characteristic absorption patterns,[5] except for (dppf)PtR_2. Here, H_1 of the phenyl group generates a very broad singlet at ambient temperature, and H_y and H_z of the cyclopentadienyl rings display slightly broadened but otherwise unresolved signals (Fig. 1). As the temperature is reduced, however, each of these peaks broadens further, and subsequently resolves into multiplets (Fig. 1). From the line widths at half-height ($\Delta\nu = b_{1/2}$), the rates (k_c) and free energies of activation ($\Delta G_c^{\ddagger}$) for the process responsible for each of these coalescence points can be calculated (Table 4 and Fig. 1).[13]

Unless the diphosphine adopts the *syn*-eclipsed

* Sila-neophyl = phenyldimethylsilylmethyl.

† Neophyl = 2-methyl-2-phenylpropyl.

Table 3. ^{1}H NMR characteristics of L_2PtR_2 complexes[a,b]

Compound	δ ^{1}H (ppm)[c]: Hydrocarbyl ligand (J_{Pt-H}) [Assignment]			δ ^{1}H (ppm): Ancillary ligands (J_{Pt-H}) [Assignment]
	Pt—CH_2	Si(CH_3)$_2$	Alkene (J_{trans}, J_{cis}, J_{gem})	
(cod)PtR_2	0.86(93.0)	0.08	6.25dd [H_A] 5.82dd [H_B] 5.59dd [H_C] (20.1, 14.6, 4.1)	4.66(41.0) [CH] 2.18(19.0)[CH_2]
(PMe_3)$_2$PtR_2	0.68(72.6)	0.41	6.57dd [H_A] 5.95dd [HB] 5.82dd [H_C] (20.2, 14.6, 4.3)	1.06(20.5) ($2J_{P-H}$ = 7.9) [Me]
(PEt_3)$_2$PtR_2	0.61(78.7)	0.33	6.53dd [H_A] 5.88dd [H_B] 5.73dd [H_C] (20.2, 14.5, 4.2)	1.49m [CH_2] 0.81m [CH_3]
(PPh_2Me)$_2$PtR_2	1.02(77.7)	0.37	6.64dd [H_A] 6.01dd [H_B] 5.83dd [H_C] (20.2, 14.5, 4.2)	1.51(20.1) ($^2J_{P-H}$ = 7.1) [Me] 7.45m [H_1] 6.97m [H_2, H_3]
(PPh_3)$_2$PtR_2	1.09(d)	0.35	6.68dd [H_A] 6.03dd [H_B] 5.84dd [H_C] (20.3, 14.5, 4.2)	7.55m [H_1] 6.90 [H_2, H_3]
(dppm)PtR_2	1.37(84.6)	0.16	6.37dd [H_A] 5.77dd [H_B] 5.66dd [H_C] (20.1, 14.6, 4.4)	3.82(21.1) ($^2J_{P-H}$ = 18.5) [CH_2] 7.45m [H_1] 6.95m [H_2, H_3]
(dppe)PtR_2	1.14(81.1)	0.05	6.26dd [H_A] 5.82dd [H_B] 5.59dd [H_C] (20.1, 14.5, 4.4)	1.70m [CH_2] 7.44m [H_1] 7.01m [H_2, H_3]
(dppp)PtR_2	0.81(80.1)	0.12	6.42dd [H_A] 5.88dd [H_B] 5.66dd [H_C] (20.2, 14.5, 4.4)	1.40m [CH_{2A}] 1.96m [CH_{2B}] 7.45m [H_1] 7.00m [H_2, H_3]
(dppb)PtR_2	0.85(77.0)	0.12	6.36dd [H_A] 5.85dd [H_B] 5.62dd [H_C] (20.1, 14.4, 4.4)	1.45br ($^2J_{P-H}$ = 20.3) [CH_{2A}] 2.13br [CH_{2B}] 7.49m [H_1] 7.04m [H_2, H_3]
(dppf)PtR_2	1.10(80.9)	0.30	6.61dd [H_A] 6.01dd [H_B] 5.82dd [H_C] (20.2, 14.5, 4.3)	3.81 [H_z] 4.17 [H_y] 7.90br [H_1] 7.08m [H_2, H_3]

[a] Recorded in benzene-d_6 at 250 MHz.
[b] Coupling constants J in Hz where observed.
[c] Referenced to internal benzene-d_5 (δ 7.15 ppm).
[d] Satellites not resolved.

Table 4. Variable temperature ^{1}H NMR data for (dppf)PtR_2

Resonance	T_c (K)[a]	Δv (H_3)[b]	k_c (s^{-1})[c]	$\Delta G_c^{\ddagger}$ (kJ mol^{-1})[d]
H_1	270	102.0	226.6	53.73
H_y	262	53.1	118.0	53.49
H_z	249	16.5	36.6	53.16

[a] Error ± 1 K.
[b] ±2%.
[c] ±2%.
[d] ±0.5%.

conformation for chelation,[14] the complex lacks a plane of symmetry. Its conformers (Fig. 2) are enantiomeric, and magnetically non-equivalent hydrogens H_y and H_y' generate distinct resonances (as do H_z and H_z'). Slow exchange between these conformers accounts for the observed low temperature spectrum (Fig. 1) representing, ideally, an $A_2B_2C_2D_2$ system (assuming that coupling between hydrogens on different rings is negligible). At higher temperatures, rapid exchange gives rise to a time-averaged spectrum ($A_2A_2'B_2B_2'$) in which single resonances represent H_y and H_z. Similarly the two phenyl substituents on each phosphorus are magnetically non-equivalent [Fig. 2(b)]. This is most prominently reflected in the behaviour of the H_1 resonances at 8.1 and 7.6 ppm (Fig. 1) which collapse to a broadened triplet at higher temperatures.[15] Assuming, reasonably, that the values of $\Delta G_c^{\ddagger}$ (Table 4) derive from the same process, then we estimate that $\Delta H^{\ddagger} \sim 46.4$ (±0.5) kJ mol^{-1} and $\Delta S^{\ddagger} \sim -27.0$ (±0.8) J mol^{-1} K^{-1}.

The *syn*-eclipsed diphosphino–ferrocene conformation would also produce the same spectroscopic patterns.[14] We favour the enantiomeric *gauche*-staggered forms as the resting conformations for dialkylplatinum(II) derivatives on the basis of established structures for related complexes with comparable metal size and coordination geometry.[15]

(ii) ^{31}P NMR (*Table* 5): the characteristically low value of ^1J(Pt—P) for (dppm)PtR_2 stems from the angular constraints around P and Pt imposed by the four-membered ring. Similar observations have

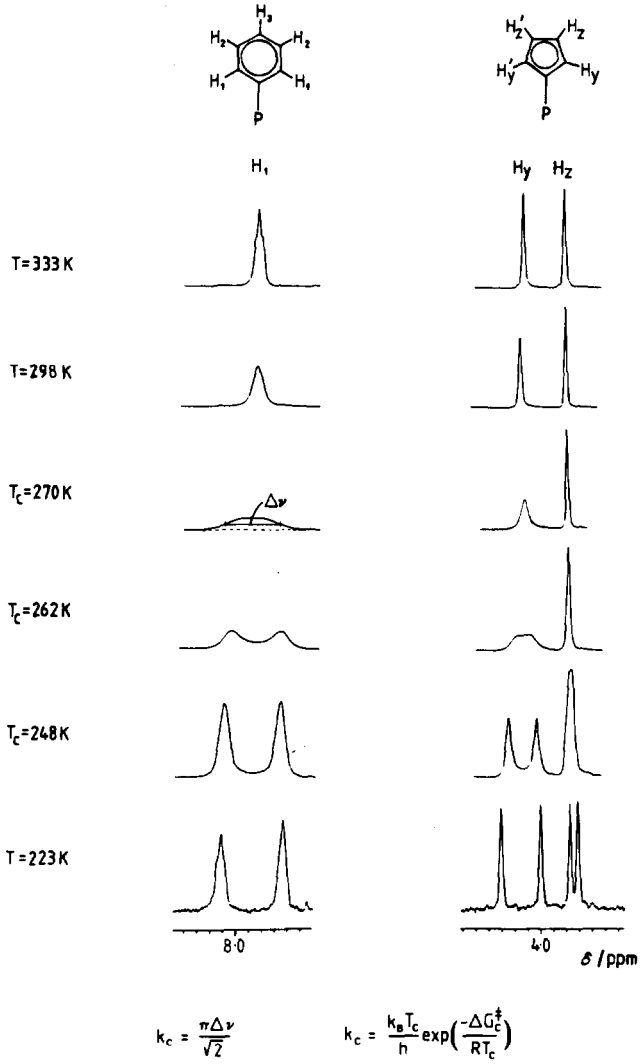

Fig. 1. Temperature dependent ^{1}H NMR spectra for (dppf)Pt($CH_2SiMe_2CH:CH_2$)$_2$.

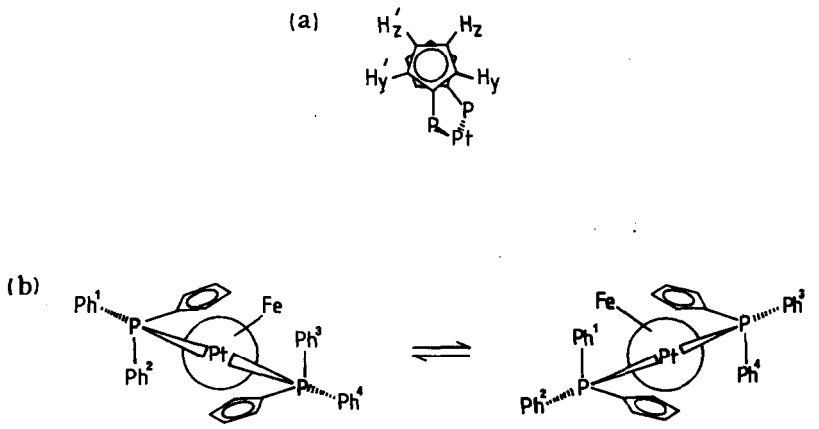

Fig. 2. Conformational projections for (dppf)Pt($CH_2SiMe_2CH:CH_2$)$_2$.

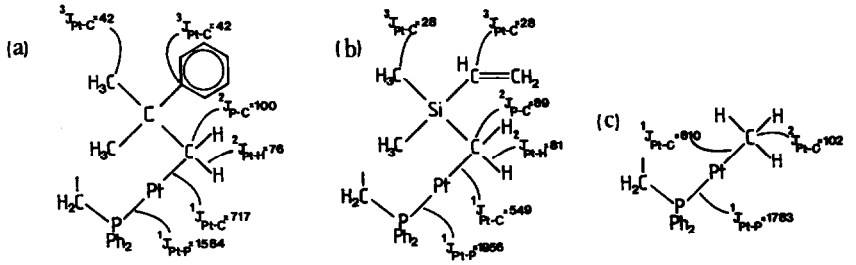

Fig. 3. Comparison of spin–spin couplings in various (dppe)PtR_2. (R = neophyl (ref. 5), methyl (ref. 20) sila-neohexenyl).

Table 5. ^{31}P NMR characteristics of L_2PtR_2 complexes[a,b]

Compound	δ ^{31}P (ppm)[c]	$^1J_{P-Pt}$
$(PMe_3)_2PtR_2$	−26.8	1976
$(PEt_3)_2PtR_2$	+4.8	2014
$(PPh_2Me)_2PtR_2$	+3.0	2020
$(PPh_3)_2PtR_2$	+25.5	2029
(dppm)PtR_2	−41.7	1600
(dppe)PtR_2	+43.6	1956
(dppp)PtR_2	+0.9	1936
(dppb)PtR_2	+14.4	1992
(dppf)PtR_2	+20.0	2051

[a] Recorded in benzene-d_6 with broad band ^1H-decoupling.
[b] Coupling constants J in Hz.
[c] With reference to external 85% H_3PO_4/D_2O.

appeared elsewhere. For example, for R = Me, J = 1434 Hz;[16] for R = Ph, J = 1392 Hz;[17] for R = 1-adamantylmethyl, J = 1236 Hz.[18]

Phosphorus nuclei incorporated in chelate rings display a ring contribution, Δ_R, to their coordination chemical shifts whose magnitude and direction depends on ring substitution and size, often useful in structural assignments. Table 6 shows the effect of ring size on coodination chemical shifts. These values agree well with those reported for L_2PtMe_2 (L_2 = dppm, dppe, dppp, dppb)[19] and confirm that these complexes have mononuclear structures rather than, for example, phosphine-bridged dimetallic configurations.

The value of ^1J(Pt—P) is *ca* 300 Hz greater in sila-neohexenyl complexes than in the neophyl analogues[5] (Fig. 3). This clearly represents some modification in Pt—P bonding and broadly indicates that sila-neohexenyl induces a notably weaker *trans*-influence than neophyl (and most other alkyl) groups as measured by this technique.[21] Discussion of the underlying reasons requires consideration of corresponding modifications in ^{13}C NMR parameters (*vide infra*).

(iii) ^{13}C NMR (*Table* 7): the doubled doublets which arise from the ligating carbons form a characteristic A_2XX' spin pattern.[5] A superimposed A_2MXX' system gives rise to ^{195}Pt satellites (A = ^{13}C, X = ^{31}P, M = ^{195}Pt, 34% abundant). Here, ^1J(Pt—C) is some 150 Hz smaller for sila-neohexenyl than for neophyl.[5] This is a general feature on comparisons of silylmethyl and alkylmethylplatinum analogues.[20,22] Indeed, for L_2 = dppe, the decrease in ^1J(Pt—C) (23.4%) almost exactly matches the increase (23.5%) in ^1J(Pt—P) (Fig. 3). It is widely accepted that these interactions are dominated by Fermi-contact con-

Table 6. Ring contributions for L_2PtR_2 complexes[a]

Compound	δP (ppm)[b]	δF (ppm)[b,c]	Δ (ppm)	Δ_R (ppm)	Chelate ring size
(dppm)PtR_2	−41.7	−22.7	−19.0	−50.1	4
(dppe)PtR_2	+43.5	−13.2	+56.7	+25.6	5
(dppp)PtR_2	+0.9	−17.3	+18.2	−12.9	6
(dppb)PtR_2	+14.4	−15.0	+29.4	−1.7	7
cis-$(Ph_2MeP)_2PtR_2$	+3.0	−28.1	+31.1	0.0	—

[a] Recorded in benzene-d_6 with broad band ^1H-decoupling.
[b] With reference to external 85% H_3PO_4/D_2O.
[c] Free phosphine chemical shifts obtained from ref. 19.

Table 7. ^{13}C NMR characteristics of L_2PtR_2 complexes[a,b]

Compound	δ ^{13}C (ppm):[c] Hydrocarbyl ligands ($^1J_{Pt—C}$) [$^2J_{P—C_{cis}}$, $^2J_{P—C_{trans}}$]				δ ^{13}C (ppm): Ancillary ligands ($J_{Pt—C}$) [Assignment]
	Pt—CH_2	Si(CH_3)$_2$	CH=CH_2	CH=CH_2	
(cod)PtR_2[d]	11.14(706.2)	1.39(31.1)	144.40(29.2)	128.38	97.51(64.2) [CH] 29.94 [CH_2]
$(PMe_3)_2PtR_2$	4.91(519.4) [8.3, 93.6]	2.53(30.3)	146.88(28.9)	127.53	17.12(29.8) ($^1J_{P—C}$ = 31.4) [Me]
$(PEt_3)_2PtR_2$	3.91(542.5) [7.9, 92.4]	3.02(29.8)	147.00(26.2)	127.41	17.42(25.3) ($^1J_{P—C}$ = 27.8) [CH_2] 8.43(18.1) [CH_3]
$(PPh_2Me)_2PtR_2$	6.42(549.7) [7.2, 91.6]	2.50(29.2)	146.59(27.6)	[e]	136.65(19.3) ($^1J_{P—C}$ = 44.6) [C1] 133.32(14.6) ($^2J_{P—C}$ = 10.9) [C2] [e] [C3] 129.52 [C4] 14.69(22.7) ($^1J_{P—C}$ = 31.7) [Me]
$(PPh_3)_2PtR_2$	7.66(569.3) [5.8, 91.4]	2.68(27.4)	146.73(26.0)	127.60	134.16(17.5) ($^1J_{P—C}$ = 44.0) [C1] 135.32(11.5) ($^1J_{P—C}$ = 12.0) [C2] [e] [C3] 129.58s [C4]
(dppm)PtR_2[d]	3.04(569.7) [6.4, 94.7]	1.47(29.5)	146.08(31.7)	126.87	132.58(19.0) ($^1J_{P—C}$ = 29.6) [C1] 133.04 [C2] 128.47s [C3] 130.26s [C4] 48.90(10.9) ($^1J_{P—C}$ = 51.0) [CH_2]
(dppe)PtR_2[d]	1.26(548.5) [5.0, 88.9]	2.14(27.7)	146.53(28.1)	126.93	133.36(24.7) ($^1J_{P—C}$ = 40.6) [C1] 133.81 [C2] [e] [C3] 130.31s [C4] 27.78m [CH_2]
(dppp)PtR_2[d]	5.14(548.3) [9.5, 91.7]	2.58(28.8)	146.85(27.9)	[e]	134.63(22.4) [C1][f] 134.05m [C2] 128.19m [C3] 129.88m [C4] 27.28m [CH_{2A}] 20.43 [CH_{2B}]
(dppb)PtR_2[d]	5.73(547.2) [7.2, 90.7]	1.70(28.7)	146.35(28.8)	126.69	135.28(22.6) ($^1J_{P—C}$ = 44.8) [C1] 133.79m [C2] 127.95m [C3] 129.45 [C4] 27.86m [CH_{2A}] 24.27br [CH_{2B}]
(dppf)PtR_2[d]	6.95(565.2) [7.3, 94.2]	2.54(28.5)	146.55(27.2)	[e]	79.39 ($^1J_{P—C}$ = 48.8) [CX] 75.33s [CY] 72.16s [CZ] 135.02(25.7) [C1] 135.67s [C2] [e] [C3] 130.07 [C4]

[a] Recorded in benzene-d_6, unless otherwise noted.
[b] Coupling constants J in Hz.
[c] Referenced to internal benzene-d_6 (δ 128.00 ppm) or chloroform-d (δ 77.00 ppm).
[d] Recorded in chloroform-d.
[e] Resonance obscured.
[f] Half of the resonance obscured.

tributions.[23–25] Consequently, any differences derive from changes in the *s*-orbital components of the respective bonds.

Compared with sila-neohexenyl, neophyl shows an enhanced ability to concentrate Pt(6*s*) character in the Pt—C bond, presumably in response to more effective overlap with the C(2*s*) component of its own donor orbital. There is also a marked increase in *trans*-^2J(P—C) in the neophyl case, further evidence of an increase in overall *s*-orbital bond order in the P—Pt—C framework.

These phenomena can most plausibly be explained in terms of a greater carbon 2*s* contribution to Pt—C bonding for the neophyl ligand. According to the propositions of isovalent hybridization, carbon will tend to direct 2*s*-character away from its most electronegative substituents.[26] Comparing neophyl and sila-neohexenyl ligands, carbon is more electronegative than silicon, while platinum remains the most electropositive of the groups bound to the methylenic carbon. The Pt—C bond is thus likely to benefit most from enhanced

carbon 2*s*-availability in the neophyl case. Significantly, for (dppe)Pt$(CH_3)_2$, both ^1J(Pt—C) at 610 Hz and ^1J(Pt—P) at 1783 Hz[27] have values intermediate between neophyl and sila-neohexenyl, consistent with the electronegativity of H, intermediate between C and Si (Fig. 3).

(iv) *IR spectroscopy*: IR data for this series of compounds are listed in the Experimental. A weak band at *ca* 1590 cm^{-1} in all these complexes is characteristic of an alkene C=C vibration.[28] When a phenyl group is present, a second, stronger band appears at *ca* 1600 cm^{-1} due to aryl C···C vibrations. The very strong doublet centred at *ca* 850 cm^{-1} is assigned to Si—C stretching. In the phenyl-substituted complexes, the two strong peaks at *ca* 750 and 700 cm^{-1} are out-of-plane C—H bending modes typical of five adjacent phenyl hydrogens.

(2) L$\overline{Pt(CH_2SiMe_2CH:CH_2)}$R. (i) ^{1}H *NMR* (*Table* 8): the most indicative features of this coordination mode are the patterns originating from the Pt-bound alkene function, comprising one doubled doublet and two eight-line patterns (all of which

Table 8. ^{1}H NMR characteristics of L$\overline{PtR(R)}$ complexes[a,b,c]

Compound	δ ^{1}H (ppm):[d] Platinacycle (J_{Pt-H}) [Assignment]		δ ^{1}H (ppm): Hydrocarbyl ligand [Assignment]		δ ^{1}H (ppm) Ancillary ligands (J_{Pt-H}) [Assignments]
	$Si(CH_3)_2$	Alkene (J_{trans}, J_{cis}, J_{gem})	$Si(CH_3)_2$	Alkene (J_{trans}, J_{cis}, J_{gem})	
$(PMe_3)\overline{PtR(R)}$	0.21	3.79(27.1) (J_{P-H} = 3.3) [H'_A] 3.71(22.8) (J_{P-H} = 4.0) [H'_B] 3.99(45.4) [H'_C] (15.9, 10.7, 3.9)	0.43	6.51dd [H_A] 5.95dd [H_B] 5.80dd [H_C] (20.2, 14.6, 4.3)	0.79(20.6) ($^2J_{P-H}$ = 8.3) [Me]
$(PEt_3)\overline{PtR(R)}$	0.21	3.77(26.4) (J_{P-H} = 2.9) [H'_A] 3.87(24.1) (J_{P-H} = 3.4) [H'_B] 3.98(46.5) [H'_C] (16.0, 11.0, 3.3)	0.43	6.52dd [H_A] 5.94dd [H_B] 5.79dd [H_C] (20.5, 14.7, 4.1)	1.27m [CH_2] 0.73m [CH_3]
$(PPh_2Me)\overline{PtR(R)}$	0.15	3.57(27.0) (J_{P-H} = 3.0) [H'_A] 3.47(23.3) (J_{P-H} = 4.1) [H'_B] 4.01(45.7) [H'_C] (16.9, 11.3, 2.6)	0.49	6.51dd [H_A] 5.97dd [H_B] 5.77dd [H_C] (20.1, 14.5, 4.3)	1.63(21.8) [Me] ($^2J_{P-H}$ = 7.8) 7.33m [H_1] 7.05m [H_5, H_3]
$(PPh_3)\overline{PtR(R)}$	0.17	3.71(23.8) (J_{P-H} = 2.6) [H'_A] 3.51(26.8) (J_{P-H} = 4.0) [H'_B] 4.14(46.9) [H'_C] (16.9, 11.3, 2.7)	0.54	6.47dd [H_A] 5.91dd [H_B] 5.70dd [H_C] (20.2, 14.6, 4.2)	7.55m [H_1] 7.06m [H_2, H_3]
$(PCy_3)\overline{PtR(R)}$	0.21	3.86(23.0) (J_{P-H} = 2.7) [H'_A] 4.01(26.0) (J_{P-H} = 2.5) [H'_B] 4.19(50.7) [H'_C] (16.5, 11.1, 2.5)	0.43	6.60dd [H_A] 5.95dd [H_B] 5.78dd [H_C] (20.2, 14.5, 4.2)	1.2–1.9m [Cy]

[a] Recorded in benzene-d_6 at 250 MHz.
[b] Coupling constants *J* in Hz.
[c] Platinum-bound methylene protons obscured.
[d] Referenced to internal benzene-d_5 (δ 7.15 ppm).

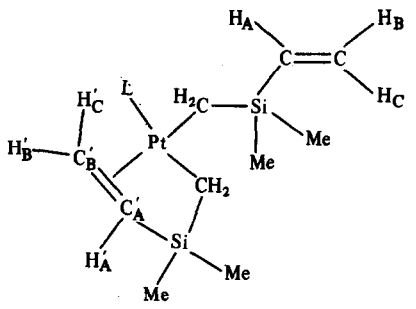

Fig. 4. ^1H and ^{13}C NMR assignments for $[(C_6H_{11})_3P]\overline{Pt(CH_2SiMe_2CH:CH_2)}(CH_2SiMe_2CH:CH_2)$.

display ^{195}Pt-satellites). By selective ^1H-decoupling, the eight-line multiplets have been assigned to H'_A and H'_B (Fig. 4) which display spin–spin coupling with ^{31}P. The four-line spectrum derives from H'_C. A shift-correlated 2D plot (Fig. 5) confirms these assignments for $L = PCy_3$. Figure 6 shows a simulation of the spectrum expected for an ABCX spin system (A,B,C = ^1H; X = ^{31}P) based on our assigned values for coupling constants in this same complex. There is close agreement between prediction and observation.

In each case the hydrogens of the η^2-alkene show

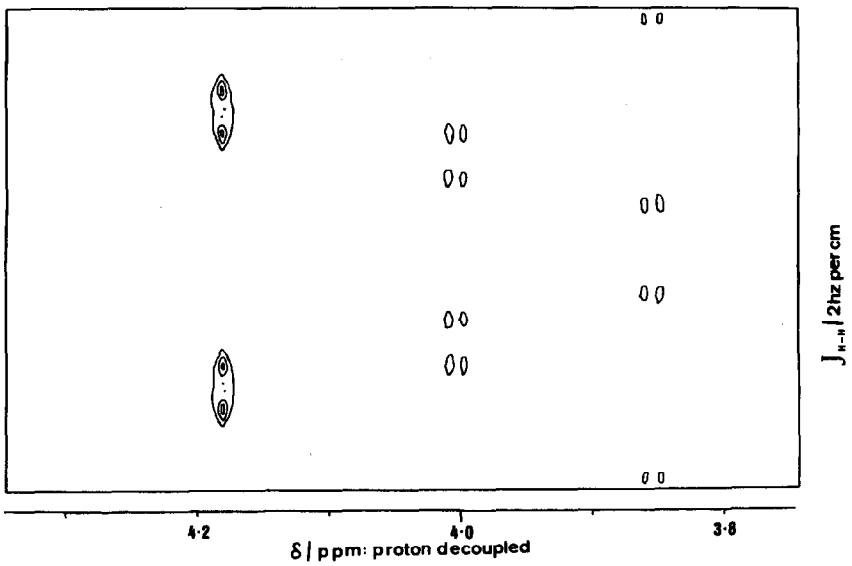

Fig. 5. Shift-correlated 2D ^1H NMR spectrum for $[(C_6H_{11})_3P]\overline{Pt(CH_2SiMe_2CH:CH_2)}$ $(CH_2SiMe_2CH:CH_2)$.

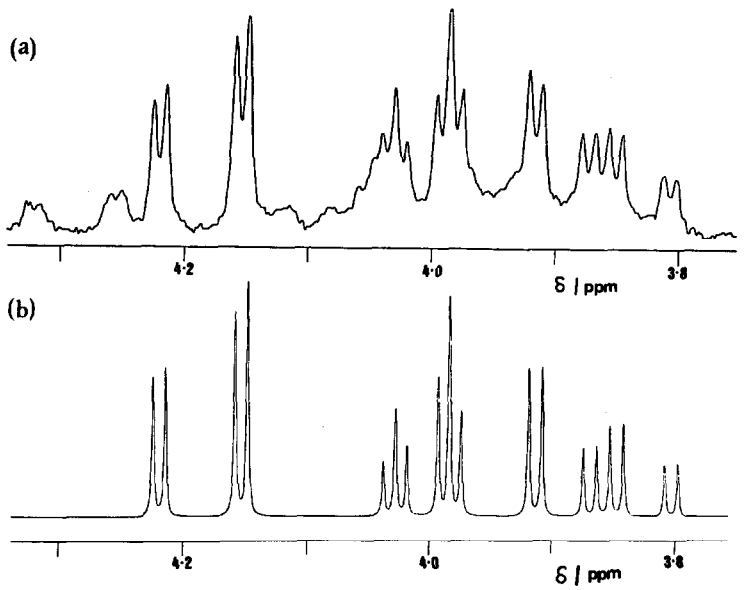

Fig. 6. (a) Observed and (b) simulated [in absence of J(Pt—H)] ^1H NMR spectra for $[(C_6H_{11})_3Pt]\overline{Pt(CH_2SiMe_2CH:CH_2)}(CH_2SiMe_2CH:CH_2)$.

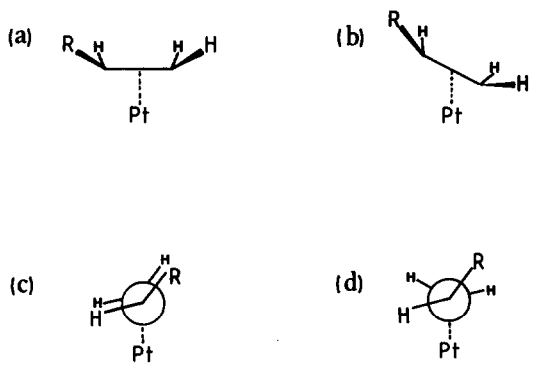

Fig. 7. Deviations from ideal η^2-alkene–Pt coordination.

the usual significant upfield coordination shift ascribed to partial rehybridization at carbon towards sp^3.[29,30] This also explains the general decrease in J(H—H) within the η^2-alkene, most marked for the geminal coupling $J(H_B—H_C)$.

There are three possible deviations from ideal, symmetrical alkene coordination (Fig. 7). The size of J(Pt—H) proposedly reflects the distance between the two nuclei.[29,31] Here, the notably larger value of $J(Pt—H'_C)$ suggests that H'_C (and Si) approach Pt more closely [cf. Fig. 7(b)], hardly surprising in view of the connection between Si and Pt via the ligating aliphatic carbon.

Irrespective of local modifications, a face-bound η^2-alkene will generate a metallacyclic ring which deprives the molecule of any axis or plane of symmetry. This might be expected to give rise to non-equivalence between several magnetic environments including the two ^{1}H nuclei of each metal-bound methylene group and between the two methyl groups on either silicon atom. In the tricyclohexylphosphine derivative the methylene signals are obscured but there is no indication of non-equivalence within distinct silicon methyl groups, each of which generates a slightly broadened single resonance (Table 8). No unequivocal conclusions can yet be drawn from other phosphine complexes, whose spectra are complicated in the regions of interest due to the presence of *cis*-$(R_3P)_2PtR_2$.

(ii) ^{31}P *NMR* (*Table* 2): all these complexes display values for ^1J(Pt—P) in the range 2014–2040 Hz, characteristic of phosphorus *trans* to alkyl ligands and in accord with the *cis*-oid structure (Fig. 4) proposed.[5] These values are consistently *ca* 20 Hz greater than for the corresponding L_2PtR_2. Steric constraints imposed by chelation may decrease the σ-donor efficiency of the ligating aliphatic carbon, resulting in a slight reduction in effective *trans*-influence.[21] The effect, however, is not spectacular.

The ^{31}P chemical shifts are generally to lower field than for L_2PtR_2, with the exception of $L = PPh_3$, which displays an upfield shift of 1.7 ppm.

(iii) ^{13}C *NMR* (*Table* 9): there are two doublet resonances with flanking satellites ascribable to ligating aliphatic carbons, at *ca* −1 and 9 ppm. The first has ^1J(Pt—C) = *ca* 410 Hz and ^2J(P—C) = *ca* 82 Hz, while the other has ^1J(Pt—C) = *ca* 720 Hz and ^2J(P—C) = *ca* 3 Hz. By comparison with corresponding data for *cis*-L_2PtR_2, the former is clearly *trans* to PR_3 and the latter is assigned *trans* to the η^2-alkene function.

The carbons of the coordinated alkene resonate 40–60 ppm to higher field than those in the free ligand. A conventional modulated spin–echo experiment has established that the lower field "triplet" [J(Pt—C) = *ca* 70 Hz] arises from the terminal carbon C'_B.

The characteristic upfield coordination shifts proposedly reflect the extent of depopulation of olefin π- with concomitant population of alkene π^*-orbitals.[32] Unequal shifts have been associated with asymmetric alkene coordination in which one carbon is nearer to platinum [Fig. 7(b)].[33] This might suggest that C'_A makes the closer approach (its coordination shift is −66.2 ppm compared with −41.8 ppm for C'_B). The apparent zero coupling between C'_A and Pt can only be attributed to self-cancellation of opposed-sign multipath coupling, also evident for the silicon-bound methyl carbons[34] (Fig. 8).

Proximity to ^{195}Pt has also been linked with larger values for ^1J(Pt—C).[33,35] Here, C'_B unequivocally displays the larger coupling constant. It seems more likely that the alkene will be tilted in this sense due to connection to the metal via the sila-alkyl chain and as suggested by the ^{1}H NMR data (*vide supra*).

Again, the inherent asymmetry of the complex might be expected to impose magnetic non-equivalence on the two methyl carbons attached to each silicon atom. No such distinction emerges.

We have been unable so far to obtain suitable crystals of any of the complexes to allow resolution of these stereochemical questions by X-ray diffractometry. Attempts to produce crystalline samples

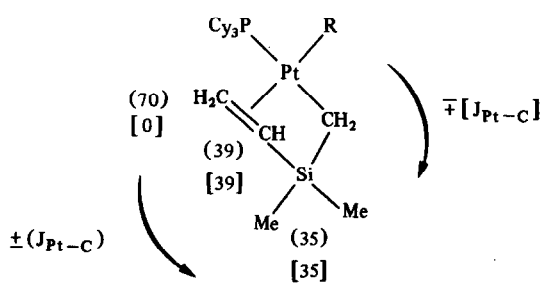

Fig. 8. Multipath Pt—C spin–spin coupling.

Table 9. ^{13}C NMR characteristics of $L\overline{PtR(R)}$[a,b]

Compound	δ ^{13}C (ppm):[c] Platinacycle ($^1J_{Pt-C}$) [$^2J_{P-C_{trans}}$] Pt—CH_2	CH_3	Alkene CH	Alkene CH_2	δ ^{13}C (ppm): Hydrocarbyl ($^1J_{Pt-C}$) [$^2J_{P-C_{cis}}$] Pt—CH_2	CH_3	Alkene CH	Alkene CH_2	δ ^{13}C (ppm): Ancillary ligands (J_{Pt-C}) [Assignment]
$(PMe_3)\overline{PtR(R)}$	−2.07 (421.3) [87.5]	1.25	81.57	82.42 (70.5)	9.26 (727.1) [3.0]	1.92 (34.5)	145.61 (38.8)	[d]	13.17(28.3) ($^1J_{P-C}$ = 27.3) [Me]
$(PEt_3)\overline{PtR(R)}$	[d]	1.38	82.07	82.75 (70.5)	[d]	2.23 (34.3)	145.79 (37.0)	128.11	13.49(24.0) ($^1J_{P-C}$ = 25.3) [CH_2] 7.79(16.4) [Me]
$(PPh_2Me)\overline{PtR(R)}$	−1.00 (413.2) [83.6]	1.37	83.65	85.96 (70.4)	9.61 (718.7) [3.0]	2.03 (34.4)	145.55 (37.2)	[d]	134.48 ($^1J_{P-C}$ = 39.8) [C1][e] 132.90 [C2] d [C3] 130.03 [C4] 11.54(35.4) ($^1J_{P-C}$ = 27.6) [Me]
$(PPh_3)\overline{PtR(R)}$	−1.86 (423.5) [81.5]	1.35	85.09	87.50 (68.8)	10.08 (721.2) [3.6]	2.29 (35.0)	145.68 (35.7)	[d]	132.18(20.4) ($^1J_{P-C}$ = 40.9) [C1] 134.65(14.2) ($^2J_{P-C}$ = 11.0) [C2] d [C3] 130.16 [C4]
$(PCy_3)\overline{PtR(R)}$	0.54 (408.7) [79.9]	1.32	83.32	85.98 (74.5)	5.46 (718.9) [3.4]	3.31 (37.6)	146.47 (39.0)	127.82	32.58(19.1) ($^1J_{P-C}$ = 18.8) [C1'] 30.05(13.3) [C2'] 28.05 ($^3J_{P-C}$ = 10.0) [C3'] 26.91 [C4']

[a] Recorded in benzene-d_6.
[b] Coupling constants J in Hz.
[c] Referenced to internal benzene-d_6 (δ 128.0 ppm).
[d] Resonance obscured.
[e] Half of the resonance obscured.

with other bulky ligands—viz. PBu^t_3 and P(2-tolyl)$_3$—have been fruitless; these phosphines did not react with $(cod)PtR_2$.

(iv) *IR spectroscopy*: the IR data for the tricyclohexylphosphine complex are listed in the Experimental. The weak band at *ca* 1590 cm^{-1} is characteristic of an alkene C=C vibration and corresponds with the L_2PtR_2 complexes. A stronger band at *ca* 1508 cm^{-1} is due to the platinum-coordinated C=C vibration; the band-lowering of *ca* 80 cm^{-1} is consistent with those reported in the literature.[28] The very strong bands at *ca* 850 and 819 cm^{-1} are Si—C stretching vibrations, as seen in the L_2PtR_2 complexes.

Acknowledgements—We thank Sue Johnson and Dick Sheppard of this Department, and Dr Geoff Hawkes and his staff at Queen Mary College, London, for NMR measurements (ULIRS); and also Dr Henry Rzepa here for most helpful discussions. We are indebted to the SERC for the award of a studentship (to R.D.K.) and are additionally grateful to Johnson Matthey plc, for their generous loan of platinum salts.

REFERENCES

1. See, for example: (a) R. R. Schrock, *Acc. Chem. Res.* 1979, **12**, 98; (b) R. R. Schrock and G. W. Parshall, *Chem. Rev.* 1976, **76**, 243; (c) P. J. Davison, M. F. Lappert and R. Pearce, *Chem. Rev.* 1976, **76**, 219; (d) G. W. Parshall and J. J. Mrwoca, *Adv. Organomet. Chem.* 1968, **7**, 157; (e) P. S. Brateman and R. J. Cross, *Chem. Soc. Rev.* 1973, **2**, 271; (f) G. M. Whitesides, J. F. Gaasch and E. R. Stedronsky, *J. Am. Chem. Soc.* 1972, **94**, 5258; (g) R. G. Nuzzo, T. J. McCarthy and G. M. Whitesides, *J. Am. Chem. Soc.* 1981, **103**, 3396; (h) S. Komiya, Y. Morimoto,

A. Yamamoto and T. Yamamoto, *Organometallics* 1982, **1**, 1528.
2. See, for example: (a) P. Foley, R. DiCosimo and G. M. Whitesides, *J. Am. Chem. Soc.* 1980, **102**, 6713; (b) R. A. Anderson, R. A. Jones and G. Wilkinson, *J. Chem. Soc., Dalton Trans.* 1978, 446; (c) P. Diversi, G. Ingrosso, A. Lucherini and D. Fasse, *J. Chem. Soc., Chem. Commun.* 1982, 945; (d) J. W. Bruno, T. J. Marks and V. W. Day, *J. Am. Chem. Soc.* 1982, **104**, 7357; (e) J. A. Duff, B. L. Shaw and B. L. Turtle, *J. Organomet. Chem.* 1974, **66**, C18; (f) S. D. Chappell, D. J. Cole-Hamilton, A. M. R. Galas and M. B. Hursthouse, *J. Chem. Soc., Dalton Trans.* 1982, 1867.
3. For reviews see: I. P. Rothwell, *Polyhedron* 1985, **4**, 2; S. D. Chappell and D. J. Cole-Hamilton, *Polyhedron* 1982, **1**, 739 and ref. 16.
4. See, for example: (a) C. S. Cundy, B. M. Kingston and M. F. Lappert, *Adv. Organomet. Chem.* 1973, **11**, 253 and refs therein; (b) J. A. Ibers, R. Di Cosimo and G. M. Whitesides, *Organometallics* 1982, **1**, 13; (c) R. Di Cosimo, S. S. Moore, A. F. Sowinski and G. M. Whitesides, *J. Am. Chem. Soc.* 1982, **104**, 124; (d) A. H. Janowicz and R. G. Bergman, *J. Am. Chem. Soc.* 1983, **105**, 3929; (e) W. D. Jones and F. J. Feher, *J. Am. Chem. Soc.* 1985, **107**, 620; (f) J. K. Hoyano, A. D. McMaster and W. A. G. Graham, *J. Am. Chem. Soc.* 1983, **105**, 7190; (g) R. H. Crabtree, *Chem. Rev.* 1985, **85**, 245; (h) P. L. Watson and G. W. Parshall, *Acc. Chem. Res.* 1985, **18**, 51 and refs therein; (i) C. M. Fendrick and T. J. Marks, *J. Am. Chem. Soc.* 1986, **108**, 425; (j) A. E. Shilov, *Activation of Saturated Hydrocarbons by Transition Metal Complexes*, Chap. 5. Reidel, Dordrecht (1984).
5. (a) D. C. Griffiths and G. B. Young, *Polyhedron* 1983, **2**, 1095; (b) D. C. Griffiths and G. B. Young, *Organometallics*, in press.
6. D. C. Griffiths, L. G. Joy, A. C. Skapski, D. J. Wilkes and G. B. Young, *Organometallics* 1986, **5**, 1744.
7. A. L. Van Geet, *Anal. Chem.* 1970, **42**, 679.
8. (a) D. F. Shriver, *The Manipulation of Air-Sensitive Compounds*. McGraw-Hill, New York (1969); (b) H. C. Brown, G. W. Kramer, A. B. Levy and M. M. Midland, *Organic Synthesis via Boranes*. Wiley, New York (1975).
9. J. X. McDermott, J. F. White and G. M. Whitesides, *J. Am. Chem. Soc.* 1976, **98**, 6521.
10. (a) M. A. Bennett, R. Bramley and I. B. Tomkins, *J. Chem. Soc., Dalton Trans.* 1973, 166; (b) M. A. Bennett, H. K. Chee, J. C. Jeffery and G. B. Robertson, *Inorg. Chem.* 1979, **18**, 1071; (c) R. Benn and A. Rufriska, *J. Organomet. Chem.* 1982, **238**, C27; (d) T. C. Flood and S. P. Bitler, *J. Am. Chem. Soc.* 1984, **106**, 6076; T. C. Flood and J. A. Statler, *Organometallics* 1984, **3**, 1795.
11. C. A. Tolman, *Chem. Rev.* 1977, **72**, 313.
12. cf. R. J. Goodfellow, M. J. Hardy and B. F. Taylor, *J. Chem. Soc., Dalton Trans.* 1973, 2450 and refs cited therein.
13. (a) H. Kessler, *Angew. Chem. Int. Ed.* 1970, **9**, 219; (b) M. Raban, *J. Chem. Soc., Chem. Commun.* 1971, 656.
14. (a) E. W. Abel, M. Booth and K. G. Orrell, *J. Organomet. Chem.* 1980, **186**, C37; (b) J. J. Bishop and A. Davison, *Inorg. Chem.* 1971, **10**, 826.
15. (a) I. R. Butler, W. R. Cullen, T-J. Kim, S. J. Rettig and J. Trotter, *Organometallics* 1985, **4**, 972; (b) W. R. Cullen, T.-J. Kim, F. W. B. Einstein and T. Jones, *Organometallics* 1983, **2**, 714.
16. T. G. Appleton, M. A. Bennett and I. B. Tomkins, *J. Chem. Soc., Dalton Trans.* 1976, 439.
17. P. S. Braterman, R. J. Cross, L. Manojlović-Muir, K. W. Muir and G. B. Young, *J. Organomet. Chem.* 1975, **84**, C40.
18. M. Bochmann, G. Wilkinson and G. B. Young, *J. Chem. Soc., Dalton Trans.* 1980, 1879.
19. P. E. Garrou, *Chem. Rev.* 1981, **81**, 229.
20. B. C. Ankianiec and G. B. Young, *Polyhedron* 1989, **8**, 57.
21. T. G. Appleton, H. C. Clark and L. E. Manzer, *Coord. Chem. Rev.* 1973, **10**, 335.
22. S. K. Thomson and G. B. Young, *Polyhedron* 1988, **7**, 1953.
23. P. S. Pregosin, *An. Rep. NMR Spectrosc.* 1986, **17**, 285 and refs therein.
24. A. Pidcock, *Adv. Chem. Soc.* 1982, **196**, 1.
25. J. A. Pople and D. P. Santry, *Mol. Phys.* 1964, **8**, 1.
26. H. A. Bent, *Chem. Rev.* 1961, **61**, 275.
27. S. Hietkamp, D. J. Strufkens and K. Vrieze, *J. Organomet. Chem.* 1979, **169**, 107.
28. (a) J. Knizek, M. Horák and V. Chvalovsky, *Coll. Czech. Chem. Commun.* 1963, **28**, 3079; (b) K. Nakamoto, *IR and Raman Spectra of Inorganic and Coordination Compounds*, Part IV. Wiley, New York (1986).
29. (a) R. Lazzaroni and C. A. Veracini, *J. Organomet. Chem.* 1971, **33**, 131; (b) M. L. Maddox, S. L. Stafford and H. D. Kaesz, *Adv. Organomet. Chem.* 1965, **3**, 1; (c) C. E. Holloway, G. Hulley, B. F. G. Johnson and J. Lewis, *J. Chem. Soc. A* 1970, 1653; (d) P. D. Kaplan and M. Orchin, *Inorg. Chem.* 1967, **6**, 1096; (e) H. P. Fritz and D. Sellmann, *Z. Naturforsch.* 1967, **22b**, 610.
30. P. S. Braterman, *Inorg. Chem.* 1966, **5**, 1085.
31. (a) H. P. Fritz, K. E. Schwarzhans and D. Sellmann, *J. Organomet. Chem.* 1966, **6**, 551; (b) B. F. G. Johnson, C. E. Holloway, G. Hulley and J. Lewis, *J. Chem. Soc., Chem. Commun.* 1967, 1143.
32. See, for example, L. E. Manzer, *Inorg. Chem.* 1976, **15**, 2354 and refs cited therein.
33. D. G. Cooper and J. Powell, *Inorg. Chem.* 1976, **15**, 1959; R. Lazzaroni and B. E. Mann, *J. Organomet. Chem.* 1979, **164**, 79.
34. J. A. Davies, *Chemistry of the* M—C *Bond*, p. 824. John Wiley, New York (1982).
35. A. C. Jesse, D. J. Stufkens and K. Vrieze, *Inorg. Chim. Acta* 1979, **32**, 87.

Polyhedron Vol. 8, No. 4, pp. 447–452, 1989
Printed in Great Britain

0277–5387/89 $3.00 + .00
© 1989 Pergamon Press plc

ELECTRONIC STATES OF HOT IONS AND THE REACTIVITY OF $[MoOCl_3(PPh_3)_2]$ TOWARDS e_s^- IN TRI-*n*-BUTYLPHOSPHATE

J. O. DZIĘGIELEWSKI* and K. FILIPEK

Department of Inorganic and Radiation Chemistry, Institute of Chemistry, Silesian University, 9 Szkolna Street, 40006 Katowice, Poland

(*Received* 1 *July* 1988; *accepted* 27 *July* 1988)

Abstract—The reactivity of Mo^V ions towards e_s^- was studied by spectroscopic analysis. The crystal field parameters $Dq = 2200\ cm^{-1}$, $Ds = -4310\ cm^{-1}$ and $Dt = 152\ cm^{-1}$ were determined and the energy terms were calculated. The electronic structure of the hot ion was determined as $(d_{xy})^1\ (d_{x^2-y^2})^1$. The decay of the hot ion leads to the excited state $(d_{xy})^1\ (d_{xz}, d_{yz})^1$ and then to the diamagnetic complex with the $(d_{xy})^2$ configuration. The rate constant of the reaction of e_s^- with $[MoOCl_3(PPh_3)_2]$ was calculated as $1.3 \times 10^{10}\ dm^3\ mol^{-1}\ s^{-1}$. The influence of the structural parameters on the radiation–chemical processes was examined.

The radiation chemistry of transition metal complexes has been extensively explored for many years.[1–6] Attention is focused, however, on the oxidation[3–15] or the reduction[1–6,16–25] of the central ions. The rate constants of redox reactions are the only results of such experiments. The central ions of complex compounds can be either reduced e.g. by e_s^-, H atoms, radicals, or oxidized e.g. by OH radicals, Cl_2^- and O^- ions. These processes lead to electronic configurations of the ions which are not stabilized by the ligand field.[26–27] The electronic states, obtained in this way, are called "hot" ones. The properties of the hot ions depend on electronic and molecular features of the irradiated complexes.[19–22] It is still difficult to make *a priori* comparison between a structural characteristic of a complex compound and its reactivity towards e_s^-, and a mechanism of its reduction. Electronic states of the hot ions and mechanisms of its decay are influenced by the structural parameters of the complex. By testing the reactivity of the complexes and the mechanisms of their radiolysis it is possible to determine energy levels of the substances acting as acceptors of electrons. In radiation chemistry this problem has been neglected so far, but it is very important in the calculation of the potential barrier between an electron trap and the e_t^- scavenger. On the other hand, it is possible to generate some new electronic states by irradiation. In this case the exact determination of the ligand field parameters and a calculation of the energy terms is comparatively easy. The sequence of the electronic configuration determined by spectroscopic methods can be supported by the analysis of the radiation yields of decomposition, i.e. the bond cleavage.[21] Other examples of the usefulness of these considerations are some possibilities of synthesis of the high purity compounds[18] as well as the formation of new complex compounds which are not stabilized by the ligand field.[19] Furthermore, it is also possible, using the radiation methods, to evaluate catalytic abilities of some complexes in the radiation processes as e.g. reduction of molecular nitrogen.[28] In this paper we try to explain the influence of some structural features on the electronic states and some properties of the hot ions. A Mo^V complex with triphenylphosphine was used as an acceptor for electrons in tri-*n*-butylphosphate (TBP) solution.

EXPERIMENTAL

$[MoOCl_3(PPh_3)_2]$ was prepared according to the literature.[29] TBP (puriss p.a., Fluka) was extracted with 10% KOH, then washed with distilled water and distilled *in vacuo*.

$[MoOCl_3(PPh_3)_2]$ solutions in TBP were saturated with Argon or N_2O for 15 min, frozen in a cryostat at 77 K then irradiated in a cobalt source

*Author to whom correspondence should be addressed.

Issledovatel (USSR) using a dose rate of 0.6×10^{16} eV cm^{-3} s^{-1} (determined with a Fricke's dosimeter and converted into the electron density of TBP).

In frozen solutions the appearance and decay of the absorption bands as a function of temperature were recorded. In irradiations (at room temperature) of solutions of the Mo^V complex in TBP the changes of the bands intensities at 230, 260, 315, 450 and 730 nm were measured.

These spectral measurements were made using a Beckman 5240 spectrophotometer. The changes in the paramagnetic susceptibility due to irradiation of the Mo^V complex in solution were determined by the ^1H NMR method described by Evans[30,31] using a Varian FT-80 A multinuclear spectrometer.

RESULTS AND DISCUSSION

Absorption bands of *t*-$[MoOCl_3(PPh_3)_2]$ in TBP are shown in Fig. 1. The characteristics of the bands are presented in Table 1. The presented spectrum is similar to those of the complexes $[MoOCl_3L_2]$ (L = phosphine) (e.g. ref. 32). The lowest energy band was attributed to a $b_2 \rightarrow e$ transition.[32-34]

Table 1. Band positions, molar extinction coefficients (ε) and assignments

Band (nm)	ε	Assignment
235	15,800	$\pi_O \rightarrow d_{xz}, d_{yz}$
260	12,000	$\pi_{phen} \rightarrow 3d_P$
315	2410	$\pi_{Cl} \rightarrow d_{xy}$
450	350	$^2B_2 \rightarrow {}^2B_1$
730	35	$^2B_2 \rightarrow {}^2E$

Assuming C_{4v} or C_{2v} symmetry of the Mo^V complex, the ligand field parameters *Dq*, *Ds* and *Dt* were determined and the energies of the terms were calculated as it is shown in Fig. 2.

On the basis of these calculations (see Fig. 2) the absorption bands appearing as a result of irradiation of the frozen solution of $[MoOCl_3(PPh_3)_2]$, in TBP saturated with argon, were quantitatively interpreted (Fig. 3). The band at 600 nm (17000 cm^{-1}) is attributed to the $^3B_1 \rightarrow {}^3A_1$ transition, whilst that at 400 nm (25000 cm^{-1}) is the $^3E \rightarrow {}^3A_1$ transition. Since these two bands

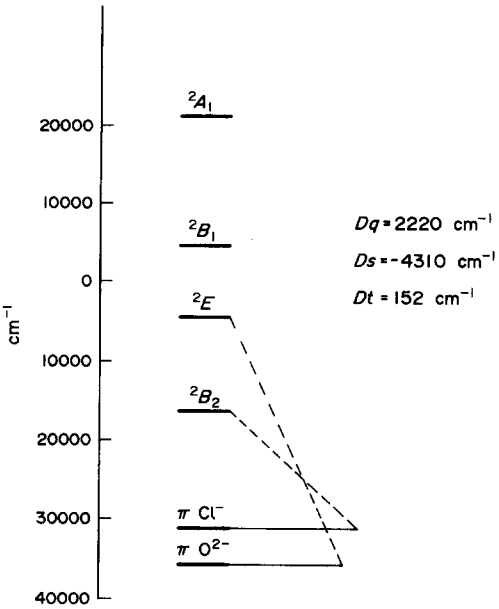

Fig. 2. Parameters of the ligand field and the energy level diagram of the central atom orbitals for the complex $[MoOCl_3(PPh_3)_2]$.

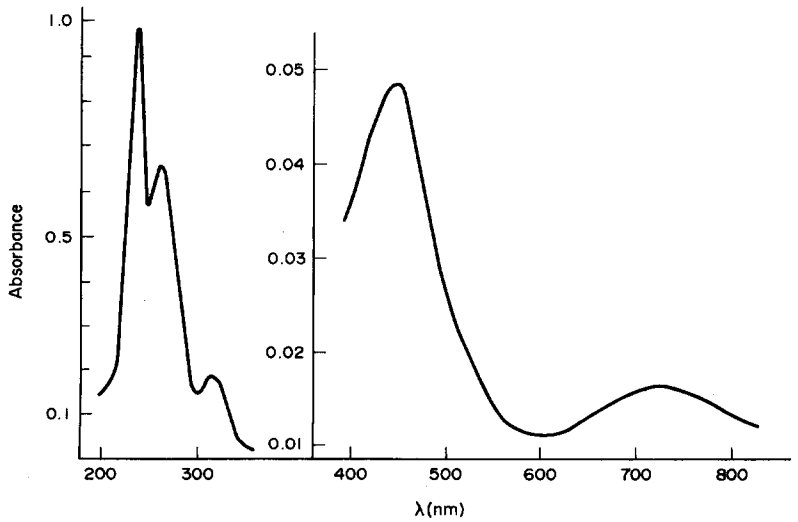

Fig. 1. Absorption bands of *t*-$[MoOCl_3(PPh_3)_2]$ in TBP.

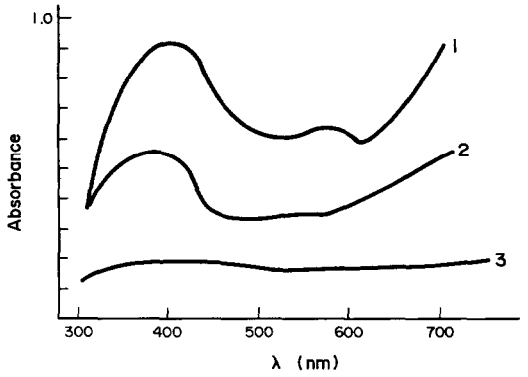

Fig. 3. Absorption bands arising after irradiation of the frozen solution of the Mo^V complex in TBP (conc = 10^{-4} mol dm^{-3}, dose = 5×10^{18} eV cm^{-3}). (1) 110 K, (2) 150 K, (3) 190 K.

appear after irradiation they are assumed to be due to the Mo^{IV} hot ion. This is regarded to be a product of the reaction of $[MoOCl_3(PPh_3)_2]$ with e_t^-, and has the $(d_{xy})^1$ $(d_{x^2-y^2})^1$ configuration. The lower intensity band (at 600 nm) disappears at 150 K, while the band at 400 nm disappears at 190 K. The lower intensity of the former band is due to the lower probability of the acceptance of e_t^- by the higher energy orbital $(d_{x^2-y^2})$ in comparison with the (d_{xz}, d_{yz}) orbitals. Moreover, the lower intensity of the band at 600 nm can be connected with the decay of the hot ion. The mechanism of this decay involves the formation of the excited state: $(d_{xy})^1$ $(d_{xz}, d_{yz})^1$ and then a transition to the ground state having the configuration $(d_{xy})^2$. The electron configuration of the excited state of Mo^{IV} is also a result of the direct acceptance of e_t^- by the (d_{xz}, d_{yz}) orbitals of Mo^V.

Knowing the electron configuration of the hot, the excited and the ground levels of the Mo^{IV} ion we can now discuss the problems of reactivity and transformations of the Mo^V complex under the influence of electrons. Hence, the cleavage of the π-bond between the Mo and Cl atoms can be attributed to the filling of the (d_{xy}) orbital. Because of the weak σ-bond, Mo—Cl, and a decrease of the oxidation number, the Cl^- ions are assumed to be released from the coordination sphere of Mo^{IV}. Simultaneously, the π-bond $Mo \overset{\pi}{\underset{\sigma}{\rightleftarrows}} PPh_3$ can be formed. It is responsible for the increasing covalency of the Mo—P bond, therefore PPh_3 should remain in the coordination sphere. The electron-transfer from the d_{xz} and d_{yz} orbitals to the d_{xy} orbital may be responsible for the Mo=O group in the Mo^{IV} complex remaining, since an electron on the (d_{xz}, d_{yz}) orbitals may weaken the π-bond between the Mo and O atoms. All these expectations have been experimentally confirmed in this work.

The magnetic susceptibility of the irradiated solution of $[MoOCl_3(PPh_3)_2]$ in TBP (conc = 6×10^{-2} mol dm^{-3}) was measured by Evans' method.[30,31] The ^1H signal of acetone was shifted from 156.5 to 166.9 Hz, while the effective magnetic moment was reduced from 1.79 to 0 BM, which is the appropriate value for a diamagnetic substance.

After irradiation we found no changes in the intensity of the bands at 235 nm or 940 cm^{-1} ($\nu_{Mo=O}$). These facts seem to confirm the presence of the Mo=O group in the reduced Mo^{IV} complex whose symmetry (C_{4v} or C_{2v}) has not been changed. The band at 260 nm is decreased slightly owing to irradiation, e.g. doses higher than 2×10^{18} eV cm^{-3} do not have any influence on the intensity, in solution of Mo^V in TBP (conc = 5.9×10^{-4} mol dm^{-3}). This fact is connected with the formation of the π-bond between the Mo^{IV} ion and the acceptor $3d$ orbitals of the P atom. Therefore, it is less likely that the π-electrons of the phenyl delocalize to the $3d$ orbitals of P atom. The removal of Cl^- ions from the coordination sphere of Mo^{IV} is supported by the intensity decrease of the band at 315 nm. The number of liberated Cl^- ions vs dose and concentration of the Mo^V complex are presented in Fig. 4.

The bands at 450 and 730 nm decreased due to irradiation. Thus, it can be concluded that the Mo^V ion is reduced. The yields of Mo^V reduction were calculated on the basis of the intensity decrease of the intensive crystal field band at 450 nm. The number of reduced molecules of the Mo^{IV} complex vs dose and concentration of the Mo^V complex are shown in Figs 5 and 6. The yields of the Mo^V reduction and the cleaved Mo—Cl bonds were

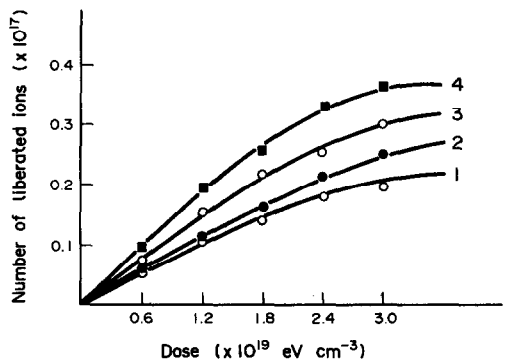

Fig. 4. Number of liberated Cl^- ions in irradiated Mo^V solution vs dose according to the following Mo^V concentrations in TBP: (1) 2.90×10^{-4}, (2) 3.25×10^{-4}, (3) 4.45×10^{-4}, (4) 5.90×10^{-4} mol dm^{-3}.

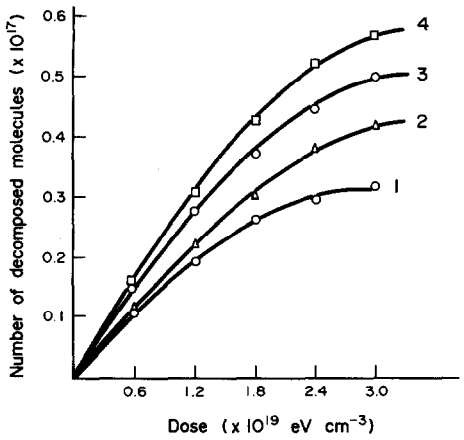

Fig. 5. Number of decomposed Mo^{V} molecules in TBP solutions saturated with Argon vs dose: (1) conc = 2.95×10^{-4}, (2) conc = 3.45×10^{-4}, (3) conc = 4.15×10^{-4}, (4) conc = 4.50×10^{-4} mol dm^{-3}.

obtained from Figs 4–6 and are presented in Table 2.

It can be noticed that Mo^{V} is reduced by e_s^-, since the yields of reduction (G) are higher in solutions saturated with argon (G_{Ar}) than in those saturated with N_2O (G_{N_2O}). The value of $\Delta G = G_{Ar} - G_{N_2O}$ corresponds to the yields of Cl^- ions liberated from the coordination sphere of the complex, which is in agreement with our predictions.

In the case of the oxalate complex of Mo^{V}, the hot ion with the $(d_{xy})^1$ $(d_{xz}, d_{yz})^1$ configuration is formed.[20] The π-bond $M\ddot{o}\underset{\sigma}{\overset{\pi}{\rightleftharpoons}}C_2O_4$ is inefficient and the σ-bond is also very weak. Therefore, the low spin state of the central ion is not stabilized by the ligand field and this fact is responsible for the change of the ground state term from $^1A_1$ to ^3E. Thus, the Mo^{IV} ion has the $(d_{xz}, d_{yz})^2$ configuration, the π-bond, $C_2\ddot{O}_4\underset{\sigma}{\overset{\pi}{\rightleftharpoons}}Mo$, is formed and $C_2O_4^{2-}$ ions

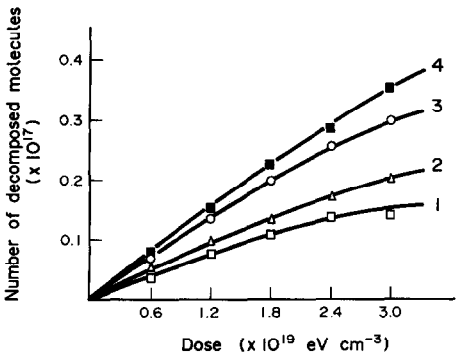

Fig. 6. Number of decomposed Mo^{V} molecules in TBP solutions saturated with N_2O vs dose: (1) conc = 2.95×10^{-4}, (2) conc = 3.45×10^{-4}, (3) conc = 4.15×10^{-4}, (4) conc = 4.50×10^{-4} mol dm^{-3}.

are stabilized in the coordination sphere of the Mo^{IV} ion. The electrons of d_{xz} and d_{yz} orbitals bring about the cleavage of the π-bond in the MoO group.[20] We can draw the conclusion that the type of π-bond, as well as the position in the spectrochemical series, exert an influence on the formation and the decay of the hot ions and, as a consequence, on the mechanisms of the complex compounds radiolysis.

In the light of the presented results the following mechanism of $[MoOCl_3(PPh_3)_2]$ radiolysis in TBP is proposed:

$$TBP \longrightarrow e_s^-, TBP^+, R, \ldots \quad (1)$$

$$e_s^- [MoOCl_3(PPh_3)_2] \longrightarrow [MoOCl_3(PPh_3)_2]^- \quad (2)$$

$$e_s^- + TBP \longrightarrow \text{radiolysis products} \quad (3)$$

$$e_s^- + N_2O \longrightarrow N_2 + O^- \quad (4)$$

$$[MoOCl_3(PPh_3)_2]^- + TBP \longrightarrow [MoOCl_2(PPh_3)_2TBP] + Cl^- \quad (5)$$

$$O^- + (C_4H_9O)P(OH)_2^+ \longrightarrow (C_4H_9O)_2P(OH) + OH \quad (6)$$

$$OH + TBP \longrightarrow H_2O + R{-}P(=O)(C_4H_9). \quad (7)$$

The formation of e_s^- in tri-*n*-alkylphosphates solutions has been known for many years.[35] The formation of the $(C_4H_9O)_2P(OH)_2^+$ cation from TBP^+ together with the simultaneous C_4H_7 group abstraction was shown previously.[36] The O^- anion-radicals and OH radicals [see reactions (4) and (6)], due to their high reactivity towards TBP,[4] do not react with the molybdenum complex but they do react with the solvent. By applying the steady state approximation to reactions (1)–(3), the following relationship was derived:

$$\frac{1}{\Delta G} = \frac{1}{G_{e_s^-}} + \frac{k_1[TBP]}{k_2 G_{e_s^-}[MoOCl_3(PPh_3)_2]}.$$

Figure 7 shows ΔG^{-1} as a function of the reciprocal of Mo^{V} concentration.

From Fig. 7 the values $G_{e_s^-} = 0.63$ and $k_1[TBP]/k_2 G_{e_s^-} = 2.3\times10^{-3}$ were found. Thus, $k_1/k_2 = 4\times10^{-4}$ and assuming $k_1 = 5\times10^6$ dm^3 mol^{-1} s^{-1} [37] we found $k_2 = 1.3\times10^{10}$ dm^3 mol^{-1} s^{-1}. On the basis of the results from Table 2, i.e. the yields of the Mo—Cl bond cleavage, the values $G'_{e_s^-} = 0.63$ and $k'_2 = 1.1\times10^{10}$ dm^3 mol^{-1} s^{-1} were calculated in a similar manner. The values of $G_{e_s^-}$

Table 2. Radiation yields of reduced Mo^{IV} molecules and cleaved Mo—Cl bonds as a function of Mo^V complex concentration TBP

Concentrations $\times 10^{-4}$ (mol dm^{-3})	Number of molecules per 100 eV Mo^{IV} Solutions saturated with Ar G_{Ar}	Solutions saturated with N_2O G_{N_2O}	ΔG $G_{Ar}-G_{N_2O}$	Mo—Cl bonds in solutions saturated with Ar
2.90				0.09
2.95	0.18	0.07	0.11	
3.25				0.10
3.45	0.21	0.09	0.12	
4.15	0.25	0.11	0.14	
4.45				0.13
4.50	0.28	0.13	0.15	
5.90				0.16

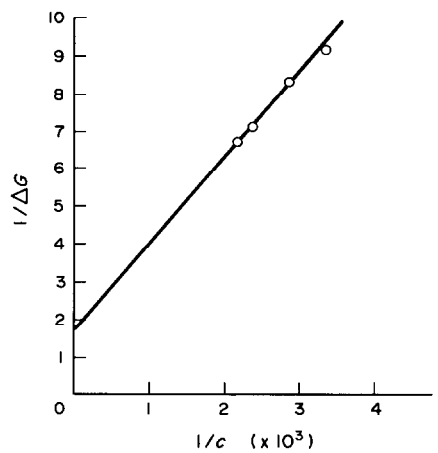

Fig. 7. Dependence of the reciprocal of $[G_{Mo^{IV}_{Ar}} - G_{Mo^{IV}_{N_2O}}]$ on the reciprocal of the concentration of the Mo^V complex.

and $G'_{e_s^-}$, and k_2 and k'_2 are nearly the same, so the expectations concerning the liberation of Cl^- ions from the coordination sphere of Mo^{IV} as a result of Mo^V reduction are confirmed. The value of k_2 is about five times higher than the rate constant of the reaction between e_s^- and the oxalate complex of Mo^V,[20] despite the fact that the acceptor orbitals of $[MoOCl_3(PPh_3)_2]$ have higher energy than those in the case of the oxalate complex. This fact seems to confirm the influence of the structural parameters of the complex on its reactivity. On the other hand, the activation energy is lower for a Mo—Cl bond cleavage (triphenylphosphine complex—more active) than for a Mo=O bond cleavage (oxalate complex—less active). The latter energy is connected with the symmetry change.

The different energetic requirements for the reactions discussed are due to the different structural parameters of the electron scavengers.

REFERENCES

1. E. Chart and M. Anbar, *Gidratirowannyj Elektron.* Moskva, Atomizdat (1973).
2. E. M. Nanobaschvili, Z. F. Chomasuridze, N. A. Razmadze, L. W. Madronina and M. B. Mamaladze, *Radiacionno-khimicheskoe Vostanovlenie Ionov Razlichnych Metallov iz Roztworov Ich Solei.* Tbilisi, Mecnereba (1978).
3. A. K. Pikaev, S. A. Kabakchi, J. E. Makarov and B. G. Yerschov, *Impulsnyj Radioliz I Evo Primienienie.* Moskva, Atomizdat (1980).
4. A. K. Pikaev and S. A. Kabakchi, *Reakcionnaa Sposobnost Pervirchnich Productov Radioliza Wody.* Moskva, Energoizdat (1982).
5. Praca zbiorowa pod redakcją J. Kroh, Wybrane zagadnienia chemii radiacyjnej, Warszawa, PWN (1986).
6. A. K. Pikaev, *Sovremennaa Radiaconnaa Chimia.* Moskva, Nauka (1986).
7. G. E. Adams, R. K. Broszkiewicz and B. D. Michael, *Trans. Faraday Soc.* 1968, **64**, 1256.
8. G. V. Buxton and R. M. Sellers, *Coord. Chem. Rev.* 1977, **22**, 195.
9. G. V. Buxton, in *The Study of Fast Processes and Transient Species by Electron Pulse Radiolysis* (Edited by J. H. Baxendale), pp. 267–282. Reidel (1982).
10. J. Lati and D. Meyerstein, *J. Chem. Soc., Dalton Trans.* 1978, 1105.
11. J. Grodkowski, P. Neta, C. J. Schlesener and J. K. Kochi, *J. Phys. Chem.* 1985, **89**, 4373.

12. S. N. Bhattacharyya and P. Netta, *J. Phys. Chem.* 1981, **85**, 1527.
13. A. W. Gogolev, W. P. Schilov, A. M. Fedoseev and A. K. Pikaev, *Iz. AN SSSR, Ser. Chim.* 1986, 456.
14. A. W. Gogolev, I. E. Makarov and A. K. Pikaev, *Iz. AN SSSR, Ser. Chim.* 1985, 690.
15. A. W. Gogolev, I. E. Makarov and A. K. Pikaev, *Chimia Vysokich Energii* 1984, **18**, 429.
16. W. P. Schilov and A. K. Pikaev, *Chimia Vysokich Energii* 1982, **16**, 468.
17. J. O. Dzięgielewski, R. Gil and P. Głowacki, *Radiochem. Radioanal. Lett.* 1982, **50**, 251.
18. H. W. Czarnik-Matusewicz and J. O. Dzięgielewski, *Radiochem. Radioanal. Lett.* 1982, **51**, 355.
19. J. O. Dzięgielewski, *Polyhedron* 1984, **3**, 1131.
20. J. O. Dzięgielewski, *Polyhedron* 1985, **4**, 1901.
21. J. O. Dzięgielewski, B. Jeżowska-Trzebiatowska, R. Gil-Bortnowska and R. Grzybek, *Polyhedron* 1986, **5**, 833.
22. J. O. Dzięgielewski, *Fizykochemia Napromienionych Roztworów Tetracykliny, Jej Pochodnych I Związków Kompleksowych* Co^{II}, Ni^{II}, Cu^{II} *Z Tetracykliną.* Katowice, Prace naukowe Uniwersytetu Śląskiego (1986).
23. C. Amado and S. Fujiwara, *Bull. Chem. Soc. Japan* 1973, **46**, 2586.
24. E. L. Evers, G. G. Jayson and A. J. Swallow, *Bull. Chem. Soc. Japan* 1978, **74**, 418.
25. A. Kumar and P. Neta, *J. Phys. Chem.* 1981, **25**, 2830.
26. C. Amado, T. Watanabe and S. Fujiwara, *J. Phys. Chem.* 1973, **46**, 1379.
27. R. Blackburn, A. J. Erkol and G. O. Philips, *J. Chem. Soc., Faraday Trans.* 1974, **70**, 1693.
28. J. O. Dzięgielewski, *Polyhedron* 1989, in press.
29. D. A. Edwards, *J. Inorg. Nucl. Chem.* 1965, **27**, 303.
30. D. P. Evans, *J. Chem. Soc.* 1959, 2003.
31. T. H. Crawford and J. Swanson, *J. Chem. Educ.* 1971, **48**, 382.
32. C. D. Garner, P. Lambert and F. E. Mabbs, *J. Chem. Soc., Dalton Trans.* 1977, 1191.
33. C. D. Garner, J. H. Hillier, F. E. Mabbs and M. F. Guest, *Chem. Phys. Lett.* 1975, **32**, 224.
34. D. P. Rilema and C. H. Brubaker, *Inorg. Chem.* 1969, **8**, 1645.
35. J. O. Dzięgielewski, J. Kaleciński and B. Jeżowska-Trzebiatowska, *Bull. Acad. Polon. Sci. Ser. Sci. Chim.* 1972, **120**, 285.
36. R. W. Wilkinson and T. F. Williams, *J. Chem. Soc.* 1961, 4098.
37. J. O. Dzięgielewski and K. Filipek, *J. Radioanal. Nucl. Chem.* 1988, **128**, 109.

Polyhedron Vol. 8, No. 4, pp. 453–455, 1989
Printed in Great Britain

0277–5387/89 $3.00+.00
© 1989 Pergamon Press plc

SPECTRAL AND MAGNETIC MOMENT STUDIES ON SOME METAL COMPLEXES WITH DIETHYLENETRIAMINE-N,N,N′,N″,N″-PENTA(METHYLENEPHOSPHONIC ACID)

B. VENKATESWARA RAO* and D. M. PURI

Department of Chemistry, Kurukshetra University, Kurukshetra, India

(*Received* 11 *September* 1986; *accepted after revision* 15 *August* 1988)

Abstract—Diethylenetriamine-N,N,N′,N″,N″-penta(methylenephosphonic acid) forms polynuclear complexes of the type $M_5L \cdot xH_2O$ (where M^{II} = Fe, Co, Ni, Cu and Cd) and $Cr_4L(OH)_2 \cdot H_2O$. Six-coordinated metal complexes are formed as inferred from their IR and electronic spectral data. Characterization has also been accompanied by an EPR study of the copper(II) complex. Antiferromagnetism in the complexes, inferred from their subnormal magnetic moments at room temperature, was confirmed by cryomagnetic data which obeyed the Curie–Weiss law. Thermoanalytical studies show the end-product to be metal oxide and phosphorous pentoxide.

Oakes *et al.*[1,2] made a comparative study of the metal complexes of diethylenetriamine pentaacetic acid (DTPA) and ethylenediamine tetraacetic acid (EDTA) with metal complexes of diethylenetriamine-N,N,N′,N″,N″ pentamethylenephosphonic acid) (DTPMP) and ethylenediamine tetrakis(methylenephosphonic acid), respectively. They studied the soluble ionic complexes in aqueous solution using a ligand-to-metal ratio of 1 : 1. However, no attempt to isolate the products and study their structures seemed to have been made by the authors.[1,2] In view of the above, we report here the isolation and structural study of some bi- and trivalent metal complexes with diethylenetriamine - N,N,N′,N″,N″ - penta(methylenephosphonic acid).

EXPERIMENTAL

Diethylenetriamine - N,N,N′,N″,N″ - penta (methylenephosphonic acid) (DTPMP) as the hexahydrate was synthesized by the method of Peck and Hudson.[3] After purification and removal of water, the ligand was obtained as a colourless highly viscous product. Found: C, 15.3; H, 5.8; N, 6.2; P, 23.1. Calc. for $C_9H_{28}O_{15}N_3P_5 \cdot 6H_2O$: C, 15.9; H, 5.9; N, 6.2; P, 22.8%.

Bivalent metal acetates (BDH AnalaR), chromium nitrate (Thomas and Thomas, India), diethylenetriamine (Sisco Chemicals, Bombay) were used as received after ascertaining their purity. 40% aqueous formaldehyde solution was used.

Preparation of the metal complexes

An aqueous solution of the ligand (0.001 mol) was added slowly with constant stirring to the metal salt solution (0.005 mol), followed by the addition of 0.0025 mol of aq. Na_2CO_3 solution, which resulted in the formation of a precipitate. A small amount of acetone was added for easy filtration. The precipitate was first washed with hot water then 50% aqueous acetone and finally with 98% acetone. It was then dried at 60–70°C. Elemental analyses are given in Table 1.

Physical measurements

PMR spectra were taken on a R-32 Perkin–Elmer (90 MHz) instrument. Magnetic susceptibility measurements at room temperature as well as at different temperatures were carried out using a Princeton applied research model 155 Vibrating Sample Magnetometer incorporating a digital read-out. The instrument and methods used for the

*Author to whom correspondence should be addressed. Present address: Department of Chemistry, V.R. Siddhartha Engineering College, Vijayawada-6, Andhra Pradesh, India.

Table 1. Colour, analytical and magnetic moment (BM) data of complexes

Serial number	Compound	Colour	Found (calc.) (%) Metal	P	N	μ_{eff}[a]	θ_{value}	Thermal analysis
(1)	$Cr_4(C_9H_{18}N_3O_{15}P_5)(OH)_2 \cdot H_2O$	Dark green	24.9 (25.3)	19.2 (18.8)	— (5.1)	1.77, 1.74, 1.72 1.71, 1.67, 1.64 1.59, 1.58, 1.151 and 1.45	−56°C	
(2)	$Fe_5(C_9H_{18}N_3O_{15}P_5) \cdot 12H_2O$	Dirty white	26.9 (26.4)	15.0 (14.7)	— (3.9)	1.76	—	
(3)	$Co_5(C_9H_{18}N_3O_{15}P_5) \cdot 16H_2O$	Purple	26.0 (25.7)	14.0 (13.5)	3.3 (3.6)	2.35, 2.30, 2.28 2.23, 2.19, 2.14, 2.08, 2.02, 1.95 and 1.92	−78°C	
(4)	$Ni_5(C_9H_{18}N_3O_{15}P_5) \cdot 20H_2O$	Light green	24.5 (24.1)	13.0 (12.7)	3.1 (3.5)	1.58, 1.57, 1.56 1.56, 1.55, 1.52 1.49, 1.47, 1.43 and 1.41	−34°C	27.3[b] (26.63%) 29.2[c] (29.6%) 40.6[d] (40.1%)
(5)	$Cu_5(C_9H_{18}N_3O_{15}P_5) \cdot 15H_2O$	Light blue	28.0 (27.6)	13.7 (13.4)	3.2 (3.6)	1.04, 1.01, 0.98 0.97, 0.92, 0.88 0.85, 0.79, 0.77 and 0.73	−118°C	
(6)	$Cd_5(C_9H_{18}N_3O_{15}P_5) \cdot 16H_2O$	White	40.0 (39.8)	11.0 (10.9)	2.8 (3.0)	Diamagnetic		29.16[d] (29.43%)

[a] The magnetic moment values are at 296, 261, 237, 189, 165, 141, 117, 93 and 77 K, respectively.
[b] Due to loss of 18 water molecules.
[c] Due to loss of 20 water molecules.
[d] Total mass loss.

remainder of the analyses were the same as described earlier.[4,5]

RESULTS AND DISCUSSION

Reactions of the bi- and trivalent metal ions and DTPMP can be represented by the following two equations.

$$5M^{2+}(aq)+H_{10}L(aq)\rightarrow M_5L\cdot xH_2O(s)+10H^+$$

$$[M^{II}=Fe, Co, Ni, Cu \text{ and } Cd]$$

$$4Cr^{3+}(aq)+H_{10}L(aq)+3H_2O \rightarrow Cr_4L(OH)_2\cdot H_2O+12H^+.$$

The complexes are insoluble in all the common organic solvents as well as water and do not melt even up to 270°C, suggesting these to be polynuclear–polymeric in nature.

The structure of the free ligand was confirmed from IR and PMR spectral studies. In the IR spectrum, a band at 1240 cm^{-1}, due to the presence of the phosphoryl group[6] was observed. The presence of other bands at 2950, 1620, 1570, 1140, 1070, 1020 and 965 cm^{-1} suggested that the ligand has a Zwitter ionic structure. The proton magnetic resonance spectrum of DTPMP in D_2O showed that methylene protons resonated at δ 2.35 indicating the presence of 18 methylene protons. Similar observations have also been made by Oakes *et al.* Another signal at δ 10.5 may either be due to some impurity but more likely due to OH (intramolecularly hydrogen bonded).

In the IR spectra of the metal complexes, the band for phosphoryl groups seemed to be absent at 1240 cm^{-1} probably due to the formation of coordination linkages. Bands were observed in the ranges 1070–1050 cm^{-1} and 1010–950 cm^{-1} which could be due to a deprotonated phosphonic acid group. New bands were observed at 410, 370, 340 and 310 cm^{-1}. The first two bands were assigned to ν(M—O) linkages as also observed by others[7] and the fourth band may be due to the coordination linkage between the metal and the nitrogen atom.[8]

Electronic absorption spectra of the complexes show that the metal ions have octahedral environments[9,10] and the results are comparable with those reported by Oakes and van Kralingen.[1,2]

Room temperature magnetic moment values of the complexes were found to be lower than those expected for free ions, suggesting the possibility of antiferromagnetism in these complexes.[11,12] Values of θ obtained from plotting $1/\chi_M$ against temperature K further comfirmed this nature, since it was observed from the graph that the complexes obeyed the Curie–Weiss law.

The EPR spectrum of a powdered sample of Cu^{II}–DTPMP complex could provide only a value of g_{av} (2.052) and no hint about individual g_x, g_y, g_z or $g_\parallel$ and $g_\perp$ values. This value favours the presence of tetragonal distortion.[13] However, this value cannot be compared with those obtained by Oakes *et al.* for their Cu^{II}–DTPMP complex because in their case, there does not seem to be much metal–metal interaction or antiferromagnetism.

Thermal analyses of $Ni_5(DTPMP)\cdot 20H_2O$ and $Cd_5(DTPMP)\cdot 16H_2O$ have been studied. They were heated in air at the rate of 10°C min^{-1} in the range 20–1000°C. It was inferred that the complexes first lost their water molecules up to 370°C and finally at higher temperatures they were found to give the final products of metal oxide and phosphorous pentoxide.[14]

Acknowledgements—One of the authors (B.V.R.) is thankful to CSIR for the award of Senior Research Fellowship. The authors thank the Director of USIC, Roorkee, for magnetic measurements and the Head, RSIC, IIT, Madras for the electronic spectra.

REFERENCES

1. J. Oakes and E. G. Smith, *J. Chem. Soc., Dalton Trans.* 1983, 601.
2. J. Oakes and C. G. van Kralingen, *J. Chem. Soc., Dalton Trans.* 1984, 1133.
3. D. R. Peck and D. Hudson, *Brit.* 1, 142, 294 (ClCo76); *Chem. Abstr.* 1969, **70**, 106650x.
4. N Palta, B. V. Rao, S. N. Dubey and D. M. Puri, *Polyhedron* 1984, **3**, 527; *Ind. J. Chem.* 1984, **23A**, 397; *Ind. Acad. Sci. Bangalore* 1985, **95**, 321.
5. B. Venkateswara Rao, N. Palta, S. N. Dubey and D. M. Puri, *J. Ind. Chem. Soc.* 1984, **61**, 951; B. Venkateswara Rao, N. Palta, S. N. Dubey and D. M. Puri, *Transition Met. Chem.* 1985, **10**, 60.
6. D. E. C. Corbridge, *Topics in Phosphorus Chemistry* (Edited by M. Crayson and E. J. Griffith), Vol. 6, p. 235. Interscience, New York (1969).
7. S. V. Tatwawadi, A. P. Singh and K. K. Narang, *Ind. J. Chem.* 1982, **21A**, 644.
8. K. Nakamoto, *Infrared Spectra of Inorganic and Coordination Compounds.* Wiley, New York (1978).
9. A. B. P. Lever, *Inorganic Electronic Spectroscopy*, pp. 275–361. Elsevier, London (1968).
10. The Nicholls, *The Chemistry of Iron, Cobalt and Nickel*, Vol. 24, pp. 1026–1035 and 1115–1161. Pergamon Press, Oxford (1973).
11. B. N. Figgis and J. Lewis, *Prog. Inorg. Chem.* 1964, **6**, 37.
12. A. El-Dissouky, G. R. Mohamed and L. S. Refaat, *Transition Met. Chem.* 1984, **9**, 23.
13. W. Low, Paramagnetic resonance in solids, Suppl. 2, in *Solid State Physics*, p. 92. Academic Press, New York (1960).
14. V. P. Khramov and A. A. Kol'tsov, *Russ. J. Inorg. Chem.* 1973, **18**, 1567.

Polyhedron Vol. 8, No. 4, pp. 457–462, 1989
Printed in Great Britain

0277–5387/89 $3.00+.00
© 1989 Pergamon Press plc

FLUORO AND MIXED-LIGAND FLUORO COMPLEXES OF COPPER(II). A NEW SYNTHESIS OF $KCuF_3$, AND SYNTHESIS AND PHYSICO-CHEMICAL STUDIES OF NEW MIXED-LIGAND FLUOROCUPRATES(II), $A[CuF(SO_4)]\cdot nH_2O$ ($A = Na$, $n = 2$; $A = K$ or NH_4, $n = 3$)

MANABENDRA N. BHATTACHARJEE, MIHIR K. CHAUDHURI* and MINAKSHI DEVI

Department of Chemistry, North-Eastern Hill University, Shillong 793 003, India

(*Received* 29 *June* 1987; *accepted after revision* 15 *August* 1988)

Abstract—White crystalline $KCuF_3$ has been synthesized from the reaction of $Cu(OH)_2$ with KHF_2 and a small amount of 40% HF at pH $\leqslant$ 4, while the synthesis of blue fluoro(sulphato)cuprates(II), $Na[CuF(SO_4)]\cdot 2H_2O$, $K[CuF(SO_4)]\cdot 3H_2O$ and $NH_4[CuF(SO_4)]\cdot 3H_2O$, has been accomplished by reacting $Cu(OH)_2$ with AF and A_2SO_4 (A = Na, K or NH_4), in the ratio of 1 : 1 : 1, in the presence of a small amount of 40% HF. Alternative synthesis of the latter involving reactions among $Cu(OH)_2$, F^-, and SCN^-, and H_2O_2 or SO_2(g) and H_2O_2 gave CuSCN and $Cu^{II}[Cu^{I}SO_3]_2\cdot 2H_2O$, respectively, instead of the desired product. The compounds have been characterized by elemental analyses, chemical determination of the oxidation state of copper, magnetic susceptibility and ESR measurements, IR, laser Raman (LR), and electronic spectroscopic studies. The complex $[CuF(SO_4)]^-$ species has a distorted octahedral polymeric structure containing both F^- and SO_4^{2-} as bridging ligands.

There has been a general interest in fluorometallates, particularly the perovskites[1–3] mainly owing to their unusual properties.[4–6] Fluorocuprates(II) form a distinct class among perovskites as regards the nature of coordination, structure and the observed colour anomaly.[7] Thus, whereas the AMF_3 (A = univalent cation; M = bivalent transition metal) complexes generally have a cubic perovskite structure, the $ACuF_3$ compounds display a lower symmetry, distorted tetragonal geometry with the Jahn–Teller effect.[8–10] Access to pure fluorometallates has been a general problem,[7] and consequently there have been instances which involve information based on impure products.[11] Moreover, information on mixed-ligand fluorocuprates(II) are restricted to a few papers.[12,13] Such complexes of transition metals enable a comparison of their properties with those of the corresponding binary fluoro complexes. In addition, mixed-fluoro complexes display some interesting properties,[14–19] some of which also have biochemical significance.[13,20]

As a part of our programme on studies of the fluoro and mixed-fluoro complexes of transition metals,[15–18,20,21] as well as the current interest in the copper(II)–fluoro chemistry,[13] we extended our investigations to fluoro and mixed fluorocuprates(II). Reported in this paper are a direct synthesis of $KCuF_3$, and synthesis, characterization and the assessment of the structure of novel mixed-ligand fluorocuprates(II): $Na[CuF(SO_4)]\cdot 2H_2O$, $K[CuF(SO_4)]\cdot 3H_2O$ and $NH_4[CuF(SO_4)]\cdot 3H_2O$. An effort has also been made to rationalize the changes in magnetic properties in going from $[CuF_3]^-$ to $[CuF(CO_4)]^-$ complexes.

EXPERIMENTAL

The chemicals used were all of reagent grade quality. IR spectra were recorded on a Perkin–Elmer model 983 spectrophotometer in KBr as well as in Nujol mull media. Laser Raman (LR) spectra were recorded on a SPEX Ramalog model 1403 spectrometer. The 5145 Å laser line from the Spectra-Physics model 165 Argon laser was used as the excitation source. The scattered light at 90° was

*Author to whom correspondence should be addressed.

detected with the aid of a cooled RCA 31034 photomultiplier tube followed by a photon count processing system. The spectra were recorded at ambient temperatures using pressed pellets of the compounds. Magnetic susceptibility measurements were made by using the Guoy method with $Hg[Co(NCS)_4]$ as the calibrant. Electronic spectra were recorded on a Cary model 2300 spectrophotometer. The pH of the reaction solutions was measured with a Systronics type 335 digital pH meter and also with pH indicator (BDH) papers. ESR spectra were recorded using a Varian E 109-ESR spectrometer (X-band) with 100 kHz field modulation.

Synthesis of potassium triflurocuprate(II), $KCuF_3$

Copper(II) hydroxide was prepared from an aqueous solution of $CuCl_2 \cdot 2H_2O$ by precipitating it with a 5% solution of NaOH. The precipitate was centrifuged and washed free from alkali and chloride.

In a typical reaction, an aqueous suspension of a freshly prepared copper(II) hydroxide, as obtained above (from 2.0 g, 11.74 mmol of $CuCl_2 \cdot 2H_2O$), was dissolved in *ca* 1 cm^3 of 40% HF. The solution was filtered to remove any traces of undissolved material. A concentrated solution of KHF_2, maintaining the molar ratio of Cu/KHF_2 at 1 : 2, was added to the above filtrate with vigorous stirring (the pH of the solution was found to be below 4). Stirring was continued until white microcrystalline $KCuF_3$ precipitated out. The product was separated by centrifugation, washed twice with ethanol and finally dried *in vacuo* over P_4O_{10}. The yield of $KCuF_3$ was 1.5 g (80%).

Synthesis of alkali-metal and ammonium monofluoro(sulphato)cuprates(II) *hydrates*, $Na[CuF(SO_4)] \cdot 2H_2O$, $K[CuF(SO_4)] \cdot 3H_2O$ *and* $NH_4[CuF(SO_4)] \cdot 3H_2O$

Freshly prepared copper(II) hydroxide was dissolved in a minimum volume of 40% HF (in a similar way to that described above). This was then treated with a concentrated solution of alkali metal or ammonium fluoride and the corresponding sulphate, with maintenance of the $Cu/AF/A_2SO_4$ molar ratio of 1 : 1 : 1. The mixture was warmed on a steambath for *ca* 15 min with occasional stirring. The light blue solution thus obtained was cooled to room temperature and filtered. The filtrate was stirred magnetically for *ca* 15 min followed by the addition of ice-cold ethanol until a precipitate just began to appear. The solution was then kept in a freezer for about 1/2 h for complete precipitation of the light blue microcrystalline $Na[CuF(SO_4)] \cdot 2H_2O$, $K[CuF(SO_4)] \cdot 3H_2O$ or $NH_4[CuF(SO_4)] \cdot 3H_2O$ compounds. The products were isolated, purified and dried in manners analogous to those described for $KCuF_3$.

Starting from 2.0 g (11.74 mmol) of $CuCl_2 \cdot 2H_2O$ in each case, the yields of $Na[CuF(SO_4)] \cdot 2H_2O$, $K[CuF(SO_4)] \cdot 3H_2O$ and $NH_4[CuF(SO_4)] \cdot 3H_2O$ were 2.1 g (75%), 2.6 g (82%) and 2.3 g (78%), respectively.

Elemental analysis

Copper was estimated iodometrically.[22a] The fluoride content of $KCuF_3$ was determined gravimetrically[22b] as lead chloride fluoride. However, for the mixed-ligand fluoro(sulphato) complexes, fluoride was first precipitated as PbClF and then the chloride was estimated by Volhard's method from which the fluoride content was calculated.[22b] Sulphate was estimated gravimetrically as $BaSO_4$.[22c] Sodium, potassium and nitrogen were determined by the methods described in our earlier papers.[23]

The analytical data and room temperature magnetic moments are reported in Table 1, while the important IR and electronic spectral bands with their assignments are summarized in Table 2.

RESULTS AND DISCUSSION

The difficulties associated with the preparation and definitive characterization of $KCuF_3$ are well known. A wide variety of colours for $KCuF_3$, from white to blue, was reported in the literature[6-9] and a correlation between the colour and composition of the compound established.[7,24] The bluest of the potassium complexes was shown to be the extreme case of $KCu(OH)F_2$. Consequently, a preparation of pure $KCuF_3$ has long been looked for since the available methods proved impractical to produce an uncontaminated product. The results of our investigations[16-18,21,25] of the fluoro chemistry of metals suggest that freshly prepared hydrated metal oxides or hydroxides are very suitable starting materials for the synthesis of fluoro and mixed-ligand fluoro complexes of the corresponding metals. Further, it was expected that use of potassium bifluoride, KHF_2, would help, not only in maintaining acidity, but also in providing a high fluoride ion concentration to facilitate formation of the pure product. Accordingly, the reaction of freshly prepared $Cu(OH)_2$ with KHF_2 in the presence of 40% HF at pH $\leqslant$ 4 led to the synthesis of a pure white microcrystalline compound, $KCuF_3$. Similar reactions at pH > 4 yielded contaminated

Table 1. Analytical data and magnetic moment values of the complexes

Compound	Colour	μ (BM) (at 298 K)	Analysis[a] A[b]	Cu	F	SO_4
$KCuF_3$	White	1.35	24.6 (24.4)	39.6 (39.8)	35.9 (35.7)	—
$Na[CuF(SO_4)]\cdot 2H_2O$	Light blue	1.60	9.4 (9.7)	26.5 (26.7)	8.1 (8.0)	40.5 (40.4)
$K[CuF(SO_4)]\cdot 3H_2O$	Light blue	1.65	14.1 (14.3)	23.6 (23.4)	7.1 (7.0)	35.1 (35.3)
$NH_4[CuF(SO_4)]\cdot 3H_2O$	Light blue	1.65	5.5 (5.6)	25.4 (25.3)	7.7 (7.5)	38.1 (38.3)

[a] Calculated values in parentheses.
[b] Alkali metal or N.

products. It may therefore be emphasized that high concentrations of both H^+ and F^- are necessary for the synthesis of pure potassium trifluorocuprate(II), $KCuF_3$.

In our endeavour to get access to the hitherto unknown mixed-ligand fluoro(sulphato) complexes of copper(II), the reaction of $Cu(OH)_2$ with 40% HF, alkali metal or ammonium fluoride, and the corresponding sulphate was carried out. This led to the synthesis of $Na[CuF(SO_4)]\cdot 2H_2O$, $K[CuF(SO_4)]\cdot 3H_2O$ or $NH_4[CuF(SO_4)]\cdot 3H_2O$ at $pH \leqslant 4$. The products isolated by conducting similar reactions at $pH > 4$ were found to be impure with inconsistent composition and colour suggesting therefore that a $pH \leqslant 4$ is conducive to the successful synthesis of the desired complexes. The role of ethanol was to precipitate the compounds.

In view of the sequence of reactions and the products obtained, it is believed that the fluorocuprate(II), CuF_3^-, ion is first formed, in the reaction of $Cu(OH)_2$ with AF and 40% HF, which subsequently undergoes a partial replacement of fluoride by SO_4^{2-} to afford the complex $[CuF(SO_4)]^-$. This certainly indicates that sulphate can compete with F^-, under the present experimental conditions, to coordinate with Cu^{II}. It is pertinent to mention that, while the mixed-ligand fluoro(sulphato)cuprates(II) can be synthesized easily, our attempted synthesis of the corresponding fluoro(oxalato)cuprates(II) has not been successful. The product was found to be a binary oxalatocuprate(II) containing chelated oxalate. It is notable that while the mixed fluoro(sulphato) complexes of Mn^{III},[16] Co^{II}[18] and Cu^{II} (present report) can be synthesized directly from the reaction of the corresponding hydroxides with alkali sulphate and hydrofluoric acid, fluoro(sulphato)ferrates(III) could not be synthesized[26] by a similar procedure. The success could be achieved[26] for the latter, only by conducting the chemical oxidation of SCN^- to SO_4^{2-} by H_2O_2 in the presence of F^- ions and Fe^{III}. In an attempt to synthesize fluoro(sulphato) cuprates(II) from the reactions of $Cu(OH)_2$ with F^-, SCN^- and SO_2(g), respectively, in the presence of H_2O_2, such reactions were carried out. Unfortunately the formation of CuSCN in the former and that of the red $Cu^{II}[Cu^{I}SO_3]_2\cdot 2H_2O$[27] in the latter precluded synthesis of the compounds looked for.

Characterization and assessment of structures

White potassium trifluorocuprate(II), $KCuF_3$ and light blue $Na[CuF(SO_4)]\cdot 2H_2O$, $K[CuF(SO_4)]\cdot 3H_2O$ or $NH_4[CuF(SO_4)]\cdot 3H_2O$ are all microcrystalline products, insoluble in common organic solvents. They decompose in water, precluding molar conductance measurements, and they result on the etching of glass slides in the presence of moisture. The compounds are stable in the dry and can be stored in polyethylene ampoules. Their stability can be ascertained by estimation of copper contents and recording of IR spectra periodically. The importance of chemical determination of oxidation states of metals capable of displaying variable oxidation states, has been emphasized in our earlier papers.[15-18,21] The results of the iodometric determination of the oxidation state of copper showed that the metal occurs in its +2 state in each of the compounds presented in this report.

The effective magnetic moment of $KCuF_3$ at 298 K was found to be 1.35 BM, in conformity with that reported by Machin *et al.*,[4] indicating a considerable antiferromagnetic interaction being operative between contiguous Cu^{2+} ions in the crystal lattice. The electronic spectrum of $KCuF_3$, recorded immediately after making its solution, showed a broad, weak and assymmetric band at 12050 cm^{-1} owing to the transition $B_{1g} \rightarrow E_g$, arising from an appreciable splitting of the ^2E_g ground state of Cu^{II} as a consequence of the Jahn–Teller effect.[28] This

Table 2. Structurally important IR and electronic spectral bands of the complexes

Compound	IR (cm^{-1})	Assignments	Electronic spectra (cm^{-1})	Assignments
$KCuF_3$	485(s)	ν(Cu—F)	12,050	$B_{1g} \rightarrow E_g$
$Na[CuF(SO_4)] \cdot 2H_2O$	485(m, br)	ν(Cu—F)	12,395	$B_{1g} \rightarrow E_g$
	1160(s), 1110(s), 1055(s)	ν_3		
	980(m)	ν_1		
	650(s), 615(s), 570(s)	ν_4		
	455(m, br)	ν_2		
		SO modes		
	3445(s)	ν(O—H)		
	1640(m)	ν(H—O—H)		
$K[CuF(SO_4)] \cdot 3H_2O$	480(m, br)	ν(Cu—F)	12,500	$B_{1g} \rightarrow E_g$
	1165(s), 1115(s), 1050(s)	ν_3		
	985(m)	ν_1		
	655(s), 615(s), 575(s)	ν_4		
	450(m, br)	ν_2		
		SO modes		
	3440(s)	ν(O—H)		
	1640(m)	ν(H—O—H)		
$NH_4[CuF(SO_4)] \cdot 3H_2O$	485(m, br)	ν(Cu—F)	12,450	$B_{1g} \rightarrow E_g$
	1160(s), 1115(s), 1050(s)	ν_3		
	980(m)	ν_1		
	645(s), 615(s), 570(s)	ν_4		
	455(m, br)	ν_2		
		SO modes		
	3440(s)	ν(O—H)		
	1640(m)	ν(H—O—H)		

in turn shows that the CuF_3^- ion has a distorted octahedral structure. The IR spectrum of $KCuF_3$ is straightforward and shows an absorption at 485 cm^{-1} assigned to the ν(Cu—F) mode.[29] A relatively lower ν(Cu—F) value points to a rather elongated Cu—F bond or enhanced ionic character. The position and broadening of the band point to the possibility of a —F—Cu—F—Cu—F— interaction in the crystal lattice leading to a polymeric structure. This agrees very well with the observed magnetic moment of the complex. The most significant aspect of the IR spectrum of the newly synthesized $KCuF_3$ is the complete absence of any absorption around 3400 cm^{-1} supporting our contention that the compound is free from OH^-.

Unlike $KCuF_3$, the fluoro(sulphato)cuprate(II) complexes are light blue in colour and contain water of crystallization. The principal features of their IR spectra are the absorptions due to coordinated sulphate and fluoride. The IR signatures for the S—O modes of sulphate, at 1160(s), *ca* 1115(s) and 1050(s) cm^{-1} assigned to ν_3, at *ca* 980m cm^{-1} due to ν_1, at *ca* 655(s), 615(s) and 570(s) cm^{-1} owing to ν_4, and at *ca* 455(m, br) cm^{-1} attributed to ν_2, attest the presence of coordinated SO_4^{2-}. The appearance of ν_1 and ν_2, as well as splitting of the ν_3 and ν_4 modes into three bands each clearly point to the bidentate nature of the sulphato ligand.[30] Further, a comparison of the IR results with those of the other sulphato complexes indicates that the ν_3 modes of the sulphato ligand of the present complexes fall in a comparatively lower region, suggesting in turn that the SO_4^{2-} is coordinated in a bridging bidentate manner.[30,31] The IR spectra of the complexes also support this view by exhibiting signals at *ca* 1150, 1110, and 1050 cm^{-1} due to ν_3, at *ca* 975 cm^{-1} due to ν_1, at *ca* 650, 610 and 570 cm^{-1} owing to ν_4, and *ca* 450 cm^{-1} due to the ν_2 mode of the coordinated sulphato ligand. Another common feature of the IR spectra of these complexes is a band at *ca* 485 cm^{-1} which has been assigned to a ν(Cu—F) mode. The broad nature of the band and its position imply the occurrence of a bridging fluoride rather than a terminal one. These observations thus suggest a double bridge arrangement involving both F^- and SO_4^{2-} leading to a situation presumably parallel to that encountered for fluoro(sulphato)manganate(III).[32] The additional bands at *ca* 3440 and 1640 cm^{-1}, observed in each of the spectra, resemble in shape and position, those of ν(O—H) and δ(H—O—H) modes of uncoordinated water.[15] Pyrolysis of $Na[CuF(SO_4)]\cdot 2H_2O$, $K[CuF(SO_4)]\cdot 3H_2O$ and $NH_4[CuF(SO_4)]\cdot 3H_2O$ at 125–130°C for 3 h led to the weight losses of 15.05%, 19.75% and 21.4%, respectively. The observed weight loss in each case corresponds to the loss of water molecules, lending further support to the presence of lattice water. The IR spectra of the compounds recorded before and after pyrolysis were similar except for the complete absence of water modes in the spectra of the pyrolysed samples. This causes us to infer that the complex ion does not undergo any apparent change on heating at 125–130°C.

The effective magnetic moments of the fluoro(sulphato)cuprate(II) hydrate at 298 K were found to lie between 1.60 and 1.65 BM. Although these values are lower than one normally expects for a Cu^{II} (d^9) system,[4] they are higher than that of $KCuF_3$. An internal comparison of observed magnetic moments of the two types of complex suggests that strong antiferromagnatism, operative in the case of $KCuF_3$, is largely controlled in the mixed-fluoro complexes in going from $[CuF_3]^-$ to $[CuF(SO_4)]^-$. Similar observations were also made in the case of some other metals.[16–18,25] Electronic spectra of the fluoro(sulphato)cuprate(II) complexes, recorded immediately after preparing their aqueous solutions, exhibited a band for each at *ca* 12400 cm^{-1} due to the transition $B_{1g} \rightarrow E_g$. This conforms with the occurrence of Cu^{II} in a distorted octahedral environment.[28] The ESR spectrum of solid $K[CuF(SO_4)]$, taken as a representative, at 298 K showed signals corresponding to three g values of 2.42, 2.20 and 2.13 with an average of 2.25. These compare very well with the literature data on Cu^{II} systems.[33] Further, the rhomic g values provide evidence for a fairly large component of low symmetry in the ligand field around the Cu^{II} centre leading to a distorted octahedral structure[33] of the complex species. Thus, it is evident from the results of physical studies that the complex $[CuF(SO_4)]^-$ has a distorted octahedral polymeric structure involving both fluoride and sulphate as bridging ligands between the contiguous Cu^{II} centres in the crystal lattice.

CONCLUSION

Pure $KCuF_3$ has been synthesized from the reaction of $Cu(OH)_2$ with KHF_2 and dilute hydrofluoric acid at pH $\leqslant$ 4. The appropriate acidity and a high concentration of F^- ions are of crucial importance. Mixed-ligand fluoro(sulphato)cuprate(II) complexes may be synthesized by reacting $Cu(OH)_2$ with 40% HF, alkali sulphate and the corresponding fluoride. Alternative routes involving oxidation of SCN^- or SO_2(g) by H_2O_2 in the presence of Cu^{II} and F^- ions have not been successful. A strong antiferromagnetism operative in the binary complex, $[CuF_3]^-$, is controlled to a large extent in the mixed-ligand $[CuF(SO_4)]^-$ complex. The results

of physical studies provide evidence for a distorted octahedral polymeric structure of the complex species with both fluoride and sulphate acting as bridging ligands in the crystal lattice.

Acknowledgements—The authors thank CSIR, New Delhi, for the award of a fellowship to M.D., and RSIC, NEHU, Shillong, for the analytical service. Helpful discussions with Prof. J. Subramanian are much appreciated.

REFERENCES

1. W. G. Palmer, *Experimental Inorganic Chemistry*. Cambridge University Press, Cambridge (1959).
2. A. Okazaki, Y. Suemune and T. Fuchikami, *J. Phys. Soc. Jpn* 1959, **14**, 1823.
3. J. Reedijk and R. W. M. ten Hoedt, *Recl. Trav. Chim. Pays-Bas.* 1982, **101**, 49: *Chem. Abstr.* **96**, 96351w.
4. D. J. Machin, R. L. Martin and R. S. Nyholm, *J. Chem. Soc.* 1963, 1490; 1500.
5. R. L. Martin, R. S. Nyholm and N. C. Stephenson, *Chem. Ind.* (Lond.) 1956, 83.
6. V. Scatturin, L. Corliss, N. Elliott and J. Hastings, *Acta Cryst.* 1961, **14**, 19; A. Okazaki and Y. Suemune, *J. Phys. Soc. Jpn* 1961, **16**, 671.
7. D. S. Crocket and H. M. Haendler, *J. Am. Chem. Soc.* 1960, **82**, 4158.
8. W. Ruedorff, G. Lincke and D. Babel, *Z. Anorg. Allg. Chem.* 1963, **320**, 150.
9. A. J. Edwards and R. D. Peacock, *J. Chem. Soc.* 1959, 4126.
10. K. Tanaka and F. Marumo, *Acta Cryst.* 1982, **B38**, 1422.
11. H. M. Haendler, F. A. Johnson and D. S. Crocket, *J. Am. Chem. Soc.* 1958, **80**, 2662.
12. R. W. M. ten Hoedt, J. Reedijk and G. C. Verschoor, *Recl. Trav. Chim. Pays-Bas.* 1981, **100**, 400: *Chem. Abstr.* **96**, 14586q.
13. J. Emsley, N. M. Reza, H. M. Dawes and M. B. Hursthouse, *J. Chem. Soc., Dalton Trans.* 1986, 313.
14. N. W. Alcock, M. M. Roberts and M. C. Chakravorti, *Acta Cryst.* 1980, **B36**, 687.
15. M. N. Bhattacharjee, M. K. Chaudhuri, H. S. Dasgupta and D. T. Khathing, *J. Chem. Soc., Dalton Trans.* 1981, 2587; M. N. Bhattacharjee and M. K. Chaudhuri, *Inorg. Synth.* 1986, **24**, 50.
16. M. N. Bhattacharjee and M. K. Chaudhuri, *Polyhedron* 1984, **3**, 399.
17. M. N. Bhattacharjee, M. K.Chaudhuri and R. N. Dutta Purkayastha, *Inorg. Chem.* 1985, **24**, 447.
18. M. N. Bhattacharjee, M. K. Chaudhuri, M. Devi and K. Yhome, *J. Chem. Soc., Dalton Trans.* 1987, 1055.
19. M. A. Soldatkina, L. B. Serezhkina and V. N. Serezhkin, *Russ. J. Inorg. Chem.* 1985, **30**, 1640.
20. S. L. Edwards, T. L. Poulos and J. Krant, *J. Biol. Chem.* 1984, **259**, 12984.
21. M. K. Chaudhuri, S. K. Ghosh and Z. Hiese, *Transition Met. Chem.* 1985, **10**, 321.
22. A. I. Vogel, *A Text Book of Quantitative Inorganic Analysis*, 4th edn, (a) p. 379; (b) p. 343; (c) p. 504. ELBS and Longman, London (1978).
23. M. K. Chaudhuri and S. K. Ghosh, *Inorg. Chem.* 1982, **21**, 4020; M. K. Chaudhuri and S. K. Ghosh, *J. Chem. Soc., Dalton Trans.* 1984, 507.
24. B. Cox and A. G. Sharpe, *J. Chem. Soc.* 1954, 1798.
25. M. N. Bhattacharjee and M. K. Chaudhuri, *Transition Met. Chem.* 1986, **11**, 193.
26. M. K. Chaudhuri and N. S. Islam, *Inorg. Chem.* 1986, **25**, 3749.
27. W. E. Dasent and D. Morrison, *J. Inorg. Nucl. Chem.* 1964, **26**, 1122.
28. D. Oelkrug, *Angew Chem. Int. Ed. Engl.* 1966, **5**, 744.
29. R. D. Peacock and D. W. A. Sharp, *J. Chem. Soc.* 1959, 2762.
30. K. Nakamoto, *Infrared and Raman Spectra of Inorganic and Coordination Compounds*, 3rd edn, p. 239. Wiley, New York (1978); A. R. Miksztal and J. S. Valentine, *Inorg. Chem.* 1984, **23**, 3548.
31. C. G. Barraclough and M. L. Tobe, *J. Chem. Soc.* 1961, 1993.
32. A. J. Edwards, *J. Chem. Soc. A.* 1971, 3074.
33. B. N. Figgis, *Introduction to Ligand Fields*, p. 218. Wiley-Eastern, New Delhi (1976).

Polyhedron Vol. 8, No. 4, pp. 463–467, 1989
Printed in Great Britain

0277–5387/89 $3.00+.00
© 1989 Pergamon Press plc

A KINETIC STUDY OF THE REACTION BETWEEN THIOUREA AND ETHYLENEDIAMINETETRAACETATO RUTHENATE(III) COMPLEX BY THE STOPPED FLOW TECHNIQUE

M. M. TAQUI KHAN* and R. M. NAIK

Discipline of Coordination Chemistry and Homogeneous Catalysis, Central Salt and Marine Chemicals Research Institute, Bhavnagar 364 002, India

(*Received* 19 *April* 1988; *accepted after revision* 15 *August* 1988)

Abstract—The kinetics of reaction between thiourea and $[Ru^{III}(H\text{-}EDTA)(H_2O)]$ (**1**) were investigated in aqueous solution as a function of pH, temperature and metal ion concentration at 0.1 M ionic strength using the stopped flow technique. It was established that the monoanionic species of complex **1**, $[Ru^{III}(EDTA)(H_2O)]^-$ (**2**) is the major reacting species over the pH range 1.5–8.5. The substitution reaction follows first-order kinetics in $[Ru(EDTA)(H_2O)]^-$ as well as in thiourea concentrations over a wide concentration range of the two reactants. The rate constant (k_1) was found to be $(2.04\pm0.17)\times10^3$ M^{-1} s^{-1} at 25°C and $\mu = 0.1$ M (KCl). From the activation parameters of the reaction it was concluded that the substitution reaction of $[Ru(EDTA)H_2O]^-$ follows an associative mechanism. The reactivities of different species of the thiourea complexes formed, have also been discussed.

The potentially hexadentate chelating agent EDTA forms complexes with many metal ions. The EDTA complexes of Ru^{III} have been known for more than a decade.[1–5] We have recently investigated the equilibrium and electrochemical and kinetic studies on the interaction of $[Ru(H\text{-}EDTA)H_2O]$ (**1**) with H_2O_2 and O_2.[6,7] The potentiometric data on **1** shows the EDTA ligand to be pentadentate in aqueous solution at low pH values.[6] The complex has a pK_a of 7.86 ± 0.02 at 30° ($\mu = 0.1$ M KCl) corresponding to the dissociation of a proton from the coordinated H-EDTA moiety. Furthermore, the single titrable proton corresponding to the above pK_a value is consistent with the presence of a water molecule bound to the metal ion. Thus, all the available experimental observations reveal that the dominant form of complex **1** contains pentadentate EDTA in aqueous solution with the sixth coordination site of the metal centre occupied by a water molecule (or by a hydroxide ion at higher pH values).

In this paper, we report the kinetics of the reaction between thiourea and complex **1** at $\mu = 0.1$ M KCl and temperature (T) = 25°C in the pH range 1.5–8.5. The equilibrium constant and the stoichiometry of the complex formed, have also been determined by the mole ratio method.[8] The activation parameters for the reaction have been evaluated and discussed. The rate constants due to different reactive species were calculated.

EXPERIMENTAL

The complex[9] $K_2[RuCl_5\cdot H_2O]$ was used as the starting material for the synthesis[10] of the complex $K[Ru(H\text{-}EDTA)H_2O]$ (**1**). A. R. grade thiourea was used as such without any purification. The ionic strength of the reactants was maintained at 0.1 M using KCl. The temperature of the reactants was maintained at the desired value by a thermostat before mixing the reactants inside the reaction chamber of a stopped flow spectrophotometer Hi-Tech coupled with an Apple data processor. The reaction was followed under pseudo-first-order conditions taking a large excess of thiourea by monitoring the peak at 468 nm which is the λ_{max} of $[Ru(EDTA)(thiourea)]^-$ complex formed.[11] The pseudo-first-order rate constants were calculated from plots of log $(A_\infty - A_t)$ vs time.

*Author to whom correspondence should be addressed.

RESULTS AND DISCUSSION

1. *Stoichiometry of the reaction of thiourea with complex* **1**

The mole ratio method was used to determine the stoichiometry of the complex formed by the displacement of water by thiourea in complex **1**. The absorbance at 468 (λ_{max} of [Ru(EDTA-H)(thiourea)]) was measured as a function of mole ratio of [Ru(H-EDTA)H_2O] to [thiourea]. The plot of absorbance vs mole ration in Fig. 1 clearly indicates that a 1:1 complex is formed immediately after mixing of the reactants. The equilibrium constant for reaction (1) was determined from the ratio of intercept to slope of the plot of

$$\frac{1}{\Delta A} \text{ vs } \frac{1}{[\text{Thiourea}]}$$

(Fig. 2). The value of equilibrium constant K determined is 9.04×10^3.

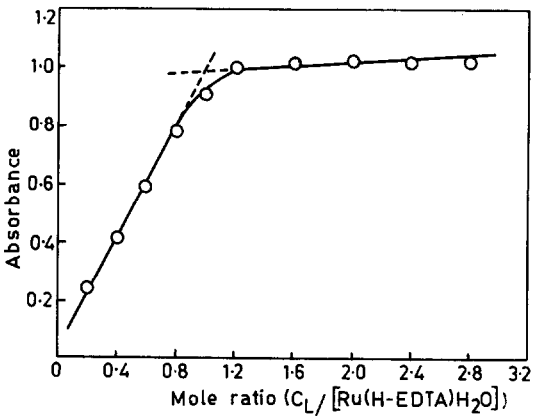

Fig. 1. Determination of stoichiometry by the mole ratio method. [Ru(H-EDTA)H_2O] = 5×10^{-4} M, μ = 0.1 KCl, pH = 3.0 and T = 25°C.

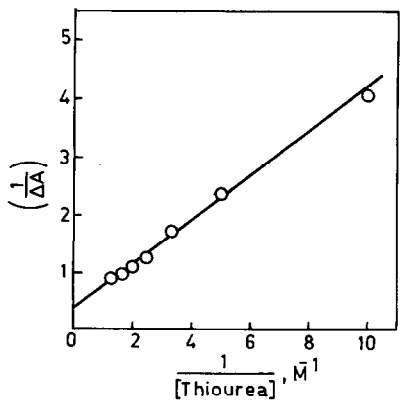

Fig. 2. Determination of the stability constant for [Ru(H-EDTA)(thiourea)] at μ = 0.1 M and T = 25°C.

Table 1. Thiourea dependence of the observed pseudo-first-order rate constant (k_{obs}) for its reaction with [Ru(H-EDTA)H_2O]$_T$, [Ru(H-EDTA)H_2O]$_T$ = 5×10^{-4} M, pH = 3.0±0.02, μ = 0.1 M (KCl) and T = 25°C

$10^2 \times$ [Thiourea] (M)	$10^{-1} \times k_{obs}$ (s^{-1})	$10^{-3} \times k_1$ ($M^{-1}s^{-1}$)
0.6	1.27	2.11
1.1	2.58	2.34
2.7	5.43	2.01
4.0	7.30	1.82
5.0	9.70	1.94

$k_1^{av} = (2.04 \pm 0.17) \times 10^3\ M^{-1}\ s^{-1}$.

2. *Kinetics of the substitution reaction*

The reaction between **1** and thiourea follows first-order dependence in **1** as well as in thiourea concentration over a wide range of concentrations. The pseudo-first-order plots of log ($A_\infty - A_t$) vs time were linear for at least three half lives of the reaction. The results in Table 1 show that the reaction is first-order in both the reactants over a wide range of concentration and pH. The values of pseudo-first-order rate constants (k_{obs}) obtained from the plot of log ($A_\infty - A_t$) vs time are plotted against thiourea concentration (Fig. 3).

3. *Dependence of rate on pH*

The kinetic measurements over a wide pH range of 1.5–8.5 (Fig. 4) (Table 2) show the pH dependence of the reaction. The rate constant of the reaction was found to increase in the pH range 1.5–4.5, remain constant in the pH range 4.5–6.5 and decrease in the higher pH range (6.5–8.5) (Fig. 4).

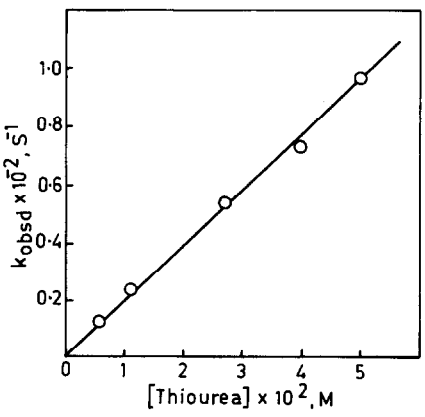

Fig. 3. Thiourea dependence of observed pseudo-first-order rate constant for the reaction of thiourea with [Ru(EDTA)H_2O]. Reaction conditions as in Table 1.

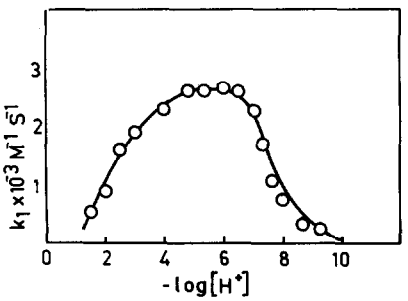

Fig. 4. pH Dependence of the reaction of thiourea with [Ru(H-EDTA)H_2O]. [Ru(H-EDTA)H_2O]$_T = 5 \times 10^{-4}$ M, [Thiourea] $= 5 \times 10^{-2}$ M, $\mu = 0.1$ M (KCl) and $T = 25°C$.

This interesting behaviour of the reaction over the entire pH range can be explained in terms of different reactivities of species **1** towards the nucleophile $SC(NH_2)_2$. Complex **1** can exist in three forms viz. protonated [Ru(H-EDTA)H_2O] **1a**, neutral [Ru(EDTA)H_2O]$^-$ **1b** and hydroxo form [Ru(EDTA)OH]$^{2-}$ **1c**. The species **1b** was found to be the most reactive species over the whole pH region. The rate constants due to these species can be calculated by an algebraic assignment of the specific rate constants outlined below. The rate of reaction (1) may be expressed by eq. (2).

$$[Ru(H\text{-}EDTA)H_2O] + [thiourea] \underset{k_{-1}}{\overset{k_1}{\rightleftharpoons}} [Ru(H\text{-}EDTA)(thiourea)] + H_2O. \quad (1)$$

$$\text{Rate} = k_1 [Ru(H\text{-}EDTA)H_2O]_T [thiourea]. \quad (2)$$

Table 2. pH Dependence of the rate constant (k_1) for the reaction of thiourea with [Ru(H-EDTA)H_2O], [Ru(H-EDTA)H_2O]$_T = 5 \times 10^{-4}$ M, [Thiourea] $= 5 \times 10^{-2}$ M $\mu = 0.1$ M (KCl) and $T = 25°C$

pH	$10^{-3} \times k_1$ ($M^{-1}\ s^{-1}$)
1.50	0.55
2.02	0.94
2.50	1.66
3.00	1.95
4.02	2.30
4.70	2.65
5.30	2.64
6.02	2.70
6.52	2.65
7.02	2.30
7.30	1.70
7.60	1.10
8.02	0.76
8.62	0.35
9.30	0.30

The total concentration of Ru^{III} complex [Ru(EDTA)(H_2O)]$_T$ can be expressed by a sum of the concentration of the three species **1a**, **1b** and **1c**.

$$[Ru(H\text{-}EDTA)H_2O]_T = \underset{\mathbf{1a}}{[Ru(H\text{-}EDTA)H_2O]} + \underset{\mathbf{1b}}{[Ru(EDTA)H_2O]^-} + \underset{\mathbf{1c}}{[Ru(EDTA)OH]^{2-}}. \quad (3)$$

Substituting the pK_{a_1} and pK_{a_2} values[6] of [Ru(EDTA)H_2O]$^-$ and [Ru(EDTA)OH]$^{2-}$, eq. (3) can be finally expressed in the form of eq. (4):

$$\frac{[Ru(H\text{-}EDTA)H_2O]_T}{[Ru(H\text{-}EDTA)H_2O]} = 1 + \frac{K_{a_1}}{[H^+]} + \frac{K_{a_1} \times K_{a_2}}{[H^+]^2}, \quad (4)$$

where K_{a_1} and K_{a_2} are expressed as follows,

$$K_{a_1} = \frac{[Ru(EDTA)H_2O][H^+]}{[Ru(H\text{-}EDTA)H_2O]} = 4.27 \times 10^{-3}\,M, \quad \text{(ref. 12)}$$

$$K_{a_2} = \frac{[Ru(EDTA)(OH)]^{2-}[H^+]}{[Ru(EDTA)H_2O]} = 2.34 \times 10^{-8}\,M. \quad \text{(ref. 12)}$$

The pH dependence of the rate constant for reaction (1) can be analysed in terms of the following reaction pathways:

$$[Ru(H\text{-}EDTA)H_2O] + L \xrightarrow{k_a} [Ru(H\text{-}EDTA)L] + H_2O, \quad (5)$$

$$[Ru(EDTA)H_2O]^- + L \xrightarrow{k_b} [Ru(EDTA)L]^- + H_2O, \quad (6)$$

$$[Ru(EDTA)(OH)]^{2-} + L \xrightarrow{k_c} [Ru(EDTA)L]^- + OH^-, \quad (7)$$

where L = thiourea.

The rate constant (k_1) given by eq. (2) can be expressed in terms of the specific rate constants k_a, k_b and k_c of the three species in the form:

$$k_1 \left(\frac{[Ru(H\text{-}EDTA)H_2O]_T}{[Ru(H\text{-}EDTA)H_2O]} \right) = k_a + k_b \left(\frac{K_{a_1}}{[H^+]} \right) + k_c \left(\frac{K_{a_1} \times K_{a_2}}{[H^+]^2} \right). \quad (8)$$

In order to simplify the evaluation of the rate parameters of eq. (8), one can consider the sections of the pH rate profile of Fig. 4.

In the pH range 1.5–4.5, it is assumed that $k_b \gg k_a$

or k_c. Thus, it is reasonable to neglect the contribution from path k_c (eq. 8) in the above pH range. Similarly, in the pH range (4.5–8.5), the contributions from path k_a (eq. 5) can be ignored.

Applying the above approximations to eq. (8), the rate expression finally reduces to eqs (9) and (10), respectively:

$$k_1\left(1+\frac{K_{a_1}}{[H^+]}\right)=k_a+k_b\left(\frac{K_{a_1}}{[H^+]}\right),$$

(at pH $\leqslant$ 4.5) (9)

$$k_1\left(1+\frac{[H^+]}{K_{a_1}}\right)=k_c+k_b\left(\frac{[H^+]}{K_{a_2}}\right).$$

(at pH $\geqslant$ 4.5) (10)

The plot of the left hand side of eq. (9) vs $1/[H^+]$, yields a straight line (Fig. 5) which gives the values of the rate constants ($k_a = 5\times10^2\,M^{-1}s^{-1}$) and ($k_b = 2.34\times10^3\,M^{-1}s^{-1}$) from the intercept and slope of the above plot, respectively. Similarly, a plot of the left hand side of eq. (10) vs $[H^+]$ gives a straight line where the values of the constants ($k_c \approx 0\,M^{-1}s^{-1}$) and ($k_b = 2.6\times10^3\,M^{-1}s^{-1}$) were calculated from the intercept and slope of the plot, respectively (Fig. 6). The intercept of Fig. 6 is almost zero within experimental error. This clearly shows that the species $[Ru(EDTA)(OH)]^{2-}$ is the least reactive of the three species. The reactivities of different species of **1** over the entire pH range, thus follow the order $[Ru(EDTA)(OH)]^{2-}$ < $[Ru(H\text{-}EDTA)H_2O]$ < $[Ru(EDTA)H_2O]^-$. The substitution of the aqua group by thiourea, thus proceeds through the major path k_b in the entire pH range studied. Similar rate vs pH profiles were observed in several other systems.[11,12]

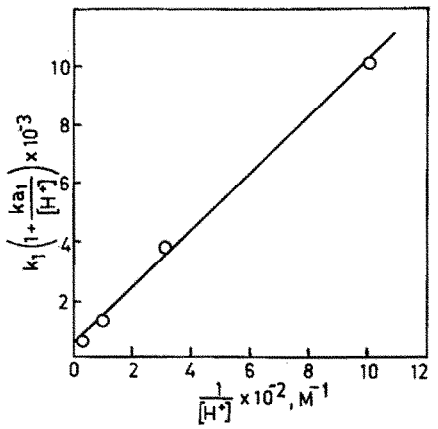

Fig. 5. Resolution of rate constants due to the reaction of $[Ru(H\text{-}EDTA)H_2O]$ and $[Ru(EDTA)H_2O]^-$ with thiourea. Plot of

$$k_1\left(1+\frac{K_{a_1}}{[H^+]}\right) \text{ vs } \frac{1}{[H^+]},$$

at $\mu = 0.1$ M and $T = 25$°C.

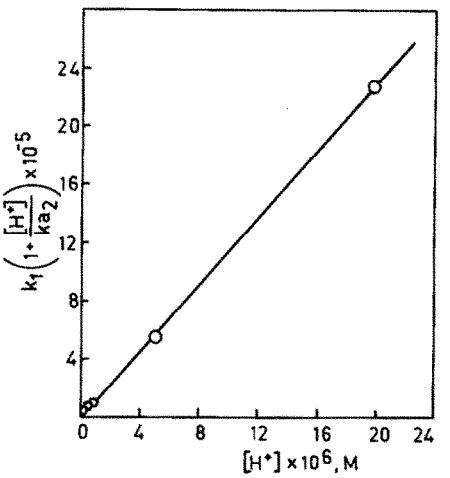

Fig. 6. Resolution of rate constant due to the reaction of $[Ru(EDTA)H_2O]^-$ and $[Ru(EDTA)(OH)]^{2-}$ with thiourea. Plot of

$$k_1\left(1+\frac{[H^+]}{K_{a_2}}\right) \text{ vs } [H^+],$$

at $\mu = 0.1$ M KCl and $T = 25$°C.

4. *Effect of temperature on reaction rate*

The reaction was studied over a wide temperature range. The activation energy E_a was calculated from the plot of log (k_1) vs $1/T$ (Fig. 7; Table 3). The enthalpy of activation, $\Delta H^{\ddagger}$ and entropy of activation, $\Delta S^{\ddagger}$ were also calculated. The values of the

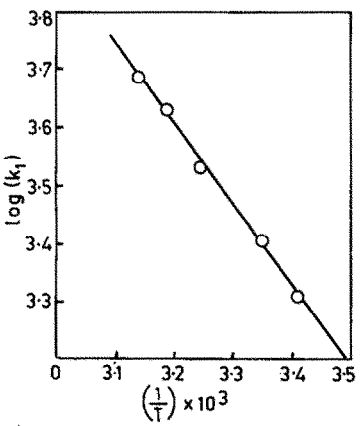

Fig. 7. Plot of log (k_1) vs $1/T$ for the determination of activation parameters E_a, $\Delta H^{\ddagger}$ and $\Delta S^{\ddagger}$. $[Ru(H\text{-}EDTA)H_2O] = 5\times10^{-4}$ M, [Thiourea] $= 5\times10^{-3}$ M, $\mu = 0.1$ M KCl, pH $= 3.0\pm0.02$.

Table 3. Temperature dependence of the rate constant (k_1) for the reaction of thiourea with [Ru(H-EDTA)H_2O], [Ru(H-EDTA)H_2O]$_T = 5\times10^{-4}$ M, [Thiourea] $= 5\times10^{-3}$ M, pH $= 3.0\pm0.02$ and $\mu = 0.1$ M (KCl)

$10^{-3}\times k_1$ ($M^{-1}s^{-1}$)	Temperature (K)
2.06	293
2.56	293
3.45	308
4.30	313
4.90	318

parameters, E_a, $\Delta H^{\ddagger}$ and $\Delta S^{\ddagger}$ were found to be 26.7 kJ mol^{-1}, 24.4 kJ mol^{-1} and -97.2 JK^{-1} mol^{-1}, respectively.

The high negative value of $\Delta S^{\ddagger}$ favours an associative S_N^2 mechanism for the displacement of water by thiourea in complex **1**. The values of enthalpies of activation for substitution reactions of Ru^{III}—OH_2 species with other ligands were found to be in the range 80–100 kJ mol^{-1}.[13,14] These data clearly indicate a high energy barrier for cleavage of the M—OH_2 bond and a dissociative nature of these reactions.

In the displacement reaction of water by thiourea in complex **1**, however, the enthalpy barrier is lowered to an appreciable extent possibly due to an associative mechanism. It is to be emphasized here that the associative mechanism is only indicative from the second-order mechanism which is always obtained by the I_d replacement of water. The reactivity of complex **1** towards substitution reaction through an associative activation is possible because of the presence of free carboxylate group in complex **1** and availability of labile coordination sites on the complex. Recently, the single crystal X-ray analysis has confirmed that EDTA is five coordinate in complex **1** and in [Ru(EDTA-H)Cl_2], EDTA is four coordinate.[15] This flexibility of coordinated EDTA in complex **1** thus allows the simultaneous coordination of thiourea and the H_2O molecule in the transition state and supports a low energy associative pathway. The space filling model of complex **1** indicates that hydrogen bonding between the free carboxylate group, the coordinated water molecule and thiourea appears favourable. The highly negative value of $\Delta S^{\ddagger}$ again supports steric crowding in the transition state and distortion in the EDTA ligand in complex **1**. Other structurally similar complexes[16,17] viz. [Fe(EDTA)H_2O]$^-$ and [Cr(EDTA)H_2O]$^-$ also follow an associative mechanism like complex **1** in their reaction with nucleophiles.

REFERENCES

1. M. M. Taqui Khan and G. Ramachandraiah, *Inorg. Chem.* 1982, **21**, 2109.
2. M. M. Taqui Khan, A. Hussain, K. Venkatasubramanian, G. Ramachandraiah and V. Oommen, *J. Mol. Catal.* 1988, **44**, 117.
3. M. Mikadia, H. Okuno and T. Ishimori, *Nippon Kagaku Zasshi* 1965, **86**, 589.
4. N. A. Ezerskaya and T. P. Solovykh, *Russ. J. Inorg. Chem.* (*Eng. Transl.*) 1966, **11**, 991.
5. J. Scherzer and L. B. Clapp, *J. Inorg. Nucl. Chem.* 1968, **30**, 1107.
6. M. M. Taqui Khan, A. Hussain, G. Ramachandraiah and M. A. Moiz, *Inorg. Chem.* 1986, **25**, 3023, and references therein.
7. M. M. Taqui Khan, H. C. Bajaj and M. R. H. Siddiqui, *J. Mol. Catal.* 1988, **44**, 279.
8. S. Brewer, *A Text Book on Analytical Chemistry*, pp. 289–294. Wiley (1980).
9. E. E. Mercer and R. R. Buckley, *Inorg. Chem.* 1965, **4**, 1692.
10. A. A. Diamantis and J. V. Dubrawaski, *Inorg. Chem.* 1981, **20**, 1142.
11. Y. Yoshino, T. Vehiro and M. Saito, *Bull. Chem. Soc. Japan* 1979, **52**, 1060.
12. T. Matsubara and C. Creutz, *Inorg. Chem.* 1979, **18**, 1956, and references therein.
13. J. A. Broomhead and L. Kane Maguire, *Inorg. Chem.* 1971, **10**, 85.
14. J. A. Broomhead, F. Basolo and R. G. Pearson, *Inorg. Chem.* 1964, **3**, 10.
15. M. M. Taqui Khan (unpublished work).
16. J. L. Hoard, M. Lind and J. V. Silverton, *J. Am. Chem. Soc.* 1961, **83**, 2770.
17. Y. Sulfab, R. S. Taylor and A. G. Skyes, *Inorg. Chem.* 1976, **15**, 2388.

Polyhedron Vol. 8, No. 4, pp. 469–472, 1989
Printed in Great Britain

0277–5387/89 $3.00+.00
© 1989 Pergamon Press plc

HOMOGENEOUS CATALYTIC HYDROGEN FORMATION USING A DITUNGSTEN CLUSTER AND LOW VALENCY METAL IONS IN AQUEOUS ACIDIC SOLUTIONS

CONSTANTINOS MERTIS* and NIKOS PSAROUDAKIS

University of Athens, Inorganic Chemistry Laboratory, Navarinou 13A 10680 Athens, Greece

(*Received* 20 *June* 1988; *accepted* 15 *August* 1988)

Abstract—The formally triply-bonded nonachlorodimetallates $[W_2(\mu\text{-}Cl)_3Cl_6]^{3-}$ (**6**) and $[Re_2(\mu\text{-}Cl)_3Cl_6]^{-}$ (**8**) undergo a two-electron homogeneous reduction by the chromous or vanadous ions to give the quadruply-bonded species $[W_2Cl_8]^{4-}$ (**4**) and $[Re_2Cl_8]^{2-}$ (**7**). In aq. HCl solutions complex **6** is an effective catalyst for the anaerobic oxidation of Cr^{II} and V^{II} to Cr^{III} and V^{III} with simultaneous dihydrogen formation.

Direct commercial production of hydrogen from water by electrolysis is uneconomic and considerable research into the possibility of splitting water using light[1] or thermal[2] energy is being carried out.

Industrially, hydrogen is produced heterogeneously from synthesis gas ($CO—H_2$) by the water–gas shift reaction. Homogeneous catalysts for this reaction are known and effective on a laboratory scale but require drastic conditions and much effort has been devoted to obtain hydride complexes[3a] operating at lower temperatures. There exist neutral, basic, and also acidic [$Rh(CO)_2I_2^-$, KI, CH_3CO_2H, HCl, H_2O or K_4PtCl_4, $SnCl_4 \cdot 5H_2O$, CH_3CO_2H, HCl, H_2O at 100°C] systems.[3b]

Although not strictly related to the above processes, relevant homogeneous hydrogen-producing acidic systems ($K_3Mo_2HCl_8$, $CrCl_2$, H_2O, HCl at 25°) have been recently reported[4] based on the ability of the dimolybdenum species to form hydrides which then react with the low-valency metal ion, equation (1):

$$[Mo_2HCl_8]^{3-} + 2Cr^{2+} + H^+ \xrightarrow{H^+} [Mo_2Cl_8]^{4-} + 2Cr^{3+} + \tfrac{1}{2}H_2. \quad (1)$$

Proton oxidative addition to the quadruply-bonded octachlorodimetallate anions $[M_2Cl_8]^{4-}$ (M = Mo, **1**; M = W, **4**) yielding the formally triply-bonded hydrides $[M_2(\mu\text{-}H)(\mu\text{-}Cl)_2Cl_6]^{3-}$ (M = Mo, **2**; M = W, **5**) coupled with diprotonation and loss of hydrogen to produce the analogous nonachloro derivatives $[M_2(\mu\text{-}Cl)_3Cl_6]^{3-}$ (M = W, **6**) are well established reactions, eqs (2) and (3):

$$[M_2Cl_8]^{4-} \xrightarrow{HCl} [M_2HCl_8]^{3-} \xrightarrow[-H_2]{HCl} [M_2Cl_9]^{3-}.$$
(2) (3)

The structures both of the reactants **1**, **4** and of the products **2**, **3**, **6** are known.[5]

However, reaction (1) requires strenuous conditions in the case of molybdenum (60°C in 12 M HCl), whereas the rhenium derivative $[Re_2Cl_8]^{2-}$ (**7**) resists protonation even after refluxing for several hours. Accordingly, $[Mo_2(\mu\text{-}Cl)_3Cl_6]^{3-}$ (**3**) and $[Re_2(\mu\text{-}Cl)_3Cl_6]^{-}$ (**8**) are best prepared by electrochemical oxidation[6] of **2** or chlorine oxidation[7] of **7**, respectively. In contrast, the isoelectronic and isostructural tungsten compound **4**, reacts[8] at −78°C giving **6**, presumably via the reactive[9] unstable hydride **5**.

Reactions (2) and (3) are easily reversible for molybdenum[4,10] and also the reduction of **8** to **7** for rhenium[7] whereas for tungsten they are not.[8,11,12] This enhanced susceptibility of W—W bonds to protons or other oxidants and the irreversibility of these reactions has been the reason for:

(a) the slow development in the chemistry of the W_2^{4+} unit and the long and numerous efforts for the isolation of **4** achieved eventually by the Na/Hg reduction[8,13] of $(WCl_4)_n$ or

*Author to whom correspondence should be addressed.

$W_2Cl_6(THF)_4$ in tetrahydrofuran, eq. (4):

$$W_2Cl_6(THF)_4 + 2Na/Hg \xrightarrow[-30°C]{THF} \tfrac{1}{2}Na_4(THF)_xW_2Cl_8 + \text{“}WCl_2\text{”}. \quad (4)$$

The product is thermally unstable at room temperature, in any solvent it dissolves,[8] eq. (5):

$$Na_4(THF)_xW_2Cl_8 \xrightarrow[\theta > 0°C]{THF} 4NaCl + 2\text{“}WCl_2\text{”}; \quad (5)$$

and

(b) the belief that these allegedly important catalytic species are in fact kinetic and thermodynamic sinks and therefore relatively uninteresting in terms of their catalytic properties.

We now describe the facile homogeneous two-electron reduction of the diamagnetic **6** and **8** to give **4** and **7**, respectively by the paramagnetic $Cr^{2+}_{(aq)}$ or $V^{2+}_{(aq)}$ ions and the low-temperature catalytic anaerobic oxidation of Cr^{II} and V^{II} to Cr^{III} and V^{III} by **6** with simultaneous hydrogen evolution in aq. HCl solutions.

EXPERIMENTAL

The potassium salts of $[Mo_2Cl_9]^{3-}$, $[W_2Cl_9]^{3-}$ and the tetra-*n*-butyl ammonium salts of $[Re_2Cl_8]^{2-}$ and $[Re_2Cl_9]^{-}$ were prepared by literature methods.[7,11,14,15] $CrCl_2$ was supplied by Ventron and $VCl_2 \cdot 4H_2O$ was prepared electrochemically.[16] All reagents were of analytical grade and thoroughly purified. Demineralized by ion exchange and doubly-distilled water was used. Solvents were very carefully deoxygenated by freeze pumping and all reactions were carried out under strictly anaerobic conditions (atmosphere of argon). Microanalyses were performed in this Laboratory and at the Research Center "Democritos". Tungsten was determined by neutron activation and chloride ions, photometrically. Electronic spectra were recorded with a Hitachi and a Carry 17; Dihydrogen was detected by gas chromatography (GC; Varian 90-P).

Reaction of tripotassium-1,1,1-*trichloro*-2,2,2-*trichloro-tris-μ-chloro-ditungsten*(III) *with* $CrCl_2$ *or* VCl_2

To a solution of $K_3W_2Cl_9$ (0.240 g, 0.298 mmol) and KCl (0.023 g, 0.309 mmol) in aq. 6 M HCl (100 cm^3), $CrCl_2$ (0.327 g, 3.02 mmol) or $VCl_2 \cdot 4H_2O$ (0.596 g, 3.07 mmol) was added at room temperature and under stirring. After *ca* 2.5 h the mixture was filtered, the solvent was removed *in vacuo* and the residues were extracted with tetrahydrofuran. The solution was removed by filtering and the residue was washed with small portions of tetrahydrofuran, dried *in vacuo*, and identified by elemental analysis and spectroscopy to be $K_3W_2Cl_9$; yield 80%.

Reaction of tripotassium 1,1,1-*trichloro*-2,2,2-*trichloro-tris-μ-chloro-dimolybdenum*(III) *with* $CrCl_2$ *or* VCl_2

The same procedure as described for $K_3W_2Cl_9$ or the corresponding $[(n\text{-}C_4H_9)_4N]_3Mo_2Cl_9$[4] was employed for the reduction of **3** to **1** (6 M HCl, $t = 2.5$ h); yield 87%.

The reaction was monitored by visible spectroscopy in 8–10 M HCl, and mixtures of **1** and **2** depending on the reaction time, were isolated following the same work-up procedure.

Reaction of tetra-n-*butylammonium*-1,1,1-*trichloro*-2,2,2-*trichloro-tris-μ-chloro-dirhenium*(IV) *with* $CrCl_2$ *or* VCl_2

To a solution of $[Bu^n_4\text{—}N]Re_2Cl_9$ (0.502 g, 0.538 mmol) and $(Bu^n_4\text{—}N)Cl$ (0.150 g, 0.541 mmol) in tetrahydrofuran (20 cm^3) was added at room temperature a solution of $CrCl_2$ (0.399 g, 3.25 mmol) or $VCl_2 \cdot 2CH_3OH$ (0.61 g, 3.28 mmol) dissolved in 6 M HCl (5 cm^3).

The mixture was left to react under stirring *ca* 2 h and a blue precipitate was formed. This was filtered, washed with methanol dried *in vacuo*, and identified by elemental analysis and spectroscopy to be $(Bu^n_4\text{—}N)_2Re_2Cl_8$; yield, 92%.

RESULTS AND DISCUSSION

When carefully deoxygenated aqueous solutions of one equivalent of $K_3W_2Cl_9$/KCl and an excess of $CrCl_2$, **9**, were mixed at room temperature or at −5°C, the colour quickly changes and a precipitate is formed. The mixture was filtered, washed with water and tetrahydrofuran leaving behind a grey–black powder insoluble in most common organic solvents.

The light green filtrate contains a mixture of $Cr^{2+}_{(aq)}$ (broad peak at 650–700 nm) and $Cr^{3+}_{(aq)}$ (peaks at 412 and 590 nm).[17] Similar results are obtained when an aq. 0.125 M HCl solution of VCl_2 (**10**) was employed. The composition of the precipitate depends on the reaction conditions (acid con-

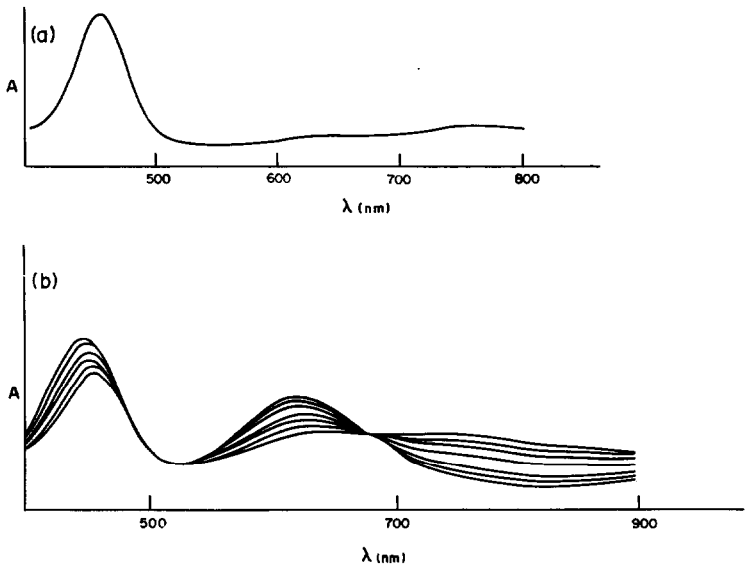

Fig. 1. (a) Spectrum of $K_3W_2Cl_9$ (6.5×10^{-4} M) in 6 M HCl at 25°C. (b) Spectral changes of a mixture of $K_3W_2Cl_9$ (6.9×10^{-4} M) and $CrCl_2$ (1.6×10^{-2} M) in 6 M HCl at 25°C recorded at 15-min intervals.

centration) and approximately analyses as "$WCl_{2-x}(OH)_x$", $x = 0 \ldots 1$.

The insolubility of various salts of **6** [K^+, $(Ph_4As)^+$, $(Bu^n_4—N)^+$] in tetrahydrofuran precluded the reaction at low temperature in this medium where the intensely blue-coloured **4** is more stable[8] (598 nm, 0°C) and attempts to detect or to isolate it as its TMEDA adduct.[13]

In mixture(s) of tetrahydrofuran–water, in which all the reactants are soluble, a transient formation of a bluish colour at −20°C is observed but it is followed by fast decomposition as described above.

However, the same reaction when carried out in aq. HCl solutions (from 6 to 12 M) produced only small amounts of the insoluble precipitate and hydrogen evolution was observed (identified by GC).

The reaction can be followed spectroscopically (Fig. 1).

The intensity of the peak at 452 nm attributed to **6** increases whereas a peak at 615 nm due to $Cr^{3+}_{(aq)}$, probably as a mixture of $[Cr(H_2O)_5Cl]^{2+}$ (peaks at 430, 605 nm) and $[Cr(H_2O)_4Cl_2]^{2+}$ (peaks at 450, 635 nm),[17] appears. Also, the peak due to $V^{2+}_{(aq)}$ (860, 560 nm) at 860 nm disappears and a shoulder at 400 nm characteristic of the $V^{3+}_{(aq)}$ ion (peaks at 588, 400, 263)[18] appears next to the peak of **6** at 452 nm.[19]

After removing the solvent *in vacuo*, the residues were extracted with tetrahydrofuran leaving behind a deep green solid identified as **6**; the filtrates contain Cr^{III} in the form of the dichloro complex $[Cr(THF)_4Cl_2]^+$ (peaks at 445 and 640 nm) or V^{III} (peaks at 502, 751 nm).[18] If a large excess of the reducing metal ion was used (from 4 to 200 mol) under identical conditions, the reaction proceeds exothermically and cooling is necessary. Again hydrogen is evolved, **6** was recovered unchanged and **9** or **10** were oxidized quantitatively to their trivalent states.

In view of the instability of **4**, expected to be even greater in water than in organic solvents, we propose that in aqueous media a two-electron reduction occurs to give **4** [eq. (6)] followed by its fast decomposition and/or hydrolysis:

$$\underset{\mathbf{6}}{[W_2Cl_9]^{3-}} + 2Cr^{2+} \xrightarrow{H_2O} \underset{\mathbf{4}}{[W_2Cl_8]^{4-}} + 2Cr^{3+} + Cl^- \quad (6)$$

In acid, decomposition is prevented because reactions (2) and (3) intercept reproducing **6**, thus the W_2^{6+}/W_2^{4+} couple participates in the catalytic cycle (Fig. 2).

The hydrogen evolved comes from reactions (2) and (3). The electrons required are provided by the low-valency metal ions which are consumed (oxidized), respectively. Parallel formation of hydrogen from the reduction of the tungsten hydride (**5**), similarly as for molybdenum [eq. (1)] is possible, and may occur to a small extent at low acid concentrations in which reaction (3) is slower.

With the potassium salt of **3** analogous results are obtained but because the rate of reaction (2) is slow, and (3) does not practically proceed under the reaction conditions, the hydrogen evolved derives from reaction (2). The Mo_2^{4+}/Mo_2^{6+} couple essen-

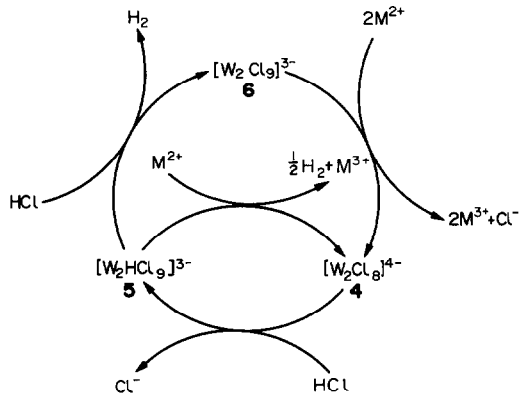

Fig. 2. The binuclear tungsten complex **6** catalyses the evolution of H_2 in HCl solutions in the presence of excess $M^{2+}_{(aq)}$, M = Cr, V.

tially catalyses reaction (7)[20] which is usually very slow even at HCl concentrations as high as 12 M,

$$M^{2+} + H^+ \longrightarrow M^{3+} + \tfrac{1}{2}H_2 \qquad (7)$$

M = Cr, V.

This cycle can be monitored by electronic spectroscopy (**3** with **10**), the interconversions $\mathbf{3} \xrightarrow{+2e^-} \mathbf{1} \underset{+2e^-}{\overset{-2e^-}{\rightleftharpoons}} \mathbf{2}$ and $V^{2+}_{(aq)} \longrightarrow V^{3+}_{(aq)}$ are discernible, and the intermediate products could be isolated by controlling the acid concentration (**3** with **9**).

Also, the rhenium complex **8** was easily converted to **7** from the room temperature interaction of one equivalent of $Re_2Cl_9(Bu^n_4—N)/(Bu^n_4—N)Cl$ in tetrahydrofuran with two equivalent of **9** or **10** in aq. HCl (6 M). The solution instantly from green turns blue and after a while blue crystals precipitate which were characterized to be the tetra-*n*-butyl ammonium salt of **7**. The Cr^{II} and V^{II} were oxidized to Cr^{III} and V^{III}, respectively, eq. (8):

$$\underset{\mathbf{8}}{[Re_2Cl_9]^-} + 2M^{2+} \xrightarrow{HCl} \underset{\mathbf{7}}{[Re_2Cl_8]^{2-}} + 2M^{3+} + Cl^- \qquad (8)$$

M = Cr, V.

The inability of the $(Re^{4}—Re)^{6+}$ core to undergo reaction (2) renders the reaction stoichiometric instead of catalytic. The mechanistic aspects of these homogeneous electron transfer reactions and the implications to chemical or biochemical catalysis are further examined.

Acknowledgement—We thank the Greek General Secretariat of Research and Technology for support.

REFERENCES

1. F. Schreiner and E. H. Appelman, *Surv. Prog. Chem.* 1977, **8**, 171; C. E. Bamberger, J. Braunstein and D. M. Richardson, *J. Chem. Ed.* 1978, **55**, 561.
2. S. M. Kuznicki and E. M. Eyring, *J. Am. Chem. Soc.* 1978, **100**, 6790; K. Kalyanasundaran, *Nouv. J. Chem.* 1979, **3**, 511.
3. (a) P. Escaffre, A. Thorez and P. Kolck, *J. Chem. Soc., Chem. Commun.* 1987, 146 and references therein; (b) J. J. Zuckerman (Ed.), *Inorganic Reactions and Methods*, Vol. 1, p. 61, and references therein. VCH, Florida (1986).
4. C. Mertis, M. Kravaritou, A. Shehadeh and D. Katakis, *Polyhedron* 1987, **6**, 1975.
5. A. Bino and F. A. Cotton, *Angew. Chem. Int. Ed. Engl.* 1979, **18**, 332; *J. Am. Chem. Soc.* 1979, **101**, 4150; F. A. Cotton and D. A. Ucko, *Inorg. Chim. Acta* 1972, **6**, 161, and references therein.
6. F. A. Cotton, *Acc. Chem. Res.* 1978, **11**, 225; M. J. Bennett, J. V. Brencic and F. A. Cotton, *Inorg. Chem.* 1969, **8**, 1060.
7. F. Bonati and F. A. Cotton, *Inorg. Chem.* 1967, **6**, 1353.
8. R. R. Schrock, L. G. Sturgeoff and P. R. Sharp, *Inorg. Chem.* 1983, **22**, 2801.
9. A. P. Sattelberger, K. W. McLaughlin and J. C. Huffman, *J. Am. Chem. Soc.* 1981, **103**, 2280.
10. A. Bino and D. Gibson, *J. Am. Chem. Soc.* 1980, **102**, 4277.
11. F. A. Cotton and A. R. Walton, *Multiple Bonds between Metal Atoms*, p. 238. Wiley, New York (1982), and references therein.
12. F. A. Cotton and G. N. Mott, *J. Am. Chem. Soc.* 1982, **104**, 5978.
13. F. A. Cotton, G. N. Mott, R. R. Shrock and L. Sturgeoff, *J. Am. Chem. Soc.* 1982, **104**, 6781.
14. A. A. Heintz, *Inorg. Synth.* 1960, **VI**, 149.
15. T. J. Barder and R. A. Walton, *Inorg. Chem.* 1967, **6**, 1497.
16. L. F. Larkwortly, K. C. Patel and D. F. Phillips, *J. Chem. Soc. A* 1970, 1095.
17. P. J. Elving and B. Zemel, *J. Am. Chem. Soc.* 1957, **79**, 1281.
18. R. J. H. Clark, *The Chemistry of Titanium and Vanadium*, pp. 166–172. Elsevier, Amsterdam (1968).
19. J. J. Lingane and L. A. Small, *J. Am. Chem. Soc.* 1949, **71**, 973.
20. D. Katakis and G. Gordon, *Mechanisms of Inorganic Reactions*. Wiley, New York (1987).

Polyhedron Vol. 8, No. 4, pp. 473-477, 1989
Printed in Great Britain

0277-5387/89 $3.00+.00
© 1989 Pergamon Press plc

ACID DISSOCIATION AND NICKEL-COMPLEX FORMATION CONSTANTS OF SOME NITROSONAPHTHOLSULPHONATE LIGANDS

S. BAJUE, P. DASGUPTA, G. C. LALOR* and H. ROBOTHAM

Department of Chemistry, University of the West Indies, Mona, Kingston 7, Jamaica

(*Received* 2 *August* 1988; *accepted* 15 *August* 1988)

Abstract—The acid dissociation constants of several 1-nitroso- and 2-nitroso-naphtholsulphonate ligands, and the formation constants of their Ni^{2+} mono-complexes are reported. The measurements were performed in the temperature range 20.0–30.0°C and ionic strength 0.1 mol dm^{-3}.

Ortho-nitrosonaphthols, like 1-nitroso-2-naphthol (**1**) and 1-nitroso-2-naphthol-3, 6-disulphonate (**2**), form complexes with many metal ions.

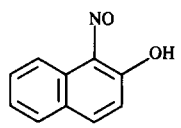

1

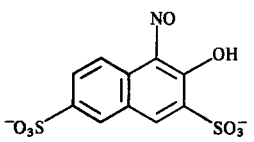

2

The formation and dissociation reactions of the cobalt and nickel complexes of these ligands have been of particular interest in our laboratories.[1-5] It has become clear that data on the various equilibria can contribute to the understanding of these reactions since the mechanism includes a number of pre-equilibria such as acid–base dissociation, ion-pair formation, and nitrosonaphthol–quinone oxime tautomerism.

Unlike keto–enol equilibria,[6] the nitrosonaphthol–quinone oxime equilibria are not amenable to measurement under the present experimental conditions. A stopped-flow spectrophotometric study on acidification of the ligands over a range of wavelengths and acid concentrations showed a single rapid change (< 2 ms) consistent with protonation and no subsequent relaxation, confirming that all equilibria are rapid. The various rate constants must be extracted by computer fittings of the data.

Although there may be significant amounts of the oxime tautomer present, the ligands are, as usual, referred to as nitrosonaphthols and abbreviated as ON-NAS-OH. The pK_a and K_f values then relate to eqs (1) and (2) respectively:

$$\text{ON-NAS-OH} \overset{K_a}{\rightleftharpoons} \text{ON-NAS-O}^- + \text{H}^+, \quad (1)$$

$$\text{ON-NAS-O}^- + \text{Ni}^{2+} \overset{K_f}{\rightleftharpoons} \text{ON-NAS-ONi}^+. \quad (2)$$

EXPERIMENTAL

Reagents

Preparation of 1-nitroso-2-naphthol-3-sulphonic acid. A published method[7] for the preparation of this compound gave very poor yields. A modified procedure using the following reaction sequence gave good yields: 2-hydroxy-3-naphthoic acid → 2-methoxy-3-naphthoic acid → 2-methoxy-3-naphthalene isocyanate → 2-methoxy-3-naphthaleneamine → 2-methoxy-3-naphthalene sulphinic acid → 2-naphthol-3-sulphonic acid → 1-nitroso-2-naphthol-3-sulphonic acid.

2-Methoxy-3-naphthoic acid. To a solution of 48 g (0.26 mol) of 2-hydroxy-3-naphthoic acid in 500 cm^3 of acetone, was added 96 g (0.7 mol) of potassium carbonate followed by 60 cm^3 (0.6 mol) of dimethyl sulphate. The flask was closed by a calcium chloride drying tube and the reaction mixture was stirred for 24 h after which time the contents were poured into 1 dm^3 of ice-cold water. About 10 g of KOH was then added and the mixture concentrated on a rotavap. After cooling the reaction mixture was adjusted to pH 4 with 50% aq. HCl at which stage 2-methoxy-3-naphthoic acid precipitated out. The product was collected, washed

*Author to whom correspondence should be addressed.

thoroughly with water and dried in a vacuum desiccator. Yield, 35 g; m.p. 131°C.

2-Methoxy-3-naphthalene isocyanate. 32 g (0.16 mol) of 2-methoxy-3-naphthoic acid was dissolved in 100 cm^3 of a 1 : 1 mixture of trifluoroacetic acid and trifluoroacetic anhydride. The flask was stoppered with a cotton wool plug, cooled to about 0°C and 15 g (0.22 mol) of sodium azide was added in portions while stirring. The reaction proceeded rapidly and after gas evolution had ceased the mixture was allowed to stand at 0–5°C while stirring for a further 15 min. The reaction mixture was then concentrated on a rotavap and on cooling the product crystallized out but it was not collected. The next step was carried out in the same flask.

3-Methoxy-2-naphthaleneamine. 260 cm^3 of 70% aq. ethanol was added to the flask containing the isocyanate. KOH pellets were added until the solution was alkaline. The mixture was then refluxed for 5 h and then poured into crushed ice whereupon the product formed as a white solid. It was filtered off, washed thoroughly with water and dried over KOH pellets in a vacuum oven at 50°C. It was recrystallized from benzene. Yield 25 g; m.p. 109°C.

2-Methoxy-3-naphthalene sulphinic acid. The above methoxyamine was diazotized and converted to the sulphinic acid derivative using chemically prepared copper powder and sulphur dioxide according to a published method.[7] It was recrystallized by dissolving it in the minimum amount of 10% aq. sodium carbonate solution, cooling in ice and then slowly adding cold dilute HCl to give the sulphinic acid as a pale pink powder. The yield was about 60%. The product is unstable and was used immediately after preparation.

2-Methoxy-3-naphthalene sulphonic acid. Finely powdered potassium permanganate (2 g) was dusted into a well-stirred solution of 2.5 g of the sulphinic acid in 100 cm^3 of acetone over a period of 30 min. The mixture was boiled for 5 min, cooled and filtered. The solid cake was extracted with 100 cm^3 of hot water in portions and the extract was evaporated to dryness to give the potassium salt of the sulphonic acid as an off-white solid. Yield 2.4 g. It was recrystallized from aq. ethanol.

2-Naphthol-3-sulphonic acid. This compound was prepared from the methoxy naphthalene sulphonic acid by refluxing it with 50% HCl for 1 h. The product was washed with ice-cold concentrated HCl and dried over NaOH in a vacuum desiccator. The compound is a very hygroscopic off-white solid.

1-Nitroso-2-naphthol-3-sulphonic acid, sodium salt. This was prepared from the 2-naphthol-3-sulphonic acid by nitrosation with $NaHO_2$ and HCl at 0°C. The resulting solution was saturated with $NaClO_4$ and on cooling the sodium salt separated as the trihydrate. It was recrystallized from an ethanol–water mixture. Recrystallization from dilute acids yielded the free sulphonic acid.

The other ligands were prepared by published methods.[8,9] The ligands were characterized by C, H and N analyses, by IR and proton NMR spectroscopy, and by equivalent weight determinations.

Stock solutions of nickel(II) perchlorate were analysed gravimetrically using dimethylglyoxime. Lithium perchlorate solutions used to maintain the ionic strength at 0.1 mol dm^{-3} were standardized by an ion exchange method. Solutions of sodium cacodylate were used for pH control.

Equilibrium measurements

The hydrogen-ion concentration was calculated from the pH of the solution. The pH and absorbances were measured with an Orion 801A pH meter and a Zeiss PMQII spectrophotometer, respectively. Temperature control was better than ± 0.1°C.

The acid dissociation constants were measured spectrophotometrically and evaluated by means of the equation

$$pK_a = pH + \log (D_L - D)/(D - D_{HL}), \qquad (3)$$

where D_{HL}, D_L and D are the absorbances of the acidic and basic forms of the ligands, and a mixture of both respectively.

The equilibrium constants were also measured spectrophotometrically using wavelengths at which there was a maximum difference in the absorbances between the ligands (HL), and the nickel complexes (NiL). To ensure that only the monochelate complex was formed the $[Ni^{2+}]$ exceeded the ligand concentration by a factor of at least 50.

The equilibrium constant according to eq. (4),

$$Ni^{2+} + HL^{n-} \underset{}{\overset{K}{\rightleftharpoons}} NiL^{(2-n)+} + H^+, \quad (n = 1 \text{ or } 2) \qquad (4)$$

was evaluated from the expression

$$K = [NiL] \times C_{H+}/\{[Ni]_0([NH]_0 - [NiL])\}, \qquad (5)$$

where C_{H+}, $[Ni]_0$, and $[HL]_0$ are the measured hydrogen ion, the initial nickel and ligand concentrations, respectively. The [NiL] was evaluated from

$$[NiL] = A - \varepsilon_{HL}[HL]/(\varepsilon_{NiL} - \varepsilon_{HL}), \qquad (6)$$

where A is absorbance measured against a Ni blank, and ε_{HL} and ε_{NiL} are the molar absorbances of HL and NiL. For any set of measurements, the $[Ni^{2+}]$

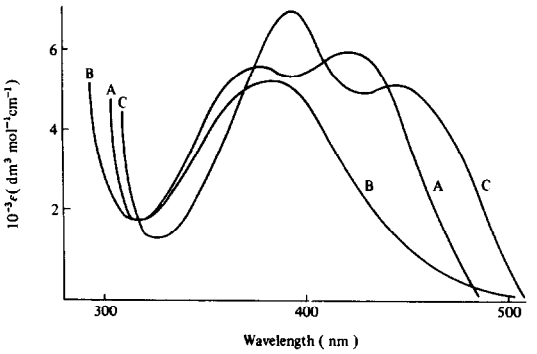

Fig. 1. UV–vis spectra of 1-nitroso-2-naphthol-3-sulphonate in pH 12 buffer (A), pH 2 buffer (B), and of Ni(1-nitroso-2-naphthol-3-sulphonate) in aqueous solution (C).

and [HL] were held constant and the $[H^+]$ varied by addition of a standard $HClO_4$ solution.

RESULTS AND DISCUSSION

Typical spectra of the 1-nitroso ligands in the acidic and basic forms, and of the NiL complex, are shown in Fig. 1. Figure 2 shows the corresponding spectra for a 2-nitroso ligand. The spectra of the base form of the ligands are similar to those of the NiL complexes, but there is a shift to lower energies of the absorption bands on coordination of the nickel.

The pK_a values measured at 20.0, 25.0 and 30.0°C are in Table 1. Table 2 shows pK_a values for several naphthols and nitrosonaphthols; in general there is good agreement between values obtained in this study and those obtained by other workers.[8] The only marked difference is with 1-nitroso-2-

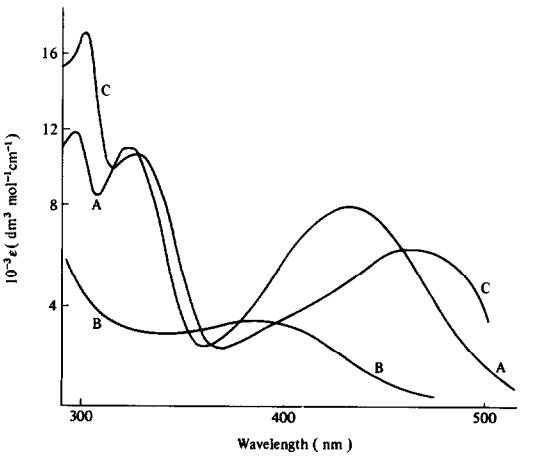

Fig. 2. UV–vis spectra of 2-nitroso-1-naphthol-5-sulphonate in pH 12 buffer (A), pH 2 (B), and of Ni(2-nitroso-1-naphthol-5-sulphonate in aqueous solution (C).

Table 1. Ligand acid dissociation constants $I = 0.1$ mol dm^{-3}

Ligand[a]					
NO	OH	SO_3	pK_a		
			20.0°C	25.0°C	30.0°C
1	2	3	7.65	7.57	7.42
1	2	4	7.26	7.20	7.15
1	2	5	7.27	7.16	7.12
1	2	7	7.35	7.29	7.26
2	1	5	—	6.94	6.91
2	1	6	7.11	7.08	7.04
2	1	7	7.07	7.04	7.00
2	1	8	—	8.10	—
2	1	4, 6	5.93	5.90	5.87

[a] Numbers give the position of the substituent on the naphthalene ring.

Table 2. Acid dissociation constant of some naphthols and nitrosonaphthols

Compound[a]				
NO	OH	SO_3	pK_a	ref.
	2		9.51	10
	2	5	9.25	11
	2	6	9.14	11
	2	7	9.35	11
	2	3, 6	9.62	11
1	2		7.42	12
1	2	3	7.57	This work
1	2	4	7.20	This work
			7.15	8
1	2	5	7.16	This work
			7.20	8
1	2	6	7.06	12
1	2	7	7.29	This work
			7.31	8
1	2	3, 6	6.94	12
	1		9.34	10
	1	5	9.11	11
	1	6	8.81	13
	1	8	13.02	11
2	1		7.17	12
2	1	4	6.10	14
2	1	5	6.94	This work
			6.91	8
2	1	6	7.08	This work
			7.02	8
2	1	7	7.04	This work
			6.97	8
2	1	8	8.10	This work
			7.74	8
2	1	4, 6	5.90	This work
2	1	4, 6	5.95	8

[a] Numbers give the position of the substituent on the naphthalene ring.

naphthol-8-sulphonate whose pK_a was reported[8] as 7.74 compared with the 8.10 obtained in this study.

In general, nitrosonaphthols are weak acids, with pK_a values ranging from 5.90 for 2-nitroso-1-naphthol-4, 6-disulphonate to 8.10 for 2-nitroso-1-naphthol-8-sulphonate. The rather high pK_a for the latter compound is unusual since the 2-nitroso-1-naphthols are otherwise stronger acids than the 1-nitroso compounds. Enhanced hydrogen bonding in the 8-sulphonate would account for its high pK_a value.

Of the 1-nitroso compounds the 3-sulphonate (pK_a = 7.57) is the least acidic, while the most acidic is the 3,6-disulphonate. The comparison of pK_a values of naphthols and corresponding nitrosonaphthols shown in Table 2 indicate that introduction of a SO_3 group in the 3-position of the naphthalene ring increases the pK_a, relative to that of the 6-SO_3 derivative, only for the 2-naphthol system. For the 1-nitroso system the pK_a decreases. This difference is probably due to reduced intramolecular hydrogen bonding with the 3-sulphonate nitrosonaphthol due to competition with the $—NO\cdots HO^-$ system or to less destabilization of the base because the O^- negative charge can be delocalized over the $(O—N—C—C—O)^-$ system.

A similar comparison can be made with the 1-naphthol derivatives. In this case the 8-SO_3 substituent causes the pK_a to increase in both the 1-naphthol and 2-nitroso-1-naphthol systems, relative to the 5-SO_3 derivative. These observations may indicate that the 2-nitroso-1-naphthols are more similar to the naphthol, and may exist more as the nitroso tautomer, than the 1-nitroso-2-naphthols in aqueous solutions. This to some extent supports the NMR results of Shono *et al.*[9] in Me_2SO–dioxane and Me_2SO–acetic acid solvents. The variation of the pK_a values (Table 1) with temperature is rather small; the change is about 0.1 pK_a units for a 10°C change in the temperature.

Values of the equilibrium constant K are shown in Table 3, together with complex formation constants, K_f, which refer to the reaction

$$Ni^{2+} + L^{n-} \rightleftharpoons NiL^{(2-n)+}, \qquad (7)$$

K and K_f are related to $K = K_a K_f$, where K_a is the acid dissociation constant of the ligand. Table 4 shows the K_f values for the nickel mono-complexes of various nitrosonapthtol ligands and it can be noted that the values obtained in this work are, again with the exception of Ni(2-nitroso-1-naphthol-8-sulphonate), in good agreement with those obtained by Saarinen *et al.*[8]

In general the K_f values are smaller for the 2-nitroso-1-naphthol derivatives when ligands of similar basicity are compared. This difference in K_f may reflect some interest, but no obvious preference in the 1-nitroso-2-naphthol system or could be ascribed to a difference in the position of the tautomeric equilibrium. If the latter is the case, then the results imply that complexing is more favourable with the oxime tautomer, which appears to be dominant for the 1-nitroso-2-naphthol ligands.

The rate expression[5] for the complexation reactions is complicated as exemplified by a possible

Table 3. Equilibrium constants for the formation of the NiL complexes. Temperature = 25.0°C, I = 0.1 mol dm^{-3}

Ligand[a]				
NO	OH	SO_3	10^2K	log K_f
1	2	3	35	7.11
1	2	4	23	6.56
1	2	5	22	6.50
1	2	7	41	6.90
2	1	4, 6	45	5.56
2	1	5	6.8	5.75
2	1	6	8.9	6.01
2	1	7	8.4	5.97
2	1	8	2.3	6.44

[a] Numbers give the position of the substituent on the naphthalene ring.

Table 4. Complex formation constants for some 1:1 nickel–nitrosonaphthol complexes

Ligand[a]				
NO	OH	SO_3	log K_f	ref.
1	2		6.7	2
1	2	3	7.11	This work
1	2	4	6.56	This work
			6.43	8
1	2	5	6.50	This work
			6.56	8
1	2	6	6.64	8
			6.55	13
1	2	7	6.90	This work
			6.73	8
1	2	3, 6	6.85	13
2	1		5.59	13
2	1	4	5.50	8
2	1	5	5.75	This work
2	1	6	6.0	This work
2	1	7	5.97	This work
			5.94	8
2	1	8	5.56	This work
			5.45	8

[a] Numbers give the position of the substituent on the naphthalene ring.

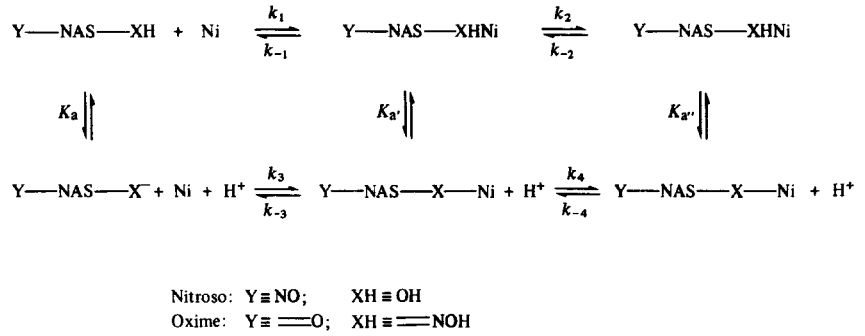

Scheme 1.

mechanism shown in Scheme 1. This explicitly involves K_a, K_aK_f, $K_{a'}$ and $K_{a''}$. We have now measured K_a and K_aK_f but there is no direct experimental evidence for $K_{a'}$ and $K_{a''}$. Computer fitting of the data appears to be the only way to obtain the numerical values of the kinetic parameters.[5] Work is now underway to complete these fits for all the NiL complexes listed in Table 3.

REFERENCES

1. G. C. Lalor, *J. Inorg. Nucl. Chem.* 1968, **30**, 1925.
2. G. C. Lalor, *Inorg. Chim. Acta.* 1975, **14**, 179.
3. T. P. Dasgupta and G. C. Lalor, *J. Ind. Chem. Soc.* 1977, **54**, 74.
4. S. A. Bajue, T. P. Dasgupta and G. C. Lalor, *Polyhedron* 1983, **2**, 431.
5. S. A. Bajue, T. P. Dasgupta, R. B. Jordan and G. C. Lalor, *Inorg. Chem.* 1985, **24**, 726.
6. M. J. Hynes and D. F. Kelly, *J. Chem. Soc., Dalton Trans.* 1988, 905.
7. S. Holt and F. A. Mason, *J. Chem. Soc.* 1931, 377.
8. H. Saarinen, *Ann. Acad. Sci. Fenn. Ser. A2* 1973, **173**.
9. E. Josephy and F. Radt (Eds), *Elseviers Encyclopaedia of Organic Chemistry, Series III*, Vol. 12B, p. 5634. Elsevier, Amsterdam (1955).
10. O. Makitie, *Suomen Kemi. B* 1966, **39**, 23.
11. J. T. Van Gemert, *Aust. J. Chem.* 1969, **22**, 1883.
12. S. Bajue, T. P. Dasgupta and G. C. Lalor, *Rev. Latinoamer. Quim.* 1979, **10**, 9.
13. O. Makitie, *Suomen Kemi. B* 1964, **37**, 17.
14. S. Bajue, Ph.D. Thesis, Univ. West Indies (1974).

Polyhedron Vol. 8, No. 4, pp. 479–482, 1989
Printed in Great Britain

0277–5387/89 $3.00+.00
© 1989 Pergamon Press plc

ELECTROCHEMICAL REACTIONS OF TRICARBONYL(CYCLOHEXADIENYLIUM)IRON SALT: REGIOCHEMISTRY DURING THE CROSS COUPLING REACTION AND TRAPPING OF THE 19-ELECTRON TRANSIENT TRICARBONYL(CYCLOHEXADIENYL RADICAL)IRON SPECIES

WEN-SHU HWANG,* RONG-LI LIAO, YI-LING HORNG and CHI WI ONG*

Department of Chemistry, National Sun Yat-Sen University, Kaohsiung, Taiwan 80424

(*Received* 18 *July* 1988; *accepted* 18 *August* 1988)

Abstract—Electrochemical reduction of the 18-electron tricarbonyl(4-methoxyl-1-methylcyclohexadienylium)iron hexafluorophosphate was found to generate a 19-electron transient species which could dimerize by cross coupling between both the C-1 and C-5 termini, or could be trapped with chloroform or benzyl bromide. The regiochemistry of reaction for the 19-electron tricarbonyl(cyclohexadienyl radical)iron complex is compared with the usual 18-electron tricarbonyl(cyclohexadienylium)iron complex during nucleophilic addition and the differences in observations are discussed.

Attention to tricarbonyl(cyclohexadienylium)iron salts has been focused mainly on the chemo-, regio- and stereo-specific nucleophilic additions, and its applications in the synthesis of a number of interesting and important natural products.[1] There have been few studies on its electrochemical properties. Pearson[2] has recently reported the electrochemical dimerization of tricarbonyl(1-methoxylcarbonylcyclohexadienyl)iron hexafluorophosphate which proceeds in a regioselective manner.

We have investigated the electrochemical behaviour of tricarbonyl(4-methoxy-1-methyl-cyclohexadienylium)iron hexafluorophosphate (**1**) and found that a one-electron reductive process takes place to generate a reactive transient 19-electron species. The titled compound **1** was chosen because nucleophilic addition occurred almost exclusively at the C-1 terminus. Any changes in regioselectivity in the reactions of the 19-electron tricarbonyl (4-methoxy-1-methylcyclohexadienyl radical)iron complex (**2**) can be readily observed. This paper will contrast the regioselection of compound **1** to that of **2**. The involvement of a free radical species in **2** was further proved by trapping experiments. Finally, the results of this study offer a possible correlation between the dienyl MO and the metal d^2sp^3 orbital.

* Authors to whom correspondence should be addressed.

RESULTS AND DISCUSSION

The single sweep cyclic voltammogram (CV) of the complex **1** was recorded with a stationary platinum microelectrode at 25°C in acetonitrile solution containing 0.1 M tetraethylammonium perchlorate (TEAP). The complex exhibited a well-defined cathodic wave, but no anodic process was detected on the reverse scan, even at sweep rates as high as 10 V s^{-1}, indicative of the existence of a fast and irreversible follow-up chemical process. Further evidence of the rapidity of the follow-up chemical process can be gained by the analysis of the sweep dependence of the cathodic wave.[3,4] Thus Fig. 1 reveals that the current in the foot of the wave is singularly independent of the sweep rate. This behaviour, originally noted by Reinmuth,[5] could indicate that the forward electron-transfer step is totally irreversible. No deterioration of the electrode response was also observed upon repeated CV scans, indicative of a cathodic reduction which cleanly leads to products without fouling the electrode surface.

Bulk electrolysis at a platinum gauze electrode of a 1.22 mM acetonitrile solution of the complex **1** at the CV peak potential (0.48 V) resulted in the passage of 1.04+0.05 faraday of charge per complex. In addition, the carbonyl IR stretching frequencies for **1** at 2070 and 2040 cm^{-1} disappeared upon

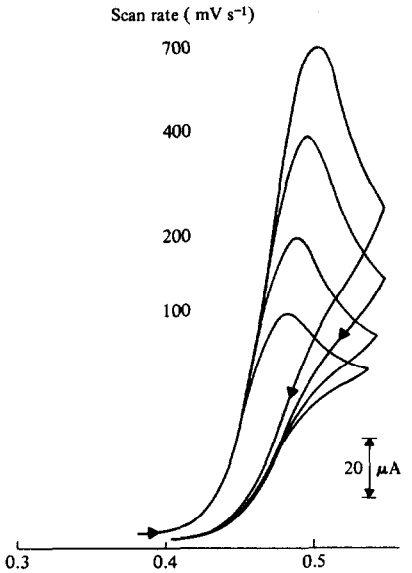

Fig. 1. First-scan cyclic voltammograms of 1.22×10^{-3} M Tricarbonyl(4 - methoxy - 1 - methylcyclohexadienylium) iron hexafluorophosphate in acetonitrile solution containing 0.1 M TEAP at a platinum microelectrode using various sweep rates. Electrode potentials in volts vs saturated Ag/AgCl.

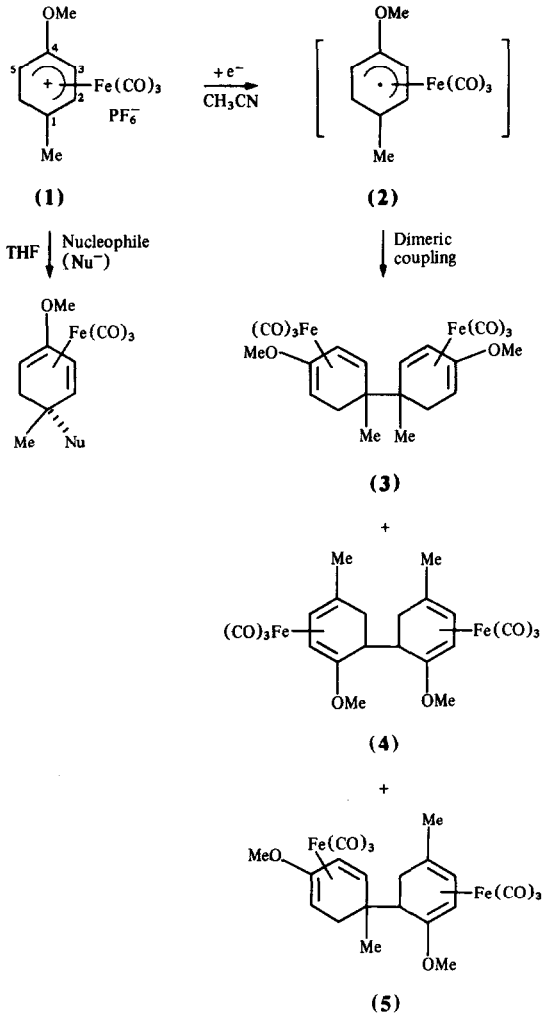

Scheme 1.

exhaustive one-electron reduction, and new bands appeared at 2010 and 1960 cm^{-1}.

When the electrochemical reduction of **1** was carried out till coulometry showed exhaustive transfer of one-electron, isolation and characterization of the product showed a mixture of complexes **3**, **4** and **5**. This result indicates that the electrochemically-generated 19-electron complex **2** undergoes reductive dimerization in a non-regioselective manner. The involvement of a free radical intermediate (**2**) was further revealed by successful trapping experiments. Trapping experiments with chloroform lead to the isolation of a new complex (**6**), together with **3**, **4** and **5**. A benzyl bromide trapping agent also gave a mixture of complexes which showed the trapping of benzyl groups and bromide.

The dimerization of electrochemical-generated radical complex **2** would be expected to be kinetically second-order. The theory applicable to EC mechanisms, predicts that the quantity $d(E_p)/d(\log v)$ will be 29.1 mV if the subsequent chemical reaction is first-order with respect to the species produced in the electrode reaction, and 19 mV if this reaction is kinetically second-order.[6] Theoretical analysis of the cyclic voltammogram, $d(E_p)/(\log v)$ in Fig. 1 gave a value of 20.8 mV which is fairly close to that predicted for the second-order mechanism.

H^1 NMR analysis of the product obtained by electroreduction of **1** revealed that **3**, **4** and **5** are formed in nearly equal amounts. This observation strongly contrasts with the results obtained from regioselective nucleophilic addition of **1** under similar conditions.[7] A plausible explanation may be arrived at if we assume that the SOMO of the 19-electron complex (**2**) is mainly the non-bonding orbital of the dienyl ψ_3 (Fig. 2) with little involvement of the iron hybrid orbitals, then we see that the methoxy substituent contribution to the orbital coefficient at the C-5 terminus is nullified to favour reductive dimerization equally well at both C-1 and C-5 termini in **2**. Electron-rich systems repel each other, thus the transfer of one electron to the dienyl of **1**, to generate **2**, will diminish the back bonding by d^2sp^3 metal orbitals. In the previous finding of the usual nucleophilic addition to **1**, the frontier orbital involved (LUMO) in the reaction is the anti-bonding orbital ψ_4.[8] In this case the methoxy substituent will deactivate nucleophilic addition to the C-5 terminus under charge control and conversely activate C-5 during orbital control.

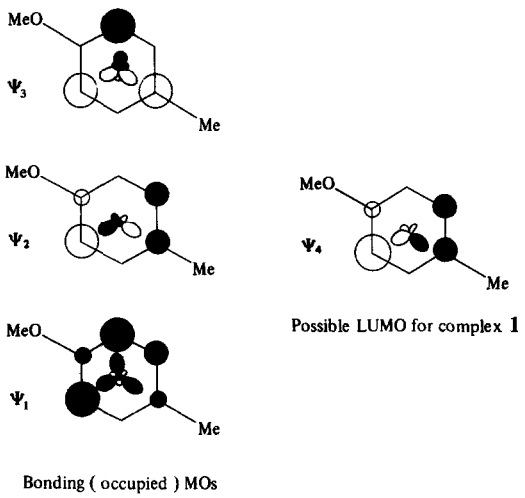

Fig. 2. Dienyl bonding to $Fe(CO)_3$ fragment. (See ref. 1 for explanation of orbital diagrams.)

In conclusion, the 19-electron dienyl–$Fe(CO)_3$ complex can be generated by a single electron reduction, electrochemically. This investigation establishes that a different overall reaction pathway takes place during electrochemical reductive dimerization as compared with nucleophilic addition to dienylium–$Fe(CO)_3$ such as **1**. The results of this study showed the importance of the relative amount of interaction between dienyl ψ_2 and the metal d^2sp^3 orbital and regioselection.

EXPERIMENTAL

General

All manipulations of air sensitive compounds were conducted under nitrogen in a drybox or *in vacuo*. Acetonitrile was refluxed over CaH_2 for several hours and then directly distilled, and redistilled twice from a 3:2 mixture of $KMnO_4$/anhydrous K_2CO_3. Finally it was distilled from P_4O_{10} before use. ^1H NMR spectra were obtained on a Bruker FT-100 or XL-400 superconducting NMR spectrometer with Me_4Si as reference. IR spectra were recorded on a Perkin–Elmer 1300 spectrophotometer, and mass spectra with AES MS 12 with GC–MS capability. Compound **1** was prepared according to the procedure described in the literature.[8]

Electrochemistry

Cyclic voltammetry was performed at ambient temperature in CH_3CN solution containing 0.1 M tetraethylammonium perchlorate (TEAP) as supporting electrolyte. A Princeton Applied Research (PAR) model 173 potentiostat equipped with a PAR 179 digital coulometer, which was provided with a feedback compensation for ohmic drop between the working and reference electrodes was used. The voltage follower amplifier (PAR 178) was mounted externally to the potentiostat with a minimum length of high impedance connection to the reference electrode for low noise pick up. CV were recorded on a PAR RE-0089 X-Y recorder and the scan rate controlled by a universal programmer (PAR 175). The electrochemical cell was constructed according to the design of Van Duyne and Reilly.[9] The distance between the platinum working electrodes and the tip of the salt bridge was 1 mm to insure a minimum ohmic drop. The platinum electrode was routinely cleaned by soaking in concentrated nitric acid for 15 min, followed by repeated rinsing with distilled water, and drying at 120°C prior to use.

The peak potential E_p of the complex **1** was independent of the concentration in the range between 10^{-4}–10^{-2} M and were always reproducible to within ± 50 mV. The repeated CV scan did not affect the appearance of the voltammogram.

Bulk electrolysis of complex **1** (500 mg, 1.22 mM) in CH_3CN with 0.1 M TEAP was conducted at 0.48 V vs a saturated Ag/AgCl reference electrode in a three compartment cell, *ca* 20 cm^3 capacity for 3 h under oxygen-free nitrogen. After exhaustive electrolysis, 122 C was consumed which amounts to the transfer of 1.04 electron per complex. The IR spectrum of an aliquot of the solution showed complete disappearance of the carbonyl stretching frequencies at 2070 and 2040 cm^{-1} with the appearance of peaks at 2010 and1960 cm^{-1}. The solvent was removed *in vacuo* and the resulting solid residue washed with water and extracted with ether, which after drying over anhydrous Na_2SO_4 and removal of solvent afforded the product (195 mg, 39%). After preparative TLC (benzene/hexane, 1:2) pure regioisomers **3**, **4** and **5** were obtained.

Trapping experiments

Experiments were carried out as above with the addition of trapping agent to the CH_3CN solution during the electrolysis and working up in the same manner. When chloroform was added as the trapping agent, a new product (**6**) was isolated together with **3**, **4** and **5** after preparative TLC separation. In the case of benzyl bromide as the trapping agent, a complex mixture was obtained with separation difficulties and was submitted directly for GC–MS analysis which showed compounds containing the incorporation of benzyl and bromine groups.

Determination of the product ratio: these were carried out on the initial mixture obtained after the electrochemical reduction of complex **1** using

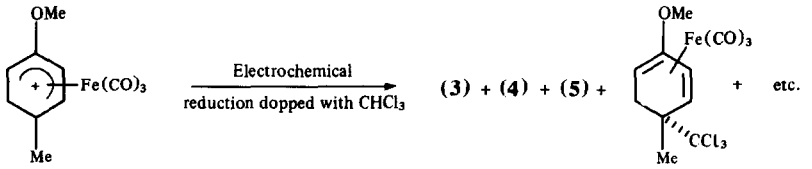

(1) (6)

Scheme 2.

expanded spectra and integral studies from the ^1H 400 MHz spectrum. They were found to be approximately in a 1:1:1 ratio. The regioisomers were separated by preparative TLC; their individual spectra are recorded as below.

All compounds were obtained as a diastereomeric mixture.

Complex **3**: $\nu_{max}(CHCL_3)$ 2045, 1975 cm^{-1}; $\delta(CDCl_3)$ 4.98 (2H, m), 3.62 (3H, s), 3.59 (3H, s), 3.18 (2H, br. m), 2.85 (2H, complex m), 2.48 (2H, dd), 1.65 (2H, dd), 1.00 (6H, 2 × s). *m/e* 528 (M^+), 356 (M^+–Fe(CO)$_3$–CO–4), 263 (M^+/2–1), 253 (M^+/2–CO–1), 122 (M^+/2–Fe(CO)$_3$–2).

Complex **4**: $\nu_{max}(CH_3Cl)$ 2040, 1965 cm^{-1}; $\delta(CDCl_3)$ 5.25 (2H, complex dd), 4.86 (2H, complex dd), 3.35 and 3.40 (6H, s each), 3.00–1.85 (6H, m), 1.55 and 1.46 (6H, s each). *m/e* 301 (M^+–Fe(Co)$_3$–(CO)$_3$–3), 263 (M^+/2–1).

Complex **5**: $\nu_{max}(CHCl_3)$ 2042, 1977 cm^{-1}; $\delta(CDCl_3)$ 5.48 (2H, d), 5.17 and 4.92 (m) (together 3H), 3.69, 3.63, 3.44 (6H, s each), 3.35–1.50 (5H, m), 1.43 and 1.23 (6H, s each). *m/e* 528 (M^+), 263 (M^+/2–1), 235 (M^+/2–CO–1), 207 (M^+/2–(CO)$_2$–1), 179 (M^+/2–(CO)$_3$–1).

Complex **6**: $\nu_{max}(CHCl_3)$ 2050, 1976, 800 cm^{-1}; $\delta(CDCl_3)$ 5.01 (1H, dd), 3.66 (3H, s), 3.35 (1H, m), 2.98 (1H, d), 2.41 (1H, dd), 1.62 (1H, dd), 1.23 (3H, s). *m/e* 310, 312 (M^+–2 × Cl), 263 (M^+–CCl_3).

Acknowledgements—We thank the National Tsing Hua University for performing the XL 400 ^1H NMR spectra. We are also indebted to the National Science Council of Taiwan for financial support.

REFERENCES

1. A. J. Pearson, *Trans. Met. Chem.* 1981, **6**, 67, and references therein.
2. A. J. Pearson, Y. S. Chen, M. C. Daroux, A. A. Tanaka and A. Zettler, *J. Chem. Soc. Chem. Commun.* 1987, 155.
3. W. H. Tamblyn, R. J. Klinger, W. S. Hwang and J. K. Kochi, *J. Am. Chem. Soc.* 1981, **103**, 3161.
4. W. S. Hwang, *Proc. NSC (ROC) Part A* 1984, **8**, 1.
5. W. H. Reinmuth, *Analyt. Chem.* 1960, **32**, 1891.
6. J. Heinze, *Angew. Chem. Int. Edn Engl.* 1984, **23**, 831.
7. W. S. Hwang, R. L. Liao and C. W. Ong, *J. Chin. Chem. Soc.* 1988, **35**, 77.
8. A. J. Pearson, P. Ham, C. W. Ong, T. R. Perrior and D. C. Rees, *J. Chem. Soc. Perkin Trans. I* 1982, 1527.
9. R. P. Van Duyne and C. N. Reilly, *Analyt. Chem.* 1972, **44**, 142.

Polyhedron Vol. 8, No. 4, pp. 483–489, 1989
Printed in Great Britain

0277–5387/89 $3.00+.00
© 1989 Pergamon Press plc

DECONTAMINANT AGENTS IN THE CATALYTIC CRACKING OF PETROLEUM. X-RAY CRYSTAL STRUCTURE OF BISMUTH-TRI-DIETHYL PHOSPHORO DITHIOATE, $Bi[(C_2H_5O)_2PS_2]_3$

M. IGLESIAS and C. DEL PINO*

Inst. de Ciencia de Materiales, CSIC, Serrano 113 28006, Madrid, Spain

and

S. MARTINEZ-CARRERA

Dto. Cristalografía. Insto. Rocasolano, CSIC, Serrano 119 28006, Madrid, Spain

(*Received* 5 *July* 1988; *accepted* 25 *August* 1988)

Abstract—We report the structure of $Bi[(C_2H_5O)_2PS_2]_3$; the compound crystallizes as yellow prisms in the monoclinic space group $p2_1$ with $a = 8.618(6)$ Å, $b = 9.698(2)$ Å, $c = 17.569(9)$ Å; β, 92.95(7)°. $D_{calc} = 1.37$ g cm^{-3} for $Z = 2$ molecules/unit cell. The structure was resolved by Patterson and Fourier methods and refined by full matrix least-squares method to a final discrepancy index based on I, of 0.085 for the 2072 independent reflections above 3σ (I). The bismuth atom is surrounded by six sulphur atoms from the three chelating phosphoro dithioate groups in a pseudo trigonally distorted octahedron (C_3 symmetry), with a lone pair positioned in one of the triangular octahedral faces. Bi—S bond lengths of the capped face (cf) are 2.799 Å (av.) longer than the Bi—S uncapped face (uf) (av. 2.758 Å). The mean S_{cf}—Bi—S_{cf} angle is 98.6° compared with 94.9° for S_{uf}—Bi—S_{uf}. Intraligand angles S—Bi—S average 72.0° and the ligand bite is 3.27 Å.

The title compound is isostructural with its analogue $Sb[(C_2H_5O)_2PS_2]_3$, and consists of discrete molecules and does not present any intermolecular contacts.

We have prepared a series of complexes of Sb^{III} and Bi^{III} with bidentate S-donor ligands, of general formula :M(S—S)$_3$, for M = Sb, Bi, and S—S = dialkyl phosphoro dithioate, dialkyl xantate, dialkyl dithiocarbamate, to be used as "passivating agents" in catalytic cracking of petroleum.[1]

The contamination of the catalysts by metals such as nickel, vanadium and iron, in the process of cracking, can be reduced by adding some compounds known as "passivating agents" with very efficient results but by a process the nature of which is still obscure. These decontaminants, are in general, compounds of non-transition elements with molecular stereochemistry governed by the valence-shell electron pair repulsion model (VSEPR).[2] These compounds are not expected to possess a regular octahedral structure with a MS_6 core, but rather one based on a 7-coordination polyhedron[3] with a lone pair of electrons occupying the seventh position. Gradually the structures of various of these decontaminants have been elucidated. There are different geometries found for these molecules: capped octahedron (CO), pentagonal bipyramid (PB) and trigonal prism (TP); the presence of the lone pair is evident from the arrangement of the nearest neighbours.

In compounds :M(S—S)$_3$ with CO structure the lone pair occupies the capping position; they present pseudo C_{3v} symmetry with three short and three long bonds, together with an avoided region ascribable to a lone pair of electrons. The long bonds are in the capped face (cf). The site of the lone pair does not appear to be equidistant from the three sulphurs of the capped face.

At present, we are studying the behaviour of the compounds mentioned above in the cracking pro-

*Author to whom correspondence should be addressed.

sesses in conjunction with the study of its thermogravimetric and thermodifferential decomposition, in order to be able to clarify the nature of the passivation process. In this paper, we present the molecular structure of $Bi[(C_2H_5O)_2PS_2]_3$.

EXPERIMENTAL

Crystalline $Bi[(C_2H_5O)_2PS_2]_3$ was prepared by treating a solution of ammonium *O,O'*-diethylphosphoro dithioate (0.97 g, 5 mM) in acetone (30 cm^3) with an acetonic solution of $BiCl_3$ (0.5 g, 16 mM, 20 cm^3 acetone). Immediately a white precipitate of NH_4Cl appeared. After 1 h of reaction (at room temperature with stirring), the solution was filtered off, concentrated and precipitated with pentane. A yellow solid was separated and washed with ethyl ether. Recrystallization from *n*-pentane gave yellow prisms suitable for X-ray study.

Crystal data

Details of the processing procedure are given in Table 1. The bismuth atom was readily found from a Patterson map and all remaining non-hydrogen atoms were located by Fourier and difference Fourier syntheses. Isotropic refinement was made by full matrix least squares. Due to thermal agitation, positions and isotropic thermal factors for atoms C_{61} and C_{62} were fixed in the last refinement. At this point an absorption correction was made by Walker and Stuart's method[5] and the structure was refined

Table 1. Crystal data, details of data collection (at room temperature) and structure refinement of $Bi[(C_2H_5O)_2PS_2]_3$

Crystal data	
Formula	$C_{12}H_{30}O_6P_3S_6Bi$
Crystal habit	Yellow, transparent, prisms
Crystal size (mm)	0.15, 0.20, 0.25
Symmetry	Monoclinic, $P2_1$
Unit cell determination	Least-squares fit from 25 reflections
Unit cell demensions	*a* 8.618(6), *b* 9.698(2), *c* 17.569(9), Å, β 92.95(7)
Cell volume, V(Å^3), Z	1466.4(1), 2
D_c(g cm^{-3}), M, F(000)	1.73, 764.63, 748
Experimental data	
Radiation and technique	Mo—K_α; Nonius CAD4 diffractometer
Monochromator	Graphite
Scan mode (W/2θ)	1.5 scan width, 1.5 min/reflection
Scanning range	$2 < \theta < 30$
Number of reflections:	
Measured	4483
Observed data ($I > 3\sigma$)	2072
Value of R_{int}	0.014
Standard reflections:	2 Reflections every 90 min, no variation I
Absorption coefficient (μ)	65.87 cm^{-1}
Solution and refinement[4]	
Solution mode	Patterson, Fourier and difference Fourier synthesis
Absorption correction[5]	Applied after isotropic refinement
Refinement mode	Least-squares of *F*s, observed reflections only, anisotropic for Bi, P, S and isotropic for O, C and fixed H-atoms
Parameters:	
Number of variables	154
H-atoms	Geometric
Final shift/error	0.10 average
w-Scheme[6]	Empirical so as to give no trends in $\langle W\Delta^2F\rangle$ vs $\langle F_0\rangle$ and $\langle \sin\theta/\lambda\rangle$
ΔF final	6.28, −2.55 eÅ^{-3}
Extinction correction	No correction applied
R, R_w	0.085, 0.084
Computer and programs	VAX11/750, XRAY80,[4] DIFABS,[5] PESOS,[6] PARST[7]
Atomic factors	Scattering factors for neutral atoms and f', f'' from *International Tables for X-Ray Crystallography* (1974)[8]

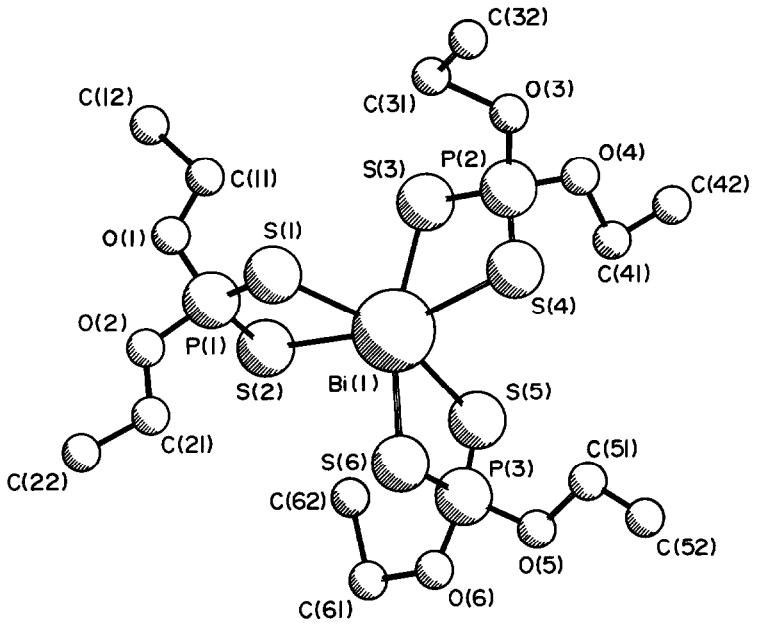

Fig. 1. Molecular structure of $Bi[(C_2H_5O)_2PS_2]_3$.

by full matrix least-squares with anisotropic thermal parameters for Bi, P and S and isotropic for O, C. The H-atoms, fixed at calculated positions, were included in the refinement with isotropic thermal parameters of the atoms to which they are attached, $R = 0.085$, $R_w = 0.084$.

RESULTS AND DISCUSSION

Description of the structure. The molecular geometry and the packing in the unit cell are depicted in Figs 1 and 2. Bond lengths and angles around the bismuth are given in Table 2.

As illustrated in Fig. 1 the coordination polyhedron of the bismuth atom can be described as a distorted capped octahedron with a stereochemically active lone pair in the capping position and approximately on a molecular pseudo-triad axis, which passes through the bismuth atom. Six sulphurs from the three anisobidentate phosphoro dithioate ligands are in the vertices of the distorted octahedron.

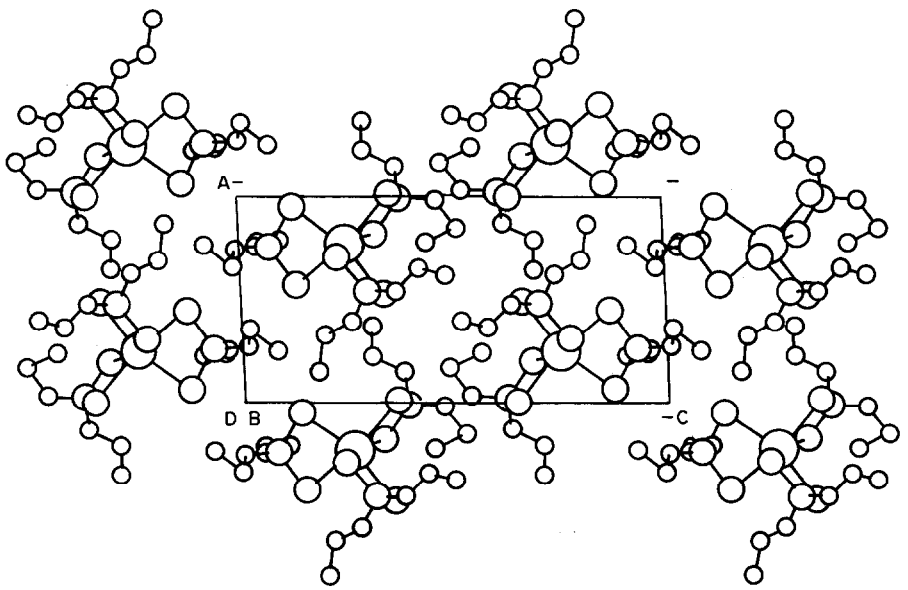

Fig. 2. [010] Projection of the primitive unit cell of $Bi[(C_2H_5O)_2PS_2]_3$.

Table 2. Selected bond distances and angles for compound $Bi[(C_2H_5O)_2PS_2]_3$

Bond distances (Å)			
Bi1—S1	2.820(16)	Bi1—S2	2.750(11)
Bi1—S3	2.778(12)	Bi1—S4	2.795(13)
Bi1—S5	2.747(14)	Bi1—S6	2.781(11)
S1—P1	1.925(16)	S2—P1	1.972(15)
S3—P2	1.972(16)	S4—P2	2.002(16)
S5—P3	1.964(15)	S6—P3	1.980(16)
P1—O1	1.497(26)	P1—O2	1.548(27)
P2—O3	1.562(29)	P2—O4	1.543(33)
P3—O5	1.551(23)	P3—O6	1.543(29)
O1—C11	1.39(6)	O2—C21	1.35(6)
O3—C31	1.62(8)	O4—C41	1.54(5)
O5—C51	1.50(6)	O6—C61	1.50(3)
C11—C12	1.60(6)	C21—C22	1.44(8)
C31—C32	1.55(9)	C41—C42	1.37(9)
C51—C52	1.36(6)	C61—C62	1.60(0)
S1···S2	3.237(19)	S3···S4	3.297(15)
S5···S6	3.271(18)		
Bond angles (°)			
S1—Bi1—S2	71.0(4)	S3—Bi1—S4	72.5(4)
S5—Bi1—S6	72.6(3)	S1—Bi1—S3	96.1(4)
S1—Bi1—S4	103.2(4)	S1—Bi1—S5	161.4(4)
S1—Bi1—S6	96.7(4)	S2—Bi1—S3	92.0(3)
S2—Bi1—S4	163.1(4)	S2—Bi1—S5	95.5(4)
S4—Bi1—S6	96.0(3)	S1—P1—S2	112.3(7)
S3—P2—S4	112.1(7)	S5—P3—S6	112.1(7)
O1—P1—O2	96.9(15)	O3—P2—O4	94.4(16)
O5—P3—O6	94.5(14)		
Torsion angles (°)			
S1—P1—O1—C11	65	S1—P1—O2—C21	−68
S2—P1—O1—C11	−61	S2—P1—O2—C21	60
S3—P2—O3—C31	37	S3—P2—O4—C41	−69
S4—P2—O3—C31	−91	S4—P2—O4—C41	58
S5—P3—O5—C51	66	S5—P3—O6—C61	−53
S6—P3—O5—C51	−62	S6—P3—O6—C61	74
O1—P1—O2—C21	177	O2—P1—O1—C11	−176
O3—P2—O4—C41	173	O4—P2—O3—C31	152
O5—P3—O6—C61	−172	O6—P3—O5—C51	−175

Lone pair–bond pair repulsions in the bismuth coordination sphere result in longer bond lengths for those bonds adjacent to the lone pair and shorter lengths for those more remote, the former averaging 2.808 Å and the latter averaging 2.749 Å; in accordance with these results, the capped face is formed by $S_1S_4S_6$. S—Sb—S angles involving long Sb—S bonds (av. 98.6°) are greater than those involving the shorter bonds (av. 95.5°). Interligand S—Sb—S angles are: 72.0° (av.) and the ligand "bite", 3.268 (av.) Å.

This type of distorted CO structure has been found in a series of As^{III}, Sb^{III} and Bi^{III} compounds. In Table 3, we have collected some data from the literature, to see in more detail the stereochemistry of these 7-coordinate compounds. Among them we have included our results. To diminish interligand repulsions, compounds :M(S—S)$_3$, with different S-donor chelating ligands have been chosen: xanthates[9] and dithiocarbamates,[10] where the groups S_2CO, S_2CN are planar, or phosphoro dithioates[12–14] with tetrahedral P surrounded by two sulphur and two oxygen atoms. In all these compounds with a MS_6 core, there are three long and three short M—S distances. The asymmetry of the M—S bond lengths is believed to arise as a result of a stereochemically active lone pair of electrons protruding from the three-fold axis, through the triangular array formed by the sulphur atoms involved in the long M—S bonds. We have chosen these ligands because the size of the ligand bite (2.97–3.28 Å) is markedly shorter than the van der

Table 3. Bond lengths and angles in molecules :M(S—S)$_3$ of trivalent elements, M (As, Sb, Bi) with thio-bidentate ligands[a]

	Molecule	Symmetry	M—S_{cf}(Å)[b]	M—S_{uf}(Å)[c]	Δ(Å)	D_s	S_{cf}—M—S_{cf}(°)	S_{uf}—M—S_{cf}(°)	Δ(0)	D_b	SMS(°) (inter-ligands)	S—S bite (intra)	S···S non-bonded (inter)
	:M(S_2COEt_2)$_3$[9]												
1.	As[d]	CO	2.94	2.28	0.66	0.78	107.6	92	15.6	0.86		2.99	3.28
2.	Sb[d]	CO	3.00	2.52	0.40	0.84	113.1	87.5	25.6	0.77		2.99	3.48
	:M(S_2CNEt_2)$_3$[10]**												
3.	As	CO	2.85	2.35	0.49	0.83	106.0	90.1	15.9	0.85	68.9	2.97	3.32
4.	Sb[e]	PB	2.92	2.58	0.30	0.89					64.8		
5.	Bi[e]	PB	2.94	2.70	0.25	0.92					63.5		
6.	:Sb(S_2CN—*n*-prop$_2$)$_3$[11]**		2.82	2.63	0.185	0.93					65.6		
7.	:Sb(S_2P(OMe)$_2$)$_3$[12]	CO	3.01	2.53	0.48		106.2	88.4	17.8	0.83	72.7		
8.	:Sb(S_2P(OEt)$_2$)$_3$[13]	CO	2.83	2.60	0.23		100.9	94.1	6.8	0.93	72.5	3.22	
9.	:Sb(S_2P(O—*i*-prop)$_2$)$_3$[12]	CO	3.02	2.52	0.49		106.6	87.5	19.1	0.82	72.1		
10.	:Bi(S_2P(OEt)$_2$)$_3$[f]	CO	2.82	2.75	0.06	0.97	98.6	95.5	3.1	0.97	72.0	3.27	
11.	:Bi(S_2P(O—*i*-prop)$_2$)$_3$[14]	CO	2.87	2.70	0.17	0.94	100(2)	91(2)	9	0.91	72.0	3.28	3.85

[a] Average values.
[b] cf, Capped face.
[c] uf, Uncapped face.
[d] Data from S. L. Lawton *et al.*, *Inorg. Chem.* 1974, **13**, 135.
[e] Reported as PB structure with lone pair in axial position (J. A. Howard, D. R. Russell and W. Santcher, *Acta Cryst.* 1975, **A31**, 3141).
** Intermolecular contacts; tendency to polimerization.
[f] This study.

Waals radius sum, so that there is enough interligand room to allow the stereochemical activity of the lone pair make itself felt.

In Table 3 the stretching deformation is given by D_S = M—S_{uf}/M—S_{cf} and the bending deformation, D_b = S_{uf}—M—S_{uf}/S_{cf}—M—S_{cf}. Certain trends are discernible if one compares the results; thus one can see that the lone pair becomes less decisive as the atomic weight of the central atom (As > Sb > Bi) increases. We also see that when ligands have the isopropyl group the stereochemistry is dominated by interligand repulsions and the lone pair is inhibited from achieving its full stereochemical activity. Apparently the absence of strong repulsive interactions between ethyl groups of neighbouring ligands allows perturbations of :M(S—S)$_3$ groups by the stereochemically active lone pair to proceed with relative ease.

It may be that the stereochemical activity of the lone pair is not necessary for the rationalization of these structures, as a trigonally distorted octahedron would be highly probable as a direct consequence of the anisobidentate character of these ligands. In fact there is a disparity in the C—S distances in xanthates and dithiocarbamates, such that the C—S distances associated with the short M—S bond are lengthened appreciably while those associated with the long M—S bond are shortened.

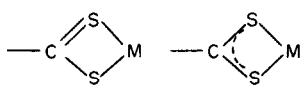

(a) (b)

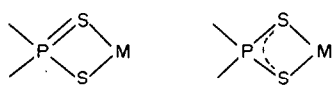

(a) (b)

In the same way, with phosphorodithioate ligands, P—S bond distances also fall into two classes: the short distances are associated with S-atoms forming long M—S interactions while the longer P—S bonds are associated with S-atoms forming short bonds to M. This situation is quite noticeable for antimony compounds but with bismuth ones as the differences in Bi—S bond lengths are smaller, the accuracy of the P—S bond distances is too low to distinguish between (a) anisobidentate or (b) isobidentate ligands, although (a) coordination is suggested.

From all the foregoing we can see that the interpretation is unclear, because of competing factors, to control the overall geometry of :M(S—S)$_3$ molecules; nuclear repulsion energies, steric requirements of the ligands and bite size, are all important factors.

The title compound is isostructural with Sb $[(C_2H_5O)_2PS_2]_3$.

At this moment we are studying the passivation power of the complexes, :M$(S_2COEt_2)_3$, :M$(S_2CNEt_2)_3$, :M$[(OEt)_2PS_2]_3$, :M$[(OC_{10}H_{21})_2S_2P]_3$, M = Sb, Bi, in the catalytic process of petroleum cracking. The accumulation of Ni, V, Fe, etc., diminishes the percentage of petrol and increases the production of hydrogen and coke. By tracing the production process of hydrogen we have been able to deduce the activity of the said passivating agents. At the same time we have prepared mixtures of nickel naphthenate with the different "passivating agents" and have gone on to study their thermo-differential and thermo-gravimetric decomposition.

The results obtained will be the subject of a separate publication.

REFERENCES

1. (a) D. L. McKay, *U.S. Pat.* 4031,002, 1977; (b) H. W. Mark, B. J. Bertus, J. S. Roberts and D. L. McKay, *U.S. Pat.* 4459,366, 1984; (c) M. W. Blaschke and R. F. Miller, *J. Link U.S. Pat.* 4609,747, 1986.
2. R. J. Gillespie and R. S. Nyholm, *Q. Rev. Chem. Soc.* 1957, **11**, 399; R. J. Gillespie, *J. Chem. Ed.* 1963, **40**, 295; R. J. Gillespie, *Adv. Chem. Ser.* 1967, **62**, 221.
3. M. G. B. Drew, *Prog. Inorg. Chem.* 1977, **23**, 67.
4. J. M. Stewart, F. A. Kundell and J. C. Baldwing, *The X-Ray System version, Computer Science Center*, University of Maryland, Coll. Park, MD (1980).
5. N. Walker and D. Stuart, *Acta Cryst.* 1983, **A39**, 158.
6. M. Martinez-Ripoll and F. H. Cano, PESOS. Insto. Rocasolano CSIC, Madrid (1975).
7. PARST, M. Nardelli, *Comput. Chem.* 1983, **7**, 95.
8. *International Tables for X-ray Crystallography*, Vol. 4. Kynoch Press, Birmingham (1974).
9. (a) G. Gottardi, *Z. Kris. Kristallogr.* 1960, **113**, 373; 1961 **115**, 451; (b) B. F. Hoskins, P. M. Piko, E. R. T. Tiekink and G. Winter, *Inorg. Chim. Acta* 1984, **84**, C13; (c) B. F. Hoskins, E. R. T. Tiekink and G. Winter, *Inorg. Chim. Acta* 1985, **97**, 217.
10. (a) M. Colapierto, A. Domenicano and L. S. Scaramuzza, *J. Chem. Soc., Commun.* 1968, 302; (b) C. L. Raston and A. H. White, *J. Chem. Soc., Dalton Trans.* 1975, 2425; (c) C. L. Raston and A. H. White, *J. Chem. Soc., Dalton Trans.* 1976,

791; (d) J. A. Howard, D. R. Russell and W. Santcher, *Acta Cryst.* 1975, **A31**, 3141.
11. C. A. Kavonnis, C. S. Kokkon and P. I. Rentzeperis, *Acta Cryst.* 1982, **B38**, 2686.
12. D. B. Sowerby, J. Haiduc, A. Barbul-Rusu and M. Salajari, *Inorg. Chim. Acta* 1983, **68**, 87.
13. R. O. Doy, M. M. Chauvin and W. E. McEwen, *Phosphorus and Sulphur* 1980, 8121.
14. S. L. Lawton, C. J. Fuhrmeister, R. G. Hass, C. S. Jarman and F. G. Lohmeyer, *Inorg. Chem.* 1974, **13**, 135.

Polyhedron Vol. 8, No. 4, pp. 491–504, 1989
Printed in Great Britain

0277–5387/89 $3.00+.00
© 1989 Pergamon Press plc

THE SYNTHESIS OF IRON(III) AND COBALT(III) COMPLEXES OF FACULTATIVE HEXADENTATE LIGANDS. THE X-RAY CRYSTAL STRUCTURE OF $[Fe\{(NC_4H_3\text{-}2\text{-}CH{=}NCH_2CH_2NHCH_2)_2\}]PF_6$

ANNE S. ROTHIN, HILARY J. BANBERY, FRANK J. BERRY, THOMAS A. HAMOR, CHRISTOPHER J. JONES* and JON A. McCLEVERTY

Department of Chemistry, University of Birmingham, P.O. Box 363, Birmingham B15 2TT, U.K.

(*Received* 28 *March* 1988; *accepted* 31 *August* 1988)

Abstract—A series of hexadentate ligands have been prepared from the condensation of 1,8-diamino-3,6-diazaoctane or 1,8-diamino-3,6-dithiaoctane with 1-hydroxy-3-methoxybenzophenone, 2-hydroxypropiophenone, 2-hydroxybenzophenone or pyrrole-2-aldehyde, and from 3-methoxysalicylaldehyde with tris(2-aminoethyl)amine. Their ability to encapsulate cobalt(III) and iron(III) in complexes of 1 : 1 ligand–metal stoichiometry is reduced by the incorporation of sulphur donor atoms, or by the replacement of the terminal six-membered chelate rings of the salicylaldehyde derivatives by a five-membered ring in the pyrrole–aldehyde derivatives. Mössbauer spectral data are reported for the iron complexes and the molecular structure of $[Fe\{(NC_4H_3\text{-}2\text{-}CH{=}NCH_2CH_2NHCH_2)_2\}]PF_6$ has been determined by single crystal X-ray diffraction techniques.

Facultative hexadentate ligands capable of octahedral coordination to a transition metal ion may encapsulate it in a 1 : 1 complex whose exterior exhibits the properties of an organic material. Such species are of interest in a variety of contexts; particularly in the production of metal containing pharmaceuticals and the formulation of selective metal ion extractants. Three basic structural types are possible for such ligands. The first is a simple linear hexadentate ligand exemplified by $HOC_6H_4CH{=}N(CH_2)_2E(CH_2)_2E(CH_2)_2N{=}CHC_6H_4OH$, in which E = NH (**1a**) or S (**1b**). The second type may be singly branched having three "arms" as in $N(CH_2CH_2N{=}CHC_6H_4OH)_3$ (**3a**) or may be derived from 1,3,5-triaminocyclohexane. The third structural type is doubly branched as, for example, in EDTA. The work described here is concerned with dinegative ligands of the first structural type. The effects of varying E, or the nature of the terminal binding sites, on the formation and properties of monocationic complexes with metal(III) ions have been assessed in a series of 11 compounds containing Fe^{III} or Co^{III} as representative metals.

*Author to whom correspondence should be addressed.

The preparation of a linear hexadentate ligand of the first type was described by Dwyer and Lions in 1950.[1] This involved the condensation of salicylaldehyde with 1,8-diamino-3,6-dithiaoctane to give **1b**. Complexes of this ligand with Fe^{II}, Co^{II}, Ni^{II}, Cu^{II}, Zn^{II} and Co^{III} were described. Subsequently, complexes of other ligands including **1a** were described.[2–11] The molecular structure of the Ni^{II} complex of **1a** has been determined[12] and confirms the ligand's ability to reach all octahedral sites on the nickel ion. Hexadentate ligands derived from the reactions of amines with 2-formylpyridine,[7,8,13,14] substituted salicylaldehydes[3,15] and pentane-2,4-dione[9,16–18] have also been reported.

More recently, complexes of Fe^{II} and Fe^{III} with certain hexadentate ligands have aroused interest because of their anomalous magnetic behaviour. The equilibria between high and low spin states in the solid state and in solution have been investigated by variable temperature, magnetic moment and Mössbauer spectroscopic measurements.[13,16–18] As part of an investigation into complexes of lipophilic ligands capable of encapsulating metal ions, we have prepared a variety of hexadentate ligands (**1c–h**; **2a**, **2b**; **3a**, **3b**; **4a**, **4b**) from the condensation

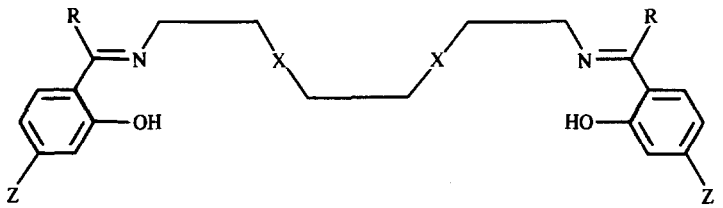

1a X = NH, R= H, Z = H $(Hsal)_2$trien
1b X = S, R = H, Z = H $(Hsal)_2$thiatrien
1c X = NH, R = Me, Z = H $(Haceph)_2$trien
1d X = S, R = Me, Z = H $(Hsal)_2$thiatrien
1e X = NH, R = Et, Z = H $(Hproph)_2$trien
1f X = S, R = Et, Z = H $(Hproph)_2$thiatrien
1g X = NH, R = Ph, Z = H $(Hbenph)_2$trien
1h X = NH, R = Ph, Z = OMe $(HMbenph)_2$trien

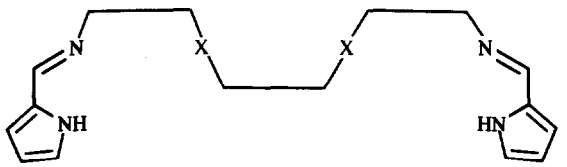

2a X = NH $(Hpyrrol)_2$trien
2b X = S $(Hpyrrol)_2$thiatrien

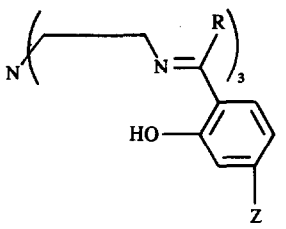

3a Z = H $(Hsal)_3$tren
3b Z = OMe $(Hvan)_3$tren

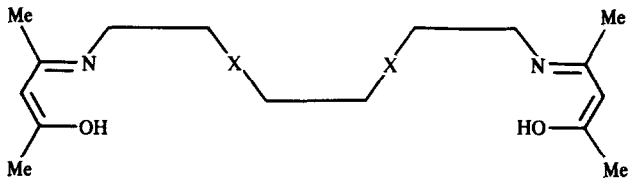

4a X = NH $(Hacac)_2$trien
4b X = S $(Hacac)_2$thiatrien

of 1,8-diamino-3,6-diazaoctane (trien) or 1,8-diamino-3,6-dithiaoctane (thiatrien) with 1-hydroxy-3-methoxybenzophenone, 2-hydroxypropiophenone, 2-hydroxybenzophenone, 2-hydroxy-4-methoxybenzophenone, pyrrole-2-aldehyde or pentane-2,5-dione. The trianionic ligand (**3b**) derived from 3-methoxysalicylaldehyde with tris(2-aminoethyl) amine (tren) has also been prepared and characterized.

EXPERIMENTAL

Synthetic studies

Technical grade 1,8-diamino-3,6-diazaoctane from Aldrich and 97% tris(2-aminoethyl)amine from Fluka were used as received. Salicylaldehyde (98%) from Aldrich was distilled from calcium carbonate before use. 3-Methoxysalicylaldehyde (*o*-vanillin, Aldrich, 98%), 2-hydroxypropiophenone

(Aldrich, 97%), 2-hydroxyacetophenone (Aldrich, 97%), pyrrole-2-carboxaldehyde (Aldrich, 99%) and 2-hydroxy-4-methoxybenzophenone (Lancaster Synthesis) were used as supplied. 2,4-Pentanedione (Fisons SLR grade) was distilled before use.

1,8-Diamino-3,6-dithiaoctane,[1] bis(salicylideneimino)-3,6-dithiaoctane,[1] bis(acetylacetonimine) 3,6-dithiaoctane,[9] $(Hsal)_2$trien,[10] $(Hsal)_3$tren,[13] [Fe{$(sal)_3$tren}],[13] [Fe{$(sal)_2$trien}]PF_6[15] and [Co{$(sal)_2$trien}]$Cl \cdot 2.5H_2O$[11b] were prepared by the methods described in the literature.

Methanol was dried over magnesium methoxide before use. All other solvents were reagent grade and used without further purification.

Physical measurements

IR spectra were recorded, as KBr discs, on a Perkin–Elmer 297 spectrophotometer. ^1H NMR spectra were obtained at 100 MHz using a Varian HA 100 instrument, or at 270 MHz (for Co^{III} complexes) using a Jeol GX 270 instrument. Me_4Si was used as the internal standard. UV–vis spectra were recorded using a Perkin–Elmer 330. Mass spectra were recorded on a Kratos MS 80 instrument by positive ion fast atom bombardment using a glycerol matrix. Elemental analyses were performed by the Microanalytical Laboratory, Department of Chemistry, University of Birmingham.

Magnetic susceptibilities in the solid state were measured by the Gouy method using Hg $[Co(NCS)_4]$[19] as a calibrant. Pascal constants (from the table given by Figgis and Lewis[20]) were used to correct for ligand and anion diamagnetism as follows: (in 10^{-9} m^3 mol^{-1}) $[(sal)_2trien]^{2-}$ 2.458; $[(aceph)_2trien]^{2-}$ 2.756; $[(proph)_2trien]^{2-}$ 3.09; $[(sal)_2thiatrien]^{2-}$ 2.62; $[(pyrrol)_2trien]^{2-}$ 1.84; $[(benph)_2trien]^{2-}$ 4.035; $[(sal)_3tren]^{3-}$ 2.99; $[(van)_3tren]^{3-}$ 3.61; $[HB(pz)_3]^-$ (pz = pyrazol-1-yl) 1.066; PF_6^- 0.8055. ^{57}Iron Mössbauer spectra were recorded with a Cryophysics MS-102 microprocessor-controlled Mössbauer spectrometer at 298 K using a $^{57}Co/Rh$ source and absorbers containing *ca* 10 mg iron cm^{-2}. The drive velocity was calibrated with a $^{57}Co/Rh$ source and a natural iron foil absorber. All the spectra were computer fitted and the ^{57}Fe chemical isomer shift data were calculated relative to the metallic iron.

Tris(3 - *methoxysalicylideneimino*)*triethylamine*, $(Hvan)_3$tren

Tris-(2-aminoethyl)amine (0.50 g, 3.4 mmol) and sodium acetate trihydrate (0.67 g, 4.9 mmol) were dissolved in a mixture of hot ethanol (4 cm^3) and water (1 cm^3). A solution of 3-methoxysalicylaldehyde (1.56 g, 10.25 mmol) in ethanol (2 cm^3) was added and the yellow solution heated for 5 min. The solution was cooled and evaporated to dryness under reduced pressure. The resulting yellow oil was triturated with diethyl ether to give the product as a yellow powder which was collected by filtration and dried *in vacuo*. Yield, 0.52 g (28%); m.p. 119–120°C.

1,8 - *Bis*(2 - *hydroxyacetophenonimine*) - 3,6 - *dithiaoctane*, $(Haceph)_2$thiatrien

1,8-Diamino-3,6-dithiaoctane (1 g, 5.5 mmol), 2-hydroxyacetophenone (1.51 g, 11.1 mmol) and 1 drop of concentrated HCl were heated together at 100°C for 90 min. The resulting yellow oil was cooled to give a yellow solid which was triturated with diethyl ether and recovered by filtration. It was dried *in vacuo*. Yield, 1.46 g (63%); m.p. 145–147°C.

1,8 - *Bis*(2 - *hydroxypropiophenonimine*) - 3,6 - *dithiaoctane*, $(Hproph)_2$thiatrien

This ligand was prepared by the previous method using 2-hydroxypropiophenone. In this case a yellow–orange oil was obtained on cooling. This was triturated with diethyl ether to give a pale yellow solid. The crude solid was recrystallized from ethanol to give the product as bright yellow crystals. Yield, 1.27 g (52%); m.p. 62–64°C.

Bis - 1,8 - (*pyrrole* - 2 - *carboxaldimino*) - 3,6 - *dithiaoctane*, $(Hpyrrol)_2$thiatrien

A solution of 1,8-diamino-3,6-dithiaoctane (0.50 g, 2.8 mmol) in warm ethanol (10 cm^3) was added to a solution of pyrrole-2-carboxaldehyde (0.53 g, 5.57 mmol) in ethanol (15 cm^3). The solution was stirred overnight at room temperature. The product precipitated as a cream solid and was recovered by filtration. It was washed with diethylether and dried *in vacuo*. Yield, 0.83 g (89%); m.p. 116–118°C.

[Fe{$(van)_3$tren}]

Tris(3 - methoxysalicylidenimino)triethylamine (0.20 g, 0.36 mmol) was dissolved in hot methanol (20 cm^3) and a solution of anhydrous iron(III) chloride (0.06 g, 0.37 mmol) in methanol (5 cm^3) added. An immediate colour change to black–purple occurred. A solution of sodium acetate trihydrate (0.19 g, 1.4 mmol) in water (20 cm^3) was next added and the mixture stirred and heated for 10 min. The volume of the resulting solution was then reduced to *ca* 5 cm^3 before cooling to 0°C to induce

precipitation of the product. The solid obtained was collected by filtration, washed with water, acetone and diethyl ether and then dried *in vacuo*. The product was obtained as a black–purple powder. Yield 0.15 g (68%); m.p. > 200°C.

$[Fe\{(pyrrol)_2trien\}]PF_6$

1,8-Diamino-3,6-diazaoctane (0.45 g, 3.08 mmol) was dissolved in dry methanol (30 cm^3) and sodium methoxide (0.33 g, 6.2 mmol) was added. Pyrrole-2-carboxaldehydc (0.59 g, 6.2 mmol) was then added and the solution refluxed for 20 min. After this time, iron(III) chloride hexahydrate (0.84 g, 3.1 mmol) was added to the hot solution and the resulting purple solution refluxed for a further 15 min, before being cooled to room temperature. The solvent was then removed under reduced pressure and the residue extracted with water. The resulting solution was filtered and NH_4PF_6 (0.60 g, 3.7 mmol) in water (5 cm^3) was added to the filtrate. The resulting purple precipitate was collected by filtration and dried. It was recrystallized twice from acetone–diethyl ether to give the product as black–purple microcrystals. Yield, 0.87 g (54%); m.p. > 200°C.

$[Fe\{(aceph)_2trien\}]PF_6$

2-Hydroxyacetophenone (0.95 g, 6.98 mmol) was added to a solution of 1,8-diamino-3,6-diazaoctane (0.50 g, 3.42 mmol) in methanol (25 cm^3). The resulting yellow solution was stirred at room temperature for 1 h. Sodium acetate trihydrate (1.3 g, 9.55 mmol) and anhydrous iron(III) chloride (0.55 g, 3.39 mmol) were then added and the red–brown solution was refluxed for 30 min. The solution was cooled, filtered and the solvent removed under reduced pressure. The residue was extracted with water, filtered and an aqueous solution of NH_4PF_6 (1 g) was added to the filtrate. The red–brown precipitate which formed was collected by filtration and recrystallized twice from acetone–diethyl ether (using $MgSO_4$ to dry the acetone solution before adding the diethyl ether). The product was obtained as red–brown microcrystals. Yield 0.58 g (30%); m.p. 155–156°C (dec).

$[Fe\{(proph)_2trien\}]PF_6$

This compound was prepared according to the previous method using 2-hydroxypropiophenone (2.57 g, 17.1 mmol), 1,8-diamino-3,6-diazaoctane (1 g, 6.8 mmol) and iron(III) chloride hexahydrate (1.85 g, 6.84 mmol). The *complex* was obtained as red–brown microcrystals. Yield, 1.32 g (32%); m.p. > 200°C.

$[Fe\{(Mbenph)_2trien\}]PF_6$

This was prepared according to the method described above for $[Fe\{(aceph)_2trien\}]PF_6$ using 2-hydroxy 4-methoxybenzophenone (0.98 g, 4.3 mmol), 1,8-diamino-3,6-diazaoctane (0.25 g, 1.71 mmol) and iron(III) chloride (0.27 g, 1.68 mmol). The *complex* was obtained as a red–brown powder. Yield, 0.57 g (44%); m.p. 155–156°C (dec).

$[Fe\{(sal)_2thiatrien\}]$

1,8-Bis(salicylideneimino)-3,6-dithiaoctane (0.20 g, 0.51 mmol) and sodium acetate trihydrate (0.05 g, 0.37 mmol) were dissolved in warm methanol (30 cm^3). NH_4PF_6 (0.16 g, 0.98 mmol) was then added, followed immediately by a solution of iron(III) chloride hexahydrate (0.14 g, 0.52 mmol) in methanol (10 cm^3). The colour immediately changed to dark purple. The solution was refluxed for 10 min, then cooled and filtered. The blue–black microcrystalline solid residue was washed with diethyl ether and air dried. The product could be recrystallized from acetone–diethyl ether. Yield, 0.16 g (53%); m.p. > 200°C.

$[Fe\{HB(pz)_3\}_2]PF_6$

A solution of anhydrous iron(III) chloride (0.18 g, 1.12 mmol) in water (5 cm^3) was added to a solution of potassium hydrotris(pyrazole-1-yl) borate (0.54 g, 2.16 mmol) in water (5 cm^3). A bright orange solid was produced. Further water was added to dissolve the solid and the solution filtered. NH_4PF_6 (0.25 g, 1.5 mmol) in water (2 cm^3) was added to the filtrate. A bright orange solid was precipitated, which was recovered by filtration and dried *in vacuo*. It was recrystallized from acetone–diethyl ether to give the product as bright red microcrystals. Yield, 0.33 g (49%); m.p. > 250°C.

$[Co\{(sal)_2thiatrien\}]PF_6$

Cobalt(II) acetate tetrahydrate (0.20 g, 0.80 mmol) in hot methanol (10 cm^3) was added to a solution of 1,8-bis(salicylideneimino)-3,6-dithiaoctane (0.26 g, 0.67 mmol) in hot methanol (15 cm^3) and the mixture was refluxed for 10 min. Air was then drawn through the solution for 30 min. Water (25 cm^3) was next added and air drawn through the solution for a further 2.5 h. NH_4PF_6 (0.14 g) in water (2 cm^3) was then added to precipitate the product as a green–brown solid. This was recovered

by filtration, washed with water, ethanol and diethyl ether and dried *in vacuo*. Yield, 0.29 g (73%); m.p. > 250°C.

$[Co\{(aceph)_2thiatrien\}]PF_6$

This compound was prepared by the previous method using cobalt(II) acetate tetrahydrate (0.2 g, 0.8 mmol) and the ligand (0.30 g, 0.72 mmol). The crude product was recrystallized from acetone–diethyl ether to give dark green microcrystals. Yield, 0.31 g (70%); m.p. 256°C (dec).

$[Co\{(proph)_2thiatrien\}]$

This was prepared according to the method described for $[Co\{(aceph)_2thiatrien\}]PF_6$ using cobalt(II) acetate tetrahydrate (0.2 g, 0.8 mmol) and the ligand (0.31 g, 0.7 mmol). The crude product was recrystallized from acetone–diethyl ether to give dark green microcrystals. Yield, 0.26 g (45%); m.p. 253°C (dec).

$[Co\{(acac)_2thiatrien\}]PF_6$

Cobalt(II) acetate tetrahydrate (0.25 g, 1 mmol) in hot methanol (10 cm^3) was added to a solution of the ligand (0.25 g, 0.73 mmol) in ethanol (5 cm^3). Immediately after this, H_2O_2 (0.6 cm^3 of 2.75%) was added and the dark green solution was refluxed for 15 min. The volume was then reduced under vacuum and NH_4PF_6 (0.35 g) in water (5 cm^3) was added. On shaking, a dark green solid precipitated; this was recovered by filtration, washed with water, ethanol and diethyl ether and air dried. It was recrystallized from acetone–diethyl ether to give dark green microcrystals which were dried *in vacuo*. Yield, 0.12 g (30%); m.p. > 250°C.

$[Co\{(aceph)_2trien\}]PF_6$

2-Hydroxyacetophenone (0.31 g, 2.28 mmol) in ethanol (15 cm^3) was added to a solution of 1,8-diamino-3,6-diazaoctane (0.15 g, 1.0 mmol) in ethanol (20 cm^3). The solution was stirred at room temperature for 4 h and then evaporated to dryness *in vacuo*. The resulting oil was dried overnight in a vacuum desiccator over silica gel.

The ligand was dissolved in acetone (20 cm^3) and the solution added to cobalt(II) chloride hexahydrate (0.24 g, 1 mmol) in water (10 cm^3). A little activated carbon was then added and air drawn through the solution for 5 h. 2 M NaOH solution (1 cm^3) was added and air drawn through the solution for a further 2 h. The mixture was then cooled in ice and filtered. The residual solid was washed with hot water (30 cm^3) and NH_4PF_6 (0.15 g) added to the filtrate. The precipitated solid was filtered off and recrystallized from acetone–diethyl ether to give the product as dark brown plates which were dried *in vacuo*. Yield, 0.16 g (25%); m.p. 192–194°C (dec).

$[Co\{(proph)_2trien\}]PF_6$

This was prepared by the previous method using 2-hydroxypropiophenone (0.59 g, 3.9 mmol), 1,8-diamino-3,6-diazaoctane (0.26 cm^3, 1.75 mmol) and cobalt(II) chloride hexahydrate (0.87 g, 3.66 mmol).

The product was obtained as red–brown crystals. Yield, 0.25 g (22%); m.p. 154–155°C (dec).

Structural studies

A crystal of $[FeC_{16}H_{22}N_6]PF_6$ (0.8 × 0.3 × 0.5 mm) was mounted on an Enraf–Nonius CAD-4 diffractometer; cell dimensions and intensities were measured by ω–2θ scans with graphite-monochromated Mo-K_α radiation.

Three standard reflections measured every 2 h showed no significant variation over the period of data collection. 5466 reflections were scanned within $2 < \theta < 25°$ covering the index ranges: h, 0–12; k, −6–16; l, −16–16. Of these, 3515 are unique (merging R_{int} 0.024), and after application of Lorentz and polarization corrections, 2714 structure amplitudes with $F > 5\sigma(F)$ were considered observed and used in the analysis.

Crystal data. $[FeC_{16}H_{22}N_6][PF_6]$, $M = 499.2$, monoclinic, space group $P2_1/c$, $a = 10.644(7)$, $b = 13.829(2)$, $c = 13.665(4)$ Å, $\beta = 91.75(2)°$, $U = 2010.5$ $Å^3$, $Z = 4$, $D_c = 1.649$ g cm^{-3}, $F(000) = 1020$, μ(Mo-K_α) = 0.927 mm^{-1}, $\lambda = 0.71069$ Å.

The structure was determined by Patterson and Fourier methods, and refined by least-squares, using anisotropic thermal parameters for all non-hydrogen atoms. Hydrogen atoms were placed in calculated positions, riding on their respective bonded atom. The weighting scheme used was $w = 1/[\sigma^2(F) + 0.0015F^2]$, and the refinement converged to $R = 0.0855$, $R' = 0.0915$ (maximum shift/error ratio in final cycle 0.244). The residual electron density in a final difference map was within the range −0.66–1.75 e $Å^{-3}$ with all main peaks close to the Fe atom.

In view of the low merging R_{int}, the rather high R values and rather large residual electron density are difficult to explain. An attempt to improve the situation by applying an empirical absorption correction[21] was not successful.

Table 1. Elemental analyses[a] and imine stretching frequencies[b]

Compound	Carbon	Hydrogen	Nitrogen	$\nu_{C=M}$ (cm^{-1})
$(Hsal)_3tren$	71.0(70.7)	6.3(6.5)	12.25(12.2)	1638
$(Hvan)_3tren$	65.5(65.6)	6.7(6.6)	10.2(10.2)	1630
$(Hsal)_2thiatrien$	61.8(61.8)	6.5(6.2)	7.4(7.2)	1638
$(Hsal)_2trien$	70.6(70.7)	6.9(6.5)	12.2(12.2)	1635
$(Haceph)_2thiatrien$	63.1(63.4)	7.0(6.7)	7.0(6.7)	1615
$(Hproph)_2thiatrien$	65.0(64.8)	7.4(7.2)	6.35(6.3)	1615
$(Hpyrrol)_2thiatrien$	57.3(57.4)	6.5(6.6)	16.5(16.7)	1642
$(Hacac)_2thiatrien$	55.5(55.7)	7.9(8.1)	7.8(8.1)	1605
$[Fe\{(sal)_2tren\}]$	63.5(63.4)	5.2(5.3)	11.1(10.9)	1625
$[Fe\{(van)_3tren\}]$	59.6(59.9)	5.4(5.5)	9.1(9.3)	1620
$[Fe\{(sal)_2thiatrien\}]PF_6$	40.7(40.9)	3.45(3.7)	5.3(4.7)	1622
$[Fe\{(sal)_2trien\}]PF_6$	43.5(43.4)	4.6(4.3)	10.4(10.1)	1630
$[Fe\{(pyrrol)_2trien\}]PF_6$	38.8(38.5)	4.2(4.4)	17.1(16.8)	1590
$[Fe\{(proph)_2trien\}]PF_6$	47.5(47.3)	5.5(5.2)	9.4(9.1)	1600
$[Fe\{(aceph)_2trien\}]PF_6$	45.7(45.4)	4.6(4.8)	9.8(9.6)	1600
$[Fe\{(Mbenph)_2trien\}]PF_6$	53.2(53.3)	5.1(4.7)	7.4(7.3)	1605
$[Co\{(sal)_2thiatrien\}]PF_6$	40.8(40.6)	3.5(3.7)	4.7(4.7)	1625
$[Co\{(aceph)_2thiatrien\}]PF_6$[c]	44.6(44.3)	4.7(4.7)	4.0(4.1)	1595
$[Co\{(proph)_2thaitrien\}]PF_6$[c]	45.7(46.0)	4.9(5.1)	4.2(3.9)	1595
$[Co\{(acac)_2thiatrien\}]PF_6$	35.2(35.1)	4.9(4.8)	5.1(5.1)	1590
$[Co\{(sal)_2trien\}]Cl \cdot 2.5H_2O$	48.6(48.8)	5.6(5.9)	11.6(11.3)	1640
$[Co\{(aceph)_2trien\}] \cdot PF_6$[c]	47.0(46.7)	5.1(5.3)	8.5(8.7)	1600
$[Co\{(proph)_2trien\}]PF_6$[c]	48.4(48.3)	5.6(5.7)	8.4(8.3)	1600

[a] Found % (Calc. %).
[b] Recorded as KBr discs.
[c] Crystallizes as a 1 : 1 solvate with acetone.

Complex neutral atom scattering factors were employed. Computations were carried out on the University of Birmingham Honeywell computer, and on the CDC 7600 at the University of Manchester Regional Computer Centre with the SHELX,[22] PLUTO[23] and DIFABS[21] programs. Final atomic coordinates, displacement factors, coefficients, full lists of bond lengths and angles and F_o/F_c values have been deposited as supplementary material with the Editor from whom copies can be obtained.*

RESULTS AND DISCUSSION

Synthetic studies

The synthesis of the hexadentate ligands follows well established precedents involving a condensation reaction of the appropriate amine, 1,8-diamino-3,6-diazaoctane, tris-(2-aminoethyl)amine or 1,8-diamino-3,6-dithiaoctane with the appropriate aldehyde or ketone to produce a Schiff base ligand. The ligands $(Hsal)_2trien$ (**1a**), $(Haceph)_2$ thiatrien (**1b**), $(Hpyrrol)_2thiatrien$ (**2b**), $(Hsal)_3$ tren (**3a**), $(Hvan)_3tren$ (**3b**) and $(Hacac)_2thiatrien$ (**4b**) were isolated as solids which were readily characterized. The other ligands were prepared *in situ* before reaction with metal ions, since they could only be isolated as oils. Although most of the hexadentate ligands reacted readily with Fe^{III} and Co^{II} (which was then oxidized to Co^{III} to form 1 : 1 complexes) attempts to prepare Fe^{III} and Co^{III} complexes of $(Hpyrrol)_2thiatrien$ and a Co^{III} complex of $(Hpyrrol)_2trien$ were not successful. Complexes of the 1,8-diamino-3,6-dithiaoctane based ligands with Fe^{III} were also difficult to prepare. Although these ligands gave colour changes with Fe^{III}, attempts to isolate and purify the complexes were only successful in the case of $[Fe\{(sal)_2thiatrien\}]PF_6$. This complex proved to be unstable in solution, as indicated by a colour change from deep red–brown to pale orange after several hours. However, it appeared to be stable in the solid state for prolonged periods. Elemental analyses for the new compounds are presented in Table 1.

* Atomic coordinates have also been deposited with the Cambridge Crystallographic Data Centre.

The IR spectra of the complexes and the free ligands all contained a strong band in the region 1590–1642 cm^{-1} (Table 1) which may be assigned to the C=N stretching vibration.[24] Complexation was accompanied by a bathochromic shift in the ligand core frequency. In the IR spectra of the ligands derived from salicylaldehyde 2-hydroxyacetophenone, 2-hydroxypropiophenone and 4-methoxybenzophenone, strong bands were observed in the region 1270–1285 cm^{-1}. These may be assigned to the C—O (phenolic) stretching vibration.[11b] Upon coordination of the ligands to metal ions these bands are shifted to high frequencies (1315–1340 cm^{-1}). One exception to this is found with [(Hsal)$_2$thiatrien] and its Fe^{III} complex, where the ν_{C-O} band is observed at the same frequency in both the ligand and the complex. In addition to these bands the ligands derived from trien or tren, and their complexes, exhibit a series of bands in the region 1130–1250 cm^{-1} which may be assigned to H_2C–N stretching vibrations. The position of these bands remains largely unchanged upon coordination of the ligands to the metal ions.

The complexes of the ligand derived from trien exhibit several bands in the 3000–3700 cm^{-1} region which may be assigned to N—H stretching vibrations.[15] An explanation for the appearance of these multiple peaks, some of which are sharp, was offered by Das Sarma and Bailar[11b] who suggested that the coordination of secondary amines to the metal results in an effect similar to that observed in amine salts, where the N—H stretching frequency is split into a number of bands.

Bands characteristic of C—H deformation for two-substituted benzene rings are observed in the range 740–780 cm^{-1} for the salicylaldehyde and substituted salicylaldehyde based ligands. The C—C stretching bands are observed in the regions 1500–1600 cm^{-1} and 1460 cm^{-1}, while C—H stretches (aliphatic) are observed in the range 2850–3000 cm^{-1}. In addition, all the complexes isolated as PF_6^- salts exhibited a strong band at *ca* 840 cm^{-1} due to the P—F stretching vibration.

The ^1H NMR spectra of the ligands and Co^{III} complexes are presented in Table 2 and are in accordance with their formulations. In the spectra of the ligands derived from salicylaldehyde, 2-hydroxyacetophenone and 2-hydroxypropiophenone, the signals at δ_{TMS} = 13–13.5 ppm are removed by shaking with D_2O and may be assigned to —OH protons. The ligands (Hsal)$_2$thiatren, (Hvan)$_3$tren, (Hsal)$_2$thiatrien, (Hsal)$_2$trien and (Hpyrrol)$_2$thiatrien exhibit a resonance of relative area two in the region δ_{TMS} 7.76–8.32 ppm which does not exchange with D_2O and may be assigned to the azamethine protons, —CH=N.[24a] In (Hacac)$_2$thiatrien, a CH resonance is observed at δ_{TMS} 5.00 ppm. For (Hpyrrol)$_2$thiatrien, the NH proton resonance is observed as a broad singlet at δ_{TMS} 11.2 ppm and is removed on shaking with D_2O.

The ^1H NMR spectra of the Co^{III} complexes are presented in Table 3. [Co{(sal)$_2$thiatrien}]PF_6 and [Co{(sal)$_2$trien}]$Cl \cdot 2.5H_2O$ exhibit two resonances at δ_{TMS} = 8.36 and 8.5 ppm, respectively, which again may be assigned to the azamethine proton. In general, little shift is observed in the positions of the NMR signals upon coordination of the ligands to the metals.

The mass spectra (Table 3) of [Fe{(sal)$_3$tren}] and [Fe{(van)$_3$tren}] were recorded by the electron impact method and exhibit molecular ions at m/z = 511[13] and 601 ^{55}Fe, respectively. All other mass spectra were recorded by fast atom bombardment using a glycerol matrix. The spectra all contain ions at an m/z value one unit higher than the molecular mass (M) corresponding with $[M+H]^+$. Such behaviour is typical of results obtained using glycerol matrices and is in accord with the formulation of the complexes as cationic 1 : 1 ligand–metal complexes.

Electronic spectral data for the complexes are summarized in Table 4. As observed by Tweedle and Wilson[15] the electronic spectrum of [Fe{(sal)$_2$trien}]PF_6 exhibits a low energy charge-transfer band centred at 610 nm (ε_{max} 1400) and a higher energy band at 490 nm (ε_{max} 3000). The lower energy band may be assigned to the low spin form and the higher energy band to the high spin form, the latter predominating at room temperature. In the complexes [Fe{(proph)$_2$trien}]PF_6, [Fe{(aceph)$_2$trien}]PF_6 and [Fe{(Mbenph)$_2$trien}]PF_6 only the higher energy bands in the range 475–490 nm are observed corresponding to the high spin form. Similarly, [Fe{(sal)$_2$thiatrien}]PF_6 exhibits an absorption band at 562 nm (ε_{max} 4100) which can be assigned to the high spin form. The complex [Fe{(pyrrol)$_2$trien}]PF_6 shows two absorption bands at 715 (ε_{max} 500) and 550 nm (ε_{max} 1820). Given that the magnetic data and ^{57}Fe Mössbauer spectra (*vide infra*) for this complex (Table 4) indicate that it exists in the low spin iron(III) state at room temperature, in the solid state the intense band at 550 nm may be due to the low spin form.

The absorption spectrum obtained of [Fe{(sal)$_3$tren}] in acetonitrile corresponds with that reported in the literature[13] and is similar to the spectrum of the new complex [Fe{(van)$_3$tren}]. All these absorption bands may be assigned to metal–ligand charge-transfer processes and no low intensity bands of purely *d–d* character were observed.

All the Co^{III} salts except [Co{(sal)$_2$trien}]$Cl \cdot 2.5H_2O$ and [Co{(aceph)$_2$trien}]PF_6 have simi-

Table 2. ^{1}H NMR spectra of ligands

Compound	δTMS[a] (ppm)	Area[b]	Assignment
$(Hsal)_3tren$	13.4[c]	1 (s,br)	OH
	7.76	1 (s)	N=CH
	7.3–6.05	4 (m)	C_6H_4
	3.49	2 (t)	CH_2
	2.79	2 (t)	CH_2
$(Hvan)_3tren$	7.85	1 (s)	N=CH
	6.94–5.84	3 (m)	C_6H_3
	3.91	3 (s)	OCH_3
	3.54	2 (t)	CH_2
	2.84	2 (t)	CH_2
$(Hsal)_2$thiatrien	13.2	1 (s,br)	OH
	8.32	1 (s)	N—H
	7.4–6.7	4 (m)	C_6H_4
	3.74	2 (t)	—SCH_2CH_2S—
	2.82	4 (m)	—NCH_2CH_2S—
$(Hsal)_2trien \cdot CHC_6H_4OH$	13.6[c]	2 (s,br)	OH
	10.6	1 (s,br)	OH
	8.21	2 (s)	CH=N
	7.4–6.6	12 (m)	C_6H_4
	3.81	1 (s)	$HC(—N)_2$
	3.68–2.42	12 (m)	CH_2
$(Hproph)_2$thiatrien	7.58–6.64	4 (m)	C_6H_4
	3.76	2 (q)	CH_2 of C_2H_5
	2.83	6 (m)	CH_2
	1.22	3 (t)	CH_3 of C_2H_5
$(Hpyrrol)_2$thiatrien	11.2[c]	2 (s,br)	NH
	8.15	2 (s)	CH=N
	6.85	2 (t)	C_4NH_3
	6.57	2 (m)	C_4NH_3
	6.24	2 (m)	C_4NH_3
	3.86	4 (t)	—SCH_2CH_2S—
	2.72	8 (m)	—NCH_2CH_2S—
$(Hacac)_2$thiatrien	10.95	1 (s,br)	OH
	5.00	1 (s)	CH=C
	3.43	2 (q)	—SCH_2CH_2S—
	2.78	4 (m)	—NCH_2CH_2S—
	2.02	3 (s)	CH_3
	1.98	3 (s)	CH_3

[a] Obtained at 100 MHz from $CDCl_3$ solutions.
[b] s = singlet, t = triplet, q = quartet, m = multiplet, br = broad.
[c] Signal removed on shaking with D_2O.

lar absorption spectra. Each exhibited an absorption in the region 635–670 nm (ε_{max} 500–1200) in addition to a strong absorption at 345–395 nm (ε_{max} 4000–7000) with a shoulder at *ca* 450 nm. The spectra of $[Co\{(sal)_2trien\}]Cl \cdot 2.5H_2O$, $[Co\{(aceph)_2trien\}]PF_6$ and $[Co\{(proph)_2trien\}]PF_6$ are similar, containing absorption maxima in the range 590–570 nm ($\varepsilon_{max} \sim 230$) and at 385 nm ($\varepsilon_{max}$ 6750).

The magnetic moments and ^{57}Fe Mössbauer parameters recorded in the solid state from the Fe^{III} complexes are presented in Table 4. All the complexes except $[Fe\{(pyrrol)_2trien\}]PF_6$ and $[Fe\{HB(pz)_3\}_2]PF_6$ (which was prepared for comparative purposes) have magnetic moments in the range 5.7–6.1 BM at 29 K, typical of high spin (^{6}A) Fe^{III} complexes.[25] The ^{57}Fe Mössbauer spectra recorded from the compounds $[Fe(sal)_2thiatren]PF_6$,

Table 3. ^1H NMR and mass spectral data for complexes

Compound	Molecular ion (m/z for ^{59}Co or ^{56}Fe)	δTMS[b] (ppm)	Area[b]	Assignment
$[Co\{(sal)_2thiatrien\}]PF_6$[c]	446[d]	8.36	1(s)	CH=N
		7.54–6.4	4(m)	C_6H_4
		4.25	2(t)	$—SCH_2CH_2S—$
		3.4–2.4	4(m)	$—NCH_2CH_2S—$
$[Co\{(aceph)_2thiatrien\}]PF_6 \cdot CH_3COCH_3$	474[e]	7.8–6.4	4(m)	C_6H_4
		4.4–3.7	2(m)	$—SCH_2CH_2S—$
		3.1–2.2	7(m)	$NCH_2CH_2S—+C—CH_3$
		2.05	3(s)	CH_3 of acetone of crystallization
$[Co\{(proph)_2thiatrien\}]PF_6 \cdot CH_3COCH_3$[c]	502[e]	7.8–6.3	4(m)	C_6H_4
		4.5–3.8	2(m)	$—SCH_2CH_2S—$
		3.4–2.3	6(m)	$NCH_2CH_2S+CH_2$ of C_2H_5
		2.05	3(s)	CH_3 of acetone
		1.17	3(t)	CH_3 of C_2H_5
$[Co\{(acac)_2thiatrien\}]PF_6$[f]	402[e]	5.18	1(s)	CH
		4.00	2(m)	$—SCH_2CH_2S—$
		3.26–2.5	4(m)	$—NCH_2CH_2S—$
		2.34	3(s)	$—CH_3$
		1.98	3(s)	$—CH_3$
$[Co\{(aceph)_2trien\}]PF_6 \cdot CH_3COCH_3$[c]	440[e]	7.8–6.4	4(m)	C_6H_4
		4.12	2(m)	central CH_2NH
		3.2 2.2	7(m)	$=NCH_2CH_2NH+CH_3$
		2.08	3(s)	CH_3 of acetone
$[Co\{(proph)_2trien\}]PF_6 \cdot CH_3COCH_3$[c]	468[e]	7.85–6.4	4(m)	C_6H_4
		3.95–4.4	2(m)	$NHCH_2CH_2NH$
		3.45–2.2	6(m)	$=NCH_2CH_2NH+CH_2$ of C_2H_5
		2.08	3(s)	CH_3 of acetone
		1.3	3(t)	CH_3 of C_2H_5
$[Co\{(sal)_2trien\}]Cl \cdot 2.5H_2O$[c]	412[e]	8.5	2(s)	CH=N
		7.55–5.8	10(m)	C_6H_4+NH
		4.55–4.05	4(m)	$HNCH_2CH_2NH$
		3.45–2.1	13(m)	$=NCH_2CH_2NH+H_2O$
$[Fe\{(sal)_3tren\}]$	511[g]			
$[Fe\{(van)_3tren\})$	601[g]			
$[Fe\{(sal)_2thiatrien\}]PF_6$	443[e]			
$[Fe\{(sal)_2trien\}]PF_6$	409[e]			
$[Fe\{(pyrrol)_2trien\}]PF_6$	355[e]			
$[Fe\{(proph)_2trien\}]PF_6$	465[e]			
$[Fe\{(aceph)_2trien\}]PF_6$	437[e]			
$[Fe\{(Mbenph)_2trien\}]PF_6$	621[e]			

[a] Obtained at 270 MHz. [b] s = singlet, t = triplet, m = multiplet.

[c] ^1H NMR from a solution in d^6-dimethylsulphoxide.

[d] Mass spectrum by fast atom bombardment (Ar) of a 5×10^{-3} mol dm^{-3} solution in acetone using a glycerol matrix.

[e] Mass spectrum by fast atom bombardment (Ar) of a 5×10^{-3} mol dm^{-3} solution in acetone–methanol 60/40 (v/v) using a glycerol matrix.

[f] ^1H NMR from a solution in d^6-acetone.

[g] Mass spectrum obtained by electron impact ionization.

Table 4. Magnetic moment, Mössbauer and electronic spectral data for complexes

Compound	Magnetic and Mössbauer data[a]	Electronic spectral data ν_{max} (cm^{-1})	ε_{max} (cm^{-1} dm^3 mol^{-1})
$[Fe\{HB(C_3N_2H_3)_3\}_2]PF_6$	δ 0.06 Δ 0.82		
$[Fe\{(sal)_3tren\}]$[b]	$\mu_{eff} = 5.76$ δ 0.45 Δ 0.78	19,417 23,000 30,770	5450 3860 13,420
$[Fe\{(van)_3tren\}]$[b]	$\mu_{eff} = 6.76$ δ 0.42 Δ 0.81	18,018 22,727 29,851 32,258	5675 3175 14,050 13,255
$[Fe\{(sal)_2thiatrien\}]PF_6$[c]	$\mu_{eff} = 6.01$ δ 0.42 Δ 0.99	17,794	4100
$[Fe\{(pyrrol)_2trien\}]PF_6$[c]	$\mu_{eff} = 2.17$ δ 0.04 Δ 2.91	13,986 18,182	500 1820
$[Fe\{(proph)_2trien\}]PF_6$[c]	$\mu_{eff} = 6.14$	21,008 23,697	3520 3350
$[Fe\{(aceph)_2trien\}]PF_6$[c]	$\mu_{eff} = 5.84$	21,053 23,474	3535 3090
$[Fe\{(Mbenph)_2trien\}]PF_6$[c]	$\mu_{eff} = 5.91$	20,325	3200
$[Co\{(sal)_2thiatrien\}]PF_6$[d]	—	14,970 22,220 25,640	663 — 4340
$[Co\{(aceph)_2thiatrien\}]PF_6 \cdot CH_3COCH_3$[c]	—	15,150 22,220 25,640	1075 — 6085
$[Co\{(proph)_2thiatrien\}]PF_6 \cdot CH_3COCH_3$[c]	—	15,105 22,220 25,315	1200 — 7045
$[Co\{(acac)_2thiatrien\}]PF_6$[c]	—	15,750 21,740 28,985	553 520 5465
$[Co\{(sal)_2trien\}]Cl \cdot 2.5H_2O$[d]	—	16,950 21,275 25,975	232 666 6221
$[Co\{(aceph)_2trien\}]PF_6 \cdot CH_3COCH_3$[c]	—	17,390 25,975	376 6750
$[Co\{(proph)_2trien\}]PF_6 \cdot CH_3COCH_3$[c]	—	17,390 25,975	278 5600

[a] μ_{eff} (BM) determined by the Gouy method using $Hg[Co(NCS)_4]$ as calibrant. δ (mm s^{-1}) maximum standard deviation 0.04 mm s^{-1} (hs = high spin, ls = low spin) with iron foil as reference. ΔE_Q (mm s^{-1}) maximum standard deviation 0.08 mm s^{-1}.

[b] Recorded in acetonitrile.

[c] Recorded in acetone.

[d] Recorded in 1 : 1 (v/v) methanol–water solution approximately 10^{-4} mol dm^{-3} in complex.

$Fe(sal)_3tren$ and $Fe(van)_3tren$ are characteristic of high spin iron(III) in near octahedral coordination and are therefore consistent with this interpretation. The larger quadrupole splitting of the $[Fe\{(sal)_2$ thiatrien$\}]PF_6$ may reflect a greater distortion of the electronic environment about iron(III) as a result of coordination to a $N_2O_2S_2$ donor set as compared to the N_3O_3 ligand.

The magnetic moments of 2.17 and 2.15 BM which were recorded from the compounds $[Fe\{(pyrrol)_2trien\}]PF_6$ and $[Fe\{HB(pz)_3\}_2]PF_6$ are characteristic of low spin (^2T) iron(III) species. All six of the donor atoms in both of these complexes, as well as in low spin $[Fe\{(pyrrol)_3tren\}]$,[25] are nitrogen atoms and their behaviour therefore contrasts with the high spin properties of other complexes reported here which contain O_2N_4, O_3N_3 or $O_2N_2S_2$ donor atom sets. The ^{57}Fe Mössbauer spectra recorded from $[Fe\{(pyrrol)_2trien\}]PF_6$ and $[Fe\{HB(pz)_3\}_2]PF_6$ are also characteristic of low spin iron(III), although the quadrupole splitting for $[Fe\{(pyrrol)_2trien\}]PF_6$ is larger than normally expected and that for $[Fe\{HB(pz)_3\}_2]PF_6$ is somewhat smaller. The crystal structure of $[Fe\{(pyrrol)_2trien\}]PF_6$ (*vide infra*) shows the iron(III) to be accommodated in a significantly distorted octahedral array of donor atoms. In contrast, iron(III) in $[Fe\{HB(pz)_3\}_2]PF_6$ is coordinated to six nitrogen atoms from two tripodal ligands and thereby enjoys a less distorted octahedral environment.

The ^{57}Fe Mössbauer spectra recorded from $[Fe\{(aceph)_2trien\}]PF_6$ and $[Fe\{(proph)_2trien\}]PF_6$ were characterized by rather broad lines and were not dissimilar from those previously recorded[16] at 298 K from $[Fe\{(acac)_2trien\}]PF_6$. The data are consistent with the magnetic measurements and show the compounds to be $S = 5/2$ high spin iron(III) species.

Structural studies

Selected bond lengths and angles from the single-crystal X-ray diffraction study on $[Fe\{(pyrrol)_2$ trien$\}]PF_6$, are listed in Table 5. The structure of the complex is illustrated in Fig. 1, which also shows the atomic numbering. The coordination about the iron atom is distorted octahedral, similar to that observed in related complexes.[12,16,26]

Table 5. Bond lengths (Å) and selected bond angles (°) with ESDs in parentheses

Lengths			
Fe(1)—N(1)	1.943(5)	N(4)—C(9)	1.489(11)
Fe(1)—N(2)	1.921(7)	N(4)—C(10)	1.510(12)
Fe(1)—N(3)	2.014(7)	N(5)—C(11)	1.445(12)
Fe(1)—N(4)	2.067(7)	N(5)—C(12)	1.319(12)
Fe(1)—N(5)	1.930(7)	N(6)—C(13)	1.377(12)
Fe(1)—N(6)	1.915(6)	N(6)—C(16)	1.372(13)
P(1)—F(1)	1.594(7)	C(1)—C(2)	1.418(11)
P(1)—F(2)	1.571(7)	C(2)—C(3)	1.389(13)
P(1)—F(3)	1.580(7)	C(3)—C(4)	1.423(10)
P(1)—F(4)	1.577(7)	C(4)—C(5)	1.391(11)
P(1)—F(5)	1.570(8)	C(6)—C(7)	1.529(13)
P(1)—F(6)	1.572(8)	C(8)—C(9)	1.529(15)
N(1)—C(1)	1.333(10)	C(10)—C(11)	1.507(14)
N(1)—C(4)	1.390(10)	C(12)—C(13)	1.420(13)
N(2)—C(5)	1.304(11)	C(13)—C(14)	1.402(12)
N(2)—C(6)	1.456(12)	C(14)—C(15)	1.347(19)
N(3)—C(7)	1.478(14)	C(15)—C(16)	1.400(14)
N(3)—C(8)	1.456(12)		
Angles			
N(1)—Fe(1)—N(2)	82.0(3)	N(3)—Fe(1)—N(5)	99.0(3)
N(1)—Fe(1)—N(3)	161.5(3)	N(4)—Fe(1)—N(5)	80.4(3)
N(2)—Fe(1)—N(3)	82.8(3)	N(1)—Fe(1)—N(6)	97.3(3)
N(1)—Fe(1)—N(4)	90.7(3)	N(2)—Fe(1)—N(6)	94.9(3)
N(2)—Fe(1)—N(4)	102.4(3)	N(3)—Fe(1)—N(6)	94.5(3)
N(3)—Fe(1)—N(4)	82.2(3)	N(4)—Fe(1)—N(6)	161.8(3)
N(1)—Fe(1)—N(5)	96.6(3)	N(5)—Fe(1)—N(6)	82.4(3)
N(2)—Fe(1)—N(5)	176.9(3)		

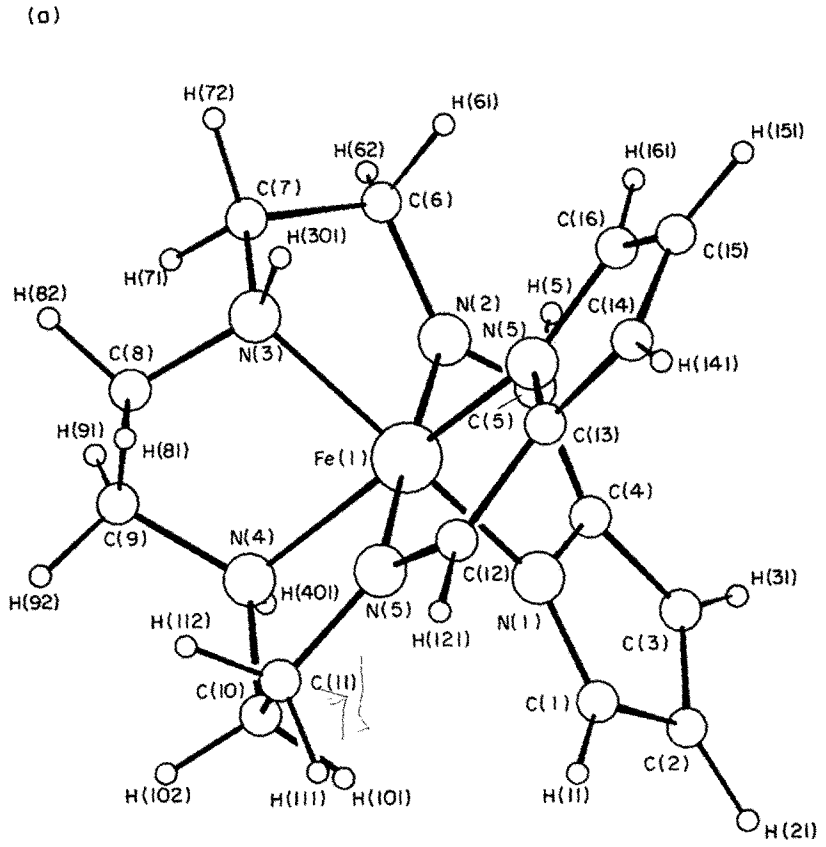

Fig. 1. (a) The structure of $[Fe\{(pyrrol)_2trien\}]^+$ showing the atom labelling. (b) A stereoview of the cation.

However, this complex cation, with a donor set of six nitrogen atoms, exhibits a greater distortion from octahedral geometry than the related cations in $[Fe\{(sal)_2trien\}]NO_3 \cdot H_2O$ and $[Fe\{(sal)_2trien\}]Cl \cdot H_2O$,[16] which have O_2N_4 donor atom sets. The angles N(1)—Fe—N(3), N(6)—Fe—N(4) and N(2)—Fe—N(5) deviate considerably from 180° (161.5, 161.8, 176.9°), whilst the 12 angles subtended at the iron atom by adjacent donor atoms range from 80.4 to 102.4°. This range may be compared to those of 83.9–95.3°, 83.9–95.2° and 83.5–96.0° for the Cl^-, Br^- and NO_3^- salts of $[Fe\{(sal)_2trien\}]^+$, respectively.[16,25]

Inspection of the Fe—N bond lengths reveals that two distinct groups are present:

(1) those between iron and a saturated, i.e. sp^3 hybridized nitrogen, 2.014 and 2.067 Å;
(2) those between iron and a pyrrolic nitrogen, or an unsaturated, i.e. sp^2 hybridized nitrogen, which are slightly shorter, range 1.915–1.943 Å.

These bond lengths are similar to the Fe—N lengths found[16] in the $[Fe\{(sal)_2trien\}]^+$ structures, wherein the iron is in the low spin ($s = \frac{1}{2}$) state. In the high spin ($s = 5/2$) $[Fe\{(acac)_2trien\}]^+$ and $[Fe\{(acac\ Cl)_2trien\}]^+$ complexes, in contrast, the Fe—N lengths are *ca* 0.17 Å longer.[16] Our structural results are, therefore, in agreement with the magnetic susceptibility and Mössbauer spectral data, indicating low spin iron in $[Fe\{(pyrrol)_2trien\}][PF_6]$ (Table 4).

The greater distortion from octahedral geometry of this complex may be a consequence of the stereochemical limitations imposed by the presence of five five-membered chelate rings, as opposed to three five-membered and two six-membered chelate rings in the $[Fe\{(sal)_2trien\}]^+$ cations. The two chelate rings adjacent to pyrrole rings are planar to within 0.01 Å. Bond lengths indicate electron delocalization over these moieties. The other three five-membered chelate rings deviate from planarity, with maximum atom displacements of −0.198, 0.298 and −0.305 Å. Thus the pyrrole ring confers considerable rigidity on the adjoining chelate ring, producing planarity at the two extremities of the ligand, and contributing to the distortion from octahedral geometry.

The PF_6^- counter ion approximates closely to octahedral geometry, maximum angular distortion, 3.1°. The P—F bond lengths are in the range 1.570(8)–1.594(7) Å in agreement with previous results.[27]

The results obtained from the structural studies show that the conversion of the six-membered terminal chelate rings in $[Fe\{(sal)_2trien\}]^+$ to five-membered rings in $[Fe\{(pyrrol)_2trien\}]^+$ is accompanied by significant additional distortions from an ideal octahedral geometry. When the Co^{III} ion is used in place of Fe^{III} the 1 : 1 complex either does not form or is of such limited stability that it cannot be isolated under similar conditions to those used to obtain the iron complex. This may reflect the inability of the ligand $(sal)_2trien$ to accommodate sufficiently the coordination requirements of the smaller Co^{III} ion. In solution at least, the incorporation of —S— donor atoms in place of —NH— in going from $[Fe\{(sal)_2trien\}]^+$ to $[Fe\{(sal)_2thiatrien\}]^+$ also results in a reduction in the stability of the complex. When both of these structural changes are combined in the ligand $(pyrrol)_2thiatrien$, the result is that 1 : 1 metal–ligand complexes with Fe^{III} or Co^{III} cannot be isolated under the conditions we have used.

Acknowledgements—We are grateful to the SERC and Amersham International plc for their support of this work, and to Mr T. Green for technical assistance.

REFERENCES

1. F. P. Dwyer and F. Lions, *J. Am. Chem. Soc.* 1950, **72**, 1545.
2. F. P. Dwyer, N. S. Gill, E. C. Gyarfas and F. Lions, *J. Am. Chem. Soc.* 1952, **74**, 4188.
3. J. Collins, F. P. J. Dwyer and F. Lions, *J. Am. Chem. Soc.* 1952, **74**, 3134.
4. F. P. Dwyer, N. S. Gill, E. C. Gyarfas and F. Lions, *J. Am. Chem. Soc.* 1953, **75**, 1526.
5. F. P. Dwyer, N. S. Gill, E. C. Gyarfas and F. Lions, *J. Am. Chem. Soc.* 1953, **75**, 2443.
6. F. P. Dwyer, N. S. Gill, E. C. Gyarfas and F. Lions, *J. Am. Chem. Soc.* 1954, 383.
7. F. P. Dwyer, N. S. Gill, E. C. Gyarfas and F. Lions, *J. Am. Chem. Soc.* 1957, **79**, 1269.
8. F. Lions and K. V. Martin, *J. Am. Chem. Soc.* 1957, **79**, 1572.
9. F. Lions and K. V. Martin, *J. Am. Chem. Soc.* 1958, **80**, 3858.
10. A. K. Mukherjee, *Sci. Cult.* 1953, **19**, 107.
11. (a) B. Das Sarma and J. C. Bailar Jr, *J. Am. Chem. Soc.* 1954, **76**, 4051; (b) B. Das Sarma and J. C. Bailar Jr, *J. Am. Chem. Soc.* 1955, **77**, 5476.
12. P. D. Cradwick, M. E. Cradwick, G. G. Dodson, D. Hall and T. N. Waters, *Acta Cryst.* 1972, **B28**, 45.
13. M. A. Hoselton, L. J. Wilson and R. S. Drago, *J. Am. Chem. Soc.* 1975, **97**, 1722.
14. L. J. Wilson and N. J. Rose, *J. Am. Chem. Soc.* 1968, **90**, 6041.
15. M. F. Tweedle and L. J. Wilson, *J. Am. Chem. Soc.* 1976, **98**, 4824.
16. E. Sinn, G. Sim, E. V. Dose, M. F. Tweedle and L. J. Wilson, *J. Am. Chem. Soc.* 1978, **100**, 3375.
17. E. V. Dose, K. M. M. Murphy and L. J. Wilson, *Inorg. Chem.* 1976, **15**, 2622.

18. J. A. Broomhead and D. J. Robinson, *Aust. J. Chem.* 1968, **21**, 1365.
19. B. N. Figgis and R. S. Nyholm, *J. Chem. Soc.* 1958, 4190.
20. B. N. Figgis and J. Lewis, in *Modern Coordination Chemistry* (Edited by J. Lewis and R. G. Wilkins), Chap. 6, p. 400. Wiley, New York (1960).
21. N. Walker and D. Stuart, *Acta Cryst.* 1983, **A39**, 158.
22. G. M. Sheldrick, SHELX, Program for Crystal Structure Determination, University of Cambridge (1978).
23. W. D. S. Motherwell, PLUTO, Program for Plotting Molecular and Crystal Structures, Report "Cambridge Crystallographic Files", University of Manchester Regional Computer Centre, Manchester (1981).
24. (a) U. Casselato, *Coord. Chem. Rev.* 1977, **23**, 31; (b) C. S. Marvel, S. A. Aspey and E. A. Dudley, *J. Am. Chem. Soc.* 1957, **78**, 4905; (c) B. Das Sarma, K. R. Ray, R. E. Sievers and J. C. Bailar Jr, *J. Am. Chem. Soc.* 1964, **86**, 14; (d) R. M. Holm, G. W. Everrett Jr and A. Charkravorty, *Prog. Inorg. Chem.* 1966, **7**, 83.
25. P. Greig Sim and E. Sinn, *Inorg. Chem.* 1978, **17**, 1288.
26. Y. Nishida, K. Kino and S. Kida, *J. Chem. Soc., Dalton Trans.* 1987, 1957.
27. H. J. Banbery and T. A. Hamor, *Acta Cryst.* 1988, **C44**, 1683.

Polyhedron Vol. 8, No. 4, pp. 505–512, 1989
Printed in Great Britain

0277–5387/89 $3.00+.00
© 1989 Pergamon Press plc

COMPLEXES OF MOLYBDENUM(0),(II) AND TUNGSTEN(0),(II) WITH SOME MACROCYCLIC POLYTHIAETHERS

D. SEVDIĆ,* M. ĆURIĆ and Lj. TUŠEK-BOŽIĆ

Rudjer Bošković Institute, Department of Chemistry, 41000 Zagreb, P.O. Box 1016, Croatia, Yugoslavia

(*Received* 16 *June* 1988; *accepted* 1 *September* 1988)

Abstract—Reactions of potentially tetradentate and hexadentate macrocyclic polythiaethers 1,4,8,11-tetrathiacyclotetradecane (TTP) and 1,4,7,10,13,16-hexathiacyclooctadecane (HTO) with $Mo(CO)_6$ and $W(CO)_6$ have been studied. The new complexes of molybdenum(0) and tungsten(0): $[Mo(CO)_3]_2[TTP]$, $[Mo(CO)_3][HTO]$, $[Mo(CO)_3]_2[HTO]$, $[W(CO)_3][TTP]$ and $[W(CO)_4]_2[HTO]$, were isolated. The interaction of these compounds with iodine afforded the seven-coordinate complexes of molybdenum(II) and tungsten(II): $[Mo(CO)_3I_2][TTP]\cdot CH_2Cl_2$, $[Mo(CO)_3I_2]_2[HTO]$ and $[W(CO)_3I_2][TTP]\cdot CH_2Cl_2$. The complexes obtained were characterized on the basis of elemental analyses, magnetic measurements and IR, ^1H NMR, ^{13}C NMR and mass spectra.

A great deal of interest has been directed to obtaining information on derivatives of molybdenum and tungsten hexacarbonyl complexes in which one or several carbonyl ligands were replaced by various ligands containing sulphur donor atoms.[1–11] Among them, macrocyclic polythiaethers have drawn less attention, and only a few complexes of molybdenum(0) and tungsten(0) with these ligands have been reported.[12–14]

Our previous studies have concentrated on complex formation of molybdenum(VI), (V), (IV) and (III) with macrocyclic polythiaethers TTP and HTO, respectively.[15,16] As an extension of these investigations, in the present report we wish to describe the synthesis and spectral properties of some carbonyl complexes of molybdenum(0), (II) and tungsten(0), (II) with these ligands (Fig. 1).

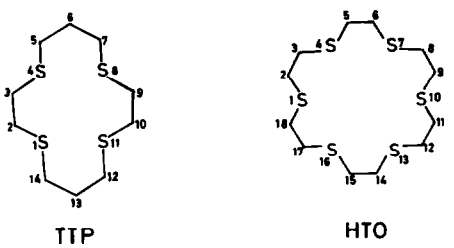

Fig. 1. Investigated ligands.

EXPERIMENTAL

Starting materials

Macrocyclic polythiaethers 1,4,8,11-tetrathiacyclotetradecane (TTP) and 1,4,7,10,13,16-hexathiacyclooctadecane (HTO) were prepared as described earlier.[17,18] The compounds $Mo(CO)_6$ and $W(CO)_6$ (Merck) were used without further purification. All solvents were purified by standard methods, dried and saturated with dry argon before use.

Preparation of complexes

All reactions were carried out under a stream of dry argon.

μ - 1,4,8,11 - *Tetrathiacyclotetradecane* - *bis[tricarbonylmolybdenum*(0)] (I). A mixture of 1.320 g (5 mmol) of $Mo(CO)_6$ and 0.268 g (1 mmol) of TTP in absolute ethanol (60 cm^3) was refluxed for 2 h with vigorous stirring. The yellow crystalline product was isolated by filtration in air of the hot solution, purified by means of repeated washings with hot ethanol and dried *in vacuo* at ambient temperature. Found: Mo, 30.2; C, 31.0; H, 3.6; S, 19.9. Calc. for $Mo_2C_{16}H_{20}S_4O_6$: Mo, 30.5; C, 30.6; H, 3.2; S, 20.4%.

*Author to whom correspondence should be addressed.

Tricarbonyl(1,4,7,10,13,16 - *hexathiacyclooctadecane*)*molybdenum*(0) (**II**). An equimolar amount of $Mo(CO)_6$ (0.264 g, 1 mmol) and HTO (0.360 g, 1 mmol) in absolute ethanol (30 cm^3) was heated under reflux for 2 h. The light yellow precipitate formed was separated by filtration of the hot solution, washed with the reaction solvent and dried. Found: Mo, 17.7; C, 33.7; H, 5.2; S, 35.8. Calc. for $MoC_{15}H_{24}S_6O_3$: Mo, 17.8; C, 33.3; H, 4.5; S, 35.5%.

μ - 1,4,7,10,13,16 - *Hexathiacyclooctadecane* - *bis*[*tricarbonylmolybdenum*(0)] (**III**). This complex was prepared similarly to **II** by using 1.056 g (0.4 mmol) of $Mo(CO)_6$ and 0.360 g (1 mmol) of HTO in 70 cm^3 of absolute ethanol and refluxing the reaction mixture for about 3 h. Found: Mo, 26.4; C, 29.7; H, 3.6; S, 26.5. Calc. for $Mo_2C_{18}H_{24}S_6O_6$: Mo, 26.6; C, 30.0; H, 3.4; S, 26.7%.

Tricarbonyl(1,4,8,11 - *tetrathiacyclotetradecane*) *tungsten*(0) (**IV**). A mixture of 0.705 g (2 mmol) of $W(CO)_6$ and 0.268 g (1 mmol) of TTP in absolute ethanol (30 cm^3) was refluxed with continuous stirring under the constant irradiation from a Camag TL-900 UV lamp for 10 h. The yellow crystals which precipitated were collected by filtration of the hot solution in air, washed with hot ethanol and dried *in vacuo* at ambient temperature. Found: W, 33.8; C, 28.9; H, 3.6; S, 24.0. Calc. for $WC_{13}H_{20}S_4O_3$: W, 34.3; C, 29.1; H, 3.7; S, 23.9%.

μ - 1,4,7,10,13,16 - *Hexathiacyclooctadecane* - *bis*[*tetracarbonyltungsten*(0)] (**V**). According to the procedure given above for **IV**, a mixture of 1.412 g (4 mmol) of $W(CO)_6$ and 0.360 g (1 mmol) of HTO in absolute ethanol (70 cm^3) was refluxed under constant irradiation from a Camag TL-900 UV lamp for 12 h. The yellow crystalline precipitate was filtered off, washed and dried. Found: W, 38.0; C, 25.8; H, 2.8; S, 20.7. Calc. for $W_2C_{20}H_{24}S_6O_8$: W, 38.6; C, 25.2; H, 2.5; S, 20.1%.

Di - iodotricarbonyl(1,4,8,11 - *tetrathiacyclotetradecane*)*molybdenum*(II)*dichloromethane*(1/1) (**VI**). The complex $[Mo(CO)_3][TTP]$ (0.78 g, 1.73 mmol) was dissolved in dichloromethane (20 cm^3) and cooled to $-10°C$. A solution of 0.50 g (1.92 mmol) of I_2 in dichloromethane (10 cm^3) was added dropwise with stirring. The mixture was vigorously stirred further for 2 h at $-10°C$. The orange crystals formed were filtered off under a stream of dry argon, washed with cool dichloromethane and dried *in vacuo*. The same product was obtained starting from complex **I**. Found: Mo, 12.5; C, 21.2; H, 3.0; S, 16.9; I, 32.3. Calc. for $MoC_{14}H_{22}S_4I_2Cl_2O_3$: Mo, 12.2; C, 21.3; H, 2.8; S, 16.3; I, 32.2%.

μ - 1,4,7,10,13,16 - *Hexathiacyclooctadecane* - *bis*[*di - iodotricarbonyl molybdenum*(II)] (**VII**). A suspension of 0.95 g (1.76 mmol) of the complex $[Mo(CO)_3][HTO]$ in dichloromethane (25 cm^3) was cooled at $-10°C$ and a solution of 0.50 g (1.92 mmol) of I_2 in dichloromethane (10 cm^3) was added slowly. The mixture was stirred for a further 2 h. The orange precipitate formed was filtered off, rinsed with the cool dichloromethane and dried. The same compound was obtained starting from complex **III**. Found: Mo, 15.4; C, 17.2; H, 2.2; S, 16.2; I, 41.1. Calc. for $Mo_2C_{18}H_{24}S_6I_4O_6$: Mo, 15.6; C, 17.6; H, 1.9; S, 15.6; I, 41.3%.

Di - iodotricarbonyl(1,4,8,11 - *tetrathiacyclotetradecane*)*tungsten*(II) *dichloromethane*(1/1) (**VIII**). This compound was prepared in an analogous manner to **VI**, starting with 0.86 g (1.59 mmol) of complex **IV** and 0.45 g (1.80 mmol) of I_2 dissolved in dichloromethane. Found: W, 21.2; C, 18.7; H, 2.4; S, 15.2; I, 29.4. Calc. for $WC_{14}H_{22}S_4I_2Cl_2O_3$: W, 21.0; C, 19.2; H, 2.5; S, 14.6; I, 29.0%.

Physical measurements

IR spectra of the complexes were recorded as KBr pellets on a Perkin–Elmer 580 B (4000–180 cm^{-1}) spectrophotometer. ^1H and ^{13}C NMR spectra were obtained in CD_2Cl_2 solutions on a JEOL FX 90Q spectrometer (90 MHz for ^1H and 22.5 MHz for ^{13}C) and on a Brucker spectrometer (300 and 360 MHz for ^1H, 70.5 and 90 MHz for ^{13}C). Tetramethylsilane was used as an internal standard. Mass spectra were obtained on a Varian CH-7 mass spectrometer, using an ionization current of 100 μA, an electron energy of 70 eV and an ion accelerating voltage of 3 kV. Magnetic susceptibilities were determined by the standard Gouy method at 295 K using $CuSO_4 \cdot 5H_2O$ as calibrant. X-ray powder patterns were obtained using an X-ray diffractometer (Philips) with a proportional counter using Cu-K_α radiation.

RESULTS AND DISCUSSION

Reactions of $Mo(CO)_6$ and $W(CO)_6$ with macrocyclic polythiaethers TTP and HTO give some tricarbonyl and tetracarbonyl complexes of molybdenum(0) and tungsten(0). These novel compounds are yellow, microcrystalline and diamagnetic solids which decompose very slowly in air, while their solutions are much less stable. By oxidation with iodine in dichloromethane they are converted to the new seven-coordinate complexes of molybdenum(II) and tungsten(II). These complexes are microcrystalline or powder-like, coloured orange, diamagnetic and less air-stable than the complexes of the zero-valent metals. They can be stored under argon only for several days.

Table 1. Conditions for preparation of the complexes

	Complex	Starting compound	Metal/ligand ratio	Solvent	Colour
I	$[Mo(CO)_3]_2[TTP]$	$Mo(CO)_6$	5:1	Ethanol	Yellow
II	$[Mo(CO)_3][HTO]$	$Mo(CO)_6$	1:1	Ethanol	Yellow
III	$[Mo(CO)_3]_2[HTO]$	$Mo(CO)_6$	4:1	Ethanol	Yellow
IV	$[W(CO)_3][TTP]$	$W(CO)_6$	1:1 2:1	Ethanol	Yellow
V	$[W(CO)_4]_2[HTO]$	$W(CO)_6$	1:1 2:1 4:1	Ethanol	Yellow
VI	$[Mo(CO)_3I_2][TTP]\cdot CH_2Cl_2$	$[Mo(CO)_3][TTP]$ $[Mo(CO)_3]_2[TTP]$	1:2	Dichloromethane	Orange
VII	$[Mo(CO)_3I_2]_2[HTO]$	$[Mo(CO)_3][HTO]$ $[Mo(CO)_3]_2[HTO]$	1:2	Dichloromethane	Orange
VIII	$[W(CO)_3I_2][TTP]\cdot CH_2Cl_2$	$[W(CO)_3][TTP]$	1:2	Dichloromethane	Orange

Conditions of preparation with some physical properties of the complexes are given in Table 1, the most important IR data are listed in Table 2, while the NMR spectra are shown in Table 3. The complexes were formulated mainly on the basis of chemical and spectral analysis. The low solubility and stability of most of the complexes in common solvents, limited their further characterization. Generally, binuclear complexes are less soluble than the mononuclear complexes, as well as are molybdenum complexes compared to those of tungsten.

Complexes of molybdenum(0) *and tungsten*(0)

Investigations of the interactions of $Mo(CO)_6$ and $W(CO)_6$ with TTP and HTO, respectively, have shown that either the mononuclear or the binuclear complexes could be formed depending on the concentration of the reactants used in the reactions. The binuclear complexes of molybdenum were obtained only when the concentration of the metal was in large excess in relation to the concentration of the ligand. So the complex $[Mo(CO)_3]_2[HTO]$ was formed with the metal–ligand ratio 4:1, and the complex $[Mo(CO)_3]_2[TTP]$ with the molar ratio 5:1. On the other hand, an equimolar metal–ligand ratio afforded the mononuclear complexes $[Mo(CO)_3][HTO]$ and $[Mo(CO)_3][TTP]$,[13] respectively.

It was observed that in the reaction of $W(CO)_6$ with HTO only the binuclear complex $[W(CO)_4]_2$ [HTO] was formed regardless of the concentration of the reactants. With the ligand TTP the mononuclear complex $[W(CO)_3][TTP]$ and the binuclear complex $[W(CO)_4]_2[TTP]$[13] could be formed depending on the metal–ligand ratio used.

The IR frequencies associated with the characteristic functional groups of the free macrocyclic polythiaethers and their metal complexes are presented in Table 2. Only for the complex $[W(CO)_3]$ [TTP] could the IR spectrum be obtained both in the solid state and in a dichloroethane solution. Its spectrum in solution has two intense bands in the carbonyl stretching region, indicating a C_{3v} local symmetry with a facial tricarbonyl configuration. In the solid state the basic two line spectrum is dominant, but almost every peak shows a shoulder due to the greater distortions of the complex molecule in the solid state packing. We can assign two carbonyl absorptions to A_1 and E vibration modes. This carbonyl IR pattern also closely resembles those obtained for some molybdenum and tungsten complexes, *fac*-$M(CO)_3L_3$[19] and *fac*-$M(CO)_3L$,[2,11,13,20] containing sulphur donor ligands. Furthermore, it is clearly apparent that the positions of the carbonyl absorptions as well as their relative intensities are very similar for all other tricarbonyl complexes of TTP and HTO (**I, II** and **III**), suggesting the same facial tricarbonyl configuration. This configuration is preferable in the metal tricarbonyl complexes with a ligand of lower π-bonding ability than the carbonyl groups.

All investigated complexes give a series of strong to medium bands between 650 and 510 cm^{-1}, characteristic of M—CO bending, and a weak band in the 490–470 cm^{-1} region due to the M—S stretching vibrations. Significant differences between the spectra of macrocyclic polythiaethers and their complexes may be noticed in the region 1220–660 cm^{-1} where

Table 2. Characteristic IR bands (cm^{-1}) of macrocyclic polythiaethers and their complexes

Compound	ν(CO)	δ(M—CO)	ν(M—S)	*trans*-CH_2 wag.	*trans*-CH_2 twist.	*gauche*-CH_2 rock.	*trans*-CH_2 rock. or ν(C—S)	*trans*-ν(C—S)
TTP		—	—	1208 vs	1140 s	—	730 w	692 s, 675 s
HTO				1195 vs	1151 s	928 w, 843 m	730 w	683 s, 660 s
I	1930 vs, 1810 vs	648 s, 615 m, 540 m	470 w	1200 m	—	930 w, 845 m	—	—
II	1922 vs, 1818 sh, 1815 sh 1795 vs	640 s, 610 m, 522 s	475 w	1220 w	1130 vw	938 m, 845 m	718 w	687 vw
III	1920 vs, 1820 sh, 1790 vs	642 vs, 606 m, 515 s	470 w	1200 vw	1170 vw	918 m, 838 m	—	—
IV	1918 sh, 1910 vs, 1820 sh 1818 sh, 1780 vs 1925vs,[a] 1815 vs[a]	630 m, 610 w, 520 s	490 w	1200 vw	1120 w	930 m, 845 m	—	—
V	2010 vs, 1975 sh, 1900 s,br 1850 s,br	615 s, 580 m	480 w	1200 w	—	925 w, 848 m	—	680 vw
VI	2040 s, 1963 s, 1925 s	582 s, 510 s	465 m	1205 w	1140 vw	930 m, 832 m	736 s	685 vw
VII	2030 s, 1950 vs,br	590 m, 525 w	485 s	1205 w	1140 vw	910 m, 850 m	735 w	682 vw
VIII	2030 s, 1955 s, 1910 s	580 m, 522 s	480 m	1210 vw	1148 w	930 vw, 835 w	738 s	670 vw

[a] Recorded in solvent.

Table 3. ^1H and ^{13}C NMR spectra of some novel complexes[a]

Complex	Nucleus	Chemical shift (δ) (ppm)[b]	Assignment
$[W(CO)_3][TTP]$	^1H	2.11 q	H(6)
		2.30–3.38 m	H(2,3), H(5), H(7), H(9,10), H(12,13,14)
	^{13}C	25.43, 26.12, 26.17, 30.23, 32.08, 33.51, 33.80, 36.58, 38.71, 46.15	C(2,3), C(5,6,7), C(9,10), C(12,13,14)
		212.72, 216.38, 216.53	CO
$[Mo(CO)_3][HTO]$	^1H	2.71–3.10 m	H(2,3), H(5,6), H(8,9), H(11,12), H(14,15), H(17,18)
	^{13}C	30.66	C(14,15)
		32.72, 33.00, 33.92, 34.04, 34.85	C(5,6), C(8,9), C(11,12), C(17,18)
		41.25	C(2,3)
		221.13	CO
$[W(CO)_3I_2][TTP]$	^1H	1.96 q	H(6), H(13)
		2.65 t overlapping	H(7), H(12)
		2.75 s	H(9,10)
		3.08 s	H(2,3)
		3.30 t	H(5), H(14)

[a] In CD_2Cl_2 relative to TMS. Protons are designated by the number of carbons to which they are attached (see Fig. 1).

[b] Abbreviations: s, singlet; t, triplet; q, quintet; m, multiplet.

bands arising from various modes of vibrations of the thiaether and methylene groups are present. Two strong bands in the IR spectra of the free ligands, TTP (692 and 675 cm^{-1}) and HTO (683 and 660 cm^{-1}), are assigned to the C—S stretching vibrations. Coordination of the sulphur atoms from the ligand to the metal atom causes both a decrease in the frequency and a lowering of the intensity of the C—S—C stretching mode. In complexes **I** and **III** the ν(C—S) bands disappeared completely indicating that all sulphur atoms are engaged in the complex. In the complex $[Mo(CO)_3]_2[HTO]$ the ligand HTO probably acts in a double tridentate bridging manner between two molybdenum units, and it can be thus presumed that molybdenum atoms have an octahedral configuration. For complex **I** where the tetradentate ligand TTP can act only in a double bidentate bridging manner between two molybdenum units, the formally five-coordinate molybdenum(0) in the complex $[Mo(CO)_3]_2$ [TTP] can be postulated. The same coordination has been found for some tricarbonylmolybdenum(0) complexes with phosphine ligands.[21,22]

IR spectra of tungsten tetracarbonyl complexes with TTP (**V**) differ substantially to those obtained for the tricarbonyl complexes. Although the optimum resolution of the carbonyl absorptions is not possible in the solid state spectrum, the four-line pattern may be recognized, suggesting the C_{2v} local symmetry with the *cis*-tetracarbonyl configuration. This pattern strongly resembles that expected for *cis*-C_{2v} disubstituted octahedral carbonyls.[4,20] Due to the disparate carbonyl ligand configuration, the great differences may also be noticed in the M—CO stretching and bending vibrations. While the former is found only in this complex as the medium band at 390 cm^{-1}, the latter gives two bands at lower frequencies (615 and 580 cm^{-1}). Furthermore, the *trans*-rocking and twisting methylene vibrations have completely disappeared, indicating a greater change in conformation of the macrocyclic ligand. In order to retain the six coordination, the HTO ligand in this complex acts as a bridge between two tungsten units in a double bidentate manner.

Unfortunately, most of the complexes are too insoluble for observing the NMR spectra. Only for the $[W(CO)_3][TTP]$ and $[Mo(CO)_3][HTO]$ complexes have the satisfactory ^1H and ^{13}C NMR spectra been obtained in dichloromethane solution. The results obtained are given in Table 3 and Fig. 2. Significant differences were observed when comparing the NMR spectra of the complexes with the spectra of the free macrocyclic polythiaethers. On the basis of spectral data it is evident that the considerable changes in conformation of the polythiaether ring occur upon complex formation. The bidentate or tridentate coordination of the macrocyclic ligands is proposed in the metal complexes.

The free TTP ligand has three sets of resonant signals for methylene protons of the polythiaether ring, a quintet at δ 1.98 ppm for the β-propanomethylene protons and overlapping triplet and

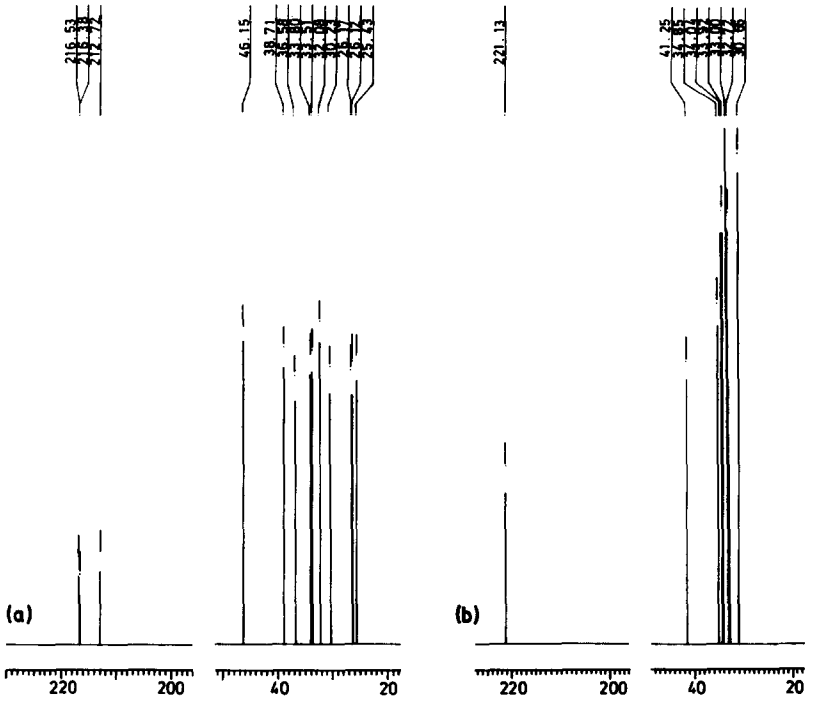

Fig. 2. ^{13}C NMR spectra of the complexes (a) $[W(CO)_3][TTP]$ and (b) $[Mo(CO)_3][HTO]$.

singlet patterns at δ 2.67 and 2.77 ppm, respectively, for the protons of α-propanomethylene and ethylene groups.[23] The ^{13}C NMR spectrum consequently shows three absorptions at δ 30.02, 30.24 and 31.49 ppm for β-, α-propano and ethano carbon atoms, respectively.

The NMR spectra of the $[W(CO)_3][TTP]$ complex are much more complex and are in agreement with the proposed unsymmetrical tridentate coordination of the ligand through the S(1), S(4) and S(11) sulphur atoms (Fig. 3). The ^1H NMR spectrum shows a well defined quintet at δ 2.11 ppm and a very complex multiplet at δ 2.30–3.38 ppm. The quintet is assigned to the protons of one β-propanomethylene group depicted as H(6). The relatively small downfield shift of these protons indicates an essentially free ligand character of the corresponding methylene group. On the other hand, the protons of the other β-propanomethylene group H(13), which is near to the S(1) and S(11) coordination sites, are shifted strongly to lower field and

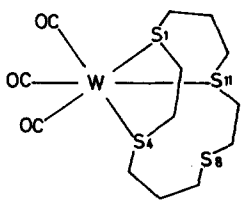

Fig. 3. Proposed structure of $[W(CO)_3][TTP]$.

overlap with the resonances of the other methylene protons. This part of the spectrum is too complex to allow precise assignments. A similar spectrum was obtained for the corresponding Mo complex of TTP, where an analogue structure of the complex was postulated.[13] Furthermore, the ^{13}C NMR spectrum of complex **IV** gives 10 resonances due to the 10 non-equivalent methylene groups (Fig. 2), confirming the unsymmetrical locked ligand coordination. The resonances corresponding to the carbonyl groups appear as three single absorptions, and no internuclear spin coupling with tungsten is observed. The chemical shift differences between the two lower field resonances is extremely small ($\Delta\delta$ = 0.17 ppm). These small deformation changes between the carbonyl groups are not visible in the spectra of the Mo complex, nor in the IR spectra of both complexes. The results obtained confirm the assumption that the ^{13}C chemical shift of the coordinated carbonyl groups is very sensitive to changes in stereochemistry and electronic environment.[24–28]

The HTO ligand having all methylene groups in identical environments, gives very simple NMR spectra. A singlet at δ 2.83 ppm is assigned to the methylene polythiaether protons, and a singlet at δ 32.56 ppm to the 12 equivalent methylene carbon atoms. The spectra of the $[Mo(CO)_3][HTO]$ complex are more complicated due to a greater number of non-equivalent thiaether fragments, as a result

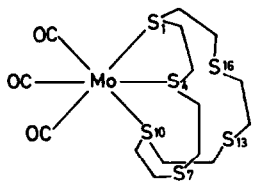

Fig. 4. Proposed structure of $[Mo(CO)_3][HTO]$.

of the non-symmetrical tridentate coordination of the ligand (Fig. 4). The ^1H NMR spectrum of complex **II** exhibits an unresolved multiplet in the δ 2.71–3.10 ppm range. More detailed information about the coordination of the polythiaether ring was provided by ^{13}C NMR spectra (Fig. 2). Seven absorptions, with one of double intensity, assigned to eight non-equivalent methylene groups, dictate the binding of the HTO ligand through the S(1), S(4) and S(10) donor sulphur atoms. Because of the close proximity to the coordinated sulphur atoms S(1) and S(4), the methylene carbons C(2) and C(3) give the resonance with the strongest downfield shift with respect to the free ligand carbon absorption. On the other hand, it may be presumed that the resonance at δ 30.66 ppm with the slight upfield shift, is derived from the methylene carbons C(14) and C(15) which are the furthest from the coordination sites. The other methylene carbon resonances could not be assigned with certainty. The presence of only one carbonyl ligand resonance indicates the fluctuation of the tricarbonyl ligand set. The same behaviour has also been observed in some carbonyl complexes of molybdenum with various macrocyclic and phosphine ligands.[13,29]

Complexes of molybdenum(II) *and tungsten*(II)

Although a wide variety of phosphine and arsine substituted halocarbonyl complexes of the type $[MX_2(CO)_3L]$ and $[MX_2(CO)_3L_2]$ (X = Cl, Br or I; M = Mo or W) have been described,[30,31] very few seven-coordinate complexes of molybdenum(II) and tungsten(II) containing sulphur donor ligands have been reported.[2,3] Iodine oxidation of molybdenum and tungsten zero-valent complexes of the macrocyclic polythiaethers TTP and HTO has been investigated. It was shown that oxidation of both molybdenum complexes of TTP, $[Mo(CO)_3][TTP]$ and $[Mo(CO)_3]_2[TTP]$, as well as of its tungsten complex $[W(CO)_3][TTP]$, with a controlled amount of iodine always leads to the formation of the 1:1 complex. Further, it is of interest that both TTP compounds obtained, $[Mo(CO)_3I_2][TTP]$ and $[W(CO)_3I_2][TTP]$, contain one molecule of dichloromethane, which is supported by elemental analyses and mass spectra. HTO complexes, $[Mo(CO)_3][HTO]$ and $[Mo(CO)_3]_2[HTO]$, react with iodine giving the 2:1 complex $[Mo(CO)_3I_2]_2$ [HTO]. It seems that with regard to the number of sulphur atoms in the ligand, as well as to the size of the macrocyclic ring, the formation of the 1:1 complex for TTP and the 2:1 complex for HTO, respectively, is sterically preferable.

Comparing the IR spectra of di-iodo metal carbonyl complexes with those obtained for the macrocyclic polythiaether complexes of zero-valent metals, it is evident that considerable changes may be noticed only in the regions which contain bands attributed to ν(CO) and δ(M—CO) vibrations. Upon oxidation with iodine the metal becomes more electropositive by forming an M—I bond, and consequently while the carbonyl stretching bands are shifted to higher frequencies, the bands associated with the M—CO bending are shifted to lower frequencies. For all other characteristic absorption bands no significant changes are observed.

The IR spectra of complexes **VI** and **VIII** show three strong bands in the carbonyl stretching region, and are very similar to those obtained earlier for seven-coordinate complexes.[2,31] As the reported X-ray crystal structures of the seven-coordinate complexes with bidentate phosphine and arsine ligands[32] reveal capped octahedral geometry with one carbonyl ligand in the unique capping position, it is highly likely that our di-iodo complexes have a similar capped octahedral structure with a C_s local symmetry. The ^1H NMR spectrum of **VIII** confirms the bidentate coordination of the macrocyclic ligand TTP in its metal complexes. On the other hand, the binuclear HTO complex **VII** exhibits only two bands associated with the carbonyl stretching absorption. Unfortunately, the extremely low solubility and stability of this complex prevent any investigation in solution, and therefore it is difficult to presume its structure with certainty.

The ^1H NMR spectrum of the complex $[W(CO)_3I_2]$ [TTP] shows five sets of resonant signals for the methylene protons of the polythiaether ring, suggesting the symmetrical bidentate ligand coordination through the S(1) and S(4) sulphur atoms (Fig. 5). One quintet is assigned to the protons of the β-propanomethylene groups, two triplets to the protons of the α-propanomethylene groups and two singlets to the ethylene protons. While the chemical shifts of both the β_1-, and one set of α-propanomethylene protons, H(7) and H(12), as well as one set of ethylene protons, H(9) and H(10), are essentially unchanged upon complex formation, the other set of α-propanomethylene protons, H(5) and H(14), and ethylene protons, H(2) and H(3), which are near to the sites of coordination, are shifted downfield by 0.63 and 0.31 ppm, respectively, due

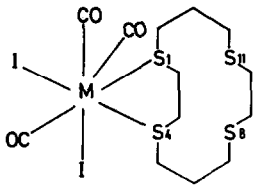

Fig. 5. Proposed structure of $[M(CO)_3I_2][TTP]$, (M = Mo or W).

to the deshielding influence of the binding sulphur atoms. As the NMR spectra were performed in CD_2Cl_2, it is impossible to assign the absorption arising from the dichloromethane molecule present in the complex. Although for the molybdenum complex with TTP, the satisfactory ^1H NMR spectrum was not obtained, an adequate structure could be proposed (Fig. 5) on the basis of IR and X-ray data. Molybdenum and tungsten complexes show the same pattern in the IR spectra and in the X-ray powder photographs, indicating that these two compounds are isomorphous.

The results obtained led us to presume that the ligand coordination modes are controlled by a combination of factors, including the metal size in relation to the size of the macrocyclic polythiaether hole, the presence of competing ligands, and the electronic nature of the metals.

Acknowledgements—The authors thank Prof. T. Cvitaš for valuable discussion and Prof. M. Klessinger for help in obtaining NMR spectra of some of the compounds. Financial support by the Foundation for Scientific Research of SR Croatia is gratefully acknowledged.

REFERENCES

1. S. G. Murray and F. R. Hartley, *Chem. Rev.* 1981, **81**, 365.
2. H. C. E. Mannerskantz and G. Wilkinson, *J. Chem. Soc.* 1962, 4454.
3. H. C. E. McFarlane and W. McFarlane, *J. Inorg. Nucl. Chem.* 1965, **27**, 1059.
4. G. R. Dobson, *Inorg. Chem.* 1969, **8**, 90.
5. G. R. Dobson and G. C. Faber, *Inorg. Chim. Acta* 1970, **4**, 87.
6. W. A. Schenk and M. Schmidt, *Z. Anorg. Allg. Chem.* 1975, **416**, 311.
7. E. W. Ainscough, E. J. Birch and A. M. Brodie, *Inorg. Chim. Acta* 1976, **20**, 187.
8. D. Sellmann and J. Schwarz, *J. Organomet. Chem.* 1983, **241**, 343.
9. E. W. Abel, M. A. Z. Chowdhury, K. G. Orrell and V. Šik, *J. Organomet. Chem.* 1984, **262**, 293.
10. M. T. Ashby and D. L. Lichtenberger, *Inorg. Chem.* 1985, **24**, 636.
11. M. T. Ashby, J. H. Enemark, D. L. Lichtenberger and R. B. Ortega, *Inorg. Chem.* 1986, **25**, 3154.
12. B. K. Balbach, A. R. Koray, A. Okur, P. Wülknitz and M. L. Ziegler, *J. Organomet. Chem.* 1981, **212**, 77.
13. C. G. Joung, J. A. Broomhead and C. J. Boreham, *J. Organomet. Chem.* 1984, **260**, 91.
14. T. Yoshida, T. Adachi, T. Ueda, M. Watanabe, M. Kaminaka and T. Higuchi, *Angew. Chem. Int. Ed. Engl.* 1987, **26**, 1171.
15. D. Sevdić and L. Fekete, *Inorg. Chim. Acta* 1982, **57**, 111.
16. D. Sevdić and L. Fekete, *Polyhedron* 1985, **4**, 1371.
17. D. Sevdić, L. Fekete and H. Meider, *J. Inorg. Nucl. Chem.* 1980, **42**, 885.
18. D. Sevdić and H. Meider, *J. Inorg. Nucl. Chem.* 1981, **43**, 153.
19. F. A. Cotton and F. Zingales, *Inorg. Chem.* 1962, **1**, 145.
20. W. A. Schenk and M. Schmidt, *J. Organomet. Chem.* 1975, **96**, 375.
21. G. J. Kubas, *J. Chem. Soc., Chem. Commun.* 1980, 61.
22. L. K. Peterson, H. B. Davis, P. Y. Leung and J. K. Hoyano, *Inorg. Chim. Acta* 1981, **48**, 259.
23. W. Rosen and D. H. Busch, *J. Am. Chem. Soc.* 1969, **97**, 4694.
24. K. Henrich and S. Wild, *J. Chem. Soc., Dalton Trans.* 1974, 2500.
25. O. A. Gansow, D. A. Schexnayder and B. Y. Kimura, *J. Am. Chem. Soc.* 1972, **94**, 3406.
26. O. A. Gansow, B. Y. Kimura, G. R. Dobson and R. A. Brown, *J. Am. Chem. Soc.* 1971, **93**, 5922.
27. L. F. Farnell, E. W. Randall and E. Rosenberg, *J. Chem. Soc., Chem. Commun.* 1971, 1078.
28. P. S. Braterman, D. W. Milne, E. W. Randall and E. Rosenberg, *J. Chem. Soc., Dalton Trans.* 1973, 1027.
29. B. E. Mann, *J. Chem. Soc., Dalton Trans.* 1973, 2591.
30. R. Colton, *Coord. Chem. Rev.* 1971, **6**, 269.
31. P. K. Baker and S. Fraser, *Inorg. Chim. Acta* 1987, **130**, 61, and refs cited therein.
32. M. G. B. Drew, *Prog. Inorg. Chem.* 1977, **23**, 67.

Polyhedron Vol. 8, No. 4, pp. 513–518, 1989
Printed in Great Britain

0277–5387/89 $3.00+.00
© 1989 Pergamon Press plc

SILVER THIOETHER CHEMISTRY: SYNTHESIS, X-RAY CRYSTAL STRUCTURE AND REDOX PROPERTIES OF $[Ag([18]aneS_6)]^+$ ($[18]aneS_6$ = 1,4,7,10,13,16-HEXATHIACYCLOOCTADECANE)

ALEXANDER J. BLAKE, ROBERT O. GOULD, ALAN J. HOLDER, TIMOTHY I. HYDE and MARTIN SCHRÖDER*

Department of Chemistry, University of Edinburgh, West Mains Road, Edinburgh EH9 3JJ, Scotland, U.K.

(*Received* 19 *July* 1988; *accepted* 8 *September* 1988)

Abstract—Reaction of $AgNO_3$ with 1 molar equivalent of $[18]aneS_6$ ($[18]aneS_6$ = 1,4,7,10,13,16-hexathiacyclooctadecane) in water–MeOH (1 : 1 v/v) affords the complex cation $[Ag([18]aneS_6)]^+$. $[Ag([18]aneS_6)]PF_6$ crystallizes in the monoclinic space group $I2/m$ with a = 5.295(4), b = 13.959(10), c = 13.951(9) Å, β = 95.15(10)°, V = 1027 Å^3, D_c = 1.983 g cm^{-3}, Z = 2. The complex cation has $C_{2h}(2/m)$ symmetry with Ag^I bound to all six thia donors of $[18]aneS_6$ with two short [Ag—S(1) = 2.6665(12) Å] and four significantly longer (Ag—S(4) = 2.7813(10) Å) Ag—S distances. This 2+4 coordination of $[18]aneS_6$ reflects the tendency of the d^{10} Ag^+ ion to increase its coordination number with soft donor ligands. Chemical oxidation of $[Ag([18]aneS_6)]^+$ and $[Ag([9]aneS_3)_2]^+$ at 293 K in highly acidic media affords the corresponding stable Ag^{II} species, which have been identified by ESR and UV–vis spectroscopy. These Ag^{II} species can only be generated electrochemically in MeCN at 293 K as transient intermediates. The enhanced stabilization of $[M([9]aneS_3)_2]^{2+}$ (M = Ag^{II}) and $[M([9]aneS_3)_2]^{3+}$ (M = Fe^{III}, Ni^{III}, Pd^{III}) under acidic conditions is discussed.

The chemistry of macrocyclic thioether complexes is of intense current interest.[1,2] This stems from the observation that, whereas non-cyclic thioether ligands are generally poor donors to metal centres,[3] a wide range of stable complexes of cyclic thioethers can be prepared. At the forefront of these studies have been complexes of the ligands 1,4,7,10,13,16-hexathiacyclooctadecane ($[18]aneS_6$)[4–6] and 1,4,7-trithiacyclononane ($[9]aneS_3$).[7–10] These ligands form a series of complexes with transition metal ions showing highly unusual stereochemical and redox characteristics.[1,4,7] As a continuation of our studies on macrocyclic thioether complexes of second and third row transition metal ions,[1] we report the synthesis, structure and redox chemistry of the Ag^I complex of $[18]aneS_6$.

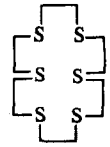

[18]ane S_6

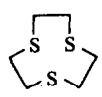

[9]ane S_3

Wieghardt and co-workers[11] and Cooper and co-workers[12] have reported recently the synthesis and structure of the complex cation $[Ag([9]aneS_3)_2]^+$. This species shows octahedral Ag^I with the two trithia ligands bound facially to the metal centre [Ag—S = 2.697(5), 2.753(4) Å]. In addition, Wieghardt and co-workers have characterized[9] a highly interesting trimeric Ag^I cation, $[Ag_3([9]aneS_3)_3]^{3+}$, incorporating bridging thioether ligands. Parallel to these works, we have been investigating the stereochemical and redox properties of the complementary $[Ag([18]aneS_6)]^+$ cation, and we describe our results herein.

RESULTS AND DISCUSSION

Reaction of $AgNO_3$ with 1 molar equivalent of $[18]aneS_6$ in refluxing water–MeOH (1 : 1 v/v) affords a colourless solution. Addition of NH_4PF_6 to the filtered solution yields $[Ag([18]aneS_6)]PF_6$

*Author to whom correspondence should be addressed.

as a colourless product. The fast atom bombardment mass spectrum of the complex shows peaks at $M^+ = 469$ and 467 corresponding to $[^{109}Ag([18]aneS_6)]^+$ and $[^{107}Ag([18]aneS_6)]^+$, respectively. IR spectral and analytical data were consistent with the formulation $[Ag([18]aneS_6)]PF_6$. A single crystal X-ray structural determination was undertaken to confirm the stereochemistry of the complex, and the connectivity of the potentially hexadentate thioether macrocycle.

Crystals of $[Ag([18]aneS_6)]PF_6$ were obtained from MeCN–Et_2O. Two views of the complex cation are shown in Fig. 1(a) and (b). The crystal structure shows the complex to have $C_{2h}(2/m)$ symmetry with a distorted octahedral stereochemistry around the Ag^I ion. All six thia donors of $[18]aneS_6$ are bound to the metal centre with two short axial bonds [Ag—S(1) = 2.6665(12) Å] and four significantly longer equatorial bond lengths [Ag—S(4) = 2.7813(10) Å, ∠S(1)AgS(4) = 80.35(3), ∠S(4)AgS(4′) = 77.43(3)°]. The structure can thus be described as 2+4 coordinate, and reflects the tendency of the d^{10} Ag^+ ion to increase its coordination number with soft donor ligands.[13] The Ag—S bond lengths in $[Ag([18]aneS_6)]^+$ are particularly long for complexes of $[18]aneS_6$, and are similar to those reported previously for $[Ag([9]aneS_3)_2]^+$ (Ag—S = 2.753(4), 2.697(5) Å).[11] It is interesting to compare the structure of $[Ag([18]aneS_6)]^+$ with that of $[Pd([18]aneS_6)]^{2+}$.[4] For the latter complex, the stereochemistry at Pd^{II} is octahedrally distorted with four short equatorial [Pd—S = 2.3114(14), 2.3067(15) Å] and two long range apical interactions (Pd···S = 3.2730(17) Å, $\angle S_{ax}PdS_{eq} = 75.06(5)°$), i.e. 4+2 coordinate.[4] Thus, on going from d^8 Pd^{II} to d^{10} Ag^I, we see a change in binding of $[18]aneS_6$ from formally tetragonally elongated to formally tetragonally compressed octahedral stereochemistry. Increases in the equatorial M—S bond lengths reflect the increase in the ionic radius of the metal centre [0.78 Å for Pd^{II}. 1.29 Å for Ag^I[14]]. The ability of $[18]aneS_6$ to encapsulate such a large metal ion as Ag^I is remarkable, and suggested to us that this system was set up for redox activity at the Ag centre; the metal free $[18]aneS_6$ is redox inactive between −2.0 and +2.0 V in MeCN.

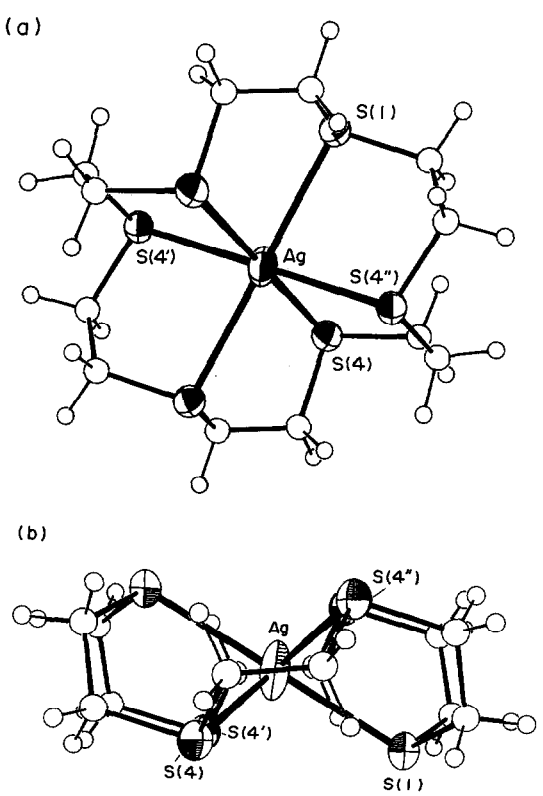

Fig. 1. Two views of the X-ray crystal structure of $[Ag([18]aneS_6)]^+$ with numbering scheme adopted.

Cyclic voltammetry of $[Ag([18]aneS_6)]^+$ in MeCN (0.1 M $^nBu_4NPF_6$) at platinum electrodes shows a sluggish oxidation near $E_{pa} = +1.00$ V vs Fc/Fc^+ which is essentially irreversible; only a small return wave is observed even at fast scan rates indicating that the oxidized product is unstable in MeCN. Importantly, a quasi-reversible reduction observed at $E_{1/2} = -0.42$ V vs Fc/Fc^+, is assigned tentatively to an $Ag^{I/0}$ couple. However, attempts to generate the reduced species by controlled potential electrolysis at 298 K were unsucessful with deposition of Ag metal occurring at the working electrode. Repeated reductive cyclic voltammetric scans of $[Ag([18]aneS_6)]^+$ in MeCN at 298 K also led to deposition of Ag metal at the electrode surface. The binding of Ag^0 to the hexathia ligand is intriguing, and occurs presumably via Ag—S bond breaking in the Ag^I precursor.

It was important to compare these results on $[Ag([18]aneS_6)]^+$ with those of the corresponding nine-membered ring system $[9]aneS_3$. The related $[Ag([9]aneS_3)_2]^+$ cation has been reported to undergo a reversible oxidation at +1.30 V vs NHE in $MeNO_2$ to afford a transient Ag^{II} species. This deep blue product could be generated as a stable species only at −70°C by chemical oxidation with Ce^{IV} in MeOH.[12] In our hands, the oxidation of $[Ag([9]aneS_3)_2]^+$ is only quasi-reversible at high scan rates at 298 K ($E_{pa} = +0.79$ V, $E_{1/2} \simeq +0.75$ V vs Fc/Fc^+), consistent with the transient nature of the oxidized product in MeCN at ambient temperatures. Electrochemically, therefore, the oxidative chemistry of $[Ag([18]aneS_6)]^+$ and $[Ag([9]aneS_3)_2]^+$ appears to be similar with the oxidized product being unstable in organic media. We also observed a reduction for $[Ag([9]aneS_3)_2]^+$

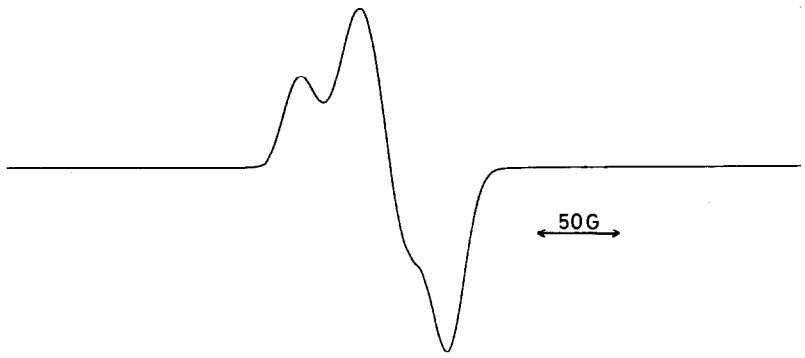

Fig. 2. *X*-Band ESR spectrum (77 K) of the Ag^{II} oxidation product of $[Ag([18]aneS_6)]^+$ in H_2SO_4 glass.

at $E_{pc} = -0.57$ V vs Fc/Fc^+ which was less reversible than for $[Ag([18]aneS_6)]^+$ suggesting that dissociation of $[9]aneS_3$ from the reduced metal centre occurs more rapidly than dissociation of $[18]aneS_6$. This is consistent with the greater denticity of the hexathia over the trithia ligand, and with the expected lability of a formally Ag^0 metal centre. Current work is aimed at trying to stabilize these reduction products.

Paramagnetic Ag^{II} complexes have been reported with a variety of donor ligands.[15] More interestingly, the stabilization of such species has been shown to be enhanced in strongly acidic, non-reducing aqueous solutions.[16] Related to this, Fabbrizzi and co-workers have noted[17] the increased stability of Cu^{III} macrocyclic complexes in acidic media, while we have found similar effects on the stability of oxidized products such as $[Pd([9]aneS_3)_2]^{3+}$.[1,7] We therefore reasoned that highly acidic, aqueous conditions might be effective in stabilizing the Ag^{II} products of $[18]aneS_6$ and $[9]aneS_3$.

Addition of concentrated (98%) H_2SO_4 solution to $[Ag([18]aneS_6)]^+$ at 298 K affords a blue solution ($\lambda_{max} = 564$ nm, $\varepsilon_{max} \simeq 5000$ M^{-1} cm^{-1}), the ESR spectrum of which, as a frozen glass at 77 K, shows a strong anisotropic signal with $g_1 = 2.063$, $g_2 = 2.028$, $g_3 = 2.007$ assigned to the formation of a Ag^{II} species (Fig. 2).[15,16] The blue solution decays to a colourless solution over a period of 2 h at 298 K. Addition of 70% $HClO_4$ solution to $[Ag([18]aneS_6)]^+$ affords the same oxidized product, although in this case the product tends to precipitate out of solution over a period of minutes. The absorption at 564 nm is assigned tentatively to a $S(p\pi) \rightarrow Ag(d)$ charge-transfer transition. Addition of these concentrated acids to $[Ag([9]aneS_3)_2]^+$ likewise affords a blue solution ($\lambda_{max} = 570$ nm, $\varepsilon_{max} = \simeq 8000$ M^{-1} cm^{-1}), the ESR spectrum of which, as a frozen glass at 77 K, shows a strong anisotropic signal with $g_1 = 2.066$, $g_2 = 2.034$, $g_3 = 2.012$ (Fig. 3). This blue Ag^{II} species is stable in solution at room temperature for several days; this contrasts with the transient nature of the

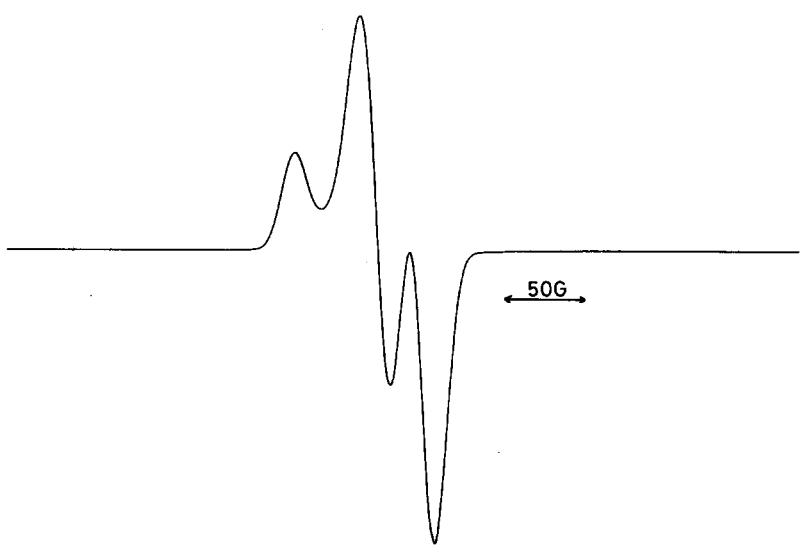

Fig. 3. *X*-Band ESR spectrum (77 K) of the Ag^{II} oxidation product of $[Ag([9]aneS_3)_2]^+$ in $HClO_4$ glass.

complex in organic solvents under ambient conditions.[12] We are currently simulating the above ESR data to identify possible ^{107}Ag and ^{109}Ag components.

We have found that the stability of other high valent metal complexes of [9]aneS$_3$ is enhanced in acidic aqueous media. Thus, the complexes $[M([9]aneS_3)_2]^{3+}$ (M = Fe^{III},[9,10] Ni^{III},[10] Pd^{III}[1,7]) are stable indefinitely in 70% $HClO_4$ solutions, and can be crystallized from them. This observation is particularly important for the complex cation $[Fe([9]aneS_3)_2]^{3+}$ which decomposes very readily in organic solvents.[9] The role of $HClO_4$ in these reactions should be commented upon. The perchlorate anion is well known to be kinetically a very poor oxidant[18] and, indeed, dilute solutions of $HClO_4$ or concentrated solutions of $NaClO_4$ do not generate the above cations from their 2+ analogues. Highly concentrated $HClO_4$ solutions ($\geqslant$ 70%) are, however, very active oxidizing agents.[19] We have not investigated the kinetics of these oxidation reactions; however, the ability of highly concentrated $HClO_4$ solutions (in vast excess to the metal complex substrate) to oxidize these species may also be due to trace oxy-chloro impurities present in solution.

EXPERIMENTAL

IR spectra were recorded as KBr and CsI discs using a Perkin–Elmer 598 spectrometer over the range 200–4000 cm^{-1}. UV–vis spectra were measured in quartz cells using Perkin–Elmer Lambda 9 and Pye Unicam SP8-400 spectrophotometers. Microanalyses were performed by the Edinburgh University Chemistry Department microanalytical service. ESR spectra were recorded as solids or as frozen glasses down to 77 K using a Bruker ER200D X-band spectrometer. Electrochemical measurements were performed on a Bruker E310 Universal Modular Polarograph. All readings were taken using a three electrode potentiostatic system in acetonitrile containing 0.1 M ^{n}Bu$_4$NPF$_6$ or ^{n}Bu$_4$BF$_4$ as supporting electrolyte. Cyclic voltammetric measurements were carried out using a double platinum electrode and an Ag/AgCl reference electrode. All potentials are quoted vs ferrocene/ferrocinium, Fc/Fc$^+$. Mass spectra were run by electron impact on a Kratos MS 902 and by fast atom bombardment on a Kratos MS 50TC spectrometer.

Synthesis of [Ag([18]aneS$_6$)]PF$_6$

To a refluxing solution of [18]aneS$_6$ (0.1 g, 2.77×10^{-4} mol) in water–MeOH (20 cm^3, 1 : 1 v/v) was added $AgNO_3$ (0.045 g, 2.64×10^{-4} mol) in water (5 cm^3). The reaction solution was refluxed for 5 min and the hot solution filtered into a solution of excess NH_4PF_6 (0.2 g, 1.23×10^{-3} mol) in water (30 cm^3). The colourless precipitate was collected and recrystallized from MeCN–Et$_2$O to give [Ag([18]aneS$_6$)]PF$_6$ (0.08 g, 49% yield). Found: C, 23.1; H, 3.68. Calc. for [Ag([18]aneS$_6$)]PF$_6$: C, 23.5; H, 3.94%. Fast atom bombardment mass spectrum: Found M$^+$ = 469, 467. Calc. for [^{109}Ag([18]aneS$_6$)]$^+$ M$^+$ = 469. Calc. for [^{107}Ag([18]aneS$_6$)]$^+$ M$^+$ = 467. IR spectrum (KBr disc): 2956, 2917, 2896, 1425, 1416, 1285, 1260, 1202, 1192, 1154, 924, 840vs,br, 733, 705, 684, 614, 555, 407 cm^{-1}.

X-Ray structure determination of [Ag([18]aneS$_6$)]PF$_6$

A colourless crystal (0.09 × 0.16 × 0.52 mm) suitable for X-ray analysis was obtained by isothermal distillation of Et$_2$O into a solution of the complex in MeCN. The crystal was mounted with its *a* axis parallel to the spindle of a STADI-2 two-circle diffractometer.

Crystal data. $C_{12}H_{24}S_6Ag^+PF_6^-$, $M = 613.46$, monoclinic, space group *I*2/*m* (an alternative setting of *C*2/*m*) with $a = 5.295(4)$, $b = 13.959(10)$, $c = 13.951(9)$ Å, $\beta = 95.15(10)°$, $V = 1027$ Å^3 [from 2θ, ω and μ values of 36 reflections; $\bar{\lambda}$(Mo-K_α) = 0.71069 Å], $D_c = 1.983$ g cm^{-3}, $Z = 2$; $F(000) = 616$, $\mu = 16.84$ cm^{-1}

Data collection and processing. STADI-2 diffractometer, graphite-monochromated Mo-K_α *X*-radiation, ω scans with scan width $(1.0+0.5\sin\mu/\tan\theta)°$, 1050 reflections measured ($2\theta_{max} = 50°$, h 0 → 5, k 0 → 16, l −16 → 16), 919 unique ($R_{int} = 0.029$), giving 829 with $F \geqslant 6\sigma(F)$. No significant crystal decay, no absorption correction.

Structure analysis and refinement. The Ag atom was fixed at the origin, and the S and P atoms located by inputting its position to DIRDIF.[20] Iterative rounds of least-squares refinement and difference Fourier synthesis[21] located all other non-H

Table 1. Bond lengths (Å) with standard deviations for [Ag([18]aneS$_6$)]$^+$

Ag—S(1)	2.6665(12)	C(3)—S(4)	1.812(4)
Ag—S(4)	2.7813(10)	S(4)—C(5)	1.824(4)
S(1)—C(2)	1.812(4)	C(5)—C(5′)	1.529(6)
C(2)—C(3)	1.519(6)		

Singly primed atoms are related to their unprimed equivalents by the operation of a crystallographic mirror plane: doubly primed atoms are related to their unprimed equivalents by the operation of a crystallographic two-fold axis.

Table 2. Bond angles (°) with standard deviations for $[Ag([18]aneS_6)]^+$

S(1)—Ag—S(4)	80.35(3)	C(2)—C(3)—S(4)	117.3(3)
S(4)—Ag—S(4″)	77.43(3)	Ag—S(4)—C(3)	100.06(13)
Ag—S(1)—C(2)	105.02(14)	Ag—S(4)—C(5)	101.19(13)
C(2)—S(1)—C(2′)	103.24(19)	C(3)—S(4)—C(5)	102.86(19)
S(1)—C(2)—C(3)	118.3(3)	S(4)—C(5)—C(5″)	110.1(3)

See footnote under Table 1.

Table 3. Torsion angles (°) with standard deviations for $[Ag([18]aneS_6)]^+$

S(4)—Ag—S(1)—C(2)	−1.93(14)	C(2′)—S(1)—C(2)—C(3)	−80.9(3)
S(4)—Ag—S(1)—C(2′)	106.58(14)	S(1)—C(2)—C(3)—S(4)	−53.1(4)
S(1)—Ag—S(4)—C(3)	−18.02(14)	C(2)—C(3)—S(4)—Ag	43.1(3)
S(1)—Ag—S(4)—C(5)	87.38(13)	C(2)—C(3)—S(4)—C(5)	−60.9(3)
S(4″)—Ag—S(4)—C(3)	−120.26(14)	Ag—S(4)—C(5)—C(5″)	52.0(3)
S(4″)—Ag—S(4)—C(5)	−14.87(13)	C(3)—S(4)—C(5)—C(5″)	155.2(3)
S(1)—Ag—S(4″)—C(5″)	−92.62(13)	S(4)—C(5)—C(5″)—S(4″)	−75.1(3)
Ag—S(1)—C(2)—C(3)	28.9(3)		

See footnote under Table 1.

atoms. Some disorder in the PF_6^- ion was modelled by placing an F atom with a site occupancy of 0.17 in a general position. Anisotropic thermal parameters were refined for all non-H atoms. Hydrogen atoms were included in fixed, calculated positions.[21] A secondary extinction parameter refined to $0.0034(5) \times 10^{-4}$; the weighting scheme, $w^{-1} = \sigma^2(F) + 0.000109F^2$ gave satisfactory analyses. At convergence, R and $R_w = 0.0411$ and 0.0564, respectively, for 73 parameters and $S = 1.407$. The maximum and minimum residues in the final ΔF syntheses were +0.61 and −1.14 eÅ^{-3}, respectively. Illustrations were prepared using ORTEP,[22] molecular geometry calculated utilized CALC,[23] and scattering factor data were taken from ref. 24. Bond lengths, angles and torsion angles are given in Tables 1–3.

Full structural parameters are available from the Director of the Cambridge Crystallographic Data Centre.

Acknowledgement—We thank the SERC for their support.

REFERENCES

1. M. Schröder, *Pure Appl. Chem.* 1988, **60**, 517 and refs therein; M. N. Bell, A. J. Blake, R. O. Gould, A. J. Holder, T. I. Hyde, A. J. Lavery, G. Reid and M. Schröder, *J. Incl. Phenom.* 1987, **5**, 169.
2. S. R. Cooper, *Accts Chem. Res.* 1988, **21**, 141.
3. S. G. Murray and F. R. Hartley, *Chem. Rev.* 1981, **81**, 365.
4. A. J. Blake, R. O. Gould, A. J. Lavery and M. Schröder, *Angew. Chem.* 1986, **98**, 282; A. J. Blake, R. O. Gould, A. J. Lavery and M. Schröder, *Angew. Chem. Int. Ed. Engl.* 1986, **25**, 274.
5. R. O. Gould, A. J. Lavery and M. Schröder, *J. Chem. Soc., Chem. Commun.* 1985, 1492; M. N. Bell, A. J. Blake, M. Schröder and T. A. Stephenson, *J. Chem. Soc., Chem. Commun.* 1986, 471.
6. D. St. C. Black and I. A. McLean, *Tetrahedron Lett.* 1969, 3961; D. St. C. Black and I. A. McLean, *Aust. J. Chem.* 1971, **24**, 1401; E. J. Hintsa, J. R. Hartman and S. R. Cooper, *J. Am. Chem. Soc.* 1983, **105**, 3739; J. R. Hartman, E. J. Hintsa and S. R. Cooper, *J. Chem. Soc., Chem. Commun.* 1984, 386; J. R. Hartman and S. R. Cooper, *J. Am. Chem. Soc.* 1986, **108**, 1202; J. R. Hartman and S. R. Cooper, *J. Am. Chem. Soc.* 1986, **108**, 1208.
7. A. J. Blake, A. J. Holder, T. I. Hyde and M. Schröder, *J. Chem. Soc., Chem. Commun.* 1987, 987.
8. R. S. Glass, W. N. Setzer, C. A. Ogle and G. S. Wilson, *Inorg. Chem.* 1983, **22**, 266; M. T. Ashby and D. L. Lichtenberger, *Inorg. Chem.* 1985, **24**, 636; D. Sellmann and P. Frank, *Angew. Chem.* 1986, **98**, 1115; D. Sellmann and P. Frank, *Angew. Chem. Int. Ed. Engl.* 1986, **25**, 1107; H-J. Küppers, A. Neves, C. Pomp, D. Ventur, K. Wieghardt, B. Nuber and J. Weiss, *Inorg. Chem.* 1986, **25**, 2400; G. S. Wilson, D. D. Swanson and R. S. Glass, *Inorg. Chem.* 1986, **25**, 3827; K. Wieghardt, H-J. Küppers, E. Raabe and C. Krüger, *Angew. Chem.* 1986, **98**, 1136; K. Wieghardt, H-J. Küppers, E. Raabe and C. Krüger, *Angew. Chem. Int. Ed. Engl.* 1986, **25**, 1101; M. T. Ashby, J. H. Enemark, D. L. Lichtenberger and R. B. Ortega, *Inorg. Chem.* 1986, **25**, 3154; R. O. Gould, A. J. Holder, T. I. Hyde, M. O. Odulate, A. J. Lavery and M. Schröder, *J. Chem. Soc., Chem. Commun.* 1987, 118; A. J. Blake, A. J. Holder, T. I. Hyde, Y. V. Roberts, A. J. Lavery and M. Schröder,

J. Organomet. Chem. 1987, **323**, 261; A. J. Holder, M. Schröder and T. A. Stephenson, *Polyhedron* 1987, **6**, 461; E. W. Abel, P. D. Beer, I. Moss, K. G. Orrell, V. Sik, P. A. Bates and M. B. Hursthouse, *J. Chem. Soc., Chem. Commun.* 1987, 978; S. C. Rawle, R. Yagbasan, K. Prout and S. R. Cooper, *J. Am. Chem. Soc.* 1987, **109**, 6181; M. N. Bell, A. J. Blake, H-J. Küppers, M. Schröder and K. Wieghardt, *Angew. Chem.* 1987, **99**, 253; M. N. Bell, A. J. Blake, H-J. Küppers, M. Schröder and K. Wieghardt, *Angew. Chem. Int. Ed. Engl.* 1987, **26**, 250; S. C. Rawle and S. R. Cooper, *J. Chem. Soc., Chem. Commun.* 1987, 308; S. C. Rawle, T. J. Sewall and S. R. Cooper, *Inorg. Chem.* 1987, **26**, 3769; E. W. Abel, P. D. Beer, I. Moss, K. G. Orrell, V. Sik, P. A. Bates and M. B. Hursthouse, *J. Organomet. Chem.* 1988, **341**, 559; A. J. Blake, A. J. Holder, Y. V. Roberts and M. Schröder, *Acta Cryst.* 1988, **C44**, 360; C. Pomp, S. Drüeke, H-J. Küppers, K. Wieghardt, C. Krüger, B. Nuber and J. Weiss, *Z. Naturforsch.* 1988, **43B**, 299.

9. H-J. Küppers, K. Wieghardt, B. Nuber, J. Weiss, E. Bill and A. X. Trautwein, *Inorg. Chem.* 1987, **26**, 3762.
10. K. Wieghardt, H-J. Küppers and J. Weiss, *Inorg. Chem.* 1985, **24**, 3067.
11. H-J. Küppers, K. Wieghardt, Y-H. Tsay, C. Krüger, B. Nuber and J. Weiss, *Angew. Chem.* 1987, **99**, 583; H-J. Küppers, K. Wieghardt, Y-H. Tsay, C. Krüger, B. Nuber and J. Weiss, *Angew. Chem. Int. Ed. Engl.* 1987, **27**, 575.
12. J. Clarkson, R. Yagbasan, P. J. Blower, S. C. Rawle and S. R. Cooper, *J. Chem. Soc., Chem. Commun.* 1987, 950.
13. R. J. Lancashire, *Comprehensive Coordination Chemistry* (Edited by G. Wilkinson, R. D. Gillard and J. A. McCleverty), Chap. 54, Vol. 5, p. 776. Pergamon Press, Oxford (1987). See also: Y. Kojima, T. Yamashita, Y. Ishino, T. Hirashima and K. Hirotsu, *Chem. Lett.* 1983, 453.
14. R. D. Shannon, *Acta Cryst.* 1976, **A32**, 751.
15. R. J. Lancashire, *Comprehensive Coordination Chemistry* (Edited by G. Wilkinson, R. D. Gillard and J. A. McCleverty), Chap. 54, Vol. 5, pp. 839–848. Pergamon Press, Oxford (1987) and refs therein; W. Levason and M. D. Spicer, *Coord. Chem. Rev.* 1987, **76**, 45 and refs therein. See also: K. B. Mertes, *Inorg. Chem.* 1978, **17**, 49; T. Ito, H. Ito and K. Toriumi, *Chem. Lett.* 1981, 1101.
16. E. Mentast, C. Baiocchi and J. S. Coe, *Coord. Chem. Rev.* 1984, **54**, 131; J. B. Kirwin, F. D. Pleat, P. J. Proll and L. H. Sutcliffe, *J. Phys. Chem.* 1963, **67**, 1617; J. C. Evans, R. D. Gillard, R. J. Lancashire and P. H. Morgan, *J. Chem. Soc., Dalton Trans.* 1980, 1277.
17. C. B. Castellani, L. Fabbrizzi, M. Licchelli, A. Perotti and A. Poggi, *J. Chem. Soc., Chem. Commun.* 1984, 806.
18. H. Taube, *Am. Chem. Soc., Symp. Ser.* 1982, **198**, 151.
19. K. Everett and F. A. Graf Jr, Handling Perchloric Acid and Perchlorates in *Handbook of Laboratory Safety*, pp. 265–276. The Chemical Rubber Company, Cleveland.
20. P. T. Beurskens, W. P. Bosman, H. M. Doesbury, Th. E. M. van den Hark, P. A. J. Prick, J. H. Noordik, G. Beurskens, R. O. Gould and V. Parthasarathia, DIRDIF: Applications of direct methods to difference structure factors, University of Nijmegen, Netherlands (1983).
21. G. M. Sheldrick, SHELX76, Program for Crystal Structure Determination. University of Cambridge, Cambridge (1976).
22. P. D. Mallinson and K. W. Muir, ORTEPII, interactive version. *J. Appl. Cryst.* 1985, **18**, 51.
23. R. O. Gould and P. Taylor, CALC, Fortran77 version, University of Edinburgh, Edinburgh (1985).
24. D. T. Cromer and J. L. Mann, *Acta Cryst.* 1968, **A24**, 321.

Polyhedron Vol. 8, No. 4, pp. 519–525, 1989
Printed in Great Britain

0277–5387/89 $3.00+.00
© 1989 Pergamon Press plc

COMPLEXES OF NAPHTHALENE-2,3-DIOL (H_2ND) WITH GROUP VI AND GROUP VIII METALS, AND THE X-RAY CRYSTAL STRUCTURE OF *CIS*-$(NH_4)_2[Mo_2O_5(ND)_2]\cdot 2H_2O$

AHMED M. EL-HENDAWY, WILLIAM P. GRIFFITH,*
CAROLINE A. O'MAHONEY and DAVID J. WILLIAMS*

Chemical Crystallography and Inorganic Chemistry Laboratories,
Imperial College of Science and Technology, London SW7 2AY, U.K.

(*Received* 28 *July* 1988; *accepted* 8 *September* 1988)

Abstract—The new naphthalene-2,3-diolato (2−) (ND) complexes *cis*-$[M_2O_5(ND)_2]^{2-}$, *cis*-$[MO_2(ND)_2]^{2-}$ (M = Mo, W), *trans*-$UO_2(ND)\cdot 3H_2O$, *trans*-$[OsO_2(ND)_2]^{2-}$ and *cis*-$M'(PPh_3)_2(ND)$ (M′ = Pd, Pt) have been isolated. The X-ray crystal structure of *cis*-$(NH_4)_2[Mo_2O_5(ND)_2]\cdot 2H_2O$ has been determined. The crystals are orthorhombic, space group *Pbca*, $a = 9.084(4)$, $b = 13.625(4)$, $c = 39.512(18)$ Å, $Z = 8$, $R = 0.041$ from 2554 observed reflections. The naphthalene-2,3-diolato ligands function as bidentate bridges, one oxygen atom of each spanning two *cis*-MoO_2 units while the other lies *trans* to a symmetric Mo—O—Mo bridge. The two naphthalene units are splayed by *ca* 18° and sheared by *ca* 24° with respect to each other. Raman, IR, ^1H and ^{13}C NMR spectra of the complexes have been recorded.

We have recently studied complexes with Group VI and VIII metals of chelating O,O′ "non-innocent" ligands such as catechol (H_2cat),[1–4] catecholamines,[5] tropolone (H trop),[6] and maltol (H malt);[7] such complexes often display unusual stereochemical or electrochemical features. We report here new complexes of molybdenum, tungsten, osmium, uranium, palladium and platinum with the ligand naphthalene-2,3-diol (H_2ND; Fig. 1) and the X-ray crystal structure of one such complex, *cis*-$(NH_4)_2[Mo_2O_5(ND)_2]\cdot 2H_2O$.

Surprisingly few complexes are known of this readily available ligand. There are solution studies on its complexation with molybdenum,[8–12] tungsten,[10–12] uranium,[13] iron, vanadium[8] and titanium,[8] niobium,[14] beryllium and aluminium.[15] The isolated complexes are *cis*-$[Ru(NH_3)_4(ND)]Cl$,[16] $Sn(ND)_2$ and $(Bu^n_4N)_2[Sn(ND)_3]$,[17] $(Et_3N)[Ph_3Sb(ND)Cl]$,[18] and $(pyH)[PhSi(ND)_2]$.[19] X-ray crystallographic studies were described for the latter two complexes.

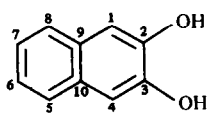

Fig. 1. Naphthalene-2,3-diol (H_2ND), with atom numbering scheme.

RESULTS AND DISCUSSION

All the complexes were prepared by the reaction of an ethanolic solution of H_2ND with the appropriate metal salt {$[MoO_4]^{2-}$, $[WO_4]^{2-}$, *trans*-$K_2[OsO_2(OH)_4]^{2-}$, *trans*-$M(PPh_3)_2Cl_2$ (M = Pd, Pt)}; the uranyl complex was made from uranyl acetate and the ligand in ethanol.

We were unable, despite many attempts, to obtain complexes with other platinum group metals with the ligand.

X-ray crystal structure of cis-$(NH_4)_2[Mo_2O_5(ND)_2]\cdot 2H_2O$

Table 1 gives selected bond lengths and angles. Figure 2 shows a perspective view of the complex

*Authors to whom correspondence should be addressed.

Table 1. Selected bond lengths (Å) and bond angles (°) with ESDs in parentheses

Bond lengths (Å)			
Mo(1)—O(1)	1.931(4)	Mo(1)—O(2)	1.703(4)
Mo(1)—O(3)	1.719(5)	Mo(1)—O(4)	1.970(5)
Mo(1)—O(5)	2.170(4)	Mo(1)—O(17)	2.405(5)
Mo(2)—O(1)	1.936(4)	Mo(2)—O(5)	2.447(5)
Mo(2)—O(15)	1.698(5)	Mo(2)—O(16)	1.704(4)
Mo(2)—O(17)	2.155(4)	Mo(2)—O(18)	1.994(4)
Bond angles (°)			
O(1)—Mo(1)—O(2)	105.1(2)	O(1)—Mo(1)—O(3)	99.9(2)
O(2)—Mo(1)—O(3)	105.3(2)	O(1)—Mo(1)—O(4)	146.4(2)
O(2)—Mo(1)—O(4)	94.4(2)	O(3)—Mo(1)—O(4)	101.1(2)
O(1)—Mo(1)—O(5)	75.1(2)	O(2)—Mo(1)—O(5)	154.9(2)
O(3)—Mo(1)—O(5)	99.3(2)	O(4)—Mo(1)—O(5)	75.8(2)
O(1)—Mo(1)—O(17)	69.8(2)	O(2)—Mo(1)—O(17)	84.4(2)
O(3)—Mo(1)—O(17)	167.6(2)	O(4)—Mo(1)—O(17)	85.5(2)
O(5)—Mo(1)—O(17)	71.9(2)	O(1)—Mo(2)—O(5)	68.6(2)
O(1)—Mo(2)—O(15)	99.3(2)	O(5)—Mo(2)—O(15)	166.1(2)
O(1)—Mo(2)—O(16)	105.7(2)	O(5)—Mo(2)—O(16)	85.2(2)
O(15)—Mo(2)—O(16)	105.3(2)	O(1)—Mo(2)—O(17)	75.5(2)
O(5)—Mo(2)—O(17)	71.3(2)	O(15)—Mo(2)—O(17)	99.5(2)
O(16)—Mo(2)—O(17)	154.5(2)	O(1)—Mo(2)—O(18)	146.9(2)
O(5)—Mo(2)—O(18)	86.3(2)	O(15)—Mo(2)—O(18)	102.0(2)
O(16)—Mo(2)—O(18)	92.8(2)	O(17)—Mo(2)—O(18)	76.2(2)
Mo(1)—O(1)—Mo(2)	109.0(2)	Mo(1)—O(5)—Mo(2)	85.8(1)
Mo(1)—O(17)—Mo(2)	87.2(1)		

anion and gives the atom numbering. The molecule has approximate non-crystallographic C_2 symmetry.

The ligand is not simply bidentate as it is in $(Et_3NH)[Ph_3Sb(ND)Cl]$[18] and in (pyH)[PhSi $(ND)_2]$[19] but adopts a rôle similar to that of the catecholato ligand in *cis*-$(NH_4)_2[Mo_2O_5(cat)_2]\cdot 2H_2O$ and $Ba[Mo_2O_5(cat)_2]\cdot 5H_2O(H_2cat)$,[20] and of the 3,5-ditertbutylcatecholato ligand (H_2DBcat) in $(Bu^n_4N)_2[Mo_2O_5(DBcat)_2]$.[21] One oxygen atom [O(4) and O(18)] of each naphthalene-2,3-diolato ligand forms a single bond to each molybdenum atom [Mo(1)—O(4) 1.970(5) Å, Mo(2)—O(18) 1.994(4) Å] while the other forms an asymmetric bridge between two molybdenum atoms [Mo(1)—O(5), Mo(2)—O(5), Mo(2)—O(17), Mo(1)—O(17): 2.170(4), 2.447(5), 2.155(4) and 2.405(4) Å, respectively]. The angles subtended by the two molybdenum atoms at O(5) and O(17) are 85.8(1) and 87.2(1)°, respectively. There is also a symmetrical oxo bridge between the two molybdenum atoms [Mo(1)—O(1) 1.931(4), Mo(2)—O(1) 1.936(4) Å; Mo(1)O(1)Mo(2) angle 109.0(2)°]. These bridge distances and angles are quite close to those observed in $(NH_4)_2[Mo_2O_5(cat)_2]\cdot 2H_2O$ and in $Ba[Mo_2O_5(cat)_2]\cdot 5H_2O$ (H_2cat).[20] Thus the triangular plane O(1), O(5), O(17) forms a common face for two substantially distorted MoO_6 octahedra, and the Mo(1)—Mo(2) distance of 3.149(1) Å does not indicate any substantial metal–metal interaction.

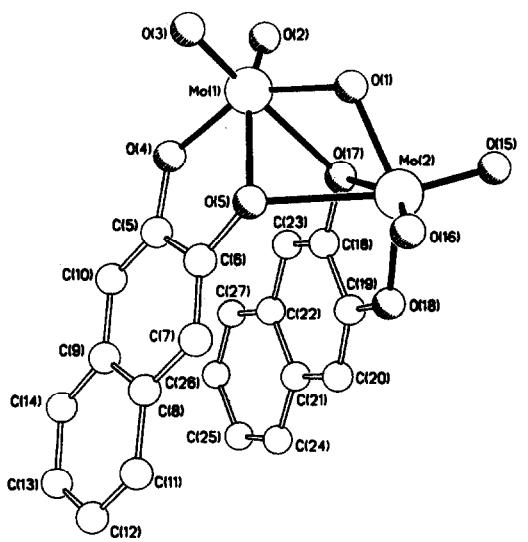

Fig. 2. Perspective view of $[Mo_2O_5(ND)_2]^{2-}$ giving atom numbering.

In addition, each Mo atom has two terminal oxo ligands *cis* to each other (mean Mo=O 1.71 Å, mean OMoO angle 105.3°) very similar to the

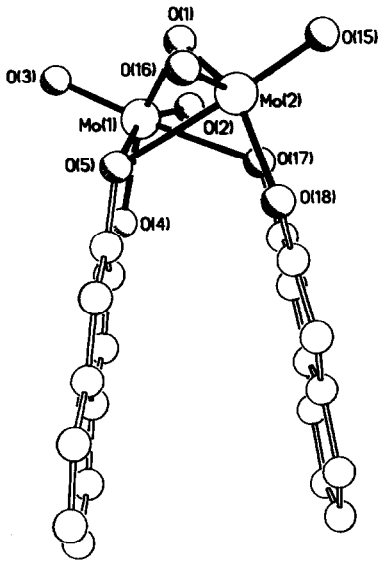

Fig. 3. View of the $[Mo_2O_5(ND)_2]^{2-}$ anion approximately in the plane of the two naphthalene units showing their splaying.

corresponding parameters in *cis*-$(NH_4)_2[Mo_2O_5(cat)_2]\cdot 2H_2O$,[20] *cis*-$K_2[MoO_2(cat)_2]\cdot H_2O$[22,23] and *cis*-$[MoO_2(trop)_2]$.[6] The *trans* effect of O(5) and O(17) gives rise to a significant lengthening (*ca* 0.2 Å) of the Mo(1)—O(5) and Mo(2)—O(17) bonds compared with Mo(1)—O(4) and Mo(2)—O(18). Analogous effects have been noted for *cis*-$[MoO_2(trop)_2]$.[6] In our complex the ligand "bite" is 76°; in $(Et_3NH)[Ph_3Sb(ND)Cl]$ it is 79.6°.[18]

The naphthalene rings are essentially planar; the splay angle between them (see Figs 3 and 4) is 18° compared with the splay angle of 20° between ligand planes in the 9,10-phenanthrenesemiquinonate (1−) (9,10-PSQ) complex $Mo_2O_5(9,10\text{-PSQ})_2$.[21]

The dianions pack "head-to-head" and "tail-to-tail" in the crystal. The ammonium cations and the water molecules create an infinite network of hydrogen bonds (Table 2) that stitch together the oxygen atoms of both adjacent and "head-to-head" molecules in the structure.

Vibrational spectra

In Table 3 we report Raman and IR spectra of the complexes. As expected, the O—H stretch [ν(O—H)] found in the free ligand at 3200–3500 cm^{-1} is not observed in the complexes, and the IR band found at 1375 cm^{-1} in the free ligand, which by analogy with catechol, we assign to an OH deformation [δ(OH)] was also not observed in the complexes. Bands near 1485 and 1270 cm^{-1} are strong in both the ligands and the complexes; the 1270 cm^{-1} mode has been assigned to ν(C=O) in $Sn(ND)_2$ and Sn(ND),[17] and that at 1485 cm^{-1} we suggest, by analogy with catecholato ligands, may arise from ν(C—C).

The molybdenum and tungsten complexes show, in addition to bands attributable to the ligand, strong Raman bands near 900 cm^{-1}, polarized in the case of aqueous solutions of $[MoO_2(ND)_2]^{2-}$ (M = Mo, W) which are weak in the IR. These we assign to $\nu_s(MO_2)$, the symmetric M=O stretch of a *cis*-MO_2 moiety. Those near 860 cm^{-1}, weak in the Raman (and depolarized in aqueous solutions of $[MO_2(ND)_2]^{2-}$) but strong in the IR we assign to $\nu_{as}(MO_2)$, the asymmetric M=O stretch of a *cis*-MO_2 moiety. Similar assignments were made for the analogous *cis*-dioxo complexes containing cat-

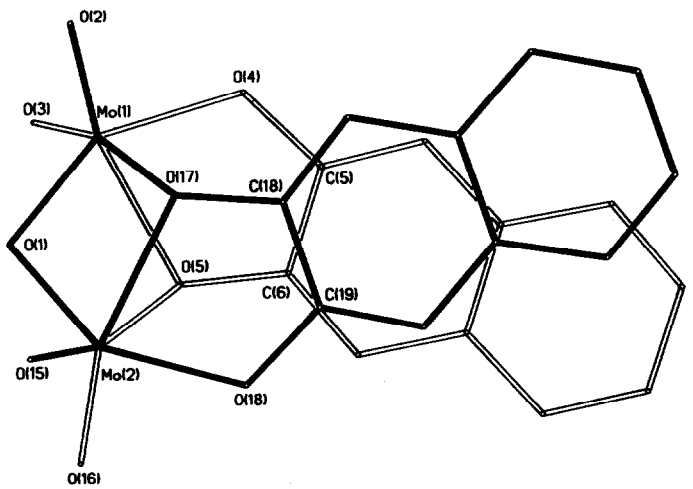

Fig. 4. Skeletal representation of the anion viewed normal to that shown in Fig. 3, showing the shearing of the naphthalene units.

Table 2. Hydrogen-bonding geometries

Atoms X—H···O	Distance (Å) X···O	H···O	Angle (°) X—H···O
N(1)—H_a···O(1)	3.14	2.21	169
N(1)—H_b···O(5)	2.99	2.07	168
N(1)—H_c···O(28)	2.91	1.98	174
N(1)—H_d···O(3)	2.98	2.24	136
N(2)—H_a···O(1)	3.04	2.12	166
N(2)—H_b···O(29)	2.83	1.92	164
N(2)—H_c···O(17)	2.95	2.02	173
N(2)—H_d···O(3)	2.98	2.08	161
O(28)—H_a···O(18)	3.02	2.20	139
O(28)—H_b···O(4)	2.85	1.97	149
O(29)—H_a···O(18)	2.85	1.93	155

echol,[1,2] catecholamine,[5] tropolone[6] and maltol[7] complexes. In $UO_2(ND)\cdot 3H_2O$ and $K_2[OsO_2(ND)_2]$, strong Raman bands at 843 and 868 cm^{-1}, respectively, have no IR counterparts, while there are strong IR bands at 930 and 830 cm^{-1}, respectively, with no Raman counterparts; these we assign, as in analogous cases[1,2,5-7] to $\nu_s(MO_2)$ and $\nu_{as}(MO_2)$ of *trans*-O=U=O ("uranyl") and *trans*-O=Os=O ("osmyl") moieties. For *cis*-$(NH_4)_2[Mo_2O_5(ND)_2]\cdot 2H_2O$, bands near 500 cm^{-1} are very tentatively assigned to modes arising from the symmetric stretch $\nu_s(M_2O)$ of the M^OM oxo bridge. Bands in all the complexes near 650 cm^{-1}, not found in the ligand, may arise from metal–oxygen stretches [ν(MO)] of the ligands; similar bands were also assigned for $Sn(ND)_2$ and $[Sn(ND)_3]^{2-}$.[17]

^1H *and* ^{13}C *NMR spectra*

The ^1H spectra of the ligand in $(C^2H_3)_2SO$ have recently been reported and assigned,[17] as has that of $[Sn(ND)_3]^{2-}$. In Table 3 we list our assignments for the ligand (see Fig. 1 for atom numbering scheme). The $H_{1,4}$ protons appear as a singlet while $H_{6,7}$ and $H_{5,8}$ are each composed of two indistinguishable doublets; protons of the hydroxy groups appear as broad singlets at δ 9.50 and 8.47 in $(C^2H_3)_2SO$ but are not observed in the complexes. For the complexes there is relatively little difference in the spectral pattern, but a shift to higher field is observed, consistent with electron withdrawal by the metal causing decreased electron density in the aromatic rings (similar effects are observed in catecholato complexes).[1]

The ^{13}C NMR spectrum of the ligand has been measured and assigned.[24] We were able to measure the ^{13}C spectra of *cis*-$K_2[MoO_2(ND)_2]\cdot 3H_2O$ and *cis*-$Na_2[W_2O_5(ND)_2]\cdot 6H_2O$ only, since they were the only complexes sufficiently soluble in ^2H_2O. The only two resonances to undergo major shifts are C_2 and C_3, those nuclei adjacent to the oxygen donor atoms; as in catecholato, catecholamine, tropolone and maltol complexes they are shifted to a lower field on coordination, and there is a similar but smaller consequential shift for C_9 and C_{10} (see Table 4).

EXPERIMENTAL

Preparations

cis-$(NH_4)_2[Mo_2O_5(ND)_2]\cdot 2H_2O$. Ammonium molybdate $(NH_4)_2[MoO_4]$ (0.4 g, 2 mmol) was dissolved in water (5 cm^3) and a solution of naphthalene-2,3-diol (0.32 g, 2 mmol) in ethanol (5 cm^3) was added. A brown–red solution was immediately formed which was left to cool for several hours. The orange–red crystals were filtered off, washed with a little water and diethyl ether, and finally dried *in vacuo*. Recrystallization was carried out from aqueous solution. Found: C, 36.2; H, 3.6; N, 4.1. $C_{20}H_{24}N_2O_{11}Mo_2$ requires: C, 36.4; H, 3.6; N, 4.2%).

cis-$M^I_2[MoO_2(ND)_2]\cdot nH_2O$ (M^I = K, n = 3; M^I = Ph_4P or Bu^n_4N, n = 0). Potassium molybdate, $K_2[MoO_4]$ (0.48 g, 2 mmol), was dissolved in water (5 cm^3) and a solution of naphthalene-2,3-diol (0.64 g, 4 mmol) in ethanol (5 cm^3) was added. The solution became brown–red on mixing. It was cooled and then evaporated until a solid was first seen to form. The orange–red precipitate was filtered off, washed with ethanol and diethyl ether, and dried in a desiccator. Found: C, 41.9; H, 2.8. $K_2[MoO_2(ND)_2]\cdot 3H_2O$ requires: C, 41.7; H, 3.2%.

The tetraphenylphosphonium or *n*-tetrabutylammonium salts of $[MoO_2(ND)_2]^{2-}$ were also made by addition of aqueous solutions of Ph_4PCl

Table 3. Vibrational and ^{1}H NMR spectroscopic data for naphthalene-2,3-diolato complexes

Compound	Vibrational spectra[a]						^{1}H NMR data[b]			
	ν(C—C)	ν(C—O)	$\nu_s(MO_2)$	$\nu_{as}(MO_2)$	ν(M—O)	$\nu_s(M_2O)$	$H_{1,4}$	$H_{5,8}$	$H_{6,7}$	Solvent
H_2(ND)	1485s	1272s					7.2s	7.6m	7.2m	$(C^2H_3)_2SO$
	1483s	1230vw					7.22s	7.64m	7.30m	C^2HCl_3
cis-$(NH_4)_2[Mo_2O_5(ND)_2]\cdot 2H_2O$	1470s	1265s	942s	883vs	635s	500m	6.82s	7.38m	7.09m	^2H_2O
	1473s	1270s	943s	886m	624m	496m				
	1467m	1254m								
cis-$K_2[MoO_2(ND)_2]\cdot 3H_2O$	1463s	1263s	900m	870s	642s		6.97s	7.66m	7.24m	^2H_2O
	1478s	1282m	918s, 902s	873m	643m					
	1466s	1266m	904s, p[c]	877w[c]						
cis-$(Ph_4P)_2[MoO_2(ND)_2]$	1463s	1275s	907m	868s	640s					
	1474s	1264w	902vs	875m	635w					
cis-$(Bu^n_4N)_2[MoO_2(ND)_2]$	1463s	1273s	902s	863vs	639s					
	1473vs	1285m	905s	869m	640b					
		1264m								
cis-$Na_2[W_2O_5(ND)_2]\cdot 6H_2O$	1473vs	1277vs	903m	870s	628s	500sh	6.92s	7.60m	7.18m	^2H_2O
	1470vs	1276m	902s	867w	630w	499m				
cis-$(Bu^n_4N)_2[WO_2(ND)_2]$	1467s, b	1273s, b	920s	865vs	642s					
	1477s		891s	868w	624w					
	1469s[c]		921s, p[c]	872w						
trans-$K_2[OsO_2(ND)_2]$	1465s	1261s			637s		7.38s	7.79m	7.30m	^2H_2O
	1461s	1266m	868vs	830s	633w					
trans-$UO_2(ND)\cdot 3H_2O$	1460s	1250s		930s	620					
	1467s	1257m	843s							
$Pd(Ph_3P)_2(ND)$	1455s	1272s			628s		6.60s	Obsc.	6.95m	C^2HCl_3
	1456s	1272m			625m					
$Pt(Ph_3P)_2(ND)$	1462s	1272s			630s		6.71s	7.45m	7.00m	C^2HCl_3
	1459vs	1269m			630w					
$(Bu^n_4N)_2[Sn(ND)_3]$							6.5s	7.2m	6.85m	$(C^2H_3)_2SO$[17]

[a] Frequencies in cm^{-1}. All data on solids; Raman data underlined.
[b] Shifts in ppm relative to $Si(CH_3)_4$.
[c] Raman data for solutions in H_2O; p = polarized.

Table 4. ^{13}C NMR resonances for $H_2(ND)$ and its complexes[a]

Compound	δ(ppm) C_2/C_3	C_9/C_{10}	C_5/C_8	C_6/C_7	C_1/C_4	Solvent
$H_2(ND)$	144.0	129.5	126.2	124.2	110.2	C^2HCl_3[20]
	146.8	130.6	127.4	125.4	111.7	[b]
cis-$K_2[MoO_2(ND)_2]\cdot 3H_2O$	160.9	132.2	128.9	125.5	109.8	^2H_2O
cis-$Na_2[W_2O_5(ND)_2]\cdot 6H_2O$	159.9	132.2	128.9	125.7	111.1	^2H_2O

[a] Shifts in ppm relative to $(CH_3)_4Si$.
[b] In 2:1 ^2H_2O–$(C^2H_3)_2SO$.

or Bu^n_4NCl such that the molar ratio of cation–metal was 2:1. Found: C, 73.0; H, 4.7. $(Ph_4P)_2[MoO_2(ND)_2]$ requires: C, 72.7; H, 4.7%. Found: C, 67.1; H, 8.6; N, 2.8. Calc. for $(Bu^n_4N)_2[MoO_2(ND)_2]$: C, 67.2; H, 9.1; N, 3.0%.

cis-$Na_2[W_2O_5(ND)_2]\cdot 6H_2O$. To sodium tungstate, $Na_2[WO_4]\cdot 2H_2O$ (0.66 g, 2 mmol) dissolved in water (5 cm^3) was added naphthalene-2,3-diol (0.32 g, 2 mmol) in ethanol (5 cm^3). A bright yellow solution was obtained which was left to stand until a yellow precipitate separated out. This was filtered off, washed with ethanol and diethyl ether, and then dried *in vacuo*. Found: C, 25.1; H, 2.6. $Na_2[W_2O_5(ND)_2]\cdot 6H_2O$ requires: C, 26.1; H, 2.6%.

The n-*tetrabutylammonium salt* $(Bu^n_4N)_2[WO_2(ND)_2]$. This was prepared by the addition of an equivalent aqueous solution of $(Bu^n_4N)Cl$ to the yellow aqueous solution of the tungsten complex. Found: C, 61.6; H, 8.1; N, 2.6. $(Bu^n_4N)_2[WO_2(ND)_2]$ requires: C, 61.4; H, 8.3; N, 2.8%.

trans-$K_2[OsO_2(ND)_2]$. Potassium osmate, *trans*-$K_2[OsO_2(OH)_4]$, was prepared by the literature method.[25]

To a solution of *trans*-$K_2[OsO_2(OH)_4]$ (0.2 g, 0.5 mmol) in water (5 cm^3), naphthalene-2,3-diol (0.16 g, 1 mmol) in ethanol (5 cm^3) was added dropwise with stirring. A dark brown colour was observed and the solution was left to cool. A fine dark precipitate separated out, and this was filtered off and treated as above. Found: C, 39.6; H, 2.2. $K_2[OsO_2(ND)_2]$ requires: C, 38.9; H, 2.0%.

trans-$UO_2(ND)\cdot 3H_2O$. To a hot solution of uranyl acetate $UO_2(CH_3COO)_2\cdot 2H_2O$ (0.84 g, 2 mmol) in ethanol (20 cm^3) was added naphthalene-2,3-diol (0.32 g, 2 mmol) in ethanol (10 cm^3). The mixture was refluxed for 2 h on a steam bath when a brown precipitate separated out, which was washed with hot ethanol and ether, and dried *in vacuo*. Found: C, 23.9; H, 2.4. $UO_2(ND)\cdot 3H_2O$ requires: C, 24.9; H, 2.5%.

$M(PPh_3)_2(ND)$ (M = Pd, Pt). Both *cis*-$Pd(PPh_3)_2Cl_2$[26] and *cis*-$Pt(PPh_3)_2Cl_2$[27] were prepared according to the literature methods. The Gandolfi[28] method was used with some modifications for the preparation of the complexes as follows: to naphthalene-2,3-diol (0.32 g, 2 mmol) in benzene (6 cm^3) and methanol (12 cm^3) was added KOH (0.22 g, 4 mmol) in methanol (12 cm^3) with stirring. To this solution *cis*-$Pd(PPh_3)_2Cl_2$ (0.85 g, 1.2 mmol) or *cis*-$Pt(PPh_3)_2Cl_2$ (0.9 g, 1.1 mmol) was added with continuous stirring at room temperature for 3.5 h, after which pink (Pd) or yellow (Pt) precipitates were isolated, washed with methanol, then water and finally with methanol followed by ether. The precipitate was dried *in vacuo*. Found: C, 69.2; H, 4.5. $Pd(PPh_3)_2(ND)$ requires: C, 70.0; H, 4.6%. Found: C, 63.1; H, 4.1. Calc. for $Pt(PPh_3)_2(ND)$: C, 62.9; H, 4.1%.

Crystal data

$C_{20}H_{24}Mo_2N_2O_{11}$, $M = 660.3$, orthorhombic, $a = 9.084(4)$, $b = 13.625(4)$, $c = 39.512(18)$ Å, $U = 4890$ Å^3, space group *Pbca*, $Z = 8$, $D_c = 1.79$ g cm^{-3}, Cu radiation, $\lambda = 1.54178$ Å, μ(Cu-K_α) = 91 cm^{-1}, $F(000) = 2639$.

Measurements

Data were measured on a Nicolet R3m diffractometer with Cu-K_α radiation (graphite monochromator) using ω-scans. A crystal of dimensions $0.23 \times 0.16 \times 0.03$ mm was used. 3029 independent reflections were measured ($2\theta \leqslant 110°$), of which 2554 had $|F_o| > 3\sigma(|F_o|)$ and were considered to be observed. The data were corrected for Lorentz and polarization factors; an empirical absorption correction based on 324 azimuthal measurements was applied.

Structure analysis

The structure was solved by the heavy-atom method. The non-hydrogen atoms were refined anisotropically. The ammonium and water pro-

tons were located from a ΔF map and refined isotropically subject to an N—H and O—H distance constraint. The positions of the remaining hydrogen atoms were idealized, C—H = 0.96 Å, assigned isotropic thermal parameters, $U(H) = 1.2\ U_{eq}(C)$, and allowed to ride on their parent carbon atoms. Refinement was by block-cascade, full-matrix least-squares to $R = 0.41$, $R_w = 0.039$ $[w^{-1} = \sigma^2(F) + 0.00024F^2]$. The maximum and minimum residual electron densities in the final ΔF map were 0.74 and -0.87 Å^{-3}, respectively. The mean and maximum shift/error in the final refinement were 0.029 and 0.295, respectively.

Computations were carried out on an Eclipse S140 computer using the SHELXTL program system.[29] Scattering factors were taken from the *International Tables for X-ray Crystallography*.*[30]

Raman spectra were measured on a Spex Ramalog 5 instrument with a Coherent Radiation Innova 90 krypton-ion laser with excitation at 6471 (red) or 5682 Å (yellow), as spinning discs with a KBr base for solids or in sealed capillaries for solutions. IR spectra were measured in liquid paraffin films between caesium iodide plates on a Perkin–Elmer 683 instrument. NMR spectra were measured on a Bruker WM-250 spectrometer.

Acknowledgements—We thank the Egyptian Ministry of Education for a grant to one of us (A.M.E.-H.) and ICI Chemicals and Polymers and the SERC for a CASE award to C.A.O'M.

We also thank Johnson Matthey Ltd for the loan of platinum group complexes.

REFERENCES

1. W. P. Griffith, C. A. Pumphrey and T. A. Rainey, *J. Chem. Soc., Dalton Trans.* 1986, 1125.
2. A. J. Nielson and W. P. Griffith, *J. Chem. Soc., Dalton Trans.* 1978, 1501.
3. M. B. Hursthouse, T. Fram, L. New, W. P. Griffith and A. J. Nielson, *Transition Metal Chem.* 1978, **3**, 253.
4. A. J. Nielson and W. P. Griffith, *J. Histochem. Cytochem.* 1978, **26**, 138.
5. A. M. El-Hendawy, W. P. Griffith and C. A. Pumphrey, *J. Chem. Soc., Dalton Trans.* 1988, 1817.
6. W. P. Griffith, C. A. Pumphrey and A. C. Skapski, *Polyhedron* 1987, **6**, 891.
7. S. J. Greaves and W. P. Griffith, *Polyhedron* 1988, **7**, 1973.
8. V. Patrovsky, *Coll. Czech. Chem. Commun.* 1970, **35**, 1599.
9. R. N. Soni and J. S. Nahata, *Ind. J. Chem.* 1972, **10**, 446.
10. S. Natansohn, J. I. Krugler, J. E. Lester, M. S. Chagnon and R. S. Finocchlaro, *J. Phys. Chem.* 1980, **84**, 2972.
11. A. V. Il'yasov, I. D. Morozova and Z. I. Usmanov, *Dokl. Akad. Nauk SSSR*, 1972, **204**, 129.
12. Z. I. Usmanov and N. A. Novosadov, *J. Struct. Chem. USSR* 1982, **24**, 128.
13. M. Bartusek, *Coll. Czech. Chem. Commun.* 1967, **32**, 757.
14. B. C. Bhuyan and S. N. Dubey, *Acta Cienc. Indica* 1984, **10**, 124.
15. A. Aleksandrov, S. Kostova and O. Nawratil, *Nauchni Trud. Plovdivski Univ.* 1983, **21**, 27 (*Chem. Abstr.* 1985, **102**, 226776).
16. R. B. Salmonsen, A. Abelleira and M. J. Clarke, *Inorg. Chem.* 1984, **23**, 385.
17. L. Soto, J. Borras and L. Perello, *Synth. React. Inorg. Met. Org. Chem.* 1982, **12**, 731.
18. R. R. Holmes, R. O. Day, V. Chandrasekhar and J. H. Holmes, *Inorg. Chem.* 1987, **26**, 157.
19. R. R. Holmes, R. O. Day, J. J. Harland and J. M. Holmes, *Organometallics* 1984, **3**, 347.
20. V. V. Tkachev and L. O. Atovmyan, *Soviet J. Coord. Chem.* (*Engl. Transl.*) 1975, **2**, 89.
21. C. G. Pierpoint and R. M. Buchanan, *Inorg. Chem.* 1982, **21**, 652.
22. L. O. Atovmyan, V. A. Sokolova and V. V. Tkachev, *Dokl. Phys. Chem.* (*Engl. Transl.*) 1975, **195**, 968.
23. V. V. Tkachev and L. O. Atovmyan, *Soviet J. Coord. Chem.* (*Engl. Transl.*) 1975, **1**, 715.
24. J. Seita, J. Sandström and T. Drakenberg, *Org. Magn. Res.* 1978, **11**, 239.
25. J. S. Malin, *Inorg. Synth.* 1980, **20**, 61.
26. R. C. Cookson and D. W. Jones, *J. Chem. Soc.* 1965, 1881.
27. J. C. Bailar and H. Itatani, *Inorg. Chem.* 1965, **4**, 1618.
28. O. Gandolfi and J. Blum, *Inorg. Chim. Acta* 1983, **80**, 103.
29. G. M. Sheldrick, SHELXTL, *An Integrated System for Solving, Refining and Displaying Crystal Structures from Diffraction Data*, Revision 4.1, University of Göttingen, F.R.G. (1983).
30. *International Tables for X-ray Crystallography*, Vol. IV, pp. 99–143. Kynoch Press, Birmingham (1974).

* Tables of atomic positional and thermal parameters have been deposited as Supplementary Data with the Editor, from whom copies are available on request. Atomic coordinates have also been deposited with the Cambridge Crystallographic Data Centre.

Polyhedron Vol. 8, No. 4, pp. 527–530, 1989
Printed in Great Britain

0277–5387/89 $3.00+.00
© 1989 Pergamon Press plc

THERMODYNAMICS OF IONIZATION OF HYPOPHOSPHOROUS AND PHOSPHOROUS ACIDS. SUBSTITUENT EFFECTS ON SECOND ROW OXY ACIDS

JOHN W. LARSON* and MARGARET PIPPIN

Department of Chemistry, Marshall University, Huntington, WV 25755-2520, U.S.A.

(*Received* 10 *June* 1988; *accepted* 28 *September* 1988)

Abstract—An NMR method has been used to determine the pK_a values for H_3PO_2 and H_3PO_3 at 5, 25, 45, 65, and 85°C. The standard enthalpies and entropies of ionization of these acids are: for H_3PO_2 −12.69 kJ and −66.3 J K^{-1}, for H_3PO_3 −14.86 kJ and −73.8 J K^{-1}, and for H_3PO_4 −7.74 kJ and −67.1 J K^{-1}. Because of its ability to participate in backbonding, substitution of OH for H leads to decreased acidity in the phosphorous oxy acid series.

Early interest in the phosphorous oxy acids H_3PO_2, H_3PO_3 and H_3PO_4 centred on the surprisingly strong acidity of lower oxidation state acids of the series. Recognition that the phosphorous acid existed in the H—$PO(OH)_2$ tautomer and hypophosphorous acid in the $H_2PO(OH)$ tautomer is a classic case of the exception proving the rule; in this case the Ricci–Pauling rules[1] of the strengths of inorganic oxy acids.

This acid series remains interesting for two reasons. First, the only interpretation of the unexpected stability of the P—H tautomers is the empirical observation[2] that "it is a general feature of phosphorous chemistry that three-valent phosphorous is never found bound to OH, but rather changes to five-valent phosphorous bound to H and =O". A more fundamental explanation grounded in bonding theory would be useful. Second, in this series the substitution of O—H for H leads to a weaker acid. This trend is opposite the inductive effect observed in other acids.

Previous studies of the acidities of hypophosphorous acid[3–7] and phosphorous acid[5–9] have resulted in widely differing values depending on the ionic strength of the solution and the temperature of the measurement. The present study was undertaken to provide pK_a values of these acids at infinite dilution and 25°C, to compare with the accurately determined value of phosphoric acid.[10] The pK_as were also determined at 5, 45, 65 and 85°C which allows calculation of the ΔH^0 and ΔS^0 of ionization of the acids. No previous experimental measurements of these quantities have been made. This additional information may help in understanding the structural dependence of the acidity of these acids.

The method used in this study is based on the work by Moedritzer[11] and Haas and Gillman[6] who observed that the NMR PH coupling constant varies with the degree of ionization of the acid.

EXPERIMENTAL

Analysis of sodium phosphite pentahydrate from BDH Chemicals and sodium hypophospite monohydrate from Fisher Scientific after heating *in vacuo* to 200°C, indicated the true formulas of $Na_2HPO_3 \cdot 4.86H_2O$ and $NaH_2PO_2 \cdot 0.79H_2O$. Stock solutions of H_3PO_2 (made by ion exchange from NaH_2PO_2), H_3PO_3 (from Aldrich) and H_3PO_4 (from Fisher Scientific) were analysed by standard acidometric titration methods. ^{31}P NMR of all pure solutions showed no oxidation of the lower valence phosphorous compounds. All solutions were made up by weight.

Proton and phosphorous magnetic resonance spectra were obtained on a Varian XL-200 spectrometer. Coupling constants were obtained for several solutions by both H and P NMR. These coupling constants were reproducible to 0.2 Hz. Temperature calibrations carried out with both a mercury in glass thermometer and using an internal

*Author to whom correspondence should be addressed.

standard of ethylene glycol indicated control to ±0.3°C.

RESULTS

Phosphorous acid

The ^{31}P NMR of phosphoric acid consists of a doublet with hydrogen–phosphorous coupling constants of 566.5 Hz for HPO_3^{-2} and 629.5 Hz for HPO_2OH^{-1} based on the direct measurements on solutions containing these species. These values are in good agreement with the values obtained by Haas and Gillman.[6] The coupling constant of 686 Hz for $HPO(OH)_2$ is based on the measured values of J_{PH} of H_3PO_3 in concentrated solutions and in 1.5 m HCl. In both cases reiterative calculations were made to correct for the degree of ionization and protonation. It is considerably higher than the value of 669 obtained previously.[6]

Determination of pK_{a_1} was made from measurements on two different series of solutions. The first series consisted of seven dilutions of a 5.294 m stock solution of pure H_3PO_3 that covered the concentration range from 4.1 to 0.09 m. The equilibrium constant for the first ionization of this acid may be calculated from the following equations

$$pK_a = -\log(m_H m_A/m_{HA}) - \log(\gamma_H\gamma_A/\gamma_{HA}) \quad (1)$$

$$m_A/m_{HA} = (686-J)/(J-629.5) \quad (2)$$

$$m_H = m_0(686-J)/56.5 \quad (3)$$

and

$$\log(\gamma_H\gamma_A/\gamma_{HA}) = 2f^\gamma + BI, \quad (4)$$

where f^γ is a function containing the Debye–Huckel limiting law and given by

$$f^\gamma = -A\{I^{1/2}/(1+1.2I^{1/2}) + (2/1.2)\ln(1+1.2I^{1/2})\} \quad (5)$$

and B is an empirical parameter. Equation (4) gives the activity coefficient to the first power in ionic strength.[10,12] Substituting these into eq. (1), gives eq. (6).

$$\log\{(686-J)^2/[56.5(J-629.5)]\} - 2f^\gamma = pK_a - BI. \quad (6)$$

Graphs of the left hand side of eq. (6) vs I yield a straight line with an intercept of pK_a at $I = 0$. A typical plot is shown in Fig. 1 for the data at 25°C.

A second series of measurements was done on a mixture of H_3PO_4, H_3PO_3 and Na_2HPO_3 in the ratio of about 1:1.75:0.5. For the proton switching reaction, eq. (7), the pK_a can be expressed by eq. (8).

$$HPO(OH)_2 + O_2P(OH)_2^{-1} = HPO_2(OH)^{-1} + OP(OH)_3 \quad (7)$$

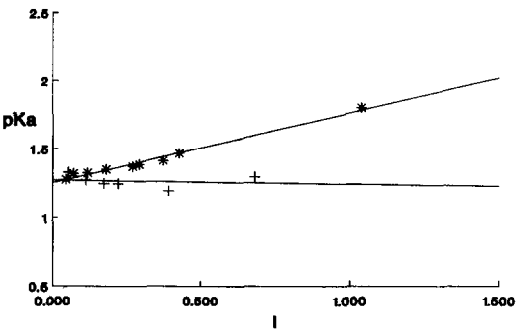

Fig. 1. Graphical determinations of the pK_a of phosphoric acid at 25°C. Values from pure H_3PO_3 (+) and from mixtures of H_3PO_3, NaH_2PO_3 and H_3PO_4 (*).

$$pK_a(HA) = pK_a(HA') - \log(m_{HA}m_{A'}/m_{HA'}m_A) - (B—B')I. \quad (8)$$

Values m_{HA}/m_A are as given in eq. (2) along with accurate temperature dependent pK_a values for phosphoric acid reported in the literature,[13] and values $m_{A'}/m_{HA'}$ calculated re-iteratively from the stoichiometry of the mixture and either acid dissociation equilibrium constant are combined to obtain values of all of the terms on the right except the last. The graphical determination of pK_a at 25°C is completed by plotting the first and second terms of this equation vs ionic strength as is shown in Fig. 1. The advantages of this second method are that no first-order correction for activity coefficients is needed for the isoelectric reaction, eq. (7), and the results are directly referenced relative to the acid to which it is most closely related.

The large slope in the plot of the second series was initially surprising. It is apparently related to the strong tendency of $H_2PO_4^-$ to H-bond with strong acids. Pitzer and Silvester[10] have discussed this characteristic in analysis of concentrated H_3PO_4 solutions. Our results indicate that the equilibrium constant is about two for reaction (9) compared to

$$HPO(OH)_2 + O_2P(OH)_2^- = HPO(OH)_2 - O_2P(OH)_2^- \quad (9)$$

the value of about 0.2 when the acid is the weaker phosphoric acid.

The agreement of the results from these two methods was excellent; always well within the uncertainty of either method. The standard deviations in pK_a values of phosphorous acid were ±0.03 by method 1 and ±0.01 by method 2. A weighted average of the two values is reported in Table 1 at 5, 25, 45, 65 and 85°C.

The most accurate previous value of pK_a is 1.29[5,7] at 18°C. This can be compared with a value of 1.19 at 18°C interpolated from the results reported here.

Table 1. pK_a values for the dissociation of H_3PO_4, H_3PO_3 and H_3PO_2 as a function of temperature

Temperature (°C)	pK_a H_3PO_4[13]	H_3PO_3	H_3PO_2
5	2.066	1.075	1.070
25	2.146	1.257	1.244
45	2.246	1.441	1.405
65	2.358	1.616	1.554
85	2.480	1.783	1.689

To obtain the most accurate relative enthalpy of ionization, a van't Hoff plot of $pK_a(H_3PO_4) - pK_a(H_3PO_3)$ vs $1/T$ led to ΔH_7^0 of -7.12 kJ mol^{-1}. This combined with the thermodynamics of ionization[13] of the reference acid, H_3PO_4, leads to the values reported in Table 2.

Hypophosphorous acid

The proton NMR of $H_2PO_2^-$ consists of a doublet with a coupling constant of 518.4 Hz that changes to a value of 575.9 Hz when protonated. Coupling constants were measured on a total of 26 different solutions between 0.5 and 1.5 in ionic strength. Six of these solutions were dilute solutions of pure H_3PO_2, 16 were buffer solutions made from either H_3PO_2 and NaH_2PO_2 or NaH_2PO_2 and HCl, and four were mixtures of H_3PO_2, NaH_2PO_2 and H_3PO_4. The results of these experiments were calculated similarly to those described in detail for phosphorous acid. As with phosphorous acid, the second virial coefficients, B, for the solutions were small except for the mixtures with phosphoric acid present, again indicating H-bonded species forming between H_3PO_2 and $H_2PO_4^-$. This data led to the pK_a values of H_3PO_2 reported in Table 1. The total uncertainty in these values is ± 0.02 and includes estimates of the uncertainties due to determination of the coupling constant for the acid and temperature calibration, as well as the 0.01 standard deviation. Our interpolated value for pK_a of 1.183 at 18°C may be compared with the literature values[5,7] of 1.10 and a value[4] of 0.99 determined at 25°C compared to our value of 1.244.

Calculation of the relative enthalpy of ionization leads to a value of 4.95 kJ more exothermic than phosphoric acid. A summary of resulting thermodynamics of ionization of all three acids is reported in Table 2. No previous enthalpy and entropy of ionization data have been reported for phosphorous and hypophosphorous acids. The uncertainties in these values are 0.9 kJ and 3 J K^{-1}, respectively.

Table 2. Thermodynamics of ionization of H_3PO_2, H_3PO_3 and H_3PO_4 at 25°C

Acid	ΔG^0 (kJ mol^{-1})	ΔH^0 (kJ mol^{-1})	ΔS^0 (J K^{-1}) (J K^{-1} mol^{-1})
H_3PO_4	12.25	−7.74	−67.1
H_3PO_3	7.15	−14.86	−73.8
H_3PO_2	7.10	−12.69	−66.3

DISCUSSION

The thermodynamic data in Table 2 reveal that the acidity trend of this series is due primarily to the change in enthalpy of ionization, while the entropy of ionization varies little within the series. The magnitudes of the entropies of ionization for all three acids are consistent with values for other acids where the first ionization results in anions with the negative charge delocalized primarily on two oxygen atoms, such as acetic acid (-92 J K^{-1}), H_3AsO_4 (-67 J K^{-1}) and $HClO_2$ (-87 J K^{-1}).

The enthalpy driven increase in the acidity of phosphorous acid compared to phosphoric acid is opposite to the direction expected based on the inductive effect of the OH group compared to H. Thus, in the series of acids of the form RCO_2H, RCH_2CO_2H, RNH_3^+, ROH and *meta*-substituted benzoic acids, the order of acidity is $CH_3O > HO > H > CH_3$. For the series of acids $RP(O)(OH)_2$, the order of acidity[5,14] is $H > CH_3O > HO > CH_3$, similar to the order found in *para*-substituted benzoic acids.[15] This pronounced acid-weakening effect of the RO and HO groups can be interpreted in terms of the conjugate electron donation, **II**, which stabilizes the acid. Comparable electron donation in the conjugate base is less important because the oxygen atoms already bear a partial negative charge.



I **II**

The importance of backbonding is also reflected in the dramatically increased basicity of the lone pair of electrons on phosphorous in the bases of phosphine and hypophosphorous acid. The equilibrium constants for eq. (10) may be compared to eq. (11)

$$PH_3 + H^+ = PH_4^+ \qquad K \sim 10^{-14} \qquad (10)$$

$$HOPH_2 + H^+ = HOPH_3^+ \qquad K \sim 10^{+9} \qquad (11)$$

calculated from the measured K_b^6 (10^{-2}) and the tautomer equilibrium constant[5,14] (10^{10}–10^{12}) for hypophosphorous acid.

REFERENCES

1. L. Pauling, *General Chemistry*. Freeman, San Francisco (1947); J. E. Ricci, *J. Am. Chem. Soc.* 1948, **70**, 109.
2. C. S. G. Phillips and R. J. P. Williams, *Inorganic Chemistry*, p. 636. Oxford University Press, Oxford (1965).
3. J. H. Espenson and D. F. Dustin, *Inorg. Chem.* 1969, **8**, 1760.
4. A. D. Mitchell, *J. Chem. Soc.* 1920, **117**, 957.
5. J. R. Wazer, *Phosphorus and Its Compounds*, Vol. I. Interscience, New York (1958).
6. T. E. Haas and H. D. Gillman, *Inorg. Chem.* 1968, **7**, 2051.
7. I. M. Kolthoff, *Recl. Trav. Chim.* 1927, **46**, 350.
8. R. O. Griffith and A. McKeown, *Trans. Faraday Soc.* 1940, **36**, 766.
9. K. Takahasi and N. Yui, *Bull. Inst. Phys. Res. (Tokyo)* 1941, **20**, 521.
10. K. S. Pitzer and L. F. Silvester, *J. Solution Chem.* 1976, **5**, 269.
11. K. Moedritzer, *Inorg. Chem.* 1967, **6**, 936.
12. A. L. Horvath, *Handbook of Aqueous Electrolyte Solutions*. Ellis Horwood Limited, Chichester (1985).
13. J. W. Larson, K. G. Zeeb and L. G. Hepler, *Can. J. Chem.* 1982, **60**, 2141.
14. J. P. Guthrie, *Can. J. Chem.* 1978, **56**, 2342.
15. A. Streitwieser Jr and C. H. Heathcock, *Introduction to Organic Chemistry*, 2nd Edn, p. 1129. Macmillan, New York (1981).
16. J. P. Guthrie, *Can. J. Chem.* 1979, **57**, 236.

Polyhedron Vol. 8, No. 4, pp. 531–532, 1989
Printed in Great Britain

0277–5387/89 $3.00+.00
© 1989 Pergamon Press plc

THE TELLURIUM ANALOGUE OF THE HYDROXIDE ION: SYNTHESES AND STRUCTURE OF $(PPh_4)TeH$

JOHN C. HUFFMAN

Molecular Structure Center, Indiana University, Bloomington, IN 47405, U.S.A.

and

ROBERT C. HAUSHALTER*

Exxon Research and Engineering Company, Annandale, NJ 08801, U.S.A.

(*Received* 24 *August* 1988; *accepted* 28 *September* 1988)

Abstract—Treatment of the ethylenediamine (en) extracts from solids of nominal composition K_2SiTe_3 and K_2GeTe_3 with $(PPh_4)Br$, gives the tetraphenylphosphonium salt of the hydrogen tellurium (1−) anion, $(PPh_4)TeH$ (**1**). Telluride (**1**) was identified by elemental analysis, IR spectroscopy and a single crystal X-ray structure determination. Crystals of **1** were isomorphous with tetragonal $(PPh_4)Br$, space group $I\bar{4}$, with cell constants at −160°C of $a = 11.945(7)$, $c = 6.867(3)$ Å, $Z = 2$ and $V = 979.8$ Å^3.

While the lighter members of the chalcogenide dianions, X^{2-}, and hydrogen chalcogenide anions, XH^-, such as the oxide and hydroxide ions, have been among the most studied species in chemistry, the corresponding heavier chalcogenide anions, particularly those of tellurium, have received very little attention. Recently, the first members of the Te_x^{2-} series with $x = 3$–5 have been structurally characterized in $Te_3^{2-}\cdot en$,[1] $Te_4^{2-}\cdot 2CH_3OH$[2] and Te_5^{2-},[3] which are very intensely coloured red–purple solids. Some confusion apparently exists concerning the simplest telluride, Te^{2-}, as it has been reported to be both red[4] and colourless.[5] The protonated telluride ion, TeH^-, has not been well characterized either, even though its preparation was first reported in 1838.[6] Since Bineau's original paper[6] there have been sketchy reports in the literature on the preparation of TeH^-, which was usually prepared by the reaction of H_2Te with ammonia. In 1939, Teichert and Klemm[7] reported the preparation and characterization of M(XH) (M = Na, K, Rb, Cs; X = S, Se) but were unable to prepare TeH^- using similar procedures. An approximate equilibrium constant for the reaction $H_2Te + NH_3 \rightarrow (NH_4)TeH$ was reported in 1950[8] but was complicated by the rapid decomposition of H_2Te near 25°C. Colourless $(NH_4)_2Te$, however, can be prepared cleanly from elemental tellurium and aluminium powder in aqueous NH_3.[9] We would like to report the synthesis and characterization of $(PPh_4)TeH$ (**1**), which to our knowledge is the first example of a well characterized solid containing the hydrogen telluride (1−) anion.

EXPERIMENTAL

All operations were performed under a high purity (< 1 ppm O_2) argon atmosphere. The metals were obtained from Cerac Inc., Milwaukee, Wisconsin. Ethylenediamine (en) was purified by stirring for 2 days with CaH_2, distillation onto K_4Sn_9 and finally vacuum transfer of the en from the red solution of K_4Sn_9. Elemental analyses were performed by Schwarzkopf Microanalytical Laboratories, Woodside, New York.

K_2SiTe_3 *and* K_2GeTe_3

These alloys were prepared by heating stoichiometric amounts of K and Ge or Si powder (−325 mesh) to 400°C for 2 min in a quartz vessel under argon. After cooling to 25°C, a stoichiometric amount of −30 mesh Te powder was added and

*Author to whom correspondence should be addressed.

the mixture carefully melted and agitated for 5 min. The black, glassy alloys were then ground to a fine powder.

$(PPh_4)TeH$ (1)

Finely powdered K_2SiTe_3 or K_2GeTe_3 were extracted with en for 8 h with vigorous stirring using ~ 5 cm^3 en/g alloy. Filtration, followed by treatment of the filtrate with an equal volume of saturated $(PPh_4)Br$ in en, gave a 10–30% yield (based on equivalents of K_2MTe_3 used) of orange crystals of **1** after standing for 48 h. In some experiments with K_2GeTe_3 the formation of Ge/Te polyanions was also observed.[10]

Table 1

Empirical formula	$TeH^-P(C_6H_5)_4^+$
Colour of crystal	Yellow–orange
Crystal dimensions	$0.08 \times 0.09 \times 0.09$ mm
Space group	$I\bar{4}$-bar
Cell dimensions (at -160°C; 32 reflections	$a = 11.945(7)$ Å $b = 11.945(7)$ Å $c = 6.867(3)$ Å
Z (molecules/cell)	2
Volume	979.80 Å^3
Calculated density	1.586 g cm^{-3}
Wavelength	0.71069 Å
Molecular weight	468.00 g mol^{-1}
Linear absorption coefficient	16.046 cm^{-1}

RESULTS AND DISCUSSION

Extraction of the low melting, black, glassy alloys of nominal composition K_2GeTe_3 and K_2SiTe_3 with ethylenediamine (en) under H_2O/O_2 free conditions, gives solutions from which $(PPh_4)TeH$ can be isolated by treatment with saturated solutions of $(PPh_4)Br$. Since en is the only proton source in the system, the TeH^- probably forms by aminolysis of Si—Te bonds or by a reaction at the alloy surface.

Crystals of **1**, which are extremely air-sensitive and instantly turn black on exposure to air, are isomorphous with $(PPh_4)I$, space group $I\bar{4}$, with $a = 11.945(7)$ and $c = 6.867(3)$ Å (at -160°C) and $Z = 2$. The crystals were identified as **1** by elemental analysis. Found: C, 61.7; H, 4.8; P, 6.6; Te, 27.5. Calc. for $C_{24}H_{21}PTe$: C, 61.5; H, 4.5; P, 6.6; Te, 27.3%. The IR absorption spectrum shows a broad absorbance centred near 1975 cm^{-1} which we assign to the Te—H stretching modes.

The single crystal X-ray data* for **1** were collected at -160°C and solved using the coordinates for the isomorphous $(PPh_4)Br$ and refined to residuals $R = 0.0312$ and $R_w = 0.0328$. The crystal data for **1** is shown in Table 1. The structure consists of isolated TeH^- and PPh_4^+ ions. The hydrogen atom in TeH^- was not located but there were several peaks with density 0.3–0.5 e Å^{-3} near the tellurium atom. No attempt was made to refine these positions.

We have consistently found crystals of $(PPh_4)TeH$ to be orange. Since pure preparations of several Te^{2-} salts have been reported to be colourless, and electrochemically generated TeH^- is reported to be colourless,[11] it is not clear that the orange colour of crystals of **1** is necessarily due to TeH^-. The orange colour may be due to the inclusion of small amounts of hydrogen ditelluride, Te_2H^-, or decomposition of the TeH^- itself. Dihydrogen telluride, H_2Te, is thermally unstable and decomposes rapidly even at 0°C, thus one might expect limited stability for the monohydrogen derivative as well. Crystals of **1** darken upon storage over several weeks while a dilute solution of **1** in en became very dark within hours at 25°C.

In summary, the TeH^- anion is stable enough to be isolated at room temperature and has been characterized as its PPh_4^+ salt. Crystals of $(PPh_4)TeH$ slowly decompose at 25°C while solutions of TeH^- have only limited stability at 25°C.

*Atomic positional parameters have been deposited with the Director, Cambridge Crystallographic Data Centre.

REFERENCES

1. A. Cisar and J. Corbett, *Inorg. Chem.* 1977, **16**, 632.
2. J. Huffman and R. Haushalter, *Z. Anorg. Allg. Chem.* 1984, **518**, 203.
3. R. Teller, L. Krause and R. Haushalter, *Inorg. Chem.* 1983, **22**, 1809.
4. D. Gruen, R. McBeth, M. Foster and C. Crouthamel, *J. Phys. Chem.* 1966, **70**, 472.
5. D. Bamberger, J. Young and R. Ross, *J. Inorg. Nucl. Chem.* 1974, **36**, 1158.
6. A. Bineau, *Annls Chim. Phys.* 1838, **67**, 230.
7. W. Teichert and W. Klemm, *Z. Anorg. Allg. Chem.* 1939, **243**, 86.
8. F. Mikero and S. Carlyon, *J. Am. Chem. Soc.* 1950, **72**, 2295.
9. R. Nitsche, *Angew. Chem.* 1957, **69**, 333.
10. R. Haushalter, unpublished results.
11. M. Pourbaix (Ed.), *Atlas of Electrochemical Equilibrium in Aqueous Solutions.* Pergamon Press, Oxford (1966).

Polyhedron Vol. 8, No. 4, pp. 533–535, 1989
Printed in Great Britain

0277–5387/89 $3.00+.00
© 1989 Pergamon Press plc

COMMUNICATION

CHARGE-TRANSFER COMPLEXES OF DIOXYGEN, LEWIS ACID HALIDES AND AROMATIC HYDROCARBONS*

SYDNEY BROWNSTEIN† and NAM FONG HAN

Division of Chemistry, National Research Council of Canada, Ottawa, Canada, K1A 0R9

(*Received* 22 *April* 1988; *accepted after revision* 5 *September* 1988)

Abstract—Ternary complexes of dioxygen with one of the following halides: BF_3, BCl_3, GeF_4, PF_5, $AlCl_3$, $SiCl_4$, $SnCl_4$ and $TiCl_4$, and one of hexamethylbenzene, mesitylene, anthracene and 9,10-dimethylanthracene have been identified by UV spectroscopy.

Since ternary charge-transfer complexes have been observed with nitric oxide, some aromatic hydrocarbons and some Lewis acid halides, it seemed worthwhile to investigate whether similar interactions would occur with dioxygen as the electron acceptor.[1] No interaction has been reported between dioxygen and the Lewis acid halides of this study under the very mild conditions which we employed. There is an extensive description of the interaction of dioxygen and aromatic compounds in solution. It can be summarized by saying that the interactions are so weak that they are only observable during chance collisions between the two species.[2] Interactions have been reported between aromatic hydrocarbons and BF_3,[3] $SnCl_4$ and $TiCl_4$.[4] All of these interactions are readily distinguishable from those which we have observed in the ternary systems of this study.

EXPERIMENTAL

Magnetic resonance spectra were obtained on a Bruker AM-400 spectrometer operating at 400 MHz for protons. Optical spectra were obtained on a Cary 210 spectrometer in CH_2Cl_2 as solvent, with concentrations expressed as moles per kg of solvent. Equilibrium constants have also been calculated using the same unit. ESR spectra were obtained at 77 K on a Varian E4 spectrometer. Microanalyses were performed by Canadian Microanalytical Service Ltd, Vancouver.

Chemicals

Boron, phosphorus and germanium fluorides, boron, silicon, tin and titanium chlorides, hexamethylbenzene, anthracene and 9,10-dimethylanthracene were used without further purification. Mesitylene, methylene chloride and aluminum chloride were purified and used as previously described.[5] Dioxygen was used directly from the supplier's cylinder. Sample preparation was always done using vacuum-line and dry box techniques.[5]

RESULTS AND DISCUSSION

A freshly prepared solution of hexamethylbenzene, boron trichloride and dioxygen darkens in colour during a few days at room temperature to a reddish-brown shade similar to that found with NO and BCl_3,[5] or $NOBCl_4$.[6] The most pronounced absorption bands, and where possible, the approximate concentrations and equilibrium constants are listed in Table 1. The concentrations of the complexes are obtained by assuming an extinction coefficient of 6800 for the long wavelength absorption since this was the value found in the analogous NO^+ and NO systems.[1,6] The absorbance is the net absorbance extrapolated to infinite time as listed in Table 2. With BF_3, PF_5 and GeF_4, absorptions corresponding to two distinct complexes are observed. One complex, which forms slowly, gradually decays and is replaced by the second. The results are listed in Tables 1 and 2. Representative spectra are presented in Fig. 1. In each case, the eventual complexes have rather similar optical spec-

* Issued as NRCC No. 29787.

†Author to whom correspondence should be addressed.

Table 1. Optical densities, concentrations and extrapolated equilibrium constants for ternary complexes of hexamethylbenzene, dioxygen and some halides

Hexamethylbenzene	Dioxygen	Halide (BCl_3)	Optical density (Å) 2780	3440	Complex	K
0.0247	0	0	0.4746	0.0432	0	—
0.0247	0	0.081	0.528	0.062	0	—
0.0219	0.0384	0.078	3.279	1.96	0.0028	4.3
		(BF_3)	2700	3300		
0.0115	0	0	0.2901	0.0341	0	—
0.0113	0.126	0.027	0.574	0.154	0.00018	5.0
		(PF_5)	2710	3340		
0.0118	0	0	0.4116	0.0341	0	—
0.0118	0	0.0308	0.6213	0.0700	0	—
0.0114	0.205	0.0303	1.065	0.300	0.00044	6.2

tra. The equilibrium constants calculated in Table 1 assume complete solution of the halide and dioxygen. A more reasonable assumption is that both the halide and dioxygen are distributed between the vapour and liquid phases according to their relative volumes. From the known cell constants, corrected equilibrium constants of 45, 200 and 140 are calculated for BCl_3, BF_3 and PF_5, respectively. The absorptions due to the GeF_4 complexes were still growing at too rapid a rate after 28 days for a reasonable extrapolation to equilibrium values. In each of the preceding cases removal of all volatile materials by pumping under vacuum gave a residue of hexamethylbenzene alone, which shows that complex formation is reversible. Similar but non-quantitative results were obtained with $AlCl_3$, $SiCl_4$, $SnCl_4$ and $TiCl_4$ as Lewis acid halides. A very broad, weak and featureless absorption extending into the visible gives these complexes their characteristic colour. In every case, proton and carbon magnetic resonance spectra had signals characteristic of hexamethylbenzene alone. This is consistent with rapid exchange of hexamethylbenzene and a low concentration of its complex. If the exchange were to occur by a dissociation mechanism, it would have to be slow, since the rate of formation is slow. Therefore, one can conclude that the exchange must occur by a displacement mechanism in which a complexed hexamethylbenzene leaves as an uncomplexed aromatic molecule approaches. The rapid exchange suggests that a species with two complexed aromatic molecules may have a limited stability.

Mesitylene, dioxygen and BF_3, BCl_3, GeF_4 and

Table 2. Net optical density as a function of time for ternary complexes of hexamethylbenzene, dioxygen and the indicated halide at the indicated wavelength maxima

BCl_3 Day	3440 Å	BF_3 Day	3300 Å	4000 Å	PF_5 Day	3340 Å	4000 Å	GeF_4 Day	3370 Å	4000 Å
1	0.124	3	0.041	0.053	1	0.093	0.171	1	0.010	0.019
2	0.443	4	0.060	0.071	2	0.167	0.401	2	0.034	0.117
3	0.783	5	0.077	0.074	3	0.212	0.502	5	0.175	0.264
6	1.284	6	0.087	0.084	6	0.299	0.402	6	0.247	0.360
8	1.512	7	0.097	0.074	7	0.317	0.372	7	0.337	0.473
9	1.604	10	0.110	0.062				8	0.441	0.562
10	1.674							9	0.520	0.648
								12	0.753	0.712
								16	1.090	0.994
								23	1.558	1.101
								28	1.857	1.164

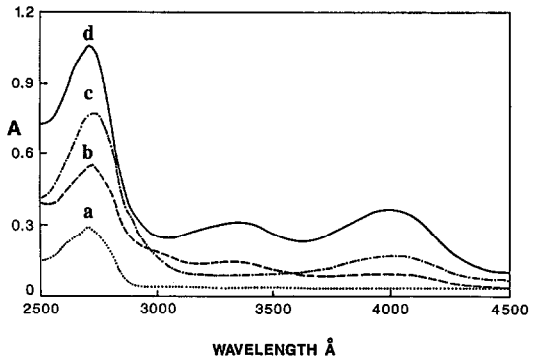

Fig. 1. UV spectra of hexamethylbenzene, dioxygen, halide systems. (a) Hexamethylbenzene alone; (b) with dioxygen and BF_3 after 10 days; (c) with dioxygen and PF_5 after 1 day; (d) with dioxygen and PF_5 after 7 days.

PF_5 form ternary charge-transfer complexes with absorption bands at 2650 and 2720 Å. The BF_3 and GeF_4 complexes also have an absorption maximum at 2920 Å while the BCl_3 complex has additional maxima at 3180 and 5140 Å, and the PF_5 complex at 3080 and 5100 Å. None of the bands were sufficiently well separated to justify equilibrium constant calculations.

Anthracene, dioxygen and BF_3 or BCl_3, but not PF_5, GeF_4 nor $SnCl_4$ react to give a dark green solid, insoluble in all the common solvents. With 9,10-dimethylanthracene as the aromatic hydrocarbon, a similar solid was obtained with BF_3, BCl_3, GeF_4 and PF_5 as Lewis acid halides. The crude product from 9,10-dimethylanthracene, BCl_3 and oxygen has: C, 64.4; H, 4.2; Cl, 11.9; O, 4.4%. The 2:1:1 complex would have: C, 68.4; H, 5.0; Cl, 19.0; O, 5.7%, which suggests that it is the primary product. These solids have a single ESR signal with a g value of 2.003. For the materials produced with BF_3 and BCl_3 there is approximately one unpaired electron for each 100 aromatic molecules.

We may conclude that in the absence of side reactions, aromatic hydrocarbons may react with dioxygen and Lewis acid halides to give charge-transfer compounds, which are weaker than the corresponding ones with NO,[1] which are weaker than those with NS^+,[7] which are weaker than those with NO^+.[5]

REFERENCES

1. S. Brownstein and B. Irish, *Polyhedron* 1988, **7**, 97.
2. E. C. Lim and V. L. Kowalski, *J. Chem. Phys.* 1962, **36**, 1729.
3. W. I. Albersberg, G. J. Hoijtink, E. L. Mackor and W. P. Weijland, *J. Chem. Soc.* 1959, 3055.
4. L. A. Burkardt, P. R. Hammond, R. H. Knife and R. R. Lake, *J. Chem. Soc.* A 1971, 3789.
5. S. Brownstein, A. Morrison and L. Tan, *Can. J. Chem.* 1986, **64**, 265.
6. S. Brownstein, E. Gabe, F. Lee and L. Tan, *J. Chem. Soc., Chem. Commun.* 1984, 1566.
7. S. Brownstein and B. Louie, *Can. J. Chem.* 1987, **65**, 1361.

Polyhedron Vol. 8, No. 4, pp. 537–539, 1989
Printed in Great Britain

0277–5387/89 $3.00 + .00
©1989 Pergamon Press plc

COMMUNICATION

SYNTHESIS AND STRUCTURAL CHARACTERIZATION OF A MIXED VALENCE OCTANUCLEAR POLYOXOMOLYBDATE, $[(C_4H_9)_4N]_4[Mo_8O_{24}(OCH_3)_2]\cdot CH_3OH\cdot H_2O$

SHUNCHENG LIU and JON ZUBIETA*

Department of Chemistry, State University of New York at Albany, Albany, NY 12222, U.S.A.

(*Received* 27 *June* 1988; *accepted* 27 *September* 1988)

Abstract—Reaction of $[(C_4H_9)_4N]_2Mo_2O_7$ with hydrazones, $R_2C{=}NNH_2$, yields the novel Mo^V/Mo^{VI} mixed valence octanuclear polyoxomolybdate, $[(C_4H_9)_4N]_4[Mo_8O_{24}(OCH_3)_2]\cdot CH_3OH\cdot H_2O$. The structure of the anionic cluster consists of a tetranuclear core $[Mo_4O_8(OR)_2]^{4+}$ of edge-sharing Mo octahedra, coordinated to two bridging dipodal $[MoO_4]^{2-}$ units and two corner sharing $[MoO_4]^{2-}$ units. Crystal data: $P2_1/n$ space group, with $a = 17.166(2)$, $b = 15.719(2)$, $c = 18.933(3)$ Å, $\beta = 95.08(1)°$, $V = 5088.9(8)$ Å^3, $Z = 2$, $D_{calc} = 1.46$ g cm^{-3}. Structure solution and refinement based on 3626 reflections, $R = 0.068$.

Recent advances in the coordination chemistry of polyoxometalate anions are largely consequences of the availability of reactive polyoxoanions which are soluble in non-aqueous, organic solvents.[1] Stimulated by the pioneering work of Klemperer and co-workers,[2] the reaction chemistry of polyoxometalate anions in non-aqueous solvents has been developed to include replacement of peripheral oxo groups by organometallic units,[3–10] by a variety of simple organic ligands with oxygen,[2,11–16] nitrogen,[17–25] and sulphur donors,[26] and by inorganic ligands such as halide and sulphido donors.[27–29] Furthermore, reactions involving redox processes, as well as simple ligand substitution, have been observed under appropriate conditions to yield mixed valence Mo^V/Mo^{VI} clusters.[26,30] Exploitation of the appropriate organic reducing agents in reactions with polyoxometalates in organic solvents should permit the development of a novel class of polymetalate clusters, a tactic we have employed in the synthesis of the title complex, $[(C_4H_9)_4N]_4[Mo_8O_{24}(OCH_3)_2]\cdot CH_3OH\cdot H_2O$.

Reaction of 4 equivalents of $[(C_4H_9)_4N]_2[Mo_2O_7]$ with 1 equivalent of a hydrazone, $R_2C{=}NNH_2$, in methanol, followed by addition of ether, yields deep red crystals of the diamagnetic complex $[(C_4H_9)_4N]_4[Mo_8O_{24}(OCH_3)_2]\cdot CH_3OH\cdot H_2O$.† The IR spectrum displays a complex pattern of features between 725 and 960 cm^{-1} associated with the presence of chemically distinct terminal Mo–oxo groups and bridging Mo–oxo groups. The single strong absorption at 957 cm^{-1} is characteristic of ν(Mo=O) for Mo^V–oxo sites, while the 729 cm^{-1} feature is assigned to triply bridging oxo groups (Mo_3O). Other absorptions in this region were not assigned. The electronic spectrum displays intense charge-transfer transitions (O → Mo) at 225 and 318 nm. The complex crystallizes in the monoclinic space group $P2_1/n$ with $a = 17.166(2)$, $b = 15.719(2)$, $c = 18.933(3)$ Å, $\beta = 95.08(1)°$, $V = 5088.9(8)$ Å^3, $Z = 2$ (based upon the octanuclear formulation), $D_{calc} = 1.46$ g cm^{-3}. A total of 5734 reflections were collected within the limits $2° \geqslant 2\theta \geqslant 45°$. Structure solution and refinement based upon 3626 reflections

*Author to whom correspondence should be addressed.

†Elemental analysis. Found: C, 35.6; H, 6.75; N, 2.25. Calc. for $C_{67}H_{156}N_4O_{28}Mo_8$: C, 36.0; H, 6.99; N, 2.51%.

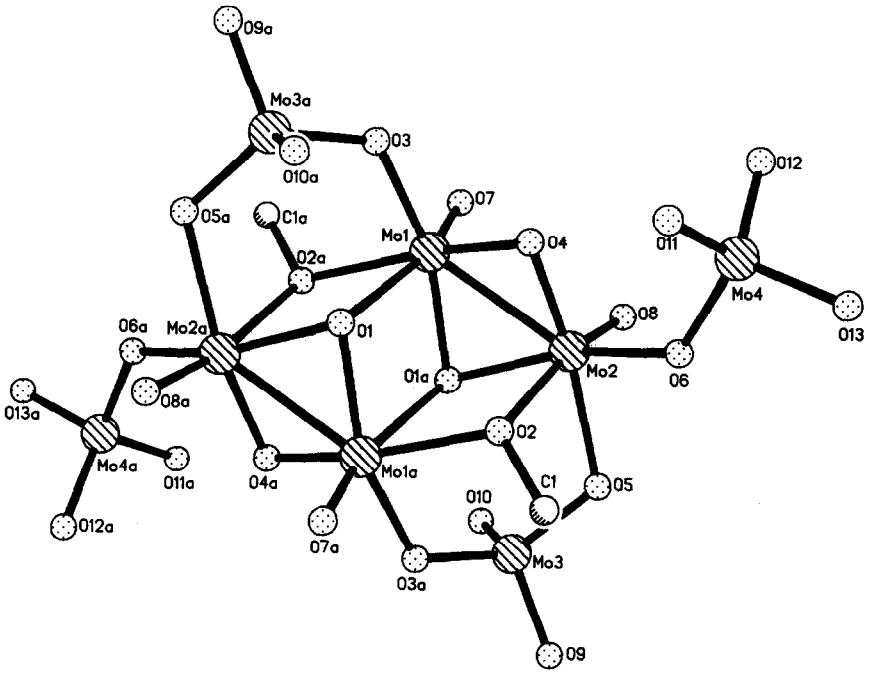

Fig. 1. Perspective view of the structure of the complex anion $[Mo_8O_{24}(OCH_3)_2]^{4-}$, showing the atom labelling scheme. Selected bond lengths (Å) and angles (°): Mo(1)—O(1), 2.362(8); Mo(1)—O(1a), 1.976(7); Mo(2)—O(1a), 2.006(7); Mo(1)—O(2a), 2.107(8); Mo(2)—O(2), 2.317(8); Mo(1)—O(4), 1.932(8); Mo(2)—O(4), 1.961(8); Mo(1)—O(3), 2.047(8); Mo(2)—O(5), 2.149(9); Mo(1)—O(7), 1.674(8); Mo(2)—O(8), 1.706(8); Mo(3)—O_t, 1.706(10); Mo(3)—O_b, 1.812(11) (av.); Mo(4)—O_t, 1.728(10) (av.); Mo(4)—O(6), 1.852(8); Mo(1)—Mo(2), 2.599(2).

with $F_o > 6\sigma(F_o)$ (Mo-K_α, $\lambda = 0.71073$ Å) converged at $R = 0.068$.*

The structure of the complex anion $[Mo_8O_{24}(OCH_3)_2]^{4-}$ is shown in Fig. 1, with selected bond lengths and angles listed in the caption. The structure consists of discrete octanuclear anions, constructed from edge- and corner-sharing Mo octahedra and tetrahedra. The central core of the structure is provided by four edge-sharing Mo octahedra associated with Mo(1), Mo(2), Mo(1a) and Mo(2a). The Mo(1) centres of this tetranuclear core exhibit coordination to two triply bridging oxo groups, two doubly bridging oxo groups, a terminal oxo group and a bridging methoxy group; while the Mo(2) centres are bonded to a single triply bridging oxo unit, three doubly bridging oxo groups, a terminal oxo group and a bridging methoxy group. The short Mo(1)—Mo(2) distance of 2.599(2) Å is characteristic of Mo^V/Mo^{VI} mixed valence complexes and consistent with direct metal–metal bonding, providing a mechanism for magnetic coupling of two Mo^V d^1 sites localized in the tetranuclear unit.[31] A most unusual feature of the structure is the presence of structurally distinct tetrahedral $[MoO_4]^{2-}$ units. While the Mo(3) groupings adopt bridging, dipodal geometry spanning opposite edges of the tetranuclear core, the tetrahedral units associated with the Mo(4) centres assume a corner-sharing linkage mode to the Mo(2) centres of the core. Although both the dipodal bridging tetrahedral groups[18,21] and the corner-sharing monodentate $[MoO_4]$ unit[32] have precedents in polyoxomolybdate chemistry, the title complex provides a unique instance of a structure displaying both coordination types.

As illustrated in Fig. 2, the tetranuclear core of $[Mo_8O_{24}(OCH_3)_2]^{4-}$ is identical to that previously reported for $[Mo_4O_8(OR)_4Cl_4]^{2-}$.[22,23] The structures are related by substitution of the terminal alkoxy and chloride ligands of $[Mo_4O_8(OR)_4Cl_4]^{2-}$ by the bridging and terminal $[MoO_4]^{2-}$ groups of $[Mo_8O_{24}(OCH_3)_2]^{4-}$, retaining the common $[Mo_4O_8(OR)_2]^{4+}$ core. This structural analysis emphasizes the ability of the $[MoO_4]^{2-}$ unit to function as a ligand, the linkage flexibility of the $[MoO_4]^{2-}$ ligand, and the ease of substitution of peripheral ligand groups associated with polymolybdate structures, while maintaining the integrity of the structural core.

*Final atomic positional and thermal parameters, bond lengths and angles, and F_o/F_c values have been deposited as supplementary material with the Editor, from whom copies are available on request. Atomic coordinates have been submitted to the Cambridge Crystallographic Data Centre.

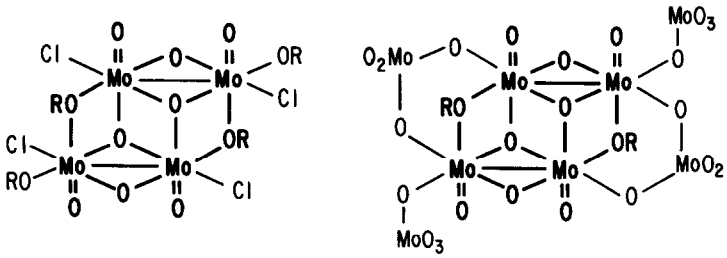

Fig. 2. Schematic representations of the structures of $[Mo_4O_8(OR)_4Cl_4]^{2-}$ and $[Mo_8O_{24}(OMe)_2]^{4-}$, showing the common tetranuclear core, $[Mo_4O_8(OR)_2]^{4+}$.

The presence of reduced Mo^V centres in the structure establishes the role of the hydrazone reagent as a reducing agent, functioning in a Wolff–Kishner type of reduction reaction.[33] The use of organic reducing agents appears to provide a facile methodology for the introduction of Mo^V sites into polymolybdate clusters,[26,33,34] which, when combined with the exploitation of the propensity toward aggregation of organic soluble $[MoO_4]^{2-}$ units, allows the synthesis of novel cluster species with unusual electronic and redox properties. Investigations of the chemical and electrochemical reduction of polyoxomolybdate species in organic solvents are currently under investigation.

Acknowledgement—This work was supported by NSF Grant CHE-8514634 to J. Zubieta.

REFERENCES

1. V. W. Day and W. G. Klemperer, *Science* 1985, **228**, 533.
2. R. D. Adams, W. G. Klemperer and R.-S. Liu, *J. Am. Chem. Soc.* 1979, **101**, 491; V. W. Day, M. R. Thompson, C. S. Day, W. G. Klemperer and R.-S. Liu, *J. Am. Chem. Soc.* 1980, **102**, 5873.
3. T. M. Che, V. W. Day, L. C. Francesconi, M. F. Fredrick, W. G. Klemperer and W. Shum, *Inorg. Chem.* 1985, **24**, 4055 and refs therein.
4. C. J. Besecker, V. W. Day, W. G. Klemperer and M. R. Thompson, *Inorg. Chem.* 1985, **24**, 44.
5. C. J. Besecker, V. W. Day, W. G. Klemperer and M. R. Thompson, *J. Am. Chem. Soc.* 1984, **106**, 4125.
6. V. W. Day, C. W. Early, W. G. Klemperer and D. J. Maltbie, *J. Am. Chem. Soc.* 1985, **107**, 8261.
7. C. J. Besecker, W. G. Klemperer and V. W. Day, *J. Am. Chem. Soc.* 1982, **104**, 6158.
8. V. W. Day, W. G. Klemperer and D. J. Maltbie, *Organometallics* 1985, **4**, 104.
9. W. G. Klemperer, V. V. Mainz, R.-C. Wang and W. Shum, *Inorg. Chem.* 1985, **24**, 1968.
10. W. G. Klemperer and R.-S. Liu, *Inorg. Chem.* 1980, **19**, 3863.
11. V. W. Day, W. G. Klemperer and C. Schwartz, *J. Am. Chem. Soc.* 1987, **109**, 6030.
12. E. M. McCarron III and R. L. Harlow, *J. Am. Chem. Soc.* 1983, **105**, 6179.
13. E. M. McCarron III, H. H. Staley and A. W. Sleight, *Inorg. Chem.* 1984, **23**, 1043.
14. E. M. McCarron and A. W. Sleight, *Polyhedron* 1986, **5**, 129.
15. B. A. Wilson, W. T. Robinson and C. J. Wilkins, *Acta Cryst.* 1983, **C39**, 54.
16. S. Liu, S. N. Shaikh and J. Zubieta, *Inorg. Chem.* 1987, **26**, 4303.
17. E. M. McCarron III, J. F. Whitney and D. B. Chase, *Inorg. Chem.* 1984, **23**, 3276.
18. T.-C. Hsieh and J. Zubieta, *Inorg. Chem.* 1985, **24**, 1287.
19. T.-C. Hsieh and J. Zubieta, *Polyhedron* 1986, **5**, 309.
20. T.-C. Hsieh and J. Zubieta, *Polyhedron* 1986, **5**, 1655.
21. S. N. Shaikh and J. Zubieta, *Inorg. Chem.* 1986, **25**, 4613.
22. T.-C. Hsieh and J. Zubieta, *J. Chem. Soc., Chem. Commun.* 1985, 1749.
23. T.-C. Hsieh, S. N. Shaikh and J. Zubieta, *Inorg. Chem.* 1987, **26**, 4079.
24. V. Chilou, P. Gouzerh, Y. Jeannin and F. Robert, *J. Chem. Soc., Chem. Commun.* 1987, 1469.
25. M. B. Hursthouse, R. L. Short, B. Piggott, A. Tucker and S. F. Wong, *Polyhedron* 1986, **5**, 2122.
26. S. Liu, X. Sun and J. Zubieta, *J. Am. Chem. Soc.* 1988, **110**, 3324.
27. Y. Do, E. D. Simhon and R. H. Holm, *Inorg. Chem.* 1985, **24**, 2827.
28. W. G. Klemperer and C. Schwartz, *Inorg. Chem.* 1985, **24**, 4459.
29. N. Buchholz and R. Mattes, *Angew. Chem. Int. Ed. Engl.* 1986, **25**, 1104.
30. M. F. Belicci, G. G. Fava and C. Pelizzi, *J. Chem. Soc.* 1983, 65.
31. B. Kamenar, B. Korpar-Colig and M. Penavic, *J. Chem. Soc., Dalton Trans.* 1981, 311.
32. P. K. Bharadwaj, Y. Ohashi, Y. Sasada, Y. Sasaki and T. Yamase, *Acta Cryst.* 1986, **C42**, 545; J. Fuchs, H. Hartl, W. D. Hunnius and S. Mahjour, *Angew. Chem. Int. Ed. Engl.* 1975, **14**, 644; P. M. Touboul, C. Idoura and P. Toledano, *Acta Cryst.* 1984, **C40**, 1652.
33. H. H. Szmant, *Angew. Chem. Int. Ed. Engl.* 1968, **7**, 120.
34. H. Kang, S. Liu, S. N. Shaikh, T. Nicholson and J. Zubieta, *Inorg. Chem.*, in press.

Polyhedron Vol. 8, No. 4, pp. 541–543, 1989
Printed in Great Britain

0277–5387/89 $3.00+.00
© 1989 Pergamon Press plc

COMMUNICATION

SYNTHESIS AND PROPERTIES OF MOLYBDENUM(VI) PEROXO COMPOUNDS WITH IMIDAZOLE AND THE X-RAY STRUCTURE OF $(C_3H_5N_2)_2[O\{MoO(O_2)_2H_2O\}_2]$, A NOVEL IMIDAZOLIUM PEROXO COMPLEX CONTAINING A μ-OXO BRIDGED DIMER

CIRILA DJORDJEVIC,* JENNIFER L. GUNDERSEN and BRADLEY A. JACOBS

Department of Chemistry, College of William and Mary, Williamsburg, VA 23185, U.S.A.

and

EKK SINN

Department of Chemistry, University of Virginia, Charlottesville, VA 22901, U.S.A.

(*Received* 2 *August* 1988; *accepted* 27 *September* 1988)

Abstract—Crystalline peroxo molybdate(VI) complexes with imidazole are reported: $(C_3H_5N_2)_2[O\{MoO(O_2)_2H_2O\}_2]$ (**1**), $MoO_2(O_2)(C_3H_4N_2)2H_2O$ (**2**) and $K_2MoO_2(O_2)_2(C_3H_4N_2)4H_2O$ (**3**). They represent the first peroxo metal compounds containing imidazole. IR spectra display characteristic ν(Mo═O) between 967 and 955 cm^{-1}, and ν(O—O) between 892 and 853 cm^{-1}. The X-ray crystal structure of (**1**) shows the presence of a μ-oxo group bridging two pentagonal bipyramidal $\{MoO(O_2)_2H_2O\}$ moieties, each hydrogen bonded to an essentially planar imidazolium cation via one of the oxygens of a coordinated peroxo group.

Peroxo molybdenum compounds are selective oxidation catalysts[1,2] and molybdenum is important in biochemistry. We report here the first peroxo complexes containing imidazole to be isolated from aqueous solutions, which are also the first molybdenum compounds with imidazole. This work demonstrates that imidazole remains unchanged in the aqueous peroxo Mo^{VI} solutions, where catalytic conversion of malic, malonic and aspartic acid to oxalates, and nicotinic acid to N-oxide has been observed.[3,4] The imidazole group of histidine side chains participates in the binding of metal atoms in many metalloproteins, and has been found to coordinate to Mo^{V} in a histidine complex.[5] In view of the presence of molybdenum at active centres of enzymes and catalysts which catalyse hydrogenation and selective oxidation,[6] it is important to discover the reactivity of imidazole in the presence of molybdenum peroxides.

Three crystalline yellow solids containing imidazole, peroxides and molybdenum were separated from aqueous solutions: the prismatic title complex (**1**), the thin needle crystals corresponding to an empirical composition $MoO_2(O_2)(C_3H_4N_2)2H_2O$ (**2**) and the microcrystalline potassium salt of composition $K_2MoO_2(O_2)_2(C_3H_4N_2)4H_2O$ (**3**). Found: C, 12.7; H, 2.1; N, 9.7; O_2^{2-}, 13.0. Calc. for (**2**), $MoC_3H_8N_2O_6$: C, 13.6; H, 3.0; N, 10.6; O_2^{2-}, 12.2%. Found: C, 7.8; H, 2.1; N, 6.0; O_2^{2-}, 16.5. Calc. for (**3**), $K_2MoC_3H_{12}N_2O_{10}$: C, 8.8; H, 2.9; N, 6.8; O_2^{2-}, 15.6%. Complexes (**1**) and (**2**) were prepared by dissolving MoO_3 (1.44 g, 10 mmol) in 30% hydrogen peroxide (10 cm^3), and adding imidazole (0.68 g, 10 mmol) dropwise and slowly, to a clear, yellow solution under stirring while maintaining the temperature between 45 and 50°C. The resulting brown–red reaction mixture was then

*Author to whom correspondence should be addressed.

stirred for 1 h, until the yellow colour returned. Prismatic crystals separated from this solution on standing at room temperature for about 24 h, at pH 4.0–4.5. They decomposed explosively at about 125°C. Rapid imidazole addition lead to overheating, and a mixture of crystals from complexes (**1**) and (**2**) was generally obtained from such preparations. Pure needle crystals of (**2**) were prepared essentially in the same manner as (**1**), but successful preparations were sparse. Faster imidazole addition, higher temperature and omission of stirring of the reaction mixture at the end, seemed to help. Although appearing over a wide pH range of 4–6, complex (**2**) precipitated best between pH 5 and 6. Complex (**3**) was synthesized by adding KOH to the reaction mixture described above, and raising the pH to about 6. The separation of a pure complex was difficult again, because of coprecipitation of various potassium oxoperoxo molybdates, having similar lattice energy and solubility, formed in solution at higher pH.

Yellow prismatic crystals of the title complex (**1**) are so far the only ones large enough for X-ray structure analysis. Crystal data: $(C_3H_5N_2)_2[O\{MoO(O_2)_2H_2O\}_2]$, monoclinic, $a = 14.516(3)$, $b = 6.802(2)$, $c = 15.187(4)$ Å, $\beta = 91.99°$, $U = 1561.7$ Å, space group $I2/a$, $Z = 4$. X-ray diffraction data were collected by standard methods on an Enraf–Nonius four-circle CAD-4 diffractometer, using Mo radiation ($\lambda = 0.71073$ Å). Of 7055 independent reflections, 3939 were used [$F_o^2 \geq 3\sigma(F_o^2)$] in the final refinement of the structural parameters; $R = 0.042$, $R_w = 0.050$. A three-dimensional Patterson synthesis was used to determine the heavy atom positions, which phased the data sufficiently well to permit location of the remaining non-hydrogen atoms from Fourier synthesis. Full-matrix least-squares refinement was carried out.

The structure of the complex is shown in Fig. 1. The coordination about each molybdenum atom is essentially that of a pentagonal bipyramid, found previously in a number of complex peroxo molybdates[VI].[1–4,7–11] The axial positions are occupied by the terminal oxo group, Mo=O, 1.682(2) Å, and the oxygen of a weakly coordinated water molecule, Mo—O, 2.441(2) Å, resembling the structures of dimeric $K_2[O\{MoO(O_2)_2H_2O\}_2]$[7] and $(pyH)_2[O\{MoO(O_2)_2H_2O\}_2]$,[8] and monomeric $MoO(O_2)_2(\alpha\text{-AA})H_2O$ (α-AA = gly, pro).[11] The equatorial plane in (**1**) is formed by four peroxo oxygens and the central bridging oxygen, with none of the atoms deviating more than 0.04 Å from the mean plane, and the molybdenum atom placed 0.37 Å above this plane. The equatorial plane is essentially orthogonal to the plane containing the symmetrically bridging oxygen (Mo—O, 1.914(2) Å; Mo—O—Mo angle, 149°), the Mo=O bond, and the water oxygen. The imidazolium ring is hydrogen bonded to an oxygen of a peroxo group, (N···O) 2.794(2) Å. The Mo—O(peroxo) and the O—O bond lengths fall in the expected range[3,4,7–11] and are 1.953(7) and 1.466(4) Å, respectively. The imidazolium cation is essentially planar, with no atom more than 0.07 Å out of the least-squares plane. A significant shortening of the C(4)—C(5), 1.298(8) Å and N(1)—C(5), 1.321(5) Å, bonds has occurred when compared with the non-protonated free or coordinated imidazole.[12–14]

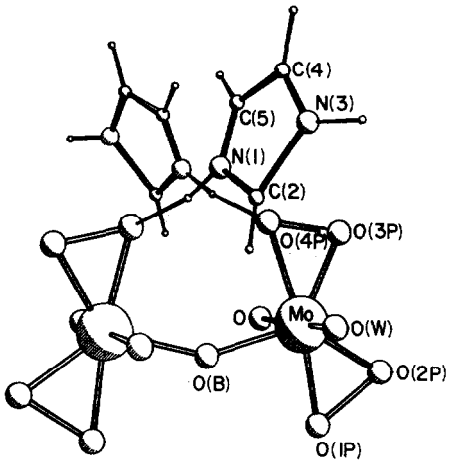

Fig. 1. The structure of $(C_3H_5N_2)_2[O\{MoO(O_2)_2H_2O\}_2]$.

IR spectra of complexes (**1**), (**2**) and (**3**) differ in a significant way. In addition to imidazole bands,[15,16] they all show strong bands assigned to ν(Mo=O) and ν(O—O),[1–4,9–11] which are distinct for each complex. Complex (**1**) only displays a strong band at 3279 cm^{-1}, assigned to ν(NH) of the imidazolium cation,[15] with ν(Mo=O) and ν(O—O) occurring at 964 and 853 cm^{-1}, respectively. In the spectrum of complex (**2**), ν(Mo=O) and ν(O—O) appear as broad and poorly resolved bands at 955 and 892 cm^{-1}, indicating the presence of a polymeric, probably very complex structure.[17] A well resolved spectrum of complex (**3**) shows ν(Mo=O) and ν(O—O) bands at 967 and 858 cm^{-1}, respectively. Additional bands appear in the spectra of complexes (**2**) and (**3**) between 350 and 300 cm^{-1}, most likely due to the ν(Mo—N) from the imidazole coordinated to molybdenum. Cyclic voltammograms of the complexes in aqueous solutions show three irreversible pH dependent cathodic (−900 to −1350 mV) and anodic (1100–1300 mV) peaks. A cathodic shift of about 75 mV was observed for complex (**1**), implying that species generated at the electrode interphase differ, and that it is more difficult to reduce molybdenum in complex (**1**).

These studies indicate that in molybdenum–peroxide–imidazole aqueous systems, complex equilibria exist among several oxoperoxo metal species involving imidazole. These equilibria depend upon the concentration of the components, the pH and the temperature. At the lowest pH (4–5) the imidazolium complex (**1**) was separated, and at only slightly higher pH (5–6) the coordination of imidazole to molybdenum induced the precipitation of complexes (**2**) and (**3**). Lattice energy and solubility of the crystals are responsible for the selection of a particular complex species to be isolated, and coprecipitation of several compounds is common because of their similar solubility. In spite of such difficulties, separation of the equilibrium species into the solid phase remains one of the best ways to understand the reactivity of such systems in the solution. Experiments to obtain crystals of (**2**) and (**3**) large enough for X-ray structure analysis are currently in progress.

Acknowledgement—Support of this work by the NSF Grant Nos CHE-8521376 and CHE-8300516 is gratefully acknowledged.

REFERENCES

1. H. Mimoun, *The Chemistry of Peroxides* (Edited by S. Patai), p. 463. Wiley, New York (1983).
2. W. Shum, *Inorg. Chem.* 1986, **25**, 4329.
3. C. Djordjevic, K. J. Covert and E. Sinn, *Inorg. Chim. Acta* 1985, **101**, L37.
4. C. Djordjevic, B. C. Puryear, N. Vuletic, C. J. Abelt and S. J. Sheffield, *Inorg. Chem.* 1988, **27**, 2926.
5. L. T. J. Delbaere and C. K. Prout, *J. Chem. Soc., Chem. Commun.* 1971, 162.
6. P. C. H. Mitchell, *J. Inorg. Biochem.* 1986, **28**, 107.
7. R. Stomberg, *Acta Chem. Scand.* 1968, **22**, 1076.
8. P. J.-M. LeCarpentier, A. Mitschler and R. Weiss, *Acta Cryst.* 1972, **B28**, 1288.
9. J. Flanagan, W. P. Griffith, A. C. Skapski and R. W. Wiggins, *Inorg. Chim. Acta* 1985, **96**, L23.
10. A. C. Dengel, W. P. Griffith, R. D. Powell and A. C. Skapski, *J. Chem. Soc., Chem. Commun.* 1986, 555.
11. C. Djordjevic, N. Vuletic and E. Sinn, *Inorg. Chim. Acta* 1985, **104**, L7.
12. R. J. Sundberg and R. B. Martin, *Chem. Rev.* 1974, **74**, 471.
13. B. K. Keppler, D. Wehe, H. Endres and W. Rupp, *Inorg. Chem.* 1987, **26**, 844.
14. B. K. Keppler, W. Rupp, U. M. Juhl, H. Endres, R. Niebl and W. Balzer, *Inorg. Chem.* 1987, **26**, 4366.
15. D. H. Bonsor, B. Borah, R. L. Dean and J. L. Wood, *Can. J. Chem.* 1976, **54**, 2458.
16. S. J. Archer, T. P. E. Auf der Heyde, G. A. Fouls and D. A. Thornton, *Transition Met. Chem.* 1982, **7**, 59.
17. I. Persdotter, L. Trysberg and R. Stomberg, *Acta Chem. Scand.* 1986, **A40**, 83.

Polyhedron Vol. 8, No. 4, pp. 545–548, 1989
Printed in Great Britain

0277–5387/89 $3.00+.00
© 1989 Pergamon Press plc

COMMUNICATION

SYNTHESIS, STRUCTURE AND PROPERTIES OF MONONUCLEAR AND DINUCLEAR MOLYBDENUM(III) BROMIDE COMPOUNDS. LIGAND-INDUCED, REVERSIBLE BREAKAGE OF A METAL–METAL BOND IN $Mo_2Br_6(dppe)_2$

BETH E. OWENS and RINALDO POLI†

Department of Chemistry and Biochemistry, University of Maryland, College Park, MD 20742, U.S.A.

(*Received* 29 *July* 1988; *accepted* 7 *October* 1988)

Abstract—$MoBr_3(THF)_3$ reacts with 1 equivalent of bis(diphenylphosphino)ethane (dppe) in THF to yield $MoBr_3(dppe)(THF)$ (**1**). The THF ligand in the latter molecule can be easily replaced by MeCN to afford $MoBr_3(dppe)(MeCN)$ (**2**). When treated in a non-donor solvent, **1** loses THF and dimerizes to one of two isomeric $Mo_2Br_6(dppe)_2$ molecules (green, **3**, kinetic product; purple, **4**, thermodynamic product) depending on experimental conditions. An X-ray analysis of **4** shows an edge-sharing bioctahedral structure and the presence of a Mo—Mo bond. Both **3** and **4** can be reconverted to the parent compound **1** by warming in the presence of excess THF. Compound **2** can also be transformed into the dinuclear compound **4**.

The chemistry of molybdenum compounds in oxidation state III is extremely vast and offers many possible applications, ranging from catalysis to materials science to biochemistry. The chemistry of molybdenum(III) is also among the richest in the field of metal–metal bonding.[1] The simple mononuclear, octahedral compounds of stoichiometry MoX_3L_3 (X = anionic ligand, L = neutral ligand) have been prepared with a variety of different neutral ligands, but most of the studies have been restricted to the trichloride system.[2] This fact can be attributed to the lack of simple preparative procedures for useful starting materials such as $MoX_3(THF)_3$ (X = Br, I; THF = tetrahydrofuran), similar to the widely used $MoCl_3(THF)_3$ where the THF ligands are easily replaced by other ligands. This is unfortunate for several reasons: a comparative study of different molybdenum(III) halide derivatives can be helpful for assessing the importance of electronic and steric factors on chemical reactivity; the bromide and iodide compounds may provide alternative and possibly better starting materials for the generation of other molybdenum(III) compounds as well as compounds of molybdenum in different oxidation states; finally, new types of reactivity and/or structural features may be found.

Cotton and Poli recently reported the synthesis, structure and THF replacement chemistry of $MoI_3(THF)_3$.[3] We successfully applied the same strategy to the large-scale preparation of the already known[4] $MoBr_3(THF)_3$.‡ We report here preliminary studies on THF substitution chemistry on $MoBr_3(THF)_3$ which led to the observation, to our knowledge unprecedented, of a ligand-induced and reversible interconversion between a mononuclear and a metal–metal bonded dinuclear compound.

A suspension of $MoBr_3(THF)_3$ in THF reacts smoothly at room temperature with an equimolar amount of bis(diphenylphosphino)ethane (dppe) to afford a clear orange solution containing $MoBr_3(dppe)(THF)$ (**1**), which can be isolated as a yellow, slightly air-sensitive microcrystalline solid in good yields by addition of diethyl ether to con-

† Author to whom correspondence should be addressed.

‡ $Mo_2Br_4(CO)_8$ and Br_2 in equimolar amounts were stirred together in THF for a few hours at 0°C, then overnight at room temperature. A 90% yield of analytically pure material was obtained.

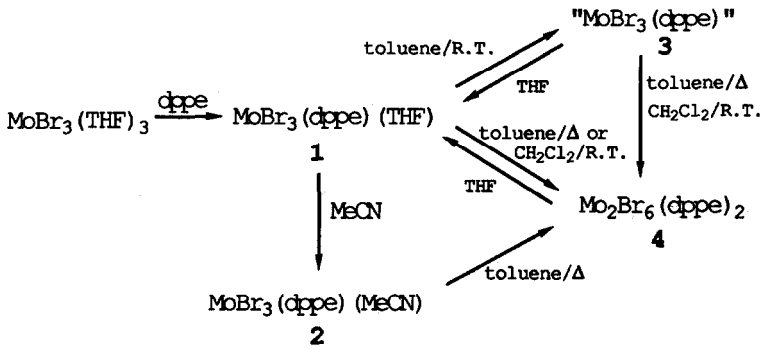

Scheme 1.

centrated solutions.† We believe **1** is a mononuclear, octahedral complex, with a *mer* arrangement of the three bromo ligands, on the basis of an X-ray crystal structure determination on the corresponding triiodide molecule[5] and the similarity of the IR spectra of the two compounds. Also, octahedral trihalide complexes of molybdenum, as well as of other metals, are known to prefer the *mer* arrangement with only a few documented exceptions.[6]

The THF molecule in **1** can be easily replaced by other ligands (see Scheme 1). Compound **2**, $MoBr_3$(dppe)(MeCN), can be obtained by adding an excess of acetonitrile to THF solutions of **1**, although better yields can be obtained by reacting the isolated **1** with pure MeCN.‡

When compound **1** is dissolved in a solvent other than THF and no other ligand is present, it slowly loses the coordinated THF molecule and converts into a different product, the nature of which depends upon the experimental conditions employed. In toluene at room temperature a green–brown compound, **3**, precipitates. In CH_2Cl_2 or in refluxing toluene a purple compound, **4**, is obtained. **3** can be converted into **4** under the same conditions where the latter is obtained directly from **1**. Both compounds **3** and **4** analyse correctly for $MoBr_3$(dppe).§ The recrystallization of **3** and **4** is rather problematic. Any attempt to recrystallize **3** results in its partial conversion to **4**. Compound **4** easily incorporates the crystallization solvent§ to afford very poorly soluble forms of the compound that are then impossible to separate from other insoluble impurities. Compound **4** is slightly soluble in polar chlorinated hydrocarbons but an attempt to recrystallize it from hot 1,1,2-trichloroethane resulted in decomposition. The change of colour from purple to orange–red and the shift of a visible absorption band, λ_{max}, from 558 to 495 nm suggest that at least partial halide exchange with the solvent may have taken place. $Mo_2Cl_6(dppe)_2$ has $\lambda_{max} = 507$ in CH_2Cl_2.[7]

Single crystals of **4** that were suitable for an X-ray analysis were obtained from $CHCl_3$.‖ The compound is dinuclear with an edge-sharing bioctahedral configuration, the six bromo ligands occupy-

† Compound **1**. Found: C, 44.4; H, 3.8; Br, 30.6. Calc. for $C_{30}H_{32}Br_3MoP_2O$: C, 44.7; H, 4.0; Br, 29.7%. IR (Nujol mull/cm^{-1}): 3055 m, 1590 w, 1575 w, 1485 m, 1440 s, 1415 w, 1345 w, 1310 vw, 1195 w, 1165 w, 1100 m, 1075 w, 1045 vw, 1030 w, 990 vw, 920 vw, 850 m, br., 745 s, 725 w, 695 s, 680 w, 650 w, 620 w, 520 s, 500 w.

‡ Compound **2**. Found: C, 43.3; H, 3.3; Br, 30.6; N, 1.8. Calc. for $C_{28}H_{27}Br_3MoNP_2$: C, 43.4; H, 3.5; Br, 30.9; N, 1.8%. IR (Nujol mull/cm^{-1}): 3055 m, 2310 w, 2275 m, 1575 w, 1490 m, 1440 s, 1415 m, 1360 w, 1345 vw, 1325 w, 1195 w, 1160 w, 1115 w, 1100 m, 1080 w, 1030 w, 1000 w, 860 m, 820 w, 765 m, 745 s, 715 m, 700 s, 695 s, 675 m, 645 m, 620 vw, 525 m, 520 m, 490 m, 475 w, 420 w.

§ Compound **3**. Found: C, 42.5; H, 3.5; Br, 30.7. Calc. for $C_{26}H_{24}Br_3MoP_2$: C, 42.5; H, 3.3; Br, 32.7%. Compound **4** typically gave analyses consistent with the incorporation of variable amounts of the crystallization solvent. An X-ray analysis confirmed the presence of interstitial solvent (see text). A sample of compound **4** obtained in **1** in refluxing toluene analysed correctly. Found: C, 42.8; H, 3.2; Br, 32.2. IR (Nujol mull/cm^{-1}): 3050 w, 1590 w, 1580 w, 1490 m, 1415 w, 1440 s, 1195 w, 1160 w, 1100 m, 1075 w, 1030 w, 1005 w, 870 w, 830 w, 815 w, 745 m, 705 m, 695 s, 675 w, 650 vw, 620 vw, 525 m, 520 m, 500 w, 475 w. UV–vis [CH_2Cl_2, R.T., λ_{max}/nm (ε)]: 345(25810), 555(2040).

‖ Crystal data for compound **4**·$4CHCl_3$: monoclinic; space group $I2/m$; $a = 15.653(2)$; $b = 19.180(4)$; $c = 13.723(2)$ Å; $\beta = 108.52(1)°$; $V = 3907(2)$ Å^3; $d_c = 1.65$ g cm^{-3}; μ(Mo-K_α) = 40.85 cm^{-1}. At the end of the structure refinement for $Mo_2Br_6(dppe)_2$, a few clusters of peaks appeared in the difference Fourier map in the proximity of the crystallographic mirror planes, but it was not possible to assign a reasonable model to any of them. The number of interstitial chloroform molecules (four per dimer) is inferred by comparison with the published isostructural $Mo_2Cl_6(dppe)_2 \cdot 4CH_2Cl_2$,[7] considering that CH_2Cl_2 and $CHCl_3$ occupy roughly the same volume. The final agreement factor reached ($R = 0.13$) is for the model not including any disordered solvent molecules.

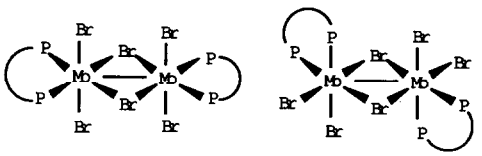

I II

ing the four axial and the two bridging positions, as illustrated in I. Because of disorder in the interstitial solvent molecules we have not been able to refine the structure to a perfectly acceptable *R* factor† and we wish to report here these crystallographic data insofar as they establish the geometry of the complex and to indicate the presence of a metal–metal interaction [Mo—Mo′ = 2.799(7) Å].

Other edge-sharing bioctahedral compounds of molybdenum(III) with bridging chloro, hydroxo and alkylsulphido ligands have been structurally characterized. They exhibit a Mo—Mo distance in the range 2.47–2.79 Å.[8] $Mo_2Cl_6(dppe)_2$ has also been recently reported,[7] having a Mo—Mo distance of 2.762(1) Å. The metal–metal interaction in this type of compound has been described in terms of either a $\sigma^2\pi^2\delta^2$ or a $\sigma^2\pi^2\delta^{*2}$ electronic configuration.[7,9]

Even at the level of structure refinement which was achieved, it seems that compound **4** has a slightly larger metal–metal distance than any of the molybdenum(III) edge-sharing bioctahedral dimers reported to date.[8] This is consistent with the higher bulk of the bridging ligand and should reflect on the strength of the metal–metal interaction and ultimately on the chemical reactivity of the compound.

Compound **4** is converted back to the parent compound **1** when warmed in neat THF or in 1,1,2-trichloroethane containing a large excess of THF, as shown by UV–vis spectroscopic monitoring of the reaction. The attainable temperature in refluxing CH_2Cl_2 is insufficient to cause the same transformation.

There are several examples in the literature of dinuclear, halide-bridged compounds that are reversibly converted to mononuclear complexes by addition/removal of donor solvent molecules[10] but, to the best of our knowledge, none of these contain a direct metal–metal interaction. $MoCl_3(PMe_3)_3$ is reported to lose one PMe_3 ligand in refluxing toluene to afford a product described as the edge-sharing bioctahedral $Mo_2Cl_6(PMe_3)_4$, but no structural data are reported for the product and the "back-reaction" has not been described.[11]

Compound **2** is stable at room temperature towards loss of the monodentate neutral ligand and dimerization to compounds **3** and/or **4**. Heating in toluene at the reflux temperature smoothly converts compound **2** into compound **4**. This observation suggests a Mo^{III}–ligand bond strength in the order THF < MeCN.

Concerning the nature of compound **3**, if we exclude the unlikely possibility of a five-coordinate monomer, the most reasonable guess is that we have a dinuclear structure as represented in II. Although most of the edge-sharing bioctahedral compounds with bis-chelating diphosphines that have been structurally characterized show an arrangement of type I,[8a] there is at least one precedent for a structure of type II, $Mo_2Cl_6(EtSCH_2CH_2SEt)_2$.[8b] Consistent with our structural assignment, compound **3** is also converted into compound **1** when heated in THF. We are planning to undertake kinetic and equilibrium studies on this system and on others containing diphosphine ligands with different steric/electronic properties.

No chemical reactivity has been reported for the chloride analogue of compound **4**, $Mo_2Cl_6(dppe)_2$,[7] but on the basis of its reported metal–metal bond distance, its conversion to the mononuclear compound $MoCl_3(dppe)(THF)$ should be harder. Conversely, the transformation of the hypothetical monomer into the dimer should be easier. With the triiodide system, however, the opposite behaviour is expected because of the higher bulk of the iodo ligands. Work is in progress in our laboratory to test these hypotheses.

Acknowledgements—We are grateful to the Department of Chemistry and Biochemistry, University of Maryland, College Park, for partial support of this work. R.P. is the recipient of a Distinguished New Faculty Award from the Camille & Henry Dreyfus Foundation. The NSF (grant CHE-84-02155) provided a portion of the funds used to purchase the X-ray diffractometer–MicroVax system. We gratefully acknowledge Dr H. Ammon for technical assistance with the X-ray diffractometer.

REFERENCES

1. (a) F. A. Cotton and R. A. Walton, *Multiple Bonds Between Metal Atoms*. Wiley, New York (1982).
2. (a) M. W. Anker, J. Chatt, G. J. Leigh and A. G. Wedd, *J. Chem. Soc., Dalton Trans.* 1975, 2639; (b) J. L. Atwood, W. E. Hunter, E. Carmona-Guzman and G. Wilkinson, *J. Chem. Soc., Dalton Trans.* 1980, 467; (c) M. Millar, Sr. S. Lincoln S.H.C.J. and S. A. Koch, *J. Am. Chem. Soc.* 1982, **104**, 288; (d) J. R. Dilworth and J. A. Zubieta, *J. Chem. Soc., Dalton Trans.* 1983, 397; (e) E. Carmona, J. M. Marin, M. L. Poveda, J. L. Atwood and R. D. Rogers, *J. Am. Chem. Soc.* 1983, **105**, 3014; (f) S.-Y. Roh and J. W. Bruno, *Inorg. Chem.* 1986, **25**, 3105.
3. (a) F. A. Cotton and R. Poli, *Inorg. Chem.* 1987, **26**, 1514; (b) F. A. Cotton and R. Poli, *Inorg. Chem.* 1987, **26**, 3310.

† See footnote ‖ on opposite page.

4. (a) E. A. Allen, K. Feenan and G. W. A. Fowles, *J. Chem. Soc.* 1965, 1636; (b) A. D. Westland and N. Muriithi, *Inorg. Chem.* 1972, **11**, 2971.
5. B. E. Owens, R. Poli and A. L. Rheingold, *Inorg. Chem.*, in press.
6. (a) A. D. Fowlie, D. A. House, W. T. Robinson and S. S. Rumbell, *J. Chem. Soc., Dalton Trans.* 1970, 803; (b) G. B. Robertson and P. A. Tucker, *Acta Cryst.* 1981, **B37**, 814; (c) G. Baumann, L. G. Marzilli, C. L. Nix II and B. Rubin, *Inorg. Chim. Acta* 1983, **77**, L35; (d) A. M. Arif, J. G. Hefner, R. A. Jones and B. R. Whittlesey, *Inorg. Chem.* 1986, **25**, 1080.
7. P. A. Agaskar, F. A. Cotton, K. R. Dunbar, L. R. Falvello and C. J. O'Connor, *Inorg. Chem.* 1987, **26**, 4051.
8. (a) F. A. Cotton, *Polyhedron* 1987, **6**, 667 and refs therein; (b) F. A. Cotton, P. E. Fanwick and J. W. Fitch III, *Inorg. Chem.* 1978, **17**, 3254.
9. F. A. Cotton, M. P. Diebold, C. J. O'Connor and G. L. Powell, *J. Am. Chem. Soc.* 1985, **107**, 7438.
10. (a) G. Wilkinson, R. D. Gillard and J. A. McCleverty (Eds) *Comprehensive Coordination Chemistry*. Pergamon Press, Oxford (1987) and refs therein; (b) G. Wilkinson, F. G. A. Stone and E. W. Abel (Eds) *Comprehensive Organometallic Chemistry*. Pergamon Press, Oxford (1982) and refs therein.
11. E. Carmona, E. Galindo, L. Sanchez, A. J. Nielson and G. Wilkinson, *Polyhedron* 1984, **3**, 347.

Polyhedron Vol. 8, No. 4, pp. 549–550, 1989
Printed in Great Britain

0277–5387/89 $3.00+.00
© 1989 Pergamon Press plc

COMMUNICATION

THE USE OF HEXAMETHYLDISILTHIANE IN THE SYNTHESIS OF TRANSITION METAL THIOHALIDES

VERNON C. GIBSON,* ALAN SHAW and DAVID N. WILLIAMS

Department of Chemistry, University Science Laboratories, South Road, Durham DH1 3LE, U.K.

(*Received* 19 *September* 1988; *accepted* 11 *October* 1988)

Abstract—The thiohalide compounds $W(S)Cl_4$, $W(S)_2Cl_2$, $Mo(S)Cl_3$, $Nb(S)Cl_3$, $Ta(S)Cl_3$, $Nb(S)Cl_3(CH_3CN)_2$, $Ta(S)Cl_3(CH_3CN)_2$, $Mo(O)(S)Cl_2$ and $W(O)(S)Cl_2$ may be obtained in high yield by low temperature treatment of the appropriate metal halide with hexamethyldisilthiane.

Transition metal thiohalides have proved accessible by a variety of methods.[1–6] However, most routes involve high temperature sealed tube/furnace procedures. The only report of a generally applicable room temperature procedure concerns the reaction of transition metal halides with Sb_2S_3 in CS_2 solvent over 1–3 days.[7]

In recent studies, we have shown that hexamethyldisiloxane is a particularly useful reagent for the mild synthesis of oxyhalide materials[8,9] according to eq. (1).

$$MCl_x + (Me_3Si)_2O \longrightarrow M(O)Cl_{x-2} + 2Me_3SiCl. \quad (1)$$

Therefore, we envisaged that the analogous sulphur reagent, $(Me_3Si)_2S$, would be suitable for the controlled, mild synthesis of related thiohalide compounds [eq. (2)] which are not conveniently accessible by other methods.

$$MCl_x + (Me_3Si)_2S \longrightarrow M(S)Cl_{x-2} + 2Me_3SiCl. \quad (2)$$

Indeed, we have found that reactions of transition metal halides with $(Me_3Si)_2S$ proceed with such exothermicity that cooling is generally required. Thus, dropwise addition of a cooled (−30°C) dichloromethane solution of $(Me_3Si)_2S$ to a suspension of the appropriate metal halide in dichloromethane at −78°C, followed by warming of the mixture to room temperature with stirring allows the high yield preparation of the known thiohalide compounds $Mo(S)Cl_3$, $W(S)Cl_4$, $W(S)_2Cl_2$, $Nb(S)Cl_3$ and $Ta(S)Cl_3$. This procedure also allows the synthesis of the mixed oxythiohalide derivatives $W(O)(S)Cl_2$ and $Mo(O)(S)Cl_2$. The tungsten compound may be obtained from WCl_6 by sequential treatment with equimolar amounts of $(Me_3Si)_2O$ and $(Me_3Si)_2S$ in either order of addition. $Mo(O)(S)Cl_2$ is obtained from the reaction of $Mo(O)Cl_4$ with $(Me_3Si)_2S$ and, to our knowledge, has not been reported previously.

If the reaction is carried out in a coordinating solvent such as acetonitrile, then solvent adducts such as $Nb(S)Cl_3(CH_3CN)_2$ and $Ta(S)Cl_3(CH_3CN)_2$ may be obtained in excellent yield [eq. (3)].

$$MCl_5 + (Me_3Si)_2S \xrightarrow{CH_3CN(s)} M(S)Cl_3(CH_3CN)_2 \quad M = Nb, Ta. \quad (3)$$

Here, we give details of the preparations of base-free $W(S)Cl_4$ and the solvent adduct $Nb(S)Cl_3(CH_3CN)_2$. Commercially available reagents can be tolerated since the solubility of the products allows their ready purification. The other less soluble thiohalide materials may be prepared by essentially analogous procedures, but it is advisable to use pure reagents e.g. locally prepared $(Me_3Si)_2S$[10] rather than commercially available material [commonly contaminated with $(Me_3Si)_2O$] since subsequent separation of oxide contaminants is less easy.

*Author to whom correspondence should be addressed.

EXPERIMENTAL

All reactions and product manipulations were performed on a conventional vacuum line using standard Schlenk techniques, or in a dry-box under an atmosphere of argon. Solvents were dried, distilled and degassed prior to use. Metal, sulphur and halide analyses were provided by the microanalytical service at Durham. IR spectra (Nujol mulls between KBr and/or CsI plates) were recorded using Perkin–Elmer 577 and 457 spectrophotometers. $MoCl_5$, WCl_6, $NbCl_5$, $TaCl_5$ (Aldrich) and $Mo(O)Cl_4$ (Alfa) were either used as received or purified, where necessary, by sublimation. $W(O)Cl_4$ was prepared by a literature procedure.[8] $(Me_3Si)_2S$ is commercially available (Fluka) or may be prepared by a literature procedure.[10]

Synthesis of $W(S)Cl_4$

A dichloromethane solution of $(Me_3Si)_2S$ (2.25 g, 12.6 mmol in 15 cm^3 CH_2Cl_2) was added dropwise with stirring to a suspension of WCl_6 (5.0 g, 12.6 mmol) in dichloromethane (20 cm^3) at $-78°C$, over a period of 15 min. An immediate reaction ensued leading to a red solution and precipitation of a brown, amorphous solid. The mixture was allowed to warm to room temperature and stirred for a further 30 min. Filtration of the supernatant solution, followed by concentration and cooling to $-78°C$ afforded red moisture sensitive crystals of $W(S)Cl_4$ (2.95 g, 65%). A second extraction of the residue with CH_2Cl_2 (20 cm^3) followed by crystallization resulted in a combined yield of 75% of analytically pure $W(S)Cl_4$. Found: W, 51.5; Cl, 39.5; S, 9.0. Calc. for Cl_4SW: W, 51.4; Cl, 39.6; S, 9.0%. IR: ν(W=S) 560 cm^{-1} (sharp, strong).

Synthesis of $[Nb(S)Cl_3(CH_3CN)_2]$

An acetonitrile solution of $(Me_3Si)_2S$ (1.97 g, 11.1 mmol in 10 cm^3 CH_3CN) was added dropwise to a suspension of $NbCl_5$ (3.0 g, 11.1 mmol) in acetonitrile (20 cm^3) at $-30°C$. The mixture was warmed to room temperature with stirring to give a green solution which gradually turned yellow with stirring overnight. The volatile components were then removed under reduced pressure and the residue was dried *in vacuo* to give a 95% yield of crude $Nb(S)Cl_3(CH_3CN)_2$. An analytically pure sample was obtained by re-extraction with CH_3CN (30 cm^3), followed by filtration, concentration to half volume and cooling to $-30°C$ to afford yellow crystals. Yield 2.26 g (65%). Found: Nb, 29.9; Cl, 32.9; S, 10.1; C, 15.1; H, 2.0; N, 8.1. Calc. for $C_4H_6N_2Cl_3NbS$: Nb, 29.7; Cl, 33.9; S, 10.2; C, 15.3; H, 1.9; N, 8.9%. IR: ν(C≡N) 2310(s), 2280(s); ν(Nb=S) 532(s) cm^{-1}.

Acknowledgement—We thank the SERC for studentships to A.S. and D.N.W.

REFERENCES

1. For two general reviews, see (a) M. J. Atherton and J. H. Holloway, *Adv. Inorg. Chem. Radiochem.* 1979, **22**, 171; (b) D. A. Rice, *Coord. Chem. Rev.* 1978, **25**, 199.
2. N. S. Fortunatov and N. I. Timoshchenko, *Ukr. Khim. Zh.* 1969, **35**, 1207.
3. K. M. Sharma, S. K. Anand, R. K. Multani and B. D. Jain, *Chemy Ind.* 1969, 1556.
4. J. P. Rannou and M. Sergent, *C.R. Acad. Sci., Paris* 1967, **C265**, 734.
5. D. Britnell, G. W. A. Fowles and D. A. Rice, *J. Chem. Soc., Dalton Trans.* 1974, 2191.
6. D. Britnell, G. W. A. Fowles and R. Mandyczewsky, *J. Chem. Soc., Chem. Commun.* 1970, 608.
7. G. W. A. Fowles, R. J. Hobson, D. A. Rice and K. J. Shanton, *J. Chem. Soc., Chem. Commun.* 1976, 552.
8. V. C. Gibson, T. P. Kee and A. Shaw, *Polyhedron* 1988, **7**, 579.
9. V. C. Gibson, T. P. Kee and A. Shaw, *Polyhedron* 1988, **7**, 2217.
10. E. W. Abel, *J. Chem. Soc.* 1961, 4933.

Polyhedron Vol. 8, No. 4, pp. 551–553, 1989
Printed in Great Britain

0277-5387/89 $3.00+.00
© 1989 Pergamon Press plc

COMMUNICATION

NEW PRECURSORS FOR CHEMICAL VAPOUR DEPOSITION OF PLATINUM AND THE HYDROGEN EFFECT ON CVD

R. KUMAR, S. ROY, M. RASHIDI and R. J. PUDDEPHATT*

Department of Chemistry, University of Western Ontario, London, Canada N6A 5B7

(*Received* 14 *August* 1988; *accepted* 24 *October* 1988)

Abstract—Volatile organoplatinum(II) complexes have been studied as precursors for low temperature chemical vapour deposition (CVD) of platinum films. The temperature of CVD and the carbon contamination of the films can both be decreased by conducting the CVD process in the presence of hydrogen. Good adherence of the films to a silicon semiconductor is obtained.

The noble metals, particularly gold, palladium and platinum, are used extensively in semiconductor device processing and are usually deposited by sputtering or electron-beam evaporation. Platinum is particularly difficult to filament-evaporate because it rapidly forms an alloy with tungsten and because its vapour pressure is low, yet it is valuable in forming platinum silicide ohmic and Schottky diode contacts to silicon and also to gallium arsenide.[1] The evaporation methods can lead to degradation of the semiconductor devices and there would therefore be advantages in using a milder deposition method, such as CVD.[2,4] This technique, operating at low temperature and pressure, has recently been the subject of intense research with special emphasis on CVD of gold films,[5–12] but with some renewed interest in platinum.[1–3,13–15]

For the noble metals, a major problem has been to find organometallic precursors for CVD which have sufficient volatility and which decompose to the pure metal under mild thermal or photochemical conditions.[1–15] Platinum precursors have been $[PtCl_2(CO)_2]$,[2,3] bis(diketonato)platinum(II) complexes,[1–3,13,15] trimethyl(β-diketonato)platinum(IV)[3] and trimethyl(η-cyclopentadienyl)platinum(IV).[3,14] The platinum films usually contain much carbon, chlorine or other impurities.[1–3] This paper describes new alkylplatinum(II) precursors and shows that CVD, in the presence of hydrogen, reduces both the pyrolysis temperature and the amount of carbon contamination.

Some results for CVD of platinum are shown in Table 1. The major new class of organoplatinum precursors comprises the alkylplatinum(II) complexes, such as *cis*-$[PtMe_2(MeNC)_2]$ and $[PtMe_2(COD)]$ (COD = 1,5-cyclooctadiene) and some known precursors are included for comparison. In all cases, when CVD was carried out at 250°C, with the precursor warmed to 40–120°C so as to give reasonably rapid deposition, the platinum films which were formed contained carbon impurities, as found in previous studies.[1–3] Analysis of platinum films deposited on silicon wafers was carried out by XPS; films were cleaned before analysis by argon sputtering since much of the surface carbon impurity was formed after CVD by adsorption of atmospheric carbon.

Now, since platinum is an excellent hydrogenation catalyst, CVD experiments in the presence of hydrogen (10^{-3} torr) were carried out (Table 1). In nearly all cases, the carbon impurities were reduced in the presence of hydrogen and in some cases the effect was dramatic. We presume that organic carbon is hydrogenated and hence the surface is continuously cleaned. Another useful effect of H_2 is to decrease the temperature required for CVD. For example, with $[PtMe_2(COD)]$, $[PtMe(\eta^1\text{-}C_5H_5)(COD)]$ and $[PtMe(\eta^5\text{-}C_5H_5)(CO)]$, CVD was observed at 135°C and was efficient at 180°C in the presence of hydrogen, but the onset of CVD occurred at 235°C in the absence of hydrogen.

* Author to whom correspondence should be addressed.

Table 1. Analytical data for platinum films formed by chemical vapour deposition at 250°C[a,b]

Complex	H_2 present	XPS analysis[c] (Element %) Pt	C	O
$[PtMe_2(MeNC)_2]$	No	88	11	—
	Yes	95	5	—
$[PtMe_2(COD)]$[d]	No	86	10	4
	Yes	94	4	2
$[PtMe(\eta^1\text{-}C_5H_5)(COD)]$	No	77	19	4
	Yes	95	5	—
[PtMeCl(COD)]	No	70	25	5
	Yes	88	9	3
$[PtMe(\eta^5\text{-}C_5H_5)(CO)]$	No	71	27	2
$[PtMe_3(\eta^5\text{-}C_5H_5)]$	No	74	25	1
$[Pt(\eta^3\text{-}C_3H_5)(\eta^5\text{-}C_5H_5)]$[e]	No	60	38	2
$[PtMe_3(acac)]_2$	No	66	30	4

[a] CVD carried out in a vertical reactor. Adherence tested by the scratch test.

[b] Known complexes were prepared according to ref. 16.

[c] After argon sputtering for 30 s.

[d] Sample purified by sublimation.

[e] ^{13}C NMR ($CDCl_3$): δ = 26.8 [^1J(PtC) = 383, CH_2]; 70.2 [^1J(PtC) = 75, CH]; 90.7 [^1J(PtC) = 32, C_5H_5].

It is likely that greater effects on both the purity of the films and the temperature of CVD could be obtained at higher hydrogen pressures, but decreased volatility of the precursors is a problem under these conditions. Low temperature CVD is particularly important for metallization of the thermally sensitive III–V semiconductors.

In summary, this work has shown that alkylplatinum(II) complexes are useful precursors for CVD of platinum, and that lower temperature CVD and a reduction in the carbon impurities in the platinum films can be accomplished by carrying out the CVD in the presence of hydrogen. Such CVD processes may have applications not only in the metallization of electronic devices but also in the preparation of heterogeneous platinum catalysts. Studies of the mechanistic basis for the CVD are in progress.

Acknowledgements—We thank NSERC (Canada) and the province of Ontario for funding through the strategic grant programme and centres of excellence (OCMR) programme, respectively. XPS analyses were carried out by Surface Science Western.

REFERENCES

1. M. J. Rand, *J. Electrochem. Soc.* 1973, **120**, 686.
2. C. F. Powell, J. H. Oxley and J. M. Blocher, Jr, *Vapor Deposition*, pp. 310–314. John Wiley, New York (1966).
3. W. Westwood, *Gmelin Handbook of Inorganic Chemistry—Supplement Vol. A1, Technology of Platinum-Group Metals*, 8th edn, pp. 43–50 (1986).
4. D. C. Bradley, *New Scientist* 1988, 38.
5. T. T. Kodas, T. H. Baum and P. B. Comita, *J. Cryst. Growth* 1988, **87**, 378.
6. C. E. Larson, T. H. Baum and R. L. Jackson, *Mater. Res. Soc. Symp. Proc.* 1987, **75**, 721; C. E. Larson, T. H. Baum and R. L. Jackson, *J. Electrochem. Soc.* 1987, **134**, 266.
7. T. H. Baum, *J. Electrochem. Soc.* 1987, **134**, 2616.
8. M. R. Aylett, *Chemtronics* 1986, **1**, 146.
9. G. M. Shedd, H. Lezec, A. D. Dubner and J. Melngailis, *Appl. Phys. Lett.* 1986, **49**, 1584.
10. T. H. Baum and C. R. Jones, *Appl. Phys. Lett.* 1985, **47**, 538.
11. T. T. Kodas, T. H. Baum and P. B. Comita, *J. Appl. Phys.* 1987, **62**, 281.
12. R. J. Puddephatt and I. Treurnicht, *J. Organomet. Chem.* 1987, **319**, 129.
13. D. Braichotte and H. van den Bergh, *Laser Process Diagn* 1986, **2**, 95.

14. J. E. Gozum, D. M. Pollina, J. A. Jensen and G. S. Girolami, *J. Am. Chem. Soc.* 1988, **110**, 2688.
15. H. H. Gilgen, R. Cacouris, P. S. Shaw, R. R. Krchnavek and R. M. Osgood, *Appl. Phys.* 1987, **42B**, 55.
16. H. C. Clark and L. E. Manzer, *J. Organomet. Chem.* 1973, **59**, 411; H. C. Clark and A. Shaver, *Can. J. Chem.* 1976, **54**, 2068; S. D. Robinson and B. L. Shaw, *J. Chem. Soc.* 1965, 1529; R. C. Menzies and H. Overton, *J. Chem. Soc.* 1933, 1290; B. E. Mann, B. L. Shaw and G. Shaw, *J. Chem. Soc. A* 1971, 3536.

Polyhedron Vol. 8, No. 4, pp. 555–558, 1989
Printed in Great Britain

0277–5387/89 $3.00+.00
Pergamon Press plc

COMMUNICATION

HETEROLEPTIC POLYPYRAZOLYLBORATE COMPLEXES OF THE LANTHANIDE IONS. THE SYNTHESIS OF CARBOXYLATE COMPLEXES AND THE MOLECULAR STRUCTURE OF $[Yb\{HB(C_3N_2H_3)_3\}_2\{O_2CPh\}]$

MICHAEL A. J. MOSS and CHRISTOPHER J. JONES*

Department of Chemistry, University of Birmingham, PO Box 363, Birmingham B15 2TT, U.K.

(*Received* 19 *August* 1988; *accepted* 31 *October* 1988)

Abstract—The heteroleptic lanthanide ion complexes $[LnL_2X]$ ($L = HB\{C_3N_2H_3\}_3$, Ln = Y, Sm, Eu, Yb, Lu and $X = O_2CPh$; Ln = Y, Yb, Lu and $X = O_2CMe$) have been prepared and characterized. They are monomeric and a single crystal X-ray diffraction study of $[YbL_2(O_2CPh)]$ shows that the molecule has a distorted square antiprismatic (SAP) coordination geometry which lies on the geometric pathway from SAP to dodecahedral. The average Yb—O distance is 2.33(2) Å and the average Yb—N distance is 2.43(4) Å. The complexes $[LnL_2(X—X)LnL_2]$ (Ln = Y, Yb, Lu and $X—X = O_2CCO_2$) have also been prepared.

In a study of the ability of uninegative bidentate co-ligands (X^-) to complete the steric saturation of the lanthanide (Ln) coordination sphere in $[LnL_2X]$ (L = hydrotrispyrazol-1-ylborate), we have shown that when X = pent-2-ene-2,4-diolate ($acac^-$) stable monomeric complexes are formed for the whole of the series of lanthanide elements from La to Lu.[1,2] However, if the size of the chelate ring formed by X is reduced from six to five by having X^- = cyclohepta-1,3,5-triene-1,7-diolate ($trop^-$), insoluble, presumably oligomeric, compounds are formed with La, Ce and Pr.[3] In order to assess the effect of further reducing the size of the chelate ring formed by X we have now prepared a series of carboxylate complexes in which four-membered chelate rings are formed.

An aqueous solution containing $MeCO_2^-$, L^- and Ln^{3+} ions in a 1:2:1 ratio rapidly produces a precipitate formulated as $[LnL_2(O_2CMe)]$ (Ln = Y, Yb, Lu) on the basis of spectroscopic data and elemental analyses. Similar complexes may be formed when Ln = Eu or Gd but in these cases substantial amounts of $[LnL_3]$ are also found in the reaction mixture. When Ln = Sm, $[SmL_2(O_2CMe)]$ may be identified in the initial precipitate but when this material is dissolved in polar organic solvents disproportionation occurs to give $[SmL_3]$ as the only isolable product. The complexes $[LnL_2(O_2CMe)]$ (Ln = Y, Yb) can also be prepared under non-aqueous conditions by reacting AgO_2CMe, KL and anhydrous $LnCl_3$ in dry THF under nitrogen. A cerium complex could also be prepared by this anhydrous route and had spectroscopic properties consistent with the formulation $[CeL_2(O_2CMe)]$. However, this material was unstable in solution and could not be isolated in a pure form.

The soluble heteroleptic benzoate complexes $[LnL_2(O_2CPh)]$ (Ln = Y, Sm, Eu, Yb, Lu) are formed readily in aqueous solution but reactions involving the larger lanthanides (Ln = La–Nd) afford only insoluble materials. A similar reaction involving 4-tertiarybutylbenzoic acid and yttrium afforded the unexpected heteroleptic complex $[YL(O_2CC_6H_4\text{-}4\text{-}CMe_3)_2]$. The interaction of oxalate, L^-, and the lanthanide ions in aqueous solution leads to the formation of insoluble products for the larger lanthanides (La–Nd). However, for the smaller lanthanides (Ln = Y, Sm–Lu) the products are soluble in polar organic solvents and, on the basis of spectroscopic and elemental analysis data may be formulated as $[(LnL_2)_2(C_2O_4)]$. All of

*Author to whom correspondence should be addressed.

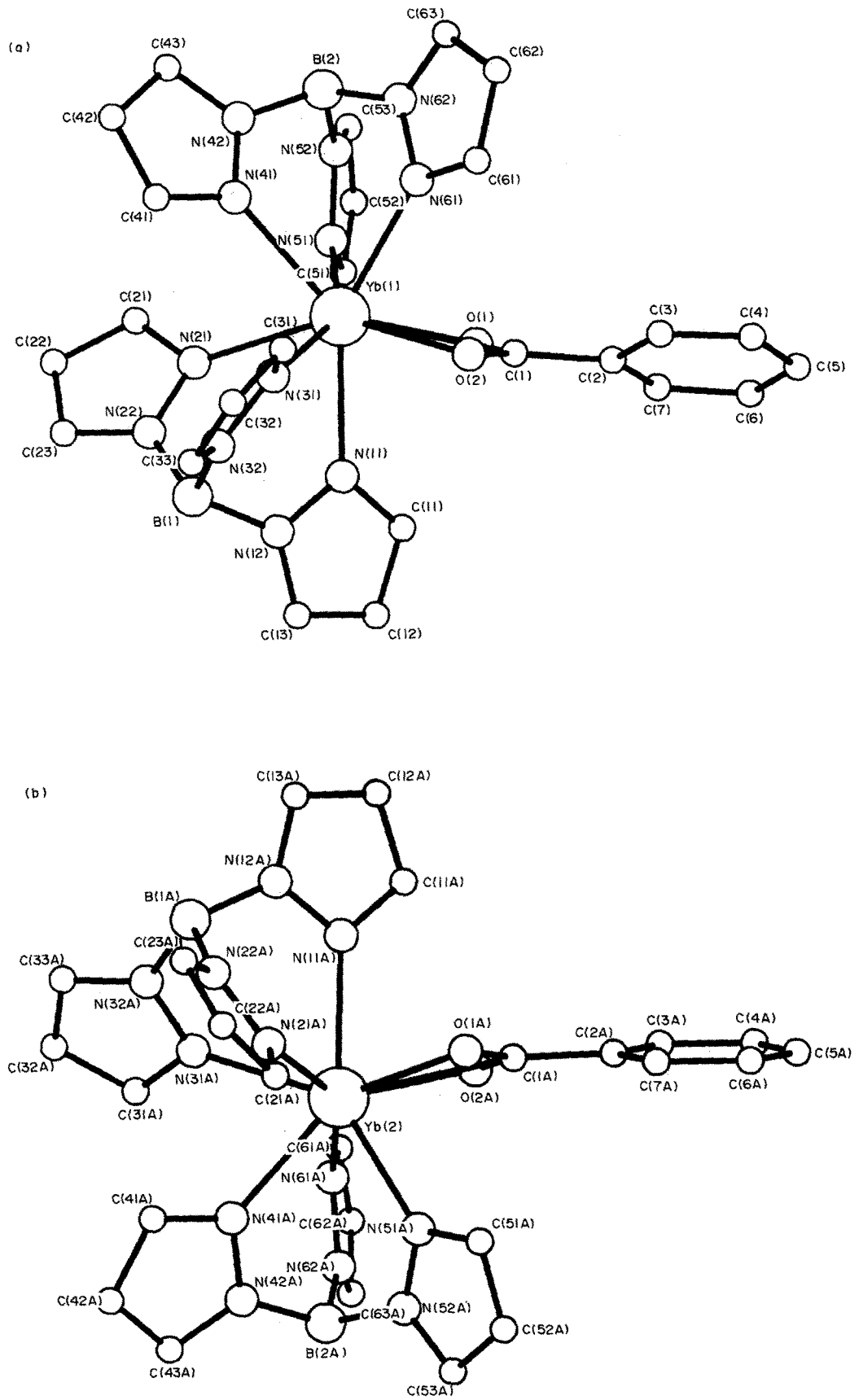

Fig. 1. The structures and atom numbering of (a) molecule (1) and (b) molecule (2).

the soluble carboxylate complexes obtained were found to exhibit dynamic ^{1}H NMR spectra as found for the related β-diketonate and tropolonate complexes,[2–4] but unlike the rigid behaviour found for $[YbL_3]$.[5]

In order to obtain more detailed structural information on an example of these carboxylate complexes, a single crystal X-ray diffraction study was carried out on $[YbL_2(O_2CPh)]$.* The crystal structure consists of discrete molecular units, there being two independent molecules in the asymmetric unit and four molecules in the unit cell. The structures and atom numbering of molecules (1) and (2) are shown in Fig. 1. Both molecules contain eight-coordinate ytterbium centres bound to one bidentate benzoate ligand and two tridentate L ligands. The coordination geometry of ytterbium in $[YbL_2(O_2CPh)]$ is best described as square antiprismatic (SAP) with the distortion of both "squares", so that it is on the geometric pathway from SAP to dodecahedral. This is in contrast to $[YbL_2(trop)]$ which had only one "square" distorted so that it is on the geometric pathway from SAP to bicapped trigonal prismatic (BCTP). At first sight the structure appears to be similar to those of $[YbL_2(acac)]$[2] and $[YbL_2(trop)]$.[3] However, there is one important difference between these structures and that of the benzoate complex. In the latter structure the coordinating nitrogen atoms of the ligands, L, are closer to the ytterbium ion, and to compensate for this the coordinating oxygen atoms of the benzoate ligand are further away. Thus the mean Yb—N bond distance is 2.43 Å (ranges: molecule (1), 2.369(6)–2.462(7) Å; molecule (2), 2.363(6)–2.481(6) Å) for this structure compared with 2.49 Å (range: 2.401(7)–2.601(6) Å for $[YbL_3]$,[6] 2.49 Å (ranges: molecule (1), 2.444(10)–2.576(11) Å; molecule (2), 2.432(14)–2.526(13) Å) for $[YbL_2(acac)]$[2] and 2.48 Å (range: 2.425(12)–2.548(10) Å) for $[YbL_2(trop)]$.[3] The mean Yb—O(benzoate) distance is 2.33 Å (ranges: molecule (1), 2.310(5)–2.360(6) Å; molecule (2), 2.319(5)–2.336(5) Å), compared with Yb—O(diketonate) distances of 2.22 Å (ranges: molecule (1), 2.199(11)–2.258(9) Å; molecule (2), 2.200(9)–2.238(9) Å) in $[YbL_2(acac)]$[2] and 2.24 Å (range: 2.222(9)–2.267(8) Å) in $[YbL_2(trop)]$.[3] Due to the shorter Yb—N bonds in $[YbL_2(O_2CPh)]$ the steric angle factor (SAF)[7] for L in $[YbL_2(O_2CPh)]$ is anomalously high. The mean SAF for L calculated from data for $[YbL_3]$, $[YbL_2(acac)]$ and $[YbL_2(trop)]$ is 0.305(3) compared to a value of 0.320 in $[YbL_2(O_2CPh)]$. The SAF value for the benzoate ligand is calculated to be 0.174. The SAS value for the complex $[YbL_2(O_2CPh)]$ is therefore 0.814, which is only slightly smaller than the values of 0.833 and 0.819 for $[YbL_2(acac)]$ and $[YbL_2(trop)]$, respectively.[8]

To our knowledge $[YbL_2(O_2CPh)]$ is the first structurally characterized lanthanide complex which has been found to contain a non-bridging, chelating bidentate benzoate ligand. The related bis(cyclopentadienyl) lanthanide acetates, benzoates and formates were first reported in 1963.[9] These were found to be dimeric containing bridging carboxylate ligands, as were $[(\eta^5\text{-}C_5H_5)_2Yb(O_2CR)]_2$ (R = Me, C_6F_5 and C_5H_4N).[10] The pentafluorobenzoate complex $[(\eta^5\text{-}C_5H_5)_2Yb(O_2CC_6F_5)]_2$ has been structurally characterized, and is a doubly carboxylate-bridged dimer.[10] The limited structural data available[11] for $[(\eta^5\text{-}C_5H_5)_2Yb(O_2CPh)]_2$ indicate that this molecule is also a doubly carboxylate-bridged dimer. In the case of pentamethylcyclopentadienyl complexes, $[(\eta^5\text{-}C_5Me_5)_2Yb(O_2CR)]_n$ is reported to be monomeric ($n = 1$) when R = CF_3, but dimeric ($n = 2$) when R = Bu^t, but no molecular structure data were obtained.[12] The only structurally characterized, simple, lanthanide benzoate complex of which we are aware is $[Dy(\mu\text{-}O_2CPh)(k'\text{-}O_2CPh)_2(H_2O)_4]\cdot H_2O$ which consists of infinite chains containing eight-coordinate Dy^{3+} ions bound to monodentate and bridging bidentate benzoate ligands.[13]

In conclusion it may be noted that, as the size of the chelate ring formed between Ln and the co-ligand X in $[LnL_2X]$ (X = acac, trop or carboxylate) is reduced from six to four, complexes containing the larger lanthanide ions become unstable with respect to disproportionation. However, the complexes in which Ln is Y, Yb or Lu remain stable as monomeric molecular species. This behaviour contrasts with that of the related cyclo-

* Crystal data. $C_{25}H_{25}B_2N_{12}O_2Yb$, $M = 720.2$, Triclinic, $a = 9.148(1)$, $b = 15.796(8)$, $c = 20.089(10)$ Å, $\alpha = 81.57(5)$, $\beta = 88.65(2)$, $\gamma = 88.15(3)°$, $U = 2870$ Å^3, $Z = 4$, $D_c = 1.67$ g cm^{-3}, space group $P\bar{1}$ (No. 2), Mo-K_α radiation ($\lambda = 0.7107$ Å, $\mu = 31$ cm^{-1}), $T = 293$ K. Data were collected on a CAD4 diffractometer at the Crystallography Unit, Universities of Aston and Birmingham. 10020 unique reflections were measured ($2 < 2\theta < 55°$) with $I > 2.5\sigma I$. The structure was solved using conventional heavy-atom methods. It was necessary to locate the atoms for the two independent molecules in the asymmetric unit. The final model with 697 parameters varied, refined to $R = 0.0504$ and $R_w\{= [\Sigma w(|F_o| - |F_c|)^2]^{1/2}\} = 0.0519$. Final Atomic coordinates, bond lengths and angles, thermal parameters and $F_o - F_c$ values have been deposited as supplementary material with the Editor, from whom copies may be obtained. Atomic coordinates have also been deposited with the Cambridge Crystallographic Data Centre.

pentadienide complexes which tend to dimerize or oligomerize and may be attributed to the greater steric demands of the trispyrazolylborate ligand.

Acknowledgements—We are grateful to Dr A. J. Edwards and Professor W. J. Evans for helpful discussions; to the SERC and BP Chemicals International for support (to M.A.J.M.); and to NATO for the provision of travel grant No. 175/84.

REFERENCES

1. M. A. J. Moss and C. J. Jones, *Abstr. XXIV Int. Conf. Coord. Chem., Chim. Chron.*, A7–488. Association of Greek Chemists (1986).
2. M. A. J. Moss, C. J. Jones and A. J. Edwards, *Polyhedron* 1988, **7**, 79.
3. M. A. J. Moss and C. J. Jones, *Polyhedron* 1988, **7**, 111.
4. W. D. Moffat, M. V. R. Stainer and J. Takats, *Inorg. Chim. Acta* 1987, **139**, 75.
5. M. V. R. Stainer and J. Takats, *J. Am. Chem. Soc.* 1983, **105**, 410.
6. M. V. R. Stainer and J. Takats, *Inorg. Chem.* 1982, **21**, 4050.
7. Feng Xi-zhang, Guo Ao-ling, Xu Ying-ting, Li Xing-fu and Sun Peng-nian, *Polyhedron* 1987, **6**, 1041.
8. M. A. J. Moss, PhD thesis. University of Birmingham, U.K. (1987).
9. R. E. Maggin, S. Manastyrskyj and M. Dubeck, *J. Am. Chem. Soc.* 1963, **85**, 672.
10. G. B. Deacon, G. D. Fallon, P. I. MacKinnon, R. H. Newnham, G. N. Pain, T. D. Tuong and D. L. Wilkinson, *J. Organomet. Chem.* 1984, **277**, C21.
11. E. C. Baker, PhD thesis. University of California, Berkeley, U.S.A. (1977).
12. T. D. Tilley, R. A. Anderson, A. Zalkin and D. H. Templeton, *Inorg. Chem.* 1982, **21**, 2644.
13. M. S. Khiyalov, I. R. Amiraslanov, F. N. Musaev and Kh. S. Mamedov, *Koord. Khim.* 1982, **8**, 548.

Polyhedron Vol. 8, No. 4, pp. 559–561, 1989
Printed in Great Britain

0277-5387/89 $3.00+.00
© 1989 Pergamon Press plc

COMMUNICATION

THE SYNTHESES AND X-RAY CRYSTAL STRUCTURES OF RHENIUM(V) COMPLEXES CONTAINING FACULTATIVE PENTADENTATE LIGANDS

HILARY J. BANBERY, FERIDA McQUILLAN, THOMAS A. HAMOR,* CHRISTOPHER J. JONES* and JON A. McCLEVERTY

Department of Chemistry, University of Birmingham, PO Box 363, Birmingham B15 2TT, U.K.

(*Received* 17 *October* 1988; *accepted* 3 *November* 1988)

Abstract—The reaction between $[ReOCl_4]^-$ and the Schiff base ligand $\{HOC_6H_4$—2-$CH{=}N(CH_2)_2\}_2S$ in ethanol, affords the monomeric complex $[ReO(OEt)\{OC_6H_4$—2-$CH{=}N(CH_2)_2\}_2S]$. However, a similar reaction using the amine ligand $\{HOC_6H_4$—2-$CH_2NH(CH_2)_2\}_2S$, obtained by reduction of the Schiff base, affords a binuclear complex $[ReO\{2\text{-}(OC_6H_4$—2-$CH_2N(CH_2)_2S(CH_2)_2NHCH_2)C_6H_4O\}_2ReO]$. The molecular structures of these complexes have been determined and show that, in the former complex, the thioether sulphur remains uncoordinated giving rise to an eight-membered chelate ring. In the latter complex each pentadentate ligand binds to both metal ions forming an amide complex with one and an amine complex with the other. The two rhenium atoms are components of a 10-membered dimetallocyclic $\{$—$ReSCH_2CH_2N$—$\}_2$ ring.

As part of a study of the complexation of rhenium by polydentate facultative ligands containing both "hard" and "soft" donor atoms, we have investigated the reactions between $[ReOCl_4]^-$ and two pentadentate ligands, each containing one sulphur, two oxygen and two nitrogen donor atoms. The first of these ligands is the Schiff base $\{HOC_6H_4$—2-$CH{=}N(CH_2)_2\}_2S$ (sal_2thimH_2), obtained from the condensation of salicylaldehyde and 1,5-diamino-3-thiapentane. The second ligand is $\{HOC_6H_4$—2-$CH_2NH(CH_2)_2\}_2S$ (sal_2thamH_4), obtained by reduction of the Schiff base with borohydride to give amine rather than imine nitrogen donor sites. The saturation of the chain linking the phenoxide moieties also results in increased ligand flexibility and we were particularly interested in the effect this change might have on the way in which the donor atom set coordinated to rhenium.

The new ligands have been fully characterized by spectroscopic methods and by elemental analyses. Both were reacted with $[ReOCl_4]^-$ in dry ethanol in the absence of air. The reaction with sal_2thimH_2 afforded a green complex which exhibited $\nu_{Re=O}$ at 944 cm^{-1} in its IR spectrum, in addition to bands attributable to the presence of the ligand sal_2thim. The ^1H NMR spectrum confirmed the presence of the ligand, and the elemental analysis data and X-ray diffraction study described below have established that the compound is the neutral complex, $[ReO(OEt)(sal_2thim)]$.

The reaction involving sal_2thamH_4 also afforded a green complex, the IR spectrum of which contained bands attributable to $\nu_{Re=O}$ at 900 and 880 cm^{-1}. Bands attributable to the pentadentate ligand were also observed. The presence of the ligand was confirmed by ^1H NMR spectroscopy, and the elemental analyses and X-ray diffraction study described below have established that the complex is $[ReO\{2\text{-}(OC_6H_4$—2-$CH_2N(CH_2)_2S(CH_2)_2NH$ $CH_2)C_6H_4O\}_2ReO]\cdot 2CH_2Cl_2$.

Crystals of $[ReO(OEt)(sal_2thim)]$ are monoclinic, $P2_1/n$, $a = 13.709(2)$, $b = 9.656(9)$, $c = 15.835(3)$ Å, $\beta = 103.55(2)°$, $Z = 4$. 3624 reflections in the range $\theta = 2$–$25°$, measured with an Enraf–Nonius CAD-4 diffractometer, 2803 having $[I > 2.5\sigma(I)]$

*Authors to whom correspondence should be addressed.

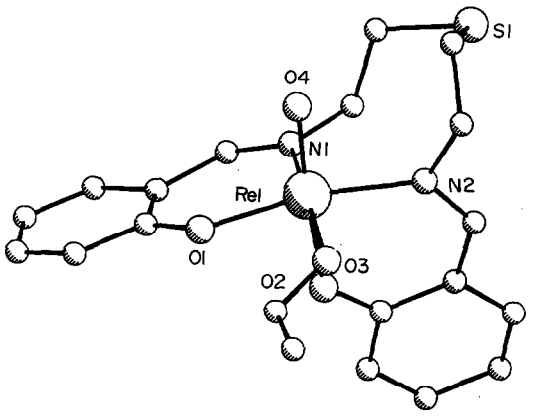

Fig. 1. The molecular structure of [ReO(OEt)(sal$_2$thim)] showing the atom labelling. Hydrogen atoms have been omitted for clarity.

were used in the analysis. The structure was solved[1] by Patterson and Fourier methods and refined[2] by least-squares using anisotropic temperature factors for the heavier atoms. Hydrogen atoms were included in calculated positions, but their parameters were not refined. The final R is 0.030; unit weights which gave a satisfactory weighting analysis were used. An empirical absorption correction was applied to the data using DIFABS.[3] The molecular structure* is shown in Fig. 1. The rhenium atom is in an approximately octahedral coordination environment, the maximum angular deviation from ideal values being 14.1°. One phenolic oxygen, O(2), of the ligand lies *trans* to the rhenyl oxo group, angle O(2)—Re—O(4) 165.9(2)°. The second phenolic oxygen, O(1), binds *cis* to the rhenyl oxo group and to the ethoxy group, which is in turn *trans* to an imine nitrogen, angle O(3)—Re—N(1) 168.3(3)°. The thioether sulphur atom does not bind to the rhenium but becomes part of an eight-membered {—ReNCH$_2$CH$_2$SCH$_2$CH$_2$N—} chelate ring. This behaviour contrasts with that found for [TcON {(CH$_2$)$_2$N=CHC$_6$H$_4$—2-O}] in which all five ligand donor atoms bind to the [TcO]$^{3+}$ moiety.[4]

Crystals of [ReO(sal$_2$thamH)]$_2$·2CH$_2$Cl$_2$ are monoclinic $P2_1/n$, $a = 11.733(3)$, $b = 9.655(3)$, $c = 18.496(2)$ Å, $\beta = 91.11(2)°$, $Z = 2$. Data collection and structure determination were as for [ReO(OEt)(sal$_2$thim)]. The final R is 0.036 for 2739 reflections. The molecular structure is shown in Fig. 2. Again, the rhenium atom is in a distorted octahedral coordination environment, maximum angular deviation from ideal values is 19.3°, in which one phenolic oxygen of the ligand lies *trans* to the rhenyl oxo group, angle O(2)—Re—O(3) 160.7(3)°. In combination with the amine nitrogen associated with the same phenyl ring, this oxygen forms part of a bidentate chelate with one rhenium atom. The

*Atomic coordinates, bond lengths and angles and thermal parameters have been deposited with the Cambridge Crystallographic Data Centre.

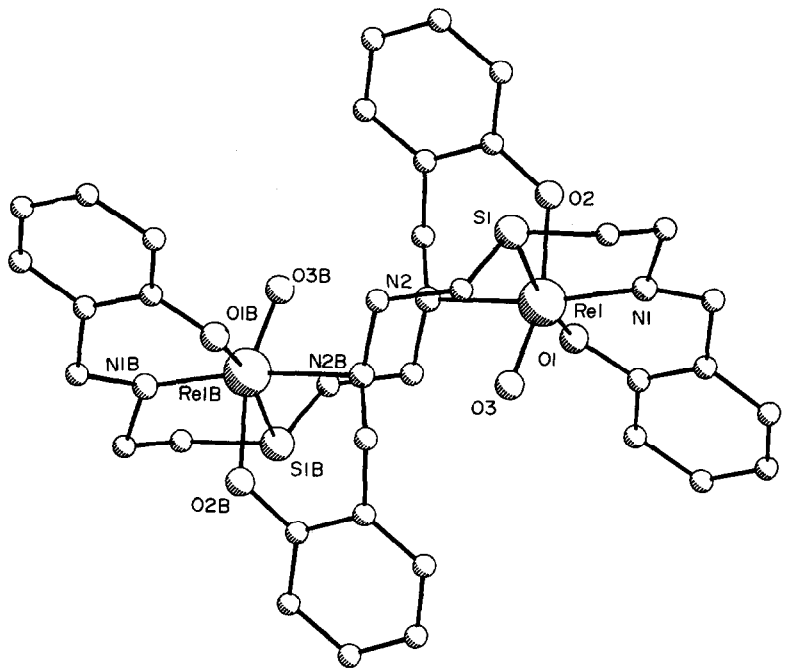

Fig. 2. The molecular structure of [ReO(sal$_2$thamH)]$_2$·2CH$_2$Cl$_2$ showing the atom labelling. Hydrogen atoms and the CH$_2$Cl$_2$ molecules have been omitted for clarity.

thioether sulphur and the remaining amide nitrogen and phenolate oxygen of the ligand, bind to *mer* sites on the other rhenium. The second ligand is bound in a complementary way to complete the dinuclear structure which contains a 10-atom bimetallocyclic ring, —Re—S—$(CH_2)_2$—NH—Re—S—$(CH_2)_2$—NH—. Although the hydrogen atoms were not located, the amido and amine nitrogen atoms, N(1) and N(2), respectively, could be clearly distinguished from their bonding geometries. Thus the angles at N(2) are close to tetrahedral, in the range 107.7–112.5°, whilst those at N(1) show a near planar geometry (sum of angles 353.3°). The Re—N distances, Re—N(1), 1.925(10) Å and Re—N(2), 2.288(9) Å, are also consistent with this, the former distance being indicative of $p\pi$–$d\pi$ electron donation from ligand to metal.

In conclusion it may be noted that, although the strategy of saturating the azomethine groups to increase ligand flexibility did lead to coordination of the thioether sulphur, the encapsulation of a single rhenium by a single ligand was still not achieved. The interplay between ligand flexibility and the preference for neutral complex formation leads to a highly complex situation in the formation of these rhenium(V) complexes. It would appear that the presence of the larger sulphur atom in the facultative ligand structure places limitations on the ability of the ligand to fully coordinate to a single metal ion. Similar effects have been noted[5] in attempts to prepare iron(III) and cobalt(III) complexes of hexadentate ligands. In these cases, stable complexes could be isolated only when oxygen or nitrogen donor atoms were present in the facultative ligand, but the incorporation of sulphur in the ligand precluded the isolation of stable 1 : 1 complexes.

Acknowledgements—We are grateful to the SERC and Amersham International plc for their support (to H.B. and F.McQ.).

REFERENCES

1. G. M. Sheldrick, SHELXS-86, Program for the Solution of Crystal Structure. University of Göttingen, F.R.G. (1987).
2. G. M. Sheldrick, SHELX-76, Program for Crystal Structure Determination. University of Cambridge, U.K. (1978).
3. N. Walker and D. Stuart, *Acta Cryst.* 1983, **A39**, 158.
4. F. Refosco, F. Tisato, U. Mazzi, G. Bandoli and M. Nicolini, *J. Chem. Soc., Dalton Trans.* 1988, 611.
5. A. S. Rothin, H. J. Banbery, F. J. Berry, T. A. Hamor, C. J. Jones and J. A. McCleverty, *Polyhedron* 1989, **8**, 491.

Polyhedron Vol. 8, No. 4, pp. 563–565, 1989
Printed in Great Britain

0277–5387/89 $3.00+.00
© 1989 Pergamon Press plc

COMMUNICATION

THE CHEMICAL MECHANISM FOR ELECTRON TRANSFER AND BRIDGE REDUCIBILITY

WILLIAM L. PURCELL

Department of Chemistry, University of Miami, Coral Gables, FL 33124, U.S.A.

(*Received* 13 *June* 1988; *accepted* 2 *November* 1988)

Abstract—One limiting mechanism proposed for bridged inner-sphere, electron transfer reactions, the chemical mechanism, involves rate-limiting reduction of the bridge to a radical by the reducing centre followed by rapid reduction of the oxidizing centre by the radical bridge. One predicted kinetic trait of such reactions is a correlation between the electron transfer rate constant and the "reducibility" of the bridge. This predicted trend is quantified here for the first time, with bridge reducibility expressed in terms of adiabatic gas-phase electron affinities. Also, a new kinetic test to distinguish outer-sphere electron transfers from those proceeding the chemical mechanism is shown to develop from the dependence of the rate constant on electron affinity.

Two limiting mechanisms are believed to occur for electron transfer reactions that proceed by an inner-sphere route, resonance transfer and the chemical (or radical) mechanism.[1] Of the two, the latter has proven much more amenable to chemical testing, and is now firmly established. The pulse radiolysis studies of Hoffman and co-workers have clearly demonstrated the viability of a mechanism in which a ligand is reduced prior to final metal cation reduction.[2–5] In a few cases, an intermediate radical species has been detected.[6–9] Finally, Gould has demonstrated for several systems that both bound and unbound ligands are reduced at similar rates.[10] Nevertheless, in the vast majority of inner-sphere electron transfer reactions, direct evidence for or against a chemical mechanism is lacking. Sadly, in many cases the mere assignment of an inner- or outer-sphere route proves impossible. Such is the case with the majority of photoredox processes.

In this paper we report on a test for the chemical mechanism based upon a predicted, but previously unobserved, relationship between bridging ligand "reducibility" and the rate constant for electron transfer. Outer-sphere reactions do not show the same trend and, thus, may be distinguished from the inner-sphere chemical mechanism reactions.

A fundamental kinetic trait predicted for inner-sphere electron transfer by the chemical mechanism is the dependence of the rate constant on the "reducibility" of the bridging ligand, since the bridge is the electron acceptor in the rate-limiting step.[11] Unfortunately, this predicted trend has not been observed except in the most qualitative terms. Cannon has compiled the most extensive set of literature data in an attempt to correlate various measures of reducibility to the experimental rate constants for electron transfer.[12] However, neither polarographic half-wave potentials, charge-transfer band maxima, nor rates of uncomplexed bridging ligand reduction reactions, have served as suitable reducibility parameters in the attempted correlations (plots (a), (b) and (c), respectively, on pp. 252–253 of ref. 12). A rough estimate of the correlation coefficients of the three plots presented by Cannon are 0.67, 0.62 and 0.31 for (a), (b) and (c), respectively. Before concluding that the predicted correlation is not followed, one should realize that the particular reactions considered by Cannon, namely chromium(II) reductions of carboxylatopentaamminecobalt(III) complexes, are known to be quite sensitive to steric effects from the carboxylate R groups (see reaction (1) below).[13] Also, inexact values for many of the reducibility parameters undoubtedly contributed to poor correlations in some of the data points. For

example, many of the carboxylate ligand parameters were estimated from methyl or ethyl esters of the acids, and in some cases the physical constants were obtained in a variety of solvents.[12] Also, as pointed out by a reviewer, some of the reactions undoubtedly do not follow a chemical mechanism.

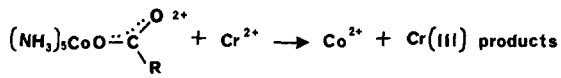

(1)

Based upon the above analysis concerning Cannon's attempt to achieve the predicted correlation for the chemical mechanism, the following minimum criteria are necessary if the expected correlation is to be observed: the electron transfer reactions should either be free of, or be subject to constant, steric factors across the series of reactant complexes, the physical constants used to express bridge reducibility should be free of variable medium (e.g. solvent) effects, and the functional groups utilized as the binding sites for the reductant and the oxidant should be invariant. This functional group requirement seems reasonable, since a significant change in the functional group attached to a cobalt(III) oxidizing centre would be expected to change the redox potential of the complex, and, thus, inject another variable into the rate constant equation. The same requirement for the reductant attack site also seems proper since experimental rate constants for electron transfer are products of two, usually inseparable, constants for the overall reaction. These are an equilibrium constant for precursor complex formation (Q_p) and the rate of internal electron transfer within this precursor (k_{et}).[14] Data now exist in the literature for a limited number of reactions which meet all the above criteria. The reactions involved are represented by eq. (2) below.[15–18] The measures of bridge reducibility are Kebarle's recently reported adiabatic gas-phase electron affinities of the organonitriles indicated in eq. (2).[19]

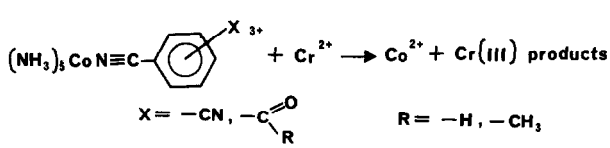

(2)

Figure 1 shows the correlation between $\ln(k_{expt})$ for reaction (2) and the electron affinities (EAs) of the six organonitrile bridging ligands whose structures are presented in Fig. 1. Also presented in Fig. 1 are points for reduction of the dicyanobenzene complexes of pentaamminecobalt(III) by both vanadium(II) and hexaammineruthenium(II).[18] Reductions by the latter reagent are necessarily outer-sphere, while the vanadium(II) reduction data will require some discussion.

The data presented in Fig. 1 deserve special comment. Clearly, the prediction of a correlation between bridging ligand reducibility and electron transfer rate constants for a chemical mechanism has been realized, at least for the six ligands in Fig. 1 and eq. (2). The displacement for the two sets of ligands (remote cyano functions vs remote carbonyl functions) was to be expected since, as mentiond above, the observed rate constants contain an equilibrium constant for precursor complex formation, which would certainly differ for chromium(II) attack at two such different functional groups. Bridged inner-sphere mechanisms were unambiguously assigned in the original kinetic studies for only three of the six chromium(II) reductions represented in Fig. 1.[15,16] Inner-sphere mechanisms were inferred for the remaining three reactions based upon the magnitudes of the rate constants[15,16] and/or rate ratio comparisons.[18]

Vanadium(II) reductions of the 1,2- and 1,3-dicyanobenzene complexes were assigned outer-sphere mechanisms by Gould[18] based upon vanadium(II) to hexaammineruthenium(II) rate ratios. However, the 1,4-dicyanobenzene complex reduction by vanadium(II) was assigned a significant inner-sphere term (45%) based upon the same rate ratio comparison. However, the rate ratio in the latter case is 0.16 which is comparable to those of the other two complexes (0.23 and 0.14). Furthermore, the rate ratio is almost identical to the 0.17 ratio obtained with the benzonitrile complex which *must* be outer-sphere with vanadium(II). Therefore, this Author believes that the assignment of a significant inner-sphere pathway for the 1,4-dicyanobenzene complex with vanadium(II) is not justified by the rate ratios. Certainly, all three vanadium(II) points in Fig. 1 mirror the behaviour of the three hexaammineruthenium(II) outer-sphere points and support an outer-sphere mechanism assignment.

The results of Fig. 1 suggest that in the absence of the chromium(III) product criterion for mechanistic assignment, a correlation (or lack thereof)

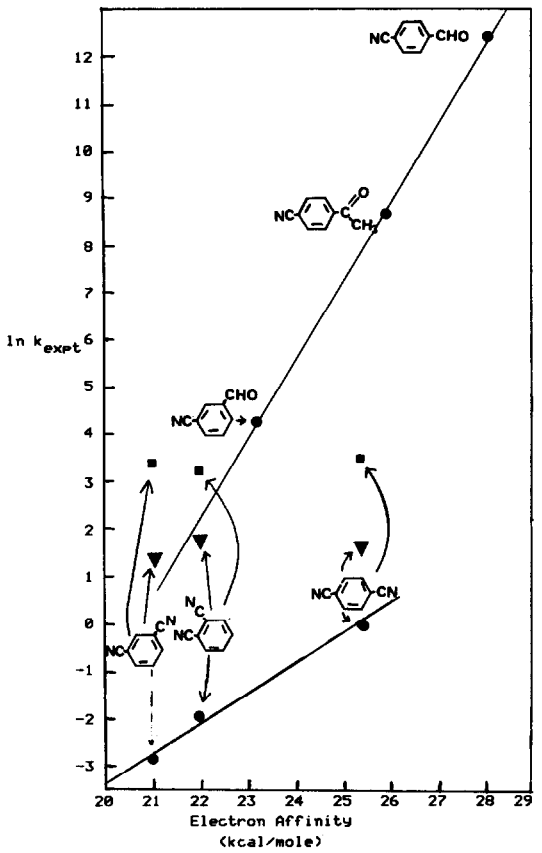

Fig. 1. Plot of $\ln(k_{expt})$ for the reduction of pentaamminecobalt(III) complexes of the organonitrile ligands indicated by various reducing agents: ●, chromium(II) reductions; ■, hexaammineruthenium(II) reductions; ▲, vanadium(II) reductions.

with potential bridging ligand electron affinities can serve to distinguish inner-sphere from outer-sphere electron transfers. The unreliable nature of the rate ratio method for such a mechanistic distinction has been discussed by Gould.[20]

The correlations noted herein do not, however, either provide for, or suggest the existence of, a distinction between the chemical and resonance transfer mechanisms from electron affinity considerations. Taube has noted that bridge reducibility should also be a factor in resonance transfer mechanisms.[11b,c,21] Still, other factors such as the donor characteristics (ionization potentials) of the bridging ligands could also be of importance in resonance transfer reactions, and, thus negate a simple, one parameter fit to the rate constants. Also, the different slopes for the two lines in Fig. 1 were unexpected and remain to be explained. Experiments are underway to clarify these points.

Acknowledgement—Support of this study by The University of Miami Research Council through a General Research Support Award to WLP is gratefully acknowledged.

REFERENCES

1. E. S. Gould and H. Taube, *J. Am. Chem. Soc.* 1964, **86**, 1318.
2. K. D. Whitburn, M. Z. Hoffman, N. V. Brezniak and M. G. Simic, *Inorg. Chem.* 1986, **25**, 3037.
3. M. Z. Hoffman and M. Simic, *J. Am. Chem. Soc.* 1972, **94**, 1757.
4. M. G. Simic, M. Z. Hoffman and N. V. Brezniak, *J. Am. Chem. Soc.* 1977, **99**, 2166.
5. K. D. Whitburn, M. Z. Hoffman, M. G. Simic and N. V. Brezniak, *Inorg. Chem.* 1980, **19**, 3180.
6. E. S. Gould, *J. Am. Chem. Soc.* 1972, **96**, 4360.
7. H. Spiecker and K. Wieghardt, *Inorg. Chem.* 1977, **16**, 1290.
8. T. G. Dunne and J. K. Hurst, *Inorg. Chem.* 1980, **19**, 1152.
9. W. F. Hollaway, V. S. Srinivasan and E. S. Gould, *Inorg. Chem.* 1984, **23**, 2181.
10. E. S. Gould, *Accts Chem. Res.* 1985, **18**, 22 and refs therein.
11. (a) A. Haim, *Prog. Inorg. Chem.* 1983, **30**, 273; (b) H. Taube and E. S. Gould, *Accts Chem. Res.* 1969, **2**, 321; (c) H. Taube, *Angew. Chem. Int. Ed.* 1984, **23**, 329.
12. R. D. Cannon, *Electron Transfer Reactions*, pp. 247–257. Butterworths, London (1980).
13. (a) M. B. Barrett, J. H. Swinehart and H. Taube, *Inorg. Chem.* 1971, **10**, 1983; (b) J. C. Chen and E. S. Gould, *J. Am. Chem. Soc.* 1973, **95**, 5539.
14. A. Haim, *Accts Chem. Res.* 1975, **8**, 264.
15. R. J. Balahura and W. L. Purcell, *Inorg. Chem.* 1975, **14**, 1469.
16. R. J. Balahura and W. L. Purcell, *J. Am. Chem. Soc.* 1976, **98**, 4457.
17. R. J. Balahura, G. B. Wright and R. B. Jordan, *J. Am. Chem. Soc.* 1973, **95**, 1137.
18. L. H-C. Hua, R. J. Balahura, Y-T. Fanchiang and E. S. Gould, *Inorg. Chem.* 1978, **17**, 3692.
19. S. Chowdhury and P. Kebarle, *J. Am. Chem. Soc.* 1986, **108**, 5453.
20. E. S. Gould, *Inorg. Chem.* 1979, **18**, 900.
21. H. Taube, *Electron Transfer Reactions of Complex Ions in Solution*. Academic Press, New York (1970).

Polyhedron Vol. 8, No. 4, pp. 567–568, 1989
Pergamon Press plc. Printed in Great Britain.

ANNOUNCEMENTS

XXVII INTERNATIONAL CONFERENCE ON COORDINATION CHEMISTRY

2–7 JULY 1989

BROADBEACH, QUEENSLAND, AUSTRALIA

Further information and copies of the Registration Brochure can be obtained from the Conference Secretariat: XXVII ICCC, UniQuest Ltd, University of Queensland, St Lucia, QLD 4067, Australia.

The following associated meetings will be held in the week preceding and the week following the ICCC meeting. Please contact the appropriate Convenor for further information and the Registration Circular.

XIV INTERNATIONAL SYMPOSIUM ON MACROCYCLIC CHEMISTRY

25–28 June 1989
Townsville, North Queensland

Convenor: Dr L. F. Lindoy
James Cook University
Department of Chemistry
and Biochemistry
Townsville, QLD 4811.
Telephone: +61 77 814 523
Facsimile: +61 77 796 371.

MARINE BIOINORGANIC CHEMISTRY SYMPOSIUM

28 June–2 July 1989
Heron Island Research Station,
North Queensland

Convenor: Professor C. J. Hawkins
University of Queensland
Department of Chemistry
St Lucia, Brisbane, QLD 4067.
Telephone: +61 7 377 2689
Facsimile: +61 7 870 4813.

BIENNIAL CONFERENCE OF THE CHEMICAL EDUCATION DIVISION OF THE ROYAL AUSTRALIAN CHEMICAL INSTITUTE

26–28 June 1989
Mt Gravatt Campus,
Brisbane College of Advanced Education

Convenor: Dr P. J. Pomery
University of Queensland
Department of Chemistry
St Lucia, Brisbane, QLD 4067.
Telephone: +61 7 377 2689
Facsimile: +61 7 870 4813.

SYMPOSIUM ON APPLIED ORGANOMETALLIC CHEMISTRY: AN ENTRY TO THE NEW TECHNOLOGY

10–12 July 1989
Peppers Guest House, Hunter Valley,
New South Wales

Convenor: Dr A. F. Masters
University of Sydney
School of Chemistry
Sydney, NSW 2006.
Telephone: +61 2 692 3743
Facsimile: +61 2 692 3329.

Continued on following page

SYMPOSIUM ON METAL COMPOUNDS IN THE DETECTION AND TREATMENT OF CANCER

10–12 July 1989
The Cumberland Hotel, Marysville, Victoria

Convenor: Dr I. A. G. Roos
Experimental Chemotherapy Laboratory
The Cancer Institute
Peter MacCallum Hospital
481 Little Lonsdale St
Melbourne, VIC 3000.
Telephone: +61 3 602 1333
Facsimile: +61 3 670 3357.

Polyhedron Vol. 8, No. 5, pp. 569–575, 1989
Printed in Great Britain

0277–5387/89 $3.00+.00
© 1989 Pergamon Press plc

THE NMR STUDY OF INVERSION AT THE METAL CENTRE AND LIGAND EXCHANGE PROCESSES OF Hg^{II} BIS-CHELATES: X-RAY CRYSTAL STRUCTURE OF $[pyr(NC_6H_{11}\text{-}c)S]_2Hg$

A. L. NIVOROZHKIN, E. V. SUKHOLENKO, L. E. NIVOROZHKIN, N. I. BORISENKO and V. I. MINKIN*

Institute of Physical Organic Chemistry, Rostov on Don State University, 344711 Rostov on Don, U.S.S.R.

Yu. K. GRISHIN

Moscow State University, Chemistry Department, 117234 Moscow, U.S.S.R.

and

O. A. DIACHENKO, T. G. TAKHIROV and D. B. TAGIEV

Department of Institute of Chemical Physics of the Academy of Science of the U.S.S.R., 142432 Chernogolovka, U.S.S.R.

(*Received* 16 *June* 1988; *accepted* 25 *August* 1988)

Abstract—Novel bis-chelate Hg^{II} complexes with a series of 1-isopropyl-3-methyl-4-N-aryl(alkyl)aminomethylene-5-thion(seleno)pyrazole derivatives $(pyr(NR)X)_2Hg$ of type (**I**) have been prepared. For the first time intramolecular reactions of tetrahedral inversion at the metal centre and degenerate ligand exchange reactions proceeding on the NMR time-scale have been observed. The activation barrier of the inversion for the complex of type (**I**) with R = C_6H_{11}-cyclo, X = S has been found by use of dynamic ^1H NMR spectroscopy (500 MHz) to be 54.3 kJ mol^{-1}. For a series of complexes (**I**) the activation barriers against intermolecular ligand exchange processes lie in the range of 65–69 kJ mol^{-1}. An X-ray study of (**I**) (R = C_6H_{11}-cyclo, X = S) revealed a pseudo-tetrahedral bond configuration of mercury, while the sulphur atoms demonstrate a tendency toward linear alignment with the angle SHgS′ of 141.0° (1).

Fifteen years ago, Eaton and Holm[1] pioneered an investigation of the stereochemical non-rigidity of the d^0,d^{10}-metal bis-chelate complexes of general type (**I**). Since then, extensive studies of the dynamic behavior of a series of related Zn^{II},[2–6] Cd^{II},[4,7–9] Be^{II},[5,10,11] and B^{III}[12–14] complexes have been undertaken.

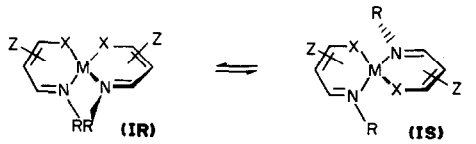

(1)

R = aryl, alkyl; X = O, S, Se;
Z = aryl, alkyl, benzo-, hetero-

The following rearrangement mechanisms are conceivable to lead to overall inversion at a metal centre (**IR**) ⇌ (**IS**):

(1) intramolecular digonal twist rearrangement proceeding without metal–ligand (M–L) bond scission;

(2) intramolecular M–L bond rupture–formation process through a tricoordinate achiral intermediate state;

(3) intermolecular ligand exchange reaction of type (2)

$$ML_2 + M^*L_2^* \rightleftharpoons ML_2^* + M^*L_2. \qquad (2)$$

The preference of one of these mechanisms, i.e. there relative rates depends mostly on the nature of the metal centre. So far Hg^{II} chelates of type (**I**) have not

*Author to whom correspondence should be addressed.

been investigated in detail, though a fairly high frequency for the type (1) process had been assumed for the complexes of type (II) on the grounds of averaging the methyl resonances of their diastereotopic isopropyl groups at low temperature (−80°C).[4] This evidence seems to be supported by the data covering organomercury compounds containing the —CSHgR unit. The rates of phenylmercury migrations are several orders of magnitude larger than those for similar lead and tin derivatives.[15,16]

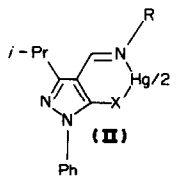

(II)

R = aryl, alkyl; X = S, Se

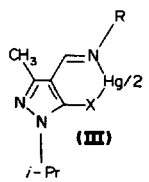

(III)

R = aryl, alkyl; X = S, Se

In the present work the novel Hg^{II} bis-chelate complexes of type (III) have been prepared and their fluctional behaviour studied in more detail thanks to the better solubility of these complexes in such solvents as CD_2Cl_2 and $CDCl_3$ which facilitated the NMR application. The X-ray structural investigation of one of the complexes (III) (R = C_6H_{11}-cyclo, X = S) has been performed.

EXPERIMENTAL

Synthesis

The ligands, 1-isopropyl-3-methyl-4-N-alkyl(aryl) aminomethylene-5-thion(seleno)pyrazoles were synthesized according to the literature.[4] The complexes of type (III) were obtained by 5 min reflux of an ethanol solution of mercury acetate and the corresponding ligand (1 : 2). Colourless crystals or powders were filtered off and purified by further crystallization from a toluene–octane (1 : 1) mixture. The yields of purified substances amount to 70–80%. Melting points and analyses are given in Table 1.

NMR spectroscopy

^1H NMR spectra were recorded using TESLA BS-567A and BRUKER AM-500 spectrometers operating at 100 and 500 MHz, ^{199}Hg spectra using JEOL FX-100 spectrometer at 17.84 MHz. ^1H and ^{199}Hg chemical shifts were measured with respect to HMDS as internal standard and $(CH_3)_2{}^{199}Hg$ as external standard. The temperature was kept within $\pm 1.5°$ accuracy, monitored by means of a thermocouple mounted in the probe and calibrated with methanol and ethylene glycol.

Computer simulated spectra were calculated according to literature methods.[7,17] Values of τ were obtained from visual comparison of computed and experimental spectra. Activation parameters were obtained from the least squares Eyring plots ($\ln(k/T)$ vs $1/T$).

For kinetic studies, commercially available solvents CD_2Cl_2, $CDCl_3$, $C_6D_5CD_3$ exposed for 24 h over 4 Å molecular sieves were used.

X-ray crystallography

Colourless crystals of bis(1-isopropyl-3-methyl-4-cyclohexylaldimino-5-pyrazolethionato) Hg^{II}

Table 1. Characterization of the complexes of type (III)

No.	X	R	M.p. (°C)	Found (calc.) % C	H	N
1	S	*t*-Bu	206	42.7 (42.6)	5.8 (5.9)	12.2 (12.4)
2	S	C_6H_{11}-cyclo	231	46.2 (46.1)	6.0 (6.1)	11.6 (11.5)
3	Se	C_6H_{11}-cyclo	157	40.6 (40.9)	5.4 (5.4)	10.1 (10.1)
4	S	C_6H_5	143	46.8 (46.9)	4.3 (4.5)	11.3 (11.7)
5	S	$C_6H_4CH_3$-*p*	189	48.4 (48.3)	4.9 (4.9)	11.5 (11.3)
6	Se	$C_6H_4CH_3$-*p*	188	43.2 (42.9)	4.1 (4.3)	9.8 (10.0)
7	S	CH_3	142	36.6 (36.4)	4.8 (4.7)	14.5 (14.2)

Table 2. Selected bond distances and valence angles of complex (III) (R = C_6H_{11}-cyclo, X = S)

Bond	D (Å)	Angle	ω (grad)
Hg—S	2.391(2)	SHgS′	141.0(1)
Hg—N(1)	2.397(8)	SHgN(1)	97.4(2)
S—C(1)	1.728(8)	S′HgN(1)	106.6(2)
N(1)—C(3)	1.278(9)	N(1)HgN(1′)	103.2(4)
N(2)—N(3)	1.385(9)	HgSC(1)	103.5(3)
N(2)—C(1)	1.345(9)	HgN(1)C(3)	121.7(6)
N(3)—C(10)	1.310(9)	HgN(1)C(4)	121.5(7)
C(1)—C(2)	1.41(1)	HgN(1)C(15)	114.1(8)
C(2)—C(3)	1.42(1)	SC(1)C(2)	134.3(5)
C(2)—C(10)	1.414(9)	C(1)C(2)C(3)	134.4(7)
		N(1)C(3)C(2)	128.0(9)

forming hexagon-based prisms were obtained by slow evaporation of the toluene–octane solution.

The crystal data: $C_{28}H_{44}HgN_6S_2$, $M_r = 729.4$; $a = 26.083(8)$; $b = 10.741(5)$; $c = 11.155(6)$ Å; $\gamma = 90.96(4)°$; $V = 3125(4)$ Å^3; $Z = 4$; $d_{calc} = 1.56$ g cm^{-3}; space group $B2/b$ (second setting). The unit-cell dimensions were refined on a DRON-1 diffractometer with a monocrystal attachment. Intensity data from 1843 independent non-zero ($I \geqslant 2\sigma(I)$) reflections of the $hk0$–$hk11$ type, crystal dimensions $0.14 \times 0.23 \times 0.14$ mm^3, were collected using a layer line registration method on a DARUM diffractometer, $0.038 \leqslant \sin\theta/\lambda \leqslant 0.600$ Å^{-1}, Cu-K_α radiation with graphite monochromator. The ESDs were introduced by Gauss integration[18] using Udelnov's program.[19] The structure was determined by direct methods and refined by least-squares on 1657 reflections with full-matrix anisotropic approximation using the Cruickshank weighting scheme to $R = 0.056$. Bond distances and valence angles are listed in Table 2. Calculations were carried out on a BESM-6 computer using the RENTGEN-75 program package.[20] The diagram of the molecular structure (Fig. 1) was obtained by use of the ELLIDS program.[21]

No shortened van der Waals contacts, with the exception of the S···C(2) distance of 3.474 Å, were found in the crystal lattice, typical of molecular crystals.

RESULTS AND DISCUSSION

X-ray data

According to the X-ray results, the mercury atom in the HgN_2S_2 moiety possesses the strongly distorted tetrahedral configuration with an angle of 95.6° between the SHgN(1) and S′HgN(1′) planes. The six-membered metallocycle is not planar, but has an envelope conformation with a 6.8° folding along the S—N axis. The mercury atom is displaced from the SC(1)C(2)C(3)N(1) plane by up to 0.188 Å. Mercury valence angles deviate considerably from the typical tetrahedral value of 109.5° and range from 97.4(2)° to 141.0(1)°. The largest SHgS′ angle exhibits a strong tendency of the mercury towards linear coordination of sulphur atoms. Another peculiarity of the molecular structure is the similarity of the Hg—S 2.391(2) Å and Hg—N 2.397(8) Å bond lengths in spite of a considerable difference between the covalent radii of sulphur (1.04 Å) and nitrogen (0.71 Å) atoms. Levelling of Hg—S and Hg—N bond distances along with the unusual valence angles at mercury are characteristic of some other mercury complexes. A comprehensive analysis of the data available[22] reveals that Hg—L bonds do not obey an additivity rule and may broadly vary even within a uniform set of ligands. For strongly electronegative donor centres such as S or Cl in tetracoordinated mercury complexes, an approxi-

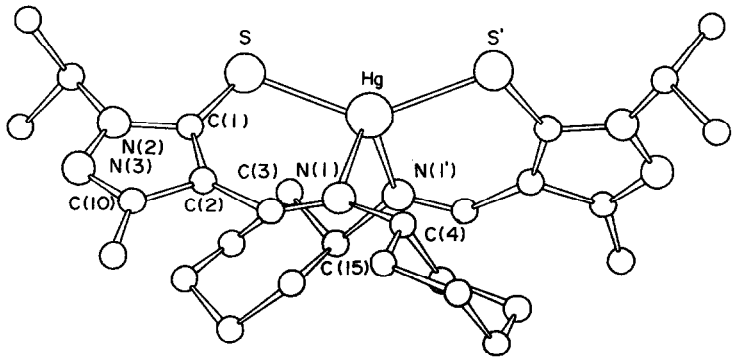

Fig. 1. Molecule of bis(1-isopropyl-3-methyl-4-cyclohexylaldimino-5-pyrazolethionato) Hg^{II}. C_6H_{11}-cyclo substituents are shown occupying one of two alternative positions.

mately linear alignment of one pair of bonds has been found accompanied by shortening of the corresponding bond lengths achieving 2.36–2.49 Å for Hg—S bonds and lengthening bond distances for another pair of bonds.[23]

In general, bond distances and valence angles at the metal centre for (III) were found to be close to those in similar mercury complexes: Hg—S 2.324; 2.327; Hg—N 2.48; 2.47 Å; SHgS′ 164°; NHgN′ 91° in bis(8-mercaptoquinolino) Hg^{II},[24] Hg—S 2.43; 2.46 Å; Hg—N 2.38; 2.32 Å; SHgS′ 122°; NHgN′ 78° in $Hg(Me_2en)SCN_2$.[25]

The electronic structure of the coordinated ligand in (III) may be approximately described in terms of the resonance hybrid (3) of iminothiolate (IV) and

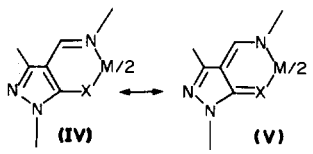

aminothionate (V) forms. As seen from the data of Table 3 for M = Zn, Cd, Ni, the first one is dominant while the last one makes the major contribution in the case of the free ligand (M/2 = H). Because of the softness of mercury in complexes (III), which favours the stronger Hg—S coordination as compared to the Hg—N one, an increasing contribution of the thiolate form should be expected. This might be viewed as shortening formally double and lengthening formally single bonds in (IV) (M = Hg) relative to (V) (M/2 = H). Nevertheless, the mercury atom in (III) causes no drastic changes in the electronic structure of the coordinated ligand, only slightly affecting the corresponding bond lengths.

NMR investigation

Even at temperatures as low as −80°C in CD_2Cl_2 solution all the complexes (III) show in their ^1H NMR spectra (100 MHz) an averaged doublet signal of diastereotopic methyls of isopropyl groups. In general, this may be accounted for by two reasons. The first one is the fast exchange process (IR) ⇌ (IS) averaging methyl resonances, while the second one, frequently ignored,[29,30] concerns rather low differences (occasional equivalence) in methyl resonance shifts $\Delta\nu$. In the latter case the use of a spectrometer operating at the higher frequency may be diagnostic. Indeed, when applying 500 MHz facilities, we succeeded in detecting the separated spectra as two spin doublets at −80°C. The value of $\Delta\nu$ is only 5 Hz (0.01 ppm) which corresponds to only 1 Hz for the 100 MHz spectrometer and this explains our previous unsuccessful attempts to freeze the inversion of Hg^{II} chelates.[4] Experimental and calculated spectra are shown in Fig. 2. The values of kinetic and activation parameters are given in Table 4.

Since the rate of inversion is not affected by varying the concentration of solution (0.03–0.006 M) and by the type of solvent, the rearrangement might be considered to occur via an intramolecular pathway. The most plausible mechanism of the process appears to be digonal twisting with inclusion of a planar transition or intermediate structure. The rate of inversion for the Hg^{II} complex is the biggest in comparison with those of analogous Zn^{II} and Cd^{II} complexes.[4] The following order of R ⇌ S interconversion rates is observed: Hg > Cd > Zn. The values of dihedral angles O formed by two SMN planes in a series of isoligand complexes (III) Zn^{II}, Ni^{II}, Cd^{II}, Hg^{II} (Table 3) might be considered as an

Table 3. Bond distances of the complexes of type (III) (R = C_6H_{11}-cyclo, X = S), Å

No.	M	C(1)—S	C(1)—C(2)	C(2)—C(3)	C(3)—N(1)	θ^a	Orbital electronegativity of M^{2+} ions[28]	Reference
1	H	1.696(2)	1.425(2)	1.396(2)	1.306(3)			26
2	Zn	1.735(3)	1.400(5)	1.420(5)	1.290(4)	80.2	−1.02	27
3	Cd	1.734(4)	1.398(6)	1.434(7)	1.280(7)	90.6	−2.04	27
		(1.738(5))	(1.421(6))	(1.411(6))	(1.279(6))[b]			
4	Ni	1.715(5)	1.388(7)	1.439(7)	1.277(7)	85.4	0.29	27
		(1.728(5))	(1.409(6))	(1.395(6))	(1.295(6))[b]			
5	Hg	1.728(8)	1.41(1)	1.42(1)	1.278(9)	95.6	−4.64	Present paper

[a] The angle between N(1)MS and N(1′)MS′ planes, grad.

[b] The values in parentheses concern the second chelate ring within the same molecule.

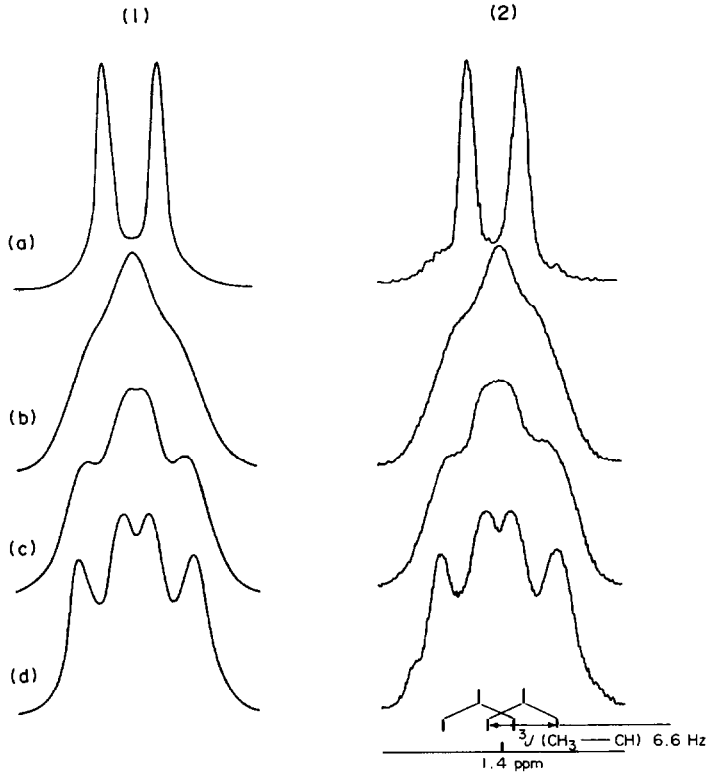

Fig. 2. Calculated (1) and experimental (2) 500 MHz ^{1}H NMR spectra of $(CH_3)_2CH$ group methyl protons of (III) (R = C_6H_{11}-cyclo, X = S) (solvent CD_2Cl_2): (a) $T = -40°C$, $k = 50\ s^{-1}$; (b) $-60°C$, $20\ s^{-1}$; (c) $-70°C$, $10\ s^{-1}$; (d) $-80°C$, $4\ s^{-1}$.

indication of a degree of the static digonal twist distortion from the pseudo-tetrahedral ($\theta = 90°$) configuration at the metal centre. However, no correlation exists between these distortions and the energy barriers (kJ mol^{-1}) against tetrahedral interconversion: Ni (40–75); Hg (54.3) < Cd (50–65) < Zn (80–95).[4,31] Interestingly, the Hg^{II} complex is the only one in this series showing the S···S *trans*-distortion.

An intramolecular bond rupture–bond closure mechanism can be invoked to explain the observed enantiomerization of Hg^{II} chelate complexes (III). This mechanism was found to operate in the case of analogous B^{III}[12–14] and Be^{II}[5] complexes with the similar chelate rings. If it occurs, it may be in principle identified by a temperature dependence of the ^{199}Hg–^{15}N spin-coupling constant as it was in the case of the isoligand $^{111}Cd^{II}$ complex.[8]

Table 4. Activation and kinetic parameters of ligand exchange process for the complexes of type (III) (X = S)[a,b]

No.	R	^3J(CH=N—^{199}Hg) (Hz)	k (s^{-1})	$\Delta H^{\ddagger}$ (kJ mol^{-1})	$\Delta S^{\ddagger}$ (J mol^{-1} K^{-1})	$\Delta G^{\ddagger}_{298}$ (kJ mol^{-1})
1	C_6H_{11}-cyclo	33	5.75	30.4±0.8	−128.3±2.3	68.7±0.1
			1.88×10^3	25.8±1.0	−95.5±5.0	54.3±0.5[c]
2	*t*-Bu	45	17.7	14.3±1.2	−173.0±4.3	65.9±0.1
3	C_6H_5	12	22.8	21.4±0.8	−147.2±2.9	65.2±0.1
4	$C_6H_4CH_3$-*p*	13	13.5	26.1±2.2	−135.5±7.9	66.5±0.2

[a] Obtained using 0.03 M concentration.
[b] Solvent toluene-d_8 (Nos 1, 2), $CDCl_3$ (Nos 3, 4).
[c] Inversion parameters.

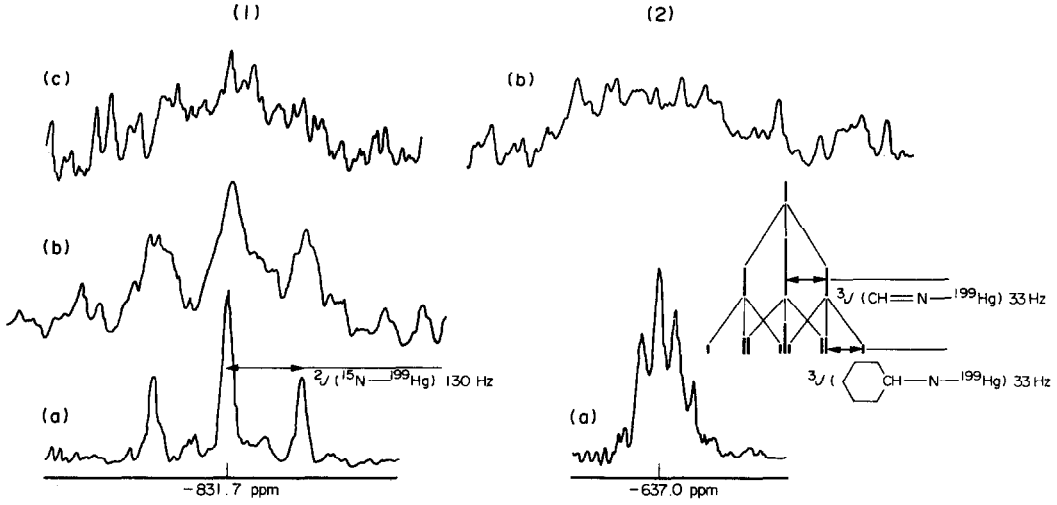

Fig. 3. ^{199}Hg NMR spectra. (1) ^{199}Hg—^{1}H spectra of (II) (R = CH_2Ph, X = Se) enriched (93%) with ^{15}N isotopes (solvent $CDCl_3$–CD_2Cl_2 (4 : 1), c = 0.03 mol dm^{-3}): (a) −61; (b) −50; (c) −36°C. (2) ^{199}Hg spectra of (III) (R = C_6H_{11}-cyclo, X = S) (solvent $C_6D_5CD_3$, c = 0.03 mol dm^{-3}): (a) 30; (b) 100°C.

The spin-coupling constant ^1J (^{199}Hg—^{15}N) in complex (II) (R = $C_6H_5CH_2$, X = Se) (for synthesis see literature[4]) was found to be equal to 130 Hz. The ^{199}Hg—{^{1}H} NMR temperature-dependent spectra are shown in Fig. 3. At elevated temperatures the triplet signal broadened and coalesced, which indicates a dissociative process due to the Hg—N bond rupture stage. Unfortunately, at the middle-exchange conditions the spectra of appropriate quality for full line shape analysis could not be recorded even though *ca* 80 000 transients were provided. The same problem occured in the case of the ^{199}Hg NMR study of (III) (R = C_6H_{11}-cyclo, X = S). At 30°C under slow-

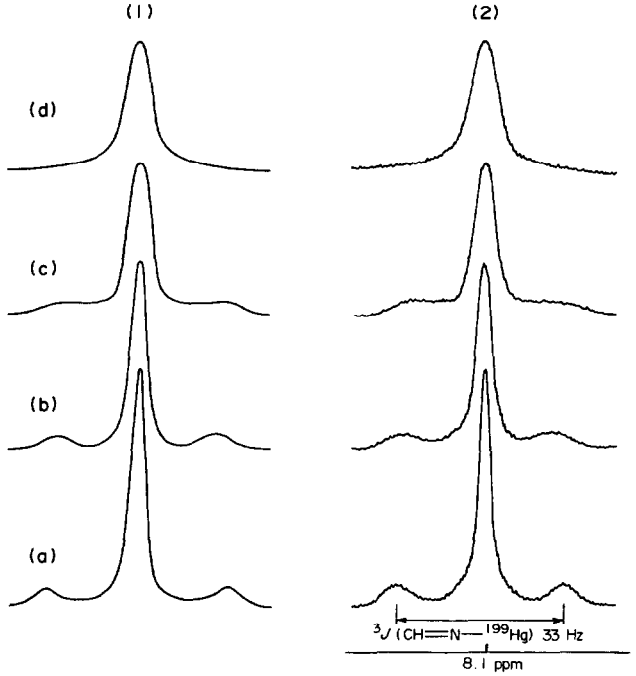

Fig. 4. Calculated (1) and experimental (2) 100 MHz ^{1}H NMR spectra of CH=N group protons of (III) (R = C_6H_{11}-cyclo, X = S): (a) T = 40°C, k = 11 s^{-1}; (b) 60°C, 22 s^{-1}; (c) 80°C, 44 s^{-1}; (d) 90°C, 65 s^{-1}.

exchange conditions, the multiplicity of the spectrum is due to the accidentally coincident couplings ^3J (CH=N—^{199}Hg) and ^3J (C_5H_{10}CH—N—^{199}Hg) of 33 Hz.

Sufficient spectral pattern was accomplished by studying the ^{1}H NMR temperature dependence of the ^{199}Hg—^{1}H coupling of the protons of the CH=N group at natural (16.9%) ^{199}Hg abundance. The typical spectra for the complex (**III**) (R = C_6H_{11}-cyclo, X = S) are given in Fig. 4. When the temperature of solution was above 30°C both the satellite signals and the central signal related to CH=N protons in isotopomers which do not contain ^{199}Hg nuclei broaden and coalesce.

The kinetic and activation parameters (Table 4) were obtained from a comparison of the experimental spectra at various temperatures with theoretically simulated ones on the grounds of the proportion of the exchange rates to the concentrations of isotopomeric molecules. The process observed may be attributed to intermolecular degenerate ligand exchange reactions of type (2) previously reported for Cd^{II}[8] and Pb^{II}[32] complexes.

As seen from Table 4, the rate of inversion at the mercury centre, found from the averaging of diastereotopic group signals, is *ca* three orders of magnitude larger than that for ligand exchange. This appears to be a general trend for the type (**I**) metal chelates. There is no significant influence of the substituents R at the nitrogen atom on the rates of ligand exchange reactions. In selenium containing complexes (**III**) (X = Se) the slow-exchange spectral pattern was not obtained as indicated by a singlet CH=N signal when the temperature of solution was as low as −80°C. This evidences faster ligand exchange reactions in these complexes as compared to that of their sulphur analogues (X = S).

REFERENCES

1. S. S. Eaton and R. H. Holm, *J. Am. Chem. Soc.* 1971, **10**, 1446.
2. V. I. Minkin, L. E. Nivorozhkin, L. E. Konstantinovsky and M. S. Korobov, *Koord. Khim.* 1977, **3**, 174.
3. L. E. Nivirozhkin, M. S. Korobov, R. Ya. Olekhnovich, L. E. Konstantinovsky and V. I. Minkin, *Koord. Khim.* 1982, **8**, 1080.
4. L. E. Nivorozhkin, M. S. Korobov, A. L. Nivorozhkin, L. E. Konstantinovsky and V. I. Minkin, *Zh. Obsch. Khim.* 1985, **55**, 1125.
5. L. E. Nivorozhkin, M. S. Korobov, N. I. Borisenko, G. S. Borodkin, Yu. E. Chernysh and V. I. Minkin, *Zh. Obsch. Khim.* 1985, **55**, 2149.
6. F. A. Bottino and P. Finocchiaro, *Polyhedron* 1985, **4**, 1507.
7. L. E. Nivorozhkin, V. I. Minkin, N. I. Borisenko, L. E. Konstantinovsky, M. S. Korobov and R. Ya. Olekhnovich, *Dokl. Akad. Nauk SSSR* 1981, **260**, 1176.
8. L. E. Nivorozhkin, G. A. Kalabin, A. L. Nivorozhkin, R. B. Valeev and V. I. Minkin, *Koord. Khim.* 1986, **12**, 608.
9. L. E. Nivorozhkin, R. Ya. Olekhnovich, M. S. Korobov, L. E. Konstantinovsky and V. I. Minkin, *Koord. Khim.* 1986, **12**, 899.
10. F. A. Bottino, A. Recca and P. Finocchiaro, *J. Organomet. Chem.* 1978, **160**, 373.
11. L. E. Nivorozhkin, L. E. Konstantinovsky, M. S. Korobov and V. I. Minkin, *Koord. Khim.* 1979, **5**, 508.
12. M. S. Korobov, L. E. Nivorozhkin, L. E. Konstantinovsky and V. I. Minkin, *J. Chem. Soc., Chem. Commun.* 1982, 169.
13. A. J. Boulton and C. S. Prado, *J. Chem. Soc., Chem. Commun.* 1981, 1008.
14. P. V. R. Schleyer and E. U. Wurthwein, *J. Chem. Soc., Chem. Commun.* 1982, 542.
15. D. N. Kravtsov, A. S. Peregudov, E. M. Rokhlina and L. A. Fedorov, *J. Organomet. Chem.* 1974, **77**, 199.
16. R. D. Bach and A. T. Weibel, *J. Am. Chem. Soc.* 1975, **97**, 2575.
17. N. I. Borisenko, L. P. Olekhnovich and V. I. Minkin, *Teor. Eksper. Khim.* 1976, **12**, 813.
18. W. R. Busing and H. A. Levy, *Acta Cryst.* 1961, **10**, 180.
19. A. I. Udelnov and Yu. T. Struchkov, *Kristallografia* 1976, **21**, 484.
20. V. I. Andrianov and Z. Sh. Safina, RENTGEN-75, Program package for the crystal structures interpretation, Chernogolovka (1975).
21. A. N. Chekhlov, *Kristallografia* 1981, **26**, 596.
22. D. Grdenic, *Q. Rev.* 1965, **19**, 303.
23. S. L. Lawton, *Inorg. Chem.* 1971, **10**, 328.
24. A. D. Ozola, Ya. K. Ozol and A. F. Ievinsh, *Izv. Akad. Nauk Latv. SSR Ser. Khim.* 1973, 8.
25. M. Cannas, A. Cristini and G. Marongiu, *Cryst. Struct. Commun.* 1978, **7**, 37.
26. A. L. Nivorozhkin, T. G. Takhirov, E. V. Sukholenko, N. I. Borisenko, V. I. Minkin and O. A. Diachenko, *Izv. Akad. Nauk SSSR Ser. Khim.* 1988, in press.
27. T. G. Takhirov, O. A. Diachenko, D. B. Tagiev, A. L. Nivorozhkin, L. E. Nivorozhkin and V. I. Minkin, *Koord. Khim.* 1988, **14**, 237.
28. G. Klopman (Ed.), *Chemical Reactivity and Reactions Paths.* Ch. 4, Wiley-Interscience, New York (1973).
29. F. A. Bottino, E. Libertini, O. Puglisi, A. Recca and G. Ronsisvalle, *J. Inorg. Nucl. Chem.* 1980, **42**, 1.
30. F. A. Bottino, A. Recca and P. Finocchiaro, *J. Inorg. Nucl. Chem.* 1980, **42**, 429.
31. L. E. Nivorozhkin, A. L. Nivorozhkin, M. S. Korobov, L. E. Konstantinovsky and V. I. Minkin, *Polyhedron* 1985, **4**, 1701.
32. L. E. Nivorozhkin, Yu. E. Chernysh, A. L. Nivorozhkin, G. S. Borodkin, N. I. Borisenko and V. I. Minkin, *Dokl. Akad. Nauk SSSR* 1987, **296**, 358.

Polyhedron Vol. 8, No. 5, pp. 577–580, 1989
Printed in Great Britain

0277-5387/89 $3.00+.00
© 1989 Pergamon Press plc

KINETICS OF THE REDUCTION OF $Ru_2(CH_3COO)_4^+$ AND OF $Ru(NH_3)_5PYRIDINE^{3+}$ BY N-(2-HYDROXYETHYL)-ETHYLENEDIAMINETRIACETATOAQUOTITANIUM(III)

MIN ZHU*

Department of Chemical Engineering, Zhengzhou Institute of Technology, Honan, People's Republic of China

and

A. OLAYINKA OYETUNJII

Department of Chemistry, Obafemi Awolowo University, Ile-Ife, Nigeria

and

KEJIAN LU and JOSEPH E. EARLEY*

Department of Chemistry, Georgetown University, Washington, DC 20047, U.S.A.

(*Received* 15 *July* 1988; *accepted after revision* 5 *September* 1988)

Abstract—The kinetics of the reaction of $Ti(HEDTA)(H_2O)$ with $Ru_2(CH_3COO)_4^+$ and with $Ru(NH_3)_5py^{3+}$ (py = pyridine) have been studied in LiCl media of 1.0 M ionic strength. Both reactions follow second-order kinetics with the rate constant dependent on acidity according to the rate law: $k_2 = kK/([H^+]+K)$, where K is close to 0.1 M [the acid-dissociation constant of $Ti(HEDTA)(H_2O)$], and k is 1.6×10^4 M^{-1} s^{-1} for $Ru_2(CH_3COO)_4^+$ at 25°C and k is 2.0×10^5 M^{-1} s^{-1} for $Ru(NH_3)_5py^{3+}$ at 4.5°C. The rate constant for reaction of $Ti(HEDTA)(OH)^-$ and $Ru_2(CH_3COO)_4^+$ is about one order of magnitude higher than the rate constant for reduction of $Ru_2(CH_3COO)_4^+$ by $Ti(OH)^{2+}$, as would be expected on the basis of the shift in Ti^{III} redox potential that is caused by ligation of HEDTA and the known influence of change in driving force on rates of outer-sphere Ru^{III}–Ti^{III} redox reactions. The rate of reduction of $Ru(NH_3)_5py^{3+}$ by $Ti(HEDTA)(OH)^-$ at 4.5°C is more than two orders of magnitude higher than the reduction rate of the same oxidant by $Ti(OH)^{2+}$ at 25°C. This non-bridging ligand effect is at least 100 times larger than can be understood on the basis of change of redox potential, and is best ascribed to a large increase in the stability constant of the precursor complex.

Ru^{III}–Ti^{III} redox reactions involve a variety of mechanisms.[1] If the Ru^{III} oxidant contains only ligands that are not good bridging groups, then outer-sphere ET occurs, with $Ti(OH)^{2+}$ acting as a reductant; if an electron-delocalized ligand is present in the coordination sphere of the oxidant, then outer-sphere ET also involves Ti^{3+} as reductant. For instance, in reactions[2] of Ti^{III} and $Ru_2(CH_3COO)_4^+$, both Ti^{3+} and its conjugate base are effective reductants, but in the case of reaction[3] of $Ru(NH_3)_5py^{3+}$ with Ti^{III}, only $Ti(OH)^{2+}$ (and not Ti^{3+}) is effective as reductant. There is a clear difference in rate law for the two reactions (two terms in the first case as against one in the second). In both cases, all observed rate constants lie along the linear free energy relationship (log second-order rate constant vs reaction driving force) that applies to outer-sphere Ru^{III}–Ti^{III} redox reactions.

If the Ru^{III} oxidant contains an effective lead-in group an inner-sphere mechanism dominates. The

*Authors to whom correspondence should be addressed.

Table 1. Kinetic data[a] for reduction of ruthenium complexes by N-(2-hydroxyethyl)-ethylenediaminetriacetatoaquotitanium(III)

$[H^+]$ (mM)	$[Ti^{III}]$ (mM)	$k_{obs} \times s^{-1}$	$k_2 \times M^{-1} s^{-1}$	$k_{2calc} \times M^{-1} s^{-1}$
(*A*) $Ru_2(CH_3COO)_4^+$ (0.63 *mM*), 25.0°*C*				
100.0	6.10	54.0	8.85	8.35
80.0	7.50	70.0	9.33	9.28
40.0	7.50	90.9	12.12	11.93
45.0	7.50	86.8	11.57	11.52
50.0	7.50	84.2	11.23	11.13
26.0	7.50	97.3	12.97	13.25
60.0	7.50	80.2	10.69	10.44
30.0	7.50	92.5	12.33	12.85
50.0	7.50	77.0	10.27	11.13
70.0	7.50	75.8	10.11	9.82
35.0	7.50	94.0	12.53	12.37
26.0	7.50	100.9	13.45	13.25
80.0	7.50	72.0	9.60	9.28
100.0	12.50	96.0	7.68	8.35
100.0	14.90	115.0	7.72	8.35
100.0	14.90	116.0	7.79	8.35
100.0	9.20	88.0	9.57	8.35
100.0	9.20	74.8	8.13	8.35
100.0	7.50	65.0	8.67	8.35
100.0	7.50	64.8	8.64	8.35
100.0	6.10	51.0	8.36	8.35
100.0	7.50	64.5	8.60	8.35
100.0	6.10	43.5	7.13	8.35
100.0	9.20	80.0	8.70	8.35
100.0	12.50	108.0	8.64	8.35
100.0	7.50	57.7	7.69	8.35
100.0	7.50	57.6	7.68	8.35
(*B*) $Ru(NH_3)_5pyridine^{3+}$ (0.4 *mM*), 4.5°*C*				
60.3	10.10	76.0	7.52	7.37
18.5	8.10	67.6	8.35	10.35
80.3	8.10	25.2	3.11	6.48
60.3	8.10	52.0	6.42	7.37
6.4	8.10	110.0	13.58	11.72
11.6	8.10	86.6	10.69	11.09
8.4	8.10	109.7	13.54	11.47
60.3	9.10	65.0	7.14	7.37
60.3	7.10	40.0	5.63	7.37
60.3	13.91	117.0	8.41	7.37
60.3	9.10	65.0	7.14	7.37
60.3	10.10	76.0	7.52	7.37
60.3	8.10	52.0	6.42	7.37
60.3	7.10	43.0	6.06	7.37
60.3	13.91	117.0	8.41	7.37
60.3	7.10	41.0	5.77	7.37
15.9	8.10	84.0	10.37	10.61
25.4	8.10	72.0	8.89	9.70
60.3	8.10	55.0	6.79	7.37
6.4	8.10	112.0	13.83	11.72
60.3	13.91	112.0	8.05	7.37
60.3	10.10	83.0	8.22	7.37
60.3	9.10	69.7	7.66	7.37
60.3	8.10	61.0	7.53	7.37
26.0	8.10	85.0	10.49	9.65
16.0	8.10	100.0	12.35	10.60

Table 1 (*continued*)

$[H^+]$ (mM)	$[Ti^{III}]$ (mM)	$k_{obs} \times s^{-1}$	$k_2 \times M^{-1} s^{-1}$	$k_{2calc} \times M^{-1} s^{-1}$
6.4	8.10	110.0	13.58	11.72
40.3	8.10	70.0	8.64	8.55
7.6	8.10	130.0	16.05	11.57
60.3	10.10	87.0	8.61	7.37
80.3	8.10	35.0	4.32	6.48
20.3	8.10	95.0	11.73	10.17
60.3	13.91	117.0	8.41	7.37
60.3	8.10	54.0	6.67	7.37
60.3	11.50	93.0	8.09	7.37
60.3	7.10	35.0	4.93	7.37
40.3	8.10	72.0	8.89	8.55
60.3	8.10	54.0	6.67	7.37
10.8	8.10	108.0	13.33	11.18
60.3	16.23	135.0	8.32	7.37
60.3	10.10	82.0	8.12	7.37
60.3	9.10	65.0	7.14	7.37
15.3	8.10	67.0	8.27	10.68
11.3	8.10	86.7	10.70	11.12
60.3	8.10	57.0	7.04	7.37
60.3	13.91	110.0	7.91	7.37

[a] 1.0 M LiCl.

presence of HEDTA as a non-bridging ligand on Ti^{III}, increases rates of inner-sphere Ru^{III}–Ti^{III} reactions, by increasing lability of Ti^{III}[4] and also by altering the stability of the precursor complex.[5] We now report kinetic studies of the influence of HEDTA as a non-bridging ligand on the rates of reductions by Ti^{III} of both the mixed valence ($Ru^{II,III}$) compound $Ru_2(CH_3COO)_4^+$ and $Ru(NH_3)_5py^{3+}$.

EXPERIMENTAL

Tetrakis(μ - acetato)diruthenium(III)chloride (hereafter, the cation of this salt will be designated $Ru_2(CH_3COO)_4^+$) was synthesized as described.[6] Elemental analysis and the extinction coefficient at 425 nM in H_2O ($\varepsilon = 695\ M^{-1}\ cm^{-1}$) agree with literature values. Pyridinepentaammineruthenium(III) perchlorate (hereafter, the cation of this salt will be designated $Ru(NH_3)_5py^{3+}$) was prepared as described by Gaunder and Taube.[7] The wavelengths of maximum absorbance (nm)/extinction coefficient ($M^{-1}\ cm^{-1}$) are $248/4.67 \times 10^3$, $256/4.71 \times 10^3$, $262/4.63 \times 10^3$, in good agreement with literature values.[8]

Titanium(III) solutions were prepared under nitrogen as described.[1] N-(2-hydroxyethyl)-ethylenediaminetriacetatoaquotitanium(III) (hereafter, Ti(HEDTA)H_2O) was prepared at least 5 min before a kinetic experiment, by mixing Ti^{3+} solution with a solution of N-(2-hydroxyethyl)-ethylenediaminetriacetic acid (hereafter, HEDTA), in 10% excess. Rates were unchanged by the presence of a 10-fold excess of HEDTA.

When Ti(HEDTA)(H_2O) was added to a solution of $Ru_2(CH_3COO)_4^+$, the colour changed from deep brown to yellow, corresponding to the decrease of an absorption peak at 425 nm. The colour of $Ru(NH_3)_5py^{3+}$ solution changed from light green to deep yellow after mixing with Ti(HEDTA)(H_2O) solutions. For both reactions, spectrophotometric titration showed that 1 mol of Ru^{III} was consumed for each mole of Ti^{III} added.

Reactions were studied in LiCl media at 1.0 M ionic strength. Kinetic experiments were carried out with Ti^{III} in at least 10-fold excess. Rates of reaction were measured using a computer-linked Durrum stopped-flow spectrophotometer. Decrease in absorbance at 425 nm, the wavelength of maximum absorbance, was monitored when Ti(HEDTA)(H_2O) was added to $Ru_2(CH_3COO)_4^+$ at $25.0 \pm 1.0°$. Reduction of $Ru(NH_3)_5py^{3+}$ by Ti(HEDTA)(H_2O) was followed by monitoring absorbance-increase at 408 nm, a wavelength close to the absorbance maximum. Since the latter reaction was too fast to follow at room temperature, the reaction cell was maintained at $4.5 \pm 2°C$. For both systems, pseudo-first-order rate plots were linear for at least three half-times. Values of the pseudo-first-order rate constant, k_{obs}, (obtained by

a linear least-squares procedure) were generally reproducible within 5% (Table 1).

Kinetic experiments in the absence of added HEDTA gave results that agreed with previously reported results[2,3] within experimental error. The presence of HEDTA increases the rate of the redox reaction for both oxidants, but the effect is much smaller for $Ru_2(CH_3COO)_4^+$ than for $Ru(NH_3)_5py^{3+}$. At constant acidity, rate constants (k_{obs}) for reduction by Ti(HEDTA)(H_2O) of both $Ru_2(CH_3COO)_4^+$ and $Ru(NH_3)_5py^{3+}$ increase linearly with Ti(HEDTA)(H_2O) concentration. Values of the second-order rate constant k_2 (k_{obs}/[Ti(HEDTA)(H_2O)]) decrease with increasing acidity. In the case of the reduction of $Ru_2(CH_3COO)_4^+$ the data are consistent with the rate law:

$$k_2 = kK/([H^+]+K).$$

For the $Ru_2(CH_3COO)_4^+$ reaction, plots of k_2 $[H^+]$ vs $[H^+]$ yielded values of second-order rate constant $k = 1.6 \times 10^4$ M^{-1} s^{-1} and $K = 0.10$ M. The value of K is the same as has been reported[4] for the acid-dissociation constant of Ti(HEDTA)(H_2O). Absence of a high-acid intercept indicates that the primary reductant is the conjugate base, Ti(HEDTA)$(OH)^-$, and suggests that the rate constant for reaction of Ti(HEDTA)(H_2O) with $Ru_2(CH_3COO)_4^+$ is not much greater than that of Ti^{3+}. The difference of rate constant between $Ti(OH)^{2+}$ and Ti(HEDTA)$(OH)^-$ is just what would be expected in view of the shift in redox potential[4] caused by the non-bridging ligand and the known dependence[1,3] of rate constant for Ru^{III}–Ti^{III} outer-sphere electron transfer reactions on reaction driving force.

In the case of the reaction of $Ru(NH_3)_5py^{3+}$, the data also can be fitted in the same way, yielding values of $k = 2.0 \times 10^5$ M^{-1} s^{-1} and $K = 0.08$ M, but the fit is less good, and it is not as clear that there is a high-acid intercept. In this case, the difference of rate constant (either k_2 or k) between $Ti(OH)^{2+}$ (measured at 25°C) and Ti(HEDTA)$(OH)^-$ (at 4.5°C) is much greater than for the other system, and it is also substantially larger than can be accounted for on the basis of shift in redox potential. It is possible that the coordinated pyridine plays a different role in the reaction that involves the organic ligand, than it does in the reaction of the simple aquo ion. A more likely rationalization of the unusually large non-bridging ligand effect is that formation constant for the precursor complex formed in the system involving the more highly-charged oxidant is more sensitive to the decreased charge of the reductant than is the system involving the oxidant with lower charge.

The presence of HEDTA on the reductant eliminates the gross rate-law difference that obtains when these two oxidants are reduced by Ti^{III} in the absence of that ligand. This in turn shows that HEDTA has a larger effect on the rate of outer-sphere electron transfer that is mediated by OH^- than on the rate of electron transfer between $Ru_2(CH_3COO)_4^+$ and $Ti(H_2O)_6^{3+}$ which is mediated[2] by the carboxylate–diruthenium molecular orbitals. Non-bridging ligand effects can give information on subtle differences in effectiveness of interactions of electron-donor and electron-acceptor orbitals.

Acknowledgement—We are grateful for travel grants from the Zhenghzou Institute of Technology and Obafemi Awolowo University.

REFERENCES

1. P. Barone and J. E. Earley, *Inorg. Chem.* 1988, **27**, 1378.
2. J. E. Earley, R. N. Bose and B. H. Berrie, *Inorg. Chem.* 1983, **22**, 1836.
3. K. M. Davies and J. E. Earley, *Inorg. Chem.* 1978, **17**, 3350.
4. R. A. Lee and J. E. Earley, *Inorg. Chem.* 1981, **20**, 1739.
5. Y. Sasaki, M. Everhart and J. E. Earley, *Polyhedron* 1985, **2**, 317.
6. R. W. Mitchell, A. Spencer and G. Wilkinson, *J. Chem. Soc., Dalton Trans.* 1973, 846.
7. E. G. Gaunder and H. Taube, *Inorg. Chem.* 1970, **9**, 2627.
8. C. Creutz and H. Taube, *J. Am. Chem. Soc.* 1973, **95**, 1087.
9. A. A. Adegite, J. E. Earley and J. F. Ojo, *Inorg. Chem.* 1979, **18**, 1537.

Polyhedron Vol. 8, No. 5, pp. 581–584, 1989
Printed in Great Britain

0277–5387/89 $3.00+.00
© 1989 Pergamon Press plc

SYNTHESIS AND REACTIONS OF DIARYL ANTIMONY(III) AMIDES

PREM RAJ,* ASHVIN K. AGGARWAL and NEELIMA MISRA

Department of Chemistry, University of Lucknow, Lucknow-226 007, India

(*Received* 23 *June* 1988; *accepted* 6 *September* 1988)

Abstract—Some new three coordinated diaryl antimony(III) amides of the type Ar_2SbL (Ar = phenyl, pentafluorophenyl and L = $—NR_2$ = —$\overline{NCOCH_2CH_2CO}$, —$\overline{NCOC_6H_4CO}$, —$\overline{NCOCOC_6H_4}$, —$\overline{NNNC_6H_4}$, —$\overline{NC(CH_3)NCH\cdot CH}$, $\overline{NC(S)SC_6H_4}$, —$\overline{NC(CH_2Cl)NC_6H_4}$, —$\overline{NC_6H_4C_6H_4}$) have been isolated and characterized by elemental analysis, solid state IR spectra, conductivity and molecular weight measurements. The amides are unaffected by water, methanol and CS_2. However, PhNCO was found to add across the Sb—N bond and Br_2 and CH_3COOH cleave the Sb—N bond in preference to the Sb—Ar bond(s).

In sharp contrast to the well documented phenylantimony(III) compounds, Ph_nSbX_{3-n} (n = 1 or 2, X = halide,[1] alkoxides,[2] carboxylate,[3] thiol,[4] dithiophosphate,[5] xanthate,[6] etc.), those containing Sb(III)—N bonds are largely limited to aminostibines, $Ph_nSb(NEt_2)_{3-n}$ (n = 1 or 2) both prepared by the reaction of lithium diethylamide with halo or dihalo stibine at low temperatures (−80°C).[7] On the other hand organoantimony(V) nitrogen derivatives have been studied extensively in recent years.[8–10]

As a part of our research programme on organoantimony(V)[9–11] and antimony(III)[12] compounds, we have now isolated a series of diarylantimony(III) amides and studied some of their reactions.

EXPERIMENTAL

The diarylantimony(III) chlorides R_2SbCl (R=C_6H_5;[1] C_6F_5[12]) wer prepared by the redistribution reaction of R_3Sb and $SbCl_3$. The organic amides, imides and heterocyclic moieties were prepared by standard techniques and were purified by crystallization.

Molecular weights were determined cryoscopically in benzene. Conductivity data were obtained in acetonitrile with the aid of a Philips "magic eye" type PR conductivity bridge using a dip type conductivity cell. The IR spectra were recorded on a Perkin–Elmer 577 spectrophotometer in the range of 4000–200 cm^{-1} using KBr discs. ^1H NMR spectra of the compounds in $CDCl_3$ solution were determined on a Varian EM 360 L spectrophotometer using TMS as an internal standard. Special precautions were taken to exclude moisture.

Two typical examples of antimony amides preparation are described below in detail and the conditions for the other reactions are summarized in Table 1.

Reaction of Ph_2SbCl *with succinimide*

In an oxygen-free atmosphere, a solution of diphenylantimony(III) chloride (0.3112 g, 1 mmol) in benzene (30 cm^3) and succinimide (0.099 g, 1 mmol) in the same solvent (30 cm^3) were stirred together in the presence of triethylamine at room temperature for 3 h. $Et_3N\cdot HCl$ (m.p. = 248°C) was filtered off. The filtrate on concentration *in vacuo* yielded a white crystalline solid and was recrystallized from petroleum ether (40–60°C) to afford diphenylantimony(III) succinimide.

Reaction of diphenylantimony(III) *chloride with the sodium salt of phthalimide*

A solution of diphenylantimony(III) chloride (0.3112 g, 1 mmol) in benzene (25 cm^3) and a sodium salt of phthalimide (0.169 g, 1 mmol) in the same solvent were stirred together at room temperature for 3 h under nitrogen, and NaCl was filtered off.

*Author to whom correspondence should be addressed.

Table 1. Preparation, properties, elemental analysis and relevant IR data for the diarylantimony(III) amide derivatives

	Complex Ar_2SbL	Ligand Solvent (cm^3)	Ar_2SbCl (g) Solvent (cm^3)	M.P. (°C) (Colour)	Yield (%)	Recrystallization solvent	Found (Calc.) (%) C	H	N	IR (in cm^{-1}) $\nu_{asym}(CO)$	$\nu_{sym}(CO)$
	($Ar = C_6H_5$)	L =	($Ar = C_6H_5$)								
I	$Ar_2Sb(\overline{NCOCH_2CH_2CO})$	$H\overline{NCOCH_2CH_2CO}$ (0.099) C_6H_6 (30)	0.3112 C_6H_6 (30)	156 (White)	85	Petroleum ether 40–60	51.2 (51.4)	3.4 (3.7)	3.2 (3.7)	1706 vs	1308 ms
II	$Ar_2Sb(\overline{NCOC_6H_4CO})$	$Na\overline{NCOC_6H_4CO}$ (0.169) C_6H_6 (20)	0.3112 C_6H_6 (25)	215 (White)	81	Petroleum ether 40–60	56.2 (56.9)	3.2 (3.3)	3.2 (3.3)	1760 s	1311 ms
III	$Ar_2Sb(\overline{NCOCOC_6H_4})$	$H\overline{NCOCOC_6H_4}$ (0.147) C_6H_6 (30)	0.3112 C_6H_6 (25)	122 (Pink)	90	Petroleum ether 40–60	56.4 (56.9)	3.1 (3.3)	3.0 (3.3)	1720 s	1320 m
IV	$Ar_2Sb(\overline{NNNC_6H_4})$	$H\overline{NNNC_6H_4}$ (0.119) C_6H_6 (20)	0.3112 C_6H_6 (25)	98 (White)	50	Et_2O	54.1 (54.9)	3.1 (3.6)	10.2 (10.7)	—	—
V	$Ar_2Sb(\overline{NC(CH_3)NCHCH})$	$H\overline{NC(CH_3)NCHCH}$ (0.082) C_6H_6 (20)	0.3112 C_6H_6 (30)	60 (White)	65	$CHCl_3$	53.1 (53.8)	4.00 (4.2)	7.6 (7.8)	—	—
VI	$Ar_2Sb(\overline{NC(S)SC_6H_4})^a$	$Na\overline{NC(S)SC_6H_4}$ (0.0945) C_6H_6 (25)	0.1556 C_6H_6 (25)	171 (Grey)	60	Et_2O	51.2 (51.6)	3.0 (3.2	3.1 (3.2)	—	—
VII	$Ar_2Sb(\overline{NC(CH_2Cl)NC_6H_4})$	$H\overline{NC(CH_2Cl)NC_6H_4}$ (0.0822) C_6H_6 (30)	0.1156 C_6H_6 (25)	96 (Light grey)	50	Et_2O	54.2 (54.4)	3.4 (3.6)	6.1 (6.3)	—	—
VIII	$Ar_2Sb(\overline{NC_6H_4C_6H_4})$	$Na\overline{NC_6H_4C_6H_4}$ (0.189) C_6H_6 (30)	0.3112 C_6H_6 (25)	239 (White)	90	Petroleum ether 40–60	65.1 (65.2)	4.0 (4.1)	3.1 (3.2)	—	—
	($Ar = C_6F_5$)		($Ar = C_6F_5$)								
IX	$Ar_2Sb(\overline{NCOCH_2CH_2CO})$	$Na\overline{NCOCH_2CH_2CO}$ (0.121) C_6H_6 (30)	0.4912 C_6H_6 (20)	65 (White)	65	Petroleum ether 40–60	34.1 (34.7)	0.9 (0.7)	2.1 (2.5)	1732 vs	1331 ms
X	$Ar_2Sb(\overline{NCOCOC_6H_4})$	$Na\overline{NCOCOC_6H_4}$ (0.169) C_6H_6 (30)	0.4912 C_6H_6 (20)	137 (Red)	50	Petroleum ether 60–80	39.1 (39.9)	0.8 (0.7)	2.1 (2.3)	1730 ms	1330 m

[a] Hygroscopic.

The filtrate on concentration *in vacuo* afforded a white crystalline solid and was recrystallized from petroleum ether (40–60°C) to give diphenylantimony(III) phthalimide.

Reaction of $Ph_2SbNCOC_6H_4CO$ *with* Br_2

To a solution of amide (1 mmol) in $CHCl_3$ (20 cm^3), bromine (2 mmol) in the same solvent (5 cm^3) was slowly added at 0°C over 30 min. The mixture was allowed to come to room temperature and was then freed from volatiles *in vacuo*. The IR spectrum of the residue and TLC in benzene showed the presence of both diphenylantimony(III) bromide and bromophthalimide. No attempts were made to separate the products.

Reaction of $Ph_2SbNNNC_6H_4$ *with* PhNCO

A mixture containing equimolar amounts of diphenylantimony(III) 1,2,3-benzotriazole (0.3937 g, 1 mmol) and phenylisocyanate (0.119 g, 1 mmol) was heated for 4 h. The resulting brown liquid was treated with diethyl ether (40–60°C) to afford light brown crystals of the PhNCO adduct. Yield = 0.34 g (65%); m.p. = 131°C. Found: C, 58.0; H, 3.1; N, 11.2. Calc: C, 58.6; H, 3.7; N, 10.9%.

RESULTS AND DISCUSSION

Diarylantimony(III) amides can conveniently be prepared by the interaction of diarylantimony(III) chloride with an amide (succinimide, phthalimide, isatin, 2-methylimidazole, 2-chloromethylbenzimidazole, 1,2,3-benzotriazole, carbazole and benzothiazoline-2-thione) in the presence of triethylamine as hydrogen chloride acceptor [eq. (1)] or by the interaction of diarylantimony(III) chloride with the sodium salt of the corresponding ligand [eq. (2)].

$$Ar_2SbCl + HL \xrightarrow[\text{Benzene}]{Et_3N} Ar_2SbL + Et_3N \cdot HCl \quad (1)$$

$$Ar_2SbCl + NaL \xrightarrow[\text{Benzene}]{} Ar_2SbL + NaCl \quad (2)$$

Ar = C_6H_5 or C_6F_5;
L = $—NR_2$ = $—NCO(CH_2)_2CO$,
$—NCOC_6H_4CO$, $—NCOCOC_6H_4$, $—NNNC_6H_4$,
$—NC(CH_3)NCHCH$, $—NC(S)SC_6H_4$,
$—NC(CH_2Cl)NC_6H_4$, $—NC_6H_4C_6H_4$.

All the reactions were found to proceed under mild conditions and were generally quantitative. Unlike the phenyl amino stibines, $Ph_nSb(NEt_2)_{3-n}$ which are obtained as liquids,[7] are colourless solids, with sharp melting points and are monomeric in freezing benzene. They are stable towards air and moisture; the melting point of sample (III) did not change even after stirring (1 h) with water at room temperature. The molar conductance of a 10^{-3} M solution in acetonitrile ranges between 15–25 ohm^{-1} cm^2 mol^{-1} at 25°C which shows the absence of ionic species in solution.

Reactions of amides

The Sb—N bond in Ar_2SbNR_2 is cleaved in preference to Sb—Ar bonds by Br_2 to give the corresponding halide, as in eq. (3).

$$Ar_2Sb(NCOC_6H_4CO) + Br_2 \longrightarrow Ar_2SbBr + COC_6H_4CONBr. \quad (3)$$

$Sb(NMe_2)_3$ is known to react with CS_2 to give $Sb(SCSNMe_2)_3$.[13] However, Ar_2SbNR_2 failed to react with an excess of CS_2 even after prolonged refluxing. On the other hand PhNCO added to the Sb—N bond in the manner of equation below [eq. (4)].

$$Ar_2SbNR_2 + PhNCO \longrightarrow Ar_2Sb—\underset{\displaystyle Ph}{\overset{}{N}}—\overset{\displaystyle O}{\overset{\|}{C}}—NR_2. \quad (4)$$

The formation of the PhNCO adduct was confirmed by the absence of ν(NCO) at 2200 cm^{-1} and the appearance of a new medium intensity band at 1700 cm^{-1} due to ν(C=O). A medium band at 1600 cm^{-1} may be assigned to ν(C—N). The failure of the reaction of CS_2 with Ar_2SbNR_2 may partly be attributed to the weak dipole nature of the former coupled with the presence of the electron withdrawing group bonded to antimony amide. Similar reactions of CS_2, RNCS and RNCO with organometal–nitrogen bonded compounds have previously been reported.[14]

IR spectra of amides

The IR spectra of all the compounds show almost identical absorption bands due to phenyl or pentafluorophenyl groups and these bands do not differ significantly from those reported earlier for diarylantimony(III) derivatives.

Absorption frequencies having diagnostic value are given in Table 1. Absorption frequencies due to carbonyl groups, symmetric as well as asymmetric, in the amido derivatives have been assigned. The ureido derivatives show the presence of a strong band in the region 1710–1750 cm^{-1} indicating the "ester type" CO group(s).

The Sb—C vibrations in the case of phenyl and

pentafluorophenyl derivatives corresponding to the y mode consistently appear in the range 448–460 cm^{-1}.[10-11] The assignment of the Sb—N band is uncertain due to the presence of phenyl absorptions in the region. However, on the basis of previous observations it is tentatively assigned at 510–520 cm^{-1}.[7]

^1H *NMR spectra*

The ^1H NMR spectra of $Ph_2SbN(COCH_2CH_2CO)$ in $CDCl_3$ at room temperature showed a singlet at δ 2.68 ppm (due to $—CH_2CH_2$ group) and a multiplet centred at δ 7.50 ppm [due to an aromatic proton (10 H, C_6H_5)]. Similarly, the compound $Ph_2SbNC(CH_3)NCH \cdot CH$ showed a complex multiplet centred at δ 7.35 [due to an aromatic proton (10 H, C_6H_5)], a singlet at δ 2.25 (due to a CH proton) and a singlet at δ 2.4 ppm (due to Me protons). The integration of the peaks is consistent with the proposed stoichiometry.

Thus on the basis of IR, NMR spectra, molecular weight and conductance data, the newly synthesized amido derivatives may be assigned a pyramidal structure. Similar structures have previously been assigned in the case of R_2MX (R = Me, Ph; M = As, Sb and Bi; X = halide).[15]

Acknowledgements—The authors are thankful to the Head of the Department of Chemistry, Lucknow University, for laboratory facilities; the Director of the RSIC, Lucknow, for obtaining IR, NMR and elemental analysis; and the CSIR, New Delhi, for financial assistance.

REFERENCES

1. G. O. Doak and L. D. Freedman, *Organometallic Compounds of Arsenic, Antimony and Bismuth*, p. 389. Wiley-Interscience, New York (1970); M. Nunn, D. B. Sowerby and D. M. Wesolek, *J. Organomet. Chem.* 1983, **251**, C45.
2. M. Wieber and U. Baudis, *Z. Anorg. Allg. Chem.* 1978, **439**, 134.
3. M. Hall, D. B. Sowerby and C. P. Falshaw, *J. Organomet. Chem.* 1986, **315**, 321; S. P. Bone and D. B. Sowerby, *J. Organomet. Chem.* 1980, **184**, 181.
4. M. Wieber, I. Fetzer-Kremling, D. Wirth and H. G. Rüdling, *Z. Anorg. Allg. Chem.* 1985, **520**, 59.
5. R. K. Gupta, A. K. Rai, R. C. Mehrotra, V. K. Jain, B. F. Hoskins and E. R. T. Tiekink, *Inorg. Chem.* 1985, **24**, 3280.
6. R. K. Gupta, A. K. Rai and R. C. Mehrotra, *Ind. J. Chem. Sect. A* 1985, **24A**, 752.
7. H. A. Meinema and J. G. Noltes, *Inorg. Nucl. Chem. Lett.* 1970, **6**, 241.
8. J. Dahlmann and K. Winsel, *J. Prakt. Chem.* 1979, **321**, 370.
9. P. Raj, A. Ranjan, K. Singhal and R. Rastogi, *Synth. React. Inorg. Met. Org. Chem.* 1984, **14**, 269.
10. P. Raj, A. K. Saxena, K. Singhal and A. Ranjan, *Polyhedron* 1985, **4**, 251.
11. P. Raj, R. Rastogi, K. Singhal and A. K. Saxena, *Polyhedron* 1986, **5**, 1581.
12. P. Raj, A. K. Aggarwal and A. K. Saxena, *J. Fluorine Chem.* 1988, **42**, 163.
13. G. Oertel, H. Holtschmidt and H. Malz, *German Patent* 1,170,393 (1964).
14. P. Raj, A. Ranjan and K. Singhal, *Synth. React. Inorg. Met. Org. Chem.* 1984, **14**, 477.
15. J. L. Wardell, Arsenic, antimony and bismuth in *Comprehensive Organometallic Chemistry* (Edited by G. Wilkinson), Vol. 2, p. 681. Pergamon Press, Oxford (1982).

Polyhedron Vol. 8, No. 5, pp. 585–596, 1989
Printed in Great Britain

0277–5387/89 $3.00+.00
© 1989 Pergamon Press plc

SYNTHESIS AND SPECTROSCOPIC CHARACTERISTICS OF 2-METHYL-2-PHENYLPROPYL- AND DIMETHYL(PHENYL)SILYLMETHYLNICKEL(II) COMPLEXES

STEPHEN I. BLACK and G. BRENT YOUNG*

Inorganic Chemistry Laboratories, Imperial College of Science, Technology and Medicine, London SW7 2AY, U.K.

(*Received* 2 *September* 1988; *accepted* 8 *September* 1988)

Abstract—Three types of organonickel derivatives, NiR_nL_m (R = CH_2CMe_2Ph, CH_2SiMe_2Ph) have been characterized. (1) $NiCp(R)L$ [L = PPh_3, P(cyclo-$C_6H_{11})_3$]; (2) *trans*-$Ni(R)(X)L_2$ (X = Cl, L = PMe_3, PEt_3, PBu^n_3, PMe_2Ph); (3) NiR_2L_2 (L_2 = bipy, Me_2bipy, Bu^t_2bipy, Me_4phen, R = CH_2CMe_2Ph and CH_2SiMe_2Ph; L_2 = Ph_2phen, bipym, dppe and L = PMe_3, R = CH_2SiMe_2Ph only). Synthetic strategies and spectroscopic characteristics for these complexes are discussed. In general contrast to their silylmethyl analogues, neophylnickel complexes are labile. $NiCp(CH_2CMe_2Ph)(L)$ readily undergoes H-transfer isomerization to give the 2-*tert*-butylphenyl complex $NiCp(2\text{-}C_6H_4CMe_3)(L)$. NiR_2L_2 (R = CH_2CMe_2Ph, L_2 = R^t_2bipy) undergo thermolytic rearrangement also by intramolecular aromatic C—H activation to give metallacycles which react further under the prevailing conditions.

Dialkylplatinum(II) derivatives L_2PtR_2 generally favour rearrangement via H-transfer reactions.[1] Analogous nickel(II) and palladium(II) species are, however, often thermolytically more versatile and may, for example, undergo reductive elimination via C—C bond formation.[2] In parallel with our studies on a variety of neophyl-† and sila-neophylplatinum† complexes,[3d] whose preferred reaction mode is aromatic δ-C—H activation and transfer (Scheme 1), we have undertaken an investigation of corresponding organonickel and organopalladium systems in an effort to understand more fully the controls on the reactivity of this group of metals towards organic fragments. Here we report on the synthesis and characterization of three types of organonickel complex where R is neophyl or sila-neophyl: CpNiR(L) (L = P-donor); *trans*-L_2NiRX (L = monodentate P-donor, X = halide); L_2NiR_2 (L = N-donor or bidentate P-donor). Several neophylnickel complexes have been reported recently.[4] In cases of overlap, we detail new or modified synthetic routes and additional spectroscopic information. During the course of our work a brief report has appeared of metallacycle formation proposedly from a dineophylnickel(II) precursor.[4d]

EXPERIMENTAL

General

Ether, hexane and THF were distilled before use from sodium–benzophenone. Toluene was distilled from sodium. Deuterated solvents were used as received from Aldrich Chemical Company, but stored under argon in grease-free vessels. Phos-

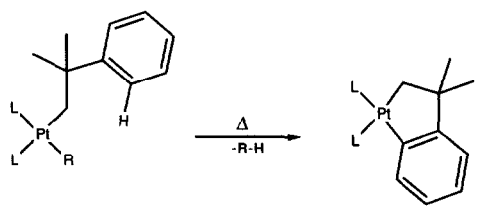

R= Me or neophyl

L_2= 2Py, COD, bipy, bipym, phen, Et_3P

Scheme 1.

* Author to whom correspondence should be addressed.

† Neophyl = 2-methyl-2-phenylpropyl; sila-neophyl = dimethyl(phenyl)silylmethyl.

phines were also stored under argon but otherwise used as received from Strem Chemicals. Pyridines (Aldrich Chemical Company) were stored over activated Linde 4 Å molecular sieves. Unless otherwise noted, all reactions were carried out under argon using standard techniques. NMR spectra were obtained using JEOL FX90Q and Bruker WM 250 instruments. Satisfactory elemental analyses were obtained for new compounds (Table 1).

Precursors

Bis(phosphine)nickel complexes were prepared by modified literature procedures,[5] by mixing solutions of $NiCl_2 \cdot 6H_2O$ in ethanol with the phosphine. This method for the triphenylphosphine and the tricyclohexylphosphine complexes, rather than those reported,[5] requires overnight reflux of the solutions, giving blue–violet and red solids, respectively.

Ni(Cp)(Cl)L (L = PCy_3, PPh_3)

These compounds were prepared via established routes, by mixing equimolar acetone solutions of the dichlorobis(phosphine)nickel(II) with nickelocene. This route is only successful for relatively bulky phosphines.[6] Attempts to prepare other compounds resulted in mixtures.

Preparation of η^5-cyclopentadienylbis(triethylphosphine)nickel(II) *chloride*

$NiCl_2(Et_3P)_2$ (1.19 g, 0.9 mmol) was reacted with CpTl (0.88 g, 0.9 mmol) in 40 cm^3 dry acetone at room temperature for 30 min. The mixture became brown then green and a pale precipitate formed. The mixture was filtered and 30 cm^3 ether added and filtration repeated. On cooling, well-formed green plates of the product separated. The product is very soluble in polar solvents, such as water, to give green solutions, but gives brown or red solutions in less polar solvents in which it is only slightly soluble. (Yield, 80%.)

Preparation of 4,4′-*bis*-tert-*butyl*-2,2′-*bipyridyl*

This was produced in *ca* 10% yield by refluxing 4-*tert*-butylpyridine (25 cm^3) and cyclohexene (10 cm^3) over degassed 5% Pd/C (1 g) for 7 days. The volatile liquids were distilled off (for recycling) and the product was extracted and recrystallized using hot toluene or ethanol. The dried product was analytically pure. Another method, using Raney nickel, has recently appeared.[7] The product is not as readily purified, however. If the reaction is conducted in the absence of cyclohexene, the yield of product approaches 80%[8] but the product is heavily contaminated with the corresponding terpyridyl from which it is difficult to separate.

Preparations of neophyl- and sila-neophenylmagnesium reagents

$Mg(CH_2SiMe_2Ph)Cl$ was prepared in the standard way from the chloroalkylsilane and magnesium in THF at ambient temperature, usually in concentrations of *ca* 1.0 mol dm^{-3}. Reaction of $PhMe_2CCH_2Cl$ with magnesium in THF is slower and the reaction requires overnight reflux to give 95% yield (also in solutions of approximately 1.0 mol dm^{-3}).

Preparation of η^5-cyclopentadienyl(neophyl)(triphenylphosphine)nickel(II)

$NiCp(PPh_3)Cl$ (0.5 g, 1.2 mmol) was dissolved in toluene (30 cm^3) at −15°C. $Mg(CH_2CMe_2Ph)Cl$ (1.3 mmol) was added rapidly, as a solution in THF and the mixture became successively green, then brown. After stirring for 1 h the solvents were removed and the residues extracted with hexane (60 cm^3) to give a green–brown solution. Crystals obtained from this solution contain two compounds (total yield up to 80%) which can be separated by chromatography on silica, eluting with hexane, into a slightly air-sensitive green compound (R = CH_2CMe_2Ph) and a brown–green compound (R = 2-$C_6H_4Bu^t$).

Preparation of η^5-cyclopentadienyl(4-tert-*butylphenyl*)(*triphenylphosphine*)*nickel*(II)

Powdered $NiCp(PPh_3)Cl$ (0.73 g, 1.7 mmol) was suspended in ether (40 cm^3) at −15°C. Mg(2-$C_6H_4Bu^t$)Br in diethyl ether (2 mmol) was added rapidly. The solution immediately became greenish-brown. The solution was stirred at ambient temperature for 4 h, depositing a pale precipitate. The ether was removed and the residue extracted with petrol to give a red–brown solution. This was passed through a short alumina column (prepared under argon) to give a brown–green solution which on removal of the solvent gave the pure product. (Yield, 50%.)

Preparation of Ni(Cp)(CH_2SiMe_2Ph)L (L = PCy_3, PPh_3)

These compounds were prepared as for the triphenylphosphine analogue. Extraction and crystallization using 40–60°C petroleum ether gave pure, air-stable green crystals. (Yield, 55% for the

PPh_3 compound and 65% for the Cy_3P compounds.)

Preparation of trans-*chloro(neophyl)bis(dimethylphenylphosphine)nickel*(II)

$NiCl_2(PMe_2Ph)_2$ (1.35 g, 3.32 mmol) was suspended in ether (20 cm^3) at −20°C. $Mg(CH_2CMe_2Ph)Cl$ (3.4 mmol) in THF, was added rapidly via syringe. The solution slowly became more orange. It was stirred as it warmed to ambient temperature (*ca* 3 h). The ether was reduced to *ca* 5 cm^3 *in vacuo*, hexane (40 cm^3) added and the solution filtered. Small, pure, air-sensitive orange needles of the product formed on cooling. (Yield, 55–65%.)

Preparations of trans-*chloro(neophyl)bis(trimethylphosphine)nickel*(II) *and* trans-*chloro(neophyl)bis(triethylphosphine)nickel*(II)

These were executed as above except that the reactions were faster and the triethylphosphine compound was isolated as an orange oil which could not be induced to crystallize. (Yields, *ca* 70%.)

Preparation of trans-*chloro(sila-neophyl)bis(trimethylphosphine)nickel*(II)

$NiCl_2(PMe_3)_2$ (0.48 g, 1.74 mmol) was suspended in ether (30 cm^3) at −20°C. $Mg(CH_2SiMe_2Ph)Cl$ (1.8 mmol in THF) was added via syringe and the mixture instantly became orange and rapidly deposited a fine, pale precipitate. This was stirred for 20 min at ambient temperture and the ether was removed under reduced pressure. The residues were extracted with 2×30 cm^3 hexane. On vacuum removal of *ca* 10–20 cm^3 of hexane and cooling, well-formed orange crystals of the analytically pure product were isolated. (Yield, 60%.)

Preparations of trans-*chloro(sila-neophyl)bis(triethylphosphine)nickel*(II) *and* trans-*chloro(sila-neophyl)bis(dimethylphenylphosphine)nickel*(II)

These were executed as above. The triethylphosphine compound could only be isolated as an orange oil, which was, however, spectroscopically pure. (Yields, 80 and 70%, respectively.)

Preparation of trans-*chloro*(4-tert-*butylphenyl)bis(dimethylphenylphosphine)nickel*(II)

$NiCl_2(PMe_2Ph)_2$ (0.70 g, 1.72 mmol) was suspended in ether (25 cm^3) at −10°C. Mg(2-$C_6H_4Bu^t$)Br (1.8 mmol in diethyl ether) was added in one portion via syringe. The mixture became orange and, on stirring and warming to ambient temperature, gave a brown solution and a pale precipitate. The ether was removed under reduced pressure and the mixture extracted with toluene (30 cm^3) to give a deep red–brown solution, which, when reduced to *ca* 5 cm^3, deposited well-formed orange–brown plates on cooling. The product did not appear to be air-sensitive as a solid, in contrast to

Table 1. Elemental analyses

Compound	Carbon Found	Carbon (Calc.)	Hydrogen Found	Hydrogen (Calc.)	Nitrogen Found	Nitrogen (Calc.)	Other Found	Other (Calc.)
bipyNi(CH_2CMe_2Ph)$_2$	74.3	(74.8)	7.1	(7.1)	5.9	(5.8)		
Me_2bipyNi(CH_2CMe_2Ph)$_2$	75.2	(75.4)	7.5	(7.5)	5.4	(5.5)		
Bu^t_2bipyNi(CH_2CMe_2Ph)$_2$	76.3	(76.9)	8.4	(8.4)	4.8	(4.7)		
CpNi(PPh_3)CH_2CMe_2Ph	77.4	(76.3)	6.9	(6.4)				
CpNi(PPh_3)4-$C_6H_4CMe_3$	76.3	(76.4)	6.4	(6.4)				
CpNi(PPh_3)CH_2SiMe_2Ph	71.1	(71.8)	6.1	(6.2)				
bipyNi(CH_2SiMe_2Ph)$_2$	64.9	(65.5)	6.5	(6.7)	5.5	(5.4)		
Me_2bipyNi(CH_2SiMe_2Ph)$_2$	66.3	(66.5)	7.2	(7.1)	5.2	(5.2)		
Bu^t_2bipyNi(CH_2SiMe_2Ph)$_2$	68.7	(69.1)	8.2	(8.0)	4.6	(4.5)		
Me_4phenNi(CH_2SiMe_2Ph)$_2$	68.1	(68.9)	7.2	(6.9)	4.7	(4.7)		
Ph_2phenNi(CH_2SiMe_2Ph)$_2$	72.4	(73.2)	6.0	(6.1)	4.6	(4.1)		
(PMe_3)$_2$Ni(Cl)CH_2SiMe_2Ph	45.3	(45.6)	7.9	(7.8)				
(PMe_2Ph)$_2$Ni(Cl)CH_2SiMe_2Ph	57.0	(57.8)	6.7	(6.7)			Cl 7.2	(6.8)
dppeNi(CH_2SiMe_2Ph)$_2$	69.7	(69.9)	6.8	(6.7)			P 7.9	(8.2)
Bu^tpy$_2$Ni(CH_2SiMe_2Ph)$_2$	67.5	(68.9)	8.2	(8.4)	4.4	(4.5)		
bipymNi(CH_2SiMe_2Ph)$_2$ · 1/2L	60.0	(60.6)	5.9	(5.9)	14.1	(14.1)		

the neophyl and sila-neophyl compounds. (Yield, 65%.)

Preparation of 4,4′-tert-*butyl*-2,2′-*bipyridylbis* (*neophyl*)*nickel*(II)

$NiCl_2Bu^tpy_4$ (1.23 g, 1.8 mmol) and Bu^t_2bipy (0.45 g, 1.7 mmol) were suspended in THF (40 cm^3) at −60°C, and *ca* 0.5 cm^3 Bu^tpy added. This mixture gives a pale violet colour characteristic of the parent complex in solution. $Mg(CH_2CMe_2Ph)Cl$ (3.8 mmol in THF) was added slowly with rapid stirring. This quickly produced a brown solution. This was stirred vigorously and allowed to warm to room temperature over 3 h to give a deep green solution. The solvent was removed under vacuum and the residues extracted with hexane (3 × 25 cm^3). The extracts were reduced to *ca* 40 cm^3, when crystal deposition was evident. Cooling produced a mass of well-formed square plates. (Yield, 60–70%.) The compound can be recrystallized from hexane or toluene as analytically pure crystals, however it appears to decompose (or isomerize) if left standing in solution or in the solid state for long periods of time even under argon.

Preparation of bis(*sila-neophyl*)*bis*(4-tert-*butylbipyridine*)*nickel*(II)

$NiCl_2Bu^tpy_4$ (1.0 g, 1.5 mmol) was suspended in ether (50 cm^3) at −70°C. Bu^tpy (1.0 cm^3) and $Mg(CH_2SiMe_2Ph)Cl$ (3.2 mmol in THF) were added rapidly with stirring. The cooling bath was removed and the solution allowed to warm to ambient temperature with vigorous stirring. After *ca* 2 h the solution was orange–brown and no precursor could be seen. The ether was then removed *in vacuo* and the residues extracted with hexane (3 × 50 cm^3). The hexane was then similarly reduced to about 50 cm^3 and cooled to give a good yield of slightly sticky but well-formed brown square plates. The compound is unstable in solution, depositing nickel metal on standing at ambient temperatures. It may also be unstable under vacuum—explaining a slightly aberrant analysis. Normally it need not be isolated and can be used directly as a hexane solution in the synthesis of further compounds. (Yield, 80%.)

Preparation of bis(*sila-neophyl*)(3,4,7,8-*tetramethylphenanthroline*)*nickel*(II)

A hexane solution of $Ni(CH_2SiMe_2Ph)_2(Bu^tpy)_2$ (1.13 mmol/40 cm^3 hexane) was added rapidly to a strongly stirred suspension of Me_4phen (0.27 g, 1.14 mmol) in ether (20 cm^3). The mixture rapidly became deep violet. It was stirred for 1 h, by which time all the starting materials had gone into solution. The solution was filtered and *ca* half the solvent removed *in vacuo*. A mass of fine violet needles separated on cooling to −20°C overnight. (Yield, 85%.)

Preparation of (2,2′-*bipyrimidyl*)*bis*(*sila-neophyl*) *nickel*(II)

Considerable difficulty was experienced in attempted preparations of this compound, apparently caused by the potential of the monometallic product to dimerize with the elimination of bipym. The reaction conditions were crucial in determining whether any of the "monomer" was isolated. Optimum conditions required that an excess of dissolved bipym was always present in the reaction mixture. A solution of $Ni(CH_2SiMe_2Ph)_2Bu^tpy_2$ (2.1 mmol) in hexane (100 cm^3) and ether (20 cm^3) was slowly (*ca* 1 h) added to a rapidly stirred solution of bipym (0.44 g, 2.8 mmol) in toluene (75 cm^3). The mixture rapidly became brown–green. The solvent was removed and the solid residue extracted with ether (50 cm^3) to give a green solution and a dark red residue (this step should remove excess insoluble bipym or dimer which appears to be only sparingly soluble in non-polar solvents). The ether was removed *in vacuo* to give a green oil. The oil was washed with hexane to give a brown solution and a green solid that analysed as $Ni(CH_2SiMe_2Ph)_2$ (bipym) · 1/2bipym. (Yield, 40%.)

RESULTS AND DISCUSSION

(1) Ni(Cp)(R)L

Synthesis. Several complexes of this type with L = Ph_3P and a variety of R groups have been reported.[9] The neophyl analogue, however, was originally reported to be labile and was not isolated.[10] Its decomposition produced mainly neophylcyclopentadiene, 2,5-dimethyl-2,5-diphenylhexane (bineophyl), *tert*-butylbenzene and traces of 1-*tert*-butyl-2-neophylbenzene. The isolation of the compound has, however, been reported more recently.[4] We have found that reaction of $NiCp(PPh_3)Cl$ with $Mg(CH_2CMe_2Ph)Cl$ in diethyl ether at −10–0°C followed by solvent evaporation and extraction into petroleum ether gives an approximately equimolar *mixture* of $NiCp(PPh_3)(CH_2CMe_2Ph)$ and its isomer $NiCp(PPh_3)(2\text{-}C_6H_4CMe_3)$, which could be separated by chromatography (previous reports appear to have neglected the isomeric product). The identity of the latter was confirmed by its indepen-

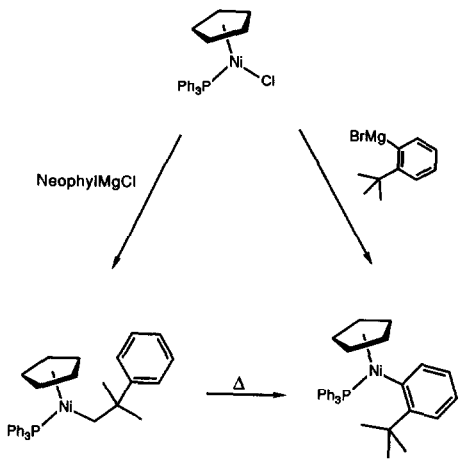

Scheme 2.

dent synthesis from $NiCp(PPh_3)Cl$ and $Mg(2\text{-}C_6H_4CMe_3)Br$. Once isolated, the neophyl complex does isomerize to the *tert*-butylphenyl species (Scheme 2), but much more slowly than would account for the amount of the aryl metal in the initial product mixture; so we conclude that the rearrangement is accelerated under the conditions that prevail in the Grignard transmetallation. These observations lend support to previous contentions on the rearrangement of neophyl metals although, oddly, this nickel system was not one of those displaying such a capacity.[10] Only rarely have the 2-*tert*-butylphenyl metal products been isolated.[1f] We are currently engaged in a mechanistic study of the H-transfer isomerization. The corresponding sila-neophyl complex, $NiCp(PPh_3)(CH_2SiMe_2Ph)$, shows no parallel reactivity in solution up to *ca* 60°C when it begins to decompose, apparently by a different route, giving paramagnetic products.

To broaden our understanding of this isomerization, we have attempted to prepare analogues with trialkylphosphines, but with little success. Mostly, the corresponding halide precursors do not behave analogously. For example two different approaches to $NiCp(Cl)(PEt_3)$—by admixture of $NiCp_2$ and $NiCl_2(PEt_3)_2$ and reaction of $NiCl_2(PEt_3)_2$ and CpTl—led ultimately to the green ionic species $[NiCp(PEt_3)_2]Cl$.[11] With the latter route the reaction was quantitative. The compound is air-stable, water-soluble and slightly soluble in acetone, in which its solutions are brown at 25°C but green at −20°C. In less polar organic solvents it is only sparingly soluble to give pale pink solutions. Presumably these media favour equilibration by phosphine dissociation to produce the neutral species $NiCp(PEt_3)Cl$. We have not been able to alkylate this compound with either $Mg(CH_2CMe_2Ph)Cl$ or $LiCH_2CMe_2Ph$. We have, however, been able to produce the analogue $NiCp(Cl)(PCy_3)$ via a similar route to the triphenylphosphine complex, but with a longer reaction period and a higher reaction temperature. This compound reacts cleanly with $Mg(CH_2SiMe_2Ph)Cl$ to give the green $NiCp(CH_2SiMe_2Ph)(PCy_3)$.

Spectroscopy. Important NMR characteristics appear in Tables 2 and 3. In their ^1H NMR spectra, the Ni—CH_2 groups show couplings to phosphorus of about 10 Hz. The Cp—H resonances occur between 5 and 6 ppm, the aryl compound showing the greatest downfield shift, as expected. This enables the compounds to be distinguished readily. The ^{31}P resonances also distinguish between the aryl and alkyl compounds; the resonances are typical of those observed in other similar compounds. In ^{13}C NMR spectra, under ideal conditions, a coupling between the phosphorus and the Cp carbons of *ca* 2 Hz can be seen. Usually, though, it is very difficult to eradicate small traces of paramagnetic and/or often insoluble impurities which prevent resolution of small couplings. (This, in addition, had hindered considerably our mechanistic studies of this group of compounds.) The resonances for the aromatic hydrogens on the sila-neophyl and neophyl groups are shifted from their position in the chloroalkanes by a marked amount depending on their proximity to nickel—the *ortho*-hydrogens show greatest shifts. They appear as a discrete doublet at lowest field in the aromatic proton range. The equivalent protons in the sila-neophyl compounds appear as a complex multiplet also at low field (*vide infra*). This effect is probably due to paramagnetic anisotropy in the metal *d*-orbitals and has been analysed in detail for nickel and palladium.[12] It is also evident in the spectra of platinum analogues.[1e,3h] IR spectra show mixtures of bands associated with the component parts of the molecules. Sila-neophyl and neophyl are easily distinguished by the distinctive bands associated with the CMe_2 and $SiMe_2$ groups at *ca* 800 and 1400 cm^{-1}, among others.

(2) *trans*-$Ni(R)(X)L_2$

Compounds of this type are among the most common for divalent nickel[13] and two such neophyl derivatives have been reported ($L = PMe_3$, $L = PMe_2Ph$).[4a] We have extended the range of phosphine ligands and of spectroscopic characteristics and have also developed the analogous sila-neophyl chemistry.

Synthesis. Optimum conditions require addition of the requisite organomagnesium halide to an ether suspension of NiX_2L_2 at −10–0°C. Less soluble halonickel precursors require 1–2 h reaction time at

Table 2. ^{1}H NMR characteristics of $L_nNi(CH_2EMe_2Ph)$ complexes[a]

Compound	$NiCH_2$	$E(CH_3)_2$ (E = C or Si)	H_1 (phenyl)	Others
$CpNi(PPh_3)(CH_2CMe_2Ph)$	1.05d (9–10 Hz)	1.08	8.05 (7 Hz)	
$CpNi(PPh_3)(2\text{-}C_6H_4Bu^t)$	—	1.45	—	1.45 (Bu^t), 5.05 (Cp), 6.4–7.4m
$CpNi(PPh_3)(CH_2SiMe_2Ph)$	−0.84d (8.7 Hz)	0.23	7.5	6.8–7.2m, 7.4–7.8m, 5.05 (Cp)
$CpNi(Cy_3P)(CH_2SiMe_2Ph)$	−0.90d (9 Hz)	0.32	7.5	6.8–7.2m, 0.9–2.1m (Cy), 4.95 (Cp)
$CpNi(Et_3P)_2Cl$[a]	—	—	—	5.6 (Cp), 1.5–1.8m (CH_2), 0.9–1.3m (CH_3)
$(PMe_3)_2Ni(Cl)(CH_2CMe_2Ph)$ (−10°C)	0.50 (~16 Hz)	2.3	7.8d	1.3 pseudt (3 Hz) P*Me*$_3$, 7.3–7.5m
$(PMe_2Ph)_2Ni(Cl)(CH_2CMe_2Ph)$ (−10°C)	0.46t (~15 Hz)	2.4	7.95d	1.26 pseudt (PC*H*$_3$), 6.9–7.1m, 7.15 (Hz), 7.3–7.4m (PPh)
$(PEt_3)_2Ni(Cl)(CH_2CMe_2Ph)$ (−10°C)	0.55t (~15 Hz)	1.7	7.7d	6.9–7.2m, 1.4m (PC*H*$_2$), 0.9m (CH_3CH_2P)
$(PMe_3)_2Ni(Cl)(CH_2SiMe_2Ph)$	−0.41t (14.1 Hz)	0.58	7.9–8.0m	1.25 pseudt (4 Hz) P*Me*$_3$, 7.3–7.5m
$(PMe_2Ph)_2Ni(Cl)(CH_2SiMe_2Ph)$	−0.60t (13.5 Hz)	0.40	7.8–8.0m	1.18 pseudt (4 Hz) P*Me*$_2$, 6.8–7.1m PPh, 7.35–7.6m PPh, 7.15 PhSi
$(PEt_3)_2Ni(Cl)(CH_2SiMe_2Ph)$	−0.71t (13.2 Hz)	0.61	7.7–7.9m	7.1–7.2m (PhSi), 0.8–1.2m (PC*H*$_2$), 1.2–1.6 (PCH_2CH_3)
$(PMe_3)_2Ni(CH_2SiMe_2Ph)_2$	−0.86t (17.6 Hz)	0.56s	7.8m	0.72d (J = 6H, *cis*), 0.91t pseudo ($J_{apparent}$ = 3 Hz, *trans*), 6.9–7.5m Ph (*cis*/*trans* = 4:1)
$(bipy)Ni(CH_2CMe_2Ph)_2$	1.62	1.77	7.6d	6.5t, 6.6d, 6.8t, 8.75d (bipy), 6.7t, 6.95t (neoph Ph)
$(Me_2bipy)Ni(CH_2CMe_2Ph)_2$	1.58	1.83	7.7d	6.3d, 6.6s, 8.6d (bipy), 6.8t, 6.9t (neophyl Ph)
$Bu^t_2bipyNi(CH_2CMe_2Ph)_2$	1.64	1.85	7.72d	1.04 (Bu^t), 6.6–7.2m, 8.8d (6 Hz), 7.4d (1 Hz) bipy
$(Ph_2phen)Ni(CH_2CMe_2Ph)_2$	1.20	1.8	7.6d	9.1d, 6.7t, 7.0–7.2m
$(bipy)Ni(CH_2SiMe_2Ph)_2$	0.40	0.32	7.90	6.4t, 6.6d, 6.8t, 8.6d (bipy) 7.1–7.8m (Ph)
$(Me_2bipy)Ni(CH_2SiMe_2Ph)_2$	0.37	0.74	7.97	1.57 (bipy*Me*), 6.2d, 6.66s, 8.6d (bipy), 7.1–7.2m (80 Ph)
$^tBu_2bipyNi(CH_2SiMe_2Ph)_2$	0.3	0.2	7.8	8.7d (6 Hz), 6.65dd (46 Hz), 7.35d (1 Hz) bipy, 0.95s Bu^t, 6.9–7.1 (m Ph)
$(Me_4phen)Ni(CH_2SiMe_2Ph)_2$[b]	−0.14	0.30	7.64	2.41, 2.58 (phenMe_4), 7.06m, 7.64m Ph, 8.65, 8.13 phen
$(Ph_2phen)Ni(CH_2SiMe_2Ph)_2$	0.15	0.38	7.7	9.28d (J = 6 Hz), 8.0s, 6.99d (6 Hz) phen, 7.6–7.8m
$(bipym)Ni(CH_2SiMe_2Ph)_2 \cdot 1/2bipym$[b]	0.27	0.55	7.64–7.7m	6.25dd, 8.1dd, 8.46dd, bipymNi, 6.26t, 8.30d bipym, 6.9–7.0m
$(dppe)Ni(CH_2SiMe_2Ph)_2$	0.85	0.32	7.6dt	0.87dd (J = 5, 15 Hz), 7.25–7.45m (Ph), 7.45br,m, 1.7br,m (CH_2P)

[a] In toluene-d_8 unless otherwise noted.
[b] In $CDCl_3$.

ambient temperatures (L = PMe_2Ph, PMe_3), while the more soluble derivatives (L = PEt_3, PBu^n_3) react almost instantly. The new compounds are highly moisture- and air-sensitive and are crystalline with the exception of $Ni(CH_2CMe_2Ph)Cl(PEt_3)_2$ which is an orange oil at ambient temperature, unlike its PMe_3 analogue.

$Mg(CH_2SiMe_2Ph)Cl$ reacted with dihalonickel precursors appreciably faster than the neophylmagnesium derivative. The sila-neophyl products were generally more soluble and easier to crystallize than their neophyl counterparts and, when pure, are notably more inert to air and moisture (though they are still very air-sensitive). $Ni(CH_2SiMe_2Ph)Cl(PEt_3)_2$ is, like its neophyl analogue, an orange oil at ambient temperature.

Spectroscopy. NMR characteristics are summarized in Tables 2 and 3. Neophyl compounds are different from their sila-neophyl counterparts in several respects. NMR indicates that the former are fluxional at room temperature; P—C and P—H couplings are not resolved for the methylene groups of the alkyl ligand. Both the ^{13}C and ^1H signals emerge as triplets at about $-10°C$ in all three complexes (in toluene-d_8), however. The sila-neophyl complexes do not show any fluxional behaviour up to moderate temperatures. It is difficult to imagine a simple, sterically promoted phosphine dissociation (of the type that has been suggested[4]) that would explain the difference between the two groups of complexes. Anyway, such systems have been observed to be less fluxional with larger halides. At reduced temperatures, the complexes also exhibit the virtual coupling typical of strongly coupled, mutually *trans*-^{31}P nuclei. This disappears along with the P—H coupling as the temperature increases. The alkyl ligands show spectroscopic characteristics similar to those in the other two groups of nickel compounds.

(3) NiR_2L_2

This is also a widely studied area of organonickel chemistry and several bis-neophyl compounds have been partially characterized (L_2 = phen, bipy).[4b] We now report modified and alternative syntheses, a broader range of ancillary ligands, additional spectroscopic information and the parallel development of a range of sila-neophyl compounds.

Synthesis (a) R = *neophyl.* Bis-neophylnickel complexes with L = bipy and phen have been synthesized previously by metathetical displacement of the diamine in the highly labile intermediate (Ni(neophyl)$_2$(tmed), obtained from alkylation of $NiCl_2(py)_4$ in the presence of tmed.[4] We have been investigating the same precursors but were seeking to proceed directly to the desired product by displacement of pyridine from NiR_2py_2, formed *in situ* but not isolated. Under conditions similar to those reported by Carmona *et al.*, only poor yields of NiR_2L_2, where L_2 = bipy, phen, could be produced. The major impediment is the thermal lability of NiR_2py_2. The insolubility of its precursor, $NiCl_2py_4$ and also of the ancillary ligands (L_2) at the requisite low temperatures, guarantees that the concentration of reactant species remains low, with a consequent high probability that thermolysis of NiR_2py_2 will occur before substitution of the pyridine by L_2. One partially successful solution to this problem was the introduction of (soluble) tmed to trap the dialkylnickel as the less labile NiR_2(tmed).[4b] We adopted an alternative strategy. First, we reasoned that perhaps higher concentrations of, ideally, a more inert dialkylnickel precursor could be introduced into solution via related, but more soluble, $NiCl_2L'_4$ complexes. These precursors were readily prepared (from a range of readily available starting materials) by addition of an excess of the ligand L′ to solutions of $NiCl_2 \cdot 6H_2O$ or $NiBr_2 \cdot 3H_2O$ in ethanol. We explored derivatives where L′ was 4-phenylpyridine, 4-*tert*-butylpyridine (Bu^{t}py), 2,6-dimethylpyridine (2,6-lutidine), 2,5-lutidine, 2,4-lutidine, 2,3-lutidine, 3,4-lutidine and 3,5-lutidine. Only Bu^{t}py had a pronounced effect on the solubility of the halide derivative and hence the rate of transalkylation. It may also improve the thermolytic inertness of the intermediate.

$Mg(CH_2CMe_2Ph)Cl$ reacts readily with $NiCl_2(Bu^tpy)_4$ above $-30°C$; little alkylation is apparent below this temperature and decomposition of the dialkyl is appreciable above 0°C. The reaction is unsatisfactory if conducted in ether with ethereal MgRX but is faster in THF or in THF–ether mixtures. The ancillary ligands can be present initially or can be added after transalkylation at $-30°C$ (yields are poor if the mixture is allowed to warm too much). In the absence of L_2, the blue colour (the parent complex is only slightly soluble in THF giving a pale blue–violet solution) of $NiCl_2(Bu^tpy)_4$ rapidly becomes green on addition of MgRCl, and the solution then slowly becomes brown as the concentration of NiR_2L_2 increases. In the presence of L_2 the only colour observed is that of the product—substitution of L′ appears to be as rapid as the formation of the intermediate dialkyl. Substitution is, however, slow in the absence of Grignard.

The best success with this route has been obtained by using ligands, L_2, which have sufficient solubility under the prevalent conditions to ensure a rate of displacement of Bu^{t}py faster than the decay of the dialkyl. Bipy and phen have very limited solubility,

Table 3. ^{13}C and ^{31}P characteristics of $L_nNi(CH_2EMe_2Ph)$ complexes[a]

Compound	Ni—CH_2	C(Si)—$(CH_3)_2$	Distinguishable Ph carbons	Others [J(P—C)]	$^{31}P\{^1H\}$
$CpNi(PPh_3)(CH_2CMe_2Ph)$	[b]	[b]	[b]	[b]	46
$CpNi(PPh_3)(2\text{-}C_6H_4CMe_3)$	[b]	[b]	[b]	[b]	33
$CpNi(PPh_3)(CH_2SiMe_2Ph)$	−32 (20)	2.0		83 (C_5H_5)	
$CpNi(PCy_3)(CH_2SiMe_2Ph)$	−41 (20)	2.5	129, 128, 144	90.6 (C_5H_5); 26.9, 27.8, 28.2, 30.1 (Cy)	45
$CpNi(PEt_3)_2Cl$	—	—	—	96 (Cp); 21 [pseudo t, J = 15 Hz] (CH_2); 10 (CH_3)	32
$CpNi(PMe_2Ph)(CH_2SiMe_2Ph)$	−34 (12)	1.0	127, 128, 132, 144	89 [2 Hz] (C_5H_5); 15 [29 Hz] $P(CH_3)_3$	9
$(PMe_3)_2Ni(Cl)(CH_2CMe_2Ph)$ (−10°C)	[b]	[b]	[b]	[b]	
$(PMe_2Ph)_2Ni(Cl)(CH_2CMe_2Ph)$ (−10°C)	24 (20)	13	[c]	139, 129, 127, 126.5, 122, 121, 118, 27 (PMe_2)	−9
$(PEt_3)_2Ni(Cl)(CH_2CMe_2Ph)$ (−10°C)	12 (22)	33.4	153 (C_1), 137 (C_2)	41.2 (CMe_2), 14.9 (PCH_2CH_3), [J = 11], 8.5 (CH_3CH_2P)	1
$(PMe_3)_2Ni(Cl)(CH_2SiMe_2Ph)$	[b]	[b]	[b]	[b]	−12
$(PMe_2Ph)_2Ni(Cl)(CH_2SiMe_2Ph)$	−9.7 (20)	1.8	[c]	12.3 ($P(CH_2)$), 143.5, 138, 137.5, 135, 131.5	12

$(PEt_3)_2Ni(Cl)(CH_2SiMe_2Ph)$	20.4 (21)	2.6	144, 137, 133, 128	8.5 (Me), 14.6 (PCH_2)"t" [11 Hz]	0.5
$(PMe_3)_2Ni(CH_2SiMe_2Ph)_2$	25 (10) 19 (17)	−4.0		−1 (*trans*-PMe_3), 8 (*cis*-PMe_3)	−13 (*trans*) −16 (*cis*)
$bipyNi(CH_2CMe_2Ph)_2$	[d]	[d]	[d]	[d]	
$Me_2bipyNi(CH_2CMe_2Ph)_2$	21	33	153, 144	42 (bipy-CH_3) (155), 153, 147 (144), 128, 127, 126, 125, 120	
$Bu^t_2bipyNi(CH_2SiMe_2Ph)_2$	31.5	33.6		29.9 (CCH_3), 42 (CCH_3)	
$bipyNi(CH_2SiMe_2Ph)_2$	[d]	[d]	[d]	[d]	
$Me_2bipyNi(CH_2SiMe_2Ph)_2$	3	−1		30.5 (bipy-CH_3); 121, 126, 128.5, 129, 137.5, 145, 146, 148, 154	
$Bu^t_2bipyNi(CH_2SiMe_2Ph)_2$		2.6	148	30, 35 (CMe_3); 158, 154, 146, 116	
$Me_4phenNi(CH_2SiMe_2Ph)_2$	[d]	[d]	[d]	[d]	
$Ph_2phenNi(CH_2SiMe_2Ph)_2$	[d]	[d]	[d]	[d]	
$bipym(NiCH_2SiMe_2Ph)_2 \cdot 1/2L$	−3	2	121, 127, 145, 156	164, 154, 153, 134, 131	
$(dppe)Ni(CH_2SiMe_2Ph)_2$	2.01 (65,15)	2.7	133.5, 128.5, 127, 130	25.3 (CH_2—P) [21 Hz]; 146, 134, 127	49

[a] In benzene-d_6.
[b] Not measured.
[c] Obscured.
[d] Insufficiently soluble.

although green, crystalline $Ni(CH_2CMe_2Ph)_2(bipy)$ can be obtained in this way in poor yield (*ca* 25%). More amenable are the various substituted homologues of bipy and phen. Good yields of $Ni(CH_2CMe_2Ph)_2L_2$ where $L_2 = Me_2bipy$ (60%) and Bu^t_2bipy (75%) were recovered. These green, crystalline compounds are extremely air- and moisture-sensitive as solids and in solution.

These ligands endow appreciably greater solubility on their complexes than bipy and this suits them better for spectroscopic and mechanistic studies. Bu^t_2bipy is especially notable in this respect, and we have developed an efficient synthesis of the ligand which does not suffer from the drawback of extensive terpyridyl formation (which is common in this type of reaction).[8]

By the same route, $Ni(CH_2CMe_2Ph)_2(Ph_2phen)$ is recovered in low yield as an intensely blue oil (the phen compound is known to be blue) which we have been unable to crystallize or purify further, although ^1H NMR suggests it is essentially pure.

$Ni(CH_2CMe_2Ph)_2(dppe)$, on the other hand, is labile at or below ambient temperature, and we were unable to isolate it. The yellow compound can, however, be observed at temperatures below 0°C but it becomes red on warming to ambient temperature and we have failed to isolate any products from the resulting mixture. Derivatives with monodentate phosphines appear to be equally reactive.

Some of these compounds are also accessible by direct *trans*-alkylation of $NiCl_2L_2$ by $Li(CH_2CMe_2Ph)$. For example, $Ni(CH_2CMe_2Ph)_2(bipy)$ can be isolated in high yield (>80%) via treatment of $NiBr_2(bipy)$ with $Li(CH_2CMe_2Ph)$ in ether at low temperatures. Although a rarely used procedure for $NiR_2(bipy)$ complexes,[14] this can be a more reliable route since it avoids the problem of the poor solubility of bipy or the possible instability of any intermediate. The main drawbacks are the less convenient synthesis of $NiBr_2bipy$ and, in this instance, neophyl lithium. The latter is produced in *ca* 30% yield by interaction of 2% Na/Li alloy and neophyl chloride at −70°C. Little rearranged by-product $LiCMe_2CH_2Ph$ is observed (<5% by GC).

$NiBr_2(dppe)$ also reacts with neophyl lithium to give an orange solution, but the mixture decomposes on warming to a red solution from which none of the desired product could be isolated.

Synthesis (b) $R = CH_2SiMe_2Ph$. Reaction of $NiCl_2L_4$ (L = py, Bu^{t}py) with $Mg(CH_2SiMe_2Ph)Cl$ occurs much more readily than with the neophylmagnesium reagent. Like the previously reported $Ni(CH_2CMe_3)_2py_2$, both sila-neophyl derivatives are essentially inert at ambient temperature when pure, but both are unstable in a vacuum and in solution at room temperature. Both are extremely air- and moisture-sensitive, although the Bu^{t}py compound is much more convenient to handle as it is highly crystalline, forming large square plates. Usually, though, the compound was not isolated but was reacted with other ligands, L_2, *in situ*.

By this route $Ni(CH_2SiMe_2Ph)_2L_2$ complexes were prepared, where L_2 = bipy, Me_2bipy, Bu^t_2bipy, dppe, tmed and dppm. The dppm complex could only be isolated as a dark orange oil, however, and was characterized by NMR alone. All the bipyridyl complexes give green crystals, the tmed complex is a brown, semi-crystalline solid and the dppe complex forms well shaped yellow cubes. Complexes with phenanthroline ligands are not so readily formed because of the insolubility of the ligands under the reaction conditions. A simple modification, though, gives some of them in high yields: the pyridine intermediate is extracted into toluene or petrol and is added to a toluene solution of the ligand; the complexes form immediately. Me_4phen produces violet needles and Ph_2phen produces a blue–violet solid.

Due to its versatility as a ligand, an increasing number of metallo-derivatives of 2,2′-bipyrimidyl are emerging,[15] although none has so far featured nickel. Tractable products are only obtained by slow addition of a solution of $NiR_2(Bu^tpy)_2$ in petrol to an excess of bipym fully dissolved in toluene. Otherwise, inseparable mixtures result. The ultimate product is a green, highly air- and moisture-sensitive solid whose analytical and spectroscopic characteristics indicate $Ni(CH_2SiMe_2Ph)_2(bipym)\cdot 1/2bipym$. This formulation is apparently stable in acetone solution at ambient temperature, but in toluene, further bipym is released with the formation of a brown complex which we believe contains $R_2Ni(\mu\text{-bipym})NiR_2$, on the basis of comparisons with platinum-analogues.[15]

During the course of our work Carmona *et al.* have reported the formation of a nickelaindan from the reaction of $Mg(CH_2CMe_2Ph)Cl$ and $NiCl_2(PM_3)_2$ in the presence of iodide.[4d] This was proposedly formed by ready elimination of Me_3CPh from dineophylnickel(II). Other studies have suggested that silicon-containing compounds of the form of Si-neophyl are much less susceptible to these cyclization reactions. We attempted a similar procedure with $Mg(CH_2SiMe_2Ph)Cl$ and $NiCl_2(PMe_3)_2$. On NMR evidence, a dialkyl complex is produced which does not crystallize readily. The indications are, though, that the previous contention is correct.[4d]

Spectroscopy. NMR measurements on these complexes have been hindered previously by the insoluble nature of many of this class of compound. We have been able to overcome these difficulties to

some extent because both the alkyl ligands and the bidentate nitrogen donors chosen have better solubilizing properties than those previously studied. Our observations are summarized in Tables 2 and 3. The ^{13}C resonances can be difficult to assign unambiguously and the spectra are broadly similar to those observed previously for analogous platinum compounds. The alkyl groups appear with the same distinctive patterns as they have in the other two organonickel series. When the aromatic protons are all visible, the neophyls show an apparent A_2M_2X pattern with a doublet at low field and two triplets in a 2:2:1 ratio. The sila-neophyls show only two complex multiplets; the *ortho*-protons are nevertheless, always shifted significantly downfield. These differences in fine structure arise from the actual complexity of the AA'MM'X system which can produce greatly differing line shapes for only slightly different couplings or shifts. It is not clear whether these differences are caused by differing electronic influences on the aromatic rings of carbon and silicon or by steric effects (resulting in different distances from nickel and hence different shifts due to the paramagnetic anisotropy of the metal orbitals). The position of the Ni—CH_2 resonances are similar to those observed for a range of neopentyl and trimethylsilylmethyl compounds before, as are the positions of the CH_3 resonances.

CONCLUSIONS

We have extended the synthetic range of three major types of organonickel(II) compounds using the neophyl and Si-neophyl ligands. The reactions leading to sila-neophyl species tend to be cleaner, and the products significantly more air- and moisture-stable and thermolytically inert than their neophyl counterparts.

In the NiCp(R)L series, the neophyl compounds are, contrary to some previous reports,[10] isolable, but are susceptible to H-transfer isomerization, while the sila-neophyl compounds are not.

In the series, *trans*-$Ni(R)XL_2$, the neophyl complexes are again more sensitive to temperature and to the atmosphere, although we have not yet identified the primary decomposition products. Similar δ-H-transfer isomerization has, however, been excluded, as requisite *ortho-tert*-butylphenyl compounds have been synthesized directly. These are very inert and readily identifiable by NMR, and are not observed in sealed tube thermolyses of the neophyl compounds.

For the dialkylnickel complexes, once more it is the neophyl ligand that imparts much greater lability in all reactivity which we have observed. The compounds decay rapidly in the presence of O_2, ROH and chlorocarbons (CCl_4, $CHCl_3$ or CH_2Cl_2), to generate mixtures of *tert*-butylbenzene and the coupling product 2,5-dimethyl-2,5-diphenylhexane (bineophyl) in varying proportions. There is evidence, supported by previous work on other complexes,[16] that some of the reactions may occur via one-electron steps. For example, the reaction with CCl_4 gives considerable amounts of Cl_3CCCl_3, which is rapidly formed as the coupling product of $^{\bullet}CCl_3$ radicals. The organic product distribution, though, is *not* indicative of a radical reaction as neophyl radicals are known to give rearrangement products. This suggests a possible first step in the reaction of, possibly halide transfer from CCl_4 to nickel accompanied by electron transfer from nickel to give the $Cl_3C^{\bullet}$ radical and a nickel(II) intermediate which then has a choice of further reactions. Some neophyl chloride is detected as a product of these reactions, so one of the options may be reductive elimination of RCl; the other major path might be reductive elimination of RR. The complexes are not as chemically inert as some earlier reports have supposed,[10] and the previously reported thermolytic product distributions should be interpreted with some caution in the light of the compounds' reactivity with oxygen, water and solvents.

Our preliminary results suggest that Ni(neophyl)$_2$L$_2$ (L$_2$ = bipy, Me$_2$bipy, Bu$^t_2$bipy) undergo thermal metallacyclization via δ-H activation yielding Ni(2-$C_6H_4CMe_2CH_2$)L$_2$ (Scheme 3) and Bu^{t}Ph, similar to the platinum compounds. Either, because the mechanism is more complex in the nickel case or because further, secondary reactions take place under the prevailing conditions, an insoluble residue and a hydrocarbon product identified

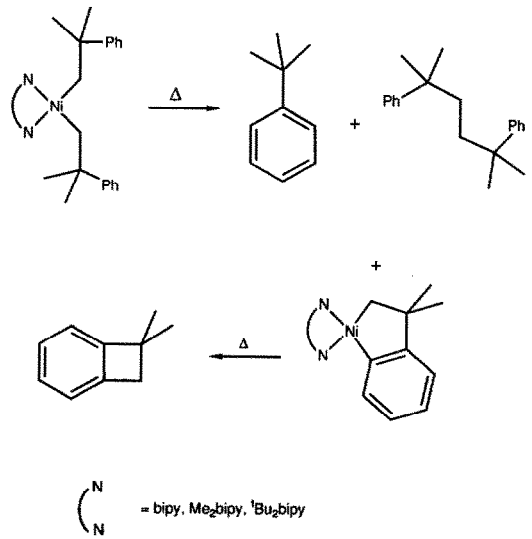

Scheme 3.

by GC–MS as 2,2-dimethyl-1,4-benzocyclobutane, are produced in addition to the expected products (Scheme 3). The mechanistics of these reactions are being explored currently in greater depth. We have also observed the metallacyclization of the PMe_3 compound reported recently by Carmona *et al.*[4] The $Ni(CH_2SiMe_2Ph)_2$ skeleton is clearly more robust and the range of accessible compounds is, consequently, greater, including the unusual bipym derivative. The reactivities of this series of compounds under more vigorous conditions has still to be investigated fully, but no metallacyclizations have been observed in preliminary studies. The inertness of silylmethyl compounds relative to alkylmethyl analogues has been observed elsewhere.[17] An unequivocal explanation has yet to be found.[18] Steric differences may play a part, but there are clealry also electronic differences as demonstrated by the spectroscopic characteristics of these compounds and their relatives.[3] Current mechanistic work on complexes containing these ligands will clarify the issues.

Acknowledgements—We are grateful to the Department of Education for Northern Ireland for the award of a postgraduate studentship (to SIB), and to the Royal Society and the University of London Central Research Fund for Equipment grants in support of some of this work. The Apple Macintosh programme Chemdraw 2, used in illustrations, is licensed to Prof. Steve Ley of this department, whom we thank. In addition, we thank Sue Johnson and Dick Sheppard for some of our high field NMR data.

REFERENCES

1. (a) R. di Cosimo, S. S. Moore, A. F. Sowinski and G. M. Whitesides, *J. Am. Chem. Soc.* 1982, **104**, 124; (b) P. Foley and G. M. Whitesides, *J. Am. Chem. Soc.* 1979, **101**, 2732; (c) P. Foley, R. Di Cosimo and G. M. Whitesides, *J. Am. Chem. Soc.* 1980, **102**, 6713; (d) D. C. Griffiths and G. B. Young, *Polyhedron* 1983, **2**, 1095; (e) D. C. Griffiths and G. B. Young, *Organometallics*, in press; (f) D. C. Griffiths, L. G. Joy, A. C. Skapski, D. J. Wilkes and G. B. Young, *Organometallics* 1986, **5**, 1744.
2. S. Komiya, Y. Abe, A. Yamamoto and T. Yamamoto, *Organometallics* 1983, **2**, 1466; R. H. Grubbs, A. Miyashita, M. Liu and P. Burk, *J. Am. Chem. Soc.* 1978, **100**, 2148; G. Smith and J. K. Kochi, *J. Organomet. Chem.* 198, **198**, 199; T. Kohara, T. Yamamoto and A. Yamamoto, *J. Organomet. Chem.* 1980, **192**, 265; T. T. Tsou and J. K. Kochi, *J. Am. Chem. Soc.* 1979, **101**, 7547; D. G. Morrell and J. K. Kochi, *J. Am. Chem. Soc.* 1975, **97**, 7262.
3. (a) B. C. Ankianiec and G. B. Young, *Polyhedron*, in press; (b) R. D. Kelly and G. B. Young, *Polyhedron* 1989, **8**, 57; (c) S. K. Thomson and G. B. Young, *Polyhedron* 1988, **7**, 1953.
4. (a) E. Carmona, F. Gonzalez, M. L. Poveda, J. L. Atwood and R. D. Rogers, *J. Chem. Soc., Dalton Trans.* 1980, 2108; (b) F. Carmona, F. Gonzalez, M. L. Poveda, J. L. Atwood and R. D. Rogers, *J. Chem. Soc., Dalton Trans.* 1981, 777; (c) E. Carmona, M. Paneque, M. L. Poveda, R. D. Rogers and J. L. Atwood, *Polyhedron* 1984, **3**, 317; (d) E. Carmona, M. L. Poveda, P. Palma, M. Paneque, E. Gutierrez-Puebla and A. Monge, *J. Am. Chem. Soc.* 1986, **108**, 6424.
5. K. A. Jensen, P. H. Nielsen and C. T. Pedersen, *Acta Chem. Scand.* 1963, **17**, 1115; L. M. Venanzi, *J. Chem. Soc.* 1958, 719.
6. C. A. Tolman, *Chem. Rev.* 1977, **77**, 313.
7. A. von Zelewsky and P. Belser, *Helv. Chim. Acta* 1980, **63**, 1675.
8. F. A. Hart and J. E. Newbery, *J. Inorg. Nucl. Chem.* 1969, **31**, 1725.
9. M. C. Baird and J. Thompson, *Can J. Chem.* 1970, **48**, 3443; M. C. Baird and J. Thompson, *Inorg. Chim. Acta* 1973, **7**, 105.
10. B. Åkermark and A. Ljungqvist, *J. Organomet. Chem.* 1978, **149**, 97; B. Åkermark and A. Ljungqvist, *J. Organomet. Chem.* 1979, **182**, 47.
11. L. A. Kaempfe and K. W. Barnett, *Inorg. Chem.* 1973, **12**, 2578.
12. D. R. Fahey, R. G. Miller, R. D. Stauffer and D. R. Parnell, *J. Am. Chem. Soc.* 1970, **92**, 1510.
13. P. W. Jolly, in *Comprehensive Organometallic Chemistry* (Edited by G. Wilkinson), Vol. 6, p. 37. Pergamon Press, Oxford (1981).
14. M. Bochman, G. Wilkinson and G. B. Young, *J. Chem. Soc., Dalton Trans.* 1980, 1879.
15. See, for example, V. F. Sutcliffe and G. B. Young, *Polyhedron* 1984, **3**, 87; J. D. Scott and R. J. Puddephatt, *Organometallics* 1986, **5**, 1538 and refs cited therein.
16. G. Smith and J. K. Kochi, *J. Organomet. Chem.* 1980, **198**, 199; J. K. Kochi and T. T. Tsou, *J. Am. Chem. Soc.* 1979, **101**, 7547.
17. See, for example, T. H. Tulip and D. L. Thorn, *J. Am. Chem. Soc.* 1981, **103**, 2448; For a review, see T. H. Tulip and G. B. Young, in *Inorganic Reactions and Methods* (Edited by J. J. Zuckerman). Springer-Verlag, Berlin (1989), in press; M. F. Lappert, P. J. Davidson and R. Pearce, *Chem. Rev.* 1976, **76**, 218.
18. B. Wozniak, J. D. Ruddick and G. Wilkinson, *J. Chem. Soc. A* 1971, 3116; M. F. Lappert, D. S. Patil and J. B. Pedley, *J. Chem. Soc., Chem. Commun.* 1975, 830.

Polyhedron Vol. 8, No. 5, pp. 597–602, 1989
Printed in Great Britain

0277–5387/89 $3.00+.00
Pergamon Press plc

CARBONYLATION OF OSMIUM AND RUTHENIUM OXO COMPLEXES. X-RAY CRYSTAL STRUCTURES OF $[Me_4N]_2[Os(O)_2(COOMe)_2(\mu\text{-}OMe)]_2$ AND $[^nPr_4N][fac\text{-}Ru(O_2CMe)_3(CO)_3]$

JOHN ARNOLD and GEOFFREY WILKINSON*

Department of Chemistry, Imperial College, London SW7 2AY, U.K.

and

BILQUIS HUSSAIN and MICHAEL B. HURSTHOUSE*

Department of Chemistry, Queen Mary College, London E1 4NS, U.K.

(*Received* 3 *August* 1988; *accepted* 28 *September* 1988)

Abstract—Insertion of CO into the Os—OMe bonds in $[Os(O)_2(OMe)_4]^{2-}$ leads to the formation of methoxide bridged dimers, $[Os(O)_2(COOMe)_2(\mu\text{-}OMe)]_2^{2-}$, as their K^+, Me_4N^+ and $^nBu_4N^+$ salts. The X-ray structure of the $^nBu_4N^+$ derivative is reported. Reduction of RuO_4^- in acetic acid by CO gives the anion $[fac\text{-}Ru(O_2CMe)_3(CO)_3]^-$, which has been structurally characterized as the $^nPr_4N^+$ salt. IR, NMR and conductivity data are also reported.

There has been considerable study of high oxidation state complexes of ruthenium and osmium.[1a,b,2] We now report carbonylation reactions of the anion $[Os(O)_2(OMe)_4]^{2-}$ and of the anion $[RuO_4]^-$ in acetic acid solution.

RESULTS AND DISCUSSION

Osmium

The complex $K_2[Os(O)_2(OMe)_4]$ (**1**) is a useful synthetic reagent.[1b,3] Since this salt has very limited solubility properties, we sought a more soluble derivative. Unfortunately, metathesis reactions with alkylammonium halides were unsuccessful, but substitution of alkylammonium hydroxides for KOH in the synthesis of the anion gave the same bright blue–green methanol solutions characteristic of **1**, which we propose contain $[NR_4]_2[Os(O)_2(OMe)_4]$ (**2**, R = Me; **3**, R = ^{n}Bu). Attempts to isolate these materials as solids failed due to the decomposition to brown oils on evaporation or precipitation—their reaction chemistry was, therefore, examined *in situ*.

Carbonylation of methanolic solutions of **1–3** gradually results in a colour change from blue to yellow. Crystalline complexes were subsequently isolated by either cooling (**1** and **2**) or evaporation followed by recrystallization from THF (**3**). These reactions proceed as in eq. (1).

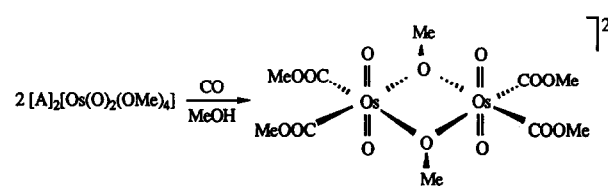

4, A = K; 5, A = Me_4N; 6, A = $^nBu_4N$ (1)

Complexes **4–6** result from insertion of CO into two Os—OMe bonds, followed by methoxide elimination and dimerization. Each pseudo-octahedral osmium(VI) centre thereby attains an 18-electron configuration.

*Authors to whom correspondence should be addressed.

These hygroscopic, diamagnetic salts have been characterized by elemental analysis, IR and NMR spectroscopy and, in the case of **5**, by X-ray crystallography.

The carbomethoxy ligands display two strong IR stretches at 1660 and 1640 cm^{-1} (for **4**) and the intense $Os(O)_2$ band has moved from 825 cm^{-1} (in **1**) to 870 cm^{-1} (in **4**). Conductivity data for **6** in MeCN accord for a 2 : 1 electrolyte. NMR spectra serve to differentiate between the two different types of —OMe groups: the ^1H NMR spectrum of **6** in $CDCl_3$ shows two singlets at δ 4.70 and 4.30 (relative intensities 1 : 2). Corresponding peaks in the ^{13}C NMR spectrum are found at δ 50.27 and 58.87, respectively. In addition, a single ^{13}C resonance at δ 181.0 is assigned to the osmium-bound carbonyl carbon of the —COOMe group. NMR data for **4** and **5** were inaccessible due to their limited solubilities.

Attempts to extend this chemistry to other alkoxides have met with little success. Repeating the synthesis of **1–3** in alcohols other than MeOH (or in mixtures with MeOH) resulted in decomposition to oily brown mixtures. Interestingly, no reaction was observed on attempted carbonylation of the chelating alkoxide complex $K_2[Os(O)_2(C_2H_4O_2)_2]$.[4] Reaction of the hydroxo species $K_2[Os(O)_2(OH)_4]$[5] with CO in water resulted in decomposition to a black insoluble powder. Finally, treatment of OsO_4 with CO in acetic acid at 100°C gave a black precipitate. The IR spectrum of this material showed bands assignable to $—O_2CMe$ and Os—CO groups, but further characterization was impossible due to the complete insolubility of the compound in common solvents; repeating the reaction in the presence of $^nBu_4NO_2CMe$ failed to yield tractable complexes.

The structure of the dimeric anion in **5**, which lies on a centre of symmetry, is shown in Fig. 1; selected bond lengths and angles are given in Table 1. The bridging methoxides are pyramidal at the oxygen and the presence of the centre of symmetry results in a *trans* arrangement of the C—O bonds. The Os—O bridge bonds are equal within experimental error. The dioxo-osmium unit is essentially linear, and the Os=O bonds are slightly longer than those in the tetrahedral osmium(VI) oxo-aryl, $Os(O)_2(mesityl)_2$.[6] The Os—C(acyl) bonds, which lie *trans* to the Os—O bonds of the methoxy bridge, are slightly shorter than that to the formyl carbon in $Os(CO)(CHO)(dppe)_2$.[7]

Ruthenium

Heating an acetic acid solution of $[^nPr_4N][RuO_4]$[8] under a CO atmosphere results in a colour change from green, through black, to clear yellow. Work-up of this solution gave a mixture of products as judged by IR and NMR spectroscopy. However, one complex was isolated in crystalline form and has been identified by elemental analysis, IR and NMR spectroscopy and, unequivocally, by X-ray crystallography. Yellow crystals of $[^nPr_4N][fac\text{-}Ru(O_2CMe)_3(CO)_3]$ (**7**) were isolated in 13% yield after crystallization from THF.

In the IR spectrum, **7** exhibits strong bands at 2104, 2035 and 2019 cm^{-1} for the Ru—CO ligands, and absorptions due to the unidentate acetate groups at 1612 and 1596 cm^{-1} (ν_{asym}) and 1363 and 1314 cm^{-1} (ν_{sym}). The methyl groups in these ligands show a singlet at δ 2.02 in the ^1H NMR spectrum in $CDCl_3$. This complex would appear to be the only example of a monomeric ruthenium carbonyl acetate, however, $Ru(O_2CCF_3)_2(CO)_3(THF)$,[9] $[Ru(O_2CMe)(CO)_3]_2$,[10] $[Ru(O_2CMe)(CO)_2]_n$,[10] and various $[Ru(O_2CMe)(CO)_2L]_2$[10] and $Ru(O_2CMe)_2(CO)_2(L)_2$[11] complexes (L = tertiary phosphine or arsine, C_5H_5N or MeCN) have been reported.

The crystal structure of **7** contains two symmetry independent units which are, however, chemically equivalent. A diagram of one of the anions is given

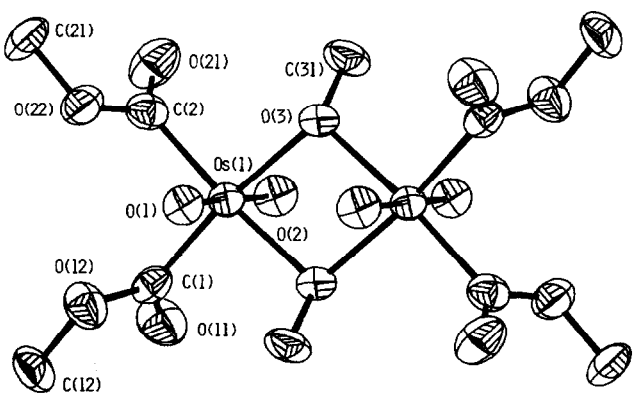

Fig. 1. The structure of the anion in $[Me_4N]_2[Os(O)_2(COOMe)_2(\mu\text{-}OMe)]_2$ (**5**).

Table 1. Selected bond lengths and angles for compound **5**

Bond lengths (Å)			
O(1)—Os(1)	1.728(5)	O(2)—Os(1)	1.722(5)
C(2)—Os(1)	2.071(7)	C(1)—Os(1)	2.070(7)
O(3)—Os(1)	2.178(5)	O(3)—Os(1a)	2.173(5)
C(31)—O(3)	1.426(7)	O(12)—C(1)	1.346(7)
O(11)—C(1)	1.200(7)	C(12)—O(12)	1.442(8)
O(21)—C(2)	1.198(7)	O(22)—C(2)	1.363(7)
C(21)—O(22)	1.446(8)	Os(1)—Os(1a)	3.385(4)
Bond angles (°)			
O(2)—Os(1)—O(1)	175.8(2)	O(3)—Os(1)—O(1)	88.7(2)
O(3)—Os(1)—O(2)	88.6(2)	C(1)—Os(1)—O(1)	93.5(3)
C(1)—Os(1)—O(2)	88.9(3)	C(1)—Os(1)—O(3)	172.8(2)
C(2)—Os(1)—O(1)	91.5(3)	C(2)—Os(1)—O(2)	92.0(3)
C(2)—Os(1)—O(3)	96.2(2)	C(2)—Os(1)—C(1)	90.6(3)
Os(1)—O(3)—Os(1a)	102.3(3)	C(31)—O(3)—Os(1)	116.3(4)
O(3)—Os(1)—O(3a)	77.7(3)	O(12)—C(1)—Os(1)	115.0(4)
O(11)—C(1)—Os(1)	125.0(5)	O(11)—C(1)—O(12)	120.0(5)
C(12)—O(12)—C(1)	116.7(6)	O(21)—C(2)—Os(1)	127.7(5)
O(22)—C(2)—Os(1)	112.7(4)	O(22)—C(2)—O(21)	119.5(6)
C(21)—O(22)—C(2)	116.3(6)	C(31)—O(3)—Os(1a)	116.4(4)

Key to symmetry operations relating designated atoms to reference atoms at (x, y, z): (a) $-x, -y, -z$.

in Fig. 2, selected bond lengths and angles for both in Table 2. The anions have a *fac* octahedral structure and within the limits of experimental error equivalent bond lengths are equal. The accuracy of the structure is not high, due to a large degree of thermal motion and/or disorder in all components. Accordingly, it is not possible to discuss in detail any special features of the structure. However, it is perhaps worth noting that the Ru—O—C angles to the monodentate acetates are all very similar and close to 120°.

EXPERIMENTAL

Microanalyses were carried out by Imperial College or Pascher Laboratories. Melting points were

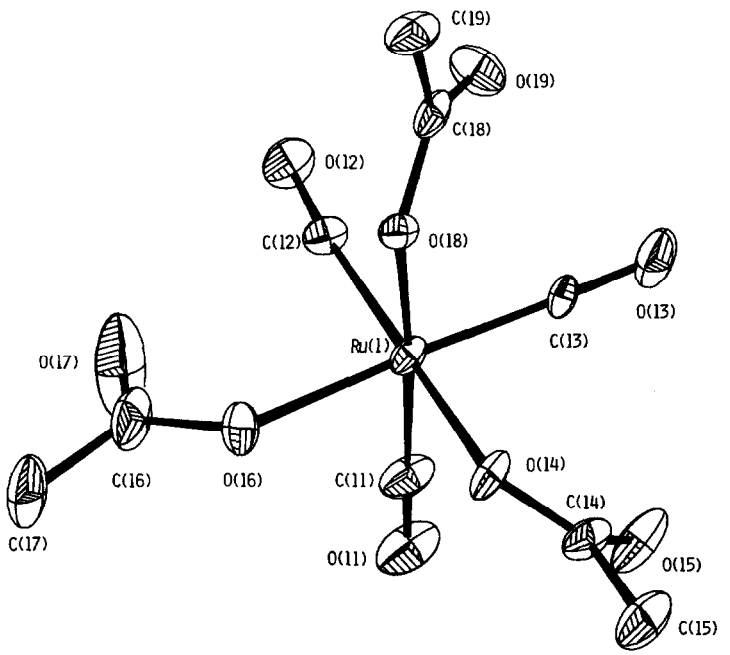

Fig. 2. The structure of one of the anions in [^{n}Pr$_4$N][*fac*-Ru(O$_2$CMe)$_3$(CO)$_3$] (**7**).

Table 2. Selected bond lengths and angles for compound 7

	Molecule 1 (n = 1)	Molecule 2 (n = 2)
Bond lengths (Å)		
C(n1)—Ru(n)	1.893(19)	1.884(19)
C(n2)—Ru(n)	1.936(19)	1.861(17)
C(n3)—Ru(n)	1.853(19)	1.915(24)
O(n4)—Ru(n)	2.068(12)	2.092(10)
O(n6)—Ru(n)	2.078(12)	2.066(14)
O(n8)—Ru(n)	2.080(11)	2.077(12)
O(n1)—C(n1)	1.122(22)	1.131(22)
O(n2)—C(n2)	1.095(21)	1.126(20)
O(n3)—C(n3)	1.141(23)	1.121(29)
C(n4)—O(n4)	1.270(23)	1.266(19)
O(n5)—C(n4)	1.267(21)	1.207(23)
C(n5)—C(n4)	1.522(28)	1.511(24)
C(n6)—O(n6)	1.319(29)	1.285(21)
O(n7)—C(n6)	1.193(29)	1.227(23)
C(n7)—C(n6)	1.500(28)	1.459(34)
C(n8)—O(n8)	1.294(17)	1.301(26)
O(n9)—C(n8)	1.248(19)	1.239(26)
C(n9)—C(n8)	1.536(24)	1.431(25)
Bond angles (°)		
C(n2)—Ru(n)—C(n1)	90.4(8)	90.0(8)
C(n3)—Ru(n)—C(n2)	89.7(8)	90.4(9)
O(n4)—Ru(n)—C(n1)	94.1(7)	92.9(6)
O(n4)—Ru(n)—C(n3)	92.3(7)	94.7(7)
O(n4)—Ru(n)—C(n2)	175.1(5)	174.2(7)
O(n6)—Ru(n)—C(n1)	89.2(8)	93.6(8)
O(n6)—Ru(n)—C(n3)	176.4(6)	177.5(6)
O(n6)—Ru(n)—C(n2)	93.9(7)	89.8(8)
C(n3)—Ru(n)—C(n1)	91.5(9)	88.9(9)
O(n6)—Ru(n)—O(n4)	84.1(5)	85.1(5)
O(n8)—Ru(n)—C(n1)	175.1(6)	176.4(6)
O(n8)—Ru(n)—C(n2)	90.8(6)	92.7(7)
O(n8)—Ru(n)—C(n3)	93.3(7)	93.3(7)
O(n8)—Ru(n)—O(n4)	84.6(5)	84.2(4)
O(n8)—Ru(n)—O(n6)	86.0(5)	84.1(5)
O(n1)—C(n1)—Ru(n)	178.0(20)	173.2(17)
O(n2)—C(n2)—Ru(n)	173.6(15)	176.7(17)
O(n3)—C(n3)—Ru(n)	178.2(15)	176.8(16)
C(n4)—O(n4)—Ru(n)	121.6(10)	121.0(10)
O(n5)—C(n4)—O(n4)	124.8(16)	124.7(15)
C(n5)—C(n4)—O(n4)	118.6(16)	114.7(15)
C(n5)—C(n4)—O(n5)	116.6(18)	120.6(16)
C(n6)—O(n6)—Ru(n)	120.9(11)	121.1(12)
O(n7)—C(n6)—O(n6)	126.7(19)	124.4(21)
C(n7)—C(n6)—O(n6)	112.7(18)	115.0(16)
C(n7)—C(n6)—O(n7)	120.5(24)	120.3(19)
C(n8)—O(n8)—Ru(n)	122.3(9)	123.6(11)
O(n9)—C(n8)—O(n8)	122.1(14)	121.9(16)
C(n9)—C(n8)—O(n8)	114.5(13)	114.8(20)
C(n9)—C(n8)—O(n9)	123.3(14)	123.1(21)

determined in sealed capillaries and are uncorrected. Spectrometers. IR: Perkin–Elmer 683 (values in cm^{-1}); NMR: Jeol FX 90Q (in $CDCl_3$, 20°C, referenced to $SiMe_4$ at δ 0.00). All operations were carried out under argon using dry, degassed solvents. Conductivities were determined on a Data Scientific PTI-18 instrument.

$[Me_4N][Os(O)_2(OMe)_4]$ (2)

A solution of NMe_4OH in MeOH (2.3 cm^3 of a 20% solution) was added to OsO_4 (0.25 g, 1.0 mmol) in MeOH (10 cm^3) at −78°C. The orange solution was warmed to 20°C to give a bright blue solution of **2**.

$[^nBu_4N]_2[Os(O)_2(OMe)_4]$ (3)

Prepared as for **2** but using a 1M solution of $^nBu_4NOH$.

$K_2[Os(O)_2(COOMe)_2(\mu\text{-}OMe)]_2 \cdot (MeOH)$ (4)

Complex **1** (0.27 g, 0.55 mmol) in MeOH (20 cm^3) was pressured with CO (20 psi). After 20 h, the golden-yellow solution was cooled to −15°C for 8 h to afford **4** (0.20 g, 88%) as yellow needles (m.p. > 340°C). Found: C, 14.5. Calc. for $C_{11}H_{22}K_2O_{15}Os_2$: C, 15.5%. Due to the compound's insolubility in common solvents, our attempts at recrystallization (in order to obtain a better analysis) were unsuccessful. IR: 3500br, 1660s, 1640s, 1420m, 1180m, 1100br, 1060s, 942m, 868s, 477m.

$[Me_4N]_2[Os(O)_2(COOMe)_2(\mu\text{-}OMe)]_2$ (5)

Carbon monoxide was bubbled through the MeOH solution of **2** described above. Cooling to −78°C for 6 h gave yellow plates (m.p. 165–170°C) in 60% yield. Yellow prisms suitable for X-ray crystallography were obtained by recrystallization from MeCN at −15°C. Found: C, 24.8; N, 3.12. Calc. for $C_{19}H_{46}N_2O_{14}Os_2$: C, 25.1; N, 3.09%. IR: 1645s, 1630s, 1490m, 1420m, 1175m, 1094s, 1065s, 1032s, 944m, 863s, 785w, 689w, 468s.

$[^nBu_4N]_2[Os(O)_2(COOMe)_2(\mu\text{-}OMe)]_2$ (6)

After carbonylation of the MeOH solution of **3** above, the yellow solution was evaporated under reduced pressure and the residue recrystallized from THF. Yield *ca* 70%, yellow needles (m.p. 118–122°C). Found: C, 41.4, N, 2.32. Calc. for $C_{41}H_{90}N_2O_{14}Os_2$: C, 41.4; N, 2.28%. IR: 1673s, 1642m, 1415w, 1072s, 1050s, 953w, 879s, 477m. ^1H NMR: 1.51 (br, 12H), 2.08 (br, 16H), 3.78 (br, 8H),

4.30 (s, 6H), 4.70 (s, 3H). $^{13}C\{^1H\}$ NMR: 13.65(s), 19.63(s), 24.15(s), 50.27(s), 58.87(s), 181.0(s). Conductivity: $\Lambda_M = 94$ ohm^{-1} cm^2 mol^{-1} (in MeCN, 0.01M).

[^{n}Pr$_4$N][*fac*-Ru(O$_2$CMe)$_3$(CO)$_3$] (7)

A solution of [^{n}Pr$_4$N][RuO$_4$] (0.50 g, 1.4 mmol) in acetic acid (10 cm^3) was heated to 100°C under CO (50 psi) for 10 h. The yellow solution was evaporated *in vacuo* and the sticky residue extracted into THF (50 cm^3). After filtration through Celite, the volume of solvent was reduced to *ca* 10 cm^3 and the solution was cooled to −15°C overnight. Pale yellow prisms (m.p. 162–163°C, decomp.) were obtained after filtration (0.10 g, 13%). Found: 44.4; H, 6.65; N, 2.87. Calc. for $C_{21}H_{37}NO_9Ru$: C, 46.0; H, 6.80; N, 2.55%. IR: 2104s, 2035s, 2019s, 1974w, 1612s, 1596s, 1490s, 1363s, 1315s, 1005w, 754m, 677m, 626m, 575w. ^{1}H NMR: 1.00 (t, 12H), 2.73 (m, 8H), 2.02 (s, 9H), 3.17 (t, 8H).

X-ray crystallography

Crystals of both compounds were sealed in thin-walled glass capillaries under argon. Following preliminary photography, unit cell and intensity data were obtained using a CAD4 diffractometer with graphite monochromated Mo-K_α radiation ($\lambda = 0.71069$ Å), according to previously detailed procedures.[12] The structures were solved via standard heavy atom methods and refined by full-matrix least-squares. For **5**, non-hydrogen atoms were refined anisotropically, hydrogens isotropically. For **7**, the structure was refined in two blocks, one containing parameters for the anions, the other for the cations. Non-hydrogen atoms were refined anisotropically, and hydrogens inserted in idealized positions and refined as components of rigid groups with group U_{iso} values. The refinement was not very satisfactory due almost certainly to high thermal motion (or disorder) in both cations and anions. Experimental data and details of the analyses are given in Table 3.

Atomic coordinates, displacement factor coefficients, full lists of bond lengths and angles, and lists of F_o/F_c values have been deposited as supplementary data with the Editor, from whom copies are available on request. Atomic coordinates have also been deposited with the Cambridge Crystallographic Data Centre.

Acknowledgements—We thank the SERC for support and Johnson Matthey for a loan of ruthenium and osmium.

Table 3. Crystal data, details of intensity measurements and structure refinements for compounds **5** and **7**

Chemical formula	$[C_5H_9O_7Os]_2 \cdot 2[C_4H_{12}N]$	$[C_9H_9O_9Ru][C_{12}H_{28}N]$
Formula weight	890.936	1097.184
Crystal system	Monoclinic	Monoclinic
a (Å)	9.265(1)	17.483(1)
b (Å)	12.483 (3)	18.444(1)
c (Å)	12.591(2)	19.486(3)
α (°)	90.0	90.0
β (°)	96.75(1)	114.94(4)
γ (°)	90.0	90.0
Volume (Å^3)	1446.12	5697.31
Space group	$P21/n$	$P21/a$
Z	4	8
D_c (g cm^{-3})	2.045	1.279
μ	88.45	5.79
F(000)	856	2288
h,k,l, range	$0 \rightarrow 11$	$0 \rightarrow 18$
	$0 \rightarrow 14$	$0 \rightarrow 19$
	$-15 \rightarrow 15$	$-20 \rightarrow 20$
Total no. of reflections	2838	7529
No. of unique reflections	2533	6973
No. of reflections used	2095	3412
Significance test	$[F > 3\sigma(F)]$	$[F > 6\sigma(F)]$
No. of parameters	247	357
Weighting scheme parameter g in $w = 1/[\sigma^2(F)+gF^2]$	0.000201	0.008682
Final R	0.0206	0.0616
Final R_w	0.0205	0.0661

REFERENCES

1. (a) F. A. Cotton and G. Wilkinson, *Advanced Inorganic Chemistry*, 5th edn. John Wiley, New York (1988); (b) W. P. Griffith, M. Schröder and T. A. Stephenson, *Comprehensive Coordination Chemistry* (Edited by G. Wilkinson, R. D. Gillard and J. A. McCleverty), Vol. 4, pp. 277, 519. Pergamon Press, Oxford (1987).
2. (a) T. C. Lau and J. K. Kochi, *J. Chem. Soc., Chem. Commun.* 1987, 798; (b) C.-M. Che, T.-F. Lai and K.-Y. Wong, *Inorg. Chem.* 1987, **26**, 2289.
3. (a) T. Behling, G. S. Girolami, G. Wilkinson, R. G. Somerville and M. B. Hursthouse, *J. Chem. Soc., Dalton Trans.* 1984, 877; (b) A. J. Nielson and W. P. Griffith, *J. Chem. Soc., Dalton Trans.* 1978, 1501.
4. W. P. Griffith and R. Rossetti, *J. Chem. Soc., Dalton Trans.* 1972, 1449.
5. J. M. Malin, *Inorg. Synth.* 1980, **20**, 61.
6. P. Stavropoulos, P. G. Edwards, T. Behling, G. Wilkinson, M. Motevalli and M. B. Hursthouse, *J. Chem. Soc., Dalton Trans.* 1987, 169.
7. G. Smith, D. J. Cole-Hamilton, M. Thornton-Pett and M. B. Hursthouse, *Polyhedron* 1983, **2**, 1241.
8. W. P. Griffith, S. V. Ley, G. P. Whitcombe and A. D. White, *J. Chem. Soc., Chem. Commun.* 1987, 1625.
9. A. J. Lindsay, G. Wilkinson, M. Motevalli and M. B. Hursthouse, *J. Chem. Soc., Dalton Trans.* 1987, 2723.
10. G. R. Crooks, B. F. G. Johnson, J. Lewis, I. G. Williams and G. Gamlen, *J. Chem. Soc.* A 1969, 2761.
11. P. Frediani, M. Bianchi, F. Piacenti, S. Ianelli and M. Nardelli, *Inorg. Chem.* 1987, **26**, 1592.
12. R. A. Jones, K. M. A. Malik, M. B. Hursthouse and G. Wilkinson, *J. Am. Chem. Soc.* 1979, **101**, 4128; S. J. Sherlock, M. Cowie, E. Singleton and M. M. de V. Steyne, *Organometallics* 1988, **7**, 1663.

Polyhedron Vol. 8, No. 5, pp. 603–611, 1989
Printed in Great Britain

0277–5387/89 $3.00+.00
© 1989 Pergamon Press plc

INTERACTION OF IRON CARBONYLS WITH LEWIS BASES

YU. A. BELOUSOV,* T. A. KOLOSOVA and V. N. BABIN

A. N. Nesmeyanov Institute of Organoelement Compounds, USSR Academy of Sciences, 28 Vavilov Str., 117813 Moscow, U.S.S.R.

(*Received* 16 *February* 1988; *accepted* 28 *September* 1988)

Abstract—The interaction of $Fe_n(CO)_m$ ($n = 1$, $m = 5$; $n = 2$, $m = 9$; $n = 3$, $m = 12$) with Lewis bases taken in the anionic form (as NaL salts, where L = azolide, OR, SR, NR_2, NO_2; $R_2C = NO_2$, where R = H or alkyl) and in the neutral form (dimethyl sulphoxide, dimethyl formamide, pyridine, *o*-phenanthroline) was studied. The first stage of the reaction is the formation of an iron carbonyl–Lewis base complex. In the second stage one-electron transfer from this activated complex to the free iron carbonyl gives rise to both the Fe^I complexes and the anion radicals $Fe_2(CO)_8^-$, $Fe_3(CO)_{11}^-$, $Fe_4(CO)_{13}^-$ and $Fe_3(CO)_{12}^-$. The latter species are active particles prone to interconversions and are capable of participating in cluster-formation processes. A Water Gas Shift Reaction (WGSR) mechanism involving iron carbonyl radical anions is proposed.

The iron carbonyl–Lewis base (L) system is responsible for a variety of both catalytic and non-catalytic conversions involving carbon monoxide. Interest in the CO-based syntheses and metal carbonyls used as catalysts is attributed to the recent development of C_1-chemistry permitting the use of resources alternative to petroleum.

Owing mainly to the studies of Hieber and coworkers[1] it is known that the predominant route of the iron carbonyl–Lewis base reaction is a two-electron redox disproportionation to give carbonyl ferrates, eq. (1)

$$Fe_{n'}(CO)_{m'} + kL \rightarrow [FeL_k]^{2+} + [Fe_n(CO)_{m-1}]^{2-} \quad (1)$$

or hydridocarbonyl ferrates $[FeL_k]^{2+}[HFe_n(CO)_{m-1}]_2^-$, where $n = 1$, $m = 5$; $n = 2$, $m = 9$; $n = 3$, $m = 12$; $n = 4$, $m = 14$, and $n' = 1$, $m' = 5$; $n' = 2$, $m' = 9$; $n' = 3$, $m' = 12$, and $2 \leqslant k \leqslant 6$.

The interpretation of redox disproportionation as a two-electron process underlies various mechanisms of reactions involving the iron carbonyl–Lewis base system and, in particular, catalytic cycles.[2,3]

All these mechanisms are based on a common idea of a preliminary formation of complexes where the Lewis base is bonded to the CO ligand. Then it is assumed that there occurs either elimination of the carbonylated product to give a 16-electron species "$Fe(CO)_4$"[2] or a two-electron reduction to give a carbonyl (hydridocarbonyl) ferrate anion with a subsequent (at the stage of hydrogen evolution) backward two-electron oxidation to generate the same $Fe(CO)_4$. Both types of the anions are stable enough to be isolated in the form of salts, and the adducts with a



bond can sometimes be detected in the course of the reaction.[4,5] However, formation of the coordinatively unsaturated and electron-deficient species $Fe(CO)_4$ was hypothesized from the fact that it was detected by IR spectroscopy in the inert gas matrix at temperatures around 20 K.[6] It is quite clear that this postulate is a weak point in the traditional approach to the mechanism of catalytic conversions. The formation of such ideas seems to be influenced by the Tolman rule[7] for determining the predominant routes of the reaction of the homogeneous catalysis via 16- and 18-electron complexes.

On the other hand, there exists an independent branch of carbonyl chemistry dealing with the odd-electron Fe^{-1} derivatives, i.e. iron carbonyl rad-

*Author to whom correspondence should be addressed.

ical anions[8–11] which can be generated either electrochemically or with the use of strong reducing agents such as a sodium mirror and sodium benzophenone ketyl.[10,12]

By studying iron carbonyl reactions with various anionic Lewis bases such as azolides,[13] nitronates,[14,15] sodium thiolates[16] and other N- and O-bases[17] directly in the ESR spectrometer cavity, we have found that the common feature of all these reactions is the formation of iron carbonyl radical anions at the initial stages, with small conversions. Their concentration was found to be fairly high (as great as 10^{-5}–10^{-2} M). The existence of such radical species in high concentrations is indicative of the presence of one-electron stages as the iron carbonyls react with the Lewis bases. Therefore, the main purpose of this study is to establish the role of one-electron processes and radical anions in iron carbonyl–Lewis base reactions.

EXPERIMENTAL

IR spectra were taken with a UR-10 instrument, and ESR spectra with an ERS-221 instrument (ZWG–DDR), in the *X*-band range with a high frequency of 100 kHz modulation. The parameters of the spectra are given for a temperature of −80°C. The reactions were conducted directly in an ampoule placed in the ESR spectrometer cavity at the equimolar reagents ratio and *ca* 0.1 M concentrations in THF. The samples were conditioned in a vacuum of 10^{-4} torr, and the THF was bulb-to-bulb distilled into the ampoule containing the reagents. The THF was dehydrated over sodium benzophenone ketyl and the iron pentacarbonyl was purified by distillation. The dimethylformamide, dimethylsulphoxide and pyridine, were purified by the known methods[18] and degassed *in vacuo* by multiple freeze–pump–thaw cycles. The compounds $^{57}Fe(CO)_5$,[19] $Na_2Fe(CO)_4 \cdot 1.5$ diox[20] $(PPN)_2[Fe_2(CO)_8]$,[21,22] $(PPN)_2[Fe_3(CO)_{11}]$,[23] $(PPN)_2[Fe_4(CO)_{13}]$,[24] $[(C_2H_5)_4N]_2[Fe_5C(CO)_{14}]$,[25] $Fe_5C(CO)_{15}$,[25] $[(C_2H_5)_4N]_2[Fe_6C(CO)_{16}]$,[25] $PPN[Fe(CO)_4COOCH_3]$,[4] $PPN[Fe(CO)_3NO]$[26] and $Fc^+PF_6^-$, where Fc^+ is ferricenium,[27] were synthesized by the known methods. The sodium salts of nitroparaffines, thiols and alcohols were synthesized from the corresponding compounds and sodium hydride in THF.

RESULTS AND DISCUSSION

(1) *Reactions of iron carbonyls with Lewis bases*

(1.1) *Anionic Lewis bases.* Iron carbonyls were found to react faster with the anionic Lewis bases than with the neutral ones. Therefore a variety of N-, O- and S-containing compounds were used as the bases in the form of sodium salts such as azolides (AzNa), amides ($NaNR_2$), alcoholates (NaOR), thiolates (NaSR), nitronates [$Na(R_2CNO_2)$] and nitrite ($NaNO_2$), where R = H or alkyl. When the reaction takes place in THF solution at −80°C, one can observe the appearance of signals from the radical species. Comparison with the data reported by Krusic *et al*[9] suggests that these signals correspond to the iron carbonyl radical anions $Fe_2(CO)_8^-$ **(I)** ($g = 2.0385$), $Fe_3(CO)_{11}^-$ **(II)** ($g = 2.0498$), $Fe_4(CO)_{13}^-$ **(III)** ($g = 2.0135$) and $Fe_3(CO)_{12}^-$ **(IV)** ($g = 2.0013$).

It was only natural to interpret these data as indicating a one-electron reduction of the starting carbonyl species, occurring in these systems. There is a vivid analogy with the iron carbonyl reduction processes taking place in the electrochemical conditions or under the effect of strong reducing agents such as sodium mirror or benzophenone ketyl.[11,12]

However, we are inclined to think that the Lewis bases used by us, especially, for example, nitrite and nitronate ions, can hardly be regarded as reducing agents. On the one hand, it follows from the reduction potentials of the anionic Lewis bases (if they are known), and on the other hand, a small probability of the one-electron reduction by eq. (2) is suggested by the absence of L˙ radicals:

$$Fe_n(CO)_m + L^- \not\rightarrow Fe_n(CO)_m^- + L^\cdot. \qquad (2)$$

We believe that the stage of the one-electron transfer is preceded by that of complexing to bring about the activation of the base and carbonyl species:

$$Fe_n(CO)_m + L^- \xrightarrow[-xCO]{} \underset{\mathbf{A}}{[Fe_n(CO)_{m-x} \cdot L]^-} \qquad (3)$$

$x = 0, 1, 2.$

The one-electron transfer then directly occurs from the anionic complex **A** to the next iron carbonyl molecule. Thus in Fe^I and Fe^{-I} complexes the degrees of oxidation are formal and appear as:*

$$[Fe_n(CO)_{m-x} \cdot L]^- + Fe_n(CO)_m \rightarrow [Fe_n(CO)_{m-x} \cdot L]^\cdot + Fe_n(CO)_m^- \xrightarrow{-CO} Fe_n(CO)_{m-1}^- \qquad (4)$$

$x = 0, 1, 2.$

* Strictly speaking, the degrees of oxidation should be designated as $1/n$ and $-1/n$, i.e. by the number of atoms in the corresponding complex. The designation used by us should be considered with this reservation.

Table 1. IR data for the complexes $Na[Fe(CO)_4C(O)L]$

L	ν(CO), THF (cm^{-1})					References
C_2H_5S	2031	1959	1913	1900	1661	This work
n-C_4H_9S	2022	1941	1912	1899	1651	This work
t-$C_5H_{11}S$	2023	1931	1904	1889	1621	This work
CH_3O	2023	1929	1913	1901	1585	4

The value of x is governed by the order in which the elimination of the first CO group and electron-transfer take place. This depends on the structure of complex **A** and electron-transfer conditions.

Adduct **A** appearing at the first stage of the process may represent firstly, the charge-transfer complex $[Fe_n(CO)_m \ldots L]^-$, second, a product resulting from the addition of a base at the carbonyl group, $[Fe_n(CO)_{m-1}C(O)—L]^-$ and third, substitution of one or more carbonyl ligands to give a direct Fe—L bond. The formation of such complexes in solution has been described earlier,[5] and some of them can be isolated in a pure form.[4]

Moreover, IR studies of the reactions of iron pentacarbonyl with sodium thiolates in THF show that with excess thiolate in these systems there appears an absorption band in the region between 1620 and 1670 cm^{-1}, typical of the "acyl"-type carbonyl group (Table 1).

It is thought that, depending on the specific conditions, all the above forms are realizable. The question is, which of them can act as a reducing agent. In particular, in our case, the role of the direct reducing agent seems to be played by the type **A** complexes.

Such complexes were synthesized in the form of salts with the bis(triphenylphosphine)iminium cation, $(PPN)[Fe(CO)_4COOCH_3]$[4] and $(PPN)[Fe(CO)_3NO]$.[26] ESR studies of the reactions of methoxycarbonyl tetracarbonyl ferrate and tricarbonyl nitrosyl ferrate with iron pentacarbonyl indicate that in this case, a fast reduction of $Fe(CO)_5$ readily occurs to give rise to the iron carbonyl radical anions **I–IV** even at temperatures below −80°C. Moreover, the entire set of the radical species detected in the reaction with $Fe(CO)_4COOCH_3^-$ was identical to that obtained in the reaction of $Fe(CO)_5$ with sodium methylate.

Thus the reaction systems involving the iron carbonyl–anionic Lewis base, at their initial stages, and small conversions, give rise to two groups of radicals, one of which is represented by the Fe^{-I} derivatives, i.e. iron carbonyl radical anions, and the other by the Fe^{I} carbonyl derivatives containing a base fragment. The second group will be discussed in more detail in sub-clause 2. The redox stage where these radicals are formed is preceded by the activated complexing of the anionic base with the iron carbonyl molecule.

(1.2) *Neutral Lewis bases.* Redox disproportionation can also occur in the case when a Lewis base had a neutral form (L′). We believe that the general scheme of the process is, in principle, similar to that discussed in the preceding section [eqs (3) and (4)]. However, in this case [eqs (5) and (6)] the process, at the same reagent concentrations, occurs far slower, probably due to the lower rates of the activating complex-formation process which may represent a limiting stage. The lower reaction rate can also be caused by charge generation [eq. (6)]. In particular, the reactions of iron pentacarbonyl with the neutral bases (ROH, RSH, R_2NH) yielding a set of radicals practically identical to that resulting from the reactions involving the anionic forms, occur far slower and at elevated temperatures only.

The ESR method was used by us to study the reactions of iron carbonyls with traditional solvents exhibiting donor properties and representing Lewis bases in the neutral form. Consideration was given to reactions with pyridine, dimethylformamide, dimethylsulphoxide and *o*-phenanthroline:

$$Fe_n(CO)_m + L' \rightleftharpoons \underset{\mathbf{A}}{[Fe_n(CO)_m \cdot L']} \qquad (5)$$

$$[Fe_n(CO)_m \cdot L'] + Fe_n(CO)_m \rightarrow \underset{\mathbf{B}}{[Fe_n(CO)_{m-x} \cdot L']^+} + Fe_n(CO)_m^-$$

$$[Fe_n(CO)_m \cdot L'] \xrightarrow[-CO]{L',\ -e^-} [Fe(L')_k]^{2+}$$

$$Fe_n(CO)_m^- \xrightarrow{-CO} Fe_n(CO)_{m-1}^-$$

$$[Fe(L')_k]^{2+} + Fe_n(CO)_{m-1}^- \xrightarrow{+e^-} [Fe(L')_k]^{2+}[Fe_n(CO)_{m-1}]^{2-}$$

L′ = Py, DMF, DMSO; $k = 6$
L′ = *o*-Phen; $k = 3$. (6)

It was shown that in all cases, at fairly small conversions, one can observe the generation of the iron carbonyl radical anions **I–IV**. Further, these radical anions give rise to carbonyl ferrate dianions with the subsequent appearance of the salts, $[Fe(L')_k][Fe_n(CO)_{m-1}]$.

Comparison of the reaction rates in the series $Fe(CO)_5$–$Fe_2CO)_9$–$Fe_3(CO)_{12}$ indicates that the easiest reaction is observed for $Fe_3(CO)_{12}$ and the most difficult one for $Fe(CO)_5$. This can be attributed to the fact that the reductive potential of $Fe_3(CO)_{12}$, $E_{1/2\,red} = -0.32$ to -0.44 V[8,11] and that of $Fe(CO)_5$, $E_{1/2\,red} = -1.64$ to -1.77 V.[11] Therefore, the electron-transfer stage [eq. (6)] is most readily realizable in the first case.

Thus, the mechanism involving the stage of activating complex-formation and the subsequent stage of a one-electron transfer from the donor-activated carbonyl complex to the carbonyl, can be regarded as a fairly general mechanism in iron carbonyl disproportionation reactions under the effect of Lewis bases.

To explain the one-electron processes occurring with participation of iron carbonyls, the conception of the activating complex-formation has been used by us for the first time. However, this approach is based on the ideas put forward by Abakumov[28] as applied to the reactions of quinones and their complexes. He was the first to express the idea of the applicability of such considerations to organometallic systems.

(2) *Radical* Fe^I *carbonyl complexes and their conversion paths*

While iron carbonyl radical anions **I–IV**, being essentially stable radicals, are detected readily, the same procedure for type **B** radicals resulting from eq. (4) is much more complicated. The Fe^I complexes (d^7 iron atom configuration) are usually very unstable and, on losing carbonyl ligands, they rapidly convert to inorganic Fe^{II} derivatives. Therefore, they can only be detected in separate cases, e.g. in reactions of $Fe(CO)_5$ with NO_2^- and $R_2CNO_2^-$.[15]

Sometimes such species can be detected in the form of spin adducts with 2-methyl-2-nitrosopropane (in reactions of iron carbonyls with $L^- = R_2CNO_2^-$).[15] An additional reason for the problem associated with the detection of mononuclear carbonyl Fe^I complexes lies in the fact that the corresponding signals including the reported ones[29–31] are located in the g region between 2.035 and 2.050, with the result that they overlap the most intense signals from **I** and **II**.

A more favourable situation is observed with the reactions of $Fe(CO)_5$ with thiolates and sodium hydrosulphide. From the outset of these reactions one can detect the broad signals from the **B** type radicals: $g = 2.0463$ (L = S—n-C_4H_9), $g = 2.0465$ (L = S—t-C_5H_{11}) and $g = 2.0459$ (L = SH).

The set of Fe^I complexes also includes two more groups of radical species with the signals within $2.020 \leqslant g \leqslant 2.022$ and $2.017 \leqslant g \leqslant 2.019$. These species always appear at the outset of the $Fe(CO)_5$—L reactions. The representatives of the latter group also appear in the reaction of $Fe_3(CO)_{12}$, but the intensities of the corresponding signals are far smaller than those in the reactions of iron pentacarbonyl.

The radicals that show up in the region $g = 2.020$–2.022 are unstable and are rapidly consumed at the initial process stages. The corresponding signals are small in intensity. This group includes, *inter alia*, a radical resulting from the $Fe(CO)_5$—NaL reaction, where $L^- = NO_2^-$ and $CH_2NO_2^-$ and giving a signal with $g = 2.0217$, and a quintet splitting on two nitrogen nuclei, $a_N = 1.6$ G (1:2:3:2:1).[15]

The radicals with $g = 2.017$–2.019 are more stable. Irrespective of the type of Lewis base, the corresponding signals have a singlet form in reactions with $Fe(CO)_5$ and are split into a quartet (1:3:3:1), $a_{^{57}Fe} = 1.8$–1.9 G, in those with $^{57}Fe(CO)_5$. The latter fact suggests the presence of three irons in each of the radicals of these groups. The higher stability of such radicals is likely due to a greater delocalization of an unpaired electron on the metallocycle.

In some cases the spectra show the presence of signals from an additional, fourth, group ($g = 2.033$–2.034), e.g. $g = 2.0338$ (L = SH); $g = 2.0337$ (L = SC_2H_5); $g = 2.0336$ (L = S—n-C_4H_9), and $g = 2.0333$ (L = S—n-C_8H_{17}). These radicals are characterized by us by the formula $Fe_2(CO)_6L_2^-$ since similar species, i.e. $Fe_2(CO)_6(N—t\text{-}Bu)_2^-$ ($g = 2.0335$, $a_N = 2.9$ G, 1:2:3:2:1)[15] and $Fe_2(CO)_6(SR)_2^-$,[16] were obtained by us from the corresponding neutral complexes by reduction on a sodium mirror in a THF solution. The signals with $g = 2.033$–2.034 are always present in reactions of iron pentacarbonyl with S-bases, sometimes in those with N-bases and never in the case of alkalis and alcoholates. This trend, defined by the stability of the radical anions $Fe_2(CO)_6L_2^-$, correlates well with the dependence of the $Fe_2(CO)_6L_2$ yields in various iron carbonyl reactions on the nature of a heteroatom in a Lewis base. The latter fact is known from the literature. Thus, for example, in the reactions of $Fe_2(CO)_9$ with thiols, alkyl sulphides and dialkyl disulphides, the $[Fe_2(CO)_6L_2]$ yields are at least 50%,[32] and in those

with N-bases, a few per cent.[33] The existence of such complexes in the case of $L = OR^-$, OH^- is unknown. It has led us to believe that the radical Fe^I carbonyl-containing complexes of the above types are intermediates resulting from the conversion of the initially formed **B** species [at the stage of one-electron transfer, eqs (4) and (6)] to the final diamagnetic compounds.

We believe that the conversion scheme can be represented as follows: the initially formed radical complex **B** reacts either with the parent iron carbonyl or the next molecule of the base. For example, in the case of $Fe(CO)_5$ and the anionic base, the following reactions are possible:

$$[Fe(CO)_4C(O)L]^- + Fe(CO)_5 \xrightarrow[-CO]{} [Fe_2(CO)_7L]^- \quad (7)$$

$$[Fe(CO)_4C(O)L]^- + L^- \xrightarrow[-CO]{} [Fe(CO)_3L_2]^{\cdot-}. \quad (8)$$

As stated above, the signal with $g = 2.0217$ in the reaction with the N-base has a quintet splitting, which corresponds to the presence of two nitrogens in this radical. The remaining radicals of this group ($g = 2.020$-2.022) also seem to contain two fragments of the base L and can have a structure of the type $[Fe(CO)_3L_2]^{\cdot-}$.

If L is a hard base (N- or O-type), it destabilizes the coordination sphere of the carbonyl complex so that the iron is readily oxidized to Fe^{2+}, to give rise to either the coordination complexes of the type $[FeL_2]_x$ (if L = anion) or a cation $[FeL'_k]^{2+}$ salts (if L′ is in the neutral form).

If L^- is a mild base (thiols and their sodium salts), one can observe stabilization of the coordination sphere within the iron carbonyl fragment:

$$[Fe(CO)_3L_2]^{\cdot-} + Fe(CO)_5 \xrightarrow[-CO]{} [Fe_2(CO)_6L_2]^{\cdot-} \quad (9)$$

$$[Fe_2(CO)_7L]^- + L^- \xrightarrow[-CO]{} [Fe_2(CO)_6L_2]^{\cdot-}. \quad (10)$$

Further clusterization can take place at this stage:

$$[Fe_2(CO)_6L_2]^{\cdot-} + Fe(CO)_5 \xrightarrow[-CO]{} [Fe_3(CO)_9L_2]^{\cdot-} \rightarrow \text{etc.} \quad (11)$$

The radicals $[Fe_2(CO)_6L_2]^{\cdot-}$ and $[Fe_3(CO)_9L_2]^{\cdot-}$ are oxidized to the neutral complexes and are thus stabilized, retaining their d^7-electron configuration. The radical-based approach to the conversion mechanism for the Fe^I complexes allows the explanation for the formation and stabilization of the various compounds of the type $[Fe_2(CO)_6L]$ and $[Fe_3(CO)_9L]$ incorporating reduced[34] or rearranged[35,36] ligands or unusually coordinated ones, e.g., via a carbon skeleton.[36]

However, in conclusion of this sub-clause we must stress that much work has to be done in the future for elucidating the composition and structure of the radicals described above.

(3) *Iron carbonyl radical anions and ways for their conversion*

As stated in sub-clause 1, in reactions of iron carbonyls with Lewis bases we detect the iron carbonyl radical anions **I**–**IV**. As a rule, they are observed in reactions with all iron carbonyls, but the sequence of the appearance of these anions, the rate of their accumulation and consumption are dependent on the parent iron carbonyl nuclearity.

Starting with $Fe_3(CO)_{12}$, the first signals to appear are those from the trinuclear radical anions, $Fe_3(CO)^{\cdot-}_{12}$ (**IV**) and $Fe_3(CO)^{\cdot-}_{11}$ (**II**), and then from $Fe_4(CO)^{\cdot-}_{13}$ (**III**) and $Fe_2(CO)^{\cdot-}_8$ (**I**). In the case of precursors in the form of the mono- and binuclear iron carbonyls $Fe(CO)_5$ and $Fe_2(CO)_9$, there first appear signals from the binuclear radical anion **I**, then from **II** and **IV**, and finally from the tetranuclear species **III**. Usually, the intensity of the latter species is low. A similar order in which the iron carbonyl radical anions are generated has been reported for the reduction of the iron carbonyls on a sodium mirror.[9]

Although in reactions involving $Fe(CO)_5$ the first usually detectable radical anions are $Fe_2(CO)^{\cdot-}_8$, it is known from the literature[37] that low-temperature matrices may contain the mononuclear $Fe(CO)^{\cdot-}_5$ and $Fe(CO)^{\cdot-}_4$ species, too. In our case, in reactions involving $Fe(CO)_5$, they also seem to appear first, being precursors of $Fe_2(CO)^{\cdot-}_8$. Therefore, the redox disproportionation eqs (3) and (4) for $Fe(CO)_5$ are expected to have the following form:

$$Fe(CO)_5 + L^- \rightarrow [Fe(CO)_4C(O)L]^- \quad (12)$$

$$[Fe(CO)_4C(O)L]^- + Fe(CO)_5 \rightarrow [Fe(CO)_4C(O)L]^{\cdot} + Fe(CO)^{\cdot-}_5 \quad (13)$$

$$Fe(CO)^{\cdot-}_5 \rightarrow Fe(CO)^{\cdot-}_4 + CO \quad (14)$$

$$Fe(CO)^{\cdot-}_4 + Fe(CO)_5 \rightarrow Fe_2(CO)^{\cdot-}_8 + CO. \quad (15)$$

When the process takes place in a closed system, as for instance, in our case, in sealed ampoules, some of the stages are distinguished by an equilibrium which is shifted towards "the heavier" iron carbonyl radical anions (a nuclearity growth phenomenon):

$$Fe_2(CO)^{\cdot-}_8 + Fe(CO)_5 \rightarrow Fe_3(CO)^{\cdot-}_{12} + CO \quad (16)$$

$$Fe_3(CO)^{\cdot-}_{12} \rightarrow Fe_3(CO)^{\cdot-}_{11} + CO \quad (17)$$

$$Fe_3(CO)^{\cdot-}_{11} + Fe(CO)_5 \rightarrow Fe_4(CO)^{\cdot-}_{13} + 3CO, \quad (18)$$

It is likely that in this case we are confronted with a kind of "oligocondensation" of iron pentacarbonyl.

Iron carbonyl radical anions **I–III** have an open electronic shell with 33, 47 and 59 cluster valence electrons, respectively. Radical metallo complex species are known to frequently possess a stereochemical non-rigidity. The coordination sphere of the radical anions **I–IV** also seems to be fairly labile and capable of skeleton rearrangement, as well as a fast ligand and electron exchange. All this favours a rapid growth of the radical ion clusters.

Similar processes in the gaseous phase have already been described.[38] However, as applied to solutions, there is a widely spread method by which the growth of the number of nuclei in iron carbonyl clusters takes place by a nucleophile substitution mechanism involving diamagnetic carbonyl ferrate dianions,[39] for example:

$$Na_2Fe(CO)_4 + Fe(CO)_5 \xrightarrow[-CO]{} Na_2Fe_2(CO)_8. \quad (19)$$

Therefore, such reactions have been also studied by an ESR method.

In fact, the interaction of $Na_2Fe(CO)_4 \cdot 1.5$diox and $(PPN)_2[Fe_2(CO)_8]$ with $Fe(CO)_5$ and $Fe_3(CO)_{12}$ appeared to occur readily, the usual set of iron carbonyl radical anions **I–IV** being formed at the outset of the process. In reactions involving salts of tri- and tetranuclear anions, such as $(PPN)_2[Fe_3(CO)_{11}]$ and $(PPN)_2[Fe_4(CO)_{13}]$, with the trinuclear carbonyl $Fe_3(CO)_{12}$, the binuclear radical anion **I** is formed in trace amounts only, the predominant products being the heavier radical anions **II–IV**. These data indicate that at small conversions the carbonyl ferrate–iron carbonyl reactions involve a one-electron transfer with the participation of these species. Such a process can be regarded as a direct one-electron reduction:

$$Fe_n(CO)_{m-1}^{2-} + Fe_{n'}(CO)_{m'} \rightarrow Fe_n(CO)_{m-1}^{-} + Fe_{n'}(CO)_{m'-1}^{-} + CO. \quad (20)$$

Generally speaking, the situation can be discussed alternatively within the frameworks of the above proposed eqs (3) and (4), if $L^- = Fe_n(CO)_{m-1}^{2-}$. Then:

$$Fe_n(CO)_{m-1}^{2-} + Fe_{n'}(CO)_{m'} \rightarrow [Fe_{n'}(CO)_{m'}Fe_n(CO)_{m-1}]^{2-} \quad (21)$$

$$[Fe_{n'}(CO)_{m'}Fe_n(CO)_{m-1}]^{2-} + Fe_{n'}(CO)_{m'} \xrightarrow[-CO]{} [Fe_{n'}(CO)_{m'}Fe_n(CO)_{m-1}]^{-} + Fe_{n'}(CO)_{m'-1}^{-}. \quad (22)$$

It should be noted, however, that the salts of the carbonyl ferrate anions, i.e. $[Fe_3(CO)_{11}]^{2-}$ and $[Fe_4(CO)_{13}]^{2-}$ do not react with $Fe(CO)_5$ at $-80°C$. The traces of iron carbonyl radical anions in this case can only be detected at room temperature in a few tens of minutes,* which is inconsistent with the stages of the activating complex formation process [eqs (21) and (22)]. Therefore, we believe, the most suitable process will be that described by eq. (20) for the direct reduction of the iron carbonyls.†

Thus one of the major properties of iron carbonyl radical anions is their ability to react with neutral iron carbonyl molecules to give rise to such radical anions with large nuclearity. There then arises a problem concerning the limits of the cluster growth process.

The literature contains data on the large iron carbonyl clusters also incorporating a carbide carbon, such as $[Fe_4C(CO)_{11}]^{2-}$, $Fe_5C(CO)_{15}$, $[Fe_5C(CO)_{14}]^{2-}$ and $[Fe_6C(CO)_{16}]^{2-}$.[25,40] Therefore it is natural to pose a question about the feasibility of carbide clustering in the reactions of iron carbonyls with Lewis bases and the associated problem concerning the assignment of the signals of the paramagnetic particles in the ESR spectra.

To solve this problem, we have studied the oxidation reactions of the salts $(PPN)_2[Fe_5C(CO)_{14}]$ and $(PPN)_2[Fe_6C(CO)_{16}]$ with ferricenium hexafluorophosphate, as well as the reduction of $Fe_5C(CO)_{15}$ on a sodium mirror in THF solution at $-80°C$. The first stages of these reactions give signals which were assigned to the carbide radical anions:

$Fe_5C(CO)_{14}^{-}$ $g = 2.0780$ $\Delta H \approx 11$ G

$Fe_5C(CO)_{15}^{-}$ $g = 2.0274$ $\Delta H \approx 3$ g

$Fe_6C(CO)_{16}^{-}$ $g = 2.0091$ or $g = 2.0017$ $\Delta H \approx 20$ G.

(Probably, the signal with $g = 2.0017$ can be assigned to $Fe_6C(CO)_{17}^{-}$.)

At larger conversions the spectra show the presence of signals from the iron carbonyl radical anions **I–IV**. Thus the carbide radical anion clusters are divided into smaller units. This suggests the existence of a common (in terms of mechanism) principle governing the formation of iron carbonyl clusters with and without the carbon ligand. As this takes place, the temperature factor produces a significant effect on the mutual conversions of ordinary and carbide radical anions.

In the reactions of iron carbonyls with Lewis bases

*In the case of $Fe_2(CO)_9$, poor solubility of both reagents in THF makes it difficult to quantitatively interpret the low-temperature spectra.

†Equation (20) can be regarded as an alternative of the redox disproportionation eq. (4), if "an extra" electron pair in the dianion is identified with the donor ligand. The same considerations can be applied to the analysis of the iron carbonyl–hydrocarbonyl anion $[HFe_n(CO)_{m-1}]^-$ formally taking $L^- = H^-$.

in the temperature region between −90 and +20°C we have not discovered any signals belonging to the carbonyl carbide clusters containing five and six irons. The process of their formation is essentially a catalytic variation of the Bell–Boudouard reaction, $2CO \rightarrow C + CO_2$, occurring at higher temperatures. This problem will be discussed in a separate communication.

Iron carbonyl radical anions **I–III**, being electron-deficient species, show a trend towards completion of the electronic shell; therefore their future in the reactions of iron carbonyls with Lewis bases is conversion to the corresponding 34-, 48- and 60-electron carbonyl ferrate anions. We believe that the role of the reducers of radical anions **I–IV** is played by unstable intermediate Fe^{I} complexes which were discussed in sub-clause 2 of this paper. The possibility of such a redox process is due to the accumulation of donor ligands in the coordination sphere of the Fe^{I} complexes, on the one hand, and formation of thermodynamically stable final products, on the other. For example, for the anionic base L^-:

$$Fe_n(CO)^{-}_{m-1} + [Fe(CO)_3L_2]^- \xrightarrow[-CO]{} Fe_n(CO)^{2-}_{m-1} + 1/x(FeL_2)_x \quad (23)$$

$$Fe_n(CO)^{-}_{m-1} + Fe_2(CO)_6L_2^- \longrightarrow Fe_n(CO)^{2-}_{m-1} + Fe_2(CO)_6L_2 \quad (24)$$

$$Fe_n(CO)^{-}_{m-1} + Fe_3(CO)_9L_2^- \longrightarrow Fe_n(CO)^{2-}_{m-1} + Fe_3(CO)_9L_2 \quad (25)$$

and for the neutral L′:

$$Fe_n(CO)^{-}_{m-1} + [Fe(CO)_3L'_2]^+ \xrightarrow[-CO]{L'} Fe_n(CO)^{2-}_{m-1} + [Fe(L')_k]^{2+}. \quad (26)$$

Thus, the final result will be the occurrence of a two-electron disproportionation scheme. The products resulting from reactions (23)–(26) are stable and usually terminate the reactions under discussion. They can be isolated preparatively, in high yields, in the form of the salts of the carbonyl ferrate anions of the type $Na_2[Fe_n(CO)_{m-1}]$ or $[Fe(L')_k][Fe_n(CO)_{m-1}]$,[1] the coordination complexes $(FeL_2)_x$,[41] as well as the diamagnetic bi- or trinuclear complexes $Fe_2(CO)_6L_2$ and $Fe_3(CO)_9L_2$.[32,33]

CONCLUSIONS

Thus the one-electron processes and radical ion complexes play an important role in the stoichiometric reactions of iron carbonyls with various Lewis bases. Moreover, these complexes are universal in that there exists practically no systems such as iron carbonyl–Lewis bases, in which they would not be formed at the early stages in fairly high steady-state concentrations.

The incompleteness of the electronic shell of the iron carbonyl radical anions and Fe^{I} radical derivatives facilitates the occurrence of the reactions of electron exchange, ligand substitution,[12] deoxygenation[15] and clusterization [for the latter case see eqs (15)–(18)]. In proton media the iron carbonyl radical anions are capable of converting to iron carbonyl hydride radicals.[11] Taking into account their universal nature and ability to undergo ready conversions at a relative stability, only these radical anions, iron carbonyl hydride radicals and Fe^{I} derivatives were assumed to be catalytically active species in a host of iron carbonyl-catalysed reactions. As far as various even-electron complexes, for example, carbonyl ferrate anions, are concerned, they represent either precursors or products of radical conversions, frequently being outside the catalytic cycles.

It would be interesting to discuss, in terms of the radical mechanism, such an important and typical kind of conversion as a WGSR mechanism: $CO + H_2O \rightleftharpoons CO_2 + H_2$.

The majority of researchers dealing with the WGSR mechanism[3] advocate either eq. (27) or a more sophisticated eq. (4) relying on a two-electron redox disproportionation process which is not always suitable for the interpretation of the experimental data.

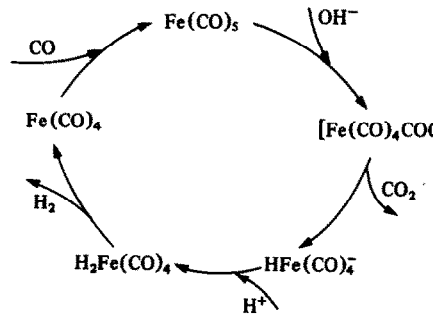

(27)

The one-electron transfer processes disclosed by us in the system "base activated carbonyl–free carbonyl" [eqs (3) and (4)] warrant another approach to the interpretation of the WGSR mechanism.

For example, for a reaction involving $Fe(CO)_5$ the first two stages coincide with the known eq. (27):

$$H_2O \rightleftharpoons H^+ + OH^- \quad (28)$$

$$OH^- + Fe(CO)_5 \rightleftharpoons [Fe(CO)_4COOH]^-. \quad (29)$$

However, a one-electron transfer stage then occurs to give rise to the iron carbonyl radical anions:

$$[Fe(CO)_4COOH]^- + Fe(CO)_5 \rightarrow$$
$$[Fe(CO)_4COOH]^{\cdot} + Fe(CO)_5^{\cdot-}$$
$$\downarrow -CO$$
$$Fe(CO)_4^{\cdot-}$$
$$\downarrow Fe(CO)_5$$
$$Fe_2(CO)_8^{\cdot-},\ Fe_3(CO)_{11}^{\cdot-},$$
$$Fe_4(CO)_{13}^{\cdot-},\ Fe_3(CO)_{12}^{\cdot-}. \quad (30)$$

In a proton media, these radical anions give iron carbonyl hydride radicals such as $HFe(CO)_4^{\cdot}$, $HFe_2(CO)_8^{\cdot}$ and $HFe_3(CO)_{11}^{\cdot}$.[42]

$$Fe_n(CO)_{m-1}^{\cdot-} + H^+ \rightleftharpoons HFe_n(CO)_{m-1}^{\cdot}. \quad (31)$$

They, like iron carbonyl radical anions,[15] can deoxygenate water in their coordination sphere to give radicals of the type $H_3Fe_n(CO)_{m-2}^{\cdot}$ such as $H_3Fe(CO)_3^{\cdot}$ and $H_3Fe_2(CO)_7^{\cdot}$.[42] The hydrogen molecule is then replaced by CO.

Thus the catalytic cycle includes reactions involving various carbonyl hydride radicals and can be presented as shown in eq. (32)

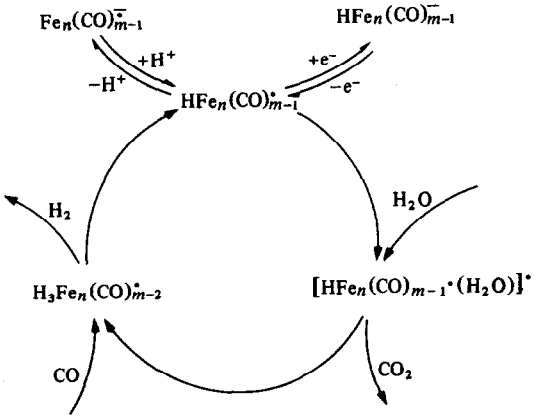

(32)

This equation makes it possible to explain the many facts which cannot be interpreted very well with the use of the traditional mechanism.[3,4] The WGSR process can be subdivided into three groups of elementary stages. The first group consists of four stages and plays a preparatory role:

—activating complex-formation of iron carbonyls and the Lewis base (H_2O, OH^-);

—one-electron transfer with the formation of coordinatively unsaturated iron carbonyl radical anions, i.e. derivatives;

—rearrangement of the radical ion species to give a set of iron carbonyl radical anions of various nuclearity;

—proton transfer between the water and the iron carbonyl radical anions to give iron carbonyl hydride radicals.

The second group of three elementary stages, according to eq. (32), represents the catalytic cycle including the reduction of water in the coordination sphere of the Fe^{-I} carbonyl radical anions at the expense of the CO ligands of the complex.

The third group consists of the carbonyl hydride radicals leaving the catalytic cycle as a result of their reduction to hydrydocarbonyl ferrate anions.

Thus, the key role in the reactions of the iron carbonyls with the Lewis bases is played by the activating complex-formation process and a subsequent one-electron transfer from the iron carbonyl–donor complex to the iron carbonyl. This gives rise to Fe^{I} and Fe^{-I} compounds which then undergo further conversions: the iron carbonyl radical anions are clusterized and the Fe^{-I} complexes are stabilized due both to the growing number of donor ligands and iron nuclei. At the later stages, the disproportionation process becomes more profound to give rise to the final products, i.e. Fe^{II} salts, the counterions of which are represented by carbonyl ferrate anions or hydridocarbonyl ferrate anions.

The specificity of the metal is frequently displayed by the behaviour of organometallic compounds. However such one-electron disproportionation reactions proceeding under the effect of Lewis bases, can be expected to take place for other metal carbonyls, including those of Ru,[43] Os[44] (iron subgroup) as well as nickel tetracarbonyl.[45]

REFERENCES

1. D. F. Shriver and K. H. Whitmire, in *Comprehensive Organometallic Chemistry* (Edited by G. Wilkinson), Vol. 4, p. 243. Pergamon Press, Oxford (1982).
2. B. D. Dombek and R. J. Angelici, *J. Catal.* 1977, **48**, 433.
3. K. R. Lane, R. E. Lee, L. Sallans and R. R. Squires, *J. Am. Chem. Soc.* 1984, **106**, 5767 and refs therein.
4. R. J. Trautman, D. C. Gross and P. C. Ford, *J. Am. Chem. Soc.* 1985, **107**, 2355.
5. D. C. Gross and P. C. Ford, *J. Am. Chem. Soc.* 1985, **107**, 585.
6. J. K. Burdett, *Coord. Chem. Rev.* 1978, **27**, 1.
7. C. A. Tolman, *Chem. Soc. Rev.* 1972, **1**, 337.
8. P. Miholova, J. Klima and A. A. Vlcek, *Inorg. Chim. Acta*, 1978, **27**, 467.
9. P. J. Krusic, J. San Filippo Jr, B. Hutchinson, R. L. Hance and L. M. Daniels, *J. Am. Chem. Soc.* 1981, **103**, 2129.
10. P. A. Dauson, B. M. Peake, B. H. Robinson and J. Simpson, *Inorg. Chem.* 1980, **19**, 465.
11. N. E. Murr and A. A. Chaloyard, *Inorg. Chem.* 1982, **21**, 2206.

12. M. Arewgoda, B. H. Robinson and J. Simpson, *J. Am. Chem. Soc.* 1983, **105**, 1893.
13. V. N. Babin, Yu. A. Belousov, V. V. Gumenyuk, R. M. Salimov, R. B. Materikova and N. S. Kochetkova, *J. Organomet. Chem.* 1983, **241**, C41.
14. Yu. A. Belousov and E. I. Mysov, *IV International Symposium on Homogeneous Catalysis*, Vol. 4, p. 3. Leningrad (1984).
15. Yu. A. Belousov and T. A. Kolosova, *Polyhedron* 1987, **6**, 1959.
16. Yu. A. Belousov, T. A. Kolosova, V. N. Babin, E. A. Viktorova and V. A. Sergeyev, *Izv. Akad. Nauk SSSR, Ser. Khim.* 1987, **7**, 1652.
17. Yu. A. Belousov, T. A. Kolosova, V. N. Babin, *VI International Conference on Organic Synthesis*, p. 231. Moscow (1986).
18. A. J. Gordon and R. A. Ford, *The Chemist's Companion*. Wiley-Interscience, New York (1972).
19. B. Bernard, L. Daniels, R. Hance and B. Hutchinson, *Snyth. React. Inorg. Met.-Org. Chem.* 1980, **10**, 1.
20. R. G. Finke and J. N. Sorrebl, *Org. Synth.* 1979, **59**, 102.
21. K. Farmery, M. Kilner, R. Greatrex and N. N. Greenwood, *J. Chem. Soc. A* 1969, **16**, 2339.
22. H. B. Chin, M. B. Smith, R. D. Wilson and R. R. Rau, *J. Am. Chem. Soc.* 1974, **96**, 5285.
23. H. A. Hodali and D. F. Shriver, *Inorg. Snyth.* 1980, **20**, 212.
24. K. Whitmire, J. Ross, C. B. Cooper and D. F. Shriver, *Inorg. Synth.* 1983, **21**, 66.
25. M. Tachikawa, R. L. Geerts and E. L. Muetterties, *J. Organomet. Chem.* 1981, **213**, 11.
26. N. G. Connelly and C. J. Gardner, *J. Chem. Soc., Dalton Trans.* 1976, 1525.
27. I. R. Lyatifov, S. P. Solodovnikov, V. N. Babin and R. B. Materikova, *Z. Naturf.* 1979, **34b**, 863.
28. G. A. Abakumov, in *Organometallic Compounds and Radicals*, p. 85. Nauka, Moscow (1985).
29. P. J. Krusic, W. J. Cote and A. Grand, *J. Am. Chem. Soc.* 1984, **106**, 4642.
30. R. G. Gasanov, L. V. Ivanova and R. Kh. Freidlina, *Izv. Akad. Nauk SSSR, Ser. Khim.* 1983, **5**, 1043.
31. P. K. Baker, N. G. Connelly, B. M. R. Jones and J. P. Maher, *J. Chem. Soc., Dalton Trans.* 1980, 579.
32. N. S. Nametkin, V. D. Turin and M. A. Kukina, *J. Organomet. Chem.* 1978, **149**, 355.
33. A. N. Nesmeyanov, M. I. Rybinskaya and L. V. Rybin, *Usp. Khim.* 1979, **48**, 393.
34. H. Alper, *J. Organomet. Chem.* 1973, **50**, 209.
35. M. M. Bagga, W. T. Flannigan and G. R. Knox, *J. Chem. Soc. C* 1969, 1534.
36. I. Omae, *Coord. Chem. Rev.* 1979, **28**, 97.
37. B. M. Peake, M. C. R. Symons and J. L. Wyatt, *J. Chem. Soc., Dalton Trans.* 1983, 1171.
38. J. Wronka and D. P. Ridge, *J. Am. Chem. Soc.* 1984, **106**, 67.
39. J. P. Collman, R. G. Finke, P. L. Matlock, R. Wahren, R. G. Komoto and J. I. Brauman, *J. Am. Chem. Soc.* 1978, **100**, 1119.
40. M. Tachikawa and E. L. Muetterties, *J. Am. Chem. Soc.* 1980, **102**, 4541.
41. A. N. Nesmeyanov, M. I. Rybinskaya, N. S. Kochetkova, V. N. Babin and G. B. Schulpin, *Dokl. Akad. Nauk SSSR, Ser. Khim.* 1968, **181**, 1397.
42. P. J. Krusic, D. J. Jones and D. C. Roe, *Organometallics* 1986, **5**, 456.
43. M. I. Bruce, in *Comprehensive Organometallic Chemistry* (Edited by G. Wilkinson), Vol. 4, p. 889. Pergamon Press, Oxford (1982).
44. R. D. Adams and J. P. Selegue, in *Comprehensive Organometallic Chemistry* (Edited by G. Wilkinson), Vol. 4, p. 967. Pergamon Press, Oxford (1982).
45. P. W. Jolly, in *Comprehensive Organometallic Chemistry* (Edited by G. Wilkinson), Vol. 6, p. 10. Pergamon Press, Oxford (1982).

Polyhedron Vol. 8, No. 5, pp. 613–625, 1989
Printed in Great Britain

0277–5387/89 $3.00+.00
© 1989 Pergamon Press plc

TRANSITION METAL COMPLEXES WITH SULPHUR LIGANDS—XLI.* RHODIUM HYDRIDE COMPLEXES WITH COORDINATION SPHERES DOMINATED BY SULPHUR: SYNTHESIS AND PROPERTIES OF COMPLEXES OF THE TYPE $[Rh(H)(PPh_3)_n(L)]$ (L = "$^{bu}S_4$"$^{2-}$ = (TETRA-*t*-BUTYL)-2,3,8,9-DIBENZO-1,4,7,10-TETRATHIADECANATE (2−), "S_4"$^{2-}$ = 2,3,8,9-DIBENZO-1,4,7,10-TETRATHIADECANATE (2−), "MeS_2"$^-$ = *o*-METHYLTHIOBENZENETHIOLATE (1−); $n = 1, 2$); X-RAY CRYSTAL STRUCTURES OF $[Rh(H)(PPh_3)("MeS_2")_2]$ AND $[RhCl(PPh_3)("MeS_2")]_2$

DIETER SELLMANN,† ANDREA FETZ, MATTHIAS MOLL and FALK KNOCH

Institut für Anorganische Chemie der Universität Erlangen–Nürnberg, Egerlandstr. 1, D-8520 Erlangen, F.R.G.

(*Received* 31 *May* 1988; *accepted* 28 *September* 1988)

Abstract—Oxidative additions of the neutral sulphur ligands (tetra-*t*-butyl)-2,3,8,9-dibenzo-1,4,7,10-tetrathiadecane (= "$^{bu}S_4$"—H_2), 2,3,8,9-dibenzo-1,4,7,10-tetrathiadecane (= "S_4"—H_2) and *o*-methylthiobenzenethiol (= "MeS_2"—H) to $[RhCl(PPh_3)_3]$, lead to S-coordinated Rh^{III}–hydride complexes with only one or two PPh_3 co-ligands. Reaction with "$^{bu}S_4$"—H_2 gives $[\mu$-"$^{bu}S_4$"$\{Rh(H)Cl(PPh_3)_2\}_2]$ (**1**) and $[Rh(H)(PPh_3)("^{bu}S_4")]$ (**2**); $[Rh(H)(PPh_3)("S_4")]$ (**3**) is obtained with "S_4"—H_2 and $[Rh(H)(PPh_3)_2("S_4")]$ (**5**) can be detected as intermediate. $[Rh(H)(PPh_3)("MeS_2")_2]$ (**6**) and $[Rh(H)Cl(PPh_3)_2("MeS_2")]$ (**8**) form with "MeS_2"—H; in solution, **8** transforms into $[Rh(H)Cl(PPh_3)(MeS_2)]_2$ (**9b**) and $[RhCl(PPh_3)("MeS_2")]_2$ (**10**). **3** and **6** react with $CHCl_3$ and HCl to give $[RhCl(PPh_3)("S_4")]$ (**5**) and $[RhCl(PPh_3)("MeS_2")_2]$ (7), respectively. **6** and **10** were characterized by X-ray structure analyses.

The interaction between hydrogen and transition metals in order to form metal hydrogen bonds is the basis of many catalytic reactions. The formation of metal hydrogen bonds is taken for granted in technical process,[2] in the photolysis of water, in the presence of transition metal compounds[3] and as well in the H/D exchange between water and H_2 which is catalysed by hydrogenases.[4]

The prevailing co-ligands of isolable hydride complexes are phosphines;[5] in contrast, hydride complexes with sulphur co-ligands (and this holds even for thioethers which are isoelectronic to phosphines), have been much less investigated. The few hydride complexes with sulphur ligands usually also contain phosphine as well as other ligands, as it is found in, for example, $[Rh(H)Cl(PPh_3)_2(SC_6H_4CH_3)]$, $[Rh(H)Cl(PPh_3)_2(SH)]$,[6] $[(triphos)(H)Rh(\mu\text{-}SH)_2Rh(H)(triphos)](BPh_4)_2$,[7] $[Ir(H)X(CO)(PPh_3)(SR)]$ (X = halide, R = alkyl or aryl),[8] $[Ir(H)(CO)(Ph_2PCH_2CH_2SH)]^+$,[9] $[Ru(H)(PPh_3)_2(SR)]$[10] or $[Mo(H)_2(S_2C_6H_3R)(PMePh_2)_3]$ (R = H, Me).[11] In fact, hydride complexes with exclusively sulphur co-ligands seem to be very rare species and to our knowledge the only described examples are the crownthioether complex $[Rh(H)(TTP)](BF_4)_2$ (TTP = 1,4,8,11-tetrathiacyclotetradecane)[12] and the thiolate complex $[Li(THF)_4]_3[Mo(H)(S_2C_6H_4)_3]$.[13] It is difficult to assess the reason for the rarity of such complexes, although in some cases the easy elimination of thiols is thought to be responsible for the instability of thiolate metal hydrides.[14]

* For part XL, see ref. 1.

†Author to whom correspondence should be addressed.

The rarity of transition metal sulphur hydride complexes is particularly surprising with respect to hydrogenases[15] and nitrogenase, which also shows hydrogenase activity.[16] Here, the activation of hydrogen is assumed to take place at transition metal sulphur centres, implying that transition metal hydride complexes are particularly potent hydrogen catalysts.

In order to assess the influence of sulphur ligands on transition metal hydrogen bonds we have tried to synthesize transition metal hydride complexes with a high degree of sulphur coordination and included it in our investigations of complexes of rhodium. By oxidative additions of the bi- and tetradentate thioether–thiols "MeS_2"—H =

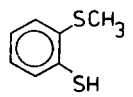

"MeS_2"—H

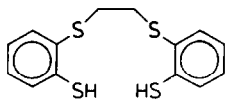

"S_4"—H_2

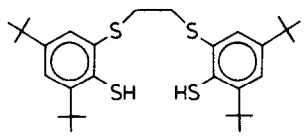

"$^{bu}S_4$"—H_2

o-methylthiobenzenethiol, "S_4"—H_2 = 2,3,8,9-dibenzo-1,4,7,10-tetrathiadecane and "$^{bu}S_4$"—H_2 = (tetra-*t*-butyl)-2,3,8,9-dibenzo-1,4,7,10-tetrathiadecane to rhodium(I) centres we have obtained rhodium(III) hydride complexes with two and more sulphur donor atoms whose syntheses and properties will be reported here.

EXPERIMENTAL

All operations were carried out under gaseous nitrogen at room temperature unless otherwise noted; solvents were dried and distilled before use. Spectra were run on the following instruments: IR, Zeiss IMR 16 IR spectrometer (solids in KBr tablets, solutions in CaF_2 cuvettes with compensation of solvent bands); NMR, Jeol JNM PMX 60 and FT JNM-GX 270 spectrometer; mass spectra, Varian MAT 212 mass spectrometer (EI and FD mode). Starting materials were prepared as described in the literature: "MeS_2"—H,[17] "S_4"—H_2,[18] "$^{bu}S_4$"—H_2[19] and $[RhCl(PPh_3)_3]$.[20] $RhCl_3 \cdot 3H_2O$ was purchased from Ventron, Karlsruhe.

Syntheses

$[\mu$-"$^{bu}S_4$" $\{Rh(H)Cl(PPh_3)_2\}_2]$ (**1**). "$^{bu}S_4$"—H_2 (170 mg, 0.31 mmol) in 10 cm^3 of THF was added to the red solution of $[RhCl(PPh_3)_3]$ (290 mg, 0.31 mmol) in 25 cm^3 of THF. After 12 h the precipitating orange–yellow solid was filtered off, washed with THF and dried for 2 h *in vacuo*. Yield: 150 mg, 52%. Found: C, 66.2; H, 6.0; S, 6.4. Calc. for $C_{102}H_{106}Cl_2P_4Rh_2S_4$ (1860.45): C, 65.9; H, 5.7; S, 6.9%.

$[Rh(H)(PPh_3($"$^{bu}S_4$"$)]$ (**2**). The orange filtrate of **1** was evaporated, and the oily residue extracted with petrol ether until a yellow solid formed; it was separated, washed with petrol ether and dried for 4 h *in vacuo*. Yield: 120 mg, 43%. Found: C, 64.5; H, 7.1%. Calc. for $C_{48}H_{60}PRhS_4$ (899.15): C, 64.1; H, 6.7%.

$[Rh(H)(PPh_3)($"S_4"$)]$ (**3**). A solution of "S_4"—H_2 (310 mg, 1 mmol) in 10 cm^3 of THF was added to the red solution of $[RhCl(PPh_3)_3]$ (925 mg, 1 mmol) in 50 cm^3 of THF and refluxed for *ca* 2 h. The resulting yellow–brown solution was evaporated to dryness, and the yellow residue washed with petrol ether and dried for 4 h *in vacuo*. Yield: 590 mg, 87%. Found: C, 56.7; H, 3.9. Calc. for $C_{32}H_{28}PRhS_4$ (674.71): C, 57.0; H, 4.2%.

Recrystallization from THF–petrol ether (1:2) at 20°C gave red crystals of the solvate $[Rh(H)(PPh_3)($"S_4"$)] \cdot$THF (**3a**). Found: C, 57.8; H, 4.2. Calc. for $C_{36}H_{36}OPRhS_4$ (746.82): C, 57.9; H, 4.9%.

$[RhCl(PPh_3)($"S_4"$)]$ (**4**). Recrystallization of **3** from $CDCl_3$ at 20°C gave red crystals of **4** $\cdot CDCl_3$. Found: C, 48.0; H, 3.3. Calc. for $C_{33}H_{27}Cl_4DPRhS_4$ (829.55): C, 47.8; H, 3.3%.

$[Rh(H)(PPh_3)_2($"S_4"$)]$ (**5**). A solution of "S_4"—H_2 (150 mg, 0.48 mmol) in 10 cm^3 of THF was added to the red solution of $[RhCl(PPh_3)_3]$ (450 mg, 0.48 mmol) in 30 cm^3 of THF. After stirring for 2 h the resulting orange–brown solution was evaporated to dryness, the orange residue being washed with petrol ether and dried for 2 h *in vacuo*. Yield: 340 mg, 76%. Found: C, 64.0; H, 4.7. Calc. for $C_{50}H_{43}P_2RhS_4$ (937.01): C, 64.1; H, 4.6%.

$[Rh(H)(PPh_3)($"MeS_2"$)_2]$ (**6**). (a) A solution of "MeS_2"—H (585 mg, 3.78 mmol) and $[RhCl(PPh_3)_3]$ (875 mg, 0.94 mmol) in 60 cm^3 of THF was stirred for 2 h. Evaporation of the solvent gave an oily residue, which was extracted with MeOH–petrol ether (1:1). The resulting orange product was filtered off, washed with petrol ether and dried for 2 h *in vacuo*. Yield: 585 mg, 92%.

Found: C, 56.8; H, 4.4. Calc. for $C_{32}H_{30}PRhS_4$ (676.73): C, 56.8; H, 4.5%.

(b) A solution of $[Rh(PPh_3)_2(\text{"}MeS_2\text{"})]$ (**11**) (135 mg, 0.17 mmol) and "MeS_2"—H (30 mg, 0.2 mmol) in 30 cm^3 of THF was stirred for 16 h. Evaporation of the solvent gave an oily brown residue, which was extracted with MeOH. The resulting solution was filtered and evaporated to dryness again. The orange residue was washed with acetone and petrol ether and dried for 3 h *in vacuo*. Yield: 60 mg, 52%. Found: C, 56.8; H, 4.4. Calc. for $C_{32}H_{30}PRhS_4$ (676.73): C, 56.8; H, 4.5%.

$[RhCl(PPh_3)(\text{"}MeS_2\text{"})_2]$ (**7**). (a) "MeS_2"—H (310 mg, 2 mmol) was added to the red solution of $[RhCl(PPh_3)_3]$ (925 mg, 1 mmol) in 70 cm^3 of acetone and stirred for 2 h under air. The resulting orange suspension was filtered; after *ca* 4 days red crystals precipitate from the filtrate, which are separated and dried for 2 h *in vacuo*. Yield: 575 mg, 81%. Found: C, 54.1; H, 4.0. Calc. for $C_{32}H_{29}ClPRhS_4$ (711.18): C, 54.0; H, 4.1%.

(b) Concentrated HCl (1.2 cm^3) was added to a suspension of $[Rh(H)(PPh_3)(\text{"}MeS_2\text{"})_2]$ (**6**) (135 mg, 0.2 mmol) in 30 cm^3 of acetone. After stirring for 12 h the red solution was filtered and evaporated to dryness. The residue was washed with MeOH and petrol ether, and recrystallized from $CHCl_3$. Yield: 105 mg, 75%. Found: C, 54.4; H, 3.9. Calc. for $C_{32}H_{29}ClPRhS_4$ (711.18): C, 54.0; H, 4.1%.

$[Rh(H)Cl(PPh_3)_2(\text{"}MeS_2\text{"})]$ (**8**). "MeS_2"—H (140 mg, 0.8 mmol) in 20 cm^3 of acetone was added to a red suspension of $[RhCl(PPh_3)_3]$ (740 mg, 0.8 mmol) in 80 cm^3 of acetone. After stirring for 2 h the yellow precipitate which forms was filtered off, washed with petrol ether and dried for 4 h *in vacuo*. Yield: 440 mg, 67%. Found: C, 63.0; H, 4.6; S, 7.8. Calc. for $C_{43}H_{38}ClP_2RhS_2$ (819.22): C, 63.0; H, 4.7; S, 7.8%.

$[Rh(H)Cl(PPh_3)(\text{"}MeS_2\text{"})]_2$ (**9b**). (a) Gaseous HCl (4.5 cm^3) was added to a red solution of $[Rh(PPh_3)_2(\text{"}MeS_2\text{"})]$ (**11**) (155 mg, 0.2 mmol) in 30 cm^3 of THF. After stirring for 12 h a yellow precipitate formed, which was separated by filtration, washed with THF and dried for 4 h *in vacuo*. Yield: 45 mg, 38%.

(b) "MeS_2"—H (475 mg, 3.07 mmol) was added to a red solution of $[RhCl(PPh_3)_3]$ (2.84 g, 3.07 mmol) in 100 cm^3 of THF. After refluxing for 3 h a yellow precipitate formed which was separated by filtration from the hot solution, washed with THF and dried for 2 h *in vacuo*. Yield: 700 mg, 41%. Found: C, 53.6; H, 4.0; S, 12.0. Calc. for $C_{50}H_{46}Cl_2P_2Rh_2S_4$ (1113.84): C, 53.9; H, 4.2; S. 11.5%.

$[RhCl(PPh_3)(\text{"}MeS_2\text{"})]_2 \cdot CH_2Cl_2$ (**10**). The green filtrate of **9** was evaporated to dryness and the green residue dissolved in 50 cm^3 of CH_2Cl_2, which was covered by a layer of petrol ether. After 6 weeks the resulting black crystals were filtered off and dried for 4 h *in vacuo*. Yield: 385 mg, 21%. Found: C, 52.0; H, 3.7; S, 11.0. Calc. for $C_{52}H_{46}Cl_4P_2Rh_2S_4$ (1196.76): C, 51.2; H, 3.9; S, 10.7%.

X-ray data collection and structure determinations

Single crystals of **6** were obtained by a two-fold recrystallization from THF solutions which were covered by a layer of petrol ether; those of **10** were obtained in the same way from CH_2Cl_2 solutions. The single crystals were sealed under nitrogen in glass capillaries; the structures were solved by direct methods. The non-hydrogen atoms were refined anisotropically and the aromatic hydrogen atoms were placed at calculated positions and refined as rigid groups. The hydrogen atoms of the methyl groups were placed in ideal tetrahedral positions and rotated around their central carbon atoms during refinement; the hydride hydrogen atom of **6** was found by difference Fourier synthesis and refined as a rigid group. Table 1 summarizes the data and information relating to data collection and structure refinement.

RESULTS AND DISCUSSION

The reaction of the sterically demanding tetradentate thioether thiol "$^{bu}S_4$"—H_2 with $[RhCl(PPh_3)_3]$ yields two hydride complexes according to eq. (1).

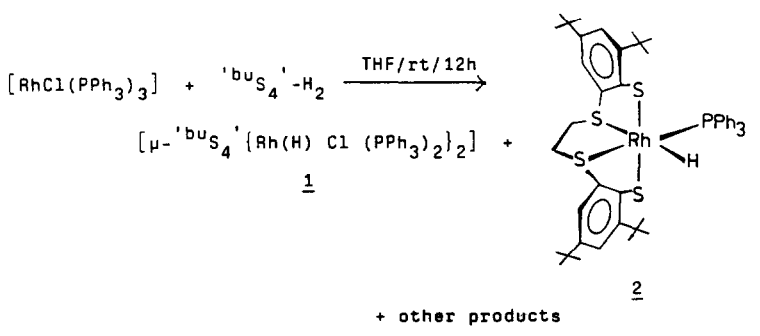

(1)

Table 1. Summary of crystallographic data and data collection procedures

Formula	[Rh(H)(PPh$_3$)("MeS$_2$")$_2$]	[RhCl(PPh$_3$)("MeS$_2$")]$_2$
	$C_{32}H_{30}PRhS_4$	$C_{50}H_{44}Cl_2P_2Rh_2S_4$
Molecular weight	676.73	1111.83
Space group	$C2/c$	$P\bar{1}$
Crystal system	Monoclinic	Triclinic
a (pm)	2078.0(19)	1206.4(6)
b (pm)	947.7(13)	1311.2(7)
c (pm)	3289.4(20)	3415.9(23)
α (°)	90.00(0)	74.12(5)
β (°)	104.23(6)	80.42(5)
γ (°)	90.00(0)	76.64(4)
V (pm^3)	$6072(9) \times 10^6$	$5026(5) \times 10^6$
Z	8	4
$\rho_{calc.}$ (g cm^{-3})	1.49	1.58
μ (cm^{-1})	8.3	9.7
Diffractometer	Nicolet R3m/V	Nicolet R3m/V
Radiation (pm)	Mo-K_α (71.073)	Mo-K_α (71.073)
Temperature (K)	213	213
Cryst. dimens. (mm)	$0.60 \times 0.30 \times 0.30$	$0.50 \times 0.20 \times 0.20$
Scan technique	ω-scan	ω-scan
2θ range (°)	3–54	4–50
Scan speed (° min^{-1})	3.0–15	3.0–15
Measured reflections	7925	21054
Unique reflections	6725	17716
Observed reflections	5360	12651
Sigma-criterion	$F > 4\sigma(F)$	$F > 6\sigma(F)$
Absorption correction	None	None
R; R_w (%)	6.3; 5.1	6.9; 5.9
Weight	$1/\sigma^2$	$1/\sigma^2$
No. of parameters	354	1118
Calculation program	SHELXTL-PLUS	SHELXTL-PLUS

Oxidative addition of SH groups to the rhodium(I) centre gives the binuclear [μ-"^{tbu}S$_4$"{Rh(H)Cl(PPh$_3$)$_2$}$_2$] (**1**) as well as the mononuclear [Rh(H)(PPh$_3$)("^{tbu}S$_4$")] (**2**). The yellow compound **2** becomes the major product if the [RhCl(PPh$_3$)$_3$] solution is slowly added to the solution of the ligand; vice versa, the orange **1** preferably forms if the ligand is added to the Rh-complex in the ratio 1 : 2.

In contrast to all other "^{tbu}S$_4$" complexes known at present, **1** is insoluble in most organic solvents and hence it could be identified only by elemental analyses and by its IR spectrum, which shows a characteristic ν(Rh—H) band at 2140 cm^{-1}. Mononuclear **2** is very soluble in organic solvents, e.g. CH_2Cl_2, $CHCl_3$ or THF. In the KBr IR spectrum, the ν(Rh—H) band is observed at 1990 cm^{-1}, and in the ^{1}H NMR spectrum the hydride signal appears at -10.25 ppm, being split into a pseudo-triplet by coupling to the rhodium and phosphorus atoms (Fig. 1).

The *t*-butyl groups yield four sharp singlets; this indicates the *cis* position of the hydride and PPh$_3$ ligands, and the structure of **2** shown in eq. (1), which has only C_1 symmetry.

The analogous reaction of [RhCl(PPh$_3$)$_3$] with the unsubstituted parent ligand "S$_4$"—H$_2$ likewise yields the hydride complex [Rh(H)(PPh$_3$)("S$_4$")] (**3**), but heating in refluxing THF is notably needed to achieve the complete coordination of the sulphur ligand, see eq. (2).

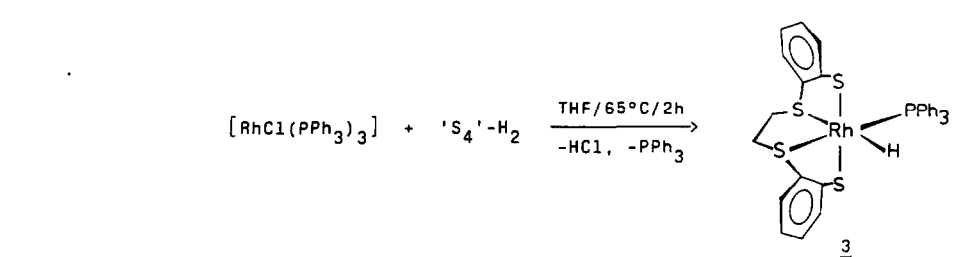

(2)

Table 2. Selected NMR, IR and MS data of the complexes

Complex	^{1}H NMR	δ (ppm)[a]	^{31}P NMR δ (ppm)	$^1J_{(Rh—P)}$ (Hz)	ν(Rh—H) (cm^{-1}) in KBr	MS (*m/e*)
1	[b]				2140	[c]
2	8.1–6.0 m	(19, ArH)[d]	43.26d	129.4	1990	899 (FD)
	3.3–1.8m	(4, C_2H_4)				
	1.47s, 1.40s,	(36, *t*-bu)				
	1.26s, 1.20s					
	−10.25	(1, RhH)[e]				
3	8.0–6.6m	(23, ArH)[d]	45.65d	142.35	2020	675 (FD)
	3.3–1.8m	(4, C_2H_4)				
	−10.98	(1, RhH)[e]				
4	8.1–6.3m	(23, ArH)[f]	19.31d	111.4		709 (FD)
	2.7s	(4, C_2H_4)				
5	8.1–6.4m	(38, ArH)[d]	[b]		1980 (broad)	[c]
	3.4–2.0m	(4, C_2H_4)				
	10.98	(1, RhH)[e]				
6	7.9–6.7 m	(23, ArH)[f]	44.25d	129.4	2060 (broad)	676 (FD)
	2.15s, 3.00m	(6, Me)				
	−12.60	(1, RhH)[e]				
7	8.1–6.6m	(23, ArH)[f]	27.84d	114.7		711 (FD)
	2.70s, 2.55m	(6, Me)	25.22d	113.6		
8	7.8–6.7m	(34, ArH)[f]	[b]		2120	[c]
	3.1–2.0m	(3, Me)				
	−15.35	(1, RhH)[g]				
9b					2040	[c]
10	8.0–6.9m	(38, ArH)[f]	−1.5m			
	3.10s	(6, Me)				

m = multiplet; d = doublet; s = singlet.
[a] Relative intensities in parentheses.
[b] See text.
[c] No M^+ ion observed.
[d] In d_8-THF.
[e] Overlapping doublets of doublets giving a pseudo-triplet.
[f] In $CDCl_3$.
[g] Overlapping doublet of triplets giving a pseudo-quartet.

3 is obtained after recrystallization from THF–petrol ether as **3**·THF; its characteristic ν(Rh—H) band appears at a slightly higher frequency, at 2020 cm^{-1} (in KBr). In the ^{1}H NMR spectrum (in d_8-THF) a pseudo-triplet is again observed for the hydride ligand at −10.98 ppm (Table 2).

The Rh—H bond of **3** is relatively stable towards acids, for example HCl/H_2O or HBF_4/Et_2O, but it is highly reactive towards chlorinated alkanes. This was noticed when **3** was dissolved in $CDCl_3$ in order to run a ^{1}H NMR spectrum; no hydride signal was observed at −10.98 ppm, but instead a multiplet appeared at 5.25 ppm due to the formation of $CHDCl_2$. From this solution, the chloro complex [Rh(Cl)(PPh_3)("S_4")] (**4**) was isolated, which had formed according to eq. (3).

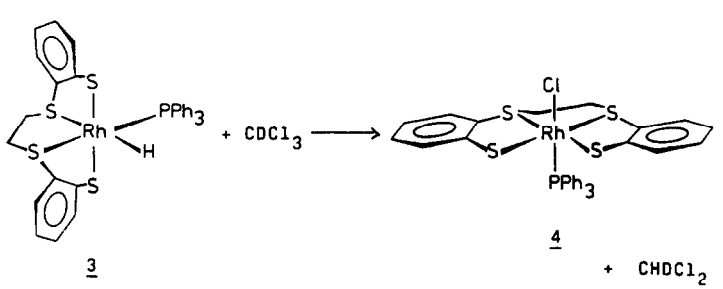

3 4 (3)

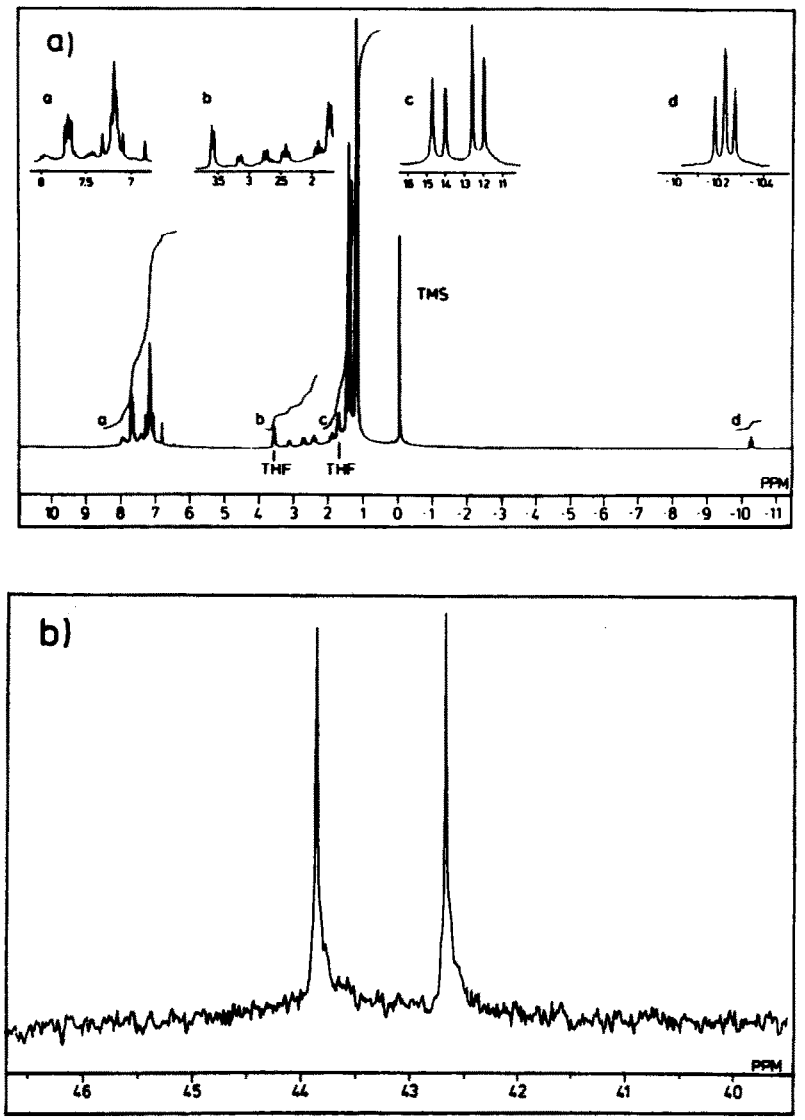

Fig. 1. NMR spectra of [Rh(H)(PPh$_3$)("^{bu}S$_4$")]: (a) ^{1}H NMR spectrum in d_8-THF (270 MHz), (b) ^{31}P NMR spectrum.

The ^{1}H NMR spectra of **3** and **4** differ remarkably. **3** shows an asymmetric multiplet for the C_2H_4 bridge between 3.3 and 2.0 ppm which is typical of six-coordinate "S_4" complexes with C_1 symmetry. **4**, however, gives only a slightly broadened singlet for the C_2H_4 bridge in $CDCl_3$. This might indicate that the chloro-complex **4** has a higher symmetry (C_2) than the hydride **3**, as illustrated by the figures of eq. (3); the necessary rearrangement may take place via the five-coordinated intermediate [Rh(PPh$_3$)("S_4")]. Evidence for the facile formation of such a fragment is seen in the FD mass spectrum of **4** which shows an intensive peak at $m/e = 674$ in addition to the M^+ ion at $m/e = 709$.

Halogenation of hydride complexes by halogen alkanes is a common reaction[21] and reaction (3) shows that in this respect hydride complexes with a coordination sphere dominated by sulphur do not behave differently; for example, the reactions between [CpMo(H)(CO)$_3$] and CCl_4,[22] [Rh(H)(PPh$_3$)$_4$] and CH_3I[23] or [Pt(H)Cl{P(OEt)$_3$}$_2$] and CCl_4[24] lead also to a H/X exchange, and in the latter case even a concomitant *trans* → *cis* rearrangement takes place.

As expected, the coordination of "S_4"—H_2 to the rhodium centre of [RhCl(PPh$_3$)$_3$] takes place stepwise. The reaction was carried out at room temperature according to eq. (4)

$$[RhCl(PPh_3)_3] + \text{"}S_4\text{"}—H_2 \xrightarrow[-HCl,\,-PPh_3]{THF/RT/2\,h} [Rh(H)(PPh_3)_2(\text{"}S_4\text{"})] \quad (4)$$

(5)

After 2 h of reaction the intermediate [Rh(H)$(PPh_3)_2$("S_4")] (**5**) can be isolated as an orange–yellow solid. It contains two PPh_3 ligands and the "S_4"$^{2-}$ ligand might act tridentately only; **5** was characterized by elemental analyses, its ν(Rh—H) band at 1980 cm^{-1} and a hydride signal at −10.98 ppm in the ^{1}H NMR spectrum. The ^{31}P NMR spectrum shows the signals of **3**, of the free PPh_3 ligand as well as of other PPh_3—Rh complexes, indicating that in solution the reaction slowly continues, finally yielding **3**.

The chelate effect and generation of three chelate rings certainly favours the coordination and oxidative addition, respectively, of the tetradentate "S_4"—H_2 to the rhodium(I) centre of [$RhCl(PPh_3)_3$]. Although these effects are expected to be less pronounced with bidentate ligands, two "MeS_2"—H can also be coordinated, yielding complexes of the type [Rh(H)(PPh_3)("MeS_2")$_2$] (**6**). In this case, however, a much larger number of stereoisomers is possible and unambiguous structure assignment on the basis of spectroscopic data becomes difficult. Scheme 1 shows a selection of these isomers, which differ with respect to the position of the hydride and PPh_3 ligands as well as that of the thioether and thiolate donors.

In order to obtain **6** according to eq. (5)

$$[RhCl(PPh_3)_3] + 4\,\text{"}MeS_2\text{"}\text{—}H \xrightarrow[-2PPh_3,\,-HCl]{THF/RT/2h} [Rh(H)(PPh_3)(\text{"}MeS_2\text{"})_2] + 2\,\text{"}MeS_2\text{"}\text{—}H \quad (5)$$

(**6**)

an excess of "MeS_2"—H is needed, even if the stoichiometry does not demand it; as will be described below, the reaction takes a different course, if only stoichiometric amounts of "MeS_2"—H or less are used.

The large number of CH_3 and ^{31}P signals in the ^{1}H and ^{31}P NMR spectra, respectively, of the raw product indeed indicates the formation of several isomers, but after recrystallization, **6** yields yellow crystals which obviously contain mainly one isomer. It shows a characteristic ν(Rh—H) band at 2060 cm^{-1} in the KBr IR spectrum and the hydride signal at −12.60 ppm in the ^{1}H NMR spectrum,

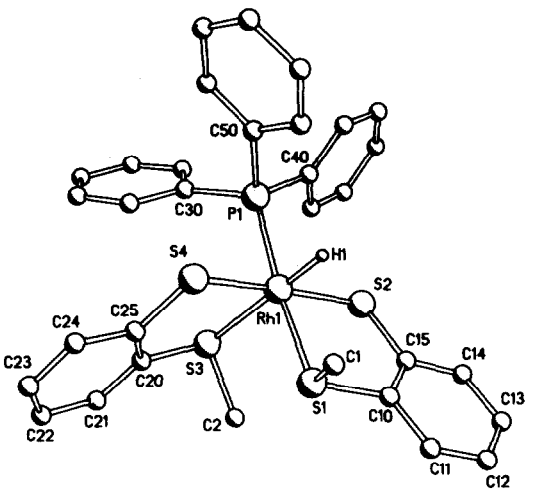

Fig. 2. Molecular structure of **6** (H atoms omitted).

which is split again into a pseudo-triplet due to rhodium and phosphorus coupling. The two methyl groups give rise to two equally intensive signals at 2.15 and 3.00 ppm; the former one appears as a singlet and the latter one is slightly split. These data are compatible e.g. with the isomers c or d of Scheme 1. This structure assignment is corroborated by the ^{31}P{^{1}H} NMR spectrum: it shows as the major signal, only one doublet ($^1J_{(Rh-P)}$ = 129.4 Hz).

The X-ray structure analysis of **6** allowed the unequivocal structure assignment. Figure 2 shows the molecular structure, and Table 3 lists selected bond distances and angles. The rhodium atom is pseudo-octahedrally surrounded by four S, one P and one H atom. The thiolato sulphur atoms occupy *trans* positions and the Rh—S(thioether) distance *trans* to the hydride ligand is a remarkable 10 pm longer than the other Rh—S distances; this is certainly due to the large well-known *trans* influence of hydride ligands. The Rh—P distance of 228.6(2) pm lies in the range of other complexes where the PPh_3 is *trans* to a thioether sulphur atom, e.g. [Rh(CO)(PPh_3)("MeS_2")] (Rh—P: 227.6 pm).[1]

As was mentioned above, **3** with the tetradentate "S_4"$^{2-}$ ligand, showed no observable reaction with acids such as hydrochloric acid or HBF_4–Et_2O at normal conditions. **6** is much more reactive and

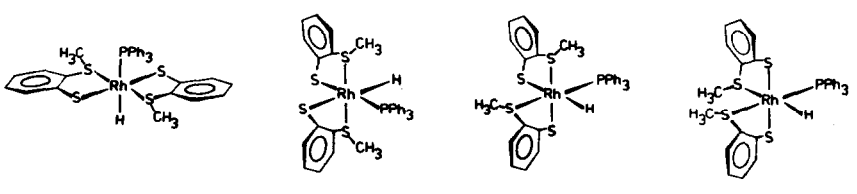

Scheme 1. Selection of stereoisomers of [Rh(H)(PPh_3)("MeS_2")$_2$] (**6**).

Table 3. Selected bond distances and angles of **6**

Bond distances (pm)		Angles (°)	
Rh(1)—S(1)	236.0(2)	S(2)—Rh(1)—S(1)	86.4(1)
Rh(1)—S(2)	235.9(2)	S(3)—Rh(1)—S(1)	93.0(1)
Rh(1)—S(3)	245.1(2)	S(3)—Rh(1)—S(2)	96.4(1)
Rh(1)—S(4)	236.2(2)	S(4)—Rh(1)—S(1)	87.9(1)
Rh(1)—P(1)	228.6(2)	S(4)—Rh(1)—S(2)	173.5(1)
S(1)—C(1)	182.4(7)	S(4)—Rh(1)—S(3)	86.9(1)
S(1)—C(10)	178.6(7)	P(1)—Rh(1)—S(1)	171.0(1)
S(2)—C(15)	174.7(7)	P(1)—Rh(1)—S(2)	94.6(1)
S(3)—C(2)	180.7(8)	P(1)—Rh(1)—S(3)	95.8(1)
S(3)—C(20)	179.0(8)	P(1)—Rh(1)—S(4)	90.6(1)
S(4)—C(25)	176.3(8)	C(1)—S(1)—Rh(1)	108.1(3)
P(1)—C(30)	185.2(7)	C(10)—S(1)—Rh(1)	105.1(3)
P(1)—C(40)	183.8(7)	C(10)—S(1)—C(1)	99.6(3)
P(1)—C(50)	184.0(7)	C(15)—S(2)—Rh(1)	104.1(3)
C(15)—C(14)	139.5(10)	C(2)—S(3)—Rh(1)	109.8(3)
C(14)—C(13)	139.9(11)	C(20)—S(3)—Rh(1)	103.6(3)
C(13)—C(12)	138.4(12)	C(20)—S(3)—C(2)	101.9(4)
C(12)—C(11)	134.4(11)	C(25)—S(4)—Rh(1)	104.1(3)
C(11)—C(10)	142.1(10)	C(30)—P(1)—Rh(1)	117.9(2)
C(10)—C(15)	140.5(10)	C(40)—P(1)—Rh(1)	113.8(2)
C(25)—C(24)	142.6(10)	C(40)—P(1)—C(30)	102.3(3)
C(24)—C(23)	139.4(11)	C(50)—P(1)—Rh(1)	112.6(2)
C(23)—C(22)	143.5(13)	C(50)—P(1)—C(30)	103.0(3)
C(22)—C(21)	137.9(12)	C(50)—P(1)—C(40)	105.7(3)
C(21)—C(20)	139.9(10)		
C(20)—C(25)	144.2(10)		

yields the chlorocomplex **7** under smooth conditions according to eq. (6):

$$[Rh(H)PPh_3)(\text{“}MeS_2\text{”})_2] + HCl \xrightarrow[-H_2]{\text{acetone/RT/24 h}} [RhCl(PPh_3)(\text{“}MeS_2\text{”})_2]. \quad (6)$$

(7)

7 also forms directly, if $[RhCl(PPh_3)_3]$ is reacted under aerobic conditions according to eq. (7):

$$[RhCl(PPh_3)_3] + 2\,\text{“}MeS_2\text{”}—H \xrightarrow[-\text{other products}]{\text{acetone/air/RT/2 h}} [RhCl(PPh_3)(\text{“}MeS_2\text{”})_2]. \quad (7)$$

(7)

Although **7** crystallizes as small red cubes, the ^1H NMR spectrum again shows several methyl signals. A singlet at 2.70 ppm and a multiplet at 2.55 ppm prove that **7** is formed as stereoisomers and accordingly in the $^{31}P\{^1H\}$ NMR spectrum, two doublets with an intensity ratio of 4 : 1 with $^1J_{(Rh—P)} = 114.7$ and 113.6 Hz are observed.

In order to obtain **6** according to eq. (5) an excess of "MeS_2"—H is necessary. This became understandable when we investigated the reaction between $[RhCl(PPh_3)_3]$ and only 1 equivalent of "MeS_2"—H, in order to synthesize $[Rh(H)Cl(PPh_3)_2(\text{“}MeS_2\text{”})]$ (**8**).

$$[RhCl(PPh_3)_3] + \text{“}MeS_2\text{”}—H \xrightarrow[-PPh_3]{\text{acetone/RT/2 h}} [Rh(H)Cl(PPh_3)_2(\text{“}MeS_2\text{”})]. \quad (8)$$

(8)

The isolation of **8** in pure form is only possible if the synthesis is carried out in solvents in which **8** is insoluble, e.g. acetone. Here, the suspended $[RhCl(PPh_3)_3]$ slowly dissolves upon addition of "MeS_2"—H and **8** precipitates simultaneously. **8** is unstable in any solvent in which is dissolves, e.g. THF, because it then immediately undergoes further reactions leading to the intermediates **9a** and **9b**, resulting ultimately in the binuclear rhodium(II) complex **10** according to eq. (9).

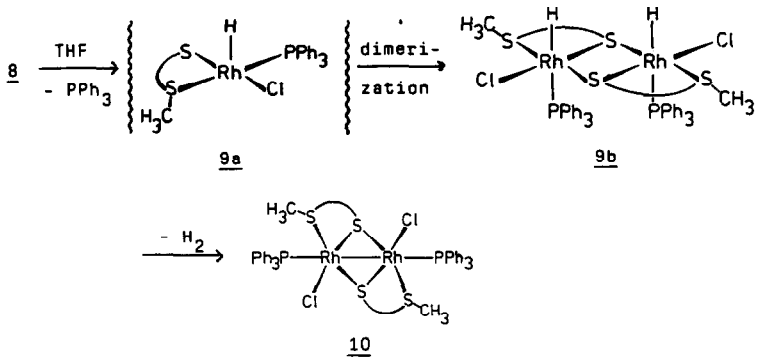

(9)

The structure of **10** could be determined by X-ray structure analysis (see below); **10** seems to be the most stable complex in this system.

The lability of **8** was detected when we tried to obtain the NMR spectra in $CDCl_3$. In the ^1H NMR spectrum, a hydride signal was observed at -15.35 ppm, which is split into a pseudo-quartet by coupling to the rhodium and two phosphorus atoms. The methyl region shows several signals between 2.0 and 3.1 ppm indicating the presence of at least two complexes. By integration and taking the hydride signal as reference, the singlet at 2.20 ppm can be assigned to **8**, whereas the singlet at 3.10 ppm stems from the rhodium(II) complex **10**. In the ^{31}P NMR spectrum, two doublets of doublets resulting from the two non-equivalent phosphorus atoms of **8** show that at least a few minutes after dissolution, **8** is still the major species in solution. Several smaller phosphorus signals, including the signal of free PPh_3 at -6.50 ppm, however, indicate the formation of new species. The lability of **8** might also be responsible for the fact that in the FD mass spectrum no molecular ion, but only two signals at $m/e = 555$ ($[M—PPh_3]^+$) and $m/e = 782$ ($[M—HCl]^+$) can be observed.

The loss of PPh_3 leads from **8** to [Rh(H)Cl(PPh_3)("MeS_2")] (**9a**), whereas the loss of HCl yields formally [Rh(PPh_3)$_2$("MeS_2")] (**11**); these two compounds seem to play key roles when [RhCl(PPh_3)$_3$] is reacted with either the neutral "MeS_2"—H or the anion "MeS_2"$^-$, and subsequently with different reagents, giving rise to a large number of reactions and complexes, which are summarized in Scheme 2.

[Rh(PPh_3)$_2$("MeS_2")] (**11**) had been characterized before,[1] all other compounds were found here and, except complex **9a**, they were all isolated and characterized; the [Rh(PPh_3)("MeS_2")]-fragment is common to all reactions and complexes.

Thus, by heating **8** in THF, according to eq. (10), the coordinatively unsaturated and 16 e$^-$-configurated **9a** forms. It is, however, unstable and dimerizes in order to give binuclear **9b**, which precipitates in yellow microcrystals from the green solution.

$$[Rh(H)Cl(PPh_3)_2(\text{“}MeS_2\text{”})] \xrightarrow{THF/65°C/4\,h} \mathbf{9b} + \mathbf{10} + \text{other products.} \quad (10)$$

The same complex **9b** forms directly if [RhCl(PPh_3)$_3$] and "MeS_2"—H are heated in boiling THF:

$$[RhCl(PPh_3)_3] + \text{“}MeS_2\text{”}—H \xrightarrow{THF/65°C/4\,h} \mathbf{9b} + \mathbf{10} + \text{other products.} \quad (11)$$

It is again obtained, if HCl adds oxidatively to [Rh(PPh_3)$_2$("MeS_2")] (**11**) at room temperature:

$$[Rh(PPh_3)_2(\text{“}MeS_2\text{”})] + HCl \xrightarrow[\mathbf{(11)}]{THF/RT/12\,h} \mathbf{9b}. \quad (12)$$

In all three cases a green solution forms, from which **9b** precipitates as yellow crystals. **9b** is insoluble in all common organic solvents and it could thus be characterized only by elemental analyses, its IR spectrum showing a sharp ν(Rh—H) band of medium intensity at 2040 cm^{-1}.

The intermediate formation of coordinatively unsaturated **9a** explains why it is necessary to apply an excess of "MeS_2"—H in reaction (5) in order to obtain **6**. Only in the presence of sufficient "MeS_2"—H is the dimerization of **9a** prevented, and **6** forms by the addition of a second "MeS_2"—H and the loss of HCl. Finally, Scheme 2 explains also, the ultimate formation of the binuclear rhodium(II) complex **10** from **9b** by a bicentric reductive elimination of H_2 and concomitant Rh—Rh bond formation. This species is observed only if the unsaturated species **9a** can form, but it is no longer detected as soon as two "MeS_2" ligands have coordinated to the Rh centre.

X-ray structure determination of [RhCl(PPh_3)("MeS_2")]$_2 \cdot CH_2Cl_2$ (**10**)

The elucidation of the molecular structure of **10** was possible by X-ray structure determination. The

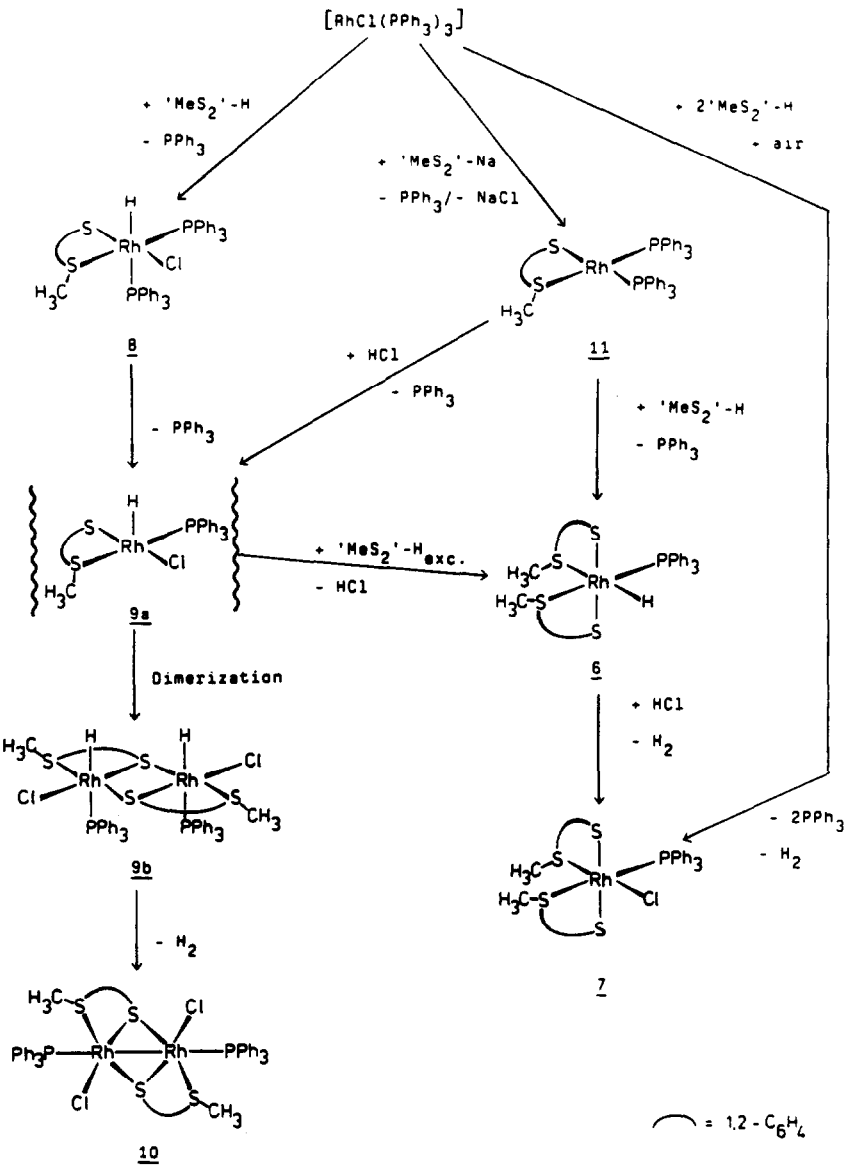

Scheme 2. Reactions and complexes in the system $[RhCl(PPh_3)_3]$/"MeS_2"—H.

asymmetric unit of the cell contains two independent molecules of **10**, the bond distances and angles of which differ only marginally. Figure 3 shows a view of one of the molecules, and Table 4 lists selected bond distances and angles of the two molecules. In the binuclear complex, each Rh atom is pseudo-octahedrally coordinated by three sulphur, one phosphorus, and one chlorine in addition to the neighbouring rhodium atom. The two thiolato sulphur atoms function as bridges connecting the two $[RhCl(PPh_3)(\text{"}MeS_2\text{"})]$ fragments in such a manner that the Rh_2S_2 unit has a dihedral angle of 71.4° along the S—S edge. The Rh—Rh distance of 268.9 pm suggests a single bond between the two rhodium centres;[25] Rh—Rh double bonds are usually assumed to be in the range of 250 pm.[26]

Taking the Rh—Rh bond into account, the structure of **10** may also be described as two facially connected octahedral $[RhCl(PPh_3)(\text{"}MeS_2\text{"})]$ fragments; this suggests, eventually, a bent Rh—Rh bond as has been postulated for $Co_2(CO)_8$.[27]

CONCLUSIONS

The oxidative addition of bi- and tetradentate thioether thiol ligands to rhodium(I) centres leads to sulphur-coordinated rhodium hydride complexes. The chelate effect of these ligands prevents the elimination of thiols and is responsible for the stability of the rhodium(III) hydride complexes.

Table 4. Selected bond distances and angles of **10**

Bond distances (pm)		Angles (°)	
Rh(1)—Rh(2)	268.9(1)	Cl(1)—Rh(1)—Rh(2)	107.3(1)
Rh(1)—Cl(1)	241.5(3)	P(1)—Rh(1)—Rh(2)	153.4(1)
Rh(1)—P(1)	240.4(4)	P(1)—Rh(1)—Cl(1)	93.3(1)
Rh(1)—S(1)	226.2(3)	S(1)—Rh(1)—Rh(2)	55.7(1)
Rh(1)—S(2)	231.0(5)	S(1)—Rh(1)—Cl(1)	161.6(1)
Rh(1)—S(3)	233.3(4)	S(1)—Rh(1)—P(1)	105.0(1)
Rh(2)—Cl(2)	241.0(5)	S(2)—Rh(1)—Rh(2)	104.6(1)
Rh(2)—P(2)	237.5(4)	S(2)—Rh(1)—Cl(1)	89.8(1)
Rh(2)—S(1)	234.2(4)	S(2)—Rh(1)—P(1)	91.8(1)
Rh(2)—S(3)	226.3(4)	S(2)—Rh(1)—S(1)	88.5(1)
Rh(2)—S(4)	233.0(4)	S(3)—Rh(1)—Rh(2)	53.0(1)
S(1)—C(10)	179.1(18)	S(3)—Rh(1)—Cl(1)	95.9(1)
S(2)—C(15)	179.2(15)	S(3)—Rh(1)—P(1)	109.5(1)
S(2)—C(1)	180.8(16)	S(3)—Rh(1)—S(1)	79.3(1)
S(3)—C(20)	177.7(14)	S(3)—Rh(1)—S(2)	157.6(1)
S(4)—C(25)	175.0(17)	Cl(2)—Rh(2)—Rh(1)	106.8(1)
S(4)—C(2)	180.7(15)	P(2)—Rh(2)—Rh(1)	151.8(1)
C(15)—C(10)	138.9(21)	P(2)—Rh(2)—Cl(2)	95.1(1)
C(15)—C(14)	142.8(27)	S(1)—Rh(2)—Rh(1)	52.9(1)
C(14)—C(13)	137.6(23)	S(1)—Rh(2)—Cl(2)	93.2(1)
C(13)—C(12)	136.8(28)	S(1)—Rh(2)—P(2)	109.6(1)
C(12)—C(11)	134.1(28)	S(3)—Rh(2)—Rh(1)	55.4(1)
C(11)—C(10)	139.9(20)	S(3)—Rh(2)—Cl(2)	161.8(1)
C(25)—C(20)	140.2(20)	S(3)—Rh(2)—P(2)	103.0(1)
C(25)—C(24)	139.1(22)	S(3)—Rh(2)—S(1)	79.1(1)
C(24)—C(23)	144.9(28)	S(4)—Rh(2)—Rh(1)	105.8(1)
C(23)—C(22)	140.5(24)	S(4)—Rh(2)—Cl(2)	93.2(1)
C(22)—C(21)	139.2(23)	S(4)—Rh(2)—P(2)	90.0(1)
C(21)—C(20)	143.6(24)	S(4)—Rh(2)—S(1)	158.7(1)
		S(4)—Rh(2)—S(3)	88.6(1)
Rh(1′)—Rh(2′)	269.6(2)	Cl(1′)—Rh(1′)—Rh(2′)	106.8(1)
Rh(1′)—Cl(1′)	241.9(4)	P(1′)—Rh(1′)—Rh(2′)	154.0(1)
Rh(1′)—P(1′)	240.0(5)	P(1′)—Rh(1′)—Cl(1′)	91.8(1)
Rh(1′)—S(1′)	226.6(4)	S(1′)—Rh(1′)—Rh(2′)	55.1(1)
Rh(1′)—S(2′)	230.4(4)	S(1′)—Rh(1′)—Cl(1′)	160.9(2)
Rh(1′)—S(3′)	234.4(4)	S(1′)—Rh(1′)—P(1′)	107.3(1)
Rh(2′)—Cl(2′)	242.1(4)	S(2′)—Rh(1′)—Rh(2′)	104.5(1)
Rh(2′)—P(2′)	236.5(4)	S(2′)—Rh(1′)—Cl(1′)	91.0(1)
Rh(2′)—S(1′)	232.8(5)	S(2′)—Rh(1′)—P(1′)	93.0(2)
Rh(2′)—S(3′)	227.0(4)	S(2′)—Rh(1′)—S(1′)	88.5(1)
Rh(2′)—S(4′)	233.5(4)	S(3′)—Rh(1′)—Rh(2′)	53.0(1)
S(1′)—C(10′)	177.7(14)	S(3′)—Rh(1′)—Cl(1′)	95.2(1)
S(2′)—C(15′)	177.6(15)	S(3′)—Rh(1′)—P(1′)	108.4(1)
S(2′)—C(1′)	183.1(16)	S(3′)—Rh(1′)—S(1′)	78.6(1)
S(3′)—C(20′)	176.4(15)	S(3′)—Rh(1′)—S(2′)	157.4(2)
S(4′)—C(25′)	182.8(15)	Cl(2′)—Rh(2′)—Rh(1′)	108.7(1)
S(4′)—C(2′)	180.8(13)	P(2′)—Rh(2′)—Rh(1′)	149.4(1)
C(15′)—C(10′)	138.5(21)	P(2′)—Rh(2′)—Cl(2′)	93.8(1)
C(15′)—C(14′)	139.5(21)	S(1′)—Rh(2′)—Rh(1′)	53.0(1)
C(14′)—C(13′)	138.8(23)	S(1′)—Rh(2′)—Cl(2′)	94.2(1)
C(13′)—C(12′)	141.6(24)	S(1′)—Rh(2′)—P(2′)	106.2(1)
C(12′)—C(11′)	136.4(22)	S(3′)—Rh(2′)—Rh(1′)	55.5(1)
C(11′)—C(10′)	136.9(21)	S(3′)—Rh(2′)—Cl(2′)	163.8(2)
C(25′)—C(20′)	138.6(23)	S(3′)—Rh(2′)—P(2′)	102.2(1)
C(25′)—C(24′)	142.7(23)	S(3′)—Rh(2′)—S(1′)	78.9(1)
C(24′)—C(23′)	141.9(26)	S(4′)—Rh(2′)—Rh(1′)	105.3(1)
C(23′)—C(22′)	133.3(30)	S(4′)—Rh(2′)—Cl(2′)	93.1(1)
C(22′)—C(21′)	135.9(24)	S(4′)—Rh(2′)—P(2′)	93.7(2)
C(21′)—C(20′)	140.8(21)	S(4′)—Rh(2′)—S(1′)	158.3(2)
		S(4′)—Rh(2′)—S(3′)	88.6(1)

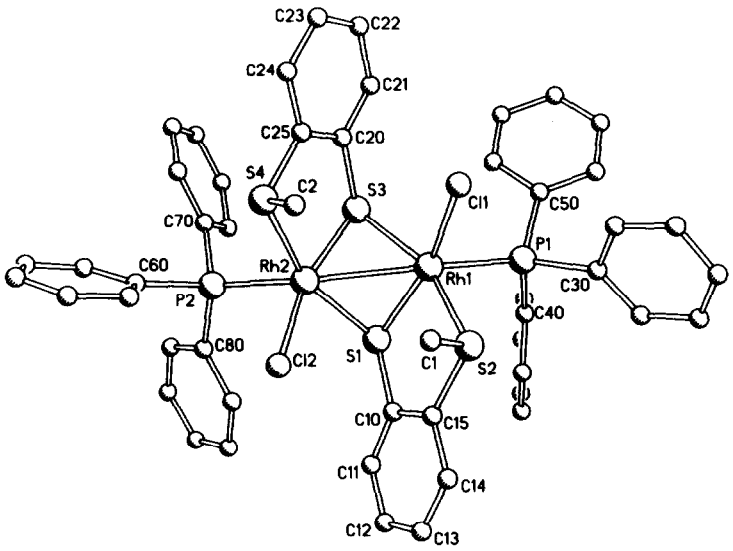

Fig. 3. Molecular structure of **10** (H atoms omitted).

In the system $[RhCl(PPh_3)_3]$/"MeS_2"—H, the coordinatively unsaturated $[Rh(PPh_3)$("MeS_2")] fragment plays a key role and the binuclear rhodium(II) complex $[RhCl(PPh_3)$("MeS_2")$]_2$ (**10**) is the ultimate product. In some cases, the hydride ligands may be easily substituted by chloride: $[Rh(H)(PPh_3)$("S_4")] (**3**) reacts with $CDCl_3$ to give $[RhCl(PPh_3)$("S_4")] (**4**), and $[Rh(H)(PPh_3)$("MeS_2")$_2$] (**6**) reacts with HCl to give $[RhCl(PPh_3)$("MeS_2")$_2$] (**7**).

Supplementary material

The atomic positional and thermal vibration parameters, plus complete distance, angle and structure factor tables have been deposited with the Editor, from whom copies are available on request. Atomic coordinates have also been deposited with the Cambridge Crystallographic Data Centre.

Acknowledgements—These investigations were supported by the Deutsche Forschungsgemeinschaft and the Fonds der Chemischen Industrie.

REFERENCES

1. D. Sellmann, A. Fetz, M. Moll and F. Knoch, *J. Organomet. Chem.* 1988, **355**, 495.
2. (a) F. H. Jardine, *J. Chem. Soc. A* 1976, 1711; (b) B. R. James, *Coord. Chem. Rev.* 1966, **1**, 505.
3. T. A. Ryan, *Coord. Chem. Rev.* 1982, **41**, 251.
4. (a) W. Newton, J. R. Postgate and C. Rodriguez-Barvueco, *Recent Developments in Nitrogen Fixation.* Academic Press, London (1977); (b) T. Yagi, M. Tsuda and H. Inokuchi, *J. Biochem. (Tokyo)* 1973, **73**, 1069.
5. E. L. Muetterties (Ed.), *Transition Metal Hydrides.* Marcel Dekker, New York (1971).
6. H. Singer and G. Wilkinson, *J. Chem. Soc. A* 1968, 2516.
7. C. Bianchini and A. Meli, *Inorg. Chem.* 1987, **26**, 4268.
8. T. Gaines and M. D. Roundhill, *Inorg. Chem.* 1974, **13**, 2521.
9. D. W. Stephen, *Inorg. Chem.* 1984, **23**, 2207.
10. B. Chassdret and R. Poilblanc, *Inorg. Chim. Acta* 1979, **34**, L209.
11. N. L. Lazarowych and R. H. Morris, *J. Chem. Soc., Chem. Commun.* 1987, 1865.
12. W. D. Lemke, K. E. Travis, N. E. Takvoryan and D. H. Busch, *Adv. Chem. Ser.* 1976, **150**, 358.
13. D. Sellmann and L. Zapf, *Z. Naturfor.* 1985, **40b**, 380.
14. R. A. Henderson, D. L. Hughes, R. L. Richards and C. Shortman, *J. Chem. Soc., Dalton Trans.* 1987, 1115.
15. J. Okura, *Coord. Chem. Rev.* 1985, **68**, 53.
16. R. W. F. Hardy, F. Bottomley and R. C. Burns (Ed.), *A Treatise on Dinitrogen Fixation.* John Wiley, New York (1979).
17. D. Sellmann, P. Kreutzer and E. Unger, *Z. Naturfor.* 1982, **37b**, 1026.
18. D. Sellmann and E. Böhlen, *Z. Naturfor.* 1982, **37b**, 1026.
19. D. Sellmann, G. Freyberger, R. Eberlein, E. Böhlen, G. Huttner and L. Zsolnai, *J. Organomet. Chem.* 1987, **323**, 21.
20. J. A. Osborn and G. Wilkinson, *Inorg. Synth.* 1967, **10**, 67.
21. R. A. Schunn, in *Transition Metal Hydrides* (Edited

by E. L. Muetterties), Chap. 5, pp. 203–258. Marcel Dekker, New York (1971).
22. T. S. Piper and G. Wilkinson, *J. Inorg. Nucl. Chem.* 1956, **3**, 104.
23. B. Ilmaier and R. S. Nyholm, *Naturwissenschaften* 1969, **56**, 415.
24. J. Chatt and B. L. Shaw, *J. Chem. Soc.* 1965, 7391.
25. A. M. Arif, R. A. Jones, M. H. Seeberger, B. R. Whittlesey and T. C. Wright, *Inorg. Chem.* 1986, **25**, 3943.
26. (a) R. A. Jones, N. C. Norman, M. H. Seeberger, J. L. Atwood and W. E. Hunter, *Organometallics* 1983, **2**, 1629; (b) R. A. Jones and T. C. Wright, *Organometallics* 1983, **2**, 1842.
27. G. G. Sumner, H. P. Klug and L. E. Alexander, *Acta Cryst.* 1964, **17**, 732.

Polyhedron Vol. 8, No. 5, pp. 627–632, 1989
Printed in Great Britain

0277–5387/89 $3.00+.00
© 1989 Pergamon Press plc

SYNTHESIS AND CHARACTERIZATION OF MOLYBDENUM(0) AND TUNGSTEN(0) CARBONYL DERIVATIVES OF METHYLENEBIS[DIPHENYLPHOSPHINE OXIDE] AND BIS[(DIPHENYLPHOSPHINYL)METHYL]PHENYLPHOSPHINE OXIDE

P. PLANINIĆ* and H. MEIDER

Rudjer Bošković Institute, Department of Physical Chemistry, Zagreb, Croatia, Yugoslavia

(*Received* 3 *May* 1988; *accepted after revision* 29 *September* 1988)

Abstract—The reaction of molybdenum and tungsten hexacarbonyls with the ligands $[(C_6H_5)_2P(O)]_2CH_2$ (MDPO) and $[(C_6H_5)_2P(O)CH_2]_2P(O)C_6H_5$ (RPPh) has been investigated. The new compounds *cis*-$M(CO)_4$MDPO, *cis*-$M(CO)_4$RPPh, *fac*-$M_2(CO)_6(MDPO)_3$ and *fac*-$M(CO)_3$RPPh, where M = Mo^0 or W^0, have been prepared. All complexes isolated are diamagnetic with an octahedral geometry. Results of IR, Raman and NMR spectra have been discussed.

Substituted carbonyl complexes of the group VI metals have been the subject of interest for many years.[1] The most examined ligands in the metal carbonyl chemistry have been various types of substituted phosphines which rather easily displace carbon monoxide from $M(CO)_6$.[2–5] Considerably less attention has been paid to phosphine oxides as ligands toward chromium, molybdenum and tungsten carbonyls. Tricarbonyl and tetracarbonyl complexes of molybdenum(0) and tungsten(0) with different monodentate phosphine oxides, as well as complexes of the $M_2(CO)_6L_3$ type, where M = Mo or W, and L = bidentate ligand, i.e. ethylenebis[diphenylphosphine oxide], were reported and characterized by IR spectroscopy a couple of decades ago.[6–8] From that time little work has been carried out on molybdenum and tungsten carbonyl complexes with phosphine oxide ligands.

Our interest has been focused on the synthesis and investigation of the complexing ability of some phosphine oxide derivatives which are potentially tridentate ligands since they contain three PO groups bridged by two CH_2 groups. These compounds proved to be good complexing agents for a number of transition metals.[9–11] The present work describes the isolation and characterization of some carbonyl complexes of molybdenum(0) and tungsten(0) with methylenebis[diphenylphosphine oxide] (MDPO) and bis[(diphenylphosphinyl) methyl]phenylphosphine oxide (RPPh). The bidentate ligand MDPO has been widely used as a complexing agent for a great number of transition metals,[12] but its carbonyl complexes have not been reported until now. The obtained RPPh compounds represent the first carbonyl complexes with a trisphosphine oxide ligand.

RESULTS AND DISCUSSION

Thermal reaction of the appropriate metal hexacarbonyl with MDPO and RPPh ligands in benzene, toluene or xylene yielded the corresponding molybdenum(0) and tungsten(0) complexes of the general type: $M(CO)_4L$ (L = RPPh, MDPO), $M(CO)_3$RPPh and $M_2(CO)_6(MDPO)_3$, where M = Mo^0, W^0. Analytical data are given in Table 1.

MDPO and RPPh ligands form tetracarbonyl complexes with molybdenum and tungsten of the same stoichiometry. It was noticed that MDPO as a bidentate ligand formed this type of complex more readily than the RPPh ligand. The tungsten tetracarbonyl complex with MDPO was obtained from xylene after 1 h of refluxing the components in the molar ratio of 1 : 1. The replacement of tungsten with molybdenum under the same reaction conditions yielded a precipitation of a mixture of

* Author to whom correspondence should be addressed.

Table 1. Analytical data for the complexes

Complex	Colour	C (%) Calc.	C (%) Found	H (%) Calc.	H (%) Found	Metal (%) Calc.	Metal (%) Found	P (%) Calc.	P (%) Found
$Mo(CO)_4MDPO$	Yellow–brown	55.8	55.9	3.5	3.5	15.4	15.1	9.2	9.1
$W(CO)_4MDPO$	Yellow–brown	48.9	49.0	3.1	3.0	25.8	25.9	8.7	8.5
$Mo(CO)_4RPPh$	Yellow–brown	56.7	56.9	3.8	3.6	12.6	12.4	12.2	12.0
$W(CO)_4RPPh$	Yellow–brown	50.8	51.0	3.4	3.2	21.6	21.6	10.9	10.6
$Mo_2(CO)_6(MDPO)_3$	Yellow	60.5	60.7	4.1	4.0	11.9	11.8	11.5	11.3
$W_2(CO)_6(MDPO)_3$	Orange–yellow	54.5	54.6	3.7	3.6	20.6	20.7	10.4	10.3
$Mo(CO)_3RPPh$	Light-yellow	57.2	57.4	4.0	3.8	13.1	13.1	12.6	12.7
$W(CO)_3RPPh$	Yellow	51.1	51.3	3.5	3.4	22.4	22.1	11.3	11.0

different carbonyl species. In order to isolate the corresponding molybdenum complex we had to take an excess of metal hexacarbonyl (2 : 1 ratio) and use lower temperatures (120°C) and a shorter reaction time (30 min). Tetracarbonyl complexes with RPPh could be obtained only if the metal–ligand ratio was at least 3 : 1 for molybdenum and 2 : 1 for tungsten, along with a rather short reaction time.

The first step in the course of preparation of tricarbonyl complexes was tetracarbonyl again, as evidenced by IR spectra. Continued heating, however, caused a decrease of the IR absorptions due to tetracarbonyl species and an increase of absorption of the tricarbonyls. The reaction was readily accomplished in 2 h for molybdenum and in about 4 h for tungsten. In general, the yield was very good for the tricarbonyl species (80–90%) and rather low for the tetracarbonyl complexes (10–17%).

The isolated compounds are diamagnetic, yellow or yellow–brown, air-sensitive solids. They are crystalline as evidenced by X-ray diffraction. The molybdenum complexes are more stable than the tungsten ones, but they can all be kept in a dry argon atmosphere for several months. The complexes are insoluble in most of the usual organic solvents, although they dissolve in DMF and DMSO with decomposition. The insolubility of the obtained complexes makes their isolation from the reaction mixture rather simple, but prevents their investigation by certain physical and spectroscopic techniques.

IR spectra

The IR spectral data of the examined complexes are presented in Table 2. Tricarbonyl and tetracarbonyl complexes show a marked difference in both the ν(CO) and ν(PO) region of the spectra. Figure 1 shows IR spectra of $W(CO)_4RPPh$ and $W(CO)_3RPPh$ complexes in the range 2100–900 cm^{-1}.

For the complexes $M(CO)_4L$ (L = RPPh or MDPO ligands), four absorption bands appear in the CO stretching region of the spectra [2000–1800 cm^{-1}, Fig. 1(a)] indicating that these species possess a C_{2v} symmetry of ligands around the central metal.[13] The absorption bands belong to four IR active carbonyl stretching modes ($2A_1+B_1+B_2$). The bands were assigned and used for calculations

Table 2. IR and Raman spectral data of the ligands and complexes

Compound	ν(CO) (cm^{-1}) IR	ν(CO) (cm^{-1}) Raman	ν(PO) (cm^{-1}) IR
MDPO			1211m, 1194s, 1175sh
cis-$Mo(CO)_4MDPO$	2015w, 1890vs, 1852s, 1808m		1160s
cis-$W(CO)_4MDPO$	1998w, 1870vs, 1845s, 1800m		1155s
fac-$Mo_2(CO)_6(MDPO)_3$	1899s, 1760s, 1724vs	1928, 1768, 1722	1200sh, 1173s
fac-$W_2(CO)_6(MDPO)_3$	1887vs, 1751vs, 1716s	1908, 1766, 1721	1191sh, 1165s
RPPh			1215s, 1192vs, 1163s
cis-$Mo(CO)_4RPPh$	2012w, 1895vs, 1850s, 1805m		1200sh, 1162vs
cis-$W(CO)_4RPPh$	2000w, 1868vs, 1845s, 1802m		1200sh, 1160vs
fac-$Mo(CO)_3RPPh$	1896vs, 1747vs, 1729vs	1893, 1780, 1712	1189vs, 1163s
fac-$W(CO)_3RPPh$	1885s, 1738vs, 1719vs	1880, 1792, 1716	1184vs, 1160vs

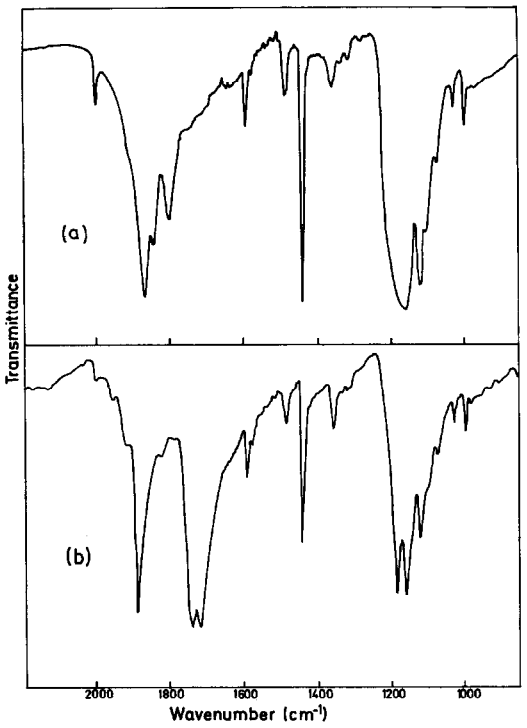

Fig. 1. IR spectra of (a) *cis*-W(CO)$_4$RPPh and (b) *fac*-W(CO)$_3$RPPh complexes

of the force constants according to the Cotton–Kraihanzel secular equations.[14] Since intermolecular interactions in the solid state can have appreciable effects upon the frequencies, the obtained values must be interpreted with caution, but they may be of interest as there are no complete data for other phosphine oxide derivatives of the group VI metal carbonyls in the literature. The calculated force constants of M(CO)$_4$MDPO and M(CO)$_4$RPPh complexes are presented in Table 3. They can be compared to those obtained for the corresponding complexes with some N-donor ligands which like phosphine oxides, are considerably poorer π-acceptors than the phosphines.[14b,c,15]

In addition to the carbonyl region, the section of the IR spectra from 1250–1100 cm^{-1} where bands due to PO stretching vibrations occur, is characteristic. These absorption bands are, in the spectra of the complexes, shifted to lower wavenumbers with regard to the free ligands (Table 2), thus indicating coordination of the phosphoryl oxygen.[16] Instead of three bands being present in the spectra of both ligands (at 1211, 1194 and 1175 cm^{-1} for MDPO, and at 1215, 1192 and 1163 cm^{-1} for RPPh), only one band at $\sim$1160 cm^{-1} appears in the spectra of all tetracarbonyl species (Table 2). Spectra of RPPh complexes show an additional shoulder on the higher energy side of the ν(PO) band. Since IR spectra of M(CO)$_4$MDPO and M(CO)$_4$RPPh complexes are nearly identical, especially in the CO stretching region, the RPPh ligand probably acts as bidentate in these complexes. The third phosphoryl oxygen from the ligand must be free, or involved in some kind of hydrogen bond.[11]

IR spectra of M(CO)$_3$RPPh and M$_2$(CO)$_6$(MDPO)$_3$ complexes show very close similarity in both shape and position of the characteristic bands. The spectra of tungsten(0) complexes exhibit the usual slight lowering of the ν(CO) absorption bands ($\sim$10 cm^{-1}) with regard to the spectra of the corresponding molybdenum(0) complexes. In all these spectra, two main strong bands, corresponding to the CO stretching vibrations, are present: a sharper band at around 1900 cm^{-1}, and a broader, split one at 1730–1740 cm^{-1}, Fig. 1(b). A spectrum with nearly identical CO stretching vibrations was reported for the trisubstituted molybdenum carbonyl complex with triphenylphosphine oxide.[7] These results are compatible with the formation of facial tricarbonyl complexes (C_{3v} local symmetry, A_1+E modes).[13] Splitting of the lower energy band into two components may arise from the lowering of the C_{3v} to C_s symmetry,[17] with regard to the polydentate structure of the ligands or in some instances, from the crystal effects in the solid state.[17]

The interesting feature of these spectra is that the ν(CO) frequency of the lower energy band appears in what is usually considered to be the bridging carbonyl region. The CO stretching vibrations in phosphine oxide complexes in general, appear at

Table 3. Carbonyl stretching frequencies and force constants for *cis*-M(CO)$_4$MDPO and *cis*-M(CO)$_4$RPPh complexes

Complex	ν(CO) (cm^{-1})				Force constants (mdyn Å^{-1})		
	A_1	A_1	B_1	B_2	k_1	k_2	k_i
Mo(CO)$_4$MDPO	2015	1890	1852	1808	14.25	15.22	0.40
Mo(CO)$_4$RPPh	2012	1895	1850	1805	14.20	15.26	0.38
W(CO)$_4$MDPO	1998	1870	1845	1800	14.14	14.92	0.40
W(CO)$_4$RPPh	2000	1868	1845	1802	14.16	14.91	0.41

lower wavenumbers than in the analogous derivatives having tertiary phosphines as ligands. This is a consequence of the lower π-accepting ability of the oxygen compared to phosphorus. A decrease of ν(CO) values in facial tricarbonyl complexes may also be enhanced by the *trans* effect of the oxygen donor ligands,[18,19] since in these species all three CO groups are in a *trans* position to the oxygen.

At the same time as ν(CO) decreases with subsequent substitution of the CO groups, ν(PO) increases as a consequence of the redistribution of the negative charge on the metal atom. Thus, in the tricarbonyl complexes ν(PO) absorption bands are shifted to higher wavenumbers with regard to the tetracarbonyls (Table 2, Fig. 1).

The similarity of the spectra of $M(CO)_3RPPh$ and $M_2(CO)_6(MDPO)_3$ suggests the same local symmetry of three facial carbonyls and three phosphoryl oxygens around the metal atoms in both types of complexes (Structures **1**, **2** and **3**).

Raman spectra

Raman spectra of facial tricarbonyl complexes are similar in shape to the corresponding IR spectra. Inspection of Table 2 shows in addition some IR–Raman coincidences. In particular, for the RPPh

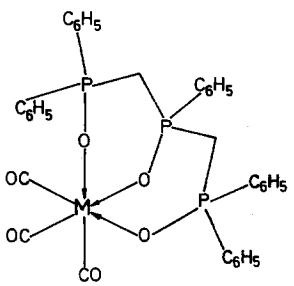

Structure 1. *fac*-$M(CO)_3RPPh$; M = Mo, W.

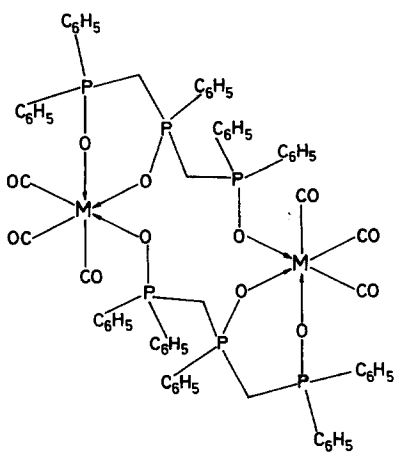

Structure 2. *fac*-$[M(CO)_3RPPh]_2$; M = Mo, W.

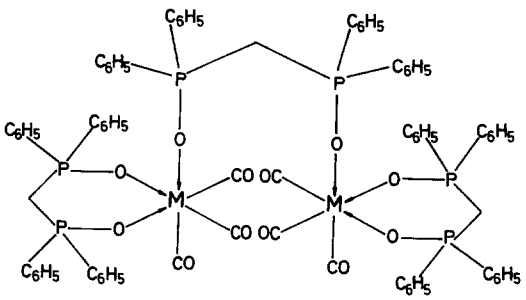

Structure 3. *fac*-$M_2(CO)_6(MDPO)_3$; M = Mo, W.

complexes the strong IR line at ~ 1900 cm^{-1} matches within experimental error the medium Raman band at approximately the same position. Splitting of the lower energy bands is considerably greater in Raman (~ 75 cm^{-1}) than in IR spectra (~ 20 cm^{-1}) of these complexes. For tricarbonyl MDPO complexes coincidences have been observed for the absorption bands at ~ 1720 cm^{-1}. According to the exclusion rule, a centre of symmetry in the crystal units of these complexes has to be excluded.[20,21] Tetracarbonyl complexes decompose under laser beams, and therefore, Raman spectra could not be recorded.

NMR spectra

^{13}C and ^{31}P NMR data for the RPPh ligand and $Mo(CO)_3RPPh$ complex are given in Table 4.

The CP MAS ^{13}C NMR spectrum of the $Mo(CO)_3RPPh$ complex exhibits several peaks from 126 to 135 ppm assigned to carbons from the phenyl rings.[22] In addition, the spectrum shows two signals, at 38.89 and 29.07 ppm, corresponding to the CH_2 groups of the ligand.[22] The difference between the two CH_2 absorptions suggests that these two CH_2 groups of the ligand are not equivalent in the complex. The absence of CO signals in the ^{13}C NMR spectrum of the complex is probably due to the long relaxation time of carbonyls.

In the CP MAS ^{31}P NMR spectrum of the RPPh ligand, we observed three absorption peaks in the approximate ratio of 1 : 1 : 1. Chemical shifts are consistent with those obtained for similar phosphine oxide ligands.[23–25] The resonance at 29.70 ppm is assigned to the central phosphorus atom. The higher field signals corresponding to the terminal PO groups appear at 27.69 and 26.57 ppm. Slight differences in the C—P—C bond angles or the presence of some kind of hydrogen bond may cause this inequivalence of the two terminal PO groups of the ligand in the solid state NMR.

The CP MAS ^{31}P NMR spectrum of the Mo $(CO)_3RPPh$ complex exhibits three well-resolved

Table 4. ^{13}C and ^{31}P NMR data of the RPPh ligand and *fac*-$Mo(CO)_3$ RPPh complex

Compound	$\delta(C)^a$ (CH_2)	$\delta(P)^a$
RPPh	Not measured	29.70, 27.69, 26.57
$Mo(CO)_3$RPPh	38.89, 29.07	35.13, 31.75, 26.91

[a] Chemical shift values [δ(C) and δ(P)] in ppm relative to tetramethylsilane and trimethylphosphate, respectively, with positive values downfield from references.

resonances at: 35.13, 31.75 and 26.91 ppm in a ratio of 1:1:1. On the other hand, in a monomeric facial complex with two PO groups occupying chemically equivalent sites, one would expect two absorption peaks in the ^{31}P NMR spectrum in a ratio of 2:1. The inequivalence of the terminal PO groups can arise from a rigid conformation of the bicyclic metal–chelate system. However, the NMR signals and the insolubility of the complexes suggest that a dimer structure with the bridging RPPh ligand is more likely (Structures **1** and **2**).

EXPERIMENTAL

Materials

The ligands, methylenebis[diphenylphosphine oxide] (MDPO) and bis[diphenylphosphinyl)-methyl]phenylphosphine oxide (RPPh) were prepared according to the data in the literature.[12,26] Metal hexacarbonyls were used directly as obtained commercially (p.a. Merck). The solvents were purified, dried over the appropriate drying agents and freshly distilled under argon prior to use. All manipulations were performed under a dry argon atmosphere.

Physical measurements

IR spectra were recorded on KBr pellets using a Perkin–Elmer Model 580B spectrophotometer.

Raman spectra were taken on solid samples in sealed capillaries, with a Coherent Radiation Model Innova 100-15 spectrometer with 20 mW power, with the sample in the 514.5 nm line of an argon ion laser as the exciting radiation. Spectra were recorded using a Dilor Z-24 triple monochromator.

Magnetic susceptibilities were measured by the Gouy method at 22°C using $CuSO_4 \cdot 5H_2O$ as calibrant.

Magnetic resonance CP MAS spectra were recorded by the Bruker, Analitische Messtechnik, GMBH, Karlsruhe, on a Bruker MSL 400 spectrometer operating at 100.63 MHz for ^{13}C and 161.98 MHz for ^{31}P. Chemical shifts were measured at 22°C with tetramethylsilane as internal standard (^{13}C) and trimethylphosphate as external standard (^{31}P). Because some of the complexes are unstable, the NMR data (^{13}C and ^{31}P) were measured only for the RPPh ligand and the $Mo(CO)_3$RPPh complex.

Preparation of complexes

$Mo(CO)_3$RPPh was obtained by mixing 0.264 g (1 mmol) of $Mo(CO)_6$, 0.554 g (1 mmol) of RPPh and 25 cm^3 of benzene, which were boiled under reflux for 3 h, in a two-neck flask, on an oil bath, with stirring. A light yellow precipitate separated out. The solution was cooled to room temperature, and the microcrystalline solid filtered off, washed with a few cm^3 of benzene and dried in the vacuum of a water suction-pipe. The yield was 0.670 g (90%). The complex is stable in air for several days.

$W(CO)_3$RPPh was prepared by refluxing a mixture of 0.352 g (1 mmol) of $W(CO)_6$ and 0.665 g (1.2 mmol) of RPPh in 30 cm^3 of toluene for 5 h. A yellow product (0.658 g 80%) was filtered off, washed with toluene and dried as above. The complex is much less stable than the corresponding molybdenum compound.

$Mo_2(CO)_6(MDPO)_3$ was obtained by mixing 0.264 g (1 mmol) of $Mo(CO)_6$, 0.624 g (1.5 mmol) of MDPO and 30 cm^3 of xylene. These were heated at 120°C with stirring for 2 h. A yellow product separated out. The complex was isolated as outlined above. The yield was 0.725 g (90%).

$W_2(CO)_6(MDPO)_3$. A mixture of 0.176 g (0.5 mmol) of $W(CO)_6$ and 0.312 g (0.75 mmol) of MDPO in 12 cm^3 of toluene was boiled under reflux for 3 h. The orange–yellow, highly air-sensitive precipitate separated out in a yield of 0.350 g (80%).

$Mo(CO)_4$RPPh was obtained after the mixture of 3 mmol of $Mo(CO)_6$ (0.792 g) and 1 mmol of RPPh (0.554 g) was refluxed in 40 cm^3 of benzene for 20 min. The yellow–brown product, which separated on the sides of the flask, was collected by filtration, washed with a few cm^3 of benzene and dried. The yield was 0.075 g (9.8%).

$W(CO)_4RPPh$ was obtained by mixing 0.704 g (2 mmol) of $W(CO)_6$ and 0.554 g (1 mmol) of RPPh. These were boiled under reflux in 40 cm^3 of xylene for 40 min. A yellow–brown compound (0.102 g) (12%) was obtained, which was filtered off, washed with xylene and dried as above.

$Mo(CO)_4MDPO$ was obtained by mixing an amount of 0.528 g (2 mmol) of $Mo(CO)_6$ with 0.416 g (1 mmol) of MDPO. These were heated in 35 cm^3 of xylene at 120°C for 30 min. A yellow–brown solid separated out in a yield of 0.090 g (14%).

$W(CO)_4MDPO$ was obtained by refluxing equimolar amounts of $W(CO)_6$ (0.352 g, 1 mmol) and MDPO (0.416 g, 1 mmol) in 35 cm^3 of xylene for 2 h. The precipitate was filtered off, washed with xylene and dried. The yield was 0.121 g (17%).

Acknowledgements—The financial support from the Foundation of Scientific Research of SR Croatia is gratefully acknowledged. We are also grateful to Dr V. Formaček of Bruker for measuring the NMR spectra.

REFERENCES

1. L. M. Haines and M. H. B. Stiddard, *Adv. Inorg. Chem. Radiochem.* 1969, **12**, 53 and refs therein.
2. R. J. Puddephatt, *Chem. Soc. Rev.* 1983, **12**, 99 and refs therein.
3. (a) R. B. King and T. W. Lee, *Inorg. Chem.* 1982, **21**, 319; (b) R. B. King and K. S. RaghuVeer, *Inorg. Chem.* 1984, **23**, 2482; (c) R. B. King and N. D. Sadanani, *Inorg. Chem.* 1985, **24**, 3136.
4. J. A. Iggo and B. L. Shaw, *J. Chem. Soc., Dalton Trans.* 1985, 1009.
5. K. R. Birdwhistell, T. L. Tonker and J. L. Templeton, *J. Am. Chem. Soc.* 1987, **109**, 1401.
6. F. Canziani, F. Zingales and U. Sartorelli, *Gazz. Chim. Ital.* 1964, **94**, 841.
7. L. Chandrasegaran and G. A. Rodley, *Inorg. Chem.* 1965, **4**, 1360.
8. H. Bock and H. Tom Dieck, *Z. Naturfor.* 1966, **21b**, 739.
9. P. Bronzan-Planinić and H. Meider, *Polyhedron* 1983, **2**, 69.
10. P. Bronzan-Planinić and H. Meider, *Croat. Chem. Acta* 1984, **57**, 477.
11. M. Herceg, P. Bronzan-Planinić, H. Meider and B. Matković, *Polyhedron* 1986, **5**, 2013.
12. C. R. White and M. D. Joesten, *J. Inorg. Nucl. Chem.* 1976, **38**, 2173 and refs therein.
13. (a) R. Poilblanc and M. Bigorgne, *Bull. Soc. Chim. Fr.* 1962, 1301; (b) P. S. Braterman, *Metal Carbonyl Spectra.* Academic Press, New York (1975).
14. (a) F. A. Cotton and C. S. Kraihanzel, *J. Am. Chem. Soc.* 1962, **84**, 4432; (b) C. S. Kraihanzel and F. A. Cotton, *Inorg. Chem.* 1963, **2**, 533; (c) F. A. Cotton, *Inorg. Chem.* 1964, **3**, 702.
15. W. Kaim and S. Kohlmann, *Inorg. Chem.* 1987, **26**, 68.
16. F. A. Cotton, R. D. Barnes and E. Bannister, *J. Chem. Soc.* 1960, 2199.
17. L. W. Houk and G. R. Dobson, *Inorg. Chem.* 1966, **5**, 2119.
18. (a) F. A. Cotton, D. J. Darensbourg and B. W. S. Kolthammer, *J. Am. Chem. Soc.* 1981, **103**, 398; (b) F. A. Cotton, D. J. Darensbourg, B. W. S. Kolthammer and R. Kudaroski, *Inorg. Chem.* 1982, **21**, 1656.
19. D. J. Darensbourg, M. Pala, D. Simmons and A. L. Rheingold, *Inorg. Chem.* 1986, **25**, 3537.
20. J. B. Lambert, *Organic Structural Analysis.* Macmillan, New York (1976).
21. K. Nakamoto, *Infrared and Raman Spectra of Inorganic and Coordination Compounds.* Wiley, New York (1978).
22. P. S. Braterman, D. W. Milne, E. W. Randall and E. Rosenberg, *J. Chem. Soc., Dalton Trans.* 1973, 1027.
23. P. A. W. Dean and M. K. Hughes, *Can. J. Chem.* 1980, **58**, 180.
24. (a) S. O. Grim, J. Del Gaudio, R. P. Molenda, C. A. Tolman and J. P. Jesson, *J. Am. Chem. Soc.* 1974, **96**, 3416; (b) S. O. Grim, L. C. Satek, C. A. Tolman and J. P. Jesson, *Inorg. Chem.* 1975, **14**, 656.
25. E. I. Sinyavskaya, S. A. Pisareva, N. I. Cokur, T. I. Ignatjeva and M. P. Komarova, *Zh. Neorg. Khim.* 1981, **26**, 1274.
26. T. Ya. Medved, Yu. M. Polikarpov, S. A. Pisareva, E. I. Matrosov and M. I. Kabacnik, *Izv. Akad. Nauk SSSR, Ser. Khim.* 1968, 2062.

Polyhedron Vol. 8, No. 5, pp. 633–639, 1989
Printed in Great Britain

0277-5387/89 $3.00+.00
© 1989 Pergamon Press plc

SYNTHESIS, CHARACTERIZATION AND STRUCTURAL ELUCIDATION OF INDIUM(III) COMPLEXES OF 2-ALKYLAMINOCYCLOPENTENE-1-CARBODITHIOIC ACID AND OF ITS ESTERS

SHAILENDRA K. SINGH, YASHPAL SINGH, AUDHESH K. RAI and RAM C. MEHROTRA*

Chemical Laboratories, University of Rajasthan, Jaipur-302004, India

(*Received* 13 *June* 1988; *accepted* 29 *September* 1988)

Abstract—Reactions of $InCl_3$ and the sodium salts of 2-alkylaminocyclopentene-1-carbodithioic acids, R(H)NC$^{\frown(CH_2)_3\frown}$CC(S)SH (where R = H, Me, Et and *n*-Bu) and esters of the parent acid, H_2NC$^{\frown(CH_2)_3\frown}$CC(S)SR^1 (where R^1 = Me and CH_2NEt_2) in 1:3 molar ratios, yield derivatives with the general formulae, In[S(S)C$^{\frown(CH_2)_3\frown}$CN(H)R]$_3$ and In[N(H)C$^{\frown(CH_2)_3\frown}$CC(S)SR^1]$_3$, respectively. These complexes have been characterized by elemental analyses, molecular weight determinations and conductometric measurements, as well as on the basis of their IR and NMR (^{1}H, ^{13}C and ^{14}N) spectral data. The bonding of indium with the acids is through SS$^-$, whereas with esters bonding occurs from the N—S sites.

Complexes of N- and S-bonded, N-alkyl and ester derivatives of 2-aminocyclopentene-1-carbodithioic acid with different transition metals exhibit[1–6] a remarkable diversity in coordination patterns, some of which may be illustrated by the formulae below (**A–C**).

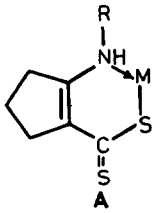

A

M = Ni^{II}, Pd^{II}, Pt^{II}, Fe^{II}, Rh^{I}, Cu^{I}, Hg^{I}; R = H, Et.

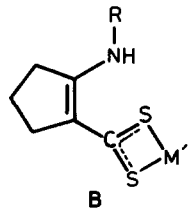

B

M^1 = Co^{II}, Co^{III}, Cr^{III}.

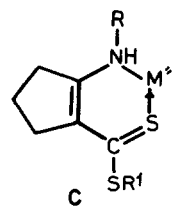

C

M^{11} = Ni^{II}, Pd^{II}; R^1 = Me, CH_2NEt_2.

A survey of the literature reveals that no attempt has been made to synthesize metal complexes of these ligands with non-transition elements, except for some organotin derivatives[7] of the ACDA esters. In view of the interesting results reported for transition metal complexes, it has been considered worthwhile to synthesize a few substituted ACDA ligands and investigate the nature of their complexation reactions and of bonding with indium.

EXPERIMENTAL

Chemicals

All the chemicals used were of reagent grade. Cyclopentanone (Sisco) was distilled (b.p., 130°C) before use and indium trichloride (Fluka) was used

*Author to whom correspondence should be addressed.

as such. All the solvents used were dried by standard methods. The ligand ACDA and its substituted derivatives have been synthesized by the literature methods[8,9] and have been characterized by melting point determination, elemental analysis, IR, ^{1}H and ^{13}C NMR spectral analyses.

General method of preparation of the complexes

All the complexes have been synthesized by the reactions of indium trichloride and the sodium salts of ligands in 1 : 3 molar ratios in hot benzene solution. The sodium salts of the ligands were obtained by their reactions with calculated amounts of sodium methoxide in hot benzene solution after constant stirring for 1 h. Since, a similar method has been followed for the synthesis of all indium derivatives, the preparation of only one compound is described here for the sake of brevity.

The benzene solution of the freshly prepared sodium salt of BuACDA (1.38 g, 5.83 mmol) was added dropwise to a stirred suspension of indium trichloride (0.43 g, 1.93 mmol) and stirring was continued for about 2 h. During the course of the reaction, the temperature was maintained below 60°C. Sodium chloride thus obtained was filtered off and removal of the solvent under reduced pressure, yielded a yellow coloured solid compound which was recrystallized from benzene–hexane, yield 93%.

Some indium complexes were found to be sparingly soluble in benzene. In these cases the solvent was distilled off and the sodium chloride was removed by washing with aqueous ethanol, leaving the insoluble compound which was finally washed with *n*-hexane and dried *in vacuo*.

Analyses

Indium was estimated gravimetrically as indium oxide. Nitrogen and sulphur were estimated by Kjeldahl's[10] and Messenger's method,[10] respectively.

Physical measurements

Molecular weights were determined on a Knauer vapour pressure osmometer in dimethylsulphoxide solution at 45°C, and conductivity measurements were carried out using a Systronics conductivity meter, type 302 SR No. 475, in nitrobenzene solution.

The IR spectra as Nujol mulls or KBr pellets were recorded with Perkin–Elmer 577 and Philips Pye–Unicam, SP 3-300, spectrophotometers. The ^{1}H and ^{13}C NMR spectra of the ligands were recorded on a 270 MHz Bruker spectrometer, at ambient temperatures, and the ^{1}H, ^{14}N and ^{13}C NMR spectra of the complexes were recorded in $CDCl_3$ or DMSO-d_6 solution, on a JEOL FX 90 Q spectrometer using TMS as an internal reference. For ^{14}N spectra, ammonium nitrate was used as an external reference.

Table 1. Analytical data of the indium(III) complex of 2-alkylaminocyclopentene-1-carbodithioic acid and its esters

	Reactants (g)			Product	Elemental analyses (%). Found (calc.)			Molecular weight in DMSO at 45°C
	$InCl_3$	LH[a]	Na	yield (%)	In	N	S	Found (calc.)
1.	0.37	ACDA	0.12	$In(ACDA)_3$[b]	19.3	7.2	32.1	580.2
		0.79		92	(19.5)	(7.1)	(32.5)	(589.6)
2.	0.38	MeACDA	0.12	$In(MeACDA)_3$[c]	18.0	6.5	30.1	—
		0.88		94	(18.2)	(6.6)	(30.4)	
3.	0.36	EtACDA	0.11	$In(EtACDA)_3$[c]	16.9	6.3	28.2	—
		0.91		95	(17.0)	(6.2)	(28.5)	
4.	0.43	BuACDA	0.14	$In(BuACDA)_3$[d]	15.2	5.4	25.1	752.4
		1.26		93	(15.1)	(5.5)	(25.3)	(757.6)
5.	0.42	$ACDE_1$	0.13	$In(ACDE_1)_3$[d]	18.4	6.4	30.0	638.7
		0.98		94	(18.2)	(6.6)	(30.4)	(631.6)
6.	0.38	$ACDE_2$	0.11	$In(ACDE_2)_3$[d]	13.4	9.8	22.6	828.2
		1.20		91	(13.7)	(10.0)	(22.9)	(838.6)

[a] LH ligands.
[b] Sparingly soluble.
[c] Insoluble.
[d] Highly soluble in common organic solvents.

RESULTS AND DISCUSSION

The metal complexes were obtained by the reactions of indium trichloride with the sodium salts of the ligands in 1 : 3 molar ratio in benzene solution:

$$InCl_3 + 3R(H)NC(=CH_2)_3=CC(S)SNa \longrightarrow In[S(S)CC(=CH_2)_3=CN(H)R]_3 + 3NaCl$$

(where R = H, —CH_3, —C_2H_5, *n*-C_4H_9)

$$InCl_3 + 3Na(H)NC(=CH_2)_3=CC(S)SR^1 \longrightarrow In[(H)NC(=CH_2)_3=CC(S)SR^1]_3 + 3NaCl$$

(where R^1 = —CH_3, —$CH_2N(C_2H_5)_2$).

The stoichiometry of the compounds has been confirmed by their analytical data (Table 1). Some of these complexes are fairly soluble in common organic solvents like chloroform, benzene and THF, whereas others are found to be insoluble. The soluble metal complexes are found to be non-electrolytic in nitrobenzene solution and monomeric in dimethylsulphoxide solution at 45°C.

Following earlier suggestions,[3,9] the ligands may be assumed to exist in the following six tautomeric forms (I–VI).

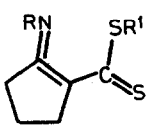

(I)

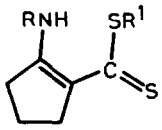

(II)

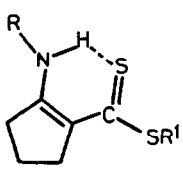

(III)

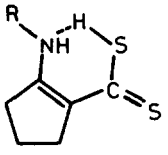

(IV)

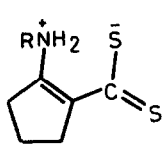

(V)

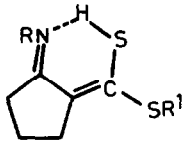

(VI)

(where R = H; R^1 = —CH_3, —$CH_2N(C_2H_5)_2$.
R = —CH_3, —C_2H_5, *n*-C_4H_9; R^1 = H).

On the basis of IR and ^{1}H NMR spectral data, Takeshima *et al.*[8] proposed structure **I**, whereas Bordas *et al.*[9] suggested structure **III** for these ligands. However, Nag and Joardar[3] reported the existence of structure **III** exclusively in DMSO-d_6 solution, while in $CDCl_3$ solution a partial contribution of structure **VI** was also proposed. The assignments for SH/NH proton signals are also inconsistent in the existing literature.[3,8,9]

In order to establish the position of NH and SH signals, low temperature ^{1}H NMR spectra of two representative derivatives, 2-butylaminocyclopentene-1-carbodithioic acid (BuACDA) and the methyl ester ($ACDE_1$) of ACDA have been recorded. The room temperature spectrum of BuACDA, in $CDCl_3$ solution, exhibits a broad signal at δ 12.8 ppm which splits into a multiplet at −50°C due to the coupling of the proton attached to the nitrogen atom with CH_2 protons of the butyl group attached to the nitrogen atom, confirming that the signal appearing at δ 12.8 ppm is due to the —NH proton of the ligand BuACDA. However, in the ^{1}H NMR spectrum of $ACDE_1$ in which the SH proton of ACDA is replaced by a methyl group and where the two protons are bound to the nitrogen atom, two broad signals at δ 11.2 and 6.2 ppm have been observed. The SCH_3 protons appear at δ 2.6 ppm as a sharp singlet. In the low temperature (−70°C) ^{1}H NMR spectrum, both the broad signals at δ 11.2 and 6.2 ppm split into multiplets. The above low temperature ^{1}H NMR spectral data confirm the existence of tautomeric form **III** exclusively for ACDA and its alkyl and ester derivatives.

IR spectral study of the ligands and the indium complexes

Following earlier observations,[3,5,8,9] broad bands observed at ≈2550 and ≈3400 cm^{-1} in the IR spectra of ACDA and its N-alkyl derivatives can

be assigned to SH and NH/NH_2, respectively. The disappearance of the former and the unaltered position of the latter in the indium complexes confirm that the bonding occurs only through S in these derivatives. The strong bands observed at 1605–1590 cm^{-1}, 1490–1480 cm^{-1}, 1360–1310 cm^{-1} and1280–1270 cm^{-1} in the ligands and their metal complexes may be assigned to the combination of $\nu_{NH+C=C}$, $\nu_{CH_2+C=C}$, $\nu_{C=N+C=S}$, and mixing of $\nu_{C=S+C=N}$ modes, respectively.

The occurrence of an asymmetric CSS stretching frequency around 1000 cm^{-1} has been reported in the case of metal dithiocarbamate[11] and dithiocarbazate[12] complexes for disulphur chelation, whereas for the involvement of only one sulphur atom, this band splits[11] into two. The appearance of only a single band in the range 1010–910 cm^{-1} in the indium complexes of ACDA and its N-alkyl substituted derivatives, therefore, indicates involvement of both sulphur atoms in these complexes. The band at $\approx$610 cm^{-1} in the ligands and the corresponding metal complexes has been assigned to either a symmetrical CSS or C—S. A new band appearing at 350–335 cm^{-1} may be assigned to ν_{In-S}.

In the IR spectrum of the free ligand $ACDE_1$, an absorption band has been observed at $\approx$3250 cm^{-1} which can be assigned[5,7] to a ν_{NH_2} vibration. A downward shift of $\approx$50 cm^{-1} of this band in the spectrum of $In(ACDE_1)_3$ indicates the deprotonation of one of the NH_2 protons on complexation. This is confirmed by a smaller ($\approx$15 cm^{-1}) downward shift of the absorptions observed in the ranges 1270 ± 5 and 1150 ± 5 cm^{-1} which have been ascribed to $\nu_{C=N+C=S}$ and $\nu_{C=S+C=N}$ modes, respectively.

The appearance of two bands for asymmetric CSS at 940 and 910 cm^{-1} clearly indicates the involvement of the sulphur atom during chelation. Further, the appearance of both M—N and M—S absorption frequencies at 550 and 350–325 cm^{-1}, respectively, indicate the participation of both the nitrogen and sulphur atoms of the ligand in bonding.

^1H *NMR spectral studies of the ligands and their complexes*

A sharp singlet observed for the —SH proton in the spectra of the ligands (Table 2) is found to be absent in the corresponding metal derivatives, indicating the removal of a —SH proton and the formation of In—S bonds.

In the ^1H NMR spectrum of ACDA, two broad signals assigned to the $—NH_2$ protons have been observed at δ 6.1 and 11.2 ppm, showing the non-equivalence of the protons of the amino groups. This may be attributed to the involvement of one of the $—NH_2$ protons in hydrogen bonding through the sulphur atom (C=S, structure **III**) of the ligand. In the spectrum of the indium complex, $In(ACDA)_3$, one of the two signals (δ 6.1 ppm) appears almost in the same region while the second signal, observed at δ 11.2 ppm in the free ligand, shifts upfield to δ 7.8 ppm. This may be due to the breaking of the hydrogen bond (N—H $\cdots$ S=) during complexation. However, the existence of two signals for the $—NH_2$ protons, instead of one signal even on complexation, indicate the probability of some weak interaction between one of the NH_2 protons and the sulphur atom (—C=S) of the dithiocarboxylate group. A similar phenomenon has been observed in the ^1H NMR spectra of the free BuACDA and its indium complex.

In the ^1H NMR spectra of indium complexes of S-alkyl or ester derivatives of ACDA (Table 2), the signal observed at δ 11.2 ppm in the ligand and assigned to hydrogen bonded (—N—H $\cdots$ S=), disappears and the —NH signal observed at δ 6.1 ppm is shifted downfield to δ 8.4 ppm, indicating the removal of one of the protons of the amino group on complexation. The signals at δ 11.2 ppm observed by us in these ligands (ester derivatives) have not been reported by earlier workers.[5–7]

A perusal of the ^1H NMR spectral data of the ligand (methyl ester) reveals that the signal at δ 2.61 ppm due to $S—CH_3$ shifts downfield (by 0.6 ppm) on complexation, which supports the participation of the C=S group on bonding with indium.

^{13}C *NMR spectral studies of the ligands and their complexes*

The signals in the ^{13}C NMR spectra of the ligand and their corresponding complexes are summarized in Table 3.

In the spectrum of BuACDA, the signal for the C(6) atom attached to the thiol group appears at δ 191.5 ppm, which shifts downfield and is observed at δ 199.9 ppm. Such a large shift of 8.4 ppm [for C(6)] may be due to the deshielding of the carbon atom because of the deprotonation of one thiol group and coordination through the other sulphur atom.

However, in the spectrum of $ACDE_1$, signals observed at δ 165.3, 201.5 and 13.8 ppm ascribed to the carbon atoms, C(2), C(6) and C(α), respectively, shift downfield and appear at δ 166.5, 203.9 and 16.9 ppm, respectively, in the corresponding indium complexes. These data further confirm the presence

Table 2. ^{1}H NMR data of indium(III) complexes of 2-alklaminocyclopentene-1-carbodithioic acid and its allied derivatives

	Compound	Solvent	Chemical shift values (δ) in ppm
1.	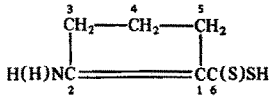 ACDA	$CDCl_3$	$CH_{2(4)}$, q, 1.7–2.0; $CH_{2(3\text{ and }5)}$, m, 2.6–2.8; $NH_{(free)}$, bs, 6.1; $NH_{(chelated)}$, bs, 11.2; SH, s, 5.1
2.	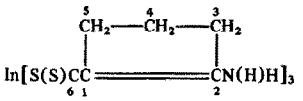 $In(ACDA)_3$	$DMSO\text{-}d_6$	$CH_{2(4)}$, q, 1.5–1.9; $CH_{2(3\text{ and }5)}$, m, 2.5–2.9[a]; $NH_{(free)}$, bs, 7.4; $NH_{(interaction)}$, bs, 8.6
3.	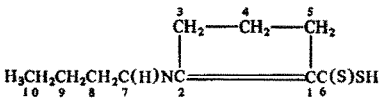 BuACDA	$CDCl_3$	$CH_{2(4)}$, q, 1.9–2.1; $CH_{2(3)}$, t, 2.6–2.8; $CH_{2(5)}$, t, 3.0–3.2; $NH_{(chelated)}$, bs, 12.6; $CH_{2(7)}$, m, 3.3–3.4; $CH_{2(8)}$, m, 1.5–1.7; $CH_{2(9)}$, m, 1.4–1.5; $CH_{3(10)}$, t, 0.8–0.9; SH, 1.5[b]
4.	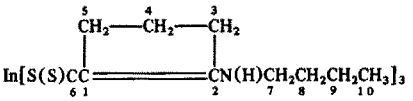 $In(BuACDA)_3$	$CDCl_3$	$CH_{2(4,8\text{ and }9)}$, m, 1.2–2.1; $CH_{2(3\text{ and }5)}$, m, 2.5–3.0 $CH_{2(7)}$, m, 3.2–3.5; $CH_{2(10)}$, t, 0.8–1.1; $NH_{(interaction)}$, bs, 9.3
5.	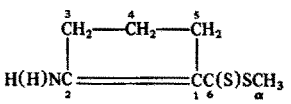 $ACDE_1$	$CDCl_3$	$CH_{2(4)}$, m, 1.9; $CH_{2(3\text{ and }5)}$, m, 2.6–2.9; $CH_{3(\alpha)}$, s, 2.6; $NH_{(free)}$, bs, 6.2; $NH_{(chelated)}$, bs, 11.2
6.	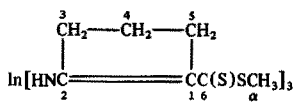 $In(ACDE_1)_3$	$DMSO\text{-}d_6$	$CH_{2(4)}$, m, 1.6–2.0; $CH_{2(3\text{ and }5)}$, m, 2.4–2.9; $NH_{(free)}$, 8.4; $CH_{3(\alpha)}$, s, 3.2
7.	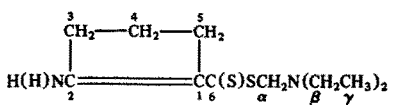 $ACDE_2$	CCl_4	$CH_{2(4)}$, m, 1.9–2.4; $CH_{2(3,5\text{ and }\beta)}$, m, 2.7–3.3; $CH_{2(\alpha)}$, s, 5.2; $NH_{(free)}$, bs, 5.8; $NH_{(chelated)}$, bs, 11.4; $CH_{3(\gamma)}$, t, 1.5
8.	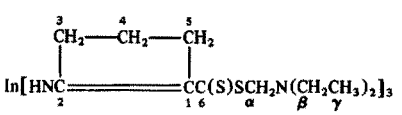 $In(ACDE_2)_3$	$DMSO\text{-}d_6$	$CH_{2(4)}$, m, 1.4–1.8; $CH_{2(3,5\text{ and }\beta)}$, m, 2.2–2.8; $CH_{2(\alpha)}$, s, 4.3; $NH_{(free)}$, bs, 8.5; $CH_{3(\gamma)}$, t, 0.7–1.2

s = Singlet, bs = broad signal, t = triplet, q = quintet and m = multiplet.

[a] Merged with the $DMSO\text{-}d_6$ peak.

[b] Mixed with $CH_{2(8)}$.

Table 3. ^{13}C spectral data of indium(III) complexes of 2-alkylaminocyclopentene-1-carbodithioic acid and its ester

	Compound	Solvent	Chemical shift values (δ) in ppm
1.	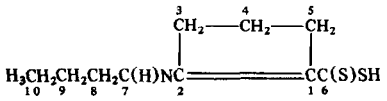 BuACDA	$CHCl_3$	$C_{(1)}$, 118.3; $C_{(2)}$, 170.9; $C_{(3)}$, 32.9; $C_{(4)}$, 18.4; $C_{(5)}$, 32.5; $C_{(6)}$, 191.5; $C_{(7)}$, 45.2; $C_{(8)}$, 31.7; $C_{(9)}$, 21.1; $C_{(10)}$, 13.5
2.	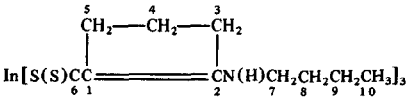 $In(BuACDA)_3$	$CHCl_3$	$C_{(1)}$, 119.2; $C_{(2)}$, 168.8; $C_{(3)}$, 35.9; $C_{(4)}$, 19.6; $C_{(5)}$, 33.8; $C_{(6)}$, 199.9; $C_{(7)}$, 46.2; $C_{(8)}$, 31.8; $C_{(9)}$, 19.9; $C_{(10)}$, 13.6
3.	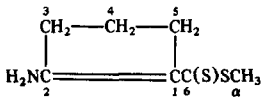 $ACDE_1$	C_6H_6	$C_{(1)}$, 116.2; $C_{(2)}$, 165.3; $C_{(3)}$, 34.6; $C_{(4)}$, 16.5; $C_{(5)}$, 30.9; $C_{(6)}$, 201.5; $C_{(\alpha)}$, 13.8
4.	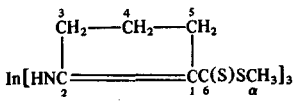 $In(ACDE_1)_3$	C_6H_6	$C_{(1)}$, 117.8; $C_{(2)}$, 166.5; $C_{(3)}$, 36.1; $C_{(4)}$, 20.5; $C_{(5)}$, 33.1; $C_{(6)}$, 203.9; $C_{(\alpha)}$, 16.9

of nitrogen and sulphur atoms along with indium in a six-membered ring (**VII**).

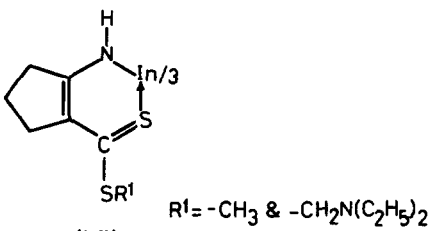

(VII) $R^1 = -CH_3$ & $-CH_2N(C_2H_5)_2$

involved in the bonding and that the indium atom is bonded through the sulphur atoms only (**VIII**).

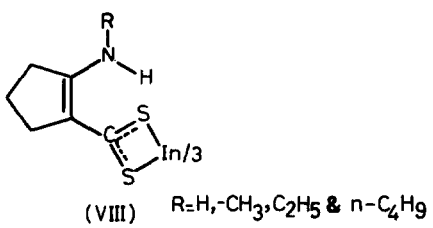

(VIII) R=H, $-CH_3$, C_2H_5 & $n-C_4H_9$

^{14}N *NMR spectral studies*

In order to confirm the mode of bonding proposed on the basis of IR, ^1H and ^{13}C NMR spectral evidence, ^{14}N NMR spectra of BuACDA and its indium complex have been recorded in chloroform solution, using ammonium nitrate as external reference. The spectrum of BuACDA exhibits two signals for the nitrogen at δ −65.3 and −64.4 ppm (J = 7.3 Hz) due to the coupling of the attached proton. The unaltered position of these signals even in the corresponding indium complex, further confirm our assumption that the nitrogen is not

Attempts to record the ^{14}N NMR spectra of N-bonded complexes of esters were not successful, which may be due to the quadrupole moment of ^{14}N and the coupling of nitrogen (I = 1) and indium (I = 9/2) resulting in a very broad signal which may escape detection.

Acknowledgements—Thanks are due to Mr Suman K. Gupta for taking a keen interest in recording all the NMR spectra. One of us (S.K.S.) is grateful to the State Government of Rajasthan and U.G.C., New Delhi, for financial support under the Special Assistance Programme.

REFERENCES

1. K. Nag and D. S. Joardar, *Can. J. Chem.* 1976, **54**, 2827.
2. K. Nag and D. S. Joardar, *Inorg. Chim. Acta* 1976, **17**, 111.
3. K. Nag and D. S. Joardar, *Inorg. Chim. Acta* 1975, **14**, 133.
4. K. Nag and D. S. Joardar, *Z. Naturf.* 1975, **30b**, 107.
5. D. S. Joardar, S. K. Mondal and K. Nag, *Bull. Chem. Soc. Jpn* 1977, **50**, 1489.
6. B. Singh and V. D. Gupta, *J. Ind. Chem. Soc.* 1982, **59**, 244.
7. (a) B. Singh and V. D. Gupta, *J. Ind. Chem. Soc.* 1982, **59**, 793; (b) B. Singh and V. D. Gupta, *Ind. J. Chem.* 1981, **20A**, 526.
8. T. Takeshima, M. Yokoyama, T. Imamoti, M. Akano and H. Asaba, *J. Org. Chem.* 1969, **34**, 730.
9. B. Bordas, P. Sohar, G. Matolcsy and P. Berencsi, *J. Org. Chem.* 1972, **34**, 1727.
10. A. I. Vogel, *A Text Book of Quantitative Inorganic Analysis*. Longman, London (1974).
11. F. Bonati, S. Genini and R. Ugo, *J. Organomet. Chem.* 1967, **9**, 395.
12. M. Akbar Ali, S. E. Livingstone and D. J. Philips, *Inorg. Chim. Acta* 1971, **5**, 119.

Polyhedron Vol. 8, No. 5, pp. 641–645, 1989
Printed in Great Britain

0277–5387/89 $3.00+.00
Pergamon Press plc

THE STEPWISE COMPLEX FORMATION IN THE COBALT(III)–AZIDE SYSTEM

NINA COICHEV and EDUARDO ALMEIDA NEVES*

Instituto de Química, Universidade de São Paulo, Cx. Postal 20780, CEP 01498, São Paulo, Brazil

(*Received* 27 *July* 1988; *accepted* 29 *September* 1988)

Abstract—Measurements of conditional potential of the Co^{III}/Co^{II} system in several sodium azide solutions (0.30–1.78 M) of ionic strength 2.0 M, held with sodium perchlorate, in aqueous medium at 25°C, lead to the following overall formation constants: $\beta_1 = 3\times10^8\ M^{-1}$, $\beta_2 = 1\times10^{15}\ M^{-2}$, $\beta_3 = 7\times10^{19}\ M^{-3}$, $\beta_4 = 1.5\times10^{23}\ M^{-4}$, $\beta_5 = 1.3\times10^{23}\ M^{-5}$ and $\beta_6 = 1.0\times10^{24}\ M^{-6}$. Calculations require introduction of the stepwise formation constants of the cobalt(II) complexes and $E^{0\prime}$ for Co^{III}/Co^{II} in non-complexing media, from literature data, in order to calculate the Leden's function, $F^0(L)$, referred to Co^{III} complexes. The first three formation constants were estimated from the linear plot of $(\log\beta_n)/n$ vs n (number of ligands) with β_4, β_5 and β_6 data.

The cobalt(III) stabilization in concentrated sodium azide solution was first mentioned by Senise[1] who observed a slow colour change of the cobalt(II) solutions, containing the blue $[Co(N_3)_4]^{2-}$ anion, due to oxidation, to the brown mixture of azide complexes of cobalt(III): the solid, explosive compound $Tl_3[Co(N_3)_6]$, was isolated from this medium. The induced oxidation of sulphur(IV), by dissolved oxygen, markedly accelerates this reaction and a spot test was developed for sulphite.[1,2]

Due to the high molar absorptivity of cobalt(III) in the azide medium, a method for determination of this element in trace levels in nickel salts was presented.[3]

This high spectrophotometric sensitivity led to the development of a method for the determination of sulphur(IV) in rain water,[4] based on the formerly described induced reaction.[2] It has been found that the best conditions for this quantitative method[4] is by performing in a 0.5 M sodium azide solution in a pH 5.5–6.5 range. In order to better understand mechanisms and to make thermodynamic considerations about this induced reaction, this paper deals with potentiometric measurements in $Co^{III}/Co^{II}/N_3^-$ solutions for obtaining equilibrium constants in the cobalt(III)/azide system.

* Author to whom correspondence should be addressed.

EXPERIMENTAL

Reagents and standard solutions

All reagents were from AR or CP specification, from Merck or Mallincrodt brands.

Sodium azide was recrystallized from water, washed with ethanol to remove traces of hydroxide, vacuum dried and then placed in an oven at 110°C until constant weight. Under these conditions it can be used as a primary standard.

Cobalt(II) perchlorate was prepared from the direct reaction of excess carbonate with 2.0 M perchloric acid for 3 days, under stirring at room temperature. After filtering, free perchloric acid was added up to 0.010 M, in order to avoid hydrolysis. Standardization was carried out electrogravimetrically.

Sodium perchlorate (5 M) used for making up the ionic strength of working solutions, was standardized after dilution to a 0.1 M concentration level, by titrating the strong acid eluted from a cationic exchanger column.

Standard perchloric acid was used in the working solutions to displace hydrazoic acid, HN_3, from the azide ions. In order to keep such working solutions free from oxygen, without losing the volatile hydrazoic acid, all standard solutions were previously bubbled with purified nitrogen, before mixing.

Working solutions

The following working solution (**I**) was prepared in a 100 cm^3 volumetric flask: 0.02000 M $Co(ClO_4)_2$, 2.000 M NaN_3 and 0.1500 M $HClO_4$ (to form HN_3). Lead dioxide was added directly to this solution to form cobalt(III), according to the following stoichiometry:

$$PbO_2 + 2[Co(N_3)_4]^{2-} + 4HN_3 + 2N_3^- \longrightarrow Pb(N_3)_2 + 2H_2O + 2[Co(N_3)_6]^{3-}.$$

This final solution (**I**) contained 5.00 mM Co^{III} and 15.0 mM Co^{II}. The free azide concentration was estimated to be 1.90 M, after discounting its consumption to form hydrazoic acid and complexes. In this procedure, nitrogen evolution was not observed in the presence of cobalt(II), due to the oxidation of hydrazoic acid by lead dioxide.

A solution (**II**) was prepared without oxidation: $[Co^{II}] = 0.01500$ M, $[HN_3] = 0.2000$ M, $[N_3^-] = 0.1790$ M and 1.76 M $NaClO_4$.

A solution (**III**) contained: $[Co^{2+}] = 0.01500$ and 1.96 M $NaClO_4$.

Potentiometric measurements

The following cell was used, thermostated at 25.0 ± 0.1°C:

$$Hg \mid Hg_2Cl_2, \text{NaCl sat.} \vdots 0.015 \text{ M } Co(ClO_4)_2, 1.96 \text{ M } NaClO_4 \vdots \text{working solution} \mid Pt.$$

The reference electrode from Micronal has a small compartment for the salt bridge, which was filled immediately before use. Measurements were carried out with a potentiometer sensitive to 0.1 mV.

10.00 cm^3 of the working solution (**II**) was potentiometrically titrated with solution (**I**), up to 20.00 cm^3. The potential of the cell shifted with the change of the $[Co^{III}]/[Co^{II}]$ ratio and free azide concentration. Another series of measurements was taken by titrating 10.00 cm^3 of solution (**I**) with solution (**III**).

Three sets of measurements were taken by repetition of the two titrations. The average of three potentiometric measurements of each particular solution formed during the titrations, was used to calculate the conditional potential, $E_x^{0'}$, for each estimated free azide concentration.

RESULTS AND DISCUSSION

Equations and treatment of data

The measured potential of the Co^{III}/Co^{II} system in complexing media of constant ionic strength, E_x, leads to the following conditional potential, $E_x^{0'}$ for each free azide concentration at the experimental conditions described herein:

$$E_x^{0'} = E_x - 0.05916 \log([Co^{III}]/[Co^{II}]). \quad (1)$$

These $E_x^{0'}$ values are slightly lower than the measured value in the non-complexing medium, $E_s^{0'}$, due to the preferential complexation of cobalt(III) cations by azide with regard to the cobalt(II) cations. The potential shift due to complexation in this system, with the element in two oxidation states, leads to the calculation of the ratio of Leden's functions[5-7] for cobalt(III), F_{III}^0, and cobalt(II), F_{II}^0:

$$E_{xs}^{0'} = E_x^{0'} - E_s^{0'} = -0.05916 \log(F_{III}^0/F_{II}^0). \quad (2)$$

Rearranging:

$$F_{III}^0 = \{10 \exp[(E_s^{0'} - E_x^{0'})/0.05916]\} \times F_{II}^0. \quad (3)$$

The Leden's function for the mononuclear cobalt(II) complexes in azide media of ionic strength 2.0 M, from the literature,[8] can be calculated as:

$$F_{II}^0 = 1 + 5.7[N_3^-] + 19[N_3^-]^2 + 7[N_3^-]^3 + 16[N_3^-]^4 + 4.4[N_3^-]^5. \quad (4)$$

The calculated F_{II}^0 data for each azide concentration was used to calculate F_{III}^0 using eq. (3).

From a series of data available from Bard,[9] a Warnqvist's[10] datum is the most reliable to use as $E_s^{0'}$ in eq. (3). This conditional potential, +1.85 V vs the normal hydrogen electrode, was measured in acidic sodium perchlorate media of ionic strength 3.5 M, higher than that used in this paper (i.e. 2.0 M). However, the potential shift due to complexation with azide is so high (more than 1 V), that an uncertainty of a few hundreds of volts corresponds to a small relative error. Discounting 0.24 V for the reference electrode, the value of +1.61 V was actually used in eq. (3).

The average ligand number (Bjerrum's function)[6,7] for cobalt(III), can be calculated from the following equation where potentials refer to small increments in azide concentrations, from the titration curves:

$$\bar{n}_{III} = \{(E_{x1}^{0'} - E_{x2}^{0'})/0.05916(\log[N_3^-]_2 - \log[N_3^-]_1)\} + \bar{n}_{II}. \quad (5)$$

Derivation of the potentiometric curve from titrations leads to differences in the average ligand number for the two oxidation states. The values for cobalt(II), $\bar{n}_{II}$, can be calculated with the known formation constants[8] and introduced into eq. (5). The calculated $\bar{n}_{III}$ and $\bar{n}_{II}$ were useful to calculate the free azide concentration from the analytical

one, $C_{N_3^-}$, after corrections were made from the dilutions during the titrations. The following equation was used to iteratively find the free azide concentration:

$$[N_3^-] = C_{N_3^-} - [HN_3] - \bar{n}_{II}[Co^{II}] - \bar{n}_{III}[Co^{III}]. \quad (6)$$

Table 1 contains the experimental and calculated data used to obtain the equilibrium constants. A number of calculation steps were considered in the treatment of the potentiometric data, in order to obtain the equilibrium constants:

(1) The first estimate of free azide concentration

Table 1. Potentiometric data (vs the calomel electrode) of the Co^{III}/Co^{II} system in several azide concentrations, from two titrations (see Experimental)

$[N_3^-]$ (mol dm^{-3})	$E_x^{0'}$ (V) (Exp)	$E_x^{0'}$ (V) Smoothed	$F_{III}^0 \times 10^{-21}$	$E_x^{0'}$ (V) (Calc.)	$\bar{n}_{III}$ (Calc.)	$C_{Co^{III}}/C_{Co^{II}}$ ($\times 10^3$)
0.3031	0.3803	0.3793	3.0581	0.3858	4.79	22.97
0.3385	0.3733	0.3720	4.7324	0.3760	4.88	30.30
0.3413	0.3701	0.3715	4.8829	0.3752	4.89	30.85
0.3726	0.3646	0.3652	7.1076	0.3675	4.97	37.04
0.4052	0.3596	0.3590	10.322	0.3600	5.04	43.49
0.4364	0.3538	0.3533	14.569	0.3536	5.10	49.65
0.4484	0.3494	0.3512	16.561	0.3512	5.12	52.04
0.4662	0.3481	0.3481	20.001	0.3478	5.16	55.55
0.5225	0.3392	0.3389	35.281	0.3380	5.25	66.67
0.5746	0.3319	0.3313	57.169	0.3298	5.32	76.93
0.6229	0.3240	0.3248	87.082	0.3230	5.38	86.40
0.6679	0.3203	0.3193	125.60	0.3173	5.43	95.27
0.7096	0.3142	0.3146	173.07	0.3123	5.47	103.5
0.7488	0.3098	0.3105	230.42	0.3080	5.51	111.1
0.7852	0.3064	0.3070	296.33	0.3042	5.54	118.3
0.8196	0.3040	0.3039	372.12	0.3009	5.56	125.0
0.8518	0.3019	0.3012	456.20	0.2979	5.58	131.3
0.8822	0.2997	0.2986	553.27	0.2952	5.60	137.3
0.9109	0.2970	0.2963	659.03	0.2928	5.62	142.9
0.9340	0.2941	0.2945	756.53	0.2909	5.63	166.7
0.9378	0.2942	0.2943	770.96	0.2906	5.63	148.1
0.9584	0.2927	0.2927	871.10	0.2890	5.64	170.9
0.9635	0.2924	0.2924	894.42	0.2886	5.65	153.1
0.9838	0.2911	0.2909	1005.1	0.2871	5.66	175.5
0.9878	0.2905	0.2906	1028.6	0.2868	5.66	157.9
1.011	0.2882	0.2890	1169.2	0.2851	5.67	180.2
1.033	0.2885	0.2875	1318.6	0.2835	5.68	166.7
1.040	0.2865	0.2870	1371.0	0.2830	5.68	185.2
1.070	0.2846	0.2850	1610.4	0.2810	5.69	190.5
1.102	0.2825	0.2829	1907.2	0.2790	5.71	196.1
1.137	0.2802	0.2807	2283.0	0.2768	5.72	202.0
1.173	0.2783	0.2785	2736.2	0.2747	5.73	208.3
1.211	0.2763	0.2763	3291.5	0.2725	5.74	215.1
1.252	0.2738	0.2740	3999.1	0.2703	5.75	222.2
1.296	0.2718	0.2716	4905.7	0.2680	5.77	229.9
1.344	0.2696	0.2692	6064.7	0.2657	5.78	238.1
1.394	0.2673	0.2669	7486.9	0.2634	5.79	246.9
1.449	0.2649	0.2645	9365.2	0.2610	5.80	256.4
1.508	0.2625	0.2623	11,697	0.2585	5.81	266.7
1.572	0.2597	0.2601	14,728	0.2560	5.82	277.8
1.643	0.2574	0.2578	18,833	0.2534	5.83	289.9
1.679	0.2563	0.2566	21.327	0.2521	5.84	296.3
1.719	0.2551	0.2551	24,615	0.2508	5.84	303.0
1.759	0.2583	0.2535	28,485	0.2495	5.85	310.1

Standard deviation (potential), $S = 3.5 \times 10^{-3}$.

was made by considering in eq. (6), $\bar{n}_{III} = 6$ and $\bar{n}_{II}$[6,7] calculated from the formation constants from the literature[8] and with the azide concentration from which $[HN_3]$ was discounted.

(2) The use of eq. (5) has shown that $\bar{n}_{III}$ is not constant along the azide range and changes from 4.8 to 5.8, which suggests stepwise complex formation. On this basis, three iterative corrections in eq. (6) have been found sufficient to obtain the free azide.

(3) The use of eq. (3) leads to the F^0_{III} data in Table 1. Conventional treatment of the data[6,7] or solution of weighted simultaneous equations[11] has been found to be inadequate to obtain the equilibrium constants, due to the non-existence of potentiometric data at lower ligand concentrations. Instability of cobalt(III) solutions provides unreliable measurements with a free azide concentration of less than 0.22 M. F^0_{III} data is a polynomial with the sum of $\beta_n[N_3^-]^n$ terms.[5-7] Estimation of the last constant was taken from the limiting value of F^0_{III} towards the higher ligand concentration:

$$\beta_6 = (F^0_{III})/[N_3^-]^6. \quad (7)$$

This has been found to be a reasonable approach to show that β_6 is of the order 10^{24}. Discounting these preliminary data of the F^0_{III} values, in the range of 5–5.5 for $\bar{n}_{III}$, β_5 was first estimated as being of the order 10^{23} from:

$$\beta_5 = (F^0_{III} - \beta_6[N_3^-]^6)/[N_3^-]^5. \quad (8)$$

Similarly, estimation of β_4 in the 4.7–5 $\bar{n}_{III}$ range, also leads to the order 10^{23}, after discounting $\beta_5[N_3^-]^5$ and $\beta_6[N_3^-]^6$ in several F^0_{III} values.

(4) A linear plot of $(\log\beta_n)/n$ vs n (number of azide ligands)[12] leads to the estimation of β_1, β_2 and β_3, as 10^8, 10^{15} and 10^{19}, respectively. This estimation is based on values proportional to the average free energy involved in ligand attachment to the higher complexes.

(5) The whole process was repeated and the following final values for the overall formation constants were found: $\beta_1 = 3\times10^8\ M^{-1}$, $\beta_2 = 1\times10^{15}\ M^{-2}$, $\beta_3 = 7\times10^{19}\ M^{-3}$, $\beta_4 = 1.5\times10^{23}\ M^{-4}$, $\beta_5 = 1.3\times10^{23}\ M^{-5}$ and $\beta_6 = 1.0\times10^{24}\ M^{-6}$.

Combination of eqs (1) and (2) leads to the following equation which permits the calculation of the potential E_x at any free azide concentration, and the $C_{Co^{III}}/C_{Co^{II}}$ concentration ratio of the complexes, at 25°C:

$$E_x = E_s^{0'} + 0.05916\log(C_{Co^{III}}/C_{Co^{II}}) - 0.05916\log(F^0_{III}/F^0_{II}). \quad (9)$$

F^0_{II} is calculated by eq. (4) and F^0_{III} by a similar equation in which the first three exponential terms can be neglected for azide concentrations higher than 0.1 M.

Interpretation of results

The calculated $E_x^{0'}$ data values from eq. (2) gave an uncertainty of ±3.5 mV, as compared with the experimental data. This prevision is better than the expected uncertainty introduced by the $E_s^{0'}$ value, 1.85 V[11] (or 1.61 vs the calomel electrode) in eq. (3).

Figure 1 shows the distribution diagram of the complexes. Even at a free azide concentration of 10^{-4} M, the contributions of the $[CoN_3]^{2+}$ and $[Co(N_3)_2]^+$ species are fairly negligible. In the studied azide concentration range (0.2–1.8 M) the $[Co(N_3)_6]^{3-}$ species predominates but with significant contribution from the $[Co(N_3)_5]^{2-}$ and $[Co(N_3)_4]^-$ anions.

The magnitude of equilibrium constants in the Co^{III}/N_3^- system is considerably higher than that of the Co^{II}/N_3^- one [see eq. (4)] and shows a marked tendency of the azide ions to behave as a "hard type" base.[13] Destruction of these cobalt(III) complexes takes place easily by acidification of the medium or dilution, with a return to cobalt(II) levels; alkalinization causes $Co(OH)_3$ precipitation. This behaviour reveals a great lability which is not found in many cobalt(III) complexes, as with cyanide or ammonium complexes.

Charge transfer from ligand to metal is feasible, as occurs with the Cu^{II}/N_3^-[14] and Fe^{III}/N_3^-[15-16] systems. In fact, a broad band with high molar absorptivities is observed, with one peak at 365 nm (Fig. 2). This spectral characteristic shows virtually no change as a function of the azide concentration until 0.5 M.

The azide ion is thermodynamically unstable and is potentially a very powerful reducing agent, as

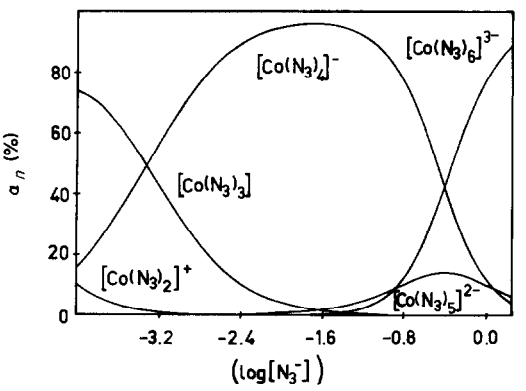

Fig. 1. The distribution diagram of the cobalt(III)–azide complexes calculated from the equilibrium constants.

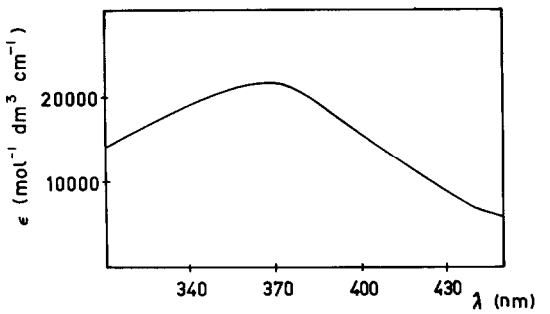

Fig. 2. UV–vis absorption spectrum of 1.00×10^{-5} M cobalt(III) in 1.90 M N_3^-, 0.10 M HN_3 and 0.050 M H_2O_2.

inferred from the standard reduction potential of the N_2/N_3^- system of -3.4 V.[17] In spite of that, the reactivity of the ligand toward oxidizing agents is fairly low under a variety of conditions and in the absence of a catalyst. The ligand is not oxidized by permanganate or hydrogen peroxide in alkaline media.[14] Hydrazoic acid is much more reactive and can be oxidized by strong oxidizing agents such as permanganate, cerium(IV) and dichromate. The stabilization of cobalt(III) is possible only due to the inertia of the azide ions towards oxidation, a behaviour quite different from that observed with thiocyanate.

The oxidation of cobalt(II) (1 mM) to cobalt(III) by the dissolved oxygen, catalysed by sulphur(IV), is convenient for analytical purposes at a 0.50 M free azide concentration, with 0.1–0.01 M free hydrazoic acid.[18] Calculations with present potential data using eq. (9) show that for a wide azide concentration range, the $O_2,H^+/H_2O_2$ system ($E^{0'} = +0.695$ V) seems thermodynamically unable to provide the cobalt(III) concentration levels experimentally found by the induced oxidation, at lower azide concentrations. The $O_2,H^+/H_2O$ system ($E^0 = +1.23$ V) is the only system really capable of performing such catalysed oxidations at 0.2–0.7 M azide concentrations. Interpretation of this induced reaction, with the participation of free radicals, will subsequently be reported with several conditional equilibrium constants, calculated for this redox process.

Acknowledgements—The authors are greatly indebted to the CNPq and FAPESP (Brazilian agencies) for their support.

REFERENCES

1. P. Senise, *Mikrochim. Acta* 1957, **5**, 640.
2. F. Feigl and V. Anger, *Spot-tests in Inorganic Analysis*, 6th edn, p. 447. Elsevier, Amsterdam (1972).
3. E. A. Neves and T. V. Silva, 184th ACS Nat. Meet.—CHAS 059. Kansas City, Missouri (1982).
4. E. A. Neves, J. Gebert and D. Klockow, 3rd Int. Cong. Analyt. Techniques Environ. Chem. and 14th Ann. Symp. Analyt. Chem. Pollutants, p. 117. Barcelona (1984).
5. I. Leden, *Z. Phys. Chem.* 1941, **A188**, 160.
6. F. J. C. Rossotti and H. S. Rossotti, *The Determination of Stability Constants*. McGraw-Hill, New York (1961).
7. K. B. Yatsimirkii and V. P. Vasil'ev, *Instability Constants of Complex Compounds*. Pergamon Press, Oxford (1960).
8. E. A. Neves, R. Tokoro and M. E. V. Suarez, *J. Chem. Res.* 1979, **11M**, 4401.
9. N. Maki and N. Tanaka, in *Encyclopedia of Electrochemistry of the Elements* (Edited by A. J. Bard), Vol. 3, pp. 43–46. Marcel Dekker, New York (1975).
10. B. Warnqvist, *Inorg. Chem.* 1970, **9**, 682.
11. E. A. Neves, I. R. G. Gutz and R. G. Tavares, *J. Electroanal. Chem. Interfacial Electrochem.* 1984, **179**, 91.
12. M. T. Beck, *Chemistry of Complex Equilibria*, pp. 38–45. Van Nostrand Reinhold, London (1970).
13. R. G. Pearson, *J. Chem. Educ.* 1968, **45**, 581.
14. E. A. Neves, E. Oliveira and Z. L. Santos, *Talanta* 1980, **27**, 609.
15. J. F. Andrade, E. A. Neves and G. Chierice, *Anal. Chim. Acta* 1983, **155**, 269.
16. E. A. Neves, J. F. Andrade and G. O. Chierice, *Anal. Lett.* 1985, **18**(A6), 707.
17. J. T. Maloy, in *Standard Potentials in Aqueous Solutions* (Edited by A. J. Bard, R. Parsons and J. Jordan), p. 133. Marcel Dekker, New York (1985).
18. E. A. Neves, J. Gebert and D. Klockow, *Fresenius Z. Anal. Chem.* 1988, **331**, 260.

Polyhedron Vol. 8, No. 5, pp. 647–651, 1989
Printed in Great Britain

0277–5387/89 $3.00+.00
© 1989 Pergamon Press plc

CUPRIC ION BINDING BY DIHYDROXYBENZOIC ACIDS

TAMAS KISS

Department of Inorganic and Analytical Chemistry, Kossuth University, 4010 Debrecen, Hungary

and

HENRYK KOZLOWSKI

Institute of Chemistry, University of Wroclaw, Joliot-Curie 14, 50-383, Wroclaw, Poland

and

GIOVANNI MICERA* and LILIANA STRINNA ERRE

Dipartimento di Chimica, Università di Sassari, Via Vienna 2, 07100 Sassari, Italy

(*Received* 18 *August* 1988; *accepted* 29 *September* 1988)

Abstract—A potentiometric and spectroscopic study has been carried out on the copper(II) complexes formed by 2,*x*-dihydroxybenzoic acids ($x = 4$, 5 or 6) in aqueous solution. It has been found that, in the low pH range, the ligands coordinate through the carboxylate group. At above pH 5 the major species are chelated complexes in which one or two ligands bind the metal ion through the carboxylate and adjacent phenolate groups. The results are compared to earlier literature data available for copper(II) dihydroxybenzoate and salicylate complexes.

The modelling of the interactions of metal ions with soil organic matter, as well as the study on the bioavailability to plants of metal ions, have started much interest in the elucidation of the behaviour of phenolic ligands.[1] Dihydroxybenzoic acids (DHB) and their analogues were found to be interesting low molecular weight models with very efficient binding ability, especially the ligands having two aromatic hydroxyls in *ortho* positions.[2–6] In the copper(II)-3,4-dihydroxybenzoic acid system, rather complicated coordination equilibria were observed.[6] In dilute aqueous solutions the bidentate catechol part of this ligand predominates as the binding site for the metal ion, although the carboxyl group may also participate in the metal ion binding. This leads to the formation of the polynuclear species.

Earlier solid-state studies have shown that at low pH, the carboxylic group could be the main donor in the formed complexes with several other diphenolic acids such as 2,4- 2,5- and 2,6-dihydroxybenzoic acids,[7–10] though the phenolate oxygen binding was also clearly indicated.[2,3,6] In this communication, we report the potentiometric and spectroscopic findings obtained for the systems containing copper(II) and 2,4-, 2,5-, and 2,6-dihydroxybenzoic acids in aqueous solutions.

EXPERIMENTAL

Potentiometric studies

Stability constants for complexes containing proton and copper(II) were determined by pH-metric titration of 25 cm^3 samples. The concentration of the ligand in the samples was 0.004 or 0.002 M. Metal-to-ligand molar ratios of 1:1, 1:2, 1:4, 1:6.6 and 1:10 were used in the titrations and the ionic strength was adjusted to 0.2 M with KCl. The titrations were performed in the pH range from 2.5 to 11, or until precipitate, depending on the molar ratio used, occurred. The pH was measured with a Radiometer pHM 64 instrument with G2040B glass

* Author to whom correspondence should be addressed.

and K4040 calomel electrodes. Since the ligands tend to undergo oxidation, all measurements were performed in a TTA 80 titration unit under an argon atmosphere. The electrode system was calibrated by the method of Irving *et al.*[11] so the pH-meter readings could be converted into hydrogen ion concentrations. In all cases, the temperature was 25°C. The calculations of the stability constants were made with PSEQUAD computer program.[12]

Spectroscopic studies

Absorption spectra were recorded on a Beckman Acta M IV spectrophotometer and EPR spectra were measured on a Varian E 9 spectrometer (X band) at 110 K. The measurements were performed under argon for the concentrations of samples similar to those used in the potentiometric studies.

RESULTS AND DISCUSSION

Proton complexes

All ligands studied have two measurable protonation constants (see Table 1). The acidity of the phenolic groups in position two is very weak, thus their dissociation was studied at high ligand concentration (0.08 M) up to high pH (~13.4). It was found that the ligand titration curves run together with the titration curve for the strong acid of the same concentration. Accordingly, the phenolic groups do not undergo dissociation in the measurable pH range; this is distinctly different from that reported earlier.[2] The high dissociation constants of these hydroxyl groups were proved also by spectrophotometric titration. The UV spectrum of the ligands remained unchanged over the pH range 11–13.2, showing the lack of deprotonation of phenolic hydroxyls. The very weak acidity of these OH groups in the *ortho* position to carboxylate, can be explained by the strong intramolecular hydrogen bond between COO^- and phenolic groups.

Copper(II) complexes

The calculated copper(II) complex formation constants, together with the earlier literature data, are given in Table 2. These three ligands behave as the hydroxy-salicylic acids (derived equilibrium constants for salicylic acid calculated from literature data[13] are also included in Table 2). The data for the 2,4- and 2,5-DHB are in fairly good agreement with those presented earlier.[2] The fitting of the experimental pH-metric data by the PSEQUAD program can be slightly improved by the introduction of the species in which the metal ion binds the DHB molecule only via the carboxylate oxygen, i.e. when the formation of the CuAH or $Cu(AH)_2$ species is assumed. The species distribution vs pH, see Figs 1–3, indicates that the total concentration of each of these species is rather low (10% or less), except in the case of the copper(II)–2,6-DHB system. In the latter case the concentrations of the CuAH and $Cu(AH)_2$ complexes approach 25 and 15%, respectively. It has to be mentioned, however, that the pH-metric determinability of these species is poor, since metal ion coordination and proton dissociation take place in the same pH range, hence the copper(II)–carboxylate coordination has only minor pH effects. The EPR spectra prove unambiguously, the formation of these minor species at a pH below 5 in all the cases studied (Table 3). The formation of the complexes with monodentate carboxylate coordination was also proposed earlier for the cupric complexes with salicylic acid.[14]

The major species formed at above pH 5 is the CuA chelated complex in which the metal ion is bound to the DHB ligand through COO and the phenolate oxygen (O^-) being in the *ortho* position to the carboxylate (2-OH). A further increase of pH leads to the formation of the other chelated species, the CuA_2 complex, in which two ligands are bound in the mode described above. The equilibrium constants characteristic to the part-processes of complex formation (see Table 2) clearly indicate the salicylate-type coordination in the complexes CuA and CuA_2. Thus, their stoichiometric compositions are more precisely $Cu(HAH_{-1})$ and $Cu(HAH_{-1})_2$.

Table 1. Proton dissociation constants for 2,*x*-DHB (*x* = 4, 5 or 6)

Ligand	p*K* (COOH)	p*K* (*x*-OH)	p*K* (2-OH)	Reference
2,4-DHB	3.11±0.02	8.68±0.02	>14.0	This work
	3.12	8.62	13.03	2
2,5-DHB	2.73±0.02	10.05±0.02	>14.0	This work
2,6-DHB	1.0±0.1	13.10±0.14	>14.0	This work
	0.91	12.57	13.0	2

Table 2. Stability constants for copper(II) complexes with 2,*x*-DHB (*x* = 4, 5 or 6)

Species	2,4-DHB	2,5-DHB	2,6-DHB	Sal[a]
Log β values				
CuAH	10.31±0.07	11.52±0.05	15.20±0.08	—
$Cu(AH)_2$	21.46±0.09	23.97±0.05	30.45±0.09	—
CuA	5.97±0.01	7.18±0.01	10.19±0.01	10.6
CuA_2	9.80±0.04	11.65±0.03	18.47±0.03	18.5
CuA_2H_{-1}	0.98±0.07	1.26±0.07	6.45±0.17	—
CuA_2H_{-2}	−8.41±0.07	−9.67±0.09	—	—
Log *K* values				
p*K* (CuA_2)	8.82	10.39	12.02	—
p*K* (CuA_2H_{-1})	9.39	10.93	—	—
$Cu+HA \rightleftarrows CuA+H^+$	−2.72	−2.87	−2.91	−2.8
	−3.07[b]	—	−2.97[b]	—
$CuA+HA \rightleftarrows CuA_2+H^+$	−4.88	−5.58	−4.82	−5.5
	−5.00[b]	—	−4.77[b]	—
log [*K* (CuA)/*K* (CuA_2)]	2.16	2.71	1.91	2.7
	1.93[b]	—	1.79[b]	—

[a] Sal = salicylic acid (ref. 13).
[b] Ref. 2.

In the more basic solutions, the deprotonation of the unbound hydroxyl at positions four, five or six takes place. The stepwise deprotonation constants (Table 2) obtained for the 2,4- and 2,5-DHB complexes are higher than the p*K* values of these groups obtained for the respective free ligands, probably due to the strong electron-releasing effect of the coordinated phenolate. This value for the copper(II)–2,6-DHB system was too high to be evaluated reliably. The differences between the two stepwise p*K*'s obtained for the CuA_2 complexes is equal to 0.6 log units, corresponding to the stat-

Table 3. Spectroscopic data for copper(II) complexes of 2,*x*-DHB (*x* = 4, 5 or 6)

Species	ESR		Absorption	Donor set
	$g_\parallel$	$A_\parallel$ (10^{-4} cm^{-1})	λ (nm) [ε]	
2,4-DHB				
CuAH	2.371	155		COO^-
CuA	2.327	168	735[a] [40]	$\{COO^-, O^-\}$
			380[b] [130]	
CuA_2	2.304	176	650[a] [102]	$2\times\{COO^-, O^-\}$
2,5-DHB				
CuAH	2.371	155		COO^-
CuA	2.327	166	720[a] [63]	$\{COO^-, O^-\}$
			420[b] [207]	
CuA_2	2.299	172	620[a] [140]	$2\times\{COO^-, O^-\}$
			425[b] [352]	
2,6-DHB				
CuAH	2.378	147		COO^-
Cu	2.333	163	740[a] [48]	$\{COO^-, O^-\}$
			410[b] [184]	
CuA_2	2.299	172	645[a] [110]	$2\times\{COO^-, O^-\}$

[a] *d–d* transition.
[b] Phenolate oxygen-to-copper(II) charge-transfer transition.

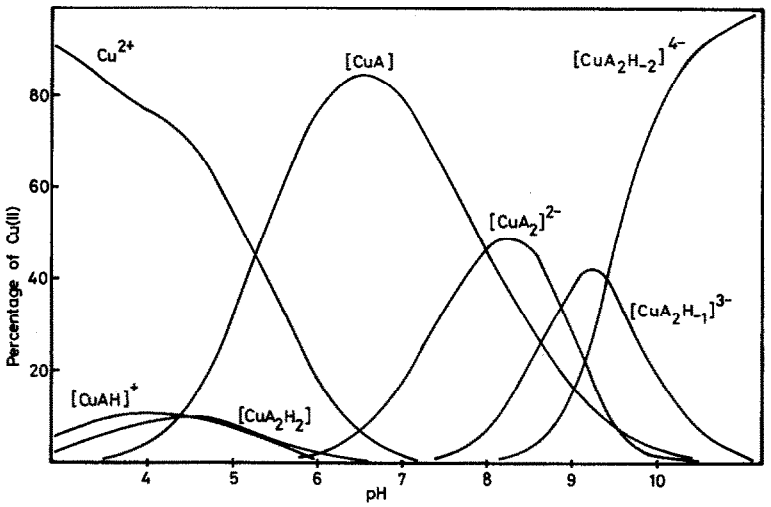

Fig. 1. Concentration distribution curves of the complexes formed in the copper(II)–2,4-DHB system as a function of pH. $C_{Cu} = 0.002$ M and $C_{ligand} = 0.004$ M.

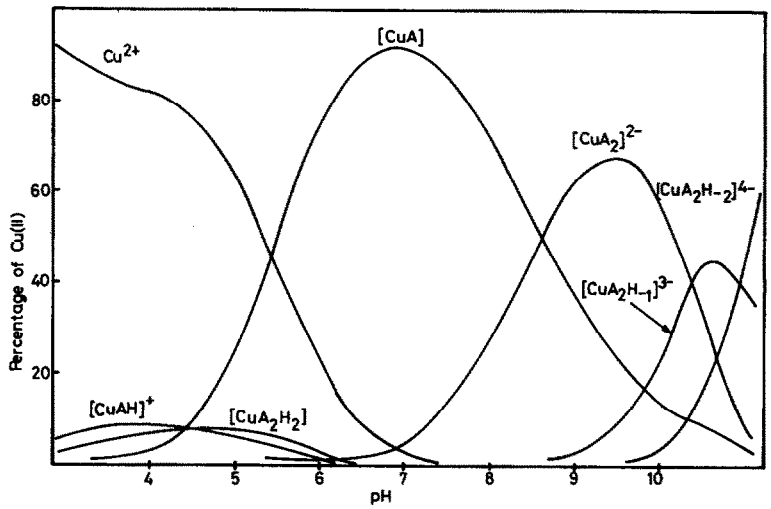

Fig. 2. Concentration distribution curves of the complexes formed in the copper(II)–2,5-DHB system as a function of pH. Details as in Fig. 1.

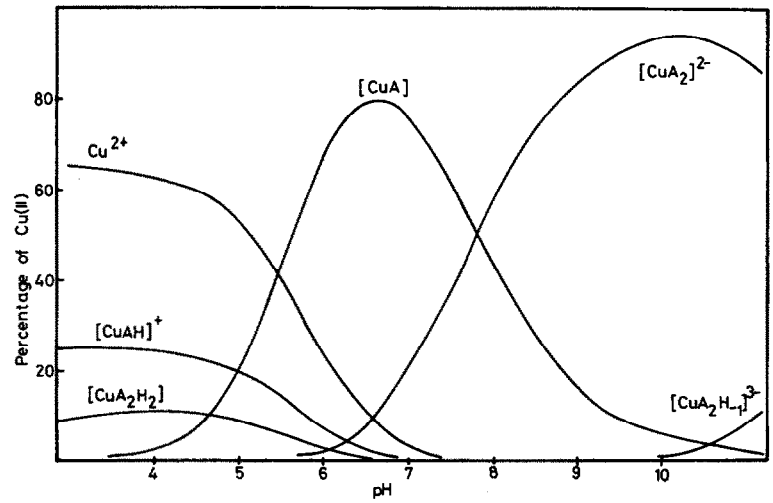

Fig. 3. Concentration distribution curves of the complexes formed in the copper(II)–2,6-DHB system as a function of pH. Details as in Fig. 1.

istical case of the dissociations of two protonated groups with the same acidity.

The spectroscopic data fit very well with the potentiometric results and the assignment of the respective complexes is presented in Table 3. The coordination of the phenolate oxygen is clearly seen, due to the charge transition between this donor and the cupric ion, which is observed in the 380–430 nm range.[15,16] The coordination of the phenolic hydroxyl groups is also clearly indicated by the distinct increase in energy of the *d–d* transitions observed for the respective complexes (see for example, ref. 6).

CONCLUSIONS

The binding ability of the dihydroxybenzoic acids strongly depends on the position of their donors. The most effective seems to be the set of two hydroxyls which are in *ortho* positions (catechol like) as was found in the case of 3,4-dihydroxybenzoic acid.[6] The ligands with carboxyl and hydroxyl groups placed on the adjacent aromatic ring carbons are also very effective chelating ligands which form complexes with the (COO^-, O^-) donor set. In all cases, the involvement of the carboxylic function seems to be basic at low pH range, but phenolic groups and their positions are of primary importance for the structures and the stability of the formed complexes.

Acknowledgements—Thanks are due to Mrs Á. Gönczy for her participation in the experimental work. This work was supported by Consiglio Nazionale delle Ricerche (Rome), the Polish Academy of Sciences (Project 01.12) and by the Hungarian Ministry of Education (Project 46/1986).

REFERENCES

1. G. Hurst and N. A. Burges in *Soil Biochemistry* (Edited by A. D. McLaren and G. H. Peterson), Vol. I, Chapt. 5, p. 260. Marcel Dekker, New York (1967).
2. M. Aplincourt, A. Debras-Bee, C. Gerard and R. P. Hugel, *J. Chem. Res.* 1986, 134.
3. C. Gerard, R. Njomnang, J.-C. Pierrard, J. Rimbault and R. Hugel, *J. Chem. Res.* 1987, 294.
4. F. Cariati, S. Deiana, L. Erre, G. Micera and P. Piu, *Inorg. Chim. Acta* 1982, **64**, L213.
5. P. W. Linder and A. Voye', *Polyhedron* 1987, **6**, 53.
6. K. Gerega, T. Kiss, H. Kozlowski, G. Micera, L. Strinna Erre and F. Cariati, *Inorg. Chim. Acta* 1987, **138**, 31.
7. F. Cariati, L. Erre, G. Micera, A. Panzanelli, G. Ciani and A. Sironi, *Inorg. Chim. Acta* 1983, **80**, 57.
8. G. Micera, L. Strinna Erre, F. Cariati, D. A. Clemente, A. Marzotto and M. Biagini Cingi, *Inorg. Chim. Acta* 1985, **109**, 173.
9. G. Micera, L. Strinna Erre, P. Piu, F. Cariati, G. Ciani and A. Sironi, *Inorg. Chim. Acta* 1985, **107**, 223.
10. G. Micera, L. Strinna Erre, F. Cariati, G. Ciani and A. Sironi, *Inorg. Chim. Acta* 1985, **100**, L1.
11. H. Irving, M. G. Miles and L. D. Pettit, *Analytica Chim. Acta* 1967, **38**, 475.
12. L. Zekany and I. Nagypal, in *Computational Methods for the Determination of Stability Constants* (Edited by D. Leggett), Plenum Press, New York (1985).
13. A. E. Martell and R. M. Smith, *Critical Stability Constants*, Vol. 5. Plenum Press, New York (1982).
14. C.-H. O'Young and S. J. Lippard, *J. Am. Chem. Soc.* 1980, **102**, 4920.
15. A. Gergely and T. Kiss, *Inorg. Chim. Acta* 1976, **16**, 51.
16. H. Kozlowski, M. Bezer, L. D. Pettit, M. Bataille and B. Hecquet, *J. Inorg. Biochem.* 1983, **18**, 231 and refs therein.

Polyhedron Vol. 8, No. 5, pp. 653–657, 1989
Printed in Great Britain

0277–5387/89 $3.00+.00
© 1989 Pergamon Press plc

REACTION OF THE HYDRIDO-BRIDGED, GROUP 6 METAL CARBONYL DIMERS WITH ORGANIC ALKOXIDES. AN APPARENT BETA-HYDRIDE ELIMINATION REACTION PERTINENT TO CATALYSIS

P. L. GAUS,* LISA M. JONES and LORETTA A. ZAMISKA

Department of Chemistry, The College of Wooster, Wooster, OH 44691, U.S.A.

(*Received* 31 *May* 1988; *accepted* 3 *October* 1988)

Abstract—IR spectroscopic and GC–MS studies have been made of the reaction between the Group 6 metal carbonyl dimers $[\mu\text{-}HM_2(CO)_{10}]^-$ (where M = Cr and W) and organic alkoxides, $R^1R^2CHO^-$, both as the PPN^+ salts. Where $R^1 = R^2$ = Ph or Me, the reactions result in the oxidation of the alkoxide to benzophenone and acetone, respectively, as determined by GC–MS. IR spectroscopic studies indicate that the reaction involves cleavage of the hydrido-bridged dimer reactants to give the hydride monomers, $[HM(CO)_5]^-$, and an intermediate alkoxo complex, $[R^1R^2CHO—M(CO)_5]^-$. The overall rate of oxidation of a given alkoxide is slower when M = W than when M = Cr. It is proposed that the alkoxo intermediate is responsible for the formation of the ketone products.

The organometallic chemistry of the alkoxide anion is especially well developed in systems where the alkoxide ligand is either bulky or stabilized against beta elimination.[1] The chemistry of simple, mononuclear organometallic alkoxides containing non-bulky alkoxide ligands that are capable of beta elimination reactions is less well developed. This is true for two reasons. Firstly, the organometallic complexes that contain non-bulky alkoxide ligands are prone to condensation reactions that produce clusters or solid state structures having bridging alkoxide groups.[1,2] Secondly, those alkoxide ligands having a hydrogen atom attached to the proper carbon atom, i.e. $R^1R^2CHO^-$, can undergo an apparently facile, simple, unimolecular beta-hydride elimination reaction[3] that is entirely analogous to the well known counterpart among the metal alkyls.[3a,4] Until very recently, it was held that such beta-hydride elimination reactions of the organometallic alkoxides were characteristically more facile than for the organometallic alkyls, because it was thought that the metal–oxygen bond was intrinsically weaker than the metal–carbon bond, which would destabilize a metal–alkoxide towards a unimolecular elimination process. However, the elegant studies of Bercaw and co-workers,[3b] in which beta-hydride elimination reactions of platinum alkoxo complexes have been compared in detail with the well known platinum alkyls of Whitesides and co-workers,[5] have made it clear that although the alkoxo complexes undergo beta-hydride elimination at a much lower temperature than do the corresponding alkyls, this is not likely due to an inherent difference in metal–oxygen vs metal–carbon bond strengths.

Because of the importance of beta-hydride elimination reactions of organometallic alkoxides in catalysis (in particular in catalytic hydrogenations,[6] catalytic formation of alkyl formates[7] and higher alcohol processes[8]), we have undertaken a study of the reaction of organic alkoxides with those organometallic compounds that should be capable of offering chances to study the beta-hydride elimination chemistry of organometallic alkoxides. We report here on the initial results of our study into the reactions of the hydrido-bridged, Group 6 metal carbonyl dimers, $[\mu\text{-}HM_2(CO)_{10}]^-$ (where M = Cr or W), with alkoxide anions containing a beta-hydrogen atom, viz. $R^1R^2CHO^-$ (where $R^1 = R^2$ = Ph or Me).

EXPERIMENTAL

All reactions were performed under an atmosphere of dry argon gas using standard Schlenk

*Author to whom correspondence should be addressed.

techniques. The THF solvent was freshly distilled from purple Na–benzophenone, and all transfers were made either via cannula or syringe.

IR spectra were recorded in 0.1 mm CaF_2 liquid cells on a Perkin–Elmer 1800 FTIR instrument. Identification of the volatile products was performed by GC–MS on a Hewlett Packard 5890 gas chromatograph equipped with an HP 5970 mass selective detector.

The dimeric reactants, $[\mu\text{-}HM_2(CO)_{10}]^-$, were prepared as the PPN^+ salts using the literature procedure.[9] The PPN^+ salts of the organic alkoxides were prepared from the sodium salts by room temperature metathesis with PPN^+Cl^-, using the THF–hexane mixtures. We did not observe attack on the PPN^+ cation, as has been reported for methoxide at high temperatures.[10]

Reactions were performed using various mole ratios of the two reactants, by transferring a solution of known concentration (typically 10^{-2}–10^{-3} M) of $PPN[\mu\text{-}HM_2(CO)_{10}]$ onto a dry, gravimetric sample of the organic alkoxide. The solutions were stirred gently at 25°C for up to 7 days, and IR spectra were recorded periodically by withdrawing a sample using syringe techniques. At the conclusion of the IR study, the solutions were exposed to the atmosphere, filtered through alumina, and analysed using GC–MS techniques. Acetone was separated at 20°C from THF on a methylsilicone column, whereas benzophenone was separated at 150°C. In some reactions, the acetone was lost due to entraining with the argon purge gas; its positive identification (significant, increasing absorbance in the IR spectrum at 1716 cm^{-1}) as a reaction product was most facilitated when the reactions were performed under a static argon pressure, rather than a continuous sweep.

RESULTS AND DISCUSSION

The reactions of the dimeric, hydrido-bridged reactants $[\mu\text{-}HCr_2(CO)_{10}]^-$ and $[\mu\text{-}HW_2(CO)_{10}]^-$ with either diphenyl methoxide, Ph_2CHO^-, or isopropoxide, $(CH_3)_2CHO^-$, have been studied using mole ratios of organometallic reactants to organic alkoxide reactants ranging from 1:1 to 1:10. Although the oxidized organic product (either acetone or benzophenone) was observed in most reactions, the greatest amounts were observed in reactions that employed an excess of the alkoxide reactant. We therefore present the following results in categories depending on the ratios of $[\mu\text{-}HM_2(CO)_{10}]^-$ to $R^1R^2CHO^-$ that were employed in the various experiments. Additionally, each reaction was accompanied by a slow, steady deposition of solid material, which caused the overall IR absorbances arising from the organometallic materials to decrease with time. Thus the IR spectra must be interpreted in light of these overall decreasing ν_{CO} IR absorbances. The spectra shown in the figures are labelled so that this general and steady loss of organometallic reactant to solids is apparent. The amount of solid that typically formed over the course of a given reaction was less when the proportions of the organic alkoxide reactant were high, i.e. in experiments employing 1:10 mole ratios of $[\mu\text{-}HM_2(CO)_{10}]^-$ to $R^1R^2CHO^-$. The rate of appearance of acetone or benzophenone became negligible in every case where the IR spectrum indicated that all of the hydrido-bridged dimer reactant had been consumed.

When a dry, anaeorbic THF solution of a 1:10 mole ratio of $PPN^+[\mu\text{-}HCr_2(CO)_{10}]^-$ and $PPN^+Ph_2CHO^-$ was stirred at 25°C under an argon atmosphere, there was no immediate change in the colour or appearance of the solution as first mixed, or in the IR spectrum of the solution. Over the next 7 days, however, there occurred a gradual and uniform change in the IR spectrum of the solution, as depicted in Fig. 1. The IR spectrum that was obtained soon after mixing is shown in Fig. 1(A). This is essentially the IR spectrum in the ν_{CO} region of the dimeric, hydrido-bridged, organometallic reactant, $[\mu\text{-}HCr_2(CO)_{10}]^-$. The values of the three characteristic frequencies[9,11] were found to be: ν_{CO} = 2030 (w), 1940 (s), 1878 (m) cm^{-1}. With the passage of time, the IR spectrum in the ν_{CO} region changed in the manner shown in Fig. 1. After 24 h [Fig. 1(B)], the ν_{CO} absorbances characteristic of $[\mu\text{-}HCr_2(CO)_{10}]^-$ were less intense, and a small peak appeared at 1664 cm^{-1}. This absorbance at 1664 cm^{-1} continued to increase in intensity over the next 6 days. An authentic sample of benzophenone was found to have the same ν_{CO} IR spectrum. The product was also determined to be benzophenone using GC–MS techniques after the IR experiments shown in Fig. 1 were completed. Thus the sole volatile organic product that was found in the reaction mixture after 7 days (other than unreacted Ph_2CHO^-, converted in work-up to Ph_2CHOH) was found to have a GC retention time and a mass spectrum that was identical to that of a known sample of $Ph_2C{=}O$. In addition, as shown in Fig. 1, there appeared only one other soluble organometallic material during the course of the reaction. This is the material having ν_{CO} IR absorbances at 1882 (s) and 1852 (m) cm^{-1}, and it was the only soluble carbonyl-containing organometallic product. This material obviously formed in conjunction with the disappearance of $[\mu\text{-}HCr_2(CO)_{10}]^-$ and with the appearance of benzophenone. Thus the single, soluble, organometallic

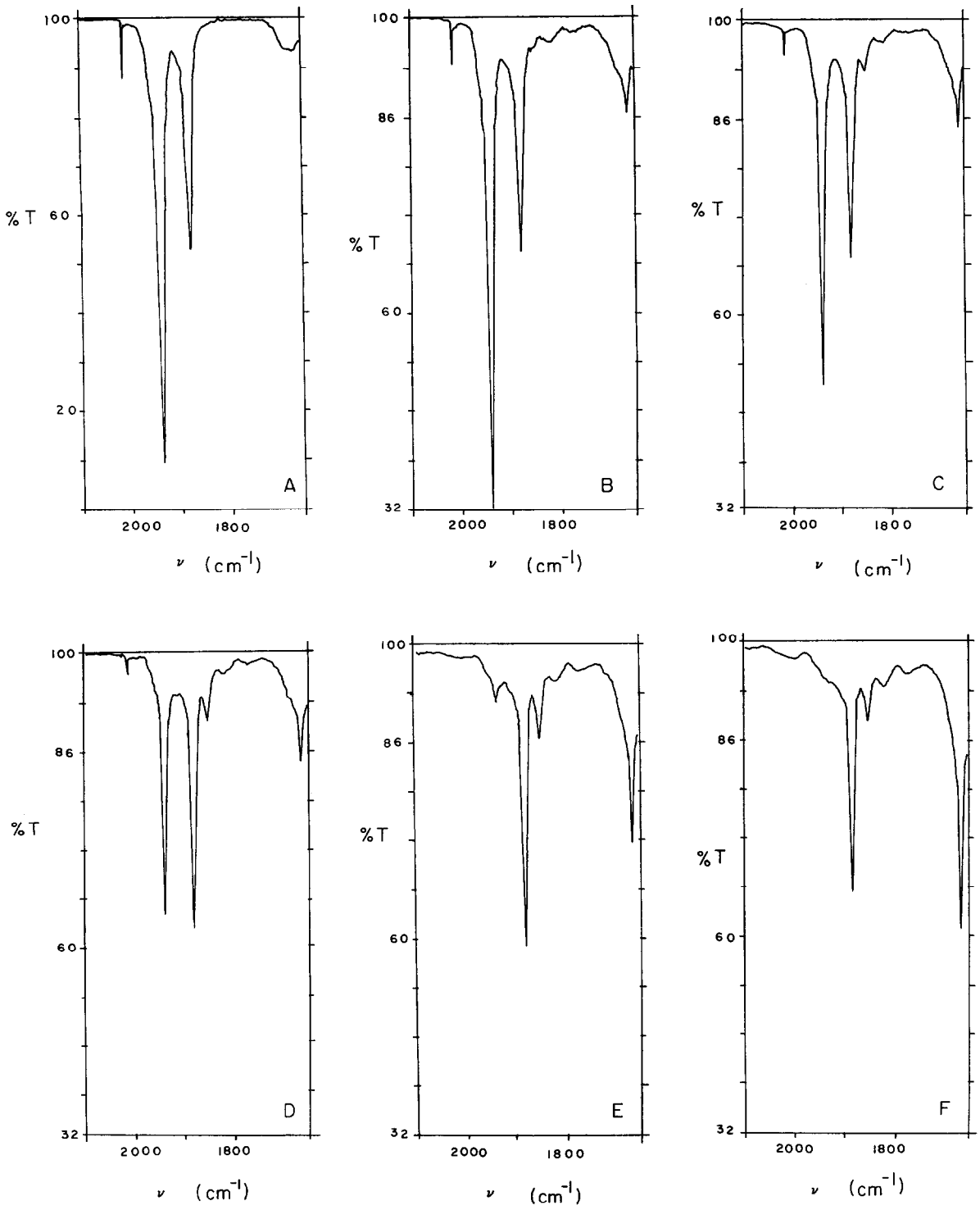

Fig. 1. IR spectra recorded at various times in the reaction of a 1:10 mole ratio of $[\mu\text{-}HCr_2(CO)_{10}]^-$ and Ph_2CHO^- in THF at 25°C. (A) At the time of mixing; (B) after 24 h; (C) after 36 h; (D) after 64 h; (E) after 136 h; (F) after 160 h.

product of the reaction was the monomeric hydride, $[HCr(CO)_5]^-$, whose IR spectrum[11] is known and matches the ν_{co} frequencies that were observed here.

The above results differ in significant ways from those that were obtained with reactions that employed a 1:1 mole ratio of reactants. The reaction of $[\mu\text{-}HCr_2(CO)_{10}]^-$ and Ph_2CHO^- in a 1:1 mole ratio did not result in complete disappearance of the ν_{co} absorbances of $[\mu\text{-}HCr_2(CO)_{10}]^-$, nor in the formation of as much benzophenone as did the

reaction described above. Additionally, although the reaction did give some monomeric hydride, $[HCr(CO)_5]^-$, there was another ν_{co} IR absorption observed at 1920 cm^{-1}. This frequency is typical of those given by monomeric alkoxo derivatives[12] of the type $[RO—Cr(CO)_5]^-$, and we conclude that this constitutes evidence for the intermediate $[Ph_2CHO—Cr(CO)_5]^-$. This is substantiated by the results obtained from the reaction of the chromium dimer with isopropoxide.

In a manner entirely analogous to the reaction of diphenyl methoxide as described above, the reaction of $[\mu\text{-}HCr_2(CO)_{10}]^-$ and $(CH_3)_2CHO^-$ in a 1:10 mole ratio resulted in the formation of acetone (ν_{co} = 1716 cm^{-1}) over the course of several days. The concomitant disappearance of ν_{co} IR absorbances characteristic of the dimer reactant, and the formation of ν_{co} IR absorbances characteristic of $[HCr(CO)_5]^-$ also occurred. When the reaction was performed using a 1:1 mole ratio of reactants, the amount of acetone that was formed was less, the disappearance of the dimeric reactant was incomplete, and an intermediate was found to appear in conjunction with the disappearance of $[\mu\text{-}HCr_2(CO)_{10}]^-$. The most typical IR spectrum is shown in Fig. 2. Thus after 122 h of reaction at 25°C, some dimeric reactant remained (ν_{co} = 2030 (w), 1940 (s), 1880 (m) cm^{-1}). Also, both acetone

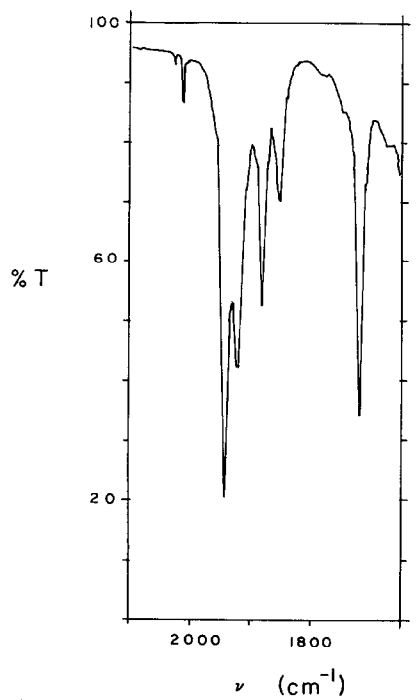

Fig. 2. The IR spectrum recorded after 122 h during the reaction of a 1:1 mole ratio of $[\mu\text{-}HCr_2(CO)_{10}]^-$ and $(CH_3)_2CHO^-$ in THF at 25°C.

(ν_{co} = 1716 cm^{-1}) and $[HCr(CO)_5]^-$ (ν_{co} = 1880, 1850 cm^{-1}) had clearly formed. Most importantly, two of the three absorbances characteristic[7,10,12] of alkoxo pentacarbonyls of chromium, namely ν_{co} = 1920 (s) and 2055 (w) cm^{-1} are present, which we assign to the intermediate $[(CH_3)_2CHO—Cr(CO)_5]^-$.

Although a number of mechanistic possibilities exist, it seems reasonable that the above evidence should be taken to indicate that the reaction of $[\mu\text{-}HCr_2(CO)_{10}]^-$ with either diphenylmethoxide or isopropoxide results first in the rate-determining formation of both the monomeric hydride $[HCr(CO)_5]^-$ and an intermediate alkoxo pentacarbonyl, as shown in eq. (1):

$$[\mu\text{-}HCr_2(CO)_{10}]^- + R^1R^2CHO^- \rightleftarrows [HCr(CO)_5]^- + [R^1R^2CHO—Cr(CO)_5]^- \quad (1)$$

Since such alkoxo complexes are known to be substitution labile,[6a,7,10,12] this intermediate is capable of being responsible for the condensations that were found to give solids. In fact, such mononuclear chromium alkoxides are known[13] to give rise to clusterification, giving polynuclear alkoxides such as $[Cr_4(CO)_{12}(\mu_3\text{-}OR)_4]^{4-}$. Most importantly, the substitution lability of the intermediate, $[R^1R^2CHO—Cr(CO)_5]^-$, satisfies one important criterion for beta-hydride elimination, and we conclude that the second step of the process studied here constitutes simple, unimolecular beta-hydride elimination, as shown in eq. (2):

$$[R^1R^2CHO—Cr(CO)_5]^- \rightleftarrows [HCr(CO)_5]^- + R^1R^2C{=}O. \quad (2)$$

The ability of such alkoxo complexes to undergo beta-hydride elimination has been previously documented.[12a] Obviously there are a number of intriguing mechanistic subtleties that may develop, including cooperative effects arising from multimetal systems, as has been discussed by Norton.[14] We are presently examining the mechanism of the reaction in more detail.

It should also be reported that reactions of $[\mu\text{-}HCr_2(CO)_{10}]^-$ and *n*-butoxide gave results that were similar to those reported above, except that the oxidized organic products were apparently aldol condensation products of *n*-butoxide and butanal. An intermediate, presumably $(CH_3CH_2CH_2CH_2O\,Cr(CO)_5]^-$, was also observed, ν_{co} = 1919 cm^{-1}.

The corresponding reactions of the organic alkoxides with the hydrido-bridged tungsten dimer proceeded more slowly, and ultimately gave less oxidized organic products. Thus the reaction of $[\mu\text{-}HW_2(CO)_{10}]^-$ and Ph_2CHO^- in a 1:10 mole ratio gave a small amount of benzophenone. No

intermediates were detected, and attempts to perform the reaction at a higher temperature resulted in the formation of solids and significant amounts of $W(CO)_6$. Reactions employing a 1:1 mole ratio gave no products. Similarly, with isopropoxide, $[\mu\text{-}HW_2(CO)_{10}]^-$ was found to give small amounts of acetone, more slowly than with the chromium analogue.

Finally, it should be noted that these results are consistent with the reversible nature of the beta-hydride elimination process. The facile reversibility of beta-hydride elimination has been indicated by certain exchange experiments,[12a] and it is required if such a reaction is to function effectively in a catalytic cycle. The reversible nature of the reaction is indicated in the results reported here by the fact that the amount of oxidized organic product, and the presence of an alkoxo pentacarbonyl intermediate, depend on both the nature and the amount of organic alkoxide reactant that is employed.

Acknowledgement—The authors gratefully acknowledge advice and assistance of Dr Richard H. Bromund, concerning the GC–MS work.

REFERENCES

1. (a) R. C. Mehrotra, *Adv. Inorg. Chem. Radiochem.* 1983, **26**, 269; (b) F. A. Cotton and G. Wilkinson, *Advanced Inorganic Chemistry*, 5th edn. Wiley, New York (1988); (c) I. P. Rothwell, *Accts Chem. Res.* 1988, **21**, 153; (d) M. Akiyama, D. Little, M. H. Chisholm, D. A. Haitko, F. A. Cotton and M. W. Extine, *J. Am. Chem. Soc.* 1979, **101**, 2504; (e) M. H. Chisholm, F. A. Cotton, C. A. Murillo and W. W. Reichert, *Inorg. Chem.* 1977, **16**, 1801; (f) M. H. Chisholm, *Polyhedron* 1983, **2**, 681.
2. (a) A. R. Siedle and L. H. Pignolet, *Inorg. Chem.* 1982, **21**, 3090; (b) F. Giordano and A. Vitagliano, *Inorg. Chem.* 1981, **20**, 633; (c) H. C. Clark and A. B. Goel, *J. Organomet. Chem.* 1979, **178**, C27.
3. (a) J. P. Collman, L. S. Hegedus, J. R. Norton and R. G. Finke, *Principles and Applications of Organotransition Metal Chemistry*. University Science Books, Mill Valley, California (1987); (b) H. E. Bryndza, J. C. Calabrese, M. Marsi, D. C. Roe, W. Tam and J. E. Bercaw, *J. Am. Chem. Soc.* 1986, **108**, 4805; (c) L. J. Newman and R. E. Bergman, *J. Am. Chem. Soc.* 1985, **107**, 5314; (d) J. Chatt and B. L. Shaw, *J. Chem. Soc. A* 1962, 5075; (e) L. Vaska and J. W. DiLuzio, *J. Am. Chem. Soc.* 1962, **84**, 4989.
4. (a) R. J. Cross, in *The Chemistry of the Metal–Carbon Bond* (Edited by F. R. Hartley and S. Patai), Vol. 2. Wiley, New York (1985); (b) P. J. Davidson, M. F. Lappert and R. Pearce, *Chem. Rev.* 1976, **76**, 219; (c) P. S. Braterman and R. J. Cross, *Chem. Soc. Rev.* 1973, **2**, 271.
5. (a) T. J. McCarthy, R. G. Nuzzo and G. M. Whitesides, *J. Am. Chem. Soc.* 1981, **103**, 1676; (b) G. M. Whitesides, *Pure Appl. Chem.* 1981, **53**, 287.
6. (a) P. A. Tooley, C. Ovalles, S. C. Kao, D. J. Darensbourg and M. Y. Darensbourg, *J. Am. Chem. Soc.* 1986, **108**, 5465; (b) D. J. Darensbourg and G. Gibson, in *Am. Chem. Soc., Symp. Ser.* No. 357 (Edited by A. L. Wayda and M. Y. Darensbourg), Chap. 9. American Chemical Society, Washington D.C. (1987).
7. D. J. Darensbourg and C. Ovalles, *J. Am. Chem. Soc.* 1987, **109**, 3330.
8. T. J. Mazanec, *Inorg. Chem.* 1988, **27**, 1114.
9. R. G. Hayter, *J. Am. Chem. Soc.* 1966, **88**, 4376.
10. D. J. Darensbourg, M. Pala, D. Simmons and A. L. Rheingold, *Inorg. Chem.* 1986, **25**, 3537.
11. M. Y. Darensbourg, R. Bau, M. W. Marks, R. R. Burch, J. C. Deaton and S. Slater, *J. Am. Chem. Soc.* 1982, **104**, 6961.
12. (a) P. L. Gaus, S. C. Kao, K. Youngdahl and M. Y. Darensbourg, *J. Am. Chem. Soc.* 1985, **107**, 2428 and refs therein; (b) D. J. Darensbourg, K. M. Sanchez and A. L. Rheingold, *J. Am. Chem. Soc.* 1987, **109**, 290.
13. (a) T. J. McNeese, M. B. Cohen and B. M. Foxman, *Organometallics* 1984, **3**, 552; (b) T. J. McNeese, T. E. Mueller, D. A. Wierda, D. J. Darensbourg and T. DeLord, *Inorg. Chem.* 1985, **24**, 3465.
14. J. R. Norton, *Accts Chem. Res.* 1979, **12**, 139.

Polyhedron Vol. 8, No. 5, pp. 659–668, 1989
Printed in Great Britain

0277–5387/89 $3.00+.00
© 1989 Pergamon Press plc

SYNTHESIS, STRUCTURE AND PROPERTIES OF A N_3 TRIDENTATE BIS-IMIDAZOLYL LIGAND WITH COPPER(II)

K. J. OBERHAUSEN, J. F. RICHARDSON and R. M. BUCHANAN*

Department of Chemistry, University of Louisville, Louisville, KY 40292, U.S.A.

and

W. PIERCE

Department of Pharmacology, University of Louisville, Louisville, KY 40292, U.S.A.

(*Received* 17 *August* 1988; *accepted* 3 *October* 1988)

Abstract—The synthesis of a new tridentate ligand, bis[2-(1-methylimidazolyl)methyl] amine, [B-MIMA], is described. The compound has been characterized by ^1H and ^{13}C NMR spectroscopy and mass spectrometry, and forms complexes with various copper(II) salts. Crystallographic studies have been completed on the blue product from the reaction of B-MIMA with copper(II) acetate, $[Cu(B\text{-}MIMA)(CH_3COO)](ClO_4)$ (**6**). Crystal data for **6** are: triclinic, $P\bar{1}$, $a = 5.176(2)$, $b = 8.489(3)$, $c = 10.066(3)$ Å, $\alpha = 95.09(5)$, $\beta = 95.72(3)$, $\gamma = 102.37(4)$, $V = 427.1$ Å and $Z = 1$. The structure was solved using the Patterson method which revealed the position of the copper atom and successive difference Fourier syntheses which revealed the location of the remaining atoms. The atom positions were refined by least-squares methods producing a final agreement factor of $R = 0.021$ and $R_w = 0.029$ for 1897 observed reflections. The structure consists of a polymeric acetate bridged network of distorted square-pyramidal copper(II) ions. The five coordinate geometry around each metal ion is a result of the bonding of three nitrogen atoms from the B-MIMA ligand and two oxygen atoms from different acetate ions. The acetate ions act as bidentate ligands bridging different copper ions and the resulting extended bridging network extends out the crystallograhic *a* axis. Spectroscopic, magnetic and electrochemical properties of the complex are described and compared with related compounds. The solution spectroscopic properties of **6** suggest that the square-pyramidal geometry of the metal ion in the solid-state is not retained in solution.

Histidine is known to be present at the active site of numerous metalloproteins,[1] in particular, electronically coupled Type III binuclear copper proteins such as haemocyanin[2] and tyrosinase.[2] Haemocyanin[2,3,4] functions as an oxygen carrier in the haemolymph of arthropods and molluscs while tyrosinase[1,2,3,5] functions both as a monophenolase $\left(\text{phenol} \xrightarrow[Cu^+]{O_2} o\text{-diphenol}\right)$ and as a two-electron oxidase $\left(o\text{-diphenol} \xrightarrow{Cu^{2+}} o\text{-quinone}\right)$. The active sites of the oxy forms of the two proteins are thought to be very similar.[1c] A preliminary X-ray crystallographic structure of deoxyhaemocyanin (deoxy Hc)[6] isolated from *Panularis interruptus* shows that the Cu^I ions are coordinated to three imidazole residues of histidine. From various spectroscopic studies, the oxy form of haemocyanin (oxy Hc) is thought to have two[7,8] or three[8,9] imidazole residues from histidine bonded to each of the cupric ions.

There has been much effort recently to synthesize low molecular weight inorganic analogues of the active site of these copper proteins.[10–15] In several instances the spectroscopic, magnetic[10,12f] and chemical reactivity (O_2 bonding and mono-

*Author to whom correspondence should be addressed.

phenolase activity) properties[11] have been successfully duplicated. In general, the model studies have focused on preparing binucleating ligands containing pyridine,[1b,c,11,14] pyrazole,[1b,12] benzimidazole[1b,13,14] and cyclic polyaza macrocyclic ligands[16] that are capable of binding two metal ions in close proximity. Along similar lines we have begun a systematic study of the structural and magnetochemistry of the metal complexes of a new N_3 tridentate bis-imidazolyl ligand. It is our objective to use this compound to prepare new binucleating ligands containing biologically more relevant imidazole functionalities, in order to construct functional models of the binuclear centres in haemocyanin and tyrosinase.

In the present report, we describe the synthesis of the polyimidazole ligand, bis[2-(1-methylimidazolyl)methyl]amine [B-MIMA],[17] and the preparation and characterization of a polymeric copper(II) complex, [Cu(B-MIMA)(CH_3COO)](ClO_4). The results from an X-ray structural analysis on [Cu(B-MIMA)(CH_3COO)](ClO_4) and the spectroscopic, magnetic and electrochemical properties of the complex will be discussed.

EXPERIMENTAL

Materials and methods

Reagent grade chemicals were used in all experiments. Solvents were dried by standard procedures prior to use. The identity and purity of the ligand B-MIMA was determined by ^1H and ^{13}C NMR spectroscopies, and mass spectrometry. All elemental analyses were performed by either Galbraith Laboratories Inc., Knoxville, Tennessee or Desert Analytics Organic Microanalysis, Tuscon, Arizona. ^1H and ^{13}C NMR spectra were recorded on a Varian XL-300 spectrometer. Chemical shifts are reported as δ units in ppm relative to an internal standard of $(CH_3)_4Si$. Mass spectra were recorded on a VG-7035 GC-MS mass spectrometer in the EI mode at 20 eV. IR spectra were recorded as DRIFTS on a Nicolet 9000 FTIR spectrophotometer using KCl as a diluting matrix. Solid-state electronic spectra were recorded as mull transmission spectra with a Shimadzu 600 spectrophotometer. Visible absorption spectra were recorded also with a Shimadzu 600 spectrophotometer using quartz cells of 1 cm thickness. Spectroscopic grade DMF was used as a solvent for all measurements. Extinction coefficients are reported in units of M^{-1} cm^{-1}. Electrochemical measurements were made at room temperature using a PAR 173 potentiostat, a PAR 175 universal programmer, a PAR 179 digital coulometer and Houston Model 2000 X-Y recorder. Controlled-potential coulometry required the use of a platinum gauze working electrode. The three-electrode cell utilized a Ag/AgCl reference electrode, a coiled platinum wire auxillary electrode and a polished glassy-carbon working electrode.

The solid-state room temperature magnetic moment was determined with a PAR Model 155 vibrating sample magnetometer calibrated with $HgCo(NCS)_4$. Pascal constants were used to correct data for diamagnetism.[18] The EPR spectrum of a frozen solution of [Cu(B-MIMA)(CH_3COO)](ClO_4) in DMF was obtained using a Varian E-109 spectrometer equipped with an Oxford Instruments Inc. cryostat. All EPR spectra of the copper complexes were calibrated using diphenylpicrylhydrazyl (DPPH) as a standard.

Synthesis of the ligand and copper(II) complexes

1-Methyl-2-imidazolecarboxaldehyde (**1**). Compound **1** was prepared according to a procedure published previously by Iverson and Lund.[19] Under a nitrogen atmosphere, 1.6 M *n*-butyllithium (68 cm^3, 0.108 mol) was slowly added to a suspension of 1-methylimidazole (8.2 g, 0.1 mol) in 250 cm^3 of dry diethyl ether at $-45°C$. The resulting mixture was allowed to stir at $-50°C$ for 1 h, after which freshly distilled dimethylformamide (12.5 cm^3, 0.15 mol) in 20 cm^3 of diethyl ether was quickly added. The reaction mixture was stirred overnight and the temperature of the dry ice–acetone bath allowed to slowly rise to 0°C. Over a period of 15 min, 10 cm^3 of water was cautiously added to the solution, followed by 65 cm^3 of 4 N HCl. The layers were separated and the ether was washed with 5×15 cm^3 portions of 4 N HCl. The combined acid extracts were saturated with potassium carbonate and extracted with 4×30 cm^3 of chloroform. The combined chloroform extracts were dried over magnesium sulphate, filtered and evaporated. The resulting residue was distilled at reduced pressure to give 7 g (64%) of **1** as a colourless oil which crystallized on standing. Boiling point 65°C (1.0 torr), m.p. 38–39°C (Lit. b.p. 89–95 (12 torr), m.p. 38–39°C).[19] ^1H NMR ($CDCl_3$, δ): 4.01 (s, 3H), 7.16 (s, 1H), 7.27 (s, 1H), 9.79 (s, 1H).

1-Methyl-2-imidazolecarboxaldehyde oxime (**2**). Compound **2** was prepared according to the method of Gebert and von Kerékjártó.[20] A solution of **1** (2.20 g, 0.02 mol) in 10 cm^3 of ethanol was added to $NH_2OH \cdot HCl$ (1.40 g, 0.02 mol) and Na_2CO_3 (1.06 g, 0.01 mol) dissolved in 20 cm^3 of water cooled to 0°C. The resulting precipitate was filtered and washed with 30 cm^3 of cold 33% ethanol to give 2.2 g (88%) of **2**. Melting point

176°C (Lit. 176°C).[21] ^{1}H NMR ($CDCl_3$, δ): 3.8 (s, 3H), 6.95 (s, 1H), 7.2 (s, 1H), 8.0 (s, 1H), 10.1 (s, 1H).

1-Methyl-2-aminomethylimidazole dihydrochloride (**3**). A solution of **2** (1.0 g, 0.008 mol) in 50 cm^3 of methanolic hydrochloride was hydrogenated at atmospheric pressure and 65°C over 10% palladium–charcoal for 4 h. The catalyst was filtered, washed with 10 cm^3 of methanol and the filtrate cooled to −20°C for 3 h. The precipitate was filtered and washed with 2×10 cm^3 portions of methanol·HCl to give 1.20 g (82%) of **3**. Melting point 251°C. ^{1}H NMR (d_6-DMSO, δ): 4.0 (s, 3H), 4.43 (s, 2H), 7.75 (s, 1H), 7.77 (s, 1H), 8.25 (6s, 4H).

Bis(2-(1-methylimidazolyl)methyl)amine trihydrochloride (**4**). A solution of **3** (2.0 g, 0.011 mol) in 50 cm^3 of methanol containing KOH (0.6 g, 0.011 mol) was added to a solution of **1** (1.2 g, 0.011 mol) in 50 cm^3 of methanol and hydrogenated at atmospheric pressure over 10% palladium–charcoal for 4 h. The catalyst was filtered off and the solvent reduced to a volume of 25 cm^3. The KCl salt was then filtered off and 300 cm^3 of methanolic·HCl added. After cooling to −20°C for 4 h, the precipitate was filtered and washed with 2×10 cm^3 portions of methanolic·HCl to give 2.3 g (68%) of **4**. Melting point 214°C. ^{1}H NMR (d_6-DMSO, δ): 3.16 (2, 1H), 4.04 (s, 6H), 4.64 (s, 4H), 7.78 (s, 2H), 7.82 (s, 2H).

Bis(2-(1-methylimidazolyl)methyl)amine [B-MIMA] (**5**). The free base **5** was obtained by dissolving **4** (1.88 g, 0.006 mol) in a saturated aqueous K_2CO_3 solution and extracting with 5×50 cm^3 portions of chloroform. The extracts were combined, dried over magnesium sulphate, and the solvent removed to give 1.2 g (97%) of B-MIMA. Melting point 122°C. Found: C, 58.3; H, 7.2; N, 34.1. Calc. for $C_{10}H_{15}N_5$: C, 58.5; H, 7.4; N, 34.1%. Mass spectra (205.26 g mol^{-1}, M/Z): 206($M+H^+$, 7); 167(27); 139(30.7); 110(36); 95(77); 83(55); 73(15). IR (KCl; cm^{-1}): $\nu_{C=N}$ 1645 cm^{-1}, $\nu_{C=N=C=C}$ 1435 cm^{-1}, ν_{NH} 3207 cm^{-1}. ^{1}H NMR ($CDCl_3$, δ): 2.27 (s, 1H), 3.55 (s, 6H), 3.78 (s, 4H), 6.75 (s, 2H), 6.85 (s, 2H). ^{13}C NMR ($CDCl_3$, δ): 32.3 (CH_3); 44.4 (CH_2); 121.0 and 126.8 (ring CH); 145.8 (ring quart. C).

Acetato [bis(2-(1-methylimidazolyl)methyl)amino] copper(II) perchlorate, [Cu(B-MIMA)(CH_3COO)](ClO_4) (**6**). A solution of **5** (0.41 g, 0.002 mol) in 5 cm^3 of methanol was added to a solution of $Cu(CH_3CO_2)_2$ (0.4 g, 0.002 mol) and $NaClO_4$ (0.122 g, 0.001 mol) in 10 cm^3 of methanol. The resulting blue solution was filtered and allowed to stand. Large blue crystals formed and were filtered and washed with methanol to give 0.58 g (80%) of **6**. The compound was recrystallized from methanol. **Caution!** Even though the perchlorate complex isolated here was not found to be shock sensitive, care is recommended in its handling. Found: C, 33.7; H, 4.2; N, 16.3. Calc. for $C_{12}H_{18}N_5ClCuO_6$: C, 33.7; H, 4.2; N, 16.4. IR (KCl; cm^{-1}): $\nu_{C=N}$ 1625, $\nu_{C=N=C=C}$ 1445, $\nu_{CO_2(asym)}$ 1595, $\nu_{CO_2(sym)}$ 1410, ν_{NH} 3205 cm^{-1}. UV–vis [DMF; λ_{max}, nm (ε, M^{-1} cm^{-1})]: 301(1270), 682(70). (Mull; λ_{max}, cm^{-1}) 14800. EPR (DMF) $g_\parallel = 2.26$; $g_\perp = 2.05$, $A_\parallel = 0.0159$ cm^{-1} (powdered crystals); $g_\parallel = 2.24$, $g_\perp = 2.07$.

X-ray crystallography, data collection, reduction of X-ray diffraction data. The crystal chosen for data collection was an irregular plate cut from a cluster of crystals. Cell constants and orientation matrices were determined by least-squares refinement of the diffraction geometry of 25 accurately centred reflections ($8 < \theta < 14°$). The choice of space group ($P1$) was confirmed using the program TRACER[22] and by the successful solution and refinement of the structure. Data were collected at room temperature on an Enraf–Nonius CAD4 automated diffractometer using the ω–2θ scan technique. As a check on crystal and electronic stability, three representative reflections were measured every 60 min. The intensities of these reflections remained constant within experimental error throughout data collection, so no decay correction was applied. The data were corrected for Lorentz and polarization effects, and an empirical absorption correction based on a series on psi scans was applied. All data were processed and the crystal structure solved using the SDP package.[22] A summary of the crystal data, experimental details and refinement results for compound **6** are given in Table 1.

Structure solution and refinement of compound **6**

The structure was solved using the Patterson method which revealed the position of the copper atom. The remaining atoms were located in succeeding difference Fourier syntheses. All non-hydrogen atoms were refined anisotropically. Hydrogen atoms were located (range 0.88–1.05 Å) and added to the structure factor calculation with isotropic thermal parameters set to $1.3 \times B_{iso}$ of the bonded atom. Hydrogen parameters were not refined. Refinement was carried out by full-matrix least-squares on F, minimizing the function $\Sigma w(|F_o| - |F_c|)^2$, where the weight w is defined as $4F_o^2/[\sigma(F_o^2)]^2$. Scattering factors were taken from Cromer and Waber[23] and anomalous dispersion effects were included in F_c;[24] the values for $\Delta f'$ and $\Delta f''$ were those of Cromer.[25] At one stage in the refinement, the enantiomeric model was calculated and showed the initial choice to be the correct one ($R = 0.023$ vs $R = 0.033$). An isotropic extinc-

Table 1. Crystal and diffraction data of [Cu(B-MIMA)(CH_3COO)](ClO_4) (**6**)

M_r	427.3
Space group	$P\bar{1}$
a (Å)	5.176(2)
b (Å)	8.489(6)
c (Å)	10.066(3)
α (°)	95.09(5)
β (°)	95.72(3)
γ (°)	102.37(4)
V (Å^3)	427.1
Z	1
$D_{meas.}$ (Mg m^{-3})	1.65(1)
D_{calc} (Mg m^{-3})	1.66
$F(000)$	219
Diffractometer	Enraf–Nonius CAD4
Data collected	$\pm h, +k, \pm l$
Monochromator	Graphite
Radiation (λ, Å)	Mo-K_α (0.71069)
Scan technique	ω–2θ
Scan range	$1.5(0.70+0.34\tan\theta)$
Scan speed (° min^{-1})	1–3
Measured reflections	2080
Observed reflections	1897 ($I > 3\sigma(I)$)
μ (cm^{-1})	14.8
Final R value $[\Sigma(\|F_o\|-\|F_c\|)/\Sigma\|F_o\|]$	0.021
Final R_w value $[\Sigma w(\|F_o\|-\|F_c\|)^2/\Sigma w\|F_o\|^2]^{1/2}$	0.029

tion parameter could not be refined. The model converged with final agreement factors of $R = \Sigma(|F_o|-|F_c|)/\Sigma|F_o| = 0.021$ and $R_w = [\Sigma w(|F_o|-|F_c|)^2/\Sigma w|F_o|^2]^{1/2} = 0.029$. The highest peak in the final difference Fourier had a height of 0.034(4) e Å^{-3}. Plots of $\Sigma(|F_o|-|F_c|)^2$ vs $|F_o|$, reflection order in data collection, $\sin\theta/\lambda$, and various classes of indices showed no unusual trends. Tables containing structure factors, atomic positional and anisotropic thermal parameters, hydrogen coordinates, bond angles and distances, and torsion angles have been deposited as supplementary material with the Editor, from whom copies are available upon request. Atomic coordinates have also been deposited with the Cambridge Crystallographic Data Centre.

RESULTS AND DISCUSSION

Synthesis

There have been several examples of polyimidazole ligands and their metal complexes reported recently,[26–31] however, the ligands generally have a tripod shape and are not easily derivatized. We wish to report the results of our initial efforts to prepare and characterize new polyimidazole ligands. In particular, this study will focus on the preparation of the bis-imidazole ligand, B-MIMA. We have used this N_3 tridentate ligand to prepare binucleating polyimidazole ligands.[17] Similar synthetic approaches have been successfully exploited by Karlin[11] and Sorrell[12] and co-workers for the preparation of polypyridine and polypyrazole ligands, respectively.

The tridentate ligand, B-MIMA (**5**), has been prepared following the procedure outlined in Fig. 1. The procedure is a general one and has been used in the preparation of several derivatives of **5**.* The aldehyde (**1**) and corresponding oxime (**2**) intermediates, depicted in Fig. 1, have been prepared previously by others (see Experimental) and the ^{1}H, ^{13}C NMR spectra and melting points of recrystallized samples of these compounds agree with literature values. Catalytic hydrogenation of **2** affords the amine (**3**) in good yields (82%). The amine (**3**) reacts smoothly with **1** in methanol forming the Schiff base intermediate which is not isolated but rather hydrogenated *in situ* affording gram quantities of the off-white solid **4**, as the trihydrochloride. The ^{1}H and ^{13}C NMR spectra of the free base of **4** agree with the proposed structure and

*We have used this general method to prepare **2** and **4** substituted imidazole analogues of B-MIMA which contain either methylene or ethylene backbone linkages. The synthesis and properties of these compounds will be reported elsewhere.

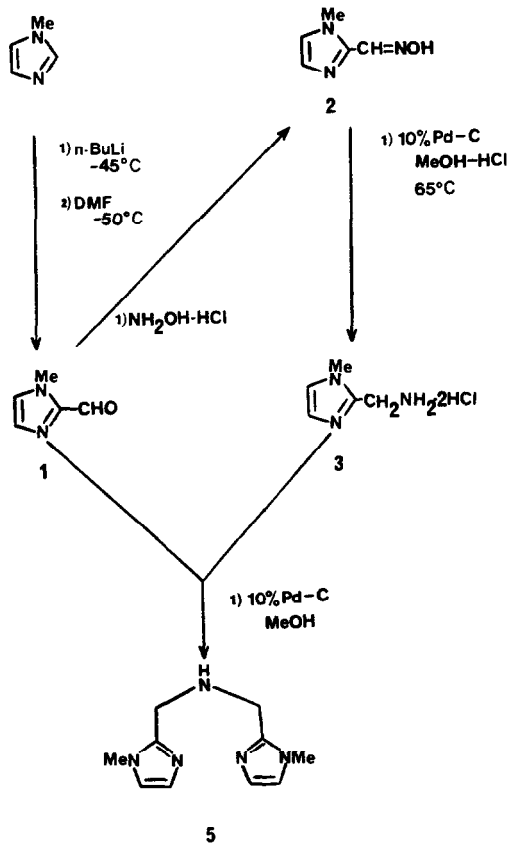

Fig. 1. Synthetic scheme for preparing the tridentate ligand, B-MIMA (**5**).

a molecular ion at 205.26 mass units has been detected by mass spectrometry. The IR spectrum of the free base **5** exhibits a ν_{NH} stretch at 3207 cm^{-1} characteristic of a secondary amine and strong stretches at 1645 and 1436 cm^{-1}, which are attributable to the C=N and —C=N—C=C— symmetric stretching modes of the imidazole ring, respectively.[32]

The blue copper(II) complex, [Cu(B-MIMA)(CH_3COO)](ClO_4) (**6**), was prepared by mixing stoichiometric amounts of copper(II) acetate and the free base of B-MIMA (**5**) in methanol, followed by precipitation of the complex with $NaClO_4$. The same complex can be isolated by reacting stoichiometric amounts of copper(II) perchlorate with **5** in methanol followed by precipitation of the metal complex with sodium acetate.

Description of the solid-state structure of [Cu(B-MIMA)(CH_3COO)](ClO_4) (**6**)

Compound **6** crystallizes from methanol in the triclinic space group $P\bar{1}$ with one molecule per unit cell. Crystal data for the complex are given in Table 1 and selected bond distances and angles are reported in Table 2.

The geometry around the copper(II) ion is best described as a distorted square-pyramid as illustrated in the packing diagram in Fig. 2. The basal plane of the square-pyramid is defined by atoms N(1), N(3), N(5) of the B-MIMA ligand and O(1) of the acetate ion. The mean displacement of the four atoms from the best least-squares plane defined by their positions is 0.012(2) Å. The axial coordination site is occupied by another oxygen atom [O(2)′] of an acetate group which is associated with an adjacent complex molecule. The copper atom is displaced from the equatorial plane towards the axial oxygen by 0.085 Å. The Cu—O(2)′ distance of 2.414(2) Å is longer than the equatorial Cu—O(1) distance of 1.928(2) Å, but is within the range of values reported for parallel stacked dimeric copper(II) complexes[33a-e] and [Cu(diethylenetriamine)X]$_2$Y$_2$ complexes.[33f-i] The intramolecular Cu—O(2) distance, on the other hand, is 3.017(2) Å which is too long to be considered as a bonding interaction.[34] The acetate group is, therefore, bridging two different metal ions and this bridging interaction extends out the crystallographic *a* axis resulting in a polymeric *syn–anti* step structure with a Cu—Cu separation of 5.176(2) Å.

In structurally similar copper(II) complexes, the second carbonylic oxygen atoms are generally greater than 2.70 Å from the metal ion and the Cu—O—C angles are approximately 50°. In **6** the carbonylic oxygen atom is 3.017(2) Å from the copper atom at an angle of 47.1°. In addition, the carbonylic oxygen atoms are usually hydrogen bonded to either solvate molecules[35-38] in the crystal lattice or coordinated imidazole N—H

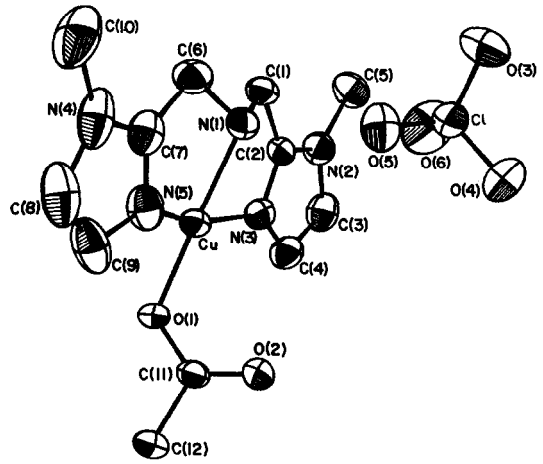

Fig. 2. Crystal packing diagram showing the *syn–anti* acetate bridging interaction in [Cu(B-MIMA)(CH_3COO)](ClO_4). Stacking interaction is along the 100-plane.

Table 2. Selected bond distances (Å) and angles (°)

Atom 1	Atom 2	Distance	Atom 1	Atom 2	Atom 3	Angle
Cu	O(2′)	2.415(2)	O(2′)	Cu	O(1)	102.41(8)
Cu	O(1)	1.928(2)	O(2′)	Cu	N(3)	93.11(9)
Cu	N(1)	2.047(2)	O(1)	Cu	N(1)	173.85(9)
Cu	N(3)	1.974(2)	O(1)	Cu	N(3)	103.0(2)
Cu	N(5)	1.967(3)	O(1)	Cu	N(5)	93.9(2)
Cl(1)	O(3)	1.417(3)	N(1)	Cu	N(3)	81.3(1)
Cl(1)	O(4)	1.424(3)	N(1)	Cu	N(5)	81.4(2)
Cl(1)	O(5)	1.448(3)	N(3)	Cu	N(5)	162.0(1)
Cl(1)	O(6)	1.425(3)	O(3)	Cl(1)	O(4)	110.2(2)
O(1)	C(11)	1.277(3)	O(3)	Cl(1)	O(5)	108.4(2)
O(2)	C(11)	1.223(4)	O(3)	Cl(1)	O(6)	111.1(2)
N(1)	C(1)	1.485(4)	O(4)	Cl(1)	O(5)	108.3(2)
N(1)	C(6)	1.479(4)	O(4)	Cl(1)	O(6)	110.2(3)
N(2)	C(2)	1.331(4)	O(5)	Cl(1)	O(6)	108.6(3)
N(2)	C(3)	1.373(5)	Cu	O(1)	C(11)	119.4(2)
N(2)	C(5)	1.469(4)	Cu	N(1)	C(1)	109.0(2)
N(3)	C(2)	1.316(4)	Cu	N(1)	C(6)	110.6(2)
N(3)	C(4)	1.380(4)	C(1)	N(1)	C(6)	115.6(2)
N(4)	C(7)	1.342(5)	C(2)	N(2)	C(3)	107.8(3)
N(4)	C(8)	1.385(6)	C(2)	N(2)	C(5)	125.5(4)
N(4)	C(10)	1.446(7)	C(3)	N(2)	C(5)	126.7(4)
N(5)	C(7)	1.326(5)	Cu	N(3)	C(2)	112.4(2)
N(5)	C(9)	1.381(5)	Cu	N(3)	C(4)	141.3(2)
C(1)	C(2)	1.491(4)	C(2)	N(3)	C(4)	106.4(2)
C(3)	C(4)	1.354(5)	O(2′)	Cu	N(1)	81.59(8)
C(6)	C(7)	1.505(5)	O(2′)	Cu	N(5)	89.4(2)
C(8)	C(9)	1.338(7)	C(7)	N(4)	C(8)	107.2(3)
C(11)	C(12)	1.510(4)	C(7)	N(4)	C(10)	127.0(4)
			C(8)	N(4)	C(10)	125.8(4)
			Cu	N(5)	C(7)	112.6(2)
			Cu	N(5)	C(9)	140.1(3)
			C(7)	N(5)	C(9)	106.0(3)
			N(1)	C(1)	C(2)	105.0(2)
			N(2)	C(2)	N(3)	111.0(3)
			N(2)	C(2)	C(1)	127.8(3)
			N(3)	C(2)	C(1)	121.2(2)
			N(2)	C(3)	C(4)	106.3(3)
			N(3)	C(4)	C(3)	108.7(3)
			N(1)	C(6)	C(7)	105.2(3)
			N(4)	C(7)	N(5)	110.8(3)
			N(4)	C(7)	C(6)	127.9(3)
			N(5)	C(7)	C(6)	121.3(3)
			N(4)	C(8)	C(9)	106.4(3)
			N(5)	C(9)	C(8)	109.7(4)
			O(1)	C(11)	O(2)	124.6(3)
			O(1)	C(11)	C(12)	115.5(2)
			O(1)	C(11)	C(12)	119.9(3)

Numbers in parentheses are estimated standard deviations in the least significant digits.

protons[37,38] associated with adjacent complex molecules.

The polymeric *syn–anti* step structure observed for **6** (Fig. 3) resembles the structure reported for $[Cu_2(ClCH_2COO)_3EtSal(C_2H_5OH)]_\infty$[36] and $[Cu(dien)X]_2Y_2$[33f-i], and has been observed in the polymeric structure of bis(L-asparinato)Zn^{II}.[39] In this later complex the second carboxylic oxygen atom of neighbouring molecules complete the octahedral coordination geometry around the metal ion with

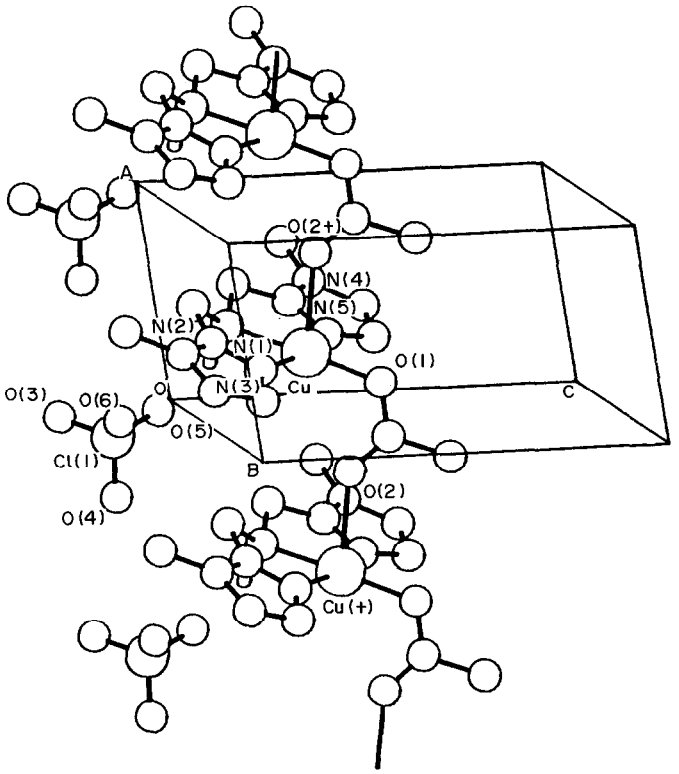

Fig. 3. ORTEP view of the complex molecule showing the atom numbering scheme and thermal motion ellipsoids (50%).

out-of-plane Zn—O distances of 2.278 and 2.481 Å.

The Cu—N bond lengths of **6** are typical of values reported previously for other copper–imidazole complexes[1b,16a,40–42] [N(1), 2.047(2), N(3), 1.947(2) and N(5), 1.967(3) Å]. The N—Cu—N angles of 81.3(1), 81.4(2) and 162.0(1)° reflect the strain imposed on the coordination environment by the five-membered chelate rings formed upon coordination of the *B-MIMA* ligand. The 1-methylimidazole rings are planar with no significant deviation from the least-squares planes through the five atoms and are nearly coplanar with a dihedral angle of 7.56°. The Cu—O bond angles are more obtuse, with the largest deviation from 90° being the O(1)—Cu—O(2') angle of 103.0(2)°. Angles closer to 90° are observed for a structurally related tridentate bis-imidazole ligand which forms eight-membered chelate rings with the copper(II) ion.[31]

The perchlorate counter ions also stack along the crystallographic *a* axis and are weakly hydrogen bonded to the N(1) proton of the complex. The HN(1)—O(5) distance is 2.030(3) Å and the N(1)—HN(1)—O(5) angle is 150.0°.

Properties

The IR spectrum of the B-MIMA changes slightly upon coordination to the copper(II) ion. Most noticeable changes are observed in the —C=N— (1645 cm^{-1}) and —C=N=C=C— (1435 cm^{-1}) symmetric stretching modes. The 1645 cm^{-1} band shifts to 1625 cm^{-1} and the 1440 cm^{-1} band shifts to 1445 cm^{-1}, implying direct coordination of imine nitrogen atoms of the ring. Carbonyl stretches for the bridging acetate ion are observed at 1595 and 1410 cm^{-1}, corresponding to the ν(COO—) asymmetric and symmetric stretches, respectively. Similar multiple bands in the region characteristic of carboxylate stretches have been reported for $\{Cu(L\text{-}Asp)(2\text{-}MeIm)\}\cdot H_2O$ and related complexes.[38]

The room temperature, solid electronic spectra of **6** exhibits a broad maximum at 14,800 cm^{-1} which is in agreement with data reported for other mixed oxygen and nitrogen ligand square-pyramidal complexes.[38] The polymeric solid-state structure of $\{Cu(B\text{-}MIMA)(CH_3COO)\}(ClO_4)$ is not retained in solution. The complex is readily soluble in polar solvents and its absorption spectrum in methanol shows a strong charge-transfer absorption at 301 nm (ε = 1270 M^{-1} cm^{-1}) and a *d–d* band at 682 nm (ε = 70 M^{-1} cm^{-1}), indicative of a square-planar geometry around the copper(II) ion.

Magnetism

At room temperature the magnetic moment of **6**

is 1.82 BM, a value that is typical of $S = 1/2$ Cu^{II}.[43] The X-band EPR spectrum recorded on a ground crystalline sample of **6** shows an axial spectrum with $g_{\|} = 2.24$ and $g_{\perp} = 2.07$ (Supplementary material). No $\Delta M_s =$ two transition has been detected in the solid-state EPR spectrum[43,44] of the complex at temperatures between 298 and 3.8 K. It appears that the acetate bridge does not promote spin–spin exchange coupling between copper(II) ions in the chain. The orthogonal nature of the acetate bridge most likely accounts for the apparent absence of exchange coupling. However, the recently reported μ-acetato bridged $[Cu(dien)(OAc)]_n(ClO_4)_n$ complex[33i] has been found to be a quasi one-dimensional complex in which the copper(II) ions are ferromagnetically coupled.

A frozen DMF solution of **6** at 77 K displays an axial EPR spectrum typical of square-planar copper(II) complexes with $g_{\|} = 2.26$, $g_{\perp} = 2.05$ and $A_{\|} = 0.0159$ cm^{-1}. Seven nitrogen superhyperfine lines have been resolved on the low field parallel component of the spectrum.

Electrochemistry

In acetonitrile and dimethylformamide, the copper(II) complex undergoes irreversible oxidation at a platinum electrode surface. Cyclic voltammetric studies indicate that the reduced species undergoes chemical decomposition, presumably due to the loss of the acetate ion at the working electrode, since no oxidation current is detected on the reverse scan. In DMF at a glassy-carbon electrode, however, the electrochemical behaviour is slightly better behaved. Cyclic voltammetry on **6** (Supplementary material) in DMF at a glassy-carbon electrode reveals a quasi-reversible one-electron reduction (relative to Fc/Fc^+) of the copper(II) ion at $E_{1/2} = -0.239$ V vs Ag/AgCl, with a peak-to-peak separation of 270 mV. The ratio of i_a/i_c is 0.89 suggesting that there is some degradation of the complex upon reduction.[45]

A similar copper(II) complex containing a N_3 bis-imidazolyl chelate has been studied by Karlin *et al.*[31] The reduction potential of their complex is approximately 0.50 V more positive than complex **6**. A possible explanation for the greater stabilization of the copper(I) species with Karlin's ligand may be that the larger (eight-membered) ring size more easily accommodates the tetrahedral geometry most likely formed upon reduction of the copper(II) ion. In addition, Karlin has reported that $Cu_2(py_2)Cl_3PF_6$[44] undergoes a quasi-reversible one-electron reduction at -0.045 V vs NHE (-0.242 V vs Ag/AgCl in DMF), which is closer to the reduction potential observed for compound **6**. Further studies correlating the effect of chelate ring size on the reduction potentials of copper(II) complexes containing tridentate N_3 bis-imidazolyl ligands are in progress.

Summary

A new N_3 tridentate bis-imidazolyl ligand (**5**) has been prepared and characterized. The ligand readily forms complexes with copper(II) and the corresponding acetate adduct is polymeric in the solid state. Solution spectroscopic properties are typical of a square-planar Cu(II) complex indicating the polymeric solid-state structure is not retained in solution. The complex ion displays quasi-reversible redox properties in DMF at glassy-carbon electrode surfaces, but irreversible electrochemistry at platinum.

Future directions

We are continuing our investigation of the chemistry of the N_3 tridentate ligand, B-MIMA (**5**), and its derivatives. In particular, we have prepared a variety of bridged binucleating derivatives[47] and are exploring their coordination and spectroscopic properties with metal ions such as: Cu, Mn, Fe and Co. Of particular interest is the copper(I) chemistry of a *m*-xylyl bridged bis(B-MIMA) analogue since a structurally similar pyridinyl[11d] compound mimics the phenolase activity observed for the redox active binuclear copper metalloprotein, tyrosinase.[1b,2] Reaction of the copper(I) complexes of polyimidazolyl ligands with biologically important molecules such as O_2, are under current investigation and will be the subject of future reports.

Supplementary material

Tables of positional parameters of non-hydrogen atoms, anisotropic thermal parameters, fractional coordinates for H atoms, bond distances and angles for H atoms, least-squares planes and torsion angles, as well as figures of the electronic spectrum, EPR spectra and cyclic voltammogram of the complex (13 pp.) are available upon request from the Editor or Author.

Acknowledgements—This research was supported with funds from the National Science Foundation (Grant No. RII-8610671) and the Commonwealth of Kentucky through the Kentucky EPSCoR Program. R.M.B. would like to acknowledge the generous support from the University of Louisville Research Foundation (Grant ID. 61-102-9626) and the College of Arts and Sciences. R.M.B. thanks Dr John L. Wong for his helpful comments and Dr Donald E. Williams for the use of his VAX-11/750.

The assistance of Mr Thompson N. Doman during the preparation of B-MIMA is also acknowledged.

REFERENCES

1. (a) C. A. Evans, R. Guevremont and D. L. Rabenstein, *Metal Ions Biol. Syst.* 1979, **9**, 41; (b) H. C. Freeman, *Inorganic Biochemistry* (Edited by G. L. Eichhorn), Vol. 1, pp. 121–166 and refs therein. Elsevier, Amsterdam (1973); (c) M. E. Winkler, K. Lerch and E. I. Solomon, *J. Am. Chem. Soc.* 1981, **103**, 7001 and refs therein.
2. (a) E. I. Solomon, K. W. Penfield and D. E. Wilcox, *Struct. Bonding (Berlin)* 1983, **53**, 1; K. D. Karlin and J. Zubieta (Eds), *Copper Coordination Chemistry: Biochemical and Inorganic Perspectives*. Adenine Press, Guilderland, New York (1983); (b) K. D. Karlin and J. Zubieta (Eds), *Biological and Inorganic Copper Chemistry*, Vols I and II. Adenine Press Guilderland, New York (1986).
3. E. I. Solomon, in *Copper Proteins* (Edited by T. G. Spiro), Vol. 3, pp. 41–88. Wiley, New York (1981).
4. (a) W. H. Vannneste and A. Zuberbuhler, in *Molecular Mechanisms of Oxygen Activation* (Edited by O. Hayaishi), pp. 371–404. Academic Press, New York (1974); (b) K. Lerch, in *Metal Ions in Biological Systems* (Edited by H. Sigel), Vol. 13, pp. 143–186. Marcel Dekker, New York (1981).
5. R. Lontie and R. Witters, in *Metal Ions in Biological Systems* (Edited by H. Sigel), Vol. 13, pp. 229–258. Marcel Dekker, New York (1981).
6. (a) W. P. J. Gaykema, W. G. J. Hol, J. M. Verijken, N. M. Soeter, H. J. Bok and J. J. Beintema, *Nature (Lond.)* 1984, **309**, 23; (b) B. Linzen, N. M. Soeter, A. F. Riggs, H.-J. Schneider, W. Schartau, M. D. Moore, E. Yokota, P. Q. Behrens, H. Nakashima, T. Takagi, T. Nemoto, J. M. Vereijken, H. J. Bak, J. J. Beintema, A. Volbeda, W. P. J. Gaykema and W. G. J. Hol, *Science* 1985, **229**, 519.
7. (a) M. S. Co and K. O. Hodgson, *J. Am. Chem. Soc.* 1981, **103**, 3200; (b) M. S. Co, K. O. Hodgson, T. K. Eccles and R. Lontie, *J. Am. Chem. Soc.* 1981, **103**, 984.
8. T. G. Spiro, G. L. Wooley, J. M. Brown, L. Powers, H. E. Winkler and E. I. Solomon, *Copper Coordination Chemistry: Biochemical and Inorganic Perspectives* (Edited by K. D. Karlin and J. Zubieta), pp. 23–47. Adenine Press, Guilderland, New York (1983).
9. J. M. Brown, L. Powers, B. Kincaid, J. A. Larrabee and T. G. Spiro, *J. Am. Chem. Soc.* 1980, **102**, 4210.
10. (a) J. V. Dagdigian, V. McKee and C. A. Reed, *Inorg. Chem.* 1982, **21**, 1332; (b) V. McKee, M. Zvagulis, J. V. Dagdigian, M. G. Patch and C. A. Reed, *J. Am. Chem. Soc.* 1984, **106**, 4765; (c) V. McKee, J. V. Dagdigian, R. Bau and C. A. Reed, *J. Am. Chem. Soc.* 1981, **103**, 7000.
11. (a) K. D. Karlin, J. C. Hayes, S. Juen, J. P. Hutchinson and J. Zubieta, *Inorg. Chem.* 1982, **21**, 4106; (b) K. D. Karlin, P. L. Dahlstrom, S. N. Cozzette, P. M. Scensny and J. Zubieta, *J. Chem. Soc., Chem. Commun.* 1981, 881; (c) K. D. Karlin, Y. Gultneh, J. P. Hutchinson and J. Zubieta, *J. Am. Chem. Soc.* 1982, **104**, 5240; (d) K. D. Karlin, J. C. Hayes, Y. Gultneh, R. W. Cruse, J. W. McKown, J. P. Hutchinson and J. Zubieta, *J. Am. Chem. Soc.* 1984, **106**, 2121; (e) K. D. Karlin, R. W. Cruse, Y. Gultneh, J. C. Hayes and J. Zubieta, *J. Am. Chem. Soc.* 1984, **106**, 3372; (f) N. J. Blackburn, K. D. Karlin, M. Concannon, J. C. Hayes, Y. Gultneh and J. Zubieta, *J. Chem. Soc., Chem. Commun.* 1984, 939; (g) K. D. Karlin, J. C. Hayes, R. W. Cruse, Y. Gultneh, J. P. Hutchinson and J. Zubieta, *Inorg. Chim. Acta* 1983, **79**, 98; (h) K. D. Karlin, J. Shi, J. C. Hayes, J. W. McKown, J. P. Hutchinson and J. Zubietta, *Inorg. Chim. Acta* 1984, **91**, L3–L7; (i) K. D. Karlin, M. S. Haka, R. W. Cruse and Y. Gultneh, *J. Am. Chem. Soc.* 1985, **107**, 5828; (j) K. D. Karlin, Y. Gultneh, J. C. Hayes and J. Zubieta, *Inorg. Chem.* 1984, **23**, 519: (k) K. D. Karlin, R. W. Cruse, M. W. Haka, Y. Gultneh and B. I. Cohen, *Inorg. Chim. Acta* 1986, **125**, L43.
12. (a) T. N. Sorrell, D. L. Jameson and C. J. O'Connor, *Inorg. Chem.* 1984, **23**, 190; (b) T. N. Sorrell and A. S. Borovik, *J. Chem. Soc., Chem. Commun.* 1984, 1489; (c) T. N. Sorrell and M. R. Malachowski, *Inorg. Chem.* 1983, **22**, 1883; (d) T. N. Sorrell and D. L. Jameson, *J. Am. Chem. Soc.* 1983, **105**, 6013; (e) T. N. Sorrell, M. R. Malachowski and D. L. Jameson, *Inorg. Chem.* 1982, **21**, 3250; (f) T. N. Sorrell, C. J. O'Connor, O. P. Anderson and J. H. Reibenspies, *J. Am. Chem. Soc.* 1985, **107**, 4199.
13. H. M. J. Hendrick, P. J. M. W. L. Birker, J. van Rijn, G. C. Verschoor and J. Reedijk, *J. Am. Chem. Soc.* 1982, **104**, 3607 and refs therein.
14. (a) Y. Nishida, K. Takahashi, H. Kuramoto and S. Kida, *Inorg. Chim. Acta* 1981, **54**, L103; (b) Y. Nishida, H. Shimo, H. Maehara and S. Kida, *J. Chem. Soc., Dalton Trans.* 1985, 1945 and refs therein.
15. (a) M. G. Simmons, C. L. Merrill, L. J. Wilson, L. A. Bottomley and K. M. Kadish, *J. Chem. Soc., Dalton Trans.* 1980, 1827; (b) H. Adams, N. A. Bailey, D. E. Fenton and R. Moody, *Inorg. Chim. Acta* 1987, **135**, L1; (c) N. A. Bailey, D. E. Fenton, R. Moody, C. O. Rodriguez deBarbarin and I. N. Scrambarella, *Inorg. Chim. Acta* 1986, **125**, L41; (d) R. J. Butcher, G. Diven, G. Erickson, G. M. Mockler and E. Sinn, *Inorg. Chim. Acta* 1986, **123**, L17; (e) J. E. Bulkowski, P. L. Burk, M.-F. Ludmann and J. A. Osborn, *J. Chem. Soc., Chem. Commun.* 1977, 498.
16. (a) P. K. Coughlin, A. E. Martin, J. C. Dewan, E.-I. Watanabe, J. E. Bulkowski, J.-M. Lehn and S. J. Lippard, *Inorg. Chem.* 1984, **23**, 1004 and refs therein; (b) R. J. Motekaitis, A. E. Martell, J.-M. Lehn and E. I. Watanabe, *Inorg. Chem.* 1982, **21**, 4253; (c) R. J. Motekaitis, A. E. Martell, B. Dietrich and J.-M. Lehn, *Inorg. Chem.* 1984, **23**, 1588.
17. A preliminary account of the synthesis and characterization of B-MIMA was reported at the

193rd Nat. Am. Chem. Soc. Meet. Denver, Colorado (1987), Abstr. No. INORG 142.
18. R. S. Drago, in *Physical Methods in Chemistry*. W. B. Saunders, Philadelphia (1977).
19. P. E. Iverson and H. Lund, *Acta Chem. Scand.* 1966, **20**, 2649.
20. U. Gebert and B. von Kerékjártó, *Leib. Ann. Chem.* 1968, **718**, 249.
21. P. Fournari, P. DeCointet and E. Laviron, *Bull. Soc. Chim. France* 1968, **6**, 2438.
22. All calculations were performed on a VAX-11/750 computer using SDP/VAX: B. A. Frenz, The Enraf–Nonius CAD4 SDP—A real-time system for concurrent X-ray data collection and crystal structure determination, in *Computing in Crystallography* (Edited by H. Schenk, R. Olthof-Hazelkamp, H. vanKonigsveld and G. C. Bassi), pp. 64–71. Delft University Press, Delft, Holland (1978).
23. D. T. Cromer and J. T. Waber, *International Tables for X-ray Crystallography*, Vol. IV, Table 2.2B. The Kynoch Press, Birmingham, U.K. (1974).
24. J. A. Ibers and W. C. Hamilson, *Acta Cryst.* 1964, **17**, 781.
25. D. T. Cromer, *International Tables for X-ray Crystallography*, Vol. IV, Table 2.3.1. The Kynoch Press, Birmingham, U.K. (1974).
26. (a) C. C. Tang, D. Davalian, P. Huang and R. Breslow, *J. Am. Chem. Soc.* 1978, **100**, 3918; (b) R. Breslow, J. T. Hunt, R. Smiley and T. Tarnowski, *J. Am. Chem. Soc.* 1983, **105**, 5337.
27. (a) A. J. Canty, E. E. George and C. V. Lee, *Aust. J. Chem.* 1983, **36**, 415; (b) P. K. Byers, A. J. Canty, N. J. Minchin, J. M. Patrich, B. W. Skelten and A. H. White, *J. Chem. Soc., Dalton Trans.* 1985, 1183; (c) P. K. Byers, A. J. Canty, L. M. Englehardt, J. M. Patrick and A. H. White, *J. Chem. Soc., Dalton Trans.* 1985, 981; (d) A. J. Canty, J. M. Patrick and A. H. White, *J. Chem. Soc., Dalton Trans.* 1983, 1873.
28. (a) H. Slebocka-Tilk, J. L. Cocho, Z. Frakman and R. S. Brown, *J. Am. Chem. Soc.* 1984, **106**, 2421; (b) R. S. Brown, D. Salmon, N. J. Curtis and S. Kusuma, *J. Am. Chem. Soc.* 1982, **104**, 3188; (c) N. J. Curtis and R. S. Brown, *J. Org. Chem.* 1980, **45**, 4038; (d) R. S. Brown and J. Huguet, *Can. J. Chem.* 1980, **58**, 889.
29. S. M. Gorun, G. C. Papaefthymiou, R. B. Frankel and S. J. Lippard, *J. Am. Chem. Soc.* 1987, **109**, 4244.
30. (a) T. N. Sorrell and A. S. Borovik, *J. Am. Chem. Soc.* 1986, **108**, 2479; (b) T. N. Sorrell and A. S. Borovik, *J. Am. Chem. Soc.* 1987, **109**, 4255.
31. K. D. Karlin, R. W. Cruse, J. W. McKown, J. C. Hayes, P. L. Dahlstrom and J. Zubieta, *Transition Met. Chem.* 1984, **9**, 404.
32. T. J. Lane, I. Nakagawa, J. L. Walter and A. J. Kandathil, *Inorg. Chem.* 1962, **1**, 267.
33. (a) E. Frasson, R. Bardi and S. Bezzi, *Acta Cryst.* 1959, **12**, 201; (b) R. M. Buchanan, C.-W. Blumenberg, C. Trapp, S. K. Larsen, D. L. Greene and C. G. Pierpont, *Inorg. Chem.* 1986, **25**, 3070; (c) G. Palenik, *Acta Cryst.* 1964, **B17**, 687; (d) F. Calderazzo, F. Marchetti, G. Dell'Amico, G. Pelizzi and A. Colligiana, *J. Chem. Soc., Dalton Trans.* 1980, 1419; (e) S. Scávnicar and B. Matković, *J. Chem. Soc., Chem. Commun.* 1967, 297; (f) S. K. Hoffmann, D. K. Towle, W. E. Hatfield, K. Weighardt, P. Chaudhari and J. Weiss, *J. Mol. Cryst. Liq. Cryst.* 1983, **107**, 161; (g) S. K. Hoffmann, D. K. Towle, W. E. Hatfield, P. Chaudhari and K. Wieghardt, *Inorg. Chem.* 1985, **24**, 1307; (h) D. K. Towle, S. K. Hoffmann, W. E. Hatfield, P. Chaudhari, P. Singh and K. Wieghardt, *Inorg. Chem.* 1985, **24**, 4393; (i) D. K. Towle, S. K. Hoffmann, W. E. Hatfield, P. Singh and P. Chaudhari, *Inorg. Chem.* 1988, **27**, 394.
34. D. S. Brown, J. D. Lee, B. G. A. Melsom, B. J. Hathaway, I. M. Procter and A. A. G. Tomlinson, *Chem. Comments* 1967, 369.
35. R. Hämäläinen, M. Ahlgren and U. Turpeinen, *Acta Cryst.* 1982, **A38**, 1571.
36. R. J. Butcher, J. W. Overman and E. Sinn, *J. Am. Chem. Soc.* 1980, **102**, 3276.
37. (a) H. A. Henriksson, *Acta Cryst.* 1977, **B33**, 1947; (b) P. Y. Boukari, A. Busnot, A. LeClaire and M. A. Bernard, *Acta Cryst.* 1982, **B38**, 2458.
38. (a) L. Menabue and M. Saladini, *Inorg. Chim. Acta* 1987, **135**, 49; (b) L. Antolini, L. P. Battaglia, A. Bonamartini Corradi, G. Marcotrigiano, L. Menabue and G. C. Pellacani, *J. Am. Chem. Soc.* 1985, **107**, 1369; (c) L. Antolini, L. Menabue, M. Saladini, M. Sola, L. P. Battaglia and A. Bonamartini Corradi, *Inorg. Chim. Acta* 1984, **93**, 61; (d) L. Antolini, G. Marcotrigiano, L. Menabue, G. C. Pellacani and H. Saladini, *Inorg. Chem.* 1982, **21**, 2263.
39. F. S. Stephens, R. S. Vagg and P. A. Williams, *Acta Cryst.* 1977, **B33**, 433.
40. S. Matsumoto, S. Ooi, Y. Nakao, W. Mori and A. Nakahara, *J. Chem. Soc., Dalton Trans.* 1981, 2045.
41. M. G. B. Drew, M. McCann and S. M. Nelson, *J. Chem. Soc., Dalton Trans.* 1981, 1868.
42. B. J. Hathaway, *Coord. Chem. Rev.* 1981, **35**, 211.
43. B. J. Hathaway and D. E. Billing, *Coord. Chem. Rev.* 1970, **5**, 143.
44. I. Bertini, D. Gatteshi and A. Scozzafava, *Coord. Chem. Rev.* 1979, **29**, 67.
45. A. J. Bard and L. R. Faulkner, *Electrochemical Methods. Fundamentals and Applications*. Wiley, New York (1980).
46. K. D. Karlin, J. W. McKown, J. C. Hayes, J. P. Hutchinson and J. Zubieta, *Transition Met. Chem.* 1984, **9**, 405.
47. R. M. Buchanan, K. J. Oberhausen and J. F. Richardson, *Inorg. Chem.* 1988, **27**, 971.

Polyhedron Vol. 8, No. 5, pp. 669–675, 1989
Printed in Great Britain

0277–5387/89 $3.00+.00
© 1989 Pergamon Press plc

THIOLATE COORDINATION IN BINUCLEAR OXOMOLYBDENUM(V) COMPLEXES. THE X-RAY CRYSTAL STRUCTURES OF THE ALKYLAMMONIUM SALTS OF $[Mo_2O_2(OCH_3)(SCH_2CH_2CH_2S)_3]^-$ AND $[Mo_2O_2(SCH_2CO_2)_4]^{2-}$

LIDUN MA,* SHUNCHENG LIU, HUIZHE ZHU and JON ZUBIETA†

Department of Chemistry, State University of New York at Albany, Albany, NY 12222, U.S.A.

(*Received* 25 *July* 1988; *accepted after revision* 5 *October* 1988)

Abstract—Reaction of $[n\text{-}Bu_4N]_2[Mo_2O_7]$ with propane-1,3-dithiol in methanol yields the triply-bridged binuclear complex $[n\text{-}Bu_4N][Mo_2O_3(OCH_3)(SCH_2CH_2CH_2S)_3]$ (**1**). Complex **1** exhibits the confacial bioctahedral geometry characteristic of this class of complexes. In contrast, the reaction of $[n\text{-}Bu_4N]_4[Mo_8O_{26}]$ with 2-mercaptoacetic acid and triethylamine in methanol results in the isolation of a complex $[Et_3NH]_2[Mo_2O_2(SCH_2CO_2)_4]$ (**2**), representing the first example of a new class of binuclear molybdenum(V) species. The structure is characterized by a "*trans*-planar" $[Mo_2O_2S_2(\text{thiolate})]^{4+}$ core and an unusually long Mo···Mo distance of 3.078(1) Å. Crystal data. Complex **1**: triclinic space group $P\bar{1}$, $a = 9.310(2)$, $b = 11.328(2)$, $c = 19.954(3)$ Å, $\alpha = 74.93(1)$, $\beta = 78.19(1)$, $\gamma = 81.53(1)°$, $V = 1979.2(10)$ Å^3, $Z = 2$, $D_{calc} = 1.369$ g cm^{-3}; structure solution and refinement based on 5292 reflections, $R = 0.0570$. Complex **2**: monoclinic space group $P2_1/n$, $a = 10.861(4)$, $b = 13.559(4)$, $c = 11.011(4)$ Å, $\beta = 104.14(2)°$, $V = 1572.1(11)$ Å^3, $Z = 2$, $D_{calc} = 1.664$ g cm^{-3}; 2133 reflections, $R = 0.0560$.

Four common structural types (**I–IV**) have been described for complexes of the oxomolybdenum(V) group coordinated to thiolate ligands.[1–6] While the binuclear structures based on the $[Mo_2O_3]^{4+}$ and $[Mo_2O_4]^{2+}$ cores, (**II**) and (**III**), are ubiquitous in the chemistry of molybdenum(V) with a range of

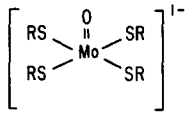

(I)

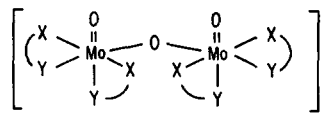

(II) XY = 5-SiMe$_3$-pyridinethiolate, $^-SCH_2CH_2NR_2$; 2XY = $^-SCH_2CH_2NRCH_2CH_2NRCH_2CH_2S^-$

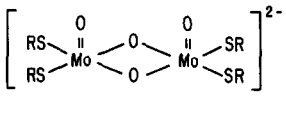

(III)

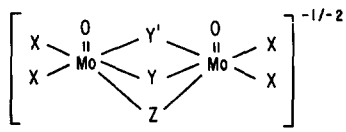

(IV) X = RS$^-$, RO$^-$
Y,Y$^-$ = RS$^-$, RO$^-$
Z = RS$^-$, RO$^-$, Cl$^-$, R_2N^-, N_3^-, O^{2-}

* Permanent address: Center of Analysis and Measurement, Fudan University, Shanghai, P.R.C.

† Author to whom correspondence should be addressed.

‡ Examples of tungsten complexes with the $[W_2O_2YY'Z]^{3+}$ core are also known.[15]

ligand donor groups and not limited to thiolate coordination, structurally characterized examples of the triply-bridged $[Mo_2O_2YY'Z]^{3+}$ core (**IV**)[7–14]‡ display some degree of thiolate coordination. Type **IV** binuclear structures may be derived geo-

metrically from the common *syn* conformer of the type **III** species, illustrated below, by addition of a third, weakly interacting, bridge donor Z. Although type **IV** structures may be described as confacial bioctahedra, the structural relationship of the $[Mo_2O_2YY']$ bridge of type **IV** structures to the $[Mo_2O_4]$ bridge of the type **III** species is apparent in the Mo—Mo distance, the folding of the $[Mo_2YY']$ rhombus along the YY′ vector, and the disposition of the terminal oxo groups. Type **IV** complexes containing the 2-mercaptoethanolate ligand exhibit some structural diversity while retaining the $[Mo_2O_2(SCH_2CH_2O)Y']^{3+/2+}$ core, in which the $(SCH_2CH_2O)^{2-}$ ligand assumes a bidentate doubly-bridging mode, spanning the Y to Z bridge positions.[11,13] Reaction conditions, such as stoichiometry, solvent and counter ions, were found to have pronounced effects on the ligation modes adopted by the additional mercaptoethanolate groups required to complete the molybdenum coordination requirements in the type **IV** complexes.

As part of our continuing investigations of the chemistry of organic solvent soluble polyoxomolybdate anions with thiolate ligands,[16] we have studied the reactions of $[n\text{-}Bu_4N]_2[Mo_2O_7]$ with 1,3-dimercaptopropane and mercaptoacetic acid in an effort to evaluate donor group influences on the degree of complex aggregation and on the coordination geometry. In contrast to the class **IV** triply-bridged structure of the propane-1,3-dithiolate complex $[Mo_2O_2(OCH_3)(SCH_2CH_2CH_2S)_3]^-$, the 2-mercaptoacetate complex $[Mo_2O_2(SCH_2CO_2)_4]^{2-}$ was found to display a $[Mo_2O_2(SCH_2CO_2)_2]^{2+}$ core with the unique features of a planar $[Mo_2S_2]$ bridge, with an *anti* disposition of the terminal oxo groups and an unusually long Mo···Mo distance. Structure **V** illustrates the structural framework for this class of binuclear complexes.

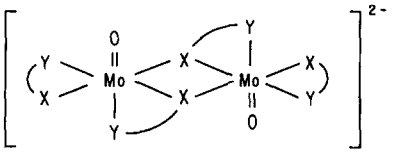

(V) XY = $^-SCH_2CO_2^-$

RESULTS AND DISCUSSION

Synthesis and spectroscopic properties

Under the synthetic conditions of a large excess of thiolate and mononuclear oxomolybdate precursors,[1,17] reactions of thiols with molybdenum(VI) yield a class of dark blue–green mononuclear molybdenum(V) complexes of the general formulation $[MoO(SR)_4]^-$:

$$[MoO_2(CH_3CHOHCHOMe)_2] \cdot 2CH_3CHOHCHOHMe + 5HSR \rightarrow [MoO(SR)_4]^- + 1/2RSSR + 4CH_3CHOHCHOHMe + H_2O + R_3NH^+.$$

Similarly, reactions of polyoxomolybdates with an excess of thiolate ligand yield mononuclear or binuclear oxomolybdate(V) complexes of classes **I** and **III**, respectively.[17]

$$[Mo_8O_{26}]^{4-} + 40HSR \rightarrow 8[MoO(SR)_4]^- + 4RSSR + 18H_2O + 4R_3NH^+$$

$$[Mo_8O_{26}]^{4-} + 24HSR \rightarrow 4[Mo_2O_4(SR)_4]^{2-} + 4RSSR + 10H_2O + 4R_3NH^+.$$

However, modifications in the nature of the molybdate precursor, in counter ions and solvents have been shown to have profound consequences on the products isolated in reactions of molybdates with thiolate ligands. Thus, $[Mo_8O_{26}]^{4-}$ reacts with 2-mercaptoethanol as the limiting reagent to yield $[Mo_{10}O_{28}(SCH_2CH_2O)_2(HOCH_3)_2]^{4-}$,[16] rather than the class **IV** dimers which constitute the major products under conventional reaction conditions.

While reaction of $[MoO_2(acac)_2]$ with excess propane-1,3-dithiol yields $[MoO(SCH_2CH_2CH_2S)_2]^-$, complex **1**, $[Mo_2O_2(OCH_3)(SCH_2CH_2CH_2S)_3]^-$, may be synthesized directly from the reaction of $[Mo_2O_7]^{2-}$ with the dithiol in methanol solution. Under appropriate reaction conditions, class **I** mononuclear species have been demonstrated to be unstable with respect to class **IV** binuclear complexes,[13] such that treatment of $[MoO(SR)_4]^-$ with a source of methoxy, amido or azido ligands yields triply-bridged analogues of type **IV**. The reaction conditions employed in the preparation of **1** favour the incorporation of the methoxy group and hence the triply-bridged geometry.

The IR spectrum of **1** exhibits features at 2958 and 1062 cm^{-1} associated with ν(C—H) and ν(C—O) for the coordinated methoxy group. The intense band at 930 cm^{-1} is characteristic for ν(Mo—O_t), while the 460 and 370 cm^{-1} bands are presumably due to the [Mo(μ-S thiolate)$_2$(μ-OCH_3)Mo] bridge.[7]

Since modification of donor groups may dramatically affect the coordination geometry of oxomolybdenum thiolate complexes, the reaction of $[Mo_8O_{26}]^{4-}$ with 2-mercaptoacetic acid was investigated. The cherry-red diamagnetic product of the reaction analysed for $[(C_2H_5)_3NH][MoO(SCH_2CO_2)_2]$, and a subsequent X-ray structural

study confirmed the binuclear structure $[(C_2H_5)_3NH]_2[Mo_2O_2(SCH_2CO_2)_4]$ (**2**).

The IR spectrum of **2** displays two strong bands at 1670 and 1610 cm^{-1} assigned to ν(C=O) of the ligand and bands in the 920–950 cm^{-1} region characteristic of ν(Mo=O_t). No bands attributable to bridging oxo groups or to a triply-bridged geometry were observed, leading to the conclusion that the coordination geometry of **2** must be unusual.

The ^1H NMR spectrum of **2** revealed two AB four-line multiplets associated with the methylene groups of the 2-mercaptoacetate ligands, indicating the presence of two distinct ligand environments. Furthermore, within each methylene unit, the protons are inequivalent to give rise to the observed AB patterns.

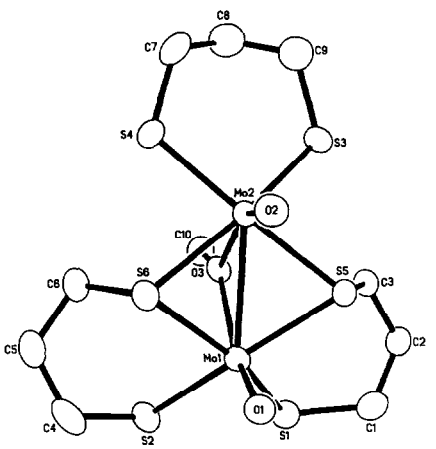

Fig. 1. ORTEP view of the structure of $[Mo_2O_2(OCH_3)(SCH_2CH_2CH_2S)_3]^-$, showing the atom-labelling scheme.

Structural studies

As shown in Fig. 1, the structure of the anion of **1** consists of discrete binuclear species $[Mo_2O_2(OCH_3)(SCH_2CH_2CH_2S)_3]^-$ with two non-equivalent pseudooctahedral molybdenum atoms sharing a face defined by two bridging thiolate sulphur donors and the oxygen atom of the bridging methoxy group. The unusual asymmetry in the molybdenum geometries is imposed by the odd number of dithiolate ligands, Mo(1) being ligated by two dithiolates which also provide bridging sulphurs for Mo(2), which is additionally ligated by a chelating but non-bridging dithiolate. The structure is essentially identical to that of $[Mo_2O_2(N_3)(SCH_2CH_2CH_2S)_3]^-$ [17] with the azido bridge replaced by the methoxy group of **1**. The $[Mo_2O_2(SCH_2CH_2CH_2S)_3]^0$ core has an analogy in Tc chemistry, the neutral $[Tc_2O_2(SCH_2CH_2S)_3]$, which may be described as two Tc square pyramids sharing a common edge defined by sulphur donors from two ethanedithiolate ligands.[18] A significant structural difference is the long Tc···Tc distance of 3.654(1) Å, which is consistent with the absence of a direct metal–metal interaction. The presence of the bridging methoxy group in **1** leads to the description of the structure in terms of two confacial octahedra, with a short Mo···Mo distance common to molybdenum(V) binuclear complexes (Table 1). The structural parameters of the bridge are very similar to those of other class **IV** complexes, which have been discussed in detail in several recent publications.[6,7] A comparison of the bridge parameters of **1** to those of selected class **IV** complexes is presented in Table 2. The non-equivalence of the molybdenum geometries is reflected in the unsym-

Table 1. Selected bond lengths (Å) and angles (°) for $[(n\text{-}C_4H_9)_4N][Mo_2O_2(OCH_3)(SCH_2CH_2CH_2S)_3]$ (**1**)

Mo(1)—Mo(2)	2.875(1)	Mo(2)—O(2)	1.699(6)
Mo(1)—O(1)	1.704(7)	Mo(2)—O(3)	2.134(6)
Mo(1)—O(1)	2.155(7)	Mo(2)—S(3)	2.390(2)
Mo(1)—S(1)	2.419(3)	Mo(2)—S(4)	2.406(3)
Mo(1)—S(2)	2.433(3)	Mo(2)—S(5)	2.514(3)
Mo(1)—S(5)	2.452(3)	Mo(2)—S(6)	2.516(3)
Mo(1)—S(6)	2.476(3)		
S(1)—Mo(1)—S(5)	87.0(1)	S(3)—Mo(2)—S(4)	91.3(1)
S(2)—Mo(1)—S(6)	86.4(1)	S(3)—Mo(2)—S(5)	80.1(1)
O(1)—Mo(1)—O(3)	155.0(3)	S(4)—Mo(2)—S(6)	81.4(1)
S(1)—Mo(1)—S(6)	159.0(1)	O(2)—Mo(2)—O(3)	150.0(3)
S(2)—Mo(1)—S(5)	158.2(1)	S(3)—Mo(2)—S(6)	166.3(1)
Mo(1)—O(3)—Mo(2)	84.4(1)	S(4)—Mo(2)—S(6)	166.3(1)
Mo(1)—S(6)—Mo(2)	70.3(1)		
Mo(1)—S(5)—Mo(2)	70.7(1)		

Table 2. Comparison of selected parameters for triply-bridged binuclear complexes of molybdenum[a]

Complex	Mo—Mo	Mo—Y[b]	Mo—Y′	Mo—Z	Mo—Y—Mo	Mo—Y′—Mo	Mo—Z—Mo	Reference
$[Mo_2O_2(OMe)(SC_6H_4Me)_6]^-$	2.919(5)	2.47(2)[SR]	2.47(2)[SR]	2.11(2)[OR]	72.6(5)	72.6(5)	87.6(6)	7
$[Mo_2O_3(SCH_2CH_2O)_3]^{2-}$	2.676(1)	1.957(12)[O^{2-}]	2.506(16)[SR]	2.215(15)[OR]	86.3(2)	64.5(1)	74.3(2)	10
$[Mo_2O_2(SPh)_2Cl(SCNR_2)_2]^+$	2.677(5)	2.045(31)[O^{2-}]	2.491(7)[SR]	2.688(11)[SR]	81.8(16)	65.0(5)	59.7(9)	12
$[Mo_2O_2Cl_5(SPh)_2]^-$	2.195(1)	2.445(3)[SR]	2.449(3)[SR]	2.651(3)[Cl]	73.2(1)	73.0(1)	67.7(1)	14
$[Mo_2O_2(N_3)(SCH_2CH_2CH_2S)_3]^-$	2.893(3)	2.473(8)[SR]	2.472(8)[SR]	2.21(2)[N]	71.6(2)	71.6(2)	81.6(6)	17
$[Mo_2O_2(OCH_3)(SCH_2CH_2CH_2S)_3]^-$	2.875(1)	2.452(3)[SR]	2.476(3)[SR]	2.145(10)[OR]	70.7(1)	70.3(1)	84.4(1)	This work
		2.514(3)[SR]	2.516(3)[SR]					

[a] Bond lengths (Å); bond angles (°).
[b] Y, Y′ and Z identified in brackets.

metrical Mo—S bridge distances, 2.464(6) Å (av.) for Mo(1)—S_b and 2.515 Å (av.) for Mo(2)—S_b.

The structure of the molecular anion of **2** is shown in Fig. 2 and seen to consist of discrete binuclear units $[Mo_2O_2(SCH_2CO_2)_4]^{2-}$ with a crystallographic centre of symmetry at the midpoint of the Mo(1)—Mo(1a) vector, relating the unique halves of the binuclear complex. The overall geometry may be described as two molybdenum octahedra sharing an edge defined by the S(1)—S(1a) vector. As suggested by the ^1H NMR studies, the 2-mercaptoacetate ligands assume two distinct coordination modes: terminal chelating through S(2) and O(4), and bridge chelating with S(1) bridging the molybdenum centres and O(1) ligated to a single molybdenum site.

The *trans* influence of the oxo group is reflected in the long Mo—O(1) bond distance of 2.145(4) Å, compared to the more normal Mo—O(4) distance of 2.052(4) Å and in the displacement of the molybdenum atom from the S(1)—S(1a)—O(1)—S(2) plane by 0.24 Å in the direction of the terminal oxo group O(3). The terminally chelating 2-mercaptoacetate group S(2)—C(3)—C(4)[O(5)]—O(4) is planar, with unexceptional bonding parameters reflected in the short C(4)—O(5) distance, relative to C(4)—O(4), indicating localization of multiple bond character in the C(4)—O(5) unit. The ligand bite distance S(4)···O(4) of 2.902(4) Å is characteristic for five-membered rings of this type. In contrast, the bridging 2-mercaptoacetate ligand is distinctly non-planar, with S(1a) *ca* 0.44 Å out of the C(2a)—C(1)—O(2)—O(1) plane. Furthermore, the S(1a)···O(1) bite distance has expanded to 3.235(4) Å. The distortions of the chelate geometry are attributed to the geometric constraints imposed on the ligand, as a consequence of spanning bridge and

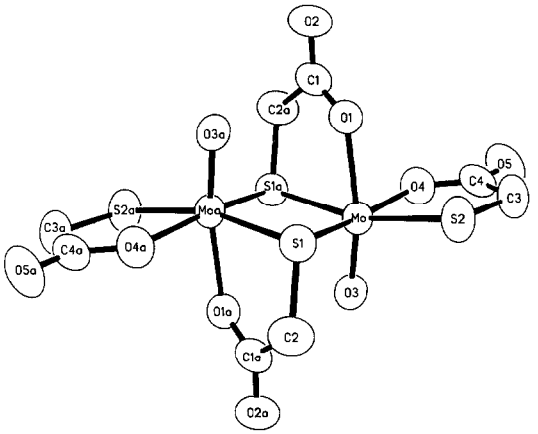

Fig. 2. Perspective view of the structure of $[Mo_2O_2(SCH_2CO_2)_4]^{2-}$, showing the atom-labelling scheme.

terminal coordination sites of the molybdenum centres.

The bridge geometry is characterized by crystallographically imposed planarity of the Mo_2S_2 rhombus and an *anti* orientation of the oxo groups. The Mo(1)—Mo(1a) distance of 3.078 Å is extremely unusual in view of the range of 2.65–2.95 Å generally observed for binuclear molybdenum(V) complexes of types **III** and **IV**. The long Mo—Mo distance implies the absence of a direct metal–metal interaction in **2**, suggesting that the observed diamagnetism of the complex is a consequence of effective antiferromagnetic coupling of the molybdenum(V) d^1 sites through the $[Mo_2S_2]$ bridge, in a fashion similar to that observed for class **II** $[Mo_2O_3]^{4+}$ bridged binuclear systems.

The "*trans* planar" geometry of the $[Mo_2O_2S_2]$ core is grossly analogous to the di-μ-sulphido bridged core of $[(\eta^5\text{-}C_5H_5)_2Mo_2O_2S_2]$[19] with certain significant differences. Whereas the structure of $[(\eta^5\text{-}C_5H_5)_2Mo_2O_2S_2]$ consists of edge-sharing tetragonal pyramids, the structure of **2** is characterized by edge-sharing octahedra. Furthermore, *anti* fusion of the basal edges of two tetragonal pyramids results in Mo–oxo vectors displaced away from the Mo_2S_2 rhombus, characterized by Mo—Mo—O angles greater than 90°.[20] In contrast, the Mo–oxo vectors of **2** are displaced towards the Mo_2S_2 rhombus, with an Mo—Mo—O angle of 78.1° and a O(1)···O(3a) distance of 2.77 Å which is well within the sum of van der Waals radii (Table 3).

Although, for binuclear complexes of type **III** and the related di-μ-sulphido bridged complexes, the *syn* conformer is predicted to be more stable[21] and is indeed most often observed,[22–26] we have no evidence for the existence of a *syn* conformer for **2**. To our knowledge, the geometry described for **2** is unique for binuclear molybdenum(V) complexes, representing a new class of bridged binuclear molybdenum(V) species.

EXPERIMENTAL

Materials and methods

All reactions were performed in freshly dried and distilled solvents. Dichloromethane was technical grade and was redistilled from $CaCl_2$ and P_4O_{10}. All other solvents were reagent grade, and were obtained from standard commercial sources without further purification. $[(n\text{-}C_4H_9)_4N]_2[Mo_2O_7]$ was prepared according to the published method.[27]

The following instruments were used in this work: IR, Perkin–Elmer 283B IR spectrophotometer; ^{1}H NMR, Bruker T-90 spectrometer; UV–vis spectra, Varian DMS 90 UV-Visible spectrophotometer; X-ray crystallography, Nicolet R3m/V diffractometer.

Preparation of compounds

$[(n\text{-}C_4H_9)_4N][Mo_2O_2(OCH_3)(SCH_2CH_2CH_2S)_3]$ (**1**). $[(n\text{-}C_4H_9)_4N][Mo_2O_7]$ (3.10 g, 5.7 mmol) was dissolved in methanol (30 cm^3) and added to a stirred solution of $HSCH_2CH_2CH_2SH$ (2.2 g, 20.3 mmol) in methanol (20 cm^3). After refluxing for 24 h at 50–60°C, the resultant red solution was filtered and concentrated to 15 cm^3. Upon addition of 20 cm^3 of anhydrous ether and standing at room temperature for 7 days, dark red crystals of **1** appeared

Table 3. Selected bond lengths (Å) and angles (°) for $[(C_2H_5)_3NH]_2[Mo_2O_2(SCH_2CO_2)_4]$ (**2**)

Mo—Mo(a)	3.078(1)	Mo—O(1)	2.145(4)
Mo—S(1)	2.471(1)	Mo—O(3)	1.676(4)
Mo—S(2)	2.374(2)	Mo—O(4)	2.052(4)
Mo—S(1a)	2.490(1)		
S(2)···O(4)	2.902(4)	C(1)—O(2)	1.244(7)
S(1a)···O(1)	3.235(4)	C(1)—O(2)	1.227(7)
		C(1)—C(2a)	1.536(11)
		C(4)—O(4)	1.297(8)
		C(4)—O(5)	1.221(8)
		C(3)—C(4)	1.476(11)
O(1)—Mo—O(3)	164.3(2)	Mo—S(1)—C(2)	103.3(6)
S(2)—Mo—O(4)	81.6(1)	Mo—S(2)—C(3)	99.0(6)
S(1)—Mo—O(4)	163.4(1)		
S(1)—Mo—S(1a)	103.3(1)		
S(2)—Mo—S(1a)	164.7(1)		
Mo—S(1)—Mo(a)	76.7(1)		

Table 4. Summary of experimental details for the X-ray diffraction studies of $[(n\text{-}C_4H_{94}N][Mo_2O_2(OCH_3)(SCH_2CH_2CH_2S)_3]$ (1) and $[(C_2H_5)_3NH]_2[Mo_2O_2(SCH_2CO_2)_4]$ (2)

Crystal parameters at 296 K[a]	1	2
a (Å)	9.310(2)	10.861(4)
b (Å)	11.328(2)	13.559(4)
c (Å)	19.954(3)	11.011(4)
α (°)	74.93(1)	90.0
β (°)	78.19(1)	104.14(2)
γ (°)	81.53(1)	90.0
V (Å^3)	1979.2(10)	1572.1(11)
Space group	$P\bar{1}$	$P2_1/n$
Z	2	2
ρ_{calc} (g cm^{-3})	1.369	1.664
Number of reflections collected:	5292 ($\pm h, \pm k, +l$)	2752 ($\pm h, +k, +l$)
Number of reflections used in solution:[b-d]		
$F_0 > 6\sigma(F_0)$:	3108	2133
Final discrepancy factor[e]		
R	0.056	0.057
R_w	0.059	0.062
Goodness-of-fit[f]	1.432	1.783

[a] From a least-squares fitting of the setting angle of 25 reflections.

[b] All calculations were performed on a Data General Nova 3 computer with 32K of 16-bit words using local versions of the Nicolet SHELTEX interactive crystallographic software package as described in G. M. Sheldrick, *Nicolet SHELTEX Operations Manual*. Nicolet XRD Corporation, Cupertino, California (1979).

[c] D. T. Cromer and J. B. Mann, *Acta Cryst.* 1968, **A24**, 321.

[d] *International Tables for X-ray crystallography*, Vol. III. Kynoch Press, Birmingham (1962).

[e] $R = \Sigma[|F_0| - |F_c|/\Sigma|F_0|]$

$R_w = [\Sigma w(|F_0| - |F_c|)^2/\Sigma w|F_0|^2]^{1/2}$

$w = 1/\delta^2(F_0) + g^*(F_0), g = 0.005.$

[f] Goodness - of - fit $= [\Sigma w(|F_0| - |F_c|)^2/(NO - NV)]^{1/2}$ where NO is the number of observations and NV is the number of variables.

on the walls of the flask (15% yield). Found: C, 37.9; H, 6.72; N, 1.83. Calc. for $C_{26}H_{57}Mo_2NO_3S_6$: C, 38.3; H, 7.00; N, 1.72%. IR (KBr pellet, cm^{-1}): 2958(m), 1463(m), 1452(w), 1296(m), 1264(m), 1062(s), 930(vs), 801(w), 645(m), 665(m), 460(s), 370(m), 322(m).

* Supplementary materials available. Fractional coordinates have been deposited with the Director, Cambridge Crystallographic Centre. Complete listings of bond distances and angles are available from the Editor, Queen Mary College, London.

$[(C_2H_5)_3NH]_2[Mo_2O_2(SCH_2CO_2)_4]$ (2). A mixture of 2-mercaptoacetic acid (4.60 g, 50 mmol) and triethylamine (10.1 g, 100 mmol) was added dropwise with stirring to a solution of $[(n\text{-}C_4H_9)_4N]_4[Mo_8O_{26}]$ (6.45 g, 3 mmol) in methanol (30 cm^3). After overnight stirring, the resultant orange solution was concentrated to 5 cm^3 and layered with 30 cm^3 of diethyl ether. Upon standing for 2 weeks, orange–red crystals deposited in 10–15% yield. Found: C, 30.5; H, 5.24; N, 3.46. Calc. for $C_{20}H_{40}N_2MoO_{10}S_4$: C, 30.5; H, 5.08; N, 3.55%. IR (KBr, cm^{-1}): 1670(s), 1610(s), 1348(m), 1253(s), 950(s), 932(m), 920(s), 375(n). UV–vis [CH_2Cl_2, λ_{max}, nm (ε, cm^{-1} M^{-1})]: 372 (1.2×10^3), 299 (4.8×10^2), 231 (2.7×10^3), 222 (2.56×10^3). ^{1}H NMR (300 MHz, D_2O): δ 1.27 (triplet, $J = 7.3$ Hz), 3.19 (quartet, $J = 7.3$ Hz), 3.67 (doublet, $J = 25$ Hz), 3.80 (d, $J = 25$ Hz), 3.96 (d, $J = 11$ Hz), 4.41 (d, $J = 11$ Hz).

X-ray crystallography

The details of the crystal data, data collection methods and refinement procedures are given in Table 4. (Supplementary Tables S.1 and S.7 provide atomic positional parameters for the structures reported. Tables of bond lengths and angles, anisotropic thermal parameters and calculated and observed structure factors for all complexes are available.)* Full details of the crystallographic methodologies may be found in ref. 28.

In no instance was an extinction correction applied for the data. Idealized hydrogen atom positions were used throughout the analyses, with the C—H and N—H distances set at 0.96 and 0.94 Å, respectively.

Acknowledgement—This research was supported by a grant from the National Science Foundation (CHE8514634).

REFERENCES

1. I. W. Boyd, I. G. Dance, K. S. Murray and A. G. Wedd, *Aust. J. Chem.* 1978, **31**, 279.
2. I. G. Dance, A. G. Wedd and I. W. Boyd, *Aust. J. Chem.* 1978, **31**, 519.
3. J. R. Bradbury, M. F. Mackay and A. G. Wedd, *Aust. J. Chem.* 1978, **31**, 2423.
4. E. I. Stiefel, *Prog. Inorg. Chem.* 1977, **22**, 1.
5. B. Spivack and Z. Dori, *Coord. Chem. Rev.* 1975, **17**, 99.
6. T.-C. Hsieh, T. Nicholson and J. Zubieta, *Inorg. Chem.* 1988, **27**, 241.
7. I. Buchanan, W. Clegg, C. D. Garner and G. M. Sheldrick, *Inorg. Chem.* 1983, **22**, 3657.
8. J. T. Huneke, K. Yamanouchi and J. H. Enemark, *Inorg. Chem.* 1978, **17**, 3695.

9. J. I. Gelder, J. H. Enemark, G. Wolterman, D. A. Boston and G. P. Haight, *J. Am. Chem. Soc.* 1975, **97**, 1616.
10. I. G. Dance and E. E. Landers, *Inorg. Chem.* 1979, **18**, 3487.
11. K. Yamanouchi, J. H. Enemark, J. W. McDonald and W. E. Newton, *J. Am. Chem. Soc.* 1977, **99**, 3529.
12. G. Bunzey, J. H. Enemark, J. I. Gelder, K. Yamanouchi and W. E. Newton, *J. Less-common Met.* 1977, **54**, 101.
13. I. W. Boyd, I. G. Dance, A. E. Landers and A. G. Wedd, *Inorg. Chem.* 1979, **18**, 1875.
14. J. R. Dilworth, B. D. Neaves, P. Dahlstrom, J. Hyde and J. Zubieta, *Transition Met. Chem.* (*Weinheim, Ger.*) 1982, **7**, 257.
15. G. R. Hanson, A. A. Brunnetti, A. C. McDonnell, K. S. Murray and A. G. Wedd, *J. Am. Chem. Soc.* 1981, **103**, 1953; J. R. Bradbury, A. F. Masters, A. C. McDonnell, A. A. Brunnetti, A. M. Bond and A. G. Wedd, *J. Am. Chem. Soc.* 1981, **103**, 1959; V. D. Patel, P. M. Boorman, K. A. Kerr and K. J. Moynihan, *Inorg. Chem.* 1982, **21**, 1385; J. M. Ball, P. M. Boorman, K. J. Moynihan and J. R. Richardson, *Acta Cryst.* 1985, **C41**, 47.
16. S. Liu, X. Sun and J. Zubieta, *J. Am. Chem. Soc.* 1988, **110**, 3324.
17. P. T. Bishop, J. R. Dilworth, J. Hutchinson and J. A. Zubieta, *J. Chem. Soc., Chem. Commun.* 1982, 1052.
18. A. Davison, B. V. DePamphilis, R. Faggiani, A. G. Jones, C. L. J. Locke and C. Orvig, *Can. J. Chem.* 1985, **63**, 319.
19. D. L. Stevenson and L. F. Dahl, *J. Am. Chem. Soc.* 1987, **89**, 3712.
20. G. Bunzey and J. H. Enemark, *Inorg. Chem.* 1978, **17**, 682.
21. T. Chandler, D. L. Lichtenberger and J. H. Enemark, *Inorg. Chem.* 1981, **20**, 75.
22. B. Spivack, Z. Dori and E. I. Stiefel, *Inorg. Nucl. Chem. Lett.* 1975, **11**, 501.
23. M. G. B. Drew and A. Kay, *J. Chem. Soc. A.* 1971, 1851.
24. D. H. Brown and J. A. B. Jeffreys, *J. Chem. Soc., Dalton Trans.* 1973, 732.
25. B. Spivack, A. P. Gaughan and Z. Dori, *J. Am. Chem. Soc.* 1971, **93**, 5265.
26. B. Spivack and Z. Dori, *J. Chem. Soc., Dalton Trans.* 1973, 1173.
27. V. W. Day, M. F. Fredrich, W. G. Klemperer and W. Shum, *J. Am. Chem. Soc.* 1977, **99**, 6146.
28. A. Bruce, J. L. Corbin, P. L. Dahlstrom, J. R. Hyde, M. Minelli, E. I. Stiefel, J. T. Spence and J. Zubieta, *Inorg. Chem.* 1982, **21**, 917.

Polyhedron Vol. 8, No. 5, pp. 677–688, 1989
Printed in Great Britain

0277–5387/89 $3.00+.00
© 1989 Pergamon Press plc

CHEMICAL AND X-RAY STRUCTURAL CHARACTERIZATION OF DIPHENYLCARBAZONE AND DIPHENYLTHIOCARBAZONE COMPLEXES OF MOLYBDENUM(VI), (n-Bu_4N)[$MoO_2(C_6H_5NNC(X)NNC_6H_5)(C_6H_5NNC(X)NN(H)C_6H_5)$] (X = O OR S) AND ($n$-$Bu_4N$)[$MoOCl_3(C_6H_5NNC(O)NNC_6H_5)$]; ISOLATION OF 2,3-DIPHENYLTETRAZOLIUM-5-THIOLATE, $C_6H_5NNC(S)NNC_6H_5$, FROM THE REACTION OF DIPHENYLTHIOCARBAZONE WITH MOLYBDATE

SHUNCHENG LIU and JON ZUBIETA*

Department of Chemistry, State University of New York at Albany, Albany, NY 12222, U.S.A.

(*Received* 1 *August* 1988; *accepted* 5 *October* 1988)

Abstract—Reaction of α-$(Bu_4N)_4[Mo_8O_{26}]$ with diphenylcarbazone ($dpcH_2$) yields the red crystalline complex $(Bu_4N)[MoO_2(C_6H_5NNC(O)NNC_6H_5)(C_6H_5(H)NNC(O)NNC_6H_5)]$ (**I**), a complex displaying two distinct chelate ring types. Treatment of **I** with HCl yields $(Bu_4N)[MoOCl_3(C_6H_5NNC(O)NNC_6H_5)]$ (**III**), a pseudo-octahedral complex with the $[MoOCl_3]^+$ core. The reaction of α-$(Bu_4N)_4[Mo_8O_{26}]$ with diphenylcarbazone ($dptcH_2$) gave a complex analogous to **I**, $(Bu_4N)[MoO_2(C_6H_5NNC(S)NNC_6H_5)(C_6H_5(H)NNC(S)NNC_6H_5)]$ (**II**) and, surprisingly, 2,3-diphenyltetrazolium-5-thiolate, $C_6H_5NNC(S)NNC_6H_5$ (**IV**). Complex **I** displays a pseudo-octahedral geometry with MoO_4N_2 coordination and presents distinct geometries for the chemically inequivalent ligand types $(dpc)^{2-}$ and $(dpcH)^-$. The structure of **II** is analogous to that of **I** with $MoO_2N_2S_2$ coordination geometry but, more significantly, reveals the site of protonation of the $(dptcH)^-$ ligand as the terminal *exocyclic* nitrogen. Crystal data: **I**, monoclinic space group $P2_1/n$, $a = 11.026(3)$, $b = 21.600(5)$, $c = 18.851(4)$ Å, $\beta = 98.04(1)°$, $V = 4445.1(12)$ Å^3, 2804 reflections, $R = 0.065$; **II**, monoclinic space group $P2_1/c$, $a = 12.209(3)$, $b = 20.090(4)$, $c = 19.097(2)$ Å, $\beta = 96.45(1)°$, $V = 4654.4(9)$ Å^3, 3835 reflections, $R = 0.047$; **III**, $P2_1/n$, $a = 14.853(2)$, $b = 15.698(4)$, $c = 17.062(4)$ Å, $\beta = 90.10(1)°$, $V = 3978.2(10)$ Å^3, 3128 reflections, $R = 0.082$; **IV**, $C2/c$, $a = 14.755(2)$, $b = 12.193(2)$, $c = 6.958(2)$ Å, $\beta = 97.42(2)°$, $V = 1241.3(8)$, 1055 reflections, $R = 0.047$.

The current interest in the transition metal chemistry of organohydrazines derives in part from their potential relationship to intermediates in the reduction of coordinated dinitrogen[1] and has been stimulated by the variety of structural types identified for terminally bonded, edge-on bonded and chelating ligand modes, illustrated in Fig. 1.[2–13] In the specific case of the chemistry of organohydrazines with oxomolybdates, a variety of mononuclear[14,15] and polynuclear complexes[16] have been isolated depending upon reaction conditions.

In the course of our investigations of the chemistry of polyoxomolybdates with organonitrogen ligands in non-aqueous solvents, the reactions of α-$(NBu_4)_4[Mo_8O_{26}]$ with diphenylcarbazone and diphenylthiocarbazone have been explored. Although dithizone or diphenylcarbazone, $C_6H_5NNC(O)NHNHC_6H_5$, has long been employed in photometric determinations of molybdenum,[17] the intensely coloured organohydrazidomolybdate complexes which are formed have re-

* Author to whom correspondence should be addressed.

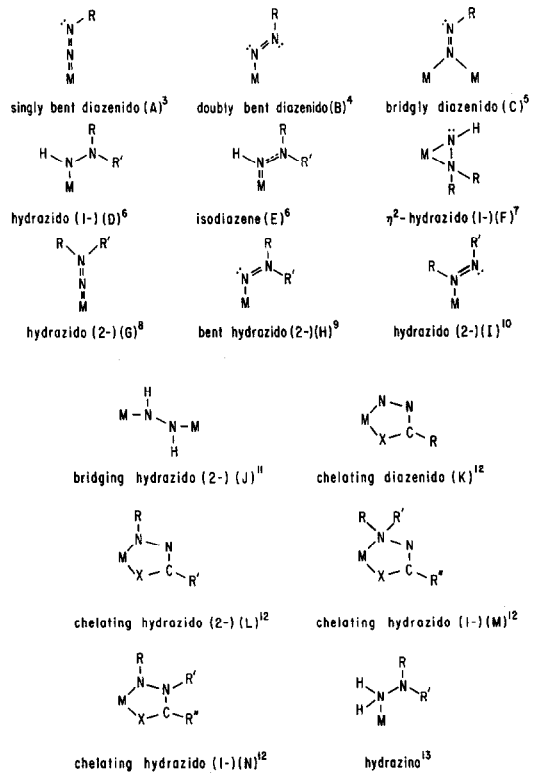

Fig. 1. Schematic representations of various structural types identified for metal–organohydrazine interactions. Superscripts refer to literature references.

mained uncharacterized. Furthermore, organocarbazone ligands represent a type of potentially multidentate and ambidentate ligand capable of a variety of bonding modes.

In this paper we report the structures of the products of the reactions of polyoxomolybdate anions with diphenylcarbazone and diphenylthiocarbazone, $[MoO_2(C_6H_5NNC(X)NNC_6H_5)(C_6H_5(H)NNC(X)NNC_6H_5)]^-$ [X = O (**I**) and X = S (**II**)]. The complexes **I** and **II** provide unique examples of species exhibiting chemically and structurally distinct dithizonate chelate ring types (L) as a consequence of protonation of an exocyclic substituent. Attempts to protonate the coordinated dithizonate ligands yielded a complex exhibiting the $[MoOCl_3]^+$ core, $[MoOCl_3(C_6H_5NNC(O)NNC_6H_5)]^-$ (**III**).

In the course of these investigations, several metal-mediated organic transformations were also observed. Reaction of **I** with organic bases yielded complexes incorporating the *o*-amidophenol ligand, while the unusual organic heterocycle $C_6H_5NNC(S)NNC_6H_5$ (**IV**) was isolated from preparations of **II** and structurally characterized.

RESULTS AND DISCUSSION

Preparations and properties of complexes

Reactions of polyoxomolybdates with simple organohydrazines and certain functionalized organohydrazines capable of chelation to the metal, yield a variety of polyoxomolybdate coordination complexes, displaying tetranuclear or octanuclear cores.[16] On the other hand, under similar reaction conditions benzoylhydrazine and thiobenzoylhydrazine react with polymolybdates to yield only tris-chelate species $[Mo(HNNCSPh)_3]$[12e] or polyoxomolybdate aggregates which do not incorporate the ligand unit. Appropriate modification of the $H_2NN(H)C(X)R$ unit (X = O or S) has been demonstrated to provide ligands capable of reaction with molybdate solutions to yield intensely coloured solutions suitable for spectroanalytical studies.[17] The diphenylcarbazone derivatives $C_6H_5NHNHC(X)NNC_6H_5$ (X = O $dpcH_2$; X = S $dptcH_2$) have been employed extensively in colorimetric studies of molybdenum.

Reaction of a suitable organic solvent soluble polymolybdate, such as $(Bu_4N)_2[Mo_2O_7]$[18] or $(Bu_4N)_4[Mo_8O_{26}]$, with $dpcH_2$ yields exclusively the mononuclear molybdenum(VI) complex $(Bu_4N)[MoO_2(dpcH(dpc)]$ (**I**). The dark purple, diamagnetic complex displays an IR band at 1595 cm^{-1} characteristic of ν(N=N), associated with the uncoordinated (N=NPh) unit of the ligand, and a second band at 1540 cm^{-1} which may be associated with ν(N=N) within the chelate ring. The strong bands at 903 and 872 cm^{-1} are assigned to ν_s and ν_{as} of the *cis*-dioxomolybdate(VI) group, respectively. The sharp medium intensity feature at 3296 cm^{-1}, associated with ν(N—H), confirms that one of the ligands is singly deprotonated $(dpcH)^-$. The appearance of a resonance at 9.82 ppm in the ^1H NMR spectrum of **I** confirms the presence of the protonated $(dpcH)^-$ ligand. Since complex **I** is formally described as a molybdenum(VI) species, the second dithizonate ligand must be present in the doubly deprotonated form $(dpc)^{2-}$, as the chelating hydrazido(2−) type (L). Although complexes **I** and **II** are unique examples of species presenting chemically and structurally distinct dithizonate chelating ligands, formally of type (L), there are a number of examples of complexes exhibiting mixed coordination to both terminally bound hydrazido(2−) and hydrazido(1−) groups of types (D) and (G)[6,8] or to mixed diazenido-hydrazido(2−) chelating ligands of the (K) and (L) structural prototypes.[12]

The electronic spectrum of **I** is characterized by intense ligand centred charge-transfer bands at

225 and 380 nm, and a less intense transition at 535 nm which appears to be associated with the [Mo—N—N] chromophore of molybdenum(VI)–hydrazido complexes.[16] Upon slow addition of HCl to an acetonitrile solution of **I**, the characteristic purple colour of the solution is discharged to yield a bright red solution, from which crystals of $(Bu_4N)[MoOCl_3(dpc)]$ (**III**) deposit upon standing for several days. The stoichiometry of the reaction and the isolation of free ligand as a major product of the reaction are consistent with the protonation of one ligand site and a single oxo group, resulting in displacement of the ligand and H_2O by three chloride donors [see eq. (1)].

$$[MoO_2(dpc)(dpcH)]^{1-}\ (I) + 3HCl \longrightarrow [MoOCl_3(dpc)]^{1-}\ (III) + dpcH_2 + H_2O \quad (1)$$

The visible spectrum of **III** exhibits features similar to those of **I** at 235 and 278 nm, assigned to a ligand based change-transfer process, and at 533 nm assigned to a ligand-to-metal charge-transfer associated with the [Mo—N—N] chromophore. In addition, a new band at 449 nm may be associated with the $[MoOCl_3]^+$ unit; a similar feature appears in the electronic spectrum of $[MoOCl_3(PhNNC(O)Ph)]^-$.[19] The IR spectrum of **III** exhibits bands at 1620 and 965 cm^{-1} which are characteristic of $\nu(N{=}N)$ and $\nu(Mo{=}O)$, respectively.

The oxo groups of **I** are also substitution labile in the common condensation-type reactions, exploited in the synthesis of *cis*-diazenidomolybdenum complexes.[16] Reaction of **I** with a stoichiometric amount of phenylhydrazine in methanol [eq. (2)], yielded a dark purple solution, from which dark prismatic crystals of $(Bu_4N)_2[Mo_4O_6(OCH_3)_2(OC_6H_4NH)_2(NNC_6H_5)_4]$ were isolated in low yield. This tetranuclear complex displays the structural core characteristic of a class of *cis*-bisdiazenidomolybdenum species,[16] and will be discussed in detail in a subsequent article.[20] Although the mechanism of complex formation has not been elucidated, the reaction may proceed through coordination of the terminal hydrazido nitrogen of the diphenylcarbazone ligand to the molybdenum–oxo unit, followed by oxo group attack on the *ortho* position of the phenyl substituent and a 1,3-proton shift, in a manner reminiscent of quinone–methide chemistry [eq. (3)].

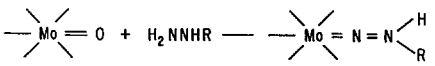

(2)

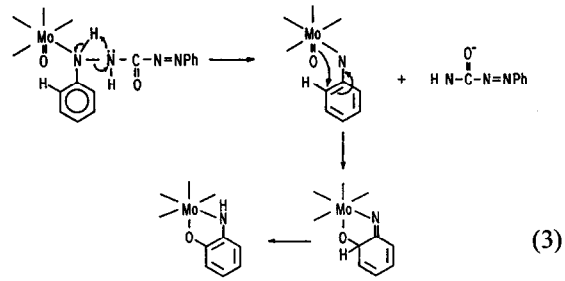

(3)

In contrast to the chemistry observed for $(dpcH_2)$, reaction of $[Mo_8O_{26}]^{4-}$ with diphenylthiocarbazone $(dptcH_2)$ yields a mixture of products, a complex anologous to **I**, $(Bu_4N)[MoO_2(dptc)(dptcH)]$ (**II**), and an organic species identified as 2,3-diphenyltetrazolium-5-thiolate, (Ph)NNC(S)NN(Ph) (**IV**).[21] The isolation of **IV** in high yield suggests that the process may exploit the ambidentate nature of the $(dptcH_2)$ ligand, which can potentially ligate through the nitrogen donors, as illustrated by structure (P) for the $(dptcH)^-$ form of the ligand.[22] Although the cyclization of this form of the ligand appears feasible, the fate of the hydrogen atoms is not obvious, nor are the details of the mechanism of formation.

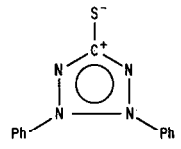

(IV)

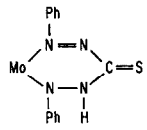

(P)

Complex **II** displays IR bands at 1600 and 1535 cm^{-1} associated with $\nu(N{=}N)$ of the $(dptc)^{2-}$ and $(dptcH)^-$ ligands. The bands assigned to ν_s and ν_{as} for Mo=O of the *cis*-dioxomolybdenum(VI) group are observed at 885 and 860 cm^{-1}, respectively, a shift of *ca* 15 cm^{-1} to lower energy than that observed for **I**. This observation is consistent with the greater π-accepting properties of the sulphur ligated dptc-chelates relative to the oxygen donor dpc groups, and the concomitant increased competition with the oxo groups for the metal t_{2g} type electrons, resulting in a relatively weaker Mo=O interaction. The electronic spectrum of **II** displays features at 259 and 476 nm, assigned to internal ligand charge-transfer and to the [Mo—N—N] chromophore, respectively. The additional band at 604 nm is characteristic of thiohydrazido type chelate complexes of molybdenum[12d,e] and is ten-

tatively assigned to the [Mo—S] chromophore. A broad feature at 9.95 ppm in the ^{1}H NMR spectrum of **II** is assigned to the proton associated with the singly deprotonated $(dptcH)^-$ ligand. The NMR spectrum of **II** is analogous to that of **I** indicating that the species are isostructural in solution.

Attempts to protonate the chelate ligands of **II** or to react **II** in the conventional condensation type reactions, yielded mixtures of intractable materials and uncomplexed molybdates, $[Mo_8O_{26}]^{4-}$ or $[Mo_6O_{19}]^{2-}$.

Description of the structures of (**I**), (**II**), (**III**) *and* (**IV**)

The structure of the complex anion of **I** is illustrated in Fig. 2, and selected bond lengths and angles are presented in Table 1. The structure of **I** consists of discrete mononuclear anions possessing pseudo-octahedral geometry with the oxo groups of the common *cis*-dioxomolybdenum $[MoO_2]^{2+}$ unit and the N and O donors of two chelating diphenylcarbazone derived ligands defining the MoO_4N_2 coordination. An unusual feature of the structure

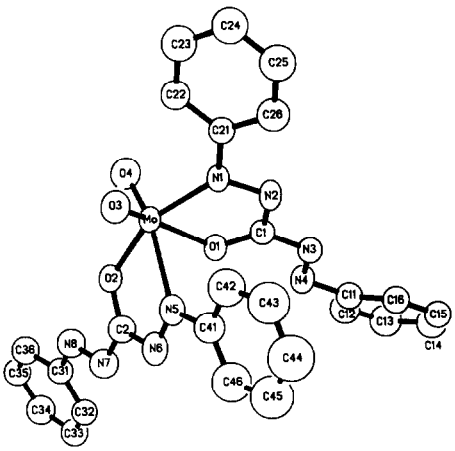

Fig. 2. ORTEP view of the structure of $[MoO_2(dpc)(dpcH)]^-$ (**I**), showing the atom labelling scheme.

is the presence of both $(dpc)^{2-}$ and $(dpcH)^-$ ligands, which necessarily display significantly different bond length and angle parameters, both for the endocyclic [Mo—NNCO] units and the exocyclic [CNNPh] moieties. As illustrated in Fig. 3(a), a comparison of the bonding parameters of the

Table 1. Selected bond lengths (Å) and angles (°) for $(Bu_4N)[MoO_2(dpc)(dpcH)]$ (**I**)

Mo(1)—O(3)	1.704(7)	Mo(1)—O(4)	1.701(7)
Mo—$(dpc)^{2-}$	chelate ring	Mo—$(dpcH)^-$	chelate ring
Mo(1)—N(1)	2.068(8)	Mo(1)—N(5)	2.432(8)
Mo(1)—O(1)	2.059(6)	Mo(1)—O(2)	2.030(8)
O(1)—C(1)	1.308(10)	O(2)—C(2)	1.319(13)
N(1)—N(2)	1.386(10)	N(5)—N(6)	1.285(14)
N(2)—C(1)	1.313(12)	N(6)—C(2)	1.355(14)
N(3)—C(1)	1.386(13)	N(7)—C(2)	1.329(13)
N(3)—N(4)	1.268(14)	N(7)—N(8)	1.345(13)
N(4)—C(11)	1.418(14)	N(8)—C(31)	1.418(13)
O(1)—Mo(1)—O(2)	85.2(3)	O(1)—Mo(1)—O(3)	149.4(3)
O(2)—Mo(1)—O(3)	106.7(3)	O(1)—Mo(1)—O(4)	102.5(2)
O(2)—Mo(1)—O(3)	91.5(3)	O(3)—Mo(1)—O(4)	105.1(3)
O(1)—Mo(1)—N(1)	72.4(3)	O(2)—Mo(1)—N(1)	156.1(3)
O(3)—Mo(1)—N(5)	89.6(2)	O(4)—Mo(1)—N(5)	101.2(3)
O(1)—Mo(1)—N(5)	72.4(2)	O(2)—Mo(1)—N(1)	67.7(3)
O(3)—Mo(1)—N(5)	86.0(3)	O(4)—Mo(1)—N(5)	158.7(3)
N(1)—Mo(1)—N(5)	96.9(3)		
Mo—$(dpc)^{2-}$	chelate ring	Mo—$(dpcH)^-$	chelate ring
M(1)—O(1)—C(1)	117.1(5)	Mo—O(2)—C(2)	122.6(6)
O(1)—C(1)—N(2)	120.9(8)	O(2)—C(2)—N(6)	122.1(9)
C(1)—N(2)—N(1)	108.7(7)	C(2)—N(6)—N(5)	110.5(10)
Mo—N(1)—N(2)	120.1(6)	Mo—N(5)—N(6)	115.2(6)
O(1)—C(1)—N(3)	125.7(8)	O(2)—C(2)—N(7)	121.8(9)
C(1)—N(3)—N(4)	114.1(9)	C(2)—N(7)—N(8)	113.8(9)
N(3)—N(4)—C(11)	111.8(9)	N(7)—N(8)—C(31)	119.4(9)

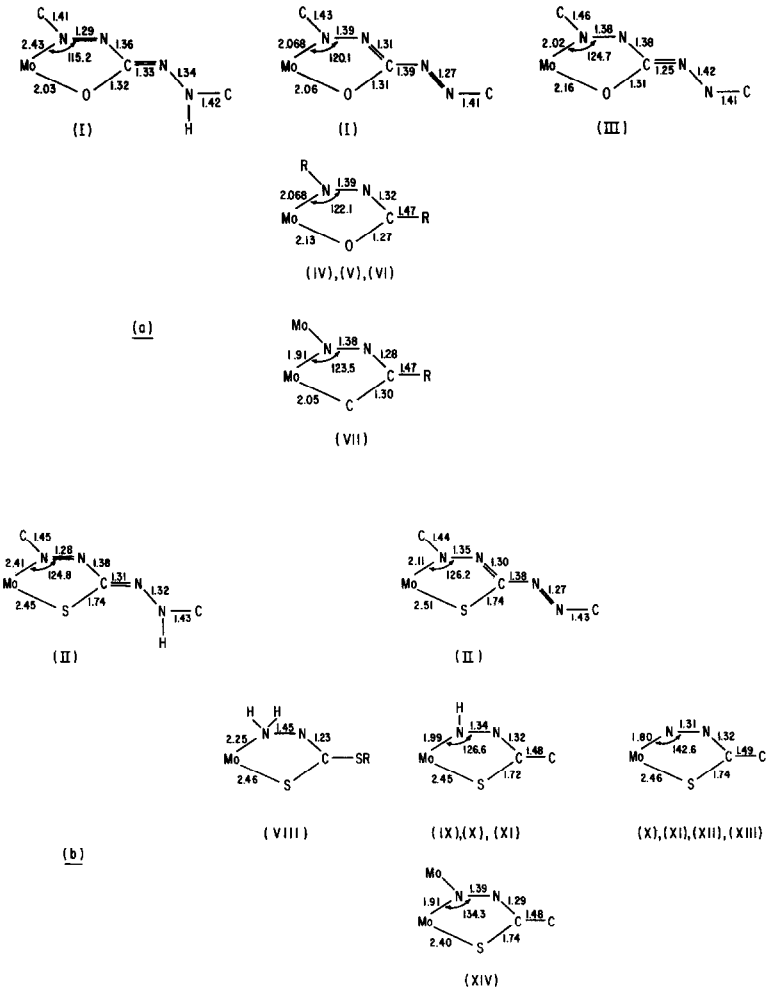

Fig. 3. (a) Schematic representation of the various [MoNNCO] chelate ring types observed for the structures of **I** and **III**, and a comparison with average structural parameters for similar chelates in previously reported structures. **IV**, $[MoCl_3O(ArNNCOPh)]^-$ (ref. 19); **V**, $[MoCl_2(NAr)(ArNNCOPh)]$ (ref. 23); **VI**, $[MoCl(NNCOPh)(HNNCOPh)(PR_3)_2]$ (ref. 24); **VII**, $[MoO(S_2CNEt_2)_2(NNCOPh)_2]$ (ref. 12d). (b) Schematic representation of the two [MoNNNCS] chelate ring types observed for **II** and a comparison with average structural parameters for similar chelate ring types. **VIII**, $[Mo(NNC(S)SEt)(H_2NNC(S)SEt)(S_2CNR_2)]$ (ref. 12e); **IX**, $[Mo(HNNNCSPh)_3]$ (ref. 12a); **X**, [Mo(NNCSAr)(HNNCSAr)(Me_2CNNCSAr)] and **XI**, [Mo(NNCSAr′)(HNNCSAr′)(Me_2CNNCSAr′)] (ref. 12c); **XII**, $[Mo(NNCSPh)(HNNCSPh)(ON(CH_3)CSPh)]$ (ref. 6a); **XIII**, [Mo(NNC(S)SR)(Me_2CNNC(S)SR)(MeSC(S)NNC(S)SMe)] (ref. 25); **XIV**, $[Mo_2O(S_2CNEt_2)_2(NNCSPh)_2]$ (ref. 12d).

[Mo—N(1)N(2)C(1)O(1)] ring with those of previously reported benzoylhydrazido(2−) molybdenum chelates[12] of type (L) establishes a geometry consistent with this assignment. The second chelate moiety [Mo—N(5)N(6)C(2)O(2)] must then be assigned as the singly deprotonated species $(dpcH)^-$, although the site of protonation cannot be assigned unambiguously. The unusually long Mo—N(5) bond distance of 2.432(8) Å results from the *trans* influence of the O(4) oxo group and the significant double bond character of the N(5)—N(6) bond drawing electron density from the Mo—N(5) interaction.

A comparison of the structure of **I** with that of the analogous diphenylthiocarbazone derivative $(Bu_4N)[MoO_2(dptc)]$ **(II)** reveals similar structural trends, illustrated in Fig. 4 and tabulated in Table 2. The bond lengths and angles for the chelated ligands once again confirm the inequivalence of ring geometries due to the presence of both $(dptc)^{2-}$ and $(dptcH)^-$ chelating ligands. The metrical parameters associated with the [Mo—S(2)C(2)N(6)

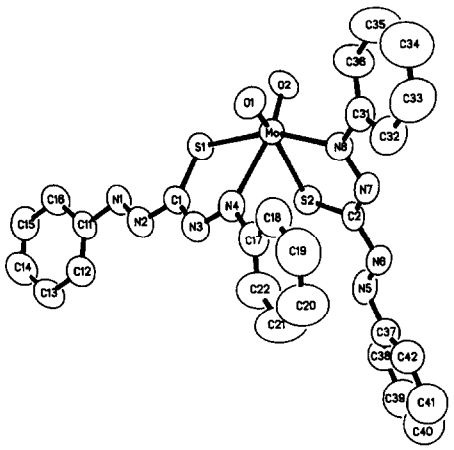

Fig. 4. A view of the structure of $[MoO_2(dptc)(dptcH)]^-$ (II), showing the atom labelling scheme.

N(5)] ring are similar to those observed for [Mo—O(1)C(1)N(2)N(1)] in **I** and conform to structural trends for previously cited examples of thiohydrazido(2−) molybdenum heterocycles,[16] as shown in Fig. 3(b). The second ring [Mo—S(1)C(1)N(2)N(1)] displays a pattern of ligand parameters identical to that observed for [Mo—O(2)C(2)N(6)N(5)] of **I** and associated with the protonated $(dptcH)^-$ ligand type. Furthermore, the low temperature data collected for **II** allowed identification of the protonation site as N(1). It is instructive that examples are available for molybdenum complexes incorporating thiohydrazido(1−), thiohydrazido(2−) and thiohydrazido(3−) chelating ligands, presented schematically in Fig. 3(b). It is clear that the chelate geometry of the [Mo—S(2)C(2)N(6)N(5)] ring of **II** is distinct from that observed for the thiohydrazido(1−) molybdenum chelate of $[Mo(N_2C(S)SC_2H_5)(H_2NNC(S)SC_2H_5)(S_2CNMe_2)]$[12a] which presents a hydrazido(1−) chelate of type (M). The ring parameters allow differentiation of the two chelate types without recourse to location of the protonation site in X-ray studies. It is also evident from the structural analysis of Fig. 3(b) that the chelating hydrazido(1−) and diazenido groups of [Mo(NNCSPh)(HNNCSPh)(ON(CH$_3$)CSPh)][6a] were incorrectly identified in ref. 6a and that the assignments should be exchanged as indicated in

Table 2. Selected bond lengths (Å) and angles (°) for $(Bu_4N)[MoO_2(dptc)(dptcH)]$ (II)

Mo(1)—O(1)	1.719(9)	Mo(1)—O(2)	1.720(9)
Mo—$(dptc)^{2-}$	chelate ring	Mo—$(dptcH)^-$	chelate ring
Mo—S(2)	2.513(1)	Mo—S(1)	2.452(1)
Mo—N(8)	2.108(4)	Mo—N(4)	2.409(5)
S(2)—C(1)	1.740(7)	S(1)—C(1)	1.739(6)
N(7)—N(8)	1.345(7)	N(4)—N(3)	1.284(6)
N(7)—C(2)	1.300(7)	N(3)—C(1)	1.383(7)
N(6)—C(2)	1.380(9)	N(2)—C(1)	1.314(7)
N(6)—N(5)	1.275(7)	N(2)—N(1)	1.319(8)
N(5)—C(37)	1.429(10)	N(1)—C(11)	1.425(7)
S(1)—Mo—S(2)	85.9(1)	S(1)—Mo(1)—N(4)	73.1(1)
S(2)—Mo—N(8)	75.1(1)	S(1)—Mo—N(8)	158.8(1)
S(2)—Mo—N(4)	74.5(1)	N(4)—Mo—N(8)	92.5(2)
S(1)—Mo—O(1)	105.8(1)	S(2)—Mo(1)—O(1)	152.0(2)
N(4)—Mo—O(1)	84.4(2)	N(8)—Mo—O(1)	87.7(2)
S(1)—Mo—O(2)	86.6(1)	S(2)—Mo—O(2)	100.9(1)
N(1)—Mo—O(2)	159.4(2)		
O(1)—Mo—O(2)	105.1(2)		
Mo—$(dptc)^{2-}$	chelate ring	Mo—$(dptcH)^-$	chelate ring
Mo—S(2)—C(2)	97.2(5)	Mo—S(1)—C(1)	103.6(5)
S(2)—C(2)—N(6)	122.1(11)	S(1)—C(1)—N(2)	123.7(11)
C(2)—N(6)—N(5)	115.1(12)	C(1)—N(2)—N(1)	114.7(11)
Mo—N(5)—N(6)	127.6(9)	Mo—N(1)—N(2)	125.5(8)
S(2)—C(2)—N(7)	125.1(12)	S(1)—C(1)—N(3)	124.6(10)
C(2)—N(7)—N(8)	113.3(13)	C(1)—N(3)—N(4)	118.7(11)
N(7)—N(8)—C(41)	110.4(15)	N(3)—N(4)—C(21)	117.3(11)

Fig. 3 to conform to the structural analysis presented herein.

The observation of the protonation site as the exocyclic nitrogen N(1), demonstrates that effects of protonation are transmitted through the ligand π-system to the chelate ring. Thus, the significant bond length differences between the chelate rings associated with $(dptc)^{2-}$ and $(dptcH)^{-}$ are not consequences of protonation of a *chelate* ring nitrogen site, as in (M) or (N) type hydrazido(1−) chelates, but of the exocyclic nitrogen.[26]* The $(dpcH)^{-}$ and $(dptcH)^{-}$ ligands may be considered as derived from the enol form of the singly deprotonated ligand (Q), coordinating through the sulphur and the imido nitrogen, while the doubly deprotonated ligands, $(dpc)^{2-}$ and $(dptc)^{2-}$, conform to structural trends established for hydrazido (2−) chelates. Although extensive delocalization throughout the Ph—N—N—C—N—N—Ph backbones and the chelate rings of both ligand forms is indicated by the bond length and angle data summarized in Fig. 3, valence structure (Q) makes a major contribution to the overall structure of the $(dptcH)^{-}$ ligand, while canonical form (R) is dominant in the structure of $(dptc)^{2-}$. Bond order calculations, based upon Pauling's method[27] and corrected for hybridization,[28] yield the approximate bond characters shown below. Although many factors influence bond lengths, making bond order–bond length relationships difficult to quantify, the general trends are apparent.

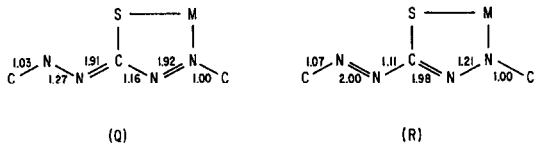

(Q) (R)

The structure of the molecular anion of $(Bu_4N)[MoOCl_3(dpc)]$ (**III**) is shown in Fig. 5 and selected bond lengths and angles are tabulated in Table 3. The pseudo-octahedral coordination geometry about the molybdenum atom is defined by the three chloride donors, the oxo group and the O, N donors of the chelating $(dpc)^{2-}$ ligand. The parameters associated with the hydrazido(2−) ligand are similar to those observed for $[MoOCl_3(ClC_6H_4CONNPh)]^{-}$ and consistent with the doubly deprotonated $(dpc)^{2-}$ form of the ligand. Further discussion of the ligand geometry is limited by the lack of precision in parameters.

The structure of the 2,3-diphenyltetrazolium-5-thiolate (**IV**) is shown in Fig. 6. The planarity of the S—C(7)—N(2)—N(1)[C(1)]—N(1a)[C(1a)]—N(2a) grouping is consistent with the aromaticity of the molecule. The short C—N and N—N bond distances within the heterocyclic ring are also indicative of extensive delocalization throughout the ring. The bond parameters tabulated in Table 4 are similar to those observed for analogous heterocyclic structures.[21]

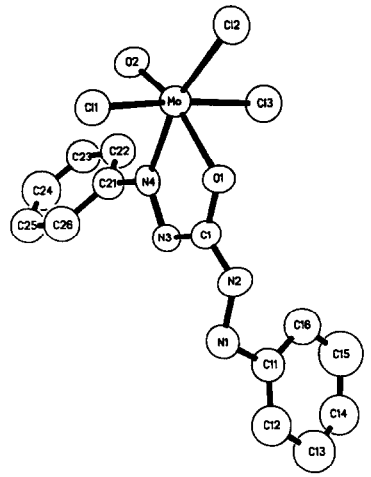

Fig. 5. ORTEP view of the structure of $[MoOCl_3(dpc)]^{-}$ (**III**), showing the atom labelling scheme.

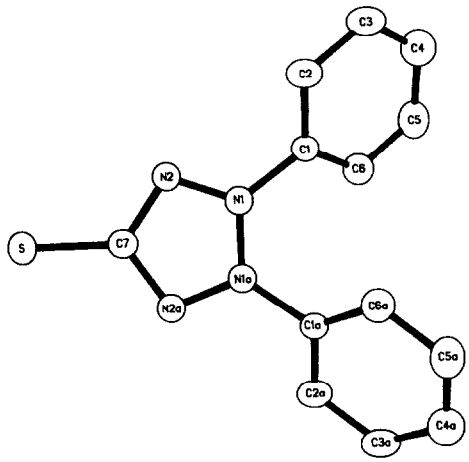

Fig. 6. The structure of $C_6H_5NNC(S)NNC_6H_5$ (**IV**), showing the atom labelling scheme.

CONCLUSIONS

The organohydrazine derivatives, diphenylcarbazone ($dpcH_2$) and diphenylthiocarbazone ($dptcH_2$), react with oxomolybdate(VI) anions in organic solvents to give mononuclear anionic complexes of the type $[MoO_2(PhNNC(X)NNPh)$

*The protonation site had also been established for organomercury(II) dithizonates in ref. 26.

Table 3. Selected bond lengths (Å) and angles (°) for $(Bu_4N)[MoOCl_3(dpc)]$ (**III**)

Mo—C(11)	2.406(5)	Mo—C(13)	2.384(6)
Mo—C(12)	2.404(6)	Mo—O(2)	1.654(11)
Mo—O(1)	2.164(10)	Mo—N(4)	2.024(12)
N(3)—N(4)	1.383(18)	N(3)—C(1)	1.376(21)
O(1)—C(1)	1.305(20)	C(1)—N(2)	1.248(22)
N(1)—N(2)	1.420(20)	N(2)—C(21)	1.457(21)
C(11)—Mo—C(12)	86.3(2)	C(11)—Mo—C(13)	167.4(2)
C(12)—Mo—C(13)	87.1(2)	C(11)—Mo—O(1)	83.6(3)
C(12)—Mo—O(1)	87.7(3)	C(13)—Mo—O(1)	85.4(3)
C(11)—Mo—O(2)	93.9(4)	C(12)—Mo—O(2)	108.4(4)
C(13)—Mo—O(2)	98.4(4)	O(1)—Mo—O(2)	163.5(5)
C(11)—Mo—N(4)	91.3(4)	C(12)—Mo—N(4)	159.1(4)
C(13)—Mo—N(4)	91.1(4)	O(1)—Mo—N(4)	71.4(5)
O(2)—Mo—N(4)	92.4(5)	Mo—O(1)—C(1)	116.6(10)
Mo—N(4)—N(3)	124.7(9)	N(4)—N(3)—C(1)	108.2(12)
N(3)—C(1)—O(1)	119.0(14)	N(3)—C(1)—N(2)	120.8(15)
C(1)—N(2)—N(1)	123.1(15)	N(2)—N(1)—C(11)	115.9(14)

Table 4. Selected bond lengths (Å) and angles (°) for $[C_{13}H_{10}N_4S]$ (**IV**)

S—C(7)	1.692(4)	C(7)—N(2)	1.368(3)
N(2)—N(1)	1.316(3)	N(1)—N(1a)	1.328(4)
N(1)—C(1)	1.440(4)		
S—C(7)—N(2)	125.0(2)	C(7)—N(2)—N(1)	104.7(2)
N(2)—N(1)—N(1a)	110.3(1)	N(2)—N(1)—C(1)	122.8(2)
C(1)—N(1)—N(1a)	126.6(1)		

$(Ph(H)NNC(X)NNPh)]^-$, X = O (**I**) or S (**II**). The intensely coloured complexes **I** and **II** are unusual in that each presents two structurally distinct dithizonate chelate rings, based on the chelating hydrazido (L) geometric prototype. Detailed structural studies and comparisons with previously reported examples of organohydrazidomolybdenum(VI) chelate structures reveal systematic geometric patterns associated with the various ligand types and establish that the site of protonation of the $(dpcH)^-$ or $(dptcH)^-$ ligands is the terminal exocyclic nitrogen rather than a ring nitrogen, N_α or N_β. Whereas the distinctive metrical parameters associated with chelating organohydrazine derived ligands of types (K) to (N) are direct consequences of protonation or alkyl substitution of chelate ring nitrogen atoms, N_α or N_β, the geometries associated with the inequivalent chelate types of this study result from transmission through the ligand π-backbone effects of protonation of a substituent group (exocyclic) nitrogen atom.

Whereas **I** undergoes protonation reactions in acid to yield $[MoOCl_3(dpc)]^-$ (**III**) and conventional condensation reactions to give polynuclear species, **II** yields only decomposition products and intractable materials under similar reaction conditions. The isolation of 2,3-diphenyltetrazolium-5-thiolate (**IV**) as a major by-product in the synthesis of **II** suggests that $(dptcH_2)$ may function as a ambidentate ligand coordinating through the terminal nitrogen donors to give (N,N′) hydrazido coordination. However, no examples of (N,N′) organocarbazone coordination were isolated.

EXPERIMENTAL

Materials and methods

All preparations were carried out in freshly distilled, dry solvents, and unless otherwise noted, no precautions to eliminate atmospheric oxygen were taken. Reagent grade solvents were used throughout. $(n\text{-}Bu_4N)_4[Mo_8O_{26}]$ was prepared by the literature method. All other reagents were obtained from standard commercial sources and used without further purification.

The following instruments were used in this

Table 5. Summary of crystal data and experimental details for the X-ray diffraction studies of $(Bu_4N)[MoO_2(dpc)(dpcH)]$ (I), $[Bu_4N][MoO_2(dptc)(dptcH)]$ (II), $(Bu_4N)[MoOCl_3(dpc)]\cdot CH_2Cl_2$ (III) and $C_6H_5NNC(S)NNC_6H_5$ (IV)

	(I)	(II)	(III)	(IV)
Crystal parameters[a]				
T (K)	294	243	294	294
a (Å)	11.026(3)	12.208(3)	14.853(2)	14.755(2)
b (Å)	21.600(5)	20.090(4)	15.698(4)	12.193(2)
c (Å)	18.851(4)	10.097(2)	17.062(4)	6.958(2)
α (°)	90.00	90.00	90.00	90.00
β (°)	98.04(1)	96.45(1)	90.10(2)	97.42(2)
γ (°)	90.00	90.00	90.00	90.00
V (Å^3)	4445.1(12)	4654.4(9)	3978.2(10)	1241.3(8)
Space group	$P2_1/n$	$P2_1/c$	$P2_1/n$	$C2/c$
Z	4	4	4	4
ρ_{calc} (g cm^{-3})	1.27	1.33	1.31	1.35
Measurement of intensity data				
Crystal colour and shape	Dark red prism	Dark brown prism	Purple prism	Orange needle
Crystal dimensions (mm)	0.25 × 0.31 × 0.25	0.25 × 0.24 × 0.19	0.31 × 0.30 × 0.29	0.24 × 0.65 × 0.29
Instrument	Nicolet R3m diffractometer			
Radiation	Mo-K_α (λ = 0.71973 Å)			
Scan mode	Coupled θ (cryst)–2θ (counter)			
Scan rate (° min^{-1})	5–30	2–15	7–30	5–30
Scan range (°)	$2 \leqslant 2\theta \leqslant 45$	$2 \leqslant 2\theta \leqslant 45$	$2 \leqslant 2\theta \leqslant 45$	$2 \leqslant 2\theta \leqslant 65$
Scan length (°)	From 2θ ($K\alpha_1$) − 1.0 to 2θ ($K\alpha_2$) + 1.0			
Background measurement	Stationary crystal, stationary counter, at beginning and end of each 2θ scan, each for the time taken for the scan			
Standards	3 collected every 200 reflections			
Number of reflections collected	6450	7956	5749	2054
Number of reflections used in solution $F_o > 6\sigma(F_o)$	2804	3835	3128	1055
Reduction of intensity data and summary of structure solution and refinement[b]				
Absorption coefficient (cm^{-1})	3.24	3.76	6.21	7.15
Absorption correction	None applied			
T_{max}/T_{min}	1.10	1.05	1.03	1.12
Structure solution	Patterson synthesis yielded the molybdenum position; all remaining non-hydrogen atoms via standard Fourier techniques			Direct methods
Atom scattering factors[c]	Neutral atomic scattering factors were used throughout the analysis			
Anomalous dispersion[d]	Applied to all non-hydrogen atoms			
Final discrepancy factors,[e] R	0.065	0.047	0.082	0.047
R_w	0.068	0.053	0.086	0.047
Goodness-of-fit[f]	1.304	1.689	1.843	1.247

[a] From a least-squares fitting of the setting angle of 25 reflections.

[b] All calculations were performed on a MICROVAX II computer using local versions of the Nicolet SHELXTL interactive crystallographic software package as described in G. M. Sheldrick, *Nicolet SHELXTL Operations Manual.* Nicolet XRD Corporation, Cupertino, California (1979).

[c] D. T. Cromer and J. B. Mann, *Acta Cryst.* 1968, **A24**, 321.

[d] *International Tables for X-ray crystallography*, Vol. III. Kynoch Press, Birmingham, U.K. (1962).

[e] $R = \Sigma[|F_o| - |F_c|/\Sigma|F_o|]$; $R_w = [\Sigma w(|F_o| - F_c|)^2/\Sigma w|F_o|^2]^{1/2}$; $w = 1/\delta^2(F_o) + g^*(F_o)$; $g = 0.002$.

[f] G.O.F. = $[\Sigma w(|F_o| - |F_c|)^2/(NO—NV)]^{1/2}$ where NO is the number of observations and NV is the number of variables.

work: IR, Perkin–Elmer 283B IR spectrophotometer; UV–vis, Varian DMSO90 UV–vis spectrophotometer; electrochemistry, BAS100 electroanalytical system; X-ray crystallography, Nicolet R3m/V diffractometer and the MicroVAX II mounted solution package. Elemental analyses were performed by Desert Analytics, Tucson, Arizona.

Preparation of compounds

$[(n\text{-}C_4H_9)_4N][MoO_2(C_6H_5NNC(O)NNC_6H_5)(C_6H_5(H)NNC(O)NNC_6H_5)]$ (**I**). α-$(Bu_4N)_4[Mo_8O_{26}]$ (2.15 g, 1.0 mmol) was dissolved in 80 cm^3 of warm CH_2Cl_2 and, after cooling to room temperature, diphenylcarbazone (3.8 g, 16.0 mmol) was added. After overnight stirring, followed by concentration to 30 cm^3, the deep red solution was layered with 30 cm^3 of anhydrous ether. After standing for 2 weeks, dark, prismatic crystals were obtained. Filtration followed by ether washing and air drying at room temperature yielded 0.96 g of product (Yield: 15%). Found: C, 59.3; H, 7.14; N, 14.5. Calc. for $C_{42}H_{57}N_9O_2Mo$: C, 59.5; H, 6.78; N, 14.8%. IR (KBr, cm^{-1}): 3296(m), 2960(m), 1595(m), 1502(s), 1485(s), 1382(m), 1228(s), 1192(s), 1020(s), 900(s), 872(s), 760(m). UV–vis [CH_3CN; λ max, nm (ε, cm^{-1} M^{-1})]: 535 (4.1×10^2), 380 (6.2×10^2); 225 (6.0×10^2). ^1H NMR (300 MHz, $CDCl_3$, δ in ppm): alkyl protons (C_4H_9—): 0.74, 1.21, 1.36, 3.05; phenyl protons: 7.34, 7.61; —NH: 9.82.

$[(n\text{-}C_4H_9)_4N][MoO_2(C_6H_5NNC(S)NNC_6H_5)(C_6H_5(H)NNC(S)NNC_6H_5)]$ (**II**). α-$(Bu_4N)_4[Mo_8O_{26}]$ (2.15 g, 1.0 mmol) was dissolved in 80 cm^3 of warm CH_2Cl_2. After cooling to room temperature, diphenylthiocarbazone (4.0 g, 16.0 mmol) was added. After overnight stirring and concentration to 30 cm^3, the deep purple solution was layered with 30 cm^3 of anhydrous ether. After 2 weeks, purple crystals of **II** were obtained in 20% yield. Found: C, 57.1; H, 6.49; N, 14.6. Calc. for $C_{42}H_{57}N_9O_2S_2Mo$: C, 57.3; H, 6.53; N, 14.3%. IR (KBr, cm^{-1}): 3300(w), 2960(m), 1600(m), 1530(m), 1485(s), 1365(s), 1320(s), 1180(s), 1160(s), 1100(s), 955(m), 880(m), 855(m), 760(s), 680(m). UV–vis [CH_3CN; λ max, nm (ε, cm^{-1} M^{-1})]: 604 (4.3×10^2), 476 (2.3×10^3); 366 (7.0×10^2), 259 (2×10^3), 222 (1.2×10^3). ^1H NMR (300 MHz, $CDCl_3$; δ in ppm): alkyl protons (C_4H_9—): 0.74, 1.22, 1.36, 3.05; phenyl protons: 7.40, 7.61; —NH, 9.95.

Dehydrotithiazone, $C_6H_5NNC(S)NNC_6H_5$ (**IV**). The filtrate from the preparation of **II** was allowed to stand for 2 weeks, whereupon bright orange crystals of **IV** deposited in 23% yield. Alternatively, the methanol solution from the preparation of **II** may be passed through a silica gel column, after concentration but prior to addition of ether, and eluted with methanol–CH_2Cl_2. Complex **II** is eluted initially as a dark purple solution, followed by an intense orange band of **IV** (Yield, 35%). Found: C, 61.0; H, 3.82; N, 21.9. Calc. for $C_{13}H_1N_4S$: C, 61.4; H, 3.97; N, 22.0%. IR (KBr, cm^{-1}): 3000(m), 1490(s), 1370(m), 1320(vs), 1250(m), 1220(m), 980(s), 760(s), 690(s). UV–vis [CH_3CN; λ max, nm (ε, cm^{-1} M^{-1})]: 260 (2.8×10^3).

$[(n\text{-}C_4H_9)_4N][MoOCl_3(C_6H_5NNC(O)NNC_6H_5)]\cdot CH_2Cl_2$ (**III**). Addition of concentrated HCl (1 cm^3) to a solution of α-$(Bu_4N)_4[Mo_8O_{26}]$ (2.15 g, 1.0 mmol) and diphenylcarbazone (3.8 g, 16 mmol) in 80 cm^3 of CH_3OH, results in a bright red solution. After stirring for 12 h, the solution was evaporated to dryness and the resultant red powder was dissolved in 30 cm^3 of CH_2Cl_2, layered with anhydrous ether, and allowed to stand for 8 days. A total of 1.4 g of purple crystals was collected (Yield, 22%). Alternatively, treatment of **I** with an excess of HCl in CH_2Cl_2 yields **III** in quantitative amounts. Found: C, 45.4; H, 6.24; N, 9.05. Calc. for $C_{30}H_{49}N_5O_2Cl_5Mo$: C, 45.9; H, 6.24; N, 8.92%. IR (KBr, cm^{-1}): 2960(m), 1610(s), 1480(m), 1420(m), 1240(s), 1020(w), 960(m), 690(m), 450(w). UV–vis [CH_3CN; λ max, nm (ε, cm^{-1} M^{-1})]: 448 (8.8×10^2), 389 (3.8×10^2), 275 (1.4×10^3), 233 (2.5×10^3). ^1H NMR (300 MHz, CD_3OD; δ in ppm): alkyl protons (C_4H_9—): 0.95, 1.33, 1.56, 3.20; phenyl protons: 6.80, 7.11.

X-ray crystallographic studies

The details of the crystal data, data collection methods and refinement procedures are given in Table 5. Atomic positional parameters for **I**, **II**, **III** and **IV** are given in Supplementary Tables A1, A2, A3 and A4, respectively. Tables of bond lengths and angles, anisotropic temperature factors and calculated and observed structure factors are available.*

The $[(n\text{-}C_4H_9)_4N]^+$ cations of structures **I**, **II** and **III** exhibited some degree of disorder. A model assigning carbon positions to the major peaks consistent with likely atomic positions was adequate as judged by final Fourier maps which exhibit residuals of electron density of 1.0–1.5 e $Å^{-3}$ in the region of the cations. These were the major

*Supplementary material available. Fractional coordinates have been deposited with the Director, Cambridge Crystallographic Centre. Complete listings of bond distances and angles are available from the Editor, Queen Mary College.

excursions of electron density on a scale of 0.8–1.3 e $Å^{-3}$ for hydrogen atoms.

Acknowledgements—We are grateful to the National Science Foundation for financial support (Grant No. CHE8514634). We thank Prof. David Carrillo of the Universidad Catolica de Valparaiso for useful discussions and information.

REFERENCES

1. J. Chatt, J. R. Dilworth and G. J. Leigh, *J. Chem. Soc., Dalton Trans.* 1973, 612; M. W. Bishop, G. Butler, J. Chatt and J. R. Dilworth, *J. Chem. Soc., Dalton Trans.* 1979, 1843; P. L. Dahlstrom, J. R. Dilworth, P. Shulman and J. Zubieta, *Inorg. Chem.* 1982, **21**, 933.
2. T. Nicholson and J. Zubieta, *Polyhedron* 1988, **7**, 171.
3. D. Sutton, *Chem. Soc. Rev.* 1975, **4**, 443; G. Avitabile, P. Ganis and M. Nemiroff, *Acta Cryst.* 1971, **B27**, 725; U. F. Duckworth, P. G. Douglas, R. Mason and B. L. Shaw, *J. Chem. Soc., Chem. Commun.* 1970, 1083; W. E. Carroll and F. J. Lalor, *J. Chem. Soc., Dalton Trans.* 1973, 1754; J. A. Ibers and B. L. Haymore, *Inorg. Chem.* 1975, **14**, 1369; J. V. McArdle, A. J. Schultz, B. J. Corden and R. Eisenberg, *Inorg. Chem.* 1973, **12**, 1676; M. Cowie, B. L. Haymore and J. A. Ibers, *Inorg. Chem.* 1975, **14**, 2617; B. L. Haymore and J. A. Ibers, *Inorg. Chem.* 1975, **14**, 1369.
4. A. P. Gaughan and J. A. Ibers, *Inorg. Chem.* 1975, **14**, 352.
5. E. W. Abel, C. A. Burton, M. R. Churchill and K.-K. G. Lin, *J. Chem. Soc., Chem. Commun.* 1974, 268.
6. (a) M. D. FitzRoy, J. M. Fredericksen, K. S. Murray and M. R. Snow, *Inorg. Chem.* 1985, **24**, 3265; (b) J. A. McCleverty, A. E. Rae, I. Wolochowicz, N. A. Bailey and J. M. A. Smith, *J. Chem. Soc., Dalton Trans.* 1983, 71; (c) C. F. Barrientos-Penna, C. F. Campana, F. W. B. Einstein, T. Jones, D. Sutton and A. S. Tracey, *Inorg. Chem.* 1984, **23**, 363; (d) T. Nicholson and J. Zubieta, *J. Chem. Soc., Chem. Commun.* 1985, 367.
7. P. D. Frisch, M. M. Hunt, W. G. Kita, J. A. McCleverty, G. E. Rae, D. Siddon, D. Swann and J. Williams, *J. Chem. Soc., Dalton Trans.* 1979, 1819; A. B. Gilchrist and D. Sutton, *Inorg. Chem.* 1977, **16**, 677; J. A. Carroll and D. Sutton, *J. Chem. Soc., Dalton Trans.* 1980, **19**, 3142; J. Chatt, J. R. Dilworth, P. L. Dahlstrom and J. Zubieta, *J. Chem. Soc., Chem. Commun.* 1980, 786; J. R. Dilworth and J. Zubieta, *J. Transition Met. Chem.* 1984, **9**, 39; J. Chatt, M. Fakley, P. B. Hitchcock, R. L. Richards and N. T. Luong-Thi, *J. Chem. Soc., Dalton Trans.* 1982, 345; N. A. Bailey, P. D. Frisch, J. A. McCleverty, N. W. Walker and J. Williams, *J. Chem. Soc., Chem. Commun.* 1975, 350; J. R. Dilworth, I. A. Latham, G. J. Leigh, G. Huttner and I. Jibril, *J. Chem. Soc., Chem. Commun.* 1983, 1360.
8. P. G. Douglas, A. R. Galbraith and B. L. Shaw, *Transition Met. Chem.* 1975, **1**, 17; R. Mason, K. M. Thomas, J. A. Zubieta, P. G. Douglas, A. R. Galbraith and B. L. Shaw, *J. Am. Chem. Soc.* 1974, **96**, 265; J. Chatt, M. E. Fakley, P. B. Hitchcock, R. L. Richards, N. T. Luong-Thi and D. L. Hughes, *J. Organomet. Chem.* 1979, **172**, C55 (see also ref. 8 for reformulation); V. W. Day, T. A. George, S. D. A. Iske and S. D. Wagner, *J. Organomet. Chem.* 1976, **112**, C55; F. C. March, R. Mason and K. M. Thomas, *J. Organomet. Chem.* 1975, **96**, C43.
9. F. W. B. Einstein, T. Jones, A. J. L. Hanlan and D. Sutton, *Inorg. Chem.* 1982, **21**, 2585.
10. S. D. Ittel and J. A. Ibers, *J. Am. Chem. Soc.* 1974, **96**, 4804.
11. R. R. Schrock, R. Blum and K. H. Theopold, *Proc. Int. Conf. Coord. Chem. 23rd* 1984, 525.
12. (a) R. Maates and H. Scholand, *Angew. Chem., Int. Ed.* 1983, **22**, 245; (b) M. W. Bishop, G. Butler, J. Chatt, J. R. Dilworth and G. J. Leigh, *J. Chem. Soc., Dalton Trans.* 1979, 1843; (c) J. R. Dilworth, P. L. Dahlstrom, J. R. Hyde, K. Kustyn, P. A. Vella and J. Zubieta, *Inorg. Chem.* 1980, **19**, 3562; (d) M. W. Bishop, J. Chatt, J. R. Dilworth, J. R. Hyde, S. Kim, K. Venkatasubramanian and J. Zubieta, *Inorg. Chem.* 1978, **17**, 2917; (e) J. R. Dilworth, J. R. Hyde, P. Lyford, P. Vella, K. Venkatasubramanian and J. Zubieta, *Inorg. Chem.* 1979, **18**, 268; (f) J. Chatt, J. R. Dilworth and G. J. Leigh, *J. Chem. Soc. A* 1970, 2239.
13. J. R. Dilworth, *Coord. Chem. Rev.* 1976, **21**, 29.
14. S. Liu and J. Zubieta, *Polyhedron* 1988, **7**, 431.
15. S. N. Shaikh and J. Zubieta, *Inorg. Chim. Acta* 1988, **144**, 147.
16. T.-C. Hsieh and J. Zubieta, *Inorg. Chem.* 1985, **24**, 1287; T.-C. Hsieh and J. Zubieta *Polyhedron* 1986, **5**, 309; T.-C. Hsieh and J. Zubieta, *Polyhedron* 1986, **5**, 1655; T.-C. Hsieh and J. Zubieta, *J. Chem. Soc., Chem. Commun.* 1985, 1749; S. N. Shaikh and J. Zubieta, *Inorg. Chem.* 1986, **25**, 4613; S. Liu, S. N. Shaikh and J. Zubieta, *Inorg. Chem.* 1987, **26**, 4303.
17. A. K. Babko and T. E. Get'man, *Ukrain. Khim. Zh.* 1961, **27**, 807; F. J. de Silva and L. de Moura, *Tecnica (Lisbon)* 1959, **34**, 437: *Chem. Abstr.* 1960, **54**, 1930.
18. V. W. Day, M. F. Fredrich, W. G. Klemperer and W. Shum, *J. Am. Chem. Soc.* 1977, **99**, 6146.
19. M. W. Bishop, J. Chatt, J. R. Dilworth, M. B. Hursthouse and M. Motevalli, *J. Chem. Soc., Dalton Trans.* 1979, 1603.
20. H. Kang, S. Liu, S. N. Shaikh, T. Nicholson and J. Zubieta, *Inorg. Chem.*, submitted for publication.
21. R. N. Hanley, W. D. Ollis, C. A. Ramsden and I. S. Smith, *J. Chem. Soc., Perkin II* 1979, 744; P. N. Preston, K. K. Tiwan and K. Turnbull, *J. Chem. Soc., Chem. Commun.* 1976, 343.
22. M. F. Perpinan, L. Ballester, A. Santos, A. Monge, C. Ruiz-Valero and E. Gutierrez Puebla, *Polyhedron* 1987, **6**, 1523.

23. M. W. Bishop, J. Chatt, J. R. Dilworth, M. B. Hursthouse, S. A. A. Jayaweera and A. Quick, *J. Chem. Soc., Dalton Trans.* 1979, 914.
24. A. V. Butcher, J. Chatt, J. R. Dilworth, G. J. Leigh, M. B. Hursthouse, S. A. A. Jayaweera and A. Quick, *J. Chem. Soc., Dalton Trans.* 1979, 921.
25. R. Maates and U. Mikloweit, *Inorg. Chim. Acta* 1986, **122**, L19.
26. A. T. Hutton and H. M. N. H. Irving, *J. Chem. Soc., Dalton Trans.* 1982, 2299.
27. L. Pauling, in *Nature of the Chemical Bond*, 3rd edn, pp. 232–239. Cornell University Press, New York (1960).
28. H. A. Bent, *Chem. Rev.* 1961, **61**, 275.

Polyhedron Vol. 8, No. 5, pp. 689–693, 1989
Printed in Great Britain

0277–5387/89 $3.00+.00
© 1989 Pergamon Press plc

SYNTHESIS AND X-RAY CRYSTAL STRUCTURES OF 1:1 COMPLEXES OF NICKEL(II) NITRATE WITH 1,10-PHENANTHROLINE AND WITH 2,2′-BIPYRIDYL

FRANK WALMSLEY, A. ALAN PINKERTON and JUDITH A. WALMSLEY*

Department of Chemistry, University of Toledo, Toledo, OH 43606, U.S.A.

(*Received* 27 *August* 1988; *accepted* 5 *October* 1988)

Abstract—Blue crystals of $[Ni(phen)(H_2O)_4](NO_3)_2 \cdot H_2O$ (where phen = 1,10-phenanthroline) and of $[Ni(bipy)(H_2O)_3(NO_3)]NO_3$ (where bipy = 2,2′-bipyridyl) were prepared and their structures determined by single crystal X-ray crystallography. In the phenanthroline complex, the nitrates are not coordinated to the nickel but in the bipyridyl complex, one nitrate is coordinated to the nickel as a monodentate ligand. The IR spectra and magnetic susceptibilities are reported.

Transition metal complexes of 1,10-phenanthroline (phen) and 2,2′-bipyridyl (bipy) have been of interest for many years. Among other uses, these complexes have been part of an effective method for metal analysis. Additional knowledge about the structure of complexes that may exist in aqueous solution is of potential value in understanding intermediates in ligand exchange reactions in aqueous solution. Nickel(II) complexes have been of special interest including reports of spectral and magnetic properties[1] and of formation constants.[2] With three ligands per nickel, the complexes are usually red, with two per nickel they are usually pink or violet, and with one per nickel, blue; there are, of course, numerous exceptions to these generalities.[1] While structures of 1:1 complexes of nickel(II) sulphate with these ligands have been reported,[3,4] little is known about 1:1 nickel(II) nitrate complexes. We report the preparation and structure of two such complexes, including IR and magnetic susceptibility data.

EXPERIMENTAL

Synthesis

$[Ni(phen)(H_2O)_4](NO_3)_2 \cdot H_2O$. Reagent grade $Ni(NO_3)_2 \cdot 6H_2O$ (5.81 g, 20 mmol) was dissolved in 5 cm^3 of deionized distilled H_2O. 1,10-Phenanthroline monohydrate (0.80 g, 4 mmol) was added to the $Ni(NO_3)_2$ solution with stirring. The solid phenanthroline slowly dissolved. Initially, some pink solid formed which subsequently dissolved forming a blue solution. A small amount of unreacted phenanthroline was filtered off. The solution was allowed to evaporate slowly until blue crystals formed. Under a microscope it was possible to see two types of crystals. The major component was blue rods and these were the crystals used in this study. The minor component appeared as blue needles. A few purple crystals (probably bis or tris complexes) were observed and were removed prior to use for measurements requiring bulk samples.

$[Ni(bipy)(H_2O)_3(NO_3)]NO_3$. Reagent grade $Ni(NO_3)_2 \cdot 6H_2O$ (5.81 g, 20 mmol) was dissolved in 5 cm^3 of deionized distilled H_2O. 2,2′-Bipyridyl (0.63 g, 4 mmol) was added to the $Ni(NO_3)_2$ solution with stirring and slight warming. The solid bipyridyl slowly dissolved with some of the solid turning pink before dissolving to give a blue–green solution. The solution was allowed to evaporate slowly until blue plate-like crystals formed.

IR and magnetic susceptibility

IR spectral measurements were made as reflectance spectra, using KBr as diluent, on a Nicolet SX-60 FTIR instrument under standard operating conditions (4 cm^{-1} resolution). Magnetic susceptibility measurements were made by the Gouy method at 20°C as previously reported.[5]

*Author to whom correspondence should be addressed. Present address: Division of Earth and Physical Sciences, University of Texas at San Antonio, San Antonio, TX 78285, U.S.A.

Table 1. Summary of the crystal data and refinement results

	$[Ni(phen)(H_2O)_4](NO_3)_2 \cdot H_2O$	$[Ni(bipy)(H_2O)_3(NO_3)]NO_3$
Molecular formula	$C_{12}H_{18}NiN_4O_{11}$	$C_{10}H_{14}NiN_4O_9$
Formula weight	435.01	392.95
Space group	$P2_1/c$	$P2_1/c$
a (Å)	8.745(1)	11.459(3)
b (Å)	13.591(2)	9.433(2)
c (Å)	15.336(3)	14.809(3)
β (°)	94.61(1)	109.88(2)
V (Å^3)	1816.8	1505.2
Z	4	4
d_{calc} (g cm^{-3})	1.66	1.73
μ(Mo-K_α) (cm^{-1})	11.3	13.5
Crystal dimensions (mm)	$0.12 \times 0.18 \times 0.21$	$0.32 \times 0.22 \times 0.08$
Temperature (°C)	21 ± 1	21 ± 1
Reflections measured	4303 (3722 unique)	3303 (3145 unique)
Maximum 2θ (°)	53.0	52.0
Agreement factor, R:		
unweighted	0.049	0.039
weighted	0.053	0.050

Crystal structures

Preliminary examination and X-ray intensity data collections were performed on an Enraf–Nonius CAD4 automatic kappa axis diffractometer equipped with a graphite crystal, incident beam monochromator (Mo-K_α, $\lambda = 0.71073$ Å). Calculations were carried out on a VAX 11/750 computer using VLXSDP. Both structures were solved using conventional Patterson and Fourier techniques and refined by full-matrix least-squares. A summary of the crystallographic data is given in Table 1.*

RESULTS AND DISCUSSION

$[Ni(phen)(H_2O)_4](NO_3)_2 \cdot H_2O$

The X-ray crystal structure results as shown in Fig. 1 reveal an octahedral environment of ligands around the nickel composed of one bidentate 1,10-phenanthroline molecule and four water molecules. The nitrate ions are not coordinated to the nickel and are thus considered to be ionic. The bond lengths of the atoms bonded to the nickel are listed in Table 2, and the bond angles which include the nickel atom are listed in Table 3.

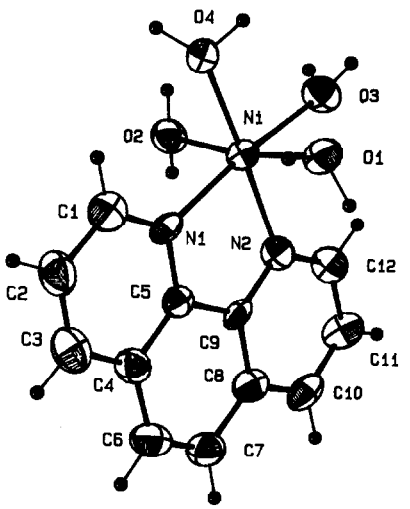

Fig. 1. ORTEP view of the nickel environment in $[Ni(phen)(H_2O)_4](NO_3)_2 \cdot H_2O$. Atoms are represented by 50% probability ellipsoids.

Table 2. Selected bond distances (Å) for $[Ni(phen)(H_2O)_4](NO_3)_2 \cdot H_2O$

Atom 1	Atom 2	Distance
Ni	N(1)	2.062(5)
Ni	N(2)	2.051(6)
Ni	O(1)	2.099(5)
Ni	O(2)	2.095(5)
Ni	O(3)	2.064(5)
Ni	O(4)	2.041(5)

Numbers in parentheses are estimated standard deviations in the least significant digits.

* Final positional and thermal parameters, a list of all bond lengths and angles, a table of some geometrical features, and a list of the observed and calculated structure factors have been deposited as supplementary material with the Editor, from whom copies are available on request. Atomic coordinates have also been deposited with the Cambridge Crystallographic Data Centre.

Table 3. Selected bond angles (°) for [Ni(phen)$(H_2O)_4$][$(NO_3)_2 \cdot H_2O$

Atom 1	Atom 2	Atom 3	Angle
N(1)	Ni	N(2)	81.3(2)
N(1)	Ni	O(2)	92.2(2)
N(1)	Ni	O(4)	95.7(2)
N(1)	Ni	O(3)	174.0(2)
N(1)	Ni	O(1)	92.6(2)
N(2)	Ni	O(1)	95.4(2)
N(2)	Ni	O(3)	92.8(2)
N(2)	Ni	O(4)	177.0(2)
N(2)	Ni	O(2)	92.4(2)
O(1)	Ni	O(2)	171.4(2)
O(1)	Ni	O(3)	87.2(2)
O(1)	Ni	O(4)	84.4(2)
O(2)	Ni	O(4)	88.1(2)
O(2)	Ni	O(3)	88.8(2)
O(3)	Ni	O(4)	90.2(2)

Numbers in parentheses are estimated standard deviations in the least significant digits.

The bond lengths and angles are in agreement with those reported for other phenanthroline complexes of nickel.[6] It has been suggested that the bite of the phenanthroline molecule is inflexible; thus the N—M—N angle changes only as a result of a change in the M—N distance due to a change in the radius of the metal.[6] This inverse relationship between the M—N distance and N—M—N angle has been documented.[6] In comparison with the $Ni(phen)_3^{2+}$ ion, the average Ni—N distance in $Ni(phen)(H_2O)_4^{2+}$ is less (2.056 vs about 2.090 Å) and the average N—Ni—N angle is greater (81.3 vs about 79.4°). Thus the nickel atom with one phenanthroline attached appears to be smaller than a nickel atom with three phenanthrolines attached. This may be due to the bulk of three phenanthroline molecules causing steric repulsions, resulting in each phenthroline moving away from the nickel atom to reduce the repulsions. This may also be due to metal–ligand back bonding. With one phenanthroline molecule, the amount of back bonding to the phenanthroline will be greater. When there are three phenanthroline molecules, the electron density donated from the nickel must be distributed among the three ligands, resulting in a lesser amount of back bonding per phenanthroline. A greater amount of back bonding increases the metal–ligand bond order and reduces the bond length in the case with one phenthroline compared to the case with three phenanthrolines.

The magnetic moment of [Ni(phen)$(H_2O)_4$][$(NO_3)_2 \cdot H_2O$ is 3.11 BM at 20°C, which is typical for octahedral nickel(II).

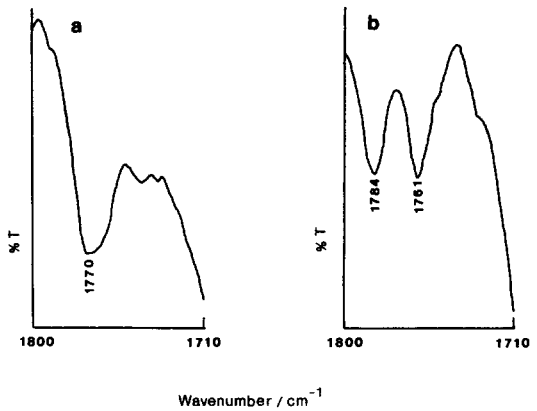

Fig. 2. IR absorptions in the 1700–1800 cm^{-1} region: (a) [Ni(phen)$(H_2O)_4$][$(NO_3)_2 \cdot H_2O$ and (b) [Ni(bipy)$(H_2O)_3(NO_3)$]NO_3.

Nitrate groups exhibit absorptions in the IR region of 1700–1800 cm^{-1} which are due to combinations of fundamental frequencies. The absorptions in this region have been used to distinguish among the various coordination modes of the nitrate group: ionic, monodentate, bidentate and bridging.[7] Ionic nitrates are expected to have a single absorption in the IR spectrum in this region.[7] As shown in Fig. 2(a), this compound has an expected single absorption at 1770 cm^{-1}. This single absorption indicates the presence of ionic nitrate which is in agreement with the X-ray crystal structure which shows no coordinated nitrates.

[Ni(bipy)$(H_2O)_3(NO_3)$]NO_3

The X-ray crystal structure results as shown in Fig. 3 reveal an octahedral environment of ligands

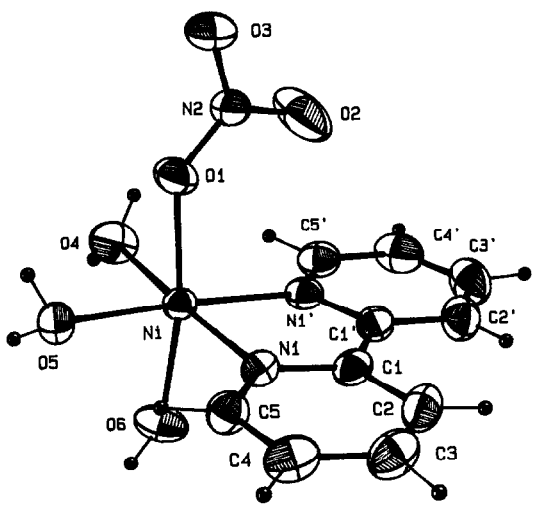

Fig. 3. ORTEP view of the nickel environment in [Ni(bipy)$(H_2O)_3(NO_3)$]NO_3. Atoms are represented by 50% probability ellipsoids.

Table 4. Selected bond distances (Å) for [Ni(bipy)$(H_2O)_3(NO_3)]NO_3$

Atom 1	Atom 2	Distance
Ni	N(1)	2.045(2)
Ni	N(1′)	2.061(3)
Ni	O(1)	2.103(2)
Ni	O(4)	2.038(2)
Ni	O(5)	2.072(2)
Ni	O(6)	2.056(3)

Numbers in parentheses are estimated standard deviations in the least significant digits.

around the nickel, composed of one bidentate 2,2′-bipyridyl molecule, three water molecules, and one monodentate nitrate ligand. The second nitrate is not coordinated to the nickel and is thus considered to be ionic. The bond lengths of atoms bonded to nickel are listed in Table 4 and the bond angles which include the nickel atom are listed in Table 5.

The bond lengths and angles are in agreement with those reported for other 2,2′-bipyridyl complexes of nickel.[3,4] It has been reported that coordinated metal–water distances are shorter when the water is trigonal rather than tetrahedral.[4] Of the three coordinated water molecules in this structure, one [O(4)] has a distinctly shorter bond distance than the other two and similar to the short bond distance in the compound of Healy.[4] Coordinated water molecules referred to as trigonal water are actually planar or nearly planar. By comparing deviations from planarity, it is possible to distinguish between trigonal and tetrahedral water

Table 5. Selected bond angles (Å) for [Ni(bipy)$(H_2O)_3(NO_3)]NO_3$

Atom 1	Atom 2	Atom 3	Angle
N(1)	Ni	N(1′)	79.5(1)
N(1)	Ni	O(1)	92.54(9)
N(1′)	Ni	O(1)	98.9(1)
N(1)	Ni	O(4)	176.2(1)
N(1)	Ni	O(5)	92.81(9)
N(1)	Ni	O(6)	89.9(1)
N(1′)	Ni	O(4)	96.8(1)
N(1′)	Ni	O(5)	172.30(8)
N(1′)	Ni	O(6)	91.1(1)
O(4)	Ni	O(5)	90.9(1)
O(4)	Ni	O(6)	91.0(1)
O(5)	Ni	O(6)	89.3(1)
O(1)	Ni	O(4)	87.2(1)
O(1)	Ni	O(5)	80.86(9)
O(1)	Ni	O(6)	170.0(1)
O(4)	Ni	O(6)	91.0(1)

Numbers in parentheses are estimated standard deviations in the least significant digits.

Table 6. Deviations (Å) from the best plane for each Ni---OH_2 in [Ni(bipy)$(H_2O)_3(NO_3)]NO_3$

	O(4)	O(5)	O(6)
Ni	−0.013	−0.043	−0.020
O	0.084	0.248	0.115
H	−0.027	−0.102	−0.044
H	−0.044	−0.103	−0.051

molecules. The data in Table 6 indicate the deviations from the best plane for each of the three water molecules including the nickel atom in the plane. The water labelled O(4) has a small deviation from planarity and is presumably trigonal. This water molecule also has a short Ni—O distance (2.038 Å) in agreement with the previous report.[4] The other two water molecules have larger deviations from planarity with the water containing O(6) being more planar than the water containing O(5). The bond orders also increase in the same way that planarity decreases; that is, the Ni—O(6) distance is shorter than the Ni—O(5) distance. Another way to consider this is to compare the H—O—H angles, although this is less sensitive due to the greater uncertainty in locating the hydrogen atoms. The H—O—H angles decrease from 112° for H—O(4)—H, to 111° for H—O(6)—H, to 97° for H—O(5)—H, the same order as the changes in the Ni—O distances.

The X-ray crystal structure shows that one of the two nitrate groups is bonded to the nickel through one oxygen—a monodentate nitrate group. Monodentate nitrate ligands bonded to nickel are expected to have two absorptions in the IR region between 1700 and 1800 cm^{-1} with a separation of about 20–25 cm^{-1}.[7] As shown in Fig. 2(b), the IR spectrum in this region has absorptions at 1761 and 1784 cm^{-1}, a separation of 23 cm^{-1}. The X-ray crystal structure also shows that one of the nitrate groups is not coordinated to the nickel—an ionic nitrate. An ionic nitrate normally would be expected to have a single absorption in this region, just as in the phenanthroline complex. Thus, a monodentate nitrate plus an ionic nitrate would normally give three absorptions in this region. Only the two absorptions due to the monodentate nitrate are observed. Why is the ionic nitrate absorption missing? Some compounds with ionic nitrates that do not have any absorptions in this region have been reported.[7] These compounds are all hydrates, as opposed to anhydrous salts such as $NaNO_3$ and $Sr(NO_3)_2$, and it was suggested[7] that extensive hydrogen bonding may be responsible. The X-ray data show that all the oxygens of the ionic nitrate group receive hydrogen bonds in the bipyridyl complex, which is in agreement with the suggestion.

The magnetic moment of $[Ni(bipy)(H_2O)_3(NO_3)]NO_3$ is 3.51 BM at 20°C. This is slightly high for octahedral nickel(II), but deviations from a regular octahedron as exhibited by this complex tend to raise the magnetic moment.

REFERENCES

1. C. M. Harris and E. D. McKenzie, *J. Inorg. Nucl. Chem.* 1967, **29**, 1047.
2. W. A. E. McBryde, *Can. J. Chem.* 1967, **45**, 2093.
3. J.-C. Tedenac and E. Philippot, *Acta Cryst.* 1974, **B30**, 2286.
4. P. C. Healy, J. M. Patrick and A. H. White, *Aust. J. Chem.* 1984, **37**, 921.
5. A. G. Menke and F. Walmsley, *Inorg. Chim. Acta* 1976, **17**, 193.
6. B. A. Frenz and J. A. Ibers, *Inorg. Chem.* 1972, **11**, 1109.
7. A. B. P. Lever, E. Mantovani and B. S. Ramaswamy, *Can. J. Chem.* 1971, **49**, 1957.

Polyhedron Vol. 8, No. 5, pp. 695–700, 1989
Printed in Great Britain

0277–5387/89 $3.00+.00
© 1989 Pergamon Press plc

SYNTHESIS AND X-RAY CRYSTAL STRUCTURE OF THE TUNGSTEN–RUTHENIUM COMPOUND $[WRu(\mu\text{-}\sigma,\eta^2\text{-}CH{=}CH_2)(CO)_4(cis\text{-}Ph_2PCH{=}CHPPh_2)(\eta\text{-}C_5H_5)]$

STEPHEN A. BREW, JOHN C. JEFFERY and F. GORDON A. STONE†

Department of Inorganic Chemistry, The University of Bristol, Bristol BS8 1TS, U.K.

(*Received* 23 *September* 1988; *accepted* 24 *October* 1988)

Abstract—The compounds $[W(\equiv CMe)(CO)_2(\eta\text{-}C_5H_5)]$ and $[Ru(CO)_3(cdpe)]$ (cdpe = *cis*-$Ph_2PCH{=}CHPPh_2$) react in tetrahydrofuran at reflux temperatures to give in *ca* 70% yield the dimetal compound $[WRu(\mu\text{-}\sigma,\eta^2\text{-}CH{=}CH_2)(CO)_4(cdpe)(\eta\text{-}C_5H_5)]$. The structure of the latter has been established by X-ray diffraction. The W—Ru bond [2.973(1) Å] is spanned by the vinyl group which is σ-bonded to the ruthenium atom (Ru—C 2.095(5) Å) and η^2-coordinated to the tungsten (W—C 2.209(5) and 2.313(5) Å). The two metal atoms are each ligated by two carbonyl groups, but one CO attached to tungsten semi-bridges the metal–metal bond (W—C—O 169.2(5)°). The cyclopentadienyl group is η^5-bonded to the tungsten, and the *cis*-$Ph_2PCH{=}CHPPh_2$ ligand is coordinated to the ruthenium (Ru—P 2.300(1) and 2.396(1) Å).

The alkylidyne–tungsten compounds $[W(\equiv CR)(CO)_2(\eta\text{-}C_5H_5)]$ (R = alkyl or aryl), as well as related species in which the cyclopentadienyl ligand is replaced by the groups $\eta\text{-}C_5Me_5$, $HB(pz)_3$ (hydrotris(pyrazol-1-yl)borate), or $\eta^5\text{-}C_2B_9H_9Me_2$, are versatile reagents for preparing dimetal or polynuclear metal complexes containing bonds between tungsten and other transition elements.[1] The methodology involves a combination of a low-valent metal–ligand fragment with the C≡W moiety present in the alkylidyne–tungsten species. The metal–ligand fragment is derived from a complex containing a labile group (CO, NCMe, C_2H_4, or THF, etc.). Indeed, the scope of this synthetic procedure is so wide that there are very few transition metals which have not been attached to a tungsten atom via reactions of this type.

Recently we have shown[2] that depending on the stoichiometry employed, the reaction between the compounds $[W(\equiv CC_6H_4Me\text{-}4)(CO)_2(\eta\text{-}C_5H_5)]$ and $[Ru(CO)_4(\eta\text{-}C_2H_4)]$ affords, respectively, the complexes $[W_2Ru\{\mu_3\text{-}C_2(C_6H_4Me\text{-}4)_2\}(CO)_7(\eta\text{-}C_5H_5)_2]$ or $[WRu_3(\mu_3\text{-}CC_6H_4Me\text{-}4)(CO)_{11}(\eta\text{-}C_5H_5)]$. Formation of these tri- and tetranuclear metal compounds, rather than a dimetal complex, prompted us to study the reaction between $[W(\equiv CC_6H_4Me\text{-}4)(CO)_2(\eta\text{-}C_5H_5)]$ and $[Ru(CO)_3(cdpe)]$ (cdpe = *cis*-$Ph_2PCH{=}CHPPh_2$). It was anticipated that this combination of reagents might yield $[WRu(\mu\text{-}CC_6H_4Me\text{-}4)(CO)_4(cdpe)(\eta\text{-}C_5H_5)]$, since the presence of the cdpe group in the ruthenium precursor should deactivate the system, thereby inhibiting the formation of products containing more than two metal atoms. Unfortunately, no appreciable reaction occurred between $[Ru(CO)_3(cdpe)]$ and $[W(\equiv CC_6H_4Me\text{-}4)(CO)_2(\eta\text{-}C_5H_5)]$ in toluene, until the mixture had been refluxed for *ca* 24 h. Even under these vigorous conditions only insignificant quantities of product were obtained, consisting of a mixture of complexes each in an amount too small to be characterized. Accordingly, the more reactive ethylidyne species $[W(\equiv CMe)(CO)_2(\eta\text{-}C_5H_5)]$ was employed. The latter with $[Ru(CO)_3(cdpe)]$ in THF gave a dimetal compound in high yield, but the product was not the expected μ-ethylidyne complex $[WRu(\mu\text{-}CMe)(CO)_4(cdpe)(\eta\text{-}C_5H_5)]$.

RESULTS AND DISCUSSION

Mixtures of $[W(\equiv CMe)(CO)_2(\eta\text{-}C_5H_5)]$ and $[Ru(CO)_3(cdpe)]$ in THF at reflux temperatures gave an orange complex, **1**, which was isolated pure after column chromatography on alumina. It was not possible to identify **1** from the spectroscopic data. In particular, the $^{13}C\text{-}\{^1H\}$ NMR spectrum

† Author to whom correspondence should be addressed.

showed no signal in the region δ 300–400 ppm characteristic for a μ-*C*Me nucleus bridging a dimetal centre.[3] Moreover, in the ^{1}H NMR spectrum there was no resonance for a methyl group. Fortunately, suitable crystals of **1** could be grown, enabling an X-ray diffraction study to be carried out. The structure of the molecule is shown in Fig. 1, and selected bond distances and angles are listed in Table 1.

The compound was thus identified as the μ-vinyl complex, [WRu(μ-σ,η^2-CH=CH$_2$)(CO)$_4$(cdpe)(η-C$_5$H$_5$)] (**1**), in which the bridging ligand is σ-bonded to the ruthenium (C(5)—Ru 2.095(5) Å) and η^2-coordinated to the tungsten (C(5)—W 2.209(5), C(6)—W 2.313(5) Å). Numerous homodinuclear metal complexes are known in which a vinyl group adopts the μ-σ,η^2 bonding mode found in **1**. Indeed, the first compounds having this structural feature were discovered over 25 years ago.[4] We have recently determined the crystal structure of the trimetal complex [WRu$_2$\{μ-σ,η^2-*trans*-CH=C(H)C$_6$H$_4$Me-4\}(μ-CO)(CO)$_3$(η-C$_5$H$_5$)$_2$(η-C$_5$Me$_5$)] in which a substituted-vinyl group bridges a W—Ru bond. However, in contrast with **1**, the vinyl group in the trimetal species is σ-bonded to the tungsten and η^2-coordinated to the ruthenium.[5] Moreover, the W—Ru distance (2.771(1) Å) is appreciably shorter than that in **1** (2.973(1) Å). This is also true of the W—Ru separation (2.769(1) Å) in the

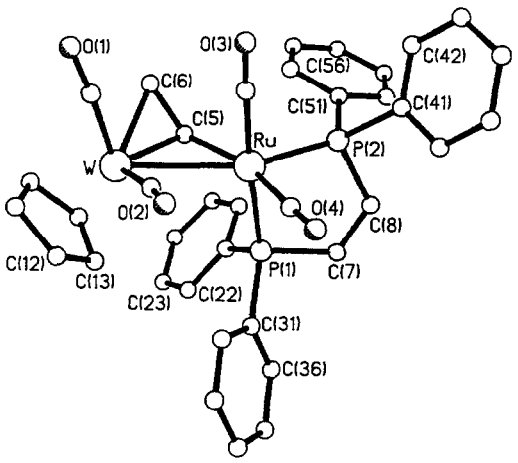

Fig. 1. The molecular structure of [WRu(μ-σ,η^2-CH=CH$_2$)(CO)$_4$(cdpe)(η-C$_5$H$_5$)].

Table 1. Selected internuclear distances (Å) and angles (°) for [WRu(μ-σ,η^2-CH=CH$_2$)(CO)$_4$(cdpe)(η-C$_5$H$_5$)] (**1**) with ESDs in parentheses

W—Ru	2.973(1)	W—C(1)	1.916(6)
W—C(2)	1.939(6)	W—C(5)	2.209(5)
W—C(6)	2.313(5)	Ru—P(1)	2.396(1)
Ru—P(2)	2.300(1)	Ru—C(3)	1.878(5)
Ru—C(4)	1.940(6)	Ru—C(5)	2.095(5)
P(1)—C(7)	1.820(5)	P(2)—C(8)	1.815(5)
C(1)—O(1)	1.181(8)	C(2)—O(2)	1.180(7)
C(3)—O(3)	1.145(6)	C(4)—O(4)	1.134(7)
C(5)—C(6)	1.430(7)		
C(1)—W—Ru	108.0(2)	C(2)—W—Ru	67.0(2)
C(2)—W—C(1)	81.7(2)	C(5)—W—Ru	44.7(1)
C(5)—W—C(1)	106.1(2)	C(5)—W—C(2)	110.8(2)
C(6)—W—Ru	71.3(1)	C(6)—W—C(1)	73.0(2)
C(6)—W—C(2)	120.5(2)	C(6)—W—C(5)	36.8(2)
P(1)—Ru—W	99.3(1)	P(2)—Ru—W	153.6(1)
P(2)—Ru—P(1)	82.4(1)	C(3)—Ru—W	84.6(2)
C(3)—Ru—P(1)	175.0(2)	C(3)—Ru—P(2)	92.8(2)
C(4)—Ru—W	112.5(2)	C(4)—Ru—P(1)	90.3(2)
C(4)—Ru—P(2)	93.7(2)	C(4)—Ru—C(3)	91.0(2)
C(5)—Ru—W	47.9(1)	C(5)—Ru—P(1)	91.2(1)
C(5)—Ru—P(2)	105.9(1)	C(5)—Ru—C(3)	89.1(2)
C(5)—Ru—C(4)	160.3(2)	C(7)—P(1)—Ru	106.2(2)
C(8)—P(2)—Ru	108.6(2)	W—C(1)—O(1)	178.1(5)
W—C(2)—O(2)	169.2(5)	Ru—C(3)—O(3)	177.7(5)
Ru—C(4)—O(4)	175.4(5)	Ru—C(5)—W	87.3(2)
W—C(5)—C(6)	75.6(3)	Ru—C(5)—C(6)	123.9(4)
W—C(6)—C(5)	67.6(3)	P(1)—C(7)—C(8)	118.7(4)
P(2)—C(8)—C(7)	118.9(4)		

complex [WRu(μ-Cl)(μ-CMe)(Cl)(CO)₂(PPh₃)₂(η-C₅H₅)], in which the metal–metal bond is spanned by ethylidyne and chlorido groups.[6]

The ruthenium atom in **1** carries two terminal CO groups and the cdpe ligand (P(1)—Ru 2.396(1), P(2)—Ru 2.300(1) Å). As expected, the tungsten atom is bonded by the cyclopentadienyl ring and two CO ligands. However, one of the latter groups semi-bridges the W—Ru bond (W—C(2)—O(2) 169.2(5)°).

Compound **1** adds to the growing number of tungsten–ruthenium species which may be obtained by adding low-valent ruthenium fragments to the C≡W bonds in alkylidyne–tungsten complexes. However, the great majority of the products obtained by this method are not dimetal species but complexes containing the core fragments WRu_2,[5] W_2Ru,[2,6,7] W_3Ru[2,8] and WRu_3.[2] Apart from compound **1**, only two dimetal species have been prepared; the aforementioned complex [WRu(μ-Cl)(μ-CMe)(Cl)(CO)₂(PPh₃)₂(η-C₅H₅)] and the complex [WRu(μ-Cl)(μ-CMe)(Cl)(CO)₂(PPh₃)(η-C₂Me₂)(η-C₅H₅)], the structure of which is as yet unresolved.[6]

The origin of the μ-CH=CH₂ group in **1** is clearly the μ-CMe fragment present in the precursor [W(≡CMe)(CO)₂(η-C₅H₅)]. This rearrangement is of interest in the context of the reactivity of ethylidyne, vinyl and vinylidene fragments when bonded to di- or trimetal centres. There are several well documented examples of the conversion of μ-CMe groups into μ-C=CH₂ fragments when ligating metal atoms.[9,10] This transformation can be accomplished by deprotonation of the μ-CMe ligand with base,[11–13] or by a thermally induced hydrogen migration process in which the hydrogen atom transferred usually but not always ends up bridging two metal centres.[14,15] Almost certainly in the conversion of a μ-CMe fragment into the ligands μ-C=CH₂ and μ-H, intermediates are traversed containing a μ-CH=CH₂ group, and it is in this context that the formation of **1** is of interest. A possible pathway is indicated in Scheme 1. From previous work[1] it may reasonably be anticipated that the reaction between [W(≡CMe)(CO)₂(η-C₅H₅)] and [Ru(CO)₃(cdpe)] would initially form the intermediate **A**, which under the reaction conditions is evidently unstable. It is possible that the strong *trans* influence of the ethylidyne group leads to dissociation of a ligated group at the ruthenium centre. This might involve release of a CO molecule, or the cdpe ligand becoming monodentate, as indicated in Scheme 1. The presence of a vacant site coupled with the electronic unsaturation at the ruthenium atom, would then facilitate an agostic C—H→Ru interaction, thereby providing a mechanism for hydrido group transfer as shown. Hence the pathway B → C → D, and finally to **1**, could be readily traversed.

Prior to the results reported herein there appears to be no precedent for the synthesis of a μ-vinyl compound from a μ-ethylidyne complex via a thermal reaction of the type described. However, Casey *et al.*[13] have observed that at *ca* 90°C the cationic pentylidyne complex [Fe₂(μ-CBuⁿ)(μ-CO)(CO)₂(η-C₅H₅)₂]⁺ is converted in essentially quantitative yield into the bridging pentenyl species [Fe₂{μ-σ,η²-CH=C(H)C₃H₇}(μ-CO)(CO)₂(η-C₅H₅)₂]⁺. In contrast, the ethylidyne complex [Fe₂(μ-CMe)(μ-CO)(CO)₂(η-C₅H₅)₂]⁺ does not rearrange even at 120°C. Our results thus suggest that the μ-CMe

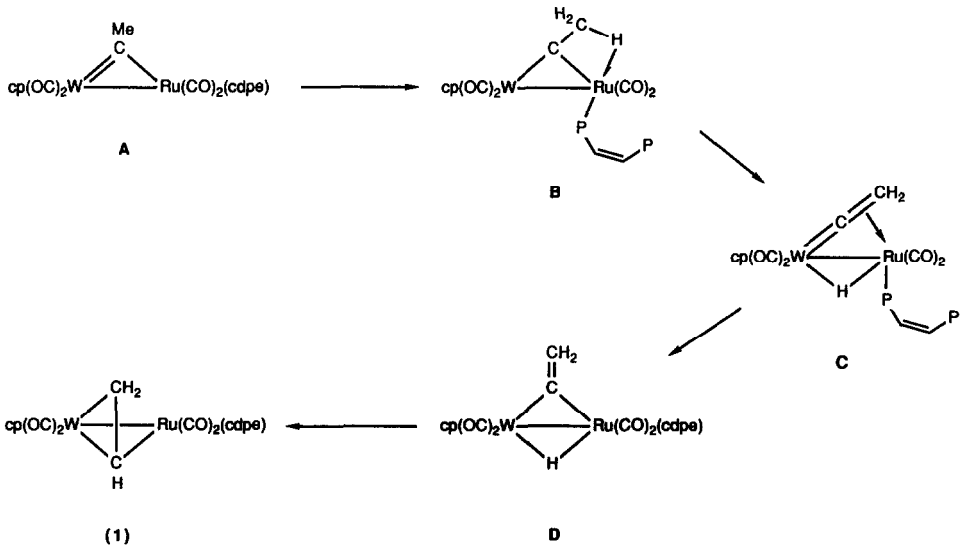

Scheme 1. cp = η-C₅H₅, *cis*-Ph₂PCH=CHPPh₂ = cdpe = P⌒P.

group is more readily activated for hydrogen migration when bridging a heteronuclear W—Ru bond than when bridging a homonuclear Fe—Fe linkage.

Once the structure of **1** was established by X-ray diffraction, it was possible to interpret the spectroscopic data for the complex (see Experimental). The IR spectrum in the carbonyl region showed four bands at 2015, 1956, 1862 and 1779 cm^{-1}. The latter peak may be assigned to the semi-bridging CO group. Examination of the NMR spectra at room temperature revealed the presence of two closely related isomers, and the slightly broadened peaks observed suggested that these might be interconverting slowly. The data given below were obtained from spectra measured at −80°C, at which temperature sharp peaks due to the major and the minor isomers (2:1) were observed. Only signals for the major isomer are discussed.

The ^1H NMR spectrum revealed three resonances at 2.44, 2.69 and 5.63 ppm, each corresponding to one proton, and these may be assigned to the μ-CH=CH_2 ligand in **1**.[16–19] The signal at δ 5.63 due to the CH group was a multiplet and coupling constants could not be determined. However, the resonances for the CH_2 group at δ 2.44 (J(HH) 11 Hz) and 2.69 (J(HH) 8 Hz) were doublets, the values of the coupling constants falling in the range expected for *trans*- and *cis*-CH=CH configurations, respectively.

In the ^{13}C-{^1H} NMR spectrum there are four CO resonances at δ 231.9, 228.5 (WCO), 201.4 (br, RuCO) and 197.9 ppm (d, RuCO, J(PC) 15 Hz). Peaks at δ 148.2 (d of d, J(PC) 37, 37 Hz) and 145.6 ppm (d of d, J(PC) 27, 39 Hz) may be assigned to the PCH=CHP moiety. The μ-CH=CH_2 group displays signals at δ 137.6 (d, J(PC) 49 Hz) and 43.0 ppm which may be tentatively assigned to the CH and CH_2 nuclei, respectively. In the spectrum of the compound [WPt(μ-σ,η^2-CH=CH_2)(CO)$_2$(PMe_3)$_2$(η-C_5H_5)] the corresponding signals are at δ 129.9 and 37.2 ppm.[19] The other peaks in the spectrum of **1** are as expected for the presence of the η-C_5H_5 and Ph groups. The ^{31}P-{^1H} NMR spectrum showed two singlet resonances at δ 71.7 and 65.1 ppm, as expected for the presence of two non-equivalent phosphorus nuclei.

The NMR properties of **1** in solution might be due to site-exchange of the ligands at the ruthenium centre, pivoting of the μ-CH=CH_2 group about the W—Ru bond with an exchange of the σ- and π-interactions between the two metal centres,[16–18,20] or a process similar to that invoked to explain the fluxionality of the π-allyl complex [W(CO)$_2$(η^3-CH_2CHCH_2)(η-C_5H_5)].[21] The latter complex is mapped with **1** since the Ru(CO)$_2$(cdpe) fragment is isolobal with a CH_2 group.[22] Hence it is attractive to consider that **1** undergoes the exchange process shown in Scheme 2(1) which is analogous to that proposed to account for the variable temperature NMR properties of [W(CO)$_2$(η^3-CH_2CHCH_2)(η-C_5H_5)]. Isomer **A** in Scheme 2(1) is the form established by the X-ray diffraction study and is assumed to be the major isomer. Alternatively, the NMR data do not exclude site-exchange at the ruthenium

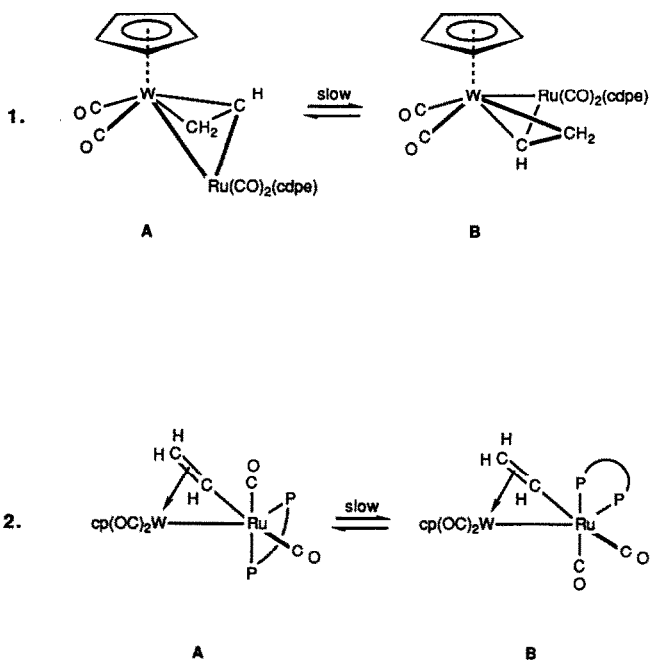

Scheme 2.

centre, as depicted in Scheme 2(2). Intuitively we regard pivoting of the μ-CH=CH$_2$ group about the W—Ru bond to be less likely than the processes shown in Scheme 2.

EXPERIMENTAL

All experiments were carried out under nitrogen. Solvents were rigorously dried before use. Light petroleum refers to that fraction of b.p. 40–60°C. NMR spectra were recorded with JNM FX90Q, GX200 or GX400 instruments, and IR spectra were measured with Nicolet MX10 or MX5 spectrophotometers. For NMR data all chemical shifts are in ppm and coupling constants are in Hz. The ^{13}C-{^1H} NMR chemical shifts are positive to high frequency of $SiMe_4$, and the ^{31}P-{^1H} chemical shifts are positive to high frequency of 85% H_3PO_4 (external). The compounds [W(≡CMe)(CO)$_2$(η-C$_5$H$_5$)][23] and [Ru(CO)$_4$(η-C$_2$H$_4$)][2,24] were prepared by methods previously reported. The complex [Ru(CO)$_3$(cdpe)] was obtained as described below.

Synthesis of the complex [Ru(CO)$_3$(cdpe)]

A sample of [Ru$_3$(CO)$_{12}$] (0.30 g, 0.47 mmol) in light petroleum (*ca* 250 cm^3) contained in a water-cooled, round-bottom flask was irradiated with light from two 100 W light bulbs, while a slow stream of ethylene was continually passed through the mixture. After several hours the solution became colourless signifying complete conversion of the [Ru$_3$(CO)$_{12}$] into [Ru(CO)$_4$(η-C$_2$H$_4$)] (ν_{CO} (max) at 2104w, 2023s and 1998s cm^{-1}).[2] The light petroleum solution of [Ru(CO)$_4$(η-C$_2$H$_4$)] was then added slowly (*ca* 30 min) to a CH_2Cl_2 (15 cm^3) solution of cdpe (0.61 g, 1.53 mmol), the mixture being continuously stirred and purged with nitrogen. If the solution of [Ru(CO)$_4$(η-C$_2$H$_4$)] is added too rapidly to the cdpe the yield of desired product is reduced, due to the formation of side-products including [Ru$_2$(μ-cdpe)(CO)$_6$].[25] Stirring was continued for *ca* 9 h before solvent was removed *in vacuo*. The yellow residue was dissolved in CH_2Cl_2–light petroleum (8 cm^3, 1 : 3) and chromatographed on an alumina column (3 × 20 cm). Elution with the same solvent mixture afforded a yellow fraction. Removal of solvent *in vacuo* give pale yellow *microcrystals* of [Ru(CO)$_3$(cdpe)] (0.18 g, 65%) (Found: C, 59.9; H, 3.8. $C_{29}H_{22}O_3P_2Ru$ requires: C, 59.9; H, 3.8%). ν_{max}(CO) at 2007s, 1936m and 1910vs cm^{-1} (in CH_2Cl_2). NMR (in $(CD_3)_2CO$): ^1H, δ 7.36–7.56 (m, 22 H, CH and Ph); ^{13}C-{^1H}, δ 211.6 (t, CO, *J*(PC) 11), 147.3 (m, CH=CH), 137.4 [m, C^1(C$_6$H$_5$)], 132.6, 130.9 and 129.4 (m × 3, Ph); ^{31}P-{^1H}, δ 78.5s.

Chloroform solutions of [Ru(CO)$_3$(cdpe)] slowly decompose at room temperature affording quantitatively the ruthenium(II) species [RuCl$_2$(CO)$_2$(cdpe)] (Found: C, 53.7; H, 3.8. $C_{28}H_{22}Cl_2O_2P_2Ru$ requires: C, 53.8; H, 3.6%). ν_{max} (CO) at 2081m and 2014s cm^{-1}. ^{31}P-{^1H} NMR (in $CDCl_3$), δ 67.5 [d, *J*(PP) 7] and 47.7 [d, *J*(PP) 7], with weak signals due to minor isomers observed.

Synthesis of the complex [WRu(μ-σ,η²-CH=CH$_2$)(CO)$_4$(cdpe)(η-C$_5$H$_5$)]

A mixture of [Ru(CO)$_3$(cdpe)] (0.20 g, 0.34 mmol) and [W(≡CMe)(CO)$_2$(η-C$_5$H$_5$)] (0.11 g, 0.34 mmol) was refluxed for 48 h in THF (30 cm^3). The solvent was removed *in vacuo*, and the residue was dissolved in CH_2Cl_2–light petroleum (1 : 4), and chromatographed on an alumina column (3 × 15 cm). Elution with the same solvent mixture removed initially a trace of an unidentified product. Further elution gave an orange fraction which after removal of solvent *in vacuo* yielded orange *microcrystals* of [WRu(μ-σ,η²-CH=CH$_2$)(CO)$_4$(cdpe)(η-C$_5$H$_5$)] (**1**) (0.21 g, 70%) (Found: C, 49.4; H, 3.7. $C_{37}H_{30}O_4P_2RuW$ requires: C, 50.2; H, 3.4%). ν_{max} (CO) at 2015m, 1956vs, 1862s and 1779m cm^{-1} (in CH_2Cl_2). NMR (in CD_2Cl_2 at −80°C): ^1H (major isomer), δ 2.44 (d, 1 H, CH_2, *J*(HH) 11), 2.69 (d, 1 H, CH_2, *J*(HH) 8), 4.43 (s, 5 H, C_5H_5), 5.63 (m, 1 H, CH), and 6.64–8.16 (m br, 22 H, CH=CH and Ph); ^{13}C-{^1H} (peaks for minor isomer indicated by an asterisk), δ 231.9, *231.5, 228.5, *227.0 (WCO), 201.4 (m br), *199.6, *198.5 [d, *J*(PC) 8], 197.9 [d, RuCO, *J*(PC) 15], *150.2 [d of d, *J*(PC) 27, 39], 148.2 [d of d, *J*(PC) 37, 37], *147.2 [d of d, *J*(PC) 39, 42], 145.6 [d of d, PCH=CHP, *J*(PC) 27, 39], 137.6 [d, *J*(PC) 49], *136.8 [d, *C*H=CH$_2$, *J*(PC) 46], 134.9 – 123.9 (Ph), *89.0, 87.6 (η-C$_5$H$_5$), *45.4 and 43.0 (CH=*C*H$_2$). ^{31}P-{^1H} (peaks for minor isomer indicated by an asterisk), δ 71.7, 65.1, *60.0 [d, *J*(PP) 28] and *58.7 [d, *J*(PP) 28].

X-ray crystallographic data

Orange crystals of **1** were grown from CH_2Cl_2–light petroleum (1 : 4). Diffraction data were collected on a Nicolet R3m/μ diffractometer at 298 K using a crystal of dimensions *ca* 0.52 × 0.40 × 0.20 mm. Of the 4825 intensities measured (ω-scans, $2\theta \leqslant 45°$), 3881 unique intensities had $F \geqslant 5\sigma(F)$, and only these were used in the solution and refinement of the structure. Intensity data were corrected for Lorentz, polarization and X-ray absorption effects. The latter by a procedure based upon azimuthal scan data.

Crystal data. $C_{37}H_{30}O_4P_2RuW$, $M = 885.5$,

monoclinic, $a = 10.340(2)$, $b = 26.525(4)$, $c = 12.105(2)$ Å, $\beta = 95.44(2)°$, $U = 3305(1)$ Å^3, $Z = 4$, $D_c = 1.78$ g cm^{-3}, $F(000) = 1728$, space group $P2_1/n$, μ(Mo-K_α) = 41.01 cm^{-1}, Mo-K_α X-radiation ($\bar{\lambda} = 0.71073$ Å graphite monochromator).

The structure was solved and all non-hydrogen atoms were located by conventional heavy-atom and difference Fourier methods. The vinyl hydrogen atoms could not be located with certainty and were not included in the refinement. All remaining hydrogen atoms were included in calculated positions with common refined isotropic thermal parameters. Refinement by full-matrix least-squares converged at $R = 0.025$ ($R_w = 0.029$) with a weighting scheme of the form $w^{-1} = [\sigma^2(F) + 0.001|F|^2]$.† The final electron density difference synthesis showed no peaks greater than 0.68 or less than -0.94 e Å^{-3}. Scattering factors were from ref. 26. All calculations were carried out on a DEC Microvax computer using the *SHELXTL* system of programs.[27]

Acknowledgement—We thank Dr M. L. Williams for helpful discussions.

REFERENCES

1. F. G. A. Stone, *Pure Appl. Chem.* 1986, **58**, 529; F. G. A. Stone, *Am. Chem. Soc., Symp. Ser.* 1983, **211**, 383; F. G. A. Stone, *Angew. Chem., Int. Ed. Engl.* 1984, **23**, 89.
2. F. G. A. Stone and M. L. Williams, *J. Chem. Soc., Dalton Trans.* 1988, 2467.
3. S. J. Dossett, A. F. Hill, J. C. Jeffery, F. Marken, P. Sherwood and F. G. A. Stone, *J. Chem. Soc., Dalton Trans.* 1988, 2453; J. A. Abad, L. W. Bateman, J. C. Jeffery, K. A. Mead, H. Razay, F. G. A. Stone and P. Woodward, *J. Chem. Soc., Dalton Trans.* 1983, 2075.
4. R. B. King, P. M. Treichel and F. G. A. Stone, *J. Am. Chem. Soc.* 1961, **83**, 3600.
5. D. L. Davies, M. J. Parrott, P. Sherwood and F. G. A. Stone, *J. Chem. Soc., Dalton Trans.* 1987, 1201.
6. J. A. K. Howard, J. C. V. Laurie, O. Johnson and F. G. A. Stone, *J. Chem. Soc., Dalton Trans.* 1985, 2017.
7. L. Busetto, M. Green, B. Hessner, J. A. K. Howard, J. C. Jeffery and F. G. A. Stone, *J. Chem. Soc., Dalton Trans.* 1983, 519.
8. L. J. Farrugia, J. C. Jeffery, C. Marsden, P. Sherwood and F. G. A. Stone, *J. Chem. Soc., Dalton Trans.* 1987, 51.
9. M. I. Bruce and A. G. Swincer, *Adv. Organomet. Chem.* 1983, **22**, 59.
10. R. D. Adams and I. T. Horváth, *Prog. Inorg. Chem.* 1985, **33**, 127.
11. M. R. Awang, J. C. Jeffery and F. G. A. Stone, *J. Chem. Soc., Dalton Trans.* 1983, 2091.
12. R. E. Colborn, D. L. Davies, A. F. Dyke, A. Endesfelder, S. A. R. Knox, A. G. Orpen and D. Plaas, *J. Chem. Soc., Dalton Trans.* 1983, 2661 and refs cited therein.
13. C. P. Casey, P. J. Fagan, W. H. Miles and S. R. Marder, in *Organometallic Compounds: Synthesis, Structure and Theory* (Edited by B. L. Shapiro), pp. 86–114. Texas A&M University Press, U.S.A. (1983).
14. J. C. Jeffery, M. J. Parrott, U. Pyell and F. G. A. Stone, *J. Chem. Soc., Dalton Trans.* 1988, 1121; E. Delgado, J. C. Jeffery and F. G. A. Stone, *J. Chem. Soc., Dalton Trans.* 1986, 2105.
15. M. Lourdichi and R. Mathieu, *Nouv. J. Chim.* 1982, **6**, 231; M. Lourdichi and R. Mathieu, *Organometallics* 1986, **5**, 2067.
16. P. O. Nubel and T. L. Brown, *J. Am. Chem. Soc.* 1984, **106**, 644.
17. C. P. Casey, S. R. Marder and B. R. Adams, *J. Am. Chem. Soc.* 1985, **107**, 7700.
18. A. F. Dyke, S. A. R. Knox, M. J. Morris and P. J. Naish, *J. Chem. Soc., Dalton Trans.* 1983, 1417.
19. M. R. Awang, J. C. Jeffery and F. G. A. Stone, *J. Chem. Soc., Dalton Trans.* 1986, 165.
20. J. R. Shapley, S. I. Richter, M. Tachikawa and J. B. Keister, *J. Organomet. Chem.* 1975, **94**, C43.
21. J. W. Faller, C. C. Chen, M. J. Mattina and A. Jakubowski, *J. Organomet. Chem.* 1973, **52**, 361 and refs cited therein.
22. R. Hoffmann, *Angew. Chem., Int. Ed. Engl.* 1982, **21**, 711.
23. W. Uedelhoven, K. Eberl and F. R. Kreissl, *Chem. Ber.* 1979, **112**, 3376.
24. B. F. G. Johnson, J. Lewis and M. V. Twigg, *J. Organomet. Chem.* 1974, **67**, C75.
25. M. I. Bruce, M. L. Williams, B. W. Skelton and A. H. White, *J. Organomet. Chem.* 1986, **306**, 115.
26. *International Tables for X-Ray Crystallography*, Vol. 4. Kynoch Press, Birmingham (1974).
27. G. M. Sheldrick, *SHELXTL programs for use with the Nicolet X-Ray System Revision 5.1.* Göttingen (1986).

†Atomic positional and thermal parameters, bond lengths and angles, and structure factor values have been deposited as supplementary material with the Editor. Atomic coordinates have also been submitted to the Cambridge Crystallographic Data Centre.

Polyhedron Vol. 8, No. 5, pp. 701–703, 1989
Printed in Great Britain

0277–5387/89 $3.00+.00
© 1989 Pergamon Press plc

COMMUNICATION

GROUP 10 TELLURIDE AND POLYTELLURIDE COMPLEXES: SYNTHESIS AND STRUCTURES OF $Pd(Te_4)_2^{2-}$ AND $(Ph_3P)_2Pt(\mu\text{-}Te)_2Pt(PPh_3)_2$

RICHARD D. ADAMS* and THOMAS A. WOLFE

Department of Chemistry, University of South Carolina, Columbia, SC 29208, U.S.A.

and

BRYAN W. EICHHORN and ROBERT C. HAUSHALTER*

Exxon Research and Engineering Company, Annandale, NJ 08801, U.S.A.

(*Received* 19 *September* 1988; *accepted* 4 *November* 1988)

Abstract—$PdCl_2$ reacts with K_2Te_4 in DMF to produce $Pd(Te_4)_2^{2-}$, which was isolated as a bis-PPh_4^+ salt. The X-ray structure of this compound revealed a square-planar palladium atom with two chelated Te_4^{2-} ligands. $Pt(PPh_3)_4$ reacts with $(Bu_4N)_4Hg_4Te_{12}$ in DMF to produce $(Ph_3P)_2Pt(\mu\text{-}Te)_2Pt(PPh_3)_2$ which was also characterized by single-crystal X-ray diffraction.

There is a growing interest in the synthesis of new telluride and polytelluride complexes for use as IR sensory materials,[1] superconducting solids[2] and amorphous spin glasses with tunable conducting properties.[3,4] Several new pseudo-binary polytelluride complexes have recently been prepared that could serve as precursors to metastable materials, that are inaccessible by other synthetic methods.[4] These compounds include $Mo_4Te_{16}(en)_4^{2-}$,[5] $NbTe_{10}^{3-}$,[6] $Hg_4Te_{12}^{4-}$,[7] $^1_\infty[Hg_2Te_5^{2-}]$,[7] $Cr(\eta^2\text{-}Te_2)_2(CO)_2^{2-}$,[8] $Fe_2Te_3(CO)_6^{2-}$[9] and $Cr_3Te_{24}^{3-}$,[10] to name a few. We report here the synthesis and structures of two new telluride complexes, namely $Pd(Te_4)_2^{2-}$†[11] and $(Ph_3P)_2Pt(\mu\text{-}Te)_2Pt(PPh_3)_2$.

The $Pd(Te_4)_2^{2-}$ ion, **1**, was prepared by reacting anhydrous $PdCl_2$ with a DMF extract of a melt of nominal composition K_2Te_4 (*ca* 2 equiv of K_2Te_4 per $PdCl_2$) followed by the addition of excess PPh_4Br in ethylenediamine (en) according to eq. (1)

$$PdCl_2 + 2K_2Te_4 \xrightarrow[DMF/en]{\text{excess } PPh_4Br} Pd(Te_4)_2(PPh_4)_2 + 2KCl + 2KBr. \quad (1)$$

The palladium–telluride complex was isolated as a crystalline bis-tetraphenylphosphonium salt of formula $Pd(Te_4)_2(PPh_4)_2$ in a *ca* 30% yield based on $PdCl_2$. The crystals were small opaque rectangles that would not redissolve in en at room temperature. The compound was characterized by microprobe analysis and single-crystal X-ray diffraction.‡

Two views of the $Pd(Te_4)_2^{2-}$ ion are given in Fig. 1. The top view shows the two chelating Te_4^{2-} chains that form the familiar square-planar coordination geometry about palladium. The ion has D_2 point symmetry with three, mutually orthogonal, two-fold rotation axes passing through the palladium

* Authors to whom correspondence should be addressed.

† Just prior to the submission of this manuscript, we discovered that Kanatzidis had apparently made the same compound.[11]

‡ Crystal data for $Pd(Te_4)_2(PPh_4)_2$: triclinic, space group $P\bar{1}$, $a = 11.035(2)$, $b = 23.394(5)$, $c = 10.529(4)$ Å; $\alpha = 102.73(2)$, $\beta = 100.46(3)$, $\gamma = 97.21(2)°$, $V = 2568(1)$ Å^3, $Z = 2$, Mo-K_α radiation ($\lambda = 0.71069$ Å) at 23°C. An empirical absorption correction was applied ($\mu = 49.19$ cm^{-1}). The structure was solved by a combination of direct methods and difference Fourier syntheses, and successfully refined by full-matrix least-squares with $R = 0.056$ and $R_w = 0.071$ for 4899 reflections with $(I) > 4\sigma(I)$.

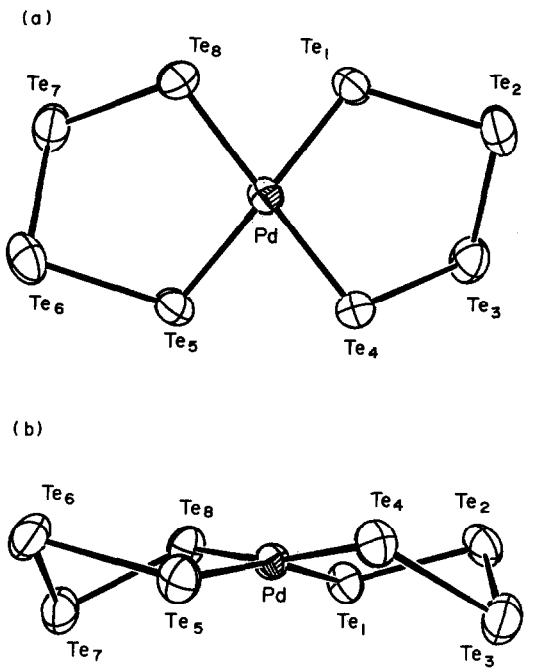

Fig. 1. Two views of the $Pd(Te_4)_2^{2-}$ anion. Pertinent bond distances (Å) and angles (°) are: Pd—Te(1), 2.600(2); Pd—Te(4), 2.585(2); Pd—Te(5), 2.603(2); Pd—Te(8), 2.586(2); Te(6)—Te(7), 2.714(3); Te(2)—Te(3), 2.716(3); other intrachain Te—Te distances, 2.76(2) (av); Te(1)—Te(8), 3.214(2); Te(4)—Te(5), 3.256(2). Te(4)—Pd—Te(1), 104.57(7); Te(4)—Pd—Te(5), 77.76(7); Te(5)—Pd—Te(8), 104.59(8); Te(8)—Pd—Te(1), 76.60(7).

atom. The side view [Fig. 1(b)] illustrates the puckered nature of the $PdTe_4$ rings which are quite similar to the MS_4 rings in the $M(S_4)_2^{2-}$ sulphur analogues (where M = Ni, Pd).[12] The Pd—Te distances average 2.59(2) Å and are indicative of single bonds based on expectations from the covalent radius of Pd^{2+} [13] and M—Te distances in other polytelluride complexes.[5,7,14] The Te—Te contacts within the Te_4 chains average 2.74(4) Å, which are typical single bond distances.[5,7,14] The Te—Pd—Te angles are distorted from 90°, with obtuse angles within the $PdTe_4$ rings [104.6(1)° (av)] and acute angles between rings [77(1)° (av)]. The Te(1)—Te(8) and Te(4)—Te(5) separations are non-bonding at 3.24(4) Å (av).

We have also been investigating the reactions between zero-valent, unsaturated transition-metal fragments (ML_n) with homo- and heteropolyatomic anions. These studies have produced the remarkable compounds $Sn_9Cr(CO)_3^{4-}$ [15] and $As_7Cr(CO)_3^{3-}$ [16] but we have been unsuccessful in isolating transition-metal complexes that contain intact heteropolyatomic anionic fragments such as $SnTe_4^{4-}$ [17] or $Au_4Te_4^{4-}$.[18] For example, the reaction between $Cr(CO)_3(\eta^6$-mesitylene) and an en extract of KAuTe (which presumably contains $K_2Au_4Te_4^{2-}$ anions in solution[18]) in the presence of excess 2,2,2-crypt yields $Cr(\eta^2\text{-}Te_2)_2(CO)_2^{2-}$ with two disordered K^+/Au^+ cations [$(K_xAu_{1-x}$-2,2,2-crypt) where $x < 1$].[8] Clearly, complex equilibria are

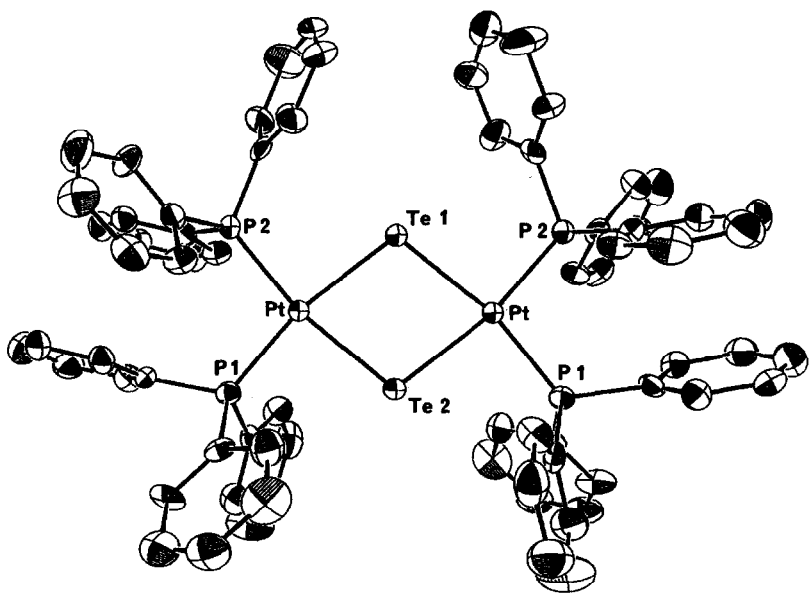

Fig. 2. A perspective of the $(Ph_3P)_2Pt(\mu\text{-}Te)_2Pt(PPh_3)_2$ molecule as viewed perpendicular to the Pt_2Te_2 plane. Pertinent bond distances (Å) and angles (°) are: Pt—Te(1), 2.612(1); Pt—Te(2), 2.628(1); Pt—P(1), 2.308(4); Pt—P(2), 2.276(3); Te(1)—Te(2), 3.258(2). Te(1)—Pt—Te(2), 76.90(3); Te(2)—Pt—P(1), 90.78(9); P(1)—Pt—P(2), 100.4(1); Te(1)—Pt—P(2), 91.86(2); Pt—Te(2)—Pt, 102.66(5); Pt—Te(1)—Pt, 103.54(5).

established when these polyatomic anions are dissolved and subsequent reactions are not straightforward. Such is the case for the reaction between $(Bu_4N)_4Hg_4Te_{12}$[7] and $Pt(PPh_3)_4$.

A 1 : 1 (mol %) mixture of $(Bu_4N)_4Hg_4Te_{12}$[7] and $Pt(PPh_3)_4$ in DMF results in the formation of $(Ph_3P)_2Pt(\mu\text{-}Te)_2Pt(PPh_3)_2 \cdot 3DMF$ (**2**). Compound **2** was isolated as brown parrallellogram-shaped crystals in *ca* 20% yield based on platinum. The fate of the mercury in this reaction is currently unknown. The molecular structure* of **2**, shown in Fig. 2, comprises two edge-shared square-planar platinum fragments bridged by two Te^{2-} ligands with a planar Pt_2Te_2 core. The Pt—Te distances are 2.62(2) Å (av), with a non-bonding Te—Te separation of 3.26(1) Å. The molecule sits on a crystallographic two-fold rotation axis defined by the Te—Te vector and is most likely isostructural with sulphur and selenium analogues.[19] Two of the solvate DMF molecules are crystallographically equivalent, whereas the third unique solvate molecule is disordered about the two-fold axis. The solvate molecules do not interact with the $(Ph_3P)_2Pt(\mu\text{-}Te)_2Pt(PPh_3)_2$ complex in the solid state.

It is interesting to compare the structure of **2** with that of (triphos)Ni(μ-η^2-Te_2)Ni(triphos) [triphos = $MeC(CH_2PPh_2)_3$] which has a Te—Te separation of 2.802(1) Å.[20] The latter molecule appears to have a "neutral" Te_2 fragment that bridges two zero-valent nickel atoms, whereas compound **2** clearly has two non-interacting Te^{2-} ligands that bridge two Pt^{2+} centres.

* Crystal data for $(Ph_3P)_2Pt(\mu\text{-}Te)_2Pt(PPh_3)_2$; monoclinic, space group $C2/c$, $a = 18.150(8)$, $b = 17.587(6)$, $c = 29.916(5)$ Å; $\beta = 92.20(3)°$, $V = 7628.4$ Å^3, $Z = 4$, Mo-K_α radiation ($\lambda = 0.71073$ Å) at 23°C. An empirical absorption correction was applied ($\mu = 47.7$ cm^{-1}). The structure was solved by a combination of direct methods and full-matrix least-squares with $R = 0.049$ and $R_w = 0.065$ for 3452 reflections with $(I) > 3\sigma(I)$.

REFERENCES

1. R. Korenstein, W. E. Hoke, P. J. Lemonias, K. T. Higa and D. C. Harris, *J. Appl. Phys.* 1987, **62**, 4929. Also see, *J. Crystal Growth* 1987, **81**, 97, 483, 501, 505, 506, 508, 543.
2. M. Potel, P. Gougion, R. Chevrel and M. Sergent, *Rev. Chim. Minerale*, 1984, 509.
3. R. C. Haushalter, C. M. O'Conner, J. P. Haushalter, A. M. Umarji and G. K. Shenoy, *Angew. Chem. Int. Ed. Engl.* 1984, **23**, 169.
4. R. C. Haushalter, D. P. Goshorn, M. G. Sewchock and C. B. Roxlo, *Mat. Res. Bull.* 1987, **22**, 761.
5. B. W. Eichhorn, R. C. Haushalter, F. A. Cotton and B. Wilson, *Inorg. Chem.* 1988, **27**, 4084.
6. W. A. Flomer, J. W. Kolis, *J. Am. Chem. Soc.* 1988, **110**, 3682.
7. R. C. Haushalter, *Angew. Chem. Int. Ed. Engl.* 1985, **24**, 433.
8. B. W. Eichhorn, R. C. Haushalter, W. Pennington, results to be published.
9. J. Merola, B. W. Eichhorn and R. C. Haushalter, manuscript in preparation.
10. J. W. Kolis, personal communication.
11. M. G. Kanatzidis, *196th ACS Meet.* Los Angeles, California (25–30 September 1988); *Abstr.*; INOR 469.
12. A. Muller, E. Krickemeyer, H. Bogge, W. Clegg and G. Sheldrick, *Angew. Chem. Int. Ed. Engl.* 1983, **22**, 1006.
13. James E. Huheey, *Inorganic Chemistry: Principles of Structure and Reactivity*, 2nd edn. Harper and Row, New York (1978).
14. W. A. Flomer, S. C. O'Neal, J. W. Kolis, D. Jeter and A. W. Cordes, *Inorg. Chem.* 1988, **27**, 969.
15. B. W. Eichhorn, R. C. Haushalter and W. Pennington, *J. Am. Chem. Soc.* 1988, **110**, 8704.
16. B. W. Eichhorn and R. C. Haushalter, J. C. Huffman, *Angew. Chem.*, submitted.
17. R. G. Teller, L. J. Krause and R. C. Haushalter, *Inorg. Chem.* 1983, **22**, 1809.
18. R. C. Haushalter, *Angew. Chem. Int. Ed. Engl.* 1985, **24**, 432.
19. R. Ugo, G. LaMonica, S. Cenini and F. Conti, *J. Chem. Soc. A* 1971, 522.
20. M. DiVaira, M. Peruzzini and P. Stoppioni, *J. Chem. Soc., Chem. Commun.* 1986, 374.

Polyhedron Vol. 8, No. 5, pp. 705–706, 1989
Pergamon Press plc. Printed in Great Britain

BOOK REVIEW

Advanced Inorganic Chemistry: A Comprehensive Text. 5th edn. F. Albert Cotton and Geoffrey Wilkinson. John Wiley, New York, 1988. xvii + 1455 pp, Figures and tables, 16 × 23.5 cm, $44.95.

Inasmuch as my reviews of the first four editions of this popular standard reference text have appeared in *J. Chem. Educ.* (1963, **40**, 230; 1967, **44**, A240; 1973, **50**, A347; 1981, **58**, A204), I shall concern myself here primarily with the differences between the 4th and 5th editions of a book which successfully accomplishes its purpose—" to provide the [senior-year or first-year graduate] student with the background necessary to comprehend current research literature in inorganic and certain aspects of organometallic chemistry". At first sight the new edition appears to conform to the unfortunate trend of texts to become longer and longer, being a full 2.1 cm (more than 3/4 in) thicker than the previous edition. In this case, however, appearance is deceptive, for the 5th edition is a mere 60 pages longer than the 4th edition. The increase in thickness is largely due to the use of heavier paper, which, together with larger and darker type, make this new edition more legible and attractive than the previous one. The book has been completely revised, updated (most of the references are from primary journals from mid-1979 to mid-1987), and expanded to emphasize the latest developments (1472 vs 1412 pp.) by the judicious rearrangement and careful rewriting of chapters and of material within sections, as well as by the meticulous insertion of new material.

The authors' trend toward decreasing the amount of theoretical material in previous editions has continued because "the continuing rapid growth of the chemistry... required the addition of important new facts to all of the descriptive material", "much of the theoretical background has found its way into textbooks used at a lower (American undergraduate) level" and "we have, over the years, become less persuaded of the value of certain types of theory" ("Theories come and go. Twenty-five years ago, when we began writing these books, there were widely accepted ideas about bonding that have by now fallen into disuse, and even disrepute").

Part 1, "Survey of Principles" (formerly titled "Introductory Topics") has been condensed from five chapters (209 pp.) to two chapters (83 pp.). Former Chapters 1, 2 and 4—"Monomolecular Solids" (25 pp.), "Symmetry and Structure" (33 pp.) and "Classification of Ligands by Donor Atoms" (88 pp.), respectively—have been eliminated, and some of their material has been placed elsewhere. Chapter 1, "Concepts in Stereochemistry and Bonding" (32 pp.) is an expanded version of the former Chapter 5, "Stereochemistry and Bonding in Main Group Compounds" (17 pp.). Chapter 2, "Introduction to Ligands and Complexes" (49 pp.) is an updated version of former Chapter 3 of the same title (46 pp.).

Part 2, "The Chemistry of the Main Group Elements", now the longest part of the book, has been expanded from 402 to 535 pages by the addition of new sections such as "Alkali Metal Salts of Complex Anions", "Compounds with Element–Element Double Bonds", "Ligands Formed by the Group VA (15) Elements" (The new IUPAC group numbering system as well as the familiar Mendeleev system is used throughout the book), "Oxygen and Oxygen Compounds as Ligands", "Sulfur and Sulfur Compounds as Ligands" and "Halide Ions and Halogen Compounds as Ligands". Expanded and updated sections include "Alkali Metal Complexes", "Carbon and Carbon Compounds as Ligands", "Dinitrogen and Nitrogen Compounds as Ligands", "Chemical Properties of Dioxygen", "Singlet Oxygen" and "Oxo Acids of Sulfur". Substantially expanded chapters include those on "Boron: Group IIIA (13)" (from 63 to 72 pp.), "Carbon . . ." (from 22 to 31 pp.), "Nitrogen . . ." (from 31 to 77 pp.), "The Group VA (15) Elements . . ." (from 45 to 62 pp.), "Oxygen . . ." (from 19 to 47 pp.), "The Group VIA (16) Elements . . ." (from 40 to 53 pp.) and "The Group VIIA (17) Elements . . ." (from 35 to 43 pp.). The chapter on "The Group IVA (14) Elements . . ." has been substantially condensed (from 55 to 40 pp.).

Part 3, "The Chemistry of the Transition Elements", formerly the longest part of the book, has been condensed from 428 to 393 pages. Former Chapter 20,"The Transition Elements and the Electronic Structures of Their Compounds" (70 pp.), has been severely compressed into Chapter 17, "Survey of the Transition Metals" (24 pp.), by deletion of the sections on "The Molecular Orbital Theory", "Electronic Absorption Spectra" and "Structural and Thermodynamic Consequences of Partly Filled *d* Shells". Chapter 19, "The Elements of the Second and Third Transition Series", has been expanded from 159 to 179 pages. New sections in Part 3 include "Spin-State Crossovers", "Mixed Oxidation States and Other Topics", "Niobium and Tantalum Cluster Complexes" and "Triple and Quadruple M—M Bonds", while the sections on "Magnetic Properties of Transition Metal Compounds", platinum metals and organometallic compounds have been expanded.

Part 4, "Survey of Selected Areas . . ." (formerly "Special Topics"), has been expanded from 297 to 356 pages. Former Chapter 25, "Metal Carbonyls and Other Complexes with π-Acceptor Ligands", retitled "Transition Metal Carbon Monoxide Compounds", has been rearranged and rewritten but not increased in length (31 pp.). Former Chapter 26, "Metal-to-Metal Bonds and Metal Atom Clusters", has been expanded from 33 to 45 pages by the addition of much new material. Former

Chapter 27, "Transition Metal Compounds with Bonds to Hydrogen and Carbon" (70 pp.), has been completely rewritten and expanded (89 pp.) into three separate chapters: "Transition Metal Compounds with Bonds to Hydrogen" (25 pp.), "Compounds with Transition Metal Single, Double, and Triple Bonds to Carbon" (30 pp.), and "Compounds of Transition Metals with Alkenes, Alkynes, and Delocalized Hydrocarbon Systems" (34 pp.). Former Chapter 28, "Reaction Mechanisms and Molecular Rearrangements in Complexes" (51 pp.), retitled "Reaction Mechanisms of Transition Metal Complexes" (52 pp.), has remained virtually unchanged in length. Former Chapter 29, "Transition Metal to Carbon Bonds in Synthesis" (31 pp.), has been rewritten and expanded to "Oxidative-addition and Migration (Insertion) Reactions" (38 pp.), while former Chapter 30, "Transition Metal to Carbon Bonds in Catalysis" (45 pp.), has been expanded to "Homogeneous Catalytic Synthesis of Organic Chemicals by Transition Metal Complexes" (59 pp.). Once again, the text ends with a chapter on "Bioinorganic Chemistry", now expanded from 36 to 42 pages.

The useful appendices have been expanded from 19 to 31 pages. Those on "Atomic Orbitals" (3 pp.), "The Quantum States Derived from Electronic Configurations" (5 pp.) and "Magnetic Properties of Chemical Compounds" (4 pp.) have been deleted, and new appendices on "Ionic Radii" (4 pp.), taken largely from former Chapter 1, and on "Basic Concepts of Molecular Symmetry; Character Tables" (21 pp.), taken largely from former Chapter 2, have been added. The detailed index has been expanded from 30 to 45 pages.

Although the introductory quotation is ascribed to Marcelin (rather than the correct Marcellin) Berthelot, the book is virtually free of errors, and the date of the discovery of Zeise's salt, the earliest known organotransition metal complex, has been corrected from 1845 (4th edn) to 1827 (p. 71). In short, in this 5th edition, Al Cotton and Geoff Wilkinson have continued their comprehensive and authoritative coverage of modern inorganic chemistry, while incorporating the latest developments and changes in areas of research activity, without allowing the size of their book to get out of hand. Considering the wide scope of this text, its price makes it a "best buy".

GEORGE B. KAUFFMAN
California State University, Fresno
Fresno, CA 93740, U.S.A.

Polyhedron Vol. 8, No. 6, pp. 707–726, 1989
Printed in Great Britain

0277–5387/89 $3.00+.00
© 1989 Pergamon Press plc

POLYHEDRON REPORT NUMBER 28

PHOSPHORANE IMINATO COMPLEXES OF TRANSITION METALS

KURT DEHNICKE*

Fachbereich Chemie der Philipps-Universität Marburg, Hans Meerwein-Straße, D-3550 Marburg, F.R.G.

and

JOACHIM STRÄHLE

Institut für Anorganische Chemie der Universität, Auf der Morgenstelle 18, D-7400 Tübingen, F.R.G.

CONTENTS

1. INTRODUCTION 707

2. SYNTHESES 708
2.1. Syntheses from nitrido complexes 708
2.2. Syntheses from azido complexes of transition metals 710
2.3. Syntheses from nitrosyl complexes 711
2.4. Syntheses from metal halides and iminophosphoranes 712
2.5. Miscellaneous syntheses 714

3. REACTIONS 715

4. CRYSTAL STRUCTURES 716

5. SPECTROSCOPIC PROPERTIES 720
5.1. IR spectra 720
5.2. NMR spectra 722

6. BONDING IN THE M—N—P MOIETY 723

REFERENCES 724

1. INTRODUCTION

Phosphorane iminato complexes of the transition metals are compounds with the ligand NPR_3^- (A), which is not known as a free ion. The group is isoelectronic with the corresponding, mostly very stable phosphorane oxide (B). Both types of compounds form stable complexes with Lewis acidic metal halides. Whereas in the case of the phosphorane oxide ligand (B) only compounds of the

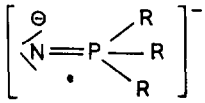

(A)

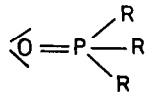

(B)

* Author to whom correspondence should be addressed.

donor–acceptor type (D) are known, the transition metal is connected by the nitrogen atom of the anion (A) via a short distance that can be interpreted as a double bond (C). The substituent R

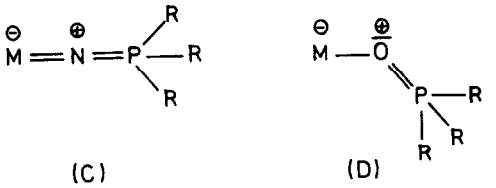

(C) (D)

bound to the P atom, are usually organic residues, rarely halogen atoms for complexes of type (C). The sequence MNP is generally linear, though, compounds with smaller bond angles down to 130° are known as well. Independent of these bond angles, the observed bond distances always represent double bonds. For the case of a bent MNP group, the situation is best described by the resonance formulae (E). Among cyclic diphosphorane iminato complexes the bent arrangement is forced by

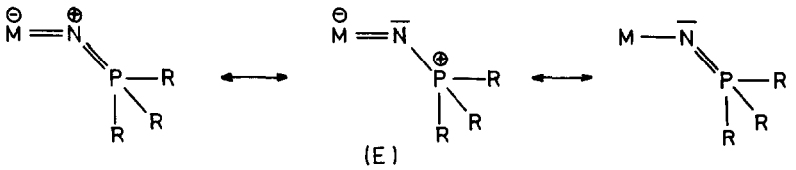

(E)

the geometry of the ring; the M—N—P bond angles are, however, in these cases also close to 139°. Less common are arsane iminato complexes. Nevertheless, spectroscopic findings allow the conclusion that a similar bonding situation is present.

2. SYNTHESES

2.1. *Syntheses from nitrido complexes*

Nitrido complexes of molybdenum, tungsten, rhenium, ruthenium and osmium in which the nitrido ligand acts as a terminal ligand of the type M≡N or as a bridging type $M{\equiv}\overset{\oplus}{N}{-}\overset{\ominus}{M}$, respectively,[1] are frequently able to react with suitable phosphanes to yield phosphorane iminato complexes.

The first examples of phosphorane iminato complexes of molybdenum and tungsten were prepared in 1970 by the reaction of triphenylphosphane with molybdenum or tungsten nitride chloride,[2] respectively, in boiling dichloromethane:[3]

$$\underset{M = Mo, W}{MNCl_3 + PPh_3} \longrightarrow \underset{\textbf{(I)}}{M(NPPh_3)Cl_3}. \qquad (1)$$

Compounds **I** are linked by chloro bridges. The constitution of these complexes however was not revealed until later. When reaction (1) is carried out with an excess of PPh_3 in CCl_4 at a higher temperature, the dimeric complex $[Mo(NPPh_3)Cl_3(PPh_3)]_2$ **(II)**[4] is obtained which has chlorine bridges. The additional molecule of PPh_3 is coordinated to the molybdenum atom. Reaction (1) is accompanied by a simultaneous redox reaction in which the transition metal is reduced from +VI to +IV and correspondingly the phosphorus is oxidized to the phosphorane imine ligand.

In 1973, Griffith and co-workers found productive syntheses for various phosphorane iminato complexes of ruthenium and osmium.[5] The reactions of the tetrachloro and tetrabromo nitrido osmates, $AsPh_4[OsNX_4]$, with PPh_3 in cold acetone, proceeded according to eq. (2):[5]

$$\underset{(X = Cl, Br)}{AsPh_4[OsNX_4] + 3PPh_3} \xrightarrow{OCMe_2} \underset{\textbf{(III)}}{[Os(NPPh_3)X_3(PPh_3)_2] \cdot Me_2CO} + AsPh_4X. \qquad (2)$$

Whereas the analogous reaction with $AsPh_4[RuNCl_4]$ only leads to the formation of $AsPh_4[RuCl_4(PPh_3)_2]$, complexes of type **III** with the general formula $[M(NPR_3)Cl_3(PR_3)_2]$ (M = Ru or Os; PR_3 = PPh_3, PPh_2Et, $PPhEt_2$ or PPh_2Me), could be obtained in high yields by the reaction of excess

PR_3 with $[MNCl_3(AsPh_3)_2]$ in cold acetone:[5]

$$[MNCl_3(AsPh_3)_2]+3PR_3 \longrightarrow [M(NPR_3)Cl_3(PR_3)_2]+2AsPh_3. \quad (3)$$

In the case of $PR_3 = PPhMe_2$, the intermediately formed complexes, $[M(NPPhMe_2)Cl_3(AsPh_3)_2]$, could be isolated.[5] Compounds **III** usually are orange–brown crystalline powders, the effective magnetic moments of which are ~ 1.8 BM for the osmium complexes and approximately 2.8 BM for the ruthenium complexes, corresponding to metal atoms in the oxidation state +IV.[5]

The mechanism of the synthesis of the phosphorane iminato complexes from nitrido compounds, can be interpreted as a nucleophilic attack of the phosphorus atom of the phosphane on the nitrido nitrogen atom.[5] Apparently, two factors are of importance: the ligands at the phosphorus atom of the phosphane as well as the electron density of the nitrogen atom which is influenced by the transition metal atom of the nitrido component. Finally, the capability of reducing the transition metal is also one condition for the synthesis of phosphorane iminato complexes. Examples in which the Lewis basic properties predominate are the nitrido complexes of rhenium(V) and rhenium(VI). This is obvious from the formation of donor–acceptor complexes with boron trihalides like $[Re(NBX_3)Cl_2(PR_3)_3]$,[6] $[Re(NBCl_3)Cl_2(PMe_2Ph)_3]$[7] and $AsPh_4[Re(NBBr_3)Br_4]$,[8] as well as with gold(I) chloride, $[Re(NAuCl)Cl_2(PMe_2Ph)_3]$.[7] The reaction of PPh_3 with $ReNCl_4$—a nitrido complex of rhenium(VII) that forms a columnar structure with alternating $Re^{\ominus}\equiv N^{\oplus}—Re^{\ominus}\equiv N^{\oplus}$ bonds[9]—however, occurs without problems at $-20°C$ in CH_2Cl_2 solution:[10]

$$ReNCl_4+2PPh_3 \longrightarrow [(PPh_3)Cl_4Re(NPPh_3)]. \quad (4)$$

On the other hand, $ReNCl_3$ or $[ReNCl_4]^-$ only react with PPh_3 on forming adducts,[10] presumably because the reduction potential of PPh_3 does not suffice to reduce rhenium(VI) to rhenium(IV). Dilworth *et al.*[11] reported a similar observation in the synthesis of $[Re(NPPh_3)(SPh)_4]$ from $ReNCl_2(PPh_3)_2$ and SPh^- in acetonitrile, which only proceeds upon exposure to oxygen and wherein the first formed $[ReN(SPh)_4]^{2-}$ is oxidized intermediately to the rhenium(VII) complex, which then reacts with PPh_3 yielding the phosphorane iminato complex:[11]

$$[ReNCl_2(PPh_3)_2] \xrightarrow{SPh^-} [ReN(SPh)_4]^{2-} \xrightarrow{O_2} [ReN(SPh)_4] \xrightarrow{PPh_3} [Re(NPPh_3)(SPh)_4]. \quad (5)$$

In the case of the reaction of the diimine complex $[MoNCl_4]_2$ with triphenyl phosphane, the synthesis of the phosphorane iminato complex proceeds because of the cleavage of the N=N bond without any change in the +V oxidation state of the molybdenum atom:[4]

$$Cl_4Mo^{\ominus}=N^{\oplus}=N^{\oplus}=Mo^{\ominus}Cl_4+4PPh_3 \longrightarrow 2[MoCl_4(NPPh_3)(PPh_3)]. \quad (6)$$

The same compound is also obtained by the reaction of PPh_3 with the chloro thionitrene complex $[MoCl_4(NSCl)]_2$,[4] whereby a reduction of molybdenum(VI) to molybdenum(V) occurs:[4]

$$[MoCl_4(NSCl)]_2+7PPh_3 \longrightarrow 2[MoCl_4(NPPh_3)(PPh_3)]+2SPPh_3+Cl_2PPh_3. \quad (7)$$

The course of reaction (8) also underlines the importance of the redox potential of the reactants for the formation of phosphorane iminato complexes from nitrido compounds. Whereas the treatment of $PPh_4[MoNCl_4]$ with PCl_5[12] does not yield a phosphorane iminato complex, the chlorine substituted product is easily formed by the presence of phosphorus trichloride:[4]

$$2PPh_4[MoNCl_4]+PCl_3+PCl_5 \longrightarrow 2PPh_4[MoCl_5(NPCl_3)]. \quad (8)$$

Reaction (9), however, proceeds with the preservation of the +VI oxidation state at the tungsten atom. The reaction of tungsten nitride chloride with bis(trichlorophosphorane)iminium chloride, primarily leads to the tetrachloro nitrido tungstate, which, however, already reacts further at room temperature in CH_2Cl_2 solution to yield the phosphorane iminato complex:[13]

$$WNCl_3+[Cl_3PNPCl_3]Cl \longrightarrow [Cl_3PNPCl_3][WNCl_4] \longrightarrow Cl_5WNP(Cl_2)NPCl_3. \quad (9)$$

The astonishing formation of the molecule $Cl_5WNP(Cl_2)NPCl_3$ from the ionic precursor complex can be explained by the continuously conjugated chain of the framework WNPNP, which is obvious from the almost planar arrangement and the only slightly different P—N bonds (see Section 4).

According to the NMR spectrum, the compound has to be understood as a zwitter-ion.[13]

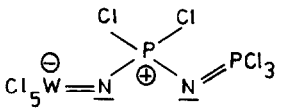

2.2. *Syntheses from azido complexes of transition metals*

The first example of this type of synthesis was found by Strähle and co-workers by the reaction of niobium tetrachloride azide, $[NbCl_4N_3]_2$,[14] with triphenylphosphane in 1,2-dichloromethane:[15]

$$[NbCl_4N_3]_2 + 2PPh_3 \longrightarrow [Nb(NPPh_3)Cl_4]_2 + 2N_2. \quad (10)$$

The reaction proceeds rapidly and nearly completely at room temperature. Later, it was also possible to apply this reaction to the corresponding tantalum compound $[TaCl_4N_3]_2$.[14] In this case, however, the reaction with triphenylphosphane takes a more complex course. Besides the formation of the phosphorane iminato complex $[Ta(NPPh_3)Cl_4]_2$,[16] the monomeric phosphorane iminato complex $[Ta(NPPh_3)Cl_4(HNPPh_3)]$,[16] solvated by the phosphorane imine $HNPPh_3$, is additionally obtained by the involvement of the solvent:

$$[TaCl_4N_3]_2 + 2PPh_3 + C_2H_4Cl_2 \longrightarrow [TaCl_4(NPPh_3)(HNPPh_3)] + TaCl_5 + C_2H_3Cl + 2N_2. \quad (11)$$

The reaction proceeds rapidly above 0°C. At lower temperatures, first the intensely yellow "phosphazide"[16] is formed, which in the case of the niobium compound [eq. (10)] is indicated by the transient red colour of the solution arising from a short lived intermediate only.[15]

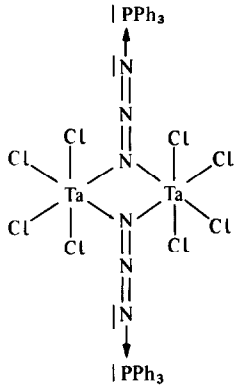

For the mechanism of formation of phosphorane iminato complexes from transition metal azides, an analogous picture to the well investigated Staudinger reaction therefore arises. Primary attack of the triphenylphosphane at the γ-N atom has been proved for this reaction by the aid of ^{15}N labelled *p*-toluene sulphone acid azide.[17] Such an adduct was isolated in the form of the complex

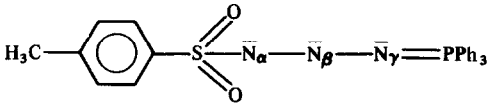

$[CH_3—C_6H_4—N=N—N=PPh_3 \cdot WBr_2(CO)_3]$ and confirmed by a crystal structure determination.[18] The decomposition can be understood in terms of the elimination of the β-N and the γ-N atom as N_2 after an additional bond to the α-N atom was formed:[19]

$$R—\bar{N}=\underline{N}—\bar{N}=PPh_3 \longrightarrow R—\bar{N}(/\bar{N}=\bar{N}/)—PPh_3 \longrightarrow R—\bar{N}=PPh_3 + N_2. \quad (12)$$

Triphenylphosphane also reacts outright and with complete conversion with the pentachloro azido metallates of niobium and tantalum (in CH_2Cl_2 solution),[20] or with the corresponding pentabromo metallates (in CH_2Br_2 solution),[21] to yield the anionic phosphorane iminato complexes:

$$[MX_5N_3]^- + PPh_3 \longrightarrow [X_5M{=}N{=}PPh_3]^- + N_2. \quad (13)$$
$$(M = Nb, Ta;\ X = Cl, Br)$$

The counter ions, PPh_4^+ or $AsPh_4^+$, are used because their salts are readily soluble in CH_2X_2. In the case of the niobium compounds, spontaneous elimination of N_2 occurs. In the case of the tantalum compound the reaction needs photochemical activation. In refluxing CH_2Cl_2 under UV irradiation (several hours), the tetraphenylarsonium pentachloro azido niobate even reacts with triphenylarsane forming a triphenylarsane iminato complex,[21] which to our knowledge is the first compound of this type:

$$AsPh_4[NbCl_5N_3] + AsPh_3 \xrightarrow{h\nu} AsPh_4[Cl_5Nb{=}N{=}AsPh_3] + N_2. \quad (14)$$

The properties and the spectroscopic data for this arsane iminato complex correspond almost exactly with those of the analogous phoshorane iminato complexes.[21]

2.3. *Syntheses from nitrosyl complexes*

The reduction of nitrosyl complexes with phosphanes to form phosphorane iminato complexes has only occasionally been reported. The reactions proceed according to the stoichiometry:

$$\overset{\ominus}{M}{=}\overset{\oplus}{N}{=}\bar{O} + 2PR_3 \longrightarrow \overset{\ominus}{M}{=}\overset{\oplus}{N}{=}PR_3 + OPR_3. \quad (15)$$

They correspond formally to the uptake of six electrons for the nitrosyl nitrogen (from +III to −III). Four of the electrons come from the two phosphorus atoms of the two phosphane molecules—the residual two from the oxidation of the metal atom. Since the nitrosyl ligand NO^+ is isoelectronic with N_2, these reactions have model character for the understanding of the reduction of dinitrogen complexes, for which six electrons are also required.[22]

The reaction of $[MoCl_5(NO)]$ with dimethylphenylphosphane and with di(*n*-propyl)-phenylphosphane proceeds under very mild conditions:[23]

$$[MoCl_5(NO)] \xrightarrow{2R_3P} [MoCl_4(NPR_3)(OPR_3)]. \quad (16)$$

The reaction of triphenylphosphane with rhenium trichloride dinitrosyl[24] in dichloromethane even proceeds exothermically and spontaneously at room temperature:[25]

$$ReCl_3(NO)_2 + 2PPh_3 \longrightarrow [ReCl_3(NO)(NPPh_3)(OPPh_3)]. \quad (17)$$

The complex dissolves easily to give a deep green colour in dichloromethane. The crystal structure determination (Section 4) makes a direct comparison of the two isoelectronic species $NPPh_3^-$ and $OPPh_3$ possible.

Sellmann and co-workers found that the dinitrosyl molybdenum complex $[Mo(NO)_2(dttd)]$ [$dttd^{2-}$ = 2,3,8,9-dibenzo-1,4,7,10-tetrathia decan(2−)] reacts with various phosphanes PR_3 (PR_3 = PMe_3, PEt_3, $PMePh_2$, $PEtPh_2$, PPh_3) in THF to form the corresponding phosphorane iminato complexes:[26]

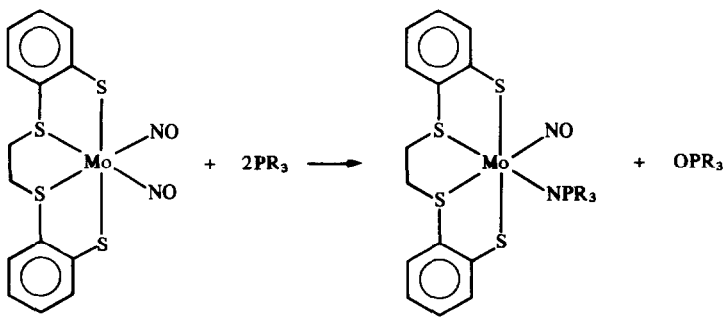

(18)

The reaction rates show a marked dependence on the phosphane substituent R. While reaction (18) with PMe_3,[26] as well as with $P(n\text{-But})_3$ and $P(Cy)_3$,[27] proceeds at room temperature within 5 min, the corresponding reactions with PPh_3[26] and with $Ph_2PC_2H_4PPh_2$[27] require 6 h in boiling THF. From this observation, Sellmann and co-workers infer a mechanism in which primary attack of the phosphorus atom occurs at the molybdenum atom, as it may be assumed that the different dimensions of the phosphane molecules are of greater influence with the already very sterically congested molybdenum atom than with the freely accessible nitrogen atom of the nitrosyl ligand. Due to the primary attack of the phosphane at the metal atom, the NO ligand could bend forming a one electron donor to maintain the 18 electron configuration at the molybdenum atom. Afterwards, deoxygenation of this NO ligand could be effected by a second phosphane molecule. Intramolecular P—N bond formation as well as isomerization eventually result in the final product:[26]

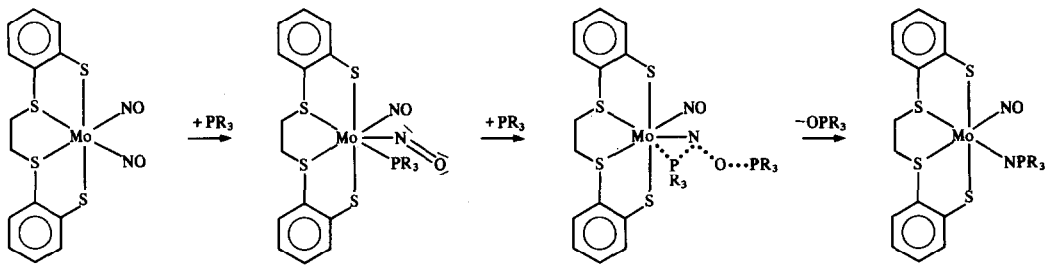

(19)

In other cases one should also discuss the possibility of a nucleophilic attack of the phosphane at the nitrosyl nitrogen atom and of a following deoxygenation by an additional phosphane molecule:

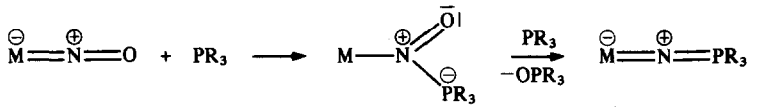

(20)

Generally predestined for a nucleophilic attack at the nitrosyl nitrogen atom are nitrosyl complexes with NO stretching vibrations in the region above $\sim 1870\ cm^{-1}$.[28] This condition is met for the nitrosyl complexes mentioned above, e.g. $[MoCl_5(NO)]$ ($2000\ cm^{-1}$)[23] and $ReCl_3(NO)_2$ (1910 and $1818\ cm^{-1}$),[24] but not, however, for the dinitrosyl complex $[Mo(NO)_2(dttd)]$ (1760 and $1665\ cm^{-1}$),[26] so that for this complex a mechanism according to reaction (19) is more likely.

Besides these two possibilities for a mechanistic course for the formation of phosphorane iminato complexes from nitrosyl complexes, the oxidation state of the central atom is also of importance. This follows for instance from the existence of the phosphane complex $[ReCl_2(NO)_2(PPh_3)_2]$ with rhenium(0), which does not show any tendency to form a phosphorane iminato complex.[29] From an analogy to the structurally investigated stibane complex $[ReCl_2(NO)_2(SbPh_3)_2]$,[30] one may conclude that the PPh_3 ligands are mutually *trans* to each other for the rhenium(0) phosphane complex. For $ReCl_3(NO)_2$ with rhenium(+I), however, spontaneous reaction with PPh_3 was observed [reaction (17)].

2.4. *Syntheses from metal halides and iminophosphoranes*

Preferred reagents for this route of synthesis are trimethylsilyl substituted iminophosphoranes, with their high tendency of forming the leaving group Me_3SiF or Me_3SiCl are used. The reactions take place according to the stoichiometry:

$$M\text{—}X + Me_3Si\text{—}N{=}PR_3 \longrightarrow M{=}N{=}PR_3 + X\text{—}SiMe_3 \qquad (21)$$
$$(X = F, Cl).$$

Occasionally hexamethyldisiloxane has also been used as a good leaving group. Thus the reaction of $VOCl_3$ with trimethylsilyltriphenyl iminophosphorane yields bis(triphenylphosphorane iminato)vanadium trichloride:[31]

$$VOCl_3 + 2Me_3SiN{=}PPh_3 \longrightarrow Cl_3V(NPPh_3)_2 + O(SiMe_3)_2. \qquad (22)$$

The reaction of osmium tetroxide with a bis(trimethylsilylated) disphosphorane, however, leads to

a trimethylsilyl group migration and to the formation of a chelate:[32]

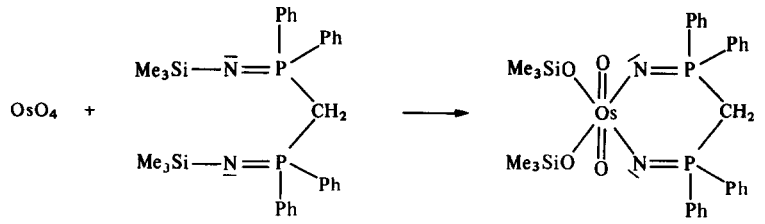

(23)

Determination of the molar mass proves the reaction product to be dimeric in solutions. Formation of a chelate is also observed with the reactions of the diphosphorane mentioned above with tungsten hexafluoride and -chloride:[33]

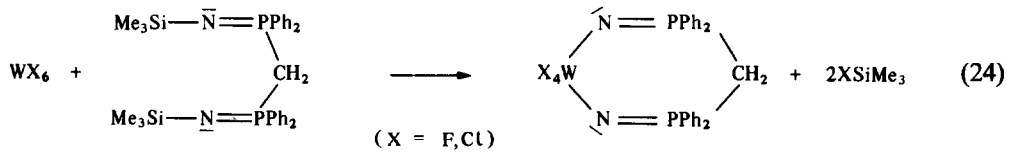

(24)

On treatment with the base DBU (1,8-diazabicyclo [5.4.0] undec-7-ene) HCl is split off from the chlorine derivative forming a conjugated heterocyclic system:[33]

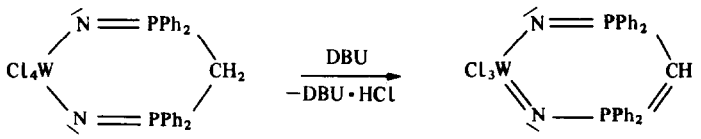

(25)

The reaction product is isoelectronic with $Cl_3W[N_2P_2(Ph_2)N]$, which is obtained by a different route (see below). It can be assumed that the initial step in the formation of the phosphorane iminato complex, according to reaction type (21), is a donor–acceptor complex, although these initial adducts cannot be isolated in general. One exception is the complex $[TiCl_4(Me_3SiNPPh_3)]$, which, however, was not fully characterized.[34]

In the case of the reaction of copper(II) chloride with trimethylsilyl triphenylphosphorane, however, a stable adduct was formed, which could be fully characterized by crystal structure determination[35] (see Fig. 1).

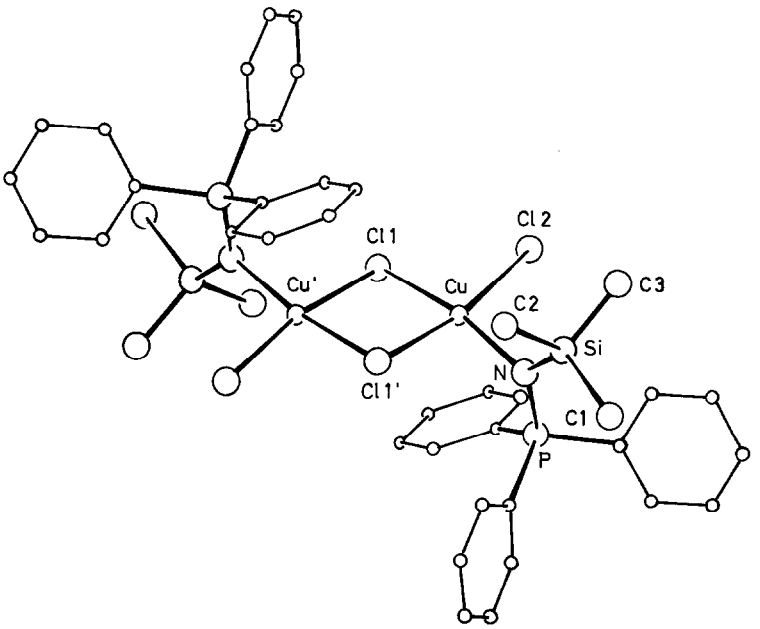

Fig. 1. Structure of the complex $[CuCl_2(Me_3SiNPPh_3)]_2$.

As expected, the nitrogen atom of the imino phosphorane is a donor atom, so that the subsequent formation of a phosphorane iminato complex is preformed. Preceding donor–acceptor complexes are also considered for the mechanism of the reactions (22) and (23), as bases like chinuclidine or chloride form complexes of the types $[VOCl_4]^-$,[36] $OsO_4 \cdot$ chinuclidine[37] and $PPh_4[OsO_4Cl]$[38] with $VOCl_3$ as well as OsO_4.

Many phosphorane iminato complexes have been synthesized according to the scheme of reaction (21). The first examples came from Dilworth and co-workers, in the reactions of cyclopentadienyl substituted titanium chloride:[34]

$$CpTiCl_3 + Me_3Si{-}N{=}PPh_3 \longrightarrow CpTiCl_2(NPPh_3) + ClSiMe_3. \quad (26)$$

Whereas $[Ti(\eta^5\text{-}C_5H_5)_2Cl_2]$ did not react and the reaction of $TiCl_4$ with $Me_3Si{-}N{=}PPh_3$ yielded the adduct mentioned above,[34] $TiCl(OR)_3$ ($R = C_3H_7$) could be converted to the bis(phosphorane iminato) complex on cleavage of the corresponding trimethylsilyl ether and simultaneous ligand exchange:[34]

$$2TiCl(OR)_3 + 2Me_3Si{-}N{=}PPh_3 \longrightarrow TiCl_2(NPPh_3)_2 + Ti(OR)_4 + 2Me_3SiOR. \quad (27)$$

Additional phosphorane iminato complexes obtaind according to the scheme of eq. (21) are:

$[TiCl(NPPh_3)(S_2CNEt_2)_2]$[34]
$[VOCl_2(NPPh_3)]$[34]
$[VOCl(NPPh_3)_2]$[34]
$[WF_4(NPPh_3)_2]$[39]
$[WF_4(NPMe_3)_2]$[40]
$[MoCl_4(NPPh_3)]_2$[41]
$[MoCl_3(NPPh_3)]_2$[42]
$[WCl_5(NPPh_3)]$[42]
$[WCl_4(NPPh_3)_2]$[42]
$[ReCl_3(NPPh_3)_2]_2$.[42]

An unexpected reaction occurred on the attempt to convert $PPh_4[MoCl_6]$ with trimethylsilyl triphenylphosphoranimine to an anionic phosphorane iminato complex. The reaction proceeds in dichloromethane at room temperature on redox disproportionation of the molybdenum, in the course of which three different products could be isolated:[42]

$$3PPh_4[MoCl_6] + 3Me_3Si{-}N{=}PPh_3 \longrightarrow (PPh_4)_2[MoCl_6] + PPh_4[MoNCl_4] + Ph_3PNPPh_3[MoCl_5(NPPh_3)] + 3ClSiMe_3. \quad (28)$$

It can be assumed that the phosphorane iminato complex $[MoCl_5(NPPh_3)]^-$, is produced first, which can also be synthesized and isolated from $[MoCl_4(NPPh_3)]_2$ and PPh_4Cl.[41] In CH_2Cl_2, however, it disproportionates in a slow reaction, when the only slightly soluble $(PPh_4)_2[MoCl_6]$ favours the course of the reaction:

$$2[MoCl_5(NPPh_3)]^- \longrightarrow [MoCl_6]^{2-} + [MoCl_4(NPPh_3)_2]. \quad (29)$$

The two phosphorane iminato ligands in $[MoCl_4(NPPh_3)_2]$, as well as in other bis(triorganophosphorane iminato) complexes, should be in a *cis* arrangement because of the strong π-bond contribution to the metal nitrogen bonds, so that the formation of the hexaphenyldiphosphazenium ion is facilitated:[42]

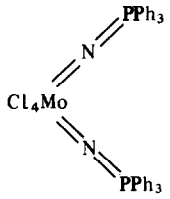

$$\longrightarrow [Ph_3PNPPh_3]^{\oplus}\,[MoNCl_4]^{\ominus} \quad (30)$$

2.5. *Miscellaneous syntheses*

Chlorothionitrene complexes, in which the $M{=}\overset{\oplus}{N}{=}\underset{\ominus}{\overset{-}{S}}{-}Cl$ moiety with the two-fold negatively charged $NSCl^{2-}$ group[43] is present, have occasionally been used as starting materials for the synthesis of phosphorane iminato complexes. This also includes the already mentioned synthesis of $[MoCl_4(NPPh_3)(PPh_3)]$ from $[MoCl_4(NSCl)]_2$ and excess triphenylphosphane [eq. (7)].[4] The

rhenium(VI) chlorothionitren complex, $[ReCl_4(NSCl)\cdot OPCl_3]$, can also be transformed with excess phosphorus trichloride into a phosphorane iminato complex:[44]

$$2[ReCl_4(NSCl)\cdot POCl_3] + 5PCl_3 \longrightarrow [ReCl_4(NPCl_3)]_2 + 2PSCl_3 + 2POCl_3 + PCl_5. \quad (31)$$

The reaction is combined with a reduction of the rhenium atom to +V. Cyclothiazeno complexes of the type

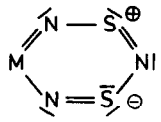

with a planar six-membered ring (see review in ref. 45) can in some cases also be decomposed to phosphorane iminato complexes on treatment with triphenylphosphane. In this way the synthesis of a bis(triphenylphosphorane iminato) complex of tungsten succeeded in addition to the formation of other products starting from cyclothiazeno tungsten trichloride[46] with excess triphenylphosphane:[47]

$$WCl_3(N_3S_2) \xrightarrow{PPh_3} WCl_4(NPPh_3)_2 + \cdots. \quad (32)$$

By analogy, the complex $[MoCl_4(NPPh_3)(Pyridine)]$ could also be prepared[48] from $[MoCl_3(N_3S_2)(Pyridine)]$[49] with triphenylphosphane and dichloromethane as solvent.

Using an analogous route, a phosphorane iminato complex of vanadium(IV)[50] is obtained by the reaction of triphenylphosphane with $[VCl_2(N_3S_2)(Pyridine)_2]$:[51]

$$[VCl_2(N_3S_2)(py)_2] + 2PPh_3 \xrightarrow{CH_2Cl_2} [VCl_3(NPPh_3)(py)_2] + \cdots. \quad (33)$$

Of special interest are the reactions of the bifunctional linear phosphazenium salt, $[H_2NPPh_2NPPh_2NH_2]^+Cl^-$, with different metal halides such as tungsten hexachloride,[52] tungsten hexafluoride and bromide,[53] rhenium pentachloride,[53] vanadium tetrachloride,[53] niobium pentachloride and molybdenum nitride chloride,[54] which according to the scheme of eq. (34) lead to cyclic phosphorane iminato complexes:[52–54]

$$WCl_6 + [H_2NPPh_2NPPh_2NH_2]Cl \xrightarrow[-4HCl]{} \quad (34)$$

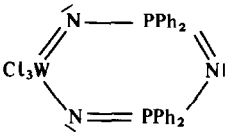

The reactions of VCl_4 and $ReCl_5$ require the oxidation by chlorine to transfer the metals into the highest possible oxidation state:[50]

$$ReCl_5 + Cl_2 + [H_2NPPh_2NPPh_2NH_2]Cl \xrightarrow[-4HCl]{} \quad (35)$$

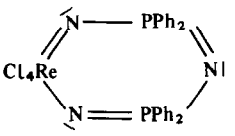

By halogen exchange of the product of eq. (34) with silver fluoride, $[F_3W(N_3P_2Ph_4)]$ could also be obtained.[50]

3. REACTIONS

Only a little is known about the chemistry of phosphorane iminato complexes. On contact with water most complexes undergo complete hydrolytic decomposition; in alkaline solution ammonia is released and the corresponding phosphoranoxide is formed. The fluoro complexes $[WF_4(NPPh_3)_2]$[39] and $[NPPh_2CH_2Ph_2PNWF_4]$[33] are remarkably unreactive toward water, which could be a kinetic phenomenon. Sellmann and co-workers showed that the velocity of the hydrolytic cleavage of the Mo—N bond in the complexes $[Mo(NO)(NPR_3)(dttd)]$ strongly depends on the residue R. Whereas the complex with R = Me reacts in THF solution at room temperature with

water within a few minutes, the corresponding reaction with R = Ph requires the addition of conc. HCl:[26]

$$2Mo(NO)(NPR_3)(dttd) \xrightarrow{H_2O} [Mo(NO)(dttd)]_2 + \text{additional products.} \quad (36)$$

The reaction of the phosphorane iminato complexes with water is presumably initiated by a proton transfer at the nitrogen atom. Experiments by Griffith and co-workers showed an example of an osmium complex that underwent protonation with $[AsPh_4][H_5O_2]Cl_2$, as well as deprotonation of the imide complex with NEt_3/PPh_3:[5]

$$[Os(NPPh_3)Cl_3(PPh_3)_2] \cdot Me_2CO \underset{Et_3N}{\overset{[AsPh_4][H_5O_2]Cl_2}{\rightleftharpoons}} [Os(NHPPh_3)Cl_4(PPh_3)] \cdot Me_2CO + PPh_3. \quad (37)$$

Treatment of the imido complex with additional hydronium ions results in the irreversible cleavage of the Os—N bond:[5]

$$[Os(NHPPh_3)Cl_4(PPh_3)] + [AsPh_4][H_5O_2]Cl \longrightarrow [Ph_3PNH_2]Cl \cdot H_2O + AsPh_4[OsCl_5(PPh_3)] + H_2O. \quad (38)$$

Oxidative splitting of the P—N bond of a phosphorane iminato complex has been observed for $[Os(NPPhMe_2)Cl_3(AsPh_3)_2]$, which can be transformed with chlorine into the osmium(VI) nitrido complex, from which the phosphorane iminato complex can again be reproduced with $PPhMe_2$:[5]

$$[Os(NPPhMe_2)Cl_3(AsPh_3)_2] \underset{PPhMe_2}{\overset{Cl_2}{\rightleftharpoons}} [OsNCl_3(AsPh_3)_2]. \quad (39)$$

When the phosphorane iminato complexes are associated by halogen bridges, the bridging bonds can be opened by coordinating solvents forming definite donor–acceptor complexes. Examples are seen in reactions of the cyclophosphorane iminato complexes $[NPPh_2NPPh_2NMCl_3]_n$ (M = Mo,[54] W[52]) with acetonitrile, which lead to the solvated complexes $[NPPh_2NPPh_2NMCl_3 \cdot CH_3CN] \cdot CH_3CN$. The complex $[MoCl_4(NPPh_3)]_2$, dimerized by $MoCl_2Mo$ bridges, could be converted upon treatment with tetraphenylphosphonium chloride in dichloromethane to the pentachloro derivative:[41]

$$[MoCl_4(NPPh_3)]_2 + 2PPh_4Cl \longrightarrow 2PPh_4[MoCl_5(NPPh_3)]. \quad (40)$$

4. CRYSTAL STRUCTURES

Table 1 provides a survey of the results of crystal structure determinations of phosphorane iminato complexes. The P—N bond distances are largely independent of the M—N bond lengths and M—N—P bond angles and lie in the narrow range of 159–166 pm. This is significantly shorter than the expected value for a P—N single bond (178 pm[56]) but somewhat longer than the P—N distances in cyclophosphazenes which are approximately 155 pm,[56] e.g. $[PNCl_2]_3$, 156 pm.[57] In phosphoranimines, $Ph_3P{=}NR$, with isolated P=N double bonds, P—N distances of approximately 157–160 pm are observed, e.g. 157.5 pm for R = α-C_5H_4N[58] and 160 pm for R = C_6H_5.[59]

The metal–nitrogen bond lengths vary within the larger range of 171–190 pm. By comparison,[1] these values too, can be interpreted roughly as M=N double bonds. Despite the uncertainties which naturally arise by the determination of the coordinates of the nitrogen atom besides the strongly scattering transition metal, it can be inferred from the data in Table 1 that a relatively short M=N distance correlates with a correspondingly long P=N distance and *vice versa*. M—N—P bond angles span a large range between 177 and 130°. In this respect it is remarkable that no drastic changes of the bond lengths M—N and N—P can be recognized even with small bond angles. As shown in Section 6 this behaviour can be explained by a simple orbital consideration. The small M—N—P bond angles of the cyclic bis(phosphorane iminato) complexes are caused by the geometry of the ring. The number of *d*-electrons at the transition metal does not seem to influence the bonding properties of the phosphorane iminato groups. With the exception of $[Re(NPPh_3)(SPh)_4]$, in which the rhenium atom has the coordination number five, the metal atoms of all other complexes are six-fold coordinated.

Table 1. Structural data for phosphorane iminato complexes of transition metals

	Space group	Number of formula units per unit cell	M—N (pm)	N—P (pm)	M—N—P (°)	Number of *d*-electrons	Reference
$[NbCl_4(NPPh_3)]_2 \cdot C_2H_4Cl_2$ (**1**)	$C2/c$	8	177.6(8)	163.7(9)	171.1(6)	0	15
$[TaCl_4(NPPh_3)]_2$ (**2**)	$P2_1/c$	4	180.1(8)	159.3(9)	176.8(7)	0	16
$[MoCl_4(NPPh_3)]_2 \cdot 2CH_2Cl_2$ (**3**)	$P2_1/n$	2	172.3(4)	165.6(4)	168.4(3)	1	41
$[MoCl_4(NPPh_3)(Pyridine)] \cdot CH_2Cl_2$ (**4**)	$P2_1/n$	4	171.9(9)	165.3(9)	176.6(6)	1	49
$[NPPh_2NPPh_2NMoCl_3(CH_3CN)] \cdot CH_3CN$ (**5**)	$P\bar{1}$	2	176.6(6); 178.9(6)	166.7(6); 163.3(6)	134.7(4); 134.3(4)	0	54
$[Mo(NO)(NPMePh_2)(dttd)]^a$ (**6**)	$P2_1/c$	4	190.4(6)	160.6(6)	129.7(4)	3	27
$[WF_4(NPPh_3)_2]$ (**7**)	$Fdd2$	8	182.5(6)	159.6(6)	157.2(4)	0	39
$[WF_4(NPMe_3)_2]$ (**8**)	$P2_1/n$	4	182.3(7); 181.6(7)	160.9(8); 163.2(7)	139.1(4); 139.1(4)	0	40
$[NPPh_2NPPh_2NWCl_3(CH_3CN)] \cdot CH_3CN$ (**9**)	$P\bar{1}$	2	177.3(5); 179.8(6)	166.3(7); 164.0(7)	134.5(4); 133.1(3)	0	52
$[WCl_5(NPCl_2NPCl_3)]$ (**10**)	$P2_1/n$	4	171(2)	166(2)	161(1)	0	13
$[Re(NPPh_3)(SPh)_4]$ (**11**)	[b]	[b]	174.3(7)	163.4(9)	163.1(6)	2	11
$[ReCl_3(NPPh_3)(NO)(OPPh_3)]$ (**12**)	$P2_1/n$	4	185.5(8)	163.0(8)	138.5(5)	4	25
$[RuCl_3(NPPhEt_2)(PPhEt_2)_2]$ (**13**)	$P2_12_12_1$	4	184.1(3)	158.6(3)	174.9(3)	4	55

[a] $dttd^{2-}$ = 2,3,8,9-dibenzo-1,4,7,10-tetrathiadecane(2−).

[b] No data published.

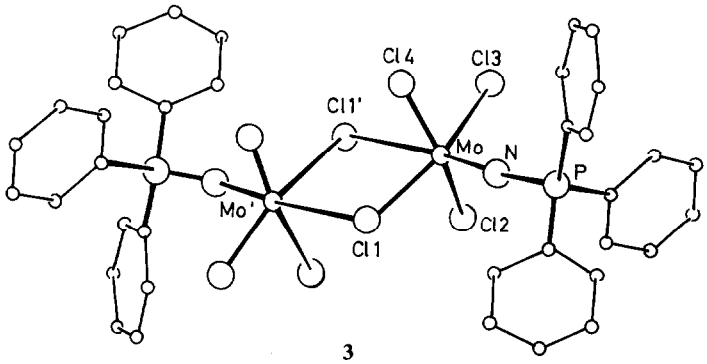

3

Fig. 2. Structure of the complex $[MoCl_4(NPPh_3)]_2$.[41]

In the dimeric tetrachlorophosphorane iminato complexes of niobium(V), tantalum(V), and molybdenum(V), the metal atoms are linked by asymmetric chloro bridges to centrosymmetric dimers[15,16,41] (see Fig. 2). The M···M distances of the three examples differ only slightly (Nb···Nb = 409.0 pm,[15] Ta···Ta = 411.2 pm,[16] Mo···Mo = 408.8 pm[41]). Therefore, a bonding interaction in the molybdenum(V) compound can be excluded. The M—Cl bond distances in the bridges MCl_2M are very different in length; they are 244 and 278 pm in the molybdenum compound. The long Mo—Cl bond is subject to the *trans*-influence of the Mo=N bond of the phosphorane iminato ligand. In its extent it corresponds to the effect of dimeric organoimido complexes with metal–nitrogen triple bonds as in $[Cl_4W{\equiv}N{-}{}^tC_4H_9]_2$, in which the bond distances in the WCl_2W bridge are 241 and 275 pm.[60] The large electron density of the M=N bonds in the phosphorane iminato ligands also causes the ligands in the *cis* position to be pushed away so that in all cases the bond angles $L_4(cis)M{=}N$ are recognizably larger than 90° and the metal atoms are above the plane of the four *cis* arranged ligands.

The *trans*-influence of the phosphorane iminato ligand is also shown by the long bonds which are formed between the metal and donor atoms on solvation with donor molecules such as pyridine in complex **4**[48] (see Fig. 3) or with acetonitrile in the isotypic complexes **5**[54] and **9** (see Fig 4).[52]

The Mo—N(pyridine) distance in **4** is 236 pm, the M—N(acetonitrile) bond lengths in **5** and **9** are 239 and 237 pm, respectively. From these distances only weak donor–acceptor bonds can be inferred in all cases. The *trans*-influence of the $(NPPh_3^-)$ group in the ruthenium(IV) complex (**13**) on the *trans* chlorine atom is interestingly only marginal. This Ru—Cl bond length is 239.7 pm, whereas both *cis* chlorine atoms exhibit Ru—Cl distance of 238.8 pm.[55] In the tungsten(VI) complex (**10**), however, a recognizable *trans*-influence of the phosphorane iminato ligand $(NPCl_2NPCl_3^-)$ is again observed. In this case the difference between the W—Cl(*trans*)/W—Cl(*cis*) bond lengths is 12 pm on average[13] (see Fig. 5). The ligand group $(NPCl_2NPCl_3^-)$ is isoelectronic with the molecular phosphazene $(OPCl_2NPCl_3)$,[61] which also has a planar skeleton OPNP with comparable bonding parameters.

The complexes **7** and **8**, contain both phosphorane iminato ligands in the *cis* position.[39,40] In

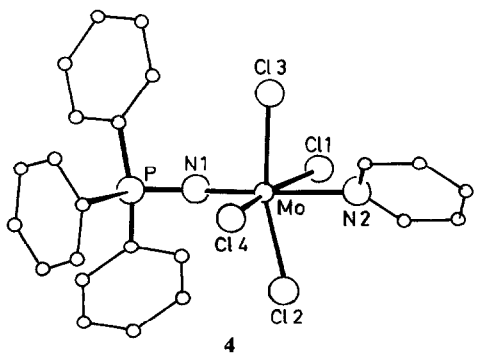

4

Fig. 3. Structure of the complex $[MoCl_4(NPPh_3)(Pyridine)]$.[49]

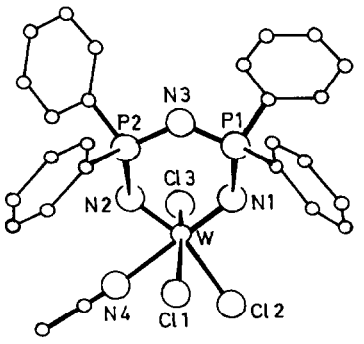

9

Fig. 4. Structure of the cyclic phosphorane iminato complex $[\overline{NPPh_2NPPh_2NW}Cl_3(CH_3CN)]$.[52]

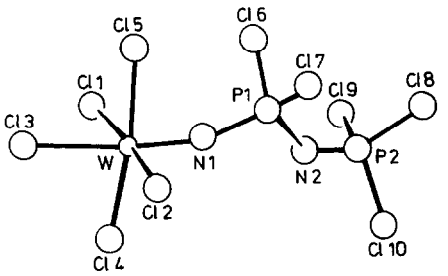

10

Fig. 5. Structure of the complex $[Cl_5W(NPCl_2NPCl_3)]$.[13]

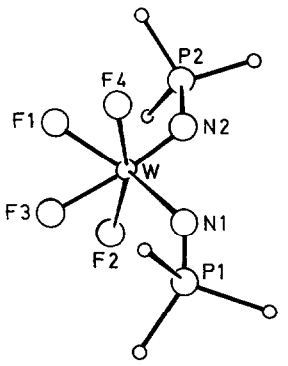

8

Fig. 6. Structure of the complex $[F_4W(NPMe_3)_2]$.[40]

this way good π-overlaps of both W—N bonds can be achieved, as is known from the *cis*-dioxo complexes of tungsten, as in the $[WO_2F_4]^{2-}$ ion,[62] for example. An indication of the high electron density of the *cis* positioned W=N bonds is also given by the large N—W—N bond angles, which are 98.5° for **7** and 99.6° for **8**.[39,40] A completely analogous situation is observed in complexes **12** and **6**, in which the phosphorane iminato ligand and the nitrosyl group are also in *cis* positions[25,27] (see Figs 7 and 8).

The N—M—N bond angles even attain values of 104.1° in complex **6** and 101.9° in complex **12**. The nitrosyl ligand is coordinated, in both examples, in a linear arrangement according to $\overset{\ominus}{M}{=}\overset{\oplus}{N}{=}\overline{O}$, so that a bond order of the M—N bond which corresponds to that of the phosphorane iminato ligand is realized.

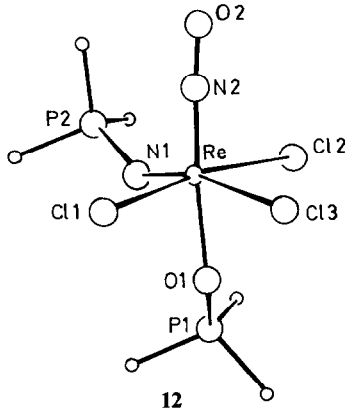

12

Fig. 7. Structure of the complex $[ReCl_3(NO)(NPPh_3)(OPPh_3)]$. (The ring carbon atoms of the phenyl groups are omitted.)

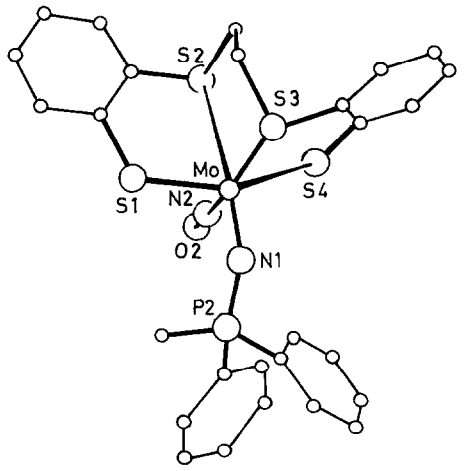

6

Fig. 8. Structure of the complex $[Mo(NO)(NPMePh_2)(dttd)]$.[27]

5. SPECTROSCOPIC PROPERTIES

5.1. *IR spectra*

In the IR spectra of the phosphorane iminato complexes a characteristic strong absorption appears in the range of *ca* 1100 cm^{-1}, which is assigned as the antisymmetric stretching vibration of the MNP group (Table 2). The corresponding symmetrical stretching vibration has only been assigned for a few examples; it generally lies slightly below 600 cm^{-1}. Both vibrations are maximally coupled by a linear arrangement (A)[64] so that the difference in the wave numbers is the largest.



One example is $[MoCl_4(NPPh_3)(pyridine)] \cdot CH_2Cl_2$ which has a bond angle, Mo—N—P, of 177° and the two stretching vibrations at 1130 and 560 cm^{-1}, corresponding to a difference of 570 cm^{-1}. In the case of the rhenium complex, $[Re(NO)(NPPh_3)Cl_3(OPPh_3)]$, with a Re—N—P bond angle of 139°, corresponding to form (B), both stretching vibrations are at 1017 and 627 cm^{-1}. Thus, the difference decreases to a value of 390 cm^{-1} because they are not as strongly coupled due to the smaller bond angle.[64]

Table 2. IR spectra

	ν_{as}(MNP) (cm^{-1})	ν_s(MNP) (cm^{-1})	Reference
$[TiCl(NPPh_3)(S_2CNEt_2)]$	1115, 1135		31
$[TiCl_2(NPPh_3)_2]$	1090, 1110		31
$[CpTiCl_2(NPPh_3)]$	1150		34
$[CpTiCl_2(NPPh_2Me)]$	1150		34
[Me—$CpTiCl_2(NPPh_3)$]	1150		34
$[VOCl(NPPh_3)_2]$	1095, 1120		31
$[VOCl_2(NPPh_3)]$	1095, 1115		31
$[VCl_3(NPPh_3)_2]$	1080, 1110		31
$[VCl_3(NPPh_3)(Pyridine)_2]$	1115	520	50
$[Cl_2\overline{VNPh_2PNPh_2PN}]$	1140–1280		53
$[Cl_2\overline{NbNPh_2PNPh_2PN}]$	1180, 1240		54
$[NbCl_4(NPPh_3)]_2$	1177		15
$PPh_4[NbCl_5(NPPh_3)]$	1138	580	20
$PPh_4[NbBr_5(NPPh_3)]$	1131	575	21
$AsPh_4[NbCl_5(NAsPh_3)]$	1155[a]	525[a]	21
$PPh_4[TaCl_5(NPPh_3)]$	1160, 1170[b]	570	20
$PPh_4[TaBr_5(NPPh_3)]$	1155	573	21
$[MoCl_3(NPPh_3)]_n$	1109		3
$[Cl_3\overline{MoNPh_2PNPh_2PN}]$	1175, 1250		54
$[MoCl_4(NPPh_3)]_2$	1119, 1137[b]	572	41
$[MoCl_4(NPPhMe_2)(OPPhMe_2)]$	1125		23
$[MoCl_4(NPPh_2^nPr)(OPPh_2^nPr)]$	1128 (^{15}N: 1120)		23, 63
$[MoCl_4(NPPh_3)(PPh_3)]$	1118	570	4
$[MoCl_4(NPPh_3)(Pyridine)] \cdot CH_2Cl_2$	1130	560	49
$PPh_4[MoCl_4(NPPh_3)(PPh_3)] \cdot 2CCl_4$	1120	564	4
$PPh_4[MoCl_5(NPPh_3)] \cdot CH_2Cl_2$	1122, 1132[b]	579	41
$PPh_4[MoCl_5(NPCl_3)]$	1130	585	4
$[Mo(NO)(NPMe_3)(dttd)]$[c]	1025		26
$[Mo(NO)(NPEt_3)(dttd)]$	1020		26
$[Mo(NO)(NPMePh_2)(dttd)]$	1050		26
$[Mo(NO)(NPEtPh_2)(dttd)]$	1050		26
$[Mo(NO)(NPPh_3)(dttd)]$	1040		26
$[WCl_3(NPPh_3)]_n$	1135		3
$[WF_4(NPMe_3)_2]$	1065–1110		40
$[WCl_4(NPPh_3)_2]$	1110, 1160[b]; 1220 (A_1, B_1)		42
$[WCl_5(NPPh_3)]$	1120, 1165[b]		42
$[WCl_5(NPCl_2NPCl_3)]$	1168		13
$[Re(NPPh_3)(SPh)_4]$	1120		11
$[ReCl_4(NPPh_3)(PPh_3)]$	1126		10
$[ReCl_4(NPCl_3)]_2$	1110		44
$[ReCl_3(NPPh_3)_2]_2$	1032, 1110[b]		42
$[Cl_4\overline{ReNPh_2PNPh_2PN}]$	1130–1270		53
$[Re(NO)(NPPh_3)Cl_3(OPPh_3)]$	1017	627	25
$[RuCl_3(NPPh_3)(PPh_3)_2] \cdot Me_2CO$	1108		5
$[RuCl_3(NPPh_2Et)(PPh_2Et)_2] \cdot Me_2CO$	1063		5
$[RuCl_3(NPPhEt_2)(PPhEt_2)_2]$	1165		5
$[RuCl_3(NPPh_2Me)(PPh_2Me)_2]$	1114		5
$[RuCl_3(NPPhMe_2)(AsPh_3)_2]$	1055		5
$[RuCl_3(NPEt_3)(PEt_3)_2]$	1099		5
$[OsCl_3(NPPh_3)(PPh_3)_2] \cdot Me_2CO$	1127 (^{15}N: 1104)		5
$[OsBr_3(NPPh_3)(PPh_3)_2] \cdot Me_2CO$	1125		5
$[OsCl_3(NPPh_2Et)(PPh_2Et)_2] \cdot Me_2CO$	1085		5
$[OsBr_3(NPPh_2Et)(PPh_2Et)_2] \cdot Me_2CO$	1090		5

Table 2—*continued*

	ν_{as}(MNP) (cm^{-1})	ν_s(MNP) (cm^{-1})	Reference
$[OsCl_3(NPPhEt_2)(PPhEt_2)_2]$	1204		5
$[OsBr_3(NPPhEt_2)(PPhEt_2)_2]$	1160		5
$[OsCl_3(NPPh_2Me)(PPh_2Me)_2]$	1128		5
$[OsCl_3(NPPhMe_2)(PPhMe_2)_2]$	1165		5
$[OsCl_3(NPPhMe_2)(AsPh_3)_2]$	1081		5
$[OsCl_3(NPEt_3)(PEt_3)_2]$	1125		5

[a] ν_{as}, ν_s(NbNAs).
[b] Splitting by Fermi-resonance.
[c] $dttd^{2-}$ = 2,3,8,9-dibenzo-1,4,7,10-tetrathiadecane(2−).

The available structural and spectroscopic information is not sufficient to draw up a correlation diagram of these effects. The value of ν_{as}(MNP) alone, however, gives in many cases an indication of the M—N—P bond angle. In this way ν_{as} is observed for $[MoCl_4(NPPh_3)]_2$ (with a Mo—N—P bond angle of 166°) at 1128 cm^{-1}, but for [Mo(NO)(NPMePh$_2$)(dttd)] (with a Mo—N—P bond angle of 130°) at 1050 cm^{-1}. In the spectra of cyclic phosphorane iminato complexes, the conditions are more complicated because of the peculiarities of the ring vibrations.

The influence of the negative charge in the anionic complexes on the MNP stretching vibrations is small compared to the spectra of the corresponding uncharged complexes. Thus the ν_{as}(MoNP) of $[MoCl_4(NPPh_3)]_2$ hardly changes at all by the transition to the ion $[MoCl_5(NPPh_3)]^-$; in the case of the two examples $[NbCl_4(NPPh_3)]_2$ and $[NbCl_5(NPPh_3)]^-$, ν_{as}(NbNP) is shifted to smaller wave numbers i.e. from 1177 to 1138 cm^{-1}.

Some of the phosphorane iminato complexes are associated by halogen bridges. The complexes $[MCl_4(NPPh_3)]_2$ (M = Nb, Ta, Mo) for instance, form centrosymmetric dimers with the molecular symmetry C_{2h}. The MCl_2M rings are planar; the M—Cl bond distances differ in length with values of 244 and 278 pm, because of the *trans* influence of the $(NPPh_3)^-$ groups, whereas the lengths of the terminal M—Cl bonds are significantly shorter, being 235 pm. In the IR spectra, the stretching vibrations of the terminal M—Cl bonds (~ 350 cm^{-1}) and of the bridging type bond (~ 275 cm^{-1}) can be clearly distinguished. Two IR active vibrations of the B_u mode are expected according to the selection rules for MCl_2M rings of C_{2h} symmetry;[64] in many cases, however, these vibrations are accidentally degenerate so that only one band can be observed.

On the formation of halogeno complexes as the ion $[MoCl_5(NPPh_3)]^-$,[41] the negative charge causes a weakening of the M—Cl bonds, which is shown by the shift of the MCl stretching vibration to smaller wave numbers by approximately 30 cm^{-1}. The halogen *trans* to the phosphorane iminato ligand is subject to its *trans*-influence, which can be observed in the IR spectrum by the appearance of another M—Cl stretching vibration at lower wave numbers. This stretching vibration appears to be close to the range of the above mentioned stretching vibrations of the MClM bridge; for the ion $[MoCl_5(NPPh_3)]^-$, for instance, this band is observed at 282 cm^{-1}.[41] The extent of the *trans*-influence of the phosphorane iminato group is comparable with the effect of other π-bonded ligands and ligand groups such as $M{=}\underline{\bar{O}}$, $M{\equiv}N|$, $M{\equiv}\overset{\ominus}{\underline{N}}\overset{\oplus}{R}$, $M{=}\underline{\overset{\ominus}{N}}{=}\underline{\bar{S}}$, $M{=}\underline{\overset{\ominus}{N}}{=}\underline{\overset{\oplus}{O}}$ etc., for which extensive spectroscopic data for comparisons are available.[65]

5.2. *NMR spectra*

NMR spectroscopic investigations for phosphorane iminato complexes are relatively small at present. In addition to the ^{31}P NMR spectra, some ^{14}N NMR spectra have also been measured, as well as ^{95}Mo and ^{51}V NMR (Table 3). ^1H NMR spectra are of secondary importance for the present problem of the phosphorane iminato complexes, they will therefore not be discussed.

In complexes of the type $[Mo(NO)(NPR_3)(dttd)]$,[26] the chemical shifts in the ^{14}N NMR spectra verify the oxidation state (−III) for the nitrogen, and the chemical shifts of the ^{95}Mo NMR spectra verify the oxidation state (+III) for the molybdenum.[26] This corresponds to a transfer of five electrons to one of the nitrosyl nitrogen atoms in the course of reaction (18)—two originate from

Table 3. NMR spectra

	Solvent	^{31}P (ppm) (relative to H_3PO_4)	Other nuclei (ppm) (in addition to ^1H NMR)	Reference
[Mo(NO)(NPMe$_3$)(dttd)][a]	CD_2Cl_2	37.3	^{14}N:[b] −333 ^{95}Mo:[c] 410(490 Hz)[d]	26
[Mo(NO)(NPEt$_3$)(dttd)]	CD_2Cl_2	50.6	−332 393(704 Hz)	26
[Mo(NO)(NPMePh$_2$)(dttd)]	CD_2Cl_2	29.6	−330	26
[Mo(NO)(NPEtPh$_2$)(dttd)]	CD_2Cl_2	31	−340 420(761 Hz)	26
[Mo(NO)(NPPh$_3$)(dttd)]	CD_2Cl_2	24	−380 430(673 Hz)	26
[Cl$_3$MoNPh$_2$PNPh$_2$PN]	CH_3CN, C_6D_6	42.4(s)	1105.7	54
[Cl$_3$WNPh$_2$PNPh$_2$PN]	CH_3CN, C_6D_6	39.2(s)		52
[F$_3$WNPh$_2$PNPh$_2$PN]	CH_3CN, CD_3CN	22.5(s)		53
[Br$_3$WNPh$_2$PNPh$_2$PN]	CH_3CN, CD_3CN	43.8(s)		53
[F$_4$WNPh$_2$PCH$_2$Ph$_2$PN]	DMF	29.7(m)		33
[Cl$_4$WNPh$_2$PCH$_2$Ph$_2$PN]	DMF	32.6(s)		33
[Cl$_3$WNPh$_2$PCHPh$_2$PN]	DMF	49.2(s)		33
[Cl$_4$ReNPh$_2$PNPh$_2$PN]	CH_3CN, CD_3CN	46.2(s)		53
[Cl$_2$VNPh$_2$PNPh$_2$PN]	CH_3CN, CD_3CN	43.7(s)	^{51}V:[e] 46.8(s)	53
[Cl$_2$NbNPh$_2$PNPh$_2$PN]	CH_3CN, CD_3CN	40.1(s)		54

[a] dttd^{2-} = 2,3,8,9-dibenzo-1,4,7,10-tetrathiadecane(2−).
[b] Relative to NH_4NO_3.
[c] Relative to $(NH_4)_6[Mo_7O_{24}]$.
[d] Half-width.
[e] Relative to $VOCl_3$.

the oxidation to the (NPR_3^-) ligand and two to the OPR_3 molecule, one follows from the oxidation of Mo(+II) to Mo(+III).[26] The chemical shifts of the ^{95}Mo NMR signal of [Cl$_3$MoNPh$_2$PNPh$_2$PN][54] and the ^{51}V NMR signal of [Cl$_2$VNPh$_2$PNPh$_2$PN][53] in contrast, prove the oxidation states of (+VI) and (+V), respectively.

The ^{31}P NMR spectra of the phosphorane iminato complexes exhibit a recognizable downfield shift in comparison with the non-metallated species like PhNPPh$_3$ (δ = 17.5 ppm[66]) or $N_3P_3Ph_6$ (δ = 14.3 ppm[67]). The deshielding of the phosphorus nuclei may be a consequence of the electron withdrawing influence of the metal centres, which is also expressed in the short metal–nitrogen bond distances.

In the case of compounds of the type [X$_n$MNPh$_2$PNPh$_2$PN] (X = halogen, n = 2, 3), which are associated by halogen bridges, it can be assumed that monomeric donor–acceptor complexes are formed by treatment with polar solvents like CH_3CN and dimethylformamide. The data of Table 3 for the mentioned types of compounds therefore refer to the corresponding donor–acceptor complexes.

6. BONDING IN THE M—N—P MOIETY

Table 1 shows that most phosphorane iminato complexes fall into two groups, one with an almost linear M—N—P arrangement and bond angles between 161 and 177°, and another with a bent M—N—P moiety and bond angles between 130 and 140°. Two different descriptions of the bonding in the M—N—P groups are therefore necessary. For the more common linear arrangement a possible bonding scheme was already suggested by Phillips and Skapski.[55] The bonding in the bent M—N—P group was briefly explained by Mronga *et al.*[25]

In the case of the almost linear M—N—P arrangement an *sp* hybridization must be assumed for the nitrogen atom, whereas the phosphorus atom is sp^3 hybridized, and the distorted octahedral coordinated metal atom has a d^2sp^3 hybridization using its d_{z^2} and $d_{x^2-y^2}$ orbitals. The M—N—P σ-bonds therefore result from an overlap of these hybrid orbitals leaving the metal d_{xz} and d_{yz} orbitals and the orbitals p_x and p_y of the N atom for the M—N π-bonding. For the P—N π-bonding in a linear arrangement only the d_{z^2} orbital of the P atom is available. The alternative orbital

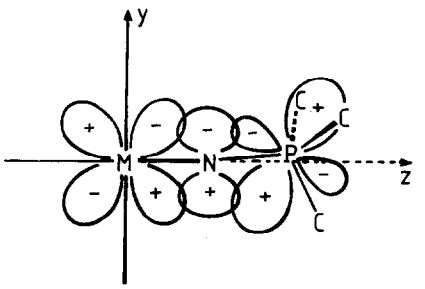

Fig. 9. Bonding situation in phosphorane iminato complexes with a nearly linear arrangement of the group M=N=P. The system of axes refers to the metal and nitrogen atoms only.[55]

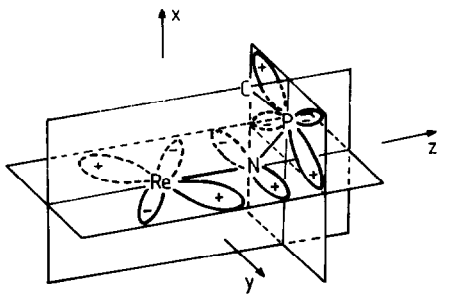

Fig. 10. Bonding scheme in a phosphorane iminato complex with a non-linear arrangement of the group M=N=P. The system of axes of the phosphorus atom is rotated by 45° around the z axis with respect to the system of axes of the metal and nitrogen atom.[25]

$d_{x^2-y^2}$, which could be involved in π-bonding in a tetrahedral coordination, is in this case not correctly disposed to interact with the nitrogen p_x or p_y orbitals.

In Figure 9, a schematic representation of the overlap in the M—N—P π-bonding is given. It results in a three-centre π-bond. In addition to that another perpendicular two-centre M—N π-bond can be formed by the d_{xz} orbital of the metal and the p_x orbital of the nitrogen atom.

A slight displacement of the phosphorus atom from the M—N axis leads to a better overlap of its d_{z^2} orbital with the p_y orbital of the nitrogen atom (Fig. 9). And in fact, such a displacement is always observed, resulting in a bond angle M—N—P between 161 and 177° (Table 1).

In the case of a bent M—N—P arrangement, an sp^2 hybridized N atom can be supposed using the s, p_x and p_z orbitals. An overlap of the p_y orbital of the nitrogen atom with the d_{z^2} orbital of the phosphorus atom to form a N—P π-bond is no longer possible in a bent M—N—P group. Therefore, only the $d_{x^2-y^2}$ orbital remains for π-overlap, as is schematically shown in Fig. 10. Together with the d_{yz} orbital of the metal a three-centre π-bonding again is formed.

However, for an additional two-centre M—N π-bond as in the case of the linear M—N—P group, no suitable orbital is available at the sp^2 hybridized nitrogen atom.

This difference between the bonding in the linear and in the bent M—N—P groups does not strongly influence the M—N and N—P bond lengths, which are in the same range in both arrangements. Therefore steric requirements may be responsible for the different geometries.

REFERENCES

1. K. Dehnicke and J. Strähle, *Angew. Chem.* 1981, **93**, 451; K. Dehnicke and J. Strähle, *Angew. Chem. Int. Ed. Engl.* 1981, **20**, 413.
2. K. Dehnicke and J. Strähle, *Z. Anorg. Allg. Chem.* 1965, **339**, 171.
3. W. Kolitsch and K. Dehnicke, *Z. Naturforsch.* 1970, **25b**, 1080.
4. I. Schmidt, U. Kynast, J. Hanich and K. Dehnicke, *Z. Naturforsch.* 1984, **39b**, 1248.
5. W. P. Griffith and D. Pawson, *J. Chem. Soc., Chem. Commun.* 1973, 418; D. Pawson and W. P. Griffith,

Inorg. Nucl. Chem. Lett. 1974, **10**, 253; D. Pawson and W. P. Griffith, *J. Chem. Soc., Dalton Trans.* 1975, 417.
6. J. Chatt and B. T. Heaton, *J. Chem. Soc. A* 1971, 705.
7. R. Dantona, E. Schweda and J. Strähle, *Z. Naturforsch.* 1984, **39b**, 733; G. Beuter, U. Englert and J. Strähle, *Z. Naturforsch.* 1988, **43b**, 145.
8. W. Kafitz, F. Weller and K. Dehnicke, *Z. Anorg. Allg. Chem.* 1982, **490**, 175.
9. W. Liese, K. Dehnicke, I. Walker and J. Strähle, *Z. Naturforsch.* 1979, **34b**, 693.
10. K. Dehnicke, H. Prinz, W. Kafitz and R. Kujanek, *Lieb. Ann. Chem.* 1981, 20.
11. J. R. Dilworth, B. D. Neaves, J. P. Hutchinson and J. A. Zubieta, *Inorg. Chim. Acta* 1982, **65**, L223.
12. B. Knopp, K.-P. Lörcher and J. Strähle, *Z. Naturforsch* 1977, **32b**, 1361; K. Dehnicke and W. Kolitsch, *Z. Naturforsch.* 1977, **32b**, 1485; U. Müller, E. Schweda and J. Strähle, *Z. Naturforsch* 1983, **38b**, 1299.
13. U. Müller, U. Patt-Siebel, A. Khabou, K. Dehnicke and E. Fluck, *Chem. Z.* 1987, **111**, 371.
14. J. Strähle, *Z. Anorg. Allg. Chem.* 1974, **405**, 139.
15. H. Bezler and J. Strähle, *Z. Naturforsch.* 1979, **34b**, 1199.
16. H. Bezler and J. Strähle, *Z. Naturforsch.* 1983, **38b**, 317.
17. H. Bock and M. Schmöller, *Chem. Ber.* 1969, **102**, 38.
18. G. L. Hillhouse, G. V. Goeden and B. L. Haymore, *Inorg. Chem.* 1982, **21**, 2064.
19. J. E. Leffler and R. D. Temple, *J. Am. Chem. Soc.* 1967, **89**, 5235.
20. R. Dübgen, U. Müller, F. Weller and K. Dehnicke, *Z. Anorg. Allg. Chem.* 1980, **471**, 89.
21. U. Müller, R. Dübgen and K. Dehnicke, *Z. Anorg. Allg. Chem.* 1981, **473**, 115.
22. J. Chatt, J. R. Dilworth and R. L. Richards, *Chem. Rev.* 1978, **78**, 589.
23. F. King and G. J. Leigh, *J. Chem. Soc., Dalton Trans.* 1977, 429.
24. N. Mronga, U. Müller and K. Dehnicke, *Z. Anorg. Allg. Chem.* 1981, **482**, 95.
25. N. Mronga, F. Weller and K. Dehnicke, *Z. Anorg. Allg. Chem.* 1983, **502**, 35.
26. D. Sellmann, J. Keller, M. Moll, H. P. Beck and W. Milius, *Z. Naturforsch.* 1986, **41b**, 1551.
27. D. Sellmann, J. Keller, M. Moll, C. F. Campana and M. Haase, *Inorg. Chim. Acta* 1988, **141**, 243.
28. F. Bottomley, W. V. F. Brooks, S. G. Clarkson and S. B. Tong, *J. Chem. Soc., Chem. Commun.* 1973, 919.
29. M. Freni, D. Giusto and V. Valenti, *Gazz. Chim. Ital.* 1964, **94**, 797.
30. D. Fenske, N. Mronga and K. Dehnicke, *Z. Anorg. Allg. Chem.* 1983, **498**, 131.
31. R. Choukroun, D. Gervais and J. R. Dilworth, *Transition Met. Chem.* 1979, **4**, 249.
32. K. V. Katti, H. W. Roesky and M. Rietzel, *Z. Anorg. Allg. Chem.* 1987, **553**, 123.
33. K. V. Katti, U. Seseke and H. W. Roesky, *Inorg. Chem.* 1987, **26**, 814.
34. J. R. Dilworth, H. J. de Liefde Meijer and J. H. Teuben, *J. Organomet. Chem.* 1978, **159**, 47.
35. D. Fenske, E. Böhm, K. Dehnicke and J. Strähle, *Z. Naturforsch.* 1988, **43b**, 1.
36. G. Beindorf, J. Strähle, W. Liebelt and K. Dehnicke, *Z. Naturforsch.* 1980, **35b**, 522.
37. M. J. Cleare, P. C. Hydes, W. P. Griffith and M. J. Wright, *J. Chem. Soc.* 1977, 941; W. P. Griffith, A. C. Skapski, K. A. Woode and M. J. Wright, *Inorg. Chim. Acta* 1978, **31**, L413.
38. R. Weber, K. Dehnicke, U. Müller and D. Fenske, *Z. Anorg. Allg. Chem.* 1984, **516**, 214.
39. H. W. Roesky, U. Seseke, M. Noltemeyer, P. G. Jones and G. M. Sheldrick, *J. Chem. Soc., Dalton Trans.* 1986, 1309.
40. H. W. Roesky, K. V. Katti, U. Seseke, U. Scholz, R. Herbst, E. Egert and G. M. Sheldrick, *Z. Naturforsch.* 1986, **41b**, 1509.
41. K. Hösler, F. Weller and K. Dehnicke, *Z. Naturforsch.* 1987, **42b**, 1563.
42. K. Hösler and K. Dehnicke, unpublished.
43. K. Dehnicke and U. Müller, *Comments Inorg. Chem.* 1985, **4**, 213.
44. H. G. Hauck, Dissertation, Universität Marburg, F. R. G. (1986).
45. T. Chivers and F. Edelmann, *Polyhedron* 1986, **5**, 1661.
46. U. Kynast, E. Conradi, U. Müller and K. Dehnicke, *Z. Naturforsch.* 1984, **39b**, 1680.
47. U. Kynast, Dissertation, Universität Marburg, F.R.G. (1984).
48. K. Völp, F. Weller and K. Dehnicke, *Z. Naturforsch.* 1987, **42b**, 947.
49. K. Völp, W. Willing, U. Müller and K. Dehnicke, *Z. Naturforsch.* 1986, **41b**, 1196.
50. R. Christophersen, Dissertation, Universität Marburg, F.R.G. (1987).
51. R. Christophersen, P. Klingelhöfer, U. Müller, K. Dehnicke and D. Rehder, *Z. Naturforsch.* 1985, **40b**, 1631.
52. H. W. Roesky, K. V. Katti, U. Seseke, M. Witt, E. Egert, R. Herbst and G. M. Sheldrick, *Angew. Chem. Int. Ed. Engl.* 1986, **25**, 477.
53. K. V. Katti, H. W. Roesky and M. Rietzel, *Inorg. Chem.* 1987, **26**, 4032.
54. H. W. Roesky, K. V. Katti, U. Seseke, H.-G. Schmidt, E. Egert, R. Herbst and G. M. Sheldrick, *J. Chem. Soc., Dalton Trans.* 1987, 847.
55. F. L. Phillips and A. C. Skapski, *J. Chem. Soc., Dalton Trans.* 1976, 1448.

56. A. F. Wells, *Structural Inorganic Chemistry*, 5th edn. Clarendon Press, Oxford (1984).
57. G. J. Bullen, *J. Chem. Soc. A* 1971, 1450.
58. S. Kulpe, I. Seidel, J. Bödeker and P. Köckritz, *Cryst. Res. Technol.* 1984, **19**, 655.
59. E. Böhm, K. Dehnicke, J. Beck, W. Hiller, J. Strähle, A. Maurer and D. Fenske, *Z. Naturforsch.* 1988, **43b**, 138.
60. K. Stahl, F. Weller, K. Dehnicke and P. Paetzold, *Z. Anorg. Allg. Chem.* 1986, **534**, 93.
61. H. R. Allcock, N. M. Tollefson, R. A. Arcus and R. R. Whittle, *J. Am. Chem. Soc.* 1985, **107**, 5166.
62. Y. A. Buslaev, Y. Y. Kharitonov and R. L. Davidovich, *Izv. Nauk SSSR, Neorgan. Mater.* 1967, **3**, 589; G. Pausewang, R. Schmitt and K. Dehnicke, *Z. Anorg. Allg. Chem.* 1974, **408**, 1.
63. D. Scott and A. G. Wedd, *J. Chem. Soc., Chem. Commun.* 1974, 527.
64. J. Weidlein, U. Müller and K. Dehnicke, *Schwingungsspektroskopie*. G. Thieme, Stuttgart (1982).
65. J. Weidlein, U. Müller and K. Dehnicke, *Schwingungsfrequenzen II*. G. Thieme, Stuttgart (1986).
66. G. S. Reddy and C. D. Weis, *J. Org. Chem.* 1963, **28**, 1822.
67. H. P. Latscha, *Z. Anorg. Allg. Chem.* 1968, **362**, 7.

Polyhedron Vol. 8, No. 6, pp. 727–730, 1989
Printed in Great Britain

0277–5387/89 $3.00+.00
© 1989 Pergamon Press plc

SEMICARBAZONES AND THIOSEMICARBAZONES—VII.* REACTIVITY OF COORDINATED THIOSEMICARBAZIDE, MOLECULAR AND CRYSTAL STRUCTURE OF *cis*-[Ni^{II}(ACETONETHIOSEMICARBAZONATE)$_2$]

J. VALDÉS-MARTÍNEZ,† R. A. TOSCANO, M. SORIANO-GARCÍA, M. RUBIO, J. GÓMEZ-LARA and M. A. VÁZQUEZ-M.

Instituto de Química, U.N.A.M., Circuito exterior, Ciudad Universitaria, Coyoacán 04510, México, D.F.

and

S. CARRANZA

Escuela de Ciencias Quimicobiologicas, Universidad Autonoma de Sinaloa Culiacan, Sin., México

(*Received* 3 *November* 1987; *accepted after revision* 15 *August* 1988)

Abstract—From the reaction between *trans*-Ni^{II} bis-thiosemicarbazidate and acetone in basic medium, a brown compound has been shown to be *cis*-Ni^{II} bis-acetone-thiosemicarbazonate by single crystal X-ray determination. The complex consists of two acetonethiosemicarbazonate ligands bonded to the central Ni atom, through S atoms and hydrazinic N atoms, in a *cis*-distorted square structure.

Reactivity of coordinated thiosemicarbazones is thought to be closely related to its biological activity as a chelating agent for trace metals. For instance, Petering *et al.*[1] demonstrated that certain Cu^{II} complexes of thiosemicarbazones were the cytotoxic agents themselves and suggested that the metallic complex could promote the ligand activity. Therefore, studies of chemical reactivity of coordinated thiosemicarbazides (TSC) and thiosemicarbazones are of interest, as they can give information on the mechanism of cytotoxic action.

Several authors have studied the reactivity of coordinated TSC, either by increasing the complexity of the coordination compound,[2] by alkylating[3] or acylating[4] the S atom in Ni derivatives.

Here we report the reaction of [Ni(TSC-H)$_2$] with acetone in basic medium and the molecular and crystal structure determination of the product of the reaction. The obtained brown diamagnetic powder has an IR spectrum corresponding to the product obtained by direct reaction of acetone-thiosemicarbazone (ATSC) with Ni^{II} salts. This suggests that the coordinated TSC gave place to the corresponding thiosemicarbazone by Schiff base condensation of the acetone on the already coordinated hydrazinic nitrogen. Slow evaporation of the mother liquors of the reaction mixture of [Ni(TSC-H)$_2$] with acetone, afford the appropriate crystals for an X-ray diffraction study. The IR spectrum of the crystals is identical with that of the precipitated brown powder. Theoretical calculations using the CNINDO method were carried out, trying to explain the apparent *cis*-structure preference of the product.

EXPERIMENTAL

Compound preparation: TSC and nickel acetate (Aldrich) were used without purification. ATSC was prepared according to Jensen.[5] Ni^{II} bis-thiosemicarbazidate [Ni(TSC-H)$_2$] and Ni^{II} bis-acetonethiosemicarbazonate [Ni(ATSC-H)$_2$] were prepared according to Nardelli.[6] The latter compound was also obtained by the following procedure. A suspension of 1 mmol of [Ni(TSC-H)$_2$] in 50 cm^3 of acetone and 2 cm^3 of 1:5 NaOH in H_2O, was

* Part VI: J. Valdés-Martínez, A. Berruecos and R. A. Toscano to be published in *Afinidad*.

†Author to whom correspondence should be addressed.

refluxed with stirring. After the powder colour changed from brown-greenish to dark brown the reflux was maintained for one more hour. The product was collected by filtration, washed with acetone, ethanol and water and dried *in vacuo* overnight.

A Nicolet FT-SX instrument was used to record the IR spectra on KBr pellets.

The theoretical calculations were carried out with the CNINDO method,[7] using the reported X-ray data for TSC[8] and ATSC,[9] taking out the proton on N(2) and performing a 180° rotation on the N(2)—C bond in order to have the molecules in the chelating geometry.

Crystal data for *cis*-[Ni^{II}(acetonethiosemicarbazonate)$_2$] at 20°C; $a = 16.642(5)$, $b = 6.959(2)$, $c = 12.295(3)$ Å, $\beta = 107.28(2)°$, $V_c = 1359.6(9)$ Å^3, $D_{calc} = 1.56$ g cm^{-3}, $F(000) = 664$, μ(Mo-K_α) = 17.17 cm^{-1}, $Z = 4$, and space group C_c. Using a brown crystal, $0.12 \times 0.22 \times 0.30$ mm, lattice parameters were obtained from 25 machine-centred reflections with $5.1 < 2\theta < 22.0°$ λ(Mo-K_α) radiation, $\lambda = 0.7107$ Å). Reflections in two octants of reciprocal space were measured with an index range of h $0 \rightarrow 18$, k $0 \rightarrow 8$, 1 ± 14, on a Nicolet R3 four-circle diffractometer. Using the ω-scanning mode, variable scan speed and two standard reflections ($1\bar{1}3$; $11\bar{1}$) monitored every 50 measurements. The intensities were corrected for Lorentz and polarization effects and empirical absorption correction based on reflection intensity measurements at different azimuthal angles was carried out. Of the 1025 reflections within the two ranges of 3–45° collected, only 883 had values of $I > 2.5\sigma(I)$ and these were used in the final refinement of structural parameters. The structure was solved by the heavy atom method incorporated by G. N. Sheldrick into the SHELXTL system,[10] and refined by the least-squares technique with anisotropic temperature factors for the non-hydrogen atoms. The H atoms of CH_3 were allowed to ride on bonded C and assigned a fixed isotropic temperature factor, $U = 0.06$ Å^2, $\Sigma w(\Delta F)^2$ minimized, with a statistical weight of the form $w = [\sigma^2(F_o) + 0.0003(F_o)^2]^{-1}$. The final conventional R-factor was 0.028, $R = \Sigma (|F_o| - |F_c|)/\Sigma |F_o|$ and $R_w = 0.031$, $R_w = \{\Sigma [w^{1/2}(|F_o| - |F_c|]/\Sigma w^{1/2}|F_o|\}$ for the correct absolute configuration and $R = 0.038$ and $R_w = 0.045$ for its enantiomorph. Scattering factors and anomalous dispersion corrections for Ni, S, N, O and H were from ref. 11. In the last cycle $(\Delta/\sigma)_{max} = 0.20$; $\Delta\rho$ from -0.20 to 0.26 eÅ^{-3} and isotropic extinction parameter $X = 0.00009$. All computations were performed on a Nova 4S computer and plots drawn on a Tektronix plotter with the SHELXTL system of programs.

Crystal and molecular structure of [Ni(ATSC-H)$_2$]

An ORTEP drawing of the complex is shown in Fig. 1. Relevant bond distances and angles are shown in Table 1. The complex consists of two ATSC groups, each bound to the central Ni atom through the thiol S atoms and the hydrazinic N atoms, yielding two five-membered rings. The four atoms surrounding the Ni^{II} ion are significantly tetrahedrally distorted from the true square-planar configuration, S(1) and N(4) lie 0.287(4) and 0.306(4) Å, respectively above, whilst S(2) and N(1) lie 0.283(4) and 0.308(4) Å, respectively below the NiN_2S_2 mean plane. The Ni—S bond distances of 2.162(2) and 2.166(2) Å are in the range of 2.1–2.3 Å found in four coordinated Ni^{II} complexes, as has been pointed out by Lopez-Castro and Truter.[12] The Ni—N bond distances of 1.921(6) and 1.934(5)

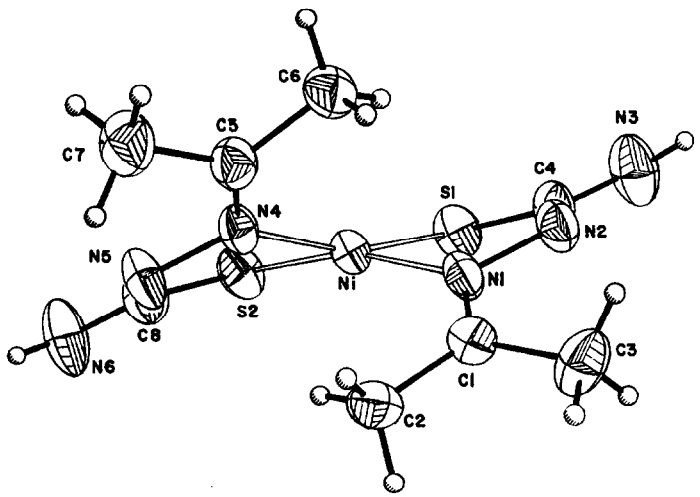

Fig. 1. ORTEP drawing of the [Ni(ATSC-H)$_2$] molecule giving the number scheme for the atoms.

Table 1. Bond lengths (Å) and angles (°) for [Ni(ATSC-H)$_2$]. The ESD's are given in parentheses

Bond lengths			
Ni—S(1)	2.166(2)	Ni—S(2)	2.162(2)
Ni—N(1)	1.921(6)	Ni—N(4)	1.934(5)
S(1)—C(4)	1.760(9)	S(2)—C(8)	1.734(7)
N(1)—N(2)	1.417(7)	Ni(1)—C(1)	1.290(8)
N(2)—C(4)	1.277(10)	N(3)—C(4)	1.369(9)
N(4)—N(5)	1.433(7)	N(4)—C(5)	1.281(8)
N(5)—C(8)	1.309(10)	N(6)—C(8)	1.373(10)
C(1)—C(2)	1.484(8)	C(1)—C(3)	1.497(11)
C(5)—C(6)	1.489(9)	C(5)—C(7)	1.493(9)
Angles			
S(1)—Ni—S(2)	93.8(1)	S(1)—Ni—N(1)	85.4(1)
S(2)—Ni—N(1)	163.1(2)	S(1)—Ni—N(4)	163.0(2)
S(2)—Ni—N(4)	86.0(2)	N(1)—Ni—N(4)	99.7(2)
Ni—S(1)—C(4)	93.5(2)	Ni—S(2)—C(8)	94.6(3)
Ni—N(1)—N(2)	118.1(4)	Ni—N(1)—C(1)	126.6(4)
N(2)—N(1)—C(1)	115.0(6)	N(1)—N(2)—C(4)	110.4(6)
Ni—N(4)—N(5)	116.6(4)	Ni—N(4)—C(5)	128.7(4)
N(5)—N(4)—C(5)	114.3(5)	N(4)—N(5)—C(8)	111.0(5)
N(1)—C(1)—C(2)	121.9(6)	N(1)—C(1)—C(3)	121.7(5)
C(2)—C(1)—C(3)	116.3(6)	S(1)—C(4)—N(2)	124.7(5)
S(3)—C(4)—N(3)	116.5(6)	N(2)—C(4)—N(3)	118.8(8)
N(4)—C(5)—C(6)	128.7(5)	N(4)—C(5)—C(7)	121.9(6)
C(6)—C(5)—C(7)	117.4(5)	S(2)—C(8)—N(5)	124.1(5)
S(2)—C(8)—N(6)	119.5(6)	N(5)—C(8)—N(6)	116.4(6)

Å are comparable with the value of 1.844(7) Å found in ammine(salicylaldehyde-4-phenylthiosemicarbazonate)nickel(II).[13] The bond distances in the five-membered chelate rings are intermediate between the usual values for single and double bonds, however, both chelate rings deviate considerably from planarity, with the maximum deviations of 0.208(4) and 0.205(4) Å for N(1) and N(4) atoms. The [Ni(ATSC-H)$_2$] molecules are held together in the crystal by both van der Waals and crystal packing forces.

DISCUSSION

To our knowledge this is the first case of a molecular structure determination of a square-planar neutral bis-chelate with *cis*-structure for the ATSC ligand, although compounds with TSC and thiosemicarbazones have been studied since 1934.[14] For example, Jensen obtained "neutral" [Ni(TSC-H)$_2$] and "ionic" [Ni(TSC)$_2$]$^{2+}$ compounds; for the ionic compounds, *cis*- and *trans*-geometries have been assigned by X-ray and IR studies.

The neutral compound [Ni(TSC-H)$_2$], which was our starting material, has a *trans*-geometry according to a single crystal X-ray diffraction study.[15] Considering this fact and the steric hindrance of the isopropylidene groups, which prevents hexacoordination in Ni^{II} and Co^{II} derivatives,[16] one would not expect the resulting product, [Ni(ATSC-H)$_2$], to have *cis*-geometry, although a *trans*-to-*cis* isomerization would be possible. It is interesting to notice, that we were not able to obtain the *trans*-isomer, regardless of the synthetic method used. This may be a consequence of the *cis*-geometry being energetically favoured.

Trying to explain this apparent *cis*-preference we carried out the theoretical calculations of the electronic density on the atoms of both molecules TSC and ATSC using the CNINDO method.[7] The ligands were studied taking out the proton on N(2) and performing a 180° rotation on the N(2)—C bond in order to have the molecules in the chelating geometry. The electronic charges obtained are shown in Fig. 2.

The Ni—S distances in complexes with the TSC ligand, are shorter in the bis-chelate compounds with *cis*-geometry.[17] This might be a result of the stronger *trans*-effect of sulphur over nitrogen which would favour a *cis*-geometry.

In agreement with this, the calculated charge on the sulphur atom is higher than that on the hydrazine nitrogen atom N(1), with a difference of 0.635

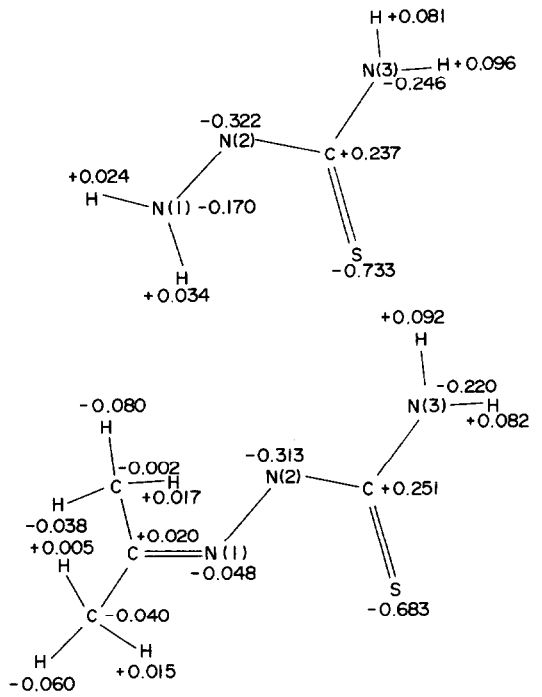

Fig. 2. Electronic charges for the TSC^- and $ATSC^-$ molecules, taking out the proton on N(2) and performing a 180° rotation on the N(2)—C bond.

between them in $ATSC^-$ and of 0.563 in TSC^-, therefore driving the sulphur atom in $ATSC^-$ more strongly than in TSC^-, to look for a geometry which would favour a stronger Ni—S bond.

Acknowledgement—We thank Mrs C. Vázquez for her technical assistance.

REFERENCES

1. H. G. Petering, H. H. Buskirk and J. A. Crim, *Cancer Res.* 1967, **27**, 1115.
2. N. V. Gerveleu and F. K. Zhovmir, *Russ. J. Inorg. Chem.* 1982, **27**, 309.
3. S. Chandra, K. B. Pandeya and R. P. Singh, *Synth. React. Inorg. Met.-Org. Chem.* 1981, **11**, 53.
4. S. Chandra, K. B. Pandeya and R. P. Singh, *Natn. Acad. Sci. Lett. (India)* 1978, **1**, 289.
5. K. A. Jensen, U. Anthoni, B. Kagi, Ch. Lansen and C. Th. Pederson, *Acta Chem. Scand.* 1968, **22**, 1.
6. M. Nardelli and P. Boldrini, *Gazz. Chim. Ital.* 1961, **91**, 280.
7. QCPE 242, *CNINDO with Bond Density Calculation.* Indiana University, Ind.
8. G. D. Andreetti, P. Domiano, G. F. Gasparri, M. Nardelli and P. Sgarabotto, *Acta Cryst.* 1970, **B26**, 1005.
9. G. J. Palenik, D. F. Redle and W. S. Carter, *Acta Cryst.* 1974, **B30**, 2390.
10. G. M. Sheldrick, *SHELXTL, Revision 3,1981. An Integrated System for Solving, Refining and Displaying Crystal Structures from Diffraction Data.* University of Gottingen, F.R.G.
11. *International Tables for X-Ray Crystallography*, Vol. IV. Kynoch Press, Birmingham (1974). Present distribution: Reidel, Dordrecht.
12. A. López-Castro and M. R. Truter, *J. Chem. Soc.* 1963, 1309.
13. M. Soriano-García, R. A. Toscano, J. Valdés-Martínez and J. M. Fernández-G., *Acta Cryst.* 1985, **C41**, 498.
14. (a) K. A. Jensen and E. Rancke-Madsen, *Z. Anorg. Allg. Chem.* 1934, **219**, 243; (b) K. A. Jensen, *Z. Anorg. Allg. Chem.* 1934, **221**, 6; (c) K. A. Jensen, *Z. Anorg. Allg. Chem.* 1934, **221**, 11.
15. (a) M. Nardelli and P. Boldrini, *Gazz. Chim. Ital.* 1961, **91**, 280; (b) L. Cavalca, M. Nardelli and G. Fava, *Acta Cryst.* 1962, **15**, 1139.
16. M. A. Malik and D. J. Phillips, *Aust. J. Chem.* 1975, **28**, 305.
17. R. G. Hazell, *Acta Chem. Scand.* 1968, **22**, 2171.

Polyhedron Vol. 8, No. 6, pp. 731–738, 1989
Printed in Great Britain

0277–5387/89 $3.00+.00
© 1989 Pergamon Press plc

REACTIONS OF FLUOROPHOSPHORANES WITH 8-TRIMETHYLSILOXYQUINOLINE AND WITH 2-(N,N-DIMETHYLAMINO)ACETOXYTRIMETHYLSILANE; X-RAY CRYSTAL STRUCTURE OF 2-(N,N-DIMETHYLAMINO)ACETOXYPHENYLTRIFLUOROPHOSPHATE, $Me_2\overline{NCH_2C(:O)OP(Ph)F_3}$*

ROLAND KREBS and REINHARD SCHMUTZLER**

Institut für Anorganische und Analytische Chemie der Technischen Universität, Hagenring 30, D-3300 Braunschweig, F.R.G.

and

DIETMAR SCHOMBURG

GBF (Gesellschaft für biotechnologische Forschung), Mascheroder Weg 1, D-3300 Braunschweig, F.R.G.

(*Received* 21 *April* 1988; *accepted* 31 *August* 1988)

Abstract—The cyclic trifluorophosphoranes, $(CH_2)_nPF_3$ (n = 4, 5; **1c** and **1d**) were found to react with 8-trimethylsiloxyquinoline (**2**) with cleavage of the Si—O bond and formation of the mono-substituted derivatives, $(CH_2)_nPF_2(Ox)$, **4** and **5** (Ox = 8-oxyquinolyl). In the case of **4**, intramolecular coordination between the nitrogen atom of the quinolyl group and phosphorus rendering phosphorus hexa-coordinate (λ^6P) has been established by NMR spectroscopy (^{31}P, ^{19}F). By contrast, this type of interaction between N and P is not observed in the case of **5** which is, therefore, a normal substituted fluorophosphorane with λ^5P. Intramolecular coordination, involving λ^6P, is observed, however, in the case of the products originating from the reaction of the trimethylsilyl ester of N,N-dimethylglycine, $Me_2NCH_2C(:O)OSiMe_3$ (**6**) with both PF_5 and $PhPF_4$; it has been indicated for both **7** and **8** by NMR spectroscopy. In the case of **8**, a single crystal X-ray structure determination has confirmed the intramolecular coordination between P and N, with the formation of hexa-coordinate phosphorus.

Fluorophosphoranes, R_nPF_{5-n}, especially tetrafluorophosphoranes (n = 1), and some trifluorophosphoranes (n = 2), and also the parent compound, PF_5, are known to react with ionic nucleophiles, such as halide or pseudohalide[1–12] ions, with the formation of ionic species, involving hexa-coordinated phosphorus.

$$R_nPF_{5-n} + X^- \longrightarrow [R_nPF_{5-n}X]^- \quad (1)$$

n = (0) 1,2.

Similar adducts have also been prepared, involving neutral Lewis bases, e.g. phosphines,[13–15] ethers,[1,16,17] and amines.[16–22]

$$R_nPF_{5-n} + B \longrightarrow R_nPF_{5-n}B \quad (2)$$

n = (0) 1,2.

For the fluorophosphoranes a decrease in the acceptor strength, as the number of the hydrocarbon groups increases, is evident; i.e. the following order has been suggested:

$(PF_5) > ArPF_4 > RPF_4 > Ar_2PF_3 > Ar(R)PF_3 > R_2PF_3$.

* Dedicated to Professor Sir Jack Lewis, FRS on the occasion of his 60th birthday.

** Author to whom correspondence should be addressed.

For the products of this Lewis acid–base interaction more or less strongly distorted octahedral geometry at phosphorus has been assumed, and has been established by NMR[1,3–12,14–16,18,20–22] and crystal structure analyses.[15,22–26]

In addition to these λ^6-fluorophosphates involving an intermolecular donor–acceptor bond some λ^6-fluorophosphates with an intramolecular N → P donor–acceptor bond have been studied. This type of interaction has been observed, e.g. for the products formed in the reaction of 8-trimethylsiloxyquinoline (**2**) (and its 2-methyl derivative) with fluorophosphoranes[27–29] [see eq. (3)]:

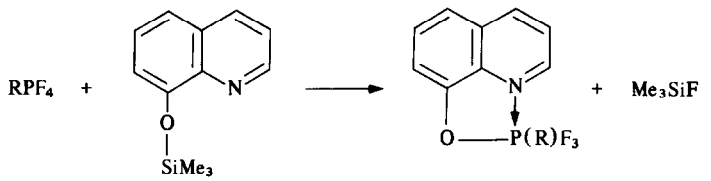

(3)

1 **2** **3**

1a R = F **3a** R = F

1b R = Me, Et, Ph **3b** R = Me, Et, Ph

The products were characterized by NMR spectroscopy[27,29] and, in two cases, by single-crystal X-ray diffraction.[27,28] For the intramolecular complexes, obtained in the reaction between PF_5 and $PhPF_4$ with 2-methyl-8-trimethylsiloxyquinoline, distorted octahedral geometry at phosphorus has been established.

RESULTS AND DISCUSSION

Reaction of 8-*trimethylsiloxyquinoline* (**2**) *with the cyclic trifluorophosphoranes,* $(CH_2)_4PF_3$ (**1c**) *and* $(CH_2)_5PF_3$ (**1d**)

For the trifluorophosphoranes, **1c** and **1d**, trigonal–bipyramidal geometry with the $(CH_2)_4$ or $(CH_2)_5$ group attached diequatorially at λ^5P has been established by electron diffraction.[30] Their reaction with **2** was studied, in order to establish if merely substitution products with λ^5P would result, or whether the same type of intramolecular interaction as in **3** would occur.

The reaction of **1c** with **2** (equimolar ratio) was found to furnish **4** in nearly quantitative yield [see eq. (4)].

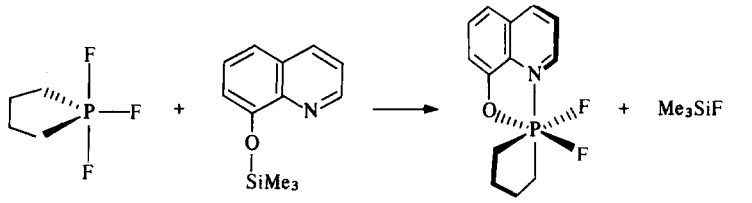

(4)

1c **2** **4**

In the ^{31}P NMR spectrum (24.3 MHz) of **4** a triplet (^1J(PF) 833) at $\delta_P = -68.3$ has been observed; a high field shift of nearly 100 ppm, compared to **1c** (δ_P 29.8).[31] High field shifts of this magnitude are considered indicative of hexa-coordination at phosphorus.[2,27] In the ^{19}F NMR spectrum of **4** two groups of signals, centred at $\delta_{F(A)} = -17.8$ and $\delta_{F(B)} = -55.2$, were observed. Since the δ_F values are different it is assumed that the two fluorine atoms are not located in *trans* positions at λ^6 phosphorus.

The lines in the ^{19}F NMR spectrum are broad and the P—F coupling constants for the two fluorine atoms are equal, of the order of 825 Hz.

^2J(FF) coupling (43 Hz) has been noted only for the low field resonance, F(A). Apparently ^3J(FH) coupling is observed only for F(B) (cf. Figs 1 and 2), coupling with protons of the CH_2 groups adjacent to phosphorus. F(B) is suggested to occupy a *cis* position, relative to the two CH_2 groups bonded to phosphorus. The smaller coupling between F(A) and the methylene protons suggests that F(A) is located *cis* to only one CH_2 group. ^3J(FH)(*trans*) coupling is not normally observed when ^{19}F and hydrocarbon groups are bonded to octahedral phosphorus.[3,16,24]

At least two possibilities must be considered, therefore, for the geometry of **4** (Figs 1 and 2).

In the X-ray structure investigations of $F_3(Ph)P(OxMe)$[28] and of $Me_2\overline{NCH_2C(:O)OP}(Ph)F_3$ (**8**) (*vide infra*), the phenyl groups were observed in the *trans* position, relative to the coordinatively bound nitrogen atoms. Assuming

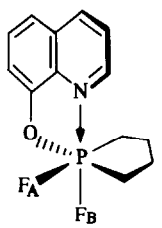

Fig. 1.

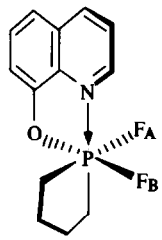

Fig. 2.

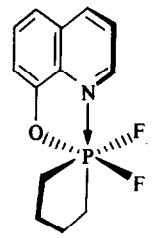

Fig. 3.

that the CH_2 groups in **4** are located *trans* to nitrogen, a geometry as shown in Fig. 3 is suggested.

Reaction of **1d** *with* **2**: *preparation of* $(CH_2)_5P(Ox)F_2$ **(5)**

In this reaction between equimolar amounts of **1d** and **2**, the formation of **5** in high yield was observed. Multiple substitution, as in the case of the reaction of aryltrimethylsilylethers with fluorophosphoranes,[32] did not occur [see eq. (5)].

Trigonal–bipyramidal geometry at phosphorus is expected for **5**, in contrast to **4**, by analogy to $Me_2P(Ox)F_2$.[27] The reason for this difference is probably the increase in Lewis acidity in **1c**, compared to **1d**, where λ^5P is part of a less strained ring system. Two structures for **5** may be considered (Figs 4 and 5); the arrangement with two axial fluorine atoms (Fig. 5) is expected to be the more stable one.

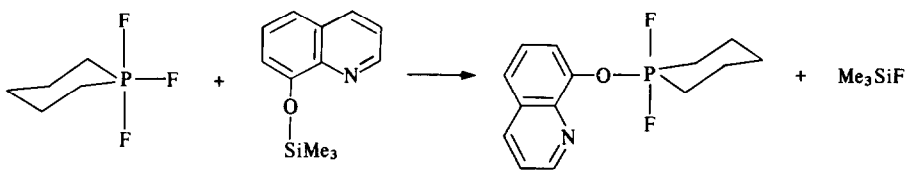

1d **2** **5** (5)

The δ_P value of **5** (−15.2), was found at only slightly higher field, compared to that of **1d** (δ_P 0.6).[33] It is assumed, therefore, at least for the solution state, that **5** is present as a fluorophosphorane, involving λ^5P, and not λ^6P (with basically octahedral geometry). N → P interactions cannot be excluded, though.

In the ^{19}F NMR spectrum of **5** only a doublet ($\delta_F = -22.4$) is seen, as expected for two equivalent fluorine atoms. The coupling constants, ^1J(PF), from the ^{31}P and ^{19}F NMR spectrum are 736 and 747 Hz, respectively.

Reaction of 2-(*N,N-dimethylamino*)*acetoxytrimethylsilane* **(6)** *with* **1a**: *preparation of* 2-(*N,N - dimethylamino*)*acetoxytetrafluorophosphate*, $Me_2\overline{NCH_2C(:O)OPF_4}$ **(7)**

The reaction occurred, in accordance with eq. (6), over 19 h at room temperature, in nearly quantitative yield,

$$\underset{\mathbf{6}}{Me_2NCH_2C(:O)OSiMe_3} + \underset{\mathbf{1a}}{PF_5} \longrightarrow \underset{\mathbf{7}}{Me_2\overline{NCH_2C(:O)OPF_4}} + Me_3SiF. \quad (6)$$

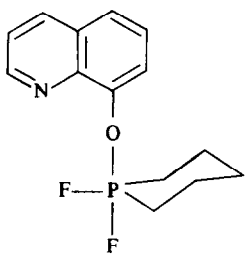

Fig. 4.

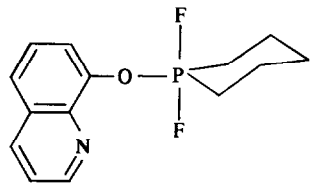

Fig. 5.

Table 1. ^{19}F NMR data of 7 and of $OxPF_4$ (3a)

	$Me_2\overline{NCH_2C(:O)OPF_4}$	$OxPF_4$
	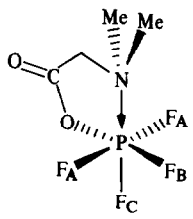	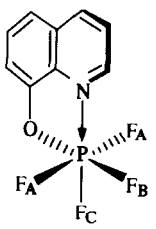
$\delta_{F(A)}$	−65.8 ppm	−51.03 ppm
$\delta_{F(B)}$	−76.8 pm	−75.17 ppm
$\delta_{F(C)}$	−81.4 ppm	−80.52 ppm
$^1J(F_AP)$	851 Hz	787.5 Hz
$^1J(F_BP)$	840 Hz	755.8 Hz
$^1J(F_CP)$	751 Hz	747.9 Hz
$^2J(F_AF_B)$	69 Hz	54.6 Hz
$^2J(F_AF_C)$	47 Hz	50.4 Hz
$^2J(F_BF_C)$	65 Hz	64.1 Hz

In the ^1H NMR spectrum of **7** (recorded at 400 MHz) two groups of signals were observed for both the Me_2N and NCH_2 protons, suggesting octahedral geometry at phosphorus. The magnitude of the HP coupling constants (11.3 and 8.9 Hz) is too high for ^6J(HP) and ^4J(HP), and is taken as an indication of ^3J(HP) coupling, via nitrogen. The fine structure of these resonances is due to coupling, ^4J(HF) to the three fluorine atoms, *cis* to nitrogen. As in the case of $Me_3N \cdot PF_5$[16], $^4J(HF_{trans})$ was not observed. The signal of the NH_2 protons is split into a doublet of quartets. The values of ^4J(HF) are equal (1.8 Hz).

The resonance of the NMe_2 protons appears as two symmetrical groups of signals. Their fine structure is suggested to be caused by the superimposition of two triplets (dt), apparently due to two different coupling constants, ^4J(HF) between the NMe_2 protons and the three *cis* fluorine atoms, as required for octahedral geometry [2.4 Hz for $^4J(HF_A)$ (triplet) and 1.7 Hz for $^4J(HF_B)$ (doublet)]. Assuming octahedral geometry, the fluorine atoms, F_A (with $^4J(HF_A)$ 2.4) should be located *trans* to each other while F_B (with $^4J(HF_B)$ 1.7) is suggested to be located *trans* to oxygen.

The ^{19}F NMR spectrum of **7** was recorded at 56.4 and 94.2 MHz. The resonances in the 94.2 MHz spectrum were assigned as an A_2BCX system. The appearance of the ^{19}F NMR spectrum was similar to that observed for the product, formed in the reaction of phosphorus pentafluoride (**1a**) with 8-trimethylsiloxyquinoline (**2**)[29] (Table 1).

The signals due to F_A and F_B are much broader than the resonance for F_C. This is due, presumably, to coupling ^4J(FH) between F_A and F_B, and NMe_2 and NCH_2 protons.

For some anions with λ^6P, e.g. $[HPF_5]^-$[11], and in the adducts, $Me_3P \cdot PF_5$,[14] $H_3N \cdot PF_5$[23,24] and $Me_3N \cdot PF_5$,[16] the coupling constants, $^2J(HF_{trans})$, $^2J(PF_{trans})$, $^2J(^{14}NF_{trans})$, as well as $^4J(HF_{trans})$ are zero. It is assumed, therefore, that there is no coupling [^4J(FH)] between F_C and NMe_2 and NCH_2 groups. This suggests that F_C is located *trans* to nitrogen.

The δ_P value of **7** (−136.8) reveals a high field shift of 56.5 ppm, compared to PF_5 (**1a**) (−80.3).[34] Similar changes have been observed for the products of the reaction of fluorophosphoranes with **2** and with nitrogen donors, e.g. acetonitrile,[20] and ammonia.[23,24] The magnitude of δ_P is characteristic of λ^6P.

Coupling constants, ^1J(PF) of 844 and 749 Hz, respectively, were observed. In view of the difference between $^1J(F_AP)$ and $^1J(F_BP)$ (11 Hz) a doublet ($^1J(PF_C)$ 749) of quartets ($^1J(PF_{A,B})$ 844) is observed.

The suggested structure of **7** is shown in Fig. 6.

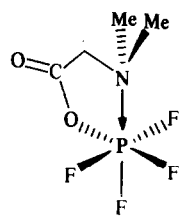

Fig. 6.

Reaction of **6** *with phenyltetrafluorophosphorane* (**1b**) (R = Ph): *preparation of* 2-(*N,N-dimethylamino*) *acetoxyphenyltrifluorophosphate*, $Me_2\overline{NCH_2C(:O)OP}(Ph)F_3$ (**8**)

The reaction was conducted under mild conditions (44 h; room temperature); **8** was obtained [eq. (7)], in nearly quantitative yield.

$$\underset{\mathbf{6}}{Me_2NCH_2C(:O)OSiMe_3} + \underset{\mathbf{1b}}{PhPF_4} \longrightarrow \underset{\mathbf{8}}{Me_2\overline{NCH_2C(:O)OP}(Ph)F_3} + Me_3SiF. \quad (7)$$

As discussed for **7** the HP coupling constants for the Me_2N and NCH_2 resonances are too large for ^6J(HP) and ^4J(HP) (8.7 and 11.1 Hz, respectively) and are caused, presumably, through coupling, ^3J(HP), via nitrogen. Besides this HP coupling, ^4J(HF) coupling (*ca* 1.8 Hz; presumably via nitrogen, too) has been observed in the ^1H NMR spectrum of **8**.

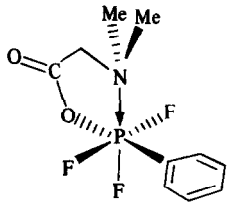

Fig. 7.

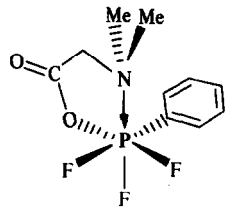

Fig. 8.

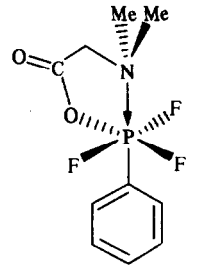

Fig. 9.

The resonances of the ^{19}F NMR spectrum have been assigned as an A_2BX system. The line assignment within the A_2B part was by comparison with published spectra:[35] $\delta_{F(A)}$ −56.1 ppm; $\delta_{F(B)}$ −59.0 ppm; $^1J(F_aP)$ 935 Hz; $^1J(F_BP)$ 935 Hz; $^2J(F_AF_B)$ 68 Hz.

The fact that the ^{19}F NMR spectrum of **8** is represented by an A_2BX spin system may be taken as an indication that the two fluorine atoms F(A), equivalent in the ^{19}F NMR spectrum, are *trans* to each other.

In the ^{31}P NMR spectrum of **8** a quartet at −119.6 ppm ($^1J(PF)$ 959 Hz) indicates a high field shift of 68 ppm, relative to $PhPF_4$ (−51.7),[2] suggesting λ^6P.

Assuming octahedral geometry at λ^6 phosphorus, the three isomers shown in Figs 7–9 are conceivable.

Since the NMR spectroscopic investigation does not allow an unequivocal decision for one of these structures, a single crystal X-ray diffraction study of **8** was conducted (Fig. 10).

The X-ray crystal structure analysis has confirmed the octahedral geometry at λ^6P in **8**, expected on the basis of the NMR investigations. Thus, the phenyl group is *trans* to nitrogen, as in the comparable compound $F_3(Ph)P(OxMe)$.[28] The coordinative P—N bond (201.3 pm) is significantly longer than in other species with λ^6P, e.g. $F_5P \cdot py$,[22] $F_5P \cdot NH_3$[24] and $F_4P(OxMe)$,[27] where bond lengths of 189.9, 184.2 and 191.1 pm, respectively, have been observed. It is suggested that the increase in the P—N bond length in **8** is due to the lower acceptor strength of the $F_3(Ph)PO$ grouping (compared to PF_5 and F_4PO). This becomes apparent upon comparing the P—N bond length in **8** and in $F_3(Ph)P(OxMe)$[28] where the acceptor groups are the same, and the observed bond length, 198.0 pm, is only marginally smaller than that in **8**. The P—F bond lengths in **8** (average 159.8 pm) are slightly increased, with respect to those in $PhPF_4$ (157.4 pm; gas-phase electron diffraction),[36] $[PF_6]^-$ (158 pm),[37] $F_5P \cdot py$,[22] $F_5P \cdot NH_3$[24] and $F_4P(OxMe)$[27] for which average values of 158.7, 159.5, and 158.8 pm, respectively, have been determined by X-ray diffraction. Average P—F bond lengths of 159.8 and 160.4 pm have been observed for the related species $F_3(Ph)P(OxMe)$.[28]

The largest deviation in the bond angles at phosphorus from those expected for ideal octahedral geometry (three 180° angles and 12 90° angles) is found for the angle O(1)—P—F(2) (9.1°).

The angles between the P—C(11) bond and P—F(1), P—F(2), P—F(3) and P—O(1) (93.5, 96.3, 94.2 and 92.7°) reveal a certain distortion of these

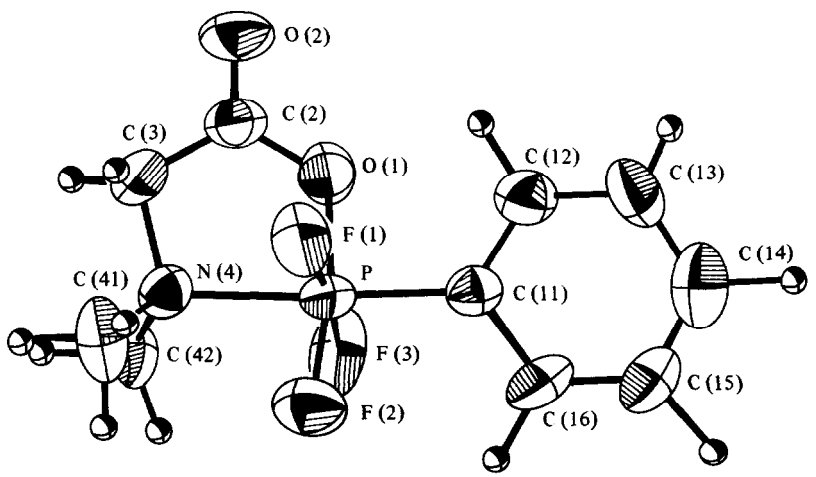

Fig. 10. Molecular structure of **8**.

Table 2. Bond lengths (pm) and angles (°) of **8**

Bond lengths			
F(1)—P	159.8(3)	F(2)—P	158.6(3)
F(3)—P	160.9(3)	C(11)—P	181.4(5)
O(1)—P	170.6(3)	N(4)—P	201.3(4)
C(12)—C(11)	138.8(7)	C(16)—C(11)	141.4(7)
C(13)—C(12)	136.5(8)	C(14)—C(13)	139.1(10)
C(15)—C(14)	137.9(10)	C(16)—C(15)	138.9(8)
C(2)—O(1)	130.5(6)	O(2)—C(2)	119.3(6)
C(3)—C(2)	150.9(10)	O(2)—C(11)	149.3(9)
C(41)—N(4)	148.9(8)	C(42)—N(4)	150.4(7)
Bond angles			
F(2)—P—F(1)	89.9(2)	F(3)—P—F(1)	172.3(2)
F(3)—P—F(2)	90.3(2)	C(11)—P—F(1)	93.5(2)
C(11)—P—F(2)	96.3(2)	C(11)—P—F(3)	94.2(2)
O(1)—P—F(1)	90.1(2)	O(1)—P—F(2)	170.9(2)
O(1)—P—F(3)	88.5(2)	O(1)—P—C(11)	92.7(2)
N(4)—P—F(1)	84.8(2)	N(4)—P—F(2)	86.7(2)
N(4)—P—F(3)	87.5(2)	N(4)—P—C(11)	176.5(2)
N(4)—P—O(1)	84.3(2)	C(12)—C(11)—P	122.6(4)
C(16)—C(11)—P	119.9(4)	C(16)—C(11)—C(12)	117.5(5)
C(13)—C(12)—C(11)	122.4(5)	C(14)—C(13)—C(12)	119.9(5)
C(15)—C(14)—C(13)	119.4(5)	C(16)—C(15)—C(14)	120.8(6)
C(15)—C(16)—C(11)	120.0(5)	C(2)—O(1)—P	122.3(3)
O(2)—C(2)—O(1)	122.6(5)	C(3)—C(2)—O(1)	112.7(4)
C(3)—C(2)—O(2)	124.0(5)	N(4)—C(3)—C(2)	106.6(6)
C(3)—N(4)—P	105.0(4)	C(41)—N(4)—P	113.9(3)
C(41)—N(4)—C(3)	107.3(6)	C(42)—N(4)—P	113.5(4)
C(42)—N(4)—C(3)	110.3(5)	C(42)—N(4)—C(41)	106.6(5)

bonds towards N(4). A similar distortion has been observed for $F_3(Ph)P(OxMe)$[28] and, to a lesser degree, in other species with λ^6P;[22,24,27] it may be rationalized in terms of Gillespie's VSEPR model.[38,39] Apparently the electron density in the dative N(4)→P bond is more localized at the lighter atom than in the P—C(11) bond (see Table 2).

EXPERIMENTAL

The usual precautions in handling highly deliquescent substances were observed in the course of this work. Solvents were dried by standard procedures.[40]

IR spectra: Beckman instrument no. 4260 A.

The NMR spectra were recorded on the following instruments: Jeol JNMC 60 HL (^{1}H at 60 MHz, ^{19}F at 56.4 MHz, and ^{31}P at 24.3 MHz); Hitachi Perkin–Elmer R 24 B (^{1}H at 60 MHz); Varian CFT 20 (^{13}C at 20.1 MHz); Bruker HM 100 (^{19}F at 94.2 MHz); Bruker WM 400 (^{1}H at 400 MHz, ^{13}C at 100.6 MHz and ^{31}P at 162 MHz). (Internal TMS, internal $CFCl_3$ and external 85% H_3PO_4 references.) High-field shifts are listed with a negative sign, low field shifts with a positive sign. Conversion of shift values:[41] ^{1}H: $\delta_{(TMS)} = \delta_{(CHCl_3)} + 7.27 = \delta_{(CH_2Cl_2)} + 5.30$; ^{19}F: $\delta_{(CFCl_3)} = \delta_{(C_6F_6)} - 163$. The following abbreviations are used in reporting the NMR data: s = singlet; d = doublet; t = triplet; q = quartet; ddt = doublet of doublets of triplets; dq = doublet of quartets; m = multiplet.

Mass spectra: these were recorded on the Varian MAT CH-7 and Finnigan MAT 8430 (direct inlet system 70, eV) instruments.

The following starting materials were synthesized by the literature procedures indicated: 8-trimethylsiloxyquinoline;[42] cyclotetramethylenetrifluorophosphorane;[43,44] cyclopentamethylenetrifluorophosphorane.[43,45]

Reaction of N,N-dimethylglycine, $Me_2NCH_2C(:O)OH$ *with hexamethyldisilazane: preparation of 2-(N,N-dimethylamino)acetoxytrimethylsilane* (**6**)

A mixture, consisting of N,N-dimethylglycine (21.9 g, 0.21 mol), hexamethyldisilazane (22.35 g, 0.14 mol), trimethylchlorosilane (0.2 g, 0.002 mol) and toluene (50 cm^3) was refluxed for 20 h. Subsequently, the mixture was fractionally distilled through a 20 cm column; yield 32.1 g (0.18 mol; 86%); b.r. 51–54°C (9 mm).

$C_7H_{17}NO_2Si$ (175.31). Found: C, 49.1; H, 9.9.

Calc.: C, 48.0; H, 9.7%. ^{1}H NMR spectrum ($CHCl_3$): $\delta_{(CH_3)_3Si}$ 0.13 (s); $\delta_{[-N(CH_3)_2]}$ 2.19 (s); $\delta_{(CH_2)}$ 2.97 (s). ^{13}C NMR spectrum ($CDCl_3$): $\delta_{N(CH_3)_2}$ 2.7 (s); δ_{NCH_3} 46.9 (s); δ_{CH_2N} 63.1 (s); $\delta_{C(:O)}$ 172.8 (s).

Reaction of 8-*trimethylsiloxyquinoline* (**2**) *with* 1.1.1-*trifluoro*-1λ^5-*phospholane*, $(CH_2)_4PF_3$ (**1c**): *preparation of the intramolecularly coordinated adduct*, **4**

A mixture of **2** (7.85 g, 0.036 mol) and 5.29 g (0.037 mol) of **1c** was heated for 14 h at 50°C. After removal of the volatile trimethylfluorosilane (3.3 g, 0.036 mol; 99%) 9.8 g (100%) of a light green solid, very soluble in dichloromethane and acetonitrile, were left. Part of this product, prior to further characterization, was recrystallized from dichloromethane–petroleum ether (40:60); m.r. 137–142°C.

$C_{13}H_{14}F_2NOP$ (269.23). Found: C, 58.1; H, 5.6; P, 11.2. Calc.: C, 58.0; H, 5.2; P, 11.5%. MS: (*m/z*) 269 $[M]^+$ (52%); 125 $[(CH_2)_4PF_2]^+$ (100%). ^{1}H NMR spectrum ($CDCl_3$): $\delta_{(CH_2)_4}$ 0.92–2.30 (m); $\delta_{aryl\text{-}H}$ 6.8–9.2 (m). ^{19}F NMR spectrum ($CDCl_3$): $\delta_{F(A)}$ −17.8, *J*(FP) 825; $\delta_{F(B)}$ −55.2, *J*(FP) 825. ^{31}P NMR spectrum (CH_2Cl_2): δ_P −68.3(t), *J*(PF) 830.

Reaction of 8-*trimethylsiloxyquinoline* (**2**) *with* 1.1.1-*trifluoro*-1λ^5-*phosphorinane*, $(CH_2)_5PF_3$ (**1d**): *preparation of* **5**

As described in the preceding experiment, a mixture of **2** (4.89 g, 0.023 mol) and of **1d** (3.68 g, 0.023 mol) was heated at 50°C for 14 h. After removal of volatile trimethylfluorosilane (2.07 g, 0.023 mol; 100%), 6.4 g (100%) of a colourless solid, very soluble in dichloromethane and acetonitrile, was obtained, part of which was recrystallized from dichloromethane–petroleum ether (40:60); m.p. 97–100°C.

$C_{14}H_{16}F_2NOP$ (283.26). Found: C, 58.2; N, 5.8; P, 10.4. Calc.: C, 59.4; H, 5.7; P, 10.9%. MS: (*m/z*) 283 $[M]^+$ (4%); 139 $[(CH_2)_5PF_2]^+$ (100%). ^{1}H NMR spectrum ($CDCl_3$): $\delta_{(CH_2)_5}$ 1.15–2.20 (m); $\delta_{aryl\text{-}H}$ 7.26–9.10 (m). ^{19}F NMR spectrum ($CDCl_3$): δ_F −22.4 (d), *J*(FP) 734. ^{31}P NMR spectrum (CH_2Cl_2): δ_P −15.2 (t), *J*(PF) 748.

Reaction of phosphorus pentafluoride with 2-(*N,N-dimethylamino*)*acetoxytrimethylsilane* (**6**): *preparation of* 2-(*N,N-dimethylamino*)*acetoxytetrafluorophosphate* (**7**)

Phosphorus pentafluoride (2.05 g, 0.16 mol) was condensed at liquid nitrogen temperature with **6** (2.89 g, 0.16 mol). The reaction mixture was allowed to warm up to room temperature, and was left standing for 19 h. Formation of a light brown solid was observed. After removal of trimethylfluorosilane (1.51 g, 0.16 mol; 99%) 3.4 g (99%) of a light brown solid were left, part of which was recrystallized from dichloromethane–acetonitrile (1:2); m.r. 116–118°C.

$C_4H_8F_4NO_2P$ (209.08). Found: C, 23.0; H, 4.0. Calc.: C, 23.0; H, 3.9%. MS: (*m/z*) 208 $[M—H]^+$ (2%); 58 $[CH_2N(CH_3)_2]^+$ (100%). ^{1}H NMR spectrum (CD_3CN) at 400 MHz: $\delta_{[-N(CH_3)_2]}$ 2.98 (ddt), ^3J(HP) 8.9, $^4J(HF_A)$ 2.4, $^4J(HF_B)$ 1.7; $\delta_{(-NCH_2-)}$ 3.93 (dq), ^3J(HP) 11.3, ^4J(HF) 1.8. ^{13}C NMR spectrum (CD_3CN); (20.1 MHz): $\delta_{[-N(CH_3)_2]}$ 52.02 (d), ^2J(CP) 10; $\delta_{(-NCH_2-)}$ 63.16 (s); $\delta_{C(:O)}$ 167.36(2). ^{19}F NMR spectrum (CD_3CN) at 94.2 MHz: see Table 1. ^{31}P NMR spectrum (CD_3CN) at 162 MHz: δ_P −136.8 (dq), $^1J(PF_{A,B})$ 844, $^1J(PF_C)$ 749.

Reaction of phenyltetrafluorophosphorane with 2-(*N,N-dimethylamino*)*acetoxytrimethylsilane* (**6**): *preparation of* 2-(*N,N-dimethylamino*)*acetoxyphenyltrifluorophosphate* (**8**)

A mixture of phenyltetrafluorophosphorane (4.26 g, 0.23 mol) and 2-(N,N-dimethylamino) acetoxytrimethylsilane (**6**) (3.98 g, 0.23 mol) was allowed to stand at room temperature for 44 h. Formation of a light brown solid was noted. After removal of the volatile product, trimethylfluorosilane (2.10 g, 0.238 mol, 100%), 5.97 g of a light brown solid were left. The product was recrystallized from dichloromethane and was obtained as colourless crystals of m.r. 125–128°C.

$C_{10}H_{13}F_3NO_2P$ (267.19). Found: C, 45.0; H, 5.1. Calc.: C, 44.9; H, 4.9%. MS: (*m/z*) 267 $[M]^+$ (4%); 58 $[(CH_3)_2NCH_2]^+$ (100%). ^{1}H NMR spectrum ($CDCl_3$) at 400 MHz: $\delta_{[N(CH_3)_2]}$ 2.89 (dq), ^3J(HP) 8.7, ^4J(HF) 2.2; $\delta_{(-NCH_2-)}$ 3.62 (dq), ^3J(HP) 11.0, ^4J(HF) 1.8; $\delta_{(aryl\text{-}H)}$ 6.92–7.55 (m). ^{13}C NMR spectrum (CD_3CN) at 20.1 MHz: $\delta_{[N(CH_3)_2]}$ 51.3 (d), ^2J(CP) 4.6; $\delta_{(-NCH_2-)}$ 62.4 (s); $\delta_{o\text{-}aryl\text{-}C}$ 127.6 (d); ^2J(CP) 19.8; $\delta_{o\text{-}aryl\text{-}C}$ 129.3 (d), ^4J(CP) 2.4; $\delta_{m\text{-}aryl\text{-}C}$ 130.8 (d), ^3J(CP) 4.2; $\delta_{ipso\text{-}aryl\text{-}C}$ 142.3 (dq), ^1J(CP) 293, ^2J(CF) 34.4; $\delta_{C(:O)}$ 164.0 (s). ^{19}F NMR spectrum ($CDCl_3$): δ_F(A) −56.1, $^1J(F_AP)$ 935; δ_F(B) −59.0, $^1J(F_BP)$ 935, $^2J(F_AF_B)$ 68. ^{31}P NMR spectrum ($CDCl_3$) at 162 MHz: δ_P −119.6 (q), *J*(PF) 959 Hz.

X-ray analysis. Crystals of **8** obtained by recrystallization from dichloromethane have monoclinic symmetry, space group $P2_1$. The unit cell which has the parameters a = 630.61(6), b = 1044.81(12), c = 937.24(9) pm, β = 108.379(12)°, contains two molecules yielding a calculated density of 1.514 g cm^{-3}. The data were collected at 293 K on a Nicolet diffractometer using graphite-monochromated Cu-

K_α radiation ($\lambda = 154.18$ pm) in the θ–2θ mode in the range $3° \leqslant 2\theta \leqslant 135°$ at a scan speed between 2.93 and 29.30° min^{-1}, depending on the intensity of the reflection.

The data were corrected for Lorentz, polarization and absorption effects ($\mu = 2.269$ mm^{-1}). The structure was solved by direct methods and difference-Fourier syntheses. Hydrogen atoms were localized from difference Fourier maps and refined, together with isotropic temperature factors. The refinement, using 969 out of 1009 measured independent reflections, ($F \geqslant 2.5\sigma(F)$) converged at $R = 0.039$. A final difference map displayed no electron density higher than 0.27×10^6 e pm^{-3}. The program SHELX-76[46] and our own programs (D. Schomburg) were used. Complex atom scattering factors[47] were employed.

Acknowledgements—This research has been aided by chemicals generously supplied by BASF AG, BAYER AG, HOECHST AG, Stauffer Chemical Company, and U.S. Agrichemicals. The support of Fonds der Chemischen Industrie, Frankfurt am Main and Deutsche Forschungsgemeinschaft, is gratefully acknowledged.

REFERENCES

1. E. L. Muetterties, T. A. Bither, M. W. Farlow and D. D. Coffman, *J. Inorg. Nucl. Chem.* 1960, **16**, 52.
2. J. F. Nixon and R. Schmutzler, *Spectrochim. Acta* 1964, **20**, 1835.
3. E. L. Muetterties and W. Mahler, *Inorg. Chem.* 1965, **4**, 119.
4. W. McFarlane, J. F. Nixon and J. R. Swain, *Molec. Phys.* 1970, **19**, 141.
5. H. Dreeskamp, C. Schumann and R. Schmutzler, *Chem. Commun.* 1970, 671.
6. J. F. Nixon and J. R. Swain, *J. Chem. Soc. A* 1970, 2075.
7. S. C. Peake, M. J. C. Hewson and R. Schmutzler, *J.* Chem. Soc. A 1970, 2364; W. Stadelmann, O. Stelzer and R. Schmutzler, *Z. Anorg. Allg. Chem.* 1971, **385**, 142.
8. Yu. A. Buslaev, E. G. Il'in and M. N. Shcherbakova, *Dokl. Akad. Nauk. SSSR* 1974, **217**, 337.
9. E. G. Il'in, M. N. Shcherbakova and Yu. A. Buslaev, *Koord. Khim.* 1975, **1**, 1179.
10. E. G. Il'in, M. N. Shcherbakova and Yu. A. Buslaev, *Dokl. Akad. Nauk. SSSR* 1976, **231**, 107.
11. A. H. Cowley, P. J. Wisian and M. Sanchez, *Inorg. Chem.* 1977, **16**, 1451.
12. B. Hupe, PhD thesis, Technische Universität Braunschweig (1980).
13. D. H. Brown, K. D. Crosbie, G. W. Fraser and D. W. A. Sharp, *J. Chem. Soc. A* 1969, 551.
14. C. W. Schultz and R. W. Rudolph, *J. Am. Chem. Soc.* 1971, **93**, 1898.
15. W. S. Sheldrick, J. A. Gibson and G.-V. Röschenthaler, *Z. Naturforsch.* 1978, **33b**, 1102.
16. L. Lunazzi and S. Brownstein, *J. Magn. Reson.* 1969, **1**, 119.
17. D. H. Brown, G. W. Fraser and D. W. A. Sharp, *J. Chem. Soc. A* 1966, 171.
18. J. S. Harman and D. W. A. Sharp, *J. Chem. Soc. A* 1970, 1138.
19. F. N. Tebbe and E. L. Muetterties, *Inorg. Chem.* 1967, **6**, 129.
20. W. Wieker, A. R. Grimmer and L. Kolditz, *Z. Chem.* 1967, **7**, 434.
21. K. P. John and R. Schmutzler, *Z. Naturforsch.* 1974, **29b**, 730.
22. W. S. Sheldrick, *J. Chem. Soc., Dalton Trans.* 1974, 1402.
23. W. Storzer, PhD thesis, Technische Universität Braunschweig (1981).
24. W. Storzer, D. Schomburg, G.-V. Röschenthaler and R. Schmutzler, *Chem. Ber.* 1983, **116**, 367.
25. W. S. Sheldrick and M. J. C. Hewson, *Z. Naturforsch.* 1978, **33b**, 834.
26. W. S. Sheldrick, *Top. Curr. Chem.* 1978, **73**, 1.
27. K. P. John, R. Schmutzler and W. S. Sheldrick, *J. Chem. Soc., Dalton Trans.* 1974, 1841.
28. K. P. John, R. Schmutzler and W. S. Sheldrick, *J. Chem. Soc., Dalton Trans.* 1974, 2466.
29. K. P. John and R. Schmutzler, unpublished results.
30. H. Oberhammer, personal communication to R. Schmutzler (1985).
31. R. Schmutzler, *Inorg. Chem.* 1964, **3**, 421.
32. S. C. Peake, M. Fild, M. J. C. Hewson and R. Schmutzler, *Inorg. Chem.* 1971, **10**, 2723.
33. W. Storzer, personal communication to R. Schmutzler (1986).
34. L. Maier and R. Schmutzler, *Chem. Commun.* 1969, 961.
35. H. Günther, *NMR-Spektroskopie*, p. 380. Georg Thième Verlag, Stuttgart (1973).
36. C. Dittebrandt and H. Oberhammer, *J. Mol. Struct.* 1980, **63**, 227.
37. H. Bode and H. Clausen, *Z. Anorg. Allg. Chem.* 1951, **265**, 229.
38. R. J. Gillespie, *Molecular Geometry*. Van Nostrand-Reinhold, New York (1972).
39. R. J. Gillespie, *Can. J. Chem.* 1960, **38**, 818.
40. D. D. Perrin, W. L. F. Armarego and D. R. Perrin, *Purification of Laboratory Chemicals*. Pergamon Press, Oxford (1966).
41. H. Günther, *NMR-Spectroskopie*, p. 52. Georg Thième Verlag, Stuttgart (1973).
42. M. Wada and R. Okawara, *Inorg. Nucl. Chem. Lett.* 1969, **5**, 355.
43. R. Schmutzler, *Inorg. Chem.* 1964, **3**, 410.
44. G. Bettermann, H. Buhl, R. Gerecke and M. Sell, personal communication (1981).
45. W. Storzer and R. Schmutzler, unpublished results (1981).
46. G. M. Sheldrick, unpublished.
47. D. T. Cromer and J. T. Waber, in *International Tables for Crystallography*, Vol. IV, p. 99 and p. 149. Kynoch Press, Birmingham (1974).

Polyhedron Vol. 8, No. 6, pp. 739–744, 1989
Printed in Great Britain

0277–5387/89 $3.00+.00
© 1989 Pergamon Press plc

INFLUENCE OF 4-TOLUENESULPHONYL GROUP ON THE COORDINATION PROPERTIES OF DL-ASPARAGINE AND L-GLUTAMINE

LEDI MENABUE* and MONICA SALADINI

Dipartimento di Chimica, University of Modena, via Campi 183, 41100 Modena, Italy

and

PAOLA MORINI

Istituto di Chimica, Facolta' di Medicina-Veterinaria, University of Bari, via Gentile 182, 70126 Bari, Italy

(*Received* 17 *March* 1988; *accepted after revision* 29 *September* 1988)

Abstract—From the interaction between N-tosyl-DL-asparagine (TsasnH), N-tosyl-L-glutamine (TsglnH) (tosyl = 4-toluenesulphonyl) and copper(II) ion in aqueous solution, compounds of formula $CuL_2 \cdot XH_2O \cdot YC_2H_5OH$ (L = tosyl-α-aminoacidate monoanion), $Cu(LH_{-1}) \cdot 2H_2O$ (LH_{-1} = tosyl-α-aminoacidate dianion) and $K_2[Cu(LH_{-1})_2]$ were isolated. By potentiometric and spectrophotometric measurements, the number and type of complex species and their cumulative formation constants were determined. The treatment of data confirmed, also in solution, the formation of the complexes separated in the solid state and defined the pH range in which they are stable. The coordination behaviour of these ligands is compared with that of parent amino acids and other N-tosyl-derivatives.

L-Asparagine and L-glutamine form, with Cu^{II} ion complexes of formulae CuL^+ and CuL_2 whose stability constants are slightly lower than those of simple amino acids like glycine, alanine etc.[1,2] and the measurements have also failed to detect stereoselectivity in the formation of bis-chelate complexes,[3,4] confirming the general trend observed for simple amino acids.[3,4] For the asparagine–Cu^{II} system, in the metal–ligand molar ratio of 1:2, above pH 10, deprotonation of the amide function occurs and the formation of a chromophore $CuN_2N_2^-O_2^-$ is supported by the shift of λ_{max} from 620 to 590 nm.[5]

This behaviour is not observed for glutamine as the chelation of the amide nitrogen requires an unfavoured hepta-atomic ring. As a result the solution coordination behaviour of N-acetyl-L-glutamine[6] closely resembles that of other N-acetyl, N-benzoyl and N-benzyloxycarbonyl amino acids and no stable solution species are formed before copper hydroxide precipitation.

On the contrary, the presence of tosyl and dansyl as N-protecting groups of amino acids leads to the formation of very stable mono- and bis(N,O-chelate) copper(II) complexes through the involvement of the carboxyl (primary ligating group) and the deprotonated sulphonamide nitrogen, at acidic or slightly alkaline pH, in aqueous and mixed-alcoholic media.[7]

Thus the introduction of the tosyl group on the amino nitrogen of asparagine and glutamine could affect their coordination properties by modifying the donor ability of the potentially active binding sites.

The results of the solid state and aqueous solution investigations on the Cu^{II}—N-tosyl-DL-asparagine and -L-glutamine are reported here and compared

*Author to whom correspondence should be addressed.

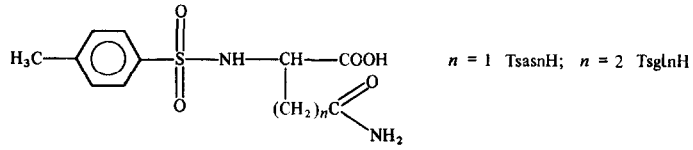

Structure 1.

with the behaviour of parent ligands as well as other N-tosyl-derivatives (see Structure 1).

EXPERIMENTAL

Reagents

TsasnH and TsglnH were recrystallized from a 1:1 ethanol–water solution and the concentrations of the solution used throughout were tested potentiometrically. Sodium hydroxide carbonate-free 0.09861 mol dm^{-3} (C.Erba) standardized against phtalate (N.B.S.) was used as titrant. Copper(II) perchlorate hexahydrate was from Fluka and the concentration of the stock solution was determined with EDTA.

Potentiometry

Potentiometric measurements were performed under a nitrogen atmosphere ($I = 0.1$ mol dm^{-3}, $NaClO_4$) at 25 ± 0.1°C with the fully automatic Orion 960 Autochemistry system using a Ross 8102SC combined electrode and a Centronics GLPII printer for recording EMF and pH readings and titration curves.[8] The standard electrode potential, E° and the ionic product K_w were determined before and after each experiment by titration of a known amount of $HClO_4$ (0.1 mol dm^{-3}) with NaOH solution.

The overall stability constants ($\beta_{pqr} = [L_pM_qH_r]/[L]^p[M]^q[H]^r$) were refined by the computer program SUPERQUAD[9] with $\sigma_E = 0.3$ (mV error) and $\sigma_V = 0.005$ (volume error). All the calculations were performed on a IBM XT286 personal computer.

Spectrophotometric measurements

Absorption spectra were obtained on a Varian Cary 2300 spectrophotometer. The solutions were scanned by varying the NaOH amount at 25°C using 10 cm cells.

Preparation of complexes

The pale blue $CuL_2 \cdot XH_2O \cdot YC_2H_5OH$ compounds were prepared by mixing 0.015 dm^3 of a hot ethanolic solution (0.2 mol dm^{-3}) of the ligands and 0.02 dm^3 of aqueous copper acetate monohydrate (0.15 mol dm^{-3}) and slowly evaporating the blue solutions. (Found: C, 40.8; H, 5.5; N, 7.4; S, 8.3; solvents, 16.0. Calc. for $Cu(Tsasn)_2 \cdot 2H_2O \cdot 2C_2H_5OH$, $C_{26}H_{42}CuN_2O_{14}S_2$: C, 40.9; H, 5.6; N, 7.3; S, 8.4; solvents, 14.8%. Found: C, 36.9; H, 5.0; N, 7.4; S, 8.2; H_2O, 14.5. Calc. for $Cu(Tsgln)_2 \cdot 6H_2O$, $C_{24}H_{42}CuN_4O_{16}S_2$: C, 37.4; H, 5.5; N, 7.3; S, 8.3; H_2O, 14.0%.)

The compounds $K_2[Cu(LH_{-1})_2]$ were prepared by suspending 1 mmol of the corresponding binary compound in 0.03 dm^3 of a mixture of C_2H_5OH and H_2O (2:1) at 50°C and alcoholic (C_2H_5OH) KOH was added until pH $\simeq$ 11. By standing the deep blue solutions for 12 h at room temperature, blue (TsasnH) and blue-violet (TsglnH) crystals separated. (Found: C, 35.3; H, 3.5; N, 7.5; S, 8.7. Calc. for $K_2[Cu(TsasnH_{-1})_2]$, $C_{22}H_{24}CuK_2N_2O_{10}S_2$: C, 37.2; H, 3.4; N, 7.9; S, 9.0%. Found: C, 38.8; H, 3.7; N, 7.5; S, 8.4. Calc. for $K_2[Cu(TsglnH_{-1})_2]$, $C_{24}H_{28}CuK_2N_2O_{10}S_2$: C, 39.0; H, 3.8; N, 7.6; S, 8.7%.)

The compound $Cu(TsasnH_{-1}) \cdot 2H_2O$ was prepared by mixing 0.005 dm^3 of a methanolic solution (0.5 mol dm^{-3}) of TsasnH with 0.02 dm^3 of aqueous copper acetate monohydrate (0.125 mol dm^{-3}) and adding aqueous NaOH solution until pH = 5.3. On standing for 12 h pale green microcrystalline compounds separated. (Found: C, 34.5; H, 4.3; N, 7.3; S, 8.1. Calc. for $C_{11}H_{16}CuNO_7S$: C, 34.5; H, 4.2; N, 7.3; S, 8.3%.) The same kind of preparation, using TsglnH, did not separate any solid compound.

Physical measurements

The electronic spectra of the solid compounds were recorded as mull transmission spectra on a Varian Cary 2300 spectrophotometer. The IR spectra were recorded with a Perkin–Elmer 180 spectrophotometer on KBr pellets in the 4000–250 cm^{-1} spectral range. The EPR spectra were recorded with a Bruker ER 200-SRC spectrometer.

Analysis

Sulphur, nitrogen, carbon and hydrogen were analysed with a Carlo Erba elemental analyser Model 1106 by Mr G. Goldoni. The water and

solvent contents were determined gravimetrically with thermal analyses performed at a rate of 10°C min^{-1} with a Mettler TA 3000 instrument.

RESULTS AND DISCUSSION

Solid state

The pale blue $CuL_2 \cdot XH_2O \cdot YC_2H_5OH$ complexes show electronic and ESR data (Table 1) which are consistent with a CuO_n ($n = 5,6$) chromophore as found for other structurally known Cu^{II}—N-protected amino acidates.[10,11] In their IR spectra (supplementary material) no changes in band position, with respect to free ligands, are observed except for $\nu(COO)_{as}$ and $\nu(COO)_{sym}$, indicating a bonding mode through the carboxylate group; the presence of coordinated solvent molecules is derived from the strong bands found in the 3550–3470 cm^{-1} spectral range, attributed to ν(OH) absorption.

The pale green $Cu(TsasnH_{-1}) \cdot 2H_2O$ complex displays spectroscopic properties in agreement with a $CuNO_4$ chromophore because of their close similarity to those of the structurally known $[Cu(Ts\text{-}\alpha\text{-}alaH_{-1})(H_2O)_2] \cdot H_2O$, where the Ts-α-alaH$_{-1}$ dianion acts as bidentate chelate in the equatorial plane through deprotonated sulphonamide nitrogen and one carboxylate oxygen.[12] In its IR spectrum, the disappearance of ν(NH) and the shift to lower energy of $\nu(SO_2)$ bands are characteristic of the deprotonated sulphonamide group.

The same holds in IR spectra of bis-potassium salts which should possess two equatorial five-membered NO-chelate rings, as found in all those previously investigated $[Cu(Ts\text{-}\alpha\text{-}aminoacidatoH_{-1})_2]^{2-}$ species,[12] but the unambiguous assignment of a *trans* or *cis* configuration is prevented by the lack of structural data, because sulphonyl and terminal peptide groups both can play a role in determining crystal packing forces; nevertheless on the basis of literature data[13–15] and by comparison with other N-tosyl-α-aminoacidate copper(II) complexes[12,16] the *trans*-configuration is the most probable. For TsglnH complex the electronic and ESR results are consistent with an essentially square-planar geometry with chromophore CuN_2O_2.[12,13] The low energy *d–d* band (640 nm) of $K_2[Cu(TsasnH_{-1})_2]$ complex, close to the value observed for the same system in 1:2 metal–ligand molar ratio, in strongly alkaline solution, is indicative of a tetragonal geometry both in solid and solution states, as found in Cu^{II}–peptide systems.[17] In fact in the IR spectrum, the appearance of a splitting in all the bands assignable to the sulphonamide group (NH, SO_2, SN) suggests a direct involvement of SO_2 in metal coordination as in the homologous tosylglycinate complex.[18]

Solution behaviour

Protonation. Several titrations of the ligands were carried out over a pH range of about 2.8–11.3, with total initial concentrations of the ligands ranging from 4.434×10^{-3} to 8.642×10^{-3} mol dm^{-3} for TsglnH and 5.265×10^{-3} mol dm^{-3} for TsasnH. The dissociation equilibria are represented as follows and the protonation constants are reported in Table 2

$$CH_3C_6H_4SO_2\tilde{N}CHCOO^- + H^+ \overset{\beta_{101}}{\rightleftharpoons} CH_3C_6H_4SO_2NHCHCOO^- \quad (2)$$
$$\quad\quad\quad

Table 2. Proton and Cu^{II} complex stability constants at 25°C and $I = 0.10$ mol dm^{-3} ($NaClO_4$), with estimated standard deviations in parentheses[a]

Complex		TsasnH	TsglnH
L	$\log \beta_{101}$	11.38(2)	11.82(3)
LH	$\log \beta_{102}$	14.58(3)	15.10(3)
	$\log K_2^H$	3.20(2)	3.28(2)
$[CuLH_{-1}]$	$\log \beta_{110}$	9.71(5)	9.03(4)
$[Cu(LH_{-1})_2]^{2-}$	$\log \beta_{210}$	16.53(4)	15.89(2)
$[CuL_2]$	$\log \beta_{212}$	27.13(4)	28.00(10)

[a] The titrations were performed at 1:1, 1:2 and 1:4 metal–ligand ratios; for both ligands, in the 1:1 ratio, the data above pH 6.5 were excluded from calculations because of $Cu(OH)_2$ precipitation.

Complexation. For the Cu^{II}–TsglnH system, all the titrations are quite superimposable on that of the free ligand up to pH 4, suggesting that no complex formation takes place before carboxylate ionization is almost complete. Otherwise, the lowering in pH, clearly observed for 1:2 metal–ligand molar ratio in the Cu^{II}–TsasnH system, suggests that a carboxylate species is formed even at pH 3. For both ligands two pH-metric equivalent points are observed according to the reactions:

$$m_{NaOH} = m_{LH} + m_{Cu}$$

$$m_{NaOH} = m_{LH} + 2m_{Cu}$$

where m is the number of moles and the second equivalent point corresponds to the deprotonation of the bonded ligand. Thus the absence of a further equivalent point excludes the deprotonation reaction of terminal amide nitrogen as well as the formation of tris-chelate complexes.

The analysis of solution spectrophotometric measurements (Table 3) in the case of the Cu^{II}–TsasnH 1:2 system, shows after addition of 1.5 equivalents of base, a band maximum at 750 nm near to the value (745 nm) observed in the solid state in the spectrum of $Cu(TsasnH_{-1})\cdot 2H_2O$. After addition of two equivalents of base, the band maximum shifts to 660 nm, close to the value of 640 nm found for the solid $K_2[Cu(TsasnH_{-1})_2]$, and remains quite constant after addition of three and four equivalents of NaOH. The coordination behaviour of TsglnH is closely similar to that of TsasnH, and is confirmed also in the metal–ligand ratio of 1:4.

The overall stability constants for the solution species taken into account are reported in Table 2 and species distribution curves are shown in Figs 1 and 2 along with those of Cu^{II}–asparagine (asnH) and –glutamine (glnH) systems.[1,19,20]

The log β for mono- and bis-chelate complexes are significantly greater than those of unsubstituted ligands[1,2,19,20] ($\Delta \log \beta = 1.3$–2.2), as found for Cu^{II}–N-tosyl-L-leucinate system,[16] because of the corresponding greater donor ability of the deprotonated sulphonamide nitrogen as compared to amino nitrogen, confirming that, in general, the tosyl group enhances the ligand field strength with respect to unsubstituted amino acids.

The greater stability in the Cu^{II}–TsasnH system as compared to the TsglnH one, may be due to the position of the terminal amide group which, since in TsasnH it is nearer to the sulphonamide nitrogen, causes an enhancement in the inductive electrophilic effect of the sulphonyl group, thus favouring even more the metal-promoted sulphonamide deprotonation. In addition, a possible cooperative contribution from a stereoselective effect of the N-substitution of a bulky group cannot be excluded.[3a] Finally, the substitution of the tosyl group on nitrogen bonded to C^{α} atom, deactivates the terminal amide nitrogen preventing its reaction, contrary to what is found in the simple Cu^{II}–asparagine system. Indeed in the present case the complex anion formed by chelation through the deprotonated terminal amide and sulphonamide nitrogen, would be very unfavoured as the stability deriving from the CuN_4 chromophore is overcome by its unbalanced four negative charges.

Table 3. Position of absorption bands [λ_{max} (nm)] of the solution Cu^{II}–N-tosyl-DL-asparaginate and –N-tosyl-L-glutaminate complexes, $C_{Cu^{2+}} = 1.66 \times 10^{-3}$ mol dm^{-3}

HL	$[HL] \times 10^3$ (mol dm^{-3})	[NaOH]/[HL] 0	1	1.25	1.50	2.00	2.50	3.00
TsasnH	3.3	800	790	765	750	660	650	650
TsglnH	3.3	800	790	770	760	665	650[a]	650[a]
	6.6	800	780	760	650	650		

[a] The solutions became turbid because of $Cu(OH)_2$ precipitation.

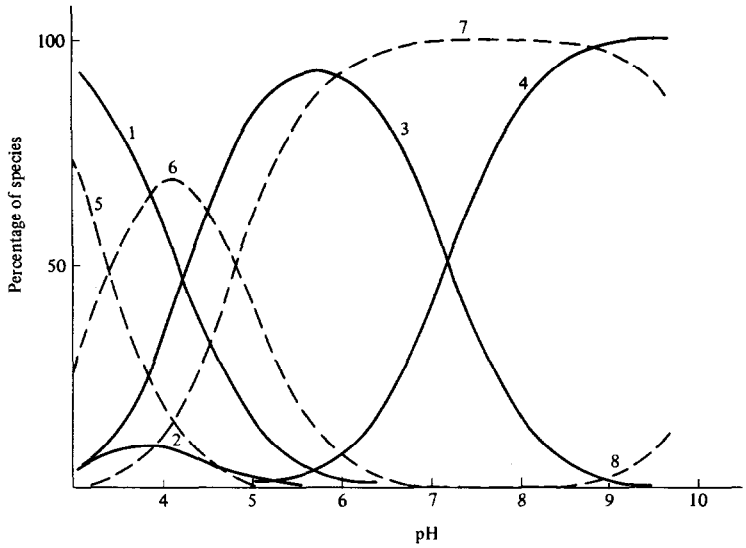

Fig. 1. Species distribution curves for the complexes by DISPO program (M. Micheloni, personal communication) at 4:1 ligand–metal molar ratio. $C_{Cu} = 8 \times 10^{-4}$ mol dm^{-3}. Solid lines: L = TsasnH, (1) = [Cu]; (2) = [CuL_2]; (3) = [$CuLH_{-1}$]; (4) = [$Cu(LH_{-1})_2$]$^{-2}$; Dashed lines: L = asnH, (5) = [Cu]; (6) = [CuL]; (7) = [CuL_2]; (8) = [CuL_2H_{-1}]$^-$; and β values are average values from refs 1 and 19.

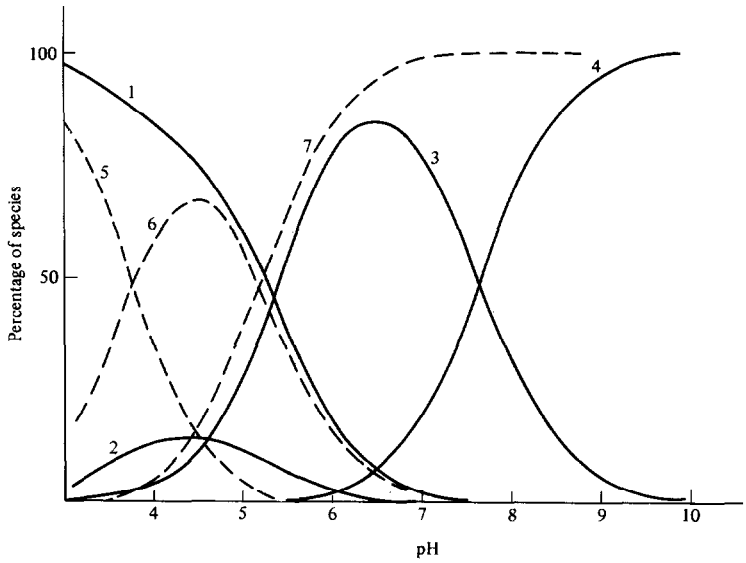

Fig. 2. Species distribution curves for the complexes by DISPO program (M. Micheloni, personal communication) at 4:1 ligand–metal molar ratio. $C_{Cu} = 8 \times 10^{-4}$ mol dm^{-3}. Solid lines: L = TsglnH, (1) = [Cu]; (2) = [CuL_2]; (3) = [$CuLH_{-1}$]; (4) = [$Cu(LH_{-1})_2$]$^{-2}$; Dashed lines: L = glnH, (5) = [Cu]; (6) = [CuL]; (7) = [CuL_2]; and β values are average values from refs 1, 19 and 20.

Acknowledgements—The authors are grateful to the Ministero della Pubblica Istruzione of Italy for financial support, the CIGS of the University of Modena for recording ESR and IR spectra. We also thank Prof. M. Micheloni (University of Florence) for kindly supplying the PC version of SUPERQUAD and DISPO programs and Mr L. Locusti for drawings.

Supplementary material—Titration curves of the ligand and metal–ligand systems and a table of IR data is available on request.

REFERENCES

1. R. B. Martin, *Met. Ions Biol. Sys.* 1979, **9**, 1 and refs therein.
2. B. E. Fischer and H. Sigel, *J. Am. Chem. Soc.* 1980, **102**, 2998.
3. (a) L. D. Pettit and R. J. Hefford, *Met. Ions Biol. Sys.* 1979, **9**, 173 and refs therein; (b) S. T. Chow and McAuliffe, *Prog. Inorg. Chem.* 1975, **19**, 51 and refs therein.
4. R. D. Gillard, H. M. Irving, R. M. Parkins, N. C.

Payne and L. D. Pettit, *J. Chem. Soc.* 1966, 1159.
5. P. M. H. Kroneck, V. Vortisch and P. Hemmerich, *Eur. J. Biochem.* 1980, **109**, 603.
6. L. Menabue and M. Saladini, *Inorg. Chim. Acta* 1987, **135**, 49 and refs therein.
7. G. Battistuzzi Gavioli, G. Grandi, L. Menabue, G. C. Pellacani and M. Sola, *J. Chem. Soc., Dalton Trans.* 1985, 2363 and refs therein.
8. "ORION 960 Autochemistry System, Instruction Manual". Orion Research (1986).
9. P. Gans, A. Sabatini and A. Vacca, *J. Chem. Soc., Dalton Trans.* 1985, 1185.
10. E. D. Estes, W. E. Estes, R. P. Scaringe, W. E. Hatfield and D. J. Hodgson, *Inorg. Chem.* 1975, **14**, 2564.
11. L. P. Battaglia, A. Bonamartini Corradi, L. Menabue, M. Saladini and M. Sola, *J. Chem. Soc., Dalton Trans.* 1987, 1333.
12. L. Antolini, L. P. Battaglia, A. Bonamartini Corradi, G. Marcotrigiano, L. Menabue and G. C. Pellacani, *J. Am. Chem. Soc.* 1985, **107**, 1369 and refs therein.
13. H. C. Freeman, *Adv. Chem. Prot.* 1967, **22**, 257.
14. F. S. Stephens, R. S. Vagg and P. A. Williams, *Acta Cryst.* 1975, **B31**, 841.
15. M. A. Hitchman, L. Kwan, L. M. Engelhardt and A. H. White, *J. Chem. Soc., Dalton Trans.* 1987, 457 and refs therein.
16. L. Antolini, L. Menabue, M. Saladini and M. Sola, *Inorg. Chim. Acta* 1988, **152**, 17.
17. J. Dehand, J. Jordanov, F. Keck, A. Mosset, J. J. Bonnet and J. Galy, *Inorg. Chem.* 1979, **18**, 1543.
18. L. Antolini, L. P. Battaglia, G. Battistuzzi Gavioli, A. Bonamartini Corradi, G. Grandi, G. Marcotrigiano, L. Menabue and G. C. Pellacani, *J. Am. Chem. Soc.* 1983, **105**, 4327.
19. A. Gergerly, I. Nagypal and E. Farkas, *J. Inorg. Nucl. Chem.* 1975, **37**, 551.
20. T. P. A. Kruck and B. Sarkar, *Can. J. Chem.* 1973, **51**, 3555.

Polyhedron Vol. 8, No. 6, pp. 745–748, 1989
Printed in Great Britain

0277–5387/89 $3.00+.00
© 1989 Pergamon Press plc

ANIONIC 2,6-PYRIDINEDICARBOXYLATE COMPLEXES WITH SOME DIVALENT FIRST-ROW TRANSITION METALS

LAWRENCE C. NATHAN,* DONALD C. ZAPIEN, ANNE M. MOORING, CHRISTINE A. DOYLE and JULIE A. BROWN

Department of Chemistry, Santa Clara University, Santa Clara, CA 95053, U.S.A.

(*Received* 19 *July* 1988; *accepted* 3 *October* 1988)

Abstract—A series of $Na_2[M(pdc)_2]\cdot nH_2O$ complexes (M = Mn^{II}, Co^{II}, Ni^{II}, Cu^{II}, and Zn^{II}; pdc^{2-} = pyridine-2,6-dicarboxylate; n = 2 or 3) have been synthesized and characterized via molar conductance, magnetic susceptibility, IR and electronic spectral measurements, and thermogravimetry. The compounds are 2 : 1 electrolytes in aqueous solution and contain six-coordinate anionic complex ions. The loss of water and the decomposition of the anhydrous salts differ from compound to compound in this series; residues consist of Na_2CO_3 and metal oxide.

Pyridine-2,6-dicarboxylic acid (also known as dipicolinic acid and abbreviated herein as H_2pdc) has been studied extensively as a Lewis base. The interest in this ligand seems to centre on the versatile yet unpredictable manner in which it coordinates to a variety of metals. For example, X-ray studies have shown that complexes such as $Ag(Hpdc)_2\cdot H_2O$[1] and $Cu(Hpdc)_2\cdot 3H_2O$[2] actually contain one neutral H_2pdc and one pdc^{2-} ligand, while $Ni(Hpdc)_2\cdot 3H_2O$[3–5] has two $Hpdc^-$ ligands. In contrast to the tridentate coordination of the ligands in the above complexes, $Hpdc^-$ is bidentate in $V(Hpdc)_3\cdot 3H_2O$.[6] Other types of complexes which have been reported, include some polymeric $M(pdc)\cdot nH_2O$ species (M = Co^{II}, Ni^{II}, Cu^{II}; n = 0, 2, or 3),[7–9] some mixed-ligand complexes with acetylacetonate, 1,10-phenanthroline, 2,2′-bipyridyl, or 2,2′,2″-terpyridyl,[9] a series of $M_2(pdc)(Hpdc)_2\cdot nH_2O$ complexes (M = Co^{II}, Ni^{II}, Cu^{II}; n = 0 or 2),[9] and a series of lanthanide complexes of the types $M(Hpdc)_3\cdot H_2O$ and $M(pdc)(Hpdc)(H_2O)_n$ (n = 4 or 6).[10,11]

Based upon the coordination number of six, commonly adopted by many transition metals, and the ability of pdc^{2-} to function as a tridentate ligand, one expects to find anionic complexes of the type $[M(pdc)_2]^{x-}$ (x = 1 or 2). A number of such complexes has been reported for trivalent metal ions, examples being $Na[M(pdc)_2]\cdot 2H_2O$ (M = Ru^{III}, Ir^{III}),[12] $Na[Cr(pdc)_2]\cdot 1.5H_2O$,[13] $Rh[Cr(pdc)_2]$[14] and some Nd^{III} and Yb^{III} complexes of the type $Na_3[M(pdc)_3]\cdot nH_2O$.[15] Apparently similar anionic complexes with divalent metal ions have not been studied. This work focuses on the series $Na_2[M(pdc)_2]$ where M = Mn^{II}, Co^{II}, Ni^{II}, Cu^{II} and Zn^{II}. Other anionic complexes previously reported included $(Ph_4As)_2[U(pdc)_3]\cdot 3H_2O$[16] and $(Ph_4As)_2[UO_2(pdc)_2]\cdot 6H_2O$.[17]

RESULTS AND DISCUSSION

Reaction of divalent metal carbonates and/or hydroxides with H_2pdc in aqueous solution in 1 : 1 or 1 : 2 mole ratios leads to $M(pdc)\cdot nH_2O$ and $M(Hpdc)_2\cdot nH_2O$, respectively,[2,7,8,18] with M = Co^{II}, Ni^{II} and Cu^{II}, and n = 0, 2, or 3. In this work, anionic complexes were prepared in aqueous solution by the reaction of divalent (hydrated) metal acetates, H_2pdc and NaOH in a 1 : 2 : 2 mole ratio. Elemental analyses and thermogravimetric data confirm the stoichiometry of the complexes as $Na_2[M(pdc)_2]\cdot nH_2O$ where M = Mn^{II} and Co^{II} with n = 2, and where M = Ni^{II}, Cu^{II} and Zn^{II} with n = 3. Conductance measurements on 0.001 M aqueous solutions (Table 1) indicate the presence of 2 : 1 electrolytes, for which Λ_M is expected to be in the 230–270 $cm^2\ ohm^{-1}\ mol^{-1}$ range.[19] While the reason for the slightly low values for the Ni^{II} and Cu^{II} complexes is unknown, the behaviour is similar to that observed for the Rh^{III} and Ir^{III}

* Author to whom correspondence should be addressed.

$Na[M(pdc)_2]$ complexes, where Λ_M values in DMF fell essentially into the non-electrolyte range.[12]

IR data on the solid $Na_2[M(pdc)_2]\cdot nH_2O$ compounds are consistent with coordination of pdc^{2-}. The $\bar{\nu}_{sym}$(COO) band is shifted as expected from the free ligand value of 1290 cm^{-1} into the range 1376–1360 cm^{-1}. Similarly, the $\bar{\nu}_{asym}$(COO) band is shifted from the free ligand value of 1658 cm^{-1} into the range 1629–1613 cm^{-1}, and no bands appear near 1700 cm^{-1} as was the case when $Hpdc^-$ or H_2pdc was also present, such as in complexes of the type $M_2(pdc)(Hpdc)_2$.[9] The shift, $\Delta\bar{\nu}_{asym}$(COO), of about 40 cm^{-1} is consistent with the absence of an extended interaction in which the >C=O group of one ligand interacts with a second metal centre.[12] In addition, the extremely broad band in the 3200–2400 cm^{-1} range due to hydrogen-bonded —COOH groups in H_2pdc is absent in the complexes, further confirming complete deprotonation of H_2pdc. The typical upward shift of major pyridine ring bands is indicative of coordination of the ring nitrogen. A broad band centred at about 3390 cm^{-1} appears in the spectrum of the Ni^{II} and Cu^{II} complexes, due to the presence of the water of hydration. The Mn^{II}, Co^{II} and Zn^{II} complexes show a similar broad band centred around 3200 cm^{-1}, but each displays an additional sharp shoulder at 3534 cm^{-1}.

A coordination number of six suggests a pseudo-octahedral coordination sphere about the metal ions. Room temperature magnetic data (Table 1) are consistent with high-spin six-coordinate $M(pdc)_2^{2-}$ species. The observed magnetic moments are similar to those of $M(Hpdc)_2\cdot 3H_2O$, $M(pdc)\cdot 3H_2O$, M(pdc) and $M_2(pdc)(Hpdc)_2\cdot nH_2O$ ($n = 0$ or 2) species: 5.25–4.54 μ_B for Co^{II}; 3.45–2.85 μ_B for Ni^{II}, and 1.93 μ_B for the latter Cu^{II} complex.[7,9]

Electronic absorption spectra of the $Na_2[M(pdc)_2]\cdot nH_2O$ complexes are summarized in Table 1. The Cu^{II} complex has the single band expected for a six-coordinate d^9 species. Spectra of the Ni^{II} and Co^{II} complexes are also typical of six-coordinate species; most of the absorption peaks have clearly defined shoulders which suggest distortion from octahedral symmetry. The spectra of the latter two complexes are very similar to those reported for the corresponding Ni^{II} and Co^{II} $M(Hpdc)_2\cdot 3H_2O$ complexes.[7]

Several pdc^{2-} and $Hpdc^-$ complexes have been studied via thermogravimetric analysis. The thermogram of $(Ph_4As)_2[UO_2(pdc)_2]\cdot 6H_2O$ showed that water was lost up to about 120°C in three steps (first one, then three, then two moles). The anhydrous salt then decomposed between 250 and 450°C in several steps, proceeding via an intermediate proposed to be UO_2(pdc-Ph)$_2$ after the loss of two moles of $AsPh_3$.[16] Thermograms of the series $M(Hpdc)_2\cdot nH_2O$ (M = Mn^{II}, Fe^{II}, Co^{II}, Ni^{II}, Cu^{II}, Zn^{II}; $n = 0$, 2, or 3) were reported by D'Ascenzo *et al.*[18] In air, the hydrates $Co(Hpdc)_2\cdot 3H_2O$, $Ni(Hpdc)_2\cdot 3H_2O$ and $Zn(Hpdc)_2\cdot 2H_2O$ lost all their moles of water in a single step, while $Fe(Hpdc)_2\cdot 2H_2O$ lost its water in two steps. All anhydrous compounds decomposed in two steps yielding the oxides Mn_3O_4, Fe_2O_3, Co_3O_4, NiO, CuO and ZnO. The order of stability was found to be Mn > Fe > Zn > Co > Ni > Cu, the reverse of the Irving–Williams sequence.

For the $Na_2[M(pdc)_2]\cdot nH_2O$ complexes studied here (Table 2 and Fig. 1), the three trihydrates (M = Zn^{II}, Ni^{II}, Cu^{II}) lose water in two steps (first two moles, then one mole). The dihydrates behave differently, with the Mn^{II} complex losing water in a single step and the Co^{II} complex losing it in two steps. There seems to be no correlation of the manner in which the water is lost and the appearance of the bands in the O—H stretching region of the aforementioned IR spectra. Decomposition of the anhydrous salts occurs in two distinct steps for Zn^{II}

Table 1. Conductance, magnetic and spectral data

Complex	Molar conductance[a] Λ_M (cm^2 ohm^{-1} mol^{-1})	Magnetic moment[b] μ_B	Electronic absorption spectra[c] λ (nm) [ε (dm^3 mol^{-1} cm^{-1})]
$Na_2[Mn(pdc)_2]\cdot 2H_2O$	260	5.65	
$Na_2[Co(pdc)_2]\cdot 2H_2O$	261	5.18	459[20], 489sh, 528sh; 580[20]; 947[7], 989[7]
$Na_2[Ni(pdc)_2]\cdot 3H_2O$	221	3.25	363sh;[d] 616[10]; 923sh, 1021[32]
$Na_2[Cu(pdc)_2]\cdot 3H_2O$	213	1.88	774[43]
$Na_2[Zn(pdc)_2]\cdot 3H_2O$	232	diam.	

[a] 0.001 M in water.
[b] At 294 K.
[c] 0.014–0.022 M in water.
[d] Shoulder on charge-transfer band.

Table 2. Thermogravimetric data

Complex	Loss of water (%) calc. (found) $-H_2O$	$-2H_2O$	$-3H_2O$	Residue (%) Composition	calc. (found)
$Na_2[Mn(pdc)_2]\cdot 2H_2O$	3.86	7.71		$Na_2CO_3+Mn_3O_4$	39.02
	—	(7.9)			(38.9)
$Na_2[Co(pdc)_2]\cdot 2H_2O$	3.82	7.65		$Na_2CO_3+Co_3O_4$	39.54
	(4.4)	(7.5)			(39.4)
$Na_2[Ni(pdc)_2]\cdot 3H_2O$	3.68	7.37	11.05	Na_2CO_3+NiO	36.96
	—	(7.5)	(11.0)		(36.3)
$Na_2[Cu(pdc)_2]\cdot 3H_2O$	3.65	7.30	10.95	Na_2CO_3+CuO	37.58
	—	(7.4)	(10.7)		(37.0)
$Na_2[Zn(pdc)_2]\cdot 3H_2O$	3.64	7.27	10.91	Na_2CO_3+ZnO	37.81
	—	(7.2)	(11.1)		(37.3)

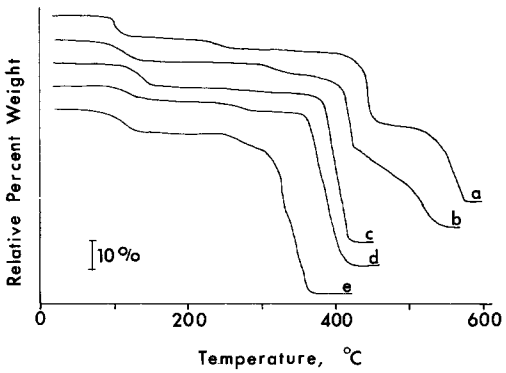

Fig. 1. Thermograms of $Na_2[M(pdc)_2]\cdot nH_2O$ complexes. (a) Zn, (b) Ni, (c) Mn, (d) Co, (e) Cu.

and Ni^{II}, in perhaps two overlapping steps for Cu^{II}, and apparently in a single step for Co^{II} and Mn^{II}. The order of stability is Zn > Ni > Mn > Co > Cu, with Ni being out of the position predicted by the reverse Irving–Williams sequence. The residues were identified based on total weight loss (Table 2) and by standard qualitative analysis tests to be mixtures of Na_2CO_3 and the respective oxides ZnO, CuO, NiO, Co_3O_4 and Mn_3O_4.

EXPERIMENTAL

Synthesis of $Na_2[M(pdc)_2]$ *complexes*

The ligand pyridine-2,6-dicarboxylic acid, sodium hydroxide and the hydrated metal acetate salts were AR-grade chemicals and were used without further purification.

Solid NaOH (20 mmol) was dissolved in 75 cm^3 of water and heated to near boiling in a 250 cm^3 round-bottom flask. The ligand H_2pdc (20 mmol) was added with stirring until solution was complete. The appropriate hydrated metal acetate (10 mmol), dissolved in 50 cm^3 of hot water, was added to the basic ligand solution and the mixture was refluxed for 1–2 h. The resulting solution was reduced in volume to less than 50 cm^3 by heating on a steam bath or using a rotary evaporator. Cooling in an ice bath induced crystallization of the crude product. Products were filtered, washed with *n*-butyl alcohol and dried in vacuum over P_2O_5. It was necessary to recrystallize the Ni^{II}, Cu^{II} and Zn^{II} complexes; each compound was dissolved in cold water, filtered to remove unreacted ligand, then evaporated to near dryness to recover the product, which was then washed and dried as described above. Yields were 85–95% for the Co^{II} and Mn^{II} complexes and 50–75% for the others.

Found: C, 35.9; H, 2.1; N, 5.8. Calc. for $Na_2Mn(C_7H_3NO_4)_2\cdot 2H_2O$: C, 36.0; H, 2.2; N, 6.0%. Colour: yellow. Found: C, 35.6; H, 2.1; N, 5.8. Calc. for $Na_2Co(C_7H_3NO_4)_2\cdot 2H_2O$: C, 35.7; H, 2.1; N, 5.9%. Colour: grey. Found: C, 35.0; H, 2.6; N, 5.9. Calc. for $Na_2Ni(C_7H_3NO_4)_2\cdot 3H_2O$: C, 34.4; H, 2.5; N, 5.7%. Colour: green. Found: C, 34.8; H, 2.9; N, 5.7. Calc. for $Na_2Cu(C_7H_3NO_4)_2\cdot 3H_2O$: C, 34.0; H, 2.4; N, 5.7%. Colour: blue. Found: C, 34.7; H, 2.5; N, 5.8. Calc. for $Na_2Zn(C_7H_3NO_4)_2\cdot 3H_2O$: C, 33.9; H, 2.4; N, 5.6%. Colour: white.

Physical and spectral measurements

Magnetic susceptibility measurements were carried out on solid samples by the Gouy method at 294 K and 5400 G. $HgCo(SCN)_4$ was used as calibrant. Diamagnetic corrections were made using Pascal's constants. The temperature-independent paramagnetism correction of 60×10^{-6} cgsu was used for the Cu^{II} complex.

Molar conductance measurements were made on 0.001 M aqueous solutions using a Markson Electromark analyser. Potassium chloride solutions were used as standards.

IR spectra were obtained as KBr pellets in the range 4000–650 cm^{-1} on a Beckman IR-8 spectrophotometer. Electronic absorption spectra were obtained as aqueous solutions (0.014–0.022 M) in the range 1300–340 nm on a Cary 14 spectrophotometer.

Thermogravimetric measurements were made in air on a home-constructed apparatus utilizing an iron-constantan thermocouple, ice-bath reference and a heating rate of 6° min^{-1}.

REFERENCES

1. M. G. B. Drew, R. W. Matthews and R. A. Walton, *J. Chem. Soc. A* 1970, 1405.
2. M. Biagini, A. Chiesi-Villa, C. Guastini and M. Nardelli, *Gazz. Chim. Ital.* 1972, **102**, 1026.
3. H. Gaw, W. R. Robinson and R. A. Walton, *Inorg. Nucl. Chem. Lett.* 1971, **7**, 695.
4. A. Chiesi-Villa, C. Guastini, A. Musatti and M. Nardelli, *Gazz.Chim. Ital.* 1972, **102**, 226.
5. P. P. Quaglieri, H. Loiseleur and G. Thomas, *Acta Cryst.* 1972, **28B**, 2583.
6. S. Ghosh, T. K. Banerjee and P. K. Ray, *J. Ind. Chem. Soc.* 1978, **55**, 610.
7. R. W. Matthews, A. D. Hamer, D. L. Hoof, D. G. Tisley and R. A. Walton, *J. Chem. Soc., Dalton Trans.* 1973, 1035.
8. M. Biagini-Cingi, A. Chiesi-Villa, C. Guastini and M. Nardelli, *Gazz. Chim. Ital.* 1971, **101**, 825.
9. D. L. Hoof and R. A. Walton, *Inorg. Chim. Acta* 1975, **12**, 71.
10. D. L. Hoof, D. G. Tisley and R. A. Walton, *J. Chem. Soc., Dalton Trans.* 1973, 200.
11. A. Anagnostopoulos, *J. Coord. Chem.* 1975, **4**, 231.
12. S. K. Sengupta, S. K. Sahni and R. N. Kapoor, *Polyhedron* 1983, **2**, 317.
13. P. E. Hoggard and H. H. Schmidtke, *Inorg. Chem.* 1973, **12**, 1986.
14. W. Furst, P. Gouzenh and Y. Jeannin, *J. Coord. Chem.* 1978, **8**, 237.
15. J. Albertsson, *Acta Chem. Scand.* 1972, **26**, 985, 1023.
16. L. Baracco, G. Bombieri, S. Degetto, E. Forsellini, R. Graziani and G. Marangoni, *Inorg. Nucl. Chem. Lett.* 1974, **10**, 1045.
17. G. Marangoni, S. Dagetto, R. Graziani, G. Bombieri and E. Forsellini, *J. Inorg. Nucl. Chem.* 1974, **36**, 1787.
18. G. D'Ascenzo, A. Marino, M. Sabbatini and T. Bica, *Thermochim. Acta* 1978, **25**, 325.
19. W. J. Gerry, *Coord. Chem. Rev.* 1971, **7**, 81.

Polyhedron Vol. 8, No. 6, pp. 749–756, 1989
Printed in Great Britain

0277–5387/89 $3.00+.00
© 1989 Pergamon Press plc

SPECTROPHOTOMETRIC STUDIES OF THE REACTIONS OF TERTIARY BISDIPHENYLPHOSPHINES $Ph_2P(CH_2)_nPPh_2$ WITH $n = 1$, 2 AND 3 ON DIBROMO-BIS(TRIPHENYLPHOSPHINE)COBALT(II), IN BENZENE SOLUTION. FORMATION OF PENTA-COORDINATED COMPLEXES

JEAN-CLAUDE PIERRARD, JEAN RIMBAULT and RENÉ P. HUGEL*

Laboratoire de Chimie Minérale, Université de Reims Champagne Ardenne, 51062 Reims, France

(*Received* 8 *April* 1988; *accepted* 4 *October* 1988)

Abstract—The reactions of $CoBr_2(PPh_3)_2$ at 25°C in benzene with $Ph_2P(CH_2)_nPPh_2$ with $n = 1$ (dpm), $n = 2$ (dpe) and $n = 3$ (dpp) have been followed spectrophotometrically and by conductivity measurements in CH_2Cl_2. The addition and substitution steps of the bidentate bisphosphines L—L on the initial cobalt complex have been identified and the equilibrium constants calculated at different wavelengths using least squares methods. With dpm, binuclear species are formed in three steps with bridging dpm molecules. With dpe and dpp, two steps are observed with the formation of the final red penta-coordinated complexes $[CoBr(L—L)_2]Br$; the intermediate complexes are different in each case. The overall constant for the equilibrium $CoBr_2(PPh_3)_2 + 2L—L \rightleftharpoons [CoBr(L—L)_2]Br + 2PPh_3$ is 1.06×10^5 for dpe and 1.20×10^3 for dpp, and depends on the size of the chelate rings.

Cobalt(II) halogenide complexes with tertiary phosphines and diphosphines are well known,[1,2] nevertheless, their solution behaviour has not been extensively investigated. After study of the substitution of triphenylphosphine ligands on $CoX_2(PPh_3)_2$ (X = Cl, Br, I and NCS) by triphenylphosphine oxide in benzene[3] or by triphenylphosphinesulphide,[4] we report here the interaction of three tertiary diphosphines $Ph_2P(CH_2)_nPPh_2$, with $n = 1$ (dpm), 2 (dpe) and 3 (dpp), on $CoBr_2(PPh_3)_2$, in benzene in order to establish the nature of the addition or substitution products, to estimate the corresponding equilibrium constants and to compare the chelating effect of the three diphosphines.

EXPERIMENTAL

Materials

$CoBr_2(PPh_3)_2$ was prepared as previously described.[5]

The $Ph_2P(CH_2)_nPPh_2$ ligands ($n = 1$, 2 and 3), purchased from Interchim, were purified by recrystallization in benzene followed by vacuum sublimation. Benzene was distilled over P_4O_{10} and deaerated with a stream of nitrogen. Handling and preparations of solutions were carried out in a glove-box.

Instrumentation

Electronic spectra were recorded on a Beckman 5240 spectrophotometer at 25 ± 0.2°C. The conductivity measurements in CH_2Cl_2 were made with a Tacussel CD 7 instrument at 1000 and 500 Hz.

General procedure

To a benzene solution of $CoBr_2(PPh_3)_2$, increasing amounts of dpm, dpe or dpp were added and the evolution of the electronic spectra followed. The initial benzene solution of $CoBr_2(PPh_3)_2$ always contains an excess of PPh_3 in order to minimize the perturbation due to traces of water, which may be present in the solvent for reasons previously explained.[3a]

*Author to whom correspondence should be addressed.

Moreover, for each equilibrium, the influence on the spectrum of dilution of a solution, with a given ratio R = diphosphine–cobalt, as well as the addition of PPh_3, respectively, gave indications on the variation of the number of involved species, and the possible interference of PPh_3 in the equilibrium.

Conductivity measurements have been made in CH_2Cl_2, (the dielectric constant of benzene being too low), in order to check the stoichiometry of the reactions, taking care in comparing the spectra in CH_2Cl_2 and benzene, to verify the presence or absence of the same species in both solvents.

Coleman, Varga and Mastin's graphical method[6] (further noted as the CVM method) was used to check the number of absorbing species involved in the equilibrium, and present in solution.

List of main symbols

C: analytical cobalt(II) concentration (mol l^{-1}).

R: ratio of analytical concentrations of diphosphine to cobalt.

B: analytical concentration of the excess of PPh_3 added in the initial solution (mol l^{-1}).

α, β, γ: proportion of cobalt engaged, respectively, in the first, second and third formed complex with exclusion of the initial $CoBr_2(PPh_3)_2$.

ε: molar absorptivity of the solution based on C, $\varepsilon = A/l \times C$.

A: absorbance.

l: optical path in cm.

ε_p, ε_1, ε_2, ε_3: molar absorptivities for $CoBr_2(PPh_3)_2$, for the first, second and third complex, respectively.

Calculations

The type of calculations carried out is illustrated in the following example of substitution equilibria between two absorbing complexes 1 and 2 with respective extinction coefficients ε_1 and ε_2. The ligands L and L′ are non-absorbing

$$\text{Complex } 1 + \text{L} \rightleftharpoons \text{Complex } 2 + \text{L}'$$

$$K = (\text{Complex } 2)(\text{L}')/(\text{Complex } 1)(\text{L}) = \frac{\alpha^2}{R(1-\alpha)^2}. \quad (1)$$

For each wavelength λ:

$$\varepsilon = A/C \times l = \varepsilon_1(1-\alpha) + \varepsilon_2\alpha,$$

ε is a linear function of α

$$\varepsilon = \varepsilon_1 + (\varepsilon_2 - \varepsilon_1)\alpha = a\alpha + b.$$

For a given solution ε, C and R are known.

K is calculated in order that the couples (ε, α) give the best straight line at a given value of λ. ε_1 and ε_2 are obtained by the extrapolation of the straight line to $\alpha = 0$ and $\alpha = 1$. Different arbitrary K values are used in relation (1) to yield, for a solution of analytical concentration C and ratio R, a value of α. We then have a series of couples (ε, α) for the n solutions.

By a least-squares method minimizing S, the best straight line going through the points (ε, α) is calculated with $S = \Sigma_1^n (1/\varepsilon^2)(\varepsilon - \varepsilon_{cal})^2$ where ε_{cal} is the calculated molar absorptivity at a given λ, from the straight line $\varepsilon_{cal} = a\alpha + b$. At the minimum of S, $\partial S/\partial a = 0$ and $\partial S/\partial b = 0$ yield a system of two relations with two unknowns, a and b:

$$\sum_1^n \frac{\alpha}{\varepsilon} = a\sum_1^n \frac{\alpha^2}{\varepsilon^2} + b\sum_1^n \frac{\alpha}{\varepsilon^2} \quad \text{and} \quad \sum_1^n \frac{1}{\varepsilon} = a\sum_1^n \frac{\alpha}{\varepsilon^2} + b\sum_1^n \frac{1}{\varepsilon^2}.$$

For each value of K the calculation of $S_{minimum}$ gives the standard deviation $\sigma = \sqrt{S/n-2}$.

The best K will be the one with the lowest σ value, so that the function $\varepsilon = f(\alpha)$ will be the best straight line. Supposing that σ, near its minimum, is at first approximation a second order function of K, the minimum of that function (pit mapping) yields the final best value of K. The K given in the text is this mean value at different wavelengths.

RESULTS AND DISCUSSION

Reaction of dpm *on* $CoBr_2(PPh_3)_2$

The conductivity variation in CH_2Cl_2 of a $CoBr_2(PPh_3)_2$ solution (1.016 mM) by addition of increasing amounts of dpm, shows an increase in conductivity with three breaks at R values of 0.5, 1.2 and 2.4, indicating the possible formation of three successive ionic species, with a dpm/Co stoichiometry of 0.5, 1 and 2, beginning with a dinuclear complex. The conductivity remains close to 20 μS cm^{-1} for $R = 1$. The spectra in CH_2Cl_2 are comparable to the spectra observed in benzene.

1st equilibrium. In benzene, the reaction is slow and the spectra are recorded 24 h after preparation of the solutions. The dilution of a $CoBr_2(PPh_3)_2$ solution ($C = 1.677 \times 10^{-4}$ mol l^{-1}, $B = 1.446 \times 10^{-3}$ mol l^{-1}) with dpm ($R = 0.255$) does not obey Beer's law and the addition of PPh_3 to the solution does not modify the spectra.

The spectra given in Fig. 1 correspond to solutions with a constant cobalt concentration and increasing quantities of dpm. The presence of several isosbestic points (610, 686 and 740 nm) and the application of the CVM method,[6] both indicate the presence of only two absorbing species in equilibrium. The spectrum of the complex formed suggests a C_{3v} symmetry about cobalt.

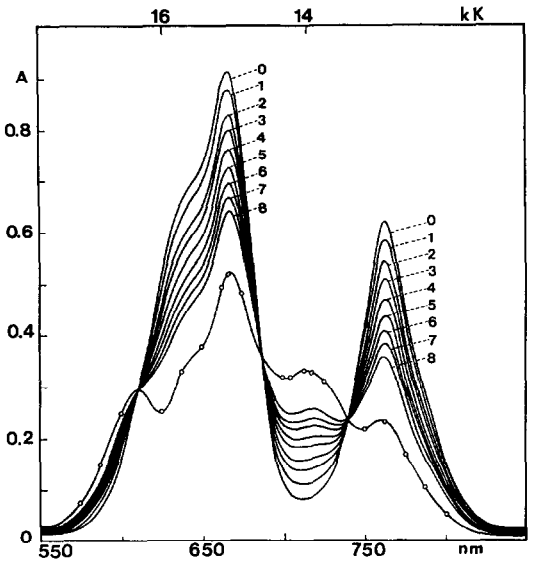

Fig. 1. Solution spectra of $CoBr_2(PPh_3)_2$ with increasing amounts of dpm in benzene ($l = 5$ cm, $T = 25°C$), $C = 0.1677$ mM, $B = 1.446$ mM. Values of R for each solution given in parentheses 0 (0), 1 (0.051), 2 (0.102), 3 (0.153), 4 (0.204), 5 (0.255), 6 (0.306), 7 (0.375), 8 (0.408). ○ calculated spectrum of $Co_2Br_4(PPh_3)_2$(dpm).

The following equilibrium yielding a dinuclear complex with a bridged dpm, agrees with the preceeding observations:

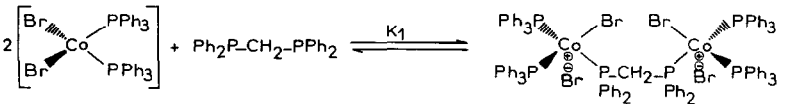

(2)

The formation of an ionic complex in benzene, undissociated in the form of an ionic pair, is likely in view of the low dielectric constant of the solvent (2.27). Hughes *et al.*[7] showed that at concentrations lower than 10^{-3} mol l^{-1}, the ionic pairs remain undissociated. In CH_2Cl_2 with a higher dielectric constant (9.08) these ionic compounds are slightly dissociated.

The conductivities of 26 different complexes, 1 : 1 electrolytes, in CH_2Cl_2 or $C_2H_4Cl_2$ are comparable (range 17–26 μS cm^{-1})[8] with those observed for our compounds calculated on the basis of one metal atom (22.5 μS cm^{-1}).

Further evidence in favour of the existence of the ionic pairs is the fact that even if the dinuclear complex can be obtained in benzene and remains soluble, it becomes insoluble after it has been crystallized as an ionic compound,.

The expression of the equilibrium constant K_1 is:

$$K_1 = \alpha/C^2(2R-\alpha)(1-\alpha)^2. \quad (3)$$

The molar absorptivities of the solutions are:

$$\varepsilon = A/l \times C = \varepsilon_p(1-\alpha)+\varepsilon_1(\alpha/2). \quad (4)$$

ε is a linear function of the ratio α of the dinuclear compounds formed

$$\varepsilon = (\varepsilon_1/2-\varepsilon_p)\alpha+\varepsilon_p. \quad (5)$$

A least-squares method gives the value of K_1 at several wavelengths (see Table 1). The mean value is $\bar{K}_1 = (1.73 \pm 0.14) \times 10^9$ mol^{-2} l^2.

From the value of $\bar{K}_1$, the concentrations of the absorbing species in solution are calculated as well as the spectrum of $Co_2Br_4(PPh_3)_2$(dpm) (Fig. 1).

2nd equilibrium. The recorded spectra of solutions with $C = 1.749 \times 10^{-4}$ mol l^{-1}, $B = 1.293 \times 10^{-3}$ mol l^{-1} and different values for $R = 0.766$, 0.958, 1.149 and 1.341, show an isosbestic point at 598 nm. The microsymmetry around cobalt is C_{3v} for the two absorbing species, but their molar absorptivities are close, so dilution of the solution with $0.7 < R < 1.4$ and the addition of PPh_3 are not conclusive. The calculation carried out for the 1st equilibrium is not possible here.

The proposed equilibrium is shown in eq. (6)

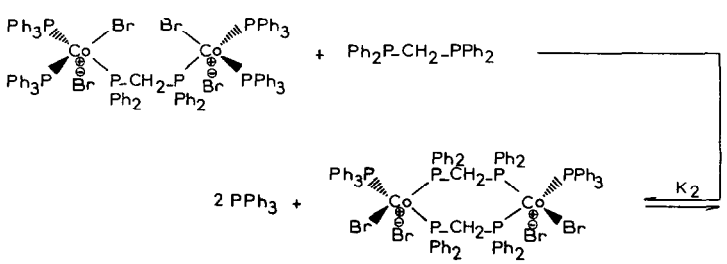

(6)

with

$$K_2 = \frac{2C\beta((B/C)+\beta)^2}{(1-\beta)(2R-1-\beta)}. \quad (7)$$

The molar absorptivities of the solutions are:

$$\varepsilon = A/l \times C = \varepsilon_1\left(\frac{1-\beta}{2}\right)+\varepsilon_2\frac{\beta}{2}. \quad (8)$$

ε_1 is known, and ε_2 will be calculated from the next equilibrium (*vide infra*). β is obtained from the experimental ε value, using (8) and K_2 is given by

Table 1. Values of K_1 at various wavelengths

λ (nm)	637	650	665	703	715	762.5
K_1 (mol^{-2} l^2)	1.93×10^9	1.61×10^9	1.60×10^9	1.65×10^9	1.94×10^9	1.64×10^9

(7). For four solutions with $\beta = 0.388, 0.567, 0.708$ and 0.795, $\bar{K}_2 = (9.4\pm0.5)\times10^{-2}$ mol l^{-1}.

3rd equilibrium. The spectra of solutions with $5.6 < R < 30.6$ are given in Fig. 2. Application of the CVM method[6] indicates the presence of one equilibrium between two absorbing species. Dilution of solution 4 (Fig. 2) obeys Beer's law. The spectrum of the first species is characteristic for a C_{3v} symmetry, whereas the dark red second species is C_{4v} (square pyramid).

The equilibrium is shown in eq. (9)

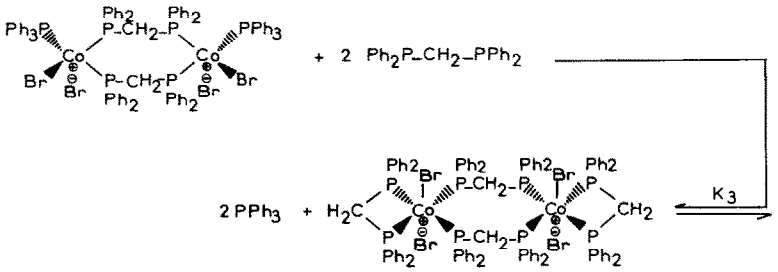

(9)

with the following relations

$$K_3 = \frac{\gamma(1+\gamma)^2}{(1-\gamma)(R-1-\gamma)^2} \qquad (10)$$

$$\varepsilon = A/l\times C = \varepsilon_2\left(\frac{1-\gamma}{2}\right)+\varepsilon_3\frac{\gamma}{2} \qquad (11)$$

$$\varepsilon = \frac{(\varepsilon_3-\varepsilon_2)}{2}\gamma+\frac{\varepsilon_2}{2}. \qquad (12)$$

The calculation on eight solutions is similar to that carried out for the first equilibrium. The values at several wavelengths (given in parentheses and in nm) are: K_3: 1.02×10^{-2} (450); 1.01×10^{-2} (462.5); 1.03×10^{-2} (475); 1.05×10^{-2} (487.5); 1.01×10^{-2} (500); 1.03×10^{-2} (512.5); 1.09×10^{-2} (525); 9.84×10^{-3} (537.5); 9.24×10^{-3} (550); 1.02×10^{-2} (625); 1.22×10^{-2} (637.5); 1.20×10^{-2} (650); 1.02×10^{-2} (750) and therefore $\bar{K}_3 = (1.05\pm0.08)\times10^{-2}$.

The spectra of $Co_2Br_2(dpm)_4$ and $Co_2Br_4(PPh_3)_2(dpm)_2$ are then calculated (Fig. 2). ε_2 is used to estimate K_2 (*vide supra*).

Reactions of dpe *on* $CoBr_2(PPh_3)_2$

The conductivity in CH_2Cl_2 of $CoBr_2(PPh_3)_2$ solution (9.861×10^{-4} mol l^{-1}) increases rapidly with the addition of dpe: ionic complexes are

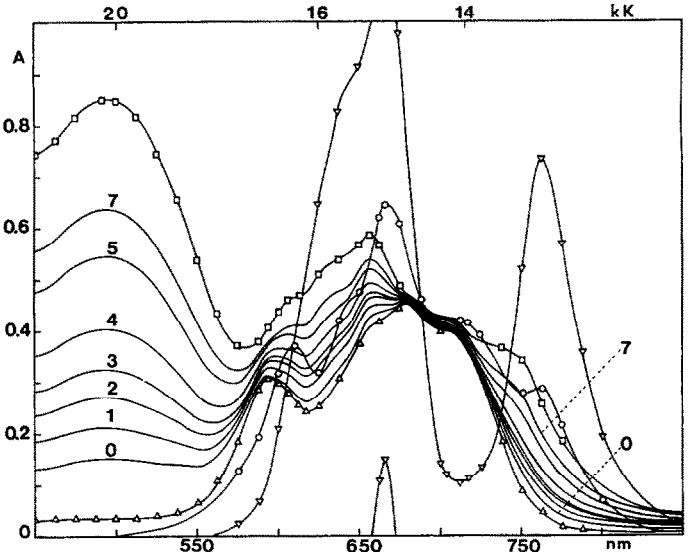

Fig. 2. Solution spectra of $CoBr_2(PPh_3)_2$ with increasing amounts of dpm in benzene ($l = 5$ cm, $T = 25$°C), $C = 0.2119$ mM, $B = 0$. Values of R for each solution in parentheses 0 (5.627), 1 (7.411), 2 (9.196), 3 (10.980), 4 (14.549), 5 (21.687), 6 (25.256), 7 (30.609). ▽: observed spectrum of $CoBr_2(PPh_3)_2$; ○, △, □: calculated spectra for $Co_2Br_4(PPh_3)_2(dpm)$, $Co_2Br_4(PPh_3)_2(dpm)_2$ and $Co_2Br_4(dpm)_4$, respectively.

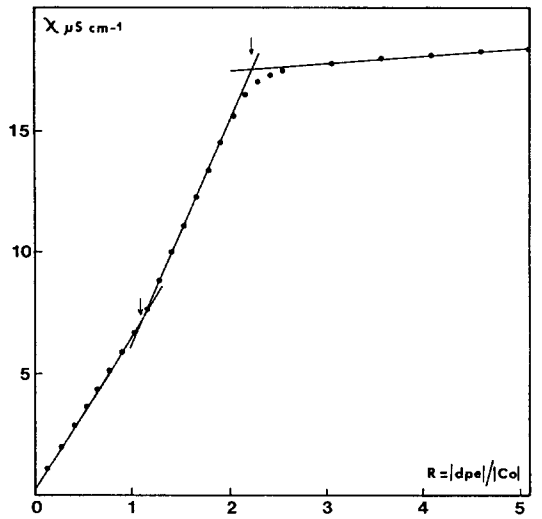

Fig. 3. Conductivity of a 0.9861 mM solution of $CoBr_2(PPh_3)_2$ vs R in CH_2Cl_2 (5000 Hz).

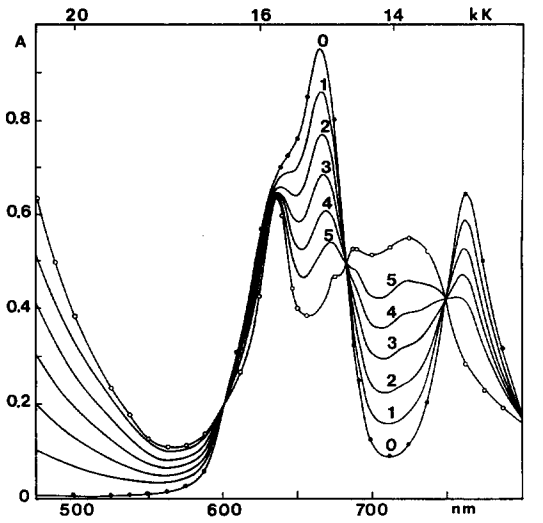

Fig. 4. Solution spectra of $CoBr_2(PPh_3)_2$ with increasing amounts of dpe (l = 5 cm, T = 25°C), C = 0.1789 mM, B = 1.158 mM. Values of R in parentheses 0 (0), 1 (0.161), 2 (0.321), 3 (0.482), 4 (0.643), 5 (0.804), 6 (0.964), 7 (1.125), 8 (1.286). Spectra of solutions 6, 7 and 8 are omitted for clarity of the graph. ● experimental spectrum of $CoBr_2(PPh_3)_2$; ○ calculated spectrum of $CoBr_2(PPh_3)$ (dpe).

formed (Fig. 3). Breaks are observed at R values close to 1 and 2. The conductivity then remains practically constant for $R > 2.2$ (~ 18 μS cm^{-1}). This implies the formation of complexes with a stoichiometry of 1 and 2 dpe per cobalt. The spectrum in CH_2Cl_2 for the final green complex (R = 2.0) is similar to the one observed by Horrocks *et al.*,[9] with a trigonal bipyramidal coordination around the cobalt. The spectrum of the intermediate complex in CH_2Cl_2 is similar to the one observed in C_6H_6.

1st equilibrium. The spectra for solutions with $0 < R < 1.286$ are given in Fig. 4. Dilution of solution 5 obeys Beer's law; the addition of PPh_3 in this same solution moves the equilibrium towards the formation of the initial reagent $CoBr_2(PPh_3)_2$. The isosbestic points at 601, 683 and 700 nm and the CVM method[6] indicate a simple equilibrium between two absorbing complexes. The proposed equilibrium is:

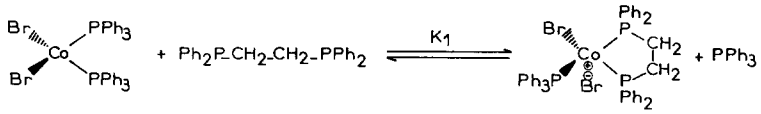

(13)

with

$$K_1 = \frac{\alpha((B/C)+\alpha)}{(1-\alpha)(R-\alpha)} \qquad (14)$$

and

$$\varepsilon = A/l \times C = \varepsilon_p(1-\alpha)+\varepsilon_1\alpha. \qquad (15)$$

ε is a linear function of α

$$\varepsilon = (\varepsilon_1-\varepsilon_p)\alpha+\varepsilon_p. \qquad (16)$$

The values of K_1 obtained by linear regression on nine solutions are (wavelengths in parentheses and in nm) K: 886 (662.5); 897 (700); 899 (712.5); 890 (725) and 895 (762.5) and a mean value $\bar{K}_1 = 893 \pm 5$. $\bar{K}_1$ allows the calculation of the spectrum of $CoBr_2(PPh_3)$(dpe) (Fig. 4).

2nd equilibrium. The spectra of solutions with $1.344 < R < 4.703$ are given in Fig. 5. The final red complex is square-pyramidal. Again the isosbestic points at 622, 647, 685 and 757 nm and the CVM method[6] indicate a simple equilibrium. The equilibrium is concentration independent (solution 5 on Fig. 5 obeys Beer's law) whereas addition of PPh_3 regresses the equilibrium. It can be written as:

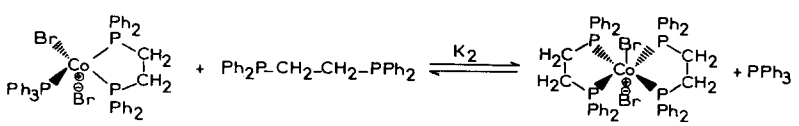

(17)

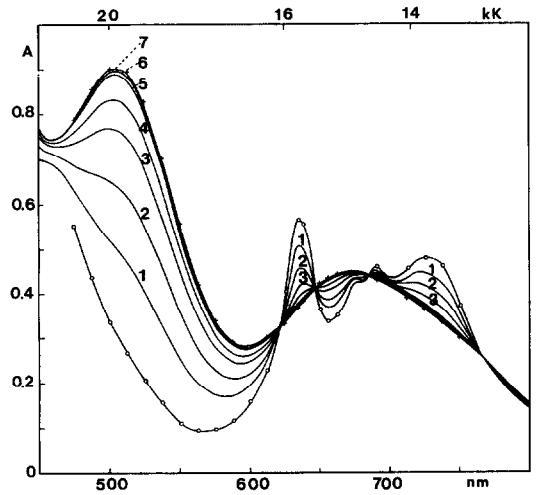

Fig. 5. Solution spectra of $CoBr_2(PPh_3)_2$ with increasing amounts of dpe ($l = 5$ cm, $T = 25°C$), $C = 0.1565$ mM, $B = 1.125$ mM. Values of R given in parentheses 1 (1.344), 2 (1.680), 3 (2.015), 4 (2.351), 5 (3.359), 6 (4.031), 7 (4.703). ○ calculated spectrum of $CoBr_2(PPh_3)$(dpe); + calculated spectrum of $CoBr_2(dpe)_2$.

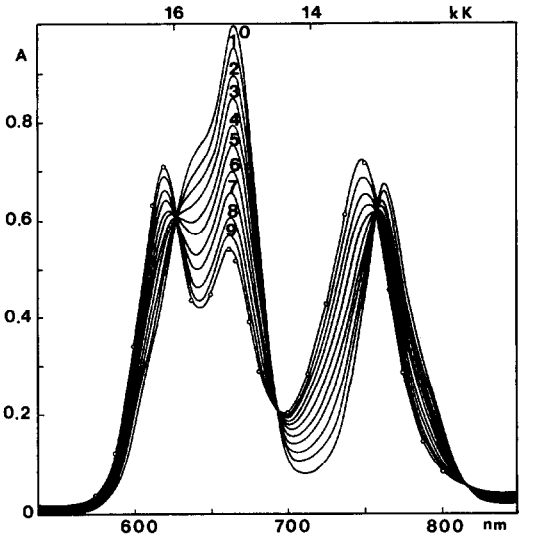

Fig. 6. Solution spectra of $CoBr_2(PPh_3)_2$ with increasing amounts of dpp ($l = 5$ cm, $T = 25°C$), $C = 0.1875$ mM, $B = 1.209$ mM. Values of R given in parentheses 0 (0), 1 (0.106), 2 (0.212), 3 (0.318), 4 (0.425), 5 (0.531), 6 (0.637), 7 (0.743), 8 (0.849), 9 (0.955), 10 (1.062). Spectrum of solution 10 is omitted for clarity of the graph. ○ calculated spectrum of $CoBr_2$(dpp).

with

$$K_2 = \frac{\beta(1+\beta+(B/C))}{(1-\beta)(R-1-\beta)} \tag{18}$$

and

$$\varepsilon = A/l \times C = (\varepsilon_2 - \varepsilon_1)\beta + \varepsilon_1. \tag{19}$$

A linear regression on seven solutions gives the following K_2 values (with wavelengths in parentheses and in nm) K_2: 114 (500); 110 (512.5); 127 (525); 130 (635); 119 (725) and 114 (737.5) and a mean value $\bar{K}_2 = 119 \pm 8$.

$\bar{K}_2$ allows the calculation of the spectra of the two complexes (Fig. 5). The spectrum of the intermediate $CoBr_2(PPh_3)$(dpe) is the same as the one calculated for the 1st equilibrium (Fig. 4).

complex corresponds to a green trigonal-bipyramidal complex, whereas the intermediate complex has a spectrum similar to the one observed in benzene solution.

1st equilibrium. The spectra for solutions with $0 < R < 1.062$ are shown in Fig. 6. Dilution of solution 7 shifts the equilibrium forward and the addition of PPh_3 shifts the equilibrium towards the starting product, $CoBr_2(PPh_3)_2$.

Again the presence of isosbestic points at 627.5, 694, 758 and 817.5 nm as well as the CVM method[6] indicate an equilibrium involving two absorbing species. The spectrum of the final product corresponds to the same C_{2v} microsymmetry as the starting material.

The equilibrium is:

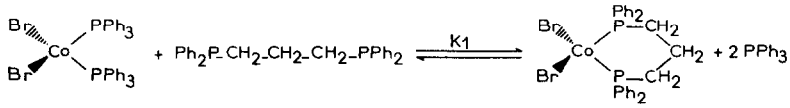

(20)

Reaction of dpp *with* $CoBr_2(PPh_3)_2$

The conductivity measurements in CH_2Cl_2 show at the beginning, the formation of a non-ionic complex. Starting with $R = 1$, an ionic complex, only slightly dissociated, is formed and a break for $R = 2$ is observed. dpp/Co stoichiometries of 1 and 2 can be proposed. The spectrum in CH_2Cl_2 of the final

with a constant

$$K_1 = \frac{\alpha(2\alpha+(B/C))^2 C}{(R-\alpha)(1-\alpha)} \tag{21}$$

and

$$\varepsilon = A/l \times C = (\varepsilon_1 - \varepsilon_p)\alpha + \varepsilon_p. \tag{22}$$

A linear regression method gives α and K_1 on 10 solutions.

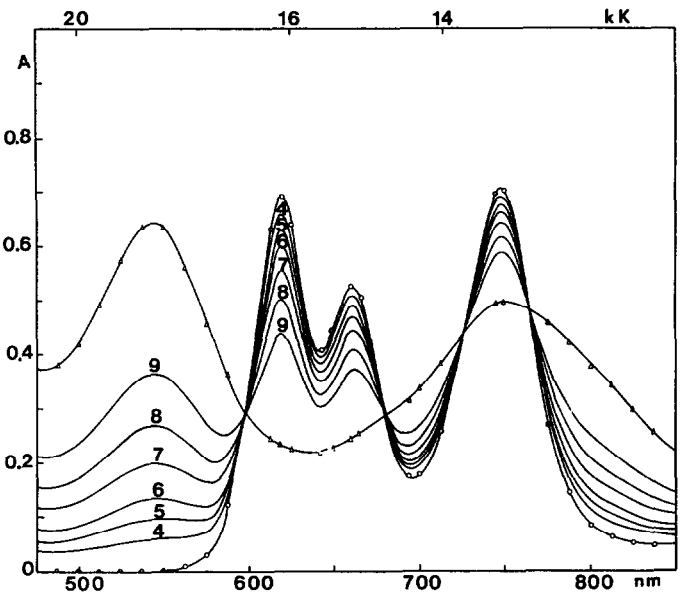

Fig. 7. Solution spectra of $CoBr_2(PPh_3)_2$ with increasing amounts of dpp ($l = 5$ cm, $T = 25°C$), $C = 0.1762$ mM. Values of R given in parentheses 1 (1.103), 2 (1.274), 3 (1.787), 4 (2.812), 5 (4.520), 6 (6.228), 7 (9.645), 8 (14.770), 9 (25.020). Spectra of solutions 1, 2 and 3 are omitted for reasons of clarity. ○ calculated spectrum of $CoBr_2(dpp)$; △ calculated spectrum of $CoBr_2(dpp)_2$.

K_1: 3.75 (640 nm); 3.91 (650 nm); 3.62 (662.5 nm) and 4.02 (664 nm) with a mean value $\bar{K}_1 = 3.83 \pm 0.25$ mol l^{-1}.

The spectra calculated using $\bar{K}_1$ are given in Fig. 6.

2nd equilibrium. Spectra of solutions with $1.103 < R < 25.02$ are shown in Fig. 7. Dilution of solution 5 shifts the equilibrium toward the starting material whereas the addition of PPh_3 has no influence on the spectrum.

A new equilibrium between two absorbing species is observed by the presence of isosbestic points at 597.5, 680, 726 and 765 nm and the application of the CVM method.[6] The final spectrum corresponds to a square-pyramidal complex of C_{4v} microsymmetry.

The equilibrium inferred from the preceding observations is:

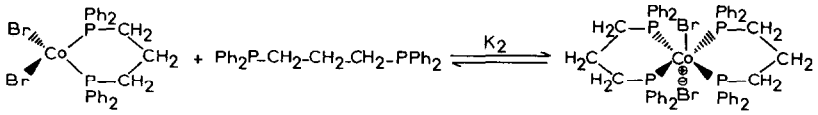

(23)

with

$$K_2 = \frac{\beta}{(1-\beta)(R-1-\beta)C}. \qquad (24)$$

ε is a linear function of β.

$$\varepsilon = A/l \times C = (\varepsilon_2 - \varepsilon_1)\beta + \varepsilon_1. \qquad (25)$$

The values of K_2 for seven solutions are shown in Table 2, with a mean value $\bar{K}_2 = 312 \pm 10$ mol^{-1} l.

This $\bar{K}_2$ value allows the calculation of the spectrum of the two complexes involved in equilibrium (23). The spectrum of $CoBr_2(dpp)$ is identical to the spectrum calculated for the 1st equilibrium.

CONCLUSIONS

The three bidentate ligands show a different behaviour when they react with $CoBr_2(PPh_3)_2$ in benzene. With a long hydrocarbonic chain, as in dpp ($n = 3$) or in dpe ($n = 2$), coordination around the metal with a six- or five-membered ring is favoured, whereas with a short one as in dpm ($n = 1$), a bridging mode of coordination on two metal atoms occurs, followed by the formation of a four-mem-

Table 2. Values of K_2 at various wavelengths

λ (nm)	525	537.5	550	619	640	662.5	664	748	750	812.5	825
K_2 (mol^{-1} l)	298	289	284	329	323	340	272	312	329	312	335

bered ring without breaking of the established bridges.

The steric hindrance of the diphosphines cannot explain the difference in reactivity. The Tolman cone angles[10] increase only slightly from dpm to dpp (dpm: 121°, dpe 125° and dpp 127°). Nevertheless, dpm is less favoured for chelation than dpe or dpp, because the four-membered ring produced on chelation is considerably strained.

The values of the equilibrium constants, $K_T = K_1 \times K_2$, corresponding to the formation of the final penta-coordinated complex starting with $CoBr_2(PPh_3)_2$ are, respectively, 1.06×10^5 for dpe and 1.20×10^3 for dpp. This order is that expected based on the size of the chelating rings.

In all cases, the final red complex is penta-coordinated with a square-pyramidal geometry containing the $CoBrP_4$ chromophore. These red compounds, obtained in benzene, are no longer soluble after they have been crystallized, owing to their ionic nature in $[CoBr(diphos)_2]^+Br^-$. The square-pyramidal structure allows a close approach of the halogen ion in benzene favouring ion-pair formation.

The interpretation of the electronic spectra will be given in a later publication.

REFERENCES

1. C. A. McAuliffe and W. Levason, *Phosphine, Arsenic and Stibine Complexes of the Transition Elements*. Elsevier, Amsterdam (1979).
2. C. A. McAuliffe, *Transition Metal Complexes of Phosphorus, Arsenic and Antimony Ligands*. Macmillan, London (1973).
3. (a) J. C. Pierrard, J. Rimbault and R. P. Hugel, *J. Inorg. Nucl. Chem.* 1977, **19**, 1625; (b) J. Rimbault, J. C. Pierrard and R. P. Hugel, *J. Chem. Res.* (*S*) 1982, 330; J. Rimbault, J. C. Pierrard and R. P. Hugel, *J. Chem. Res.* (*M*) 1982, 3401; (c) J. C. Pierrard, J. Rimbault and R. P. Hugel, *J. Chem. Res.* (*S*) 1982, 332; J. C. Pierrard, J. Rimbault and R. P. Hugel, *J. Chem. Res.* (*M*) 1982, 3420; (d) J. Rimbault, J. C. Pierrard and R. P. Hugel, *Nouv. J. Chim.* 1983, **7**, 653.
4. J. Rimbault, J. C. Pierrard and R. P. Hugel, *J. Chem. Res.* (*S*) 1978, 74; J. Rimbault, J. C. Pierrard and R. P. Hugel, *J. Chem. Res.* (*M*) 1978, 1037.
5. J. Rimbault, J. C. Pierrard and R. P. Hugel, *Bull. Soc. Chim. France* 1976, 1705.
6. J. Coleman, L. Varga and S. Mastin, *Inorg. Chem.* 1970, **9**, 1015.
7. E. D. Hughes, C. K. Ingold, S. Patai and Y. Pocker, *J. Chem. Soc.* 1957, 1206.
8. (a) L. Sacconi and R. Morassi, *J. Chem. Soc. A* 1969, 2036; (b) P. Ugnagliati, G. Deganelle, L. Busetto and U. Belluco, *Inorg. Chem.* 1969, **8**, 1625.
9. W. D. Horrocks Jr, G. R. Van Hecke and D. D. Hall, *Inorg. Chem.* 1967, **6**, 694.
10. C. A. Tolman, *Chem. Rev.* 1977, **3**, 313.

Polyhedron Vol. 8, No. 6, pp. 757–762, 1989
Printed in Great Britain

0277–5387/89 $3.00+.00
© 1989 Pergamon Press plc

METAL-MEDIATED ADDITION OF ALCOHOLS TO DICYANDIAMIDE

R. K. RAY*

Department of Chemistry, Rama Krishna Mission Vivekananda Centenary College, Rahara 743186, 24 Parganas (North), West Bengal, India

and

M. K. BANDYOPADHYAY

Department of Physics, Rama Krishna Mission Vivekananda Centenary College, Rahara 743186, 24 Parganas (North) West Bengal, India

and

GEORGE B. KAUFFMAN

Department of Chemistry, California State University, Fresno, Fresno, CA 93740, U.S.A.

(*Received* 10 *March* 1988; *accepted after revision* 5 *October* 1988)

Abstract—The syntheses of 1-amidino-O-alkylurea sulphates and their corresponding copper(II) and nickel(II) complexes are described. These compounds exhibit bi-univalent electrolyte conductances in aqueous solution. The electronic spectra and magnetic moments of the copper(II) and nickel(II) complexes are characteristic of square planar stereochemistry. Vibrational spectra provide useful information regarding ligand bonding sites.

Dicyandiamide (**1**) contains an active nitrile (C≡N) group. In the presence of dilute acid it combines with a molecule of water and is converted into guanylurea, which is also known as dicyandiamidine (**2**), while in the presence of ammonia and amines, biguanide (**3**), a strongly coordinating ligand, is formed.[1] If dicyandiamide is refluxed with alcohol in the presence of a copper(II), nickel(II), or palladium(II) salt, the addition of alcohols to dicyandiamide occurs with the formation of 1-amidino-O-alkylureas (**4**), which are also powerfully coordinating ligands.[2,3]

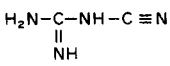

(**1**)

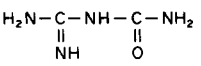

(**2**)

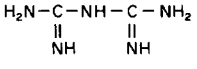

(**3**)

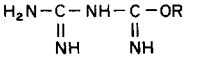

(R = alkyl group)

(**4**)

In this article we report a study of the preparation and properties of copper(II) and nickel(II) complexes of 1-amidino-O-alkylurea (**4**) (R = C_2H_5 $(CH_3)CH$, *n*-C_5H_{11}, and *n*-C_3H_7).

EXPERIMENTAL

1-*Amidino*-O-n-*propylurea sulphate*, $[AP^nUH]_2 \cdot H_2SO_4 \cdot 2.5H_2O$

The copper(II) complex, $[Cu(AP^nUH)_2](CH_3COO)_2$, was obtained by refluxing dicyandiamide (25 g), copper(II) acetate (25 g), and *n*-propanol (200 cm^3). The solution was cooled in a refrigerator, and the resulting complex acetate was separated by filtration. The rose-red precipitate was dissolved in ethanol, and the resulting solution was treated with an aqueous solution of ammonium sulphate, whereupon the dark red complex sulphate was precipitated. The precipitate was washed and suspended in water (150 cm^3). The copper was removed by precipitation with hydrogen sulphide, and the excess H_2S was removed by passing air through the

* Author to whom correspondence should be addressed.

suspension, which was then filtered. The filtrate was then concentrated to a volume of about 50 cm^3 on a steam bath and cooled in an ice bath. Excess acetone was then added with stirring, whereupon a white crystalline precipitate formed. The sulphate is very soluble in water, sparingly soluble in ethanol, and insoluble in acetone. The sample was dried over $CaCl_2$ at room temperature (yield, 23 g; 36%). Found: C, 28.0; H, 7.2; N, 26.0; SO_4, 22.4. Calc. for $[AA^nUH]_2 \cdot H_2SO_4 \cdot 2.5H_2O$: C, 28.2; H, 7.2; N, 26.2; SO_4, 22.5%.

1-*Amidino*-O-n-*amylurea sulphate* $[AA^nUH]_2 \cdot H_2SO_4 \cdot 3H_2O$

This compound was prepared by refluxing *n*-amyl alcohol (1-pentanol) (200 cm^3), copper(II) acetate (25 g), and dicyandiamide (25 g) as described above for the *n*-propyl derivative (yield, 16 g; 22%). Found: C, 33.9; H, 8.1; N, 22.6; SO_4, 19.2; H_2O, 10.6. Calc. for $[AA^nUH]_2 \cdot H_2SO_4 \cdot 3H_2O$: C, 33.8; H, 8.0; N, 22.5; SO_4, 19.3; H_2O, 10.8%.

1-*Amidino*-O-sec-*butylurea sulphate* $[AB^{sec}UH]_2 \cdot H_2SO_4 \cdot 2H_2O$

This compound was prepared by refluxing *sec*-butanol (150 cm^3), copper(II) acetate (25 g), and dicyandiamide (25 g) as described above for the *n*-propyl derivative (yield, 15 g; 22%). Found: C, 32.1; H, 7.3; N, 24.7; SO_4, 21.3; H_2O, 7.9. Calc. for $[AB^{sec}UH]_2 \cdot H_2SO_4 \cdot 2H_2O$: C, 32.0; H, 7.5; N, 24.6; SO_4, 21.3; H_2O, 8.0%.

Bis(1-*amidino*-O-n-*propylurea*)*copper*(II) *chloride*, $[Cu(AP^nUH)_2]Cl_2 \cdot 2H_2O$

Copper(II) chloride dihydrate (2 g), dicyandiamide (2 g), and *n*-propanol (20 cm^3) were refluxed for 6 h on a steam bath. The violet solution was filtered hot and allowed to stand in a refrigerator for 1 or 2 days, whereupon rose-violet crystals separated. These were collected by suction-filtration and recrystallized either from hot water or from hot ethanol and air-dried (yield, 2.5 g; 46%). Found: Cu, 13.8; Cl, 15.4; N, 24.5; C, 26.5; H, 6.6; H_2O, 7.8. Calc. for $[Cu(AP^nUH)_2]Cl_2 \cdot 2H_2O$: Cu, 13.9; Cl, 15.6; N, 24.6; C, 26.4; H, 6.6; H_2O, 7.9%.

Bis(1-*amidino*-O-n-*propylurea*)*copper*(II) *sulphate*, $[Cu(AP^nUH)_2]SO_4 \cdot 2H_2O$

To an aqueous solution of bis(1-amidino-O-*n*-propylurea)copper(II) chloride, an aqueous solution of potassium sulphate was added dropwise with constant stirring, followed by filtration. After the filtrate was concentrated by evaporation and cooled, reddish crystals separated, which were recrystallized from water and air-dried (yield, 2.5 g; 48%). Found: Cu, 13.2; C, 25.0; H, 6.2; N, 23.4; SO_4, 20.1; H_2O, 7.3. Calc. for $[Cu(AP^nUH)_2]SO_4 \cdot 2H_2O$: Cu, 13.1; C, 24.8; H, 5.8; N, 23.2; SO_4, 20.0; H_2O, 7.5%.

Bis(1-*amidino*-O-n-*propylurea*)*copper*(II) *nitrate*, $[Cu(AP^nUH)_2](NO_3)_2 \cdot 3H_2O$

This compound in the form of rose-violet crystals was prepared in the same way as the chloride compound, except that copper(II) nitrate was used instead of copper(II) chloride (yield, 2.3 g; 30%). Found: Cu, 12.0; C, 22.6; H, 5.6; N, 26.7; H_2O, 10.2. Calc. for $[Cu(AP^nUH)_2](NO_3)_2 \cdot 3H_2O$: Cu, 12.0; C, 22.8; H, 5.7; N, 26.6; H_2O, 10.2%.

Bis(1-*amidino*-O-sec-*butylurea*)*copper*(II) *chloride*, $[Cu(AB^{sec}UH)_2]Cl_2 \cdot 1.5H_2O$

This rose-red compound was prepared in the same way as $[Cu(AP^nUH)_2]Cl_2$ except that *sec*-butanol was used instead of *n*-propanol (yield, 2.4 g; 40%). Found: Cu, 13.2; C, 30.2; H, 6.6; N, 23.3; Cl, 14.9. Calc. for $[Cu(AB^{sec}UH)_2]Cl_2 \cdot 1.5H_2O$: Cu, 13.2; C, 30.1; H, 6.5; N, 23.4; Cl, 14.8%.

Bis(1-*amidino*-O-sec-*butylurea*)*copper*(II) *sulphate*, $[Cu(AB^{sec}UH)_2]SO_4$

This compound in the form of rose-red crystals was prepared like $[Cu(AB^{sec}UH)_2]Cl_2 \cdot 1.5H_2O$ with appropriate modification (yield, 2.6 g; 40%). Found: Cu, 13.3; C, 30.1; H, 6.5; N, 23.6; SO_4, 20.0. Calc. for $[Cu(AB^{sec}UH)_2]SO_4$: Cu, 13.3; C, 30.2; H, 6.5; N, 23.5; SO_4, 20.1%.

Bis(1-*amidino*-O-n-*amylurea*)*copper*(II) *chloride*, $[Cu(AA^nUH)_2]Cl_2 \cdot H_2O$

This compound in the form of rose-violet crystals was prepared in the same way as $[Cu(AP^nUH)_2]Cl_2 \cdot 2H_2O$ except that *n*-amyl alcohol (1-pentanol) was used instead of *n*-propanol (yield, 2.6 g; 46%). Found: Cu, 12.8; C, 33.9; H, 6.9; N, 22.4; Cl, 14.3. Calc. for $[Cu(AA^nUH)_2]Cl_2 \cdot H_2O$: Cu, 12.8; C, 33.8; H, 6.8; N, 22.5; Cl, 14.3%.

Bis(1-*amidino*-O-n-*propylurea*)*nickel*(II) *chloride*, $[Ni(AP^nUH)_2]Cl_2 \cdot 2H_2O$

An aqueous solution of 1-amidino-O-*n*-propylurea sulphate (2.5 g) and nickel(II) sulphate heptahydrate ($NiSO_4 \cdot 7H_2O$) (1.2 g) was made strongly

basic with sodium hydroxide solution, whereupon a yellow complex nickel base was precipitated. This precipitate was filtered and washed several times with water until free of base. The complex nickel base was then triturated with 2 N hydrochloric acid until neutral to litmus paper, and the product was recrystallized as bright yellow crystals from ethanol (yield, 2.3 g; 45%). Found: Ni, 12.8; C, 26.8; H, 6.3; N, 24.8; Cl, 15.8. Calc. for $[Ni(AP^{n}UH)_2]Cl_2 \cdot 2H_2O$: Ni, 13.0; C, 26.6; H, 6.2; N, 24.8; Cl, 15.7%.

Bis(1-*amidino*-O-sec-*butylurea*)*nickel*(II) *chloride*, $[Ni(AB^{sec}UH)_2]Cl_2 \cdot H_2O$

This compound in the form of yellow crystals was prepared like the previous compound with $[AB^{sec}UH]_2 \cdot H_2SO_4 \cdot 2H_2O$ substituted for $(AP^{n}UH]_2 \cdot H_2SO_4 \cdot 2.5H_2O$ (yield, 2.2 g; 40%). Found: Ni, 12.1; C, 25.0; H, 6.3; N, 23.1; Cl, 14.8. Calc. for $[Ni(AB^{sec}UH)_2]Cl_2 \cdot H_2O$: Ni, 12.1; C, 24.9; H, 6.2; N, 23.2; Cl, 14.7%.

Bis(1-*amidino*-O-sec-*butylurea*)*nickel*(II) *hydroxide*, $[Ni(AB^{sec}UH)_2](OH)_2 \cdot 2H_2O$

This yellow compound was prepared by digesting $[Ni(AB^{sec}UH)_2]Cl_2$ with sodium hydroxide solution (yield, 2 g; 80%). Found: Ni, 13.1; C, 32.4; H, 7.5; N, 25.1. Calc. for $[Ni(AB^{sec}UH)_2](OH)_2 \cdot 2H_2O$: Ni, 13.1; C, 32.1; H, 7.6; N, 25.1%.

Bis(1-*amidino*-O-n-*amylurea*)*nickel*(II) *chloride*, $[Ni(AA^{n}UH)_2]Cl_2 \cdot H_2O$

This yellow compound was prepared by triturating $[Ni(AB^{sec}UH)_2](OH)_2$ with dilute (2 N) hydrochloric acid until neutral to litmus and recrystallizing the product from ethanol (yield, 2.1 g; 50%). Found: Ni, 11.9; N, 22.7; C, 34.3; H, 4.5; Cl, 14.3. Calc. for $[Ni(AA^{n}UH)_2]Cl_2 \cdot H_2O$: Ni, 11.9; N, 22.7; C, 34.17; H, 4.4; Cl, 14.3%.

Analysis

The metals were analysed by standard analytical procedures: nitrogen, by the combustion method; carbon and hydrogen, by the Alfred Bernhardt Mikro-Analytische Laboratorium, West Germany; chlorine was determined as silver chloride. Electrical conductances were measured with a Philips PR 9500 conductivity bridge. IR spectra were recorded at the Central Drug Research Institute (Lucknow, India). Magnetic moments were obtained from corrected χ_M values determined by using a Gouy balance with $CuSO_4 \cdot 5H_2O$ as the calibrant. Solution spectra were obtained with a Hilger Uvispec spectrophotometer over the range of 350–1000 nm.

RESULTS AND DISCUSSION

Bis(ligand)copper(II) bases (hydroxides) are rose-red compounds which conform to the anhydro base formulation, indicating that the ligand can behave as a monoprotic acid. All these basic compounds liberate ammonia on treatment with ammonium chloride and can be neutralized with dilute HCl, H_2SO_4, or HNO_3 in alcohol to yield the corresponding salts, i.e. protonation of the free $—NH_2$ group of 1-amidino-O-alkylurea occurs even after complex formation.[1,2] Care was taken in the preparation of the salts with acids; otherwise, the compounds hydrolysed to give the corresponding aqua compound.[1,2]

It is now well established that the metal ion-promoted addition of alcohol to dicyandiamide leads to the formation of 1-amidino-O-alkylurea complexes.[2–6] All the copper(II) and nickel(II) complex bases (hydroxides) were insoluble in water, but the corresponding salts (chloride, bromide, nitrate and sulphate) are soluble in water as well as in methanol, ethanol, N,N-dimethylformamide, dimethyl sulphoxide, and pyridine. As the size of the alkyl group of the ligand increases, the solubility of the complexes in water decreases, while in organic solvents the solubility increases.

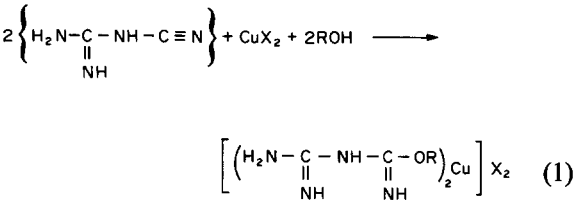

The present study shows that the copper(II) ion initiates alcohol (R = $C_2H_5(CH_3)CH$, *n*-C_3H_7, *n*-C_5H_{11}) addition, and the formation of complexes of the types $[CuL_2]X_2$ (X = Cl, NO_3, $0.5SO_4$, CH_3COO, etc.) is evident from the IR spectra of $[CuL_2]X_2$ and other related complexes. There are no typical nitrile bands (—C≡N) due to dicyandiamide at 2176 and 2222 cm^{-1}; instead, we observed a characteristic C—O—R (R = C_2H_5, $CH_3(CH)$, *n*-C_3H_7, and *n*-C_5H_{11}) stretch at about 1200 cm^{-1} and a C—H symmetrical deformation vibration at about 1400 cm^{-1}. There was no >C=O stretch at 1740 cm^{-1}, indicating that the products are not substituted guanylureas.[3]

IR bands appearing around ~ 540 cm^{-1} (s) assigned to ν(Ni—N) and ~ 530 cm^{-1} due to

ν(Cu—N) indicate the coordinate nature of guanidine nitrogen atoms.[7] The non-coordinating nature of the water molecules is confirmed by the absence of any recognized bands for rocking and wagging modes of vibration. Instead, a broad diffuse band around 3500 cm^{-1} indicates the lattice nature of the water molecules. The fact that the anhydrous compound, which shows no such band at about 3500 cm^{-1}, is obtained by heating at 100°C further substantiates this conclusion. In the IR spectra of all the nickel(II) and copper(II) complexes, the bands in the 3μ region arising due to ν_{asy}(N—H) (3300–3390 cm^{-1}) and ν_{sy}(N—H) (3100–3140 cm^{-1}) modes of vibration of the guanyl group[8] are observed almost in the same positions as those in the original ligand molecules, with a slight decrease in intensities, suggesting the participation of ligands in complex formation without deprotonation. The ν(C=N) stretching bands of the guanidine part of all the ligands appearing at 1650 cm^{-1} have been found to experience an average shift of (10±5) cm^{-1}, pointing to the probable participation of the imino nitrogen (=NH) of the guanyl moiety of the ligands in complex formation with the metal(II).[9–11] The IR spectral bands for these three ligands and their probable assignments are given in Table 1. No reaction occurs between dicyandiamide and an alcohol in the absence of copper(II), nickel(II), or palladium(II) ions. In fact, dicyandiamide can be recovered unchanged even after 50 h of refluxing in alcohols.[3,12–14]

Complexes of empirical formula $[CuL_2]X_2$ are biunivalent electrolytes since they exhibit conductance values of the order of 200 Ω^{-1} cm^2 mol^{-1} in aqueous solution at 25°C.[15] All copper(II) complexes show effective magnetic moment values of about 1.73 BM. The electronic spectra of bis(ligand)copper(II) salts show typical absorption bands characteristic of a square planar $[CuN_4]$ chromophore. The data show that the introduction of higher alkyl groups into the ligand has almost no effect on the spectra of either the copper(II) or nickel(II) complexes. For square planar geometry three transitions:

$$d_{xy} \rightarrow d_{x^2-y^2}; \quad d_{xz}, d_{yz} \rightarrow d_{x^2-y^2};$$
$$\text{and} \quad d_{z^2} \rightarrow d_{x^2-y^2},$$

are likely. In most copper(II) chelates these transitions are covered in a somewhat broad envelope. Other square planar $[CuN_4]$ chromophores appear in bis(biguanide)copper(II) (19.2 kK, $\varepsilon = 38.5$ in water),[1,16,17] bis(phenylbiguanide)copper(II) (18.2 kK, $\varepsilon = 65.5$ in water),[1,16] ethylenedibiguanidecopper(II) (19.2 kK, $\varepsilon = 50.5$ in water),[1,16,18] bis(ethylenediamine)copper(II) (18.2 kK, $\varepsilon = 63$

Table 1. IR group frequencies (cm^{-1}) of amidinourea, 1-amidino-O-*n*-propylurea, 1-amidino-O-*n*-amylurea, and 1-amidino-O-*sec*-butylurea sulphates and their band assignments

Amidinourea sulphate	1-amidino-O-*n*-propylurea sulphate	1-amidino-O-*n*-amylurea sulphate	1-amidino-O-*sec*-butylurea sulphate	Nature of vibration	Reference
1125 vs	1120 vs	1120 vs	1120 vs	Sulphate	3, 29
	1200 vs	1200 vs	1200 vs	C—O—R stretching vibration	
1350 vs	1350 vs	1350 vs	1355 vs	C—N stretching vibration	20, 29–31
	1400 vs	1405 vs	1400 vs	C—H symmetrical deformation vibration	
1465 vs	1490 vs	1490 vs	1485 vs		
1530 w	1540 s	1545 vs	1545 vs	$-NH_3^+$ symmetrical band	29
1580 s	1565	1585 vs	1590 vs	N—H deformation vibration	
	1605				
1625 w	1650 vs	1650 vs	1650 vs	C=N vibration amide band	20, 29–31
1680 vs	—	—	—		
1740 vs	—	—	—	>C=O absorption band	
3180 s	3205 vs	3200 vs	3205 vs	N—H and NH_2 stretching vibrations	20, 29–31
3320 s	3310 sh	3310 sh	3310 sh		
3350 s	3360 vs	3355 vs	3355 vs		

vs, Very strong; w, weak; s, strong; sh, shoulder.

Table 2. Colours, electronic spectra, conductances, IR spectra, and effective magnetic moments of some 1-amidino-O-alkylurea copper(II) and nickel(II) complexes

Complex	Solvent	Colour in solution	Absorption bands (kK)	Molar conductance in aqueous solution at 25°C (Ω^{-1} cm^2 mol^{-1})	IR spectra ν(C—O—C) (cm^{-1})	μ_{eff} at 300 K (BM)
$[Cu(AP^{n}UH)_2]Cl_2$	Water	Rose-red	18.8	201	1205 s	1.82
	Ethanol	Rose-red	18.6			
	DMF	Light violet	18.5			
	DMSO	Bluish green	17.2			
	Py	Light green	16.4			
$[Cu(AB^{sec}UH)_2]Cl_2$	Water	Rose-red	18.8	182	1205 s	1.79
	Ethanol	Rose-red	18.6			
	DMF	Light green	18.5			
	DMSO	Bluish green	17.2			
	Py	Light green	16.4			
$[Cu(AA^{n}UH)_2]Cl_2$	Water	Rose-red	18.8		1205 s	1.79
	Ethanol	Rose-red	18.6	167	1205 s	1.77
	DMF	Light green	18.5			
	DMSO	Bluish green	17.2			
	Py	Light green	16.4			
$[Ni(AP^{n}UH)_2]Cl_2$	Water	Orange-yellow	22.2		1208 s	Diamagnetic
	Ethanol	Orange-yellow	21.9	238		
	DMF	Orange-yellow	22.7			
	DMSO	Orange-yellow	23.2			
	Py	Orange-yellow	20.0 sh, 24.3			
$[Ni(AB^{sec}UH)_2]Cl_2$	Water	Orange-yellow	22.2	214	1207 s	Diamagnetic
	Ethanol	Orange-yellow	21.9			
	DMF	Orange-yellow	22.7			
	DMSO	Orange-yellow	23.2			
	Py	Orange-yellow	24.3			

DMF, N,N-dimethylformamide; DMSO, dimethylsulphoxide; Py, pyridine; s, strong; sh, shoulder; vs, very strong.

in water),[19] bis(1-amidino-O-alkylurea)copper(II) (18.5 kK, $\varepsilon = 43$ in water),[2,20] tetrakis(benzamidazole)copper(II) perchlorate (19.0 kK, solid state).[21] The absorption bands of bis(1-amidino-O-alkylurea)copper(II) (18.5 kK) indicate that these ligands exert similar crystal field effects on copper(II).[2,19–22] However, in the spectrum of the present bis(ligand)copper(II) chloride, a considerable shift of band positions occurs with change of solvents; the following tetragonality order was observed: water > ethanol > N,N-dimethylformamide (DMF) > dimethyl sulphoxide (DMSO) > pyridine (Py), in agreement with Dutta and De's results.[23]

The spectra of the bis(ligand)nickel(II) compounds in aqueous solution show absorption bands at 22.2 kK (Table 2).[2,18,24] The diamagnetism and band positions of these complexes indicate a square planar configuration.[25–27] In donor solvents such as DMSO, Py, etc., there is a shift of band position compared to that in water (Table 1), unlike that observed in square planar ethylenedibiguanidenickel(II) compounds.[4(a),28]

Since there are no changes in the band maxima of ethylenedibiguanidenickel(II) compounds, the d_{z^2} orbital, which must receive the donor solvents in the *trans* apical sites, is not the orbital immediately lower in energy than the $d_{x^2-y^2}$ orbital. The ordering proposed is $d_{x^2-y^2} > d_{xy} > d_{z^2} > d_{xz}, d_{yz}$. In the present series of complexes the band shift indicates a tetragonality of the complex, and a different *d* orbital order, which is $d_{x^2-y^2} > d_{z^2} > d_{xy} > d_{xy}, d_{zx}$, with a 22.2 kK band representing a $d_{z^2} \rightarrow d_{x^2-y^2}$ transition.

Acknowledgements—The senior author (R.K.R.) wishes to thank Professor R. L. Dutta, former Head of the Department of Chemistry, Burdwan University, India,

for his interest and for providing some facilities for research. They also thank the referee for his constructive suggestion for improving this article.

REFERENCES

1. P. Rây, *Chem. Rev.* 1961, **61**, 313.
2. R. L. Dutta and A. Syamal, *Coord. Chem. Rev.* 1967, **2**, 441.
3. R. L. Dutta and R. K. Ray, *J. Indian Chem. Soc.* 1976, **53**, 507; R. L. Dutta and A. M. Singh, *J. Indian Chem. Soc.* 1975, **52**, 1000.
4. V. Rasmussen and W. A. Baker Jr, *J. Chem. Soc. A* 1967, (a) 580; (b) 1712.
5. A. Syamal, *Z. Anorg. Allg. Chem.* 1976, **419**, 189.
6. W. R. Wasson and C. Trapp, *J. Phys. Chem.* 1969, **73**, 3763.
7. N. Saha and D. Mukherjee, *Polyhedron* 1986, **5**, 1317.
8. A. Albert and E. Spinner, *J. Chem. Soc.* 1960, 1221.
9. N. Nakanishi and P. H. Solomon, *Infrared Absorption Spectroscopy*, 2nd edn, p. 257. Holden-Day, San Francisco (1977).
10. S. P. Ghosh and P. Battacharjee, *J. Inorg. Nucl. Chem.* 1970, **23**, 573.
11. S. P. Ghosh, P. Battacharjee, L. Dubey and L. K. Mishra, *J. Indian Chem. Soc.* 1977, **54**, 234.
12. T. C. Creitz, R. G. Sell and D. L. Wampler, *J. Chem. Soc., Chem. Commun.* 1969, 1371.
13. F. H. S. Curd and F. L. Rose, *J. Chem. Soc.* 1946, 733.
14. S. N. Poddar and P. Rây, *J. Indian Chem. Soc.* 1952, **29**, 381.
15. W. J. Greay, *Coord. Chem. Rev.* 1971, **7**, 81.
16. A. Syamal, *J. Sci. Ind. Res.* 1978, **61**, 313.
17. A. Chakravarty and S. Basu, *J. Inorg. Nucl. Chem.* 1961, **17**, 55.
18. D. Banerjea, *Transition Met. Chem.* 1982, **7**, 22.
19. K. Sone and S. Utsuno, *Bull. Chem. Soc. Japan* 1966, **39**, 1813.
20. R. L. Dutta and A. M. Singh, *J. Inorg. Nucl. Chem.* 1978, **40**, 417.
21. M. Goodgame and L. I. B. Haines, *J. Chem. Soc. A* 1966, 174.
22. M. M. Ray and P. Rây, *J. Indian Chem. Soc.* 1959, **36**, 849.
23 R. L. Dutta and D. De, *J. Indian Chem. Soc.* 1969, **46**, 70.
24. R. N. Banerjee, S. Gangopadhyay, A. K. Banerjee and D. Banerjea, *J. Coord. Chem.* 1983, **12**, 287.
25. R. S. Nyholm, *Chem. Rev.* 1953, **53**, 263.
26. J. R. Miller, *Adv. Inorg. Radiochem.* 1962, **2**, 157.
27. R. G. Hayter and F. S. Humiec, *Inorg. Chem.* 1965, **4**, 1701.
28. D. J. MacDonald, *Inorg. Chem.* 1967, **6**, 2269.
29. R. L. Dutta and A. Syamal, *J. Indian Chem. Soc.* 1967, **44**, 571.
30. R. M. Silverstein and G. C. Bassler, *Spectrometric Identification of Organic Compounds*, 2nd edn, p. 97. Wiley, New York (1967).
31. R. K. Ray, *Chromatographic Studies on Metal Complexes*, D. Phil. Thesis, Univ. of Burdwan, India (1976).

Polyhedron Vol. 8, No. 6, pp. 763–767, 1989
Printed in Great Britain

0277–5387/89 $3.00+.00
© 1989 Pergamon Press plc

PREPARATION AND CHARACTERIZATION OF *n*- AND *i*-BUTYLINDIUM THIOLATE*

RYOKI NOMURA,† SHIN'JI INAZAWA, KOUICHI KANAYA and HARUO MATSUDA

Department of Applied Chemistry, Faculty of Engineering, Osaka University, Yamada-Oka, Suita, Osaka 565, Japan

(*Received* 25 *May* 1988 : *accepted after revision* 11 *October* 1988)

Abstract—Butylindium thiolates $Bu^n_xIn(SR)_{3-x}$ ($x = 0$, R = Pr^n, Ph; $x = 1$, R = Pr^i, Hex^c, Ph; $x = 2$, R = Pr^n, Pr^i, Hex^c, Ph) and $Bu^i_xIn(SR)_{3-x}$ ($x = 1$, R = Ph; $x = 2$, R = Pr^n, Pr^i, Ph) are prepared in the reaction of Bu_3In and corresponding thiols in ether. Monothiolates can be obtained from all Bu_3In–alkanethiol combinations, but di- and trithiolates are isolated only from less hindered ones such as Bu^n_3In–Pr^nSH. While, more acidic benzenethiols can give mono-, di- and trithiolates. The mono- and dialkylthiolates, are distillable liquids and they are charactrized by means of NMR spectroscopy (^1H and ^{13}C). In contrast, the phenylthiolates are solids and have poor solubility in organic solvents. The molecular weight measurements show that the dithiolates are generally monomeric in solution.

Recent advances in the technique of OMCVD for fabricating III/V compound semiconductor materials have prompted work to investigate the nature of trialkyls of indium and their adducts with pnictogen compounds such as phosphines etc.[1–5] However, other fields of organoindium chemistry have remained insufficiently explored. Especially, only limited and non-systematic information is available for organoindium thiolates. Meanwhile, an intense interest has arisen in metal chalcogenides as photovoltaic or optoelectric device materials,[6–9] and we believe that the organometallic thiolates will be the most useful precursors for such chalcogenide materials.

Numerous research groups have reported the preparation of the organoindium thiolates since Coates and Whitecombe synthesized dimethylindium methylthiolate for the first time.[10–15] However, dithiolates were rarely obtained with the exception of dithiochelates.[16,17] In general, it has been found that the only product from the reaction of trialkyls of indium with even excess amounts of acids such as carboxylic acids, was the dialkylindium derivatives.[1] In some cases the elimination of three alkyl groups was possible under forcing conditions but monoalkylindium derivatives could not be obtained. However, the brief report from Kocheshkov *et al.*, where phenylindium derivatives were discussed, indicated that both dialkyl and monoalkylindium thiolates could be synthesized.[18] Also the organoindium thiolates already reported possessed high melting points and were sometimes insoluble in organic solvents. These properties may give rise to difficulties in purification. With the aim of obtaining soluble and/or volatile organoindium thiolates, we report the reactions of Bu^n_3In and Bu^i_3In with several thiols, carried out systematically, and analytical and spectrometric properties of the butylindium thiolates thus obtained.

EXPERIMENTAL

General

^1H and ^{13}C NMR spectra were recorded on a Hitachi R90H FT spectrometer, and the common acquisition conditions were described in the previous papers.[19,20] Coupling constants $^1J(^{13}C–^1H)$ were measured by means of the gated decoupling J-spin modulation mode of the instrument. Molecular weights were measured by cryoscopy in benzene solution. Analytical GLC was carried out with a

* Part of this work was presented at the 52nd annual meeting of the Chemical Society of Japan in Kyoto, 1 April 1986, Abstr. No. 1K27, p. 590.

† Author to whom correspondence should be addressed.

Shimadzu GC-8A connected with a glass column (2 mm × 3 m) packed with Porapack N. All the reactions were carried out under a dry N_2 atmosphere unless otherwise noted.

Trialkylindiums

Bu^n_3In and Bu^i_3In were synthesized by the Grignard method as reported previously.[21] Yields of Bu^n_3In and Bu^i_3In were 93 and 68%, respectively. Their boiling points and NMR data are indicated in Table 1.

Butylindium thiolates

Into a solution of the indium trialkyl (5 mmol) in 30 cm^3 absolute ether was added slowly, thiol (5 or 10 mmol) in ether (5 cm^3) at −78°C with stirring. The mixture was then allowed to warm up to room temperature and was stirred for another 6–24 h. If necessary, the solution was heated under reflux for an additional 2–6 h. Solvent and unreacted thiol were removed *in vacuo* and the crude thiolates were purified by vacuum distillation or by recrystallization from ether–hexane. The alkylthiolates were obtained as colourless, viscous oils, while indium tri(phenylthiolate) appeared to be a white powder insoluble in organic solvents. In contrast, Tuck *et al.* have reported that the reaction of indium trichloride with benzenethiol,[23] or of indium with diphenyl disulphide[24] gave soluble indium tri(phenylthiolate).

The prepared alkylindium thiolates are relatively stable in air, compared with the trialkylindiums and alkylindium alkoxides, but have some disagreeable odour. They became glassy in appearance along with a decrease of C and H contents after weeks under moist air.

RESULTS AND DISCUSSION

The reactions of Bu^n_3In and Bu^i_3In with several thiols were carried out as described above and the products and their yields are summarized in Table 2. Additionally, the spectral and analytical data of the isolated thiolates are also displayed in Tables 1 and 3, respectively.

$$R_3In + nR'SH \longrightarrow R_{3-n}In(SR')_n.$$

A dropwise addition of equimolar amounts of thiols into the ether solutions of the trialkyls of indium resulted in a gradual evolution of the corresponding butane isomer which was checked by GLC analysis and dialkylindium thiolates were

Table 1. B.p. (m.p.) and NMR data of butylindium thiolates

		δ ^{1}H					δ ^{13}C				
		Bu					Bu				
Compounds[a]	B.p., °C/mmHg (m.p., °C)[b]	α	β	γ	δ	In—S—CH	α	β	γ	δ	In—S—C
$Bu^n In$	81/1[c]	0.92	1.39	1.72	0.92		22.5	30.1	28.7	13.8	
$Bu^n_2InSPr^n$	70/10^{-3}	0.97	1.1–1.8		0.92	2.73	16.6	30.0	28.4	13.8	29.7
$In(SPr^n)_3$	(167)										
$Bu^n_2InSPr^i$	78/10^{-3}	0.95	1.1–1.8		0.85	3.28	17.5	30.0	28.6	13.8	33.8
$Bu^n In(SPr^i)_2$	148/10^{-3}	1.00	165	1.40	0.93	3.46	17.9	29.9	28.3	13.7	34.1
$Bu^n_2In(SHex^c)$	78/0.02		1.0–1.9		0.93	3.10	16.6	29.9	28.2	13.8	41.9
$Bu^n In(SHex^c)_2$	91/0.04		1.3–2.2		0.94	3.17	19.2	26.7	25.3	13.7	42.6
Bu^n_2InSPh	(160 dec)	0.98	1.54	1.21	0.83		19.5	29.6	28.2	13.6	[d]
$Bu^n In(SPh)_2$	(150 dec)	[e]					[e]				
$Bu^n In$ 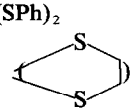	(117–118)	1.41	1.69	1.33	0.93	3.16	19.6	29.8	28.2	13.8	34.8
Bu^i_3In	81/7	1.14	2.40	1.14			24.7	37.6	27.9		
$Bu^i_2InSPr^n$	132/10^{-3}	1.03	2.14	0.99		2.75	26.1	29.8	27.8		29.8
$Bu^i_2InSPr^i$	100/10^{-3}	0.95	2.08	0.93		3.25	30.5	28.0	27.8		33.7
Bu^i_2InSPh	> 190/10^{-3}	1.01	2.00	0.86			32.7	27.6	27.0		154.2

[a] Hex^c means cyclohexyl.
[b] Melting points were measured by TG.
[c] Ref. 22, 86–87°C/0.4 mmHg.
[d] Signals for *ipso* carbon were fairly broadened and the accurate chemical shifts of them could not be read.
[e] The solubility of this thiolate was too low to record a NMR spectrum.

Table 2. Preparation of butylindium thiolates

Bu	R′	*n*	Reaction time (h) rt	Reflux	Product	Yield (%)
Bu^n	Pr^n	1	18		$Bu^n_2InSPr^n$	87
		2	15	2	$In(SPr^n)_3$	13
		3	20	3	$In(SPr^n)_3$	96
	Pr^i	1	20	3	$Bu^n_2InSPr^i$	81
		2	20	3	$Bu^nIn(SPr^i)_2$	44
		3	20	6	$Bu^nIn(SPr^i)_2$	58
	Hex[c]	1	20		$Bu^n_2InSHex^c$	96
		2	20	2	$Bu^n_2InSHex^c$	85
		3	20	6	$Bu^nIn(SHex^c)_2$	56
	Ph	1	6		Bu^n_2InSPh	87
		2	6	2	$Bu^nIn(SPh)_2$	67
		3	6	6	$In(SPh)_3$	42
	CH_2CH_2SH	1	24		Bu^nIn 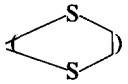	71
	$SCNEt_2$	1	6		$In(S_2CNEt_2)_3$	33
Bu^i	Pr^n	1	20		$Bu^i_2InSPr^n$	88
		2	20	3	$Bu^i_2InSPr^n$ +	47
					$Bu^iIn(SPr^n)_2$[b]	40
		3	20	5	$Bu^i_2InSPr^n$ +	20
					$Bu^iIn(SPr^n)_2$[b]	50
	Pr^i	1	20		$Bu^i_2InSPr^i$	92
		2	20	3	$Bu^i_2InSPr^i$	83
		3	20	6	$Bu^i_2InSPr^i$	78
	Ph	1	20		Bu^i_2InSPh	89
		2	20		$Bu^iIn(SPh)_2$	64

[a] Hex^c means cyclohexyl.

[b] Could not be isolated by distillation and NMR yields are presented here.

obtained in good yields. The monoalkylthiolates appeared as viscous liquids and were distillable under reduced pressures. On the other hand, the dialkylindium phenylthiolates were waxy or gummy solids at room temperature which melted as they decomposed. In contrast, more acidic diethyldithiocarbamic acid gave no butylindium derivatives, but a symmetrical indium(III) dithiocarbamate complex was formed as the sole product. It was reported that dialkylindium dithiocarbamates which were synthesized via the metathesis reaction between dialkylindium halides and sodium dithiocarbamate salts were spontaneously converted into the bis(dithiocarbamate) complex.[14] Therefore, in our case, the dialkylindium diethyldithiocarbamate is presumably formed initially and then the tris(dithiocarbamate) complex is obtained via subsequent disproportionation. However, tributylindium could not be detected as a final product as would be predicted by this scheme.

In the reactions where more than two molar equivalents of thiol were employed, the degree of substitution was found to be strongly dependent upon the isomer of the butyl group and/or those of the thiol moieties. Benzenthiol gave Bu^n_2InSPh, $Bu^nIn(SPh)_2$ and $In(SPh)_3$ in the reactions with Bu^n_3In in the molar ratios of 1 : 1, 2 : 1 and 3 : 1, respectively; and Bu^i_2InSPh, and $Bu^iIn(SPh)_2$ in the reactions with Bu^i_3In in 1 : 1 and 2 : 1 molar ratio, respectively. These phenylthiolates are solids at room temperature and poorly soluble in organic solvents.

In contrast, for some reactions with alkylthiols the product expected from reactant stoichiometry was not always obtained. For example, $Bu^n_2InSPr^n$ and $In(SPr^n)_3$ were formed in the reaction of Bu^n_3In with *n*-propanethiol in 1 : 1 and 2–3 : 1 molar ratio, respectively, but $Bu^nIn(SPr^n)_2$ could not be formed with any mole ratio of the starting materials. However, dibutylindium thiolates from the secondary alkanethiols seemed not to react with further thiol nucleophiles. Consequently, it was necessary to use more than the stoichiometric amounts of the thiols in order to prepare the dithiolates. Especially for the bulky triisobutylindium, the replacement of more than two butyl groups did not occur.

These phenomena could not be explained by the

Table 3. Analytical data and molecular weights of butylindium thiolates

Compounds[a]	Found, % (calc., %) C	H	Formula (FW)	Molecularity (concn, wt%)
$Bu^n_2InSPr^n$	42.9 (43.4	8.0 8.3)	$C_{11}H_{25}InS$ (304.2)	1.6 (0.31)
$In(SPr^n)_3$	31.4 (31.8	6.1 6.2)	$C_9H_{21}InS_3$ (340.3)	
$Bu^n_2InSPr^i$	43.2 (43.4	8.2 8.3)	$C_{11}H_{25}InS$ (304.2)	1.2 (0.30)
$Bu^nIn(SPr^i)_2$	41.8 (41.0	8.0 8.0)	$C_{10}H_{23}InS_2$ (322.2)	1.1 (0.50), 1.4 (2.9)
$Bu^n_2InSHex^c$	49.5 (48.8	8.5 8.5)	$C_{14}H_{29}InS$ (344.3)	1.6 (2.9)
$Bu^nIn(SHex^c)_2$	47.9 (47.8	8.2 8.5)	$C_{16}H_{31}InS_2$ (402.4)	1.0 (0.35), 1.0 (2.2)
Bu^n_2InSPh	49.7 (49.7	6.4 6.9)	$C_{14}H_{23}InS$ (338.2)	
$Bu^nIn(SPh)_2$	49.7 (49.2	4.4 4.9)	$C_{16}H_{19}InS_2$ (390.3)	
$In(SPh)_3$	48.2 (48.9	3.7 3.4)	$C_{18}H_{15}InS_3$ (442.3)	
Bu^nIn 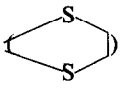	26.9 (27.3	4.9 5.0)	$C_6H_{13}InS_2$ (264.1)	2.0 (0.08)
$Bu^i_2InSPr^n$	42.6 (43.4	8.2 8.3)	$C_{11}H_{25}InS$ (304.2)	1.1 (0.30)
$Bu^i_2InSPr^i$	43.1 (43.4	8.4 8.3)	$C_{11}H_{25}InS$ (304.2)	1.0 (0.26)
Bu^i_2InSPh	49.7 (49.7	6.9 6.9)	$C_{14}H_{23}In$ (338.2)	

[a] Hex^c means cyclohexyl.

reported bond energy ordering: e.g. $D_1 > D_3 > D_2$ observed for trimethylindium.[17] Perhaps such a disagreement may be related to steric crowding around the indium centre from both alkyl groups bound to the indium atom and the alkyl groups in the thiolate moieties. Therefore, the bulkiness of both alkyl groups and thiolates synergistically affects the degree of the substitution.

Generally the In—S bond is considered to have less dipolar effects than its oxygen analogue and its weak coordination ability has been reported.[1] Thus, several organoindium thio-derivatives are found to be monomeric in solutions. Therefore, we have observed the molecular weights of the following thiolates in benzene solution: $Bu^n_2InSPr^n$, $Bu^n_2InSPr^i$, $Bu^nIn(SPr^i)_2$, $Bu^n_2InSHex^c$, $Bu^nIn(SHex^c)_2$, $Bu^i_2InSPr^n$, and $Bu^i_2InSPr^i$. The observed molecularity is presented in Table 3. These data show that dithiolates are approximately monomeric in the concentration range 0.5–3.0 wt% in benzene but monothiolates of *n*-butylindium have some degree of association. In addition, it is very interesting that 1,2-ethanedithiol gave cyclic dithioindate as a sole product without the formation of the polymers consisting of a dithiol bridge. This cyclic compound was solid at room temperature and although only slightly soluble in most organic solvents, was found to be a dimer in benzene.

The degree of association seemed to depend upon the degree of branching in the indium alkyls and thiolate moieties. Therefore, among the monothiolates the molecularity decreased in the series for the following metal ligand–sulphur ligand combinations: Bu^n–Pr^n > Bu^n–Hex^c > Bu^n–Pr^i = Bu^i–Pr^n > Bu^i–Pr^i. Similarly, it has been reported that alkylzinc thiolates which have branches are liquid and almost monomeric in solution at room temperature, in comparison with the straight chain analogues

which were found to be dimeric to hexameric.[25] In the indium cases, this tendency was also dependent upon the alkyl groups bound to the indium centre.

NMR spectroscopy

^{1}H and ^{13}C NMR data of the compounds are summarized in Table 1. All the measurements were obtained in chloroform-*d* solution (10 wt%). For the solid samples, it was necessary to use more diluted solutions (0.1–1 wt%) because of their low solubilities. In the ^{1}H NMR spectra, the signals due to the α-protons in the butyl groups were generally superimposed on those of terminal methyl protons in the monothiolate compounds. However, those α-proton signals were down field of the terminal signals in dithiolates.

In ^{13}C NMR spectra, the signals due to the α-carbons in the *n*-butyl groups appeared at a slightly higher field than those in the starting Bu^n_3In. While the signals of α-carbons in the *i*-butyl groups appeared at lower fields by *ca* 10 ppm compared with Bu^i_3In. In contrast, an opposite tendency was found in the signals due to the β-carbons. Since isobutylindium thiolates are believed to be monomeric in solution from the molecularity measurements, it can be said that the chemical shifts in the isobutyl group may be affected only by the covalently-bonded sulphur ligands. However, since in the *n*-butyl cases some self-association was observed, the *n*-butyl chemical shifts have been further affected. The above mentioned effect was further supported by the spectrum of thiolate moieties. In this case the signal due to the δ Cl and C2 of the thiolate ligand resembled those of sulphides, not of thiolate anions.[26] These results also indicate the less polar and more covalent nature of In—S bonding in the compounds.

CONCLUSION

In conclusion, *n*- and *i*-butylindium thiolates were easily prepared from the corresponding trialkylindium and thiols. Benzenethiol was found to give mono-, di- and trithiolates. However, it was difficult to control the stoichiometry of the reactions with some alkanethiols and not all substitution products could be isolated.

REFERENCES

1. D. G. Tuck, *Comprehensive Organometallic Chemistry* (Edited by G. Wilkinson), Vol. 1, pp. 694–701 and 712–719. Pergamon Press, Oxford (1982).
2. C. H. Chen, C. A. Larsen, G. B. Stringfellow, D. W. Brown and A. J. Robertson, *J. Cryst. Growth* 1986, **77**, 11.
3. A. H. Moore, M. D. Scott, J. I. Davies, D. C. Bradley, M. M. Faktor and H. Chudzynska, *J. Cryst. Growth* 1986, **77**, 19.
4. F.-W. Reier, P. Wolframm and H. Schumann, *J. Cryst. Growth* 1986, **77**, 23.
5. J. Haigh and S. O'Brien, *J. Cryst. Growth* 1984, **68**, 550.
6. A. N. Tiwari, D. K. Pandya and K. L. Chopra, *Sol. Energy Mater.* 1987, **15**, 121.
7. Y. Ueno, H. Kaigawara, T. Sugiura and H. Minoura, *Denki Kagaku* 1987, **55**, 263.
8. K. Kuriyama and T. Saitoh, *Thin Solid Films* 1984, **111**, 331.
9. W.-T. Kim, C.-S. Yan, H.-M. Jeong and C.-D. Kim, *J. Appl. Phys.* 1986, **60**, 2357.
10. G. E. Coates and R. A. Whitecombe, *J. Chem. Soc.* 1956, 3351.
11. H. Tada, K. Yasuda and R. Okawara, *Inorg. Nucl. Chem. Lett.* 1967, **3**, 315.
12. H. Tada and R. Okawara, *J. Organomet. Chem.* 1970, **28**, 21.
13. J. Weidlein, *J. Organomet. Chem.* 1971, **32**, 181.
14. T. Maeda and R. Okawara, *J. Organomet. Chem.* 1972, **39**, 87.
15. H. D. Hausen and H. J. Guder, *J. Organomet. Chem.* 1973, **57**, 243.
16. A. F. Berniuz and D. G. Tuck, *J. Organomet. Chem.* 1972, **46**, 243.
17. J. G. Contreras and D. G. Tuck, *J. Organomet. Chem.* 1974, **66**, 405.
18. I. M. Viktorova, N. I. Sheverdina and K. A. Kocheshkov, *Dokl. Akad. Nauk SSSR* 1971, **198**, 94.
19. R. Nomura, A. Takabe and H. Matsuda, *Polyhedron* 1987, **6**, 411.
20. R. Nomura, M. Yamamoto, A. Takabe and H. Matsuda, *Polyhedron* 1987, **6**, 1161.
21. R. Nomura, S.-J. Inazawa, H. Matsuda and S. Saeki, *Polyhedron* 1987, **6**, 507.
22. H. Raymond and J.-P. Laurent, *Bull. Soc. Chim. Fr.* 1966, 3454.
23. R. K. Chadha, P. C. Hayes, H. E. Marbrouk and D. G. Tuck, *Can. J. Chem.* 1987, **65**, 804.
24. R. Kumar, H. E. Mabrouk and D. G. Tuck, *J. Chem. Soc., Dalton Trans.* 1988, 1045.
25. G. E. Coates and D. Ridley, *J. Chem. Soc.* 1965, 1870.
26. E. Bretmaier and W. Voelter, *Carbon-13 NMR Spectroscopy*, 3rd edn, pp. 233–235. VCH Verlag. mbH, Weinheim (1987).

Polyhedron Vol. 8, No. 6, pp. 769–774, 1989
Printed in Great Britain

0277–5387/89 $3.00+.00
© 1989 Pergamon Press plc

COPPER COMPLEXES OF 2-α-HYDROXYBENZYLBENZIMIDAZOLE (HL) AND THE CRYSTAL AND MOLECULAR STRUCTURES OF $[Cu(HL)_2(NCS)_2]\cdot 2Me_2CO$ AND $[Cu_2(HL)_2(L)_2(NO_3)_2]\cdot 4Me_2SO$

BRIAN PIGGOTT*

Inorganic Chemistry Research Laboratory, School of Natural Sciences, Hatfield Polytechnic, Hatfield AL10 9AB, U.K.

and

MICHAEL B. HURSTHOUSE* and RICHARD L. SHORT

Department of Chemistry, Queen Mary College, London E1 4NS, U.K.

(*Received* 5 *July* 1988; *accepted* 11 *October* 1988)

Abstract—The preparation and properties of copper(II) complexes of the title ligand (HL) are described and the X-ray crystal structures of $[Cu(HL)_2(NCS)_2]\cdot 2Me_2CO$ and $[Cu_2(HL)_2(L)_2(NO_3)_2]\cdot 4Me_2SO$ where L is the deprotonated form of HL. The crystal structure of $[Cu(HL)_2(NCS)_2]\cdot 2Me_2CO$ shows that HL chelates such that two nitrogen and two oxygen donors are mutually *trans* giving a centrosymmetric structure. The acetone molecules are strongly hydrogen bonded to the hydroxyl protons. In $[Cu_2(HL)_2(L)_2(NO_3)_2]\cdot 4Me_2SO$ the copper atoms are bridged by the O^- of two of the deprotonated ligands, each of which are also chelating. The two copper atoms and two bridging ligands define a plane with the other two ligands lying on the same side of this plane in such a way that the hydroxyl groups point towards each other. This dimeric cation is sited on a two-fold axis. One of the nitrate ions is positioned on the two-fold axis and bridges the hydroxyl groups, but in a disordered way. It is presumably this hydrogen bonding that holds the molecule in such an unusual conformation. The second nitrate ion occupies a cavity in the structure and is hydrogen bonded to an amino hydrogen of the deprotonated ligand.

Our original interest in 2-α-hydroxybenzylbenzimidazole (HL) was based on its reported antiviral activity and the suggestion that this might be related to chelation with trace metals.[1] We therefore synthesized a number of cobalt and nickel complexes with HL.[2] Several of these complexes adopted interesting structures and so it was decided to extend our study and investigate the coordination chemistry of HL with a variety of copper salts.

EXPERIMENTAL

HL was synthesized as described in the literature.[3] Analytical data for the complexes are given in Table 1. Yields of the complexes depended on the extent of solvent evaporation. In all cases the products were filtered off when approximately 2 g had crystallized.

$Cu(HL)_2Cl_2(EtOH)_2$

HL (4.5 g, 0.02 mol) was dissolved in ethanol (50 cm^3) and to this was added a solution of $CuCl_2\cdot 2H_2O$ (1.7 g, 0.01 mol) in ethanol (10 cm^3). On standing in an open flask, bright green crystals formed after several days. These were filtered off and air dried. After analysis a sample of this complex was desolvated by vacuum drying at 80°C to give a dark green solid.

*Authors to whom correspondence should be addressed.

Table 1. Analytical data for the complexes

Complex	Found (%) C	H	N	X	Calculated (%) C	H	N	X
$Cu(HL)Cl_2(EtOH)_2$	57.1	5.4	8.3	10.9	56.9	5.3	8.3	10.5
Weight loss study	12.4				13.6			
$Cu(HL)_2Br_2(EtOH)_2$	50.4	5.0	7.6	21.0	50.3	4.8	7.3	21.0
Weight loss study	11.5				12.1			
$Cu(HL)_2I_2$	43.4	3.8	7.4	32.1	43.9	3.2	7.3	33.1
$[Cu(HL)_2(NCS)_2]\cdot 2Me_2CO$	57.5	4.9	11.3		58.1	4.9	11.3	
Weight loss study	15.2				15.7			
$Cu(HL)_2(NCS)_2$	57.5	4.1	13.7		57.4	3.9	13.4	
$Cu(HL)_2(NO_3)_2$	52.9	3.9	13.5		52.9	3.8	13.2	
$[Cu_2(HL)_2(L)_2(NO_3)_2]\cdot 4Me_2SO$	58.3	4.2	12.8		58.7	4.1	12.2	

X is Cl, Br or I.

$Cu(HL)_2Br_2(EtOH)_2$

Prepared as for the chloride but using $CuBr_2$ (2.2 g, 0.01 mol) to give green crystals. The desolvated form of this complex is very dark green.

$Cu(HL)_2I_2$

HL (4.5 g, 0.02 mol) and $Cu(ClO_4)_2\cdot 6H_2O$ (3.7 g, 0.01 mol) were dissolved in ethanol (50 cm^3). To this green solution was added KI (3.2 g, 0.02 mol) to give a deep yellow–green solution. This solution was filtered and the filtrate on standing overnight at 0°C produced dark green crystals which were filtered and crushed to give a dark red–brown powder. After analysis, this material was recrystallized from ethanol and the resulting dark brown crystals crushed and dried *in vacuo*.

$[Cu(HL)_2(NCS)_2]\cdot 2Me_2CO$

HL (4.5 g, 0.02 mol) and $Cu(ClO_4)_2\cdot 6H_2O$ (3.7 g, 0.01 mol) were dissolved in acetone (10 cm^3) and to the blue solution was added a solution of KSCN (2 g, 0.02 mol) in acetone (25 cm^3). After standing overnight at 0°C the precipitated $KClO_4$ was filtered off and the filtrate allowed to evaporate in an open petri dish. The green crystals that formed were filtered and recrystallized from acetone. One of these crystals was suitable for the X-ray study. A sample of this complex was vacuum dried at 100°C to give a greenish-brown, acetone-free solid.

$Cu(HL)_2(NO_3)_2$

$Cu(NO_3)_2\cdot 3H_2O$ (2.4 g, 0.01 mol) was dissolved in acetone (20 cm^3) and the solution shaken with 5 g of anhydrous Na_2SO_4. After standing for 1 h this solution was filtered onto HL (2.3 g, 0.01 mol). The resulting clear green solution on standing for several days produced a mass of needle-like green crystals which were filtered and dried *in vacuo* at 100°C. Any attempt to recrystallize this product resulted in the immediate precipitation of a blue solid.

$[Cu_2(HL)_2(L)_2(NO_3)_2]\cdot 4Me_2SO$

As for $CuHL_2(NO_3)_2$, but using only half the quantity of $Cu(NO_3)_2\cdot 3H_2O$ (1.2 g, 0.05 mol) and dissolving HL (2.3 g, 0.01 mol) in acetone (150 cm^3). The blue solid formed was recrystallized from dimethylsulphoxide and one of the crystals used for the X-ray study.

The diffuse reflectance spectra were recorded on a Beckman DK2 spectrophotometer and are given in Table 2. Magnetic measurements (Table 2) were carried out at room temperature on a Gouy balance of conventional design. IR spectra were recorded as Nujol mulls on a Grubb Parsons Mark I grating spectrometer (Table 3). Electrolytic conductances were measured with a Philips PR 9500 Bridge and standard cell (Table 3).

X-ray crystallography

Crystals of both compounds were sealed in thin-walled glass capillaries to guard against solvent loss. Following preliminary photography, unit cell and intensity data were obtained using a CAD4 diffractometer, graphite monochromated Mo-K_α radiation ($\lambda = 0.70169$ Å) according to previously detailed procedures.[4] The structures were solved via

Table 2. Electronic spectral and magnetic data

Complex	Absorption maxima (cm^{-1})	Magnetic moment (BM)
$Cu(HL)_2Cl_2$	12,100	1.75
$Cu(HL)_2Cl_2(EtOH)_2$	11,800	1.94
$Cu(HL)_2Br_2$	12,400	1.72
$Cu(HL)_2Br_2(EtOH)_2$	12,300	1.96
$Cu(HL)_2I_2$	—	Diamagnetic
$[Cu(HL)_2(NCS)_2]\cdot 2Me_2CO$	16,700—broad on low energy side	1.88
$Cu(HL)_2(NCS)_2$	19,000 sh; 17,300; 14,300 sh	1.43
$Cu(HL)_2(NO_3)_2$	12,500 sh; 10,400	1.97
$[Cu_2(HL)_2(L)_2(NO_3)_2]\cdot 4Me_2SO$	15,400	0.47

BM = Bohr magneton; sh = shoulder.

standard Patterson and heavy atom methods and refined via full-matrix least-squares methods, using programs listed previously.[4]

Crystallograhic data

Compound **1**. $C_{36}H_{36}N_6O_4S_2Cu_2$, $M_r = 744.39$, monoclinic, $a = 8.696(9)$, $b = 11.052(4)$, $c = 19.105(7)$ Å, $\beta = 85.24(5)°$, $U = 1829.7$ Å^3, space group $P2_1/n$, $Z = 2$, $D_c = 1.35\,g\,cm^{-3}$, $\mu(Mo\text{-}K_\alpha) = 7.0\,cm^{-1}$. 3627 reflections measured ($1.5 \leqslant \theta \leqslant 25$), 3219 unique, 2123 observed [$I > 1.5\sigma(I)$]. Final R, R_w values were 0.047 and 0.045, for 237 parameters; non-hydrogen atoms were anisotropic, hydrogens in fixed positions with group U_{iso} values.

Compound **2**. $C_{64}H_{70}N_{10}O_{14}S_4Cu_2$, $M_r = 1442.62$, monoclinic, $a = 15.932(8)$, $b = 9.227(1)$, $c = 21.180(2)$ Å, $\beta = 98.51(3)°$, $U = 3079.2$ Å^3, space group $P2_1/n$, $Z = 2$, $D_c = 1.40$ g cm^{-3} $\mu(Mo\text{-}K_\alpha) = 7.9\,cm^{-1}$. 5340 reflections measured ($1.5 \leqslant \theta \leqslant 24$), 4813 unique, 2725 observed [$I > 1.5\sigma(I)$]. Final R, R_w values were 0.069 and 0.057, for 436 parameters. Non-hydrogen atoms were refined anisotropically, hydrogens inserted in ideal positions and refined with group U_{iso} values, riding on parent C or N atom. The nitrates are both disordered and component atoms were assigned relevant fractional occupancy (see Discussion). Sources of scattering factor data and computer programs used are as in ref. 4. Tables of atomic positional and thermal parameters, bond lengths and angles and F_o/F_c values have been deposited as supplementary data with the Editor, from whom copies are available on request. Atomic coordinates have also been deposited with the Cambridge Crystallographic Data Centre.

RESULTS AND DISCUSSION

The structure of $[Cu(HL)_2(NCS)_2]\cdot 2Me_2CO$ is shown in Fig. 1. The molecule lies on a centre of symmetry with the O, N chelate ligands thus arranged to give mutually *trans*-O, O and -N, N and with *trans*-N-bonded thiocyanates. Selected bond lengths and angles are given in Table 4. The Cu—N bond lengths to HL are slightly longer than those to the thiocyanates. The usual Jahn–Teller distortion for the octahedral copper(II) species results in considerable lengthening of the Cu—O bonds. It is possible that this lengthening in also aided by the

Table 3. IR spectral and molar conductance data

Complex	Band position (cm^{-1})	Molar conductance[a]
$Cu(HL)_2Cl_2$		4.3
$Cu(HL)_2Cl_2(EtOH)_2$	Strong broad peak from 3600 to 2500	2.4
$Cu(HL)_2Br_2$		5.3
$Cu(HL)_2Br_2(EtOH)_2$	Strong broad peak from 3600 to 2500	4.4
$Cu(HL)_2I_2$		18.0
$[Cu(HL)_2(NCS)_2]\cdot 2Me_2CO$	2084; 1684	Insoluble
$Cu(HL)_2(NCS)_2$	2111	Insoluble
$Cu(HL)_2(NO_3)_2$		Insoluble
$[Cu_2(HL)_2L_2(NO_3)_2]\cdot 2Me_2SO$		Insoluble

[a] At room temperature in nitrobenzene. Units: S cm^2 mol^{-1}.

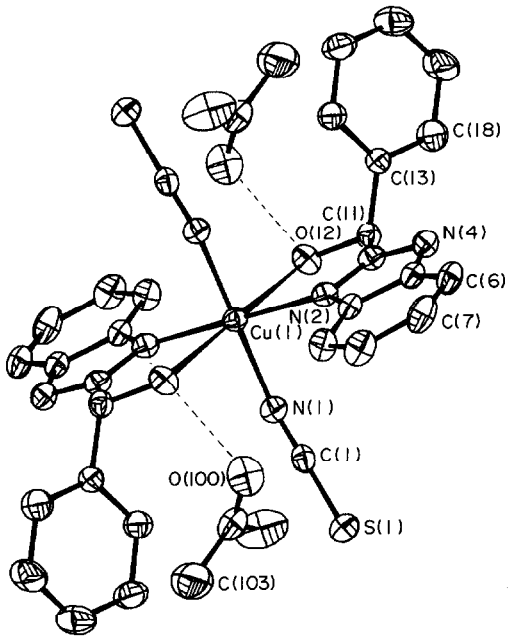

Fig. 1. A view of the centrosymmetric molecule $Cu(HL)_2(NCS)_2$ with associated acetone molecules of solvation.

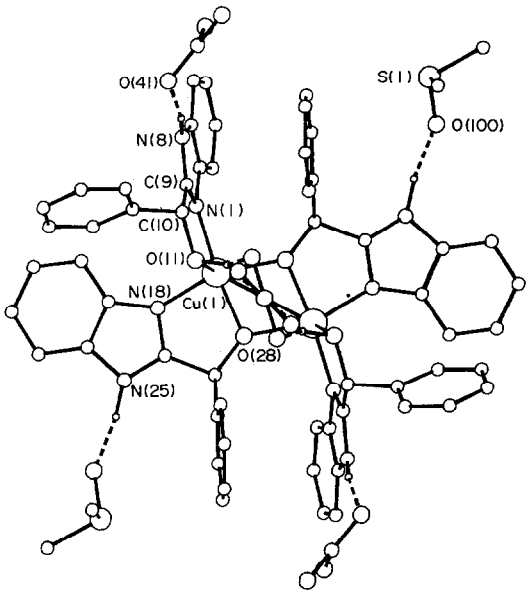

Fig. 2. A view of the dimer $[Cu_2(HL)_2(L)_2(NO_3)_2]\cdot 4Me_2SO$ down the two-fold axis.

formation of hydrogen bonding interactions between the hydroxy hydrogens and the oxygens of acetone solvate molecules (see Fig. 1). The material obtained by desolvation of the acetonate has different electronic, spectral and magnetic properties (Table 2) and IR spectra (Table 3). These would seem to indicate a complex with a structure more radically different from Fig. 1 than just the absence of acetone, for example, a magnetic moment of 1.43 BM is indicative of some interaction between the copper ions. However, during the preparation of $[Cu(HL)_2(NCS)_2]\cdot 2Me_2CO$ it was observed that

Table 4. Selected bond lengths (Å) and angles (°) for $[Cu(HL)_2(NCS)_2]\cdot 2Me_2CO$

(a) Bond lengths			
Cu(1)—N(1)	1.956(5)	Cu(1)—N(2)	1.995(5)
Cu(1)—O(12)	2.575(6)	C(1)—N(1)	1.155(6)
C(1)—S(1)	1.630(7)	N(2)—C(3)	1.317(6)
N(2)—C(10)	1.391(6)	C(3)—N(4)	1.341(6)
C(3)—C(11)	1.496(7)	N(4)—C(5)	1.394(6)
C(5)—C(6)	1.387(7)	C(5)—C(10)	1.384(6)
C(6)—C(7)	1.373(7)	C(7)—C(8)	1.395(7)
C(8)—C(9)	1.378(7)	C(9)—C(10)	1.398(7)
C(11)—O(12)	1.419(6)		
(b) Bond angles			
N(1)—Cu(1)—N(2)	88.1(2)	N(1)—Cu(1)—O(12)	93.3(2)
N(2)—Cu(1)—O(12)	70.9(2)	Cu(1)—N(1)—C(1)	153.1(4)
N(1)—C(1)—S(1)	179.2(4)	Cu(1)—N(2)—C(3)	125.1(4)
Cu(1)—N(2)—C(10)	129.3(4)	C(3)—N(2)—C(10)	105.6(4)
N(2)—C(3)—N(4)	112.2(5)	N(2)—C(3)—C(11)	125.2(5)
N(4)—C(3)—C(11)	122.5(5)	C(3)—N(4)—C(5)	107.9(5)
N(4)—C(5)—C(6)	132.3(4)	N(4)—C(5)—C(10)	104.7(5)
C(6)—C(5)—C(10)	123.0(5)	C(5)—C(6)—C(7)	115.9(5)
C(6)—C(7)—C(8)	122.2(5)	C(7)—C(8)—C(9)	121.3(5)
C(8)—C(9)—C(10)	117.2(5)	C(5)—C(10)—N(2)	109.7(5)
C(9)—C(10)—N(2)	130.1(4)	C(5)—C(10)—C(9)	120.2(5)
C(3)—C(11)—O(12)	107.3(5)	C(3)—C(11)—C(13)	113.4(4)
C(13)—C(11)—O(12)	112.7(4)	Cu(1)—O(12)—C(11)	111.0(3)

decomposition took place if the solution was left standing for more than 2 or 3 days, and it could be that during desolvation at 100°C partial decomposition takes place to give a copper(I) species.

The structure of $[Cu_2(HL)_2(L)_2(NO_3)_2]\cdot 4Me_2SO$ is shown in Fig. 2. Selected bond lengths and angles are given in Table 5. The dimeric cation has a structure analogous to that found in the perchlorate complex.[5] On each copper atom, an anionic ligand is chelating through an imino nitrogen and the deprotonated hydroxy oxygen. This oxygen also bridges to the other copper atom, and two such interactions lead to the formation of a four-membered $[CuO]_2$ ring. The second ligand on each copper is then chelating such that one imino nitrogen lies in the dimer plane and completes a distorted square coordination, and the hydroxy oxygen coordinates through an axial site to give

Table 5. Selected bond lengths (Å) and angles (°) for $[Cu_2(HL)_2(L)_2(NO_3)_2]\cdot 4Me_2SO$

(a) Bond lengths			
Cu(1)—Cu(1a)[a]	3.017(5)	Cu(1)—N(1)	1.955(7)
Cu(1)—O(11)	2.447(8)	Cu(1)—N(18)	1.967(7)
Cu(1)—O(28)	1.937(6)	Cu(1a)—O(28)	1.938(6)
N(1)—C(2)	1.411(11)	N(1)—C(9)	1.313(12)
C(2)—C(3)	1.383(13)	C(2)—C(7)	1.378(12)
C(3)—C(4)	1.386(13)	C(4)—C(5)	1.381(14)
C(5)—C(6)	1.368(15)	C(6)—C(7)	1.408(12)
C(7)—N(8)	1.377(13)	N(8)—C(9)	1.344(11)
C(9)—C(10)	1.506(13)	C(10)—O(11)	1.430(10)
C(10)—C(12)	1.500(13)	N(18)—C(19)	1.404(10)
N(18)—C(26)	1.338(9)	C(19)—C(20)	1.382(12)
C(19)—C(24)	1.394(10)	C(20)—C(21)	1.356(12)
C(21)—C(22)	1.393(13)	C(22)—C(23)	1.403(14)
C(23)—C(24)	1.390(11)	C(24)—N(25)	1.390(10)
N(25)—C(26)	1.326(9)	C(26)—C(27)	1.493(11)
C(27)—O(28)	1.396(8)	C(27)—C(29)	1.536(14)
(b) Bond angles			
N(1)—Cu(1)—O(11)	74.1(3)	N(1)—Cu(1)—N(18)	105.3(3)
O(11)—Cu(1)—N(18)	95.9(3)	N(1)—Cu(1)—O(28)	170.2(2)
O(11)—Cu(1)—O(28)	99.5(3)	N(18)—Cu(1)—N(18)	82.6(3)
O(28)—Cu(1)—O(28a)	77.3(3)	Cu(1)—O(28)—Cu(1a)	102.3(4)
Cu(1)—N(1)—C(2)	130.1(5)	Cu(1)—N(1)—C(9)	122.9(6)
C(2)—N(1)—C(9)	105.3(7)	N(1)—C(2)—C(3)	130.0(8)
N(1)—C(2)—C(7)	108.3(8)	C(3)—C(2)—C(7)	121.6(8)
C(2)—C(3)—C(4)	118.2(9)	C(3)—C(4)—C(5)	119.3(9)
C(4)—C(5)—C(6)	123.9(9)	C(5)—C(6)—C(7)	116.1(9)
C(2)—C(7)—C(6)	120.8(10)	C(2)—C(7)—N(8)	106.5(7)
C(6)—C(7)—N(8)	132.6(7)	C(7)—N(8)—C(9)	107.1(8)
N(1)—C(9)—N(8)	112.8(8)	N(1)—C(9)—C(10)	124.0(7)
N(8)—C(9)—C(10)	123.2(8)	C(9)—C(10)—O(11)	107.2(7)
C(9)—C(10)—C(12)	113.2(7)	C(12)—C(10)—O(11)	110.7(6)
Cu(1)—O(11)—C(10)	111.2(5)	Cu(1)—N(18)—C(19)	141.8(4)
Cu(1)—N(18)—C(26)	112.0(5)	C(19)—N(18)—C(26)	105.9(6)
N(18)—C(19)—C(20)	131.5(6)	N(18)—C(19)—C(24)	107.5(7)
C(20)—C(19)—C(24)	121.0(7)	C(19)—C(20)—C(21)	117.0(8)
C(20)—C(21)—C(22)	122.7(9)	C(21)—C(22)—C(23)	121.5(8)
C(22)—C(23)—C(24)	114.9(8)	C(19)—C(24)—C(23)	122.8(8)
C(19)—C(24)—N(25)	106.7(7)	C(23)—C(24)—N(25)	130.4(6)
C(24)—N(25)—C(26)	107.4(6)	N(18)—C(26)—N(25)	112.5(7)
N(18)—C(26)—C(27)	119.5(6)	N(25)—C(26)—C(27)	127.9(7)
C(26)—C(27)—O(28)	106.8(6)	C(26)—C(27)—C(29)	112.6(6)
C(29)—C(27)—O(28)	111.4(7)	Cu(1)—O(28)—C(27)	117.8(5)

[a] Atoms Cu(1a) and O(28a) are related to the parent atoms by the symmetry operation $2-x, -y, 1-x$.

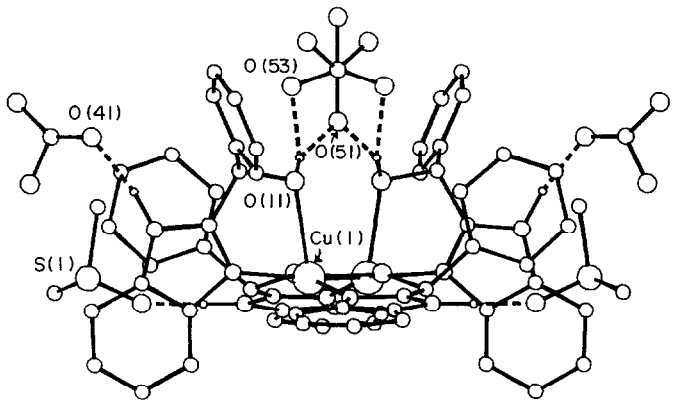

Fig. 3. A view of the dimer $[Cu_2(HL)_2(L)_2(NO_3)_2]\cdot 4Me_2SO$ perpendicular to the two-fold axis.

distorted square pyramidal geometry. The two axial CuO bonds lie on the same side of the dimer plane and the dimer has C_2 symmetry. One of the nitrate groups lies on the dimer (and crystallographic) two-fold axis and hydrogen bonds to the coordinating hydroxy groups' hydrogens, but in a disordered manner so that in half of the molecules the two OH hydrogens are bridged by one nitrate oxygen and in the other half by two nitrate oxygens. This is shown in Fig. 2. An analogous situation occurred with the perchlorate,[5] and it is quite possible that this is a structure-determining feature. The second nitrate is also disordered and is sited close to a further two-fold axis in the lattice. Oxygen atoms of this nitrate seem to be involved in H-bonding to the hydrogen of the amino nitrogen of the chelate/bridging ligand. Dimethyl sulphoxide molecules of solvation are also present in the lattice, but do not seem to be involved in any significant interactions. The mechanism of the rapid conversion of $Cu(HL)_2(NO_3)_2$ into $[Cu_2(HL)_2(L)_2(NO_3)_2]$ in solution is intriguing and a knowledge of the structure of $Cu(HL)_2(NO_3)_2$ would certainly help in elucidation of this mechanism. Unfortunately, apart from probably being monomeric, little else can be deduced about the structure of $Cu(HL)_2(NO_3)_2$ and attempts to grow crystals suitable for an X-ray study have not been successful.

The magnetic moments of $Cu(HL)_2X_2(EtOH)_2$ and $Cu(HL)_2X_2$ (where X is Cl^- or Br^-) show them to be magnetically dilute, and a reasonable structure to propose is one which is similar to that shown in Fig. 1 but with SCN^- replaced by Cl^- or Br^- and acetone replaced by ethanol. The molar conductance of these complexes is consistent with the coordinated halide ion (Table 3). However, a puzzling feature of the ethanolates is the spectral and magnetic changes on desolvation (Table 2). The spectral change is most readily observed since the solvates are bright green whereas the desolvated complexes are very much darker green. It is not possible to decide from the IR spectra where the ethanol is coordinated or hydrogen bonded.

The electronic spectrum, magnetic moment (Table 2) and ESR spectrum all indicate that the copper in $Cu(HL)_2I_2$ is present as copper(I). The molar conductance in nitrobenzene gives a value typical for uni–univalent electrolytes (Table 3). These observations can be rationalized on the basis of the formula $[Cu(C_{14}H_{11}N_2OI)(HL)]I$, in which one of the ligands has been iodinated. It is known, for example, that iodination of 2,4,5-trimethylimidazole gives 1-iodo-2,4,5-trimethylimidazole.[6,7]

REFERENCES

1. D. G. O'Sullivan and P. W. Sadler, *Nature* 1961, **192**, 341.
2. M. Goodgame and B. Piggott, *J. Chem. Soc. A* 1971, 826.
3. M. A. Phillips, *J. Chem. Soc.* 1928, 2395.
4. R. A. Jones, M. B. Hursthouse, K. M. A. Malik and G. Wilkinson, *J. Am. Chem. Soc.* 1979, **101**, 4128.
5. B. Piggott, M. B. Hursthouse, P. Thornton and N. P. C. Walker, *Polyhedron* 1988, **7**, 323.
6. K. Hofmann, *The Chemistry of Heterocyclic Compounds; Imidazole and Derivatives*, Pt 1, p. 122. Interscience, New York (1953).
7. H. Pauly, *Ber.* 1910, **41**, 2243.

Polyhedron Vol. 8, No. 6, pp. 775–792, 1989
Printed in Great Britain

0277–5387/89 $3.00+.00
© 1989 Pergamon Press plc

SOLVOLYSES OF THIOCYANATES BY TRIFLUOROETHANOIC ACID

R. D. GILLARD,* NORDIN GARIF† and JULIO PEDROSA DE JESUS‡

Department of Chemistry, University College, P.O. Box 78, Cardiff CF1 1XL

(*Received* 19 *July* 1988; *accepted* 11 *October* 1988)

Abstract—The solvolyses by trifluoroethanoic ("trifluoroacetic" TFA) acid of several known and new thiocyanates have been studied using proton magnetic resonance. For the organic linkage isomers of RNCS (R = alkyl groups) isothiocyanates react (via N-alkyl monothiocarbamato trifluoroethanoates) to form alkylamines RNH_2, whereas the thiocyanates RSCN yield thiols, RSH and ammonia. The coordinated thiocyanates include isomers (some new) of dithiocyanatobisdiaminoethanerhodium(III) salts, characterized spectroscopically and through their reactions (additions of mercury(II) ions, reductions of iodate(V), isomerizations). Both linkage isomeric forms of coordinated thiocyanate with TFA formed ammonia (showing a sharp triplet at $\delta = 6.6$ ppm).

The thiocyanate group can bond to metal ions to form mononuclear complexes either through its nitrogen atom or through its sulphur atom. We synthesized[1] a series of complexes; *cis*- and *trans*-$[Rh(en)_2(NCS)_2]X$ (we have italicized the atom actually attached to the metal ion), where X is an anion which may be SCN^-.

Many methods comment upon the linkage isomers of thiocyanates. The application of NMR spectroscopy as a tool to elucidate the bonding mode of the thiocyanate ligand has gained widespread popularity. These experiments have utilized direct measurement for ^{13}C,[2] ^{14}N[3] and ^{15}N[4] of the ligand and the indirect measurement for ^1H,[5,6] ^1H with lanthanide induced shift,[7] $^1H\{^{195}Pt\}$ INDOR,[8] ^{31}P[9–13] and ^{195}Pt.[4] Following our success[14] (using a medium which slowed exchange) in analysing ^{14}N: ^{15}N ratios in ^{15}N-labelled ammine complexes $[Co(NH_3)_5X]Y_2$ by proton magnetic resonance, we sought a similar simple distinction (using proton resonance) between M—*N*CS and M—*S*CN moieties, where M represents a metal ion in a kinetically inert oxidation state.

We anticipated that the products of reaction (1)

$$R—NCS + HOOC\cdot CF_3 \rightleftharpoons R—NCSH^+ + \bar{O}OC\cdot CF_3 \quad (1)$$

should show no coupling to the ^{14}N of the proton of the coordinated isothiocyanic acid, whereas, in the products of reaction (2), such coupling

$$R—SCN + HOOC\cdot CF_3 \rightleftharpoons RSCNH^+ + \bar{O}OC\cdot CF_3 \quad (2)$$

in coordinated thiocyanic acid (kinetics permitting) should give a triplet ^1H signal. Solid complexes containing coordinated nitrous acid have been isolated,[15] such as $[Co(en)_2(ONOH)X]^{n+}$, and similarly, there is excellent evidence[16,17] for the persistence in solution during lengthy periods of coordinated thiocyanic acid, in protonated adducts of $[M(NH_3)_5(SCN)]^{2+}$ (M = Co, Rh), or $[Co(en)_2(SCN)_2]^+$. (The solid acid adducts of $[M(NCS)_6]^{3-}$ salts, e.g. $(NH_4)_3[(Mo(NCS)_6]CH_3CO_2H$[18] and $[Cr(NCS)_6]^{3-}$[19] are of a different type.)

We report here our findings on the compounds with R = alkyl and various kinetically inert inorganic moieties, like $[M(NH_3)_5]^{3+}$ (M = Co, Rh).

RESULTS AND DISCUSSION

Thiocyanate ions in TFA

Sodium and potassium thiocyanates dissolve readily in neat trifluoroacetic acid (TFA hereafter).

* Author to whom correspondence should be addressed.
† Present address: Universiti Teknologi Malaysia, Skudai 80990, Johor, Malaysia.
‡ Present address: University of Aveiro, 3800 Aveiro, Portugal.

The solution turns yellow and occasionally bubbles as the salt starts to dissolve. The ^1H NMR of the resulting solution shows a sharp triplet centred at $\delta = 6.67$ ppm [Fig. 1(a)]. The ^1H NMR spectrum of ammonium thiocyanate after dissolution in TFA also shows only this triplet, the signal[14] of the proton in quaternary ammonium ions. The identical ^1H NMR spectrum of NH_4Cl in TFA proves this finding [Fig. 1(b)]. Ogg and Ray reported[20] that anhydrous liquid ammonia furnished a triplet signal with $J_{^{14}NH} = 46$ Hz compared to $J_{^{14}NH} = 53$ Hz for NH_4^+ ions in TFA found in the present work.

The ^1H NMR spectrum of a proton attached to a nitrogen atom is always very broad and sometimes unobservable, for two reasons, intermolecular proton exchanges and quadrupolar relaxation. As in anhydrous ammonia,[20] the quadrupolar mechanism is dominant[21] in the acidic solution of NH_4^+ ions. The linewidth of NH_4^+ in TFA decreases with increasing temperature and *vice versa* [Fig. 1(c)], as expected for any quadrupolar mechanism. The behaviour is opposite to that expected for chemical exchange.[22]

The study of such reactions between thiocyanate ions and mineral acid was a matter of interest some years ago. The initial step is protonation, which, theoretically, can occur at the sulphur atom to produce thiocyanic acid H—*S*—C≡N, or at the nitrogen atom to produce isothiocyanic acid H—*N*=C=S, which predominates over its isomer in the vapour state,[23] or in solution.[24,25,*] ^1H NMR spectra of isothiocyanic acid in CCl_4 have been reported[26] (δ 4.95 ppm): cf. isocyanic acid H*N*CO (3.35, $J_{^{14}NH} = 64$ Hz) and hydrazoic acid HN_3 (4.10). Isothiocyanic acid H*N*CS is unstable[27] in *mineral* acid. The overall hydrolysis may be presented as in eq. (3); ammonium ions are a final product.

$$H^+ + HNCS + 2H_2O \longrightarrow H_2S + CO_2 + NH_4^+. \quad (3)$$

Thiocyanate salts in conc. H_2SO_4 (98%) (in the present work) show a sharp triplet centred at δ 5.45 ppm in comparison to the proton signals of NH_4^+ in TFA at δ 6.67 ppm.

A number of intermediates are involved in the hydrolysis. One is carbonyl sulphide OCS, which is reasonably stable in acid but slowly hydrolyses[27] to CO_2 and H_2S. Another (postulated by Klason[28]) is thiocarbamic acid $HSCONH_2$ [eq. (4)]:

$$NCS^- + H^+ + H_2O \longrightarrow H—S—\overset{\overset{O}{\|}}{C}—NH_2. \quad (4)$$

* The salt $[Ph_4As]H(NCS)_2$ was isolated by M. F. A. Dove from solutions of sulphur dioxide (see M. F. A. Dove, *Chem. Comm.* 1965, 23).

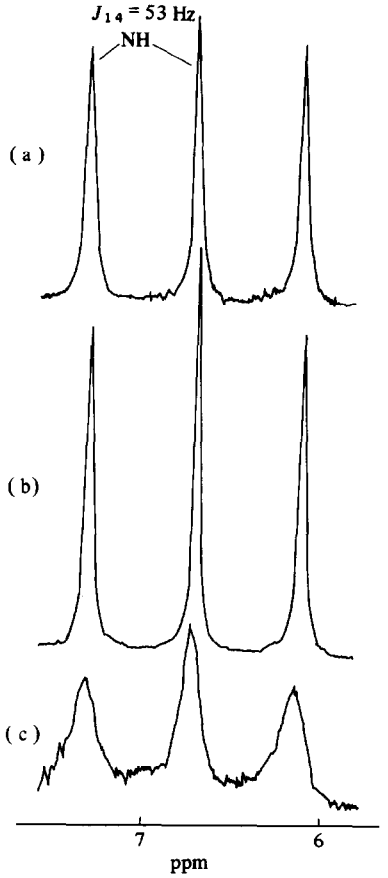

Fig. 1. Proton resonance spectra in TFA of (a) KSCN at 35°C; (b) NH_4Cl at 35°C; (c) KSCN at −5°C.

The free acid is unknown, but the ammonium salt decomposes[29] in acidic solution to produce CO_2 and H_2S via OCS. Stedman and his students have made detailed kinetic and spectroscopic studies[30,31] of the reaction of thiocyanate ions in various concentrations of H_2SO_4.

Drawing the analogy to such hydrolysis of thiocyanate ions in mineral acid solution, its solvolysis in TFA [pK_a (25°C) 0.25] is initiated by protonation to form isothiocyanic acid. The intermediate is probably monothiocarbamatotrifluoroacetate formed as in eq. (5)

$$SCN^- + HOOCCF_3 \rightleftharpoons SCNH \overset{H^+}{\rightleftharpoons} H_2N—\overset{\overset{S}{\|}}{C}—OOC \cdot CF_3. \quad (5)$$

However, reaction of SCN^- in TFA followed by ^1H NMR spectroscopy, failed to detect the proton signal of this thiocarbamato compound; only the triplet signal of NH_4^+ was obtained. This rapid solvolysis of thiocyanic acid has been briefly mentioned.[26] The isothiocyanic acid formed, polymerized and eventually produced the yellow iso-

perthiocyanic acid, as in eq. (6).

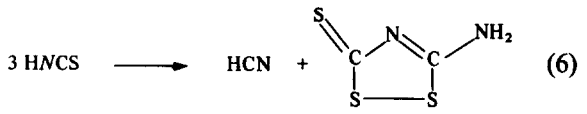

(6)

Organic isothiocyanates in TFA

The isothiocyanates R*N*CS (R = CH_3, C_2H_5, $C_6H_5CH_2$) were studied by ^1H NMR using TFA as the solvent. In a typical example, methyl isothiocyanate, H_3CNCS, the simplest, was dissolved in TFA. The solution immediately turned yellow. The course of the reaction was followed against time by means of ^1H NMR spectroscopy. Some of the spectra and δ values are given in Figs 2(a)–(g) and Table 1.

Table 1. ^1H NMR results for the reaction of CH_3NCS with TFA at 35°C (and see Fig. 2)

Time (min)	Multiplicity	δ (ppm),	J (Hz)
0[a]	Singlet	3.24	—
2	Singlet	3.24	—
	Doublet	3.09	$J_{HH} \sim 5$
47	Singlet	3.24	
	Doublet	3.09	$J_{HH} \sim 5$
	Quartet	2.60[b]	$J_{HH} \sim 5$
292	Broad triplet	6.75	$J_{^{14}NH} \sim 53$
	Broad triplet	6.75	$J_{^{14}NH} \sim 53$
	Quartet	2.93[b]	$J_{HH} \sim 5$

[a] Measured in CCl_4.
[b] Measured at the centre of the quartet.

At the beginning, a doublet centred at δ 3.09 ppm emerged slowly, in addition to the singlet at δ 3.24 ppm from the parent methyl isothiocyanate. We interpret this doublet ($J_{HH} \sim 5$ Hz) as the signal of the methyl group split by a proton attached to the nitrogen atom of the N-methylmonothiocarbamatotrifluoroacetate, $CH_3NH—CS—OOCCF_3$, the suggested intermediate. This decomposes to

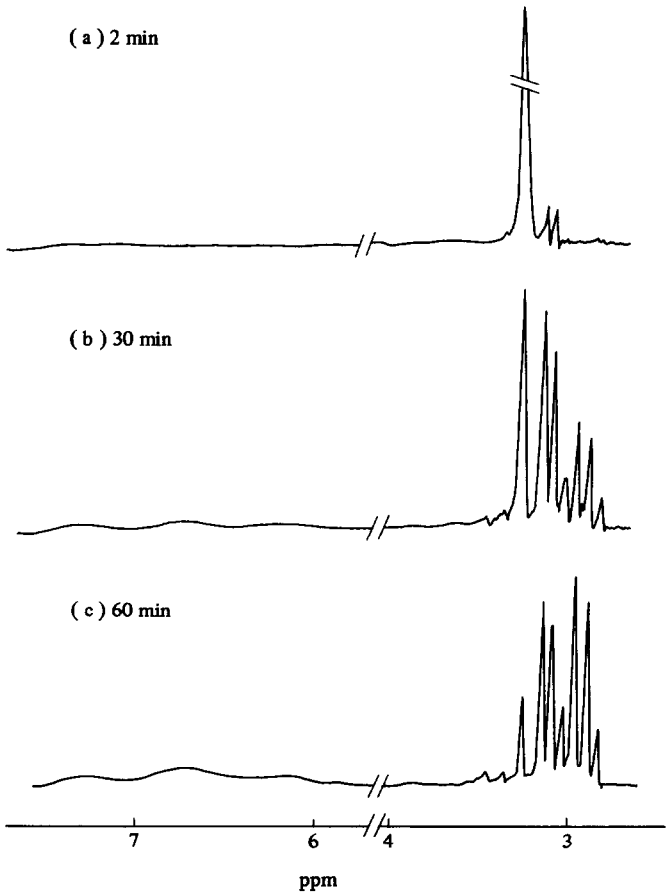

contd overleaf

Fig. 2. Proton magnetic resonance of methyl isothiocyanate $H_3C \cdot NCS$ dissolved in TFA after increasing times (min) of reaction: (a) 2; (b) 30; (c) 60; (d) 90; (e) 150; (f) 210; (g) 1440 (1 day)—"infinity"; (h) for comparison, $H_3C \cdot NH_2$ (in ethanol) dissolved in TFA, was used.

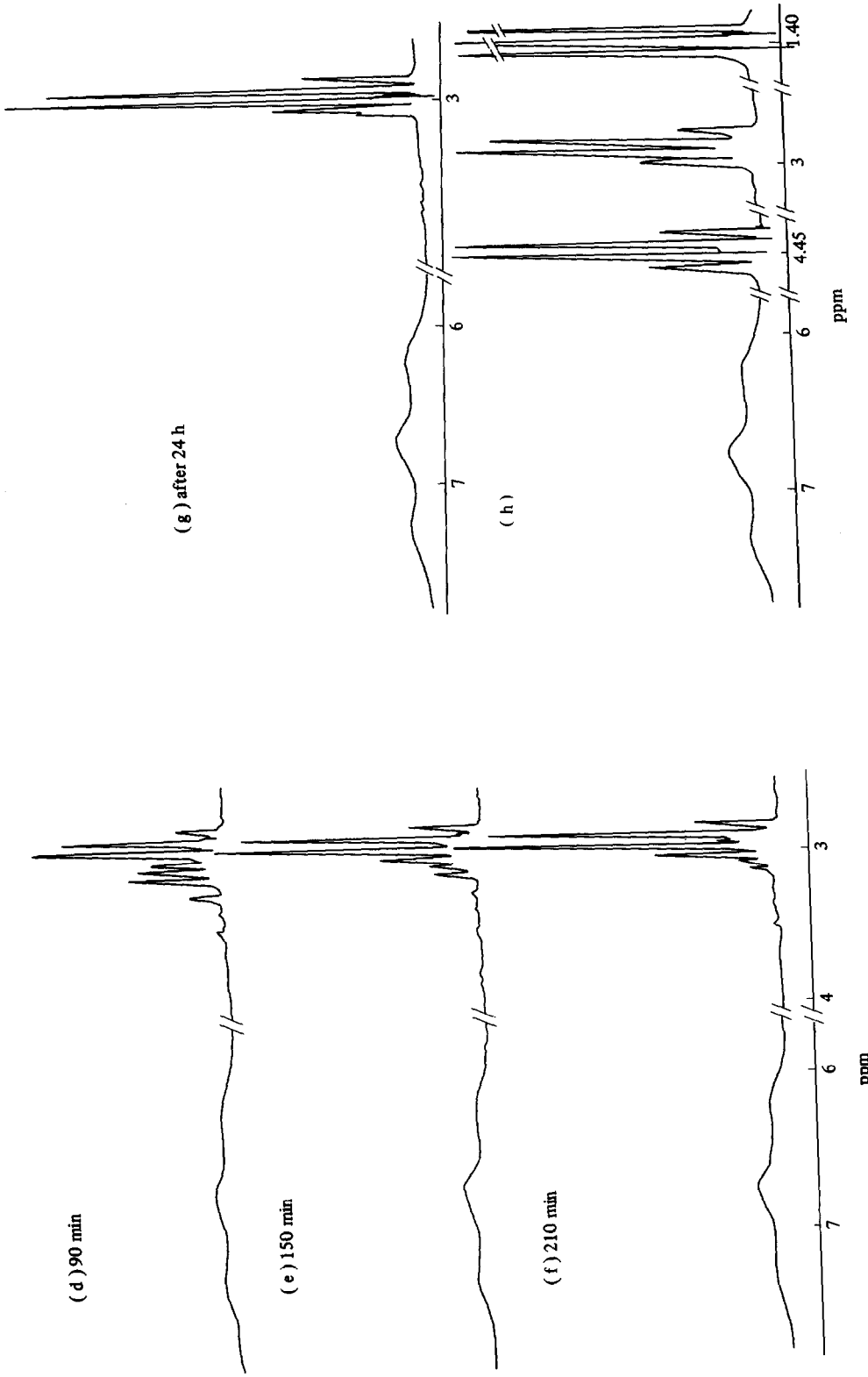

Fig. 2 (*continued*).

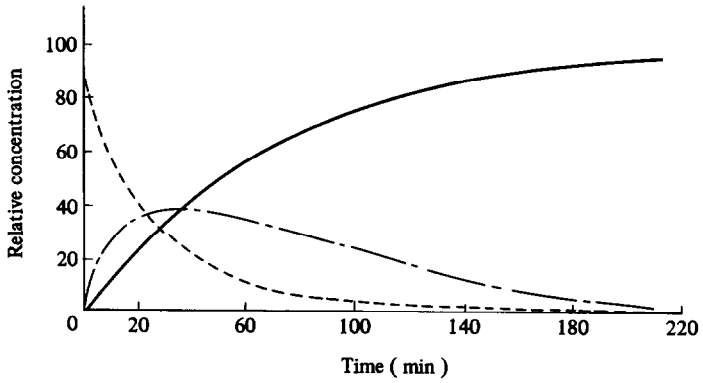

Fig. 3. Relative concentrations of various species in the reaction of $H_3C \cdot NCS$ with TFA: (———) $(H_3C \cdot NH_3)^+(F_3C \cdot COO)^-$; (— · — · —) $H_3CNHC(S)OCOCF_3$; (— — — —) $H_3C \cdot NCS$.

products. One has a quartet (1 : 3 : 3 : 1) centred at δ 2.90 ppm and a broad triplet centred at δ 6.75 ppm. This set is the ^1H NMR spectrum of the methylammonium ion, confirmed by comparison with the signal of the authentic methylamine (in alcohol) dissolved in TFA [see Figs 2(g,h)]. Under our experimental conditions (the concentration of H_3CNCS in TFA is 0.739 M at 35°C), the reaction goes to completion. The relative concentrations (reminiscent of a consecutive reaction) of various species during the course of the reaction were calculated from the proton integration and are plotted in Fig. 3.

The reaction of ethyl isothiocyanate CH_3CH_2NCS was also followed by ^1H NMR spectroscopy: examples of the spectra are shown in Figs 4(a)–(e). The intermediate (with a slightly more complicated splitting pattern) is believed to be

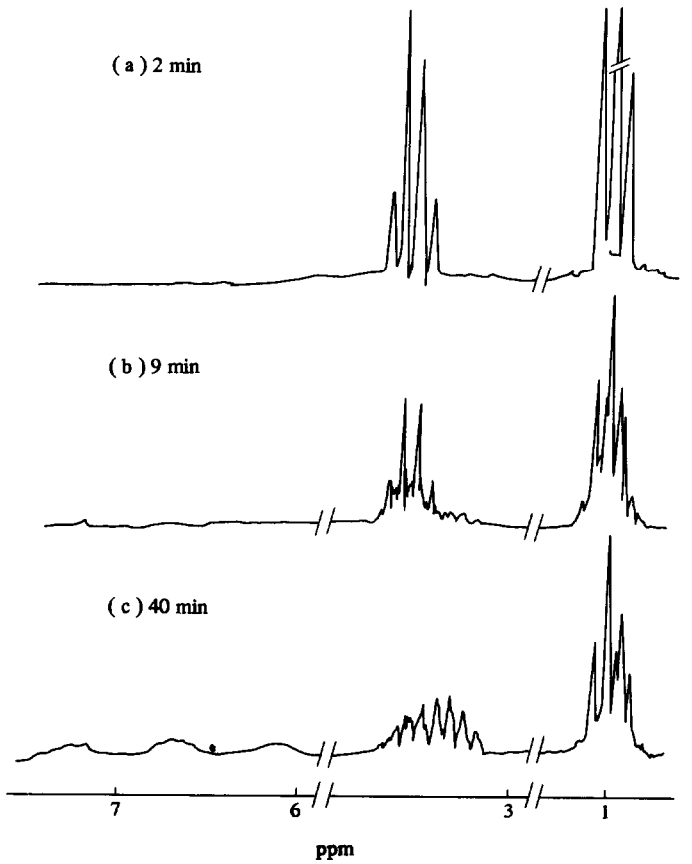

contd overleaf

Fig. 4. Proton resonance spectra of ethyl isothiocyanate, C_2H_5NCS, in TFA, after varying times of reaction (min): (a) 2; (b) 9; (c) 40; (d) 80; (e) 1440 (1 day)—"infinity"; (f) for comparison, aqueous ethylamine in TFA was used.

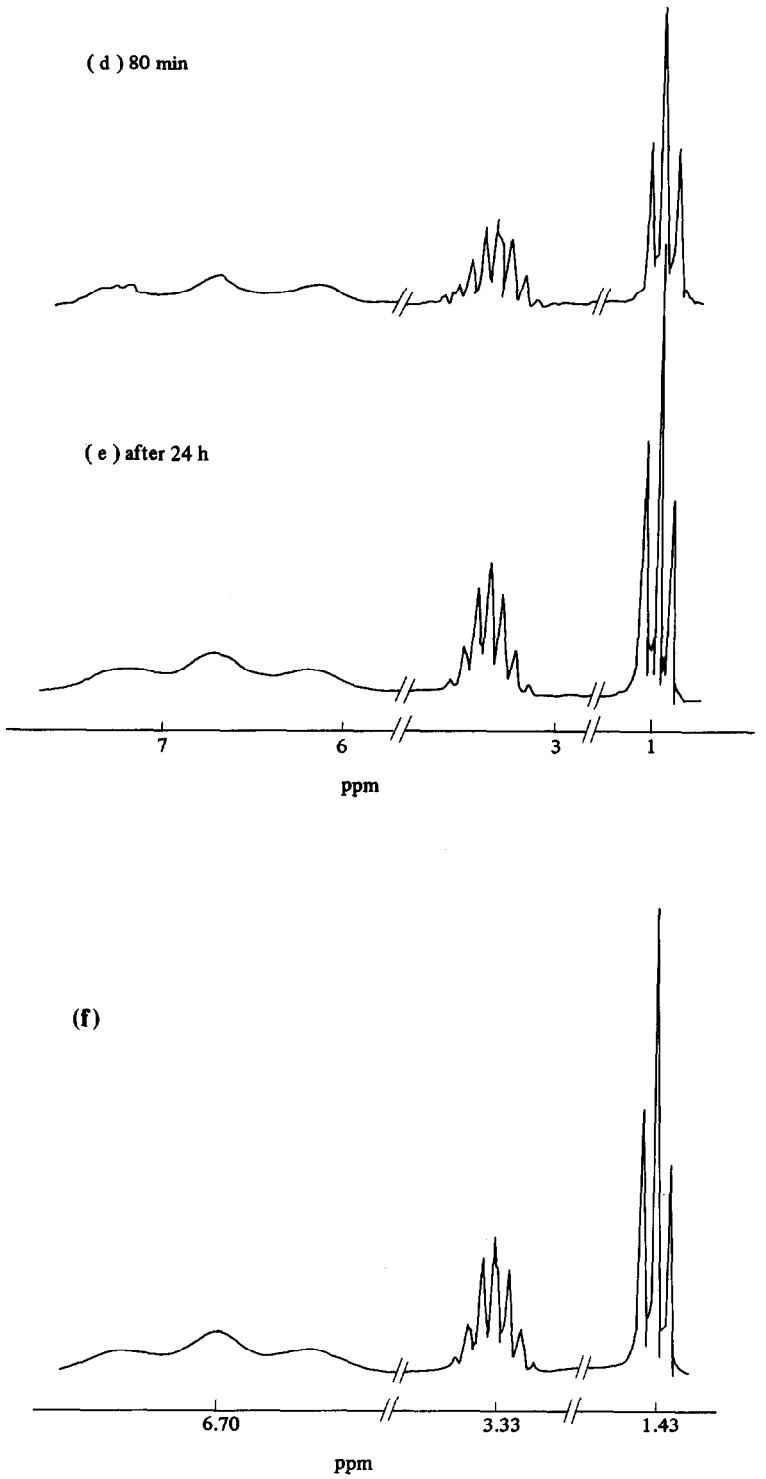

Fig. 4 (*continued*).

N-ethylmonothiocarbamatotrifluoroacetate. The intermediates then decomposed to the ethylammonium ion as one of the products [see Fig. 4(e)], again confirmed by comparing with authentic ethylamine in TFA [Fig. 4(f)].

Mechanism of the reactions between organic isothiocyanate and TFA. The rate and mechanism of hydrolysis of isothiocyanic acid by mineral acids has received adequate attention.[30,31] In contrast, the kinetics and mechanism of the hydrolysis of the

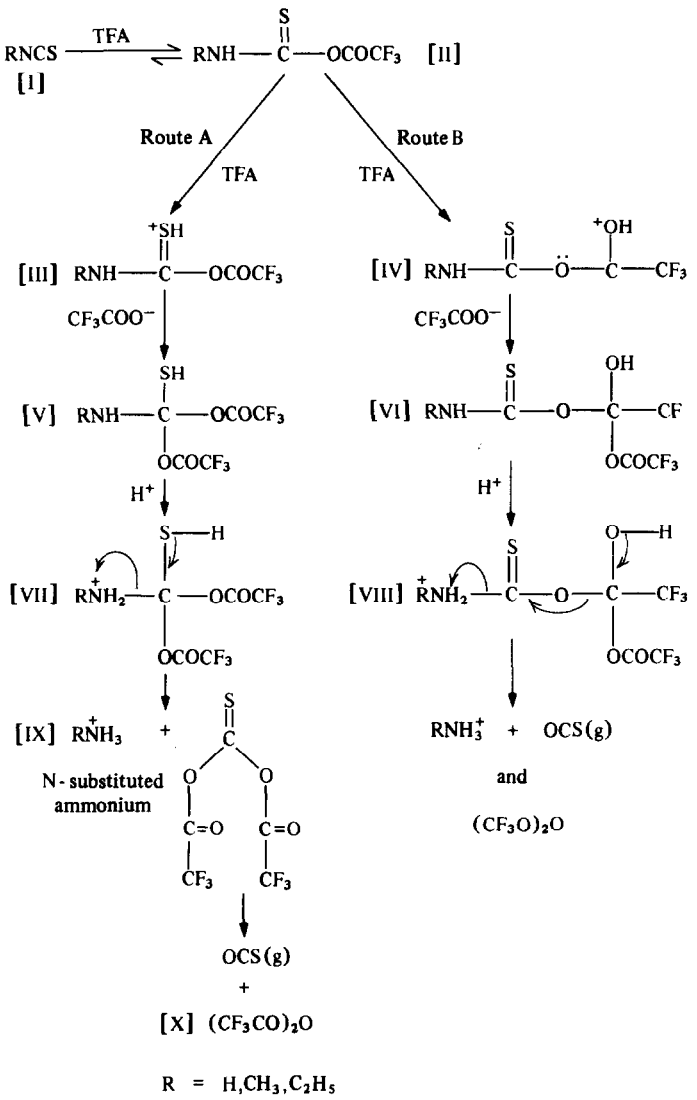

Scheme 1. Mechanisms for solvolysis of thiocyanates.

organic isothiocyanate derivatives has been little studied. However, simple organic isothiocyanates should[32] resemble isothiocyanic acid with respect to ready hydrolysis, giving an amine and carbonyl sulphide, which is in turn hydrolysed to CO_2 and H_2S. Mechanisms for solvolysis of organic isothiocyanates with TFA are shown in Scheme 1. From ^{1}H NMR spectra, the N-substituted monothiocarbamatotrifluoroacetate (**II**) is the common intermediate. This finding also indirectly confirms the proposed mechanism of solvolysis of isothiocyanic acid by TFA.

Subsequent decomposition (Scheme 1) of the intermediate is initiated either by further addition of TFA to C=S (route A) or to C=O (route B). The choice depends on (a) relative basicities, and (b) relative electrophilicities of the protonated form of intermediates (**III**) and (**IV**). Decomposition via either route A or B, will produce N-substituted ammonium ions (**IX**), carbonyl sulphide (OCS) and trifluoroacetic anhydride (**X**). The broad triplet signal of N-substituted ammonium ions is due to its lower symmetry compared to tetrahedral NH_4^+. The decomposition of simpler N-substituted monothiocarbamate formed from the reaction of RNCS with OH^- had been proposed[33] as in Scheme 2. So, it is possible that **V** of route A decomposes without further protonation on the nitrogen atom, as shown in Scheme 3.

Reaction of organic thiocyanate (RSCN) *with* TFA. Solutions of organic thiocyanates (RSCN) (R = CH_3, C_2H_5, ϕCH_2) do not exhibit a ^{1}H NMR signal other than that from the parent. Never-

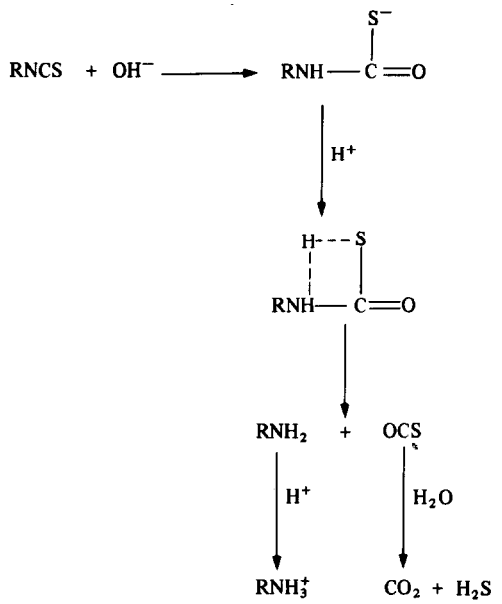

Scheme 2. Possible intermediates of base hydrolysis.

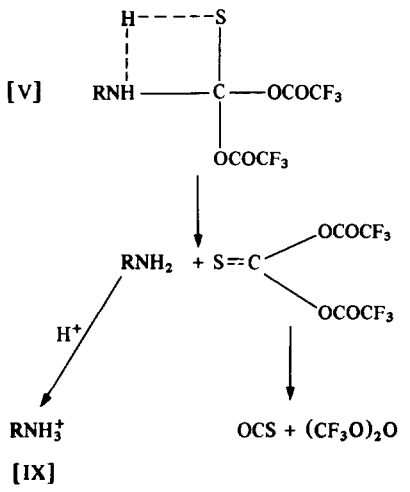

Scheme 3. Possible alternative decomposition of intermediate (V) of Scheme 1.

theless, the protonation shown in eq. (2) probably occurs, but the NMR signal of the proton attached to the quadrupolar nitrogen atom is too broad to be observed.

Organic thiocyanates are hydrolysed by *mineral* acid, to give a thiol RSH, CO_2 and NH_3 as shown in reactions (7)–(10). The initial step (7) is the protonation of the thiocyanate group.

$$R—S—C\equiv N \overset{H^+}{\rightleftharpoons} R—S—C\equiv\overset{+}{N}H \qquad (7)$$

$$R—S—C\equiv\overset{+}{N}H + 2H_2O \longrightarrow RS—C(OH)NH + H_3O^+ \qquad (8)$$

$$RSC(OH)=NH \longrightarrow RSC(O)NH_2 \longrightarrow RSH + CO_2 + NH_3 \qquad (9)$$

$$NH_3 + H^+ \longrightarrow NH_4^+. \qquad (10)$$

A typical example of the reaction of ethyl thiocyanate with conc. H_2SO_4 is shown in Fig. 5. The sharp triplet is obviously due to the ammonium ion. The broad singlet at δ 7.9 ppm is most probably due to the proton attached to the nitrogen atom of the $RSC(O)NH_2$ molecule. The signals centred at δ 1.0 and 2.8 ppm are due to the ethyl group of the thiol compound.

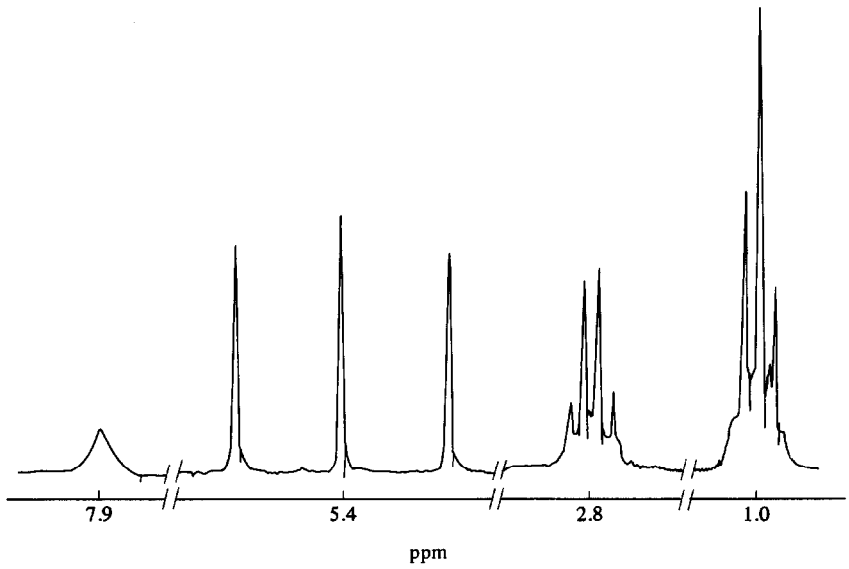

Fig. 5. Proton magnetic resonance spectrum of ethyl thiocyanate in 98% H_2SO_4.

Metal–thiocyanate complexes in TFA

To distinguish between reactivities of coordinated isothiocyanic acid and thiocyanic acid, a range of metal complexes containing linkage isomeric thiocyanates was needed. We used some well-known examples {such as[34] $[Pd(bipy)(NCS)_2]$ and $[Pd(bipy)(SCN)_2]$} and have also made[1] a number of isomers of $[Rh(en)_2(SCN)_2]^+$. We comment briefly on these compounds. Analytical results are given in Table 2 and some spectroscopic properties in Table 3 (supporting assignment of linkage isomers[39,40]) and Table 4 (confirming assignment of geometric isomerism, from the—chiefly hydrogenic—modes of the chelating ligands, at frequencies greater than 1000 cm^{-1}). A feature, which we re-

Table 2. Conductometric and analytical results for isomeric thiocyanato complexes of rhodium(III), $[Rh(en)_2(NCS)_2]X$

Compound	Λ_{H_2O}[a]	C		H		N		Ionic NCS^-	
		Calc.	Found	Calc.	Found	Calc.	Found	Calc.	Found[b]
cis-$[Rh(en)_2(NCS)_2]Cl \cdot H_2O$	129	18.3	18.4	4.6	4.3	21.4	21.9	—	—
cis-$[Rh(en)_2(NCS)_2](NCS) \cdot H_2O$		20.2	20.6	4.3	4.2	23.6	23.2	14.0	13.9
cis-$[Rh(en)_2(NCS)(SCN)](NCS) \cdot H_2O$	126	20.2	19.4	4.3	4.5	23.6	23.2	14.0	13.4
trans-$[Rh(en)_2(NCS)_2](NCS) \cdot H_2O$		20.2	20.7	4.3	4.3	23.6	23.1		
trans-$[Rh(en)_2(NCS)(SCN)](NCS) \cdot H_2O$	144	20.2	19.4	4.3	4.3	23.6	23.2		
trans-$[Rh(en)_2(SCN)_2](NCS) \cdot H_2O$		20.2	19.7	4.3	4.2	23.6	23.2		

[a] Molar conductivities (Ω^{-1} cm^2 mol^{-1}) for *ca* 10^{-3} M solutions at 293 K; *trans*-$[Rh(en)_2Cl_2]Cl$ gave $\Lambda = 116\ \Omega^{-1}\ cm^2\ mol^{-1}$.

[b] By Volhard titration.

Table 3. IR absorption bands associated with the thiocyanate ligand in complexes of rhodium(III) (cm^{-1})

Compound	ν_{CN}	ν_{CS}	δ_{NCS}	Reference
$[Rh(NH_3)_5(NCS)](ClO_4)_2$	2145(s,b)	815(s)		[a]
trans-$[Rh(en)_2(NCS)Cl](ClO_4)$		835		[b]
cis-$[Rh(cyclam)(NCS)_2](ClO_4)$	2100	835		[c]
	2080	820		
cis-$[Rh(en)_2(NCS)_2]Cl$	2125(sh)	820(w)	—	[d]
cis-$[Rh(en)_2(NCS)_2](NCS)$	2125(s)	820(w)	485(w)	[d]
trans-$[Rh(en)_2(NCS)_2](NCS)$	2110(vb,s)	835(m)	470(m)	[d]
	2045(vb,s)	710(w)	430(w)	
cis-$[Rh(en)_2(NCS)(SCN)]Cl$	2120(s)	830(vw)	450(m)	[d]
		735(vw)	430(sh)	
		700(vw)		
cis-$[Rh(en)_2(NCS)(SCN)](NCS)$	2140	835(w)	470(sh)	[d]
	2120(sh)	750(w)	460(m)	
	2060(s)	730(w)		
trans-$[Rh(en)_2(NCS)(SCN)](NCS)$	2140(s)	835(w)	470(m)	[d]
	2060(s)	735(m)	455(m)	
		710(w,b)	450(sh)	
			420(vw)	
			400(vw)	
trans-$[Rh(cyclam)(SCN)_2](ClO_4)$	2090	830		[c]
$[Rh(NH_3)_5(SCN)](ClO_4)_2$	2115(s,sp)	730(w,b)		[a]

[a] Reference 38.

[b] Reference 36.

[c] Reference 37.

[d] This work; the range of such frequencies is well known, but may be exemplified by isomers of $[Os(NCS)_6]^{3-}$ studied by W. Preetz and G. Peters, *Z. Naturforsch.* 1979, **34b**, 1243.

Table 4. IR absorption bands for isomers of $[Rh(en)_2(NCS)_2](NCS)$

Isomer	X	Y	Z	ν_{NH_2}	ν_{CH_2}	$\delta_{d(NH_2)}$	$\nu_{bend(NH_2)}$	$\delta_{s(NH_2)}$	$\nu_{wag(CH_2)}$	$\nu_{twist(CH_2)}$	ν_{C-N}	Others
cis-	*N*CS	*S*CN	NCS	3280(s) 3220(s) 3120(s)	2980(s) 2940(m) 2880(m)	1580(s) 1560(sh) 1545(sh)	1460(sh) 1450(m) 1440(sh)	1390(m) 1365(m,sp) 1360(sh)	1315(m) 1285(m,s) 1270(sh)	1145(sh) 1130(s) 1120(s)	1055(s)	1220(m)
trans-	*N*CS	*S*CN	NCS	3290(s) 3210(s) 3120(s)	2990(sh) 2945(s,sp) 2925(s,sp) 2855(s,sp) 2780(w)	1580(s) 1560(sh)	1450(m)	1395(m) 1385(w) 1380(m) 1360(m)	1315(m) 1290(m,sp) 1270(w)	1130(s) 1110(sh)	1060(s,sp)	1215(m)
trans-	*S*CN	*S*CN	NCS	3260(sh) 3220(s,b) 3120(s,b)	2980(m) 2970(m) 2950(m) 2880(w) 2800(w)	1605(m) 1585(s,b)	1445(m)	1400(m) 1385(m) 1362(m) 1367(m)	1320(sh) 1315(m-w) 1285(m,sp) 1280(sp)	1145(sh) 1130(s) 1115(sh)	1055(s,sp)	1210(m)
cis-	*N*CS	*N*CS	NCS	3200(s,b) 3100(s,b)	2960(m) 2900(sh)	1580(sh) 1570(s,b) 1560(sh)	1450(m)	1400(m) 1370(m)	1320(m) 1300(m)	1160(sh) 1150(s) 1120(m) 1110(sh)	1055(s)	1220(m) 1210(m)
trans-	*N*CS	*N*CS	NCS	3140(s,b)	2980 2950 2890(sh) 2790(sh)	1570(s,b)	1445(s) 1360(m)	1390(m) 1285(s,sh) 1280(sh)	1320(m)	1125(s,b)	1050(s)	1210(s)

KBr pellets. (s) = strong; (m) = medium; (w) = weak; (sp) = sharp; (b) = broad; (sh) = shoulder.

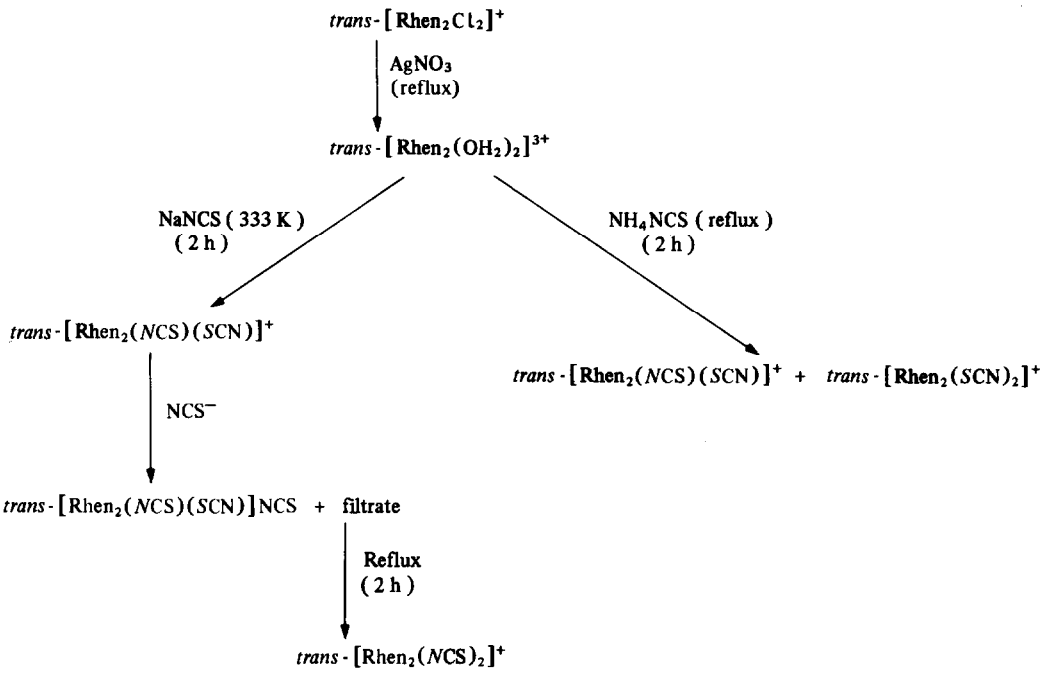

Scheme 4. Formation of linkage isomers of *trans*-$[Rh(en)_2(NCS)_2]^+$.

mark on separately,[35] is the Christiansen filter effect commonly found in these (and other) thiocyanato complexes. Because of this, care is needed to establish numbers and positions of vibrational bands in the ν_{CN} region.

Johnson and Basolo showed[36] that the reaction of *trans*-$[Rh(en)_2Cl_2](NO_3)$ with NaNCS gives *trans*-$[Rh(en)_2Cl(NCS)]^+$ and no disubstituted product. We therefore started here with silver-promoted aquation to *trans*-$[Rh(en)_2(OH_2)_2]^{3+}$: this, with an excess of NaNCS at 333 K, gives mainly *trans*-$[Rh(en)_2(NCS)(SCN)]^+$ (isolated as its thiocyanate). Further reaction of the mother liquor gives *trans*-$[Rh(en)_2(NCS)_2]^+$. Scheme 4 summarizes the *trans* isomers.

Among the *cis* isomers, we have made two, one being the known compound obtained by following the method[36] of Johnson and Basolo. Here, the major product was the thiocyanato–isothiocyanato thiocyanate.

$$cis\text{-}[Rh(en)_2Cl_2](NO_3) + KNCS \longrightarrow cis\text{-}[Rh(en)_2(NCS)(SCN)](NCS). \quad (11)$$

This analysed well (Volhard: cf. Table 2) for ionic thiocyanate. Using the chloride of the chloro factor, under reflux with an excess of KNCS, we obtained a new isomer:

$$cis\text{-}[Rh(en)_2Cl_2]Cl + KNCS \longrightarrow cis\text{-}[Rh(en)_2(NCS)_2](NCS). \quad (12)$$

In general, salts of our S-bonded isomers are more water soluble than the isomeric isothiocyanato complex salts. In the same way, the solid chlorides of the thiocyanato salts are hygroscopic, but their N-bonded isomers are not.

The IR spectra, 250–1000 cm^{-1}, recorded in Table 5, give further good evidence for the retention of *cis* or *trans* geometry in products and need no further discussion. (Diagrams are available.)[1(a)] Among other properties of these isomeric $[Rh(en)_2(NCS)_2]^+$ ions, we studied isomerizations (Scheme 4), addition of mercury(II), and oxidations by trioxoiodate(V) in acidic solution (i.e. iodic acid). These, being slow at room temperature, go to completion in a few hours at 333 K. Essentially (see Experimental) $[Rh^{III}—NCS]^{2+} \rightarrow [Rh^{III} \rightarrow NH_3]^{3+}$ + some $[Rh(CN)]^{2+}$; whereas $[Rh—SCN]^{2+}$ is unreactive.

Addition of aqueous mercury(II) chloride to aqueous *cis*-$[Rh(en)_2(NCS)_2]^+$ gave the clear-cut results of Fig. 6: similar findings for the *trans* species are given in Fig. 7. Additions of mercury(II) and silver(I) ions to pendant pseudo-halide (e.g. cyanides) or sulphur atoms of coordinated isothiocyanates, have been well studied.[41,42] Mercury ions also promote the solvolysis in water of halo–rhodium bonds, and the *cis*-$[M(en)_2Cl_2]^+$ ions (M = Co, Rh) show[43] a kinetic pattern arising from a long-lived stable chloride-bridged dinuclear intermediate, as in eq. (13).

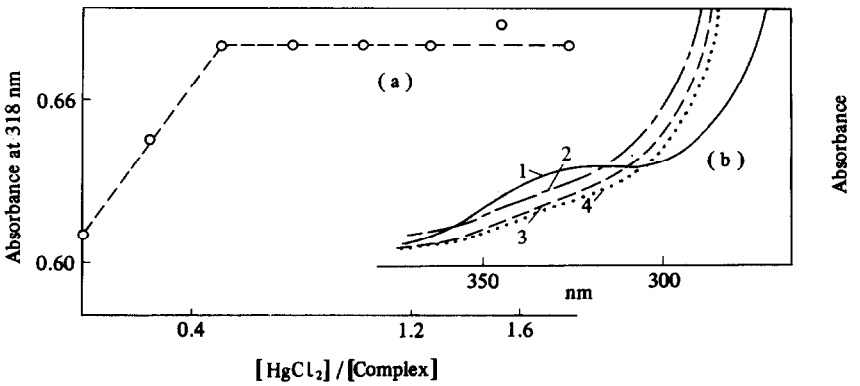

Fig. 6. Effect on the electronic absorption spectrum (———) of *cis*-$[Rh(en)_2(NCS)_2]^+$ of adding aqueous $HgCl_2$: (a) absorbance at 318 nm as f $[HgCl_2]$: [complex ion]; (b) addition in excess: 10 M (—·—·—), 20 M (— — — —), 30 M (·····).

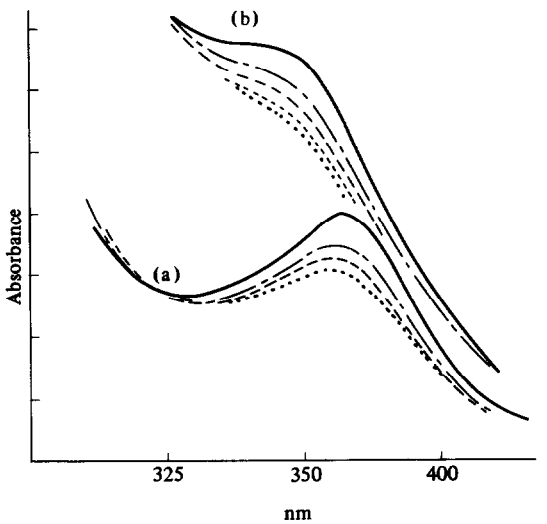

Fig. 7. Effect of adding an excess of aqueous $HgCl_2$ (a) *trans*-$[Rh(en)_2(NCS)(SCN)]^+$ (———) with: 5 M $HgCl_2$ (—·—·—), 10 M (— — — —) and 15 M (·····); (b) *trans*-$[Rh(en)_2(NCS)_2]^+$ (———) with: 5 M $HgCl_2$ (—·—·—), 10 M (— — — —) and 15 M (·····).

$$cis\text{-}[Rh(en)_2Cl_2]^+ + Hg^{2+} \longrightarrow cis\text{-}[Rh(en)_2Cl_2Hg]^{3+} \longrightarrow \text{products.} \quad (13)$$

After periods ranging from several hours to several days, all the complexes studied, whether S-bonded (thiocyanate–metal complexes), or N-bonded (isothiocyanate–metal complexes), exhibit the same triplet signal in TFA centred at $\delta \sim 6.6$ ppm due to NH_4^+. In addition, the signals from other ligands appear (e.g. from bipy in the Pd compounds, and at δ 3.3 and 5 ppm from the ethylenediamine ligands of Rh^{III} complexes, Fig. 8). Clearly, in TFA, the complexes solvolyse; thiocyanate groups dissociated from the complexes eventually produce NH_4^+. This finding requires amplification (in a kinetic framework) to be useful in studies of linkage isomerism, but is directly useful in the analysis of N-isotopic abundance in thiocyanates, via the ^{14}N: ^{15}N coupling method.[14]

Larsson showed[16] that *cis*-$[Co(en)_2(NCS)_2]ClO_4$, dissolved in concentrated sulphuric acid, produces *cis*-$[Co(en)_2(NCSH)_2]^{4+}$, responsible for the colour change from red to bright yellow. Similar protonation is also observed[16] for $[Co(NH_3)_5NCS](ClO_4)_2$. The lifetime of the species are unknown, although Gillard and Maskill were able[17] to measure circular dichroism spectra for the resolved ion (+)-$[Co(en)_2(NCSH)_2]^{4+}$ in such solutions, so that racemization is slow and salts can indeed be crystallized.

^1H NMR spectra of these compounds in conc. H_2SO_4 were taken. Within 2 h of dissolution, hydrolysis had taken place and a triplet at δ 5.3 ppm was observed (see Fig. 9). The solvolysis of $[Co(NH_3)_5X]^{2+}$ (X = CN^-, ONO^-, NO_2^-, Cl^-, Br^-, F^-, NCS^-) by H_2SO_4 has been studied by ^1H NMR.[44-46] In every case, the anionic ligand is rapidly replaced by the $HOSO_3^-$ anion. However, the triplet signal for the particular case of the hydrolysis of $[Co(NH_3)_5NCS]^{2+}$ was not mentioned, and it may not have been observed because of quadrupolar relaxation.

The sharp triplet obtained here at 5.3 ppm and in TFA centred at $\delta = 6.6$ ppm, is due to the proton attached to the ^{14}N of NH_4^+, formed by solvolysis of N- or S-coordinated and free thiocyanate.

EXPERIMENTAL

Electronic spectra were recorded on a Pye-Unicam SP.8000 or on a Beckman DK-2A spectrophotometer. Values of pH were measured using

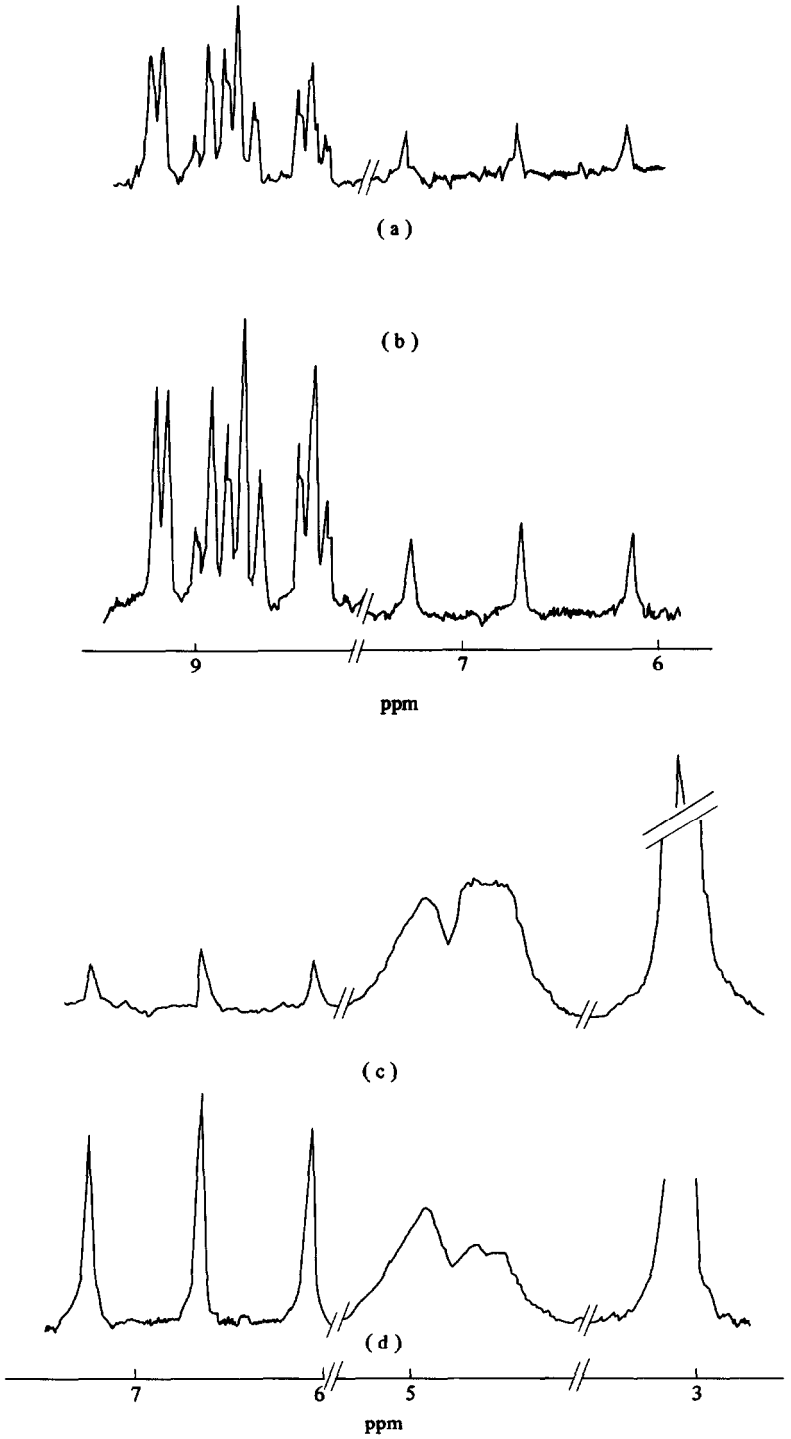

Fig. 8. Typical ^{1}H proton magnetic resonance spectra in TFA: (a) isothiocyanato species, Pd(bipy)(*N*CS)$_2$, after 1 day; (b) the same after 14 days; (c) thiocyanato species, *trans*-[Rh(en)$_2$(*S*CN)$_2$]X, X = Cl, after 1 day; (d) X = (NCS)$^-$, after 8 days.

a Corning digital pH-meter, model PT.15. IR spectra were recorded on a Perkin–Elmer 257 or Pye-Unicam SP200 spectrophotometer. Thermogravimetric analyses were performed using a Stanton–Redcroft TG-750 thermogravimetric balance. ^{1}H NMR spectra were obtained on a 90 MHz Perkin–Elmer R-32 spectrophotometer fitted with a digital signal analyser. Chemical shifts were measured relative to TSS [$NaMe_3Si(CH_2)_3SO_3$] or TMS ($SiMe_4$), as an internal standard. The temperature for ^{1}H NMR experiments was 35°C unless otherwise stated.

Table 5. IR spectra (300–1000 cm^{-1}) of geometric isomers of $[Rh(en)_2(NCS)_2]^+$

$[Rh(en)_2(NCS)_2](NCS)$		$[Rh(en)_2(NCS)_2]Cl$		$[Rh(en)_2(SCN)_2]X$		
cis-	*trans-*	*cis-*	*trans-*	*cis-* (X = NCS)	*cis-* (X = Cl)	*trans-* (X = NCS)
	320(w)				335(w)	
	345(w)			348(m)	345(m)	345(m)
	370(w)					
				375(vw)	400(vw)	375(w)
			430(sh)	400(w)		400(wm)
400(wm)	430(wm)		445(mb)			420(w)
				460(m)	452(m)	450(sh)
				470(sh)		458(m)
455(sh)	450(sh)					470(m)
468(m)	460(m)					
485(w)	470(m)					
	480(sh)					
	502(ms)		500(ms)	505(ms)	503(ms)	500(ssp)
518(m)						
510(ws)	560(w)		555(mw)	560(wm)	558(wm)	558(wm)
578(ms)	570(sh)		575(mw)	580(ms)	518(ms)	580(msp)
	580(msp)					
			695(vw)		670(w)	
	710(w)		705(vw)		695(w)	700(wb)
730(w)	735(m)			732(w)	735(w)	735(m)
750(w)	740(ms)			750(sh)		
	750(m)					
785(mw)						
800(m)	790(sh)		800(mb)	800(m)	800(m)	800(m)
820(mw)	800(m)					
				835(w)	840(w)	835(m)
	835(w)					
	875(w)		878(m)	880(w)	880(w)	880(w)
	875(w)		878(m)	880(w)	880(w)	880(w)
875(m)	890(m)	890(sh)	895(w)	890(wm)	895(m)	
	895(wm)					
	920(wm)			930(w)		915(m)
970(w)	940(wm)			940(w)		935(m)
1010(mb)						
	1000(ms)		995(ms)	995(m)	100(m)	995(s)

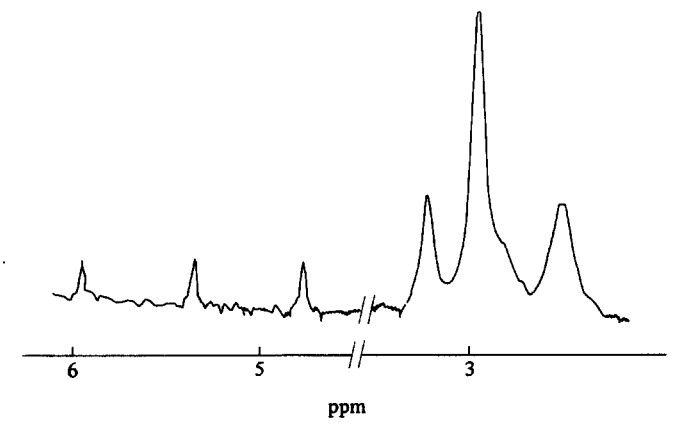

Fig. 9. Proton resonance of $[Co(NH_3)_5(NCS)](ClO_4)_2$ in 98% H_2SO_4.

Purification of organic thiocyanates and isothiocyanates

Some minor impurities in phenyl isothiocyanate, C_6H_5NCS, and ethyl isothiocyanate, C_2H_5NCS, were observed by means of ^1H NMR spectroscopy in CCl_4. Purification was by distillation under reduced pressure (10–14 mm Hg). The purity was checked by ^1H NMR in CCl_4 and refractive indexes, at the sodium yellow lines, presented as: formula, literature[47] (20°C), observed (20.5°C): C_2H_5NCS: 1.5130, 1.5140; C_6H_5NCS: 1.6477, 1.6465; CH_3SCN: 1.4582, 1.4586; CH_3CH_2SCN: 1.4670, 1.4690; $C_6H_5CH_2SCN$: 1.5480, 1.5488.

^1H *NMR in* TFA

The ^1H NMR spectra of thiocyanate salts (Na^+, K^+, NH_4^+ etc.) were recorded on small amounts (15–20 mg) with about 0.5 cm^3 of TFA, and those of organic isothiocyanates were obtained by dissolving a small amount ($\sim$ 20 mg) of liquid in TFA; the spectra were recorded immediately and then at intervals. The concentrations in the reaction mixture of methyl isothiocyanate with TFA shown in Fig. 3 were deduced from the proton integration of the spectra.

TFA hardly dissolves most metal thiocyanate complexes. TFA was added to a capped sample bottle containing the metal complex, and the clear increasingly yellow solution was withdrawn from time to time to record spectra.

Rhodium^{III} complexes

trans-$[Rh(en)_2Cl_2]NO_3$. Following the method of Johnson and Basolo,[36] 2.0 g of $RhCl_3 \cdot 3H_2O$ gave 0.98 g of *trans*-$[Rh(en)_2Cl_2]NO_3$. Found: C, 13.1; H, 4.5; N, 19.2. Calc. for $[Rh(en)_2Cl_2]NO_3$: C, 13.5; H, 4.5; N, 19.7%. λ 406 nm ($\varepsilon = 763$ mol^{-1} dm^2) and 286 nm ($\varepsilon = 1280$ mol^{-1} dm^2) literature:[36] λ (406, 750) and λ (288, 1300). The present SI units for ε differ from those usually given.

The preparations of the thiocyanato complexes of the bis(1,2-diaminoethane)/rhodium(III) moiety are given here in some detail because they deviate from the original method[36] of Johnson and Basolo, who obtained a substance of composition $[Rh(en)_2(NCS)_2](NCS)$ by refluxing $[Rh(en)_2Cl_2]^+$ in sodium thiocyanate. However, they reported[36] that their product failed Gladstone's test (giving no coloration with aqueous ferric ions). Our products, containing ionic thiocyanate gegen-ions, give the blood-red colour instantly. In the present context of substitution at rhodium(III) centres by thiocyanate, it is worth recalling the fact[48] that, despite forcing conditions, only one of the two chloro ligands of *cis*-α-$[Rh(trien)Cl_2]^+$ could be substituted.

Electronic spectra are given in Table 6, chiefly as a further means of characterization: the intensities for these isotropic absorptions are high, like those of other thiocyanatorhodium(III) species, whether N- or S-bonded.

Titration of ionic thiocyanate. The Volhard method was used. Typically 10 cm^3 of a 3.2×10^{-3} M solution of the complex was titrated with 0.1 M $AgNO_3$ using an acidic Fe^{2+} solution as the indicator. Values from the direct and back titration were taken.

trans-$[Rh(en)_2(NCS)_2]X$ (X = NCS, Cl). 0.620 g (1.7 mmol) of *trans*-$[Rh(en)_2Cl_2]NO_3$ in 50 cm^3 of H_2O and 0.590 g of $AgNO_3$ was set to reflux for 2 h, and the silver chloride formed was carefully removed. To the filtrate, which contained *trans*-$[Rh(en)_2(OH_2)_2]^{3+}$ (checked by visible spectrum), 1.5 g of NaNCS was added. The solution was heated (in a steam bath) at 70°C for about 2 h, during which time a new absorption band grew at *ca* 350 nm. The volume was reduced to about 20 cm^3, and all was cooled in ice. The solid obtained was collected, washed with ice-cold water, ethanol and ether. This solid is *trans*-$[Rh(en)_2(NCS)(SCN)]$ (NCS); yield 0.11 g; λ 364 and 275 nm. IR spectroscopy shows strong sharp absorptions at 2140 and 2060 cm^{-1}.

The filtrate was again allowed to reflux for about 1 h, cooled and concentrated in vacuum to 10 cm^3 and finally kept overnight in the refrigerator. The resulting yellow precipitate was collected, washed with ice water, acetone and ether; yield 60 mg. Found: C, 19.6; H, 4.0; N, 22.8. Calc. for $[Rh(en)_2(NCS)_2](NCS) \cdot H_2O$: C, 20.2; H, 4.3; N, 23.6%. λ 340, 270 and 220 nm. IR: a strong sharp absorption at 2110 cm^{-1} was observed, characteristic of an N-bonded thiocyanate and at 2045 cm^{-1} due to ionic thiocyanate. *trans*-$[Rh(en)_2(NCS)_2]Cl$: *trans*-$[Rh(en)_2(NCS)_2](NCS)$ was suspended in water and moist anion-exchange resin (Amberlite IRA-400 in the chloride form) was added. The mixture was stirred (magnetically) until all dissolved. The solution was filtered several times and the yellow filtrate taken to dryness. IR shows only a single, broad, strong absorption at 2110 cm^{-1}.

trans-$[Rh(en)_2(SCN)_2]X$ (X = NCS, Cl). An aqueous solution (30 cm^3) of *trans*-$[Rh(en)_2Cl_2]NO_3$ (620 mg, 1.7 mmol) was refluxed with 590 mg (3.4 mmol) of $AgNO_3$ for 2 h and precipitated AgCl was removed by careful filtration. NH_4NCS (0.9 g) was added to the filtrate and the whole mixture was

Table 6. Electronic spectra in aqueous solution of some compounds of thiocyanate and rhodium(III), $[Rh(en)_2(NCS)_2]X$

Compound	λ (nm)	$\nu(10^3\ cm^{-1})^a$	$\varepsilon(dm^2\ mol^{-1})^b$ $(\times 10^{-3})$
cis-$[Rh(en)_2(NCS)_2](NCS)\cdot H_2O$	318	31.45	8.8
	238(sh)	42.02	89.6
cis-$[Rh(en)_2(NCS)_2]Cl\cdot H_2O$	318	31.45	6.0
	238	42.02	119.3
	2.5(sh)	46.51	127.5
cis-$[Rh(en)_2(SCN)(NCS)](NCS)\cdot H_2O$	350	28.57	2.65
	274(sh)	36.50	21.1
	240(sh)	41.67	52.1
trans-$[Rh(en)_2(NCS)_2](NCS)\cdot H_2O$	340	29.41	4.1
	220	45.45	168.0
trans-$[Rh(en)_2(NCS)(SCN)](NCS)\cdot H_2O$	364	27.47	4.45
	275(sh)	36.36	28.7
	250(sh)	40.00	40.8
trans-$[Rh(en)_2(SCN)_2](NCS)\cdot H_2O$	400(sh)	25.00	1.1
	350	28.57	2.8
	275	36.36	105.0
trans-$[Rh(en)_2(NCS)Cl](NCS)$	363[c]	27.55	3.4

[a] The reciprocal of the measured wavelength (± 1 nm).
[b] Note units.
[c] From ref. 36.

refluxed for about 1 h. The yellow solution was then reduced to about 10 cm^3 and left overnight in a refrigerator. The yellow–orange solid formed was collected, washed with ice-water, ethanol, ether and air-dried. This solid (140 mg) is again *trans*-$[Rh(en)_2(NCS)(SCN)](NCS)$, which was recrystallized from hot water. The volume of the filtrate F was reduced (*in vacuo*; 40°C) to about 5 cm^3 and it was left overnight in a refrigerator. The yellow solid obtained was collected, washed with ice–water, ethanol and ether; yield 70 mg. Found: C, 19.6; H, 4.2; N, 22.8. Calc. for *trans*-$[Rh(en)_2(SCN)_2](NCS)\cdot H_2O$: C, 20.2; H, 4.3; N, 23.3%. ν_{CN} at 2045(s, sp); 2110(s), 2130(s), 2140(sh). In an alternative treatment of F, it was taken to dryness, *in vacuo* at 40°C, and the product was redissolved in *ca* 3 cm^3 of hot water, allowed to cool to room temperature, and left at 2°C overnight. The yield was 95 mg.

The chloride salt was prepared by anion exchange as described previously. Its IR spectrum shows a single sharp strong absorption at 2110 cm^{-1} (ν_{CN}).

Isomerization of *trans*-$[Rh(en)_2(NCS)(SCN)]^+$ (*Scheme* 4). On refluxing a solution of *trans*-$[Rh(en)_2(NCS)(SCN)]^+$ in H_2O, the electronic spectrum changes to that of the *trans*-diisothiocyanate. The lower energy absorption band moves from 364 to around 340 nm, and two well defined shoulders are also observed at 270 and 220 nm. The product could not be isolated, although a few reactions have been studied.

Reactions with $HgCl_2$(aq): adding $HgCl_2$ (aq) to aqueous *cis*-$[Rh(en)_2(NCS)_2]^+$ changed the electronic spectrum (Fig. 6). Absorbance at 318 nm increases linearly from $[HgCl_2]/[Complex] = 0$–0.5 and then stays constant (up to $[HgCl_2]/[Complex] = 1.8$); Fig. 6(a). When a large excess of $HgCl_2$ is added, the changes shown in Fig. 6(b) are observed. The first absorption band moves to higher energy and the intensity at 320 nm decreases.

Reactions with IO_3^-: solid $NaIO_3\cdot H_2O$ (4.5 mg, 0.02 mmol) was added to 10 cm^3 of a solution of the complex (typically 2×10^{-3} M) previously acidified with $HClO_4$ (so that $[H^+] = 0.02$ M), at room temperature (when reaction was very slow) or at 333 K (reaction time *ca* 3 h) in a water bath. The I_2 formed was usually extracted with CCl_4. *cis*-$[Rh(en)_2(NCS)_2]^+$ with IO_3^- at room temperature gave a mixture of products, with, after anion exchange to the chloride, a new absorption at 2191 cm^{-1}, (CN^-) a broadening in the N—H stretching, bending and rocking regions (NH_3 ligand) and again the band at 2140 cm^{-1} (NCS^-). The lower energy absorption in the electronic spectrum moves to higher energies. Chromatography (cation ex-

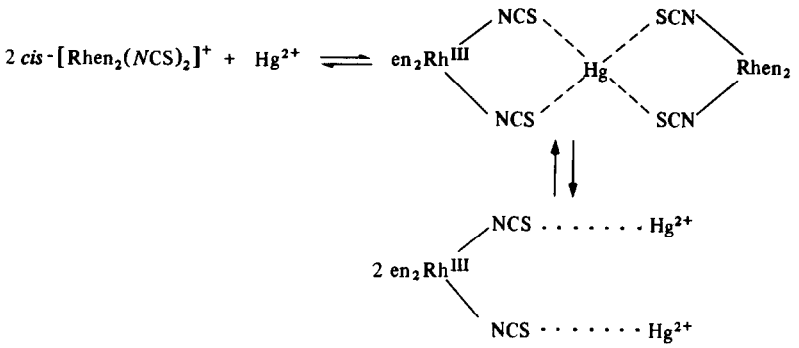

Scheme 5. Adducts of mercury(II) with the *cis*-bis-isothiocyanate complex.

change resin, H^+ form) developed two main bands, one eluted with 0.1 M HCl {singly charged, *cis*-$[Rh(en)_2(NCS)(CN)]^+$} and the other with 0.5 M HCl {doubly charged, *cis*-$[Rh(en)_2(NH_3)(NCS)]^{2+}$, *cis*-$[Rh(en)_2(NH_3)(CN)]^{2+}$}.

The products from *cis*-$[Rh(en)_2(SCN)(NCS)]^+$ with IO_3^-, under the same conditions, were also analysed. On comparing the IR spectrum of the product (impure $[Rh(en)_2(SCN)(NH_3)]^{2+}$) with that of factor, there is no evidence for CN^- (absorption at 2191 cm^{-1}), but the changed NH_2 vibrations also occurred here. The absorption around 2120 cm^{-1} (associated with C—N stretching of the thiocyanate ligand) was observed. Two new, broad, strong bands are observed at ~ 2450 and ~ 840 cm^{-1}. In the electronic spectrum, the main feature is a new well defined band at around 245 nm.

The reaction of *trans*-$[Rh(en)_2(NCS)(SCN)]^+$ with IO_3^- at 333 K was followed: the products again involve coordinated NH_3, CN^- and NCS^- moieties. However, the reaction at room temperature produces no CN^-, although coordinated NCS^- and NH_3 are still present: the mixture of products is more complex than in the reactions of the other isomers.

Addition of an excess of $HgCl_2$(aq) to solutions of *trans*-$[Rh(en)_2(NCS(SCN)]^+$ and *trans*-$[Rh(en)_2(NCS)_2]^+$ was followed in a similar way.

The results of the titration of *cis*-$[Rh(en)_2(NCS)_2]^+$ with $HgCl_2$(aq), Fig. 6(a), suggest that the first association between the rhodium(III) complex and the mercuric ions, probably involves two moles of complex to one of Hg^{2+}(aq). When this ion is then added in excess, it associates in a 2:1 ratio (Hg–Complex), Scheme 5. This would explain the increase in intensity observed in the quantitative titration [Fig. 6(a)], as a new chelate ring is formed around the rhodium(III) centre. In addition, at this concentration of Hg^{2+}, and also when Hg^{2+} is present in excess, there is a shift of the bands to lower energies, both in this instance and with the *trans* compound.

Cobalt(III) *complexes*

cis-$[Co(en)_2(NCS)_2](ClO_4)$. This was prepared according to Gillard and Maskill.[17] Found: C, 17.0; H, 4.6; N, 19.9. Calc. for *cis*-$[Co(en)_2(NCS)_2](ClO_4)\cdot H_2O$: C, 17.5; H, 4.4; N, 20.4%. IR spectra contain a single broad ν_{CN} at 2105 cm^{-1}. λ 508 and 314 nm correspond to published values.

$[Co(NH_3)_5NCS](ClO_4)_2$. This was prepared as described in ref. 49 by reacting NaNCS with an aqueous solution of $[Co(NH_3)_5H_2O]^{3+}$ to form $[Co(NH_3)_5NCS](NCS)_2$. The perchlorate salt was prepared by dissolving the thiocyanate salt in water and a saturated solution of $NaClO_4$ was added. The resulting orange–red precipitate was collected, washed with water, ethanol, ether and sucked dry. Found: C, 3.0; H, 3.9; N, 19.3. Calc. for $[Co(NH_3)_5NCS](ClO_4)_2\cdot H_2O$: C, 2.9; H, 4.0; N, 20.1%. λ 496 and 306 nm correspond to known values.

Palladium(II) *complexes*

Pd(bipy)$(SCN)_2$. The compound (0.5 g) was prepared according to Basolo and Burmeister, from 0.84 g $K_2Pd(SCN)_4$. Found: C, 38.4; H, 2.3; N, 14.1. Calc. for Pd(bipy)$(SCN)_2$: C, 38.0; H, 2.1; N, 14.8%. IR spectra (Nujol) contain sharp, strong bands at 2114 and 2091 cm^{-1}.

Pd(bipy)$(NCS)_2$. The compound (0.21 g) was prepared from $K_2Pd(SCN)_4$ (0.84 g) with 0.32 g of 2,2′-bipyridyl. Found: C, 37.7; H, 2.4; N, 14.2. Calc. for Pd(bipy)$(NCS)_2$: C, 38.0; H, 2.1; N, 14.8%. IR spectra (Nujol) contain a single, broad, strong absorption at 2100 cm^{-1}.

Acknowledgements—This paper is based on the PhD theses of Nordin Garif (1983)[1(b)] and Julio Pedrosa de Jesus (1977),[1(a)] who respectively, thank the Universiti Teknologi Malaysia and the University of Aveiro for leave. We also thank Dr Neil Burford and Mr Gareth Phillips for some preliminary confirmatory work carried out by

them while undergraduates in Cardiff. We thank Prof. E. Whittle for advice on fluoro–organic chemistry and Dr D. A. Wilson for valued discussion of the resonance spectra.

REFERENCES

1. (a) J. D. Pedrosa de Jesus, Stereochemical aspects and photochemistry of compounds of rhodium(III), PhD thesis, University of Wales (1977); (b) N. Garif, Reactions of nitrogenous ligands in metal complexes, PhD thesis, University of Wales (1983).
2. (a) J. A. Kargol, R. W. Crecely and J. L. Burmeister, *Inorg. Chim. Acta* 1977, **25**, L109; (b) J. A. Kargol, R. W. Crecely and J. L. Burmeister, *Inorg. Chem.* 1979, **18**, 2532.
3. (a) C. F. William, J. L. Burmeister, C. P. Cheng and T. L. Brown, *Inorg. Chem.* 1981, **20**, 1734; (b) O. W. Howarth, R. E. Richards and L. M. Venanzi, *J. Chem. Soc.* 1964, 3335.
4. P. S. Pregosin, H. Sterit and L. M. Venanzi, *Inorg. Chim. Acta* 1980, **38**, 237.
5. L. G. Marzilli, R. C. Stewart, L. A. Epps and J. B. Allen, *J. Am. Chem. Soc.* 1973, **95**, 5796.
6. J. A. Kargol, K. D. Lavin, R. W. Crecely and J. L. Burmeister, *Inorg. Chem.* 1980, **19**, 1515.
7. S. J. Anderson and A. H. Norbury, *J. Chem. Soc., Chem. Commun.* 1975, 48.
8. S. J. Anderson and R. J. A. Goodfellow, *J. Chem. Soc., Chem. Commun.* 1975, 443.
9. J. A. Carty and S. E. Jacobson, *J. Chem. Soc., Chem. Commun.* 1975, 175.
10. J. A. Carty, *Inorg. Chem.* 1976, **15**, 1956.
11. J. J. MacDougall, J. H. Nelson, M. W. Babich, C. C. Fuller and R. A. Jacobson, *Inorg. Chim. Acta* 1978, **27**, 201.
12. J. J. MacDougall, A. W. Verstuyft, L. W. Cary and J. H. Nelson, *Inorg. Chem.* 1980, **19**, 1036.
13. C. T. Hunt and A. L. Balch, *Inorg. Chem.* 1982, **21**, 1242.
14. I. G. Browning, R. D. Gillard, J. R. Lyons and P. R. Mitchell, *J. Chem. Soc.* 1974, 373.
15. K. Garbett, R. D. Gillard and R. Ugo, *J. Chem. Soc. A* 1966, 1137.
16. R. Larsson, *Acta Chem. Scand.* 1962, **16**, 931 and refs therein.
17. R. D. Gillard and R. Maskill, *J. Chem. Soc. A* 1971, 2813.
18. K. Eriks and J. R. Knox, *Acta Cryst.* 1966, **21** (supplement), Abstract 9.19, p. A140 (1966).
19. R. D. Gillard, N. C. Payne and W. O. Davies, *J. Inorg. Nucl. Chem.* 1968, **30**, 2759.
20. R. A. Ogg Jr. and J. D. Ray, *J. Chem. Phys.* 1957, **26**, 1515.
21. J. Mason, *Chem. Rev.* 1981, **81**, 205.
22. J. D. Roberts, *J. Am. Chem. Soc.* 1956, **78**, 4495.
23. I. Beard and B. P. Dailey, *J. Chem. Phys.* 1950, **71**, 938.
24. J. Goubeau and O. Gott, *Chem. Ber.* 1940, **73**, 127.
25. T. M. Barakat, N. Legge and A. D. E. Pullin, *Trans. Faraday Soc.* 1963, **59**, 764.
26. J. Nelson, R. S. Pratt and S. M. Nelson, *J. Chem. Soc. A* 1970, 583.
27. H. W. Thompson, C. F. Kearton and S. A. Lamb, *J. Chem. Soc.* 1935, 1033.
28. P. K. Klason, *J. Prakt. Chem.* 1887, **36**, 57.
29. A. Pinner and W. Schauman, *Chem. Ber.* 1881, **14**, 1082.
30. T. D. B. Morgan, G. Stedman and P. A. Whincup, *J. Chem. Soc.* 1965, 4813.
31. T. D. B. Morgan, E. D. Phillips and G. Stedman, *J. Chem. Soc. A* 1969, 2318.
32. M. N. Hughes, in *The Chemistry and Biochemistry of Thiocyanic Acid and its Derivatives* (Edited by A. A. Newman). Academic Press, London (1975).
33. The Chemistry of the —NCS Group, by L. Drobnica, P. Kristian and J. Augustin, in *The Chemistry of Cyanates and their Thio Derivatives, Part 2* (Edited by Saul Patai). John Wiley, New York (1977).
34. Cf. T. Moeller, *Inorganic Chemistry*, p. 400. John Wiley, New York (1982), though the stoichiometry given there is incorrect.
35. R. D. Gillard and J. D. Pedrosa de Jesus, *Polyhedron*, in press.
36. S. A. Johnson and F. Basolo, *Inorg. Chem.* 1962, **1**, 925.
37. E. J. Bounsall and S. R. Kopprich, *Can. J. Chem.* 1970, **48**, 1481.
38. H. H. Schmidtke, *J. Am. Chem. Soc.* 1965, **87**, 2522.
39. A. H. Norbury, *Adv. Inorg. Chem. Radiochem.* 1975, **17**, 231.
40. J. Lewis, R. S. Nyholm and P. W. Smith, *J. Chem. Soc.* 1961, 4590.
41. K. Garbett, PhD thesis, University of Sheffield (1967).
42. D. N. Purohit and J. Bjerrum, *J. Inorg. Nucl. Chem.* 1971, **33**, 2067.
43. J. L. Armstrong, M. J. Blandamer, J. Burgess and A. Chew, *J. Inorg. Nucl. Chem.* 1981, **43**, 173 and refs therein.
44. W. L. Jolly, A. D. Harris and T. S. Briggs, *Inorg. Chem.* 1965, **4**, 1064.
45. D. N. Hendrickson and W. L. Jolly, *Inorg. Chem.* 1970, **9**, 1197.
46. H. Yoneda and Y. Nakashima, *Bull. Chem. Soc. Japan* 1974, **47**, 669.
47. E. E. Reid, *Organic Chemistry of Bivalent Sulphur*, Vol. 6. Chemical Publishing, New York (1966).
48. P. M. Gidney, R. D. Gillard, B. T. Heaton, P. S. Sheridan and D. H. Vaughan, *J. Chem. Soc., Dalton Trans.* 1973, 1462.
49. L. C. Falk and R. G. Link, *Inorg. Chem.* 1971, **10**, 215.

Polyhedron Vol. 8, No. 6, pp. 793–800, 1989
Printed in Great Britain

0277–5387/89 $3.00+.00
© 1989 Pergamon Press plc

METAL–(PHENYLTHIO)ALKANOIC ACID INTERACTIONS—X.* THE CRYSTAL STRUCTURES OF THALLIUM(I) (PHENYLTHIO)ACETATE(PHENYLTHIO)ACETIC ACID ADDUCT, CAESIUM (2,4-DICHLORO-5-METHYLPHENYLTHIO)ACETATE(2,4-DICHLORO-5-METHYLPHENYLTHIO)ACETIC ACID ADDUCT, CAESIUM (PHENYLTHIO)ACETATE(PHENYLTHIO)ACETIC ACID ADDUCT AND CAESIUM 2-(PHENYLTHIO)PROPIONATE MONOHYDRATE

THOMAS C. W. MAK and WAI-HING YIP

Department of Chemistry, The Chinese University of Hong Kong, Shatin, New Territories, Hong Kong

and

WING-HONG CHAN

Department of Chemistry, Hong Kong Baptist College, Kowloon, Hong Kong

and

COLIN H. L. KENNARD

Department of Chemistry, University of Queensland, Brisbane, Queensland 4067, Australia

and

GRAHAM SMITH† and ERIC J. O'REILLY

Department of Chemistry, Queensland University of Technology, Brisbane, Queensland 4000, Australia

(*Received* 16 *August* 1988; *accepted* 11 *October* 1988)

Abstract—Crystal structures of four univalent metal complexes with (phenylthio)acetic acid (PTAH), (2,4-dichloro-5-methylphenylthio)acetic acid (DCMPTAH), and 2-(phenylthio)propionic acid (PTPAH) have been determined using X-ray diffraction. The thallium complex, $[Tl(PTA)(PTAH)]_n$, (**1**) is orthorhombic, space group *Pccn*, $Z = 4$, $a = 10.466(6)$, $b = 26.75(1)$, $c = 6.013(2)$ Å. $[Cs(DCMPTA)(DCMPTAH)]_n$, (**2**) is triclinic, space group $P\bar{1}$, $Z = 1$, $a = 5.159(3)$, $b = 6.898(3)$, $c = 16.500(8)$ Å, $\alpha = 90.04(4)$, $\beta = 94.22(4)$ and $\gamma = 103.27(4)°$. PTAH forms an adduct $[Cs(PTA)(PTAH)]_n$, (**3**) which is monoclinic, space group *Cc* with $Z = 4$, $a = 35.88(1)$, $b = 7.201(2)$, $c = 6.907(1)$ Å, $\beta = 91.19(2)°$. PTPAH forms a conventional hydrated complex, $[Cs(PTPA)(H_2O)]_n$, (**4**), which is orthorhombic, *Pbca*, with $Z = 8$, $a = 8.849(4)$, $b = 9.500(3)$, $c = 29.78(1)$ Å. The structures (**1–4**) were refined to residuals of 0.078, 0.087, 0.030 and 0.036 for 1353, 1571, 2225, 1807 "observed" reflections, respectively. Both **1** and **2** are examples of acid salts of the type, MHX_2, where

* For Part IX, see ref. 1.

† Author to whom correspondence should be addressed.

X^- and HX are crystallographically equivalent. The molecules are polymeric and have bonded ligands as well as adducted acid species. **3** is an example of a type B ($M^+X^- \cdot HX$) salt with X^- and HX crystallographically different. **4** is an example of a normal Cs salt. The Tl compound (**1**) is disordered with only half the general position sites occupied by the metal atom. Each site is at the centre of a distorted MO_5S octahedron with very short bonds to both asymmetric bidentate and bridging carboxylate groups [Tl—O, 2.22, 2.44(1) Å] and to the thioether S [Tl—S, 2.517(4) Å]. In **2**, the Cs atom is at the centre of symmetry of a distorted MO_6 octahedron. It has a polymer structure with acetate bridges linking consecutive Cs atoms and carboxylate oxygen also bifurcated between two Cs atoms. The Cs—O distances are 3.123(10), 3.152(8) and 3.237(8) Å. Complex **3** has an irregular MO_8 polyhedron about Cs with bonds from both PTA and PTAH ligands [Cs—O range, 3.03–3.45(1) Å; mean, 3.23(1) Å], and extends into a 2-D polymer structure. Compound **4** is also polymeric but with distorted octahedral MO_6 coordination, bridging through both carboxylate and water oxygens [Cs—O range, 3.02–3.33(1) Å; mean, 3.20(1) Å].

As part of a general investigation into the metal-coordination chemistry of (phenylthio)alkanoic acids, a group of disordered compounds have been isolated in the solid state. These crystalline compounds have a general formula ($M^+X^- \cdot HX$). Speakman[2,3] classifies two fundamental types of acid–salt ($M^+X^- \cdot HX$) structures: type A, where the two X-units are crystallographically equivalent and type B, where the two X-units are crystallographically non-equivalent and occur as an anion and a neutral molecule. An aqueous solution of such an acid salt, MHX_2, is an optimum buffer with a pH very close to the pK_a of the acid HX. In all the type A cases quoted by Speakman, the intercarboxyl hydrogen bond occurs about either an inversion centre or a two-fold axis. This paper deals with both type A and B structures. These are $[Tl(PTA)(PTAH)]_n$ (**1**), $[Cs(DCMPTA)(DCMPTAH)]_n$ (**2**) (type A) and $[Cs(PTA)(PTAH)]_n$ (**3**) (type B), [PTA = (phenylthio)acetate; DCMPTA = (2,4-dichloro-5-methylphenylthio)acetate]. Also reported is the structure of a conventional caesium salt with the ligand 2-(phenylthio)propionic acid (PTPAH) which forms $[Cs(PTPA)(H_2O)]_n$ (**4**).

EXPERIMENTAL

Preparation

Complexes were made by reacting the appropriate acid in aqueous ethanol with an excess of metal carbonate.[4] After digesting for about 1 h, the excess carbonate was filtered off, and the solutions, on standing, yielded suitable crystals for diffraction.

Analysis: For **1**, found: C, 35.2; H, 3.29. Calc. for $C_{16}H_{15}O_4S_2Tl$: C, 35.6; H, 2.80% (anhydrous). $C_{16}H_{17}O_5S_2Tl$: C, 34.5; H, 3.07%, (monohydrate). For **2**, found: C, 34.0; H, 2.46; Cl, 22.0. Calc. for $C_{18}H_{15}Cl_4CsO_4S_2$: C, 34.1; H, 2.38; Cl, 22.4.

Crystal data, X-ray data collection and structure refinement

Table 1 lists details of cell parameters, data acquisition and structure solution. Data were processed using the profile fitting procedure of Diamond[5] and were corrected for absorption. Structures were solved by Patterson methods and refined using SHELX-76[6] on the University of Queensland's IBM 3083 computer (**1**, **3** and **4**) or SHELXTL[7] (**2**). For all structures, blocked-matrix anisotropic refinement (100 variable maximum) was used for all non-hydrogen atoms. Hydrogens were located from difference-Fourier syntheses and included at fixed positions with their isotropic U values set invariant at 0.05 $Å^2$. Residuals R and R_w are defined as: $R = [\Sigma ||F_o| - |F_c||/\Sigma |F_o|]$ and $R_w = [\Sigma w(||F_o| - |F_c||^2/\Sigma w|F_o|^2)^{0.5}]$. Neutral atom scattering factors were used.

Bond distances and angles are given in Table 2. Final atomic parameters, lists of anisotropic thermal parameters, intramolecular bond distances and angles, and observed and calculated structure factors are available from the Authors.

The Patterson-heavy atom method was used to solve the structure of **1**. The measured density (2.16 g cm^{-3}) indicates that there are four molecules of formula $C_{16}H_{15}O_4S_2Tl$ in the unit cell. For the space group *Pccn*, this implies that the Tl atoms lie at special positions, either at (0,0,0) (point symmetry $\bar{1}$) or (0,0,0.5) (point symmetry 2). The sharpened Patterson synthesis gave seven major vectors confirming the space group *Pccn* (D_{2h}^{10}, No. 56) ($0kl$, $l = 2n+1$ absent; $h0l$, $l = 2n+1$; $hk0$, $h+k = 2n+1$), with Tl at general positions (site occupancy = 0.5). This model refined successfully. To balance the charge of the univalent cation, the ligand must be disordered over two sites with half being present as the anion (PTA) and the other as the acid (PTAH).

Table 1. Experimental data for [Tl(PTA)(PTAH)]$_n$ (**1**), [Cs(DCMPTA)(DCMPTAH)]$_n$ (**2**), [Cs(PTA)(PTAH)]$_n$ (**3**) and [Cs(PTPA)(H_2O)]$_n$ (**4**)

	1	**2**	**3**	**4**
Formula	$C_{16}H_{15}O_4S_2Tl$	$C_{18}H_{15}Cl_4CsO_4S_2$	$C_{16}H_{15}CsO_4S_2$	$C_{10}H_{14}CsO_3S$
M_r	539.8	634.16	468.32	346.18
Space group	*Pccn* (No. 56)	$P\bar{1}$ (No. 2)	*Cc* (No. 9)	*Pbca* (No. 61)
a (Å)	10.466(6)	5.159(3)	35.88(1)	8.849(4)
b (Å)	26.75(1)	6.898(3)	7.201(2)	9.500(3)
c (Å)	6.013(2)	16.500(8)	6.907(1)	29.78(1)
α (°)	90	90.04(4)	90	90
β (°)	90	94.22(4)	91.19(2)	90
γ (°)	90	103.27(4)	90	90
V (Å^3)	1683.4(1)	569.9(4)	1784.2(7)	2503(1)
Z	4	1	4	8
D_c (g cm^{-3})	2.12	1.847	1.743	1.837
D_m (g cm^{-3})	2.16	1.849	1.716	1.831
F(000)	1024	310	920	1336
μ(Mo-K_α) (cm^{-1})	99.1	23.2	23.0	30.8
Data collection				
a Diffractometer	Nicolet R3m	Nicolet R3m	Nicolet R3m	Nicolet R3m
b Radiation	Mo-K_α	Mo-K_α	Mo-K_α	Mo-K_α
c Wavelength (Å)	0.71069	0.71069	0.71069	0.71069
d $2\theta_{max}$ (deg)	54	50	62	55
e Crystal size (mm)	0.04 × 0.46 × 0.46	0.12 × 0.24 × 0.28	0.20 × 0.36 × 0.38	0.16 × 0.20 × 0.24
f Transmission factors	0.03–0.06	0.41–0.53	0.41–0.59	0.49–0.66
g Unique data	1745	1755	2629	2439
Structure refinement				
R[a]	0.078	0.087	0.030	0.036[d]
R_w[b]	0.087	0.109	0.035	—
w[c] (A)	1	1	2.5	—
(B)	1.2×10^{-3}	1.8×10^{-3}	3.5×10^{-3}	—
Data used	1353	1571	2225	1807
Discrimination	$I > 3\sigma(I)$	$I > 3\sigma(I)$	$I > 2.5\sigma(I)$	$I > 2.5\sigma(I)$

[a] $R = [\Sigma ||F_o| - |F_c|| / \Sigma |F_o|]$.
[b] $R_w = [(\Sigma w||F_o| - |F_c||^2 / \Sigma w|F_o|^2)^{0.5}]$.
[c] $w = A/(\sigma^2 F_o + BF_o^2)$.
[d] Unit weights used.

Table 2. Bond distances and angles about the coordination spheres in **1**, **2**, **3** and **4**

(a) *Distances* (Å)

1

Tl—O(10)	2.506(8)	Tl—O(11)[a]	2.218(10)
Tl—S(7)	2.517(4)	Tl—O(10)[b]	2.444(8)
Tl—O(10)[a]	3.148(8)	Tl—O(11)[c]	2.987(9)
Tl—Tl[a]	3.427(2)	Tl—Tl[b]	3.825(2)

[a] $(\frac{1}{2}+x, -y, \frac{1}{2}-z)$
[b] $(-x, -y, -z)$
[c] $(-x, -y, 1-z)$

2

Cs—O(10)[a]	3.123(10)	Cs—O(10)[b]	3.237(8)
Cs—O(11)	3.152(8)		

[a] $(x, -1+y, z)$
[b] $(-1+x, -1+y, z)$

Table 2—*continued*

		3	
Cs—O(10)A	3.277(5)	Cs—O(10)B	3.447(5)
Cs—O(10)A[a]	3.305(6)	Cs—O(10)B[d]	3.140(5)
Cs—O(11)A[b]	3.029(5)	Cs—O(11)B[d]	3.069(6)
Cs—O(11)A[c]	3.371(5)	Cs—O(11)B[e]	3.167(5)
[a] $(x, 1-y, -\frac{1}{2}+z)$			
[b] $(x, y, -1+z)$			
[c] $(x, -y, -\frac{1}{2}+z)$			
[d] $(x, 1-y, \frac{1}{2}+z)$			
[e] $(x, -1+y, z)$			
		4	
Cs—O(10)	3.019(5)	Cs—O(11)[c]	3.273(6)
Cs—O(10)[a]	3.241(5)	Cs—Ow	3.215(6)
Cs—O(11)[b]	3.110(6)	Cs—Ow[d]	3.333(6)
[a] $(\frac{1}{2}-x, \frac{1}{2}+y, z)$			
[b] $(\frac{1}{2}+x, \frac{1}{2}-y, -z)$			
[c] $(-x, -y, -z)$			
[d] $(\frac{1}{2}-x, \frac{1}{2}+y, z)$			
	(b) *Angles* (degrees)		
		1	
O(10)—Tl—S(7)	75.0(2)	S(7)—Tl—O(11)[c]	100.3(2)
O(10)—Tl—O(10)[a]	137.5(2)	O(10)[a]—Tl—O(11)[a]	45.4(2)
O(10)—Tl—O(11)[a]	133.3(2)	O(10)[a]—Tl—O(10)[b]	132.0(2)
O(10)—Tl—O(10)[b]	78.8(2)	O(10)[a]—Tl—O(11)[c]	63.6(2)
O(10)—Tl—O(11)[c]	74.8(2)	O(11)[a]—Tl—O(10)[b]	87.8(2)
S(7)—Tl—O(10)[a]	103.1(2)	O(11)[a]—Tl—O(11)[c]	76.6(2)
S(7)—Tl—O(11)[a]	146.8(2)	O(10)[b]—Tl—O(11)[c]	124.2(2)
S(7)—Tl—O(10)[b]	119.0(2)		
		2	
O(11)—Cs—O(10)[a]	114.4(2)	O(10)[a]—Cs—O(10)[b]	71.6(2)
O(11)—Cs—O(10)[b]	116.1(2)		
		3	
O(10)A—Cs—O(10)A[a]	80.2(3)	O(11)A[b]—Cs—O(10)B	125.6(3)
O(10)A—Cs—O(11)A[b]	123.7(3)	O(11)A[b]—Cs—O(10)B[d]	63.4(3)
O(10)A—Cs—O(11)A[c]	70.0(3)	O(11)A[b]—Cs—O(11)B[d]	144.8(3)
O(10)A—Cs—O(10)B	77.7(3)	O(11)A[b]—Cs—O(11)B[e]	79.5(3)
O(10)A—Cs—O(10)B[d]	160.3(3)	O(11)A[c]—Cs—O(10)B	147.4(3)
O(10)A—Cs—O(11)B[d]	60.0(3)	O(11)A[c]—Cs—O(10)B[d]	128.4(3)
O(10)A—Cs—O(11)B[e]	127.9(3)	O(11)A[c]—Cs—O(11)B[d]	75.8(3)
O(10)A[a]—Cs—O(11)A[b]	88.3(3)	O(11)A[c]—Cs—O(11)B[e]	74.8(3)
O(10)A[a]—Cs—O(11)A[c]	126.5(3)	O(10)B—Cs—O(10)B[d]	83.7(3)
O(10)A[a]—Cs—O(10)B	42.8(3)	O(10)B—Cs—O(11)B[d]	89.5(3)
O(10)A[a]—Cs—O(10)B[d]	82.7(3)	O(10)B—Cs—O(11)B[e]	129.7(3)
O(10)A[a]—Cs—O(11)B[d]	124.8(3)	O(10)B[d]—Cs—O(11)B[d]	126.7(3)
O(10)A[a]—Cs—O(11)B[e]	151.5(3)	O(10)B[d]—Cs—O(11)B[e]	69.7(3)
O(11)A[b]—Cs—O(11)A[c]	74.3(3)	O(11)B[d]—Cs—O(11)B[e]	75.2(3)
		4	
O(10)—Cs—O(10)[a]	152.3(2)	O(10)[a]—Cs—Ow[d]	75.1(2)
O(10)—Cs—O(11)[b]	73.4(2)	O(11)[b]—Cs—O(11)[c]	98.6(2)
O(10)—Cs—O(11)[c]	125.4(2)	O(11)[b]—Cs—Ow	63.3(2)
O(10)—Cs—Ow	79.9(2)	O(11)[b]—Cs—Ow[d]	139.8(2)
O(10)—Cs—Ow[d]	91.1(2)	O(11)[c]—Cs—Ow	145.2(2)
O(10)[a]—Cs—O(11)[b]	132.0(2)	O(11)[c]—Cs—Ow[d]	60.4(2)
O(10)[a]—Cs—O(11)[c]	68.4(2)	Ow—Cs—Ow[d]	151.4(2)
O(10)[a]—Cs—Ow	100.7(2)		

DISCUSSION

$[Tl(PTA)(PTAH)]_n$ (1)

The Tl^I compound (**1**) is most unusual with the metal atom having half occupancy. If, on the other hand, Tl atoms were at all the eight equivalent positions, the Tl—Tl separations would be short [3.426 Å, $(0.5-x, y, 0.5+z, c$ glide about a at $x = 0.25)$ or 3.824 Å $(-x, -y, -z$, inversion centre)]. The shorter distance would disappear if water replaced the metal in half the Tl sites. This would make Tl seven coordinate with a long Tl—H_2O distance of 3.426(1) Å. As a result the water molecule would be likewise surrounded by the equivalent ligands. This is consistent with chemical analysis and density measurement. Somewhat analogous compounds have been reported[8] (although not of Tl), with water at a central site of an 18-crown-6 ether.

Another possibility could be the presence of Tl^{III}, in a structure such as $Tl^I_2(PTA)_2 \cdot Tl^{III}_2(PTA)_6$. This would explain the presence of identical PTA ligands but with half occupancy of four of the eight sites by Tl^I and two by Tl^{III}. This could also explain the short Tl–ligand distances, e.g. Tl—$O(11)^I$, 2.218(10) Å, which is comparable to typical Tl^{III}—O distances [$CsTl^{III}(SO_4)\cdot 2H_2O$,[9] Tl—O, 2.21–2.28 Å]. Tl^I—O distances are more typically 2.6–3.4 Å as found in Tl_2CO_3.[10] The Tl—S(7) distance in **1** [2.517(4) Å] is also short compared to the more typical values in diethyldithiophosphinatothallium(I)[11] of 3.06 Å.

Although the former possibility appears more tenable, the presence of water at this site cannot be confirmed crystallographically because of the magnitude of the electronic effect due to Tl.

In **1**, the metal is incompletely surrounded by its ligands. This is probably due to $6s^2$ electrons of Tl acting as a stereochemical lone pair occupying part of the coordination sphere and producing a distorted MO_5S octahedron with both very short asymmetric bonds to oxygens of bidentate and bridging carboxylate groups and to the thioether S. The linear polymer extends along the a axis at $x = 0$, 0.5. van der Waals' interactions appear to locate the rows of hydrophobic phenyl groups at $y = 0.25$, 0.75 (Figs 1 and 2).

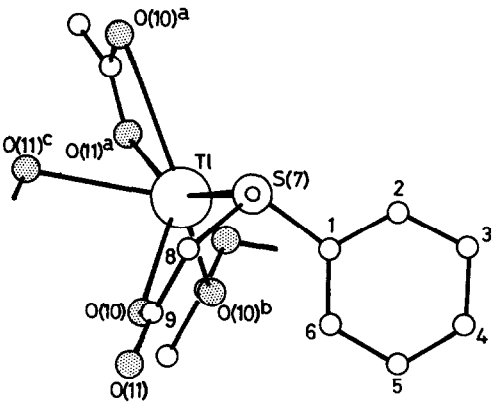

Fig. 1. $[Tl(PTA)(PTAH)]_n$, (**1**).

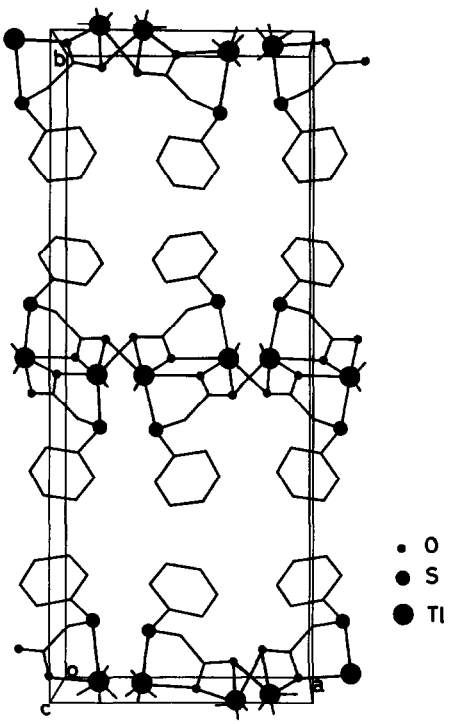

Fig. 2. The packing of **1** in the cell viewed perpendicular to ab. Alternate Tl sites are unoccupied.

$[Cs(DCMPTA)(DCMPTAH)]_n$ (2)

2 crystallizes in the space group $P\bar{1}$ with one molecule per unit cell. This indicates that the DCMPTA and DCMPTAH groups (the anion and the acid) are crystallographically identical giving a typical type A structure.[2] The Tl complex (**1**) also fits this category. Statistical tests indicate a centrosymmetric space group although these tests are not entirely definitive.[12,13]

2 has a distorted centrosymmetric MO_6 octahedral coordination around the Cs (Fig. 3). The metal is linked to alternate Cs atoms along the b axis through acetate bridges and down the a axis through another acetate bridge with O(10) bifurcated between consecutive Cs atoms (Fig. 4). There is no bonding between Cs and S. The results found for the ligand in complex **2** are comparable to that found in DCMPTA complexes of Cu^{II}.[14,15] The

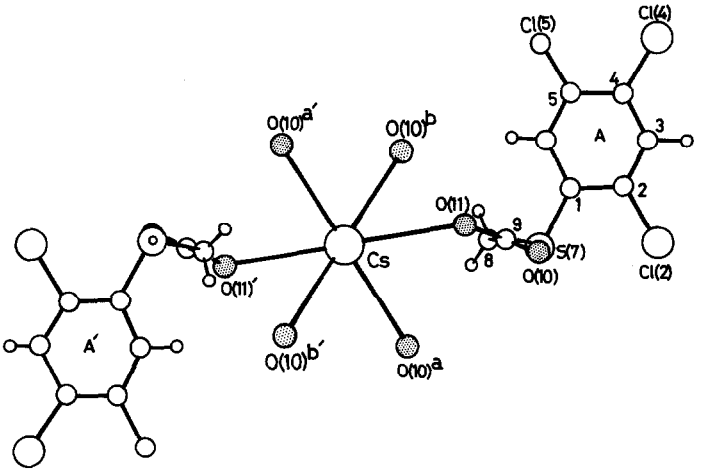

Fig. 3. [Cs(DCMPTA)(DCMPTAH)]$_n$, (2).

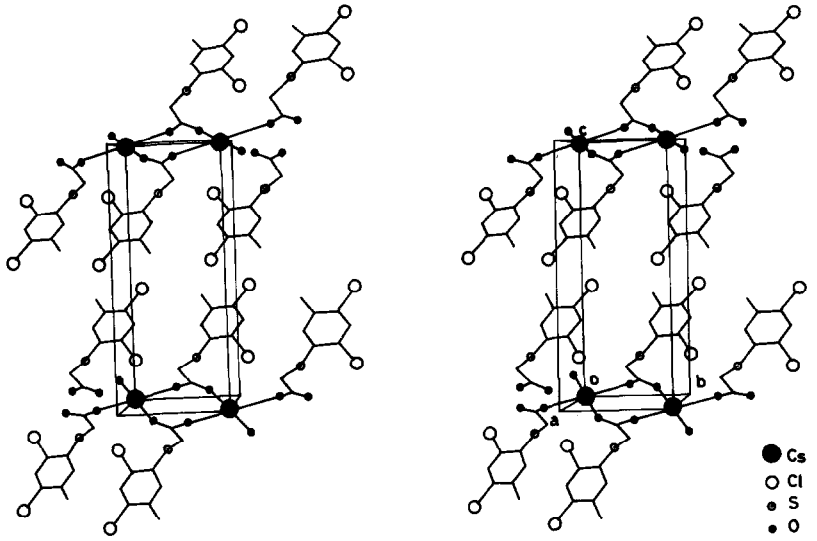

Fig. 4. Stereoview of the packing of **2** in the unit cell. The polymer chains extend down the *a* axis via carboxyl oxygens.

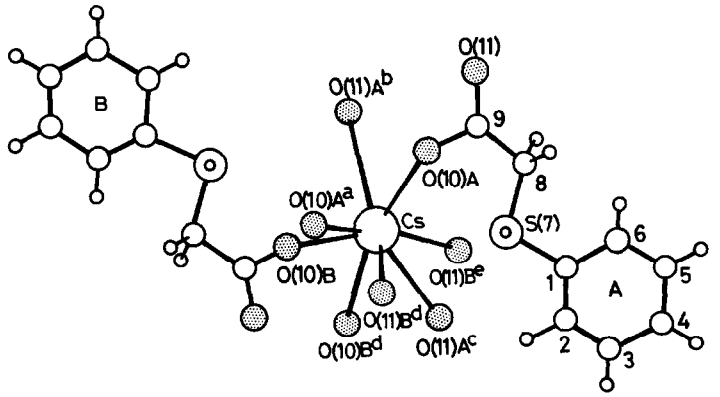

Fig. 5. [Cs(PTA)(PTAH)]$_n$, (3).

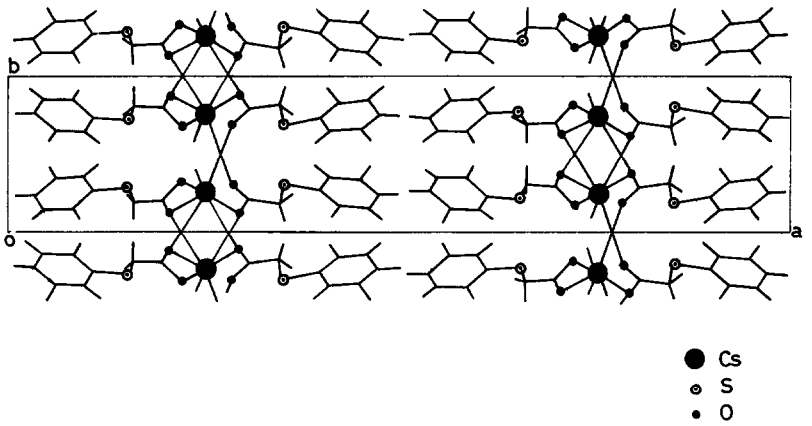

Fig. 6. The packing of **3** in the unit cell viewed down *c*.

Cs—O distances are quite typical of compounds considered to contain ionic Cs, e.g. 3.20(1) Å in $[Cs_2[Cu(H_2O)_6](SO_4)_2]$.[16]

[Cs(PTA)(PTAH)]$_n$ (3)

3 has irregular eight-coordination about Cs, comprising carboxylate oxygens from both PTA, (A) and PTAH, (B) ligands (Fig. 5). It is not possible to distinguish between these types, which are related by pseudo-two-fold symmetry. The packing of **3** in the unit cell (Fig. 6) shows a 2-D polymer which extends through the *b* direction in the cell. Hydrophilic centres involving the Cs—O network are located at $x = 0.25, 0.75$ in the cell while the hydrophobic phenyl rings of the PTA ligands are centred at $x = 0$, 0.5 with no significant intermolecular associations. The PTA and PTAH ligands are also similar and are essentially planar, the conformation of the parent acid.[4]

[Cs(PTPA)(H$_2$O)]$_n$ (4)

4 is also a polymer (Fig. 7) but unlike the type A and type B examples found for **1**, **2** and **3**, no acid molecules are found in the structure. Furthermore, the coordination involves a water ligand, completing a distorted octahedral polyhedron about Cs. The Cs—O range and mean are 3.02–3.33(1) and 3.20(1) Å, respectively. The water is involved in bridging Cs centres in the polymer structure, together with other carboxyl oxygens. The resulting polymer chains pack in the unit cell as a 2-D polymer (Fig. 8). The thiopropionate side chains of the PTPA ligands are convoluted, similar to the conformations of both 2-methyl-2-(phenylthio)propionate and 2-methyl-3-(phenylthio)propionate ligands in their metal complexes.[17]

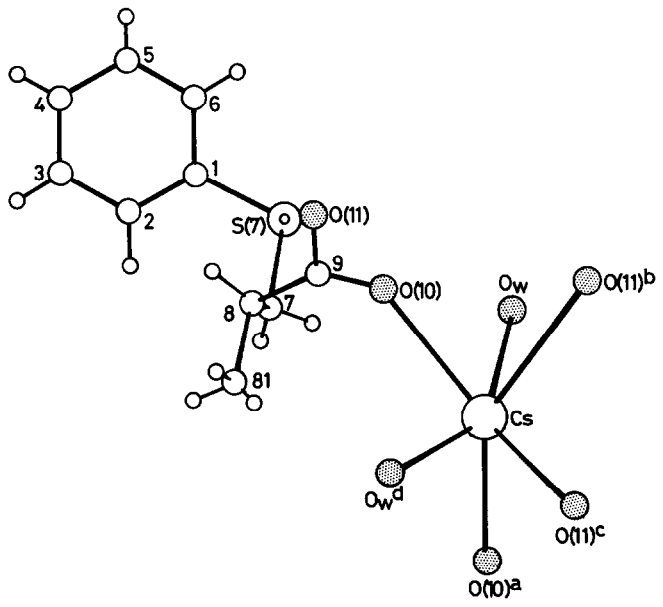

Fig. 7. [Cs(PTPA)(H$_2$O)]$_n$, (**4**).

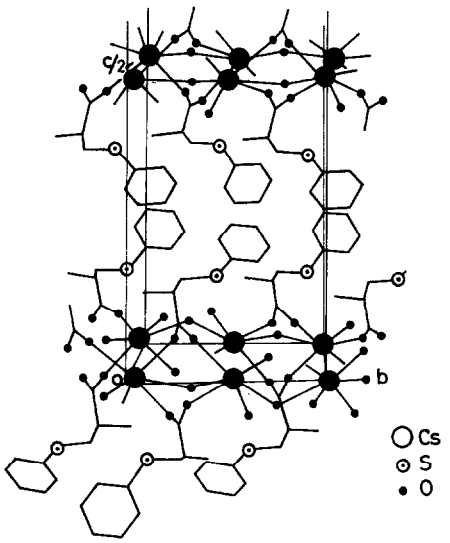

Fig. 8. The packing of **4** in the unit cell viewed down *a*.

Acknowledgements—The authors thank Dr John D. Cotton for constructive comments, the Chinese University of Hong Kong for provision of data collection facilities, and the Queensland Institute of Technology for data preparation and computing facilities.

REFERENCES

1. W.-H. Chan, T. C. W. Mak, W.-H. Yip, C. H. L. Kennard, G. Smith and E. J. O'Reilly, *Aust. J. Chem.* 1987, **40**, 981.
2. J. C. Speakman, *Struct. Bond.* 1972, **12**, 141.
3. H. N. Shrivastava and J. C. Speakman, *J. Chem. Soc.* 1961, 1151.
4. T. C. W. Mak, W.-H. Yip, G. Smith, E. J. O'Reilly and C. H. L. Kennard, *Inorg. Chim. Acta* 1984, **88**, 35.
5. R. Diamond, *Acta Cryst.* 1969, **A24**, 43.
6. G. M. Sheldrick, *SHELX76, Program for Crystal Structure Determination*, Univ. of Cambridge, England (1976).
7. G. M. Sheldrick, *SHELXTL, Revision 3.* Nicolet XRD Corp. (1981).
8. C. B. Shoemaker, D. P. Shoemaker, L. V. McAfee and W. De Kock, *Acta Cryst.* 1985, **C41**, 347.
9. J. H. C. Hogg, H. H. Sutherland and D. J. Williams, *J. Chem. Soc., Chem. Commun.* 1971, 1568.
10. R. Marchand, Y. P. Piffard and M. Tournoux, *Can. J. Chem.* 1975, **53**, 2454.
11. S. Esperas and S. Husebye, *Acta Chem. Scand.* (*A*) 1974, **28**, 1015.
12. G. A. Sim, *Acta Cryst.* 1948, **11**, 123.
13. H. Lipson and W. Cochran, *The Crystalline State, Vol. III: The Determination of Crystal Structures*, p. 56. Bell, London (1966).
14. G. Smith, E. J. O'Reilly, C. H. L. Kennard, T. C. W. Mak and W.-H. Yip, *Polyhedron* 1985, **4**, 451.
15. C. H. L. Kennard, G. Smith, E. J. O'Reilly, T. C. W. Mak and W.-H. Yip, *Inorg. Chim. Acta* 1985, **98**, L31.
16. J. M. Whitnall and C. H. L. Kennard, *J. Solid State Chem.* 1977, **22**, 379.
17. W.-H. Chan, T. C. W. Mak, W.-H. Yip, G. Smith, E. J. O'Reilly and C. H. L. Kennard, *Polyhedron* 1987, **6**, 881.

Polyhedron Vol. 8, No. 6, pp. 801–804, 1989
Printed in Great Britain

0277–5387/89 $3.00+.00
© 1989 Pergamon Press plc

A PRESSURE TUNING SPECTROSCOPIC STUDY OF THE SULPHIDO–METAL CLUSTERS, $M_6(\mu_3\text{-}S)_8(PEt_3)_6^{n+}$ (M = Fe, $n = 2$; M = Co, $n = 1$)

JEFFERY L. COFFER, JOHN R. SHAPLEY* and HARRY G. DRICKAMER*

School of Chemical Sciences, Department of Physics, and Materials Research Laboratory, University of Illinois, Urbana-Champaign, Urbana, IL 61801, U.S.A.

(*Received* 11 *August* 1988; *accepted after revision* 13 *October* 1988)

Abstract—The effect of pressure on the visible absorption spectra of the sulphido–metal clusters, $M_6(\mu_3\text{-}S)_8(PEt_3)_6^{n+}$ (M = Fe, $n = 2$; M = Co, $n = 1$) has been measured in both crystalline and polymethylmethacrylate environments up to 171 kbar. The broad absorption at *ca* 15.4 kK (650 nm) for each cluster has been deconvoluted into three separate peaks. In the case of the iron cluster, tentative assignments of the transitions are made on the basis of their shifts with pressure in conjunction with a previously-reported SCF-Xα calculation. The cobalt cluster shows a much weaker pressure dependence, which is attributed to weaker metal–metal interactions and more delocalized ligand character in the frontier orbitals.

Extensive interest in the chemistry of sulphido–metal clusters has developed in recent years, due mainly to their significance as models for heterogeneous metal–sulphide catalysts[1] or the active sites of certain redox proteins.[2] In particular, Ghilardi and co-workers have succeeded in the synthesis and structural characterization of octahedral, paramagnetic clusters of the type $M_6(\mu_3\text{-}S)_8(PEt_3)_6^{n+}$ (M = Fe, $n = 2$; M = Co, $n = 1, 0$).[3,4] These clusters are specifically noteworthy due to their structural similarity to clusters present in the bulk metal sulphides known as the Chevrel phases, some of which become superconducting upon the application of modest pressures.[5]

The electronic structure of these molecular clusters is an active issue. For $Fe_6(\mu_3\text{-}S)_8(PEt_3)_6^{2+}$, magnetic susceptibility and EPR measurements suggest a ground state electron configuration with six unpaired electrons.[3] This is at odds with a SCF-Xα calculation that indicates only four unpaired spins, with the highest occupied level predominantly Fe—Fe bonding. The analogous cobalt cluster, with seven additional valence electrons, is also paramagnetic[4] but details of its magnetic properties or electronic structure are presently unknown.

In an effort to cast light on the nature of the bonding in these systems, a study of the effects of pressure on the visible electronic spectra of $M_6(\mu_3\text{-}S)_8(PEt)_6^{n+}$ (M = Fe, $n = 2$; M = Co, $n = 1$) was undertaken. Pressure tuning spectroscopy (PTS) has been demonstrated to be a powerful means of probing the electronic structure of various molecules, including metal clusters.[6] Changes in static pressure may effect dramatic changes in the electronic energy levels, with such changes highly dependent upon the nature of the orbital interactions in the molecule.

EXPERIMENTAL

$[M_6(\mu_3\text{-}S)_8(PEt_3)_6][B(C_6H_5)_4]_n$ (M = Fe, $n = 2$; M = Co, $n = 1$) were prepared by literature methods.[3,4] Crystalline samples of each were examined using Nujol as a pressure transmitting medium. Both compounds were also studied in a polymeric environment by dissolution in polymethylmethacrylate (PMMA). Each sample was loaded into a diamond anvil cell (DAC). All runs were reproduced at a minimum of two separate loads. The ruby fluorescence method was utilized for pressure calibration.[7] The light source employed was an Oriel tungsten halogen lamp, dispersed by a Kratos 1/4 m monochromator using either a 1000 or 450 blaze grating. Light in the visible region was detected by EMI 9558 or 9658 photomultiplier tubes, along with an Ortec photon counting system. Further details concerning the optical system may be found elsewhere.[8]

*Authors to whom correspondence should be addressed.

The resulting spectra were fit with a series of symmetric Gaussian peaks by means of a computer program that varied the values for each peak's height, location, and full width at half-maximum in order to achieve the minimum variance.

RESULTS AND DISCUSSION

The effect of increasing pressure on the visible spectrum of $Fe_6(\mu_3\text{-}S)_8(PEt_3)_6^{2+}$ dissolved in PMMA is illustrated in Fig. 1. For each spectrum, the broad absorption at *ca* 15.4 kK (620 nm) is most accurately deconvoluted into three separate peaks. The effect of pressure on these three peaks is graphically represented in Fig. 2, both for molecules of the cluster dissolved in PMMA as well as for the crystalline material. Two points should be noted from these shifts. The first is that qualitatively the shifts are the same in both media. This implies that the effects of pressure are intramolecular in nature. The second point is that for each peak there is an initial dramatic blue shift of 10–15 cm^{-1}/kbar, up to approx. 100 kbar. At that point, the slopes of the shifts decrease by an order of magnitude.

Tentative assignments of the three peaks resolved for the Fe_6 cluster may be made by utilizing the above pressure shift data in conjunction with a previously reported SCF-Xα calculation. In Table 1, a comparison of the observed E_{max} values with possible symmetry-allowed one-electron transitions from the Xα calculation is given. From this comparison, it can be seen that the lowest energy peak most closely matches energetically the computed $6t_{2g} \rightarrow 10t_{1u}$ transition, an excitation originating from an MO of mostly Fe—P bonding character to a virtual level of delocalized P—Fe—S interactions. The next experimental absorption peak may be interpreted in terms of either $3t_{1g} \rightarrow 10t_{1u}$ or $4t_{2u} \rightarrow 6e_g$ transitions. The former transition both originates and terminates in MOs involving delocalized P—Fe—S bonding, while the latter originates from an MO primarily Fe—Fe bonding and ends in a delocalized P—Fe—S energy level. Finally, the highest energy band, closely matching the computed $4t_{2u} \rightarrow 7t_{2g}$ transition, involves a level of Fe—Fe interactions as its origin and terminates in a more delocalized Fe—S orbital.

Given the similar shifts of all peaks with increasing pressure, the above assignments are consistent with experimental observations. These assignments reflect pairs of transitions that either originate or terminate in molecular orbitals of identical symmetry (i.e. $4t_{2u}$ or $10t_{1u}$). In the case of the middle-energy peak, one cannot definitely distinguish

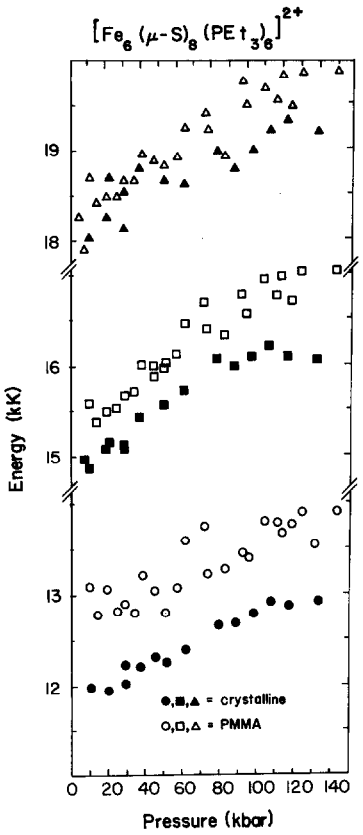

Fig. 2. The effect of pressure on the three visible absorption peaks of $Fe_6(\mu_3\text{-}S)_8(PEt_3)_6^{2+}$ in crystalline and PMMA environments.

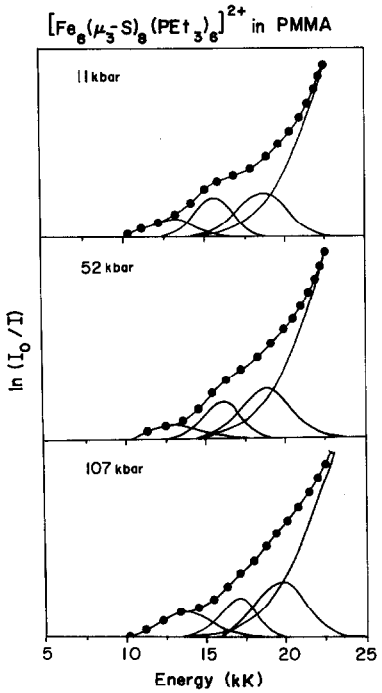

Fig. 1. The visible spectrum of $Fe_6(\mu_3\text{-}S)_8(PEt_3)_6^{2+}$, dissolved in PMMA, at 11, 52 and 117 kbar.

Table 1. Observed and calculated E_{max} values of $Fe_6(\mu_3\text{-}S)_8(PEt_3)_6^{2+}$ and the transition type

E_{max} (kK) Crystalline[a]	PMMA[a]	Calcd[b]	Transition type
12.1	13.0	13.7	$6t_{2g} \rightarrow 10t_{1u}$ (Fe—P → P—Fe—S)
14.9	15.5	15.7	$3t_{1g} \rightarrow 10t_{1u}$ (P—Fe—S → P—Fe—S)
		16.0	$4t_{2g} \rightarrow 6e_g$ (Fe—Fe → P—Fe—S)
18.0	18.5	17.5	$4t_{2u} \rightarrow 7t_{2g}$ (Fe—Fe → Fe—S)

[a] Experimental E_{max} values extrapolated to 1 atm.
[b] Ref. 3.

between the two possibilities given, although the $3t_{1g} \rightarrow 10t_{1u}$ assignment is somewhat closer energetically to the observed value. It should be emphasized also that these assignments concur with the ground state electronic configuration suggested by EPR and magnetic susceptibility data.[3]

The shifts with increasing pressure for the analogous peaks in the case of the cobalt cluster in both crystalline form and PMMA are illustrated in Fig. 3. While the scatter in the polymer data is substantial, it is apparent from consideration of the data from both media that there is an absence of a noteable blue shift for the two lowest energy bands in $Co_6(\mu_3\text{-}S)_8(PEt_3)_6^+$. This effect is most pronounced if one compares, for example, the shifts obtained for the crystalline Fe_6 cluster with the analogous Co_6 molecule (Fig. 4). While there is no detailed theoretical study available to assist in spectral assignments of this cobalt cluster, some qualitative explanations for the differences between the iron and cobalt analogues are possible. Consideration of structural data reveals that the average metal–metal bond lengths in the cobalt cluster are considerably

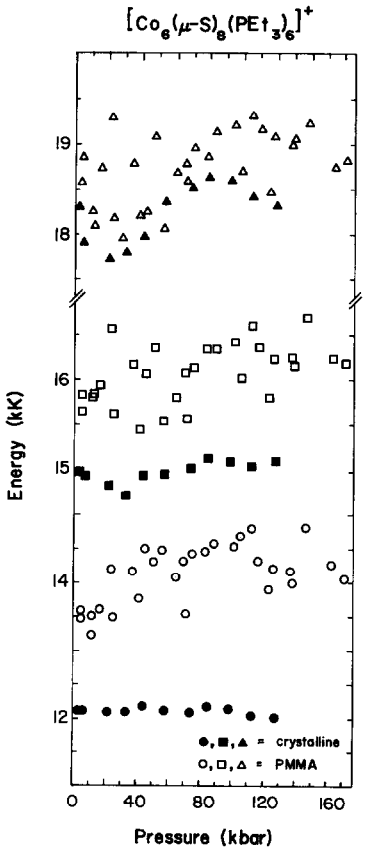

Fig. 3. The effect of pressure on the three visible absorption peaks of $Co_6(\mu_3\text{-}S)_8(PEt_3)_6^+$ in crystalline and PMMA environments.

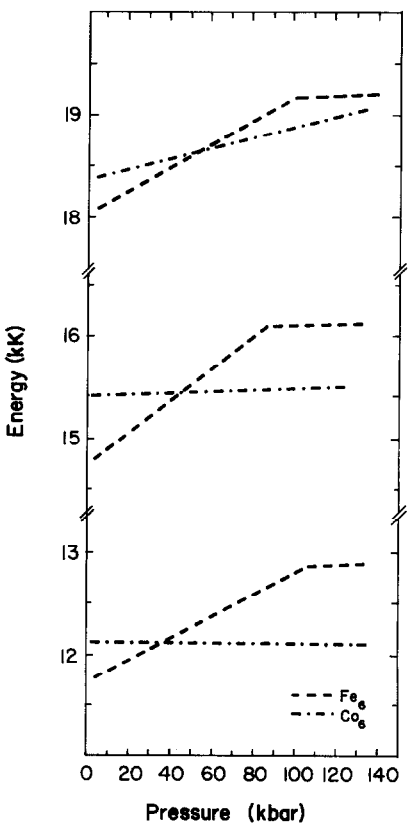

Fig. 4. Comparison of the shifts in crystalline $Fe_6(\mu_3\text{-}S)_8(PEt_3)_6^{2+}$ and $Co_6(\mu_3\text{-}S)_8(PEt_3)_6^+$ (least-squares fit).

longer than in the Fe_6 analogue and also longer than those in other large cobalt clusters. These relatively long Co—Co bonds are presumably related to the high valence electron count (97) in this cluster, and reflect weaker metal–metal interactions as a consequence. It should also be noted that the metal–sulphur and metal–phosphorus distances are shorter in this cluster, and the balance between M—M and P—M—S energy levels will be affected as a result. Recall that in the case of the Fe_6 cluster, two of the assigned peaks are transitions from energy levels primarily of M—M character to more delocalized metal–ligand orbitals. Thus the absence of a substantial blue shift with increasing pressure for the visible absorption bands of this Co_6 cluster suggests that their transitions arise and terminate in electronic energy levels which are more delocalized throughout the entire cluster than the iron analogue.

Finally, it should be noted that the highest energy absorption of the Co_6 cluster in a crystalline environment does appear to mimic somewhat the analogous band in the Fe_6 cluster in terms of a blue shift. This result is taken albeit with some suspicion, since the intensity of this band is extremely close to an intense absorption in the UV (a band not accessible with our equipment). Thus it is doubtful if the measured shift is quantitatively meaningful.

In summary, the observations reported here provide a tentative assignment of the visible electronic spectrum of $Fe_6(\mu_3\text{-}S)_8(PEt_3)_6^{2+}$, an assignment which is consistent with previously reported experimental data. Distinct differences between the optical properties of the iron and cobalt analogues are present, due presumably to differences in their frontier electronic levels. Further experiments, in particular a rigorous theoretical study of $Co_6(\mu_3\text{-}S)_8(PEt_3)_6^{+}$, are needed to clarify these differences.

Acknowledgements—This work was supported in part by the Materials Science Division of the Department of Energy under contract DE-AC02-76ER01198 and in part by the National Science Foundation Grant DMR 86-12860.

REFERENCES

1. J. M. Berg and R. H. Holm, *Iron–Sulfur Proteins* (Edited by T. G. Spiro), Vol. 4. Wiley, New York (1982).
2. B. Bogdanovich, P. Gottsch and M. Rubach, *J. Mol. Cat.* 1981, **11**, 135.
3. A. Agresti, M. Bucci, F. Cecconi, C. Ghilardi and S. Midollini, *Inorg. Chem.* 1985, **24**, 689; F. Cecconi, C. Ghilardi and S. Midollini, *J. Chem. Soc., Chem. Commun.* 1981, 640.
4. F. Cecconi, C. Ghilardi, S. Midollini and A. Orlandini, *Polyhedron* 1986, **5**, 2021; F. Cecconi, C. Ghilardi and S. Midollini, *Inorg. Chim. Acta* 1982, **64**, L47.
5. R. Chevrel, H. Hirrien and M. Sergent, *Polyhedron* 1986, **5**, 87, and references therein; Y. Yao, R. Guertin, D. Jenks, J. Jorgensen and D. Capone, *Phys. Rev. B* 1988, **37**, 5032.
6. H. G. Drickamer, *Accts Chem. Res.* 1986, **19**, 329.
7. J. D. Barnett, S. Block and C. J. Piermanini, *Rev. Sci. Instrum.* 1973, **44**, 1.
8. C. W. Jurgensen and H. G. Drickamer, *Phys. Rev. B* 1984, **30**, 7202.

Polyhedron Vol. 8, No. 6, pp. 805–811, 1989
Printed in Great Britain

0277–5387/89 $3.00+.00
© 1989 Pergamon Press plc

CHARGE DISTRIBUTION IN ICOSAHEDRAL CARBORANES: A UV PHOTOELECTRON SPECTROSCOPIC STUDY

TOMÁŠ VONDRÁK*

ESCA Centre, The J. Heyrovský Institute of Physical Chemistry and Electrochemistry, Czechoslovak Academy of Sciences, Dolejškova 3, 182 23 Prague 8, Czechoslovakia

and

JAROMÍR PLEŠEK, STANISLAV HEŘMÁNEK and BOHUMIL ŠTÍBR

Institute of Inorganic Chemistry, Czechoslovak Academy of Sciences, 250 68 Řež near Prague, Czechoslovakia

(*Received* 15 *August* 1988; *accepted* 20 *October* 1988)

Abstract—The UV photoelectron (PE) investigation of dicarba-*closo*-dodecaboranes 1,12-$C_2B_{10}H_{12}$, 1-SH-1,12-$C_2B_{10}H_{11}$, 2-SH-1,12-$C_2B_{10}H_{11}$, 1-X-1,2-$C_2B_{10}H_{11}$ (X = SH, phenyl), 3-phenyl-1,2-$C_2B_{10}H_{11}$, 4-X-1,2-$C_2B_{10}H_{11}$, 8-X-1,2-$C_2B_{10}H_{11}$, 9-X-1,2-$C_2B_{10}H_{11}$, 9-X-1,7-$C_2B_{10}H_{11}$ (X = SH, CH_3S) and 1-SH-1,7-$C_2B_{10}H_{11}$ is reported. The first two band systems in the PE spectrum of 1,12-$C_2B_{10}H_{11}$ are assigned to cluster π-bonding orbitals and σB—H(C—H)-bonding orbitals, respectively. The interaction between exo-substituent and cluster π-orbitals is weak and the sulphur lone pair ionization energy depends simply on the mutual position of substituent and carbon atoms. The electron density at particular vertices in 1,2-$C_2B_{10}H_{12}$ decreases in the order $9 \gtrsim 8 > 4 > 3 > 1$.

Cluster compounds of boron have been the subject of extensive experimental and theoretical investigation.[1,2] The bonding in heteroboranes and perturbations of the electron densities brought about by heteroatoms or substituents are still not clearly understood. The rationalization of the electron structure and chemistry of polyhedral borane compounds contribute to the general understanding of electron deficient systems. The interest in these compounds is also stimulated by the analogy with the transition metal cluster species through the isolobal principle.[3,4] The separation of the skeletal bonding from the exo-skeletal bonding is useful for the rationalization of the cluster bonding and of Wade's electron counting rules,[5] but any endo–exo separation is not rigorous and thus the equatorial–apex approach and tensor surface harmonics (TSH) methods[6–11] are of limited use for the interpretation of the UV–PE spectra. Moreover, the carbon atoms substituting boron vertices in *closo* structures (deltahedral regular polyhedron) introduce a distortion of spherical symmetry inherent to the TSH approach. Within the Stone TSH approach, the molecular orbitals (MOs) of a cluster are built up from the orbitals of B—H groups. Three orbitals are available for the endo-cluster bonding, namely two *p* orbitals perpendicular to the B—H bond and an inward-pointing, radially oriented, *sp* hybrid. In the limit of spherical symmetry, the resulting MOs are labelled *S*, *P*, *D*, *F* etc. The MOs composed of the *sp* hybrid are labelled by the superscript σ, and the MOs composed of the *p* orbitals have the properties of vector surface harmonics and are labelled P^π, D^π etc. The correlation of some irreducible representations of the full rotation group with those of its I_h and D_{5d} subgroups is shown in Table 1.

Some carboranes were the subject of semi-empirical[12–19] and *ab initio*[20,21] calculations. The MNDO MO energies in a series of *closo*-boranes are in reasonable agreement with the results of TSH calculations involving the cage σ–π interaction[22] and with the *ab initio* results.[23] The MNDO calculated orbital energies were used for the interpretation of the HeI PE spectra of *closo*-carboranes, 1,2-

* Author to whom correspondence should be addressed.

Table 1. Correlation of some irreducible representations of the full rotation group (R_3) and those of I_h and D_{5d} point groups

R_3 ⟶	I_h ⟶	D_{5d}
S	A_g	A_{1g}
P	T_{1u}	$E_{1u}+A_{2u}$
D	H_g	$E_{2g}+E_{1g}+A_{1g}$
F	$T_{2u}+G_u+H_u$	$T_{2u}\rightarrow A_{2u}+E_{2u}$
		$G_u\rightarrow E_{1u}+E_{2u}$
		$H_u\rightarrow E_{2u}+E_{1u}+A_{1u}$

$C_2B_{10}H_{12}$ and 1,7-$C_2B_{10}H_{12}$.[24] The PE spectra of 1,12-$C_2B_{10}H_{12}$ and smaller carboranes were interpreted by means of the equatorial–apex model.[25,26] The exo-substitution proved useful for the determination of the π-ionizations in PE spectra of pentaborane.[27] The substituent effect is a particularly suitable tool for the interpretation of PE spectra, since the changes of IEs are approximately proportional to the MO localization at the point of substitution.[28] In the following, we report HeI PE spectra of a series of mercapto-, methylthio-, and phenylderivatives of dicarba-*closo*-dodecaboranes (Fig. 1) with the aim to gain more information on the bonding in icosahedral carborane species.

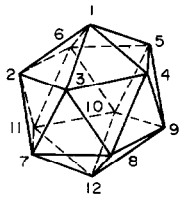

(1) 1,12-$C_2B_{10}H_{11}$
(2) 1-SH-1,12-$C_2B_{10}H_{11}$
(3) 2-SH-1,12-$C_2B_{10}H_{11}$
(4) 1-SH-1,2-$C_2B_{10}H_{11}$
(5) 4-SH-1,2-$C_2B_{10}H_{11}$
(6) 4-CH_3S-1,2-$C_2B_{10}H_{11}$
(7) 8-SH-1,2-$C_2B_{10}H_{11}$
(8) 8-CH_3S-1,2-$C_2B_{10}H_{11}$
(9) 9-SH-1,2-$C_2B_{10}H_{11}$
(10) 9-CH_3S-1,2-$C_2B_{10}H_{11}$
(11) 1-C_6H_5-1,2-$C_2B_{10}H_{11}$
(12) 3-C_6H_5-1,2-$C_2B_{10}H_{11}$
(13) 1-SH-1,7-$C_2B_{10}H_{11}$
(14) 9-SH-1,7-$C_2B_{10}H_{11}$
(15) 9-CH_3S-1,7-$C_2B_{10}H_{11}$

Fig. 1. Structures of derivatives of *closo*-1,2-$C_2B_{10}H_{12}$, 1,7-$C_2B_{10}H_{12}$ and 1,12-$C_2B_{10}H_{12}$.

EXPERIMENTAL

The photoelectron spectrometer used was the VG Scientific UVG 3 instrument. The working resolution was 30–40 meV throughout the whole scanned range, since the analyser was operated in the constant passing energy mode. The HeI PE spectra were calibrated by an Ar–Xe mixture added to the measured sample. The temperature of evaporation varied in the 80–140°C range. The samples (**1–15**) (Fig. 1) were prepared by original methods[29–31] or according to already known procedures.[32–34] The MNDO program developed by W. Thiel[35] was used. The experimental coordinates of heavy atoms were fixed,[36] whereas the internal coordinates of the hydrogen atoms were allowed to relax. For the *closo*-$B_{12}H_{12}^{2-}$ species the I_h symmetry and B—B and B—H distances of 1.782 and 1.166 Å were adopted, respectively.

RESULTS AND DISCUSSION

1,12-*dicarbadodecaborane* (1) *and derivatives* (2, 3)

The PE spectrum of (**1**) is similar to the spectra of isomeric 1,2-$C_2B_{10}H_{12}$ and 1,7-$C_2B_{10}H_{12}$.[24] The higher symmetry of (**1**) (D_{5d} point group) brings about a smaller number and a better resolution of PE bands observed in the spectrum (Fig. 2). For the assignment of the photoelectron bands, the validity of the Koopmans' theorem,[37] i.e. equating of ionization energies to the negative of orbital energies, is assumed. In the PE spectrum, four overlapping bands are observed within the 10.5–12.1 eV interval (region A) and another three bands are found in the 13.5–14.3 eV interval (region B). The high energy region of the spectrum (region C) consists of two bands at 16.01 and 17.22 eV, and of a shoulder on the low energy side of the band peaking at 16.01 eV. The MNDO calculation provides a picture consistent with the PE spectrum: the five outermost occupied levels lie within the 1 eV interval (Fig. 3). These levels are the g_u and h_g symmetry species (in the I_h point group). The inspection of the composition of these levels shows that those belonging to the F species ($2e_{2u}$ and $3e_{1u}$ in D_{5d} point group) are composed purely of the boron and carbon p-orbitals which combine in lobes directed tangentially to the sphere circumscribing the cluster (Table 2). These levels which belong to the D representation, namely $2e_{2g}$, $2e_{1g}$ and $4a_{1g}$, have a considerable contribution from hydrogen s-orbitals. These levels are also of the π-type but the axes of the resulting surface orbitals are not perpendicular to the exo-bonds and thus they have a non-zero overlap with the hydrogen s-orbitals. The mixing of

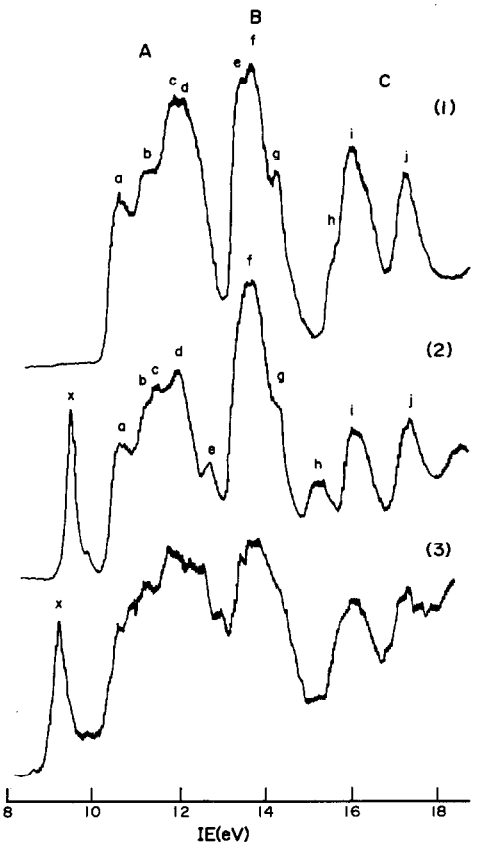

Fig. 2. HeI PE spectrum of 1,12-$C_2B_{10}H_{12}$ (**1**), 1-SH-1,12-$C_2B_{10}H_{11}$ (**2**) and 2-SH-1,12-$C_2B_{10}H_{11}$ (**3**).

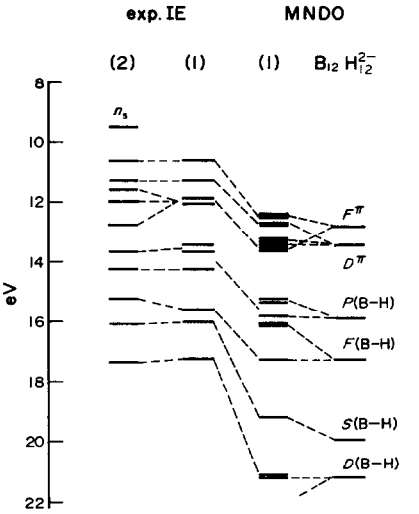

Fig. 3. Diagram of vertical IEs of 1,12-$C_2B_{10}H_{12}$ (**1**) and MNDO orbital energies for (**1**) and $B_{12}H_{12}^{2-}$. The scale is shifted by 10 eV to lower energy for $B_{12}H_{12}^{2-}$.

hydrogen *s*-orbitals with the *D* species is symmetrically allowed since the 12 hydrogen *s*-orbitals transform as a_g, t_{1u}, t_{2u} and h_g. Carborane (**1**) does not strictly have the I_h symmetry. Calculation of the regular icosahedral anion, $B_{12}H_{12}^{2-}$ (Table 3), shows that the deviation from the I_h symmetry does not affect to a significant extent the contribution of the hydrogen *s*-orbitals in the *D* surface levels.

Table 2. Experimental vertical IEs for (**1**) and (**2**), and calculated MO energies and composition of MOs for (**1**)

1-SH-1,12-$C_2B_{10}H_{11}$ (**2**) IE (eV)	1,12-$C_2B_{10}H_{12}$ (**1**) IE (eV)	$-\varepsilon$ (eV)	C[a] (%)	H[b] (%)	D_{5d}	I_h	R_3	Character
9.50 *x*								n_S
10.67 *a*	10.61 *a*	12.44	0	0	$2e_{2u}$	g_u	*F*	π
11.32 *b*	11.26 *b*	12.75	0	37	$2e_{2g}$	h_g	*D*	π
11.56 *c*	11.87 *c*	13.27	22	35	$2e_{1g}$	h_g	*D*	π
12.00 *d*	12.00 *d*	13.39	30	33	$4a_{1g}$	h_g	*D*	π
12.75 *e*	13.45 *e*	13.57	39	3	$3e_{1u}$	g_u	*F*	π
13.66 *f*	13.67 *f*	15.25	7	39	$2e_{1u}$	t_{1u}	*P*	σ-BH
14.23 *g*	14.26 *g*	15.80	31	38	$3a_{2u}$	t_{1u}	*P*	σ-BH
15.23 *h*	15.63 *h*	16.10	0	43	$1e_{2u}$	t_{2u}	*F*	σ-BH
16.08 *i*	16.01 *i*	17.25	27	42	$2a_{2u}$	t_{2u}	*F*	σ-BH
17.37 *j*	17.22 *j*	19.17	13	35	$3a_{1g}$	a_g	*S*	σ-BH
		21.17	0	13	$1e_{2g}$	h_g	*D*	σ-BH
		21.53	18	13	$1e_{1g}$	h_g	*D*	σ-BH
		24.45	34	15	$2a_{1g}$	h_g	*D*	σ-BH
		29.59	6	5	$1e_{1u}$	t_{1u}	*P*	σ
		36.49	50	7	$1a_{2u}$	t_{1u}	*P*	σ
		46.05	30	2	$1a_{1g}$	a_g	*S*	σ

[a] The sum of squares of atomic orbital coefficients over both carbon atoms.
[b] The sum of squares of atomic orbital coefficients over all hydrogen atoms.

Table 3. Calculated MO energies and composition of MOs for *closo*-$B_{12}H_{12}^{2-}$

I_h	R_3	$-\varepsilon$ (eV)	H^a (%)	Character
$1g_u$	F	2.8	0	π
$2h_g$	D	3.43	38	π
$2t_{1u}$	P	5.84	44	σ-BH
$1t_{2u}$	F	7.22	48	σ-BH
$2a_g$	S	9.92	40	σ-BH
$1h_g$	D	11.81	18	σ-BH
$1t_{1u}$	P	19.8	7	σ
$1a_g$	S	31.27	7	σ

[a] The sum of squares of atomic orbital coefficients over all hydrogen atoms.

The following five levels ($2e_{1u}$, $3a_{2u}$, $1e_{2u}$, $2a_{2u}$ and $3a_{1g}$) have a σ-exo bonding character. Within the Stone notation these levels belong to the P, F and S species. Thus on the basis of the MNDO calculated MO energies, the bands *a–d* in region A of the spectrum of (**1**) can be assigned to the F and D cluster π-levels and three observed bands *e–g* in region B to the F and P σ-BH orbitals. The band *i* and the shoulder *h* on its low energy side may be tentatively assigned to the a_{2u} component of the F σ-BH and to the S σ-BH level, respectively. The remaining band *j* may arise from the ionization of the highest component of the D σ-BH level but the agreement of the vertical IEs and the relative spacings of MO energies is rather poor in region C.

The substitution of the C(1) hydrogen by the SH-group lowers the symmetry of 1,12-$C_2B_{10}H_{12}$ to C_{5v} (if the non-linearity of the SH-group is neglected) and thus the number of the endo-bonding levels is conserved. The PE spectrum of the 1-SH-derivative (**2**) differs markedly in the band envelope within region A. Two bands (*b*, *c*) are observed instead of band *b* in (**1**) and the ionizations *c* and *d* of the parent compound seem to fall within band *d* and a new weak band *e* appears. The narrow peak *x* appearing at 9.50 eV is unambiguously due to the ionization of the sulphur lone pair (n_S). Since the π-conjugative interactions between skeletal π-orbitals and substituent *p*-orbitals were found to be weak,[24] the effect of the substituent is predominantly of the inductive nature. The n_S vertical IE is equal to that in methanethiol[38] and thus a similar electron density on the carbon atom may be anticipated.

The position of the first two π-ionizations is not affected by the substituent. This agrees with the calculated MO localizations. The two highest occupied π-levels have no contribution from the carbon orbitals and thus the SH substituent has only a slight effect on their IEs. On the other hand, the $2e_{1g}$, $4a_{1g}$ and $3e_{1u}$ π-levels have considerable contributions from the carbon orbitals. These levels may be more sensitive to the substitution and this may rationalize the changes of the band envelope within bands *c* and *d*, and the appearance of band *e* at 12.75 eV. The latter band may be assigned to the $4a_{1g}$ level for which the σ-overlap with sulphur orbitals is symmetry allowed and the calculation of parent (**1**) provides a high contribution of carbon bonded hydrogen *s*-orbitals. The same argument supports the assignment of band *h* to the $2a_{2u}$ exo-bonding level which seems significantly destabilized in (**2**).

The PE spectrum of 2-SH-1,12-$C_2B_{10}H_{11}$ (**3**) exhibits at least six transitions within region A. The higher number of bands observed is clearly due to the loss of the five-fold axis. The n_S ionization is shifted by 0.27 eV to lower IEs.

Phenyl derivatives (**11**, **12**)

The two sharp bands (*x*, *x'*) which appear before the onset of skeletal π-ionizations come from the ionization of the $e_{1g}(\pi)$-level of phenyl (Fig. 4). As is observed in the PE spectra of benzene derivatives, this level is split into the b_1 and a_2 orbitals (in C_{2v} point group). The splitting is a measure of the π–π interaction.[39] The observed splitting (0.29 eV) is lower than that found for methylbenzene[40] (0.52 eV) where only the hyperconjugative and the inductive effects work. It corroborates the conclusion that the π–π interaction between the cluster and exo-substituent is weak.

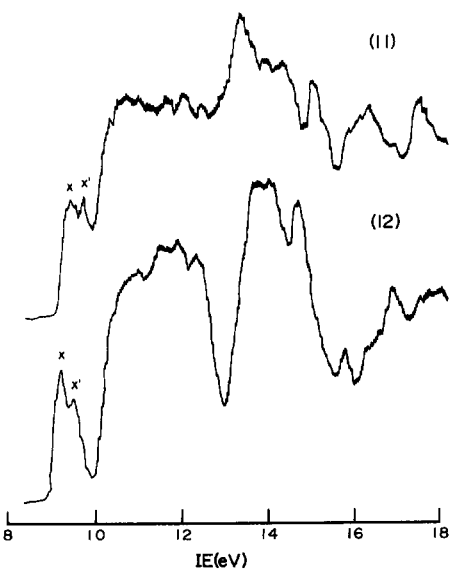

Fig. 4. HeI PE spectra of phenylcarboranes (**11**) and (**12**).

Mercapto and methylthio derivatives (**4–10, 13–15**)

Examples of PE spectra of the SH and CH_3 derivatives are shown in Fig. 5. The shape of the PE spectra of the parent 1,2-$C_2B_{10}H_{12}$ and 1,7-$C_2B_{10}H_{12}$ is conserved. A new band (x') emerges in the spectra of (**8**) and (**10**). It arises probably from the ionization of the sulphur angle determining orbital ($\tilde{n}_S$), rather than from the skeletal π-ionizations. The IEs of sulphur localized orbitals are summarized in Table 4. The n_S IE of CH_3S derivatives is 0.66–0.69 eV lower than that of corresponding SH derivatives.

The n_S IE decreases with an increase in the number of edges connecting the B—S(H, CH_3) vertex (denoted B_x) with the carbon vertices. When the number of edges between the carbon atoms and the B_x vertex are the same, then IEs are identical (within the experimental error) as follows from the comparison of pairs (**3**)–(**5**), (**7**)–(**14**) and (**8**)–(**15**) (see Table 4). The increase of one $C\cdots B_x$ distance in the 1,2-isomer from one to two edges (denoted $1 \rightarrow 2$) brings about a destabilization of 0.48 eV, as follows from the comparison of (**5**) and (**7**). A further increase in the $C\cdots B_x$ distance to three edges ($2 \rightarrow 3$) results in the destabilization by 0.04 eV in (**9**).

For the phenyl derivatives the destabilization of the phenyl $e_{1g}(\pi)$ level amounts to 0.26 eV on going

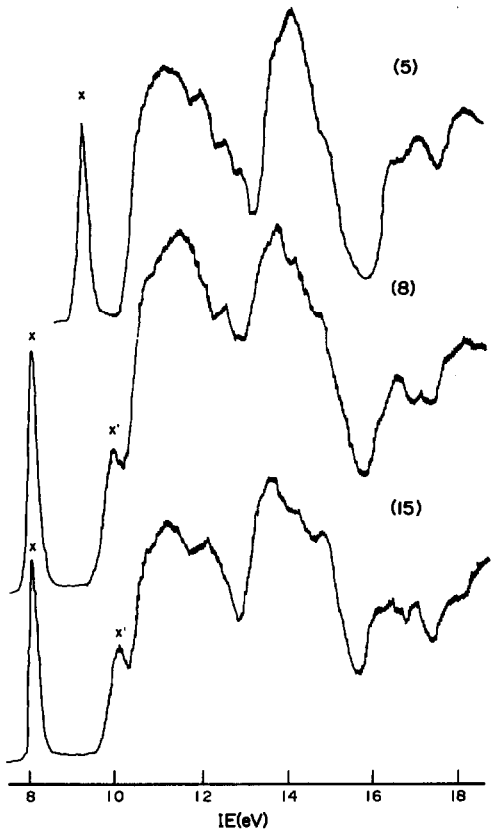

Fig. 5. HeI PE spectra of mercapto- and methylthiocarboranes (**5**), (**8**) and (**15**).

Table 4. n_S, $\tilde{n}_S$ and phenyl $e_{1g}(\pi)$ vertical IEs in substituted carboranes[a] (eV)

Distance (edges)[b]		HS—		CH_3S—		Phenyl $e_{1g}(\pi)$		
C(1)	C(x)	n_S	$\tilde{n}_S$	n_S	$\tilde{n}_S$	a_2	b_1	M[c]
				(eV)				
0	1	9.99 [4]				9.77	9.48	9.63 [11]
0	2	9.58 (9.51) [13]						
0	3	9.50 (9.47) [2]						
1	1	9.73[d]				9.51	9.22	9.37 [12]
1	2	9.25 (9.25) [5]		8.58 (8.56) [6]				
		9.24 (9.25) [3]						
2	2	8.77 (8.77) [7]		8.08 (8.09) [8]	10.01			
		8.77 (8.77) [14]	10.65	8.11 (8.09) [15]	10.14			
2	3	8.73 (8.73) [9]		8.03 (8.04) [10]	10.04			

[a] The values in parentheses are the calculated IEs if the destabilization of the substituent orbital is taken as 0.26, 0.48 and 0.04 eV for the increase in the number of edges separating the substituted skeletal atom from carbon atom from $0 \rightarrow 1$, $1 \rightarrow 2$ and $2 \rightarrow 3$, respectively. The compound's number is in brackets. The effect of both carbon atoms is assumed additive and [4] is taken as the reference point. In the MeS derivatives [6, 8, 10 and 15], the destabilization of the n_S orbital by 0.68 eV induced by the methyl group is assumed.

[b] The number of edges separating the substituted skeletal atom from carbon atoms C(1) and C(x); $x = 2, 7, 12$.

[c] The mean value of a_2 and b_1 IEs.

[d] Estimated value for 3-SH-1,2-$C_2B_{10}H_{11}$.

from the 1- to the 3-derivative, i.e. when the $C\cdots B_x$ distance increases by one C—B edge (denoted $0 \rightarrow 1$). We can assume the same destabilization of the SH derivative and thus the n_S IE of 9.73 eV can be estimated for 3-SH-1,2-$C_2B_{10}H_{11}$. This value is consistent with the n_S IE of (**5**) which can be formally derived from the 3-SH derivative by an increase of one $C\cdots B_x$ distance from one to two edges.

If the additivity of the effects of carbon atoms is assumed, the relative destabilization of the sulphur lone pair in the derivatives of 1,7-$C_2B_{10}H_{12}$ and 1,12-$C_2B_{10}H_{12}$ can be estimated. Derivative (**13**) is formally derived from (**4**) by the $(1 \rightarrow 2)$ shift. The estimated IE of 9.51 eV agrees well with the experimental one (9.58 eV). Compound (**14**) can be derived from (**4**) by the $2\times(1 \rightarrow 2)+(0 \rightarrow 1)$ shift which corresponds to the destabilization of 1.22 eV. The calculated IE agrees with the experimental value (8.77 eV). For derivatives (**2**) and (**3**), the destabilization can be calculated in the same way. It is equal to $(1 \rightarrow 2)+(2 \rightarrow 3) = 0.52$ eV for (**2**) and $(0 \rightarrow 1)+(1 \rightarrow 2) = 0.74$ eV for (**3**). These estimates, 9.47 and 9.25 eV, are consistent with the experimental values (9.50 and 9.25 eV, respectively).

The sulphur lone pair IE is influenced by the electron density at the point of substitution. The relative changes in n_S IE show that the electron density in 1,2-$C_2B_{10}H_{12}$ decreases in the order $9 \gtrsim 8 > 4 > 3 > 1$, and the electron density in the B(9) position in 1,7-$C_2B_{10}H_{12}$ is approximately equal to that in the B(8) position in 1,2-$C_2B_{10}H_{12}$, and position two in 1,12-$C_2B_{10}H_{12}$ is equivalent to the position four in 1,2-$C_2B_{10}H_{12}$. The observed decrease of the n_S IE correlates well with the site selectivity of the electrophillic attack,[41,42] electron densities inferred from the pK_a values of carborane thiols[43] and with the *ab initio* calculated charges.[21]

CONCLUSIONS

The exo-substitution proved to be a suitable probe for the experimental assessment of electron distribution in perturbed icosahedral cluster species. The electron densities seem to depend only on the number of edges separating the respective vertex from the skeletal heteroatoms. The effect of the two carbon atoms is additive. The MNDO calculated MO picture is consistent with the PE spectra and the observed substitution effect. Although the hydrogen *s*-orbitals' participation seems to differ from Stone's assumption of the complete exo–endo bonding separation, the proposed sequence of the highest occupied levels π-endo, σ-exo seems justified by the interpretation of PE spectra.

REFERENCES

1. W. N. Lipscomb, *Boron Hydrides*. Benjamin, New York (1963).
2. R. N. Grimes, *Carboranes*. Academic Press, New York (1970).
3. B. F. G. Johnson (Ed.), *Transition Metal Clusters*. Wiley, New York (1980).
4. R. W. Rudolph, *Accts Chem. Res.* 1976, **9**, 446.
5. K. Wade, *Adv. Inorg. Chem. Radiochem.* 1976, **18**, 67.
6. R. Hoffmann and W. N. Lipscomb, *J. Chem. Phys.* 1962, **36**, 2179.
7. A. J. Stone, *Molec. Phys.* 1980, **41**, 1339.
8. A. J. Stone, *Inorg. Chem.* 1981, **20**, 563.
9. A. J. Stone and M. J. Alderton, *Inorg. Chem.* 1982, **21**, 2297.
10. A. J. Stone, *Polyhedron* 1984, **3**, 1299.
11. P. W. Fowler and W. Portefield, *Inorg. Chem.* 1985, **24**, 3511.
12. M. D. Newton, F. P. Boer and W. N. Lipscomb, *J. Am. Chem. Soc.* 1966, **88**, 2353.
13. M. D. Newton, F. P. Boer, W. E. Palke and W. N. Lipscomb, *Proc. Nat. Acad. Sci. Wash.* 1965, **53**, 1086.
14. H. Hart and W. N. Lipscomb, *Inorg. Chem.* 1968, **7**, 1070.
15. T. F. Koetzle, F. E. Scarborough and W. N. Lipscomb, *Inorg. Chem.* 1968, **7**, 1076.
16. T. F. Koetzle and W. N. Lipscomb, *Inorg. Chem.* 1970, **9**, 2743.
17. C. C. Cheung, R. A. Beaudet and G. A. Segal, *J. Am. Chem. Soc.* 1970, **92**, 4158.
18. D. A. Dixon, D. A. Kleier, T. A. Halgren, J. H. Hall and W. N. Lipscomb, *J. Am. Chem. Soc.* 1977, **99**, 6226.
19. J. MacCurtain, P. Brint and T. R. Spalding, *J. Chem. Soc., Dalton Trans.* 1985, 2591.
20. I. R. Epstain, T. F. Koetzle, R. M. Stevens and W. N. Lipscomb, *J. Am. Chem. Soc.* 1970, **92**, 7019.
21. M. F. Guest and I. H. Hillier, *Molec. Phys.* 1973, **26**, 435.
22. P. Brint, J. P. Cronin, E. Seward and T. Whelan, *J. Chem. Soc., Dalton Trans.* 1983, 975.
23. M. J. S. Dewar and M. L. McKee, *Inorg. Chem.* 1980, **19**, 2662.
24. T. Vondrák, *Polyhedron* 1987, **6**, 1559.
25. T. P. Fehlner, M. Wu, B. J. Menengheli and R. W. Rudolph, *Inorg. Chem.* 1980, **19**, 49.
26. J. A. Ulman and T. P. Fehlner, *J. Am. Chem. Soc.* 1978, **100**, 449.
27. J. A. Ulman and T. P. Fehlner, *J. Am. Chem. Soc.* 1976, **98**, 1119.
28. A. M. Beez, G. Bieri, H. Bock and E. Heilbronner, *Helv. Chim. Acta* 1973, **56**, 1028.
29. J. Plešek and S. Heřmánek, *Chem. Ind (Lond.)* 1977, 360.
30. J. Plešek and S. Heřmánek, *Coll. Czech. Chem. Commun.* 1981, **46**, 678.
31. J. Plešek, T. Jelínek, S. Heřmánek, F. Mareš and B.

Štíbr, *Coll. Czech. Chem. Commun.*, to be published.
32. T. L. Heyling, J. W. Ager, S. L. Clark, D. J. Mangold, H. L. Goldstein, M. Hillman, R. J. Polak and J. W. Szymanski, *Inorg. Chem.* 1963, **2**, 1089.
33. S. Papetti, C. O. Obenland and T. L. Heying, *Ind. Engng Chem., Prod. Res. Devel.* 1966, **5**, 334.
34. M. F. Hawthorne and P. A. Wegner, *J. Am. Chem. Soc.* 1965, **87**, 4392.
35. W. Thiel, MNDO program. Fachbereich Chemie der Phillips Universität, Marburg.
36. R. K. Bohn and M. D. Bohn, *Inorg. Chem.* 1971, **10**, 350.
37. T. Koopmans, *Physica* 1934, **1**, 104.
38. S. Craddock and R. A. Whiteford, *J. Chem. Soc., Faraday Trans. II* 1972, **68**, 281.
39. R. S. Brown and F. S. Jørgensen, *Electron Spectroscopy*, Vol. 5, p. 66. Academic Press, London (1984).
40. T. P. Debies and J. W. Rabalais, *J. Electron Spect. Relat. Phenom.* 1973, **1**, 355.
41. J. Plešek, Z. Plzák, J. Stuchlík and S. Heřmánek, *Coll. Czech. Chem. Commun.* 1981, **46**, 1748.
42. J. Plešek and S. Heřmánek, *Coll. Czech. Chem. Commun.* 1981, **46**, 687.
43. J. Plešek and S. Heřmánek, *Coll. Czech. Chem. Commun.* 1979, **44**, 24.

Polyhedron Vol. 8, No. 6, pp. 813–818, 1989
Printed in Great Britain

0277–5387/89 $3.00+.00
© 1989 Pergamon Press plc

THE CHEMISTRY OF IRON IN BIOSYSTEMS—III. COMPLEX FORMATION BETWEEN Fe^{III} AND MALONIC ACID IN AQUEOUS SOLUTIONS

V. SALVADÓ and X. RIBAS

Departament de Química, Col.legi Universitari de Girona (U.A.B.), Pça. Hospital 6, E 17071 Girona, Catalonia, Spain

V. ZELANO and G. OSTACOLI

Dipartimento di Chimica Analitica, Università di Torino, Via Bidone 36, I 10125 Torino, Italy

and

M. VALIENTE*

Departament de Química, Química Analítica, Universitat Autònoma de Barcelona, E 08193 Bellaterra, Catalonia, Spain

(*Received* 16 *August* 1988; *accepted* 20 *October* 1988)

Abstract—Complex formation between Fe^{3+} ions and malonic acid (H_2L), in acidic aqueous solutions containing 0.5 M $NaNO_3$ as inert ionic medium at 25°C, has been studied potentiometrically. The data were consistent with the following reactions and related stability constants:

$$Fe^{3+} + L^{2-} = FeL^{+} \quad \log \beta_{0,1,1} = 7.52$$
$$Fe^{3+} + 2L^{2-} = FeL_2^{-} \quad \log \beta_{0,1,2} = 13.29$$
$$Fe^{3+} + 3L^{2-} = FeL_3^{3-} \quad \log \beta_{0,1,3} = 16.93$$

which agree partially with previous models. No mixed complexes were detected, i.e. hydrolytic complex species. A suggestion of possible structures for the complex species formed is briefly discussed. In separate experiments and in the absence of Fe^{III}, protolytic reactions of malonic acid were studied under the same experimental conditions. A numerical comparison of these results with those already published was carried out by means of the Specific Interaction Theory (SIT).

The biological activity of metal ions depends to a great extent on the interactions with those metal complexing agents present in the environment[1] and the formation of strong soluble complexes between Fe^{III} and ligands bearing carboxylic groups which are present in nature, is widely known. A systematic study including chemical characterization of these agents is currently being carried out in our laboratories. Results on the complexation of Fe^{III} with tartrate have been published.[2] We have also investigated iron(III)–malonate complexes in acidic solutions. The presence of malonic acid retards to lower pH the precipitation of ferric hydroxide in aqueous solutions. These differences with respect to tartaric acid excited our curiosity to ascertain the role of side hydroxyl groups in similar ligands.

Iron(III)–malonate complexes have been studied by several authors using different techniques and thermodynamic conditions[3–9] (see Table 1). Thus, a kinetic study carried out by Cavasino[4] found

* Author to whom correspondence should be addressed.

Table 1. Summary of literature data on Fe^{III}–malonate complexes in aqueous solutions

Model	Ionic media	Method	References
FeL, FeL_2	—	Spectrophotometric	3
FeL	0.5 ($NaClO_4$)	Kinetic	4
FeL, HFeL	1.0 ($NaClO_4$)	Amperometric	5
FeL	0.5 ($LiClO_4$)	Potentiometric and spectrophotometric	6
FeL_3	0.5 ($NaClO_4$)	Polarographic	7
FeL, FeL_2	0.1 ($NaClO_4$)	Potentiometric	8
FeL, FeL_2, FeL_3	1.0 ($NaClO_4$)	Potentiometric and calorimetric	9
FeL, FeL_2, FeL_3	0.5 ($NaNO_3$)	Potentiometric	This work

the species FeL. Gordienko,[5] using amperometric measurements, postulates the species FeL and FeHL. In a polarographic study, Schaap *et al.*[6] suggested the species FeL_3. Alternatively, Ramamoorthy and Manning,[8] from potentiometric data, give a model with the species FeL and FeL_2 to exlain the behaviour of the iron(III)–malonate system. Finally Dellien,[9] working in very acidic media and employing both potentiometric and calorimetric techniques, found the complex species FeL, FeL_2 and FeL_3. All these studies were performed at 25°C and different ionic media were employed. A careful and systematic study of the chemical interactions between Fe^{3+} and malonic acid in aqueous solutions has been carried out in the present work. Potentiometric data obtained in a wide concentration range of the reacting species were analysed to quantitatively characterize the complex species and related stability constants.

EXPERIMENTAL

Reagents, solutions and apparatus

Malonic acid (Scharlau, AR) was used with no further purification, its purity was verified by potentiometric titration. Ferric nitrate (Merck, AR) was used as supplied to prepare stock solutions in 0.5 M NO_3^-. The Fe^{III} content was determined as described in ref. 10. The free acidity, h, in iron solutions was obtained following ref. 11. $NaNO_3$ (Probus, AR), purified as described in ref. 12, was used as the ionic media. Solutions of carbonate-free NaOH were prepared and determined as described elsewhere.[12] Stock solutions of malonic acid, $Fe(NO_3)_3$, HNO_3 and NaOH were conditioned in $NaNO_3$ to achieve an ionic strength of 0.5 M.

A digital voltimeter (Crison Digilab 517) of 0.1 mV precision interfaced to an Epson HX 20 computer was used to control the potentiometric experiments. A glass electrode (Metrohm 1028) connected against a double junction reference electrode (Orion 9020) were employed to generate the EMF data.

Method of investigation

Continuous EMF measurements have been performed in order to analyse the equilibrium state of the system. The hydrogen ion concentration, h, has been experimentally determined in a number of solutions prepared from stock solutions of $Fe(NO_3)_3$, malonic acid, HNO_3 and $NaNO_3$.

Measurements of EMF were performed by titrations using the galvanic cell I formulated by:

$$RE//TS/GE, \qquad (I)$$

where GE indicates a glass electrode and RE represents a double junction reference electrode. Stability criteria of the EMF measurements considered the potential to be stable when the variation was less than 0.1 mV within 10 min.

For each experiment, the analytical concentrations of Fe^{III} (**B**) and malonate (**L**) were varied in the range 2.0–6.0 mM and 5.0–20.0 mM, respectively. Values of pH varied from 1.5 to 5.5, where precipitation of ferric hydroxide was observed.

The experimental data are collected in Fig. 1 in the form Z vs $-\log h$ at the different **B** and **L** levels. Z represents the number of H^+ bound to the total malonate and is defined by:

$$Z = (\mathbf{H} - h + Kw/h)/\mathbf{L} \qquad (1)$$

where **H** represents the analytical concentration of hydrogen ion.

In order to verify our equilibrium data, experimental points obtained in back titrations are plotted in Fig. 1 by means of full symbols. The good agreement between the forward and back titration data shows that only reversible processes take part in the

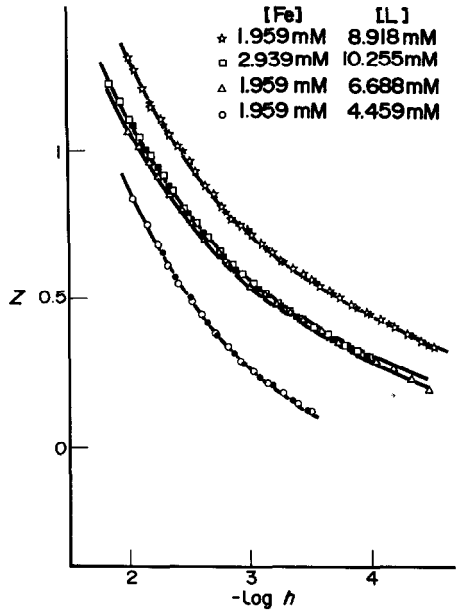

Fig. 1. Z plotted vs $-\log h$ for the different sets of experiments. Full points represent back titrations. Solid lines have been calculated by the model proposed in the present work.

complexation reactions. All the experiments were performed at 25 ± 0.2°C.

RESULTS

Analysis of the experimental information is based on the complex formation between ferric ions, Fe^{3+}, and malonic acid, expressed by the general equation:

$$pH + qFe + rL = H_pFe_qL_r; \quad \beta_{p,q,r} \qquad (2)$$

where $\beta_{p,q,r}$ represents the formation constants of the complex species with different p, q and r values. Charges are omitted for simplicity.

The stoichiometry of the complexes, and the constant $\beta_{p,q,r}$ have been determined by means of a numerical analysis of the experimental data. For this purpose, the computer programs LETAGROP[13] and SUPERQUAD[14] were used. In both cases, the treatment is based on the minimization of an error square sum U, defined by:

$$U = \sum_{N_p} (E_{calc} - E_{exp})^2 \qquad (3)$$

where E_{exp} represents the experimental EMF values, E_{calc} is a corresponding magnitude calculated by the program, assuming a determined model of species formed and related stability constants, and N_p is the number of experimental points.

As has been discussed previously,[2,15] a systematic analysis of such ternary systems (three reacting components) requires a well established knowledge of the binary interactions, i.e. the protolysis of malonic acid and hydrolysis of Fe^{III}. In our case, data for Fe^{III} hydrolysis has been taken from a previous work,[16] which was performed under the same experimental conditions. With respect to malonic acid, the following study was carried out.

Protolytic equilibria of malonic acid

Experiments in the absence of Fe^{III} were carried out in order to quantitatively characterize malonic acid protolysis in the desired thermodynamic conditions.

In this case, the EMF data have been treated both by the Rossotti's graphical method[17] and numerically by the programs LETAGROP and SUPERQUAD. Table 2 gives the results for these treatments, which are found to be in good agreement.

On the other hand and for the sake of comparison with other results reported in the literature,[4,5,18–20] the different values of stability constants have been correlated using the Specific Interaction Theory, SIT.[21,22] Such a treatment of the data can be summarized by the expression:

$$\beta_1^I = \beta_1^0 \gamma_H \gamma_L / \gamma_{HL} \qquad (4)$$

where β_1^I represents the protolytic constant at the ionic strength I, β_1^0 is the value of this constant at $I = 0$ and γ_H, γ_L, γ_{HL} the activity coefficients of H, L and HL species. The activity coefficients follow the expression:

$$\log \gamma_i = -z_i^2 D + \sum_k \varepsilon_{ik} m_k \qquad (5)$$

where D is the Debye–Huckel term, k represents the species with opposed charge to i in the ionic media, m_k represents their molality and ε_{ik} are the specific interaction coefficients between the corresponding species present in the aqueous solution. Applying SIT and rearranging eq. (4), the following expressions can be written for each one of the proto-

Table 2. Results obtained for the behaviour of malonic acid in aqueous 0.5 M $NaNO_3$, by different graphical and numerical methods. $K_{a1} = \beta_2 \beta_1^{-1}$, $\beta_1 = K_{a2}^{-1}$ where K_{a1} and K_{a2} are the corresponding acidic constants

Method	$\log \beta_1$	$\log \beta_2$	$\log K_2$
Rossotti[a]	5.05	7.62	2.57
LETAGROP[b]	5.06 ± 0.008	7.62 ± 0.016	2.56
SUPERQUAD[b]	5.05 ± 0.004	7.61 ± 0.010	2.56

[a] Graphical (ref. 17).
[b] Numerical.

lytic constants ($X = NO_3^-$):

$$Y_1 = \log \beta_1^I + 4D - \varepsilon_{H,X} m_X = \log \beta_1^0 + (\varepsilon_{L,M} - \varepsilon_{HL,M}) m_M \quad (6)$$

$$Y_2 = \log \beta_2^I + 6D - 2\varepsilon_{H,X} m_X = \log \beta_2^0 + \varepsilon_{L,M} m_M. \quad (7)$$

In Fig. 2, Y_1 and Y_2 vs I are represented for the different data considered. As seen, our results show a good fit in such a correlation.

Numerical treatment of the ternary system

With respect to the Fe^{III}–malonate system, a numerical analysis of data has been carried out, starting from previous results[3–9] to fit to our experimental data. The results of the calculation are collected in Table 3. As seen in this table, the best fit to the experimental data corresponds to the model where the species FeL, FeL_2 and FeL_3 are formed. This result is expressed by the following reaction equations, and the corresponding $\beta_{p,q,r}$ values are given:

$$Fe^{3+} + L^{2-} = FeL^+ \quad \log \beta_{0,1,1} = 7.52 \quad (8)$$

$$Fe^{3+} + 2L^{2-} = FeL_2^- \quad \log \beta_{0,1,2} = 13.29 \quad (9)$$

$$Fe^{3+} + 3L^{2-} = FeL_3^{3-} \quad \log \beta_{0,1,3} = 16.93 \quad (10)$$

Further analysis of the results, including polynuclear and mixed species (i.e. protolytic species) has shown that such species do not fit the experimental data.

Figure 3 shows the individual values of $(E_{calc} - E_{exp})$ mV in the acidic range studied. As seen, the proposed model shows no systematic deviations with respect to the experimental data.

Table 3. Results obtained on the numerical treatment of the experimental data for the system Fe^{III}–malonic acid

Model	(p, q, r)	U	σ (mV)	$\log \beta_{p,q,r}$
1	(0, 1, 1)	0.44×10^4	6.89	6.46±0.14
	(0, 1, 2)			11.75±0.06
2	(0, 1, 1)	0.44×10^4	6.85	6.52±0.13
	(0, 1, 2)			11.73±0.07
	(1, 1, 1)			Rejected
3	(0, 1, 1)	0.43×10^3	2.12	7.65±0.15
	(0, 1, 2)			13.35±0.14
	(0, 1, 3)			16.83±0.15
	(−2, 2, 2)			Rejected
4[a]	(0, 1, 1)	0.77×10	0.29	7.52±0.01
	(0, 1, 2)			13.29±0.01
	(0, 1, 3)			16.93±0.01

[a] After correction of possible analytical errors.

DISCUSSION

The results obtained in the present work correspond to the formation of a complex between Fe^{III} and malonic acid in aqueous solutions of 0.5 M $NaNO_3$ as the ionic medium.

The experimental data have verified the equilibrium state of the system as well as that no irreversible or sideways process is taking part in the reactions studied.

The complex species formed are represented by eqs (8)–(10). From the numerical treatment of the data, no polynuclear or protonated species were detected. This fact indicates a different behaviour of this system with respect to the Fe^{III}–tartrate system studied previously[2] in which the formation of polynuclear complexes has been postulated. On the other hand, the stability of the Fe^{III}–tartrate com-

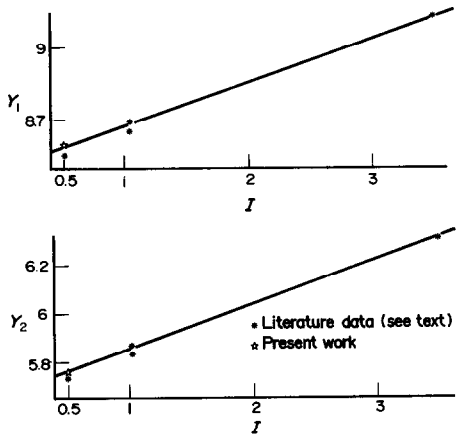

Fig. 2. Correlation of the protolytic constants of malonic acid by means of the Specific Interaction Theory (SIT).

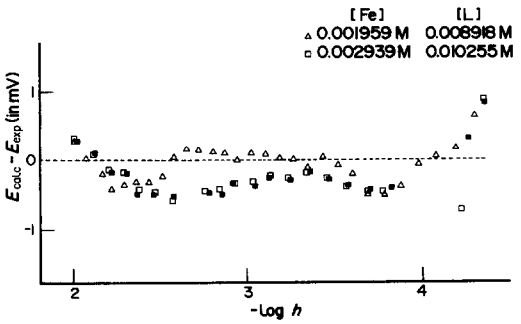

Fig. 3. $(E_{calc} - E_{exp})$ mV vs $-\log h$ for the different experimental values analysed. E_{calc} correspond to the EMF values calculated by the program on the basis of the proposed model.

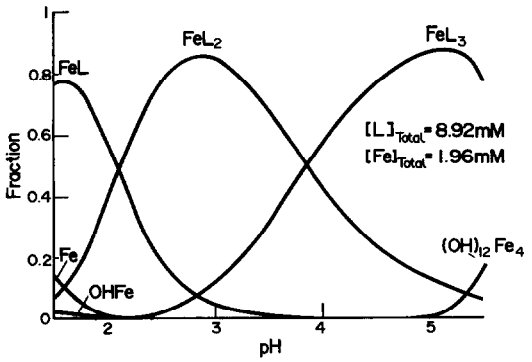

Fig. 4. Fraction diagram of the Fe^{III}–malonate complex species as a function of $-\log h$.

plexes is higher than the Fe^{III}–malonate, thus precipitation of ferric hydroxide is observed at a pH > 5.5, while in the presence of tartaric acid this does not occur. These differences may be explained by the contribution of the hydroxyl groups of the tartaric acid to form more stable complexes.

In Fig. 1 the solid lines represent calculated values of Z vs $-\log h$ using the model given by eqs (8)–(10). The agreement with experimental values shows a high confidence level on this model.

Figure 4 shows the distribution diagram of the species, calculated by the program HALTAFALL,[23] in the acidic range studied. As seen, a step-wise formation of complexes is observed.

The proposed model in the present work corresponds to species of stoichiometry 1 : 1, 1 : 2 and 1 : 3 respectively. For these stoichiometries, and taking into account that Fe^{III} complexes usually have an octahedral co-ordination geometry,[24] it is possible to speculate on probable structures of the proposed species. In Fig. 5, possible structures for the species FeL, FeL_2 and FeL_3 are suggested. These speculations are consistent with the absence of both polynuclear and protolytic complex species in the Fe^{III}–malonate system. At any rate, further experimental information would be needed to properly determine such structures, i.e. direct spectroscopic measurements of the related solutions.

Taking into account the information summarized in Table 1, a correlation between our results and those obtained by Dellien[9] is observed. It is found that the differences in the respective constant values are small in spite of the different media utilized (see Table 4). The work of Dellien shows, in the case of FeL_3 species, that the uncertainty in β_3 is rather large $[(4\pm2)\times10^{16}]$. This may be a consequence of the experimental information, which has been obtained in a very acidic range (the acid content, h, ranges from 30 to 150 mM). In this sense, it is interesting to observe the concentrations of the

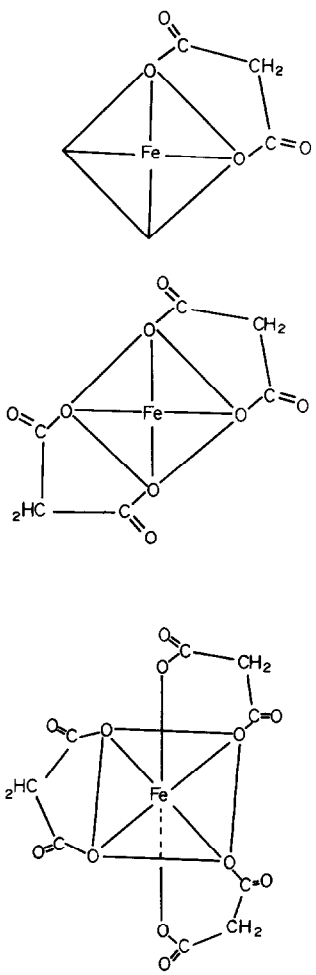

Fig. 5. Suggested structures for the Fe^{III}–malonate soluble complexes assuming an octahedral co-ordination of Fe^{III}.

complex species as a function of pH. Thus, in Fig. 4 it is observed that the presence of FeL_3 is less than 1% at pH < 1, while this species is the most abundant at pH 3.5. It is difficult to see how under such experimental conditions one can differentiate between species of such low concentration. In our case the work was extended up to pH ⩽ 5 where the different species, and especially FeL_3, can be easily distinguished.

Table 4. Differences between the values of stability constants for the Fe^{3+}–malonate equilibria obtained by Dellien[9] and the respective values proposed in this work

Species	$\log\beta$ (ref. 9)	$\log\beta$ (this work)
FeL	7.50	7.52
FeL_2	13.04	13.29
FeL_3	16.60	16.93

On the other hand, the slight differences observed between the constants derived in both investigations may explain that Fe^{3+}–NO_3^- interactions[25] are negligible under our experimental conditions.

Acknowledgements—Thanks are due to Professor P. G. Daniele from the Università di Torino for help and advice. The "Patronat del Col. legi Universitari de Girona" and the Spanish–Italian Co-operation Programme provided financial support for this joint work.

REFERENCES

1. I. M. Harrison and R. J. Hoare, *Metals in Biochemistry*. Chapman and Hall, London (1980).
2. V. Salvadó, X. Ribas and M. Valiente, *Inorg. Chim. Acta* 1987, **137**, 155.
3. F. F. Grigorenko and L. M. Sidler, *Vest. Kiev Univ.* 1969, **10**, 11.
4. F. P. Cavasino and E. Di Dio, *J. Chem. Soc. A.* 1971, 3176.
5. V. I. Gordienko, I. Yu. Mikhailyuk and V. I. Sidorenko, *Zh. Obshch. Khim.* 1971, **41**, 3, 507.
6. W. B. Schaap, H. A. Laitinien and J. C. Bailar, *J. Am. Chem. Soc.* 1954, **76**, 5868.
7. M. Deneux, R. Meiller and R. L. Benoit, *Can. J. Chem.* 1968, **46**, 1383.
8. S. Ramamoorthy and P. G. Manning, *J. Inorg. Nucl. Chem.* 1973, **35**, 1571.
9. I. Dellien, *Acta Chem. Scand. A* 1977, **31**, 473.
10. A. I. Vogel, *Quantitative Inorganic Analysis*. Longman, London (1963).
11. G. Charlot, *Chimie Analytique Générale*. Masson & Cie, Paris (1969).
12. *Some Laboratory Methods*. Mimeograph, Dept. of Inorganic Chemistry, The Royal Institute of Technology, Stockholm (1956).
13. L. G. Sillén and B. Warnquist, *Ark. Kemi* 1969, **31**, 377.
14. A. Vacca and A. Sabatini, *Proceedings of The International School of Metal Complexes in Solution*. Palermo, Italy 1983.
15. X. Ribas, V. Salvadó and M. Valiente, submitted.
16. X. Ribas, Doctoral thesis. Universitat Autònoma de Barcelona (1987).
17. F. J. C. Rossotti and H. S. Rossotti, *Acta Chem. Scand.* 1955, **9**, 1166.
18. I. Grenthe and E. Hansson, *Acta Chem. Scand.* 1969, **23**, 611.
19. S. Ito, H. Tomiyasu and H. Ohtari, *Bull. Chem. Soc. Japan* 1973, **46**, 2238.
20. I. Dellien and I. Grenthe, *Acta Chem. Scand.* 1971, **25**, 1387.
21. L. Ciavatta, *Annali Chim.* 1980, **70**, 551.
22. C. F. Baes and R. E. Mesner, *The Hydrolysis of Cations*, John Wiley, New York (1976).
23. N. Ingri, W. Kakolowicz, L. G. Sillén and B. Warnquist, *Talanta* 1967, **14**, 1261.
24. F. A. Cotton and G. Wilkinson, *Advanced Inorganic Chemistry: A Comprehensive Text*. John Wiley, New York (1980).
25. IUPAC, *Stability Constants of Metal Ion Complexes* (1973).

Polyhedron Vol. 8, No. 6, pp. 819–826, 1989
Printed in Great Britain

0277–5387/89 $3.00+.00
© 1989 Pergamon Press plc

PREPARATION AND CHARACTERIZATION OF MOLECULAR SIEVES BASED ON ALUMINIUM PHOSPHATE

YAN XU, PETER J. MADDOX and JOHN M. THOMAS*

Davy Faraday Research Laboratory, The Royal Institution, 21 Albemarle Street, London W1X 4BS, U.K.

(*Received* 27 *September* 1988; *accepted* 20 *October* 1988)

Abstract—An improved synthetic procedure for the preparation of MAPO-5 molecular sieves (M = Mg, Co, Mn, Ni, Cr) is reported. These compounds are shown to be monophasic by X-ray powder diffractometry and have surface areas between 250 and 270 $m^2\ g^{-1}$. Results of thermogravimetric analyses, scanning electron microscopy and *in situ* X-ray diffractometry are presented. Structural modification of the framework by the metal component is also discussed in the light of these data.

Of late, largely as a result of the work carried out by Flanigen, Lok, Wilson and co-workers,[1–6] many new types of open framework structures have been brought to light. Most of these have alternating trivalent aluminium and pentavalent phoshorus as the predominant occupants of the tetrahedral sites in their structures, with other elements such as lithium, beryllium, magnesium, boron, silicon and some transition elements[1] capable of being incorporated into the framework. These aluminium phosphates, metal aluminophosphates and metal–silicon–aluminophosphates (AlPO's, MAPO's and MSAPO's using the nomenclature of Flanigen *et al.*[1]) can also take up some of the structures previously identified among the zeolitic aluminosilicates (e.g. erionite, chabazite, faujasite). These materials are particularly promising as adsorbents especially for effecting difficult separations, but their catalytic properties have yet to be fully explored. As part of a larger investigation of novel catalytic reactions using these microporous aluminium phosphates, we focus in this paper on straightforward, improved methods of preparing some MAPO-5 molecular sieves, which contain *ca* 0.8 nm diameter, one-dimensional channels. We also report upon their characterization using a combination of X-ray diffractometry, thermogravimetry and other procedures, and comment on the extra-framework species which tend to occur in such microcrystalline samples.

* Author to whom correspondence should be addressed.

EXPERIMENTAL

Synthesis

(i) *Materials.* Phosphoric acid (85%) was obtained from Aldrich Chemical Co. Ltd and aluminium hydroxide from Fluka Chemicals Ltd. Triethylamine (AR), hydrofluoric acid (40% AR), manganese(II) chloride tetrahydrate (AR), nickel(II) chloride hexahydrate (AR), cobalt(II) chloride hexahydrate and magnesium(II) chloride were obtained from BDH Chemical Co. Ltd. Chromium(III) nitrate nonohydrate was obtained from Alfa Products. Water was distilled and deionized before use.

(ii) *Preparation of aluminium phosphate solution.* Equimolar proportions of phosphoric acid and aluminium hydroxide were heated above 150°C for about 1 h, during which, small aliquots of water were continually added to maintain the reaction. Then extra water was added, and the mixture was filtered to remove unreacted aluminium hydroxide. The resulting filtrate is an aluminium phosphate solution with an Al–P molar ratio of 0.6, and this was employed for the synthesis of the MeAPO-5's.

(iii) *Preparation of* MAPO-5's (M = Mg, Co, Mn, Ni, Cr). The amount of each reactant used is based on the following molar ratios: 1.0 P_2O_5: 0.6 Al_2O_3: (0–0.3) $M^{2+/3+}$: (1.5–2.2) Et_3N: (40–100) H_2O: (0.2–1.0) F^-.

The metal chloride was dissolved in the aluminium phosphate solution in a plastic beaker.

Dropwise addition of triethylamine to this vigorously stirred solution, followed by addition of hydrofluoric acid resulted in a perfectly homogeneous solution of pH 5.5–7.0 after several hours. This reaction mixture was heated in a PTFE lined autoclave at 190°C for periods of up to 16 h. The product mixture was filtered, washed with copious amounts of water, dilute hydrochloric acid and water again. The resultant crystalline material was dried at 110°C for 2 h in air. ($AlPO_4$-5 was prepared if no metal salt was added to the reaction mixture.)

These samples contained the trapped triethylamine templating agent, and this could be removed by heating between 550 and 600°C for 3 h in air.

Characterization

XRD patterns were collected on a conventional Siemens D500 diffractometer using nickel filtered Cu-K_α radiation (0.02 step size, 2 s per point). *In situ* XRD experiments were performed using a specially designed cell from GTP Engineering Co. Ltd (Swindon, Wilts, U.K.) by heating the samples in a flow of dry air (50 cm^3 min^{-1}).

Surface area measurements were carried out using static BET conditions using nitrogen as adsorbent at 77 K. Chemical analyses were obtained from Butterworth Laboratories Ltd (Teddington, Middx, U.K.). Scanning electron microscopy/energy dispersive X-ray emission analysis data were collected at the JEOL Laboratories (London, U.K.). Simultaneous thermal gravimetric, differential thermogravimetry and differential thermal analyses were performed on a Stanton Redcroft STA780 machine (heating rate = 10° min^{-1} in nitrogen to 270°C, in air above 270°C). Diffuse reflectance spectra were collected on a Perkin–Elmer/Hitachi 200 spectrophotometer.

RESULTS AND DISCUSSION

(i) *Features of* MAPO-5 *synthesis*

The MAPO-5 molecular sieves were prepared by hydrothermal crystallization from a metal cation-doped, aluminophosphate gel containing an organic template. One of the important steps employed in our synthetic procedure is the preparation of an aluminium phosphate solution, which is free of unreacted aluminium hydroxide. $AlPO_4$-5 and MAPO-5's are, like all zeolites, metastable, and consequently their crystallization times are restricted. Previous syntheses[3–5] use aluminium hydroxide or alumina directly as the aluminium source, and since these reactants are thermodynamically stable, it takes a long time for aluminium to enter the zeolite phase, and as a result other non-zeolitic byproducts are formed in these syntheses. In our preparation, however, both the aluminium and the phosphorus exist mainly as active polymerized ions in solution prior to addition of the metal salt and templating agent. This modification results in highly shortened crystallization times and more crystalline samples.

The use of hydrofluoric acid is another feature in our syntheses. The advantages of fluoride anion involvement in the preparation of ZSM-5 have been demonstrated,[7] and it seems likely that it assists in the solubility of the aluminium and metal species. It probably also plays a minor role as a weak acid keeping the pH of the solution between 5.5 and 7.0. If too much hydrofluoric acid is added to the reaction mixture, however, the aluminium and metal species do not transfer completely to the zeolite phase, probably because of the stability of the soluble fluoride complexes (Table 1). Other fluoride sources, in particular, ammonium fluoride and potassium fluoride, were also used successfully in MAPO-5 synthesis.

Table 1. Syntheses conditions of $AlPO_4$-5 and MAPO-5 aluminium phosphates[a]

	$[Et_3N]/[P_2O_5]$	$[F^-]/[Al_2O_3+MeO_x]$[a]	Time at 190°C (h)	pH	Calcination temperature (°C)
$AlPO_4$-5	1.5–1.9	0.0–1.0	2–9	5.5–7.0	550
MgAPO-5	1.5–1.9	0.0–1.0	7–16	5.5–7.0	550–700
CoAPO-5	1.5–2.2	0.3–1.0	2–7	6.0–7.0	550–700
MnAPO-5	1.5–2.2	0.3–1.0	7–16	6.0–7.0	550–700
NiAPO-5	1.5–2.2	0.3–1.0	7–14	6.0–7.0	550–700
CrAPO-5	1.5–2.2	0.3–1.0	7–14	6.0–7.0	550

[a] MeO_x = substituted metal oxide equivalent.

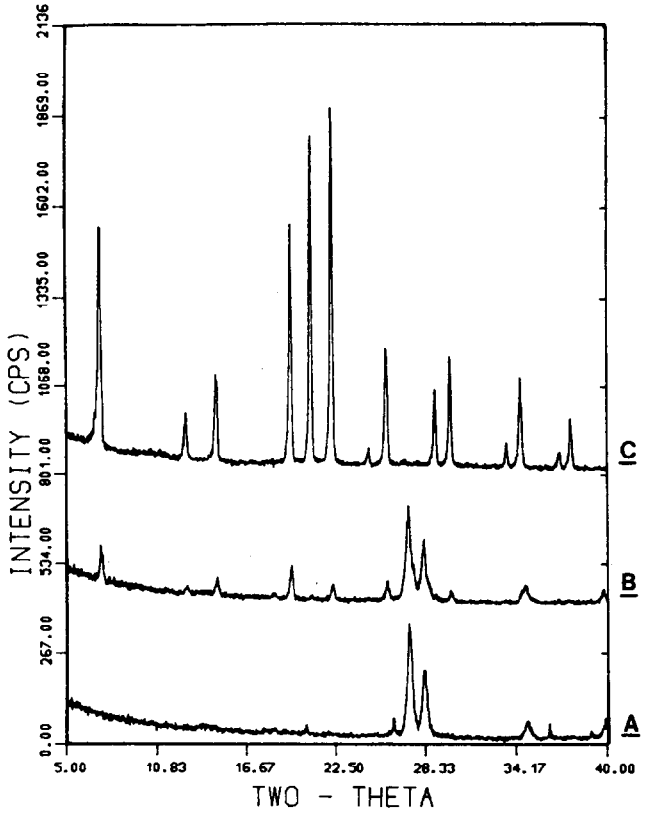

Fig. 1. Effect of the $[Et_3N]/[P_2O_5]$ ratio on crystalline products in CoAPO-5 synthesis: **A** $[Et_3N]/[P_2O_5] = 1.17$, **B** = 1.33, **C** = 1.60.

The organic template, triethylamine, plays a critical structure-directing role in the formation of the channels in the MAPO-5's. Tri-*n*-propylamine and tetra-*n*-propylammonium hydroxide are the templates usually employed for these particular molecular sieves, but we find triethylamine equally effective. The amount of triethylamine in the reaction mixture is crucial as shown in Table 1, and is further demonstrated by XRD patterns of the reaction products in the attempted synthesis of CoAPO-5 with different template/P_2O_5 molar ratios in Fig. 1.

Finally, the time of crystallization is an important variable because of the metastable nature of these compounds (Table 1); overlong crystallization times result in a major impurity. This has been identified by powder diffraction as an aluminium phosphate dense phase corresponding to one of the structural forms of silica, tridymite,[6] as illustrated in Fig. 2 for some NiAPO-5 syntheses.

(ii) *Structure and composition of* MAPO-5's

In metal substituted aluminium phosphate molecular sieves, the metal seems to substitute for the aluminium rather than the phosphorus atoms. This results in a negatively charged framework when the metal is divalent, and such materials have Brønsted acid sites and hence are potential cracking catalysts.[8-10]

The preparations of MgAPO-5, CoAPO-5, MnAPO-5 and NiAPO-5, in which the metal is formally divalent, are described above; only the magnesium, cobalt and manganese variants have previously been characterized and observed in high purity.[1,9] In addition, CrAPO-5 was synthesized, in which chromium is trivalent (Cr^{3+}ZSM-5 has been reported[11]); this material was expected to have a net neutral framework charge like $AlPO_4$-5 (assuming substitution of chromium for aluminium).

The subsequent discussion focuses on those synthesized samples with the highest metal substitution, which are monophasic by XRD; these are shown in Fig. 3 for the calcined samples in which the template has been removed from the channels. The XRD patterns indicate that they all have the structure of the aluminium phosphate molecular sieve number 5, reported by Bennett and coworkers.[7] The calculated unit cell parameters from these XRD patterns are given in Table 2. Smaller unit cell volumes are observed for $AlPO_4$-5 and

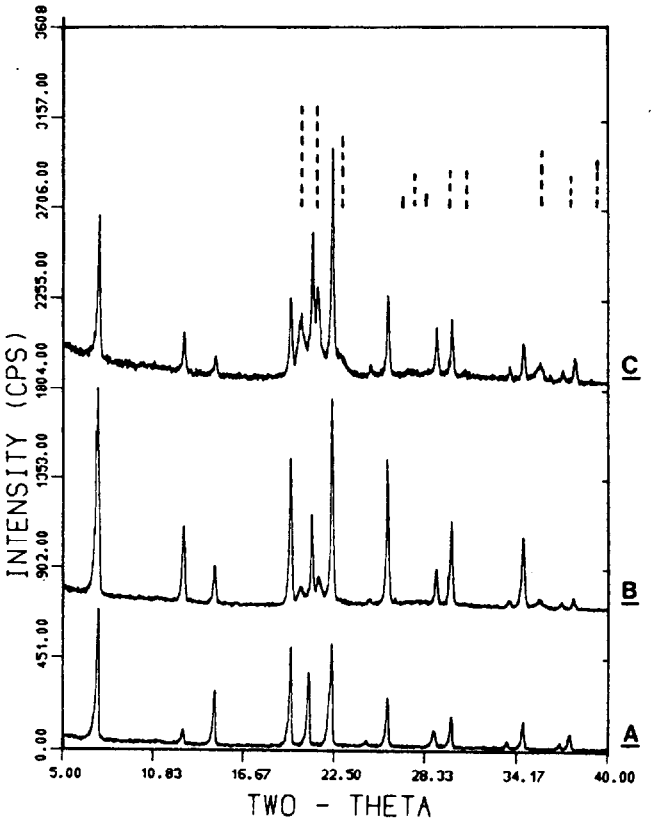

Fig. 2. Effect of reaction time on crystalline products in NiAPO-5 synthesis: **A** 12 h, **B** 16 h, **C** 20 h. Dotted lines show an aluminium phosphate dense phase reproduced from the JCPDS library.

CrAPO-5 than for divalent metal substituted variants, and this is related to the ionic radii of the metals (Table 2). Among the *transition* metal substituted MAPO-5's, the unit cell volume increases with increasing ionic radius. It is difficult, however, to fully explain all the subtle variations, and although the heteroatom content of each aluminophosphate is slightly different, these parameters are supporting evidence for isomorphic substitution of M^{n+} for Al^{3+}.

These molecular sieves contain one-dimensional channels of pore size 0.8 nm, along the *c* axis. Nitrogen adsorption isotherms were measured at 77 K, indicating that all the samples have surface areas between 250 and 270 $m^2\ g^{-1}$. This demonstrates that these molecular sieves contain open channels; furthermore, their metallic component cannot be blocking the pores of the structure, for instance, as an amorphous metal chloride, and is evidence for the substitution of the metal into the framework.

Chemical formulae based on elemental analyses of the aluminophosphates are given in Table 3. At first sight, these values are disconcerting because for MgAPO-5, NiAPO-5, CoAPO-5 and MnAPO-

Table 2. Unit cell parameter refinements of $AlPO_4$-5 and MAPO-5 aluminium phosphates

	Unit cell parameters			Cation radii	
	a (Å)	*c* (Å)	*V* (Å^3)	(Å)	
$AlPO_4$-5	13.683	8.483	1371.5	Al^{3+}	0.51
MgAPO-5	13.741	8.430	1380.5	Mg^{2+}	0.66
CoAPO-5	13.748	8.439	1381.2	Ca^{2+}	0.72
MnAPO-5	13.783	8.467	1392.9	Mn^{2+}	0.80
NiAPO-5	13.697	8.475	1377.1	Ni^{2+}	0.69
CrAPO-5	13.669	8.460	1369.0	Cr^{3+}	0.63

Table 3. Chemical formulae of $AlPO_4$-5 and MAPO-5 aluminium phosphates from elemental analysis (H_2O and template from thermal analysis)

	Chemical formulae (per unit cell)
$AlPO_4$-5	$P_{12}Al_{12}O_{48}(H_2O)_{4.3}(Et_3N)_{1.2}$
MgAPO-5	$P_{12}Al_{10.9}Mg_{1.3}O_{48}(H_2O)_{4.0}(Et_3N)_{1.2}$
CoAPO-5	$P_{12}Al_{11.1}Co_{1.0}O_{48}(H_2O)_{4.8}(Et_3N)_{1.0}$
MnAPO-5	$P_{12}Al_{11.3}Mn_{1.0}O_{48}(H_2O)_{4.3}(Et_3N)_{1.1}$
NiAPO-5	$P_{12}Al_{11.6}Ni_{0.5}O_{48}(H_2O)_{4.4}(Et_3N)_{1.1}$
CrAPO-5	$P_{12}Al_{11.6}Cr_{0.4}O_{48}(H_2O)_{4.2}(Et_3N)_{1.2}$

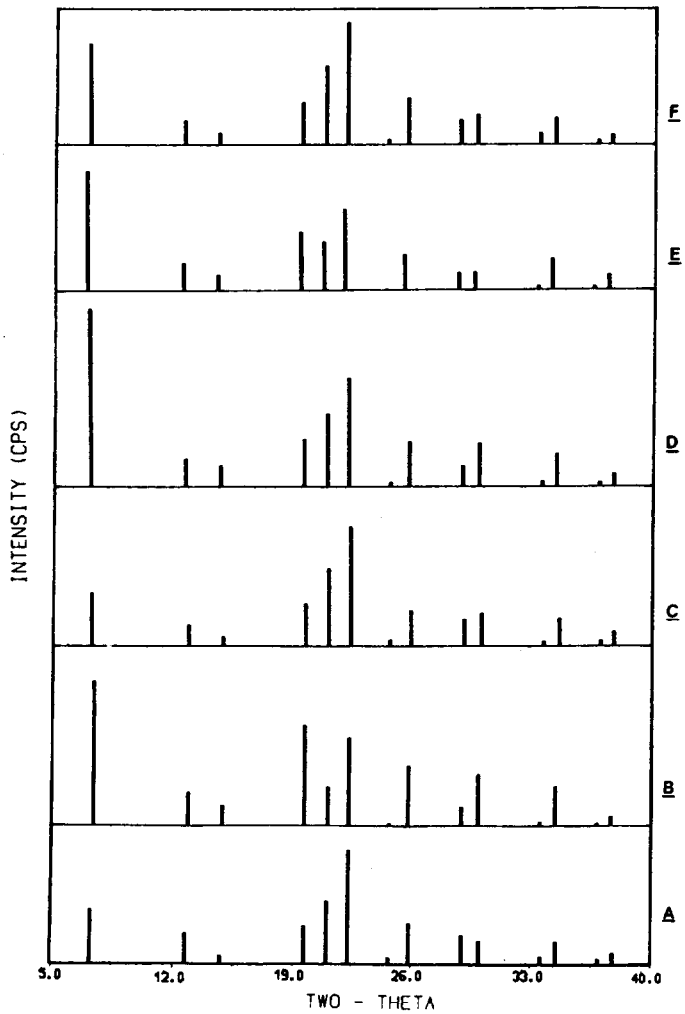

Fig. 3. X-ray powder diffraction patterns of calcined aluminium phosphates: **A** $AlPO_4$-5, **B** MgAPO-5, **C** CoAPO-5, **D** MnAPO-5, **E** NiAPO-5, **F** CrAPO-5.

5, the metal content is greater than the difference in phosphorus and aluminium content. These four molecular sieves, however, possess ion exchange properties as a result of the divalent metal substitution at the aluminium sites. An explanation for the observed analyses is that the metal occupies both framework (Al) sites and extra-framework positions. This was supported by ion exchange experiments on MnAPO-5 in which Mn^{2+} cations were displaced by Na^+ [12] by stirring in 0.2 M NaCl solution, with no resultant loss in crystallinity of the sample by XRD. MgAPO-5, CoAPO-5, MnAPO-5 and NiAPO-5 can be regarded as having both extra-framework metal cations and Brønsted acid sites, although in different proportions; this can be illustrated by idealized chemical formulae: $Mg^{2+}_{0.2}H^+_{0.7}$ $(Mg_{1.1}Al_{10.9}P_{12}O_{48})^{1.1-}$, $Co^{2+}_{0.1}H^+_{0.7}$ $(Co_{0.9}Al_{11.1}P_{12}O_{48})^{0.9-}$, $Mn^{2+}_{0.3}H^+_{0.1}$ $(Mn_{0.7}Al_{11.3}P_{12}O_{48})^{0.7-}$ and $Ni^{2+}_{0.1}H^+_{0.2}$ $(Ni_{0.4}Al_{11.6}P_{12}O_{48})^{0.4-}$ where the parentheses indicate the framework compositions. In contrast, this does not arise for CrAPO-5, because the chromium is trivalent and the net-framework charge is neutral. Hence, CrAPO-5 is unlike the other four MAPO-5's and more like $AlPO_4$-5, as other experiments will demonstrate.

It was mentioned above that the synthetic procedures used resulted in highly crystalline samples. Scanning electron micrographs of $AlPO_4$-5, MgAPO-5, NiAPO-5, MnAPO-5 and CoAPO-5 showed that they consist mainly of hexagonal prisms, with very few intergrowths and no aggregates. The MnAPO-5 prisms were about 300 μm long and 30 μm in diameter, whereas MgAPO-5, CoAPO-5 and NiAPO-5 prisms were shorter, between 50 and 100 μm in length. The CrAPO-5 sample, however, was made up of aggregates. Energy dispersive X-ray emission analysis on all

Table 4. Thermogravimetry results of $AlPO_4$-5 and MAPO-5 aluminium phosphates

	Template (I)		Template (II)		Structure
	Weight loss (%)	Temperature (°C)	Weight loss (%)	Temperature (°C)	collapse (°C)
$AlPO_4$-5	8.1	400	—	—	1200
MgAPO-5	4.6	385	3.7	570	750
CoAPO-5	2.3	370	4.6	550	770
MnAPO-5	3.8	377	3.2	580	—
NiAPO-5	4.3	350	3.0	588	—
CrAPO-5	7.7	390	—	—	—

the MAPO-5's showed that the metallic component is homogeneously distributed, and that there are no metal rich phases.

The structural differences between the MAPO-5's of different metal valency, mentioned above, was highlighted by careful thermogravimetric studies of the template-containing precursors. All samples released surface water below 100°C and a smaller amount of zeolitic water at about 250°C. For the magnesium, cobalt, manganese and nickel substituted aluminium phosphates, their templates are relased at two distinct temperatures; this has been noted previously in the case of cobalt,[9] and is a result of the template first evolving as free amine, and then by degradation of the proton or metal-complexed amine at a higher temperature (Table 4). CrAPO-5 and $AlPO_4$-5, however, have only one template weight loss, which is consistent with the neutral framework charge of these two structures. These differences are illustrated by differential thermal gravimetry and differential thermal analysis of $AlPO_4$-5, MgAPO-5 and NiAPO-5 in Fig. 4.

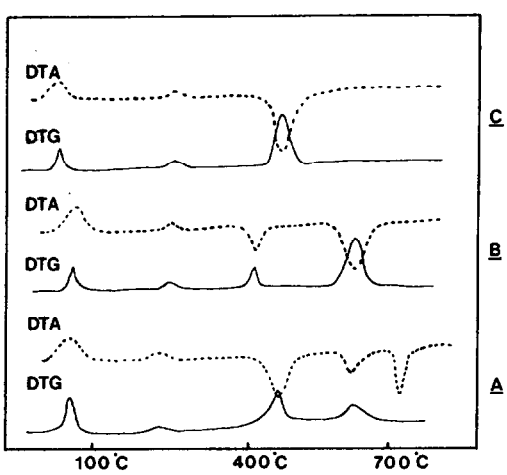

Fig. 4. Differential thermal analysis (DTA) and differential thermal gravimetric analysis (DTG) of some aluminium phosphates: **A** MgAPO-5, **B** NiAPO-5, **C** $AlPO_4$-5.

In situ X-ray diffraction was employed to observe the changes as the residual water and template were driven from the channels of $AlPO_4$-5 and NiAPO-5. Samples were heated in a flow of dry air and were allowed to equilibrate for 0.5 h at each particular temperature, before a diffraction pattern was collected. Figure 5 shows the result for the case of $AlPO_4$-5; heating to 100°C removes most of the water and causes an increase in crystallinity. Evolution of free triethylamine up to 300°C dramatically changes the relative intensities of the (110) and (200) reflections and slightly increases the unit cell size; further heating has little effect on the peak intensities. The identical experiment for NiAPO-5 has similar characteristics as water and free templates are removed from the channels as shown in Fig. 6. On heating to 550°C, however, these is another change corresponding to the loss of the complexed template (from thermogravimetric analysis). This is a unit cell contraction and a change in the relative intensities of the (210), (002) and (211) reflections.

Preliminary ^{27}Al and ^{31}P solid-state NMR of the aluminium phosphates were carried out, but the results are not discussed at length here, as they are somewhat puzzling. This may be related to the fact that the field strength at which the NMR is collected may affect the appearance of the spectra of these materials as reported recently.[13]

The results described above provide evidence for the incorporation of the metal component into the frameworks of the MAPO-5 aluminium phosphates. X-ray powder diffraction establishes the absence of non-MAPO-5 phases and the different lattice parameters suggest metal framework substitution. Adsorption measurements indicate that they contain unblocked channels and scanning electron microscopy shows a homogeneous heteroatom distribution. In the case of CoAPO-5, further evidence is the intense blue colour of the crystals, which is characteristic of divalent cobalt in

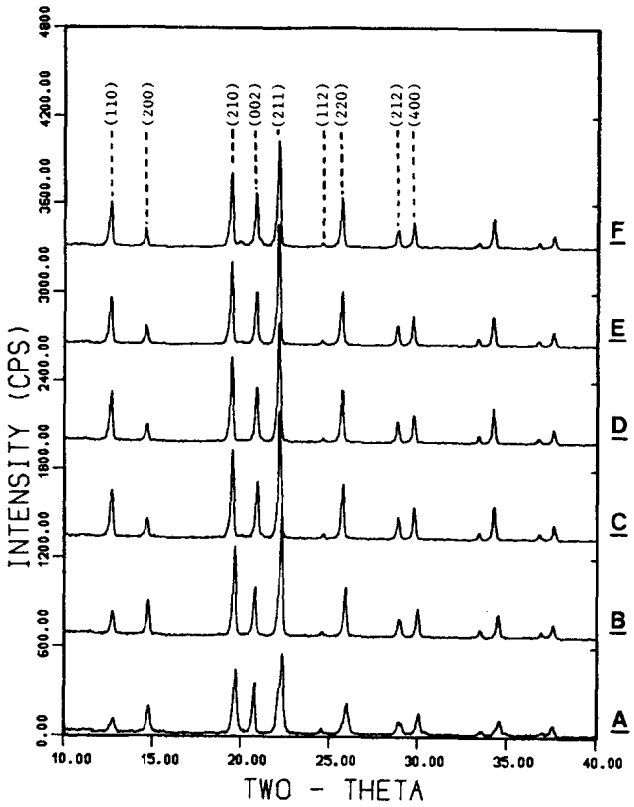

Fig. 5. High temperature *in situ* X-ray diffraction patterns of $AlPO_4$-5: **A** 25°C, **B** 100°C, **C** 300°C, **D** 400°C, **E** 450°C, **F** 550°C (Miller indices indicated at the top of the figure).

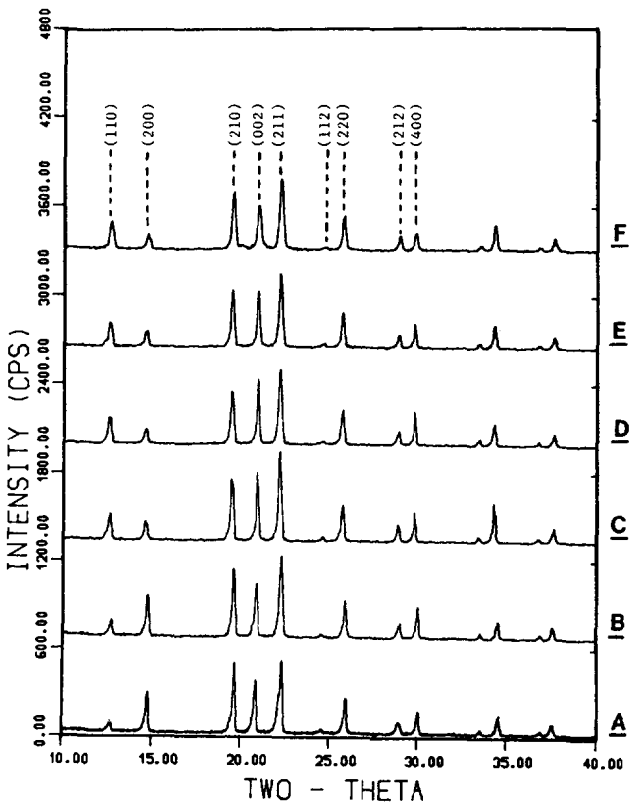

Fig. 6. High temperature *in situ* X-ray diffraction patterns of NiAPO-5: **A** 25°C, **B** 100°C, **C** 300°C, **D** 400°C, **E** 450°C, **F** 550°C (Miller indices indicated at the top of the figure).

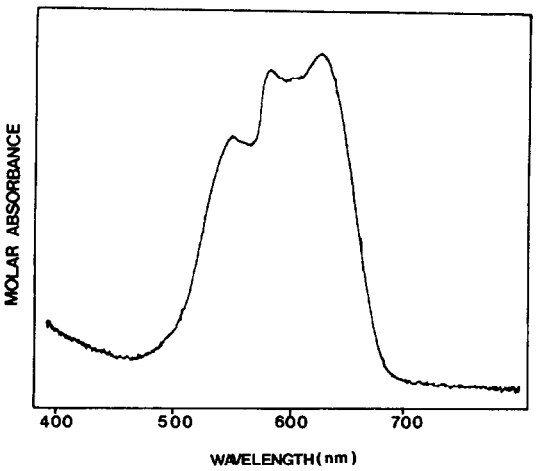

Fig. 7. Diffuse reflectance spectrum of CoAPO-5.

a tetrahedral environment; the diffuse reflectance spectrum of CoAPO-5 is shown in Fig. 7.[14] The new variants discussed in this paper, NiAPO-5 and CrAPO-5, still require further investigation to prove conclusively that framework incorporation has indeed taken place. Although trivalent chromium prefers an octahedral coordination, Cr^{3+}–ZSM-5 has been prepared and evidence for tetrahedral Cr^{3+} in the framework has been previously presented.[11] Recent work, based on magnetic susceptibility, has demonstrated that divalent nickel may have a tetrahedral coordination (though distorted) in a pollucite-like structure.[15]

Future work will focus on the precise nature of the metal substitution in MAPO-5 and some catalytic testing of these materials.

Acknowledgements—Support from the Science and Engineering Research Council (to P.J.M.) and a Studentship from the Chinese Government (to Y.X.) are gratefully acknowledged. We thank Dr A. R. West, Aberdeen University, for use of thermal analysis equipment, and Prof. A. K. Cheetham, Oxford University, for the electron microscopy measurements. Y.X. thanks Prof. Ruren Xu and Prof. W. Q. Pang and their colleagues at the Department of Chemistry, Jilin University, for their advice concerning zeolite synthesis before coming to the Royal Institution.

REFERENCES

1. E. M. Flanigen, B. M. Lok, R. L. Patton and S. T. Wilson, *Proc. 7th Intl. Zeolite Conf.*, p. 103 (1986).
2. S. T. Wilson, B. M. Lok, C. A. Messina, T. R. Cannan and E. M. Flanigen, *J. Am. Chem. Soc.* 1982, **104**, 1146.
3. S. T. Wilson, B. M. Lok and E. M. Flanigen, *U.S. Patent* 4,310,440 (1982).
4. C. A. Messina, B. M. Lok and E. M. Flanigen, *U.S. Patent* 4,544,143 (1985).
5. S. T. Wilson and E. M. Flanigen, *U.S. Patent* 4,567,029 (1986).
6. J. M. Bennett, J. P. Cohen, E. M. Flanigen, J. J. Pluth and J. V. Smith, *Am. Chem. Soc., Symp. Ser.* 1983, **218**, 109.
7. J. L. Guth, H. Kessler and R. Wey, *Proc. 7th Intl. Zeolite Conf.*, p. 121 (1968).
8. V. R. Choudhary and D. B. Akolekar, *J. Catal.* 1987, **103**, 115.
9. N. J. Tapp, N. B. Milestone and L. J. Wright, *J. Chem. Soc., Chem. Commun.* 1985, 1801.
10. D. R. Pyke, P. Whitney and H. Houghton, *Appl. Catal.* 1985, **18**, 173.
11. W. Q. Pang, Y. Yue and S. J. Li, *J. Phys. Sci.* 1986, **3**, 108.
12. P. Cumming and D. A. Kay, *Quantitative Chemical Analysis*, 11th edn. Oliver and Boyd, London (1956).
13. C. S. Blackwell and R. L. Patten, *J. Phys. Chem.* 1988, **92**, 3965.
14. F. A. Cotton and G. Wilkinson, *Advanced Inorganic Chemistry*, 3rd edn, p. 772. Wiley, New York (1972).
15. J. H. Binks, private communication.

Polyhedron Vol. 8, No. 6, pp. 827–830, 1989
Printed in Great Britain

0277–5387/89 $3.00+.00
© 1989 Pergamon Press plc

INFLUENCE OF OXIDATION STATE ON SUBSTITUTION BY ISOCYANIDE AND PHOSPHITE NUCLEOPHILES IN BIS(2,2′-BIPYRIDINE)DICARBONYLTUNGSTEN

JOSEPH A. CONNOR* and JOSEPHINE M. A. WALSHE

Chemical Laboratory, University of Kent, Canterbury, Kent CT2 7NH, U.K.

(*Received* 29 *September* 1988; *accepted* 20 *October* 1988)

Abstract—Purple crystals of *cis,trans*-$[W(CO)_2\{P(OMe)_3\}_2(bipy)]$ (bipy = 2,2′-bipyridine) are obtained in good yield by heating *cis*-$[W(CO)_2(bipy)_2]$ in trimethylphosphite. Substitution by isocyanides in *cis*-$[W(CO)_2(bipy)_2][BF_4]_2$ produces purple–red six-coordinate tungsten(II) salts, *cis,cis*-$[W(CO)_2(CNR)_2(bipy)][BF_4]_2$ (R = C_6H_{11}, CH_2Ph, Ph) in moderate yields. Further substitution by isocyanide produces the known seven-coordinate complexes $[W(CNR)_5(bipy)][BF_4]_2$ and $[W(CNR)_7][BF_4]_2$. The new complexes have been characterized by microanalysis and spectroscopy (IR, ^1H, ^{13}C, ^{31}P NMR and electronic absorption). A comparison with the physical properties of isostructural analogues of tungsten(II) or tungsten(0), as appropriate, is made.

There are few examples of complex compounds containing more than two different types of ligand attached to a metal in a low formal oxidation state in which a two-electron oxidation or reduction does not result in either isomerization or a change in coordination number, or both. Recently we have observed that substitution in the six-coordinate *cis*-$[W(CO)_2(bipy)_2]^{2+}$ ion by neutral monodentate phosphine and phosphite ligands, L, results in the displacement of 2,2′-bipyridine and formation of six-coordinate *cis,trans*-$[W(CO)_2L_2(bipy)]^{2+}$ ions. These results stand in contrast to those obtained when the same ligands react with the seven-coordinated molybdenum(II) complex ion *cis*-$[Mo(CO)_2(bipy)_2(NCMe)]^{2+}$. Substitution by the same ligands in the six-coordinate metal(0) complexes, *cis*-$[M(CO)_2(bipy)_2]$ (M = Mo, W), may result in the displacement of either one or both bipy ligands depending on the conditions and the particular ligand used.[1] The stereochemistry of the product in which only one bipy ligand is substituted, is also dependent on the nucleophile. Taken together, these observations have indicated that we could learn more about the influence of oxidation state on the properties of isostructural metal complexes, than has been clear previously.

* Author to whom correspondence should be addressed.

RESULTS AND DISCUSSION

Heating *cis*-$[W(CO)_2(bipy)_2]$ with pure trimethylphosphite at 100°C for 13 h produces a good (89%) yield of purple crystals of *cis,trans*-$[W(CO)_2\{P(OMe)_3\}_2(bipy)]$. The product is much more soluble in a range of solvents than the starting material. The product is characterized by two strong absorptions in the IR spectrum at 1825 and 1750 cm^{-1} (Nujol) assigned to *cis*-carbonyl ligands. Comparison of the $\nu(CO)$ values in $[W(CO)_2(bipy)L_2]$ indicates that the acceptor strength of L decreases in the order $P(OMe)_3 \geq EtNC > bipy$: the discrimination between phosphite and isocyanide is much less marked than in the analogous molybdenum(0) complexes.[1] The ^{31}P NMR spectrum shows one signal only at δ +58.55 ppm ($^1J(WP)$ 369 Hz) produced by *trans*-phosphite ligands. The lowest energy absorption of the complex at 530 nm (CH_3CN solution), which may have contributions from both metal-to-ligand charge-transfer and localized *d–d* (ligand field) transitions, exhibits solventochromism in a manner which is similar to $[W(CO)_4(bipy)]$; the value of the λ_{max} decreases by more than 100 nm as the polarity of the solvent increases from carbon tetrachloride to dimethylsulphoxide.

In acetonitrile solution the complex *cis*-$[W(CO)_2(bipy)_2][BF_4]_2$ reacts at room temperature with 2

molar equivalents of isocyanide, RNC (R = C_6H_{11}, CH_2Ph, Ph), to form deep red solutions from which the six-coordinate salts *cis,cis*-$[W(CO)_2(CNR)_2(bipy)][BF_4]_2$ were isolated with some difficulty in a crystalline form and characterized by microanalysis. The addition of excess isocyanide to *cis*-$[W(CO)_2(bipy)_2][BF_4]_2$ or, alternatively, to *cis, cis*-$[W(CO)_2(CNR)_2(bipy)][BF_4]_2$, in acetonitrile at room temperature produces the seven-coordinate salts $[W(CNR)_5(bipy)][BF_4]_2$. Previously, examples of these seven-coordinate complexes (R = *i*-Pr, *t*-Bu, C_6H_{11}, CH_2Ph) have been prepared[2] from the oxidative addition reaction of *cis*-$[W(CO)_4(bipy)]$ with $PhICl_2$ in the presence of the isocyanide. Reaction with a further excess of isocyanide in acetonitrile at reflux completed displacement of the original ligands from the metal and $[W(CNR)_7][BF_4]_2$ was obtained.

The IR spectra of $[W(CO)_2(CNR)_2(bipy)][BF_4]_2$ complexes show two pairs of absorptions in the 2200–1800 cm^{-1} range which are assigned to CO and CN stretching vibrations. These establish the *cis*-orientation of these ligands. Comparison of the values of ν(CO) in *cis*-$[W(CO)_2(bipy)_2][BF_4]_2$, *cis,trans*-$[W(CO)_2\{P(OMe)_3\}_2(bipy)][BF_4]_2$,[3] and *cis,cis*-$[W(CO)_2(CNR)_2(bipy)][BF_4]_2$ indicates that, in a six-coordinate $[W(CO)_2(bipy)L_2]^{2+}$ ion, the ligands L (0.5(bipy), $P(OMe_3)$ and RNC), have similar donor–acceptor properties with reference to the tungsten(II) centre. This conclusion is reinforced by the observation that the positions of the bipy proton resonances in these compounds are also similar. The increasing pressure on the isocyanide ligands to accept electron density as a result of ($5d \rightarrow \pi^*$) π-bonding is indicated by the change in the chemical shift of the protons on the α-carbon atoms of the isocyanide ligand, as first CO and then bipy is replaced by isocyanide in the seven-coordinate fluxional dications $[W(CNR)_5(bipy)]^{2+}$ and $[W(CNR)_7]^{2+}$. The isocyanide ^{13}C resonances in the $[W(CNR)_5(bipy)][BF_4]_2$ complexes were observed as broad singlets without resolution of the ^{13}C–^{183}W coupling. In each case, the resonance is shifted to lower field ($\Delta\delta$ *ca* 2 ppm) from the free ligand value, which is evidence of significant (M → CNR) π-back-bonding in these complexes. This is in contrast to the usual shift to higher fields observed,[4] for example, in $[W(CO)_5(CNC_6H_{11})]$ ($\Delta\delta$ −16.2 ppm). All the other isocyanide ligand carbon resonances in the $[W(CNR)_5(bipy)]^{2+}$ complexes are shifted down field from those of the free ligand. The largest coordination shift, $\Delta\delta$, is experienced by the alkyl carbon adjacent to the isocyanide group when R = C_6H_{11} (5.44 ppm) or R = CH_2Ph (4.91 ppm).

The reactions described for $[W(CO)_2(bipy)_2]^{2+}$ are in contrast to the result obtained when isocyanides react with the analogous $[Mo(CO)_2(bipy)_2(NCMe)][BF_4]_2$. In the molybdenum system, substitution by isocyanide produces,[5] first, $[Mo(CNR)_3(bipy)_2][BF_4]_2$ (R = Et, *p*-tolyl) and subsequently, $[Mo(CNR)_5(bipy)][BF_4]_2$. Further substitution to give the known $[Mo(CNR)_7][BF_4]_2$ could not be achieved by heating with excess isocyanide at reflux, although $[Mo(CNC_6H_{11})_7]^{2+}$ reacts[6] with bipy to give $[Mo(CNC_6H_{11})_5(bipy)]^{2+}$. There is a delicate balance between different ligand environments in these analogous molybdenum(II) and tungsten(II) systems. Tungsten(II) preserves bonds to CO in preference to isocyanide: this order is reversed for molybdenum(II), consistent with the greater Lewis basicity of tungsten(II) towards the ligand of lower σ-donor/π-acceptor ratio. The change of coordination number at tungsten(II) which occurs between the six-coordinate *cis,cis*-$[W(CO)_2(CNR)_2(bipy)][BF_4]_2$ and seven-coordinate $[W(CNR)_5(bipy)][BF_4]_2$, is clearly an index of the steric properties of the isocyanide. There is evidence from IR spectra that the donor–acceptor (electronic) properties of alkyl isocyanide and trialkyl phosphite ligands are similar, but *cis,trans*-$[W(CO)_2\{P(OMe)_3\}_2(bipy)][BF_4]_2$ will not react[3] with excess phosphite to produce a seven-coordinate complex such as $[W\{P(OMe)_3\}_5(bipy)][BF_4]$ in the manner of an isocyanide. The cone angle[7] of trimethyl phosphite ($107 \pm 2°$) is significantly greater than that estimated (*ca* 78°) for cyclohexyl isocyanide. In contrast to the reactions with bidentate phosphine ligands,[3] it should be noted that seven-coordination at tungsten(II) is not achieved by fluoride abstraction in the presence of isocyanides.

The information obtained for the two pairs of tungsten complexes, *cis,cis*-$[W(CO)_2(CNCH_2R)_2(bipy)]^z$ ($z = 0$, R = Me; $z = 2^+$, R = Ph) and *cis,trans*-$[W(CO)_2\{P(OMe)_3\}(bipy)]^z$, shows a consistent pattern of the influence of oxidation state of the metal on spectroscopic properties. The frequency of absorption of both ν(CO) and, in the isocyanide complexes, of ν(CN) increases on oxidation; the frequency difference between these pairs of absorptions decreases in the higher oxidation state. Oxidation of the metal results in a shift of the bipy ligand proton resonances to lower field, particularly for H(4) and H(5) (*ca* 0.4 ppm). The methylene protons adjacent to the isocyanide group are also strongly (1.9 ppm) shifted to lower field. In the phosphite complexes, the ^{31}P resonance moves to lower field and the value of ^1J(WP) decreases as a result of oxidation, in a manner reminiscent of phosphine complexes of platinum.[8] The lowest energy absorption in the

visible region increases in energy with oxidation, consistent with the decrease in electron density at the metal atom involved in a MLCT process. Whereas this absorption in the tungsten(0) complexes displays very significant solvatochromism, this is not observed in the analogous tungsten(II) complex.

EXPERIMENTAL

Materials and methods were in general similar to those described in other papers from this laboratory.[3] All operations were carried out under dry, deoxygenated dinitrogen atmospheres. Solvents were dried, deaerated and distilled prior to use.

Preparation of cis,trans-2,2′-*bipyridinedicarbonylbis(trimethylphosphite)tungsten*

Trimethyl phosphite (30 cm^3, 0.25 mol) was added to *cis*-$[W(CO)_2(bipy)_2]$ (0.95 g, 1.72 mmol) and the mixture was heated at 373 K overnight (13 h). The dark green solution which formed was allowed to cool to room temperature, whereupon purple crystals precipitated. The solution was left at room temperature for 2 days. The crystalline product was isolated by filtration and washed with diethyl ether (0.99 g, 89% yield). Found: C, 33.5; H, 3.9; N, 4.1; P, 8.7; W, 29.5. Calc. for $C_{18}H_{26}N_2O_8P_2W$: C, 33.6; H, 4.1; N 4.4; P, 9.1; W, 28.5%. IR (Nujol) 1825s, 1750s, 1592m, 1300m, 1263w, 1050br, 767w, 725w, 705w, 519m cm^{-1}. ^1H NMR (CD_3CN): δ 9.24t (H6), 8.63d (H3), 8.05 (H4), 7.46t (H5) (bipy protons), 3.31m (OCH_3) ppm. λ_{max} 510 (DMSO); 540 (Me_2CO); 570 (THF); 590 (C_6H_6); 622 (CCl_4) nm.

Preparation of 2,2′-*bipyridinedicarbonylbis(cyclohexylisocyanide)tungsten*(II) *bis(tetrafluoroborate)*

Cyclohexyl isocyanide (0.36 cm^3, 3.44 mmol) was added to acetonitrile (10 cm^3) and the solution was added dropwise via a syringe to a vigorously stirred solution of *cis*-$[W(CO)_2(bipy)_2][BF_4]_2$ (1.25 g, 1.72 mmol) in acetonitrile (50 cm^3). The colour of the reaction mixture became orange–red on addition of the isocyanide solution. The reaction mixture was stirred at room temperature for 11 h (overnight) to ensure completion of the reaction. The solvent was then removed under reduced pressure to yield a dark red oil. Attempts to precipitate this as a solid from acetone–diethyl ether, acetone–hexane, dichloromethane–hexane and THF–hexane solvent mixtures were unsuccessful. The oil was stirred with diethyl ether (100 cm^3) for a period of typically 4–5 days, the diethyl ether being replaced by fresh solvent two or three times. The product was isolated as a purple–red solid (0.95 g, 70% yield). Found: C, 40.5; H, 4.5; N, 7.1; W, 25.4. Calc. for $C_{26}H_{30}N_4B_2F_8O_2W$: C, 39.9; H, 3.8; N, 7.1; W, 23.3%. IR (Nujol) 2190s, 2130s, 1980m, 1910s, 1605m, 1315m, 1060br, 768m, 730m, 521w cm^{-1}. ^1H NMR (CD_3CN): δ 9.22d (H6), 8.66d (H3), 8.40t (H4), 7.86t (H5) (bipy protons), 4.50s, 1.72–1.36m ($C_6H_{11}NC$) ppm. The complex $[W(CO)_2(CNCH_2Ph)_2(bipy)][BF_4]_2$ was prepared in a similar manner. Found: C, 42.3; H, 2.6; N, 7.2; W, 22.4. Calc. for $C_{28}H_{22}N_4B_2F_8O_2W$: C, 41.8; H, 2.8; N, 7.0; W, 22.9%. IR (Nujol) 2175s, 2117s, 1973m, 1900s, 1607m, 1498m, 1060br, 818w, 770m, 730m, 698m, 603m, 523m, 493w cm^{-1}. ^1H NMR (CD_3CN): δ 9.10d (H6), 8.60d (H3), 8.34t (H4), 7.70t (H5) (bipy protons), 7.48–7.24m ($C_6H_5CH_2NC$), 5.36s ($C_6H_5CH_2NC$) ppm. The complex $[W(CO)_2(CNPh)_2(bipy)][BF_4]_2$ was also prepared. Found: C, 40.7; H, 2.8; N, 7.9; F, 18.4; W, 25.3. Calc. for $C_{26}H_{18}N_4B_2F_8O_2W$: C, 40.2; H, 2.3; N, 7.2; F, 19.6; W, 23.7%. IR (Nujol) 2130m, 2040s, 1940s, 1860s, 1597m, 1583m, 1310w, 1280w, 1050br, 865m, 810m, 750m, 725m, 679m, 650w, 632w, 535w, 515w cm^{-1}. IR (CH_3CN) ν(CO) 1965, 1867 cm^{-1}. ^1H NMR (CD_3CN): δ 9.54d (H6), 8.64d (H3), 8.34t (H4), 7.84t (H5) (bipy protons), 7.56–7.12m (C_6H_5NC) ppm.

Preparation of 2,2′-*bipyridinepentakis(benzylisocyanide)tungsten*(II) *bis(tetrafluoroborate)*

Excess benzyl isocyanide (1 cm^3, 8.28 mmol) was added dropwise via a syringe to a rapidly stirred solution of *cis*-$[W(CO)_2(bipy)_2][BF_4]_2$ (0.82 g, 1.49 mmol) in acetonitrile (40 cm^3). The solution turned red immediately. The reaction mixture was left stirring at room temperature for 48 h to ensure completion of the reaction. The solvent was then evaporated under reduced pressure to give a red oil. This was stirred in diethyl ether (100 cm^3) for a period of typically 4–5 days, with the diethyl ether being replaced with fresh solvent two or three times. The product was isolated as a free-flowing bright red powder (1.29 g, 79% yield). Found: C, 54.6; H, 4.0; N, 8.6; W, 12.0. Calc. for $C_{50}H_{43}N_7B_2F_8W$: C, 54.6; H, 3.9; N, 8.9; W, 16.7%. IR (Nujol) 2190m, 2120s, 1598m, 1495m, 1348m, 1151w, 1050br, 803w, 772m, 742m, 727m, 693m, 597m, 519w, 490 cm^{-1}. ^1H NMR (CD_3CN): δ 8.89d (H6), 8.42d (H3), 8.16t (H4), 7.54t (H5) (bipy protons), 7.35–7.16m ($C_6H_5CH_2NC$), 5.14s ($C_6H_5CH_2NC$) ppm. ^{13}C NMR (CD_3CN): δ 155.40 (C2), 153.99 (C6), 141.08 (C4), 128.53, 125.29 (C3,C5) (bipy carbons); 159.98 (NC) 135.89 (C1), 130.08 (C2,C6), 129.56, 127.98 (C3–C5), 50.21 (CH_2) (benzyl isocyanide carbons) ppm. λ_{max} (CH_3CN)

510 nm. The complexes $[W(CNPh)_5(bipy)][BF_4]_2$ and $[W(CNC_6H_{11})_5(bipy)][BF_4]_2$ were prepared as purple–red powders by a similar procedure. $[W(CNC_6H_{11})_7][BF_4]_2$ was obtained as yellow crystals (95% yield) from the reaction between cyclohexyl isocyanide (4.65 mmol) and $[W(CNC_6H_{11})_5(bipy)][BF_4]_2$ (0.33 mmol) in acetonitrile (reflux, 84 h). Found: C, 52.2; H, 6.9; N, 8.6. Calc. for $C_{49}H_{77}N_7B_2F_8W$: C, 52.5; H, 6.9; N, 8.7%. IR and ^1H NMR spectra were in agreement with published values.

Acknowledgements—We thank SERC and ICI New Science Group for the provision of a CASE studentship, and Dr R. A. Head for his interest.

REFERENCES

1. J. A. Connor and C. Overton, *J. Chem. Soc., Dalton trans.* 1982, 2397.
2. A. Bell and R. A. Walton, *J. Organomet. Chem.* 1984, **263**, 359.
3. J. A. Connor, E. J. James, C. Overton, J. M. A. Walshe and R. A. Head, *J. Chem. Soc., Dalton Trans.* 1986, 511.
4. D. L. Cronin, J. R. Wilkinson and L. J. Todd, *J. Mag. Res.* 1975, **17**, 353.
5. J. A. Connor, E. J. James, C. Overton and N. el Murr, *J. Chem. Soc., Dalton Trans.* 1984, 255.
6. A. Bell, S. J. Lippard, M. Roberts and R. A. Walton, *Organometallics* 1983, **2**, 1562.
7. C. A. Tolman, *Chem. Rev.* 1977, **77**, 313.
8. G. G. Mather, A. Pidcock and G. J. N. Rapsey, *J. Chem. Soc., Dalton Trans.* 1973, 2095.

Polyhedron Vol. 8, No. 6, pp. 831–834, 1989
Printed in Great Britain

0277–5387/89 $3.00+.00
© 1989 Pergamon Press plc

ADDUCTS OF TRIMETHYLALUMINIUM WITH PHOSPHINE LIGANDS: X-RAY CRYSTAL STRUCTURES OF Me_3AlPPh_3 AND $Me_3AlP(o\text{-tolyl})_3$

DERK A. WIERDA and ANDREW R. BARRON*

Department of Chemistry, Harvard University, Cambridge, MA 02138, U.S.A.

(*Received* 31 *August* 1988; *accepted* 24 *October* 1988)

Abstract—The crystal and molecular structures of two phosphine adducts of trimethylaluminium are reported. Compound **1**, Me_3AlPPh_3, crystallizes in the rhombohedral space group R_3(obv), $a = b = 14.344(4)$, $c = 16.503(7)$ Å, $V = 2944(2)$ Å^3, $Z = 6$, $R = 0.0436$, $R_w = 0.0532$. Compound **2**, $Me_3AlP(o\text{-tolyl})_3$, crystallizes in the rhombohedral space group R_3C, $a = b = 14.978(1)$, $c = 34.195(5)$ Å, $V = 6643(1)$ Å^3, $Z = 4$, $R = 0.0574$, $R_w = 0.0601$. Structural features are discussed with reference to the ^{13}C and ^{31}P NMR spectroscopic data.

We have recently shown[1] that the dominant factor influencing the NMR chemical shifts in Me_3AlPR_3 complexes is steric repulsion between the aluminium methyl groups and the phosphine substituents. The ^{13}C chemical shifts of the Al—CH_3 groups may be used as an indication of the distortion from an idealized planar, monomeric $AlMe_3$, and the change in ^{31}P chemical shift (Δ)† of the phosphines on coordination to $AlMe_3$ correlates with the difference in R—P—R angles between free and coordinated phosphine.

The complex, $Me_3AlP(o\text{-tolyl})_3$, does not fit the trends found in ^{31}P Δ or Al—CH_3 ^{13}C chemical shifts. Based on a calculated cone angle for $P(o\text{-tolyl})_3$[2] of 194° a negative ^{31}P Δ is expected if the angle R—P—R decreases on coordination. The observed value, however, is positive (+7.7 ppm)[1] indicating that the C—P—C angle is opened on coordination. This observation suggests that the $P(o\text{-tolyl})_3$ ligand adopts a conformation so as to relieve steric strain between the *o*-tolyl and aluminium methyl groups.

In order to test the validity of the NMR data as a structural probe for Me_3AlPR_3 complexes we have undertaken an X-ray crystallographic study of Me_3AlPPh_3 and $Me_3AlP(o\text{-tolyl})_3$.

RESULTS AND DISCUSSION

Me_3AlPPh_3

The molecular structure of Me_3AlPPh_3 (**1**) is shown in Fig. 1 and selected bond lengths are given in Table 1. The complex contains a crystallographically-imposed C_3 axis coincident with the Al—P bond. The aromatic rings of the triphenylphosphine ligand adopt a propeller-like conformation, with the phenyl groups pitched 38.5° from the plane defined by Al, P and C(1). As a consequence of this the Al—C and P—C bonds are only partly staggered with a dihedral angle of 39.8°.

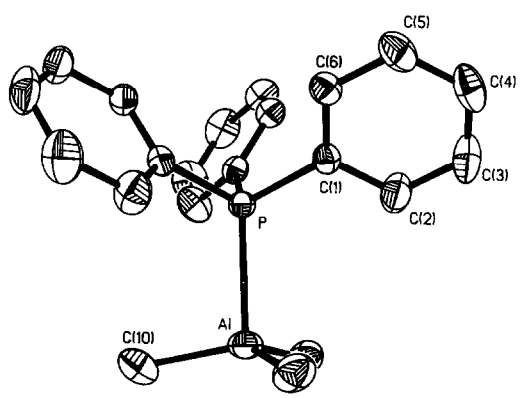

Fig. 1. X-ray crystal structure of Me_3AlPPh_3 (**1**) showing the numbering scheme.

* Author to whom correspondence should be addressed.
† ^{31}P $\Delta = \delta_{complex} - \delta_{free\ phosphine}$.

Table 1. Selected bond lengths (Å) and angles (°) for **1**

Al—P	2.535(1)	Al—C(10)	1.981(2)
P—C(1)	1.820(2)	C(1)—C(2)	1.391(3)
C(2)—C(3)	1.385(3)	C(3)—C(4)	1.377(3)
C(5)—C(6)	1.395(3)	C(6)—C(1)	1.394(2)
Al—P—C(1)	114.0(1)	P—Al—C(10)	100.6(1)
P—C(1)—C(2)	122.7(1)	P—C(1)—C(6)	119.0(2)
C(1)—C(2)—C(3)	120.1(2)	C(2)—C(3)—C(4)	120.8(2)
C(3)—C(4)—C(5)	119.8(2)	C(4)—C(5)—C(6)	120.2(2)
C(5)—C(6)—C(1)	120.1(2)		

The shortest non-bonding distances between the phenyl ring and aluminium methyl group are C(2)—C(10b) = 3.819(2) Å and C(2)—C(10A) = 3.993(2) Å. These contacts are emphasized by viewing the molecule along Al—P (Fig. 2). The Al—P distance, 2.535(1) Å, does not vary significantly from that found in Me_3AlPMe_3 (2.53(4) Å)[3] or $(Me_3Al)_2 \cdot (Ph_2PCH_2)_2$ (2.544(4) Å).[4]

A comparison of the structure of **1** and free monomeric $AlMe_3$[5] (see Table 2) shows that the lengths of the Al—C bonds increase, and that the C—Al—C angles decrease on coordination. Both changes are in the direction predicted by an increased aluminium *p*-character in the Al—C bonds on changing from a planar to tetrahedral geometry. From NMR results[1] the aluminium centre should be distorted further from planarity in Me_3AlPPh_3 than in Me_3AlPMe_3, this is indeed the case.

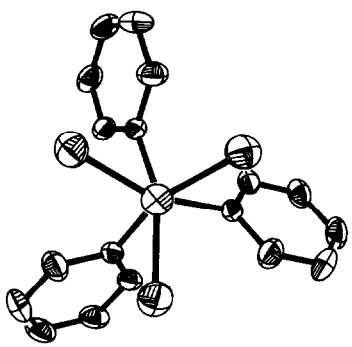

Fig. 2. The structure of Me_3AlPPh_3 (**1**) viewed down the Al—P vector.

The changes in PPh_3 geometry[6] on coordination are not so marked (see Table 2). The only appreciable change is an opening of the C—P—C angle by *ca* 1.6°. This is in contrast to the results from ^{31}P NMR spectroscopy[1] which predict that the C—P—C angle is reduced slightly on coordination. It is likely that this discrepancy between solid state and solution is a consequence of the distortions observed in the crystal structure of PPh_3.[6]

The unit cell of Me_3AlPPh_3 is comprised of six molecules with no unduly close intermolecular contacts.

$Me_3AlP(o\text{-tolyl})_3$

The molecular structure of $Me_3AlP(o\text{-tolyl})_3$ (**2**) is shown in Fig. 3; selected bond lengths and angles are given in Table 3. The complex contains a crys-

Table 2. Selected bond lengths (Å) and angles (°) of $AlMe_3$, Me_3AlPR_3 complexes and free phosphines, PR_3

Compound	Al—P	Al—C	P—C	C—Al—C	C—P—C
Me_3Al[a]		1.957		120.0	
Me_3AlPMe_3[b]	2.53	1.973	1.822	117.1	103.4
PMe_3[b]			1.846		97.54
Me_3AlPPh_3	2.535	1.981	1.820	116.6	104.6
PPh_3[c]			1.828 (av)		102.9 (av)
$Me_3AlP(o\text{-tolyl})_3$	2.584	1.874	1.834	113.9	105.1
$P(o\text{-tolyl})_3$[d]			1.86 (av)		102.8 (av)

[a] Reference 5.
[b] Reference 3.
[c] Reference 6.
[d] Reference 7.

Table 3. Selected bond lengths (Å) and angles (°) for **2**

Al—C(10)	1.974(6)	Al—P	2.584(2)
P—C(1)	1.834(4)	C(1)—C(2)	1.402(6)
C(1)—C(6)	1.400(5)	C(2)—C(3)	1.384(7)
C(3)—C(4)	1.376(6)	C(4)—C(5)	1.381(9)
C(5)—C(6)	1.377(7)	C(6)—C(7)	1.512(7)
C(10)—Al—P	104.5(1)	Al—P—C(1)	113.6(1)
P—C(1)—C(2)	119.3(2)	P—C(1)—C(6)	120.9(3)
C(2)—C(1)—C(6)	119.7(4)	C(1)—C(2)—C(3)	120.3(3)
C(2)—C(3)—C(4)	120.1(5)	C(3)—C(4)—C(5)	119.2(5)
C(4)—C(5)—C(6)	122.6(4)	C(1)—C(6)—C(5)	118.1(4)
C(1)—C(6)—C(7)	123.1(4)	C(5)—C(6)—C(7)	118.7(3)

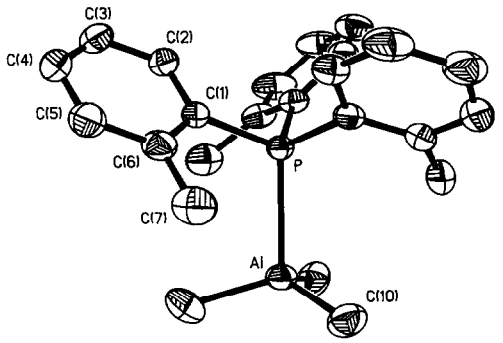

Fig. 3. X-ray crystal structure of $Me_3AlP(o\text{-tolyl})_3$ (**2**) showing the numbering scheme.

tallographically-imposed C_3 axis along the Al—P bond. The aromatic rings of the *o*-tolyl groups adopt a propeller-like arrangement, with a pitch of 50.2° from the plane defined by Al, P and C(1). As a consequence of this, the Al—C and P—C bonds are nearly eclipsed, with a dihedral angle of 10.5°. This conformation allows the *o*-tolyl methyl groups to be staggered with respect to the aluminium methyl groups (Fig. 4). The shortest non-bonding distances between the *o*-tolyl methyl and the aluminium methyl groups are C(7)—C(10) = 3.481(4) Å and C(7)—C(10) = 3.872(5) Å. The Al—P distance, 2.584(2) Å, is significantly longer than Al—P distances previously reported.[3,4]

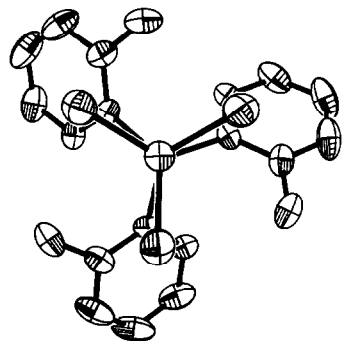

Fig. 4. The structure of $Me_3AlP(o\text{-tolyl})_3$ (**2**) viewed down the Al—P vector.

The changes in the Al—C bond distance and C—Al—C angle on coordination of $AlMe_3$ to $P(o\text{-tolyl})_3$ (see Table 2) are consistent with increased aluminium *p*-character in the Al—C bonds on changing from a planar to tetrahedral geometry. From ^{13}C NMR data it was predicted[1] that the C—Al—C angle for **2** should be smaller than that found for **1**; this is observed (Table 2). The ^{31}P Δ value for **2**[1] suggested a larger C—P—C angle on coordination than in free phosphine,[7] which is confirmed by the crystal structure (see Table 2).

It is of course possible that the conformation of the *o*-tolyl rings observed in the crystal structure is not retained in solution. It is clear, however, that changes in the geometry of **2** predicted by NMR are consistent with those observed in the solid state.

The unit cell of $Me_3AlP(o\text{-tolyl})_3$ is comprised of four molecules with no unduly close intermolecular contacts. All the intermolecular distances correspond to, or are greater than, normal van der Waals contacts.

CONCLUSIONS

The X-ray structural data reported here confirm that ^{13}C and ^{31}P NMR data can be used as an indication of changes in geometry around aluminium and phosphorus on coordination of phosphines to $AlMe_3$. There is no evidence, however, that NMR can be used to predict either the Al—P bond length, or the energy of dissociation of the complexes Me_3AlPR_3.

EXPERIMENTAL

Crystals were prepared as described in ref. 1 and sealed under nitrogen in Lindemann capillaries.

Table 4. Crystal data, details of intensity measurement and structure refinement for Me_3AlPPh_3 (**1**) and $Me_3AlP(o\text{-tolyl})_3$ (**2**)

Compound	(**1**)	(**2**)
Formula	$C_{21}H_{24}AlP$	$C_{24}H_{30}AlP$
M_r	334.38	376.40
Crystal dimensions (mm)	$0.4 \times 0.5 \times 0.7$	$0.5 \times 0.3 \times 0.3$
Crystal system	Rhombohedral	Rhombohedral
a, b (Å)	14.344(4)	14.978(1)
c (Å)	16.503(7)	34.195(5)
V (Å^3)	2944(2)	6643(1)
Space group	R_3 (obv)	R_3C
D_c (g cm^{-3})	1.13	1.13
Z	6	4
λ (cm^{-1})	1.34	1.64
Minimum, maximum (°)	4.0, 45.0	4.0, 45.0
T (K)	193	193
Total data	1792	8171
Total unique data	1507	974
Total observed data	1171	778
Significance test	$F_o > 6\sigma(F_o)$	$F_o > 6\sigma(F_o)$
Number of parameters	70	80
Weighting scheme		
Parameter g in $1/[(F_o)^2+gF_o^2]$	0.0001	0.0001
Final R	0.0436	0.0574
Final R_w	0.0532	0.0601

Unit-cell parameters and intensity data were obtained by following previously detailed procedures,[8] using a Nicolet R3m/v diffractometer operating in the θ–2θ scan mode with graphite-monochromated Mo-K_α radiation ($\lambda = 0.71069$ Å). Empirical absorption corrections were applied to the data using the program PSICOR. Further experimental data are giving in Table 3.

The structures were solved using the direct methods program XS,[9] which revealed the positions of the aluminium and phosphorus atoms. The remainder of the atoms were found using standard difference map techniques. Most, but not all of the hydrogens were visible in the final difference map. Hydrogens were included as fixed atom contributors in the final cycle (C—H = 0.96 Å).

Details of the refinements are given in Table 4. Bond lengths and angles are given in Tables 1 and 3. Atomic scattering factors and anomalous scattering parameters are as given in ref. 9.

Acknowledgements—We thank the Petroleum Research Fund and the Milton Fund for financial support. Andrew R. Barron is a 1987–1988 Du Pont Young Faculty Fellow.

REFERENCES

1. A. R. Barron, *J. Chem. Soc., Dalton Trans.* 1988, 3047.
2. C. A. Tolman, *Chem. Rev.* 1977, **77**, 313.
3. A. Almenningen, L. Fernholt and A. Haaland, *J. Organomet. Chem.* 1978, **145**, 109.
4. D. C. Bradley, H. Chundzynska, M. M. Factor, D. M. Frigo, M. B. Hursthouse, B. Hussain and L. M. Smith, *Polyhedron* 1988, **7**, 1289.
5. G. A. Anderson, F. R. Forgaard and A. Haaland, *Acta Chem. Scand.* 1972, **26**, 1947.
6. J. J. Daly, *J. Chem. Soc.* 1964, 3799.
7. T. S. Cameron and B. Dahlen, *J. Chem. Soc., Perkin II* 1975, 1737.
8. M. D. Healy, D. A. Wierda and A. R. Barron, *Organometallics* 1988, **7**, 2543.
9. G. M. Sheldrick, SHELXTL.PLUS. Nicolet Corporation, Madison, Wisconsin, U.S.A. (1986).

Polyhedron Vol. 8, No. 6, pp. 835–839, 1989
Printed in Great Britain

0277–5387/89 $3.00+.00
© 1989 Pergamon Press plc

PREPARATION AND LIGAND PROPERTIES OF BIS-THIONYLIMINO COMPLEXES OF THE TYPE $M(NSO)_2(PR_3)_2$. X-RAY STRUCTURE OF $Pt(NSO)_2(PMe_3)_2$

IVAN P. PARKIN, ALEXANDRA M. Z. SLAWIN, DAVID J. WILLIAMS and J. DEREK WOOLLINS*

Department of Chemistry, Imperial College of Science and Technology, South Kensington, London SW7 2AY, U.K.

(*Received* 21 *September* 1988; *accepted* 27 *October* 1988)

Abstract—Reaction of $S(NSO)_2$ with *cis*-$MCl_2(PR_3)_2$ (M = Pt, PR_3 = PMe_3, PEt_3, PPr^n_3, PBu^n_3, PPh_3, $PMePh_2$, PMe_2Ph and dppe; M = Pd, PR_3 = dppe) in liquid ammonia gives *cis*-$M(NSO)_2(PR_3)_2$ quantitatively by ^{31}P NMR and in 60% isolated yield. The new compounds have been characterized by microanalyses, IR, ^1H and ^{31}P NMR, mass spectrometry and in the case of $Pt(NSO)_2(PMe_3)_2$, X-ray crystallography. The molecule has *cis* square-planar geometry with approximate C_2 symmetry.

Compounds containing the NSO^- ligand have been the subject of recent work;[1,2] reaction of $Rh(CO)H(PPh_3)_3$ with $CsNSO_2$ gives $Rh(NSO)(CO)(PPh_3)_2$, whilst treatment of $Ti(Cp)_2Cl_2$ with KNSO yields the bis compound $Ti(Cp)_2(NSO)_2$.[3] The *cis* and *trans* isomers of $Pt(NSO)_2(PPh_3)_2$ have been made from $Pt(C_2H_4)(PPh_3)_2$; reaction with $Hg(NSO)_2$ gives the *trans* product[4] whilst with $PhAs(NSO)_2$ the *cis* isomer is obtained.[5] Reaction of $Hg(NSO)_2$ with *cis*-$PtCl_2(PR_3)_2$ has also been claimed[4] to give *cis*-$Pt(NSO)_2(PR_3)_2$ on the basis of ^{31}P NMR only, but there are discrepancies between the data reported in refs 4 and 5. In the light of these problems we have now developed a general synthetic route for the formation of $M(NSO)_2(PR_3)_2$.

We are currently investigating the synthetic potential of various sulphur–nitrogen reagents with metal complexes using liquid ammonia as solvent.[6,7] Here, we report the synthesis and spectroscopic characterization of the new complexes, $M(NSO)_2(PR_3)_2$ and $Ti(Cp)_2(NSO)_2$ from the reaction of $S(NSO)_2$ in liquid ammonia. The X-ray crystal structure of $Pt(NSO)_2(PMe_3)_2$ is also reported.

EXPERIMENTAL

All manipulations were performed under an inert atmosphere (argon or nitrogen). Solvents were dried before use: CH_2Cl_2 was distilled from CaH_2 and petroleum ether (60–80) distilled from sodium benzophenone. The ^{31}P NMR and some ^1H NMR were recorded using a JEOL FX90Q spectrometer operating at 36.21 and 89.55 MHz, and referenced to external 85% H_3PO_4 and internal $SiMe_4$, respectively. The other ^1H NMR were obtained on a Bruker WM 250 MHz operating at 250.13 MHz referenced to $CHCl_3$ at 7.24 ppm. IR spectra were obtained from KBr discs using a Perkin–Elmer 1720 spectrophotometer. Mass spectra were obtained both by EI and FAB (using thiodiethanol matrix) on a VG 2020 machine. Microanalyses were performed by the departmental service.

The compounds $PtCl_2(PR_3)_2$ (PR_3 = PMe_3, PEt_3, PPr^n_3, PBu^n_3, PMe_2Ph, $PMePh_2$, PPh_3 and dppe) and $PdCl_2$(dppe) were made as previously described.[8] $Ti(C_5H_5)_2Cl_2$ (Aldrich) and anhydrous ammonia (BOC) were used as supplied. $S(NSO)_2$ was prepared by the literature method.[9]

Preparation of $M(NSO)_2(PR_3)_2$

All these complexes (Table 1) were made by the same general method illustrated here for $Pt(NSO)_2(PPr^n_3)_2$ (**3**). *cis*-$PtCl_2(PPr^n_3)_2$ (0.080 g, 0.137 mmol) was added to a stirred red solution of $S(NSO)_2$ (0.021 g, 0.137 mmol) in liquid ammonia at −78°C. The resultant suspension was stirred for 30 min at −78°C and then the ammonia blown off by a stream of argon. The resultant yellow solid was

* Author to whom correspondence should be addressed.

Table 1. Microanalytical data

Compound	C	H	N	Melting point (°C)	Yield (%)
$Pt(NSO)_2(PMe_3)$ (**1**)	14.8 (15.3)	4.5 (3.8)	5.7 (5.9)	154–157	62
$Pt(NSO)_2(PEt_3)_2$ (**2**)	25.9 (25.9)	5.4 (5.4)	5.0 (5.0)	124–125	54
$Pt(NSO)_2(PPr^n_3)_2$ (**3**)	33.5 (33.8)	6.6 (6.6)	4.3 (4.4)	110–113	50
$Pt(NSO)_2(PMe_2Ph)_2$ (**4**)	32.3 (32.3)	4.5 (3.7)	4.9 (4.7)	107–110	65
$Pt(NSO)_2(PMePh_2)_2$ (**5**)	42.9 (43.4)	3.5 (3.6)	3.9 (3.9)	121–123	57
$Pt(NSO)_2(PPh_3)_2$ (**6**)	46.7 (46.7)	3.3 (3.3)	3.2 (3.0)		62
$Pt(NSO)_2(dppe)\cdot CDCl_3$ (**7**)	38.3 (38.6)	3.8 (3.4)	3.6 (3.4)		43
$Pd(NSO)_2(dppe)$ (**8**)	48.9 (49.6)	4.2 (4.5)	4.5 (4.7)		32
$Ti(Cp)_2(NSO)_2$ (**9**)	39.1 (39.7)	3.2 (3.3)	9.3 (9.3)		75

extracted into CH_2Cl_2 (5 cm^3), filtered through a celite/glass wool plug and layered with petroleum ether 60–80 (50 cm^3). Cooling of the solution to −20°C yielded crystals of (**3**) (0.044 g, 0.068 mmol, 59%). Microanalytical data are given in Table 1, NMR data in Table 2, and MS and selected IR data in Table 3.

Preparation of $Ti(Cp)_2(NSO)_2$ was carried out

Table 2. ^{31}P and ^1H NMR data for compounds of the type $ML_2(NSO)_2$ and $Pt(NSO)Cl(PR_3)_2$

Compound	^{31}P NMR δ (ppm)	^{31}P NMR ^1J (Hz)	^1H NMR
1	−32.6	3027	1.17 [d, ^2J(P—H) 10.8, ^3J(Pt—H) 34.1 Hz]
2	1.1	3070	1.15 [d of t, ^3J(P—H) 17.4, ^2J(H—H) 7.1 Hz (18H)], 1.78 (m, 12H)
3	−7.8	3069	1.61 (m, 24H), 1.00 [t, ^2J(H—H) 7.0 Hz, (18H)]
4	−22.1	3088	1.48 [d, ^2J(P—H) 10.9, ^3J(Pt—H) 32.3 Hz, (12H)], 7.42 (m, 10H)
5	−8.1	3119	1.76 [d, ^2J(P—H) 10.2, ^3J(P—H) 33.0 Hz, (6H)], 7.4 (m, 20H)
6	8.8	3190	7.3 (m)
7	33.9	3112	7.8 (m, 8H), 7.4 (m, 12H), 2.28 (m, 4H)
8	53.4		7.6 (m, 8H), 7.3 (m, 12H), 2.4 (m, 4H)
9			6.37 (s)
10[a]	−7.0	3072	

	^{31}P NMR δ_a	δ_x	^1J_a	^1J_x	$^2J_{ax}$
$Pt(NSO)Cl(PEt_3)_2$ (**11**)	7.4	0.2	3640	2734	20
$Pt(NSO)Cl(PBu^n_3)_2$ (**12**)	−0.6	−6.3	3695	2944	20
Pt(NSO)Cl(dppe) (**13**)	39.8	33.8	3700	3003	8

[a] (**10**) = $Pt(NSO)_2(PBu^n_3)_2$.

Table 3. Mass spectral and selected NSO IR vibrations

Compound	ν_{asym}	ν_{sym}	Def.	M^+	M^+—NSO	M^+—$(NSO)_2$
1	1245s	1061m	567w	471	409	346
	1230vs	1047vs				
2	1243vs	1057s	567m	555	493	
	1228vs	1050s	554m			
3	1249vs	1058vs	545m	639	576	513
	1221m					
4	1242vs	1055vs	555w	596	533	
		1020m				
5	1242vs	1062s	569w	720	658	596
6	1243vs	1062m	547m			
	1228s	1092m				
7	1239vs	1057s	562w			
		1012m				
8	1250vs	1054s				
		1010m				
9	1235vs	1075s	525m	302	246	

under the same experimental conditions as above except that the crystals were grown by slow diffusion of *n*-hexane (15 cm^3) into a CH_2Cl_2 (5 cm^3) solution at room temperature.

Crystal data. $C_6H_{18}N_2O_2P_2S_2Pt$, $M = 471.4$, monoclinic, $a = 9.963(2)$, $b = 13.903(2)$, $c = 11.406(2)$ Å, $\beta = 109.85(2)°$, $U = 1486$ Å^3, space group $P2_1/n$, $Z = 4$, $D_c = 2.11$ g cm^{-3}. Yellow, air-stable prisms, dimensions $0.03 \times 0.20 \times 0.23$ mm, μ(Cu-K_α) = 225 cm^{-1}, $\lambda = 1.54178$ Å, $F(000) = 896$.

Data collection and processing. A Nicolet R3m diffractometer, ω-scan method, ($2\theta \leqslant 100°$), graphite-monochromated Cu-K_α radiation; 1523 independent measured reflections of which 1387 were observed [$|F_o| > 3\sigma(|F_o|)$], corrected for Lorentz and polarization factors; empirical absorption correction based on 362 azimuthal measurements (laminar correction (100) prominent). Minimum and maximum transmission factors were 0.018 and 0.097.

Structure analysis and refinement. The structure was solved by the heavy atom method and all the non-hydrogen atoms refined anisotropically. The hydrogen atoms were idealized (C—H = 0.96 Å), assigned isotropic thermal parameters $U(H) = 1.2U_{eq}(C)$ and allowed to ride on their parent carbons. The methyl groups were refined as rigid bodies. Refinement was by block-cascade full-matrix least-squares to $R = 0.052$, ($R = \Sigma[|F_o| - |F_c|]/\Sigma|F_o|$), $R_w = 0.055$ ($w^{-1} = \sigma^2(F) + 0.00130F^2$). The maximum and minimum residual electron density in the final ΔF map were 1.47 and −1.46 eÅ^{-3}, respectively. The mean and maximum shifts/error in the final refinement cycle were 0.004 and 0.052, respectively. Computations were carried out on an Eclipse S140 computer using the SHELXTL program system[10] and published scattering factors.

RESULTS AND DISCUSSION

Reaction between $PtCl_2(PR_3)_2$ and $S(NSO)_2$ gives $Pt(NSO)_2(PR_3)_2$ in good yield, *ca* 60% [eq. (1)]

$$Pt(PR_3)_2Cl_2 + S(NSO)_2 \longrightarrow Pt(NSO)_2(PR_3)_2 + SCl_2. \quad (1)$$

^{31}P NMR shows that the reaction proceeds almost quantitatively with the only other observable phosphorus-containing species being $PtS_2N_2(PR_3)_2$ (*ca* 5%). The observed disulphurdinitrido complex is probably formed from the products of the reaction between the eliminated SCl_2 and liquid ammonia [eq. (2)]

$$6SCl_2 + 18NH_3 \longrightarrow 3S_2N_2^{2-} + 12NH_4Cl + 6H^+$$

$$S_2N_2^{2-} + PtCl_2(PR_3)_2 \longrightarrow Pt(S_2N_2)(PR_3)_2 + 2Cl^-. \quad (2)$$

We have shown previously that reaction of an ammonia solution of SCl_2 with $PtCl_2(PR_3)_2$ gives exclusively $Pt(S_2N_2)(PR_3)_2$.[11] When a slight excess of $PtCl_2(PR_3)_2$ to $S(NSO)_2$ is used (1.2 : 1.0 molar ratio), *ca* 25% $Pt(S_2N_2)(PR_3)_2$ is observed by ^{31}P NMR. Further increasing the molar ratio to (2 : 1) gives $Pt(NSO)_2(PR_3)_2$ (25%), $Pt(NSO)Cl(PR_3)_2$ (50%) and $Pt(S_2N_2)(PR_3)_2$ (25%).

The ^{31}P NMR spectra of **1**–**7** (Table 2) consist of singlets with platinum satellites indicating that the

phoshines are equivalent. The magnitude of the ^{31}P–^{195}Pt coupling constant (*ca* 3100 Hz) is appropriate for platinum(II) and suggests nitrogen rather than oxygen bound NSO^- ligands. (2850 Hz for phosphorus *trans* to nitrogen in $Pt(S_2N_2)(PR_3)_2$, 3250 Hz in $Pt(S_2N_2H)(PR_3)_2^+X^-$.)[8,11] An oxygen bound ligand would be expected to have a greater coupling constant. Detailed analysis of the fragmentation pattern of the mass spectra shows peaks corresponding to $Pt(NSO)(NS)(PR_3)_2^+$ and $Pt(NS)_2(PR_3)_2^+$, both of which could not be readily accounted for if the complex was oxygen bound. Finally, nitrogen bound NSO^- ligands are more likely, as nitrogen is expected to formally carry the negative charge. The ^{31}P chemical shifts and ^1J couplings are dependant on the phosphine. The observed shifts in the complexes mirror the shifts in the uncoordinated phosphine. For example, on increasing the number of methyl groups from PPh_3 through to PMe_3 the chemical shift becomes more negative and the magnitude of ^1J is reduced. Methyl groups are better σ-donors than phenyl groups and poorer π-acceptors. Thus, increasing the number of methyl groups results in greater electron density on the phosphorus atoms, better shielding and more negative chemical shifts.

The ^{31}P NMR spectra of **11**–**13** are of the AX type with ^2J ^{31}P—^{31}P couplings of 20 Hz, typical for platinum(II).[8,11] The ^{195}Pt–^{31}P coupling constants of 3650 and 2850 Hz are typical of phosphorus *trans* to chlorine and nitrogen in platinum(II) complexes, leading us to postulate the existence of these $PtCl(NSO)(PR_3)_2$ complexes (N.B. no solid compounds of this formula have been isolated to date). Further evidence for our formulation comes from the position of the resonances in **11**. For example, phosphorus *trans* to nitrogen occurs at 0.2 ppm compared to 1.5 ppm in **2**, and phosphorus *trans* to chlorine occurs at 7.4 ppm compared to 9.1 ppm in $PtCl_2(PEt_3)_2$.

^1H NMR (Table 2) for **1**, **4** and **5** reveal methyl resonances split by both $^2J_{P—H}$ of 11 Hz and $^3J_{Pt—H}$ of *ca* 34 Hz. This again indicates identical phosphine groups in a symmetric environment. For the other complexes (**2**, **3**, **6**, **7**) the small differences in chemical shifts hide the couplings.

Compounds **1** and **9** exhibit characteristic NSO vibrations in the regions 1250–1200 cm^{-1} and 1090–1040 cm^{-1} corresponding to the asymmetric and symmetric stretching modes, respectively. Previous IR studies of RNSO compounds suggest that these two modes are not strongly coupled. Individual modes were assigned to ν(NS) or ν(SO) although the subject of disagreement in these compounds has been largely resolved with the higher frequency mode being assigned as the ν(NS). In this study compounds **1** and **2** both show two ν_{asym} and ν_{sym} vibrations and in the absence of coupled modes suggests two inequivalent NSO groups. This cannot be reconciled with the crystal structure which shows a symmetric environment and similarly with the ^{31}P NMR. For compounds **4**, **5**, **7** and **8** only one band for the ν_{asym} is observed although this is broadened relative to the ν_{asym} observed in **1** and **2**. However, the ν_{sym} shows two modes although these are partially covered by ligand modes.

The X-ray structure of **1** is shown in Fig. 1 with bond lengths and angles in Table 4. The molecule

Table 4. Bond lengths and angles for $Pt(NSO)_2(PMe_3)_2$ (**1**)

Pt—P(1)	2.262(3)	Pt—P(2)	2.264(4)
Pt—N(1)	2.049(11)	Pt—N(2)	2.049(10)
P(1)—C(1)	1.788(26)	P(1)—C(2)	1.796(16)
P(1)—C(3)	1.797(18)	P(2)—C(4)	1.763(23)
P(2)—C(5)	1.786(25)	P(2)—C(6)	1.818(19)
N(1)—S(1)	1.492(13)	S(1)—O(1)	1.456(19)
N(2)—S(2)	1.465(14)	S(2)—O(2)	1.442(18)
P(1)—Pt—P(2)	96.3(1)	P(1)—Pt—N(1)	88.5(3)
P(2)—Pt—N(1)	174.7(3)	P(1)—Pt—N(2)	173.1(4)
P(2)—Pt—N(2)	90.2(4)	N(1)—Pt—N(2)	85.1(5)
Pt—P(1)—C(1)	113.1(7)	Pt—P(1)—C(2)	119.8(5)
C(1)—P(1)—C(2)	105.5(11)	Pt—P(1)—C(3)	113.1(7)
C(1)—P(1)—C(3)	103.2(11)	C(2)—P(1)—C(3)	100.3(8)
Pt—P(2)—C(4)	116.9(7)	Pt—P(2)—C(5)	116.4(8)
C(4)—P(2)—C(5)	103.2(12)	Pt—P(2)—C(6)	113.6(7)
C(4)—P(2)—C(6)	102.0(11)	C(5)—P(2)—C(6)	102.8(11)
Pt—N(1)—S(1)	129.5(9)	N(1)—S(1)—O(1)	123.3(8)
Pt—N(2)—S(2)	132.6(8)	N(2)—S(2)—O(2)	121.4(8)

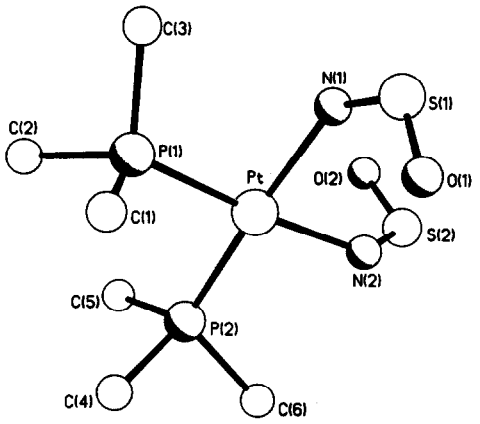

Fig. 1. The X-ray structure of **1**.

has slightly distorted *cis* square-planar geometry with local non-crystallographic C_2 symmetry and the expected bond lengths and angles. The Pt—N(1)—N(2) and Pt—P(1)—P(2) planes are rotated *ca* 3° with respect to each other about an axis bisecting the P(1)—Pt—P(2) angle. The two Pt—N—S—O planes are rotated 85° from the coordination plane. There is no crystallographic evidence to explain the complexity of the IR spectrum; there are no significant intermolecular contacts.

REFERENCES

1. H. W. Roesky, K. K. Pandey, B. Krebs and M. J. Dartmann, *J. Chem. Soc., Dalton Trans.* 1984, 2271.
2. H. Dieno, H. W. Roesky, M. Noltemeyer and G. M. Sheldrick, *J. Chem. Soc., Chem. Commun.* 1987, 1483.
3. M. Hebberhold, F. Neumann, G. S. Fink and U. Thewalt, *Inorg. Chem.* 1987, **26**, 3612.
4. R. Short, M. B. Hursthouse, T. G. Purcell and J. D. Woollins, *J. Chem. Soc., Chem. Commun.* 1987, 407.
5. T. Chivers, K. S. Dhathathreyan, C. Lensink and J. F. Richardson, *Inorg. Chem.* 1988, **27**, 1570.
6. I. P. Parkin, P. S. Belton, J. D. Woollins and D. J. Williams, *J. Chem. Soc., Chem. Commun.*, submitted.
7. I. P. Parkin, J. D. Woollins and D. J. Williams, *J. Chem. Soc., Dalton Trans.*, submitted.
8. R. Jones, C. P. Warrens, D. J. Williams and J. D. Woollins, *J. Chem. Soc., Dalton Trans.* 1987, 907.
9. D. A. Armitiage and A. W. Sinder, *Inorg. Chem.* 1972, **11**, 1151.
10. G. M. Sheldrick, SHELXTL, An Integrated System for Solving, Refining and Displaying Crystal Structures from Diffraction Data. University of Göttingen, F.R.G. (1978) (revision 4.1 1983).
11. I. P. Parkin, unpublished results.

Polyhedron Vol. 8, No. 6, pp. 841–844, 1989
Printed in Great Britain

0277–5387/89 $3.00 + .00
© 1989 Pergamon Press plc

THE PREPARATION AND X-RAY STRUCTURE OF $[Et_4N][Pt(CN)_2(S_2N_2H)]$

PAUL F. KELLY, ALEXANDRA M. Z. SLAWIN, DAVID J. WILLIAMS and J. DEREK WOOLLINS*

Department of Chemistry, Imperial College of Science and Technology, South Kensington, London SW7 2AY, U.K.

(*Received* 21 *September* 1988; *accepted* 27 *October* 1988)

Abstract—Reaction of $Pt(COD)(S_2N_2)$ (**1**) with KCN gives $K_2[Pt(CN)_2(S_2N_2)]$ (**2**) which can be protonated using HCl. The X-ray structure of $[Et_4N][Pt(CN)_2(S_2N_2H)]$ (**3**) is reported. The anion has *cis* square-planar geometry with characteristic bond lengths and angles for the $S_2N_2H^-$ ligand.

As part of a continuing study into the chemistry of metal–sulphur–nitrogen systems we have recently reported on the preparation of the disulphur–dinitrido complex $Pt(COD)(S_2N_2)$ (**1**)[1] (COD = 1,5-cyclooctadiene), which we suggested had great promise as a starting material for the synthesis of previously unobtainable complexes of the type $PtL_2(S_2N_2)$. Here we report on the reaction of **1** with 2 equivalents of KCN which readily yields salts of $[Pt(CN)_2(S_2N_2)]^{2-}$ and, after protonation with HCl, $[Pt(CN)_2(S_2N_2H)]^-$. The structure of the latter anion, the nickel analogue of which has been known for some 30 years, has been confirmed by X-ray crystallography.

EXPERIMENTAL

General conditions and preparation of starting materials were as previously reported; a variation upon the preparation of $Pt(COD)(S_2N_2)$ is included below as it results in a product of higher purity than the earlier method.[1]

$Pt(COD)(S_2N_2)$ (1)

A mixture of $Pt(COD)Br_2$ (0.597 g, 1.3 mmol) and $[Me_2Sn(S_2N_2)]_2$ (0.31 g, 0.65 mmol) in CH_2Cl_2 (50 cm^3) was stirred for 4 h, after which time the volume of the solvent was reduced to 10 cm^3 *in vacuo* and the resulting solution treated with $[^nBu_4N]OH$ (1.3 cm^3 of a 1 M solution in MeOH, 1.3 mmol). After stirring for 1 min the solution was evaporated to dryness and the residue washed with water (50 cm^3), then dried and extracted into CH_2Cl_2 (20 cm^3). After filtration, the volume of the solution was reduced to 5 cm^3 and the product obtained as well-formed micro-crystals by slowly stirring hexane (50 cm^3) into the mixture. After further washings with hexane (30 cm^3) and Et_2O (50 cm^3) the solid was dried *in vacuo*. Micro-analysis. Found: C, 25.1; H, 3.2; N, 6.5. Calc. C, 24.3; H, 3.1; N, 7.1%. Typical yield ≈ 80%.

Crude $K_2[Pt(CN)_2(S_2N_2)]$

$Pt(COD)(S_2N_2)$ (0.2 g, 0.5 mmol) and KCN (66 mg, 1.0 mmol) were mixed as solids and, with the mixture cooled to 0°C using an ice bath, ethanol (15 cm^3) was added with stirring. After a few minutes just enough CH_2Cl_2 (*ca* 5–10 cm^3) was added to dissolve the remaining solid, while the temperature was maintained at 0°C. The resulting solution was stirred overnight with the ice bath allowed to slowly melt and the temperature to reach RT. The resulting mixture consisted of an orange solution with some unreacted KCN as precipitate; the solvent was evaporated *in vacuo* until enough CH_2Cl_2 had been removed to allow the unreacted $Pt(COD)(S_2N_2)$ to start to crystallize out. At this point more ethanol (*ca* 15 cm^3) was added and the suspension stirred for 10 min, followed by addition of CH_2Cl_2 (*ca* 1 cm^3) to dissolve any remaining precipitate. The resulting solution was stirred for a further 6 h then reduced in volume to *ca* 10 cm^3. Hexane (50 cm^3) was added giving crude

* Author to whom correspondence should be addressed.

$K_2[Pt(CN)_2(S_2N_2)]$ as a yellow precipitate, which was filtered and dried *in vacuo*. Yield 150 mg (72%).

$[Et_4N][Pt(CN)_2(S_2N_2H)]$

Crude $K_2[Pt(CN)_2(S_2N_2)]$ (84 mg, 0.2 mmol) was dissolved in degassed water (1 cm^3) and treated with dilute HCl (1 cm^3 of a 0.2 M solution) giving a green coloured solution with some precipitate. The water was removed *in vacuo* and the residue extracted into THF (20 cm^3). After filtration the volume of the THF was reduced and crude $K[Pt(CN)_2(S_2N_2H)]$ precipitated as a yellow–orange solid by addition of hexane (70 cm^3). Yield 50 mg.

This product was stirred with $[Et_4N]Br$ (30 mg, 0.14 mmol) in 1 : 1 EtOH–CH_2Cl_2 (20 cm^3) for 20 min, then the solvent was removed *in vacuo* and the residue extracted with CH_2Cl_2 (20 cm^3) followed by filtration through celite. The celite was washed with further amounts of CH_2Cl_2 ($\approx 5 \times 30$ ml) until the washings were colourless; the combined filtrate was reduced to 20 cm^3 and the product obtained as a green precipitate by addition of hexane.

Yield 53 mg (56% based upon $K_2[Pt(CN)_2(S_2N_2)]$ or 40% based upon **1**. Microanalysis. Found: C, 25.4; H, 4.4; N, 14.5. Calc. for $[(CH_3CH_2)_4N][Pt(CN)_2(S_2N_2H)]$: C, 25.5; H, 4.5; N, 14.9%.

Crystals suitable for X-ray crystallography were obtained by slow hexane diffusion into an EtOH solution.

Crystal data. $C_{10}H_{21}N_5PtS_2$, $M = 470.5$, orthorhombic, $a = 14.231(5)$, $b = 14.508(3)$, $c = 16.081(4)$ Å, $U = 3320$ $Å^3$, space group *Pcab*, $Z = 8$, $D_c = 1.88$ g cm^{-3}, Cu radiation, $\lambda = 1.54178$ Å, $\mu(Cu\text{-}K_\alpha) = 183$ cm^{-1}, $F(000) = 1807$.

Data collection and processing. Data were measured on a Nicolet R3m diffractometer with Cu-K_α radiation (graphite monochromator) using the ω-scan method. A crystal of dimensions $0.13 \times 0.20 \times 0.33$ mm was used. 2235 independent reflections were measured ($2\theta \leqslant 116°$), of which 1921 had $|F_o| > 3\sigma(|F_o|)$ and were considered to be observed. The data were corrected for Lorentz and polarization factors; an empirical absorption correction (ellipsoidal) based on 376 azimuthal measurements was applied (maximum and minimum transmission factors were 0.070 and 0.008).

Structure analysis. The structure was solved by the heavy-atom method. The non-hydrogen atoms were refined anisotropically. The amine proton on N(1) was placed in a calculated trigonal position and then allowed to refine isotropically subject to a N—H distance constraint of 0.98 Å. The positions of the remaining hydrogen atoms were idealized, C—H = 0.96 Å, assigned isotropic thermal parameters, $U(H) = 1.2\ U_{eq}(C)$, and allowed to ride on their parent carbons. The methyl groups were refined as rigid bodies. Refinement was by block-cascade full-matrix least-squares to $R = 0.041$ ($R = \Sigma[|F_o| - |F_c|]/\Sigma|F_o|$), $R_w = 0.045$ ($w^{-1} = \sigma^2(F) + 0.00043F^2$). The maximum and minimum residual electron densities in the final ΔF map were 1.20 and -0.54 e $Å^{-3}$, respectively. The mean and maximum shifts/error in the final refinement were 0.019 and 0.214, respectively. Computations were carried out on an Eclipse S140 computer using the SHELXTL program system.[2]

RESULTS AND DISCUSSION

The anion $[Ni(CN)_2(S_2N_2H)]^-$ was first prepared in 1957 by reaction of the dimeric nickel species $K_4[Ni_2(CN)_6]$ with S_4N_4,[3] and has subsequently been shown to be available from a similar reaction with $K_2[Ni(CN)_4]$[4] and from reaction of $Ni(S_2N_2H)_2$ with KCN.[5] However, despite the fact that the nickel species is so well known there have been no reports of salts of the platinum analogue, $[Pt(CN)_2(S_2N_2H)]^-$. This is primarily due to the fact that the platinum cyano complex $K_2[Pt(CN)_4]$ does not react with S_4N_4 in a similar manner to its nickel counterpart. Furthermore, while it is quite possible that $Pt(S_2N_2H)_2$ reacts with KCN to give the substituted species, no investigations into this reaction have been reported (possibly due to the difficulty of preparing bulk amounts of the starting material). Here we report on the preparation of $[Pt(CN)_2(S_2N_2H)]^-$ by a method which circumvents these problems, utilizing the recently discovered organometallic complex Pt(COD)(S_2N_2) (**1**).

Reaction of **1** with 2 equivalents of KCN in EtOH–CH_2Cl_2 results in the replacement of the labile COD group by two cyanides [eq. (1)]

$$\underset{(1)}{Pt(COD)(S_2N_2)} + 2KCN \longrightarrow \underset{(2)}{K_2[Pt(CN)_2(S_2N_2)]} + COD. \quad (1)$$

The solvent system in which the reaction is performed is crucial, for a number of reasons. One important consideration is the solubility of the reactants; KCN requiring EtOH, in which **1** is only poorly soluble. For this reason the reaction is performed in the presence of just enough CH_2Cl_2 to allow **1** to dissolve, although this often means that some KCN is precipitated during the course of the

reaction (see Experimental). Also, the reaction is performed at low temperature (at least initially), since heating mixtures of KCN and **1** much above room temperature results in the production of a highly coloured species, which is also apparent if the reaction is performed in MeOH instead of EtOH. It is possible that this coloured species may be a salt of the dimeric anion $[Pt(CN)(S_2N_2)]_2^{2-}$ although we have yet to confirm this.

Crude $K_2[Pt(CN)_2(S_2N_2)]$ (**2**), obtained in the above manner, is a yellow solid which appears to be air-stable and dissolves only in water and polar solvents. The IR of this product shows the expected S—N bands at 1055, 693 and 373 cm^{-1}, together with cyanide stretches at 2110 and 2124 cm^{-1} (cf. 2135 and 2124 cm^{-1} in $K_2[Pt(CN)_4]$). Also present are rather broad peaks in the region around 1100 cm^{-1}, typical of S=O stretches. Such impurities are common in complexes of the type $Pt(S_2N_2)(PR_3)_2$, which we have prepared by a variety of routes,[6] but can easily be washed out with water. In the case of **2**, which is water soluble, this is obviously not possible and it is for this reason that we have yet to prepare analytically pure samples; a typical microanalysis shows C, 6.5; N, 11.5%, compared to calculated values of 5.8 and 13.4%, respectively. However, the nature of the compound can be unequivocally deduced from the IR spectrum and, by inference, from the crystal structure of the protonated species.

Protonation of $[Pt(CN)_2(S_2N_2)]^{2-}$ is easily achieved and in some situations unavoidable. Thus attempts to prepare $[Et_4N]_2[Pt(CN)_2(S_2N_2)]$ by reaction of **2** with $[Et_4N]Br$ in CH_2Cl_2–EtOH lead to mixtures of an intractable oil together with green crystals of $[Et_4N][Pt(CN)_2(S_2N_2H)]$ (**3**). The latter is, however, best prepared by treatment of **2** with dil. HCl in H_2O, which gives crude samples of $K[Pt(CN)_2(S_2N_2H)]$ that can be converted to the tetraethylammonium salt by reaction with $[Et_4N]Br$ [eq. (2)]. Extraction of the product of this reaction into CH_2Cl_2, in which it is fairly soluble, yields samples of a high analytical purity. Typically, the overall yield of this final product, based upon the amount of $Pt(COD)Br_2$ initially used, is in the order of 30–35%. The IR spectrum of the compound includes bands at 2986 (ν[N—H]), 2139/2127 (ν[CN]) and 1048/689 cm^{-1} (ν[N—S]). It is noteworthy that, as we have previously observed for phosphine complexes, the relative intensities of the latter two bands is changed as a result of protonation. Thus, whereas in **2** the higher frequency band is the more intense of the two, in **3** the opposite is true.

$$\underset{(2)}{K_2[Pt(CN)_2(S_2N_2)]} + HCl \longrightarrow K[Pt(CN)_2(S_2N_2H)] + KCl$$
$$\Big\downarrow + [Et_4N]Br$$
$$[Et_4N][Pt(CN)_2(S_2N_2H)] + KBr. \qquad (2)$$
$$(3)$$

Attempts to prepare $K[Pt(CN)_2(S_2N_2H)]$ by reaction of $K_2[Pt(CN)_4]$ with S_4N_4 in MeOH seems to invariably fail. Thus, refluxing the platinum species with S_4N_4 (1 : 1) for 3 h, followed by evaporation of the solvent *in vacuo*, yields a pale yellow, hygroscopic residue. The IR of this residue shows bands due to unreacted $K_2[Pt(CN)_4]$ together with sulphur oxyanions such as thiosulphate, but none of the bands observed in the crude $K[Pt(CN)_2(S_2N_2H)]$ prepared as above. The absence of this product is also confirmed by the fact that the residue dissolves in H_2O to give a colourless solution. If the residue is extracted with CH_2Cl_2 this yields unreacted S_4N_4 (typically 70 mg from a reaction initially involving 120 mg).

Similarly, attempts to prepare salts of **2** by displacement of the phosphine groups in $Pt(S_2N_2)(PMe_2Ph)_2$ by cyanide (present as the $[^nBu_4N]^+$ salt) prove unsuccessful, although we have preliminary evidence to suggest that a monosubstituted species, in which one of the phosphines has been replaced, may be formed. On this point it is worth noting that cyanide deprotonates complexes of the type $[Pt(S_2N_2H)(PR_3)_2]X$; thus treatment of $[Pt(S_2N_2H)(PMe_2Ph)_2]BF_4$ with 1 equivalent of $[^nBu_4N]CN$ results in the formation of $Pt(S_2N_2)(PMe_2Ph)_2$, as observed by ^{31}P NMR.

Slow diffusion of hexane into an EtOH solution of **3** yields very well-formed crystals, suitable for X-ray crystallography. The anion has the expected square-planar geometry (Fig. 1, Table 1), with a maximum deviation from planarity of 0.03 Å [for N(3)]. It is noteworthy that, as in previously studied transition metal $S_2N_2H^-$ complexes,[7] the N—H proton lies significantly out of the plane of the metallocycle (0.25 Å). The bond lengths and angles in the PtS_2N_2 ring are consistent with previous results for protonated complexes, with characteristic angles at N(1), N(2) and S(1) in accord with the presence of a proton on N(1).[7] The bond lengths for the Pt—$(CN)_2$ unit are normal. There is an intermolecular N(1)—H···N(4) hydrogen bond (N(1)—N(4) 2.93 Å, H···N(4) 2.02 Å; N—H···N

Table 1. Bond distances (Å) and angles (°) in $[Et_4N][Pt(CN)_2(S_2N_2H)]$

Pt—N(1)	2.020(8)	N(1)—S(1)	1.587(8)
S(1)—N(2)	1.518(9)	N(2)—S(2)	1.682(9)
S(2)—Pt	2.261(3)		
Pt—N(1)—S(1)	119.0(5)	N(1)—S(1)—N(2)	110.8(5)
S(1)—N(2)—S(2)	120.3(5)	N(2)—S(2)—Pt	103.8(3)

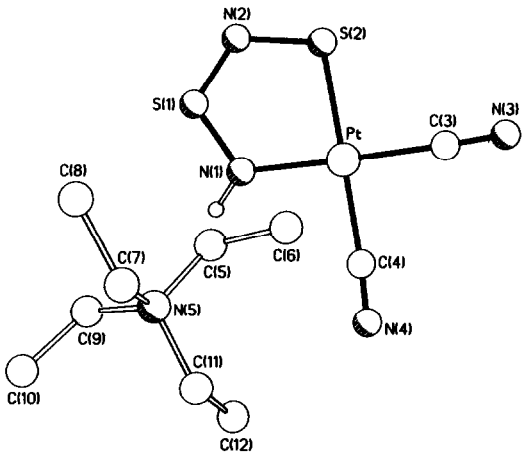

Fig. 1. X-ray structure of $[Et_4N][Pt(CN)_2(S_2N_2H)]$.

angle 154°). Despite the planarity of the anions they do not display stacking properties in the crystal in this case, in contrast to previously studied phosphine complexes.[7] This is undoubtedly due to the very bulky nature of the cation and the absence of any potential hydrogen-bonding acceptor sites. Work on the preparation of crystalline samples containing smaller cations is underway.

Acknowledgement—We are grateful to Johnson Matthey Chemicals for loans of precious metals.

REFERENCES

1. P. F. Kelly, A. M. Z. Slawin, D. J. Williams and J. D. Woollins, *Polyhedron* 1988, **7**, 1925.
2. G. M. Sheldrick, SHELXTL, An Integrated System for Solving, Refining and Displaying Crystal Structures from Diffraction Data. University of Göttingen, F.R.G. (1978) (Revision 4.1 1983).
3. J. Weiss, *Z. Naturfor.* 1957, **12B**, 481.
4. D. T. Haworth and R. S. Czernuszewicz, *Spectrosc. Lett.* 1980, **13**, 765.
5. K. Hornemann and J. Weiss, *Angew. Chem. Int. Ed. Engl.* 1982, **21**, 633.
6. P. F. Kelly and J. D. Woollins, *Transition Met. Chem.*, in press.
7. R. Jones, P. F. Kelly, D. J. Williams and J. D. Woollins, *J. Chem. Soc., Dalton Trans.* 1988, 803.

Polyhedron Vol. 8, No. 6, pp. 845–847, 1989
Printed in Great Britain

0277–5387/89 $3.00+.00
© 1989 Pergamon Press plc

COMMUNICATION

THE SYNTHESIS OF SOME TRIS-(3,5-DIMETHYLPYRAZOL-1-YL) BORATOTRISARYLOXOZIRCONIUM(IV) COMPLEXES. THE MOLECULAR STRUCTURE OF $[Zr\{HB(3,5\text{-}Me_2C_3N_2H)_3\}\{OC_6H_4(NO_2)\}_3]$

ROMAN A. KRESINSKI, THOMAS A. HAMOR,* LLOYD ISAM, CHRISTOPHER J. JONES* and JON A. McCLEVERTY

Department of Chemistry, University of Birmingham, PO Box 363, Birmingham B15 2TT, U.K.

(*Received* 8 *July* 1988; *accepted* 25 *November* 1988)

Abstract—The air- and moisture-stable complexes $[Zr\{HB(3,5\text{-}Me_2C_3N_2H)_3\}\{OC_6H_4Z\}_3]$ (Z = H, 3-NO_2, 4-NO_2, 2-F, 3-F, 4-F, 4-Bu^t), have been prepared by the reaction of the appropriate phenol with the known complex $[Zr\{HB(3,5\text{-}Me_2C_3N_2H)_3\}Cl_3]$, in the presence of a base. The molecular structure of $[Zr\{HB(3,5\text{-}Me_2C_3N_2H)_3\}(OC_6H_4\text{-}4\text{-}NO_2)_3]$ was determined by X-ray diffraction techniques. The complex has near C_{3v} point symmetry. The Zr—O(4-nitrophenoxide) distance is 1.978(1) Å and the Zr—O—C(4-nitrophenyl) angle is 161.4(1)°. The phenyl rings are oriented to lie in the clefts between the pyrazolyl rings.

The complex $[ZrLCl_3]$ (I) (L = $HB(3,5\text{-}Me_2C_3N_2H)_3$), is a precursor to a variety of complexes in which the projecting methyl groups of the $HB(3,5\text{-}Me_2C_3N_2H)_3$ ligand strongly favour an octahedral environment around the zirconium atom.[1] These include methoxide[1] and *t*-butoxide[2] derivatives as well as organometallic compounds,[3] but to our knowledge no reports of aryloxide complexes have appeared. In the course of our investigations[4–6] into the ability of sterically demanding tripodal ligands to regulate the chemistry at metal centres, we have prepared a series of trisphenoxide derivatives containing the $\{Zr\{HB(3,5\text{-}Me_2C_3N_2H)_3\}\}^{3+}$ moiety.

The reaction of I with HOC_6H_4Z (Z = H, 3-NO_2, 4-NO_2, 2-F, 3-F, 4-F, 4-Bu^t) in dichloromethane containing triethylamine, afforded the air-stable tris-phenoxide complexes $[ZrL(OC_6H_4Z)_3]$, even when only a 2 : 1 stoichiometric ratio of HOC_6H_4Z to I was used. When 3 : 1 HOC_6H_4Z–I ratios were used yields of $[ZrL(OC_6H_4Z)_3]$ in the range 51–88% were obtained depending upon Z. These compounds were all soluble in dichloromethane and polar organic solvents but insoluble in water. They were characterized by ^{1}H NMR, IR and MS and all gave satisfactory elemental analyses for C, H and N. The ^{1}H NMR spectra of the complexes exhibited signals which were consistent with C_{3v} point symmetry for the molecules. In the case of $[ZrL(OC_6H_4\text{-}4\text{-}NO_2)_3]$, and the other four-substituted phenoxides, the NMR spectrum showed that both edges of the aryl ring were equivalent indicating that, at room temperature, rotation of the aryl ring about the C—O bond was rapid on the NMR timescale. An electrochemical investigation of $[ZrL(OC_6H_4\text{-}2\text{-}F)_3]$ by cyclic voltammetry at a platinum bead electrode in THF or acetonitrile revealed only highly irreversible reduction processes. No well defined product waves were apparent and it is likely that the reduction processes in these solvents lead to decomposition of the complex.

In order to obtain more detailed structural information about an example of these species a single crystal X-ray diffraction study was carried out on $[ZrL(OC_6H_4\text{-}4\text{-}NO_2)_3]$. Crystals of this complex are trigonal, $R\bar{3}$, a = 12.211(3) Å, α = 93.85(4)°, Z = 2.

* Authors to whom correspondence should be addressed.

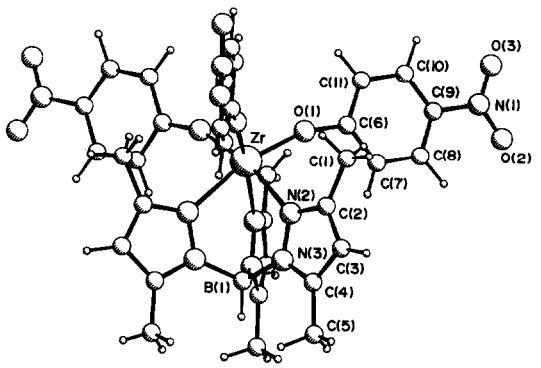

Fig. 1. A view of the complex showing the atom numbering.

Cell dimensions and intensities were measured with an Enraf–Nonius CAD-4 diffractometer using Mo-K_α radiation. 1767 reflections in the range $\theta = 2$–24° having $I > 2.5\sigma(I)$ were used in the analysis. The structure was solved by direct methods[7] and refined by least-squares using anisotropic temperature factors for the heavier atoms and isotropic temperature factors for the hydrogens. The calculations[8] were terminated when all shifts were $< 0.01\sigma$, and R and R_w were 0.027 and 0.038, respectively, $w = 1/\sigma^2(F)$.

A view of the complex* drawn with PLUTO[9] is shown in Fig. 1. The molecule exhibits C_3 symmetry with the zirconium, boron and the hydrogen atom bonded to the boron lying on a crystallographic three-fold axis. The approximation to C_{3v} symmetry is evident, the 4-nitrophenyl rings being twisted only slightly, by 4.3(2)°, out of the putative mirror plane. The basically octahedral coordination geometry at zirconium shows significant trigonal distortion. The three N—Zr—N angles are 79.4(1)° and the O—Zr—O angles, 98.6(1)°. The *cis*-N—Zr—O angles are close to 90° while the *trans* angles are 166.4(1)°. Noteworthy is the large (161.4(1)°) Zr—O—C(phenoxy) angle indicating a considerable degree of $p\pi \rightarrow d\pi$ donation from the ligand to the metal.

In the crystal structure of the analogous [ZrL(OBu^t)(η^2-C(Me)NCMe$_3$)Me][3] where zirconium is seven-coordinate, the Zr—N(pyrazolyl) bond distances are significantly greater, averaging 2.414 Å compared with our value of 2.301(2) Å. This difference may be attributed to the steric effect of the bulky *t*-butyliminoethyl group interacting with a methyl group of a pyrazolyl ring.[3] The Zr—O—C(butoxy) moiety has Zr—O = 1.924, O—C = 1.45 Å and an angle at oxygen of 174.4°. These compare with values of 1.978(1), 1.338(2) Å and 161.4(1)°, respectively, in the Zr—O—C(4-nitrophenoxy) moiety of our complex. In neither structure do intermolecular contacts appear to affect the geometry and these differences may be a manifestation of the additional electron delocalization involving the aromatic ring. The bonding geometry at such an oxygen atom, however, shows considerable flexibility. Thus in the crystal structure of [Zr(η^5-C$_5$H$_5$)$_2$(OC$_6$H$_4$-4-Cl)]$_2$O[10] the two chemically equivalent Zr—O—C(aryloxy) angles (153.1 and 177.3°) differ by 24°. In 13 Zr—O(aryloxy) residues whose geometries have been determined[10–14] by X-ray crystallography the Zr—O lengths range from 1.90 to 2.07 Å, mean 1.984 Å, the O—C lengths, from 1.305 to 1.40 Å, mean 1.361 Å, and the angles at oxygen from 148 to 177°, mean 165.5°, in reasonable agreement with our values. Interestingly there is a weak inverse correlation ($r = -0.60$) between the Zr—O length and Zr—O—C angle.

It is notable that in the structure described here the phenyl rings are oriented to lie between the 3-methyl groups of the ligand L. This behaviour contrasts with that found in mono- and bis-phenoxy, or arylamide, complexes containing the {Mo(NO)L} moiety in which the aryl rings are oriented away from the ligand L.[4] Thus, while L is highly sterically demanding in the region of the pyrazolyl rings, it is far less so in the region between the pyrazolyl rings, provided that relatively flat co-ligand substituents are involved.

Acknowledgements—We are grateful to Dr N. J. Hazel for helpful discussions and to the SERC and BP Chemicals International for support (to R.A.K.).

REFERENCES

1. D. L. Reger and M. E. Tarquini, *Inorg. Chem.* 1982, **21**, 840.
2. D. L. Reger and M. E. Tarquini, *Inorg. Chem.* 1983, **22**, 1064.
3. D. L. Reger, M. E. Tarquini and L. Lebioda, *Organometallics* 1983, **2**, 1763.
4. J. A. McCleverty, *Chem. Soc. Rev.* 1983, **12**, 331.
5. M. A. J. Moss, C. J. Jones and A. J. Edwards, *Polyhedron* 1988, **7**, 79.
6. C. J. Jones, J. A. McCleverty and S. S. Salam, *J. Chem. Soc., Dalton Trans.* 1988, 2769.
7. G. M. Sheldrick, SHELXS-86, Program for the solution of crystal structures. University of Göttingen (1987).

* Tables of atomic positional and thermal parameters, bond lengths and angles, and observed and calculated structure factors have been deposited as supplementary data with the Editor. Atomic coordinates have also been deposited with the Cambridge Crystallographic Data Centre.

8. G. M. Sheldrick, SHELX-76, Program for crystal structure determination. University of Cambridge (1978).
9. W. D. S. Motherwell, PLUTO, Program for plotting molecular and crystal structures, Report "Cambridge Crystallographic Files". University of Manchester Regional Computer Centre, Manchester (1981).
10. Y. Qingchuan, J. Xianglin, X. Xiaojie, L. Genpei, T. Youqi and C. Shoushan, *Sci. Sin.* 1982, Ser. B, **25**, 356.
11. C. Wenrai, D. Jinbi and C. Shoushan, *J. Struct. Chem.* 1982, **1**, 73.
12. D. Jinbi, L. Meizhen, Z. Jiping and C. Shoushan, *J. Struct. Chem.* 1982, **1**, 63.
13. A. K. McMullen, I. P. Rothwell and J. C. Huffman, *J. Am. Chem. Soc.* 1985, **107**, 1072.
14. S. L. Latesky, A. K. McMullen, G. P. Niccolai, I. P. Rothwell and J. C. Huffman, *Organometallics* 1985, **4**, 902.

Polyhedron Vol. 8, No. 6, pp. 849–850, 1989
Printed in Great Britain

0277–5387/89 $3.00+.00
© 1989 Pergamon Press plc

COMMUNICATION

THE CLEAVAGE OF A PHOSPHA-ALKYNE AT A REDUCED TANTALUM CENTRE. POSSIBLE INTERMEDIACY OF A TANTALUM PHOSPHIDE

ALAN H. COWLEY* and STEPHEN W. HALL

Department of Chemistry, The University of Texas at Austin, Austin, TX 78712, U.S.A.

(*Received* 27 *October* 1988; *accepted* 3 *November* 1988)

Abstract—The reaction of $Ta(OAr)_2Cl_3$ (Ar = 4-Me,2,6-*t*-$Bu_2C_6H_2$) with 3.0 equivalents of Na/Hg, followed by treatment with 3.0 equivalents of *t*-BuC≡P results in the formation of the 2,5-di-*t*-butyl-1,3,4-triphosphacyclopentadienyl (**1**) and 2,4,5-tri-*t*-butyl-1,3-diphosphacyclopentadienyl (**2**) anions. It is speculated that the formation of **1** involves the phosphide intermediate, $(ArO)_2Ta{\equiv}P$.

There have been recent reports of the cyclotrimerization of phospha-alkynes.[1] Arguing by analogy with the cyclotrimerization of alkynes it seemed reasonable to suggest the intermediacy of a metalladiphosphapentadiene. Given that metallacyclopentadienes have been isolated recently from the reaction of alkynes with reduced tantalum species,[2] we were prompted to undertake a comparable reaction using the phospha-alkyne, *t*-BuC≡P. However, the reaction took an unexpected course and resulted in the formation of di- and triphosphacyclopentadienide anions.

EXPERIMENTAL

The tantalum aryloxide, $Ta(OAr)_2Cl_3$ was prepared by treatment of $TaCl_5$ with 2.0 equivalents of LiOAr in C_6H_6 solution. The procedure was similar to that described for the synthesis of other tantalum(V) compounds of this type.[2] The $Ta(OAr)_2Cl_3$ was reduced with 3.0 equivalents of Na/Hg prior to the addition of 3.0 equivalents of *t*-BuC≡P.[3] After filtration of the reaction mixture, the solvent and volatiles were removed *in vacuo* and the resulting pale yellow solid was washed with *n*-hexane and toluene. Fractional crystallization from DME or THF afforded compounds **1** and **2** in isolated yields of 42 and 37%, respectively.

$^{31}P\{^1H\}$ NMR (121.5 MHz, 85% H_3PO_4 external THF) **1**: δ 245.5 (d, $^2J_{PP}$ = 47 Hz) 252.5 (t, $^2J_{PP}$ = 47 Hz); **2**: δ 187.6(s). ^1H NMR (300.0 MHz, Me_4Si, CD_3CN) **1**: δ 1.57(s); **2**: δ 1.46 (s, 9H), 1.62 (s, 18H). ^{13}C NMR (75.5 MHz, Me_4Si, THF-d_8), **1**: δ 37.4 (d of d of d, $^3J_{PC}$ = 10.6, $^3J_{PC}$ = 5.3 Hz); **2**: 36.7 (t, $^3J_{PC}$ = 9.8 Hz), 37.0 (d of d, $^3J_{PC}$ = 10.1; $^4J_{PC}$ = 8.3 Hz). Negative ion mass spectroscopy, **1**: *m/z* 231 (M^-); **2**: *m/z* 269 (M^-).

RESULTS AND DISCUSSION

The ^{31}P NMR data for **1** are in satisfactory agreement with those reported for the 2,5-di-*t*-butyl-1,3,4-triphosphacyclopentadienyl anion.[4] The 2,4,5-tri-*t*-butyl-1,3-diphosphacyclopentadienyl anion (**2**) has been suggested previously as a by-product in the preparation of **1**.[5] This structure assignment is confirmed by ^1H and $^{13}C\{^1H\}$ NMR, and negative ion mass spectroscopy.

Becker *et al.*[4] have demonstrated that **1** is formed via the reaction of *t*-BuC≡P with the phosphide

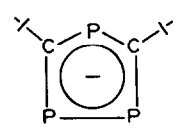

1

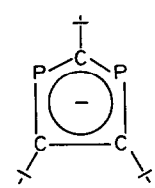

2

*Author to whom correspondence should be addressed. Present address: Department of Chemistry, Imperial College, South Kensington, London SW7 2AY, U.K.

source, $LiP(SiMe_3)_2$. It therefore seems reasonable to imply a phosphide intermediate in the present case. One possibility is that *t*-Bu≡P is cleaved by the reduced tantalum species to afford the intermediates $(ArO)_2Ta{\equiv}P$ (**3**) and $(ArO)_2Ta{\equiv}C$-*t*-Bu (**4**). In turn, each of these species could react with 2 moles of *t*-BuC≡P to produce **1** and **2**, respectively. Consistent with this view is the observation that **1** and **2** are produced in an equimolar ratio. The source of the extra electrons for **1** and **2** is presumably the alkali metal. We note that the intermediate $(t\text{-}BuCH_2O)_3W{\equiv}P$, a very similar species to **3**, has been postulated recently by Chisholm *et al.*[6] Moreover, cleavage of *t*-BuC≡P by WCl_6 and $MoCl_5$ in the presence of $POCl_3$ has been reported by Becker and co-workers.[7] In both cases, a *t*-BuC≡CBu-*t* complex was formed but the phosphide-derived product(s) was not isolated.

Acknowledgements—Support by the National Science Foundation and the Robert A. Welch Foundation is greatly appreciated.

Note Added in Proof

A 1,4-diphospha-2-rhodacyclopentadiene complex has been isolated very recently. See P. Binger, B. Biedenbach, R. Mynott, C. Krüger, P. Betz and M. Regitz, *Angew. Chem. Int. Ed. Engl.* 1988, **27**, 1157.

REFERENCES

1. A. R. Barron and A. H. Cowley, *Angew. Chem. Int. Ed. Engl.* 1987, **26**, 907; R. Milczarek, W. Rüsseler, P. Binger, K. Jonas, K. Angermund, C. Krüger and M. Regitz, *Angew. Chem. Int. Ed. Engl.* 1987, **26**, 908.
2. M. A. Bruck, A. S. Copenhaver and D. E. Wigley, *J. Am. Chem. Soc.* 1987, **109**, 6525.
3. G. Becker, G. Gressner and U. Uhl, *Z. Naturfor.* 1981, **B36**, 16; G. Becker, *Z. Anorg. Allg. Chem.* 1974, **430**, 66.
4. G. Becker, W. Becker, R. Knebl, H. Schmidt, U. Weeber and M. Westerhausen, *Nova Acta Leopold* 1985, **59**, 55.
5. R. Bartsch, P. B. Hitchcock and J. F. Nixon, *J. Chem. Soc., Chem. Commun.* 1987, 1146.
6. M. H. Chisholm, K. Folting and J. W. Pasterczyk, *Inorg. Chem.* 1988, **27**, 3057.
7. G. Uhl, E. Hey, G. Becker, F. Weller and K. Dehnicke, *Z. Anorg. Allg. Chem.* 1983, **497**, 213; E. Hey, F. Weller, B. Simon, G. Becker and K. Dehnicke, *Z. Anorg. Allg. Chem.* 1983, **501**, 61.

Polyhedron Vol. 8, No. 7, pp. 851–858, 1989
Printed in Great Britain

0277–5387/89 $3.00+.00
© 1989 Pergamon Press plc

AXIAL LIGAND SUBSTITUTION REACTIONS OF PHOSPHINE DERIVATIVES OF RUTHENIUM(II) AND RUTHENIUM(III) BENZOQUINONE DIOXIME COMPLEXES

MOHAMED A. KHALIFA*

Department of Chemistry, Faculty of Science Alexandria University, Alexandria, Egypt

(*Received* 12 *April* 1988; *accepted after revision* 6 *September* 1988)

Abstract—The synthetic, spectral and kinetic studies of ruthenium(II) macrocyclic complexes, $Ru(BQDH)_2L_2$ (where BQDH = benzoquinone dioximate), are reported. Axial ligands include nitrogen, phosphorus and sulphur donors. An oxidized species, $Ru(BQDH)(BQD)(PPh_3)_2$, formed via one-electron oxidation followed by loss of a bridging hydrogen, was characterized as a ruthenium(III) complex. Kinetic and thermodynamic data of axial ligand substitution showed that the reaction mechanism is dissociative (D) and that the five-coordinate intermediate possesses little or no ability to discriminate between nucleophiles. The ruthenium(II) complexes were found to be more labile than the corresponding ruthenium(III) complexes. *Trans*-group and leaving-group effects are discussed. The BQDH ruthenium complexes differ from the DMGH analogues in that the former are much more labile, owing to the high delocalization of the conjugated π-system of the BQDH. The ruthenium BQDH complexes were also found to be much more inert than the analogous iron complexes implying that the $M \rightarrow L$ π-back bonding is more important for ruthenium.

The chemistry of macrocyclic complexes and their closely related porphyrin and phthalocyanine-type complexes of ruthenium are relatively well known.[1–15] Kinetic studies of the ruthenium(II) complexes show different lability in the axial ligand substitution reactions. In carbonyl ruthenium(II) porphyrins, RuP(CO)(L), a remarkable lability of the nitrogen donors L *trans* to CO has been reported.[16,17] Similar labilization is observed for isocyanide derivatives of ruthenium porphyrins.[18] However, the corresponding $RuP(MeIm)_2$ and $RuP(Py)_2$ complexes are very inert.[19]

Sweigart[20,21] has reported the kinetic comparisons of axial ligand lability in the FePc and RuPc complexes of phosphines and phosphite. Recently, the kinetics of the reactions of a series of labile iron macrocyclic complexes have been reported[22] and the reaction mechanism was found to be dissociative (D). More recently, extensive kinetic studies of $Ru(DMGH)_2L_2$ bis-adducts have shown a substantially different lability in the axial ligation dynamics leading to a number of mechanistic considerations.[23] Dissociative (D), interchange dissociative "I_d" and associative "I_a" pathways were reported.

Furthermore, the electrochemistry of the ruthenium complexes of the BQDH has been studied[24] and reveals the isolation of two different products namely $Ru^{II}(BQDH)_2L_2$ and $Ru^{III}(BQDH)(BQD)L_2$. In the former the $(BQDH)_2$ acts as a dibasic macrocyclic ligand while in the latter (BQDH)(BQD) acts as a tribasic ligand. These findings prompted the interest to study the kinetic behaviour of these complexes towards axial ligation. This may demonstrate the effect of the structural differences of the in-plane ligand as well as the oxidation states of the central metal ion on the nucleophilic substitution reactions of axial ligands. Herein, the synthetic, spectral and kinetic data for the bis-adducts of ruthenium(II) and (III) complexes of BQDH are reported.†

* Present address: Department of Chemistry, Science and Mathematics Center, Makkah, P.O. Box 2064, Saudi Arabia.

† Ligand abbreviations: BQDH = benzoquinone dioximate (3,5-cyclohexadiene-1,2-dionedioximate); DMGH = dimethylglyoximate; P = porphyrin; Pc = phthalocyanine; MeIm = 1-methylimidazole; Py = pyridine; Pip = piperidine, PPh_3 = triphenylphosphine; $P(OBu)_3$ = tri-*n*-butylphosphite; DMSO = dimethylsulphoxide.

EXPERIMENTAL

Synthesis

Preparation of $Ru(BQDH)(BQD)(PPh_3)_2$. A solution of benzoquinone dioxime (0.58 g) and sodium hydroxide (0.174 g) in methanol (80 cm^3) was purged under a stream of Ar for 30 min in a Schlenk flask. Tris(triphenylphosphine)dichlororuthenium(II) (1.74 g) was then added and the reaction mixture was refluxed for 14 h. The intensely purple powder was collected, washed with deaerated water and methanol and dried *in vacuo* (yield 40%). Found: C, 64.2; H, 4.1; N, 5.8; P, 7.3. Calc. for $C_{48}H_{39}N_4O_4P_2Ru$: C, 64.1; H, 4.5; N, 6.2; P, 6.9%.

This complex can also be prepared by admitting oxygen to a solution of the $Ru(BQDH)_2(PPh_3)_2$ as previously reported.[24]

Other compounds. The complexes of $Ru(BQDH)_2(PPh_3)_2$ and $Ru(BQDH)_2(PPh_3)$(MeIm) were prepared according to the method of Bond and Khalifa.[24]

Tris(triphenylphosphine)dichlororuthenium(II), was prepared as reported previously by Hallman *et al.*[25] Benzoquinone dioxime was prepared by borohydride reduction of benzofurazan oxide.[26,27]

Ruthenium trichloride dihydrate (Matthey–Bishop, Inc.), tri-*n*-butylphosphite (Aldrich), triphenylphosphine (Aldrich), piperidine (Aldrich), dimethylsylphoxide (Aldrich) and N-methylimidazole (Aldrich) were used without further purification. Pyridine (Fisher) was distilled from KOH prior to use. Toluene (Aldrich) was freshly distilled from CaH_2 before use.

Kinetic measurements. Reactions were monitored spectrophotometrically using an Aminco DW-2a UV–vis spectrophotometer or a Perkin–Elmer Hitachi 340 recording spectrophotometer. Deaerated solutions in 1 cm quartz cells were thermostated in a close-fitting brass block. The temperature of the block was maintained by a constant flow of circulating water by means of a Lauda circulator (K-21 R). Solutions were thermostated for approximately 15 min prior to the reaction measurements. The slower reactions were followed by periodically scanning the spectrum between 350–800 nm. Chart speeds were adjusted to suit the rate of the reaction.

Concentrations of ruthenium complexes were typically about 1.0×10^{-4} M. Reactions were run under pseudo-first-order conditions with the added nucleophile in large excess. The nucleophile was injected into the serum-capped cell, containing the ruthenium complex, with a Hamilton gas tight syringe. All the reactions were followed until the absorbance at infinite time could be correctly read off or calculated. Final spectra were recorded. Plots of $\log(A - A_\infty)$ vs time were linear over 3 half-lives. Reproducibility of separate runs was typically $\pm 5\%$ or less. The observed rate constant $k_{obs} = 2.303 \times$ slope of the line. Plots of $\log k/T$ vs $1/T$ gave straight lines. The activation parameters, $\Delta H^\ddagger$ and $\Delta S^\ddagger$, were calculated from the slopes and the intercepts of the lines, respectively.

RESULTS AND DISCUSSION

Spectral data

The spectral data of $Ru(BQDH)_2(PPh_3)_2$ and its oxidized product are quite different (Table 1). The ruthenium(II) complex exhibits two well defined sharp bands at 457 and 402 nm. The oxidized species shows a broad band at 456 nm with a shoulder on the higher energy side at 415 nm. Similar behaviour has been reported by Canon and co-workers[28,29] for N,N′-ethylene bis(salicylideneaminato)bis(triphenylphosphine)ruthenium(II) complex. Under nitrogen, two bands with λ_{max} at 770 and 505 nm, were observed. However, on admitting oxygen, a well defined band appeared at 800 nm with a shoulder on the higher energy side at $\simeq$ 690 nm. Such behaviour was also observed by West *et al.*[30] and the oxidized complex was reported to be the corresponding ruthenium(III) species. Accordingly, the spectral behaviour for the $Ru(BQDH)_2(PPh_3)_2$ suggested that the oxidized species is a ruthenium(III) complex.

As mentioned in the Experimental, the oxidized species can be obtained either by admitting oxygen to the ruthenium(II) complex solution or by carrying out the synthesis in methanol. Even

Table 1. Electronic absorption spectra of ruthenium macrocyclic complexes in toluene

Complex	λ_{max} (nm)
$Ru(BQDH)_2(PPh_3)_2$	457,402
$Ru(BQDH)_2(PPh_3)$(MeIm)	496,406
$Ru(BQDH)_2(PPh_3)$(Py)	487,407
$Ru(BQDH)_2(PPh_3)$(Pip)	495,410
$Ru(BQDH)_2(PPh_3)(P(OBu)_3)$	434,390
$Ru(BQDH)_2(PPh_3)$(DMSO)	443,397
$Ru(BQDH)(BQD)(PPh_3)_2$	456
$Ru(DMGH)_2(PPh_3)_2$	362[a]
$Ru(DMGH)_2(PPh_3)$(MeIm)	396[a]
$Ru(DMGH)_2(PPh_3)$(Py)	390[a]
$Ru(DMGH)_2(PPh_3)(P(OBu)_3)$	338[a]

[a] Ref. 23.

under careful conditions of oxygen-free argon, the synthesis in methanol yields the ruthenium(III) complex. Such oxidizing power of methanol was previously reported by Cannon *et al.*[28,29] for closely related ruthenium complexes.

A summary of electronic spectral data for the macrocyclic complexes investigated in this study is given in Table 1. Data for $Ru(DMGH)_2(PPh_3)_2$ are also given for the purpose of comparison. The lower energy band for the BQDH ruthenium complexes as well as the band for the DMGH complexes were assigned as charge transfers from ruthenium to the in-plane macrocyclic ligand. Such assignment was also proposed by Taube *et al.*[2] for some ruthenium macrocyclic complexes.

An inspection of the spectral data reveals a systematic variation in properties according to the variation in the structure. Thus, λ_{max} depends on the ligand field exerted by the equatorial macrocyclic ligand and both σ- and π-effects of the axial ligands. The much lower energy of the M → L charge transfer transition in BQDH complexes relative to DMGH complexes is consistent with a lowering of the π^*-level of the dioxime moiety as a result of conjugation with the hexadiene group. On replacement of PPh_3, a good σ-donor and π-acceptor by either of MeIm, Py or Pip; which are only good σ-donors to give the mixed complexes, the long wavelength band shifts to lower energy. The shift is greater with the formation of the bis-MeIm, Py or Pip adducts. However, when DMSO is coordinated *trans* to PPh_3 in the ruthenium complex of BQDH, a shift to a higher energy relative to the bis-PPh_3 complex is observed. This is an indication that the DMSO is a better π-acid ligand than the PPh_3. Remarkably, when $P(OBu)_3$ was used to replace PPh_3, the long wavelength band shifts to a much higher energy. This indicates that $P(OBu)_3$ is a better π-acid ligand than both DMSO and PPh_3. Thus, being a good π-acceptor ligand, tributylphosphite accepts electron density from filled t_{2g} orbitals. Therefore reducing the ease of charge transfer from ruthenium to BQDH. On the other hand, MeIm, Py and Pip, would increase the ease of such transfer since they are good σ-donors. Thus, for the mixed phosphite phosphine complexes, more energy is required to perform such charge transfer; and hence gives lower wavelengths for absorption maxima. These results show that the energy of the $Ru(BQDH)_2L_2$ bis-adducts complexes decreases in the following order: $Ru(BQDH)_2(PPh_3)(P(OBu)_3)$ > $Ru(BQDH)_2(PPh_3)(DMSO)$ > $Ru(BQDH)_2(PPh_3)_2$ > $Ru(BQDH)_2(PPh_3)(MeIm)$. That the tributylphosphite is a strong π-acid and electron withdrawing ligand was also reported by Sweigart *et al.*[20]

Using the data in Table 1, it is now possible to arrange the axial ligands involved in this study according to their σ-donating or π-accepting ability. The σ-donor power of these ligands decrease in the following order: MeIm ~ Pip > Py > PPh_3. On the other hand, the π-accepting ability of the π-acid ligands decreases in the following sequence: $P(PBu)_3$ > DMSO > PPh_3. Hence, triphenylphosphine is known to be a σ-donor and π-acceptor ligand.[31]

Kinetic data

The reactions investigated in this study can be classified as follows:

$$Ru(BQDH)_2(PPh_3)_2 + MeIm \longrightarrow Ru(BQDH)_2(PPh_3)(MeIm) + PPh_3 \quad (1)$$

$$Ru(BQDH)_2(PPh_3)(MeIm) + PPh_3 \longrightarrow Ru(BQDH)_2(PPh_3)_2 + MeIm \quad (2)$$

$$Ru(BQDH)_2(MeIm)(PPh_3) + MeIm \longrightarrow Ru(BQDH)_2(MeIm)_2 + PPh_3 \quad (3)$$

$$Ru(BQDH)(BQD)(PPh_3)_2 + X \longrightarrow Ru(BQDH)(BQD)(PPh_3)(X) + PPh_3, \quad (4)$$

X = MeIm, Py, Pip, DMSO and $P(OBu)_3$.

Reactions (1), (2) and (4) were followed spectrophotometrically in toluene (Table 2). The successive spectra, for each system, pass through a sharp fixed isosbestic point(s), implying that these reactions proceed cleanly to completion. The spectra of the final products are almost identical to those of the prepared authentic samples in the appropriate solvents. Typical spectral changes with time on the addition of MeIm to $Ru(BQDH)_2(PPh_3)_2$ solution in toluene at 40°C are given in Fig. 1. As the reaction proceeds to completion, the absorbance of $Ru(BQDH)_2(PPh_3)_2$ at 457 and 402 nm decreases and the peaks at 496 and 406 nm due to the mixed complex $Ru(BQDH)_2(PPh_3)(MeIm)$ increase. Analysis of the absorbance at 457 and 496 nm gave consistent rate constants (Table 2).

As stated earlier, the spectra of the oxidized species of BQDH ruthenium complex changes drastically from that of the corresponding ruthenium(II) complex. Interestingly enough, the triphenylphosphine off rate for the oxidized species is also much slower compared with that for the corresponding ruthenium(II) complex under the same conditions (Table 2). Typical spectral changes with time on the addition of piperidine to a solution of the oxidized ruthenium complex in toluene at 70°C are shown in Fig. 2, reaction (4), X = Pip.

Table 2. Kinetic data for the reaction: (T)Ru(N_4)L + X → (T)Ru(N_4)X + L, in toluene

Macrocycle (N_4)	*Trans* group (T)	Leaving group (L)	Nucleophile (X)	Temperature (°C)	k_1[a] (s^{-1})
$(BQDH)_2$	PPh_3	PPh_3	MeIm	40	3.40×10^{-4}
	PPh_3	PPh_3	MeIm	50	1.12×10^{-3}
	PPh_3	PPh_3	MeIm	60	2.70×10^{-3}
	PPh_3	MeIm	PPh_3	60	9.30×10^{-5}
	PPh_3	MeIm	PPh_3	70	4.40×10^{-4}
	PPh_3	MeIm	PPh_3	80	1.22×10^{-3}
(BQDH)(BQD)	PPh_3	PPh_3	MeIm	60	2.80×10^{-4}
	PPh_3	PPh_3	MeIm	70	5.17×10^{-4}
	PPh_3	PPh_3	MeIm	80	1.50×10^{-3}
	PPh_3	PPh_3	MeIm	90	2.80×10^{-3}
	PPh_3	PPh_3	Py	70	5.01×10^{-4}
	PPh_3	PPh_3	Py	80	1.38×10^{-3}
	PPh_3	PPh_3	Py	90	2.77×10^{-3}
	PPh_3	PPh_3	Pip	60	3.02×10^{-4}
	PPh_3	PPh_3	Pip	70	6.20×10^{-4}
	PPh_3	PPh_3	Pip	80	1.45×10^{-3}
	PPh_3	PPh_3	$P(OBu)_3$	70	4.70×10^{-4}
	PPh_3	PPh_3	$P(OBu)_3$	80	1.26×10^{-3}
	PPh_3	PPh_3	$P(OBu)_3$	90	2.61×10^{-3}
	PPh_3	PPh_3	DMSO	70	5.50×10^{-4}
	PPh_3	PPh_3	DMSO	80	1.20×10^{-3}
	PPh_3	PPh_3	DMSO	90	2.51×10^{-3}
$(DMGH)_2$	PPh_3	PPh_3	MeIm	70.5	8.93×10^{-5}[b]
	PPh_3	MeIm	PPh_3	80	1.43×10^{-4}[b]
	MeIm	PPh_3	MeIm	90	6.40×10^{-5}[b]

[a] The errors in the values of k are within ±5%. [b] Ref. 23.

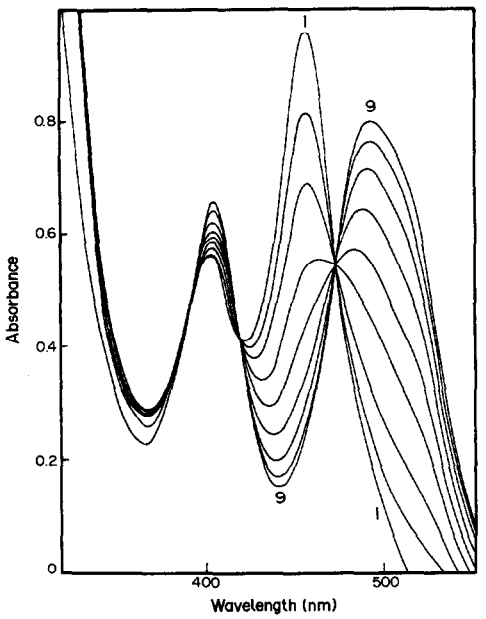

Fig. 1. Spectrophotometric changes with time for the reaction: $Ru(BQDH)_2(PPh_3)_2 + MeIm \rightarrow Ru(BQDH)_2(PPh_3)(MeIm) + PPh_3$, in toluene at 40°C. Spectra 1–9 were recorded at time 0, 5, 15, 35, 65, 115, 205, 320 and 505 min, respectively. Intervening spectra have been omitted for clarity.

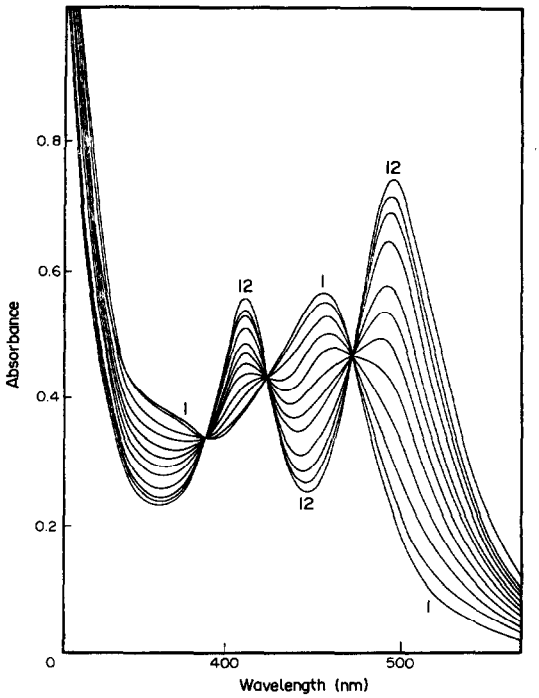

Fig. 2. Spectrophotometric changes with time for the reaction: $Ru(BQDH)(BQD)(PPh_3)_2 + Pip \rightarrow Ru(BQDH)(BQD)(PPh_3)(Pip) + PPh_3$, in toluene at 70°C. Spectra 1–12 were recorded at times 0, 5, 10, 15, 20, 25, 30, 35, 45, 60, 75 and 180 min, respectively.

The reaction proceeds cleanly to completion. The spectral changes are consistent with the formation of the mixed phosphine piperidine complex, λ_{max} 495 and 410 nm; and the disappearance of the bis-phosphine complex, λ_{max} 456 nm. The shift towards lower energy is consistent with Pip being a good σ-donor. Analyses of the spectral data at 495 or 456 nm gave excellent linear log plots and consistent rate constants (Table 2).

The reaction of the oxidized complex with good π-acid ligands such as tributylphosphite was also investigated. A shift of the absorption bands towards higher energy side was observed. Typical absorption changes are given in Fig. 3. The reaction proceeds smoothly to completion, showing two excellent isosbestic points. The formation of the mixed complex Ru(BQDH)(BQD)(PPh_3)–($P(OBu)_3$) was characterized by the increase of the absorbance at 434 and 390 nm. Analysis of the absorbance at 434 nm gave excellent linear log plots. The kinetic results and the activation parameters are listed in Tables 2 and 3, respectively.

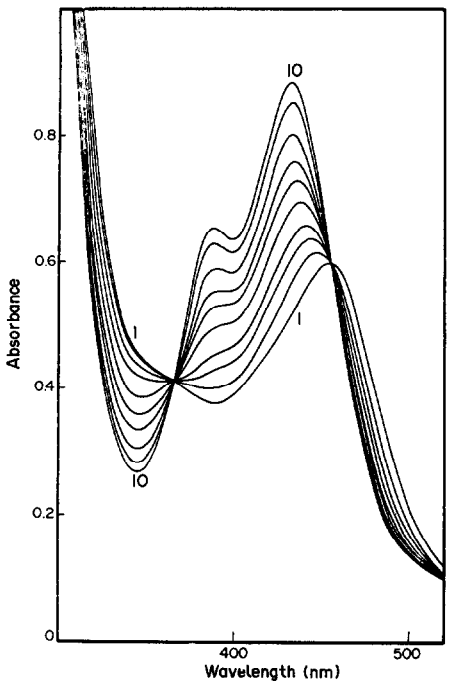

Fig. 3. Spectrophotometric changes with time for the reaction: Ru(BQDH)(BQD)(PPh_3)$_2$+$P(OBu)_3$ → Ru(BQDH)(BQD)(PPh_3)($P(OBu)_3$)+PPh_3, in toluene at 70°C. Spectra 1–10 were recorded at times 0, 4, 9, 14, 24, 34, 44, 64, 105 and 185 min, respectively.

The formation of the bis-amine complex, Ru(BQDH)$_2$(MeIm)$_2$, from the mixed phosphine methylimidazole complex, reaction (3), was found to be very slow. Such reactions were followed qualitatively by refluxing the reaction mixture in toluene. The rate constant was found to be several orders of magnitude slower than those listed in Table 2.

The general pattern of reactivity of the BQDH ruthenium complex parallel that of the DMGH ruthenium systems[23] and that of the TIM, Pc, DMGH and BQDH iron complexes[22] described previously. For the reaction

$$(T)Ru(N_4)L+X \longrightarrow (T)Ru(N_4)X+L, \quad (5)$$

where T is the *trans*-group; L the leaving group; X the nucleophile and N_4 represents the in-plane macrocyclic ligand, proceeding via a dissociative mechanism (D),

$$(T)Ru(N_4)L \underset{k_{-1}}{\overset{k_1}{\rightleftharpoons}} (T)Ru(N_4)+L \quad (6)$$

$$(T)Ru(N_4)+X \xrightarrow{k_2} (T)Ru(N_4)X. \quad (7)$$

The pseudo-first-order rate constant neglecting the reverse reaction is given by

$$k_{obs} = \frac{k_1 k_2[X]}{k_{-1}[L]+k_2[X]}. \quad (8)$$

For [L] negligible and [X] large, expression (8) reduces to:

$$k_{obs} = k_1 \quad (9)$$

and the reaction proceeds with the formation of 100%

Table 3. Activation parameters for axial ligand substitution reactions of (T)Ru(N_4)L complexes in toluene[a]

Complex	Nucleophile (X)	$\Delta H^{\ddagger}$ (Kcal mol^{-1})	$\Delta S^{\ddagger}$ (cal mol^{-1} deg^{-1})
(PPh_3)Ru(BQDH)(BQD)PPh_3	MeIm	19±2	10±3.5
	Py	21±2	5.0±2.5
	Pip	18±1	10±3
	$P(OBu)_3$	21±1	5.0±3
	DMSO	18.7±0.2	7.3±0.4
(PPh_3)Ru(BQDH)$_2$$PPh_3$	MeIm	21±1	5.0±3
(PPh_3)Ru(BQDH)$_2$MeIm	PPh_3	30±2	25±5

[a] L is the leaving group and T is the *trans*-ligand.

(T)Ru(N_4)X with a rate independent of the concentration or nature of the entering group X. These conditions are used to obtain "off rates" as previously described.[16-23]

The PPh_3 off rate for the BQDH ruthenium(II) bis-triphenylphosphine complex, $k_1 = 2.7 \times 10^{-3}$ s^{-1} at 60°C (Table 2). However, the PPh_3 off rate for the corresponding DMGH complex, $k_1 = 8.93 \times 10^{-5}$ s^{-1} at 70.5°C. This is clearly indicative that the BQDH complexes are much more labile toward PPh_3 loss than the DMGH complexes. This difference in lability can be rationalized on the basis that BQDH is a ligand with a delocalized π-system while DMGH is not. Thus, the higher the conjugation in the equatorial macrocyclic ligand, the more labile the system. The high delocalization of the conjugated π-system would produce a strong ligand field from the equatorial in-plane-macrocycle and thus results in weak long axial bonds. Thus, BQDH being a better π-acceptor than the DMGH ligand would result in more labile complexes for the former than the latter. Similar *cis*-effect was previously reported for analogous iron(II) macrocyclic complexes.[22]

From the experimental conditions it can be deduced that the equilibrium constants K_{eq} must be large. The reaction of $Ru(BQDH)_2(PPh_3)_2$ and MeIm was studied in both directions. For this case $k_f > k_r$, and for the conditions used the forward reaction went essentially to completion. Data in Table 2 allowed the equilibrium constant to be calculated. A value of $K_{eq} = 29$ for this reaction at 60°C implies that the reaction lies heavily to the right and greatly favours the formation of the mixed $Ru(BQDH)_2(PPh_3)$(MeIm) complex. This means that synergic π-bonding occurs in the mixed complex with the result that MeIm is extremely inert *trans* to PPh_3.

The kinetic behaviour of the oxidized ruthenium complex of the BQDH came as a surprise. Data in Table 2 showed that the oxidized species is $\simeq 10$ times slower towards the loss of PPh_3 than that for the ruthenium(II) complex. This kinetic inertness is a general feature of the ruthenium(III) amine complex and was previously reported.[32-34] If the oxidation is a ligand centred process to produce the cation radical, the kinetic results would have been the same for the oxidized species and the ruthenium(II) complex. Even more surprising are the results of the elemental analytical data. Analytical data for the ruthenium(II) complex of the BQDH were within experimental error, identical with those for the ruthenium(III) complex. Moreover, the data showed no evidence for coordinated chloride in the ruthenium(III) complex. These results indicate that the oxidation of the ruthenium(II) to ruthenium(III) complex takes place with loss of a proton.

The benzoquinoid structure is very stable and its protons are held strongly. On the other hand, a bridging hydrogen atom is weakly bonded and can easily be lost. Thus, the mechanism by which the ruthenium(II) complex of the BQDH is converted to ruthenium(III) species can be considered as follows: firstly, oxidation of the ruthenium(II) metal centre to ruthenium(III) proceeds to form an unstable cationic complex. Secondly, the high charge density at the new ruthenium(III) centre results in pulling the electron density from the nitrogen donor atoms. Thus producing a decrease of the electron density at the oxygens and increase in the acid–base properties of a bridging hydrogen atom. Such a process is strongly facilitated by the highly conjugated extended π-system of the BQDH.[35] This would lead to the loss of the bridging hydrogen atom producing the trinegative tetradentate macrocyclic ligand (BQDH)(BQD). Thus the final stable ruthenium(III) complex has zero charge. This mechanism can be represented by eqs (10) and (11). The two axial triphenylphosphine groups have been omitted for clarity.

Structure **(iii)** is the only structure which not only would fit the elemental analytical and spectral data, but also explains the electrochemical and kinetic behaviour that the oxidation site is a metal-centred rather than a ligand-centred process. Similar structure was previously suggested by Wilkinson and coworkers[36] for the $Ru(bdo_2en)(PPh_3)$ complex (where bdo = butan-2,3-dionemonooxime and en = ethylenediamine). Thus, the spectral, electrochemical, kinetic and elemental analytical results are conclusive evidence that the oxidized species is a ruthenium(III) complex of the BQDH and almost certainly does not contain the π-cation radical.

An alternative mechanism by which oxidation of $Ru(BQDH)_2(PPh_3)_2$ by molecular oxygen proceeds probably with an outer-sphere formation of the superoxide ion followed by its reaction with a second Ru^{II} ion to yield hydrogen peroxide and two molecules of $Ru(BQDH)(BQD)(PPh_3)_2$. A similar mechanism was proposed for the oxidation of $Ru(NH_3)_6^{2+}$ and $Ru(NH_3)_6^{3+}$ by molecular oxygen.[37]

Stabilization of unusual oxidation states is one of the most fascinating properties of the macrocyclic ligands. Electrochemical investigations suggest the formation of readily accessible thermodynamically stable ruthenium(IV) complexes of the BQDH and several other structurally related macrocyclic ligands.[24] Combination of the electrochemical and kinetic data reveals that the ruthenium(IV) complexes formed with a further oxidation step of the ruthenium(III) complexes, followed by

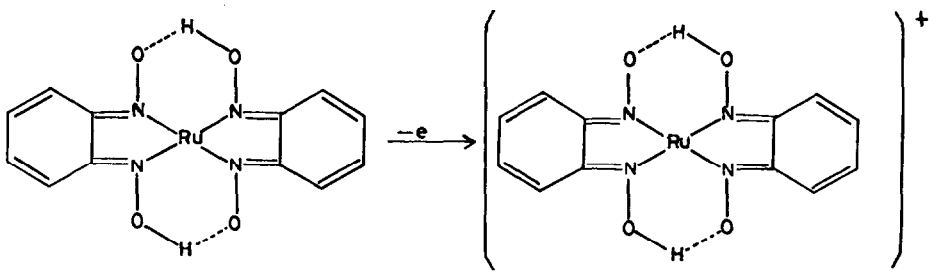

(10)

i ii

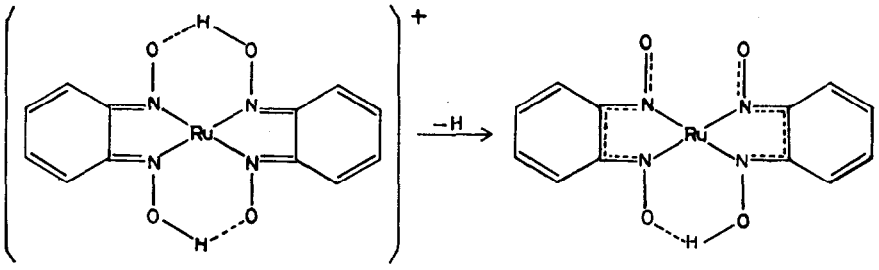

(11)

ii iii

a loss of the second bridging hydrogen to produce the tetranegative macrocyclic ligand. Thus the final ruthenium(IV) complex has zero charge. Similarly copper(0) complexes were previously reported for neutral macrocyclic ligands.[38]

Comparison of the axial ligand lability as measured by k_1 for the ruthenium macrocyclic complexes involved in this study with those previously reported for iron macrocyclic complexes[22] indicate that the ruthenium complexes are much more inert. This is probably due to the well-known superior π-backbonding ability of the ruthenium, leading to increased bond strength between the ruthenium and the axial ligands.

Remarkably, these results are in excellent agreement with the electrochemical data reported for a series of copper(II),[38] ruthenium(II) and (III),[24] and iron(II)[39] macrocyclic complexes. Polarographic studies showed stripping of the axial ligands from the copper(II) and iron(II) complexes. However, the axial ligands were strongly bound to the ruthenium ion of the ruthenium macrocyclic complexes. This is indicative that the copper(II) and iron(II) complexes are kinetically labile, while the ruthenium(II) and (III) complexes are kinetically inert. Thus the electrochemical data do not support the kinetic results.

Acknowledgements—Helpful discussions with Professor M. F. Iskander, Dr N. J. Lees-Gayed and Dr S. S. Massoud are gratefully acknowledged.

REFERENCES

1. S. S. Isied, *Inorg. Chem.* 1970, **19**, 911.
2. D. D. Walker and H. Taube, *Inorg. Chem.* 1981, **20**, 2828.
3. A. R. Chakravarty and A. Chakravarty, *J. Chem. Soc., Dalton Trans.* 1983, 961, and references cited therein.
4. C. K. Poon, T. C. Lau, C. L. Wong and Y. P. Kan, *J. Chem. Soc., Dalton Trans.* 1983, 1641.
5. C. K. Poon, T. C. Lau and C. M. Che, *Inorg. Chem.* 1983, **22**, 3893.
6. C. K. Poon, T. W. Tang and T. C. Lau, *J. Chem. Soc., Dalton Trans.* 1982, 865.
7. C. K. Poon, T. W. Tang and T. C. Lau, *J. Chem. Soc., Dalton Trans.* 1981, 2556.
8. C. K. Poon and C. M. Che, *J. Chem. Soc., Dalton Trans.* 1981, 1019, and references cited therein.
9. M. H. Barley, D. Dolphin and B. R. James, *J. Chem. Soc., Chem. Commun.* 1984, 1499.
10. B. R. James, D. Dolphin, T. W. Leung, F. W. B. Einstein and A. C. Willis, *Can. J. Chem.* 1984, **62**, 1238.
11. M. Barley, J. Y. Becker, G. Domazetis, D. Dolphin and B. R. James, *J. Chem. Soc., Chem. Commun.* 1981, 982.
12. R. H. Felton, in *The Porphyrins* (Edited by D. Dolphin), Vol. 5, p. 53. Academic Press, New York (1978)
13. D. P. Rillema, J. K. Nagle, L. F. Barringer Jr and T. J. Meyer, *J. Am. Chem. Soc.* 1981, **103**, 56.
14. D. Dolphin, B. R. James, A. J. Murray and J. R. Thornback, *Can. J. Chem.* 1980, **58**, 1125.

15. G. M. Brown, F. R. Hoff, T. J. Meyer and D. G. Whitten, *J. Am. Chem. Soc.* 1975, **97**, 5385.
16. S. S. Eaton and R. G. Eaton, *Inorg. Chem.* 1977, **10**, 72.
17. S. S. Eaton and R. G. Eaton, *Inorg. Chem.* 1976, **15**, 134.
18. C. E. Holloway, D. V. Stynes and C. P. J. Vuik, *J. Chem. Soc., Dalton Trans.* 1982, 95.
19. G. M. Brown, F. R. Hopf, J. A. Ferguson, T. J. Meyer and D. G. Whitten, *J. Am. Chem. Soc.* 1973, **95**, 5939.
20. J. Martinsen, M. Miller, D. Trojan and D. A. Sweigart, *Inorg. Chem.* 1980, **19**, 2162.
21. M. M. Doeff and D. A. Sweigart, *Inorg. Chem.* 1981, **20**, 1683.
22. M. A. Khalifa, *Inorg. Chim. Acta* 1987, 126.
23. M. A. Khalifa and A. El-Awady, *Ind. J. Chem.*, in press.
24. A. M. Bond and M. A. Khalifa, *Aust. J. Chem.* 1988, **41**, 000.
25. P. S. Hallman, T. A. Stephenson and G. Wilkinson, *Inorg. Synth.* 1970, **12**, 237.
26. P. A. Smith and J. H. Boyer, *Org. Synth.* 1951, **14**, 31.
27. J. H. Boyer and S. E. Ellzey Jr, *J. Am. Chem. Soc.* 1960, **82**, 2525.
28. H. Doine, F. F. Stephens and R. D. Cannon, *Inorg. Chim. Acta* 1984, **82**, 149.
29. H. Doine, F. F. Stephens and R. D. Cannon, *Bull. Chem. Soc. Jpn* 1985, **58**, 1327.
30. K. S. Murray, A. M. Van den Bergen and B. O. West, *Aust. J. Chem.* 1978, **31**, 203.
31. F. A. Cotton and G. Wilkinson, *Advanced Inorganic Chemistry*, 4th edn, p. 87. Wiley-Interscience, New York (1980).
32. D. Waysbort and G. Navon, *Inorg. Chem.* 1979, **18**, 9.
33. J. A. Broomhead, F. Basolo and R. G. Pearson, *Inorg. Chem.* 1964, **3**, 826.
34. L. A. P. Kane-Maguire and G. Thomas, *J. Chem. Soc., Dalton Trans.* 1975, 1324.
35. M. Chw, C. Creutz and N. Sutin, *J. Am. Chem. Soc.* 1977, **99**, 5615.
36. A. R. Middleton, J. R. Thornback and G. Wilkinson, *J. Chem. Soc., Dalton Trans.* 1980, 174.
37. D. M. Stanbury, O. Haas and H. Taube, *Inorg. Chem.* 1980, **19**, 518.
38. A. M. Bond and M. A. Khalifa, *Inorg. Chem.* 1987, **26**, 413.
39. A. M. Bond and M. A. Khalifa, to be submitted.

Polyhedron Vol. 8, No. 7, pp. 859–864, 1989
Printed in Great Britain

0277–5387/89 $3.00+.00
Pergamon Press plc

COMPARISON OF COMPLEXIBILITY ON INORGANIC COBALT(II) COMPLEXES BETWEEN ION-EXCHANGER AND AQUEOUS SOLUTION MEDIA

HIROHIKO WAKI* and YOSHINOBU MIYAZAKI

Department of Chemistry, Faculty of Science, Kyushu University, Hakozaki, Higashiku, Fukuoka, Japan

(*Received* 1 *September* 1988; *accepted* 20 *October* 1988)

Abstract—The formation of cobalt(II) complexes with inorganic ligands in ion-exchanger solid phases has been investigated by direct spectrophotometric measurements. It was found that the stability constants of the one-to-one cobalt(II)–thiocyanate complex in the cation-exchanger phase are in all cases intrinsically higher than those in the solutions of the corresponding condition. This result can be ascribed to a low dielectric constant and high internal pressure as characteristic properties of the ion-exchanger phase, in comparison with the solution phase. This fact must be taken into consideration in using a conventional cation-exchange method for the determination of stability constants, in which the complex formation with anionic ligands in cation-exchangers has often been neglected for simplification in analysis.

Although a large number of studies on complex formation in solutions using an ion-exchange method have so far been reported,[1–4] little has been noted on complex formation within the ion-exchanger phase itself. It is known that the very high complexation of metal ions in the anion-exchanger phase is due to the high ligand anion concentration and that the very low complexation in the cation-exchanger phase is due to the exclusion of ligand anions. We considered that there should also be other factors such as dielectric constant and internal pressure etc. influencing complexation in the ion-exchanger phase, and attempted to find an intrinsic difference in complexation between the ion-exchanger phase and ordinary solution phase. We studied cobalt(II)–chloride and cobalt(II)–thiocyanate complex systems by applying absorption spectrophotometry to the solid phase.[5,6]

EXPERIMENTAL

Apparatus, reagents and ion-exchangers

A Hitachi Recording spectrophotometer EPS-3T was employed for absorbance measurements. All reagents used were of commercially available reagent grade. Cation-exchangers of different cross-linking degrees, Dowex 50W-X2, -X4 and -X8 (100–200 mesh) of the sodium form; and a cross-linked dextran gel-type cation-exchanger, SP-Sephadex C-25 of sodium form; were used in determining the stability constant of the one-to-one cobalt(II)–thiocyanate complex in each ion-exchanger phase.

Establishment of absorption spectra

A technique for the absorbance measurements of an ion-exchanger layer and its quantitative treatment have already been developed.[5,6] The ion-exchanger beads in which the complexes were sorbed were packed into a 2 mm quartz cell with a small amount of equilibrated solution, and the absorption spectrum was measured using a Hitachi Recording spectrophotometer EPS-3T. A net absorption spectrum on the sorbed chemical components was obtained by subtracting the absorbance of the interstitial solution from the observed overall absorbance of the sample layer. In order to make a correct spectral analysis, the net light path length of the ion-exchanger solid phase in the cell, as well as that of the interstitial solution, must be known. They were experimentally determined separately as follows.

* Author to whom correspondence should be addressed.

A potassium ferricyanide solution was used to determine the light path length of the interstitial solution. Since highly-charged anions such as $Fe(CN)_6^{3-}$ are almost entirely excluded from the cation-exchanger phase, the visible absorption spectrum of the cation-exchanger layer containing a potassium ferricyanide solution should be ascribed to that of the interstitial solution. The light path length of the interstitial solution in this cell can be obtained (in mm) by

$$l_i = 2\frac{A_i}{A_s} \quad (1)$$

where A_s and A_i are the absorbances of the equilibrated solution (using a 2 mm cell) and of the cation-exchanger layer (for a 2 mm cell), respectively.

In obtaining the light path length of the cation-exchanger phase in the same cell, a praseodymium chloride solution was used. The molar absorptivity of the praseodymium cation may be almost constant irrespective of its solution environment, that is, the molar absorptivity of the metal ion in the cation-exchanger phase is considered to be the same as that in the solution. Thus the light path length of the cation-exchanger phase (in mm) in the cell can be calculated by

$$l = \frac{\bar{A}^* - A_i}{\varepsilon_{Pr}\bar{C}_{Pr}} \quad (2)$$

where $\bar{A}^*$ is the overall absorbance of the ion-exchanger layer, A_i the absorbance of the interstitial equilibrium solution calculated using eq. (1), ε_{Pr} the molar absorptivity of the praseodymium ion and $\bar{C}_{Pr}$ the praseodymium ion concentration in the cation-exchanger phase expressed in mol dm^{-3}.

RESULTS AND DISCUSSION

Light path parameters for the ion-exchanger particle layer

The absorption spectrum for the cation-exchanger layer of Dowex 50W-X4 (100–200 mesh) equilibrated with a solution containing 0.004 M potassium ferricyanide and 0.5 M hydrochloric acid is shown in Fig. 1. The light path length of the interstitial solution was found to be 0.755 mm for a 2 mm cell using eq. (1), by comparison with the equilibrated solution spectrum.

The absorption spectrum for the cation-exchanger phase of the same resin, equilibrated with a 0.05 M praseodymium chloride–0.5 M perchloric acid solution using a 2 mm cell, is given in Fig. 2. The net light path length of the cation-exchanger phase was found to be 1.25 mm, using eq. (2).

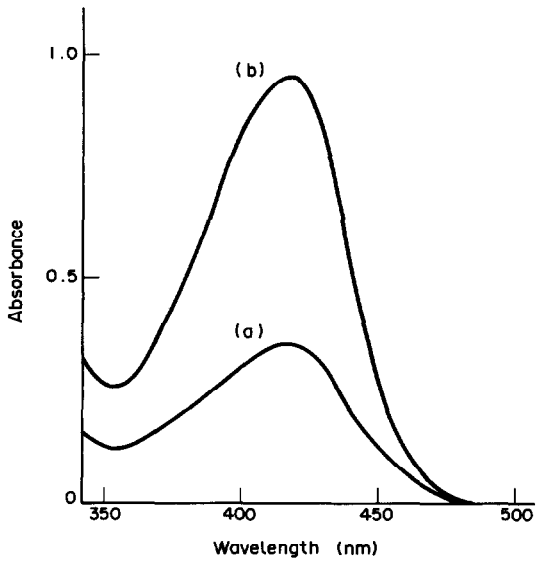

Fig. 1. Determination of the partial light path length for an interstitial solution in a 2 mm cell. (a) The absorption spectrum for a Dowex 50W-X4 layer equilibrated with a 0.004 M $K_3Fe(CN)_6$–0.5 M HCl solution. (b) The solution spectrum of the equilibrium solution.

In the same way, the light path parameters of a SP-Sephadex C-25 layer in a 2 mm cell were determined to be 1.02 mm for interstitial and 0.865 mm for solid phase.

These values were used in obtaining a correct

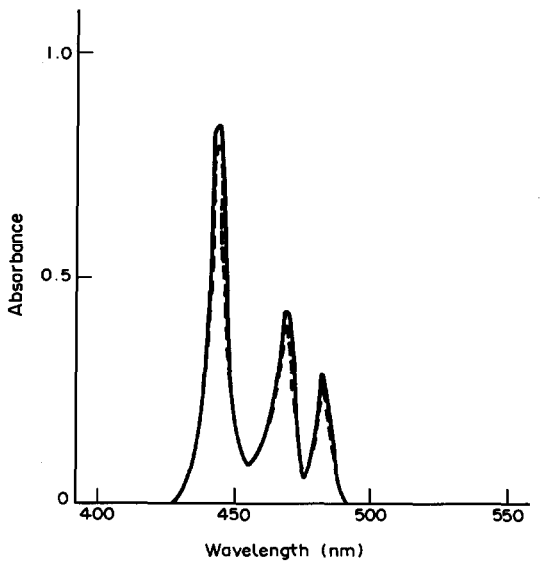

Fig. 2. Determination of net absorbance by praseodymium in the ion-exchanger phase in a 2 mm cell. Solid line: overall absorption spectrum for a Dowex 50W-X4 layer equilibrated with a 0.05 M $PrCl_3$–0.5 M $HClO_4$ solution. Dashed line: net cation-exchanger phase absorption spectrum after subtracting the interstitial solution absorbance.

absorption spectrum of the sorbed chemical components within the ion-exchanger phase in further studies.

Absorption spectra of the ion-exchanger phase in the cobalt(II)–chloride system

The absorption spectrum of the cation-exchanger Dowex 50W-X4 phase equilibrated with a 0.476 M cobalt(II) chloride–5.4 M hydrochloric acid solution is shown in Fig. 3. The total chloride ion concentration in this cation-exchanger phase was calculated to be 2.64 M from the amount of chloride ions sorbed and the net volume of the ion-exchanger phase. For comparison, the absorption spectrum of a 0.290 M cobalt(II) chloride–2.06 M hydrochloric acid solution which has the same total chloride concentration is shown in the figure. Furthermore, the spectrum of the anion-exchanger AG 1-X4 phase equilibrated with a 0.290 M cobalt(II) chloride–1.84 M hydrochloric acid solution is also shown, the counter-chloride concentration in the solid phase is again 2.64 M.

Both cation- and anion-exchanger phase spectra had characteristic peaks at 520 nm (due to octahedral complexes) and 600–700 nm (due to tetrahedral higher complexes). On the other hand, the solution spectrum had a peak at 520 nm only. No peaks at longer wavelengths were observed.

Absorption spectra of the ion-exchanger phase in the cobalt(II) thiocyanate system

The absorption spectrum for the cation-exchanger Dowex 50W-X4 phase equilibrated with a 0.10 M cobalt(II) chloride–0.70 M sodium thiocyanate solution is shown in Fig. 4. The total thiocyanate ion concentration in this cation-exchanger phase was calculated to be 0.155 M from the amount of thiocyanate ion sorbed and the net volume of the ion-exchanger phase. For comparison, the absorption spectrum of a 0.10 M cobalt(II) chloride–0.155 M sodium thiocyanate solution which has the same total thiocyanate concentration is shown in the figure. The absorption spectrum for the ion-exchanger phase showed two characteristic peaks at wavelengths, 520 and 620 nm, although the solution again had a single peak at 520 nm, similar to the chloride system.

The comparison of these absorption spectra at the same ligand concentration, indicates that the complexibility in the ion-exchanger phase is intrinsically higher than that in the ordinary solution.

Determination of cation-exchanger corresponding solutions on complexation

In the foregoing sections, it was spectroscopically indicated that complexibility in the cation- or anion-

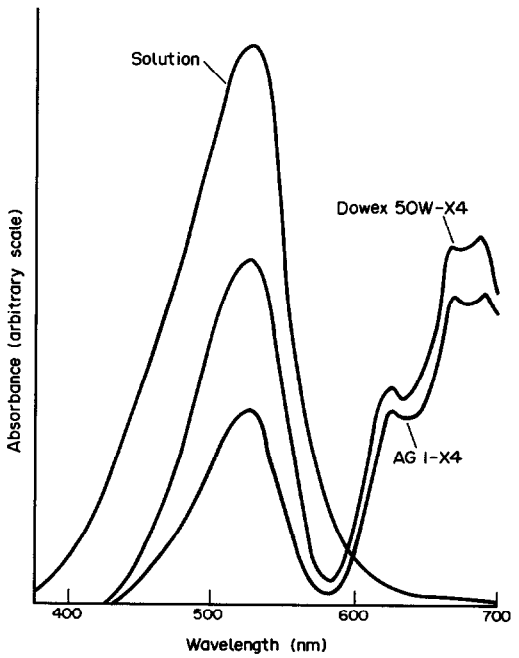

Fig. 3. Absorption spectra of the ion-exchanger phases and solution for the cobalt(II)–chloride system compared at the same ligand concentration (2.64 M).

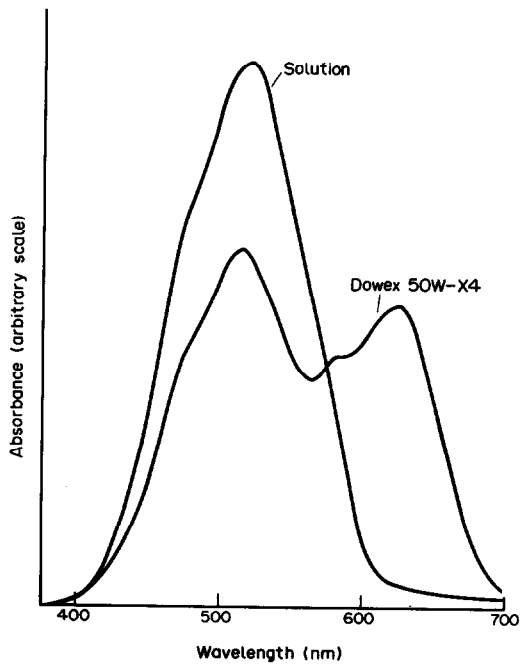

Fig. 4. Absorption spectra of the ion-exchanger phase and solution for the cobalt(II)–thiocyanate system compared at the same ligand concentration (0.155 M).

exchanger solid phase is much higher than in aqueous solutions of the same ligand concentration. We next tried to find which solution may correspond to the cation-exchanger phase in terms of complexation.

In comparing the complexation for different media, a spectral parameter A_r was conveniently introduced, which is defined as the ratio of absorbance at a wavelength for tetrahedral complexes (686 nm for the cobalt(II)–chloride system and 620 nm for the cobalt(II)–thiocyanate system) to that for octahedral complexes (520 nm for both systems), a higher A_r value indicating a higher complexation environment. The A_r for Dowex 50W-X4 of the chloride system was 1.06 (see Fig. 3) and that of the thiocyanate system was 0.89 (see Fig. 4).

Next, the A_r values for hydrochloric acid or sodium thiocyanate solutions of different concentrations containing cobalt(II) chloride were measured from their absorption spectra and plotted against each total ligand concentration (Figs 5 and 6). Interpolation has indicated that the Dowex 50W-X4 phase, equilibrated with a 0.476 M cobalt (II) chloride–5.4 M hydrochloric acid solution (internal chloride concentration is 2.64 M) has the same A_r value as that of the cobalt(II) solution with 5.81 M total chloride concentration. Furthermore, it was found that the resin phase, equilibrated with 0.10 M cobalt(II) chloride–0.70 M sodium thiocyanate solution (the internal thiocyanate concentration is 0.155 M) has the same A_r value as that of the cobalt(II) solution with 2.20 M total thiocyanate concentration. In all cases, the cation-exchange resin phase corresponded to a solution with a much higher ligand concentration in terms of complex formation.

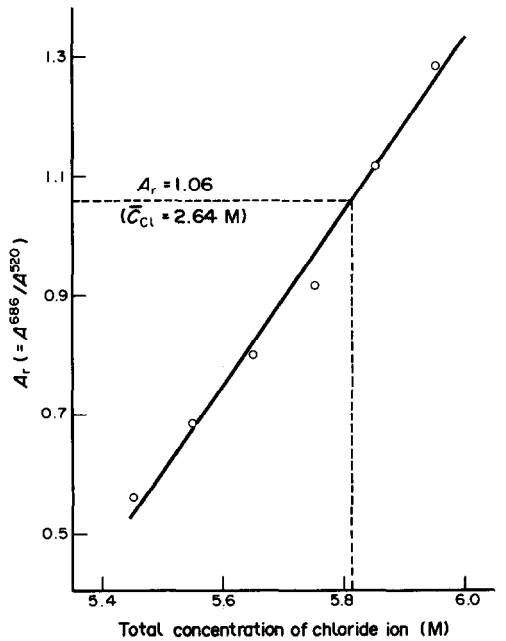

Fig. 5. Establishment of the ion-exchanger corresponding solution of the same complexation for the cobalt(II)–chloride system.

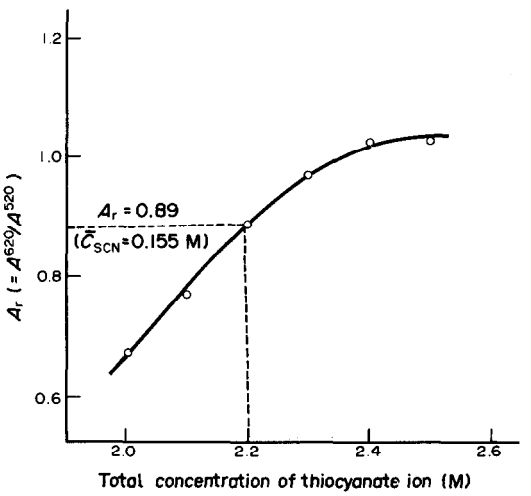

Fig. 6. Establishment of the ion-exchanger corresponding solution of the same complexation for the cobalt(II)–thiocyanate system.

Method for evaluating the stability constant of a complex in a cation-exchanger phase

When the reaction of M^{m+} and L^- forms only $ML^{(m-1)+}$, the apparent absorptivity in the ion-exchanger phase $\bar{\varepsilon}$ can be expressed as

$$\bar{\varepsilon} \equiv \frac{\bar{A}}{\bar{C}_M l} = \frac{\bar{\epsilon}_0[\overline{M^{m+}}]+\bar{\epsilon}_1[\overline{ML^{(m-1)+}}]}{[\overline{M^{m+}}]+[\overline{ML^{(m-1)+}}]} = \frac{\bar{\epsilon}_0+\bar{\epsilon}_1\bar{K}_1[\overline{L^-}]}{1+\bar{K}_1[\overline{L^-}]}, \quad (3)$$

where the upper bar refers to an ion-exchanger phase, $\bar{\epsilon}_0$ and $\bar{\epsilon}_1$ are the molar absorptivities of free M^{m+} and $ML^{(m-1)+}$, respectively, l is the light path length, $\bar{C}_M$ the total concentration of the sample metal and $\bar{K}_1$ the stability constant of $ML^{(m-1)+}$ in the ion-exchanger phase

$$\bar{K}_1 = \frac{[\overline{ML^{(m-1)+}}]}{[\overline{M^{m+}}][\overline{L^-}]}. \quad (4)$$

The following equation was derived from eqs (3) and (4) for the graphical analysis of the $\bar{K}_1$ value.

$$\bar{\phi} \equiv \frac{\bar{\varepsilon}-\bar{\epsilon}_0}{[\overline{L^-}]} = \bar{K}_1\bar{\epsilon}_1 - \bar{K}_1\bar{\varepsilon} \quad (5)$$

which is of the same form as the equation for the conventional solution analysis:

$$\phi \equiv \frac{\varepsilon - \epsilon_0}{[L^-]} = K_1\epsilon_1 - K_1\varepsilon. \quad (6)$$

Using a Donnan relation, $[\overline{L^-}]$ in eq. (5) is written in the form

$$[\overline{L^-}] = \frac{y_{B^+}y_{L^-}[B^+]}{\bar{y}_{B^+}\bar{y}_{L^-}[\overline{B^+}]}[L^-] = k[L^-], \quad (7)$$

where B^+ is a supporting cation in large excess. When the ionic strength and the concentration of B^+ in the equilibrating solution are constant, $\bar{y}_{B^+}$ or $\bar{y}_{L^-}$ may also be constant as well as y_{B^+} or y_{L^-}. Thus $[\overline{L^-}]$ can be evaluated by $[L^-]$ and a proportional constant k which had been determined using a known system. Accordingly, the stability constant of the one-to-one complex in the cation-exchanger phase can be determined from the slope of $\bar{\phi}$ vs $\bar{\varepsilon}$ plots of eq. (5), in analogy to the ϕ vs ε plot for the solution analysis.

Evaluation of stability constants of the cobalt(II)–thiocyanate complex in the cation-exchanger phase

In order to give more quantitative information about the above observation that the complexibility in an ion-exchanger phase is higher than that in an ordinary aqueous solution, we evaluated stability constants of the $CoSCN^+$ complex within cation-exchangers of different cross-linking degrees by a direct spectrophotometric technique.

Necessary data for evaluating the stability constants are listed in Table 1, where $[\overline{SCN^-}]$ was obtained using proportional constants in eq. (7), $k = 0.279$ (Dowex 50W-X2), 0.202 (-X4), 0.0837 (-X8) and 0.506 (SP-Sephadex C-25) which had been determined by a separate column equilibration experiment.

The graphical analysis for stability constants of the $CoSCN^+$ complex are shown in Fig. 7. For comparison, the stability constants of the same complex in aqueous solutions, prepared so that the ionic strengths were the same as those within the ion-exchanger phase, were also determined. An example of the solution analysis is also given in Fig. 7. The stability constant values obtained are shown in Table 2.

As can be seen from the table, the stability constants for the cation-exchanger phase were always larger than those for the aqueous solution of the same ionic strength. One of the reasons is undoubtedly a lower dielectric constant for the ion-exchanger phase due to the presence of organic components. Although the stability constant of

Table 2. Stability constants of the $CoSCN^+$ complex in cation-exchanger phases and aqueous solutions at $25 \pm 1°C$

Ion-exchanger			Aqueous solution	
	$\bar{I}$	$\bar{K}_1$	I	K_1
SP-Sephadex C-25	0.42	9.6	0.5	5.3
Dowex 50W-X2	1.7	8.9	1.7	5.3
-X4	2.0	11	2.0	5.2
-X8	3.4	28	3.4	6.0

$\bar{I}$: ionic strength in the ion-exchanger phase.

Table 1. Data for evaluating stability constants of the $CoSCN^+$ complex in ion-exchanger phases

Dowex 50W-X2	$\bar{A}$	0.256	0.253	0.240	0.212	0.193	0.171
	$\bar{C}_{Co}$	0.452	0.360	0.285	0.234	0.200	0.174
	$[\overline{SCN^-}]$	0	0.0236	0.0490	0.0754	0.102	0.129
Dowex 50W-X4	$\bar{A}$	0.315	0.321	0.297	0.267	0.231	0.203
	$\bar{C}_{Co}$	0.495	0.385	0.318	0.247	0.199	0.165
	$[\overline{SCN^-}]$	0	0.0172	0.0357	0.0548	0.0743	0.0941
Dowex 50W-X8	$\bar{A}$	0.442	0.377	0.313	0.243	0.201	0.158
	$\bar{C}_{Co}$	0.751	0.587	0.461	0.353	0.277	0.210
	$[\overline{SCN^-}]$	0	0.0071	0.0147	0.0226	0.0307	0.0388
SP-Sephadex C-25	$\bar{A}$	0.056	0.108	0.131	0.136	0.137	0.138
	$\bar{C}_{Co}$	0.155	0.132	0.119	0.110	0.100	0.090
	$[\overline{SCN^-}]$	0	0.0344	0.0716	0.110	0.149	0.189

Equilibrating solutions are $NaSCN + NaClO_4$ ($I = 0.5$) containing 0.05 M $Co(ClO_4)_2$. The absorbance for the ion-exchanger phase is taken as $\bar{A} = \bar{A}^{514} - \bar{A}^{570}$, $\bar{C}_{Co}$ was obtained by dividing the total amount of cobalt(II) sorbed by the net volume of ion-exchanger phase, expressed in mol dm^{-3}.

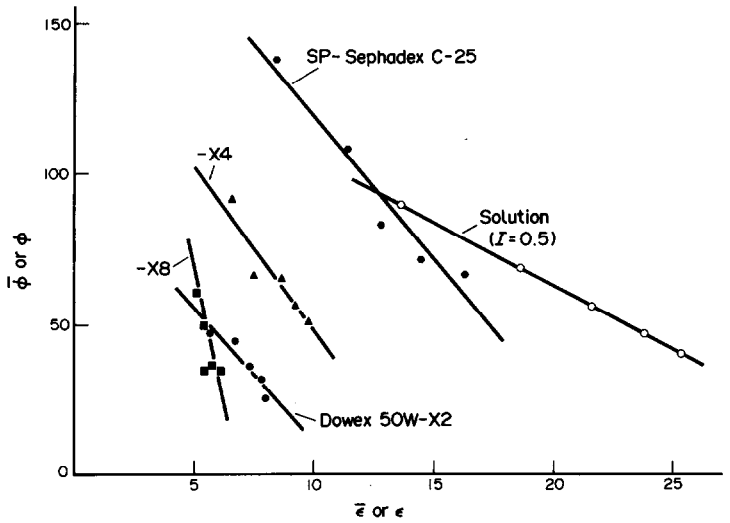

Fig. 7. Determination of stability constants of the one-to-one cobalt(II)–thiocyanate complex in cation-exchanger phases and aqueous solutions at 25 ± 1°C.

the aqueous solution was nearly constant, irrespective of ionic strength, that for the cation-exchange resin increased with an increase in the degree of cross-linking, that is, with an increase in ionic strength.

Another reason of higher complexibility for the ion-exchanger phase may be the presence of a high internal pressure produced by the resin network. When the following reaction occurs in the ion-exchange resin,

$$Co^{2+}(aqua) + SCN^{-}(aqua) \rightleftharpoons CoSCN^{+}(aqua) + nH_2O \quad (8)$$

some of the water molecules librated through the complexation reaction may be excluded from the resin phase. When water molecules are transferred to the solution phase from the highly-pressured ion-exchange resin phase, the energy $\pi\Delta V$ is released, π being the swelling pressure and ΔV the volume contraction of the resin phase through reaction. The higher the degree of cross-linking, the higher the internal pressure and the larger $\pi\Delta V$, thus the complexation increases.

In spite of the lower internal pressure and lower ionic strength of SP-Sephadex C-25 than the ion-exchange resins, the stability constant for SP-Sephadex C-25 is found to be somewhat larger than that for Dowex 50W-X2. This could probably be due to an attraction between the π-electrons of the thiocyanate ion and those of the benzene ring of the Dowex resins, which somewhat weakens the ligand activity of the thiocyanate ion.

In any case, these facts on the high complexation ability of the cation-exchanger phase should be sufficiently considered when using conventional cation-exchange methods for evaluating stability constants, where complexation with anionic ligands has frequently been neglected without any evidence for simplification.[7,8]

REFERENCES

1. R. M. Smith and A. E. Martell (Eds), *Critical Stability Constants, Inorganic Complexes*, Vol. 4. Plenum Press, New York (1976).
2. E. Högfeldt (Ed.), *Stability Constants of Metal–Ion Complexes*, Part A: Inorganic ligands. Pergamon Press, Oxford (1982).
3. L. G. Sillen and A. E. Martell (Eds), *Stability Constants of Metal–Ion Complexes*, Special Publication No. 17. London (1964).
4. L. G. Sillen and A. E. Martell (Eds), *Stability Constants of Metal–Ion Complexes*, Special Publication No. 25. London (1971).
5. H. Waki, S. Takahashi and S. Ohashi, *J. Inorg. Nucl. Chem.* 1973, **35**, 1259.
6. K. Yoshimura, H. Waki and S. Ohashi, *Talanta* **23**, 449.
7. J. Schubert, *J. Phys. Chem.* 1948, **52**, 340.
8. J. Schubert and A. Lindenbaum, *J. Am. Chem. Soc.* 1952, **74**, 3529.

Polyhedron Vol. 8, No. 7, pp. 865–871, 1989
Printed in Great Britain

0277–5387/89 $3.00+.00
© 1989 Pergamon Press plc

THE PROPERTIES AND STRUCTURES OF TRIS(BENZENETHIOLATO)INDIUM(III)-BIS-PYRIDINE ADDUCT, AND OF TRIS(BENZENESELENOLATO)INDIUM(III)

THEODORE A. ANNAN, RAJESH KUMAR, HASSAN E. MABROUK and DENNIS G. TUCK*

Department of Chemistry and Biochemistry, University of Windsor, Windsor, Ontario, Canada N9B 3P4

and

RAJ K. CHADHA

Department of Chemistry, University of Manitoba, Winnipeg, Manitoba, Canada R3T 2N2

(*Received* 27 *September* 1988; *accepted* 27 *October* 1988)

Abstract—The bis-pyridine adduct of $In(SC_6H_5)_3$ has been prepared. A crystal structure determination shows that the molecule has two different conformations in the solid state, related to the orientations of the phenyl rings of the SC_6H_5 ligand. The crystalline form of $In(SeC_6H_5)_3$ is a homopolymer in which six-coordinate indium atoms are linked through bridging selenium atoms. The phenyl groups of the SeC_6H_5 ligand show an interesting disorder pattern. The structure of $In(SC_6H_5)_3$ is discussed in this context.

Recent papers[1–3] from this laboratory have described three different preparative routes to tris (benzenethiolato)indium(III). The compound is apparently a homopolymer, whose structure can be broken down by neutral or anionic donor ligands to give the appropriate mononuclear adducts; an X-ray crystallographic study of the tetraphenylphosphonium salt of $[InBr(SPh)_3]^-$ has also been reported.[1] The selenium analogue has similar properties, extending to its behaviour as a Lewis acid.[2]

We have now been able to obtain $In(SeC_6H_5)_3$ in crystalline form, and to show that this compound has a homopolymeric structure in the solid state. It has not been possible to carry out similar studies with $In(SC_6H_5)_3$, but the neutral adduct $In(SC_6H_5)_3py_2$ (py = pyridine) has been investigated, and the X-ray results confirm previous arguments based on spectroscopic studies.[1] The results are compared with those for other indium(III) compounds, and with certain other selenolato derivatives of d^{10} metal ions.

EXPERIMENTAL

Preparative

(i) *Tris(benzenethiolato)indium*(III)-*bis-pyridine.* Tris(benzenethiolato)indium(III) was prepared by the reaction of indium metal with diphenyldisulphide in refluxing toluene.[2] $In(SC_6H_5)_3$ (1 g) was dissolved in warm pyridine (5 cm^3), and the resultant solution allowed to evaporate slowly at room temperature. The crystals obtained after *ca* 2 months were collected and dried. The IR and ^1H NMR spectra confirmed the presence of both pyridine and SC_6H_5 ligand (Found: C, 55.7; H, 4.23. Calc. for $C_{28}H_{25}N_2S_3In$: C, 56.0; H, 4.20%).

(ii) *Tris(benzeneselenolato)indium*(III). $In(SeC_6H_5)_3$ was prepared by the reaction of indium metal with diphenyldiselenide in refluxing toluene.[2] Crystals suitable for X-ray crystallography were obtained by the slow evaporation of a dilute

* Author to whom correspondence should be addressed.

solution in toluene (0.1 g in 100 cm^3) under a slow stream of nitrogen over a period of 10 days.

Structure determinations

Suitable crystals of either $In(SC_6H_5)_3py_2$ (**1**) or $In(SeC_6H_5)_3$ (**2**) were sealed in thin-walled glass capillaries and mounted and aligned on a Syntex $P2_1$ automated diffractometer. Data collection followed the procedures described previously.[4] The intensities of three monitor reflections were measured after every 100 reflections, and did not change significantly during data collection. The intensities were corrected for Lorentz and polarization effects. No absorption corrections were used in the refinement of **1**, because of the low absorption coefficient; in **2**, subsequent accidental loss of the crystal prevented the application of an absorption correction, but in the event this appears to have had little effect (see below). Details of cell constants and other relevant experimental data are given in Table 1.

For **1**, there were no systematic absences, and the space group $P\bar{1}$ was used in the refinement, and taken to be correct in view of the successful refinement. The position of the indium atoms was found by direct methods, and the structure was refined by block matrix methods, using the program SHELX.[6] At this point, two different forms of the molecule were identified, and both indium atoms [In(1), In(2)] were included in each block; in addition, block 1 contained six sulphur atoms, four nitrogen and 16 carbon atoms [C(11)—C(34)] and a scale factor (173 parameters), and block 2 contained In(1), In(2), 40 carbon atoms [C(35)—C(90)] and a scale factor (179 parameters). Indium, sulphur and nitrogen atoms were refined anisotropically, and carbon atoms isotropically. Hydrogen atoms were subsequently included in ideal positions [r(C—H) = 0.95 Å], and assigned U-values 1.10 × those of the carbon atoms attached to the hydrogen in question. The function minimized during the least-squares refinement was $(|F_o|-|F_c|)^2$, and a weighting scheme $1/[\sigma^2(F)+pF^2]$ was employed ($p = 0.00001$). The small residual electron density in the final difference map was not at any chemically significant position, and there was not secondary extinction.

For **2**, the systematic absences (hkl, $h+k = 2n+1$; $h0l$, $l = 2n+1$) indicated the space group $C2/c$ or Cc, but the systematic weakness suggested $C2/c$. Eventual structural solution and refinement in $C2/c$, together with a failure to obtain significantly improved results in Cc, confirmed the former as being the correct space group. The structure was solved by direct methods, using MULTAN 78. The indium atom was constrained to lie on an inversion centre, and Se(1) on a two-fold axis (see Fig. 1). When anisotropic refinement of In and Se atoms converged, the presence of large thermal ellipsoids for the carbon atoms, plus the fact that the asymmetric unit contains one and one half phenyl rings as indicated by the elemental analyses, suggested disorder in the phenyl rings. The phenyl group bonded to Se(1) requires two-fold symmetry within the ring, but is disordered about the two-fold axis

Table 1. Summary of crystal data, intensity collection and structural refinement for **1** and **2**

	1	**2**
Formula, *fw*	$C_{28}H_{25}N_2S_3In$, 600.4	$C_{18}H_{15}Se_3In$, 582.7
Cell constants at 22°C	*a*, 9.552(2) Å; α, 91.92(3)°	*a*, 12.565(5) Å
	b, 15.314(5) Å; β, 93.58(2)°	*b*, 20.095(14) Å; β, 112.58(3)°
	c, 19.370(6) Å; γ, 106.12(2)°	*c*, 7.250(3) Å
Cell volume (Å^3)	2713(1)	1690(2)
Space group	$P\bar{1}$	$C2/c$
Z	4	4
d (calc.), d (exp.) (g cm^{-3})	1.47, 1.45	2.29, 2.25
Absorption coefficient (cm^{-1})	10.21	31.86
Radiation	Mo-K_α ($\lambda = 0.71069$ Å)	Mo-K_α ($\lambda = 0.71069$ Å)
2θ (max) for data collection	45°	50°
Scan width	$K_{\alpha_1}-0.8°$ to $K_{\alpha_2}+0.8°$	$K_{\alpha_1}-0.8°$ to $K_{\alpha_2}+0.8°$
Total reflections measured	5397 ($+h$, $\pm k$, $\pm l$)	1762 ($+h$, $+k$, $\pm l$)
Unique "observed" reflections [$I \geq 3\sigma(I)$]	4275	706
$R = (\Sigma\|\|F_o\|-\|F_c\|\|)/\Sigma\|F_o\|)$	0.0457	0.0605
$R_w = (\Sigma_w(\|F_o\|-\|F_c\|)^2/(\Sigma_w\|F_o\|^2)^{1/2}$	0.0568	0.0675
Shift/esd (max) in the final cycle	0.04	0.02
Max (eA^{-3}) in the final dimap	0.91	1.6

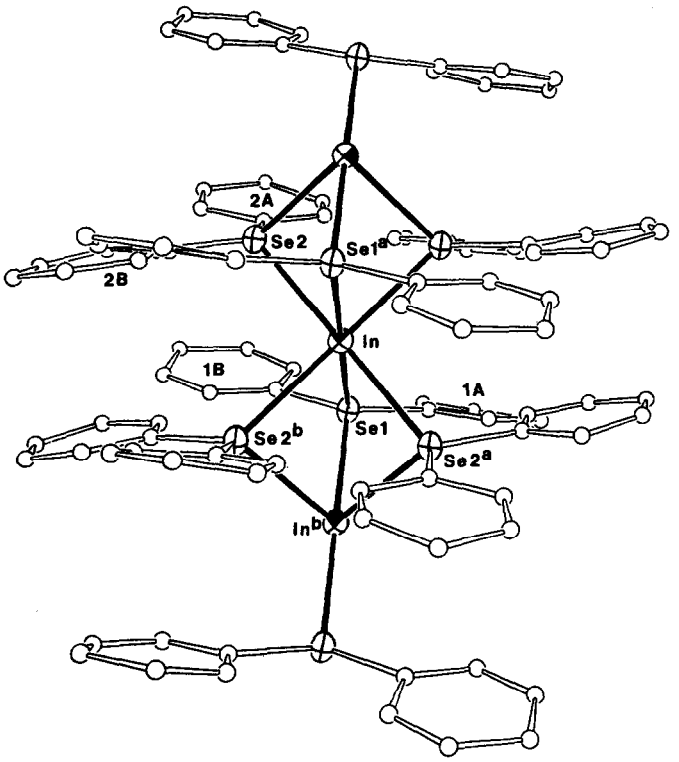

Fig. 1. ORTEP diagram showing a chain of $In(SeC_6H_5)_3$ parallel to the *a* axis. The Se and In atoms are drawn with 50% probability ellipsoids; and C atoms are arbitrarily small, and have 50% occupancy. Hydrogen atoms have been omitted for the sake of clarity. For symmetry related positions, see footnotes to Table 2.

passing through Se(1), and this axis generates the carbon atoms of ring 1B from those of 1A, with all of the carbon sites having 50% occupancy. The ring bonded to Se(2), which is the selenium atom on the general position, is also disordered, and was therefore divided into two sets "2A" and "2B", with each set having 50% occupancy. The carbon atoms were refined isotropically, and no attempt was made to include hydrogen atoms. The function minimized during full-matrix least-squares refinement was $w(|F_o|-|F_c|)^2$ and in the final cycles, a weighting scheme of the form $w = 1/[\sigma^2(F)+0.00001F^2]$ was employed. No evidence of secondary extinction was noticed. A final difference Fourier map contained a few peaks of the order of 1–1.5 $eÅ^{-3}$ in the vicinity of the indium and selenium atoms, which may be due to uncorrected absorption effects (see above).

Selected bond distances and angles for **1** and **2** are given in Tables 2 and 3, respectively, and Figs 1–3 show the molecular structures with the atomic numbering schemes. Tables of atomic coordinates, anisotropic thermal parameters, and observed and calculated structure factors for each compound are available as supplementary material from the Editor.

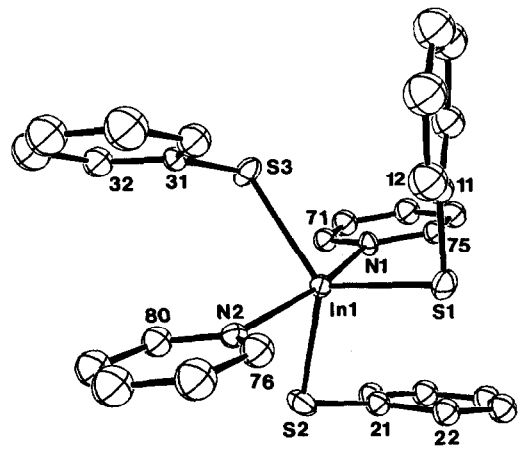

Fig. 2. ORTEP diagram of form A of $In(SC_6H_5)_3py_2$, showing the atomic numbering scheme. Atoms identified by numbers are carbons.

RESULTS AND DISCUSSION

The structure of $In(SC_6H_5)_3py_2$

The results of the X-ray crystallographic studies show that the bis-pyridine adduct of $In(SC_6H_5)_3$ is

Table 2. Bond lengths (Å) and bond angles (deg) for $In(SC_6H_5)_3(C_5H_5N)_2$

In(1)—S(1)	2.448(3)	S(1)—In(1)—S(2)	111.5(1)
In(1)—S(2)	2.472(3)	S(1)—In(1)—S(3)	119.9(1)
In(1)—S(3)	2.455(3)	S(2)—In(1)—S(3)	128.3(1)
In(1)—N(1)	2.408(7)	S(1)—In(1)—N(1)	97.3(2)
In(1)—N(2)	2.374(8)	S(2)—In(1)—N(1)	88.6(2)
In(2)—S(4)	2.447(3)	S(3)—In(1)—N(1)	79.7(2)
In(2)—S(5)	2.468(3)	S(1)—In(1)—N(2)	97.7(2)
In(2)—S(6)	2.459(3)	S(2)—In(1)—N(2)	85.7(2)
In(2)—N(3)	2.390(6)	S(3)—In(1)—N(2)	93.0(2)
In(2)—N(4)	2.390(7)	N(1)—In(1)—N(2)	165.0(3)
S(1)—C(11)	1.77(1)	S(4)—In(2)—S(5)	109.4(1)
S(2)—C(21)	1.77(1)	S(4)—In(2)—S(6)	118.9(1)
S(3)—C(31)	1.77(1)	S(5)—In(2)—S(6)	131.6(1)
S(4)—C(41)	1.77(1)	S(4)—In(2)—N(3)	102.5(2)
S(5)—C(51)	1.77(1)	S(5)—In(2)—N(3)	88.6(2)
S(6)—C(61)	1.77(1)	S(6)—In(2)—N(3)	81.3(2)
N(1)—C(71)	1.33(1)	S(4)—In(2)—N(4)	94.8(2)
N(1)—C(75)	1.33(1)	S(5)—In(2)—N(4)	83.8(2)
N(2)—C(76)	1.33(1)	S(6)—In(2)—N(4)	92.1(2)
N(2)—C(80)	1.32(1)	N(3)—In(2)—N(4)	162.6(3)
N(3)—C(81)	1.32(1)	In(1)—S(1)—C(11)	100.8(3)
N(3)—C(85)	1.33(1)	In(1)—S(2)—C(21)	100.8(4)
N(4)—C(86)	1.33(1)	In(1)—S(3)—C(31)	108.6(3)
N(4)—C(90)	1.32(1)	In(2)—S(4)—C(41)	108.3(3)
Ring C(11)—C(16)		In(2)—S(5)—C(51)	101.9(4)
Mean C—C	1.37(8)	In(2)—S(6)—C(61)	108.7(3)
Mean C—C—C	120(4)	In(1)—N(1)—C(71)	117.2(7)
		In—N(1)—C(75)	125.3(5)
Ring C(21)—C(26)		C(71)—N(1)—C(75)	117.2(8)
Mean C—C	1.37(4)	In(1)—N(2)—C(80)	118.6(9)
Mean C—C—C	120(3)	In(2)—N(3)—C(81)	123.7(6)
Ring C(31)—C(36)		In(2)—N(3)—C(85)	117.2(6)
Mean C—C	1.36(8)	C(81)—N(3)—C(85)	118.4(7)
Mean C—C—C	120(4)	In(2)—N(4)—C(86)	123.0(7)
Ring C(41)—C(46)		In(2)—N(4)—C(90)	118.0(6)
Mean C—C	1.37(4)	C(86)—N(4)—C(90)	118.7(8)
Mean C—C—C	120(3)	S(1)—C(11)—C(12)	119.3(9)
Ring C(51)—C(56)		S(1)—C(11)—C(16)	122.7(8)
Mean C—C	1.38(4)	S(2)—C(21)—C(22)	120.9(7)
Mean C—C—C	120(2)	S(2)—C(21)—C(26)	121.7(8)
Ring C(61)—C(66)		S(3)—C(31)—C(32)	118.8(7)
Mean C—C	1.38(3)	S(3)—C(31)—C(36)	120.3(9)
Mean C—C—C	120(1)	S(4)—C(41)—C(42)	119.2(8)
Ring N(1), C(71)—C(75)		S(4)—C(41)—C(46)	120.0(8)
Mean C—C	1.36(2)	S(5)—C(51)—C(52)	120.7(8)
Mean C—C—C	120(3)	S(5)—C(51)—C(56)	120.6(6)
Ring N(2), C(76)—C(80)		S(6)—C(61)—C(62)	117.8(6)
Mean C—C	1.36(4)	S(6)—C(61)—C(66)	122.7(7)
Mean C—C—C	120(4)		
Ring N(3), C(81)—C(85)			
Mean C—C	1.36(2)		
Mean C—C—C	120(2)		
Ring N(4), C(86)—C(90)			
Mean C—C	1.37(3)		
Mean C—C—C	120(3)		

[a] Esd's on average values are calculated with the use of the "scatter" formula:

$$\sigma = [\sum (d_i - \bar{d})^2/(N-1)]^{1/2},$$

where d_i is the ith, and $\bar{d}$ the mean, of N equal measurements.

Table 3. Bond distances (Å) and angles (deg) for $In(SeC_6H_5)_3$

In—Se(1)	2.772(2)	Se(1)—In—Se(2)	97.9(1)
In—Se(2)	2.766(2)	Se(1[a])—In—Se(2)	82.1(1)
In—Se(2[b])	2.789(2)	Se(1)—In—Se(2[b])	81.7(1)
Se(1)—C(1A)	1.90(3)	Se(1[a])—In—Se(2[b])	98.3(1)
Se(2)—C(11A)	1.94(3)	Se(2)—In—Se(2[b])	97.8(1)
Se(2)—C(11B)	1.93(3)	Se(2[a])—In—Se(2[b])	82.2(1)
Ring 1A, C(1A)—C(6A)		In—Se(1)—C(1A)	117.3(8)
Mean C—C	1.43(6)	In—Se(1)—C(1B)	110.9(8)
Mean C—C—C	120(5)	C(1A)—Se(1)—C(1B)	114.8(9)
Ring 2A, C(11A)—C(16A)		In—Se(2)—C(11A)	110.0(9)
Mean C—C	1.40(5)	In—Se(2)—C(11B)	117.2(9)
Mean C—C—C	120(4)	C(11A)—Se(2)—C(11B)	114(1)
Ring 2B, C(11B)—C(16B)		Se(2)—C(11A)—C(12A)	120(2)
Mean C—C	1.42(5)	Se(2)—C(11A)—C(16A)	123(3)
Mean C—C—C	120(2)	Se(2)—C(11B)—C(12B)	122(2)
In···In[b]	3.625	Se(2)—C(11B)—C(16B)	115(2)

1. The symmetry related positions are: a, $-x$, $-y$, $-z$; b, x, $-y$, $z-\frac{1}{2}$.
2. The carbon atoms of ring 1A are related to those of 1B by $-x$, y, $\frac{1}{2}-z$ and all the carbon atoms have 50% occupancy.
3. Esd's on average values have been calculated as in Table 2.

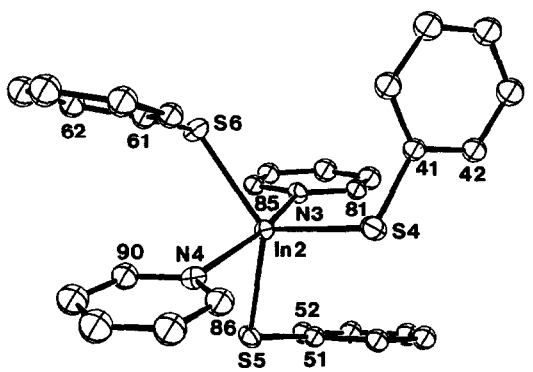

Fig. 3. ORTEP diagram of form B of $In(SC_6H_5)_3py_2$, showing the atomic numbering scheme. Atoms identified by numbers are carbons.

indeed a mononuclear species. The molecular structure is essentially based on a distorted trigonal bipyramidal InS_3N_2 kernel, with the sulphur atoms of the benzenethiolate ligands occupying the equatorial sites and the pyridine nitrogens in the axial positions. This compound then joins the increasingly large group of five-coordinate inorganic and organometallic compounds of indium(III), and this coordination state, which includes both trigonal bipyramidal and square-based pyramidal, must now be regarded as of equal importance with the longer established tetrahedral and octahedral stereochemistries.[6,7]

The structure consists of two independent molecules 1A and 1B which differ in the arrangement of the phenyl rings of the $-SC_6H_5$ ligands. In molecule 1A (Fig. 2), these three phenyl groups are in a cyclic arrangement, with ring C(11)—C(16) approximately normal to the other two. The dihedral angle between the plane of this ring and that of ring C(21)—C(26) is 90.3(2)°, and that between C(11)—C(16) and C(31)—C(36) is 84.4(2)°. The planes of C(21)—C(26) and C(31)—C(36) are then almost parallel, with a dihedral angle of 9.9(2)°. In 1B, the ring C(41)—C(46) is again almost normal to the other two phenyl rings, with dihedral angles of 98.9(2)° to C(51)—C(56), and 95.7(2)° to C(61)—C(66) and the latter two are at a dihedral angle of 8.2(2)°. Another way of describing the difference between 1A and 1B is in terms of the torsion angles involved at the In—S—C_6H_5 sites; in 1A, the angle In(1)—S(1)—C(11)—C(12) is 107.0(2)°, whereas in 1B the corresponding In(2)—S(4)—C(41)—C(46) angle is 67.2(2)°, and similarly, we find In(1)—S(1)—C(11)—C(16) at −75.0(2)°, and In(2)—S(4)—C(41)—C(42) at −117.8(2)°, a difference of about 40°.

Despite these significant differences in the orientation of the phenyl groups, the InS_3N_2 kernels of the two molecules are essentially identical, as are the $-SC_6H_5$ ligands in terms of their internal geometries. The N—In—N angle in 1A is 165.0(3)°, and in 1B, 162.6(3)°, both significantly less than the

180° required for trigonal bipyramidal stereochemistry. Although the S—In—S angles in 1A range from 111.5(1) to 128.3(1)°, the average is 120(3)°, while in 1B the average of 120(4)° arises from a range of 109.4(1)–131.6(1)°. Despite the two different orientations, the average In—S bond distance is the same in both structures, namely 2.458(8) Å, very close to the average value[1] of 2.450(4) Å in the anion $[BrIn(SC_6H_5)_3]^-$. A brief review of other In—S bond lengths has been given elsewhere,[1] with distances > 2.59 Å being reported, but differences in coordination number and ligand type between the various molecules studied prevent any detailed analysis at this point. The average S—C distance in the ligand is 1.77(1) Å, with all ligands being identical within experimental error in this respect, and this value is close to that of 1.75(2) Å in the structure previously reported.[1]

The average In—N bond distance is also identical in 1A and 1B, at 2.39(1) Å. In the molecule $Cl_2In(O_2CC_6H_5)py_2$, which also can be described as having a distorted trigonal bipyramidal structure with apical pyridine ligands,[8] the relevant In—N bond lengths are 2.250(5) and 2.300(6) Å, and a brief discussion of the results for other indium(III) complexes involving neutral aromatic nitrogen donors lead to an average value for In—N over a small group of compounds of 2.28 Å, with a range of 2.238(3)–2.514(19) Å. In general then, the present results are in keeping with previous work, but the significant difference between $In(SC_6H_5)_3py_2$ and $Cl_2In(O_2CC_6H_5)py_2$ is not easily understood.

We return below to the relationship between this compound and the parent $In(SC_6H_5)_3$.

The structure of $In(SeC_6H_5)_3$

Figure 3 confirms that $In(SeC_6H_5)_3$ is indeed a homopolymeric structure in the solid state, with linear chains formed by indium and selenium atoms running parallel to the *a* axis of the unit cell. Each indium is coordinated by six selenium atoms, and each selenium bridges two indium atoms. Crystallographically, each indium is on a centre of inversion; Se(1) lies on a two-fold axis and Se(2) on a general position, so that In and $Se(2^{a,b})$ form a planar chain, with Se(1) lying alternately above and below this plane. The four atoms In, In^b, Se(1) and $Se(1^a)$ also define a plane, perpendicular to the *b* axis, and this plane is at an angle of 89.7(1)° to a third plane involving In, Se(2), $Se(2^b)$, $Se(2^a)$ and $Se(2^c)$.

The geometry of the $InSe_6$ kernel is a highly distorted octahedral, with Se—In—Se angles which vary between 81.7(1)–98.3(1)°, with an average of 90° which is imposed by the symmetry relationships. The average In—Se bond length is 2.776(8) Å, and this appears to be the first such distance to be reported in a complex of this type. The In—Se distances in the adamantane-like $In_4Se_{10}^{8-}$ anion[9] are 2.543(2) for In—Se_t, and 2.565(2) Å for In—Se_{br}, but obviously the presence of the pendant phenyl groups must have some effect on the bond length in the present structure. The average In ··· In separation is 3.625 Å, much larger than the known In—In bonding distance[10] of 2.775(2) Å.

The geometry about each selenium atom is pyramidal, but the important feature of the ligand arrangement is that the phenyl rings are disorded, with each ring shown in Fig. 1 having an occupancy of 50%. The average Se—C distance is 1.92(3) Å, similar to that in $[Pb(SeC_6H_5)_3]^-$ [average value 1.91(1) Å],[11] $(C_6H_5)_2Se_2$ [1.93(5) Å][12] and $(C_6F_5)_2Se_2$ [1.910(15) Å].[12] Leaving aside the polymeric structure of **2**, the M—SeC_6H_5 geometry is quite similar to that in $[Pb(SeC_6H_5)_3]^-$.

Relationship between structure and properties

The most satisfying conclusion is that the structure of $In(SeC_6H_5)_3$ is indeed the homopolymer predicted from the chemical properties of the compound, although the details of the cross-linking could not be deduced from the general insolubility of the compound in non-donor solvents, or from its reaction with neutral or anionic donors.[2] Cross-linking by M ← S(Se) donation has frequently been proposed for the solid state structure of metal thiolates and selenolates, and the present work is in keeping with studies of $[Hg(SeCH_3)_2]_n$ and related compounds.[13]

Despite repeated attempts involving a variety of solution and vaporization techniques, we were unable to produce crystals of $In(SC_6H_5)_3$, and it is interesting to consider the possible reasons, given the relative ease with which the selenium analogue yielded good crystals. It seems certain that In—S bonds are thermodynamically stronger than In—Se bonds, which means that a homopolymeric $In(SC_6H_5)_3$ structure would be more stable to dissociation than $In(SeC_6H_5)_3$, and hence less soluble in organic solvents. In fact, the sulphur compound is soluble only in strong donors such as pyridine, or in refluxing benzene,[1] and complexation is clearly significant in the case of the donor solvents. A suitable solvent for crystallization is therefore lacking. Another factor acting against the formation of an ordered lattice may be the short In—S bonds, which as the present results show, are approx. 0.3 Å shorter than In—Se, so that a regular structure such as that in Fig. 1 may be difficult to replicate for $In(SC_6H_5)_3$, since the phenyl groups of one plane

may face considerable steric hindrance in packing with those of the next layer. Thus attempts to grow crystals of $In(SC_6H_5)_3$ from the vapour phase may be vitiated by irregular growth of the homopolymer, in contrast with the regular arrangement which is obviously possible for $In(SeC_6H_5)_3$.

A final conclusion to be drawn from the structure of $In(SeC_6H_5)_3$ is that the formation of adducts, such as $In(SeC_6H_5)_3L$ (L = 2,2′-bipyridine, 1,10-phenanthroline, or two triphenylphosphines) or $[InBr(SePh)_3]^-$, must involve a major rearrangement of the InSe kernel, assuming that these species are isostructural with the analogous SC_6H_5 compounds. The molecularity and stereochemistry of the species present in toluene, or in donor solvents, are clearly of importance in this context, and will be the subject of future investigations.

Acknowledgement—This work was supported in part by Operating Grants (to D.G.T.) from the Natural Sciences and Engineering Research Council of Canada.

REFERENCES

1. R. K. Chadha, P. C. Hayes, H. E. Mabrouk and D. G. Tuck, *Can. J. Chem.* 1987, **65**, 804.
2. H. E. Mabrouk, R. Kumar and D. G. Tuck, *J. Chem. Soc., Dalton Trans.* 1988, 1045.
3. J. H. Green, R. Kumar, N. Seudeal and D. G. Tuck, *Inorg. Chem.*, in press.
4. M. A. Khan, R. S. Steevensz, D. G. Tuck, J. G. Noltes and P. W. R. Corfield, *Inorg. Chem.* 1980, **19**, 3407.
5. G. M. Sheldrick, *Computing in Crystallography* (Edited by G. Shlenk), pp. 34–42. Delft Univ. Press (1978).
6. D. G. Tuck, *Comprehensive Organometallic Chemistry* (Edited by G. Wilkinson, F. G. A. Stone and E. W. Abel), Vol. 1, Chap. 7, pp. 683–723. Pergamon Press, Oxford (1982).
7. D. G. Tuck, *Comprehensive Coordination Chemistry* (Edited by G. Wilkinson, R. D. Gillard and J. A. McCleverty), Vol. 3, Chap. 25.2, pp. 153–182. Pergamon Press, Oxford (1987).
8. M. A. Khan, C. Peppe and D. G. Tuck, *Acta Cryst.* 1983, **C39**, 1339.
9. E. Krebs, D. Voelker and K. O. Stiller, *Inorg. Chim. Acta* 1982, **65**, L101.
10. M. A. Khan, C. Peppe and D. G. Tuck, *Can. J. Chem.* 1984, **62**, 601.
11. P. A. W. Dean, J. J. Vittal and N. C. Payne, *Inorg. Chem.* 1984, **23**, 4232.
12. C. M. Woodward, D. S. Brown, J. D. Lee and A. G. Massey, *J. Organometal. Chem.* 1976, **121**, 333.
13. A. P. Arnold, A. J. Canty, B. W. Skelton and A. H. White, *J. Chem. Soc., Dalton Trans.* 1982, 607.

Polyhedron Vol. 8, No. 7, pp. 873–877, 1989
Printed in Great Britain

0277–5387/89 $3.00+.00
© 1989 Pergamon Press plc

INFLUENCE OF 3-METHYL SUBSTITUTION ON THE ABILITY OF 2-PYRROLIDONE TO FORM HETEROMETALLIC POLYMERIC STRUCTURES; SYNTHESIS AND X-RAY CRYSTAL STRUCTURE OF $[HgCu(C_5H_8NO)_2(CH_3O)(NO_3)]_2$, WHERE C_5H_8NO IS THE ANION OF 3-METHYL-2-PYRROLIDONE

DAVID M. L. GOODGAME,* DAVID J. WILLIAMS and RICHARD E. P. WINPENNY

Chemistry Department, Imperial College of Science, Technology and Medicine, London SW7 2AY, U.K.

(*Received* 28 *September* 1988; *accepted* 27 *October* 1988)

Abstract—Reaction of $Hg(C_5H_8NO)_2$ (where C_5H_8NO is the anion of 3-methyl-2-pyrrolidone) with copper(II) nitrate in methanol yields $[HgCu(C_5H_8NO)_2(CH_3O)(NO_3)]_2$ which has been characterized by X-ray diffraction. The crystals are triclinic, $P\bar{1}$, $a = 7.041(3)$, $b = 11.343(4)$, $c = 11.427(4)$ Å, $\alpha = 69.13(3)$, $\beta = 76.08(3)$, $\gamma = 84.17(3)°$, $V = 828$ Å^3, $Z = 1$. The structure was refined on 1338 reflections to $R = 0.074$. The compound has pairs of copper atoms bridged by two methoxide ions. Each copper atom has a square pyramidal coordination geometry formed by five oxygen atoms, two from methoxide ions, one from NO_3^-, and one from each of two different $Hg(C_5H_8NO)_2$ units. These last two provide additional bridges between the basal and apical coordination sites of the bridged copper atoms and, in so doing, form 10-membered macrocyclic rings. Adjacent dimers are linked by pairs of Hg···O(nitrate) interactions, forming a loosely bound polymeric structure.

We have recently shown that $Hg(C_4H_6NO)_2$, the product of the reaction between mercury(II) acetate and 2-pyrrolidone (C_4H_7NO) in methanol, forms an extensive series of heterometallic complexes with diverse and unusual polymeric structures. These polymers have been found to form chains, e.g. $\{[Hg_3Co(C_4H_6NO)_6](NO_3)_2\}_n$,[1] $[Hg_2Eu(C_4H_6NO)_4(NO_3)_3]_n$,[2] $[Hg_3Tb_2(C_4H_6NO)_6(NO_3)_6]_n$,[2] and $[Hg_2Th(C_4H_6NO)_4(NO_3)_4]_n$,[3] corrugated sheets, e.g. $[Hg_2Cu(C_4H_6NO)_4(NO_3)_2]_n$,[4] or three-dimensional networks, e.g. $[Hg_3Zn_2(C_4H_6NO)_6(NO_3)_{3.33}(CH_3O)_{0.67}]_n$.[5]

The adoption of a particular structural type appears to be influenced by two main factors: (a) the preferred coordination number and geometry of the heterometal binding to the oxygen atoms of the $Hg(C_4H_6NO)_2$ unit; and (b) the ability of that unit to adopt many different conformational modes by ligand rotation about the N—Hg—N bonds, without any significant departure from linearity at the mercury centre.

We have also been exploring the effects of the presence of alkyl groups adjacent to the donor atoms in the pyrrolidone ring, as the resulting increase in steric requirements would be expected to modify the structures of the corresponding heterometallic complexes in ways that are not easy to predict, because of the conformational possibilities of the HgL_2 units.

We report here the structure of a tetranuclear (Hg_2Cu_2) complex obtained with 3-methyl-2-pyrrolidone as the bridging ligand.

EXPERIMENTAL

Preparation

Bis(3-methyl-2-pyrrolidonato)mercury(II) (0.8 g, 2 mmol), prepared by an analogous method to that used[1] for the 2-pyrrolidone analogue, was dis-

* Author to whom correspondence should be addressed.

solved in methanol (40 cm^3) and a solution of $Cu(NO_3)_2 \cdot 3H_2O$ (0.24 g, 1 mmol) in methanol (5 cm^3) was added. The solution was filtered and allowed to evaporate at 3°C. After 3 weeks, small, blue, plate-like crystals had formed above the level of the solution. Found: C, 23.2; H, 3.2; N, 7.6. Calc. for $HgCu(C_5H_8NO)_2(CH_3O)(NO_3)$: C, 23.9; H, 3.5; N, 7.6%. In addition to these blue crystals a large quantity of colourless $Hg(C_5H_8NO)_2 \cdot H_2O$ separated from the bulk solution. Found: C; 28.4; H, 4.3; N, 6.8. Calc. for $Hg(C_5H_8NO)_2H_2O$: C, 29.0; H, 4.4; N, 6.8%. Evaporation at room temperature gave only this latter compound.

X-ray study

$[HgCu(C_5H_8NO)_2(CH_3O)(NO_3)]_2$ crystallizes as pale blue plates. The crystal data are: triclinic, $a = 7.041(3)$, $b = 11.343(4)$, $c = 11.427(4)$ Å, $\alpha = 69.13(3)$, $\beta = 76.08(3)$, $\gamma = 84.17(3)°$, $V = 828$ Å^3, space group $P\bar{1}$, $Z = 1$ (the molecule is disposed about a centre of symmetry), $M_r = 1106$, $D_c = 2.14$ g cm^{-3}, μ(Cu-K_α) = 195 cm^{-1}. Refined unit cell parameters for a crystal of approximate dimensions $0.03 \times 0.06 \times 0.09$ mm were obtained by centring 18 reflections on a Nicolet R3m diffractometer. 1692 independent reflections ($\theta \leqslant 50°$) were measured with graphite monochromated Cu-K_α radiation using the omega-scan measuring routine. Of these, 1338 had $|F_o| > 3\sigma(|F_o|)$ and were considered observed. Lorentz, polarization and a numerical absorption correction (face indexed crystal, minimum and maximum transmission factors 0.25 and 0.58) were applied.

The structure was solved by the heavy-atom method which revealed the position of the mercury atom. The remaining non-hydrogen atoms were located from subsequent ΔF maps. Both 3-methyl-2-pyrrolidone ligands were severely disordered; for the first ligand it was possible to distinguish two geometries due to a conformational folding of the C(11) to C(14) portion of the ring; for the second, inversion of the methyl group [C(25)] occurs, giving two partial occupancy positions for this carbon, also high thermal motion for the remaining carbons of this ligand. For these reasons C(12a,b), C(13a,b), C(15a,b), C(21) and C(25a,b) were refined isotropically. The remaining atoms in the structure were refined anisotropically. No hydrogen atoms were included in the refinement. Refinement was by block-cascade full-matrix least-squares to $R = 0.074$, $R_w = 0.072$ [$w^{-1} = \sigma^2(F) + 0.001F^2$].

Computations were carried out on an Eclipse S140 computer using the SHELXTL program system.[6] Scattering factors were from ref. 7. Important bond lengths and angles are listed in Table 1.

Spectroscopy

The EPR spectrum was recorded on a polycrystalline sample at room temperature using a Q-band (*ca* 34 GHz) spectrometer comprising a Varian Q-band microwave bridge and a Newport 12-in type F magnet powered by a C905 rotary generator and post stabilizer.

Table 1. Bond lengths (Å) and angles (°) for **A**

Hg—Cu	3.180(4)	Hg—N(1)	1.975(16)
Hg—N(2′)	2.050(19)	Cu—O(1)	2.002(20)
Cu—O(2)	2.249(22)	Cu—O(3)	1.982(17)
Cu—O(6)	1.907(16)	Cu—Cu′	2.957(6)
Cu—O(6′)	1.903(17)		
Cu—Hg—N(1)	78.5(7)	Cu—Hg—N(2′)	101.3(7)
N(1)—Hg—N(2′)	174.6(9)	Hg—Cu—O(1)	74.3(6)
Hg—Cu—O(2)	157.7(5)	O(1)—Cu—O(2)	88.4(8)
Hg—Cu—O(3)	111.4(6)	O(1)—Cu—O(3)	89.4(8)
O(2)—Cu—O(3)	81.8(7)	Hg—Cu—O(6)	94.3(6)
O(1)—Cu—O(6)	168.5(9)	O(2)—Cu—O(6)	102.7(8)
O(3)—Cu—O(6)	94.7(7)	Hg—Cu—Cu′	77.6(1)
O(1)—Cu—Cu′	135.2(6)	O(2)—Cu—Cu′	106.9(6)
O(3)—Cu—Cu′	133.7(5)	O(6)—Cu—Cu′	39.0(5)
Hg—Cu—O(6′)	65.9(7)	O(1)—Cu—O(6′)	96.9(8)
O(2)—Cu—O(6′)	103.3(8)	O(3)—Cu—O(6′)	172.0(6)
O(6)—Cu—O(6′)	78.2(8)	Cu′—Cu—O(6′)	39.2(5)
Cu—O(6)—Cu′	101.8(8)		

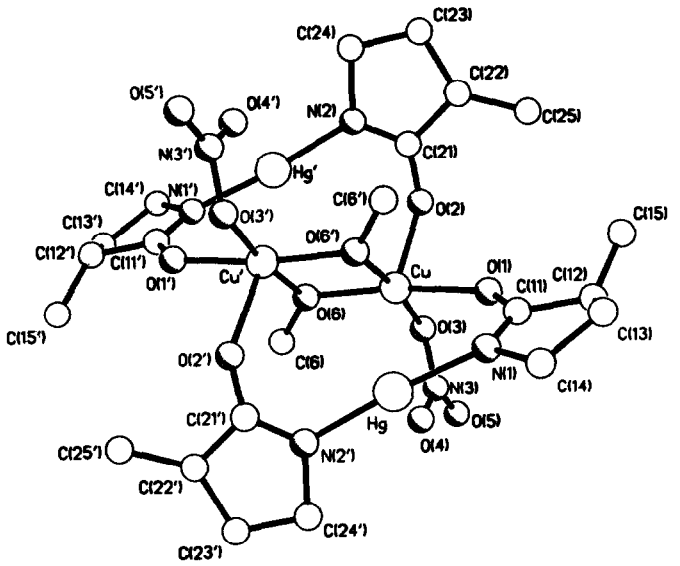

Fig. 1. Molecular structure of $[HgCu(C_5H_8NO)_2(CH_3O)(NO_3)]_2$ (where C_5H_8NO = the anion of 3-methyl-2-pyrrolidone) showing the crystallographic numbering scheme.

RESULTS AND DISCUSSION

The X-ray structural analysis on the blue crystals obtained from methanolic solutions of $Hg(C_5H_8NO)_2$ and copper(II) nitrate show that the compound has the stoichiometry $HgCu(C_5H_8NO)_2(CH_3O)(NO_3)$ (**A**), and that two such units are bridged by the methoxide ions to form the tetranuclear (Cu_2Hg_2) complex shown in Fig. 1.

The copper atoms are five-coordinate with distorted square pyramidal geometry. The atoms comprising the base are: one oxygen from 3-methyl-2-pyrrolidone, one from a nitrate ion, and two from the bridging methoxide ions. Deprotonation of methanol to form such methoxide bridges is well-known.[8-10] The apical oxygen comes from the second pyrrolidone ligand within the asymmetric unit.

The Cu—O bond lengths differ, the shortest being those involved in the formation of the Cu_2O_2 ring (*ca* 1.90 Å). The next shortest are the remaining basal Cu—O bonds (*ca* 1.99 Å) and, as expected, the longest bond is to the apical oxygen [2.25(2) Å]. A similar variation occurs in $Cu_2[o\text{-}Ph_2PC_6H_4C(O)CHC(O)C(CH_3)]_2(OCH_3)_2$ (**B**). There the bridging oxygens have Cu—O distances of *ca* 1.92 Å, the remaining basal oxygens *ca* 1.94 Å, and the apical Cu—O bond = 2.42(1) Å.

Symmetry requires that the Cu_2O_2 ring in **A** is planar; the Cu—O—Cu′ angle is 102°. The Cu—Cu′ distance (2.96 Å) is very similar to that in related compounds, e.g. in **B**, Cu—Cu = 2.98 Å, and in $Cu_2Cl_2(pyridine)_2(OCH_3)_2$[9] Cu—Cu = 3.04 Å. The Cu···Cu interactions in **A** are sufficient to remove any ^{63}Cu hyperfine splitting from the EPR spectrum of the compound, but they are not strong enough to produce an $S = 1$ type of spectrum. Instead, a normal $S = 1/2$ spectrum ($g_z = 2.34$, $g_{xy} = 2.08$) was observed at room temperature at Q-band frequency.

A sixth coordination position of each Cu^{II} ion is occupied by a mercury atom (Fig. 2). The Hg···Cu distance (3.18 Å), although fairly short, is probably too long to be considered as a formal Hg—Cu bond. The presence of the mercury atom prevents the approach of any other potential ligands. The Hg coordination is very similar to that seen in complexes of 2-pyrrolidone,[1-5] with Hg—N bonds of

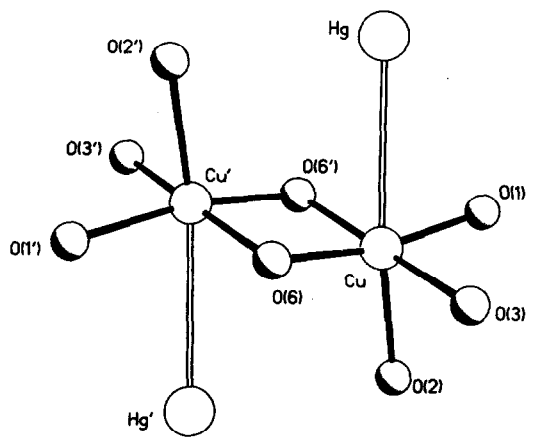

Fig. 2. The coordination environments of the two copper atoms in the dimeric unit.

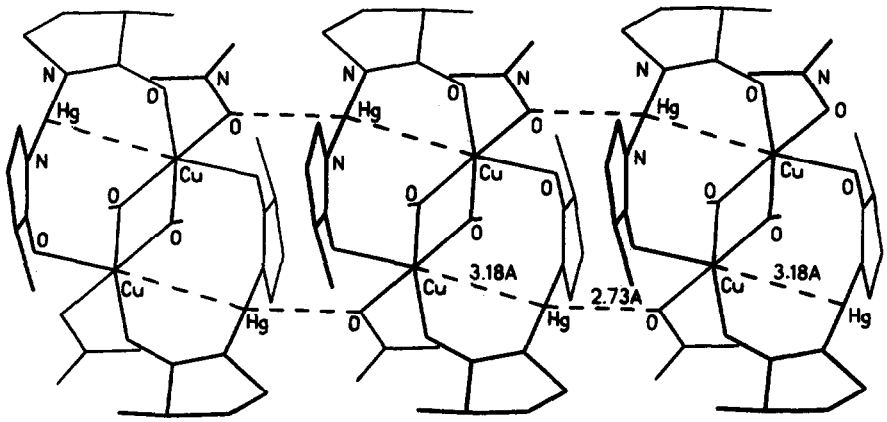

Fig. 3. Linking of adjacent dimers in the *a* direction *via* pairs of weak Hg···O(nitrate) interactions.

1.99 and 2.03 Å and an approximately linear N—Hg—N unit (175°). The slight departure from linearity is probably caused by inter-dimer interactions between a nitrate oxygen O(3) in one dimer and Hg′ in another [Hg′—O(3) = 2.73 Å]. Interestingly, the Hg′···O(3) vector makes a trigonal approach to the nitrate oxygen, with Cu, O(3), N(3), and Hg′ coplanar within 0.05 Å. Though these are the only inter-dimer links they do result in the formation of a loosely linked polymer (Fig. 3). A related, but more extensive, anion mediated network exists in $[HgAg(C_4H_6NO)_2(NO_3)]_2$, a dimeric complex involving 2-pyrrolidone.[11]

An important feature of the structures of the heterometallic complexes formed by 2-pyrrolidone is the presence of macrocyclic rings: 8-membered,[11] 16-membered,[1-3] or 32-membered.[4] In the present complex 10-membered rings are formed by each HgL_2 unit spanning the two copper centres, with basal coordination to one and apical coordination to the other. To achieve this there is a noticeable twist of the ligands about the mercury atom, with the angle between the mean planes of the two ligands being 74.2°.

The way in which dimerization is achieved in **A**, viz. methoxide bridges supplemented by the spanning action of the 3-methyl-2-pyrrolidone across the two copper centres, contrasts markedly with the situation in $[HgAg(C_4H_6NO)_2(NO_3)]_2$.[11] In that case, each HgL_2 unit binds to a silver atom in a chelating fashion, but with one of the oxygen atoms additionally serving as a bridging atom to the other silver atom of the dimer, forming an Ag_2O_2 ring.[11] It is tempting to ascribe the absence of this dimerization mode in **A** to the preferred geometry at copper which, for *cis*-binding at copper, requires a much smaller O_{bridge}—Cu—$O_{terminal}$ angle (*ca* 96° in **A**) than the corresponding O—Ag—O angles (*ca* 135 and 142°) in the Hg–Ag complex. This angle reduction would require bending of the HgL_2 unit.

However, this problem would not arise if the oxygens of HgL_2 were to occupy *trans*-positions about copper in forming an $O_{bridging}$—Cu—$O_{terminal}$ ring system. Therefore, it seems more likely that the dimerization mode adopted in **A** reflects the ease of methoxide bridge formation by Cu^{II} ions. Indeed, it might be more fruitful to regard these HgL_2 "ligands" as being able to span appropriate dinuclear metal units in uncommon ways, as well as forming extended polymers.

The drastic structural change from the sheet polymer formed[4] by the reaction of Hg(2-pyrrolidone)$_2$ and copper(II) nitrate, to the tetranuclear structure of **A** by the use of 3-methyl-2-pyrrolidone, suggests that these substituted analogues merit further attention, particularly in view of the diversity of structural types found so far for the unsubstituted ligand upon metal variation.

Acknowledgement—We thank the SERC for the diffractometer, the EPR spectrometer, and for a Research Studentship (to R.E.P.W.).

REFERENCES

1. D. M. L. Goodgame, D. J. Williams and R. E. P. Winpenny, *Angew. Chem. Int. Ed. Engl.* 1988, **27**, 261.
2. D. M. L. Goodgame, D. J. Williams and R. E. P. Winpenny, *J. Chem. Soc., Chem. Commun.* 1988, 437.
3. D. M. L. Goodgame, D. J. Williams and R. E. P. Winpenny, *Polyhedron* 1988, **7**, 1807.
4. D. M. L. Goodgame, D. J. Williams and R. E. P. Winpenny, *Angew. Chem. Int. Ed. Engl* 1987, **26**, 1044.
5. R. E. P. Winpenny, Ph.D. Thesis, London Univ., 1988.
6. G. M. Sheldrick, SHELXTL (Revision 4.1), An Integrated System for Solving, Refining, and Displaying

Crystal Structures from Diffraction Data, Univ. of Göttingen, F.R.G. (1983).
7. *International Tables for X-ray Crystallography*, Vol. IV, pp. 99, 149. Kynoch Press, Birmingham, U.K. (1974).
8. D. A. Wrobleski, J. B. Rauchfuss, A. L. Rheingold and K. A. Lewis, *Inorg. Chem.* 1984, **23**, 3124.
9. R. Willett and G. L. Breneman, *Inorg. Chem.* 1983, **22**, 326.
10. M. Yanashita, H. Ito and T. Ito, *Inorg. Chem.* 1983, **22**, 2101.
11. D. M. L. Goodgame, D. J. Williams and R. E. P. Winpenny, *Polyhedron* 1988, **7**, 1299.

Polyhedron Vol. 8, No. 7, pp. 879–886, 1989
Printed in Great Britain

0277–5387/89 $3.00+.00
© 1989 Pergamon Press plc

THE SYNTHESIS, COORDINATION AND ELECTROCHEMICAL STUDIES OF METALLOCENE BIS(CROWN ETHER) RECEPTOR MOLECULES. SINGLE-CRYSTAL X-RAY STRUCTURE OF A FERROCENE BIS(CROWN ETHER) POTASSIUM COMPLEX

PAUL D. BEER* and HARRISON SIKANYIKA

Department of Chemistry, University of Birmingham, P.O. Box 363, Birmingham B15 2TT, U.K.

and

ALEXANDRA M. Z. SLAWIN and DAVID J. WILLIAMS

Chemical Crystallography Laboratory, Department of Chemistry, Imperial College, London SW7 2AY, U.K.

(*Received* 3 *October* 1988; *accepted* 31 *October* 1988)

Abstract—The condensation of 1,1′-bis(chlorocarbonyl)ferrocene and 1,1′-bis(chlorocarbonyl)ruthenocene with 4-aminobenzo-15-crown-5 gives the metallocene bis(crown ether) ligands 1,1′-bis[(2,3,5,6,8,9,11,12-octahydro-1,4,7,10,13-benzopentaoxacyclopentadecin-15-yl)amino]carbonylferrocene (**4**) and the ruthenocene analogue (**5**). ^{13}C NMR titrations of **4** and **5** with Na^+, K^+ and Cs^+ alkali metal salts lead to titration curves interpreted as suggesting 1 : 1 stoichiometry. The single-crystal X-ray structure of [**4**K]$PF_6 \cdot$ 4MeOH reveals an intramolecular sandwich complex with the potassium guest cation in the solid state. Competition fast atom bombardment (FAB) mass spectrometry selectivity experiments show **4** and **5** to exhibit exclusive K^+ selective complexation over either Na^+ or Cs^+.

Responsive macrocyclic receptor molecules whose binding strength and/or selectivity towards guest species can be influenced by physical and chemical means, have been the subject of many recent reports in the chemical literature.[1–5] Examples include pH-responsive crown ethers,[2,3,6,7] which change their cation binding ability in response to medium pH and photoresponsive crown ethers,[1,8] azoarene-capped oxygen macrocycles which undergo photo-induced reversible interconversion between the *trans* and *cis* azo linkages resulting in substantial changes in their cation binding properties.

Particular attention has been focused on the synthesis of redox-responsive macrocycles that contain redox-active functions such as quinone,[9–14] nitrobenzene[15] and metallocene moieties[16–23] in close proximity to a cation binding site. We are currently interested in preparing metallocene redox-active macropolycyclic host molecules designed to be *selective* as well as being redox-responsive to the host binding of inorganic and organic guest species.[19–22] One application of such receptors lies in their potential development as components of new chemical sensory devices.

We report here the synthesis, coordination and electrochemical studies of two new metallocene bis-benzo-crown ethers, **4** and **5**, and the single-crystal X-ray structure of [**4**K]$PF_6 \cdot$ 4MeOH, which, to our knowledge, is the *first* structural example of a bis-benzo-crown ether potassium intramolecular sandwich complex. A preliminary report on this work has recently been published.[19]

* Author to whom correspondence should be addressed.

RESULTS AND DISCUSSION

Synthesis of 4 *and* 5

The condensation of respective 1,1′-bis(chlorocarbonyl)metallocenes **1** and **2**[24] with 2 mol of 4-aminobenzo-15-crown-5 (**3**)[25] in the presence of triethylamine gave, after column chromatography (alumina, 99% CH_2Cl_2, 1% MeOH), the ferrocene bis(crown ether) (**4**: 80% yield) and the ruthenocene analogue (**5**: 75% yield), Scheme 1 (preparative details are given in the Experimental).

The structures of both new air-stable metallocene bis(crown ethers) were characterized by elemental analysis, mass spectrometry and ^1H (Tables 1 and 2) and ^{13}C NMR spectroscopy (Tables 3 and 4).

Coordination studies

^{13}C NMR spectroscopy was used initially to investigate the complexation of **4** and **5** with alkali metal cations sodium, potassium and caesium.[26] The stepwise addition of an alkali metal nitrate salt to a methanol (65%)–acetone (35%) solution of **4** and a methanol (65%)–dichloromethane (35%) solution of **5** led to considerable shifts of the OCH_2 carbons of the respective bis(crown molecules). In all cases the $\Delta\delta$ ppm versus [alkali metal salt]/[metallocene bis(crown ether)] titration curves can

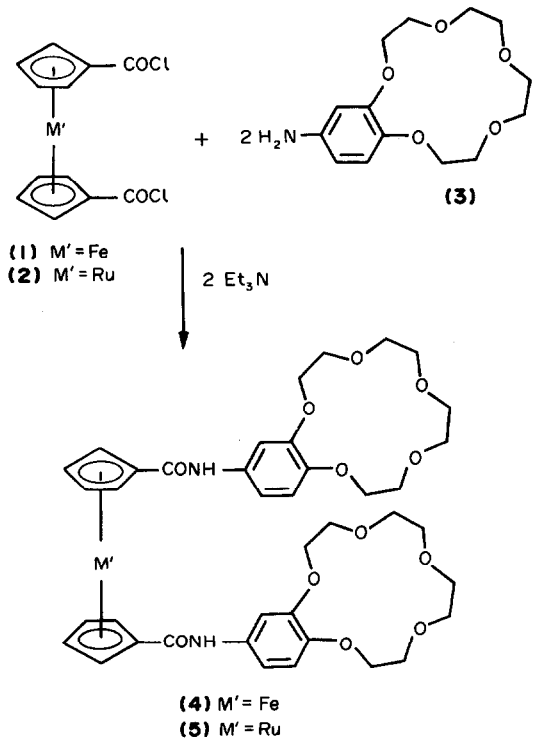

Scheme 1.

Table 1. ^1H NMR data for **4** (solvent $CDCl_3$; reference TMS)

δ (ppm)		Assignment
3.73–4.13	(*m*, 32 H)	Crown protons
4.39[a]	(*t*, *J* 1.8 Hz, 4H)	Ferrocenyl
4.60[a]	(*t*, *J* 1.8 Hz, 4H)	
6.82	(*d*, *J* 8.7 Hz, 2H)	
7.20	(*d* of *d*, *J* 8.7 Hz, *J* 2 Hz, 2H)	Aromatics
7.55	(*d*, *J* 2 Hz, 2H)	
8.87	(*s*, broad, 2H)	NH

[a] 'Apparent triplet' assigned as an AA′BB′ system.

Table 2. ^1H NMR data for **5** (solvent $CDCl_3$; reference TMS)

δ (ppm)		Assignment
3.72–4.10	(*m*, 32H)	Crown protons
4.72[a]	(*t*, *J* 1.7 Hz, 4H)	Ruthenocenyl
5.01[a]	(*t*, *J* 1.7 Hz, 4H)	
6.75	(*d*, *J* 8.7 Hz, 2H)	
7.09	(*d* of *d*, *J* 8.7 Hz, *J* 2 Hz, 2H)	Aromatics
7.42	(*d*, *J* 2 Hz, 2H)	
8.38	(*s*, broad, 2H)	NH

[a] 'Apparent triplet' assigned as an AA′BB′ system.

Table 3. ^{13}C NMR data for **4** from broad band decoupled and DEPT spectra (solvent $CDCl_3$; reference TMS)

δ (ppm)	Assignment
68.83	OCH_2
69.39	
69.62	
69.71	
70.38	
70.53	
70.88	
70.96	
71.07 (**4**)[a]	Ferrocene-C
79.27	Ferrocene-C(ipso)
107.01	Aromatics
112.32	
114.94	
132.78	
145.60	
149.30	
168.65	C=O

[a] Relative integration.

Table 4. ^{13}C NMR data for **5** from broad band decoupled and DEPT spectra (solvent $CDCl_3$; reference TMS)

δ (ppm)	Assignment
68.74	OCH_2
69.38	
69.61	
69.65	
70.36	
70.52	
70.87	
70.96	
72.66 (**2**)[a]	Ruthenocene-C
73.25 (**2**)[a]	
83.35	Ruthenocene-C(ipso)
107.01	Aromatics
112.38	
114.78	
132.53	
145.54	
149.19	
167.05	C=O

[a] Relative integration.

be interpreted as suggesting 1 : 1 stoichiometry of metallocene bis(crown ether) to guest alkali metal cation (Fig. 1). This result may lead to the proposition that both **4** and **5**, in solution, are adopting a conformation in which the amido-benzo-15-crown-5 units are lying either cofacial or in close proximity to one another and are acting co-operatively to form intramolecular sandwich complexes with the alkali metal cation guest species. In contrast to this observation, a recent publication reports the 18-crown-6 units of a related ferrocene bis(crown ether) to be acting independently of one another and complexing two alkali metal guest ions.[27]

Refluxing aqueous-methanolic solutions of **4** with an excess amount of sodium or potassium hexafluorophosphate led to the successful isolation of the respective [**4**M]$PF_6 \cdot H_2O$, M = Na, K, complexes (see Table 5 for elemental analyses).

The single-crystal structure of [**4**K]$PF_6 \cdot 4MeOH$ is illustrated in Fig. 2 with the space-filling representation of the structure in Fig. 3. The structure confirms the intramolecular sandwich complex with the potassium guest cation in the solid state. Selected bond lengths and bond angles are listed in Tables 6 and 7, respectively. The torsional angles associated with the crown ether rings are shown in Table 8. These values are similar to those of benzo-15-crown-5 itself[28] and one conformer in the $NaClO_4$ (benzo-15-crown-5)$_2$ sandwich.[29] The potassium guest cation is coordinated to all 10 oxygen atoms of the two benzo-crown ether moieties in an irregular pentagonal antiprismatic configuration with K—O contact distances ranging

Table 5. Microanalytical (%)[a] data

Compound	C	H	N
4	59.9(59.7)	5.8(6.0)	3.3(3.5)
5	56.6(56.4)	5.8(5.6)	3.4(3.3)
[**4**K]$PF_6 \cdot H_2O$	47.7(47.7)	5.0(4.9)	2.8(2.9)
[**4**Na]$PF_6 \cdot H_2O$	48.5(49.4)	5.5(5.5)	2.7(2.8)

[a] Calculated values are in parentheses.

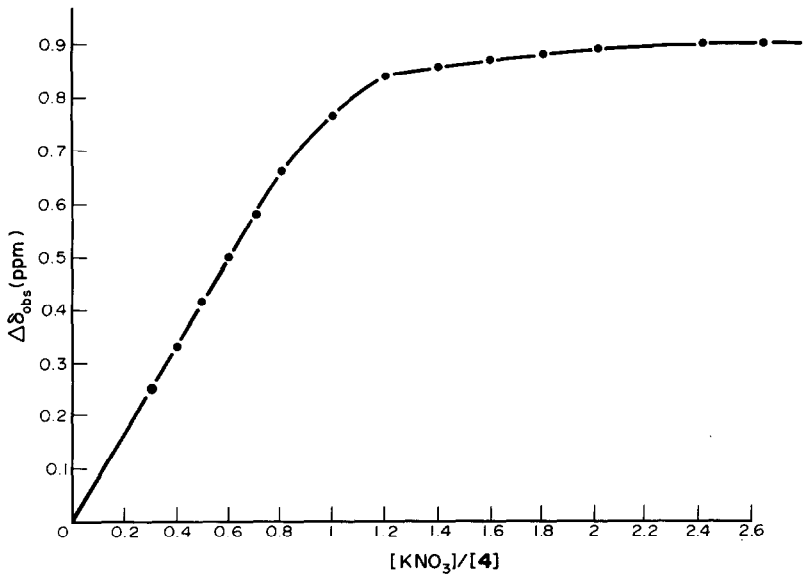

Fig. 1. ^{13}C NMR titration curve of **4** and potassium nitrate.

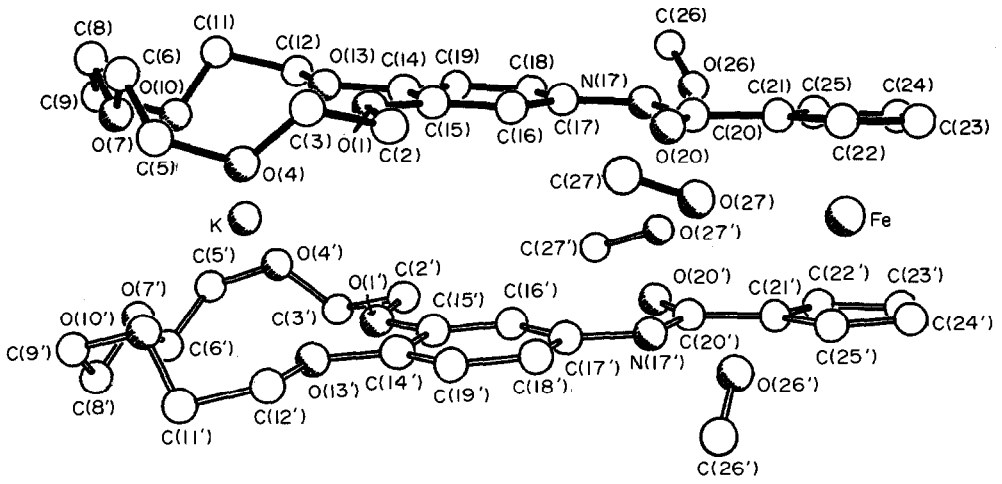

Fig. 2. The skeletal representation of the solid-state structure of [**4**K]PF_6·4MeOH.

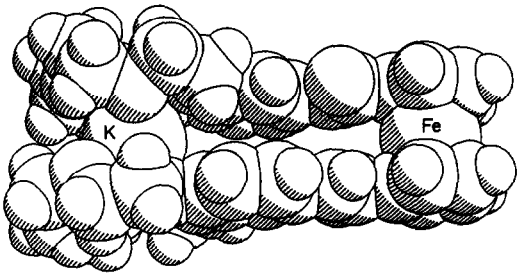

Fig. 3. The space-filling representation of the solid-state structure of the 1 : 1 complex formed between **4** and potassium.

from 2.82 to 2.97 Å (Table 9). These distances compare with 2.78–2.96 Å in the KI (benzo-15-crown-5)$_2$ crystal structure reported by Truter.[30] In contrast to Truter's structure, it is noteworthy that the two shortest K—O contact distances are *not* those from the catechol oxygens but are from K—O(4) and K—O(7) (Table 9). Unlike the centrosymmetrical arrangement of the two benzo-crown ligands in the KI (benzo-15-crown-5)$_2$ structure,[30] here the two components of the sandwich are related by a two-fold axis that passes through the Fe and K atoms with the benzo-crown moieties of **4** being *gauche* to each other. The cyclo-

Table 6. Bond lengths (Å) with ESDs in parentheses

Fe—C(21)	2.043(4)	Fe—C(22)	2.038(5)
Fe—C(23)	2.043(5)	Fe—C(24)	2.020(5)
Fe—C(25)	2.040(4)	Fe—C(21a)	2.043(4)
Fe—C(22a)	2.038(5)	Fe—C(23a)	2.043(5)
Fe—C(24a)	2.020(5)	Fe—C(25a)	2.040(4)
O(1)—C(2)	1.412(5)	O(1)—C(15)	1.377(5)
C(2)—C(3)	1.503(7)	C(3)—O(4)	1.416(6)
O(4)—C(5)	1.416(6)	C(5)—C(6)	1.465(7)
C(6)—O(7)	1.436(7)	O(7)—C(8)	1.411(6)
C(8)—C(9)	1.484(9)	C(9)—O(10)	1.435(6)
O(10)—C(11)	1.416(6)	C(11)—C(12)	1.487(7)
C(12)—O(13)	1.435(6)	O(13)—C(14)	1.356(5)
C(14)—C(15)	1.399(6)	C(14)—C(19)	1.380(7)
C(15)—C(16)	1.367(6)	C(16)—C(17)	1.407(7)
C(17)—C(18)	1.379(7)	C(17)—N(17)	1.404(6)
C(10)—C(19)	1.388(7)	N(17)—C(20)	1.355(6)
C(20)—O(20)	1.224(6)	C(20)—C(21)	1.483(7)
C(21)—C(22)	1.413(7)	C(21)—C(25)	1.435(7)
C(22)—C(23)	1.418(7)	C(23)—C(24)	1.399(7)
C(24)—C(25)	1.413(7)	O(26)—C(26)	1.396(8)
O(27)—C(27)	1.391(10)	P—F(1)	1.576(5)

Table 7. Bond angles (°) with ESDs in parentheses

C(2)—O(1)—C(15)	119.4(3)	O(1)—C(2)—C(3)	105.7(4)
C(2)—C(3)—O(4)	109.3(4)	C(3)—O(4)—C(5)	114.3(4)
O(4)—C(5)—C(6)	113.9(4)	C(5)—C(6)—O(7)	108.7(4)
C(6)—O(7)—C(8)	110.7(4)	O(7)—C(8)—C(9)	109.3(4)
C(8)—C(9)—O(10)	113.3(4)	C(9)—O(10)—C(11)	113.1(4)
O(10)—C(11)—C(12)	109.5(4)	C(11)—C(12)—O(13)	106.1(4)
C(12)—O(13)—C(14)	118.6(3)	O(13)—C(14)—C(15)	115.5(4)
O(13)—C(14)—C(19)	125.9(4)	C(15)—C(14)—C(19)	118.5(4)
O(1)—C(15)—C(14)	113.5(4)	O(1)—C(15)—C(16)	124.4(4)
C(14)—C(15)—C(16)	122.1(4)	C(15)—C(16)—C(17)	119.0(4)
C(16)—C(17)—C(18)	119.0(4)	C(16)—C(17)—N(17)	123.5(4)
C(18)—C(17)—N(17)	117.4(4)	C(17)—C(18)—C(19)	121.4(5)
C(14)—C(19)—C(18)	119.8(4)	C(17)—N(17)—C(20)	128.6(4)
N(17)—C(20)—O(20)	123.0(4)	N(17)—C(20)—C(21)	116.3(4)
O(20)—C(20)—C(21)	120.7(4)	C(20)—C(21)—C(22)	123.2(4)
C(20)—C(21)—C(25)	129.6(4)	C(22)—C(21)—C(25)	107.2(4)
C(21)—C(22)—C(23)	108.9(4)	C(22)—C(23)—C(24)	107.2(4)
C(23)—C(24)—C(25)	109.6(4)	C(21)—C(25)—C(24)	107.0(4)

Table 8. Torsional angles (°) associated with the crown ether rings with ESDs in parentheses

C(15)	O(1)	C(2)	C(3)	167.8(4)
C(2)	O(1)	C(15)	C(14)	176.5(4)
C(2)	O(1)	C(15)	C(16)	−5.0(6)
O(1)	C(2)	C(3)	O(4)	61.3(4)
C(2)	C(3)	O(4)	C(5)	−163.5(4)
C(3)	O(4)	C(5)	C(6)	85.3(6)
O(4)	C(5)	C(6)	O(7)	66.9(6)
C(5)	C(6)	O(7)	C(8)	−177.7(4)
C(6)	O(7)	C(8)	C(9)	172.1(4)
O(7)	C(8)	C(9)	O(10)	−64.1(5)
C(8)	C(9)	O(10)	C(11)	−79.8(5)
C(9)	O(10)	C(11)	C(12)	165.5(4)
O(10)	C(11)	C(12)	O(13)	−62.5(5)
C(11)	C(12)	O(13)	C(14)	−168.2(4)
C(12)	O(13)	C(14)	C(15)	178.2(4)
C(12)	O(13)	C(14)	C(19)	−2.3(6)
O(13)	C(14)	C(15)	O(1)	0.1(5)
O(13)	C(14)	C(15)	C(16)	−178.4(4)
C(19)	C(14)	C(15)	O(1)	−179.4(4)
C(19)	C(14)	C(15)	C(16)	2.0(7)
O(13)	C(14)	C(19)	C(18)	178.9(4)
O(1)	C(15)	C(16)	C(17)	−178.3(4)
C(14)	C(15)	C(16)	C(17)	0.0(6)
C(15)	C(16)	C(17)	C(18)	−2.5(6)
C(16)	C(17)	C(18)	C(19)	3.0(7)
C(17)	C(18)	C(19)	C(14)	−0.9(7)

Table 9. K—O contact distances (Å)

K—O(1)	2.97(1)
K—O(4)	2.88(1)
K—O(7)	2.82(1)
K—O(10)	2.86(1)
K—O(13)	2.91(1)

pentadienyl rings of the ferrocene unit are almost parallel (3.4° between their mean planes and a mean inter-ring separation of 3.3 Å) and rotated from an eclipsed orientation by *ca* 7° (Fig. 4). Similar geometries are found in low temperature triclinic,[29] orthorhombic[30] forms of ferrocene, 1-acetyl-1′-benzoyl-ferrocene,[31] acetyl-ferrocene,[32] diacetyl-ferrocene[33] and ferrocene–carboxylic acid[34] where ring orientations range from eclipsed (0°) to 14° from eclipsed.[31] The cyclopentadienyl ring, the amide group and the benzo ring are not all coplanar there being small torsional rotations about the C(20)—C(21) [N(17), C(20), C(21), C(22) torsion angle 174.1(4)°] and the C(17)—N(17) [C(18), C(17), N(17), C(20) torsion angle −176.8(4)°] bonds.

There are four molecules of methanol for each molecule of the complex, forming strong hydrogen bonds to each other and more weakly to the amido linkages of the ligand. It is noteworthy that X-ray quality crystals of the complex rapidly degrade in air indicating that the methanol molecules are essential to the structure of the crystal.

Fast atom bombardment mass spectrometry selectivity studies

Fast atom bombardment (FAB) mass spectrometry, a new powerful semi-quantitative technique, has been used to study the selectivity of *monocyclic* crown ethers for metal cations in competition experiments.[37] It seemed reasonable to apply this method for the first time to bis(crown) ethers.

Individual FAB mass spectrometric experiments

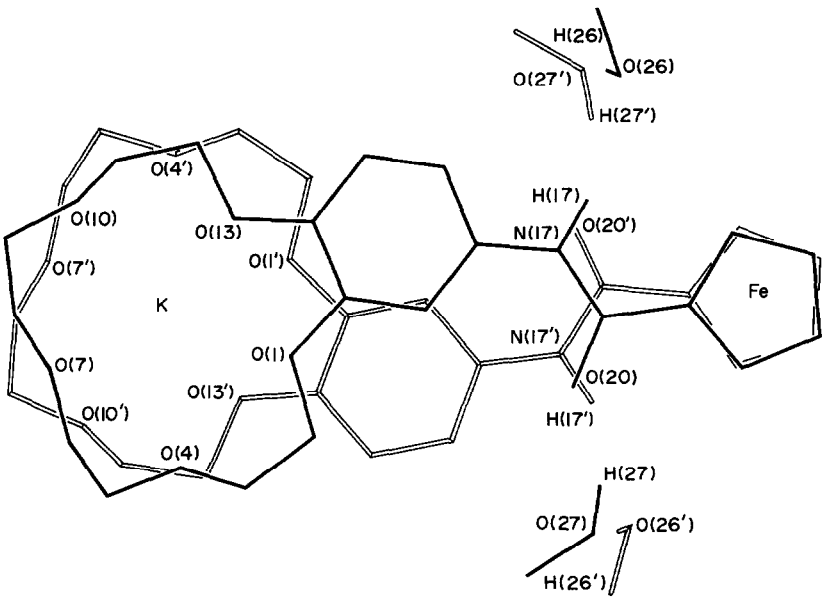

Fig. 4. View of the complex normal to the plane of the upper ("heavy bonds") cyclopentadienyl ring. Hydrogen bonding geometries: $O_{20}\cdots O_{27}$ 2.71 Å, $O_{20}\cdots H_{27}$ 1.79 Å, O···H—O < 154°, $O_{26}\cdots O_{27}$ 2.71 Å, $H_{26}\cdots O_{27}$ 1.73 Å, O···H—O < 175°, $N_{17}\cdots O_{26}$ 3.13 Å, $H_{17}\cdots O_{26}$ 2.19 Å, N—H···O < 161°.

of **4** (5×10^{-3} M; 0.5 cm^3 65% methanol–35% acetone) and **5** (5×10^{-3} M; 0.5 cm^3 65% methanol–35% dichloromethane) with the nitrates of sodium, potassium and caesium (5×10^{-3} M; 0.5 cm^3 water–1.0 cm^3 glycerol) gave gas-phase [bis(crown ether)+metal]$^+$ ions at *m/z* values of 1 : 1 stoichiometric formulations. Analogous competition experiments of **4** and **5** with an aqueous solution of sodium, potassium and caesium nitrates each at a concentration of 5×10^{-3} M gave the respective [**4**+potassium]$^+$ ion (*m/z* 843) and [**5**+potassium]$^+$ ion (*m/z* 889), exclusively.

The exclusive selectivity exhibited by both **4** and **5** towards potassium suggests that a well-defined cavity exists between the amido-benzo-15-crown-5 units which provides an optimal spatial fit[38] for the potassium guest cation (see Figs 2 and 3).

It is interesting to note that related bis(benzo-15-crown-5) and bis(benzo-18-crown-6) ether ligands linked together by various alkyl and alkoxy moieties, preferentially extract alkali metal cations larger than the hole size of the respective benzo-crown ether unit[39,40] (K^+ and Cs^+, respectively); this change of selectivity has been called the "bis crown effect".[41]

Electrochemical studies

The results of cyclic voltammetry measurements in acetonitrile of **4** and **5** are reported in Table 10. Addition of one or more equivalents of sodium or potassium hexafluorophosphate to the electrochemical acetonitrile solutions of **4** had little effect ($\Delta E_{1/2} \leqslant 20$ mV) on the reversible ferrocenyl oxidation wave. This result implies that the alkali metal cation complexed at the benzo-crown ether coordinating sites, is too far away to influence the electron density at the ferrocene iron atom, either inductively or through space.

Table 10. Electrochemical data

Compound	$E_{1/2}$[a] (V)	ΔE_p[b] (mV)
4	0.79	100(70)
5	0.55[c]	—

[a] Obtained from cyclic voltammetry studies in acetonitrile solvent containing 0.2 M $[Bu^n_4N]BF_4$ as supporting electrolyte. Solutions were *ca* 2×10^{-3} M in the compound and measurements were made at 21 ± 1°C at 0.2 V s^{-1} scan rate using a Pt bead working electrode with ferrocene internal reference. Values are quoted relative to the saturated calomel reference electrode.

[b] Separation between anodic and cathodic peak potentials, values for ferrocene under the same conditions in parentheses. No compensation was made for internal cell resistance.

[c] Anodic peak potential for an irreversible process.

We are currently synthesizing related Group 1A selective metallocene receptor molecules designed to have the cation binding site in closer proximity to the redox-active centre.

EXPERIMENTAL

Reactions were carried out under an atmosphere of dry nitrogen and solvents were distilled prior to use from an appropriate drying agent. ^{1}H NMR spectra were recorded at 400 MHz and ^{13}C NMR spectra at 100 MHz using tetramethylsilane (TMS) as internal standard. Electrochemical measurements were performed on a PAR 174A polarographic analyser. Positive ion FAB mass spectrometry was performed using a primary atom beam of Ar (6 keV) on a Kratos MS80 RF mass spectrometer coupled to a Kratos DS55 data system.

1,1′-Bis(chlorocarbonyl)ferrocene, 1,1′-bis(chlorocarbonyl)ruthenocene and 4-aminobenzo-15-crown-5 were prepared according to literature procedures.[24,25]

1,1′-*Bis*{[(2,3,5,6,8,9,11,12-*octahydro*-1,4,7,10,13-*benzopentaoxacyclopentadecin* - 15 - *yl*) - *amino*]-*carbonyl*}*ferrocene* (4)

A solution of 1,1′-bis(chlorocarbonyl)ferrocene (**1**) (0.5 g, 1.61 mmol) in dry toluene (70 cm^3) was added dropwise over 30 min to a stirred solution of 4-aminobenzo-15-crown-5 (**3**; 0.91 g, 3.2 mmol) in toluene (100 cm^3) containing triethylamine (0.32 g, 3.2 mmol). When addition was complete stirring was continued for 1 h and the solution filtered. After removal of solvent the crude product was chromatographed on a column of alumina using 99% dichloromethane–1% methanol eluant. An orange band was collected and after solvents were removed recrystallization from dichloromethane–hexane gave **4** (1.03 g, 80%) as orange crystals, m.p. 198–199°C; *m/z* 804.

1,1′-*Bis*{[(2,3,5,6,8,9,11,12-*octahydro*-1,4,7,10,13-*benzopentaoxacyclopentadecin* - 15 - *yl*) - *amino*]-*carbonyl*}*ruthenocene* (5)

The procedure for the preparation of **5** followed that described for **4**. A solution of 1,1′-bis(chlorocarbonyl)ruthenocene (**2**) (0.6 g, 1.68 mmol) in dry toluene (50 cm^3) was added dropwise over 30 min to a stirred solution of 4-aminobenzo-15-crown-5 (0.95 g, 3.3 mmol) in toluene (70 cm^3) containing triethylamine (0.34 g, 3.3 mmol). When addition was complete stirring was continued for 1 h and the solution filtered. Removal of solvent gave the crude product which was chromatographed on an alumina column using 99% dichloromethane–1% methanol. A pale yellow band was collected and removal of solvents followed by recrystallization from dichoromethane–hexane gave **5** (0.98 g, 75%) as pale yellow crystals, m.p. 206–207°C; *m/z* 850.

Preparation of sodium and potassium complexes of 4

To a methanolic solution of **4** (1 mmol) was added an excess amount of alkali metal hexafluorophosphate salt (5 mmol). The resulting solution was refluxed for 30 min and upon cooling an orange precipitate was collected and dried *in vacuo*. Recrystallization from methanol gave the respective complexes in quantitative yields.

^{13}C *NMR titration experiments*

The experimental procedure consisted of measuring $\Delta\delta_{obs}$ as a function of changing alkali metal nitrate salt concentrations while the metallocene bis(crown ether) ligand's concentration was kept constant. In a typical experiment, **4** (30 mg, 0.373 mmol) was dissolved in 65% methanol–35% acetone (4 cm^3) and the resulting solution transferred to a ^{13}C NMR tube. The ^{13}C NMR chemical shifts were measured versus tetramethylsilane (TMS) as internal standard after each addition of $NaNO_3$, KNO_3 and $CsNO_3$, respectively. Titration curves were obtained by plotting $\Delta\delta_{obs}$ (ppm) versus $[MNO_3]/[\mathbf{4}]$. See Fig. 1 in Results and Discussion.

*Crystal data**

$C_{40}H_{48}N_2O_{12}KFe \cdot PF_6 \cdot (CH_3OH)_4$, $M = 1116.9$, monoclinic, space group $C2/c$, $a = 14.283(3)$, $b = 25.726(5)$, $c = 14.438(2)$ Å, $\beta = 101.53(2)°$, $V = 5198$ Å^3, $Z = 4$ (the complex is disposed about a two-fold axis), $D_c = 1.43$ g cm^{-3}, $\mu = 41$ cm^{-1}, $F(000) = 2332$.

Data collection. 2672 unique independent reflections ($2\theta \leqslant 100°$C) were measured on a Nicolet R3m diffractometer with Cu-K_α radiation (graphite monochromator, $\lambda = 1.54178$ Å) using the ω-scan measuring routine. Of these, 2022 had $[|F_o| > 3\sigma(|F_o|)]$ and were considered observed.

Structure solution and refinement. The structure was solved by direct methods. A numerical absorption correction, based on a face-indexed crystal, was applied. The non-hydrogen atoms were refined anisotropically. The PF_6^- group was disordered, and refined as two distinct orientations, of occupancy 70 and 30%, respectively. The hydroxy hydrogen atoms on the methanols and the amide

* The atomic co-ordinates for this work are available on request from the Director of the Cambridge Crystallographic Data Centre, University Chemical Laboratory, Lensfield Road, Cambridge CB2 1EW, U.K.

proton were located from a ΔF map and refined isotropically. The leading hydrogen atoms on the methyls of the methanols were also located from a ΔF map, and the groups refined as rigid bodies. The positions of the remaining hydrogen atoms were idealized (C—H 0.96 Å), assigned isotropic thermal parameters $U(H) = 1.2\ U_{eq}$ (C), and allowed to ride on their parent carbon atoms. Refinement converged to $R = 0.051$, $R_w = 0.046$ [$w^{-1} = \sigma^2(F) + 0.00032F^2$]. Refinement was by block-cascade full-matrix least-squares, carried out on an Eclipse S140 computer using the SHELXTL program system.[40]

Acknowledgements—We thank the British Council for financial support (to H.S.), NATO, the Research Corporation Trust for additional financial support and the SERC for use of the high field NMR service at the University of Warwick.

REFERENCES

1. S. Shinkai and O. Manabe, *Top. Curr. Chem.* 1984, **121**, 67.
2. H. Stetter and W. Frank, *Angew. Chem., Int. Ed. Engl.* 1976, **15**, 686.
3. J. P. Desvergne and H. Bouas-Laurent, *J. Chem. Soc., Chem. Commun.* 1978, 403.
4. S. Shinkai, K. Inuzuka, O. Miyazaki and O. Manabe, *J. Am. Chem. Soc.* 1985, **107**, 3950.
5. S. Shinkai, S. Nakamura, S. Tachiki, O. Manabe and T. Kgiyama, *J. Am. Chem. Soc.* 1985, **107**, 3363.
6. W. Wierenga, B. R. Evans and J. A. Woltersom, *J. Am. Chem. Soc.* 1979, **101**, 1334.
7. L. A. Frederick, T. M. Fyles, V. A. Malik-Diemer and D. M. Whitfield, *J. Chem. Soc., Chem. Commun.* 1980, 1211.
8. H. L. Ammon, S. K. Bhattacharjee, S. Shinkai and Y. Honda, *J. Am. Chem. Soc.* 1984, **106**, 262.
9. R. E. Wolf Jr and S. R. Copper, *J. Am. Chem. Soc.* 1984, **106**, 4646.
10. H. Bock, B. Hierholzer, F. Voegtle and G. Hollman, *Angew. Chem. Int. Ed. Engl.* 1984, **23**, 57.
11. L. Echegoyen, D. A. Gustowski, V. J. Gatto and G. W. Gokel, *J. Chem. Soc., Chem. Commun.* 1986, 220.
12. D. A. Gustowski, M. Delgado, V. J. Gatto, L. Echegoyen and G. W. Gokel, *J. Am. Chem. Soc.* 1986, **108**, 7553.
13. K. Maruyama, H. Sohmiya and H. Tsukube, *J. Chem. Soc., Perkin Trans. 1* 1986, 2069.
14. F. Dietl, G. Gierer and A. Merz, *Synthesis* 1986, 626.
15. A. Kaifer, D. A. Gustowski, L. Echegoyen, V. J. Gatto, R. A. Schultz, T. P. Clearly, C. R. Morgan, D. M. Goli, A. M. Rios and G. W. Gokel, *J. Am. Chem. Soc.* 1985, **107**, 1958.
16. S. Akabori, Y. Habata, M. Sato and S. Ebine, *Bull. Chem. Soc. Jpn* 1983, **56**, 1459.
17. B. Czech and A. Ratajczak, *Pol. J. Chem.* 1980, **54**, 767.
18. T. Saji, *Chem. Lett.* 1986, 275.
19. P. D. Beer, *J. Chem. Soc., Chem. Commun.* 1985, 1115.
20. P. D. Beer, *J. Organomet. Chem.* 1985, **297**, 313.
21. P. D. Beer and A. D. Keefe, *J. Organomet. Chem.* 1986, **306**, C10.
22. P. D. Beer, C. G. Crane, A. D. Keefe and A. R. Whyman, *J. Organomet. Chem.* 1986, **314**, C9.
23. P. D. Beer, P. J. Hammond, C. Dudman, I. P. Danks and C. D. Hall, *J. Organomet. Chem.* 1986, **306**, 367.
24. H. J. Lorkowski, R. Pannier and A. Wende, *J. Prakt. Chem.* 1967, **35**, 149.
25. R. Ungaro, B. El Haj and J. Smid, *J. Am. Chem. Soc.* 1977, **98**, 5198.
26. E. Amble and E. Amble, *Polyhedron* 1983, **2**, 1063.
27. B. Czech, A. Czech, S. I. Kang and R. A. Bartsch, *Chem. Lett.* 1984, 37.
28. I. R. Hanson, *Acta Crystallogr.* 1978, **B34**, 1026.
29. J. D. Owen, *J. Chem. Soc., Dalton Trans.* 1980, 1066.
30. P. R. Mallinson and M. R. Truter, *J. Chem. Soc., Perkin Trans. 2* 1972, 1818.
31. P. Seiler and J. D. Dunitz, *Acta Crystallogr.* 1979, **B35**, 2020.
32. P. Seiler and J. D. Dunitz, *Acta Crystallogr.* 1982, **B38**, 1741.
33. G. Calvarin and D. Weigel, *Acta Crystallogr.* 1971, **B27**, 1253.
34. K. Sato, M. Katada, H. Sano and M. Kono, *Bull. Chem. Soc. Jpn* 1984, **57**, 2361.
35. G. J. Palenik, *Inorg. Chem.* 1970, **9**, 2424.
36. F. A. Cotton and A. H. Reid Jr, *Acta Crystallogr.* 1985, **C41**, 686.
37. R. A. W. Johnstone and M. E. Rose, *J. Chem. Soc., Chem. Commun.* 1983, 1268.
38. E. Weber and F. Vogtle, *Top. Curr. Chem.* 1981, **98**, 1.
39. M. Bourgoin, K. H. Wong, J. Y. Hui and J. Smid, *J. Am. Chem. Soc.* 1975, **97**, 3462.
40. K. Kikukawa, G. X. He, A. Abe, T. Goto, R. Arata, T. Ikeda, F. Wada and T. Matsuda, *J. Chem. Soc., Perkin Trans. 2* 1987, 135.
41. K. Kimura, H. Sakamoto, Y. Koseki and T. Shono, *Chem. Lett.* 1985, 1241.
42. G. M. Sheldrick, SHELXTL, An Integrated System for Solving, Refining and Displaying Crystal Structures from Diffraction Data. University of Göttingen (1978); revised version (1984).

Polyhedron Vol. 8, No. 7, pp. 887–891, 1989
Printed in Great Britain

0277–5387/89 $3.00+.00
© 1989 Pergamon Press plc

CIS-1,4-CYCLOHEXADIENEBISEPISULPHIDE COMPLEXES OF CHROMIUM, MOLYBDENUM AND TUNGSTEN CARBONYLS: THE X-RAY CRYSTAL STRUCTURE OF $[Cr(CO)_4(\overline{CHSCHCH_2CHSCHCH_2})]$

EDWARD W. ABEL,* NEIL A. COOLEY, KENNETH KITE, KEITH G. ORRELL and VLADIMIR ŠIK

Department of Chemistry, The University, Exeter EX4 4QD, U.K.

and

MICHAEL B. HURSTHOUSE and HELEN M. DAWES

Department of Chemistry, Queen Mary College, Mile End Road, London E1 4NS, U.K.

(*Received* 3 *October* 1988, *accepted* 31 *October* 1988)

Abstract—The first metal carbonyl derivatives of a coordinated episulphide ring are reported. Two classes of complex have been obtained wherein the bisepisulphide behaves either as a bridging ligand between two metal pentacarbonyl moieties as in for example $[\{W(CO)_5\}_2(\overline{CHSCHCH_2CHSCHCH_2})]$, or as a chelating ligand in a mononuclear metal pentacarbonyl complex such as $[Cr(CO)_4(\overline{CHSCHCH_2CHSCHCH_2})]$, for which the X-ray crystal structure is reported.

The chemistry of organic episulphides is essentially dominated by the reactivity of the three-membered $\overline{C—S—C}$ ring. The ring strain present in such compounds, although less than their epoxide analogues, accounts for much of their known chemistry,[1] exemplified by the polymerization of ethylene sulphide in sunlight.[2]

Among the classes of reaction of episulphides is that of desulphurization by low oxidation state metal complexes. The first of such observations was the desulphurization of 3-chloropropylene episulphide and cyclohexene episulphide by di-iron-nonacarbonyl.[3] A subsequent study of episulphide desulphurization by $Fe_2(CO)_9$ showed the reactions to be highly stereospecific and a sulphur–metal coordinated intermediate has been proposed.[4] A wide variety of transition metal compounds has now been shown to desulphurize episulphides, but the mechanisms of such reactions are poorly understood.[1]

To date, only one transition metal–episulphide complex has been reported in which the episulphide retains its integrity.[5] This complex $[PtCl_2(\overline{SCMe_2CMe_2})_2]$ is not very stable in solution, and the palladium analogue could not be prepared. We have sought to investigate the reactions of the potential ligand (L), *cis*-1,4-cyclohexadiene bisepisulphide, Fig. 1. This has been already shown to participate in a template type of polymerization reaction;[6] it does however have sulphur atoms in a suitable conformation for the production of chelated complexes. We report herein the syntheses of the compounds $[\{Cr(CO)_5\}_2L]$, $[\{W(CO)_5\}_2L]$, $[Cr(CO)_4L]$ and $[Mo(CO)_4L]$ and the X-ray crystal structure of $[Cr(CO)_4L]$.

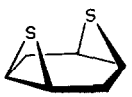

Fig. 1. *cis*-1,4-cyclohexadienebisepisulphide, $\overline{CHSCHCH_2CHSCHCH_2}$.

* Author to whom correspondence should be addressed.

EXPERIMENTAL

Materials

cis - 1,4 - cyclohexadienebisepisulphide (L),[6] $[M(CO)_4(nbd)]$ (M = Cr, Mo[7] and W[8]), $[NEt_4][W(CO)_5Br]$,[9] Et_3OBF_4[10] and $Fe_2(CO)_9$[11] were prepared using literature procedures.

Complexes

$[Cr(CO)_4L]$. A cooled (−5°C) solution of $[Cr(CO)_4(nbd)]$ (0.16 g, 0.64 mmol) in toluene (20 cm^3) was added to a suspension of L (0.14 g, 0.94 mmol) in toluene (10 cm^3). The mixture was stirred for 3 h producing a bright yellow precipitate. After removal of solvent under low pressure the crude product was extracted into cold THF (20 cm^3) and filtered. The cloudy solution was then filtered through a pad of celite and the solvent removed under reduced pressure. This residue was dissolved in dichloromethane (15 cm^3) and hexane (7 cm^3). This solution was chilled to −20°C to yield deep yellow crystals of $[Cr(CO)_4L]$ (0.02 g).

$[Mo(CO)_4L]$. This was prepared in an analogous manner, except that dichloromethane replaced THF for the initial extraction of the crude product from the reaction mixture.

$[\{Cr(CO)_5\}_2L]$. Chromium hexacarbonyl (0.5 g, 2.27 mmol) in THF (20 cm^3) was subjected to UV irradiation through quartz for 8 h to produce an orange solution of $[Cr(CO)_5(THF)]$. Approximately one half of this solution was cooled to −20°C and added over a period of 40 min to L (0.23 g, 1.59 mmol). The reaction mixture was allowed to achieve ambient temperature and stirring was continued for a further 3 h. Solvent was removed *in vacuo* and the resulting oily residue was extracted into dichloromethane (10 cm^3). Chromatography on alumina with dichloromethane elution gave one bright yellow band. The volume of this band eluate was reduced to *ca* 4 cm^3 and the solution cooled to −20°C. The product $[\{Cr(CO)_5\}_2L]$ (0.2 g) was collected by filtration as small golden needles.

$[\{W(CO)_5\}_2L]$. This compound was obtained from the mixing of L (0.15 g, 1.04 mmol) and $[W(CO)_5Br][NEt_4]$ (0.54 g, 1.00 mmol) in the presence of an excess of triethyloxonium tetrafluoroborate in dichloromethane (30 cm^3). Chromatography of the crude product on alumina, with dichloromethane–hexane (1 : 1 by volume) elution gave a single, pale yellow band. Reduction of the eluate volume under reduced pressure to 10 cm^3 and cooling to −10°C produced yellow crystals of $[\{W(CO)_5\}_2L]$ (0.03 g).

All complexes synthesized were more or less air-sensitive, and all operations were performed under dry nitrogen using Schlenk techniques. Characterization data for the products are reported in Table 1.

Spectra

^1H NMR spectra were recorded on a Bruker AM250 spectrometer, operating at 250 MHz. IR spectra were recorded using either a Perkin–Elmer 299B or 398 spectrophotometer with 0.5 mm NaCl solution cells.

X-ray crystallography

The crystal used for X-ray work was mounted under nitrogen in a capillary. Following preliminary photography, unit cell and intensity data

Table 1. Characterization of the group 6a metal carbonyl complexes of *cis*-1,4-cyclohexadienebisepisulphide (L)

Complex	Yield (%)	Melting point (°C)	Colour	Analysis (%) C[a]	H[a]	C[b]	H[b]	ν_{CO} (cm^{-1})
$[Cr(CO)_4L]$ (1)	11	135–137(d)	Yellow	38.9	2.6	38.9	2.6	2010(m),[c] 1903(vs,br), 1859(s)
$[Mo(CO)_4L]$ (2)	48	115–121(d)	Yellow	34.2	2.3	34.1	2.3	2021(m),[d] 1907(vs,br), 1871(s)
$[\{Cr(CO)_5\}_2L]$ (3)	67	51–53(d)	Yellow	36.0	1.6	36.3	1.5	2067(w),[d] 1970(w), 1915(s)
$[\{W(CO)_5\}_2L]$ (4)	8	—	Yellow	24.2	1.0	24.3	1.0	2072(w),[c] 1965(w), 1937(vs), 1919(s)

[a] Obtained.
[b] Calculated.
[c] In dichloromethane.
[d] In THF.

were obtained using a CAD4 diffractometer and graphite monochromatized Mo-K_α radiation ($\lambda = 0.71069$ Å), following standard procedures.[12a] The structure was solved via use of the heavy-atoms method and refined by full-matrix least-squares; non-hydrogen atoms were assigned anisotropic thermal parameters, hydrogen atoms were experimentally located and freely refined with group U_{iso} values.

Crystallographic data are as follows: $C_{10}H_8CrO_4S_2$, $M_r = 308.28$, orthorhombic, $a = 13.256(3)$, $b = 9.201(1)$, $c = 9.746(1)$ Å, $V = 1188.71$ Å^3, space group *Pnma*, $Z = 4$, $D_c = 1.722$ g cm^{-3}, μ(Mo-K_α) = 12.73 cm^{-1}, $T = 295$ K. 1236 data were recorded giving 1105 unique and 714 observed [$I > 1.5\sigma(I)$]. Empirical absorption correction was carried out as described in ref. 12b. Number of parameters in least-squares, 106 and weighting scheme $w = [\sigma^2(F) + 0.0002F_o^2]^{-1}$. Final R, $R_w = 0.0385$, 0.0377. Atomic scattering factors were calculated from the data in ref. 12c. Final atomic positional parameters, displacement factor coefficients and lists of F_o/F_c values have been deposited as supplementary material with the Editor, from whom copies are available on request. Atomic coordinates have also been deposited with the Cambridge Crystallographic Data Centre.

RESULTS AND DISCUSSION

General properties

The reactions of *cis*-1,4-cyclohexadienebisepisulphide (L) with [M(CO)$_4$(nbd)] (M = Cr and Mo) gave the tetracarbonyl products [M(CO)$_4$L], but attempts to prepare the analogous tungsten product have not been successful.

[{Cr(CO)$_5$}$_2$L] and [{W(CO)$_5$}$_2$L] have been synthesized by the action of L upon [Cr(CO)$_5$(THF)] and [W(CO)$_5$Br], respectively.

Whilst all four products were sensitive to oxygen in solution, the tetracarbonyl complexes were considerably more unstable than the pentacarbonyls.

X-ray studies

The novelty of a chelating bisepisulphide prompted us to make a single crystal X-ray structural determination of [Cr(CO)$_4$(CHSCH CH$_2$CHSCHCH$_2$)]. The molecular structure is illustrated in Fig. 2, and a selection of bond lengths and bond angles is given in Table 2. The molecule is an octahedral chelated species and possesses a crystallographic mirror plane which bisects the S—S vector and contains C(2), C(4), Cr, C(13), O(13), C(11) and O(11). The bisepisulphide ligand has retained its integrity after complexation. The sulphur-to-metal bonds are in the manner of thioethers, with Cr—S bond lengths of 2.339(3) Å. These are short compared[13,14] with the sum of the covalent radii of these atoms of 2.52 Å, supporting the suggestion[15] of an element of multiple bond π-character in the chromium–sulphur linkage. What appears to be a remarkably small C—S—C bond angle of 47.3(2)° in the coordinated bisepisulphide is nevertheless within the expected[1] range for the

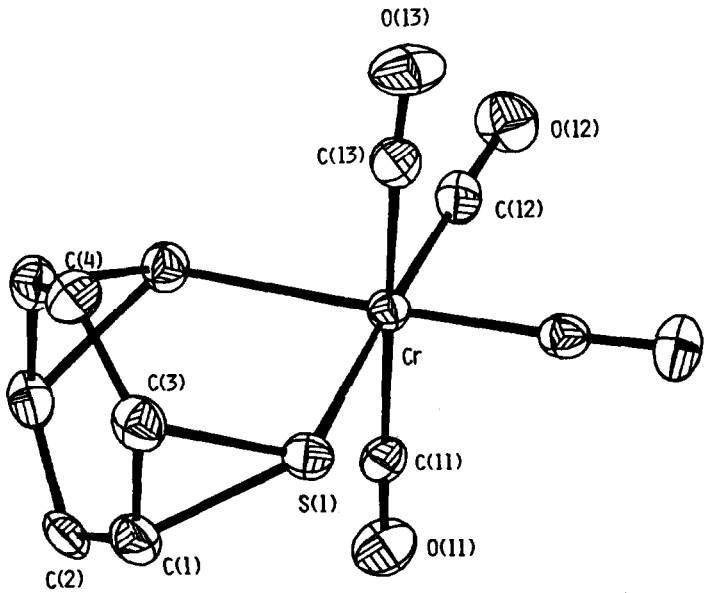

Fig. 2. Crystal structure of chromium tetracarbonyl *cis*-1,4-cyclohexadienebisepisulphide, [Cr(CO)$_4$(CHSCHCH$_2$CHSCHCH$_2$)].

Table 2. Bond lengths and angles for the complex $[Cr(CO)_4(\overline{CHSCHCH_2}\ \overline{CHSCHCH_2})]$

Bond lengths (Å)			
Cr—S(1)	2.339(3)	Cr—S(1)[a]	2.339(3)
Cr—C(11)	1.969(9)	Cr—C(12)	1.814(7)
Cr—C(12)[a]	1.814(7)	Cr—C(13)	1.932(10)
S(1)—C(1)	1.915(7)	S(1)—C(3)	1.856(7)
S(1)[a]—C(1)[a]	1.915(7)	S(1)[a]—C(3)[a]	1.856(7)
C(2)—C(1)	1.456(7)	C(3)—C(1)	1.513(9)
C(4)—C(3)	1.448(7)	C(2)—C(1)[a]	1.456(7)
C(4)—C(3)[a]	1.448(7)	C(3)[a]—C(1)[a]	1.513(9)
C(11)—O(11)	1.171(8)	C(12)—O(12)	1.157(6)
C(13)—O(13)	1.188(9)		
Bond angles (°)			
S(1)—Cr—S(1)[a]	88.4(2)	C(11)—Cr—S(1)	87.4(2)
C(11)—Cr—S(1)[a]	87.4(3)	C(12)—Cr—S(1)	177.4(2)
C(12)—Cr—S(1)[a]	94.2(3)	C(12)[a]—Cr—S(1)	94.2(3)
C(13)—Cr—S(1)	93.2(3)	C(13)—Cr—S(1)[a]	93.2(3)
C(12)—Cr—C(11)	93.3(3)	C(13)—Cr—C(11)	179.1(3)
C(13)—Cr—C(12)	86.0(3)	C(11)—Cr—C(12)[a]	93.4(3)
C(12)—Cr—C(12)[a]	83.2(4)	C(13)—Cr—C(12)[a]	86.0(4)
O(11)—C(11)—Cr	178.8(6)	O(12)—C(12)—Cr	176.9(4)
O(13)—C(13)—Cr	176.3(6)	C(1)—S(1)—Cr	118.9(3)
C(3)—S(1)—Cr	117.8(3)	C(3)—S(1)—C(1)	47.3(2)
C(2)—C(1)—S(1)	122.4(5)	C(3)—C(1)—S(1)	64.3(4)
C(1)—C(3)—S(1)	68.4(4)	C(4)—C(3)—S(1)	119.3(5)
C(3)—C(1)—C(2)	124.0(6)	C(4)—C(3)—C(1)	123.6(6)
C(1)—C(2)—C(1)[a]	110.2(6)	C(3)—C(4)—C(3)[a]	111.4(6)
C(2)—C(1)[a]—C(3)[a]	124.0(6)	C(4)—C(3)[a]—C(1)[a]	123.6(6)

Key to symmetry operations relating designated atoms to reference atoms at x, y, z: [a] $x, -0.5-y, z$.

episulphide ring system. More notable are the C—S bond lengths of 1.915(7) Å, which appear to be the longest observed to date in episulphide rings.

^{1}H *NMR studies*

Despite their very different stoichiometries the NMR spectra of the complexes $[M(CO)_4L]$ and $[\{M(CO)_5\}_2L]$ have similar features. In both types of complex, the methylene group protons give signals characteristic of the AB part of an ABX_2 spin system, while the methine protons give essentially singlet signals. The partially resolved vicinal couplings of the methylene signals are an aid to the individual assignment of the latter. The Karplus rules predict[16] that the coupling constant between H_a and H_c (Fig. 3) will be larger than between H_a and H_b. Thus, the protons showing the larger vicinal couplings will be H_c. It is striking that in the mononuclear chelate ligand complexes, **1** and **2**, these protons appear to the lower frequency side of the H_b protons, whereas in the dinuclear bridging ligand

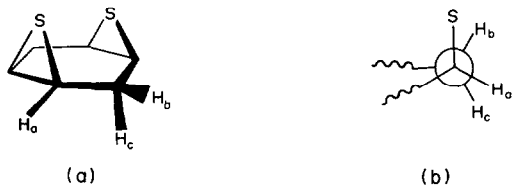

Fig. 3. The relationship between the vicinal protons in *cis*-1,4-cyclohexadienebisepisulphide and its metal complexes.

complexes, **3** and **4**, the relative chemical shifts of H_b and H_c are reversed (Table 3). In all cases the geminal coupling constants $^3J(H_b—H_c)$ are of the order of 18.5 Hz and the vicinal coupling constants $^3J(H_a—H_c)$ and $^3J(H_a—H_b)$ are *ca* 3.5 and 1 Hz, respectively. As these latter couplings were not fully resolved, their magnitudes were not known with any accuracy and therefore could not be used to provide any reliable information concerning the conformations of the six-membered carbocyclic rings in the two types of complex.

Table 3. ^{1}H NMR spectroscopic data for the group 6a metal complexes of *cis*-1,4-cyclohexadienebisepisulphide (L)

Complex	Solvent	Temperature (°C)	$\delta(H_a)$ (ppm)	$\delta(H_b)$ (ppm)	$\delta(H_c)$ (ppm)	$J(H_b—H_c)$ (Hz)
$[Cr(CO)_4L]$ (1)	CD_2Cl_2	25	3.16	3.02	3.01	18.6
$[Mo(CO)_4L]$ (2)	$C_6D_5NO_2$	25	3.47	3.22	2.99	18.7
$[\{Cr(CO)_5\}_2L]$ (3)	$CDCl_3$	25	3.24	3.08	3.21	18.2
$[\{W(CO)_5\}_2L]$ (4)	CD_2Cl_2	25	3.55	3.01	3.34	18.4

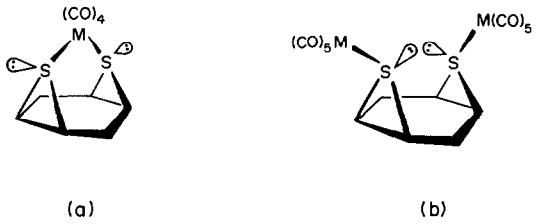

Fig. 4. The use of the "inner" and "outer" lone pairs of sulphur electrons in the formation of $[M(CO)_4L]$ and $[\{M(CO)_5\}_2L]$, respectively.

The isochronous nature of the CH group protons indicates the very high degree of symmetry in all four complexes. The structure determination of **1** demonstrates that the tetracarbonyl products can be thought of as utilizing the two inner lone pairs of the episulphide ligand as illustrated in Fig. 4(a). Model studies show that steric requirements make it impossible for the bis-metal pentacarbonyl species, **3** and **4**, to do other than use the two outer lone pairs of the ligand as in Fig. 4(b).

OTHER REACTIONS

Solutions of compounds **1** and **2** in several solvents, were heated to 45°C in sealed tubes, whereupon extensive decomposition took place. We were, however, unable to characterize any molecular product from the residues.

Ligand L reacted smoothly with di-ironnonacarbonyl in dichloromethane to give $[Fe_3(\mu_3\text{-}S)_2(CO)_9]$ in good yield. This product has been obtained previously by the desulphurization of episulphides[3] and other thioethers.[17] We have reacted $[Cr(CO)_4(nbd)]$ and $[W(CO)_4(nbd)]$ with ethylene sulphide and find no evidence for formation of isolable new metal complexes.

REFERENCES

1. D. C. Dittmer, in *Comprehensive Heterocyclic Chemistry* (Edited by A. R. Katritzky and C. W. Rees), Section 5.06. Pergamon Press, London (1984).
2. P. P. Perkins and M. A. Youtz, *J. Am. Chem. Soc.* 1929, **51**, 3508.
3. R. B. King, *Inorg. Chem.* 1963, **2**, 326.
4. B. M. Trost and S. D. Ziman, *J. Org. Chem.* 1973, **38**, 932.
5. E. W. Abel, M. Booth and K. G. Orrell, *J. Chem. Soc., Dalton Trans.* 1979, 1994.
6. F. Haviv and B. Belleau, *Can. J. Chem.* 1978, **56**, 2677.
7. M. A. Bennett, L. Pratt and G. Wilkinson, *J. Chem. Soc.* 1961, 2037.
8. R. B. King and A. Fronzaglia, *Inorg. Chem.* 1966, **5**, 1837.
9. E. W. Abel, I. S. Butler and J. G. Reid, *J. Chem. Soc.* 1963, 2068.
10. H. Meerwein, *Org. Synth.* 1966, **46**, 113.
11. R. B. King, *Organometal. Synth.* 1965, **1**, 93.
12. (a) R. A. Jones, K. M. A. Malik, M. B. Hursthouse and G. Wilkinson, *J. Am. Chem. Soc.* 1979, **101**, 4128; (b) A. C. T. North, D. C. Phillips and F. S. Mathews, *Acta Cryst.* 1968, **24A**, 351; (c) *International Tables for X-ray Crystallography*, Vol. 4. Kynoch Press, Birmingham (1974).
13. F. A. Cotton and D. C. Richardson, *Inorg. Chem.* 1966, **5**, 1851.
14. L. Pauling, *The Nature of the Chemical Bond*, 3rd edn, p. 225. Cornell University Press, Ithaca, New York (1960).
15. E. N. Baker and N. G. Larson, *J. Chem. Soc., Dalton Trans.* 1976, 1769.
16. M. Karplus, *J. Chem. Phys.* 1959, **30**, 11.
17. A. J. Bard, A. H. Cowley, J. K. Leland, G. J. N. Thomas, N. C. Norman, P. Jutzi, C. P. Morley and E. Schlütter, *J. Chem. Soc., Dalton Trans.* 1985, 1303.

Polyhedron Vol. 8, No. 7, pp. 893–896, 1989
Printed in Great Britain

0277–5387/89 $3.00+.00
© 1989 Pergamon Press plc

THE PREPARATION AND X-RAY STRUCTURE OF [dbuH][$PtBr_5(PPh_3)$]

MAJID MOTEVALLI and MICHAEL B. HURSTHOUSE*

Department of Chemistry, Queen Mary College, Mile End Road, London E1 4NS, U.K.

and

PAUL F. KELLY and J. DEREK WOOLLINS*

Department of Chemistry, Imperial College of Science and Technology, South Kensington, London SW7 2AY, U.K.

(*Received* 3 *October* 1988; *accepted* 31 *October* 1988)

Abstract—In contrast to analogous complexes of smaller phosphines, which react with bromine to give platinum(IV) dibromo species, [$Pt(S_2N_2H)(PPh_3)_2$]BF_4 (**1**) reacts to give a mixture of $PtBr_2(PPh_3)_2$, $PtBr_4(PPh_3)_2$ and, if performed in the presence of [dbuH]Cl, the pentabromo complex [dbuH][$PtBr_5(PPh_3)$] (**2**). The X-ray crystal structure determination of the latter represents the first such analysis of a complex of this class.

We have recently reported on the reactions of [$Pt(S_2N_2H)(PR_3)_2$]BF_4 (PR_3 = PMe_2Ph and PMe_3) with stoichiometric quantities of bromine which lead to platinum(IV) dibromo complexes of the type [$Pt(S_2N_2H)(Br)_2(PR_3)_2$]$BF_4$, which in turn spontaneously decompose to the platinum(II) complexes $Pt(S_2N_2H)(Br)(PR_3)$.[1]

This type of reaction is sensitive to the nature of the phosphine present; here we report upon the reaction of the triphenylphosphine complex, [$Pt(S_2N_2H)(PPh_3)_2$]BF_4 (**1**), with bromine which leads, via loss of the sulphur–nitrogen fragment, to simple platinum–triphenylphosphine–bromo complexes. If the reaction is performed in the presence of [dbuH]Cl (a by-product of the preparation of the starting materials) a salt of the pentabromo anion [$PtBr_5(PPh_3)$]$^-$ is formed. Although complexes of this type have been made previously, the X-ray crystal structure of the latter is the first to be reported.

RESULTS AND DISCUSSION

Complexes of the type [$Pt(S_2N_2H)(PR_3)_2$]BF_4 are readily formed by reaction of BF_3 with the analogous $S_2N_2^{2-}$ complexes, which in turn are prepared in high yield by treatment of a mixture of *cis*-$PtCl_2(PR_3)_2$ and $S_4N_4H_4$ with the base dbu.[2] One by-product of the latter reaction is [dbuH]Cl which can only be completely removed by thoroughly washing the products with water. During our early investigations into the reaction of [$Pt(S_2N_2H)(PMe_2Ph)_2$]BF_4 with bromine, which yields the platinum(IV) dibromo complex [$Pt(S_2N_2H)(Br)_2(PMe_2Ph)_2$]$BF_4$,[1] the undoubted presence of small amounts of [dbuH]Cl as contaminants did not appear to affect the course of the reaction. However, upon extending the range of reactions to include the PPh_3 complex, it soon became clear that in this case the purity of the starting materials is more important.

The reaction of **1** with bromine proceeds much more slowly than that of the PMe_2Ph analogue; thus the ^{31}P NMR spectrum of the product after 30 min shows $\approx$ 50% of the platinum species unreacted. Also present in this solution is $PtBr_2(PPh_3)_2$, indicating that the reaction proceeds via a different route to that observed in the other cases, one which involves loss of the $S_2N_2H^-$ ligand. In addition, if the reaction is performed upon starting material which is contaminated with [dbuH]Cl, then another species is seen in the ^{31}P NMR spectrum. This new complex appears as a singlet at $\delta = -7.0$ ppm, together with ^{195}Pt sat-

* Authors to whom correspondence should be addressed.

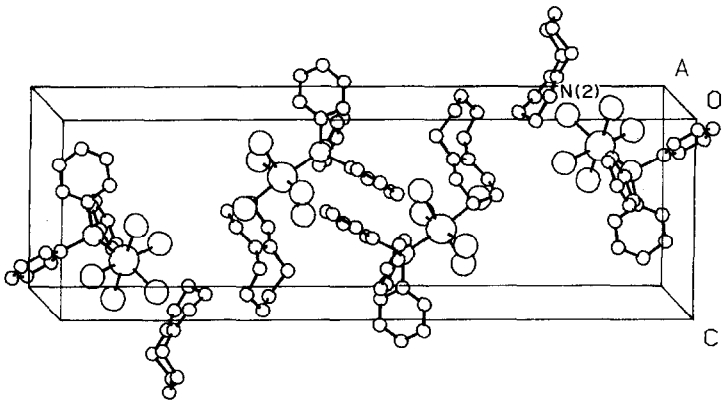

Fig. 1. X-ray structure of [dbuH][$PtBr_5(PPh_3)$] showing the unit cell contents.

ellites ($^1J(^{195}Pt—^{31}P)$ 2140 Hz). The low value of the ^1J coupling suggests the presence of platinum(IV). By slow diffusion into $CHCl_3$ solutions the platinum(IV) complex can be obtained as well-formed red crystals.

On first obtaining crystals of this complex we hoped that it would prove to be a platinum–sulphur–nitrogen species; however their IR spectrum showed none of the expected S—N stretches, and showed a peak at ≈ 1650 cm^{-1}, typical of dbu. Micro-analysis and X-ray crystallography confirmed the complex to be [dbuH][$PtBr_5(PPh_3)$].

A diagram of the unit cell contents is given in Fig. 1. Selected bond lengths and angles are listed in Table 1. The anion has the expected octahedral geometry with the unique Pt—Br distance being

Table 1. Selected bond lengths and angles for [dbuH][$PtBr_5(PPh_3)$]

Bond lengths (Å)

Br(1)—Pt(1)	2.465(4)	Br(2)—Pt(1)	2.466(4)
Br(3)—Pt(1)	2.470(4)	Br(4)—Pt(1)	2.470(4)
Br(5)—Pt(1)	2.533(5)	P(1)—Pt(1)	2.364(6)
C(11)—P(1)	1.819(13)	C(21)—P(1)	1.817(13)
C(31)—P(1)	1.811(15)	C(1)—N(1)	1.442(26)
C(4)—N(1)	1.351(23)	C(9)—N(1)	1.496(23)
C(2)—N(2)	1.467(27)	C(4)—N(2)	1.324(25)
C(3)—C(1)	1.522(29)	C(3)—C(2)	1.493(28)
C(5)—C(4)	1.530(32)	C(6)—C(5)	1.581(34)
C(7)—C(6)	1.525(32)	C(8)—C(7)	1.540(34)
C(9)—C(8)	1.535(30)		

Bond angles (°)

Br(2)—Pt(1)—Br(1)	172.8(1)	Br(3)—Pt(1)—Br(1)	90.1(2)
Br(3)—Pt(1)—Br(2)	95.5(2)	Br(4)—Pt(1)—Br(1)	86.6(2)
Br(4)—Pt(1)—Br(2)	87.4(2)	Br(4)—Pt(1)—Br(3)	174.5(1)
Br(5)—Pt(1)—Br(1)	86.2(2)	Br(5)—Pt(1)—Br(2)	89.6(2)
Br(5)—Pt(1)—Br(3)	86.3(2)	Br(5)—Pt(1)—Br(4)	89.1(2)
P(1)—Pt(1)—Br(1)	94.7(2)	P(1)—Pt(1)—Br(2)	90.1(2)
P(1)—Pt(1)—Br(3)	87.4(2)	P(1)—Pt(1)—Br(4)	97.3(2)
P(1)—Pt(1)—Br(5)	173.6(1)	C(11)—P(1)—Pt(1)	114.4(5)
C(21)—P(1)—Pt(1)	116.9(4)	C(21)—P(1)—C(11)	102.3(6)
C(31)—P(1)—Pt(1)	112.2(5)	C(31)—P(1)—C(11)	106.4(6)
C(31)—P(1)—C(21)	103.3(6)	C(4)—N(1)—C(1)	123.4(18)
C(9)—N(1)—C(1)	116.6(16)	C(9)—N(1)—C(4)	119.9(20)
C(4)—N(2)—C(2)	125.4(17)	C(3)—C(1)—N(1)	111.4(17)
C(3)—C(1)—N(2)	107.3(18)	C(2)—C(3)—C(1)	109.9(17)
N(2)—C(4)—N(1)	117.8(21)	C(5)—C(4)—N(1)	122.0(20)
C(5)—C(4)—N(2)	120.2(18)	C(6)—C(5)—C(4)	108.6(20)
C(7)—C(6)—C(5)	113.0(21)	C(8)—C(7)—C(6)	114.7(20)
C(9)—C(8)—C(7)	113.2(19)	C(8)—C(9)—N(1)	110.7(17)

0.06 Å longer than the four equivalent "equatorial" Pt—Br distances, as a result of the *trans* influence of the phosphine. The hydrogen atoms on the dbu cation were not located and we cannot identify the point of protonation in this way. However, the bridgehead nitrogen, N(1), is nearly planar (sum of angles = 359.9°) so it is likely that N(2) carries the proton.

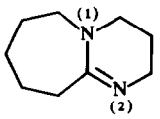

Complexes of this class have been reported previously; treatment of halogen-bridged complexes of the type [PtX$_2$(PR$_3$)]$_2$ with [^{n}Pr$_4$N]X yields salts of [PtX$_3$(PR$_3$)]$^-$ which can be oxidized with the appropriate halogen to give the corresponding platinum(IV) species.[3] This technique has been used to produce complexes of PMe$_3$, although to our knowledge none of the products has been analysed by X-ray crystallography.

The precise mechanism for the production of **2** in this case is unclear, as is the reason for the contrast between the reactions of the PMe$_2$Ph and PPh$_3$ complexes. However, the role of the [dbuH]Cl is crucial; if the reaction is performed upon a compound known to be completely free of the latter then no [PtBr$_5$(PPh$_3$)]$^-$ is formed. In this case, addition of excess bromine, followed by slow hexane diffusion yields a mass of micro-crystals which analyse as a mixture of PtBr$_2$(PPh$_3$)$_2$ and PtBr$_4$(PPh$_3$)$_2$. Possibly [dbuH]Cl can react with the latter platinum(IV) species to yield a salt of [PtBr$_4$Cl(PPh$_3$)]$^-$, via loss of triphenylphosphine, and this in turn reacts with the bromine in the system to give the final product. It is worth noting that although the precise mechanism for the reaction is unclear, and obviously our first preparation of **2** was totally fortuitous, the reaction is reproducible so long as care is taken to leave [dbuH]Cl in the system.

We have yet to fully characterize the products of the reaction of [Pt(S$_2$N$_2$H)(PPh$_2$Me)$_2$]BF$_4$ with bromine; ^{31}P NMR reveals the presence of a platinum(IV) complex, consistent with [Pt(S$_2$N$_2$H)(Br)$_2$(PPh$_2$Me)$_2$]BF$_4$, but this rapidly decomposes in a matter of minutes to give a mixture with a similar ^{31}P NMR spectrum to that of the decomposition products from the PMe$_2$Ph analogue. Thus, there appears to be two distinct effects brought about by the introduction of more phenyl groups into the phosphines present. The first of these is the destabilizing effect upon the resulting platinum(IV) dibromo species, as witnessed by the greater instability of the PPh$_2$Me complex, which is stable only for minutes, compared to the PMe$_3$ and PMe$_2$Ph analogues which are stable for days.

Another effect appears to be at work in the PPh$_3$ case, since ^{31}P NMR shows no evidence for the presence of [Pt(S$_2$N$_2$H)(Br)$_2$(PPh$_3$)$_2$]BF$_4$, even as a short lived species. Rather, it would seem that in this case the reaction proceeds via an entirely different mechanism, since it is slower and eventually results in the loss of the sulphur–nitrogen ligand. It may well be that the crucial factor is the steric influence of the bulky triphenylphosphine groups, although it is unclear why this should have the effect of labilizing the S$_2$N$_2$H$^-$ ligand.

EXPERIMENTAL

General reaction conditions and techniques were as described previously.[1] Compound **1** was prepared from Pt(S$_2$N$_2$)(PPh$_3$)$_2$, the latter from PtCl$_2$(PPh$_3$)$_2$ and S$_4$N$_4$H$_4$/dbu.[2] The bromine solution used consisted of 0.2 cm^3 of Br$_2$ in 20 cm^3 CH$_2$Cl$_2$ (i.e. 0.195 M w.r.t. Br$_2$).

Reaction of **1** *with* Br$_2$ *in the absence of* [dbuH]Cl

A solution of **1** (0.25 g, 0.28 mmol) in CH$_2$Cl$_2$ (20 cm^3) was treated with Br$_2$ in CH$_2$Cl$_2$ (1.5 cm^3, 0.29 mmol) and stirred for 30 min, during which time the solution gradually darkened from orange to light red and deposited some pale solid. The volume of the solvent was reduced to ≈ 5 cm^3 *in vacuo* and Et$_2$O (40 cm^3) added giving a bright orange precipitate. ^{31}P NMR of a CDCl$_3$ solution of the product showed the presence of the starting material together with PtBr$_2$(PPh$_3$)$_2$ (ratio ≈ 1 : 1.2).

The solution was treated with more bromine solution (0.75 cm^3, 0.15 mmol) and stirred overnight. The resulting red solution was reduced in volume and hexane (30 cm^3) layered on top. Slow diffusion of the hexane resulted in a mass of yellow microcrystals. Micro-analysis suggested a mixture of PtBr$_2$(PPh$_3$)$_2$ and PtBr$_4$(PPh$_3$)$_2$. Found: C, 47.2; H, 3.2. Calc. for dibromide: C, 49.2; H, 3.4 and for tetrabromide C, 41.6; H, 2.9%.

Reaction in the presence of [dbuH]Cl

A solution of **1** (0.25 g, 0.28 mmol), known to be contaminated with [dbuH]Cl, in CH$_2$Cl$_2$ (10 cm^3) was treated with bromine solution (1.5 cm^3, 0.29 mmol). After stirring for 30 min the solvent was reduced in volume; the ^{31}P NMR spectrum of the product showed the presence of PtBr$_2$(PPh$_3$)$_2$ and a platinum(IV) complex (ratio 2 : 1). The mixture was taken up in CH$_2$Cl$_2$ (10 cm^3) and treated with

toluene (20 cm^3). The rest of the CH_2Cl_2 was removed *in vacuo* and the resulting orange solid filtered off and washed with cold toluene followed by Et_2O. The solid obtained was redissolved in CH_2Cl_2 (3 cm^3) and hexane layered on top; slow diffusion yielded **2** as well-formed orange–red crystals. Found: C, 32.0; H, 3.0; N, 2.8. Calc. C, 32.1; H, 3.2; N, 2.8%.

Crystal data. $C_{27}H_{32}N_2Br_5Pt$, $M = 1010.1$, monoclinic, $a = 9.583(6)$, $b = 32.523(6)$, $c = 10.115(3)$ Å, $\beta = 94.74(4)°$, $U = 3141.7$ $Å^3$, space group $P2_1/n$, $Z = 4$, $D_c = 2.14$ g cm^{-3}, μ(Mo-K_α) 108.8, $\lambda = 0.71069$ Å, $F(000) = 1904$.

Data collection and processing. ($1.5\theta \leqslant 25°$), graphite monochromated Mo-K_α radiation; 5518 independent measured reflections, 3677 observed [$|F_o| > 6\sigma(|F_o|)$], corrected for Lorentz and polarization factors; empirical absorption correction.

Structure analysis and refinement. The structure was solved by the heavy-atom method and all the non-hydrogen atoms refined anisotropically. The hydrogen atoms were idealized (C—H = 0.96 Å), assigned group isotropic thermal parameters $U(H) = 1.2U\text{eq}(C)$ and allowed to ride on their parent carbons. Refinement was by full-matrix least-squares to $R = 0.045$, ($R = \Sigma[|F_o| - |F_c|]/\Sigma|F_o|$), $R_w = 0.046$ ($w^{-1} = \sigma^2(F) + 0.00035F^2$). Computations were carried out on a VAX 11/750 computer using the SHELX76 program system.*

* Atomic coordinates, thermal parameters, full lists of bond lengths and angles and lists of F_o/F_c values have been deposited as supplementary data with the Editor, from whom copies are available on request. Atomic coordinates have also been deposited with the Cambridge Crystallographic Data Centre.

REFERENCES

1. R. Jones, P. F. Kelly, D. J. Williams and J. D. Woollins, *J. Chem. Soc., Dalton Trans.* 1988, 1569.
2. R. Jones, P. F. Kelly, D. J. Williams and J. D. Woollins, *Polyhedron* 1987, **6**, 1541.
3. P. L. Goggin, R. J. Goodfellow, S. R. Haddock, J. R. Knight, F. J. S. Reed and B. F. Taylor, *J. Chem. Soc., Dalton Trans.* 1974, 523.

Polyhedron Vol. 8, No. 7, pp. 897–907, 1989
Printed in Great Britain

0277–5387/89 $3.00+.00
© 1989 Pergamon Press plc

REDISTRIBUTION REACTIONS OF PLATINUM(II) AND PALLADIUM(II) PHOSPHINE COMPLEXES

JEFFREY A. RAHN, MARK S. HOLT and JOHN H. NELSON*

Department of Chemistry, University of Nevada, Reno, NV 89557-0020, U.S.A.

(*Received* 28 *August* 1988; *accepted* 31 *October* 1988)

Abstract—Anion redistribution equilibria of the type $(R_3P)_2MX_2+(R_3P)_2MY_2 \leftrightarrows 2(R_3P)_2MXY$ (X, Y = Cl, Br, I, CN, N_3; R_3P = Me_2PhP, $MePh_2P$, $(Bzl)_3P$, $(CH_2{=}CH)_2PhP$, $(CH_2{=}CH)Ph_2P$ and 1-phenyl-3,4-dimethylphosphole; M = Pd, Pt) have been studied by $^{31}P\{^1H\}$ and in some cases $^{195}Pt\{^1H\}$ NMR spectroscopy. It was found that except for the two cases when R_3P = $MePh_2P$, M = Pd, X = Cl, Y = Br and R_3P = Me_2PhP, M = Pd, X = Cl, Y = Br, redistribution was in general instantaneous. The $(R_3P)_2PdCl_2+(R_3P)_2Pd(CN)_2$ reactions were slow but proceeded to completion. In contrast, when one of the anions is CN^- no anion redistribution was observed for the platinum complexes even after a month. The thermodynamic stabilities of the mixed anion species relative to the symmetric species is anion dependent showing that these are not random processes. The $(R_3P)_2PdXY$ complexes possess the *trans* geometry. The $(R_3P)_2PtXY$ complexes are generally *cis* but in some cases both the *cis* and *trans* isomers are present in solution. A mechanism is proposed for these reactions. Phosphine redistribution of the type $(R_3P)_2MX_2+(R'_3P)_2MX_2 \leftrightarrows 2(R_3P)(R'_3P)_2MX_2$ is general for palladium. It did not occur for platinum unless one or more of the R and R′ groups on each phosphine was unsaturated (allyl, vinyl or the butadiene moiety of a phosphole). In most of these cases the $(R_3P)(R'_3P)MX_2$ complexes underwent intramolecular [4+2] Diels–Alder cycloaddition reactions.

Ligand redistribution reactions [eq. (1)] are common for typical element compounds.[1]

$$MA+M'B \rightleftharpoons MB+M'A. \quad (1)$$

The theoretical aspects,[1,2] experimental methods for their study[1–4] and the various systems which undergo this class of reaction have been reviewed.[1–4] Redistribution reactions of transition metal complexes, although less studied,[4] may not be less common. We reported earlier[5,6] that neutral ligand redistribution is a general reaction for palladium(II) complexes. In this paper we extend that study to analogous platinum(II) complexes and consider as well, anionic ligand redistribution for both palladium(II) and platinum(II) phosphine complexes. This type of reaction is of fundamental importance to our understanding of the solution chemistry of "inert" transition metal complexes.

*Author to whom correspondence should be addressed.

EXPERIMENTAL

Reagents and physical measurements

All chemicals used were reagent grade and were used as received or synthesized as described below. All solvents, when necessary, were dried by standard procedures and stored over Linde 4 Å molecular sieves. All reactions involving phosphines were conducted under a nitrogen atmosphere.

The $^{31}P\{^1H\}$ and $^{195}Pt\{^1H\}$ NMR spectra were recorded at 40.26 and 21.28 MHz, respectively, on a JEOL FX-100 spectrometer in the FT mode. Phosphorus chemical shifts were relative to external 85% H_3PO_4, with a positive value being downfield of the reference. ^{195}Pt chemical shifts are referenced to a standard frequency of 21.4 MHz relative to the proton resonance of TMS at 100 MHz.[7,8] Concentration values for calculating "k_{eq}" were obtained by integration of the areas of the ^{31}P res-

onances, or by measurement of the peak heights. When both methods could be used, the "k_{eq}" values were within 5% of each other.

Synthesis

Most $(R_3P)_2MCl_2$ complexes were prepared by reacting 2 equivalents of the phosphine or phosphole with one equivalent of the $(PhCN)_2MCl_2$ complex in CH_2Cl_2 under a nitrogen atmosphere as reported previously.[9] When R_3P was Bu_3P or Et_3P, 2 equivalents of the phosphine were reacted with 1 equivalent of K_2PtCl_4 as described previously.[10] The bromide,[11] iodide,[11] cyanide[12] and azide[13] complexes were prepared by metathesis of the chloride complexes in a CH_2Cl_2–CH_3OH–H_2O solvent mixture for 1 to 7 days for the palladium and platinum complexes, respectively. Except for cyanide, a 4:1 molar ratio of NaX to chloride complex was employed. For the cyanide complexes, a 2:1 molar ratio of NaCN to chloride complex was employed. The $^{31}P\{^1H\}$ NMR data for the palladium and platinum complexes is contained in Tables 1 and 2, respectively. The physical properties of all complexes agreed with the literature data.[9–26]

Redistribution reactions

These were performed by dissolving a 1:1 molar ratio of the two complexes, 20–60 mg each, in approximately 3 cm^3 of $CDCl_3$. The resultant solution was then placed in a 10 mm NMR tube and spectra were recorded immediately at 300 K, after 2 and 48 h, then again after a week or more.

RESULTS AND DISCUSSION

Anion redistribution

Reaction of complexes containing two different anions, X and Y [eq. (2)], was generally very rapid.

Table 1. ^{31}P NMR data for reactions of the type $(R_3P)_2PdX_2+(R_3P)_2PY_2 \rightleftharpoons 2(R_3P)_2PdXY$

	$(MePh_2P)_2PdX_2$ $\delta^{31}P^a$			$(MePh_2P)_2PdY_2$ $\delta^{31}P^a$			
X	*cis*	*trans*	Y	*cis*	*trans*	$\delta^{31}P^a$ XY	K_{eq}
Cl	18.0(B)[b]	6.9	Br	5.9	4.2	—	—
Cl	18.0	6.9	I	—	−5.7	3.5	4.2
Cl	—	—	CN	—	—	7.1	∞
Cl	17.9	6.9	N_3	16.6	7.3	7.6	0.3
Br	5.9	4.2	I	3.5	−5.7	0.3	4.7
Br	6.0	4.2	CN	7.2	6.8	5.7	21.2
Br	5.8	4.1	N_3	7.2	—	6.4	—
I	—	−5.7	CN	—	6.8	2.4	21.9
I	—	−5.7	N_3	16.3	7.3	4.9	1.7
CN	—	6.9	N_3	16.4	7.3	7.7	79.1
	$(Me_2PhP)_2PdX_2$ $\delta^{31}P^a$			$(Me_2PhP)_2PdY_2$ $\delta^{31}P^a$			
X	*cis*	*trans*	Y	*cis*	*trans*	$\delta^{31}P$ XY	K_{eq}
Cl	4.7	−6.0	Br	7.8	−10.1	—	—
Cl	5.0	−6.0	I	—	−20.4	−10.9	3.2
Cl	—	—	CN	—	—	−5.5	∞
Cl	4.6(B)[b]	−5.9	N_3	4.6(B)	−3.7	−4.5	—
Br	−7.7	−10.1	I	−10.8	−20.4	−14.3	4.0
Br	—	−10.1	CN	—	−5.5	−7.5	490
Br	−7.7	−10.1	N_3	−3.5	−3.8	−5.7	0.1
I	—	−20.4	CN	—	−5.7	−11.2	29.9
I	—	−20.4	N_3	2.9	−3.7	−7.7	0.3
CN	—	−5.7	N_3	3.7	—	−4.2	112

[a] In ppm in $CDCl_3$ at 300 K.
[b] B = broad.

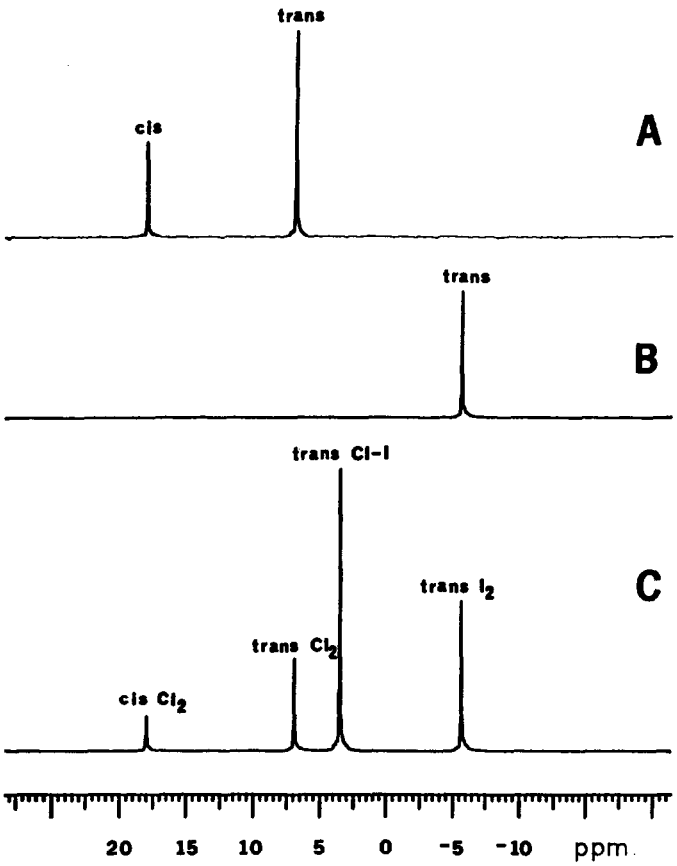

Fig. 1. 40.26 MHz $^{31}P\{^1H\}$ NMR spectra of (A) $(MePh_2P)_2PdCl_2$, (B) $(MePh_2P)_2PdI_2$ and (C) a 1 : 1 molar mixture of the two (all) in $CDCl_3$ at 300 K.

$$(R_3P)_2MX_2+(R_3P)_2MY_2 \rightleftharpoons 2(R_3P)_2MXY. \quad (2)$$

In most cases, an equilibrium mixture of starting materials and either a *cis* or *trans* (in some cases both) mixed anion complex was formed. Equilibrium constants for eq. (2) were calculated from the equation:

$$K_{eq} = \frac{[(R_3P)_2MXY]^2_{total}}{[(R_3P)_2MX_2][(R_3P)_2MY_2]}$$

where $[(R_3P)_2MXY]_{total}$ is the total concentration of the *cis* and *trans* isomers of the mixed anion products.

Palladium reactions. The $(R_3P)_2PdX_2$ complexes generally exist as temperature dependent equilibrium mixtures of *cis* and *trans* isomers in solution.[11,14-20] Their $^{31}P\{^1H\}$ NMR spectra contain two resonances, one for each isomer, with that of the *trans* isomer generally being upfield of that for the *cis* isomer. The $^{31}P\{^1H\}$ NMR spectrum of a typical reaction mixture is shown in Fig. 1(C). The spectrum of the mixture contains, in addition to the resonances expected for the starting materials, a new singlet whose chemical shift lies between those of the *trans*-Cl_2 and *trans*-I_2 complexes. This resonance is assigned to the *trans*-$(MePh_2P)_2PdClI$ complex since the *cis* isomer should show two ^{31}P chemical shifts (*vide infra*). Similar spectra were observed for the 20 reactions listed in Table 1. The *trans* mixed anion complex formed in every case studied, except for the two Cl/Br combinations where only the two starting materials were present in solution after several days.

In several cases where the redistribution occurred, the K_{eq} values differ substantially from the statistical value of four, indicating that these equilibrium constants are influenced by the strengths of the Pd—X bonds[4] and are not random processes.

The reactions between the $(R_3P)_2PdCl_2$ and $(R_3P)_2Pd(CN)_2$ complexes were slower, but proceeded to completion. The *trans*-$(R_3P)_2Pd(CN)Cl$ complex was the only species present in solution after 1 week. Exchanges between the cyanide complexes and the complexes of other anions (Br, I, and N_3) all had equilibrium constants (K_{eq} = 21.1–490) that are much greater than for the non-cyanide containing exchanges. Reaction of the

Table 2. ^{31}P NMR data on exchange reactions of the type $(R_3P)_2PtX_2+(R_3P)_2PtY_2 \rightleftharpoons 2(R_3P)_2PtXY$

Number	R_3P	X	$\delta^{31}P^a$	J(Pt—P)^b	Y	$\delta^{31}P$	J(Pt—P)	$\delta^{31}P$ mixed X	$\delta^{31}P$ mixed Y	J(Pt—P) mixed X	J(Pt—P) mixed Y	J(PP)^b	K_{eq}
1	Me_2PhP	Cl	−16.0	3547	Br	−16.0	3500	−14.0	−18.0	3519	3524	17	2.6
2	Me_2PhP	Cl	−16.0	3546	I	−23.3	3364	−13.3	−16.3	3359	3520	15	
						−18.1	2316	−14.5		2375		—	0.9
3	Me_2PhP	Cl	−16.0	3547	CN	−13.8	2192	—	—	—	—	—	—
4	Me_2PhP	Cl	−16.0	3546	N_3	−16.9	3370	−13.0	−19.2	3748	3218	24	13.7
5	Me_2PhP	Br	−16.1	3500	I	−18.1	3364	−15.3	−18.7	3348	3503	12	
						−23.3	2316	−18.0		2346		—	1.9
6	Me_2PhP	Br	−16.0	3499	CN	−13.8	2190	—	—	—	—	—	—
7	Me_2PhP	Br	−16.0	3501	N_3	−16.9	3370	−11.9	−21.2	3724	3204	23	16.7
8	Me_2PhP	I	−18.2	3364									
			−23.3	2314	CN	−13.8	2190	—	—	—	—	—	—
9	Me_2PhP	I	−18.1	3364	N_3	−16.9	3370	−12.9	−23.9	3567	3203		
								−10.6		2483		21	5.4
10	Me_2PhP	CN	−13.8	2190	N_3	−16.9	3369	—	—	—	—	—	—
11	$MePh_2P$	Cl	−1.8	3623	Br	−2.2	3572	−0.4	−3.7	3589	3602	16	3.7
12	$MePh_2P$	Cl	−1.8	3623	I	−4.8	3423						
						−7.5	2397	−0.5	−6.3	3414	3604	12	0.064
13	$MePh_2P$	Br	−2.2	3572	I	−4.8	3423	−2.3	−4.8	3401	3579	12	1.8
						−7.5	2397	−2.7		2429		0	
14	$MePh_2P$	Cl	−1.7	3624	N_3	−3.5	3440	0.1	−4.4	3818	3300	23	14.6
15	$MePh_2P$	Br	−2.3	3572	N_3	−3.8	3440	0.2	−6.4	3787	3293	22	28.4

16	$MePh_2P$	I	−4.7	3424									
			−7.3	2396	N_3	−3.5	3440	−2.2	−8.9	3610	3295	20	8.1
17	$PhVy_2P$[c]	Cl	−5.4	3573	Br	−6.0	3520	−4.6	−6.8	3540	3552	15	4.6
						−7.8	2408						
18	$PhVy_2P$	Cl	−5.1	3573	I	−8.3	3369	−5.2	−8.3	3362	3553	13	1.5
						−7.9	2408						
19	$PhVy_2P$	Br	−5.8	3522	I	−8.4	3369	−6.5	−7.5	3348	3534	12	2.9
20	DMPP[d]	Cl	7.7	3348	Br	7.4	3285	5.7	9.4	3317	3315	17	3.8
21	DMPP	Cl	7.7	3345	I	5.1	3120						
						4.7	2336	10.4	2.9	3144	3301	15	—
22	DMPP	Br	7.5	3286	I	5.2	3120						
						4.8	2336	8.5	4.6	3120	3276	15	4.1
23	Bzl_3P	Cl	5.1	2461	Br	−1.4	2393	−2.0		2424		0	3.7
24	Bzl_3P	Cl	5.1	2461	I	−10.5	2339	−1.8		2385		0	4.9
25	Bzl_3P	Br	−1.4	2393	I	−10.5	2339	−5.6		2361		0	3.4
26	Ph_2VyP	Cl	2.7	3633	Br	2.2	3583	3.2	1.6	3591	3620	15	4.1
27	Ph_2VyP	Cl	2.8	3632	I	0.6	2452	2.0	0.3	3405	3634	12	1.9
						−0.1	3434						
28	Ph_2VyP	Br	2.4	3583	I	0.6	2452	1.08	1.07	3401	3614	11	1.8
						−0.1	3434						

[a] In ppm in $CDCl_3$ at 300 K.
[b] In Hz.
[c] Vy = $CH{=}CH_2$.
[d] DMPP = 1-phenyl-3,4-dimethylphosphole.

azide complexes with the chloride, bromide and iodide complexes, except for the $(MePh_2P)_2PdI_2$+ $(MePh_2P)_2Pd(N_3)_2$ reaction ($K_{eq} = 1.7$), all had equilibrium constants which were less than one. The equilibrium constants for the chloride with iodide and bromide with iodide reactions were near the statistical value, ranging from 3.2 to 4.2. It should also be noted that the nature of the phosphine affects the value of the equilibrium constant, but that there is no regular trend that is easily discernible relating to either the size or the basicity of the phosphine.

Platinum reactions. The geometry of the $(R_3P)_2PtX_2$ complexes may be easily determined from the magnitude of the platinum–phosphorus coupling constant. For *cis* complexes ^1J(Pt—P) is generally greater than 3000 MHz, while for *trans* compounds ^1J(Pt—P) is generally less than 2500 Hz.[21,27-29] The $(R_3P)_2PtI_2$ complexes exist as temperature-dependent equilibrium mixtures of *cis* and *trans* isomers in solution. The chloride, bromide and azide complexes are wholly *cis* and the cyanide complexes wholly *trans* in solution.

The $^{31}P\{^1H\}$ NMR spectrum of a typical reaction mixture is shown in Fig. 2. This spectrum contains an AB quartet, in addition to the resonances expected for the starting materials. This AB pattern is assigned to the *cis*-$(R_3P)_2PtXY$ complex. The magnitudes of the two ^1J(Pt—P)s and ^2J(PP)[30,31] are all consistent with the *cis* geometry. In all cases, when both the symmetric complexes were *cis*, the mixed anion complex was also *cis*. If both the symmetric complexes were *trans*, then the mixed anion complex which formed was also *trans* [reactions (23), (24), (25)]. In some cases, when one of the symmetric complexes was an iodide complex, a mixture of *cis* and *trans* isomers of $(R_3P)_2PtXI$ [reactions (2), (5), (9), (13)] was formed, with the major species being the *cis* isomer. A similar study[32] with *cis*-$(MePh_2P)_2Pt(NO_3)_2$ and *cis*-$(MePh_2P)_2Pt(CH_3)_2$ showed that the *cis*-$(MePh_2P)_2Pt(NO_3)(CH_3)$ isomer was formed first and that it slowly isomerized to the *trans* isomer.

Most of the equilibrium constants for the anion redistribution reactions of the platinum complexes do not differ markedly from the statistical value of four. The redistribution occurs to the greatest extent when one of the anions is the pseudo-halide N_3^-. Anion redistribution does not occur when one of the anions is cyanide (even after a month) which is in stark contrast to the results of the palladium reactions where the cyanide reactions occurred to the greatest extent. Also, redistribution between chloride and bromide complexes occurred for platinum but not for palladium. Clearly, the metal has an influence on K_{eq}.

The $(Bzl_3P)_2PtX_2$ (X = Cl, Br and I) complexes are each *trans* isomers, probably because of the

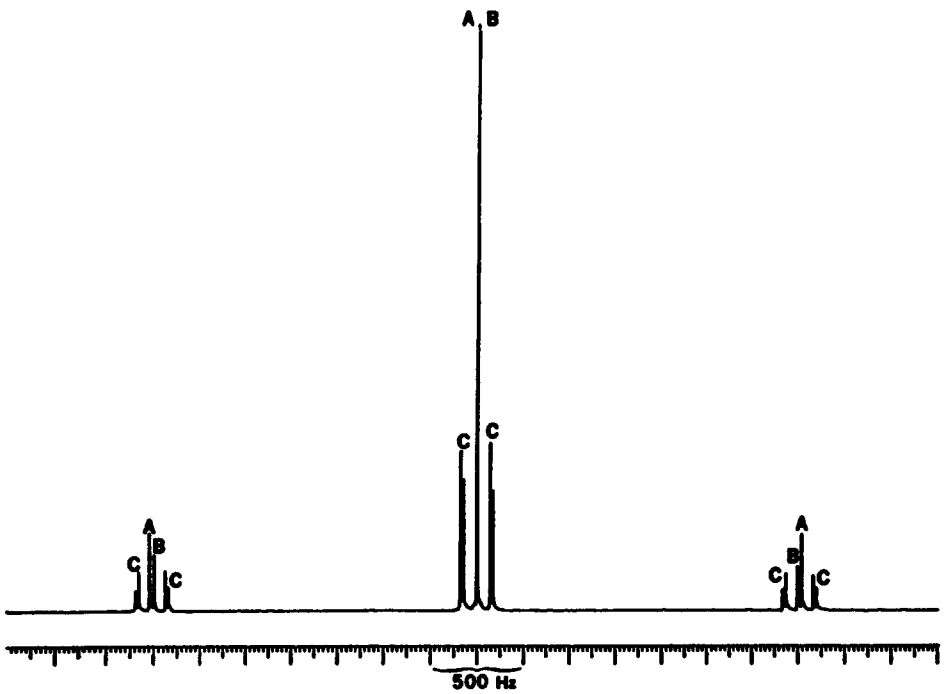

Fig. 2. 40.26 MHz $^{31}P\{^1H\}$ NMR spectrum of an equilibrium mixture of (A) $(Me_2PhP)_2PtCl_2$, (B) $(Me_2PhP)_2PtBr_2$ and (C) $(Me_2PhP)_2PtClBr$ in $CDCl_3$ at 300 K.

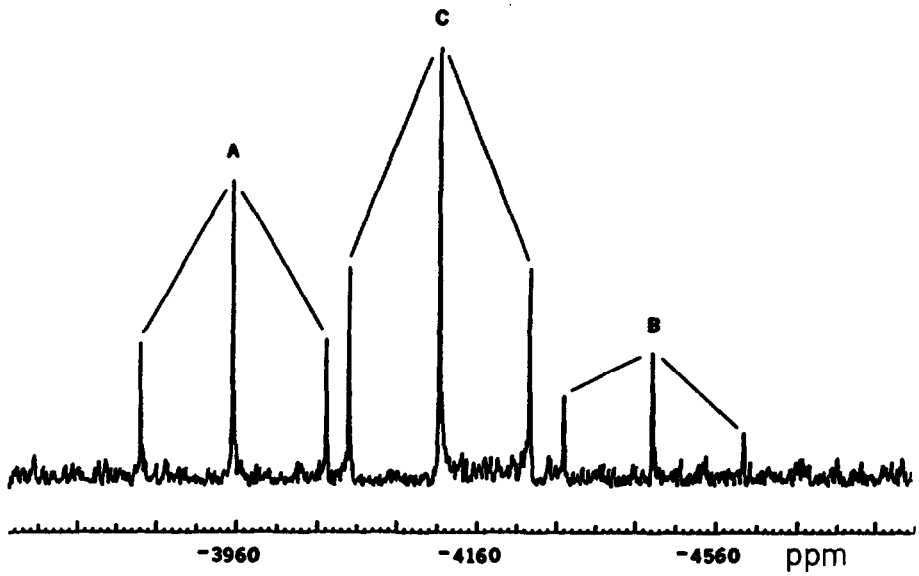

Fig. 3. 21.28 MHz $^{195}Pt\{^1H\}$ NMR spectrum of an equilibrium mixture of (A) $(Bzl_3P)_2PtCl_2$, (B) $(Bzl_3P)_2PtBr_2$ and (C) $(Bzl_3P)_2PtBrCl$ in $CDCl_3$ at 300 K.

steric bulk of Bzl_3P. Formation of *trans*-$(Bzl_3P)_2PtXY$ would then be expected. The $^{195}Pt\{^1H\}$ NMR spectrum for the reaction of $(Bzl_3P)_2PtCl_2$ with $(Bzl_3P)_2PtBr_2$ is shown in Fig. 3. For *trans*-$(Bzl_3P)_2PtCl_2$, $\delta^{195}Pt = -3954$ ppm and for *trans*-$(Bzl_3P)_2PtBr_2$, $\delta^{195}Pt = -4478$ ppm. The ^{195}Pt chemical shift of *trans*-$(Bzl_3P)_2PtBrCl$ is, as anticipated[33] due to the rough additivity of the halide influence on $\delta^{195}Pt$, intermediate between these two values ($\delta^{195}Pt = -4210$ ppm). Figure 4 shows the $^{195}Pt\{^1H\}$ NMR spectrum for the reaction of $(MePh_2P)_2PtBr_2$ with $(MePh_2P)_2PtI_2$ which displays the presence of both *cis*- ($\delta = -4931$ ppm) and *trans*- ($\delta = -5120$ ppm) $(MePh_2P)_2PtBrI$.

An unexpected trend was noted concerning the platinum–phosphorus coupling constants for the *cis* mixed halide complexes produced in reactions involving the chloride, bromide and iodide

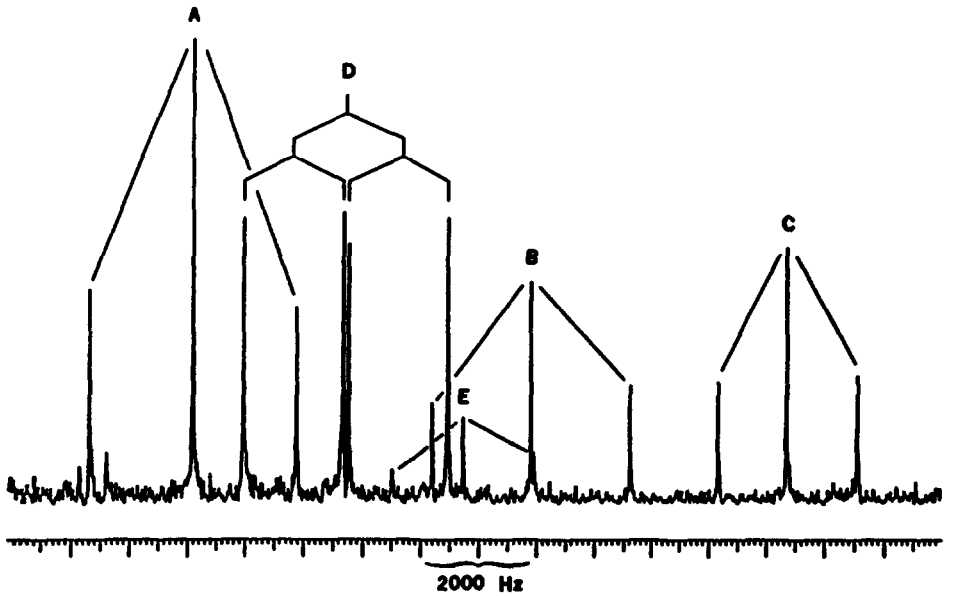

Fig. 4. 21.28 MHz $^{195}Pt\{^1H\}$ NMR spectrum of an equilibrium mixture of (A) *cis*-$(MePh_2P)_2PtBr_2$ ($\delta = -4685$ ppm), (B) *cis*-$(MePh_2P)_2PtI_2$ ($\delta = -5230$ ppm), (C) *trans*-$(MePh_2P)_2PtI_2$ ($\delta = -5648$ ppm), (D) *cis*-$(MePh_2P)_2PrBrI$ ($\delta = -4931$ ppm) and (E) *trans*-$(MePh_2P)_2PtBrI$ ($\delta = -5120$ ppm) in $CDCl_3$ at 300 K.

complexes. In most cases, there is a reversal in the magnitude of J(Pt—P). Reaction (5) is a typical example. For *cis*-$(Me_2Ph)_2PtBr_2$ and *cis*-$(Me_2PhP)_2PtI_2$, ^1J(Pt—P) is, respectively, 3500 and 3364 Hz. For the *cis*-$(Me_2PhP)_2PtBrI$ complex, the resonance assigned to the phosphorus *trans* to bromide has ^1J(Pt—P) of 3348 Hz and that assigned to the phosphorus *trans* to iodide has ^1J(Pt—P) of 3503 Hz. This is just opposite to our expectations. A reversal in the assignment of the phosphorus resonances for the *cis*-$(R_3P)_2PtXY$ complexes would give ^1J(Pt—P) coupling constants that are consistent with expectations, but then the chemical shifts would be difficult to explain.[34] Hence, the exact assignment of the chemical shifts in these cases is uncertain but the conclusions regarding the reactions remain the same, independent of the assignment.

Mechanism of anion redistribution. As with geometrical isomerizations[35] of L_2MX_2 complexes, both associative and dissociative mechanisms are possible for the anion redistribution reactions. We believe that the associative mechanism illustrated in eq. (3), which has been previously proposed,[36–38] is the most likely process. We do not wish to imply anything regarding the coordination geometry of the anion-bridged intermediate (i.e. either square-based pyramidal (SBP) or trigonal-bipyramidal (TBP)), or of the actual location of the ligands not involved in bridging. Based upon the limited amount of structural data[39] on L_3MX_2 complexes the geometry may be distorted between SBP and TBP.

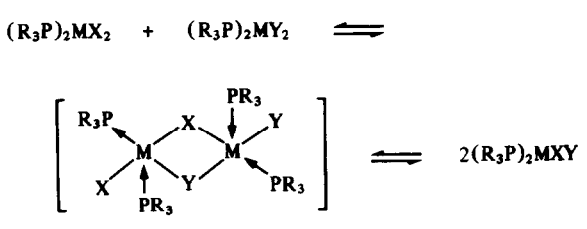

(3)

Phosphine redistribution

Palladium reactions. We have previously reported[5,6] on the neutral ligand redistribution of palladium complexes and found it to be fairly general. Six new reactions, all involving phosphines with unsaturated substituents, were carried out between pairs of palladium(II) phosphine complexes (Table 3). In each case, the $(R_3P)(R'_3P)PdX_2$ complex was in equilibrium with $(R_3P)_2PdX_2$ and $(R'_3P)PdX_2$, but also in each case this mixed ligand complex underwent a subsequent Diels–Alder [4+2] cycloaddition reaction[40] as illustrated in eq. (4). For the chloride complexes, only the *cis* mixed

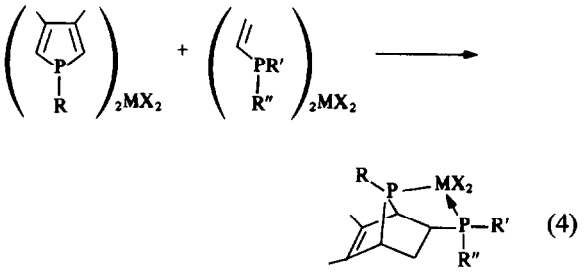

(4)

Table 3. ^{31}P NMR data on reactions of the type $(R_3P)_2PdX_2 + (R'_3P)_2PdX_2 \rightleftharpoons 2(R_3P)(R'_3P)PdX_2$, [4+2] cycloaddition product

Number	X	R_3P^a	R'_3P^b	$\delta^{31}P^c$ Mixed ligand	$\delta^{31}P^c$ Geometry	J(PP)^d	$\delta^{31}P^c$ [4+2] product^e	J(PP)
29	Cl	$PhVy_2P$	DMPP	26.9, 15.7	*cis*	4.9	123.8, 35.4	4.9
30	Cl	Ph_2VyP	DMPP	27.4, 23.4	*cis*	0	124, 34.6	7.3
31	Br	$PhVy_2P$	DMPP	24.4, 13.7	*cis*	22	124.5, 35.5	1.5
				17.3, 4.5	*trans* AB	544	—	—
32	Br	Ph_2VyP	DMPP	21.9, 15.2	*cis*	0	123.9, 35.4	0
				14.0	*trans*	0	—	—
33	I	$PhVy_2P$	DMPP	6.5, −1.0	*trans* AB	540	120.7, 33.2	2.3
34	I	Ph_2VyP	DMPP	6.7	*trans*	0	121.4, 34.6	0

[a] Vy = CH=CH$_2$.
[b] DMPP = 1-phenyl-3,4-dimethylphosphole.
[c] In PPM in $CDCl_3$ at 300 K.
[d] In Hz.
[e] See ref. 40.

Table 4. Attempted exchange reactions of platinum(II) phosphine complexes of the type $L_2PtX_2 + L'_2PtX_2 \rightleftharpoons$ No reaction

L	L′	X
$MePh_2P$	Me_2PhP	Cl
$MePh_2P$	Me_2PhP	Br
$MePh_2P$	Me_2PhP	I
Me_2PhP	Ph_2Vyp	Cl
Me_2PhP	$PhVy_2P$	Cl
Bzl_3P	Bu_3P	Cl
Bzl_3P	Bu_3P	Br
Bzl_3P	Bu_3P	I
cis-Et_3P	Bu_3P	Cl
trans-Et_3P	Bu_3P	Cl

ligand complex was formed. For the bromide complexes, both the *cis* and *trans* mixed ligand complexes were formed and for the iodide complexes, only the *trans* mixed ligand complex was formed. This is in agreement with previous observations that the *cis* isomer stability decreases with increasing size of the halide.[11] In each case, ligand redistribution was instantaneous and the following Diels–Alder cycloaddition relatively slow. Because of the following Diels–Alder cycloaddition reaction, K_{eq} for the ligand redistribution could not be measured. We also observed slow Diels–Alder [4+2] reactions [eq. (5)] in reactions (20), (21) and (22) of Table

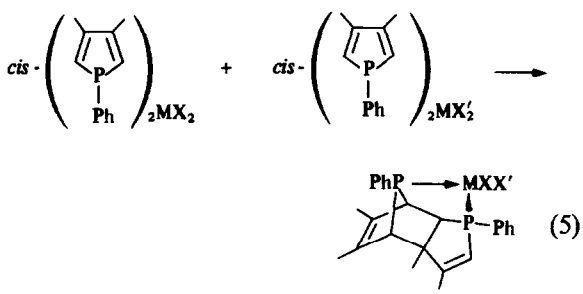

(5)

2. Details of these Diels–Alder reactions will be described in subsequent publications.

Platinum reactions. For all the platinum reactions listed in Table 4 there was no evidence of phosphine redistribution in $CDCl_3$ over a period of 4 weeks. In contrast, for each of the reactions listed in Table 5, phosphine redistribution not only occurred but did so instantaneously. It should be noted that all of the phosphines which participated in the redistribution reaction bear unsaturated substituents (allyl, vinyl, or the butadiene moiety of the phosphole ring). Most of the $(R_3P)(R'_3P)PtX_2$ complexes have the *cis* geometry. Reactions (39) and possibly (40) (both iodides) showed *trans* mixed ligand species. For reactions (35) and (36), equilibrium constants could be measured. For all other cases, [4+2] Diels–Alder cycloaddition occurred and equilibrium constants could not be measured.

Mechanism of phosphine redistribution. It is tempting to suggest that the mechanism for phos-

Table 5. ^{31}P NMR data on reactions of the type $(R_3P)_2PtX_2 + (R'_3P)_2PtX_2 \rightleftarrows 2(R_3P)(R'_3P)PtX_2 \rightarrow$ [4+2] cycloaddition product

Number	X	R_3P^a	R'_3P^a	$\delta^{31}P^b$ (J(Pt—P))^c Mixed ligand	J(PP)^c	[4+2] cycloaddition products $\delta^{31}P$	J(Pt—P)	$\delta^{31}P$	J(Pt—P)	J(PP)
35[d]	Cl	Ph_2VyP	$PhVy_2P$	3.4(3649), −5.6(3562)	17	—	—	—	—	—
36[e]	Cl	DMPP	$Ph(allyl)_2P$	8.5(3363), −2.8(3584)	17	—	—	—	—	—
37	Cl	$PhVy_2P$	DMPP	8.1(3325), 3.1(3613)	19	96.1	3254	21.4	3420	17
38	Cl	Ph_2VyP	DMPP	8.8(3350), 4.3(3652)	17	96.0	3237	20.7	3474	17
39	I	$PhVy_2P$	DMPP	3.3(2300), −6.1(2446)	450	98.5	2957	23.1	3188	10
40	I	Ph_2VyP	DMPP	2.8[f]	—	99.1	2932	24.5	3274	10

[a] Vy = CH=CH_2; DMPP = 1-phenyl-3,4-dimethylphosphole.
[b] In ppm in $CDCl_3$ at 300 K.
[c] In Hz.
[d] $K_{eq} = 5.3$.
[e] $K_{eq} = 57.3$.
[f] Concentration too low to observe additional NMR parameters.

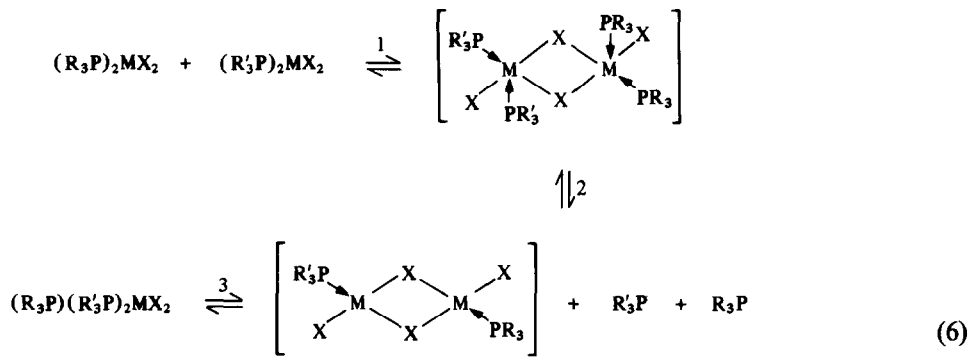

(6)

phine ligand redistribution is similar to that of anion redistribution. We propose the mechanism shown in eq. (6). This is not dissimilar from dimer formation and phosphine dissociation which has been proposed to occur in similar systems.[41,42] Platinum(II) is more inert than palladium(II) and platinum–ligand bond strengths are generally greater than palladium–ligand bond strengths for the same ligands. Hence, one may anticipate the equilibrium constant for equilibrium (2) [eq. (6)] to be smaller for platinum than for palladium and we propose then that neutral ligand redistribution should only occur with platinum for weakly bound ligands. We have shown that redistribution reactions, contrary to our initial expectations, are not only common but unexpectedly rapid for "inert" square-planar palladium(II) and platinum(II) complexes. It seems most likely that they occur by associative processes involving bridged intermediates. The spontaneous *cis–trans* isomerizations which are common[11,14,20] for $(R_3P)_2PdX_2$ complexes, may occur by similar processes.

Acknowledgement—Acknowledgement is made to the donors of the Petroleum Research Fund, administered by the American Chemical Society, for financial support.

REFERENCES

1. J. C. Lockhart, *Redistribution Reactions*. Academic Press, New York (1970).
2. K. Moedritzer, *Adv. Organomet. Chem.* 1968, **6**, 171.
3. M. D. Curtis and P. S. Epstein, *Adv. Organomet. Chem.* 1981, **19**, 213.
4. P. E. Garrou, *Adv. Organomet. Chem.* 1984, **23**, 95.
5. A. W. Verstuyft and J. H. Nelson, *Syn. React. Inorg. Met.-Org. Chem.* 1975, **5**, 69.
6. A. W. Verstuyft, D. A. Redfield, L. W. Cary and J. H. Nelson, *Inorg. Chem.* 1976, **15**, 1128.
7. P. S. Pregosin, *Ann. Rep. NMR Spectrosc.* 1986, **17**, 285.
8. R. K. Harris and B. E. Mann, *NMR and the Periodic Table*, p. 251. Academic Press, New York (1978).
9. F. R. Hartley, *The Chemistry of Platinum and Palladium*. Wiley, New York (1973).
10. G. B. Kauffman and L. A. Teter, *Inorg. Synth.* 1963, **7**, 245.
11. (a) J. J. MacDougall, J. H. Nelson and F. Mathey, *Inorg. Chem.* 1982, **21**, 2145; (b) M. S. Holt, J. H. Nelson and N. W. Alcock, *Inorg. Chem.* 1986, **25**, 2288; (c) J. A. Rahn, M. S. Holt, M. O'Neil-Johnson and J. H. Nelson, *Inorg. Chem.* 1988, **27**, 1316.
12. A. W. Verstuyft, L. W. Cary and J. H. Nelson, *Inorg. Chem.* 1976, **15**, 3161.
13. A. W. Verstuyft and J. H. Nelson, *Inorg. Chem.* 1975, **14**, 1501.
14. D. A. Redfield and J. H. Nelson, *Inorg. Chem.* 1973, **12**, 15.
15. D. A. Redfield and J. H. Nelson, *J. Am. Chem. Soc.* 1974, **96**, 6219.
16. D. A. Redfield and J. H. Nelson, *Inorg. Nucl. Chem. Lett.* 1974, **10**, 931.
17. D. A. Redfield, L. W. Cary and J. H. Nelson, *Inorg. Chem.* 1975, **14**, 50.
18. A. W. Verstuyft, D. A. Redfield, L. W. Cary and J. H. Nelson, *Inorg. Chem.* 1977, **16**, 2776.
19. J. J. MacDougall, F. Mathey and J. H. Nelson, *Inorg. Chem.* 1980, **19**, 1400.
20. J. J. MacDougall, J. H. Nelson, F. Mathey and J. J. Mayerle, *Inorg. Chem.* 1980, **19**, 709.
21. S. O. Grim, R. L. Keiter and W. McFarlane, *Inorg. Chem.* 1967, **6**, 1133.
22. J. M. Jenkins and B. L. Shaw, *J. Chem. Soc. A* 1966, 770.
23. W. J. Louch and D. R. Eaton, *Inorg. Chim. Acta* 1978, **30**, 243.
24. A. J. Mukhedkar, M. Green and F. G. A. Stone, *J. Chem. Soc. A* 1970, 947.
25. J. M. Bowman and Z. Dori, *Inorg. Chem.* 1970, **2**, 395.
26. G. G. Mather, G. J. N. Rapsey and A. Pidcock, *Inorg. Nucl. Chem. Lett.* 1973, **9**, 567.
27. A. Pidcock, R. E. Richards and L. M. Venanzi, *Proc. Chem. Soc. Lond.* 1962, 184.
28. A. Pidcock, in *Catalytic Aspects of Metal Phosphine Complexes* (Edited by E. C. Alyea and D. W. Meek), pp. 1–22. ACS Advances in Chemistry Series 196, American Chemical Society, Washington DC (1982).

29. J. F. Nixon and A. Pidcock, *Ann. Rev. NMR Spectrosc.* 1969, **2**, 345.
30. P. S. Pregosin and R. W. Kunz, ^{31}P *and* ^{13}C *NMR of Transition Metal Phosphine Complexes*, pp. 28–34. Springer, New York (1979).
31. K. R. Dixon, in *Multinuclear NMR* (Edited by J. Mason), pp. 394–396. Plenum Press, New York (1987).
32. P. J. Thompson and R. Puddephatt, *J. Chem. Soc., Chem. Commun.* 1975, 841.
33. P. L. Goggin, R. J. Goodfellow, S. R. Haddock and B. F. Taylor, *J. Chem. Soc., Dalton Trans.* 1976, 459.
34. B. E. Mann, C. Masters, B. L. Shaw, R. M. Slade and R. E. Stainbank, *Inorg. Nucl. Chem. Lett.* 1971, **7**, 881; A. W. Verstuyft, J. H. Nelson and L. W. Cary, *Inorg. Nucl. Chem. Lett.* 1976, **12**, 53; J. H. Nelson and F. Mathey, in *Phosphorus-31 NMR Spectroscopy in Stereochemical Analysis: Organic Compounds and Metal Complexes* (Edited by J. G. Verkade and L. D. Quin), pp. 665–694. VCH Publishers, Deerfield Beach, Florida (1987).
35. G. K. Anderson and R. J. Cross, *Chem. Soc. Rev.* 1980, 185.
36. M. Wada and K. Nishiwaki, *J. Chem. Soc., Dalton Trans.* 1983, 1841.
37. J. D. Scott and R. J. Puddephatt, *Organometallics* 1983, **2**, 1643.
38. A. A. Kiffen, C. Masters and J. P. Visser, *J. Chem. Soc., Dalton Trans.* 1975, 1311.
39. W. J. Louw, D. J. A. de Waal and G. J. Kruger, *J. Chem. Soc., Dalton Trans.* 1976, 2364; K. M. Chui and H. M. Powell, *J. Chem. Soc., Dalton Trans.* 1974, 2117; K. M. Chui and H. M. Powell, *J. Chem. Soc., Dalton Trans.* 1974, 1879.
40. M. S. Holt, J. H. Nelson, P. Savignac and N. W. Alcock, *J. Am. Chem. Soc.* 1985, **107**, 6396; J. A. Rahn, M. S. Holt, G. A. Gray, N. W. Alcock and J. H. Nelson, *Inorg. Chem.* 1989, **28**, 217.
41. K. Tamaka and S. Kawaguchi, *Inorg. Chim. Acta* 1981, **54**, L201.
42. W. J. Louw and R. VanEldick, *Inorg. Chem.* 1981, **20**, 1939.

Polyhedron Vol. 8, No. 7, pp. 909–915, 1989
Printed in Great Britain

0277–5387/89 $3.00+.00
© 1989 Pergamon Press plc

COPPER(II) AND NICKEL(II) COMPLEXES WITH A LINEAR PENTADENTATE LIGAND. THE X-RAY CRYSTAL STRUCTURE OF [CuL][CuCl$_4$] (L = 1,9-BIS-(2-PYRIDYL)-2,5,8-TRIAZANONANE)

M. J. ROSALES* and R. A. TOSCANO

Instituto de Química, Universidad Nacional Autónoma de México, Circuito Exterior, Ciudad Universitaria, Coyoacán 04510, Mexico, D. F.

and

M. A. LUNA-CANUT and M. E. SOSA-TORRES*

División de Estudios de Posgrado, Facultad de Química, Universidad Nacional Autónoma de México, Ciudad Universitaria, Coyoacán 04510, Mexico, D. F.

(*Received* 3 *May* 1988; *accepted* 31 *October* 1988)

Abstract—Reactions between Cu^{II} and Ni^{II} salts and the ligand 1,9-bis-(2-pyridyl)-2,5,8-triazanonane at different stoichiometric relations produced two different complexes in the case of Cu^{II} and only one with Ni^{II}. The spectral properties of these complexes are discussed and the X-ray crystal structure of one of the Cu^{II} products is described. The compound consists of a Cu^{II} pentacoordinated complex cation (all the donor atoms in L are coordinated) and a tetrahedral $[CuCl_4]^{2-}$ group. The coordination geometry of the cation can be described as a distorted square-based pyramid.

Although the study of the coordination chemistry of macrocyclic polyamine ligands, especially the quadridentate, has received much attention, linear polydentate chelators have not been studied so extensively. Pentadentate ligands are stereochemically important both for the interest in the structural behaviour of pentacoordinate complexes in solution and in the solid state,[1] as well as for being potential sources for the synthesis of seven-coordinate transition metal complexes.[2,3]

A number of transition metal complexes with linear pentadentate ligands have been prepared and several spectroscopic structural, electrochemical and kinetic studies have been carried out with them.[4,5]

Various metal complexes of the potential pentadentate ligand 1,9-bis-(2-pyridyl)-2,5,8-triazanonane (PICDIEN) have been prepared. The acid dissociation and stability constants of the Co^{II}, Ni^{II}, Cu^{II} and Zn^{II} complexes[6] and the oxygenation constants of the cobaltous chelates have been determined[7] and a series of Co^{III} isomeric complexes of PICDIEN have been characterized by X-ray diffraction.[8–10] In these last compounds, it can be observed that all five possible coordination sites of the ligand are bonded to the metal atom which has a near regular octahedral coordination sphere.

In this paper we report the reaction of Cu^{II} and Ni^{II} salts with PICDIEN using several M–L stoichiometric relations, the spectral properties of the products and the X-ray crystal structure of one of the copper complexes.

RESULTS AND DISCUSSION

The reactions between PICDIEN and the metal salts were first carried out in 1:1 stoichiometric relationships using nickel(II) and copper(II) chlorides and perchlorates. In the case of nickel, a violet complex was produced regardless of the salt used while both cupric salts yielded a blue compound.

* Authors to whom correspondence should be addressed.

Table 1. Some physical and spectroscopic data for complexes **1–5**

Compound	Colour	μ_{eff} (BM)	Far-IR 200–300 (cm^{-1})		
[Cu(PICDIEN)][$CuCl_4$], **1**	Blue	1.94	295	285	
[Cu(PICDIEN)](ClO_4)$_2$, **2**	Blue	2.03	—	—	—
[Ni(PICDIEN)][$NiCl_4$], **3**	Pink-greyish	3.78	290	275	256
[Ni(PICDIEN)](ClO_4)$_2$, **4**	Pinkish	3.02	—	—	—
[Cu(PICDIEN)][Cu_xCl_y], **5**	Green	3.22[a]	295	270	260
				245	235
				218	212

[a] Based on a molecular formula $x = 5$, $y = 12$.

Table 1 lists some spectroscopic results for the compounds synthesized.

From the analytical and spectroscopic information, the complexes derived from the chlorides were assigned the formulae [CuL][$CuCl_4$], **1**, and [NiL][$NiCl_4$], **3**, and those obtained from the perchlorates [CuL][ClO_4]$_2$, **2**, and [NiL][ClO_4]$_2$, **4**. Compound **2** had been previously prepared but very little information about it was given.

The IR spectra of the complexes show all the bands expected for both the ligand and the counterion. The electronic spectra both in solution and in the solid state were measured for all complexes, and the results are given in Table 2. Figure 1 shows the spectra of **1** and **2**.

The diffuse reflectance spectra are equivalent for both [Cu(PICDIEN)][$CuCl_4$] and [Cu(PICDIEN)][ClO_4]$_2$, indicating that the absorbing species in this region is the cation [Cu(PICDIEN)]$^{2+}$, which is in agreement with the data reported,[11] while the anionic species $[CuCl_4]^{2-}$ is described as absorbing at lower energies.[12]

Hathway *et al.*, in a series of papers,[11,13,14] have determined the absorbing region for copper(II) complexes in a variety of geometries. In this case the spectra obtained suggest that the complex has a square-based pyramid structure distorted towards a trigonal bipyramid.

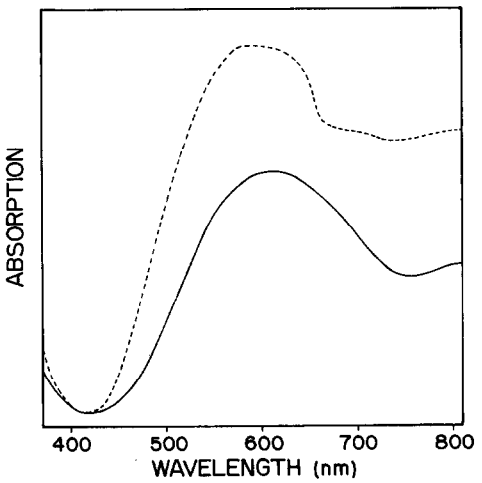

Fig. 1. Diffuse reflectance spectra of **1** (solid line) and **2** (dashed line).

Table 2. Electronic absorption (nm) in solution and in the solid state

	Aqueous solution 0.1 N HCl								Diffuse reflectance			
	λ_{max}	ε_{max}	λ_{min}	ε_{min}	λ_{max}	ε_{max}	λ_{min}	ε_{min}	λ_{max}	λ_{min}	λ_{max}	λ_{min}
[Cu(PICDIEN)][$CuCl_4$]	600	68	425	0					600			
[Cu(PICDIEN)](ClO_4)$_2$	595	119	425	5					580			
[Ni(PICDIEN)][$NiCl_4$][a]	[b]		650	VS[c]	525	11	450	6	[b]	580	520	430
[Ni(PICDIEN)](ClO_4)$_2$[a]	[b]		655	VS	535	14	400	8	[b]	640	520	420
[Ni(PICDIEN)][$NiCl_4$]	716	< 2	652	4	390	[b]						
[Ni(PICDIEN)](ClO_4)$_2$	716	VS	653		393							
[Cu(PICDIEN)][Cu_xCl_y]	619								700			

[a] In H_2O.

[b] There is a broad band near 800 nm.

[c] VS, very small.

Compounds **1** and **2** also give the same electronic spectra when they are dissolved in water or in 0.1 N HCl. This is indicative of the complex being stable and inert enough as to maintain their structure in solution even in an acidic medium.

The diffuse reflectance spectra of the two nickel complexes, **3** and **4**, are very similar. Even though it was not possible to run our spectra in the range of the visible spectrum which has been used as diagnostic of five-coordinate species ($\sim 7700\ cm^{-1}$), the part of the spectra that we can compare is similar to that reported by Sacconi *et al.*[15,16]

The spectra of an aqueous solution remains the same. However, when the complexes are dissolved in 0.1 N HCl, the originally pink tone solutions change to pale green and the UV–vis spectra change. This might be caused by a chloride ligand entering into the sixth coordinating position forming an octahedral complex. The final spectra support this suggestion since they are very similar to those reported for octahedral species.[17,18]

The magnetic moments for **1** and **2** are 1.94 and 2.03 BM, respectively, which are the normal values for Cu^{II} complexes indicating that, in the case of **1**, there is negligible spin–spin coupling. Nickel complexes **3** and **4** have magnetic moments of 3.78 and 3.0 BM, respectively. The first higher value might be due to an orbital contribution to the moment from the tetrahedral counterion $[NiCl_4]^{2-}$. The magnetic moment observed for tetrahedral species such as $[NiCl_4]^{2-}$,[19] or [Ni(hexamethyl phosphoramide)]$^{2+}$,[20] is above 4 BM. Pentacoordinate nickel complexes can assume both high or low spin configurations, regardless of the geometry attained. In the case of the complexes $[Ni\{((CH_3)_2NCH_2CH_2)_3N\}X]^{2+}$ prepared by Ciampolini,[21] the magnetic moment has a value of 3.42 BM and the complex has a trigonal bipyramid structure.[22] We are therefore proposing a similar structure for the cation in **3** and **4**.

Spectroscopic and magnetic data then suggested pentacoordinate complexes for the cations in **1** to **4**. The two idealized geometries for this coordination number are square-based pyramid, symmetry groups C_{4v} and trigonal bipyramidal, symmetry group D_{3h}. Many complexes in fact show geometries that are intermediate between these two.[23] In order to determine which was the case for the copper complex cation prepared in this work an X-ray crystal structure determination of **1** was undertaken.

Crystal structure of **1**

The structure of the compound consists of discrete $[Cu(PICDIEN)]^{2+}$ cations and $[CuCl_4]^{2-}$ anions. The structures of both cation and anion are shown in Fig. 2 together with the atom numbering scheme. Bond lengths and angles are given in Tables 3 and 4.

The cation is a five-coordinated species in which the five coordinating positions of the ligand are bonded to the copper atom in a distorted square-based pyramidal structure. N(1) and N(4) could be considered to occupy the axial positions of a trigonal bipyramid [N(1)—Cu—N(4) 176.2(2)°], indicating that the structure is really intermediate between these two geometries.

The Cu—N bond lengths, with the exception of Cu—N(2) (mean 2.0463 Å), are within the range of values reported in other similar complexes.[23,24] The distance Cu—N(2) of 2.243(4) Å is significantly

Table 3. Bond lengths (Å) for **1**

Cu(1)—Cl(1)	2.260(1)	Cu(1)—Cl(2)	2.255(1)
Cu(1)—Cl(3)	2.292(1)	Cu(1)—C(4)	2.271(1)
Cu(2)—N(1)	2.035(3)	Cu(2)—N(2)	2.243(4)
Cu(2)—N(3)	2.073(4)	Cu(2)—N(4)	2.048(4)
Cu(2)—N(5)	2.029(4)	N(1)—C(1)	1.340(6)
N(1)—C(5)	1.332(6)	N(2)—C(6)	1.464(6)
N(2)—C(7)	1.466(6)	N(3)—C(8)	1.480(6)
N(3)—C(9)	1.485(7)	N(4)—C(10)	1.467(6)
N(4)—C(11)	1.468(6)	N(5)—C(12)	1.330(6)
N(5)—C(16)	1.356(6)	C(1)—C(2)	1.394(7)
C(2)—C(3)	1.372(8)	C(3)—C(4)	1.377(7)
C(4)—C(5)	1.375(6)	C(5)—C(6)	1.514(7)
C(7)—C(8)	1.529(7)	C(9)—C(10)	1.502(8)
C(11)—C(12)	1.503(7)	C(12)—C(13)	1.381(7)
C(13)—C(14)	1.376(9)	C(14)—C(15)	1.374(9)
C(15)—C(16)	1.360(8)		

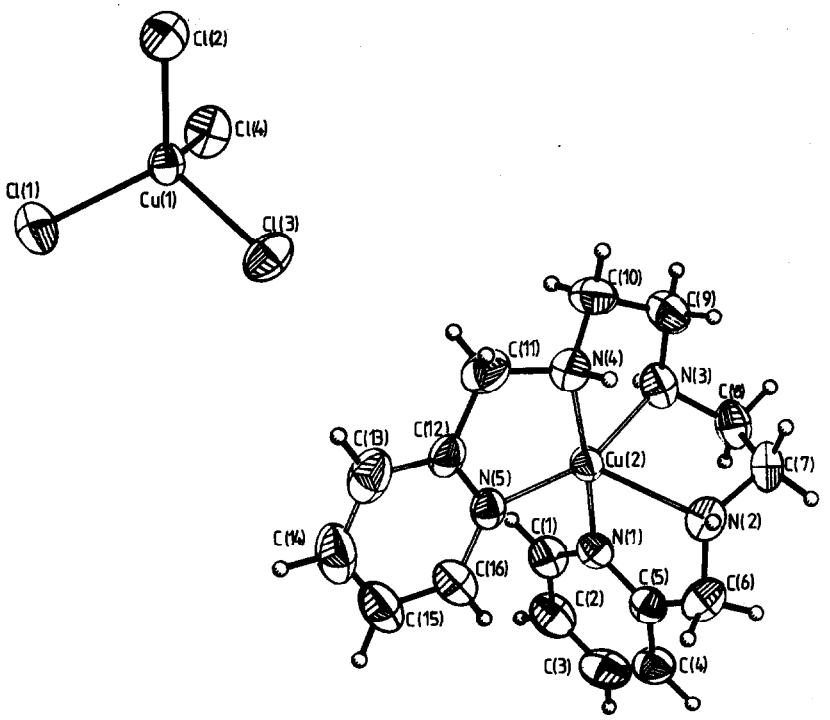

Fig. 2. View of both cation and anion of **1** including numbering scheme

Table 4. Bond angles (deg) for **1**

Cl(1)—Cu(1)—Cl(2)	114.3(1)	Cl(1)—Cu(1)—Cl(3)	110.7(1)
Cl(2)—Cu(1)—Cl(3)	106.7	Cl(1)—Cu(1)—Cl(4)	107.7(1)
Cl(2)—Cu(1)—Cl(4)	108.1	Cl(3)—Cu(1)—Cl(4)	109.2
N(1)—Cu(2)—N(2)	79.3(1)	N(1)—Cu(2)—N(3)	97.9(1)
N(2)—Cu(2)—N(3)	81.7(1)	N(1)—Cu(2)—N(4)	176.2(2)
N(2)—Cu(2)—N(4)	104.3(2)	N(3)—Cu(2)—N(4)	83.9(2)
N(1)—Cu(2)—N(5)	95.8(1)	N(2)—Cu(2)—N(5)	115.5(1)
N(3)—Cu(2)—N(5)	159.9(1)	N(4)—Cu(2)—N(5)	81.6(2)
Cu(2)—N(1)—C(1)	124.1(3)	Cu(2)—N(1)—C(5)	117.2(3)
C(1)—N(1)—C(5)	118.6(4)	Cu(2)—N(2)—C(6)	106.6(3)
Cu(2)—N(2)—C(7)	107.1(3)	C(6)—N(2)—C(7)	114.9(4)
Cu(2)—N(3)—C(8)	108.4(3)	Cu(2)—N(3)—C(9)	108.5(3)
C(8)—N(3)—C(9)	113.3(4)	Cu(2)—N(4)—C(10)	108.0(3)
Cu(2)—N(4)—C(11)	111.0(3)	C(10)—N(4)—C(11)	116.3(4)
Cu(2)—N(5)—C(12)	115.0(3)	Cu(2)—N(5)—C(16)	126.1(3)
C(12)—N(5)—C(16)	118.6(4)	N(1)—C(1)—C(2)	122.1(5)
C(1)—C(2)—C(3)	118.4(5)	C(2)—C(3)—C(4)	119.3(5)
C(3)—C(4)—C(5)	119.2(5)	N(1)—C(5)—C(4)	122.4(4)
N(1)—C(5)—C(6)	117.9(4)	C(4)—C(5)—C(6)	119.7(4)
N(2)—C(6)—C(5)	112.7(4)	N(2)—C(7)—C(8)	111.3(4)
N(3)—C(8)—C(7)	109.9(4)	N(3)—C(9)—C(10)	110.2(4)
N(4)—C(10)—C(9)	109.0(4)	N(4)—C(11)—C(12)	111.7(4)
N(5)—C(12)—C(11)	117.0(4)	N(5)—C(12)—C(13)	121.6(4)
C(11)—C(12)—C(13)	121.4(4)	C(12)—C(13)—C(14)	118.9(5)
C(13)—C(14)—C(15)	119.9(5)	C(14)—C(15)—C(16)	118.2(5)
N(5)—C(16)—C(15)	122.8(5)		

longer than the other Cu—N distances. Although values similar, or longer, to this one are not common, they have been observed in some complexes.[23] It is difficult to explain the reasons for this long bond although it has been reported[25] that a peculiar behaviour of the square-based pyramidal copper complexes is a relatively long bond between copper and the apical coordinating atom with bond lengths ranging from 2.41 to 2.76 Å. If we take N(2) as the apical vertex of a square-based pyramid, an examination of the angles between the remaining donor atoms clearly shows the distortions from the ideal geometry.

The spatial arrangement of the PICDIEN ligand in **1** is diffirent from those observed in the cobalt complexes of PICDIEN, for which crystal structures have been described.[8-10] This must be a consequence of the different steric requirements of the Cu^{II} ion where a pentadentate complex is preferred to the Co^{III} compounds where near regular octahedtral structures are favoured. The torsion angles about the non-rigid bonds of the PICDIEN ligand are presented in Table 5.

There are no significant distortions in the polyamine skeleton. C—C and C—N bond lengths are practically the same as the ones observed in other complexes of PICDIEN. Two of the three secondary nitrogen atoms of the ligand exhibit chirality, the configuration of N(2) is *S* while that of N(4) is *R* (or *R* and *S*).

The anionic group consists of a $CuCl_4$ tetrahedral group with Cu—Cl bond lengths ranging from 2.255(1) to 2.292(1) Å. Cl—Cu—Cl angles are all very close to the ideal value of 109° [106.7–114.3(1)°]. These results contrast with the flattened tetrahedral structure observed for several [alkylammonium]$_2$[$CuCl_4$] salts.[26,27] Those distorted structures have been related to N···Cl short interactions.

Table 5. Torsion angles (deg) for **1**

N(1)—C(5)—C(6)—N(2)	−17.8(6)
C(7)—N(2)—C(6)—C(5)	−92.4(5)
C(6)—N(2)—C(7)—C(8)	90.3(5)
N(2)—C(7)—C(8)—N(3)	50.8(5)
C(9)—N(3)—C(8)—C(7)	73.7(5)
C(8)—N(3)—C(9)—C(10)	−151.7(4)
N(3)—C(9)—C(10)—N(4)	49.9(6)
C(11)—N(4)—C(10)—C(9)	−168.3(4)
C(10)—N(4)—C(11)—C(12)	143.1(4)
N(4)—C(11)—C(12)—N(5)	−10.0(6)

In the case of **1** there are some short intermolecular contacts between some of the amine protons and the chlorine atoms of the anion. Distances for these contacts are given in Table 6.

It has been reported[28] that some linear polydentate ligands can conform so that the same ligand molecule coordinates to two metal atoms. With PICDIEN having a relatively long saturated chain, the ligand has a large flexibility and we decided to carry out reactions in which there was an excess of metal ions as to see if a polynuclear complex could also be obtained.

These reactions with the nickel(II) and copper(II) chlorides were carried out using metal–ligand stoichiometric ratios of 4 : 1. In the case of nickel, **3** was again obtained but in the case of copper a green compound resulted, **5**. It has not been possible to determine with certainty the exact formulation for this compound but we believe it to contain a polynuclear, halogen-bridged anion. A general formula would then be [CuPICDIEN][Cu_xCl_y]. Polynuclear species of this type have been reported.[27,29,30] The same reaction was also carried out with copper(II) acetate and adding $NaClO_4$ in order to precipitate the complex, but **2** was then obtained thus supporting the suggestion of a different anionic species causing the difference in analytical and spectroscopic results.

The diffuse reflectance spectrum of **5** shows a broad band which is believed to be formed by two unresolved overlapping bands. One should correspond to the cation and the other to the anion which could have either tetrahedral or square-based pyramidal geometries around the copper atoms.

When **5** is dissolved in water or in 0.1 N HCl, the electronic spectrum is the same as the one observed for **1**. However if the complex is dissolved in ethanol or dimethylformamide, the spectrum remains the same as that for the solid state.

Table 6. Short intermolecular contacts (Å)

				Symmetry relation		
H(3a)—Cl(1)	2.688	N(3)—Cl(1)	3.532	1.00−x	1.00−y	−z
H(4a)—Cl(3)	2.450	N(4)—Cl(3)	3.398	0.5−x	0.5+y	0.5−z
H(2a)—Cl(2)	2.817	N(2)—Cl(2)	3.419	0.5−x	0.5+y	0.5−z

The magnetic moment for **5** is 3.22 BM which is a very high value for a d^9 species. On the other hand, such a high value could be explained in terms of ferromagnetic interactions such as those reported for $[Cu_2Cl_6]^{2-}$.[31,32] Ferromagnetic or antiferromagnetic interactions can occur in polynuclear structures but further studies are necessary to determine if such effects are present in our complex.

EXPERIMENTAL

Elemental analyses were carried out on a Perkin–Elmer 240B microanalyzer and in Butterworth Ltd Laboratories in the U.K. The metal contents were measured, after decomposition of the complexes, by atomic absorption analyses on a Varian 475 equipment.

IR spectra in the range 4000–200 cm^{-1} were recorded in KBr pellets on a Perkin–Elmer 599B spectrophotometer. Far-IR spectra were obtained on a Perkin–Elmer 1330.

UV-vis spectra in solution and in the solid state were obtained on Bausch Lomb 2000 and Cary 17-D spectrophotometers, respectively.

Magnetic moments were measured at room temperature (23°C) by the Gouy method with a Cahn electromagnet, Model 6685 and a Cahn 2000 electrobalance.

Preparation of the compounds

The ligand 1,9-bis-(2-pyridyl)-2,5,8-triazanonane, L, was prepared as described in the literature.[7]

[CuL][$CuCl_4$]. The ligand, L (1.1107 g, 1 mmol) was dissolved in 25 cm^3 of ethanol and added to a solution of $CuCl_2 \cdot 2H_2O$ (0.6647 g, 1 mmol) in 10 cm^3 of ethanol. The precipitate formed was filtered off, washed with ethanol and dried under vacuum. Found: C, 35.3; H, 4.25; N, 11.5; Cu, 24.5. Analysis calculated for $C_{16}H_{23}N_5Cl_4Cu_2$: C, 34.5; H, 4.13; N, 12.6; Cu, 22.9%.

[CuL][ClO_4]$_2$. $Cu(CH_3COO)_2$ (0.2683 g, 1.47 mmol) was dissolved in 10 cm^3 of ethanol and added to a solution of the ligand (0.4213 g, 1.47 mmol) in ethanol. The complex was precipitated by adding some drops of perchloric acid. The resulting precipitate was filtered, washed and dried. Found: C, 35.5; H, 4.28; N, 12.4; Cu, 12.0. Analysis calculated for $C_{16}H_{23}N_5Cl_2O_8Cu$: C, 35.0; H, 4.23; N, 12.8; Cu, 11.6%.

[CuL][Cu_xCl_y]. This compound was prepared in the same way as the first complex, although 2.226 g (13.05 mmol) of $CuCl_2 \cdot H_2O$ and 0.9303 g (3.2 mmol) of ligand were used. The green precipitate was treated as the previous compounds. Found: C, 17.9; H, 2.71; N, 6.3; Cl, 35.7; Cu, 39.8. Analysis calculated for $C_{16}H_{23}N_5Cl_{12}Cu_6$: C, 17.6; H, 2.10; N, 6.4; Cl, 39.0; Cu, 34.9%.

[NiL][$NiCl_4$]. Same procedure as above using 0.5346 g, 2.2 mmol of $NiCl_2 \cdot 4H_2O$ and 0.627 g, 2.2 mmol of ligand. Found: C, 33.0; H, 4.65; N, 12.1. Analysis calculated for $C_{16}H_{23}N_5Cl_4Ni_2$: C, 33.3; H, 4.4; N, 12.0%.

[NiL][ClO_4]$_2$. $Ni(ClO_4)_2 \cdot 6H_2O$, (0.345 g, 0.94 mmol) and the ligand (0.268 g, 0.94 mmol) were made to react following the same procedure as above. Found: C, 34.2; H, 4.48; N, 12.2. Analysis calculated for $C_{16}H_{23}N_5Cl_2O_8Ni$: C, 34.3; H, 4.46; N, 12.3%.

Crystal structure determination

Crystal data. $Cu_2C_{16}H_{23}N_5Cl_4$, molecular weight = 554, monoclinic, $a = 11.822(2)$, $b = 13.845(3)$, $c = 13.619(3)$ Å, $\beta = 93.17(2)°$, $V = 2225.5(1.9)$ Å^3. Space groups $P2_{1/n}$, $Z = 4$; $\rho_c = 1.653$ g cm^{-3}; $F(000) = 1120$, $\lambda = 0.71069$ Å; μ(Mo-K_α) = 24.14 cm^{-1}.

Data collection and solution

Intensity data were collected on a crystal of dimensions $0.32 \times 0.36 \times 0.4$ mm using ω scans ($3 < 2\theta < 45.0°$) with a variable scan rate from 4 to 30 deg min^{-1} and a scan width of 1.0° on a Nicolet R3m four-circle diffractomer with graphite-monochromated Mo-K_α radiation. From a total of 2910 measured reflections, 2395 with [$F > 3\sigma(F)$] were considered observed and used in the structure solution and refinement. Two monitor reflections with constant intensity, $R_{merge} = 0.0164$ from merging equivalent reflections. Data were corrected for Lorentz and polarization effects. Maximum and minimum transmission factors for absorption corrections were 0.268 and 0.244, respectively.

The structure was solved by direct methods and Fourier difference maps using SHELXTL.[34] The refinement was carried out by the full-matrix least-squares method using anisotropic thermal parameters for all non-hydrogen atoms. Amine protons were localized in a Fourier map and included in the refinement. All the remaining hydrogen atoms were placed in idealized positions and included in the refinement. The weighting scheme used was $[\sigma^2(F_o) + G(F_o^2)]^{-1}$, where σ is the estimated standard deviation based on counting statistics, and G an adjustable variable; the final G value was 0.00028. A final difference Fourier synthesis indicated maximum residuals of 0.6 eÅ^{-3}. Scattering factors were taken from the *International Tables for X-Ray Crystallography*.[35] The calculations were performed on a Nova 4S computer. Final

$R = 0.0361$ and $R_w = 0.034$. Final atomic coordinate and other crystallographic data have been deposited with the Editor and atomic coordinates have been sent to the Cambridge Crystallographic Data Centre.

REFERENCES

1. H. Gampp, D. Haspra, M. Maeder and A. Zuberbuehler, *Inorg. Chem.* 1984, **23**, 3724.
2. S. M. Nelson and D. H. Busch, *Inorg. Chem.* 1969, **8**, 1859.
3. C. W. G. Ansell, J. Lewis, P. R. Raithby, J. N. Ramsden and M. Schröeder, *J. Chem. Soc., Chem. Commun.* 1982, 546.
4. J. H. Timmons, W. R. Harris, I. Murase and A. E. Martell, *Inorg. Chem.* 1978, **17**, 2192.
5. P. Zanello, R. Cini and A. Cinquantini, *Inorg. Chim. Acta* 1983, **74**, 89.
6. W. R. Harris, I. Murase, J. H. Timmons and A. E. Martell, *Inorg. Chem.* 1978, **17**, 889.
7. J. H. Timmons, R. H. Niswander, A. Clearfield and A. E. Martell, *Inorg. Chem.* 1979, **18**, 2977.
8. G. Bombieri, E. Forsellini, A. del Pra, M. L. Tobe, C. Chatterjeer and C. J. Cooksey, *Inorg. Chim. Acta* 1983, **75**, 93.
9. G. Bombieri, E. Forsellini, A. del Pra and M. L. Tobe, *Inorg. Chim. Acta* 1981, **51**, 177.
10. G. Bombieri, E. Forsellini, A. del Pra, M. L. Tobe and C. Chatterjee, *Inorg. Chim. Acta* 1983, **68**, 205.
11. B. J. Hathaway, *J. Chem. Soc., Dalton Trans.* 1972, 1196.
12. A. B. P. Lever, *Inorganic Electronic Spectroscopy*, Chap. 9, p. 359. Elsevier, New York (1968).
13. B. J. Hathaway and A. G. Tomlinson, *Coord. Chem. Rev.* 1970, **5**, 1.
14. B. J. Hathaway and D. E. Billing, *Coord. Chem. Rev.* 1970, **5**, 143.
15. L. Sacconi, P. Nannelli, N. Nardi and V. Campigli, *Inorg. Chem.* 1965, **4**, 943.
16. L. Sacconi, P. L. Orioli and M. Di Vaira, *J. Am. Chem. Soc.* 1965, **87**, 2059.
17. A. B. P. Lever, *Inorganic Electronic Spectroscopy*, Chap. 9, p. 333. Elsevier, New York (1968).
18. W. March and W. Conrad-Fernelius, *J. Chem. Educ.* 1961, **38**, 192.
19. N. S. Gill and R. S. Nyholm, *J. Chem. Soc.* 1959, 3997.
20. J. T. Donoghue and R. S. Drago, *Inorg. Chem.* 1962, **1**, 866.
21. M. Ciampolini and N. Nardi, *Inorg. Chem.* 1966, **5**, 41.
22. M. D. Vaira and P. L. Orioli, *Inorg. Chem.* 1967, **6**, 955.
23. R. R. Holmes, *Prog. Inorg. Chem.* 1984, **32**, 119.
24. B. J. Hathaway, L. Hulett, N. J. Ray and R. Sheahan, *J. Chem. Soc., Dalton Trans.* 1981, 1463.
25. E. L. Muetterties and R. A. Schunn, *Q. Rev.* 1966, **20**, 245.
26. J. Lamotte-Brasseur, L. Dupont and O. Dideberg, *Acta Cryst. Sect. B.* 1973, **29**, 241.
27. L. P. Battaglia, A. Bonamartini-Corradi, G. Marcotrigiano, L. Menabue and G. C. Pellacani, *Inorg. Chem.* 1979, **18**, 148.
28. M. Kimura, S. Suzuki, W. Mori and A. Nakahara, *Inorg. Chim. Acta* 1981, **56**, 83.
29. F. A. Cotton and G. Wilkinson, *Advanced Inorganic Chemistry*, 4th. Edn, p. 812. Wiley, New York (1980).
30. J. R. Wasson, J. W. Hall, H. W. Richardson and W. E. Hatfield, *Inorg. Chem.* 1977, **16**, 458.
31. C. Chow, R. Caputo, R. D. Willet and B. Gerstein, *J. Chem. Phys.* 1974, **61**, 271.
32. D. B. Brown, J. W. Hall, M. F. Scott and W. Hatfield, *Inorg. Chem.* 1977, **16**, 1813, and references therein.
33. O. Yamauchi, H. Seki and T. Shoda, *Bull. Chem. Soc. Jpn* 1983, **56**, 3258.
34. G. M. Sheldrick, SHELXTL Version 3. An Integrated System for Solving, Refining and Displaying Crystal Structures from Diffraction Data. Univ. of Göttingen, F.R.G. (1981).
35. *International Tables for X-Ray Crystallography*, Vol. IV, p. 72. Kynoch Press, Birmingham (1974).

Polyhedron Vol. 8, No. 7, pp. 917–920, 1989
Printed in Great Britain

0277–5387/89 $3.00+.00
© 1989 Pergamon Press plc

REACTIONS OF THE MOLYBDENUM COMPLEX $[MoCl(SnCl_3)(CO)_3(NCMe)_2]$ WITH ONE EQUIVALENT OF L {L = PPh_3, $AsPh_3$, $SbPh_3$, py, 3Br—py, 4Br—py AND $P(OPh)_3$} TO GIVE $[Mo(\mu\text{-}Cl)(SnCl_3)(CO)_3L]_2$. BRIDGE CLEAVAGE REACTIONS OF $[Mo(\mu\text{-}Cl)(SnCl_3)(CO)_3(PPh_3)]_2$

PAUL K. BAKER* and ADRIAN BURY

Department of Chemistry, University College of North Wales, Bangor, Gwynedd LL57 2UW, U.K.

(*Received* 6 *July* 1988; *accepted after revision* 8 *November* 1988)

Abstract—The seven-coordinate molybdenum complex $[MoCl(SnCl_3)(CO)_3(NCMe)_2]$ reacts rapidly with 1 equivalent of L [L = PPh_3, $AsPh_3$, $SbPh_3$, py, 3Br—py, 4Br—py and $P(OPh)_3$], in acetone at room temperature, to afford the chloro-bridged compounds $[Mo(\mu\text{-}Cl)(SnCl_3)(CO)_3L]_2$. The triphenylphosphine dimer $[Mo(\mu\text{-}Cl)(SnCl_3)(CO)_3(PPh_3)]_2$ reacts with 2 equivalents of L′ [L′ = PPh_3, $SbPh_3$, py and $P(OPh)_3$] to give the bridge-cleaved mononuclear compounds $[MoCl(SnCl_3)(CO)_3LL']$.

Recent interest in seven-coordinate complexes has been highlighted by Bencze *et al.*[1,2] They showed the seven-coordinate complexes $[MX_2(CO)_3L_2]$ (M = Mo or W; X = Cl or Br; L = PPh_3 or $AsPh_3$) to be active alkene metathesis catalysts for the ring-opening polymerization of norbornene and norbornadiene.[1,2] Although many examples of seven-coordinate dihalo complexes of the type $[MX_2(CO)_3L_2]$ (M = Mo or W; X = Cl, Br or I; L = neutral donor ligands) have been prepared,[3–11] very few analogous halotin compounds such as $[MX(SnX_3)(CO)_3L_2]$ have been reported.[12–14] Very recently we have described the preparation of the reactive seven-coordinate halotin complex, $[MoCl(SnCl_3)(CO)_3(NCMe)_2]$, from reaction of the zero-valent complex $[Mo(CO)_3(NCMe)_3]$ *in situ* with an equimolar quantity of $SnCl_4$.[15]

In this paper we wish to describe the reactions of $[MoCl(SnCl_3)(CO)_3(NCMe)_2]$ with 1 equivalent of monodentate neutral donor ligand (L) to rapidly give the chloro-bridged complexes $[Mo(\mu\text{-}Cl)(SnCl_3)(CO)_3L]_2$. The bridge cleavage reactions of $[Mo(\mu\text{-}Cl)(SnCl_3)(CO)_3L]_2$ are also described herein.

EXPERIMENTAL

All reactions described in this paper were carried out under an atmosphere of dry nitrogen using standard Schlenk line techniques.

The complex $[MoCl(SnCl_3)(CO)_3(NCMe)_2]$ was prepared by the published method.[15] $[Mo(CO)_6]$ was generously donated by Amax Speciality Metals U.K. Ltd. All other chemicals were purchased from commercial sources.

Elemental analyses for carbon, hydrogen and nitrogen were recorded on a Carlo Erba Elemental Analyser MOD 1106 (using helium as a carrier gas). IR spectra were recorded on a Perkin–Elmer 1430 ratio recording IR spectrophotometer. Magnetic susceptibilities of the complexes were measured on a Johnson-Matthey Magnetic Susceptibility balance. The molecular weight of $[Mo(\mu\text{-}Cl)(SnCl_3)(CO)_3(py)]_2$ (**4**) was determined by Rast's method[16] using camphor as the solvent.

$[Mo(\mu\text{-}Cl)(SnCl_3)(CO)_3(PPh_3)]_2$ (**1**)

To $[MoCl(SnCl_3)(CO)_3(NCMe)_2]$ (4.03 g, 7.7 mmol) dissolved in acetone (50 cm^3) with continuous stirring under a stream of dry nitrogen, was added PPh_3 (2.02 g, 7.7 mmol). After stirring for 30 s, filtration and removal of the solvent *in vacuo* gave light brown crystals of $[Mo(\mu\text{-}Cl)(SnCl_3)(CO)_3(PPh_3)]_2$ (**1**) (yield = 5.31 g, 98%), which were recrystallized from acetone.

Similar reactions of $[MoCl(SnCl_3)(CO)_3(NCMe)_2]$ with 1 equivalent of L [L = $AsPh_3$, $SbPh_3$, py, 3Br—py, 4Br—py and $P(OPh)_3$] in ace-

* Author to whom correspondence should be addressed.

Table 1. Physical and analytical[a] data for the complexes $[Mo(\mu\text{-}Cl)(SnCl_3)(CO)_3L]_2$ and $[MoCl(SnCl_3)(CO)_3LL']$

Complex	Colour	Yield	C	H	N
$[Mo(\mu\text{-}Cl)(SnCl_3)(CO)_3(PPh_3)]_2$ (1)	Orange–brown	98	36.1	3.1	—
			(35.9)	(2.2)	—
$[Mo(\mu\text{-}Cl)(SnCl_3)(CO)_3(AsPh_3)]_2$ (2)	Light brown	75	34.2	2.7	—
			(33.8)	(2.0)	—
$[Mo(\mu\text{-}Cl)(SnCl_3)(CO)_3(SbPh_3)]_2$ (3)	Light brown	80	31.5	2.1	—
			(31.8)	(1.9)	—
$[Mo(\mu\text{-}Cl)(SnCl_3)(CO)_3(py)]_2$ (4)	Brown	92	18.3	1.4	2.9
			(18.5)	(1.0)	(2.7)
$[Mo(\mu\text{-}Cl)(SnCl_3)(CO)_3(3Br—py)]_2$ (5)	Brown	78	16.4	1.0	2.2
			(16.1)	(0.7)	(2.3)
$[Mo(\mu\text{-}Cl)(SnCl_3)(CO)_3(4Br—py)]_2$ (6)	Brown	80	15.3	0.8	2.2
			(16.1)	(0.7)	(2.3)
$[Mo(\mu\text{-}Cl)(SnCl_3)(CO)_3\{P(OPh)_3\}]_2$ (7)	Brown	64	34.2	2.6	—
			(33.6)	(2.0)	—
$[MoCl(SnCl_3)(CO)_3(PPh_3)_2]$ (8)	Yellow	69	48.4	3.4	—
			(48.5)	(3.1)	—
$[MoCl(SnCl_3)(CO)_3(PPh_3)(SbPh_3)]$ (9)	Orange–yellow	74	45.3	3.0	—
			(44.4)	(2.9)	—
$[MoCl(SnCl_3)(CO)_3(py)(PPh_3)]$ (10)	Orange–yellow	90	40.6	2.2	1.8
			(39.9)	(2.6)	(1.8)
$[MoCl(SnCl_3)(CO)_3(PPh_3)\{P(OPh)_3\}]$ (11)	Brown	88	45.7	3.2	—
			(46.2)	(3.0)	—

[a] Calculated values in parentheses.

tone at room temperature after stirring for 30 s, afforded the analogous chloro-bridged complexes $[Mo(\mu\text{-}Cl)(SnCl_3)(CO)_3L]_2$ (**2–7**) (see Table 1 for colour and yields). Molecular weight determination for $[Mo(\mu\text{-}Cl)(SnCl_3)(CO)_3(py)]_2$: Found: 872, Calc: 1039.

Reaction of $[Mo(\mu\text{-}Cl)(SnCl_3)(CO)_3(PPh_3)]_2$ *with 2 equivalents of* PPh_3

To $[Mo(\mu\text{-}Cl)(SnCl_3)(CO)_3(PPh_3)]_2$ (0.70 g, 0.5 mmol) dissolved in acetone (15 cm^3) with continuous stirring under a stream of dry nitrogen, was added PPh_3 (0.26 g, 1 mmol). After stirring for 30 min, filtration and removal of the solvent *in vacuo* gave bright yellow crystals of $[MoCl(SnCl_3)(CO)_3(PPh_3)]_2$ (**8**) (yield = 0.66 g, 69%), which were recrystallized from acetone.

Similar reactions of $[Mo(\mu\text{-}Cl)(SnCl_3)(CO)_3(PPh_3)]_2$ with 2 equivalents of L′ [L′ = $SbPh_3$, py and $P(OPh)_3$] gave $[MoCl(SnCl_3)(CO)_3(PPh_3)L]$ (**8–11**) (see Table 1 for colours and yields).

RESULTS AND DISCUSSION

Equimolar quantities of the bisacetonitrile complex $[MoCl(SnCl_3)(CO)_3(NCMe)_2]$ and L [L = PPh_3, $AsPh_3$, $SbPh_3$, py, 3Br—py, 4Br—py and $P(OPh)_3$] react in acetone at room temperature to give good yields of the new chloro-bridged dimers $[Mo(\mu\text{-}Cl)(SnCl_3)(CO)_3L]_2$ (**1–7**). The triphenylphosphine dimer $[Mo(\mu\text{-}Cl)(SnCl_3)(CO)_3(PPh_3)]_2$ (**1**) reacts with 2 equivalents of L′ [L′ = PPh_3, $SbPh_3$, py and $P(OPh)_3$] in acetone at room temperature, to give the symmetrical bridge-cleaved products $[MoCl(SnCl_3)(CO)_3LL']$ (**8–11**). The complexes, **1–11**, were characterized by elemental analysis (C, H and N) (Table 1) and IR spectroscopy (Table 2). All the complexes were found to be diamagnetic, which was expected since the complexes obey the effective atomic number rule. The dimers **1–7** are photosensitive and thermally unstable, however they can be stored in the dark under a nitrogen atmosphere at 0°C for several days. The monomeric complexes, **8–11**, are more stable than the dimers, but are still stored in Schlenk tubes under nitrogen. The complexes, **1–11**, are only slightly soluble in chlorinated solvents such as $CHCl_3$ or CH_2Cl_2, however they are much more soluble in acetone (see Experimental).

Reaction of $[MoCl(SnCl)_3(CO)_3(NCMe)_2]$ with 1 equivalent of L [L = PPh_3, $AsPh_3$, $SbPh_3$, py, 3Br—py, 4Br—py and $P(OPh)_3$] probably initially affords the monoacetonitrile complexes $[MoCl(SnCl_3)(CO)_3(NCMe)L]$. Several attempts

Table 2. IR data[a] for the complexes $[Mo(\mu\text{-}Cl)(SnCl_3)(CO)_3L]_2$ and $[MoCl(SnCl_3)(CO)_3LL']$

Complex	ν(CO) (cm^{-1})
(1)	2077, 2051, 1959, 1941, 1873 and 1708
(2)	2050, 2040, 1966, 1959, 1945 and 1879
(3)	2040, 1937 and 1868
(4)	2034, 1948 and 1940
(5)	2025, 1946, 1940, 1927, 1919 and 1915
(6)	2025, 1947, 1940, 1929, 1927 and 1916
(7)	2002, 1959, 1929 and 1902
(8)	1964, 1950 and 1882
(9)	1947, 1941 and 1877
(10)	1958, 1946 and 1940
(11)	1980, 1945 and 1881

[a] Spectra recorded as $CHCl_3$ thin films between NaCl plates.

were made to isolate these monoacetonitrile intermediates by rapid work-up procedures without success. Evidence to support the initial formation of these monoacetonitrile intermediates comes from related work we have carried out on the related diiodo system $[MI_2(CO)_3(NCMe)_2]$ (M = Mo and W). The complexes $[MI_2(CO)_3(NCMe)_2]$, react with 1 equivalent of L [L = PPh_3, $AsPh_3$, $SbPh_3$, PPh_2Cy and $P(OPh)_3$] in CH_2Cl_2 to give the monoacetonitrile complexes $[MI_2(CO)_3(NCMe)L]$, which were isolated and fully characterized.[17] The apparent greater ease of dimerization of $[MoCl(SnCl_3)(CO)_3(NCMe)L]$ compared to the diiodo analogues, may be due to the steric bulk of the $SnCl_3$ group. Seven-coordinate complexes of molybdenum(II) and tungsten(II) are highly crowded and coordinatively saturated, hence it is highly likely that the substitution reactions go via a dissociative mechanism. Hence, the bulky $SnCl_3$ group attached to the metal should facilitate easy loss of acetonitrile from $[MoCl(SnCl_3)(CO)_3(NCMe)L]$ to give the dimers $[Mo(\mu\text{-}Cl)(SnCl_3)(CO)_3L]_2$. The dimeric nature of the complexes $[Mo(\mu\text{-}Cl)(SnCl_3)(CO)_3L]_2$ was confirmed by molecular weight measurements on $[Mo(\mu\text{-}Cl)(SnCl_3)(CO)_3(py)]_2$ (**4**) by Rast's method[16] (see Experimental).

It is highly likely that the dimeric complexes, **1**–**7**, are bridged via the chloride ion rather than the $SnCl_3$ group, since $SnCl_3$ does not possess a dative lone pair on the tin (apart from the attached chlorine atoms) to coordinate to the other molybdenum atom. It is improbable that chloride groups on the tin bridge, since there are no precedents for this type of behaviour. Several attempts were made to grow a single crystal for X-ray crystallography of the dimers $[Mo(\mu\text{-}Cl)(SnCl_3)(CO)_3L]_2$ (**1**–**7**), but due to the instability of these complexes no success was achieved. However, since the structure of the bromide-bridged dimer $[W(\mu\text{-}Br)Br(CO)_4]_2$ shows the two tungsten atoms to be in capped octahedral environments,[18] it is highly likely that these $[Mo(\mu\text{-}Cl)(SnCl_3)(CO)_3L]_2$ (**1**–**7**) complexes have this type of geometry.

Symmetric cleavage of the chloride bridges in the complexes $[Mo(\mu\text{-}Cl)(SnCl_3)(CO)_3(PPh_3)]_2$ (**1**), by L′ to give monomeric seven-coordinate complexes of the type $[MoCl(SnCl_3)(CO)_3(PPh_3)L']$, are similar to the symmetric bridge cleavage reactions carried out on the octacarbonyl halo-bridged dimers of the type $[M(\mu\text{-}X)X(CO)_4]_2$ (M = Mo or W; X = Cl, Br or I) described by Colton and his coworkers.[19] Since the IR spectra of the compounds $[MoCl(SnCl_3)(CO)_3(PPh_3)L']$ (**8**–**11**) show three carbonyl stretching bands (Table 2) with a similar pattern to analogous dihalo complexes of the type $[MX_2(CO)_3L_2]$ which have been shown to have capped octahedral geometry by X-ray crystallography,[20–28] it is likely that complexes **8**–**11** have this geometry.

Acknowledgements—We wish to thank Amax Speciality Metals Ltd for their generous gift of $[Mo(CO)_6]$, and we thank Mr A. Quinlan for measuring the molecular weight of $[Mo(\mu\text{-}Cl)(SnCl_3)(CO)_3(py)]_2$ by Rast's method.

REFERENCES

1. L. Bencze and A. Kraut-Vass, *J. Molec. Catal.* 1985, **28**, 369.
2. L. Bencze, A. Kraut-Vass and L. Prókai, *J. Chem. Soc., Chem. Commun.* 1985, 911.
3. M. H. B. Stiddard, *J. Chem. Soc. A.* 1962, 4712.
4. R. Colton and I. B. Tomkins, *Aust. J. Chem.* 1966, **19**, 1143.
5. J. Lewis and R. Whyman, *J. Chem. Soc. A.* 1967, 77.
6. W. S. Tsang, D. W. Meek and A. Wojcicki, *Inorg. Chem.* 1968, **7**, 1263.
7. J. R. Moss and B. L. Shaw, *J. Chem. Soc. A.* 1970, 595.
8. L. Bencze, *J. Organomet. Chem.* 1972, **37**, C37.
9. A. D. Westland and N. Muriithi, *Inorg. Chem.* 1973, **12**, 2356.
10. S. C. Tripathi, S. C. Srivastava and A. K. Shrimal, *Inorg. Chim. Acta.* 1976, **18**, 231.
11. J. A. Bowden and R. Colton, *Aust. J. Chem.* 1969, **22**, 905.
12. K. Edgar, B. F. G. Johnson, J. Lewis and S. B. Wild, *J. Chem. Soc. A.* 1968, 2851.
13. M. Panizo and M. Cano, *J. Organomet. Chem.* 1985, **287**, 221.
14. A. Bell and R. A. Walton, *J. Organomet. Chem.* 1985, **290**, 341.

15. P. K. Baker and A. Bury, *J. Organomet. Chem.* 1989, **359**, 189.
16. F. G. Mann and B. C. Saunders (Eds), *Practical Organic Chemistry*, pp. 342–344. Longman Green, London (1954).
17. P. K. Baker and S. G. Fraser, *Transition Met. Chem.* 1987, **12**, 560.
18. F. A. Cotton, L. R. Falvello and J. H. Meadows, *Inorg. Chem.* 1985, **24**, 514.
19. R. Colton, *Coord. Chem. Rev.* 1971, **6**, 269.
20. M. G. B. Drew, A. W. Johans and A. P. Wolters, *J. Chem. Soc., Chem. Commun.* 1971, 819.
21. M. G. B. Drew and J. D. Wilkins, *J. Chem. Soc., Dalton Trans.* 1973, 2664.
22. A. Mawby and G. E. Pringle, *J. Inorg. Nucl. Chem.* 1972, **34**, 517.
23. M. G. B. Drew, *J. Chem. Soc., Dalton Trans.* 1972, 1329.
24. G. Schmid, R. Boese and E. Welz, *Chem. Ber.* 1975, **108**, 260.
25. M. G. B. Drew and J. D. Wilkins, *J. Chem. Soc., Dalton Trans.* 1975, 1984.
26. R. Boese and U. Müller, *Acta Cryst.* 1977, **B33**, 582.
27. M. G. B. Drew and A. P. Wolters, *Acta Cryst.* 1977, **B34**, 205.
28. M. G. B. Drew and J. D. Wilkins, *J. Chem. Soc., Dalton Trans.* 1977, 557.

Polyhedron Vol. 8, No. 7, pp. 921–924, 1989
Printed in Great Britain

0277–5387/89 $3.00+.00
© 1989 Pergamon Press plc

A ^{95}Mo NMR STUDY OF ELECTRONIC EFFECTS IN TETRACARBONYL–MOLYBDENUM COMPLEXES OF AROMATIC α-DIIMINE CHELATE LIGANDS

ELMER C. ALYEA† and JOHN MALITO

Guelph-Waterloo Centre for Graduate Work in Chemistry, Department of Chemistry and Biochemistry, University of Guelph, Guelph, Ontario, Canada N1G 2W1

and

SYLVIA D. ERNST, WOLFGANG KAIM† and STEPHAN J. KOHLMANN

Institute für Anorganische Chemie der Universität, Pfaffenwaldring 55, D-7000 Stuttgart 80, F.R.G.

(*Received* 7 *April* 1988; *accepted* 8 *November* 1988)

Abstract—Studies of nine (α-diimine)Mo(CO)$_4$ complexes demonstrate the importance of metal-to-ligand charge-transfer contributions for the chemical shift in ^{95}Mo NMR spectroscopy. The $\delta(^{95}Mo)$ values, which occur in the range −847 to −1164 ppm, correlate with the calculated LUMO coefficients c_N^2 at the coordinating (chelate) nitrogen centres, with the McLachlan π-spin populations ρ_N^{ML} and with ESR coupling constants $a(^{14}N)$ of the anion radical complexes.

^{95}Mo NMR spectroscopy has already proven to be a very valuable tool for various areas of molybdenum chemistry[1,2] with the shift scale for this nucleus ($I = 5/2$, 15.7% natural abundance) encompassing more than 7000 ppm. There are usually relatively narrow lines [$Q = -0.015(4)\ 10^{-28}$ m^2] observed with coordination complexes, so that a number of structural and electronic effects can be studied by this method; e.g. long range electronic interactions,[3–5] stereochemistry in chiral complexes,[6] or chelate ring size contributions.[7] Chemical shift and coupling constant data are now available for an extensive range of substituted molybdenum carbonyl complexes.[1,8]

In order to gain an even more detailed understanding as to what factors influence the ^{95}Mo NMR chemical shift, we have now studied isostructural complexes between the Mo(CO)$_4$ fragment and a number of α-diimine chelate ligands, whose characteristics in terms of calculated molecular orbital and various related experimental data are well established.[9–17] Particularly interesting is the series of four isomeric bidiazine complexes complexes which have already allowed some insight into the mechanisms and consequences of charge-transfer interactions in coordination compounds.[9,11,17]

RESULTS AND DISCUSSION

The structures of the ligands employed are shown in Fig. 1: bpdz = 3,3′-bipyridazine, bpm = 4,4′-bipyrimidine, bpz = 2,2′-bipyrazine, bpym = 2,2′-bipyrimidine, abpy = 2,2′-azobipyridine, bptz = 3,6-bis(2′-pyridyl)-1,2,4,5-tetrazine. Spectroscopic results and relevant data for the ligands are summarized in Table 1, with the $\delta(^{95}Mo)$ data for the 2,2′-bipyridine (bpy) complex being taken from ref. 7. Starting with the most revealing comparison of the four isomeric bidiazine systems, these complexes exhibit a familiar pattern:[9] while the two mononuclear bipyrimidine compounds show spectra very similar to that of the bpy system, the two other complexes display a distinct low field shift and a detectable narrowing of the absorption signal. This result clearly rules out the ligand field strength as being solely responsible for the chemical shift. The HOMO–LUMO difference follows the order bpm < bpdz ~ bpz < bpym, as experimentally[9] indicated by metal-to-ligand (d–π^*) charge-transfer (MLCT) absorptions and by the respective differ-

† Authors to whom correspondence should be addressed.

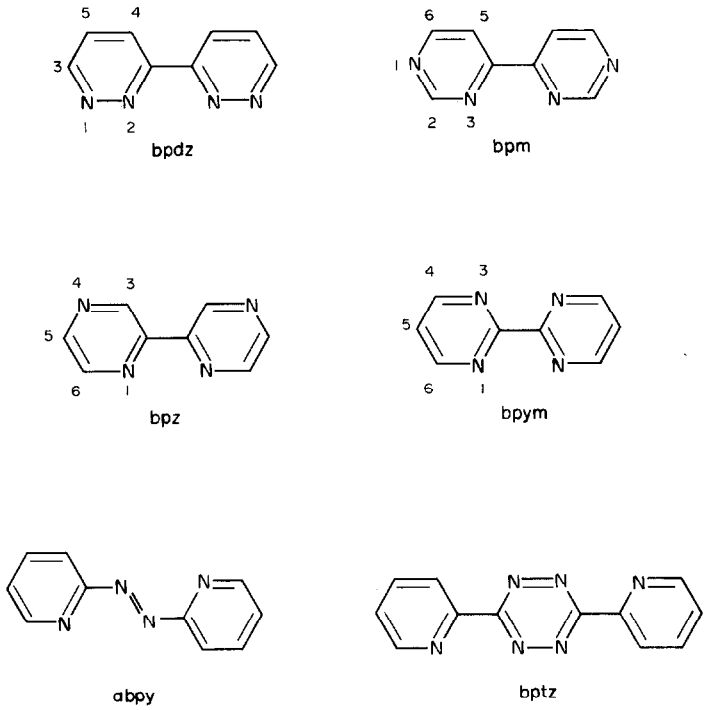

Fig. 1.

ences between the oxidation and reduction potentials. The observed $\delta(^{95}Mo)$ values also do not directly parallel the changes in the ground state basicity K_b of the ligand (bpz < bpm < bpym < bpdz),[9,16] which in any case is not expected to dominate the magnitude of the chemical shift.[1,8]

Instead, this observed pattern correlates with the calculated LUMO coefficients c_N^2 at the coordinating (chelate) nitrogen centres,[9] with the McLachlan π-spin populations ρ_N^{ML} and ^{14}N ESR coupling constants, a, of the anion radical complexes.[13] Although the $^{95,97}Mo$ coupling constants in the anion radicals could be observed in but a few cases, because of the low natural abundance of these isotopes (^{97}Mo: $I = 5/2$, 9.6%),[13-15] it may be safely assumed on the basis of the direct cor-

Table 1. ^{95}Mo NMR parameters and reference data for (α-diimine)$Mo(CO)_4$ complexes

Complex	$\delta(^{95}Mo)$ [$\Delta\nu_{1/2}$(Hz)]	c_N^{2a}	$\rho_N^{ML b}$	$a(^{14}N)$ (mT)	Reference
(bpy)$Mo(CO)_4$	−1164 (60)	0.139	0.173	0.36	7, 19, 20
(bpym)$Mo(CO)_4$[c]	−1162 (64)	0.095	0.104	0.228	9, 13, 21
(bpym)$[Mo(CO)_4]_2$	−1162 (58)				
(bpm)$Mo(CO)_4$	−1162 (67)	0.104	0.128	0.26	9, 13
(bpz)$Mo(CO)_4$	−1112 (41)	0.170	0.208	0.468	9, 13
(bpdz)$Mo(CO)_4$	−1102 (28)	0.163	0.230	0.550	9, 13
(abpy)$Mo(CO)_4$[c]	−936 (4)	0.251, 0.078[d]	0.319, 0.085[d]	~ 0.6, 0.24[d]	10, 14
(bptz)$Mo(CO)_4$[c]	−904 (12)	0.250, 0.000[d]	0.297, −0.009[d]	0.640, < 0.02[d]	10,14
(bptz)$[Mo(CO)_4]_2$	−847(22)				

[a] Coulomb integral parameters $h_N = 0.5$.

[b] Coulomb integral parameter of coordinating nitrogen centres $h_N = 0.8$, of non-coordinating centres $h_{N'} = 0.5$ (bidiazines) or $h_{N'} = 0.8$ (bptz); McLachlan parameter $\lambda = 1.2$.

[c] ESR data and ρ_N^{ML} for the binuclear $Mo(CO)_4$ complex.

[d] Pyridine nitrogen centre.

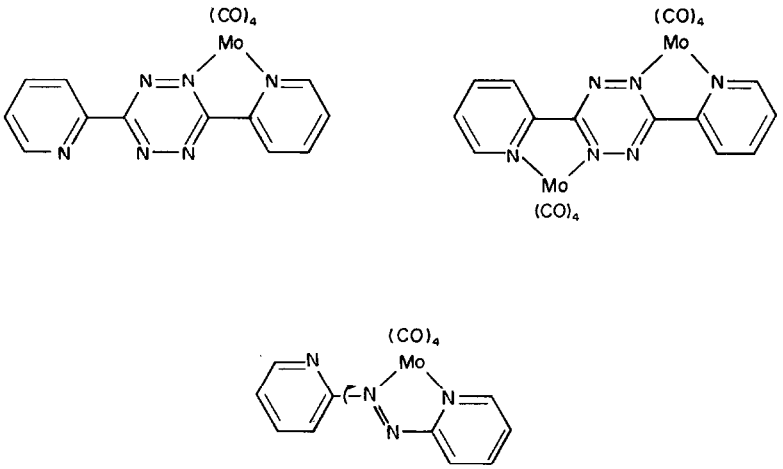

Fig. 2.

relation between $a(^{14}N)$ and $a(^{95,97}Mo)$[14] that the chemical shift correlates with the coupling constant of the metal in the singly reduced complex (see Table 1).

This relation also holds for complexes of the other two ligands, abpy and bptz (see Fig. 2). Large c_N^2, ρ_N^{ML} and $a(^{14}N)$ values for the coordinating azo nitrogen centres[10,14,15] correlate qualitatively with more deshielded values of $\delta(^{95}Mo)$. The value for the mononuclear abpy complex is a little more shielded than that for the bptz system, since the former cannot adopt a coplanar conformation,[10,18] thereby reducing the π-interaction as is also evident from a cathodically shifted reduction potential.[10] A double metal–ligand interaction in the binuclear bptz complex results in a further low field shift for the metals, in agreement with a strongly lowered LUMO, facilitated reduction and a very low-lying metal-to-ligand charge-transfer (MLCT) transition.[10] In the bpym series, on the other hand, the second coordination of $Mo(CO)_4$ does not cause a detectable shift in $\delta(^{95}Mo)$ (Table 1); bpym is a ligand with relatively poor π-acceptor capability.[9,10]

The line width $\Delta\nu_{1/2}$ seems to relate to the nearness of the second nitrogen atom to the coordinated nitrogen centre, the complex with the α-iminoazo ligand abpy, exhibiting a very low value of only 4 Hz. The narrowness of this line is surprising when compared to other *cis*-$Mo(CO)_4L_2$ values,[1,8] especially since the bite angle in $Mo(CO)_4$(abpy) (70.9°) is even less than that in α-diimine complexes (72.8°).[22] This lowering of the electric field gradient at the molybdenum nucleus is enhanced by the proximity of the second nitrogen atom and is consistent with the greater charge delocalization, but such a correlation with the line width must remain tentative.

CONCLUSION

The results obtained in this study of qualitatively isostructural $Mo(CO)_4$ complexes illustrate the significance of charge-transfer interactions for the ^{95}Mo NMR chemical shift. The factors affecting the magnitude of $\delta(^{95}Mo)$ are normally discussed with reference to a modified Ramsey expression for the paramagnetic term[1,8] that includes spectrochemical (ΔE) and nephelauxetic ($k'\langle r^{-3}\rangle$) factors. In the present case, neither the ground-state basicities of the ligands nor the MLCT absorption energies of the complexes properly account for the observed trends of $\delta(^{95}Mo)$; it is the amount of charge transferred from the low valent metal to the π-accepting ligand via the N(chelate) coordination centres which correlates with the chemical shift of the metal. This study has thus shown a correlation of NMR chemical shift data with ESR coupling constants in the singly reduced complexes,[23] an observation which may be of significance for other metal complexes as well.[24]

EXPERIMENTAL

Preparation of the ligands and complexes has been described previously.[9,10,15]

The ^{95}Mo NMR spectra were recorded at 26.08 MHz frequency on a Bruker WH 400 spectrometer at Guelph, using 10 mm sample tubes and dichloromethane solutions at ambient temperatures and with aq. 2 M K_2MoO_4 at pH 11 as external standard. The pulse width was normally 47 μs for the 90° pulse, with the resolution being better than 13 Hz per point.

Acknowledgements—Support for this work has come from Deutsche Forschungsgemeinshaft, Fonds der Chemischen Industrie and Flughafen Frankfurt/Main AG (to W.K.), from N.S.E.R.C. (Canada) and from an Imperial Oil University Research Grant (to E.C.A.).

REFERENCES

1. M. Minelli, J. H. Enemark, R. T. C. Brownlee, M. J. O'Connor and A. G. Wedd, *Coord. Chem. Rev.* 1985, **68**, 169.
2. E. C. Alyea, A. Malek and J. Malito, *Polyhedron* 1986, **5**, 403; C. G. Young, M. Minelli, J. H. Enemark, G. Miessler, N. Janietz, H. Kauermann and J. Wachter, *Polyhedron* 1986, **5**, 407; R. A. Grieves and J. Mason, *Polyhedron* 1986, **5**, 415.
3. S. Donovan-Mtunzi, M. Hughes, G. J. Leigh, J. Mason, H. M. Ali and R. L. Richards, *J. Organomet. Chem.* 1983, **246**, C1.
4. R. T. C. Brownlee, A. F. Masters, M. J. O'Connor, A. G. Wedd, H. A. Kimlin and J. D. Cotton, *Org. Magn. Res.* 1982, **20**, 73.
5. E. C. Alyea and J. Topich, *Inorg. Chim. Acta* 1982, **65**, L95.
6. M. Minelli, T. W. Rockway, J. H. Enemark, H. Brunner and M. Muschiol, *J. Organomet. Chem.* 1981, **217**, C34.
7. E. C. Alyea and A. Somogyvari, *Magn. Res. Chem.* 1986, **24**, 357.
8. E. C. Alyea and A. Somogyvari, *Transition Met. Chem.* 1987, **12**, 306; E. C. Alyea and A. Somogyvari, *Can. J. Chem.* 1988, **66**, 397.
9. S. Ernst and W. Kaim, *J. Am. Chem. Soc.* 1986, **108**, 3578.
10. W. Kaim and S. Kohlmann, *Inorg. Chem.* 1987, **26**, 68.
11. S. Ernst, Y. Kurth and W. Kaim, *J. Organomet. Chem.* 1986, **302**, 211.
12. W. Kaim and S. Kohlmann, *Inorg. Chem.* 1986, **25**, 3306.
13. W. Kaim and S. Ernst, *J. Phys. Chem.* 1986, **90**, 5010.
14. W. Kaim and S. Kohlmann, *Inorg. Chem.* 1986, **25**, 3442.
15. W. Kaim, S. Ernst and S. Kohlmann, *Polyhedron* 1986, **5**, 445.
16. S. Ernst and W. Kaim, *Inorg. Chim. Acta* 1986, **114**, 123.
17. W. Kaim and B. Olbrich-Deussner, *J. Organomet. Chem.* 1988, **340**, 71.
18. D. Fenske, W. Kaim and S. Kohlmann, unpublished structural results.
19. H. tom Dieck, K. D. Franz and F. Hohmann, *Chem. Ber.* 1975, **108**, 163.
20. W. Kaim, *Chem. Ber.* 1981, **114**, 3789; *J. Am. Chem. Soc.* 1982, **104**, 3833.
21. W. Kaim, *Inorg. Chem.* 1984, **23**, 3365.
22. R. S. L. Bruce, M. K. Cooper, H. C. Freeman and B. G. McGrath, *Inorg. Chem.* 1974, **13**, 1032.
23. W. Kaim, *Coord. Chem. Rev.* 1987, **76**, 187.
24. J. Mason, *Chem. Rev.* 1987, **87**, 1299, or D. Rehder, *Bull. Magn. Res.* 1982, **4**, 33.

Polyhedron Vol. 8, No. 7, pp. 925–927, 1989
Printed in Great Britain

0277–5387/89 $3.00+.00
© 1989 Pergamon Press plc

ADDUCT FORMATION BY NICKEL(II) COMPLEXES OF S-METHYL HYDRAZINE CARBODITHIOATE SCHIFF BASES WITH 2,2′-BIPYRIDYL AND 1,10-PHENANTHROLINE

ALY M. A. HASSAAN,* EZZAT M. SOLIMAN and AHMED M. EL-ROUDI

Chemistry Department, Faculty of Science, Minia University, Minia, Egypt

(*Received* 11 *April* 1988; *accepted after revision* 8 *November* 1988)

Abstract—The base-adducts of nickel(II) complexes of S-methyl hydrazine carbodithioate Schiff bases with 2,2′-bipyridyl and 1,10-phenanthroline are prepared and isolated in benzene and acetonitrile, and analysed. Structures are suggested on the basis of IR and electronic spectra. Adduct formation with 2,2′-bipyridyl has been studied in a dichloroethane solution, spectrophotometrically. The results obtained suggest the formation of the *cis*-octahedral monoadduct.

Schiff bases derived via the condensation of S-methyl hydrazine carbodithioate with some ketones and aromatic aldehydes were found to behave as monobasic bidentate ligands, giving bis-neutral complexes with the nickel(II) salt (**1**).[1] It was deduced that these complexes possess a square-planar structure with the basic coordination unit NiN_2S_2. The square-planar arrangement around nickel(II), as well as its coordinative unsaturation, make these complexes good Lewis acids.[1,2] These chelates were found to form different base-adducts with Lewis bases depending on the substituents (R_1 and R_2).[1,3]

In the present work, base-adducts of nickel(II) chelates of the type (**1**) with 2,2′-bipyridyl and 1,10-phenanthroline have been isolated as solids in benzene and acetonitrile and their structures studied. In solution, adduct formation with 2,2′-bipyridyl has been studied in dichloroethane. Attention has been focused on the effect of both the solvents used and the substituents on the base-adduct formation.

RESULTS AND DISCUSSION

Reactions of neutral diamagnetic square-planar nickel(II) chelates of the type (**1**) ($R_1 = H$, $R_2 = C_6H_5$, *p*-BrC_6H_4 and *p*-$NO_2C_6H_4$) with 2,2′-bipyridyl or 1,10-phenanthroline, in benzene yield the corresponding crystalline solid bis-adducts (**3**) independent of the nickel chelate–base molar ratio. In the case of (**1**) ($R_1 = H$, R_2 = *p*-$OCH_3C_6H_4$ and *p*-$CH_3C_6H_4$), reaction with 2,2′-bipyridyl in benzene gives rise to mono- and bis-base-adducts (**2** and **3**, respectively) depending on the nickel chelate–base molar ratio. This disparity may be ascribed to the ability of *p*-Br, *p*-NO_2 and unsubstituted chelate derivatives to accept two molecules of bidentate Lewis base, due to their electron withdrawing substituent effects which can lead to rupture of the Ni ← N bond. Therefore, the N-arylidene S-methyl hydrazine carbodithioate acts as a monodentate ligand (Structure **3**). However, in the case of the electron releasing groups (CH_3, OCH_3), the Ni ← N bond is much stronger and resists the bond rupture.

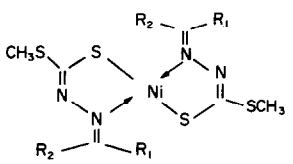

(**1**)

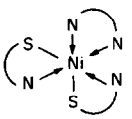

(**2**)

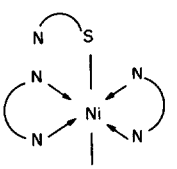

(**3**)

Reaction of (**1**) ($R_1 = CH_3$, $R_2 = CH_3$) with 1,10-phenanthroline in benzene yields bis-adducts

* Author to whom correspondence should be addressed.

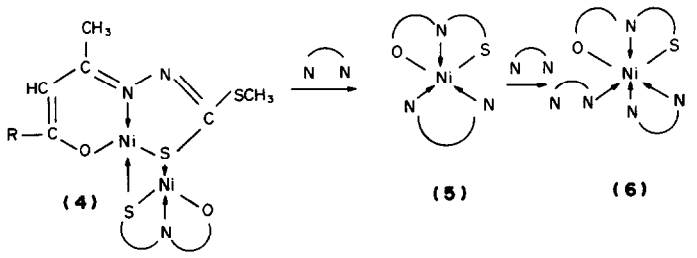

(4) (5) (6)

(3) whether the nickel chelate–base molar ratio used is either 1 : 1 or 1 : 2, whereas reaction of this chelate with 2,2′-bipyridyl in benzene yields mono- and bis-adducts (**2** and **3**, respectively) depending on the molar ratio used. Such disparity in behaviour may be attributed to the high reactivity of 1,10-phenanthroline compared to 2,2′-bipyridyl.

Reaction of a dimeric molecule of the nickel(II) chelate of the S-methyl hydrazine carbodithioate Schiff base of acetyl and benzoyl acetone (**4**; R = CH_3 and C_6H_5, respectively) with 2,2′-bipyridyl in benzene, affords only the bis-adduct (**6**). This reaction is found experimentally to be independent of the chelate–base molar ratio used. The same reaction in acetonitrile gives only the mono-adduct (**5**) whatever the molar ratio used. An attempt to prepare the bis-adduct in acetonitrile was unsuccessful. This implies that acetonitrile retards the addition reaction of 2,2′-bipyridyl to these chelates, while benzene leads to the reverse situation. The bis-adduct of these chelates is only obtained in acetonitrile in the case of the reaction with the more reactive 1,10-phenanthroline. The bis-adduct molecule (**6**) may be suggested to contain two molecules of bidentate Lewis base, but one of them acts as a unidentate ligand. The different isolated base-adducts, together with their elemental analysis results, are listed in Table 1.

Table 1. The analytical data of 2,2′-bipyridyl and 1,10-phenanthroline adducts of S-methyl hydrazine carbodithioate Schiff base nickel(II) complexes of the general formula

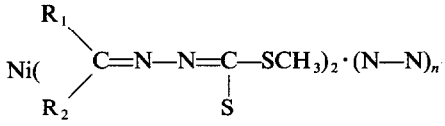

R_1	R_2	Solvent	Bidentate Lewis bases (N—N)	n	Ni (%) Calc.	Ni (%) Found	N (%) Calc.	N (%) Found
H	C_6H_5	Benzene	2,2′-bipy	2	7.4	7.5	14.2	14.0
H	C_6H_5	Benzene	1,10-phen	2	6.7	6.5	13.3	13.8
H	*p*-BrC_6H_4	Benzene	2,2′-bipy	2	6.2	6.8	11.8	12.3
H	*p*-BrC_6H_4	Benzene	1,10-phen	2	5.9	5.6	11.2	11.0
H	*p*-$NO_2C_6H_4$	Benzene	2,2′-bipy	2	6.6	6.7	12.7	12.9
H	*p*-$NO_2C_6H_4$	Benzene	1,10-phen	2	6.3	6.1	12.0	12.3
H	*p*-$OCH_3C_6H_4$	Benzene	2,2′-bipy	1	8.4	8.5	12.1	11.9
H	*p*-$OCH_3C_6H_4$	Benzene	2,2′-bipy	2	6.9	7.2	13.1	12.9
H	*p*-$CH_3C_6H_4$	Benzene	2,2′-bipy	1	8.9	8.7	12.7	12.5
H	*p*-$CH_3C_6H_4$	Benzene	2,2′-bipy	2	7.2	7.0	13.7	13.8
CH_3	CH_3	Benzene	1,10-phen	2	7.5	7.5	15.1	15.6
CH_3	CH_3	Benzene	2,2′-bipy	1	10.9	10.4	15.6	15.2
CH_3	CH_3	Benzene	2,2′-bipy	2	8.4	7.9	16.1	16.0
(**4**)	R = CH_3	Benzene	2,2′-bipy	2	10.2	10.9	14.6	14.2
	CH_3	CH_3CN	2,2′-bipy	1	14.0	14.3	13.4	13.0
	CH_3	CH_3CN	1,10-phen	2	8.9	8.1	13.5	13.3
	C_6H_5	Benzene	2,2′-bipy	2	9.3	9.6	13.4	13.5
	C_6H_5	CH_3CN	2,2′-bipy	1	12.4	12.2	11.9	11.2
	C_6H_5	CH_3CN	1,10-phen	2	8.7	8.4	12.4	12.7

IR spectra

The mesomeric effect of the carbodithioate group adjacent to a nitrogen atom will give rise to a band due to (C=N), namely the thioureide band.[4] S-methyl hydrazine carbodithioate shows such an absorption at 1520 cm^{-1}. This band appears at 1510 cm^{-1} in the spectra of (**1**) $R_1 = CH_3$, $R_2 = CH_3$ and at 1490 cm^{-1} in the spectra of (**1**) $R_1 = H$, $R_2 = C_6H_5$, *para*-substituted C_6H_4 complexes. This band is found to shift to a lower frequency of 1480 cm^{-1} with splitting, in the corresponding base-adducts of 2,2′-bipyridyl or 1,10-phenanthroline with (**1**) $R_1 = CH_3$, $R_2 = CH_3$ and to 1440 cm^{-1} for the corresponding base-adducts with (**1**) $R_1 = H$, $R_2 = C_6H_5$, *para*-substituted C_6H_4. This may be attributed to the rearrangement of the in-plane ligand as a result of *cis*-octahedral formation. The band at 1600 cm^{-1} may be assigned to the azomethine group, C=N. This band is not shifted in the base-adducts, but its intensity is increased with splitting. This may be assigned to a contribution to the C=N stretching from the 2,2′-bipyridyl or 1,10-phenanthroline.

Electronic spectra

The electronic spectra of the isolated solid base-adducts of (**1**) ($R_1 = H$, $R_2 = C_6H_5$, *para*-substituted C_6H_4 and $R_1 = CH_3$, $R_2 = CH_3$) with 2,2′-bipyridyl and 1,10-phenanthroline recorded in the solid state as Nujol mulls are consistent with an octahedral coordination geometry. The spectra exhibit one broad band in the vicinity of 15,000–20,000 cm^{-1} due to the ν_2-transition, $^3A_{2g} \rightarrow {}^3T_{1g}(F)$ in an octahedral configuration. However, the appearance of a high intensity band in the region 23,000–28,000 cm^{-1} in the electronic spectra of the above base-adducts may be argued to be due to a charge-transfer transition rather than an $^3A_{2g} \rightarrow {}^3T_{1g}(P)$ transition.[5] The ν_1-transition, $^3A_{2g} \rightarrow {}^3T_{2g}(F)$, lies outside the range of the spectrophotometer used.

In an attempt to study the base-adduct formation by means of spectrophotometric titration,[6] it was found that the addition of 2,2′-bipyridyl to a dichloroethane solution of (**1**) ($R_1 = H$, $R_2 = p$-$CH_3C_6H_4$, p-$OCH_3C_6H_4$, C_6H_5 and p-$NO_2C_6H_4$) results in profound spectral changes (Fig. 1). The spectrophotometric results obtained suggest that the reaction of the above chelates with 2,2′-bipyridyl in dichloroethane affords the hexacoordinate monoadduct (**2**). The values of $\log K$ measured at 25°C ± 0.1 are 3.3, 4.0, 4.3 and 6.1, respectively. These values of $\log K$ have been found to be slightly greater than those measured in benzene.[7]

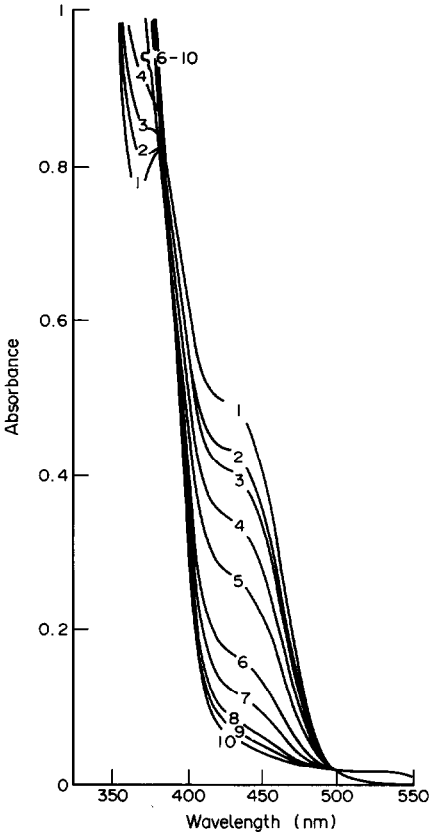

Fig. 1.

EXPERIMENTAL

Different molar ratios of 2,2′-bipyridyl or 1,10-phenanthroline were reacted with nickel(II) chelates of S-methyl hydrazine carbodithioate Schiff bases in benzene and acetonitrile to obtain the corresponding isolated solid base-adducts. The nickel content was determined gravimetrically. Electronic spectra and spectrophotometric titrations were recorded using a Spectronic 2000 spectrophotometer. A Shimazu 408 spectrophotometer was used for recording the KBr IR spectra.

REFERENCES

1. L. El-Sayed, M. F. Iskander, A. El-Toukhy and S. E. Zayan, *Inorg. Chim. Acta* 1972, **6**, 663.
2. D. P. N. Satchell, *Q. Rev.* 1963, **XVII**, 160.
3. L. El-Sayed, M. F. Iskander and A. El-Toukhy, *J. Inorg. Nucl. Chem.* 1974, **36**, 1739.
4. J. Chatt, L. A. Duncanson and L. M. Venanzi, *Nature* 1956, **177**, 1042.
5. K. J. Cavell, R. J. Magee and J. O. Hill, *J. Inorg. Nucl. Chem.* 1979, **41**, 1281.
6. J. S. Coleman, L. P. Verga and S. H. Mastin, *Inorg. Chim. Acta* 1970, **9**, 1015.
7. M. F. Iskander, L. El-Sayed, L. Labib and A. El-Toukhy, *Inorg. Chim. Acta* 1984, **86**, 187.

Polyhedron Vol. 8, No. 7, pp. 929–932, 1989
Printed in Great Britain

0277–5387/89 $3.00+.00
© 1989 Pergamon Press plc

PREPARATION AND X-RAY CRYSTAL STRUCTURE OF THE BIS(η^5-CYCLOPENTADIENYL)CHLORO(4-OXOFERROCENEBUTANOYLOXY)ZIRCONIUM(IV) COMPLEX

MA YONGXIANG,* ZHU YING and WANG XIN

Department of Chemistry, Lanzhou University, Lanzhou 730000, China

and

MA CHUNLIN

Department of Chemistry, Liaocheng Teachers College, Shandong, China

(*Received* 21 *April* 1988; *accepted after revision* 8 *November* 1988)

Abstract—Bis(η^5-cyclopentadienyl)chloro(4-oxoferrocenebutanoyloxy)zirconium(IV), η^5-$Cp_2ZrCl(OCOCH_2CH_2COFc)$ ($Cp = C_5H_5$, $Fc = C_5H_5FeC_5H_4$), has been synthesized by reaction of zirconocene dichloride with sodium 4-oxoferrocenebutanoate and has been characterized by elemental analysis, PMR and IR spectroscopy. The X-ray crystal structure of the title complex was determined using 2593 independent reflections with $I > 3\sigma(I)$. The complex crystallizes in the monoclinic space group $P2_1/c$ with four monomeric molecules in a cell of dimensions $a = 11.952(6)$, $b = 13.104(3)$, $c = 14.547(3)$ Å, $\beta = 108.2(3)°$, $V = 2164.5$ Å^3, $D_{calc} = 1.666$ g cm^{-3} and $\mu(K_\alpha) = 12.912$ cm^{-1}. The structure has been solved by direct methods and refined by Fourier and full-matrix least-squares methods to a conventional $R = 0.0465$. The carboxyl group in this complex is a bidentate ligand and the atoms, Zr, Cl, O(2), O(3), C(4) and C(3) lie in a quasi-mirror plane.

The chemistry, electronic structures and molecular geometries of bis(η^5-cyclopentadienyl) transition metal complexes, η^5-Cp_2ML_n have been widely studied.[1–8] A large number of metallocene derivatives of group IVB elements are 16-electron complexes with additional ligands.[9] But a small number of five-, six- and seven-coordinate complexes of zirconium(IV) have also been prepared.[7,8,10–13] The structure of some of the five-coordinate complexes, η^5-Cp_2ZrL_3, that contain chelating ligands has been determined by X-ray diffraction,[7,8,14,15] but the crystal and molecular structures of those complexes containing carboxyl ligands have not been studied so far. In this paper, a new five-coordinate, 18-electron complex of zirconium containing a carboxyl group (I) has been synthesized and the molecular geometry established by X-ray crystallography.

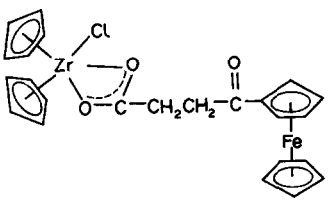

(I)

EXPERIMENTAL

Preparation of (I)

This complex was prepared by reaction of equimolar amounts of η^5-Cp_2ZrCl_2 and $FcCOCH_2CH_2COONa$ in anhydrous benzene under argon. The $FcCOCH_2CH_2COONa$ was obtained by the method described in the literature.[16] Recrystallization from a benzene–hexane solvent afforded orange crystals. Found: C, 53.7; H, 4.3; Cl, 7.1. Calc. for $C_{24}H_{23}ClFeO_3Zr$: C, 53.2; H, 4.3; Cl,

* Author to whom correspondence should be addressed.

Table 1. Crystal data

Formula: $C_{24}H_{23}ClFeO_3Zr$	$c = 14.547(4)$ Å
Molecular weight: 541.97	$\beta = 108.20(3)°$
Crystal system: monoclinic	$V = 2164.5$ Å^3
Space group: $P2_1/c$	$Z = 4$
$F(000) = 1096$	$D_{calc} = 1.666$ g cm^{-3}
$a = 11.952(6)$ Å	μ(Mo-K_α) = 12.912 cm^{-1}
$b = 13.104(3)$ Å	Number of parameters refined 367

6.6%. The complex decomposes without melting at 196°C. IR (KBr discs, cm^{-1}): ν(C=O) 1665s, ν(C···O) 1527s, ν(Zr—O) 485s, other bands 1454s, 1400s, 1078m, 1022s, 811s, 725m, 633m, 532m, and 414m. PMR (in $CDCl_3$, ppm): 6.23 (C_5H_5Zr); 4.23 (C_5H_5Fe); 4.43–4.52 and 4.73–4.82 (C_5H_4Fe); 2.43–2.63 and 2.97–3.17 (—CH_2CH_2—).

Crystal structure determination

Several clear, orange cubic crystals of dimensions $0.4 \times 0.25 \times 0.20$ mm, which were obtained by slow crystallization from benzene–hexane, were selected for the X-ray diffraction analysis. The data were collected on an Enraf–Nonius CAD-4 automatic four-circle diffractometer with graphite monochromated Mo-K_α radiation ($\bar{\lambda} = 0.71073$ Å), using the ω–2θ scan technique in the range $4° < 2\theta < 54°$ at *ca* 293 K. Three standard reflections were monitored every 3600 s to check both crystal and apparatus stability. The intensity data were converted to structure factor amplitudes by corrections for Lorentz, polarization and absorption effects. Of the 4897 independent reflections measured, 2593 reflections had net intensities I greater than $3\sigma(I)$ and were used in the subsequent analysis. The cell constants and other crystal data are shown in Table 1.

The structure was solved by direct methods and Fourier techniques. The 30 non-hydrogen atoms were refined by block-diagonal-matrix least-squares techniques using anisotropic thermal parameters. A difference Fourier synthesis revealed the positions of all the hydrogen atoms. These were assigned a fixed isotropic thermal parameter in the final refinement by full-matrix least-squares techniques. The discrepancy indices $R = \Sigma||F_o|-|F_c||/\Sigma|F_o|$ and $R_w = [\Sigma w(|F_o|-|F_c|)^2/\Sigma w|F_o|^2]^{1/2}$ ($w = 1/\sigma^2$) were 0.046 and 0.053, respectively. In the final cycle, the parameter shift converged almost to zero, except for those of hydrogen atoms which were less than the corresponding standard deviations. A final difference Fourier map showed no extra peaks.*

* Supplementary material available: a listing of structure factors and anisotropic thermal parameters (25 pages) has been deposited with the Editor at Queen Mary College and also with the Cambridge Crystallographic Data Centre.

RESULTS AND DISCUSSION

The geometry of the molecule and the atom numbering scheme for η^5-$Cp_2ZrCl(OCOCH_2CH_2COFc)$ are shown in Fig. 1. The bond distances and bond angles are given in Table 2. The results of selected mean plane calculations are summarized in Table 3 and selected dihedral angles are listed in Table 4.

In this complex, the zirconium atom attaches to each carbon atom of two cyclopentadienyl rings, to the chlorine atom and two oxygen atoms of the 4-oxoferrocenebutanoyloxy group. Due to the crowding in the coordination group, the Zr—Cl bond length, 2.518(1) Å, is significantly longer

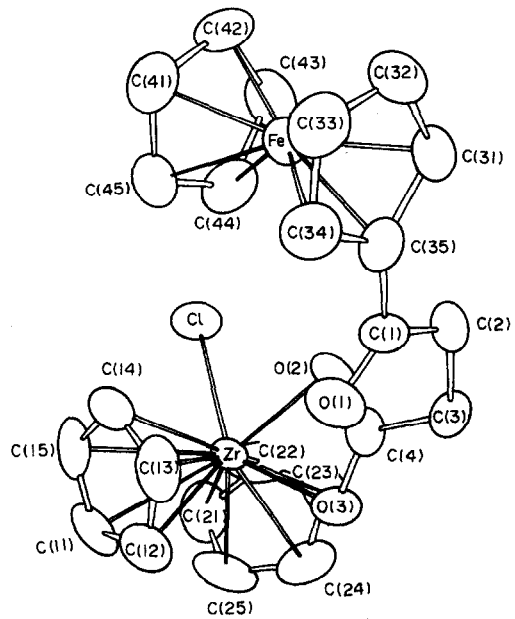

Fig. 1. A perspective drawing of the $Cp_2ZrCl(OCOCH_2CH_2COFc)$ molecule. Each atom is represented by an ellipsoid consistent with the thermal parameters.

Table 2. Bond distances and bond angles in (η^5-$C_5H_5)_2ZrCl(OCOCH_2CH_2COFc)$

Lengths (Å)			
Zr—Cl	2.518(1)	Fe—C_{31}	2.024(5)
Zr—O_2	2.248(3)	Fe—C_{32}	2.051(5)
Zr—O_3	2.287(3)	Fe—C_{33}	2.054(5)
Zr—C_{11}	2.500(6)	Fe—C_{34}	2.008(6)
Zr—C_{12}	2.480(6)	Fe—C_{35}	1.988(5)
Zr—C_{13}	2.500(5)	O_1—C_1	1.213(6)
Zr—C_{14}	2.521(6)	O_2—C_4	1.280(6)
Zr—C_{15}	2.531(6)	O_3—C_4	1.253(6)
Zr—C_{21}	2.478(6)	C_1—C_2	1.521(7)
Zr—C_{22}	2.528(6)	C_1—C_{35}	1.473(8)
Zr—C_{23}	2.522(6)	C_2—C_3	1.521(7)
Zr—C_{24}	2.535(6)	C_3—C_4	1.495(7)
Zr—C_{25}	2.487(6)		

Angles (°)			
Cl—Zr—O_2	77.24(9)	C_2—C_3—C_4	113.0(5)
Cl—Zr—O_3	134.2(1)	O_2—C_4—O_3	117.5(4)
O_2—Zr—O_3	57.0(1)	O_2—C_4—C_3	119.7(5)
O_1—C_1—C_2	120.4(5)	O_3—C_4—C_3	122.7(5)
C_1—C_2—C_3	113.0(5)		

Numbers in parentheses are estimated standard deviations in the last significant figure.

than the distance of 2.441 Å in η^5-Cp_2ZrCl_2.[5] The Zr—O(2) and Zr—O(3) bond lengths 2.248(3) Å and 2.287 Å, respectively, are longer than the Zr—O bond length in eight-coordinate $Zr[SOCN(C_2H_5)_2]_4$ (2.190 Å),[17] $[Zr(C_2O_4)_4]^{4-}$ (2.199 Å)[18] and $Zr(acac)_4$ (2.198 Å).[19] They are also much longer than Zr—O distances in the four-coordinate oxo-bridged dimeric complexes, $[\eta^5$-$Cp_2ZrCl]_2O$ (1.94 Å)[20] and $[\eta^5$-$Cp_2Zr(SC_6H_5)]_2O$ (1.968 Å).[21] The Zr—O(2) and Zr—O(3) bond lengths are equal to those in η^5-$Cp_2ZrCl[SOCN(CH_3)_2]$ (2.249 Å) and η^5-$Cp_2Zr(COCH_3)(CH_3)$ (2.290 Å),[22] respectively. The bond lengths of O(2)—C(4) and O(3)—C(4), which are almost equal (1.280 and 1.253 Å, respectively). are longer than the normal C=O distance (1.22 Å) and shorter than the C—O distance (1.43 Å). The C(1)—C(35) bond length, 1.473 Å, is shorter than standard C—C single bond (1.54 Å). It is shown that the double bond between C(1) and O(1) has been conjugated with the cyclopentadienyl ring in ferrocene.

The four molecules per unit cell occupy general positions of the space group $P2_1/c$ and are not required to have any symmetry. It can be seen from

Table 4. Dihedral angles between planes

Plane numbers		Dihedral angle (°)	Plane numbers		Dihedral angle (°)
1	2	53.5	2	6	98.5
1	3	23.1	3	4	93.7
1	4	88.4	3	5	93.6
1	5	87.2	3	6	91.6
1	6	87.1	4	5	2.9
2	3	30.4	4	6	2.7
2	4	101.2	5	6	5.0
2	5	102.5			

Table 3. Least-squares mean planes of the form $AX+BY+CZ=D$ where A, B, C and D are constants and X, Y, Z are orthogonalized coordinates

Plane numbers	Atoms	A	B	C	D
1	C_{11}, C_{12}, C_{13}, C_{14}, C_{15}	−0.4856	0.6794	−0.5501	−6.2720
2	C_{21}, C_{22}, C_{23}, C_{24}, C_{25}	−0.8256	−0.1539	−0.5426	−1.1092
3	Zr, O_2, O_3, C_4, Cl, C_3	−0.7016	0.3497	−0.6209	−4.2531
4	C_{31}, C_{32}, C_{33}, C_{34}, C_{35}	0.7052	−0.0282	−0.7085	−5.8584
5	C_{41}, C_{42}, C_{43}, C_{44}, C_{45}	0.7168	0.0193	−0.6970	−8.7825
6	C_{31}, C_{32}, C_{33}, C_{34}, C_{35}, C_1, C_2, O_1	0.6725	−0.0428	−0.7389	−6.3887

Atoms and their displacement from planes (Å)

Plane 1	C_{11}, −0.008; C_{12}, 0.008; C_{13}, −0.005; C_{14}, −0.000; C_{15}, 0.005
Plane 2	C_{21}, −0.005; C_{22}, 0.005; C_{23}, −0.004; C_{24}, 0.001; C_{25}, 0.003
Plane 3	O_2, −0.043; O_3, 0.008; C_4, −0.020; Cl, 0.022; C_3, 0.033; Zr, −0.056
Plane 4	C_{31}, −0.001; C_{32}, 0.002; C_{33}, −0.002; C_{34}, 0.002; C_{35}, −0.001
Plane 5	C_{41}, 0.001; C_{42}, −0.000; C_{43}, −0.001; C_{44}, 0.001; C_{45}, −0.001
Plane 6	C_{31}, 0.033; C_{32}, −0.029; C_{33}, −0.043; C_{34}, 0.021; C_{35}, 0.064; C_1, 0.016; C_2, −0.039; O_1, −0.023

Table 3 that the dihedral angle between two cyclopentadienyl ligands in the ferrocenyl group equals 2.9°, that is to say, planes 4 and 5 are parallel. It should be pointed out that the Fe—C(35) distance is the shortest in all of Fe—C bonds in the ferrocenyl group. The dihedral angles between planes 1 and 3, and 2 and 3 are 23.1 and 30.4°, respectively, and the sum of the two dihedral angles is 53.5°, which equals the dihedral angle between planes 1 and 2. It is shown that plane 3 inserts between planes 1 and 2.

The ferrocenyl group bends towards the zirconocenyl group and the chlorine atom is close to the iron atom. The Cl—Zr—O(3) bond angle (134.2°) is 37° larger than the Cl—Cr—Cl bond angle in η^5-Cp_2ZrCl_2,[5] but is 3° and 4° smaller than the Cl—Zr—S(2) (137.5°) in η^5-$Cp_2ZrCl[S_2CN(C_2H_5)_2]$ and Cl—Zr—O (138.1°) in η^5-$Cp_2ZrCl[SOCN(CH_3)_2]$, respectively. The average distances between the zirconium and the carbon atoms of the two cyclopentadienyl rings is equal to that in η^5-Cp_2ZrCl_2. The Cl···O(2) distance (2.982 Å) is 0.22 Å less than the sum of the van der Waals radii (3.20 Å).[23] Specifically, the O(2)···O(3) contact (2.166 Å) is 0.64 Å less than the van der Waals contact (2.80 Å). The C(3)—C(4) bond length, 1.495 Å, is shorter than that of normal C—C single bond. It can be seen from the above that the arrangement of atoms or coordination groups in this molecule is suitable and more crowded.

REFERENCES

1. J. E. Bercaw, *J. Am. Chem. Soc.* 1974, **96**, 5087.
2. C. A. Bertelo and J. Schwartz, *J. Am. Chem. Soc.* 1975, **97**, 288.
3. J. C. Green, M. L. H. Green and C. K. Prout, *J. Chem. Soc., Chem. Commun.* 1972, 421.
4. J. W. Lauher and R. Hoffman, *J. Am. Chem. Soc.* 1976, **98**, 1729.
5. C. K. Prout, T. S. Cameron, R. A. Forder, S. R. Critchley, B. Denton and G. V. Rees, *Acta Cryst.* 1974, **30B**, 2290.
6. J. L. Peterson and L. F. Dahl, *J. Am. Chem. Soc.* 1974, **96**, 2248.
7. M. E. Silver, O. Eisenstein and R. C. Fay, *Inorg. Chem.* 1983, **22**, 759.
8. M. E. Silver and R. C. Fay, *Organometallics* 1983, **2**, 44.
9. P. C. Wailes, R. S. P. Coutts and H. Weigold, in *Organometallic Chemistry of Titanium, Zirconium and Hafnium*. Academic Press, New York (1974).
10. R. D. Wilson, T. F. Koetzle, D. W. Hart, A. Kvick and D. L. Tipton, *J. Am. Chem. Soc.* 1977, **99**, 1775.
11. F. A. Cotton and G. Wilkinson, in *Advanced Inorganic Chemistry*. Wiley, New York (1980).
12. M. L. H. Green, J. A. McCleverty, L. Pratty and G. Wilkinson, *J. Chem. Soc.* 1961, 4854.
13. A. H. Bruder, R. C. Fay, D. F. Lewis and A. A. Sayler, *J. Am. Chem. Soc.* 1976, **98**, 6932.
14. T. Don Tilley, *Organometallics* 1985, **4**, 1452.
15. S. K. Sengupta and B. P. Baranwal, *Rev. Roum. Chim.* 1983, **28**, 487.
16. K. L. Rinehart, Jr., K. L. Motz and S. Moon, *J. Am. Chem. Soc.* 1957, **79**, 2749.
17. W. L. Steffen and R. C. Fay, *Inorg. Chem.* 1978, **17**, 2120.
18. G. L. Glen, J. V. Silverton and J. L. Hoard, *Inorg. Chem.* 1963, **2**, 250.
19. J. V. Silverton and J. L. Hoard, *Inorg. Chem.* 1963, **2**, 243.
20. J. F. Clarke and M. B. Drew, *Acta Cryst.* 1974, **30B**, 2267.
21. J. L. Petersen, *J. Organomet. Chem.* 1979, **166**, 179.
22. G. Fachinetti, C. Floriani, F. Marchetti and S. Merlino, *J. Chem. Soc., Chem. Commun.* 1976, 522.
23. D. Van Der Helm, A. E. Lessor, Jr. and L. L. Merritt, Jr., *Acta Cryst.* 1962, **15**, 1227.

Polyhedron Vol. 8, No. 7, pp. 933–934, 1989
Printed in Great Britain

0277–5387/89 $3.00+.00
© 1989 Pergamon Press plc

PREPARATION AND X-RAY CRYSTAL STRUCTURE OF BIS(1,8-NAPHTHYRIDINE-N-MONOXIDE)COPPER(II) NITRATE

GAN XINMIN, TANG NING, WANG XIN, ZHU YIN and TAN MINYU*

Department of Chemistry, Lanzhou University, Lanzhou, P.R.C.

(*Received* 24 *May* 1988; *accepted after revision* 8 *November* 1988)

Abstract—The title compound $Cu(napyo)_2(NO_3)_2$ was formed by the reaction of copper(II) nitrate with 1,8-naphthyridine-N-monoxide (napyo) in methanol. The complex crystallizes in the monoclinic space group $P2_1/n$ with $Z = 2$, $a = 7.768(2)$, $b = 13.976(2)$, $c = 9.045(3)$ Å, $\beta = 113.12(3)°$. The structure was determined from 1579 observed reflections and refined to $R = 0.035$. The copper atoms show a tetragonally distorted octahedral configuration, being bonded to two oxygen atoms (Cu—O, 1.951 Å) and two nitrogen atoms (Cu—N, 1.963 Å) of the two napyo ligands and to two oxygen atoms (Cu—O, 2.410 Å) of two nitrate groups.

A number of copper complexes with some aromatic amine N-oxides have been investigated,[1] but the copper complex with 1,8-naphthyridine-N-monoxide (napyo), which belongs to this kind of aromatic amine N—oxide, has never been reported. We recently synthesized this compound and determined its crystal and molecular structure.

EXPERIMENTAL

Preparation of $Cu(napyo)_2(NO_3)_2$

Copper nitrate hexahydrate (0.030 g, 0.1 mmol) and napyo[2] (0.029 g, 0.2 mmol) were dissolved in methanol (40 cm^3). The solution was placed in a desiccator with $CaCl_2$ at room temperature. After about 2 weeks dark blue needle-like crystals of the title compound were obtained. Found: C, 39.7; H, 2.9; N, 17.1; Cu, 13.1. Calc. for $C_{16}H_{12}CuN_6O_8$: C, 40.1; H, 2.5; N, 17.5; Cu, 13.2%.

Crystal structure determination of $Cu(napyo)_2(NO_3)_2$

Crystal data. $C_{16}H_{12}CuN_6O_8$, $M = 479.85$, monoclinic, space group $P2_1/n$, $a = 7.768(2)$, $b = 13.976(2)$, $c = 9.045(3)$ Å, $\beta = 113.12(3)°$. $V = 903.3$ $Å^3$, $Z = 2$, $D_c = 1.764$ g cm^{-3}, D_o (flotation in CCl_4/CH_2I_2) = 1.756 g cm^{-3}, λ(Mo-K_α) = 0.7109 Å, $\mu = 12.7$ cm^{-1}, $F(000) = 486$.

A single crystal of dimensions $0.2 \times 0.2 \times 0.4$ mm was selected for the data collection on an Enraf–Nonius CAD4 diffractometer with graphite-monochromated Mo-K_α radiation, ω–2θ scan. 2183 reflections were collected in the range of $2° \leqslant 2\theta \leqslant 52°$, 1579 reflections with $I \geqslant 3\sigma(I)$ were used in the structure determination and refinement. Lorentz polarization and absorption correction were applied. The structure was solved by direct method and Fourier techniques, refined by full-matrix least-squares with anisotropic temperature parameters for all non-hydrogen atoms and isotropic thermal parameters for hydrogen atoms. Final $R = 0.035$, $R_w = 0.045$.

RESULTS AND DISCUSSION

Selected bond lengths and bond angles are given in Tables 1 and 2. Figure 1 shows the structure of the complex molecule and Fig. 2 shows the molecular packing arrangement in the unit cell. Final atomic coordinates, anisotropic thermal

Table 1. Bond lengths (Å)

Cu—O	1.951(3)	C(5)—C(6)	1.357(6)
Cu—O(1)	2.410(3)	C(6)—C(7)	1.391(6)
Cu—N(2)	1.963(3)	C(7)—N(2)	1.328(5)
N(1)—O	1.335(4)	N(2)—C(8)	1.343(5)
N(1)—C(1)	1.324(5)	C(8)—N(1)	1.387(4)
C(1)—C(2)	1.388(6)	C(8)—C(4)	1.394(5)
C(2)—C(3)	1.369(6)	N(3)—O(1)	1.263(5)
C(3)—C(4)	1.403(6)	N(3)—O(2)	1.221(5)
C(4)—C(5)	1.428(5)	N(3)—O(3)	1.233(5)

* Author to whom correspondence should be addressed.

Table 2. Bond angles (°)

O—Cu—O(1)	89.5(1)	C(8)—N(1)—C(1)	120.6(4)
O—Cu—O(1′)	90.5(1)	C(4)—C(5)—C(6)	119.2(4)
O—Cu—N(2)	83.2(1)	C(5)—C(6)—C(7)	120.3(4)
O—Cu—N(2′)	96.8(1)	C(6)—C(7)—N(2)	122.5(4)
O(1)—Cu—N(2)	87.0(1)	C(7)—N(2)—C(8)	117.3(3)
O(1)—Cu—N(2′)	93.0(1)	N(2)—C(8)—C(4)	125.2(3)
O—N(1)—C(1)	120.7(3)	C(8)—C(4)—C(5)	115.5(4)
O—N(1)—C(8)	118.7(3)	C(3)—C(4)—C(5)	125.2(4)
N(1)—C(1)—C(2)	121.0(4)	N(1)—C(8)—N(2)	115.1(3)
C(1)—C(2)—C(3)	120.5(4)	O(1)—N(3)—O(2)	119.8(4)
C(2)—C(3)—C(4)	118.9(4)	O(1)—N(3)—O(3)	119.2(4)
C(3)—C(4)—C(8)	119.3(4)	O(2)—N(3)—O(3)	121.0(4)
C(4)—C(8)—N(1)	119.7(4)		

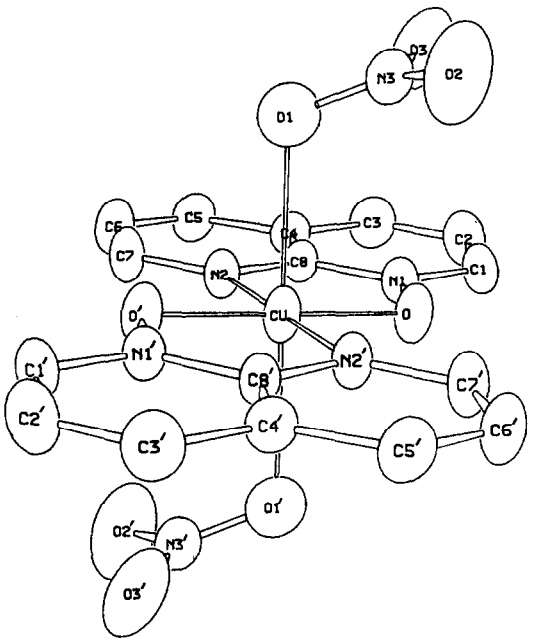

Fig. 1. The structure of the complex molecule.

parameters and lists of F_o/F_c values have been deposited with the Editor as supplementary material.

It can be seen from Fig. 1 that the copper atom is located on the inversion centre of the complex molecule and is bonded to two oxygen atoms (Cu—O, 1.951 Å) and two nitrogen atoms (Cu—N(2), 1.963 Å) of two napyo ligands and to two oxygen atoms (Cu—O(1), 2.410 Å) of two unidentate nitrate groups. The latter two distances are much greater than the other four and this phenomenon doubtlessly results from the Jahn–Teller effect of the Cu^{2+} ion with a d^9 electronic configuration. So the coordination configuration of the copper atom is a lengthened octahedron.

REFERENCES

1. N. M. Karayannis, A. N. Speca, D. E. Chasan and L. L. Pytlewski, *Coord. Chem. Rev.* 1976, **20**, 37.
2. Y. Kobayashi, I. Kumadaki, H. Stao, Y. Sekine and T. Hara, *Chem. Pharm. Bull.* 1974, **22**, 2097.

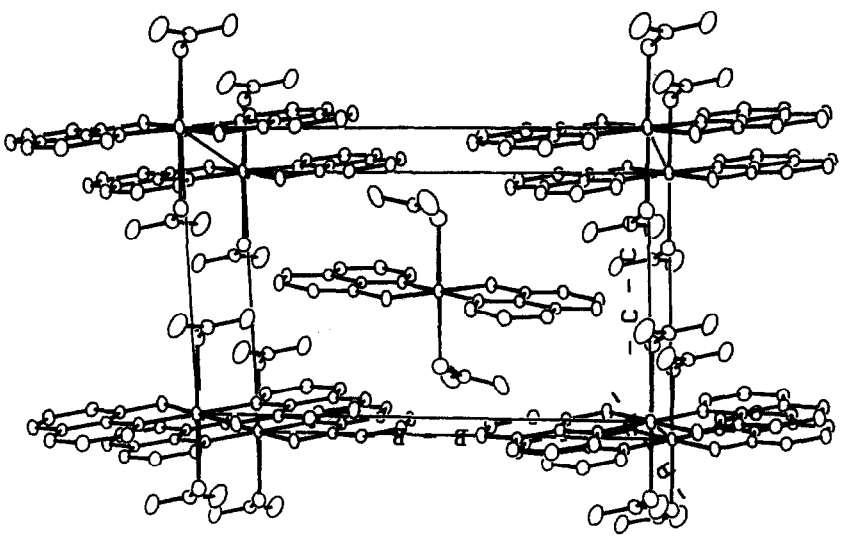

Fig. 2. The packing arrangement of molecule in unit cell.

Polyhedron Vol. 8, No. 7, pp. 935–940, 1989
Printed in Great Britain

0277–5387/89 $3.00+.00
© 1989 Pergamon Press plc

SPECTROSCOPIC STUDIES ON Cu(3-AMINOISOXAZOLE)$_n$X$_2$ · mH$_2$O COMPLEXES

K. MADHUKAR, B. MADHU and B. A. SASTRY*

Solid State and Molecular Physics Laboratory, Physics Department, Osmania University, Hyderabad-500 007, India

and

G. PONTICELLI and M. MASSACESI

Istituto Chimica Generale, Inorganica ed Analitica, Universita di Cagliari, vis Ospedale 72, 09100 Cagliari, Italy

(*Received* 16 *May* 1988; *accepted after revision* 8 *November* 1988)

Abstract—The 3-aminoisoxazole (3-AI) copper(II) complexes, Cu(3-AI)$_n$X$_2$ · mH$_2$O (where $n = 2$, X = Cl, Br, NO$_3$, $m = 0$; $n = 4$, X = ClO$_4$, $m = 1$) have been synthesized and their IR, electronic and ESR spectral properties have been studied to obtain stereochemical information of these complexes both in solid and solution states. The metal appears to be four-coordinate in the bis-complexes and hexa-coordinate in the case of the tetrakis-complex. In DMF (N,N′-dimethylformamide) solutions two species are found to form, unlike in the solutions of pyridine.

From our previous IR, ESR and electronic spectral studies on isoxazolamine derivatives with metal ions, it was found that there is a competition between N_{ring}, O_{ring} and N of the exocyclic amino group atom, depending on the aminic and methylic group positions and the nature of the metal ion.[1–6] It was also found that some of the above copper(II) complexes possess fluxional geometry.[7] In view of the above important observations, we have synthesized and extended the studies to the polycrystalline and solute specimens of copper(II) complexes of unmethylated 3-aminoisoxazole

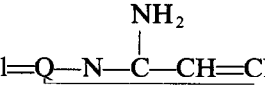

(3-Al=O—N—C—CH=CH), using the above three techniques to obtain information on the stereochemistry and solute–solvent interactions. The complex chosen for the present work has the general formula, Cu(3-AI)$_n$X$_2$ · mH$_2$O where $n = 2$ and $m = 0$ when X = Cl, Br, NO$_3$ and $n = 4$ and $m = 1$ when X = ClO$_4$.

* Author to whom correspondence should be addressed.

EXPERIMENTAL

Materials

3-AI, CuCl$_2$ · 2H$_2$O, Cu(NO$_3$)$_2$ · 3H$_2$O were commercially available. CuBr$_2$, Cu(ClO$_4$)$_2$ · 6H$_2$O were prepared using literature methods.

Preparation of the complexes

The complexes were prepared from the reaction of the methanolic solutions of the ligand and the metal salt in the required stoichiometrical ratio. The precipitation is promoted by adding isopropanol. The compounds were purified by means of repeated washing with isopropanol. The dried complexes are either crystalline or powder-like. Nitrogen, carbon and hydrogen were analysed with a Perkin–Elmer 240 Elemental Analyser.

Physical measurements

Physical measurements were carried out as described earlier.[8]

RESULTS AND DISCUSSION

IR and electronic spectral studies

The analytical data and physical properties of these complexes are reported in Table 1. Table 2 gives the principal IR bands of nitrate and perchlorate compounds along with their assignment. The far IR bands are listed in Table 3. In the compound $Cu(3\text{-}AI)_4(ClO_4)_2 \cdot H_2O$, the absorption bands at 3580 cm^{-1} ν(OH) and at 1620 cm^{-1} δ(HOH) and the loss of water at 110°C show the presence of water of crystallization. The molar conductivity values are typical of non-conducting compounds. In the solid state the perchlorate and nitrate derivatives exhibit IR bands indicative of unidentate groups.[1] The bands at 316 cm^{-1} are assigned to the ν(Cu—$OClO_3$) stretching frequency and the bands at 306 cm^{-1} to the ν(Cu—ONO_2). The ν(Cu—X) band of the halide compounds is in good agreement with the terminal metal halide mode for square-planar stereochemistry.[9] The band present in these complexes in the 259–232 cm^{-1} range is attributed to ν(Cu—N_{ring}) vibrations. This confirms that 3-AI is monodentate N_{ring}-bonded. On the basis of reflectance spectra (Table 4), the $Cu(3\text{-}AI)_2X_2$ compounds have square-planar (CuN_2X_2) stereochemistry,[10] while the $Cu(3\text{-}AI)_4(ClO_4)_2 \cdot H_2O$ is distorted hexa-coordinate (CuN_4O_2).[11] On the other hand, in the bis-complexes of 3-AMI (3-amino-5methylisoxazole), this ligand acts as a bridging (N- and O-bonded) bidentate ligand and the complexes are found to be polymeric.[1] In the case of tetrakis-complexes of 3-AMI, this ligand acts as an N_{ring}-bonded monodentate ligand.

ESR data

Polycrystalline spectra. Figures 1 and 2 show the X-band ESR spectra of the present complexes at

Table 1. Analytical data and physical properties

Complex	Colour	Analysis (%)[a] C	H	N	Λ_M in MeOH ($cm^2\,\Omega^{-1}\,mol^{-1}$)
$Cu(3\text{-}AI)_2Cl_2$	Light green	24.0 (23.8)	2.9 (2.7)	18.6 (18.5)	4
$Cu(3\text{-}AI)_2Br_2$	Dark brown	18.2 (18.4)	2.1 (2.4)	14.3 (14.3)	6
$Cu(3\text{-}AI)_2(NO_3)_2$	Blue–green	20.3 (20.3)	2.4 (2.3)	23.7 (23.6)	8
$Cu(3\text{-}AI)_2(ClO_4)_2 \cdot H_2O$	Dark green	23.2 (23.4)	3.2 (2.9)	18.2 (18.2)	12

[a] Calculated values are given in parentheses.

Table 2. Principal IR bands in the 4000–400 cm^{-1} range (solid phase)

Complex	ν_1	ν_2	ν_3	ν_6	$\nu_2+\nu_3$
$Cu(3\text{-}AI)_2(NO_3)_2$	1290vsbr	1055ssh	705m	810ms	1730w
	ν(OH)	δ(HOH)	ν_1	ν_3	ν_4
$Cu(3\text{-}AI)_4(ClO_4)_2 \cdot H_2O$	3580m	1620vs	935ms	1110vs, 1090vs	620s, 410m

Table 3. Far IR spectra (400–200 cm^{-1})

Complex	ν(Cu—X)	ν(Cu—N)	Other bands
$Cu(3\text{-}AI)_2Cl_2$	283vsbr	250m	350w
$Cu(3\text{-}AI)_2Br_2$	229vs	235s	248ms, 273m
$Cu(3\text{-}AI)_2(NO_3)_2$		232ms	386sh, 351w, 306vs (Cu—ONO_2), 216w
$Cu(3\text{-}AI)_4(ClO_4)_2 \cdot H_2O$		259s	382sh, 370sh, 360sh, 338w, 316 (Cu—$OClO_3$)

Table 4. g and electronic reflectance spectral (ΔE) values of polycrystalline samples of 3-AI and 3-AMI complexes of copper(II)

Complex	Temperature (K)	g_1	g_2	g_3	A_3 (G)	G	R	ΔE (cm^{-1})	Reference
Cu(3-AI)$_2$Cl$_2$	300	2.036	2.080	2.274	—	4.7	0.23	14360	Present study
	77	2.034	2.083	2.273	—	4.7	0.26		
Cu(3-AI)$_2$Br$_2$	300	2.037	2.090	2.234	—	3.7	0.37	14450	
Cu(3-AI)$_2$(NO$_3$)$_2$	300	2.074	2.074	2.319	—	4.3	0.00	15150	
	77	2.063	2.063	2.312	—	4.9	0.00		
Cu(3-AI)$_4$(ClO$_4$)·H$_2$O	300	2.059	2.059	2.276	—	4.7	0.00	16070	
Cu(3-AMI)$_2$Br$_2$	300	2.036	2.073	2.218	—	4.0	0.25	20800, 13000	6 and 1
Cu(3-AMI)$_2$(NO$_3$)$_2$	300	2.055	2.055	2.270	—	4.9	0.00	25000, 17800, 13900	
Cu(3-AMI)$_4$Cl$_2$	300	2.030	2.070	2.260	—	5.2	0.21	24000, 15600, 14000	
Cu(3-AMI)$_4$(ClO$_4$)$_2$	273	2.064	2.181	2.278	165			26100, 18000, 13600 11100sh	7 and 1
	90	2.071	2.194	2.280	147				
	4.2	2.070	2.174	2.281	153				
Cu(3-AMI)$_4$(NO$_3$)$_2$	273	2.051	2.166	2.274	150			25500, 18200, 13400	
	90	2.055	—	2.274	150				
	4.2	2.058	2.191	2.278	151				

300 and 77 K and Q-band spectrum of Cu(3-AI)$_4$(ClO$_4$)$_2$·H$_2$O at 300 K respectively. In none of the present complexes, at both the above temperatures, are copper(II) hyperfine lines resolved at X-band, indicating strong dipolar and exchange interactions between copper(II) ions in the unit cell. The asymmetric ESR line obtained in perchlorate complex at X-band (Fig. 1) has been resolved partially at Q-band (Fig. 2), indicating that the order of exchange interaction among copper(II) ions is about 1 cm^{-1}. The principal g values are calculated using the procedure of Kneubuhl[12] and these values, along with the values of $G\{(g_3-2)/[(g_1+g_2/2)-2]\}$ and $R[(g_2-g_1)/(g_3-g_2)]$, are given in Table 4. From the value of G it is possible to know whether or not exchange coupling effects invalidate the use of observed g values to reflect the local copper(II) environment.[13] In the present studies, in all the complexes the G values lie between 3.5 and 5, which indicates that the influence of exchange effects to deviate the crystal g values from molecular g values is less. Hence, it appears that the magnetic misalignment of the molecules in the unit cell in all the complexes is not much.[13-16] In the nitrate and perchlorate complexes, since the chromophore around copper(II) has axial symmetry ($R = 0$) and $g_1 > 2.04$, the ground state of copper(II) is $d_{x^2-y^2}$. The rhombic g values and the values of R in the range 0.2–0.4 in the chloro and bromo complexes indicate that the ground state of copper(II) in the CuN_2X_2 entities is dominated by $d_{x^2-y^2}$ with a slight admixture of d_{z^2}. These g values are comparable to the values obtained in other N_{ring}-bonded copper(II) complexes of other heterocyclic ligands.[16-21] But before drawing conclusions on the slight temperature variations of the g values, one has to take into consideration the increased errors in the g values brought about by the broadening effects due to dipolar, exchange and unresolved hyperfine interactions.[13] Therefore these temperature variations in the g value may arise due to the fluxional

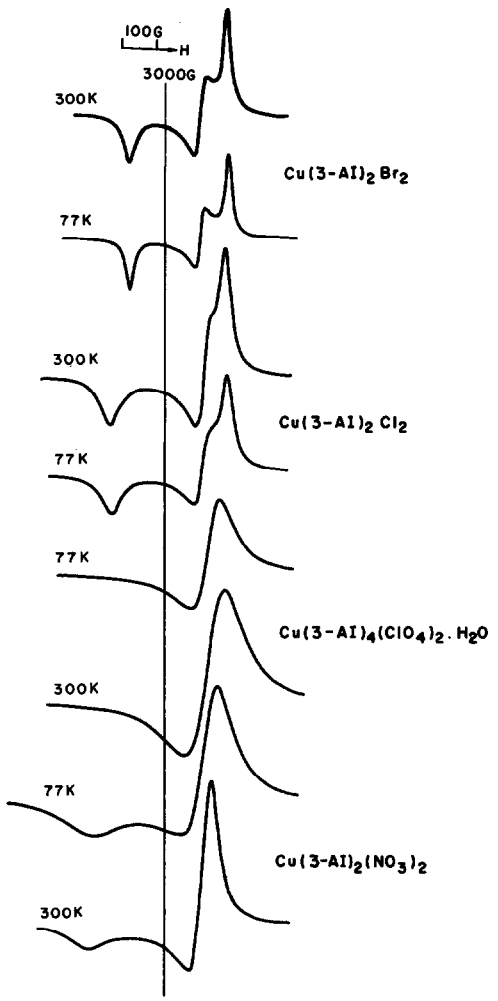

Fig. 1. ESR spectra of polycrystalline 3-AI copper(II) complexes of 9.07 GHz.

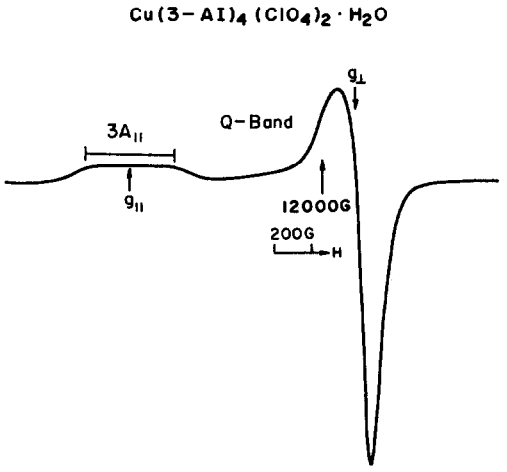

Fig. 2. ESR spectrum of polycrystalline $Cu(3\text{-AI})_4(ClO_4)_2 \cdot 2H_2O$ at 35.4 GHz.

nature of the geometries[22] or due to the inaccuracies in the g values induced by the above line broadening factors. A comparison of the g values of the bis-complexes of 3-AI and 3-AMI (Table 4) indicates that these values in the former complexes are more than in the latter complexes, which may arise probably due to the difference in the nature of coordination of 3-AI (monodentate N_{ring}-bonded) and 3-AMI (bridging bidentate) ligands. Since, in the case of the tetrakis-complex of 3-AI and 3-AMI, both the ligands are monodentate N_{ring}-bonded and hence g and A values of these complexes are comparable,[5] the difference in the symmetries (axial and rhombic) in the chromophores of $Cu(3\text{-AI})_4(ClO_4)_2 \cdot H_2O$ and $Cu(3\text{-AMI})_4(ClO_4)_2$ (Table 4) may arise most probably due to the fact that the former complex is hexa-coordinate (CuN_4O_2) and the latter one is penta-coordinate (CuN_4O).[1]

Solution spectra

Figures 3 and 4 show the ESR spectra in the frozen solutions of these complexes in DMF (dimethylformamide) and pyridine, respectively. Table 5 gives the g and A values obtained from these

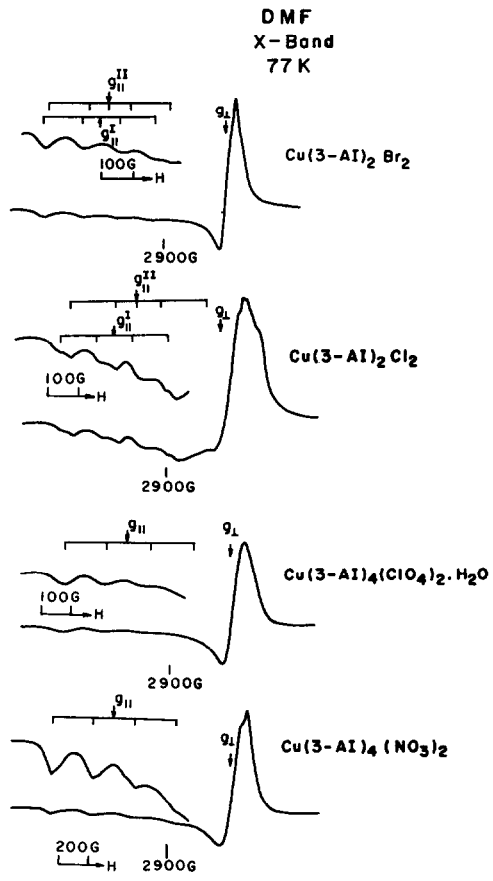

Fig. 3. ESR spectra of 3-AI copper(II) complexes in frozen DMF solutions.

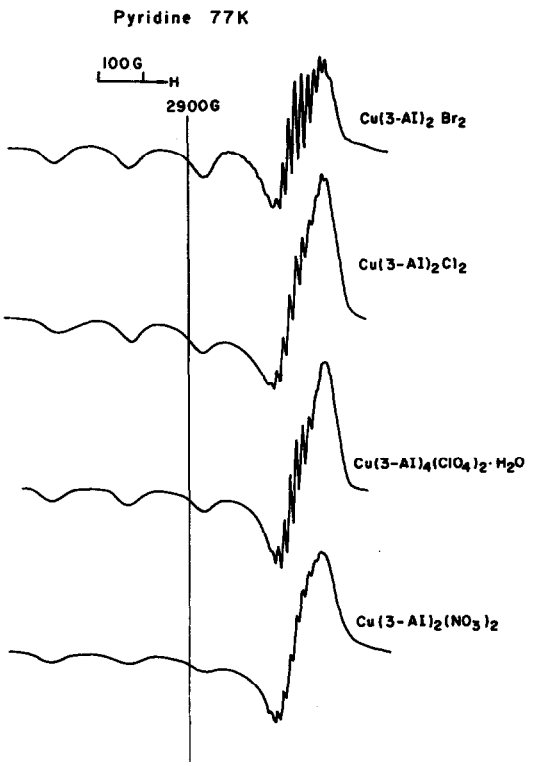

Fig. 4. ESR spectra of 3-AI copper(II) complexes in frozen pyridine solutions.

spectra. In the DMF solutions of chloro and bromo complexes, two species with different g and A values similar to 3-AMI complexes[6] are found to exist. The two species observed in the other two complexes are very close (Fig. 3) and hence only average g and A values of the two species are given in Table 5. In the case of the chloro complex the g and A values of species I and II are indicating oxygen and nitrogen coordinations, respectively.[16] Also the g values of species II of the above complex are comparable to the polycrystalline values: On the other hand the g (2.40–2.35) and A values (120–140 G) of the DMF species of the remaining complexes are indicating oxygen coordination. In pyridine solutions, the g and A values of all the species are the same within experimental error and indicate nitrogen coordination, which is supported by the ligand hyperfine structure on the perpendicular features. The above information suggests that the 3-AI ligands may most probably have been replaced by the solvent molecules in these solutions. This type of solute–solvent interaction is also observed in the copper(II) complexes of 3-AMI.[6]

CONCLUSIONS

Copper(II) complexes of 3-aminoisoxazole with general formula Cu(3-AI)$_n$X$_2$·mH$_2$O have been synthesized and their IR, electronic and ESR data obtained in polycrystalline and solution forms yielded the following information.

(a) IR and electronic spectral studies indicated that in all complexes 3-AI acts as a monodentate N$_{ring}$-bonded ligand, unlike the 3-AMI ligand which acts as a monodentate ligand in tetrakis-complexes and a bridging ligand (N- and O-bonded) in bis-complexes. The bis-complexes of 3-AI are mono-

Table 5. Spin-Hamiltonian constants obtained in DMF and pyridine solutions of 3-AI and 3-AMI copper(II) complexes

Complexes		Solvent	$g_\parallel$	$g_\perp$	$A_\parallel$ (G)	Reference
Cu(3-AMI)$_2$Cl$_2$	DMF	Species I	2.348	2.044	124	Present study
		Species II	2.288		152	
	Pyridine		2.268	2.037	160	
Cu(3-AI)$_2$Br$_2$	DMF	Species I	2.397	2.062[a]	121	
		Species II	2.378		128	
	Pyridine		2.268		170	
Cu(3-AI)$_2$NO$_3$	DMF[b]		2.369	2.049	136	
	Pyridine		2.270	2.037	175	
Cu(3-AI)$_4$(ClO$_4$)$_2$·H$_2$O	DMF[b]		2.348	2.048	140	
	Pyridine		2.271	2.032	173	
Cu(3-AMI)$_4$(ClO$_4$)$_2$	Pyridine		2.288	2.027	181	5
Cu(3-AMI)$_2$(NO$_3$)$_2$	DMF	Species I	2.393	—	120	6
		Species II	2.373		131	
Cu(3-AMI)$_2$Br$_2$	Pyridine		2.267	2.072	173	6

[a] The $g_\perp$ value is the average value of the two species.
[b] The g and A values are the average values of the two species.

meric with CuN_2X_2 ($X = Cl^-$, Br^- and NO_3^-) geometries, unlike the corresponding 3-AMI complexes which are polymeric. The tetrakis-complexes of 3-AI are hexa-coordinate (CuN_4O_2), unlike the corresponding 3-AMI complexes which are penta-coordinate (CuN_4O).

(b) The G values calculated from the g values obtained in polycrystalline samples, indicate that the magnetic misalignment of molecules in the unit cell is only small. The partial resolution of the copper(II) hyperfine lines at Q-band in the case of $Cu(3\text{-AI})_4(ClO_4)_2 \cdot H_2O$ indicates that the exchange interaction amongst copper(II) ions in the unit cell is of the order of 1 cm^{-1}. The g values of the bis-complexes in the present case are found to be greater than that of the corresponding values in the 3-AMI complexes, indicating that the metal–ligand bond is weaker in the present complexes than in the 3-AMI complexes.

(c) Two species are found to exist in the DMF solutions of all the complexes unlike in the pyridine solutions. Large changes induced in the g values of the species in these solutions indicate that the coordinate positions in the complexes are occupied by solvent molecules.

Acknowledgement—One of the authors (B.M.) is grateful to CSIR, New Delhi for financial assistance.

REFERENCES

1. G. Devoto, M. Massacesi, R. Pinna and G. Ponticelli, *Transition Met. Chem.* 1977, **2**, 236.
2. M. Biddau, M. Massacesi, R. Pinna and G. Ponticelli, *Transition Met. Chem.* 1978, **3**, 153.
3. M. Biddau, G. Devoto, M. Massacesi and G. Ponticelli, *Transition Met. Chem.* 1976, **1**, 295, 99, 173.
4. G. Ponticelli, *J. Inorg. Nucl. Chem.* 1977, **39**, 45.
5. B. A. Sastry, S. Md. Asadullah, G. Ponticelli and M. Massacesi, *J. Inorg. Nucl. Chem.* 1981, **43**, 1521.
6. B. A. Sastry, S. Md. Asadullah, G. Ponticelli and R. Pinna, *J. Molec. Struct.* 1981, **73**, 195.
7. B. A. Sastry, B. Balaiah, R. Subramanian, G. Ponticelli, G. Devoto and M. Massacesi, *Ind. J. Pure Appl. Phys.* 1985, **23**, 279.
8. B. A. Sastry, B. Balaiah, K. V. G. Reddy, B. Madhu, G. Ponticelli and M. Massacesi, *Polyhedron* 1987, **6**, 1053.
9. D. M. L. Goodgame, M. Goodgame and G. W. Rayner Canham, *Inorg. Chim. Acta* 1969, **3**, 393.
10. E. J. Duff and M. N. Hughes, *J. Chem. Soc. A.* 1968, 2144.
11. D. M. L. Goodgame and F. A. Cotton, *J. Chem. Soc.* 1961, 2298.
12. F. K. Kneubuhl, *J. Chem. Phys.* 1960, **33**, 1074.
13. I. M. Proctor, B. J. Hathaway and P. Nicholis, *J. Chem. Soc. A.* 1968, 1678.
14. M. J. Beu, B. J. Hathaway and R. J. Fereday, *J. Chem. Soc. A.* 1972, 1229.
15. A. A. G. Tomlinson and B. J. Hathaway, *J. Chem. Soc. A.* 1968, 1905.
16. B. J. Hathaway, *J. Chem. Soc., Dalton Trans.* 1972, 1196.
17. K. V. R. Chary, K. V. G. Reddy, B. A. Sastry, G. Ponticelli and R. Pinna, *Ind. J. Pure Appl. Phys.* 1983, **21**, 698.
18. B. A. Sastry, B. Balaiah, K. V. G. Reddy, B. Madhu, G. Ponticelli, M. Massacesi and G. Puggioni, *Ind. J. Pure Appl. Phys.* 1986, **24**, 460.
19. M. Massacesi, G. Ponticelli, C. Ramachary and V. G. Krishnan, *Transition. Met. Chem.* 1980, **5**, 353.
20. M. Massacesi, G. Ponticelli, V. A. Buddha and V. G. Krishnan, *J. Molec. Struct.* 1979, **51**, 27.
21. M. Massacesi, G. Ponticelli, V. A. Buddha and V. G. Krishnan, *J. Molec. Struct.* 1978, **48**, 55.
22. B. J. Hathaway, *Coord. Chem. Rev.* 1982, **41**, 423.

Polyhedron Vol. 8, No. 7, pp. 941–945, 1989
Printed in Great Britain

0277–5387/89 $3.00+.00
© 1989 Pergamon Press plc

PREFERENTIAL SOLVATION EFFECTS IN THE SUBSTITUTION KINETICS OF THE (2,6 DIMETHYL PYRAZINE)PENTACYANOFERRATE(II) COMPLEX

HENRIQUE E. TOMA*

Instituto de Química, Universidade de São Paulo, Caixa Postal 20780, São Paulo, SP, Brazil

and

MARIA S. TAKASUGI

Departamento de Química, Universidade de Fed. Parana, Caixa Postal 1963, Curitiba, PR, Brazil

(*Received* 7 *June* 1988; *accepted* 8 *November* 1988)

Abstract—The spectroscopic behaviour and the substitution kinetics of the (2,6 dimethyl pyrazine)pentacyanoferrate(II) complex in mixed water–organic solvents are strongly influenced by preferential solvation effects. The dissociation rate constants, obtained in the presence of a high excess of dimethyl sulphoxide as the incoming ligand, exhibit a linear dependence with respect to the acceptor number scale.

The solvent can play an extraordinary rôle in the kinetics and mechanisms of ligand substitution processes. These reactions usually proceed at overall rates much slower than the diffusion limits, and the diffusional encounter of the reactants can be treated as a pseudo-equilibrium followed by the rate determining step involving ligand exchange within the precursor complex.[1] The formation of the precursor complex and the substitution step are strongly influenced by the solvent composition, which may induce general changes in the free energies, or specific changes on the structure–reactivity behaviour of the reactants and activated complexes. On the other hand, in mixed solvents, the composition and reactivity of the precursor complex will depend on the extent of preferential solvation. We have previously shown[2] that this type of interaction has a dramatic influence in the solvatochromic properties of cyanoiron(II) complexes. We now report a detailed study of the preferential solvation effects in the substitution kinetics of the (2,6 dimethyl pyrazine)pentacyanoferrate(II) complex.

EXPERIMENTAL

The $Na_3[Fe(CN)_5(dmpz)]\cdot 3H_2O$ (dmpz = 2,6 dimethyl pyrazine) complex was synthesized and characterized previously.[3] $H_3Fe(CN)_5(dmpz)\cdot 3H_2O$ was obtained as a yellow solid, by rapidly mixing a saturated aqueous solution of $Na_3[Fe(CN)_5(dmpz)]\cdot 3H_2O$ with an equal volume of hydrochloric acid (37%), at 0°C, in a well-ventilated hood. The solid was collected on a filter, washed with diethyl ether and stored in a sealed flask, in the freezer. The tetrabutylammonium (TBA) salt was prepared by reacting $H_3Fe(CN)_5(dmpz)\cdot 3H_2O$ with stoichiometric amounts of tetrabutylammonium hydroxide in methanol, followed by the evaporation of the solvent under low pressure.

The electronic spectra of the complexes were recorded on a Cary 17 or a Hewlett–Packard model 8451-A diode-array spectrophotometer. The solvents were saturated with dry argon and transferred into the spectrophotometric cell with calibrated syringes. Serum caps or Teflon stoppers were used for syringe transfer, with special care to prevent the contact of the rubber with the solvents. The kinetics were carried out under an argon atmosphere, by monitoring spectrophotometrically the dissociation of the complex in the presence of a high excess of dimethyl sulphoxide (dmso) as the entering ligand.

RESULTS AND DISCUSSION

The $[Fe(CN)_5(dmpz)]^{3-}$ complex undergoes a dissociation reaction in solution, according to eq.

* Author to whom correspondence should be addressed.

(I), leading to a partial decay of the strong charge transfer band in the visible region (Fig. 1). The spectra are greatly influenced by the solvent, as observed in many cyanoiron(II) complexes.[2,5-8] The dissociation process can be repressed in the presence of an excess of the dmpz ligand, or driven to completion by adding an appropriate ligand, such as dmso, which has strong affinity for the pentacyanoferrate(II) ion.[9]

$$[Fe(CN)_5(dmpz)]^{3-} + S \rightleftharpoons [Fe(CN)_5S]^{3-} + dmpz. \quad (1)$$

In general, the substitution reactions in pentacyanoferrate(II) complexes proceed via a dissociative mechanism. The kinetics exhibit a saturation behaviour where the observed rate constants and the corresponding activation parameters are independent of the concentration and nature of the entering ligand.[10] Additional evidence for the dissociative mechanism has been obtained for the (3,5 dimethyl pyridine)pentacyanoferrate complex, based on measurements of the activation volumes.[11]

The kinetic constant measured at the saturation point, (versus [dmso]) for the dissociation of the $[Fe(CN)_5(dmpz)]^{3-}$ complex is 6.3×10^{-4} s^{-1}, in comparison to 1.3×10^{-3} s^{-1} (25°C) for the analogous 3,5 dimethyl pyridine complex.[10,11]

The substitution kinetics for the pentacyano(3,5 dimethylpyridine)ferrate(II) complex have already been investigated[12] in binary aqueous mixtures containing up to 40% by volume of methanol, ethanol, *t*-butyl alcohol, glycerol and tetrahydrofuran. The kinetics were consistent with the operation of a dissociative mechanism under all the conditions studied. The rates were also correlated with the Grunwald–Winstein *Y* values, showing only a low sensitivity to the solvent composition.

In the case of the pentacyano(2,6 dimethyl pyrazine) complex, the kinetics of substitution with dmso exhibited saturation behaviour in methanol, as illustrated in Fig. 2, with only 20% increase in the observed rate constants. In acetone and in acetonitrile, however, the rates were enhanced by two orders of magnitude. These results were unexpected, in view of the preceding results for the 3,5 dimethyl pyridine complex.[10] For this reason, we examined the detailed kinetic behaviour of the

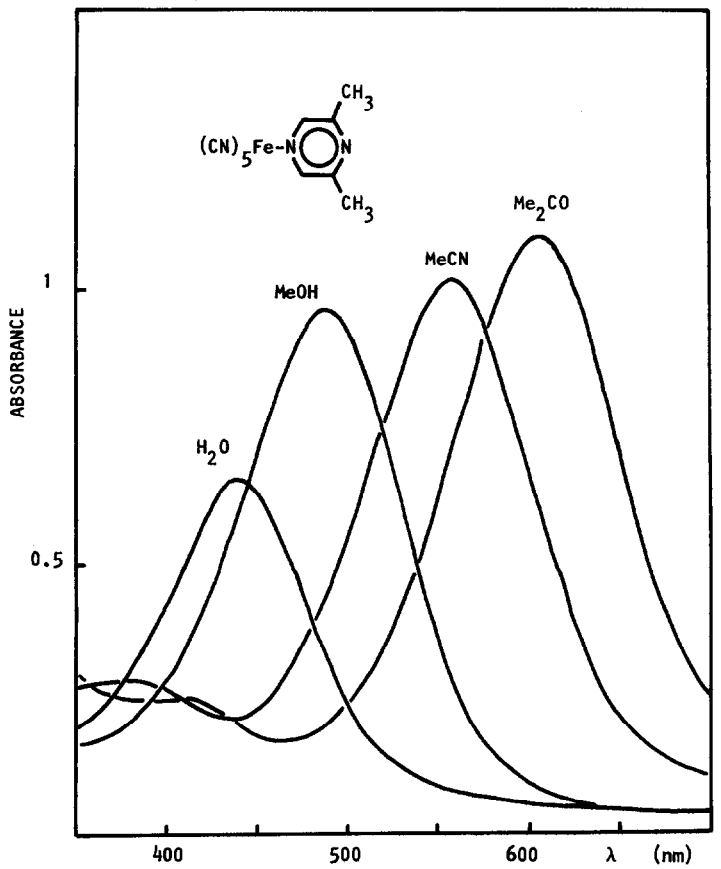

Fig. 1. Electronic spectra of $[Fe(CN)_5(dmpz)]^{3-}$, 1.4×10^{-4} mol dm^{-3}, in water, methanol, acetonitrile and acetone.

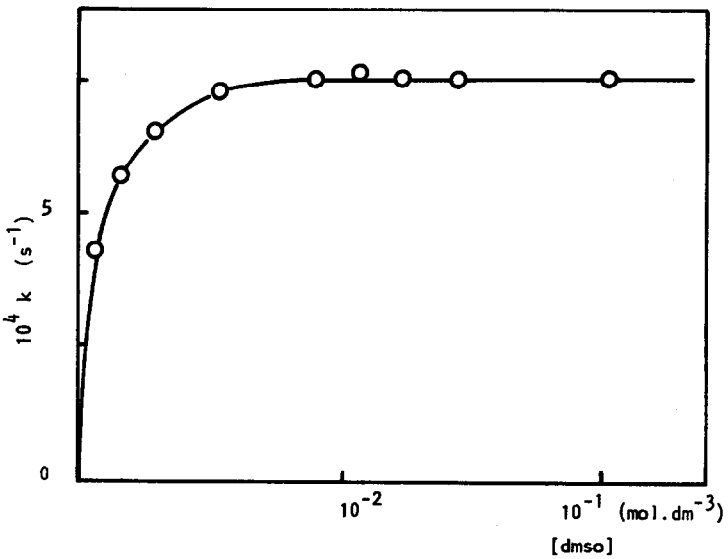

Fig. 2. Plots of the observed rate constants for the dissociation reaction of $[Fe(CN)_5(dmpz)]^{3-}$ in methanol, showing saturation behaviour with respect to the concentration of the entering ligand, dmso.

dmpz complex in binary aqueous mixtures containing methanol, acetone and acetonitrile. Typical results are shown in Table 1.

The spectra of the $[Fe(CN)_5(dmpz)]^{3-}$ complex were also obtained under the conditions employed for the kinetics, for comparison purposes. The spectroscopic behaviour is strongly influenced by preferential solvation in the mixed solvents, as one can see in Fig. 3. When no preferential solvation occurs, the composition of the solvation shell should reflect

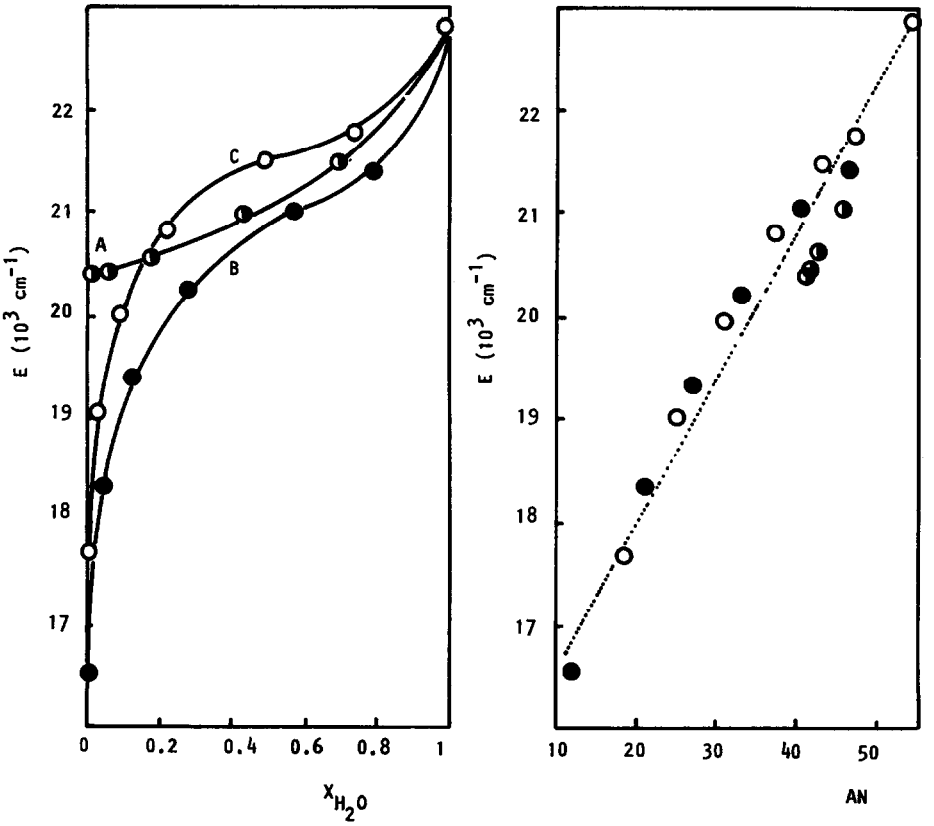

Fig. 3. Plots of the spectral charge transfer energies for the $[Fe(CN)_5(dmpz)]^{3-}$ complex versus the mole fraction of water (left) and the acceptor number (right) of aqueous methanol (A), acetone (B) and acetonitrile (C) mixed solvents.

Table 1. Dissociation rate constants for the $[Fe(CN)_5(dmpz)]^{3-}$ complex in binary mixed solvents[a]

H_2O–MeOH $10^4 k$ (s^{-1}) (X)	H_2O–Me_2CO $10^4 k$ (s^{-1}) (X)	H_2O–MeCN $10^4 k$ (s^{-1}) (X)
7.6 (0)	187 (0)	700 (0)
7.6 (0.02)	128 (0.04)	400 (0.03)
7.6 (0.07)	86 (0.12)	155 (0.09)
7.5 (0.18)	33 (0.29)	80 (0.22)
7.0 (0.43)	17.6 (0.57)	22.7 (0.49)
6.4 (0.70)	9.2 (0.80)	13.0 (0.74)
6.3 (1.00)	6.3 (1.00)	6.3 (1.00)

[a] 25°C, mole fraction of water in parentheses.

the composition of the bulk solvent, and the spectroscopic data are expected to follow a linear dependence with respect to the mole fraction of the mixture.[12] The deviation from the linear behaviour shown in Fig. 3(A) is consistent with a strong preferential solvation of the cyanoiron complex, with the water molecules predominating in the solvation shell in aqueous acetone or acetonitrile mixed solvents. A similar deviation from the ideal behaviour is observed in the plots of partial vapour pressure of water in acetonitrile solutions versus the mole fraction.[1] This means that water is transferred more easily from the bulk solvent to the complex solvation shell when it is in a weakly interacting medium, such as in acetonitrile.

The preferential solvation effects can be dealt with by means of the acceptor number scale (AN),[13–15] which is a combined measure of solvent polarity or polarizability and hydrogen bond donor ability.[16] As one can see in Fig. 3(B) the spectroscopic data for the pentacyano(2,6 dimethyl pyrazine)ferrate(II) complex are linearly correlated with AN.

The kinetic constants (k) for the dissociation reactions (Fig. 4) follow the trends observed for the spectroscopic behaviour, indicating strong preferential solvation effects. A linear correlation with the acceptor number scale is observed for each series of mixed solvents, as expressed by eq. (2):

$$\ln k = \ln k_o - b \cdot (AN), \qquad (2)$$

where $\ln k_o = -6.51$, -2.70, 0.16, and $b = -0.016$, -0.087, -0.140, for aqueous methanol, acetone and acetonitrile, respectively.

The $[Fe(CN)_5(dmpz)]^{3-}$ complex can interact strongly with the solvent via the cyanide and pyrazine ligands. The acceptor properties of the solvents

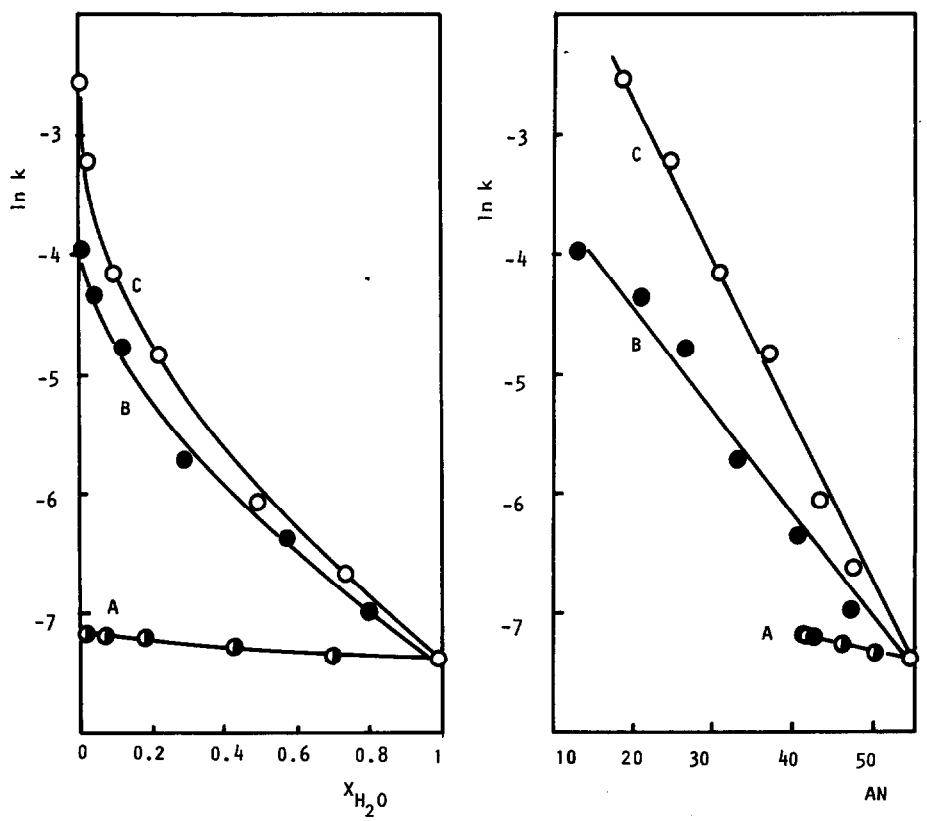

Fig. 4. Plots of $\ln k$ for the dissociation of $[Fe(CN)_5(dmpz)]^{3-}$ versus the mole fraction (left) and the acceptor number (right) of aqueous methanol (A), acetone (B) and acetonitrile (C) mixed solvents.

should enhance the backbonding capability of both ligands, leading to a greater stabilization of the solvated precursor complex, with respect to the pentacoordinated activated complex, decreasing the rates of the dissociation reactions. On the other hand, the solvent effects are probably not restricted to the stabilization of the precursor complex, otherwise the data in Fig. 4(B) would fit a single correlation with the acceptor number scale, as in the case for the spectroscopic behaviour.[2] The different slopes in Fig. 4(B) are associated with the kinetic behaviour in the pure solvents, which show some scattering in the correlation with the acceptor number scale. We presume that the scattering arises from solvent effects in the activated complexes, assisting the transfer of the leaving ligand to the solvation shell.

Acknowledgements—We thank CNPq, FAPESP and FINEP for financial support.

REFERENCES

1. C. H. Langford and J. P. K. Tong, *Pure Appl. Chem.* 1977, **49**, 93.
2. H. E. Toma and M. S. Takasugi, *J. Sol. Chem.* 1983, **12**, 657.
3. H. E. Toma and E. Stadler, *Inorg. Chem.* 1985, **24**, 3085.
4. H. E. Toma and J. M. Malin, *Inorg. Chem.* 1973, **12**, 1039.
5. J. Burgess, *Spectrochim. Acta* 1970, **26A**, 1369.
6. J. Burgess, *Spectrochim. Acta* 1970, **26A**, 1957.
7. J. Burgess and S. F. N. Norton, *J. Chem. Soc., Dalton Trans.* 1972, 1712.
8. J. Burgess and M. V. Twigg, *J. Chem. Soc., Dalton Trans.* 1974, 2032.
9. H. E. Toma, J. M. Malin and E. Giesbrecht, *Inorg. Chem.* 1973, **12**, 2084.
10. M. J. Blandamer, J. Burgess and R. I. Haines, *J. Chem. Soc., Dalton Trans.* 1976, 1293.
11. T. R. Sullivan, D. R. Stranks, J. Burgess and R. I. Haines, *J. Chem. Soc., Dalton Trans.* 1977, 1460.
12. L. S. Frankel, C. H. Langford and T. R. Stengle, *J. Phys. Chem.* 1970, **74**, 1376.
13. U. Mayer, V. Gutmann and W. Gerger, *Monatsh. Chem.* 1975, **106**, 1235.
14. U. Mayer, W. Gerger and V. Gutman, *Monatsh. Chem.* 1977, **108**, 489.
15. V. Gutmann, *Pure Appl. Chem.* 1979, **51**, 2197.
16. R. W. Taft, N. J. Pienta, M. J. Kamlet and E. M. Arnett, *J. Org. Chem.* 1981, **46**, 661.

Polyhedron Vol. 8, No. 7, pp. 947–951, 1989
Printed in Great Britain

0277–5387/89 $3.00+.00
© 1989 Pergamon Press plc

COMPARATIVE STUDY OF TUNGSTEN(V) COMPLEXES WITH 8-QUINOLINOL AND 2-METHYL-8-QUINOLINOL

R. LOZANO,* J. ROMÁN and F. DE JESUS

Departamento de Química Inorgánica, Facultad de Farmacia, Universidad Complutense, 28040 Madrid, Spain

(*Received* 20 *June* 1988; *accepted* 8 *November* 1988)

Abstract—The present paper reports a comparative study of a number of oxo- and sulphido bridge tungsten(V) oxo-complexes with 8-quinolinol and 2-methyl-8-quinolinol as ligands. The results obtained permit us to assign the following formulae to the complexes: $W_2O_3(LL)_4$, $W_2O_4(LL)_2$, $W_2O_2S_2(LL)_2$ and $W_2O_3S(LL)_2$. All these complexes present very low values of the magnetic moment, according to a dimer structure with monoxo, dioxo, disulphido and oxo-sulphido bridges. We suggest that the low magnetic moments observed are due, at least in part, to intramolecular metal–metal interactions.

Oxo-complexes of the group (VI) elements play a central rôle in a variety of industrial and biological oxidation processes.[1]

In previous communications we have reported the isolation and study of monomeric and dimeric molybdenum(V) complexes with different ligands,[2–4] but such binuclear compounds are not so numerous in tungsten chemistry. However, recently we have reported the characterization of tungsten(V) dimeric complexes with dithiocarbamates as ligands.[5,6]

The object of the present study has been to obtain compounds of tungsten(V) with 8-quinolinol and 2-methyl-8-quinolinol as ligands, so as to observe the steric effect exercised by the methyl group.

The systematic changes upon bridge modification are useful in characterizing the compounds and in clarifying assignments of W—O and W—S bridge stretching frequencies. The results are discussed on the basis of structural information available for tungsten complexes.

These complexes were characterized by IR and electronic spectroscopy, magnetic susceptibility measurements and analytical data. The results obtained permit us to assign the following formulae to the complexes: $W_2O_3(LL)_4$, $W_2O_4(LL)_2$, $W_2O_2S_2(LL)_2$ and $W_2O_3S(LL)_2$.

* Author to whom correspondence should be addressed.

EXPERIMENTAL

(a) *Materials*

$Na_2WO_4 \cdot 2H_2O$, 8-quinolinol and 2-methyl-8-quinolinol were Merck commercial products.

The solvents used to prepare and to recrystallize the complexes were Carlo Erba or Merck. The solutions for absorption spectra were prepared using dimethylsulphoxide (DMSO) spectral grade (Merck–Uvasol).

(b) *Analytical procedures*

Elemental analyses were performed on a Perkin–Elmer model 240 B elemental analyser.

Tungsten was determined by atomic absorption with a Perkin–Elmer model 430 atomic absorption spectrophotometer, after decomposing the complexes with a 1 : 1 mixture of concentrated nitric and sulphuric acid.

The analytical data are given in Table 1. Results conform to proposed formulae.

(c) *Methods*

Magnetic susceptibility was determined by the Gouy method at room temperature using a Mettler H-51 AR balance and a type C Newport electromagnet. Molar susceptibilities have been cor-

Table 1. Elemental analyses and magnetic moments of tungsten(V) oxo-complexes

Compound	Calculated (%) C	H	N	W	Found (%) C	H	N	W	μ (BM)
$W_2O_3(C_9H_6NO)_4$	43.5	2.4	5.7	37.1	44.0	2.5	5.5	37.1	0.8
$W_2O_4(C_9H_6NO)_2$	30.0	1.7	3.9	51.1	30.8	2.0	3.9	51.2	0.3
$W_2O_2S_2(C_9H_6NO)_2$	28.7	1.6	3.7	48.9	29.0	1.7	3.7	49.0	0.0
$W_2O_3S(C_9H_6NO)_2$	29.3	1.6	3.8	50.0	29.4	1.7	3.8	50.1	0.2
$W_2O_3(C_{10}H_8NO)_4$	45.8	3.0	5.3	35.2	46.0	3.1	5.4	35.1	1.3
$W_2O_4(C_{10}H_8NO)_2$	32.1	2.1	3.7	49.2	32.1	2.2	3.8	49.2	0.6
$W_2O_2S_2(C_{10}H_8NO)_2$	30.8	2.1	3.6	47.2	31.0	2.1	3.6	47.0	0.4
$W_2O_3S(C_{10}H_8NO)_2$	31.4	2.1	3.7	48.2	31.4	2.1	3.6	48.1	0.0

rected for diamagnetism. Table 1 shows the results obtained.

The IR spectra were measured on a Perkin–Elmer recording spectrophotometer model 283 using KBr pellets. Important IR absorption peaks for the compounds prepared in this study are listed in Table 2.

The vis–near UV spectra of the compounds were measured in the range 220–1000 nm, on a Beckman recording spectrophotometer model 554, using complex solutions in DMSO. The results obtained are given in Table 3.

(d) *Preparation of the complexes*

$W_2O_3(C_9H_6NO)_4$. (3.30 g, 10 mmol) of $Na_2WO_4 \cdot 2H_2O$ was dissolved in 30 cm^3 of water and depolymerized with NaOH. Another solution of 8-quinolinol (2.90 g, 20 mmol) in 60 cm^3 of hot absolute ethanol was prepared. Once it was cold, this solution was added to the previous one, taking on a yellow colour—the resulting solution. A solution of 1 g of sodium dithionite was added, changing from yellow to green. Glacial acetic acid was added drop by drop and with vigorous stirring till reaching pH 5.

A brown solid was precipitated, which separated by filtration *in vacuo* and was washed repeatedly with a boiling water–ethanol mixture (50%). The residue was filtered hot and *in vacuo* so as to obtain a brown powder which was dried over P_4O_{10} (yield, 67%).

$W_2O_4(C_9H_6NO)_2$. A solution of $Na_2WO_4 \cdot 2H_2O$ (3.30 g, 10 mmol) in 50 cm^3 of water was prepared. 2 N NaOH was added till reaching pH 10, and the solution was heated by boiling for 10 min.

A second solution, 8-quinolinol (0.45 g, 10 mmol) dissolved in 40 cm^3 of hot absolute ethanol, was

Table 2. IR absorption maxima of tungsten(V) oxo-complexes

Compound	ν W=O (cm^{-1})	ν W—Ob (cm^{-1})	ν W—Sb (cm^{-1})	ν W—N (cm^{-1})	ν W—O—C (cm^{-1})
$W_2O_3(C_9H_6NO)_4$	925	ν_a 835 ν_s 463	—	340	1117
$W_2O_4(C_9H_6NO)_2$	930	ν_a 825 ν_s 455	—	332	1112
$W_2O_2S_2(C_9H_6NO)_2$	943	—	ν_a 470 ν_s 368	335	1105
$W_2O_3S(C_9H_6NO)_2$	935	ν_a 820 ν_s 448	ν_a 473 ν_s 372	332	1110
$W_2O_3(C_{10}H_8NO)_4$	957	ν_a 812 ν_s 450	—	335	1110
$W_2O_4(C_{10}H_8NO)_2$	960	ν_a 810 ν_s 440	—	324	1103
$W_2O_2S_2(C_{10}H_8NO)_2$	962	—	ν_a 460 ν_s 360	318	1090
$W_2O_3S(C_{10}H_8NO)_2$	958	ν_a 805 ν_s 430	ν_a 465 ν_s 363	320	1100

Table 3. Electronic absorption spectra of tungsten(V) oxo-complexes

Compound	ν in kK (ε in M^{-1} cm^{-1})
$W_2O_3(C_9H_6NO)_4$	14.0 (158); 17.9 (316); 20.5 (6,527); 27.7 (7,432); 30.3 (15,728); 35.5 (45,106)
$W_2O_4(C_9H_6NO)_2$	15.3 (97); 18.3 (248); 20.5 (3,726); 27.4 (5,133); 30.1 (18,532); 35.9 (35,414)
$W_2O_2S_2(C_9H_6NO)_2$	15.1 (195); 17.9 (471); 20.4 (2,429); 22.4 (3,987); 27.5 (7,419); 30.5 (19,018); 35.7 (47,826)
$W_2O_3S(C_9H_6NO)_2$	15.3 (136); 18.1 (306); 20.6 (4,831); 22.3 (6,147); 26.5 (5,329); 30.7 (16,401); 34.9 (43,538)
$W_2O_3(C_{10}H_8NO)_4$	14.0 (226); 18.0 (417); 20.6 (3,587); 27.4 (5,219); 31.4 (14,721); 35.9 (37,126)
$W_2O_4(C_{10}H_8NO)_2$	15.1 (84); 17.9 (324); 20.4 (2,980); 29.6 (6,432); 30.7 (16,748); 34.6 (49,586)
$W_2O_2S_2(C_{10}H_8NO)_2$	15.4 (65); 18.2 (163); 20.2 (1,535); 22.5 (2,146); 27.9 (4,434); 30.1 (17, 823); 34.3 (63,586)
$W_2O_3S(C_{10}H_8NO)_2$	15.3 (149); 18.1 (431); 20.4 (4.482); 22.6 (7,313); 27.6 (8,436); 31.1 (20,347); 34.8 (52,406)

prepared. The two solutions were combined and the resulting one was yellow in colour. A solution of 0.5 g of sodium dithionite in 20 cm^3 of water was added to it and the resulting solution turned green. Lastly, 2N HCl was added, drop by drop, and with continuous stirring till reaching pH 2 so that a greenish precipitate was obtained which was separated by filtration *in vacuo*.

The solid obtained was washed with a mixture of 20 cm^3 of water and 20 cm^3 of boiling ethanol, and filtered hot and *in vacuo* so as to obtain a greenish powder which was dried over P_4O_{10} (yield, 54%).

$W_2O_2S_2(C_9H_6NO)_2$. $Na_2WO_4 \cdot 2H_2O$ (3.30 g, 10 mmol) was dissolved in 50 cm^3 of water, and a concentrated sodium hydroxide solution was added, heating the solution by boiling for 10 min to avoid polymerization.

At the same time, 8-quinolinol (1.45 g, 10 mmol) was dissolved in 35 cm^3 of hot absolute ethanol. Once it was cold, this solution was added to the previous one and a new solution of 1 g of sodium dithionite in 40 cm^3 of water was added. The resulting solution changed from yellow to green. Hydrogen sulphide was passed through the resulting solution with simultaneous cooling in a freezing mixture for about 30 min. Glacial acetic acid was added, drop by drop, till reaching pH 6 and total precipitation. The solution was filtered and an orange residue was obtained which was washed with an acetic acid–ethanol mixture and was dried over P_4O_{10} (yield, 71%).

$W_2O_3S(C_9H_6NO)_2$. A solution of sodium tungstate (3.30 g, 10 mmol) dihydrated in 50 cm^3 of water was prepared, adding 10 cm^3 of concentrated boiling NaOH and dropping 2 N HCl until reaching pH 2. Another solution of 1 g of sodium dithionite in 40 cm^3 of water was added to the previous one. The resulting solution was heated lightly for 15 min. Once it was cold, hydrogen sulphide was bubbled slowly through the solution for about 60 min, changing it to a dark brown colour.

Another solution of 8-quinolinol (1.45 g, 10 mmol) in 60 cm^3 of hot absolute ethanol was prepared. The two solutions were combined and glacial acetic acid was added to it, drop by drop, till reaching pH 5 and total precipitation.

The solid precipitate was washed with a 2 N ethanol–acetic acid mixture (1 : 1), obtaining a brown-coloured powder which was dried over P_4O_{10} (yield, 68%).

Similar preparations for the tungsten(V) oxo-complexes with 2-methyl-8-quinolinol as the ligand were performed.

DISCUSSION

(a) *Structures of the complexes*

According to the results of the analytical, magnetic and spectroscopic data, the synthesized oxo-complexes are dimeric.

When precipitation occurred at pH 5 with acetic acid, the complexes had a monoxo bridge, the stoichiometry was 2 : 1 and the tungsten was six-coordinated. The formula which was most closely square with the analyses is $W_2O_3(LL)_4$. However, when

precipitation was carried out at pH 2, the stoichiometry of the compounds was 1 : 1, the tungsten was five-coordinated and the complexes had a dioxo bridge. The formula we assign to these complexes is $W_2O_4(LL)_2$.

By bubbling hydrogen sulphide through $Na_2WO_4 \cdot 2H_2O$ solution and the corresponding ligand, complexes were obtained with a 1 : 1 stoichiometry, and tungsten was five-coordinated with the formula $W_2O_2S_2(LL)_2$.

When the hydrogen sulphide was bubbled through $Na_2WO_4 \cdot 2H_2O$ solution in dil. HCl with posterior addition of the ligand, the union between the tungsten atoms is realized by means of an oxo-sulphido bridge, the formula of the complexes being $W_2O_3S(LL)_2$.

(b) *Magnetic properties*

All the complexes studied present very low values for the magnetic moments (1.3–0.0 BM), as occurs in similar tungsten(V) complexes,[5,6] which can probably be attributed to an interaction through the bridge atoms or the possible formation of a direct metal–metal bond, as has been proved for similar molybdenum(V) oxo-complexes.[7,8]

(c) *IR spectra*

The IR spectra show, in all cases, a very strong band in the range 962–925 cm^{-1}, which we attribute to the vibration of the terminal W=O bond.

If we compare the complexes of 2-methyloxine with the tungsten(V) complexes of oxine (see Table 2), we observe that the first ones exhibit the band of the symmetric stretching mode of the W=O bond, displaced to greater frequencies. This difference is due to the steric effect of the methyl group, which weakens the union of the 2-methyloxine ligand with the tungsten atom, strengthening the tungsten terminal oxygen bond.

Since the W=O bond is stronger in the 2-methyloxine complexes than in the oxine ones, the bonding of the tungsten atom to the oxygen bridge atoms should be less in the dimeric 2-methyloxine complexes.

In the IR spectra of the compounds with monoxo-, dioxo- and oxo-sulphido bridges, we assign the bands corresponding to the W—O—W bridge at 835–805 and 463–430 cm^{-1} which we attribute to the vibration of the antisymmetric and symmetric stretching modes, respectively, of the W—O bridge bond. These bands are displaced to lower frequencies in the 2-methyloxine complexes, in comparison with the analogous complexes with oxine.

Another two bands, which appear in the IR spectra of the complexes with disulphido and oxo-sulphido bridges in the regions of 470–465 and 372–360 cm^{-1}, can be attributed to the vibration of the antisymmetric and symmetric stretching mode, respectively, of the W—S bridge bond. These bands are displaced to lower frequencies in the 2-methyloxine complexes as occurs with the W—O bridge bands, previously discussed.

All the complexes studied exhibit two bands in the IR spectra in the 1115 and 330 cm^{-1} regions. We attribute the first one to a C—O—W vibration mode and the second one to the W—N bond stretching as has been observed in other tungsten(V) complexes.[9–11]

(d) *Visible and UV spectra*

The electronic spectra (Table 3) for all the complexes present two bands in the 14,005–14,455 and 17,921–18,315 cm^{-1} regions, which we attribute to *d–d* transitions. We assign the two bands to $^2B_2 \rightarrow {}^2E(I)$ and $^2B_2 \rightarrow {}^2B_1$ transitions, respectively, for a distorted octahedral structure[12] for the monoxo bridge complexes and for a square pyramidal structure[13] for the complexes with dioxo-, disulphido and oxo-sulphido bridges.

In the visible region we can detect two other bands over 20,000 and 27,000 cm^{-1} that we attribute to charge-transfer transitions.

In the complexes with disulphido and oxo-sulphido bridges another band appears in the visible region over 22,000 cm^{-1} that can be attributed to a charge-transfer:

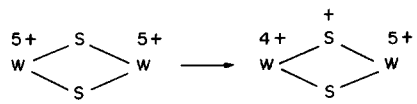

as has been observed in other transition metal complexes with a sulphur bridge.[14,15]

In the UV region, two transitions are detected at 30,000 and 35,000 cm^{-1} attributable to intraligand transitions.

We have made these compounds which, on the basis of our physical measurements, are analogous to similar molybdenum compounds.

REFERENCES

1. B. K. Burgess, D. B. Jacobs and E. I. Steifel, *Biochim. Biophys. Acta* 1980, **614**, 196.
2. R. Lozano, A. L. Doadrio and A. Doadrio, *Polyhedron* 1982, **1**, 163.
3. R. Lozano, J. Román, E. Alarcón, A. L. Doadrio and A. Doadrio, *Rev. Chim. Miner.* 1983, **20**, 173.

4. R. Lozano, J. Román, M. D. Armada and A. Doadrio, *Polyhedron* 1985, **4**, 1563.
5. R. Lozano, E. Alarcón, J. Román and A. Doadrio, *Polyhedron* 1984, **3**, 1021.
6. R. Lozano, J. Román, M. D. Armada and E. Parrondo, *Eur. J. Solid State Inorg Chem.* 1989, in press.
7. L. Ricard, C. Martin, R. Wiest and R. Weiss, *Inorg. Chem.* 1975, **14**, 2300.
8. L. Ricard, J. Stienne, P. Karagiannidis, P. Toledano, J. Fisher and A. Mitschler, *J. Coord. Chem.* 1974, **3**, 277.
9. V. C. Gibson, T. P. Kee and A. Shaw, *Polyhedron* 1988, **7**, 579.
10. M. A. Ansari, J. Chandrasekaran and S. Sarkar, *Polyhedron* 1988, **7**, 471.
11. M. H. Chisholm, J. C. Huffman and J. W. Pasterczyk, *Polyhedron* 1987, **6**, 1551.
12. C. J. Ballhausen and H. B. Gray, *Molecular Orbital Theory*. Benjamin, New York (1965).
13. H. B. Gray and C. B. Hare, *Inorg. Chem.* 1962, **1**, 363.
14. I. G. Dance and A. E. Landers, *Inorg. Chem.* 1979, **18**, 3487.
15. A. Kay and P. C. H. Mitchell, *J. Chem. Soc. A* 1970, 2421.

Polyhedron Vol. 8, No. 7, pp. 953–958, 1989
Printed in Great Britain

0277–5387/89 $3.00+.00
© 1989 Pergamon Press plc

NITROSOTHIOUREA: ITS REACTIVITY WITH METAL IONS AND THEIR COMPLEXES

D. S. PANDEY and U. C. AGARWALA*

Department of Chemistry, Indian Institute of Technology, Kanpur 208 016, India

(*Received* 21 *June* 1988; *accepted* 8 *November* 1988)

Abstract—Reactions of nitrosothiourea with different metal ions in the presence of pyridine, 2,2′-bipyridyl, 1,10 phenanthroline and a few complexes of ruthenium, rhodium, iridium, palladium and platinum have been carried out under varying reaction conditions. Physical methods such as IR, magnetic measurements, melting points, mixed melting points and elemental analyses have been used for the identification of reaction products.

Werner[1] and Stedman *et al.*[2] have shown that the unstable S-nitrosothiourothonium ion formed during the reaction of HNO_2 with thiourea, dissociates according to mechanism (1) in low acidic conditions and mechanism (2) under higher acidic conditions:

$$H^+ + HNO_2 + SC(NH_2)_2 \rightleftharpoons (NH_2)_2CSNO$$

$$(NH_2)_2CSNO \rightleftharpoons NH_2CSNHNO \longrightarrow NH_2CS{-}N{=}NOH$$

$$NH_2C{-}S{-}N{=}NOH \longrightarrow H^+ + HNCS + N_2 + OH^- \quad (1)$$

$$2H^+ + HNO_2 + 2SC(NH_2)_2 \longrightarrow (NH_2)_2CSSC(NH_2)_2 + 2NO + 2H_2O. \quad (2)$$

Since the NO group in both mechanisms either migrates from sulphur to nitrogen, eq. (1), or is generated, during reaction (2), there is a possibility of it being trapped by the metal ions to form their nitrosyls. However, the preferential ligation of the ambidentate NCS^-, forming simultaneously in the reaction, may create a problem in the "*in situ* trapping" of NO. It will, therefore, be interesting to examine the reactivity of S-nitrosothiourothonium (NTU) as the nitrosylating agent, over a range of acidities (from 2 M to pH 7) with various metal ions. The metal ions chosen for the reactions are those whose nitrosyls are stable and are synthesized at room or at low temperatures only. Since these metal ions are also potential thiocyanate scavengers, the relative overall efficacy of "NO group trapping" by the metal ions to that of the thiocyanate group under given experimental conditions may also be compared. The present note reports some work in this area.

EXPERIMENTAL

Analar grade chemicals and freshly distilled solvents were used in the reactions. NTU and the complexes of Ru, Rh, Ir, Pd and Pt were prepared and purified by the literature methods.[3–7] Microanalytical measurements, IR spectra (KBr), m.p. and room temperature magnetic susceptibilities of the complexes were carried out as described elsewhere.[8,9]

(A) *Reaction of* NTU *with* Co^{II} *acetate in presence of pyridine*

A methanolic solution (25 cm^3) containing Co^{II} acetate (1.0 mmol) was cooled to about 0°C using an ice–salt bath. To this, 15 cm^3 of an aqueous solution of NTU (freshly prepared) and 4.5 mmol of pyridine were added with stirring and left for about 0.5 h at 0°C. A pink compound separated out which was filtered and washed with water and a little methanol. It was extracted with excess alcohol, and the deep blue alcoholic extract was slowly evaporated on a waterbath whereby pink needle shaped crystals crystallized out. These were filtered, washed with ether and dried *in vacuo*. They were analysed for $[Co(py)_3(NCS)_2]$.

Reactions of NTU with Cr^{II}, Mn^{II}, Fe^{II}, Ni^{II}, Cu^{II}, Ag^{I}, Zn^{II}, Cd^{II} and Hg^{II} salts in presence of pyridine; Co^{II}, Ni^{II} and Cu^{II} salts in presence of 2,2′-bipyridyl

* Author to whom correspondence should be addressed.

Table 1. Reaction carried out, reactants, products, colour, melting point analyses and major IR bands

Sl. No.	Reactants	Reaction	Product
1	Cr^{II} acetate + NTU + py	(A)	$[Cr(NCS)_3(py)_2]\cdot H_2O$
2	Mn^{II} chloride + py + NTU	(A)	$[Mn(py)_4(NCS)_2]1/2MeOH$
3	Co^{II} acetate + py + NTU	(A)	$[Co(py)_3(NCS)_2]$
4	Fe^{II} sulphate + py + NTU	(A)	$[Fe(py)_4(NCS)_2]$
5	$[Co(py)_3(NCS)_2]$ + TMAC	(B)	$[Co(NCS)_2Cl_2][(CH_3)_4N]_2$
6	$[Co(py)_3(NCS)_2]$ + TEAC	(B)	$[Co(NCS)_2Cl_2][(C_2H_5)_4N]_2$
7	$Cp(py)_3(NCS)_2$ + TBAC	(B)	$[Co(NCS)_4][(C_4H_9)_4N]_2$
8	Co^{II} acetate/sulphate + bipy + NTU	(A)	$[Co(bipy)_2(NCS)_2]$
9	Co^{II} acetate/sulphate + phen + NTU	(A)	$[Co(phen)_2(NCS)_2]$
10	Ni^{II} nitrate + py + NTU	(A)	$[Ni(py)_4(NCS)_2]$
11	Ni^{II} nitrate + bipy + NTU	(A)	$[Ni(bipy)_2(NCS)_2]$
12	Ni^{II} nitrate + phen + NTU	(A)	$[Ni(phen)_2(NCS)_2]$
13	Cu^{II} sulphate + py + NTU	(A)	$[Cu(py)_2(NCS)_2]$
14	Cu^{II} sulphate + bipy + NTU	(C)	$[Cu(bipy)_2(NCS)_2]$
15	Cu^{II} sulphate + phen + NTU	(A)	$[Cu(phen)_2(NCS)_2]$
16	Zn^{II} chloride + py + NTU	(A)	$[Zn(py)_3(NCS)_2]\cdot H_2O$
17	$[RuCl_2(PPh_3)_3]$ + NTU	(C)	$[Ru(NO)(NCS)_2Cl(PPh_3)_2]1/2CH_2Cl_2$
18	$[Ru(NH_3)_5Cl]Cl_2$ + NTU	(A)	$[Ru(NO)(NH_3)_4NCS]Cl_2$
19	$[RhCl(PPh_3)_3]$ + NTU	(C)	$[Rh(NO)Cl(PPh_3)NCS]$
20	$AgNO_3$ + py + NTU	(A)	$[Ag(py)_2(NCS)_2]$
21	$CdSO_4$ + py + NTU	(A)	$[Cd(py)_2(NCS)_2]$
22	$IrCl_3(PPh_3)_3$ + NTU	(C)	$[Ir(PPh_3)_2(NCS)_2Cl(thio)]$
23	$Pd(PPh_3)_4$ + NTU	(A)	$[Pd(NCS)_2(PPh_3)_2]$
24	$Pt(PPh_3)_4$ + NTU	(A)	$[Pt(NCS)_2(PPh_3)_2]$
25	Hg^{II} chloride + py + NTU	(A)	$[Hg(py)_2(NCS)_2]$

py, pyridine; bipy, 2,2′-bipyridyl; phen, 1,10-phenanthroline; TMAC, tetramethylammonium chloride; TEAC, tetraethyl ammonium chloride; TBAC, tetrabutyl ammonium chloride.

Colour	M.p.	Analyses (found, calculated) C	H	N	S	X(Cl)	Major IR bands ν_{CN}	ν_{CS}	δ_{NCS}	ν_{NO}
White	260°C	38.5	3.2	16.7	23.1	—	2060	760	468	
		(38.8)	(3.0)	(17.4)	(23.8)					
White	—	52.2	3.6	15.0	12.4	—	2066	798	480	
		(53.6)	(4.3)	(16.6)	(12.7)					
Pink	190°C	51.5	3.6	16.8	16.2	—	2090	760	468	
		(49.6)	(3.6)	(17.0)	(15.5)			770		
Dark brown (needles)	—	54.5	4.8	17.5	12.9	—	2068	804	470	
		(54.1)	(4.1)	(17.2)	(13.1)					
Blue	—	29.7	5.9	15.0	16.5	—	2090	760	468	
		(30.5)	(6.1)	(14.2)	(16.3)					
Blue	—	32.5	4.8	14.3	16.0	17.5	2090	760	468	
		(31.9)	(5.2)	(14.6)	(16.7)	(18.6)				
Blue	—	54.9	5.2	10.5	17.2	—	2090	750	470	
		(55.9)	(4.1)	(10.9)	(16.6)					
Violet–pink	—	52.8	2.7	16.4	12.4	—	2080	762	470	
							2065			
Violet	—	57.2	3.3	14.2	10.6	—	1066	762	470	
		(58.2)	(3.7)	(15.7)	(11.8)		2079			
Light blue	—	54.2	4.4	17.4	12.8	—	2079	800	468	
		(53.7)	(4.1)	(17.1)	(13.0)					
Green	—	52.8	4.2	17.5	12.3	—	2080	760	465	
		(53.7)	(4.1)	(17.1)	(13.1)		2092			
Green	—	58.2	3.5	16.2	11.6	—	2080	770	465	
			(3.1)	(15.7)	(11.9)		2095			
Green	—	42.6	3.9	13.5	16.3	—	2065	770	405	
		(41.7)	(4.9)	(13.9)	(15.9)					
Pale green	190°C	52.4	4.5	15.7	11.8	—	2070	765	462	
		(53.3)	(4.0)	(16.7)	(12.9)		2083			
Dark green	Does not melt	57	3.0	14.2	10.5	—	2070	780	464	
		(57.8)	(3.7)	(15.6)	(11.9)					
White	—	45.6	3.7	16.4	14.8	—	2100	847	485	
		(46.6)	(3.9)	(16.0)	(14.7)		2075			
Yellow–orange	—	54.2	4.5	4.8	7.8	9.1	2085	855	470	1875
		(54.4)	(3.7)	(4.9)	(7.6)	8.4				
Orange–yellow	—	5.96	7.1	25.2	18.8	18.1	2080	860	470	1875
		(3.6)	(3.6)	(25.1)	(19.2)	21.2				
Orange	—	46.5	4.2	5.9	6.9	9.0	2120	730		1635
		(46.5)	(3.1)	(7.3)	(7.3)	6.5				
White	—	37.2	2.4	15.8	15.8	—	2090	755	430	
		(37.7)	(2.6)	(14.6)	(16.8)					
White	190°C	38.9	2.9	13.0	15.2	—	2090	770	469	
		(37.5)	(2.6)	(14.5)	(16.5)					
Orange–yellow	260°C	48.9	3.4	11.6	12.1	4.1	2120	765	470	
		(48.8)	(6.5)	(6)	(10.8)					
Yellow–orange	—	60.5	3.9	3.7	8.2	—	2100	860	—	
		(61.1)	(4.0)	(3.7)	(8.5)					
Yellow–orange	—	54.6	3.8	3.3	8.5	—	2090	860	—	
		(53.2)	(3.7)	(3.3)	(9.8)					
White	80°C	30.0	2.5	11.7	12.8	—	2130	780	460	
		(30.4)	(2.1)	(11.9)	(13.5)		2025			

and 1,10-phenanthroline and with $[Ru(NH_3)_5Cl]Cl_2$, $[Pd(PPh_3)_4]$ and $[Pt(PPh_3)_4]$ were carried out by the procedure similar to that described in the previous paragraph.

(B) *Reaction of* $[Co(py)_3(NCS)_2]$ *with* $[(CH_3)_4N]Cl$

The refluxing of 30 cm^3 of a methanolic solution containing $[Co(py)_3(NCS)_2]$ (1 mmol) with $[(CH_3)_4N]Cl$ (2 mmol) for 30 min followed by concentration of the resulting mixture to half its volume on a water bath, and finally cooling to room temperature, resulted in a deep blue oil. On repeated crystallization using CH_2Cl_2–petroleum ether, the oil afforded a deep blue complex which was filtered, washed with alcohol and ether and dried *in vacuo*. It was analysed for $[(CH_3)_4N]_2[CoCl_2(NCS)_2]$.

Reactions of tetraethyl and tetrabutyl ammonium chloride were also carried out by the same procedure.

(C) *Reaction of* NTU *with* $[RuCl_2(PPh_3)_3]$

An aqueous solution of NTU (15 cm^3; freshly prepared) was added to a refluxing solution (25 cm^3, 1:1 ethanol/CH_2Cl_2) containing $[RuCl_2(PPh_3)_3]$ (0.26 g). The resulting mixture was refluxed for 1.5 h. On cooling, a yellow–orange microcrystalline compound was precipitated which was filtered, washed with ethanol and diethyl ether and dried *in vacuo*. It was recrystallized from CH_2Cl_2–petroleum ether, and analysed for $[Ru(NO)(NCS)_2(PPh_3)_2Cl]1/2CH_2Cl_2$.

Reactions of $[RhCl(PPh_3)_3]$ and $[IrCl_3(PPh_3)_3]$ with NTU were carried out by the same procedure.

RESULTS AND DISCUSSION

The results (Table 1) show the formation of metal thiocyanato complexes in reasonably good yields (*ca* 60%). All products reported in the literature have been identified by their elemental analyses and by comparing their colours, melting points, mixed melting points, the IR spectra and the magnetic susceptibility data, with those of the authentic samples.

Reactions of NTU with the salts of Mn^{II}, Fe^{II}, Ni^{II}, Ag^{I}, Cd^{II} and Hg^{II} [10–17] in presence of pyridine; those of Co^{II}, Ni^{II} and Cu^{II} ions in the presence of 2,2′-bipyridyl and 1,10-phenanthroline,[18] and $[Pd(PPh_3)_4]$ and $[Pt(PPh_3)_4]$,[19] strictly under the reaction conditions used for their nitrosyl synthesis, yielded the literature-known thiocyanato complexes. Co^{II}, Cr^{II} and Zn^{II} under similar conditions yielded different complexes. Chromium(II) acetate in the presence of pyridine formed a white complex $[Cr(NCS)_3(py)_2 \cdot H_2O]$ whose IR spectrum displayed an intense split band around 1965 cm^{-1} (ν_{CN}), weak to medium intense bands around 760 cm^{-1} (ν_{CS}) and 450 cm^{-1} (δ_{NCS}) besides the characteristic bands of pyridine. The positions of these bands suggested the linkage of the NCS group through its nitrogen end.[20] Reactions with Co^{II} and Zn^{II} yielded $[Co(py)_3(NCS)_2]$ or $[Co(py)_6][Co(NCS)_4]$ and $[Zn(py)_3(NCS)_2 \cdot H_2O]$, respectively. The deep blue ethanolic solution of the cobalt complex gave, on slow evaporation, pink needle-shaped crystals containing cobalt in the anion. $[(CH_3)_4N]_2[CoCl_2(SCN)_2]$, $[(C_2H_5)_4N]_2[CoCl_2(SCN)_2]$ and $[(C_4H_9)_4N]_2[Co(SCN)_4]$ were obtained on treating the tetramethyl, tetraethyl or tetrabutyl ammonium chloride with the eluent which was obtained by passing a solution of the pink crystals through a column of cation exchanger in ethanol or methanol.

Although the formation of thiocyanato complexes by all the metal ions suggested the generality of the reaction course, the reactions of ruthenium and rhodium ions and their complexes which picked up NO along with SCN groups are of interest here. Considering the remarkable affinities of these metal ions for NO,[21] the products were not unexpected. $[Ru(NO)(NCS)_2Cl(PPh_3)_2]$ is the first mixed nitrosyl derivative of ruthenium of this type.

The bright yellow–orange crystalline diamagnetic Ru^{II} complex, $[Ru(NO)(NCS)_2Cl(PPh_3)_2]1/2CH_2Cl_2$, exhibited in its IR spectrum, intense bands at 1875 cm^{-1} (ν_{NO}) and 2080 cm^{-1} (ν_{CN}), and other characteristic bands of the NCS group around 860 cm^{-1} ($\nu_{C=S}$) and 470 cm^{-1} (δ_{NCS}), respectively. These positions suggested the bonding of the NCS group in the complex through its nitrogen atoms. Furthermore NO^+, being strongly *trans* directing,[22] will prefer to coordinate to the metal ion *trans* to a ligand having the weakest *trans* effect viz. Cl^- ion.[22] It is, therefore, suggested that NO^+ is bonded *trans* to the chloride ion. Besides under reaction conditions, the formation of $[Ru(NO)Cl(NCS)_2(PPh_3)_3]$ will be favoured over that of $[Ru(NO)(NCS)_3(PPh_3)_2]$. Since ν_{CN} and $\nu_{C=S}$ appeared as single bands, this indicated the *trans* positions of the NCS groups, and phosphine molecules in $[Ru(NO)Cl_3(PPh_3)_2]$.[23] The following structure is therefore tentatively suggested.

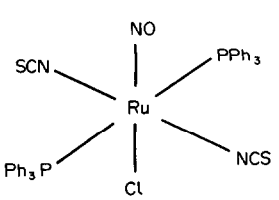

The reaction of $[Ru(NH_3)_5Cl]Cl_2$ with NTU in aqueous medium led to the formation of a yellow nitrosyl, $[Ru(NO)(NCS)(NH_3)_4]Cl_2$. In view of (1) the elemental analyses; (2) the IR spectra bands, [ν_{NO}, 1875 cm^{-1}, ν_{CN} 2080 cm^{-1} (strong sharp); ν_{CS} 860 cm^{-1} weak; δ_{NCS} (medium intensity) 880 cm^{-1} and the characteristic NH_3 bands]; (3) the ion exchange studies indicating the presence of the NCS group inside, the Cl^- outside the coordination sphere; and (4) the NO being a strong *trans* directing group, preferring to coordinate *trans* to the NH_3 molecule (weak *trans* directing group), the following structure is proposed.

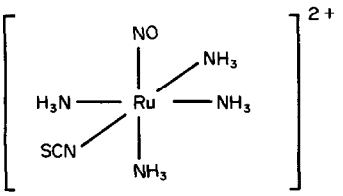

However, other alternating structures may also be possible. The IR spectrum of the rhodium complex, $[Rh(NO)(NCS)Cl(PPh_3)]$, exhibited a band at 1630 cm^{-1} indicating the presence of coordinated NO^-. The reaction thus proceeds with the oxidation of Rh from +1 to +3. Presumably NO^+, the only oxidizing species present in the system, might have been picked up by Rh^I during the intramolecular *trans* migration of NO^+ from sulphur to nitrogen (cf. reaction 1) and oxidized the metal ion. During the process it also coordinated to the metal centre.

Since the preferred geometry of Rh^{III} complexes is octahedral, four coordination around the metal centre in $[Rh(NO)Cl(NCS)(PPh_3)]$ is highly unexpected. However, the position of the ν_{CN} band (2110 cm^{-1}) which appeared at relatively higher wave numbers along with the positions of $\nu_{C=S}$ and δ_{NCS}, span the range of the bridging NCS group. It is unfortunate that we are not in a position to confirm the ν_{Rh-Cl} band because of a large number of ligand bands present in the region. In view of these arguments, an octahedral geometry of the rhodium complex with bridging NCS^- and Cl^- ions, and with terminal NO^- and PPh_3 molecules in *trans* positions have been tentatively proposed. NO^- could also coordinate *trans* to bridging Cl^-. We do not, however, wish to decide in favour of any of the alternative structures possible for the complex.

The presence of the coordinated thiourea in the octahedral iridium complex, $[Ir(PPh_3)_2(NCS)_2Cl$ (thiourea)], have been confirmed by recrystallizing it a number of times from different solvents and allowing it to pass through Sephadex G-10 column (25 × 2 cm). In every case the complex was found to be identical to the starting material. As expected, the IR band positions of the NCS group (Table 1) suggested S-bonded thiocyanate because of the "b" character of the metal ion.

In all the reactions, a point of interest is the invariable coordination of the NCS group irrespective of NO being linked with the metal ion or not. This is understandable in the case of Pd and Pt complexes which have more tendency to form complexes in the zero valent state rather than their nitrosyls.[24] Besides, they (in +2 oxidation state) prefer to form $(N_2O_2)^{2-}$ complexes[25] which should be relatively unstable with respect to those of their thiocyanates, and particularly, when the NCS concentration is very high in the medium. The same argument may be put forward for the formation of NCS complexes by the first row transition metal ions. In most cases, the NO group is introduced only under special conditions in the first transition elements. It is therefore assumed that the greater affinity of the NCS group compared with that of NO for the first transition series elements may be one of the reasons why the NO group is not trapped by them.

CONCLUSION

The conclusion from the previous Results and Discussion is that NTU does not seem to have favourable potential for nitrosylation, except when the metal ion has relatively higher affinity for the NO group. The possible reason for this could be the very high rate of reaction (1) under these conditions. The NO group before being picked up by the metal ions, migrates to the nitrogen atom of thiourea which subsequently decomposes to NCS^- by destroying NO^+. Thus due to very large NCS concentration, the latter preferentially attacks the metal centre and forms thiocyanato complexes rather than nitrosyls.

Acknowledgement—Thanks are due to CSIR, New Delhi, India for award of a Senior Research Fellowship to one of the authors (D.S.P.).

REFERENCES

1. E. A. Werner, *J. Chem. Soc.* 1912, **101**, 2180.
2. K. Al-Mallah, P. Callings and G. Stedman, *J. Chem. Soc., Dalton Trans.* 1974, 2469.
3. T. A. Stephenson and G. Wilkinson, *J. Inorg. Nucl. Chem.* 1966, **28**, 945.
4. J. A. Osborn and G. Wilkinson, *Inorg. Synth.* 1967, **10**, 67.
5. J. E. Fergusson and J. L. Love, *Inorg. Synth.* 1971, **13**, 208.

6. R. Ugo, F. Cariati and G. La Monica, *Inorg. Synth.* 1968, **11**, 105.
7. D. R. Coulson, *Inorg. Synth.* 1970, **13**, 121.
8. A. I. Vogel, *A Text Book of Quantitative Inorganic Chemistry*, p. 399. Longman, London (1961).
9. A. I. Vogel, *A Text Book of Quantitative Inorganic Chemistry*, p. 407. Longman, London (1951).
10. M. Schafer and C. Curran, *Inorg. Chem.* 1965, **4**, 623.
11. R. J. H. Clark and C. S. Williams, *Spectrochim. Acta* 1966, **22**, 1081.
12. I. S. Ahuja and A. Garg, *J. Inorg. Nucl. Chem.* 1972, **34**, 1929.
13. R. H. Toeniskoetter and S. Saloman, *Inorg. Chem.* 1968, **7**, 617.
14. M. A. Bennett, R. J. H. Clark and A. D. J. Goodwin, *Inorg. Chem.* 1967, **6**, 1625.
15. S. M. Nelson and T. M. Shepherd, *Inorg. Chem.* 1965, **4**, 803.
16. C. K. Jorgensen, *Inorganic Complexes*, p. 71. Academic Press, London (1963).
17. A. H. Norbury, *Adv. Inorg. Chem. Radiochem.* 1975, **17**, 231.
18. A. A. Scholt and K. Fritsch, *J. Inorg. Nucl. Chem.* 1966, **28**, 2677.
19. A. Sabatini and I. Bertine, *Inorg. Chem.* 1965, **4**, 1665; C. Pecile, *Inorg. Chem.* 1966, 5.
20. L. H. Jones, *J. Chem. Phys.* 1965, **25**, 1069; and 1958, **28**, 1234.
21. B. F. G. Johnson and J. A. McCleverty, *Progress Inorg. Chem.* 1966, **7**, 277.
22. D. A. Snyder and D. L. Weaver, *Chem. Commun.* 1969, 1425.
23. D. Hall and A. A. Taggart, *J. Chem. Soc.* 1965, 1359; D. Dale and D. C. Hodgkin, *J. Chem. Soc.* 1364.
24. J. J. Levison and S. D. Robinson, *J. Chem. Soc. A* 1970, 2947.
25. S. Cenini, R. Ugo, G. La Monica and S. D. Robinson, *Inorg. Chim. Acta* 1972, **6**, 182.

Polyhedron Vol. 8, No. 7, pp. 959–967, 1989
Printed in Great Britain

0277–5387/89 $3.00+.00
© 1989 Pergamon Press plc

NEUTRAL AND CATIONIC OXO-METHYL COMPLEXES OF RHENIUM(V); X-RAY STRUCTURE OF $ReOMe_2Cl(PMe_3)_2$

DAVID M. HOFFMAN* and DERK A. WIERDA

Department of Chemistry, Harvard University, 12 Oxford Street, Cambridge, MA 02138, U.S.A.

(*Received* 27 *August* 1988; *accepted* 9 *November* 1988)

Abstract—Reaction of $ReO(OEt)Cl_2(py)_2$ with 1 equivalent of $AlMe_3$ in the presence of 2 equivalents of PMe_3 or PMe_2Ph produces $ReOMe_2Cl(PMe_2R)_2$ (R = Me or Ph) and reaction of $ReOMe_2Cl(PMe_2R)_2$ with dmpe gives $ReOMe_2Cl(dmpe)$. Spectroscopic studies and an X-ray structure of the PMe_3 derivative show that the compounds are octahedral with a *trans*-[Cl—Re═O] group and *cis*-methyl ligands. Reactions of an excess of $ZnMe_2$ with $ReOMe_2Cl(PMe_2R)_2$ and $ReOMe_2Cl(dmpe)$ give square-pyramidal $ReOMe_3(PMe_2R)$ (R = Me and Ph) and octahedral $ReOMe_3(dmpe)$, respectively. The trimethyl complexes are unstable at room temperature ($t_{1/2} \approx 3$ h for $ReOMe_3(PMe_3)$ in C_6D_6). The complexes $ReOMe_2Cl(PMe_2R)_2$ and $ReOMe_2Cl(dmpe)$ react with $[Ag(CH_3CN)_2][BF_4]$ to give $[ReOMe_2(PMe_2R)_2(CH_3CN)][BF_4]$ (R = Me and Ph) and $[ReOMe_2(dmpe)(CH_3CN)[BF_4]$, respectively. The cations are octahedral and contain a *trans*-$[CH_3CN—Re═O]$ moiety. Both the PMe_3 and PMe_2Ph derivatives exist in solution as a mixture of *cis*- and *trans*-phosphine isomers; variable temperature NMR studies show that the *trans* isomer predominates at low temperatures.

We have established that d^2 square-pyramidal $ReO(CH_2SiMe_3)_3(PMe_3)$ reacts with a variety of small molecules, including CO,[1] HCCH,[2] CN^-, CH_2N_2 and bipyridine (bipy),[3] Scheme 1. Surprisingly, however, $ReO(CH_2SiMe_3)_3(PMe_3)$ does not react with ethylene.[1] This may be due to the large steric bulk of the trimethylsilylmethyl ligand. These observations prompted us to prepare d^2 oxo-methyl complexes in order to test the reactivity of the less hindered complexes with ethylene and other small organic molecules. Reported here are the results of our initial synthetic work which includes the preparation of $ReOMe_2Cl(PMe_2R)_2$ (R = Me and Ph); $ReOMe_2Cl(dmpe)$ (dmpe = $Me_2PCH_2CH_2PMe_2$); $ReOMe_3(PMe_2R)$ (R = Me and Ph); $ReOMe_3(dmpe)$; $ReOMe_3(bipy)$; $[ReOMe_2(CH_3CN)(PMe_2R)_2]^+$ (R = Me and Ph); and $[ReOMe_2(CH_3CN)(dmpe)]^+$.

RESULTS AND DISCUSSION

Neutral oxo-dimethyl rhenium(V) *complexes*

The reaction of $ReO(OEt)Cl_2(py)_2$ (**1**)[4] with 1 equivalent of $AlMe_3$ in the presence of 2 equivalents of trimethylphosphine or dimethylphenylphosphine gives $ReOMe_2Cl(PMe_3)_2$ (**2a**, yield 62%) and $ReOMe_2Cl(PMe_2Ph)_2$ (**2b**, yield 56%), respectively [eq. (1)]. If 1/3 equivalent of $AlMe_3$ is used in reaction (1), a mixture of starting material, and mono- and dimethylated products is obtained. Reaction of **1** with 1 equivalent of $AlMe_3$ in the absence of phosphine, or with 2 or 3 equivalents of $AlMe_3$ in presence of PMe_2Ph or PMe_3, gives paramagnetic products which have not yet been characterized.

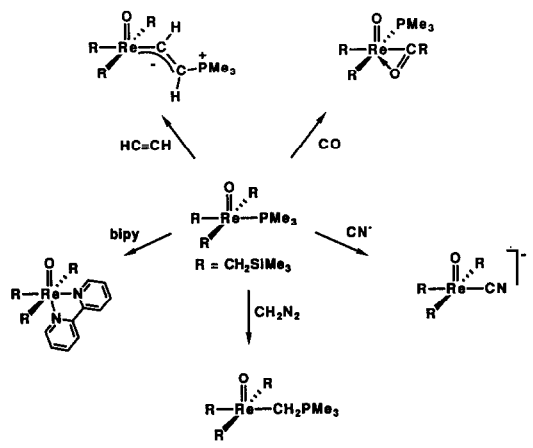

Scheme 1.

* Author to whom correspondence should be addressed.

These are presumably oxo-free complexes.

$$\underset{(\mathbf{1})}{ReO(OEt)Cl_2(py)_2} + AlMe_3 + 2PMe_2R \xrightarrow[CH_2Cl_2]{75°C\,12\,h}$$

$$ReOMe_2Cl(PMe_2R)_2 + Al(OEt)ClMe + 2py. \quad (1)$$

[R = Me (**2a**) and Ph (**2b**)]

Reaction of **2a** or **2b** with dmpe at room temperature gives $ReOMe_2Cl(dmpe)$ (**2c**) quantitatively by ^1H NMR (vs internal standard) and in 62 and 73% isolated yields, respectively [eq. (2)]. Surprisingly, the reaction of **1** with $AlMe_3$ and dmpe [cf. eq. (1)] does not give **2c**.

$$ReOMe_2Cl(PMe_2R)_2 + dmpe \xrightarrow[1\,h]{Toluene}$$

$$\underset{(\mathbf{2c})}{ReOMe_2Cl(dmpe)} + 2PMe_2R. \quad (2)$$

The compounds **2a**, **2b** and **2c** are red–brown crystalline solids, which are sparingly soluble in hexane and soluble in toluene and CH_2Cl_2. They are moderately air-sensitive, more so in solution than in the solid state.

The structure of **2a** has been determined by an X-ray crystallographic study; an ORTEP plot of the molecule is given in Fig. 1. Bond lengths and angles are presented in Table 1. The molecular geometry of **2a** is distorted octahedral. The Re=O,[1,2,5] Re—CH_3,[6] and Re—P[1,7] distances are normal, but the Re—Cl distance (2.607(3) Å) is long [e.g. it is 0.17 and 0.16 Å longer than the Re—Cl distances (Cl *trans* to Re=O) in $ReOCl_3(CNBu^t)_2$ and $ReOCl_3(PEt_2Ph)_2$, respectively].[5b,c] A possible explanation for the longer than normal Re—Cl distance is that electron donation from the strongly σ donating methyl groups makes an electron contribution from the chloride unnecessary and, given this, that steric interactions are minimized by pushing chlorine away from the rhenium centre.

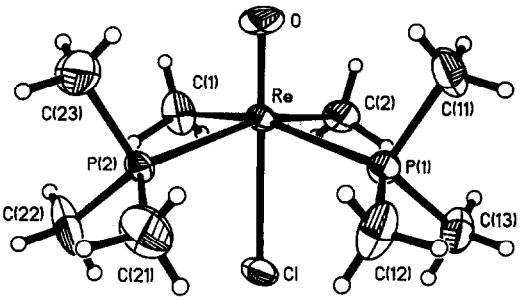

Fig. 1. ORTEP plot of $ReOMe_2Cl(PMe_3)_2$ (**2a**) showing the atom numbering scheme (50% probability level).

In **2a** the methyl groups are closer to the rhenium than the phosphines ($d_{Re-P} - d_{Re-C} = 0.25$ Å) and, because of this, the oxo and chloride ligands are repelled more by the methyl groups than the phos-

Table 1. Complete listing of bond lengths (Å) and angles (°) for $ReOMe_2Cl(PMe_3)_2$ (**2a**)

Bond distances			
Re—O	1.673(6)	P(1)—C(11)	1.828(11)
Re—C(1)	2.184(9)	P(1)—C(12)	1.813(11)
Re—C(2)	2.193(9)	P(1)—C(13)	1.809(10)
Re—Cl	2.607(3)	P(2)—C(21)	1.805(11)
Re—P(1)	2.459(3)	P(2)—C(22)	1.780(10)
Re—P(2)	2.449(3)	P(2)—C(23)	1.800(12)
Angles			
O—Re—C(1)	102.0(3)	P(2)—Re—Cl	76.6(1)
O—Re—C(2)	103.3(3)	Re—P(1)—C(11)	108.0(3)
O—Re—P(1)	96.6(2)	Re—P(1)—C(12)	122.1(3)
O—Re—P(2)	97.0(2)	Re—P(1)—C(13)	118.0(3)
O—Re—Cl	169.9(2)	C(11)—P(1)—C(12)	101.4(5)
C(1)—Re—C(2)	81.5(3)	C(11)—P(1)—C(13)	103.4(5)
C(1)—Re—P(1)	159.5(3)	C(12)—P(1)—C(13)	101.5(4)
C(1)—Re—P(2)	84.9(2)	Re—P(2)—C(21)	122.2(4)
C(1)—Re—Cl	85.4(3)	Re—P(2)—C(22)	117.0(4)
C(2)—Re—P(1)	86.0(2)	Re—P(2)—C(23)	108.3(4)
C(2)—Re—P(2)	157.5(2)	C(21)—P(2)—C(22)	102.3(5)
C(2)—Re—Cl	84.5(2)	C(21)—P(2)—C(23)	99.8(5)
P(1)—Re—P(2)	101.4(1)	C(22)—P(2)—C(23)	104.8(5)
P(1)—Re—Cl	77.3(1)		

phine ligands, even though the phosphines are larger. This is indicated in the structure by angular distortions from an octahedral geometry. For instance, the O—Re—C angles [102.0(3) and 103.3(3)°] are slightly larger than the O—Re—P angles [96.6(2) and 97.0(2)°]. Also, the O—Re—Cl angle is 10° from linear and bent in the direction of a line bisecting the P—Re—P angle.

Spectroscopic data for **2a**, **2b** and **2c** are similar and consistent with the solid state structure of **2a**. For instance, in **2a** the protons of the Re—*Me* groups appear as a doublet in the ^{1}H NMR spectrum, and the carbons appear as a doublet of a doublet in the $^{13}C\{^1H\}$ NMR spectrum ($^2J_{CP}$ = 48 and 8 Hz). By analogy to what has been reported for $ReO(CH_2SiMe_3)_3(PMe_3)$,[1] the $^{31}P—^1H$ coupling observed for **2a** is attributed to the *cis*-[P—Re—CH_3] groups, and the large and small $^2J_{PC}$ values are assigned to the *trans*- and *cis*-[P—Re—CH_3] moieties, respectively. The methyl protons of the PMe_3 ligands in **2a** give rise to a doublet in the ^{1}H NMR spectrum, but the carbons appear as a complex multiplet in the $^{13}C\{^1H\}$ spectrum. To a first approximation the latter can be interpreted as one half of an AA′XX′ spectrum, but in order to simulate the spectrum successfully it is necessary to use an AXY spin system (Fig. 2). This takes into account that $ReO(^{12}CH_3)_2Cl[^{31}P(^{13}CH_3)(^{12}CH_3)_2][^{31}P(^{12}CH_3)_3]$ is the isotopomer actually observed by $^{13}C\{^1H\}$ NMR. A complete listing of all coupling constants is given in the Experimental.

^{18}O labelling studies show that the Re=O stretching bands for **2a**, **2b** and **2c** occur at 1004, 999 and 1000 cm^{-1}, respectively. These are normal values for neutral rhenium(V) mono-oxo complexes.[8] The ^{18}O labelled compounds were prepared by stirring the unlabelled complexes with an excess of degassed $H_2{}^{18}O$ (100 equivalents) for 24 h in toluene.

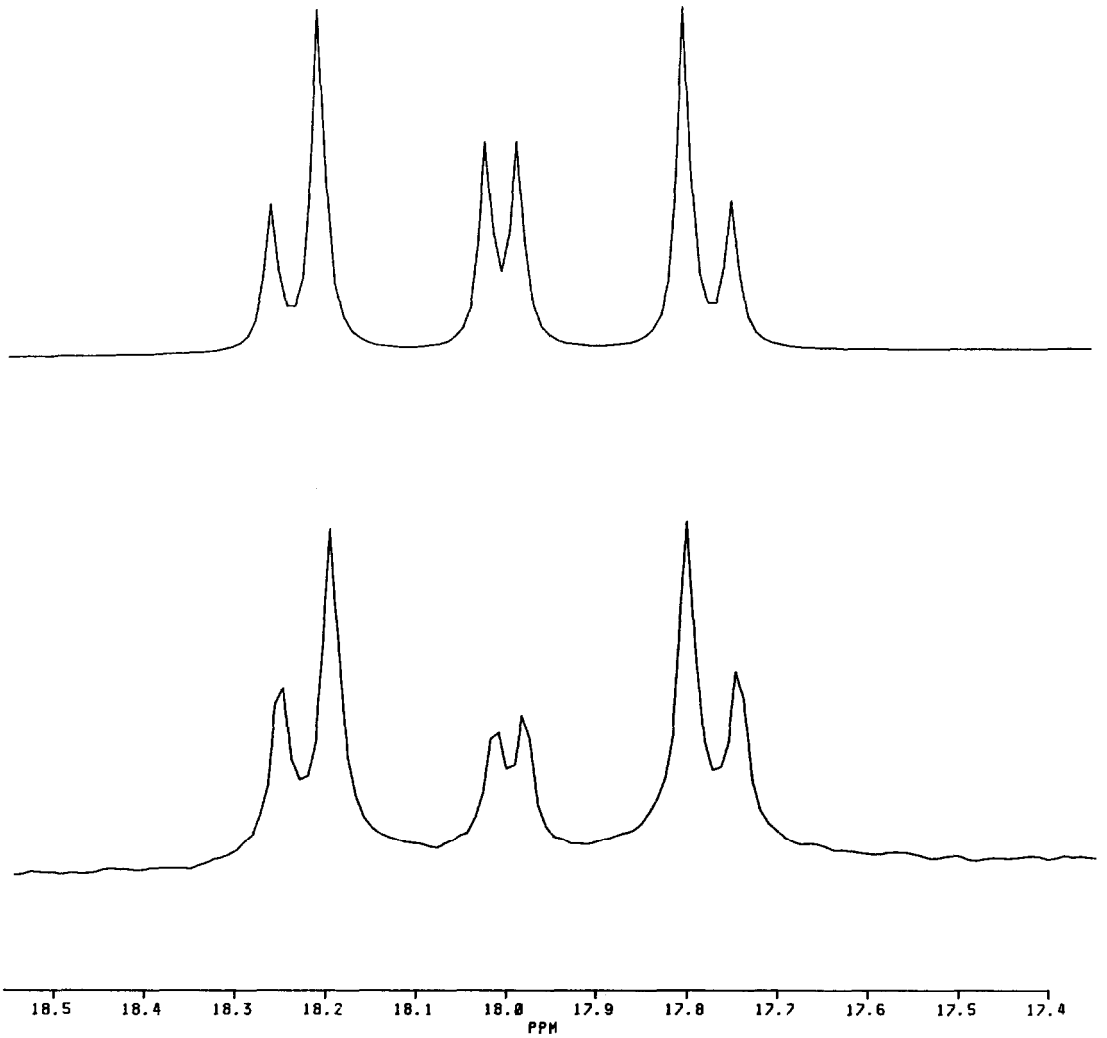

Fig. 2. Simulated (top) and experimental (bottom) $P(CH_3)_3$ region of the 75.5 MHz $^{13}C\{^1H\}$ spectrum for $ReOMe_2Cl(PMe_3)_2$ (**2a**).

Neutral oxo-trimethyl rhenium(V) complexes

Reactions of **2a**, **2b** and **2c** with an excess of $ZnMe_2$ at 0°C give the corresponding trimethyl derivatives, $ReOMe_3(PMe_2R)$ [R = Me (**3a**) and Ph (**3b**)] and $ReOMe_3$(dmpe) (**3c**), eqs (3) and (4). Reactions (3) and (4) are quantitative by ^1H NMR (vs internal standard), and the isolated yields are 47, 51 and 31% for **3a**, **3b** and **3c**, respectively.

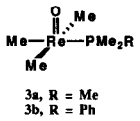

3a, R = Me
3b, R = Ph

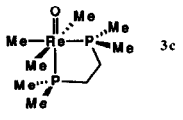

3c

Complex **3b** can also be prepared by the reaction of $Re_2(\mu\text{-}O)O_2Me_6$[6a,c] with PMe_2Ph [eq. (5)], and complex **3c** by the reactions of dmpe with **3a** or **3b**.

$$ReOMe_2Cl(PMe_2R)_2 + ZnMe_2 \xrightarrow[\text{Toluene}]{0°C} ReOMe_3(PMe_2R) + ZnMeCl + PMe_2R \quad (3)$$

[R = Me (**3a**) and Ph (**3b**)]

$$ReOMe_2Cl(\text{dmpe}) + ZnMe_2 \xrightarrow[\text{Toluene}]{0°C} ReOMe_3(\text{dmpe}) + ZnMeCl \quad (4)$$

(**3c**)

$$Re_2(\mu\text{-}O)O_2Me_6 + 3PMe_2Ph \longrightarrow 2ReOMe_3(PMe_2Ph) + P(O)Me_2Ph. \quad (5)$$

Compounds **3a** and **3b** are green oils, and **3c** is a red solid. All of the compounds decompose at room temperature ($t_{1/2} \approx 3$ h for **3a** in C_6D_6) to give as yet, uncharacterized products. The decomposition rates depend qualitatively on the phosphine ligand, with the dmpe ligand complex being the slowest to decompose and the PMe_3 complex being fastest.

The facile decomposition of **3a**, **3b** and **3c** has hampered their complete characterization. In particular, chemical analyses could not be obtained for any of the compounds and reliable IR data have been collected only for **3c** (ν(Re=O) 1018 cm^{-1}). NMR data sets have been obtained for all three compounds, however, and they are consistent with the structures shown. The proposed structures for **3a** and **3b** are analogous to the structure reported for $ReO(CH_2SiMe_3)_3(PMe_3)$.[1]

Compounds **3a** and **3b** are fluxional on the NMR time scale at room temperature. In low temperature limiting ^1H NMR spectra recorded at −66°C, the methyl ligands in **3a** give rise to a doublet, which by the integral intensity is assigned to the methyl ligands *cis* to PMe_3, and a singlet (methyl ligand *trans* to PMe_3). The observation of P—H coupling due to the *cis*-[P—Re—CH_3] and not the *trans*-[P—Re—CH_3] groups is consistent with an earlier study of $ReO(CH_2SiMe_3)_3(PMe_3)$.[1]

In contrast to compounds **3a** and **3b**, **3c** is not fluxional on the NMR time scale. In the $^{31}P\{^1H\}$ NMR spectrum recorded for **3c**, two doublets are observed indicating that the phosphorus atoms are in different chemical environments and are both bound to the metal. The ^1H NMR spectrum also shows evidence for two bound phosphorus atoms in that each methyl ligand (2:1 integral ratio) appears as a doublet of a doublet. Doublet of doublet resonances are also observed for the carbons of the methyl ligands in the $^{13}C\{^1H\}$ NMR spectrum.

In addition to $ReO(CH_2SiMe_3)_3(PMe_3)$, two other compounds related to **3a**, **3b** and **3c**, $Re(NPh)Me_3(PMe_3)_2$[9] and $ReOEt_3(PPh_3)_2$,[10] have been reported in the literature. The existence of these two compounds, each containing two phosphine ligands, suggested to us that the bis-phosphine complexes $ReOMe_3(PMe_2R)_2$, R = Me and Ph, should exist.

In an effort to observe a bis-phosphine adduct, we recorded a low-temperature limiting ^1H NMR spectrum (−73°C, $C_6D_5CD_3$) for a mixture of **3a** and 5 equivalents of PMe_3. This spectrum was consistent with the presence of *cis,mer*-$ReOMe_3(PMe_3)_2$ and free PMe_3 in solution. An attempt to isolate the bisphosphine complex by reacting an excess of PMe_3 with **3a** on a large scale, however, resulted in recovery of only **3a** after work-up. Thus, two phosphine ligands do coordinate to **3a** at low temperature in solution, but the isolable species contains only *one* phosphine ligand. Obviously, two phosphine centres coordinate in **3c** because of the chelate effect, but it is unclear why two phosphines coordinate in $Re(NPh)Me_3(PMe_3)_2$ and $ReOEt_3(PPh_3)_2$, whereas only one coordinates in **3a** and **3b**.

In addition to the NMR studies, there is also indirect evidence that the mono-phosphine formulation of **3b** is correct. The reaction of **3b** with bipyridine, carried out in an NMR tube and monitored by ^1H NMR, gave *one* free phosphine molecule and $ReOMe_3$(bipy) (**4**) [eq. (6), 80% yield by integration vs internal standard]. A large-scale reaction produced **4** in 35% isolated yield.

$$ReOMe_3(PMe_2Ph) + \text{bipy} \xrightarrow{C_6D_6} ReOMe_3(\text{bipy}) + PMe_2Ph. \quad (6)$$

(**4**)

Complex **4** is a blue crystalline solid which is air-stable in solution and in the solid state. The IR spectrum has a strong band at 970 cm^{-1} which can be assigned to the Re=O stretch. The ^1H NMR

spectrum reveals two methyl resonances in the integral ratio 2:1 as well as eight different resonances attributable to coordinated bipyridine. These data are consistent with the structure shown below.

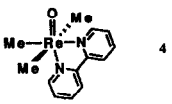

4

Cationic oxo-methyl rhenium(V) *complexes*

Reactions of **2a**, **2b** and **2c** with $[Ag(CH_3CN)_2][BF_4]$ in acetonitrile give the cationic rhenium(V) complexes $[ReOMe_2(PMe_2R)_2(CH_3CN)]$ [R = Me (**5a**, yield 71%) and R = Ph (**5b**, yield 65%)], eq. (7) and $[ReOMe_2(dmpe)(CH_3CN)][BF_4]$ (**5c**, yield 68%), eq. (8), respectively. The cationic complexes are thermally stable red oils or oily solids which are insoluble in hydrocarbon solvents.

$$ReOMe_2Cl(PMe_2R)_2 + [Ag(CH_3CN)_2][BF_4] \xrightarrow{CH_3CN} [ReOMe_2(PMe_2R)_2(CH_3CN)][BF_4] + AgCl \quad (7)$$

[R = Me (**5a**) and Ph (**5b**)]

$$ReOMe_2Cl(dmpe) + [Ag(CH_3CN)_2][BF_4] \xrightarrow{CH_3CN} [ReOMe_2(dmpe)(CH_3CN)][BF_4] + AgCl. \quad (8)$$

(**5c**)

Variable temperature ^1H and ^{13}C NMR studies (CD_3COCD_3) reveal that **5a** and **5b** exist in solution as an equilibrium mixture of the *cis*- and *trans*-phosphine isomers shown below. For **5a** at 23°C, the ratio of *cis* to *trans* isomers (*cis–trans*) is approximately 1:1. At −33°C the *trans* isomer is dominant (1:6) and at +39°C the *cis* isomer is slightly favoured (1.7:1). The spectral changes are fully reversible. The solution behaviour of **5b** is similar to that of **5a** but, as expected on steric grounds, PMe_2Ph has a greater preference to be *trans* to PMe_2Ph (as opposed to *cis*) in comparison to the PMe_3 case.



5a, R = Me
5b, R = Ph

If the variable temperature ^1H NMR studies of **5a** and **5b** are repeated using CD_3CN as a solvent, the *cis–trans* ratio remains constant at temperatures below 23°C. This suggests that the isomerization is a two-step process involving acetonitrile dissociation followed by an intramolecular rearrangement of the resulting five-coordinate intermediate.

The *cis*- and *trans*-phosphine isomers of **5a** and **5b** are readily distinguished in ^1H NMR spectra. For instance, the *cis* isomer of **5a** gives rise to a doublet of a doublet for $ReCH_3$ and a doublet for the PMe_3 protons, whereas the *trans* isomer gives a triplet for $ReCH_3$ and a virtual triplet for the PMe_3 protons.

In contrast to **5a** and **5b**, NMR spectra recorded for **5c** are invariant with temperature. Two separate proton resonances for the dmpe methyl groups and only one ^{31}P resonance are observed for **5c**, and the ^1H NMR spectrum in the Re*Me* region resembles the spectra of *cis* **5a** and **5b**. These findings, as well as $^{13}C\{^1H\}$ NMR data, are consistent with the structure shown below.

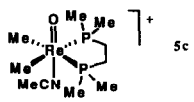

5c

IR spectra recorded for **5a**, **5b** and **5c** show broad overlapping bands in the 950–1050 cm^{-1} region. This has prevented a definitive identification by labelling studies of the bands arising from the Re=O stretches. Oxo ligands are present, however, because the cations can be converted in the absence of air or water to their respective neutral compounds (**2a**, **2b** and **2c**) via reactions (9) and (10). It is noteworthy that only *cis*-dimethyl *cis*-diphosphine $ReOMe_2Cl(PMe_2R)_2$ complexes are obtained from eq. (9).

$$[ReOMe_2(PMe_2R)_2(CH_3CN)][BF_4] + NaCl \xrightarrow[1\,h]{CH_3CN} ReOMe_2Cl(PMe_2R)_2 + NaBF_4 \quad (9)$$

$$[ReOMe_2(dmpe)(CH_3CN)][BF_4] + NaCl \xrightarrow[1\,h]{CH_3CN} ReOMe_2Cl(dmpe) + NaBF_4. \quad (10)$$

CONCLUSION

We have prepared the neutral rhenium oxo-methyl complexes $ReOMe_2Cl(PMe_2R)_2$ (R = Me, Ph) and $ReOMe_2Cl(dmpe)$, and the cationic rhenium oxo-methyl complexes $[ReOMe_2(PMe_2R)_2(CH_3CN)]^+$ (R = Me, Ph) and $[ReOMe_2(dmpe)(CH_3CN)]^+$, in moderate yields. The latter compounds are the first examples of rhenium(V) mono-oxo cations.

The original synthetic targets of this study, $ReOMe_3(PMe_2R)$ compounds, are thermally unstable. This is in contrast to $ReO(CH_2SiMe_3)_3(PMe_3)$, which is stable at 23°C in the absence of air for months.[1] A related compound, $ReOEt_3(PPh_3)_2$, is also reported to be unstable at room temperature, but in this case the instability is

probably due to the presence of β-hydrogens in the molecule.[10] We are studying the decomposition reactions of $ReOMe_3(PMe_2R)$ in order to determine the ultimate products. Reactivity studies using $ReOMe_3(PMe_2R)$, which can be generated quantitatively *in situ*, are also in progress.

EXPERIMENTAL

Microanalyses were performed by Dornis and Kolbe, F.R.G. IR data were collected on a Perkin–Elmer 598 spectrophotometer (Nujol mulls (cm^{-1}), referenced externally to the 1601 cm^{-1} band of polystyrene). NMR data were collected using Bruker AM-500, AM-300, AM-250 and WM-300-WB (^{31}P NMR) spectrometers. ^1H NMR spectra were referenced to the ^1H impurities in the deuterated solvents (benezene-d_6, δ 7.15; acetonitrile-d_3, δ 1.93), ^{13}C NMR spectra to the ^{13}C triplet of benzene-d_6 (δ 128.0) or the septet of acetonitrile-d_3 (δ 1.3), and ^{31}P spectra to external H_3PO_4, with upfield shifts taken as negative. Molecular weights were determined by isothermal distillation (vs ferrocene).[11]

All operations were performed under oxygen-free nitrogen, argon or *in vacuo*. Solvents were purified by standard techniques and were dry and oxygen-free.

$^{13}C\{^1H\}$ NMR spectra obtained for the carbons of the phosphine ligands in **2a**, **2b**, **2c**, **3c**, **5a**, **5b** and **5c** were simulated using the program PANIC (Bruker). Initial ^{13}C coupling constants for **2a**, **2b**, **2c**, **5a**, **5b** and **5c** were obtained analytically by approximating the spin systems as AA′XX′ ($J_{CC'} = 0$).[12] Simulations with PANIC were carried out using an AXY spin system. In all cases, simulated and analytically determined coupling constants were in close agreement. The methyl region of the ^1H NMR spectrum of $ReOMe_3$(dmpe) (**3c**) was simulated as well.

(1) *Chlorodimethyloxobis(trimethylphosphine)rhenium*(V), $ReOMe_2Cl(PMe_3)_2$ (**2a**)

To a cold solution (−78°C) of $ReO(OEt)Cl_2(py)_2$ (1.50 g, 3.15 mmol) in methylene chloride (75 cm^3) $AlMe_3$ (1.6 cm^3, 3.20 mmol, 2.0 mol dm^{-3} in toluene) was added dropwise. The resulting green solution was frozen (−196°C) and the flask evacuated. PMe_3 (6.50 mmol) was then condensed into the flask via a calibrated vacuum manifold. After the mixture was allowed to warm to room temperature, the blue solution was heated (**Caution**: closed flask heating) at 75°C for 12 h. The volatiles were then removed *in vacuo*, and the residue was extracted with toluene (4 × 75 cm^3); the extracts were filtered and then evaporated to dryness *in vacuo*, and the residue was extracted with warm hexane (6 × 75 cm^3, 45°C). The hexane solution was filtered, reduced in volume, and cooled to −60°C to give red blocks. If necessary, the compound can be recrystallized from toluene. (Yield 0.82 g, 1.97 mmol, 62%.) Found: C, 23.1; H, 5.9; mol. wt (CH_2Cl_2) 404(30). Calc. for $ReClP_2OC_8H_{24}$: C, 22.9; H, 5.8%; mol. wt calc. 419.9.

^1H NMR (C_6D_6): δ 3.8 (d, 6, *cis*-J_{PH} = 7.4 Hz, Re*Me*), 1.6 (d, 18, J_{PH} = 9.2 Hz, P*Me*$_3$). $^{13}C\{^1H\}$ NMR (C_6D_6): δ 19.4 (dd, 2, *trans*-J_{CP} = 48 Hz, *cis*-J_{CP} = 8 Hz, Re*Me*), 18.0 (AXY, J_{CP} = 27.3, $^3J_{CP}$ = 2.7, J_{PP} = −11.4 Hz, $\Delta P_X - \Delta P_Y$ = 1.9 Hz, P*Me*$_3$). $^{31}P\{^1H\}$ (C_6D_6): δ −47.1 (s). IR: ν(Re═O) 1004 s [ν(Re═^{18}O) 949], 1433(sh), 1420(m), 1368(sh), 1305(m), 1281(s), 958(s), 944(s), 859(m), 850(m), 747(s), 671(m), 510(m), 500(m), 351(w), 301(w), 268(w).

(2) *Chlorodimethyloxobis(dimethylphenylphosphine) rhenium*(V), $ReOMe_2Cl(PMe_2Ph)_2$ (**2b**)

This compound was prepared by a procedure analogous to the one used for the preparation of $ReOMe_2Cl(PMe_3)_2$. (Yield 54%.) Found: C, 39.4; H, 4.9; mol. wt (benzene) 520(30). Calc. for $ReClP_2OC_{18}H_{28}$: C, 39.7; H, 5.2%; mol. wt calc. 544.0.

^1H NMR (C_6D_6): δ 7.33 (m, 4, PMe_2*Ph*), 7.00 (m, 6, PMe_2*Ph*), 4.05 (d, 6, *cis*-J_{PH} = 7.1 Hz, Re*Me*), 1.47 (d, 6, J_{PH} = 8.9 Hz, P*Me*$_a$Me$_b$Ph), 1.41 (d, 6, J_{PH} = 9.5 Hz, PMe$_a$*Me*$_b$Ph). $^{13}C\{^1H\}$ NMR (C_6D_6): δ 131.50 (d, 1, J_{CP} = 3.3 Hz, PMe_2*Ph*), 131.47 (d, 1, J_{CP} = 3.3 Hz, PMe_2*Ph*), 130.9 (s, 1, PMe_2*Ph*), 129.54 (d, 1, J_{CP} = 3.3 Hz, PMe_2*Ph*), 129.51 (d, 1, J_{CP} = 3.3 Hz, PMe_2*Ph*), 18.7 (dd, 2, *trans*-J_{CP} = 44 Hz, *cis*-J_{CP} = 7 Hz, Re*Me*), 15.7 (AXY, J_{CP} = 33.7 Hz, $^3J_{CP}$ = 4.9 Hz, J_{PP} = −6.9 Hz, $\Delta P_X - \Delta P_Y$ = 1.7 Hz, P*Me*$_a$Me$_b$Ph), 14.5 (AXY, J_{CP} = 36.2 Hz, $^3J_{CP}$ = 4.5 Hz, J_{PP} = −5.0 Hz, $\Delta P_X - \Delta P_Y$ = 2.4 Hz, PMe$_a$*Me*$_b$Ph). $^{31}P\{^1H\}$ NMR (C_6D_6): δ −39.5 (s). IR: ν(Re═O) 999(s) [ν(Re═^{18}O) 948], 1438(m), 1419(w), 1370(w), 1315(w), 1307(w), 1290(m), 1279(w), 1239(w), 1161(w), 1109(m), 987(sh), 948(s), 912(sh), 907(s), 839(m), 752(m), 741(s), 711(w), 697(m), 679(w), 679(w), 510(w), 502(w), 489(m), 417(m), 404(m), 345(w), 327(w), 311(w), 301(w).

(3) *Chlorodimethyloxo(bis(dimethylphosphino)ethane)rhenium*(V), $ReOMe_2Cl(Me_2PCH_2CH_2PMe_2)$ (**2c**)

To a solution of $ReOMe_2Cl(PMe_2Ph)_2$ (0.275 g, 0.51 mmol) in toluene (25 cm^3) dmpe (0.106 cm^3,

0.58 mmol) was added via syringe. The brown solution was stirred (1 h), filtered and concentrated *in vacuo* (to *ca* 3 cm^3). Cooling (−20°C) produced brown crystals. (Yield 0.162 g, 0.39 mmol, 76%.) This compound was also prepared from $ReOMe_2Cl(PMe_3)_2$ in 62% yield by an analogous procedure. A satisfactory carbon analysis was not obtained. Found: C, 25.5; H, 5.4. Calc. for $ReClP_2OC_8H_{22}$: C, 23.0; H, 5.3%.

^1H NMR (C_6D_6): δ 3.76 (d, 6, *cis*-J_{PH} = 6.8 Hz, Re*Me*), 1.79 (m, 2, —C*H*$_2$PMe$_2$), 1.40 (d, 6, J_{PH} = 11.4 Hz, —CH$_2$P*Me*$_2$), 1.07 (d, 6, J_{PH} = 8.0 Hz, —CH$_2$P*Me*$_2$), 0.93 (m, 2, —C*H*$_2$PMe$_2$). $^{13}C\{^1H\}$ NMR (C_6D_6): δ 32.9 (AXY, 2, J_{CP} = 41.0 Hz, $^3J_{CP}$ = 3.3 Hz, J_{PP} = −12 Hz, —*C*H$_2$PMe$_2$), 16.7 (AXY, 2, J_{CP} = 28.2 Hz, $^3J_{CP}$ = 10.1 Hz, J_{PP} = −4.3 Hz, $\Delta P_X - \Delta P_Y$ = 3.4 Hz, —CH$_2$P*Me*$_2$), 11.8 (AXY, 2, J_{CP} = 39.8 Hz, $^3J_{CP}$ = 7.1 Hz, J_{PP} = −5 Hz, $\Delta P_X - \Delta P_Y$ = 1.9 Hz, —CH$_2$P*Me*$_2$), 11.35 (AXY, 2, *trans*-J_{CP} = 37.5 Hz, *cis*-J_{CP} = 12.5 Hz, J_{PP} = −3.4 Hz, Re*Me*). $^{31}P\{^1H\}$ NMR (C_6D_6): δ 16.1 (s). IR: ν(Re═O) 1000(s) [ν(Re═^{18}O) 948], 1827(w), 1799(m), 1420(w), 1409(w), 1302(sh), 1288(m), 1246(w), 1180(br), 1107(w), 940(s), 919(w), 901(m), 867(w), 844(w), 748(m), 713(m), 650(m), 636(m), 510(m), 453(w), 362(w), 349(w).

(4) *Trimethyloxo(trimethylphosphine)rhenium*(V), $ReOMe_3(PMe_3)$ (**3a**)

To a cold solution (0°C) of $ReOMe_2Cl(PMe_2Ph)_2$ (0.050 g, 0.12 mmol) in toluene (20 cm^3) a toluene solution (5 cm^3) of $ZnMe_2$ (0.020 cm^3, 0.21 mmol) was added dropwise via an addition funnel over a period of 10 min. The solvent was then removed at 0°C under reduced pressure. The residue was extracted with cold pentane. Removal of the pentane under reduced pressure yielded a green oil. The yield was quantitative by ^1H NMR vs internal standard. The isolated yield was 47%. The material decomposed within days when stored at −20°C.

^1H NMR (C_7D_8, −57°C): 3.56 (s, 3, Re*Me*), 2.57 (d, 6, J_{PH} = 8.2 Hz, Re*Me*), 0.61 (d, 9, J_{PH} = 8.2 Hz, P*Me*$_3$). $^{13}C\{^1H\}$ NMR (C_7D_8, −66°C): 32.2 (d, 1, J_{CP} = 25.3 Hz, Re*Me*), 18.0 (s, 2, Re*Me*), 12.6 (d, 2, J_{CP} = 31.3 Hz, P*Me*$_3$). $^{31}P\{^1H\}$ NMR (C_7D_8, −23°C): δ −0.7 (s).

(5) *Trimethyloxo(dimethylphenylphosphine)rhenium*(V), $ReOMe_3(PMe_2Ph)$ (**3b**)

This compound was prepared by a procedure analogous to the one used for the preparation of $ReOMe_3(PMe_3)$. The yield was quantitative by ^1H NMR vs internal standard. The isolated yield was 51%.

^1H NMR (C_7D_8, −66°C): δ 7.26 (m, 2, PMe$_2$*Ph*), 7.04 (m, 3, PMe$_2$*Ph*), 3.66 (s, 3, Re*Me*), 2.62 (d, 6, J_{PH} = 8.7 Hz, Re*Me*), 0.85 (d, 6, J_{PH} = 9.1 Hz, P*Me*$_2$Ph). $^{13}C\{^1H\}$ NMR (C_7D_8, −66°C): δ 131.6 (d, 2, J_{CP} = 10.7 Hz, PMe$_2$*Ph*), 130.8 (s, 1, PMe$_2$*Ph*), 129.1 (2, PMe$_2$*Ph*), 31.8 (d, 1, J_{CP} = 24.9 Hz, Re*Me*), 18.9 (s, 2, Re*Me*), 12.5 (d, 2, J_{CP} = 30.7 Hz, P*Me*$_2$Ph). $^{31}P\{^1H\}$ NMR (C_7D_8, 23°C): δ −0.8 (s).

(6) *Trimethyloxo(bis(dimethylphosphino)ethane) rhenium*(V), $ReOMe_3$(dmpe) (**3c**)

This compound was prepared by a procedure similar to the one used for the preparation of $ReOMe_3(PMe_3)$. The compound is a red solid. (Yield 31%.)

^1H NMR (C_6D_6): δ 3.25 (dd, 3, J_{P_XH} = 7.8 Hz, J_{P_YH} = 6.6 Hz, Re*Me*), 2.94 (dd, 6, J_{P_XH} = 13.7 Hz, J_{P_YH} = 5.7 Hz, Re*Me*), 1.39 (d, 6, J_{PH} = 9.9 Hz, —CH$_2$P*Me*$_2$), 1.02 (m, 2, —C*H*$_2$PMe$_2$), 0.55 (m, 2, —C*H*$_2$PMe$_2$), 0.20 (d, 6, J_{PH} = 7.5 Hz, —CH$_2$P*Me*$_2$). $^{13}C\{^1H\}$ NMR (C_6D_6): δ 28.8 (m, 1, —*C*H$_2$PMe$_2$), 25.9 (dd, 1, J_{CP_X} = 20.5 Hz, J_{CP_Y} = 17.5 Hz, Re*Me*), 24.7 (m, 1, —*C*H$_2$PMe$_2$), 17.2 (m, 2, CH$_2$P*Me*$_2$), 17.0 (dd, 2, J_{CP_X} = 17.5 Hz, J_{CP_Y} = 12.5 Hz, Re*Me*), 7.7 (m, 2, CH$_2$P*Me*$_2$). $^{31}P\{^1H\}$ NMR (C_6D_6): δ −3.0 (d, J_{PP} = 29 Hz), −34.7 (d, J_{PP} = 29 Hz). IR: ν(Re═O) 1018(s), 1419(m), 1360(sh), 1299(m), 1283(m), 1239(m), 1252(m), 1221(m), 980(m), 938(s), 927(sh), 910(m), 894(m), 835(m), 793(w), 703(m), 649(w).

(7) *Trimethyloxo(bipyridine)rhenium*(V), $ReOMe_3$(bipy) (**4**)

To a cold (0°C) solution of $ReOMe_2Cl(PMe_2Ph)_2$ (0.050 g, 0.09 mmol) in toluene (30 cm^3) a toluene solution (5 cm^3) of $ZnMe_2$ (0.020 cm^3, 0.21 mmol) was added dropwise via an addition funnel. After the addition was complete, the solvent was removed at 0°C *in vacuo*. The residue was extracted with cold pentane, and the pentane solution added to a flask containing an excess of bipy (0.050 g, 0.32 mmol). The mixture slowly changed colour from green to blue (2 h). Solvent and the excess bipy were then removed *in vacuo*. Crystallization from pentane (−50°C) gave blue crystals. (Yield 0.013 g, 0.03 mmol, 35%.)

^1H NMR (C_6D_6): δ 8.81 (m, 1, *bipy*), 7.77 (d, 1, bipy), 7.25 (m, 1, bipy), 6.79 (d, 1, bipy), 6.50 (dt, 1, bipy), 6.23 (dq, 2, bipy), 5.34 (m, 1, bipy), 3.92 (s, 3, Re*Me*), 2.83 (s, 6, Re*Me*). IR: ν(Re═O) 970(s), 1602(m), 1588(m), 1579(sh), 1562(w), 1419(sh),

1312(m), 1260(m), 1239(m), 1150(w), 1010(w), 990(w), 957(sh), 900(m), 752(s), 511(w).

(8) *Dimethyloxo(acetonitrile)bis(trimethylphosphine) rhenium*V) *tetrafluoroborate*, $[ReOMe_2(PMe_3)_2(CH_3CN)][BF_4]$ (**5a**)

To a mixture of $ReOMe_2Cl(PMe_3)_2$ (0.100 g, 0.24 mmol) and $[Ag(CH_3CN)_2][BF_4]$ (0.065 g, 0.24 mmol) cold acetonitrile (25 cm^3, 0°C) was added. A white powder formed immediately. The solution was stirred (1 h), filtered, and then the solvent removed *in vacuo* to yield a red oil. (Yield 0.086 g, 0.17 mmol, 71%.) Two isomers were observed in solution (the *cis–trans* ratio at 24°C in CD_3CN is 3:1). Found: C, 23.4; H, 5.1; N, 2.9. Calc. for $ReP_2F_4ONC_{10}BH_{27}$: C, 23.4; H, 5.3; N, 2.7%.

IR: 2287(w), 1314(sh), 1292(m), 1235(s), 1120(br), 1030(br), 1010(m), 950(m), 905(m), 848(w), 761(w).

cis isomer. ^1H NMR (CD_3CN): δ 3.0 (dd, 6, *cis*-J_{PH} = 7.3 Hz, *trans*-$J_{P'H}$ = 2.3 Hz, Re*Me*), 1.9 (s, 3, C*H*$_3$CN), 1.83 (d, 18, J_{PH} = 10.3 Hz, P*Me*$_3$). $^{13}C\{^1H\}$ NMR (CD_3CN): δ 18.0 (AXY, 2, J_{CP} = 23 Hz, $^3J_{CP}$ = 10.5 Hz, J_{PP} = −17 Hz, $\Delta P_X - \Delta P_Y$ = 1.9 Hz, P*Me*$_3$), 14.4 (dd, 2, *trans*-J_{CP} = 15 Hz, *cis*-J_{CP} = 9 Hz, Re*Me*). $^{31}P\{^1H\}$: δ −36.1 (s).

trans isomer. ^1H NMR (CD_3CN): δ 3.73 (t, 6, J_{PH} = 6.3 Hz, Re*Me*), 1.95 (s, 3, C*H*$_3$CN), 1.73 (virtual triplet, 18, $J_{PH} = J_{P'H}$ = 5.1 Hz, P*Me*$_3$). $^{13}C\{^1H\}$ NMR (CD_3CN): 14.72 (virtual triplet, 6, $J_{CP} = {}^3J_{CP}$ = 17 Hz, P*Me*$_3$), −6.1 (t, 2, J_{CP} = 5 Hz, Re*Me*). $^{31}P\{^1H\}$ (CD_3CN): δ −32.9 (s).

(9) *Dimethyloxo(acetonitrile)bis(dimethylphenylphosphine)rhenium*(V) *tetrafluoroborate*, $[ReOMe_2(PMe_2Ph)_2(CH_3CN)][BF_4]$ (**5b**)

This compound was prepared by a procedure similar to the one used for the preparation of $[ReOMe_2(PMe_3)_2(CH_3CN)][BF_4]$. The compound was isolated as a red–orange oil. (Yield 65%.) Two isomers were observed in solution (the *cis–trans* ratio at 24°C in CD_3CN is 2:1).

IR: 2255(w), 2240(m), 1440(sh), 1308(m), 1289(w), 1236(m), 1060(vbr), 980(br), 956(w), 895(m), 870(sh), 838(w), 740(s), 690(m), 675(w), 518(m), 483(s), 412(m), 397(sh).

cis isomer. ^1H NMR (CD_3CN): δ 7.62 (m, 2, PMe_2*Ph*), 7.51 (m, 3, PMe_2*Ph*), 3.08 (dd, 6, *cis*-J_{PH} = 9.4 Hz, *trans*-$J_{P'H}$ = 2.0 Hz, Re*Me*), 1.95 (s, 3, C*H*$_3$CN), 1.90 (d, 6, J_{PH} = 10 Hz, P*Me*$_2$Ph), 1.85 (d, 6, J_{PH} = 9.9 Hz, P*Me*$_2$Ph). $^{13}C\{^1H\}$ NMR (CD_3CN): δ 132.1 (s, 2, PMe_2*Ph*), 131.82 (d, 2, J_{PC} = 3.5 Hz, PMe_2*Ph*), 131.77 (d, 2, J_{CP} = 3.5 Hz, PMe_2*Ph*), 131.46 (d, 2, J_{CP} = 3.7 Hz, PMe_2*Ph*), 131.41 (d, 2, J_{CP} = 3.7 Hz, PMe_2*Ph*), 130.15 (d, 2, J_{CP} = 4.5 Hz, PMe_2*Ph*), 16.25 (AXY, 2, J_{CP} = 30 Hz, $^3J_{CP}$ = 2.2 Hz, J_{PP} = −12.2 Hz, $\Delta P_X - \Delta P_Y$ = 2.0 Hz, P*Me*$_a$Me$_b$Ph), 14.96 (AXY, 2, J_{CP} = 32.2 Hz, $^3J_{CP}$ = 1.3 Hz, J_{PP} = −12.2 Hz, $\Delta P_X - \Delta P_Y$ = 2.4 Hz, PMe$_a$*Me*$_b$Ph), 16.5 (dd, 2, *trans*-J_{CP} = 16 Hz, *cis*-J_{CP} = 2 Hz, Re*Me*). $^{31}P\{^1H\}$ NMR (CD_3CN): δ −28.1 (s).

trans isomer. ^1H NMR (CD_3CN): δ 7.62 (m, 2, PMe_2*Ph*), 7.51 (m, 3, PMe_2*Ph*), 3.65 (t, 6, J_{PH} = 6.4 Hz, Re*Me*), 2.02 (virtual triplet, 12, $J_{P'H} = J_{PH}$ = 4.6 Hz, P*Me*$_2$Ph), 1.95 (s, 3, C*H*$_3$CN). $^{13}C\{^1H\}$ NMR (CD_3CN): δ 132.1 (s, 2, PMe_2*Ph*), 131.82 (d, 2, J_{PC} = 3.5 Hz, PMe_2*Ph*), 131.77 (d, 2, J_{PC} = 3.5 Hz, PMe_2*Ph*), 131.46 (d, 2, J_{PC} = 3.7 Hz, PMe_2*Ph*), 131.41 (d, 2, J_{PC} = 3.7 Hz, PMe_2*Ph*), 130.0 (t, 2, J_{PC} = 4.5 Hz, PMe_2*Ph*), 13.87 (virtual triplet, 4, $J_{CP} = {}^3J_{CP}$ = 17.2, P*Me*$_2$Ph), −3.1 (t, 2, J_{CP} = 4.5 Hz, Re*Me*). $^{31}P\{^1H\}$ NMR (CD_3CN): δ −23.4 (s).

(10) *Dimethyloxo(acetonitrile)(bis(dimethylphosphino)ethane)rhenium*(V) *tetrafluoroborate*, $[ReOMe_2(Me_2PCH_2CH_2PMe_2)(CH_3CN)][BF_4]$ (**5c**)

This compound was prepared by a procedure similar to the one used for the preparation of $[ReOMe_2(PMe_3)_2(CH_3CN)][BF_4]$. The compound was isolated as a red–brown solid. (Yield 68%.) Found: C, 23.6; H, 5.1; N, 2.5. Calc. for $ReP_2F_4ONC_{10}BH_{25}$; C, 23.5; H, 4.9; N, 2.7%.

^1H NMR (CD_3CN): δ 2.96 (dd, 6, *cis*-J_{PH} = 5.8 Hz, *trans*-$J_{P'H}$ = 2.5 Hz, Re*Me*), 2.20 (m, 4, —C*H*$_2$PMe$_2$), 1.91 (d, 6, J_{PH} = 11.5 Hz, —CH$_2$ P*Me*$_2$), 1.69 (d, 6, J_{PH} = 11.5 Hz, —CH$_2$P*Me*$_2$). $^{13}C\{^1H\}$: δ 31.5 (AXY, 2, J_{CP} = 42 Hz, $^3J_{CP}$ = 1 Hz, J_{PP} = −16 Hz, $\Delta P_X - \Delta P_Y$ = 1.7 Hz, —*C*H$_2$ PMe$_2$), 15.8 (AXY, 2, J_{PC} = 27.2 Hz, $^3J_{CP}$ = 1 Hz, J_{PP} = −10.8 Hz, $\Delta P_X - \Delta P_Y$ = 3.3 Hz, —CH$_2$ P*Me*$_a$Me$_b$), 10.6 (AXY, 2, J_{CP} = 36 Hz, $^3J_{CP}$ = 2.3 Hz, J_{PP} = −12.8 Hz, $\Delta P_X - \Delta P_Y$ = 3.7 Hz, —CH$_2$PMe$_a$*Me*$_b$), 4.9 (m, 2, Re*Me*). $^{31}P\{^1H\}$ NMR (CD_3CN): δ 22.6 (s). IR: 1421(sh), 1302(m), 1297(m), 1250(w), 1210(w), 1186(w), 1135(sh), 1095(s), 1055(s), 1040(s), 1010(s), 955(s), 940(s), 921(sh), 906(sh), 870(s), 851(m), 793(w), 755(m), 651(m), 520(m), 500(sh), 450(m), 355(w), 335(w).

Crystallographic studies

Crystal data. $ReOClMe_2(PMe_3)_2$ at −80(1)°C: M = 419.9; monoclinic, space group $P2_1/n$, a = 6.632(4), b = 12.729(4), c = 17.495(6) Å, β = 93.08(4)°, Z = 4, D_c = 1.891 g cm^{-3}, μ(Mo-K_α) = 87.21 cm^{-1}.

Data collection. X-ray data were collected on a

Nicolet R3 four-circle diffractometer equipped with a LT-1 low-temperature device. Data collection was controlled using the Nicolet program P3. Raw diffractometer data were processed using the program XDISK. An empirical absorption correction was performed with the program PSICOR. $4 \leqslant 2\theta \leqslant 45°$, $T = 193$ K, 4366 data measured, 1930 unique, 1741 observed [$F_o > 6\sigma(F_o)$].

Structure solution and refinement. The structure was solved and refined using the SHELXTL-PLUS (microVax II) packages of programs. The rhenium atom was found by use of a Patterson synthesis. Standard difference map techniques were used to find the remaining non-hydrogen atoms. After all of the non-hydrogen atoms were located and refined anisotropically, a difference map revealed approximately one half of the hydrogen positions. The hydrogen atoms were therefore placed in calculated positions on the appropriate carbon atoms ($U_{iso}(H) = 1.2U_{iso}(C)$; d_{C-H} 0.96 Å) for refinement. Refinement was performed to convergence [$\Delta/\sigma(\max) < 0.001$] with this model. The values of R, R_w were 0.0335 and 0.0401, respectively, and the weighting scheme was $w = [\sigma^2(F) + 0.0018F^2]^{-1}$. The final difference map contained two peaks (1.63 and 1.44 eÅ^{-3}) within 1.00 Å of the rhenium. All other peaks were less than 0.90 eÅ^{-3}.

Final atomic coordinates, a table of anisotropic thermal parameters and a F_o/F_c listing have been deposited with the Editor as supplementary material.

Acknowledgement—The authors thank the Petroleum Research Fund, administered by the American Chemical Society, for the support of this research.

REFERENCES

1. S. Cai, D. M. Hoffman, D. Lappas and H.-G. Woo, *Organometallics* 1987, **6**, 2273.
2. D. Lappas, D. M. Hoffman, K. Folting and J. C. Huffman, *Angew. Chem. Int. Ed. Engl.* 1988, **27**, 587; D. Lappas, D. M. Hoffman, K. Folting and J. C. Huffman, *Angew. Chem.* 1988, **100**, 585.
3. D. Lappas and D. M. Hoffman, unpublished results.
4. N. P. Johnson, F. I. M. Taha and G. Wilkinson, *J. Chem. Soc.* 1964, 2614.
5. (a) A. M. Arif, T. A. Bright and R. A. Jones, *J. Coord. Chem.* 1987, **16**, 45; M. Fernanda, N. N. Carvalho, A. J. L. Pombeiro, D. L. Hughes and R. L. Richards, *J. Organomet. Chem.* 1987, **335**, C23; G. Ciani, A. Sironi, T. Beringhelli, G. D'Alfonso and M. Freni, *Inorg. Chim. Acta* 1986, **113**, 61; G. Gilli, M. Sacerdoti, V. Bertolasi and R. Rossi, *Acta Cryst.* 1982, **38**, 100; C. J. L. Lock and C. Wan, *Can. J. Chem.* 1975, **53**, 1548; G. F. Ciani, G. D'Alfonso, P. F. Romiti, A. Sironi and M. Freni, *Inorg. Chim. Acta* 1983, **72**, 29; C. J. L. Lock and G. Turner, *Can. J. Chem.* 1977, **55**, 333; M. B. Hursthouse, S. A. A. Jayaweera and A. Quick, *J. Chem. Soc., Dalton Trans.* 1979, 279, (b) J. C. Bryan, R. E. Stenkamp, T. H. Tulip and J. M. Mayer, *Inorg. Chem.* 1987, **26**, 2283, (c) V. S. Sergienko, M. A. Porai-Koshits, V. E. Mistryukov and K. V. Kotegov, *Koord. Khim.* 1982, **8**, 230.
6. (a) P. Stavropoulos, P. G. Edwards, G. Wilkinson, M. Motevalli, K. M. Abdul Malik and M. B. Hursthouse, *J. Chem. Soc., Dalton Trans.* 1985, 2167, (b) P. Edwards, K. Mertis, G. Wilkinson, M. B. Hursthouse and K. M. A. Malik, *J. Chem. Soc., Dalton Trans.* 1980, 334, (c) W. A. Herrmann, J. G. Kuchler, J. K. Felixberger, E. Herdtweck and W. Wagner, *Angew. Chem. Int. Ed. Engl.* 1988, **27**, 394; W. A. Herrmann, J. G. Kuchler, J. K. Felixberger, E. Herdtweck and W. Wagner, *Angew. Chem.* 1988, **100**, 420.
7. P. G. Edwards, A. C. Skapski, A. M. Z. Slawin and G. Wilkinson, *Polyhedron* 1984, **3**, 1083; P. G. Edwards, G. Wilkinson, M. B. Hursthouse and K. M. A. Malik, *J. Chem. Soc., Dalton Trans.* 1980 2467.
8. G. Rouschias, *Chem. Rev.* 1974, **74**, 531.
9. K. W. Chiu, W.-K. Wong, G. Wilkinson, A. M. R. Galas and M. B. Hursthouse, *Polyhedron* 1982, **1**, 31.
10. W. K. Rybak and J. J. Ziolkowski, *J. Mol. Catal.* 1987, **42**, 347.
11. E. P. Clark, *Ind. Eng. Chem. Anal. Ed.* 1941, **13**, 820.
12. H. Günther, *Angew. Chem. Int. Ed. Engl.* 1972, **11**, 861; H. Günther, *Angew. Chem.* 1972, **84**, 907.

Polyhedron Vol. 8, No. 7, pp. 969–975, 1989
Printed in Great Britain

0277–5387/89 $3.00+.00
© 1989 Pergamon Press plc

STRUCTURES AND ENERGIES OF THE [BH_2P] ISOMERS AND INTERACTION OF BORYLPHOSPHINIDENE WITH METAL COMPLEXES

M. C. KERINS and N. J. FITZPATRICK†

Department of Chemistry, University College, Belfield, Dublin 4, Ireland

and

MINH THO NGUYEN

Department of Organic Chemistry, University of Groningen, 9747 AG Groningen, The Netherlands

(*Received* 23 *September* 1988; *accepted* 9 *November* 1988)

Abstract—A portion of the potential energy surface of the [BH_2P] system has been studied in both the singlet and triplet electronic states using *ab initio* methods. Local minima corresponding to borylphosphinidene (H_2BP), boraphosphene (HBPH) and phosphinoborene (BPH_2) were obtained at the HF/6–31G** level. Transition structures linking these species via 1,2-hydrogen shifts were also located. Relative energies were estimated at the MP4/6–31++G**+ZPE level. The singlet HB=PH is the global minimum, while H_2B—P is the lowest energy on the triplet surface. Calculated results suggest that these two species are probably the only stable ones with respect to unimolecular rearrangement. Comparison between Iterative Extended Hückel (IEH) calculations on $(H_3CP)Fe(CO)_3$, $(H_2NP)Fe(CO)_3$ and $(H_2BP)Fe(CO)_3$ also suggests that the latter complex is somewhat weaker than the former, but complexation with a d^8 metal system might be a means of examining boraphosphinidenes.

Being members of the family of phosphorus compounds with lower coordination states, the boraphosphenes **I** (or phosphaborenes) featuring a boron–phosphorus double bond are of considerable current interest. In 1986, Cowley and co-workers[1] reported the first vapour phase synthesis of **I** (with R_1 = 2,2,6,6-tetramethylpiperidino; R_2 = 2,4,6-tri-*t*-butylphenyl) from thermolysis of the dimeric form **II** (diphosphadiboretanes) at 250°C.

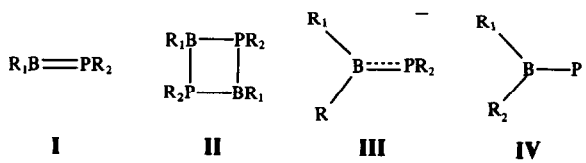

I **II** **III** **IV**

The lithium salts of **I**, giving phosphinidene–borate anions **III**, have been described simultaneously by Power and co-workers[2] and Couret *et al.*[3] The transient existence of **I** during the synthesis of **II** has also been postulated by Nöth and collaborators.[4]

On the other hand, the isomeric forms **IV** (borylphosphinidenes), belong to a class of reactive species whose interactions with transition metal fragments have been studied extensively.[5,6]

As far as we know, apart from some preliminary SCF calculations[1] comparing linear and bent forms of the parent HB=PH species (with the split-valence 6–31G basis set), no theoretical work on these species has as yet been undertaken. As part of our continuing efforts on theoretical studies of low-coordinated phosphorus compounds[7] we now describe *ab initio* molecular orbital calculations on the potential energy surface of the simplest system, [BH_2P]. The latter was considered in both the lowest-lying singlet and triplet electronic states in order to obtain useful information on the relative stabilities between isomers with respect to 1,2-hydrogen shifts.

† Author to whom correspondence should be addressed.

In addition, the possibility of trapping borylphosphinidenes in a metal complex is also worth examining. Therefore, the second part of the present work consists of a comparative Iterative Extended Hückel (IEH) study of the ability of borylphosphinidene (H_2BP) to coordinate to a tricarbonylmetal moiety relative to amino- and methylphosphinidenes (H_2NP and H_3CP, respectively).

RESULTS AND DISCUSSION

(1) Ab initio *calculations on the* [BH_2P] *potential energy surface*

Ab initio calculations were carried out using the GAUSSIAN 82 package[8] on a VAX 11/780 computer. The equilibrium and transition structures were located using analytical energy derivatives at the single determinantal SCF level with the polarized 6–31G** basis set.[9] Harmonic vibrational frequencies were computed at the HF/6–31G** level in order to characterize stationary points and to estimate zero-point vibrational contributions to relative energies. The latter were obtained from single-point calculations (with HF/6–31G** geometries) at the Møller–Plesset perturbation theory[10] level employing an additional basis set, namely the 6–31++G** (++ denotes a set of diffuse *s* functions on H and *sp* functions on B and P).[11] The unrestricted formalism (UHF, UMP) was used for the triplet states.

(a) *Singlet states.* Five stationary points on the singlet [BH_2P] energy surface were located. These consisted of three minima including borylphosphinidene **1** (H_2B—P), boraphosphene **3** (HB=PH) and phosphinoborene **5** (B—PH_2), and the transition structures **2** and **4** for the 1,2-hydrogen shift connecting the isomers. The HF/6–31G** optimized geometries are displayed in Fig. 1, while the total and relative energies are collected in Table 1.

As seen in Table 1, the boraphosphene **3** has the lowest energy. At the HF level, there is a very small energy barrier between **1** and **3**. At higher levels, this barrier disappears indicating that the borylphosphinidene **1** does not exist as a discrete species in the closed-shell singlet state. A similar situation has previously been observed for the isovalent borylnitrene (H_2B—N).[12] For its part, the phosphinoborene **5** is calculated to be a high-level minimum lying 48.7 kcal mol^{-1} above **3**. The energy barrier for the **5**–**3** conversion amounts to only 9.2 kcal mol^{-1}. This value is thus much smaller than that of 18 and 33 kcal mol^{-1} previously obtained for the H_2P—CH → HP=CH_2[13] and H_2P—N → HP=NH[14] conversions, respectively, at similar levels of theory. Accordingly, boraphosphene **3** is probably the only observable species on the singlet potential energy surface.

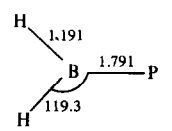

1

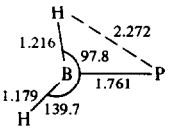

ν_i = 377 i

2

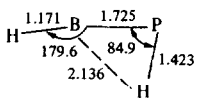

3

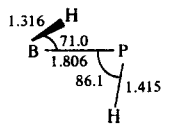

HBPH = 87.8

ν_i = 1478 i

4

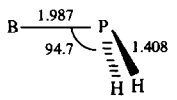

HBPH = 97.3

5

Fig. 1. HF/6–31G** geometries of stationary points on the singlet energy surface. Bond lengths in Å and bond angles in degrees. ν_i are imaginary frequencies, associated with transition structures, given in cm^{-1}.

At the HF/6–31G** level, the harmonic B=P stretching frequency in **3** is 1043 cm^{-1}. This value lies close to those of 1260 cm^{-1} for P=N in HP=NH[14] and 1114 cm^{-1} for C=P in H_2C=PH[13] at a similar level. In contrast, it is larger than the stretching frequency of 709 cm^{-1} computed for P=P in HP=PH.[15] This indicates that the boron–phosphorus bond in boraphosphenes has a rather strong double bond character. In view of the systematic overestimation of vibrational frequencies at the HF level (by 10–15%), it can be expected that the B—P stretching frequencies of R_1B=PR_2 compounds lie in the region of 900–950 cm^{-1}.

It is also worth noting that the HOMO in **3** is B—P π-bonding, whereas the second HOMO is B—P σ-bonding. These orbitals are pictured in structures **3a** and **3b**, respectively.

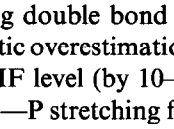

1st HOMO

3a

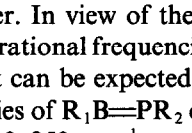

2nd HOMO

3b

Table 1. Calculated total (hartrees) zero-point vibrational (ZPE, kcal mol^{-1}) and relative (kcal mol^{-1}) energies of singlet structures

Level[a]	1	2	3	4	5
	Total and zero-point energies				
HF/6–31G**	−366.48731	−366.48647	−366.50275	−366.38942	−366.43306
MP2/6–31G**	−366.66352	−366.66668	−366.69261	−366.58660	−366.60365
MP4SDTQ/6–31G**	−366.70291	−366.70585	−366.72948	−366.62822	−366.64631
MP2/6–31++G**	−366.66685	−366.67002	−366.69577	−366.59606	−366.61192
ZPE[b]	11.2	10.7	10.7	9.0	10.4
	Relative energies				
HF/6–31G**	9.7	10.2	0.0	71.1	43.7
MP2/6–31G**	18.2	16.3	0.0	66.5	55.8
MP4SDTQ/6–31G**	16.7	14.8	0.0	63.5	52.2
MP2/6–31++G**	18.1	16.2	0.0	62.6	52.6
MP4SDTQ/6–31++G**[c]	16.6	14.7	0.0	59.6	49.0
Estimated[d]	17.1	14.7	0.0	57.9	48.7

[a] Using HF/6–31G** geometries given in Fig. 1.

[b] Values at HF/6–31G** and scaled by 0.9.

[c] Estimated values using the additivity approximation: ΔE(MP4/6–31++G**) ≈ ΔE(MP4/6–31G**) + ΔE(MP2/6–31++G**) − ΔE(MP2/6–31G**).

[d] Including ΔE(MP4SDTQ/6–31++G**) and Δ(ZPE).

(b) *Triplet states.* The UHF/6–31G** optimized geometries for the triplet species **6**–**10** considered are recorded in Fig. 2. The total and relative energies are collected in Table 2. In order to facilitate the comparison, the final energy profile for both singlet and triplet electronic states is shown schematically in Fig. 3 (values at MP4SDTQ/6–31++G**+ZPE level).

At all levels of theory considered, the borylphosphinidene **6** (H_2B—P) turns out to be the triplet global minimum lying 31.1 and 53.7 kcal mol^{-1} below **8** (HB=PH) and **10** (B—PH_2), respectively. The triplet phosphinidene **6** possesses a C_{2v} symmetry ($^3A_2$ state) while the triplet boraphosphene **8** is planar and *cis*-bent ($^3A'$). The phosphinoborene **10** exhibits a flatter pyramidal configuration about phosphorus than that in the singlet **5**.

Parallel to the decrease of the B—P distances in the three minima (from **6** via **8** to **10**, Fig. 2), the corresponding harmonic stretching frequencies also increase monotonically from 696 cm^{-1} in **6** via 727 cm^{-1} in **8** to 833 cm^{-1} in **10**. The change occurring in the B—P distances of the triplets with respect to the singlets is thus in line with the orbital picture. For example, the triplet boraphosphene **8** is formally formed by taking an electron away from the B—P π-bonding orbital **3a** (becoming the orbital **8b** in structure **8**) and placing it in an orbital which

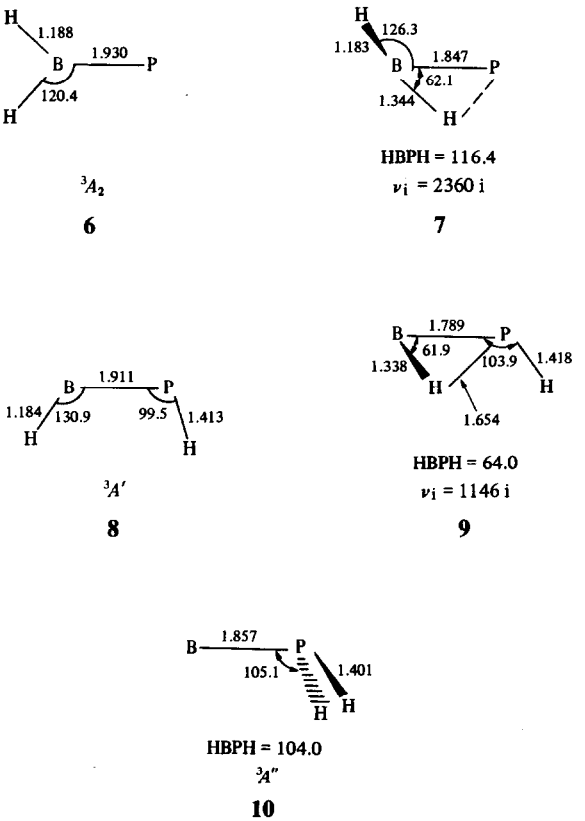

Fig. 2. UHF/6–31G** geometries of stationary points on the triplet energy surface. Bond lengths in Å and bond angles in degrees. ν_i are imaginary frequencies in cm^{-1}.

Table 2. Calculated total (hartrees), zero-point vibrational (ZPE, kcal mol^{-1}) and relative (kcal mol^{-1}) energies of triplet structures

Level[a]	6	7	8	9	10
	Total and zero-point energies				
UHF/6–31G**	−366.52015	−366.42719	−366.46805	−366.39909	−366.43467
UMP2/6–31G**	−366.67235	−366.59637	−366.61819	−366.56472	−366.58538
UMP4SDTQ/6–31G**	−366.70770	−366.63298	−366.65379	−366.59944	−366.61851
UMP2/6–31++G**	−366.67467	−366.60086	−366.62256	−366.56929	−366.58981
ZPE[b]	11.8	9.2	10.4	9.4	11.1
$\langle s^2 \rangle$[c]	2.0176	2.0306	2.0132	2.1149	2.0087
	Relative energies				
UHF/6–31G**	0.0	58.3	32.7	76.0	53.6
UMP2/6–31G**	0.0	47.7	34.0	67.5	54.8
UMP4SDTQ/6–31G**	0.0	46.9	33.8	67.9	56.0
UMP2/6–31++G**	0.0	46.3	32.7	66.1	53.2
UMP4SDTQ/6–31++G**[d]	0.0	45.2	32.5	66.5	54.4
Estimated[d]	0.0	42.6	31.1	64.1	53.7

[a] Using UHF/6–31G** geometries given in Fig. 1.
[b] Values at UHF/6–31G** and scaled by 0.9.
[c] Expectation values of the S^2-operator for UHF wavefunctions.
[d] See footnote in Table 1.

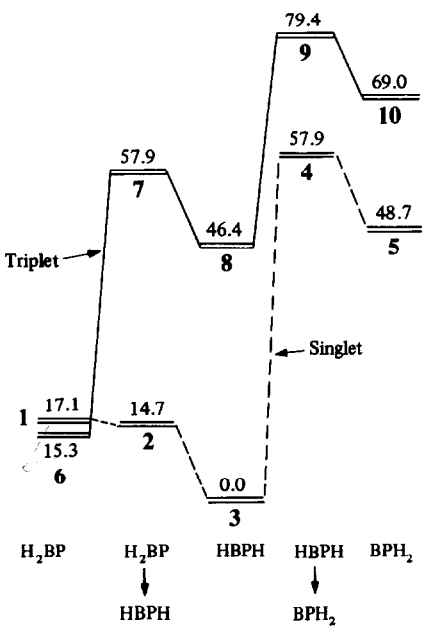

Fig. 3. Relative energies in kcal mol^{-1}, of the pathway for isomerization of the singlet and triplet [BH_2P] species.

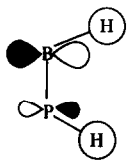

1st HOMO

8a

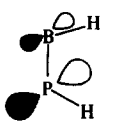

2nd HOMO

8b

is primarily localized on boron and with B—P antibonding components (the orbital **8a**). This consequently reduces the B—P bond order in **8** and the stretching frequency by 316 cm^{-1} (with respect to that of the singlet **3**).

The three minima interconvert, respectively, through the two transition structures **7** and **9**. In the latter, the B—P distances are more contracted than in the equilibrium structures. Both conversions proceed via an out-of-plane migration with rather similar H—B—P angles (62.1° in **7** and 61.9° in **9**).

Our best energetic estimates (Table 2) suggest that the triplet borylphosphinidene **6** is quite stable with respect to unimolecular rearrangement. For instance, the conversion H_2B—P (**6**) → HB=PH (**8**) via the transition structure **7** requires a large barrier energy of 42.6 kcal mol^{-1}. In contrast, the conversion of either HB=PH (**8**) or B—PH_2 (**10**) to the more stable and directly connected isomer is a rather facile process, requiring only 10.4 kcal mol^{-1} for **10** and 11.5 kcal mol^{-1} for **8**. Accordingly, the "cascade effect" in the triplet potential energy surface (see Fig. 3) appears to favour the formation of borylphosphinidene **6** as the only stable triplet species. It is noted that the energy difference

Table 3. Net charges and overlap population in species considered (IEH calculations)

	H_2NP	H_3CP	H_2BP	$H_2NPFe(CO)_3$	$H_3CPFe(CO)_3$	$H_2BPFe(CO)_3$
Atomic charges						
P	−0.55	−0.12	0.04	0.15	0.12	0.10
X(N,C,B)	0.47	0.05	−0.11	−0.04	0.02	0.04
H	0.04	0.04	0.03	0.06	0.01	−0.06
Fe	—	—	—	0.07	0.09	0.14
C(O)	—	—	—	0.07	0.08	0.09
O	—	—	—	−0.17	−0.16	−0.14
Overlap populations						
P—X(σ)	0.66	0.76	0.87	0.74	0.75	0.87
P—X(π)	0.34	0.08	0.46	0.11	0.00	0.33
P—X($\sigma+\pi$)	1.00	0.84	1.33	0.85	0.75	1.20
P—Fe	—	—	—	1.11	1.15	0.98
Fe—C(O)	—	—	—	0.54	0.55	0.56
C—O	—	—	—	1.49	1.49	1.49

between the most stable triplet structure **6** and the most stable singlet one, **3** (which is also the global minimum of the species considered), is calculated to be 15.3 kcal mol^{-1} (Fig. 3). This is slightly larger than the values of 10 and 6 kcal mol^{-1} previously obtained for the $CH_3P \rightarrow CH_2PH$[13] and $NH_2P \rightarrow HNPH$[16] systems, respectively (at comparable levels of theory).

In summary, the most significant chemical result of the present study of the $[BH_2P]$ potential energy surface is a prediction that the boraphosphene **3** and borylphosphene **6** are stable discrete species in the lowest-lying singlet and triplet electronic states, respectively. The remaining isomers are high-energy species and unstable with respect to unimolecular rearrangement.

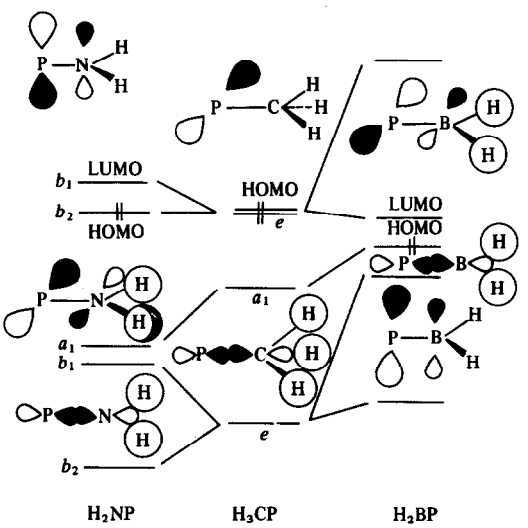

Fig. 4. Molecular orbital correlation digram for H_2NP, H_3CP and H_2BP.

(2) *Comparative extended Hückel study of the complexation of phosphinidenes with the* d^8 *metal fragment* $Fe(CO)_3$

In order to examine whether borylphosphinidenes are possible candidates for metal complexation, we also performed IEH calculations on the interaction of the model species NH_2P, CH_3P and BH_2P with the d^8 $Fe(CO)_3$ moiety. The three phosphinidenes are interesting because of the difference between them, with a π-donor in the α-position in H_2NP, almost none in H_3CP and a π-acceptor in the α-position in H_2BP. We used the *Forticon-8*[17] program for the IEH calculations. Details of the choice of semi-empirical parameters used are given in the Appendix. Calculations on the isolated ligands (Fig. 4) show that the HOMO–LUMO gap in borylphosphinidene (H_2BP) is quite similar to that in aminophosphinidene (H_2NP). From nitrogen to carbon to boron, the gap between the first and second HOMOs decreases, with the second HOMO moving to higher energy as the p_z(P) coefficient increases. A population analysis (Table 3) also indicates that there is greatest P—X charge-transfer in BH_2P. The P—X bond is strongest for X = B, with stronger σ- and π-components than in amino- and methylphosphinidenes. Such a difference obviously affects the interaction with metal fragments.

The interaction between CH_3P and $Fe(CO)_3$ has previously been discussed in some detail by Trinquier and Bertrand.[5a] However, for the purpose of comparison, we display again the interaction dia-

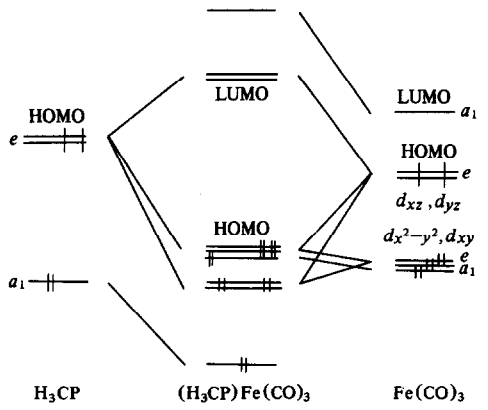

Fig. 5. Molecular orbital interaction diagram for $(CH_3P)Fe(CO)_3$.

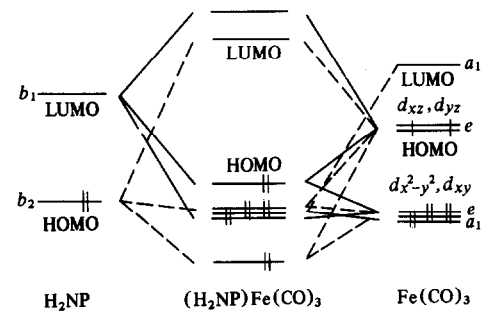

Fig. 6. Molecular orbital interaction diagram for $(NH_2P)Fe(CO)_3$.

gram in Fig. 5 along with that for $(H_2NP)Fe(CO)_3$ and $(H_2BP)Fe(CO)_3$ in Figs 6 and 7, respectively.

As seen in Fig. 7, the HOMO (e) of $Fe(CO)_3$ can overlap with the LUMO (b_2) of H_2BP. The analogous interaction in $(H_2NP)Fe(CO)_3$ is that with the empty b_1-orbital of H_2NP. The overlap is not as good in the former as in the latter. The HOMO and LUMO of H_2BP are at lower energy than those of H_2NP which should favour the H_2BP (LUMO)–$Fe(CO)_3$ (HOMO) interaction and operate against the H_2BP (HOMO)–$Fe(CO)_3$ (LUMO) one. Thus, the orbital overlap trend reduces Fe—P donation in going from H_2NP to H_2BP, while the molecular orbital energy trend favours it. In H_2BP, the HOMO (a_1) can also interact with the LUMO (a_1) of $Fe(CO)_3$, although the energy difference is large. The HOMO–LUMO gap in the complexes is largest in $(H_3CP)Fe(CO)_3$ (≈ 3 eV), smaller in $(H_2NP)Fe(CO)_3$ (≈ 2.5 eV) and further reduced to ≈ 1.5 eV in $(H_2BP)Fe(CO)_3$, suggesting a decreasing kinetic stability.

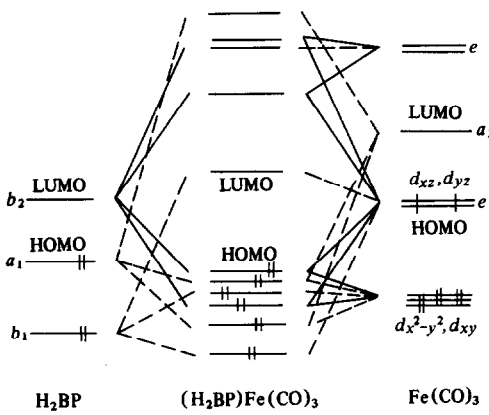

Fig. 7. Molecular orbital interaction diagram for $(H_2BP)Fe(CO)_3$.

The population analysis (Table 3) shows that there is greatest Fe → P electron transfer in the H_2BP complex (although boron retains little of this extra charge). In addition, the P—X ($\sigma+\pi$) and P—X (π) overlap populations *decrease* on complexation in all cases. These values are largest in $(H_2BP)Fe(CO)_3$. In contrast, the Fe—P overlap population is smallest in the latter. Thus, despite considerable Fe—P donation, the Fe—P turns out to be slightly weaker in the borylphosphinidene complex.

In summary, the IEH calculations suggest that the $(H_2BP)Fe(CO)_3$ complex is somewhat less stable than either $(H_2NP)Fe(CO)_3$ or $(H_3CP)Fe(CO)_3$, though the HOMO–LUMO gap is by no means negligible. The Fe—P bond is weaker, but the X—P becomes stronger for $X = BH_2$ than for $X = NH_2$ or CH_3. Thus complexation with a d^8 metal moiety might be a means of examining boraphosphinidenes. This is certainly better than complexation with other fragments such as d^6 systems.

Acknowledgements—We are indebted to the Department of Education (Ireland) for financial support. The computer facilities provided by the U.C.D. Computer Centre are gratefully acknowledged.

REFERENCES

1. (a) A. M. Arif, J. E. Boggs, A. H. Cowley, J. G. Lee, M. Pakulski and J. M. Power, *J. Am. Chem. Soc.* 1986, **108**, 6083; (b) A. H. Cowley, *Phosphorus Sulfur* 1987, **30**, 129.
2. (a) X. Feng, M. M. Olmstead and P. P. Power, *Inorg. Chem.* 1985, **25**, 4615; (b) R. A. Bartlett, X. Feng and P. P. Power, *J. Am. Chem. Soc.* 1986, **108**, 6817; (c) R. A. Bartlett, X. Feng, M. M. Olmstead and P. P. Power, *Phosphorus Sulfur* 1987, **30**, 245.
3. C. Couret, J. Escudié, B. Garrigues, M. Lazraq and J. Satgé, *Can. J. Chem.* 1987, **65**, 1230.

4. (a) P. Kölle, H. Nöth and R. T. Paine, *Chem. Ber.* 1986, **119**, 2681; (b) P. Kölle, G. Linti, H. Nöth, G. L. Wood, C. K. Narula and R. T. Paine, *Chem. Ber.* 1988, **121**, 871.
5. (a) G. Trinquier and G. Bertrand, *Inorg. Chem.* 1985, **24**, 3842; (b) J. G. Lee, J. E. Boggs and A. H. Cowley, *Polyhedron* 1986, **5**, 1027; (c) D. Gonbeau, G. Pfister-Guillouzo, A. Marinetti and F. Mathey, *Inorg. Chem.* 1985, **24**, 4133.
6. (a) F. Mathey, *Angew. Chem. Int. Ed. Engl.* 1987, **26**, 275; (b) G. Huttner and K. Knoll, *Angew. Chem. Int. Ed. Engl.* 1987, **26**, 743; (c) A. Cowley, *Accts Chem. Res.* 1988, **21**, 81.
7. (a) M. T. Nguyen, *Chem. Phys.* 1987, **117**, 91; (b) M. T. Nguyen and N. J. Fitzpatrick, *Polyhedron* 1988, **7**, 223; (c) M. T. Nguyen and N. J. Fitzpatrick, *Chem. Phys. Lett.* 1988, **146**, 524.
8. J. S. Binkley, M. J. Frisch, R. A. Whiteside, K. Raghavachari, R. Seeger, D. J. DeFrees, H. B. Schlegel, E. M. Fluder and J. A. Pople, *Gaussian 82*. Carnegie–Mellon University (1983).
9. P. C. Hahiharan and J. A. Pople, *Theoret. Chim. Acta* 1973, **28**, 213.
10. R. Krishnan and J. A. Pople, *Int. J. Quant. Chem.* 1978, **14**, 91.
11. M. J. Frisch, J. A. Pople and J. S. Binkley, *J. Chem. Phys.* 1984, **80**, 3265.
12. M. T. Nguyen, *J. Chem. Soc., Chem. Commun.* 1987, 342.
13. M. T. Nguyen, M. A. McGinn and A. F. Hegarty, *Inorg. Chem.* 1986, **25**, 2185.
14. M. T. Nguyen, M. A. McGinn and A. F. Hegarty, *J. Am. Chem. Soc.* 1985, **107**, 8029.
15. M. T. Nguyen, *Chem. Phys.* 1986, **109**, 277.
16. K. Ito and S. Nagase, *Chem. Phys. Lett.* 1986, **126**, 531.
17. J. Howell, A. Rossi, D. Wallace, K. Haraki and R. Hoffmann, *Forticon-8*, Q.C.P.E. No. 344.
18. N. J. Fitzpatrick and G. H. Murphy, *Inorg. Chim. Acta* 1984, **81**, 41.
19. F. Herman and S. Skillman, *Atomic Structure Calculations*. Prentice–Hall, New Jersey (1963).
20. H. Basch, A. Viste and H. B. Gray, *Theoret. Chim. Acta* 1965, **3**, 463.
21. J. H. Ammeter, H. B. Burgi, J. C. Thibeault and R. Hoffmann, *J. Am. Chem. Soc.* 1978, **100**, 3686.

APPENDIX

Parameters used in the IEH calculations

Geometrical parameters. For BH_2P, the geometry is given in Fig. 2. For CH_3P and NH_2P, the geometries were taken from refs 13 and 14, respectively. The $Fe(CO)_3$ fragment was assumed to be octahedral with r(Fe—C) = 1.820 Å and r(C—O) = 1.150 Å. The Fe—P distance used was fixed at 2.00 Å for all complexes.

Basis sets and diagonal coulomb terms. The basis set for iron consisted of valence Slater-type 3*d*, 4*s* and 4*p* atomic orbitals; for the first-row atoms, 2*s* and 2*p* atomic orbitals, and for phosphorus, 3*s* and 3*p* atomic orbitals, were used. 1*s* orbitals were included on hydrogen atoms. The radial wavefunctions computed by Fitzpatrick and Murphy[18] as a least-squares fit to the SCF functions of Herman and Skillman[19] were chosen (double-zeta functions were used to represent *d* orbitals). A value of 1.3 was used as the exponent for the hydrogen 1*s* orbitals. Valence orbital ionization energies of the atoms were taken from Basch *et al.*[20] as approximations to the diagonal terms of the coulomb matrix. Off-diagonal terms were calculated using the "weighted" Wolfsberg–Helmholz parameterization.[21]

Polyhedron Vol. 8, No. 7, pp. 977–981, 1989
Printed in Great Britain

0277-5387/89 $3.00+.00
© 1989 Pergamon Press plc

PEROXO COMPLEXES OF Zr^{IV}, Th^{IV}, Mo^{VI} AND U^{VI} IONS CONTAINING SOME BIDENTATE ORGANIC LIGANDS

M. T. H. TARAFDER,* M. B. H. HOWLADER, B. NATH, R. KHAN and A. A. M. ANOWARUL ISLAM

Department of Chemistry, University of Rajshahi, Rajshahi, Bangladesh

(*Received* 27 *September* 1988; *accepted* 9 *November* 1988)

Abstract—Several new organoperoxo complexes of Zr^{IV}, Th^{IV}, Mo^{VI} and U^{VI} have been synthesized and characterized. The complexes have the general formulae, $[Zr(O_2)C_6H_4(CO_2)_2 \cdot 2C_5H_5NO]$, $[Th(O_2)_2L]$, $[Th(O_2)C_6H_4(CO_2)_2 \cdot 2OPPh_3]$, $[Th(O_2)L'_2]$, $[MO(O_2)_2L]$, $[MO(O_2)L'_2]$ and $[MO(O_2)L''H_2O]$ [L = bidentate, neutral; L′ = bidentate, uninegative and L″ = bidentate, dinegative ligands; M = Mo^{VI} and U^{VI}], respectively. The complexes were found to oxidize PPh_3 and $AsPh_3$ to their oxides. The IR spectra of the complexes indicate that the frequency of the ν_1 mode of the $M(O_2)$ grouping, which is essentially an O—O stretch, decreases with the increase in the atomic number of metals in a particular group.

The general field of peroxo complexes of transition metals has attracted considerable attention in recent years.[1–9] By introducing different ligands into metal peroxides, its properties can be modified so that more stable complexes are formed. In general, peroxo complexes containing multidentate ancillary ligands stabilize the metal peroxo moiety which precludes the transfer of active oxygens to organic and inorganic substrates.[5,9] In addition, the reactivity of peroxo complexes can be greatly modified by introducing metals of different sizes.[2,4–6,9,10] We have been interested in extending such a study to peroxo complexes of Zr^{IV}, Th^{IV}, Mo^{VI} and U^{VI} containing a number of bidentate organic ligands. We report here the synthesis of these complexes and their possible oxygen transfer reactions.

EXPERIMENTAL

Reagents

All chemicals used were of reagent grade and were used as supplied by Merck.

Physical measurements and elemental analyses

IR spectra (as KBr pellets) were recorded on a Pye-Unicam SP3-300 IR spectrophotometer. Conductivities of 10^{-3} M solutions in dimethyl sulphoxide (DMSO) were recorded at 298 K using a WPA CM35 conductivity meter and a dip-type cell with platinized electrodes.

Metals[4,6–8] were determined gravimetrically. Carbon and hydrogen analyses were carried out by Mikroanalytisches Labor Pascher, F.R.G.

Preparation of complexes: General method for the preparation of complexes **1** *and* **4**: $[M(O_2)C_6H_4(CO_2)_2 \cdot 2L]$ (M = Zr^{IV} *and* Th^{IV}; L = C_5H_5NO *or* $OPPh_3$)

$M(NO_3)_4 \cdot 4H_2O$ (0.005 mol) in water (25 cm^3) was added to a solution of phthalic acid (0.005 mol) in methanol (20 cm^3). To the mixture, 25 cm^3 of 30% H_2O_2 was added followed by the addition of a solution of L (0.01 mol) in acetone (50 cm^3). The resulting precipitate which separated out was filtered, washed with ethanol and dried *in vacuo* over P_4O_{10}.

Preparation of complexes **2** *and* **3**: $[Th(O_2)_2L]$ (L = $C_6H_4(NH_2)_2$ *and* $C_5H_4NNH_2$)

$Th(NO_3)_4 \cdot 4H_2O$ (0.005 mol) in water (25 cm^3) was added to a solution of the ligand L (0.005 mol) in ethanol (25 cm^3). To the mixture, 30 cm^3 of 30% H_2O_2 was added. The resulting mixture was heated on a steam bath for 10 min. The precipitate so obtained was processed and collected as before.

* Author to whom correspondence should be addressed. Present address: Department of Chemistry, University of St. Andrews, St. Andrews, Fife KY16 9AJ, Scotland, U.K.

Preparation of **5**: $[Th(O_2)(C_6H_4NH_2O)_2]$

The same procedure was applied to $Th(NO_3)_4 \cdot 4H_2O$ (0.005 mol), $C_6H_4NH_2OH$ (0.01 mol) and 20 cm^3 of 30% H_2O_2, which gave the product **5**.

Preparation of **6**: $[Mo(O)(O_2)_2C_6H_4(NH_2)_2]$

MoO_3 (0.005 mol) was stirred and heated in 30% H_2O_2 (60 cm^3) at 50°C for 48 h. The solution was filtered and the filtrate added to a solution of $C_6H_4(NH_2)_2$ (0.005 mol) in ethanol (30 cm^3). The precipitate obtained was separated and stored as above.

Preparation of complexes **7–9**: $[Mo(O)(O_2)(NH_2CH_2CH_2O)_2]$ *and* $[Mo(O)(O_2)L''H_2O]$ ($L'' = CH_2CH_2O_2$ *and* $CH_2(CO_2)_2$]

These complexes were prepared similarly from MoO_3 (0.005 mol) in 50 cm^3 of 30% H_2O_2 and a stoichiometric amount of organic ligands in ethanol (25 cm^3).

Preparation of **10** *and* **11**: $[U(O)(O_2)_2L]$ ($L = C_6H_4(NH_2)_2$ *and* $C_5H_4NNH_2$)

To a solution of $UO_2(NO_3)_2 \cdot 6H_2O$ (0.005 mol) in ethanol (20 cm^3), was added successively a solution of L (0.005 mol) in the same solvent (25 cm^3) and 20 cm^3 of 30% H_2O_2. The product was separated and stored as above.

Preparation of complexes **12** *and* **13**: $[U(O)(O_2)L'_2]$ ($L' = NH_2CH_2CH_2O^-$ *and* $C_6H_4NH_2O^-$)

The same procedure was applied to $UO_2(NO_3)_2 \cdot 6H_2O$ (0.005 mol), L′ (0.01 mol) and 25 cm^3 of 30% H_2O_2, which yielded products **12** and **13**.

Preparation of **14**: $[U(O)(O_2)CH_2(CO_2)_2H_2O]$

Complex **14** was prepared similarly, from $UO_2(NO_3)_2 \cdot 6H_2O$ (0.005 mol), $CH_2(COOH)_2$ (0.005 mol) and 20 cm^3 of 30% H_2O_2.

Reaction of **10** *with triphenylphosphine* [*Reaction* (*a*)]

Triphenylphosphine (1.05 g, 0.004 mol) was added to a solution of **10** (0.85 g, 0.002 mol) in tetrahydrofuran (THF) (40 cm^3). The mixture was heated to 60°C for 72 h. TLC indicated that the reaction was complete. The solution was filtered and the residue collected. A yellowish-white product was recovered from the filtrate which was identified as $OPPh_3$, m.p. 156–157°C (literature 157°C).

Reaction of **6** *with triphenylarsine* [*Reaction* (*b*)]

A solution of triphenylarsine (0.28 g, 0.0009 mol) in THF (25 cm^3) was added to a suspension of **6** (0.13 g, 0.00045 mol) in the same solvent (50 cm^3). The mixture was refluxed for 48 h. TLC indicated that arsine was converted entirely into arsine oxide. The solution was filtered and the residue collected. Evaporation of the filtrate yielded the product, m.p. 186–188°C (literature 189°C).

Attempted reaction of **8** *and* **14** *with allyl alcohol* [*Reaction* (*c*)]

Refluxing **8** with allyl alcohol in a 1 : 1 molar ratio in THF medium for 48 h failed to produce any reaction. **8** was recovered unchanged. Refluxing of **14** with allyl alcohol in the presence of a large excess of 30% H_2O_2 in dioxane medium for 48 h at 90°C also failed to produce any reaction. The unaltered complex **14** was recovered.

RESULTS AND DISCUSSION

Elemental analyses and conductivity data of the complexes (**1–14**) are presented in Table 1. The conductivity data for solutions in DMSO indicate that **1–14** are non-electrolytes. IR spectral data are shown in Table 2. Complexes of phthalic acid, **1** and **4**, show a decrease in ν(C=O) by 22 and 45 cm^{-1}, respectively, compared to the free ligand value (1680 cm^{-1}), and those of malonic acid, **9** and **14**, show a decrease in ν(C=O) by 95 and 87 cm^{-1}, respectively, compared to the free ligand value (1725 cm^{-1}), indicating carboxylate binding in the complexes. In complex **1**, complexing causes a decrease in ν(N—O) by 32 cm^{-1} compared to the free pyridine oxide (1242 cm^{-1}).[11] In **4**, the ν(P=O) mode is decreased by 67 cm^{-1} from the free ligand value (1192 cm^{-1}).[12] Ethyleneglycol is potentially bidentate, dinegative. The ν(OH) mode, observed as a broad band at 3200–3600 cm^{-1}, disappears upon coordination in **8** which indicates deprotonation and coordination at the oxygen site. Complexes **2**, **3**, **5–7** and **10–13** show two bands (**2**, 3340 and 3280; **3**, 3280 and 3180; **5**, 3320 and 3200; **6**, 3210 and 3100; **7**, 3200 and 3140; **10**, 3160 and 3120; **11**, 3240 and 3100; **12**, 3100 and 3000; **13**, 3220 and 3165 cm^{-1}—significantly lower than the values for O-phenylenediamine (3400, 3380 cm^{-1}) (in **2**, **6** and **10**); 2-aminopyridine (3350, 3200 cm^{-1}) (in **3** and **11**); 2-aminophenol (3414,

Table 1. Analytical data and other physical properties of the peroxo complexes[a]

Number	Compound	Colour	% Metal		% Carbon		% Hydrogen		Molar conductance (Ω^{-1} cm^2 mol^{-1})
			Calc.	Found	Calc.	Found	Calc.	Found	
1	$[Zr(O_2)C_6H_4(CO_2)_2 \cdot 2C_5H_5NO]$	Ash	19.1	19.1	45.3	45.2	2.9	2.9	0
2	$[Th(O_2)_2C_6H_4(NH_2)_2]$	Ash	57.4	57.2	17.8	17.5	1.9	2.0	1.5
3	$[Th(O_2)_2(C_5H_4NNH_2)]$	Yellow	59.5	59.1	15.4	15.4	1.5	1.5	0
4	$[Th(O_2)C_6H_4(CO_2)_2 \cdot 2OPPh_3]$	Yellow	23.6	23.4	53.6	53.3	3.4	3.4	3
5	$[Th(O_2)(C_6H_4NH_2O)_2]$	Ash	48.3	47.8	29.9	29.8	2.5	2.5	1.0
6	$[Mo(O)(O_2)_2C_6H_4(NH_2)_2]$	Brown	33.8	33.6	25.5	25.4	2.8	2.8	0
7	$[Mo(O)(O_2)(NH_2CH_2CH_2O)_2]$	Yellow	36.3	36.4	18.2	18.1	4.5	4.4	0
8	$[Mo(O)(O_2)(CH_2CH_2O_2)H_2O]$	Black	43.2	43.3	10.8	10.8	2.7	2.7	2.5
9	$[Mo(O)(O_2)CH_2(CO_2)_2 \cdot H_2O]$	Ash	36.3	36.2	13.6	13.5	1.5	1.5	2.0
10	$[U(O)(O_2)_2C_6H_4(NH_2)_2]$	Ash	55.9	55.8	16.9	16.7	1.9	1.8	1.0
11	$[U(O)(O_2)_2(C_5H_4NNH_2)]$	Yellow	57.8	57.5	14.6	14.5	1.5	1.5	0
12	$[U(O)(O_2)(NH_2CH_2CH_2O)_2]$	Yellow	58.6	58.4	11.8	11.6	2.9	2.8	2.0
13	$[U(O)(O_2)(C_6H_4NH_2O)_2]$	Yellow	47.4	47.5	28.7	28.7	2.4	2.4	1.5
14	$[U(O)(O_2)CH_2(CO_2)_2H_2O]$	Yellow	58.6	58.7	8.9	8.8	0.98	0.9	0

[a] The organic moieties for the compounds indicated are:

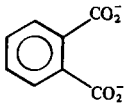

1 and **4**

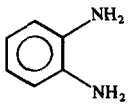

2,**6** and **10**

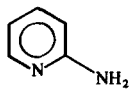

3 and **11**

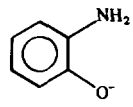

5 and **13**

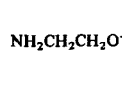

7 and **12**

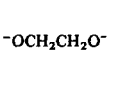

8

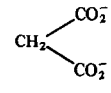

9 and **14**

3342 cm^{-1}) (in **5** and **13**); ethanolamine (3380, 3290 cm^{-1}) (in **7** and **12**), which indicate coordination by the amino nitrogen. This is also evident from the appearance of bands at 255–320 cm^{-1} which are tentatively attributed to the ν(M—N) mode[4–9] (M = Zr^{IV}, Th^{IV}, Mo^{VI} and U^{VI}).

Further, in complexes **3** and **11**, the ν(C=N) mode appears at 1570 and 1560 cm^{-1}, respectively, indicating that the ring nitrogen is coordinated to the metal atom.[10] In addition, the far IR spectra of **1**, **4**, **5**, **7–9**, **12–14** display bands at 360–460 cm^{-1} (Table 2) which are tentatively attributed to the ν(M—O′) modes[4–9] (O′ = oxygen in organic ligand). The metal peroxo grouping (local C_{2v} symmetry) gives rise to three IR- and Raman-active vibrational modes. These are predominantly (O—O) stretching (ν_1), the symmetric M—O stretch (ν_2) and the antisymmetric M—O stretch (ν_3). The characteristic ν_1(O—O) modes of **1–14** appear at 800–875 cm^{-1} (Table 2). In particular, the ν_1 mode of the present thorium peroxo complexes (**2–5**) occur at slightly lower frequencies than the zirconium analogue (**1**). This is more discernible in the peroxo complexes of the elements of group 6A; there is a decrease in ν_1 upon passing from molybdenum complexes (**6–9**) (865–875 cm^{-1}) to the corresponding uranium peroxo complexes (**10–14**) (800–830 cm^{-1}). The present data, thus show that for the M(O_2) grouping, the ν_1(O—O) modes decrease with the increase in the atomic number of metals in a particular group. In the present examples, the ν_3 and ν_2 modes appear at 600–695 and 500–555 cm^{-1}, respectively. These assignments are based on comparisons with other peroxo complexes of zirconium, thorium, molybdenum and uranium.[5–9,13,14] The complexes **6–14** display ν(M=O) modes[3,7] at 900–925 cm^{-1}. Complexes **8**, **9** and **14** show broad bands at 3160 cm^{-1} arising from coordinated water molecules.

Reactivity

So that the possible reactivity of the present peroxo complexes could be explored, compounds **10** and **6** were allowed to react with PPh_3 and $AsPh_3$, respectively. The reactions produced $OPPh_3$ and $OAsPh_3$. The products showed IR bands at 1192 and 880 cm^{-1}, assigned to ν(P=O) and ν(As=O) modes, respectively.[12,15] IR spectra of the metal residues of reactions (a) and (b) showed the disappearance of ν_1(O—O) bands, thereby indicating the transfer of peroxo oxygens to the substrates. In reaction (c), compounds **8** and **14** were allowed to react with allyl alcohol. These compounds failed to

Table 2. IR spectral data for the Zr^{IV}, Th^{IV}, Mo^{VI} and U^{VI} complexes[a] [band maxima (cm^{-1})]

Compound	ν(O—H)	$\nu(NH_2)$	ν(C=O)	ν(C=N)	ν(E=O)	ν(M=O)	ν_1(O—O)	ν_3 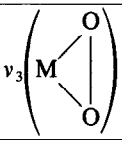	ν_2 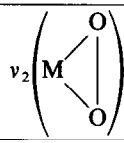	ν(M—O′)	ν(M—N)
1			1658vs		1210sh		832vs	675vs	555vs	425vs	
2		3340w 3280w					828vs	600w	525w		320sh
3		3280w 3180w		1570w			830s	600w	525w		310sh
4			1635s		1125vs		828vs	695vs	545vs	400w	
5		3320w 3200sh					828m	600w	525br	405w	300s
6		3210w 3100w				900m	865w	600s	520m		310w
7		3200w 3140m				900vs	870sh	635m	530m	400w	350w
8	3160br					925vs	870sh	635vs	530vs	390s	
9	3160br		1630vs			915vs	875sh	620vs	530vs	360vs	
10		3160w 3120w				920vs	815w	600w	500w		260sh
11		3240m 3100sh		1560w		905vs	800w	600sh	520w		250s
12		3100w 3000sh				900vs	830m	600sh	525w	425w	255s
13		3220w 3165w				905vs	810w	600sh	540w	640br	260sh
14	3160br		1638vs			920vs	815m	600br		405m	

[a] Relative band intensities are denoted by vs, s, m, w, sh and br, meaning very strong, strong, medium, weak, shoulder and broad, respectively.

oxidize allyl alcohol even when refluxing at 90°C was continued for 48 h. The negative results outline the enhanced stability of the metal peroxo moiety in the presence of bidentate, dinegative chelating ligands. We observed similar negative results with other peroxo complexes containing tridentate, bidentate–dinegative and quadridentate ligands.[5,6,9,16]

Acknowledgement—We thank the University Grants Commission, Bangladesh for funding this research.

REFERENCES

1. H. Mimoun, *J. Mol. Catal.* 1980, **7**, 1.
2. D. A. Muccigrosso, S. E. Jacobson, P. A. Apgar and F. Mares, *J. Am. Chem. Soc.* 1978, **100**, 7063.
3. A. D. Westland, F. Haque and J. M. Bouchard, *Inorg. Chem.* 1980, **19**, 225.
4. A. D. Westland and M. T. H. Tarafder, *Inorg. Chem.* 1981, **20**, 3992.
5. A. D. Westland and M. T. H. Tarafder, *Inorg. Chem.* 1982, **21**, 3228.
6. M. T. H. Tarafder and M. A. L. Miah, *Inorg. Chem.* 1986, **25**, 2265.
7. M. T. H. Tarafder and A. R. Khan, *Polyhedron* 1987, **6**, 275.
8. M. T. H. Tarafder and A. Ahmed, *Ind. J. Chem.* 1986, **25A**, 729.
9. M. T. H. Tarafder, *Ind. J. Chem.* 1987, **26A**, 874.
10. H. Mimoun, M. Postel, F. Casabianca, J. Fischer and A. Mitschles, *Inorg. Chem.* 1982, **21**, 1303.
11. P. V. Balakrisnan, S. K. Patil and H. V. Venkatesetty, *J. Inorg. Nucl. Chem.* 1966, **28**, 540.
12. D. Brown, J. Hill and C. E. F. Rickard, *J. Chem. Soc. A* 1970, 499.
13. E. Wendling, *Bull. Soc. Chim. Fr.* 1967, 16.
14. W. P. Griffith, *J. Chem. Soc.* 1964, 5428.
15. J. Burnstein, M. Halman, S. Pinchas and D. Samuel, *J. Chem. Soc.* 1964, 821.
16. M. T. H. Tarafder and A. A. M. Anowarul Islam, *Polyhedron*, 1989, **8**, 109.

Polyhedron Vol. 8, No. 7, pp. 983–989, 1989
Printed in Great Britain

0277–5387/89 $3.00+.00
© 1989 Pergamon Press plc

THE HYDROLYSIS OF THE PRASEODYMIUM(III) ION, Pr^{3+}, IN 3 m (Li)ClO_4 AT 60°C

LIBERATO CIAVATTA,† RAFFAELLA PORTO and ERMANNO VASCA

Dipartimento di Chimica dell'Università, Via Mezzocannone, 4, 80134 Napoli, Italy

(*Received* 28 *September* 1988; *accepted* 9 *November* 1988)

Abstract—The reaction of the Pr^{3+} ion with water has been studied at 60°C in 3 m (molal) (Li)ClO_4 ionic medium by measurements of the hydrogen ion concentration with a glass electrode. The metal concentration ranged from 0.03 to 1 m, while the acidity was varied from high values, where hydrolysis is negligible, to low enough values for a precipitate of praseodymium(III) hydroxide to form. Hydrolysed solutions were conveniently prepared by coulometric generation of OH^- ions. The potentiometric data, which indicate that less than 1% of the metal ion can be transformed into reaction products in clear solutions, have been explained in terms of $Pr(OH)^{2+}$, $Pr_2(OH)^{5+}$, $Pr_2(OH)_2^{4+}$ and $Pr_3(OH)_5^{4+}$ species. Their formation constants in the inert 3 m $LiClO_4$ medium are reported.

This work is part of a general programme aiming at the elucidation of the reaction with water of the tripositive lanthanide ions. In two previous investigations,[1,2] the hydrolysis equilibria of the La^{3+} ion at 60°C and of the Ce^{3+} at 50°C have been studied. Temperatures higher than 25°C, generally accepted as standard, were chosen in order to favour species of nuclearity lower than $La_5(OH)_9^{6+}$ and $Ce_3(OH)_5^{4+}$, which are the main complexes at room temperature.[3,4] In both cases, evidence was produced for intermediate complexes, $La_2(OH)_3^{3+}$ and $Ce(OH)^{2+}$. For easy comparison with previous results, we have adopted in the present study a temperature of 60°C.

Very little quantitative information has been reported as yet on the hydrolysis of the Pr^{3+} ion. The only attempt seems to be that made in 1946 by Moeller[5] who measured, at 25°C with a glass electrode, the acidity of $Pr_2(SO_4)_3$ solutions and concluded that mononuclear hydrolytic complexes cannot be the main reaction products. While sulphate complexing and medium changes prevented an accurate analysis of the data, the measurements in dilute solutions were explained by assuming the formation of $Pr(OH)^{2+}$ with $\log^* \beta_{11} = -9.0$. This result was based on the postulate that there were no appreciable amounts of protolytic impurities, as sulphuric acid, in the praseodymium(III) sulphate which he had prepared.

* Author to whom correspondence should be addressed.

Symbols

- a_w activity of water;
- $^*\beta_{pq}$ equilibrium constant for the formation of $Pr_q(OH)_p^{3q-p}$ considering H_2O and not OH^- as reagent;
- m_H proton analytical excess, $=[ClO_4^-]+m_X-3m_M-[Li^+]$;
- m_M total concentration of the Pr^{3+} ion;
- m_X total concentration of the Cl^- ion;
- $\bar{n}$ average number of hydrogen ions set free per praseodymium atom, $=([H^+]-m_H)/m_M$;
- y_H, y_M, y_{pq} activity coefficients, respectively, of H^+, Pr^{3+}, $Pr_q(OH)_p^{3q-p}$.

Concentrations and equilibrium constants, if not otherwise stated, are expressed on the molal scale, m (mol/kg H_2O).

METHOD

The investigation was performed by measuring, with a glass electrode, the $[H^+]$ of a series of $Pr(ClO_4)_3$ solutions of various acidity. The concentration of ClO_4^- in all the test solutions was made up to 3 m by the addition of $LiClO_4$. Since the hydrolysis reaction becomes measurable at $\log[H^+] < -5$ and less than 1% of the praseodymium(III) can be transformed into hydrolysis products before the precipitation of solid hydroxides, rather concentrated metal solutions, in the

range from 0.03 to 1 m, were studied in order to attain sufficiently high buffer capacities. At the low values of $\bar{n}$ that need be measured, < 0.01, the deleterious effect of protolytic impurities, introduced in the system with strong base solutions, was minimized by coulometric generation of OH^- ions. The inherent accuracy of the coulometric method allowed the low $\bar{n}$ values to be affected by uncertainties not exceeding 1%.

The test solutions, abbreviated by TS in the following discussion, were of the general composition:

$$Pr^{III}\ m_M,\ H^+ m_H,\ Cl^-\ m_X,$$

$$Li^+\ (3-3\ m_M - m_H + m_X),\ ClO_4^-\ 3.00\ m,$$

where m_H in most of the hydrolysed solutions studied was negative. The auxiliary chloride ion, in the range $5 \times 10^{-3} \leqslant m_X \leqslant 0.05$ m, served the purpose of avoiding salt bridges in the electrolysis cell (I), employed for the coulometric generation of OH^-, as well as in the galvanic cell (II) for measuring $[H^+]$. Practically coinciding results, within the limits of experimental error, were obtained in experiments carried out at different m_X but constant m_M, thus indicating the negligible influence of Cl^- ions on the hydrolytic equilibria.

The acidity of TS was decreased in a stepwise fashion by the electrolysis cell (I), connected to a constant-current source

$$-Pt/TS/Ag+. \qquad (I)$$

When current is passed through (I), the reaction $Ag(s) + Cl^- + H_2O \rightarrow AgCl(s) + OH^- + (1/2)H_2(g)$ takes place on the right. However, small amounts of silver ions are reduced on the platinum cathode, proportional to the electrolysis duration. The side process occurs at a rate of $(5 \pm 1) \times 10^{-10}$ mol s^{-1}, thus an efficiency of OH^- generation better than 99.9% can be achieved only with currents exceeding 50 mA. On the other hand, at such high intensities it becomes difficult to avoid a local excess of base which might promote premature precipitation of praseodymium(III) hydroxides. Good results were attained with intensities in the interval 1–20 mA. To prevent the accumulation of strong base in the vicinity of the cathode, generations of less than 30 s were alternated with pauses of at least 60 s. The moles of electrons passed were corrected for the amount of silver ion reduced. For each experiment, the correction term was evaluated from the total silver deposited on the platinum cathode, which was determined afterwards as described previously.[1] The values of m_H could then be assessed with an uncertainty of less than 1%.

The hydrogen ion concentration in TS was determined using cell (II)

$$-Ag/AgCl/TS/GE+ \qquad (II)$$

where GE denotes the glass electrode. The EMF of cell (II) can be expressed at 60°C as eq. (1)

$$E = E'_0 + 0.06610 \log([H^+] m_X y_{HCl}^2), \qquad (1)$$

in which E'_0 is a constant in each experiment and y_{HCl} denotes the activity coefficient of hydrochloric acid. The standard states are so chosen that the activity of a solute species tends to its molality as the composition of TS approaches 3 m $LiClO_4$.

During a series of measurements, carried out conveniently at constant m_M as a potentiometric titration, the variations of y_{HCl}, owing to the small $\bar{n}$ values reached, are negligible. Therefore data of the same titration can be calculated using eq. (2)

$$E = E_0 + 0.06610 \log([H^+] m_X). \qquad (2)$$

The value of E_0 was determined in each titration by measurements in solutions with $m_H > 10^{-4}$ m, where hydrolysis is suppressed and, consequently, $[H^+] = m_H$. E_0 and m_H^*, the proton excess in the starting solution, were assessed simultaneously on the basis of Gran plots.[6] In each case, data in the acidity range from 2×10^{-3} to 10^{-4} m gave E_0 values constant to better than 0.05 mV and m_H^* values within $\pm 0.2\%$.

In constructing the $\bar{n}(\log[H^+])$ function, which forms the basis for the deduction of the composition of the main reaction products, we had to consider the effect of small but unavoidable amounts of protolytic impurities introduced with the reagents, mostly $LiClO_4$, present in high concentration. The acidity constant of the protolytic impurity as well as its concentration was determined by a potentiometric procedure developed recently.[7] The contaminant, supposed to be a monoprotic acid, was found to have $pK_a = 5.5 \pm 0.2$ at 60°C and a concentration of about 20×10^{-6} m in 3 m $LiClO_4$, the salt being purified by double crystallization. The quality of the preparation did not improve in subsequent crystallizations. However, better results were obtained by prolonged purging of the solutions with purified nitrogen gas. Hence, after two days of bubbling, the impurity level from 20×10^{-6} m recorded after 2 h purging, sank to $(5 \pm 1) \times 10^{-6}$ m in 3 m $LiClO_4$. Very likely, the impurity is carbon dioxide, whose last traces are removed sluggishly by the nitrogen stream.

On the basis of these figures we estimate that the $\bar{n}$ values for the lowest m_M are uncertain to about 1%. However, the error is less in the remaining reaction range.

Most of the measurements were performed by gradually decreasing the acidity of TS. Therefore doubts may arise whether a true equilibrium was

attained. To answer this essential question, experiments were also made by acidification of partially hydrolysed solutions with perchloric acid. The data (back titrations in Table 1) are seen to agree in Fig. 1 within the limits of experimental error with those of the forward titrations, thus indicating a real equilibrium.

EXPERIMENTAL

Materials and analysis

Praseodymium(III) *perchlorate solutions.* These were made from the oxide, Pr_6O_{11}, a Fluka product of 99.9% purity, and $HClO_4$, Merck p.a. The oxide was added portionwise to a hot, 4 m $HClO_4$ solution, until a pH value of 3 was reached. In acid media, the mixed Pr^{III}–Pr^{IV} oxide dissolves completely with a distinct ozone smell, indicating that the Pr^{IV} ion is reduced by water. In order to remove heavy metal impurities present in the reagents, the solution of Pr^{III} was made alkaline with OH^- ions, produced electrolytically on a platinum cathode, until a permanent precipitate of Pr^{III} hydroxide appeared. The solution, after standing for a week, was filtered and re-acidified to about pH = 3. No traces of the Pr^{IV} ion could be detected by the iodine–starch test.

The Pr concentration was established by titration with EDTA, using xylenol orange as the visual indicator.[8] The results agreed to 0.1%. The proton analytical excess was determined by coulometric acid–base titration with a glass electrode. The perchlorate ion concentration was calculated as the sum: $m_H + 3m_M$.

Lithium perchlorate, perchloric acid and lithium chloride solutions. These were prepared and analysed as described previously.[1,2]

Table 1. The experimental $\bar{n}(-\log[H^+], m_M)$ data

$\bar{n} \times 10^3$ $(-\log[H^+])$
$m_M = 0.9988$
(a) 0.175 (4.631); 0.40 (4.968); 0.675 (5.147); 0.985 (5.264); 1.33 (5.350); 1.67 (5.413); 2.02 (5.462); 2.36 (5.502); 2.70 (5.536); 3.05 (5.565); 3.39 (5.591); 4.08 (5.634); 4.77 (5.670).
(b) 0.47 (5.045); 0.75 (5.188); 1.02 (5.278); 1.335 (5.352); 1.68 (5.414); 2.03 (5.462); 2.375 (5.501); 2.72 (5.535); 3.07 (5.565); 3.42 (5.591); 3.83 (5.619); 4.28 (5.645); 4.77 (5.669); 5.29 (5.691); 5.845 (5.711).
(c) 0.45 (5.046); 1.26 (5.354); 2.28 (5.511).
$m_M = 0.3000$
0.41 (5.217); 0.63 (5.363); 0.91 (5.478); 1.22 (5.563); 1.545 (5.633); 1.90 (5.692); 2.27 (5.742); 2.65 (5.782); 3.03 (5.815); 3.405 (5.845); 3.78 (5.870); 4.16 (5.892); 4.55 (5.913); 4.93 (5.929); 5.31 (5.949); 5.68 (5.964); 6.06 (5.978); 6.44 (5.990); 6.82 (5.999).
$m_M = 0.1000$
(a) 0.61 (5.450); 0.95 (5.608); 1.33 (5.723); 1.71 (5.807); 2.13 (5.878); 2.55 (5.933); 3.05 (5.985); 3.61 (6.033); 4.25 (6.078); 4.96 (6.119); 5.74 (6.156); 6.59 (6.191).
(b) (Back titration) 6.02 (6.163); 5.55 (6.142); 4.89 (6.109); 4.24 (6.075); 3.69 (6.037); 3.14 (5.993); 2.59 (5.940); 2.14 (5.883); 1.42 (5.752); 0.98 (5.616).
(c) (Back titration) 5.83 (6.163); 5.08 (6.126); 4.52 (6.093); 3.97 (6.058); 3.41 (6.015); 2.78 (5.962); 2.33 (5.906); 1.845 (5.832); 1.52 (5.770); 1.125 (5.669); 0.81 (5.555); 0.485 (5.347).
$m_M = 0.0300$
(a) 1.49 (5.849); 1.98 (5.956); 2.47 (6.042); 2.97 (6.111); 3.475 (6.167); 3.98 (6.215); 4.48 (6.256); 4.99 (6.290); 5.50 (6.320); 6.01 (6.347); 6.58 (6.373); 7.15 (6.396); 7.73 (6.416); 8.30 (6.435); 8.875 (6.451); 10.0 (6.465).
(b) 1.33 (5.775); 1.80 (5.917); 2.29 (6.018); 2.78 (6.096); 3.32 (6.162); 3.87 (6.214); 4.42 (6.257); 4.99 (6.295); 5.56 (6.326); 6.12 (6.353); 6.69 (6.376); 7.26 (6.397); 7.83 (6.415); 8.47 (6.434); 9.10 (6.451); 9.80 (6.468).

Experimental details of the EMF measurements

The potentiometric titrations were carried out by immersing the vessel, containing the test solution, in a silicone oil thermostat kept at 60.00 ± 0.03°C. Glass electrodes manufactured by Jena Glasswerk were employed. They took 20 min after the addition of OH^- to acquire a steady value, which remained constant to ± 0.1 mV for several hours. Silver–silver chloride electrodes were obtained according to Brown.[9] Platinum gauze electrodes, 2×2 cm, were boiled in 1 : 1 HNO_3 and ignited in an alcohol flame. Platinum gauze, coated by a thick layer of silver, was used as the anode in cell (I). It was prepared by electrolysis from 0.05 m AgCl in 16 m LiCl. The electrodes were washed with concentrated ammonia, and then soaked for several days in water.

The sequence of operations: stepwise addition of OH^- by constant-current coulometry and EMF measurements was performed with an all automatic data acquisition system furnished by the Hewlett and Packard Company. The number of coulombs could be determined with an error of less than 0.02%. The EMF values were established to within ± 0.02 mV.

Before a titration was started, a stream of purified and presaturated nitrogen was passed for 2 days through the solutions kept at room temperature. Throughout the measurements at 60°C, the solution was protected from atmospheric contamination by

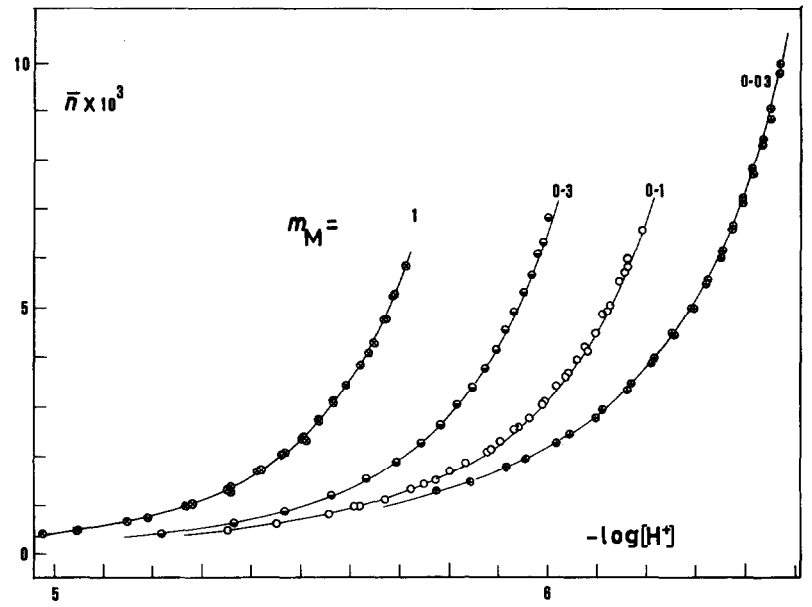

Fig. 1. $\bar{n}$, the average number of OH^- ions bound per praseodymium atom, as a function of $\log[H^+]$. The curves were calculated using the constants of Table 3 and expressions (9) and (10) for medium changes.

placing it in vessels fitted with high-vacuum ground glass stoppers.

In the back titrations, the test solution was acidified by stepwise addition of a standard $HClO_4$ solution.

THE COMPOSITION OF THE HYDROLYSIS PRODUCTS

The $\bar{n}(\log[H^+], m_M)$ data, which are given in Table 1 and are graphically represented in Fig. 1, were treated as follows. First, the number of OH ions, p, bound in the $Pr_q(OH)_p^{3q-p}$ complexes, and the conditional constants K_p, eq. (6), were deduced for each set at constant m_M. Subsequently, the main q values and the $^*\beta_{pq}$ constants were determined by examining the dependence of K_p on m_M. Medium changes, caused by the replacement of large portions of the solvent lithium ion with Pr^{3+}, were accounted for by the Specific Interaction Theory, SIT.[10] Finally, the equilibrium constants were refined with numerical procedures based on the principle of least-squares.

Evaluation of the prevailing p *values*

In solutions where a series of $Pr_q(OH)_p^{3q-p}$ complexes is formed, the concentration of OH^- ions bound in the hydrolysis products, is expressed as

$$\bar{n}m_M = [H^+] - m_H = \sum_p \sum_q p[Pr_q(OH)_p^{3q-p}]$$

$$= \sum_p \sum_q p^*\beta_{pq}[Pr^{3+}]^q[H^+]^{-p}a_w^r y_M^q y_H^{-p} y_{pq}^{-1}, \quad (3)$$

where the exponent r is a function of p, q and the structure of the $Pr_q(OH)_p^{3q-p}$ species. Since $\bar{n}$ could never be made to exceed 0.01, the composition of TS at constant m_M varies only slightly upon alkalification and hydrolysis. Therefore, as long as m_M is maintained constant, the changes in activity coefficients and water activity may be neglected. Furthermore, the calculations can be simplified by putting

$$[Pr^{3+}] \simeq m_M(1-\bar{n}). \quad (4)$$

Approximation (4) becomes exact either when $p = q$ or for $\bar{n} \to 0$. As the results of the next section will show, we are not very far from these conditions, so that no appreciable error is introduced by using eq. (4). Hence eq. (3) can be written with good approximation, as eq. (5)

$$\bar{n}m_M = \sum_p pK_p x^p, \quad (5)$$

where the conditional m_M-dependent constant K_p is defined by

$$K_p = \sum_q {}^*\beta_{pq} m_M^q y_M^q y_H^{-p} y_{pq}^{-1} a_w^r \quad (6)$$

and

$$x = (1-\bar{n})[H^+]^{-1}. \quad (7)$$

Comparison of the experimental points with normalized functions,[11] based on eq. (5) and representing various hypotheses, suggested the presence of complexes with $p = 1$ and 2, at the lowest $\bar{n}$. However, at least another value of p,p' must be

Table 2. Survey of the K_p constants

m_M	$-\log K_1$	$-\log K_2$	$-\log K_5$	p'
0.9988	8.56±0.02	14.15±0.02	32.4_4±0.1	4.9±0.5
0.3000	9.27±0.02	15.21±0.02	34.24±0.05	4.8±0.5
0.1000	9.74±0.02	16.19±0.02	35.7±0.1	4.6±0.5
0.0300	10.25±0.02	17.35±0.02	37.3±0.1	5.3±0.5

assumed to explain the systematic deviations at the highest $\bar{n}$. We postulated the formation of species with a single p' and analysed the function

$$\log R = \log(\bar{n}m_M - K_1x - 2K_2x^2) = \log(p'K_{p'}) + p'\log x. \quad (8)$$

First, from the plots $\bar{n}m_M x^{-1}$ vs x for the lowest $\bar{n}$, preliminary values of K_1 and K_2 were evaluated, which when introduced into eq. (8) yielded p' as slope of the $\log R$ against $\log x$. Then, temporary $K_{p'}-s$ values were estimated by taking for p' the nearest integer value, and better K_1 and K_2 constants were calculated after correcting $\bar{n}m_M$ for $p'K_{p'}x^{p'}$. The cycle was repeated until convergence. The final results summarized in Table 2 indicate the presence of a species with $p' = 5$, in addition to complexes with one and two OH^- ions. The uncertainties of the K_p constants represent maximum deviations from mean values.

Calculation of q

To find the main q values we have to confront data of different m_M, thus involving the estimate of the variations of the activity coefficients as well as of the water activity. Corrections for medium effects were made by SIT.[10] According to theory, as reagents and products are all positively charged and the anionic composition of the medium is essentially constant, the activity coefficient y_i of the "i" species of charge z_i in our medium scale, may be expressed as a function of the ionic strength, I, by

$$\log y_i = -z_i^2\{0.5452I^{0.5}/(1+1.5I^{0.5}) - 0.2624\} = -z_i^2 D. \quad (9)$$

Concerning the a_w variations, we assumed a linear dependence of $\log a_w$ with m_M between the value in 3 m $LiClO_4$, where $a_w = 1$ according to our choice of standard states, and that in 1 m $Pr(ClO_4)_3$ at 60°C. We get, using the isopiestic data published by Pitzer,[12]

$$\log a_w = 0.0199 m_M. \quad (10)$$

To deduce q and $^*\beta_{pq}$ from eq. (6) we have to make guesses about the coefficients r. For mononuclear $Pr(OH)_p^{3-p}$ species we set $r = 4p$, which means that H^+ is solvated by $4H_2O$, as suggested by experimental[13,14] and theoretical[15] evidence, and that the Pr^{3+} ion maintains its coordination in the hydrolysis products. The formation of hydroxide or oxide bridges in polynuclear complexes implies the removal of water from the coordination sphere of the metal ion. Consequently, r is less than $4p$ and its estimate requires some information on the structure of the complexes. At any rate, as the a_w values are not very different from unity, rough estimates of r seem adequate for the interpretation of data with the present accuracy.

For species with $p = 1$, eq. (6) gives

$$K_1 m_M^{-1} 10^{4D} a_w^{-4} = {}^*\beta_{11} + {}^*\beta_{12} m_M 10^{12D} a_w^{-1} + \cdots, \quad (11)$$

where we use $r = 3$ for the formation of $Pr_2(OH)^{5+}$. Within the limits of experimental error the left-hand side of eq. (11) was found to be constant for $m_M \leqslant 0.3$. On the other hand, a systematic deviation which greatly exceeds the estimated uncertainty of the data, was recorded at $m_M = 1$. This has been ascribed to the presence, in addition to $Pr(OH)^{2+}$, of small amounts of $Pr_2(OH)^{5+}$. The values of $^*\beta_{11}$ and $^*\beta_{12}$ are reported in Table 3.

Equation (6) yields for $p = 2$

$$K_2 = {}^*\beta_{21} m_M 10^{-6D} a_w^8 + {}^*\beta_{22} m_M^2 a_w^6 + \cdots. \quad (12)$$

The value of $r = 6$ for the $Pr_2(OH)_2^{4+}$ ion stems

Table 3. Values of the formation constants, $^*\beta_{pq}$

	$-\log {}^*\beta_{11}$	$-\log {}^*\beta_{12}$	$-\log {}^*\beta_{22}$	$-\log {}^*\beta_{53}$
Graphical	8.75±0.02	9.2±0.1	14.25±0.05	32.7±0.1
Least-squares	8.74±0.01	9.34±0.06	14.23_3±0.01_5	32.76±0.09

from the assumption that a double bridge of OH^- links the metal ions. Over the entire concentration range studied, the quantity $\log(K_2 m_M^{-2} a_w^{-6})$ is independent of m_M within ± 0.05 units. We may thus infer that the $Pr_2(OH)_2^{4+}$ species is formed. The mean $*\beta_{22}$ value is shown in Table 3.

An exploratory examination of the dependence of K_5 on m_M suggested that the main q is equal to three. The value of $\log *\beta_{53} = \log(K_5 m_M^{-3} 10^{6D} a_w^{-15})$ (Table 3) was found to be constant to within ± 0.1 units. The value of $r = 15$ was chosen according to a model in which three metal atoms are arranged in an equilateral triangle around a central O^{2-} ion, equivalent to two OH^-. Each of the remaining three OH^- groups links a pair of praseodymiums. Of the 20 water molecules bound to the five protons set free in the formation of $Pr_3(OH)_5^{4+}$, five originate from the water coordinated by the metal ions.

Refinement of the equilibrium constants

The calculations of the previous sections have furnished evidence for the presence of $Pr(OH)^{2+}$, $Pr_2(OH)_2^{4+}$ and $Pr_3(OH)_5^{4+}$ species and for small amounts of the $Pr_2(OH)^{5+}$ ion in the most concentrated praseodymium(III) solutions. As a check, the equilibrium constants $*\beta_{pq}$ were deduced by procedures founded on the principle of least-squares. The computation consisted in the minimization of the sum

$$U = \sum \{(\bar{n}_i - \bar{n}_c)/\bar{n}_i\}^2, \qquad (13)$$

where $\bar{n}_i$ stands for an experimental datum and $\bar{n}_c$ denotes a calculated $\bar{n}$ value with a given set of $*\beta_{pq}$s. Medium changes were accounted for by using eqs (9) and (10).

The minimum of U was found with the constants listed in Table 3. These are seen to agree fairly well with those evaluated above using graphical procedures based on approximation (4). The uncertainties of the constants are three times the standard deviation, defined by the "D-boundary",[16] and are smaller than maximum errors estimated by graphical procedures.

The method originating from the least-squares principle offers a quantitative measure of the fit between experimental data and proposed model. Of a total of 116 data points, 54 have shown positive deviations, whereas 62 have shown negative ones. The average of the positive deviations amounts to 2.8%, that of the negative ones to 2.1%. The magnitude and sign of the deviations do not exhibit appreciable trends with $\bar{n}$ and m_M.

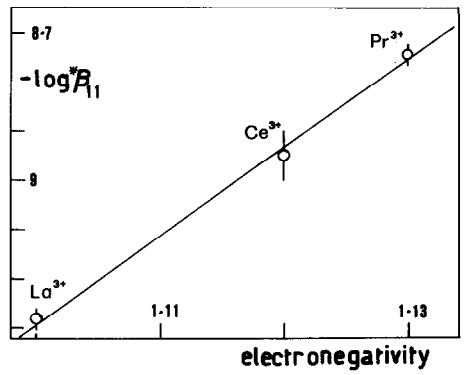

Fig. 2. The linear dependence of $\log *\beta_{11}$ on the electronegativity (χ) for the first lanthanide ions. The line expresses: $-28.85 \pm 17.79\ \chi$.

DISCUSSION

The main conclusion of the present investigation is that the hydrolytic complexes $Pr(OH)^{2+}$, $Pr_2(OH)^{5+}$, $Pr_2(OH)_2^{4+}$ and $Pr_3(OH)_5^{4+}$, are formed in the narrow reaction region, $\bar{n} < 0.01$, which connects the Pr^{3+} ion with colloidal praseodymium hydroxides. The short discussion is dedicated to trends and irregularities in the behaviour of the cations La^{3+} and Ce^{3+}, studied previously,[1,2] and Pr^{3+}.

An exact linear relation is verified between $\log *\beta_{11}$ and electronegativities, χ. This is illustrated in Fig. 2 where against χ values, taken from Allred's study,[17] are plotted the log of the constants of the initial hydrolysis step at 60°C in 3 m (Li)ClO_4. For Ce^{3+}, $\log *\beta_{11} = -8.95 \pm 0.05$ was calculated from the value determined at 50°C, -9.13, and the enthalpy change $\Delta *H_{11} = 33$ kJ mol^{-1}, estimated for $La^{3+} + H_2O \leftrightarrows LaOH^{2+} + H^+$. At increasing electronegativity the drainage of charges from the ligand oxygen to the metal ion raises the positive charge density on the periphery of the hydrated cation. The greater the charge density, the lower is the work required to remove a proton and to transfer it to a water molecule. A clear correlation seems to exist between aquo acidity and electronegativity within the same group, including cations of the same charge and of the same coordination number.

The difference in electronegativity within the same group provides a plausible explanation also in the trend of $*\beta_{12}/*\beta_{11}$, the equilibrium constant of the dimerization with a single hydroxo bridge. Below, along with electronegativity values[17] are summarized the $*\beta_{12}/*\beta_{11}$ constants for the first three lanthanides, 60°C and 3 m $LiClO_4$, and for dipositive cations of group 2b at 25°C in the specified media: $\log(*\beta_{12}/*\beta_{11})$ (χ): La^{3+} 0.36(1.10);

Ce^{3+} −0.35(1.12); Pr^{3+} −0.60(1.13); Zn^{2+} (3.2 m NaCl) 1.72(1.65); Cd^{2+} (3.47 m $LiClO_4$) 1.04(1.69); Hg^{2+} (3.5 m $NaClO_4$) 0.81(2.00). The constants for Zn^{2+}, Cd^{2+} and Hg^{2+} were obtained from ref. 18. The drainage of electrons from the oxygen donor atom by the more electronegative Pr^{3+} and Hg^{2+} ions will render the formation of a second oxygen–metal bond less probable.

Concerning the formation of $Pr_2(OH)_2^{4+}$ and $Pr_3(OH)_5^{4+}$, expressed as the polymerization from $Pr(OH)^{2+}$

$$Pr(OH)^{2+} \rightleftharpoons 1/2Pr_2(OH)_2^{4+}, \qquad \log(*\beta_{22}^{1/2}/*\beta_{11}) = 1.6$$

$$Pr(OH)^{2+} \rightleftharpoons 1/5Pr_3(OH)_5^{4+} + 2/5Pr^{3+}, \qquad \log(*\beta_{53}^{1/5}/*\beta_{11}) = 2.2,$$

the constants do not sensibly differ from those found for several cations of different charge, ion size and electronic structure.[19] As pointed out on many occasions,[19,20] the polymerization reaction is primarily a property of the oxygen atom and the hydroxide ion as ligand.

Apart from these similarities, some irregularities still persist in the behaviour of the lanthanide series. We recall that the dinuclear complexes, $La_2(OH)_2^{4+}$ as well as $Ce_2(OH)_2^{4+}$, do not attain detectable concentration levels under experimental conditions identical to those chosen for praseodymium(III). Presently, the limited amount of fairly reliable information on the hydroxide complexes of tripositive lanthanides does not allow definite conclusions on these anomalies.

Acknowledgement—This work has been financially supported by the Ministero della Pubblica Istruzione, Rome.

REFERENCES

1. L. Ciavatta, M. Iuliano and R. Porto, *Polyhedron* 1987, **6**, 1283.
2. L. Ciavatta, R. Porto and E. Vasca, *Polyhedron* 1988, **7**, 1355.
3. G. Biedermann and L. Ciavatta, *Acta Chem. Scand.* 1961, **15**, 1347.
4. G. Biedermann and L. Newmann, *Arkiv kemi* 1964, **22**, 303.
5. T. Moeller, *J. Phys. Chem.* 1946, **50**, 242.
6. G. Gran, *Analyst* 1952, **77**, 661.
7. L. Ciavatta, R. Porto and E. Vasca, to be published.
8. I. M. Kolthoff and P. J. Elving, *Treatise on Analytical Chemistry*, Part 2, Vol. 8, p. 57. John Wiley, New York (1963).
9. A. S. Brown, *J. Am. Chem. Soc.* 1934, **56**, 646.
10. L. Ciavatta, *Ann. Chim. (Rome)* 1980, **70**, 551.
11. L. G. Sillén, *Acta Chem. Scand.* 1956, **10**, 186.
12. K. S. Pitzer, in *Activity Coefficients in Electrolyte Solutions* (Edited by R. M. Pytkowicz), Vol. 1. CRC Press, Boca Raton, Florida (1979).
13. D. G. Tuck and R. M. Diamond, *J. Phys. Chem.* 1961, **65**, 193.
14. D. S. Terekhova, *Zh. Strukt. Khim.* 1970, **11**, 530.
15. R. Grahn, *Arkiv Fys.* 1962, **21**, 13.
16. L. G. Sillén, *Acta Chem. Scand.* 1962, **16**, 159.
17. A. L. Allred, *J. Inorg. Nucl. Chem.* 1961, **17**, 215.
18. (a) L. G. Sillén and E. A. Martell, *Stability Constants*. The Chemical Society, London, Special Publication No. 17 (1964) and No. 25 (1971); (b) E. Högfeldt, *Stability Constants*. Pergamon Press, Oxford (1982).
19. C. F. Baes and R. E. Mesmer, *The Hydrolysis of Cations*. John Wiley, New York (1976).
20. G. Biedermann and D. Ferri, *Acta Chem. Scand.* 1982, **A36**, 611.

Polyhedron Vol. 8, No. 7, pp. 991–996, 1989
Printed in Great Britain

0277-5387/89 $3.00+.00
© 1989 Pergamon Press plc

COPPER(II) HALIDE COMPLEXES OF 4-AMINOBENZOPHENONE; SYNTHESIS AND X-RAY CRYSTAL STRUCTURE OF THE COPPER(II) POLYMERIC COMPLEXES: (4-AMINOBENZOPHENONE)DICHLOROCOPPER(II)·0.5S (S = ETHANOL OR METHANOL)

IDA MARIA VEZZOSI and ALINE FRANCA ZANOLI

Department of Chemistry, University of Modena, Via Campi 183, 41100 Modena, Italy

and

ELEONORA FORSELLINI and FRANCO BENETOLLO†

Institute of Chemistry and Technology of Radioelements C.N.R., Corso Stati Uniti 4, 35100 Padova, Italy

and

GABRIELLA BOMBIERI

Institute of Pharmaceutical Chemistry, University of Milano, Viale Abruzzi 42, 20131 Milano, Italy

(*Received* 29 *September* 1988; *accepted* 9 *November* 1988)

Abstract—The compounds of the formula $CuCl_2$(4-aminobenzophenone) (hereinafter L) 0.5S (S = ethanol or methanol) were synthesized and characterized by means of thermogravimetric, electronic, IR spectra and magnetic susceptibility measurements. For the ethanol derivative, the structure was determined by a single crystal X-ray diffraction analysis. It crystallizes in the monoclinic system, space group $P2_1/a$ with $Z = 4$ in a unit cell having $a = 29.903(4)$, $b = 6.202(2)$, $c = 8.195(2)$ Å, $\beta = 92.88(4)°$. The structure is polymeric and consists of infinite chains of chlorine bridged copper(II) ions along the b axis: the repeating unit is $(L—CuCl_2—EtOH—CuCl_2—L)_n$. Although the two coppers are related through crystallographic inversion centres, they have different coordination geometries owing to the statistical positioning of the ethanol molecule. One is octahedrally coordinated to three chlorines in the square plane and to the nitrogen of L, while in the apical positions are the ethanol oxygen and a fourth chlorine atom; the second has a pyramidal coordination geometry, because of the missing ethanol oxygen in one apical position. (The same structure has been deduced for the methanol derivative.) Relevant bond distances are Cu—Cl(1), 2.593(5); Cu—Cl(1)′, 2.294(4); Cu—Cl(2)″, 2.450(4); Cu—N, 2.03(1); Cu—O, 2.06(2) Å.

Benzophenone and its derivatives have considerable chemical, physical and medical interest.

Of particular relevance are their applications in the pharmaceutical industry as starting products in the synthesis of cardiovascular[1] and hypotensive[2] drugs, and as intermediates for the preparation of psychotropic[1] and analgesic drugs.[3]

In addition, benzophenone has played an important role in the development of synthetic and mech-

† Author to whom correspondence should be addressed.

anistic photochemistry, since it is a good triplet sensitizer.[4] This characteristic property can be strongly affected by structural and environmental effects. The introduction of a one electron donor group, such as NH_2, into the aromatic ring, "switches" the reactive state $n\pi^*$ to a less reactive $\pi\pi^*$, or charge-transfer (CT) state,[5] and strongly decreases the coordinative reactivity of the carbonyl group.

In order to clarify the influence of the position of the NH_2 group on the coordinative ability of the benzophenones, we have previously studied the complexes of 2-aminobenzophenone with copper(II) halides.[6] In this paper we report the preparation and structural, magnetic and spectroscopic characterization of the title compounds.

EXPERIMENTAL

4-Aminobenzophenone in hexane solution was purified by chromatography on neutral alumina. AnalaR grade anhydrous copper chloride was used.

Synthesis of $CuCl_2$(4-*aminobenzophenone*)·0.5EtOH

An absolute ethanolic solution of copper(II) chloride was added slowly under continuous stirring to an ethanolic solution of 4-aminobenzophenone with metal-to-ligand molar ratios ranging from 1 : 1 to 1 : 2. Red–orange crystals separated out after 4–5 days. (Found: C, 47.3; H, 3.9; N, 4.0. Calc. for $C_{14}H_{14}NO_{1.5}Cl_2Cu$: C, 47.3; H, 3.9; N, 3.9%.)

Synthesis of $CuCl_2$(4-*aminobenzophenone*)·0.5MeOH

This compound was prepared as described above by using methanol in place of ethanol. (Found: C, 46.5; H, 3.8; N, 4.0. Calc. for $C_{13.5}H_{13}NO_{1.5}Cl_2Cu$: C, 46.6; H, 3.7; N, 4.0%.)

Physical measurements

IR spectra in Nujol mulls in KBr pellets as support, in KBr pellets (4000–250 cm^{-1}), in Nujol mulls in polythene as support and in polythene pellets (600–100 cm^{-1}), were recorded on a Perkin–Elmer 180 spectrophotometer. The electronic spectra of the solid samples were recorded on a Shimadzu MPS 50-L spectrophotometer. Samples were prepared by grinding the compounds on filter paper as support. The thermogravimetric analysis was performed at a rate of 10°C min^{-1} with a Netzsch Sta 409 thermobalance. The room temperature magnetic moments were measured by the Gouy method using $Ni(tu)_3S_2O_3$ as the calibrant and correcting for diamagnetism using Pascal's constants.

X-ray measurements and structure determination

A transparent red, prismatic, single crystal of $0.05 \times 0.15 \times 0.20$ mm was centred on a four-circle Philips PW 1100 diffractometer. Using graphite-monochromated Mo-K_α radiation, 2569 reflections ($2\theta_{max} = 46°$) were measured which, when merged, gave 996 unique reflections with $I \geqslant 3\sigma(I)$. The intensity data were corrected for Lorentz-polarization effects and for absorption.[7]

The structure was solved using three-dimensional Patterson and Fourier techniques and refined by full-matrix least-squares. Hydrogen atoms were introduced at calculated positions and were allowed to ride on associated carbon atoms during the least-squares refinement ($d_{C-H} = 0.95$ Å and $U_{iso} = 0.06$ $Å^2$). Atomic scattering factors were taken from ref. 8. Data processing and computation were carried out by using the *SHELX 76* program package.[9]

The refinement of the $CuCl_2L$ moiety reached convergency at $R = 0.065$. At this point three residual peaks in the range 2–3 e $Å^{-3}$ were evident in the Fourier difference map. They were interpreted as a statistically distributed one-half ethanol molecule per $CuCl_2L$ unit. The introduction of the ethanol molecule in the positions indicated by the electron density residuals, with a population factor of 0.5, gave the most significant lowering of the R value: $R = 0.053$. Geometrical calculations were made by using the *PARST* program,[10] while the structure illustrations were from *PLUTO*[11] and *ORTEP*.[12]

Tables of atomic coordinates, atomic thermal vibrations and calculated structure amplitudes are available as supplementary material; atomic coordinates have also been deposited at the Cambridge Crystallographic Data Centre.

Crystal data

$C_{14}H_{14}NO_{1.5}Cl_2Cu$, $M = 354.2$, monoclinic space group $P2_1/a$, $a = 29.903(4)$, $b = 6.202(2)$, $c = 8.195(2)$ Å, $\beta = 92.88(4)°$, $U = 1517.9$ $Å^3$, $Z = 4$, $D_c = 1.55$ Mg m^{-3}, $F(000) = 720$, μ(Mo-K_α) = 17.05 cm^{-1}.

RESULTS AND DISCUSSION

The solid complexes were obtained by treating a solution of $CuCl_2$ in ethanol (or methanol) with the ligand in the same solvent. Features of thermogravimetric analysis, electronic and IR spectra of the two compounds are summarized in Table 1.

The thermogravimetric analysis shows a sharp

Table 1. Room temperature (298 K), electronic (10^{-3} cm^{-1}) and IR (cm^{-1}) results for the ligand and the complexes in the solid state. Weight loss temperature range (K) and magnetic moments are also included

	Ligand	$CuCl_2L \cdot 0.5EtOH$	$CuCl_2L \cdot 0.5MeOH$
μ_{eff}/μ_B		1.84	1.84
Weight loss temperature range		369–400	336–369
d–d band		13.70br	13.070br
CT band		22.47sbr	13.070br
ν(OH)		3460mbr	3460mbr
$\nu(NH_2)$	3420m	3298m	3320m
	3338m	3266m	3300m
	3225m	3210m	3260m
		3135m	3240m
ν(CO)	1630vs	1650vs	1645vs
$\delta(NH_2)$	1588vs	1600vs	1600vs
δ(OH)		1300s	1300s
ν(Cu—Cl)		274vs	274vs

maximum in the temperature ranges 369–400 and 336–369 K, without decomposition, for the ethanol and methanol adducts, respectively, corresponding to the complete loss of the respective alcohol.

The room-temperature solid-state electronic and IR data of the methanol and ethanol derivatives are identical, suggesting the same structure for both complexes. In particular, the unresolved broad band, centred at 13,070 cm^{-1}, can be assigned to the simultaneous presence of two different chromophores, $CuCl_4NO$ and $CuCl_4N$, which present very small absorption energy differences. The very strong and broad CT bond at 22,470 cm^{-1} can be considered as responsible for the red colour of these unusual polymeric species.

The IR spectra in the low energy region show a strong band at about 274 cm^{-1}, which is in the region typically associated with the bridging Cu—Cl stretching mode.[13]

The structure is polymeric and consists of infinite chains where the repeating unit is (L—$CuCl_2$—EtOH—L—$CuCl_2$).

The chlorine bridged copper(II) ions run parallel to the *b* axis as shown in Fig. 1. The asymmetric unit is formed by the L—$CuCl_2$(ethanol)$_{0.5}$ moiety which is presented in Fig. 2 with the atom numbering scheme used. The crystallographic inversion centres at 1/2,0,1/2 and 0,1/2,1/2, connect the two copper ions which are bridged through Cl(1) and its equivalent, while O(1) of the ethanol molecule coordinated to a metal ion, must be considered statistically distributed between the two coppers around the crystallographic inversion centres and then assigned to only one of the two in order to avoid chemically impossible contacts between the carbon atoms of the ethyl groups. The crystallographic centres at 0,0,1/2 and 1/2,1/2,1/2 connect the copper ions bridged through Cl(2) and its equivalent. The 4-aminobenzophenone ligand coordinated via the nitrogen atom completes in one case (where the ethanol oxygen is bound to the metal) an octahedral coordination geometry, and in the second case a square pyramidal coordination

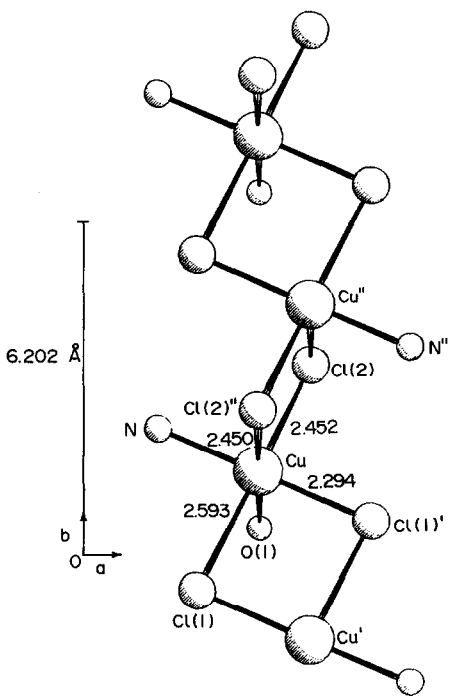

Fig. 1. View of the copper coordination polyhedrons along *b*. Neighbouring coppers are related by the crystallographic inversion centres at 1/2,0,0 (Cu···Cu' 3.434(3) Å) and 1/2,1/2,1/2 (Cu···Cu'' 3.403(3) Å). (' $1-x, -y, 1-z$ and '' $1-x, 1-y, 1-z$.)

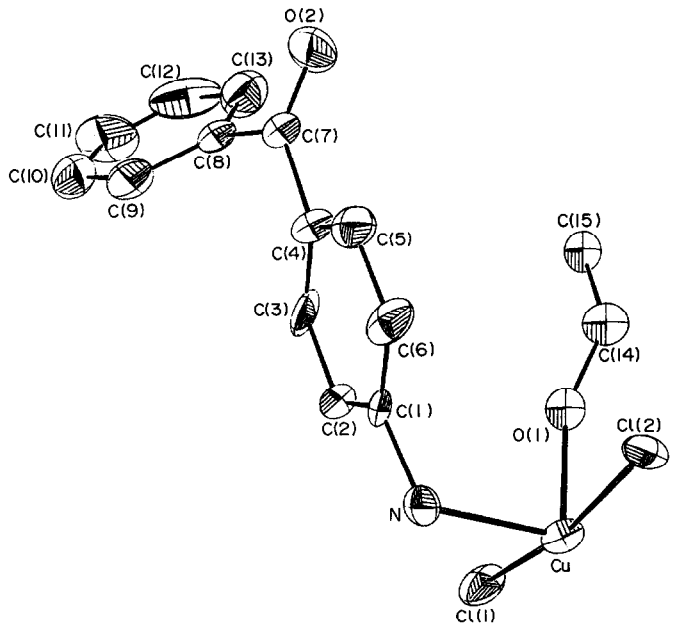

Fig. 2. The asymmetric unit, with H atoms omitted and 50% probability thermal ellipsoids.

geometry (the ethanol oxygen is missing here) as is shown in Fig. 1.

The square plane of both the octahedron and square pyramid coordination polyhedra comprise three chlorines and one nitrogen, while the ethanol oxygen and chlorine in the first polyhedron are in the apical positions and only a chlorine in the second polyhedron.

Representative bond lengths and angles are given in Table 2. The Cu—Cl bond distances, which are all bridging, range from 2.294(4) to 2.593(5) Å. In particular, the Cl(2) bridges are symmetrical, Cu—Cl(2) 2.452(6) and Cu—Cl(2)″ 2.450(4) Å, and a Cl(2)—Cu—Cl(2)″ angle of 92.1(3) and Cu—Cl(2)—Cu″ 87.9(3)°. The Cl(1) bridging distances are significantly different, Cu—Cl(1) 2.593(5) (the longest Cu—Cl distance) and Cu—Cl(1)′ 2.294(4) Å (the shortest) (Cu—Cl(1)—Cu′

Table 2. Selected bond lengths (Å) and angles (°) with ESDs in parentheses

(a) Bond lengths			
Cu—Cl(1)	2.593(5)	N—C(1)	1.45(1)
Cu—Cl(2)	2.452(6)	O(2)—C(7)	1.22(2)
Cu—O(1)	2.059(17)	C(4)—C(7)	1.51(2)
Cu—N	2.030(10)	C(7)—C(8)	1.49(2)
Cu—Cl(1)′	2.294(4)	C(14)—C(15)	1.57(4)
Cu—Cl(2)″	2.450(4)		
O(1)—C(14)	1.43(3)		
(b) Bond angles			
O(1)—Cu—N	92.2(5)	Cu—O(1)—C(14)	156(2)
Cl(2)—Cu—N	89.2(3)	N—C(1)—C(6)	120(1)
Cl(2)—Cu—O(1)	91.1(5)	N—C(1)—C(2)	118(1)
Cl(1)—Cu—N	88.4(3)	O(1)—C(14)—C(15)	140(2)
Cl(1)—Cu—O(1)	79.8(5)	O(2)—C(7)—C(4)	120(1)
Cl(1)—Cu—Cl(2)	170.4(1)	O(2)—C(7)—C(8)	121(1)
Cu—Cl(2)—Cu″	87.9(1)	C(4)—C(7)—C(8)	118(1)
Cl(2)—Cu—Cl(2)″	92.1(2)	Cu—Cl(1)—Cu′	89.1(2)
Cu—N—C(1)	117.0(8)	Cl(1)—Cu—Cl(1)′	91.0(2)

Equivalent positions: ′ $1-x, -y, 1-z$; ″ $1-x, 1-y, 1-z$.

is 89.1(2)°) are higher than the Cu—Cl(2)—Cu″ previously reported and consequently Cl(1)—Cu—Cl(1)′ 90.9(2)° is slightly smaller than the corresponding angle, Cl(2)—Cu—Cl(2)″. The two contact distances, Cu···Cu″ and Cu···Cu′ are 3.403(3) and 3.434(3) Å, being shorter when the Cu—Cl(2)—Cu″ angle is smaller. The octahedron square planes are distorted towards tetrahedral, the deviations with respect to the best mean plane calculated through N, Cl(1)′, Cl(1), Cl(2) being N −0.251(10), Cl(1)′ −0.028(4), Cl(1) 0.030(4), Cl(2) 0.038(4) Å. The copper deviates from this plane by −0.166(2) Å in the same direction as Cl(2)″, which is −2.613(4) Å away from the plane (O(1) is 1.88(2) Å distant in the opposite direction). The two *trans*-Cl(1) and -Cl(2) atoms form an angle Cl(1)—Cu—Cl(2) of 170.4(1)° and the bending is in the direction of the ethanol oxygen opposite to the Cl(2)″ position. The shorter Cu—Cl(1) bridging distance of 2.294(4) Å is *trans* to nitrogen and is close to the values of 2.270(3) and 2.318(3) Å for non-bridging distances in the di-μ-chloro-dodecachlorotricuprate(II) anion[14] and to the values of 2.297(1) and 2.278(1) Å for non-bridging chlorine in bis(2-aminobenzophenone)dichlorocopper(II);[6] while the other values for Cu—Cl bond distances which range from 2.450(4) to 2.593(5) Å are in agreement with the values normally found for chlorine bridges.[15] The Cu—N bond distance of 2.03(1) Å has a value comparable to that found for Cu—N(1) (2.028(3) Å) and Cu—N(2) (2.020(4) Å) in the bis(2-aminobenzophenone)dichlorocopper(II) complex[6] (where the two 2-aminobenzophenone ligands are, respectively, monodentate via N(1) and bidentate via N(2) and O(2) to the copper ion), and to the value of 1.984(4) Å in copper(2-aminobenzophenone)$_2$$(BF_4)_2$ where the two neutral ligands are both bidentate through nitrogen and oxygen donor atoms[16] and to the value of 1.992(5) Å in bis(4-chloro-1,2-benzoquinone-2-oximato)(methanol)copper(II).[17] The Cu—O(ethanol) bond distance of 2.059(17) Å is somewhat shorter when compared, for example, to the Cu—O(methanol) distance of 2.274(4) Å found in the previously quoted compound, or to the Cu—O distances in a series of N,N-bis(benzimidazol-2-ylmethyl) amine copper derivatives[18] which range from 2.266(6) to 2.461(6) Å. This is indicative of a relatively strong interaction between copper(II) and ethanol. The 4-aminobenzophenone ligand (see Fig. 2) has the two benzene rings rotated with respect to each other by 112.1(4)°, while the dihedral angles between the phenyls and the plane through C(7), C(8), O(2), C(4) are 19.9(5)° (for the 4-aminobenzene ring) and 125.8(5)° for the second phenyl. The two benzene rings ($C_1 \rightarrow C_6$) and ($C_8 \rightarrow C_{13}$) are rotated by 63.6(3) and 62.2(3)°, respectively, with respect to the copper coordination plane. The bond distances and angles in the ligand are generally close to those reported for the free 4,4′-diaminobenzophenone,[19] with the exception of the C(1)—N bond length which is, in the present case (1.45(1) Å), longer with respect to the value of 1.370(3) Å in the free ligand, due to the metal coordination. The twisted conformation of the ligand is maintained, but with different torsion of the two phenyls with respect to the previously quoted plane containing the C=O bond (24 and 33° in 4,4′-diaminobenzophenone).

There is a short intermolecular contact between N(1) and O(2)‴ at $x, y, 1+z$, N(1)···O(2)‴ 2.91(1) Å, N(1)—H(18)···O(2)‴ 1.96(1) Å, and the angle N(1)—H(18)···O(2)‴ is 174(1) °; the short distance between the NH_2 hydrogen and the ketonic oxygen is comparable to the value of 1.99 Å found in bis(2-aminobenzophenone)dichlorocopper(II)[6] for the intramolecular contact, ketonic oxygen–amine hydrogen. This contact, which can be considered as a hydrogen bond, connects the polymeric chains in the direction of the *c* axis, giving rise to a layer polymer as shown in Fig. 3.

In conclusion, we note that with respect to the 2-

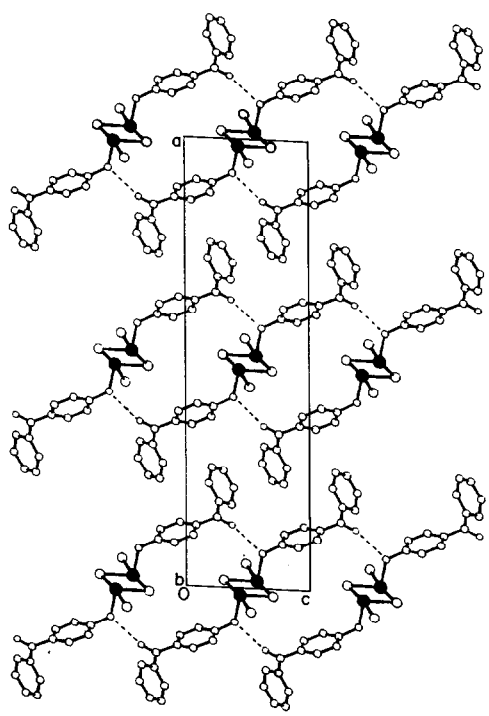

Fig. 3. Crystal packing down *b*, the polymeric columns are connected via hydrogen bonds between the carboxylic oxygen and one adjacent amino proton (one column is shown in Fig. 1), black circles are copper atoms.

aminobenzophenone ligand, the *para* position of the amino group is unfavourable for bidentate behaviour of the ligand itself. The amino coordination is preferred to the carbonyl coordination, and the possibility of polymeric chains being formed by the coordination of both the possible donor atoms (oxygen and nitrogen) on different copper ions, is overcome by the better donor ability of the chlorines which realize the polymeric structure just described.

The loss of the alcohol molecule in the sixth coordinative position of the copper inner sphere does not involve molecular rearrangements. In fact, the new coordination sphere around copper is the stable, square planar pyramidal geometry shown by the $CuCl_4N$ chromophore.

The stability of this type of environment can activate coordinative reactions at the sixth apical position, but it is rather rare that this is found only for one half of the copper ions, taking account also of the relatively strong Cu—O(ethanol) bond, probably because the driving force of the crystal packing is the formation of polymeric structures through the chlorine bridges. Indeed, copper halides with the simultaneous presence of octahedral six-coordinated and square pyramidal pentacoordinated species are known in the literature.[14]

REFERENCES

1. U. A. Wittcoff and B. G. Reuben, *Industrial Organic Chemical in Perspective*, Part two: Technology, formulation and use. John Wiley, New York (1981).
2. D. M. Wankankar and B. D. Hosangadi, *Ind. J. Chem.* 1980, **19B**, 703 and refs therein.
3. D. A. Walsh, I. R. Shanklin Jr and D. A. Shamblee, *Ger. Offen.* 3035,688 (CL C 07C103/28); *Chem. Abstr.* 1981, **95**, 42702x.
4. A. A. Lamola and N. J. Turro, *Techniques of Organic Chemistry* (Edited by P. A. Leermakas and A. Wessberg), Vol. XIV. Interscience, New York (1969).
5. G. Favaro and F. Masetti, *J. Photochem.* 1981, **15**, 241 and refs therein.
6. I. M. Vezzosi and L. Antolini, *Inorg. Chim. Acta* 1984, **85**, 155.
7. A. C. T. North, D. C. Phillips and F. Mathews, *Acta Cryst.* 1968, **A24**, 351.
8. *International Tables for X-Ray Crystallography*, 2nd edn, Vol. 4, p. 101. Kynoch Press, Birmingham (1974).
9. G. M. Sheldrick, *SHELX 76*. University of Cambridge, U.K. (1976).
10. M. Nardelli, *Comput. Chem.* 1983, **7**, 95.
11. W. D. S. Motherwell and W. Clegg, *PLUTO 78. A program for plotting and crystal structures*. University of Cambridge, U.K. (1978).
12. C. K. Johnson, *ORTEP Report ORNL–5138*, Oak Ridge National Laboratory, Oak Ridge, Tennessee (1976).
13. R. L. Harlow, J. Welles, G. W. Watt and S. H. Simonsen, *Inorg. Chem.* 1974, **13**, 2860.
14. L. Antolini, G. Marcotrigiano, L. Menabue and G. C. Pellacani, *J. Am. Chem. Soc.* 1980, **102**, 5506.
15. L. Antolini, G. Marcotrigiano, L. Menabue and G. C. Pellacani, *J. Am. Chem. Soc.* 1980, **102**, 1303.
16. I. M. Vezzosi, F. A. Zanoli, L. P. Battaglia and A. Bonamartini Corradi, *Inorg. Chim. Acta* 1985, **105**, 13.
17. C. Bisi Castellani, O. Carugo and A. Coda, *Acta Cryst.* 1988, **C44**, 267.
18. Y. Nishida and K. Takahashi, *J. Chem. Soc., Dalton Trans.* 1988, 691.
19. G. P. M. Van Der Velden and J. H. Noordik, *J. Cryst. Molec. Struct.* 1980, **10**, 83.

Polyhedron Vol. 8, No. 7, pp. 997–998, 1989
Printed in Great Britain

0277–5387/89 $3.00+.00
© 1989 Pergamon Press plc

COMMUNICATION

THE PREPARATION AND X-RAY STRUCTURE OF $PtCl_2(S_4N_4)(PMe_2Ph)$, AN OCTAHEDRAL COMPLEX CONTAINING A MERIDIONAL TRIDENTATE $S_4N_4^{2-}$ LIGAND

MICHAEL B. HURSTHOUSE and MAJID MOTEVALLI

Department of Chemistry, Queen Mary College, Mile End Road, London E1 4NS, U.K.

and

PAUL F. KELLY and J. DEREK WOOLLINS*

Department of Chemistry, Imperial College of Science and Technology, South Kensington, London SW7 2AY, U.K.

(*Received* 12 *December* 1988; *accepted* 11 *January* 1989)

Abstract—Reaction of $[PtCl_2(PMe_2Ph)]_2$ (**1**) with S_4N_4 in CH_2Cl_2 leads to the platinum(IV) complex $PtCl_2(S_4N_4)(PMe_2Ph)$ (**2**), which contains the tridentate meridional $S_4N_4^{2-}$ ligand coordinating via two sulphurs and one nitrogen atom.

As part of a continuing study into metalla–sulphur–nitrogen chemistry, we have recently reported[1–3] on the preparation of complexes of $S_2N_2^{2-}/S_2N_2H^-$ and S_3N^-, starting from platinum–phosphine complexes of the type *cis*-$[PtCl_2(PR_3)]_2$. The variety of these reactions indicates the versatility of the latter complexes as starting materials. However, despite their ability to react with a range of reagents, such as $Na(S_3N_3)$, $[Me_2Sn(S_2N_2)]_2$ etc., they are inert towards S_4N_4 at room temperature. In contrast, we have found that dimeric complexes of the type $[PtCl_2(PR_3)]_2$ readily react with S_4N_4 to give a variety of species, the precise nature of which depends upon both the stoichiometry of the reaction and the nature of the phosphine group. Here we report on the reaction of $[PtCl_2(PMe_2Ph)]_2$ (**1**) with S_4N_4, in the molar ratio 1 : 2, which yields the platinum(IV) complex, $PtCl_2(S_4N_4)(PMe_2Ph)$ (**2**). This is only the second example of a complex containing the $S_4N_4^{2-}$ ligand, which in this case adopts a unique coordination geometry as established by X-ray crystallography.

In a typical reaction, a solution of **1** (0.12 mmol) in CH_2Cl_2 (20 cm^3) was slowly added to a solution of S_4N_4 (0.25 mmol) in CH_2Cl_2 (15 cm^3) with stirring. After 15 min the volume of the CH_2Cl_2 was reduced to 10 cm^3 and the red solution was passed down a bio-bead gel-permeation column. Elution with CH_2Cl_2 revealed an intense dark red band between two paler bands; this was collected and the volume reduced to 5 cm^3 *in vacuo*. Addition of hexane (60 cm^3) yielded a dark red solid which was filtered from the pale yellow solution and dried. Crystals suitable for X-ray crystallography were obtained by slow hexane diffusion into a CH_2Cl_2 solution.† Found: C, 16.5; H, 2.1; N, 9.1. Calc. for

* Author to whom correspondence should be addressed.

† *Crystal data.* $C_8H_{11}N_4Cl_2S_4PPt$, monoclinic, a = 13.170(4), b = 11.616(3), c = 10.924(2) Å, β = 91.15(2)°, U = 1670.8 Å^3, space group $P2_1/n$, Z = 4, M = 517.5, D_c = 2.05 g cm^{-3}. Data were measured on a Nonius CAD4 diffractometer with graphite monochromated Mo-K_α radiation (λ = 0.71069 Å) using 2θ scans. The structure was solved by the heavy atom method and refined anisotropically using absorption corrected data to give R = 0.052, R_w = 0.050, for 2064 independent observed reflections [$|F_o| > 3\sigma(|F_o|)$, $1.5 < \theta \leqslant 25°$]. The atomic coordinates are available on request from the Director of the Cambridge Crystallographic Data Centre, University Chemical Laboratory, Lensfield Rd, Cambridge CB2 1EW. Any request should be accompanied by a full literature citation for this communication.

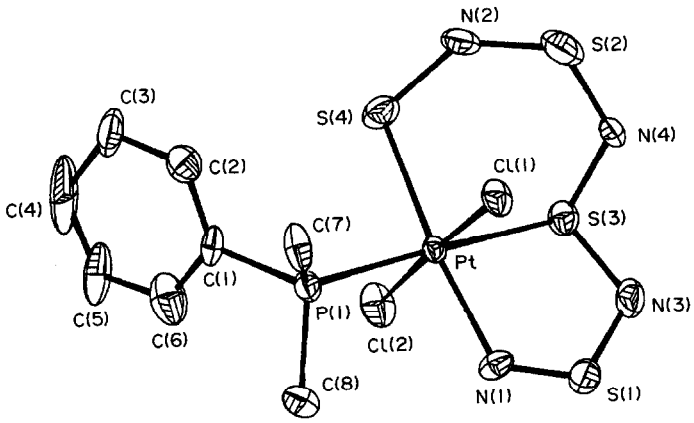

Fig. 1. The X-ray crystal structure of $PtCl_2(S_4N_4)(PMe_2Ph)$ (**2**). Important bond distances and angles: N(1)—S(1) 1.461(15), S(1)—N(3) 1.598(18), N(3)—S(3) 1.674(19), S(3)—N(4) 1.664(17), N(4)—S(2) 1.553(18), S(2)—N(2) 1.565(18), N(2)—S(4) 1.664(17), Pt—N(1) 2.105(15), Pt—S(4) 2.335(7), Pt—S(3) 2.394(6), Pt—Cl(1) 2.319(6), Pt—Cl(2) 2.324(6), Pt—P 2.345(6) Å; Pt—S(4)—N(2) 108.7(7), S(4)—N(2)—S(2) 133.9(10), N(2)—S(2)—N(4) 123.2(9), S(2)—N(4)—S(3) 121.8(11), N(4)—S(3)—N(3) 101.2(9), S(3)—N(3)—S(1) 114.9(10), N(3)—S(1)—N(1) 119.6(9), S(1)—N(1)—Pt 115.9(9), N(1)—Pt—S(4) 174.6(4), N(4)—S(3)—Pt 108.1(7), N(3)—S(3)—Pt 102.8(7), S(3)—Pt—S(4) 90.1(3), N(1)—Pt—S(3) 85.0(5)°.

$[PtCl_2S_4N_4\{P(CH_3)_2(C_6H_5)\}]$: C, 16.3; H, 1.9; N, 9.5%. ^{31}P NMR; singlet δ 5.0, $^1J(^{195}Pt-^{31}P)$ 2170 Hz.

The $^1J(^{195}Pt-^{31}P)$ coupling constant in the ^{31}P NMR spectrum of **2** is typical of compounds of platinum(IV), and this conclusion is confirmed by the X-ray structure of the compound (Fig. 1) which reveals an octahedral geometry, with the $S_4N_4^{2-}$ ligand coordinating through two sulphurs and one nitrogen in a meridional fashion. The ligand can be regarded as fused S_2N_2 and S_3N_2 groups. Comparison with the structure of $IrCl(CO)(S_4N_4)(PPh_3)$ (**3**), which can be prepared[4] by reacting $IrCl(CO)(PPh_3)_2$ with S_4N_4 and is the only previously reported complex of this ligand, reveals that although in both cases the ligand is coordinated through the same atoms, there is an important difference in the geometry of the ligand. Whereas in **3** the S_4N_4 undergoes relatively little reorganization upon coordination, in **2** a much more open geometry is adopted. The ligand in **2** deviates significantly from planarity and can be considered to comprise of one chelating S_2N_2 group forming a PtS_2N_2 metallacycle (as in $Pt(S_2N_2)(PMe_3)_2$)[2] fused at the Pt—S bond with a PtS_3N_2 metallacycle. The two rings are not coplanar but result in an overall *mer*-coordination, indicating that the $S_4N_4^{2-}$ ligand is potentially stable in a variety of conformations.

We have yet to establish a mechanism for the reaction of **1** with S_4N_4. However, it is interesting to note that under identical conditions the analogous palladium complex, $[PdCl_2(PMe_2Ph)]_2$, is inert to S_4N_4. It is possible that the first stage of the reaction involves oxidative addition of the S_4N_4 across an S—N bond, followed by cleavage of the chloro bridge by a second sulphur atom.

Acknowledgement—We are grateful to Johnson Matthey for loans of K_2PtCl_4.

REFERENCES

1. R. Jones, P. F. Kelly, C. P. Warrens, D. J. Williams and J. D. Woollins, *J. Chem. Soc., Chem. Commun.* 1986, 711.
2. P. A. Bates, M. B. Hursthouse, P. F. Kelly and J. D. Woollins, *J. Chem. Soc., Dalton Trans.* 1986, 2367.
3. R. Jones, C. P. Warrens, D. J. Williams and J. D. Woollins, *J. Chem. Soc., Dalton Trans* 1987, 907.
4. F. Edelmann, H. W. Roesky, C. Spang, M. Noltemeyer and G. M. Sheldrick, *Angew. Chem. Int. Ed. Engl.* 1986, 931.

Polyhedron Vol. 8, No. 7, p. 999, 1989
Pergamon Press plc. Printed in Great Britain

CORRIGENDA

Transition metal complexes with the thiosemicarbazide-based ligands—V. Synthesis, crystal and molecular structure, and spectra of S-methyl-N(1)-salicylidene-N(4)-α-methoxypicolyl-isothiosemicarbazidonickel(II). V. M. Leovac, V. I. Češljević and N. Galešić (*Polyhedron* Vol. 7, No. 24, pp. 2641–2647, 1988).

(i) On p. 2643 of this paper, in the second complete paragraph, the first sentence should be: "Full-matrix least-squares refinement on F was performed for 2060 reflections with $I>3\sigma(I)$ varying separately and successively coordinates of non-H atoms, their anisotropic temperature factors and coordinates of H atoms (73, 145 and 49 parameters refined, respectively)."; i.e. the originally printed "successive" should read "successively" and "were determined" should be deleted.
(ii) On p. 2645, in the third paragraph of the *Description of the structure,* the third sentence should be: "The N(4)—C(4) bond length of 1.443(7) Å involving the C(sp^3) picoline atom is slightly shortened"; i.e. the originally printed "also greatly" should read "slightly".

Polyhedron Vol. 8, No. 8, pp. 1001–1005, 1989
Printed in Great Britain

0277–5387/89 $3.00+.00
© 1989 Pergamon Press plc

SYNTHESIS AND X-RAY CRYSTAL STRUCTURE OF A NOVEL CERIUM(IV) ARYLSILOXIDE

P. S. GRADEFF* and K. YUNLU

Rhône-Poulenc Inc., CN 5266, Princeton, NJ 08543, U.S.A.

and

A. GLEIZES* and J. GALY

Laboratoire de Chimie de Coordination du CNRS, Unité n° 8241, 205 route de Narbonne, 31077 Toulouse cédex, France

(*Received* 20 *June* 1988; *accepted* 11 *October* 1988)

Abstract—$Ce(OSiPh_3)_4 \cdot x$DME ($0.5 < x < 1$) was prepared from $Ce(OPr^i)_4$ by exchange reaction with Ph_3SiOH in dimethoxyethane (DME). Crystallization from a toluene–ether mixture yielded monocrystals of $Ce(DME)(OSiPh_3)_4 \cdot C_6H_5CH_3$, the crystal structure of which was determined by X-ray single-crystal techniques. It crystallizes in the monoclinic system, sp.gr. = $P2_1/c$, $a = 28.078(6)$ Å, $b = 14.628(2)$ Å, $c = 18.739(5)$ Å, $\beta = 92.24(2)°$, $V = 7.691$ Å^3, $Z = 4$, $R = 0.074$ for 4406 observations with $I > 3\sigma(I)$ and 319 variables. The Ce^{IV} ion exhibits a (4+2) coordination by oxygen atoms with four short metal–silyloxy bonds ($2 \times 2.10(1)$ Å; $2 \times 2.13(1)$ Å) and two long metal–DME bonds (2.58(1) Å; 2.59(1) Å).

Compounds of the type $M(OSiR_3)_n$, where $n = 3$ or 4, have been prepared first for Ti.[1] A more comprehensive study was made by Bradley and Thomas related to Ti, Zr, Nb and Ta.[2] The silyloxides of Gd and Er were reported in 1970[3] and they seem to be the only examples with the lanthanides.

The outcome of organic reactions involving tetravalent cerium being difficult to predict, we have undertaken a broad range study that began with the development of a simplified method for the synthesis of ceric alkoxides from ceric ammonium nitrate[4] and centred recently on the Ce^{IV} alkanoatoamine derivatives[5] and ceric silyloxides.

Among several Ce—O—Si bond compounds prepared in our Laboratory,[6] the tetrakis(triphenylsiloxy)cerium gave a good monocrystal suitable for crystal X-ray examination. We wish to report here on the synthesis and structural characterization of this product.

* Authors to whom correspondence should be addressed.

EXPERIMENTAL

Reagents and physical measurements

All manipulations were carried out under the exclusion of oxygen and moisture either in a N_2-filled, recirculating glove box or by the usual Schlenk technique using argon as an inert gas. The anhydrous solvents, dimethoxyethane (DME) and diethylether were purchased from Aldrich and were used without further purification. Ph_3SiOH was purchased from Petrarch Systems and was used without further purification. Ceric isopropoxide was prepared according to the published method.[4] ^1H, ^{13}C and ^{29}Si NMR spectra were recorded on a JEOL FX 90Q FT NMR spectrometer and the IR spectrum on a Perkin–Elmer 567 Grating IR spectrophotometer.

Preparation of $Ce(OSiPh_3)_4 \cdot x$DME (1)

Ceric isopropoxide (16 g, 42.5 mmol) was dissolved in 50 cm^3 of DME. Under stirring, 46.97 g

of triphenylsilanol (169 mmol) in 50 cm^3 DME was added slowly via a syringe. A white precipitate appeared after 10 s and stirring was continued during the next 15 min. The precipitate was filtered and washed with two portions of 50 cm^3 diethylether. After drying for 1 h *in vacuo* at 30°C, 50 g of a fine, white powder was obtained. It appears that depending on the extent of drying the amount of the coordinated DME varies from 0.5 to 1 mol. Found: C, 69.2; H, 4.7; Si, 9.1; Ce, 11.2. Calc. for $Ce(OSiPh_3)_4 \cdot 0.5DME$: C, 69.1; H, 5.0; Si, 8.7; Ce, 10.9. ^1H NMR ($CHCl_3$-d): 2.9 (s, CH_3); 3.0 (s, CH_2CH_2); 6.9; 7.0; 7.1; 7.86; 7.87 (phenyl). ^{13}C NMR ($CHCl_3$-d): 60.24 (—CH_3); 71.83 (—CH_2CH_2); 127.41; 128.83; 135.27; 138.47 (phenyl). ^{29}Si NMR (C_6H_6-d_6/THF: 1/2) 24.14 (s). IR (KBr, cm^{-1}): 3030 (w, —C—H, ring); 2950 (w, —C—H, DME); 1420 (m, Si—Ph); 1251 (m, C—O); 1090 (vs, C—O); 1010 (s, Si—Ph); 880 (vs, Ce—O—Si); 692 and 505 (s, C—H, ring).

Preparation of single crystals and X-ray structure analysis

Single crystals suitable for X-ray structure analysis were grown by dissolving 4 g of $Ce(OSiPh_3)_4$ (**1**) in a mixture of 60 cm^3 toluene and 25 cm^3 ether, and storing the solution for 24 h at −12°C, after which time, shiny, hexagonal-shaped crystals had been formed. After filtration via a Schlenk frit, the crystals were dried carefully by passing argon through the frit for *ca* 10 min.

A single crystal was sealed under dry nitrogen in a Lindeman-glass capillary and mounted on an Enraf-Nonius CAD4 computer-controlled four-circle diffractometer, using graphite-monochromatized Cu-K_α-radiation. Accurate unit-cell constants were derived from the setting angles of 25 reflections (Table 1). The intensity data were collected at room temperature up to a maximum Bragg angle $\theta = 53°$ (Table 1). The space group $P2_1/c$ was uniquely determined from the relevant systematic absences. The crystal was automatically reoriented each time the agreement factor between caculated and measured indices was larger than 0.12. The data were corrected for the corresponding periodic variations in intensity of about 5%, and for Lorentz and polarization effects. At the end of the data collection, the faces of the crystal were no longer smooth but covered with imbricated white shiny microcrystals.

The structure was solved by Patterson synthesis followed by alternating cycles of least-squares refinements and electron density calculations by means of Fourier and difference-Fourier synthesis, using the SHELX-76, SDP and ORTEP chains of programs.[7] The atomic scattering factors were taken from the usual tabulation,[8] and the effects of anomalous scattering were taken into account by using Cromer and Ibers' values of $\Delta f'$ and $\Delta f''$.[9] Throughout the refinements, the function minimized was $\Sigma w(F_o - |F_c|)/\Sigma F_o$, where F_o and $|F_c|$ are the observed and calculated structure factor amplitudes and w the weight. The phenyl groups were

Table 1. Crystallographic data for $Ce(DME)(OSiPh_3)_4 \cdot C_6H_5CH_3$

Physical and crystal data

Formula: $CeSi_4O_6C_{83}H_{78}$	Mol. wt. = 1424.01
Crystal system: monoclinic	$V = 7.691$ Å^3
Space group: $P2_1/c$	$Z = 4$
$a = 28.078(6)$ Å	ρ_{exp} was not measured
$b = 14.628(2)$ Å	$\rho_x = 1.230$ g cm^{-3}
$c = 18.739(5)$ Å	$\mu_{Cu\text{-}K_\alpha} = 56.7$ cm^{-1}
$\beta = 92.24(2)°$	Morphology: trapezoid plaquette (0.62 × 0.38 × 0.14) mm
	Transmission range: 0.19–0.48

Data collection

Temperature: 298 K	Radiation: λ(Cu-K_α) = 1.5418 Å
Crystal-detector: 208 mm	Detector window: height = 4 mm; width = 4 mm
Take-off angle = 5.5°	Scan mode: θ–2θ
Max. Bragg angle: $\theta = 53°$	Scan angle: $\Delta\theta = \Delta\theta_0 + B \tan\theta$, $\Delta\theta_o$[a] = 1.10; B[a] = 0.15

Scan speed parameters: SIGPRE[a] = 0.75; SIGMA[a] = 0.018; VPRE[a] = 10° min^{-1}; TMAX[a] = 60 s
Standard intensity reflections: 3 3 −1, 1 3 0, 1 0 2 measured every 3600 s
Standard orientation reflections; 2 12 0, 19 0 0, 0 0 12 checked every 100 reflections
Independent recorded reflections: 8944

[a] These parameters have been described in: A. Mosset, J. J. Bonnet and J. Galy, *Acta Crystallogr.* 1977, **B33**, 2633.

treated as rigid groups (C—C = 1.395 Å) with individual isotropic thermal parameters.

It rapidly appeared that besides four $OSi(C_6H_5)_3^-$ ligands, one DME molecule was coordinated to the cerium atom. Refining the non-H atoms using anisotropic thermal parameters for the Ce atom only and unit weights yielded a conventional agreement factor $R = 0.116$. After numerical absorption corrections were applied using a grid size of $4 \times 10 \times 18$, the R factor lowered to 0.094. At this stage of refinement, the difference-Fourier map showed two independent benzene rings which were attributed to solvent toluene molecules. Since they were lying at close proximity to inversion centres, they were given 50% occupancy factors. They were refined as rigid groups with free individual temperature parameters. Only one of the two corresponding methyl groups could be identified. Each H atom except for the "amputated" toluene molecule was located and introduced as a fixed contributor with an idealized position (C—H = 0.97 Å) and a thermal parameter equal to that of the atom to which it is attached. The methyl groups of both the toluene and DME molecules were treated as rigid bodies. The last cycles of refinement were run with anisotropic thermal parameters for all non-H and non-phenyl atoms. The unit weights were replaced by a non-Poisson contribution weighting scheme with a p factor of 0.01. In the final cycle of refinement, the largest (variable shift)/(esd) ratio was 0.26 for the atoms of the Ce $(DME)(OSiPh_3)_4$ molecule, and 0.90 for the atoms of the solvent molecules; the reliability factors stabilized at $R = 0.074$, $R_w = 0.082$, and the error in an observation of unit weight was $s = 1.02$ electron, for 4406 observations with $I > 3\sigma(I)$ and 319 variables. The final difference-Fourier map showed no significant peak. Final atomic positional and thermal parameters and lists of F_o/F_c values have been deposited as supplementary material with the Editor from whom copies are available on request.

SYNTHESIS AND PROPERTIES OF $Ce(OSiPh_3)_4$

Although ceric alkoxides were prepared by Bradley *et al.* as early as 1957,[2] the exchange reaction with silanols does not seem to have been carried out. Reaction of ceric isopropoxide with 4 moles of triphenylsilanol in DME resulted in the formation of a white, air stable powder:

$$Ce(OPr^i)_4 + 4Ph_3SiOH \longrightarrow Ce(OSiPh_3)_4 + 4i\text{-PrOH}. \quad (1)$$

NMR results and elemental analysis are in agreement with the expected formula for **1**. The product appears to be air stable and resistant towards hydrolysis. Reaction with acetylacetone forms immediately, dark red cerium(IV) acetylacetonate complex. The product is soluble in THF, $CHCl_3$ or toluene and not soluble in hydrocarbons. In close analogy to the corresponding Ti-complex, $Ti(OSiPh_3)_4$ (**1**), is heat resistant with a melting temperature of 330°C.

As shown by elemental analysis and NMR and IR spectroscopy, **1** contains variable amounts of DME which was used as solvent. Depending on the drying conditions the (DME)/Ce molar ratio varies between 0.5–1. The single crystals of **1** obtained from a mixture of 60 cm^3 toluene and 25 cm^3 ether, revealed to have the formula $Ce(DME)(OSiPh_3)_4 \cdot C_6H_5CH_3$ from the X-ray structure determination.

CRYSTAL AND MOLECULAR STRUCTURE OF $Ce(DME)(OSiPh_3)_4 \cdot C_6H_5CH_3$

The unit-cell has a volume of 7691 $Å^3$ and contains four $Ce(DME)(OSiPh_3)_4$ molecules located at about (1/4, 0, 3/8), (3/4, 0, 5/8), (1/4, 1/2, 7/8), (3/4, 1/2, 1/8) and four toluene molecules (t1 and t2) statistically distributed around the inversion centres at (0, 0, 0), (0, 1/2, 1/2), (1/2, 0, 0), (1/2, 1/2, 1/2) with 50% site occupancies. A stereoscopic view of the cell content is given in Fig. 1. A simplified view of the $Ce(DME)(OSiPh_3)_4$ molecule emphasizing the coordination geometry of the Ce^{IV} ion and showing the atom numbering scheme is shown in Fig. 2. The main bond lengths and angles are presented in Table 2. All the phenyl bond lengths and angles are equal to 1.395 Å and 120°, respectively, according to the rigid body mode of refinement.

The Ce^{IV} ion is bound to four triphenylsiloxy groups with oxygen atoms O1, O2, O3, O4 at distances ranging from 2.10(1) to 2.13(1) Å, and two chelating DME oxygen atoms (O5, O6) about 0.5 Å further: 2.58(1) and 2.59(1) Å. Muetterties' pairing dihedral angle criterion[10] did not allow to locate this six-fold coordination symmetry somewhere between octahedral and trigonal prismatic, even by using the modified version by Kouba and Wreford[11] to take into account large discrepancies in metal-to-ligand distances. The coordination would rather be considered as a (4+2) environment derived from a tetrahedral geometry. The part of environment reminiscent of a tetrahedron comprises the four siloxy oxygen atoms (O1 → O4). They are equidistant from the Ce atom within experimental error and define two perpendicular planes with the Ce atom: CeO1O3 and

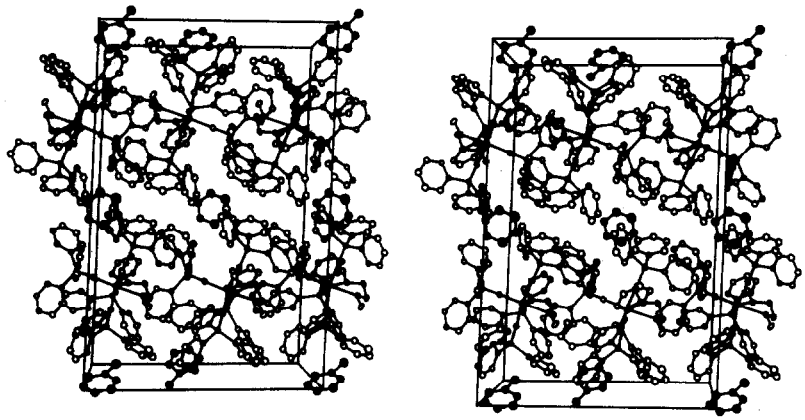

Fig. 1. Stereoscopic ORTEP view down the *b* axis (*a* is vertical) of the molecular packing of $Ce(DME)(OSiPh_3)_4 \cdot C_6H_5CH_3$. The origin of the represented unit-cell was translated by (0, −1/4, 0) with respect to the conventional one. Solvent toluene molecules t1 and t2 are blackened. Only one set of the positions they are statistically distributed on is represented. The methyl group was not located for t2. Atoms are drawn with their 10% probability thermal ellipsoids.

Table 2. Main bond lengths (Å) and angles (deg.) in $Ce(DME)(OSiPh_3)_4$

Around Ce					
Ce—O(1)	2.098(10)	O(1)—Ce—O(2)	95.3(4)	O(1)—Ce—O(5)	162.5(4)
Ce—O(2)	2.133(10)	O(1)—Ce—O(3)	107.7(4)	O(1)—Ce—O(6)	98.0(4)
Ce—O(3)	2.100(11)	O(1)—Ce—O(4)	95.1(4)	O(2)—Ce—O(5)	84.1(4)
Ce—O(4)	2.128(10)	O(2)—Ce—O(3)	96.7(4)	O(2)—Ce—O(6)	80.2(4)
		O(2)—Ce—O(4)	160.5(4)	O(3)—Ce—O(5)	89.8(3)
		O(3)—Ce—O(4)	95.7(4)	O(3)—Ce—O(6)	154.3(4)
Ce—O(5)	2.575(10)			O(4)—Ce—O(5)	81.0(4)
Ce—O(6)	2.587(10)	O(5)—Ce—O(6)	64.6(3)	O(4)—Ce—O(6)	82.1(4)
Triphenylsiloxanolate ligand					
Si(1)—O(1)	1.618(11)	Ce—O(1)—Si(1)	173.0(7)	O(3)—Si(3)—C(1a3)	110.1(5)
Si(2)—O(2)	1.607(11)	Ce—O(2)—Si(2)	178.6(7)	O(3)—Si(3)—C(1b3)	111.8(5)
Si(3)—O(3)	1.624(11)	Ce—O(3)—Si(3)	170.1(6)	O(3)—Si(3)—C(1c3)	110.1(5)
Si(4)—O(4)	1.611(11)	Ce—O(4)—Si(4)	175.7(7)	C(1a3)—Si(3)—C(1b3)	107.4(5)
Si(1)—C(1a1)[a]	1.874(13)	O(1)—Si(1)—C(1a1)	108.3(6)	C(1a3)—Si(3)—C(1c3)	108.6(6)
Si(1)—C(1b1)	1.866(13)	O(1)—Si(1)—C(1b1)	111.6(6)	C(1b3)—Si(3)—C(1c3)	108.8(5)
Si(1)—C(1c1)	1.894(11)	O(1)—Si(1)—C(1c1)	108.7(5)	O(4)—Si(4)—C(1a4)	109.6(6)
Si(2)—C(1a2)	1.905(13)	C(1a1)—Si(1)—C(1b1)	107.4(5)	O(4)—Si(4)—C(1b4)	109.7(6)
Si(2)—C(1b2)	1.881(15)	C(1a1)—Si(1)—C(1c1)	111.2(5)	O(4)—Si(4)—C(1c4)	109.7(6)
Si(2)—C(1c2)	1.887(12)	C(1b1)—Si(1)—C(1c1)	109.6(5)	C(1a4)—Si(4)—C(1b4)	108.2(6)
Si(3)—C(1a3)	1.867(15)	O(2)—Si(2)—C(1a2)	112.5(6)	C(1a4)—Si(4)—C(1c4)	110.3(5)
Si(3)—C(1b3)	1.858(11)	O(2)—Si(2)—C(1b2)	109.8(6)	C(1b4)—Si(4)—C(1c4)	109.3(5)
Si(3)—C(1c3)	1.892(13)	O(2)—Si(2)—C(1c2)	107.7(5)		
Si(4)—C(1a4)	1.895(13)	C(1a2)—Si(2)—C(1b2)	109.0(6)		
Si(4)—C(1b4)	1.903(16)	C(1a2)—Si(2)—C(1c2)	106.3(5)		
Si(4)—C(1c4)	1.889(13)	C(1b2)—Si(2)—C(1c2)	111.5(5)		
DME ligand					
O(5)—C(51)	1.464(20)	Ce—O(5)—C(51)	116.7(9)	C(61)—O(6)—C(62)	114.0(13)
O(5)—C(52)	1.407(23)	Ce—O(5)—C(52)	120.9(10)	O(5)—C(51)—C(61)	105.1(14)
O(6)—C(61)	1.444(20)	C(51)—O(5)—C(52)	109.6(13)	O(6)—C(61)—C(51)	110.1(14)
O(6)—C(62)	1.429(21)	Ce—O(6)—C(61)	113.9(9)		
C(51)—C(61)	1.501(26)	Ce—O(6)—C(2)	122.6(9)		

[a] C(1aj), C(1bj), C(1cj) are the three phenyl C atoms attached to atom Si(j).

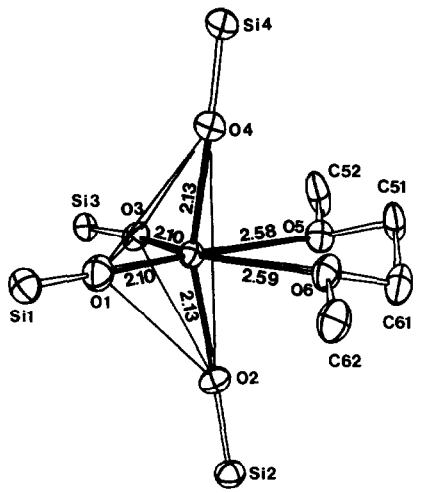

Fig. 2. The (4+2) coordination geometry of cerium(IV) in $Ce(DME)(OSiPh_3)_4$. For the sake of clarity the phenyl groups were not drawn. 20% Probability thermal ellipsoids are shown.

CeO2O4 make an angle of 89.8(4)°. All the relevant six O—Ce—O angles, which would equal 109.5° in an ideal tetrahedron, are indeed markedly larger than 90°: as a result of the intervention of the O5, O6 DME bite which occurs between atoms O2 and O4, right in the plane defined by atoms Ce, O1, O3 (the angle between planes CeO1O3 and CeO5O6 is 2°), the O2—Ce—O4 angle opens to 160.5(4)° and the other five "tetrahedral" angles shrink to 95–96° (Table 2).

The Ce—O—Si angles are nearly straight, ranging from 170.1(6) to 178.6(7)°. The Si—O and Si—C bond lengths ranging from 1.61(1) to 1.62(2) Å and 1.86(1) to 1.90(1) Å, respectively do not show unusual features, nor do bond lengths and angles in the DME chelating ligands.

The molecular packing may be described as layered with layers of $Ce(DME)(OSiPh_3)_4$ molecules at mean levels $x = 1/4$ and $x = 3/4$ alternating with layers of toluene molecules at mean levels $x = 0$ and $x = 1/2$ (Fig. 1).

REFERENCES

1. W. D. English and L. H. Sommer, *J. Am. Chem. Soc.* 1955, **77**, 170.
2. D. C. Bradley and I. M. Thomas, *J. Chem. Soc.* 1959, 3404.
3. J. M. Batwara and R. C. Mehrotra, *J. Inorg. Nucl. Chem.* 1970, **32**, 411.
4. P. S. Gradeff and F. G. Schreiber, *Inorg. Chem.* 1985, **24**, 1110; P. S. Gradeff, F. G. Schreiber and H. Mauermann, *J. Less-Common Met.* 1986, **126**, 335.
5. P. S. Gradeff and H. Mavermann, *J. Less-Common Met.*, to be published.
6. P. S. Gradeff and K. Yunlu, *J. Less-Common Met.*, to be published.
7. G. M. Sheldrick, Computer: DEC VAX 11-730. Programs: SHELX-76, program for crystal structure determination, Univ. of Cambridge, England (1976); SDP structure determination package, Enraf-Nonius, Delft (1979); C. K. Johnson, ORTEP, a Fortran thermal-ellipsoid plot program for crystal structure illustrations, report ORNL-3794, Oak-Ridge National Laboratory, Tennessee (1965).
8. D. T. Cromer and J. T. Waber, *International Tables for X-ray Crystallography*, Vol. 4. Kynoch Press, Birmingham (1974).
9. D. T. Cromer, *International Tables for X-ray Crystallography*, Vol. 4. Kynoch Press, Birmingham (1974).
10. E. L. Muetterties and L. J. Guggenberger, *J. Am. Chem. Soc.* 1974, **96**, 5751.
11. J. K. Kouba and S. S. Wreford, *Inorg. Chem.* 1976, **15**, 1463.

Polyhedron Vol. 8, No. 8, pp. 1007–1014, 1989
Printed in Great Britain

0277–5387/89 $3.00+.00
© 1989 Pergamon Press plc

SYNTHESIS AND X-RAY CRYSTALLOGRAPHIC CHARACTERIZATION OF THE DECAMETHYLSAMAROCENE SOLVATES $(C_5Me_5)_2Sm(OC_5H_8)_2$ AND $(C_5Me_5)_2Sm(OC_5H_{10})$

WILLIAM J. EVANS* and TAMARA A. ULIBARRI

Department of Chemistry, University of California, Irvine, Irvine, CA 92717, U.S.A.

(*Received* 22 *July* 1988; *accepted* 31 *October* 1988)

Abstract—The bis(dihydropyran) and mono(tetrahydropyran) solvates of $(C_5Me_5)_2Sm$ have been prepared by displacing THF from $(C_5Me_5)_2Sm(THF)_2$ and have been studied by X-ray diffraction. $(C_5Me_5)_2Sm(OC_5H_8)_2$ crystallizes from C_5H_8O in space group $P2_1/c$ with $a = 11.819(6)$, $b = 14.192(10)$, $c = 17.838(6)$ Å, $\beta = 95.26(4)°$ and $D_{calc} = 1.313$ g cm^{-3} for $Z = 4$. Least-squares refinement on the basis of 3168 observed reflections led to a final R value of 0.047. $(C_5Me_5)_2Sm(OC_5H_{10})$ crystallizes from hexane in space group $P2_1/a$ with $a = 14.900(5)$, $b = 16.263(7)$, $c = 10.732(3)$ Å, $\beta = 70.32(2)°$ and $D_{calc} = 1.376$ g cm^{-3} for $Z = 4$. Least-squares refinement of 3660 observed reflections led to a final R value of 0.046. Structural variations in the $(C_5Me_5)_2Sm(ether)_x$ series where $x = 0$, 1 and 2 are analysed.

Due to the strong reduction potential of samarium(II) ($Sm^{III}/Sm^{II} = -1.5$ V vs NHE[1]), divalent organosamarium chemistry is one of the major areas of study in the organolanthanide field.[2–4] Reactivity with a variety of substrates including organic halides, epoxides, ketones, alkynes, alkenes, azo compounds, CO, NO, N_2O and C_5H_5NO among others, has been observed.[2–4] To fully understand organosamarium(II) reactivity, it is important to know how similar this class is to trivalent lanthanide complexes. For example, is the special reactivity of samarium(II) species due just to the strong reduction potential, or are special metal–ligand bonding interactions present in these complexes which also affect the chemistry?

One source of information on this topic is X-ray crystal structure data. However, only a few organosamarium(II) complexes have been studied. The first structurally characterized organosamarium(II) complex was the disolvate $(C_5Me_5)_2Sm(THF)_2$ (**1**).[5,6] Subsequently, the unusual, bent, solvent-free $(C_5Me_5)_2Sm$ (**2**)[7,8] and the mono-ring complex $[(C_5Me_5)(THF)_2Sm(\mu\text{-}I)]_2$ (**3**),[6] were studied by X-ray diffraction. In the course of our studies on samarium(II) chemistry, we have obtained X-ray crystal structures on two additional $(C_5Me_5)_2Sm^{II}$ complexes, a bis(dihydropyran) derivative and a mono(tetrahydropyran) complex. These compounds, along with **1** and **2**, provide the data needed for a structural analysis of the complete series $(C_5Me_5)_2SmL_x$ where L = ether, $x = 0$–2.

EXPERIMENTAL

The complexes described below are extremely air- and moisture-sensitive. Therefore, both the syntheses and subsequent manipulations of these compounds were conducted under nitrogen with rigorous exclusion of air and water using Schlenk, vacuum line and glovebox (Vacuum/Atmospheres HE-553 Dri-Lab) techniques. Solvents were purified and physical measurements were obtained as previously described.[9] $(C_5Me_5)_2Sm(THF)_2$ was prepared according to the literature.[6]

$(C_5Me_5)_2Sm(OC_5H_8)_2$ (4)

In the glovebox, $(C_5Me_5)_2Sm(THF)_2$ (0.170 g, 0.300 mmol) was placed in a 50 cm^3 flask equipped with a Teflon stir bar and dissolved in *ca* 15 cm^3 of toluene. The toluene was removed by rotary evaporation and the process was repeated to yield a dark brownish-green solid which, by complexometric analysis, was the monosolvate, $(C_5Me_5)_2Sm(THF)$. The solid was then dissolved in *ca* 10 cm^3 of 3,4-dihydro-2H-pyran and the brownish-green–black solution was stirred for 30 min. The solvent was

* Author to whom correspondence should be addressed.

removed by rotary evaporation to yield a purple–black microcrystalline solid, $(C_5Me_5)_2Sm(OC_5H_8)_2$ (**4**), in quantitative yield. Found: Sm, 25.9. Calc. for $SmC_{30}H_{46}O_2$: Sm, 25.5%. $(C_5Me_5)_2Sm(OC_5H_8)_2$ can be recrystallized from a concentrated solution of 3,4-dihydro-2H-pyran by cooling to −32°C. ^1H NMR (benzene-d_6, 0.11 mM) δ 3.585 (s, C_5Me_5), definitive assignment of resonances associated with the dihydropyran group have not been made. ^{13}C NMR (benzene-d_6, 0.11 mM) δ 95.65 (q, C_5Me_5, $J = 120$ Hz), −94.01 (s, C_5Me_5). IR (KBr) 2915(s), 2860(s), 1665(w), 1450(m), 1420(w), 1230(w), 1195(w), 1060(w), 1040(m), 885(w), 860(w), 830(w), 810(w), 750(w), 725(w) cm^{-1}; $\chi_M = 5840 \times 10^{-6}$ (cgs); $\mu_{eff} = 3.75\ \mu_B$.

$(C_5Me_5)_2Sm(OC_5H_{10})$ (**5**)

In the glovebox, $(C_5Me_5)_2Sm(THF)$ (0.142 g, 0.288 mmol) was placed in a 20 cm^3 vial and dissolved in *ca* 8 cm^3 of tetrahydropyran to yield a deep maroon solution. The reaction was shaken vigorously. After 90 min, the solvent was removed by rotary evaporation to yield a dark maroon–brown solid. The maroon solid was dissolved in 10 cm^3 of toluene. The toluene was removed by rotary evaporation and this procedure was repeated to yield the dark brown solid, $(C_5Me_5)_2Sm(OC_5H_{10})$, in quantitative yield. Found: Sm, 30.5. Calc. for $SmC_{25}H_{40}$: Sm, 29.7%. This complex can be recrystallized from hexane. ^1H NMR (benzene-d_6, 0.05 mM) δ 4.05 (s, C_5Me_5), 9.15 v br s, −0.35 br s, −2.27 (br s, OC_5H_{10}). ^{13}C NMR (benzene-d_6, 0.05 mM) δ 96.23 (q, C_5Me_5, $J = 125$ Hz), −96.42 (s, C_5Me_5). IR (KBr) 2920(s), 2860(s), 1445(w), 1030(w), 915(w), 805(w) cm^{-1}; $\chi_M = 5143 \times 10^{-6}$ (cgs); $\mu_{eff} = 3.52\ \mu_B$.

X-ray data collection, structure determination and refinement for $(C_5Me_5)_2Sm(OC_5H_8)_2$

General procedures for data collection and reduction have been described previously.[10] A dark purple–black crystal measuring $0.62 \times 0.38 \times 0.042$ mm was sealed under nitrogen in a glass capillary and mounted on a Syntex $P2_1$ diffractometer. Lattice parameters were obtained from the settings of 15 computer-centred reflections. Monoclinic symmetry was indicated by the interaxial angles and confirmed by axial rotation photography. Data were collected by the θ–2θ scan technique in bisecting geometry. The p factor in the expression[11] for the standard deviation of the observed intensities was given a value of 0.05. Relevant crystal and data collection parameters are given in Table 1. All computations were carried out with a local version of the UCLA Crystallographic Computing Package.[12] The space group was determined as $P2_1/c$ (No. 14) from the systematic absences, $h0l$, $l \neq 2n$, and $0k0$, $k \neq 2n$.

During the data collection, the intensities of three standard reflections exhibited only random fluctuations within ±2%. Data were corrected for Lorentz, polarization and absorption effects. Patterson and difference Fourier techniques were used to locate all non-hydrogen atoms which were refined with anisotropic thermal parameters by the use of full-matrix least-squares methods. Hydrogen atoms were not included in the refinement. Atomic scattering factors were taken from ref. 13. A final difference map containing no recognizable features; its largest peak was of height 1.12 $eÅ^{-3}$ at a distance of 1.03 Å from the samarium atom.

X-ray data collection, structure determination and refinement for $(C_5Me_5)_2Sm(OC_5H_{10})$

A dark brown crystal measuring $0.40 \times 0.26 \times 0.26$ mm was handled as described above. Lattice parameters for a monoclinic cell were obtained from the settings of 15 computer-centred reflections. Relevant crystal and data collection parameters are given in Table 1. The space group was determined as $P2_1/a$ (alternate setting of $P2_1/c$, No. 14) from the systematic absences, $h0l$, $h \neq 2n$, and $0k0$, $k \neq 2n$. During the data collection, the intensities of three standard reflections measured every 100 reflections showed a linear decay of 8%. Data were corrected for Lorentz, polarization and absorption effects and for the decay of standards. Patterson and difference Fourier techniques were used to locate all non-hydrogen atoms which were refined with anisotropic thermal parameters by the use of full-matrix least-squares methods. Hydrogen atoms were not included in the refinement. The high thermal parameters for C(16) to C(20) indicate the presence of a large amount of thermal motion in the form of in-plane wagging for these pentamethylcyclopentadienyl methyl groups. A model containing two carbons at half occupancy for these methyl carbons was tried. The single site model presented in this paper was found to be a better model for the system. A final difference map contained no recognizable features; its largest peak was of height 2.69 $eÅ^{-3}$ at a distance of 1.10 Å from the samarium atom.

RESULTS AND DISCUSSION

Synthesis and characterization

Rotary evaporation of toluene solutions of $(C_5Me_5)_2Sm(THF)_2$ (**1**) reduces the amount of sol-

Table 1. Crystal data and summary of intensity data collection and structure refinement for $(C_5Me_5)_2Sm(OC_5H_8)_2$ (**4**) and $(C_5Me_5)_2Sm(OC_5H_{10})$ (**5**)

	(**4**)	(**5**)
Compound	$SmC_{30}H_{46}O_2$	$SmC_{25}H_{40}O$
Molecular weight	589.046	506.944
Space group	$P2_1/c$	$P2_1/a$
Cell constants, a (Å)	11.819(6)	14.900(5)
b (Å)	14.192(10)	16.263(7)
c (Å)	17.838(6)	10.732(3)
β (°)	95.26(4)	70.32(2)
Cell volume (Å^3)	2979	2448
Molecules/unit cell	4	4
D(calc.) (g cm^{-3})	1.313	1.376
Temperature (K)	298	298
μ(calc.) (cm^{-1})	20.0	24.2
Radiation	Mo-K_α, $\lambda = 0.71073$ Å	Mo-K_α, $\lambda = 0.71073$ Å
Transmission factor range	0.76–0.96	0.66–0.77
Maximum crystal dimensions (mm)	$0.62 \times 0.38 \times 0.042$	$0.40 \times 0.26 \times 0.26$
Scan width	$-1.2°$ in 2θ from $K\alpha_1$ to $+1.2°$ from $K\alpha_2$	$-1.2°$ in 2θ from $K\alpha_1$ to $+1.2°$ from $K\alpha_2$
Scan rate (° min^{-1})	Variable, 3.0–16.0	Variable, 4–16
Background counting	Estimated from 96 step peak profile	Estimated from 96 step peak profile
Standard reflections	1,−1,−2; 3,1,−5; −3,−3,−2	2,0,2; −1,6,0; −1,1,4
Decay of standards	±2%, oscillation—no correction done	8%
2θ range (°)	4–50	4.0–55.0
Total unique data	5604	5921
Unique data with $I \geqslant 3\sigma(I)$	3168	3660
Number of parameters varied	298	244
G.O.F.	1.47	1.62
R	0.047	0.046
R_w	0.057	0.058
Maximum Δ/σ in final cycle	0.02	0.02

vated THF and forms the monosolvated species $(C_5Me_5)_2Sm(THF)$. This complex dissolves in 3,4-dihydro-2H-pyran, C_5H_8O, presumably to form a mixture of disolvated species $(C_5Me_5)_2Sm(OR_2)(OR'_2)$. Rotary evaporation of this solution removes the lower boiling THF preferentially and leaves $(C_5Me_5)_2Sm(OC_5H_8)_2$ (**4**). X-ray quality crystals of **4** recrystallize from C_5H_8O. The THF in **1** can be similarly displaced by tetrahydropyran. Rotary evaporation of toluene solutions of this product gives $(C_5Me_5)_2Sm(OC_5H_{10})$ (**5**). Recrystallization from hexane gives X-ray quality crystals.

The physical properties of **4** and **5** are consistent with the presence of samarium(II). The intense, dark colours are similar to those of other organosamarium(II) species and differ from the typical light yellow–orange colours of samarium(III) species.[2] The room temperature magnetic susceptibilities of **4** and **5** are in the samarium(II) range.[14] The ^{13}C NMR spectra of **4** and **5** are similar to those of **1–3** but different from $(C_5Me_5)_2Sm^{III}$ spectra in that the methyl carbon signals are at low field, ~ 96 ppm, and the ring carbon signals are at high field, −94 to −96 ppm. The complexometric analyses of **4** and **5** were consistent with their formulations as $(C_5Me_5)_2Sm(OC_5H_8)_2$ and $(C_5Me_5)_2Sm(OC_5H_{10})$, respectively, and definitive identification was made by X-ray crystallography.

X-ray crystal structures

Figures 1 and 2 show the molecular structures of **4** and **5**, respectively, and bond distances and angles are given in Tables 2 and 3. In complex **4**, the two C_5Me_5 ring centroids and the two OC_5H_8 oxygen atoms comprise a distorted tetrahedral geometry around the samarium atom. The six angles describing these five positions in **4** are very similar to the analogous angles in **1**. The O(1)—Sm—O(2) angle in **4** is 82.2(2) vs 82.7(4)° in **1**. The Cn(1)—Sm—Cn(2) angles [Cn(1) = ring centroid

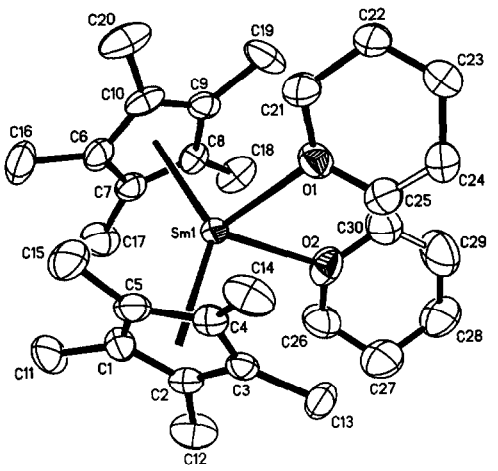

Fig. 1. Molecular structure of $(C_5Me_5)_2Sm(OC_5H_8)_2$ (**4**).

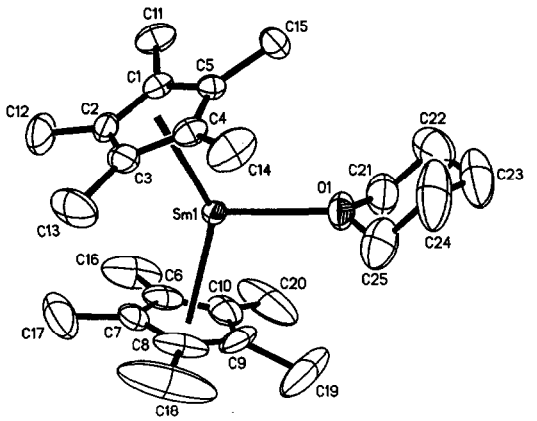

Fig. 2. Molecular structure of $(C_5Me_5)_2Sm(OC_5H_{10})$ (**5**).

for the C_5Me_5 ring comprised of carbon atoms (1)–(5)] are 138.2° in **4** and 136.5° in **1**. The four Cn—Sm—O angles in **4** are 103.0, 104.5, 106.9 and 107.9° compared to 103.8, 104.5, 107.8 and 108.3° in **1**.

As shown in Table 4, the Sm—C(C_5Me_5) average distance in **4** is slightly smaller than that in **1**, and the Sm—O distances are slightly longer than those in **1**. However, the differences are not statistically significant. The double bonds in the dihydropyran rings, C(24)—C(25) and C(29)—C(30), are both located on the inside of the O—Sm—O wedge although neither are oriented toward the samarium atom or toward each other.

In $(C_5Me_5)_2Sm(OC_5H_{10})$, the tetrahydropyran ligand is positioned almost symmetrically between the C_5Me_5 rings as shown by the C_5Me_5 centroid—Sm—O angles of 107.0 and 107.4°. The samarium atom lies 0.34 Å out-of-the plane defined by the two ring centroids and the oxygen atom. Hence, the formal coordination geometry is not perfectly trigonal planar. The (ring centroid)—Sm—(ring centroid) angle of 140.0° is slightly larger than those observed for the eight-coordinate complexes **1** and **4**. This is consistent with the smaller steric demand placed on the metal by the single solvate molecule. The average Sm—C(C_5Me_5) distance of 2.816(3) Å is smaller than those in **1** and **4**, which again is consistent with the lower coordination number in **5**. The Sm—O distance in **5** is between the two values found in $(C_5Me_5)_2Sm(THF)_2$ and is smaller than the analogous distances in $(C_5Me_5)_2Sm(OC_5H_8)_2$. The tetrahydropyran ligand adopts a chair conformation with normal bond distances and angles.[15]

Structural comparisons

Table 4 consists of a compilation of crystallographic data on divalent samarium complexes containing the C_5Me_5 ligand. The complexes are arranged in order of decreasing coordination number. For the six samarium complexes, a diminishing progression of average Sm—C(C_5Me_5) distances is observed as the coordination number decreases. This is sterically reasonable since fewer ligands can get closer to the metal. The trend follows the change in effective ion radius observed for metals, as a function of coordination number in halides and chalcogenides.[16] The difference in the averages in going from formal eight coordination to six coordination, 2.86(1)–2.79(1) Å, is not large and the ranges of individual values for complexes with different coordination numbers often overlap. For example, six-coordinate $(C_5Me_5)_2Sm$ and eight-coordinate $(C_5Me_5)_2Sm(THF)_2$ both have a 2.81 Å Sm—C(C_5Me_5) bond length. In comparison, Shannon shows that the ionic radius of Sm^{2+} varies from 1.22 to 1.27 to 1.32 Å in seven-, eight- and nine-coordinate samarium(II) complexes, respectively.[16]

The (ring centroid)–Sm–(ring centroid) angles also follow a regular pattern which is understandable in terms of steric factors. The increase in angle as coordination number decreases is reasonable since the additional ligands in the higher coordinate complexes will force the C_5Me_5 rings closer together (smaller angle). As was found in the Sm—C(C_5Me_5) distances, the range of samarium complexes is small, 136.5–140.5°.

In contrast to the data discussed above, the Sm—O distances do not follow a regular pattern with respect to coordination number. Given that the overall range is again small, that different ether ligands are involved and that only two coordination numbers can be compared, this may not be too surprising.

Table 2. Bond distance (Å) and angle (°) data on $(C_5Me_5)_2Sm(OC_5H_8)_2$

Sm(01)—O(01)	2.655(6)	C(04)—C(05)	1.411(13)
Sm(01)—O(02)	2.699(7)	C(04)—C(14)	1.510(14)
Sm(01)—C(07)	2.819(9)	C(05)—C(15)	1.562(14)
Sm(01)—C(05)	2.826(10)	C(06)—C(07)	1.385(13)
Sm(01)—C(01)	2.827(10)	C(06)—C(10)	1.416(14)
Sm(01)—C(08)	2.831(9)	C(06)—C(16)	1.546(14)
Sm(01)—C(09)	2.838(9)	C(07)—C(08)	1.414(13)
Sm(01)—C(06)	2.851(9)	C(07)—C(17)	1.538(14)
Sm(01)—C(10)	2.853(9)	C(08)—C(09)	1.407(12)
Sm(01)—C(02)	2.853(9)	C(08)—C(18)	1.522(13)
Sm(01)—C(04)	2.859(9)	C(09)—C(10)	1.420(14)
Sm(01)—C(03)	2.867(8)	C(09)—C(19)	1.544(13)
O(01)—C(25)	1.394(13)	C(10)—C(20)	1.547(14)
O(01)—C(21)	1.465(11)	C(21)—C(22)	1.498(15)
O(02)—C(30)	1.407(14)	C(22)—C(23)	1.514(15)
O(02)—C(26)	1.477(13)	C(23)—C(24)	1.480(16)
C(01)—C(05)	1.390(14)	C(24)—C(25)	1.319(16)
C(01)—C(02)	1.419(13)	C(26)—C(27)	1.454(18)
C(01)—C(11)	1.528(13)	C(27)—C(28)	1.521(19)
C(02)—C(03)	1.437(12)	C(28)—C(29)	1.477(19)
C(02)—C(12)	1.551(13)	C(29)—C(30)	1.379(19)
C(03)—C(04)	1.399(12)	Sm(01)—Cn(1)	2.581
C(03)—C(13)	1.529(12)	Sm(01)—Cn(2)	2.573

O(01)—Sm(01)—O(02)	82.2(2)	C(09)—C(08)—C(07)	106.7(8)
C(25)—O(01)—C(21)	114.5(8)	C(09)—C(08)—C(18)	127.2(10)
C(30)—O(02)—C(26)	115.4(9)	C(07)—C(08)—C(18)	125.9(9)
C(05)—C(01)—C(02)	107.3(8)	C(08)—C(09)—C(10)	108.6(9)
C(05)—C(01)—C(11)	129.3(11)	C(08)—C(09)—C(19)	125.2(10)
C(02)—C(01)—C(11)	122.8(11)	C(10)—C(09)—C(19)	126.1(10)
C(01)—C(02)—C(03)	107.4(9)	C(06)—C(10)—C(09)	107.0(9)
C(01)—C(02)—C(12)	126.0(10)	C(06)—C(10)—C(20)	125.1(11)
C(03)—C(02)—C(12)	126.1(9)	C(09)—C(10)—C(20)	127.2(11)
C(04)—C(03)—C(02)	108.0(8)	O(01)—C(21)—C(22)	109.2(9)
C(04)—C(03)—C(13)	127.1(9)	C(21)—C(22)—C(23)	110.0(10)
C(02)—C(03)—C(13)	124.6(9)	C(24)—C(23)—C(22)	108.8(10)
C(03)—C(04)—C(05)	107.3(8)	C(25)—C(24)—C(23)	124.9(12)
C(03)—C(04)—C(14)	126.5(9)	C(24)—C(25)—O(01)	122.0(11)
C(05)—C(04)—C(14)	125.7(9)	C(27)—C(26)—O(02)	111.5(11)
C(01)—C(05)—C(04)	110.0(8)	C(26)—C(27)—C(28)	112.6(12)
C(01)—C(05)—C(15)	125.2(10)	C(29)—C(28)—C(27)	110.2(11)
C(04)—C(05)—C(15)	124.8(10)	C(30)—C(29)—C(28)	124.7(14)
C(07)—C(06)—C(10)	108.1(9)	C(29)—C(30)—O(02)	119.0(13)
C(07)—C(06)—C(16)	127.6(11)	Cn(1)—Sm(01)—Cn(2)	138.2
C(10)—C(06)—C(16)	123.7(12)	Cn(1)—Sm(01)—O(01)	103.0
C(06)—C(07)—C(08)	109.4(9)	Cn(1)—Sm(01)—O(02)	106.9
C(06)—C(07)—C(17)	125.9(10)	Cn(2)—Sm(01)—O(01)	107.9
C(08)—C(07)—C(17)	124.3(10)	Cn(2)—Sm(01)—O(02)	104.5

Table 3. Bond distance (Å) and angle (°) data on $(C_5Me_5)_2Sm(OC_5H_{10})$

Sm(01)—O(01)	2.630(6)	C(03)—C(13)	1.553(12)
Sm(01)—C(09)	2.770(9)	C(04)—C(05)	1.418(10)
Sm(01)—C(08)	2.791(8)	C(04)—C(14)	1.503(12)
Sm(01)—C(10)	2.794(9)	C(05)—C(15)	1.519(10)
Sm(01)—C(03)	2.803(8)	C(06)—C(10)	1.364(15)
Sm(01)—C(07)	2.811(7)	C(06)—C(07)	1.369(13)
Sm(01)—C(06)	2.817(7)	C(06)—C(16)	1.531(14)
Sm(01)—C(04)	2.821(7)	C(07)—C(08)	1.376(16)
Sm(01)—C(05)	2.835(6)	C(07)—C(17)	1.529(16)
Sm(01)—C(02)	2.853(7)	C(08)—C(09)	1.386(19)
Sm(01)—C(01)	2.858(6)	C(08)—C(18)	1.508(17)
O(01)—C(25)	1.410(14)	C(09)—C(10)	1.356(18)
O(01)—C(21)	1.469(14)	C(09)—C(19)	1.559(16)
C(01)—C(02)	1.391(10)	C(10)—C(20)	1.509(17)
C(01)—C(05)	1.416(9)	C(21)—C(22)	1.508(20)
C(01)—C(11)	1.546(10)	C(22)—C(23)	1.476(26)
C(02)—C(03)	1.406(12)	C(23)—C(24)	1.421(25)
C(02)—C(12)	1.521(11)	C(24)—C(25)	1.491(19)
C(03)—C(04)	1.405(11)	Sm(01)—Cn(1)	2.569
		Sm(01)—Cn(2)	2.542

C(25)—O(01)—C(21)	111.6(8)	C(06)—C(07)—C(08)	107.6(10)
C(02)—C(01)—C(05)	109.1(6)	C(06)—C(07)—C(17)	126.1(13)
C(02)—C(01)—C(11)	126.3(7)	C(08)—C(07)—C(17)	125.9(14)
C(05)—C(01)—C(11)	124.0(7)	C(07)—C(08)—C(09)	106.5(10)
C(01)—C(02)—C(03)	107.6(6)	C(07)—C(08)—C(18)	123.4(18)
C(01)—C(02)—C(12)	125.3(9)	C(09)—C(08)—C(18)	129.9(19)
C(03)—C(02)—C(12)	126.8(9)	C(10)—C(09)—C(08)	109.6(10)
C(04)—C(03)—C(02)	108.7(7)	C(10)—C(09)—C(19)	125.2(24)
C(04)—C(03)—C(13)	125.5(9)	C(08)—C(09)—C(19)	124.8(23)
C(02)—C(03)—C(13)	125.3(9)	C(09)—C(10)—C(06)	106.9(11)
C(03)—C(04)—C(05)	107.7(7)	C(09)—C(10)—C(20)	126.0(19)
C(03)—C(04)—C(14)	125.4(8)	C(06)—C(10)—C(20)	126.8(18)
C(05)—C(04)—C(14)	126.9(8)	O(01)—C(21)—C(22)	106.1(11)
C(01)—C(05)—C(04)	106.9(6)	C(23)—C(22)—C(21)	111.6(15)
C(01)—C(05)—C(15)	126.1(7)	C(24)—C(23)—C(22)	108.1(13)
C(04)—C(05)—C(15)	126.8(7)	C(23)—C(24)—C(25)	110.8(13)
C(10)—C(06)—C(07)	109.4(10)	O(01)—C(25)—C(24)	108.8(13)
C(10)—C(06)—C(16)	123.8(14)	Cn(1)—Sm(01)—Cn(2)	140.0
C(07)—C(06)—C(16)	126.6(13)	Cn(1)—Sm(01)—O(01)	107.4
		Cn(2)—Sm(01)—O(01)	107.0

Comparison of the data in Table 4 with data on trivalent $(C_5Me_5)_2Sm$ complexes is also informative. In the past, average Sm—C(C_5Me_5) distances in trivalent $(C_5Me_5)_2Sm(X)(Y)$ complexes ranged from 2.72 to 2.77 Å[17] and did not overlap with averages of eight-coordinate Sm^{II}—C(C_5Me_5) lengths, 2.812(4)–2.86(1) Å (Table 4). Recently, however, the range for $(C_5Me_5)_2Sm(X)(Y)$ complexes has been extended from 2.68(1) Å for $[(C_5Me_5)_2Sm(\mu\text{-}Me)_2AlMe_2]_2$[18] to 2.80(1) Å for sterically crowded $[(C_5Me_5)_2Sm(CNCMe_3)]_2(\mu\text{-}O)$.[19] Hence, there is no longer such a clean distinction between the ranges. In general, however, for comparable coordination environments, Sm—C(C_5Me_5) distances can be valuable indicators of the valence of the metal centre.

The Sm—O distances also fall in distinct ranges for divalent vs trivalent $(C_5Me_5)_2Sm$ complexes. Table 4 shows a range of 2.62(2)–2.699(7) Å, whereas in published trivalent $(C_5Me_5)_2Sm(X)(THF)$ systems, Sm—O bonds range from 2.44(2)[20] to 2.511(4) Å.[21] The (ring centroid)–Sm–(ring centroid) angles, on the other hand, are not specific to the metal valence state. The samarium(II) range of 136.5–140.1° overlaps considerably with the 127[17]–141°[22] range observed for trivalent $(C_5Me_5)Sm$ complexes.

SUMMARY

Analysis of the structural data now available on the series $(C_5Me_5)_2Sm(OR_2)_x$, $x = 0$–2, shows that

Table 4. Comparative structural data on divalent bis(pentamethylcyclopentadienyl) lanthanide complexes

Complex	Formal coordination number	Average Ln—C(ring) distance (Å)	Range of Ln—C(ring) distance (Å)	Sm—O distance (Å)	Ring centroid–Sm–ring centroid angle (°)	Reference
$(C_5Me_5)_2Sm(THF)_2$	8	2.86(1)	2.81(2)–2.91(1)	2.62(1) 2.64(1)	136.5	6
$(C_5Me_5)_2Sm(OC_5H_8)_2$	8	2.842(4)	2.819(9)–2.867(8)	2.655(6) 2.699(7)	138.2	This work
$(C_5Me_5)_2Sm^{II}(\mu\text{-}C_5H_5)Sm^{III}(C_5Me_5)_2$	8[a]	2.812(4)	2.782(10)–2.847(9)	—	139.7	17
$(C_5Me_5)_2Sm(OC_5H_{10})$	7	2.816(3)	2.770(9)–2.858(6)	2.630(6)	140.0	This work
$[(C_5Me_5)(THF)_2Sm(\mu\text{-}I)]_2$	7	2.81(2)	2.77(2)–2.84(3)	2.66(1) 2.62(2)	—	6
$(C_5Me_5)_2Sm$	6	2.79(1)	2.775(6)–2.815(6)	—	140.1	8

[a] Two of the metal ligand distances are quite long.

organosamarium(II) complexes show reasonable structural trends based on coordination number. Both the Sm—C(C_5Me_5) and the Sm—O(THF) distances have characteristic values for samarium(II) complexes which are distinct from trivalent values in complexes of comparable coordination environment. These data are similar to the structural trends found in trivalent organolanthanide complexes.[23]

Acknowledgements—We thank the National Science Foundation for support of this research and Professor R. J. Doedens and D. K. Drummond for crystallographic help.

REFERENCES

1. L. R. Morss, *Chem. Rev.* 1976, **76**, 827.
2. W. J. Evans, *Polyhedron* 1987, **6**, 803 and refs therein.
3. H. B. Kagan and J. L. Namy, in *Handbook on the Physics and Chemistry of Rare Earths* (Edited by K. A. Gschneidner Jr and L. Eyring), Vol. 6, Chap. 50 and refs therein. Elsevier, Amsterdam (1984).
4. H. B. Kagan and J. L. Namy, *Tetrahedron* 1986, **42**, 6573 and refs therein.
5. W. J. Evans, I. Bloom, W. E. Hunter and J. L. Atwood, *J. Am. Chem. Soc.* 1981, **103**, 6507.
6. W. J. Evans, J. W. Grate, H. W. Choi, I. Bloom, W. E. Hunter and J. L. Atwood, *J. Am. Chem. Soc.* 1985, **107**, 941.
7. W. J. Evans, L. A. Hughes and T. P. Hanusa, *J. Am. Chem. Soc.* 1984, **106**, 4270.
8. W. J. Evans, L. A. Hughes and T. P. Hanusa, *Organometallics* 1986, **5**, 1285.
9. W. J. Evans, J. W. Grate and R. J. Doedens, *J. Am. Chem. Soc.* 1985, **107**, 1671.
10. D. B. Sams and R. J. Doedens, *Inorg. Chem.* 1979, **18**, 153.
11. P. W. R. Corfield, R. J. Doedens and J. A. Ibers, *Inorg. Chem.* 1967, **6**, 197.
12. C. E. Strouse, personal communication to R. J. Doedens.
13. *International Tables for X-ray Crystallography*, Vol. IV, p. 72. Kynoch Press, Birmingham, U.K. (1974).
14. W. J. Evans and M. A. Hozbor, *J. Organomet. Chem.* 1987, **326**, 299.
15. S. M. Johnson, J. Herrin, S. J. Liu and I. C. Paul, *J. Am. Chem. Soc.* 1970, **92**, 4428.
16. R. D. Shannon, *Acta Cryst.* 1976, **A32**, 751.
17. W. J. Evans and T. A. Ulibarri, *J. Am. Chem. Soc.* 1987, **109**, 4292.
18. W. J. Evans, L. R. Chamberlain, T. A. Ulibarri and J. W. Ziller, *J. Am. Chem. Soc.* 1988, **110**, 6423.
19. W. J. Evans, D. K. Drummond, L. A. Hughes, H. Zhang and J. L. Atwood, *Polyhedron* 1988, **7**, 1693.
20. W. J. Evans, J. W. Grate, K. R. Levan, I. Bloom, T. T. Peterson, R. J. Doedens, H. Zhang and J. L. Atwood, *Inorg. Chem.* 1986, **25**, 3614.
21. W. J. Evans, I. Bloom, W. E. Hunter and J. L. Atwood, *Organometallics* 1985, **4**, 112.
22. W. J. Evans and D. K. Drummond, *J. Am. Chem. Soc.* 1988, **110**, 2772.
23. K. N. Raymond and C. W. Eigenbrot Jr, *Accts Chem. Res.* 1980, **13**, 276.

Polyhedron Vol. 8, No. 8, pp. 1015–1018, 1989
Printed in Great Britain

0277–5387/89 $3.00+.00
© 1989 Pergamon Press plc

MIXED LIGAND COMPLEXES—I. (AMINO ACIDATO)ETHYLENEDIBIGUANIDECOBALT(III) SALTS

R. K. RAY*

Department of Chemistry, Rama Krishna Mission Vivekananda Centenary College, Rahara 743186, 24 Parganas (North), West Bengal, India

and

GEORGE B. KAUFFMAN

Department of Chemistry, California State University, Fresno, CA 93740, U.S.A.

(*Received* 19 *July* 1988; *accepted after revision* 8 *November* 1988)

Abstract—(Amino acidato)dibiguanidecobalt(III) salts of the type $[Co(AB)en(bigH)_2]^{2+}$ have been prepared and characterized (ABH = DL-α-alanine, β-alanine, L-leucine, DL-valine and L-histidine; $en(bigH)_2 = N^1,N^1$-ethylenedibiguanide). A number of salts of each cation have been prepared, and their ionic nature has been confirmed by conductance measurements. IR spectra have furnished positive information regarding the bonding sites of the title ligands. Electronic spectra revealed expected trends. In the case of the $[Co(hist)en(bigH)_2]^{2+}$ cation, the histidinate (hist) anion behaves as a bidentate NN donor not as an NO donor.

Biguanide (**1**) and ethylenedibiguanide (**2**) are extremely powerful and formidable coordinating ligands which have played important roles in elucidating many interesting aspects of coordination chemistry.[1,2] Furthermore, by stabilizing many otherwise unfamiliar oxidation states of metal ions, these ligands have played significant roles in the development of ideas on the mechanism of racemization and on interesting reaction kinetics.[1–5] Dutta and his students[6–8] have prepared and characterized some cobalt(III) mixed chelates of the type $[Co(AB)(bigH)_2]^{2+}$ (ABH = glycine, DL-α-alanine, β-alanine, etc.; bigH = biguanide). A survey of metal dibiguanide complexes shows that although a number of studies have been made of homo-(dibiguanide) complexes of a variety of transition metal ions, none has been devoted to hetero-(dibiguanide) complexes.[1–5,7,9–11] In this paper we report a study of several mixed chelates of cobalt (III) containing one bidentate amino acid (with a donor set, NO for alanine, leucine and valine, and an NN donor set or NO donor set for histidine) and one quadridentate ligand (N^1,N^1-ethylenedibiguanide) in order to aid in the elucidation of the structure of $[Co(AB)en(bigH)_2]^{2+}$.

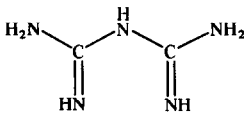

Biguanide (**1**)

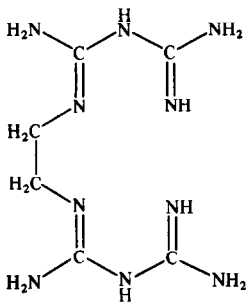

Ethylenedibiguanide (**2**)

EXPERIMENTAL

Ethylenedibiguanide hydroxide sulphate and diamineethylenedibiguanidecobalt(III) hydroxide sulphate were prepared following known methods.[1,2]

Analysis

Cobalt and nitrogen were determined as $CoSO_4$ and by the combustion method, respectively. Carbon and hydrogen were analysed by CDRI (Lucknow, India). Chlorine, bromine and iodine were determined as the silver salts. Electrical conductances were measured with a Philips PR 9500 conducti-

* Author to whom correspondence should be addressed.

vity bridge. IR spectra were recorded at CDRI (Lucknow). Solution spectra were obtained with a Hilger Uvispec spectrophotometer over the range 320–600 nm.

DL - α - *Alaninatoethylenedibiguanidecobalt(III) sulphate*

Diamine ethylenedibiguanidecobalt(III) hydroxide sulphate-4-hydrate (1 g) was dissolved in water (15 cm^3), heated with α-alanine (0.2 g in 10 cm^3 of water), and the mixture digested on the steam bath. When evolution of ammonia had ceased, the solution was cooled, neutralized with cold, dilute H_2SO_4 (1 : 4) and filtered. After concentration and cooling, the filtrate deposited red–violet crystals, which were recrystallized from hot water and dried over $CaCl_2$ (yield, 0.8 g). Found: Co, 11.6; C, 20.8; H, 4.8; N, 30.4. Calc. for $[Co(\alpha\text{-alan-}\bar{O})en(bigH)_2](SO_4)\cdot 2H_2O$: Co, 11.6; C, 21.3; H, 5.12; N, 30.3%.

DL - α - *Alaninatoethylenedibiguanidecobalt(III) chloride*

The above sulphate salt (1 g) was dissolved in water (15 cm^3) and treated with excess aqueous barium chloride solution, whereupon insoluble barium sulphate was formed, which was removed by filtration. The filtrate was concentrated to a small volume and then cooled, whereupon red-violet crystals separated. These were purified by recrystallization from hot water (yield, 0.7 g). Found: Co, 11.8; C, 21.5; H, 5.3; N, 30.6. Calc. for $[Co(\alpha\text{-alan-}\bar{O})en(bigH)_2]Cl_2\cdot 3H_2O$: Co, 11.7; C, 21.5; H, 5.5; N, 30.7%.

DL-α-*Alaninatoethylenedibiguanidecobalt(III) iodide*

The above chloride salt (1 g) was dissolved in water (15 cm^3), and KI solution was added to this solution to precipitate red–violet crystals, which were purified by two recrystallizations, twice from hot water (yield, 0.9 g). Found: Co, 8.9; C, 16.3; H, 3.7; N, 23.3. Calc. for $[Co(\alpha\text{-alan-}\bar{O})en(bigH)_2]I_2\cdot 1.5H_2O$: Co, 8.9; C, 16.4; H, 3.8; N, 23.4%.

The following compounds were obtained by procedures similar to those for DL-α-alaninatoethylenedibiguanidecobalt(III) chloride and iodide.

β-Alaninatoethylenedibiguanidecobalt(III) chloride

Reddish-violet crystals, recrystallized from hot water. Found: Co, 11.7; C, 21.4; H, 5.3; N, 30.7. Calc. for $[Co(\beta\text{-alan-}\bar{O})en(bigH)_2]Cl_2\cdot 3H_2O$: Co, 11.7; C, 21.5; H, 5.5; N, 30.7%.

β-Alaninatoethylenedibiguanidecobalt(III) iodide

Reddish-violet crystals, recrystallized from hot water. Found: Co, 8.8; C, 16.2; H, 3.6; N, 23.4. Calc. for $[Co(\beta\text{-alan-}\bar{O})en(bigH)_2]I_2\cdot 1.5H_2O$: Co, 8.9; C, 16.4; H, 3.8; N, 23.4%.

L-*Leucinatoethylenedibiguanidecobalt(III) chloride*

Reddish-violet crystals, recrystallized from a (1 : 1) alcohol/water mixture. Found: Co, 11.3; C, 27.8; H, 6.0; N, 29.9. Calc. for $[Co(l\text{-leuc-}\bar{O})en(bigH)_2]Cl_2\cdot 1.5H_2O$: Co, 11.4; C, 27.9; H, 6.0; N, 29.9%.

DL-*Valinatoethylenedibiguanidecobalt(III) sulphate*

Reddish-violet crystals, recrystallized from a hot (1 : 1) alcohol/water mixture. Found: Co, 10.8; C, 23.8; H, 5.5; N, 28.3. Calc. for $[Co(val\text{-}\bar{O})en(bigH)_2](SO_4)\cdot 2.5H_2O$: Co, 10.8; C, 24.2; H, 5.7; N, 28.3%.

DL-*Valinatoethylenedibiguanidecobalt(III) chloride*

Reddish-violet crystals, recrystallized from a hot (1 : 1) alcohol/water mixture. Found: Co, 10.9; C, 24.3; H, 6.0; N, 28.7; Cl, 13.1. Calc. for $[Co(val\text{-}\bar{O})en(bigH)_2]Cl_2\cdot 3.5H_2O$: Co, 10.9; C, 24.5; H, 6.1; N, 28.6; Cl, 13.2%.

L - *Histidinatoethylenedibiguanidecobalt(III) sulphate*

Orange–red crystals, recrystallized from hot water. Found: Co, 9.8; C, 24.0; H, 4.8; N, 30.8. Calc. for $[Co(hist\text{-}\bar{O})en(bigH)_2](SO_4)\cdot 3H_2O$: Co, 9.9; C, 24.3; H, 5.0; N, 30.8%.

L-*Histidinatoethylenedibiguanidecobalt(III) chloride*

Orange–red crystals, recrystallized from hot water. Found: Co, 10.6; C, 26.1; H, 4.9; N, 33.1; Cl, 13.0. Calc. for $[Co(hist\text{-}\bar{O})en(bigH)_2]Cl_2\cdot 2H_2O$: Co, 10.7; C, 26.2; H, 5.1; N, 33.2; Cl, 12.9%.

L - *Histidinatoethylenedibiguanidecobalt(III) bromide*

Orange–red crystals, recrystallized from hot water. Found: Co, 9.1; C, 22.3; H, 4.1; N, 28.6; Br, 26.0. Calc. for $[Co(hist\text{-}\bar{O})en(bigH)_2]Br_2\cdot 2H_2O$: Co, 9.2; C, 22.6; H, 4.3; N, 28.5; Br, 25.0%.

L-*Histidinatoethylenedibiguanidecobalt(III) iodide*

Orange–red crystals, recrystallized from hot water. Found: Co, 8.3; C, 19.8; H, 3.4; N, 25.4; I,

Table 1. Colours, conductances and electronic spectra of the mixed chelates

Complex	Colour	Molar conductance (Ω^{-1} cm^2 mol^{-1} at 25°C)	Electronic spectra Band I (nm)	Band II (nm)
[Co(α-alan)en(bigH)$_2$]Cl$_2$·3H$_2$O	Reddish-violet	209	490(173)[a]	360(322)[a]
[Co(α-alan)en(bigH)$_2$]I$_2$·1.5H$_2$O	Reddish-violet	211	490(175)	360(325)
[Co(β-alan)en(bigH)$_2$]Cl$_2$·3H$_2$O	Reddish-violet	215	490(171)	360(320)
[Co(β-alan)en(bigH)$_2$]I$_2$·1.5H$_2$O	Reddish-violet	207	490(169)	360(318)
[Co(leuc)en(bigH)$_2$]Cl$_2$·1.5H$_2$O	Reddish-violet	205	490(174)	360(319)
[Co(val)en(bigH)$_2$]Cl$_2$·3H$_2$O	Reddish-violet	208	490(178)	360(326)
[Co(hist)en(bigH)$_2$]Cl$_2$·2H$_2$O	Orange–red	215	490(175)	—
[Co(hist)en(bigH)$_2$]Br$_2$·2H$_2$O	Orange–red	217	490(180)	—
[Co(hist)en(bigH)$_2$]I$_2$·H$_2$O	Orange–red	219	490(178)	—

α-alanH = α-alanine; β-alanH = β-alanine; en(bigH)$_2$ = ethylenedibiguanide; histH = histidine; leucH = leucine; valH = valine.

[a] Values in parentheses indicate extinction coefficients.

35.4. Calc. for [Co(hist-Ō)en(bigH)$_2$]I$_2$·H$_2$O: Co, 8.2; C, 20.2; H, 3.6; N, 25.5; I, 35.6%.

RESULTS AND DISCUSSION

It is not known whether diamineethylenedibiguanidecobalt(III) hydroxide sulphate has a *cis* or *trans* configuration.[1,2] When the compound was treated with an amino acid, ammonia was not immediately evolved, but on warming the mixture, ammonia was evolved, and a reddish solution resulted. On concentrating the solution to a small volume and neutralizing it, the cations could be isolated. All the salts are highly crystalline, appear homogeneous under the microscope, and are very stable in aqueous solution. The molar conductances (Table 1) in aqueous solution at 25°C are 205–219 Ω^{-1} cm^2 mol^{-1}, which are within the range for bi-univalent electrolytes.[2]

In the IR spectra of all the cobalt(III) complexes, the bands in the 3 μ region, arising due to ν_{asy}(N–H) (3310–3385 cm^{-1}) and ν_{asy}(N–H) (3100–3150 cm^{-1}) modes of vibration of the guanyl group,[12] are observed almost in the same positions as those in the original ligand molecules, with slight decreases in intensities, suggesting participation of the ligand in complex formation without deprotonation. In the region of 1645–1660 cm^{-1}, the complexes exhibit strong bands, and these are assigned to ν(C=N) stretch, ν(N—H) deformation, and ν(O—H) deformation vibration.[13–15] In ethylenedibiguanide sulphate, the ν(C=N) stretch occurs at 1695 cm^{-1}, and the ν(N—C—N) stretch at 1585 cm^{-1}. A similar N—C—N stretching frequency of other cobalt(III) biguanide complexes was observed at ~1580 cm^{-1}.[15] The lowering of the ν(C=N) stretch (1660 cm^{-1}) and the ν(N—C—N) stretch (1545 cm^{-1}) in metal complexes is due to coordination with nitrogen atoms of =NH groups. The ν(C—N) stretch of the C—NH$_2$ group of both the ligand and the complexes, is assigned to about 1345–1375 cm^{-1}. A strong band in the region of 1190–1315 cm^{-1} corresponds to the formation of the chelate ring, which is absent in this region in the particular ligand.[16] Since the —C=N— stretch of the biguanide is in the region of antisymmetrical carboxyl stretching,[17] it frustrated attempts to demonstrate whether the carboxyl group is free or not. Attempts to protonate COO$^-$ by HCl to produce [Co(histH)en(bigH)$_2$]$^{3+}$, led to decomposition of the complex,[2,9,18] As expected for cobalt(III) complexes,[19] all the chelates exhibit two *d–d* absorption bands I and II (Table 1). The higher energy band, II, of the [Co(hist)en(bigH)$_2$]$^{2+}$ ion could not be located, presumably because it was covered by the charge-transfer transition arising from an interaction between cobalt(III) and the imidazole moiety.[20] Such a high energy band, II, was also not observed in compounds of ions like [Co(pic)(bigH)$_2$]$^{2+}$ [picH = picolinic acid (pyridine 2-carboxylic acid); bigH = biguanide], [Cu(lut)(bigH)$_2$]$^+$ [lutH$_2$ = lutidinic acid (pyridine 2,6-dicarboxylic acid)], [Co(DMG)(bigH)$_2$]$^+$ (DMGH$_2$ = dimethylglyoxime), [Co(en)(bigH)$_2$]$^{3+}$, and [Co(hist)(bigH)$_2$]$^{2+}$ (histH = histidine) ions.[8,21] Although histidine may act either as a bidentate NN[22,23] or as an NO donor,[24] the spectrum of the [Co(hist)en(bigH)$_2$]$^{2+}$ ion reveals that the histidinate ion functions in this particular complex as a bidentate NN ligand. Interestingly enough, band I for the [Co(hist)en(bigH)$_2$]$^{2+}$ ion is comparable to transitions in cobalt(III) complexes with [CoN$_6$] chromophores, e.g. [Co(bigH)$_3$]$^{3+}$ (λ_{max}, 495 nm; ε = 235), [Co(en)$_3$]$^{3+}$ (λ_{max}, 470 nm; ε = 72.5),

$[Co(en)(bigH)_2]^{3+}$ (λ_{max}, 475 nm; $\varepsilon = 165$), $[Co(en)_2(bigH)]^{3+}$ (λ_{max}, 480–490 nm; $\varepsilon = 158$), $[Co(o\text{-phen})(bigH)_2]^{3+}$ (λ_{max}, 470 nm; $\varepsilon = 177$), $[Co(dipy)(bigH)_2]^{3+}$ (λ_{max}, 465 nm; $\varepsilon = 172$), $[Co(dipy)en(bigH)_2]^{3+}$ (λ_{max}, 480–490 nm; $\varepsilon = 175$); (en = ethylenediamine, dipy = α,α′-dipyridyl).[8,21,25] It thus appears that the histidinate ion behaves as an NN bidentate donor in this mixed chelate, using the imidazole and NH_2 nitrogen for linking to cobalt (III).[2,8,23]

Acknowledgements—The senior author (R.K.R.) wishes to thank Professor R. L. Dutta (Department of Chemistry, Burdwan University), Professor D. Banerjea (Department of Chemistry, University College of Science, Calcutta), Dr R. N. Banerjee (Department of Chemistry, Jadavpur University), and Dr P. Banerjee (Department of Chemistry, Indian Association for the Cultivation of Science, Calcutta) for helpful suggestions, for providing some facilities, and for constant encouragement during the course of this investigation. One of us (G.B.K.) is indebted to Professor Helen J. Gigliotti and Wendy M. Wheat (California State University, Fresno) for technical assistance.

REFERENCES

1. P. Rây, *Chem. Rev.* 1961, **61**, 313.
2. A. Syamal, *J. Sci. Ind. Res.* 1978, **37**, 661.
3. R. N. Banerjea and D. Banerjea, *Ind. J. Chem.* 1979, **17A**, 246.
4. D. Banerjea, *Transition Met. Chem.* 1982, **7**, 22.
5. R. K. Ray, *Polyhedron* 1989, **8**, 7.
6. R. L. Dutta and S. Sarkar, *J. Ind. Chem. Soc.* 1967, **44**, 832.
7. R. L. Dutta and I. Malik, *J. Ind. Chem. Soc.* 1967, **44**, 866.
8. R. L. Dutta and A. Bhattacharya, *J. Ind. Chem. Soc.* 1976, **52**, 1002.
9. A. Das, S. Gangopadhyay and D. Banerjea, *Transition Met. Chem.* 1987, **12**, 18.
10. A. Syamal, *J. Ind. Chem. Soc.* 1987, **64**, 719.
11. D. J. MacDonald, *J. Inorg. Nucl. Chem.* 1967, **29**, 1271.
12. A. Albert and E. Spinner, *J. Chem. Soc.* 1960, 1221.
13. P. V. Babykutty, C. P. Prabhakaran, R. Anantanaranan and C. G. R. Nair, *J. Inorg. Nucl. Chem.* 1974, **36**, 3685.
14. D. Sen, *J. Chem. Soc., Dalton Trans.* 1975, 1701.
15. R. H. Skabo and P. W. Smith, *Aust. J. Chem.* 1969, **22**, 659.
16. A. Syamal and V. D. Ghakekar, *J. Inorg. Nucl. Chem.* 1978, **40**, 1606.
17. K. Nakamoto and P. J. McCarthy, *Spectroscopy and Structure of Chelate Compounds*, p. 221. Wiley, New York (1968).
18. D. Banerjea and B. Chakraborty, *J. Inorg. Nucl. Chem.* 1964, **26**, 1233.
19. F. A. Cotton and G. Wilkinson, *Advanced Inorganic Chemistry*, p. 572. Interscience, New York (1962).
20. L. J. Zompa, *Chem. Commun.* 1969, 783.
21. R. L. Dutta, S. Sarkar and K. K. Bhattacharyya, *J. Ind. Chem. Soc.* 1973, **50**, 1235.
22. K. Nakamoto and P. J. McCarthy, *Spectroscopy and Structure of Chelate Compounds*, p. 358. Wiley, New York (1968).
23. R. H. Kretsinger, F. A. Cotton and R. F. Brayan, *Acta Cryst.* 1963, **16**, 651.
24. B. Evertsson, *Acta Cryst.* 1969, **25**, 30.
25. R. L. Dutta, *J. Ind. Chem. Soc.* 1967, **44**, 863.
26. J. Hidaka and B. E. Douglas, *Inorg. Chem.* 1964, **3**, 1180.

Polyhedron Vol. 8, No. 8, pp. 1019–1027, 1989
Printed in Great Britain

0277-5387/89 $3.00+.00
© 1989 Pergamon Press plc

COPPER(II) COMPLEXES WITH ASPARTATE AND GLUTAMATE

EMILIO BOTTARI*

Dipartimento di Chimica dell'Università di Roma "La Sapienza", P.le. A.Moro 5, Città Universitaria 00185 Roma, Italy

and

MARIA ROSA FESTA and RENATA JASIONOWSKA

Università del Molise, Campobasso, Italy

(*Received* 27 *September* 1988; *accepted* 9 *November* 1988)

Abstract—Aspartic and glutamic acids have been studied as ligands (L) for copper(II) at 25°C and in 1.00 M $NaClO_4$ (as a constant ionic medium), by measuring the electromotive force of galvanic cells containing glass and copper amalgam electrodes in a wide concentration range of the reagents, to elucidate the formation of the protonated species. The experimental data have accounted for the species CuL, CuL_2, CuHL, $CuHL_2$, CuH_2L_2, CuH_2L and, for aspartate, CuH_4L_2. The relative stability constants have been determined and compared with those of glycine and serine. The protonation constants of aspartate have also been determined under the same experimental conditions using an H_2 electrode.

The behaviour of amino acids as ligands (L) towards cations represents a subject of research in our laboratory. In previous papers, glycine[1] and serine[2,3] were studied, and experimental data were also explained by assuming the presence of protonated species.

In this paper the results obtained for the copper(II)–aspartate and copper(II)–glutamate systems are reported. These two amino acids, containing one amino and two carboxylic groups, can act as tridentate ligands.

Stability constants[4,5] and critical stability constants[6] represent the most important studies published until 1973. More recently, both systems have been more thoroughly investigated,[7–14] although equilibria involving glutamate have been studied in less detail than those with aspartate. Generally, from the limited amount of available data on the concentration ranges of the reagents, it seems that all the studies were carried out in only limited ranges. However, disagreement exists on the protonated species which are assumed to explain the experimental data.

Liang and Olin[14] have performed the most complete research on the copper(II)–aspartate system and accounted for their measurements of the electromotive force (e.m.f.) of cells containing glass electrodes by assuming the species CuL, CuHL, CuL_2, $CuHL_2$, CuH_2L_2 to exist. The system did not exhibit stereoselectivity.

Although Brookes and Pettit[9] studied the copper(II)–glutamate system in a very restricted reagent concentration range, they pointed out small quantities of protonated species, not found by other authors. To extend the study of Liang and Olin and to determine the existence and the stability constants of the protonated species, we planned to study both systems in a wide range of reagents by measuring the e.m.f. of cells containing glass and amalgam electrodes, so that it would be possible to obtain data on the existence of species not found previously, like CuH_2L, CuH_3L_2 and CuH_4L_2.[14]

The results will be used to compare the behaviour of aspartate, glutamate, serine and glycine as ligands towards copper(II).

* Author to whom correspondence should be addressed.

METHOD

Method of investigation

The ions Cu^{2+}, H^+ and aspartate (asp^{2-}) or glutamate (glu^{2-}) are considered to be independent reagents at 25°C in solutions of the following general composition: B M in Cu^{2+}; H M in H^+; A M in L; $(1-2B-H)$ M in Na^+; $(1-A)$ M in ClO_4^-, where L indicates one of the ligands, B and A represent the total concentrations of copper(II) and ligands, respectively, H is the analytical excess of hydrogen ions with respect to 1 M $NaClO_4$, H_2O and asp^{2-} or glu^{2-}, respectively.

To study equilibria occurring in the above described solution S, the e.m.f. of the cells:

$$\text{R.E.}|\text{Solution } S|\text{G.E.} \qquad \text{(I)}$$

$$\text{Cu(Hg)}|\text{Solution } S|\text{R.E.} \qquad \text{(II)}$$

was measured at 25°C, R.E., G.E. and Cu(Hg) are reference, glass and copper amalgam electrodes, respectively.

According to Biedermann and Sillén,[15] in a constant ionic medium (1 M $NaClO_4$), the e.m.f. of cells (I) and (II) at 25°C and in mV units can be expressed as a function of h (free hydrogen ions concentration) and b (free Cu^{2+} concentration):

$$E_I = E_I^0 + 59.16 \log h + E_j$$

$$E_{II} = E_{II}^0 - 29.58 \log b - E_j.$$

E_I^0 and E_{II}^0 are two constants determined in the absence of the ligand, so that $H = h$ and $B = b$. The liquid junction potential $= E_j$, and, under the selected experimental conditions, we found $E_j = -62h$. The values of b and h for each point were obtained by a procedure similar to that described previously.[16] For each set of measurements B and H were kept constant, while A and consequently $-\log h$ gradually increased. Titrations were terminated at $-\log h \leqslant 8$ and back titrations agreed well with the direct ones.

EXPERIMENTAL

Chemicals and apparatus

Copper(II) perchlorate, perchloric acid, sodium hydroxide, sodium perchlorate were prepared and analysed as described in ref. 17. Copper amalgam ($\approx 0.01\%$ weight) was prepared by dissolving electrolytic copper (freshly deposited) in a weighed amount of mercury in the measurement vessel. L-Aspartic and L-glutamic acids (both C.Erba and Fluka p.a.) were recrystallized twice from double-distilled water and then dried at 110°C. The absence of water and the stoichiometric composition were checked by TGA (Thermo gravimetric analysis). All solutions were purged of O_2 by bubbling purified N_2 through them as described previously. The H_2 electrode and the apparatus were described in ref. 18.

CALCULATIONS AND RESULTS

Knowledge of the protonation constants of aspartate and glutamate was necessary in order to account for the e.m.f. data in terms of complex formation. The equilibrium

$$asp^{2-} + nH^+ \rightleftharpoons H_n asp^{+n-2} \quad \text{where } n = 1, 2, 3,$$

defined by the relationship

$$[H_n asp] = k_n h [H_{n-1} asp] \quad \text{(charges omitted)},$$

was investigated at 25°C and 1 M $NaClO_4$, by measuring the e.m.f. of the cell

$$Pt,H_2|\text{Solution } S_1|\text{R.E.} \qquad \text{(III)}$$

as a function of H and A in the ranges $0 \leqslant H \leqslant 0.1$ M and $5 \times 10^{-3} \leqslant A \leqslant 0.02$ M.

The results of e.m.f. measurements of cell (III), elaborated as described in ref. 19, gave the following values of the protonation constants: $\log k_1 = 9.625 \pm 0.01$; $\log k_1 k_2 = 13.31 \pm 0.02$; $\log k_1 k_2 k_3 = 15.42 \pm 0.03$. The error limits were estimated from the maximum shift possible for which agreement was still acceptable.

The k_n values of the glutamate, determined in another paper,[20] under the same experimental conditions, are $\log k_1 = 9.52 \pm 0.01$; $\log k_1 k_2 = 13.69 \pm 0.02$; $\log k_1 k_2 k_3 = 16.00 \pm 0.03$.

For both systems (copper(II)–aspartate and copper(II)–glutamate) e.m.f. measurements were performed at different H values (0.025, 0.035, 0.050, 0.070 and 0.100 M) and B values (0.5, 1.0 and 2.0×10^{-3} M). As the e.m.f. of cells (I) and (II) gave b and h, and B was analytically known, it was possible to calculate η ($= \log(B/b)$) and the data could be presented in the form $\eta\ (-\log h)_{H,B}$.

Figures 1 and 2 show the dependence of η on $-\log h$ for copper(II) aspartate and glutamate, respectively. In both cases, as expected, η is independent of B, and therefore polynuclear complexes in Cu^{2+} are not present in appreciable concentration. The prevailing species are of the type CuH_pL_r with the relative stability constants $\beta_{1,p,r}$, where $p \neq 0$ and $r \geqslant 1$. To evaluate the predominant values assumed by p and r the free concentration of the ligand, a, can be obtained from the material balance of H, written in the following form:

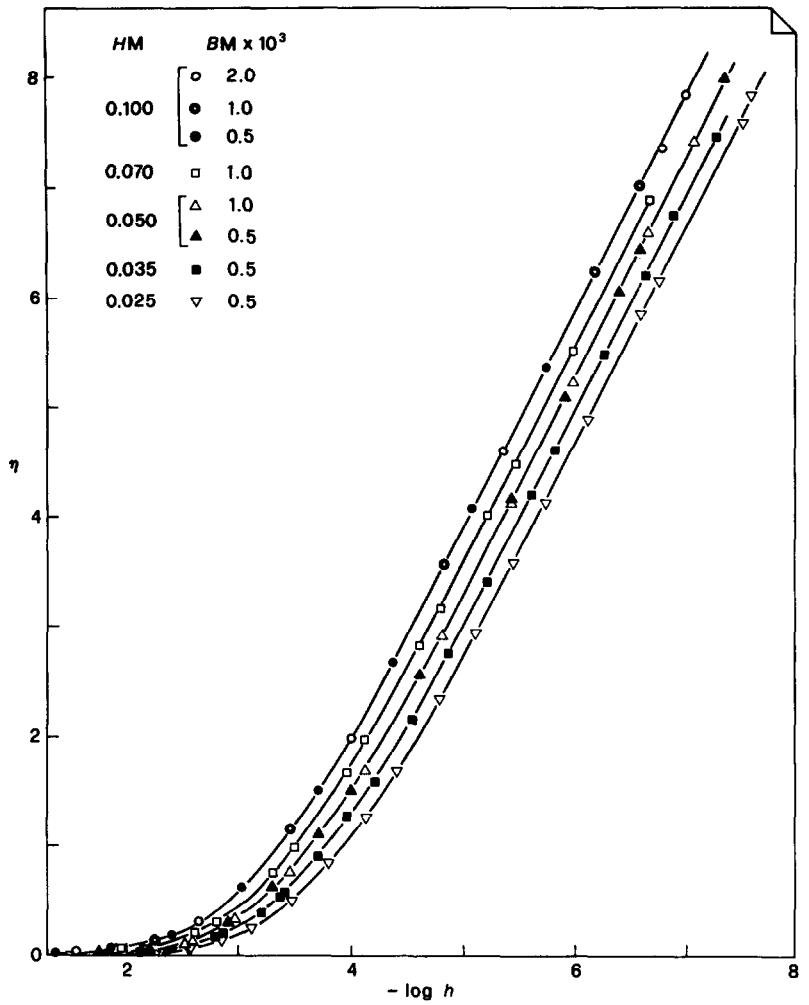

Fig. 1. Experimental data for the copper(II)–aspartate system plotted in the form η ($= \log(B/b)$) vs $-\log h$. Curves are calculated by means of the values collected in Table 1a.

$$H = h + k_1 ha + 2k_1k_2h^2a + 3k_1k_2k_3h^3a + \Sigma_p\Sigma_r p\beta_{1,p,r} bh^p a^r. \quad (1)$$

In eq. (1) and in those that follow, hydrolytic species of copper(II) are neglected on the basis of the obtained b and h and of the results of Berecki-Biedermann.[21] Since for all the points $H \geqslant 0.02B$, first approximation values of a can be calculated by neglecting the last term of eq. (1). It will be verified below that the first approximation and refined $\log a$ values coincide within ± 0.01.

In Figs 3 and 4, η is plotted against $\log a$ for aspartate and glutamate, respectively. As points obtained at different H fall on different curves, η is an increasing function of H, so that protonated species with $p \geqslant 0$ are present. However, in both cases, in the range $7 \leqslant -\log h \leqslant 8$, η is independent of H, so that species formed with loss of protons can be excluded.

At $-\log h \geqslant 5.5$, the quantity $\log[(10^{\eta}-1)b^{-1}a^{-2}]$ was constant within ± 0.03 and independent of B and H, so that the data could be explained by supposing the presence of CuL_2 alone (L is the aspartate or the glutamate, respectively) and the average value of the above quantity represented is its stability constant (see Table 1).

At a more acidic range ($2.5 \leqslant -\log h \leqslant 5$ for aspartate and $3.5 \leqslant -\log h \leqslant 5.5$ for glutamate), to find the prevailing values of p and r, the methods described for serine were applied.[2,3]

In these ranges, for both systems, the experimental data could be explained by assuming the presence of CuHL, CuL, $CuHL_2$ and CuH_2L_2 (where L indicates alternatively aspartate or glutamate). For all these complexes the stability constants were calculated.

Systematic deviations were observed for both systems at $-\log h \leqslant 2.5$ for aspartate and $-\log h \leqslant 3.5$ for glutamate. To verify the presence

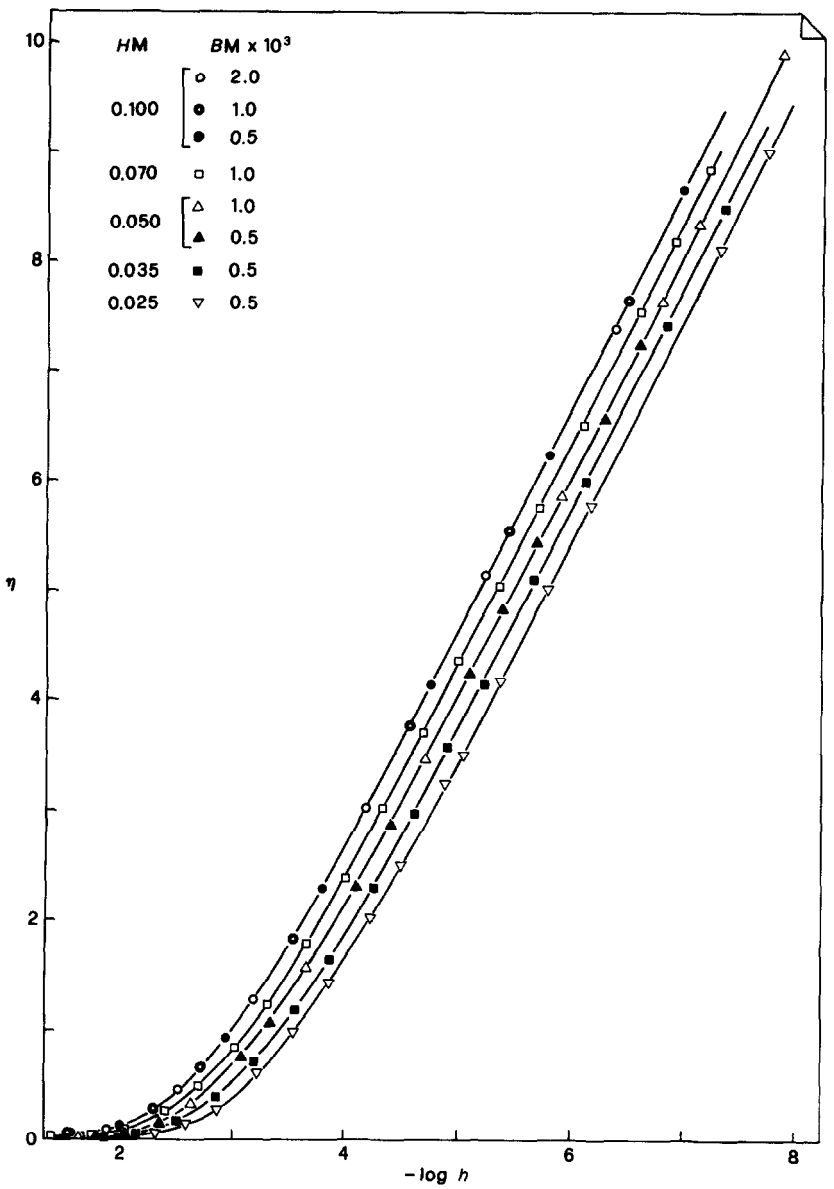

Fig. 2. Experimental data for the copper(II)–glutamate system plotted in the form η vs $-\log h$. Curves are calculated by means of the values collected in Table 1b.

of other species, the contribution of the complexes found at higher $-\log h$ was calculated by means of the already obtained constants assumed as correct and, by subtracting it from B, the following quantity was calculated for each point and for both systems:

$$B_c = B - \beta_{1,0,1}ba - \beta_{1,1,1}bha - \beta_{1,0,2}ba^2 - \beta_{1,1,2}bha^2 - \beta_{1,2,2}bh^2a^2. \quad (2)$$

Since in the $-\log h$ range reported above, the presence of other complexes was confirmed for all points $B_c > b$. To find the prevailing p' and r' of the species CuH_p, L_r present in this range, and their stability constants, η_c ($= \log(B_c/b)$) was calculated from eq. (2) and plotted against $-\log(h^2a)$.

In Fig. 5, the trend of η_c vs $-\log(h^2a)$ is shown for the system copper(II)–aspartate. Since the existence of CuH_2L alone does not explain the data, the hypothesis of the presence of CuH_2L and CuH_4L_2 was formulated, so that eq. (2) can be written as follows:

$$\eta_c = \log(1 + \beta_{1,2,1}h^2a + \beta_{1,4,2}h^4a^2).$$

According to the method of normalized curves proposed by Sillén,[22] the points of Fig. 5 were superimposed to a family of curves of equation:

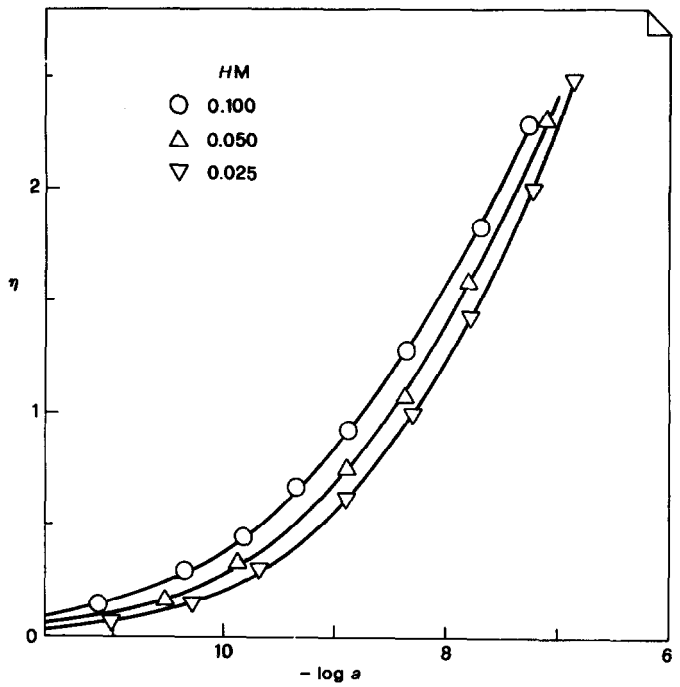

Fig. 3. The dependence of η on $-\log a$ at different H values, for the complexes formed by aspartate. Curves are calculated by means of the constants in Table 1a.

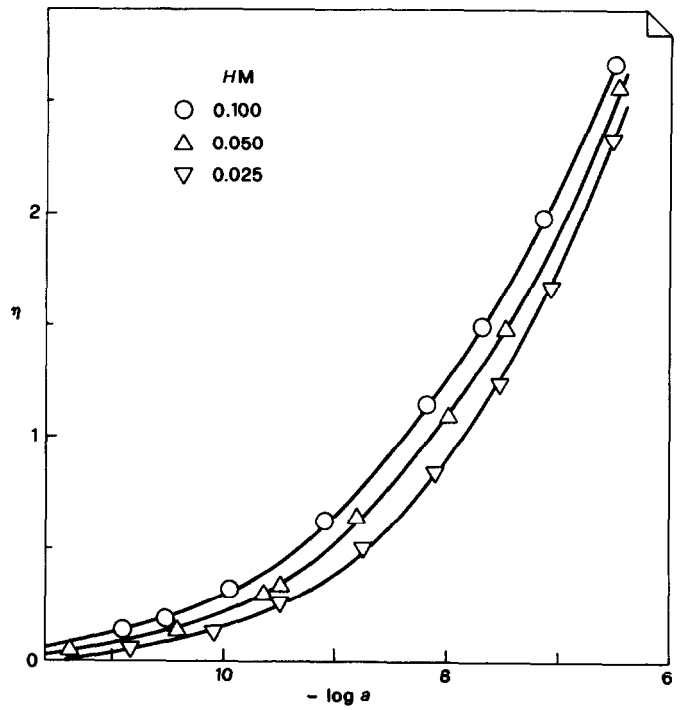

Fig. 4. The dependence of η on $-\log a$ at different H values, for the complexes formed by glutamate. Curves are calculated by means of the values in Table 1b.

Table 1. Values of the stability constants

(a) Copper(II)–aspartate Species	Approach I	Approach II	Proposed value
CuL	8.41±0.05	8.40±0.01	8.40±0.01
CuHL	12.44±0.04	12.38±0.02	12.40±0.02
CuH_2L	14.35±0.10	14.25±0.05	14.25±0.05
CuL_2	15.89±0.02	15.90±0.01	15.90±0.01
$CuHL_2$	20.10±0.10	20.16±0.05	20.15±0.05
CuH_2L_2	24.02±0.07	24.08±0.05	24.08±0.05
CuH_4L_2	28.34±0.15	28.26±0.07	28.26±0.07
(b) Copper(II)-glutamate Species	Approach I	Approach II	Proposed value
CuL	8.25±0.10	8.20±0.03	8.20±0.03
CuHL	12.34±0.07	12.42±0.05	12.40±0.05
CuH_2L	14.8±0.15	14.68±0.07	14.65±0.05
CuL_2	14.93±0.03	14.93±0.01	14.93±0.01
$CuHL_2$	19.62±0.08	19.57±0.04	19.60±0.04
CuH_2L_2	23.85±0.10	23.90±0.04	23.90±0.04

$$y = \log(1+\alpha u+u^2)$$

where $u = h^2a\sqrt{\beta_{1,4,2}}$ and $\alpha = \beta_{1,2,1}/\sqrt{\beta_{1,4,2}}$. From the point of best fit obtained by moving experimental and theoretical plots parallel to the abscissa, the values of $\beta_{1,2,1}$ and $\beta_{1,4,2}$ were obtained. The good agreement between the normalized curve and points (Fig. 5) confirm the above hypothesis.

The same procedure was applied to the points obtained for copper(II)–glutamate. In this case the assumption of CuH_2L alone satisfactorily explains the experimental data. The value of the corresponding stability constant $\beta_{1,2,1}$ was obtained in a similar manner to the case for aspartate.

The data obtained in the whole $-\log h$ range studied could be explained by assuming the following species for the system copper(II)–aspartate:

CuL, CuHL, CuH_2L, CuL_2,

$CuHL_2$, CuH_2L_2 and CuH_4L_2,

and for the system copper(II)–glutamate:

CuL, CuHL, CuH_2L, CuL_2, $CuHL_2$ and CuH_2L_2.

The stability constants found above were refined by an iterative treatment and the obtained values are collected in Table 1 as results of approach I.

In approach II, the experimental data B, H, A and b and h were elaborated by means of a computer graphic program described in another paper[23] and the species found, with their corresponding stability constants, are collected in Table 1. The results show that for both approaches the same species explain the experimental data and the values of the stability constants are practically coincident.

The $\beta_{1,p,r}$ values collected in Table 1 explain data obtained at higher B (till $B = 0.01$ M) as well.

DISCUSSION

Experimental data relating to equilibria occurring at 25°C and in 1 M $NaClO_4$ between copper(II)

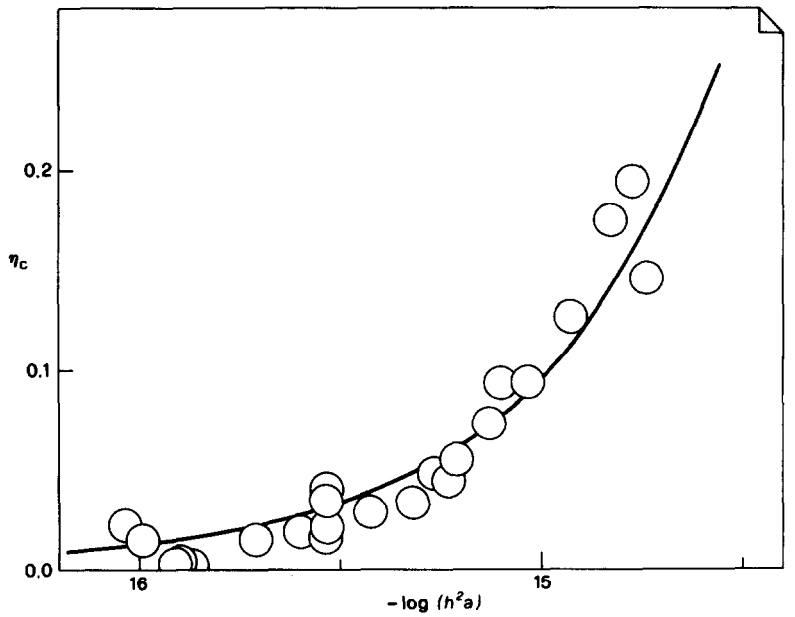

Fig. 5. The system copper(II)–aspartate. The plot η_c ($= \log(B_c/b)$ vs $-\log(h^2a)$ shows the presence of CuH_2L and CuH_4L_2. The curve is that normalized in the position of best fit.

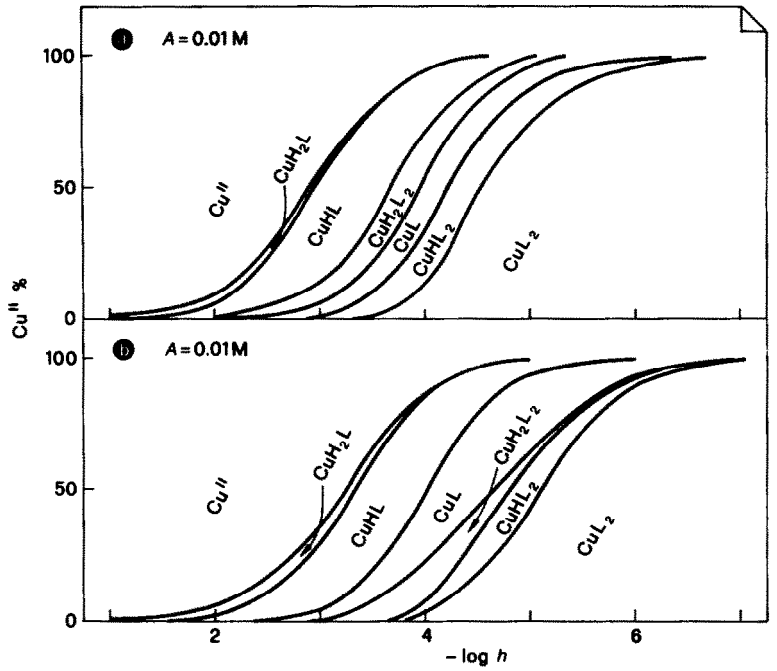

Fig. 6. Distribution of complexes as a function of $-\log h$ at $A = 0.01$ M and at $B = 0.5 \times 10^{-3}$ M for aspartate (a) and glutamate (b). Curves at higher B are practically coincident.

and aspartate or glutamate are well explained by assuming the species and relative stability constants collected in Table 1. Furthermore, the protonation constants of aspartate have been determined in the same experimental conditions.

From Table 1 and Fig. 6, it can be seen that aspartate is able to form several protonated species with copper(II). The first five complexes were found by Liang and Olin[14] and by Brookes and Pettit,[9] whereas CuH_2Asp and $CuH_4(Asp)_2$ were not found. By taking into account the different ionic medium, the stability constant for CuL here proposed approximately agrees with that proposed by Brookes and Pettit, that of CuHL agrees with the value proposed by Liang and Olin, while the other constants disagree with both works.[14,9]

Moreover, the constants of complexes containing two aspartates per species, do not agree with each other[9,14] probably because of either the limited concentration range investigated for the reagents or for the values of k_n determined by glass electrode or because the free concentration of the central group (*b*) was not measured.

By means of the observed $\beta_{1,p,r}$ distribution curves of the species existing in aqueous solutions of copper(II)–aspartate were calculated as a function of $-\log h$ at $A = 0.01$ M and plotted in Fig. 6. From the distribution curves relative to aspartate it is apparent that at $A = 0.01$ M, CuH_2L is only 2% of total copper(II) and CuH_4L_2 does not appear. By increasing A, their quantity increases so that CuH_2L reaches 5% at $A = 0.025$ M, whereas CuH_4L_2 appears at $A \geqslant 0.025$ (at $A = 0.025$ M it is about 1%).

To explain equilibria occurring between copper(II) and glutamate, the species CuL, CuL_2, CuHL, $CuHL_2$, CuH_4L_2 and CuH_2L have been proposed. No appreciable evidence for the existence of CuH_4L_2 was found. Our values cannot be compared with those of others because of the different experimental conditions, the limited ($\approx 1 \times 10^{-3}$ M) concentration ranges of the reagents and the values of the protonation constants of the ligand. At last no information is given on the way used to determine k_1, k_2 and k_3. The distribution curves of complexes found for copper(II)–glutamate are plotted in Fig. 6 at $A = 0.01$ M.

Only Brookes and Pettit[9] found the same species (except CuH_2L) but they calculated that CuH_2L_2 and $CuHL_2$, present in the range $3 \leqslant -\log h \leqslant 4.5$, constitute only 3–5% of total copper(II). This disagreement can be explained by taking into account that these researchers studied solutions containing copper(II) and glutamate only in a 1:1 ratio ($\approx 1 \times 10^{-3}$ M) and then the stability constants relative to the species containing two ligands are affected by a higher error.

Figure 6 shows that at $-\log h \approx 4$, $CuHL_2$ is $\approx 5\%$, CuH_2L_2 is 15%, and CuHL reaches 35%. At $-\log h = 3$, CuH_2L represents 5–6% of total

Table 2. A comparison between the values of $\log \beta_{1,p,r}$ for glycine, serine, aspartate and glutamate as ligands towards copper(II)

Species	Glycine	Serine	Aspartate	Glutamate
CuL	8.39	8.55	8.40	8.20
CuHL	10.62	10.90	12.40	12.40
CuH_2L	—	—	14.25	14.67
CuL_2	16.96	16.02	15.90	14.93
$CuHL_2$	—	—	20.15	19.60
CuH_2L_2	—	—	24.08	23.90
CuH_4L_2	—	—	28.26	—

The constants relative to glycine were earlier determined under the same experimental conditions,[24] while those corresponding to serine[2] were found in 3 M $NaClO_4$.

copper(II). It seems interesting to compare the behaviour of aspartate, glutamate, glycine and serine as ligands towards copper(II) (Table 2). All four ligands form with copper(II) CuL, CuL_2 and CuHL with differing stabilities.

Serine seems to be the strongest ligand and glutamate the weakest, whereas glycine and aspartate show approximately the same strength. The protonated complexes formed by the last two ligands of Table 2 are more stable than those that correspond to glycine and serine. The formation of CuH_2L, $CuHL_2$, CuH_2L_2 and CuH_4L_2 is reasonably attributed to the additional carboxylic group existing in the side chain of aspartic and glutamic acids.

To propose an explanation for the formation of protonated species, it is helpful to compare the constants relative to the following equilibria of the stepwise protonation of CuL and CuHL:

$$CuL + H^+ \rightleftharpoons CuHL \qquad (3)$$

with constant $K_1^H = [CuHL]h^{-1}[CuL]^{-1}$.

$$CuHL + H^+ \rightleftharpoons CuH_2L. \qquad (4)$$

with constant $K_2^H = [CuH_2L]h^{-1}[CuHL]^{-1}$.

Both (3) and (4) occur with aspartate and glutamate, while only equilibrium (3) can be formulated for serine and glycine. Completely different values of $\log K_1^H$ (2.2, 2.4, 4.0, 4.2, respectively) are obtained for all four ligands. On the contrary the values of $\log K_1^H$ obtained for serine and glycine (2.2 and 2.4) are similar and homogeneous with those of $\log K_2^H$ relative to aspartate and glutamate (1.9 and 2.3). As the $\log K_1^H$ and $\log K_2^H$ are determined by thermodynamic stability and by the kind of bond, it seems reasonable to suggest the following mechanism for the formation of the complexes.

For all the four ligands, first of all copper(II) is bound to the ligands through the amine group and the next carboxylic group to form CuL and CuL_2. In moderately acidic solutions ($-\log h \approx 5$) the carboxylic group of the side chain of aspartic and glutamic acids is protonated and the species CuHL, $CuHL_2$ and CuH_2L_2 are formed. Their respective quantities depend on the ratio ligand : copper(II) and on the $-\log h$ value. By further decreasing $-\log h$ (≈ 3), the proton displaces copper(II) from its bond with the $-NH_2$ group to form CuH_2L with the aspartic and glutamic acids, while CuHL appears in the case of glycine and serine. The formation of CuHL corresponds, in the case of glycine and serine, to the protonation of the aminic group, while for aspartate and glutamate, it relates to the protonation of the additional carboxylic group. Finally, the apparent higher stability of CuH_2L formed by glutamate can be explained by taking into account the basicity of the ligands, stronger for glutamate than aspartate.

Acknowledgements—This work was supported by Italian Consiglio Nazionale delle Ricerche (CNR) and by Italian Ministero della Pubblica Istruzione.

REFERENCES

1. E. Bottari and R. Jasionowska, *Ann. Chim., Roma* 1978, **68**, 517.
2. E. Bottari, M. R. Festa and R. Jasionowska, *Ann. Chim., Roma* 1987, **77**, 837.
3. E. Bottari, M. R. Festa and R. Jasionowska, *J. Coord. Chem.* 1988, **17**, 245.
4. A. E. Martell and L. G. Sillén, *Stability Constants.* Special Publications Nos 17(1964), and 25(1971), The Chemical Society, London.
5. D. D. Perrin, *Stability Constants of Metal Ion Complexes* Part B: Organic ligands. IUPAC Chemical data, Series No. 22, Pergamon Press (1979).
6. A. E. Martell and R. M. Smith, *Critical Stability Constants.* Plenum Press, New York (1974).
7. I. Nagypàl, A. Gergely and E. Farkas, *J. Inorg. Nucl. Chem.* 1974, **36**, 699.
8. J. H. Ritsma, *Recl. Trav. Chim. Pays-Bas* 1975, **94**, 210.
9. G. Brookes and L. D. Pettit, *J. Chem. Soc., Dalton Trans.* 1977, 1918.
10. T. Sakurai, O. Yamanchi and A. Nakahara, *Bull. Chem. Soc. Japan* 1978, **51**, 3203.
11. G. A. Boos, T. F. Solov'eva and A. V. Zakharov, *Russ. J. Inorg. Chem.* 1979, **24**, 1060.
12. R. F. C. Claridge, J. J. Kilpatrick and H. K. J. Powell, *Aust. J. Chem.* 1980, **33**, 2757.
13. L. Lomozik, A. Wojciechowska and M. Jaskolski, *Mh. Chemie* 1983, **114**, 1185.
14. Yi-Chang Liang and Å. Olin, *Acta Chem. Scand.* 1984, **38A**, 247.

15. G. Biedermann and L. G. Sillén, *Ark. Kemi* 1953, **5**, 425.
16. E. Bottari, *Mh. Chemie* 1975, **106**, 451.
17. E. Bottari, A. Liberti and A. Rufolo, *J. Inorg. Nucl. Chem.* 1968, **30**, 2173.
18. E. Bottari and R. Jasionowska, *Ann. Chim., Roma* 1979, **69**, 153.
19. E. Bottari, *Ann. Chim., Roma* 1976, **66**, 677.
20. E. Bottari, M. R. Festa and R. Jasionowska, *J. Coord. Chem.*, to be published.
21. C. Berecki-Biedermann, *Ark. Kemi* 1956, **9**, 175.
22. L. G. Sillén, *Acta Chem. Scand.* 1956, **10**, 186.
23. E. Bottari, T. Coccitto, G. Curzio, M. R. Festa and R. Jasionowska, *Ann. Chim., Roma* 1988, **78**, 635.
24. E. Bottari, R. Jasionowska and R. Porto, *Ann. Chim., Roma* 1983, **73**, 15.

Polyhedron Vol. 8, No. 8, pp. 1029–1032, 1989
Printed in Great Britain

0277–5387/89 $3.00+.00
© 1989 Pergamon Press plc

SYNTHESIS AND CHARACTERIZATION OF SOME OXO-BRIDGED TRI- AND TETRANUCLEAR MANGANESE(III) SCHIFF BASE COMPLEXES

BANGLIN CHEN and KE CHEN*

Chemistry Department of Zhejiang University, Hangzhou, China

(*Received* 3 *October* 1988; *accepted* 9 *November* 1988)

Abstract—Some oxo-bridged tri- and tetranuclear manganese(III) Schiff base complexes $[Mn_3O(bzacipa)_2(O_2CCH_3)_3]$, $[Mn_3O(bzacipa)_2(O_2CCH_3)_2NCS\cdot H_2O]$, and $[Mn_4O_2(bzacipa)_2(O_2CCH_3)_2(NCS)_2\cdot 2H_2O]$, where $bzacipa^{2-}$ is the dianion of 2-(β-hydroxy-β-methylethyl-imine)-4-phenyl-butanone(4), have been synthesized and characterized by elemental analyses, IR and electronic spectra, and thermal analyses. The possible structures of the complexes are suggested.

It is generally believed that four atoms of manganese per photosystem II reaction centre are essential for oxygen evolution in green plants and photosynthetic bacteria.[1-2] The Mn_4 aggregate is capable of cycling between five oxidation levels (S_0–S_4) during the catalytic cycle,[3-6] but can also adopt an additional "super-reduced" oxidation level, labelled S_{-1}, under certain conditions.[7] It was recently reported that the complexes containing the $[Mn_4O_2]$ core have structural features similar to the enzyme and are isolable in three oxidation levels corresponding to the native S_{-1}, S_0 and S_1 levels.[8,9] Oxo-bridged trinuclear centres are likely intermediates in the formation of large polynuclear aggregates for manganese and iron complexes.[8-11] In the preceding report we have synthesized some trinuclear manganese(III) complexes containing the tridentate Schiff base ligand $bzacea^{2-}$, where $bzacea^{2-}$ is the dianion of 2-(β-hydroxyethylimine)-4-phenyl-butanone(4).[12] In this paper we describe the synthesis and characterization of $[Mn_3O(bzacipa)_2(O_2CCH_3)_2]$, $[Mn_3O(bzacipa)_2(O_2CCH_3)_2NCS\cdot H_2O]$ and $[Mn_4O_2(bzacipa)_2(O_2CCH_3)_2(NCS)_2\cdot 2H_2O]$, where $bzacipa^{2-}$ is the dianion of 2-(β-hydroxy-β-methylethyl-imine)-4-phenyl-butanone (4)

EXPERIMENTAL

Materials

The Schiff base $H_2bzacipa$ was prepared similarly to $H_2bzacea$.[13] $Mn(O_2CCH_3)_3\cdot 2H_2O$ was prepared according to ref. 14, then dried *in vacuo* over KOH. All other chemicals and solvents were reagent grade and used without further purification.

Preparation of $[Mn_3O(bzacipa)_2(O_2CCH_3)_3]$

The ligand $H_2bzacipa$ (3.0 g, 1.37×10^{-2} mol), dissolved in 15 cm^3 of hot 2-C_3H_7OH was added to a solution of $Mn(O_2CCH_3)_3\cdot 2H_2O$ (5.4 g, 2.06×10^{-2} mol) in 80 cm^3 of hot 2-C_3H_7OH. The resulting mixture was allowed to stand at 40°C for 3 h. The precipitated solids were collected on a filter, washed with small volumes of 2-C_3H_7OH and dried *in vacuo*. Yield: 2.7 g; 50% based on the $Mn(O_2CCH_3)_3\cdot 2H_2O$ used. Found: C, 48.7; H, 5.0; N, 3.2; Mn, 20.2. Calc. for $C_{32}H_{39}Mn_3N_2O_{11}$: C, 48.5; H, 5.0; N, 3.5; Mn, 20.8%.

Preparation of $[Mn_3O(bzacipa)_2(O_2CCH_3)_2NCS\cdot H_2O]$

The complex $[Mn_3O(bzacipa)_2(O_2CCH_3)_3]$ (0.7 g, 8.84×10^{-4} mol) in 10 cm^3 CH_3OH was treated with 50 cm^3 of aqueous solution of KNCS (8.84×10^{-3} mol). The precipitate was formed after stirring for several minutes. The solids were isolated on a filter, washed with 3×10 cm^3 of distilled water and dried *in vacuo* over silica gel. Yield: 5 g; 70% based on $[Mn_3O(bzacipa)_2(O_2CCH_3)_3]$ used. Found: C, 46.2; H, 4.9; N, 4.6; Mn, 19.7. Calc. for $C_{31}H_{38}Mn_3O_{10}S$: C, 46.0; H, 4.7; N, 5.2; Mn, 20.4%.

* Author to whom correspondence should be addressed.

Preparation of $[Mn_4O_2(bzacipa)_2(O_2CCH_3)_2(NCS)_2 \cdot 2H_2O]$

The complex $[Mn_3O(bzacipa)_2(O_2CCH_3)_3]$ (0.7 g, 8.84×10^{-4} mol) in 10 cm^3 CH_3OH was treated with 50 cm^3 of aqueous solution of KNCS (8.84×10^{-3} mol). The precipitate was formed after stirring for several minutes and was extracted with 2×30 cm^3 of chloroform. The chloroform solution of the complexes was re-extracted into 2×50 cm^3 of distilled water. The chloroform phase was filtered and the pure solid was crystallized by the addition of petroleum ether. The solids were isolated on a filter, washed with ether and dried *in vacuo* over silica gel. Yield: 0.25 g; 40% based on the $[Mn_3O(bzacipa)_2(O_2CCH_3)_3]$ used. Found: C, 40.2; H, 4.3; N, 5.5; Mn, 22.6. Calc. for $C_{32}H_{40}Mn_4N_4O_{12}S_2$: C, 40.2; H, 4.2; N, 5.9; Mn, 23.0%.

Physical measurements

Carbon, hydrogen and nitrogen analyses were carried out with a Perkin–Elmer 240 microanalyser. The manganese analysis was carried out by the formaldoxime method.[15] Electronic spectra were recorded with a Shimadzu UV-240 type spectrophotometer using CH_3OH solutions of the complexes. The IR spectra were obtained using KBr discs (4000–400 cm^{-1}) on a Nicolet 5DX IR spectrophotometer, and polyethylene discs (500–200 cm^{-1}) on a Nicolet 170SX IR spectrophotometer. The thermal analyses studies were obtained using a Peking PCT-1 thermobalance. Thermogravimetry and differential thermal analyses curves were obtained at a heating rate of 10°C min^{-1} in static air. The intermediate products isolated for $[Mn_3O(bzacipa)_2(O_2CCH_3)_2NCS \cdot H_2O]$ and $[Mn_4O_2(bzacipa)_2(O_2CCH_3)_2(NCS)_2 \cdot 2H_2O]$ were obtained by heating these compounds on the thermobalance until the weight loss is 63 and 55%, respectively.

RESULTS AND DISCUSSION

Synthetic method

When the method of synthesizing $[Mn_3O(bzacea)_2(O_2CCH_3)_3]$[12] was used to synthesize $[Mn_3O(bzacipa)_2(O_2CCH_3)_3]$ (the solutions of H_2bzacipa and $Mn(O_2CCH_3)_3 \cdot 2H_2O$ in 2-propanol were refluxed and stirred for 3 h), only mixtures of large polynuclear manganese complexes were isolated (%Mn > 25) and the synthesis was difficult to repeat. Synthesis under mild conditions (the solutions were kept at 40°C for 3 h) produced $[Mn_3O(bzacipa)_2(O_2CCH_3)_3]$. The tendency of H_2bzacipa to form larger polynuclear manganese complexes was also found in the formation of $[Mn_4O_2(bzacipa)_2(O_2CCH_3)_2(NCS)_2 \cdot 2H_2O]$. The complexes are slightly soluble in methanol and DMSO, but insoluble in other solvents.

IR spectra

The ligand H_2bzacipa shows a sharp O—H stretching vibration at 3320 cm^{-1} and exists mainly in the ketamine structure[16] (Fig. 1). When the complexes are formed, the ν(O—H) disappears and ν(C=O) shifts to a lower frequency, indicating the coordination of the oxygens in the ligand. The complex $[Mn_3O(bzacipa)_2(O_2CCH_3)_3]$ shows $\nu_{as}(CO_2^-)$ at 1610 cm^{-1} and $\nu_s(CO_2^-)$ at 1395 cm^{-1}, $\Delta\nu = 215$ cm^{-1}, indicating the existence of monodentate $CH_3CO_2^-$.[17] The complexes $[Mn_3O(bzacipa)_2(O_2CCH_3)_2NCS \cdot H_2O]$ and $[Mn_4O_2(bzacipa)_2(O_2CCH_3)_2(NCS)_2 \cdot 2H_2O]$ show ν(CN) at 2060 cm^{-1} indicating the presence of the N-bonded NCS^-.[18] Johnson *et al.*[19] have analysed the IR and Raman spectra of a series of complexes $[M^{III}_3O(O_2CR)_6L_3]X \cdot xH_2O$. The $\nu_{asym}(M_3O)$ would be expected to lie in the region 500–700 cm^{-1}. The complex $[Mn_3O(O_2CCH_3)_6Py_3]ClO_4$ shows $\nu_{asym}(Mn_3O)$ at 590 cm^{-1} and $\delta_s(Mn_3O)$ at 289 cm^{-1}. The complexes reported here show $\nu_{asym}(Mn_3O)$ at *ca* 530 cm^{-1} and $\delta_s(Mn_3O)$ at *ca* 280 cm^{-1}, indicating the presence of μ_3-O atoms. The trinuclear manganese complexes contain a Mn_3O unit and the complex $[Mn_4O_2(bzacipa)_2(O_2CCH_3)_2(NCS)_2 \cdot 2H_2O]$ contains a Mn_4O_2 unit which includes two Mn_3O units sharing one edge. The Mn_4O_2 unit was found in tetranuclear manganese complexes such as $[Mn_4O_2(O_2CCH_3)_6(bpy)_2]$,[9] $[Mn_4O_2(O_2CCH_3)_7(bipy)_2]ClO_4 \cdot 3H_2O$ and $[Mn_4O_2(O_2CPh)_7(bipy)_2]$.[8] The IR spectral data are listed in Table 1.

Electronic spectra

The ligand H_2bzacipa shows two absorptions at 41.5×10^3 cm^{-1} (I) and 29.4×10^3 cm^{-1} (II) in CH_3OH and tentative assignments are made to the

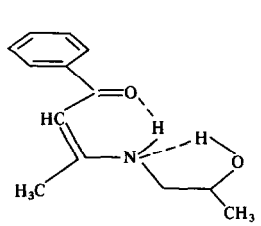

Fig. 1. The ketamine structure of H_2bzacipa.

Table 1. IR spectral data (cm^{-1}) of the complexes

Complex	C=O	C=C (aromatic)	C=C (non-aromatic)	Mn_3O (ν_{asym})	Mn_3O (δ_s)
H_2bzacipa	1600	1579	1540	—	—
$[Mn_3O(bzacipa)_2(O_2CCH_3)_3]$	1590	1576	1511	540	284.5, 278.6
$[Mn_3O(bzacipa)_2(O_2CCH_3)_2NCS\cdot H_2O]$	1596	1570	1509	527	292, 272
$[Mn_4O_2(bzacipa)_2(O_2CCH_3)_2(NCS)_2\cdot 2H_2O]$	1590	1571	1508	524	286, 272

$\pi \rightarrow \pi^*$ transition of the benzene ring conjugated with carbonyl, and the $\pi \rightarrow \pi^*$ transition of C=C—C=O conjugated with benzene, respectively.[12] The complexes show two new absorptions at ca 27.0×10^3 cm^{-1} (III) and ca 21.5×10^3 cm^{-1} (IV) having similar energy to the $[Mn_3O(bzacea)_2(O_2CCH_3)_3]$ type complexes[12] and are tentatively assigned to charge-transfer and ligand-field transitions, respectively. The energy of band (IV) is comparable to that of the $^5E_g \rightarrow {}^5T_{2g}$ transition in the $[Mn_3O(O_2CCH_3)_6CH_3CO_2H]ClO_4$ and $[Mn_3O(O_2CCH_3)_6Py_3]ClO_4$ complexes.[20] The electronic spectral data and their assignments are listed in Table 2.

Thermal analysis

Figure 2 displays the TG and DTA curves of $[Mn_3O(bzacipa)_2(O_2CCH_3)_3]$. The thermal decomposition products are suggested and are listed in Table 3. The observed weight losses for these processes compare favourably with the theoretical values. The intermediate thermal decomposition products of $[Mn_3O(bzacipa)_2(O_2CCH_3)_2NCS\cdot H_2O]$ (weight loss: 62%) and $[Mn_4O_2(bzacipa)_2(O_2CCH_3)_2(NCS)_2\cdot 2H_2O]$ (weight loss: 57%) show ν(S=O) absorptions at 1120 cm^{-1}.[21] The thermal decomposition processes of the complexes show some similarity with the trinuclear manganese(III) carboxylic acid complexes.[22] The processes are as follows: reduce to the polymanganese complexes first, and then change to Mn_3O_4 (see Table 3). The residues from the thermal analyses of the complexes are confirmed to be Mn_3O_4 by manganese analyses and IR spectra, which show absorptions at 610, 490 and 415 cm^{-1}.[23]

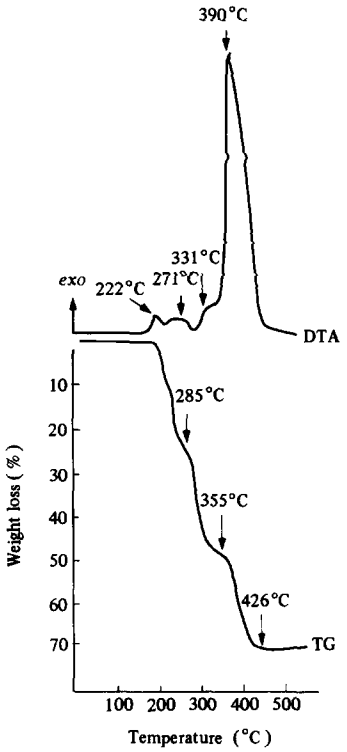

Fig. 2. TG and DTA curves of $[Mn_3O(bzacipa)_2(O_2CCH_3)_3]$.

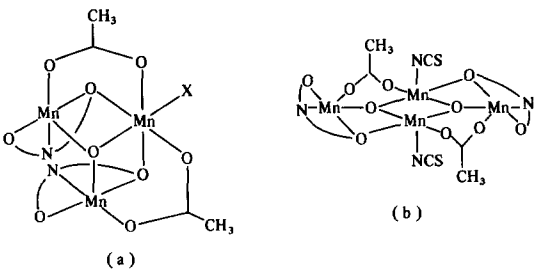

Fig. 3. Possible structures of the complexes: (a) trinuclear complexes and (b) the tetranuclear complex.

Table 2. Electronic spectral data ($\times 10^3$ cm^{-1}) of the complexes

Complex	$\pi \rightarrow \pi^*$	Charge-transfer	Ligand-field
$[Mn_3O(bzacipa)_2(O_2CCH_3)_3]$	40.0	26.7	20.6(sh)
$[Mn_3O(bzacipa)_2(O_2CCH_3)_2NCS\cdot H_2O]$	40.8	26.3	21.5(sh)
$[Mn_4O_2(bzacipa)_2(O_2CCH_3)_2(NCS)_2\cdot 2H_2O]$	40.3	26.4	21.6(sh)

Table 3. Thermal decomposition products of the complexes

Complex	Temperature range (°C)	Peak temperature (°C)	Possible intermediate product	Weight loss (%) obs.	calc.
$[Mn_3O(bzacipa)_2(O_2CCH_3)_3]$	20–285	222(exo), 271(exo)	$[Mn_3O_2(bzacipa)_2(O_2CCH_3)_3]$	25.7	25.4
	285–355	331(exo)	$1/2[Mn_6O_4(bzacipa)_2(O_2CCH_3)_4]$	47.6	46.6
	355–426	390(exo)	Mn_3O_4	71.6	71.1
$[Mn_3O(bzacipa)_2(O_2CCH_3)_2NCS \cdot H_2O]$	20–178	—	$1/2[Mn_6O_2(bzacipa)_4(O_2CCH_3)_3(NCS)_2]$	5.8	5.9
	178–478	—	$1/2[Mn_6O_4(bzacipa)(O_2CCH_3)_3(NCS)_2]$	45.3	44.1
	478–626	538(exo)	$Mn_3O_3SO_4$	61.9	61.8
	626–873	—	Mn_3O_4	71.3	71.7
$[Mn_4O_2(bzacipa)_2(O_2CCH_3)_2(NCS)_2 \cdot 2H_2O]$	20–158	97(endo)	$[Mn_4O_2(bzacipa)_2(O_2CCH_3)_2(NCS)_2]$	4.2	3.8
	158–461	207(exo), 433(exo)	$[Mn_4O_4(bzacipa)(NCS)_2]$	35.5	35.5
	461–680	510(exo)	$4/3Mn_3O_3SO_4$	57.1	56.9
	680–892	—	$4/3Mn_3O_4$	67.5	68.1

It is common for manganese(III) to be five- or six-coordinate and the possible structures of the be Mn_3O_4 by manganese analyses and IR spectra, see Fig. 3, where $\overset{\frown}{O}\,\overset{\frown}{N}\,\overset{\frown}{O}$ denotes a bridging tridentate ligand; water coordination was not assumed.

REFERENCES

1. J. Amesz, *Biochim. Biophys. Acta* 1983, **726**, 1.
2. G. C. Dismukes, *Photochem. Photobiol.* 1986, **43**, 99.
3. J. P. Dekker, H. J. Van Gorkum, M. Brok and L. Ouwehand, *Biochim. Biophys. Acta* 1984, **767**, 301.
4. D. B. Goodin, V. K. Yachandra, R. D. Britt, K. Sauer and M. P. Klein, *Biochim. Biophys. Acta* 1984, **767**, 209.
5. B. Kok, B. Forbush and M. McGloin, *Photochem. Photobiol.* 1970, **11**, 457.
6. A. N. Scrinnasan and R. R. Sharp, *Biochim. Biophys. Acta* 1986, **850**, 211.
7. E. K. Pistorius and G. H. Schmid, *Biochim. Biophys. Acta* 1987, **890**, 352.
8. J. B. Vincent, C. Christmas, J. C. Huffman, G. Christou, H.-R. Chang and D. N. Hendrickson, *J. Chem. Soc., Chem. Commun.* 1987, 236.
9. C. Christmas, J. B. Vincent, J. C. Huffman, G. Christou, H.-R. Chang and D. N. Hendrickson, *J. Chem. Soc., Chem. Commun.* 1987, 1303.
10. C. Christmas, J. B. Vincent, J. C. Huffman, G. Christou, H.-R. Chang and D. N. Hendrickson, *Angew. Chem. Int. Ed. Engl.* 1987, **26**, 915.
11. S. J. Lippard, *Chem. Brit.* 1986, **22**, 222.
12. K. Chen and B. L. Chen, *K. Tongbao*, accepted.
13. E. Jäger, *Z. Chem.* 1966, **6**, 111.
14. E. I. Heiba, R. M. Dessau and W. J. Koehl Jr, *J. Am. Chem. Soc.* 1969, **91**, 138.
15. Z. Marczenko, *Spectrophotometric Determination of Elements*. Wydawnictwa Naukowo Techniczne, Warsaw (1976).
16. G. O. Dudek and R. H. Holm, *J. Am. Chem. Soc.* 1961, **83**, 2099.
17. K. Nakamoto, *Infrared Spectra of Inorganic and Coordination Compounds*, 2nd edn. John Wiley, New York (1970).
18. K. Nakamoto, *Coordination Chemistry* (Edited by A. E. Martell), Vol. 1. Van Nostrand, New York (1971).
19. M. B. Johnson, D. B. Powell and R. D. Cannon, *Spectrochim. Acta* 1981, **37A**, 995.
20. T. Shchiman'ski-buzar and Yu. Yu. Eyulkovski, *Koord. Khim.* 1976, **2**, 1172.
21. L. J. Bellamy, *The Infrared Spectra of Complex Molecules*, Vol. 1, 3rd edn. Chapman and Hall, London (1975).
22. I. V. Arkhangel'skii *et al.*, *Zh. Neorg. Khim.* 1985, **30**, 3078.
23. *Gmelins Handbuch Der Anorganischenchemie*, Mangan Teil Cl. Springer, Berlin (1974).

Polyhedron Vol. 8, No. 8, pp. 1033–1037, 1989
Printed in Great Britain

0277–5387/89 $3.00+.00
© 1989 Pergamon Press plc

CHELATE COMPLEXES CONTAINING THE {Mo(NO)HB(3,5-$Me_2C_3N_2H)_3$} MOIETY AND AN EXAMPLE OF A PYRAZOLE SUBSTITUTION REACTION INVOLVING THE HB(3,5-$Me_2C_3N_2H)_3$ LIGAND

NAJAT ALOBAIDI

Department of Physics, College of Education, AlMustansiriyah University, Baghdad, Iraq

and

CHRISTOPHER J. JONES* and JON A. McCLEVERTY

Department of Chemistry, University of Birmingham, PO Box 363, Birmingham B15 2TT, U.K.

(*Received* 19 *October* 1988; *accepted* 10 *November* 1988)

Abstract—Toluene-3,4-dithiol ($TDTH_2$) reacts with [Mo(NO)LX_2] (X = OEt or I; L = HB(3,5-$Me_2C_3N_2H)_3$) to produce the chelate complex [Mo(NO)L(TDT)]. This complex is reduced at a potential more anodic than its non-chelated counterpart [Mo(NO)L$(SPh)_2$]. The reaction between [Mo(NO)LI_2] and 1,2-diaminobenzene affords the bimetallic complex [{Mo(NO)LI}$_2$(1,2-$(NH)_2C_6H_4$)]. This reaction and that of [Mo(NO)LI_2] with 2-aminobenzenethiol also produce products in which partial degradation of the tripodal ligand L has occurred with one dimethyl pyrazolyl group being lost.

The sterically demanding tripodal ligand hydrotris(3,5-dimethylpyrazolyl)borate (L) may be used to restrict both molybdenum(II), in the form of $\{Mo(NO)\}^{3+}$, and molybdenum(V), in the form of $\{MoO\}^{3+}$, to octahedral six-coordination.[1,2] In the case of the $\{Mo(NO)L\}^{2+}$ moiety, this results in the formation of formally 16-electron complexes of the general formula [Mo(NO)LXY] (X, Y are halide alkoxide, aryloxo, organoamide or thiolate). These coordinatively unsaturated species are stabilized by both steric and electronic factors.[1,3]

A surprising observation on the chemistry of the {MoL} moiety is that, whilst several examples of molybdenum(V) species containing five-membered chelate rings attached to the $\{Mo(O)L\}^{2+}$ core have been characterized,[2] no such examples have been reported for the molybdenum(II) $\{Mo(NO)L\}^{2+}$ core. Thus [Mo(O)L(Chel)] (Chel = OCH_2CH_2O, 1,2-$O_2C_6H_4$, 1,2-$ONHC_6H_4$, 1,2-$SNHC_6H_4$ or 3,4-$S_2C_6H_4Me$) have been prepared,[2] but the reaction of [Mo(NO)LI_2] with 1,2-NH_2—EH—C_6H_4 (E = NH, S or O) affords complexes of the formula [Mo(NO)L{NHC_6H_4EH}], in which only one donor atom of the bifunctional aryl ligand is bound to molybdenum. In the case of catechol, the reaction with [Mo(NO)LI_2] results in the destruction of the ligand L by deboronation to give [Mo(NO)(3,5-$Me_2C_3N_2H)_3(O_2$—$C_6H_4)$].[4] In addition, all attempts to prepare a chelate complex of {Mo(NO)L} with glycol have thus far failed;[5] although complexes containing large polyethylene glycol chelate rings are known.[6] A comparison of the structural data for [Mo(E)L$(SPh)_2$] (E = O or NO) reveals[2,7] that the Mo—N—(L) bond distances are slightly longer in the complex with E = O than with E = NO (averages: 2.243 Å for E = O and 2.222 Å for E = NO). This effect is especially pronounced if only the Mo—N(L) bonds *trans* to the E ligands are considered (2.367 Å for E = O and 2.244 Å for E = NO). The Mo—S distances are also longer (averages: 2.382 Å for E = O and 2.358 Å for E = NO). It would seem possible that in the nitrosyl complexes the reduced bond distances result in a closer approach of the non-donor chelate ring atoms to a 3-Me substituent in L. This in turn might give rise to a stronger interligand repulsion

* Author to whom correspondence should be addressed.

than occurs in the {Mo(O)} derivatives. The use of larger donor atoms such as sulphur in toluene-3,4-dithiol ($TDTH_2$) might relieve this interaction, allowing chelation to occur in the nitrosyl complex as well as the oxo complex.

In addition to these steric considerations, the formation of chelate rings with the $\{Mo(NO)L\}^{2+}$ moiety will have electronic consequences. In [Mo(NO)LXY], $p\pi$–$d\pi$ donation from the donor atoms of X and Y to the unfilled molybdenum *d* orbital can alleviate the electron deficiency of the molybdenum centre.[1] A similar situation arises in the related complex $[Mo(NO)(\eta^5\text{-}C_5H_5)(SPh)_2]$. Ashby and Enemark have shown[3] that the interaction between filled sulphur 3*p* orbitals and the molybdenum d_{xy} orbital elevates the energy of the LUMO, thus reducing the nucleophilic character of the complex. This accounts for the finding that $[Mo(NO)(\eta^5\text{-}C_5H_5)(SPh)_2]$ remains monomeric rather than dimerizing via sulphur bridges to give a formally 18-electron compound. The solid state structure[3] of this complex reveals that the thiophenolate ligands are orientated so as to maximize the overlap between sulphur 3*p* orbitals and the molybdenum d_{xy} orbital. The incorporation of a bridging group between the sulphur donor atoms to form a chelate would change the orientation of the sulphur 3*p* orbitals, thus reducing opportunities for their interaction with the unfilled molybdenum *d* orbital. The effect of this would be a destabilization of the higher energy filled orbitals and a stabilization of the LUMO.[3] This latter effect would be expected to give rise to an anodic shift in the reduction potential of a chelate complex as compared to a non-chelated analogue.

In order to examine the points raised above we have re-investigated the synthesis of chelate complexes containing the $\{Mo(NO)L\}^{2+}$ moiety. The ligands selected for this study were toluene-3,4-dithiol ($TDTH_2$) to provide two large donor atoms and 1,2-diaminobenzene ($DABH_2$) to provide two small donor atoms but reduce the risk of boron sequestration which arises with oxygen donors,[4] and finally 2-aminobenzenethiol ($ABTH_2$) to represent the intermediate situation.

EXPERIMENTAL

Synthetic studies

All reagents were used as supplied, $[Mo(NO)\{HB(3,5\text{-}Me_2C_3N_2H)_3\}I_2]$ and $[Mo(NO)\{HB(3,5\text{-}Me_2C_3N_2H)_3\}(OEt)_2]$ were prepared according to previously described methods.[8,9] Silica gel 60 (70–230 mesh) was used as the stationary phase for column chromatography unless otherwise stated. All reactions were carried out under nitrogen but purification procedures were carried out in air. Elemental analyses were carried out by the Microanalytical Laboratory, University of Birmingham.

IR spectra were recorded using a PE 297 spectrometer as KBr discs unless otherwise stated. ^1H NMR spectra were obtained as solutions in $CDCl_3$ using Varian HA 100 or Jeol GX 270 (270 MHz) instruments. Cyclic voltammetric measurements were made using a Hitek PPR 1 waveform generator and DT 2101 potentiostat or a PAR 174A polarograph. Solutions in CH_2Cl_2 were *ca* 10^{-3} mol dm^{-3} in complex and 0.2 mol dm^{-3} in $[Bu^nN]BF_4$ as the base electrolyte. A platinum bead test electrode was used with an SCE reference electrode and ferrocene as internal standard. Potentials are quoted relative to the SCE and under these conditions E_f for the oxidation of ferrocene was found to be 0.56 V with a ΔE_p of 100 mV. The number of electrons associated with electrode processes was estimated by comparison with $[Mo(NO)LCl_2]$ and confirmed by coulometry where specified in the text.

[Mo(NO)L(TDT)]

Method I. A mixture of $[Mo(NO)LI_2]$ (0.5 g, 0.75 mmol) and toluene-3,4-dithiol (0.32 g, 1 mmol) was heated for 24 h in CH_2Cl_2 (100 cm^3) containing NEt_3 (10 drops) under reflux. The deep blue solution which formed was evaporated to dryness under reduced pressure and the solid obtained was purified by recrystallization from CH_2Cl_2–hexane mixtures. Further purification was effected by column chromatography using CH_2Cl_2 as the eluant. Yield 0.24 g (55%).

Method II. A mixture of $[Mo(NO)L(OEt)_2]$ (1 g, 1.95 mmol) and toluene-3,4-dithiol (0.32 g, 1 mmol) was heated for 24 h in toluene (60 cm^3) under reflux. The deep blue solution which formed was evaporated to dryness under reduced pressure and the solid obtained was purified by recrystallization from CH_2Cl_2–hexane mixtures. Further purification was effected by column chromatography using CH_2Cl_2 as the eluant. Yield 0.5 g (45%). This material was spectroscopically (^1H NMR and IR) identical to that obtained by method I. Found: C, 46.1; H, 5.0; N, 17.2. Calc. for $C_{22}H_{28}N_7BMoOS_2$: C, 45.8; H, 4.9; N, 17.0%.

[Mo(NO){HB(3,5-$Me_2C_3N_2H)_2$}(ABT)I]

A solution of $[Mo(NO)LI_2]$ (1 g, 1.5 mmol) and 2-aminobenzenethiol (185 mg, 1 mmol) was heated under reflux in toluene (30 cm^3) containing NEt_3 (10 drops) for 48 h. The red–brown reaction mixture

was evaporated to dryness under reduced pressure and the solid obtained was purified by recrystallization from CH_2Cl_2–hexane mixtures. Further purification was effected by column chromatography using CH_2Cl_2 as the eluant and collecting the principle purple fraction. Yield 0.4 g (47%). Found: C, 33.1; H, 3.7; N, 14.5; I, 21.4. Calc. for $C_{16}H_{20}N_6BIMoOS$: C, 33.2; H, 3.5; N, 14.5; I, 22.0%.

[{Mo(NO){HB(3,5-$Me_2C_3N_2H)_3$}I}$_2$(DAB)]

A solution of [Mo(NO)LI_2] (1 g, 1.5 mmol) and 1,2-diaminobenzene (160 mg, 1 mmol) was heated under reflux in toluene (100 cm^3) containing NEt_3 (10 drops) for 3 days. The red–purple reaction mixture was evaporated to dryness under reduced pressure and the solid obtained was purified by recrystallization from CH_2Cl_2–hexane mixtures. Further purification was effected by column chromatography using CH_2Cl_2 as the eluant and collecting the purple fraction. Yield 0.30 g (34%). Found: C, 36.2; H, 4.3; N, 17.7. Calc. for $C_{36}H_{52}N_{16}B_2I_2Mo_2O_2$: C, 35.8; H, 4.3; N, 18.6%.

[Mo(NO){HB(3,5-$Me_2C_3N_2H)_2$(DAB)}I]

A solution of [Mo(NO)LI_2] (1 g, 1.5 mmol) and 1,2-diaminobenzene (160 mg, 1 mmol) was heated under reflux in toluene (60 cm^3) containing NEt_3 (10 drops) for 24 h. The red–purple reaction mixture was evaporated to dryness under reduced pressure and the solid obtained purified by recrystallization from CH_2Cl_2–hexane mixtures. Further purification was effected by column chromatography using CH_2Cl_2 as the eluant and collecting the magenta fraction. Yield 0.25 g (30%). Found: C, 33.9; H, 4.3; N, 15.1. Calc. for $C_{16}H_{21}N_7BIMoO$: C, 34.2; H, 3.8; N, 17.5%.

RESULTS AND DISCUSSION

Synthetic studies

The previously reported[4] reaction between [Mo(NO)LI_2] and $TDTH_2$ in the absence of added base afforded a complex, [Mo(NO)LI{SC_6H_3(Me)SH}], containing a monodentate thiolate ligand. The reaction between [MO(NO)LI_2] and EtOH similarly produces the monoalkoxide [Mo(NO)LI(OEt)] under such conditions. However, if NEt_3 is added the bis-alkoxide, [Mo(NO)L$(OEt)_2$] is produced instead. Accordingly, we have repeated the reaction between [Mo(NO)LI_2] and $TDTH_2$ in the presence of NEt_3 and obtained a purple complex, **1**, in which both iodide ligands have been displaced. A spectroscopically (^{1}H NMR and IR) identical material may be obtained from the reaction between [Mo(NO)L$(OEt)_2$] and $TDTH_2$ in toluene under reflux. In this case the more acidic thiolate ligand serves to displace the alkoxide group in the form of EtOH, which is then displaced from the reaction mixture in boiling toluene. This reaction parallels the use of [Mo(O)L{OCH_2CH_2O}] as a precursor to complexes containing the {Mo(O)L}$^{2+}$ moiety.[2] The IR spectrum of **1** contained ν_{NO} at 1660 cm^{-1} and ν_{BH} at 2550 cm^{-1}. The ^{1}H NMR spectrum contained six singlets of relative areas 6 : 3 : 3 : 3 : 3 : 3 at δ_{TMS} = 2.51, 2.49, 2.43, 2.32, 2.29 and 1.53, which may be assigned to the six pyrazolyl methyl groups in L and the methyl group in the TDT ligand. The pyrazolyl 4-H signals appeared as two signals of relative area 1 : 2 at δ_{TMS} = 5.67 and 6.06 ppm, while the aryl protons of the TDT ligand appeared as an area 1 singlet at δ_{TMS} = 7.88 and two area 1 doublets at δ_{TMS} = 7.17 and 7.93 ppm (J_{HH} = 8 Hz). The mass spectrum of **1** contained a molecular ion envelope based at m/z = 579 (^{98}Mo, ^{11}B), in addition to an ion at m/z = 549 attributable to {M—(NO)}$^+$. On the basis of these data and the elemental analysis results we formulate **1** as the complex [Mo(NO)L(TDT)] in which both iodide or ethoxide ligands in the starting material have been replaced by a chelating TDT ligand.

A similar material containing ABT could not be prepared from [Mo(NO)LI_2] and $ABTH_2$. Instead a product, **2**, was isolated in which the ligand L was no longer present. The reaction between [Mo(NO)L$(OEt)_2$] and $ABTH_2$ in toluene afforded only intractable materials. The IR spectrum of **2** contained ν_{NO} at 1676 cm^{-1} and ν_{NH} at 3200 cm^{-1}. However, ν_{BH} appeared at 2485 cm^{-1} rather than the normal value of 2550 cm^{-1} generally found in complexes containing the {Mo(NO)L}$^{2+}$ moiety. The ^{1}H NMR spectrum of **2** revealed that one 3,5-dimethylpyrazolyl group had been lost from L. Only three pyrazolyl methyl resonances of relative areas 3 : 3 : 6 were observed at δ_{TMS} = 2.14, 2.25 and 2.36 ppm. The pyrazolyl 4-H protons appeared as two area 1 singlets at δ_{TMS} = 5.62 and 5.85 ppm, while the aryl protons of the ABT ligand appeared as two multiplets of relative areas 3 : 1 at δ_{TMS} = 7.3 and 7.7 ppm. A broad area 1 resonance attributable to the remaining NH proton in the ABT ligand was observed at δ_{TMS} = 4.6 ppm. The elemental analyses for **2** established the presence of iodine in the molecule and were in accord with the formulation [Mo(NO){HB(3,5-$Me_2C_3N_2H)_2$}(ABT)I]. The mass spectrum contained an ion envelope based at m/z = 580 (^{98}Mo, ^{127}I, ^{11}B) consistent with this formula, along with an ion at m/z = 550 attributable to {M—(NO)}$^+$. However, there was also an

ion at $m/z = 610$ which might be attributed to $\{M+(NO)\}^+$.

The spectroscopic data cannot fully define the structure of this compound and as yet crystals suitable for an X-ray diffraction study have not been obtained. A variety of structures may be proposed for **2** but we favour one in which a dimethylpyrazole moiety in L has been replaced by ABT. It might be expected that a B—N interaction would be of higher stability than a B—S one, and we would propose that the sulphur atom of the ABT ligand is bound to the molybdenum atom. This is in accord with the observed chemical shift of the aryl-NH proton which is not in the region associated with molybdenum arylamide derivatives of this type. As it stands, the formulation [Mo(NO){HB(3,5-$Me_2C_3N_2H)_2$(ABT)}I] would leave the boron atom coordinatively saturated but the molybdenum centre would be formally five-coordinate. The complex might thus be expected to oligomerize through the formation of iodide or thiolate bridges and thus increase the molybdenum coordination number to six. An osmometric solution molecular weight determination,* carried out in $CHCl_3$, gave a value of 1633 which may be compared with the expected values for [Mo(NO){HB(3,5-$Me_2C_3N_2H)_2$(ABT)}I]$_n$ of 1155 ($n = 2$) and 1733 ($n = 3$). This result confirms the oligomeric nature of the complex and is more closely in accord with a trimeric rather than a dimeric formulation.

The reaction between [Mo(NO)LI_2] and $DABH_2$ affords two major products. The first of these is the bimetallic complex, **3**, and the second a magenta material, **4**, which proved difficult to obtain in a pure form. The reaction between [Mo(NO)L$(OEt)_2$] and $DABH_2$ afforded only intractable materials. The IR spectrum of **3** contained ν_{NO} at 1665 cm^{-1}, ν_{BH} at 2550 cm^{-1} and ν_{NH} at 3300 cm^{-1}. The ^1H NMR spectrum contained five singlets of relative area 6:6:6:12:6 at $\delta_{TMS} = 1.55$, 1.94, 2.35, 2.44 and 2.58 ppm attributable to the pyrazolyl methyl protons. The pyrazolyl 4-H protons appeared as three singlets of relative areas 2:2:2 at $\delta_{TMS} = 5.37$, 5.84 and 5.86 ppm and the aryl protons of the DAB moiety appeard as two multiplets each of relative areas 2 at $\delta_{TMS} = 7.53$ and 8.34 ppm; the NH protons of the DAB ligand were observed as a single broad resonance of relative area 2 at $\delta_{TMS} = 12.44$ ppm. On the basis of this data we formulate **3** as [{Mo(NO)LI}$_2$(DAB)].

The IR spectrum of **4** contained ν_{BH} at 2480 cm^{-1} and ν_{NH} at 3240 cm^{-1}. The ^1H NMR spectrum contained only four resonances, each of relative area 3, at $\delta_{TMS} = 2.18$, 2.32, 2.63 and 2.42 ppm attributable to the pyrazolyl methyl groups. Two area 1 resonances at $\delta_{TMS} = 5.63$ and 5.84 ppm were assigned to the pyrazolyl 4-H protons. A broad area 2 resonance at $\delta_{TMS} = 4.0$ ppm was assigned to the NH protons of the DAB ligand and the aryl protons of the DAB ligand appeared as multiplets of relative area 1:2:1 at $\delta_{TMS} = 6.74$, 7.06 and 7.42 ppm. However, in contrast to that of **2**, the solid state IR spectrum of **4** contained two ν_{NO} bands at 1670 and 1660 cm^{-1}. The mass spectrum of **4** contained an ion envelope based at $m/z = 563$ (^{98}Mo, ^{127}I, ^{11}B) attributable to a molecular ion for a complex of formula [Mo(NO){HB(3,5-$Me_2C_3N_2H)_2$(DAB)}I], although this was not fully confirmed by the microanalytical data. It seems likely that **4** is similar in nature to **2**, but difficulties in obtaining analytically pure materials precluded a definitive characterization of this material.

Electrochemical studies

The cyclic voltammogram (CV) of [Mo(NO)L(TDT)] contained a reversible one-electron reduction wave at $E_f = -0.35$ V, with a separation between the cathodic and anodic peak potentials of $\Delta E_p = 130$ mV (CH_2Cl_2, SCE, F_c/F^+ 0.56 V, ΔE_p 120 mV). This may be compared with the value of −0.64 V reported for the reduction of [Mo(NO)L$(SPh)_2$] (MeCN, SCE).[10] The CV of [{Mo(NO)LI}$_2$(DAB)] contained a reversible reduction wave with $E_f = -0.44$ V and $\Delta E_p = 80$ mV (CH_2Cl_2, SCE, F_c/F^+ 0.55 V with $\Delta E_p = 80$ mV), which was shown by coulometry to be a one-electron process. A second irreversible two-electron wave was also observed at $E_p^c = -1.32$ V.

The electrochemical properties of the complexes containing the degraded polypyrazolylborate ligand were also investigated. Both exhibited a single formally one-electron reduction process in the range 0 to −1.5 V. In the case of [Mo(NO){HB(3,5-$Me_2C_3N_2H)_2$(ABT)}I] this appeared at $E_f = -0.30$ V with $\Delta E_P = 60$ mV (MeCN, SCE, F_c/F^+ $E_f = 0.42$ V, $\Delta E_p = 60$ mV), while for [Mo(NO){HB(3,5-$Me_2C_3N_2H)_2$(DAB)}I] this appeared at $E_f = -0.80$ V with $\Delta E_p = 80$ mV (MeCN, SCE). The more cathodic reduction potential found for this latter compound is in accord with its formulation as an analogue of [Mo(NO){HB(3,5-$Me_2C_3N_2H)_2$(ABT)}I] since the replacement of a thiophenolate ligand by an aryl amide ligand in [Mo(NO)LClX] (X = SPh, NHPh) similarly produces a cathodic shift of 480 mV.[10]

*We are indebted to Mrs S. Bradshaw, Department of Chemistry, University of Sheffield, for making this measurement.

CONCLUSION

The formation of the chelate ring in [Mo(NO)L(TDT)] establishes that, with larger donor atoms, five-membered chelate rings may form with the $\{Mo(NO)L\}^{2+}$ moiety. However, in the case of [Mo(NO)L(TDT)] this is associated with a substantial anodic shift in reduction potential compared to the non-chelate analogue,[10] [Mo(NO)L$(SPh)_2$]. This observation is in accord with the expected electronic consequences of the structural changes brought about by the incorporation of a bridging aryl group between the ligating sulphur atoms. In [Mo(NO)L$(SPh)_2$] the phenyl rings can orientate themselves so that filled sulphur $3p$ orbitals can lie in the xy plane. These filled sulphur $3p$ orbitals can then interact strongly with the unfilled molybdenum d_{xy} orbital as illustrated in Fig. 1. By analogy with [Mo(NO)$(\eta^5$-$C_5H_5)(SPh)_2$], S $p\pi \rightarrow$ Mo $d\pi$ charge donation would be expected to raise the energy of the LUMO which is largely d_{xy} in character.[3] In contrast, the formation of a chelate ring with the TDT ligand requires the rotation of the sulphur atoms about the Mo—S bond to give a C—S—Mo—NO torsion angle substantially different from 0 or 180°. This results in a rotation of the sulphur p orbitals out of the xy plane, reducing opportunities for the overlap of the sulphur p orbitals with the molybdenum d_{xy} orbital. This in turn leads to some destabilization of the complex as a whole, but to the stabilization of the LUMO as compared to the situation in the non-chelate complex.[3] These changes in the stability of the LUMO are reflected in the reduction potentials of the complexes, with the chelate complex exhibiting the more anodic potential.

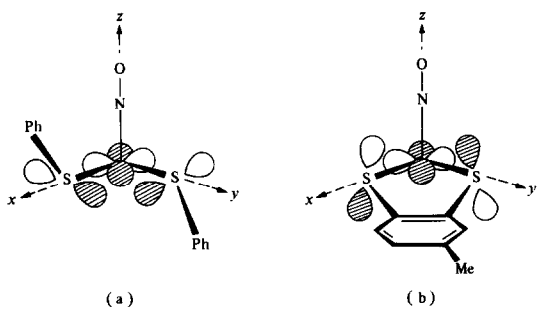

Fig. 1. A schematic representation of the orbital orientation in the $\{Mo(NO)Y_2\}$ ($Y_2 = (SPh)_2$ or TDT) fragment. (a) The situation in [Mo(NO)L$(SPh)_2$] where the phenyl rings are orientated so as to place the filled sulphur $3p$ orbitals in the xy plane. (b) The situation in [Mo(NO)L(TDT)] in which the chelate ring enforces a rotation of the sulphur $3p$ orbitals out of the xy plane and reduces the overlap with the unfilled molybdenum d_{xy} orbital.

The reactions between [Mo(NO)LI_2] and $DABH_2$ or $ABTH_2$, in the presence of base, result in some degradation of the ligand L. In these cases complete removal of the boron does not occur as found with catechol, **4**, and it seems likely that the compounds **2** and **4** represent intermediates in the deboronation reaction which goes to completion with catechol. It would appear that the $\{Mo(NO)L\}$ core does not readily form five-membered chelate rings when ligand donor atoms smaller than sulphur are involved. This contrast with the behaviour of the $\{Mo(O)L\}$ moiety could arise from steric effects or from differences in the reactivity of the two different molybdenum centres. The finding that chelate complexes of the $\{Mo(NO)L\}$ fragment form when two large sulphur donor atoms are involved in a five-membered chelate ring, or when smaller oxygen donor atoms are involved in a large chelate ring, would be consistent with the steric effect argument. However, the results described here also show that, for ligands with oxygen or nitrogen donor atoms, both boron and molybdenum represent potential reaction sites within the $\{Mo(NO)L\}$ moiety.

Acknowledgements—We are grateful to Mr T. Green for experimental assistance and to Mustansirigh University of Iraq for support (to N.AlO).

REFERENCES

1. J. A. McCleverty, *Chem. Soc. Rev.* 1983, **12**, 331.
2. W. E. Cleland Jr, K. M. Barnhart, K. Yamanouchi, D. Collison, F. E. Mabbs, R. B. Ortega and J. H. Enemark, *Inorg. Chem.* 1987, **26**, 1017.
3. M. T. Ashby and J. H. Enemark, *J. Am. Chem. Soc.* 1986, **108**, 730.
4. H. Adams, N. A. Bailey, A. S. Drane and J. A. McCleverty, *Polyhedron* 1983, **2**, 465.
5. N. AlObaidi, C. J. Jones and J. A. McCleverty, unpublished results.
6. N. AlObaidi, P. D. Beer, J. P. Bright, C. J. Jones, J. A. McCleverty and S. S. Salam, *J. Chem. Soc., Chem. Commun.* 1986, 239.
7. S. A. Roberts and J. H. Enemark, personal communication.
8. S. J. Reynolds, C. F. Smith, C. J. Jones, J. A. McCleverty, D. C. Bower and D. H. Templeton, *Inorg. Synth.* 1985, **23**, 4.
9. J. A. McCleverty, A. E. Rae, I. Wolochowicz, N. A. Bailey and J. M. A. Smith, *J. Chem. Soc., Dalton Trans.* 1982, 951.
10. N. AlObaidi, M. Chaudhury, D. Clague, J. C. Pearson, C. J. Jones, J. A. McCleverty and S. S. Salam, *J. Chem. Soc., Dalton Trans.* 1987, 1733.

Polyhedron Vol. 8, No. 8, pp. 1039–1043, 1989
Printed in Great Britain

0277–5387/89 $3.00+.00
© 1989 Pergamon Press plc

THE KINETIC COORDINATION TEMPLATE EFFECT OF AN *ORTHO*(2,2′-BIPYRIDYL) SUBSTITUENT IN THE METAL ION-CATALYSED FORMATION OF ARYLPHOSPHONIUM SALTS FROM AN ARYL HALIDE. X-RAY CRYSTALLOGRAPHIC CONFIRMATION AND AN UNUSUAL ASPECT OF LIGAND REACTIVITY IN COORDINATION COMPOUNDS

DAVID W. ALLEN,* PAUL E. CROPPER and IAN W. NOWELL†

Department of Chemistry, Sheffield City Polytechnic, Pond Street, Sheffield S1 1WB, U.K.

(*Received* 21 *September* 1988; *accepted* 10 *November* 1988)

Abstract—The reaction of 3-(2,4-dibromo-5-methylphenyl)-2,2′-bipyridyl with triphenylphosphine or tributylphosphine in the presence of either copper(II) acetate or nickel(II) bromide in ethanol, proceeds with regiospecific replacement of the bromine in the *ortho* position with respect to the 2,2′-bipyridyl group, which provides a kinetic coordination template for the metal catalyst. An intermediate bromocopper(I) complex derived from the aryl halide and bromo(triphenylphosphine)copper(I) has been characterized and shown to undergo conversion to the arylphosphonium salt on heating. An X-ray crystal structure of one of the arylphosphonium salts is also reported, providing unequivocal proof of the position of halogen replacement.

The reactions of aryl halides with tertiary phosphines to form arylphosphonium salts only proceed at high temperatures (150–200°C) and in the presence of a transition metal halide, e.g. $Ni^{II}Br_2$, as catalyst.[1–4] However, we have shown that when the aryl halide bears an *ortho* substituent which is able to provide an appropriate coordination template for the metal ion, the displacement of the halide by the phosphine proceeds in good yield under much less severe conditions in refluxing ethanol. Among effective kinetic template systems are the dyestuffs (**1**; X = Cl, Br, I; R = H or NHAc),[5] the Schiff's bases (**2**; X = Cl, Br, I)[6] and the benzimidazole (**3**).[7] In this paper, we report a study of the related reactions of the aryl halide (**4**), which bears a 2,2′-bipyridyl unit as the potential template system, together with an X-ray study of a phosphonium salt (**5**, R = Ph) derived therefrom.

RESULTS AND DISCUSSION

The bipyridyl template (**4**) was of interest in view of earlier observations made in studying the nickel(II) catalysed reactions of the above dyestuff (**1**) and Schiff's base systems (**2**) with phosphines which revealed that, when such template systems involved a *second* donor centre capable of interacting with the metal ion in a chelating manner, the formation of the phosphonium salt was significantly retarded or inhibited completely, presumably a consequence of the diversion of the metal ion in a mode of coordination inappropriate to the key catalytic steps. On this basis it was expected that the bipyridyl system (**4**) would not prove to be an effective template.

However, when the aryl halide (**4**) was heated with *either* triphenylphosphine *or* tributylphosphine in ethanol containing nickel(II) bromide, the related phosphonium salts (**5**, R = Ph or Bu) were formed in good yield over several hours. The reactions did not occur in the absence of the nickel(II) halide. The phosphonium salt formation reactions were also catalysed by copper(II) acetate, and in this respect the reactions of the halide (**4**) resemble those of the dyestuffs (**1**), rather than those of the Schiff's bases (**2**) or the benzimidazole (**3**), for which nickel(II) halides were found to be the only effective catalysts.

^{31}P NMR studies indicated that the products were free of phosphorus-containing impurities (e.g. $R_3P{=}O$ or R_3P), the salts having ^{31}P chemical

* Author to whom correspondence should be addressed.
† Present address: Department of Chemistry, Robert Gordon's Institute of Technology, School Hill, Aberdeen AB9 1FR, Scotland, U.K.

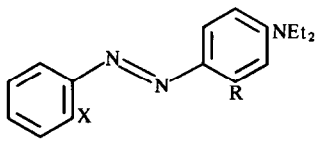

(1)

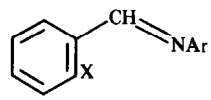

(2)

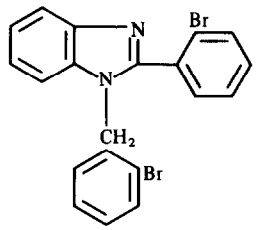

(3)

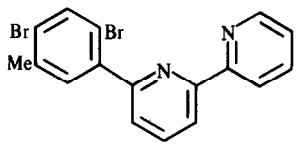

(4)

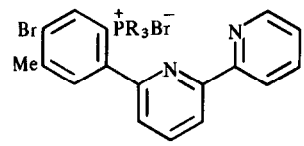

(5)

shifts of 23.8 ppm (**5**, R = Ph) and 32.6 ppm (**5**, R = Bu), respectively. ^{1}H NMR spectra were also consistent with the formation of a mono-phosphonium salt, thus implying that regiospecific replacement of the halogen *ortho* to the donor group had occurred, the *para*-halogen remaining unaffected. Proof of the structures of these compounds rests on microanalytical data, ^{1}H and ^{31}P NMR studies, and the results of an X-ray crystallographic study of (**5**, R = Ph) (see below).

The reaction of the halide (**4**) (1 mol equiv) with the preformed copper(I) complex (**6**) (1 mol equiv), together with triphenylphosphine (1 mol equiv), also gave the corresponding colourless phosphonium salt (**5**, R = Ph) in good yield (*ca* 60%).

$[Ph_3PCuBr]_4$

(6)

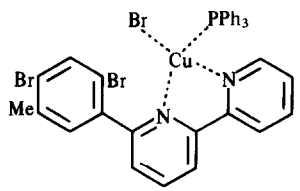

(7)

When this reaction was carried out using equimolar amounts of the halide (**4**) and the complex (**6**), but excluding the additional mole of triphenylphosphine, a red solution resulted, which, on standing overnight, deposited orange–red crystals. On the basis of microanalytical data, and the ^{31}P NMR spectrum which exhibited a signal at $\delta = -4.96$ ppm (indicating the presence of a PPh_3 ligand), it is proposed that this product is the tetrahedral copper(I) complex (**7**) formed from the halide (**4**) with the bromo(triphenylphosphine) copper(I) complex. Related copper(I) complexes of simple bipyridyl ligands and phosphines have been prepared by Jardine *et al.*[8] Prolonged heating of the red solution also led to the formation of the phosphonium salt (**5**, R = Ph) (isolated in 26% yield) and thus it would seem that the complex (**7**) is an early intermediate on the pathway to the phosphonium salt. An X-ray crystal structure of the complex (**7**) has been attempted, but was frustrated by the instability of the crystals in the X-ray beam.

In none of the other *ortho*-(template) aryl halides studied so far have we observed the formation of arylphosphonium salts from the reaction of the aryl halide with a halogen(triphenylphosphine) copper(I) complex. Thus, the isolation and subsequent conversion of the complex (**7**) into the phosphonium salt (**5**) is quite significant, and provides the first example of an isolable intermediate complex in reactions of this type.

The mechanism of subsequent conversion of the complex into the phosphonium salt remains unclear, but is likely to involve a coordination-assisted oxidative insertion of copper(I) into the carbon–halogen bond to form the related coordinatively stabilized arylcopper(III) complex (**8**).

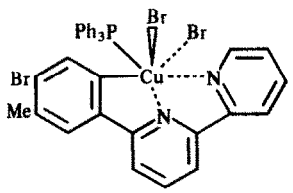

(8)

Reductive elimination of the arylphosphonium salt from (**8**) would regenerate the copper(I) halide, which in the presence of additional phosphine would reform the initial halogeno(phosphine) copper(I) complex. Prior to the above reaction of the halide (**4**) with the copper(I) complex, all other reactions of template halides (**1**)–(**3**) were promoted by copper(II) and/or nickel(II), it being assumed that an initial electron transfer step occurred (probably via a phosphine molecule usually present in excess), leading to the generation of a copper(I) or nickel(I) species *in situ*.[6]

These kinetic coordination template reactions therefore provide an interesting group of examples which demonstrate the pronounced effect on the organic reactivity of the ligand as a result of its coordination to a metal ion, and contribute to the current discussion[9] of the principles of ligand reactivity in coordination compounds.

X-ray structural study of 3-(2-*triphenylphosphonio*-4-*bromo*-5-*methylphenyl*)-2,2′-*bipyridyl bromide dihydrate* (**5**, R = Ph)

Crystal data. $C_{35}H_{31}Br_2N_2O_2P_1$. $M_r = 701.8$. Monoclinic, space group $P2_1/c$, $a = 8.743(5)$, $b = 22.398(4)$, $c = 15.669(3)$ Å, $\beta = 94.0(0)$, $\alpha = \gamma = 90°$. $U = 3061.2$ Å^3, Mo-K_α $\lambda = 0.71069$ Å, $D_m = 1.52$, $D_c = 1.54$ g cm^{-3}, $Z = 2$, μ(Mo-K_α) = 13.25 cm^{-1}, $F(000) = 712$.

Data collection and recovery. Intensities were measured for a crystal, approximate dimensions 0.20 × 0.12 × 0.12 mm, mounted on a glass fibre rod with the *c* axis coincident with the rotation (ω) axis of a two circle Stoe Stadi 2 diffractometer. Monochromatic Mo-K_α radiation was used and the background-ω-scan background technique employed. Sixteen layers were collected giving 3169 independent reflections, of which 1704 had $I > 3\sigma(I)$ and were used for subsequent analysis. Corrections for Lorentz and polarization effects were applied, but no corrections for absorption were made.

Structure determination and refinement. The space group and unit cell parameters were obtained from oscillation and Weissenberg photographs. Systematic absences when $h0l$, $l = 2n+1$ and $0k0$, $k = 2n+1$, and density measurements indicate that the space group is $P2_1/c$. The approximate positions of the two bromine atoms were calculated using a three-dimensional Patterson synthesis. Multi-solution direct methods using *SHELX*[10] enabled the position of all non-hydrogen atoms to be readily located. Scattering factors were calculated using an analytical approximation[11] and the weighting scheme $w = 1.000[\sigma^2(F_o)+0.001265(F_o)^2]$ adopted. Full-matrix least-squares refinement for the ordered non-hydrogen atoms gave final $R = 0.0951$ and $R' = 0.0958$. Selected bond distances are listed in Table 1, and selected bond angles in Table 2. Full atomic parameters, thermal parameters, bond lengths, bond angles and mean plane data have been deposited at the Cambridge Crystallographic Data Centre (CCDC).

Discussion of the structure. Although it has not proved possible to gain detailed structural data for this phosphonium salt, it is quite clear that the bromine atom in the *ortho* position with respect to the bipyridyl system has been replaced by phosphorus, and that the *para*-bromine atom contained in the same aryl ring remains unaffected.

The geometry around the phosphorus atom (Fig. 1) is approximately tetrahedral, with the bond angles ranging from 106 to 114° (Table 2). Both pyridine rings of the bipyridyl system are planar and are inclined to one another at an angle of 22.1°. The twisting of these rings to each other might be explained by the accommodation of the large triphenylphosphine group.

A feature worth noting in this crystal structure is that the pyridine ring C(51)—C(55) is inclined to the C(41)—C(46) phenyl ring, so that the overall configuration is such that the nitrogen atom N(1) is closely approached by the positively charged phosphorus atom, giving a N(1)—P distance of 3.03 Å, which is within the sum of their van der Waals'

Table 1. Selected bond distances (bond distances in (Å) and ESDs in parentheses)

C(43)—Br(1)	1.92(2)
C(44)—C(7)	1.51(3)
C(46)—C(51)	1.48(3)
C(55)—N(1)	1.36(2)
N(1)—C(51)	1.33(3)
C(55)—C(61)	1.50(3)
C(65)—N(2)	1.28(3)
N(2)—C(61)	1.28(3)
P—C(11)	1.81(2)
P—C(21)	1.79(2)
P—C(31)	1.75(2)
P—C(41)	1.83(2)

Table 2. Selected bond angles (bond angles in (°) and ESDs *ca* 2°)

C(42)—C(43)—Br(1)	117	P—C(11)—C(12)	122
C(44)—C(43)—Br(1)	121	P—C(11)—C(16)	119
C(43)—C(44)—C(7)	124	P—C(21)—C(22)	125
C(45)—C(44)—C(7)	118	P—C(21)—C(26)	115
C(45)—C(46)—C(51)	120	P—C(31)—C(32)	120
C(41)—C(46)—C(51)	122	P—C(31)—C(36)	121
C(46)—C(51)—N(1)	119	P—C(41)—C(42)	114
C(52)—C(51)—N(1)	122	P—C(41)—C(46)	127
C(54)—C(55)—N(1)	121	C(11)—P—C(21)	106
C(54)—C(55)—C(61)	120	C(11)—P—C(31)	108
C(61)—C(55)—N(1)	120	C(11)—P—C(41)	107
C(55)—N(1)—C(51)	117	C(21)—P—C(31)	113
C(55)—C(61)—C(62)	117	C(21)—P—C(41)	114
C(55)—C(61)—N(2)	120	C(31)—P—C(41)	109
C(62)—C(61)—N(2)	123		
C(64)—C(65)—N(2)	125		
C(65)—N(2)—C(61)	117		

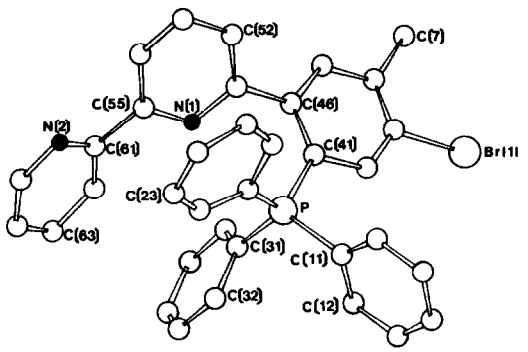

Fig. 1. X-ray structure of 3-(2-triphenylphosphonio-4-bromo-5-methylphenyl)-2,2′-bipyridyl bromide.

radii (N = 1.55, P = 1.85 Å).[12] Such an interaction between N(1) and P may also be indicated by the increase in the P—C(41)—C(46) bond angle to 127.0° (compared to the other exocyclic angle P—C(41)—C(42), 114.1°).

Positions for the anionic bromide, Br(2), and two oxygens, O(1) and O(2), were identified and have subsequently been omitted from the crystal structure for clarity. No other atoms were identified as associating with the oxygen atoms and although no hydrogen atoms could be located on these atoms, it is believed that they are water molecules entrapped in the crystal lattice (confirmed by microanalysis). Although the bromide anion, Br(2), shows no sign of interaction with the cation ($P^+ \cdots Br^-$ 4.6 Å), it has been located within the sum of the van der Waals' radii ($Br \cdots O$ = 3.35 Å) for both O(1)—Br(2), 2.58 Å and O(2)—Br(2), 3.27 Å.

EXPERIMENTAL

^{31}P NMR spectra were recorded on a Bruker WP80 SY instrument. Chemical shifts are reported with respect to 85% *ortho*-phosphoric acid as external standard; shifts to high frequency are positive in sign. ^1H NMR spectra were recorded on the same instrument, and chemical shifts are reported on the δ scale with respect to tetramethylsilane as internal standard in deuteriochloroform solution. Mass spectra were recorded using a VG Micromass 305 Spectrometer.

3-(2,4-Dibromo-5-methylphenyl)-2,2′-bipyridyl (**4**) was obtained as a gift from Dr R. Price, ICI Organics Division, Blackley, Manchester. Tetrakis[bromo(triphenylphosphine)copper(I)] was prepared as previously described.[8]

Reaction of the halide (**4**) *with phosphines*

The halide (10^{-3} mol), tertiary phosphine (3×10^{-3} mol) and *either* nickel(II) bromide *or* copper(II) acetate (0.2×10^{-3} mol) were heated together under reflux in ethanol (10 cm^3) under nitrogen for 5–8 h. The reaction mixture was then poured into water (50 cm^3) containing potassium bromide (0.5 g) and extracted with ether to remove non-ionic impurities. The aqueous layer was then extracted with chloroform (3×10 cm^3). The chloroform extract was dried ($MgSO_4$) and evaporated. The oily residue was then triturated several times with sodium-dried ether until it solidified. The crude salts were then recrystallized. The following were characterized.

3 - (2 - *Triphenylphosphonio* - 4 - *bromo* - 5 - *methylphenyl*)-2,2′-*bipyridyl bromide* (**5**; R = Ph). (40%), m.p. 272°C (from $CHCl_3$–EtOAc). (Found: C, 60.5; H, 4.2; N, 4.0. $C_{35}H_{27}N_2Br_2P_1 \cdot 2H_2O$ requires C, 59.8; H, 4.1; N, 4.0%.) $\delta^{31}P(CDCl_3)$: 23.89 ppm; $\delta^1H(CDCl_3)$: 8.2–7.0 (m, 24ArH) 2.7 (s,3H) ppm. (Found: $(M—^{81}Br)^+$ 585.1079. $C_{35}H_{27}N_2Br_2P_1$ requires $(M—^{81}Br)^+$ 585.1095.)

3 - (2 - *Tributylphosphonio* - 4 - *bromo* - 5 - *methylphenyl*)-2,2′-*bipyridyl bromide* (**5**; R = Bu). (42%), m.p. 134°C (from $CHCl_3$–ether). (Found: C, 56.4; H, 6.4; N, 4.6. $C_{29}H_{39}N_2Br_2P_1 \cdot H_2O$ requires C, 55.8; H, 6.6; N, 4.5%.) $\delta^{31}P(CDCl_3)$: 32.79 ppm; $\delta^1H(CDCl_3)$: 8.8–7.4 (m,9ArH) 2.6 (m,9H) 1.4 (m,12H) 0.9 (m,9H) ppm.

Reaction of the halide (**4**) *with* $[Ph_3PCuBr]_4$

The halide (0.25 g) and the copper(I) phosphine complex (0.25 g) were heated together in ethanol (10 cm^3) to form an orange–red solution. On standing overnight, red crystals were isolated and recrystallized from ethanol to give bromo(triphenylphosphine)[3-(2,4-dibromo-5-methylphenyl)-2,2′-bipyridyl]copper(I) (**8**) (0.34 g, 62%), m.p. 202–204°C (Found: C, 51.5; H, 3.2; N, 3.4. $C_{35}H_{27}CuBr_3N_2$ requires C, 51.9; H, 3.3; N, 3.4%.) $\delta^{31}P(CDCl_3)$: −4.96 ppm; $\delta^1H(CDCl_3)$: 8.2–7.1 (m,24ArH) and 2.4 (s,3H) ppm.

REFERENCES

1. Y. Hirusawa, M. Oku and R. Yamamoto, *Bull. Soc. Chem. Jpn* 1957, **30**, 667.
2. L. Horner, G. Mummenthey, H. Moses and P. Beck, *Chem. Ber.* 1966, **99**, 2782.
3. L. Horner and U. M. Duda, *Tetrahedron Lett.* 1970, 5177.
4. P. Beck, in *Organic Phosphorus Compounds* (Edited by G. M. Kosolapoff and L. Maier), Vol. 2 and refs therein. Wiley-Interscience, New York (1972).
5. D. W. Allen, I. W. Nowell, L. A. March and B. F. Taylor, *J. Chem. Soc., Perkin Trans. 1* 1984, 2523.
6. D. W. Allen, P. E. Cropper, P. G. Smithurst, P. R. Ashton and B. F. Taylor, *J. Chem. Soc., Perkin Trans. 1* 1986, 1989.
7. D. W. Allen, P. E. Cropper and I. W. Nowell, *J. Chem. Res.* (S) 1987, 298; D. W. Allen, P. E. Cropper and I. W. Nowell, *J. Chem. Res.* (M) 1987, 2562.
8. F. H. Jardine, I. Rule and A. G. Vohra, *J. Chem. Soc. A* 1970, 238.
9. E. C. Constable, *Inorg. Chim. Acta* 1988, **145**, 49.
10. G. M. Sheldrick, *SHELX, Program for Crystal Structure Determination.* University of Cambridge, U.K. (1976).
11. *International Tables for X-ray Crystallography*, Vol. 4. Kynoch Press, Birmingham (1974).
12. J. E. Huheey, *Inorganic Chemistry—Principles of Structure and Reactivity*, 2nd edn, p. 7. Harper and Row, London (1978).

Polyhedron Vol. 8, No. 8, pp. 1045–1052, 1989
Printed in Great Britain

0277–5387/89 $3.00+.00
© 1989 Pergamon Press plc

SYNTHESIS AND REACTIVITY OF PALLADIUM(I) DERIVATIVES WITH BIS(DIPHENYLPHOSPHINO)AMINE. X-RAY CRYSTAL STRUCTURE OF $Pd_2(\mu\text{-dppa})_2Cl_2 \cdot (CH_3)_2CO$

R. USON,* J. FORNIES, R. NAVARRO, M. TOMAS, C. FORTUÑO and J. I. CEBOLLADA

Departamento de Química Inorgánica, Instituto de Ciencia de Materiales de Aragón, Universidad de Zaragoza-C.S.I.C. 50009 Zaragoza, Spain

and

A. J. WELCH

Department of Chemistry, University of Edinburgh, Edinburgh EH9 3JJ, U.K.

(*Received* 21 *September* 1988; *accepted* 10 *November* 1988)

Abstract—$ClPd(\mu\text{-dppa})_2PdCl$ [dppa = bis(diphenylphosphino)amine] (**1**) has been prepared by treating $PdCl_2(NCPh)_2$ with $Pd_2(dba)_3 \cdot CHCl_3$ (dba = dibenzylideneacetone) and dppa in CH_2Cl_2. Substitution reactions allow the synthesis of the neutral $BrPd(\mu\text{-dppa})_2PdBr$ (**2**) and the cationic $[Ph_3PPd(\mu\text{-dppa})_2PdPPh_3](BPh_4)_2$ (**4**) derivatives. Complex **1** reacts with $SnCl_2$ yielding $Cl_3SnPd(\mu\text{-dppa})_2PdSnCl_3$ (**3**). The species R_2N^+ and SO_2 insert into the Pd—Pd bond of **1** to give the appropriate A-frame Pd^{II}–Pd^{II} complexes. Extrusion of SO_2 takes place at room temperature. CO does not react with **1** in CH_2Cl_2 at room temperature. The insertion–elimination reactions of **1** with isonitriles RNC (R = *p*-Tol, Cy) have been studied.

The molecular structure of $ClPd(\mu\text{-dppa})_2PdCl \cdot (CH_3)_2CO$ has been established by a single crystal X-ray study. The crystals are monoclinic, space group $P2_1/c$, with $a = 13.540(3)$, $b = 16.943(2)$, $c = 21.082(15)$ Å, $\beta = 105.257(42)°$ and $Z = 4$. The final R factor was 0.033 for 5091 observed reflections. The Pd—Pd distance is 2.6378(6) Å.

Bis(diphenylphosphino)amine (dppa) has received very little attention in palladium coordination chemistry. We have recently described the synthesis of dppa-containing Pd^{II} and Pd^{I} complexes in which the P-donor ligand acts as a terminal monodentate or bidentate chelating ligand, or bridges between two metal centres.[1] Here we report the synthesis of the homo binuclear Pd^{I} derivatives $XPd(\mu\text{-dppa})_2PdX$ (X = Cl, Br, $SnCl_3$) and the reactivity of $ClPd(\mu\text{-dppa})_2PdCl$ in respect to the formation of cationic complexes and insertion reactions into the Pd—Pd bond. The reactions of $ClPd(\mu\text{-dppa})_2PdCl \cdot (CH_3)_2CO$ with RNC (R = *p*-Tol, Cy) have also been studied.

The molecular structure of $ClPd(\mu\text{-dppa})_2PdCl \cdot (CH_3)_2CO$ has been established by a single crystal X-ray diffraction study. As far as we know, the molecular structures of only two dppa-containing transition metal complexes $Rh_2(\mu\text{-CO})(\mu\text{-Cl})(\mu\text{-dppa})_2(CO)_2 \cdot CH_3OH$[2] and $(C_6F_5)ClAu(\mu\text{-dppa})AuCl(C_6F_5)$[3] have been previously reported.

RESULTS AND DISCUSSION

The reaction of $PdCl_2(NCPh)_2$ with $Pd_2(dba)_3 \cdot CHCl_3$ (dba = dibenzylideneacetone) and dppa (molar ratio 2 : 1 : 4), in oxygen-free CH_2Cl_2 yields the homo-binuclear Pd^{I} derivative $ClPd(\mu\text{-dppa})_2PdCl$ (**1**):

$$PdCl_2(NCPh)_2 + \tfrac{1}{2}Pd_2(dba)_3 \cdot CHCl_3 + 2dppa \longrightarrow ClPd(\mu\text{-dppa})_2PdCl + 3/2dba + 2NCPh + CHCl_3. \quad (1)$$

* Author to whom correspondence should be addressed.

Table 1. Analytical and conductivity data

Complex	C	N	H	Λ_M ohm^{-1} cm^2 mol^{-1}
$[Pd_2(\mu\text{-dppa})_2Cl_2]$ **1**	54.6 (54.7)	2.7 (2.6)	4.3 (4.0)	
$[Pd_2(\mu\text{-dppa})_2Cl_2]CH_3COCH_3$ **1a**	54.4 (55.1)	2.6 (2.5)	4.3 (4.3)	
$[Pd_2(\mu\text{-dppa})_2Cl_2]2NCCH_3$ **1b**	53.9 (54.9)	4.7 (4.9)	4.2 (4.2)	
$[Pd_2(\mu\text{-dppa})_2Br_2]$ **2**	49.6 (50.4)	2.3 (2.4)	3.7 (3.7)	
$[Pd_2(\mu\text{-dppa})_2(SnCl_3)_2]$ **3**	40.1 (40.2)	1.9 (1.9)	2.9 (2.9)	
$[Pd_2(\mu\text{-dppa})_2(PPh_3)_2][BPh_4]_2$ **4**	73.0 (73.8)	1.3 (1.3)	5.3 (5.2)	195
$[Pd_2(\mu\text{-}N_2C_6H_4\text{-}o\text{-}NO_2)(\mu\text{-dppa})_2Cl_2][BF_4]$ **5**	50.2 (50.2)	5.2 (5.4)	3.6 (3.6)	105
$[Pd_2(\mu\text{-}N_2C_6H_4\text{-}p\text{-}CH_3)(\mu\text{-dppa})_2Cl_2][BF_4]$ **6**	51.8 (52.4)	4.4 (4.4)	3.8 (3.9)	108

Solutions of complex **1** in donor solvents give the corresponding $[ClPd(\mu\text{-dpa})_2PdCl]\cdot nS$ [S = acetone, $n = 1$ (**1a**); S = acetonitrile, $n = 2$ (**1b**)] which are slightly soluble in the solvent S. The thermogravimetric analyses of complexes **1a** and **1b** confirm the indicated stoichiometry; they loose solvent at 155 and 115°C, respectively. The structure of complex **1a** has been established by a single crystal X-ray diffraction study and is discussed below. Analytical and conductivity data are collected in Table 1.

Complex **1** reacts with $[NBu^n_4]Br$ in CH_2Cl_2 to give $BrPd(\mu\text{-dppa})_2PdBr$ (**2**); treatment of **1** with $SnCl_2$ in CH_2Cl_2 (molar ratio 1:2) produces insertion of $SnCl_2$ into the Pd—Cl bonds, yielding $Cl_3SnPd(\mu\text{-dppa})_2PdSnCl_3$ (**3**).

The IR spectra of complexes **1**, **2** and **3** show an absorption due to ν(N—H) [3310 cm^{-1} (**1**), 3310 cm^{-1} (**2**) and 3285 cm^{-1} (**3**)], *i.e.* at higher energies than in the spectrum of the free ligand [dppa = ν(N—H) 3230 cm^{-1}].

The ν(N—H) absorption appears in complex **1b** at 3220 cm^{-1}, shifted to lower energy than that of the free ligand and of complex **1**, probably due to the interaction between the $NCCH_3$ molecules and the N—H group of the bridging dppa.[4,5] Complex **1a** shows two ν(N—H) absorptions located at 3315 and 3185 cm^{-1} since only one of the two bridging dppa's is linked to acetone (see below, structure of **1a**). Complexes **1**, **1a** and **1b** show ν(Pd—Cl) absorptions in the 255–245 cm^{-1} region, in the same range as found for ν(Pd—Cl) in $ClPd(\mu\text{-dppm})_2PdCl$[6] and at lower energies than ν(Pd—Cl) for the Pd^{II} derivative $PdCl_2$(dppa) (290, 280 cm^{-1}),[7] suggesting a fairly high *trans* influence of the Pd—Pd bond. Complex **1a** shows a strong absorption at 1710 cm^{-1} corresponding to ν(CO) of the $(CH_3)_2CO$, while an absorption at 2255 cm^{-1} observed in the IR spectrum of **1b** is assigned to ν(C≡N) of the $NCCH_3$. Complex **3** shows absorptions at 315, 308 and 299 cm^{-1} due to ν(Sn—Cl).[8]

The $^{31}P\{^1H\}$ NMR spectra of complexes **1–3** in $CDCl_3$ show singlet signals at 58.96, 57.26 and 56.29 ppm respectively, due to the presence of four equivalent phosphorus atoms.

Addition of PPh_3 to a suspension of **1** in methanol (molar ratio 2:1) results in complete dissolution of the solid and, by adding $NaBPh_4$, the cationic $[Ph_3PPd(\mu\text{-dppa})_2PdPPh_3](BPh_4)_2$ (**4**) can be isolated:

$$ClPd(\mu\text{-dppa})_2PdCl + 2PPh_3 + 2NaBPh_4 \longrightarrow [Ph_3PPd(\mu\text{-dppa})_2PdPPh_3](BPh_4)_2 + 2NaCl. \quad (2)$$

The IR spectrum of complex **4** shows an absorption at 610 cm^{-1} due[9] to BPh_4^- and the $^{31}P\{^1H\}$ NMR spectrum shows two signals at 58.88 and 29.85 ppm, corresponding to the P(dppa) and $P(PPh_3)$ atoms.

Insertion reactions

Complex **1** reacts (in acetone at −30°C) with diazonium salts $[N_2R]BF_4$ (R = C_6H_4-*o*-NO_2, C_6H_4-*p*-CH_3) yielding the "A-frame" homo-bimetallic compounds $[ClPd(\mu\text{-dppa})_2(\mu\text{-}N_2R)PdCl]BF_4$ [R = C_6H_4-*o*-NO_2 (**5**), C_6H_4-*p*-CH_3 (**6**)]

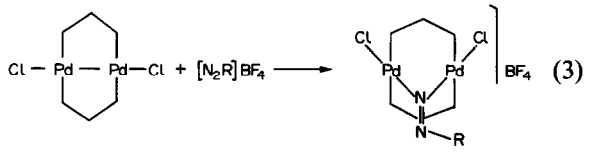

(3)

in which the $[NNR]^+$ moiety inserted into the Pd—Pd bond.

The $^{31}P\{^1H\}$ NMR spectra of complexes **5** and **6** show two multiplets (**5** 61.06, 56.56; **6** 61.77, 59.20 ppm) corresponding to an AA'BB' system, consistent with a bridging diazenide ligand with an NNC angle less than 180°C.

The IR spectra of complexes **5** and **6** show a strong and broad absorption at ~ 1100 cm^{-1} due to the counterion BF_4;[10] complex **5** shows an absorption at 1530 cm^{-1} due to $\nu_{as}(NO_2)$ of the $[N_2(C_6H_4\text{-}o\text{-}NO_2)]^+$ group.[11]

When SO_2 is bubbled through a CH_2Cl_2 solution of complex **1** (orange), a green solution is obtained, and by adding diethylether in the presence of SO_2 a green precipitate is obtained. This solid seems to be the A-frame derivative with SO_2 inserted into the Pd—Pd bond [ClPd(μ-dppa)$_2$(μ-SO_2)PdCl]; however, even in the solid state, it decomposes very rapidly, yielding the orange starting material **1**, and we have not been able to observe absorptions $\nu(SO_2)$ due to inserted SO_2. The $^{31}P\{^1H\}$ NMR spectrum of a $CDCl_3$ solution at room temperatue shows the signal due to the starting material **1** and a small singlet at 66.35 ppm which could be due to the SO_2 derivative.

The instability of ClPd(μ-dppa)$_2$(μ-SO_2)PdCl contrasts with the stability of the dppm derivative; in fact ClPd(μ-dppm)$_2$(μ-SO_2)PdCl has been prepared[12] and SO_2 is evolved when a CH_2Cl_2 solution of the complex is refluxed under N_2.

In contrast, although ClPd(μ-dppm)$_2$ PdCl reacts with CO in CH_2Cl_2 yielding ClPd(μ-dppm)$_2$(μ-CO)PdCl,[6] complex **1**, ClPd(μ-dppa)$_2$PdCl, does not react with CO under similar conditions.

Reactions with isonitriles

Palladium(I) and platinum(I) complexes of this type react with isonitriles and the nature of the reaction product (terminal **A**, **B**; bridging **C** or both **D**) is dependent on the starting M^I complex, the isonitrile and the solvent used.[6,9,13]

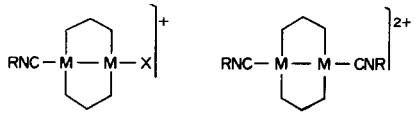

(A) (B)

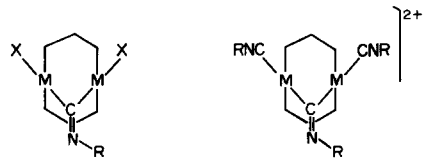

(C) (D)

The reactions between ClPd(μ-dppa)$_2$PdCl·$(CH_3)_2CO$ (**1a**) and CNTol-*p* or CNCy have been studied and the results are different to those of ClPd(μ-dppm)$_2$PdCl.[6]

Complex **1a** reacts in dichloromethane with a stoichiometric amount of *p*-TolNC (molar ratio 1 : 1) giving a pale-orange solution and when benzene is added the colour of the solution turns red-orange (as far as we know, this change in colour could indicate the transformation of species **A** into species **C**). In a few seconds the colour of the solution fades (**C** → **A**) and a yellow solid precipitates. The IR spectra of this solid shows an absorption at 2170 cm^{-1} [ν(C≡N)] indicating that the isonitrile is coordinated as a terminal ligand to the metal centre (**A** or **B**) and that no inserted isonitrile (species **C**, **D**) is present. The analytical [found (calculated) for [ClPd(μ-dppa)$_2$PdCNR]Cl (**A**), C: 56.4(57.4); N: 3.5(3.6), H: 3.9(4.2)] and conductivity (Λ_M 57 ohm^{-1} cm^2 mol^{-1}) data indicate that the yellow solid could be a mixture of the starting material and the cationic species [ClPd(μ-dppa)$_2$CNR]Cl (**A**). However, the $^{31}P\{^1H\}$ NMR spectrum of a $CDCl_3$ solution of the yellow solid shows two singlets (58.86 and 49.34 ppm) and two complicated multiplets (centred at 56.67 and 53.77 ppm). The singlet at δ 58.86 ppm is assignable to the starting material (**1**); the multiplets, which corresond to an AA'BB' system, can be assigned to [ClPd(μ-dppa)$_2$PdCNR]Cl (**A**), and the other singlet (δ 49.34 ppm) seems to indicate the presence of [(RNC)Pd(μ-dppa)$_2$Pd(CNR)]Cl_2 (**B**), so that in solution ClPd(μ-dppa)$_2$PdCl and species **A** and **B** seem to be present.

By reacting **1a** with an excess of CNTol-*p* (molar ratio 1 : 30) in CH_2Cl_2 and in the presence of $NaClO_4$ (to facilitate the formation of the cationic complex) a red solid is obtained. The IR spectrum of this solid shows absorptions at 2160 cm^{-1} [ν(C≡N)] and 1620 cm^{-1} [ν(C=N)] indicating the presence of terminal and bridging isonitriles. The analytical data of the red solid are in agreement with the calculated values for [(RNC)Pd(μ-dppa)$_2$(μ-CNR)Pd(CNR)]$(ClO_4)_2$ [found (calculated), C: 56.3(56.4); N: 4.4(4.6); H: 4.1(4.1)]. The solution of this solid in $CHCl_3$ is orange-yellow with a perceptible smell of isonitrile, and the $^{31}P\{^1H\}$ NMR spectrum shows only a singlet

(δ 51.93 ppm), assignable to [(RCN)Pd(μ-dppa)$_2$Pd(CNR)](ClO$_4$)$_2$. These data indicate that in solution elimination of isonitrile takes place:

$$[(RNC)Pd(\mu\text{-dppa})_2(\mu\text{-CNR})Pd(CNR)](ClO_4)_2 \xrightarrow{CHCl_3} [(RNC)Pd(\mu\text{-dppa})_2Pd(CNR)](ClO_4)_2 + CNR. \quad (4)$$

The reaction between complex **1a** and CNCy (molar ratio 1 : 1) in CH_2Cl_2 shows a similar behaviour to that observed for CNTol-*p*. An orange-yellow solid can be isolated: [ClPd(μ-dppa)$_2$Pd(CNCy)]Cl [ν(C≡N) 2175 cm^{-1}], analytical data [found (calculated) C: 56.5(56.8); N: 3.7(3.6); H: 4.7(4.6)]; however, the $^{31}P\{^1H\}$ NMR spectrum ($CDCl_3$) shows two singlets (δ 58.85 ppm and 49.88 ppm) and two complicated multiplets (centred at 56.79 ppm and 54.25 ppm), indicating that in solution the starting material and species **A** and **B** are present. If this reaction is carried out in the presence of $NaClO_4$, a yellow solid [ν(C≡N) 2175 cm^{-1}; analytical results: Found (calculated for [ClPd(μdppa)$_2$Pd(CNR)](ClO$_4$) C: 53.4(53.8); N: 3.5(3.4); H: 4.5(4.3)] is obtained. The $^{31}P\{^1H\}$ NMR spectrum shows a similar pattern to that observed for [ClPd(μ-dppa)$_2$Pd(CNR)]Cl [58.84(s); 52.62(s); 57.67(m); 54.97(m) ppm] indicating the presence of starting material and species **A** and **B**.

No complexes containing both inserted and coordinated isonitriles have been obtained even using a large excess (molar ratio 1 : 40) of CNCy, showing minimal tendency of CNCy to insert into the Pd—Pd bond.[13]

Structure of [Pd(μ-Cl)(dppa)]$_2$ · CH_3COCH_3 (**1a**)

The structure of complex **1a** has been solved by single crystal X-ray diffraction. Bond distances and angles are given in Table 2; Fig. 1 shows the molecular structure of the complex **1a**. Figure 2 shows the unit cell. The presence of an acetone molecule associated with only one of the NH ends of the [Pd$_2$(μ-dppa)$_2$Cl$_2$] should be noted.

The molecular structure involves two palladium centres with a Pd—Pd bond [2.6378(6) Å]; two dppa ligands bridge the metal–metal bond and there is one Cl ligand per palladium atom. The environment around each palladium is almost square planar with small tetrahedral distortions (*e.g.* the dihedral angles between the planes Cl(1)Pd(1)P(2), P(1)Pd(1)Pd(2) and Cl(2)Pd(2)P(3), P(4)Pd(2)Pd(1) are 4.93(4) and 3.03(4)° respectively. The angles between mutually *cis*-Pd(1)–ligand bonds are in the range 83.4–92.1°; the same parameters corresponding to the Pd(2) centre are in the range 88.1–

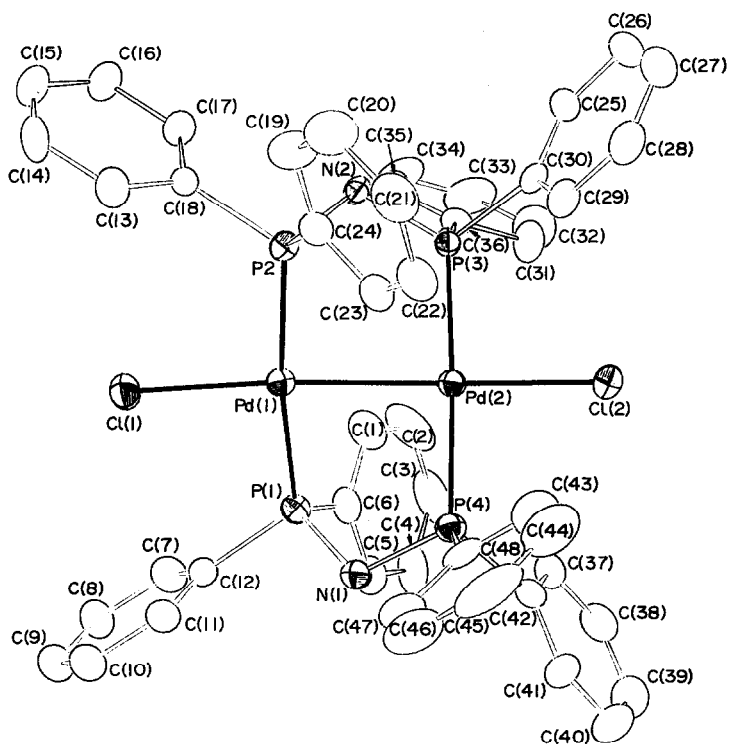

Fig. 1. Plan view of **1a**, excluding hydrogen atoms for the sake of clarity. Thermal ellipsoids are drawn at the 30% probability level.

Table 2. Interatomic distances (Å) and interbond angles (deg) in **1a**

Pd(1)—Pd(2)	2.6378(6)	P(2)—C(24)	1.830(4)
Pd(1)—P(1)	2.2629(14)	P(3)—N(2)	1.690(4)
Pd(1)—P(2)	2.2808(13)	P(3)—C(30)	1.825(3)
Pd(1)—Cl(1)	2.3991(13)	P(3)—C(36)	1.818(4)
Pd(2)—P(3)	2.2800(13)	P(4)—N(1)	1.702(5)
Pd(2)—P(4)	2.2917(14)	P(4)—C(42)	1.827(4)
Pd(2)—Cl(2)	2.4153(15)	P(4)—C(48)	1.810(4)
P(1)—N(1)	1.700(5)	N(1)—H(N1)	0.82(7)
P(1)—C(6)	1.816(4)	N(2)—H(N2)	0.83(7)
P(1)—C(12)	1.797(3)	C(49)—C(50)	1.490(9)
P(2)—N(2)	1.690(4)	C(49)—C(51)	1.474(9)
P(2)—C(18)	1.827(3)	C(49)—O	1.238(8)

Pd(2)—Pd(1)—P(1)	83.44(4)	Pd(2)—P(4)—N(1)	111.89(16)
Pd(2)—Pd(1)—P(2)	89.34(3)	Pd(2)—P(4)—C(42)	117.56(12)
Pd(2)—Pd(1)—Cl(1)	175.61(4)	Pd(2)—P(4)—C(48)	113.68(13)
P(1)—Pd(1)—P(2)	171.90(5)	N(1)—P(4)—C(42)	101.44(19)
P(1)—Pd(1)—Cl(1)	93.91(5)	N(1)—P(4)—C(48)	105.72(20)
P(2)—Pd(1)—Cl(1)	93.52(5)	C(42)—P(4)—C(48)	105.23(16)
Pd(1)—Pd(2)—P(3)	88.14(3)	P(1)—N(1)—P(4)	112.7(3)
Pd(1)—Pd(2)—P(4)	89.46(4)	P(1)—N(1)—H(N1)	116.9(49)
Pd(1)—Pd(2)—Cl(2)	177.88(4)	P(4)—N(1)—H(N1)	114.8(49)
P(3)—Pd(2)—P(4)	176.41(5)	P(2)—N(2)—P(3)	116.09(25)
P(3)—Pd(2)—Cl(2)	90.42(5)	P(2)—N(2)—H(N2)	116.8(48)
P(4)—Pd(2)—Cl(2)	92.05(5)	P(3)—N(2)—H(N2)	124.3(48)
Pd(1)—P(1)—N(1)	108.12(16)	P(1)—C(6)—C(1)	118.6(3)
Pd(1)—P(1)—C(6)	116.55(13)	P(1)—C(6)—C(5)	121.1(3)
Pd(1)—P(1)—C(12)	118.59(12)	P(1)—C(12)—C(7)	120.50(23)
N(1)—P(1)—C(6)	106.38(20)	P(1)—C(12)—C(11)	119.44(23)
N(1)—P(1)—C(12)	101.19(19)	P(2)—C(18)—C(13)	119.89(24)
C(6)—P(1)—C(12)	104.39(16)	P(2)—C(18)—C(17)	120.10(24)
Pd(1)—P(2)—N(2)	107.80(15)	P(2)—C(24)—C(19)	122.9(3)
Pd(1)—P(2)—C(18)	116.83(12)	P(2)—C(24)—C(23)	116.6(3)
Pd(1)—P(2)—C(24)	118.00(12)	P(3)—C(30)—C(25)	121.58(23)
N(2)—P(2)—C(18)	101.38(18)	P(3)—C(30)—C(29)	118.07(23)
N(2)—P(2)—C(24)	106.43(19)	P(3)—C(36)—C(31)	119.09(25)
C(18)—P(2)—C(24)	104.73(16)	P(3)—C(36)—C(35)	120.90(25)
Pd(2)—P(3)—N(2)	115.59(15)	P(4)—C(42)—C(37)	117.61(24)
Pd(2)—P(3)—C(30)	114.23(11)	P(4)—C(42)—C(41)	121.85(25)
Pd(2)—P(3)—C(36)	113.88(12)	P(4)—C(48)—C(43)	117.5(3)
N(2)—P(3)—C(30)	102.24(18)	P(4)—C(48)—C(47)	122.5(3)
N(2)—P(3)—C(36)	104.68(19)	C(50)—C(49)—O	120.1(6)
C(30)—P(3)—C(36)	104.87(15)	C(51)—C(49)—O	119.8(6)

92.1°. The square planar environment around the Pd(1) centre is more distorted than around the Pd(2) centre. The angles between mutually *trans*-palladium–ligand bonds are: 171.9°, 175.6° for Pd(1) and 176.4°, 177.9° for Pd(2) respectively. The chain Cl(1)Pd(1)Pd(2)Cl(2) is almost linear, the angle between the Cl(1)Pd(1) line and the Pd(2)Cl(2) line is 2.8°.

The Pd—P distances are in the range 2.263–2.292 Å, similar to those in dinuclear Pd—Pd derivatives with two bridging dppm ligands $BrPd(\mu\text{-dppm})_2PdBr$,[14] $ClPd(\mu\text{-dppm})_2PdSnCl_3$,[15] $(C_6Cl_5)Pd(\mu\text{-dppm})_2Pd(C_6Cl_5)$.[13b]

The Pd(1)—Cl(1) and Pd(2)—Cl(2) distances are 2.3991(13) and 2.4153(15) Å respectively.

The Pd—Pd distance, [2.6378(6) Å], is in the same range or somewhat shorter than the distances found in other Pd^I—Pd^I derivatives with two dppm's as bridging ligands; 2.644(2) Å in $ClPd(\mu\text{-dppm})_2PdSnCl_3$,[15] 2.670(2) Å in $(C_6Cl_5)Pd(\mu\text{-dppm})Pd(C_6Cl_5)$[13b] and 2.699(2) Å in $BrPd(\mu\text{-dppm})_2PdBr$.[14]

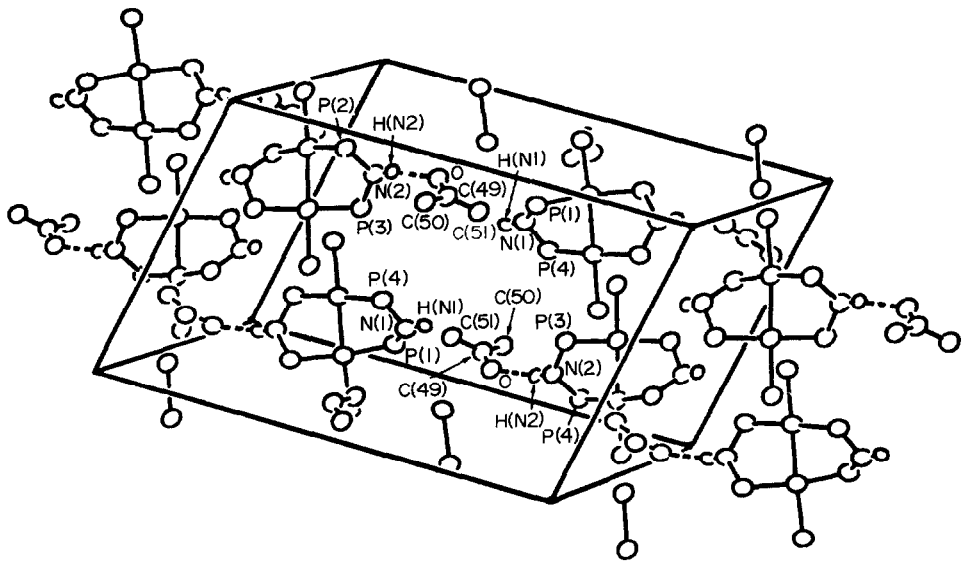

Fig. 2. Unit cell contents for **1a** · Me_2CO.

The environment around each N atom is almost trigonal planar. The PNP angles around N(1) and N(2) are 112.7(3) and 116.1(3)° respectively. The four P—N distances are similar [1.702(4)–1.690(4) Å]; these distances are shorter than the sum of the N and P covalent radii (1.80 Å), and this fact may suggest that the N—P bonds in the coordinated dppa ligands have partial double bond character.

The distance between the two P atoms of the same dppa group [P(1)—P(4) or P(2)—P(3)] are approximately 0.2 Å longer than the Pd(1)—Pd(2) distance.

The two coordination planes around the Pd atoms are twisted about the Pd(1)—Pd(2) bond, so that the dihedral angle between them is 36.83(4)° (see Fig. 3).

There is an acetone molecule for each ClPd(μ-dppa)PdCl molecule; the O atom of the solvent molecule is situated at only 2.10(9) Å from the H atom bonded to N(2) and 2.915(7) Å from the N(2) atom indicating the presence of typical hydrogen bond.[16] No analogous interaction is present for the H atom bonded to N(1).

EXPERIMENTAL

C, H and N analyses were carried out on a Perkin–Elmer 240 microanalyser. Conductivities were measured in approx. 5×10^{-4} M acetone solutions with a Philips PW 9501/01 conductimeter. The IR spectra were recorded (in the 4000–200 cm^{-1} range) on a Perkin–Elmer spectrophotometer. $^{31}P\{^1H\}$ NMR spectra were recorded on a Varian XL-200. Thermogravimetric studies have been carried out using a TGS-2 Perkin–Elmer system.

Standard methods were used to prepare the following complexes: $Ph_2PNHPPh_2$(dppa),[17] $PdCl_2(PhCN)_2$[18] and $Pd_2(dba)_3 \cdot CH_3Cl$.[19]

ClPd(μ-dppa)$_2$PdCl (1)

To a solution of dppa (0.600 g, 1.55 mmol) in 30 cm^3 of CH_2Cl_2, $PdCl_2(NCPh)_2$ (0.298 g, 0.78 mmol) and $Pd_2(dba)_3 \cdot CHCl_3$ (0.402 g, 0.39 mmol) were added; the mixture was refluxed for 1 h. After filtration the resulting red solution was evaporated to

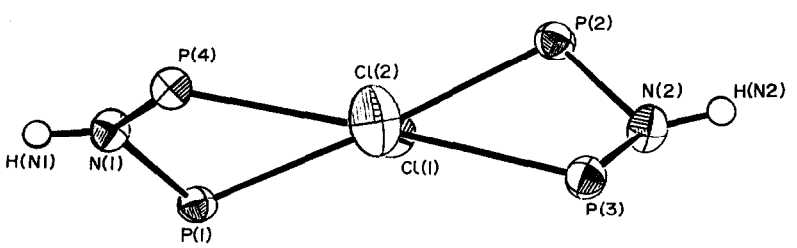

Fig. 3. View along the Pd—Pd bond showing the relative inclination of the two five-atom rings.

$\simeq 5\ cm^3$ and Et_2O (30 cm^3) was added. The orange-brown solid which separated was filtered off and this solid was stirred in 60 cm^3 of Et_2O for 3 h at room temperature (68% yield).

$[ClPd(\mu\text{-dppa})_2PdCl]\cdot(CH_3)_2CO$ (**1a**), $[ClPd(\mu\text{-dppa})_2PdCl]\cdot 2NCCH_3$ (**1b**). Complex **1** (0.4 g, 0.38 mmol) was dissolved in 20 cm^3 of acetone and stirred at room temperature. After a few minutes a yellow precipitate was formed. The solid was filtered off, and air dried (**1a**, 82% yield).

Complex **1b** was obtained in a similar way by using acetonitrile as solvent (65% yield).

$BrPd(\mu\text{-dppa})_2PdBr$ (**2**)

To a solution of $ClPd(\mu\text{-dppa})_2PdCl$ (0.200 g, 0.19 mmol) in 20 cm^3 of CH_2Cl_2, NBu^n_4Br (1.00 g, 3.10 mmol) was added. The mixture was stirred at room temperature overnight and then evaporated to dryness. The orange residue was washed with water ($2\times 10\ cm^3$) and extracted with CH_2Cl_2. The dichloromethane solution was evaporated almost to dryness and the addition of Et_2O (30 cm^3) renders an orange solid which was recrystallized from acetone/diethyl ether (**2**, 44% yield).

$SnCl_3Pd(\mu\text{-dppa})_2PdSnCl_3$ (**3**)

To a solution of $ClPd(\mu\text{-dppa})_2PdCl$ (**1**) (0.200 g, 0.19 mmol) in 20 cm^3 of CH_2Cl_2, a solution of $SnCl_2$ (0.189 g, 1.00 mmol) in 20 cm^3 of MeOH was added. The mixture was stirred for 4 h at room temperature. The solution was evaporated to 10 cm^3 giving a red precipitate, which was filtered, and air dried. Complex **3** (72% yield).

$[(Ph_3P)Pd(\mu\text{-dppa})_2Pd(PPh_3)]BPh_4$ (**4**)

PPh_3 (0.105 g, 0.40 mmol) was added to a suspension of $ClPd(\mu\text{-dppa})_2PdCl$ (**1**) (0.200 g, 0.189 mmol) in 15 cm^3 MeOH; stirring at room temperature for 10 min resulted in complete dissolution. After addition of $NaBPh_4$ (0.136 g, 0.4 mmol), an orange solid precipitated. The resulting solid was filtered off and air dried. Complex **4** (60% yield).

$[ClPd(\mu\text{-dppa})_2(\mu\text{-}N_2R)PdCl]$ $R = C_6H_4\text{-}o\text{-}NO_2$ (**5**), $C_6H_4\text{-}p\text{-}CH_3$ (**6**)

To a solution of $ClPd(\mu\text{-dppa})_2PdCl$ (**1**) (0.263 g, 0.25 mmol) in acetone (25 cm^3) (−30°C), $[o\text{-}NO_2C_6H_4N_2]BF_4$ was added. The solution was stirred at −30°C for 15 min and then allowed to reach room temperature over *ca.* 30 min. The resulting red solution was filtered and evaporated to *ca.* 5 cm^3. The addition of Et_2O (30 cm^3) afforded **5** (55% yield).

Complex **6** was obtained similarly by using $[p\text{-}CH_3\text{-}C_6H_4N_2]BF_4$ (57% yield).

Crystallographic study of (**1a**)

Crystal data (*at* 185 K). $Pd_2P_4Cl_2ON_2C_{50}H_{48}$, $M = 1100.54$. Monoclinic, $a = 13.540(3)$, $b = 16.943(2)$, $c = 21.082(15)$ Å, $\beta = 105.257(42)°$, $U = 4671(4)\ Å^3$, space group $P2_1/c$ (No. 14). $Z = 4$, $D_c = 1.565\ g\ cm^{-3}$, $F(000) = 2224$, graphite-monochromated Mo-K_α radiation, $\lambda = 0.71069$ Å, $\mu(\text{Mo-}K_\alpha) = 10.49\ cm^{-1}$, yellow crystal, $0.2\times 0.25\times 0.3$ mm.

Data collection and processing. CAD4 diffractometer with low temperature unit, ω–2θ scans, ω scan width $0.8+0.35\tan\theta$, 6145 reflections measured (θ_{max} 22°; h $-14\rightarrow 14$, k $0\rightarrow 17$, l $0\rightarrow 22$), giving 5091 reflections with $F \geqslant 5\sigma(F)$ for structure solution and refinement. No significant crystal movement or decay over 78 X-ray hours.

Structure analysis and refinement. Solution by Patterson and difference syntheses was followed by full-matrix least-square refinement with anisotropic thermal parameters for all atoms except H, using the SHELX 76 program system.[20] Empirical absorption correction[21] applied after isotropic convergence. The phenyl rings were refined as rigid groups with H atoms in calculated positions. H atoms bonded to N located and freely refined. Those of the solvent molecule set in idealized positions. Group U's for all H atoms [0.067(3) $Å^2$ at convergence]. Refinement of 476 parameters converged at $R = 0.0333$ and $R_w = 0.0486$ (weighting scheme $w^{-1} = [\sigma^2(F)+0.000006F^2]$. Largest peak 1.53 $e/Å^3$ at 1.07 from Pd(1).

Acknowledgements—We thank the Dirección General de Investigación Cientifica y Técnica for financial support (project PB85-0128) and the Scientific Office of NATO for a travel grant.

REFERENCES

1. (a) R. Usón, J. Forniés, R. Navarro and J. I. Cebollada, *J. Organometal. Chem.* 1986, **304**, 381 and references therein; (b) J. Forniés, F. Martínez, R. Navarro, A. Redondo, M. Tomás and A. J. Welch, *J. Organometal. Chem.* 1986, **316**, 351 and references therein.
2. G. Liehr, G. Szucsanyi and J. Ellermann, *J. Organometal. Chem.* 1984, **265**, 95.
3. R. Usón, A. Laguna, M. Laguna, M. N. Fraile, P. G. Jones and G. M. Sheldrick, *J. Chem. Soc., Dalton Trans.* 1986, 291.

4. H. Schmidbaur, E. F. Wagner and A. Wohleben-Hummer, *Chem. Ber.* 1979, **112**, 496.
5. J. Ellermann and W. Wend, *J. Organometal. Chem.* 1983, **258**, 21.
6. L. S. Benner and A. L. Balch, *J. Am. Chem. Soc.* 1978, 6099.
7. R. Usón, J. Forniés, R. Navarro and J. I. Cebollada. Own observations.
8. D. F. Schriver and M. P. Johnson, *Inorg. Chem.* 1967, 1265.
9. R. Usón, J. Forniés, P. Espinet and C. Fortuño, *J. Chem. Soc., Dalton Trans.* 1986, 1849.
10. K. Nakamoto, *Infrared Spectra of Inorganic and Coordination Compounds*, 2nd edn, p. 187. Wiley Interscience, New York (1970).
11. M. Francel, *J. Am. Chem. Soc.* 1952, **74**, 1265.
12. L. S. Benner, M. M. Olmstead, H. Hope and A. L. Balch, *J. Organometal. Chem.* 1978, **153**, C31.
13. (a) R. Usón, J. Forniés, P. Espinet, F. Martínez, C. Fortuño and B. Menjón, *J. Organometal. Chem.* 1983, **256**, 365; (b) P. Espinet, J. Forniés, C. Fortuño, G. Hidalgo, F. Martínez, M. Tomás and A. J.Welch, *J. Organometal. Chem.* 1986, **317**, 105.
14. (a) R. G. Holloway, B. R. Renfold, R. Colton and J. McCormick, *J. Chem. Soc., Chem. Commun.* 1976, 485; (b) R. Colton, M. J. McCormick and D. Pannan, *Aust. J. Chem.* 1978, **31**, 1425.
15. M. M. Olmstead, L. S. Benner, H. Hope and A. L. Balch, *Inorg. Chim. Acta.* 1979, **32**, 193.
16. N. N. Greenwood and A. Earnshaw, *Chemistry of the Elements*, p. 65. Pergamon Press, Oxford (1984).
17. H. Nöth and L. Meinel, *Z. Anorg. Chem.* 1967, **349**, 225.
18. J. R. Doyle, P. E. Slade and H. B. Jonassen, *Inorg. Synth.* 1960, **6**, 218.
19. T. Ukai, H. Kawazin and T. Ishii, *J. Organometal. Chem.* 1974, **65**, 253.
20. G. M. Sheldrick, SHELX-76 Program System. University of Cambridge (1976).
21. N. G. Walker and D. Stuart, *Acta Cryst., Sect A* 1983, **39**, 158.

Polyhedron Vol. 8, No. 8, pp. 1053–1059, 1989
Printed in Great Britain

0277–5387/89 $3.00+.00
© 1989 Pergamon Press plc

ION-PAIR EXTRACTION OF THE GALLIUM(III) ION FROM HYDROCHLORIC ACID WITH VARIOUS METHOXY-SUBSTITUTED TRIARYLPHOSPHINES

YUKO YAMASHOJI,* TAKAYUKI MATSUSHITA, MINORU TANAKA and TOSHIYUKI SHONO

Department of Applied Chemistry, Faculty of Engineering, Osaka University, Yamadaoka 2-1, Suita, Osaka 565, Japan

and

MASANORI WADA

Department of Industrial Chemistry, Faculty of Engineering, Tottori University, Koyamacho-minami, Tottori 680, Japan

(*Received* 17 *September* 1988; *accepted* 10 *November* 1988)

Abstract—A series of methoxy-substituted triarylphosphines $R_nPh_{3-n}P$ (n = 1–3), where R may be 2-(MeO)C_6H_4, 4-(MeO)C_6H_4, 2,6-(MeO)$_2C_6H_3$ and 2,4,6-(MeO)$_3C_6H_2$, have been prepared and employed as extractants for the gallium(III) ion from hydrochloric acid solutions. The extractabilities of these compounds are found to become more effective with an increase in their basicities, which are determined by non-aqueous titrimetry. Highly basic compounds, $\{(2,6\text{-}(MeO)_2C_6H_3)\}_3P$ and $\{(2,4,6\text{-}(MeO)_3C_6H_2)\}_3P$, possess the highest extractability amongst the triarylphosphines. The extraction mechanism is discussed on the basis of the ^1H and ^{31}P NMR spectroscopic data.

Triphenylphosphine (Ph_3P) is one of the most popular ligands which can coordinate with noble metal ions. Thus it has been applied to the extraction of such metal ions as gold, platinum and palladium from acidic media.[1–5] In these cases, triphenylphosphine acts as a neutral ligand or its phosphonium salt of hydrogen chloride, depending on both the nature of the metal ions and the concentration of hydrochloric acid.

In a previous paper,[6] we described that the basicities of the methoxy-substituted triarylphosphines, $R_nPh_{3-n}P$ [R = 2-(MeO)C_6H_4, 4-(MeO)C_6H_4, 2,6-(MeO)$_2C_6H_3$ and 2,4,6-(MeO)$_3C_6H_2$ (abbreviations: 2-MeOPh, 4-MeOPh, 2,6-MeOPh and 2,4,6-MeOPh, respectively); n = 1, 2 and 3], increase with increasing numbers of the introduced methoxy groups on the phenyl rings, and that tris(2,4,6-trimethoxyphenyl)phosphine (2,4,6-MeOPh)$_3P$ (pK_a = 11.02) possesses the highest basicity amongst them, which is comparable to that of piperidine (pK_a = 11.2).[7] In addition, this phosphine shows the most effective extractability for the gallium(III) ion from hydrochloric acid solutions. In this system, we have proposed that the gallium(III) ion is extracted through an anion-exchange mechanism.

In this paper, we describe the extraction behaviour of a series of methoxy-substituted triarylphosphines for the gallium(III) ion from acidic media and the relationship between their extractabilities and basicities. Moreover, the extraction mechanism will be discussed from the chemical shifts obtained in ^1H and ^{31}P NMR spectroscopy.

EXPERIMENTAL

Preparation of methoxy-substituted triarylphosphines

Triarylphosphines, $R_nPh_{3-n}P$, where R is 2,6-MeOPh and 2,4,6-MeOPh (n = 1–3), were prepared according to the method described in a previous paper.[8]

* Author to whom correspondence should be addressed.

$R_nPh_{3-n}P$, where R is 2-MeOPh and 4-MeOPh (n = 1–3), were prepared as follows. $(2\text{-MeOPh})_3P$: a tetrahydrofuran (THF) solution (10 cm^3) of chlorodiphenylphosphine (5.7 g) was added to a THF solution (30 cm^3) of Grignard reagent, $o\text{-}CH_3OC_6H_4MgBr$ at 0°C, which was prepared from *o*-bromoanisole (5.0 g). The mixture was refluxed for 3 h. After the reaction was complete, distilled water (25 cm^3) containing conc. H_2SO_4 (2.5 cm^3) was added to decompose an excess of the Grignard reagent. The reaction mixture was extracted twice with benzene (100 cm^3). The benzene extracts were washed with an aqueous solution of diluted $NaHCO_3$ (5%) and then several times with distilled water, and dried over Na_2SO_4. The benzene solution was evaporated to dryness under reduced pressure, and the residue was recrystallized from ethanol.

Other triarylphosphines were prepared by a similar method to the one described above. These compounds were obtained in 60–70% yield. Their analytical data, melting points, mass spectral data and pK_a values are listed in Table 1.

Reagents

An aqueous gallium(III) chloride solution was prepared by dissolving gallium metal (99.99%), which was obtained from Wako Chemical Co. Ltd, in conc. HCl and diluting with deionized water to the required concentration. Other reagents were of analytical grade.

Extraction and analytical procedure

Equal volumes (5 cm^3) of a chloroform solution of an extractant and a HCl solution of the gallium(III) ion were placed in a centrifuge glass tube (10 cm^3), followed by shaking for 15 min at 25 ± 0.1°C and centrifuging until phase separation. The concentration of the gallium(III) ion remaining in the aqueous phase was determined by atomic absorption spectrometry. The concentration of the gallium(III) ion transferred into the organic phase was calculated from mass balance, using that in the aqueous phase. Deuterochloroform was used as the organic phase for NMR measurements in place of chloroform.

pK_a *Measurements of phosphines*

The basicities of the triarylphosphines were measured by non-aqueous titrimetry in nitromethane according to the method reported by Streuli.[9] A standard HCl solution (0.004 mol dm^{-3}) and a glass calomel electrode system were used. Diphenylguanidine was used as the reference standard for all of the non-aqueous titrations. The pK_a (H_2O) values were calculated from the half-neutralization potential values obtained in the non-aqueous titrimetry.

Physical measurements

Atomic absorption measurements were made on a Nippon Jarrell Ash AA-8500 Mark II spectrometer using a $N_2O\text{–}C_2H_2$ flame. IR spectra were recorded on a JASCO 910 grating spectrophotometer between caesium iodide plates. A Horiba pH meter F-8 DP equipped with a glass calomel electrode was used for titrimetry. ^1H NMR spectra were obtained on a JNM-PS-100 spectrometer operating at 100 MHz using tetramethylsilane (TMS) as the internal standard. ^{31}P

Table 1. Elemental analyses and some properties of triarylphosphines

Compound	Mass [M^+]	Melting point (°C)	Elemental analyses Found (Calc.) (%) C	H	pK_a
$(2\text{-MeOPh})Ph_2P$	292	124–125	77.6(78.1)	5.9(5.8)	3.33
$(2\text{-MeOPh})_2PhP$	322	167–168	75.1(74.5)	6.1(5.9)	4.01
$(2\text{-MeOPh})_3P$	352	205–207	71.5(71.6)	6.1(6.0)	4.47
$(4\text{-MeOPh})Ph_2P$	292	65–67	77.8(78.1)	5.9(5.8)	3.67
$(4\text{-MeOPh})_2PhP$	322	80–82	74.7(74.5)	6.0(5.9)	4.06
$(4\text{-MeOPh})_3P$	352	134–135	71.5(71.6)	6.0(6.0)	4.75
$(2,6\text{-MeOPh})Ph_2P$	322	127–128	74.4(74.5)	6.0(5.9)	5.39
$(2,6\text{-MeOPh})_2PhP$	382	123–124	68.5(69.1)	6.0(6.0)	7.28
$(2,6\text{-MeOPh})_3P$	442	158–160	64.8(65.2)	6.2(6.1)	9.33
$(2,4,6\text{-MeOPh})Ph_2P$	352	105–106	71.4(71.6)	6.1(6.0)	5.77
$(2,4,6\text{-MeOPh})_2PhP$	442	150–151	64.8(65.2)	6.2(6.1)	8.22
$(2,4,6\text{-MeOPh})_3P$	532	166–168	60.6(60.9)	6.3(6.2)	11.02

NMR spectra were taken on a JEOL-GSX-270S spectrometer operating at 270 MHz using 85% H_3PO_4 as the external standard.

RESULTS AND DISCUSSION

Basicities of methoxy-substituted triarylphosphines

Previously, Streuli and Fritz and co-workers have determined the pK_a values of organic acids and bases such as substituted phosphines,[9] phenols,[10] and amines[11] by non-aqueous titrimetry. We determined the pK_a values of the methoxy-substituted triarylphosphines using almost the same procedure as described by them. These numerical data are summarized in Table 1. It can be seen that the pK_a values of the triarylphosphines are increased with an increase in the number of introduced methoxy groups on the phenyl rings. However, they are affected by the substituted position of the methoxy group on the phenyl ring: the substitution of the four-position on the phenyl ring resulted in a slightly higher basicity compared with that for the substitution of the two-position, and the pK_a value of (2,6-MeOPh)Ph_2P is higher than that of (2-MeOPh)$_2$PhP, in spite of involving two methoxy groups per one phosphine molecule. This pK_a difference between (2,6-MeOPh)Ph_2P ($pK_a = 5.39$) and (2-MeOPh)$_2$PhP ($pK_a = 4.01$) may arise from steric effects in addition to electronic effects. The 2,6-MeOPh group is more bulky than the 2-MeOPh group, so that free rotation, in solution, of the methoxy-substituted phenyl ring around the P—C bond might be more restricted for the former compared with the latter. Thus, (2,6-MeOPh)Ph_2P may statistically adopt a more effective configuration for electron releasing from the methoxy group on the phosphorus atom than (2-MeOPh)$_2$PhP.

The extraction isotherm

The extraction behaviour of the gallium(III) ion with the triarylphosphines from various concentrations of HCl is shown in Figs 1–4, where the concentration of the extractants in the organic phase is equal to the initial concentration of the gallium(III) ion in the aqueous phase (5.0×10^{-4} mol dm^{-3}). Figures 1 and 2 show the extraction isotherms obtained by using (2-MeOPh)$_n$Ph$_{3-n}$P and (4-MeOPh)$_n$Ph$_{3-n}$P ($n = 1$, 2 and 3), respectively. Figure 1 also includes the extraction isotherm obtained by using Ph_3P for comparison. It can be seen in both cases that maximum extractions of the gallium(III) ion are achieved at lower concentrations of HCl in the order of $n = 1 < 2 < 3$. This order is fairly consistent with the increasing

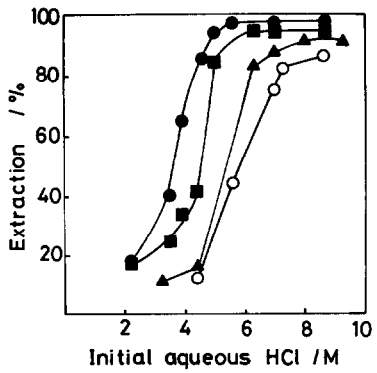

Fig. 1. Effects of HCl concentration on extraction of Ga^{III} (5×10^{-4} M) with (2-MeOPh)$_n$Ph$_{3-n}$P and Ph_3P (5×10^{-4} M). (▲): $n = 1$; (■): $n = 2$; (●): $n = 3$; (○): Ph_3P.

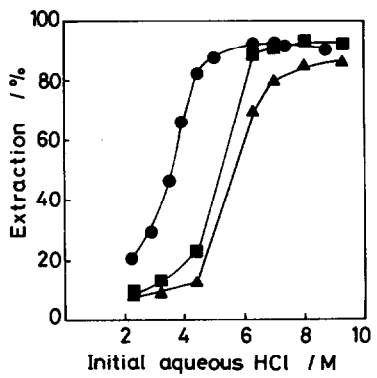

Fig. 2. Effects of HCl concentration on extraction of Ga^{III} (5×10^{-4} M) with (4-MeOPh)$_n$Ph$_{3-n}$P (5×10^{-4} M). (▲): $n = 1$; (■): $n = 2$; (●): $n = 3$.

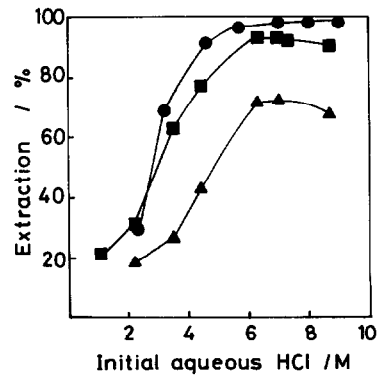

Fig. 3. Effects of HCl concentration on extraction of Ga^{III} (5×10^{-4} M) with (2,6-MeOPh)$_n$Ph$_{3-n}$P (5×10^{-4} M). (▲): $n = 1$; (■): $n = 2$; (●): $n = 3$.

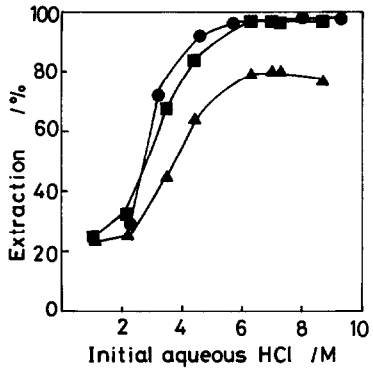

Fig. 4. Effects of HCl concentration on extraction of Ga^{III} (5×10^{-4} M) with (2,4,6-MeOPh)$_n$Ph$_{3-n}$P (5×10^{-4} M). (▲): $n = 1$; (■): $n = 2$; (●): $n = 3$.

order of their basicities. The percentage extraction of the gallium(III) ion with Ph_3P was only about 80% more than with 7.3 M HCl. The pK_a value of Ph_3P is 2.73,[9] being the lowest basicity examined in the present work.

Figures 3 and 4 show the extraction isotherms obtained by using (2,6-MeOPh)$_n$Ph$_{3-n}$P and (2,4,6-MeOPh)$_n$Ph$_{3-n}$P (n = 1, 2 and 3), respectively. A similar relationship was observed between their extractabilities and basicities. Moreover, extractions nearly equal to 100% were obtained in the cases of (2,6-MeOPh)$_3$P and (2,4,6-MeOPh)$_3$P, which are highly basic as shown in Table 1. These results indicate that they are the most effective extractants among the triarylphosphines investigated here.

^{1}H *and* ^{31}P *NMR*

In the extractions of platinum(II) and palladium(II) with Ph_3P from acidic media, it has been proposed[4] that Ph_3P can act as both a neutral ligand and an anion exchanger by forming its phosphonium cation [Ph_3P^+H].

In order to clarify the extraction mechanism for the present systems, we have measured the following ^{1}H and ^{31}P NMR spectra: (I) the $CDCl_3$ solutions of the triarylphosphines themselves, (II) those after shaking with conc. HCl and (III) those after extraction of gallium(III) from 6.0 M HCl, for which data are summarized in columns I, II and III, respectively, in Table 2 for the ^{1}H NMR spectra and in Table 3 for the ^{31}P NMR spectra.

^{1}H *NMR study*. The phenyl proton signals of the methoxy-substituted triarylphosphines split as expected, and those at the *ortho* and *para* positions vs methoxy group are observed at higher magnetic fields than those at the *meta* position. The ^{1}H NMR data for (2,6-MeOPh)$_3$P and (2,4,6-MeOPh)$_3$P, which are already reported in a previous paper,[8] are listed again in Table 2 for comparison. When the $CDCl_3$ solutions of the triarylphosphines were shaken with conc. HCl, all the proton signals shifted to lower magnetic fields as shown in column II in Table 2. This may be caused by the formation of their phosphonium salts from hydrogen chloride. The shift values of the phenyl protons are larger than those of the methyl protons of the methoxy groups; the former lies in the range 0.20–0.48 ppm and the latter in the range 0.08–0.24 ppm. However, the shift value of the phenyl protons of Ph_3P is the smallest amongst the triarylphosphines investigated here. On the other hand, when the $CDCl_3$ solutions of the triarylphosphines were shaken with a gallium(III) solution in 6.0 M HCl, their chemical shifts are observed at almost the same magnetic fields as those observed after shaking with conc. HCl, except for Ph_3P, whose proton signals are shifted to lower magnetic fields by *ca* 0.21 ppm. In particular, all the proton signals for (2,6-MeOPh)$_3$P and (2,4,6-MeOPh)$_3$P are observed at the same positions. These results will be discussed later in combination with those obtained in the ^{31}P NMR spectroscopy.

^{31}P *NMR study*. As shown in column I in Table 3, the ^{31}P chemical shifts of the triarylphosphines lie within a wide range of −4.84 ppm for Ph_3P to −69.36 ppm for (2,4,6-MeOPh)$_3$P, and are shifted to higher magnetic fields with an increase in the number of introduced methoxy groups per triarylphosphine molecule.

It should be noted that the chemical shifts of the triarylphosphines having a methoxy group in the two-position on the phenyl ring, are observed at higher magnetic fields than those in the four-position. A higher magnetic field shift like this has been reported for the compound (2-MeOPh)Ph_2P and explained in terms of an anisotropic effect.[12] It is particularly interesting that the shift values increase almost proportionally with an increase in the number of methoxy groups. For example, when the ^{31}P chemical shift of Ph_3P is a standard, the difference in the chemical shifts between Ph_3P and (2-MeOPh)Ph_2P is 11.28 ppm. That between (2-MeOPh)Ph_2P and (2-MeOPh)$_2$PhP is 11.18 ppm and that between (2-MeOPh)$_2$PhP and (2-MeOPh)$_3$P is 11.70 ppm. A similar behaviour is observed for a series of the 4-MeOPh derivatives, of which the shift values, however, are smaller than those of the 2-MeOPh derivatives.

The ^{31}P chemical shifts of the $CDCl_3$ solutions of the triarylphosphines after shaking with conc. HCl are given in column II (Table 3), and the differences in chemical shifts before and after shaking with it

Table 2. ^1H NMR data for methoxy-substituted triarylphosphines[a]

Compound	Proton	Chemical shift (ppm) I[b]	II[c]	III[d]
Ph_3P	Ph(15H)	7.36–7.30(m)	7.62–7.44(m)	7.84–7.58(m)
(2-MeOPh)Ph_2P	CH_3(3H)	3.72(s)	3.82(s)	3.90(s)
	3-H,5-H,6-H(3H)	6.96–6.62(m)	7.28–7.02(m)	7.30–7.08(m)
	Ph(10H),4-H(1H)	7.36–7.24	7.92–7.54(m)	7.84–7.60(m)
(2-MeOPh)$_2$PhP	CH_3(6H)	3.72(s)	3.83(s)	3.86(s)
	3-H,5-H,6-H(6H)	6.96–6.64(m)	7.38–7.06(m)	7.34–7.10(m)
	Ph(5H),4-H(2H)	7.34–7.24(m)	7.90–7.44(m)	7.88–7.58(m)
(2-MeOPh)$_3$P	CH_3(9H)	3.73(s)	3.88(s)	3.90(s)
	3-H,5-H,6-H(9H)	6.97–6.72(m)	7.42–7.12(m)	7.29–7.14(m)
	4-H(3H)	7.41–7.24(m)	7.89–7.71(m)	7.94–7.74(m)
(4-MeOPh)Ph_2P	CH_3(6H)	3.78(s)	3.89(s)	3.90(s)
	3-H,5-H(2H)	6.90(d)	7.15(dd)	7.14(dd)
		$[8]_H$	$[8]_H$, $[2]_P$	$[8]_H$, $[2]_P$
	Ph(10H),2-H,6-H(2H)	7.36–7.19(m)	7.84–7.50(m)	7.94–7.74(m)
(4-MeOPh)$_2$PhP	CH_3(6H)	3.80(s)	3.89(s)	3.91(s)
	3-H,5-H(2H)	6.90(d)	7.15(dd)	7.16(dd)
		$[8]_H$	$[8]_H$, $[2]_P$	$[8]_H$, $[2]_P$
	Ph(5H),2-H,6-H(4H)	7.34–7.19(m)	7.90–7.52(m)	7.76–7.52(m)
(4-MeOPh)$_3$P	CH_3(9H)	3.80(s)	3.88(s)	3.89(s)
	3-H,5-H(6H)	6.90(d)	7.15(dd)	7.16(dd)
		$[8]_H$	$[8]_H$, $[2]_P$	$[8]_H$, $[2]_P$
	2-H,6-H(6H)	7.24(t)	7.76(dd)	7.66(dd)
		$[8]_H$, $[8]_P$	$[8]_H$, $[14]_P$	$[8]_H$, $[14]_P$
(2,6-MeOPh)$_3$P	CH_3(18H)	3.46(s)	3.72(s)	3.72[e]
	3-H,5-H(6H)	6.51(dd)	6.72(dd)	6.72(dd)
		$[8]_H$, $[4]_P$	$[8]_H$, $[5]_P$	not clear
	4-H(3H)	7.15(t)	7.61(t)	7.61(t)
		$[8]_H$	$[8]_H$	$[8]_H$
	P^+—H	—	7.80(d)	not clear
			$[80]_P$	
(2,4,6-MeOPh)$_3$P	2-CH_3,6-CH_3(18H)	3.47(s)	3.73(s)	3.72(s)[e]
	4-CH_3(9H)	3.78(s)	3.91(s)	3.90[e]
	3-H,5-H(6H)	6.04(d)	6.20(d)	6.20(d)
		$[3.5]_P$	$[6]_P$	$[6]_P$
	P^+—H	—	7.91(d)	not clear
			$[82]_P$	

[a] Measured in $CDCl_3$.
[b] Phosphines themselves.
[c] After shaking with conc. HCl.
[d] After extraction of Ga^{III} from 6.0 M HCl.
[e] Slightly split signals were observed (s = singlet, d = doublet, t = triplet, dd = double doublets).

are also given in column (II–I). It can be seen that relatively large, lower magnetic field shifts are observed for (2,6-MeOPh)$_3$P, (2,4,6-MeOPh)$_3$P and the 2-MeOPh derivatives. On the contrary, the ^{31}P chemical shift of Ph_3P changes slightly, and the shift values for the 4-MeOPh derivatives are relatively small compared with those for the above 2-MeOPh derivatives. This trend is consistent with that observed in ^1H NMR spectroscopy. Such differences in the shift values between the 2- and 4-methoxy-substituted compounds may be ascribed to the difference in the anisotropic magnetic field effect between them, because their basicities are comparable, as shown in Table 1. In addition, the ^{31}P NMR spectra of the $CDCl_3$ solutions of (2,6-MeOPh)$_3$P and (2,4,6-MeOPh)$_3$P were observed as

Table 3. ^{31}P NMR data of methoxy-substituted triarylphosphines[a]

Compound	Chemical shift (ppm) I[b]	II[c]	III[d]	(II–I)	(III–II)
Ph_3P	−4.84	−4.82	4.87	0.02	9.69
$(2\text{-MeOPh})Ph_2P$	−16.12	−9.48	−3.75	6.64	5.73
$(2\text{-MeOPh})_2PhP$	−27.30	−11.87	−8.51	15.43	3.36
$(2\text{-MeOPh})_3P$	−39.00	−17.18	−16.94	21.82	0.24
$(4\text{-MeOPh})Ph_2P$	−6.47	−4.03	0.61	2.44	4.64
$(4\text{-MeOPh})_2PhP$	−8.14	−3.31	3.97	4.83	7.28
$(4\text{-MeOPh})_3P$	−9.60	−4.05	3.60	5.55	7.65
$(2,6\text{-MeOPh})_3P$	−66.38	−50.18	−50.18	16.20	0
$(2,4,6\text{-MeOPh})_3P$	−69.36	−52.14	−52.21	17.22	−0.07

The ppm values are relative to an external standard (85% H_3PO_4).
[a] Measured in $CDCl_3$.
[b] Phosphines themselves.
[c] After shaking with conc. HCl.
[d] After extraction of Ga^{III} from 6.0 M HCl.

clearly split signals after shaking with conc. HCl, as shown in Fig. 5. These split signals may arise from coupling with the proton nucleus (^1H), by the formation of their phosphonium salts with HCl. However, such a clearly split signal was not observed for $(2\text{-MeOPh})_2PhP$ and $(2\text{-MeOPh})_3P$, although their shift values are comparable with those observed for $(2,6\text{-MeOPh})_3P$ and $(2,4,6\text{-MeOPh})_3P$. This may be related to the difference in their basicities: the latter two compounds have such high basicities that they can easily form their stable phosphonium salts with HCl.

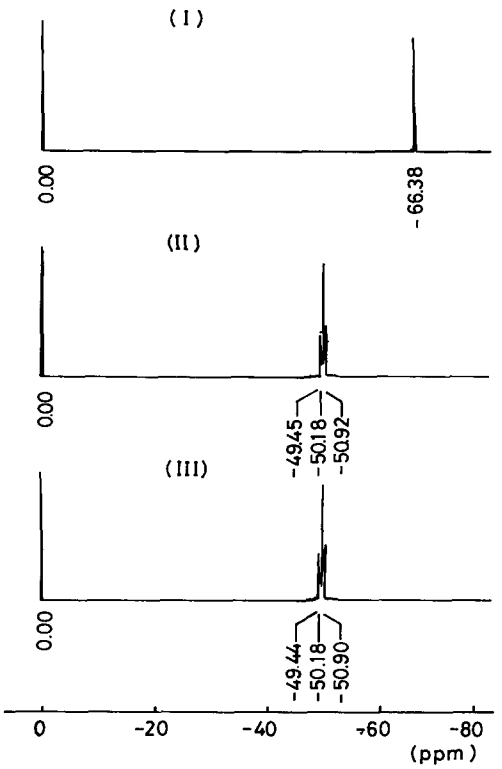

Fig. 5. ^{31}P NMR spectra of $(2,6\text{-MeOPh})_3P$ in $CDCl_3$. (I): $(2,6\text{-MeOPh})_3P$; (II): after shaking with conc. HCl; (III): after extraction of Ga^{III} ion. 0.00 ppm is for the external standard (85% H_3PO_4).

Next, the ^{31}P chemical shifts of the $CDCl_3$ solutions of the triarylphosphines after extraction of gallium(III) from 6.0 M HCl are given in column III (Table 3), and also the differences in the chemical shifts between columns II and III are presented in column (III–II). The differences in column (III–II) are almost zero for the compounds $(2\text{-MeOPh})_3P$, $(2,6\text{-MeOPh})_3P$ and $(2,4,6\text{-MeOPh})_3P$. Moreover, as shown in Fig. 5, the spectral features of $(2,6\text{-MeOPh})_3P$ between after shaking with conc. HCl and after extraction of gallium(III) are very similar. From these results, it can be concluded that the extraction of gallium(III) with these compounds proceeds via the ion-pair formation in which they act as an anion-exchanger, as shown in the following equation;

$$R_3P + HCl \rightleftharpoons [R_3P^+H][Cl^-]$$

$$[R_3P^+H][Cl^-] + H[GaCl_4] \rightleftharpoons [R_3P^+H][GaCl_4^-] + HCl,$$

where R_3P denotes a triarylphosphine.

On the other hand, with other triarylphosphines, relatively large lower magnetic field shifts are observed after the extraction of gallium(III). The following two reasons, responsible for the lower magnetic field shifts, are considered: (1) these triarylphosphines react with $H[GaCl_4]$, which is a main species in 6.0 M HCl, to give their phosphonium salts with a tetrachlorogallate(III) ion,

$[R_3P^+H][GaCl_4^-]$ and (2) they coordinate to the gallium(III) ion as a neutral ligand.

$$(R_3P) + H[GaCl_4] \rightleftharpoons [R_3P^+H][GaCl_4^-] \quad (1)$$

$$n(R_3P) + H[GaCl_4] \rightleftharpoons H[GaCl_4(R_3P)_n]. \quad (2)$$

From only the shift values, we can not conclude that either of the above two processes takes place in the extraction of gallium(III) with this group of triarylphosphines. However, in the extraction of H_2PtCl_6 with (2,6-MeOPh)$_3$P in $CDCl_3$ from neutral aqueous solution (not hydrochloric acid), its ^{31}P NMR spectrum shows a close similarity to that for the $CDCl_3$ extract of gallium(III); the chemical shift of the ^{31}P signals is observed at -50.13 ppm with splitting. This result may support the extraction process of the ion-pair formation (1), rather than the coordination of the extractant (2). However, the ^{31}P NMR spectra of the $CDCl_3$ extracts of this group of triarylphosphines show a single peak which is different from those of (2-MeOPh)$_3$P, (2,6-MeOPh)$_3$P and (2,4,6-MeOPh)$_3$P. These ambiguous data might be explained by taking the existence of the following rapid equilibrium, which is beyond the NMR time scale, into consideration: $[R_3P^+H][GaCl_4^-] \rightleftharpoons [H][GaCl_4(R_3P)]$. In addition, the coupling constants (J_{P^+-H}) observed for the extraction systems with (2,6-MeOPh)$_3$P or (2,4,6-MeOPh)$_3$P are calculated to be *ca* 80 Hz, which are smaller than those observed for the isolated phosphonium salts; 546 Hz for [(2,6-MeOPh)$_3P^+H$][ClO_4^-] and [(2,6-MeOPh)$_3P^+H$][Cl^-]. This may be caused by hydration of the extracted phosphonium salts, because the $CDCl_3$ extracts always include the saturated H_2O.

In the present work, the extraction mechanisms for the methoxy-substituted triarylphosphines–gallium(III) systems are discussed on the basis of ^1H and ^{31}P NMR spectroscopic data in connection with their basicities and extractabilities. It can be concluded that highly basic compounds, (2,6-MeOPh)$_3$P and (2,4,6-MeOPh)$_3$P, act as anion-exchangers by forming their phosphonium salts with hydrogen chloride in the extraction of gallium(III) from hydrochloric acid.

Acknowledgements—The authors wish to thank Professor N. Sonoda and his co-workers, Osaka University, for ^{31}P NMR measurements and their helpful suggestions.

REFERENCES

1. P. Senise and F. Levi, *Anal. Chim. Acta* 1960, **30**, 422.
2. P. Senise and F. Levi, *Anal. Chim. Acta* 1960, **30**, 509.
3. M. Mojski and M. Plesinska, *Microchem. J.* 1979, **24**, 117.
4. M. Mojski, *Talanta* 1980, **27**, 7.
5. K. R. Koch and J. E. Yates, *Anal. Chim. Acta* 1983, **147**, 235.
6. Y. Yamashoji, T. Matsushita, M. Wada and T. Shono, *Chem. Lett.* 1987, 43.
7. M. Wada and S. Higashizaki, *J. Chem. Soc., Chem. Commun.* 1984, 482.
8. M. Wada, S. Higashizaki and A. Tsuboi, *J. Chem. Res. (M)* 1985, 467.
9. C. A. Streuli, *Anal. Chem.* 1960, **32**, 985.
10. J. S. Fritz and S. S. Yamamura, *Anal. Chem.* 1957, **29**, 1079.
11. C. A. Streuli, *Anal. Chem.* 1959, **31**, 1652.
12. W. E. McEwen, Wen-I Shiau, Young-Ing Yeh, D. N. Schutz, R. U. Pagilagan, J. B. Levy, C. Symmes Jr, G. O. Nelson and I. Granoth, *J. Am. Chem. Soc.* 1975, **97**, 1787.

Polyhedron Vol. 8, No. 8, pp. 1061–1067, 1989
Printed in Great Britain

0277–5387/89 $3.00+.00
© 1989 Pergamon Press plc

SYNTHESIS AND THERMAL DECOMPOSITION OF MAGNESIUM HYDROXIDE NITRATES

K. PETROV,* A. LYUBCHOVA and L. MARKOV

Institute of General and Inorganic Chemistry, Bulgarian Academy of Sciences, 1040 Sofia, Bulgaria

(*Received* 1 *August* 1988; *accepted* 10 *November* 1988)

Abstract—A magnesium hydroxide nitrate, $Mg_2(OH)_3NO_3$, with lattice parameters $a_0 = 3.16$ and $c_0 = 6.98$ Å has been prepared by precipitation from $Mg(NO_3)_2$ and NaOH solutions. Its hydrothermal treatment in the mother liquor at 150°C leads to crystallization of a new phase with lattice parameters $a_0 = 5.46$ and $c_0 = 6.96$ Å. Transmission electron microscope and selected area electron diffraction studies have shown that the formation of the MgO phase during the decomposition of $Mg_2(OH)_3NO_3$, is a topotactic process. On the basis of the general formulae, lattice parameters and decomposition mechanisms, it has been assumed that the structures of the magnesium hydroxide nitrates are related to the single-layered brucite-like type.

In previous studies[1] on the formation of mixed crystals of Mg—Co hydroxide nitrates it was established that $Co_2(OH)_3NO_3$ is tolerant with respect to the isomorphous replacement of Co^{II} by Mg^{II} ions. The possibility of obtaining a pure magnesium hydroxide nitrate by precipitation, on which there are no data in the literature, was also considered. It should be noted that there are only a few investigations on the conditions of preparation, composition and structure of magnesium hydroxide nitrates.[2–5]

Recently, the interest in the decomposition mechanism of the hydroxide nitrates of divalent metals has considerably increased. The crystal structures of the largest part of these compounds proved to be of a layered, brucite-like type.[6–9] The strong cation–anion intralayer interaction and the weak interlayer hydrogen bonding in these structures facilitate the diffusionless formation of the final oxide product during thermal treatment.[10,11] In this connection, the preparation of each new hydroxide nitrate phase and the study of its decomposition is of definite interest.

The present paper contains results from studies of the preparation, characterization and thermal decomposition of magnesium hydroxide nitrate synthesized by precipitation.

* Author to whom correspondence should be addressed.

EXPERIMENTAL

Magnesium hydroxide nitrate was prepared by adding a 0.5 M NaOH solution with intense stirring to a boiling 3 M $Mg(NO_3)_2$ solution saturated with respect to $NaNO_3$. The initial volume in the reaction vessel was maintained constant during the precipitation by evaporation and regulation of the rate with which the NaOH solution was added. The suspension obtained was cooled to 0°C, then washed with iced water until the elimination of nitrate ions in the washing water, and subsequently washed with ethanol. The precipitate was first dried at room temperature, then at 60°C for 1 h.

To elucidate the ageing processes of the magnesium hydroxide nitrate in its mother liquor, the following experiments were carried out: on stopping the addition of the precipitant, the suspension was subjected to hydrothermal treatment in an autoclave (described in ref. 12), then at 150°C for 96 h.

The magnesium content of the samples was determined complexometrically, the nitrate ions content, by the method of Dewarda, and the hydroxide, acidimetrically. XRD analyses were carried out with a powder diffractometer using Co-K_α radiation and a scintillation counter. The diffraction patterns were indexed by the method of Lipson.[13] The unit cell parameters were calculated using the least-

squares method. The IR spectra of the samples were obtained on a KBr tablet. DT and TG analyses were carried out in air with a heating rate of 10°C min^{-1}. Transmission electron microscope (TEM) and selected area electron diffraction (SAED) studies were performed on samples deposited on a carbon substrate. The decomposition of the samples under electron irradiation in the microscope chamber was also examined.

RESULTS AND DISCUSSION

During precipitation of Mg^{II} ions from a $Mg(NO_3)_2$ solution with alkaline hydroxide, unstable magnesium hydroxide nitrates were formed which readily hydrolysed to $Mg(OH)_2$ during the precipitation. Complete hydrolysis was hindered by increasing the concentration of nitrate ions in the initial solution of $Mg(NO_3)_2$ with the addition of $NaNO_3$. When the hydroxyl ratio (moles of NaOH added to those of $Mg(NO_3)_2$ in the initial solution) varied in the range $0.3 < OH/NO_3 < 1.5$, an unknown magnesium hydroxide nitrate phase was precipitated. With a hydroxyl ratio above 1.5, the precipitate obtained was two-phase, i.e. a second phase of $Mg(OH)_2$ appeared.

The hydrothermal treatment of precipitated magnesium hydroxide nitrate proved to be accompanied by structural changes leading to the formation of a new crystalline phase.

Figure 1 presents TEM photographs of samples

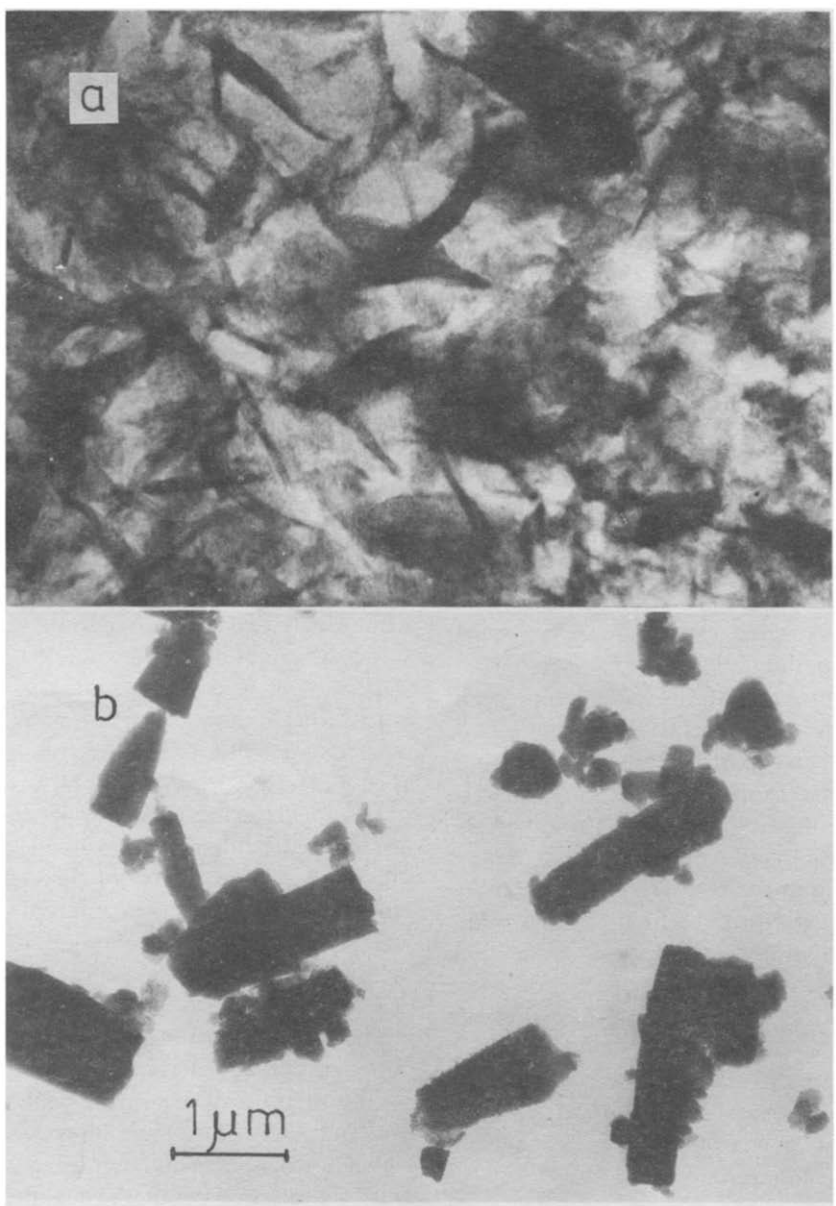

Fig. 1. TEM photographs of the magnesium hydroxide nitrate samples I and II, (a) and (b), respectively.

Table 1.

d_{obs} (Å)	d_{calc} (Å)	$(I/I_1)_{obs}$	*hkl*
6.99	6.98	100	001
3.47	3.49	19	002
2.74	2.74	9	100
2.55	2.55	41	101
2.31	2.33	1	003
2.15	2.15	30	102
1.77	1.77	12	103
1.58	1.58	9	110
1.54	1.54	9	111
1.468	1.472	6	104
1.441	1.441	1	112
1.398	1.396	1	005
1.343	1.343	2	201
1.275	1.275	2	202
1.239	1.244	2	105
1.172	1.172	2	114
1.075	1.071	1	106
1.024	1.024	1	211

of the two phases. The crystals of freshly precipitated hydroxide nitrate are needles and have no well-shaped faces. After the hydrothermal ageing, crystallization processes take place which lead to the growth of ribbon-like crystals.

The chemical analyses of the two phases obtained in a series of experiments, show that magnesium hydroxide nitrates are non-stoichiometric compounds with varying compositions. Further studies were carried out with samples having the following compositions: $Mg_2(OH)_{3.24}(NO_3)_{0.76}(H_2O)_{0.24}$ for the fresh phase, sample I; and $Mg_2(OH)_{3.14}(NO_3)_{0.86}(H_2O)_{0.19}$ for the hydrothermally obtained phase, sample II.

Both kinds of magnesium hydroxide nitrate are indexed on the basis of a hexagonal unit cell, space group $P3m1$ ($a_0 = 3.165 \pm 0.003$ and $c_0 = 6.982 \pm 0.001$ Å for sample I; and $a_0 = 5.460 \pm 0.0017$ and $c_0 = 6.958 \pm 0.005$ Å for sample II).

The interlayer spacings, the relative intensities and the diffraction indices of both kinds of hydroxide nitrates (the freshly precipitated and the hydrothermally treated) are presented in Tables 1 and 2, respectively.

The lattice parameters of magnesium hydroxide nitrates are very close to those of the hydroxide nitrates of cobalt, nickel and copper with the composition $M_2(OH)_3NO_3$,[8,14,15] for which a layered brucite-type structure is found.

On the basis of data from chemical analysis, the similarity of unit cells, and the maximum hydroxyl ratio (1.5) up to which a single phase product is precipitated, the magnesium hydroxide nitrates are to be considered as salts with an idealized composition, $Mg_2(OH)_3NO_3$. They might have structures similar to the brucite. In this case, the interlayer spacings would correspond to the values of the parameter c_0, i.e. 6.982 and 6.958 Å for samples I and II, respectively.

The IR spectra of magnesium hydroxide nitrates are presented in Fig. 2. The bands at 770 (ν_4), 835 (ν_2), 1022 (ν_1), 1333, 1384 and 1488 cm^{-1} (ν_3) correspond to the stretching modes of the NO_3 groups of sample I. The appearance of the band ν_1 and the splitting of ν_3 show that the symmetry of nitrate groups is lower than D_{3h} which is characteristic of a free nitrate ion.[16] Hence, oxygen atoms from the nitrate groups participate in the formation of the oxygen surroundings of magnesium ions which is established for isotypic hydroxide nitrates.[8] The

Table 2.

d_{obs} (Å)	d_{calc} (Å)	$(I/I_1)_{obs}$	*hkl*	d_{obs} (Å)	d_{calc} (Å)	$(I/I_1)_{obs}$	*hkl*
7.00	6.96	100	001	1.468	1.467	7	114
4.73	4.73	14	100	1.436	1.435	1	302
3.92	3.91	20	101	1.340	1.339	4	221
3.48	3.48	19	002	1.271	1.270	4	222
2.80	2.80	5	102	1.240	1.239	2	115
2.73	2.73	3	110	1.227	1.227	1	312
2.54	2.54	76	111	1.177	1.176	3	223
2.15	2.15	50	112	1.074	1.073	2	224
2.08	2.08	1	103	1.045	1.047	1	314
1.77	1.77	16	113	1.020	1.021	3	411
1.74	1.74	1	004	0.989	0.989	3	412
1.73	1.73	1	211	0.974	0.974	1	225
1.58	1.58	18	300	0.944	0.945	3	500
1.54	1.54	16	301				

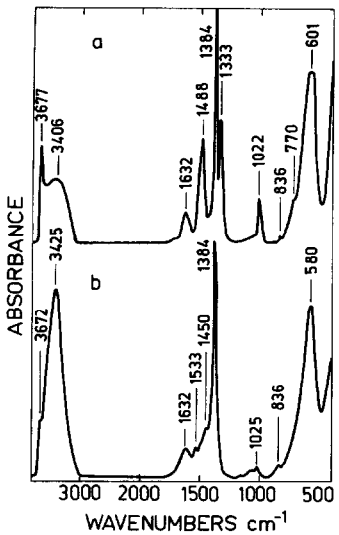

Fig. 2. IR spectra of the magnesium hydroxide nitrate samples I and II, (a) and (b), respectively.

remaining spectral bands are attributed to the following vibrations: 609 (ν_{Mg-O}), 1632 (δ_{H_2O}), 3677 and 3703 cm^{-1} (ν_{OH}). Sample II has an analogous spectrum.

DTA, TG and DTG curves of decomposition of the two samples are shown in Fig. 3. The thermal destruction of the samples was also studied by X-ray phase analysis of intermediate products obtained by isothermal treatment of the initial phases at 150, 300 and 400°C for 1 h.

Both samples decompose endothermally in two steps at 250–450°C. From the studies of the isothermally treated phases, it is established that up to 150°C the intercalated water is eliminated. At this step the OH/NO_3 ratio does not change. No alterations can be observed in the X-ray diffraction patterns either. At 300°C, i.e. in the region of the endoeffects, nitrogen oxides and water evolve. The X-ray diffraction patterns indicate the presence of MgO. The complete decomposition of both samples to MgO ends at 400°C.

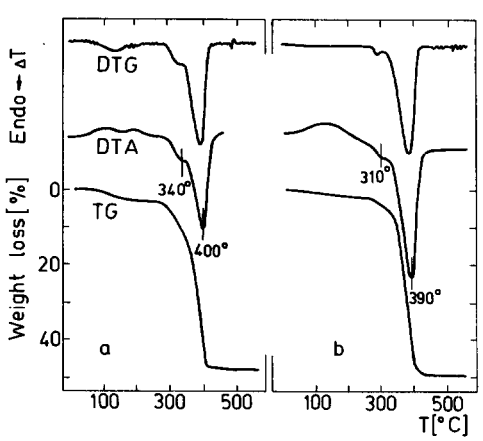

Fig. 3. DTA, TG and DTG curves of the magnesium hydroxide nitrate samples I and II, (a) and (b), respectively.

The assumption about a brucite-like structure of the magnesium hydroxide nitrates and the relatively low decomposition temperatures (below 400°C) presuppose the proceeding of structural transformations of a shear-collapse type with conservation of the two-dimensional metal–oxygen layers. In a number of cases of this kind of structural transformations there is a definite crystallographic relationship between the crystal structures of parent and product phases.[17]

TEM and SAED studies *in situ* were performed with sample II due to the higher morphological perfection of this hydroxide nitrate (see Fig. 1). Figure 4 shows TEM photographs of an initial crystal and another one decomposed under electron beam irradiation, as well as the SAED pattern of the decomposed crystal. The initial crystals of the sample proved to be very unstable towards irradiation, owing to which it was impossible to obtain the SAED pattern of an initial crystal. The diffraction spots on the SAED pattern of the decomposed crystal are smeared probably due to the disorientation of the subcrystallites, which makes exact crystallographic indexing impossible.

The above difficulties imposed the use of an indirect approach to the elucidation of the orientation relationship during the decomposition process. This approach was based on the following facts known from the literature: (1) hydrolysis of the hydroxy salts to the corresponding hydroxides under mild conditions, e.g. in a weakly alkaline medium, is a topotactic process leading to the formation of a pseudomorphous product;[17] (2) the structural transformation of $Mg(OH)_2$ to MgO is also topotactic

$$\langle 111\rangle_{MgO} \| \langle 001\rangle_{Mg(OH)_2},$$

$$\langle 110\rangle_{MgO} \| \langle 001\rangle_{Mg(OH)_2}.$$[10]

Taking into consideration these facts, some additional experiments were carried out on the hydrolysis of magnesium hydroxide nitrate to $Mg(OH)_2$ and the decomposition of the latter in the microscope chamber.

It was established that the hydroxide nitrate was hydrolysed in water medium to a hydroxide. Figure 5 shows TEM photographs and a SAED pattern of the $Mg(OH)_2$ obtained. Obviously, the hydrolysis

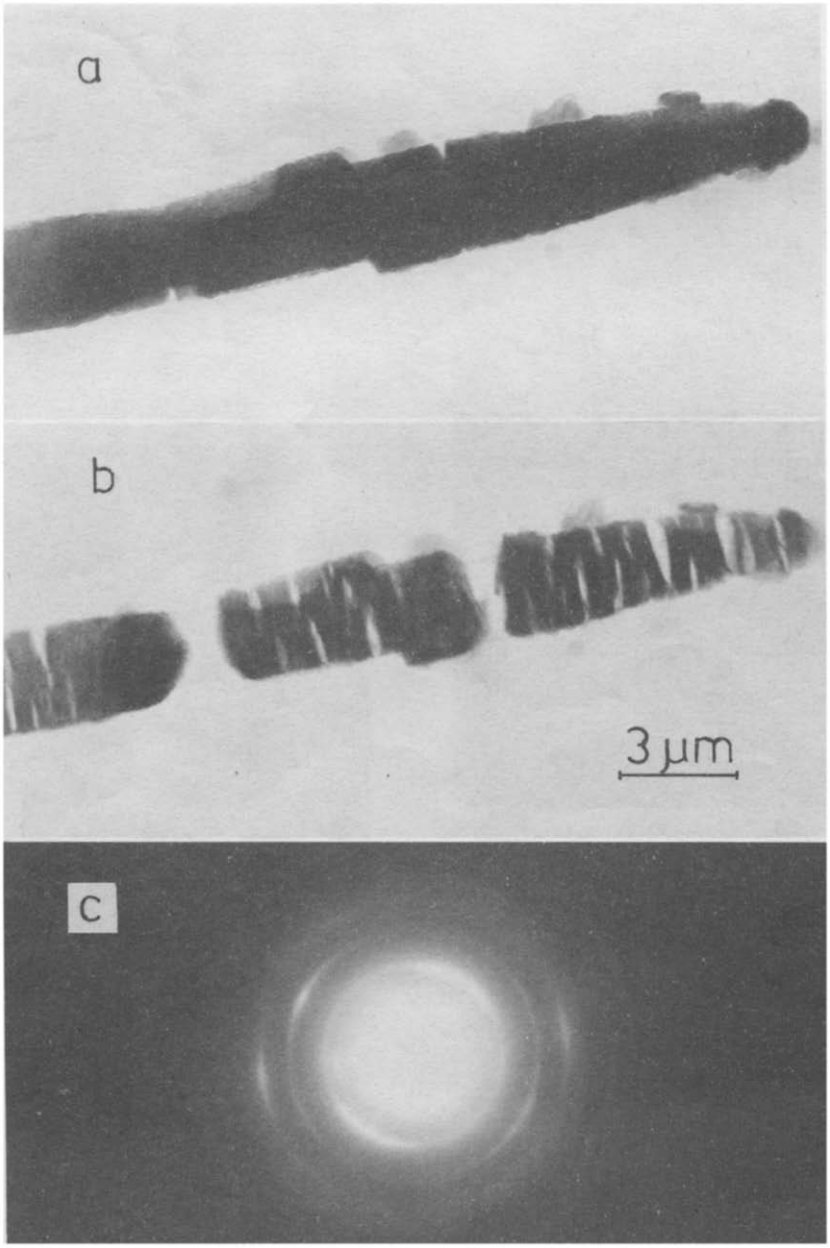

Fig. 4. TEM photographs of sample II: (a) initial, (b) decomposed crystal, (c) SAED pattern of the product.

in this case leads to no change in crystal habit, i.e. the product is pseudomorphous. The SAED pattern contains only (001) reflections of the hexagonal lattice. Therefore, the long axis of the crystals coincides with the crystallographic direction ⟨001⟩. The absence of spots with indices hkl, $0kl$ and $hh0$ indicates a pronounced turbostratic disorder in the structure of magnesium hydroxide.

The decomposition of $Mg(OH)_2$ in the microscope chamber proceeds similarly to that of the hydroxide nitrate (Fig. 6). The SAED pattern of the sample shows spots which can be indexed on the basis of a cubic unit cell with a lattice parameter $a_0 = 4.20$ Å. These data show that $Mg(OH)_2$ is decomposed to MgO. The crystallites of the product were oriented along the direction ⟨110⟩ which is parallel to the electron beam, and again, the dependence

$$\langle 001\rangle_{Mg(OH)_2} \| \langle 111\rangle_{MgO},$$

is established.

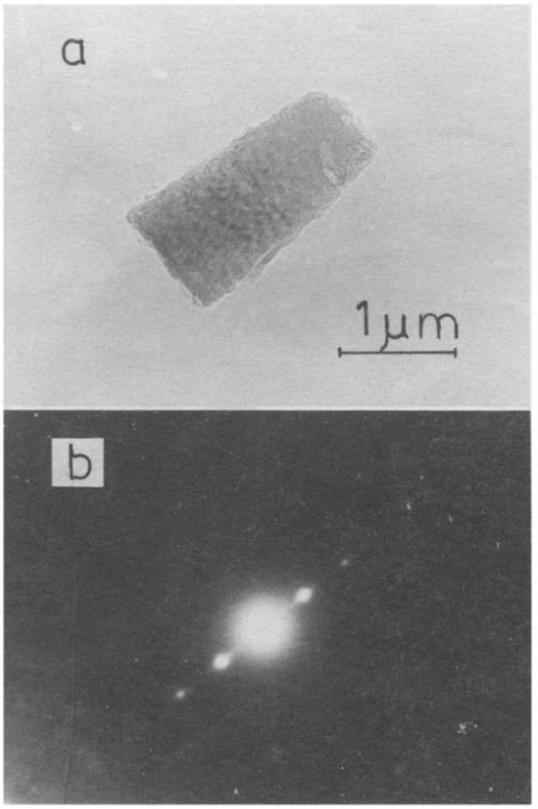

Fig. 5. (a) TEM photograph and (b) SAED pattern of magnesium hydroxide obtained by hydrolysis of sample II.

The SAED pattern of decomposed magnesium hydroxide nitrate is similar to that of the hydroxide obtained. Hence, the above crystallographic correlations can also be valid for magnesium hydroxide nitrate and the oxide obtained from it, i.e.

$$\langle 001\rangle_{Mg_2(OH)_3NO_3} \| \langle 111\rangle_{MgO}.$$

This means that for the hydroxide nitrate phase the direction $\langle 001\rangle$ coincides with the long axis of the crystals. This assumption is confirmed by the TEM photograph of the decomposed initial crystal [Fig. 4(b)]. The evolution of water and nitrogen oxides during the decomposition produces strains in the decomposing crystal, which leads to the appearance of cracks spreading in the (001) plane.

On the basis of the experimental results, the magnesium hydroxide nitrates obtained can be regarded as brucite derivatives. This conclusion is confirmed by comparison of the lattice parameters and the IR spectroscopy data with those concerning the hydroxide nitrates with the formula $M_2(OH)_2NO_3$ and by the decomposition mechanism. Similarly to $Mg(OH)_2$, the magnesium hydroxide nitrates form the lattice of the oxide product by a diffusionless shear-collapse mechanism.

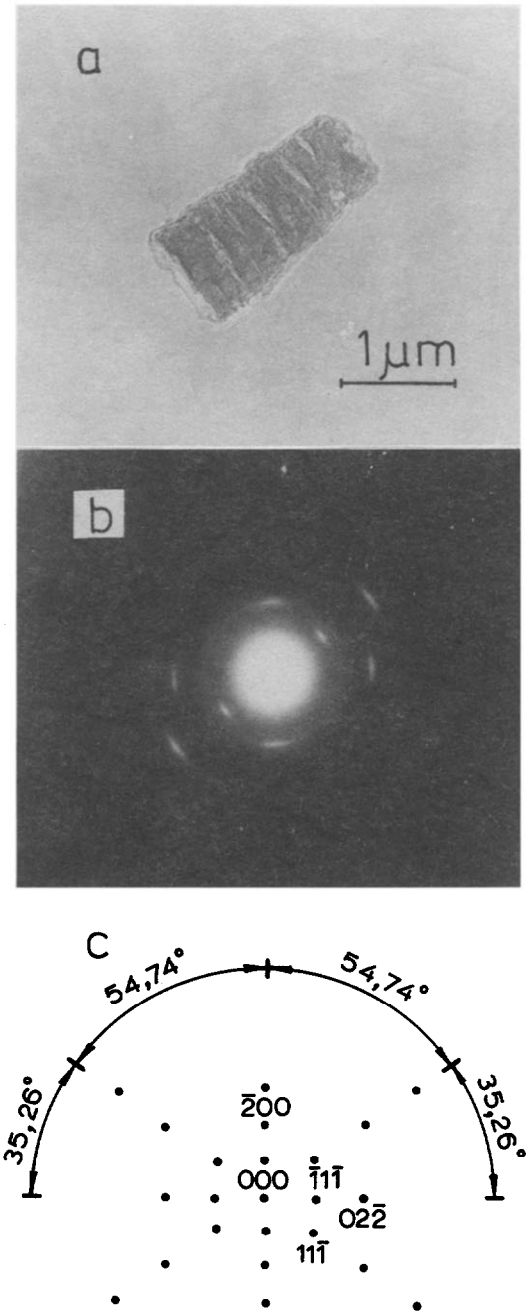

Fig. 6. TEM photograph, SAED pattern and scheme of the SAED pattern of the decomposition product of magnesium hydroxide, (a), (b) and (c), respectively

Acknowledgements—Thanks are due to Professor Dr Dr.h.c. H.-H. Emons and his collaborators from the Bergakademie, Freiberg, G.D.R., for their help with the performance of the hydrothermal experiments.

REFERENCES

1. K. Petrov, L. Markov and R. Rachev, *React. Solids* 1987, **3**, 67.

2. *Gmelin's Handbook*. Syst. No. 27, Section B4 (1953).
3. I. P. Vyrodov, *Zh. Prikl. Khim.* 1961, **34**, 208.
4. I. A. Kudrenko and Yu. G. Dorokhov, *Zh. Neorg. Khim.* 1973, **18**, 35.
5. C. E. Holcombe, *J. Mater. Sci. Lett.* 1978, **13**, 2736.
6. W. Feitknecht, *Fortschr. Chem. Forsch.* 1953, **2**, 670.
7. M. Louer, D. Louer and D. Grandjean, *Acta Cryst.* 1973, **B29**, 1696.
8. H. Effenberger, *Z. Krist.* 1983, **165**, 127.
9. M. Louer, D. Grandjean and D. Weigel, *Acta Cryst.* 1973, **B29**, 1703.
10. J. Green, *J. Mater. Sci.* 1983, **18**, 673.
11. J. P. Auffredic, D. Louer and M. Louer, *J. Therm. Anal.* 1979, **16**, 329.
12. W. Voigt, Th. Fanghanel and H. H. Emons, *Z. Phys. Chem.* 1985, **266**, 523.
13. H. Lipson and H. Steeple, *Interpretation of X-ray Powder Diffraction Patterns*. Macmillan, London (1970).
14. W. Feitknecht and A. Kummer, *Z. Anorg. Allg. Chem.* 1955, **282**, 41.
15. P. Gallezot and M. Prettre, *Bull. Chim. Fr.* 1969, 407.
16. K. Nakamoto, *Spectroscopy of Metal Chelate Compounds*. Wiley, New York (1967).
17. H. R. Oswald and J. R. Gunter, in: 1976 *Crystal Growth and Materials*, p. 415. North Holland, Amsterdam (1977).

Polyhedron Vol. 8, No. 8, pp. 1069–1075, 1989
Printed in Great Britain

0277-5387/89 $3.00+.00
© 1989 Pergamon Press plc

SUBSTITUTION REACTIONS IN CYCLOMETALLATED COMPLEXES. CRYSTAL AND MOLECULAR STRUCTURE OF $[(C_5H_5N)(Me_3P)\overline{Ni(CH_2CMe_2\text{-}o\text{-}C_6H_4)}]$

ERNESTO CARMONA,† MARGARITA PANEQUE and MANUEL L. POVEDA

Departamento de Química Inorgánica, Instituto de Ciencia de Materiales, Universidad de Sevilla-CSIC, 41071 Sevilla, Spain

and

ENRIQUE GUTIERREZ-PUEBLA and ANGELES MONGE

Instituto de Ciencia de Materiales, Sede D, CSIC. Serrano 113, 28006 Madrid, Spain and Facultad de Ciencias Químicas, Universidad Complutense de Madrid, 28040 Madrid, Spain

(*Received* 19 *September* 1988; *accepted* 10 *November* 1988)

Abstract—The interaction of the cyclometallated complex $[(Me_3P)_2\overline{Ni(CH_2CMe_2\text{-}o\text{-}C_6H_4)}]$ with the mono or bidentate N- and P-donor ligands C_5H_5N (py), $Me_2NCH_2CH_2NMe_2$ (tmen), PMe_2Ph and $Me_2PCH_2CH_2PMe_2$ (dmpe), has been studied. Of these, only py and dmpe afford the substitution products, $[(C_5H_5N)(Me_3P)\overline{Ni(CH_2CMe_2\text{-}o\text{-}C_6H_4)}]$ (**2**) and $[(dmpe)\overline{Ni(CH_2CMe_2\text{-}o\text{-}C_6H_4)}]$ (**4**), in clean, high yield reactions. Isolation of the tmen derivative has proved unattainable, while the PMe_2Ph complex $[(PhMe_2P)_2\overline{Ni(CH_2CMe_2\text{-}o\text{-}C_6H_4)}]$ (**3**), is best obtained by alkylation of $[NiCl_2(PMe_2Ph)_2]$ with $Mg(CH_2CMe_2Ph)Cl$, in the presence of I^-. The new compounds **2–4** have been characterized by analytical and spectroscopic studies, and in the case of **2**, an X-ray structural determination has also been undertaken. Compound **2** is monoclinic, space group $P2_1/c$, with unit cell parameters $a = 9.154(2)$, $b = 10.810(2)$, $c = 19.240(10)$ Å, $\beta = 102.3(1)°$ and $D_{calc} = 1.23$ g cm^{-3} for $Z = 4$. The nickel centre is in a slightly distorted square-planar environment, with Ni—C(aryl) and Ni—C(alkyl) distances of 1.917(5) and 1.935(5) Å, respectively.

Transition metal–metallacycles have been subjected to numerous studies in recent years, due mainly to their intermediacy in a number of catalytic reactions,[1] e.g. alkene metathesis,[2] diene oligomerization,[3] telomerization of butadiene and carbon dioxide,[4] etc. In addition, use of cyclometallated compounds allows the study of some transformations of transition metal complexes which undergo facile decomposition reactions. Work by Whitesides and co-workers has demonstrated that for many such systems[5] the β-hydrogen elimination reaction can be suppressed by constraining the M—C_α—C_β—H dihedral angle to values far from the optimal 0°. Other metallacycles undergo decomposition by this well-known pathway, but their thermal stability is generally much higher than that displayed by their acyclic analogues.

We have reported recently[6a] the formation of the nickelacyclopentene complex $[(Me_3P)_2\overline{Ni(CH_2CMe_2\text{-}o\text{-}C_6H_4)}]$ (**1**). Many cyclometallated complexes of nickel are known[7–10] and the simplest of the nickelacyclopentane units, $\overline{Ni(CH_2CH_2CH_2CH_2)}$, is known to undergo[11] three major decomposition pathways: β-hydrogen elimination, carbon–carbon bond cleavage to ethylene, and reductive elimination. Since the latter process is very often favoured in L_nNiRR' compounds (R,R′ = alkyl or aryl groups) by addition of a phosphine or other ligand,[12] we have attempted the elimination of cyclobutene by addition to compound **1** of N- and P-containing ligands. Instead we have found that the nickelacyclopentene complex **1**, $[(Me_3P)_2\overline{Ni(CH_2CMe_2\text{-}o\text{-}C_6H_4)}]$, undergoes sub-

† Author to whom correspondence should be addressed.

stitution of one of the two PMe_3 ligands. This substitution chemistry is the subject of this paper, which describes also the results of a single-crystal X-ray structural determination, carried out with the mixed PMe_3–py derivative, $[(C_5H_5N)(Me_3P)Ni(CH_2CMe_2\text{-}o\text{-}C_6H_4)]$ (**2**).

RESULTS AND DISCUSSION

We have recently shown that the cyclometallated complex **1** can be readily prepared by reacting $[NiCl_2(PMe_3)_2]$ with 2 equiv of $Mg(CH_2CMe_2Ph)Cl$, in the presence of I^- as a catalyst. Since this metallacyclic compound exhibits a very rich insertion chemistry, the synthesis of similar cyclic units, containing different co-ligands, has been undertaken.

An X-ray structural determination carried out on compound **1** has shown[6b] that, in spite of the different *trans*-influence of the alkyl and aryl groups, the two Ni—P bonds have nearly equal lengths. Both groups have good *trans*-directing properties and indeed the fluxional behaviour observed for **1** can be explained in terms of a fast intermolecular exchange between coordinated and traces of free PMe_3. NMR data suggest the interchange process to be faster for the PMe_3 ligand *trans* to the Ni—C(alkyl) bond. On this basis, it is reasonable to expect facile substitution of one of the two PMe_3 ligands, with formation of new metallacycles. Since, on the other hand, cyclometallated **1** is stable towards reductive elimination of the organic fragment, even in the presence of added phosphine ligands, simple substitution reactions should provide access to the desired compounds. We have studied the interaction of **1** with two N-containing ligands, pyridine (py) and tmen ($Me_2NCH_2CH_2NMe_2$) and with two P-donors, PMe_2Ph and dmpe ($Me_2PCH_2CH_2PMe_2$). Clean reactions are only observed for py and dmpe, while tmen fails to give the corresponding substitution product and the PMe_2Ph derivative is best prepared by direct alkylation of $[NiCl_2(PMe_2Ph)_2]$, as discussed below.

Reaction of **1** *with pyridine. Formation of* **2** *and its molecular structure*

Treatment of **1** with an excess of py at room temperature, affords, after work-up, a yellow crystalline material of composition $[(C_5H_5N)(Me_3P)Ni(CH_2CMe_2\text{-}o\text{-}C_6H_4)]$ (**2**). The new complex has solubility and reactivity towards oxygen and moisture very similar to those of **1**, but at variance with the behaviour found for the latter complex, it has rigid structure in solution. NMR data strongly suggest that the py ligand is occupying the position *trans* with respect to the Ni—CH_2 bond. In accord with this, the methylene carbon nucleus, Ni—CH_2, gives rise to a doublet in the $^{13}C\{^1H\}$ NMR spectrum, with a coupling constant, $^2J_{CP}$, of 13.7 Hz. In the related metallacyclobutene $[(R_3P)_2Ni(CH_2\text{-}o\text{-}C_6H_4)]$,[13] values of *ca* 23 and 55 Hz are found for *cis*- and *trans*-$^{13}CH_2$—Ni—^{31}P couplings, respectively. Formation of **2** can therefore be represented as indicated in eq. (1). The reaction can be readily reversed by addition of PMe_3 to solutions of **2**. As already mentioned, the facile substitution of the ligand which is *trans* with respect to the Ni—alkyl bond is not unexpected and follows from the higher *trans* effect of this group, as compared with the aryl ligand. Note however, that this kinetic effect does not seem to be related to any appreciable weakening of the corresponding bond in the ground state of the molecule, since the Ni—P bonds in **1** have nearly equal lengths.[6b]

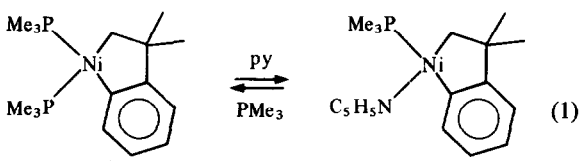

(1)

1 **2**

The geometry proposed for **2** on the basis of spectroscopic data has been confirmed by a single-crystal X-ray study. Figure 1 shows an ORTEP view of the molecule of **2** and Tables 1 and 2 include relevant structural data. The coordination around nickel is slightly distorted square-planar, with some distortion being imposed by the relatively small bite angle of the chelating organic ligand which constrains the C(1)—Ni—C(6) angle to 82.4(2)°. The remaining angles between pairs of *cis*-ligands are close to the ideal 90° value (Table 2). The square-planar arrangement is further emphasized by angles between *trans*-ligands, C(6)—Ni—P and C(1)—Ni—N of 172.4(2) and 175.2(2)°, respectively. The Ni—P distance is somewhat longer than the corresponding distance in **1** (2.197(1) vs 2.192(4) Å), but the Ni—C(alkyl) bond length of 1.935(5) Å and the Ni—C(aryl) separation of 1.917(5) Å, are slightly shorter than the corresponding values of 1.96(1) and 1.93(1) Å, found respectively in the parent complex **1**. These bond lengths are not exceptional and fall in the range observed for other alkyl and aryl complexes of nickel(II).[14] The Ni—N separation, 1.963(4) Å, is close to the 1.957(8) Å value reported for $[Ni(CH_2SiMe_3)_2(py)_2]$,[15] and appreciably smaller than the distance of *ca* 2.08 Å observed in bis(pyridine) octahedral complexes of nickel(II).[16–18]

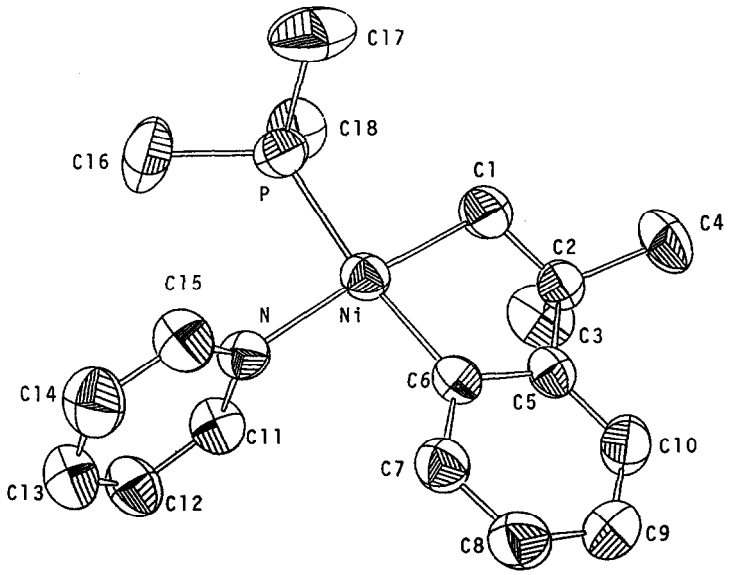

Fig. 1. ORTEP view of the molecule of **2**.

Table 1. Crystal and refinement data for **2**

Empirical formula	$C_{18}H_{26}PNNi$
Crystal system	Monoclinic
Space group	$P2_1/c$
Cell dimensions	
a (Å)	9.154(2)
b (Å)	10.810(2)
c (Å)	19.24(1)
β (°)	102.30(2)
Z	4
V (Å^3)	1860(1)
D_{calc} (g cm^{-3})	1.24
Temperature (°C)	22
Mol wt	346.094
Linear absorption coefficient (cm^{-1})	11.25
$F(000)$	736
Crystal dimensions (mm)	0.3 × 0.4 × 0.6
Diffractometer	Enraf–Nonius CAD4-F
Radiation	Graphite monochromated Mo-K_α (λ = 0.7107 Å)
Scan technique	ω–2θ
2θ range (°)	1–50
Data collected	(−10,0,0) to (10,12,22)
Reflections collected	3478
Unique data	3367
Data with [$I \geqslant 3\sigma(I)$]	2221
R int (%)	8.5
Standard reflections	3 standards/111 reflections
Decay	⩽ 42% variation
R(F) (%)	4.5
R_w(F) (%)	5.0
Average shift/error	0.0035
Data/parameter	11

Reaction of **1** *with the phosphine ligands*, PMe_2Ph *and* dmpe

Two synthetic routes can in principle be used for the preparation of the metallacyclic derivatives containing PMe_2Ph and dmpe ligands: reaction of the chlorides, $[NiCl_2P_2]$ (P = PMe_2Ph; P_2 = dmpe), with an excess of the Grignard reagent, $Mg(CH_2CMe_2Ph)Cl$, in the presence of I^-, and substitution of the PMe_3 ligands in **1** by the corresponding phosphine. Rather interestingly, the PMe_2Ph complex, $[(PhMe_2P)_2Ni(CH_2CMe_2\text{-}o\text{-}C_6H_4)]$ (**3**), can only be obtained in good yields by the first procedure, while formation of $[(dmpe)Ni(CH_2CMe_2\text{-}o\text{-}C_6H_4)]$ (**4**), is only accomplished by dmpe substitution of the PMe_3 groups in **1**, eqs (2) and (3).

$$NiCl_2(PMe_2Ph)_2 + 2Mg(CH_2CMe_2Ph)Cl \xrightarrow{[I^-]} (PhMe_2P)_2Ni(CH_2CMe_2\text{-}o\text{-}C_6H_4) + C_6H_5CMe_3 + MgCl_2 \quad (2)$$

$$(Me_3P)_2Ni(CH_2CMe_2\text{-}o\text{-}C_6H_4) + dmpe \longrightarrow (dmpe)Ni(CH_2CMe_2\text{-}o\text{-}C_6H_4) + 2PMe_3. \quad (3)$$

Reaction (2) affords high yields of cyclometallated **3**, which can be isolated as a yellow, moderately air-stable, crystalline solid. Its characterization as a metallacycle analogous to **1** follows from microanalysis, and IR and NMR spectroscopy. As for the PMe_3 analogue, it is reasonable to assume[6]

Table 2. Selected bond distances (Å) and angles (°) for **2**

Ni—C(1)	1.9353(59)	C(8)—C(9)	1.3707(93)
Ni—C(6)	1.9167(54)	C(9)—C(10)	1.3808(87)
Ni—N	1.9632(43)	N—C(11)	1.3254(71)
Ni—P	2.1974(19)	N—C(15)	1.3409(67)
C(1)—C(2)	1.5238(85)	C(11)—C(12)	1.3783(88)
C(2)—C(3)	1.5145(79)	C(12)—C(13)	1.3704(90)
C(2)—C(4)	1.5441(86)	C(13)—C(14)	1.3715(107)
C(2)—C(5)	1.4994(74)	C(14)—C(15)	1.3690(93)
C(5)—C(6)	1.4166(72)	P—C(16)	1.8106(68)
C(5)—C(10)	1.3921(82)	P—C(17)	1.7971(59)
C(6)—C(7)	1.4024(73)	P—C(18)	1.8073(87)
C(7)—C(8)	1.3814(87)		
N—Ni—P	94.30(14)	C(6)—C(7)—C(8)	122.14(54)
C(6)—Ni—P	172.39(17)	C(7)—C(8)—C(9)	120.59(57)
C(6)—Ni—N	93.16(20)	C(8)—C(9)—C(10)	119.46(60)
C(1)—Ni—P	90.22(18)	C(5)—C(10)—C(9)	120.56(55)
C(1)—Ni—N	175.19(22)	Ni—N—C(15)	123.30(36)
C(1)—Ni—C(6)	82.36(24)	Ni—N—C(11)	118.25(35)
Ni—C(1)—C(2)	111.60(39)	C(11)—N—C(15)	118.43(48)
C(1)—C(2)—C(5)	105.59(44)	N—C(11)—C(12)	122.90(49)
C(1)—C(2)—C(4)	111.79(49)	C(11)—C(12)—C(13)	118.18(59)
C(1)—C(2)—C(3)	110.86(48)	C(12)—C(13)—C(14)	119.38(62)
C(4)—C(2)—C(5)	111.45(47)	C(13)—C(14)—C(15)	119.25(61)
C(3)—C(2)—C(5)	109.05(48)	N—C(15)—C(14)	121.84(53)
C(3)—C(2)—C(4)	108.09(51)	Ni—P—C(18)	113.28(28)
C(2)—C(5)—C(10)	125.08(49)	Ni—P—C(17)	117.20(23)
C(2)—C(5)—C(6)	113.86(46)	Ni—P—C(16)	118.88(26)
C(6)—C(5)—C(10)	121.06(50)	C(17)—P—C(18)	102.53(36)
Ni—C(6)—C(5)	115.46(38)	C(16)—P—C(18)	102.01(37)
C(5)—C(6)—C(7)	116.11(48)	C(16)—P—C(17)	100.50(34)
Ni—C(6)—C(7)	128.43(41)		

that the cyclometallation proceeds through an unstable dialkyl intermediate, $[Ni(CH_2CMe_2Ph)_2(PMe_2Ph)_2]$, which undergoes a rapid δ-hydrogen abstraction reaction.

Complex **3** is fluxional; the room temperature $^{31}P\{^1H\}$ NMR spectrum consists of two broad singlets centred at 4.3 and 0.2 ppm. Upon cooling, the spectrum somewhat narrows, but no coupling between the two anisochronous ^{31}P nuclei can be observed, even at -80°C. These and other observations suggest the existence of a phosphine-exchange process and, as for **1**, the NMR spectra can be explained in terms of an exchange between coordinated and traces of free phosphine, by means of a five-coordinate intermediate species, as shown in Scheme 1. In the $^{13}C\{^1H\}$ NMR spectrum, recorded at 20°C, the two phosphine ligands give well-resolved doublets, and the Ni—CH_2 resonance also appears as a doublet ($^2J_{CP}$ = 16 Hz), as a result of the coupling with only one of the ^{31}P nuclei. These results contrast with those found for **1**, whose room temperature ^{13}C NMR spectrum exhibits a broad

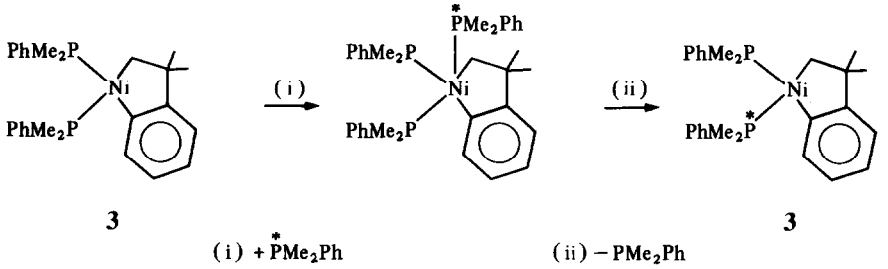

3 **3**

(i) + $\overset{*}{P}Me_2Ph$ (ii) − PMe_2Ph

Scheme 1.

signal for the two PMe_3 ligands and a singlet for the Ni—CH_2 nucleus. It can therefore be concluded that the phosphine exchange process is faster for the PMe_3 derivative **1**. The low value of 16 Hz found for $^2J_{CP}$ is typical of a *cis*-coupling (*trans*-^{13}C–^{13}P coupling constants in complexes of this type have much higher values (*ca* 40–70 Hz), see refs 6 and 13 and the discussion of the NMR spectra of **4**). This suggests that at this temperature the PMe_2Ph ligand *trans* to the Ni—C(alkyl) bond is undergoing fast exchange with traces of free PMe_2Ph via a phosphine association–dissociation process, while for the other coordinated phosphine ligand the rate of exchange is slow on the NMR time scale. These observations are in agreement with the already mentioned higher *trans*-effect of the alkyl group, as compared with the aryl ligand, and are also in accord with the behaviour reported for **1**.[6b] Cooling to −50°C and below causes broadening of the Ni—CH_2 resonance, but the expected doublet of doublets is not observed even at −80°C.

As already indicated, complex **1** undergoes a smooth reaction with dmpe, with complete replacement of the PMe_3 ligands [eq. (3)]. The resulting compound **4** is a highly crystalline material, sparingly soluble in petroleum and diethyl ether, but readily soluble in other common organic solvents. As with the related metallacycles, **1–3**, complex **4** displays high thermal stability, which contrasts with the propensity of complexes of the type [(dmpe)Ni(alkyl)(aryl)] to undergo reductive elimination reactions.[19] The metallacyclic nature of **1–4** is doubtless responsible for this enhanced stability.

In contrast with **1** and **3**, and clearly due to the chelating nature of the dmpe ligand, **4** is a rigid molecule whose structure can be readily deduced from NMR studies. Thus, the $^{31}P\{^1H\}$ NMR consists of an AX pattern (δ_A 26.9, δ_X 34.8, $^2J_{AX}$ 9 Hz), in accord with the existence of two different moieties in the metallacyclic unit. In the ^{13}C NMR spectrum, the methylene group gives rise to the expected doublet of doublets, with *trans* and *cis*, $^2J_{CP}$, coupling constants of 65.8 and 18 Hz, respectively. Similar features are observed for the aromatic quaternary carbon bound to nickel, which also appears as a doublet of doublets.

As discussed above, complex **4** cannot be prepared by direct cyclometallation, but occurs by dmpe replacement of the PMe_3 ligands in **1**. This is not surprising since the putative dialkyl intermediate, [(dmpe)$Ni(CH_2CMe_2Ph)_2$], which can be obtained[20] by addition of dmpe to the unstable tmen derivative [$Ni(CH_2CMe_2Ph)_2$(tmen)],[15] does not metallate by moderate heating (60°C, 4 days, toluene solution). These results are in accord with those found previously by other workers[21] in related platinum systems and may be accounted for by reference to the chelating nature of the dmpe ligand.

EXPERIMENTAL

Microanalyses were carried out by the Pascher Microanalytical Laboratory, Bonn, and the Microanalytical Service of the University of Sevilla. The spectroscopic instruments used were Perkin–Elmer models 557 and 684 for IR spectra and Varian XL-200 for ^1H, ^{13}C and ^{31}P NMR spectra. All preparations and other operations were carried out under oxygen-free nitrogen, following conventional Schlenk techniques. Solvents were dried and degassed before use. The light petroleum used had b.p. 40–60°C. Complex **1** was prepared according to ref. 6.

Synthesis of [$(C_5H_5N)(Me_3P)\overline{Ni(CH_2CMe_2\text{-}o\text{-}C_6H_4)}$] (**2**)

0.34 g of complex **1** (1 mmol) were dissolved in 10 cm^3 of Et_2O and to the resulting solution pyridine (2 cm^3, excess) was added. The mixture was stirred for 2 h at room temperature, during which time it was occasionally exposed to vacuum to remove the replaced PMe_3 from the solution. The solvent was then pumped-off and the residue extracted with Et_2O (25 cm^3). Cooling at −20°C furnished yellow–orange crystals of the desired compound (0.24 g, 70% yield). Found: C, 61.4; H, 7.6; N, 3.8. Calc. for $C_{18}H_{26}NPNi$: C, 62.5; H, 7.5; N, 4.0%. ^1H NMR (C_6D_6, 200 MHz): δ 0.63 (d, J_{HP} = 6 Hz, PMe_3), 1.48 (d, J_{HP} = 11 Hz, Ni—CH_2), 1.82 (s, CMe_2), 6.31–7.29 (m, aromatics). $^{13}C\{^1H\}$ NMR (C_6D_6): δ 13.1 (d, J_{CP} = 19 Hz, PMe_3), 38.9 (d, J_{CP} = 14 Hz, Ni—CH_2), 35.0 (s, CMe_2), 121.4, 123.4, 123.5, 134.3, 134.7, 150.7, 168.1 (aromatics). $^{31}P\{^1H\}$ NMR (C_6D_6): δ −15.0 s.

Reaction of [$(C_5H_5N)(Me_3P)\overline{Ni(CH_2CMe\text{-}o\text{-}C_6H_4)}$] (**2**) *with* PMe_3

To a suspension of [$(C_5H_5N)(Me_3P)\overline{Ni(CH_2CMe_2\text{-}o\text{-}C_6H_4)}$] (**2**) (0.34 g, 1 mmol) in Et_2O (10 cm^3), PMe_3 (0.5 cm^3, 5 mmol, excess) was added and the mixture stirred at room temperature for 2 h. Evaporation of the solvent until a final volume of 2 cm^3 and cooling at −20°C provided 0.28 g of [$(Me_3P)_2\overline{Ni(CH_2CMe_2\text{-}o\text{-}C_6H_4)}$].[6] This crystalline material may sometimes contain small amounts of the unreacted pyridine derivative, that can be separated by fractional crystallization or additionally reacted with more PMe_3.

Synthesis of [$(PhMe_2P)_2\overline{Ni(CH_2CMe_2\text{-}o\text{-}C_6H_4)}$] (**3**)

To a stirred suspension of [$NiCl_2(PMe_2Ph)_2$] (1.84 g, 4.5 mmol) in 60 cm^3 of Et_2O, cooled to −30°C, $Mg(CH_2CMe_2Ph)Cl$ was added (7.2 cm^3 of a 1.25 N solution in Et_2O, 9 mmol). The mixture was stirred at low temperature for 15 min and then warmed and stirred at 30°C for an additional 3 h. The solvent was removed *in vacuo* and the residue extracted with a petroleum ether–diethyl ether mixture (20:70 cm^3). After centrifugation, concentration to 30 cm^3 and cooling at −20°C for 10 h, 1 g of the crude product was obtained. This material was purified by extraction with Et_2O and filtration. Partial evaporation of the solvent and cooling at −30°C provided pure samples of the title compound as yellow needles (Yield 40%). Found: C, 67.01; H, 7.32. Calc. for $C_{26}H_{34}P_2Ni$: C, 66.85; H, 7.28%. ^1H NMR (C_6D_6, 200 MHz): δ 0.99 (d, J_{HP} = 15.8 Hz, P—Me), 1.84 (s, CMe_2), 1.95 (d, J_{HP} = 9.3 Hz, Ni—CH_2), 6.9–7.5 (m, aromatics). $^{13}C\{^1H\}$ NMR (THF–CD_3COCD_3): δ 13.8 (d, J_{CP} = 22 Hz, P_A—Me), 16.4 (d, J_{CP} = 21 Hz, P_B—Me), 34.4 (s, CMe_2), 50.8 (d, J_{CP} = 11 Hz, CMe_2), 53.0 (d, J_{CP} = 16 Hz, Ni—CH_2), 119.9, 121.9, 122.2 and 138.4 (s, s, d, J_{CP} = 6 Hz, and s, nickelacycle CH aromatics), 167.0 (s, C_{Ar}—CMe_2), 169.6 (d, J_{CP} = 79 Hz, Ni—$C_{aromatic}$). $^{31}P\{^1H\}$ NMR (THF–CD_3COCD_3): δ 4.3 (s, P_A), 0.2 (s, P_B).

Preparation of [(dmpe)$\overline{Ni(CH_2CMe_2\text{-}o\text{-}C_6H_4)}$] (**4**)

Complex **1** (0.64 g, 1.87 mmol) was dissolved in Et_2O (15 cm^3) and the solution cooled at −20°C. Dmpe (0.37 cm^3, 1.87 mmol) was then added. After stirring at this temperature for a few minutes, a yellow crystalline product precipitated. The mixture was warmed and stirred at room temperature for 30 min, the solvent partially evaporated to half of the initial volume and the resulting suspension cooled to −30°C and filtered. The title compound was obtained in almost quantitative yield. Recrystallization from Et_2O provided yellow crystals of analytical purity. Found: C, 55.8; H, 8.2. Calc. for $C_{16}H_{28}P_2Ni$: C, 56.3; H, 8.2%. ^1H NMR (C_6D_6, 200 MHz): δ 0.91 (d, J_{HP} = 8 Hz, P_A—Me), 1.01 (d, J_{HP} = 7 Hz, P_B—Me), 0.80–1.00 (m, P—CH_2), 1.69 (s, CMe_2), 1.88 (dd, J_{HP_A} = 11 Hz, J_{HP_B} = 3 Hz, Ni—CH_2), 7.2–7.3 (m, aromatics). $^{13}C\{^1H\}$ NMR (C_6D_6): δ 11.9 (d, J_{CP} = 22 Hz, P_A—Me), 13.2 (d, J_{CP} = 15 Hz, P_B—Me), 27.1 (dd, J_{CP_A} = 25 Hz, J_{CP_B} = 20 Hz, P_A—CH_2), 28.6 (dd, J_{CP_B} = 27 Hz, J_{CP_A} = 21 Hz, P_B—CH_2), 35.8 (d, J_{CP} = 5 Hz, CMe_2), 48.3 (dd, J_{CP_A} = 66 Hz, J_{CP_B} = 18 Hz, Ni—CH_2), 51.0 (dd, J_{CP_A} = 9 Hz, J_{CP_B} = 3 Hz, CMe_2), 122.1, 122.2, 123.5 and 140.0 (s, s, s and dd, J_{CP_A} = 14 Hz, J_{CP_B} = 4 Hz, CH aromatics), 167.3 (dd, J_{CP_B} = 85 Hz, J_{CP_A} = 14 Hz, Ni—$C_{aromatic}$), 169.4 (d, J_{CP} = 5 Hz, C_{Ar}—CMe_2). $^{31}P\{^1H\}$ NMR (C_6D_6): δ 26.9 (d, P_A), 34.8 (d, P_B, J_{PP} = 9 Hz).

Structure solution and refinement

The crystal data and the parameters used during the collection and refinement of the diffraction data are summarized in Table 1. A yellow crystal was coated with an epoxy resin and mounted on the diffractometer. The cell dimensions were refined by a least-squares fit of the θ values of 25 reflections. There was appreciable change in the periodically monitored standard reflections because the crystal became damaged by radiation. The intensities were corrected for decay and for Lorentz and polarization effects.

Scattering factors for neutral atoms and anomalous dispersion corrections for nickel and phosphorus were taken from the *International Tables for X-ray Crystallography*.[22]

The structure was solved by Patterson and Fourier methods, and an empirical absorption correction[23] was applied at the end of the isotropic refinement.

The final refinement was made with anisotropic thermal motion for the non-hydrogen atoms and fixed isotropic temperature factors and calculated coordinates for hydrogen atoms.†

Most of the calculations were carried out with *XRAY80* system.[24]

Acknowledgements—Generous support of this work by the Agencia Nacional de Evaluación y Prospectiva is very gratefully acknowledged. M.P. thanks the Ministerio de Educación y Ciencia for support by a research grant.

REFERENCES

1. E. Lindner, *Adv. Heterocycl. Chem.* 1986, **39**, 237; S. D. Chappel and D. J. Cole-Hamilton, *Polyhedron* 1982, **1**, 739.
2. J. Kress, J. A. Osborn, R. M. E. Greene, K. J. Ivin and J. J. Rooney, *J. Am. Chem. Soc.* 1987, **109**, 899.
3. H. M. Colquhoun, J. Holton, D. J. Thompson and M. V. Twigg, *New Pathways for Organic Synthesis.* Plenum Press, New York (1984).
4. P. Braunstein, D. Matt and D. Nobel, *J. Am. Chem. Soc.* 1988, **110**, 3207.
5. J. X. McDermott, J. F. White and G. M. Whitesides,

† Supplementary material available. Tables of fractional coordinates, thermal parameters, bond distances and angles, and observed and calculated structure factors for **2** (26 pp.).

J. Am. Chem. Soc. 1976, **98**, 6521; J. X. McDermott, M. E. Wilson and G. M. Whitesides, *J. Am. Chem. Soc.* 1976, **98**, 6529.

6. (a) E. Carmona, P. Palma, M. Paneque, M. L. Poveda, E. Gutiérrez-Puebla and A. Monge, *J. Am. Chem. Soc.* 1986, **108**, 6424; (b) E. Carmona, E. Gutiérrez-Puebla, J. M. Marín, A. Monge, M. Paneque, M. L. Poveda and C. Ruiz, *J. Am. Chem. Soc.*, in press.
7. M. A. Bennett, T. W. Hambley, N. K. Roberts and G. B. Robertson, *Organometallics* 1985, **4**, 1992.
8. H. Hoberg, Y. Peres, C. Krüger and Y-H. Tsay, *Angew. Chem. Int. Ed. Engl.* 1987, **26**, 771.
9. G. Wilke, *Angew. Chem. Int. Ed. Engl.* 1988, **27**, 185.
10. R. H. Grubbs and A. Miyashita, *J. Organomet. Chem.* 1978, **161**, 371.
11. R. H. Grubbs, A. Miyashita, M. Liu and P. Burk, *J. Am. Chem. Soc.* 1978, **100**, 2418.
12. K. Tatsumi, A. Nakamura, S. Komiya, A. Yamamoto and T. Yamamoto, *J. Am. Chem. Soc.* 1984, **106**, 8181; A. Yamamoto, *Organotransition Metal Chemistry*, p. 243. Wiley Interscience, New York (1986).
13. R. Neidlein, A. Rufińska, H. Schwager and G. Wilke, *Angew. Chem. Int. Ed. Engl.* 1986, **25**, 640.
14. P. W. Jolly, *Comprehensive Organometallic Chemistry* (Edited by G. Wilkinson, F. G. A. Stone and E. W. Abel), Vol. 6. Pergamon Press, Oxford (1982).
15. E. Carmona, F. González, M. L. Poveda, J. L. Atwood and R. D. Rogers, *J. Chem. Soc., Dalton Trans.* 1981, 777.
16. M. Bonamico, G. Dessy, V. Fares, A. Flamini and L. Scaramuzza, *J. Chem. Soc., Dalton Trans.* 1976, 1743.
17. J. I. Bullock, M. F. C. Ladd and D. C. Povey, *J. Chem. Soc., Dalton Trans.* 1977, 2242.
18. M. M. Borel, A. Geffronais and M. Ledésert, *Acta Cryst.* 1976, **32B**, 2385.
19. S. Komiya, Y. Abe, A. Yamamoto and T. Yamamoto, *Organometallics* 1983, **2**, 1466.
20. E. Carmona, M. Paneque, M. L. Poveda, R. D. Rogers and J. L. Atwood, *Polyhedron* 1984, **3**, 317.
21. D. C. Griffiths and G. B. Young, *Polyhedron* 1983, **2**, 1095.
22. *International Tables for X-ray Crystallography*, Vol. IV. Kynoch Press, Birmingham, U.K. (1974).
23. N. Walker and D. Stuart, *Acta Cryst.* 1983, **A39**, 158.
24. J. M. Stewart, *The X-ray System.* Computer Science Center, University of Maryland, College Park (1985).

Polyhedron Vol. 8, No. 8, pp. 1077–1083, 1989
Printed in Great Britain

0277–5387/89 $3.00+.00
© 1989 Pergamon Press plc

CRYSTAL STRUCTURE AND SPECTROSCOPIC STUDY OF $[Cu(BPCA)(OH_2)(O_2CCH_3)]\cdot H_2O$ COMPLEX; BPCA = *N*-2-PYRIDINYLCARBONYL-2-PYRIDINECARBOXIMIDATE ANION

JOSÉ V. FOLGADO, EDUARDO MARTÍNEZ-TAMAYO, AURELIO BELTRÁN-PORTER and DANIEL BELTRÁN-PORTER*

UIBCM, Departament de Química Inorgánica, Universitat de Valencia, Dr. Moliner 50, 46100 Burjassot, Valencia, Spain

and

AMPARO FUERTES and CARLES MIRAVITLLES

Institut de Ciencia de Materials de Barcelona, Martí i Franqués s/n, 08028 Barcelona, Spain

(*Received* 19 *September* 1988; *accepted* 10 *November* 1988)

Abstract—The crystal and molecular structure of the $[Cu(BPCA)(OH_2)(O_2CCH_3)]\cdot H_2O$ complex (BPCA = *N*-2-pyridinylcarbonyl-2-pyridinecarboximidate anion) has been determined by X-ray diffraction methods. It crystallizes in the triclinic space group $P\bar{1}$ with two formula units in a cell of dimensions: $a = 7.416(2)$, $b = 8.632(4)$, $c = 13.034(3)$ Å, $\alpha = 74.55(3)$, $\beta = 84.84(3)$, $\gamma = 81.04(5)°$. Least-squares refinement of 2534 reflections with $I > 2.5\sigma(I)$ and 218 parameters gave a final $R = 0.047$ and $R_w = 0.049$. The structure consists of discrete $[Cu(BPCA)(OH_2)(O_2CCH_3)]$ neutral units linked through hydrogen bonding. The coordination geometry around copper ions can be described as tetragonal square pyramidal, the oxygen atom from the coordinated water molecule occupying the axial position. The compound loses both coordinated and lattice water upon heating, and quickly rehydrates to the initial form when it cools down to room temperature. The powder X-band ESR spectra of both the hydrated and the anhydrous forms exhibit the $\Delta M_s = 2$ absorption, indicating magnetic exchange between two copper(II) ions. The nature of this coupling is discussed on the basis of the structural features.

In the course of our study of the interactions between copper(II) and easily stackable ligands,[1] we have recently reported the synthesis and characterization of a set of copper(II)–BPCA (BPCA = *N*-2-pyridinylcarbonyl-2-pyridinecarboximidate anion) complexes which include di- and polynuclear species.[2,3] BPCA is a tridentate rigid quasi-planar N-donor ligand whose monoanionic character makes it different from other related ligands like terpy (2,2′:6′,2″-terpyridine), paphy (pyridine-2-aldehyde-2′-pyridyl hydrazone), or TPT [2,4,6-tris(2-pyridyl)-1,3,5-triazine].[1–5] This renders possible the isolation of neutral Cu(BPCA)X entities (X = monoanion). When X is a potentially bridging ligand, condensed systems may result.[2,3] Such an ability is well established for simple carboxylates,[6] and we have analysed it in the copper(II)–terpy system.[7] To progress on this subject, we are now approaching the study of the interactions between carboxylate monoanions and the $[Cu(BPCA)]^+$ entities. In this work we present the results concerning the Cu(BPCA)–acetate system.

EXPERIMENTAL

Preparation of $[Cu(BPCA)(OH_2)(O_2CCH_3)]\cdot H_2O$

A blue solution of $Cu(O_2CCH_3)\cdot 2H_2O$ (1 mmol) in water (12 cm^3) was mixed while stirring with a

* Author to whom correspondence should be addressed.

colourless solution of TPT (1 mmol) in ethanol (10 cm^3). The deep green colour of the resulting solution is consistent with the formation of a copper(II)–TPT complex.[5] This solution was heated to gentle boiling and became blue after *ca* 1 h, thus indicating TPT hydrolysis and consequent formation of $[Cu(BPCA)]^+$ entities.[2] The solution was allowed to stand at room temperature and dark blue crystals appeared after several days. These were separated by filtration, washed with small portions of cold ethanol and stored in a desiccator over silica gel. Found: C, 44.0; H, 4.0; Cu, 16.5; N, 11.0. Calc. for $C_{14}H_{15}CuN_3O_6$: C, 43.7; H, 3.9; Cu, 16.5; N, 10.9%.

Physical measurements

IR spectra were obtained on KBr pellets in the 4000–250 cm^{-1} region using a Pye Unicam SP 2000 spectrophotometer. Diffuse reflectance electronic spectra were recorded on a Perkin–Elmer Lambda 9 UV/VIS/NIR spectrophotometer. ESR spectra were recorded on a Bruker ER 200D X-band spectrometer equipped with a variable temperature device. Water was determined thermogravimetrically using a Setaram B70 simultaneous TGA–DTA thermobalance. X-Ray powder diffraction patterns ($2° < 2\theta < 50°$) were performed in a Kristalloflex 810 Siemens diffractometer, equipped with a variable temperature device, using Cu-K_α radiation and silicon powder as internal reference.

Crystallographic study

Crystal data. Blue prismatic crystals of $C_{14}H_{15}CuN_3O_6$, M = 384.5, triclinic, space group $P\bar{1}$, $a = 7.416(2)$, $b = 8.632(4)$, $c = 13.034(3)$ Å, $\alpha = 74.55(3)$, $\beta = 84.84(3)$, $\gamma = 81.04(5)°$, $V = 793.4(9)$ $Å^3$, $Z = 2$, $D_c = 1.609$ g cm^{-3}, $F(000) = 390$, μ(Mo-K_α) = 13.8 cm^{-1}.

Data collection. A well formed crystal of dimensions $0.16 \times 0.18 \times 0.20$ mm was selected and mounted on an Enraf–Nonius CAD-4 diffractometer equipped with a graphite monochromator. The cell dimensions were obtained by least-squares refinement of 25 well-centred reflections ($14° < 2\theta < 27°$) using Mo-K_α radiation ($\lambda = 0.70926$ Å). The space group $P\bar{1}$ was assumed throughout the structure analysis and was confirmed by the successful refinement of the structure. Examination of four standard reflections, monitored after each 50 reflections, showed no substantial intensity decay. A total of 2926 reflections were measured ($2° < 2\theta < 50°$; $-8 < h < 8$, $-10 < k < 10$, $0 < l < 15$) with the variable-speed ω–2θ technique, of which 2534 were unique with $I > 2.5\sigma(I)$ and used in the determination of the structure. Lorentz and polarization corrections were applied, but not for absorption.

Structure solution and refinement. The position of copper and 14 non-hydrogen atoms were obtained by direct methods (*MULTAN* 11/84).[8] The remaining non-hydrogen atoms were located from subsequent Fourier syntheses. The model obtained was refined with the *SHELX76* system[9] by weighted anisotropic full-matrix least-squares methods. After refinement of positional and anisotropic thermal parameters for all non-hydrogen atoms, difference maps indicated the positions of all the hydrogen atoms (excepting one associated to one water molecule and another associated to the BPCA ligand), and were included in the final refinement with common fixed isotropic thermal parameters ($U = 0.075$ $Å^2$). The final R values were $R = 0.047$ and $R_w = 0.049$ (218 parameters refined); $\Sigma w(|F_o| - |F_c|)^2$ was minimized, where $w = 1/[\sigma^2(F_o) + 0.028834(F_o^2)]$ with $\sigma^2(F_o)$ from counting statistics. In the final difference map the residual maxima were less than 0.65 e $Å^{-3}$. Atomic scattering factors and corrections for anomalous dispersion for the copper atom were taken from ref. 10. The geometrical calculations were performed with *XANADU*[11] and *DISTAN*[12] and molecular illustrations were drawn with *PLUTO*.[13] Final atomic coordinates, thermal parameters and F_o/F_c values have been deposited with the Editor as supplementary data.

RESULTS AND DISCUSSION

Crystal structure

Figure 1 shows a perspective view of the molecule with the atomic numbering scheme, and Fig. 2 shows a view of the crystal packing in the solid. Selected bond distances and angles are listed in Table 1. The coordination sphere of copper(II) is best described as a tetragonal square pyramid. The basal positions are occupied by the three nitrogen atoms from the BPCA ligand and one oxygen atom from the monodentate acetate anion, while the apical position is occupied by the oxygen atom from the coordinated water molecule. The Cu—N bond distances, ranging from 1.947 to 2.000 Å, are very similar to those found in the Cu(BPCA)Br and other copper(II) complexes with related *N*-heterocyclic ligands,[1,2] while the Cu—O(basal) and the Cu—O(apical) bond distances are 1.942(2) and 2.338(3) Å, respectively. The four basal atoms are coplanar within ±0.01 Å, and the copper atom is

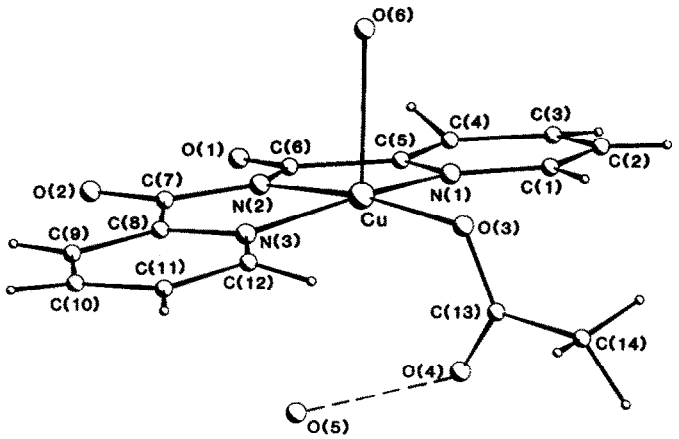

Fig. 1. Perspective view of [Cu(BPCA)(O$_2$CCH$_3$)(OH$_2$)]·H$_2$O with atomic numbering.

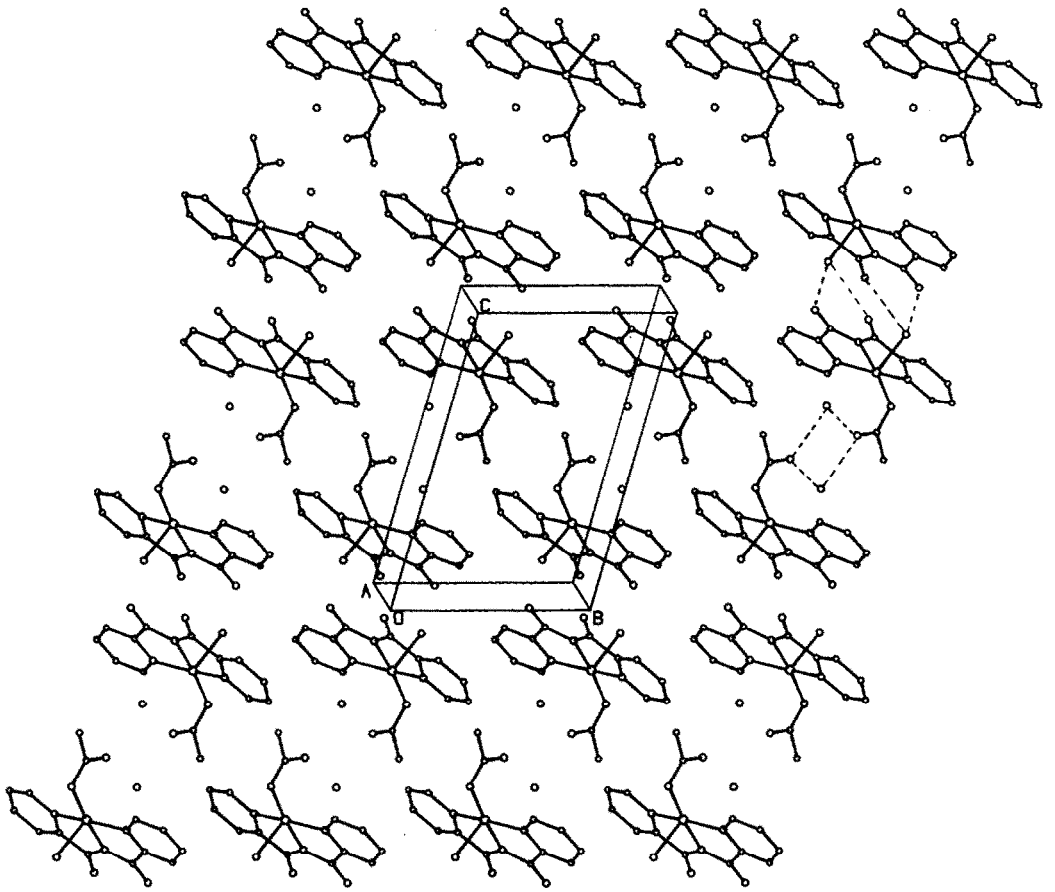

Fig. 2. Crystal packing of [Cu(BPCA)(O$_2$CCH$_3$)(OH$_2$)]·H$_2$O. Only a part of the hydrogen bonding network is shown (broken line) for clarity.

displaced 0.15 Å above the mean plane. The plane defined by the Cu, O(3) and O(6) atoms makes an angle of 87.4° with the basal plane. If the second oxygen atom of the acetate group is considered as "semicoordinated" [Cu—O(4) = 2.790(3) Å], the environment of the copper(II) could be described as an elongated and strongly distorted octahedron because the O(3)—Cu—O(4) angle is 51.4(1)°. This kind of coordination has been also found in other carboxylate, nitro and nitrite copper(II) complexes.[7,14–16] Otherwise, the oxygen atom of the second water molecule is located 3.506(4) Å below

Table 1. Selected bond distances (Å) and angles (°) for [Cu(BPCA)(O_2CCH_3)(OH_2)]·H_2O: standard deviations are given in parentheses

Cu—N(1)	1.998(2)	Cu—N(2)	1.947(2)
Cu—N(3)	2.000(2)	Cu—O(3)	1.942(2)
Cu—O(6)	2.338(2)	C(13)—O(3)	1.270(4)
C(13)—O(4)	1.234(5)		
O(3)—Cu—O(6)	91.5(1)	N(1)—Cu—O(6)	92.4(1)
N(1)—Cu—O(3)	97.3(1)	N(2)—Cu—O(6)	96.5(1)
N(2)—Cu—O(3)	172.0(1)	N(2)—Cu—N(1)	82.3(1)
N(3)—Cu—O(6)	97.5(1)	N(3)—Cu—O(3)	97.4(1)
N(3)—Cu—N(1)	162.0(1)	N(3)—Cu—N(2)	81.6(1)
O(6)—Cu—N(1)	92.4(1)	O(6)—Cu—N(2)	96.5(1)
O(6)—Cu—N(3)	97.5(1)	O(6)—Cu—O(3)	91.5(1)
O(4)—C(13)—O(3)	121.8(3)	C(5)—C(6)—O(1)	121.2(2)
C(5)—C(6)—N(2)	110.4(2)	N(2)—C(6)—O(1)	128.4(3)
C(8)—C(7)—O(2)	121.1(2)	C(8)—C(7)—N(2)	110.6(2)
N(2)—C(7)—O(2)	128.3(2)		
Hydrogen bonding[a]			
O(5)···O(4)‴	2.782(5)	O(5)—H(*w*50)—O(4)‴	167(2)
O(5)···O(4)	3.052(6)	O(6)—H(*w*60)—O(1)′	131(1)
O(6)···O(1)′	2.977(5)	O(6)—H(*w*60)—O(2)′	142(2)
O(6)···O(2)′	2.989(5)	O(6)—H(*w*61)—O(2)″	167(3)
O(6)···O(2)″	2.890(5)		

[a] O(1)′ and O(2)′ from O(1) and O(2) after $1-x$, $-y$, $2-z$.
O(2)″ from O(2) after $-1+x$, y, z.
O(4)‴ from O(4) after $1-x$, $-y$, $1-z$.

the copper(II) atom in the apical direction. Owing to this rather large distance, the second water molecule could not be considered coordinated to the copper atom.

The BPCA ligand is nearly planar (within ±0.12 Å), although if the two pyridinylcarbonyl halves are viewed separately, the respective deviations from planarity are less then 0.04 Å, with their mean planes making an angle of 6.6°. Another feature to note in the conformation of the BPCA ligand is the values of the angles around the carbon atoms involved in the carbonyl groups (see Table 1). As previously noted,[17] the need for short copper–nitrogen bonds introduces such a large angular strain.

As the contact distances shown in Table 1 indicate, the crystal packing is achieved by intermolecular hydrogen bonding. Indeed, the non-coordinated water molecule is hydrogen bonded to oxygen atoms [O(4) and O(4)‴] from two acetate groups (related by an inversion centre) belonging to adjacent molecules (see Fig. 2). On the other hand, the coordinated water molecule is hydrogen bonded simultaneously to two [O(1)′ and O(2)′] and one [O(2)″] carbonyl-oxygen atoms from two different BPCA ligands (see Table 1). Therefore, it is to be noted that this extended hydrogen bonding network gives rise to a lamellar structure. Thus, every pair of [Cu(BPCA)(O_2CCH_3)] entities linked through the coordinated water molecules yields a double layer unit which, in turn, is interconnected with the adjacent ones by means of the hydrogen bonds involving the non-coordinated water molecules. Then a sequence of alternate H_2O and [Cu(BPCA)(O_2CCH_3)] layers result.

Vibrational and electronic spectra

Concerning the IR bands due to BPCA ligand, we note the presence of a strong band assignable to the ν(C=O) vibrations of the imide group located at 1710 cm^{-1}, which agrees with that observed for other Cu^{II}–BPCA derivatives.[2] Between 3200 and 3700 cm^{-1} there appears a relatively broad and medium-intensity absorption showing well defined maxima at 3430 and 3500 cm^{-1} and a shoulder at 3300 cm^{-1}. These bands can be assigned to the O—H stretching vibrations of hydrogen-bonded, not clustered, water molecules.[18] Bands corresponding to $\nu_{as}(CO_2)$ and $\nu_s(CO_2)$ from the acetate group are identified at 1590 and 1415 cm^{-1}, respectively, in spite of the complexity of the vibrational spectrum or BPCA in the 1200–1700 cm^{-1} region.

The reflectance electronic spectrum exhibits one broad unresolved band in the visible region with

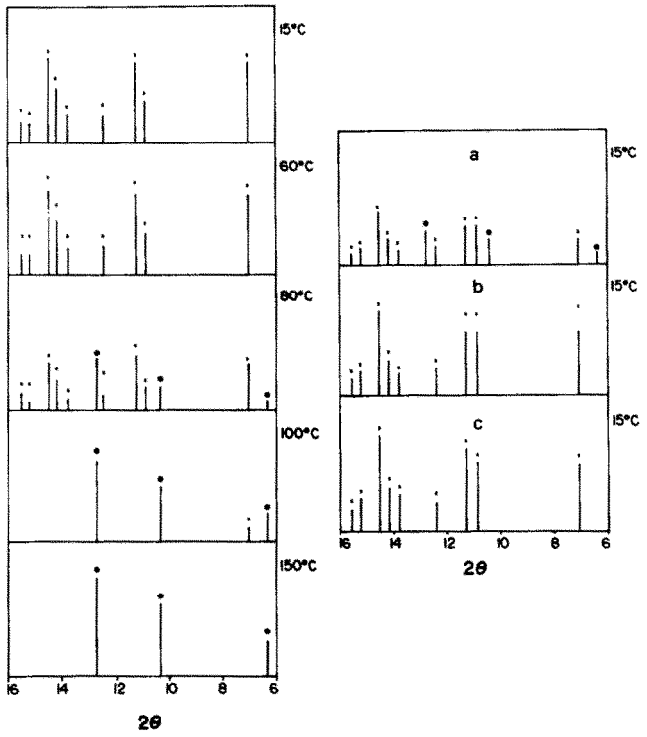

Fig. 3. Temperature variation of polycrystalline powder X-ray patterns of [Cu(BPCA)(O$_2$CCH$_3$)(OH$_2$)]·H$_2$O (left), and time variable polycrystalline powder X-ray patterns of [Cu(BPCA)(O$_2$CCH$_3$)] at (a) $t = 0$, (b) $t = 5$ min and (c) $t = 10$ min (right). (▮) Peaks of [Cu(BPCA)(O$_2$CCH$_3$)(OH$_2$)]·H$_2$O, (●) peaks of [Cu(BPCA)(O$_2$CCH$_3$)].

the maximum in the absorption envelope located near 16,200 cm^{-1}, in agreement with the geometry of the [CuN$_3$OO'] chromophore.[19]

Dehydration–rehydration processes

An unexpected result is that concerning the thermal behaviour of the title compound. In fact, TGA–DTA curves show a single endothermic dehydration step (peak temperature = 115°C) in which two water molecules per mol of complex are evolved in a single step. Moreover, variable temperature X-ray powder diffraction patterns (Fig. 3) do not show the formation of any crystalline intermediate phase between the starting [Cu(BPCA)(OH$_2$)(O$_2$CCH$_3$)]·H$_2$O complex and the resulting anhydrous product. On the other hand, the anhydrous phase quickly rehydrates at room temperature to give again the initial phase (Fig. 3). Thus it seems that the reversible equilibrium

$$[Cu(BPCA)(OH_2)(O_2CCH_3)]\cdot H_2O(s) \overset{\Delta T}{\rightleftharpoons} [Cu(BPCA)(O_2CCH_3)](s) + 2H_2O(g)$$

would occur through a concerted process in whose evolution it is not possible to discern non-coordinated and coordinated water molecules.

The X-ray powder diffraction pattern of the anhydrous derivative can be indexed[20] to a triclinic cell of dimensions $a = 6.38(4)$, $b = 8.80(8)$, $c = 14.26(8)$ Å, $\alpha = 85.0(6)$, $\beta = 91.8(7)$, $\gamma = 88.9(3)°$, $V = 797(1)$ Å^3. The main changes with respect to the initial cell are observed in the *ac* plane, in accordance with the directionality of the hydrogen bonding network. At this stage, it would be unreliable to argue about the actual structure evolution. Notwithstanding, given that dehydration occurs without appreciable colour change, it may be thought that the copper(II) environment remains essentially "4+1" in the anhydrous phase. This might be achieved through the apical coordination of the O(4) oxygen atom from the acetate group (see below), although the formation of acetate bridges could not be fully excluded *a priori*. Nevertheless, this last possibility seems unlikely because of the great structural changes required and the easiness of water displacement.

In short, such a pseudo-topotactic reversible water dissociation could be described as an acid–base intercalation reaction in the interlayer space of the [Cu(BPCA)(O$_2$CCH$_3$)] host lattice.

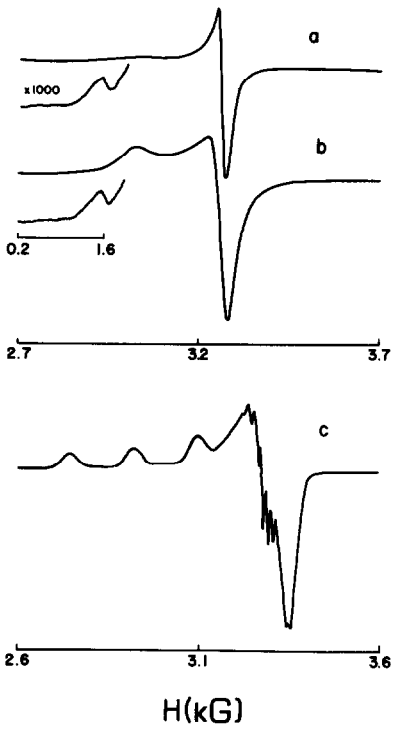

Fig. 4. X-Band ESR spectra of (a) polycrystalline powder samples of $[Cu(BPCA)(O_2CCH_3)(OH_2)]\cdot H_2O$, (b) $[Cu(BPCA)(O_2CCH_3)]$, and (c) frozen solution (ethanol, 125 K) of $[Cu(BPCA)(O_2CCH_3)(OH_2)]\cdot H_2O$.

ESR spectroscopy

X-Band ESR spectra of polycrystalline $[Cu(BPCA)(OH_2)(O_2CCH_3)]\cdot H_2O$ samples show axial-type signals which remain unchanged from room temperature down to 125 K [Fig. 4(a)]. The resulting g values ($g_\parallel = 2.23$, $g_\perp = 2.06$) indicate a mainly copper(II) $d_{x^2-y^2}$ orbital ground state, which agrees with the above statements. The spectra show also a weak absorption at half field value associated to a $\Delta M_s = 2$ forbidden transition. This implies a magnetic interaction between two copper(II) ions. Most dimeric copper(II) complexes of known structure, exhibiting exchange interactions, contain a bridging atom or group of atoms through which a magnetic interaction may be propagated. However, a few examples have been recently reported where the exchange pathway must be considered as purely dipolar ("through space") in origin.[21,22] In our case, the "dimeric spectra" could be then understood on the basis of two potential interaction pathways: (i) a "through space" dipolar path, and (ii) a superexchange path through an extended bridging network involving the hydrogen bonded water molecules. Actually, the possibility of the propagation of the magnetic exchange between copper(II) ions through hydrogen bond frameworks has been previously shown.[1,23] From the hydrogen bonding scheme in Table 1 it might be thought of three possible superexchange dimeric pathways connecting Cu—Cu′, Cu—Cu″ and Cu—Cu‴, which involve spin–spin distances of 6.75, 7.42 and 8.28 Å, respectively (the symmetry relations are indicated in Table 1). The only additional pair involving a comparable copper–copper distance (6.93 Å) is the Cu—Cu^{iv} (Cu^{iv} is generated from Cu after $-x, -y, 2-z$). In any case, the Cu—Cu′ pair shows both the shortest intermetallic distance and a simple hydrogen bonding network. Accordingly, it is reasonable to assume that the interaction in this pair causes the $\Delta M_s = 2$ signal.

On the other hand, the ESR spectrum of the anhydrous form $[Cu(BPCA)(O_2CCH_3)]$ [Fig. 4(b)], also shows the weak intensity $\Delta M_s = 2$ absorption. Besides, this spectrum is axial and leads to g values identical to those corresponding to the hydrated form. Whereas this last observation is clearly consistent with the above statement on the "4+1" copper(II) coordination mode in the anhydrous form, it is evident that now the magnetic exchange cannot proceed through any hydrogen bonding network. In this case, a "through space" dipolar path would be the only way to propagate the magnetic interaction if, as suggested above, dimerization through acetate bridges does not occur.

Finally, the $[Cu(BPCA)(OH_2)(O_2CCH_3)]\cdot H_2O$ solution ESR spectra (nitromethane, ethanol, chloroform) do not show signs of coupling apart from the copper and nitrogen hyperfine structure. The room temperature spectrum yields isotropic $g = 2.11$ and $A(Cu) = 0.0074$ cm^{-1} parameters. The frozen-solution spectrum (ethanol or chloroform, 125 K) shows an axial signal [Fig. 4(c)] leading to $g_\parallel = 2.24$, $g_\perp = 2.06$ ($g_{ave} = 2.12$). The copper hyperfine splitting in the $g_\parallel$ part is well defined yielding $[A_\parallel(Cu)] = 0.018$ cm^{-1}, whereas the $[A_\perp(Cu)]$ is not resolved, although it can be estimated to be less than 0.0025 cm^{-1}. On the $g_\perp$ component, a seven line superhyperfine structure due to the three nitrogen atoms from BPCA ligand is detected. This structure is also present but poorly resolved in the high-field hyperfine component of $g_\parallel$. Since the principal direction of the superhyperfine ^{14}N tensor is along the Cu—N bond, we can estimate values of $A_\parallel(^{14}N) = 0.0016$ cm^{-1} and $A_\perp(^{14}N) = 0.0011$ cm^{-1}. According to the literature,[24] all these values are those expected for a monomeric copper(II) complex with a basically $d_{x^2-y^2}$ orbital ground state.

In the light of these results, the determination of the structure of the anhydrous species becomes a very interesting challenge because this compound might constitute one of the scarce examples of pair-

wise dipolar coupling in copper(II) systems. In this sense, new experiments on the structure and the Lewis acid–base intercalation chemistry in the [Cu(BPCA)(O$_2$CCH$_3$)] host lattice are in progress.

Acknowledgements—We thank the CAICYT and the CSIC for partial support of this research and for a fellowship to A.F. J.V.F. thanks the Spanish Ministerio de Educación y Ciencia for a FPI fellowship. We are grateful to M. Caldés for helpful discussions.

REFERENCES

1. J. V. Folgado, R. Ibáñez, E. Coronado, D. Beltrán-Porter, J. M. Savariault and J. Galy, *Inorg. Chem.* 1988, **27**, 19 and refs cited therein.
2. J. V. Folgado, E. Escrivá, A. Beltrán-Porter and D. Beltrán-Porter, *Transition Met. Chem.* 1987, **12**, 306.
3. J. V. Folgado, E. Coronado, D. Beltrán-Porter, R. Burriel, A. Fuertes and C. Miravitlles, *J. Chem. Soc., Dalton Trans.* 1988, 3041.
4. J. V. Folgado, E. Coronado and D. Beltrán-Porter, *J. Chem. Soc., Dalton Trans.* 1986, 1061.
5. J. V. Folgado, E. Escrivá, A. Beltrán-Porter and D. Beltrán-Porter, *Transition Met. Chem.* 1986, **11**, 485.
6. R. C. Mehrotra and R. Bohra, *Metal Carboxylates.* Academic Press, New York (1983).
7. J. V. Folgado, E. Escrivá, A. Beltrán-Porter, D. Beltrán-Porter, A. Fuertes and C. Miravitlles, *Polyhedron* 1987, **6**, 1533.
8. P. Main, G. Germain and M. M. Woolfson, *MULTAN 11/84, A System of Computer Programs for the Automatic Solutions of Crystal Structures from X-Ray Diffraction Data.* University of York, U.K., and Louvain, Belgium (1984).
9. G. M. Sheldrick, *SHELX76, Program for Crystal Structure Determination.* University of Cambridge, U.K. (1976).
10. *International Tables for X-Ray Crystallography*, Vol. 4, pp. 72–99. Kynoch Press, Birmingham (1974).
11. P. Roberts and G. M. Sheldrick, *XANADU, Program for Crystallographic Calculations.* University of Cambridge, U.K. (1975).
12. J. Burzlaff, V. Bohme and M. Gomm, *DISTAN.* University of Erlangen, F.R.G. (1977).
13. W. D. S. Motherwell and W. Clegg, *PLUTO78, Program for Plotting Molecular and Crystal Structures.* University of Cambridge, U.K. (1978).
14. A. Fuertes, C. Miravitlles, E. Escrivá, E. Coronado and D. Beltrán, *J. Chem. Soc., Dalton Trans.* 1987, 1847.
15. B. J. Hathaway, *Struct. Bonding* 1984, **57**, 55, and references cited therein.
16. J. M. Savariault, T. Rojo, M. I. Arriortua and J. Galy, *C.R. Acad Sci.* 1983, **297**, 895.
17. E. I. Lerner and S. J. Lippard, *Inorg. Chem.* 1977, **16**, 1546.
18. J. R. Ferraro, *Low-frequency Vibrations of Inorganic and Coordination Compounds*, p. 65. Plenum Press, New York (1971).
19. A. B. P. Lever, *Inorganic Electronic Spectroscopy*, 2nd edn., p. 568. Elsevier, Amsterdam (1985).
20. E. Werner, *TREOR-4, Trial and Error Program for Indexing of Unknown Powder Patterns.* University of Stockholm, Sweden (1984).
21. P. J. Barker and S. R. Stobart, *J. Chem. Soc., Chem. Commun.* 1980, 969.
22. A. W. Addison, P. J. Burker and K. Henrick, *Inorg. Chem.* 1982, **21**, 60.
23. D. N. Hendrickson, in *Magneto-structural Correlations in Exchange-coupled Systems* (Edited by D. Gatteschi, O. Kahn and R. D. Willet). NATO-ASI Series, Reidel, Dordrecht (1985).
24. M. Tirant, T. D. Smith, J. R. Pilbrow, G. Hanson and G. R. Sinclair, *J. Chem. Soc., Dalton Trans.* 1987, 1755.

Polyhedron Vol. 8, No. 8, pp. 1085–1092, 1989
Printed in Great Britain

0277–5387/89 $3.00+.00
© 1989 Pergamon Press plc

α-PYRIDINE CARBOXYLATE COMPLEXES OF RHODIUM(III) WITH Rh—Hg AND Hg—Rh—Sn BONDS—II*

M. CANO,† J. V. HERAS, M. MARTÍNEZ-AZNAR and E. PINILLA

Departamento de Química Inorgánica, Facultad de Ciencias Químicas, Universidad Complutense, 28040 Madrid, Spain

and

C. ALVAREZ

Departamento de Química Orgánica, Facultad de Ciencias Químicas, Universidad Complutense, 28040 Madrid, Spain

(*Received* 21 *July* 1988; *accepted* 11 *November* 1988)

Abstract—New complexes with an Rh—Hg bond of the type $RhX(HgX)(pyC)PR_3$ (**A**) and $RhCl(HgPh)(pyC)(CO)(PR_3)$ (**A′**) (X = Cl, Br, I; pyC = 2-C_5NH_4COO; R = 4-$CH_3OC_6H_4$, 4-$CH_3C_6H_4$, 4-FC_6H_4, 4-ClC_6H_4) have been prepared by the reaction of $Rh(pyC)(CO)(PR_3)$ with HgX_2 (X = Cl, Br, I) and PhHgCl.

The reactivity of the above bimetallic derivatives towards $SnCl_2$ yielding new complexes with Hg—Rh—Sn bonds is also reported.

Synthetic and structural aspects of the chemistry of complexes containing bonds between dissimilar metal atoms are of continuing interest.[1,2] In particular, the reactions of mercury(II) compounds with complexes of transition metals have been extensively studied[2] and different types of reactions have been found. Thus, when the transition metal complex is an electron-rich one, a donor–acceptor complex with mercuric derivatives is usually formed.[3–5] However, when the transition metal complex is less nucleophilic and amenable to oxidation, oxidative addition products were obtained. For this reason, Vaska's complex is easily oxidized by mercury(II) halides or pseudohalides,[6] but a similar reaction does not occur for analogous Rh^I complexes.

Nevertheless, a series of Rh—Hg bonded compounds has been prepared by oxidation of $RhCl(CO)(L)_2$ complexes with $HgCl_2$, with more basic ligands than PPh_3, such as L = PPh_2Et, PPh_2Pr^i, L_2 = Ph_2PCH_2SPh and $Ph_2PCH_2CH_2SPh$.[7] Recently, the reactivity of $HgCl_2$ towards binuclear rhodium–rhodium complexes was studied yielding new compounds with Rh—Hg—Rh bonds.[7,8]

In previous work,[9] we have reported the high basicity of the $Rh(pyC)(CO)(PR_3)$ complexes in their reactions with I_2, Br_2 and ICH_3. Herein we report the analogous reactions with Hg^{II} derivatives HgX_2 (X = Cl, Br, I) and PhHgCl, to form six-coordinated Rh^{III} complexes, $RhX(HgX)(pyC)(CO)(PR_3)$ (**A**; **I–XII**) and $RhCl(HgPh)(pyC)(CO)(PR_3)$ (**A′**; **XIII–XVI**) with HgX and X or HgPh and Cl as the additional ligands. It is noteworthy that for Rh^I complexes containing N—O ligands, only one related compound, Rh(moq)(CO)[P(4-$CH_3C_6H_4)_3$]$HgCl_2$ has been described.[10]

In the second part of this study we have synthesized trimetallic complexes, $Rh(SnCl_3)(HgCl)(pyC)(CO)(PR_3)$ (**B**; **XVII–XX**) and $Rh(SnCl_3)(HgPh)(pyC)(CO)PR_3$ (**B′**; **XXI–XXIV**), by insertion reactions of $SnCl_2$ in the above Rh—Hg complexes.

EXPERIMENTAL

IR spectra were recorded on a 1300 Perkin–Elmer spectrophotometer (over the 4000–200 cm^{-1} range) with KBr pellets.

* For part I, see ref. 9.

† Author to whom correspondence should be addressed.

Conductance measurements were performed in $\sim 3 \times 10^{-4}$ M acetone solution with a Philips PR 9500 conductimeter. Analyses (C, H, N) were carried out by Elemental Microanalyses Laboratories Ltd (Devon, England). ^{31}P-NMR spectra were recorded on a Varian XL-200 spectrometer at room temperature using 85% H_3PO_4 as the external standard. The reactions were carried out normally at room temperature.

Complexes of Rh(pyC)(CO)(PR_3) were prepared by our published methods.[9] The solvents were distilled before use. The other reagents were commercially obtained.

RhCl(HgCl)(pyC)(CO)(PR_3)·$2HgCl_2$ (R = 4-$CH_3OC_6H_4$, 4-$CH_3C_6H_4$, 4-FC_6H_4, 4-ClC_6H_4) *complexes* (**I–IV**)

A slight excess over the Rh/Hg (1 : 3) stoichiometric ratio of mercury(II) chloride was added to an acetone solution (15 cm^3) of the corresponding Rh(pyC)(CO)(PR_3)[9] (0.1 mmol) complex. The starting yellow solution immediately changed to a deep yellow colour. The stirring was continued for 5 min. Addition of cold Et_2O lead to the complete precipitation of the yellow complex, which was filtered off, recrystallized from CH_2Cl_2/Et_2O (10 : 20 cm^3), washed with acetone–diethylether and dried *in vacuo* (yield, $\sim$ 75%).

The analogous compounds, RhBr(HgBr)(pyC)(CO)(PR_3)·$HgBr_2$ (**V–VIII**), were prepared by a procedure similar to the above. In these cases the time of reaction changes depending on the phosphine ligand and it is 6 to 10 h for P(4-$CH_3OC_6H_4)_3$ and P(4-$ClC_6H_4)_3$, respectively.

RhI(HgI)(pyC)(CO)(PR_3)·HgI_2 (R = 4-$CH_3OC_6H_4$, 4-$CH_3C_6H_4$, 4-FC_6H_4, 4-ClC_6H_4) *complexes* (**IX–XII**)

In these cases, the reaction occurred in absolute ethanol (10 cm^3) and the mixture was stirred for 24 h, at room temperature in darkness. The solvent was reduced to *ca* 2 cm^3 and cooled light petroleum (15 cm^3) was added. The orange precipitate was filtered off, washed with ethanol (5 cm^3) and dried *in vacuo* (yield, 60%).

RhCl(HgPh)(pyC)(CO)(PR_3) (R = 4-$CH_3OC_6H_4$, 4-$CH_3C_6H_4$, 4-FC_6H_4, 4-ClC_6H_4) *complexes* (**XIII–XVI**)

Rh(pyC)(CO)(PR_3)[9] (0.15 mmol) was dissolved in ethanol (20 cm^3), and PhHgCl (0.45 mmol) was added. The solution was stirred and refluxed for 15 min. It was then filtered through Kieselguhr, to eliminate the metallic mercury forming during the reaction. The solvent was removed and the crude solid was recrystallized from dichloromethane–light petroleum giving a yellow solid (yield, 92%).

Rh($SnCl_3$)(HgX)(pyC)(CO)(PR_3) (R = 4-CH_3OC_6H, 4-$CH_3C_6H_4$, 4-FC_6H_4, 4-ClC_6H_4, X = Cl, Ph) *complexes* (**XVII–XXIV**)

A slight excess ($\sim$ 10%) of $SnCl_2$ was added to an acetone solution of the corresponding bimetallic compound (**I–IV** and **XIII–XVI**). Immediately the colour changed from yellow to red–orange. The solution was stirred for 5 min, then the solvent was removed and the solid was dissolved in dichloromethane (10 cm^3) and reduced in volume to 5 cm^3. Addition of cold light petroleum (10 cm^3) gave, quantitatively, the orange solid, which was recrystallized from acetone–diethylether (1 : 2). The Rh($SnBr_3$)(HgBr)(pyC)(CO)(4-$CH_3OC_6H_4$) complex is prepared by a procedure similar to the above, by addition of $SnBr_2$ to the RhBr(HgBr)(pyC)(CO)(4-$CH_3OC_6H_4$) complex.

RESULTS AND DISCUSSION

Reactions of Rh(pyC)(CO)PR_3 *complexes with* HgX_2 (X = Cl, Br, I) *and* ClHgPh

In contrast to the lack of reaction of $HgCl_2$ with *trans*-RhCl(CO)($PRh_3)_2$[6,7] in acetone, solutions of the Rh(pyC)(CO)(PR_3) complexes reacted with HgX_2 to form by oxidative addition, the RhX(HgX)(pyC)(CO)(PR_3) (**A**) complexes (**I–XII**) (Table 1).

The reaction is complete only when a Rh/Hg molar ratio of 1 : 3 or higher is employed. The compounds are air-stable for long periods, but show very low solubility in the most common solvents, in which partial decomposition to Hg^0 and decarbonylated products is observed. The conductivity measurements of freshly prepared acetone solutions are consistent with the neutral character of the compound (Table 1).

Analogous reactions with PhHgCl were carried out in refluxing ethanol under nitrogen atmosphere for short reaction times. New yellow microcrystalline products were obtained and characterized as the oxidative addition complexes, RhCl(HgPh)(pyC)(PR_3) (**A′**, **XIII–XVI**) (Table 1). These compounds are air-stable, soluble in common organic solvents, and non-electrolytic in acetone solution.

The IR spectra of all complexes of type (**A**) and (**A′**) (Table 2) exhibit a strong band in the carbonyl stretching region, 2075–2033 cm^{-1}. This band is shifted $\sim$ 100–70 cm^{-1} towards higher frequencies, with respect to the parent compounds,[9]

Table 1. Analytical data and some physical properties for the (**I–XXIV**) compounds

Complexes	Yield (%)	M.p.[a] (°C)	Λ^b (Ω^{-1} cm^2 mol^{-1})	Found (Calc.) (%) C	H	N
I $RhCl(HgCl)(pyC)(CO)\|P(4\text{-}CH_3OC_6H_4)_3\|\cdot 2HgCl_2$	78	180	3.9	24.0 (23.7)	1.8 (1.8)	1.0 (0.9)
II $RhCl(HgCl)(pyC)(CO)\|P(4\text{-}CH_3C_6H_4)_3\|\cdot 2HgCl_2$	71	174	7.8	23.9 (24.5)	1.7 (1.8)	1.0 (1.0)
III $RhCl(HgCl)(pyC)(CO)\|P(4\text{-}FC_6H_4)_3\|\cdot 2HgCl_2$	75	123	2.9	21.2 (21.7)	1.2 (1.2)	1.0 (1.0)
IV $RhCl(HgCl)(pyC)(CO)\|P(4\text{-}ClC_6H_4)_3\|\cdot 2HgCl_2$	73	220–225	9.0	20.3 (20.9)	1.0 (1.1)	1.0 (1.0)
V $RhBr(HgBr)(pyC)(CO)\|P(4\text{-}CH_3OC_6H_4)_3\|\cdot HgBr_2$	59	129	10.1	25.3 (25.4)	2.0 (1.9)	1.1 (1.0)
VI $RhBr(HgBr)(pyC)(CO)\|P(4\text{-}CH_3C_6H_4)_3\|\cdot HgBr_2$	79	184–189	7.9	25.9 (26.3)	2.1 (2.0)	1.2 (1.1)
VII $RhBr(HgBr)(pyC)(CO)\|P(4\text{-}FC_6H_4)_3\|\cdot HgBr_2$	64	147	8.9	22.9 (23.3)	1.3 (1.2)	0.9 (1.1)
VIII $RhBr(HgBr)(pyC)(CO)\|P(4\text{-}ClC_6H_4)_3\|\cdot HgBr$	67	152–156	8.0	22.2 (22.4)	1.3 (1.2)	1.2 (1.0)
IX $RhI(HgI)(pyC)(CO)\|P(4\text{-}CH_3OC_6H_4)_3\|\cdot HgI_2$	32	142–145	4.0	22.5 (22.2)	1.9 (1.7)	1.1 (0.9)
X $RhI(HgI)(pyC)(CO)\|P(4\text{-}CH_3C_6H_4)_3\|\cdot HgI_2$	40	109	8	22.3 (22.9)	1.6 (1.7)	0.9 (0.9)
XI $RhI(HgI)(pyC)(CO)\|P(4\text{-}FC_6H_4)_3\|\cdot HgI_2$	28	160–166	5.8	20.9 (20.3)	1.1 (1.1)	1.0 (0.9)
XII $RhI(HgI)(pyC)(CO)\|P(4\text{-}ClC_6H_4)_3\|\cdot HgI_2$	31	128–131	3.6	20.0 (19.7)	1.2 (1.1)	1.1 (0.9)
XIII $RhCl(HgPh)(pyC)(CO)\|P(4\text{-}CH_3OC_6H_4)_3\|$	92	94–100	2.4	44.2 (44.4)	3.2 (3.3)	1.2 (1.5)
XIV $RhCl(HgPh)(pyC)(CO)\|P(4\text{-}CH_3C_6H_4)_3\|$	94	85	5.1	47.1 (46.9)	3.3 (3.4)	1.7 (1.6)
XV $RhCl(HgPh)(pyC)(CO)\|P(4\text{-}FC_6H_4)_3\|$	96	103–106	8.8	42.2 (42.2)	2.2 (2.4)	1.7 (1.6)
XVI $RhCl(HgPh)(pyC)(CO)\|P(4\text{-}ClC_6H_4)_3\|$	87	119	3.8	40.1 (39.9)	2.3 (2.3)	1.7 (1.5)
XVII $Rh(SnCl_3)(HgCl)(pyC)(CO)\|P(4\text{-}CH_3OC_6H_4)_3\|$	96	111	0.7	31.1 (31.5)	2.3 (2.4)	1.3 (1.3)
XVIII $Rh(SnCl_3)(HgCl)(pyC)(CO)\|P(4\text{-}CH_3C_6H_4)_3\|$	98	110–118	3.4	33.2 (33.0)	2.4 (2.5)	1.5 (1.4)
XIX $Rh(SnCl_3)(HgCl)(pyC)(CO)\|P(4\text{-}FC_6H_4)_3\|$	93	98–110	6.2	29.2 (29.1)	1.4 (1.6)	1.5 (1.3)
XX $Rh(SnCl_3)(HgCl)(pyC)(CO)\|P(4\text{-}ClC_6H_4)_3\|$	92	105–108	4.4	27.1 (27.8)	1.6 (1.5)	1.2 (1.3)
XXI $Rh(SnCl_3)(HgPh)(pyC)(CO)\|P(4\text{-}CH_3OC_6H_4)_3\|$	94	122–124	1.6	36.6 (36.8)	2.8 (2.7)	1.2 (1.3)
XXII $Rh(SnCl_3)(HgPh)(pyC)(CO)\|P(4\text{-}CH_3C_6H_4)_3\|$	85	89–91	7.3	37.9 (38.5)	2.5 (2.9)	1.5 (1.3)
XXIII $Rh(SnCl_3)(HgPh)(pyC)(CO)\|P(4\text{-}FC_6H_4)_3\|$	87	145–149	0.9	34.2 (34.7)	1.8 (2.0)	1.4 (1.3)
XXIV $Rh(SnCl_3)(HgPh)(pyC)(CO)\|P(4\text{-}ClC_6H_4)_3\|$	78	153	7.1	32.5 (33.2)	2.0 (1.9)	1.4 (1.2)

[a] Decompose without melt.
[b] In acetone *ca* 10^{-3} M.

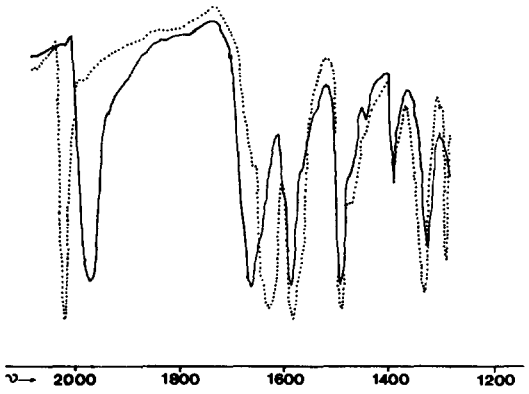

Fig. 1. IR spectra of: ——, Rh(pyC)(CO)[P(4-$FC_6H_4)_3$]; ···, RhCl(HgCl)(pyC)(CO)[P(4-$FC_6H_4)_3$]·$2HgCl_2$.

and is consistent with a carbonyl ligand in an oxidized Rh^{III} complex. An example is shown in Fig. 1.

The presence of a single sharp $\nu(C{\equiv}O)$ absorption seems to point to the presence of only one isomer in the solid state. It can be reasonably argued that the isomer obtained comes from the *trans* addition of the X and HgX groups to the square-planar Rh(pyC)(CO)(PR_3) complexes,[9] as a result of the considerable bulkiness of these groups.[11]

However, for the *trans* oxidative addition of PhHgCl, two isomers are possible depending upon the dissociation of the organomercuric derivative in HgCl and Ph or HgPh and Cl, respectively. A possible explanation is considered below.

In the lower frequency region, the addition products with $HgCl_2$ (**I–IV**) exhibit three new bands with respect to monocarbonyl starting compounds (Table 2). A band at *ca* 370 cm^{-1}, assigned to ν(Hg—Cl), is attributed to the presence of additional lattice molecules of $HgCl_2$ in the compounds.[3,12–15]

The bands at *ca* 300 and 260 cm^{-1}, are consistent with ν(metal–halogen) vibrations. In a tentative assignment it is possible to consider the band at 260 cm^{-1} as due to the ν(Hg—Cl) of HgCl group bonded to transition metal, while the band at *ca* 300 cm^{-1} is attributed to the ν(Rh—Cl). A value of ~ 300 cm^{-1} for ν(Rh—Cl) vibration is also found in Rh^{III} complexes.[16,17] On the other hand, in hexacoordinate Ir^{III} halocomplexes[18] it has been shown that the ν(Ir—Cl) is only modified by the nature of the ligand *trans* to the halogen, the influence of the *cis* ligands being negligible.

If the above assignment for ν(Rh—Cl) is correct, the value of these vibrations is only very slightly modified for the different phosphine ligands, the assignment would be consistent with the above proposed *trans* addition of the groups HgCl and Cl to the parent compounds.

The assignment of metal–halogen vibration bands for the derivatives with PhHgCl is complicated by the numerous bands which appear in this region. However, it is noteworthy that absorption at ~ 260 cm^{-1} attributed to ν(Hg—Cl) is absent in all cases.

As expected, the derivatives with $HgBr_2$ and HgI_2 did not show bands in the region studied above.

The presence of the asymmetric ν(OCO) band (1670–1625 cm^{-1}) and the corresponding symmetric ν(OCO) band (1345–1330 cm^{-1}) show that the carboxylic group would be monodentate for all the above-mentioned complexes, as it is in the parent compounds.[9,19,20]

A shift of the asymmetric ν(OCO) band by *ca* 30–15 cm^{-1} towards the lower frequency region, with respect to the parent compounds, is observed for derivatives with HgX_2 (X = Cl, Br, I) (**I–XII**). This result may be due to interactions with the additional mercury halide molecules through the free oxygen of the carboxylate group. Figure 1 shows this shift in the IR spectra of the Rh(pyC)(CO)[P(4-$FC_6H_4)_3$] complex.

Reactions of RhCl(HgCl)(pyC)(CO)(PR_3) *and* RhCl(HgPh)(pyC)(CO)(PR_3) *with* $SnCl_2$

We have synthesized trimetallic complexes of composition Rh($SnCl_3$)(HgCl)(pyC)(CO)(PR_3) (**B**, **XVII–XX**) and Rh($SnCl_3$)(HgPh)(pyC)(CO)(PR_3) (**B′**, **XXI–XXIV**) (Table 1).

The insertion reactions of $SnCl_2$ in haloorganometallic complexes provide a useful method for the synthesis of M—Sn compounds.[21]

For the above Rh—Hg compounds (**A** and **A′**) we have proposed a *trans* disposition of groups HgX and X in which two kinds of M—halogen bonds (M = Rh, Hg) are present. First of all the insertion of $SnCl_2$ should be possible in both kinds of bonds, however, we have no previous evidence of this insertion into the Hg—X bond.[21]

The new compounds are yellow–orange solids, air-stable, and sparingly soluble in common organic solvents. Analytical data and some of their properties are listed in Table 1.

The IR spectra (Table 2) show only a carbonyl band whose position is not substantially different from that of the parent complexes. This fact suggests that the addition of $SnCl_2$ does not appreciably modify the rhodium oxidation state. On the other hand, the ν_{as}(OCO) band is shifted *ca* 50 cm^{-1} towards the higher frequency region, with respect to the mercuric derivatives, coming back to an analogous position to the starting Rh^{I} derivatives. This fact is consistent with the absence of interactions between the carboxylic group and the mercury of

Table 2. IR data of the (I–XXIV) complexes

Complexes		ν(C≡O)	pyC		ν(Hg—Cl)lattice	ν(Rh—Cl)	ν(Hg—Cl)	ν(Sn—Cl)
			ν_{as}(OCO)	ν_{sym}(OCO)				
I	$RhCl(HgCl)(pyC)(CO)\|P(4\text{-}CH_3OC_6H_4)_3\|\cdot 2HgCl_2$	2035	1635	1335	360	290	255	
II	$RhCl(HgCl)(pyC)(CO)\|P(4\text{-}CH_3C_6H_4)_3\|\cdot 2HgCl_2$	2033	1625	1335	373	300	260	
III	$RhCl(HgCl)(pyC)(CO)\|P(4\text{-}FC_6H_4)_3\|\cdot 2HgCl_2$	2040	1630	1330	370	295	260	
IV	$RhCl(HgCl)(pyC)(CO)\|P(4\text{-}ClC_6H_4)_3\|\cdot 2HgCl_2$	2038	1630	1330	370	301	262	
V	$RhBr(HgBr)(pyC)(CO)\|P(4\text{-}CH_3OC_6H_4)_3\|\cdot HgBr_2$	2050	1645	1340				
VI	$RhBr(HgBr)(pyC)(CO)\|P(4\text{-}CH_3C_6H_4)_3\|\cdot HgBr_2$	2053	1645	1340				
VII	$RhBr(HgBr)(pyC)(CO)\|P(4\text{-}FC_6H_4)_3\|\cdot HgBr_2$	2050	1645	1340				
VIII	$RhBr(HgBr)(pyC)(CO)\|P(4\text{-}ClC_6H_4)_3\|\cdot HgBr_2$	2048	1640	1340				
IX	$RhI(HgI)(pyC)(CO)\|P(4\text{-}CH_3OC_6H_4)_3\|\cdot HgI_2$	2050	1645	1330				
X	$RhI(HgI)(pyC)(CO)\|P(4\text{-}CH_3C_6H_4)_3\|\cdot HgI_2$	2055	1650	1335				
XI	$RhI(HgI)(pyC)(CO)\|P(4\text{-}FC_6H_4)_3\|\cdot HgI_2$	2050	1640	1330				
XII	$RhI(HgI)(pyC)(CO)\|P(4\text{-}ClC_6H_4)_3\|\cdot HgI_2$	2048	1645	1330				
XIII	$RhCl(HgPh)(pyC)(CO)\|P(4\text{-}CH_3OC_6H_4)_3\|$	2060	1660	1330		290		
XIV	$RhCl(HgPh)(pyC)(CO)\|P(4\text{-}CH_3C_6H_4)_3\|$	2065	1660	1330		290		
XV	$RhCl(HgPh)(pyC)(CO)\|P(4\text{-}FC_6H_4)_3\|$	2070	1665	1335		290		
XVI	$RhCl(HgPh)(pyC)(CO)\|P(4\text{-}ClC_6H_4)_3\|$	2075	1670	1345		295		
XVII	$Rh(SnCl_3)(HgCl)(pyC)(CO)\|P(4\text{-}CH_3OC_6H_4)_3\|$	2045	1675	1345			300	330
XVIII	$Rh(SnCl_3)(HgCl)(pyC)(CO)\|P(4\text{-}CH_3C_6H_4)_3\|$	2050	1675	1345			300	330
XIX	$Rh(SnCl_3)(HgCl)(pyC)(CO)\|P(4\text{-}FC_6H_4)_3\|$	2045	1680	1345			290	320
XX	$Rh(SnCl_3)(HgCl)(pyC)(CO)\|P(4\text{-}ClC_6H_4)_3\|$	2050	1680	1340			300	330
XXI	$Rh(SnCl_3)(HgPh)(pyC)(CO)\|P(4\text{-}CH_3OC_6H_4)_3\|$	2065	1650	1350				330
XXII	$Rh(SnCl_3)(HgPh)(pyC)(CO)\|P(4\text{-}CH_3C_6H_4)_3\|$	2075	1650	1350				330
XXIII	$Rh(SnCl_3)(HgPh)(pyC)(CO)\|P(4\text{-}FC_6H_4)_3\|$	2070	1650	1345				330
XXIV	$Rh(SnCl_3)(HgPh)(pyC)(CO)\|P(4\text{-}ClC_6H_4)_3\|$	2075	1645	1350				330

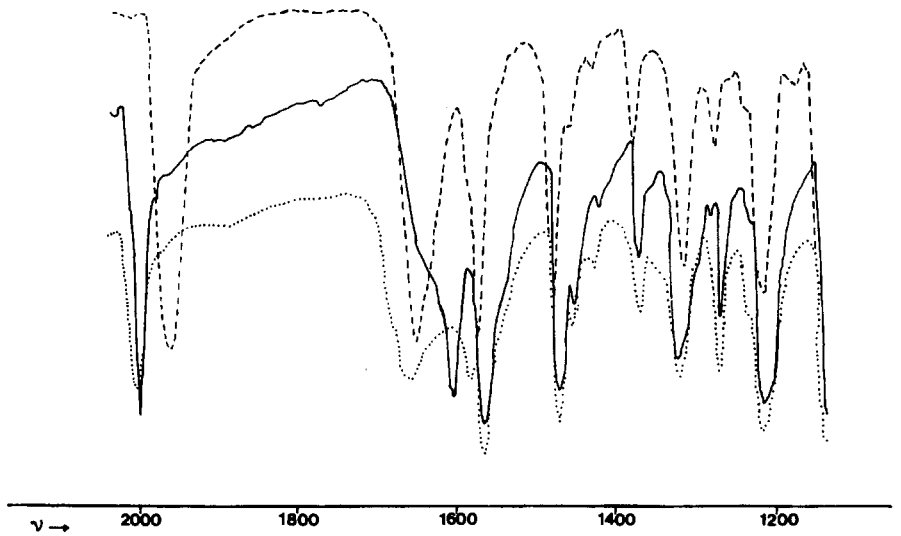

Fig. 2. IR spectra of: ---, $Rh(pyC)(CO)|P(4\text{-}FC_6H_4)_3|$; ——, $RhCl(HgCl)(pyC)(CO)|P(4\text{-}FC_6H_4)_3|\cdot 2HgCl_2$; ···, $Rh(SnCl_3)(HgCl)(pyC)(CO)|P(4\text{-}FC_6H_4)_3|$.

the additional molecules which are not present in **B** and **B′** compounds. An example of this behaviour is illustrated in the IR spectra of Fig. 2.

In the low frequency region some other differences are also observed. One broad band, centred at 330 cm^{-1}, is tentatively assigned to the sum of asymmetric and symmetric ν(Sn—Cl) vibrations of the $SnCl_3$ group. This value is similar to that found for ν(Sn—Cl) in the $Ir(SnCl_3)(HgCl)(CO)(PR_3)$[22,23] complex. One other band appears as a shoulder at *ca* 298–290 cm^{-1}. This value is not substantially different from those ν(Hg—Cl) of the above **A** complexes.

Based on these observations, it is reasonable to formulate the **B** and **B′** complexes as the products of the hypothetical oxidative addition of $SnCl_3$ and HgCl or HgPh groups to the $Rh(pyC)(CO)(PR_3)$ complexes. This interpretation is also supported by the linear relation between ν(C≡O) and the sum of the electron affinities of both groups (Table 3).

Table 3. ν(C≡O) and electron affinities of X and Y in oxidative addition products $(Rh(X)(Y)(pyC)(CO)|P(4\text{-}CH_3C_6H_4)_3|$

X—Y	ν(C≡O) (cm^{-1})	X	EA[a] (eV)	Y	EA[a] (eV)	EA[b] (eV)
CH_3I	2050	I	3.06	CH_3	1.13	4.19
I_2	2085	I	3.06	I	3.06	6.12
Br_2	2097	Br	3.36	Br	3.36	6.72
$HgCl_2$	2033	Cl	3.61	HgCl	−0.34[c]	3.27
		Cl	3.61	HgCl	−0.60[d]	3.01
$HgBr_2$	2053	Br	3.36	HgBr	1.00[c]	4.36
HgI_2	2055	I	3.06	HgI	1.41[c]	4.47
PhHgCl	2065	Cl	3.61	HgPh	1.40[c]	5.01
		Ph	2.21	HgCl	−0.60[d]	1.61[e]
$ClHgSnCl_3$	2050	HgCl	−0.34[c]	$SnCl_3$	4.54[c]	4.20
		HgCl	−0.60[d]	$SnCl_3$	4.80[d]	4.20[d]
$PhHgSnCl_3$	2075	HgPh	1.40[c]	$SnCl_3$	4.54[c]	5.55 (5.94[f])

[a] Electron affinities from *Handbook of Chemistry and Physics* 50th edn E-73. CRC, Cleveland (1970).

[b] Sum of EAs obtained from Fig. 5.

[c] EAs estimated by us from the figure.

[d] EAs estimated by Pregosin *et al.* ref. 23.

[e] EAs obtained if a Ph—HgCl break was supposed.

[f] Sum of EAs estimated by us. The error between this value and that obtained from the figure (0.4 eV) corresponds to an error of 3 cm^{-1} in the ν(C≡O) frequency.

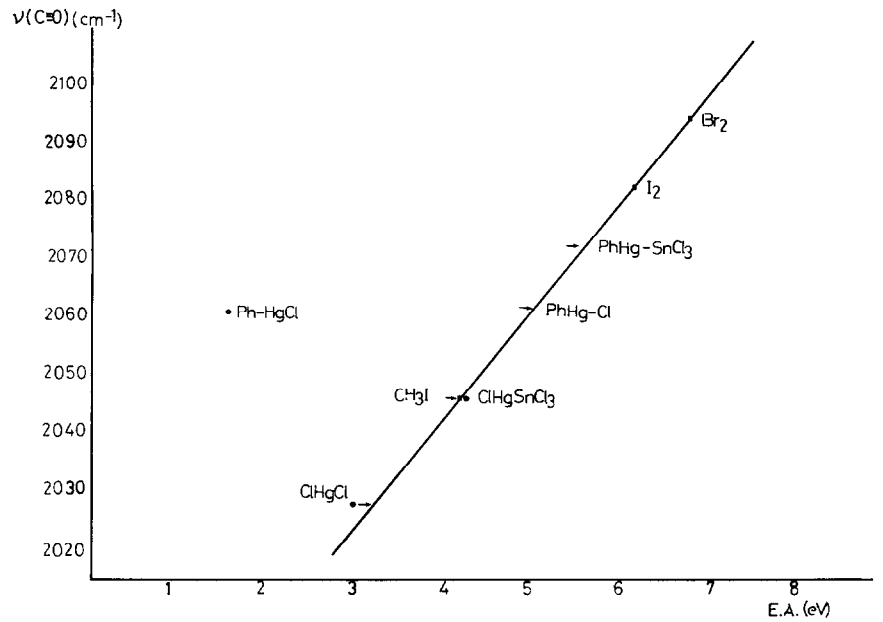

Fig. 3. Linear relation between the ν(C≡O) and the sum of electron affinities values given in Table 3.

Vaska[24] found a singular behaviour of the ν(CO) frequencies on oxidative addition of X—Y molecules, when the addition occurs with breaking of the X—Y bond to form *trans* adducts.[23] For these reactions a linear correlation between the sum of electron affinities (EA) of X and Y and the ν(CO) was found. Using this correlation, Pregosin *et al.*[23] estimated the EAs of $HgCl^+$ and $SnCl_3^-$ groups based on the ν(C≡O) of $IrCl_2(HgCl)(CO)(PPh_3)_2$ and $IrH(SnCl_3)Cl(CO)(PPh_3)_2$, giving values of −0.61 and 4.80 eV, respectively. The sum of these values compares favourably with the estimated values obtained by us in the **B** and **B′** complexes by the correlation shown in Fig. 3.

Also, the sum of the values for electron affinities of HgCl and Cl in the Pregosin complexes, is in good accordance with those estimated by us for the complexes of type **A**. In the same way, the behaviour of the ν(CO) for the addition complexes with PhHgCl is consistent with the addition of PhHg and Cl groups to the rhodium. These facts also support the view that the suggested *trans* addition of (Cl)(HgCl) and (PhHg)(Cl) groups to the complexes $Rh(pyC)(CO)(PR_3)$ really occurs.

The reaction products with $SnCl_2$ can similarly be formulated as the result of a *trans* addition of hypothetical $ClHgSnCl_3$ or $PhHgSnCl_3$ species to the rhodium(I) starting complexes.

^{31}P-*NMR*

The ^{31}P-NMR spectra are a source of information about the coordinated phosphorus ligands. The chemical shifts,[25] and especially, the *J*(Rh—P) coupling constants, are very sensitive to electron density variations on the rhodium atom.

We have recorded the ^{31}P-NMR of Rh(pyC)(CO)(PR_3) complexes in Cl_3CD and C_6D_6, and the data are given in Table 4.

In the case of oxidative addition products with $HgCl_2$, the very low solubility prevents the utilization of this technique, however, we have some results for the complexes with PhHgCl, $HgBr_2$ and some tin derivatives (Table 4). The data indicate that in the starting Rh(pyC)(CO)(PR_3) complexes, the changes in the phosphine ligand, or in the solvent used, cause only a small modification in the coupling constants. In all cases the *J*(Rh—P) are *ca* 160 Hz, representative of Rh^I square-planar complexes.

For the complex with $P(4\text{-}FC_6H_4)_3$, the spectrum exhibits two doublets of almost identical *J*(Rh—P) coupling constant values. Since only one $P(4\text{-}FC_6H_4)_3$ molecule is present, this fact could be attributed to the presence of two isomers. Although the highest *trans* influence of the nitrogen to oxygen in the N—O ligand would be responsible in the formation of only one isomer, we have observed two isomers in related Rh^I complexes with 2-quinaldinate as the N—O ligand, only when the phosphine ligand exhibits a lower basicity.

The observation that the values in *J*(Rh—P) for the addition products with HgX_2 or PhHgCl is lower than in the parent four coordinate complexes, is consistent with an increase in the oxidation state of the rhodium atom.

It is remarkable that in the mercury–tin deriva-

Table 4. ^{31}P-NMR data of some of the obtained complexes[a]

	Complexes	δ_P	J(Rh—P)	Solvent
I	$Rh(pyC)(CO)\|P(4\text{-}CH_3OC_6H_4)_3\|$	35.9 d	160.3	$CDCl_3$
		33.4 d	162.5	C_6D_6
II	$Rh(pyC)(CO)\|P(4\text{-}CH_3C_6H_4)_3\|$	37.7 d	160.6	$CDCl_3$
		38.0 d	163.2	C_6D_6
III	$Rh(pyC)(CO)\|P(4\text{-}FC_6H_4)_3\|$	37.9 d	164.4	$CDCl_3$
		38.0 d	166.1	C_6D_6
VI	$RhBr(HgBr)(pyC)(CO)\|P(4\text{-}CH_3C_6H_4)_3\|\cdot HgBr_2$	30.4 d	121	Acetone
XIII	$RhCl(HgPh)(pyC)(CO)\|P(4\text{-}CH_3OC_6H_4)_3\|$	25.2 d	110.5	$CDCl_3$
XIV	$RhCl(HgPh)(pyC)(CO)\|P(4\text{-}CH_3C_6H_4)_3\|$	27.1	111.1	$CDCl_3$
		27.9	112.3	C_6D_6
XVIII	$Rh(SnCl_3)(HgCl)(pyC)(CO)\|P(4\text{-}CH_3C_6H_4)_3\|$	42.4	111.8	$CDCl_3$
XXII	$Rh(SnCl_3)(HgPh)(pyC)(CO)\|P(4\text{-}CH_3C_6H_4)_3\|$	41.8	139.4	$CDCl_3$
		34.5	136.0	Acetone

[a] 1H decoupled: chemical shifts in ppm downfield from 85%H_3PO_4, coupling constants in Hz.

tives (**B** and **B'**) the coupling constant values exceeded those of the mercuric derivatives (**A** and **A'**). This fact could be attributed to the highest oxidative character of chlorine with respect to $SnCl_3$ ligands. However, the J(Rh—P) is not substantially different for complexes of the types **A** and **B**, and this fact is indicative that the Rh oxidation state hardly varies.

Acknowledgement—We are grateful to the Comision Asesora de Investigación Científica y Técnica (CAICYT, Spain) for financial support (Proyect PR84-0367).

REFERENCES

1. D. L. Kepert and K. Vrieze, In *Comprehensive Inorganic Chemistry* (Edited by J. C. Bailar Jr, H. J. Emeleus, Sir R. Nyholm and A. F. Trotman-Dickenson), Vol. 4, Chap. 47. Pergamon Press, Oxford (1973).
2. Sir G. Wilkinson, F. G. A. Stone and E. W. Abel, (Eds), *Comprehensive Organometallic Chemistry*, Vol. 6, Chaps 40–43. Pergamon Press, Oxford (1982).
3. D. J. Cook, J. L. Dawes and R. D. W. Kemmitt, *J. Chem. Soc. A* 1967, 1547.
4. J. L. Dawes and R. D. W. Kemmitt, *J. Chem. Soc. A* 1968, 1072.
5. J. L. Dawes and R. D. W. Kemmitt, *J. Chem. Soc. A* 1968, 2093.
6. R. S. Nyholm and K. Vrieze, *J. Chem. Soc. A* 1965, 5337.
7. A. R. Sanger, *Can. J. Chem.* 1984, **62**, 822.
8. A. R. Sanger, *Inorg. Chim. Acta* 1985, **99**, 95.
9. J. V. Heras, E. Pinilla and M. Martínez, *Polyhedron* 1983, **2**, 1009.
10. R. Usón, L. A. Oro, M. Sanaú, P. Lahuerta and K. Hildebrand, *J. Inorg. Nucl. Chem.* 1981, **43**, 419.
11. P. D. Brotherton, C. L. Rastón and A. H. White, *J. Chem. Soc., Dalton Trans.* 1976, 1799.
12. A. M. Ciplys, R. J. Gelle and M. Snow, *J. Chem. Soc., Dalton Trans.* 1976, 35.
13. W. H. Morrison Jr and D. N. Hendrickson, *Inorg. Chem.* 1972, **11**, 2912.
14. M. P. Pardo and M. Cano, *J. Organomet. Chem.* 1983, **247**, 293.
15. M. A. Lobo, M. F. Perpiñán, M. P. Pardo and M. Cano, *J. Organomet. Chem.* 1983, **254**, 325.
16. R. Usón, L. A. Oro, M. A. Ciriano and R. González, *J. Organomet. Chem.* 1981, **205**, 259.
17. A. R. Sanger, *J. Chem. Soc., Dalton Trans.* 1977, 120.
18. J. M. Jenkins and B. L. Shaw, *Proc. Chem. Soc.* 1963, 279.
19. J. A. Leipoldt, J. G. Lamprecht and D. E. Graham, *Inorg. Chim. Acta* 1985, **101**, 123.
20. A. J. Growe, R. Hill, P. J. Smith, J. S. Brooks and R. Fornstone, *J. Organomet. Chem.* 1981, **204**, 47.
21. K. M. Mackay and B. K. Nicholson, *Comprehensive Organometallic Chemistry* (Edited by G. Wilkinson, F. G. A. Stone and E. W. Abel), Vol. 6, p. 1092. Pergamon Press, Oxford (1982).
22. R. Usón, L. A. Oro, M. J. Fernández and M. T. Pinillos, *Inorg. Chim. Acta* 1980, **39**, 57.
23. H. K. Kretschmer, P. S. Pregosin, P. Faure and W. Schaepfer, *J. Organomet. Chem.* 1983, **253**, 17.
24. L. Vaska, *Acc. Chem. Res.* 1968, **1**, 335.
25. P. Diechl, E. Pluck and R. Koskelf (Eds), in *Basic Principles and Progress*. Springer, Berlin (1979).

Polyhedron Vol. 8, No. 8, pp. 1093–1097, 1989
Printed in Great Britain

0277-5387/89 $3.00+.00
© 1989 Pergamon Press plc

ENTHALPY OF SUBLIMATION OF ADDUCTS—AN EVALUATION INVOLVING $MX_2 \cdot nL$ (M = Zn, Cd, Hg; X = Cl, Br, I; n = 1, 2, 3; L = ORGANIC BASE CONTAINING CO OR PO GROUPS) ADDUCTS

AÉCIO PEREIRA CHAGAS* and CLAUDIO AIROLDI

Instituto de Química, Universidade Estadual de Campinas, 13081 Campinas (SP), Brazil

(*Received* 30 *August* 1988; *accepted* 11 *November* 1988)

Abstract—The approximation that the molar enthalpy of sublimation of an adduct is equal to the molar enthalpy of sublimation or vaporization of the ligand, has been applied to the calculation of the mean enthalpy of dissociation of the metal–ligand bond, $\bar{D}$(MO), for adducts of the type $MX_2 \cdot nL$ (M = Zn, Cd, Hg; X = Cl, Br, I; n = 1, 2, 3; L = ligand containing PO or CO groups) and for other similar compounds. Based on a thermochemical cycle, a linear equation $\bar{D}(MO) = A\,\Delta_r H(a) + B$ was obtained, with $A = 1/n$ and $\Delta_r H$(a) derived from the enthalpy of the reaction $MX_2 \cdot nL(s) = MX_2(g) + nL(g)$, whose thermochemical value was calculated from experimental data. By using data from nearly 80 compounds and calculating $\bar{D}$(MO) for various approximations, it was verified through linear regression that the cited approximation is the one which correlates the best with the stoichiometries of the compounds. This result is a good argument for the use of this approximation in $\bar{D}$(MO) calculations.

Knowledge of the interactions of metal ions with ligand atoms of nitrogen and oxygen groups is of great importance in the understanding of biological and industrial processes. Thus, a simple illustration is shown by haemoglobin, where the nitrogen atoms of the porphyrin ring hold the iron atom in forming iron–nitrogen bonds. Moreover, the photosynthetic process in green plants is carried out by chlorophyll, which has a magnesium atom centred in a ring, very similar to the porphyrin system. Nitrogen fixation in plants by microorganisms involving enzymes, has as an active centre, the Mo—S—Fe group. DNA polymerase and a series of enzymes, such as carbonic anhydrase, carboxypeptidase A, etc., the so-called zinc enzymes, have an active site on the metal, which is free to accept a pair of electrons from a donor atom of the substrate, leading the reaction to a determined function. Normally, this process is dependent on the formation of a zinc–oxygen bond.[1–3]

These few examples illustrate models of a huge class of enzymes, whose activity can be better understood if the energies involved in the formation or breakage of bonds during the process of the reaction are known. However, there is a shortage of available thermochemical data for such complexes which could be applied to the enzyme. In addition, the majority of these data were obtained in aqueous solution and the suitable energies for metal–ligand interactions should be calculated from gaseous data.[1]

For a less complex system comprising a generic compound $MX_2 \cdot nL$ (M = metal, X = halogen, L = organic ligand), the enthalpy of dissociation in the gaseous phase is given by:

$$MX_2 \cdot nL(g) \longrightarrow MX_2(g) + nL(g). \qquad (1)$$

The enthalpy of this reaction is a measure of the strength of the metal–ligand bond, whose value can be given by:

$$\Delta H(1) = n\bar{D}(MY)$$

where $\bar{D}$(MY) is the mean enthalpy of dissociation of MY, with Y being the donor atom bonded to M.

A thermochemical cycle (Cycle 1) might be established to determine $\Delta H(1)$ or $\bar{D}$(MY) for solid complexes.

* Author to whom correspondence should be addressed.

$$\begin{array}{ccc} MX_2 \cdot nL(g) & \xrightarrow{\Delta H(1)} & MX_2(g) + nL(g) \\ \uparrow \Delta_{sub}H(a) & & \uparrow \Delta_{sub}H(h) \quad \uparrow n\Delta^g_{cd}H(l) \\ MX_2 \cdot nL(s) & \xrightarrow{\Delta H(2)} & MX_2(s) + nL(cd) \end{array}$$

(Cycle 1)

$\Delta H(2)$ is experimentally determined through solution–reaction calorimetry. Normally, $\Delta_{sub}H(h)$ and $\Delta^g_{cd}H(l)$ are determined from various techniques such as calorimetry, vapour pressure measurements, etc. and are available in the literature. The term $\Delta_{sub}H(a)$ is not usually available experimentally, since the adducts are not stable outside of the solid state.

The main purpose of this publication is to further the discussion initiated by Burkinshaw and Mortimer[1,4] and to present some empirical correlations which support the method utilized to determine $\Delta_{sub}H(a)$.

An extra thermodynamic assumption has been used for non-sublimable complexes. In this approximation, it is established that the enthalpy of sublimation of the adduct is equal to the enthalpy of sublimation or vaporization of 1 mol of ligand,[1,5] i.e.: $\Delta_{sub}H(a) = \Delta^g_{cd}H(l)$. The validity of this approximation is shown to be reasonable, as, from the few complexes of this kind which do sublime, the enthalpy values displayed are close to those of the ligand, varying within a 10 kJ mol^{-1} range. (Table 1 lists some examples.) The sparse data show that the assumption is valid within the experimental error. It is concluded that this approximation is valid since the intermolecular forces in the complex and the ligand are very similar; namely, the crystalline structures of the ligand complex remain virtually unchanged.[4]

Table 1. Sublimation enthalpies at 298 K of some adducts and their respective ligands

Compound	$\Delta_{sub}H$ (kJ mol^{-1})	Reference
Cytosine (cyt)	147.2±2.6	4
1-Methylcytosine (mcyt)	141.8±8.8	4
Thiourea (tu)	93.7±10[a]	6
$MnCl_2 \cdot 2cyt$	153±21	4
$CdCl_2 \cdot 2mcyt$	145±20	4
$HgCl_2 \cdot 2mcyt$	159±19	4
$ZnCl_2 \cdot 4tu$	90±20[a]	6
$CdCl_2 \cdot 4tu$	75±20[a]	6
$HgCl_2 \cdot 4tu$	101±20[a]	6

[a] The deviation of ref. 6 was re-evaluated.

Correlations

An interesting thermochemical cycle (Cycle 2) similar to Cycle 1, which is very useful to the acquisition of correlations, is presented below:

$$\begin{array}{ccc} MX_2 \cdot nL(g) & \xrightarrow{\Delta H(1)} & MX_2(g) + nL(g) \\ \uparrow \Delta_{sub}H(a) \quad \nearrow \Delta_rH(a) & & \uparrow \Delta_{sub}H(h) \quad \uparrow n\Delta^g_{cd}H(l) \\ MX_2 \cdot nL(s) & \xrightarrow{\Delta H(2)} & MX_2(s) + nL(cd) \end{array}$$

(Cycle 2)

The application of Hess' law to this cycle gives:

$$\bar{D}(MY) = 1/n[\Delta_rH(a)] + 1/n\Delta_{sub}H(a) \qquad (1)$$

with $\bar{D}(MY) = 1/n\,\Delta H(1)$ and $\Delta_rH(a) = \Delta H(2) + \Delta_{sub}H(h) + n\Delta^g_{cd}H(l)$. All the parameters on the right-hand side of this last equality are experimentally determined and, consequently, $\Delta_rH(g)$ is an exact parameter calculated without approximation. $\bar{D}(MY)$ is calculated from eq. (1), by means of the approximation

$$\Delta_{sub}H(a) = \Delta^g_{cd}H(l). \qquad (A\text{-}1)$$

The experimental and calculated data can be fit to a straight line equation $y = ax + b$, where $y = \bar{D}(MY)$; $a = 1/n$; $X = \Delta_rH(a)$ and $b = 1/n\,\Delta_{sub}H(a)$.

If one considers eq. (1) not as a functional relationship but as a statistical relationship, it makes sense to find a correlation between $\bar{D}(MY)$ and Δ_rH, as indicated by eq. (1) itself. Other approximations can be found to estimate $\Delta_{sub}H(a)$, as will be described further.

The correlation shown in Fig. 1 was obtained from published data, by using the compounds $MX_2 \cdot nL$, with M = Zn, Cd, Hg; X = Cl, Br, I; n = 1, 2 or 3; and L an organic ligand containing a CO or PO group. The compounds and references are in Table 2. Table 3 lists the parameters calculated by the least-squares method.[18]

Taking into account the approximation

$$\Delta_{sub}H(a) = \Delta_{sub}H(h) \qquad (A\text{-}2)$$

used to calculate $\bar{D}(MY)$, the same correlation can be seen in Fig. 2. The parameters obtained are listed in Table 3. Other approximations were also employed:

$$\Delta_{sub}H(a) = [n\Delta^g_{cd}H(l) + \Delta_{sub}H(h)]/n + 1 \qquad (A\text{-}3)$$

and

$$\Delta_{sub}H(a) = \{[\Delta^g_{cd}H(l)]^n\,\Delta_{sub}H(h)\}^{1/n+1}. \qquad (A\text{-}4)$$

In these approximations, the arithmetic and geometric means of the enthalpies of vaporization or sublimation of the ligands and of the halides were

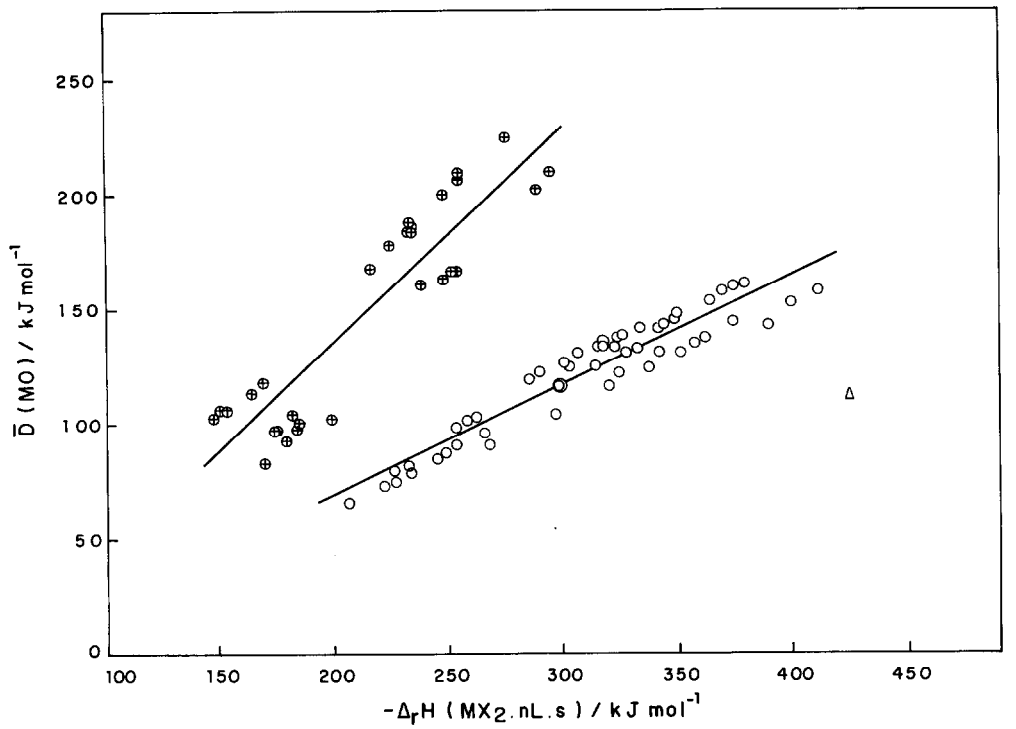

Fig. 1. Correlation between $\bar{D}$(MO) vs $\Delta_r H$(a) for the (A-1) approximation. Compounds with one, ⊕; two, ○; and three, △, metal–oxygen bonds.

Table 2. Compounds used for the correlation between $\bar{D}$(MO) vs $\Delta_r H$(a)

Compound	M	X	Reference	Non-isolated adducts
Compound with one MO bond				
MX_2·dmf	Zn, Cd, Hg	Cl, Br, I	7	HgI_2
MX_2·dma	Cd, Hg	Cl, Br	8, 16	
MX_2·tmu	Cd, Hg	Cl, Br	9	
MX_2·dmu	Cd, Hg	Cl, Br	10	
MX_2·mu	Cd, Hg	Cl, Br	11	
MX_2·ur	Cd, Hg	Cl, Br, I	12	HgI_2
Compound with two MO bonds				
MX_2·2tepo	Zn, Cd, Hg	Cl	13	
MX_2·2tppo	Zn, Cd, Hg	Cl, Br, I	5, 14	
$ZnCl_2$·2tbpo	Zn	Cl	13	
MX_2·2hmpo	Zn, Cd, Hg	Cl, Br, I	15	
MX_2·2dmf	Zn, Cd	Cl, Br, I	7	$CdBr_2$
MX_2·2dma	Zn, Cd	Cl, Br, I	8, 16	$CdCl_2$ and $CdBr_2$
MX_2·da	Zn, Cd	Cl, Br, I	17	
HgX_2·2da	Hg	Cl, Br	17	
MX_2·2tmu	Zn, Cd	Cl, Br, I	9	$CdCl_2$ and $CdBr_2$
MX_2·2dmu	Zn, Hg	Cl, Br	10	$HgBr_2$
ZnX_2·2mu	Zn	Cl, Br	11	
MX_2·2ur	Zn, Cd	Cl, Br, I	12	$CdCl_2$
Compound with three MO bonds				
$CdBr_2$·3dmu	Cd	Br	10	

dmf = N,N-dimethylformamide; dma = N,N-dimethylacetamide; tmu = tetramethylurea; dmu = dimethylurea; mu = methylurea; ur = urea; tepo = triethylphosphineoxide; tppo = triphenylphosphineoxide; tbpo = tribenzylphosphineoxide; hmpo = hexamethylphosphoramide; da = diacetamide.

Table 3. Calculated parameters for the correlations between $\bar{D}$(MO) vs $\Delta_r H$(a) for all approximations [see eq. (1)]

Compound (approximation)	Number of compounds	$1/n$	Number of ligands in $MX_2 \cdot nL$ compounds	$1/n \cdot [\Delta_{sub}H(a)]$	Correlation coefficient
$MX_2 \cdot 2L$(A-1)	52	0.48 ± 0.07	0.5	-26 ± 22	0.9527
$MX_2 \cdot L$ (A-1)	30	0.95 ± 0.19	1	-55 ± 42	0.9116
$MX_2 \cdot 2L$(A-2)	52	0.37 ± 0.07	0.5	-27 ± 22	0.7684
$MX_2 \cdot L$ (A-2)	30	0.15 ± 0.06	1	$+58 \pm 13$	0.4695
$MX_2 \cdot 2L$(A-3)	52	0.46 ± 0.07	0.5	-32 ± 21	0.9518
$MX_2 \cdot L$ (A-3)	30	0.64 ± 0.14	1	-16 ± 29	0.8825
$MX_2 \cdot 2L$(A-4)	52	0.46 ± 0.07	0.5	-31 ± 21	0.9509
$MX_2 \cdot L$ (A-4)	30	0.67 ± 0.14	1	-19 ± 30	0.8973

used. The calculated parameters are given in Table 3.

DISCUSSION

From an inspection of the correlations obtained, it is noted that the best correlation was that of the (A-1) approximation, which reproduced practically all the stoichiometric relationships of the complexes ($1/n = 0.5$) within the estimated standard deviation. The same behaviour was not observed for the (A-2) approximation. Although the (A-3) and (A-4) approximations gave reasonable results, these values are not better than those of the (A-1) approximation. All adducts are metal–oxygen bonded ligands, having halide–ligand stoichiometries in the proportions 1 : 1, 1 : 2 and 1 : 3. With the exception of diacetamide (da), all other ligands are monodentate. Therefore, the above stoichiometries are associated with the presence of one, two or three metal–oxygen bonds in the adducts, respectively. However, for these compounds there are always two metal–oxygen bonds. An interesting conclusion can be extracted from the (A-1) results

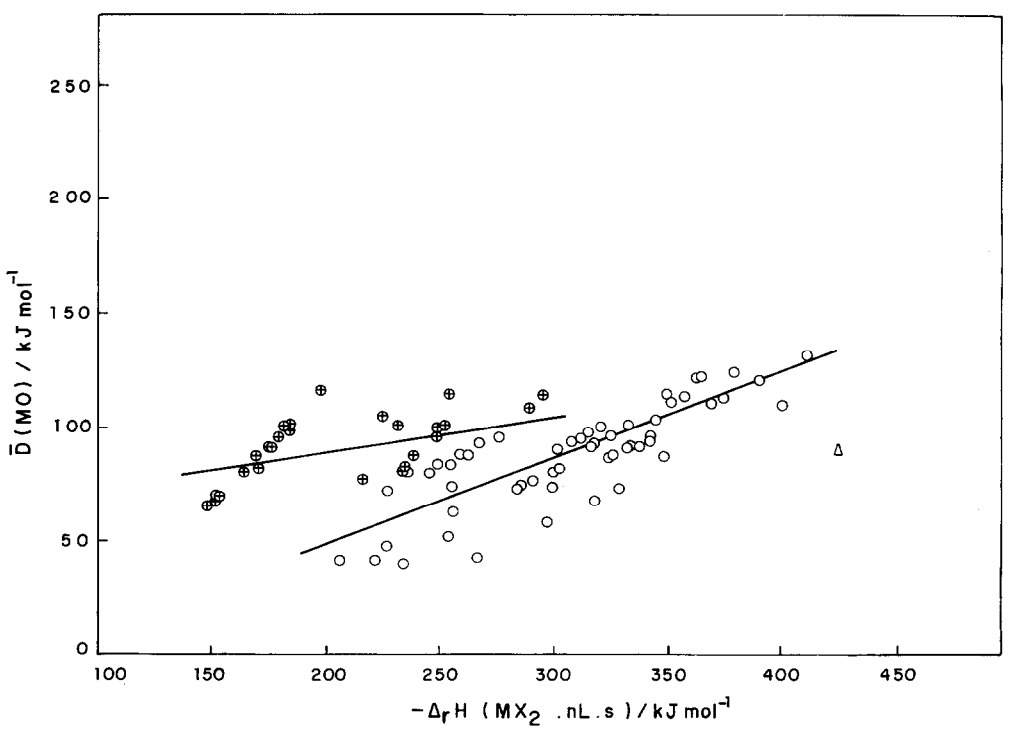

Fig. 2. Correlation between $\bar{D}$(MO) vs $\Delta_r H$(a) for the (A-2) approximation. Compounds with one, ⊕; two, ○; and three, △, metal–oxygen bonds.

Table 4. Some $\bar{D}$(MY) values in $MCl_2 \cdot nL$ compounds

Bond	n[a]	$\bar{D}$(MY)[b] (kJ mol^{-1})	N[c]
ZnO	2	146±10	10
ZnO	1	201	1
ZnN[d]	2	152±1	2
ZnS[e]	4	117	1
CdO	2	142±9	4
CdO	1	178±41	6
HgO	2	101±10	9
HgO	1	92	1

[a] n = number of Y atoms bonded to M, which is the same as number of ligands.

[b] Mean value ± standard deviation.

[c] N = number of compounds utilized for the mean calculation.

[d] References 19 and 20.

[e] Reference 6.

in Fig. 1, which still permit the distinguishing of two separate sets, with one and with two metal–oxygen bonds. However, the tris-adduct is represented as a single point (triangle in Fig. 1). Consequently, the diacetamide compounds are fitted into the two metal–oxygen bonds set. On the other hand, from the (A-2) approximation (Fig. 2) this kind of discernment is not possible, since, there is an overlapping of the plotted points.

All these correlations can be considered as a strong argument in favour of the (A-1) approximation, and certainly the differences and variations in $\bar{D}$(MY) values for all these series of compounds, more than 80, are corrected, except in case of a constant term.

In addition, a summary of the selected values of $\bar{D}$(MY) are given in Table 4, calculated by considering that the (A-1) approximation is valid. This table lists the mean values of bonds for some compounds and the respective standard deviations of the mean. Except for the cadmium–oxygen bond ($n = 1$), the standard deviation of the mean is of the order of the quantity of the calculated values of $\bar{D}$(MY), estimated as ±8 kJ mol^{-1}. Note also that, in general, $\bar{D}$(MY, $n = 1$) is bigger than half of $\bar{D}$(MY, $n = 2$), characterizing a competitive interaction between the halide and ligand. For comparison, $\bar{D}$(ZnN) and $\bar{D}$(ZnS) values are also included. An inspection of $\bar{D}$(MY) values (Table 4) suggests the sequence: Zn ≃ Cd > Hg for the mean enthalpy of the metal–ligand bond.

REFERENCES

1. P. M. Burkinshaw and C. T. Mortimer, *Coord. Chem. Rev.* 1983, **48**, 101.
2. M. A. V. R. da Silva (Ed.), *Thermochemistry and its Applications to Chemical and Biochemical Systems*. D. Reidel, Dordrecht, Holland (1984).
3. R. J. P. Williams, *Polyhedron* 1987, **6**, 61.
4. P. M. Burkinshaw and C. T. Mortimer, *J. Chem. Soc., Dalton Trans.* 1984, 75.
5. R. A. Jorge, C. Airoldi and A. P. Chagas, *J. Chem. Soc., Dalton Trans.* 1978, 1102.
6. S. J. Ashcroft, *J. Chem. Soc. A* 1970, 1020.
7. O. A. de Oliveira, A. P. Chagas and C. Airoldi, *Inorg. Chem.* 1983, **22**, 136.
8. J. de A. Simoni, A. P. Chagas and C. Airoldi, *J. Chem. Soc., Dalton Trans.* 1980, 156.
9. C. Airoldi, A. P. Chagas and F. P. Assunção, *J. Chem. Soc., Dalton Trans.* 1980, 1823.
10. F. P. Assunção, A. P. Chagas and C. Airoldi, *J. Chim. Phys.* 1982, **79**, 253.
11. F. P. Assunção, A. P. Chagas and C. Airoldi, *Can. J. Chem.* 1982, **60**, 2132.
12. M. R. M. C. Santos and C. Airoldi, *Thermochim. Acta* 1988, **125**, 295.
13. J. C. Queiroz, C. Airoldi and A. P. Chagas, *J. Inorg. Nucl. Chem.* 1981, **43**, 1207.
14. J. C. Queiroz, C. Airoldi and A. P. Chagas, *J. Chem. Thermodyn.* 1986, **18**, 709.
15. J. C. Queiroz, C. Airoldi and A. P. Chagas, *J. Chem. Soc., Dalton Trans.* 1985, 1103.
16. J. de A. Simoni, C. Airoldi and A. P. Chagas, *An. Acad. Brasil. Ciênc.* 1983, **55**, 254.
17. C. Airoldi, A. P. Chagas and M. Namora Fo., *J. Inorg. Nucl. Chem.* 1981, **43**, 89.
18. G. L. Squires, *Practical Physics*. McGraw-Hill, London (1968).
19. C. Airoldi, M. L. C. P. Silva and A. P. Chagas, *J. Chem. Soc., Dalton Trans.* 1986, 1913.
20. A. V. Ablov, Z. P. Burnasheva and T. B. Konunova, *Russ. J. Inorg. Chem.* 1965, **10**, 1243.

Polyhedron Vol. 8, No. 8, pp. 1099–1102, 1989
Printed in Great Britain

0277–5387/89 $3.00+.00
© 1989 Pergamon Press plc

IDENTIFICATION OF A LOWEST EXCITED STATE IN THE $Cr(CO)_5PBu_3$ COMPLEX

C. DÍAZ† and N. YUTRONIC

Department of Chemistry, Faculty of Sciences, University of Chile, Casilla 653, Santiago, Chile

(*Received* 5 *October* 1988; *accepted* 11 *November* 1988)

Abstract—Electronic absorption data are reported for the $Cr(CO)_5PBu_3$ complex. The absorption band at the lowest energy value is assigned to a metal → ligand charge-transfer transition (MLCT) on the basis of the solvent effect. Data for this effect on $M(CO)_5PBu_3$ (M = Mo and W) are also discussed.

The UV–vis absorption spectra of the $M(CO)_5L$ complexes (M = Cr, Mo and W, L = neutral donor ligand) have been extensively studied.[1–4] The lowest absorption energy in these compounds has been assigned to the ligand field transition $^1A(e^2b_2^2) \rightarrow {}^1E(e^1b_2^2a_1^1)$.[4,5] As we have shown recently,[4] this transition is sensitive to the π-acceptor ability of the L ligand. For phosphine ligands, the band corresponding to this transition appears in the range 310–360 nm[6] and hence the compounds $M(CO)_5PR_3$ are generally colourless or pale yellow.[7,8] In contrast to this, the $Cr(CO)_5PBu_3$ complex presents a strong red-wine (Chartreuse) colour, suggesting an unusual absorption behaviour.

In this article we discuss the assignment of the absorption band at the lowest energy for the $Cr(CO)_5PBu_3$ complex using solvent effect. Data for the $M(CO)_5PBu_3$ complexes are also reported.

RESULTS AND DISCUSSION

In Fig. 1 the absorption spectrum of $Cr(CO)_5PBu_3$ in *n*-hexane is shown. Evidently the band at 555 nm explains the red colour of the complex. This band shows a characteristic displacement to higher energy as the polarity of the solvent is increased (Table 1). The band moves within a range of 85 nm on going from *n*-hexane to acetonitrile, as is shown in Fig. 2.

For the hydroxylic solvents, in addition to the polarity effects, hydrogen bond interactions must also be considered. From Table 1, a displacement

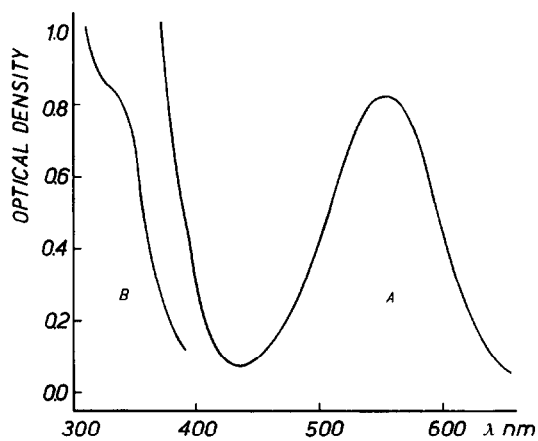

Fig. 1. Absorption spectra of $Cr(CO)_5PBu_3$ in *n*-hexane solution; curve (B) is a diluted sample.

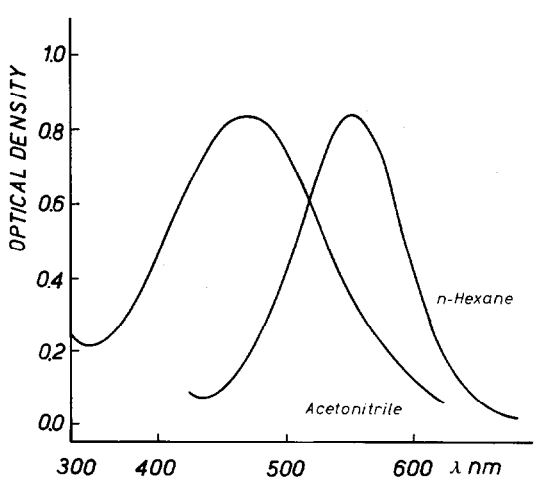

Fig. 2. Solvent dependence of the low-energy absorption band of $Cr(CO)_5PBu_3$.

† Author to whom correspondence should be addressed.

Table 1. Solvent[a] dependence of electronic absorption bands of $M(CO)_5PBu_3$ complexes

Complex	Solvent	Dielectric constant[b]	λ_{max} MLCT	λ_{max} LF
$Cr(CO)_5PBu_3$	*n*-Hexane	1.9	555	332 (sh)
	Chloroform	4.8	528	
	Chlorobenzene	5.7	523	
	t-Butanol	1.5	520	
	n-Butanol	17.5	516	
	Acetone	20.7	495	
	Ethanol	34.6	508	
	Acetonitrile	37.5	470	328 (sh)
$W(CO)_5PBu_3$	*n*-Hexane	1.9	427	351
	Acetonitrile	37.5	419 (sh)	350
$Mo(CO)_5PBu_3$	*n*-Hexane	1.9	< 350[c]	350
	Acetonitrile			350

[a] At room temperature; λ in nm; MLCT and LF designate the $M \rightarrow PBu_3$ charge-transfer and ligand field absorption, respectively; sh: shoulder.
[b] Dielectric constant values from ref. 24.
[c] Probably hidden under $M \rightarrow (CO)^*$MLCT.

to higher energy is observed for alcohol solvents. This can be understood by considering the limiting structures **I** and **II** given below, usually applied to describe carbonyl compounds:

$$O{=}C{=}M{-}L \qquad \overset{\delta+}{O}{\equiv}C{-}M{-}\overset{\delta-}{L}.$$
(I) **(II)**

Hydroxylic solvent should stabilize the oxygen lone pair electron in the carbonyl ground state through structure **I**, by hydrogen bonding:

$$\begin{matrix} & & H\cdots O{=}C{=}M{-}PR_3. \\ RO & \diagup & \end{matrix}$$

The solvent dependence is comparable to the shift of 59 nm observed for the lowest CTML transition in $Cr(CO)_5(RN{=}NR)$ complexes[9] on substituting *n*-hexane for acetonitrile. Thus, the transition is strongly dependent on the metal; for the $M(CO)_5PBu_3$ complexes, see Table 1, the energy varies in the order Mo > W > Cr, the behaviour is similar to that observed for the lowest absorption band in the complexes, $M(CO)_5(RN{=}NR)$[9] and $M(CO)_4$(1,10-phen).[10]

† Although this band has a low extinction coefficient ($\varepsilon = 302$), it can be assigned to a charge-transfer transition. These bands are generally, but not always very intense. For instance rhodium(I) and iridium(I) complexes exhibit charge-transfer transitions of relatively low intensity (see refs 11 and 12).

On the basis of the above observations we have assigned the lowest energy band in the solution spectra of $Cr(CO)_5PBu_3$ to a metal–ligand charge-transfer transition.†

The next lowest energy absorption band observed as a shoulder in the spectra of $Cr(CO)_5PBu_3$ is only slightly influenced by the polarity of the solvent (see Fig. 1 and Table 1). This behaviour is typical of *d–d* bands as observed for other complexes.[9] Thus, we have estimated a value of $\lambda = 328$ nm for the ligand field transition from the relation $\varepsilon_{max} = -137.7\pi + 407.2$ valid for *d–d* transition in $Cr(CO)_5L$ complexes.[4] This value is very close to that observed in Fig. 1 at $\simeq 332$ nm. Therefore, it is possible to assign this absorption band to a metal centred $d_{yz,xz} \rightarrow d_{x^2-y^2,z^2}$ transition. For the complexes, $M(CO)_5PBu_3$ (M = Mo and W), this band is observed at about 350 nm and shows no shift by solvent effects.

Now the question is why $Cr(CO)_5PBu_3$ exhibits a lowest excited state that is not observed in other $Cr(CO)_5PR_3$ compounds. Comparison of IR,[7,8] ^{31}P NMR[8] and ESCA[13] spectral data of tributylphosphine chromium complexes with other alkylphosphine complexes does not reveal significant differences that could be used to explain such behaviour. The steric effect of PR_3 appears not to be related to the absorption differences mentioned above; the steric parameter of Tolman[14] for PBu_3 and other phosphines such as PMe_3, PEt_3, PPr_3, etc. are similar. Nonetheless, we have noted that tributylphosphine is a much stronger σ-

donor than trimethylphosphine, triethylphosphine and other alkylphosphines. This is also evidenced by Valence Photoelectron Spectroscopy,[15] as well as by ^{95}Mo NMR spectroscopy of $Mo(CO)_{5-n}(PR_3)_n$ complexes.[16] Also, the ionization potential of the free phosphine ligands is consistent with PBu_3 having a higher donor ability than PR_3 ($R = C_2H_5$, C_6H_5, CH_3, H) and PX_3 compounds ($X = OC_2H_5$, OC_4H_9, OCH_3, Br, Cl, F).[17]

The fact that alkylphosphines have a weaker donor ability than PBu_3 can considerably affect the energy of the metal–ligand antibonding orbitals. Figure 3 shows a partial view of MO levels for the C_{4v} $M(CO)_5L$ complexes;[9,18,19] the levels are labelled according to their metal *d* orbital character. The greatest donor ability of PBu_3 should destabilize the a_1 MO. The π^*-level indicated in the diagrams, has a higher energy than the a_1 and b_1 MOs in the majority of the $M(CO)_5L$ complexes.[9,20] However, when the L ligand has a low energy vacant orbital, this π^*-level decreases in energy in some cases[20] to the level between the *e*, b_2 and b_1, a_1 orbitals. For the $Cr(CO)_5PBu_3$ complex, a low energy π^*-level is postulated as is shown in Fig. 3. This level probably arises from contributions of filled metal *d* orbitals and the LUMO of tributylphosphine. Comparison of ionization data,[17,18] as well as theoretical studies[21,22] for PX_3, PH_3, PR_3 (R = other than butyl) with those of PBu_3, certainly suggests that the LUMO of tributylphosphine may have a lower energy. In the $Cr(CO)_5PR_3$ ($R \neq n$-Bu) and $Cr(CO)_5PX_3$ compounds, the LUMO of the phosphorus compounds is too high in energy[18] and hence a low energy π^*-state is not possible. In fact the pentacarbonylchromium complexes with PR_3 ($R \neq n$-Bu) and PX_3 ligands[5,6] do not absorb above 360 nm.

The lowest energy excited state in the $Cr(CO)_5PBu_3$ complex also should be π^*-(CO) in nature, but this is improbable because the Cr → (CO)* charge-transfer transition for complexes $Cr(CO)_5L$ (L = N donor, P donor) appears in the range 220–290 nm.[5,6]

With regard to the current interest in low-lying MLCT states of transition metal compounds, we note that the $Cr(CO)_5PBu_3$ complex constitutes the fourth class of the compound type $M(CO)_5L$ having MLCT lowest excited states.

The other examples known are $W(CO)_5$(4-R-pyridine),[20] $Cr(CO)_5ArC(OCH_3)$[23] and $M(CO)_5$(RN=NR).[9]

EXPERIMENTAL

Preparation of $Cr(CO)_5PBu_3$

A solution of 3 mmol $Cr(CO)_6$ in *ca* 60 cm^3 of THF was irradiated (UV lamp Hanau medium pressure 150 W) for 90 min at room temperature. A solution of 3 mmol of tributylphosphine in *ca* 20 cm^3 of THF was then added and the mixture stirred for 20 min. After removing the solvent under reduced pressure, the excess of hexacarbonyl was sublimed from the residue *in vacuo* at room temperature. The oily residue was then redissolved in an *n*-pentane–benzene mixture (10 : 1), filtered through kieselguhr, and the solvent evaporated *in vacuo*. The product obtained was a wine-red liquid. Found: C, 52.2; H, 7.6. Calc. for $C_{17}H_{27}O_5PCr$; C, 51.8; H, 6.8%. ^1H NMR; $\delta_H(CCl_4$, from TMS) 1.0 (3H, m, CH_3), 1.6 (6H, m, $(CH_2)_3$). IR: ν(CO) *n*-hexane

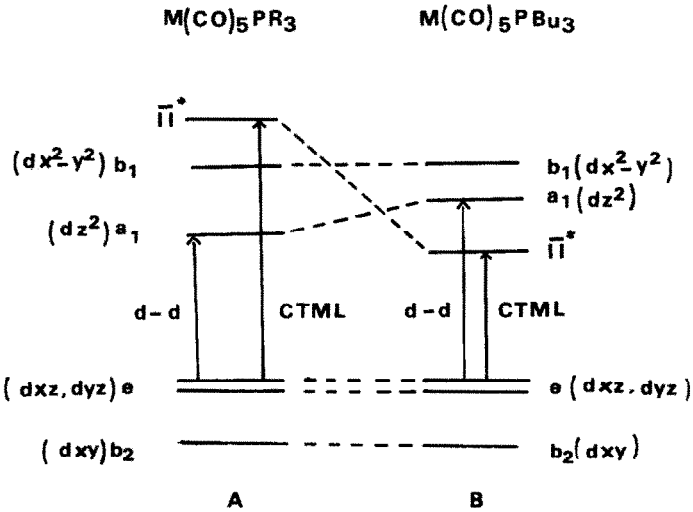

Fig. 3. Partial MO diagram for $Cr(CO)_5PBu_3$ complexes: (A) L = PR_3, (B) L = PBu_3.

solution 2061 s (A_1^2), 1985 vw (B_1), 1944 vs, 1930 vs (E), 1915 m,sh (A_1^1); δ(MCO) 671 s (E), 650 s (A_1). The main bands in the ligand region (liquid between plates) were 2960 vs, 2937 vs, 2878 vs, 1460 s, 1416 m, 1089 m, 905 m, 790 w, 770 w, 718 m. For comparison, the spectral data for the free tributylphosphine are: ^{1}H NMR: δ_H 0.96 (3H, m, CH_3); 1.55 (6H, m $(CH_2)_3$). IR: 2959 vs, 2924 vs, 2878 vs, 1465 s, 1415 m, 1091 m, 895 m, 785 w,br, 721 m.

The $M(CO)_5PBu_3$ complexes (M = Mo, W) were prepared in a similar way and their ^{1}H NMR and IR spectral properties were in agreement with those cited in the literature for authentic samples.[8] UV–vis absorption spectra were recorded with Cary 17 and Varian-DMS 90 spectrophotometers.

Acknowledgement—Financial support received by Departamento Técnico de Investigación of Universidad de Chile is gratefully acknowledged.

REFERENCES

1. M. Wrighton, *Chem. Rev.* 1974, **74**, 401.
2. M. S. Wrighton, D. L. Morse, H. B. Gray and D. K. Ottesen, *J. Am. Chem. Soc.* 1976, **98**, 1976.
3. G. Boxhoorn, A. Oskam, E. P. Gibson, R. Narayaswamy and A. J. Rest, *Inorg. Chem.* 1981, **20**, 783.
4. C. Díaz and N. Yutronic, *Polyhedron* 1987, **6**, 503.
5. G. Boxhoorn, D. J. Studkens, P. J. P. Coolwijk and A. M. F. Hazemans, *Inorg. Chem.* 1981, **20**, 2778.
6. N. Yutronic, *XVII Congreso Latinoamer. Quím.*, Colombia, Bogotá, Res. P-CI-285-B3.
7. T. A. Magee, C. N. Matthews, T. Seng Wang and J. Wotiz, *J. Am. Chem. Soc.* 1961, **83**, 3200.
8. S. O. Grim, D. A. Wheatland and W. McFarlane, *J. Am. Chem. Soc.* 1967, **89**, 5573.
9. C. C. Frazier III and H. Kisch, *Inorg. Chem.* 1978, **17**, 2737.
10. M. S. Wrighton and D. Morse, *J. Organomet. Chem.* 1975, **97**, 405.
11. G. L. Geoffroy, M. S. Wrighton, G. S. Hammond and H. B. Gray, *J. Am. Chem. Soc.* 1974, **96**, 3105.
12. R. Brady, B. R. Flynn, G. L. Geoffroy, H. B. Gray, J. Peone and L. Vaska, *Inorg. Chem.* 1977, **15**, 1485.
13. W. S. Mialki and R. A. Walton, *Inorg. Chem.* 1982, **21**, 2791.
14. C. A. Tolman, *Chem. Rev.* 1977, **77**, 313.
15. B. E. Burstein, D. J. Darensbourg, G. E. Kellogg and D. I. Lichtenberger, *Inorg. Chem.* 1984, **23**, 4361.
16. E. C. Alyea, R. E. Lenkinski and A. Somogyvari, *Polyhedron* 1982, **1**, 130.
17. G. Distefano, G. Innorta, S. Pignataro and A. Foffani, *J. Organomet. Chem.* 1968, **14**, 165.
18. L. W. Yarbrough and M. B. Hall, *Inorg. Chem.* 1978, **17**, 2269.
19. T. F. Block, R. F. Fenske and Ch. P. Casey, *J. Am. Chem. Soc.* 1976, **98**, 441.
20. M. S. Wrighton, H. B. Abrahamson and D. L. Morse, *J. Am. Chem. Soc.* 1976, **98**, 4105.
21. I. H. Hillier and V. R. Saunders, *J. Chem. Soc. A* 1970, 2457.
22. I. H. Hillier and V. R. Saunders, *Trans. Faraday Soc.* 1970, **66**, 2401.
23. E. O. Fisher, H. J. Kollmeier, G. C. Kreiter, J. Muller and D. R. Fisher, *J. Organomet. Chem.* 1970, **22**, C39.
24. T. R. Griffiths and D. C. Pugh, *Coord. Chem. Rev.* 1970, **29**, 129.

Polyhedron Vol. 8, No. 8, pp. 1103–1109, 1989
Printed in Great Britain

0277–5387/89 $3.00+.00
© 1989 Pergamon Press plc

COPPER(I) BROMIDE COMPLEXES WITH HETEROCYCLIC THIONES AND TRIPHENYLPHOSPHINE AS LIGANDS. THE X-RAY CRYSTAL STRUCTURE OF COPPER(I) PYRIMIDINE-2-THIONE BIS (TRIPHENYLPHOSPHINE) BROMIDE [$Cu(PPh_3)_2$(PymtH)Br]

C. LECOMTE* and St. SKOULIKA

Laboratoire de Minéralogie et Cristallographie (UA n° 809), Faculté des Sciences, Centre de 2ème Cycle, B.P. n° 239, 54506 Vandoeuvre les Nancy, France

and

P. ASLANIDIS, P. KARAGIANNIDIS* and St. PAPASTEFANOU

Laboratory of Inorganic Chemistry, Department of Chemistry, Aristotle University of Thessaloniki, Thessaloniki, Greece

(*Received* 19 *October* 1988; *accepted* 11 *November* 1988)

Abstract—Reactions of copper(I) bromide with heterocyclic thiones (L) [L = pyridine-2-thione (py2SH), pyridine-4-thione (py4SH), pyrimidine-2-thione (pymtH), 1,3-thiazolidine-2-thione (tzdtH), 1-methyl-1,3-imidazoline-2-thione (meimtH), benz-1,3-imidazoline-2-thione ($bzimtH_2$), benz-1,3-oxazoline-2-thione (bzoxtH), 5-nitro-2-benz-1,3-imidazoline-2-thione ($nbzimtH_2$), benz-1,3-thiazoline-2-thione (bztzH) and quinazolinone-2-thione ($qnotH_2$)] in the presence of triphenylphosphine yields mononuclear complexes of the general formula $[Cu(L)(PPh_3)_2Br]$. The complexes have been characterized by elemental analysis, IR, UV-vis and NMR spectroscopy. The crystal structure of $[Cu(PPh_3)_2$(pymtH)Br] has been determined by single-crystal X-ray diffraction methods. The yellow–orange crystals are monoclinic, space group $P2_1/n$ with $a = 13.035(2)$, $b = 43.660(9)$, $c = 13.446(2)$ Å, $\beta = 90.68(2)°$, and $D_{calc} = 1.352$ g cm^{-3}, $V = 7652$ Å^3, $R(F) = 0.067$; $R_w(F) = 0.069$, $GOF = 1.19$. In both molecules of the asymmetric unit, the pymtH molecule acts as a monodentate ligand through the S atom (Cu—S = 2.352(3) Å).

Heterocyclic thiones as ligands are potentially ambidentate or multi-functional donors with either the exocyclic S or heterocyclic N (or S or O) atom available for coordination.[1] The aim of the present paper is to further our present knowledge in the field of these ligands which exhibit a thione–thiol (—N=C—SH ⇋ —NH—C=S) equilibrium. Recently, the complexing properties of these ligands with copper(I) in the presence of triphenylphosphine have been studied, and a variety of interesting complexes (monomeric or dimeric) with the thione ligands acting as S-donors have been obtained.[2,3] More recently, monomeric complexes formulated as $[Cu(PPh_3)_2(L)_2]NO_3$ have been obtained via a simple method of preparation by direct reaction of $Cu(PPh_3)_2NO_3$ with the ligands investigated.[4] As a part of the examination of the ligation behaviour of these ligands, we report in this paper the preparation and characterization of a series of mononuclear Cu^I complexes of general formula $[Cu(PPh_3)_2(L)Br]$.

EXPERIMENTAL

Physical measurements

Elementary analyses were performed on a Perkin–Elmer 240 B elemental analyser. IR spectra

* Authors to whom correspondence should be addressed.

Table 1. Experimental conditions

Formula	$CuBrSP_2N_2C_{40}H_{33}$
Formula weight	778.9
Space group	Monoclinic $P2_1/n$
Lattice parameters	$a = 13.035(2)$ $b = 43.660(5)$ $c = 13.446(2)$ Å
	$\beta = 90.68(2)°$ $V = 7651.7$ Å^3 $Z = 8$ $\rho_{cal} = 1.352$ g cm^{-3}
Diffractometer	Enraf–Nonius CAD4F (room temp)
Radiation	Cu-K_α $\lambda = 1.54051$ Å
Scan type θ_{min}–θ_{max}	ω–2θ 1–70°
Scan range, speed	$1+0.45\tan\theta$ $0.5 < v < 2°$ min^{-1}
Aperture, mm	4
hkl limits	$-15 < h < 14$ $0 < k < 49$ $0 < l < 16$
Number of reflections measured	15120
Number of reflections used $I > 2\sigma(I)$	$N = 6998$
Number of parameters N_p	836
N/N_p	8.3
Program used	SDP,[5] SHELX,[6] PLUTO[5]
$R(F)$, $R_w(F)$, *GOF*	0.067; 0.069; 1.16
w	$[\sigma^2_{count}+0.0025F^2]^{-1}$

were recorded in the 4000–250 cm^{-1} region on a Perkin–Elmer 467 spectrophotometer using KBr pellets. Electronic spectra in chloroform solutions were obtained on a Cary 17 DX spectrophotometer. NMR spectra were recorded on a Brucker AW 80 spectrometer. Conductivity measurements were taken in a Wheatstone bridge Model RC 216 B2 using 10^{-3} M solutions in acetonitrile or chloroform. Melting points were determined with a Büchi apparatus and are uncorrected. Magnetic susceptibility measurements were taken employing the Faraday technique at different magnetic field strengths. $Hg[Co(SCN)]_4$ was used as the calibrand.

Starting materials

All thione ligands, supplied by EGA or Aldrich, were purified by recrystallization from ethanol. Anhydrous copper(I) bromide, triphenylphosphine and all solvents were of reagent grade and were used without further purification in synthetic work.

Preparation of the complexes

CuBr (1 mmol) was suspended in 10 cm^3 THF and treated with a 40 cm^3 solution of 1 mmol of the appropriate ligand and 2 mmol PPh_3 in the same solvent. The reaction mixture was stirred for 1 h at 40°C, filtered and cooled to room temperature. Slow evaporation of the solvent at room temperature gave a microcrystalline solid, which was filtered off, washed with ethanol and ether and dried *in vacuo*. The yield in this procedure was about 65–85%.

Crystal and molecular structure determination

A suitable crystal of $[Cu(PPh_3)_2(PymtH)Br]$ was obtained from recrystallization of the complex in THF. Preliminary Weissenberg photographs revealed a monoclinic cell and systematic conditions (*h*0*l*: $h+l = 2n$, 0*k*0: $k = 2n$) led to space group $P2_1/n$. The experimental conditions are given in Table 1. The scattering factors were taken from refs 6 and 7. The structure was solved by the heavy atom method by interpretation of the Patterson map and was refined by standard least-squares and Fourier techniques. Due to thermal motion or disorder problems, the C(31)—C(36) phenyl ring was refined as a rigid group; all the coordinates of the hydrogen atoms linked to the carbon atoms were calculated and kept fixed during the refinement process. The two N—H hydrogen atom coordinates used were those found in the difference Fourier map in order to distinguish between the two nitrogens of the pyrimidine ring. Main bond distances and angles are given in Table 2. Fractional coordinates, standard deviations, equivalent temperature factors, anisotropic thermal parameters of the atoms, least-squares planes, other bond lengths and structure factors have been deposited as supplementary material with the Editor from whom copies are available on request.*

RESULTS AND DISCUSSION

Recently, the mononuclear complex, $[Cu(PPh_3)_2(py2SH)Br]$, has been isolated by the reaction

*Atomic coordinates have also been deposited with the Cambridge Crystallographic Data Centre.

Table 2. Main bond distances (Å) and angles (°)

Molecule 1		Molecule 2	
Distances			
Cu(1)—Br(1)	2.519(1)	Cu(2)—Br(2)	2.512(2)
Cu(1)—S(1)	2.345(3)	Cu(2)—S(2)	2.359(3)
Cu(1)—P(1)	2.303(2)	Cu(2)—P(3)	2.304(3)
Cu(1)—P(2)	2.306(2)	Cu(2)—P(4)	2.267(3)
S(1)—C(37)	1.695(8)	S(2)—C(79)	1.68(1)
P(1)—C(1)	1.820(8)	P(3)—C(43)	1.80(1)
P(1)—C(7)	1.825(8)	P(3)—C(49)	1.829(9)
P(1)—C(3)	1.815(8)	P(3)—C(55)	1.822(9)
P(2)—C(19)	1.826(9)	P(4)—C(61)	1.80(1)
P(2)—C(25)	1.822(9)	P(4)—C(67)	1.83(1)
P(2)—C(31)	1.820(8)	P(4)—C(73)	1.817(8)
C(37)—N(1)	1.33(1)	C(79)—N(3)	1.35(1)
N(1)—C(39)	1.31(1)	N(3)—C(81)	1.33(2)
C(39)—C(40)	1.37(1)	C(81)—C(82)	1.35(2)
C(40)—C(41)	1.33(1)	C(82)—C(83)	1.32(2)
C(41)—N(2)	1.34(1)	C(83)—N(4)	1.38(1)
N(2)—C(37)	1.34(1)	N(4)—C(79)	1.36(1)
Angles			
Br(1)—Cu(1)—P(1)	108.0(1)	Br(2)—Cu(2)—P(3)	101.1(1)
Br(1)—Cu(1)—P(2)	111.0(1)	Br(2)—Cu(2)—P(4)	107.1(1)
Br(1)—Cu(1)—S(1)	108.2(1)	Br(2)—Cu(2)—S(2)	110.5(1)
P(1)—Cu(1)—P(2)	112.9(1)	P(3)—Cu(2)—P(4)	124.3(1)
P(1)—Cu(1)—S(1)	106.5(1)	P(3)—Cu(2)—S(2)	106.1(1)
P(2)—Cu(1)—S(1)	110.0(1)	P(4)—Cu(2)—S(2)	107.3(1)
Cu(1)—S(1)—C(37)	114.6(3)	Cu(2)—S(2)—C(79)	108.6(4)

of $Cu(PPh_3)_3Br$ with $Zr(py2S)_4$ in THF.[3] However, we report in this study a more simple and general method for the preparation of such complexes, namely, the reaction between the heterocyclic thiones and a 1 : 2 mixture of CuBr and PPh_3. Table 3 lists the compounds with their colours, melting points and analytical data. The results of the elemental analyses for all complexes show good agreement with the formula $[Cu(PPh_3)_2(L)Br]$. The magnetic susceptibility measurements at room temperature indicate that the complexes are diamagnetic, consistent with a d^{10} configuration. They can be handled in air without evident decomposition, decompose slowly in water, are soluble in chloroform, acetone and acetonitrile, slightly soluble in methanol and benzene but insoluble in ether. Their conductivity measurements in chloroform or acetonitrile show, as expected, a non-electrolytic nature.

Description of the crystal structure

A stereographic projection of the two molecules of the asymmetric unit is given in Fig. 2. Figure 1 is a PLUTO drawing of the molecule with the numbering scheme used for the main atoms. In both molecules the Cu atom is four-coordinated by a bromide atom, two triphenylphosphine ligands and one monodentate pymtH molecule coordinating through the sulphur atom; the Cu—L bond lengths in both molecules are similar (Table 2). However, the coordination polyhedra of both molecules of the asymmetric unit are different due to the P—Cu—P coordination angles: The Cu(1) coordination polyhedron is close to a regular tetrahedron ($106.5 \leqslant L—Cu—L' \leqslant 112.9°$), whereas in the Cu(2) polyhedron, the $P_3—Cu_2—P_4$ angle is 124.3(1)°. This demonstrates the flexibility of these coordination angles in this class of compounds. However, all these angles fall within the range reported for other tetrahedral complexes of copper(I).[8–12] A possible explanation for the large value of the $P_3—Cu—P_4$ angle is the π–π interaction between the phenyl ring C(49)···C(54) and the pymtH ($N_3 \cdots N_4$) entity: the angles between their least-squares planes is 16° and the distances of atoms C(51), C(50), C(49), C(52) are, respectively, 3.04, 3.02, 3.35 and 3.34 Å from the pymtH plane.

The average Cu—S bond length is 2.352 Å as usually found for tetrahedrally coordinated copper(I) complexes with thione–sulphur donors.[4,13]

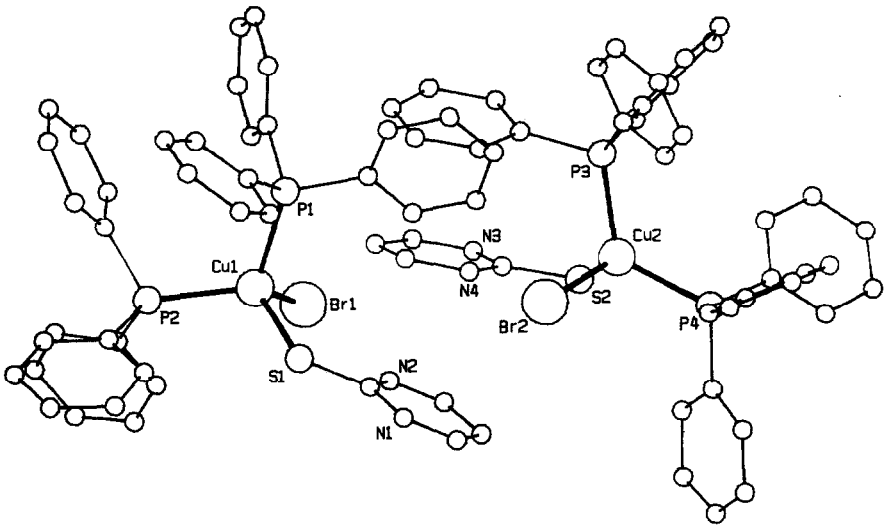

Fig. 1. PLUTO drawing of the two molecules of the asymmetric unit.

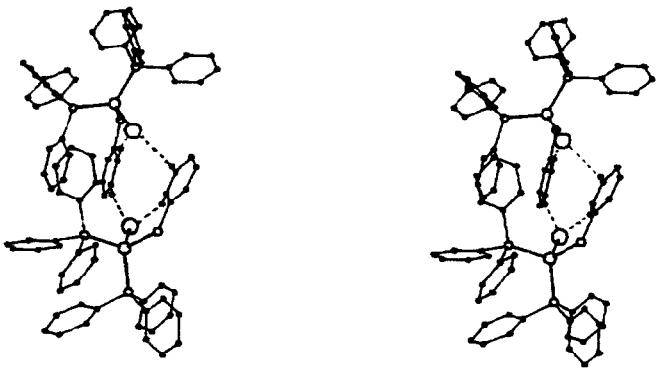

Fig. 2. ORTEP stereoview of the molecules.

The Cu—P bond lengths are normal (see, for example refs 4, 14, 15). The average Cu—Br bond lengths of 2.515 Å are significantly longer than those observed in $Cu(PPh_3)_3Br$ (2.35 Å).[15] Moreover, it is slightly longer than the corresponding Cu—Br distance of 2.462 Å in $Cu(PPh_3)_2$ (py2SH)Br_3, and it compares well with that found in $(TTTCu_2Br_4)$[16] (TTT = tetrathiotetracene) (2.490 Å) and in $[Cu(PPh_3)Br]_4$[17] (2.495 Å).

Hydrogen bonds and intermolecular contacts

As described in the Experimental section, the hydrogen atoms linked to N_2 and N_4 were found in difference Fourier maps and no peak at a distance of about 1 Å of N_1, N_3 was visible. Furthermore, the bond distances in the pymtH ring agree with this assignment (Table 2) and are close to those found in most pyrimidine-2-thione complexes.[18,19] As shown in Fig. 2, intramolecular hydrogen bonds between the bromide atoms (Br_1, Br_2) and the HN_2, HN_4 hydrogen occur ($Br_1 \cdots N_2 = 3.205(7)$ Å, $Br_2—N_4 = 3.300(8)$ Å). These hydrogen bonds are of different strength, as shown also by the least-squares planes formed by the Cu, Br, S, C, N atoms (Table 4). Furthermore, short van der Waals contacts exist between one H—C hydrogen atom of the pymtH ring of one molecule, with the bromide atom of the other molecule, giving rise to an almost dimeric molecule (Br_1—C(83) = 3.67(1) Å, Br_2—C(41) = 3.462(9) Å). Then the strongest hydrogen bond to one bromide atom is associated with the weakest van der Waals contact. As a consequence of this dimer formation, Br_1, Br_2, N_2, N_4, C(83), C(41) form a plane within 0.6 Å (Table 4). Finally, no other intermolecular contact is smaller than 3.5 Å.

Table 3. Some physical properties and analytical data of the complexes

Compound	Yield (%)	Colour	M.p. (°C)	%C[a]	%H[a]	%N[a]	%Cu[a]
I [Cu(py2SH)(PPh$_3$)$_2$Br]	72	Yellow	191	62.26(63.20)	4.14(4.52)	2.10(1.80)	8.18(8.15)
II [Cu(py4SH)(PPh$_3$)$_2$Br]	60	Yellow	186–187	62.85(63.20)	4.27(4.52)	2.02(1.80)	8.26(8.15)
III [Cu(pymtH)(PPh$_3$)$_2$Br]	85	Orange	178	61.91(61.58)	5.02(4.39)	3.51(3.59)	8.23(8.14)
IV [Cu(tzdtH)(PPh$_3$)$_2$Br]	75	Pale yellow	163	59.80(59.44)	4.48(4.47)	1.62(1.78)	7.90(8.07)
V [Cu(meimtH)(PPh$_3$)$_2$Br]	66	White	215–216	61.83(61.26)	4.27(4.88)	3.25(3.57)	8.22(8.10)
VI [Cu(bzoxtH)(PPh$_3$)$_2$Br]	82	White	176	63.27(63.04)	4.19(4.30)	1.79(1.71)	7.60(7.75)
VII [Cu(bztzH)(PPh$_3$)$_2$Br]	71	Pale yellow	191–193	61.15(61.83)	4.32(4.22)	1.51(1.67)	7.58(7.61)
VIII [Cu(bzimtH$_2$)(PPh$_3$)$_2$Br]	74	White	215–216	62.88(63.12)	4.22(4.43)	3.31(3.42)	7.56(7.76)
IX [Cu(qnotH$_2$)(PPh$_3$)$_2$Br]	68	Pale yellow	220	62.07(62.39)	4.09(4.25)	2.91(3.31)	7.65(7.51)
X [Cu(nbzimtH$_2$)(PPh$_3$)$_2$Br]	70	Yellow	102–103	60.07(59.78)	4.42(4.05)	4.43(4.86)	7.46(7.36)

[a] Calculated values in parentheses.

IR spectra

IR spectra, in the region 4000–250 cm^{-1}, provide information concerning the mode of coordination. Some selected bands and their assignments are given in Table 5.

The solid-state IR spectra of complexes studied, exhibit the dominance of the thione form of the ligands investigated with the presence of ν(NH) bands at 3180–3130 cm^{-1},[20–22] the absence of any evidence for ν(SH) bands in the 2500–2600 cm^{-1} region,[23–24] and the production of characteristic "thioamide" bands.[23]

All the pymtH ligands are bonded to the metal through the sulphur atom, as shown by the shifts of the "thioamide" bands observed by comparing the IR spectra of the complexes with those of the free ligands. Of the four "thioamide" bands, those showing the most significant changes upon coordination are (III) and (IV). "Thioamide(III)" undergoes downward shifts ranging from 10 to 60 cm^{-1}. "Thioamide(IV)" shows similar behaviour, although here, the shifts are generally greater (30–100 cm^{-1}), and the absorptions are in many cases pertly masked by strong triphenylphosphine bands.

In agreement with the X-ray crystal structure there is no positive evidence that in the complexes discussed here, the ligands behave as bidentate. In fact, "thioamide(I)" occurred at the same wavenumbers, or showed small ($\pm$5 cm^{-1}) shifts, signifying that the ligands are not N-bonded to the metal.

The N—H stretching frequency in the complexes tends to lie at a lower wavenumber than in the free ligands, but the shifts of this band are small, suggesting that the nitrogen atoms are not involved in bonding.[24] The directions of the shifts in the position of all the bands in the spectra of the complexes are the same, indicating that the binding pattern in all the complexes must be similar.

The monodentate nature of the ligands is further confirmed by the presence of a band around 350 cm^{-1}, which is assigned to the ν(Cu—S) vibration.[25]

Electronic and NMR spectra

The UV-vis spectra of the compounds in $CHCl_3$ solutions, as expected, show only two absorption bands at 310–360 and 240–280 nm, which can be assigned as intraligand transitions.

The ^{1}H NMR spectra of the complexes in $CDCl_3$ solution also provided proof that ligands are (NH) protonated. The absence of any evidence for the thiol (SH) proton (δ 3–5 ppm) and the presence of a peak for the NH group at $\sim$ 10–14 ppm (sometimes very broad) indicate the thione tautomer as the dominant species in the complexes studied.

Table 4. Equation and distances from the least-squares planes

Plane 1	$0.6087x$	$-0.5544y$	$-0.5676z$	$= 8.9479$		
Br_1	Cu_1	S_1	C_{37}	N_2		
−0.120	0.173	0.170	0.024	0.094		
Plane 2	$0.3576x$	$-0.0576y$	$-0.9321z$	$= 8.0309$		
Br_2	Cu_2	S_2	C_{79}	N_4	Br_1[a]	
−0.234	0.360	−0.348	0.060	0.162	0.119	
Plane 3	$0.6953x$	$+0.0044y$	$-0.7187z$	$= -4.4328$		
Br_1	Br_2	N_2	N_4	C_{83}	C_{41}	Cu_2[a]
0.372	0.584	0.049	−0.310	−0.140	−0.555	0.587
Angles between	1–2	38.9°				
	1–3	23.3°				
	2–3	34.0°				

[a] Atom not included in the least-squares calculations.

Table 5. Selected NMR and IR spectroscopic data

Compound	^{1}H NMR δ(N—H) (ppm)	IR (cm^{-1}) ν(N—H)	"Thioamide(II)"	"Thioamide(III)"	ν(Cu—S)
I	13.6	3150	1305	1025	360
II	[a]	3180	1310	1020	[b]
III	[a]	3140	1320	1020	355
IV	11.2	3140	1305	1022	[b]
V	13.1	3140	1285	1030	[b]
VI	[a]	3140	1250	990	255
VII	14.1	3135	1325	1000	[b]
VIII	11.3	3133	1310	1025	360
IX	13.2+9.0	3130	1330	1020	360
X	11.8	3160	1300	1025	380

[a] No associated N—H activity was observed.
[b] No absorption attributable to Cu—S vibration was observed.

REFERENCES

1. E. S. Raper, *Coord. Chem. Rev.* 1985, **61**, 115.
2. M. Belicchi Ferrari, G. Gaspari Fava, C. Pelizzi and P. Tarasconi, *Inorg. Chim. Acta* 1985, **97**, 99.
3. P. Karagiannidis, P. Aslanidis, D. Kessissoglou, B. Krebs and M. Dartmann, *Inorg. Chim. Acta* (accepted for publication).
4. P. Karagiannidis, P. Aslanidis, S. Papastefanou and A. Terzis, *Inorg. Chim. Acta* 1989, **156**, 277.
5. *SDP: Structure Determination Package*. Enraf Nonius, Delft, The Netherlands (1977).
6. G. Sheldrick, *SHELX76*. University of Göttingen, Germany (1976).
7. *International Tables for X-Ray Crystallography*, Vol. IV. Kynoch Press, Birmingham (1974).
8. S. J. Lippard and K. M. Melmed, *Inorg. Chem.* 1967, **6**, 2223.
9. S. J. Lippard and K. M. Melmed, *Inorg. Chem.* 1969, **8**, 2755.
10. G. G. Messmer and G. J. Palenik, *Inorg. Chem.* 1969, **8**, 2750.
11. S. J. Lippard and G. J. Palenik, *Inorg. Chem.* 1971, **10**, 1322.
12. L. M. Engelhardt, C. Pakawatchai and A. H. White, *J. Chem. Soc., Dalton Trans.* 1985, 125.
13. S. C. Kokkou, V. Schramm and P. Karagiannidis, *Acta Cryst.* 1985, **C41**, 1040.
14. I. G. Dance, P. J. Guerney, A. D. Rae and M. L. Scudder, *Inorg. Chem.* 1983, **22**, 2883.
15. P. H. Davis, R. L. Belford and I. C. Paul, *Inorg. Chem.* 1973, **12**, 213.
16. R. P. Shibaeva and V. F. Kaminkii, *Kristallografiya* 1981, **26**, 332.
17. R. D. Bereman, M. R. Churchill, P. M. Schaber and M. E. Winkler, *Inorg. Chem.* 1977, **18**, 3122.

18. F. A. Cotton and W. H. Ilsley, *Inorg. Chem.* 1981, **20**, 614.
19. C. Chieh, *Can. J. Chem.* 1977, **56**, 560.
20. P. P. Singh and R. Rivest, *Can. J. Chem.* 1968, **46**, 2361.
21. B. Singh, M. M. P. Rukhaivar and R. J. Sinha, *J. Inorg. Nucl. Chem.* 1977, **39**, 29.
22. A. W. McLellan and G. A. Melson, *J. Chem. Soc. A* 1967, 137.
23. C. N. R. Rao and P. Venkataraghavan, *Spectrochim. Acta* 1962, **18**, 541.
24. E. S. Raper and J. L. Brooks, *J. Inorg. Nucl. Chem.* 1977, **39**, 2163.
25. L. J. Bellamy, *The Infrared Spectra of Complex Molecules*. Wiley, New York (1966).

Polyhedron Vol. 8, No. 8, pp. 1111–1116, 1989
Printed in Great Britain

0277–5387/89 $3.00+.00
Pergamon Press plc

STUDIES ON EXTRACTION OF LANTHANUM(III), CERIUM(III), EUROPIUM(III), THORIUM(IV) AND URANIUM(VI) WITH 3-PHENYL-4-ACETYL-5-ISOXAZOLONE (HPAI)

A. JYOTHI and G. N. RAO*

Department of Chemistry, Indian Institute of Technology, New Delhi-110016, India

(*Received* 21 *September* 1988; *accepted* 23 *November* 1988)

Abstract—The extraction of lanthanum(III), cerium(III), europium(III), thorium(IV) and uranium(VI) from aqueous solutions into 4-methyl-2-pentanone (MIBK), containing 3-phenyl-4-acetyl-5-isoxazolone (HPAI), has been investigated. The mechanism of extraction and the species extracted have been identified. Extraction constants in each system have been calculated and compared with those of the corresponding systems using 1-phenyl-3-methyl-4-benzoyl-5-pyrazolone (HPMBP) and thenoyltrifluoroacetone (HTTA). It is found that, in general, HPAI extracts these metals better than HPMBP and HTTA. Solid complexes of these metals with HPAI have been isolated and characterized by using elemental analysis, IR and NMR spectroscopic techniques.

β-Diketones have been used extensively for the extraction of metals. Thenoyltrifluoroacetone (HTTA) has received special attention in the separation of elements like uranium, thorium and zirconium.[1] However, it is difficult to prepare and rather unstable during storage. Acyl pyrazolones have been found effective for the efficient extraction of lanthanides,[2,3] actinides[4,5] and other metals.[6–8] Similar to acyl pyrazolones, β-diketones derived from 4-acyl derivatives of isoxazolones are considered to be attractive as chelating reagents. Recently we have reported the extraction of manganese(II), iron(II), nickel(II), cobalt(II), copper(II), zinc(II), palladium(II) and cadmium(II) with 3-phenyl-4-acyl-5-isoxazolones.[9,10] We now report on the extraction of lanthanum(III), cerium(III), europium(III), thorium(IV) and uranium(VI) with 3-phenyl-4-acetyl-5-isoxazolone (HPAI). The solid complexes isolated were characterized by elemental analysis, IR and ^{1}H NMR spectral studies. HPAI can exist in four tautomeric forms (Fig. 1) and has been shown to behave like a bidentate enol forming neutral metal complexes of the type shown in Fig. 2. The effectiveness of the ligand HPAI in the separation of metals is discussed.

* Author to whom correspondence should be addressed.

EXPERIMENTAL

Reagents

All the reagents used were of analytical grade. The ligand HPAI was prepared according to the method of Korte and Storiko,[11] using 3-phenyl-5-isoxazolone and acetic anhydride in the presence of sodium acetate and its purity checked by elemental analysis. 4-Methyl-2-pentanone (MIBK) was used as solvent for the extraction. Stock solutions of metals were prepared by using spec-pure quality metal oxide/nitrate and standardized by titration with EDTA or gravimetrically. A constant ionic strength in the aqueous phase was maintained by using potassium nitrate solution. The pH of the aqueous phase was maintained by using mixtures of potassium chloride–hydrochloric acid for pH 1–3 and sodium acetate–acetic acid for pH 3–6.

Extraction procedure

10 cm^3 of the aqueous phase containing an aliquot of metal solution, 5 cm^3 of buffer solution and 1 cm^3 of 1 M KNO_3 was equilibrated with 10 cm^3 of MIBK, containing the required concentration of HPAI, in a stoppered bottle. The mixture was shaken in a mechanical shaker for 1 h at 25 ± 1°C.

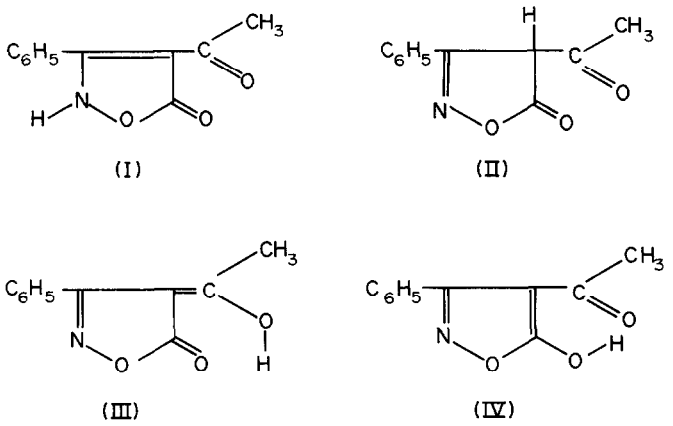

Fig. 1.

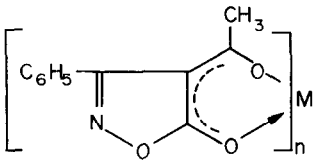

Fig. 2.

Preliminary studies showed that this period is sufficient for attaining the equilibrium. After equilibration, the two phases were separated and the pH of the aqueous phase was measured by using ELICO MODEL L1-120 digital pHmeter. The concentration of metal ion in the aqueous phase was determined spectrophotometrically by developing colour with Alizarin Red-S[12] for lanthanum(III), cerium(III) and europium(III), thoran for thorium(IV)[13] and dibenzoylmethane (DBM) for uranium(VI),[14] using a Pye Unicam SP-500 visible spectrophotometer. Preliminary experiments showed that the colour of Alizarin Red-S metal ion is very sensitive to changes in the hydrogen ion concentration, hence it was necessary to destroy the acetate ion which makes it difficult to attain the desired pH. A 5 cm^3 aliquot of the aqueous phase was evaporated and fused twice with perchloric acid to destroy the acetate ion, and the residue was dissolved in distilled water and the metal content was determined spectrophotometrically by developing colour with Alizarin Red-S.[12] Occasionally the organic phase was back-extracted with 2 M HNO_3 and the metal content was similarly determined.

Preparation of metal complexes

The metal complexes were prepared by the following general procedure: an ethanolic solution of the ligand prepared by dissolving 5 mmol in a minimum quantity of 95% ethanol was added dropwise, with stirring, to a hot solution of 1 mmol of metal nitrate or chloride in water. The reaction mixture was heated on a water bath for 10 min. The precipitates formed were filtered, washed with a 1 : 1 ethanol and water mixture and dried in a desiccator over fused calcium chloride. Analytical data, colour and melting points of the complexes prepared are given in Table 1.

Table 1. Physical and analytical data of HPAI and its metal complexes

Molecular formula	Colour	Decomposition temperature (°C)	Calculated (%) C	H	N	Found (%) C	H	N
$C_{11}H_9O_3N$	Yellow	140 (m.p.)	65.0	4.4	6.9	64.9	4.5	6.7
$C_{33}H_{28}O_{11}N_3La$	Cream	216	50.7	3.6	5.4	50.4	3.3	5.0
$C_{33}H_{28}O_{11}N_3Ce$	Cream	203	50.6	3.6	5.4	50.5	3.4	5.0
$C_{33}H_{28}O_{11}N_3Eu$	Cream	210	49.9	3.5	5.3	50.0	3.4	5.3
$C_{44}H_{32}O_{12}N_4Th$	Cream	168	50.8	3.8	5.4	51.1	3.9	5.2
$C_{22}H_{16}O_8N_2U$	Yellow	189	39.2	2.4	4.1	40.3	2.4	4.6

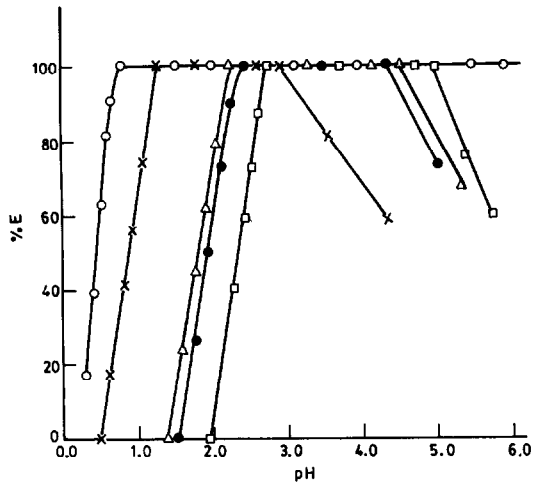

Fig. 3. Plot of $\%E$ vs pH: ○ = Th^{4+}; × = UO_2^{2+}; △ = Eu^{3+}; ● = Ce^{3+}; □ = La^{3+}; 0.01 M HPAI in MIBK.

RESULTS AND DISCUSSION

The extraction of La^{3+}, Ce^{3+}, Eu^{3+}, Th^{4+} and UO_2^{2+} as a function of the pH of the aqueous phase is shown in Fig. 3. The extraction behaviour of these metals can be understood by the variation of the distribution ratio "K_d" (defined as the concentration of metal ion in the organic phase divided by the concentration of metal ion in the aqueous phase) as a function of the aqueous phase acidity and as a function of the extractant concentration. The plots of $\log K_d$ vs pH (Fig. 4), at constant ligand concentration (0.01 M), gave straight lines with a slope around two for UO_2^{2+}, three for La^{3+}, Ce^{3+} and Eu^{3+}, while the slope is four for Th^{4+}. This suggests the release of two, three and four hydrogen ions, respectively, during the extraction process.

To calculate the number of ligand molecules coordinated with the extracted species, the concentration of HPAI was varied at constant pH. The log–log plots of distribution ratio vs ligand concentration (Fig. 5) were linear with slopes

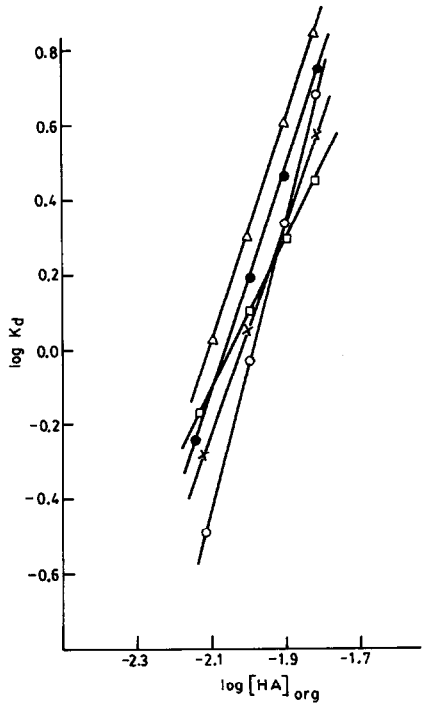

Fig. 5. Plot of $\log K_d$ vs $\log[HA]_{org}$: ○ = Th^{4+}; □ = UO_2^{2+}; △ = Eu^{3+}; × = Ce^{3+}; ● = La^{3+}.

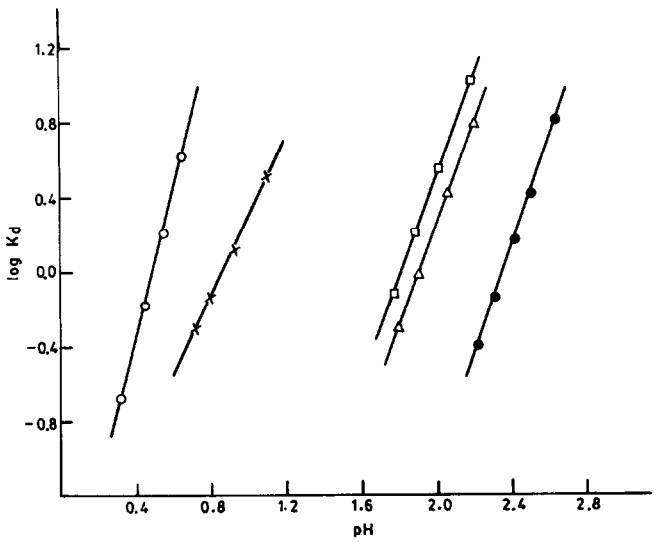

Fig. 4. Plot of $\log K_d$ vs pH: ○ = Th^{4+}; × = UO_2^{2+}; □ = Eu^{3+}; △ = Ce^{3+}; ● = La^{3+}; 0.01 M HPAI in MIBK.

around two for UO_2^{2+}, three for La^{3+}, Ce^{3+} and Eu^{3+}, and four for Th^{4+}, indicating that two, three and four molecules of the ligand, respectively, are incorporated in the extracted species. Hence, the extraction equilibria can be represented as

$$Ln^{3+} + 3HPAI \rightleftharpoons Ln(PAI)_3 + 3H^+$$

$$Th^{4+} + 4HPAI \rightleftharpoons Th(PAI)_4 + 4H^+$$

$$UO_2^{2+} + 2HPAI \rightleftharpoons UO_2(PAI)_2 + 2H^+$$

where, Ln represents lanthanum, cerium and europium, and PAI is the anion of 3-phenyl-4-acetyl-5-isoxazolone. The extraction constant K_{ex} is given as:

$$\log K_{ex} = \log K_d - n\text{pH} - n \log [\text{HPAI}]_{org}$$

where, $n = 2$, 3 or 4 for UO_2^{2+}, La^{3+}, Ce^{3+}, Eu^{3+} and Th^{4+}, respectively.

The values of the extraction constants ($\log K_{ex}$) have been calculated for all the systems and are summarized in Table 2. The extraction constant values obtained for the present systems have been compared with those available in the literature using HPMBP and HTTA (Table 2). It can be seen from the table that HPAI gives much higher extraction constant values than HPMBP and HTTA. This can be attributed to the lower pK_a value of this reagent (1.31) as compared to those of HTTA (6.23)[1] and HPMBP (4.10).[17]

In order to understand the mechanism of the extraction process and nature of the species extracted, physico-chemical studies on solid complexes of these metals have been carried out. Analytical data, together with some physical properties of the complexes, are given in Table 1. The elemental analyses correspond to the general formula $M(PAI)_n \cdot xH_2O$, where, for M = La, Ce and Eu, $n = 3$ and $x = 2$; for M = Th, $n = 4$ and $x = 0$; for $M = UO_2$, $n = 2$ and $x = 0$. The presence or absence of coordinated water molecules in the metal complexes was confirmed by IR and ^1H NMR spectral studies.

Table 2. Comparison of extraction constant values (log K_{ex}) of metal–HPAI systems with metal–HPMBP and metal–HTTA systems

Metal	Ligand HPAI[a]	HPMBP[b]	HTTA[c]
Lanthanum	−0.88	−7.28	−9.90
Cerium	+0.21	−6.71	−9.60
Europium	+0.69	−5.33	−8.99
Thorium	+5.93	−1.00	+1.00
UO_2	+2.36	−1.15	−2.40

[a] Present work.
[b] References 3 and 4.
[c] References 1, 15 and 16.

IR spectra

IR spectra were recorded on a Unicam SP-1200 IR spectrophotometer and Nicolet 5-DX-FTIR spectrophotometer. The chelates of lanthanum, cerium and europium showed a broad peak in the 3300–3500 cm^{-1} region, which is assigned to the ν(O—H) of coordinated water. This region is free of absorption for the complexes of thorium and UO_2^{2+}, indicating the absence of coordinated water. Of interest are the C=O and C=C stretching frequencies of the chelate ring; these are known to be very sensitive to substitution in β-diketonates.[18] The intense band located between 1680 and 1640 cm^{-1}, in the spectra of chelates, are assigned to the ν_{as}(C=O) mode. The other strongest absorption occurring around 1515–1480 cm^{-1} in the spectra, are assigned to the ν_{as}(C=C). These agree well with the similar assignments in acetylacetonates[19] and acyl pyrazolones.[20] The chelate of UO_2^{2+} showed an intense band at 935 cm^{-1}, which is assigned to the ν(O=U=O).

The following points are of structural significance:

(i) The intense broad band centred around 2600 cm^{-1}, which is assigned to the ν(O—H) in the spectrum of the ligand, is absent in the spectra of complexes, indicating the ionization of the enolic O—H group and the involvement of oxygen of the hydroxyl group in chelation.

(ii) The stretching frequencies of the C=O group have shifted from 1780 cm^{-1} in the ligand to ν(C=O): 1660 (La)–1648 cm^{-1} (Th) in the complexes, which suggests that the carbonyl group is involved in bonding.

(iii) The absence of any band between 3100 and 3600 cm^{-1} in the anhydrous complexes (e.g. Th), indicates the absence of ν(N—H). Thus the possibility of any amino–diketo tautomeric form or reacting only through the carbonyl groups, or forming a coordinate link to metal through the nitrogen of its secondary amino group, is eliminated.

(iv) The presence of bands in the 400–500 cm^{-1} region, typical of metal-β-diketonates ν(M—O), suggests that the bonding of the metal to the ligand is through the oxygen atoms.

Proton NMR spectra

The ^1H NMR spectral data of the ligand and some of its metal complexes are shown in Table 3.

Table 3. ^{1}H NMR spectral data of HPAI and its metal complexes[a]

Compound	Phenyl protons	Methyl protons	Water molecule protons	Hydroxyl proton	Solvent
HPAI	7.03–7.51(m)	2.49(s)	—	11.6	$CDCl_3$
$C_{33}H_{28}O_{11}N_3La$	7.43–7.10(m)	2.02(s)	3.38(s)	—	DMSO-d_6
$C_{44}H_{32}O_{12}N_4Th$	7.81–6.42(m)	2.10(s)	—	—	DMSO-d_6
$C_{22}H_{16}O_8N_2U$	7.53–6.74(m)	2.27(s)	—	—	DMSO-d_6

[a] Chemical shifts in δ (ppm) relative to TMS.
m—multiplet; s—singlet.

The spectra were obtained using a JEOL-JNM-FX-100 FT-NMR spectrometer.

The spectrum of the ligand showed a sharp singlet at δ 2.49 ppm relative to TMS, which is assigned to the methyl protons, a multiplet at δ 7.93–7.51 ppm due to the phenyl protons and a broad peak at δ 11.6 ppm assigned to a hydroxyl proton, indicating that the ligand exists in the enolic form. The enolic ^{1}H resonance present in the ligand is absent in the spectra of metal chelates, indicating that the hydroxyl proton has been lost and the enolic form of the ligand is involved in chelation. In the spectra of metal chelates, both the methyl and phenyl proton signals have been shifted upfield compared to that of the ligand, and a slight broadening of the signals was observed. The shift of these signals may be attributed to contact and pseudocontact interactions, while the broadening may be attributed to spin–spin relaxation processes. The spectrum of the lanthanum complex shows a resonance attributable to coordinated water molecules.

Thus, the results of elemental analysis, IR and ^{1}H NMR spectral studies confirm that the ligand HPAI in these metal chelates is behaving as a bidentate, forming the extractable species of the type depicted in Fig. 2.

Separations

The possibility of utilizing the reagent HPAI for the separation of metals, has been investigated by calculating the separation factor "S", which is the ratio of the distribution coefficients of the elements to be separated.[21] A separation in which not more than 1% of one element is co-extracted, will be obtained if $S \geqslant 10^4$ and the product of distribution coefficient is unity.[21] The separation of thorium from lanthanum, cerium and europium is perfect around pH 1.0, where the separation factor is "∞", because the extraction of lanthanum, cerium and europium is negligible around pH 1.0 (Fig. 3). Similarly, UO_2^{2+} can be separated from lanthanum, cerium and europium around pH 1.0, where the separation factor is "∞". Thus under these conditions, it is possible to separate the actinides (thorium and uranium) from the lanthanides studied. It is evident from the results presented in the text, that these acyl isoxazolones represent a new group of chelating reagents which have great potential in solvent extraction.

Acknowledgement—The financial assistance provided by the Council of Scientific and Industrial Research, New Delhi, India is gratefully acknowledged.

REFERENCES

1. Y. Marcus and A. S. Keretes, *Ion Exchange and Solvent Extraction of Metal Complexes*. Wiley Interscience, New York (1967).
2. Z. Kolarik, *J. Inorg. Nucl. Chem.* 1971, **33**, 1135.
3. A. Roy and K. Nag, *J. Inorg. Nucl. Chem.* 1978, **40**, 331.
4. G. N. Rao and H. C. Arora, *Ind. J. Chem.* 1982, **21A**, 335.
5. M. K. Chmutova, G. A. Pribylova and B. F. Myasoedov, *J. Anal. Chem. USSR* 1973, **28**, 2076.
6. M. Y. Mirza and F. I. Nwabue, *Talanta* 1981, **28**, 49.
7. O. Navratil and B. S. Jensen, *J. Radio. Anal. Chem.* 1970, **5**, 313.
8. Y. Akama, K. Sato and T. Nakai, *Polyhedron* 1985, **4**, 1259.
9. A. Jyothi and G. N. Rao, *Chem. Script.* 1987, **27**, 367.
10. A. Jyothi and G. N. Rao, *Bull. Chem. Soc. Jpn*, in press.
11. F. Korte and K. Storiko, *Chem. Ber.* 1961, **4**, 1956.
12. R. W. Rinehart, *Anal. Chem.* 1954, **26**, 1820.
13. A. Mayer and G. Bradshaw, *Analyst* 1952, **77**, 154.
14. J. H. Yoe, F. Will III and R. A. Black, *Anal. Chem.* 1953, **25**, 1200.
15. A. M. Poskanzer and B. M. Foreman, *J. Inorg. Nucl. Chem.* 1961, **16**, 323.
16. T. Sekine and D. Dyrssen, *J. Inorg. Nucl. Chem.* 1967, **29**, 1457.

17. N. T. Sizonenko and Yu. A. Zolotov, *Zh. Anal. Khim.* 1969, **24**, 1305.
18. K. Nakamoto, *Infrared Spectra of Inorganic and Coordination Compounds*, p. 247. Wiley Interscience, London (1970).
19. H. Musumi and N. Iwasaki, *Bull. Chem. Soc. Jpn* 1967, **40**, 550.
20. E. C. Okafor, *J. Inorg. Nucl. Chem.* 1980, **42**, 1155.
21. Yu. A. Zolotov, *Extraction of Chelate Compounds*, p. 26. Humphrey Science, Ann Arbor, Michigan (1970).

Polyhedron Vol. 8, No. 8, pp. 1117–1121, 1989
Printed in Great Britain

0277–5387/89 $3.00+.00
© 1989 Pergamon Press plc

AN UNUSUAL EXAMPLE OF INTERMOLECULAR COUPLING BETWEEN METAL–METAL BONDED DIMERS: CRYSTAL AND MOLECULAR STRUCTURE OF $Rh_2(O_2CCH_3)_2(CF_3C(O)CHC(O)CH_3)_2 \cdot C_5H_5N$

HOLLY J. McCARTHY and DEREK A. TOCHER*

Department of Chemistry, University College London, 20 Gordon Street, London WC1H 1AJ, U.K.

(*Received* 24 *October* 1988; *accepted* 24 *November* 1988)

Abstract—The reaction of $Rh_2(O_2CCH_3)_4$ with 1,1,1-trifluoro-2,4-pentanedionate in water, gives two isomers of $Rh_2(O_2CCH_3)_2(CF_3C(O)CHC(O)CH_3)_2 \cdot 2H_2O$. Addition of pyridine and elution from a silica column gives isomerically pure $Rh_2(O_2CCH_3)_2(CF_3C(O)CHC(O)CH_3)_2 \cdot C_5H_5N$. The structure of the crystalline product was obtained by X-ray diffraction. The crystals belong to the monoclinic space group $P2_1/n$ with $a = 9.660(2)$, $b = 19.976(3)$, $c = 13.202(2)$ Å, $\beta = 106.54(2)°$, $V = 2442(1)$ Å^3 and $z = 4$. The structure was refined on 2708 independent reflections to $R_w = 0.0604$. The asymmetric unit contains a single dinuclear unit in which only one rhodium atom is bound by an axial pyridine molecule. The Rh—Rh bond is 2.534(1) Å and the Rh—N bond, 2.133(10) Å. Surprisingly, pairs of dinuclear units are linked together in the solid state via two long, 3.106 Å, Rh—C interactions, between the axial site on the metal and the γ-carbon atom of the β-diketonate ligand.

The vast majority of the classical metal–metal bonded dimers of the type $M_2(XYZ)_4$ (where XYZ is a monoanionic three-atom bridging ligand) exist as discrete dinuclear units, or simple bis-adducts $M_2(XYZ)_4L_2$ (L = pyridine, H_2O, PR_3 etc.), both in the solid state and in solution. Relatively few of these compounds exist as polymeric materials, the best characterized examples being the ruthenium compounds $Ru_2(O_2CR)_4Cl$ and $Ru_2(HN(O)CR)_4Cl$, in which dinuclear cations are linked in chains by bridging axial chloride ions,[1–4] and the so-called "unsolvated" $Cr_2(O_2CR)_4$ molecules, which associate in the solid state via oxygen bridge bonding.[5,6] In the course of our studies into the products formed on reaction of dirhodium(II) tetracarboxylate molecules with a number of β-diketone ligands, we have encountered an unusual molecule $Rh_2(O_2CCH_3)_2(CF_3C(O)CHC(O)CF_3)_2 \cdot C_5H_5N$, which in the solid state dimerizes through a pair of weak rhodium–carbon interactions.

EXPERIMENTAL

Synthesis

$Rh_2(O_2CCH_3)_4 \cdot 2CH_3OH$ (0.156 g, 0.31 mmol) was refluxed in H_2O (20 cm^3) with $CF_3C(O)CH_2C(O)CH_3$ (0.5 cm^3) for 6 h. The green precipitate formed was filtered off and air-dried. The solid was suspended in CH_3OH (10 cm^3) to which C_5H_5N (0.1 cm^3) was added. The mixture was stirred for 1 h, in which time a red solution was obtained. The CH_3OH was removed under reduced pressure and the red gum redissolved in CH_2Cl_2 (5 cm^3). This was loaded onto a silica gel (60–120 mesh) column and a green band eluted with a mixture of CH_2Cl_2 (80%), *n*-hexane (12%) and diethyl ether (8%). Slow evaporation of this solution resulted in the deposition of a homogeneous mass of green crystalline material. Yield 0.167 g, 70%. Found: C, 32.2; H, 2.7; N, 1.8. Calc. for $C_{19}H_{19}NO_8F_6Rh_2$: C, 32.2; H, 2.7; N, 2.0%. IR spectrum (KBr disc): 3449(w), 1607(m), 1542(s), 1512(m), 1481(m) 1443(s), 1420(w), 1340(m),

*Author to whom correspondence should be addressed.

1267(s), 1210(s), 1198(s), 1152(s), 1137(s), 1095(m), 1064(w), 1003(w), 946(w), 819(w), 789(m), 754(w), 697(s), 624(w), 598(w), 530(w), 350(w) cm^{-1} (key: s, strong; m, medium; w, weak). Mass spectrum: m/z 630, $[Rh_2(O_2CCH_3)_2(CF_3C(O)CHC(O)CH_3)_2]^+$. Proton NMR ($CD_2Cl_2$ solvent, $(CH_3)_4Si$ reference): 17°C, pyridine, δ 8.48, 7.96, 7.52 ppm; $CF_3C(O)CHC(O)CH_3$, 5.54 ppm; O_2CCH_3, 2.08 ppm; $CF_3C(O)CHC(O)CH_3$, 1.90 ppm; −79°C, pyridine, δ 8.41, 7.97, 7.53 ppm; $CF_3C(O)CHC(O)CH_3$, 5.63 and 5.44 ppm; O_2CCH_3, 2.10 and 2.06 ppm; $CD_3C(O)CHC(O)CH_3$, 1.89 and 1.84 ppm.

X-ray studies

Green needle crystals were obtained as described above.

Crystal data. $C_{19}H_{19}NO_8F_6Rh_2$, monoclinic, space group $P2_1/n$, $a = 9.660(2)$, $b = 19.976(3)$, $c = 13.202(2)$ Å, $\beta = 106.54(2)°$, $U = 2442$ Å^3, $z = 4$, $M = 709.20$, $D_c = 1.93$ g cm^{-1}, μ(Mo-K_α) = 13.8 cm^{-1}, $F(000) = 1392$.

Measurements. Refined unit cell parameters were obtained by centring 50 reflections on a Nicolet R3mV diffractometer. A total of 4322 unique data were measured in the range $5° \leqslant 2\theta \leqslant 50°$ with Mo-K_α radiation (graphite monochromator). Of these, 2708 reflections had $I > 2.0\sigma(I)$ and were considered to be observed. Three standard reflections were remeasured every 97 scans and showed no significant loss (< 2%) in intensity during the data collection. The data were corrected for Lorentz and polarization factors, and an empirical absorption correction was applied.

Structure analysis. The positions of the two rhodium atoms were derived using direct methods and the remaining non-hydrogen atoms were found by iterative application of difference Fourier synthesis and least-squares refinement. The fluorine atoms are disordered over two sites. A satisfactory model for the disorder was found by assuming a 75% occupancy of one site [fluorines F(1a)—F(6a) attached to C(9) and C(14)] and a 25% occupancy of the alternative site [fluorines F(1b)—F(6b) attached to C(8) and C(13)]. No attempt was made to locate the hydrogen atoms. All atoms [except F(3b)] were refined anisotropically. The final cycle of refinement included 374 parameters and converged to give $R = 0.0776$ and $R_w = 0.0604$ ($w^{-1} = \sigma^2(F) + 0.00088F^2$), and did not shift any parameter by more than 0.026 times its estimated standard deviation. The final difference Fourier map was featureless with the largest peak being 1.01 e Å^{-3}. Computations were carried out on a Microvax II computer using the SHELXTL PLUS program package.

Final atomic coodinates, thermal parameters and structure factor tables have been deposited with the Editor and with the Cambridge Crystallographic Data Centre, as supplementary material.

RESULTS AND DISCUSSION

Some 20 years ago, the reaction of $Rh_2(O_2CCH_3)_4$ with β-diketones was reported to give complexes with the stoichiometry $[Rh(O_2CCH_3)(\beta\text{-diketonato})L]_2$, where L is the neutral donor ligand, H_2O or pyridine.[7] Several structures were proposed for these molecules. However, the most likely one contained a $[Rh_2]^{4+}$ core, two cisoid bridging acetato ligands, one chelating β-diketonato ligand on each metal ion, and one donor ligand, L, on each metal ion in the coordination site *trans* to the rhodium–rhodium single bond. We have recently confirmed this geometry for the molecule $Rh_2(O_2CCH_3)_2(CF_3C(O)CHC(O)CF_3)_2 \cdot 2C_5H_5N$.[8]

When $Rh_2(O_2CCH_3)_4$ is treated with an aqueous solution of the unsymmetrical β-diketone, $CH_3C(O)CH_2C(O)CF_3$, two isomers of the compound $Rh_2(O_2CCH_3)_2(CF_3C(O)CHC(O)CH_3)_2 \cdot 2H_2O$ are formed.[7] Although these isomers were not separated by Cenini *et al.* they were identified by ^1H NMR spectroscopy. In the *cis* isomer the β-diketonate ligands are arranged such that the $—CF_3$ substituents are approximately eclipsed, leading to inequivalent acetato ligands, while in the *trans* isomer each $—CF_3$ group is eclipsed with the $—CH_3$ substituent on the other β-diketonate, giving rise to an equivalence of the two acetato ligands in the NMR spectrum.

If the crude reaction mixture described earlier is treated with pyridine, which displaces the axially coordinated water molecules, and is then eluted from a silica column, an efficient separation of the two isomers can be effected.

The first fraction to be eluted from the column was shown, by ^1H NMR spectroscopy, to be the *trans* isomer. Surprisingly however, integration of the ^1H NMR spectrum was in the ratio pyridine–acetate–β-diketonate of 1:2:2. Given the propensity for the $[Rh_2]^{4+}$ unit to interact strongly with two axial ligands, this observation could not be easily rationalized and therefore we deemed it necessary to determine unequivocally the structure of this molecule in the solid state by X-ray crystallography.

Green needle crystals of $Rh_2(O_2CCH_3)(CF_3C(O)CHC(O)CH_3)_2 \cdot C_5H_5N$ are readily obtained

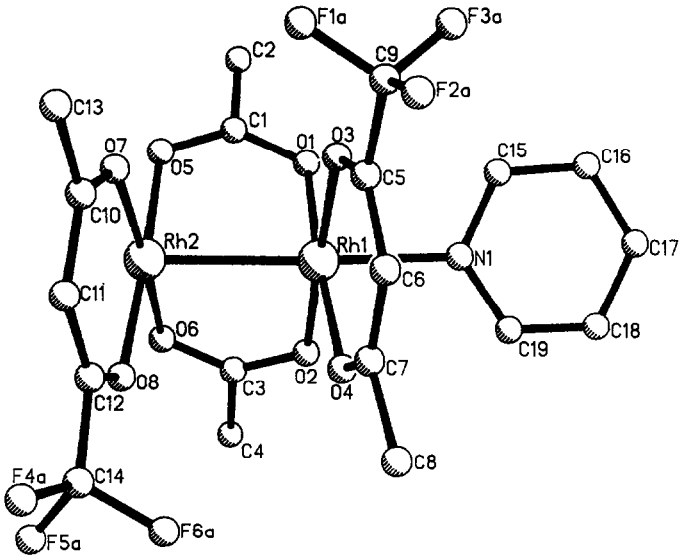

Fig. 1. Molecular structure of $Rh_2(O_2CCH_3)_2(CF_3C(O)CHC(O)CH_3)_2 \cdot C_5H_5N$ defining the atom labelling scheme.

by the slow evaporation of the solvent mixture used to elute the chromatography column. Data collection, structure solution and refinement used routine procedures described previously.[9]

The molecular structure of $Rh_2(O_2CCH_3)_2(CF_3C(O)CHC(O)CH_3)_2 \cdot C_5H_5N$ is shown in Fig. 1, while the coupling of the dinuclear units is illustrated in Fig. 2. Selected bond lengths and angles are presented in Table 1. The two rhodium atoms in the dinuclear core are bridged by two acetate ligands and each rhodium is also coordinated by a chelating $[CF_3C(O)CHC(O)CH_3]^-$ ligand. The coordination site on Rh(1) *trans* to the Rh—Rh bond is occupied by a pyridine molecule. The Rh—Rh bond length, 2.534(1) Å, is very similar to the one observed in $Rh_2(O_2CCH_3)_2(CF_3C(O)CHC(O)CF_3)_2 \cdot 2C_5H_5N$, 2.523(2) Å,[8] and is much greater than that observed for the tetracarboxylate complex, $Rh_2(O_2CCH_3)_4 \cdot 2C_5H_5N$, 2.396(1) Å.[10] This Rh—Rh bond distance is not dissimilar to that observed in $Rh_2(O_2CCH_3)_2(phen)_2$ complexes (mean: 2.558(3) Å), which also contain only two acetate ligands bridging the metal–metal single bond.[11] One closely related molecule, $Rh_2(O_2CCH_3)_2(dmg)_2 \cdot 2PPh_3$, has been observed to have a significantly longer Rh—Rh bond, 2.618(5) Å.[12] The Rh—Rh and Rh—N bonds are not colinear: angle Rh(2)—Rh(1)—N(1) =

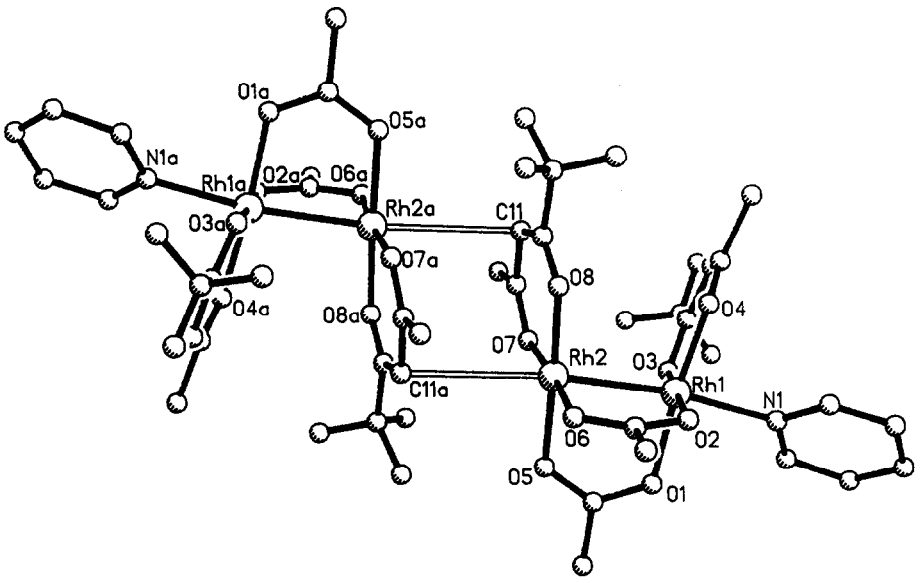

Fig. 2. Coupling of the dinuclear units (atoms labelled "a" are generated by an inversion centre).

Table 1. Selected bond lengths (Å) and bond angles (°) for $Rh_2(O_2CCH_3)_2(CF_3C(O)CHC(O)CH_3)_2 \cdot C_5H_5N$

Rh(1)—O(1)	2.022(8)	Rh(1)—Rh(2)	2.534(1)
Rh(1)—O(2)	2.023(8)	Rh(2)—O(5)	2.039(9)
Rh(1)—O(3)	2.008(9)	Rh(2)—O(6)	2.033(9)
Rh(1)—O(4)	1.998(8)	Rh(2)—O(7)	2.001(9)
Rh(1)—N(1)	2.133(10)	Rh(2)—O(8)	1.993(9)
O(1)—C(1)	1.272(15)	O(2)—C(3)	1.268(16)
C(1)—O(5)	1.262(15)	C(3)—O(6)	1.249(15)
C(1)—C(2)	1.500(19)	C(3)—C(4)	1.532(18)
O(3)—C(5)	1.266(18)	O(7)—C(10)	1.241(16)
C(5)—C(9)	1.547(19)	C(10)—C(13)	1.505(19)
C(5)—C(6)	1.395(21)	C(10)—C(11)	1.413(19)
C(6)—C(7)	1.414(19)	C(11)—C(12)	1.415(18)
C(7)—C(8)	1.527(21)	C(12)—C(14)	1.487(18)
C(7)—O(4)	1.258(15)	C(12)—O(8)	1.238(15)
O(1)—Rh(1)—Rh(2)	86.1(2)	O(2)—Rh(1)—Rh(2)	86.4(3)
O(2)—Rh(1)—O(1)	91.7(4)	O(3)—Rh(1)—Rh(2)	95.5(2)
O(3)—Rh(1)—O(1)	86.9(4)	O(3)—Rh(1)—O(2)	177.5(4)
O(4)—Rh(1)—Rh(2)	98.2(2)	O(4)—Rh(1)—O(1)	175.0(4)
O(4)—Rh(1)—O(2)	86.1(4)	O(4)—Rh(1)—O(3)	95.2(4)
N(1)—Rh(1)—Rh(2)	171.8(3)	N(1)—Rh(1)—O(1)	86.9(4)
N(1)—Rh(1)—O(2)	89.5(4)	N(1)—Rh(1)—O(3)	88.4(4)
N(1)—Rh(1)—O(4)	88.7(4)	O(5)—Rh(2)—Rh(1)	84.9(3)
O(6)—Rh(2)—Rh(1)	84.5(3)	O(6)—Rh(2)—O(5)	90.2(4)
O(7)—Rh(2)—Rh(1)	99.8(2)	O(7)—Rh(2)—O(5)	88.8(4)
O(7)—Rh(2)—O(6)	175.5(4)	O(8)—Rh(2)—Rh(1)	97.8(2)
O(8)—Rh(2)—O(5)	176.0(4)	O(8)—Rh(2)—O(6)	87.1(4)
O(8)—Rh(2)—O(7)	93.6(4)		

171.8(3)°. This angle is similar to those observed in $Rh_2(O_2CCH_3)_2(CF_3C(O)CHC(O)CF_3)_2 \cdot 2C_5H_5N$[8] and $Rh_2(O_2CC(CH_3)_3)_2(CF_3C(O)CHC(O)CF_3)_2 \cdot 2C_5H_5N$,[13] and can almost certainly be attributed to unfavourable steric interactions between the axial ligands and the $-CF_3$ substituent(s) on the chelating β-diketonate ligands. Although the deviation from linearity is significant, it is markedly less than that observed in $Rh_2(O_2CR)_2[(C_6H_4)PR'R'']_2 \cdot 2L$ molecules, which also exhibit similarly distorted structures.[14,15] The rhodium–carboxylate–oxygen bonds are longer than those to the β-diketonate oxygen atoms (mean values of 2.029 and 2.000 Å, respectively). In addition, the Rh—Rh—O(carboxylate) angles average 85.5°, while those involving the β-diketonate ligands average 97.8°. The dihedral angle between the least-square planes defined by the atoms Rh(1)—O(3)—C(5)—C(6)—C(7)—O(4) and Rh(2)—O(7)—C(10)—C(11)—C(12)—O(8) is 29.3°. These distortions from the idealized octahedral geometry about the metal ions must be attributed to the unfavourable steric interactions between the substituent groups on the two chelating β-diketonate ligands. The two β-diketonate ligands are rotated about the Rh—Rh axis by *ca* 7° from the eclipsed configuration (torsion angles O(3)—Rh(1)—Rh(2)—O(7) 7.6°; O(4)—Rh(1)—Rh(2)—O(8) 6.6°). Similarly, the two bridging acetate ligands are distorted with torsion angles about the Rh—Rh bond of 6.2 and 7.4°. This twisting of one end of the dinuclear molecule with respect to the other is much reduced from that observed in $Rh_2(O_2CCH_3)_2(CF_3C(O)CHC(O)CF_3)_2 \cdot 2C_5H_5N$,[8] where the four independent torsion angles fall in the range 11–15°.

Initial inspection of the molecular structure indicated that one rhodium atom per molecule was coordinatively unsaturated. However, when the crystal packing was examined, it became apparent that in the solid state the binuclear units are associated in pairs, see Fig. 2. The open site on Rh(2) is blocked by a γ-carbon atom of a β-diketonate ligand on an adjacent molecule. The rhodium-to-carbon distance, 3.106 Å, is too long to be considered as a formal bond. However, the interaction must be relatively strong, otherwise we would expect to observe the axial ligation of a second pyridine molecule. Similar long metal–carbon interactions have been observed in the homoleptic β-diketonate com-

pounds of mercury(II) and iron(II).[16,17] We believe that the separation between the two metallocyclic rings is principally a function of the unfavourable steric interactions. There is no evidence of metal–metal interactions between the dinuclear units, the Rh(2)—Rh(2a) distance being > 4.8 Å.

The ^1H NMR spectra recorded in CD_2Cl_2 at 290 K (see Experimental), show only averaged β-diketonate and acetate ligands. When spectra were recorded at 194 K, each class of ligand has two sets of resonances consistent with a steady-state structure in which only one rhodium ion is ligated by pyridine. The low temperature NMR data do not conclusively establish that binuclear units are linked in pairs in solution. However, even though neither signal due to the proton on the γ-carbon atom exhibits resolved coupling to rhodium, we believe that the chemical shift difference, which is much larger than that for any other pair of proton environments, may be attributed to a structure in solution closely similar to that which is observed in the crystal lattice.

Acknowledgements—We thank Johnson Matthey plc for their generous loans of rhodium trichloride and the SERC for provision of the X-ray equipment.

REFERENCES

1. M. J. Bennett, K. G. Caulton and F. A. Cotton, *Inorg. Chem.* 1969, **8**, 1.
2. A. Bino, F. A. Cotton and T. R. Felthouse, *Inorg. Chem.* 1979, **18**, 2599.
3. A. R. Chakravarty, F. A. Cotton and D. A. Tocher, *Polyhedron* 1985, **4**, 1097.
4. A. R. Chakravarty and F. A. Cotton, *Polyhedron* 1985, **4**, 1957.
5. F. A. Cotton, M. W. Extine and G. W. Rice, *Inorg. Chem.* 1978, **17**, 176.
6. F. A. Cotton, C. E. Rice and G. W. Rice, *J. Am. Chem. Soc.* 1977, **99**, 4704.
7. S. Cenini, R. Ugo and F. Bonati, *Inorg. Chim. Acta* 1967, **1**, 443.
8. H. J. McCarthy and D. A. Tocher, *Inorg. Chim. Acta* 1988, **145**, 171.
9. E. C. Morrison, C. A. Palmer and D. A. Tocher, *J. Organomet. Chem.* 1988, **349**, 405.
10. Y.-B. Koh and G. G. Christoph, *Inorg. Chem.* 1978, **17**, 2590.
11. M. Calligaris, L. Campana, G. Mestroni, M. Tornatore and E. Alessio, *Inorg. Chim. Acta* 1987, **127**, 103.
12. J. Halpern, E. Kimura, J. Molin-Case and C. S. Wong, *J. Chem. Soc., Chem. Commun.* 1971, 1207.
13. H. J. McCarthy and D. A. Tocher, to be published.
14. A. R. Chakravarty, F. A. Cotton, D. A. Tocher and J. H. Tocher, *Organometallics* 1985, **4**, 8.
15. E. C. Morrison and D. A. Tocher, *Inorg. Chim. Acta* 1989, **157**, 139.
16. W. Depmeier, K. Dietrich, K. Konig, H. Musso and W. Weiss, *J. Organomet. Chem.* 1986, **314**, C1.
17. F. A. Cotton and G. W. Rice, *Nouv. J. Chim.* 1977, **1**, 301.

Polyhedron Vol. 8, No. 8, pp. 1123–1134, 1989
Printed in Great Britain

0277–5387/89 $3.00+.00
© 1989 Pergamon Press plc

CLUSTER CONDENSATIONS. THE DECARBONYLATION AND DIMERIZATION OF THE SULPHUR-BRIDGED CLUSTER COMPLEXES $Ru_3(CO)_8L(\mu_3\text{-}HC_2Ph)(\mu_3\text{-}S)$ (L = CO AND PMe_2Ph). X-RAY CRYSTAL STRUCTURES OF $Ru_3(CO)_8(PMe_2Ph)(\mu_3\text{-}HC_2Ph)(\mu_3\text{-}S)$, $[Ru_3(CO)_8(\mu_3\text{-}HC_2Ph)(\mu_4\text{-}S)]_2$ AND TWO ISOMERS OF $[Ru_3(CO)_7(PMe_2Ph)(\mu_3\text{-}HC_2Ph)(\mu_4\text{-}S)]_2$

RICHARD D. ADAMS,* JAMES E. BABIN and THOMAS A. WOLFE

Department of Chemistry, University of South Carolina, Columbia, SC 29208, U.S.A.

(*Received* 21 *October* 1988; *accepted* 30 *November* 1988)

Abstract—The compounds $Ru_3(CO)_9(\mu_3\text{-}HC_2Ph)(\mu_3\text{-}S)$ (**1**) and $Ru_3(CO)_8(PMe_2Ph)(\mu_3\text{-}HC_2Ph)(\mu_3\text{-}S)$ (**2**) are decarbonylated when heated to 68°C and condense to form the dimers $[Ru_3(CO)_8(\mu_3\text{-}HC_2Ph)(\mu_4\text{-}S)]_2$ (**3**) and two isomers of $[Ru_3(CO)_7(PMe_2Ph)(\mu_3\text{-}HC_2Ph)(\mu_4\text{-}S)]_2$ (**4**) and (**5**), respectively. Compounds **2**, **3**, **4** and **5** were characterized by single-crystal X-ray diffraction. Compounds **1** and **2** are open clusters that have a triply bridging sulphido ligand and a triply bridging HC_2Ph ligand. Compounds **3**, **4** and **5** are dimers of the decarbonylated forms of **1** and **2** that are joined by two S → Ru donor–acceptor bonds, one from each cluster to the other. Compounds **3** and **4** are centrosymmetric and were formed by the combination of enantiomers of the cluster precursors. Compound **5** is chiral but has overall C_2 symmetry and was formed by the combination of enantiomerically similar monomeric units. Compound **5** is converted to **4** when heated, but the reverse does not occur.

Recent studies have demonstrated the value of bridging sulphido ligands in facilitating the addition of metal containing groups to cluster complexes[1–9] [e.g. eq. (1)[10]]. In the absence of addition reagents, ligand elimination processes may result in self-condensation of the clusters, (e.g. dimerization, eq. (2);[11] cyclotrimerization, eq. (3)[12]). This is facilitated by coordination of the lone pair of electrons of the bridging sulphido ligand to the vacant site on the metal atom of a second cluster. Further ligand elimination can lead to the formation of metal–metal bonds between the clusters.[11]

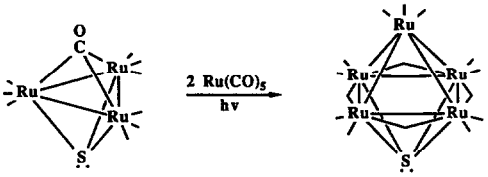

(1)

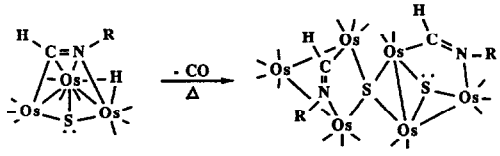

(2)

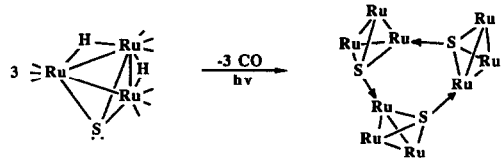

(3)

We have recently reported the preparation and structural characterization of the sulphur- and alkyne-bridged cluster complex, $Ru_3(CO)_9(\mu_3\text{-}HC_2Ph)(\mu_3\text{-}S)$ (**1**), from the reaction of $Ru_3(CO)_9(\mu_3\text{-}CO)(\mu_3\text{-}S)$ with HC_2Ph.[13] Compound **1** is easily enlarged by the sequential addition of ruthenium carbonyl fragments generated from $Ru(CO)_5$.[14] We have now found that **1** and its PMe_2Ph derivative, **2**, readily undergo the elim-

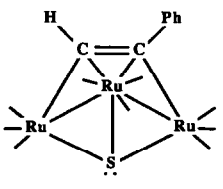

1

* Author to whom correspondence should be addressed.

ination of 1 mole of CO when heated and the resultant ligand deficient species will combine with a second cluster to yield dimers joined by bridging sulphido ligands. The results of this study are reported herein.

EXPERIMENTAL

General data

All reactions were performed under a nitrogen atmosphere, unless otherwise specified. Reagent grade solvents were dried over 4 Å molecular sieves. $Ru_3(CO)_{12}$ was purchased from Strem Chemical Co. and was used as received. Phenylacetylene was purchased from Aldrich Chemical Co. and was vacuum distilled before use. Dimethylphenylphosphine was purchased from Aldrich Chemical Co. and used as received. CP grade carbon monoxide was purchased from Linde Co. and was used without further purification. $Ru_3(CO)_9(\mu_3\text{-}\eta^2\text{-}HC_2Ph)(\mu_3\text{-}S)$ (**1**) was prepared as previously reported.[13]

All chromatographic separations were performed in air. TLC separations were performed on plates of 0.25 mm Kieselgel 60 F_{254}, E. Merck, F.R.G. IR spectra were recorded on a Nicolet 5DXB FT-IR spectrophotometer. ^1H NMR spectra were recorded on a Brüker AM-300 spectrometer operating at 300 MHz. Elemental analyses were performed by Desert Analytics, Tucson, Arizona.

Preparation of $Ru_3(CO)_8(\mu_3\text{-}\eta^2\text{-}HC_2Ph)(PMe_2Ph)(\mu_3\text{-}S)$ (**2**)

100 mg (0.145 mmol) of compound **1** and 0.022 cm^3 (0.154 mmol) of PMe_2Ph were dissolved in cyclohexane (75 cm^3). The reaction solution was then stirred for 30 min at 25°C, and the solvent was removed *in vacuo*. The residue was dissolved in a minimum of CH_2Cl_2 and was chromatographed by TLC by using a hexane–CH_2Cl_2, 8:2 solvent mixture. Yield: 74.3 mg of $Ru_3(CO)_8(PMe_2Ph)[\mu_3\text{-}HC_2Ph](\mu_3\text{-}S)$ (**2**), 64% as a yellow band. IR for **2**: (ν(CO) cm^{-1} in hexane) 2082(s), 2050(vs), 2018(vs), 1997(w,br), 1982(m), 1974(w,sh), 1967(w,sh). ^1H NMR (δ in $CDCl_3$) 8.95 (s, 1H), 7.40–6.66 (m, 10H), 1.88 (d, 3H, J_{PH} = 9.54 Hz), 1.72 (d, 3H, J_{PH} = 10.47 Hz). Found: C, 36.5; H, 2.1. Calc. for $Ru_3PSO_8C_{24}H_{17}$: C, 36.0; H, 2.1%.

Decarbonylation of $Ru_3(CO)_9(\mu_3\text{-}HC_2Ph)(\mu_3\text{-}S)$ (**1**)

50 mg (0.0725 mmol) of compound **1** was dissolved in hexane (50 cm^3) and then heated to a reflux for 30 min. During this time, the yellow solution changed to a cloudy orange colour. The hexane was removed *in vacuo*, the residue was dissolved in a minimum of CH_2Cl_2 and was chromatographed by TLC, using a hexane–CH_2Cl_2, 95:5, solvent mixture. Yield: 47.0 mg of orange $[Ru_3(CO)_8(\mu_3\text{-}HC_2Ph)(\mu_4\text{-}S)]_2$ (**3**), 98%. IR for **3**: (ν(CO) cm^{-1} in hexane) 2087(vs), 2060(vs), 2041(vs), 2024(m), 2016(w), 2010(vw), 2001(w), 1974(w). ^1H NMR (δ in $CDCl_3$) 8.30 (s, 1H), 7.16–6.87 (m, 5H). Found: C, 29.0; H, 0.90. Calc. for $Ru_6S_2O_{16}C_{32}H_{12}$: C, 29.0; H, 0.91%.

Reaction of **3** *with* CO

9.0 mg (0.0068 mmol) of compound **3** was dissolved in heptane (10 cm^3). The solution was heated to reflux (98°C) for 30 min under a CO purge. Work-up as described above yielded 9.1 mg of **1**, 97%, as a yellow band.

Reaction of **3** *with* PMe_2Ph

5.0 mg (0.0038 mmol) of **3** was dissolved in CH_2Cl_2 (10 cm^3). To this solution was added 1 equivalent of PMe_2Ph. The reaction mixture was then stirred for 30 min at 25°C and the solvent was removed *in vacuo*. The residue was dissolved in a minimum of CH_2Cl_2 and was chromatographed by TLC, using a hexane–CH_2Cl_2, 8:2, solvent mixture. Yield: 5.1 mg of **2**, 84%.

Decarbonylation of **2**

51.8 mg (0.075 mmol) of compound **2** was dissolved in hexane (50 cm^3) and was then heated to a reflux for 3.5 h. The solution turned from bright yellow to orange. The hexane was removed *in vacuo*. The residue was dissolved in a minimum of CH_2Cl_2 and was chromatographed by TLC using a hexane–CH_2Cl_2, 75:25, solvent mixture. This yielded 2.7 mg of compound **2**, 21.2 mg of *R,S*-$[Ru_3(CO)_7(PMe_2Ph)(\mu_3\text{-}HC_2Ph)(\mu_4\text{-}S)]_2$ (**4**), 45% as an orange band, and 24.5 mg of *R,R*- and *S,S*-$[Ru_3(CO)_7(PMe_2Ph)(\mu_3\text{-}HC_2Ph)(\mu_4\text{-}S)]_2$ (**5**), 52.0% as a bright orange band. For **4**: IR (ν(CO) cm^{-1} in hexane) 2052(s), 2028(vs), 1996(w), 1972(m), 1953(w). ^1H NMR (δ in $CDCl_3$) 7.59–6.57 (m, 11H), 1.98 (d, 3H, J_{PH} = 10.83 Hz), 1.96 (d, 3H, J_{PH} = 10.86 Hz). Found: C, 36.0; H, 2.2. Calc. for $Ru_6P_2S_2O_{14}C_{46}H_{34}$: C, 35.8; H, 2.2%. For **5**: IR (ν(CO) cm^{-1} in hexane) 2067(s), 2054(m), 2029(vs), 2006(vw), 1982(m), 1971(w), 1967(w,sh), 1951(m). ^1H NMR (δ in $CDCl_3$) 7.64–6.57 (m, 11H), 2.04 (d, 3H, J_{PH} = 10.29 Hz), 2.01 (d, 3H, J_{PH} = 10.47 Hz). Found: C, 35.7; H, 1.93. Calc. for $Ru_6P_2S_2O_{14}C_{46}H_{34}$: C, 35.8; H, 2.22%. The yields of

compounds **4** and **5** were calculated from the amount of **2** that was consumed.

Isomerization of **5** *to* **4**

48.8 mg (0.0369 mmol) of compound **5** was heated to reflux in octane (50 cm^3). The reaction solution was refluxed for 2.5 h. Work-up as described above yielded 27.1 mg of compound **4**, 60%, and 3.8 mg of compound **5**. The yield of compound **4** was calculated from the amount of **5** consumed.

Crystallographic analyses

Crystals of **2** were grown by slow evaporation of hexane solutions at −20°C. Crystals of **3** were grown by slow evaporation of solvent from hexane–CH_2CL_2, 8 : 2, solutions at 25°C. Crystals of **4** and **5** were grown by slow evaporation of benzene solutions at 25°C. The data crystals were mounted in thin-walled glass capillaries. Diffraction measurements were made on a Rigaku AFC6 automatic diffractometer by using Mo-K_α radiation. Unit cells were determined and refined from 25 randomly selected reflections obtained by using the AFC6 automatic search, centre, index and least-squares routines. Crystal data and results of the analyses are listed in Table 1. All data processing was performed on a Digital Equipment Corp. MICROVAX II computer by using the TEXSAN structure solving program library (v 2.0) obtained from the Molecular Structure Corp., College Station, Texas. Neutral atom scattering factors were obtained from the standard sources.[15a] Anomalous dispersion corrections were applied to all non-hydrogen atoms.[15b] Full-matrix least-squares of refinements minimized the function:

$$\sum_{hkl} w(|F_{obs}| - |F_{calc}|)^2 \quad \text{where}$$

$$w = 1/\sigma(F)^2, \quad \sigma(F) = \sigma(F^2_{obs})/2F_{obs}$$

$$\text{and} \quad \sigma(F^2_{obs}) = [\sigma(I_{raw})^2 + (PF^2_{obs})^2]^{1/2}/Lp.$$

Table 1. Crystal data for the structural analyses of compounds **2–5**

Compound	**2**	**3**	**4**	**5**
Formula	$Ru_3SPO_8C_{24}H_{17}$	$Ru_6S_2O_{16}C_{32}H_{12}$	$Ru_6S_2P_2O_{14}C_{46}H_{34}$	$Ru_6S_2P_2O_{14}C_{46}H_{34}$
Formula weight	799.48	1322.86	1543.25	1543.25
Crystal system	Triclinic	Triclinic	Triclinic	Triclinic
Lattice parameters				
a (Å)	10.0315(9)	13.469(2)	11.221(3)	12.982(1)
b (Å)	15.394(1)	15.750(4)	13.099(3)	20.395(3)
c (Å)	9.902(1)	9.930(2)	10.148(4)	10.649(1)
α (°)	106.542(7)	90.27(2)	93.62(3)	102.01(1)
β (°)	106.978(9)	96.72(2)	116.56(2)	93.564(9)
γ (°)	96.154(8)	73.57(2)	78.11(2)	101.85(1)
V (Å^3)	1371.4(6)	2006(1)	1304.9(7)	2683.0(6)
Space group	$P\bar{1}$ (No. 2)	$P\bar{1}$ (No. 2)	$P\bar{1}$ (No. 2)	$P\bar{1}$ (No. 2)
Z value	2	2	1	2
D_{calc} (g cm^{-3})	1.94	2.19	1.96	1.91
μ(Mo-K_α) (cm^{-1})	17.68	23.16	18.51	18.01
Radiation	Mo-K_α	Mo-K_α	Mo-K_α	Mo-K_α
Absorption of correction	Numerical	Numerical	Empirical	Empirical
Transmission coefficient (Max.; Min)	0.59; 0.49	0.94; 0.67	1.00; 0.58	1.00; 0.82
Temperature (°C)	23	23	23	23
$2\theta_{max}$ (°)	50.0	45.0	46.0	42.0
Number of observations [$I > 3\sigma(I)$]	4415	3796	2776	3453
Number of variables	402	511	316	331
Residuals: R; R_w	0.021; 0.026	0.026; 0.029	0.043; 0.047	0.047; 0.044
Goodness-of-fit indicator	1.82	1.01	2.02	1.47
Maximum shift in final cycle	0.08	0.02	0.08	0.00
Largest peak in final difference map (e$^-$ Å^3)	0.36	0.37	1.57	0.94

All four compounds crystallized in the triclinic crystal system.

The space group $P\bar{1}$ was assumed and confirmed in each case by the successful solution and refinement of the structure.

For **2**, the structure was solved by a combination of Patterson and difference Fourier syntheses. All non-hydrogen atoms were refined with anisotropic thermal parameters. All hydrogen atoms were located and refined with isotropic thermal parameters.

The structures of compounds **3**–**5** were solved by combinations of direct methods and difference Fourier syntheses. Compound **3** contains two symmetry independent molecules in the unit cell, and each molecule contains a crystallographically imposed centre of symmetry. Compound **4** contains only one complete molecule in the unit cell and it contains a crystallographically imposed centre of symmetry. For **3** and **4**, all non-hydrogen atoms were refined with anisotropic thermal parameters. For **3**, the acetylenic hydrogen atoms were located and refined. The hydrogen atom positions of the phenyl groups were calculated and included in the structure factor calculations, but they were not refined. For **4**, all hydrogen atom coordinates were calculated and their scattering contributions were added to the structure factor calculations, but their positions were not refined. For **5**, only the atoms larger than oxygen were refined with anisotropic thermal parameters. Hydrogen atom coodinates were calculated and their scattering contributions were included in the structure factor calculations, but their positions were not refined.*

RESULTS AND DISCUSSION

Compounds **1** and **2** undergo decarbonylation when solutions in hexane solvent are refluxed. The decarbonylated species then couple in pairs to yield the hexaruthenium complexes **3**, and **4** and **5** in reasonably good yield from **1** and **2**, respectively. Compound **3** can be reconverted to **1** by treatment with CO at 97°C, and converted to **2** by treatment with PMe_2Ph at 25°C. As determined from the crystallographic characterizations, *vide infra*, compounds **4** and **5** are isomers. It was found that **5** is converted to **4** when refluxed in octane solutions, but the reverse does not occur. This is in accord with the finding that the yield of **4** relative to **5** increases as the reaction period decreases.

Description of the structures

$Ru_3(CO)_8(PMe_2Ph)(\mu_3\text{-}HC_2Ph)(\mu_3\text{-}S)$ (**2**). An ORTEP diagram of the molecular structure of **2** is shown in Fig. 1. Selected bond distances and angles are listed in Tables 2 and 3. The molecule consists of an "open" triangular cluster of three ruthenium atoms that contains two ruthenium–ruthenium bonds. Structurally, compound **2** is very similar to that of **1**.[13] However, unlike **1**, in which the two ruthenium–ruthenium bonds are nearly equal in length, 2.798 vs 2.776 Å,† the Ru(2)—Ru(3) bond that lies approximately *trans* to the phosphine ligand in **2** is significantly longer than the Ru(1)—Ru(2) bond, 2.8077(5) vs 2.7482(4) Å. A similar difference that was attributed to a σ-inductive effect of the phosphine ligand was observed between the two open osmium cluster complexes $Os_3(CO)_9(\mu_3\text{-}S)_2$ and $Os_3(CO)_8(PMe_2Ph)(\mu_3\text{-}S)_2$.[16] Compound **2** contains a triply bridging sulphido ligand and a triply bridging HC_2Ph ligand analogous to **1**. The alkyne ligand has adopted the $2\sigma+\pi$ or μ_3-|| bonding mode and serves as a four electron donor.[17] The hydrogen atom on the alkyne ligand was located and refined. In the ^1H NMR spectrum of **2**, it was observed in the characteristically low-field shift region at $\delta = 8.95$. The carbonyl ligands on Ru(2) differ from the relative positions observed in **1**. In **2**, one carbonyl ligand C(23)—O(23) lies essentially in the plane of the three metal atoms and displays a weak semibridg-

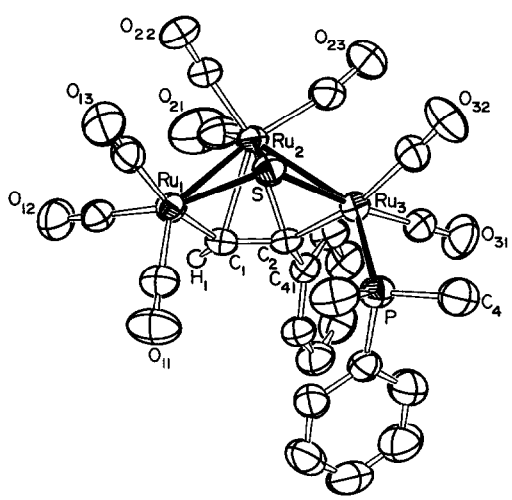

Fig. 1. An ORTEP diagram of $Ru_3(CO)_8(PMe_2Ph)(\mu_3\text{-}HC_2Ph)(\mu_3\text{-}S)$ (**2**).

*Complete tables of bond lengths, angles, atomic positional and thermal parameters, and observed and calculated structure factors for **2**–**5** have been deposited as supplementary material with the Editor, from whom copies are available on request. Atomic coordinates have been submitted to the Cambridge Crystallographic Data Centre.

† These are averaged values.

Table 2. Intramolecular distances for $Ru_3(CO)_8(PMe_2Ph)(\mu_3\text{-}HC_2Ph)(\mu_3\text{-}S)$ (**2**)

Atom	Atom	Distance	Atom	Atom	Distance
Ru(1)	C(11)	1.878(3)	Ru(2)	Ru(3)	2.8077(5)
Ru(1)	C(12)	1.912(3)	Ru(3)	C(31)	1.888(3)
Ru(1)	C(13)	1.973(3)	Ru(3)	C(32)	1.936(3)
Ru(1)	C(1)	2.053(3)	Ru(3)	C(2)	2.076(2)
Ru(1)	S	2.3691(8)	Ru(3)	P	2.2785(8)
Ru(1)	Ru(2)	2.7482(4)	Ru(3)	S	2.3680(7)
Ru(2)	C(22)	1.896(3)	P	C(3)	1.796(4)
Ru(2)	C(23)	1.907(3)	P	C(51)	1.815(3)
Ru(2)	C(21)	1.910(4)	P	C(4)	1.822(4)
Ru(2)	C(1)	2.290(3)	C(1)	C(2)	1.399(4)
Ru(2)	C(2)	2.320(2)	O	C(av)	1.131(4)
Ru(2)	S	2.4082(7)	C	C(ring)	1.376(6)

Distances are in angstroms. Estimated standard deviations in the least significant figure are given in parentheses.

Table 3. Intramolecular bond angles for $Ru_3(CO)_8(PMe_2Ph)(\mu_3\text{-}HC_2Ph)(\mu_3\text{-}S)$ (**2**)

Atom	Atom	Atom	Angle	Atom	Atom	Atom	Angle
C(11)	Ru(1)	S	104.3(1)	S	Ru(2)	Ru(1)	54.22(2)
C(11)	Ru(1)	Ru(2)	145.4(1)	S	Ru(2)	Ru(3)	53.33(2)
C(12)	Ru(1)	C(13)	92.8(1)	Ru(1)	Ru(2)	Ru(3)	90.85(1)
C(12)	Ru(1)	S	159.2(1)	C(31)	Ru(3)	Ru(2)	116.96(9)
C(12)	Ru(1)	Ru(2)	104.37(9)	C(32)	Ru(3)	S	90.86(9)
C(13)	Ru(1)	S	90.39(9)	C(32)	Ru(3)	Ru(2)	111.6(1)
C(13)	Ru(1)	Ru(2)	111.3(1)	C(2)	Ru(3)	P	101.20(7)
C(1)	Ru(1)	S	83.92(8)	C(2)	Ru(3)	S	85.13(7)
C(1)	Ru(1)	Ru(2)	54.67(7)	C(2)	Ru(3)	Ru(2)	54.26(6)
S	Ru(1)	Ru(2)	55.55(2)	P	Ru(3)	S	97.86(3)
C(22)	Ru(2)	S	86.8(1)	P	Ru(3)	Ru(2)	140.84(2)
C(22)	Ru(2)	Ru(1)	82.60(9)	S	Ru(3)	Ru(2)	54.66(2)
C(22)	Ru(2)	Ru(3)	132.8(1)	Ru(3)	S	Ru(1)	113.35(3)
C(23)	Ru(2)	S	100.2(1)	Ru(3)	S	Ru(2)	72.01(2)
C(23)	Ru(2)	Ru(1)	154.4(1)	Ru(1)	S	Ru(2)	70.23(2)
C(23)	Ru(2)	Ru(3)	71.3(1)	C(2)	C(1)	Ru(1)	130.23(2)
C(21)	Ru(2)	S	163.1(1)	C(2)	C(1)	Ru(2)	73.5(1)
C(21)	Ru(2)	Ru(1)	109.2(1)	Ru(1)	C(1)	Ru(2)	78.31(8)
C(21)	Ru(2)	Ru(3)	130.9(1)	C(1)	C(2)	C(41)	114.7(2)
C(1)	Ru(2)	C(2)	35.33(9)	C(1)	C(2)	Ru(3)	125.8(2)
C(1)	Ru(2)	S	78.26(7)	C(1)	C(2)	Ru(2)	71.1(1)
C(1)	Ru(2)	Ru(1)	47.02(6)	C(41)	C(2)	Ru(3)	119.6(2)
C(1)	Ru(2)	Ru(3)	74.36(7)	C(41)	C(2)	Ru(2)	124.2(2)
C(2)	Ru(2)	S	79.15(6)	Ru(3)	C(2)	Ru(2)	79.18(8)
C(2)	Ru(2)	Ru(1)	76.37(6)	O(23)	C(23)	Ru(2)	170.6(3)
C(2)	Ru(2)	Ru(3)	46.56(6)	O	C(av)	Ru	176(1)

Angles are in degrees. Estimated standard deviations in the least significant figure are given in parentheses.

ing character to Ru(3), Ru(2)—C(23)—O(23) = 170.6(3)°. This ligand lies in the region approximately *trans* to the phosphine ligand on Ru(3). The development of the semibridging character could be a result of the greater concentration of electron density on Ru(3) due to the substitution of a carbonyl ligand with the PMe_2Ph ligand. All the other carbonyl ligands are linear. Overall, the molecule contains no symmetry and the crystal consists of a racemic mixture of the two enantiomers.

$[Ru_3(CO)_8(\mu_3\text{-}HC_2Ph)(\mu_4\text{-}S)]_2$ (**3**). An ORTEP drawing of the molecular structure of **3** is shown in Fig. 2. Selected bond distances and angles are listed in Tables 4 and 5. In the crystal, compound **3** contains two symmetry independent dimers of the monomeric unit $Ru_3(CO)_8(\mu_3\text{-}HC_2Ph)(\mu_3\text{-}S)$ and each dimer contains a crystallographically-imposed centre of symmetry. The basic monomeric unit is structurally very similar to that of its parent **1**. Unlike **1**, **3** does not have a carbonyl ligand on the metal atom Ru(3), at the site approximately *trans* to the phenyl-substituted end of the bridging alkyne ligand. Instead, this site is filled by the donation of a lone pair of electrons from the sulphido ligand of the second monomeric unit of the dimer. This S → Ru donor–acceptor bond is significantly longer,

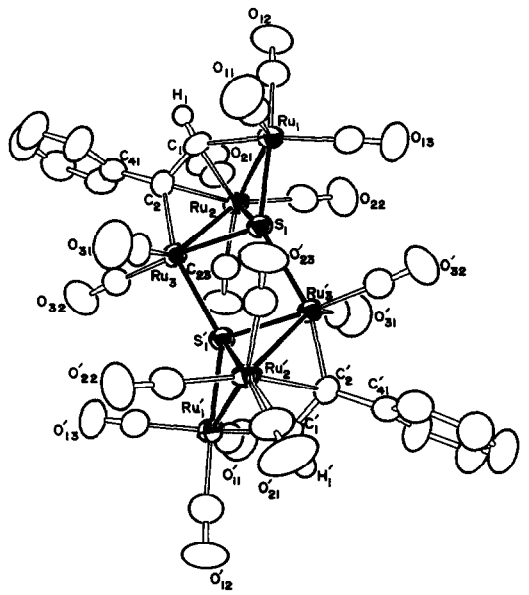

Fig. 2. An ORTEP diagram of the molecular structure of $[Ru_3(CO)_8(\mu_3\text{-}HC_2Ph)(\mu_4\text{-}S)]_2$ (**3**).

2.478(2) Å, than the Ru—S bonds within the monomeric unit which range from 2.337(2) to 2.418(2) Å. A similar difference in Ru—S bonding was observed in the cyclotrimer $[Ru_3(CO)_8(\mu\text{-}H)_2(\mu_4\text{-}S)]_3$ (**6**) in

Table 4. Intramolecular distances for **3**

Atom	Atom	Distance	Atom	Atom	Distance
Ru(1A)	C(11A)	1.895(9)	Ru(2B)	C(1B)	2.266(7)
Ru(1A)	C(12A)	1.907(9)	Ru(2B)	C(2B)	2.310(7)
Ru(1A)	C(13A)	1.977(9)	Ru(2B)	S(1B)	2.418(2)
Ru(1A)	C(1A)	2.049(8)	Ru(2B)	Ru(3B)	2.817(1)
Ru(1A)	S(1A)	2.337(2)	Ru(3A)	C(31A)	1.837(8)
Ru(1A)	Ru(2A)	2.777(1)	Ru(3A)	C(32A)	1.895(9)
Ru(1B)	C(11B)	1.86(1)	Ru(3A)	C(2A)	2.038(7)
Ru(1B)	C(12B)	1.895(8)	Ru(3A)	S(1A)	2.346(2)
Ru(1B)	C(13B)	1.990(9)	Ru(3A)	S(1A′)	2.478(2)
Ru(1B)	C(1B)	2.055(7)	Ru(3B)	C(31B)	1.828(8)
Ru(1B)	S(1B)	2.342(2)	Ru(3B)	C(32B)	1.910(8)
Ru(1B)	Ru(2B)	2.788(1)	Ru(3B)	C(2B)	2.038(6)
Ru(2A)	C(22A)	1.88(1)	Ru(3B)	S(1B)	2.347(2)
Ru(2A)	C(21A)	1.899(9)	Ru(3B)	S(1B′)	2.486(2)
Ru(2A)	C(23A)	1.944(9)	C(1B)	C(2B)	1.41(1)
Ru(2A)	C(1A)	2.253(7)	C(1A)	C(2A)	1.40(1)
Ru(2A)	C(2A)	2.330(7)	C(2B)	C(41B)	1.483(9)
Ru(2A)	S(1A)	2.410(2)	C(2A)	C(41A)	1.49(1)
Ru(2A)	Ru(3A)	2.803(1)	C(1A)	H(1A)	0.88(7)
Ru(2B)	C(21B)	1.896(8)	C(1B)	H(1B)	0.98(7)
Ru(2B)	C(22B)	1.902(9)	O	C(av)	1.13(1)
Ru(2B)	C(23B)	1.914(9)	C	C(av)	1.37(1)

Distances are in angstroms. Estimated standard deviations in the least significant figure are given in parentheses.

Table 5. Intramolecular bond angles for **3**

Atom	Atom	Atom	Angle	Atom	Atom	Atom	Angle
C(11A)	Ru(1A)	S(1A)	98.7(3)	C(23A)	Ru(2A)	Ru(3A)	72.2(2)
C(11A)	Ru(1A)	Ru(2A)	140.8(3)	C(1A)	Ru(2A)	S(1A)	76.6(2)
C(12A)	Ru(1A)	S(1A)	161.2(2)	C(1A)	Ru(2A)	Ru(1A)	46.7(2)
C(12A)	Ru(1A)	Ru(2A)	105.9(2)	C(1A)	Ru(2A)	Ru(3A)	73.4(2)
C(13A)	Ru(1A)	S(1A)	92.9(2)	C(2A)	Ru(2A)	S(1A)	77.8(2)
C(13A)	Ru(1A)	Ru(2A)	113.9(2)	C(2A)	Ru(2A)	Ru(1A)	76.1(2)
C(1A)	Ru(1A)	S(1A)	82.2(2)	C(2A)	Ru(2A)	Ru(3A)	45.6(2)
C(1A)	Ru(1A)	Ru(2A)	53.1(2)	S(1A)	Ru(2A)	Ru(1A)	52.98(5)
S(1A)	Ru(1A)	Ru(2A)	55.43(5)	S(1A)	Ru(2A)	Ru(3A)	52.85(5)
C(11B)	Ru(1B)	S(1B)	98.5(3)	Ru(1A)	Ru(2A)	Ru(3A)	89.78(3)
C(11B)	Ru(1B)	Ru(2B)	139.0(3)	C(21B)	Ru(2B)	S(1B)	165.1(2)
C(12B)	Ru(1B)	S(1B)	165.2(3)	C(21B)	Ru(2B)	Ru(1B)	114.2(2)
C(12B)	Ru(1B)	Ru(2B)	109.7(3)	C(21B)	Ru(2B)	Ru(3B)	126.4(2)
C(13B)	Ru(1B)	S(1B)	92.5(2)	C(22B)	Ru(2B)	S(1B)	92.4(3)
C(13B)	Ru(1B)	Ru(2B)	112.8(2)	C(22B)	Ru(2B)	Ru(1B)	83.3(3)
C(1B)	Ru(1B)	S(1B)	82.6(2)	C(22B)	Ru(2B)	Ru(3B)	139.0(3)
C(1B)	Ru(1B)	Ru(2B)	53.2(2)	C(23B)	Ru(2B)	S(1B)	99.3(2)
S(1B)	Ru(1B)	Ru(2B)	55.43(5)	C(23B)	Ru(2B)	Ru(1B)	151.9(2)
C(22A)	Ru(2A)	S(1A)	90.8(3)	C(23B)	Ru(2B)	Ru(3B)	73.1(2)
C(22A)	Ru(2A)	Ru(1A)	80.5(3)	C(1B)	Ru(2B)	S(1B)	76.8(2)
C(22A)	Ru(2A)	Ru(3A)	138.3(2)	C(1B)	Ru(2B)	Ru(1B)	46.6(2)
C(21A)	Ru(2A)	S(1A)	168.2(2)	C(1B)	Ru(2B)	Ru(3B)	73.1(2)
C(21A)	Ru(2A)	Ru(1A)	116.1(3)	C(2B)	Ru(2B)	S(1B)	78.4(2)
C(21A)	Ru(2A)	Ru(3A)	128.3(3)	C(2B)	Ru(2B)	Ru(1B)	76.5(2)
C(23A)	Ru(2A)	S(1A)	97.6(2)	C(2B)	Ru(2B)	Ru(3B)	45.5(2)
C(23A)	Ru(2A)	Ru(1A)	150.2(2)	S(1B)	Ru(2B)	Ru(1B)	52.89(5)
S(1B)	Ru(2B)	Ru(3B)	52.59(5)	Ru(1B)	S(1B)	Ru(3B)	114.01(7)
Ru(1B)	Ru(2B)	Ru(3B)	89.11(3)	Ru(1B)	S(1B)	Ru(2B)	71.68(5)
C(31A)	Ru(3A)	S(1A)	102.6(2)	Ru(1B)	S(1B)	Ru(3B′)	143.55(8)
C(31A)	Ru(3A)	S(1A′)	98.9(2)	Ru(3B)	S(1B)	Ru(2B)	72.47(6)
C(31A)	Ru(3A)	Ru(2A)	141.8(2)	Ru(3B)	S(1B)	Ru(3B′)	102.44(7)
C(32A)	Ru(3A)	S(1A)	166.0(2)	Ru(2B)	S(1B)	Ru(3B)	122.26(7)
C(32A)	Ru(3A)	S(1A′)	98.8(2)	Ru(1A)	S(1A)	Ru(3A)	114.48(7)
C(32A)	Ru(3A)	Ru(2A)	114.3(2)	Ru(1A)	S(1A)	Ru(2A)	71.59(5)
C(2A)	Ru(3A)	S(1A)	85.3(2)	Ru(1A)	S(1A)	Ru(3A′)	142.74(8)
C(2A)	Ru(3A)	S(1A′)	158.5(2)	Ru(3A)	S(1A)	Ru(2A)	72.20(6)
C(2A)	Ru(3A)	Ru(2A)	54.8(2)	Ru(3A)	S(1A)	Ru(3A′)	102.66(7)
S(1A)	Ru(3A)	S(1A′)	77.34(7)	Ru(2A)	S(1A)	Ru(3A)	119.95(7)
S(1A)	Ru(3A)	Ru(2A)	54.95(5)	C(2B)	C(1B)	Ru(1B)	132.1(5)
S(1A′)	Ru(3A)	Ru(2A)	104.23(5)	C(2B)	C(1B)	Ru(2B)	73.8(4)
C(31B)	Ru(3B)	S(1B)	103.3(2)	Ru(1B)	C(1B)	Ru(2B)	80.2(2)
C(31B)	Ru(3B)	S(1B′)	97.8(2)	C(2A)	C(1A)	Ru(1A)	132.6(5)
C(31B)	Ru(3B)	Ru(2B)	141.4(3)	C(2A)	C(1A)	Ru(2A)	75.3(4)
C(32B)	Ru(3B)	S(1B)	166.6(2)	Ru(1A)	C(1A)	Ru(2A)	80.3(3)
C(32B)	Ru(3B)	S(1B′)	97.7(2)	C(1B)	C(2B)	C(41B)	113.6(6)
C(32B)	Ru(3B)	Ru(2B)	115.8(2)	C(1B)	C(2B)	Ru(2B)	70.3(4)
C(2B)	Ru(3B)	S(1B)	85.7(2)	Ru(3B)	C(2B)	Ru(2B)	80.5(2)
C(2B)	Ru(3B)	S(1B′)	159.6(2)	C(1A)	C(2A)	C(41A)	115.7(6)
C(2B)	Ru(3B)	Ru(2B)	54.0(2)	C(1A)	C(2A)	Ru(3A)	124.3(5)
S(1B)	Ru(3B)	S(1B′)	77.56(6)	C(1A)	C(2A)	Ru(2A)	69.3(4)
S(1B)	Ru(3B)	Ru(2B)	54.94(5)	Ru(3A)	C(2A)	Ru(2A)	79.5(2)
S(1B′)	Ru(3B)	Ru(2B)	106.19(5)	O	C	Ru(av)	176.6(8)

Angles are in degrees. Estimated standard deviations in the least significant figure are given in parentheses.

which the monomeric units were also joined by S → Ru donor–acceptor bonds.[12] The sulphido ligand in the first monomeric unit is similarly coordinated to the corresponding ruthenium atom of the second cluster and this completes joining of the two clusters. A planar Ru—S—Ru—S ring is formed. The alkyne hydrogen atoms were located and refined. It exhibits the characteristic low-field shift, $\delta = 8.30$, but is shifted upfield slightly (0.53 ppm) from that observed in **1**.

R,S-$[Ru_3(CO)_7(PMe_2Ph)(\mu_3\text{-}HC_2Ph)(\mu_4\text{-}S)]_2$ (**4**). An ORTEP drawing of the molecular structure of **4** is shown in Fig. 3. Selected bond distances and angles are listed in Tables 6 and 7. The unit cell contains one formula unit of **4** and like **3** it contains a crystallographically-imposed centre of symmetry. Thus **4** consists of a combination of the *R*- and *S*-enantiomers of the monomeric cluster unit. The configuration of the cluster can be defined uniquely from the configuration of the chiral sulphido ligand. The monomeric unit, $Ru_3(CO)_7(PMe_2Ph)(\mu_3\text{-}HC_2Ph)(\mu_3\text{-}S)$, is structurally very similar to that of its parent **2**, *vide supra*, except that the two Ru—Ru bond distances are nearly equal, Ru(1)—Ru(2) by TLC, using a hexane–CH_2Cl_2, 95:5, solvent = 2.803 (1) Å and Ru(2)—Ru(3) = 2.799(2) Å. The dimer is linked through two S → Ru donor–acceptor bonds similar to those in **3**. As in **3**, these donor–acceptor bonds are significantly longer, 2.500(3) Å, than those within the monomeric cluster unit, range 2.348(3)–2.427(3) Å. As in **3**, the Ru—S—Ru—S ring is planar by symmetry.

R,R- and S,S-$[Ru_3(CO)_7(PMe_2Ph)(\mu_3\text{-}HC_2Ph)(\mu_4\text{-}S)]_2$ (**5**). An ORTEP drawing of the molecular struture of **5** is shown in Fig. 4. Selected bond distances and angles are listed in Tables 8 and 9. Compound **5** is an isomer of **4**. It is also a dimer of **2**, but was formed by the coupling of two enantiomerically similar monomers. The structure of the monomeric unit, $Ru_3(CO)_7(PMe_2Ph)(\mu_3\text{-}HC_2Ph)(\mu_3\text{-}S)$, in **5** is essentially the same as that in **4**. The two monomeric units are joined by two S → Ru donor–acceptor bonds, Ru(3)—S(2) and Ru(6)—S(1), that are similar in length to those in **4**, 2.490(4) and 2.510(4) Å, and are significantly longer than the Ru—S bonds within the cluster unit. Overall, the molecule has C_2 symmetry (not crystallographically imposed). The Ru—S—Ru—S ring is not planar but has a slight fold. The dihedral angle is 16.5°. Since the crystal of **5** is centrosymmetrical, it must contain an equal mixture of the two enantiomeric dimers (i.e. the *R,R* and *S,S* combinations of the monomers).

The irreversible isomerization of **5** to **4** indicates that **5** is a kinetically stable product of the decarbonylation of **2**. Evidently, for reasons that are not apparent to us, enantiomerically similar monomeric units undergo dimerization more readily than enantiomerically dissimilar monomeric units, but the *meso* isomer **4** is thermodynamically more stable.

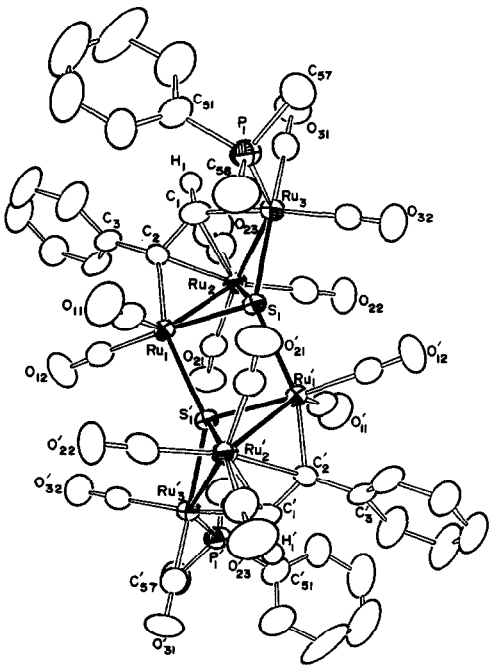

Fig. 3. An ORTEP diagram of *R,S*-$[Ru_3(CO)_7(PMe_2P)(\mu_3\text{-}HC_2Ph)(\mu_4\text{-}S)]_2$ (**4**).

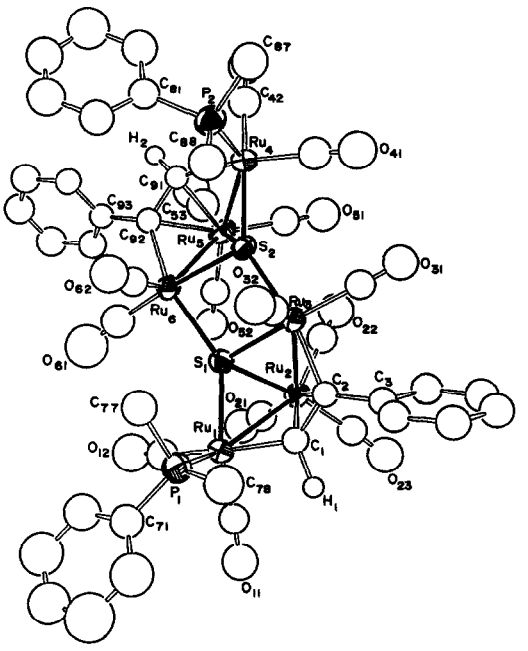

Fig. 4. An ORTEP diagram of $[Ru_3(CO)_7(PMe_2Ph)(\mu_3\text{-}HC_2Ph)(\mu_4\text{-}S)]_2$ (**5**). The *R,R*-enantiomer is shown.

Table 6. Intramolecular distances for **4**

Atom	Atom	Distance	Atom	Atom	Distance
Ru(1)	C(11)	1.83(1)	Ru(2)	Ru(3)	2.799(2)
Ru(1)	C(12)	1.90(1)	Ru(3)	C(31)	1.87(1)
Ru(1)	C(2)	2.05(1)	Ru(3)	C(32)	1.93(1)
Ru(1)	S(1)	2.355(3)	Ru(3)	C(1)	2.07(1)
Ru(1)	S(1′)	2.500(3)	Ru(3)	P(1)	2.274(3)
Ru(1)	C(21)	2.85(1)	Ru(3)	S(1)	2.348(3)
Ru(1)	Ru(2)	2.802(1)	P(1)	C(58)	1.79(1)
Ru(2)	C(23)	1.87(1)	P(1)	C(57)	1.80(1)
Ru(2)	C(22)	1.90(1)	P(1)	C(51)	1.82(1)
Ru(2)	C(21)	1.92(1)	C(1)	C(2)	1.41(1)
Ru(2)	C(1)	2.29(1)	C(2)	C(3)	1.50(1)
Ru(2)	C(2)	2.30(1)	O	C(av)	1.13(1)
Ru(2)	S(1)	2.427(3)	C	C(av)	1.37(1)

Distances are in angstroms. Estimated standard deviations in the least significant figure are given in parentheses.

Table 7. Intramolecular bond angles for **4**

Atom	Atom	Atom	Angle	Atom	Atom	Atom	Angle
C(11)	Ru(1)	S(1)	98.2(4)	C(2)	Ru(2)	Ru(1)	46.2(2)
C(11)	Ru(1)	S(1′)	98.4(3)	S(1)	Ru(2)	Ru(3)	52.82(6)
C(11)	Ru(1)	Ru(2)	139.1(4)	S(1)	Ru(2)	Ru(1)	52.93(6)
C(12)	Ru(1)	S(1)	171.1(3)	Ru(3)	Ru(2)	Ru(1)	90.17(4)
C(12)	Ru(1)	S(1′)	97.9(3)	C(31)	Ru(3)	P(1)	91.0(3)
C(12)	Ru(1)	Ru(2)	118.2(3)	C(31)	Ru(3)	S(1)	160.3(3)
C(2)	Ru(1)	S(1)	84.9(3)	C(31)	Ru(3)	Ru(2)	105.5(3)
C(2)	Ru(1)	S(1′)	158.9(3)	C(32)	Ru(3)	P(1)	92.4(3)
C(2)	Ru(1)	Ru(2)	53.9(3)	C(32)	Ru(3)	S(1)	91.4(3)
S(1)	Ru(1)	S(1)	79.2(1)	C(32)	Ru(3)	Ru(2)	119.0(3)
S(1)	Ru(1)	Ru(2)	55.34(7)	C(1)	Ru(3)	P(1)	93.8(3)
S(1′)	Ru(1)	Ru(2)	105.14(7)	C(1)	Ru(3)	S(1)	82.3(3)
C(23)	Ru(2)	S(1)	161.8(4)	C(1)	Ru(3)	Ru(2)	53.6(3)
C(23)	Ru(2)	Ru(3)	109.7(4)	P(1)	Ru(3)	S(1)	107.4(1)
C(23)	Ru(2)	Ru(1)	130.3(4)	P(1)	Ru(3)	Ru(2)	142.22(9)
C(22)	Ru(2)	S(1)	89.8(3)	S(1)	Ru(3)	Ru(2)	55.43(7)
C(22)	Ru(2)	Ru(3)	83.4(3)	Ru(3)	S(1)	Ru(1)	115.0(1)
C(22)	Ru(2)	Ru(1)	135.0(3)	Ru(3)	S(1)	Ru(2)	71.76(8)
C(21)	Ru(2)	S(1)	102.4(3)	Ru(3)	S(1)	Ru(1′)	144.0(1)
C(21)	Ru(2)	Ru(3)	155.2(3)	Ru(1)	S(1)	Ru(2)	71.73(8)
C(21)	Ru(2)	Ru(1)	71.5(3)	Ru(1)	S(1)	Ru(1′)	100.8(1)
C(1)	Ru(2)	S(1)	76.4(2)	Ru(2)	S(1)	Ru(1′)	118.9(1)
C(1)	Ru(2)	Ru(3)	46.8(3)	C(58)	P(1)	Ru(3)	115.0(4)
C(1)	Ru(2)	Ru(1)	73.8(3)	C(57)	P(1)	Ru(3)	114.8(4)
C(2)	Ru(2)	S(1)	78.2(2)	C(51)	P(1)	Ru(3)	115.1(3)
C(2)	Ru(2)	Ru(3)	76.6(2)	C(2)	C(1)	Ru(3)	131.6(7)
C(2)	C(1)	Ru(2)	72.6(6)				
Ru(3)	C(1)	Ru(2)	79.7(4)				
C(1)	C(2)	C(3)	116.3(9)				
C(1)	C(2)	Ru(1)	125.1(7)				
C(1)	C(2)	Ru(2)	71.7(6)				
C(3)	C(2)	Ru(1)	118.4(6)				
C(3)	C(2)	Ru(2)	126.9(6)				
Ru(1)	C(2)	Ru(2)	79.9(3)				
O	C	Ru(av)	178(1)				

Angles are in degrees. Estimated standard deviations in the least significant figure are given in parentheses.

Table 8. Intramolecular distances for **5**

Atom	Atom	Distance	Atom	Atom	Distance
Ru(1)	C(11)	1.84(2)	Ru(5)	C(53)	1.82(2)
Ru(1)	C(12)	1.92(2)	Ru(5)	C(51)	1.86(2)
Ru(1)	C(1)	2.06(1)	Ru(5)	C(52)	1.87(2)
Ru(1)	P(1)	2.273(5)	Ru(5)	C(91)	2.27(1)
Ru(1)	S(1)	2.355(4)	Ru(5)	C(92)	2.30(1)
Ru(1)	Ru(2)	2.790(2)	Ru(5)	S(2)	2.431(4)
Ru(2)	C(21)	1.85(2)	Ru(5)	Ru(6)	2.798(2)
Ru(2)	C(23)	1.87(2)	Ru(6)	C(62)	1.81(2)
Ru(2)	C(22)	1.88(2)	Ru(6)	C(61)	1.82(2)
Ru(2)	C(1)	2.26(1)	Ru(6)	C(92)	2.07(1)
Ru(2)	C(2)	2.33(1)	Ru(6)	S(2)	2.333(4)
Ru(2)	S(1)	2.447(4)	Ru(6)	S(1)	2.510(4)
Ru(2)	Ru(3)	2.806(2)	P(1)	C(71)	1.79(2)
Ru(3)	C(32)	1.80(2)	P(1)	C(78)	1.80(2)
Ru(3)	C(31)	1.89(2)	P(1)	C(77)	1.82(2)
Ru(3)	C(2)	2.05(1)	P(2)	C(87)	1.79(2)
Ru(3)	S(1)	2.340(4)	P(2)	C(88)	1.79(2)
Ru(3)	S(2)	2.490(4)	P(2)	C(81)	1.81(2)
Ru(4)	C(42)	1.83(2)	C(1)	C(2)	1.39(2)
Ru(4)	C(41)	1.92(2)	C(2)	C(3)	1.48(2)
Ru(4)	C(91)	2.06(1)	C(91)	C(92)	1.40(2)
Ru(4)	P(2)	2.272(5)	C(92)	C(93)	1.52(2)
Ru(4)	S(2)	2.334(4)	O	C(av)	1.16(2)
Ru(4)	Ru(5)	2.814(2)	C(Ph)	C(av)	1.38(2)
C(1)	H(1)	1.01	C(91)	H(2)	1.0

Distances are in angstroms. Estimated standard deviations in the least significant figure are given in parentheses.

Table 9. Intramolecular bond angles for **5**

Atom	Atom	Atom	Angle	Atom	Atom	Atom	Angle
C(11)	Ru(1)	P(1)	91.1(5)	C(2)	Ru(2)	Ru(3)	45.9(3)
C(11)	Ru(1)	S(1)	166.2(5)	S(1)	Ru(2)	Ru(1)	53.0(1)
C(11)	Ru(1)	Ru(2)	110.3(5)	S(1)	Ru(2)	Ru(3)	52.4(1)
C(12)	Ru(1)	P(1)	95.6(5)	Ru(1)	Ru(2)	Ru(3)	89.84(5)
C(12)	Ru(1)	S(1)	92.5(5)	C(32)	Ru(3)	S(1)	100.2(5)
C(12)	Ru(1)	Ru(2)	114.1(5)	C(32)	Ru(3)	S(2)	94.6(5)
C(1)	Ru(1)	P(1)	97.2(4)	C(32)	Ru(3)	Ru(2)	139.5(5)
C(1)	Ru(1)	S(1)	81.8(4)	C(31)	Ru(3)	S(1)	166.0(5)
C(1)	Ru(1)	Ru(2)	52.9(4)	C(31)	Ru(3)	S(2)	97.1(5)
P(1)	Ru(1)	S(1)	101.4(2)	C(31)	Ru(3)	Ru(2)	113.8(5)
P(1)	Ru(1)	Ru(2)	141.7(1)	C(2)	Ru(3)	S(1)	85.7(4)
S(1)	Ru(1)	Ru(2)	56.0(1)	C(2)	Ru(3)	S(2)	163.6(4)
C(21)	Ru(2)	S(1)	92.6(5)	C(2)	Ru(3)	Ru(2)	54.8(4)
C(21)	Ru(2)	Ru(1)	78.7(6)	S(1)	Ru(3)	S(2)	79.6(1)
C(21)	Ru(2)	Ru(3)	140.9(5)	S(1)	Ru(3)	Ru(2)	55.9(1)
C(23)	Ru(2)	S(1)	166.0(5)	S(2)	Ru(3)	Ru(2)	110.0(1)
C(23)	Ru(2)	Ru(1)	115.1(5)	C(42)	Ru(4)	P(2)	90.8(6)
C(23)	Ru(2)	Ru(3)	126.7(5)	C(42)	Ru(4)	S(2)	162.6(6)
C(22)	Ru(2)	S(1)	101.3(5)	C(42)	Ru(4)	Ru(5)	107.8(6)
C(22)	Ru(2)	Ru(1)	153.6(5)	C(41)	Ru(4)	P(2)	93.2(5)
C(22)	Ru(2)	Ru(3)	75.2(5)	C(41)	Ru(4)	S(2)	91.4(5)
C(1)	Ru(2)	S(1)	76.0(4)	C(41)	Ru(4)	Ru(5)	118.0(5)

Table 9—*Continued*

Atom	Atom	Atom	Angle	Atom	Atom	Atom	Angle
C(1)	Ru(2)	Ru(1)	46.7(4)	C(91)	Ru(4)	P(2)	95.2(4)
C(1)	Ru(2)	Ru(3)	73.2(4)	C(91)	Ru(4)	S(2)	82.2(4)
C(2)	Ru(2)	S(1)	77.6(3)	C(91)	Ru(4)	Ru(5)	52.7(4)
C(2)	Ru(2)	Ru(1)	76.3(4)	P(2)	Ru(4)	S(2)	105.5(2)
P(2)	Ru(4)	Ru(5)	141.6(1)	C(92)	Ru(6)	S(2)	85.0(4)
S(2)	Ru(4)	Ru(5)	55.4(1)	C(92)	Ru(6)	S(1)	161.0(4)
C(53)	Ru(5)	S(2)	162.8(6)	C(92)	Ru(6)	Ru(5)	53.9(4)
C(53)	Ru(5)	Ru(6)	128.8(6)	S(2)	Ru(6)	S(1)	79.3(1)
C(53)	Ru(5)	Ru(4)	111.9(6)	S(2)	Ru(6)	Ru(5)	55.7(1)
C(51)	Ru(5)	S(2)	92.5(5)	S(1)	Ru(6)	Ru(5)	107.8(1)
C(51)	Ru(5)	Ru(6)	138.6(5)	Ru(3)	S(1)	Ru(1)	114.6(2)
C(51)	Ru(5)	Ru(4)	82.6(5)	Ru(3)	S(1)	Ru(2)	71.7(1)
C(52)	Ru(5)	S(2)	101.0(5)	Ru(3)	S(1)	Ru(6)	99.2(1)
C(52)	Ru(5)	Ru(6)	70.5(5)	Ru(1)	S(1)	Ru(2)	71.0(1)
C(52)	Ru(5)	Ru(4)	153.3(5)	Ru(1)	S(1)	Ru(6)	144.4(2)
C(91)	Ru(5)	S(2)	76.1(4)	Ru(2)	S(1)	Ru(6)	133.8(2)
C(91)	Ru(5)	Ru(6)	74.1(4)	Ru(6)	S(2)	Ru(4)	115.4(2)
C(91)	Ru(5)	Ru(4)	46.3(3)	Ru(6)	S(2)	Ru(5)	71.9(1)
C(92)	Ru(5)	S(2)	78.1(4)	Ru(6)	S(2)	Ru(3)	99.9(1)
C(92)	Ru(5)	Ru(6)	46.8(4)	Ru(4)	S(2)	Ru(5)	72.4(1)
C(92)	Ru(5)	Ru(4)	76.0(4)	Ru(4)	S(2)	Ru(3)	143.3(2)
S(2)	Ru(5)	Ru(6)	52.4(1)	Ru(5)	S(2)	Ru(3)	131.6(2)
S(2)	Ru(5)	Ru(4)	52.2(1)	C(71)	P(1)	Ru(1)	116.0(6)
Ru(6)	Ru(5)	Ru(4)	89.35(5)	C(78)	P(1)	Ru(1)	113.1(6)
C(62)	Ru(6)	S(2)	99.4(5)	C(77)	P(1)	Ru(1)	113.3(6)
C(62)	Ru(6)	S(1)	96.3(5)	C(87)	P(2)	Ru(4)	114.5(6)
C(62)	Ru(6)	Ru(5)	139.4(5)	C(88)	P(2)	Ru(4)	114.9(6)
C(61)	Ru(6)	S(2)	170.2(6)	C(81)	P(2)	Ru(4)	114.4(5)
C(61)	Ru(6)	S(1)	96.2(6)	C(2)	C(1)	Ru(1)	134(1)
C(61)	Ru(6)	Ru(5)	118.6(6)	C(2)	C(1)	Ru(2)	75.3(9)
Ru(1)	C(1)	Ru(2)	80.3(5)				
C(1)	C(2)	Ru(3)	123(1)				
C(1)	C(2)	Ru(2)	69.4(9)				
C(1)	C(2)	C(3)	118(1)				
Ru(3)	C(2)	Ru(2)	79.3(5)				
C(92)	C(91)	Ru(4)	132(1)				
C(92)	C(91)	Ru(5)	73.6(8)				
Ru(4)	C(91)	Ru(5)	81.0(5)				
C(91)	C(92)	Ru(6)	124(1)				
C(91)	C(92)	Ru(5)	70.8(8)				
Ru(6)	C(92)	Ru(5)	79.3(5)				
C(91)	C(92)	C(93)	117(1)				
O	C	Ru(av)	175(2)				
C(Ph)	C	C(av)	120(2)				

Angles are in degrees. Estimated standard deviations in the least significant figure are given in parentheses.

This study clearly shows the importance of the bridging sulphido ligand to the first step in cluster self-condensation. Unfortunately, our attempts to induce further condensation by the formation of metal–metal bonds between the two triruthenium groups have not yet been successful. In the osmium system, eq. (2), further condensation was achieved.[11] These two systems seem to differ from that of the decarbonylation and dimerization of $Os_3(CO)_9(\mu_3\text{-}S)_2$.[18] In the dimer, $[Os_3(CO)_8(\mu_3\text{-}S)_2]_2$ (7), the monomeric units are joined by metal–metal bonds only. However, it is possible that unobserved sulphur-bridged intermediates were traversed en route to 7.

Acknowledgements—These studies were supported by the National Science Foundation under Grant CHE-8612862. NMR measurements were made on a Brüker AM-300 spectrometer purchased with funds from the National Science Foundation under Grant No. CHE-8411172.

REFERENCES

1. R. D. Adams, *Polyhedron* 1985, **4**, 2003.
2. R. D. Adams, J. E. Babin and M. Tasi, *Inorg. Chem.* 1986, **25**, 4514.
3. R. D. Adams, J. E. Babin and M. Tasi, *Inorg. Chem.* 1987, **26**, 2807.
4. R. D. Adams, J. E. Babin and M. Tasi, *Inorg. Chem.* 1986, **25**, 4460.
5. R. D. Adams, I. T. Horváth and S. Wang, *Inorg. Chem.* 1985, **22**, 1728.
6. R. D. Adams, I. T. Horváth and P. Mathur, *J. Am. Chem. Soc.* 1984, **106**, 6292.
7. R. D. Adams, T. S. A. Hor and I. T. Horváth, *Inorg. Chem.* 1984, **23**, 4733.
8. D. J. Darensbourg, D. J. Zalewski, K. M. Sanchez and T. Delord, *Inorg. Chem.* 1988, **27**, 821.
9. A. Winter, I. Jibril and G. Huttner, *J. Organomet. Chem.* 1983, **247**, 259.
10. R. D. Adams, J. E. Babin and M. Tasi, *Organometallics* 1988, **7**, 503.
11. R. D. Adams, Z. Dawoodi, D. F. Foust and B. E. Segmüller, *J. Am. Chem. Soc.* 1983, **105**, 831.
12. R. D. Adams, D. Mannig and B. E. Segmüller, *Organometallics* 1983, **2**, 149.
13. R. D. Adams, J. E. Babin, M. Tasi and T. A. Wolfe, *Organometallics* 1987, **6**, 2228.
14. R. D. Adams, J. E. Babin, M. Tasi and T. A. Wolfe, *Polyhedron* 1988, **7**, 1071.
15. *International Tables for X-ray Crystallography*, Vol. IV. Kynoch Press, Birmingham (1975): (a) Table 2.2B, pp. 99–101; (b) Table 2.3.1, pp. 149–150.
16. R. D. Adams, I. T. Horváth, B. E. Segmüller and L. W. Yang, *Organometallics* 1983, **2**, 144.
17. (a) E. Sappa, A. Tiripicchio and P. Braunstein, *Chem. Rev.* 1983, **83**, 203; (b) P. R. Raithby and M. J. Rosales, *Adv. Inorg. Radiochem.* 1985, **29**, 169.
18. R. D. Adams and I. T. Horváth, *J. Am. Chem. Soc.* 1984, **106**, 1869.

Polyhedron Vol. 8, No. 8, pp. 1135–1138, 1989
Printed in Great Britain

0277–5387/89 $3.00+.00
© 1989 Pergamon Press plc

MOLECULAR ORBITAL STUDY OF THE COMPLEXATION OF P_5 AND P_6 RINGS WITH ARENEMETAL FRAGMENTS

M. C. KERINS and N. J. FITZPATRICK*

Department of Chemistry, University College, Belfield, Dublin 4, Ireland

and

MINH THO NGUYEN

Department of Organic Chemistry, University of Groningen, 9747 AG Groningen, The Netherlands

(*Received* 8 *November* 1988; *accepted* 12 *December* 1988)

Abstract—Extended Hückel calculations on the model complexes $(C_6H_6)_2Cr$, $(C_6H_6)CrP_6$, $(C_5H_5)_2Cr^{2-}$, $(C_5H_5)CrP_5^{2-}$, $(C_5H_5)_2Fe$ and $(C_5H_5)FeP_5$ showed that the complexes containing P_5 and P_6 ring systems may show stabilities comparable to, or even stronger than, their carbon analogues, despite large differences between the free cyclic fragments. Although the HOMO–LUMO energy gaps in both P and C complexes are often similar, the pattern of MO interactions differ significantly for P and C rings and there is less distinct MO binding in P complexes.

It is now established that the P_x units can act as two, four, six and eight electron donors to metal fragments.[1] Among those P-containing complexes recently synthesized are several triple- and double-decker sandwich complexes with cyclic and planar P_6[2] and P_5[3] layers which lie parallel to other arene ligands. While the existence of the *free* hexaphosphabenzene (**I**) is, up to now, only theoretically postulated,[4] the cyclic anion (**II**), the all-phosphorus analogue of the cyclopentadienide anion ($C_5H_5^-$), has recently been generated in solution and characterized spectroscopically.[5] The shape of the experimental UV spectrum, which exhibits two $\pi^* \leftarrow \pi$ absorption bands and a $\pi^* \leftarrow n$ band, suggests a strongly aromatic character for **II**.



(I)



(II)

In this context, an interesting problem is to consider to what extent can the P_x rings, **I** and **II**, be compared with their carbon analogues in complexation with metal fragments. In this particular work we attempt to consider this question in a simple way by carrying out self-consistent charge and configuration extended Hückel[6] calculations on the double-decker complexes formed from the interaction of P_6 and C_6H_6 with $(C_6H_6)Cr$, and of P_5^- and $C_5H_5^-$ with both $(C_5H_5)Cr^-$ and $(C_5H_5)Fe^+$, respectively. Such a comparative study enables some qualitative information about the P_x complexes to be found.

The calculations were carried out using the FORTICON-8 program[7] and the MO correlation diagrams were constructed using a program developed in our laboratory. The calculation on the moieties were non-iterative, using the coulomb terms from the self-consistent results. Details of the choice of semi-empirical parameters used for the iterative calculations were given in previous papers.[8] The geometries employed were derived from the crystal structures where possible and the following distances were taken (values in Å):

(a) $(C_6H_6)Cr$, $(C_6H_6)_2Cr$ and $(C_6H_6)CrP_6$: r(Cr—C) = 2.19; r(C—C) = 1.38; r(Cr—P) = 2.54 and r(P—P) = 2.17 (refs 2 and 9).

* Author to whom correspondence should be addressed.

(b) $(C_5H_5)Cr^-$, $(C_5H_5)_2Cr^{2-}$ and $(C_5H_5)CrP_5^{2-}$: r(Cr—C) = 2.30; r(C—C) = 1.43; r(P—P) = 2.17 and r(Cr—P) = 2.30 (refs 3(a) and 10);

(c) $(C_5H_5)Fe^+$, $(C_5H_5)_2Fe$ and $(C_5H_5)FeP_5$: r(Fe—C) = 2.03; r(C—C) = 1.43; r(P—P) = 2.10 and r(Fe—P) = 2.34 (refs 3(c) and 11).

Molecular orbital correlation diagrams are displayed in Figs 1–3.

The $(C_6H_6)_2Cr$ *and* $(C_6H_6)CrP_6$ *complexes*

From Fig. 1, it can be seen that there is a considerable difference between the free P_6 and C_6H_6 moieties. There is in fact a large HOMO–LUMO separation ($\approx$ 5 eV) in the latter, while in P_6 the gap is only about 1.2 eV. In both, the LUMO is of π^*-character (2e).

The $(C_6H_6)Cr$ moiety has a small HOMO–LUMO gap (0.5 eV). In $(C_6H_6)_2Cr$, the gap becomes larger (1.8 eV). The principal interaction (which is well known) is that of the LUMO-(C_6H_6) with the 2nd-HOMO-(C_6H_6)Cr. The latter is mainly of Cr($d_{x^2-y^2}$, d_{xy}) origin. There is also interaction between the filled π-(C_6H_6) level and the empty 1st-LUMO-(C_6H_6)Cr. The resulting antisymmetric MO thus constitutes the complex LUMO. The HOMO-$(C_6H_6)_2Cr$ is essentially the HOMO-(C_6H_6)Cr with strong Cr(d_{z^2}) character.

In the P_6 complex, the HOMO–LUMO separation is somewhat smaller (1.5 eV). Here, as with C_6H_6, a strong interaction between the 2nd-HOMO-(C_6H_6)Cr and LUMO-P_6 occurs, with mixing-in of the HOMO-P_6 level. These interacting MOs lie closer in energy than those in $(C_6H_6)_2Cr$, so that the resulting interaction is expected to be stronger.

The charges on benzene in the two complexes differ little. In $(C_6H_6)CrP_6$, the P charge is -0.029 and the C and H charges are -0.031 and -0.034. Thus, the overall Cr $\rightarrow$ P_6 charge-transfer is less than the Cr $\rightarrow$ CH transfer. The atomic populations reveal that the metal gives electrons to the vacant π^*-hexaphosphabenzene orbitals. The results also show large donation to the metal from the P_6 ring.

In summary, it may be said that both $(C_6H_6)_2Cr$

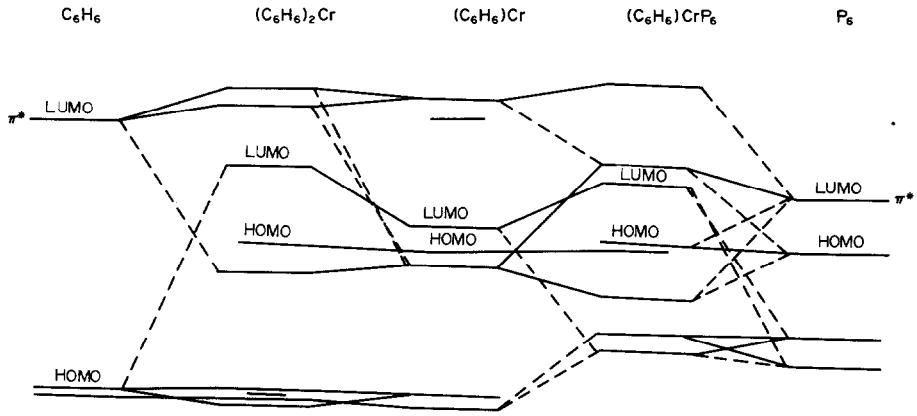

Fig. 1. MO correlation diagram comparing the $(C_6H_6)_2Cr$ and $(C_6H_6)CrP_6$ complexes.

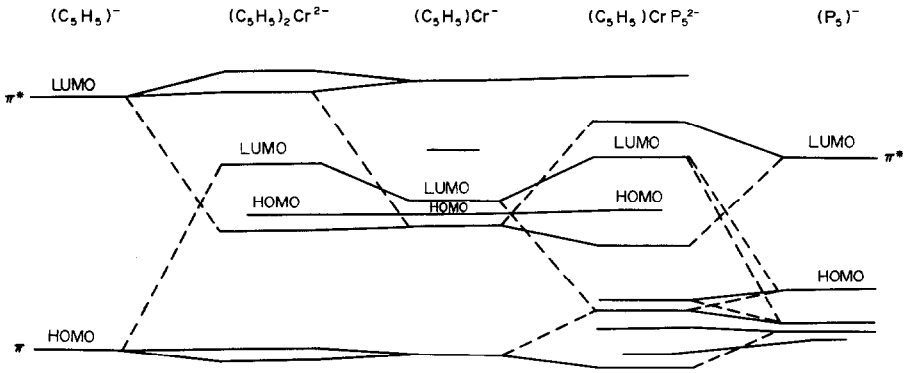

Fig. 2. MO correlation diagram comparing the $(C_5H_5)_2Cr^{2-}$ and $(C_5H_5)CrP_5^{2-}$ complexes.

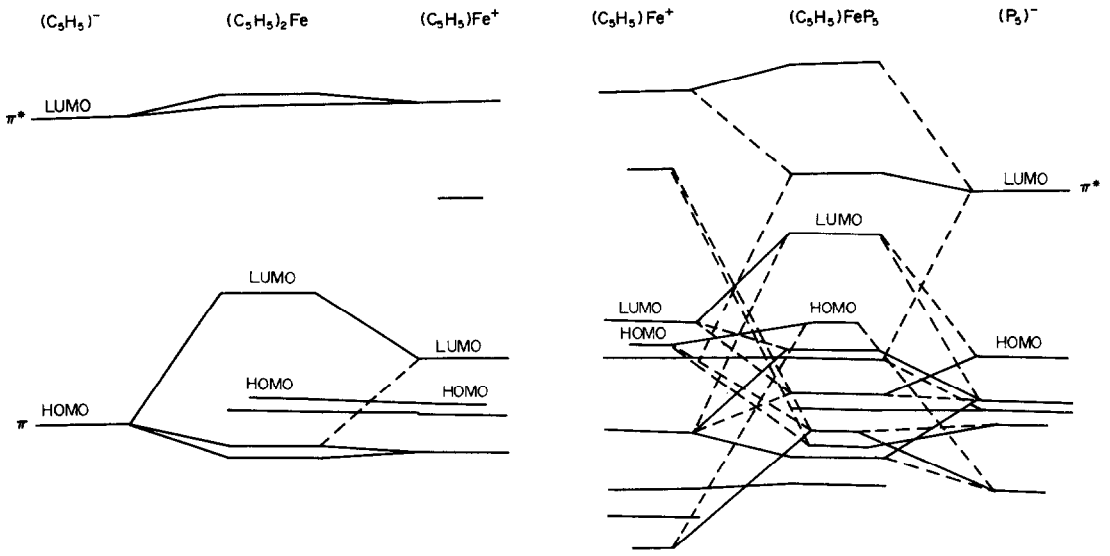

Fig. 3. MO correlation diagram comparing the $(C_5H_5)_2Fe$ and $(C_5H_5)FeP_5$ complexes.

and $(C_6H_6)CrP_6$ have a number of similarities. In particular, the LUMO–HOMO energy separation is of the same order in both, which suggests comparable kinetic stabilities. In the P_6-complex, the main interaction is $P(\sigma) \rightarrow Cr$ donation with weaker $Cr \rightarrow P(\pi^*)$ donation than in the C_6H_6 case. Overall, while free P_6 is much less stable than free benzene,[4] it appears that with such systems as a d^6 arenechromium fragment, the P_6 ring may be trapped.

The $(C_5H_5)_2Cr^{2-}$ *and* $(C_5H_5)CrP_5^{2-}$ *complexes*

There are some differences between the free $C_5H_5^-$ and P_5^- moieties. The HOMO–LUMO gap in the former is large ($\approx$ 5.5 eV) and is smaller in the latter ($\approx$ 2.5 eV). The LUMO is of π^*-character (2e) in both, but in $C_5H_5^-$, the HOMO is π, whereas in P_5^-, the HOMO is not and the π (1e) orbital lies less than 1 eV lower in energy. Thus, the LUMO of $C_5H_5^-$ lies higher in energy than that of P_5^- while a reverse ordering occurs for the HOMOs (Fig. 2). Despite such differences, the HOMO–LUMO energy gap levels becomes similar in both complexes ($\approx$ 1 eV).

In $(C_5H_5)CrP_5^{2-}$, the principal stabilization arises from a strong interaction between the LUMO-$(P_5)^-$ and the 2nd-HOMO-$(C_5H_5)Cr^-$ giving rise to the 2nd-HOMO of the complex. Owing to the more favoured HOMO–LUMO energy separation, this interaction is stronger than the corresponding one in $(C_5H_5)_2Cr^{2-}$. The non-bonding HOMO of $(C_5H_5)Cr^-$ remains the principal contribution to the HOMOs of both complexes. There is also an additional stabilizing interaction between the HOMO-$(P_5)^-$ and the LUMO-$(C_5H_5)Cr^-$ (Fig. 2). This would enhance the stability of the P_5 system. In going from the $C_5H_5^-$ to the P_5^- complex, a decreasing overlap thus does not operate against a greater interaction with the metal as much as with the six-membered ring analogues discussed above.

From a population analysis, we note that the $Cr \rightarrow$ ring charge-transfer occurs in both complexes. The $C_5H_5^-$ ring charges become more negative and that of Cr more positive in $(C_5H_5)_2Cr^{2-}$. The two way electron flow in $(C_5H_5)CrP_5^{2-}$ also involves a larger amount of electrons than that in the C_5H_5 counterpart. In $(C_5H_5)CrP_5^{2-}$ the $d_{x^2-y^2}/d_{zy}$ populations are 1.506, and in $(C_5H_5)_2Cr^{2-}$ the corresponding value is 1.754, thus increased donation from Cr is indicated in the P complex. Also in the P complex the $d_{xz/yz}$ population is 0.445, while in $(C_5H_5)_2Cr^{2-}$ it is 0.274. Thus in the P complex there is more donation to the Cr. This is a further illustration of the difference between the complexes and indicates appreciable stability for $(C_5H_5)CrP_5^{2-}$.

An investigation of the eclipsed forms of the complexes showed very similar interactions and energies to those for the staggered complexes examined here.

In summary, the calculations indicate that donation to and from the metal are larger in $(C_5H_5)CrP_5^{2-}$ than in $(C_5H_5)_2Cr^{2-}$. As the HOMO–LUMO energy separations differ little, the kinetic stability of both complexes may be expected to be similar. Thus, the existence of cyclo-P_5^- in the complexed form is perhaps not as surprising as originally thought. However, this complex is di-anionic, therefore a consideration of the corres-

ponding neutral Fe complex was undertaken for comparative purposes.

The $(C_5H_5)_2Fe$ *and* $(C_5H_5)FeP_5$ *complexes*

The isolated $C_5H_5Fe^+$ moieties in the two complexes differ slightly, thus in Fig. 3 they are represented separately. Firstly, we note that the LUMOs of the cyclopentadienide rings are not involved in bonding in ferrocene. The HOMO–LUMO energy differences amount to about 2.0 eV in both complexes, which are larger (Fig. 3) than in the anionic chromium species. As previously, there is significant mixing-in of lower-lying orbitals into the HOMO-$(P_5)^-$ and LUMO-$(C_5H_5)Fe^+$ interaction. The $C_5H_5^-/P_5^-$ donation to the $(C_5H_5)Fe^+$ fragment is the major feature in both complexes, and there is little evidence (from a population analysis) for Fe → C or Fe → P charge-transfer. The pronounced charge drift in $(C_5H_5)FeP_5$ can be seen in the transfer of electron from the P(s, p_x, p_y) orbitals to the Fe(d_{xy}, d_{yz}) ones, which in turn increases the Fe → C donation. Because the HOMO-$(P_5)^-$ lies closer energetically to the LUMO of $(C_5H_5)Fe^+$ than does the HOMO-$(C_5H_5)^-$, the P_5 complex is expected to be somewhat more stable.

In conclusion, it may be deduced from this preliminary study that complexes containing P_5^- and P_6 ring systems may, in a number of cases, show stabilities comparable to (or even better than) their C analogues, despite large differences between the free ring fragments. This study also suggests that the pattern of MO interactions signficantly differ for P and C rings.

Acknowledgement—The authors are indebted to the Department of Education (Irish Government) for financial support.

REFERENCES

1. (a) O. J. Scherer, *Angew. Chem. Int. Ed. Engl.* 1985, **24**, 924; (b) O. J. Scherer, *Comments Inorg. Chem.* 1987, **6**, 1.
2. (a) O. J. Scherer, H. Sitzmann and G. Wolmershäuser, *Angew. Chem. Int. Ed. Engl.* 1985, **24**, 351; (b) O. J. Scherer, I. Bach, J. Schwalb, H. Sitzmann, G. Wolmershäuser, W. Kaim and R. Gross, *Phosphorus Sulfur* 1987, **30**, 269; (c) O. J. Scherer, J. Schwalb, H. Swarowsky, G. Wolmershäuser, W. Kaim and R. Gross, *Chem. Ber.* 1988, **121**, 443.
3. (a) O. J. Scherer, J. Schwalb, G. Wolmershäuser, W. Kaim and R. Gross, *Angew. Chem. Int. Ed. Engl.* 1986, **25**, 363; (b) O. J. Scherer and T. Brück, *Angew. Chem. Int. Ed. Engl.* 1987, **26**, 59; (c) O. J. Scherer, T. Brück and G. Wolmershäuser, *Chem. Ber.* 1988, **121**, 935.
4. (a) N. C. Baird, *Can. J. Chem.* 1984, **62**, 341; (b) M. T. Nguyen and A. F. Hegarty, *J. Chem. Soc., Chem. Commun.* 1986, 383; (c) S. Nagase and K. Ito, *Chem. Phys. Lett.* 1986, **126**, 43.
5. M. Baudler, S. Akpapoglou, D. Ouzounis, F. Wasgestian, B. Meinigke, H. Budzikiewicz and H. Münster, *Angew. Chem. Int. Ed. Engl.* 1988, **27**, 280.
6. (a) R. Hoffmann and W. N. Lipscomb, *J. Chem. Phys.* 1962, **32**, 2872, 3179, 3489; (b) R. Hoffmann, *J. Chem. Phys.* 1963, **39**, 1397.
7. J. Howell, A. Rossi, D. Wallace, K. Haraki and R. Hoffmann, FORTICON-8, Q.C.P.E. No. 344.
8. (a) M. T. Nguyen, M. A. McGinn, A. F. Hegarty and J. Elguero, *Polyhedron* 1985, **4**, 1721; (b) M. C. Kerins, N. J. Fitzpatrick and M. T. Nguyen, *Polyhedron* 1989, **8**, 969.
9. E. Weiss and E. O. Fisher, *Z. Anorg. Chem.* 1958, **285**, 142.
10. E. Weiss and E. O. Fisher, *Z. Anorg. Chem.* 1958, **284**, 69.
11. J. D. Dunitz, L. E. Orgel and A. Rich, *Acta Cryst.* 1956, **9**, 373.

Polyhedron Vol. 8, No. 9, pp. 1149–1155, 1989
Printed in Great Britain

0277–5387/89 $3.00+.00
© 1989 Pergamon Press plc

REACTIONS OF CARBONYL SULPHIDE AND CARBON DISULPHIDE WITH RUTHENIUM COMPLEXES

KRISHNA KUMAR PANDEY* and SHARAD KUMAR TEWARI

Department of Chemistry, Devi Ahilya University, Indore 452001, India

(*Received* 20 *May* 1988; *accepted* 6 *July* 1988)

Abstract—The reaction of COS with $[Ru(CH_3CN)_2Cl_2(PPh_3)_2]$ under various experimental conditions resulted in the formation of chloro-bridged complexes $[(Ph_3P)Cl(CO)Ru(\mu\text{-}Cl)_2Ru(CO)Cl(PPh_3)]$ and $[(PPh_3)_2Cl(CO)Ru(\mu\text{-}Cl)_2Ru(CO)Cl(PPh_3)_2]$ which reacted with excess PPh_3 under reflux to form $[Ru(CO)Cl_2(PPh_3)_3]$. CS_2 reacted with $[Ru(CH_3CN)_2Cl_2(PPh_3)_2]$ in the presence of PPh_3 to give $[(Ph_3P)_2Cl(CS)Ru(\mu\text{-}Cl)_2Ru(CS)Cl(PPh_3)_2]$. Reactions of COS with $[RuH(CH_3COO)(PPh_3)_3]$, $[Ru(CO)Cl(CH_3COO)(PPh_3)_2]$, $[RuH(CO)Cl(AsPh_3)_3]$ and $[Ru(CO)Cl_2(AsPh_3)_3]$ resulted in the formation of the complexes $[Ru(CO)(CH_3COO)(PPh_3)_2]_2(\mu\text{-}S)$, $[(Ph_3P)_2Cl(CO)Ru(\overset{O}{\overset{\|}{C}})S\text{—}Ru(CO)Cl(PPh_3)_2]$, $[RuH(CO)_2Cl(AsPh_3)_2]$ and $[Ru(CO)_2Cl_2(AsPh_3)_2]$, $[(Ph_3As)_2Cl(CO)Ru(\mu\text{-}Cl)_2Ru(CO)Cl(AsPh_3)_2]$, respectively. CS_2 reacted with $[RuH(CH_3COO)(PPh_3)_3]$ and $[RuH(CO)Cl(AsPh_3)_3]$ to give $[Ru(CS)(CH_3COO)(PPh_3)_2]_2(\mu\text{-}S)$ and $[RuH(CO)(CS)Cl(AsPh_3)_2]$, respectively. The complexes were characterized by elemental analysis, magnetic measurements, IR and electronic spectral studies.

The coordination properties of triatomics such as CO_2, COS and CS_2, which are the potential source of C_1 chemistry, are interesting, especially from a synthetic view point. The interesting reactions, especially of CO_2 and CS_2, are those which are related to (a) the formation of organometallic compounds, (b) the facile insertion into the M—H, M—C, M—N etc. bonds and (c) the catalytic synthesis of various types of organic compounds.[1–20] Since the first report of the reaction of COS, which is structurally similar to CO_2 and CS_2, with a metal complex by Baird and Wilkinson,[21] it has received little attention.[22] Herein, we wish to report the reactions of COS and CS_2 with ruthenium complexes.

EXPERIMENTAL

All the reagents were of analytical or chemically pure grade. Benzene, toluene, hexane and diethyl ether were dried over sodium, dichloromethane over P_4O_{10} and methanol over CaO. All the solvents were purged with nitrogen and distilled immediately before use. All reactions were performed under pure dry nitrogen atmosphere. $[Ru(CH_3CN)_2Cl_2(PPh_3)_2]$, $[RuH(CH_3COO)(PPh_3)_3]$, $[RuH(CO)ClL_3]$ (L = PPh_3, $AsPh_3$), $[Ru(CO)Cl_2(AsPh_3)_3]$ and COS were prepared by literature methods.[23–27]

The analyses for sulphur and chloride in the complexes were carried out by the standard methods.[28] Carbon and hydrogen analyses were performed using a Carlo Erba 1106 Thomas CH Analyser 35. For the estimation of phosphorus and arsenic, samples were decomposed with sodium peroxide, sugar and sodium nitrate in the ratio 20 : 1 : 3 in a Parr bomb crucible and extracted with water. Then the solution was neutralized with dilute H_2SO_4 and an excess of concentrated H_2SO_4 (0.5 cm^3) added. It was heated until the evolution of SO_3 fumes ceased, then cooled and diluted with water. From the filtrate of the solution, phosphorus and arsenic were estimated by standard methods.[29] The results are reported in Table 1.

The IR spectra were recorded in the range 4000–250 cm^{-1} with a Perkin–Elmer 580 spectrophotometer from the R.S. Instrument Centre at the Indian Institute of Technology, Bombay. Samples were prepared as KBr pellets. Important IR frequencies are given in Table 2. The electronic

*Author to whom correspondence should be addressed.

Table 1. Elemental analyses of the complexes

Compounds	[Found (calc.)] (%)				
	C	H	Cl	S	P/As
$[Ru(CO)Cl(PPh_3)]_2(\mu\text{-}Cl)_2$	49.2 (49.3)	3.3 (3.2)	15.5 (15.3)	—	6.9 (6.7)
$[Ru(CO)Cl(PPh_3)_2]_2(\mu\text{-}Cl)_2$	61.2 (61.3)	4.3 (4.1)	9.9 (9.8)	—	8.7 (8.5)
$[Ru(CO)Cl_2(PPh_3)_3]$	66.8 (66.9)	4.7 (4.5)	7.3 (7.2)	—	9.6 (9.4)
$[Ru(CS)Cl(PPh_3)_2]_2(\mu\text{-}Cl)_2$	59.8 (60.0)	4.2 (4.0)	9.7 (9.5)	4.4 (4.3)	8.5 (8.3)
$[Ru(CO)(CH_3COO)(PPh_3)_2]_2(\mu\text{-}S)$	64.4 (64.3)	4.6 (4.5)	—	2.2 (2.1)	8.6 (8.5)
$[Ru(CS)(CH_3COO)(PPh_3)_2]_2(\mu\text{-}S)$	62.8 (62.9)	4.6 (4.4)	—	6.5 (6.4)	8.5 (8.3)
$[Ru(CO)Cl(PPh_3)_2]_2(\mu\text{-}COS)$	62.5 (62.6)	4.3 (4.1)	5.0 (4.9)	2.2 (2.2)	8.7 (8.6)
$[RuH(CO)_2Cl(AsPh_3)_2]$	56.5 (56.6)	4.0 (3.8)	4.6 (4.4)	—	18.8 (18.6)
$[RuH(CO)(CS)Cl(AsPh_3)_2]$	55.4 (55.5)	3.9 (3.7)	4.2 (4.3)	3.8 (3.9)	18.4 (18.2)
$[Ru(CO)_2Cl_2(AsPh_3)_2]$	54.2 (54.3)	3.5 (3.6)	8.6 (8.4)	—	18.0 (17.8)
$[Ru(CO)Cl(AsPh_3)_2]_2(\mu\text{-}Cl)_2$	54.8 (54.6)	3.6 (3.0)	8.8 (8.7)	—	18.6 (18.4)

Table 2. Colour, melting point and important IR frequencies of the complexes

Compounds	Colour	M.p. (°C)	ν(CO) (cm^{-1})	ν(CS) (cm^{-1})	ν(Ru—Cl) (cm^{-1})	ν(Ru—S) (cm^{-1})
$[Ru(CO)Cl(PPh_3)]_2(\mu\text{-}Cl)_2$	Green	180	1950	—	330 260	—
$[Ru(CO)Cl(PPh_3)_2]_2(\mu\text{-}Cl)_2$	Orange	268	1960	—	330 255	—
$[Ru(CO)Cl_2(PPh_3)_3]$	Orange	70	2025 1982 1945	—	—	—
$[Ru(CS)Cl(PPh_3)_2]_2(\mu\text{-}Cl)_2$	Red	212	—	1290	335 265	—
$[Ru(CO)(CH_3COO)(PPh_3)_2]_2(\mu\text{-}S)$	Green	150	1940	—	—	460
$[Ru(CS)(CH_3COO)(PPh_3)_2]_2(\mu\text{-}S)$	Green	125	—	1290	—	460
$[Ru(CO)Cl(PPh_3)_2]_2(\mu\text{-}COS)$	Yellow	230	1950	—	—	—
$[RuH(CO)_2Cl(AsPh_3)_2]$	White	280	2065 2005	—	340	—
$[RuH(CO)(CS)Cl(AsPh_3)_2]$	Yellow	250	2030	1320	340	—
$[Ru(CO)_2Cl_2(AsPh_3)_2]$	Cream–white	140	2060 2000	—	—	—
$[Ru(CO)Cl(AsPh_3)_2]_2(\mu\text{-}Cl)_2$	Red	160	1970	—	350 275	—

spectra have been recorded with Shimadzu 160 spectrophotometer. Magnetic measurements were carried out by Gouy's method at room temperature (25°C) using mercury tetrathiocyanato cobaltate(II) as calibrant. All the complexes were found to be dimagnetic. Melting points were determined by the capillary method and are uncorrected.

Synthesis of $[(Ph_3P)Cl(CO)Ru(\mu\text{-}Cl)_2Ru(CO)Cl(PPh_3)]$ (**1**)

COS was bubbled into a solution of $[Ru(CH_3CN)_2Cl_2(PPh_3)_2]$ (0.2 g) in toluene (30 cm^3) for 30 min and the reaction mixture was stirred for 1 h. This was then evaporated to 5 cm^3 under reduced pressure. On the addition of *n*-hexane (40 cm^3), a green complex (**1**) precipitated which was centrifuged, washed with *n*-hexane and dried *in vacuo* (yield 0.08 g, 67%).

Synthesis of $[(Ph_3P)_2Cl(CO)Ru(\mu\text{-}Cl)_2Ru(CO)Cl(PPh_3)_2]$ (**2**)

COS was bubbled into a solution of $[Ru(CH_3CN)_2Cl_2(PPh_3)_2]$ (0.2 g) and PPh_3 (0.4 g) in toluene (40 cm^3) for 30 min and the reaction mixture was refluxed for 2 h. This was evaporated to 5 cm^3 and slow addition of *n*-hexane (40 cm^3) precipitated a red complex (**2**) which was centrifuged, washed with *n*-hexane and dried *in vacuo* (yield 0.065 g, 34%).

Synthesis of $[Ru(CO)Cl_2(PPh_3)_3]$ (**3**)

A solution of $[(Ph_3P)Cl(CO)Ru(\mu\text{-}Cl)_2Ru(CO)Cl(PPh_3)]$ (0.2 g) and PPh_3 (0.4 g) in benzene (30 cm^3) was refluxed for 8 h whereby the colour of the solution changed from green to orange. The resulting orange solution was reduced in volume and *n*-hexane was added to give orange crystals of **3**.

Synthesis of $[(Ph_3P)_2Cl(CS)Ru(\mu\text{-}Cl)_2Ru(CS)Cl(PPh_3)_2]$ (**4**)

A solution of $[Ru(CH_3CN)_2Cl_2(PPh_3)_2]$ (0.2 g) and PPh_3 (0.6 g) in CS_2 (20 cm^3) was refluxed for 3 h. The colour of the solution changed to red. The solution was diluted with diethyl ether (80 cm^3) and cooled to 5°C. The red precipitate of **4** that formed was collected by filtration, washed with diethyl ether and dried *in vacuo* (yield 0.1 g, 52%).

Synthesis of $[Ru(CO)(CH_3COO)(PPh_3)_2]_2(\mu\text{-}S)$ (**5**)

COS was bubbled into a solution of $[RuH(CH_3COO)(PPh_3)_3]$ (0.2 g) in toluene (20 cm^3) for 30 min and the reaction mixture was stirred for a further 1 h. Complex **5** was isolated by a similar procedure to that given for complex **1** (yield 0.12 g, 78%).

Synthesis of $[Ru(CS)(CH_3COO)(PPh_3)_2]_2(\mu\text{-}S)$ (**6**)

A mixture of CS_2 (2 cm^3) and $[RuH(CH_3COO)(PPh_3)_3]$ (0.2 g) in toluene (20 cm^3) was allowed to reflux for 1 h. The reaction mixture was evaporated to 5 cm^3 under reduced pressure. On addition of 40 cm^3 of *n*-hexane, complex **6** was precipitated which was centrifuged, washed with *n*-hexane and dried *in vacuo* (yield 0.1 g, 64%).

Synthesis of $[Ru(CO)Cl(PPh_3)_2]_2(\mu\text{-}COS)$ (**7**)

COS was bubbled into a solution of $[Ru(CO)Cl(CH_3COO)(PPh_3)_2]$ (0.2 g) in toluene (30 cm^3) for 30 min and the reaction mixture was stirred for 1 h. Complex **7** was isolated by a similar procedure to that given for complex **1** (yield 0.13 g, 67%).

Synthesis of $[RuH(CO)_2Cl(AsPh_3)_2]$ (**8**)

COS was bubbled into a solution of $[RuH(CO)Cl(AsPh_3)_3]$ (0.2 g) in toluene (30 cm^3) for 30 min and the reaction mixture was stirred for 1 h. Complex **8** was isolated by a similar procedure to that given for complex **1** (yield 0.08 g, 54%).

Synthesis of $[RuH(CO)(CS)Cl(AsPh_3)_2]$ (**9**)

A solution of $[RuH(CO)Cl(AsPh_3)_3]$ (0.2 g) in toluene (30 cm^3) was treated with CS_2 (4 cm^3) for 3 h. Complex **9** was isolated by a similar procedure to that given for complex **5** (yield 0.1 g, 65%).

Reaction of COS *with* $[Ru(CO)Cl_2(AsPh_3)_3]$

COS was bubbled into a solution of $[Ru(CO)Cl_2(AsPh_3)_3]$ (0.2 g) in toluene (30 cm^3) for 30 min. The reaction mixture was refluxed for 1 h. The solvent was removed under reduced pressure and the residue was dissolved in a minimum of dichloromethane. On the addition of methanol, a cream white complex $[Ru(CO)_2Cl_2(AsPh_3)_2]$ (**10**) separated, which was filtered, washed with methanol and diethyl ether and dried *in vacuo* (yield $\approx$ 5%).

The filtrate was reduced to half the volume and cooled to 5°C. The red complex $[(Ph_3As)_2Cl(CO)Ru(\mu\text{-}Cl)_2Ru(CO)Cl(AsPh_3)_2]$ (**11**) which separated was centrifuged, washed with *n*-hexane and dried *in vacuo* (yield 0.04 g, 43%).

RESULTS AND DISCUSSION

COS reacts with $[Ru(CH_3CN)_2Cl_2(PPh_3)_2]$ at room temperature to give a green complex (**1**):

$$2Ru(CH_3CN)_2Cl_2(PPh_3)_2 + 2COS \rightarrow [(Ph_3P)Cl(CO)Ru(\mu\text{-}Cl)_2Ru(CO)Cl(PPh_3)] + 2SPPh_3.$$

The reaction of COS with $[Ru(CH_3CN)_2Cl_2(PPh_3)_2]$ under reflux in the presence of PPh_3 yields an orange complex (**2**):

$$2Ru(CH_3CN)_2Cl_2(PPh_3)_2 + 2COS + 2PPh_3 \rightarrow [(Ph_3P)_2Cl(CO)Ru(\mu\text{-}Cl)_2(CO)Cl(PPh_3)_2] + 2SPPh_3.$$

The green complex (**1**) or orange complex (**2**) reacts with excess PPh_3 under reflux to give orange complex $[Ru(CO)Cl_2(PPh_3)_3]$ (**3**).

$[Ru(CH_3CN)_2Cl_2(PPh_3)_2]$ in CS_2 under reflux in the presence of PPh_3 affords a red complex (**4**).

$$Ru(CH_3CN)_2Cl_2(PPh_3)_2 + 2CS_2 + 2PPh_3 \rightarrow [(Ph_3P)_2Cl(CS)Ru(\mu\text{-}Cl)_2(CS)Cl(PPh_3)_2] + 2SPPh_3.$$

Reaction of $[RuH(CH_3COO)(PPh_3)_3]$ with COS and CS_2 results in the formation of sulphur bridged carbonyl and thiocarbonyl complexes, respectively:

$$[RuH(CH_3COO)(PPh_3)_3] + SCX \rightarrow [Ru(CX)(CH_3COO)(PPh_3)_2]_2(\mu\text{-}S) + \cdots$$

(**5**), X = O; (**6**), X = S.

COS reacts with $[Ru(CO)Cl(CH_3COO)(PPh_3)_2]$ to give the bridged carbonyl sulphide complex (**7**):

$$2Ru(CO)Cl(CH_3COO)(PPh_3)_2 + COS \rightarrow (Ph_3P)_2Cl(CO)Ru{-}\overset{\overset{O}{\|}}{C}{-}S{-}Ru(CO)Cl(PPh_3)_2 + \cdots$$

Reactions of SCX with $[RuH(CO)Cl(AsPh_3)_3]$ give hydridodicarbonyl ruthenium complexes:

$$RuH(CO)Cl(AsPh_3)_3 + SCX \rightarrow RuH(CO)(CX)Cl(AsPh_3)_2 + \cdots$$

(**8**), X = O; (**9**), X = S.

COS reacts with $[Ru(CO)Cl_2(AsPh_3)_3]$ to give a cream–white complex, $[Ru(CO)_2Cl_2(AsPh_3)_2]$ (**10**) and a red complex, $[(Ph_3As)_2Cl(CO)Ru(\mu\text{-}Cl)_2Ru(CO)Cl(AsPh_3)_2]$ (**11**).

IR spectra

Important IR data are summarized in Table 2. The IR spectrum of the green complex, $[Ru(CO)Cl_2(PPh_3)]_2$, shows absorption bands at 1950, 330 and 260 cm^{-1} in addition to the characteristic bands of triphenylphosphine.[30] The band at 1950 cm^{-1} is due to the characteristic stretching frequencies of the terminal carbonyl group. The band at 330 cm^{-1} is typical of ν(Ru—Cl) (Cl *trans* to Cl) while the band at 260 cm^{-1} could be due to either ν(Ru—Cl) (Cl *trans* to P) or to bridging chlorine modes, or to both.[31] The green complex (**1**) may, therefore, be dimeric in the solid state with bridging chlorines.

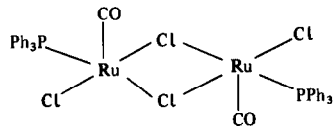

(**1**)

The IR spectrum of the orange complex $[Ru(CO)Cl_2(PPh_3)_2]_2$ shows absorption bands at 1960 cm^{-1} due to ν(CO),[32] 330 cm^{-1} due to ν(Ru—Cl) and 255 cm^{-1} due to ν(Ru—Cl) (bridging Ru—Cl modes). The IR spectrum of $[Ru(CO)Cl_2(PPh_3)_3]$ contains carbonyl bands at 2025, 1982 and 1945 (same as the literature values)[32] indicating the presence of two isomers which could not be separated. One isomer of complex (**3**) has been reported previously with ν(CO) at 1950 cm^{-1}.[33,34] The IR spectrum of the thiocarbonyl complex $[Ru(CS)Cl_2(PPh_3)_2]_2$ shows absorption bands at 1290 cm^{-1} due to ν(CS) (literature value 1290 cm^{-1}),[35] and at 335 and 265 cm^{-1} due to ν(Ru—Cl). The IR spectra of sulphide bridged complexes, $[Ru(CX)(CH_3COO)(PPh_3)_2]_2(\mu\text{-}S)$ (X = O, S), exhibit absorption bands at 1940 cm^{-1} due to ν(CO), at 1290 cm^{-1} due to ν(CS), at *ca* 460 cm^{-1} due to ν(Ru—S) and in the regions 1510, 1460 cm^{-1} due to ν(CO) of the acetate group, suggesting that the acetato ligand present is bidentate.[36] The IR spectrum of the carbonyl sulphide complex $[(Ph_3P)_2Cl(CO)Ru{-}\overset{\overset{O}{\|}}{C}{-}S{-}Ru(CO)Cl(PPh_3)_2]$ contains a broad band at 1950 cm^{-1} due to ν(CO), a broad band at 1540 cm^{-1} and a weak band at 850 cm^{-1} due to the ν(CO) and ν(CS) of the COS group, respectively.[37] The IR spectrum of $[RuH(CO)_2Cl(AsPh_3)_2]$ shows absorption bands at 2065 and 2005 cm^{-1} due to ν(CO) (literature: 2060, 200 cm^{-1}), the bands at 1985 cm^{-1} may be due to ν(Ru—H) and those at 340 cm^{-1} are due to ν(Ru—Cl). The IR spectrum of $[RuH(CO)(CS)Cl(AsPh_3)_2]$ contains bands at 2030 cm^{-1} due to ν(CO), at 1320 cm^{-1} due to ν(CS), the

one at 1985 cm^{-1} may be due to ν(Ru—H) and the one at 340 cm^{-1} is due to ν(Ru—Cl). The ν(Ru—Cl) at 340 cm^{-1} in these complexes indicates a chloride *trans* to carbonyl rather than to triphenylarsine. Therefore structures of complexes **8** and **9** tentatively may be given.

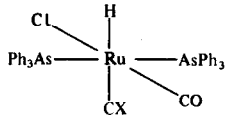

(8) X = O
(9) X = S

The structure for $[RuH(CO)_2Cl(AsPh_3)_2]$ has been established by Harris and Robinson,[26] and for the analogous triphenylphosphine complex $[RuH(CO)_2Cl(PPh_3)_2]$ by James and Markham.[38] $[Ru(CO)Cl_2(AsPh_3)_2]$ contains strong bands at 2060 and 2000 cm^{-1} due to ν(CO) which are in the range reported previously for a *cis–trans–cis* type of isomer.[33,39-41] The IR spectrum of the complex, [di - μ - chlorobis(chlorocarbonylbistriphenylarsine) ruthenium], exhibits absorption bands at 1970 cm^{-1} (broad) due to ν(CO) and at 350 and 275 cm^{-1} due to ν(Ru—Cl). One isomer of this complex has been previously reported with ν(CO) at 1955 cm^{-1}.[26]

Electronic spectra

The ground state of Ru^{II} in an octahedral field (t_{2g}^6 configuration) is $^1A_{1g}$. The excited states corresponding to the $t_{2g}^5 e_g^1$ configuration are $^3T_{1g}$, $^3T_{2g}$, $^1T_{1g}$ and $^1T_{2g}$ in increasing order of energy. Thus one should expect four transitions, $^1A_{1g} \rightarrow {}^3T_{1g}$; $^1A_{1g} \rightarrow {}^3T_{2g}$; $^1A_{1g} \rightarrow {}^1T_{1g}$ and $^1A_{1g} \rightarrow {}^1T_{2g}$. In the electronic spectra of Ru^{II} complexes, three bands in some cases, four or five bands in other cases, appear in the visible region (Fig. 1). The positions of these bands and their respective assignments are given in Table 3. From the band positions, the

Table 3. Electronic spectral data of the complexes

Compounds	Band position nm (ε)	(cm^{-1})	Assignments	$10Dq$ (cm^{-1})	B (cm^{-1})	C (cm^{-1})	β
$[Ru(CO)Cl(PPh_3)]_2(\mu\text{-}Cl)_2$	785(240)	12738	$^1A_{1g} \rightarrow {}^3T_{1g}$	22476	293	3246	0.47
	520(508)	19230	$^1A_{1g} \rightarrow {}^1T_{1g}$				
	418(1606)	23923	$^1A_{1g} \rightarrow {}^1T_{2g}$				
	295(13636)	33898	Charge-transfer				
$[Ru(CO)Cl(PPh_3)_2]_2(\mu\text{-}Cl)_2$	778(205)	12853	$^1A_{1g} \rightarrow {}^3T_{1g}$	22036	295	3061	0.47
	527(477)	18975	$^1A_{1g} \rightarrow {}^1T_{1g}$				
	422(1205)	23696	$^1A_{1g} \rightarrow {}^1T_{2g}$				
	298(12525)	33557	Charge-transfer				
$[Ru(CS)Cl(PPh_3)_2]_2(\mu\text{-}Cl)_2$	510(751)	19607	$^1A_{1g} \rightarrow {}^1T_{1g}$	22007	299	2400	0.48
	410(956)	24390	$^1A_{1g} \rightarrow {}^1T_{2g}$				
	295(10327)	33898	Charge-transfer				
$[Ru(CO)(CH_3COO)(PPh_3)_2]_2(\mu\text{-}S)$	558(271)	17921	$^1A_{1g} \rightarrow {}^1T_{1g}$	20321	316	2400	0.51
	435(683)	22988	$^1A_{1g} \rightarrow {}^1T_{2g}$				
	297(14177)	33670	Charge-transfer				
$[Ru(CS)(CH_3COO)(PPh_3)_2]_2(\mu\text{-}S)$	567(429)	17636	$^1A_{1g} \rightarrow {}^1T_{1g}$	20036	344	2400	0.55
	432(709)	23148	$^1A_{1g} \rightarrow {}^1T_{2g}$				
	298(13776)	33557	Charge-transfer				
$[Ru(CO)Cl(PPh_3)_2]_2(\mu\text{-}COS)$	529(187)	18903	$^1A_{1g} \rightarrow {}^1T_{1g}$	21303	279	2400	0.45
	428(706)	23364	$^1A_{1g} \rightarrow {}^1T_{2g}$				
	298(16125)	33557	Charge-transfer				
$RuH(CO)_2Cl(AsPh_3)_2$	530(213)	18867	$^1A_{1g} \rightarrow {}^1T_{1g}$	21267	309	2400	0.49
	420(592)	23809	$^1A_{1g} \rightarrow {}^1T_{2g}$				
	298(12232)	33557	Charge-transfer				
$RuH(CO)(CS)Cl(AsPh_3)_2$	536(144)	18656	$^1A_{1g} \rightarrow {}^1T_{1g}$	21056	274	2400	0.44
	434(520)	23041	$^1A_{1g} \rightarrow {}^1T_{2g}$				
	300(10444)	33333	Charge-transfer				
$[Ru(CO)Cl(AsPh_3)_2]_2(\mu\text{-}Cl)_2$	529(308)	18903	$^1A_{1g} \rightarrow {}^1T_{1g}$	21303	255	2400	0.41
	435(756)	22988	$^1A_{1g} \rightarrow {}^1T_{2g}$				
	300(13761)	33333	Charge-transfer				

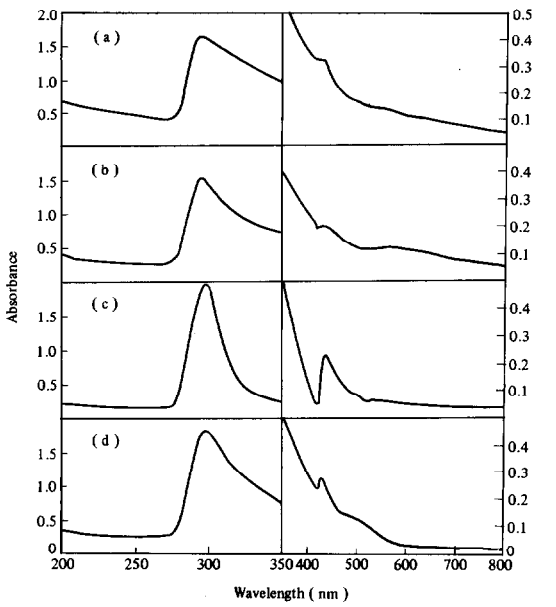

Fig. 1. Electronic absorption spectra of: (a) $[Ru(CO)(CH_3COO)(PPh_3)_2]_2(\mu\text{-}S)$; (b) $[Ru(CS)(CH_3COO)(PHh_3)_2]_2(\mu\text{-}S)$; (c) $[Ru(CO)Cl(PPh_3)_2]_2(\mu\text{-}COS)$; (d) $[Ru(CO)Cl(AsPh_3)_2]_2(\mu\text{-}Cl)_2$.

values of $10Dq$, B, β and C have been calculated.[42] The values of the molar extinction coefficients for the bands in the range 400–500 nm were found to be more than those of the usual *d–d* transitions. This may be due to: (i) mixing of the energy levels with those corresponding to the neighbouring intense charge-transfer bands, (ii) the covalent nature of the complexes and (iii) the lowering of the symmetry to the molecule whereby the centre of symmetry is lost.

Acknowledgement—We thank the Council of Scientific and Industrial Research, New Delhi for financial assistance (Project No. 1(1026)/85-EMR-II).

REFERENCES

1. J. Tsuji, *Organic Synthesis by Means of Transition Metal Complexes*, Vol. 1. Springer, Berlin (1975).
2. V. J. Choy and C. J. O'Connor, *Coord. Chem. Rev.* 1973, **9**, 145.
3. I. S. Butler and A. E. Fenster, *J. Organomet. Chem.* 1974, **66**, 161.
4. P. V. Yaneff, *Coord. Chem. Rev.* 1977, **23**, 183.
5. I. S. Butler, *Acc. Chem. Res.* 1977, **10**, 359.
6. I. S. Kolomnikor and M. Kh. Grigoryan, *Russ. Chem. Rev.* 1978, **47**, 334.
7. M. E. Vol'pin and I. S. Kolomnikov, *Pure Appl. Chem.* 1973, **33**, 567.
8. M. E. Vol'pin and I. S. Kolomnikov, *Organometallic Reactions*, Vol. 5. Wiley Interscience, New York (1975).
9. J. A. Ibers, *Chem. Soc. Rev.* 1982, **11**, 57.
10. H. Werner, *Coord. Chem. Rev.* 1982, **43**, 165.
11. M. Ebner, H. Otto and H. Werner, *Angew. Chem. Int. Ed. Engl.* 1985, **24**, 518.
12. H. Werner, M. Ebner and W. Bertleft, *Z. Naturforsch.* 1985, **40B**, 1351.
13. E. G. Lundquist, K. Folting, J. G. Huffman and K. G. Caulton, *Inorg. Chem.* 1987, **26**, 205.
14. C. R. Langnick, P. G. Pringle and B. L. Shaw, *J. Chem. Soc., Dalton Trans.* 1985, 1015.
15. A. Behr, in W. Keim(Herausg), *Catalysis in* Cl *Chemistry*, p. 169. D. Reidel, Dordrecht (1983).
16. S. Cenini, F. Porta, M. Pizzotti and C. Crotti, *J. Chem. Soc., Dalton Trans.* 1985, 163.
17. S. Cenini, F. Porta, M. Pizzotti and G. LaMonica, *J. Chem. Soc., Dalton Trans.* 1984, 355.
18. H. G. Raubenheimer, G. J. Kruger and H. W. Viljoen, *J. Chem. Soc., Dalton Trans.* 1985, 1963.
19. M. L. Kullberg and C. P. Kubiak, *Inorg. Chem.* 1986, **25**, 26.
20. C. Bianchini, C. A. Ghilardi, A. Meli, S. Midollini and A. Orlandini, *Inorg. Chem.* 1985, **24**, 924.
21. M. C. Baird and G. Wilkinson, *J. Chem. Soc. A* 1967, 865.
22. K. K. Pandey and H. L. Nigam, *Rev. Inorg. Chem.* 1984, **6**, 69.
23. J. D. Gilbert and G. Wilkinson, *J. Chem. Soc. A* 1969, 1749.
24. A. Dobson, S. D. Robinson and M. F. Uttley, *Inorg. Synth.* 1977, **17**, 124.
25. N. Ahmad, J. J. Levison, S. D. Robinson and M. F. Uttley, *Inorg. Synth.* 1975, **15**, 45.
26. A. D. Harris and S. D. Robinson, *Inorg. Chim. Acta* 1980, **42**, 25.
27. G. Brauer, *Handbook of Preparative Inorganic Chemistry*, Vol. I, 2nd edn. Academic Press, New York (1963).
28. A. I. Vogel, *A Textbook of Quantitative Inorganic Analysis*, 3rd edn. Longmans, London (1961).
29. K. K. Pandey, *Spectrochim. Acta A* 1983, **39**, 925.
30. J. C. Sheldon and S. Y. Tyree Jr., *J. Am. Chem. Soc.* 1958, **80**, 2120.
31. D. M. Adam, *Metal Ligand and Related Vibrations*. Edward Arnold, London (1967).
32. L. Ruiz-Ramuez and T. A. Stephenson, *J. Chem. Soc., Dalton Trans.* 1974, 1640.
33. T. A. Stephenson and G. Wilkinson, *J. Inorg. Nucl. Chem.* 1966, **28**, 945.
34. J. Halpern, B. R. James and A. L. W. Kemp, *J. Am. Chem. Soc.* 1966, **88**, 5142.
35. T. A. Stephenson, E. S. Switkes and P. W. Armit, *J. Chem. Soc., Dalton Trans.* 1974, 1134.
36. F. A. Cotton and G. Wilkinson, *Advanced Inorganic Chemistry, A Comprehensive Text*, 4th edn, p. 170. Wiley-Interscience, New York (1980).
37. S. Datta, K. K. Pandey and U. C. Agrwala, *Inorg. Chim. Acta* 1980, **40**, 65.

38. B. R. James and L. D. Markham, *Inorg. Nucl. Chem. Lett.* 1971, **7**, 373.
39. W. Hieber and P. John, *Chem. Ber.* 1970, **103**, 2178.
40. M. I. Bruce, C. W. Gibbs and F. G. A. Stone, *Z. Naturforsch.* 1968, **32B**, 1543.
41. C. F. J. Barnard, J. A. Daniels, J. Teffery and R. J. Mawby, *J. Chem. Soc., Dalton Trans.* 1976, 953.
42. A. B. P. Lever, *Inorganic Electronic Spectroscopy*, p. 305. Elsevier, Amsterdam (1968).

Polyhedron Vol. 8, No. 9, pp. 1157–1161, 1989
Printed in Great Britain

0277–5387/89 $3.00+.00
© 1989 Pergamon Press plc

SYNTHESIS OF RHODIUM(II) HYDROCINNAMATE AND SOME COMPLEXES WITH NITROGEN LIGANDS

RENATO NAJJAR,* WANDA DE OLIVEIRA and JOÃO BATISTA CARDUCCI

Instituto de Química, Universidade de São Paulo, CP 20.780, CEP 01498, São Paulo, SP, Brazil

and

MAKOTO WATANABE

Department of Industrial Chemistry, Chubu University, Kasugi, Aichi 487, Japan

(*Received* 30 *June* 1988; *accepted* 8 *November* 1988)

Abstract—Rhodium(II) hydrocinnamate has been prepared by the reaction of hydrocinnamic acid with rhodium(II) acetate and has been used to prepare complexes of probable formula $[Rh_2(C_6H_5CH_2CH_2CO_2)_4L_2]$ (L = imidazole, 2-methylimidazole, pyridine, dimethylamine). IR, Raman, electronic, XPE and NMR (^1H) spectra and magnetochemical and thermal analysis data are reported.

Interest in the synthesis of new rhodium carboxylates has existed since the discovery, by Bear *et al.*, of the anti-tumor properties of those compounds in 1972.[1] Many studies on the catalytic activity of the rhodium carboxylates have already been reported, as for example hydrogenation of olefins;[2] the synthesis of aza-β-lactams from diazo compounds[3] and the synthesis of the benzyl ketones from benzene and α-diazoketones[4] are some of the applications of the rhodium carboxylates in this field. Cotton and co-workers have contributed with a notable number of articles with regard to binuclear complexes, not only concerning the structures, but also the synthesis of new compounds.[5–8] In this paper, we describe the synthesis and the characterization of rhodium hydrocinnamate and some of its adducts.

EXPERIMENTAL

Reagents

$RhCl_3 \cdot 3H_2O$ was purchased from Aldrich Chemical Co. Diethyl ether (Merck) was distilled and dried over sodium. Chloroform, ethanol and other chemicals were analytical grade and used as supplied. Hydrocinnamic acid[9] and rhodium(II) acetate[10] were prepared by literature methods.

Synthesis

$Rh_2(HCin)_4$. Anhydrous rhodium(II) acetate (0.5 g, 1.1 mmol) and hydrocinnamic acid (1.8 g, 12 mmol) were ground in a mortar and transferred to a test tube, which was maintained between 90–94°C for 3 h. Afterwards, the resultant solid was washed several times with hot water until the supernatant was colourless. The residual green solid was dissolved in anhydrous ethyl ether (100 cm^3). After filtering, the ether was evaporated and the product dried in a vacuum desiccator over anhydrous calcium chloride. Finally, it was heated *in vacuo* at 78°C for 24 h. The excess of hydrocinnamic acid was sublimed and condensed (yield, 65–70%).

$Rh_2(HCin)_4(Im)_2$. Rhodium hydrocinnamate (0.1 g, 0.12 mmol) was dissolved in 30 cm^3 of ether. This solution was added to another containing 0.017 g (0.25 mmol) of imidazole in 2 cm^3 of acetone. During the reaction, the initially pink solution gradually gave a suspension of a pink solid. After some hours, the supernatant was removed with a pipette and the solid residue was washed

*Author to whom correspondence should be addressed.

several times with ether and dried in a vacuum desiccator, over anhydrous calcium chloride (yield, ~ 95%).

$Rh_2(HCin)_4(mIm)_2$. Rhodium hydrocinnamate (0.1 g, 0.12 mmol) was dissolved in 30 cm^3 of ethanol and added slowly to a suspension containing 0.021 g (0.25 mmol) of 2-methylimidazole in 10 cm^3 of ethanol, under stirring. The colour of the resulting solution changed from green to pink and a pink solid precipitated. The supernatant was removed with a pipette, the solid residue was washed with ethanol and ether and the final product was dried in a vacuum desiccator, over calcium chloride (yield, ~ 90%).

$Rh_2(HCin)_4(py)_2$. Pyridine (0.03 cm^3, 0.3 mmol) was added slowly with stirring to 0.1 g (0.12 mmol) of $Rh_2(HCin)_4$ dissolved in 20 cm^3 of ether and the solvent was removed by evaporation. The residue was washed with water several times and dried in a vacuum desiccator, over anhydrous calcium chloride (yield, ~ 92%).

$Rh_2(HCin)_4(DMA)_2$. Rhodium hydrocinnamate (0.1 g, 0.12 mmol) was dissolved in 30 cm^3 of anhydrous ethyl ether and slowly added, under stirring, to a 40% aqueous solution of dimethylamine. The precipitate was washed with water and afterwards with ether. Finally, it was dried in a vacuum desiccator, over calcium chloride (yield, ~ 65%).

Elemental analyses were carried out by the Microanalytical Laboratory (Instituto de Química, Universidade de São Paulo). The solid state IR absorption spectra were obtained using a Perkin–Elmer 180 spectrometer with fluorolube mulls between KBr windows or KBr discs.

The Raman spectra were obtained with a Jarrell–Ash 25-300 double monochromator fitted with a photomultiplier tube detector (ITT-Fw 130) and using a rotating-sample cell. The exciting radiation was 514.5 nm for rhodium acetate and rhodium hydrocinnamate, while for the adducts, 647.1 nm was used, with 30–35 mW of power. The emergent radiation was detected perpendicular to the laser beam. The spectral resolution in all measurements was 10 cm^{-1}. The electronic spectra were recorded on a Zeiss DMR-10 spectrometer, using millimolar $CHCl_3$ solutions. ^1H NMR measurements were obtained on a Bruker AC 80 spectrometer. The samples were dissolved in $CDCl_3$ and the chemical shifts were referred to Me_4Si as an internal standard. X-ray photoelectron spectra (XPE) were obtained using a Shimadsu ESCA 750 with Mg-K_α exciting irradiation. The magnetic susceptibility at 298 K was measured using the Gouy method. Mercury tetrathiocyanocobaltate(II) was used as the calibrant, and diamagnetic corrections were estimated from Pascal's constants. The effective magnetic moment was calculated from the expression: $\mu_{eff} = 2.84(X_M \cdot T)^{1/2}$. X-ray powder patterns were obtained using a Norelco apparatus and diffractometer from Philips Electronic Instruments with Cu-K_α radiation. The thermogravimetric studies were carried out on a Perkin–Elmer TGS-1 apparatus, at a heating rate of 10 deg min^{-1} under a nitrogen atmosphere.

RESULTS AND DISCUSSION

Table 1 shows the elemental analyses for rhodium hydrocinnamate and its adducts. These results are in compliance with the general formula $Rh_2(HCin)_4 \cdot 2L$. The rhodium hydrocinnamate is an amorphous (according to X-ray powder pattern) green solid, water insoluble but soluble in acetone, chloroform, ethyl ether, methanol, ethanol and tetrahydrofuran. Thermogravimetric analyses indicated that the compound and its adducts are stable up to *ca* 100°C. At higher temperatures, fast decomposition occurs which is not so clear for the adducts but in all cases the final product is Rh_2O_3.

IR spectra

The IR spectra show bands in the region of 1405–1413 cm^{-1} (ν_{sym} OCO) and 1560–1591 cm^{-1} (ν_{asym} OCO). These absorptions are not very conclusive with regard to the coordination mode of the carboxylate group, but allow us to exclude

Table 1. Analytical data

	Carbon		Hydrogen		Nitrogen	
	Calc.	Found	Calc.	Found	Calc.	Found
$Rh_2(HCin)_4$	53.9	53.9	4.5	4.8	—	—
$Rh_2(HCin)_4(Im)_2$	53.7	52.9	4.7	4.6	6.0	6.1
$Rh_2(HCin)_4(mIm)_2$	54.8	54.6	5.2	5.1	5.8	6.0
$Rh_2(HCin)_4(py)_2$	57.5	57.9	4.8	5.2	3.9	4.2
$Rh_2(HCin)_4(DMA)_2$	53.8	53.8	5.6	5.1	3.1	3.4

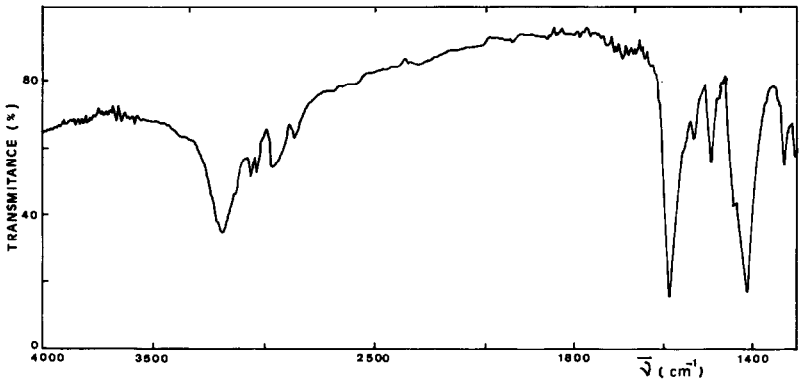

Fig. 1. IR spectrum of the imidazole adducts.

the monodendate hypothesis of coordination, because in this case the difference between the asymmetric and symmetric stretching modes is generally $\geqslant 200$ cm^{-1}.[11] In all spectra we can observe a medium sharp band at 1490 cm^{-1} that may be assigned to ring vibrations. In the adducts, the band that refers to the asymmetric stretching is shifted to higher wave numbers relative to anhydrous rhodium hydrocinnamate ($\Delta \simeq 25$–30 cm^{-1}, Fig. 1).

Raman spectra

Raman spectroscopy has been used to study the Rh—Rh bond, but the complexity of the spectra in the region below 500 cm^{-1} and the low intensity bands expected for such interactions prevent a clear assignment. The rhodium hydrocinnamate Raman spectrum presents a medium line at 179 cm^{-1} and a weak line in the 345 cm^{-1} region, respectively, assigned to the Rh—Rh and Rh—O vibrations.[12–14] In the adducts, the region at *ca* 170 cm^{-1} could not be studied due to the presence of strong plasma lines. When the axial ligands are changed, we can see a shift from 345 cm^{-1} in the anhydrous rhodium hydrocinnamate to 334, 330 and 322 cm^{-1} in the pyridine, imidazole and 2-methylimidazole adducts, respectively. Those shifts are probably related to the increased donor strength of the axial ligands, as had been observed by Ketteringham and Oldham.[15]

Electronic spectra

The absorptions in chloroform solutions for rhodium hydrocinnamate and its adducts confirm the behaviour expected for such typical dimeric rhodium carboxylates, with two bands (or one band and a shoulder) in this region, the lower energy one sensitive to the change of the axial ligands.[16] It is interesting to observe that the change is according to the rhodium cinnamate derivatives,[17] where the λ_1 shifts to higher frequencies with axial ligands of increasing acceptor power. It becomes evident from the less intense shift of the λ_1 band for the methylimidazole than for imidazole. The hyper-conjugative effect of the methyl group which reduces

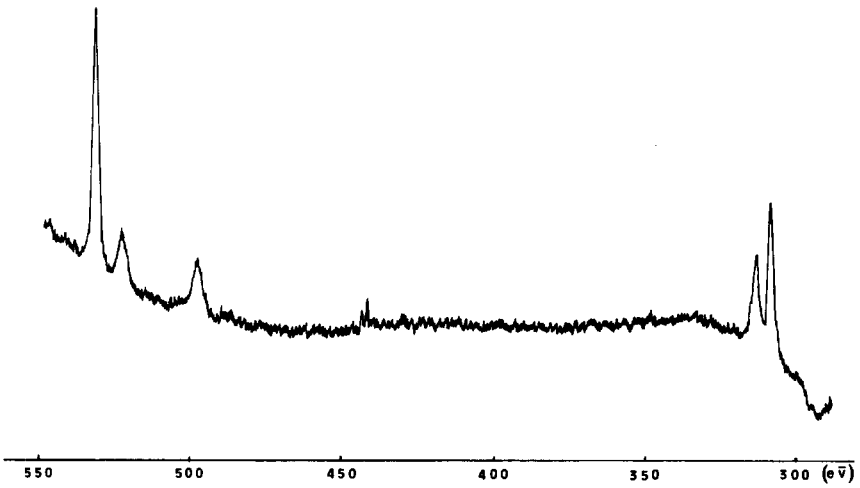

Fig. 2. X-ray photoelectron spectrum of $Rh_2(HCin)_4$.

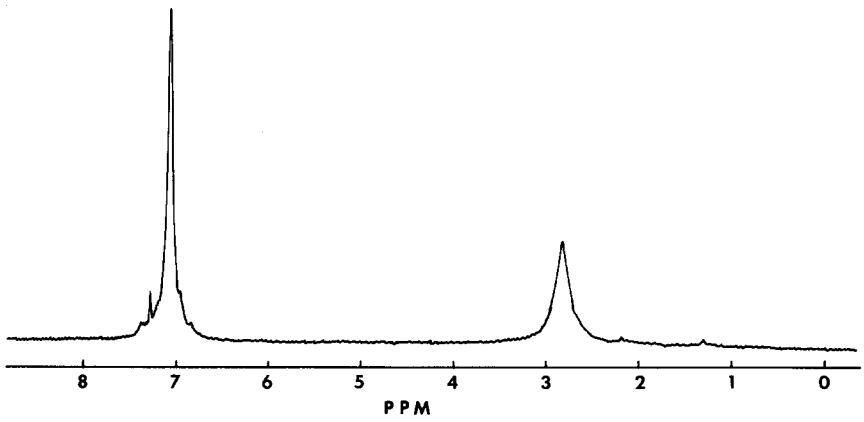

Fig. 3. ^{1}H NMR of rhodium hydrocinnamate.

the π-acceptor capability of the imidazole ring is probably responsible for this effect.

XPE

Changes in the electron density about an atom are reflected in changes in the binding energies of the core electrons. Larger binding energies are associated with smaller electron densities, so, Rh^{III} has larger $3d_{5/2}$ energy than Rh^{II}, and the latter larger than Rh^{I}. The rhodium(II) carboxylates have generally the $3d_{5/2}$ binding energy in the range of 308.5–309 eV.[18,19] The photoelectron spectrum of the rhodium hydrocinnamate (Fig. 2) shows a single Rh $3d_{5/2}$ peak at 308.5 eV, consistent with identical rhodium ions in each dimeric unit and a single O_{1s} peak at 331 eV, indicating eight equivalent oxygen atoms.

^{1}H *NMR*

The ^{1}H NMR spectrum of the anhydrous rhodium hydrocinnamate (Fig. 3) does not show any signals at 11.4 ppm, indicating the absence of the hydroxylic proton of the carboxylic group and a single line at *ca* 7.05 ppm, suggesting that all the phenyl groups are equivalent. The broad line at 2.7 ppm corresponds to the multiplet of the hydrocinnamic acid in the 2.6–3.0 ppm region, and the weak peak at *ca* 7.2 ppm should be an impurity of $CHCl_3$.

Magnetic susceptibility

Rhodium carboxylates are generally characterized by the coupling of spins between two rhodium(II) ions, giving rise to magnetic moments lower than those expected for a magnetically dilute Rh^{II} (d^7) compound. Rhodium hydrocinnamate is essentially diamagnetic, with $\mu_{eff} = 0.4$ BM.

CONCLUSION

All the measurements we have made suggest that rhodium hydrocinnamate and its adducts have the typical structure of the rhodium(II) carboxylates, with two rhodium ions held together by bridging carboxylate groups, and the core presenting a D_{4h} symmetry.

Acknowledgements—We thank the Fundação de Amparo à Pesquisa de Estado de São Paulo (FAPESP) and the Conselho Nacional de Desenvolvimento Científico e Tecnológico (CNPq) that supported, in part, this work. J.B.C. is indebted to FAPESP for a fellowship.

REFERENCES

1. R. G. Hughes, J. L. Bear and A. P. Kimball, *Proc. Am. Assoc. Cancer Res.* 1972, **13**, 120.
2. T. J. Pinnavaia, R. Raythatha, J. G. S. Lee, L. J. Halloran and J. F. Hoffman, *J. Am. Chem. Soc.* 1979, **101**, 6891.
3. C. J. Moody, C. J. Pearson and G. Lawton, *Tetrahedron Lett.* 1985, **26**, 3171.
4. M. A. McKervey, D. N. Russell and M. F. Twohig, *J. Chem. Soc., Chem. Commun.* 1985, 491.
5. B. E. Bursten and F. A. Cotton, *Inorg. Chem.* 1981, **20**, 3042.
6. F. A. Cotton and J. L. Thompson, *Inorg. Chim. Acta* 1985, **81**, 193.
7. A. R. Chakravarty, F. A. Cotton, D. A. Tocher and J. H. Tocher, *Inorg. Chim. Acta* 1985, **101**, 185.

8. P. A. Agaskar, F. A. Cotton, R. Falvello and S. Han, *J. Am. Chem. Soc.* 1986, **108**, 1214.
9. S. Gabriel and J. Zimmerman, *Berichte* 1880, 1680.
10. G. A. Rempel, P. Legzdins, H. Smith and G. Wilkinson, *Inorg. Syn.* 1972, **13**, 90.
11. G. B. Deacon and F. Huber, *Inorg. Chim. Acta* 1985, **104**, 41.
12. J. San Filippo Jr and H. J. Sniadoch, *Inorg. Chem.* 1973, **12**, 2326.
13. I. K. Kireeva, G. Ya. Mazo and R. N. Shchelokov, *Russ. J. Inorg. Chem.* 1979, **24**, 220.
14. V. M. Miskowski, W. P. Schaefer, B. Sadeghi, B. D. Santarsiero and H. B. Gray, *Inorg. Chem.* 1984, **23**, 1154.
15. A. P. Ketteringham and C. Oldham, *J. Chem. Soc., Dalton Trans.* 1973, 1067.
16. S. A. Johnson, H. R. Hunt and H. M. Neumann, *Inorg. Chem.* 1963, **2**, 960.
17. R. Najjar, E. R. Netto and I. Takano, *Inorg. Chim. Acta* 1984, **89**, 53.
18. A. M. Dennis, R. A. Howard, K. M. Kadish and J. L. Bear, *Inorg. Chim. Acta* 1980, **44**, L139.
19. M. Q. Ahsan, I. Bernal and J. L. Bear, *Inorg. Chem.* 1986, **25**, 260.

Polyhedron Vol. 8, No. 9, pp. 1163–1171, 1989
Printed in Great Britain

0277-5387/89 $3.00+.00
© 1989 Pergamon Press plc

OPTICALLY ACTIVE COORDINATION COMPOUNDS—XLIX.* THE *CIS*-BIS-AQUO-BIS-1,2-DIAMINOETHANERHODIUM(III) SYSTEM

R. D. GILLARD† and JULIO D. PEDROSA DE JESUS‡

Inorganic Research Laboratories, University College, P.O. Box. 78, Cardiff CF1 1XL, Wales, U.K.

(*Received* 18 *July* 1988; *accepted after revision* 8 *November* 1988)

Abstract—Resolved *cis*-$[Rh(en)_2(OH)_2]^+$ or *cis*-$[Rh(en)_2(OH_2)_2]^{3+}$ were formed by base or acid hydrolysis, respectively, of resolved oxalato bisethylenediamine rhodium(III); acid dissociation constants, determined using circular dichroism, are given by $pK_1 = 5.02$ and $pK_2 = 9.04$, and these are compared with values from pH titration. *Cis*-$[Rh(en)_2(H_2O)(OH)]^{2+}$ shows marked enhancement of circular dichroism in solution (relative to its own conjugate acid and base) similar to that for its cobalt(III) analogue. The possible micro-species responsible are discussed in terms of bridging by $(H_3O_2)^-$.

Isomeric compounds of the type $[M(en)_2XY]^{n+}$, where en signifies 1,2-diaminoethane and M = Co^{III}, Cr^{III}, Rh^{III} or Ir^{III} have been well studied. For M = Rh^{III}, the current situation is fully summarized.[2] The optical activity of the *cis* isomers has not been so extensively used as for homologues with M = Co, so here we report some applications of the stereochemical method for determining solution properties for M = Rh^{III}.

A good way of making *cis* complexes is through the oxalato species, $[Rh(en)_2(C_2O_4)]^+$, itself best made by a catalytic route developed here,[3] and widely validated[4] as giving high yields. Also in high yield, the anations of this oxalato ion with hydrohalic acids (presumably via hydrolysis) have been used[5,6] to prepare *cis*-dichloro and dibromo ions. These hydrolyses themselves have been explored as routes to other *cis* compounds of rhodium(III), in particular to those containing ions of the type *cis*-$[Rh(en)_2X_2]^{n+}$, where X = OH or OH_2.

EXPERIMENTAL

The apparatus and detailed findings are described in the Ph.D. thesis of J. D. P. D. Jesus ("Stereochemical Aspects and Photochemistry of Compounds of Rhodium(III)", University of Wales, at University College, Cardiff (1977)). The parent oxalato-compound was prepared[3] and resolved[5] optically by established methods. Its hydrolysis was studied by spectrophotometry and circular dichroism (CD).

When the perchlorate of the oxalato complex was used in basic hydrolysis, the final CD spectrum was that of a solution of (−)-*cis*-$[Rh(en)_2(OH)_2]^+$ at the same concentration as the starting solution. However, when the *chloride* was treated in the same manner in sodium hydroxide solution, a different final CD spectrum was observed. Tipping also produced[7] anomalous behaviour for the CD spectra of similar aquorhodium(III) complexes in the presence of chloride ions. This is perhaps due to strong ion pairing between the complexed cation and the Cl ions, although Poë and Vuik[8] thought that the values of K_{IP} for the ion pairs *trans*-$[Rh(en)_2Cl_2]Cl$ and *cis*-$[Rh(trien)Cl_2]Cl$ at concentrations of 25 and 60 M^{-1} derived[9] from radiochloride exchange rates, were "unreasonably large" for an aqueous solution.

Reaction with NO_2^-

(a) *Cis*-diaquobis(ethylenediamine)rhodium(III), treated with an excess of nitrite ion at 100°C gave the *cis*-dinitro-bis(ethylenediamine)rhodium(III)

* For part XLVIII see ref. 1.

† Author to whom correspondence should be addressed.

‡ Present address: Chemistry Department, University of Aveiro, Aveiro 3800, Portugal.

ion, whose circular dichroism spectrum has a lowest energy absorption at 300 nm.

(b) *Cis-O*-nitrito-aquo-bis(ethylenediamine)rhodium(III) was obtained by addition of sodium nitrite to the cold (4°C) acidic (pH 3.5) solution of the diaquo compound (molar ratio of complex: NO_2^- = 1 : 1). A new band immediately developed around 335 nm; this increased in intensity on heating (333 K) to a maximum after 30 min. The pH changed from 3.50 to 4.35.

(c) Acid–base properties. The pK_a was 8.5 ± 0.4, by titration against NaOH. The conjugate base, *cis*-$[Rh(en)_2(ONO)(OH)]^+$ at pH = 11.1 shows a CD band at a lower energy (345 nm) than for the corresponding conjugate acid (as expected for aquo ⇌ hydroxo ligand). Another well defined absorption appears (for pH 11.1) in the region (297 nm) where a shoulder was observed for the *O*-nitritoaquo parent at pH = 4.35. On reacidification to pH = 4.3, the CD spectrum of the starting solution (at the same pH) is restored.

(d) *Cis*-$[Rh(en)_2(H_2O)_2]^{3+}$ reacted with NO_2^- (in a 1 : 1 ratio as in part (b)) at pH 6, but at a slower rate than at pH 3. On reacting the resultant solution of *cis*-$[Rh(en)_2(ONO)(OH_2)]^{2+}$ with an excess of NaCl, the lower energy CD band moves to 335 nm and a better defined absorption develops around 300 nm, characteristic of *cis*-$[Rh(en)_2(NO_2)Cl]^+$.

(e) The reacidified solution from (c) was treated with more nitrite, at 330 K. The CD band at 340 nm, which is due to *cis*-$[Rh(en)_2(ONO)_2]^+$, decreases in intensity relative to the shoulder around 300 nm, which then develops into the well-defined absorption of *cis*-$[Rh(en)_2(NO_2)_2]^+$ with an approximately two-fold increase in the intensity, at 345 nm. Scheme 2 represents the probable reactions taking place.

Reaction with IO_3^-

(a) Aqueous *cis*-diaquobis(ethylenediamine)rhodium(III) nitrate, at pH = 2.6 (adjusted with HNO_3) has a CD maximum at 322 nm; on adding sodium iodate, a very fast shift to 337 nm occurs. On leaving the solution at room temperature for 24 h, the band moves to 342 nm.

(b) The addition of IO_3^- to a starting solution of diaquo rhodium(III) ion acidified to pH = 1.0 with HNO_3, also causes a very fast CD shift to 342 nm, which does not change significantly over 24 h at room temperature.

(c) The reaction is more rapid as the concentration of H^+ increases.

(d) We assume that the rapidly formed species with a CD absorption maximum at 342 nm is *cis*-$[Rh(en)_2(OH_2)(OIO_2)]^{2+}$, akin to the *cis*-$[Co(en)_2(OH_2)(OIO_2)]^{2+}$ complex known to form from a similar rapid addition of iodate to the racemic cobalt(III) congener.

RESULTS AND DISCUSSION

Hydrolysis

Scheme 1 shows several hydrolyses centred on this accessible oxalato-ion.

The $[Rh(en)_2(C_2O_4)]^+$ ion reacts quite rapidly with nitric acid.[10] It gives *cis*-$[Rh(en)_2(OH_2)_2]^{3+}$ on reaction with either nitric or perchloric acid. The reaction of $[Rh(en)_2(C_2O_4)]^+$ with hydroxide gives *cis*-$[Rh(en)_2(OH)_2]^+$. The corresponding aquo-

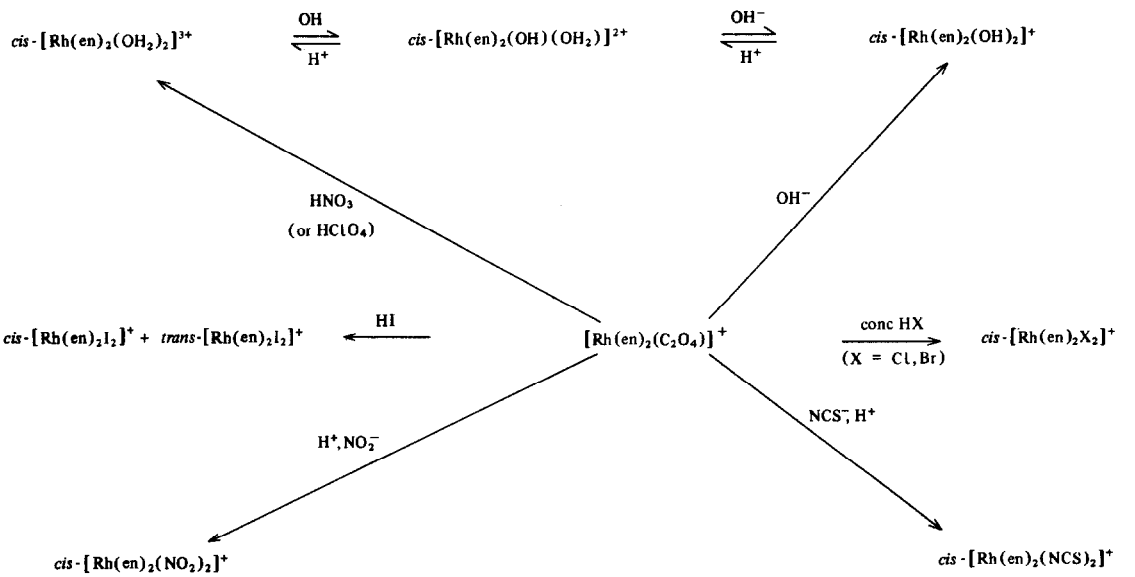

Scheme 1.

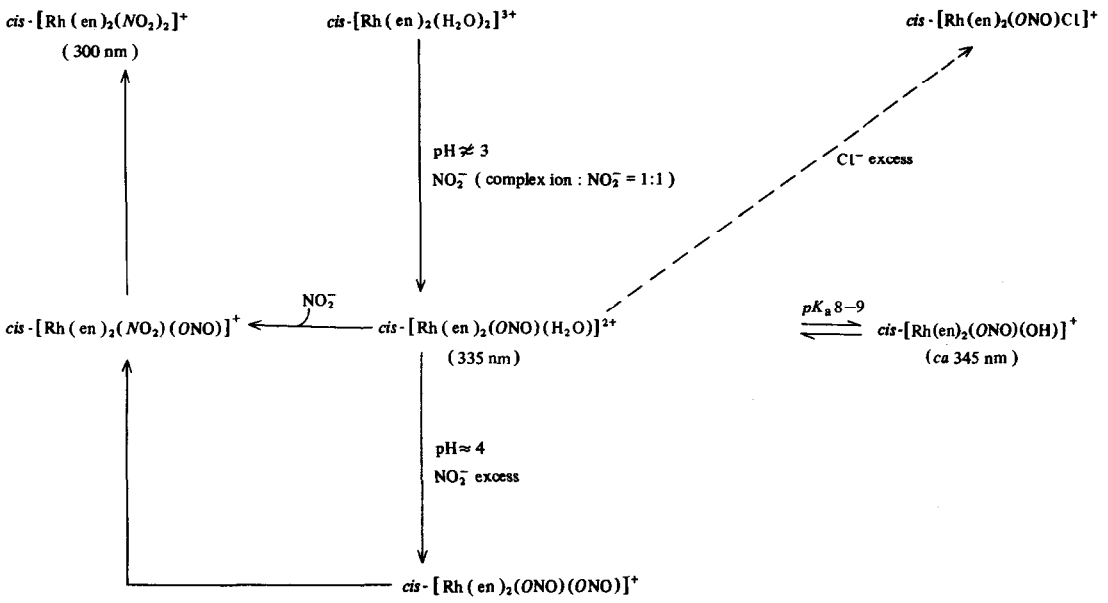

Scheme 2.

complexes were obtained by acidifying the solution of dihydroxo-[Rh^{III}] ion.

Although the preparation of *cis*-$[Rh(en)_2(NO_2)_2]^+$ involves[11] reacting *cis*-$[Rh(en)_2Cl_2]^+$ with nitrite, we find that $[Rh(en)_2(C_2O_4)]^+$ is nevertheless a suitable starting material. This reaction can be performed obtaining very good yields, by reacting the oxalato-complex with $NaNO_2$ in acid (pH ~ 4). Details of intermediates and their circular dichroism changes are given in the Experimental section and in Scheme 2. Similar reactions with NaI result[11] in a mixture of *cis*- and *trans*-$[Rh(en)_2I_2]^+$ ions. In similar acidic conditions (pH 4), NCS^- also gives some *cis*-$[Rh(en)_2(NCS)_2]^+$. However, this reaction is not straightforward and the yield was poor. A better synthesis, along with the properties of this thiocyanate and its linkage isomers are discussed in detail elsewhere.[12] All these reactions (see Scheme 1) take place with 100% retention of the *cis* configuration with the mentioned exception[11] of the reaction with iodide (where *cis–trans* isomerization is swift). The products, *cis*-$[Rh(en)_2X_2]^{n+}$, from the optically active oxalato-species, are also optically active, for all X = OH^-, H_2O, NO_2^-, Cl^-, Br^-.

Base hydrolysis of $[Rh(en)_2(C_2O_4)]^+$

Aquo and hydroxo compounds containing the *cis*- or *trans*-$[Rh(en)_2]^{3+}$ moiety have been prepared using various routes.[5,10,13,14] Since $[Co(en)_2(C_2O_4)]^+$ is known[15,16] to undergo hydrolysis in a wide range of basic conditions, we studied the reactivity of the Rh^{III} analogue in alkaline solution. The reaction of the rhodium(III) oxalato ion with OH^- gives *cis*-$[Rh(en)_2(OH)_2]^+$, and is first order with respect to the hydroxide and the complex at 333 K, for $0.05\,M < [OH^-] < 0.2$ M. Using optically active $[Rh(en)_2(C_2O_4)]^+$, no isomerization occurred. The *cis*-aquohydroxo and the diaquo ions could then be prepared in solution by appropriate adjustment of the pH of the solution containing *cis*-$[Rh(en)_2(OH)_2]^+$. The *cis*-$[Rh(en)_2(OH_2)_2]^{3+}$ ion could of course also be prepared by a reaction of $[Rh(en)_2(C_2O_4)]^+$ with $HOClO_3$ or $HONO_2$, and isolated as *cis*-$[Rh(en)_2(OH_2)_2](NO_3)_2ClO_4$. The other salt usually isolated as a solid was *cis*-$[Rh(en)_2(OH)(OH_2)](ClO_4)_2$, which has been synthesized by a laborious route (via the *cis*-dichloro ion) by Palmer *et al.*[17] via:

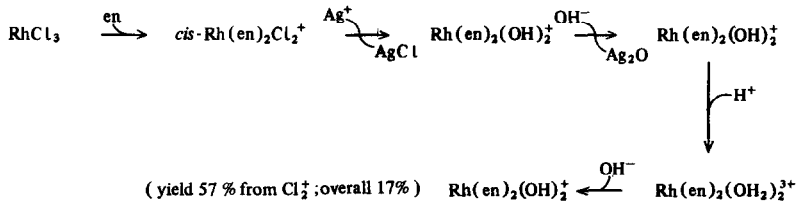

Those authors did succeed in increasing the notoriously low yield of the *cis*-dichloro ion made by this older method[11] to 30%, giving an overall yield around 17%.

The reaction of $[Rh(en)_2(C_2O_4)]^+$ with the base can be easily followed spectrophotometrically. The product, *cis*-$[Rh(en)_2(OH)_2]^+$, was identified by its electronic spectrum in the final solution, by the spectrum of *cis*-$[Rh(en)_2(OH_2)_2]^{3+}$ resulting from the acidification of that solution, and by measuring the CD spectrum when optically active $[Rh(en)_2(C_2O_4)]ClO_4$ was employed; the reaction then took place with the conservation of optical activity. The overall reaction can thus be described by

$$(-)\text{-}[Rh(en)_2(C_2O_4)]^+ + 2OH^- \rightleftharpoons (-)\text{-}[Rh(en)_2(OH)_2]^+ + C_2O_4^{2-}.$$

Values of absorbance at 285 (and 325 nm) were used to obtain pseudo-first order rate constants for four different concentrations of hydroxide (Table 1): the reaction is first order with respect to the hydroxide ion. The rate law can then be written as

$$\text{Rate} = k[OH^-][Rh(en)_2(C_2O_4)]^+$$

with $k = 4.55 \times 10^{-3}$ mol^{-1} dm^3 s^{-1} at 333 K.

There is no *cis–trans* isomerization in the basic hydrolysis of $(-)$-$[Rh(en)_2C_2O_4]^+$; this is as expected from the higher stereo-inertness of *cis*-Rh^{III} relative to *cis*-Co^{III} compounds. However, a scheme similar to that offered for the cobaltic compound[15,16] (also where rate = k[complex][OH^-], with $k = 2.8(\pm 0.5) \times 10^{-2}$ mol^{-1} dm^3 s^{-1}) would be expected for the reaction of $[Rh(en)_2(C_2O_4)]^+$, *viz*

$$cis\text{-}[Rh(en)_2(C_2O_4)]^+ + OH^- \longrightarrow cis\text{-}[Rh(en)_2(C_2O_4)(OH)]^0$$

$$cis\text{-}[Rh(en)_2(C_2O_4)(OH)]^0 + OH^- \longrightarrow cis\text{-}[Rh(en)_2(OH)_2]^+ + C_2O_4^{2-},$$

Table 1. Observed pseudo-first order rate constants for the base hydrolysis of $[Rh(en)_2(C_2O_4)]^+$ at 333 K

$[OH^-]^a$	[Complex]^b	$k_{obs.} \times 10^4$ (s^{-1}) ^{c}	^{d}
0.05	7.30	2.3	2.1
0.10	3.50	4.5	4.2
0.15	3.30	6.0	6.1
0.20	3.76	8.8	9.0

[a] Molar concentrations of hydroxide.
[b] Molar concentrations of $[Rh(en)_2(C_2O_4)]^+$, $\times 10^3$.
[c] From change in absorption at 285 nm.
[d] From change in absorption at 325 nm.

where the ring opening is the rate determining step.

Acidic properties of cis-$[Rh(en)_2(OH_2)_2]^{3+}$

Cis-$[Rh(en)_2(OH_2)_2]^{3+}$ in aqueous solution is a diprotic acid, with acidity constants K_1 and K_2.

$$n H_2O + cis\text{-}[Rh(en)_2(OH_2)_2]^{3+} \overset{K_1}{\rightleftharpoons} cis\text{-}[Rh(en)_2(OH)(OH_2)]^{2+} + H^+(OH_2)_n$$

$$cis\text{-}[Rh(en)_2(OH)(OH_2)]^{2+} + n H_2O \overset{K_2}{\rightleftharpoons} cis\text{-}[Rh(en)_2(OH)_2]^+ + H^+(OH_2)_n.$$

Previously reported values are given in Table 2. Values of pK_a have been measured for the *trans* and *cis* isomers. One set of results for the *cis* compounds was most likely obtained from compounds which were not geometrically pure, as the value of pK_1 obtained was abnormally small.[5] We have therefore repeated the determination of the two acidity constants for the *cis*-$[Rh(en)_2(OH_2)_2]^{3+}$ ion, using circular dichroism (and, for comparison, a pH titration).

Figure 1 shows how the circular dichroism of a solution of *cis*-$[Rh(en)_2(OH)_2]^+$ varies as titration

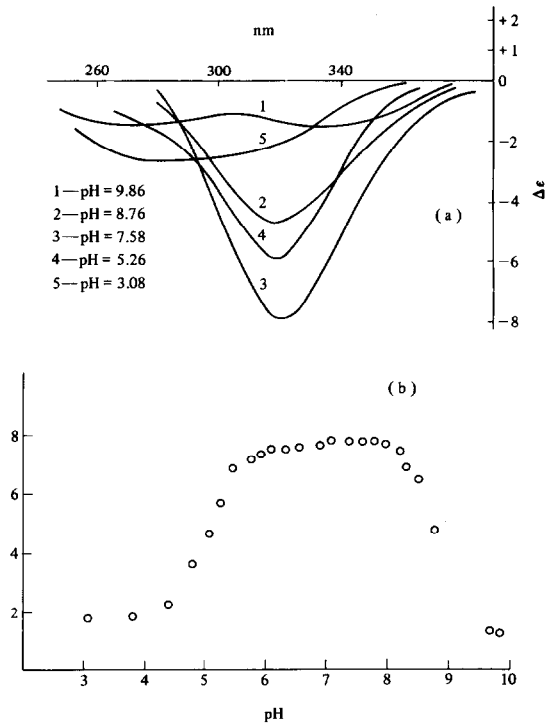

Fig. 1. CD spectra during titration of *cis*-$[Rh(en)_2(OH)_2]^+$ with 5 M HNO_3. (a) Typical spectra measured at: (1) pH 9.86; (2) pH 8.76; (3) pH 7.58; (4) pH 5.26; and (5) pH 3.08. (b) The variation with pH of molar circular dichroism, $\Delta\varepsilon$, at 320 nm. From measurements as in (a) $\Delta\varepsilon_{320}$ has been multiplied by -1.

Table 2. Measured acid dissociation constants for *cis*-$[Rh(en)_2(OH_2)_2]^{3+}$

Method[a]	pK_1	pK_2	Ref.
Pot.	6.09	8.08	[b]
	5.82	7.98	[b]
	5.85	7.95	[c]
	6.72	7.64	[d]
	3.2	6.9	[e]
	4.8	8.5	[f]
CD (291 K)	5.02	9.04	[f]

[a] Potentiometric (Pot.) titration (pH); CD, via the spectrophotometric method, using circular dichroism.

[b] Ref. 17.

[c] Klabunde, Ph.D. thesis, Northwestern University (1967), quoted in [b], and said at that time (1980) to be (*sic*) the "only available values".

[d] Ref. 18.

[e] Ref. 5.

[f] This work.

with HNO_3 progresses. By following the change in intensity of the CD spectra at 320 nm, as in Fig. 1b, the presence of three species is clear. Until pH ~ 9.5, the intensity (i.e. the molar circular dichroism per mole of rhodium ion, in whatever form) is about the same as that of the starting *cis*-$[Rh(en)_2(OH)_2]^+$ solution. Between pH 9.5 and pH 8, the intensity increases substantially and then stays constant until *ca* pH 5.5. This region of pH, between 8 and 5.5, corresponds stoichiometrically to the presence of mainly *cis*-$[Rh(en)_2(OH)(OH_2)]^{2+}$. Below pH ~ 5.5, there is again a very pronounced change (decrease) in intensity until pH 4.5. This corresponds to the protonation of the intermediate ion(s) to give the diaquo complex. The changes in intensity were used to calculate the pK_a values. This effect, that the circular dichroism of the aquohydroxo ion was larger than that for either the diaquo or the dihydroxo ion, was previously found for the analogous cobalt(III) system.[19] The *g*-factor ($\Delta\varepsilon/\varepsilon$) increases because, roughly speaking, chirality at the metal ion has increased more than has distortion of the local centrosymmetry which increases the intensity of the *d–d* transitions in isotropic spectra. This can arise from the formation of an additional flexible ring, and, in species containing the *cis*-$M(H_2O)(OH)$ moiety, such a formation of new rings has indeed been suggested as a general phenomenon,[20] occurring by dimerization through strong hydrogen bonds in $\mu(HOHOH)^-$ as shown (L is any ligand, here $\frac{1}{2}$en).

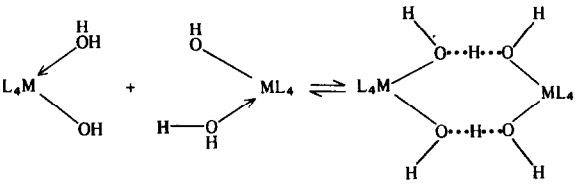

Such a dimerization would have little effect upon the allowedness of *d–d* bands in the metal ions (which are rather remote from each other) but confers an extra element of conformational flexibility in the dimer.

Among existing cases of effects attributed to a bridging by $(H_3O_2)^-$, are several in systems reminiscent of the present one:

(i) pK_{A1} and pK_{A2} of the ol-bridged *meso*-dimer (**I**) are very well separated; Hancock attributes[21] the anomalous stability of the first conjugate base (**II**) to the structure shown:

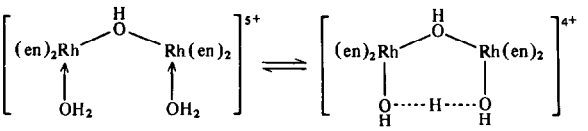

(**I**) (**II**)

This suggestion recalls an earlier debate[22,23] attempting to distinguish between the oxygen ligands in (**III**) and (**IV**):

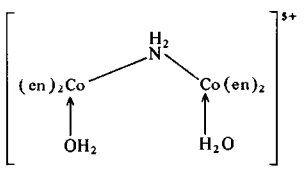

III

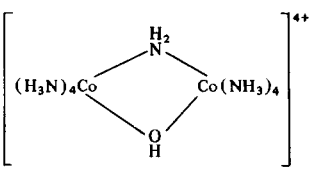

IV

(ii) In addition to crystallographic proof[24] of the existence of the centric species in its tetra-iodide dihydrate, where bipy = 2,2′-bipyridyl, vapour tensiometry also supported[25] the reality of the species in aqueous solutions.

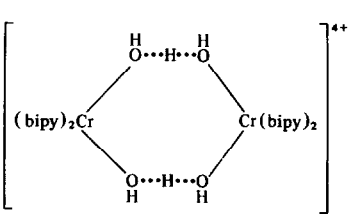

(iii) The bridging role of $(H_3O_2)^-$ in tri-tungsten species has been demonstrated by X-ray methods,[20,26] not only in the crystalline phase but also in aqueous solution[27] by employing differential anomalous X-ray scattering.

(iv) To account for an extra Mössbauer active species, Meagher[28] has very recently suggested the possibility that the well known hydrolysed dimers of aquo-iron(III) include some novel ones with $\mu(H_3O_2^-)$. In a similar way, an extra Mössbauer signal in the more complicated system Fe(EHGS) had been assigned to the $Fe^{III}\mu(H_3O_2)Fe^{III}$ fragment.[29]

(v) A recent example is perhaps provided by the system $[Pd(phen)(OH_2)_2]^{2+}$. Discrepancy between the interpretation of the careful titrations by Anderegg and Wanner[30] and later magnetic resonance experiments[31] may arise from the presence of the dimeric $\mu(H_3O_2)^-$ species under the greater concentration found in spectrometry.

Ardon and Bino[24] point out that the major difficulty in proving the presence of the $\mu(H_3O_2)^-$ species in solution lies in distinguishing it from its anhydride, the μ(OH) species. The instant enhancement of molar circular dichroism on crossing the pK_A observed for (+)-*cis*-$[Rh(en)_2(H_2O)(OH)]^{2+}$ and, several years ago,[19] for (+)-*cis*-$[Co(en)_2(H_2O)(OH)]^{2+}$, offer a novel method for making this distinction, at least for kinetically inert resolvable compounds.

While, in monomeric complex ions, the possibility of such bridging through strong hydrogen bonds is greatest in the *cis*-hydroxo-aquo systems, (because of the relative strength of OHO bonds), any other *cis* arrangement of a hydrogen bond donor and a hydrogen bond acceptor may give rise to similar bridging, as in the *cis*-diammine species or the *cis*-aquo-ammines, as shown below.

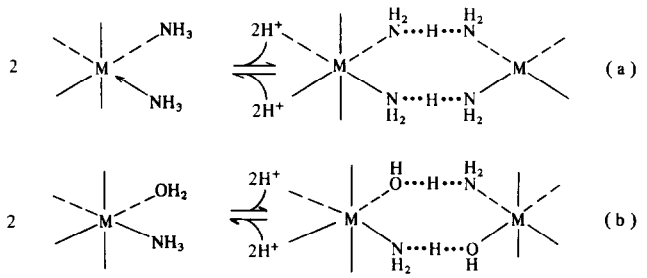

Many similar situations involving substituted hydroxo or amido species, are possible. Indeed, for any unidentate protic ligand (which is a hydrogen bond donor), in the position *cis* to its own conjugate base (which is a hydrogen bond acceptor) the bridge may form.

Grinberg[32] pointed out the special effects on pK_A of the *cis*-diammine platinum(IV) moiety; and (a) above may now help to account for these.

Quite apart from such anomalies in the absolute size of acidity constants, the extra equilibrium involving dimerization may also have an effect upon measured pK_A, as shown schematically below (for clarity, charges are omitted).

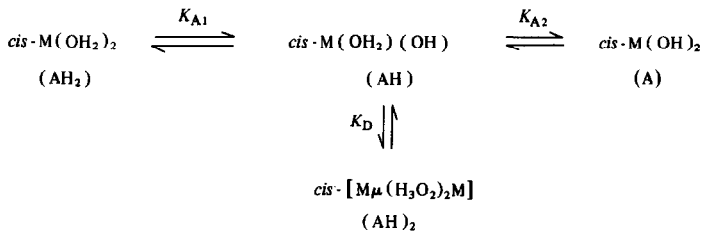

The apparent values of pK_A will vary with concentration (this may help to explain the large spread in results of Table 2); properties like circular dichroism will not vary linearly with total metal concentration; and there may be stereoselective effects in racemic as against optically active systems (as observed[33] for other dimeric bridged complexes like tartrato-vanadate(IV) or copper(II) tartrates). For example, in (+)-*cis*-$[M(en)_2H_2O)(OH)]^{2+}$, the only possible dimer is non-centric $(+)(\mu H_3O_2)(+)$, whereas for the (±) complex ion, the possible dimers comprise the non-centric pair $(+)(\mu H_3O_2)(+)$ and its enantiomer $(-)(\mu\text{-}H_3O_2)(-)$, and the centric (*meso*) isomer $(+)(\mu\text{-}H_3O_2)(-)$ which should have quite different properties from the racemate. Experiments are in hand on this stereoselectivity.

The classical analogy between protonation of a Bronsted base and its co-ordination extends to $(H_3O_2)^-$, as in Scheme 4:

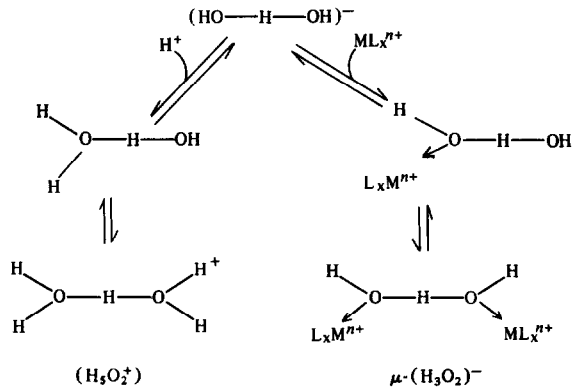

The transformation from the short O–O contact (2.29 Å) of free $(H_3O_2)^-$ to the much larger separation (*ca* 2.5 Å) of $(H_5O_2)^+$ or that in the $\mu(H_3O_2)^-$ bridge linking two metal ions, is in line with many other changes of O–O distance from two co-ordinated oxygen systems like $[(DMSO)_2H]^+$ to three co-ordinated oxygen atoms, as in $[(R_2O)_2H]^+$. In addition, and at present unique to the aquo system, there is the charge effect on O–O distance.

Reactions with carbon dioxide

It is convenient to summarize our CD results on the resolved compounds in the light of the careful work by Palmer *et al.*[17] on the racemic system. They showed that, in rapid reactions with carbon dioxide, *cis*-$[Rh(en)_2(OH)_2]^+$ and *cis*-$[Rh(en)_2(OH)(OH_2)]^{2+}$ formed *cis*-$[Rh(en)_2(CO_3)(OH)]^0$ and *cis*-$[Rh(en)_2(CO_3)(OH_2)]^+$ respectively: these were related by a pK_a of 8.45. $[Rh(en)_2(CO_3)]^+$ had $\lambda = 327$ (312 M^{-1} cm^{-1}) (cf. the oxalato-species; Table 3).

In the titration of carbonato-free solutions of *cis*-$[Rh(en)_2(OH_2)_2]^{3+}$ with sodium hydroxide, the circular dichroism spectra change through formation of aquohydroxo- and dihydroxo-Rh^{III} species. In the presence of CO_2, the changes in spectra

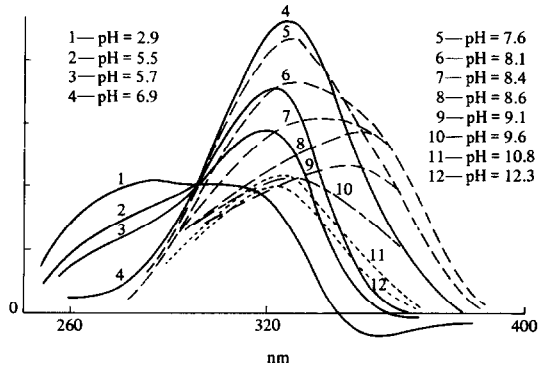

Fig. 2. Variation of circular dichroism for (−)-$[Rh(en)_2(OH_2)_2]^{3+}$ during titration (in the presence of CO_2) with NaOH. Spectra were measured at the following pHs: (1) 2.9; (2) 5.5; (3) 5.7; (4) 6.9; (5) 7.6; (6) 8.1; (7) 8.4; (8) 8.6; (9) 9.1; (10) 9.6; (11) 10.8; and (12) 12.3.

Table 3. Electronic absorption spectra (isotropic and CD) of interconvertible species *cis*-$[Rh(en)_2XY]^{n+}$

		Isotropic absorption				Circular dichroism		
		Band I		Band II				
X	Y	λ	ε	λ	ε	λ	$\Delta\varepsilon$	Ref.
OH^-	OH^-	330	192	275	185	410	+0.03	[a,b]
		329	184	280	179			17
						335	−0.38	[a,b]
OH	OH_2	323	199	283	155(sh)			17
		322	215	271	160	320	−0.99	[a,c]
OH_2	OH_2	313	185	268	161	314	−0.63	[a]
		318	174	271	148			17
CO_3^{2-}	OH_2[e]	332	224					17
						350[d]	−0.92	[a]
CO_3^{2-}	OH^-	330	300					17
						330[d]	−0.6[d]	[a]

[a] This work.
[b] pH 8.85.
[c] pH 7.1.
[d] These values are approximate, based on an analysis of spectra like those in Fig. 3.
[e] This species may have one or more of a variety of possible structures, including aquocarbonato—as preferred in ref. 17—or the tautomeric hydroxo-hydrogencarbonato-, or some hydrogen bonded (intra- or intermolecular) variant.

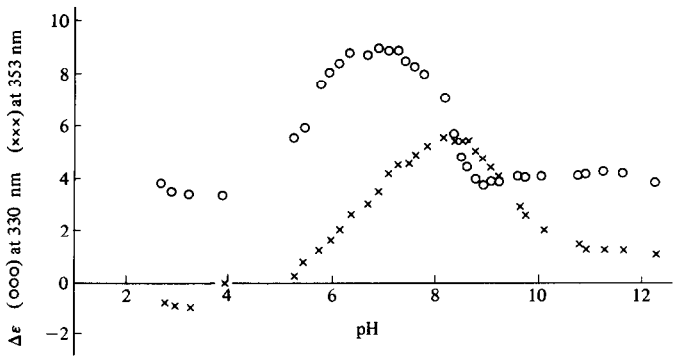

Fig. 3. Variation of $\Delta\varepsilon_{330}$ (○○○) and $\Delta\varepsilon_{353}$ (× × ×) for (−)-$[Rh(en)_2(OH_2)_2]^{3+}$ during titration with NaOH in CO_2.

(Fig. 2) are similar to those in the carbonate-free situation until pH ~ 7 (cf. Fig. 1a). But, as the pH is increased above 7, a new band develops around 350 nm. This is better shown in Fig. 3, where the intensities at 330 and 353 nm are plotted as a function of pH. Up to pH ~ 4.5, the intensity at 330 nm is about equal to that of the starting solution of *cis*-$[Rh(en)_2(OH_2)_2]^{3+}$. At the same time, the intensity at 350 nm changes slightly from a negative value to approximately zero. From pH 4.5 to 6, the intensity at 330 nm increases substantially to its maximum value, whereas the intensity at 350 nm shows a much smaller increase. The intensity at 330 nm does not then change significantly until pH 7, although the Cotton effect at 350 nm continues to increase until it reaches a maximum at pH 8.5. From pH 7 to 8.5 the intensity at 330 nm again changes very substantially and then maintains an approximately constant value for pH > 8.5. The intensity of the band at 350 nm decreases from pH 8.5 to 10.5 and then stays constant at higher pH. The spectrum of the final solution is distinctly different from that of *cis*-$[Rh(en)_2(OH)_2]^+$ obtained in the titration of carbonate-free solutions. It shows only one absorption band with $\lambda \simeq 330$ nm, instead of two (less intense) bands shown by the *cis*-dihydroxo compound, at 340 and 270 nm. If that final alkaline solution is titrated back with acid, the new band at 350 nm is even more clear. The solution finally obtained for pH 3.06 gives the circular dichroism spectrum of *cis*-$[Rh(en)_2(OH_2)_2]^{3+}$. The development of the band around 350 nm is observed between pH 5.5 and 8.5. The dominant aquorhodium(III) species in this range of pH is the *cis*-$[Rh(en)_2(OH)(OH_2)]^{2+}$ ion. Therefore, the compound responsible for the highly intense absorption at 350 nm arises from the reaction of this complex ion with HCO_3^-. As the titration proceeds, both the carbonato complex and the aquohydroxo ion are titrated, and the final product is not *cis*-$[Rh(en)_2(OH)_2]^+$ alone. It shows a CD spectrum of higher intensity than would be expected for this compound. The reactions suggested by these features are in Scheme 3, which is, in essence, the same as that derived for the racemic system.[17]

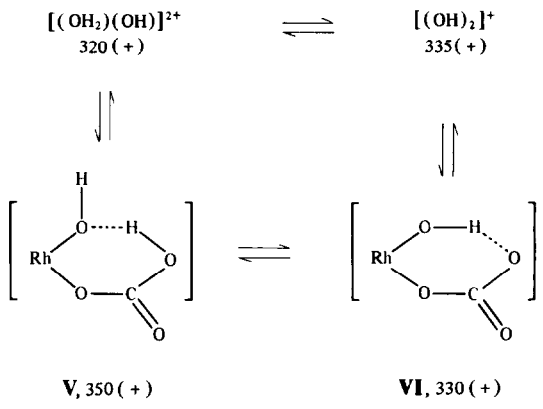

Scheme 3.

The formation of compound (V) explains the very high intensity of the new band at 350 nm, even stronger than that corresponding to the aquohydroxo compound (itself anomalously high). In fact, the six membered chelate ring formed within the molecule is expected to contribute strongly to the optical activity.[34] All the reactions are fast, as expected for reactions not involving M–O bond cleavage, so all species involving the unidentate ligands OH^-, OH_2 CO_3^{2-} of Table 3 and Scheme 3 have chemically correlated optical configurations.

Acknowledgements—We wish to thank the University of Aveiro, Portugal, for granting leave (J.D.P.D.J.), and the Instituto Nacional de Investigacao Cientifica and University College Cardiff for financial support.

REFERENCES

1. M. Fujita and R. D. Gillard, *Polyhedron* 1988, **7**, 2731.
2. P. S. Sheridan and F. H. Jardine, in *Comprehensive Coordination Chemistry* (Edited by G. Wilkinson, R. D. Gillard and J. A. McCleverty), Vol. 4. Pergamon Press, Oxford (1987).
3. R. D. Gillard, J. P. de Jesus and P. S. Sheridan, *Inorg. Synth.* 1980, **20**, 57.
4. M. P. Hancock, *Acta Chem. Scand.* 1979, **33A**, 15.
5. R. D. Gillard and L. R. H. Tipping, *J. Chem. Soc., Dalton Trans.* 1977, 1241.
6. A. W. Addison, R. D. Gillard, P. S. Sheridan and L. R. H. Tipping, *J. Chem. Soc., Dalton Trans.* 1974, 709.
7. L. R. H. Tipping, Ph.D. Thesis, University of Wales (at University College Cardiff) (1977).
8. A. J. Poë and C. P. J. Vuik, *Inorg. Chem.* 1980, **19**, 1771.
9. K. M. Bowker, E. R. Gardner and J. Burgess, *Trans. Faraday Soc.* 1971, **62**, 3576.
10. C. Burgess, F. R. Hartley and D. E. Rogers, *Inorg. Chim. Acta* 1975, **13**, 35.
11. S. N. Anderson and F. Basolo, *Inorg. Synth.* 1963, **7**, 217.
12. N. Garif, R. D. Gillard and J. P. de Jesus, *Polyhedron* 1989, **8**, 775.
13. F. N. S. Rowan, R. M. Milburn and T. P. Dasgupta, *Inorg. Chem.* 1976, **15**, 1477.
14. A. J. Poë and E. Shaw, *J. Chem. Soc. A* 1970, 393.
15. C. Andrade, R. B. Jordan and H. Taube, *Inorg. Chem.* 1970, **9**, 711.
16. M. E. Farago and C. F. V. Mason, *J. Chem. Soc. A* 1970, 3100.
17. D. A. Palmer, R. van Eldik, H. Kelm and G. M. Harris, *Inorg. Chem.* 1980, **19**, 1009.
18. S. Y. Drurechenskaya, A. V. Belyaev and B. J. Peshchevtakki, *Russ. J. Inorg. Chem.* (Eng. transl.) 1974, **19**, 427.
19. R. D. Gillard, *J. Chem. Soc. A* 1968, 1945.
20. A. Bino and D. Gibson, *J. Am. Chem. Soc.* 1982, **104**, 4383.
21. M. Hancock, B. Nielsen and J. Springborg, *Acta Chem. Scand.* 1982, **36A**, 313 and cf. ref. 2.
22. (a) K. Garbett and R. D. Gillard, *J. Chem. Soc., Chem. Commun.* 1965, 45; (b) *Idem., J. Chem. Soc. A* 1968, 1725.
23. R. D. Mast and A. G. Sykes, *J. Chem. Soc. A* 1967, 784.
24. A. Bino and D. Gibson, *Inorg. Chem.* 1984, **223**, 109 and refs therein.
25. M. Ardon and B. Magyar, *J. Am. Chem. Soc.* 1986, **106**, 3359.
26. A. Bino and D. Gibson, *J. Am. Chem. Soc.* 1981, **103**, 6741.
27. R. D. Lorentz, A. Bino and J. E. Penner-Hahn, *J. Am. Chem. Soc.* 1986, **108**, 8116.
28. A. Meagher, *Inorg. Chim. Acta* 1988, **146**, 19.
29. C. J. Carrano and K. Spartahari, *Inorg. Chem.* 1984, **23**, 1993.
30. G. Anderegg and H. Wanner, *Inorg. Chim. Acta* 1986, **113**, 101.
31. S. Wimmer, P. Castan, F. L. Wimmer and N. P. Johnson, *Inorg. Chim. Acta* 1988, **142**, 13.
32. O. N. Adrianova and T. N. Fedorova, *Russ. J. Inorg. Chem.* (Engl. Edn) 1980, **25**, 105 (and refs therein).
33. J. H. Dunlop, D. F. Evans, R. D. Gillard and G. Wilkinson, *J. Chem. Soc.* 1966, 1260.
34. R. D. Gillard, *J. Inorg. Nucl. Chem.* 1964, **26**, 657.

Polyhedron Vol. 8, No. 9, pp. 1173–1199, 1989
Printed in Great Britain

0277–5387/89 $3.00+.00
© 1989 Pergamon Press plc

OXOVANADIUM(IV) AND AMINO ACIDS—II.* THE SYSTEMS L-SERINE AND L-THREONINE+VO^{2+}. A POTENTIOMETRIC AND SPECTROSCOPIC STUDY

J. COSTA PESSOA and L. F. VILAS BOAS

Centro de Química Estrutural, Complexo Interdisciplinar, Instituto Superior Tecnico, 1096 Lisboa, Portugal

and

R. D. GILLARD†

School of Chemistry and Applied Chemistry, University of Wales, Cardiff College, P.O. Box 912, Cardiff CF1 3TB, U.K.

(*Received* 30 *August* 1988; *accepted* 11 *November* 1988)

Abstract—The equilibria in aqueous solution in the systems L-serine and L-threonine $+VO^{2+}$ have been studied by a combination of pH-potentiometric and spectroscopic methods (EPR, visible absorption and circular dichroism) in the pH range 1.5–13.6. For pH > 4, high ligand-to-metal ratios were used. The results of the various methods are made self-consistent, then rationalized assuming an equilibrium model including species, MLH, ML, MLH_{-2}, MLH_{-3}, ML_2H_2, ML_2H, ML_2, ML_2H_{-1}, ML_2H_{-2}, $M_2L_2H_{-2}$ and $M_2L_2H_{-3}$ (where HL denotes L-serine or L-threonine) and several hydrolysis products; their formation constants and individual electronic spectra (isotropic and circular dichroism) are given. Plausible isomeric structures for each of the stoichiometries are discussed.

Knowledge of the complex equilibria of VO^{2+} in the presence of amino acids is relevant in understanding its possible interaction with likely biological ligands; few reliable data exist.

The first part of this study[1] introduced our work and gave detailed results for the system L-Ala+VO^{2+} in the pH range 2–12. This work involves the study of the L-serine and L-threonine+VO^{2+} systems by combining the results of potentiometric and spectroscopic techniques. A part of this has been presented in a preliminary form.[2] No other reliable data have been published for these systems.[3] Several general experimental difficulties in the study of oxovanadium(IV) +amino acid systems were discussed in Part I.[1]

The L-Ser and L-Thr systems have an additional coordinating group (–CHROH, hereafter designated by –ROH) but—to our knowledge—no reliable data for pK_{a3} of the –ROH group are available. Examples of published values for this pK_a(–ROH) (= pK_{a3}) of L-Ser include: 11.02 (I = 0.10 M KNO_3),[4] 11.45 (I = 1 M $NaClO_4$),[5] 13.6 (I = ?)[6] and 16 (I = ?).[7] However, pH potentiometric titrations performed in this work suggest that (at least for I = 2.25 M $NaNO_3$ and t = 25°C) the pK_{a3} of L-Ser is greater than 12. NMR experiments even suggest that pK_{a3} may be in the range 13–14.

Our results suggest that for pH > 6.5, several species form that involve the coordination of the $-RO^-$ group of L-Ser and L-Thr. Since pK_{a3} is not available, exactly as for the *bidentate* L-Ala+VO^{2+} system, the formation constants calculated[1] correspond to the general reaction:

$$xVO^{2+} + yL^- + zH^+ \rightleftharpoons (VO)_x(L)_y(H^+)_z. \quad (1)$$

In common with biochemical studies, we abbreviate L-alanine as HA, L-serine as HS and L-threonine as HT, and their conjugate bases, the singly charged alaninate, serinate and threoninate ions are then A^-, S^- and T^-, respectively. L^- will denote both S^- and T^-.

* For Part I, see ref. 1.

† Author to whom correspondence should be addressed.

EXPERIMENTAL

Reagents

All solutions were prepared in an inert atmosphere (high purity dinitrogen passed through soda lime and glass wool). All measurements were performed at 25°C with solutions containing 2.25 M $NaNO_3$.

L-Serine (BDH), L-threonine (BDH) and L-serine methyl ester hydrochloride (Sigma) were dried for several days (vacuum desiccator with silica gel). All results refer to optically pure amino acids only.

Instrumentation

The instruments used were described in Part I.[1] Several potentiometric titrations were made with a Metrohm 655 Dosimat, instead of the Radiometer Autoburet ABU12.

Calibration procedure for pH measurements

This was described in Part I.[1] The maximum pH value for the titration curves of solutions containing L-Ser (and L-Thr)+VO^{2+} was 7.5. Several visible and circular dichroism spectra recorded in the pH range 10.5–13.6, and a combined electrode (Radiometer GK2351B—low sodium-error electrode) was used for this purpose. The interference of the Na^+ was corrected using factors supplied by the manufacturer. The accuracy of these pH measurements is obviously not as good as for pH < 10.

General experimental conditions

Five titration curves ($C_{\text{amino-acid}} = 3\text{–}10 \times 10^{-2}$ M) were obtained for each amino acid to determine the protonation constants in 2.25 M $NaNO_3$; NaOH (2.2 M) was used.

For both L-Ser (and L-Thr)+VO^{2+}, 10 titration curves were measured with initial total concentrations of oxovanadium(IV) in the range 2.6–50×10^{-3} M and L-amino acid 0.012–0.36 M. Titrations involving pH measurements in the pH range 2–4 and 4.0–7.5 were performed using ligand-to-metal (L/M) ratios of 0.5–6.4 and 30–113.

A total of 40 visible spectra and 80 CD spectra (visible region) were recorded for each system, with total concentrations of oxovanadium(IV) and amino acid in the range $1.5\text{–}26 \times 10^{-3}$ and 0.01–0.31 M, respectively. Ligand-to-metal ratios were in the range 4–100.

RESULTS

EPR studies

The EPR spectra recorded with frozen "solutions" containing VO^{2+} and L-Ser or L-Thr at 77 K are typical VO^{2+} axial spectra. The field region that corresponds to $A_\parallel$ and $M_I = 5/2$ and 7/2 gives more information about the type and number of species present.

In Fig. 1, we include the high-field region of the EPR spectra of frozen "solutions" containing L-Ser and VO^{2+} with ligand-to-metal ratios of 38.0 at several values of pH. The results obtained for the L-Thr+VO^{2+} system are similar. SI to SVII represent distinct components detected in the EPR spectra. Each corresponds to a given set of g and A values ($\parallel$ and $\perp$): there may of course be more than one vanadium complex with approximately the same g and A parameters.

Analysing Fig. 1, we make the following general observations:

(i) For pH $\lesssim$ 6, the spectra obtained with L-Ser+VO^{2+} and L-Thr+VO^{2+} are similar to those for the L-Ala+VO^{2+} system,[1] except that the pH range where species of the type L_I and L_{II} (L = S, T, A) predominate is narrower and is shifted by $\sim$ 0.5 pH units to lower pH.

(ii) At pH $\sim$ 6, essentially one component only is detected (designated by S_{III} or T_{III}). The EPR spectra of S_{III} and T_{III} are identical and coincide with the spectra of MA_2.[1] This suggests that, for all three systems, the same type of species is responsible for the observed spectra.

(iii) For pH $\gtrsim$ 6 the EPR spectra for the L-Ser (and L-Thr)+VO^{2+} systems differ completely from those in the L-Ala+VO^{2+} system in similar conditions, in that a clearly seen component (designated by S_{IV} or T_{IV}) for pH 6.4 has $A_\parallel(L_{III}) > A_\parallel(L_{IV})$. The component S_{IV} in Fig. 1 corresponds to at least two different species, S_{IV} and $S_{IV'}$; Their experimental spectra are indistinguishable; $S_{IV'}$ predominates for pH $\gtrsim$ 9 (see below).

As the pH increases, the intensity of the peak in the region of L_{III} decreases. The modifications with pH in these peaks also suggest that a new component (designated by L_V) forms, with $A_\parallel(L_V)$ slightly smaller than $A_\parallel(L_{III})$. For pH $\gtrsim$ 10, L_{III} has probably disappeared—the peak observed in this region may correspond to L_V only.

(iv) For pH $\gtrsim$ 11, the intensity of the peaks in the region of L_V increases, suggesting formation of a new component—L_{VI}. As pH increases above about 12, shoulders in the peaks corresponding

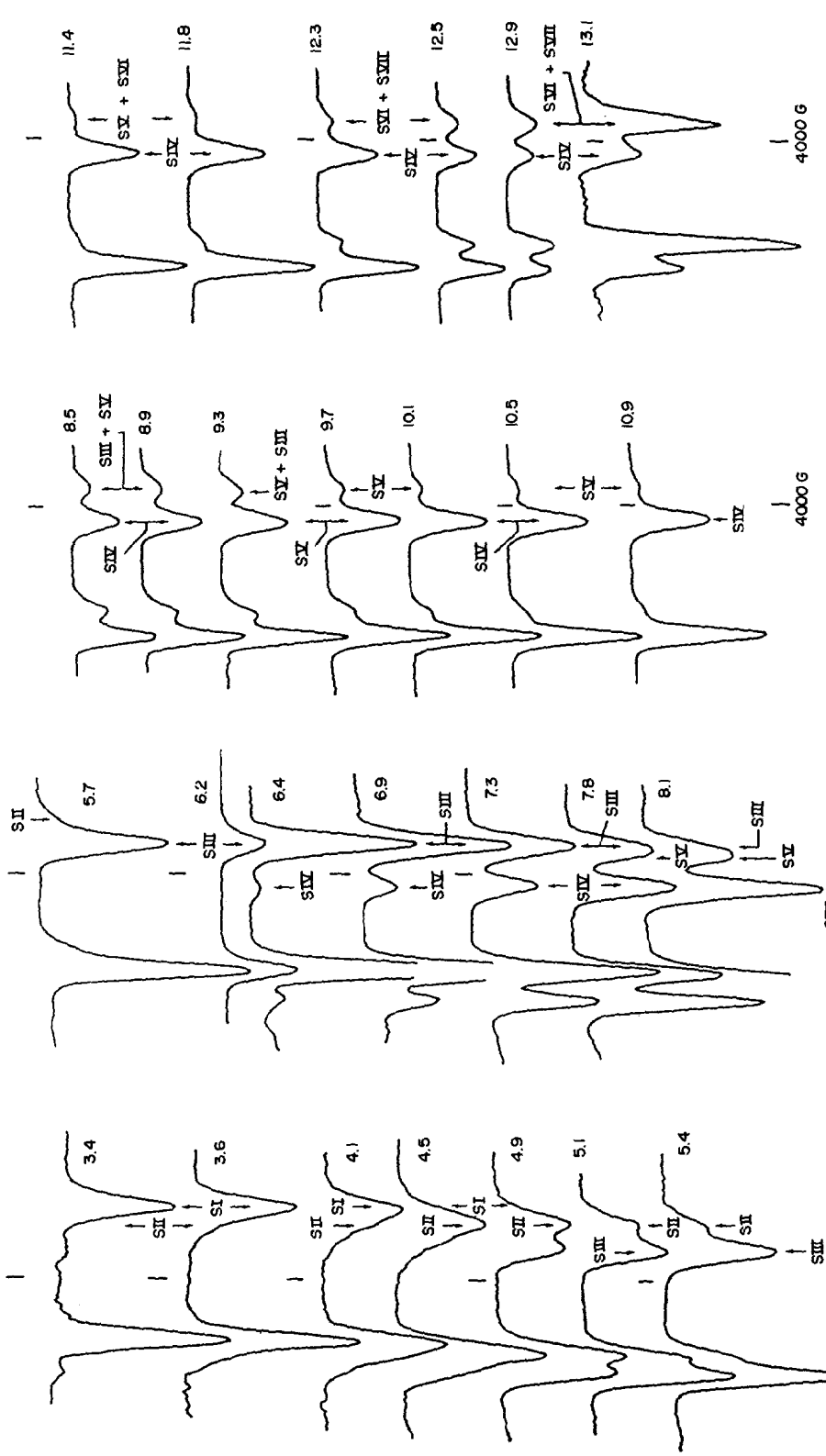

Fig. 1. High field range (3800–4200 Gauss) of the first derivative EPR spectra at 77 K of frozen "solutions" containing L-Ser and VO^{2+} with L/M = 38.0. The total vanadium concentration is in the range $1.3–2.2 \times 10^{-2}$ M. pH values are indicated.

to $M_I = 7/2$ and a slight decrease in $A_\parallel$ also suggest the formation of another component—L_{VII}. CD spectra in similar conditions also indicate at least two (probably three) distinct species.

Several spectra were recorded at fixed pH values, varying L/M by progressively adding stock VO^{2+} solution. For example, for the L-Ser + VO^{2+} system at pH 9.3, three components may be detected—S_{III}, S_V and S_{IV}, with $A_\parallel(S_{IV}) \ll A_\parallel(S_V) \lesssim A_\parallel(S_{III})$. Their positions and relative intensities are essentially unchanged as L/M varies from 38 to 10. The signal due to S_{III} appears as a shoulder on the signal of S_V.

At pH ~ 13.4, S_{IV}, and another component—S_{VI} and/or S_{III}, are detected. The relative intensity of S_{IV} may slightly decrease as L/M varies from 38 to 12.

In spectra at pH ~ 12.5 for the L-Thr + VO^{2+} system, at least two components occur: T_{IV} and T_{VI} (and/or T_{VII}), with relative intensities independent of L/M from 35 to 10. CD spectra in similar conditions point to at least three distinct species.

Circular dichroism and visible absorption spectra

As for EPR, the CD and visible spectra and their changes as the pH varies are similar for both L-Ser + VO^{2+} and L-Thr + VO^{2+} systems. We will, in the main, present results (and calculations) for the L-Ser + VO^{2+} system.

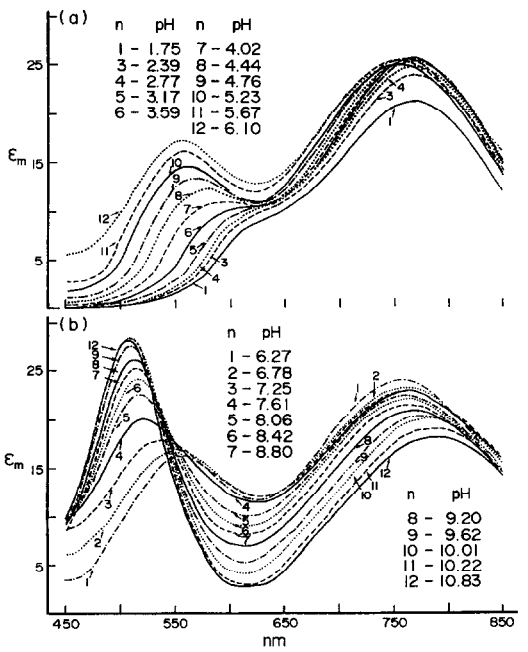

Fig. 2. Visible spectra of solutions containing L-Ser + VO^{2+} with L/M = 38.0 and $C_{VO} = 7.2$–8.3×10^{-3} M. The pH corresponding to each spectrum is indicated. The CD spectra for the same solutions are in Figs 4 and 5.

Figure 2 includes visible spectra of L-Ser + VO^{2+} solutions with an L/M ratio of 38.0. For pH $\lesssim$ 6.1 (Fig. 2a), the results are similar to those in the L-Ala + VO^{2+} system for L/M = 53.9.[1] For pH $\gtrsim$ 3, the spectra also reveal a progressive increase in the ligand field around VO^{2+}.

For pH $\gtrsim$ 6.3, on the other hand, the evolution of the visible spectra is completely different from that for the L–Ala + VO^{2+} system, with a ligand-to-metal ratio of 53.9 (Fig. 2 of ref. 1) and as pH increases:

(i) Band II increases in intensity and further shifts to lower wavelengths.
(ii) Band I shows a progressive decrease in ε_m and shifts to longer wavelengths.

Figure 3 includes visible spectra for pH $\gtrsim$ 10.7. For pH $\gtrsim$ 12.3, the general increase in ε_m (especially in the range 450–600 nm) suggests extensive hydrolysis of VO^{2+}; these spectra are akin to those observed in the L-Ala + VO^{2+} system for pH $\gtrsim$ 8.

As for the L-Ala + VO^{2+} system, the CD spectra of solutions of L-Ser (and L-Thr) + VO^{2+} vary enormously in the pH range 1–14. Up to pH 6, the spectra are relatively similar to those for L-Ala + VO^{2+}, in that $|\Delta\varepsilon_m|$ values gradually increase and band II shifts to longer wavelengths. The $|\Delta\varepsilon_m|$ values are of the same order of magnitude: e.g. at pH ~6 and ~760 nm, $\Delta\varepsilon_m$(Ser) ~ $1.4 \times \Delta\varepsilon_m$(Ala). Figure 4 includes some spectra of L-Ser + VO^{2+} solutions for pH $\lesssim$ 6.

As for EPR and visible spectra, for pH $\gtrsim$ 6 the CD spectra in the system L-Ser or L-Thr + VO^{2+} (Figs 5 and 6) differ completely from those for the L-Ala + VO^{2+} system in similar conditions. Namely:

(i) In the range 400–800 nm the $|\Delta\varepsilon_m|$ values continue to increase till pH ~ 8.8.
(ii) In the range 650–800 nm: $\Delta\varepsilon_m$(pH 8.4) ~ $3.5 \times \Delta\varepsilon_m$(pH 6.3).
(iii) In the range 450–550 nm: $\Delta\varepsilon_m$(pH 8.4) ~ $2.2 \times \Delta\varepsilon_m$(pH 6.3).

For pH $\gtrsim$ 8.5 (Fig. 5):
In the range 650–800 nm, the $\Delta\varepsilon_m$ still increase till pH ~ 10.7.
In the range 450–550 nm, the $|\Delta\varepsilon_m|$ decrease and for pH $\gtrsim$ 10, $\Delta\varepsilon_m > 0$.

For pH $\gtrsim$ 10.7 (Fig. 6), by contrast:
In the range 650–800 nm, $\Delta\varepsilon_m$ wanes and at high pH a species exists which has $\Delta\varepsilon < 0$.
In the range 450–550 nm, the $\Delta\varepsilon_m > 0$ waxes till pH ~ 12.6 (Fig. 6).
For pH $\gtrsim$ 12.6, all $|\Delta\varepsilon_m|$ decrease.

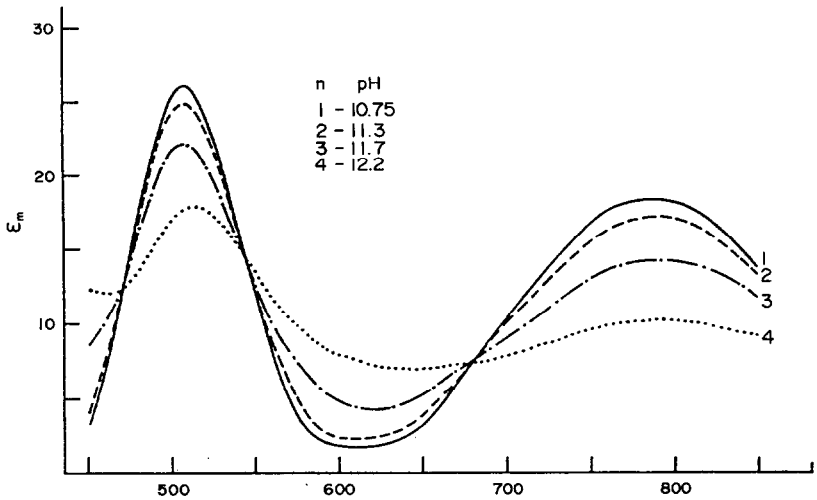

Fig. 3. Visible spectra of solutions containing L-Ser+VO^{2+} for pH $\gtrsim$ 10.7 with L/M = 38.0 and $C_{VO} = 6.7–7.7 \times 10^{-3}$ M. The pH corresponding to each spectrum is indicated and the CD spectra for the same solutions are in Fig. 6.

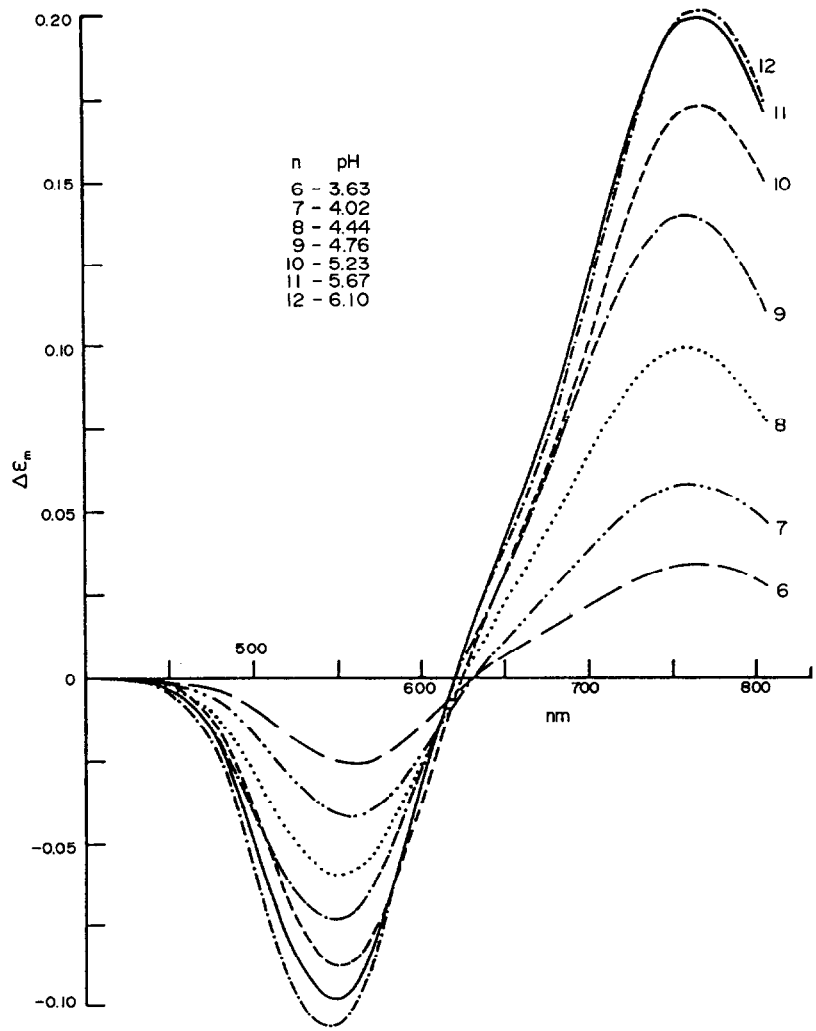

Fig. 4. CD spectra of solutions containing L-Ser+VO^{2+} with L/M = 38.0 and $C_{VO} = 7.2–7.9 \times 10^{-3}$ M. The isotropic absorption spectra of these solutions are in Fig. 2.

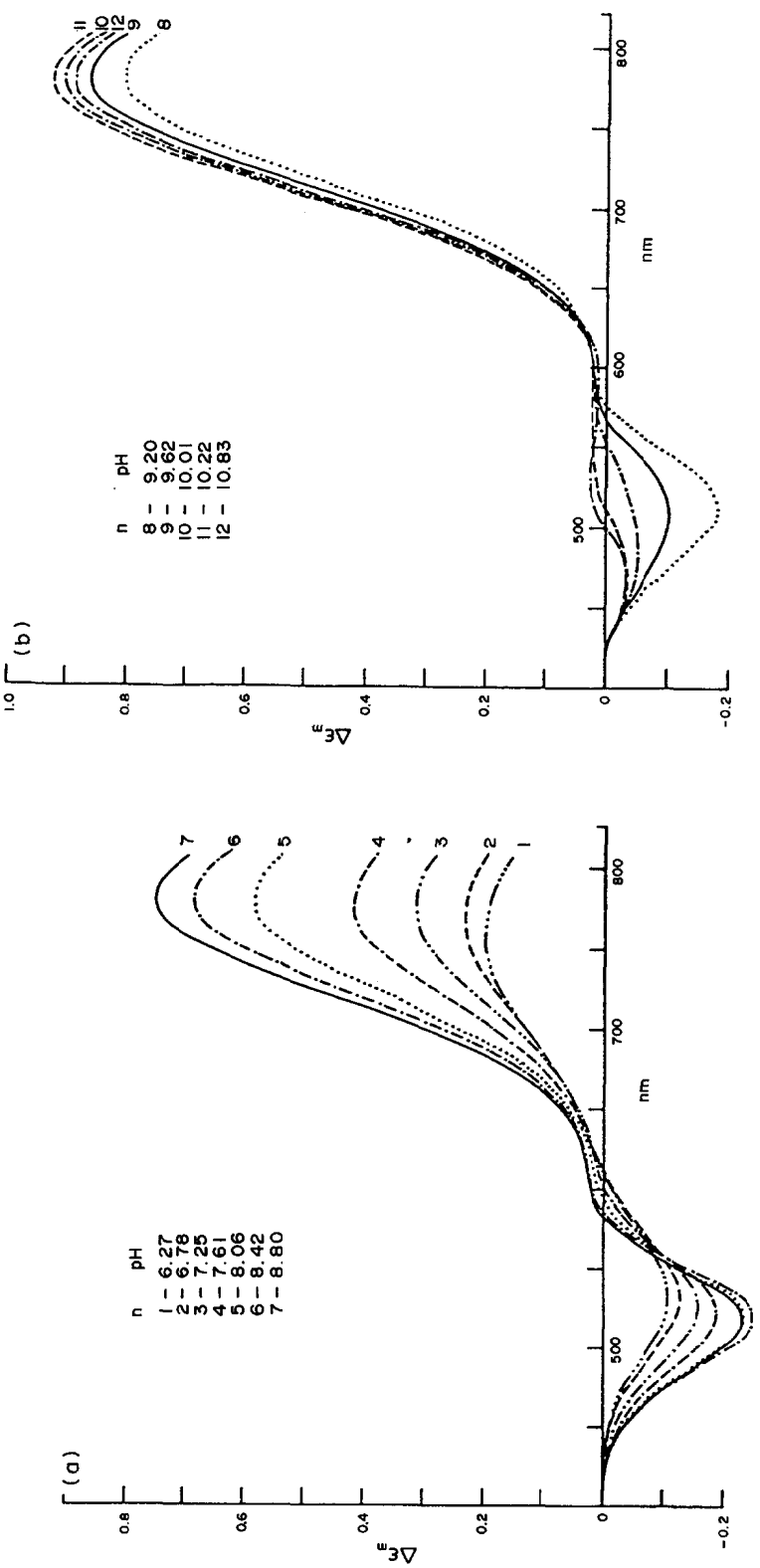

Fig. 5. CD spectra of solutions containing L-Ser + VO^{2+} with L/M = 38.0 and C_{VO} = 7.5–8.3 × 10^{-3} M. The isotropic absorption spectra of these solutions are in Fig. 2.

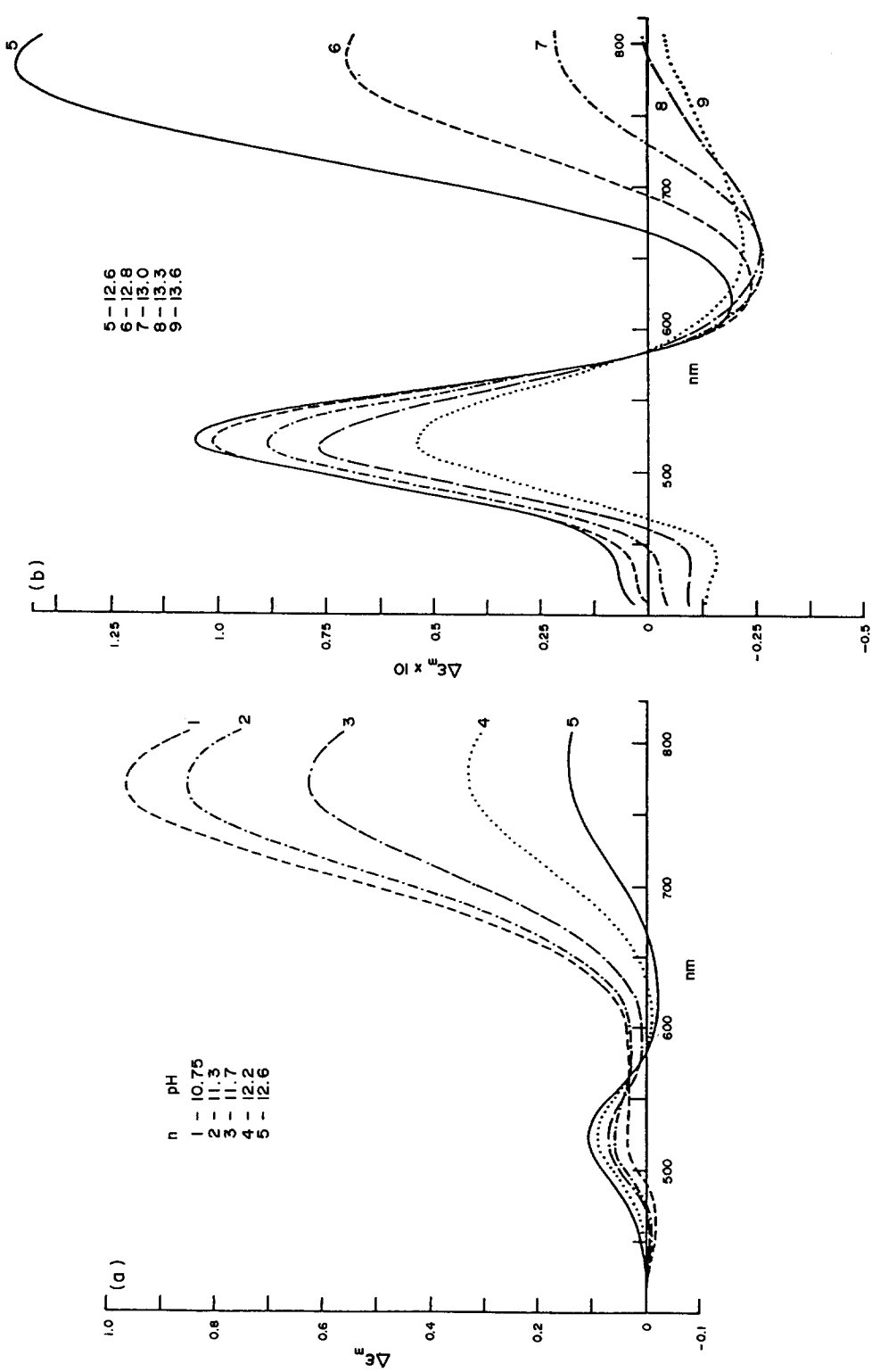

Fig. 6. CD spectra of solutions containing L-Ser + VO^{2+} with L/M = 38.0 and C_{VO} = 7.5–8.3 × 10^{-3} M. The isotropic absorption spectra of the solutions with pH < 12.3 are in Fig. 3. Note the different scales for a and b.

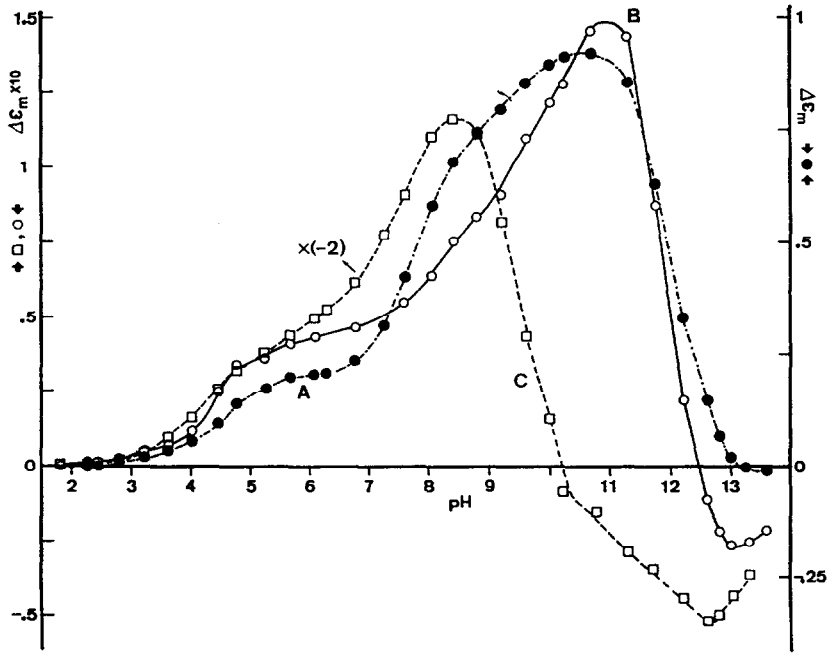

Fig. 7. Change with pH of the $\Delta\varepsilon_m$ values of L-Ser + VO^{2+} solutions with L/M = 38.0 from Figs 4–6 at three wavelengths. A: 767 nm, B: 632 nm and C: 527 nm ($\Delta\varepsilon_m \times -2$).

Between pH 4 and 8, oxovanadium(IV) must be coordinated mainly to amino acids, otherwise $VO(OH)_2$ would precipitate. However, the soluble product of hydrolysis of oxovanadium(IV) is clearly not as important for L-Ser (and L-Thr) + VO^{2+} as for L-Ala + VO^{2+} in similar conditions. Likewise, the solutions for L-Ser (and L-Thr) + VO^{2+} were violet or pink-violet in the pH range 7–13.3, and the ligand-to-metal ratios were lower, whereas L-Ala + VO^{2+} solutions with L/M ~ 54 were already brown for pH $\gtrsim$ 8.4.

Besides these qualitative observations, the EPR, visible and CD spectra show clearly that the $-RO^-$ group is involved in the coordination to VO^{2+} at pH > 7 in L-Ser (and L-Thr) + VO^{2+} solutions with high L/M ratios. The coordination of the $-CH_2O^-$ group of malate must similarly be assumed to explain the EPR, visible and CD spectra for pH > 7, in solutions containing L-malic acid and VO^{2+} with high L/M ratios.[8]

CD spectra have also been recorded at fixed pH (pH = 4.5, 7.2, 9.2 and 13.3 for solutions containing L-Ser + VO^{2+} and pH = 4.5, 7.4, 9.4, 12.4 and 13.6 for solutions containing L-Thr + VO^{2+}) at varying but high amino acid-to-vanadium ratios. For each pH, two types of experiments were performed: (i) the total concentration of the amino acid is approximately constant and that of VO^{2+} is varied or, (ii) the total vanadium concentration is kept approximately constant but that of amino acid is varied (not done for pH = 12.4 and 13.6).

At pH 4.5, the CD spectra show minor changes between amino acid : vanadium = 97 (C_{VO} ~ 0.0021 M) and 21 (C_{VO} ~ 0.0086 M) [C_{VO} = total concentration of oxovanadium(IV)]. For lower L/M, the CD spectra change more, probably due to hydrolysis. At pH 7.2 (L-Ser, Fig. 8a) and pH 7.4 (L-Thr), the CD spectra change quite drastically as L/M varies between 97 (C_{VO} = 0.0017 M) and 19 (C_{VO} = 0.0083 M). At pH 9.2 (L-Ser) and 9.4 (L-Thr), the CD spectra again show minor changes between amino acid : vanadium = 97 (C_{VO} = 0.0016 M) and 19 (C_{VO} = 0.0083 M).

At pH ~ 12.4 (L-Thr), the CD spectra show gross changes as L/M varies between 35 and 10 (Fig. 9a); similar but less marked behaviour may be observed at pH ~ 13.3 (L-Ser, Fig. 8b). At pH ~ 13.6 (L-Thr, Fig. 9b), $|\Delta\varepsilon_m|$ values decrease a little as L/M varies between 35 and 12.

At pH ~ 13.3, solutions containing L-Ser + VO^{2+} with L/M = 35 (CD spectrum 1 in Fig. 8b) are light violet. Nevertheless solutions used to record CD spectra 2 and 3 in the same figure differ, being brownish-yellow, and those used for CD spectra 4–7 were brown, becoming browner as the VO^{2+} concentration increased.

As with L-Ala + VO^{2+}, the results in Figs 8 and 9b can be explained only by assuming equilibria between at least two vanadium-containing species differing in their degree of polymerization. On the other hand, if CD spectra recorded at fixed pH and varying but high L/M ratios almost coincide, that

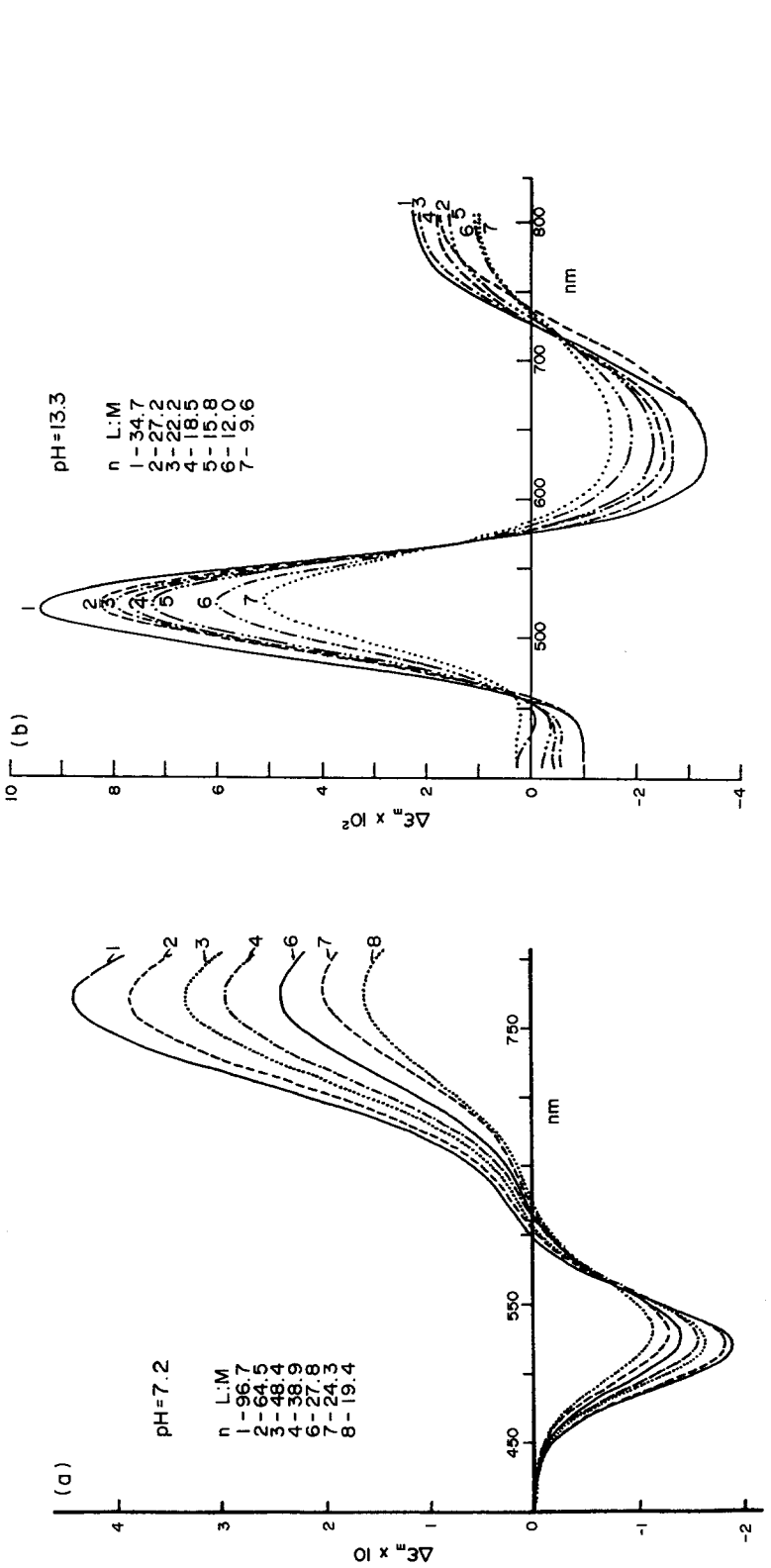

Fig. 8. CD spectra of solutions containing L-Ser and oxovanadium(IV) with (a) $C_{VO} = 1.7–8.3 \times 10^{-3}$ M and (b) $C_{VO} = 8.8–26 \times 10^{-3}$ M. The solutions were prepared by varying the volume of the VO^{2+} stock solution. For each group of spectra, the total L-Ser concentration is approximately the same.

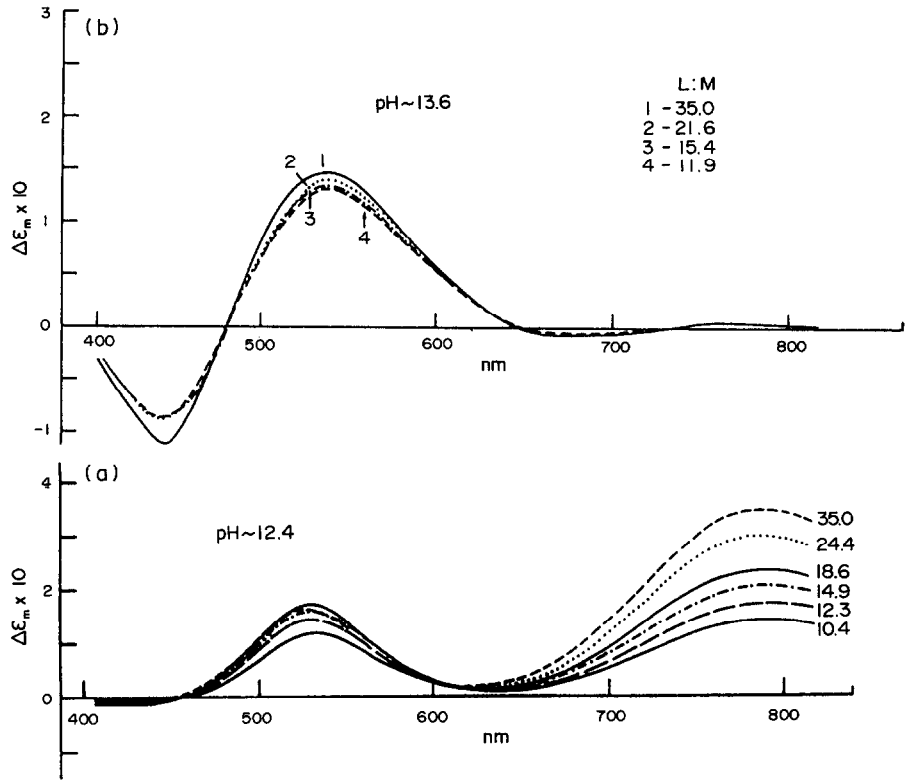

Fig. 9. CD spectra of solutions containing L-Thr and oxovanadium(IV) with (a) $C_{VO} = 8.5–25 \times 10^{-3}$ M and (b) $C_{VO} = 6.8–18 \times 10^{-3}$ M. The solutions were prepared by varying the volume of the VO^{2+} stock solution. For each group of spectra, the total L-Thr concentration is approximately the same.

can be explained only by assuming that in those conditions species predominate with the same degree of polymerization.

"Very basic" (originally brown) solutions containing L-Ser (or L-Thr)+VO^{2+} acidified to pH ~ 10–11 remain brown for some time. However, if acid is added till pH $\lesssim$ 7–8, fast equilibration occurs to the colour characteristic of that pH. More or less similar behaviour was found in the L-Ala+VO^{2+} system,[1] consistent with extensive polymerization of vanadium(IV) in brown solutions. In the conditions used for the spectra in Fig. 6, no great polymerization occurs until at least pH 13.3. Distinct from all other known amino acid+VO^{2+} systems,[1,2,9–11] L-Ser and L-Thr are unique in preventing polymerization of VO^{2+} at high pH. The malic acid+VO^{2+} system[8] behaves in a similar way.

CD spectra for solutions containing L-serine methyl ester and VO^{2+} (with total ligand and metal concentrations similar to those used in Figs 5 and 6) have shapes in the pH range 7–13 resembling those for the L-Ser (and L-Thr)+VO^{2+} systems, but values of $|\Delta\varepsilon_m|$ are some ten times lower. For pH ~ 12.3–12.8, the CD spectra are similar to spectra 8 and 9 in Fig. 6b, except that band I shifts to longer wavelengths (e.g. ~ 710 nm and ~ 760 nm for pH ~ 12.3 and 12.8, respectively). Further, while in the pH range 6–13.3 the L-Ser (and L-Thr) solutions were violet or pink-violet, in the system involving L-serine methyl ester+VO^{2+}, solutions were brownish-green with a slight bluish shade till pH ~ 9 and brown for pH > 9.7.

Hydrolysis of the methyl ester cannot be ruled out in explaining the spectra. However, from these experiments, one may at least conclude that for the L-Ser (and L-Thr)+VO^{2+} systems the carboxylate group is involved in coordination in the pH range 7–12, since the different results (much lower $|\Delta\varepsilon_m|$ values and colours of the solutions) for the L-serine methyl ester+VO^{2+} system would otherwise be inexplicable.

Potentiometry

Protonation constants calculated by the MINIQUAD[12] and SUPERQUAD[13] programs almost coincide. From SUPERQUAD, for L-serine in solutions containing 2.25 M $NaNO_3$ (at 25°C): $pK_{a1} = 2.322 \pm 0.004$ and $pK_{a2} = 9.274 \pm 0.002$ and

for L-threonine $pK_{a1} = 2.326 \pm 0.004$ and $pK_{a2} = 9.187 \pm 0.002$.

As for L-Ala the titration curves involving "low" ligand-to-metal ratios demonstrate the formation of amino acid complexes with VO^{2+}, but $VO(OH)_2$ precipitates for pH $\gtrsim$ 4.

Also as for L-Ala, the titration curves obtained using high L/M ratios show a progressive increase of pH as base is added in the pH range 4.0–7.5. In formation curves calculated for these curves:

(i) $\bar{n} \sim 2$ for the pH range 5–7; this means that ML_2 complexes make an important contribution.
(ii) The calculated formation curves do not coincide with each other but the observed differences are not as important as those found in the L-Ala system—this probably means that hydrolysis and formation of polymeric species are not as important.
(iii) In the "high" pH region $\bar{n} > 2$, an effect which is more important for curves with lower L/M ratios.
(iv) The $\bar{n}$ values for titration curves in the L-Thr+VO^{2+} system exceed those for L-Ser, especially for pH $\lesssim$ 5 and pH $\gtrsim$ 7.

As in the case of L-Ala, the systems are quite complex. Calculations involving the refinement of β_{xyz} values of all possible species (i.e. $M_xL_yH_z$ with x, y and z quite general) gave results with no physical meaning. As for the L-Ala+VO^{2+} system,[1] we therefore chose the following strategy:

(i) From titration curves of solutions with "low" L/M, "titration points" were selected to correspond to "solutions" where only MLH and ML (and VO^{2+}) co-exist. Several iterations were needed to select these "titration points" and because the pK_{a1} of L-Ser and L-Thr are $\sim$ 0.2 pH units lower than the pK_{a1} of L-Ala, this particular selection was difficult.
(ii) Taking β_{111} and β_{110} as known, the MINIQUAD and SUPERQUAD programs were used to calculate the β_{xyz} of other species now including the full set of the "complete" titration curves.

Our best model (model I) from this procedure is in Table 1. For each of the $\log \beta_{xyz}$ values, plausible ranges are also given, established by a critical examination of all the calculations.

Beside the usual criteria used to select equilibrium models for such programs (CHI[2] and R values, standard deviations, etc.) we compare with spectroscopic values. This self-consistency between

Table 1. Composition and formation constants of the species in the L-Ser (and L-Thr) systems, assuming various equilibrium models. Values for $\log \beta_{xyz}$ of eq. (1) are given[a]

Species[b]	L-Ser+VO^{2+}		L-Thr+VO^{2+}	
	Model IA	Model IIA	Model IB	Model IIB
MLH	10.37 (0.08)	10.37 (0.08)	10.30 (0.08)	10.30 (0.08)
ML	6.38 (0.10)	6.38 (0.10)	6.41 (0.14)	6.41 (0.14)
ML_2H_2[c]	20.0 (0.3)	19.9 (0.3)	20.0 (0.3)	20.0 (0.3)
ML_2H	16.44 (0.2)	16.44 (0.2)	16.43 (0.2)	16.43 (0.2)
ML_2	11.70 (0.1)	11.70 (0.1)	11.93 (0.1)	11.93 (0.1)
$M_2L_2H_{-2}$	4.99 (0.2)	4.99 (0.3)	4.98 (0.3)	4.98 (0.3)
ML_2H_{-1}	4.45 (0.1)	4.45 (0.2)	4.80 (0.1)	4.80 (0.2)
$M_2L_2H_{-3}$	−1.23 (0.2)	−1.23 (0.2)	−1.35 (0.2)	−1.35 (0.2)
ML_2H_{-2}	—	−5.0 (0.2)	—	−4.8 (0.2)
MLH_{-2}	—	−6.0 (0.2)	—	−6.0 (0.2)
MLH_{-3}	—	−18.0 (0.4)?	—	−18.0 (0.4)?
H_2L	11.596	11.596	11.513	11.513
HL	9.274	9.274	9.187	9.187

[a] The type of vanadium(IV) hydrolysis products considered and the corresponding formation constants are in Table 1 of ref. 1.

[b] In the calculations performed with MINIQUAD and SUPERQUAD, formation constants could be refined for stoichiometries like $M_2L_2H_{-4}$, ML_2H_{-2}, MLH_{-2} and MLH_{-3}. However, the calculated β substantially differ depending on the formation constants included; besides, the β values obtained in these calculations were such that it would not be possible to rationalize these with the visible and CD spectra.

[c] ML_2H_2 is specially important for solutions with high ligand-to-metal ratios for pH $\lesssim$ 4.5. This is the reason why the β_{122} values are given with a relatively high uncertainty.

thermodynamic and spectroscopic results constitutes the novelty and power of our method of speciation.

One main problem in calculations with MINIQUAD and SUPERQUAD for the L-Ala + VO^{2+} system was the importance of hydrolysis products of VO^{2+} in the pH range 5–8. The nature of such products and their formation constants are not accurately known (for a brief discussion of oxovanadium(IV) hydrolysis, see ref. 3). Hydrolysis in the L-Ser (and L-Thr) + VO^{2+} systems is much less important. Consequently, the calculations are more reliable and the χ^2 values (10–40) of the models contributing to Table 1 are quite reasonable, considering: the complexity of the systems; the many titration curves included; the several NaOH concentrations used and the two pH ranges included (2–4.0 and 4.0–7.5).

As we found in the L-Ala + VO^{2+} system, models excluding ML_2H_2 and $M_2L_2H_{-3}$ are also acceptable. The statistical parameters including $M_2L_2H_{-3}$ clearly improve but the results including ML_2H_2 are not so clear-cut. However, calculations involving CD and visible spectra in the pH ranges 2.5–4.5 and 6–9 show that both species should be included. Recent potentiometric and calorimetric measurements for the Gly + VO^{2+} system[14] for pH < 3 were also interpreted with a model including MG_2H_2.

Spectrometry

In solutions of VO^{2+} and L-Ser or L-Thr, only vanadium complexes contribute to ε_m or $\Delta\varepsilon_m$ in the visible region. This fact removes the limitation of potentiometry to those regions of pH where the ligand has no significant buffer effect. Therefore, when calculating formation constants based on visible or CD spectra, we are better off for species like ML_2H_2, which predominates in the pH range 2–4.5. Also, solutions with pH > 7.5 may be used, which are especially valuable in the L-Ser (and L-Thr) + VO^{2+} systems.

As for the L-Ala + VO^{2+} system, the SQUAD program was used to check that the visible and CD measurements were consistent with the potentiometric results in the pH range 1.8–5.3. For visible and CD spectra, calculations were performed on results for 450–830 and 405–805 nm, respectively. For the species MSH, MS_2H_2, MS, MS_2H, MS_2 and $M_2S_2H_{-2}$, ε (or $\Delta\varepsilon$) are considered as parameters to be refined, and the β_{xyz} for the several species were calculated either individually or in sets of two (except β_{22-2}, since in this pH range $M_2S_2H_{-2}$ is never an important species).

The values so calculated are within the range obtained with MINIQUAD and SUPERQUAD. Therefore, the values for β_{111}, β_{110}, β_{121} and β_{120} given in model IA in Table 1 may be accepted as correct and $\log\beta_{122} = 19.9 \pm 0.3$ taken as consistent with both potentiometry and spectrophotometry. Similar calculations in the pH range 1.8–7 but now including MS_2H_{-1} and $M_2S_2H_{-3}$ gave values for β_{12-1} and β_{22-3} also within the range in model IA (Table 1).

Taking β_{111}, β_{122}, β_{110}, β_{121}, β_{120} and β_{22-2} as known, the visible and CD spectra of MSH, MS_2H_2, MS, and MS_2H were calculated using SQUAD based on experimental spectra in the pH range 1.8–5.3. As had been done for the L-Ala + VO^{2+} system,[1] we used a step-by-step procedure, now following the order:

visible spectra:
(i) MSH and MS_2H_2, (ii) MS_2H and (iii) MS,
CD spectra:
(i) MS_2H_2 (1st iteration), (ii) MS_2H, (iii) MSH (1st iteration), (iv) MS (1st iteration), (v) MSH, (vi) MS_2H_2 and (vii) MS.

For example, in the calculation of the CD spectra of MLH [step (iii)], after including the CD spectra of MS_2H_2 (1st iteration) and MS_2H in the input file [they were calculated in steps (i) and (ii)], a set of experimental spectra was first chosen; then the CD spectra of MSH, MS, MS_2 and $M_2S_2H_{-2}$ were calculated using SQUAD. The values obtained for $\Delta\varepsilon_{111}$ were then included in the input file of SQUAD as known parameters. Step (iv) (calculation of the CD spectra of ML) was then executed. In order to get a second version of a spectrum calculated in a previous step, the 1st version is removed from the input file. The calculated visible and CD spectra are in Fig. 10.

Once the visible and CD spectra of MSH, MS_2H_2, MS and MS_2H were known and included in the input file of SQUAD, the visible spectra of MS_2, $M_2S_2H_{-2}$ and MS_2H_{-1} were also calculated by a step-by-step procedure that also involved an expansion of the pH range of the experimental spectra included. The sequence of these calculations is summarized in Table 2 and the calculated spectra are in Fig. 11a.

The calculated spectra in Fig. 12a of MS_2, $M_2S_2H_{-2}$ and $M_2S_2H_{-3}$ from a calculation with SQUAD[15] used experimental spectra in the pH range 3.6–7.2.

Once the visible and CD spectra of most of the species that may be important for pH < 7.5 are known and included in the input file of SQUAD, calculations may be performed for pH > 7.5.

One main difficulty in the calculations for pH > 11–12 is that the K_{a3} of L-Ser and L-Thr is unknown. Probably, this accounts in part for no

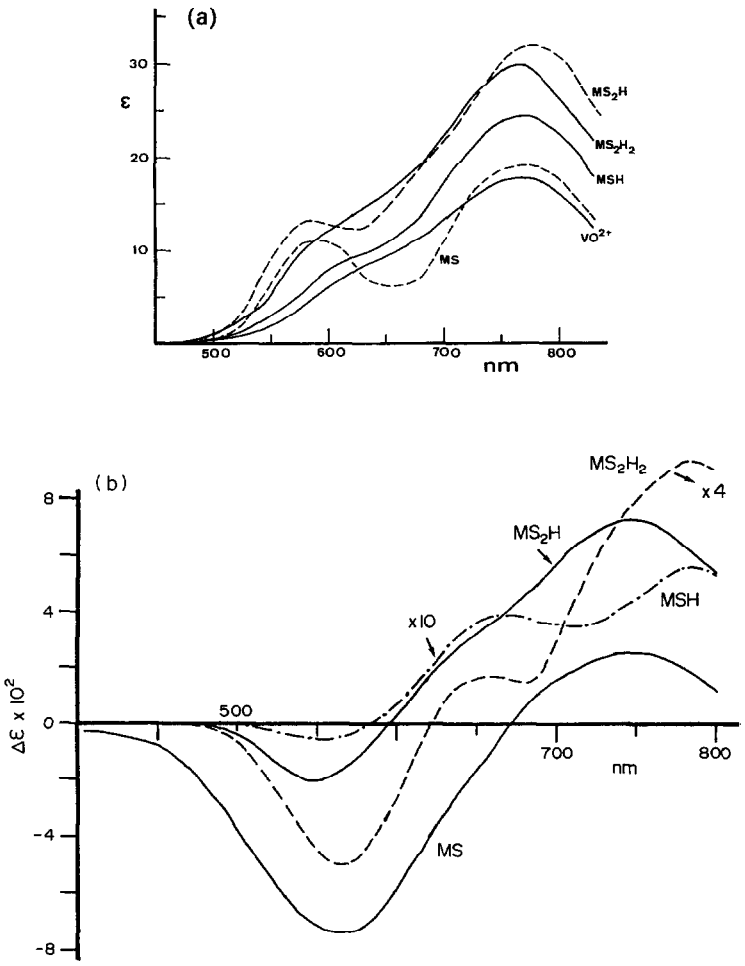

Fig. 10. Visible absorption (a) and circular dichroism (b) spectra (calculated using the SQUAD[15] program—see text for details) for species MSH, MS_2H_2, MS and MS_2H ($\log \beta_{xyz}$ in Table 1) which are only important for pH < 5.5 in solutions with high L/M ratios.

Table 2. Sequence of calculations used to obtain the visible spectra of MS_2, $M_2S_2H_{-2}$ and MS_2H_{-1}[a]

Spectra included in the input file of SQUAD	pH range of experimental spectra	Spectra calculated	Spectrum considered to be satisfactory
MSH, MS_2H_2 MS, MS_2H	1.8–5.7	MS_2 and $M_2S_2H_{-2}$	MS_2
The same and MS_2	1.8–7.2	MS_2H_{-2}, $M_2S_2H_{-2}$ and $M_2S_2H_{-3}$	$M_2S_2H_{-2}$
The same and $M_2S_2H_{-2}$	1.8–7.7	MS_2H_{-1} and $M_2S_2H_{-3}$	MS_2H_{-1}
The same and MS_2H_{-1}	Further calculations are described in the text and Table 3.		

[a]The experimental spectra used were chosen from solutions where there is no significant contribution from oxovanadium(IV) hydrolysis products and vanadium–amino acid complexes (e.g. MSH_{-2}) important for higher pH.

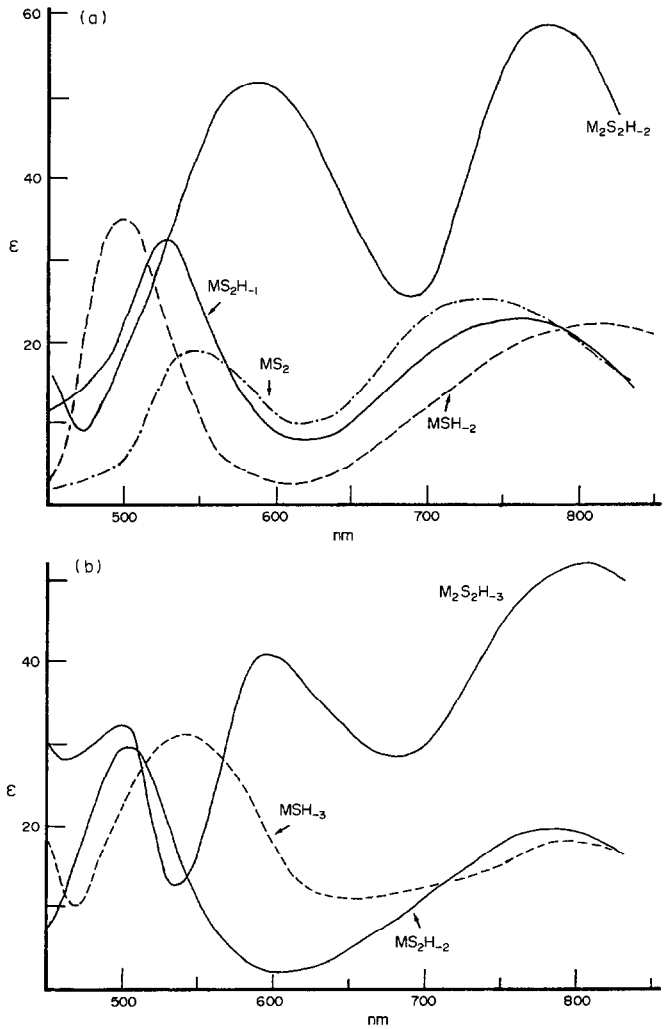

Fig. 11. Visible absorption spectra (calculated using the SQUAD[15] program—see text for details) for species that may form in solutions containing L-Ser+VO^{2+} (high L/M ratios) for pH > 6 using the formation constants in model IIA—Table 1 and experimental visible spectra in the pH range 6.4–11.7. (a) MS_2, $M_2S_2H_{-2}$, MS_2H_{-1} and MSH_{-2}. (b) $M_2S_2H_{-3}$, MS_2H_{-2} and MSH_{-3}.

results being obtained using the SQUAD program when the spectra of solutions with pH > 12.8 were included; it was impossible to pass beyond the intermediate calculations of the program. Even when pK_{a3} values were assumed (in the range 11–13.5) and all formation constants corrected accordingly, it was again not possible to get to the start of the 1st iteration cycle of SQUAD.

Tables 3–5 summarize some results obtained with SQUAD for the visible and CD spectra of L-Ser+VO^{2+} solutions and Figs 11 and 12 include the visible and CD spectra calculated for the several species assuming model IIA (Table 1) as correct.

A feature common to all calculations is that β_{12-2} (the formation constant for ML_2H_{-2}) is a constant to be refined; consistently, $\log\beta_{12-2}$ is in the range -5.0 ± 0.3. This ML_2H_{-2} is important only for pH $\gtrsim$ 8, explaining why β_{12-2} is not refined consistently with MINIQUAD and SUPERQUAD; titration curves always had pH $\lesssim$ 7.5.

While it was never possible to refine simultaneously β_{12-2}, β_{11-2} and β_{11-3} from the CD measurements, it was however possible for the visible spectra, but the value for β_{11-3} seems too high. However, plausible values may be obtained for these constants in calculations involving β_{12-2} and β_{11-2}, β_{12-2} and β_{11-3} or β_{12-2}, β_{11-3} and β_{10-3}. Results are always better if β_{11-2} is included and β_{11-3} not, than vice versa. However, excluding K_{a3} of the amino acid certainly gives more problems in calculations involving β_{11-3} than β_{11-2}.

For basic aqueous solutions, $VO(OH)_3^-$ is detected[16] from pH $\gtrsim$ 12, consistent with $\log\beta_{10-3}$ being -18 to -19.[3] Most calculations in Table 3 and involving this species agree. However, we emphasize that if a pK_{a3} for the amino acid and/or

Table 3. Calculations of visible spectra and/or formation constants of species MS_2H_{-2}, MSH_{-2}, MSH_{-3} and MH_{-3} using SQUAD,[15] based on experimental visible spectra (450–830 nm) of L-Ser + VO^{2+} solutions (high L/M ratios) in the pH range 6.4–11.3[a,b]

Calculation number	VIS1	VIS2	VIS3	VIS4
$\log\beta_{12-2}$ (SD)	−5.147 (0.023)	−5.272 (0.045)	−4.641 (0.071)	−5.162 (0.054)
$\log\beta_{11-2}$ (SD)	−5.842 (0.018)	−5.874 (0.018)	[c]	−5.792 (0.026)
$\log\beta_{11-3}$ (SD)	—	[c]	−15.72[d] (0.16)	−16.225[d] (0.091)
$\log\beta_{10-3}$ (SD)	—	−18.497 (0.42)	−15.836[e] (0.034)	—
pH range of experimental spectra (No. iteration cycles)	6.4–11.3 (4)	6.4–11.8 (7)	6.4–11.8 (14)	6.4–11.3 (7)

[a] Spectra for species MSH, MS_2H_{-3}, MS, MS_2H, MS_2, $M_2S_2H_{-2}$, $M_2S_2H_{-3}$ and MS_2H_{-1} are considered to be known and are included in the input file of SQUAD.

[b] So long as the K_{a3} of L-Ser is unknown, calculations involving the stoichiometry MSH_{-3} may have a doubtful meaning.

[c] When the four formation constants were all considered as parameters to be refined, the calculation does not converge—$\log\beta_{10-3}$ diverges.

[d] The β_{11-3} calculated seems too high.

[e] The β_{10-3} calculated is too high.

a VO^{2+} hydrolysis product that may form for pH higher than $VO(OH)_3^-$ are not included, speciations necessarily give "parallel" concentrations for MH_{-3} and MLH_{-3}. Therefore, not only is it not possible to explain the general decrease of $|\Delta\varepsilon_m|$ values for pH > 13 (this of course, clearly indicates that oxovanadium(IV)–amino acid complexes are hydrolysing to products containing no coordinated amino acid), but all calculations involving β_{11-3} are doubtful.

DISCUSSION

The proposed equilibrium model—the set of species (with plausible values for their formation constants), to explain all the experimental potentiometric and spectroscopic results is in Table 1 (model II). For low L/M ratios, other complex species might be important.

Figure 13 gives the concentration distribution estimated from EPR spectra (Fig. 1 and similar for L-Thr + VO^{2+}). Figure 11 should be compared with the distribution in the L-Ser + VO^{2+} system, Fig. 14, calculated for L/M = 38.0 and a total vanadyl concentration close to those corresponding to the EPR, visible and CD spectra of Figs 1–6.

(i) Species $S_I + S_{II}$ correspond to several stoichiometries: M, MSH, MS_2H_2, MS_2H and MS. The L-Ala + VO^{2+} system presented a similar situation.[1] The EPR peaks show only gradual (but apparent) changes in positions as H_2O in $VO(OH)_5^{2+}$ is substituted by the 1st and 2nd R–COO^- group or by a R–NH_2 group.

(ii) Species S_{III} corresponds to MS_2 ($M_2S_2H_{-2}$ is probably EPR silent). The crossing point with $S_I + S_{II}$ and S_{III} at pH 5 in Fig. 13 approximately coincides with the crossing point with $MS_2H + MS$ and MS_2 in Fig. 14.

(iii) As mentioned before, S_{IV} and $S_{IV'}$ have very similar g and A parameters and correspond to MS_2H_{-1} and MS_2H_{-2}, respectively.

(iv) S_V could correspond to $M_2S_2H_{-3}$, but there are other plausible hypotheses which are discussed below.

(v) S_{VI} could correspond to MSH_{-2} and/or MSH_{-3} and S_{VII} probably corresponds to MH_{-3} (or to MSH_{-3}).

On a semi-quantitative basis, the concentration distribution shown also explains the evolution of visible and CD spectra of Figs 2–6, namely:

(i) The increase of $|\Delta\varepsilon_m|$ until pH ~ 6, as in the L-Ala + VO^{2+} system.[1]

(ii) The further increase of $|\Delta\varepsilon_m|$ in the range 400–800 nm until pH ~ 8, which coincides with the formation of MS_2H_{-1} (and $M_2S_2H_{-3}$).

(iii) The CD spectra for pH > 8, rationalized either considering only MS_2H_{-2} and MSH_{-2} as being important for pH > 8 or taking these and MSH_{-3} as important species for pH $\gtrsim$ 9.

The spectra (visible and CD) calculated by SQUAD using the formation constants of Table 1

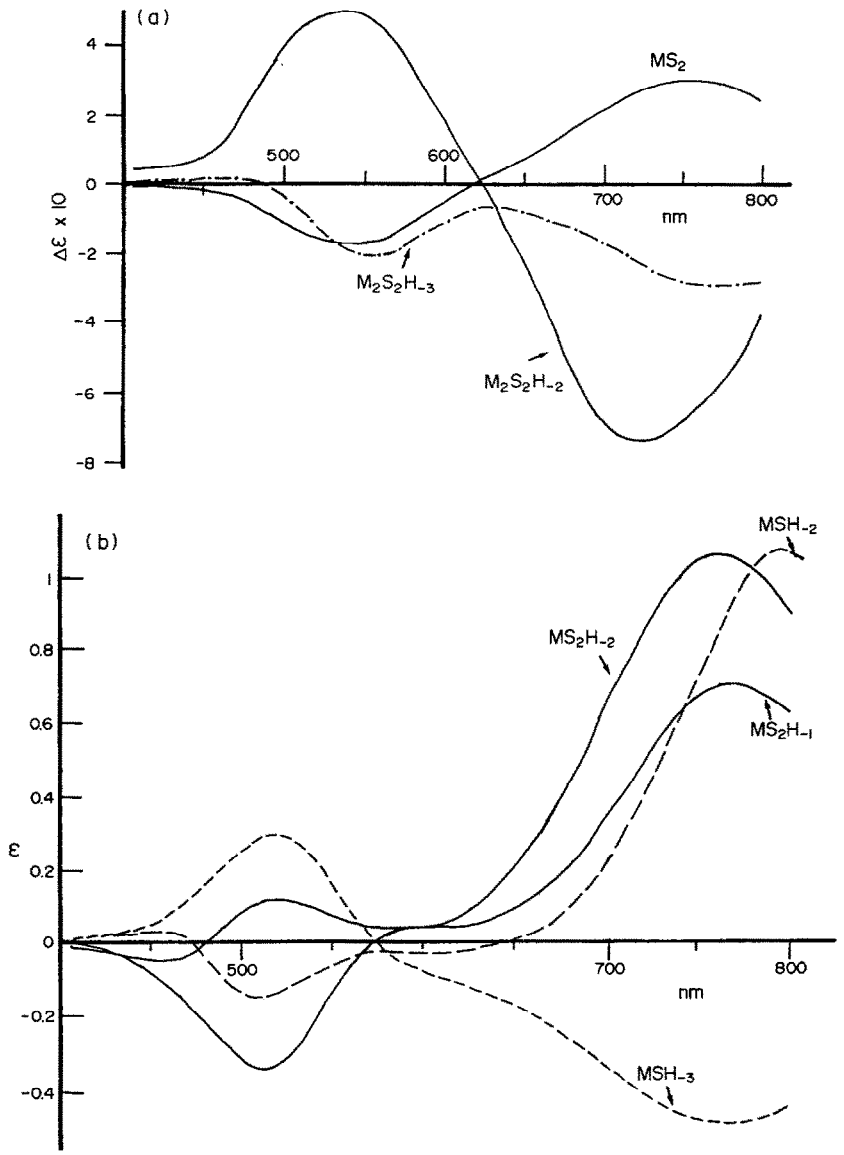

Fig. 12. Circular dichroism spectra (calculated using the SQUAD[15] program—see text for details) for species that may form in solutions containing L-Ser + VO^{2+} (high L/M ratios) for pH > 6 using the formation constants in model IIA—Table 1 and experimental CD spectra in the pH range 6.7–12.8.

and the visible and CD spectra of Figs 10–12 almost coincide with the experimental spectra.

Correlation of formation constants

Figure 15 represents $\log \beta^S$ vs $\log \beta^T$ from this work as well as $\log \beta^S$ vs $\log \beta^A$. Such linear plots are expected as long as the coordination geometry around VO^{2+} is the same for a given stoichiometry. If the plot of ($\log \beta^S_{xyz}$, $\log \beta^A_{xyz}$) is not nearly linear, this indicates that the coordination geometries in $M_xS_yH_z$ and $M_xA_yH_z$ differ.

Constants for the L-Thr + VO^{2+} system are such that its degree of complex formation is greater, and VO^{2+} hydrolysis, $M_2T_2H_{-2}$ and $M_2T_2H_{-3}$ are less important than in the other systems.

Structures

Because the vanadyl ion is lopsided, many of its chelates may form more isomers than do apparently analogous monoatomic metal centres; refs 1 and 3 briefly discuss this.

Stoichiometry MLH probably corresponds to complexes with the R–COO^- group coordinated equatorial. Writing the formation of such complexes as ($n = 1$):

$$VO^{2+} + nHL \overset{K_n}{\rightleftharpoons} VO(HL)_n^{2+}. \qquad (2)$$

K_1(L-Ser) = 12.5 and K_1(L-Thr) = 12.9, to be compared with K_1(L-Ala) = 15.6[1] and K_1(Gly) = 14.8[17] or K_1(Gly) = 11.5[14] (the Gly values in a different medium, 1 M $NaClO_4$).

Table 4. Calculations of CD spectra and/or formation constants using SQUAD, based on experimental CD spectra (405–805 nm) of L-Ser + VO^{2+} solutions (high L/M ratios) in the pH range 6.7–12.8[a]

Calculation number	CD1	CD2	CD3	CD4[b]	CD5[c]	CD6	CD7	CD8	CD9	CD10[d]	CD11
$\log\beta_{12-2}$ (SD)	[e]	[f]	[g]	−4.85 to −4.87	−5.294 (0.063)	[e]	[e]	[h]	[h]	−4.76 to −5.08	−4.932 (0.011)
$\log\beta_{11-3}$ (SD)	—	—	[g]	−17.75 to −18.76	−15.204 (0.026)	—	—	[h]	[h]	—	—
$\log\beta_{11-2}$ (SD)	—	—	—	—	—	[e]	[e]	[h]	[h]	−5.87 and −6.17	−6.199 (0.017)
$\log\beta_{10-3}$ (SD)	[e]	[f]	[g]	−17.96 to −18.73	−17.79 (0.26)	—	[e]	[h]	—	−17.62 and −18.07	—
$\log\beta_{22-5}$	[e]	—	—	—	—	[e]	[e]	—	—	—	—
$\log\beta_{12-3}$	—	[f]	[g]	—	—	—	—	—	—	—	—
pH range of experimental spectra	6.7–12.6 or 6.7–12.8	6.7 to 12.8	6.7 to 12.8	6.7 to 12.8	6.7 to 10.8	6.7 to 11.8	6.7 to 12.6	6.7 to 12.8	6.7 to 11.3	6.7 to 12.8	6.7 to 11.3
No. iteration cycles	3 or 6	7	20	20	7	5	5	6	4	14	4

[a] In all calculations included in the table, the CD spectrum of MS_2H_{-1} ($\Delta\varepsilon_{12-1}$) is one of the spectra to be obtained.
[b] Calculation did not converge, β^{11-3}, β_{12-2} and β_{10-3} always within the limits given.
[c] Calculation converged but β_{11-3} is too high. The pH region is not suitable to refine β_{10-3}. Probably a species exists that is important in the pH 8–11 that is not included and the results reflect an attempt of the system to fit the spectra with the stoichiometries being refined.
[d] Calculation did not converge. β_{12-2} is always within the limits given and β_{11-2} and β_{10-3} alternate between the values given.
[e] Calculation diverged. Main problem in β_{22-5}.
[f] Calculation diverged. Main problem in β_{12-3}.
[g] Calculation did not converge. Main problems in β_{11-3}, β_{12-3} and β_{10-3}.
[h] Calculation diverged. Main problem in β_{11-3}.

Table 5. Spectroscopic properties for each band of each $(VO)_x(S)_y(H^+)_z$ species

Species	λ_{max}	ε	$\Delta\varepsilon$	$\lvert\Delta\varepsilon/\varepsilon\rvert$[a]	λ_{max}	ε	$\Delta\varepsilon$	$\lvert\Delta\varepsilon/\varepsilon\rvert$[a]
MSH	615	~ 9	—		767	24.4	—	
								0.00023
	550	—	−0.00051	[b]	780	—	0.0056	
	667	—	0.0039					
MS	590	11.0	—		770	19.3	—	
				0.0067				0.0013
	570	—	−0.074		750	—	0.026	
MS_2H_2	~ 605	~ 12	—		777	32.8	—	
								0.0007
	567	—	−0.0125	[b]	785	—	0.023	
	658	—	0.042					
MS_2H	585	13.3	—		765	29.9	—	
				0.0015				0.0024
	537	—	−0.0206		755	—	0.0726	
MS_2	546	18.8	—		735	25.3	—	
				0.0089				0.012
	547	—	−0.168		750	—	0.308	
$M_2S_2H_{-2}$	585	51.9	—		778	59.3	—	
				0.0096				0.012
	542	—	0.50		730	—	−0.736	
MS_2H_{-1}	527	30.7	—		770	22.8	—	
				0.011				0.031
	515	—	−0.338		770	—	0.701	
MS_2H_{-2}	505	29.8	—		785	19.3	—	
								0.054
	~ 460	—	−0.045	[b]	760	—	1.05	
	520	—	0.113					
$M_2S_2H_{-3}$	~ 500	32.0	—		~ 810	51.8	—	
				0.00065[c]				0.0056
	470	—	0.0207		775	—	0.288	
	595	40.8	—	0.005[c]				
	560	—	−0.204					
MSH_{-2}	500	35.0	—		~ 815	22.0	—	
				[b]				0.048
	450	—	0.037		> 800	—	1.06	
	515	—	−0.153					
MSH_{-3}	540	31.1	—		790	17.8	—	
				0.0095				0.027
	520	—	0.297		772	—	−0.489	

[a] Approximate asymmetry factor calculated for each band according to: $\Delta\varepsilon$ (at λ_{max})/ε (at λ_{max}).

[b] Two bands are observed in the CD spectrum of opposite signs; these partly cancel each other so that no *g*-factor is presented.

[c] Presumably the bands in the visible spectrum at ~ 500 and 595 nm correspond to the CD bands at 470 and 560 nm, respectively.

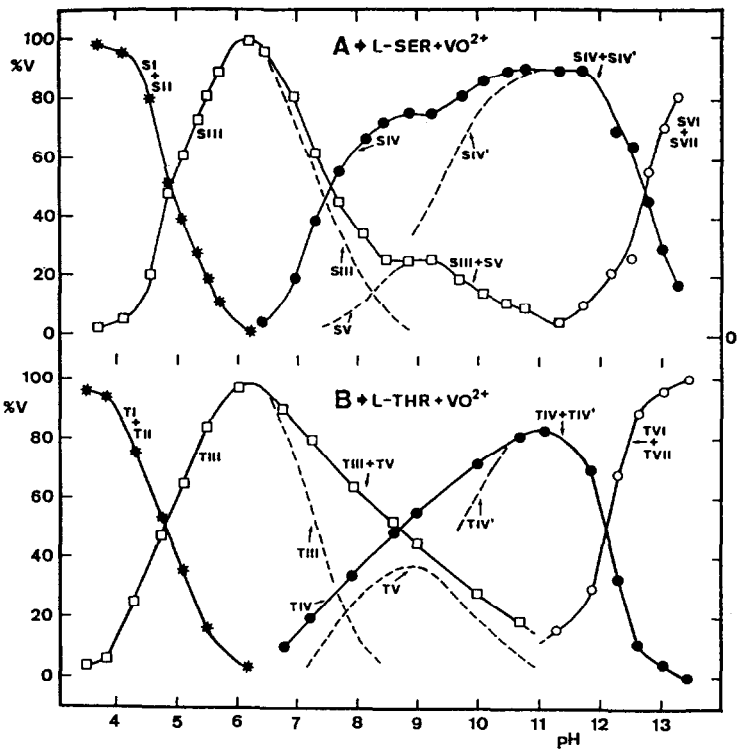

Fig. 13. Concentration distribution of the species L_I–L_{VII} detected in the EPR spectra. These distributions should be considered only as approximate. EPR silent species are obviously not included. (A) L-Ser+VO^{2+} system—estimated from the EPR spectra of Fig. 1. (B) L-Thr+VO^{2+} system—estimated from the EPR spectra of solutions containing L-Thr and VO^{2+} with L/M = 25.1 and C_{VO} in the range $1.2–1.5 \times 10^{-2}$.

The visible and CD spectra calculated for MSH (Fig. 10) and for MAH are similar; one would not expect major differences in these spectra for complexes involving different amino acids coordinated as monodentate ligands by the carboxylate group.

The calculated CD spectra and the K_1 value suggest that probably there is no such direct interaction between the oxygen of the –ROH group and the metal centre as was suggested for $Cu(HS)^{2+}$.[4] However, although there is no clear indication of it, there may be some interaction of the –ROH group and coordinated water.

The stoichiometry ML_2H_2 probably corresponds

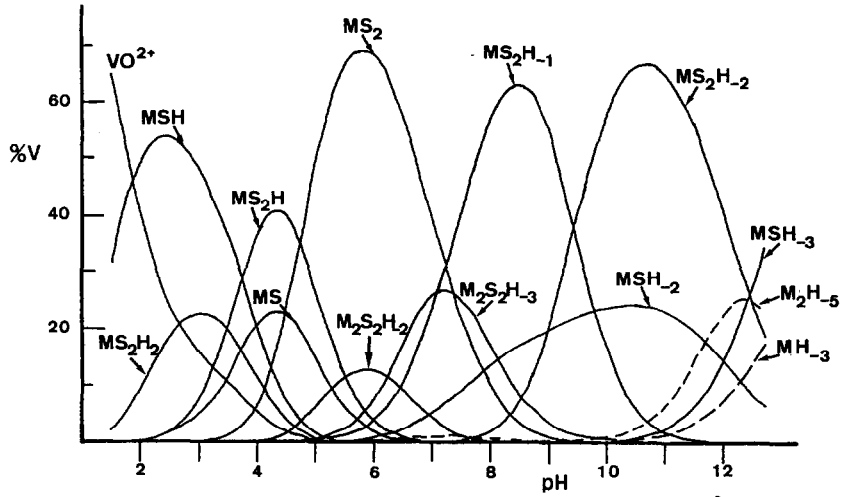

Fig. 14. Concentration distribution of the complexes formed in the L-Ser+VO^{2+} system in solutions with $C_{VO} = 8.0 \times 10^{-3}$ M and L/M = 38.0, calculated using the β_{xyz} of model IIA in Table 1 and $\log \beta_{20-5} = -22.22$ and $\log \beta_{10-3} = -18.8$. This speciation is on a molar basis, while the concentration distribution of fig. 11 in Part I[1] was calculated on an atomic basis.

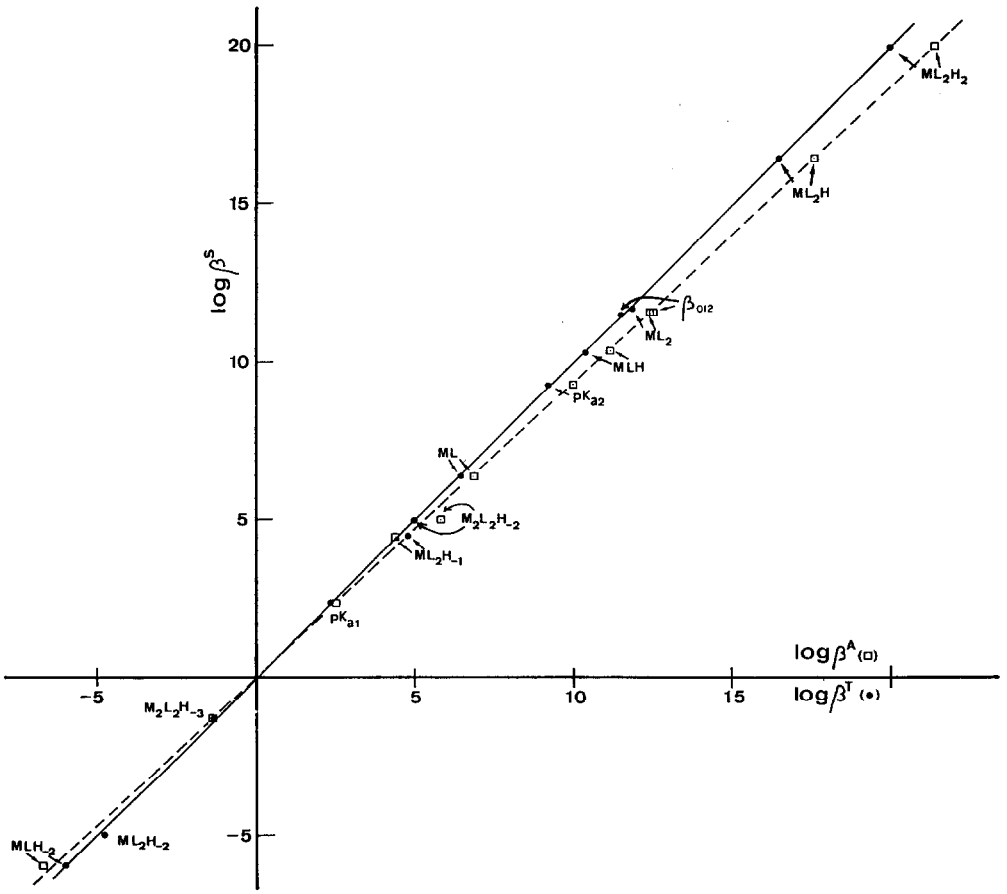

Fig. 15. Representation of $\log \beta^{S}_{xyz}$ vs $\log \beta^{T}_{xyz}$ (●) obtained in this work and of $\log \beta^{S}_{xyz}$ vs $\log \beta^{A}_{xyz}$ (□) obtained in part I[1]. The pK_{a1}, pK_{a2} and $\log \beta_{012}$ are also represented.

to complexes with two monodentate carboxylate groups coordinated equatorial. From Table 1, K_1K_2(L-Ser) ~ 24. The corresponding value for L-Ala is 30.2.[1] Apart from differences in the ε_{122} and $\Delta\varepsilon_{122}$ values, spectra calculated for MS_2H_2 (Fig. 10) are similar to those calculated for MA_2H_2.[1] The differences may be a mathematical artefact (because the systems are quite complicated), or they may originate in differing proportions of *cis* and *trans* isomers, (I) and (II), in MA_2H_2 as against MS_2H_2.

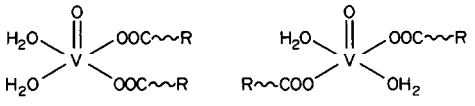

At this point, we emphasize that more than one isomer corresponds to the particular stoichiometry for each "species" $M_xL_yH_z$. Relative isomeric concentrations are independent of concentrations of metal, ligand and H^+, so our experimental techniques do not distinguish between them (in some cases, the EPR spectra could ultimately help). Therefore not only each formation constant, but also the calculated visible and CD spectra reflect the features of each isomer in proportion to its relative importance. For example, in the case of ML_2H_2 stoichiometry, the value for β_{122} is the weighted sum of $\beta_{122}(cis)+\beta_{122}(trans)$ and the calculated visible and CD spectra may involve contributions from structures (I) and (II).

Stoichiometry ML may correspond to structures (III) and (IV) (not considering the possibility of one group being axial). These are not enantiomers (as they would be if the amino acid were glycine).

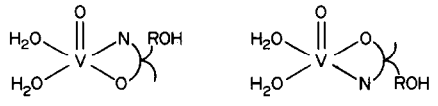

The β_{110} obtained ($\log\beta$ ~ 6.4) is the weighted sum of β_{110}(III) and β_{110}(IV). As for L-Ala we note that for L-Ser and L-Thr: $\beta_{110}(Ni^{2+}) < \beta_{110}(VO^{2+}) < \beta_{110}(Cu^{2+})$ (as $\log\beta_{110}(Ni^{2+})$ ~ 5.4 and $\log\beta_{110}(Cu^{2+})$ ~ 8).[4,5]

The visible spectrum calculated for VO(S) is very similar to that for VO(A).[1] CD spectra are also similar. The different relative intensities for bands I ($\Delta\varepsilon > 0$) and II ($\Delta\varepsilon < 0$) may be a mathematical

artefact or real: they may also reside in slightly different positions of the maxima for bands I and II.

Because the vanadyl ion is lopsided, four structures may be envisaged for MS_2H with one S^- (or T^-) bidentate and the other coordinated only via the R–COO^- group, all equatorial (monodentate coordination involving the $-NH_2$ or $-RO^-$ is unlikely). Additional structures may naturally be envisaged where one group is coordinated axial.

The visible and CD spectra calculated for MS_2H are remarkably like those for MA_2H.[1] The type and relative proportions then of species in these systems with stoichiometry MS_2H are the same. There is then practically no interaction between the oxygen of the ROH group and the metal centre or a water molecule coordinated to it.

For stoichiometry ML_2, assuming equatorially coordinated R–NH_2 and R–COO^- groups, three isomers (V)–(VII) may form in differing concentrations.

the metal centre. This would favour isomers (V) and (VII).

Two *d–d* bands are found for MS_2 in the range 500–800 nm instead of the three bands in many complexes with *trans* geometry.[3] There have been proposals that for VO^{2+} complexes the *cis* geometry is favoured. However, several stereochemical effects may operate and this argument cannot be definitive. Nevertheless, the correlation between the number of *d–d* bands detected and the geometry is reasonably established, suggesting that ML_2 (L = Ala, Ser and Thr) would be predominantly *cis* complexes.

In the L-Ser and L-Thr systems, the stoichiometry $M_2L_2H_{-2}$ is less important than for L-Ala+VO^{2+}. Several dimeric structures may be envisaged with two OH groups bridging the vanadium atoms and N, O coordination in equatorial positions, e.g. (VIII) and (IX). The V=O groups may be "parallel" or "antiparallel" and the structures might be quite distorted from those idealized as (VIII) and (IX).

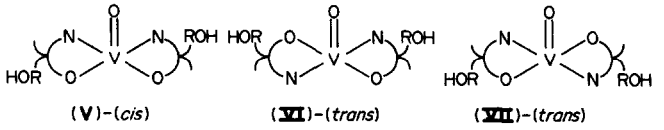

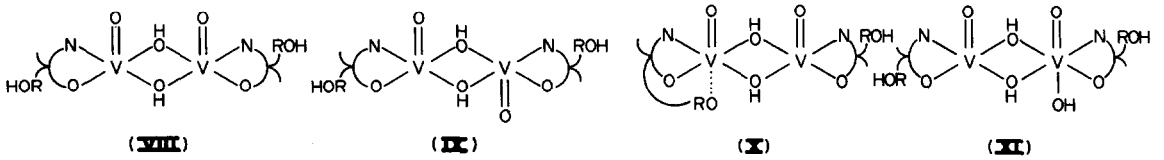

Spectra of these isomers should differ. However, not only was there no evidence in EPR spectra at pH ~ 6 for isomers, but the EPR spectra of VO(L-SerO)$_2$, VO(L-ThrO)$_2$ and VO(L-AlaO)$_2$ are identical ($g_\parallel = 1.944$, $g_\perp = 1.976$, $A_\parallel = 164$ and $A_\perp = 55 \times 10^{-4}$ cm^{-1}), within the small experimental error.

The calculated visible spectrum of MS_2 is similar to that for MA_2[1] but the ε_{120} values are normally higher. The calculated CD spectra of MS_2 and MA_2 are also similar except that $|\Delta\varepsilon_{120}$(L-Ser)$| > |\Delta\varepsilon_{120}$(L-Ala)|, especially for band II. As for other stoichiometries, this may either be a mathematical artefact or arise from a real difference in the relative importance of isomers (V)–(VII) in the two systems.

The interaction of the oxygen of $-CH_2OH$ with a water ligand (proposed for Cu(L-SerO)$_2$[4]) may also be envisaged for VO(L-SerO)$_2$. Alternatively, a ROH of L-Ser (or L-Thr) directly could interact with

High $\Delta\varepsilon$ values may be expected for such structures and are indeed observed (Fig. 12). The calculated CD spectrum for $M_2S_2H_{-2}$ (pattern: +, −) is reasonably different from that for $M_2A_2H_{-2}$ (pattern: +, −, −) and $|\Delta\varepsilon_{22-2}|$ are much higher for $M_2S_2H_{-2}$. This either originates in a mathematical artefact or may result from a different proportion of isomers. Any interaction of the O atom of the –ROH group with vanadium might either have a direct effect on the spectra, or an indirect one through the stabilization of certain isomers.

Many different dimeric structures may be envisaged for stoichiometry $M_2L_2H_{-3}$, with two bridging OH groups:

(i) With one $-RO^-$ group coordinated in either equatorial or axial position [e.g. (X)].
(ii) With no coordination of $-RO^-$, but with one OH^- group axial [e.g. (XI)] or equatorial [e.g.

(**XII**)]. Some direct or indirect effect of the –ROH group may operate as mentioned for $M_2S_2H_{-2}$.

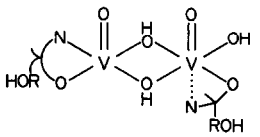

(**XIII**)

High $\Delta\varepsilon$ values would be expected for both types, as observed (Fig. 12). The calculated CD spectrum for $M_2S_2H_{-3}$ is similar to that for $M_2A_2H_{-3}$: the sign pattern is the same: (+, −, −) and the λ_{max} and $\Delta\varepsilon$ values do not differ much. This suggests that the type of complexes in the two systems is not too different, although the isomeric proportions may differ. These considerations suggest that, for the $M_2S_2H_{-3}$ stoichiometry, isomers which involve the coordination of one $-RO^-$ group [eg. (**X**)] do not form in appreciable amount.

Both $M_2S_2H_{-2}$ and $M_2S_2H_{-3}$ are probably EPR silent. Both are dimers with two OH^- as bridging groups, so ε values higher than for monomeric complexes are expected. This is indeed so, since the ε values in visible spectra of stoichiometries $M_2S_2H_{-2}$ and $M_2S_2H_{-3}$ are two or more times those for other species (namely MS).

For pH $\gtrsim$ 6.5, spectra of solutions (per metal ion) containing L-Ser (and L-Thr)+VO^{2+} differ from those of L-Ala+VO^{2+}. One most noticeable difference involves the components designated by L_{IV} and $L_{IV'}$ in the EPR (Figs 1 and 13). Components designated by L_V correspond to $A_\parallel \sim 163\times10^{-4}$ cm^{-1} and approximately coincide with L_{III}.

Comparing Figs 13 and 14, L_{IV} and L_V correspond to ML_2H_{-1}. The EPR spectra of L_{IV} and $L_{IV'}$ are indistinguishable (at least in our experimental conditions) and correspond to $A_\parallel = (150–154)\times10^{-4}$ cm^{-1} and $g_\parallel = 1.955–1.961$. This suggests that the groups involved in the coordination and their arrangement around the VO^{2+} are the same in L_{IV} and $L_{IV'}$. Notwithstanding this, the visible and CD spectra calculated for stoichiometries ML_2H_{-1} both differ.

The visible, CD and EPR spectra observed for pH $\gtrsim$ 6.5 can be explained only by assuming that the $-RO^-$ group of L-Ser (and L-Thr) coordinates to VO^{2+}. Such coordination starts around two pH units lower than for the L-Ser (and L-Thr)+Cu^{2+} systems[5,7,20,21] (note that the L/M ratios are quite different), consistent with the preference of VO^{2+}, relative to Cu^{2+}, for oxygen-containing ligands.

The stoichiometry ML_2H_{-1} probably corresponds to at least two different complexes: one involving coordination of the $-RO^-$ group, corresponding to L_{IV} in the EPR spectra and the other involving coordination of OH^- ("similar" to MA_2H_{-1} in the L-Ala+VO^{2+} system), corresponding to L_V in the EPR spectra.

The structure of ML_2H_{-2} ($L_{IV'}$ in the EPR spectra) can either be similar to the first type for ML_2H_{-1}, but involving the dissociation of the second uncoordinated –ROH group, or can involve the coordination of this group, implying quite a different structure. Alternatively, an OH^- group could be involved. For the former case one might indeed expect that the EPR spectra of L_{IV} and $L_{IV'}$ should be indistinguishable. For the two last structures mentioned, the observed similarity of the EPR spectra would be a coincidence.

Structures for ML_2H_{-1} and ML_2H_{-2} must account for:

(i) The high $\Delta\varepsilon$ values.
(ii) The high "stability" of the complexes, explaining why hydrolysis does not occur at "high" pH as it does in the case of the L-Ala+VO^{2+} system.[1]

This suggests that L_{IV} and $L_{IV'}$ do not involve coordination of OH^-, but (instead) terdentate coordination of one ligand and bidentate coordination of the other.

Using the contributions of R–COO^-, R-NH_2, RO^- and OH^- to $g_\parallel$ and $A_\parallel$ proposed by Chasteen,[19] these EPR spectral parameters may be estimated for each possible structure for ML_2H_{-1} and ML_2H_{-2}, assuming equatorial coordination. Such calculated values for $A_\parallel$ ($\times10^4$ cm^{-1}) are given hereafter for many structures. These calculations imply axially coordinated H_2O. As discussed above, this is probably not true for the complexes predominant in this pH range, and no safe conclusions can be made based on calculated $A_\parallel$.

Figure 16 gives structures for complexes corresponding to stoichiometries ML_2, ML_2H_{-1} and ML_2H_{-2}. Several other structures can be envisaged for each.

The visible and CD spectra calculated for each stoichiometry include contributions from all the structures of the complexes that may form. Thus, ML_2H_{-1} includes contributions from L_{IV} and L_V and one may note the resemblance of the CD spectra calculated for MS_2H_{-1} and the one obtained for MA_2H_{-1}.[1]

In Fig. 15, the point for [$\log\beta_{12-1}$(Ser), $\log\beta_{12-1}$(Ala)] is quite near the line, notwithstanding that one structure expected to contribute to this stoichiometry (corresponding to L_{IV}) is quite different from the structures expected for MA_2H_{-1}. This coincidental goodness-of-fit probably results from: (i) the contribution of S_V to

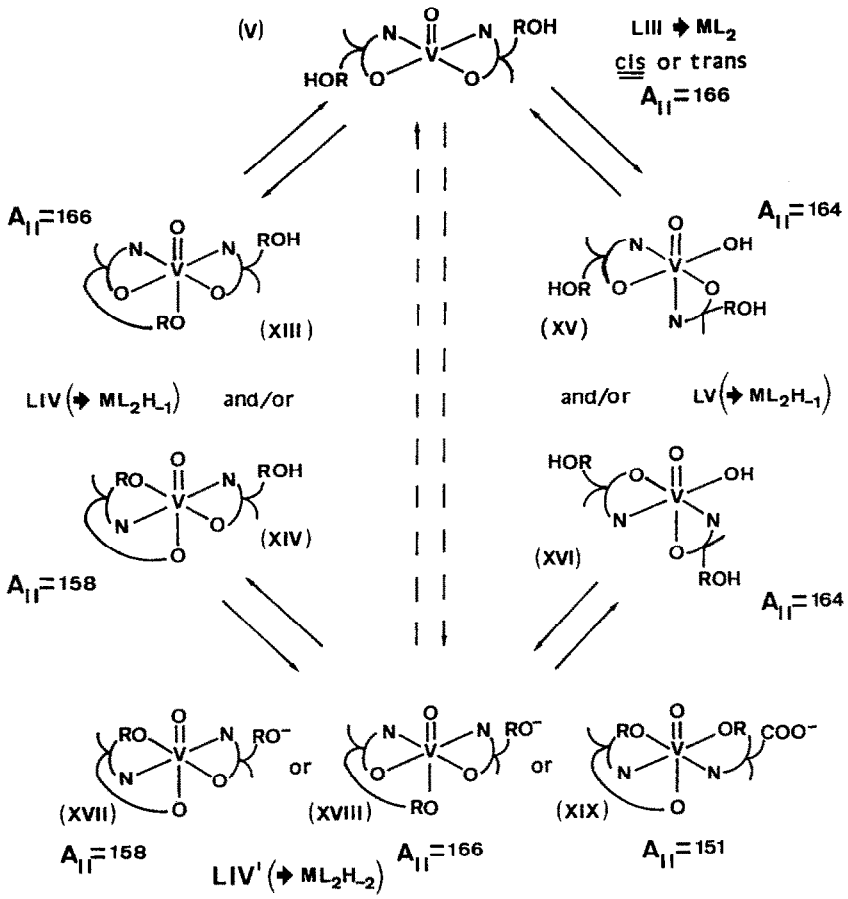

Fig. 16. Plausible structures for the main species that predominate in the pH range 7–12 in solutions containing L-Ser (and L-Thr) + VO^{2+} with high L/M ratios. Estimated values for $A_{\parallel}$ ($\times 10^4$ cm^{-1}) are also included[19] not considering the influence of the axial ligands (see text).

MS_2H_{-1}; (ii) the pK_a of the –ROH group followed by coordination of $-RO^-$ is around 8 (this may be compared with CuS_2 where the corresponding pK_a is ~ 10).[5,20,21]

Several different structures could be envisaged for the stoichiometry MLH_{-2}. The CD spectrum calculated for MSH_{-2} (Fig. 12) is reasonably similar to that for MAH_{-2} and could indicate complexes such as **(XX)**. However, the calculated visible spectrum (Fig. 11) suggests that isomers like **(XXI)** and/or **(XXII)** may be more important.

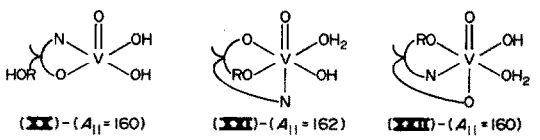

The MSH_{-3} stoichiometry may be important for pH $\gtrsim$ 11 and the calculated CD spectrum (Fig. 12) is what one would expect from the evolution of the experimental CD spectra in the high pH range (Fig. 6). As for the MSH_{-2} stoichiometry, structures like **(XXIII)** and **(XXIV)** seem more reasonable than **(XXV)** to explain the calculated visible and CD spectra and the "high" stability of the vanadium–amino acid complexes that exist for pH $\gtrsim$ 12.

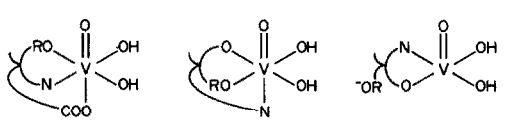

The components L_{VI} and L_{VII} in the EPR spectra at high pH (Fig. 1) correspond to $A_{\parallel} = 168$ and 164×10^{-4} cm^{-1}, respectively. The calculated $A_{\parallel}$ include only contributions from groups coordinated equatorially. As L_{VI} probably corresponds to MLH_{-2} and/or MLH_{-3} and L_{VII} to MLH_{-3} and/or MH_{-3} ($A_{\parallel}$(calc.) $= 162 \times 10^{-4}$ cm^{-1}), we assume that axial coordination of $-RO^-$, RNH_2, $RCOO^-$ or OH^- affects the EPR spectra differently from H_2O.

Although the experimental CD spectra obtained for L-Ser+VO^{2+} solutions at pH ~ 13.3 (Fig. 8b) are akin to those for L-Thr+VO^{2+} solutions at pH ~ 13.6 (Fig. 9b) and the band pattern is the same (−, +, −, +), the relative intensities of the bands are not the same and values of $|\Delta\varepsilon_m|$ are larger for the L-Thr+VO^{2+} system. Therefore, hydrolysis of ML_2H_{-2} to MLH_{-3} and other complexes not involving coordinated amino acid occurs at a higher pH in this system.

Except for differences ascribed to slightly different concentration distributions in the two systems, like that just described, no clear distinctions were noticed in the experimental CD spectra of the L-Ser+VO^{2+} and of the L-Thr+VO^{2+} solutions that could be attributed to the existence of two dissymmetric centres in L-Thr as against one in L-Ser.

While the two methylene hydrogen atoms of the alkoxo function of serinate are inequivalent in the vanadyl-bonded species, their difference is small and the $-CH_2O^-$ moiety is almost symmetrical, so we are concerned with understanding the *failure* of the corresponding asymmetric carbon atom of the threonine side chain to manifest its asymmetry in the vanadyl electronic manifold. The explanation of this failure may be electronic or steric and we consider these in turn.

This failure arises because the $-RO^-$ group is inefficient at inducing dissymmetry to the VO^{2+} bands. Restating this, the new element of chirality (arising from $-*CH(CH_3)-O^-$ of L-threoninate) may be able to influence only some orbitals of the vanadyl ion, transitions between which are of low asymmetry factor (g-factor). Recalling that the rotational strength of any electronic transition is given by $\mu_m\mu_e\cos\theta$, where μ_m and μ_e are the magnetic-dipole and electric-dipole moments of transition respectively and θ is the angle between them, we see that, if the chiral ligand $-*CH(CH_3)-O^-$ occupies a position such that d-orbitals affected by it participate only in magnetic-dipole-forbidden transitions, no great influence of this centre on CD in the visible d–d region would be expected.

For example if the $-RO^-$ groups always coordinate axially (affecting mainly the d_{z^2} level) and to a less extent d_{x^2} and d_{y^2}, the transition $d_{xy} \leftrightarrow d_{x^2-y^2}$ will be insensitive to it.

The alternative steric explanation is that for complexes forming for pH > 7, the vicinal effect is less important than effects arising from dissymmetric arrangement of the ligating atoms and a dissymmetric deviation of ligating atoms from a regular structure.[22]

For example, for the structures **A** and **B** (where vanadium is above the plane of its four equatorial ligands),

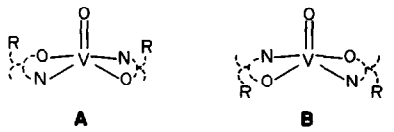

A **B**

if, for some reason, their concentrations differ, [**A**] ≠ [**B**], there is—beside the vicinal and conformational contributions—an effect resulting from these differing concentrations. Two contributions to the overall measured Cotton effect may then be considered (separating them as in ref. 22):

—dissymmetric arrangement of the ligating atoms,
—dissymmetric deviation of ligating atoms from regular structure.

According to ref. 22, the latter contribution can be as important as the configurational contribution in determining the magnitude of the Cotton effect. In the present case, for alkaline solutions where terdentate coordination is likely to occur, structure **B** is favoured. The two contributions just mentioned become dominant.

*Comments on the equilibria at high p*H

The most remarkable feature of the L-Ser (and L-Thr)+VO^{2+} systems is the existence of a relatively high proportion of vanadium(IV)–amino acid complexes in the high pH range. A similar situation is found in L-Ser (and L-Thr)+Cu^{2+} systems.[23,24]

For pH $\gtrsim$ 11, models II in Table 1 predict that vanadium(IV)–amino acid complexes with stoichiometries ML_2H_{-2}, MLH_{-2} and MLH_{-3} predominate. However, other stoichiometries could be envisaged for the high pH range, e.g. $M_2L_2H_{-4}$ and $M_2L_2H_{-5}$: if MLH_{-2} and/or MLH_{-3} are not included in the calculations with SQUAD, spectra can be obtained for such species, although the results cannot be considered as "good" as those obtained for model II. For lower L/M ratios and/or higher vanadium concentrations, $M_2L_2H_{-4}$ and $M_2L_2H_{-5}$ probably make a greater contribution. However, such solutions are not easy to study; vanadyl hydrolysis and/or oxidation and sluggish equilibration become nuisances. As the pK_{a3} of L-Ser and L-Thr are unknown, it is impossible to make accurate calculations for pH > 11–12. Thus, both experimental possibilities and good computational criteria are lacking to test the importance of such stoichiometries.

Nevertheless, some general conclusions may be drawn from CD spectra at very high pH. In fact, since in such CD spectra for high L/M ratios at pH ~ 13.3 (Fig. 8b) and 13.6 (Fig. 9b), there are differences in $\Delta\varepsilon_m$, an equilibrium is postulated between species with different degrees of poly-

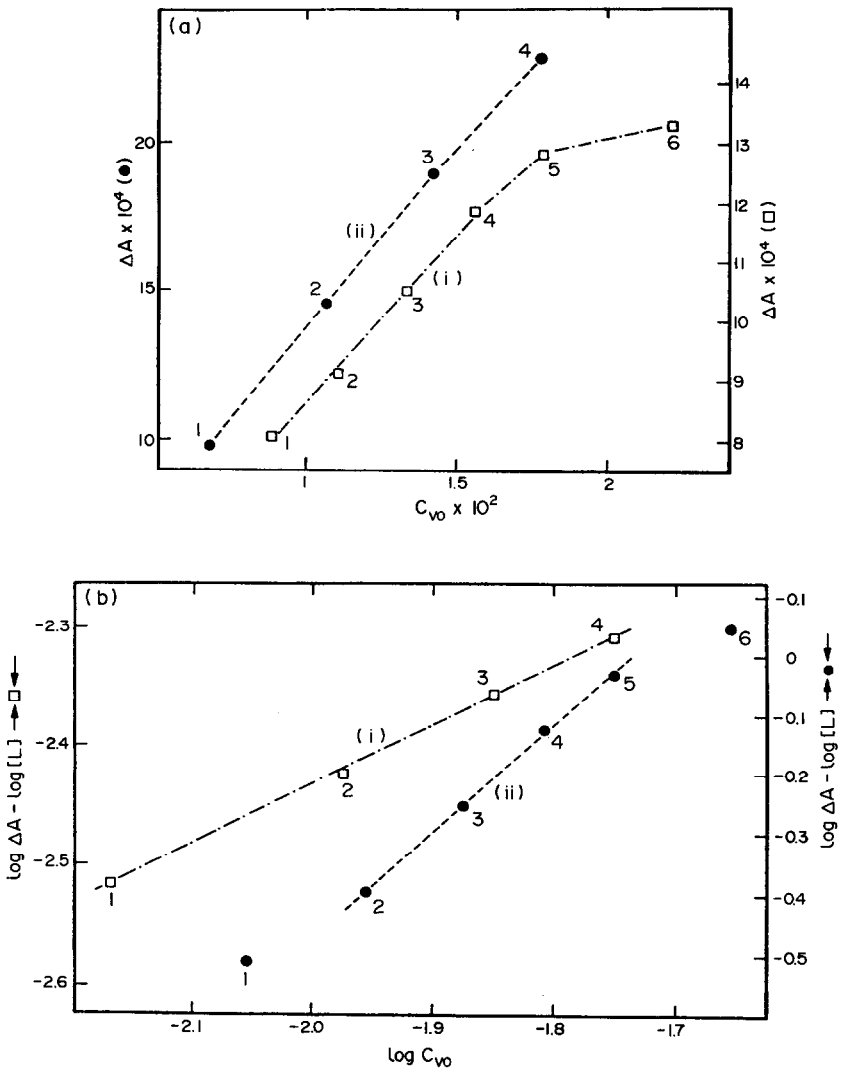

Fig. 17. Representation of: (a) ΔA vs C_{VO} for the CD spectra of (i) L-Ser+VO^{2+} solutions at pH ~ 13.3 for λ = 532 nm (□) (from Fig. 8b); (ii) L-Thr+VO^{2+} solutions at pH ~ 13.6 for λ = 527 nm (●) (from Fig. 9b). The total ligand concentration may be considered as being constant. (b) $\log \Delta A - \log [L]$ vs C_{VO} corresponding to (i) and (ii) in (a).

merization, especially for L-Ser+VO^{2-} at pH ~ 13.3.

At these pH values, a substantial amount of vanadium is uncoordinated by amino acid and this is probably one species involved in the above mentioned equilibrium.

Figure 17a gives a representation of ΔA vs C_{VO} for two wavelengths at pH 13.3 and 13.6. Two types of situations will be considered—A and B—and the corresponding models are described and discussed in Table 6.

Hypothesis A: From eq. (6A) of Table 6, the plot to test this is Y_A vs $\log C_{VO}$. However, $[M_2]$, part of Y_A is not known, so $\alpha(M_2)$ cannot be calculated. However, when C_{VO} increases, $[M_2]$ and $\sqrt{[M_2]}$ (< 1) also increase, so that $\alpha(M_2)$ and $\log \alpha(M_2)$ decrease. Therefore, if—instead of representing Y_A vs $\log C_{VO}$—we take $(\log \Delta A - \log [L])$ vs $\log C_{VO}$, a "straight line" with slope greater than 1/2 is expected and indeed found. Thus, plotting in this way $(\log \Delta A - \log [L])$ vs $\log C_{VO}$ (Fig. 17b) (or $\log \Delta A - 2 \log [L]$) vs $\log C_{VO}$ (ΔA values from Fig. 17a), gives straight lines with slopes 0.878 and 0.986 for (i) and (ii) respectively.

Hypotheses B: According to eq. (6B) of Table 6 the best plot is of Y_B vs $\log C_{VO}$. Again [M] is unknown, so α(M) cannot be calculated. However, as C_{VO} increases, α(M) and $\log \alpha$(M) increase (α(M) > 1). Again, plotting $(\log \Delta A - \log [L])$ (or $\log \Delta A - 2 \log [L]$), a slope greater than 2 would be expected.

The slopes obtained are less than 1. This suggests

Table 6. Two models for explaining CD spectra of solutions with high L/M ratios, fixed (and high) pH and variable C_{VO}[a]

Hypothesis A

dimer	$\rightleftharpoons$	monomer
("free" metal)		(responsible for the CD spectra)

$$M_2+2L \rightleftharpoons 2ML^{b}$$

$$\beta'_{ML}=\frac{[ML]^2}{[M_2][L]^2}\longrightarrow [ML]=\sqrt{\beta'_{ML}}[L]\sqrt{[M_2]}$$

Multiplying by $\Delta\varepsilon_{ML}$: $\Delta A=\sqrt{\beta'_{ML}}\Delta\varepsilon_{ML}[L]\sqrt{[M_2]}$ or

$$\Delta A=(K)_1[L]\sqrt{[M_2]} \qquad (3A)$$

Applying logarithms:

$$\log\Delta A-\log[L]=\log(K)_1+1/2\log[M_2] \qquad (4A)$$

Representing $(\log\Delta A-\log[L])$ vs $\log[M_2]$ one should obtain a straight line with slope 1/2.

$[M_2]$ is not known but

$$C_{VO}=2[M_2]+[ML]=[M_2]\underbrace{|2+(\sqrt{\beta'_{ML}}[L])/(\sqrt{[M_2]})|}_{\alpha(M_2)}$$

or: $$[M_2]=C_{VO}/\alpha(M_2) \qquad (5A)$$

Substituting (5A) in (4A), one gets:

$$\underbrace{\log\Delta A-\log[L]+1/2\log\alpha(M_2)}_{Y_A}=\log(K)_1+1/2\log C_{VO} \qquad (6A)$$

Conclusion: Representing Y_A vs $\log C_{VO}$ should give a straight line, slope 1/2.[c]

Hypothesis B

monomer	$\rightleftharpoons$	dimer
("free" metal)		(responsible for the CD spectra)

$$2M+2L \rightleftharpoons M_2L_2$$

$$\beta'(M_2L_2)=\frac{[M_2L_2]}{[M]^2[L]^2}\longrightarrow [M_2L_2]=\beta'(M_2L_2)[L]^2[M]^2$$

Multiplying by $\Delta\varepsilon(M_2L_2)$: $\Delta A=\beta'(M_2L_2)\Delta\varepsilon(M_2L_2)[L]^2[M]^2$ or

$$\Delta A=(K)_2[L]^2[M]^2 \qquad (3B)$$

Applying logarithms:

$$\log\Delta A-\log[L]=\log(K)_2+2\log[M] \qquad (4B)$$

Representing $(\log\Delta A-2\log[L])$ vs $\log[M]$ one should obtain a straight line with slope 2.

[M] is not known but

$$C_{VO}=[M]+2[M_2L_2]=[M]\underbrace{\{1+2\beta'(M_2L_2)[L]^2[M]\}}_{\alpha(M)}$$

or: $$[M]=C_{VO}/\alpha(M) \qquad (5B)$$

Substituting (5B) in (4B), one gets:

$$\underbrace{\log\Delta A-\log[L]+2\log\alpha(M)}_{Y_B}=\log(K)_2+2\log C_{VO} \qquad (6B)$$

Conclusion: Representing Y_B vs $\log C_{VO}$ should give a straight line, slope 2.

[a] For both A and B, if the equilibria are shifted towards the formation of the optically active complex, if C_{VO} varies, as one has an excess of ligand all vanadium would yield the complex, the ΔA would be proportional to C_{VO} and $\Delta\varepsilon_m$ = constant, which is not the case (although one is nearer to that situation in Fig. 9b than in Fig. 8b). Therefore, if the experimental results may be explained by either A or B, as the $\Delta\varepsilon_m$ are not constant this means that an appreciable amount of "free" metal exists.

[b] If the equilibrium is of the type $M_2+2L\rightleftharpoons 2MLH_{-3}+3H^+$, since one is considering groups of CD spectra at fixed pH, the treatment would be similar. If the equilibrium is of the type $M_2+4L\rightleftharpoons 2ML_2$, instead of eq. (3A) one would get: $\Delta A=\Delta\varepsilon_{ML_2}\sqrt{\beta'_{ML_2}}[L]^2\sqrt{[M_2]}$ and the treatment is also similar. If the equilibrium involves simultaneously ML and ML_2 complexes, as long as L/M is high their relative proportions are almost invariant with C_{VO} and the treatment is still valid.

[c] If the equilibrium is of the type $M_n+nL\rightleftharpoons nML$, the slope corresponding to eqs (4A) and (6A) would be $1/n$.

that equilibria of the type included in hypothesis B (Table 6) are unsuitable to describe the experimental CD spectra at high pH and variable C_{VO}. However, the results are consistent with expectation for hypothesis A. Therefore, at high pH, a fair description involves optically active monomeric complexes in equilibrium with dimeric (or oligomeric) non-optically active vanadium(IV) hydrolysis products. This agrees with the results obtained with SQUAD for pH $\lesssim$ 12.8 and is consistent with the present knowledge of vanadium(IV) aqueous chemistry at very high pH, where one expects to have $VO(OH)_3^-$ in equilibrium with other oligomeric species.[3]

Acknowledgements—The authors thank the British Council for grants; J.C.P. and L.F.V.B. thank the Instituto Nacional de Investigação Científica and Fundação Calouste Gulbenkian for financial support. R.D.G. acknowledges the grant of study leave by University College, Cardiff in 1982 and 1987. We acknowledge helpful comments by Dr I. Fabian of Debrecen on an obscurity in our species diagram in fig. 11 of the present ref. 1. This has been amended here (cf. Fig. 14).

REFERENCES

1. Part I of this series: J. Costa Pessoa, L. F. Vilas Boas, R. D. Gillard and R. J. Lancashire, *Polyhedron* 1988, **7**, 1245.
2. J. Costa Pessoa and L. F. Vilas Boas, 1980 *Autumn Meeting—Chemical Society*. University College, Cardiff (1980).
3. L. F. Vilas Boas and J. Costa Pessoa, Chapter on vanadium in *Comprehensive Coordination Chemistry* (Edited by G. Wilkinson, R. D. Gillard and J. A. McCleverty), Vol. 3, pp. 453–583. Pergamon Press, Oxford (1987).
4. L. D. Pettit and J. L. Swash, *J. Chem. Soc., Dalton Trans.* 1976, 2416.
5. P. Grenouillet, R. P. Martin, A. Rossi and M. Ptak, *Biochim. Biophys. Acta* 1973, **322**, 185.
6. D. A. Metzler, *Biochemistry. The Chemical Reactions of Living Cells*, p. 58. Academic Press, New York (1977).
7. A. A. Popel, A. V. Zakharov, I. I. Evgen'eva and L. V. Vasil'eva, *Russ. J. Inorg. Chem.* 1978, **23**, 1351.
8. J. Costa Pessoa, L. F. Vilas Boas and M. H. Teixeira, to be published.
9. R. D. Gillard, R. J. Lancashire, J. Costa Pessoa and L. F. Vilas Boas, Comunicação 3A11, 2° Encontro Nacional de Química, Porto (1979).
10. R. D. Gillard, J. Costa Pessoa and L. F. Vilas Boas, Comunicação C31.9, 5° Encontro Nacional de Química, Porto (1982).
11. R. D. Gillard, R. Marques, J. Costa Pessoa and L. F. Vilas Boas, Comunicação 5CP12, 9° Encontro Nacional de Química, Coimbra (1986).
12. A. Sabatini, A. Vacca and P. Gans, *Talanta* 1974, **21**, 53; P. Gans, A. Sabatini and A. Vacca, *Inorg. Chim. Acta* 1976, **18**, 237.
13. P. Gans, A. Sabatini and A. Vacca, *Inorg. Chim. Acta* 1983, **79**, 219; P. Gans, A. Sabatini and A. Vacca, *J. Chem. Soc., Dalton Trans.* 1985, 1195.
14. P. Bernardo, G. Tomat, P. Zanonato, R. Portanova and M. Tolazzi, *Inorg. Chim. Acta* 1988, **145**, 285.
15. D. J. Leggett and W. A. E. McBryde, *Analyt. Chem.* 1975, **47**, 1065; D. J. Leggett, *Analyt. Chem.* 1977, **49**, 276; D. J. Leggett, S. L. Kelly, L. R. Shine, Y. T. Wu, D. Chang and K. M. Kadish, *Talanta* 1983, **30**, 579.
16. M. M. Iannuzzi and P. H. Rieger, *Inorg. Chem.* 1975, **14**, 2895.
17. I. Fábián and I. Nagypál, *Inorg. Chim. Acta* 1982, **62**, 193.
18. R. M. Smith, R. J. Motekaitis and A. E. Martell, *Inorg. Chim. Acta* 1985, **103**, 73; R. M. Smith and A. E. Martell, *Critical Stability Constants*. Plenum Press, New York, (a) Vol. 2, 1976; (b) Vol. 5, 1982 (Suppl. 1).
19. N. D. Chasteen, in *Biological Magnetic Resonance* (Edited by L. J. Berliner and J. Reuben), Vol. 3, p. 53. Plenum Press, New York (1981).
20. A. Rossi, M. Ptak, P. Grenouillet and R. P. Martin, *J. Chim. Phys.* 1974, **71**, 1371.
21. P. Sharrock, *Can. J. Chem.* 1985, **63**, 46.
22. K. Okazaki and K. Saito, *Bull. Chem. Soc. Japan* 1982, **55**, 785.
23. R. D. Gillard and S. H. Laurie, *J. Chem. Soc. A* 1970, 59.
24. R. D. Gillard, R. J. Lancashire and P. O'Brien, *Trans. Metal Chem., Weinheim* 1980, **5**, 340 (and references therein).

Polyhedron Vol. 8, No. 9, pp. 1201–1204, 1989
Printed in Great Britain

0277–5387/89 $3.00+.00
© 1989 Pergamon Press plc

MIXED-LIGAND COMPLEXES OF TECHNETIUM—III. SYNTHESIS AND CHARACTERIZATION OF [BIS(DIPHENYLPHOSPHINO)ETHANE]TETRAKIS(TRIMETHYL PHOSPHITE)TECHNETIUM(I) HEXAFLUOROPHOSPHATE, $[Tc(DPPE)(TMP)_4]PF_6$

U. ABRAM,* R. BEYER and R. MÜNZE

Central Institute of Nuclear Research Rossendorf, PF 19, Dresden, DDR-8051, G.D.R.

and

J. STACH

Karl-Marx-University Leipzig, Department of Chemistry, Talstr. 35, Leipzig, DDR-7010, G.D.R.

and

L. KADEN, B. LORENZ and M. FINDEISEN

Central Institute of Isotopes and Radiation Research, Permoserstr. 15, DDR-7010 Leipzig, G.D.R.

(*Received* 1 *September* 1988; *accepted* 10 *November* 1988)

Abstract—The diamagnetic technetium(I) complex $[Tc(DPPE)(TMP)_4]PF_6$ was prepared from $[Tc(N_2)H(DPPE)_2]$ and characterized by elemental analysis, ^1H- and ^{99}Tc-NMR spectroscopy and fast atom bombardment mass spectrometry. $[Tc(DPPE)(TMP)_4]PF_6$ is a prototype compound for technetium complexes with mixed phosphine–phosphite coordination spheres.

In a recent report[1] we showed that hydridobis [bis(diphenylphosphino)ethane] dinitrogentechnetium(I), $[Tc(N_2)H(DPPE)_2]$,[2,3] is a useful starting material for the preparation of technetium mixed-ligand complexes with the metal in low oxidation states which may have a potential use as radiopharmaceuticals in diagnostic nuclear medicine.[1,4,5] With isocyanides (^{t}BuNC, cyclohexylNC), ligand exchange takes place by substitution of the hydride and the dinitrogen ligand to yield $[Tc(DPPE)_2(RNC)_2]^+$ cations.[1]

In this paper, we report ligand exchange reactions of this compound using trimethylphosphite (TMP).

* Author to whom correspondence should be addressed.

EXPERIMENTAL

All operations were carried out in a fume cupboard, using gloves to avoid contamination. The weak β-emission of ^{99}Tc is retained by the glass of the reaction vessels. Secondary X-rays (bremsstrahlung) only become important if handling a larger scale of ^{99}Tc.

The procedures are performed in an atmosphere of dry nitrogen.

Preparation

$[Tc(N_2)H(DPPE)_2]$ (37 mg; 40 μmol) were suspended in 10 cm^3 MeOH. After addition of 2 cm^3 TMP, the mixture was refluxed for 1 h to obtain a

clear solution. The volume was reduced in vacuum to 1 cm^3, and 0.5 cm^3 of a saturated KPF_6 solution was added. Addition of 0.5 cm^3 water and cooling results in the formation of a colourless solid which was filtered and twice washed with ether. After recrystallization from acetone–water, 36 mg (80%) of colourless crystals were obtained; m.p. 182–186°C dec. Elemental analysis: Found: C, 41.5; H, 5.5; P, 20.7; Tc, 8.3. Calc. C, 40.1; H, 5.3; P, 19.9; Tc, 8.7. ^{1}H-NMR (without ^{31}P-decoupling): phenyl, 7.3 ppm *m* (20H); CH_3, 3.86 ppm *m* (18H) and 2.86 ppm *m* (18H); CH_2, 2.22 ppm *m* (4H). ^{99}Tc-NMR: −1664 ppm *m*.

Physical measurements

Fast atom bombardment mass spectra were recorded on a VG-ZAB-HSQ spectrometer. Argon was used as primary beam gas. The ion gun was operated at 8 keV and 100 μA. Glycerol was used as matrix. CID spectra could be obtained with argon as the collision gas.

The ^{1}H- and ^{31}P-NMR spectra were obtained in acetone-d_6 on a WX 90 DS spectrometer. The ^{99}Tc-NMR spectrum was recorded in CD_2Cl_2 on a AM 250 instrument with a measuring frequency of 56.3 MHz for ^{99}Tc. The chemical shifts are relative to TMS and TcO_4^- in D_2O, respectively.

RESULTS AND DISCUSSION

In contrast to the ligand exchange reaction between $[Tc(N_2)H(DPPE)_2]$ with isocyanides,[1] the reaction with trimethylphosphite does not result in the formation of $[Tc(DPPE)_2(TMP)_2]^+$, but yields another colourless complex, $[Tc(DPPE)(TMP)_4]^+$, which can be precipitated as the hexafluorophosphate salt. The compound is soluble in polar organic solvents, sparingly soluble in ether and insoluble in hydrocarbons and water. As a solid, it is stable in air, whereas in solution, a slow decomposition occurs if allowed to stand in the atmosphere over a longer period.

In the IR spectrum there is no evidence for frequencies arising from the N_2 and H^- ligand, respectively. The vibrational frequencies due to the P—O bonds of the TMP ligands are hypsochromically shifted in the complexes (by about 40 cm^{-1}), indicating their coordination to technetium.

More detailed information about the structure of the complex can be derived from the mass spectrometric investigations. Figure 1 shows the FAB mass spectrum of the mixed-ligand complex. The peak with the highest *m/z* value, 993, which represents the complex ion, corresponds to $[Tc(DPPE)(TMP)_4]^+$ cations. The structure of the $m/z = 993$ ion is supported by the more intense peaks at *m/z* 869, 745, 621 and 497, respectively, which indicate a stepwise loss of the TMP ligands. This assumption is confirmed by MIKE (mass analysed ion kinetic energy) spectra of the corresponding ions. As illustrated in Fig. 2, each of the mass selected ions, starting with $[Tc(DPPE)(TMP)_4]^+$, decomposes under metastable conditions (without collision gas) by elimination of one TMP ligand. The decomposition of the finally formed $[Tc(DPPE)]^+$ ion yields typical fragment ions by loss of, e.g. C_2H_4 (469), C_6H_6 (419), and $P(C_6H_5)_2$ (311).

Collision activation increases the number of

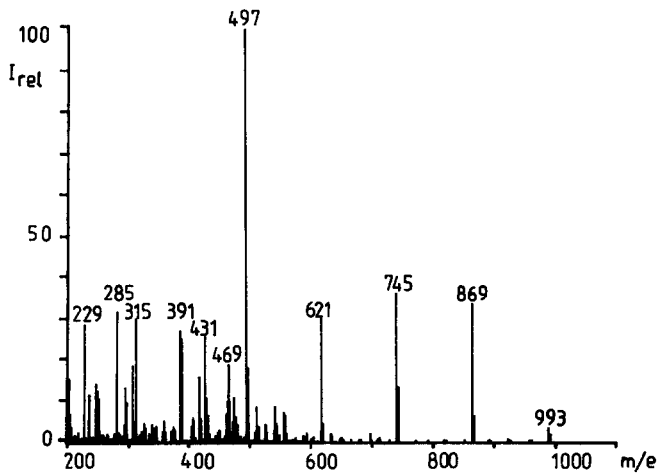

Fig. 1. Positive FAB mass spectrum of $[Tc(DPPE)(TMP)_4]^+$; matrix: glycerol.

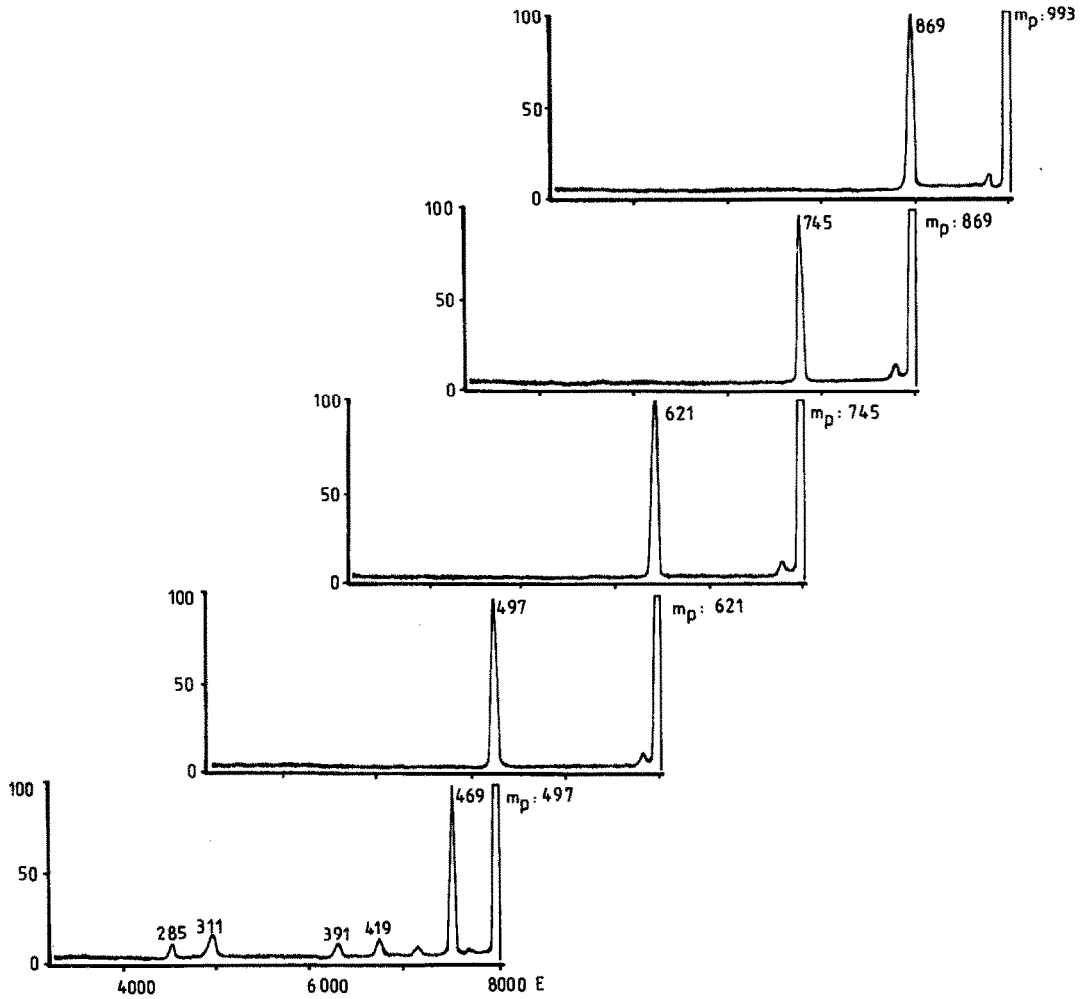

Fig. 2. MIKE spectra showing the fragmentation of metastable *m/z* 993, 869, 745, 621 and 497 ions.

ions formed. The MIKE spectrum of $[Tc(DPPE)(TMP)_4]^+$ ions recorded at 50% main beam reduction due to the collision gas (argon), contains all peaks which can be observed in the corresponding spectra obtained under metastable conditions (see Fig. 2). However, the most important fragmentation pathway, which allows the determination of the structure, is given by the loss of the ligands. This was also found in the MS–MS spectra of similar phosphine containing cationic Tc complexes.[6,7]

NMR spectroscopic results characterize $[Tc(DPPE)(TMP)_4]PF_6$ to be diamagnetic, as expected for the corresponding d^6 configuration. The proton spectrum confirms the stated structure showing two signals for the methyl protons of the differently bonded phosphite ligands. The ^{99}Tc-NMR spectrum (Fig. 3) shows a multiplet signal at -1664 ppm. This upfield chemical shift is in accordance with the values measured for $[Tc(TMP)_6]^+$ and $[Tc(DMPE)_3]^+$, which give ^{99}Tc-NMR signals at -1657 and -1837 ppm.[8] The larger line width in the $[Tc(DPPE)(TMP)_4]^+$ is due to its lower symmetry and the resulting quadrupole relaxation effects (quadrupole moment of ^{99}Tc: $Q = -0.2 \times 10^{-28}$ m^2).[9] Nevertheless, a multiplet structure of the ^{99}Tc-NMR signal could be resolved, arising from coupling with the ^{31}P nuclei of the ligands (three different groups each with two P-atoms). Individual coupling constants could not be derived due to many line overlappings. Obviously, the ^{99}Tc-^{31}P(phosphite) couplings are smaller than those found for $[Tc(TMP)_6]^+$ (910 Hz) and come in the range of corresponding ^{99}Tc-^{31}P(phosphine) values (574 Hz for $[Tc(dmpe)_3]^+$).[8,10] The ^{31}P-NMR spectrum of the mixed-ligand complex shows the expected high order pattern which is difficult to analyse.

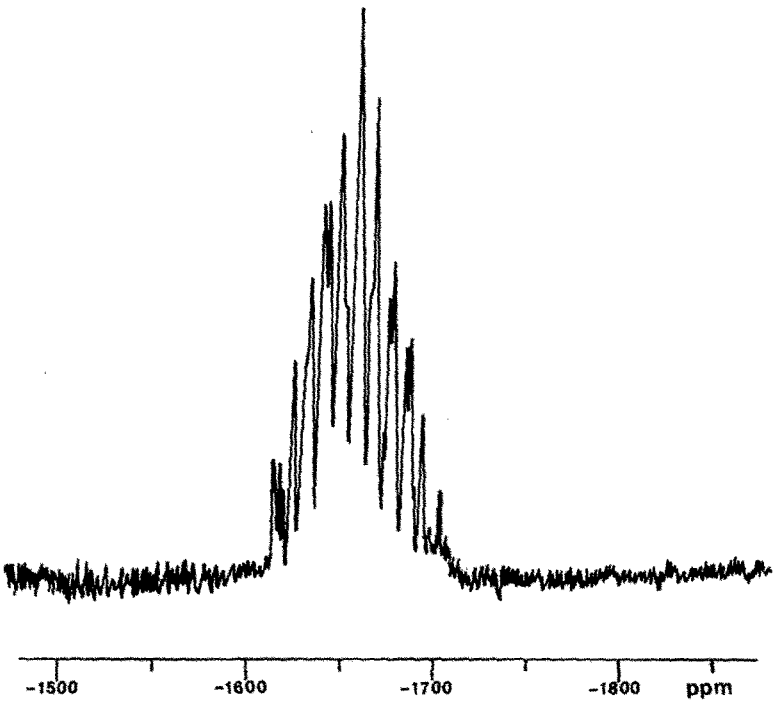

Fig. 3. ^{99}Tc-NMR spectrum of $[Tc(DPPE)(TMP)_4]PF_6$ in CD_2Cl_2.

REFERENCES

1. U. Abram, S. Abram, R. Beyer, R. Münze, L. Kaden, B. Lorenz and M. Findeisen, *Inorg. Chim. Acta* 1988, **148**, 141.
2. L. Kaden, B. Lorenz, K. Schmidt, H. Sprinz and M. Wahren, *Z. Chem.* 1979, **19**, 305.
3. Y. T. Struchkov, A. S. Bazanov, L. Kaden, B. Lorenz, M. Wahren and H. Meyer, *Z. Anorg. Allg. Chem.* 1982, **494**, 91.
4. G. D. Zanelli, A. Lahiri, N. Patel, T. Smith, F. Brady, G. Radfar, N. D. Cook, J. C. W. Crawley and D. J. Silvester, *Eur. J. Nucl. Med.* 1987, **13**, 12.
5. U. Abram, G. Kampf, S. Abram and R. Münze, *Appl. Radiat. Isot.* 1988, **39**, 385.
6. S. E. Unger, *Analyt. Chem.* 1984, **56**, 363.
7. A. I. Cohan, K. A. Glavan and J. F. Kronauge, *Biomed. Mass Spectrom.* 1983, **10**, 287.
8. M. Findeisen, B. Lorenz and U. Abram, *Z. Chem.* 1989, **29**, 29.
9. D. Wendtland, J. Bauche and P. Luce, *J. Phys. B* 1977, **10**, 1989.
10. D. W. Wester, D. H. White, F. E. Miller, R. T. Dean, J. A. Schreifels and J. E. Hunt, *Inorg. Chim. Acta* 1987, **131**, 163.

Polyhedron Vol. 8, No. 9, pp. 1205–1211, 1989
Printed in Great Britain

0277–5387/89 $3.00+.00
© 1989 Pergamon Press plc

DICHLORO AND AMINO ACID COBALT(III) COMPLEXES OF ETHYLENEDIAMINE-N,N′-di-S-α-PROPIONIC ACID

MOO-JIN JUN,* YOUN BONG PARK and SUNG RACK CHOI

Department of Chemistry, Yonsei University, Seoul, Korea

(*Received* 16 *May* 1988; *accepted* 11 *November* 1988)

Abstract—The dichloro cobalt(III) complex of ethylenediamine-N,N′-di-S-α-propionic acid (SS-eddp), [Co(SS-eddp)Cl_2], has yielded the Δ-s-*cis* isomer only. Chloro-aqua and diaqua cobalt(III) complexes of SS-eddp, Δ-s-*cis*-[Co(SS-eddp)Cl·H_2O] and Δ-s-*cis*-[Co(SS-eddp)$(H_2O)_2]^+$, have also been prepared. Reactions of the s-*cis*-[Co(SS-eddp)$Cl_2]^-$ complex with amino acids have yielded the s-*cis*-[Co(SS-eddp)(aa)]$^{n+}$ complexes (aa = L-alanine, S-methyl-L-cysteine or L-cysteine). The L-alanine or S-methyl-L-cysteine cobalt(III) complex of SS-eddp has been obtained as the s-*cis*-meridional isomer only. The S-methyl-L-cysteine is coordinated to the cobalt(III) ion via the nitrogen and oxygen donor atoms, while the cysteine is found to coordinate to the cobalt(III) ion via the nitrogen and sulphur donor atoms.

Ethylenediamine-N,N′-di-S-α-propionic acid (SS-eddp), the configuration of which is shown below, was first prepared by Liu and co-workers.[1]

The SS-eddp ligand is a flexible tetradentate ligand of the N_2O_2 system and can occupy four-coordinate sites with three geometrical isomers possible, s-*cis* (symmetric *cis*), uns-*cis* (unsymmetric *cis*) and *trans* in [Co(SS-eddp)$X_2]^{n+}$ type complexes as shown in Fig. 1. Both s-*cis* and uns-*cis* geometrical isomers can have either Δ or Λ absolute configurations.

Liu and co-workers have prepared the cobalt(III) complexes of SS-eddp, [Co(SS-eddp)L]$^{n+}$, where L is ethylenediamine (en) or *R*-propylenediamine (*R*-pn). The [Co(SS-eddp)(en)]$^+$ and [Co(SS-eddp)(*R*-pn)]$^+$ complexes have yielded Λ-s-*cis*, Δ-s-*cis*, and Δ-uns-*cis* isomers.[1] Recently, the rhodium(III) complexes of SS-eddp of the type [Rh(SS-eddp)L]$^{n+}$ (L = Cl_2, en, *R*- or *S*-alanine, glycine) have been prepared.[2–4] The dichloro complex of [Rh(SS-eddp)$Cl_2]^-$ has yielded only Δ-s-*cis* and Λ-uns-*cis* isomers. The ethylenediamine rhodium(III) complex of SS-eddp has also yielded only Δ-s-*cis* and Λ-uns-*cis* isomers.

It will be of interest to see which isomers would be obtained in the diacido cobalt(III) complexes of SS-eddp. It will be shown here that only one isomer, the Δ-s-*cis* isomer, has been yielded for the complexes of [Co(SS-eddp)$L_2]^{n+}$ (L = Cl or H_2O). There have been no reports on the SS-eddp or any N_2O_2 type tetradentate ligand cobalt(III) complexes of amino acids containing the sulphur atom. Our work on the SS-eddp cobalt(III) complexes of amino acids containing the sulphur atom, S-methyl-L-cysteine (mcy) and cysteine (cy), show rather an interesting result: the coordination of S-methyl-L-

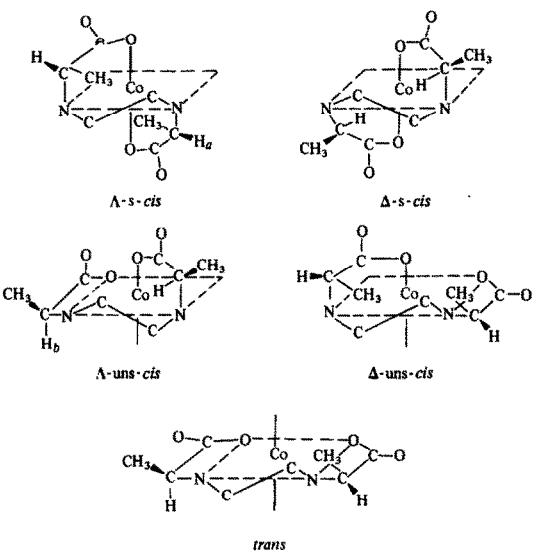

Fig. 1. The possible isomers of [Co(SS-eddp)$X_2]^{n+}$ complexes.

* Author to whom correspondence should be addressed.

cysteine in [Co(SS-eddp)(mcy)] is through the amino and carboxylate groups, whereas the cysteine is coordinated through the amino and mercaptide groups in $[Co(SS\text{-}eddp)(cy)]^+$. The synthesis of the *S*-alanine cobalt(III) complex of SS-eddp is also described.

EXPERIMENTAL

Physical measurements

Electronic absorption spectra were obtained with a Shimadzu UV-240 spectrophotometer. PMR spectra were recorded on a Varian EM 360L spectrometer. IR spectra were taken with a Shimadzu IR-435 spectrophotometer. Circular dichroism spectra were obtained with a J-500C spectropolarimeter. Elemental analyses were performed by Micro-Tech Analytical Laboratory, Skokie, Illinois.

Preparation of ethylenediamine-N,N′-*di*-S-α-*propionic acid* (SS-eddp)

This was prepared by the reported method.[1]

Preparation of s-cis-*hydrogen dichloro(ethylenediamine*-N,N′-*di*-S-α-*propionato)cobaltate*(III), s-cis-H[Co(SS-eddp)Cl_2]

To a solution of ethylenediamine-N,N′-di-S-α-propionic acid (1.0 g) in 35 cm^3 of water were added sodium hydroxide (0.4 g) and cobalt(III) chloride hexahydrate (1.2 g). The brown solution was aerated with carbon dioxide-free air for 5 h. Concentrated hydrochloric acid (20 cm^3) was added to the oxidation product and the reaction mixture was concentrated on a steam bath with continuous stirring to about 30 cm^3. The colour changed to a dark bluish-green and a dark green precipitate appeared. After cooling, the precipitate was collected on a filter, and washed with MeOH and ether. More of the green compound was obtained from the filtered solution by adding a small amount of conc. HCl and evaporating the solution. Separation of any isomers using an ion exchange resin column yielded only one isomer. Yield: 0.45 g. Found: C, 27.4; H, 4.6; N, 8.0. Calc. for H[Co(SS-eddp)Cl_2]·H_2O: C, 27.4; H, 4.8; N, 8.0%.

Preparation of s-cis-[Co(SS-eddp)Cl·H_2O] in situ

s-*cis*-H[Co(SS-eddp)Cl_2]·H_2O (15 mg) was dissolved in 20 cm^3 of 0.01 N perchloric acid. The solution was allowed to stand at 20°C for 70 min. The colour of the solution changed from dark green to blue, and at this point the electronic absorption and CD spectra were obtained.

Preparation of s-cis-$[Co(SS\text{-}eddp)(H_2O)_2]^+$ in situ

Sodium bicarbonate (0.05 g) was added to the s-*cis*-[Co(SS-eddp)Cl·H_2O] solution obtained above. The resultant solution was allowed to stand at room temperature for 30 min and the colour changed to light purple. Perchloric acid was added to the solution until the pH of the solution reached 2. The colour of the solution then changed to violet, and the electronic absorption and CD spectra were taken.

Preparation of s-cis-L-*alaninato(ethylenediamine*-N,N′-*di*-S-α-*propionato)cobalt*(III), s-cis-[Co(SS-eddp)(L-ala)]

s-*cis*-[Co(SS-eddp)Cl_2]·H_2O (0.70 g) was dissolved in 20 cm^3 of water and heated at 60°C for 20 min. L-alanine (0.19 g) was added and the pH of solution was adjusted to 8 with 1 N NaOH. After adding 0.1 g of activated charcoal, the solution was heated at 60°C in a water bath with stirring for 5 h. The activated charcoal was filtered and washed with hot water. The washings and filtrate were combined, and then concentrated on a rotatory evaporator to a volume of 5 cm^3. The resulting violet solution was poured into a column containing cation-exchange resin (Dowex 50W-X4, 200–400 mesh, H^+ form). The solution was separated into two bands using water as the eluent. The upper band, the unreacted $[Co(SS\text{-}eddp)(H_2O)_2]^+$, was retarded without elution. From the electronic absorption and ^1H NMR spectra, the eluate of the lower band was identified as the s-*cis* isomer. By fractional crystallization, the s-*cis*-[Co(SS-eddp)(*S*-ala)] was obtained. Yield: 0.49 g. Found: C, 37.9; H, 5.6; N, 11.8. Calc. for $CoC_{11}H_{20}N_3O_6$: C, 37.8; H, 5.7; N, 12.0%.

Preparation of s-cis-S-*methyl*-L-*cysteinato(ethylenediamine*-N,N′-*di*-S-α-*propionato)cobalt*(III), s-cis-[Co(SS-eddp)(mcy)]

s-*cis*-H[Co(SS-eddp)Cl_2]·H_2O (1.0 g) was dissolved in 30 cm^3 of water and heated at 60°C for 20 min. S-methyl-L-cysteine (0.4 g) was added and the pH of solution was adjusted to 10 with 1 N NaOH. Activated charcoal (0.1 g) was added and the reaction mixture was heated and stirred at 60°C on a water bath for 8 h. The charcoal was removed by filtration and washed with hot water. The combined filtrate and washings were concentrated to 5

cm^3 using a rotatory evaporator. The solution was passed through an ion-exchange column (Dowex 50W-X4, 200–400 mesh, H^+ form) with water as eluent. Two bands were formed. The upper band was the unreacted $[Co(SS\text{-}eddp)(H_2O)_2]^+$. The product was obtained by fractional crystallization of the lower band solution. Yield: 0.64 g. Found: C, 36.4; H, 5.6; N, 10.7. Calc. for $CoC_{12}H_{22}N_3O_6S$: C, 36.5; H, 5.6; N, 10.6%.

Preparation of s-cis-*sodium* S-*cysteinato(ethylenediamine*-N,N′-*di*-S-α-*propionato)cobaltate*(III), s-cis-Na[Co(SS-eddp)(cy)]

s-*cis*-H[Co(SS-eddp)Cl_2]·H_2O (1.0 g) was dissolved in 60 cm^3 of water and the solution was heated at 60°C for 20 min. The colour of solution turned from green to red–violet. After the solution was cooled to 0°C, 0.36 g of *S*-cysteine was added, and the pH of solution was adjusted to 10 by the addition of a 1 N NaOH solution. The solution was maintained at 0°C for 5 h with stirring on an ice bath. The reaction mixture was concentrated to 20 cm^3 using a rotatory evaporator. When 20 cm^3 of absolute ethanol was added, black precipitates were formed. The precipitates were removed by filtration and washed with absolute ethanol. The combined filtrate and washings were concentrated to 15 cm^3. The resulting reaction mixture was allowed to stand at 0°C for 1 day. The dark brown crystals which settled at the bottom of the beaker were filtered, washed with absolute ethanol and ether, and air-dried. More of the dark brown compound was obtained from the filtrate by evaporating the solution and adding absolute ethanol. Yield: 0.57 g. Found: C, 31.4; H, 4.9; N, 11.1. Calc. for $CoC_{10}H_{17}N_3O_6S \cdot H_2O$: C, 31.6; H, 5.0; N, 11.0%.

RESULTS AND DISCUSSION

Preparation of the dichloro cobalt(III) complex of SS-eddp has yielded only one geometrical isomer, the s-*cis* isomer. Attempts to isolate other isomers including ion-exchange chromatography have failed. In the electron absorption spectrum of $[Co(SS\text{-}eddp)Cl_2]^-$ shown in Fig. 2 bands I and II, which are due to the *d–d* transitions in the octahedral $CoN_2O_2Cl_2$ system, appear between 400 and 650 nm. The shape of the first band is nearly symmetrical, indicating an s-*cis* configuration. If the complex has the *trans* configuration a splitting of band I should be observed.[5–7] If the complex has an uns-*cis* geometry, two atoms of the same kind (Cl—Cl, N—N, O—O) are at the *cis* positions, and a very intense absorption of band II would be expected, since the ligand field around the central atom is highly unsymmetrical.

The PMR spectrum shown in Fig. 3 clearly indicates that the $[Co(SS\text{-}eddp)Cl_2]^-$ complex has a s-*cis* geometry. A single methyl doublet is shown at 1.7 ppm and a single α-carbon proton quartet is seen at 3.5 ppm. If the complex has an uns-*cis* geometry, the same methyl should show two doublets and the α-carbon proton should show two quartets, because the two carboxylate arms are not equivalent in the uns-*cis* geometry.

Figure 4 shows portions of the PMR spectra of s-*cis*-[Co(edda)(en)]$^+$, Λ-s-*cis*-[Co(SS-eddp)(en)]$^+$, Δ-s-*cis*-[Co(SS-eddp)(en)]$^+$, and Δ-s-*cis*-[Co(SS-eddp)Cl_2]$^-$, where edda is ethylenediamine-N,N′-diacetic acid. The chemical shifts of the protons of edda (labelled H_a and H_b) can be distinguished because of the magnetic anisotropic shielding of the C—N bond,[1,8,9] and the H_a protons resonate at a lower field than the H_b protons. From the known

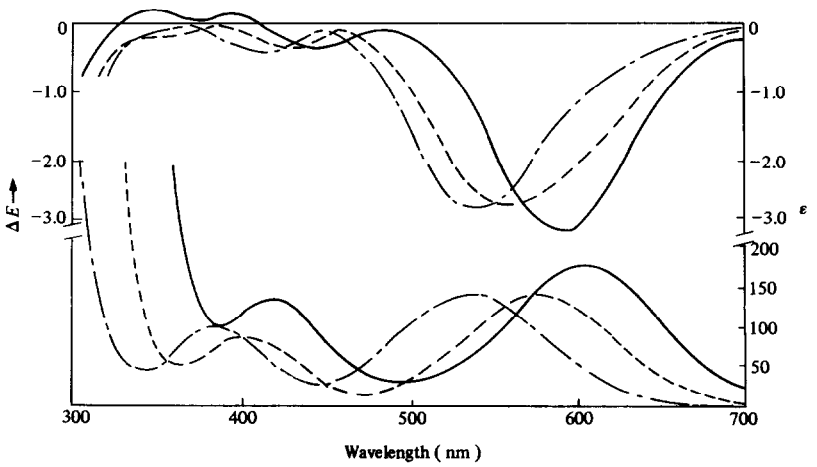

Fig. 2. Circular dichroism and electronic absorption spectra of Δ-s-*cis*-[Co(SS-eddp)Cl_2]$^-$ (——), Δ-s-*cis*-[Co(SS-eddp)Cl(H_2O)] (– – – –), and Δ-s-*cis*-[Co(SS-eddp)$(H_2O)_2$]$^+$ (—·—·—).

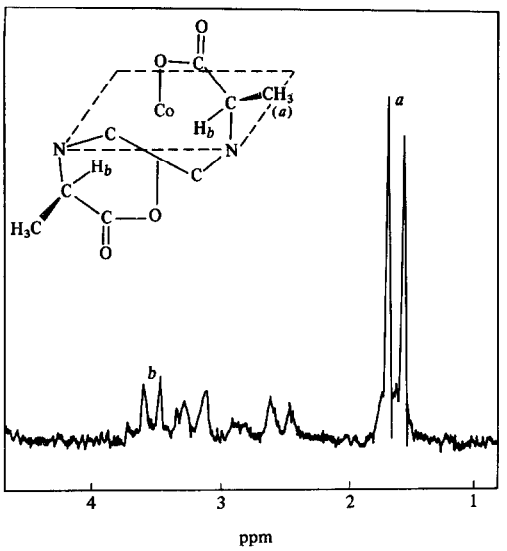

Fig. 3. PMR spectrum of Δ-s-*cis*-H[Co(SS-eddp)Cl_2] H_2O.

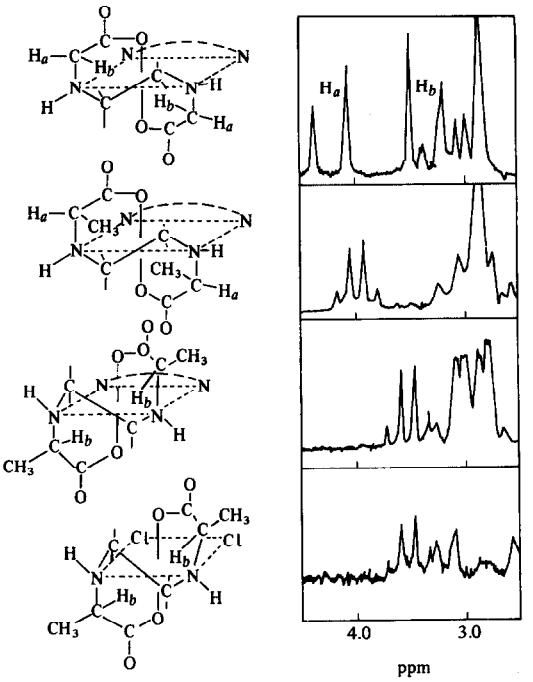

Fig. 4. PMR spectra of (from top to bottom) s-*cis*-[Co(edda)(en)]$^+$, Λ-s-*cis*-[Co(SS-eddp)(en)]$^+$, Δ-s-*cis*-[Co(SS-eddp)(en)]$^+$, and Δ-s-*cis*-[Co(SS-eddp)Cl_2]$^-$. Stereochemical representations are shown on the left.

absolute configuration of SS-eddp the absolute configuration of the s-*cis*-[Co(SS-eddp)Cl_2]$^-$ complex can be assigned based on its PMR spectrum. Only an H_a proton signal is exhibited in the Λ-s-*cis* isomer at 4.0 ppm, while only an H_b proton signal appears in the Δ-s-*cis* isomer at 3.5 ppm. The s-*cis*-[Co(SS-eddp)Cl_2]$^-$ shows only the H_b quartet at 3.5 ppm, and a Δ-absolute configuration is assigned to this complex. Such an assignment of the Δ-absolute configuration is also substantiated by its CD spectrum shown in Fig. 2. The dominant negative Cotton effect shown near 600 nm indicates the Δ-absolute configuration, as in the case for Δ-(−)-s-*cis*-[Co(SS-eddp)(en)]$^+$ or Δ-(−)-s-*cis*-[Co(SS-eddp)(*R*-Pn)]$^+$ complex.[1]

Figure 2 also indicates the electronic absorption spectra for Δ-s-*cis*-[Co(SS-eddp)Cl·H_2O] and Δ-s-*cis*-[Co(SS-eddp)$(H_2O)_2$]$^+$ and their spectra data are summarized in Table 1. Two observations can generally be made: the peaks of band I are symmetrical indicating s-*cis* configurations, and the λ_{max} is shifted towards the shorter wavelength as the chloro ligands are substituted by the aqua ligands, which is in accordance with the spectrochemical series. The CD spectra in Fig. 2 show the negative Cotton effect for the band I absorption, indicating Δ-absolute configurations for those complexes.

It is interesting to find out that only the s-*cis* isomer has been obtained during the preparation of the [Co(SS-eddp)Cl_2]$^-$ complex. In octahedral complexes of the type [M(edda-type ligand)L_2]$^{n+}$, the s-*cis* configuration is generally favoured, while the uns-*cis* configuration is also formed in low yield

Table 1. Electronic absorption spectral data for the cobalt(III) complexes with the SS-eddp ligand

Complex	$\lambda_1{}^a$ $(\varepsilon_1)^b$	λ_2 (ε_2)
Δ-s-*cis*-H[Co(SS-eddp)Cl_2]H_2O	602(172)	421(121)
Δ-s-*cis*-[Co(SS-eddp)Cl·H_2O]	578(134)	408(84)
Δ-s-*cis*-[Co(SS-eddp)$(H_2O)_2$]$^+$	536(130)	388(90)
s-*cis*-[Co(SS-eddp)(*S*-ala)]	530(93) 500sh	370(132)
s-*cis*-[Co(SS-eddp)(Smcy)]	530(99) 500sh	370(147)
Na[Co(SS-eddp)(cy)]	500sh(40)	370(250)

[a] In nm.
[b] In M^{-1} cm^{-1}.

when L_2 is a bidentate ligand.[10] Thus, only the s-*cis* isomer has been found for [Co(SS-eddiv)$(NO_3)H_2O$] and [Co(pren)$(H_2O)_2]^+$ complexes, while both s-*cis* and uns-*cis* isomers have been obtained for $[Co(SS\text{-}eddiv)(en)]^+$ and $[Co(pren)(en)]^+$ complexes,[11,12] where SS-eddiv and pren are, respectively, ethylenediamine-N,N′-di-S-α-isovaleric acid and 2S,2′S-1,1′-(ethane-1,2-diyl) bis(pyrrolidine-2-carboxylate). Ring strain and non-bonded interactions between chelate rings have been cited for the preference for the s-*cis* configuration. On the other hand, the extra stability due to the chelation effect of the bidentate ligands makes the existence of the uns-*cis* configuration possible.[10–13] Octahedral complexes of $[Co(SS\text{-}eddp)L_2]^{n+}$ have yielded both s-*cis* and uns-*cis* isomers when L is a bidentate ligand such as en or amino acid.[1,10] Diacido cobalt(III) complexes of SS-eddp prepared in this work, are the only octahedral complexes of $[Co(SS\text{-}eddp)L_2]^{n+}$ where L is a unidentate ligand.

The substitution reactions of Δ-s-*cis*-$[Co(SS\text{-}eddp)Cl_2]^-$ with L-alanine, S-methyl-L-cysteine and L-cysteine in aqueous media, have resulted in the isolation of the corresponding amino acid complexes with retention of configuration. Three geometrical isomers, s-*cis*-*mer* (meridional), uns-*cis*-*mer*, and uns-*cis*-*fac* (facial) occur (Fig. 5) when an amino acid (aa) is coordinated in the $[Co(SS\text{-}eddp)(aa)]^{n+}$ complex.

The electronic absorption spectrum is useful in differentiating between the facial and meridional isomers: the loss of symmetry from facial (cubic holohedrized symmetry) to meridional (rhombic holohedrized symmetry) is expected to cause a splitting or at least a broadening of the first absorption band.[14] In the electronic absorption spectrum of [Co(SS-eddp)(L-ala)] (Fig. 6), band I and band II appear between 350 and 550 nm. The splitting pattern of the first band having a shoulder near 500 nm indicates that the [Co(SS-eddp)(L-ala)] complex has a meridional geometry of either s-*cis* or uns-*cis*. The PMR spectrum of the [Co(SS-eddp)(L-ala)] complex (Fig. 7) clearly shows an s-*cis* geometry. The methyl regions of this complex show

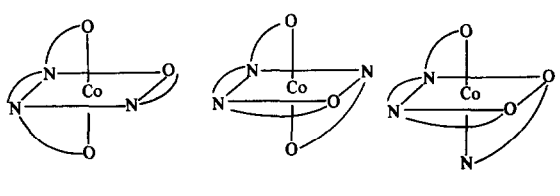

Fig. 5. The configuration isomers of [Co(edda-type)(aa)]$^{n+}$ complexes.

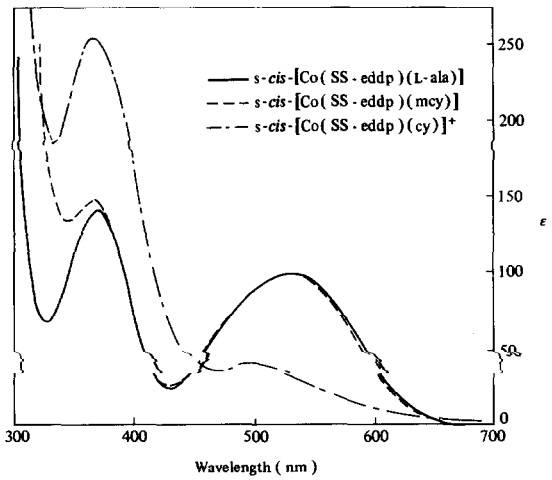

Fig. 6. Electronic absorption spectra of the amino cobalt (III) complexes of SS-eddp.

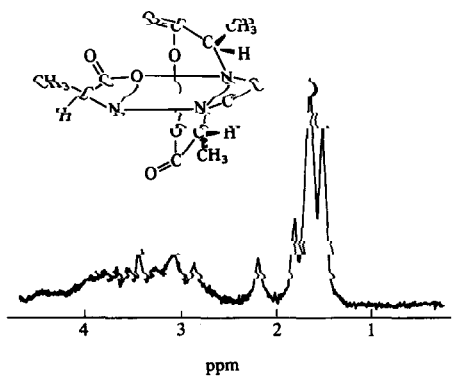

Fig. 7. PMR spectrum of s-*cis*-[Co(SS-eddp)(*S*-ala)].

two methyl doublets with a 2 : 1 intensity, indicating that the loss of C_2 symmetry going from the s-*cis* dichloro cobalt(III) complex to the s-*cis* alanine cobalt(III) complex causes two of the propionato arms of SS-eddp to be no longer equivalent. The doublets at 1.7 and 1.5 ppm are due to the methyl groups of the unequivalent propionato arms. The doublet at 1.5 ppm is distinctive of the L-alanine methyl group in this s-*cis* isomer.

Although S-methyl-L-cysteine has three donor atoms (N, O, S), the IR spectrum of the [Co(SS-eddp)(mcy)] complex shows the coordination of nitrogen and oxygen donor atoms. The C=O stretching band occurs at 1650 cm^{-1} (Table 2), as is typical of the coordinated carboxylate groups. The electronic absorption spectrum (Fig. 6) of this complex shows a similar pattern as the alanine complex; a typical CoN_3O_3 system with a meridional configuration. The PMR spectrum of the complex shown in Fig. 8 presents the methylene protons in the S-methyl-L-cysteinato chelate ring at 3.0 ppm

Table 2. The CO stretching frequencies of the SS-eddp ligand and cobalt(III) complexes

Compound	ν^a(C=O)	Group
SS-eddp	1580	$-CO_2-$
Δ-s-*cis*-H[Co(SS-eddp)Cl_2]H_2O	1620	$-CO_2Co$
s-*cis*-[Co(SS-eddp)(*S*-ala)]	1640	$-CO_2Co$
s-*cis*-[Co(SS-eddp)(Smcy)]	1650	$-CO_2Co$
Na[Co(SS-eddp)(cy)]	1610	$-CO_2-$

[a] In cm^{-1}.

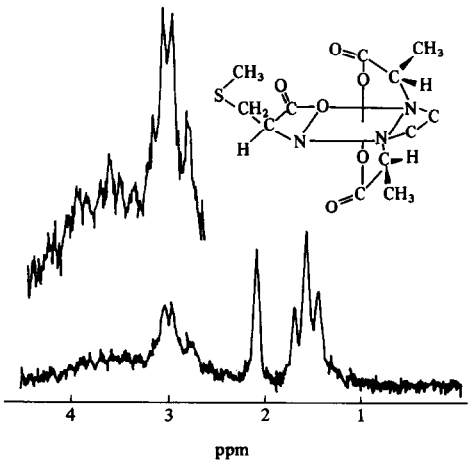

Fig. 8. PMR spectrum of s-*cis*-[Co(SS-eddp)(Smcy)].

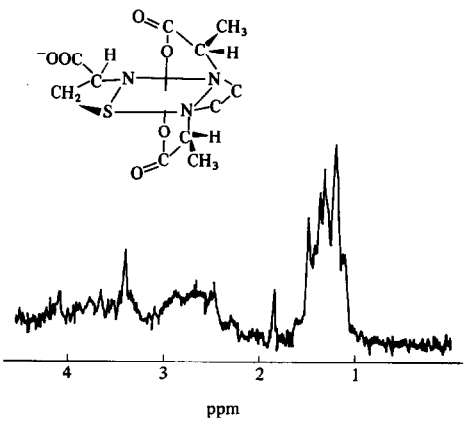

Fig. 9. PMR spectrum of Na[Co(SS-eddp)(cy)].

as a doublet along with the S-methyl protons at 2.1 ppm as a singlet. The methyl groups in the two propionato arms are shown as doublets at 1.4 and 1.6 ppm. If the complex has an uns-*cis* configuration, the PMR spectrum would have been much more complicated.

The IR spectrum provides definite evidence as to which groups of the cysteine are coordinated in Na[Co(SS-eddp)(cy)]. There is no band observed in the 2500 cm^{-1} region (S—H stretching mode), suggesting that the mercaptide group is coordinated at one of two coordination sites. The other site may be occupied by the amino or the carboxylate group. An intense C=O stretching band occurs at 1610 cm^{-1} in the IR spectrum of Na[Co(SS-eddp)(cy)]. This value is consistent with the presence of the free carboxylate ions. The presence of the strong N—H stretching band near 3200 cm^{-1} indicates the fact that the cysteine is coordinated to the cobalt(III) ion through the nitrogen and sulphur atoms.

The electronic absorption spectrum (Fig. 6) of the $[Co(SS\text{-}eddp)(cy)]^-$ complex shows the splitting pattern of the CoN_3O_2S system which is very different from that of the CoN_3O_3 system. The *d–d* spectral data of Table 1 are consistent with pseudooctahedral symmetry, band I corresponding to the low symmetry split components of $^1A_{1g}$–$^1T_{1g}$ and band II to those of $^1A_{1g}$–$^1T_{2g}(O_h)$.[15] In spite of the low position of the mercaptide ion in the spectrochemical series, it coordinates strongly to cobalt(III), but in other cobalt(III) complexes of cysteine the mercaptide group is not always coordinated and there is competition among the three functional groups.[16,17] The PMR spectrum of the $[Co(SS\text{-}eddp)(cy)]^-$ complex (Fig. 9) shows the methyl groups in the two carboxylate arms at 1.2 and 1.4 ppm as doublets, the pattern of which is consistent with the s-*cis* configuration.

REFERENCES

1. L. N. Schoenberg, D. W. Cooke and C. F. Liu, *Inorg. Chem.* 1968, **7**, 2386.
2. M. Sheridan, M. J. Jun and C. F. Liu, *Inorg. Chem.* 1984, **23**, 1485.
3. M. Sheridan, M. J. Jun and C. F. Liu, *Inorg. Chim. Acta* 1983, **69**, 183.
4. M. Sheridan, M. J. Jun and C. F. Liu, *Polyhedron* 1982, **1**, 659.
5. H. Yamatera, *Bull. Chem. Soc. Jpn* 1958, **31**, 95.

6. P. C. Harrington, S. Linke and M. Alexander, *Inorg. Chem.* 1973, **12**, 168.
7. V. Carunch, G. Illumiati and G. Ortagi, *Inorg. Chem.* 1967, **6**, 2168.
8. J. I. Legg and D. W. Cooke, *Inorg. Chem.* 1965, **4**, 1576.
9. W. A. Freeman, *J. Coord. Chem.* 1978, **7**, 197.
10. D. J. Radanovic, *Coord. Chem. Rev.* 1984, **54**, 159.
11. M. Strasak and I. Majer, *Inorg. Chim. Acta* 1983, **7**, 2368.
12. M. Strasak and F. Bachraty, *J. Coord. Chem.* 1984, **13**, 105.
13. M. J. Jun and C. F. Liu, *J. Chem. Soc., Dalton Trans.* 1976, 1031.
14. F. Basolo, C. J. Ballhausen and J. Bjerrum, *Acta Chem. Scand.* 1955, 810; Y. Shimura and R. Thuchida, *Bull. Chem. Soc. Jpn* 1956, **29**, 311.
15. R. A. Wentworth and T. S. Piper, *Inorg. Chem.* 1965, **4**, 709.
16. H. C. Freeman, C. J. Moore, W. G. Jackson and A. M. Sargeson, *Inorg. Chem.* 1978, **17**, 3513.
17. W. G. Jackson, A. M. Sargeson and P. A. Tucker, *J. Chem. Soc., Chem. Commun.* 1977, 199.

Polyhedron Vol. 8, No. 9, pp. 1213–1215, 1989
Printed in Great Britain

0277–5387/89 $3.00+.00
© 1989 Pergamon Press plc

POLYOXOMOLYBDATE–HYDROCARBON INTERACTIONS. SYNTHESIS AND STRUCTURE OF $[(n\text{-}C_4H_9)_4N][Mo_2O_5(C_8H_{13}O_5)]\cdot 0.5(C_2H_5)_2O$, FROM THE REACTION OF 3-HYDROXY-2-BUTANONE WITH $[(n\text{-}C_4H_9)_4N]_2[Mo_2O_7]$

SHUNCHENG LIU and JON ZUBIETA*

Department of Chemistry, State University of New York at Albany, Albany, NY 12222, U.S.A.

(*Received* 23 *August* 1988; *accepted after revision* 23 *November* 1988)

Abstract—Reaction of $[(n\text{-}C_4H_9)_4N]_2[Mo_2O_7]$ with 3-hydroxy-2-butanone (acetoin) in methanol yields $[(n\text{-}C_4H_9)_4N][Mo_2O_5(C_8H_{13}O_5)]\cdot 0.5(C_2H_5)_2O$, a complex with the $[Mo_2O_5]^{2+}$ core and a coordinated 2,3,4,5-tetrahydroxy-2,3,4,5-tetramethylfuranose ring, formed by Aldol condensation and oxidation of acetoin groups. Crystal data: triclinic space group $P\bar{1}$, $a = 11.824(2)$, $b = 12.033(2)$, $c = 12.677(3)$ Å, $\alpha = 83.65(1)$, $\beta = 71.30(1)$, $\gamma = 88.71(1)°$, $V = 1698.0(6)$ Å^3, $Z = 2$, $D_{calc} = 1.37$ g cm^{-3}; 3826 reflections to give $R = 0.0588$.

Coordination complexes of polyoxomolybdates are of interest as models for surface-bound intermediates in heterogeneous catalysis employing solid molybdenum oxides.[1–5] Structurally characterized examples of polyoxomolybdate complexes incorporating simple organic substrate units include $[Mo_8O_{26}(HCO_2)_2]^{6-}$,[6] $[Mo_4O_{14}(OH)CH_2]^{3-}$,[7] $[Mo_8O_{24}(OCH_3)_4]^{4-}$,[8] $[Mo_4O_8(OC_2H_5)_2\{CH_3C(CH_2O)_3\}_2]$[9] and $[Mo_4O_{10}(OCH_3)_6]^{2+}$,[10] and the alkoxy and siloxy derivatives of $[MoO_3(P_3O_9)]^{2-}$[11] and $[Mo_3O_7\{CH_3C(CH_2O)_3\}_2]^{2-}$,[12] and of the niobotungstate $[Nb_2W_4O_{19}]^{4-}$.[13] In the course of our investigations of polyoxomolybdate–carbonyl interactions,[14] we have examined the chemistry of acetoin. As anticipated, the organic substrate is incorporated into a polyoxomolybdate core; however, the acetoin group has undergone an Aldol condensation and oxidation to provide an unusual 2,3,4,5-tetrahydroxy-2,3,4,5-tetramethylfuranose ring coordinated to the $[Mo_2O_5]^{2+}$ core of the product, $[(n\text{-}C_4H_9)_4N][Mo_2O_5(C_8H_{13}O_5)]\cdot 0.5(C_2H_5)_2O$. A closely related dimolybdo–furanose structure has been reported for the lyxose–dimolybdate, $(NH_4)[Mo_2O_5(C_4H_5O_5)]$, formed by the epimerization and ligation of xylose in the presence of ammonium molybdate.[15]

Reaction of $[(n\text{-}C_4H_9)_4N]_2[Mo_2O_7]$ with an equimolar amount of acetoin in methanol, followed by addition of ether, gives colourless, transparent blocks of $[(n\text{-}C_4H_9)_4N][Mo_2O_5(C_8H_{13}O_5)]\cdot 0.5(C_2H_5)_2O$ in 55% yield.† The IR spectrum is characterized by strong bands at 952 and 940 cm^{-1} assigned to ν_s(Mo=O) and ν_{as}(Mo=O), respectively, and a number of features in the 650–900 cm^{-1} range associated with ν(Mo—O—Mo) and ν(Mo—O—alkoxy). The complex crystallizes in the triclinic space group $P\bar{1}$ with $a = 11.824(2)$, $b = 12.033(2)$, $c = 12.677(3)$ Å, $\alpha = 83.65(1)$, $\beta = 71.30(1)$, $\gamma = 88.71(1)°$, $V = 1698.0(6)$ Å^3, $D_{calc} = 1.37$ g cm^{-3}. Structure solution and refinement based on 3826 reflections with $F_o \geqslant 6\sigma(F_o)$ (Mo-K_α, $\lambda = 0.71073$ Å) converged at $R = 0.0588$.‡

The structure of $[Mo_2O_5(C_8H_{13}O_5)]^{1-}$ is shown in Fig. 1, and selected bond lengths and angles are presented in the caption. The structure of the binuclear complex monoanion consists of the well-

* Author to whom correspondence should be addressed.

† Elemental analysis: Found: C, 41.2; H, 7.1; N, 2.00. Calc. for $C_{24}H_{49}NO_{10}Mo_2$: C, 41.0; H, 7.0; N, 1.99%. Ether of crystallization is lost upon drying the crystals in vacuum at room temperature overnight.

‡ Final atomic positional and thermal parameters, bond lengths and angles, and F_o/F_c values have been deposited as supplementary material with the Editor, from whom copies are available on request. Atomic coordinates have also been submitted to the Cambridge Crystallographic Data Centre.

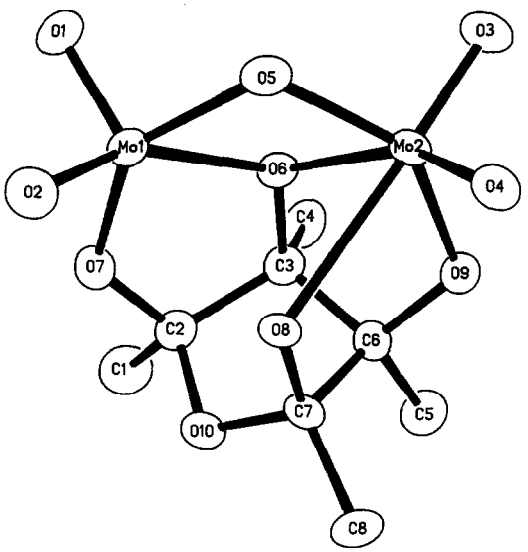

Fig. 1. ORTEP view of the structure of $[Mo_2O_5(C_8H_{13}O_5)]^-$, showing the atom labelling scheme. Selected bond lengths (Å) and angles (°): Mo(1)—O(1), 1.700(5); Mo(1)—O(2), 1.691(5); Mo(1)—O(5), 1.945(5); Mo(1)—O(6), 2.725(4); Mo(1)—O(7), 1.934(5); Mo(1)—O(8), 2.709(5); Mo(2)—O(3), 1.687(5); Mo(2)—O(4), 1.729(5); Mo(2)—O(5), 1.894(5); Mo(2)—O(6), 2.151(5); Mo(2)—O(8), 2.485(4); Mo(2)—O(9), 1.933(5); O(6)—C(3), 1.426(9); O(7)—C(2), 1.371(10); O(8)—C(7), 1.448(8); O(9)—C(6), 1.441(9); O(10)—C(2), 1.475(10); O(10)—C(7), 1.395(9). O(1)—Mo(1)—O(8), 168.8(3); O(3)—Mo(2)—O(8), 168.6(2); O(2)—Mo(1)—O(8), 168.8(3); O(3)—Mo(2)—O(8), 168.6(2); O(2)—Mo(1)—O(6), 150.6(2); O(4)—Mo(2)—O(6), 153.7(2); O(5)—Mo(1)—O(7), 141.8(2); O(5)—Mo(2)—O(9), 142.3(2); O(10)—C(2)—C(3), 104.0(6); C(2)—C(3)—C(6), 103.6(6); C(3)—C(6)—C(7), 100.6(6); C(6)—C(7)—O(10), 103.6(6); C(7)—O(10)—C(2), 109.1(5).

documented $[Mo_2O_5]^{2+}$ core,[16] ligated to an organic moiety formally derived from 2,3,4,5-tetrahydroxy-2,3,4,5-tetramethylfurane (**1**). The tetradentate

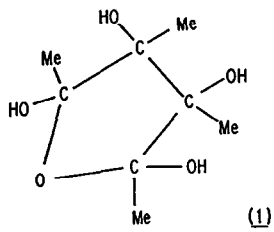

(1)

ligand coordinates to the Mo centres through four alkoxy oxygen donors, two of which, O(7) and O(9), are terminal, while O(6) and O(8) assume bridging modes.

The most unusual feature of the structure is the geometry associated with O(8), which exhibits unsymmetrical bridging with unusually long bond distances of 2.485(4) and 2.709(5) Å to Mo(2) and Mo(1), respectively. Such Mo—O bond distances are outside the range of 2.10–2.20 Å, characteristic for bridging alkoxides and clearly indicate that O(8) is present as the protonated alcohol form.[17] This observation is also consistent with the charge requirements for a mononegative anion $[Mo_2O_5(C_8H_{13}O_5)]^-$, which require that the ligand be trinegative $(C_8H_{13}O_5)^{3-}$, rather than the fully deprotonated form. The ^1H NMR spectrum of $[(n\text{-}C_4H_9)_4N][Mo_2O_5(C_8H_{13}O_5)]$ exhibits a singlet at 8.63 ppm, integrating for a single proton, which confirms the presence of the alcoholic proton.

Although the overall coordination geometry may be most simply described in terms of two $[MoO_6]$ octahedra sharing a face defined by O(5), O(6) and O(8), the detailed geometry about the molybdenum centres suggests an alternative description based on edge-sharing square-pyramids, with an additional weak axial interaction. In fact, the bond strengths associated with Mo(1)—O(8) and Mo(2)—O(8) are *ca* 0.1 and 0.2, respectively.[18]

The ligand exhibits a number of unusual bond lengths: C(2)—O(7) is significantly shorter than the average of other C—O(alkoxy) distances (1.37(1) vs 1.44(1) Å), while the C(2)—O(10) distance of 1.475(10) Å is considerably longer than C(7)—O(10), 1.395(9) Å. This observation suggests some contribution from the acyclic form (**2**) to the over-

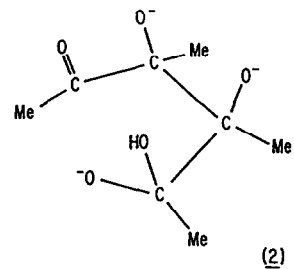

(2)

all ligand structure, a feature possibly related to the ring closure via an Aldol condensation.

It is noteworthy that acetoin undergoes spontaneous dimerization in organic solvents to give the six-membered cyclic bis-hemiacetal, 2,5-dihydroxy-2,3,5,6-tetramethyldioxane (**3**).[19] In contrast, the

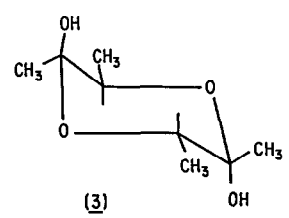

(3)

ligand moiety observed in the structure of $[(n\text{-}C_4H_9)_4N][Mo_2O_5(C_8H_{13}O_5)]$ implicates an Aldol

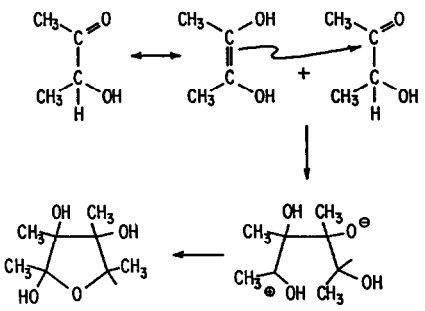

Scheme 1.

condensation mechanism to produce the furanose ring, coupled to oxidation of a carbon site by the dimolybdate precursor (see Scheme 1). Thus, the polyoxomolybdate not only serves to oxidize the ligand substrate, but also to promote the Aldol condensation pathway. We are investigating the chemistry of related α-hydroxyketones and α-diketones, where such oxidation processes and enolate mechanisms appear to be general.[6,14]

Acknowledgement—This work was supported by NSF grant CHE8514634 to J. Zubieta.

REFERENCES

1. R. K. Graselli and J. D. Burrington, *Adv. Catal.* 1981, **30**, 133.
2. H.-F. Liu, R.-S. Liu, K. Y. Liew, R. E. Johnson and J. H. Lunsford, *J. Am. Chem. Soc.* 1984, **106**, 4117.
3. C. J. Machiels, U. Chrowdry, R. H. Staley, F. Ohuchi and A. W. Sleight, in *Catalytic Conversions of Synthetic Gas and Alcohols to Chemicals* (Edited by R. G. Herman). Plenum Press, New York (1984).
4. V. W. Day and W. G. Klemperer, *Science* 1985, **228**, 533.
5. M. T. Pope, *Heteropoly and Isopoly Oxometalates.* Springer-Verlag, New York (1983).
6. R. D. Adams, W. G. Klemperer and R.-S. Liu, *J. Chem. Soc., Chem. Commun.* 1979, 256.
7. V. W. Day, M. F. Fredrich, W. G. Klemperer and R.-S. Liu, *J. Am. Chem. Soc.* 1979, **101**, 491.
8. E. M. McCarron III and R. L. Harlow, *J. Am. Chem. Soc.* 1983, **105**, 6179.
9. A. J. Wilson, W. T. Robinson and C. J. Wilkins, *Acta Cryst.* 1983, **C39**, 54.
10. S. Liu, S. N. Shaikh and J. Zubieta, *Inorg. Chem.* 1987, **26**, 4303.
11. W. G. Klemperer, V. V. Mainz, R.-C. Wang and S. Yang, *Third Chem. Cong. of North America*, June 1988, Toronto: *Inorg. Abstr.* 265; V. W. Day, W. G. Klemperer, C. Schwartz and R.-C. Wang, in *Surface Organometallic Chemistry: The Molecular Approach to Surface Science and Catalysis* (Edited by J. M. Basset and B. Gates), p. 173. Kluwer, Dordrecht (1988).
12. L. Ma, S. Liu and J. Zubieta, unpublished results.
13. V. W. Day, W. G. Klemperer and C. Schwartz, *J. Am. Chem. Soc.* 1987, **109**, 6030.
14. S. Liu, S. N. Shaikh and J. Zubieta, *Inorg. Chem.* 1989, **28**, 175.
15. G. E. Taylor and J. M. Waters, *Tetrahedron Lett.* 1981, **22**, 1277.
16. R. H. Holm, *Chem. Rev.* 1987, **87**, 1401.
17. T. C. Hsieh and J. Zubieta, *Inorg. Chim. Acta* 1987, **127**, L31.
18. J. C. Bart and V. Ragaini, in *Proceedings of the Third International Conference on the Chemistry and Uses of Molybdenum* (Edited by H. F. Barry and P. C. H. Mitchell). Climax Molybdenum Company, Ann Arbor, Michigan (1979).
19. J. C. Jochims and G. Taigel, *Tetrahedron Lett.* 1968, 5483.

Polyhedron Vol. 8, No. 9, pp. 1217–1221, 1989
Printed in Great Britain

0277-5387/89 $3.00+.00
© 1989 Pergamon Press plc

THE YTTRIUM ION AS A TEMPLATE IN THE SYNTHESIS OF THE MACROCYCLIC AND ACYCLIC COMPLEXES FORMED IN THE REACTIONS WITH 2,6-DIACETYLPYRIDINE AND HYDRAZINE*

WANDA RADECKA-PARYZEK

Faculty of Chemistry, Adam Mickiewicz University, 60-780 Poznań, Poland

(*Received* 3 *November* 1988; *accepted* 24 *November* 1988)

Abstract—The macrocyclic tetradentate NNNN donor yttrium nitrate complex of formula $[YL^1(NO_3)_3]\cdot 2H_2O$, where L^1 is 2,5,11,14-tetramethyl-3,4,12,13,19,20-hexaazatricyclo[13.3.1.1^{6,10}]eicosa-1(19),2,4,6,8,10(20),11,13,15,17-decaene, has been prepared by the condensation of 2,6-diacetylpyridine with hydrazine in the presence of a metal ion template and characterized by spectral and analytical data. Different experimental conditions (the type of counterion, ratio of starting materials) lead to the isolation of acyclic tetradentate NNNO or terdentate NNN donor complexes of yttrium with uncondensed carbonyl or amino groups. They are formulated as $[YL^2(H_2O)_2]Cl_3\cdot 2H_2O$ and $[YL^2(H_2O)_2](ClO_4)_3\cdot 2H_2O$, where L^2 is (6-acetyl-pyrid-2-yl)methyl ketone azine, and $[YL^3(NO_3)_3]\cdot 2H_2O$, $[YL^3_2]Cl_3\cdot 2H_2O$ and $[YL^3_2](ClO_4)_3\cdot 2H_2O$, where L^3 is 2,6-diacetylpyridinedihydrazone. The 2,6-diacetylpyridine (L) complexes isolated as minor products, are regarded as possible intermediates in the formation of macrocyclic L^1 and ring-opened L^2 complexes of yttrium.

Interest in exploring the encapsulation of the rare earth elements by polyoxa- and polyaza-macrocycles like coronands and cryptands, has continually increased since they can be used for lanthanide separation, for the stabilization of unusual oxidation states, for the systematic investigation of the coordinating properties of these elements and for probing the metal ion binding sites of biological macromolecules.[1]

The coordination of yttrium by polyoxa-macrocycles has been little studied. The synthetic and structural results of research on complexation of yttrium with crown ethers were recently reported.[2]

In previous papers we reported the preparation and characterization of scandium and heavier lanthanide (Tb–Lu) complexes containing the 14-membered tetradentate hexaaza macrocyclic ligand.[3] The lighter lanthanides (La–Gd) have been found to be ineffective as templates for the synthesis of this macrocycle under similar conditions, but effective in the synthesis of N donor macrocycles with greater ring size.[4] We have concluded that the important factor which must be taken into account in the synthesis of the macrocyclic compounds with the aid of a metal ion is the ratio of cation diameter to ligand cavity size. As a continuation of our studies on the effectiveness of metal ions of varying radius and electron configuration in the synthesis of polyaza-macrocyclic compounds with different ring size, we extended our investigations to the yttrium ion, which has not so far been examined in this respect. We now report what we believe to be the first example of the template action of yttrium ion (which is similar in size to Dy and Ho) in the synthesis of a macrocyclic compound. We have found that different experimental conditions lead to the isolation of macrocyclic (coronate) or acyclic (podate) complexes of yttrium.

EXPERIMENTAL

The hydrated yttrium salts (chloride, perchlorate or nitrate) were prepared by dissolving the 99.99% Y_2O_3 in the appropriate acid. The solutions were

* Presented in part at the Workshop on the Basic and Applied Aspects of Rare Earths, Venice, Italy, 26–27 May, 1988

Table 1. Analytical data for L^1, L^2, L^3 and L complexes of yttrium

Compound	Calculated %C	%H	%N	Found %C	%H	%N
$[YL^1(NO_3)_3]\cdot 2H_2O$	34.3	3.5	20.0	34.2	3.5	20.0
$[YL^2(H_2O)_2]Cl_3\cdot 2H_2O$	36.6	4.4	9.5	36.4	4.5	9.3
$[YL^2(H_2O)_2](ClO_4)_3\cdot 2H_2O$	27.6	3.3	7.2	27.6	3.3	7.0
$[YL^3(NO_3)_3]\cdot 2H_2O$	21.5	3.4	22.3	21.4	3.4	22.2
$[YL^3_2]Cl_3\cdot 2H_2O$	35.2	4.9	22.8	35.0	4.9	22.7
$[YL^3_2](ClO_4)_3\cdot 2H_2O$	26.8	3.7	17.4	26.7	3.7	17.2
$[YL(NO_3)_3]\cdot 2H_2O$	22.8	2.8	11.8	22.4	2.7	11.3
$[YL_2(H_2O)_2]Cl_3\cdot 2H_2O$	36.4	4.4	4.7	37.1	4.3	4.9
$[YL_2(H_2O)_2](ClO_4)_3\cdot 2H_2O$	27.5	3.8	3.6	27.4	3.8	3.5

evaporated and precipitates recrystallized from methanol.

Preparation of the yttrium complexes. General procedure

The complexes were prepared by the template synthesis of the yttrium chloride, perchlorate or nitrate with 2,6-diacetylpyridine and hydrazine in ethanol, in the reactant ratios 2 : 1 : 1, 1 : 1 : 2, 1 : 2 : 4 and 1 : 3 : 6. The reaction mixtures were heated under reflux with stirring for 24 h. The resulting precipitates were filtered off, washed with hot ethanol and ether, and dried under vacuum.

The macrocyclic complex of L^1 is formed only in the reaction of yttrium nitrate with 2,6-diacetylpyridine and hydrazine in the 2 : 1 : 1 molar ratio of starting materials. Under the same reaction conditions, yttrium chloride and perchlorate gave the acyclic 1 : 1 complexes (6-acetyl-pyrid-2-yl)methyl ketone azine (L^2). Small amounts of yttrium nitrate, chloride or perchlorate complexes of 2,6-diacetylpyridine (L) were also obtained from these reactions.

From the reactions of yttrium nitrate, chloride and perchlorate with 2,6-diacetylpyridine and hydrazine in the molar ratios 1 : 1 : 2, 1 : 2 : 4 and 1 : 3 : 6, the 2,6-diacetylpyridinedihydrazone (L^3) complexes were isolated with the metal-to-ligand stoichiometry of 1 : 1 for nitrate and 1 : 2 for chloride and perchlorate as counteranions, irrespective of the molar proportions of starting materials.

Table 1 reports analytical data of the compounds.

Measurements

These were as previously described.[2]

RESULTS AND DISCUSSION

The 14-membered hexaaza-macrocyclic complex of yttrium has been prepared via template condensation of 2,6-diacetylpyridine with hydrazine in the presence of $Y(NO_3)_3\cdot 6H_2O$ in the ratio of reactants 1 : 1 : 2. Less than the stoichiometric amounts of 2,6-diacetylpyridine and hydrazine were required to prevent the formation of 2,6-diacetylpyridinedihydrazone. The formulation of this complex as $[YL^1(NO_3)_3]\cdot 2H_2O$ follows from spectral data (IR, UV–vis, ^1H NMR and MS) and thermal and elemental analysis. The complex is a yellow air-stable solid, soluble in CH_3CN and DMSO.

The IR spectrum of this complex in the 4000–200 cm^{-1} region confirms the formation of the macrocyclic compound by the absence of uncondensed functional group (NH_2, C=O) stretching modes of starting materials and the appearance of a strong absorption band at 1620 cm^{-1}, attributable to the coordinated C=N stretching frequencies. The high and low energy pyridine bands are observed at 1575, 1460, 630 and 420 cm^{-1} suggesting coordination of pyridine.[5] A broad diffuse band of strong intensity in the 3700–3200 cm^{-1} region may be assigned to the O—H stretching vibration for lattice water. The

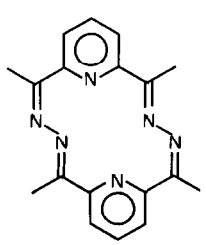

L^1

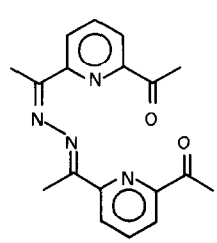

L^2

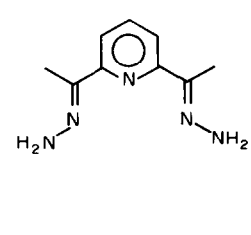

L^3

absorption characteristic of coordinated water does not appear. The thermogravimetric analysis confirms this observation indicating the loss of two molecules of water at 40–70°C.

The IR spectrum of this complex demonstrates the presence of coordinated nitrates. The band characteristic of ionic nitrates at 1390 cm^{-1} does not appear. The two new bands associated with the asymmetric stretch appear near 1320 and 1495 cm^{-1}. The magnitude of the separation (175 cm^{-1}) is typical of bidentate bonding of the nitrates.[6]

The electronic spectra of acetonitrile solution of the complex exhibit bands at *ca* 268 and 333 nm, attributable to the $\pi \rightarrow \pi^*$ transitions of coordinated macrocycle.

The ^1H NMR spectrum of the yttrium complex of L^1 obtained in DMSO-d_6 solution shows the pyridine protons at δ 7.9–8.2 and methyl protons at δ 2.28 and 2.56. The integrated relative intensities are in good agreement with the required ratio 1 : 1 : 1, consistent with the proposed formulation of this complex.

The mass spectrum of this complex provides strong evidence for the presence of a macrocyclic compound showing the highest fragment at m/z 318, corresponding to the molecular weight of the uncoordinated macrocycle.

On the basis of the spectral data and thermogravimetric analysis, along with molecular model inspection, it seems reasonable to assign the tentative coordination number of 10 for the yttrium ion in this complex. The metal ion is presumably coordinated to the four nitrogen atoms of the hexaaza 14-membered macrocycle and to oxygen atoms of three bidentate nitrate groups. The synthesis and crystal structure of the 12-membered crown ether complex of yttrium nitrate with such a high coordination number was recently reported.[7]

Attempts to prepare this macrocyclic compound with the aid of yttrium chloride or perchlorate was unsuccessful. In the reactions in which 2,6-diacetylpyridine was allowed to react with hydrazine in the presence of yttrium chloride or perchlorate, the ring closure did not occur. Instead, the ring-opened complexes of (6-acetyl-pyrid-2-yl)methyl ketone azine (L^2) were formed. The complexes are yellow solids, moderately soluble in acetonitrile. They have the composition $[YL^2(H_2O)_2]Cl_3 \cdot 2H_2O$ and $[YL^2(H_2O)_2](ClO_4)_3 \cdot 2H_2O$.

It should be noted, here, that ligand L^2 appears to be identical with the compound isolated earlier, as an intermediate in the preparative route to the free L^1 macrocycle.[8]

The IR spectra of the two complexes of L^2 are very similar and analysed similarly to that of the free ligand. The band characteristic of the C=N stretching mode, indicating the partial condensation reaction, is shifted by *ca* 30 cm^{-1} from 1600 cm^{-1} in the free ligand to lower frequencies, suggesting the coordination by the nitrogen atom. The profile of the pyridine ring vibration observed in the 1600–1400 cm^{-1} region and the strong band at 1000 cm^{-1} are characteristic of coordinated pyridine. An important feature is the occurrence of the medium absorption bands at 1700 and 1670 cm^{-1}, assigned to the C=O stretching modes. In the IR spectrum of the free ligand this absorption appears at 1695 cm^{-1}. The shift of this band to lower frequencies in the complexes indicates the coordination through the oxygen atom. The position of the other C=O band at a slightly higher frequency than in the free ligand suggests that one of the two carbonyl groups remain uncoordinated.

The ^1H NMR spectra of these complexes in acetonitrile-d_3 solution confirm this observation. The appearance of two methyl proton signals of the CH_3CO groups at δ 2.72 and 2.85, instead of one signal observed at δ 2.72 for the free ligand, and the small downfield shift of the CH_3CN methyl and pyridine proton resonances from δ 2.4 and 7.7–8.3, respectively, in the free azine to δ 2.45 and 7.9–8.4 in the complexes, is assumed to be a consequence of coordination of the ligand to the yttrium ion through the three nitrogen donor atoms and one oxygen atom of the two carbonyl groups.[9]

The presence of uncoordinated perchlorates is inferred from the absence of the degenerate stretching and bending modes of ClO_4^- at 1100 cm^{-1}. A broad diffuse band in the 3500–3200 cm^{-1} region and weak absorptions at 860 and 540 cm^{-1} suggest the presence of lattice and coordinated water. This is supported by the results of the thermogravimetric analysis, which indicates a loss of two molecules of water at 35–65°C and two water molecules at 140–190°C for these complexes.

The electronic spectra of yttrium chloride and perchlorate complexes of L^2, for solutions in acetonitrile, consist of three bands at 238–240, 258–262 and 296–300 nm. The differences in the spectra of the complexes and free ligand can be attributed to changes in energy levels of the ligand orbitals on coordination.

The tentative coordination number of six is proposed for podate yttrium chloride and perchlorate complexes of (6-acetylpyrid-2-yl)methyl ketone azine. The coordination sphere is filled by the tetradentate NNNO donor ligand with sufficient interaction of two water molecules.

The failure of the 2,6-diacetylpyridine and hydrazine system to undergo complete condensation and cyclization, in the presence of yttrium chloride and perchlorate, is presumably attributed to the greater

flexibility of the podands than coronands and to the different complexing properties of the counterions involved in the template synthesis. The nitrate ions, contrary to the chlorides and perchlorates, are known to be very good complexing agents towards the rare earth elements. The yttrium ion has therefore been found to be effective for the synthesis of the 14-membered hexaaza-macrocyclic ligand, but the interaction between the metal ion and the counteranion seems to play the decisive role in the stabilization of the macrocyclic complex.

In addition to the ring-closed and ring-opened complexes discussed above, a small number of 2,6-diacetylpyridine (L) complexes were isolated from the reactions of 2,6-diacetylpyridine with hydrazine in the presence of yttrium nitrate, chloride and perchlorate in the reactant ratio 1 : 1 : 2. They are yellow microcrystalline compounds, soluble in polar solvents. The complexes have the compositions $[YL(NO_3)_3]\cdot 2H_2O$, $[YL_2(H_2O)_2]Cl_3\cdot 2H_2O$ and $[YL_2(H_2O)_2](ClO_4)_3\cdot 2H_2O$.

The evidence for the coordination of the carbonyl oxygen atoms and pyridine nitrogen atom to the yttrium ion comes from the IR and ^1H NMR spectra of the complexes.

The most diagnostic feature is the shifting of the C=O absorption band to lower wavenumbers by about 40 cm^{-1} relative to the ligand (1700 cm^{-1}), resulting from a decrease in the C=O double bond character owing to coordination. The band assigned to the pyridine ring vibrations are shifted to higher frequencies, which is a good indication of the coordination of the heterocyclic nitrogen atom.

The signals of methyl protons at δ 2.75 and pyridine protons at δ 8.18 observed in the ^1H NMR spectrum of 2,6-diacetylpyridine appear at δ 2.88–2.90 and δ 8.2–8.6 in the spectra of yttrium complexes.

The IR spectra of the complexes indicate the presence of ionic perchlorate and chloride (unsplit band at 1100 cm^{-1} and absence of the band at *ca* 230 cm^{-1} characteristic of Ln—Cl interaction) and coordinated bidentate nitrato groups (bands at 1310 and 1465 cm^{-1}).

The absorptions characteristic of lattice water at 3700–3200 cm^{-1} occur in the IR spectra of nitrate, chloride and perchlorate complexes of yttrium. In addition, in the spectrum of the nitrate complex, a weak absorption is found at *ca* 880 and 540 cm^{-1} as expected for coordinated water. The thermogravimetic analysis confirms this observation indicating the loss of two molecules of water at 40–80°C for all the complexes and, additionally, in the case of the chloride and perchlorate complexes, the loss of two water molecules at 150–190°C.

Treatment of the yttrium complexes of L with hydrazine in ethanol at 75°C for 24 h leads to isolation of the L^1 complex of yttrium nitrate and L^2 complexes of yttrium chloride and perchlorate. Thus the yttrium complexes of 2,6-diacetylpyridine are regarded as possible intermediates in the partial or total condensation reaction leading to the formation of coronate L^1 or podate L^2 complexes. The coordination of the metal ion to the pyridine nitrogen and the two oxygen atoms of the carbonyl groups makes the carbonyl more susceptible to nucleophilic attack by the hydrazine nitrogen atom.

From the reaction of yttrium nitrate, chloride and perchlorate with 2,6-diacetylpyridine and hydrazine in 1 : 1 : 2, 1 : 2 : 4 and 1 : 3 : 6 molar ratios of starting materials, the yellow air-stable complexes of 2,6-diacetylpyridinedihydrazone (L^3) were isolated. They are formulated as $[YL^3(NO_3)_3]\cdot 2H_2O$, $[YL_2^3]Cl_3\cdot 2H_2O$ and $[YL_2^3](ClO_4)_3\cdot 2H_2O$.

The IR spectra of these complexes were analysed in comparison with that of the free ligand, which was prepared and described previously.[10] These three complexes all give very similar spectra except for anion and water vibrational modes, but they are different from the spectra of the free ligand. The C=N absorption band observed in the spectrum of the ligand at 1600 cm^{-1} is shifted by 50–60 cm^{-1} to lower wavenumbers upon complexation, suggesting the involvement of the nitrogen lone pair in coordination with the yttrium ion. The N—N frequency found at 1150 cm^{-1} in the free ligand, increased by 50 cm^{-1} in the complexes. It may be explained by the coordination of one of the nitrogen atoms from each N—N bond to the metal.[11] Bonding of the pyridine nitrogen atom is shown by the increase in frequency of higher and lower energy pyridine ring vibrations (1570, 950, 640, 400 cm^{-1}) by about 20–45 cm^{-1} in the complexes. The non-bonding of the NH_2 nitrogen atom is confirmed by the persistence of the NH_2 vibration occurring at 1635 cm^{-1} in the free ligand, and the shifting of the antisymmetric and symmetric stretching vibrations of the NH_2 groups from 3360 and 3200 cm^{-1} to higher frequencies in the metal complexes. The weak absorption band at 375–385 cm^{-1} may be assigned to the metal–nitrogen stretching vibrations.

The ^1H NMR spectra of these complexes indicate the bonding mode discussed above, showing a small downfield shift of the methyl and pyridine proton resonances from δ 2.25 and 7.82, respectively, in the free ligand, to δ 2.32–2.38 and δ 8.12–8.25 in the complexes.

The broad diffuse band in the 3600–3500 cm^{-1} region is observed for all these complexes and is assigned to the stretching and bending modes for lattice water. The thermogravimetric analysis in-

dicates for yttrium complexes of 2,6-diacetylpyridinedihydrazone, loss of two molecules of water at 30–60°C.

The spectra of the chloride and perchlorate complexes of L^3 do not show absorption bands characteristic of coordinated counterions. An IR absorption attributable to the ClO_4^- anion occurs as unsplit bands at 1100 and 626 cm^{-1}. The spectrum of the yttrium nitrate complex of L^3 indicates the presence of the nitrato groups coordinating in a bidentate fashion by the appearance of two bands at 1310 and 1480 cm^{-1}, instead of one band at 1390 cm^{-1} typical for ionic nitrates.

The electronic spectra of L^3 complexes of yttrium recorded in acetonitrile, show similar features and contain intense and medium absorption bands with maxima at 285–287 nm and 352–360 nm. The free ligand shows an intense band at 273 nm with a shoulder at 305 nm. The differences between the spectra of the complexes and free ligand can be attributed to the metal–ligand interaction.

On the basis of available evidence, it can be concluded that 2,6-diacetylpyridinedihydrazone acts as a terdentate NNN donor ligand. The stoichiometry of the complexes depends on the type of counterion. The coordination number of six is assigned for the yttrium complex of hydrazone with non-coordinating chlorides and perchlorates, assuming that the coordination sphere is filled by two molecules of ligand. With the small but strongly coordinating nitrates as counterions, the yttrium forms a complex with a 1 : 1 metal to hydrazone ratio, and the coordination number of nine is achieved by the incorporation of three bidentate nitrato groups into the coordination sphere.

Acknowledgement—Financial support from the Polish Academy of Sciences (Project CPBP No. 01.12.4.18) is gratefully acknowledged.

REFERENCES

1. J.-C. Bünzli, in *Handbook on the Physics and Chemistry of Rare Earths* (Edited by K. A. Gschneidner Jr and L. Eyring), Vol. 9. Elsevier, Amsterdam (1987).
2. R. Rogers and E. J. Voss, *J. Coord. Chem.* 1988, **16**, 405 and refs therein.
3. W. Radecka-Paryzek, *Inorg. Chim. Acta* 1979, **35**, L349; W. Radecka-Paryzek, *Inorg. Chim. Acta* 1981, **52**, 261.
4. W. Radecka-Paryzek, *Inorg. Chim. Acta* 1980, **45**, L147; W. Radecka-Paryzek, *Inorg. Chim. Acta* 1981, **54**, L251; W. Radecka-Paryzek, *Inorg. Chim. Acta* 1985, **109**, L21.
5. N. S. Gill, R. H. Nuttal and D. E. Scaife, *J. Inorg. Nucl. Chem.* 1961, **18**, 79.
6. J.-C. Bünzli and D. Wessner, *Inorg. Chim. Acta* 1980, **44**, L55.
7. R. D. Rogers and L. K. Kurihara, *J. Incl. Phenom.* 1986, **4**, 351.
8. W. Radecka-Paryzek, *Inorg. Chim. Acta* 1979, **34**, 5.
9. J. Lewis and T. D. O'Donoghue, *J. Chem. Soc., Dalton Trans.* 1980, 743.
10. W. Radecka-Paryzek and E. Jankowska, *Inorg. Chim. Acta* 1987, **134**, 179; W. Radecka-Paryzek, E. Jankowska and E. Luks, *Polyhedron* 1988, **7**, 439.
11. M. R. Harrison and D. Nicholls, *Transition Met. Chem.* 1984, **9**, 144.

Polyhedron Vol. 8, No. 9, pp. 1223–1226, 1989
Printed in Great Britain

0277–5387/89 $3.00+.00
© 1989 Pergamon Press plc

ACCELERATION OF LIGAND EXCHANGE BY COORDINATED NITRATE IN POLYPYRIDYL RUTHENIUM COMPLEXES

JERRY L. WALSH* and CREGG C. YANCEY†

Department of Chemistry, University of North Carolina at Greensboro, Greensboro, NC 27412, U.S.A.

(*Received* 19 *September* 1988; *accepted* 30 *November* 1988)

Abstract—The rate of substitution of L by a chloride ion or acetonitrile in *cis*-$[Ru(bpy)_2(L)(X)]^+$ (X = NO_3; L = pyridine, acetonitrile; bpy = 2,2′-bipyridine) in low polarity solvents, is greatly enhanced over the rates observed for complexes with X = Cl, NO_2, CF_3CO_2 and *p*-$CH_3C_6H_4SO_3$. For X = NO_3, rate constants and a mechanism for formation of the final product, *cis*-$Ru(bpy)_2Cl_2$ or *cis*-$[Ru(bpy)_2(CH_3CN)_2]^{2+}$, are presented. The rate enhancement for the nitrato complex is attributed to its ability to act as a bidentate ligand.

The influence of non-exchanging ligands on the rate of ligand substitution in coordination complexes has been studied extensively.[1] Often the influence can be related to the effect of donor or acceptor properties of the non-exchanging ligand on the electronic nature of the metal centre. The thermal and photochemical substitution reactions of polypyridyl ruthenium complexes are usually predictable and well-behaved, exhibiting trends expected in comparison to other systems.[2–4] In general, ruthenium(II) and ruthenium(III) complexes are relatively inert.[3] Facile ligand exchange occurs thermally only for solvent complexes, especially oxygen donor solvents, and complexes with weakly coordinating anions in polar solvents.[2]

The facile substitution of nitrato ligands of the complexes, $[Ru(bpy)_2(L)(NO_3)]^+$ (L = CH_3CN, pyridine (py); bpy = 2,2′-bipyridine), by anions in low polarity solvents is described here. However, surprisingly, the nitrato ligand induces rapid substitution of relatively inert ligands, such as acetonitrile and pyridine, in the subject complexes.

EXPERIMENTAL

Ruthenium complexes were prepared by literature methods.[4–6]‡ Acetonitrile and dichloromethane were purified by standard methods.[7] Other chemicals were reagent grade and used as received.

Spectral and kinetic data were obtained on a Varian DMS-100 spectrophotometer equipped with a thermostatable, programmable multicell holder and a Houston Model 164 recorder; temperature was controlled with a Neslab RTE-8 bath/circulator. Cyclic voltammetry experiments were performed with a Bioanalytical Systems model CV-1B analyzer using electrolyte solutions of 0.1 M tetraethylammonium perchlorate in acetonitrile, or 0.2 M tetrabutylammonium hexafluorophosphate in dichloromethane. All manipulations were performed under reduced light conditions because of the light sensitivity of these compounds.[4]

Rate constants at 25.0 ± 0.2°C were determined from absorbance (A) vs time (t) data taken from recorded spectra at appropriate wavelengths. Data showed that all reactions were first-order in ruthenium complex for two or more half-lives. Linear least-squares fitting at $\ln(A - A_0)$ vs t was used to obtain first-order rate constants. Where consecutive reactions occurred, the rate constants were different enough to avoid interference when data was carefully selected. Reported rate constants are the average of three or more trials with a typical standard deviation of < 20% of the reported values.

For the reaction of $[Ru(bpy)_2(py)(NO_3)]^+$ with Cl^-, the infinity values for runs with less than a stoichiometric amount of chloride were obtained

* Author to whom correspondence should be addressed.
† ACS–PRF Project SEED Fellow.
‡ Spectral analyses suggest that all ruthenium complexes involved are in the *cis* configuration.

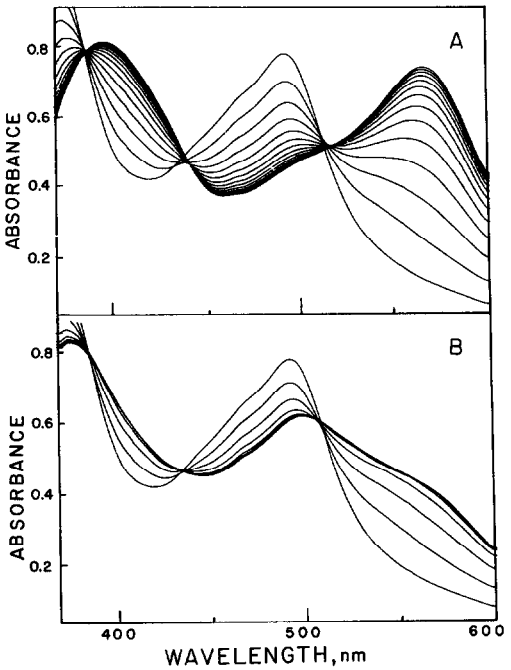

Fig. 1. Reaction of *cis*-$[Ru(bpy)_2(py)(NO_3)]^+$ with chloride ion in acetone at 25°C, recorded at 44 min intervals. Concentration of *cis*-$[Ru(bpy)_2(py)(NO_3)]^+ = 1.2 \times 10^{-4}$ M. (A) $[Cl^-] = 4.8 \times 10^{-4}$ M; (B) $[Cl^-] = 0.96 \times 10^{-4}$ M.

from identical runs with more than the stoichiometric amount of chloride, such that the infinity values are those expected for complete transformation to $Ru(bpy)_2Cl_2$. In doing so, the data fit first-order behaviour very well.

RESULTS

When tetrabutylammonium chloride is added to dichloromethane or acetone solutions of $[Ru(bpy)_2(py)(NO_3)]^+$, the solution spectrum (Fig. 1) changes smoothly from that of the nitrato complex ($\lambda_{max} = 486$ nm) to that of $Ru(bpy)_2Cl_2$ ($\lambda_{max} = 562$ nm), with isosbestic points at 365, 422 and 510 nm. This suggests that the one step transformation shown in the following equation has occurred.

$$[Ru(bpy)_2(py)(NO_3)]^+ + 2Cl^- \longrightarrow Ru(bpy)_2Cl_2 + py + NO_3^-.$$

The reaction is first-order ($k = 7.3 \times 10^{-5}$ s^{-1} at 25.0°C) in ruthenium complex but zero-order in chloride. An interesting feature of the reaction kinetics is that with less than a 1:2 mole ratio of ruthenium to chloride, the spectral changes follow typical first-order behaviour until all chloride is depleted. The reaction then comes to an immediate halt [Fig. 1(B)]. The reaction is not influenced by elimination of atmospheric oxygen, the presence of hydroquinone or ascorbic acid as reducing agents, by solvent purification, or by use of different samples of the ruthenium complex. Under the same conditions, $[Ru(bpy)_2(CH_3CN)(NO_3)]^+$ reacts extremely rapidly with the chloride ion and two well separated steps are observable. The first is complete on an ordinary mixing time scale, giving an intermediate with $\lambda_{max} = 535$ nm. This species reacts more slowly with chloride by a first-order reaction ($k = 3.0 \times 10^{-4}$ s^{-1} at 25°C) to give $Ru(bpy)_2Cl_2$. With more polar solvents, like ethanol, solvolysis of the nitrato ligand occurs rapidly and $[Ru(bpy)_2(L)(S)]^{2+}$ (S = solvent) and/or $[Ru(bpy)_2(L)Cl]^+$ are obtained as the products.

Other anions, such as Br^- and SCN^-, substitute similarly to chloride giving $Ru(bpy)_2X_2$ (X = Br, SCN) as final products. Related complexes, $[Ru(bpy)_2(py)(X)]^+$ (X = Cl, *p*-$CH_3C_6H_4SO_3$, CF_3CO_2, NO_2) are unreactive or at least much less reactive ($t_{1/2} > 5$ days) than the nitrato complex under the same conditions.

The reaction of $[Ru(bpy)_2(L)(NO_3)]^+$ (L = CH_3CN, py) with chloride in acetonitrile solution yields a mixture of products but, in pure acetonitrile, $[Ru(bpy)_2(CH_3CN)_2]^{2+}$ ($\lambda_{max} = 425$ nm) is the observed product. For L = CH_3CN, a one step reaction is observed. With L = py, two steps are observed (Fig. 2) with an intermediate which has a spectrum very similar to that of $[Ru(bpy)_2(CH_3CN)(NO_3)]^+$ in acetonitrile. The rate of the first step ($k = 7.2 \times 10^{-5}$ s^{-1}) is identical to that for chloride substitution. The rate at which the intermediate is transformed to $[Ru(bpy)_2$

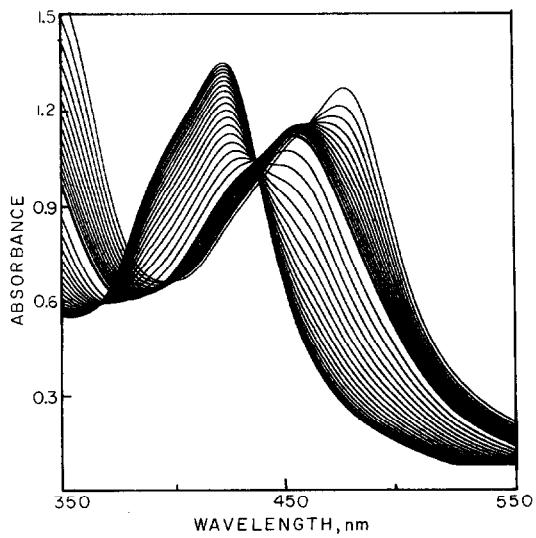

Fig. 2. Reaction of *cis*-$[Ru(bpy)_2(py)(NO_3)]^+$ with acetonitrile solvent at 25°C, recorded at 30 min, then 120 min intervals.

$(CH_3CN)_2]^{2+}$ is the same as for $[Ru(bpy)_2(CH_3CN)(NO_3)]^+$ ($k = 7.5 \times 10^{-6}$ s^{-1}).

Each of the above reactions was also monitored by cyclic voltammetry.* All species involved exhibit at least pseudo-reversible behaviour. The cyclic voltammetry results confirmed the spectral analyses. Reaction of $[Ru(bpy)_2(py)(NO_3)]^+$ ($E_{1/2} = 0.94$ V) with chloride in dichloromethane, showed a one step transformation to $Ru(bpy)_2Cl_2$ ($E_{1/2} = 0.36$ V). The same reaction for $[Ru(bpy)_2(CH_3CN)(NO_3)]^+$ exhibits an intermediate ($E_{1/2} = 0.56$ V) which then reacts to form $Ru(bpy)_2Cl_2$ at rates consistent with spectral data. In acetonitrile, $[Ru(bpy)_2(py)(NO_3)]^+$ reacts to form an intermediate ($E_{1/2} = 0.98$ V) which then produces $[Ru(bpy)_2(CH_3CN)_2]^{2+}$ ($E_{1/2} = 1.41$ V). In this case, a second product, probably $[Ru(bpy)_2(py)(CH_3CN)]^{2+}$ ($E_{1/2} = 1.3$ V) is observed, possibly the result of the higher ruthenium complex or supporting electrolyte concentration used for cyclic voltammetry compared to spectral analysis. A one step reaction is observed for the reaction of $[Ru(bpy)_2(CH_3CN)(NO_3)]^+$ ($E_{1/2} = 0.98$ V) with acetonitrile to form $[Ru(bpy)_2(CH_3CN)_2]^{2+}$ ($E_{1/2} = 1.41$ V).

In pure dichloromethane or acetone, $[Ru(bpy)_2(py)(NO_3)]^+$ is stable for days. However, $[Ru(bpy)_2(CH_3CN)(NO_3)]^+$ is reasonably stable in acetone but a significant amount of green oxo-bridged species is formed in a matter of hours in dichloromethane. Chloride ion substitution into $[Ru(bpy)_2(py)(H_2O)]^{2+}$ in acetone occurs in a reaction which is first-order in complex and zero-order in chloride ($k = 1.0 \times 10^{-3}$ s^{-1}).

DISCUSSION

The nitrato complexes $[Ru(bpy)_2(L)(X)]^+$ (L = py, CH_3CN; X = NO_3) undergo relatively rapid ($t_{1/2} < 200$ min) ligand exchange, as shown in the following equation,

$$[Ru(bpy)_2(L)(NO_3)]^+ + 2L' \longrightarrow [Ru(bpy)_2(L')_2]^{n+} + L + NO_3^-$$

[L = py, CH_3CN; L′ = Cl ($n = 0$); L′ = CH_3CN ($n = 2$)],

whereas, similar species (L = py; X = Cl, NO_2, CF_3CO_2, p-$CH_3C_6H_4SO_3$) are unreactive, showing little to no reaction in 5 days. The spectral data and kinetic results are consistent with the mechanism shown in Scheme 1.

$$[Ru(bpy)_2(L)(NO_3)]^+ \underset{k_{-1}}{\overset{k_1}{\rightleftharpoons}} \mathbf{I} + L \quad (1)$$

$$\mathbf{I} + L' \xrightarrow{k_2} [Ru(bpy)_2(L')(NO_3)]^+ \quad (2)$$

$$[Ru(bpy)_2(L')(NO_3)]^+ + L' \xrightarrow{k_3} [Ru(bpy)_2(L')_2]^{2+} + NO_3^- \quad (3)$$

Scheme 1.

Reaction (1) represents reversible formation of a short-lived intermediate, **I**. No net reaction occurs for $[Ru(bpy)_2(py)(NO_3)]^+$ when L′ is absent. For L = CH_3CN, **I** may provide a pathway for decomposition to oxo-bridged products as well as substitution. When L′ is present, reaction (1) becomes rate-controlling as **I** reacts rapidly with L′. The rate of this reaction depends on the identity of L but very little on L′. For L = py, k_1 (L′ = Cl) is 7.3×10^{-5} s^{-1} and k_1 (L′ = CH_3CN) is 7.2×10^{-5} s^{-1}. For L = CH_3CN, k_1 is very fast. For L = py and L′ = Cl, k_2 and k_3 are presumably greater than k_1, so only starting complex and final product are spectrally observable. For L = CH_3CN and L′ = Cl, k_1 and k_2 are greater than k_3, so the intermediate, $Ru(bpy)_2(Cl)NO_3$, accumulates during the reaction.

For acetonitrile substitution (L′ = CH_3CN), k_3 is slower than for chloride substitution, probably a reflection of the charge effect in low polarity solvent. In this case, steps (1) and (2) lead to no net reaction for L = CH_3CN. For L = py, steps (1) and (2) lead to the formation of $[Ru(bpy)_2(CH_3CN)(NO_3)]^+$, which then undergoes the same transformation as when this species is the starting material.

The question arises as to what feature of the nitrato ligand leads to such facile substitution of pyridine and acetonitrile in $[Ru(bpy)_2(L)(NO_3)]^+$. Since the spectral properties of $[Ru(bpy)_2(py)(NO_3)]^+$ are very similar to those of the other $[Ru(bpy)_2(py)(X)]^+$ complexes,[4] the electronic nature of the ruthenium centre in the ground state reactants appears to be similar. The rates of various reactions would be consistent with solvation of the nitrato ligand followed by anation. However, the products are not the same for the nitrato reaction as for reaction of the aquo complex. Thus, this reaction pathway can be ruled out.

Two features which distinguish nitrate from the other X ligands are its ability to act as a bidentate ligand and its behaviour as an oxidizing agent. Nitrate has been shown to be capable of oxidizing $[Ru(bpy)_2(py)(H_2O)]^{2+}$ in aqueous acidic solution.[8] Thus, a short-lived ion-paired redox species, such as $[Ru(bpy)_2(L)(O)^{2+},NO_2^-]$, may be generated. Ion pairing is undoubtedly important in the low polarity

* Reduction potentials differ by small amounts from literature values due to differences in solvent and/or added electrolyte.

solvents used. Following substitution by L′, recombination of the oxo moiety with NO_2^- would lead to the net substitution observed, including the absence of oxidized products. Substitution reactions carried out by redox intermediates are quite common in coordination chemistry.[9] Many are characterized by unusual kinetic features,[2c,9] but the net process involves unusually rapid substitution. The lack of influence by reducing agents and what appears to be a reasonably robust[5] coordination sphere in $[Ru(bpy)_2(py)(O)]^{2+}$ would argue against this mechanism.

Although nitrite and trifluoroacetate may behave as bidentate ligands, the tendency of these and other X ligands to do so is less than that of nitrate.[10] With the relatively small bite angle of the nitrato ligand, the monodentate nitrato ligand of $[Ru(bpy)_2(py)(NO_3)]^+$ may bind to produce a pseudo-seven coordinate transition state. Loss of L and formation of a bidentate nitrato ligand leads to a six coordinate intermediate, **I**. The intermediate would then accept L′ to generate $[Ru(bpy)_2(L')(NO_3)]^+$. A strongly ion-paired chloride or an acetonitrile from the solvent cage is readily available for coordination. Further substitution of the nitrato ligand by L′ would give the final product. Other examples[11,12] of nitrate acceleration of *cis* ligand substitution have been reported for chromium(III)–amine and cobalt(III)–amine and –oxalato complexes. It is not obvious in all cases that a nitrato ligand in the coordination sphere of the metal is the active species.[12] When coordinated nitrate is thought to be present, a chelating mechanism similar to that proposed for **I** in Scheme 1 was proposed. In the present case, there appears to be no doubt that nitrate is coordinated during L substitution, since it remains in the coordination sphere after L substitution, and the presence of coordinated nitrate accelerates the rate of L substitution.

In summary, the nitrato ligand induces significant labilization of the ligands *cis* to it in *cis*-$[Ru(bpy)_2(L)(NO_3)]^+$ complexes. A three step mechanism, involving an intermediate which is extremely susceptible to ligand addition, leads to facile substitution of the nitrato ligand and its neighbour.

Acknowledgement—The financial support of the donors of the American Chemical Society–Petroleum Research Fund, particularly through Project SEED, are gratefully acknowledged.

REFERENCES

1. (a) B. Douglas, D. H. McDaniel and J. J. Alexander, *Concepts and Models of Inorganic Chemistry*, 2nd edn. John Wiley, New York (1983); (b) F. Basolo and R. G. Pearson, *Mechanism of Inorganic Reactions*, 2nd edn. John Wiley, New York (1968); (c) D. Katakis and G. Gordon, *Mechanism of Inorganic Reactions*. John Wiley, New York (1987); (d) T. P. Dasgupta, *MTP Int. Rev. Sci.: Inorg. Chem.*, Series Two, 1984, **9**, 63.
2. (a) S. S. Isied and H. Taube, *Inorg. Chem.* 1976, **15**, 3070; (b) L. R. Allen, P. P. Craft, B. Durham and J. L. Walsh, *Inorg. Chem.* 1987, **26**, 53; (c) J. Chang, S. Meyerhoffer, L. R. Allen, B. Durham and J. L. Walsh, *Inorg. Chem.* 1988, **27**, 1602.
3. (a) B. Bosnich and F. P. Dwyer, *Aust. J. Chem.* 1966, **19**, 2235; (b) H. Taube, *Comments Inorg. Chem.* 1981, **1**, 17.
4. B. Durham, J. L. Walsh, C. L. Carter and T. J. Meyer, *Inorg. Chem.* 1980, **19**, 860.
5. B. Moyer and T. J. Meyer, *Inorg. Chem.* 1981, **21**, 436.
6. B. P. Sullivan, D. J. Salmon and T. J. Meyer, *Inorg. Chem.* 1978, **7**, 3334.
7. A. J. Gordon and R. A. Ford, *The Chemists's Companion*. John Wiley, New York (1972).
8. B. A. Moyer and T. J. Meyer, *J. Am. Chem. Soc.* 1979, **101**, 1327.
9. (a) M. L. Tobe, *Inorganic Reaction Mechanisms*. Thomas Nelson, London (1972); (b) D. E. Richardson and H. Taube, *Inorg. Chem.* 1979, **18**, 549.
10. F. A. Cotton and G. Wilkinson, *Advanced Inorganic Chemistry*, 4th edn. John Wiley, New York (1980).
11. (a) G. Guastalla and T. W. Swaddle, *Can. J. Chem.* 1974, **52**, 527; (b) G. Guastalla and T. W. Swaddle, *Inorg. Chem.* 1974, **13**, 61.
12. S. Aygen, H. Hanssum and R. van Eldik, *Inorg. Chem.* 1985, **24**, 2853 and refs therein.

Polyhedron Vol. 8, No. 9, pp. 1227–1232, 1989
Printed in Great Britain

0277–5387/89 $3.00+.00
© 1989 Pergamon Press plc

AMINOCARBOXYLATO CHELATE RING CONFORMATION INFLUENCE ON THE OPTICAL ACTIVITY OF COBALT(III) COMPLEXES—II.† THE OPTICAL ACTIVITY OF THE *CIS*(NO_2),*TRANS*(NH_2)-(*R*-ALANINATO)(1,3-DIAMINOPROPANE)DINITROCOBALT(III) DIASTEREOMERS AND THE CRYSTAL STRUCTURE OF THE Λ-DIASTEREOMER

N. JURANIČ, M. J. MALINAR, K. ANDJELKOVIČ and M. B. ČELAP‡

Institute of Chemistry, Faculty of Sciences, University of Beograd, 11001 Beograd, P.O. Box 550, Yugoslavia

and

R. HERAK

"Boris Kidrič" Institute of Nuclear Sciences, 11001 Beograd, P.O. Box 522, Yugoslavia

and

Lj. MANOJLOVIČ-MUIR

Chemistry Department, University of Glasgow, Glasgow G12 8QQ, U.K.

and

D. VUČELIČ and M. VUČIČ

Institute of General and Physical Chemistry, Beograd, Yugoslavia

(*Received* 25 *July* 1988; *accepted* 12 *December* 1988)

Abstract—On investigating the relation between optical activity of aminocarboxylato cobalt(III) complexes and aminocarboxylato chelate ring conformation, it was found that the diastereomers of *cis*(NO_2),*trans*(NH_2)-(*R*-alaninato)(1,3-diaminopropane)dinitrocobalt(III) exhibit almost symmetrical circular dichroic (CD) spectra, indicating a weak vicinal and conformational contribution of the *R*-alaninato ligand to the optical activity of the diastereomers. The crystal structure analyses revealed that in both diastereomers, the *R*-alaninato chelate ring adopts a strained envelope conformation, with the side methyl group in an equatorial position.

The vicinal contribution of the diastereomers of aminocarboxylatocobalt(III) complexes to the optical activity has been considered as an important one, while the conformational effect of an α-aminocarboxylato ring was considered to be of little importance.[2] However, we have recently shown[1] that in the complexes containing bulky nitro ligands, unequal steric constraints imposed on aminocarboxylato chelates in a diastereomeric pair produce quite different conformations of the chelates, which are reflected in different conformational and vicinal contributions to the optical activity. Specifically, we have established that in the Λ-*cis*(NO_2),*trans*(NH_2)-bis(*S*-aminocarboxylato)dinitrocobaltate(III) diastereomers, the δ-envelope conformation of a chelate ring and the equatorial position of the corresponding ring

† For part I, see ref. 1.

‡ Author to whom correspondence should be addressed.

side group result in a weak conformational and vicinal contribution to the optical activity. Contrary to this, in the Δ-isomer the λ-twist conformation of an *S*-aminocarboxylato chelate ring and the axial position of the corresponding ring side group induce a considerably greater contribution to the optical activity. Hence, the aminocarboxylato chelate ring conformation is of utmost importance for the optical activity of diastereomers. Therefore, we are now undertaking extensive examination of the influence of the aminocarboxylato chelate ring conformation on the optical activity of cobalt(III) complexes. In the investigation we are dealing with mixed ligand complexes which contain, in addition to an aminocarboxylato chelate, sterically demanding ligands. Such ligands are expected to force the aminocarboxylato ring to adopt a strained conformation, the geometry of which is then reasonably insensitive to intermolecular interactions. This is very necessary when the solution optical activity is going to be related to the conformation of a chelate in a solid complex.

In the present work we are investigating the *cis* (NO_2),*trans*(NH_2)-(*R*-alaninato)(1,3-diaminopropane)dinitrocobalt(III) diastereomers which contain sterically demanding nitro and 1,3-diaminopropane ligands. These complexes are closely related to the previously examined *cis*(NO_2),*trans* (NH_2)-bis(aminocarboxylato)dinitrocobaltate(III) complexes,[1] but in the former ones a greater strain is expected to be exerted on the aminocarboxylato chelate. To establish the chelate rings conformations, we have undertaken the crystal structure determination of Λ-*cis*(NO_2),*trans* (NH_2)-(*R*-alaninato)(1,3-diaminopropane)dinitrocobalt(III) dihydrate. The crystal structure of the corresponding Δ-isomer has been reported by us earlier.[3]

RESULTS

Optical activity

CD spectra in the region of the first *d–d* transition of the investigated diastereomers are presented in Fig. 1. For comparison, CD spectra of the related bis(*R*-alaninato) and bis(1,3-diaminopropane) complexes are also given. It is seen that by substituting one *R*-alaninato ligand by 1,3-diaminopropane in the *cis*(NO_2),*trans*(NH_2)-bis(*R*-alaninato)dinitrocobaltate(III) diastereomers, the optical activity of the resulting isomers is considerably reduced and the corresponding CD curves become almost symmetrical.

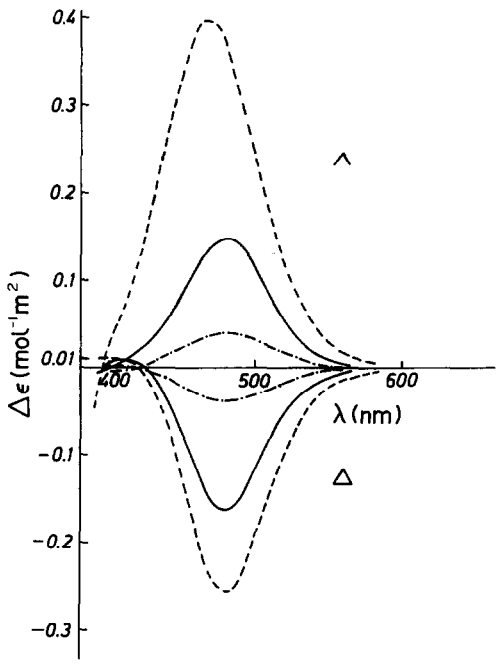

Fig. 1. CD spectra of the Λ- and Δ-isomers of the *cis*(NO_2),*trans*(NH_2)-$[Co(NO_2)_2(R\text{-ala})_2]^-$ (– – –), *cis* (NO_2),*trans*(NH_2)-$[Co(NO_2)_2(R\text{-ala})(tn)]$ (——) and *cis* (NO_2)-$[Co(NO_2)_2(tn)_2]^+$ (– · – · –) complexes.

Crystal structure

The crystal structure of Λ-*cis*(NO_2),*trans*(NH_2)-(*R*-alaninato)(1,3-diaminopropane)dinitrocobalt (III) dihydrate consists of discrete neutral complex molecules and water molecules, joined together by the system of O—H···O and N—H···O weak hydrogen bonds. An ORTEP drawing of the complex molecule with the numbering scheme of the atoms is given in Fig. 2. Bond distances and angles are given in Table 1. Atomic coordinates, anisotropic thermal parameters, intermolecular contacts involving hydrogen atoms, and observed and calculated structure factors are presented as supplementary material.

The geometry of the complex molecule is in agreement with previously reported data for related complexes.[3,4] All the bond lengths and angles in the coordination polyhedron of cobalt(III), as well as in the *R*-alaninato and 1,3-diaminopropane ligands, are unexceptional. The same holds for the nitro groups. The angle between the least-squares mean planes through the cobalt atom and the corresponding nitro group is 106°. The Co—NO_2 distance *trans* to the carboxylato oxygen is significantly shorter than this one *trans* to an amino group, in accordance with our previous observations of π-bond participation in NO_2-bonding in cobalt(III) complexes.[5]

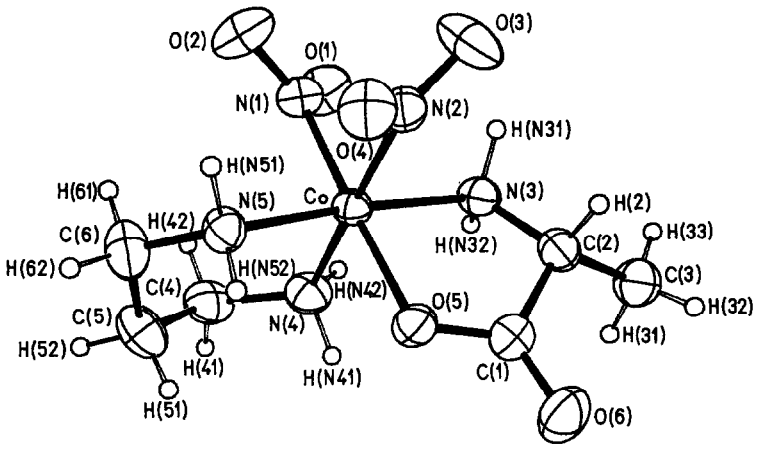

Fig. 2. ORTEP drawing of the complex molecule with the atomic numbering scheme.

The conformation of *R*-alaninato five-membered and 1,3-diaminopropane six-membered rings, expressed by the relevant conformational parameters,[6] are given in Table 2. The analysis of these data shows that *R*-alaninato chelate adopts the λ-envelope conformation, with the methyl group in the equatorial position. The same conformation of the *R*-alaninato chelate was found earlier in the Δ-diastereomer.[3]

Due to the strong repulsion between 1,3-diaminopropane and the methyl group from the *R*-alaninato ligand, the conformation of the 1,3-diaminopropane ring in the investigated Λ-isomer is a distorted highly strained chair.

DISCUSSION

From the crystal structures of the two diastereomers, it can be seen that the *R*-alaninato che-

Table 1. Interatomic distances (Å) and angles (°) with ESDs in parentheses

Co—O(5)	1.919(2)	Co—N(1)	1.899(2)
Co—N(2)	1.953(2)	Co—N(3)	1.964(2)
Co—N(4)	1.980(3)	Co—N(5)	1.963(2)
O(1)—N(1)	1.231(3)	O(2)—N(1)	1.234(3)
O(3)—N(2)	1.220(3)	O(4)—N(2)	1.234(3)
O(5)—C(1)	1.284(3)	O(6)—C(1)	1.225(4)
N(3)—C(2)	1.481(4)	N(4)—C(4)	1.477(4)
N(5)—C(6)	1.466(4)	C(1)—C(2)	1.530(4)
C(2)—C(3)	1.514(4)	C(4)—C(5)	1.490(5)
C(5)—C(6)	1.507(5)		
O(5)—Co—N(1)	177.3(1)	O(5)—Co—N(2)	91.7(1)
O(5)—Co—N(3)	83.8(1)	O(5)—Co—N(4)	88.5(1)
O(5)—Co—N(5)	88.9(1)	N(1)—Co—N(2)	88.7(1)
N(1)—Co—N(3)	93.5(1)	N(1)—Co—N(4)	91.1(1)
N(1)—Co—N(5)	93.8(1)	N(2)—Co—N(3)	88.9(1)
N(2)—Co—N(4)	179.0(1)	N(2)—Co—N(5)	88.6(1)
N(3)—Co—N(4)	90.2(1)	N(3)—Co—N(5)	172.2(1)
N(4)—Co—N(5)	92.4(1)	Co—O(5)—C(1)	116.9(2)
Co—N(1)—O(1)	118.5(2)	Co—N(1)—O(2)	121.0(2)
O(1)—N(1)—O(2)	120.5(2)	Co—N(2)—O(3)	120.0(2)
Co—N(2)—O(4)	120.3(2)	O(3)—N(2)—O(4)	119.7(2)
Co—N(3)—C(2)	109.4(2)	Co—N(4)—C(4)	121.1(2)
Co—N(5)—C(6)	122.9(2)	O(5)—C(1)—O(6)	122.8(3)
O(5)—C(1)—C(2)	115.2(2)	O(6)—C(1)—C(2)	122.0(3)
N(3)—C(2)—C(1)	108.3(2)	N(3)—C(2)—C(3)	112.9(2)
C(1)—C(2)—C(3)	114.4(2)	N(4)—C(4)—C(5)	112.7(3)
C(4)—C(5)—C(6)	112.7(3)	N(5)—C(6)—C(5)	111.9(3)

Table 2. Conformational parameters of chelate rings in the Λ-*cis*(NO_2),*trans*(NH_2)-(*R*-alaninato)(1,3-diaminopropane)dinitrocobalt(III)

(a) Puckering parameters[6]

Ring	Atoms	Puckering amplitude (Å)	ϕ(°)	θ
1	Co, O(5), C(1), C(2), N(3)	0.271	140.3	
2	Co, N(4), C(4), C(5), C(6), N(5)	0.532	358.3	159.2

(b) Torsion angles

Co—O(5)—C(1)—C(2)	3.7	N(5)—Co—N(4)—C(4)	31.2
O(5)—C(1)—C(2)—N(3)	−20.6	Co—N(4)—C(4)—C(5)	−52.7
C(1)—C(2)—N(3)—Co	26.8	N(4)—C(4)—C(5)—C(6)	68.0
C(2)—N(3)—Co—O(5)	−20.9	C(4)—C(5)—C(6)—N(5)	−67.0
N(3)—Co—O(5)—C(1)	10.0	C(5)—C(6)—N(5)—Co	51.9
		C(6)—N(5)—Co—N(4)	−31.5

(c) Displacements (Å) of the atoms from their least-squares mean planes

Ring 1	Co	−0.107	N(3)	0.169	C(2)	−0.165	C(1)	0.052
	O(5)	0.051	C(3)	0.557				
Ring 2	Co	−0.094	N(4)	0.151	C(4)	−0.260	C(5)	0.312
	C(6)	−0.254	N(5)	0.146				

late ring adopts a strained λ-envelope conformation in both. This is a consequence of the repulsion of the *R*-alaninato methyl group from the nitro group in the Δ-isomer, and from 1,3-diaminopropane in the Λ-isomer. Hence, the nitro group and 1,3-diaminopropane ligands have fixed the amino-carboxylato chelate ring conformations. This gave the opportunity for the interpretation of the solution CD spectra on the basis of the crystal structures.

CD spectra of the examined diastereomers could be well explained by means of the Quadrant Rule for the conformational and vicinal contributions to the optical activity of octahedral complexes.[7] According to the rule, the *R*-alaninato λ-envelope conformation is expected to induce a weak negative contribution to the optical activity, as it may be concluded from Fig. 3. 1,3-Diaminopropane adopts different conformations in the two diastereomers. In the investigated Λ-isomer the conformation is a highly strained distorted chair, while in the Δ-isomer it is an almost ideal chair. However, according to the same rule, no significant conformational contribution to the optical activity is expected (Fig. 3). Therefore, almost symmetrical CD spectra of the diastereomers are observed, with only slightly stronger negative dichroism of the Δ-isomer, due to the *R*-alaninato λ-envelope chelate conformation.

Especially interesting is the large change of the optical activity when in the Λ-*cis*(NO_2),*trans*(NH_2)-bis(*R*-alaninato)dinitrocobalt(III) diastereomers one *R*-alaninato ligand is substituted by 1,3-diaminopropane (Fig. 1), which is connected with the change of the *R*-alaninato conformation from the

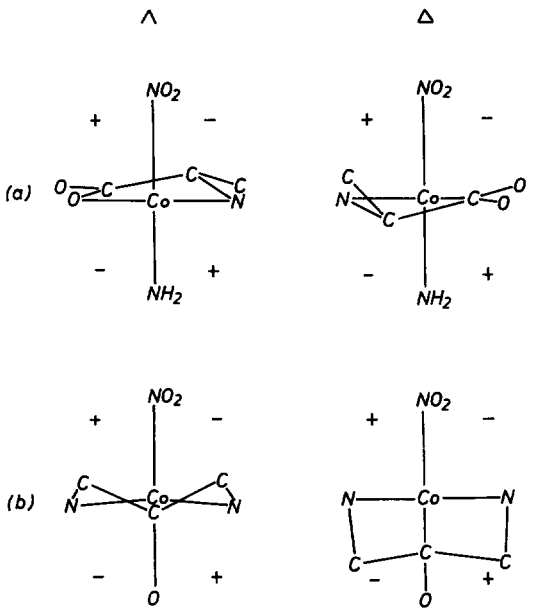

Fig. 3. Skeletal atom projection of the *R*-alaninato (a) and 1,3-diaminopropane (b) ligands in the investigated isomers according to the Quadrant Rule for ligand conformational and vicinal contributions to the optical activity of octahedral complexes.

δ-twist to λ-envelope one. This is in accordance with the findings in our previous paper,[1] in which we have concluded that the λ-twist conformation of an *S*-aminocarboxylato chelate ring induces a large negative contribution to the optical activity, or consequently, by symmetry, that the δ-twist conformation of the *R*-alaninato aminocarboxylato chelate ring has a large positive contribution.

In the Λ-isomer the λ-envelope conformation of the *R*-alaninato chelate ring is preserved upon the substitution of an *R*-alaninato by a 1,3-diaminopropane ligand, and the resulting optical activity of the Λ-*cis*(NO_2),*trans*(NH_2)-(*R*-alaninato)(1,3-diaminopropane)dinitrocobalt(III) isomer is an almost average value of those in the corresponding bis(*R*-alaninato) and bis(1,3-diaminopropane) complexes (Fig. 1).

EXPERIMENTAL

Preparation

Λ-*cis*(NO_2),*trans*(NH_2)-(*R*-alaninato)(1,3-diaminopropane)dinitrocobalt(III) dihydrate was obtained by the procedure previously described by us.[3]

CD spectra

Spectra of the investigated complexes were recorded by a JASCO Dichrograph Model 500 A, using 2×10^{-3} M aqueous solutions.

X-ray analysis

The specimen used for X-ray crystal structure analysis was an orange crystal of dimensions $1.08 \times 0.52 \times 0.68$ mm. All measurements were made at room temperature (~ 22°C) with Mo-K_α radiation, $\lambda = 0.71069$ Å, on an Enraf–Nonius CAD 4F diffractometer equipped with a graphite monochromator.

Crystal data: $[Co(NO_2)_2(C_3H_6NO_2)(C_3H_{10}N_2)] \cdot 2H_2O$, $M_r = 349.2$; orthorhombic; space group $P2_12_12_1$; $a = 9.369(1)$, $b = 10.567(1)$, $c = 14.231(1)$ Å; $U = 1408.9(2)$ Å^3; $Z = 4$; $D_o = 1.56$, $D_c = 1.657$ g cm^{-3}; $F(000) = 728$; μ(Mo-K_α) = 12.57 cm^{-1}.

Unit cell dimensions were determined by a least-squares fit to the setting angles of 23 reflections with $13 < \theta < 17°$. The space group was determined from the systematic absences and confirmed by the shape of a Patterson function and structure analysis.

The intensities of 4447 reflections with $2 < \theta < 30°$ were measured from θ–2θ scans of $(0.80 + 0.35 \tan\theta)°$ in θ, and background was estimated by extending the scans of both ends by 25%. The scans speeds were adjusted to give $\delta I/I > 0.03$ subject to a time limit of 90 s. A standard reflection remeasured every 2 h showed a continuous drop in intensity, amounting to 17% at the end of data collection. All reflections in the h range from −13 to 13, k from 0 to 14 and l from 0 to 20 were measured. Corrections were made for decomposition, Lorentz polarization and absorption effects, the latter by an empirical method,[8] which gave transmission factors on F of 0.84–1.38. Rejecting systematic absences and merging duplicate measurements gave 4082 hkl and $\bar{h}kl$ structure amplitudes, $I \geqslant \sigma(I)$, which were used in subsequent calculations.

The structure was solved by Patterson and difference Fourier methods and refined by full-matrix least-squares, minimizing the function $\Sigma w(|F_o| - |F_c|)^2$, where $w = 1/\sigma^2(|F_o|)$. After isotropic refinement of all non-hydrogen atoms, the structure amplitudes were calculated for values of polarity factor, η,[9] 1 and −1, giving R factors of 0.082 and 0.089, respectively. The model of the correct absolute configuration, which was also in accordance with the configuration deduced from the configuration of *R*-alanine, was further refined. The hydrogen atoms of the complex molecule were included in the structural model in the calculated positions, with C—H and N—H bonds of 0.96 Å, while those belonging to the water molecules were calculated at the positions from the difference Fourier map. All hydrogen atoms were allowed to ride on the atoms to which they are bonded, with $U(H) = 1.2U$ of the corresponding atom. The refinement of 183 parameters including the polarity factor, η, and extinction coefficient, r^*, defined by Larson,[10] converged at $R = 0.041$ and $R_w = 0.047$, with $\eta = 1.04(3)$ and $r^* \times 10^{-3} = 0.72(7)$, and the largest parameter/shift error ratio was 0.05. In the final difference electron density synthesis, the function values varied from −0.47 to 0.54 e Å^{-3}, with most of the largest positive peaks situated in the vicinity of the cobalt atom. Neutral atom scattering factors and complex anomalous dispersion corrections were taken from ref. 11.

All calculations were performed on a GOULD SEL 32/27 minicomputer using the GX program package.[12]

REFERENCES

1. N. Juranić, M. J. Malinar, P. N. Radivojša, S. Zarić, D. Vučelić, M. Vučić and M. B. Ćelap, *Polyhedron* 1988, **7**, 1153.
2. F. S. Richardson, *Inorg. Chem.* 1972, **11**, 2366.
3. M. J. Malinar, R. Herak, M. B. Ćelap, N. Pavlović, S. Milić and D. Stojanov, *Bull. Soc. Chim. (Beograd)* 1981, **46**, 303.
4. R. Herak, *A. Yugoslav Centre Cryst.* 1980, **15**, 1.
5. R. Herak, N. Juranić and M. B. Ćelap, *J. Chem. Soc., Chem. Commun.* 1980, 660.
6. D. Cremer and J. A. Pople, *J. Am. Chem. Soc.* 1975, **97**, 1374.

7. B. Bosnich and J. McB. Harrowfield, *J. Am. Chem. Soc.* 1972, **94**, 3425.
8. N. Walker and D. Stuart, *Acta Cryst.* 1983, **A39**, 158.
9. D. Rogers, *Acta Cryst.* 1981, **A37**, 734.
10. C. A. Larson, in *Crystallographic Computing* (Edited by F. D. Ahmed), p. 291. Munksgaard, Copenhagen (1970).
11. *International Tables for X-ray Crystallography*, Vol. IV, pp. 99, 149. Kynoch Press, Birmingham (1974).
12. P. R. Mallinson and K. W. Muir, *J. Appl. Cryst.* 1985, **18**, 51.

Polyhedron Vol. 8, No. 9, pp. 1233–1237, 1989
Printed in Great Britain

0277–5387/89 $3.00+.00
© 1989 Pergamon Press plc

ELECTRONEGATIVITY SCALE FROM X-RAY PHOTOELECTRON SPECTROSCOPIC DATA

M. HUSAIN* and ALKA BATRA

Department of Physics, Jamia Millia Islamia, New Delhi-110025, India

and

K. S. SRIVASTAVA

Department of Physics, University of Lucknow, Lucknow-226007, India

(*Received* 18 *May* 1988; *accepted after revision* 12 *December* 1988)

Abstract—Electronegativity of atoms, based on Allred and Rochow's method, has been re-estimated by calculating the effective nuclear charge by using the experimental values of the binding energies of the inner and valence states obtained from X-ray photoelectron spectroscopic data. The present method has the advantage that no arbitrary method of determining the screening constants is involved.

Pauling[1] originally defined electronegativity as "the power of an atom in a molecule to attract electrons to itself", and also set up its relative scale based on bond energies from thermochemical data. Several other workers have also correlated electronegativity with different atomic or molecular properties and have given a quantitative measure of it by several empirical relations based on ionization potential and electron affinity,[2] bond order,[3] bond stretching force constants,[4] stability ratio,[5] electrostatic force and covalent radius,[6] molecular orbital,[7] and dipole moment,[8] etc. The concept of electronegativity has been of considerable help in the calculation of a number of important parameters, such as partial ionic character of bonds,[9] effective charge per atom,[10,11] equilibrium length of polar bonds[12] and ionicity,[13] etc.

A scale of electronegativity based on the force of electrostatic attraction between the nucleus and an electron from a bonded atom has been constructed by Allred and Rochow.[6] This force of electrostatic attraction at the electron due to the nucleus and other surrounding electrons is given by

$$F = \frac{e}{r} Z_{\text{eff}} \qquad (1)$$

where r represents the distance between the electron and the nucleus and eZ_{eff} is the charge which is effective at the electron due to the nucleus and its surrounding electrons. The effective nuclear charge is always less than the actual nuclear charge due to the screening by the other electrons in the atom. Allred and Rochow[6] have made use of Slater's rule,[14] for determining the value of the screening constant and have thus estimated the $Z_{\text{eff}} = [Z - \sigma]$.

The effective force F, given by eq. (1), is an approximate measure of the extent to which an atom in a molecule attracts electrons to itself, and hence it was proposed as a measure of the absolute electronegativity of an atom. The electronegativity scale due to Allred and Rochow,[6] and that of Pauling, bear the following relation

$$Xp = a + b\frac{Z_{\text{eff}}}{r} \qquad (2)$$

where $a = 0.744$ and $b = 0.35$.

Mande and Damle[15,16] have pointed out that though the assumption of Allred and Rochow[6] is reasonable, their electronegativity values do not always compare very well with the values of Pauling, which are based on experimental values of thermochemical data. The reason for this disagreement, is because they have calculated the effective nuclear charge or screening constant by Slater's[14] method, which is simply an empirical method.

* Author to whom correspondence should be addressed.

Mande and Damle[15,16] have given a method for calculating the effective nuclear charges for different inner shells with the help of experimental X-ray term values and Dirac's relativistic equation.[17] According to Schiff,[17] the total relativistic energy of an electron in any orbital is given by

$$E = mc^2\left[1+\frac{\gamma^2}{(s+n')^2}\right]^{-1/2} \tag{3}$$

where

$$\gamma = \frac{Ze^2}{\hbar c} = \alpha Z, \quad \alpha = \frac{e^2}{\hbar c}$$

$$= \text{fine structure constant}, \tag{4}$$

where $n = n' + |k|$ = total quantum number.

$$s = \sqrt{k^2-\gamma^2} = \sqrt{k^2-\alpha^2Z^2} \tag{5}$$

and

$$k = l(l+1)-j(j+1)-1/4$$

$$= -l-1 \quad \text{for } j = l+1/2$$

$$= l \qquad \text{for } j = l-1/2. \tag{6}$$

Thus from eq. (6) for the $s_{1/2}$ term, $l = 0, j = 1/2$, $k = -1$, for the $p_{1/2}$ term, $l = 1, j = 1/2, k = 1$, for $p_{3/2}$, $l = 1$, $j = 3/2$, $k = -2$, and for $d_{3/2}$, $l = 2$, $j = 3/2, k = 2$.

Now subtracting the energy corresponding to the rest mass from eq. (3), we get

$$E = mc^2\left[1+\frac{\alpha^2Z^2}{\{(k^2-\alpha^2Z^2)^{1/2}+n-|k|\}^2}\right]^{-1/2} - mc^2.$$

Thus the energy of the electron in terms of Rydberg's constant

$$R = \frac{2me^4\pi^2}{ch^3} = \frac{\alpha^2mc}{2h}$$

is given by

$$\frac{\nu}{R} = -\frac{E}{hcR} =$$

$$-\frac{mc^2}{hcR}\left[\left\{1+\frac{\alpha^2Z^2}{\{n-|k|+(k^2-\alpha^2Z^2)^{1/2}\}^2}\right\}^{-1/2}-1\right], \tag{7}$$

but

$$\frac{mc^2}{hcR} = \frac{mc^2}{\frac{hc(\alpha^2mc)}{2h}} = \frac{2}{\alpha^2}. \tag{8}$$

Thus

$$\frac{\nu}{R} =$$

$$-\frac{2}{\alpha^2}\left[\left\{1+\frac{\alpha^2Z^2}{[n-|k|+(k^2-\alpha^2Z^2)^{1/2}]^2}\right\}^{-1/2}-1\right]. \tag{9}$$

Now introducing the screening constant, we can write Z as $[Z-\sigma]$ in eq. (9) and we get

$$\frac{\nu(nlj)}{R} =$$

$$-\frac{2}{\alpha^2}\left\{1+\frac{\alpha^2(Z-\sigma)^2}{[n-|k|+\{k^2-\alpha^2(Z-\sigma)^2\}^{1/2}]^2}\right\}^{-1/2}-\frac{2}{\alpha^2}. \tag{10}$$

Therefore, the energy of any emission line can be expressed as

$$\left(\frac{\Delta\nu}{R}\right)_{(\text{line})} = \frac{\nu(n_il_ij_i)}{R} - \frac{\nu(n_fl_fj_f)}{R}. \tag{11}$$

Let us put $|k| = j'$ and

$$K = n-|k|+\varepsilon$$

$$= n-|j'|+\varepsilon$$

where

$$\varepsilon = \sqrt{j'^2-\alpha^2(Z-\sigma)^2}.$$

Thus eq. (10) can be written as

$$\frac{\nu(n,l,j)}{R} = -\frac{2}{\alpha^2}\left\{1+\frac{\alpha^2(Z-\sigma)^2}{K^2}\right\}^{-1/2}-\frac{2}{\alpha^2}. \tag{12}$$

Mande and co-workers[16,18] have calculated $(Z-\sigma)$ for inner levels by using experimental data of X-ray spectroscopy for the ν/R term values in eq. (12), but for the valence state they have extrapolated the term values in a very crude manner to get $(Z-\sigma)$ from eq. (12) and therefore their values for the electronegativity of valence state cannot be taken as being very accurate. Their expression for electronegativity normalized to Pauling's scale is expressed by the following relation.

$$X_M = 0.778\frac{Z_{\text{eff}}}{r^2}+0.5. \tag{13}$$

In order to overcome the above mentioned shortcoming for the evaluation of the term values, we have used the binding energies of the valence states of the atoms obtained from X-ray photoelectron spectroscopic data[19] to calculate the screening constant.

To find the screening constant σ and Z_{eff}, eq. (12) has been simplified for computational convenience as

$$\sigma = Z-\sqrt{X-\frac{X^2\alpha^2}{4}}\left\{P\left(1-\frac{\alpha^2X^2}{2}\right)\right.$$

$$\left.+\sqrt{j'^2-\alpha^2p^2\left(X-\frac{X^2\alpha^2}{4}\right)}\right\}, \tag{14}$$

where Z is the atomic number of the atom concerned, $X = \nu/R$, the term values for the valence state and $p = n - |j'|$. From eq. (14) we have

$$Z - \sigma = \sqrt{X - \frac{X^2\alpha^2}{4}}\left\{P\left(1 - \frac{X^2\alpha^2}{2}\right) + \sqrt{j'^2 - \alpha^2 p^2\left(X - \frac{X^2\alpha^2}{4}\right)}\right\}. \quad (15)$$

With the help of eq. (15), Z_{eff} for atoms with Z lying in the range $1 < Z < 92$, have been computed with a computer.

The electronegativities of all those atoms for which the covalent radii[5] r are given, have been calculated by feeding the values of Z_{eff} into eq. (15) (Table 1). On calculating the electronegativities, the authors have given different values to the constants a and b, occurring in eq. (2), to fit Pauling's electronegativity values, which have been assumed by all workers to be the standard ones. The modified form of eq. (3) is as follows.

$$X = 0.77\frac{Z_{eff}}{r^2} + 0.24. \quad (16)$$

By using eq. (16), the electronegativity values of atoms have been calculated and it is found that these values are in better agreement with Pauling (Table 1).

Table 1. Electronegativities of the atoms

Z	Element	n	j'	p	$X = \frac{\nu}{R}$	Z_{eff}	r	$\frac{Z_{eff}}{r^2}$	X_{calc}	X_P	X_M	X_{AR}
3	Li	2	−1	1	0.3963	1.2593483	1.23	0.8324	0.88	1.0	1.17	0.97
4	Be	2	−1	1	0.6854	1.6557400	0.89	2.0903	1.84	1.5	2.11	1.47
5	B	2	+1	1	0.6101	1.5621462	0.82	3.3232	2.02	2.0	2.23	2.01
6	C	2	+1	1	0.8279	1.8197301	0.77	3.0692	2.60	2.5	2.73	2.50
7	N	2	+1	1	1.0684	2.0671952	0.75	3.6750	3.06	3.0	3.26	3.07
8	O	2	+1	1	1.0015	2.0014327	0.73	3.7557	3.13	3.5	3.71	3.50
9	F	2	+1	1	2.2809	2.2634406	0.72	4.3661	3.60	4.0	4.34	4.10
11	Na	3	−1	2	0.3779	1.8441654	1.54	0.7776	0.83	0.9	0.86	1.01
12	Mg	3	−1	2	0.5622	2.2493241	1.36	1.2161	1.17	1.2	1.32	1.23
13	Al	3	+1	2	0.4401	1.9901489	1.18	1.4293	1.34	1.5	1.48	1.47
14	Si	3	+1	2	0.5993	2.3223507	1.11	1.8849	1.69	1.6	1.87	1.74
15	P	3	+1	2	0.7713	2.6345889	1.06	2.3448	2.04	2.1	2.21	2.06
16	S	3	+1	2	0.7618	2.6183152	1.02	2.5166	2.17	2.5	2.63	2.44
17	Cl	3	+1	2	0.9537	2.9295596	0.99	2.9898	2.54	3.0	2.97	2.83
19	K	4	−1	3	0.3192	2.2598491	2.03	0.5485	0.66	0.8	0.62	0.91
20	Ca	4	−1	3	0.4495	2.6816862	1.74	0.8857	0.92	1.0	1.07	1.04
21	Sc	4	−1	3	0.4809	2.7737627	1.44	1.3377	1.27	1.3	1.17	1.20
22	Ti	4	−1	3	0.5015	2.8325437	1.32	1.6257	1.49	1.5	1.42	1.32
23	V	4	−1	3	0.4956	2.8158338	1.22	1.8919	1.69	1.6	1.61	1.45
24	Cr	4	−1	3	0.4974	2.8209422	1.18	2.0259	1.79	1.6	1.70	1.56
25	Mn	4	−1	3	0.5466	2.9571563	1.17	2.1602	1.90	1.5	1.75	1.60
26	Fe	4	−1	3	0.5787	3.0427410	1.17	2.2228	1.95	1.8	1.78	1.64
27	Co	4	−1	3	0.5782	3.0414264	1.16	2.2603	1.89	1.8	1.86	1.70
28	Ni	4	−1	3	0.5614	2.9969196	1.15	2.2661	1.98	1.8	1.90	1.75
29	Cu	4	−1	3	0.5681	3.0147482	1.17	2.2083	1.93	1.9	2.03	1.75
30	Zn	4	−1	3	0.6907	3.3241358	1.25	2.1274	1.87	1.6	1.94	1.66
31	Ga	4	−1	3	0.4412	2.6568141	1.26	1.6735	1.52	1.6	1.77	1.82
32	Ge	4	−1	3	0.5809	3.0485186	1.22	2.0482	1.81	1.8	2.01	2.02
33	As	4	−1	3	0.7213	3.3969632	1.20	2.3590	2.05	2.0	2.31	2.20
34	Se	4	−1	3	0.7169	3.3865878	1.17	2.4739	2.14	2.4	2.57	2.48
35	Br	4	−1	3	0.8713	3.7334457	1.14	2.8728	2.45	2.8	2.89	—
37	Rb	4	−1	3	0.3074	2.7720868	2.16	0.5942	0.69	0.8	0.61	0.89
38	Sr	4	−1	3	0.4184	3.2340392	1.91	0.8865	0.92	1.0	0.73	0.99
39	Y	5	−1	4	0.4765	3.4512629	1.62	1.3151	1.25	1.2	1.05	1.11
40	Zr	5	−1	4	0.5029	2.5455703	1.45	1.6864	1.53	1.4	1.29	—
41	Nb	5	−1	4	0.5059	3.5561298	1.34	1.9805	1.76	1.6	1.49	—
42	Mo	5	−1	4	0.5221	3.6126109	1.30	2.1376	1.88	1.9	1.66	—

[*continued*

Table 1—*continued*

Z	Element	n	l'	p	$X=\frac{\nu}{R}$	Z_{eff}	r	$\frac{Z_{eff}}{r^2}$	X_{calc}	X_P	X_M	X_{AR}
43	Te	5	−1	4	0.5353	3.6579883	1.27	2.2680	1.98	1.9	1.75	—
44	Ru	5	−1	4	0.5419	3.6804671	1.25	2.3555	2.05	2.2	1.78	—
45	Rh	5	−1	4	0.5485	3.7028094	1.25	2.3698	2.06	2.2	1.84	—
46	Pd	4	−3	1	0.6132	3.1322573	1.28	1.9118	1.71	2.2	1.79	—
47	Ag	5	−1	4	0.5574	3.7327258	1.34	2.0788	1.84	1.9	1.70	1.42
48	Cd	5	−1	4	0.6610	4.0647912	1.48	1.8557	1.66	1.7	1.68	1.46
49	In	5	+1	4	0.4272	3.2621273	1.44	1.5732	1.45	1.7	1.36	—
50	Sn	5	+1	4	0.5397	3.6729895	1.40	1.8740	1.68	1.8	1.59	1.72
51	Sb	5	+1	4	0.6353	3.9849989	1.40	2.0332	1.80	2.0	1.79	1.82
52	Te	5	+1	4	0.6625	4.0694000	1.36	2.2002	1.93	2.4	2.16	2.01
53	I	5	+1	4	0.7684	4.3825403	1.33	2.4776	2.14	2.6	2.56	2.21
55	Cs	6	−1	5	0.2860	3.2086098	2.35	2.5810	0.68	0.7	—	0.86
56	Ba	6	−1	5	0.3831	3.7135054	1.98	0.9472	0.96	0.9	—	0.97
57	La	6	−1	5	0.4103	3.8430594	1.69	1.3456	1.27	1.1	—	1.08
58	Ce	6	−1	5	0.4154	3.8668674	1.65	1.4203	1.33	1.1	—	—
59	Pr	6	−1	5	0.3985	3.7874003	1.64	1.4082	1.32	1.1	—	—
60	Nd	6	−1	5	0.4037	3.8120283	1.64	1.4173	1.33	1.1	—	—
61	Pm	6	−1	5	0.4081	3.8327437	1.63	1.4426	1.35	1.1	—	—
62	Sm	6	−1	5	0.4140	3.8603465	1.62	1.4709	1.37	1.1	—	—
63	Eu	6	−1	5	0.4176	3.87709234	1.85	1.1328	1.11	1.1	—	—
64	Gd	6	−1	5	0.4529	4.0376151	1.62	1.5385	1.42	1.1	—	—
65	Tb	6	−1	5	0.4301	3.9346840	1.61	1.5179	1.40	1.1	—	—
66	Dy	6	−1	5	0.4360	3.9615763	1.60	1.5475	1.43	1.1	—	—
67	Ho	6	−1	5	0.4426	3.9913444	1.58	1.5989	1.47	1.1	—	—
68	Er	6	−1	5	0.4485	4.0179660	1.58	1.6095	1.47	1.1	—	—
69	Tm	6	−1	5	0.4544	4.0442950	1.58	1.6201	1.48	1.1	—	—
72	Hf	6	−1	5	0.5513	4.4554392	1.44	2.1486	1.89	1.3	—	—
73	Ta	6	−1	5	0.5809	4.5726364	1.34	2.5466	2.20	1.5	—	—
74	W	6	−1	5	0.5882	4.6012735	1.30	2.7226	2.33	1.7	—	—
75	Re	6	−1	5	0.5809	4.5726364	1.28	2.7909	2.38	1.9	—	—
76	Os	6	−1	5	0.6250	4.7430030	1.26	2.9875	2.54	2.2	—	—
77	Ir	6	−1	5	0.6691	4.9064529	1.27	3.02426	2.58	2.2	—	—
78	Pt	6	−1	5	0.6618	4.8806139	1.30	2.8879	2.46	2.2	—	—
79	Au	6	−1	5	0.6787	4.9425260	1.34	2.7526	2.35	2.4	—	—
80	Hg	6	−1	5	0.7647	5.246267	1.49	2.3631	2.05	1.9	—	—
81	Tl	6	+1	5	0.4493	4.0215380	1.48	1.8359	1.65	1.8	—	—
82	Pb	6	+1	5	0.5456	4.4315464	1.47	2.0508	1.81	1.8	—	—
83	Bi	6	+1	5	0.5360	4.3923921	1.36	2.0606	1.82	1.9	—	—
84	Po	6	+1	5	0.6199	4.7236143	1.46	2.2159	1.94	2.0	—	—
85	At	6	−2	4	0.6838	4.9613287	1.54	2.3597	2.05	2.2	—	—
90	Th	7	−1	6	0.4412	4.6492607	1.65	1.7077	1.55	1.3	—	—
91	U	7	−1	6	0.4412	4.6492607	1.42	2.3057	2.01	1.5	—	—

X_{calc}—Authors' calculated values.
X_P—Pauling's[9] values.
X_M—Mande's[18] values.
X_{AR}—Allred and Rochow's[6] values.

Acknowledgement—Thanks are due to the Department of Science and Technology, New Delhi for financial assistance.

REFERENCES

1. L. Pauling, *Phys. Rev.* 1929, **34**, 956.
2. R. S. Mulliken, *J. Chem. Phys.* 1934, **2**, 782.
3. W. Gordy, *Phys. Rev.* 1946, **69**, 604.
4. A. D. Walsh, *Proc. R. Soc.* 1951, **207A**, 13.
5. R. T. Sanderon, *Inorganic Chemistry*, pp. 69, 74–78. Affiliated East West New Delhi (1971).
6. A. L. Allred and R. G. Rochow, *J. Inorg. Nucl. Chem.* 1958, **5**, 264.
7. H. O. Pritchard and H. A. Skinnar, *Chem. Rev.* 1955, **55**, 745.

8. J. G. Malone, *J. Chem. Phys.* 1933, **1**, 1976.
9. L. Pauling, *The Nature of the Chemical Bond*, 3rd edn, pp. 57, 88, 505. Cornell University Press, Ithaca, New York (1960).
10. K. Siegbahn, C. Nordling, A. Fahlman, R. Nordberg, K. Hamrin, J. Hedman, G. Johansson, T. Bergmark, S. Karlsson, I. Lindgren and B. Lindberg, *ESCA Atomic, Molecular and Solid State Structure studied by means of electron spectroscopy*. Nova Acta Ragiae Soc. Sci. UP aliensis Ser IV, 1967, **20**, 76.
11. B. J. Lindberg, K. Hammann, G. Jhonson, P. Galius, A. Fahlman, C. Nordling and K. Seigbahn, *Phys. Script.* 1970, **1**, 286.
12. V. Schomaker, *J. Am. Chem. Soc.* 1941, **63**, 37.
13. J. C. Phillips, *Rev. Mod. Phys.* 1970, **42**, 317.
14. J. C. Slater, *Phys. Rev.* 1930, **36**, 57.
15. C. Mande and P. S. Damle, *Ind. J. Pure Appl. Phys.* 1965, **3**, 142.
16. C. Mande and P. S. Damle, *Proc. Phys. Soc.* 1966, **87**, 1005.
17. L. Shiff, *Quantum Mechanics*, p. 337. McGraw-Hill, New York (1955).
18. C. Mande, Pranwa Deshmukh and Probh Deshmukh, *J. Phys.* 1977, **10B**, 2293.
19. T. A. Carlson, *Photoelectron and Auger Spectroscopy*, pp. 165, 337–343. Plenum Press, New York (1975).

Polyhedron Vol. 8, No. 9, pp. 1239–1242, 1989
Printed in Great Britain

0277–5387/89 $3.00+.00
© 1989 Pergamon Press plc

DETERMINATION OF FORMATION CONSTANTS OF COPPER(II) DI-CARBOXYLATES WITH A SOLID STATE COPPER(II) ION-SELECTIVE ELECTRODE

C. J. COETZEE

Department of Chemistry, University of the Western Cape, Private Bag X17, Bellville, 7535, South Africa

(*Received* 14 *November* 1988; *accepted* 12 *December* 1988)

Abstract—Formation constants for 1 : 1 complexes of copper(II) with oxalate, malonate, succinate, glutarate and adipate, respectively, have been determined at 25°C and 0.10 M ionic strength using a copper(II) ion-selective electrode.

Ion-selective electrodes have attained wide acceptance for analytical and general chemical measurement purposes. One of the chief advantages of these electrodes is that they respond only to free uncomplexed ions in solution. This property makes them extremely useful as analytical tools for the study of complexes and especially for the determination of formation constants. Copper(II) ion-selective electrodes of both the liquid–liquid membrane[1] and the solid membrane[2–4] design have been successfully used for the determination of formation constants of copper(II) complexes.

Although formation constant values for a large number of copper(II) complexes are known, they were determined under a variety of conditions. In this work an Orion Cupric ion electrode Model 94-29 was used for the re-evaluation of values of formation constants of 1 : 1 complexes between the copper(II) ion and oxalate, malonate, succinate, glutarate and adipate, under controlled and comparable conditions.

EXPERIMENTAL

Copper(II) solutions were prepared by the treatment of excess basic copper(II) carbonate (Merck extra pure) with a perchloric acid solution (Merck G.R.). After double filtration the solutions were diluted with distilled water obtained from an all-glass still, standardized and diluted to suitable volumes. Sodium perchlorate monohydrate, oxalic and succinic acid (Merck G.R.) were used as such, malonic acid (Merck LAB), glutaric acid (Merck ORG) and adipic acid (Merck) were twice recrystallized from water. The experimental procedure was carried out as follows: potentiometric measurements were made at 25±0.5°C using the electrochemical cell:

Cu^{2+} electrode / sample solution / saturated calomal electrode. (Beckman 39170)

EMF values were measured with a Beckman Research model pH-meter. Prior to equilibria measurements, the copper(II) electrode was calibrated by means of standard copper(II) solution prepared in sodium perchlorate medium to give an ionic strength of 0.10 M. The cell EMF is given by $E = E^{\ominus} + 0.0296 \log a_{Cu}$. The electrode gave a linear response between pCu values of 2 and 4.8. Because $E^{\ominus}$ varied from time to time, the calibration of the electrode was checked before each set of equilibrium measurements were made.

The equilibrium concentration of the free copper ion in solution was measured at a constant pH of 6 and constant ionic strength of 0.10 M after mixing appropriate volumes of solutions of a known concentration of copper ion and ligand. The pH of the solutions was adjusted by means of sodium hydroxide or perchloric acid solutions which were also 0.10 M in sodium perchlorate.

The formation constant K for the reaction $Cu^{2+} + L^{2-} \rightleftharpoons CuL$ is given by the equation

$$K = \frac{[CuL] f_{CuL}}{[Cu^{2+}][L^{2-}] f_{Cu} f_{L}}.$$

In order to calculate the K values the following must be taken into consideration. At pH 6, the copper ion in solution is hydrolysed to a certain

extent according to the reaction $Cu^{2+}+H_2O \rightleftharpoons Cu(OH)^{+}+H^{+}$. By using the known value of the hydrolysis constant[5] the calculated ratio of $[Cu(OH)^{+}]/[Cu^{2+}]$ at pH 6 is found to be equal to 0.3388, which implies that about 25% of the free copper ions in solution are hydrolysed. This has to be taken into account and cannot be ignored as in a previous study.[1] At pH 6 the ligands being diprotic carboxylic acids will also be protonated to a certain extent. The free $[L^{2-}]$ can be calculated using their respective pK_1 and pK_2 values.[6,7] The values $[Cu^{2+}]_e$, [CuL] and $[L^{-2}]$ which were used to calculate the formation constant K, were calculated as follows:

$$[Cu^{2+}]_e = \text{measured directly by potentiometry}$$

$$[CuL] = [Cu^{2+}]_{total} - 1.3388[Cu^{2+}]_e$$

$$[L^{2-}] = [L^{2-}]_{total} - [CuL] - [HL^{-}] - [H_2L].$$

Activity coefficients were calculated by using the extended Debye–Hückel equation $\log f = -0.51Z^2\mu^{1/2}(1+\mu^{1/2})^{-1}$. The values for the formation constants are listed in Tables 1–5. In Table 6 the experimental values are compared with

Table 1. Formation constants of copper oxalate complexes at $\mu = 0.10$ M and 25°C

$T_{Cu}\times 10^4$	$T_L\times 10^4$	$[Cu^{2+}]_e\times 10^4$ (mol dm^{-3})	$[CuL]\times 10^4$	$[L^{2-}]\times 10^4$	$K\times 10^{-5}$ (dm^3 mol^{-1})
6.456	6.06	0.560	5.706	0.3081	4.39
6.456	6.06	0.570	5.693	0.3198	4.14
10.76	10.10	0.780	9.716	0.3347	4.94
10.76	16.10	0.066	10.67	4.729	4.53
10.76	16.10	0.060	10.68	4.722	5.00
10.76	16.10	0.076	10.66	4.740	3.92
21.52	20.20	1.350	19.71	0.4246	4.56

Table 2. Formation constants of copper malonate complexes at $\mu = 0.10$ M and 25°C

$T_{Cu}\times 10^4$	$T_L\times 10^4$	$[Cu^{2+}]_e\times 10^4$ (mol dm^{-3})	$[CuL]\times 10^4$	$[L^{2-}]\times 10^4$	$K\times 10^{-4}$ (dm^3 mol^{-1})
10.76	19.36	0.230	10.45	7.454	8.08
10.76	19.36	0.180	10.52	8.841	8.77
10.76	19.36	0.200	10.49	7.421	9.37
10.76	19.36	0.222	10.46	7.445	8.39
21.52	29.05	0.450	20.92	6.803	9.06
21.52	29.05	0.442	20.93	6.795	9.24
21.52	38.72	0.240	21.20	14.66	7.99
21.52	38.72	0.233	21.21	14.65	8.24

Table 3. Formation constants of copper succinate complexes at $\mu = 0.10$ M and 25°C

$T_{Cu}\times 10^4$	$T_L\times 10^4$	$[Cu^{2+}]_e\times 10^4$ (mol dm^{-3})	$[CuL]\times 10^4$	$[L^{2-}]\times 10^4$	$K\times 10^{-3}$ (dm^3 mol^{-1})
10.76	9.072	6.190	2.473	5.379	9.37
10.76	9.072	6.240	2.406	5.434	9.41
10.76	9.072	6.150	2.526	5.336	10.21
10.76	9.072	6.200	2.459	5.390	9.76
21.52	15.12	11.56	6.044	7.398	9.37
21.52	15.12	11.53	6.043	7.398	9.40
21.52	20.16	10.52	7.436	10.37	9.04
21.52	20.16	10.35	7.663	10.19	9.64

Table 4. Formation constants of copper glutarate complexes at $\mu = 0.10$ M and 25°C

$T_{Cu} \times 10^4$	$T_L \times 10^4$	$[Cu^{2+}]_e \times 10^4$ (mol dm^{-3})	$[CuL] \times 10^4$	$[L^{2-}] \times 10^4$	$K \times 10^{-2}$ (dm^3 mol^{-1})
10.76	13.03	7.112	1.239	9.906	2.33
10.76	13.03	7.080	1.281	9.870	2.43
10.76	13.03	7.100	1.255	9.893	2.37
21.52	26.06	12.90	4.249	18.32	2.38
21.52	26.06	12.95	4.183	18.38	2.33
32.28	39.09	17.90	8.315	25.85	2.38

Table 5. Formation constants of copper adipate complexes at $\mu = 0.10$ M and 25°C

$T_{Cu} \times 10^4$	$T_L \times 10^4$	$[Cu^{2+}]_e \times 10^4$ (mol dm^{-3})	$[CuL] \times 10^4$	$[L^{2-}] \times 10^4$	$K \times 10^{-1}$ (dm^3 mol^{-1})
10.76	9.335	7.70	0.451	7.434	10.45
10.76	9.335	7.65	0.518	7.378	12.17
21.52	28.02	14.40	2.241	21.57	9.57
21.52	28.02	14.50	2.107	21.68	8.89
21.52	28.02	14.35	2.308	21.52	9.91
32.28	37.35	21.30	3.764	28.11	8.34
32.28	37.35	20.75	4.500	27.49	7.89

Table 6. Formation constants of copper(II) di-carboxylate (1 : 1) complexes at 25°C and ionic strength 0.10 M

Ligand	K	Standard deviation	Log K measured	Log K literature	
Oxalate	4.50×10^5	0.39×10^5	5.65	6.3	8
				4.85	9
Malonate	8.64×10^4	0.54×10^4	4.94	5.0	6
				5.55	10
Succinate	9.53×10^3	0.35×10^3	3.98	3.3	8
				2.93	10
Glutarate	2.37×10^2	0.04×10^2	2.37	2.4	6
Adipate	9.60×10	1.4×10	1.98	2.3	6

available literature data, which were determined under comparable conditions by different authors. The results show a weakening of complexation with increasing ring size of the formed chelate. The method used in this study, where free copper(II) concentrations are measured directly, is thought to be superior to the conventional methods because of its simplicity and potential applicability to a wide range of ionic media.[1]

Acknowledgements—The author thanks the Council for Scientific and Industrial Research and the University of the Western Cape for financial assistance.

REFERENCES

1. G. A. Rechnitz and Z. F. Lin, *Anal. Lett.* 1967, **1**, 23.

2. G. A. Rechnitz and N. C. Kenny, *Anal. Lett.* 1969, **2**, 395.
3. H. Wada and Q. Fernando, *Anal. Chem.* 1971, **43**, 751.
4. E. H. Hansen and J. Ruzicka, *Talanta* 1973, **20**, 1105.
5. C. W. Davies, *J. Chem. Soc.* 1951, 1256.
6. M. Yasada, K. Yamasaki and H. Ohtaki, *Bull. Chem. Soc. Jpn* 1960, **33**, 1067.
7. C. Bliefert, *pH-Wert-Berechnungen*. Verlag Chemie, Weinheim (1978).
8. E. Gelles and R. M. Hay, *J. Chem. Soc.* 1958, 3673; 3684; and 3689.
9. A. McAuley and G. H. Nancollas, *Trans. Faraday Soc.* 1960, **56**, 1165.
10. E. Campi, *Ann. Chim. (Italy)* 1963, **53**, 96.

Polyhedron Vol. 8, No. 9, pp. 1243–1246, 1989
Printed in Great Britain

0277–5387/89 $3.00+.00
© 1989 Pergamon Press plc

COMMUNICATION

AN EFFICIENT SYNTHETIC ROUTE TO PERIPHERALLY-SUBSTITUTED AND LACUNAR NICKEL(II) COMPLEXES OF DIBENZOTETRAAZA[14]ANNULENES

JULITA EILMES

Faculty of Chemistry, Jagiellonian University, Karasia 3, 30-060 Cracow, Poland

(*Received* 12 *December* 1988; *accepted* 5 *January* 1989)

Abstract—An aminolytic cleavage of γ,δ-unsaturated-δ-lactonic substituents of disubstituted nickel(II) complexes of dibenzotetraaza[14]annulenes (**1** and **2**) has been accomplished by means of aliphatic amines and diamines. The reaction led to amide groups containing derivatives having either pendant open-chain γ,γ'-substituents or γ,γ'-bridging groups. The products were characterized by ^{1}H NMR and IR data.

The synthesis of the substituted Jäger complexes, **1** and **2**, and the transformations of the lactonic rings into the new substituents carrying carboxyl and ester functions have already been described.[1,2]

Further experiments revealed that the unsaturated δ-lactonic substituents of complexes **1** and **2** are susceptible to an aminolytic cleavage, giving rise to new disubstituted derivatives.

This paper reports the results of the reactions of complexes **1** and **2** with primary and secondary aliphatic amines and diamines.

RESULTS

An aminolysis of the lactonic substituents of the macrocyclic complexes was accomplished by refluxing the starting compounds **1** and **2** in benzene solution with an excess of appropriate amine. The reaction led to the new products in reasonable yield (70–88%).

The products of the reaction with aliphatic amines have amide groups containing pendant arms on the ligand periphery (compounds **3–8**). The same synthetic route when applied to aliphatic diamines gives rise to the lacunar complexes (**9–12**), with bridging groups connected to opposite γ-positions on the macrocyclic ring.

The procedure extended to a variety of amines and diamines provides a convenient method for the macrocyclic ligand modifications.

Scheme 1 outlines the performed reactions. ^{1}H NMR and IR data are given in Table 1.

EXPERIMENTAL

Melting points are uncorrected. IR spectra were recorded in Nujol and hexachlorobutadiene on a Zeiss UR-10 spectrometer. ^{1}H NMR spectra were taken on a Brüker AM500 MHz instrument using TMS as internal standard.

Parent complexes **1** and **2** were prepared by a procedure described earlier.[1]

Syntheses of the complexes **3–12** *(general procedure)*

An appropriate amine (30 mmol) was added to a slurry of the parent complex (1 mmol) in benzene (30 cm^3). The reaction mixture was heated under gentle reflux for 30 min, then left overnight at room temperature. The solvent and excess reagent were distilled off on a rotatory evaporator. A green residue was triturated with water, filtered off and then washed carefully with water.

Further purification was accomplished according to one of the methods given below (see Table 2):

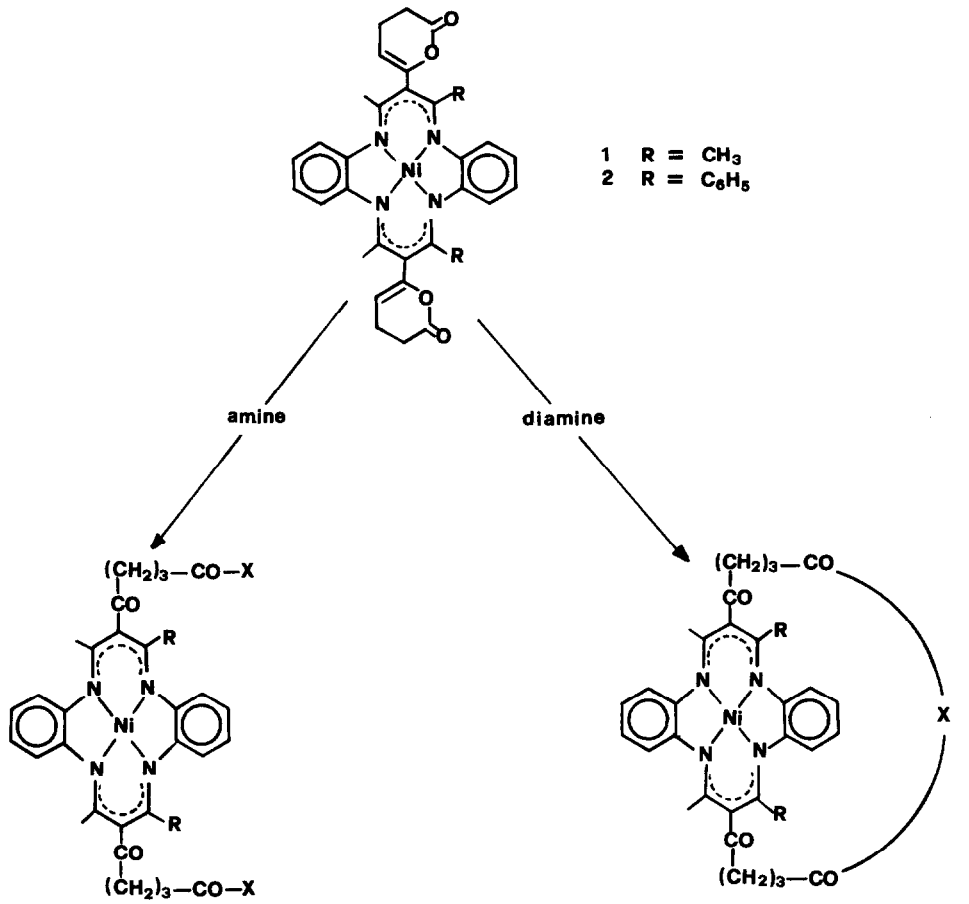

3 R = CH_3 X = NH–CH_2– 

4 R = C_6H_5 X = NH–CH_2– 

5 R = CH_3 X = NH– 

6 R = C_6H_5 X = NH– 

7 R = CH_3 X =

8 R = C_6H_5 X =

9 R = CH_3 X = NH–CH_2–C(CH_3)(CH_3)–CH_2–NH

10 R = C_6H_5 X = NH–CH_2–C(CH_3)(CH_3)–CH_2–NH

11 R = CH_3 X = 

12 R = C_6H_5 X = 

Scheme 1.

Table 1. ^{1}H NMR and IR data for the complexes **3–12**

Complex	IR data ν(C=O) ν(N—H)	^{1}H NMR data [$CDCl_3$, δ (ppm)]
3	1625s 1665s 3250m	1.94(s, 12H)CH_3, 2.0(m, 4H)$CH_2CH_2CH_2CH_2$, 2.37(t, 4H, J = 6 Hz)$COCH_2CH_2$, 2.82(t, 4H, J = 6 Hz)CH_2CON, 4.47(d, 4H, J = 5 Hz)CH_2N, 5.94(bs, 2H)NH, 6.62(bs, 8H)*o*-C_6H_4, 7.3(bs, 10H)C_6H_5
4	(1640–1660)s 3250m	[1.5(m)$CH_2CH_2CH_2$, 2.08(s)CH_3]18H, 4.39(d, 4H, J = 5 Hz)CH_2N, 5.65(mAA′BB′, 4H)*o*-C_6H_4, 5.82(bs, 2H)NH, 6.75(m, 4H)*o*-C_6H_4, 7.37(m, 20H)C_6H_5
5	1630s 1660s 3270m	[1.5(m)C_6H_{10}, 1.92(m)$CH_2CH_2CH_2$, 1.97(s)CH_3]36H, 2.28(t, 4H, J = 7 Hz)$COCH_2CH_2$, 2.88(t, 4H, J = 6.9 Hz)CH_2CON, 3.77(m, 2H)CH(cyclohexyl), 5.48(d, 2H, J = 7.2 Hz)NH, 6.65(mAA′BB′, 8H)*o*-C_6H_4
6	1630s 1650s 3270m	[2.07(s)CH_3, 1.5(m)C_6H_{10}, $CH_2CH_2CH_2$]38H, 3.67(m, 2H)CH(cyclohexyl), 5.4(d, 2H, J = 7 Hz)NH, 5.63(mAA′BB′, 4H)*o*-C_6H_4, 5.75(m, 4H)*o*-C_6H_4, 6.37(m, 10H)C_6H_5
7	1625s 1650s	1.6(m, 12H)pip.(β, γ), [1.97(s), 2.0(m)]16HCH_3, $CH_2CH_2CH_2$, 2.45(t, 4H, J = 7 Hz)$COCH_2CH_2$, 2.85(t, 4H, J = 7 Hz)CH_2CON, 3.44(t, 4H, J = 5.5 Hz)pip.(α), 3.55(t, 4H, J = 5.5 Hz)pip.(α), 6.61(mAA′BB′, 8H)*o*-C_6H_4
8	1630s 1660s	1.53(m, 12H)pip.(β, γ), 1.6(m, 4H)$CH_2CH_2CH_2$, [2.0(s), 2.1(m)]14HCH_3, $CH_2CH_2CH_2$, 3.3(t, 4H, J = 5.0 Hz)pip.(α), 3.5(bt, 4H)pip.(α), [5.41(m, 2H), 5.9(m, 2H)]*o*-C_6H_4, 6.74(mAA′BB′, 4H)*o*-C_6H_4, 7.34(m, 10H)C_6H_5
9	1625s 1675s 3250m	0.94(bs, 6H)$C(CH_3)_2$, [1.97(s), 2.0(m)]16HCH_3, $CH_2CH_2CH_2$, 2.31(bs, 4H)$COCH_2CH_2$, 2.82(bs, 4H)CH_2CON, 3.16(bs, 4H)CH_2N, 6.62(mAA′BB′, 8H) *o*-C_6H_4, 7.1(bs, 2H)NH
10	(1630–1660)s 3300	1.02(bs, 6H)$C(CH_3)_2$, 1.22(m, 4H)$CH_2CH_2CH_2$, [2.11(m), 2.17(s)]14H$CH_2CH_2CH_2$, CH_3, 3.03(bs, 4H)CH_2N, [5.41(m, 2H), 5.9(m, 2H)]*o*-C_6H_4, 6.74(mAA′BB′, 4H)*o*-C_6H_4, 7.18(s)NH, 7.26(m)C_6H_5
11	1620s 1670s	[1.98(s)CH_3, 2.01(m)$CH_2CH_2CH_2$]16H, 2.46(t, 4H)$COCH_2CH_2$, 2.85(t, 4H)CH_2CON, 3.51(bs, 4H)pip., 3.62(bs, 4H)pip., 6.62(m, 8H)*o*-C_6H_4
12	1625s 1670s	[1.9(m)$CH_2CH_2CH_2$, 2.1(s)CH_3]18H, 3.36(bs, 4H)pip., 3.54(bs, 4H)pip., [5.4(m, 2H), 5.92(m, 2H)]*o*-C_6H_4, 6.7(m, 4H)*o*-C_6H_4, 7.26(m)C_6H_5

Table 2. Physical properties of the complexes **3–12**

Complex	Molecular formula	Melting point (°C)	Colour	Purification method[a]	Yield (%)
3	$C_{46}H_{48}N_6O_4Ni$	235	Light green	(a) (butanol)	82
4	$C_{56}H_{52}N_6O_4Ni$	145	Green	(b)	78
5	$C_{44}H_{56}N_6O_4Ni$	260	Light green	(a) (acetone)	85
6	$C_{54}H_{60}N_6O_4Ni$	160	Green	(b)	79
7	$C_{42}H_{52}N_6O_4Ni$	210	Deep green	(c)	78
8	$C_{52}H_{56}N_6O_4Ni$	190	Deep green	(c)	75
9	$C_{37}H_{44}N_6O_4Ni$	225	Green	(b)	88
10	$C_{47}H_{48}N_6O_4Ni$	240	Green	(b)	86
11	$C_{36}H_{40}N_6O_4Ni$	210	Deep green	(b)	72
12	$C_{46}H_{44}N_6O_4Ni$	230	Green	(b)	70

[a] See Experimental.

(a) recrystallization;

(b) dissolving in methylene chloride, followed by reprecipitation with *n*-hexane;

(c) column chromatography (Al_2O_3 neutral, acetone).

Satisfactory elemental analyses were obtained for all synthesized complexes.

Acknowledgement—This research was financially supported by the Committee of Chemical Sciences of the Polish Academy of Sciences.

REFERENCES

1. J. Eilmes, *Polyhedron* 1987, **6**, 423.
2. J. Eilmes, *Polyhedron* 1988, **7**, 2197.

Polyhedron Vol. 8, No. 9, pp. 1247–1249, 1989
Printed in Great Britain

0277–5387/89 $3.00+.00
© 1989 Pergamon Press plc

COMMUNICATION

TETRAKIS(2,6-DI-*t*-BUTYLPHENOXY)URANIUM(IV): THE FIRST STRUCTURALLY CHARACTERIZED NEUTRAL HOMOLEPTIC ARYLOXIDE COMPLEX OF URANIUM(IV)

WILLIAM G. VAN DER SLUYS and ALFRED P. SATTELBERGER*

Inorganic and Structural Chemistry Group (INC-4), Isotope and Nuclear Chemistry Division, Los Alamos National Laboratory, Los Alamos, NM 87545, U.S.A.

and

WILLIAM E. STREIB and JOHN C. HUFFMAN

Molecular Structure Center, Indiana University, Bloomington, IN 47401, U.S.A.

(*Received* 8 *January* 1989; *accepted* 10 *February* 1989)

Abstract—The reaction of $[(Me_3Si)_2N]_2\overline{UN(SiMe_3)SiMe_2CH_2}$ with 4 equivalents of HO-2,6-$Bu^t_2C_6H_3$ in toluene at 100°C provides orange U(O-2,6-$Bu^t_2C_6H_3)_4$ in high yield. U(O-2,6-$Bu^t_2C_6H_3)_4$ has been characterized by NMR, magnetic susceptibility (μ_{eff} = 2.68 BM), and X-ray crystallography. It is the first structurally characterized homoleptic uranium(IV) aryloxide complex. The UO_4 core is nearly tetrahedral with U(1)—O(2) = 2.135(4) Å, O(2)—U(1)—O(2′) = 110.2(1)° and O(2)—U(1)—O(2″) = 108.0(2)°; the U(1)—O(2)—C_{ipso} angle is 154.0(6)°.

We recently reported the synthesis and characterization of two uranium(III) phenoxide complexes, $\{U(O\text{-}2,6\text{-}R_2C_6H_3)_3\}_x$ (R = Pr^i, $x = 2$; R = Bu^t, $x = 1$).[1] The uranium(IV) analogues of these complexes have not been reported, although $[Li(THF)_4][U(O\text{-}2,6\text{-}Pr^i_2C_6H_3)_5]$ has been isolated from the reaction of UCl_4 and LiOAr in THF and structurally characterized.[2] Lappert and co-workers[3] were unable to prepare U(O-2,6-$Bu^t_2C_6H_3)_4$ from $[U(NEt_2)_4]_2$ and excess phenol. Instead, the $U(NEt_2)$(O-2,6-$Bu^t_2C_6H_3)_3$ was isolated according to eq. (1):

$$0.5[U(NEt_2)_4]_2 + \geqslant 3HO\text{-}2,6\text{-}Bu^t_2C_6H_3 \xrightarrow{C_5H_{12}} U(NEt_2)(O\text{-}2,6\text{-}Bu^t_2C_6H_3)_3 + 3HNEt_2. \quad (1)$$

We have repeated this reaction in our laboratory and find that, even in refluxing toluene, the fourth diethylamide ligand [eq. (1)] cannot be metathesized.

Several years ago, Dormond *et al.*[4] described the reactions of the uranium(IV) metallacycle $[(Me_3Si)_2N]_2\overline{UN(SiMe_3)SiMe_2CH_2}$,[5] with both HOBu^t and HO-2,6-$Me_2C_6H_3$. They observed rapid protonation of the uranium–carbon bond and isolated two U(OR)$[N(SiMe_3)_2]_3$ complexes [eq. (2)]:

$$[(Me_3Si)_2N]_2\overline{UN(SiMe_3)SiMe_2CH_2} + HOR \xrightarrow{C_6H_6} U(OR)[N(SiMe_3)_2]_3 \quad (2)$$

(R = Bu^t, 2,6-$Me_2C_6H_3$).

They also noted that cleavage of uranium–nitrogen bonds occurred but was not competitive with attack on the metal–carbon bond.

In agreement with Dormond *et al.*, we find that the reaction of one equivalent of HO-2,6-$Bu^t_2C_6H_3$ with $[(Me_3Si)_2N]_2\overline{UN(SiMe_3)SiMe_2CH_2}$ in hexane at room temperature for 1 h, provides orange

* Author to whom correspondence should be addressed.

$U(O\text{-}2,6\text{-}Bu^t_2C_6H_3)[N(SiMe_3)_2]_3$ in essentially quantitative yield. This hydrocarbon soluble, air-sensitive compound has been characterized by elemental analyses and ^1H NMR.* The room temperature ^1H NMR spectrum shows non-equivalent silyl amide ligands indicative of restricted rotation about the U—O bond and/or U—N bonds.

The reaction of $[(Me_3Si)_2N]_2\overline{UN(SiMe_3)SiMe_2CH_2}$ with slightly greater than 4 equivalents of $HO\text{-}2,6\text{-}Bu^t_2C_6H_3$ in toluene at 100°C for 6 h provides, after solvent removal and recrystallization from hexane, an orange, air-sensitive crystalline solid in 80% yield [eq. (3)]:

$$[(Me_3Si)_2N]_2\overline{UN(SiMe_3)SiMe_2CH_2} + 4HO\text{-}2,6\text{-}Bu^t_2C_6H_3 \xrightarrow{PhCH_3,\Delta} U(O\text{-}2,6\text{-}Bu^t_2C_6H_3)_4 + 3HN(SiMe_3)_2. \quad (3)$$

The ^1H NMR spectrum shows one type of phenoxide ligand and elemental analyses were consistent with the formula $U(O\text{-}2,6\text{-}Bu^t_2C_6H_3)_4$.† The solid follows Curie–Weiss behaviour from 60 to 300 K with $\mu_{eff} = 2.68$ BM, consistent with the presence of two unpaired electrons (U^{4+} has a $5f^2$ ground-state configuration).

X-ray quality crystals, in the form of orange cubes, were grown from a concentrated THF solution at −40°C, and the structure was determined from X-ray diffraction data collected at −145°C.‡ The uranium lies on a crystallographic $\bar{4}$ site (i.e. the molecule has S_4 symmetry) and is coordinated by the oxygen atoms [U(1)—O(2) = 2.135(4) Å] of the four phenoxide ligands in a nearly tetrahedral fashion: angles O(2)—U(1)—O(2′) and O(2)—U(1)—O(2″) are 110.2(1) and 108.0(2)°, respectively (Fig. 1). The U(1)—O(2)—C(3) angle is 154.0(6)°. $U(NEt_2)[O\text{-}2,6\text{-}Bu^t_2C_6H_3]_3$, which also adopts a tetrahedral geometry, has an average U—O distance of 2.143(4) Å.[3] In the trigonal bipyramidal uranium(IV) anion, $[U(O\text{-}2,6\text{-}Pr^i_2C_6H_3)_5]^-$, the U—O distances range from 2.15(1) to 2.19(1) Å.[2]

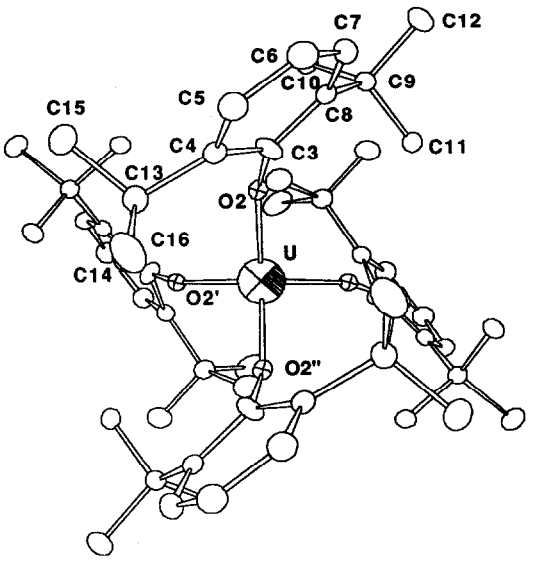

Fig. 1. ORTEP drawing of $U(O\text{-}2,6\text{-}Bu^t_2C_6H_3)_4$. U(1)—O(2) = 2.135(4) Å; O(2)—C(3) = 1.344(14) Å; U(1)—O(2)—C(3) = 154.0(6)°; O(2)—U(1)—O(2′) = 110.2(1)°; O(2)—U(1)—O(2″) = 108.0(2)°.

The reason that $U(NEt_2)(O\text{-}2,6\text{-}Bu^t_2C_6H_3)_3$ does not react with $HO\text{-}2,6\text{-}Bu^t_2C_6H_3$ to form $U(O\text{-}2,6\text{-}Bu^t_2C_6H_3)_4$ is most likely a consequence of the enhanced π-basicity of NEt_2^- relative to $N(SiMe_3)_2^-$. For the latter, N → Si $p\pi$–$d\pi$ bonding is possible and this will compete with N → U π-bonding. In this context, we note that the U—N bond length of 2.162(5) Å in $U(NEt_2)(O\text{-}2,6\text{-}Bu^t_2C_6H_3)_3$ is significantly shorter than the terminal U—N bonds of $[U(NEt_2)_4]_2$, which range from 2.21(1) to 2.24(1) Å,[6] and that the average U—N bond length in $HU[N(SiMe_3)_2]_3$ is 2.237(9) Å.[7]

Schrock and co-workers[8] have structurally characterized the d^2 tungsten(IV) phenoxide complexes, $W(O\text{-}2,6\text{-}R_2C_6H_3)_4$ (R = Me and Pr^i), and found the coordination geometries to be nearly square-planar. The latter has been explained in terms of oxygen lone-pair → tungsten π-donation, which stabilizes the square-planar geometry relative to the tetrahedral geometry.[8,9] For $U(O\text{-}2,6\text{-}Bu^t_2C_6H_3)_4$, it is unclear whether the tetrahedral geometry is the

* Found: C, 41.6; H, 8.0; N, 4.4. Calc. for $UC_{32}H_{75}N_3OSi_6$: C, 41.6; H, 8.2; N, 4.5%. ^1H NMR for $U(O\text{-}2,6\text{-}Bu^t_2C_6H_3)[N(SiMe_3)_2]_3$ (22°C, benzene-d_6): δ 16.2 (br s, *meta*); δ 15.1 (vbr s, Bu^t); δ 12.9 (br s, *para*); δ 3.4 (vbr s, TMS); δ −7.4 (vbr s, TMS); δ −20.9 (vbr s, TMS).

† Found: C, 63.5; H, 7.8; N, <0.05. Calc. for $UO_4C_{56}H_{84}$: C, 63.5; H, 8.0; N, 0.0%. ^1H NMR for $U(O\text{-}2,6\text{-}Bu^t_2C_6H_3)_4$ (22°C, benzene-d_6): δ 10.5 (d, J_{HH} = 7.3 Hz, *meta*); δ 8.3 (t, J_{HH} = 7.3 Hz, *para*); δ −1.0 (br s, Bu^t).

‡ X-ray analysis: $U(O\text{-}2,6\text{-}Bu^t_2C_6H_3)_4$ crystallizes in the tetragonal space group $I\bar{4}$ with cell constants (at −145°C): $a = b = 14.066(2)$, $c = 12.404(2)$ Å, $V = 2652.1$ Å^3, $d_{calc} = 1.327$ g cm^{-3} and $Z = 2$. The structure was solved by a combination of Patterson and Fourier techniques and refined (positional and anisotropic thermal parameters for 16 non-hydrogen atoms; positional and isotropic thermal parameters for 21 hydrogen atoms; 229 variables) by full-matrix least-squares. Final discrepancy indices were $R_F = 0.029$ and $R_{wF} = 0.030$ for those 2020 reflections with $F_o \geq 2.33\sigma(F_o)$. The limits of data collection were $6° \leq 2\theta \leq 60°$ (Mo-K_α).

result of the increased steric requirements of the phenoxide ligands, reduced oxygen → metal π-bonding, or a combination of the two. Efforts are underway in our laboratory to prepare and structurally characterize the related 2,6-diisopropyl- and 2,6-dimethylphenoxide complexes.

Acknowledgements—We wish to thank the Office of Energy Research, Division of Chemical Sciences, U.S. Department of Energy for financial support, and Dr D. L. Clark and Dr C. J. Burns for helpful discussions. We also thank Dr Clark for a preprint of ref. 9.

Supplementary Material Available. Tables of crystal data, fractional coordinates, anisotropic thermal parameters, and distances and angles have been deposited with the Cambridge Crystallographic Data Centre. A listing of observed and calculated structure factors has been deposited with the Editor at Indiana University and is also available from the Molecular Structure Center, Indiana University (Report no. 88901).

REFERENCES

1. W. G. Van Der Sluys, C. J. Burns, J. C. Huffman and A. P. Sattelberger, *J. Am. Chem. Soc.* 1988, **110**, 5924.
2. P. C. Blake, M. F. Lappert, R. G. Taylor, J. L. Atwood and H. Zhang, *Inorg. Chim. Acta* 1987, **139**, 13.
3. P. B. Hitchcock, M. F. Lappert, A. Singh, R. G. Taylor and D. Brown, *J. Chem. Soc., Chem. Commun.* 1983, 561.
4. A. Dormond, A. A. El Bouadili and C. Moïse, *J. Chem. Soc., Chem. Commun.* 1985, 914.
5. (a) S. J. Simpson, H. W. Turner and R. A. Andersen, *Inorg. Chem.* 1981, **20**, 2991; (b) S. J. Simpson and R. A. Andersen, *J. Am. Chem. Soc.* 1981, **103**, 4063.
6. J. G. Reynolds, A. Zalkin, D. H. Templeton, N. M. Edelstein and L. K. Templeton, *Inorg. Chem.* 1976, **15**, 2498.
7. R. A. Andersen, A. Zalkin and D. H. Templeton, *Inorg. Chem.* 1981, **20**, 622.
8. M. L. Listemann, R. R. Schrock, J. C. Dewan and R. M. Kolodziej, *Inorg. Chem.* 1988, **27**, 264.
9. R. H. Cayton, M. H. Chisholm, D. L. Clark and C. E. Hammond, *J. Am. Chem. Soc.*, in press.

Polyhedron Vol. 8, No. 9, pp. 1251–1252, 1989
Printed in Great Britain

0277–5387/89 $3.00+.00
© 1989 Pergamon Press plc

COMMUNICATION

A NEW TYPE OF CATENAND: INTERLOCKED MACROCYCLES HELD TOGETHER BY INTRAMOLECULAR SANDWICH BENZO-15-CROWN-5 POTASSIUM COMPLEXES

PAUL D. BEER* and ANNE S. ROTHIN

Department of Chemistry, University of Birmingham, P.O. Box 363, Birmingham B15 2TT, U.K.

(*Received* 27 *September* 1988; *accepted after revision* 10 *February* 1989)

Abstract—The synthesis of a new type of catenand ligand (**6**) containing two interlocked 6,6′-bis(benzo-15-crown-5)-2,2′-bipyridine moieties held together via intramolecular sandwich benzo-15-crown-5 potassium complexes is reported.

The catenands[1,2] are a new class of ligand that display unusual coordinating properties towards transition metals, such as the exceptional stabilization of transition metals in low oxidation states. For example nickel(I)[3] and formally copper(0)[1] catenates have both been successfully prepared. These properties are attributed to the novel molecular architecture of the catenands, the interlocking of macrocyclic ligands creating a unique topological environment favourable for a low valent transition metal. We report here the synthesis and preliminary coordination chemistry of a new type of catenand ligand (**6**) in which the interlocked macrocycles are held together by intramolecular sandwich benzo-15-crown-5 potassium complexes.

The condensation of 6,6′-bis(bromomethyl)-2,2′-bipyridine (**1**)[4] and 2 equivalents of 4-hydroxymethylbenzo-15-crown-5 (**2**)[5] in the presence of sodium hydride gave the new bis crown ether ligand (**3**) in 72% yield (Scheme 1). Its structure was characterized by elemental analysis, mass spectrometry and ^{1}H and ^{13}C NMR spectroscopy. The reaction of $Cu^I(CH_3CN)_4PF_6$[6] with 2 equivalents of **3** gave the deep orange air-stable crystalline complex, **4**. Reacting **4** with an excess amount of KPF_6 gave the new catenate, **5**.

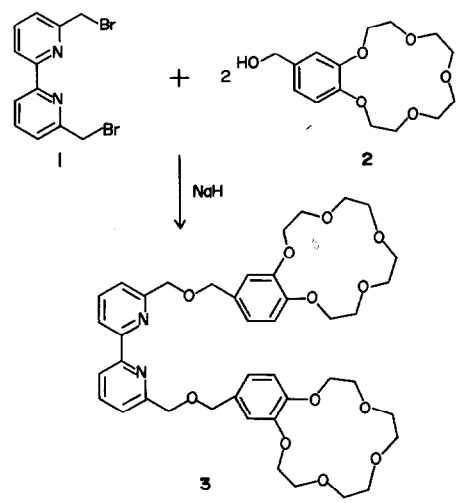

Scheme 1.

Copper(I) demetallation of **5** was achieved quantitatively on addition of either potassium or tetramethylammonium cyanide to produce the novel catenand **6** as a white solid.

The catenane structure of **6** was established by a combination of conductivity measurements (acetonitrile $\Lambda = 226\ \Omega^{-1}\ cm^2\ mol^{-1}$),† FAB mass spectrometry and ^{1}H NMR. The FAB mass spectrum of **6** displays the $[(\mathbf{6})-PF_6]^+$ molecular ion at 1776. The 270 MHz ^{1}H NMR spectrum of **5** showed the respective CH_2 absorptions at 4.35 and 4.58 ppm. These relatively high field positions may be attributed to the mutual ring current effects of the respective bipyridyl subunits in **5**. On removal of

* Author to whom correspondence should be addressed.

† Ligand **3** forms a 1 : 1 **3**·KPF_6 complex with excess KPF_6, whose conductivity (acetonitrile) $\Lambda = 118\ \Omega^{-1}\ cm^2\ mol^{-1}$ under identical experimental conditions.

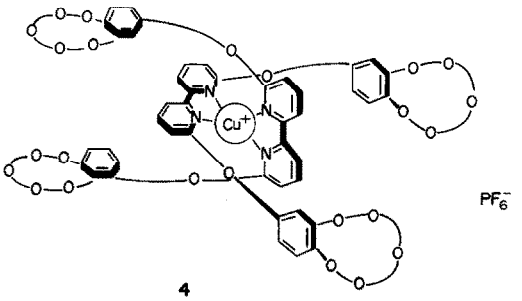

4

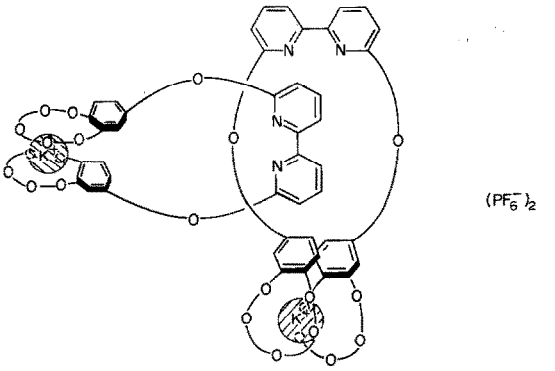

6

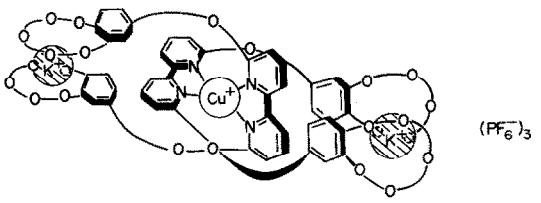

5

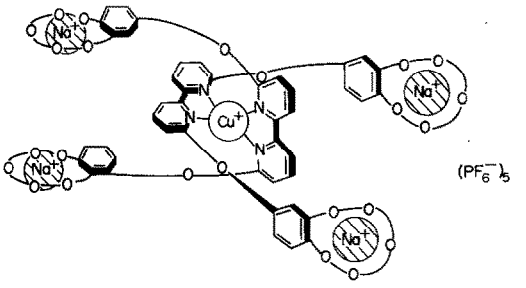

7

the copper(I) cation these ring current effects are negated and consequently the CH_2 absorptions of **6** are observed at lower field, 4.52 and 4.64 ppm, respectively. Similar ^{1}H NMR spectral characteristics are observed with the 1,10-phenanthrolene catenands and metallocatenates reported by Sauvage and co-workers.[1]

The electrochemical properties of the copper(I) complexes, **4** and **5**, were studied using cyclic voltammetry in dry DMF with SCE as reference. Neither complex could be electrochemically oxidized, the interlocked ligands stabilizing the tetrahedral coordination environment around the copper(I) metal centre. However, in contrast to the copper(I) catenates reported by Sauvage and co-workers,[1] both **4** and **5** exhibited *irreversible* reduction waves at -1.62 and -1.58 V, respectively, suggesting that copper demetallation occurs under these conditions.

In contrast to the potassium cation, Na^+ does *not* form a catenate structure with **4**, instead the polymetallic complex **7** was isolated.

Acknowledgements—We thank the SERC for a postdoctoral fellowship to A.S.R. and for use of the Mass Spectrometry Service at University College Swansea.

REFERENCES

1. C. O. Dietrich-Buchecker, J. P. Sauvage and J. M. Kern, *J. Am. Chem. Soc.* 1984, **106**, 3043.
2. C. O. Dietrich-Buchecker and J. P. Sauvage, *Chem. Rev.* 1987, **87**, 795.
3. C. O. Dietrich-Buchecker, J. M. Kern and J. P. Sauvage, *J. Chem. Soc., Chem. Commun.* 1985, 760.
4. J. C. Rodriguez-Ubis, B. Alpha, D. Plancherel and J. M. Lehn, *Helv. Chim. Acta* 1984, **67**, 2264.
5. A. H. Haines, I. Hodgkisson and C. Smith, *J. Chem. Soc., Perkin Trans. I* 1983, 311.
6. C. J. Kubas, B. Monzya and A. L. Crumbliss, *Inorg. Synth.* 1971, **19**, 90.

Polyhedron Vol. 8, No. 10, pp. 1253–1259, 1989
Printed in Great Britain

0277–5387/89 $3.00+.00
© 1989 Pergamon Press plc

PREPARATION AND X-RAY CRYSTAL STRUCTURE OF $[Ni_6\{\mu\text{-}S(CH_2)_3N(CH_3)_2\}_{12}]$, A CYCLIC HEXAMERIC HOMOTHIOLATE OF NICKEL

MERCÈ CAPDEVILA, PILAR GONZÁLEZ-DUARTE* and JOAN SOLA

Departament de Química, Universitat Autònoma de Barcelona, Bellaterra, 08193 Barcelona, Spain

and

CONCHA FOCES-FOCES, FÉLIX HERNÁNDEZ CANO and MARTÍN MARTÍNEZ-RIPOLL

UEI de Cristalografía, Instituto Rocasolano CSIC, Serrano 119, 28006 Madrid, Spain

(*Received* 21 *September* 1988; *accepted* 10 *November* 1988)

Abstract—Highly hygroscopic, black, prism-like crystals separated out from CH_3CN solutions containing $(Et_4N)_2NiCl_4$ and 3-dimethylamino-1-propanethiol at several mole ratios. Crystals of $[Ni_6\{S(CH_2)_3N(CH_3)_2\}_{12}]$ are orthorhombic, space group $P2_12_12$ with $a = 30.197(6)$, $b = 29.231(4)$, $c = 10.649(1)$ Å and $Z = 4$. The Ni_6S_{12} core of each molecular unit constitutes a hexagonal prism whose rectangular faces are NiS_4 coordination planes (Ni—S = 2.19 Å; S—Ni—S = 82.2°, 98.05°). Approximate diameters for the Ni_6 and S_6 rings are 5.85 and 6.60 Å, respectively. The allowed molecular symmetry for the Ni_6S_{12} core, D_{6h}, is reduced to D_{3d} when the axial and equatorial S—C bonds are included.

Since the report in 1965 of the hexagonal "tiara" structure of $[Ni_6(SEt)_{12}]$,[1] one of the first discrete homothiolate compounds,[2] several cyclic nickel(II) thiolate complexes with different degrees of oligomerization have been described. Thus, a square cyclic structure, $[Ni_4\{\mu\text{-}SC_5H_9N(CH_3)\}_8]$,[3] hexagonal molecular cycles, $[Ni_6(\mu\text{-}SR)_{12}]$, R = Et,[1] CH_2CH_2OH,[4] $(CH_2)_3\dot{N}H(CH_3)_2$,[5] and an octogonal cyclic molecule, $[Ni_8(\mu\text{-}SCH_2COOEt)_{16}]$[6] have been characterized structurally by X-ray diffraction prior to the recent publication of the first pentanuclear complex, $[Ni_5(\mu\text{-}SEt)_{10}]$, together with another tetrameric species, $[Ni_4(\mu\text{-}SC_6H_{11})_8]$.[7] The thiol ligand in the pentametallic complex is the same as that in the hexameric unit $[Ni_6(SEt)_{12}]$, already mentioned.

Considering the rest of the metals in the nickel group, cyclic structures have only been found in the case of palladium, and the two examples known, $[Pd(SR)_2]_n$, R = CH_2CH_2OH[4] and $CH_2CH_2CH_3$,[8] correspond to hexameric molecular units ($n = 6$). The M_nS_{2n} core of the macrocyclic molecules, $[Ni(SR)_2]_n$, $4 \leqslant n \leqslant 8$, can always be described as a regular prism with as many faces as number of metal atoms, each face having the metal atom in its centre and linking to each other by means of the doubly-bridging sulphur atoms that lie on the vertices.

By reacting different nickel compounds with 3-dimethylamino-1-propanethiol at varying metal-to-ligand ratios under anhydrous conditions and inert atmosphere, we have obtained, as a side product, a black highly hygroscopic crystalline complex of the empirical formula $[Ni\{S(CH_2)_3N(CH_3)_2\}_2]$. A compound with the same composition had already been found in this laboratory,[5] and it had been proposed that its structure could consist of hexanuclear cyclic molecules analogous to those found in $[Ni_6\{\mu\text{-}S(CH_2)_3NH(CH_3)_2\}_{12}](ClO_4)_{12}\cdot 2H_2O$.[5] The facts that the reaction medium was completely different in both syntheses of $[Ni\{S(CH_2)_3N(CH_3)_2\}_2]$, that the γ-mercaptoamine complex of known structure has the ligand in a zwitterionic form, and that rings of different nuclearity have been found for the com-

* Author to whom correspondence should be addressed.

plex $[Ni(SEt)_2]_n$,[1,7] prompted us to determine the structure of the complex $[Ni\{S(CH_2)_3N(CH_3)_2\}_2]$, synthesized in organic medium.

EXPERIMENTAL

Preparation of compounds

3-Dimethylamino-1-propanethiol was synthesized according to a known procedure[9] and purified by vacuum distillation until its purity, checked by iodometric determination of the SH group, was > 99.5%. The corresponding sodium salt was prepared by mixing a methanolic solution of NaOMe, always less than 1 cm^3, with an equivalent amount of the thiol in 20 cm^3 of CH_3CN. $(Et_4N)_2NiCl_4$ was obtained by following a standard procedure.[10] In the following preparations, degassed solvents were used and all manipulations were performed under an atmosphere of dry and pure nitrogen.

$[Ni_6\{S(CH_2)_3N(CH_3)_2\}_{12}]$. A solution of $(Et_4N)_2NiCl_4$ in 25 cm^3 of CH_3CN was slowly added with constant stirring to the sodium thiolate solution indicated above. The colour rapidly turned dark red–brown. After the mixture was stirred for 2 h, NaCl was removed by filtration. Cooling the filtrate to −20°C afforded a brown solid, which is now being characterized. Further cooling of the filtrate at −20°C for 1 week afforded large shiny black prisms of pure product, independently of whether the ligand-to-metal mole ratio in the initial reaction mixture had been 4:1, 6:1 or 8:1. The crystals were filtered very rapidly at approximately −15°C because of the strong temperature dependence of their solubility, then dried *in vacuo* and stored under nitrogen. Found: C, 39.8; N, 9.1; S, 21.2. Calc. for $C_{10}H_{24}N_2NiS_2$: C, 40.7; N, 9.5; S, 21.7%.

Physical measurements

The IR spectrum of the complex (4000–400 cm^{-1}), recorded as KBr pellet on a Perkin–Elmer 1710 spectrophotometer, shows no difference to that of the free ligand, the 3000–2700 cm^{-1} region indicating very clearly that the nitrogen atom is not involved in coordination.[5]

Microanalyses were performed with a Carlo–Erba N.A. 1500 analyser.

X-ray data collection, solution and refinement of the structure

A suitable crystal was wedged into a glass capillary and sealed under an atmosphere of nitrogen. The main characteristics of the crystallographic analysis are given in Table 1. The structure was solved, as far as the heavy atoms are concerned, by difference direct methods (DIRDIF), starting from a square planar nickel atom surrounded by four sulphur atoms. A hexanuclear Ni_6S_{12} cage has been established unambiguously as well as the corresponding geometric parameters, although the disorder present in the aliphatic chains has prevented the total completion of the structure. Atomic coordinates and thermal parameters for all nickel, sulphur and carbon atoms linked to sulphur atoms and lists of F_o and F_c values have been deposited as supplementary material with the Editor. Atomic coordinates have also been deposited with the Cambridge Crystallographic Data Centre. Selected bond distances and angles are given in Table 2.

RESULTS AND DISCUSSION

Synthesis

$[Ni_6\{S(CH_2)_3N(CH_3)_2\}_{12}]$ was always obtained as a final pure by-product when mixing nickel(II) and the sodium thiolate with excess ligand. It is extremely hygroscopic and also very soluble in all common organic solvents.

Owing to the fact that different ligand-to-metal ratios have been tried and that in all cases a significant amount of pure $[Ni(SR)_2]$ complex is collected after another solid has separated out from solution, it can be concluded that the hexameric nickel complex is very stable and probably present in solution from the time the reactants are mixed. Its very high solubility, which is consistent with the molecular structure, agrees with the facts that it appears as the final product and also that it requires low temperature while separating it from solution.

Despite the common feature for all cyclic $[Ni(SR)_2]_n$ complexes, that they show an appreciable solubility in different organic solvents, it is difficult to find a relationship between the synthetic method followed in each case ($n = 4$,[3,7] $n = 5$,[7] $n = 6$[1,4,5] and this work, $n = 8$[6]) and the nuclearity of the complex species isolated.

Description of the structure of $[Ni_6\{\mu\text{-}S(CH_2)_3N(CH_3)_2\}_{12}]$

The crystal structure of the title compound consists of neutral cyclic molecules, each of them containing a regular hexagon of nickel atoms, Table 3, bridged over the edges by pairs of doubly-bridging thiolate ligands, Fig. 1. The Ni_6S_{12} core, that shows D_{6h} symmetry, can thus be described as a hexagonal prism with nickel atoms at the centres of its rectangular faces and sulphur atoms at the vertices.

Table 1. Crystallographic data for $Ni_6[S(CH_2)_3N(CH_3)_2]_{12}$

Crystal data	
Formula	$[NiS_2N_2C_{10}H_{24}]_6$
Crystal size (mm)	$0.8 \times 0.2 \times 0.2$
Crystal habit and colour	Prismatic, black
Symmetry	$P2_12_12$
Unit cell determination	L.S. fit from 35 reflections ($\theta < 40°$)
Unit cell dimensions	30.197(6), 29.231(4), 10.649(1) Å
Packing: V (Å^3), Z, D_c (g cm^{-3}), M, $F(000)$	9399(2), 4, 1.25, 1769.7, 3792
Experimental data	
Technique	Four circle diffractometer: PW1100 Bisecting geometry Graphite oriented monochromator Radiation: Cu-K_α (1.54178 Å) ω–2θ scans, scan width: 1.5° Detector apertures $1 \times 1°$, up θ_{max} 60° 2 min./reflection
Number of reflections:	
Measured	7676
Independent	7676
Observed	3806 ($3\sigma(I)$ criterion)
Standard reflections:	2 reflections every 90 min Variation: none
Max–min transmission factors	1.38, 0.79
Solution and refinement	
Solution	Direct Difference Methods (DIRDIF[11])
Refinement	L.S. on F_{obs}
Final R	12.1[a]
Computer and programs	DIRDIF,[11] XRAY76[12]
Scattering factors and anomalous dispersion (Ni, S)	*International Tables for X-ray Crystallography*[13]

[a] The high R value is due to serious disorder and incomplete modelling in the side groups.

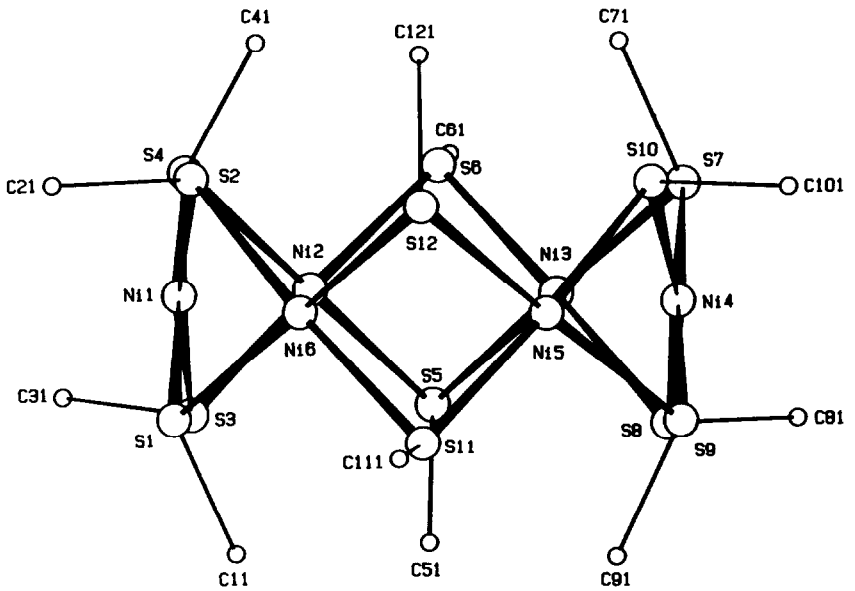

Fig. 1. Structure of the Ni_6S_{12} core and the S—C bonds of $[Ni_6\{S(CH_2)_3N(CH_3)_2\}_{12}]$ showing the atom labelling scheme.

Table 2. Selected bond distances (Å) and angles (°) for $[Ni_6\{S(CH_2)_3N(CH_3)_2\}_{12}]$

Ni···Ni		Ni···S	
Ni_1—Ni_2	2.921(9)	Ni_1—S_1	2.205(12)
Ni_2—Ni_3	2.920(9)	Ni_1—S_3	2.205(12)
Ni_4—Ni_5	2.924(9)	Ni_2—S_3	2.208(13)
Ni_1—Ni_6	2.913(9)	Ni_2—S_5	2.182(12)
Ni_3—Ni_4	2.916(9)	Ni_3—S_5	2.194(12)
Ni_5—Ni_6	2.927(9)	Ni_3—S_7	2.186(12)
		Ni_4—S_7	2.185(12)
Mean value:	2.920	Ni_4—S_9	2.205(13)
		Ni_5—S_9	2.194(13)
		Ni_5—S_{11}	2.178(13)
		Ni_6—S_1	2.165(12)
S···C		Ni_6—S_{11}	2.197(12)
S_1—C_{11}	1.882(39)	Ni_1—S_2	2.197(13)
S_3—C_{31}	1.823(46)	Ni_1—S_4	2.195(14)
S_5—C_{51}	1.843(38)	Ni_2—S_4	2.210(13)
S_7—C_{71}	1.903(45)	Ni_2—S_6	2.188(14)
S_9—C_{91}	1.838(55)	Ni_3—S_6	2.151(12)
S_{11}—C_{111}	1.811(46)	Ni_3—S_8	2.221(11)
S_2—C_{21}	1.845(51)	Ni_4—S_8	2.193(11)
S_4—C_{41}	1.850(54)	Ni_4—S_{10}	2.177(12)
S_6—C_{61}	1.824(49)	Ni_5—S_{10}	2.188(13)
S_8—C_{81}	1.817(42)	Ni_5—S_{12}	2.184(12)
S_{10}—C_{101}	1.933(44)	Ni_6—S_2	2.218(13)
S_{12}—C_{121}	1.934(45)	Ni_6—S_{12}	2.199(13)
Mean value:	1.858	Mean value:	2.193
Ni···Ni···Ni		S···Ni···S (θ_1)	
Ni_2—Ni_1—Ni_6	118.0(3)	S_3—Ni_1—S_4	82.5(5)
Ni_2—Ni_3—Ni_4	121.1(3)	S_5—Ni_2—S_6	82.6(5)
Ni_4—Ni_5—Ni_6	120.0(3)	S_7—Ni_3—S_8	81.4(4)
Ni_1—Ni_2—Ni_3	120.9(3)	S_9—Ni_4—S_{10}	81.8(5)
Ni_3—Ni_4—Ni_5	118.3(3)	S_{11}—Ni_5—S_{12}	82.8(5)
Ni_5—Ni_6—Ni_1	121.6(3)	S_{10}—Ni_5—S_9	81.8(5)
		S_{11}—Ni_6—S_{12}	82.0(5)
Mean value:	120.0	S_1—Ni_1—S_2	81.9(5)
		S_3—Ni_2—S_4	82.1(5)
		S_5—Ni_3—S_6	83.1(5)
S···Ni···S (θ_2)		S_7—Ni_4—S_8	82.0(4)
S_1—Ni_1—S_3	97.6(5)	S_1—Ni_6—S_2	82.3(5)
S_3—Ni_2—S_5	98.1(4)		
S_5—Ni_3—S_8	98.7(4)	Mean value:	82.2
S_7—Ni_4—S_{10}	98.4(5)		
S_1—Ni_6—S_{11}	97.7(5)		
S_2—Ni_1—S_4	98.0(5)		
S_4—Ni_2—S_6	97.4(5)		
S_6—Ni_3—S_7	97.1(5)		
S_8—Ni_4—S_9	98.3(5)		
S_{10}—Ni_5—S_{12}	98.4(5)		
S_{11}—Ni_5—S_9	98.3(5)		
S_2—Ni_6—S_{12}	98.8(5)		
Mean value:	98.1		

Table 3. Relevant geometric parameters for the Ni_6S_{12} core of $[Ni_6\{S(CH_2)_3N(CH_3)_2\}_{12}]$

Displacements of atoms from Ni_6 and S_6 planes (in pm)[a]						
Plane	S_4	S_2	S_{12}	S_6	S_{10}	S_7
I S_6, above	−3.22	6.54	−12.33	2.68	12.06	−5.73
Plane	Ni_1	Ni_2	Ni_3	Ni_4	Ni_5	Ni_6
II Ni_6	3.07	−0.63	−2.29	2.97	−0.45	−2.67
Plane	S_1	S_3	S_{11}	S_5	S_8	S_9
III S_6, below	6.42	−2.98	−13.02	4.14	−6.42	11.86

Angles between planes (in °)

I/II: 0.397 II/III: 0.304 I/III: 0.570

Dihedral angles between NiS_4 planes (°)		
Atoms defining the plane	Dihedral angle (°)	Nickel[b]
Ni_1—S_1—S_2—S_3—S_4	117.792	−0.0609
Ni_2—S_3—S_4—S_5—S_6		0.0505
Ni_2—S_3—S_4—S_5—S_6	123.031	
Ni_3—S_5—S_6—S_7—S_8		0.0435
Ni_3—S_5—S_6—S_7—S_8	118.750	
Ni_4—S_7—S_8—S_9—S_{10}		0.0674
Ni_4—S_7—S_8—S_9—S_{10}	116.812	
Ni_5—S_9—S_{10}—S_{11}—S_{12}		−0.0636
Ni_5—S_9—S_{10}—S_{11}—S_{12}	123.863	
Ni_6—S_1—S_2—S_{11}—S_{12}		−0.0353
Ni_6—S_1—S_2—S_{11}—S_{12}	119.534	
Ni_1—S_1—S_2—S_3—S_4		

Dihedral angle, mean value: 120°; Nickel, mean value: 0.002 Å

[a] Atom labelling is given in Fig. 1.

[b] Displacement of nickel atoms from NiS_4 planes (in Å).

Calculated mean values for distances and angles in each face, given in Fig. 2, agree very well with other literature data for cyclic $[Ni(SR)_2]$ complexes.[6,7]

Coordination around the metal is essentially square planar. The mean displacement of nickel from the S_4 coordination plane, calculated from values given in Table 3, is only 0.002 Å. Atoms corresponding to the Ni_6 hexagon, as well as those of the parallel and larger S_6 hexagons above and below, deviate very slightly from the planes they define. The mean distance between the Ni_6 and S_6 planes is 1.44 Å. These values together with the dihedral angles between adjacent NiS_4 planes are shown in Table 3.

The position of each carbon linked to a sulphur atom, Fig. 1, shows that the ligand chains depart from the S_6 hexagons alternately, according to axial and equatorial configurations. Thus, it can be assumed that six C—S vectors are practically parallel to the S_6 planes, while the others are divided into two sets, each having opposite directions roughly along the S—S lateral edges of the hexagonal prism (see Fig. 2). The idealized symmetry of the Ni_6S_{12} core after including these 12 carbon atoms is D_{3d}. Calculated mean values for the Ni—S—Ni′, Ni—S—C_{ax}, Ni—S—C_{eq}, C_{ax}—S—Ni′ and C_{eq}—S—Ni′ angles, Fig. 2, are 83.6, 110.3, 106.5, 112.5 and 106.4°, respectively.

The Ni—Ni distance between adjacent faces, 2.92 Å, precludes any metal–metal interaction. Approximate diameters for Ni_6 and S_6 rings are 5.85 and 6.60 Å, respectively. These data agree very well with the corresponding values of other hexameric nickel–thiolate complexes.[1,4,5]

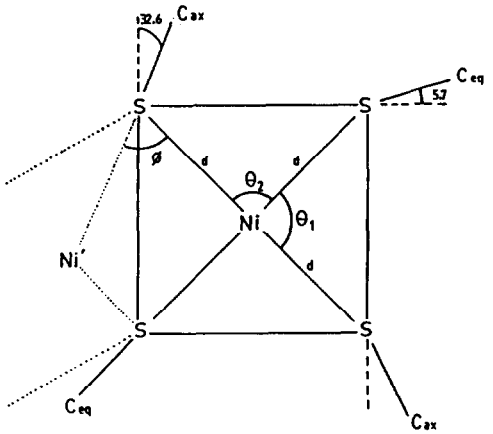

$d = 2.193$ Å (24 values)
$\theta_1 = 82.2°$ (12 values)
$\theta_2 = 98.1°$ (12 values)

Fig. 2. Relevant geometrical parameters at each face and at the edge linkage of the hexagonal prism.

Table 4. Geometric parameters, defined in Fig. 2, of several hexameric nickel(II) thiolates[a,b]

SR	d(Ni—S) (Å)	d'(Ni—Ni') (Å)	Nickel[c]	θ_1	θ_2	ϕ	Reference
SEt	2.20	2.92	[d]	≈ 83	[d]	≈ 83	1
$S(CH_2)_3NHMe_2$	2.20	2.93	0.04	81.9	98.0	83.9	5
$S(CH_2)_3NMe_2$	2.19	2.92	0.002	82.2	98.05	83.6	This work
SCH_2CH_2OH	2.21	2.92	< 0.06	82.6	97.5	82.9	4
SEt[b]	2.20	2.82	0.12	81.8	98.3	79.6	7

[a] In case there are several values, mean values are given.
[b] The pentameric cycle reported recently is included for comparison.
[c] Defined in Table 3.
[d] Not reported.

The similarity of the main geometric parameters in $[Ni(SR)_2]_6$ complexes with known structures is noteworthy, Table 4, since it clearly indicates that the substituents on the aliphatic chain of the thiol have no influence on the geometry of the Ni_6S_{12} core. This could also explain why there is no important difference between the structures of $[Ni_6\{S(CH_2)_3\overset{+}{N}H(CH_3)_2\}_{12}]^{12+}$ [5] and $[Ni_6\{S(CH_2)_3N(CH_3)_2\}_{12}]$ (this work), where the ligand is, respectively, in a zwitterionic or an anionic form. Despite the fact that complexes with a different degree of oligomeration may exist in solution,[15] and that there must be a relation between solid complex species formed and solubility in a particular medium, all existing data seem to favour the hexameric cyclic nickel(II) thiolates if steric repulsions between ligand substituents[3,7] or inclusion of coordinating groups on the toroid axis[6] are absent. However, the report on the pentanuclear $[Ni_5(SEt)_{10}]$ complex[7] enhances the need for finding an explanation for experimental data.

Acknowledgements—Financial support from CAYCIT (1058–84) and CIRIT is gratefully acknowledged.

REFERENCES

1. P. Woodward, L. F. Dahl, E. W. Abel and B. C. Crosse, *J. Am. Chem. Soc.* 1965, **87**, 5251.
2. I. G. Dance, *Polyhedron* 1986, **5**, 1037.
3. W. Gaete, J. Ros, X. Solans, M. Font-Altaba and J. L. Briansó, *Inorg. Chem.* 1984, **23**, 39.
4. R. O. Gould and M. M. Harding, *J. Chem. Soc. A* 1970, 875.
5. H. Barrera, J. C. Bayón, J. Suades, C. Germain and J. P. Declerq, *Polyhedron* 1984, **3**, 969.
6. I. G. Dance, M. L. Scudder and R. Secomd, *Inorg. Chem.* 1985, **24**, 1201.
7. M. Kriege and G. Henkel, *Z. Naturfor.* 1987, **42b**, 1121.
8. N. Kunchur, *Acta Cryst.* 1968, **B24**, 1623.
9. B. C. Cossar, J. O. Fournier, D. L. Fields and D. D. Reynolds, *J. Org. Chem.* 1962, **27**, 93.
10. N. S. Gill and F. B. Taylor, *Inorg. Synth.* 1967, **9**, 136.

11. P. T. Beurkens, W. P. Bosman, H. M. Doesburg, R. O. Gould, Th. E. M. Van der Hark, P. A. J. Prick, J. H. Noordik, G. Beurkens, V. Parthasarathi, H. J. Bruins Slot, R. C. Haltiwanger and J. M. M. Smits, DIRDIF System. Crystallography Laboratory, Toernooivel, Nijmegen, The Netherlands (1984).
12. J. M. Stewart, P. A. Machin, C. W. Dickinson, H. L. Ammon, H. Heck and H. Flack, *The X-ray system*, Technical report TR-446. Computer Science Center, University of Maryland, U.S.A. (1976).
13. *International Tables for X-ray Crystallography*, Vol. IV. Kynoch Press, Birmingham, U.K. (1974).
14. E. W. Abel and B. C. Crosse, *J. Chem. Soc. A* 1966, 1377.
15. I. G. Dance, M. L. Scudder and R. Secomb, *Inorg. Chem.* 1985, **24**, 1203.

Polyhedron Vol. 8, No. 10, pp. 1261–1277, 1989
Printed in Great Britain

0277–5387/89 $3.00+.00
© 1989 Pergamon Press plc

TUNGSTEN COMPLEXES WITH STRONG π-DONOR AND π-ACCEPTOR LIGANDS: $W(E)Cl_2(L)(PR_3)_2$ (E = O, NR, S, AND L = CO, CNR, CH_2=CHR AND O=CHMe)

FU-MIN SU, JEFFREY C. BRYAN, SOONHEE JANG and JAMES M. MAYER*

Department of Chemistry, University of Washington, Seattle, WA 98195, U.S.A.

(*Received* 17 *September* 1988; *accepted* 23 *November* 1988)

Abstract—The synthesis and characterization of a series of tungsten complexes, $W(E)Cl_2(L)(PR_3)_2$, containing both a π-donor group (E = oxo, imido, or sulphido) and a π-acceptor ligand (L = CO, CN^{t}Bu, CH_2=CHR, O=CHMe) is reported (PR_3 = PMe_3, $PMePh_2$). The compounds are prepared by substitution of a phosphine ligand in $W(E)Cl_2(PR_3)_3$ by L and by oxidative addition of heterocumulenes E=L, epoxides or episulphides to $WCl_2(PMePh_2)_4$. All of the compounds have an octahedral structure with the π-donor and π-acceptor ligands *cis*, according to spectroscopic data and X-ray crystal structures of oxo–carbonyl (**4**), oxo-ethylene (**7**) and imido–carbonyl (**25**) complexes. The ethylene ligands are oriented perpendicular to the tungsten–oxygen, –nitrogen, or –sulphur multiple bond, and are non-fluxional by NMR. These geometrical features are a direct result of the electronic structure of the d^2 metal centre. The dihapto coordination of acetaldehyde shows the substantial π-basicity of the tungsten(IV)–oxo centre. The CO stretching frequencies indicate that the donor abilities are in the order: oxo < sulphido < imido (< alkylidene < alkylidyne). Complexes **4**, **7** and **25** are significantly distorted from octahedral geometry, also due to the electronic influence of two π-bonding ligands. The structure of $WCl_2(PMePh_2)_4$ (**1**) shows smaller distortions, a result of the steric bulk of the four phosphine ligands. Crystallographic data for **1**: $P\bar{1}$, a = 11.7401(13), b = 14.2555(12), c = 17.5922(12) Å, α = 76.226(6), β = 70.891(7), γ = 83.476(8)°, Z = 2; for **25**: *Pbcn*, a = 17.764(2), b = 15.821(6), c = 23.829(3) Å, Z = 8.

Metal–ligand π-bonding can be divided into two types. π-Donor ligands, such as terminal oxo (O^{2-}), imido (NR^{2-}), and sulphido (S^{2-}) groups, form multiple bonds with transition metal centres, formally by donation of electrons to empty metal d orbitals.[1] Because of the need for empty d orbitals, these groups are found as terminal ligands predominantly in high oxidation state complexes, with d^0, d^1 or d^2 electronic configurations. In contrast, the π-acceptor (π-acid) ligands: carbon monoxide, isonitriles and olefins require filled d orbital(s) of π-symmetry for productive π-bonding.[2] The filled d_π orbital must in addition be high enough in energy to interact strongly with the ligand acceptor orbital(s), so that π-acid ligands are found mostly in low-valent complexes. Since the two classes of ligands have conflicting requirements, few examples of complexes containing both types have been reported.[3]

This report describes the synthesis and characterization of a series of tungsten(IV) complexes with both a π-donor oxo, imido, or sulphido group and a π-acid carbonyl, isonitrile or ethylene ligand.[4] These are the first isolated examples of olefin complexes with terminal oxo, sulphido or imido ligands,[5] and of oxo–carbonyl and sulphido–carbonyl species. The compounds are prepared by substitution and/or by oxidative addition to a tungsten(II) complex. The electronic structure of these compounds is discussed in light of their structure and reactivity, with the conclusion that the d^2 configuration is ideal for molecules with both classes of ligands.

The oxo- and imido–olefin complexes are of particular interest because species of this kind have been suggested as intermediates in olefin oxidation reactions by metal reagents (osmium tetroxide,

* Author to whom correspondence should be addressed.

chromyl chloride, etc.) and by metalloenzymes.[1,6] Similarly, oxo–carbonyl species may be intermediates in the oxidation of CO by metal oxides.[7] Indeed, the oxidative addition of epoxides and carbon dioxide to form oxo–olefin and oxo-carbonyl complexes reported here is the reverse of olefin or CO oxidation.

RESULTS

Synthesis

Two synthetic routes have been used to prepare the tungsten(IV) oxo, imido, and sulphido complexes: substitution of a phosphine ligand in the tris-phosphine complexes $W(E)Cl_2(PR_3)_3$ (E = O, S, NR) and oxidative addition of epoxides, episulphides and heterocumulenes to $WCl_2(PR_3)_4$ (**1**) [eq. (1)].

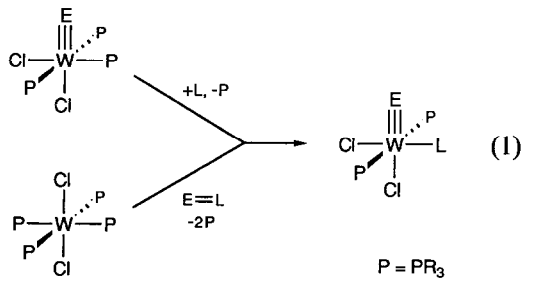

(1)

E = O, S, N^{t}Bu, NPh, N-*p*-Tol, $NSiMe_3$; PR_3 = $PMePh_2$, PMe_3; L = CO, CN^{t}Bu, $CH_2{=}CH_2$, $CH_2{=}CHR$, $PhC{\equiv}CH$.

Many of the compounds have been prepared by both routes. The molybdenum oxo–carbonyl complex $Mo(O)Cl_2(CO)(PMePh_2)_2$ is also formed by displacement of a phosphine ligand in $Mo(O)Cl_2(PMePh_2)_3$ with CO. The isolated compounds are listed in Table 1, together with the compound numbers and the method(s) of synthesis. The last column indicates the reagent used in the oxidative addition reaction.

Ligand substitution is the most straightforward procedure, since facile routes to $W(O)Cl_2(PR_3)_3$ [PR_3 = $PMePh_2$ (**2**), PMe_3 (**3**)][8] and $W(NPh)Cl_2(PR_3)_3$ [PR_3 = $PMePh_2$ (**19**), PMe_3 (**20**)][9] have been reported. Preparation of the sulphido complex $W(S)Cl_2(PMePh_2)_3$ (**13**) is reported below. Carbon monoxide, *t*-butylisonitrile and ethylene all readily displace $PMePh_2$ from $W(E)Cl_2(PMePh_2)_3$ (E = O, S, NPh). The reactions are equilibria, however, and addition of excess $PMePh_2$ to the CO, CN^{t}Bu and $CH_2{=}CH_2$ complexes in a sealed NMR tube in general forms a small amount of the tris-$PMePh_2$ complexes. The formation of PMe_3–carbonyl and –ethylene complexes from **3** is less favourable: $W(O)Cl_2(CH_2{=}CH_2)(PMe_3)_2$ has been observed in the presence of excess ethylene, but we have been unable to isolate it because the equilibrium is unfavourable. In contrast, PMe_3 is readily displaced from the imido complex **20** by ethylene.

Terminal olefins such as propylene do not bind as strongly to the tungsten–oxo centre and can be completely displaced by excess $PMePh_2$. Internal olefins do not react with $W(O)Cl_2(PMePh_2)_3$ (**2**). This pattern of binding $CH_2{=}CH_2$ > $CH_2{=}CHR$ > $RHC{=}CHR$, is typical of transition metal olefin complexes.[10] Butadiene, vinyl fluoride and allyl alcohol displace phosphine from **2**, but the electron rich olefin ethyl–vinyl–ether does not, indicating that π-backbonding is important in stabilizing the olefin complexes (see below). The π-basicity of the tungsten(IV) centre is especially evident in the formation of the η^2-acetaldehyde complex, **12**, by reaction of **2** with $O{=}CHMe$. η^2-Aldehyde complexes are rare;[11] the η^2-form is favoured over the η^1-linkage isomer only by metal centres that have a strong preference for a π-acid ligand.

The oxidative addition reactions of $WCl_2(PMePh_2)_4$ (**1**)[12] generally require a few hours at ambient temperatures in benzene solution. $PMePh_2$ is the ligand of choice because its large size favours dissociation; PMe_3 is more difficult to substitute because of its small size and greater donor ability.[13] The difference between the two ligands is observed both in the thermodynamics of the ligand substitution reactions, as described above, and in the reaction kinetics. $WCl_2(PMe_3)_4$ reacts very slowly at ambient temperatures with CO_2, and reactions of $W(NPh)Cl_2(PR_3)_3$ occur at 25°C for PR_3 = $PMePh_2$ but only at elevated temperatures for the PMe_3 derivative.

Epoxides react with **1** to give an apparent equilibrium mixture of tungsten(IV) oxo complexes. Thus ethylene oxide gives predominantly the oxo–ethylene complex **7**, propylene oxide gives a mixture of the propylene and phosphine complexes **8** and **2**, and epoxides of internal olefines (2-butene oxides, tetramethylethylene oxide) give only the tris-phosphine complex **2**. The rate of equilibration among the oxo complexes is comparable to or faster than the rate of oxidative addition. Ethylene sulphide reacts with **1** to give the sulphido ethylene complex **16** as the major product when the stoichiometry is 1 : 1, but ethylene sulphide reacts further with **16** to give unidentified tungsten product(s) and $MePh_2PS$.

Heterocumulenes X=C=Y react with **1** with cleavage of one double bond, forming a tungsten–X multiple bond and a C≡Y ligand. When X and

Table 1. Compounds prepared and synthetic procedures

Number	Compound	Prepared by: Substitution	Prepared by: Oxidative addition, $WCl_2(PMePh_2)_4$ (1)+
2	$W(O)Cl_2(PMePh_2)_3$[a,b]		
3	$W(O)Cl_2(PMe_3)_3$[a]		
4	$W(O)Cl_2(CO)(PMePh_2)_2$	√	CO_2
5	$W(O)Cl_2(CO)(PMe_3)_2$	√	CO_2
6	$W(O)Cl_2(CN^tBu)(PMePh_2)_2$	√	
7	$W(O)Cl_2(CH_2{=}CH_2)(PMePh_2)_2$	√	$\overline{OCH_2CH_2}$
8	$W(O)Cl_2(CH_2{=}CHMe)(PMePh_2)_2$	√	$\overline{OCH_2CHMe}$[c]
9	$W(O)Cl_2(CH_2{=}CHCH{=}CH_2)(PMePh_2)_2$	√	
10	$W(O)Cl_2(CH_2{=}CHCH_2OH)(PMePh_2)_2$	√	
11	$W(O)Cl_2(PhC{\equiv}CH)(PMePh_2)_2$	√	
12	$W(O)Cl_2(O{=}CHMe)(PMePh_2)_2$	√	
13	$W(S)Cl_2(PMePh_2)_3$		$MePh_2PS$
14	$W(S)Cl_2(CO)(PMePh_2)_2$	√	OCS
15	$W(S)Cl_2(CN^tBu)(PMePh_2)_2$	√	SCN^tBu
16	$W(S)Cl_2(CH_2{=}CH_2)(PMePh_2)_2$	√	$\overline{SCH_2CH_2}$[d]
17	$W(N^tBu)Cl_2(CO)(PMePh_2)_2$		OCN^tBu
18	$W(N^tBu)Cl_2(CN^tBu)(PMePh_2)_2$		$^tBuNCN^tBu$
19	$W(NPh)Cl_2(PMePh_2)_3$		
20	$W(NPh)Cl_2(PMe_3)_3$[e]		
21	$W(NPh)Cl_2(CO)(PMePh_2)_2$	√	
22	$W(NPh)Cl_2(CO)(PMe_3)_2$	√	
23	$W(NPh)Cl_2(CH_2{=}CH_2)(PMePh_2)_2$	√	
24	$W(NPh)Cl_2(CH_2{=}CH_2)(PMe_3)_2$	√	
25	$W(N\text{-}p\text{-}Tol)Cl_2(CO)(PMePh_2)_2$		OCN-*p*-Tol
26	$W(NSiMe_3)Cl_2(CO)(PMePh_2)_2$		$OCNSiMe_3$
27	$Mo(O)Cl_2(CO)(PMePh_2)_2$	√	

[a] Reference 8.
[b] Also formed from 1+ sterically crowded epoxides, see text.
[c] Formed together with **2**.
[d] A number of products are formed in the reaction.
[e] Reference 9.

Y are different the reactions are regioselective: isocyanates yield only tungsten–imido–carbonyl complexes, and SCO and SCN^tBu give the sulphido–carbonyl and sulphido–isonitrile compounds. The weaker double bond of the heterocumulene appears to be cleaved in each case. The reaction of **1** with CS_2 gave only $MePh_2PS$ and uncharacterized tungsten product(s).

The oxidative addition of heterocumulenes is an irreversible reaction. Isomeric oxo–isonitrile (**6**) and imido–carbonyl (**17**) species have been isolated and they do not interconvert, even after a week at 70°C [eq. (2)].

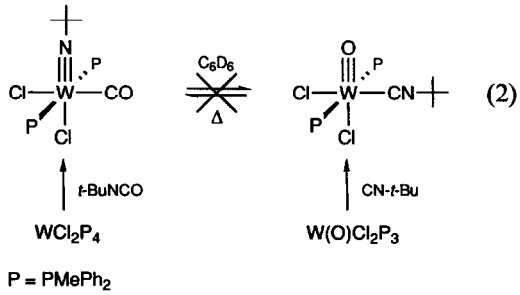

(2)

^{13}C enrichment of the oxo–carbonyl complex **4** is not observed on reaction with $^{13}CO_2$ for a week at 25°C.

The oxidative addition reaction appears to be a powerful route to high oxidation state tungsten compounds. We have, for instance, recently reported the addition of ketones to **1**, forming oxo–alkylidene compounds.[14] This route has also been used to prepare the sulphido tris(phosphine) complex **13** from the phosphine sulphide [eq. (3)]:

$$WCl_2(PMePh_2)_4 + MePh_2PS \longrightarrow \underset{\textbf{(1)}}{} \quad W(S)Cl_2(PMePh_2)_3 + 2PMePh_2. \quad (3)$$
$$\textbf{(13)}$$

Phosphinimines (e.g. $MePh_2P{=}N$-*p*-Tol) also react with **1** to form imido complexes, but oxygen atom transfer from phosphine oxides has not been observed.

Characterization

Compounds **2–27** have been characterized by NMR and IR spectroscopies (Table 2), analytical data, and by X-ray crystal structures of **4**, **7** and **25**. The data are consistent with a common geometry for all the complexes: octahedral with *trans*-phosphines, *cis*-chlorides and *cis*-π-donor and -acceptor ligands. Thus all the compounds (except those with unsymmetrical olefin, acetylene and aldehyde ligands **8–12**) show a virtual triplet for the phosphine methyl groups, indicative of two *trans*-phosphine ligands. The ^{13}C resonances for the carbonyl and isonitrile carbons are binomial triplets. The phenyl groups of $PMePh_2$ are observed to be diastereotopic (when not obscured by overlapping resonances), consistent with the only molecular symmetry element being a mirror plane that relates the two phosphines. The α-olefin, phenylacetylene and acetaldehyde complexes **8–12**, which contain no symmetry element, shown an AB pattern in the ^{31}P NMR and the phosphorus methyl groups appear as two doublets in the ^1H NMR.

The butadiene ligand in **9** is bound in an η^2-fashion, as indicated by its NMR spectra. For instance, four ^{13}C signals are observed for the butadiene, two in the olefinic region and two quite close to those observed for the propylene complex, **8**.

The ^1H NMR spectra of the ethylene complexes **7**, **16**, **23** and **24** all show two signals for the ethylene hydrogens, indicating that the ethylene ligands do not rotate on the NMR timescale. The barriers to ethylene rotation are significant, greater than 16 kcal mol^{-1} from variable temperature NMR data.[15] The phenylacetylene complex is also non-fluxional at 25°C.

The presence of a single ^{13}C resonance for the ethylene carbons shows that these carbons are related by the mirror plane. Therefore the ethylene ligands are oriented perpendicular to the metal–oxo, –sulphido and –imido multiple bonds, consistent with the structure of **7** in the solid state (Fig. 2).

The fluxionality of the complexes of α-olefins and acetaldehyde (**8–10**, **12**) cannot be determined from the NMR spectra. The substituted carbon is a chiral centre so the phosphines are diastereotopic, independent of olefin or aldehyde rotation. Two isomers are possible: the substituent can either point towards the oxo group or away. The observation of only one species by NMR seems to indicate that one isomer is strongly preferred, although it is possible that rotation, which would interconvert the isomers, is much more facile for these ligands. Rapid isomer interconversion via olefin or aldehyde dissociation is ruled out by the presence of inequivalent phosphines and by separate resonances for bound and free ligands.

The dihapto bonding mode of acetaldehyde in **12** is indicated by the lack of a high energy (> 1500 cm^{-1}) C=O stretching mode in its IR spectrum and by its NMR spectra. An η^1-structure would be expected to have free rotation about the W—OCHMe bond and would therefore show equivalent phosphine ligands, in contrast to the asymmetric structure observed. Both the aldehyde carbon and hydrogen atoms show coupling to the phosphorus atoms that are bound to tungsten, indicative of W—C bonding. The observed C—H and H—H coupling shows that the acetaldehyde group is intact in **12**, ruling out, for instance, an alternative hydrido–acyl structure.

Compounds **4**,[4b] **7**[4a] and **25** have been characterized by X-ray crystal structures (Figs 1–3): a comparison of the bond distances and angles is given in Table 3. The three complexes adopt similar octahedral structures, with an approximate mirror plane containing the tungsten and the *cis*-chlorides. The presence of this mirror plane is consistent with the spectroscopic data, which indicate equivalent phosphine ligands. The tungsten–oxygen distances of 1.689(6) (**4**) and 1.714(6) Å (**7**) are typical of mono-oxo tungsten compounds: the mean W—O distance in 34 mono-oxo structures is 1.699 Å[16] (compare also the value of 1.67(1) Å in **3**[17]). The W—N distance of 1.754(6) Å and W—N—C angle of 171.6(5)° in **25** are very similar to those in the phenylimido complex **20** (1.755(3) Å, 179.5(3)°).[18] On the basis of tungsten–chloride distances, the order of the *trans* influence appears to be: oxo > imido > carbon monoxide ≈ ethylene, consistent with previous suggestions.[19] A shorter tungsten–carbonyl distance is found in the imido complex (1.983(8) Å) than in the oxo species (2.029(9) Å),

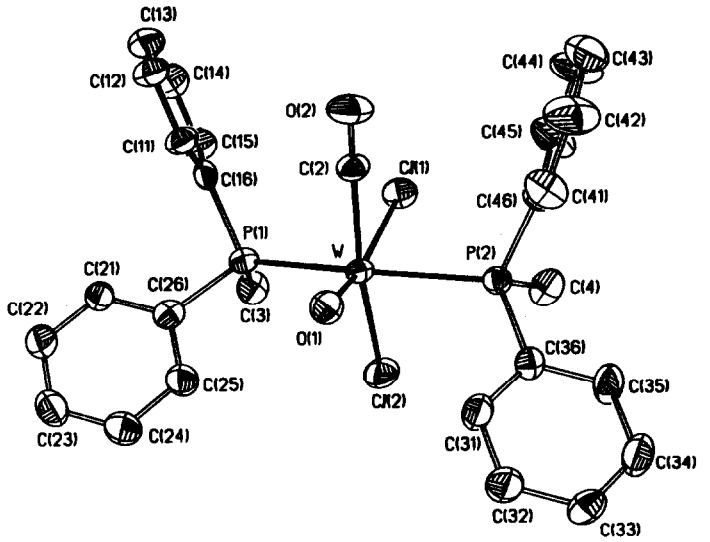

Fig. 1. Perspective drawing of $W(O)Cl_2(CO)(PMePh_2)_2$ (**4**) with hydrogen atoms omitted for clarity.

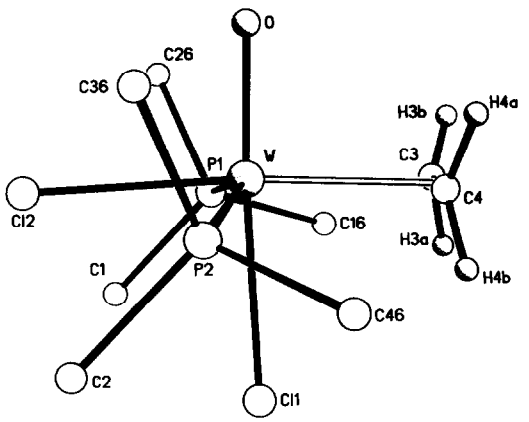

Fig. 2. Perspective drawing of $W(O)Cl_2(CH_2{=}CH_2)(PMePh_2)_2$ (**7**) with hydrogen atoms (except on the ethylene ligand) omitted and only the *ipso*-carbons of the phenyl rings shown.

indicating stronger backbonding in the imido derivative (see Discussion).

The coordination geometries in **4**, **7** and **25** are best described as distorted octahedral, with *cis* angles varying from 75.5(3) to 104.1(2)° and *trans* angles as low as 154.7(1)°. In all three structures the π-acid ligand lies almost exactly at a right angle to the metal–oxo/imido multiple bond ($\angle$E—W—L = 88.9(3)–90.7(4)°, E = oxo or imido), but the phosphines and the *cis*-chloride ligand have moved away from the oxo or imido group ($\angle$E—W—L = 93.0(2)–104.1(2)°). Thus the "*trans*" P—W—P angles are significantly less than 180° (154.7(1)–168.5(1)°). In **4** and **25** the phosphines bend primarily away from the oxo or imido ligand; in **7** the distortion is away from the ethylene as well. The Cl—W—Cl angle is approximately 90° in all three structures, presumably to keep the Cl···Cl non-bonded distance at ~3.5 Å. The movement of Cl(2) away from the oxo or imido thus results in Cl(1) being close to the carbonyl or ethylene ligands, with Cl(1)—W—$C_{carbonyl}$ angles of 75.5(3) (**4**) and 78.0(2)° (**25**).

$WCl_2(PMePh_2)_4$ (**1**) has a more regular octahedral structure, with *trans*-chlorides ($\angle$Cl—W—Cl = 179.6(1)°) and four phosphines in the equatorial plane (Fig. 4, Table 4). The steric crowding caused by the presence of four large $PMePh_2$ ligands (cone angle 136°[13]) is partially relieved by a ruffling of the four phosphines. Two phosphines lie above the equatorial plane and two below, with Cl(1)—W—P angles of 94.8, 84.7, 95.4 and 84.8(1)°. This gives an approximate S_4 axis, and the molecule as a whole has roughly D_{2d} symmetry. Similar structures have been reported for a number of $MoCl_2L_4$ molecules (L = PMe_3, L_2 = diphos, dmpe, 1,2-$C_6H_4(PPh_2)_2$) and the disordered $MCl_2(PMe_3)_4$—$M(N_2)_2(PMe_3)_4$ (M = Mo, W).[20] The facile loss of $PMePh_2$ from **1**, and therefore its high reactivity, is undoubtedly due to this steric crowding.

The $PMePh_2$ cone angle is not a good measure of the crowding in **1** because the phenyl rings interleave and stack [Fig. 4(a)]. The eight phenyls form four pairs in which the rings are roughly parallel, with interplanar distances from 3.2 to 3.5 Å. These distances indicate an attractive stacking interaction; the interlayer distance in graphite, for example, is 3.35 Å.[21]

Table 2. Selected NMR and IR data for the complexes $W(E)Cl_2L(PR_3)_2$ (**2–27**)[a]

Ligands			$^{31}P\{^1H\}$		$^{13}C\{^1H\}$ NMR				^1H NMR							IR	
									PCH_3			Others					
E	L	No.	∂	J_{WP}	∂	m	J_{PC}	Assignment	∂	m	J_{PC}	∂	m	J	Int	Assignment	ν(CX)	ν(WE)
O	$PMePh_2$	**2**[b]	0.0	340					2.22	t	4	1.67	d	8	3H	PCH_3Ph_2		945
			−16.7	413					1.67	d	8							
O	CO	**4**	4.6	331	234.4	t	5	*C*O	2.22	t	4						2006	955
					13.7	t	15	PCH_3Ph_2										
O	CO	**5**							1.31	t	4						1995	955
O	CN—*t*-Bu	**6**	0.7	339	14.4	t	15	PCH_3Ph_2	2.40	t	4	0.66	s		9H	$C(CH_3)_3$	2120	955
O	$CH_2{=}CH_2$	**7**	8.5	266	53.8[c]			$=CH_2$[c]	2.43	t	6	2.77	m		2H	CHH=CHH		960
					14.0	t	15	PCH_3Ph_2				2.24	m		2H	CHH=CHH		
O	$CH_2{=}CHMe$	**8**	9.1[d]		27.1	s		CH_3	2.40	d	8	2.39	d	3	3H	CH_3		960
			9.4[d]		60.2	s		=*C*	2.54	d	8	2.58	m		1H	=CHH		
					65.8	s		=*C*				2.78	m		1H	=CHH		
												3.45	m		1H	CHMe		
O	$CH_2{=}CHCH{=}CH_2$	**9**[e]	6.3[f]	279	12.9	d	27	PCH_3Ph_2	2.38	d	8				[e]			960
			9.2[f]	263	13.6	d	27	PCH_3Ph_2	2.52	d	8							
O	$CH_2{=}CHCH_2OH$	**10**[g]	9.4[h]						2.40	d	9				[g]			960
			9.4[h]						2.48	d	9							
O	PhC≡CH	**11**	10.5[h]	255					2.17	d	10	9.88	dd[i]		1H	≡CH		940
			12.7[h]	236					2.52	d								
O	O=CHMe	**12**	9.5[j]	273	23.2	s		CCH_3	2.48	d	11	2.50	d	5	3H	CH_3		
			14.2[j]	276	93.1	d	9	OCHMe	2.37	d	11	4.41	m			OCHMe		
S	$PMePh_2$	**13**	−22.3	270	18.6	t	15	PCH_3Ph_2	2.24	t	4							
			−37.6	320	26.6	d	33	PCH_3Ph_2	2.01	d	8							
S	CO	**14**	4.0	266	16.2	t	16	PCH_3Ph_2	2.18	t	4						1986	524
S	CN—*t*-Bu	**15**	−4.1	276	16.7	t	15	PCH_3Ph_2	2.32	t	3	0.72	s		9H	$C(CH_3)_3$	2127	519
S	$CH_2{=}CH_2$	**16**	8.1	208	14.7	t	16	PCH_3Ph_2	2.32	t	4	3.17	m		2H	CHH=CHH		515
					53.2	s		$=CH_2$				2.63	m		2H	CHH=CHH		
N—*t*-Bu	CO	**17**	4.2	298	14.6	t	15	PCH_3Ph_2	2.34	t	4	0.74	s		9H	$C(CH_3)_2$	1966	1098
					30.1	s		$NC(CH_3)_3$										
					69.7	s		$NCMe_3$										

N—*t*-Bu	CN—*t*-Bu	**18**	6.0	308					2.48	t	4	0.77 s	9H		2090[k]	
												0.99 s	9H			
N—Ph	$PMePh_2$	**19**[j]	−4.2	300					2.37	t	4	7.05 m	5H	N—*Ph*		
			1.2	386					1.88	d	8	7.31 m				
N—Ph	CO	**21**	3.2	290	240.5	s			2.30	t	4	7.03 m	5H	N—*Ph*	1964	1101
					14.5	t	15	PCH_3Ph_2								
N—Ph	CO	**22**	−20.3	288	248.8	s			1.35	t	4	6.97 m	5H	N—*Ph*	1946	1070
					15.3	t	15	$P(CH_3)_3$				6.84 m				
N—Ph	$CH_2{=}CH_2$	**23**	4.1	232	13.2	t	15	PCH_3Ph_2	2.42	t	4	2.27 m	2H	C*H*H=C*H*H		1099
					48.0	s		$=CH_2$				2.24 m	2H	CH*H*=CH*H*		
												7.05 m	5H	N—*Ph*		
												7.36 m				
N—Ph	$CH_2{=}CH_2$	**24**	2.6	232	13.9	t	15	$P(CH_3)_3$	1.39	t	4	2.25 m	2H	C*H*H=C*H*H		1156
					39.4	s		$=CH_2$				2.30	2H	CH*H*=CH*H*		
												6.79 m	5H	N—*Ph*		
N—*p*-Tol																
	CO	**25**	3.5	292	13.6	t		PCH_3Ph_2	2.32	t	4	1.76 s	3H	$C_6H_4CH_3$	1964[k]	1099
					21.5	s		$C_6H_4CH_3$								
$NSiMe_3$	CO	**26**	6.5	307					2.31	t	4	−0.33 s	9H	$NSi(CH_3)_3$	1976[k]	
Mo(O)[m]	CO	**27**							2.21	t	4				2130[k]	950

[a] Taken in C_6D_6 at ambient temperature at 500 or 300 MHz (^1H), and 121.4 MHz (^{31}P). Taken in CD_2Cl_2 or C_6D_6 at 75.4 MHz (^{13}C). Coupling constants are reported in Hz. Resonances in the aromatic region are not reported. ^1H and ^{13}C chemical shifts (∂) are in ppm downfield from TMS and are referenced to solvent resonances. ^{31}P spectra are internally referenced to $PMePh_2$, ∂ −27.6, relative to H_3PO_4. IR spectra obtained as Nujol mulls except where indicated, values given in cm^{-1}. Complete IR spectra are given in the Experimental.

[b] Reference 8.

[c] t, $^1J_{CH} = 156$.

[d] Doublet (part of an AB pattern), $^2J_{PP} = 161$.

[e] Complete ^1H and ^{13}C NMR data are given in the Experimental.

[f] Doublet (part of an AB pattern), $^2J_{PP} = 163$.

[g] Complete ^1H NMR data are given in the Experimental.

[h] Part of an AB pattern, only the two large peaks are reported, J_{PP} not determined.

[i] $J_{PH} = 17$, $J_{PH} = 5$.

[j] Doublet (part of an AB pattern), $^2J_{PP} = 175$.

[k] IR spectrum taken in C_6D_6 solution.

[l] Reference 9.

[m] *Mo*(O)Cl_2(CO)$(PMePh_2)_2$.

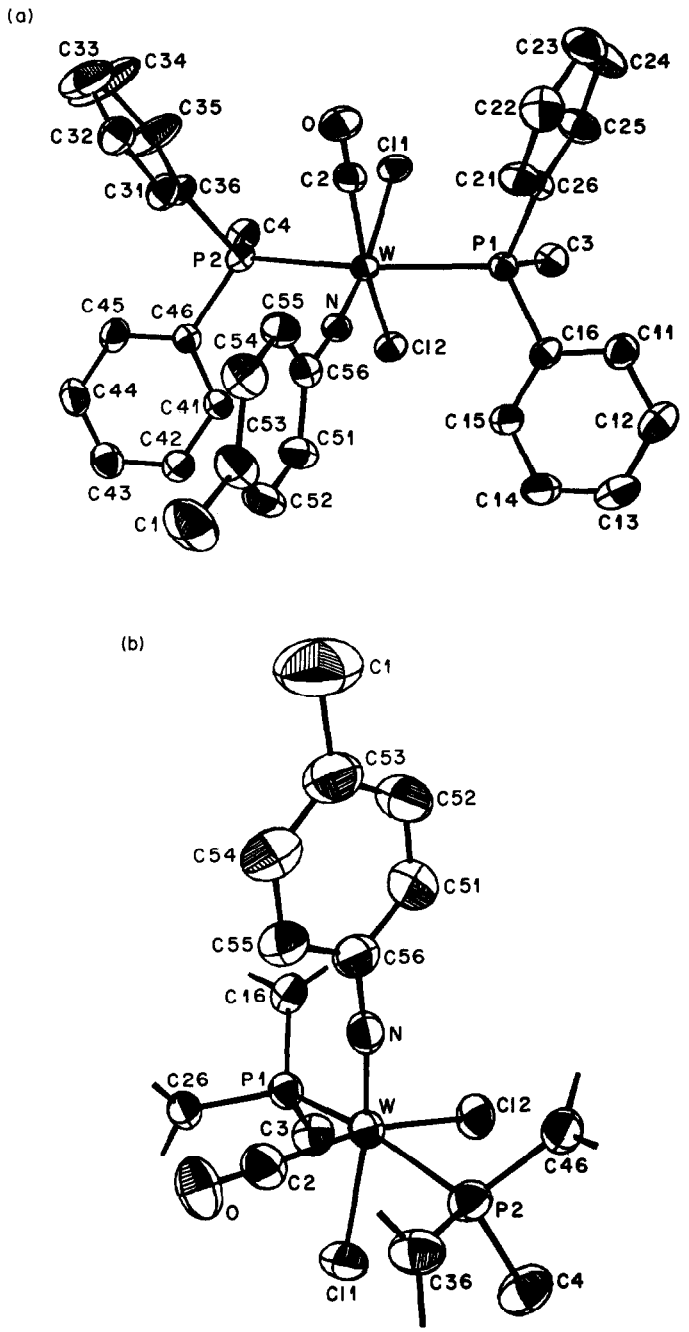

Fig. 3. Perspective drawings of W(N-*p*-Tol)Cl_2(CO)($PMePh_2$)$_2$ (**25**) with hydrogen atoms omitted; in (b) only the *ipso*-carbons of the phenyl rings are shown.

Reactions

The oxo–carbonyl, oxo–isonitrile and oxo–ethylene complexes are thermally stable, exhibiting less than 10% decomposition after a day at 90°C in C_6D_6 solution. Solutions of the α-olefin complexes, however, are substantially decomposed within 24 h at 40°C, and the acetaldehyde complex decomposes within a few hours at 25°C. These processes appear to occur via loss of the π-acid ligand. Reaction of complexes **4–10** with an excess of CO, CN^{t}Bu, or C_2H_4 results in ligand exchange, consistent with the suggestion above that the ligand exchange reactions are equilibria.

Dissociation of coordinated carbon monoxide or ethylene in **4** or **7** can also be promoted photochemically. Irradiation of **7** in the presence of $PMePh_2$, for instance, gives **2** [eq. (4)]:

Table 3. Selected bond lengths and angles in $W(O)Cl_2(CO)(PMePh_2)_2$ (**4**), $W(O)Cl_2(CH_2CH_2)(PMePh_2)_2$ (**7**) and $W(N\text{-}p\text{-}Tol)Cl_2(CO)(PMePh_2)_2$ (**25**)[a]

	$W(O)Cl_2(CO)L_2$ (**4**)	$W(O)Cl_2(C_2H_4)L_2$ (**7**)	$W(NTol)Cl_2(CO)L_2$ (**25**)
W=E	1.689(6)	1.714(6)	1.754(6)
W—Cl(1)	2.504(2)	2.495(3)	2.476(2)
W—Cl(2)	2.411(3)	2.444(3)	2.455(2)
W—P	2.538, 2.539(2)	2.594, 2.575(3)	2.521, 2.526(2)
W—C(2)	2.029(9)	2.218, 2.221(12)	1.983(8)
C(2)—O(2)	1.142(11)		1.139(8)
C(3)—C(4)		1.404(17)	
E—W—C(2)	89.6(3)	90.6, 90.7(4)	88.9(3)
E—W—P	98.3, 97.4(2)	98.8, 98.3(2)	98.3(2), 93.0(2)
E—W—Cl(1)	165.1(2)	176.1(2)	166.9(2)
E—W—Cl(2)	103.4(2)	94.2(2)	104.1(2)
P—W—Cl(1)	82.4, 83.9(1)	82.1, 82.1(1)	83.4(1), 86.2(1)
C(2)—W—Cl(1)	75.5(3)	85.8, 85.5(3)	78.0(2)
P(1)—W—P(2)	163.2(1)	154.7(1)	168.5(1)
Cl(1)—W—Cl(2)	91.6(1)	89.6(1)	89.0(1)
P—W—Cl(2)	84.2, 86.5(1)	80.4, 79.8(1)	86.9, 87.8(1)
C(2)—W—Cl(2)	166.8(3)	175.0(3)[b]	166.9(2)
P—W—C(2)	93.9, 92.0(2)	99.2, 99.2(3)[b]	90.8, 92.0(2)
W—C(2)—O(2)	177.0(7)		178.5(7)
W—N—C(56)			171.6(5)

[a] Bond distances in Å, angles in degrees; E represents O(1) in **4**, O in **7** and N in **25**. When P is given, the bond length or angle to both P(1) and P(2) is listed.

[b] Angle involving the ethylene centroid.

$$W(O)Cl_2(CH_2{=}CH_2)(PMePh_2)_2 + PMePh_2 \xrightarrow{h\nu} W(O)Cl_2(PMePh_2)_3 + CH_2{=}CH_2. \quad (4)$$
(**7**) (**2**)

No evidence of olefin oxidation or oxygen atom transfer to phosphine was obtained.

Complex **7** reacts with 1 equivalent of trimethylaluminium to form the oxo–methyl complex, **28**, which has been characterized spectroscopically [eq. (5)]:

$$W(O)Cl_2(CH_2{=}CH_2)(PMePh_2)_2 + AlMe_3 \longrightarrow W(O)(Me)Cl(CH_2{=}CH_2)(PMePh_2)_2. \quad (5)$$
(**7**) (**28**)

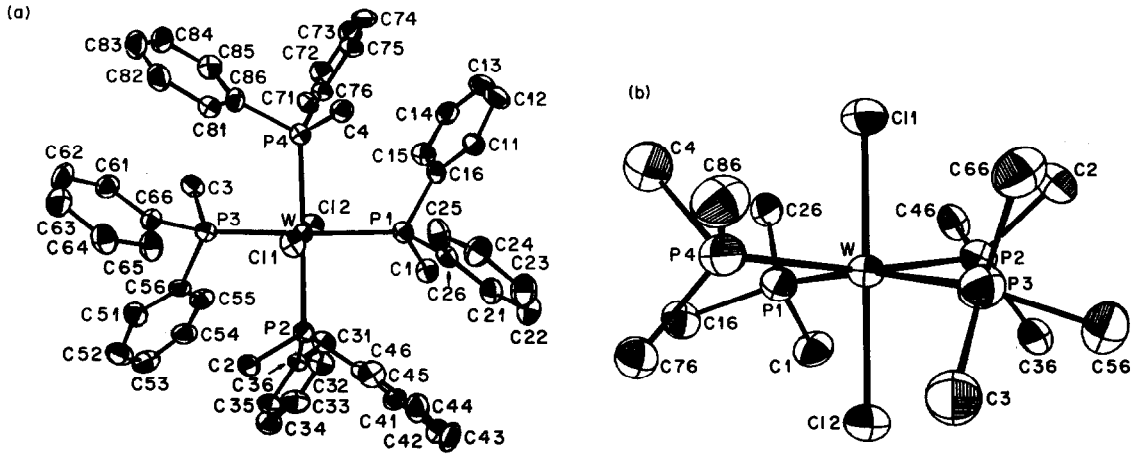

Fig. 4. Perspective drawings of $WCl_2(PMePh_2)_4$ (**1**) with hydrogen atoms omitted; in (b) only the *ipso*-carbons of the phenyl rings are shown.

Table 4. Selected bond lengths and angles in $WCl_2(PMePh_2)_4$ (1)[a]

W—Cl(1)	2.423(2)	W—C(2)	2.432
W—P(1)	2.531(3)	W—P(2)	2.539
W—P(3)	2.540(3)	W—P(4)	2.539
Cl(1)—W—Cl(2)	179.57(11)		
Cl(1)—W—P(1)	94.75(9)	Cl(2)—W—P(1)	84.82(9)
Cl(1)—W—P(2)	84.74(9)	Cl(2)—W—P(2)	95.18(9)
Cl(1)—W—P(3)	95.44(9)	Cl(2)—W—P(3)	84.99(9)
Cl(1)—W—P(4)	84.81(9)	Cl(2)—W—P(4)	95.26(9)
P(1)—W—P(2)	90.03(9)	P(1)—W—P(3)	169.80(8)
P(1)—W—P(4)	90.67(9)	P(2)—W—P(4)	169.55(8)
P(2)—W—P(3)	91.39(9)	P(3)—W—P(4)	89.79(9)

[a] Bond distances in Å, angles in degrees.

The carbonyl and isonitrile complexes **4** and **6** do not react with $AlMe_3$, although the ethylene ligand in **28** can be substituted for CO and CN^{t}Bu to form $W(O)(Me)Cl(L)(PMePh_2)_2$ [L = CO (**29**); CN^{t}Bu (**30**)]. The methyl derivatives are less stable than the dichloride analogues, decomposing in solution at ambient temperatures. A major product of the decomposition of the methyl–ethylene complex **28**, is the *di*chloride–ethylene complex, **7**. The ^{1}H NMR of **28–30** show a triplet for the tungsten methyl groups (J_{PH} = 10 Hz), in addition to resonances similar to those for **4**, **6** and **7**. The methyl group is believed to be *trans* to the oxo ligand, given the large oxo *trans* influence, but this cannot be determined from the spectral data.

DISCUSSION

The stability of this wide range of tungsten(IV) olefin and carbonyl complexes is remarkable, given that these ligands do not often form high oxidation state complexes.[3,22] The tungsten(IV)–oxo, –sulphido, or –imido centre clearly has a high affinity for a π-acid ligand. This is perhaps most evident in the formation of the η^2-acetaldehyde complex **12**. The origin of this stability lies in the electronic structure of the tungsten(IV) d^2 centre.

The electronic configuration of d^2 mono-oxo and related species is well established.[23] The two d electrons are paired in the HOMO, which is the d_{xy} orbital (the z axis is taken as coincident with the metal–ligand multiple bond, Scheme 1). The LUMO is usually the metal–ligand π^*-orbitals, the antibonding combination of the metal d_{xz} and d_{yz} with the ligand p_π orbitals. Oxo, sulphido and imido ligands form strong triple bonds in octahedral symmetry only in electron counts of d^0, d^1 or d^2, because additional d electrons would have to occupy strongly antibonding[24] π^*-orbitals.[23] The

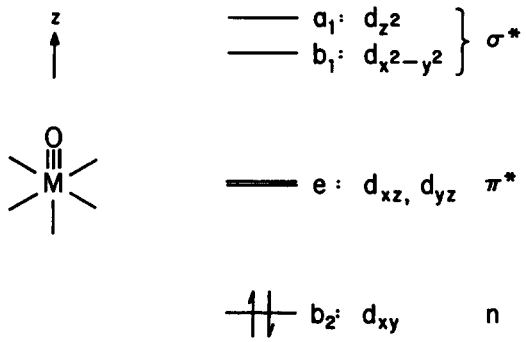

Scheme 1.

d^2 configuration is therefore ideal for the π-donor/π-acceptor molecules reported here: a W≡E triple bond can be formed and two electrons (one pair) are available for backbonding to the π-acid ligand.

Since the two d electrons are in the d_{xy} orbital, the π-acid ligand (carbon monoxide, ethylene, etc.) must bind *cis* to the tungsten–E multiple bond. In addition, an olefin ligand with only one acceptor orbital has only one orientation that allows favourable overlap with d_{xy}:



Thus, the unsaturated organic ligand lies perpendicular to the tungsten–E bond, as observed in complexes **7–12**, **16**, **23** and **24**. The large barrier to ethylene rotation is due to loss of the π-backbonding interaction on turning the ethylene 90°. This orbital description is similar to that used to explain the geometry and lack of rotation in d^2 oxo–acetylene[25] and oxo–carbene compounds,[26] and is supported by two recent theoretical studies.[27]

The high barriers to olefin rotation indicate that π-backbonding is an important interaction for these complexes. Significant backbonding is also implied by the CO stretching frequencies (Table 5). This conclusion is somewhat surprising since the tungsten centre is in the +4 oxidation state, with two chloride ligands and an oxo, sulphido, or imido group. However, the tungsten(IV) centre is a reasonable reducing agent,[28a] implying that the two *d* electrons are at fairly high energy and are available for backbonding. Weaker backbonding is seen in the molybdenum oxo–carbonyl complex **27** (compare ν(CO) = 2130 cm^{-1} for **27**, 2006 cm^{-1} for **4**), because molybdenum is a less electropositive metal and molybdenum(IV) is a poorer reducing agent than tungsten(IV).[28]

The CO stretching frequency can be used as a measure of the electron density at the metal centre. For instance, because PMe_3 is a stronger donor than $PMePh_2$, the PMe_3 complexes **5** and **22** have lower CO stretching frequencies than **4** and **21**, by 11 and 18 cm^{-1}. This enables a comparison of the electron donor abilities of the multiply bonded ligands (Table 5). The oxo ligand is the least electron donating, then sulphido, and the imido group is the most donating. This order does not simply parallel the donor atom electronegativity, O (3.5) > N (3.0) > S (2.5).[29] It is reasonable that oxygen is the weakest donor, but the poor donation from the sulphido ligand is surprising. The presence of the imido substituent may complicate the comparison, but the substituent does not seem to have a substantial influence on ν(CO). The poor donation from the sulphido ligand may indicate that π-bonding involving the third row element sulphur is not as effective as π-interactions involving oxygen and nitrogen. This is also suggested by the electronic spectra: the lowest energy transition, believed to be $d_{xy} \rightarrow d_{xz}d_{yz}$ ($n \rightarrow \pi^*$),[23] is in the range 492–544 nm in the oxo- and imido–carbonyl complexes, but is at much lower energy (696 nm) in the sulphido–carbonyl compound **14**.

Table 5. Comparison of C—O stretching frequencies

Compound	ν(CO) (cm^{-1})
$W(O)Cl_2(CO)(PMePh_2)_2$ (**4**)	2006
$W(S)Cl_2(CO)(PMePh_2)_2$ (**13**)	1986
$W(NSiMe_3)Cl_2(CO)(PMePh_2)_2$ (**26**)	1976
$W(N'Bu)Cl_2(CO)(PMePh_2)_2$ (**17**)	1966
$W(N\text{-}p\text{-}Tol)Cl_2(CO)(PMePh_2)_2$ (**25**)	1964
$W(NPh)Cl_2(CO)(PMePh_2)_2$ (**21**)	1964
$W(CPMePh_2)Cl_2(CO)(PMePh_2)_2$[a]	1903
$W(O)Cl_2(CO)(PMe_3)_2$ (**5**)	1995
$W(NPh)Cl_2(CO)(PMe_3)_2$ (**22**)	1946
$W(CHPh)Cl_2(CO)(PMe_3)_2$[b]	1939
$W(CPh)Cl(CO)[P(OMe)_3](PMe_3)_2$[b]	1919

[a] G. Hillhouse, unpublished results.

[b] A. Mayr, M. F. Asaro, M. A. Kjelsberg, K. S. Lee and D. V. Engen, *Organometallics* 1987, **6**, 432.

Table 5 also contains CO stretching frequencies for related alkylidene and alkylidyne complexes. Because of the low electronegativity of carbon (2.5), an alkylidene would be expected to be a very strong donor, but phenylimido is almost as donating as benzylidene. The difference in bond polarity is probably offset by the difference in bond order, an M≡NPh triple bond versus an M=CHPh double bond. The alkylidyne ligand provides a comparison of triple bonds but, because the alkylidyne is a trivalent group, the compounds are not strictly analogous. One of the alkylidyne complexes in Table 5 has an unusual phosphinium–alkylidyne moiety, and in the other a phosphite ligand is in place of one of the chlorides. The list of analogous compounds illustrates the similarities among metal–ligand multiple bonds. Imido and carbene or alkylidene ligands are not as different as is implied by the oxidation state formalism of NR^{2-} as a π-donor and CR_2, a neutral π-acid ligand.

The above discussion used the electronic structure of the parent oxo, sulphido or imido complex and added the π-acid ligand as a small perturbation. The solid state structures and the spectroscopic data are consistent with this approach: The molecules are not distorted towards bound epoxide, η^2-CO_2 or η^2-OCNR forms—there is no evidence for bonding between the π-donor and π-acceptor ligands. The angle between the ligands is very close to 90° in all three cases, and the carbonyl ligands are essentially linear (W—C—O = 177.0(7), 178.5(7)° for **4** and **25**).

There is, however, a short contact between the carbonyl carbon and the oxo or imido nitrogen atom in **4** and **25**, due to the short W—CO and W≡O or W≡NR bonds. These distances, O···C = 2.63 Å and N···C = 2.62 Å, are much longer than a bond (compare 1.163 Å in CO_2),[30] but are substantially shorter than the sum of the van der Waals radii (C, 1.7; N, 1.55; O, 1.5 Å).[31] Thus, there is probably overlap of the oxygen or nitrogen p_x orbital with the carbonyl π^*-orbital in the *xz* plane, in addition to the overlap with the tungsten d_{xz} (Scheme 2). One effect of this three orbital–two electron situation is to lower the energy of the filled W—O or W—N π_x-orbital compared to the π_y. This is consistent with the orientation of

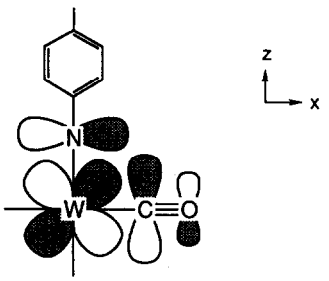

Scheme 2. A schematic drawing of the interaction of the tungsten d_{xz}, nitrogen p_x and carbonyl π^* orbitals in W(N-*p*-Tol)Cl_2(CO)$(PMePh_2)_2$ (**25**).

the tolyl group in **25**, in the *xz* plane: the empty aromatic π^*-orbital(s) of the tolyl ring overlap better with the filled M—N π_y-orbital than the lower energy π_x. This is a weak interaction, however, since rapid rotation about the C—N bond is observed in the ^{1}H NMR at $-90°C$ ($\Delta G^{\ddagger} < 9$ kcal mol^{-1}). The π-donor acetylene ligand in **11**, *cis* to the oxo, has a larger effect: in this three orbital–*four* electron case the acetylene competes for the tungsten d_{xz} orbital, as noted in other oxo–acetylene compounds.[25] As a result, the W—O bond order is lower and complex **11** has the lowest W—O stretching frequency of the oxo compounds reported here.

The presence of two π-bonding ligands also seems to be the origin of the significant distortions from octahedral geometry. Closely related d^0 dioxo[32] and d^4 dicarbonyl[33] complexes also adopt highly distorted structures, the distortions resulting from the presence of *cis*-π-bonding ligands.

EXPERIMENTAL

General considerations

All manipulations were carried out using either high vacuum line or glovebox techniques except as indicated. Solvents were vacuum transferred from sodium benzophenone (diethyl ether, THF), calcium hydride (benzene, toluene, petroleum ether, heptane and pentane), or 4 Å sieves (methylene chloride) immediately before use. Deuterated solvents were dried and transferred from activated 4 Å sieves. Gaseous reagents were obtained from Matheson and used without further purification. Complexes **1**,[12] **2**, **3**,[8] **20**,[9] and Mo(O)Cl_2(P$MePh_2)_3$[34] and $MePh_2PS$[35] were prepared following literature procedures.

Elemental analyses were performed by Canadian Microanalytical Service Ltd, Vancouver, British Columbia. NMR spectra were taken using Varian CFT-20 and VXR-300, and Bruker CXP-200 and WM-500 spectrometers. Variable temperature NMR was performed on the VXR-300. IR spectra were obtained as Nujol mulls (unless otherwise noted) using Perkin–Elmer 225, 283 or 1640 spectrometers, and are reported in cm^{-1}. Selected NMR and IR spectra are given in Table 2, the remainder below. The NMR data are reported below as: chemical shift (multiplicity, integral, coupling constant in Hz, assignment). UV–vis spectra were recorded on a Hewlett–Packard 8450A spectrophotometer, and are reported as: UV–vis: λ_{max} (ε).

W(O)Cl_2(CO)$(PMePh_2)_2$ (**4**)

This was prepared from CO in 70% yield as red–purple crystals following the procedure for **7**. Complex **4** was also observed in > 95% yield (together with < 5% **2**) by NMR when CO_2 (127 torr in 7.5 cm^3) was was exposed to **1** (27 mg) for 3 h in C_6D_6 in a sealed NMR tube. IR: ν(CO) = 2006, $\nu(^{13}CO)$ = 1985. Found: C, 46.6; H, 3.9. Calc. for $C_{27}H_{26}Cl_2O_2P_2W$: C, 46.4; H, 3.7%. UV–vis: 498 nm (86). **4**—^{13}CO was prepared in a sealed NMR tube from 10 mg of **2** in C_6D_6 and ^{13}CO (Cambridge Isotope).

W(O)Cl_2(CO)$(PMe_3)_2$ (**5**)

This was prepared in a sealed tube containing 10 mg of **3** in C_6D_6 and 20 equivalents of CO.

W(O)Cl_2(CN^{t}Bu)$(PMePh_2)_2$ (**6**)

CN^{t}Bu (0.02 cm^3, 0.26 mmol) was added to a stirred solution of **2** (0.2 g, 0.23 mmol) in benzene (15 cm^3). The purple solution was filtered and the volume was reduced to 1 cm^3. Petroleum ether (5 cm^3) was added. The purple crystals were isolated and dried *in vacuo*; yield 0.11 g (70%). ^{1}H NMR: 7.02–7.95 (br m, 12, PMe*Ph*$_2$, *p* and *m*), 7.70 (m, 4, PMe*Ph*Ph′, *o*), 8.11 (m, 4, PMePh*Ph*′, *o*). UV–vis: 552 nm (110).

W(O)Cl_2(CH_2=CH_2)$(PMePh_2)_2$ (**7**)

A suspension of **2** (0.35 g, 0.4 mmol) in benzene (20 cm^3) was stirred at 40°C under 1 atm of ethylene for 30 min. Filtration, evaporation of most of the solvent and addition of petroleum ether gave 0.25 g (74%) of yellow crystals. **7** was also formed in ~ 80% yield (together with ~ 10% of **2**, by NMR) when ethylene oxide (6 torr in 25 cm^3) was exposed to **1** (9 mg) for 3 h in C_6D_6 in a sealed NMR tube.

^{1}H NMR: 6.94 (m, 6, PMe*Ph*Ph′, *p* and *m*), 7.04 (m, 6, PMePh*Ph*′, *p* and *m*), 7.40 (m, 4, PMe*Ph*Ph′, *o*), 7.98 (m, 4, PMePh*Ph*′, *o*). Found: C, 48.5; H, 4.5. Calc. for $C_{28}H_{30}Cl_2OP_2W$: C, 48.1; H, 4.3%. UV–vis: 358 nm (240).

$W(O)Cl_2(C_2H_4)(PMe_3)_2$

The compound was detected by ^{1}H NMR in a sealed tube when $W(O)Cl_2(PMe_3)_2$ (10 mg) dissolved in C_6D_6 was exposed to 20 equivalents of C_2H_4. IR (C_6D_6): 960 br [ν(WO)]. ^{1}H NMR: 1.42 (t, J_{PH} = 4, P*Me*$_3$), 2.60 (m, 2, C*H*H′C*H*H′), 2.64 (m, 2, CH*H*′CH*H*′).

$W(O)Cl_2(CH_2{=}CHMe)(PMePh_2)_2$ (8)

Compound **8** was prepared from propylene and **2** in 65% yield as yellow crystals following the procedure for **7**. **8** was also formed in ~ 15% yield (together with ~ 75% of **2**, by NMR) when propylene oxide (10 torr in 25 cm^3, Aldrich) was exposed to **1** (9 mg) for 3 h in C_6D_6 in a sealed NMR tube. ^{1}H NMR: 6.94–7.11 (br m, 12, PMe*Ph*$_2$, *p* and *m*), 7.43 (m, 2, PMe*Ph*$_2$, *o*), 7.67 (m, 2, PMe*Ph*$_2$, *o*), 8.02 (m, 4, PMe*Ph*$_2$, *o*). Found: C, 48.8; H, 4.7. Calc. for $C_{29}H_{32}Cl_2OP_2W$: C, 48.4; H, 4.5%.

$W(O)Cl_2(CH_2{=}CHCH{=}CH_2)(PMePh_2)_2$ (9)

Compound **9** was prepared from butadiene and **2** in 50% yield as yellow crystals following the procedure for **7**. ^{1}H NMR: 2.61 (m, 1, WC*H*H′CH CHCH$_2$), 3.00 (m, 1, WCH*H*′CHCHCH$_2$), 3.68 (d, 1, J = 17, WCH$_2$CHCHC*H*H′), 4.25 (m, 1, WCH$_2$ C*H*CHCH$_2$), 4.28 (d, 1, J = 11, WCH$_2$CHCH CH*H*′), 5.97 (dt, 1, J = 17, 10, WCH$_2$CHC*H*CH$_2$), 6.94–7.11 (br m, 12, PMe*Ph*$_2$, *p* and *m*), 7.36 (m, 2, PMe*Ph*$_2$, *o*), 7.69 (m, 2, PMe*Ph*$_2$, *o*), 7.91 (m, 4, PMe*Ph*$_2$, *o*). ^{13}C{^{1}H} NMR: 57.8 (s, W*C*H$_2$ CHCHCH$_2$), 71.7 (s, WCH$_2$*C*HCHCH$_2$), 113.9 (s, WCH$_2$CHCH*C*H$_2$), 145.7 (s, WCH$_2$CH*C*HCH$_2$). Found: C, 50.3; H, 4.6. Calc. for $C_{30}H_{32}Cl_2OP_2W$: C, 49.7; H, 4.4%.

$W(O)Cl_2(CH_2{=}CHCH_2OH)(PMePh_2)_2$ (10)

Compound **10** was prepared from allyl alcohol (0.05 cm^3) in 45% yield as pale yellow crystals following the procedure for **6**. IR: 3450 (br, OH). ^{1}H NMR: 1.0 (br m, 1, CH$_2$CHCH$_2$O*H*), 2.35 (br m, 1, C*H*H′CHCH$_2$OH), 2.70 (br m, 1, CH*H*′CH CH$_2$OH), 3.52 (br m, 2, CH$_2$CHC*H*$_2$OH), 4.36 (br m, 1, CH$_2$C*H*CH$_2$OH).

$W(O)Cl_2(PhC{\equiv}CH)(PMePh_2)_2$ (11)

Compound **11** was prepared from phenylacetylene (0.05 cm^3) in 65% yield as light yellow crystals following the procedure for **6**.

$W(O)Cl_2(O{=}CHMe)(PMePh_2)_2$ (12)

Acetaldehyde (0.5 cm^3, Aldrich) was added to a suspension of **1** (0.20 g) in benzene (1 cm^3). On stirring for 2 h, some blue solids were observed to form on the reaction walls. Pentane (5 cm^3) was added and the resulting white solids filtered and dried *in vacuo* for 3 h, yielding 0.045 g (27%) of **12**. IR: 1192, 1113 vs, 1076 s, 953 s, 923 s, 896 vs, 746, 722, 692 vs.

$W(S)Cl_2(PMePh_2)_3$ (13)

Complex **1** (0.41 g) was added to $MePh_2PS$ (0.09 g) in 10 cm^3 of toluene and stirred for 3 h. The reaction mixture was concentrated to 2 cm^3 and heptane (10 cm^3) was added. The resulting solids were filtered, washed with pentane (5 cm^3) and dried *in vacuo* for 18 h, yielding 0.245 g (71%) of green **13**. Found: C, 51.9; H, 4.4. Calc. for $C_{39}H_{39}Cl_2P_2SW$: C, 52.8; H, 4.4%. IR: 1282, 1095, 1028, 1000 w, 890 vs, 741 s, 694 vs, 507 vs, 480, 441 w.

$W(S)(CO)Cl_2(PMePh_2)_2$ (14)

Carbonyl sulphide (66 torr in 25 cm^3, K&K) was added to a suspension of **1** (75 mg) in benzene (12 cm^3) and stirred for 1 h. Volatiles were pumped away and Et_2O (2 cm^3) was added to dissolve the residue, and pentane (15 cm^3) was added. The resulting solids were filtered and dried *in vacuo* for 2 h, yielding 17 mg (33%) of green **14**. Found: C, 45.0; H, 3.9. Calc. for $C_{27}H_{26}Cl_2OP_2SW$: C, 45.3; H, 3.7%. IR: 1986 [ν(CO)], 1280 w, 1092, 1034, 893 vs, 741 s, 729 s, 689 s, 524 s ν(W=S), 508 s, 480, 457 s, 291 w ν(WCl). UV–vis: 696 nm (82).

$W(S)(CN^tBu)Cl_2(PMePh_2)_2$ (15)

t-Butyl isothiocyanate (0.011 cm^3, Aldrich) was added to a suspension of **1** (89 mg) in benzene (10 cm^3) and stirred for 2.5 h. The reaction mixture was concentrated to 4 cm^3 and pentane (10 cm^3) was added. The resulting solids were filtered and dried *in vacuo* for 2 h, yielding 44 mg (68%) of yellow–green **15**. Found: C, 48.2; H, 4.6; N, 1.7; S, 4.4. Calc. for $C_{31}H_{35}Cl_2NP_2SW$: C, 48.3; H, 4.6; N, 1.8; S, 4.2%. IR: 2127 [ν(CN)], 1239, 1190, 1101, 1090, 1028, 893 vs, 795 s, 739 vs, 695 s, 519 s ν(W=S), 510 s, 488, 480, 420, 347 w, 277 ν(WCl).

$W(S)(CH_2{=}CH_2)Cl_2(PMePh_2)_2$ (**16**)

Complex **13** (0.125 g) was stirred under 1 atm of ethylene in toluene (8 cm^3) for 1 h. The reaction mixture was concentrated to 2 cm^3 and heptane (10 cm^3) was added. The resulting solids were filtered and dried *in vacuo* for 18 h, yielding 0.075 g (74%) of grey **16**. Found: C, 46.9; H, 4.2. Calc. for $C_{28}H_{30}Cl_2P_2SW$: C, 47.0; H, 4.2%. IR: 1284, 1186, 1100, 1027 w, 965 w, 901 s, 890 vs, 753, 737 s, 693 vs, 515 s, 447.

$W(N^tBu)(CO)Cl_2(PMePh_2)_2$ (**17**)

t-Butyl isocyanate (0.013 cm^3, Strem) was added to a suspension of **1** (0.14 g) in benzene (10 cm^3) and stirred for 90 min. Volatiles were pumped away and Et_2O (4 cm^3) and pentane (5 cm^3) were added. The resulting solids were filtered and dried *in vacuo* for 2 h, yielding 0.055 g (55%) of red **17**. Found: C, 49.5; H, 4.7; N, 1.6. Calc. for $C_{31}H_{35}Cl_2NOP_2W$: C, 49.4; H; 4.7; N, 1.9%. IR: 1966 vs ν(CO), 1281 w, 1252 s, 1098 ν(WNC), 1029 w br, 893 vs, 740 s, 727 s, 690 s, 508 s, 489, 454 w, 287 w, 254 w. UV–vis: 501 nm (56).

$W(N^tBu)(CN^tBu)Cl_2(PMePh_2)_2$ (**18**)

t-Butyl carbodiimide (0.002 cm^3, Aldrich) was exposed to **1** (15 mg) for 1 week in C_6D_6 in a scaled NMR tube. IR (C_6D_6): 2090 s ν(CN), 1262, 1185 br, 1120 s br, 1100 s br, 890 vs br, 740 vs, 693 vs.

$W(NPh)Cl_2(PMePh_2)_3$ (**19**)

This complex was prepared following the reported procedure for **20**.[9] Excess $PMePh_2$ (2.2 cm^3, 11.7 mmol) was added by syringe to a benzene solution of $W(NPh)Cl_4$ (1.18 g, 2.83 mmol). Sodium amalgam (Na 0.196 g, 8.52 mmol; Hg 19.8 g) was then added by syringe. The solution was stirred at room temperature for 12 h, filtered, and most of the volatiles were removed *in vacuo*. Petroleum ether was added and 2.0 g (75%) of brown **19** was isolated by filtration. IR: 1279 w, 1094 w, 1025 w, 892, 748, 738, 724, 695, 506. UV–vis: 542 nm (260).

$W(NPh)Cl_2(CO)(PMePh_2)_2$ (**21**)

Following the procedure for **22**, 0.4 g (0.43 mmol) of **19** was stirred under 1 atm of CO at room temperature for 2 days. Evaporation of the solvent and addition of petroleum ether gave 0.27 g (83%) of purple **21**. IR: 1964 ν(CO), 1101, 906, 893, 770, 746, 736, 723, 696, 505, 483, 455, 446. UV–vis: 508 nm (100).

$W(NPh)Cl_2(CO)(PMe_3)_2$ (**22**)

A suspension of **20** (0.25 g, 0.44 mmol) in benzene (25 cm^3) was stirred under 1 atm CO at 65°C for a day. Evaporation of most of the solvent and addition of Et_2O gave 0.11 g (69%) of purple **22**. IR: 1946 ν(CO), 1303, 1282, 1070, 950, 773, 743, 723, 555, 465, 379. Found: C, 29.8; H, 4.3; N, 2.5. Calc. for $C_{13}H_{23}Cl_2NOP_2W$: C, 29.7; H, 4.4; N, 2.7%. UV–vis: 492 nm (220).

$W(NPh)Cl_2(CH_2{=}CH_2)(PMePh_2)_2$ (**23**)

Following the procedure for **20**, 0.3 g (0.32 mmol) of **19** gave 0.14 g (49%) of **23**. IR: 1653, 1582, 1188, 1156, 1104, 1093, 1072, 999, 990, 891, 767, 739, 697, 618, 507, 484, 446, 437.

$W(NPh)Cl_2(CH_2{=}CH_2)(PMe_3)_2$ (**24**)

A solution of **24** (0.35 g, 0.9 mmol) in benzene (15 cm^3) was stirred at 70°C under 1 atm of ethylene for 1 h. Evaporation of most of the solvent and addition of petroleum ether gave 0.18 g (38%) of yellow **24**. IR: 1282, 1168, 1069, 1023, 950, 861, 773, 743, 723, 691, 567, 555, 542. Found: C, 31.8; H, 5.1; N, 2.6. Calc. for $C_{14}H_{27}Cl_2NOP_2W$: C, 31.9; H, 5.1; N, 2.7%.

$W(N\text{-}p\text{-}Tol)(CO)Cl_2(PMePh_2)_2$ (**25**)

p-Tolyl isocyanate (0.015 cm^3, Aldrich) was added to a suspension of **1** (105 mg) in benzene (12 cm^3) and stirred for 4 h. The volatiles were pumped away, Et_2O (1 cm^3) was added to dissolve the residue, and pentane (8 cm^3) was added. The resulting solids were filtered and dried *in vacuo* for 2 h, yielding 45 mg (57%) of purple **25**. Found: C, 51.4; H, 4.2; N, 1.7. Calc. for $C_{34}H_{33}Cl_2NOP_2W$: C, 51.8; H, 4.2; N, 1.8%. IR: 1964 vs ν(CO), 1587 w, 1158, 1099 ν(WNC), 892 vs, 821 s, 758 s, 740 s, 731 s, 720 s, 690 vs, 559 w, 515 s, 480, 450 w, 290, 255 w. UV–vis: 544 nm (160).

$W(NSiMe_3)(CO)Cl_2(PMePh_2)_2$ (**26**)

Trimethylsilyl isocyanate (0.030 cm^3, Aldrich) was added to a suspension of **1** (0.20 g) in benzene (15 cm^3) and stirred for 21 h. The volatiles were pumped away and Et_2O (1 cm^3) and pentane (15 cm^3) were added. The resulting solids were filtered and dried *in vacuo* for 2 h, yielding 0.110 g (75%) of red **26**. IR: 1976 vs ν(CO), 1249, 1129 s, 1118 s, 1098, 890 vs, 838 br, 739 s, 690 vs, 506 s, 455, 273 w, 255 w.

$Mo(O)Cl_2(CO)(PMePh_2)_2$ (**27**)

This complex was prepared from CO and $Mo(O)Cl_2(PMePh_2)_3$ in 65% yield as brown crystals following the procedure for **4**, except petroleum ether was added through the side arm of the Schlenk flask instead of by vacuum transfer. ^1H NMR: 6.94–7.03 (br m, 12, PMe*PH*$_2$, *p* and *m*), 7.55 (m, 4, PMe*Ph*Ph′, *o*), 7.92 (m, 4, PMePh*Ph*′, *o*).

$W(O)Me(Cl)(CH_2{=}CH_2)(PMePh_2)_2$ (**28**)

A solution of **7** (0.20 g, 0.28 mmol) was dissolved in benzene (20 cm^3), cooled to 10°C, and $AlMe_3$ (1.0 M in benzene, 0.33 cm^3, 0.33 mmol) was added with stirring. The mixture was filtered and the volume was reduced to 1 cm^3. Ether (10 cm^3) was added and yellow crystals were isolated upon stirring the mixture; yield 0.08 g (40%). IR: 960 *ν*(W—O). ^1H NMR: 1.35 (t, 3, $^3J_{PH}$ = 11, WC*H*$_3$), 2.23 (t, 6, J_{PH} = 4, P*Me*Ph$_2$), 2.47 (m, 2, C*H*H′C*H*H′), 2.58 (m, 2, CH*H*′CH*H*′), 6.94–7.06 (br m, 12, PMe*PhPh*′, *p* and *m*), 7.57 (m, 4, PMe *Ph*Ph′*o*), 7.78 (m, 4, PMePh*Ph*′, *o*). ^{13}C NMR: 11.5 (q of t, J_{PC} = 17, J_{CH} = 116, WCH_3), 20.65 (q of t, J_{PC} = 9, J_{CH} = 121, PCH_3Ph$_2$), 48.99 (t, J_{CH} = 158, C_2H_4). $^{31}P\{^1H\}$ NMR: 19.5 (s, J_{WP} = 274).

$W(O)Me(Cl)(CO)(PMePh_2)_2$

This complex was prepared in a sealed tube containing **28** (10 mg) in C_6D_6 and 1 atm CO. IR (C_6D_6): 1985 *ν*(CO), 960 *ν*(WO). ^1H NMR: 1.72 (t, 3, $^3J_{PH}$ = 10, WCH_3), 2.17 (t, 6, J_{PH} = 4, P*Me*Ph$_2$), 6.94–7.07 (br m, 12, PMePh*Ph*′, *p* and *m*), 7.67 (m, 4, PMe*Ph*Ph′, *o*), 7.75 (m, 4, PMePh*Ph*′, *o*). $^{13}C\{^1H\}$ NMR: 236.6 (s, J_{PC} = 5, *C*O). $^{31}P\{^1H\}$ NMR: 15.7 (s, J_{WP} = 323, J_{PC} = 4). The ^{13}C and ^{31}P spectra were determined for W(O)Me(Cl)(^{13}CO)$(PMePh_2)_2$.

$W(O)Cl(Me)(CN^tBu)(PMePh_2)_2$

CN^tBu (0.015 cm^3, 0.20 mmol) was added to a stirred solution of **28** (0.10 g, 0.23 mmol) in 15 cm^3 of benzene. The purple solution was filtered and the volume was reduced to 1 cm^3. Petroleum ether (5 cm^3) was added and the purple crystals were isolated and dried *in vacuo*; yield 0.35 g (45%). IR: 2110 *ν*(CN), 955 *ν*(WO). ^1H NMR: 0.80 (s, 9, CNC*Me*$_3$), 2.07 (t, 3, J_{PH} = 9, WCH_3), 2.40 (t, 6, J_{PH} = 4, P*Me*Ph$_2$), 6.97–7.14 (br m, 12, PMe*Ph*$_2$, *p* and *m*), 7.70 (m, 4, PMe*Ph*Ph′, *o*), 8.11 (m, 4, PMePh*Ph*′, *o*). $^{13}C\{^1H\}$ NMR: 15.35 (t, J_{PC} = 15, P*Me*Ph$_2$), 15.45 (t, J_{PC} = 6, WCH_3), 30.69 (s, CNC*Me*$_3$), 57.83 (s, CH*C*Me$_3$), 145.50 (t, J_{PC} = 19, *C*NCMe$_3$). $^{31}P\{^1H\}$ NMR: 16.8 (s, J_{WP} = 327).

X-ray structure determinations for W(N-*p*-Tol)(CO)$Cl_2(PMePh_2)_2$ (**25**) *and* $WCl_2(PMePh_2)_4$ (**1**)

Data were collected at room temperature (295 K) on a crystal sealed in a glass capillary (**25**) and on

Table 6. Crystallographic data for $WCl_2(PMePh_2)_4$ (**1**) and W(N-*p*-Tol)(CO)$Cl_2(PMePh_2)_2$ (**25**)

Complex	$WCl_2(PMePh_2)_4 \cdot (THF) \cdot (C_6H_6)_{0.5}$	W(N-*p*-Tol)(CO)$Cl_2(PMePh_2)_2$
Formula	$C_{59}H_{63}Cl_2OP_2W$	$C_{34}H_{33}Cl_2NOP_2W$
f_w	1104.86	788.35
Crystal dimensions	0.28 × 0.23 × 0.21 mm	0.17 × 0.26 × 0.58 mm
Space group	*P*1-bar	*Pbcn*
a (Å)	11.7401(13)	17.764(2)
b (Å)	14.2555(12)	15.821(6)
c (Å)	17.5922(12)	23.829(3)
α (°)	76.226(6)	
β (°)	70.891(7)	
γ (°)	83.476(8)	
V (Å^3)	2700.0(7)	6697(3)
Z	2	8
ρ_{calc} (g cm^{-3})	1.36	1.56
μ (cm^{-1})	23.8	38.1
θ limits (°)	2–25	2–28
Transmission factors		0.794–0.999; av 0.890
Total number of reflections	9954	16,110
	h, ±*k*, ±*l*	±*h*, *k*, *l*
Data $I > 3\sigma$	5734	3713
Final number of variables	564	370
R	0.054	0.028
R_w	0.065	0.031

a crystal mounted on a glass fiber (**1**) using a CAD4 diffractometer operating in the θ–2θ scan mode with graphite monochromated Mo-K_α radiation ($\lambda = 0.71069$ Å), as previously described.[36] The structures were solved using standard heavy atom methods and refined with full-matrix least-squares, with scattering factors and anomalous dispersion terms taken from standard compilations.[37] All non-hydrogen atoms were refined anisotropically, hydrogen atom positions were calculated (C—H = 0.95 Å). Crystallographic data are given in Table 6. Positional and thermal parameters, complete tabulations of bond lengths and angles, and observed and calculated structure factors are available as supplementary material from the Editor.

Acknowledgements—We would like to thank Lauren Atagi for the photochemical experiments and Don McAlister for his many contributions. This work was supported by the Donors of the Petroleum Research Fund, administered by the American Chemical Society, the University of Washington Graduate School Research Fund (GSRF), the National Science Foundation (CHE-8617965), and the Chevron Research Company. We also acknowledge support for X-ray equipment from the National Science Foundation (CHE-8617023) and the University of Washington GSRF (PHS grant PR-07096).

REFERENCES

1. W. A. Nugent and J. M. Mayer, *Metal–Ligand Multiple Bonds*. Wiley Interscience, New York (1988).
2. J. P. Collman, L. S. Hegedus, J. R. Norton and R. G. Finke, *Principles and Applications of Organotransition Metal Chemistry*, pp. 37–48. University Science Books, Mill Valley, California (1987).
3. Carbonyl–imido and carbonyl–nitrido complexes: (a) W(NAr)(CO)(S_2CNR_2)$_2$ (ν(CO) = 1912 cm^{-1}): G. L. Hillhouse and B. L. Haymore, *J. Organomet. Chem.* 1978, **162**, C23 (see also *J. Am. Chem. Soc.* 1982, **104**, 1537); (b) Re(NAr)Cl_3(CO)(PPh_3) (ν(CO) = 2040 cm^{-1}): G. La Monica and S. Cenini, *J. Chem. Soc., Dalton Trans.* 1980, 1145; G. La Monica and S. Cenini, *Inorg. Chim. Acta* 1978, **29**, 183; (c) Ru and Os^{VI} nitrido–carbonyl complexes: P. A. Belmonte, University of Illinois Chicago Circle, personal communication (1985); (d) Matrix isolation and gas phase studies: J. A. Crayston, M. J. Almond, A. J. Downs, M. Poliakoff and J. J. Turner, *Inorg. Chem.* 1984, **23**, 3051; M. J. Almond, A. J. Downs and R. N. Perutz, *Inorg. Chem.* 1985, **24**, 275; Z. H. Kafafi, R. H. Hauge, W. E. Billups and J. L. Margrave, *J. Am. Chem. Soc.* 1987, **109**, 4775; K. Lane, L. Sallans and R. R. Squires, *J. Am. Chem. Soc.* 1984, **106**, 2719; (e) There are more examples of oxo–isonitrile complexes, for instance: C. T. Lam, D. L. Lewis and S. J. Lippard, *Inorg. Chem.* 1976, **15**, 989; D. C. Bradley, M. B. Hursthouse, K. M. A. Malik, A. J. Neilson and R. L. Short, *J. Chem. Soc., Dalton Trans.* 1983, 2651; J. C. Bryan, R. E. Stenkamp, T. H. Tulip and J. M. Mayer, *Inorg. Chem.* 1987, **26**, 2283 and ref. 3c.
4. Preliminary reports of this work have appeared: (a) F.-M. Su, C. Cooper, S. J. Geib, A. L. Rheinfold and J. M. Mayer, *J. Am. Chem. Soc.* 1986, **108**, 3545; (b) J. C. Bryan, S. J. Geib, A. L. Rheinfold and J. M. Mayer, *J. Am. Chem. Soc.* 1987, **109**, 2826.
5. Imido–olefin complexes have been prepared independently by: G. R. Clark, A. J. Nielson, C. E. F. Rickard and D. C. Ware, *Polyhedron*, in press. An oxo complex containing tetracyanoethylene, an unusual olefin, has been described: P. W. Schneider, D. C. Bravard, J. W. McDonald and W. E. Newton, *J. Am. Chem. Soc.* 1972, **94**, 8640; L. Ricard and R. Weiss, *Inorg. Nucl. Chem. Lett.* 1974, **10**, 217. Spectroscopic evidence has been obtained for the interaction of OsO_4 with olefins: W. W. Nugent, *J. Org. Chem.* 1980, **45**, 4533.
6. K. B. Sharpless, A. Y. Teranishi and J.-E. Bäckvall, *J. Am. Chem. Soc.* 1977, **99**, 3120; S. G. Hentges and K. B. Sharpless, *J. Am. Chem. Soc.* 1980, **102**, 4263; J. P. Collman, J. I. Brauman, B. Meunier, T. Hayashi, T. Kodadek and S. A. Raybuck, *J. Am. Chem. Soc.* 1985, **107**, 2000 and refs therein; J. P. Collman, T. Kodadek, S. A. Raybuck, J. I. Brauman and L. M. Papazain, *J. Am. Chem. Soc.* 1985, **107**, 4343; see also: R. A. Sheldon and J. K. Kochi, *Metal-catalyzed Oxidations of Organic Compounds*. Academic Press, New York (1981); A. K. Rappé and W. A. Goddard III, *J. Am. Chem. Soc.* 1982, **104**, 448; R. Schrock, S. Rocklage, J. Wengrovius, G. Rupprecht and J. Fellmann, *J. Molec. Catal.* 1980, **8**, 73.
7. T. Engel and G. Ertl, *Adv. Catal.* 1979, **28**, 1.
8. E. Carmona, L. Sanchez, M. L. Poveda, R. A. Jones and J. G. Hefner, *Polyhedron* 1983, **2**, 797.
9. A. J. Nielson, *Inorg. Synth.* 1986, **24**, 194.
10. J. P. Collman, L. S. Hegedus, J. R. Norton and R. G. Finke, *Principles and Applications of Organotransition Metal Chemistry*, p. 149. University Science Books, Mill Valley, California (1987).
11. Y.-H. Huang and J. A. Gladysz, *J. Chem. Ed.* 1988, **65**, 298.
12. P. R. Sharp, *Organometallics* 1984, **3**, 1217; P. R. Sharp, J. C. Bryan and J. M. Mayer, *Inorg. Synth*, in press.
13. C. A. Tolman, *Chem. Rev.* 1977, **77**, 313.
14. J. C. Bryan and J. M. Mayer, *J. Am. Chem. Soc.* 1987, **109**, 7213.
15. J. Sandström, *Dynamic NMR Spectroscopy*, p. 96. Academic Press, New York (1982).
16. J. M. Mayer, *Inorg. Chem.* 1988, **27**, 3899.
17. K. W. Chiu, D. Lyons, G. Wilkinson, M. Thornton-Pett and M. B. Hursthouse, *Polyhedron* 1983, **2**, 803.
18. D. C. Bradley, M. B. Hursthouse, K. M. A. Malik, A. J. Nielson and R. L. Short, *J. Chem. Soc., Dalton Trans.* 1983, 2651.
19. W. A. Nugent and B. L. Haymore, *Coord. Chem. Rev.* 1980, **31**, 123; E. M. Shustorovich, M. A. Porai-

Koshits and Yu. A. Buslaev, *Coord. Chem. Rev.* 1975, **17**, 1.
20. E. Carmona, J. M. Marin, M. L. Poveda, J. L. Atwood and R. D. Rogers, *Polyhedron* 1983, **2**, 185; M. Nardelli, G. Pelizzi and G. Predieri, *Gazz. Chim. Ital.* 1980, **110**, 375; L. K. Fong, J. R. Fox, B. M. Foxman and N. J. Cooper, *Inorg. Chem.* 1986, **25**, 1880; M. Bakir, F. A. Cotton, M. M. Cudahy, C. Q. Simpson, T. J. Smith, E. F. Vogel and R. A. Walton, *Inorg. Chem.* 1988, **27**, 2608.
21. F. A. Cotton and G. Wilkinson, *Advanced Inorganic Chemistry*, 4th edn, p. 357. John Wiley, New York (1980).
22. High-valent olefin complexes are rare: F. W. S. Benfield and M. L. H. Green, *J. Chem. Soc., Dalton Trans.* 1974, 1324; M. L. H. Green and R. Mahtab, *J. Chem. Soc., Dalton Trans.* 1979, 262; E. J. Parsons, R. D. Larsen and P. W. Jennings, *J. Am. Chem. Soc.* 1985, **107**, 1793; High-valent carbonyl complexes are more common, for instance: M. M. Millar, T. O'Sullivan, N. deVries and S. A. Koch, *J. Am. Chem. Soc.* 1985, **107**, 3714; J. L. Davidson and G. Vasapollo, *J. Organomet. Chem.* 1985, **291**, 43; I. W. Nowell, K. Tabatabaian and C. White, *J. Chem. Soc., Chem. Commun.* 1979, 547; J. W. Faller and Y. Ma, *Organometallics* 1986, 1949 and refs therein; see also ref. 3.
23. W. A. Nugent and J. M. Mayer, *Metal–Ligand Multiple Bonds*, Section 2.3.1 and refs therein. Wiley Interscience, New York (1988).
24. J. M. Mayer, *Comm. Inorg. Chem.* 1988, **8**, 125.
25. E. A. Maatta and R. A. D. Wentworth, *Inorg. Chem.* 1979, **18**, 524; W. E. Newton, J. W. McDonald, J. L. Corbin, L. Ricard and R. Weiss, *Inorg. Chem.* 1980, **19**, 1997; J. L. Templeton, P. B. Winston and B. C. Ward, *J. Am. Chem. Soc.* 1981, **103**, 7713; J. L. Templeton, B. C. Ward, G. J.-J. Chen, J. W. McDonald and W. E. Newton, *Inorg. Chem.* 1981, **20**, 1248; M. A. Bennett and I. W. Boyd, *J. Organomet. Chem.* 1985, **290**, 165 and refs therein; G. J.-J. Chen, J. W. McDonald and W. E. Newton, *Organometallics* 1985, **4**, 422 and refs therein.
26. J. H. Wengrovius and R. R. Schrock, *Organometallics* 1982, **1**, 148; M. R. Churchill and A. L. Rheingold, *Inorg. Chem.* 1982, **21**, 1357; see also ref. 14.
27. (a) D. C. Brower, J. L. Templeton and D. M. P. Mingos, *J. Am. Chem. Soc.* 1987, **109**, 5203; (b) K. A. Jørgensen and P. Swanstrøm, *Acta Chem. Scand.* 1987, **B41**, 153.
28. (a) Z. Dori, *Prog. Inorg. Chem.* 1981, **28**, 239; (b) E. I. Stiefel, *Prog. Inorg. Chem.* 1977, **22**, 1.
29. L. Pauling, *The Nature of the Chemical Bond*, 3rd edn, p. 43. Cornell University Press, New York (1960).
30. A. F. Wells, *Structural Inorganic Chemistry*, 5th edn, p. 926. Clarendon Press, Oxford (1984).
31. A. Bondi, *J. Phys. Chem.* 1964, **68**, 441.
32. K. Tatsumi and R. Hoffmann, *Inorg. Chem.* 1980, **19**, 2656 and refs therein; ref. 27a; ref. 1, Section 5.3.3.2.
33. P. Kubacek and R. Hoffmann, *J. Am. Chem. Soc.* 1981, **103**, 4320.
34. A. V. Butcher and J. Chatt, *J. Chem. Soc. A* 1970, 2652.
35. D. Seyferth and D. E. Welch, *J. Organomet. Chem.* 1964, **2**, 1; R. A. Zingaro and R. E. McGlothlin, *J. Chem. Engng Data* 1963, **8**, 226.
36. T. K. G. Erikson, J. C. Bryan and J. M. Mayer, *Organometallics* 1988, **7**, 1930.
37. *International Tables of X-Ray Crystallography*, Vol. IV, Tables 2–2B, 2.3.1.3. Kynoch Press, Birmingham, U.K. (1974).

Polyhedron Vol. 8, No. 10, pp. 1279–1283, 1989
Printed in Great Britain

0277–5387/89 $3.00+.00
© 1989 Pergamon Press plc

REACTION OF TRIMETHYLALUMINIUM WITH A TRIDENTATE OPEN-CHAIN AMINE. SYNTHESIS AND MOLECULAR STRUCTURE OF $[Al(CH_3)]_2[C_{12}H_{28}N_6][Al(CH_3)_2]_2$

GREGORY H. ROBINSON,* FRITZ MOISE, WILLIAM T. PENNINGTON and SAMUEL A. SANGOKOYA

Department of Chemistry, Clemson University, Clemson, SC 29634-1905, U.S.A.

(*Received* 7 *November* 1988; *accepted* 5 *January* 1989)

Abstract—Reaction of 3,3′-iminobispropylamine with trimethylaluminium affords the crystalline complex $[Al(CH_3)]_2[C_{12}H_{28}N_6][Al(CH_3)_2]_2$. The title compound crystallizes in the monoclinic space group $P2_1/n$, with unit cell parameters $a = 8.334(2)$, $b = 11.099(3)$, $c = 14.264(4)$ Å, $\beta = 90.99(2)°$, $V = 1319.2$ Å^3, and $\rho = 1.14$ g cm^{-3} for $Z = 2$. Least-squares refinement based on 1018 observed reflections [$I > 3\sigma(I)$] converged at $R = 0.048$, $R_w = 0.053$. The title compound, consisting of two amine units bridged by four organoaluminium moieties, has extensive Al—N association. The two central aluminium atoms are five-coordinate residing in trigonal bipyramidal environments. The compound contains three Al_2N_2 rings with a mean Al—N distance of 1.990(4) Å. The shortest Al···Al contact of 2.830(2) Å does not suggest significant metal–metal interactions.

The utilization of organo-main group compounds as organometallic precursors to ceramic materials is currently a very popular area of study. Organoaluminium–nitrogen compounds are noteworthy as potential single source organometallic precursors to aluminium nitride. While much of the recent emphasis in this area has concerned the condensation reactions of aluminium alkyls with ammonia,[1] Smith performed a considerable amount of seminal work concerning the organoaluminium chemistry of primary and secondary monodentate amines.[2–10] The corresponding organoaluminium chemistry of nitrogen-based macrocyclic ligands and multidentate open-chain amines has received less attention. Here, we report the synthesis and molecular structure of $[Al(CH_3)]_2[C_{12}H_{28}N_6][Al(CH_3)_2]_2$ isolated from reaction of 3,3′-iminobispropylamine ($C_6H_{17}N_3$) (Fig. 1) with trimethylaluminium. The title compound is noteworthy in that it contains an extensive aluminium–nitrogen network, in addition to accommodating two five-coordinate aluminium atoms residing in trigonal bipyramidal environments.

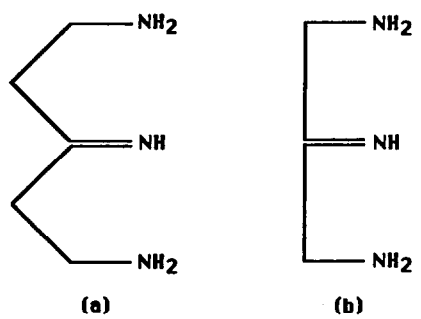

Fig. 1. (a) 3,3′-iminobispropylamine and (b) diethylenetriamine.

EXPERIMENTAL

Synthesis

Standard Schlenk techniques were employed in conjunction with an inert atmosphere dry box (Vacuum Atmospheres HE-43 Dri-Lab). Trimethylaluminium and 3,3′-iminobispropylamine, both purchased from Aldrich Chemical Company, were used as received. Single crystal, X-ray data were collected on a Nicolet R3m/V diffractometer. ^{1}H NMR data were recorded on a JOEL-FX90Q

* Author to whom correspondence should be addressed.

NMR spectrometer. Solvents were purified and degassed in the usual manner.

Inside the dry box, a reaction vessel was charged with 3,3′-iminobispropylamine (7.15 mmol) and a mixture of methylene chloride and pentane (5 cm^3: 10 cm^3, respectively). Trimethylaluminium (14.3 mmol) was slowly added via syringe. Reaction was immediate and quite exothermic. The resulting clear mixture was heated overnight in an oil bath (90°C). The system was vented frequently to allow release of CH_4. After allowing the system to stand undisturbed for several hours at room temperature, a multitude of small, colourless, extremely air-sensitive crystals were obtained. ^1H NMR ($CDCl_3$): δ −0.529 [s, 3H, Al(CH_3)], −0.665 [s, 3H, Al(CH_3)], −0.798 [s, 6H, Al(CH_3)$_2$], −0.842 [s, 6H, Al(CH_3)$_2$], −0.924 [s, 6H, Al(CH_3)$_2$], −0.943 [s, 6H, Al(CH_3)$_2$], 1.69–2.69 [m, 24H, (N(CH_2)$_3$)$_2$N]. The six peaks representing the alkyl aluminium protons are indicative of solution isomerization of the title compound.

X-ray structural solution and refinement

A single crystal of [Al(CH_3)]$_2$[$C_{12}H_{28}N_6$][Al(CH_3)$_2$]$_2$ was mounted in a thin-walled glass capillary under an inert atmosphere of argon. Cell constants and an orientation matrix for the setting angles of 26 carefully centred reflections in the range $15.07 < 2\theta < 29.61°$ corresponded to a monoclinic cell with dimensions $a = 8.334(2)$, $b = 11.099(3)$, $c = 14.264(4)$ Å, $\beta = 90.99(2)°$, $V = 1319.2$ Å^3, and $\rho = 1.14$ g cm^{-3} for $Z = 2$. The space group was determined to be $P2_1/n$. The structure was solved by direct methods and refined, based on 1018 observed reflections [$I > 3\sigma(I)$], using SHELXTL.[11] Hydrogen atoms, located from difference Fourier maps, were placed in idealized positions with fixed isotropic temperature factors. Refinement converged at $R = 0.048$, $R_w = 0.053$. Relevant crystallographic data are given in Table 1.

Table 1. Summary of crystallographic data for [Al(CH_3)]$_2$[$C_{12}H_{28}N_6$][Al(CH_3)$_2$]$_2$

Formula	$C_{18}H_{46}Al_4N_6$
Formula weight	454.62
Colour; habit	Colourless prisms
Size (mm)	0.10 × 0.15 × 0.70
Crystal system	Monoclinic
Space group	$P2_1/n$
a (Å)	8.334(2)
b (Å)	11.0990(3)
c (Å)	14.264(4)
Volume (V) (Å^3)	1319
Z (molecules/cell)	2
ρ (calc.)	1.14
Diffractometer	Nicolet R3m/V
λ(Mo-K_α) (Å)	0.71073
Temperature (°C)	21
2θ limits (°)	3.50–45.0
Number of data measured	1980
Number of data observed	1018 [$I > 3\sigma(I)$]
Goodness-of-fit	1.16
R	0.048
R_w	0.053

RESULTS AND DISCUSSION

Particularly significant in the design of organoaluminium single source aluminium nitride precursors is the optimization of Al—N interactions throughout the source molecule. We have endeavoured to address this premise by exploring the organoaluminium chemistry of macrocyclic[12–14] and multidentate open-chain amines.[15–18] Multidentate open-chain amines are notably attractive in this regard for two reasons: (1) reaction of N—H and Al—R species results in alkane elimination and reaction products with considerable Al—N association; (2) due to their inherent flexibility, multidentate open-chain amines offer various modes of coordination about an aluminium atom, thereby potentially saturating the coordination sphere via extensive Al—N contacts. The tridentate open-chain amine 3,3′-iminobispropylamine was allowed to react with trimethylaluminium; [Al(CH_3)]$_2$[$C_{12}H_{28}N_6$][Al(CH_3)$_2$]$_2$ was the only product isolated. The overall reaction is given in eq. (1). The X-ray crystal structure of the compound is given in Fig. 2.

$$4Al(CH_3)_3 + 2(H_2NCH_2CH_2CH_2)_2NH \longrightarrow [Al(CH_3)]_2[C_{12}H_{28}N_6][Al(CH_3)_2]_2 + 6CH_4. \quad (1)$$

Several points are worthy of note regarding the structure and bonding in [Al(CH_3)]$_2$[$C_{12}H_{28}N_6$][Al(CH_3)$_2$]$_2$. The title compound consists of a dimer, in that two amine units are bridged by four organoaluminium species. The molecule, residing about a crystallographic centre of symmetry, contains two dimethylaluminium species and two methylaluminium species. Furthermore, [Al(CH_3)]$_2$[$C_{12}H_{28}N_6$][Al(CH_3)$_2$]$_2$ contains three Al_2N_2 ring fragments. The coordination environment of the aluminium atoms is particularly significant. The two outermost aluminium atoms, Al(2) and Al(2a), are in the usual organoaluminium coordination of four-coordinate tetrahedral. However, the two central aluminium atoms, Al(1) and Al(1a), are clearly five-coordinate, being bonded to two nitrogen atoms of each amine

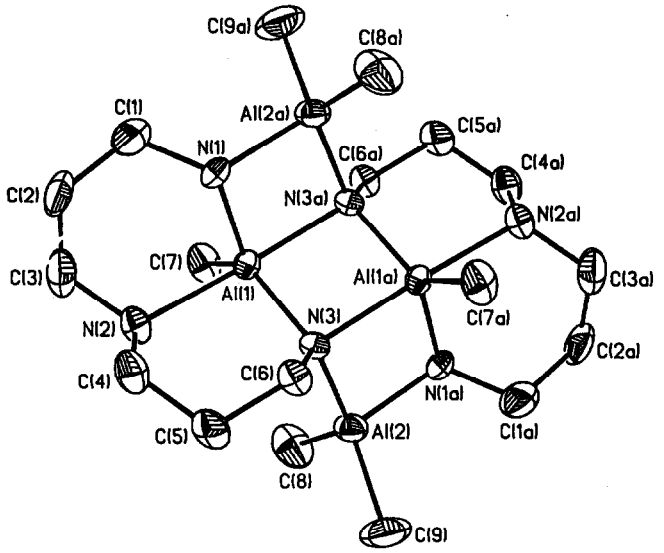

Fig. 2. A view of the $[Al(CH_3)]_2[C_{12}H_{28}N_6][Al(CH_3)_2]_2$ molecule showing the atom labelling scheme. Thermal ellipsoids show 35% probability levels; hydrogen atoms have been omitted. Selected bond distances (Å) and angles (°): Al(1)—N(1), 1.967(4); Al(1)—N(2), 2.193(4); Al(1)—N(3), 1.878(4); Al(1)—N(3a), 2.065(4); Al(1)—C(7), 1.988(6); Al(2)—N(3), 1.891(4); Al(2)—N(1a), 1.944(4); Al(2)—C(8), 1.974(7); Al(2)—C(9), 1.987(7); Al(1)···Al(2a), 2.830(2); Al(1)···Al(1a), 2.883(3). N(2)—Al(1)—N(3a), 169.0(2); N(1)—Al(1)—C(7), 117.1(2); N(3)—Al(1)—C(7), 127.9(2); N(2)—Al(1)—C(7), 89.8(2); N(2)—Al(1)—N(3), 91.6(2); N(3)—Al(2)—N(1a), 90.6(2); C(8)—Al(2)—C(9), 111.0(3); Al(1)—N(3)—C(6), 116.3(3); Al(2)—N(3)—C(6), 111.7(3); Al(2)—N(3)—Al(1a), 91.2(2); Al(1)—N(3)—Al(1a), 93.8(2).

unit in addition to a methyl carbon atom. The aluminium atom, Al(1), is coplanar with C(7), N(1), and N(3). The N(2)—Al(1)—N(3a) bond angle is 169.0(2)° while the N(2)—Al(1)—C(7), N(2)—Al(1)—N(3) and N(1)—Al(1)—N(2) are determined to be 89.8(2), 91.6(2) and 86.2(2)°, respectively. The Al(1)—N(2) and Al(1)—N(3a) bond distances are 2.193(4) and 2.065(4) Å, respectively. The coordination of both Al(1) and Al(1a) may thus be described as five-coordinate trigonal bipyramidal. A perspective view of the coordination geometry about Al(1) is given in Fig. 3.

The title compound is easily compared to the previously reported $[Al(CH_3)]_2[C_8H_{20}N_6][Al(CH_3)_2]_2$ complex[18] isolated from reaction of trimethylaluminium with diethylenetriamine (Fig. 1). While this complex bears a resemblance to the title compound in that both compounds contain two five-coordinate aluminium atoms, there are fundamental differences between the two. In the organoaluminium–diethylenetriamine complex the two five-coordinate aluminium atoms are in square-pyramidal environments, while the two five-coordinate aluminium atoms

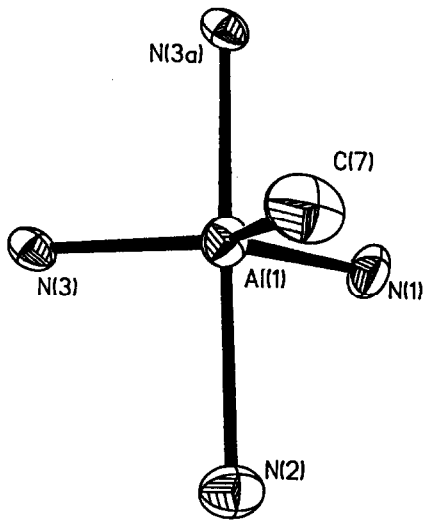

Fig. 3. A perspective view of the coordination geometry about Al(1) in $[Al(CH_3)]_2[C_{12}H_{28}N_6][Al(CH_3)_2]_2$.

in the title compound are in trigonal bipyramidal geometries. This may be viewed as a consequence of the greater inherent flexibility of 3,3′-iminobispropylamine relative to diethylenetriamine. In-

deed, in two other recently reported organoaluminium compounds containing penta-coordinate aluminium atoms, $[Al(CH_3)][C_{18}H_{19}N_4][Al(CH_3)_2]$[15] and $[Al(CH_3)][Ph_2P(O)C]_2[Al(CH_3)_2]_2$,[19] the five-coordinate aluminium atoms were found to be in trigonal bipyramidal environments. Notably, both of these compounds involved flexible multidentate ligands. It thus appears that the coordination geometry of five-coordinate aluminium species depends markedly on the associated ligand(s). It may thus be suggested that if the associated multidentate ligand(s) is sufficiently flexible, a trigonal bipyramidal coordination of aluminium may be favoured. Conversely, if the associated ligand(s) is sufficiently rigid, a square bipyramidal coordination geometry may be observed.

Another notable difference between the title compound and the organoaluminium–diethylenetriamine complex is the coordination environment of the nitrogen atoms. Each nitrogen atom in the previously reported organoaluminium–diethylenetriamine complex, including the two central nitrogen atoms, is bonded to two aluminium atoms. The single hydrogen atom on both central nitrogen atoms of the free tridentate amine was utilized in alkane elimination during the course of the reaction with trimethylaluminium. A similar situation was not observed in the title compound. Surprisingly, the central secondary amine nitrogen atoms, N(2) and N(2a) in $[Al(CH_3)]_2[C_{12}H_{28}N_6][Al(CH_3)_2]_2$, each retained their single hydrogen atom, while both hydrogen atoms of two primary amine nitrogen atoms, N(3) and N(3a), were utilized in the alkane elimination. The remaining primary nitrogen atoms, N(1) and N(1a), each donated one of their hydrogen atoms to alkane elimination. This all results in the central nitrogen atoms in the title compound being bonded to only one aluminium atom, whereas the two nitrogen atoms that lost both of their hydrogen atoms are bonded to three aluminium atoms. This appears to be a consequence of the increased length in the hydrocarbon linkages of the multidentate open-chain amines (3,3′-iminobispropylamine relative to diethylenetriamine), in that the $-(CH_2)_3-$ hydrocarbon fragments are too long to facilitate substantial interaction of the organoaluminium moieties with the central N—H units. Consequently, the terminal primary amine units are in better positions to be involved in the Al—N network. Importantly, this is the first observation by this laboratory where both hydrogen atoms of a $-NH_2$ fragment were cleaved resulting in the nitrogen atom bonding to three aluminium atoms.

The organoaluminium chemistry of multidentate open-chain amines has proven to be a particularly fruitful area of study. Small changes in the length of the hydrocarbon fragments of these amines profoundly affect the coordination geometry of aluminium. Indeed, we have recently observed a six-coordinate aluminium atom in a macrocyclic amine complex.[20] Related studies with multidentate open-chain amines and alkylaluminium halides and hydrides are forthcoming.

Acknowledgement—We are grateful to the National Science Foundation for support of this work to G.H.R. (RII-8520554).

Supplementary material available. A summary of data collection and refinement, tables of bond distances and angles, and tables of fractional coordinates, in addition to a listing of observed and calculated structure factors have been deposited with the Cambridge Crystallographic Data Centre. Complete structural information is available from the Editor.

REFERENCES

1. L. V. Interrante, L. E. Carpenter II, C. Whitmarsh and W. Lee, *Mater. Res. Soc. Proc.* 1985, **73**, 369.
2. A. W. Laubengayer, J. D. Smith and G. G. Ehrlich, *J. Am. Chem. Soc.* 1961, **83**, 542.
3. M. Cohen, J. K. Gilbert and J. D. Smith, *J. Chem. Soc.* 1965, 1092.
4. J. K. Gilbert and J. D. Smith, *J. Chem. Soc. A* 1968, 233.
5. K. Gosling, J. D. Smith and D. H. W. Wharmby, *J. Chem. Soc. A* 1969, 1738.
6. P. B. Hitchcock, J. D. Smith and K. M. Thomas, *J. Chem. Soc., Dalton Trans.* 1976, 1433.
7. G. M. McLaughlin, G. A. Sim and J. D. Smith, *J. Chem. Soc., Dalton Trans.* 1972, 2197.
8. K. J. Alford, A. K. Gosling and J. D. Smith, *J. Chem. Soc., Dalton Trans.* 1972, 2203.
9. S. Amirkhalili, P. B. Hitchcock and J. D. Smith, *J. Chem. Soc., Dalton Trans.* 1979, 1206.
10. S. Amirkhalili, P. B. Hitchcock, A. D. Jenkins, J. Z. Nyathi and J. D. Smith, *J. Chem. Soc., Dalton Trans.* 1981, 377.
11. G. M. Sheldrick, SHELXTL, Crystallographic computing system, Revision 5.1. Nicolet Instruments Division, Madison, Wisconsin (1986).
12. G. H. Robinson, E. S. Appel, S. A. Sangokoya, H. Zhang and J. L. Atwood, *J. Coord. Chem.* 1988, **17**, 373.
13. G. H. Robinson and S. A. Sangokoya, *Organometallics* 1988, **7**, 1453.
14. G. H. Robinson, A. D. Rae, C. F. Campana and S. K. Byram, *Organometallics* 1987, **6**, 1227.
15. G. H. Robinson, S. A. Sangokoya, F. Moise and W. T. Pennington, *Organometallics* 1988, **7**, 1887.
16. G. H. Robinson, F. Moise, W. T. Pennington and

S. A. Sangokoya, *J. Cryst. Spec. Res.* 1988, **18**, 387.
17. G. H. Robinson, S. A. Sangokoya and R. D. Rogers, *Polyhedron* 1988, **7**, 2727.
18. G. H. Robinson and S. A. Sangokoya, *J. Am. Chem. Soc.* 1987, **109**, 6852.
19. G. H. Robinson, B. Lee, W. T. Pennington and S. A. Sangokoya, *J. Am. Chem. Soc.* 1988, **110**, 6260.
20. G. H. Robinson, M. F. Self, S. A. Sangokoya and W. T. Pennington, *J. Am. Chem. Soc.* 1989, **111**, 1520.

Polyhedron Vol. 8, No. 10, pp. 1285–1291, 1989
Printed in Great Britain

0277–5387/89 $3.00+.00
© 1989 Pergamon Press plc

CYCLOPENTADIENYL SUBSTITUTED DIETHYLAMINOCARBYNE COMPLEXES OF TUNGSTEN IN A HIGHER OXIDATION STATE

A. C. FILIPPOU

Institut für Anorganische Chemie, Technische Universität München, Lichtenbergstraße 4, D-8046 Garching, F.R.G.

(*Received* 9 *November* 1988; *accepted* 5 *January* 1989)

Abstract—The reaction of an equimolar mixture of $(\eta^5\text{-}C_5H_5)(I)_2(CO)W{\equiv}CNEt_2$ (**1**) and $t\text{-}C_4H_9NC$ in THF at 50°C, results in the replacement of the CO ligand by isocyanide and formation of $(\eta^5\text{-}C_5H_5)(I)_2(t\text{-}C_4H_9NC)W{\equiv}CNEt_2$ (**2**). Complex **2** reacts further with $t\text{-}C_4H_9NC$ in refluxing THF with displacement of the iodide ligand from the coordination sphere to give the cationic carbyne complex $[(\eta^5\text{-}C_5H_5)(I)(t\text{-}C_4H_9NC)_2W{\equiv}CNEt_2]^+I^-$ (**3**). A new route to **2** in three steps has also been developed. The starting material, *mer*-$I(t\text{-}C_4H_9NC)_3W{\equiv}CNEt_2$ (**4**), is transformed with KC_5H_5 in refluxing THF to $(\eta^5\text{-}C_5H_5)(t\text{-}C_4H_9NC)(CO)W{\equiv}CNEt_2$ (**5**). Complex **5** is then oxidized with elemental iodine in CH_2Cl_2 to give $[(\eta^5\text{-}C_5H_5)(I)(t\text{-}C_4H_9NC)(CO)W{\equiv}CNEt_2]^+I^-$ (**6**), the first cationic, carbonyl-containing carbyne complex of tungsten in a higher oxidation state. Finally, **6** is decarbonylated thermally in boiling THF to **2**. The composition and structure of the new complexes **2**, **3**, **5** and **6** have been determined by total elemental analyses and IR, ^1H NMR, ^{13}C NMR spectroscopies, as well as by mass spectrometry. The non-ionic nature of **2** and ionic nature of **6** in solution, have been confirmed by conductivity measurements.

Complexes containing a metal–carbon triple bond are divided into two classes. Class (a) includes compounds of low valent metals, which are known as Fischer type carbyne complexes. In these complexes, the electron-rich metal is stabilized by good π-acceptor ligands such as CO, e.g. *trans*-$X(CO)_4M{\equiv}CR$ (X = halogen; M = Cr, Mo, W; R = aryl or alkyl group).[1] Class (b) contains complexes of high valent metals, i.e. Schrock type alkylidyne complexes. In these complexes, the electron-deficient metal is stabilized by good π-donor ligands, such as halogen or alkoxy ligands, e.g. $X_3(dme)W{\equiv}CCMe_3$ (X = halogen; dme = 1,2-dimethoxyethane).[2]

Striking differences in the reactivity exist between class (a) and (b) compounds. This is most impressively demonstrated by their reactions with alkynes. Fischer type carbyne complexes catalyse alkyne polymerization, while Schrock type alkylidyne complexes function as alkyne metathesis catalysts.[3,4]

In our development of the chemistry of substituted tungsten carbyne complexes with the general formula $I(CO)_2L_2W{\equiv}CNEt_2$ (L = C_5H_5N, PMe_3, $t\text{-}C_4H_9NC$, L_2 = 2,2′-bipy, *o*-phen), we have demonstrated that their oxidative decarbonylation with iodine gives $(I)_3(CO)L_2W{\equiv}CNEt_2$ in high yield.[5–8]

These complexes are unique, because they combine features of both Fischer type carbyne complexes, such as π-acceptor CO ligands, and Schrock type alkylidyne complexes, i.e. a high valent metal centre. Therefore, new, interesting reactivity patterns are expected. We first studied their reactions with nucleophiles and found two reaction pathways to be predominant: (a) Substitution of the labile CO ligand and one iodide ligand by the nucleophile to form cationic carbyne complexes, e.g. the reaction of $(I)_3(CO)L_2W{\equiv}CNEt_2$ with $t\text{-}C_4H_9NC$ to give $[(I)_2(t\text{-}C_4H_9NC)_2L_2W{\equiv}CNEt_2]^+I^-$ (L_2 = 2,2′-bipy, *o*-phen; L = $t\text{-}C_4H_9NC$)[7,8] and (b) reductive elimination of iodine to give low valent, neutral or cationic carbyne complexes, e.g. the reaction of $(I)_3(CO)(PMe_3)_2W{\equiv}CNEt_2$ or $(I)_3(CO)L_2W{\equiv}CNEt_2$ (L_2 = 2,2′-bipy, *o*-phen) with PMe_3 to give *mer*-$I(PMe_3)_3(CO)W{\equiv}CNEt_2$ or $[(PMe_3)_2(CO)L_2W{\equiv}CNEt_2]^+I^-$ (L_2 = 2,2′-bipy, *o*-phen).[5,6] To

extend our studies on cyclopentadienyl (cp) substituted carbyne complexes, we have first developed a high yield route to $(\eta^5\text{-}C_5R_5)(CO)_2W{\equiv}CNEt_2$ (R = H, Me) and subsequently decarbonylated these complexes to give $(\eta^5\text{-}C_5R_5)(X)_2(CO)W{\equiv}CNEt_2$ (R = H, Me; X = Br, I).[9,10] We have found differences in the reactivity of $(\eta^5\text{-}C_5H_5)(I)_2(CO)W{\equiv}CNEt_2$ compared to the corresponding $(I)_3(CO)L_2W{\equiv}CNEt_2$ complexes (L_2 = 2,2′-bipy, *o*-phen; L = PMe_3, *t*-C_4H_9NC). Thus a reaction with PMe_3 occurs only at elevated temperatures; it leads to the displacement of the Cp ligand and reductive elimination of iodine to form low valent trimethylphosphine-substituted carbyne complexes. The expected product, $(\eta^5\text{-}C_5H_5)(PMe_3)(CO)W{\equiv}CNEt_2$, was not observed.[11] This result has prompted us to investigate the reaction of $(\eta^5\text{-}C_5H_5)(I)_2(CO)W{\equiv}CNEt_2$ with *t*-C_4H_9NC.

RESULTS AND DISCUSSION

The reaction of **1** with *t*-C_4H_9NC (molar ratio 1 : 1.2) in THF at 50°C, yields quantitatively the substitution product **2** [eq. (1)]. This product is isolated as a purple, microcrystalline solid, which is only slightly sensitive to air and moisture, soluble in CH_2Cl_2, THF and toluene, but insoluble in Et_2O and *n*-pentane (m.p. 110°C).

Complex **2** reacts with *t*-C_4H_9NC in boiling THF with the elimination of one iodide ligand from the coordination sphere and formation of the yellow, cationic carbyne complex **3** [eq. (2)]. This product is soluble in CH_2Cl_2, sparingly soluble in cold THF and toluene, but insoluble in Et_2O and *n*-pentane. Complex **3** undergoes decomposition in a sealed capillary at 135°C. A slow halogen exchange (iodide for chloride) occurred in a solution of **3** in CH_2Cl_2 at room temperature. This reaction is accelerated in boiling CH_2Cl_2 and leads to mixed halogen substitution products.[11]

A different route to **2** has been developed requiring three steps. The first step involves the reaction of the easily available *mer*-$I(t\text{-}C_4H_9NC)_3(CO)W{\equiv}CNEt_2$ (**4**)[12] with KC_5H_5 in refluxing THF to give **5** [eq. (3)]. Complex **5** is an extremely air-sensitive, yellow oil, which is very soluble in CH_2Cl_2, THF, Et_2O and *n*-pentane. Complex **5** is then quantitatively transformed with elemental iodine to **6**, the

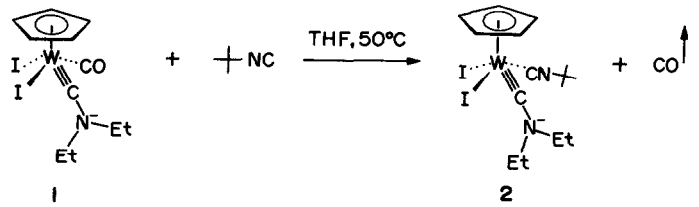

1 2 (1)

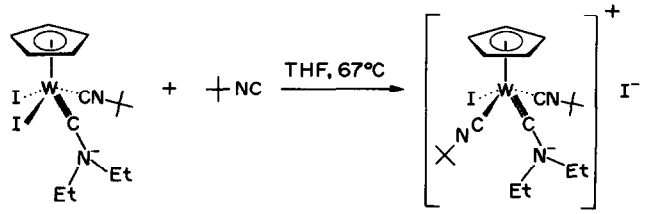

2 3 (2)

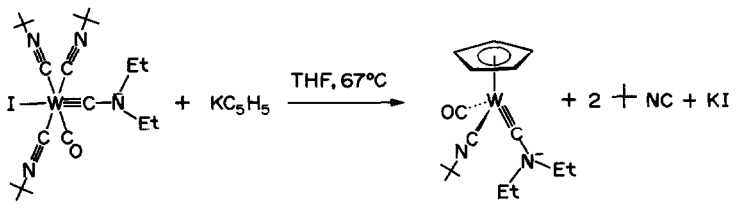

4 5 (3)

first carbonyl containing, cationic carbyne complex of tungsten in a higher oxidation state [eq. (4)]:

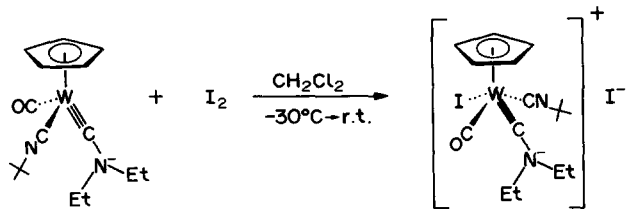

5 6 (4)

This product is obtained as an orange, microcrystalline powder, which is very soluble in CH_2Cl_2, sparingly soluble in cold THF and toluene, but insoluble in Et_2O and *n*-pentane. Decomposition of **6** is observed in a sealed capillary at 108°C.

In the last step, **6** is thermally decarbonylated to quantitatively give **2** [eq. (5)]:

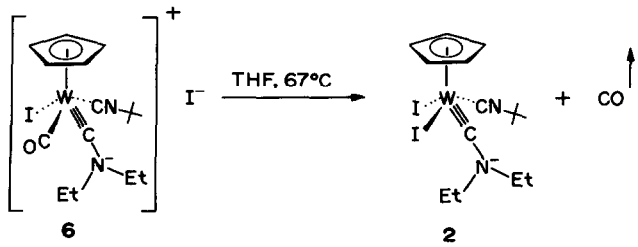

6 2 (5)

We assume a piano-stool geometry for complexes **2**, **3** and **6**, in agreement with MO-calculations on $CpML_4$ complexes, which favour energetically this structure over an alternative C_5H_5-capped trigonal bipyramidal structure.[13] The solution IR spectra of the new compounds, **2**, **3**, **5** and **6**, show characteristic absorptions for the stretching vibrations of the coordinated isonitrile and carbonyl ligands (Table 1).

A shift of the $\nu(C{\equiv}N{-})$ absorptions to higher frequency is observed when the IR data of **2**, **3** and **6** are compared. This shift can be attributed to a reduction of the electron density at the metal, and the simultaneous weakening of the metal isonitrile back-bonding. The same trend is observed for the $\nu(C{\equiv}O)$ band of compound **1** ($\nu(C{\equiv}O)$ in CH_2Cl_2, 2008 cm^{-1})[9] and **6** ($\nu(C{\equiv}O)$ in CH_2Cl_2, 2053 cm^{-1}), due to the weaker metal carbonyl back-bonding in **6** compared with **2**. In KBr, the complexes exhibit a strong band around 1600 cm^{-1}, which may be assigned to a $\nu(C{=}N)$ vibration. This

Table 1. $\nu(C{\equiv}N{-})$, $\nu(C{\equiv}O)$ and $\nu(C{=}N)$ stretching vibrations of **2**, **3**, **5** and **6** in cm^{-1}

Complex	Solvent	$\nu(C{\equiv}N{-})$	$\nu(C{\equiv}O)$	$\nu(C{=}N)^a$
2	CH_2Cl_2	2145 s	—	1604
	THF	2141 s	—	
	Toluene	2131 s	—	
3	CH_2Cl_2	2172 s	—	1615
	THF	2192 sh, 2170 s	—	
	Toluene	2192 sh, 2171 s	—	
5	CH_2Cl_2	1925 w	1829 s	—
	THF	1929 w	1845 s	
	n-Pentane	1933 m	1860 s	
6	CH_2Cl_2	2199 m	2053 s	1639
	THF	2210 m	2041 s	
	Toluene	2206 m	2041 s	

[a] $\nu(C{=}N)$ in KBr solvent.

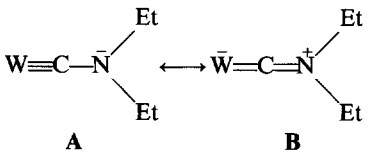

Fig. 1. Resonance forms for the bonding in the carbyne ligand.

band displays the strong interaction of the metal–carbon triple bond with the lone pair of nitrogen (Fig. 1, resonance form **B**).

The contribution of resonance form **B** to the bonding description of the carbyne ligand is diminished in **2** compared with **3** and **6**, due to an enhancement of the electron density at the metal centre. Therefore, a shift of the ν(C≡N) vibration to lower frequency is observed. A similar trend has already been reported for other diethylaminocarbyne complexes of tungsten in both lower and higher oxidation states.[5,6,8,14]

The triplets for the methyl protons of the diethylamino group observed in the ^{1}H NMR spectra of **2**, **3**, **5** and **6**, confirm the free rotation of the ethyl groups around the carbyne–carbon–nitrogen bond (Table 2). A singlet is obtained for the *t*-butyl groups of the isonitrile ligands in **3**, showing their *trans*-orientation. Complexes **5** and **6** are chiral, therefore, the protons of the methylene groups in the carbyne ligand are diastereotopic and give a signal of four overlapping quartets, which may be assigned in an ABX_3 spin system:

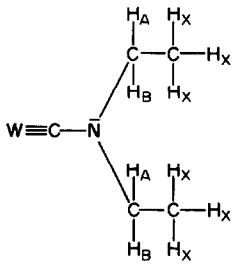

The same splitting is observed for the signals of the methylene protons in **2**, which must, therefore, also be diastereotopic. These facts suggest a structure of low symmetry with a *cis*-orientation of the iodide ligands. In contrast, the *t*-C_4H_9NC ligands in **3** are *trans*-oriented and the molecule contains a plane of symmetry; the methylene protons are therefore homotopic and give rise to a quartet.

Resonances, expected for the carbyne carbons in cyclopentadienyl-substituted diethylaminocarbyne

Table 2. ^{1}H NMR spectroscopic data of **2**, **3** and **6** in CD_2Cl_2 and **5** in C_6D_6; chemical shifts in δ, relative to the solvent ($CDHCl_2$, $\delta = 5.32$ ppm; C_6D_6, $\delta = 7.15$ ppm); relative intensities and multiplicities in parentheses, coupling constants in Hz

Complex	NCH_2CH_3	*t*-C_4H_9NC	NCH_2CH_3	C_5H_5	*T* (°C)
2	1.33 (6, t) $^3J_{HH} = 7.3$	1.53 (9, s)	3.45 (2, dq) $^2J_{H_AH_B} = 13.1$ $^3J_{H_AH_X} = 7.3$; 3.52 (2, dq) $^2J_{H_AH_B} = 13.1$ $^3J_{H_BH_X} = 7.3$	5.43 (5, s)	20
3	1.29 (6, t) $^3J_{HH} = 7.3$	1.55 (18, s)	3.48 (4, q) $^3J_{HH} = 7.3$	5.63 (5, s)	0
5	1.09 (6, t) $^3J_{HH} = 7.3$	1.24 (9, s)	2.83 (2, dq) $^2J_{H_AH_B} = 13.2$ $^3J_{H_AH_X} = 7.3$; 2.91 (2, dq) $^2J_{H_AH_B} = 13.2$ $^3J_{H_BH_X} = 7.3$	5.32 (5, s)	20
6	1.32 (6, t) $^3J_{HH} = 7.3$	1.60 (9, s)	3.59 (2, dq) $^2J_{H_AH_B} = 13.2$ $^3J_{H_AH_X} = 7.3$; 3.63 (2, dq) $^2J_{H_AH_B} = 13.2$ $^3J_{H_BH_X} = 7.3$	6.02 (5, s)	20

Table 3. ^{13}C NMR spectroscopic data of **2**, **3** and **6** in CD_2Cl_2 and **5** in C_6D_6; chemical shifts in δ, relative to the solvent (CD_2Cl_2, $\delta = 53.8$ ppm; C_6D_6, $\delta = 128.0$ ppm)

Complex	NCH_2CH_3	Me_3CNC	NCH_2CH_3	Me_3CNC	C_5H_5	Me_3CNC	W—CO	W≡C	T (°C)
2	14.7	30.9	48.9	59.3	94.7	150.3	—	305.5	20
3	14.5	30.1	49.1	59.9	93.3	136.2	—	302.3	0
5	14.4	31.6	45.6	58.7	89.7	202.8	226.7	259.9	20
6	14.3	30.1	50.1	61.0	94.9	127.8	201.5	302.3	20

complexes of tungsten, are observed in the $^{13}C\{^1H\}$ NMR spectra of **2**, **3**, **5** and **6** (Table 3).[9,10]

The isonitrile carbons appear as broad singlets, because of the quadrupol relaxation of nitrogen. Therefore any ^{13}C–^{14}N coupling cannot be resolved. Comparing the data of **2**, **3** and **6**, an upfield shift of the isonitrile carbon resonance is observed. This can be explained by the weaker metal–isonitrile back-bonding ($6 < 3 < 2$) and is in agreement with results obtained earlier for other tungsten isonitrile complexes.[8,12,14,15] For the same reason, the strong metal–isonitrile back-bonding in **5** causes an extremely large downfield shift of the isonitrile carbon signal. This is independently demonstrated by the shift of the $\nu(C\equiv N\rightarrow)$ vibration in the IR spectrum of **5** to a considerably lower frequency ($\nu(C\equiv N\rightarrow)$ in CH_2Cl_2, 1925 cm^{-1}) compared with that of the free ligand ($\nu(C\equiv N\rightarrow)$ in CH_2Cl_2, 2140 cm^{-1}).

The conductance of **6** in 1,2-dichloroethane is of the same magnitude ($c = 4.6 \times 10^{-4}$ mol dm^{-3}, $t = 19.8$°C, $\Lambda = 31\ \Omega^{-1}\ cm^2\ mol^{-1}$) as that of $NR_4^+X^-$ (R = "bu, "pr; X = Br, I, PF_6) and other ionic diethylaminocarbyne complexes of tungsten in low and high oxidation states.[6–8,16] The conductivity increases with decreasing concentration of the complex, and proves independently the ionic nature of **6** in solution. In contrast, 1,2-dichloroethane solutions of **1** and **2** are not conducting.

The mass spectral data of **2**, **3**, **5** and **6** (Table 4) reveal characteristic fragmentation patterns of isonitrile-substituted diethylaminocarbyne complexes. Loss of I or t-C_4H_9NC, elimination of isobutylene ($Me_2C{=}CH_2$) from the t-C_4H_9NC ligand or C_2H_5 from the carbyne ligand are observed. Using the SIMS method for complex **3**, the parent cation $[(\eta^5\text{-}C_5H_5)(I)(t\text{-}C_4H_9NC)_2W{\equiv}CNEt_2]^+$ (K^+: $m/z = 626$) is observed. Complex **6** decom-

Table 4. Mass spectral data of **2**, **3**, **5** and **6**

Complex	m/z (relative ^{184}W isotope)	Tentative assignment
2	543	$[M—I]^+$
	487	$[M—I—Me_2C{=}CH_2]^+$
3	626	K^+
	543	$[K—t\text{-}C_4H_9NC]^+$
	487	$[K—t\text{-}C_4H_9NC—Me_2C{=}CH_2]^+$
	458	$[K—t\text{-}C_4H_9NC—Me_2C{=}CH_2—C_2H_5]^+$
5	444	M^+
	388	$[M—Me_2C{=}CH_2]^+$
	360	$[M—Me_2C{=}CH_2—CO]^+$
	331	$[M—Me_2C{=}CH_2—CO—C_2H_5]^+$
6	670	$[M—CO]^+$
	587	$[M—CO—t\text{-}C_4H_9NC]^+$
	460	$[M—CO—t\text{-}C_4H_9NC—I]^+$
	543	$[M—CO—I]^+$
	487	$[M—CO—I—Me_2C{=}CH_2]^+$
	460	$[M—CO—I—Me_2C{=}CH_2—HNC]^+$
	431	$[M—CO—I—t\text{-}C_4H_9NC—C_2H_5]^+$
	376	$[M—CO—I—t\text{-}C_4H_9NC—C_2H_5—C_2H_5NC]^+$

poses under EI conditions with elimination of CO and formation of $[(\eta^5\text{-}C_5H_5)(I)_2(t\text{-}C_4H_9NC)W{\equiv}CNEt_2]^+$ (m/z = 670), the molecular ion of **2**. This ion could not be detected in the mass spectrum of **2** under EI conditions.

CONCLUSION

Starting from $(\eta^5\text{-}C_5H_5)(CO)_2W{\equiv}CNEt_2$, the precursor of $(\eta^5\text{-}C_5H_5)(I)_2(CO)W{\equiv}CNEt_2$, and $(\eta^5\text{-}C_5H_5)(t\text{-}C_4H_9NC)(CO)W{\equiv}CNEt_2$, we were able to isolate by high yield methods, neutral and cationic cyclopentadienyl-substituted tungsten carbyne complexes containing isocyanide ligands. The oxidative decarbonylation of the electron-rich complex $(\eta^5\text{-}C_5H_5)(t\text{-}C_4H_9NC)(CO)W{\equiv}CNEt_2$, enabled us to synthesize $[(\eta^5\text{-}C_5H_5)(I)(t\text{-}C_4H_9NC)(CO)W{\equiv}CNEt_2]^+I^-$, the first cationic diethylaminocarbyne complex of high-valent tungsten containing a carbonyl ligand. Its decarbonylation leads to the first neutral, carbonyl-free diethylaminocarbyne complex of high-valent tungsten. Based upon the spectroscopic data, the mass spectral data and the conductivity measurements, we suggest a neutral structure with a *cis*-orientation of the two iodide ligands for **2** and an ionic structure with a *trans*-orientation of the two isonitrile ligands for **3**. In both molecules an iodide ligand, acting as a π-donor, is located in the *trans*-position relative to the carbyne ligand. Therefore, we assume that the same orientation is retained in the ionic compound **6**, although we cannot exclude stereoisomers with a different orientation.

The new complexes are useful starting materials for the investigation of isonitrile carbyne coupling reactions induced by electrophiles or reducing agents.[17]

EXPERIMENTAL

KC_5H_5 was prepared from KH and C_5H_6 in THF. $(\eta^5\text{-}C_5H_5)(I)_2(CO)W{\equiv}CNEt_2$ and *mer*-$I(t\text{-}C_4H_9NC)_3(CO)W{\equiv}CNEt_2$ were synthesized as described previously.[9,12] t-C_4H_9NC was distilled and stored under nitrogen. All operations were carried out under nitrogen or argon atmospheres using Schlenk tube techniques. The solvents were dried by standard methods (*n*-pentane, toluene, Et_2O and THF over Na; CH_2Cl_2 over P_4O_{10} and Na/Pb alloy). The Al_2O_3 used for filtration (Merck Darmstadt, neutral, activity *I*, 0.063–0.2 mm) was degassed and dried at room temperature *in vacuo*, and then saturated with nitrogen. Elemental analyses were determined by the Microanalytical Laboratory of this department. IR spectra were measured with a Nicolet DX5 FT spectrophotometer, NMR spectra with a Jeol GX 270 FT instrument and mass spectra with a Varian MAT CH7 spectrometer using EI conditions for **2**, **5** and **6** and the SIMS method for **3**. Conductance measurements were carried out as described previously.[6–8,16]

$(\eta^5\text{-}C_5H_5)(I)_2(t\text{-}C_4H_9NC)W{\equiv}CNEt_2$ (2)

A purple solution of **1** (180 mg, 0.29 mmol) and t-C_4H_9NC (0.04 cm^3, 0.35 mmol) in THF (60 cm^3) was heated for 1 h at 50°C until the ν(C≡O) band in the IR spectrum of **1** at 2000 cm^{-1} disappeared. The red–purple solution was reduced in volume and an Et_2O–pentane mixture (1 : 2) was added. The supernatant, almost colourless solution was removed and the purple, microcrystalline solid dried *in vacuo* (190 mg, 97% relative to **1**). (Found: C, 27.0; H, 3.5; I, 38.1; N, 4.2; W, 28.2. $C_{15}H_{24}I_2N_2W$ (670.03) requires: C, 26.9; H, 3.6; I, 37.9; N, 4.2; W, 27.4%.)

$[(\eta^5\text{-}C_5H_5)(I)(t\text{-}C_4H_9NC)_2W{\equiv}CNEt_2]^+I^-$ (3)

A red–purple solution of **2** (140 mg, 0.21 mmol) and t-C_4H_9NC (0.032 cm^3, 0.28 mmol) in THF (50 cm^3) was refluxed for 5 h. The colour of the solution turned brown–yellow. The solvent was reduced in volume and *n*-pentane was added. The supernatant light brown solution was decanted and the yellow, microcrystalline solid dried *in vacuo* (140 mg, 89% relative to **2**). (Found: C, 31.9; H, 4.5; I, 32.6; N, 5.5; W, 24.6. $C_{20}H_{33}I_2N_3W$ (753.16) requires: C, 31.9; H, 4.4; I, 33.7; N, 5.6; W, 24.4%.)

$(\eta^5\text{-}C_5H_5)(t\text{-}C_4H_9NC)(CO)W{\equiv}CNEt_2$ (5)

A mixture of **4** (280 mg, 0.42 mmol) and KC_5H_5 (0.70 mmol) was refluxed in THF (60 cm^3) for 6 h. The solvent was then evaporated *in vacuo* and the residue extracted with Et_2O (3 × 30 cm^3). The extracts were filtered through Al_2O_3 (2 × 3 cm) and the solvent removed *in vacuo* to give a yellow oil. Upon cooling a saturated solution of the yellow oil in *n*-pentane to −78°C, yellow crystals of **5** were obtained, which melt below room temperature (150 mg, 81% relative to **4**). (Found: C, 43.0; H, 5.4; N, 6.2. $C_{16}H_{24}N_2OW$ (444.23) requires: C, 43.3; H, 5.4; N, 6.3%.)

$[(\eta^5\text{-}C_5H_5)(I)(t\text{-}C_4H_9NC)(CO)W{\equiv}CNEt_2]^+I^-$ (6)

To a yellow solution of **5** (110 mg, 0.25 mmol) in CH_2Cl_2 (30 cm^3) was added at −30°C, a purple solution of I_2 (62 mg, 0.24 mmol) in CH_2Cl_2 (20 cm^3). The colour of the iodine solution disappeared immediately and the reaction solution turned first

to red and then, upon warming up to room temperature, to orange. The solvent was reduced in volume *in vacuo* and an Et_2O–pentane mixture (1 : 2) was added. The supernatant, almost colourless liquid was decanted, and the microcrystalline, orange residue dried *in vacuo* (165 mg, 95% relative to **5**). (Found: C, 27.6; H, 3.5; I, 36.1; N, 4.0; O, 2.3; W, 26.5. $C_{16}H_{24}I_2N_2OW$ (698.04) requires: C, 27.5; H, 3.5; I, 36.4; N, 4.0; O, 2.3; W, 26.3%.)

$(\eta^5\text{-}C_5H_5)(I)_2(t\text{-}C_4H_9NC)W{\equiv}CNEt_2$ (**2**) *from* **6**

An orange suspension of **6** (140 mg, 0.20 mmol) in THF (50 cm^3) was refluxed for 1.5 h. Upon warming, **6** dissolved in THF to give first an orange solution, which then changed colour through red to red–purple. When all of **6** had been consumed (monitoring by IR) the solution was concentrated *in vacuo* and an Et_2O–pentane mixture (1 : 2) was added. The supernatant liquid was decanted and the microcrystalline, purple precipitate dried *in vacuo* (130 mg, 97% relative to **6**).

2 was characterized by the ^1H NMR and IR spectra.

Acknowledgements—I would like to thank Professor W. A. Herrmann for providing institute facilities and encouraging this work, Professor E. O. Fischer for financial support and personal discussion, M. Barth, L. Eidel and U. Graf for the elemental analyses and Professor H. G. Alt for the assistance with mass spectrometry.

REFERENCES

1. E. O. Fischer and U. Schubert, *J. Organomet. Chem.* 1975, **100**, 59.
2. R. R. Schrock, D. N. Clark, J. Sancho, J. H. Wengrovius, S. M. Rocklage and S. F. Pedersen, *Organometallics* 1982, **1**, 1645.
3. T. J. Katz, T. H. Ho, N. Y. Shih, Y. C. Ying and V. I. W. Stuart, *J. Am. Chem. Soc.* 1984, **106**, 2659.
4. J. Sancho and R. R. Schrock, *J. Mol. Catal.* 1982, **15**, 75.
5. A. C. Filippou, E. O. Fischer and J. Okuda, *J. Organomet. Chem.* 1988, **339**, 309.
6. A. C. Filippou, E. O. Fischer and H. G. Alt, *J. Organomet. Chem.* 1988, **344**, 215.
7. A. C. Filippou, E. O. Fischer and H. G. Alt, *Z. Naturfor.* 1988, **43B**, 654.
8. A. C. Filippou, E. O. Fischer and R. Paciello, *J. Organomet. Chem.* 1988, **347**, 127.
9. A. C. Filippou and E. O. Fischer, *J. Organomet. Chem.* 1988, **341**, C35.
10. A. C. Filippou and E. O. Fischer, *J. Organomet. Chem.* 1988, **349**, 367.
11. A. C. Filippou, unpublished results.
12. A. C. Filippou and E. O. Fischer, *J. Organomet. Chem.* 1988, **352**, 141.
13. P. Kubacek, R. Hofmann and Z. Havlas, *Organometallics* 1982, **1**, 180.
14. A. C. Filippou and E. O. Fischer, *J. Organomet. Chem.*, in press.
15. D. L. Cronin, J. R. Wilkinson and L. J. Todd, *J. Magn. Res.* 1975, **17**, 353.
16. A. C. Filippou, E. O. Fischer and H. G. Alt, *J. Organomet. Chem.* 1988, **340**, 331.
17. A. C. Filippou, NATO Advanced Research Workshop, Transition metal carbene complexes. Wildbad Kreuth (September 1988).

Polyhedron Vol. 8, No. 10, pp. 1293–1297, 1989
Printed in Great Britain

0277–5387/89 $3.00+.00
© 1989 Pergamon Press plc

THE INTERACTION OF $FeCl_3$ WITH PPh_3 IN CHLOROFORM. X-RAY CRYSTAL STRUCTURE OF $[Ph_3PCH_2PPh_3][FeCl_4]_2$

J. DAVID WALKER and RINALDO POLI*

Department of Chemistry and Biochemistry, University of Maryland, College Park, MD 20742, U.S.A.

(*Received* 12 *December* 1988; *accepted* 18 *January* 1989)

Abstract—Interaction of $FeCl_3$ and PPh_3 in $CHCl_3$ yields complex mixtures containing unstable adducts. The compound $[Ph_3PCH_2PPh_3][FeCl_4]_2 \cdot CHCl_3$ was isolated from the solution after the decomposed mixture had been allowed to interact with air. Crystal data: triclinic, space group $P\bar{1}$, $a = 11.459(4)$, $b = 12.102(2)$, $c = 18.109(4)$ Å, $\alpha = 105.15(2)$, $\beta = 102.14(2)$, $\gamma = 94.91(2)°$, $V = 2347(2)$ Å^3, $Z = 2$, $d_c = 1.49$ g cm^{-3}, μ(Mo-K_α) = 13.49 cm^{-1}, $R = 0.045$ ($R_w = 0.054$) for 487 parameters and 5256 observed reflections with $F_o^2 > 3\sigma(F_o^2)$.

We have recently studied the interaction of iron(III) chloride with monodentate phosphine ligands and we have obtained the mononuclear $FeCl_3(PR_3)_2$ (R = Ph, Me, Cy) derivatives.[1] These compounds exhibit a trigonal bipyramidal geometry with the phosphine ligands occupying the axial positions. We have also conducted an EPR study of the $FeCl_3$–PPh_3 interaction in different molar ratios and shown that a reactive four-coordinate $FeCl_3(PPh_3)$ compound, presumably with tetrahedral geometry, is formed when a 1 : 1 ratio is used. This compound decomposes at room temperature in aromatic solvents according to two competitive pathways, the first involving reduction to iron(II) species by the solvent, and the second being a disproportionation to an ionic iron(III) material.[1] We were interested in understanding the relationship between our reactive 1 : 1 adduct and a reported[2] yellow crystalline solid, described as $FeCl_3(PPh_3)$, that had been obtained from $Fe_3(CO)_{12}$ and PPh_3 in $CHCl_3$. An EPR spectroscopic study of the $FeCl_3$–PPh_3 interaction in $CHCl_3$ shows[1] that the $FeCl_3(PPh_3)$ species also forms in this solvent, but it subsequently decomposes according to the same pathways observed in the aromatic solvents. However, while we were trying to crystallize the ionic iron(III) product from the $CHCl_3$ solution, we obtained evidence that yet another decomposition path is available in these conditions. The results of this study are reported here.

EXPERIMENTAL

All operations were carried out under an atmosphere of dinitrogen, unless otherwise specified. Solvents were dried by conventional methods and distilled under dinitrogen prior to use. $FeCl_3$ was dehydrated by treatment in $SOCl_2$ and PPh_3 was recrystallized from absolute ethanol.

Reaction of $FeCl_3$ *with* PPh_3 *in* $CHCl_3$. *Synthesis of* $[Ph_3PCH_2PPh_3][FeCl_4]_2$

PPh_3 (0.92 g, 3.51 mmol) was added to a suspension of anhydrous $FeCl_3$ (0.85 g, 5.26 mmol) in 35 cm^3 of $CHCl_3$ and stirred at room temperature for 1 day. The black solution slowly lightened to produce a yellow solution and a greyish white solid. The solid was filtered and the solution allowed to sit for 1 week. At this point, exposure of this solution to air caused yellow crystals to form within several hours. A single crystal for the X-ray analysis was selected from this batch. The air-stable crystals were filtered and dried under vacuum, yielding 0.21 g (11%) of product, which retained one molecule of interstitial crystallization solvent ($CHCl_3$). Found: C, 43.3; H, 3.0; Cl, 36.7. Calc. for $C_{38}H_{33}Cl_{11}Fe_2P_2$: C, 43.3; H, 3.2; Cl, 37.0%. IR (Nujol mull, cm^{-1}): 1585 w, 1435 s, 1110 m, 995 s,

* Author to whom correspondence should be addressed.

810 w, 790 m, 760 m, 740 s, 685 m, 510 m, 500 m, 490 m.

X-ray crystallography for $[Ph_3PCH_2PPh_3][FeCl_4]_2 \cdot CHCl_3$

A single crystal was glued on the tip of a glass fibre and mounted on the diffractometer. The cell constant determination, data collection and reduction were routine. A semi-empirical absorption correction was applied according to the method described by North *et al.*[3] Crystal data are assembled in Table 1. The structure was solved by direct methods and refined by alternating cycles of full-matrix least-squares and difference Fourier maps. Hydrogen atoms were included at calculated positions and used for structure factor calculations, but not refined. An interstitial chloroform molecule was also found. This had the carbon atom disordered among two equally populated positions, above and below the plane containing the three chlorine atoms.

Oxidation state, ionic charge, and synthetic methodology considerations led us to believe initially that the atom bridging the two phosphine moieties in the cation was an oxygen atom. Refinement with all the non-hydrogen atoms, including those of the interstitial chloroform molecule, treated anisotropically, converged to an agreement factor $R = 0.049$ ($R_w = 0.058$). The equivalent isotropic thermal parameter for the bridging atom was 7.5(2) Å^2, much larger than those of the neighbouring atoms (around 3.00 Å^2), but still acceptable. However, the results of the elemental analysis, together with this high thermal parameter for the bridging atom, convinced us that we did not have an oxygen atom but rather a carbon atom of a methylene functionality holding together the two PPh_3 moieties. Refinement on the appropriately modified model converged to a lower agreement factor

Table 1. Crystal data for $[Ph_3PCH_2PPh_3][FeCl_4]_2 \cdot CHCl_3$

Formula	$C_{38}H_{33}Cl_{11}Fe_2P_2$
f_w	1053.30
Space group	$P\bar{1}$
Systematic absences	none
a (Å)	11.459(4)
b (Å)	12.102(2)
c (Å)	18.109(4)
α (°)	105.15(2)
β (°)	102.14(2)
γ (°)	94.91(2)
C (Å^3)	2347(2)
Z	2
d_{calc} (g cm^{-3})	1.49
Crystal size (mm)	0.5 × 0.4 × 0.3
μ(Mo-K_α) (cm^{-1})	13.49
Data collection instrument	CAD-4
Radiation (monochromated in incident beam)	Mo-K_α (λ = 0.71073 Å)
Orientation reflections: number; range (2θ) (°)	25, 20–30
Temperature (°C)	20
Scan method	ω–2θ
Data collection range (2θ) (°)	4–50
Number of unique data, total observed	8353, 5256
Number of parameters refined	487
Transmission factors: max, min	1.000, 0.8612
R^a	0.045
R_w^b	0.054
Quality-of-fit indicator[c]	2.04
Largest shift/ESD, final cycle	0.25
Largest peak (e Å^{-3})	0.574

[a] $R = \Sigma ||F_o| - |F_c|| / \Sigma |F_o|$.
[b] $R_w = [\Sigma w(|F_o| - |F_c|)^2 / \Sigma w|F_o|^2]^{1/2}$; $w = 1/\sigma^2(|F_o|)$.
[c] Quality-of-fit = $[\Sigma w(|F_o| - |F_c|)^2 / (N_{observations} - N_{parameters})]^{1/2}$.

Table 2. Selected intramolecular distances (Å) and angles (°) for $[Ph_3POPPh_3][FeCl_4]_2 \cdot CHCl_3$

Atom	Atom	Distance		Atom	Atom	Distance	
Fe(1)	Cl(1)	2.156(2)		P(1)	C(10)	1.792(4)	
Fe(1)	Cl(2)	2.209(2)		P(1)	C(20)	1.796(4)	
Fe(1)	Cl(3)	2.157(2)		P(1)	C(30)	1.783(4)	
Fe(1)	Cl(4)	2.177(2)		P(1)	C(1)	1.822(4)	
Fe(2)	Cl(5)	2.205(2)		P(2)	C(40)	1.790(4)	
Fe(2)	Cl(6)	2.177(2)		P(2)	C(50)	1.786(4)	
Fe(2)	Cl(7)	2.173(2)		P(2)	C(60)	1.801(4)	
Fe(2)	Cl(8)	2.181(2)		P(2)	C(1)	1.816(4)	
Atom	Atom	Atom	Angle	Atom	Atom	Atom	Angle
Cl(1)	Fe(1)	Cl(2)	109.34(7)	C(10)	P(1)	C(30)	112.7(2)
Cl(1)	Fe(1)	Cl(3)	111.17(8)	C(20)	P(1)	C(30)	108.6(2)
Cl(1)	Fe(1)	Cl(4)	109.10(8)	C(10)	P(1)	C(1)	110.3(2)
Cl(2)	Fe(1)	Cl(3)	109.42(7)	C(20)	P(1)	C(1)	106.7(2)
Cl(2)	Fe(1)	Cl(4)	108.88(8)	C(30)	P(1)	C(1)	110.0(2)
Cl(3)	Fe(1)	Cl(4)	108.9(1)	C(40)	P(2)	C(50)	112.1(2)
Cl(5)	Fe(2)	Cl(6)	108.06(7)	C(40)	P(2)	C(60)	107.7(2)
Cl(5)	Fe(2)	Cl(7)	110.22(7)	C(50)	P(2)	C(60)	109.6(2)
Cl(5)	Fe(2)	Cl(8)	108.79(7)	C(40)	P(2)	C(1)	110.8(2)
Cl(6)	Fe(2)	Cl(7)	108.45(7)	C(50)	P(2)	C(1)	110.7(2)
Cl(6)	Fe(2)	Cl(8)	112.48(8)	C(60)	P(2)	C(1)	105.7(2)
Cl(7)	Fe(2)	Cl(8)	108.83(7)	P(2)	C(1)	P(1)	123.4(2)
C(10)	P(1)	C(20)	108.4(2)				

Estimated standard deviations in the least significant figure are given in parentheses.

($R = 0.045$; $R_w = 0.054$) and gave a more reasonable equivalent isotropic thermal parameter for the bridging atom [3.1(1) Å^2]. Selected bond lengths and angles are listed in Table 2.*

RESULTS AND DISCUSSION

(a) *Chemical studies*

The dark brown solutions obtained at low temperature by interacting anhydrous $FeCl_3$ and PPh_3 in a 1 : 1 molar ratio, and containing the unstable $FeCl_3(PPh_3)$ species,[1] rapidly changed colour to yellow when warmed to room temperature. We repeatedly tried to work up these solutions under a dinitrogen atmosphere with the hope of crystallizing the yellow decomposition product.

This is believed to be an ionic compound with empirical formula $FeCl_3(PPh_3)$,[2] possibly $[FeCl_2(PPh_3)_2]^+[FeCl_4]^-$. These solutions show high electric conductance, consistent with the production of ionic species. In addition, most of the known derivatives of iron(III) with soft donor ligands, and also a few with hard donor ligands, are ionic. Examples are $[Fe(L—L)_2X_2][FeX_4]$ [X = Cl or Br, L—L = *o*-$C_6H_4(AsMe_2)_2$;[4] X = Cl, L—L = methylenebis(diphenylphosphine oxide) or tetramethylenebis(diphenylphosphine oxide)[5]] and $[FeCl_2L_4][FeCl_4]$ (L = N-methylimidazole,[6] pyridine-N-oxide,[7] dimethylsulphoxide[8]). Unfortunately all of these materials correspond to the empirical formula $FeCl_3L_2$ or $FeCl_3(L—L)$. No ionic compound with an empirical formula $FeCl_3L$, that is with structure $[FeCl_2L_2][FeCl_4]$, seems to have been positively characterized. Four-coordinate tetrahedral iron(III) is common in anionic species, such as $[FeX_4]^-$ (X = Cl, Br, SR[9]) and has been suggested for the neutral $FeCl_3(THF)$ compound,[10] but, to the best of our knowledge, never found in cationic complexes.

While our attempts to obtain a crystalline material under dinitrogen were unsuccessful, we sampled an aliquot of the solution for a gas chro-

* A full list of bond distances and angles, positional parameters, anisotropic displacement parameters and F_o/F_c data have been deposited with the Editor as supplementary material. The atomic coordinates have also been deposited with the Cambridge Crystallographic Data Centre.

matographic analysis[1] and observed that a crystalline material was rapidly obtained upon exposure to air. We then decided to expose the rest of the solution to air, and we obtained the product, later proven to be $[Ph_3PCH_2PPh_3][FeCl_4]_2 \cdot CHCl_3$ by elemental and X-ray structural analysis (*vide infra*), in low yield. The solution had been exposed to air 8 days after the initial $FeCl_3$–PPh_3 interaction.

We have repeated the preparation of this crystalline material several times in consistently reproducible low yields. During one of these preparations, the solution was exposed to air shortly after the change of colour to yellow was completed, and *no crystalline product was obtained.*

The presence of a methylene functionality in the cation suggests that interaction with the solvent has occurred. The interaction of PPh_3 with haloforms is documented in the literature. With CHI_3, an ill-characterized 1 : 1 adduct was obtained.[11] PPh_3 and $CHBr_3$ do not react at room temperature, but under thermal or photochemical conditions $[Ph_3PCHBr_2]^+Br^-$ is obtained.[12] The reaction of PPh_3 and $CHCl_3$ has been reported to produce $Ph_3P{=}CCl_2$ in the presence of a strong base. This reaction has been described as proceeding through the free dichlorocarbene.[13] From these data, it would appear that the nucleophilic attack of PPh_3 on $CHCl_3$ is not a facile process. However, the presence of the strong Lewis acid, $FeCl_3$, should provide additional driving force by coordinating the chloride leaving group to form the stable $FeCl_4^-$ anion [eq. (1)]:

$$PPh_3 + CHCl_3 + FeCl_3 \longrightarrow [Ph_3PCHCl_2]^+[FeCl_4]^- \quad (1)$$

This type of reactivity has also been described for the PPh_3–CCl_4 system, where $[Ph_3PCCl_3]Cl$ is obtained without the aid of a Lewis acid.[14]

$FeCl_3$ could as well promote an additional nucleophilic attack to the quaternary carbon, according to eq. (2):

$$PPh_3 + [Ph_3PCHCl_3]^+[FeCl_4]^- + FeCl_3 \longrightarrow [Ph_3PCH(Cl)PPh_3][FeCl_4]_2 \quad (2)$$

Since this reaction is in large excess of $CHCl_3$, this second nucleophilic attack will occur only if reaction 2 is faster than reaction 1.

This reactivity pattern would parallel the one observed for the interaction of PPh_3 with CH_2Br_2, where $[Ph_3PCH_2PPh_3]Br_2$ has been obtained.[15] In addition, the reaction[16] of PPh_3 and CCl_4 in a 3 : 1 ratio, reported to yield $[Ph_3PC(Cl)PPh_3]Cl$, presumably proceeds through $[Ph_3PCCl_2PPh_3]Cl_2$.

The product of eq. (2) is the closest compound to the observed product of which we can rationalize the formation. It is completely obscure to us how the action of oxygen could replace the chlorine atom with a hydrogen atom in $[Ph_3PCH(Cl)PPh_3][FeCl_4]_2$, assuming that the latter is indeed an intermediate. It initially occurred to us, in view of the synthetic methodology, that the two PPh_3 units might be bridged by an oxygen atom, but this hypothesis has been subsequently ruled out by accurate elemental analysis determinations and by the results of the crystal structure refinement (see Experimental).

We do not have a better explanation as to how the observed product is formed. The only conclusion that can be safely drawn is that the intermediate species upon which oxygen is operating is only slowly produced in the reaction conditions, since no product is obtained when oxygen is introduced promptly after the interaction of $FeCl_3$ and PPh_3 has occurred. We have not further investigated the mechanism of this curious transformation, nor have we altered the reaction conditions in an attempt to maximize the yield of the product.

(b) *Crystallographic study*

The $[Ph_3PCH_2PPh_3][FeCl_4]_2$ compound crystallizes with one formula unit plus an interstitial $CHCl_3$ molecule in the asymmetric unit. No significant intermolecular interactions are observed, and the different ions are well separated from each other.

The $FeCl_4^-$ anions display fairly regular tetrahedral geometries, the one containing Fe(2) being slightly more distorted [average Cl—Fe—Cl angles are $109.47 \pm 0.8°$ for Fe(1) and 109.47 ± 1.6 for Fe(2)]. The Fe—Cl distances (average 2.18(2) Å) compare with those found in other $FeCl_4^-$ salts, for instance 2.182(1) Å in the $AsPh_4^+$ salt, 2.175(5) (av.) Å in the PPh_3Me^+ salt and 2.184(5) (av.) in the $[Fe(MeCN)_6]^{2+}$ salt.[17]

Figure 1 shows a view of the dication. This is arranged in a conformation where the atoms P(1), P(2), C(1), C(20) and C(60) approximately lie in the same plane. This allows the P(1)—C(1)—P(2) angle to close to the observed value of 123.4(2)° without major steric repulsions between the phenyl groups on adjacent phosphorus atoms. This angle is smaller than that found in the $[Ph_3PCHPPh_3]^+$ cation [128.2(3)°],[18] albeit larger than that observed for $Ph_2P(Se)CH_2P(Se)Ph_2$ [117.9(6)°],[18] in agreement with a different hybridization state in the former case and with a decreased steric repulsion and/or with the absence of an electrostatic repulsion in the latter one. The P—C(1) distances (average 1.819(4) Å) are in the expected range for a phos-

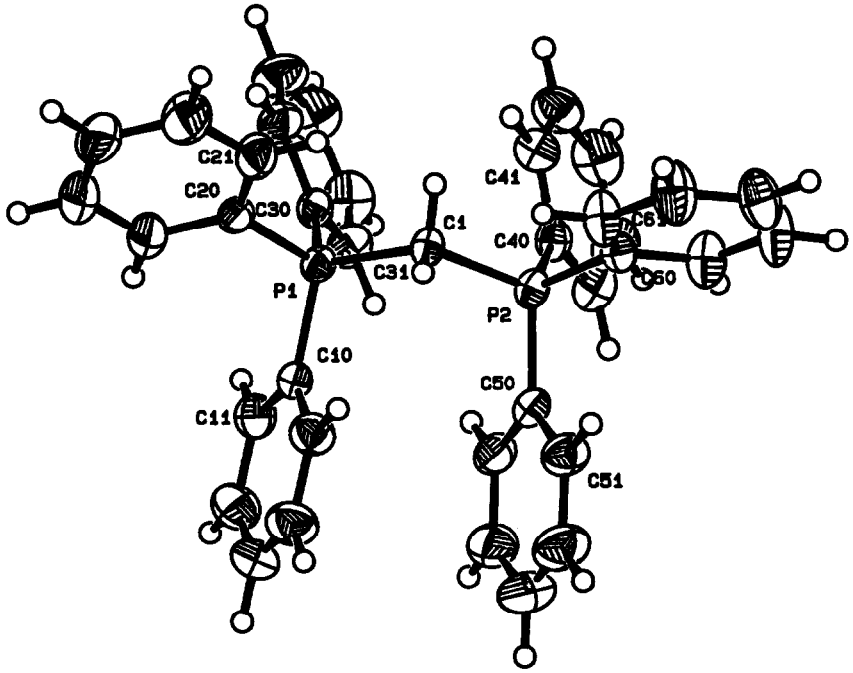

Fig. 1. An ORTEP view of the dication of compound $[Ph_3PCH_2PPh_3][FeCl_4]_2 \cdot CHCl_3$. Hydrogen atoms are drawn with arbitrary radii for the sake of clarity.

phorus–carbon (sp^3) single bond, and compare favourably with those observed in $Ph_2P(Se)CH_2P(Se)Ph_2$ (av. 1.84(1) Å), the slight decrease being consistent with the presence of positive charges.

Acknowledgements—We are grateful to the University of Maryland, College Park, (UMCP) Chemistry Department, the UMCP General Research Board, the Camille and Henry Dreyfus Foundation (through a Distinguished New Faculty Award to R.P.), and the Donors of the Petroleum Research Fund, administered by the American Chemical Society, for support of this work. The X-ray diffractometer and MicroVax computer system were purchased in part with NSF funds (CHE-84-02155). We gratefully acknowledge Professor H. Ammon for technical assistance with the X-ray diffractometer.

REFERENCES

1. J. D. Walker and R. Poli, *Inorg. Chem.*, in press.
2. P. P. Singh and R. Rivest, *Can. J. Chem.* 1968, **46**, 1773.
3. A. C. T. North, D. C. Phillips and F. S. Mathews, *Acta Cryst.* 1968, **A24**, 351.
4. (a) R. S. Nyholm, *J. Chem. Soc.* 1950, 851; (b) J. Lewis, R. S. Nyholm and G. A. Rodley, *J. Chem. Soc.* 1965, 1483; (c) G. S. F. Hazeldean, R. S. Nyholm and R. V. Parish, *J. Chem. Soc. A* 1966, 162.
5. (a) S. Lobana, H. S. Cheema and S. S. Sandhu, *Transition Met. Chem.* 1984, **9**, 119; (b) S. Lobana, H. S. Cheema and S. S. Sandhu, *J. Chem. Soc., Dalton Trans.* 1983, 2039.
6. S. A. Cotton, P. V. H. Pisani and R. Stubbs, *Inorg. Nucl. Chem. Lett.* 1976, **12**, 695.
7. S. A. Cotton and J. F. Gibson, *J. Chem. Soc., Dalton Trans.* 1970, 2105.
8. M. A. Bennett, F. A. Cotton and D. L. Weaver, *Acta Cryst.* 1967, **23**, 581.
9. (a) S. J. Lippard, *Accts Chem. Res.* 1973, **6**, 282; (b) R. H. Holm, *Accts Chem. Res.* 1977, **10**, 427; (c) S. A. Koch, L. E. Maelia and M. Millar, *J. Am. Chem. Soc.* 1983, **105**, 5944; (d) M. Millar, J. F. Lee, S. A. Koch and R. Fikar, *Inorg. Chem.* 1982, **21**, 4106.
10. L. S. Brenner and C. A. Root, *Inorg. Chem.* 1972, **11**, 652.
11. W. M. Dehn and R. B. Conner, *J. Am. Chem. Soc.* 1912, **34**, 1409.
12. F. Ramirez and N. McKelvie, *J. Am. Chem. Soc.* 1957, **79**, 5829.
13. A. J. Speziale and K. W. Ratts, *J. Am. Chem. Soc.* 1962, **84**, 854.
14. R. Appel, *Inorg. Synth.* 1986, **24**, 107.
15. J. S. Driscoll, D. W. Grisley Jr, J. V. Pustinger, J. E. Harris and C. N. Matthews, *J. Org. Chem.* 1964, **29**, 2427.
16. R. Appel, *Inorg. Synth.* 1986, **24**, 113.
17. (a) F. A. Cotton and C. A. Murillo, *Inorg. Chem.* 1975, **10**, 2467; (b) R. Glowiak, E. Durcanska, I. Ondrejkovicova and G. Ondrejovic, *Acta Cryst.* 1986, **C42**, 1331; (c) G. Constant, J.-C. Daran and Y. Jeannin, *J. Organomet. Chem.* 1972, **44**, 353.
18. P. J. Carroll and D. D. Titus, *J. Chem. Soc., Dalton Trans.* 1977, 824.

Polyhedron Vol. 8, No. 10, pp. 1299–1305, 1989
Printed in Great Britain

0277-5387/89 $3.00+.00
© 1989 Pergamon Press plc

KINETICS OF THE REDUCTION OF THE TETRAHYDROXYARGENTATE(III) ION BY SULPHITE IN AQUEOUS ALKALINE MEDIA

LOUIS J. KIRSCHENBAUM* and ISSIFOU KOUADIO

Department of Chemistry, University of Rhode Island, Kingston, RI 02881, U.S.A.

and

EDOARDO MENTASTI

Department of Analytical Chemistry, University of Torino, 10125 Torino, Italy

(*Received* 25 *October* 1988; *accepted after revision* 18 *January* 1989)

Abstract—The reduction of $Ag(OH)_4^-$ by sulphite ion to give silver(I) and sulphate in strong base has been studied by stopped-flow spectrophotometry. The reaction was found to fit a second-order rate law with a rate constant $k = (9.1 \pm 0.1) \times 10^2\ M^{-1}\ s^{-1}$ ($T = 25°C$, $\mu = 1.2$ M). The estimated enthalpy and entropy of activation are 27 kJ mol^{-1} and -153 J K^{-1} mol^{-1} respectively. Variation of rate with ionic strength is consistent with the interaction between mononegative $Ag(OH)_4^-$ and dinegative SO_3^{2-}. The redox reaction appears to proceed by a one-step oxygen atom transfer. Two kinetically indistinguishable pathways are discussed. The first involves initial attack of a sulphite oxygen at an axial silver(III) site. The second pathway involves initial interaction between sulphur(IV) and a bound hydroxyl. Sulphite oxidation by silver(III) is about 10^4 times faster than that of phosphite, while no reaction is observed with NO_2^-.

Silver(III) is a spin paired d^8 system like gold(III), copper(III), nickel(II) and palladium(II).[1,2] It forms diamagnetic square-planar complexes with ligands including hydroxide,[3] triglycine, tetraglycine,[4] dimethylglyoximate,[5] tellurate and periodate.[6] Although octahedral geometry is rare, it is found in paramagnetic complexes with the general formula M_3AgF_6[7] (M = K, Na, Rb or Cs). Diamagnetic tetragonal silver(III) fluoro complexes ($MAgF_4$) have been successfully prepared by direct fluorination of 1 : 1 mixtures of MCl and $AgNO_3$.[8] Pale yellow, diamagnetic silver(III) complexes of tetraazamacrocyclic substrates have been extensively studied.[9] Silver(III) porphyrin complexes have also been investigated. For instance, Kadish *et al.* found that oxidation of the octaethylporphynatosilver(II) leads to the corresponding silver(III) complex.[10] Ethylene-bridged biguanide complexes of silver(III) were first prepared in 1944 by Chakravorty and Ray[11] as $Ag(enBigH)_2X_3$ (X = $0.5SO_4$, NO_3, ClO_4 or H). A thorough investigation of the kinetics of formation and decomposition of these complexes has been reported.[12] Simple, stable silver(III) biguanide and methyl biguanide complexes also have been synthesized.[13] Silver(III) complexes of triglycine and tetraglycine were successfully prepared by Kirschenbaum and Rush[4] by direct mixing of $Ag(OH)_4^-$ and the ligands in aqueous basic media. There are striking spectral and kinetic similarities of these complexes with those of analogous copper(III) polypeptide systems obtained by Margerum *et al.*[14]

$Ag(OH)_4^-$ has a half life of about 1.5 h in 1.2 M hydroxide at room temperature and has a UV–vis maximum at 267 nm in aqueous alkaline media. In recent years, we have studied the reaction of $Ag(OH)_4^-$ with a number of complexing and reducing substrates.[5,15–17]

Substitution reactions of $Ag(OH)_4^-$ with various oxygen donor ligands—periodate, tellurate,[3] phosphate, borate, pyrophosphate, carbonate and arsenate[18]—have been investigated. In the case of

* Author to whom correspondence should be addressed.

periodate and tellurate ions, the kinetically stable complexes $Ag(H_2IO_6)_2^{3-}$ and $Ag(H_4TeO_6)_2^-$, respectively, were formed. However, the substitution reactions of $Ag(OH)_4^-$ with the other oxoanions were partial and occurred only at reduced OH^-.

The formation of silver(III) complexes often provides a path for $Ag(OH)_4^-$ reduction,[16,19] but offers some increased stability under conditions where the highly reactive $Ag(OH)_3(H_2O)$ ion is otherwise formed [eq. (1)][20]

$$Ag(OH)_4^- \overset{H_2O}{\rightleftharpoons} Ag(OH)_3(H_2O) + OH^- . \quad (1)$$

Redox reactions of the tetrahydroxyargentate(III) ion have been studied with reductants including ethylenediamine (en),[21] H_2O_2,[22] $Mo(CN)_8^{4-}$, $Fe(CN)_6^{4-}$, MnO_4^{2-},[19] N_3^-,[16] $S_2O_3^{2-}$ [17] and arsenites.[15] It was found that an inner-sphere two-electron transfer process was involved in the cases of azide, thiosulphate, en, and arsenite. By contrast, a silver(II) intermediate was inferred for the other substrates.

The reduction of transition metals by sulphite in aqueous alkaline medium has been studied for $Mo(CN)_8^{3-}$, $Mn(P_2O_7)_3^{9-}$, $Fe(CN)_6^{3-}$ [23,24] and deprotonated copper(III) tetraglycine ($Cu(H_{-3}G_4)^-$).[25] Margerum *et al.*[25] recently showed that the kinetics of the reaction of $Cu(H_{-3}G_4)^-$ with excess sulphite is first-order in sulphite at pH 9.2. In addition, the reduction reaction goes stoichiometrically ($\Delta Cu(H_{-3}G_4)^- : \Delta SO_3^{2-} = 2:1$) via two reversible one-electron transfer steps, generating a sulphite radical anion in the first step. Brown and Higginson[23] showed that substitution-inert complexes which behave as one-equivalent oxidants can give quantitative sulphate products. However, those substitution labile complexes which react with a lower non-integral stoichiometry, give a mixture of sulphate and dithionate. In the particular case of the ferricyanide–sulphite reaction, Swinehart[26] suggested an outer-sphere mechanism involving sulphite radicals and dithionate and sulphate as major products. On the other hand, Veprek-Siska and Wagnerova[27] favoured an inner-sphere process with sulphate the only significant sulphur-containing product. Lancaster and Murray,[24] have shown that the reaction proceeds via the intermediates $Fe(CN)_5(CNSO_3)^{5-}$ and $Fe(CN)_5(CNSO_3)^{4-}$, followed by hydrolysis of the latter to ferrocyanide and sulphate. They thought that the reaction pattern lies somewhere between inner- and outer-sphere, a compromise between the two contradictory explanations mentioned above.

The reaction of $Ag(OH)_4^-$ with thiosulphate at low concentrations ($< 1.0 \times 10^{-3}$ M) proceeds via the aquated species $Ag(OH)_3(H_2O)$, giving a monothiosulphato complex, $Ag(OH)_3S_2O_3^{2-}$, which undergoes internal redox.[17] At thiosulphate concentrations above 1×10^{-3} M, silver(III) is reduced in a five-coordinate intermediate without hydroxyl replacement. In the case of the reaction of $Ag(OH)_4^-$ with arsenite, the reaction appears to proceed by a one-step oxygen atom transfer.[15] We have studied the reaction of $Ag(OH)_4^-$ with sulphite ion to see if its reduction mechanism is similar to either the thiosulphate or arsenite systems.

EXPERIMENTAL

Reactant solutions

For all experiments, sulphite stock solutions were freshly made in doubly distilled water, or in 1.2 M base by exact weighing of reagent grade anhydrous sodium sulphite (J. T. Baker). All sulphite reactant solutions were then made by serial dilution. Sodium hydroxide solutions were prepared from 50% low carbonate NaOH (Fisher). Lithium hydroxide solutions were made from solid hydrated LiOH (Matheson Coleman and Bel). A 1.2 M $NaClO_4$ or $LiClO_4$ solution was used for ionic strength adjustment when appropriate. $NaClO_4$ was prepared from NaOH and $HClO_4$ (Fisher), adjusted to pH 7, followed by filtration. Similarly, $LiClO_4$ was obtained from LiOH and $HClO_4$. $Ag(OH)_4^-$ solutions were prepared by anodic oxidation as previously described.[4] About 200 cm^3 of 1.2 M NaOH or LiOH solution were placed in a 250 cm^3 polyethylene beaker containing a silver foil anode. Argon was bubbled through the silver(III) solution during electrolysis from a capillary placed near the anode to provide constant stirring of the solution. In order to minimize spontaneous oxidation of sulphite to sulphate[28] by atmospheric oxygen, solutions used to prepare SO_3^{2-} solutions were also degassed with argon. In addition, great care was taken to avoid trace metal and multivalent cation catalytic auto-oxidation[25] of sulphite by using very clean glassware.

For the purpose of comparison, we also studied the reduction of silver(III) by NO_2^- and HPO_3^{2-}. The nitrite stock solutions were prepared by direct weighing of reagent grade $NaNO_2$ (Mallinckrodt). The phosphite solutions were made from a 50% solution of phosphorous acid (Allied Chemical) by potentiometric titration with 1.2 M NaOH.

An Aminco–Morrow stopped-flow apparatus was used in the kinetic runs.[4] Large excesses of reductant were used for all experiments. The reactions were monitored as $Ag(OH)_4^-$ disappearance at 267 nm ($\varepsilon = 1.17 \times 10^4\ M^{-1}\ cm^{-1}$). At this wavelength, neither sulphite, nitrite, nor phosphite

showed any significant absorbance. The reactions were followed on a Tektronix 564B storage oscilloscope coupled to a Radio Shack TRS-80 computer which recorded and processed the kinetic data. All observed pseudo-first-order rate constants are reproducible within 5%. Spectral analysis was done on a Cary 15 UV–vis spectrophotometer.

Product analysis

Known concentrations of sulphite and $Ag(OH)_4^-$ were mixed together. Immediately upon completion of the reaction, a saturated solution of barium nitrate was added to precipitate the product and excess sulphite where excess reductant was used. After filtration, the precipitates were dried and their IR spectra recorded on a Perkin–Elmer 1310 spectrophotometer. Blank sulphite and sulphate solutions were also analysed to check for possible contamination. To test for reactions between reactants and products, parallel experiments were done for the systems silver(I)–sulphite and silver(II)–sulphate.

RESULTS

Identification of the reaction product

At excess $Ag(OH)_4^-$, only sulphate IR peaks were observed. When excess reductant was used, sulphate and sulphite peaks were obtained. We therefore conclude that the reaction product is sulphate.

Reaction stoichiometry

The stoichiometry of the reaction was determined at excess silver(III) by measuring the difference between initial and final absorbances in the stopped-flow apparatus. The value for $\Delta[Ag^{III}]$ thus obtained when compared with the amount of sulphite present, indicated a stoichiometry of 1 : 1.

Attempts to determine the reaction stoichiometry at excess sulphite by iodometric back titration were not conclusive. Indeed, scattered ratio values were obtained. The difficulty in getting good stoichiometric data at excess sulphite is probably due to air-oxidation of sulphite or sulphate.[29] The detection of sulphate at moderate and large excess sulphite concentrations, however, leads us to conclude that the 1 : 1 stoichiometry is also operative under the kinetic conditions.

Based on the 1 : 1 stoichiometric ratio and the product analysis at excess SO_3^{2-}, the reaction goes as follows [eq. (2)]:

$$Ag(OH)_4^- + SO_3^{2-} \xrightarrow{k} Ag(OH)_2^- + SO_4^{2-} + H_2O. \quad (2)$$

Kinetics

When an excess of sulphite is mixed with yellow $Ag(OH)_4^-$, the colour is immediately discharged. A rapid first-order decrease in absorbance in the stopped-flow apparatus over the region 230–400 nm was observed, with no indication of intermediate complex formation. The dependence of the reaction rate on the sulphite ion concentration (5×10^{-4} M $\leqslant [SO_3^{2-}] \leqslant 5\times10^{-3}$ M) was studied at 25°C and $\mu = 1.2$ M, with initial silver(III) concentrations ranging from 1×10^{-5} to 1×10^{-4} M. As illustrated in Fig. 1, the reaction shows a first-order dependence in excess sulphite as given in eq. (3):

$$-d[Ag(OH)_4^-]/dt = k_{obs}[Ag(OH)_4^-] = k[SO_3^{2-}][Ag(OH)_4^-]. \quad (3)$$

A least-squares treatment of the data gives a straight line with an intercept that is close to zero (Fig. 1). The second-order rate constant obtained from this treatment is $k = (9.1\pm0.1)\times10^2\ M^{-1}s^{-1}$. Agreement between observed and calculated pseudo-first-order rate constants is generally better than 5% (Table 1).

Temperature dependence

The reaction was carried out over the range 10–53°C with a 1×10^{-3} M sulphite solution at $[OH^-] = 1.2$ M and $\mu = 1.2$ M. A plot of the data using eq. (4)[30] is linear (Fig. 2).

$$\ln(k_{obs}Nh/RT) = -\Delta H^{\ddagger}/RT + \Delta S^{\ddagger}/R. \quad (4)$$

The enthalpy and entropy of activation calculated from the slope and intercept of the least-squares treatment of eq. (4) are 27 kJ mol^{-1} and -153 J K^{-1} mol^{-1}, respectively. The recalculated temperature dependent rate constants are in good agreement with the observed rate constants.

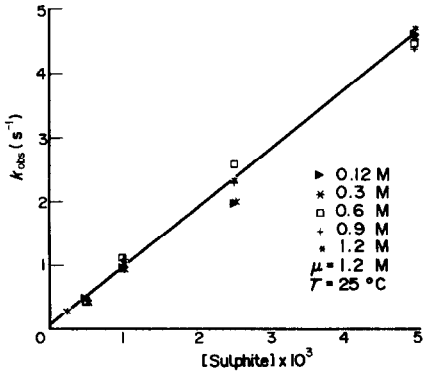

Fig. 1. Variation of the observed pseudo-first-order rate constants with sulphite at different hydroxide concentrations.

Table 1. Values of the observed pseudo-first-order rate constants for the reaction of $Ag(OH)_4^-$ with excess sulphite in different hydroxide concentrations ($\mu = 1.2$ M)

$[OH^-]$ (M)	$[SO_3^{2-}] \times 10^3$ (M)	k_{obs} (s^{-1})	k_{calc} (s^{-1})[a]
[NaOH]			
1.2	0.5	0.50	0.52
	1.0	1.03	0.98
	2.5	2.34	2.38
	5.0	4.72	4.71
0.9	0.5	0.48	0.52
	1.0	1.10	0.98
	2.5	2.31	2.38
	5.0	4.42	4.71
0.6	0.5	0.42	0.52
	1.0	1.12	0.98
	2.5	2.60	2.38
	5.0	4.50	4.71
0.3	0.25	0.27	0.28
	0.5	0.44	0.52
	1.0	0.95	0.98
	2.5	2.00	2.38
	5.0	4.60	4.71
0.12	0.5	0.49	0.52
	1.0	0.99	0.98
	2.5	2.00	2.38
	5.0	4.66	4.71
[LiOH]			
1.2	0.5	0.45	0.52
	1.0	1.04	0.98
	2.5	2.34	2.38
	5.0	4.67	4.71

[a] Calculated from the least-squares line of $k = 0.07 + 9.10 \times 10^2 [SO_3^{2-}]$.

Ionic strength dependence

The kinetics were followed in the ionic strength range from 0.12 to 1.2 M in both LiOH and NaOH at $[SO_3^{2-}] = 5 \times 10^{-3}$ M. A hydroxide concentration of 0.12 M was maintained for all reactions. A net increase of the pseudo-first-order rate constant with ionic strength was observed. A Debye–Hückel–Brönsted–Davies[31] equation plot of $\log k_{obs}$ vs $\mu^{1/2}/(\mu^{1/2}+1) - 0.05\mu$ was linear in the case of LiOH, with a slope of 1.9 (Fig. 3). This is close to the value of two predicted for the interaction of mononegative $Ag(OH)_4^-$ with dinegative SO_3^{2-}. However, at high ionic strengths (≥ 0.6 M), a small deviation from this line was observed for the NaOH data.

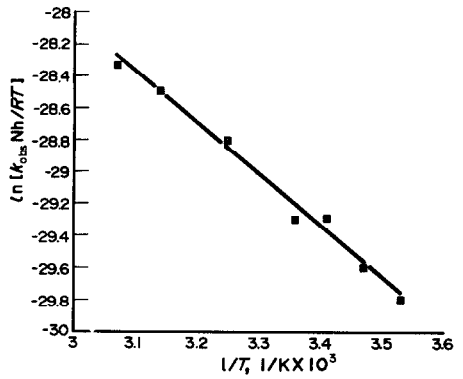

Fig. 2. Temperature dependence for the reaction between sulphite ($[SO_3^{2-}] = 1 \times 10^{-3}$ M) and $Ag(OH)_4^-$.

Reaction of silver(III) *with nitrite and phosphite*

When a nitrite solution is mixed with silver(III) in 1.2 M NaOH, the rate of decrease of the silver(III) absorbance cannot be distinguished from the expected spontaneous decomposition of $Ag(OH)_4^-$,[3,6] even at $[NO_2^-] = 1$ M.

For the system silver(III)–phosphite, the reaction was first carried out over the range 0.01–0.08 M $[HPO_3^{2-}]$, $[OH^-] = 0.96$ M, $\mu = 1.2$ M at 25°C. A slight acceleration in the decomposition of $Ag(OH)_4^-$ was observed. Attempts to account for this change by kinetic means were unsuccessful. There seems to be a competition between the spontaneous decomposition of $Ag(OH)_4^-$ and the oxidation of phosphite, which we were unable to separate because of the complex product-catalysed kinetics of the former reaction.* However, when

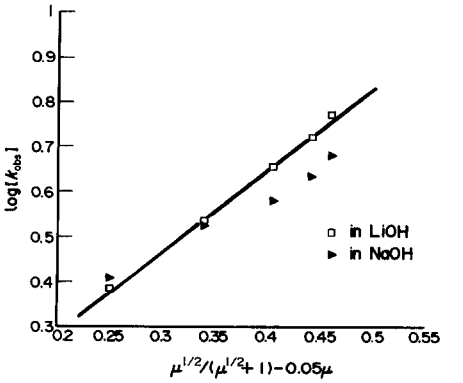

Fig. 3. Ionic strength dependence in aqueous perchlorate media at $[SO_3^{2-}] = 5 \times 10^{-3}$ M and $[OH^-] = 0.12$ M.

* The decomposition half-life of $Ag(OH)_4^-$ in electrolysed 1.2 M NaOH is about 90 min. However, when mixed in the stopped-flow apparatus with solutions which have not been pre-electrolysed to remove trace impurities, the decomposition rate of this complex is significantly faster. Therefore, higher phosphite concentrations and higher ionic strength were required in order to separate the reaction of phosphite with $Ag(OH)_4^-$ from spontaneous decomposition.

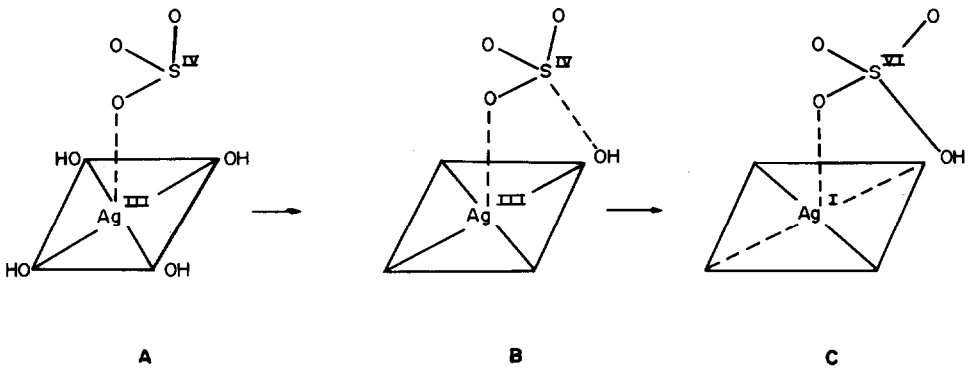

Scheme 1.

three concentrations of phosphite in the range 0.2–0.4 M (μ = 1.88 M, $[OH^-]$ = 0.72 M) were used, the decrease in absorbance at 267 nm was indeed first-order. The plot of k_{obs} vs $[HPO_3^{2-}]$ over this limited range was linear with a zero intercept. The slope of this line corresponds to a second-order rate constant of 1.0×10^{-1} M^{-1} s^{-1}.

DISCUSSION

Sulphite has been found to be an effective complexing agent for transition metal ions such as palladium(II),[32] cobalt(III),[33] and tellurium(I).[34] In the reduction of ferricyanide by sulphite, two iron sulphite intermediate complexes were reported.[4] In the present study, however, there is no kinetic or spectral evidence for a silver(III)–sulphite transient complex. In previous studies, it has been reported that the product of the reduction of transition metals by sulphite is either dithionate or sulphate, or both.[23,26,35] According to the product analysis, sulphate appears to be the only oxidation product of this reaction. The possibility of sulphate resulting from the disproportionation of the dithionate in base can be excluded. Although dithionate is thermodynamically unstable[36] in base, it is kinetically inert with respect to disproportionation.[37]

In blank experiments with $Ag^{III}+SO_4^{2-}$ and $Ag^{I}+SO_3^{2-}$, no reactions were observed, indicating that reactants and products do not react with one another. Furthermore, the stoichiometry observed in this study supports that sulphate is the only product of the reaction.

As is inferred in the two-electron transfer reaction of arsenite with $Ag(OH)_4^-$,[15] the oxidation of sulphite by silver(III) probably proceeds via a one-step oxygen atom transfer. Two kinetically indistinguishable pathways that account for our results are in Schemes 1 and 2. Scheme 1 involves attack by a sulphite oxygen on an axial site of the square-planar silver(III) complex. In Scheme 2, three-coordinate sulphur(IV) undergoes a nucleophilic attack by a hydroxyl ligand followed by oxygen transfer in either a singly-bridged or chelated (as in Scheme 1) intermediate. Both these schemes depend on the expansion of the sulphur(IV) coordination sphere with the fourth oxygen in the sulphate product deriving from $Ag(OH)_4^-$. The insignificant intercept observed in Fig. 1 indicates that there is no participation by $Ag(OH)_3(H_2O)$ in the reduction process as is in the thiosulphate reaction.[17] The lack of any hydroxide dependence on the rate, is as expected since SO_3^{2-} is the only sulphurous acid species in alkaline media (pKa_1 = 1.91,

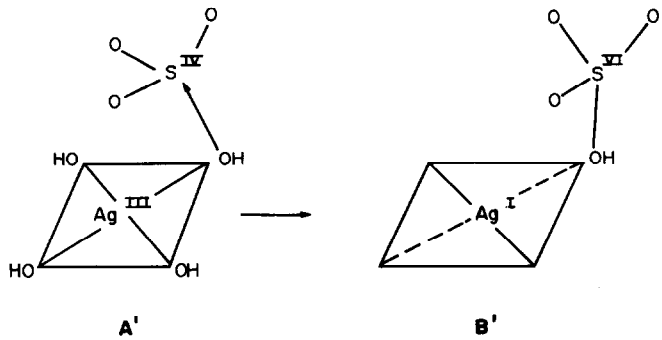

Scheme 2.

pKa_2 = 7.18).[38] The possibility of a rapid transfer of a hydroxyl ligand to sulphite, concurrent with donation of its electron pair to silver(III) via the empty $d_{x^2-y^2}$ orbital (oriented in the equatorial plane of the complex), appears reasonable. Support of the possibility that redox occurs through a five-coordinate intermediate as in Scheme 1 is provided by the results of other $Ag(OH)_4^-$ reactions. For instance, the presence of third-order terms in the reaction of en,[21] HO_2^- [22] and thiourea[39] implies the formation of five-coordinate transients.

Activation parameters for silver(III) complexation reactions have been interpreted in terms of an associative mechanism for ligand exchange. The activation parameters reported here are similar to those obtained in the reduction of silver(III) by arsenite[15] species, $H_2AsO_3^-$ and $HAsO_3^{2-}$, where a five-coordinate silver(III) intermediate was postulated. The reaction is likely to proceed by (1) ion association, (2) axial attack by negative sulphite on the positive silver(III) centre, (3) changes in bond lengths of the two reactants and reconstruction of their solvation spheres and (4) a fast electron transfer step involving the rupture of a silver–oxygen bond to yield the products. The observed rate seems to be due to the formation of a bridged precursor intermediate (A or A′) which is then followed by a fast redox process. This is consistent with a large negative entropy as is observed.

The good agreement for the ionic strength dependence in LiOH–$LiClO_4$ with expectations indicates the absence of substantial ion pairing in the intimate step of the reaction, as is reported for similar reactions.[26,40] We note that at 1.2 M OH^-, there is no difference in rate between NaOH and LiOH (Table 1). Thus sodium (but not lithium) ion pairing is probably not responsible for the deviation in Fig. 3.

If we presume that the reduction of silver(III) by phosphite is, like the sulphite reaction, independent of [OH^-] and has the expected ionic strength variation, we may correct the second-order rate constant obtained at μ = 1.88 M[31] and compare the rates of the two reactions. The rate constant corrected to μ = 1.2 M for phosphite is 9.5×10^{-2} M^{-1} s^{-1} which is about four orders of magnitude smaller than the value of 9.1×10^2 M^{-1} s^{-1} obtained for the reaction of silver(III) with sulphite (25°C). The difference in reactivity between sulphite and phosphite, which are isoelectronic, may stem from the fact that sulphite has a lone pair of electrons on sulphur that is readily available in the electron transfer process. On the other hand, there is no such pair of electrons on the phosphite phosphorus which is bound to a non-labile hydrogen.[41] Ghosh *et al.*[42] reported that although phosphite is a powerful reducing agent, the reduction of the chromium(V) chelate bis(2-ethyl-2-hydroxybutyrato) oxochromate(V) by phosphite is immeasurably slow. This is consistent with the sluggish reactivity of phosphite.

Kinetics of nitrite ion oxidation by metal ions have been recently reported.[42–44] For example, the reduction of chromium(V) by nitrite was inferred to proceed by an $NO_2^{\cdot}$ radical intermediate.[42] Wilmarth *et al.*[44] reported rate constants for oxidations of $Fe(bpy)_3^{3+}$ by nitrite and sulphite of 3.3×10^4 and 4.6×10^6 M^{-1} s^{-1}, respectively. However, there is no evidence of a nitrite–silver(III) reaction even at [NO_2^-] = 1 M. An explanation for the non-reactivity of nitrite may be found in the inability of nitrogen to accept electrons into *d* orbitals. Before the bound hydroxyl oxygen can be transferred, an additional electron pair must coordinate to the central atom of the oxoanion (*vide supra*). While the availability of *d* orbitals permits an expanded number of valence electrons in arsenite, sulphite and phosphite, nitrite cannot coordinate to oxygen while it is also bound to silver. One-electron transfer to form $NO_2^{\cdot}$ and a silver(II) intermediate, while a potential alternative to oxygen atom transfer, would have a high activation energy. The $NO_2^{\cdot}/NO_2^-$ potential is just over 1 V.[45] We have estimated the $Ag(OH)_4^-/Ag(OH)_4^{2-}$ one-electron reduction to be about 3/10 V less than this,[46] thus posing a thermodynamic barrier to the electron transfer. Therefore, the non-reactivity of NO_2^- with $Ag(OH)_4^-$ is entirely consistent with the oxidation of the other oxoanions via an atom transfer mechanism.

Acknowledgements—We wish to thank the Donors of the Petroleum Research Fund administered by the American Chemical Society for support of this Research.

REFERENCES

1. P. J. Durrant and B. Durrant, *An Introduction to Advanced Inorganic Chemistry*, 2nd edn. John Wiley, New York (1970).
2. F. A. Cotton and G. Wilkinson, *Advanced Inorganic Chemistry*, 5th edn. John Wiley, New York (1988).
3. G. L. Cohen and G. J. Atkinson, *J. Electrochem. Soc.* 1968, **12**, 1236.
4. L. J. Kirschenbaum and J. D. Rush, *J. Am. Chem. Soc.* 1984, **106**, 1003.
5. L. J. Kirschenbaum, R. K. Panda, E. T. Borish and E. Mentasti, *Inorg. Chem.*, submitted.
6. L. J. Kirschenbaum, J. H. Ambrus and G. Atkinson, *Inorg. Chem.* 1973, **12**, 2832.
7. R. Hoppe in P. Hagenmuller (Ed.), *Inorganic Solid Fluorides*, p. 276. Academic Press, New York (1985).

8. R. Hoppe and R. Homann, *Z. Anorg. Allg. Chem.* 1970, **379**, 193.
9. E. K. Barefield and M. T. Mocella, *Inorg. Chem.* 1973, **12**, 2829.
10. K. M. Kadish, D. G. Davis and J. H. Fuhrop, *J. Am. Chem. Soc.* 1974, **96**, 591.
11. K. Chakravorty and P. Ray, *Ind. Chem. Soc.* 1944, **21**, 47.
12. P. Ray, *Inorg. Synth.* 1960, **6**, 74.
13. D. Sen, *J. Chem. Soc. A* 1969, 1304.
14. D. W. Margerum and G. D. Owens, *Met. Ions Biol. Syst.* 1981, **12**, 75.
15. L. J. Kirschenbaum and J. D. Rush, *Inorg. Chem.* 1983, **22**, 3304.
16. E. T. Borish and L. J. Kirschenbaum, *Inorg. Chem.* 1984, **23**, 2355.
17. J. D. Rush and L. J. Kirschenbaum, *Inorg. Chem.* 1985, **24**, 744.
18. J. D. Rush and L. J. Kirschenbaum, *Polyhedron* 1985, **5**, 1573.
19. L. J. Kirschenbaum, E. T. Borish and J. D. Rush, *Isr. J. Chem.* 1985, **25**, 159.
20. L. J. Kirschenbaum and L. Mrozowski, *Inorg. Chem.* 1978, **17**, 3718.
21. L. J. Kirschenbaum, *J. Inorg. Nucl. Chem.* 1976, **38**, 881.
22. E. T. Borish and L. J. Kirschenbaum, *J. Chem. Soc., Dalton Trans.* 1983, 769.
23. A. Brown and W. C. E. Higginson, *J. Chem. Soc., Dalton Trans.* 1972, 166.
24. J. M. Lancaster and R. S. Murray, *J. Chem. Soc. A* 1971, 2755.
25. J. M. Anast and D. W. Margerum, *Inorg. Chem.* 1981, **20**, 2319.
26. J. H. Swinehart, *J. Inorg. Nucl. Chem.* 1967, **29**, 2313.
27. J. Veprek-Siska and D. M. Wagnerova, *Coll. Czech. Chem. Comm.* 1965, **30**, 1390.
28. H. N. Alyea and H. L. T. Backstron, *J. Am. Chem. Soc.* 1929, **51**, 90.
29. G. Nickless, *Inorganic Sulphur Chemistry*. Elsevier, Amsterdam (1968).
30. F. Basolo and R. G. Pearson, *Mechanisms of Inorganic Reactions*, 2nd edn. John Wiley, New York (1967).
31. B. Perlmutter-Hayman, in *Progress in Reaction Kinetics*, Vol. 6, p. 239. Pergamon Press, Oxford (1972).
32. G. Mahal and R. Van Eldik, *Inorg. Chem.* 1987, **26**, 2838.
33. W. G. Jackson, *Inorg. Chem.* 1988, **27**, 777.
34. L. Peter and M. Beat, *Inorg. Chem.* 1985, **19**, 3071.
35. D. W. Carlyle and O. Zeck Jr, *Inorg. Chem.* 1973, **12**, 2978.
36. A. J. Bard, R. Parsons and J. Jordan, *Standard Potentials in Aqueous Solution*, p. 106. Marcel Decker, New York (1985).
37. D. W. Carlyle, *J. Am. Chem. Soc.* 1972, **94**, 4525.
38. D. C. Harris, *Quantitative Chemical Analysis*, 2nd edn, p. 737. W. H. Freeman and Cie, New York (1987).
39. L. J. Kirschenbaum and R. K. Panda, *Polyhedron* 1988, **7**, 2753.
40. A. R. Olson and T. R. Simonson, *J. Chem. Phys.* 1949, **17**, 348.
41. H. S. Gutowski, D. W. McCall and C. P. Slichter, *J. Chem. Phys.* 1953, **21**, 279.
42. S. K. Ghosh, R. N. Bose and E. S. Gould, *Inorg. Chem.* 1987, **26**, 2688.
43. G. Stedman, *Adv. Inorg. Chem. Radiochem.* 1979, **22**, 113.
44. W. K. Wilmarth, D. M. Stanbury, J. E. Byrd, H. N. Po and C.-P. Chua, *Coord. Chem. Rev.* 1983, **51**, 155.
45. M. S. Ram and D. M. Stanbury, *J. Am. Chem. Soc.* 1984, **106**, 8136.
46. E. T. Borish, L. J. Kirschenbaum and E. Mentasti, *J. Chem. Soc., Dalton Trans.* 1985, 1789.

Polyhedron Vol. 8, No. 10, pp. 1307–1313, 1989
Printed in Great Britain

0277–5387/89 $3.00+.00
© 1989 Pergamon Press plc

LIQUID–LIQUID EXTRACTION OF SOME M^{II} AND M^{III} IONS WITH 2-ETHYLHEXYLHYDROGENPHENYLPHOSPHONATE

EMMANUEL O. OTU and ALAN D. WESTLAND*

Ottawa–Carleton Chemistry Institute, University of Ottawa, Ottawa, Ontario, Canada K1N 6N5

(*Received* 9 *November* 1988; *accepted* 18 *January* 1989)

Abstract—The extraction of zinc(II), cadmium(II), bismuth(III) and some lanthanide ions from aqueous perchloric acid into hexane solutions of 2-ethylhexylphenylphosphonic acid, HEHϕP, has been studied. The extracted species contain varying numbers of extractant molecules and phosphonate groups as ligands, depending upon the size and charge of the ions. High loadings of the extractant with the metal ion resulted in suppression of the extraction. Alkali ions were not extracted but alkali perchlorate suppressed the extraction through the effect of ionic strength on the metal ion activity.

Phosphorus-based extractants, especially tributyl phosphate, are commonly employed for the isolation of higher valent metal ions such as the lanthanides and actinides. Mono-acidic extractants such as diesters of phosphoric acid have been the subject of several studies.[1–7] Mono esters of phosphonic acids have been reported to possess high separation factors for successive members of the lanthanide and actinide series.[8–12] Despite this advantage, these have been less studied.

The highest separation factors have been observed with 2-ethylhexylhydrogenphenylphosphonate (HEHϕP).[8] We therefore decided to study the extraction parameters (acid and extractant dependencies) of this extractant. Because it shows an especial affinity for larger ions such as the lanthanides, we have compared its behaviour in complexing lanthanides with its reactivity towards other M^{III} ions as well as M^{II} ions both large and small. Having determined some of the parameters of extraction, we are able to suggest possible extraction mechanisms.

EXPERIMENTAL

Materials

Lanthanum nitrate (99.99%) was obtained from Johnson Matthey Co. Praseodymium, neodymium, samarium, gadolinium, dysprosium, erbium and lutetium atomic absorption standard solutions were obtained from Aldrich Chemical Co. Bismuth nitrate and calcium carbonate were Baker reagent grade, and technical grade zinc powder was obtained from Fisher Scientific Co. Analar grade perchloric acid was supplied by BDH Chemicals. The hexane was practical grade.

Synthesis of HEHϕP

HEHϕP was prepared according to the method of Kantipuly.[13] This entailed the alcoholysis of phenylphosphonic dichloride with 2-ethyl-1-hexanol. Both reagents were obtained from Aldrich Chemical Co. A 1:1.5 molar ratio, respectively, of the above reagents in benzene was mixed in a pressure bottle and stirred for 48 h at room temperature. The pressure was released carefully and the mixture washed several times with water to remove unesterified phenylphosphonic acid. The mixture was taken up in ether and shaken with 10% NaOH solution. The aqueous phase was scrubbed with benzene to remove alcohol and any diester, and then acidified with concentrated hydrochloric acid to liberate the monoester, HEHϕP. This was taken up in anhydrous diethyl ether, dried with $MgSO_4$ and filtered. Solvent was removed under reduced pressure. The structure and purity of the product was confirmed by ^1H and ^{13}C NMR, and mass spectrometry. Found: C, 62.1; H, 8.6. Calc. for $C_{14}H_{23}O_3P$: C, 62.2; H, 8.6%.

* Author to whom correspondence should be addressed.

Preparation of metal ion solutions

Aliquots of the metal ions in nitric acid medium were evaporated to dryness. The residues were taken up in 70% $HClO_4$ and re-evaporated to dryness. The dissolution in $HClO_4$ and evaporation was repeated and the resulting perchlorate salts were finally dissolved in $HClO_4$ and diluted with water to the required volume. The acidity was determined by titration.

Determination of the distribution ratio, K_d

The extractant phases had concentrations in the range 0.01–0.1 M HEHϕP in hexane. Normally, a 5 cm^3 volume of extractant was stirred magnetically with 5 cm^3 of metal ion solution in vials held in a thermostat bath at 25.0±0.5°C. Equilibrium was attained in 5 min but routine stirring times were rather longer than this. After equilibration, the phases were allowed to settle for 15 min before separating. Analyses of both aqueous and organic fractions yielded mass recoveries of greater than 98%. Therefore, for much of the data that follows, the aqueous phase was analysed and the metal content of the organic phase found by difference.

The lanthanides were determined by direct-coupled plasma emission spectrometry. The aqueous phases were run without treatment but the organic phases were wet-ashed with $HClO_4$ prior to analysis. Zinc and calcium were determined by atomic absorption spectrometry. Bismuth was determined by spectrophotometry as the complex, BiI_4^-.[14] Phosphate formed by wet-ashing the extractant was shown not to interfere.

Analyses were run in duplicate. Some, but not all, of the equilibrations were run in duplicate as well. The distribution ratio, K_d, was calculated by dividing the concentration of the ion in the organic phase by that in the aqueous phase.

RESULTS AND DISCUSSION

Figure 1 shows extraction isotherms for Dy^{3+} and Zn^{2+}. As the plots are not linear, it is evident that the ions do not obey Henry's Law in one or both of the phases in each case. The ionic strength of the aqueous phases is very largely determined by the fixed concentration of acid present. The aqueous phases containing rather low concentrations of metal ion should therefore obey Henry's Law to a good approximation. The situation is otherwise for

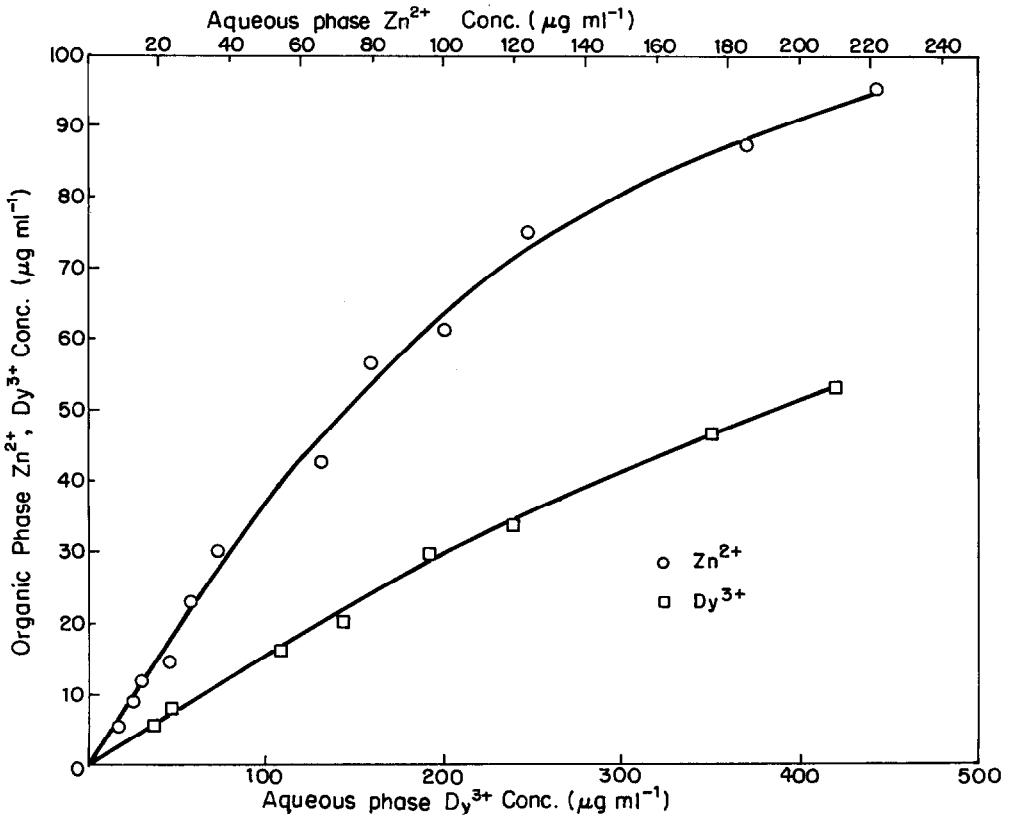

Fig. 1. Extraction isotherms for Zn^{2+} from 0.01 M $HClO_4$ and Dy^{3+} from 1.0 M $HClO_4$ into 0.01 M HEHϕP in hexane at room temperature.

the organic phase, however. It is shown later that the stoichiometric ratios of HEHϕP to Dy^{3+} and Zn^{2+} are 5:1 and 3:1, respectively, when the extractant is in large excess. As the extractant concentration was only 0.01 M, a large fraction of the extractant was bound to the metal ions in the organic phases that were relatively concentrated in metal ion. For example, in the most concentrated zinc solution (0.0015 M), with a 3:1 mole ratio of HEHϕP to zinc, 45% of the extractant would be bound to zinc. The curvature of the extraction isotherm suggests that with such a high degree of loading, the stoichiometry of the extracted species cannot be maintained at 3:1.

There is an additional reason for the curvature. As the extractant is deprotonated upon complexing, the acidity of the aqueous phase is increased. This would have a considerable effect in the case of zinc extraction where the initial acid concentration of the aqueous phase was 0.01 M. However, in the dysprosium case, the high acidity would not be changed appreciably by the complexing.

In the experiments described below, the metal ion concentrations were kept small relative to the extractant concentration so that both phases invariably obeyed Henry's Law.

Acid dependencies

Double logarithmic plots of the distribution coefficient against acid concentration appear in Figs 2 and 3. The slopes indicate that K_d is inversely second power and third power dependent upon the initial aqueous phase acidity for the M^{II} and M^{III} ions, respectively. The ionic strength was adjusted to a constant value with $NaClO_4$ throughout each series of measurements.

Peppard *et al.*[8] obtained the same third power dependence in the extraction of M^{III} ions with HEHϕP in toluene. Second power dependence has been reported for the extraction of Ca^{2+} with *n*-octyl esters of phenyl and chloromethyl phosphonic acids.[15]

The results suggest that neutral complexes enter the organic phase and the ion charge is neutralized by the extractant in anionic form. It follows that the perchlorate ion does not enter the complex.

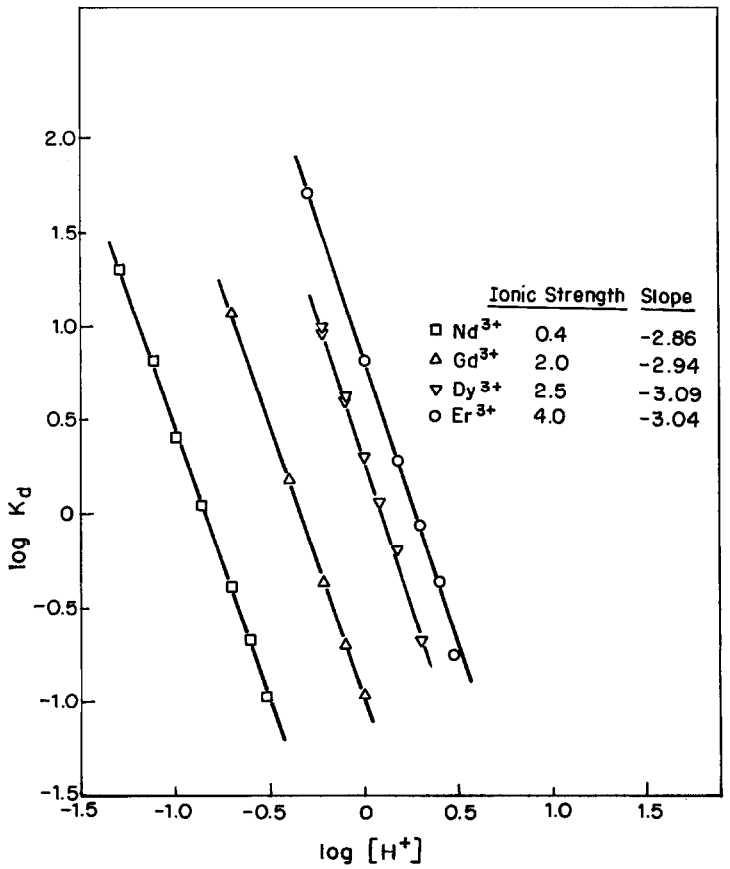

Fig. 2. Hydrogen ion dependence of the extraction of Nd^{3+}, Gd^{3+}, Dy^{3+} and Er^{3+} into 0.025 M HEHϕP in hexane; aqueous phase $HClO_4 + NaClO_4$ at 25°C.

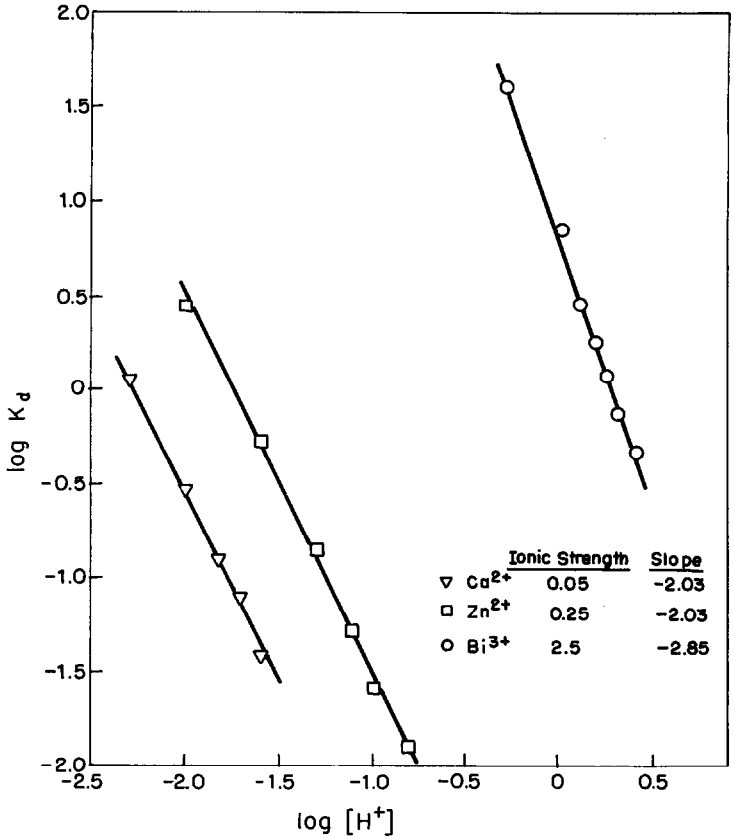

Fig. 3. Hydrogen ion dependence of the extraction of Ca^{2+}, Zn^{2+} and Bi^{3+} into 0.025 M HEHϕP in hexane; aqueous phase $HClO_4+NaClO_4$ at 25°C.

Were it to do so, the order of dependence upon acid concentration would be less than that observed.

Extractant dependencies

Studies of the dependence of extraction upon extractant concentration provide information about the composition of the extracted complexes. From the slopes of plots in Figs 4 and 5 it can be seen that the extraction of lanthanum and praseodymium is third power dependent upon extractant concentration, while the order drops to 2.5 for the heavier lanthanides. The neodymium and samarium plots are intermediate with slopes of 2.8 and 2.7, respectively. The plots in Fig. 6 indicate third order dependence for Ca^{2+} and Bi^{3+} and an order of 1.5 for Zn^{2+}. Peppard *et al.* reported third order dependence for M^{III} ions when treated with the extractants mentioned above.[8] Calcium exhibited an order of 2.5 when extracted with *n*-octylhydrogenchloromethylphosphonate and 3.0 with *n*-octylhydrogenphenylphosphonate.[15] An extractant dependence of order 1.5 has been observed for the extraction of Zn^{2+} with bis(2-ethylhexyl) phosphonic acid (HDEHP).[16] The order is thus variable, depending upon the ion charge and size and upon the particular choice of extractant.

The extractions with HEHϕP follow the equations:

$$La^{3+}(\text{or } Bi^{3+})+3(HY)_2 \rightleftharpoons M(HY_2)_3+3H^+$$

$$Ln^{3+}+2.5(HY)_2 \rightleftharpoons LnY(HY_2)_2+3H^+$$

$$Ca^{2+}+3(HY)_2 \rightleftharpoons Ca(HY_2)_2(HY)_2+2H^+$$

$$Zn^{2+}+1.5(HY)_2 \rightleftharpoons ZnY(HY_2)+2H^+,$$

in which the charged species and uncharged species are in aqueous and organic media, respectively, and $(HY)_2$ is the dimer of HEHϕP.[17,18] It is owing to the dimeric nature of the extractant that either integral or half-integral powers, n, arise in an equilibrium relation. For the reaction

$$M^{z+}+n(HY)_2 \rightleftharpoons \text{complex}+zH^+,$$

the equilibrium relation is

$$K_s=\frac{[\text{complex}][H^+]^z}{[M^{z+}][(HY)_2]^n}=\frac{K_d[H^+]^z}{[(HY)_2]^n}.$$

The number of extractant molecules that react with a given ion appears to decrease with the electric

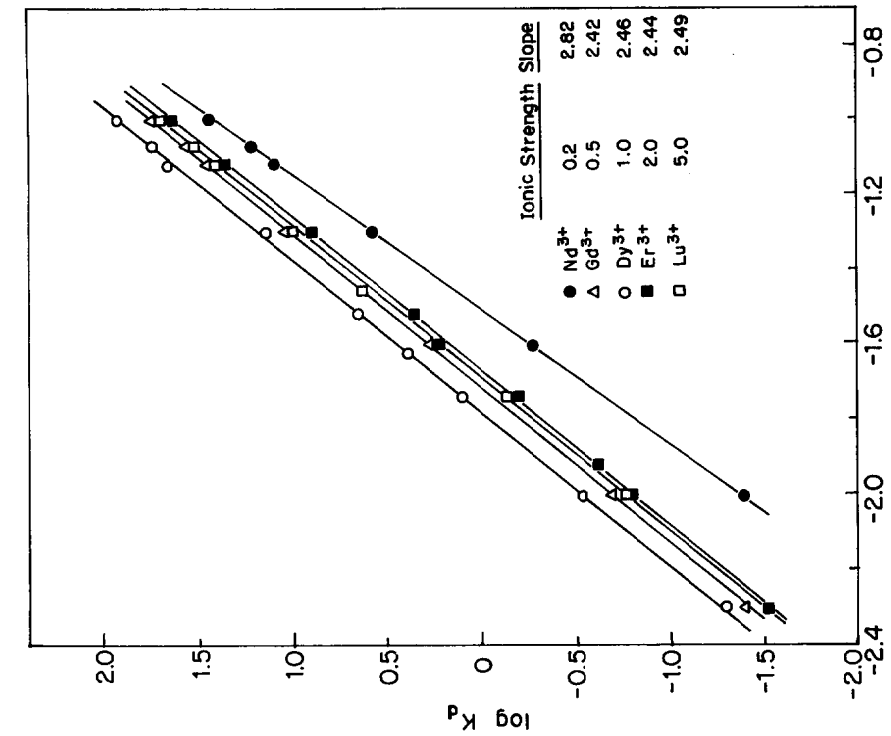

Fig. 5. Extractant dependence of the extraction of Nd^{3+}, Gd^{3+}, Dy^{3+}, Er^{3+} and Lu^{3+} from aq. $HClO_4$ into hexane containing HEHφP at 25°C.

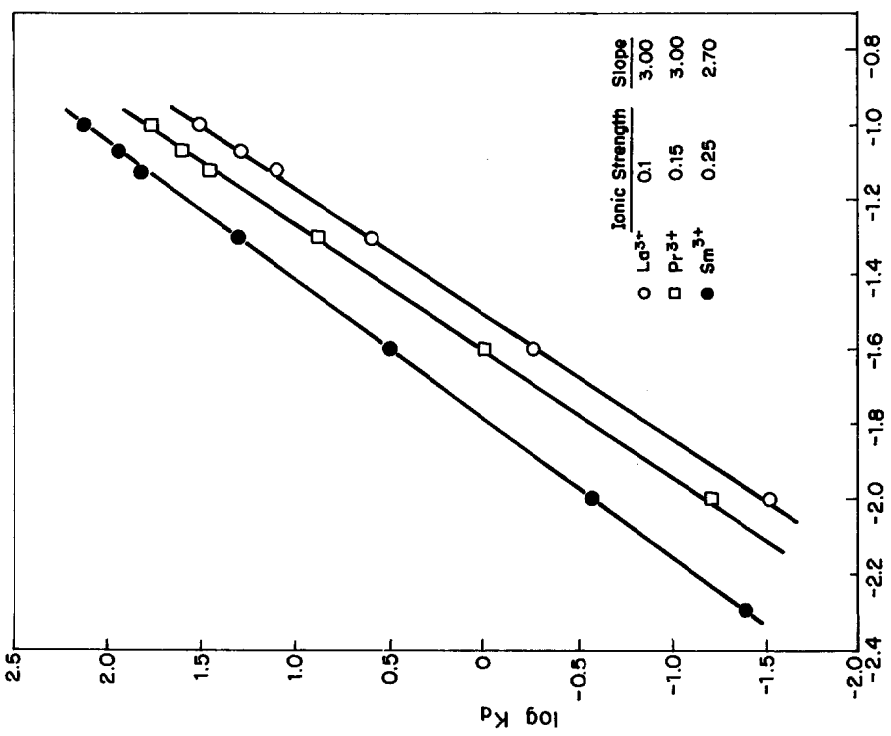

Fig. 4. Extractant dependence of the extraction of La^{3+}, Pr^{3+} and Sm^{3+} from aq. $HClO_4$ into hexane containing HEHφP at 25°C.

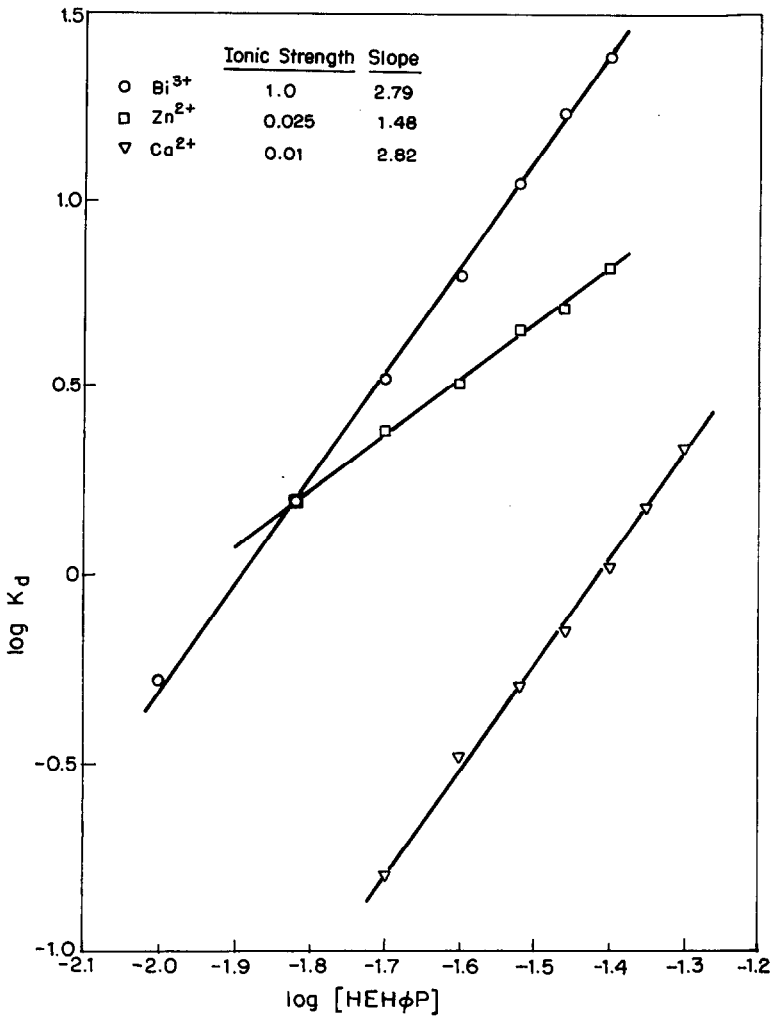

Fig. 6. Extractant dependence of the extraction of Ca^{2+}, Zn^{2+} and Bi^{3+} from aq. $HClO_4$ into hexane containing HEHϕP at 25°C.

field about that ion. The field is given approximately by the ionic function, ze/r, where ze is the charge and r the radius of that ion. Thus the largest rare earth ion, La^{3+}, binds three extractant dimers. With a decrease in radius, the later lanthanides replace one of the dimers with a monomer unit.

The radius of the calcium ion is about equal to that of Dy^{3+} but it carries only a double charge. Evidently the smaller electrical field permits the Ca^{2+} ion to react with additional, i.e. three, $(HY)_2$ molecules. The smaller radius of the Zn^{2+} ion combined with the fact that it is of the pseudo rare gas type, gives this ion a considerably stronger field. It consequently accommodates only 1.5 $(HY)_2$ molecules.

Effect of alkali salt

As HEHϕP is a liquid cation exchanger, it was thought that it might extract some of the alkali ion used in some of the experiments to adjust the ionic strength. Sodium perchlorate added to the aqueous phase at concentrations as high as 3 M had a large inhibitory effect on extractions. However, we were able to relate the effect of alkali salt solely to the reduction of the activity of the other ions in solution. The influence is quite large as can be seen from Fig. 7, which shows the effect of ionic strength on the distribution coefficient of Nd^{3+}. The solutions are too concentrated to allow the use of the Debye–Hückel equation, but the behaviour is compatible with plausible values of the activity of Nd^{3+} ion. Organic phases that had been equilibrated with 1 M alkali perchlorate in 0.01 M perchloric acid were found to contain less than 1 $\mu g\ cm^{-3}$ of alkali ion.

The phosphonate half ester shows extremely little affinity for univalent ions but a strong affinity for trivalent and quadrivalent ions. This difference is much less pronounced with sulphonate-type ion

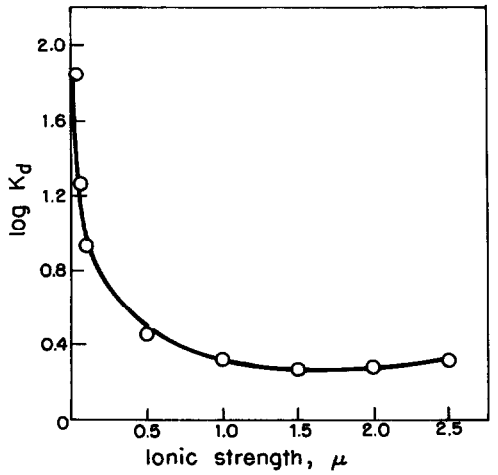

Fig. 7. Effect of ionic strength, $\mu(HClO_4+NaClO_4)$, on the extraction of Nd^{3+} into 0.025 M HEHϕP in hexane at 25°C.

exchangers. It follows that the phosphonate will display better selectivity between ions of differing charge. It is to be expected that there will also be better selectivity between ions of the same formal charge but differing effective charge. This is indeed observed in the separation factors for successive members of the lanthanide and actinide series.

We have measured enthalpies and entropies of extraction for a selection of ions of various effective charges by both HEHϕP and dinonylnaphthalene sulphonic acid. In all cases, there was a greater difference in free energy in the extraction of a given pair of ions when the phosphonate extractant was used. The results will appear elsewhere.

REFERENCES

1. D. F. Peppard, G. W. Mason, J. L. Maier and W. J. Driscoll, *J. Inorg. Nucl. Chem.* 1957, **4**, 334.
2. D. F. Peppard, G. W. Mason, W. J. Driscoll and R. J. Sironen, *J. Inorg. Nucl. Chem.* 1958, **7**, 276.
3. D. F. Peppard, G. W. Mason, W. J. Driscoll and S. McCarty, *J. Inorg. Nucl. Chem.* 1959, **12**, 141.
4. B. Ceccaroli, J. Alstad and M. J. F. Leroy, *Polyhedron* 1982, **1**, 257.
5. D. Li, Z. Wang, Y. Xie, C. Shen, C. Zhung and S. Le, *New Front. Rare Earth Sci. Appl., Proc. Int. Conf. Rare Earth Dev. Appl.* 1985, **1**, 463.
6. G. Xie and G. Chen, *Jinan Liyi Xuebao* 1986, **3**, 60.
7. X. Wang, Department of Chem., Xinjiang University, China, personal communication.
8. D. F. Peppard, G. W. Mason and I. Hucher, *J. Inorg. Nucl. Chem.* 1961, **18**, 245.
9. D. F. Peppard, G. W. Mason and I. Hucher, *Radioisotopes Phys. Sci. Ind, Proc. Conf. Use.* 1962, **2**, 541. Copenhagen (1960).
10. B. Weaver and R. R. Shourr, *J. Inorg. Nucl. Chem.* 1971, **33**, 1909.
11. G. Gershini, *J. Chromatogr.* 1974, **102**, 299.
12. R. D. Baybarz, *Nucl. Sci. Engng* 1963, **17**, 463.
13. C. J. Kantipuly, PhD thesis, University of Ottawa (1984).
14. E. B. Sandell, *Colorimetric Determination of Traces of Metals*, 2nd edn, p. 216. Interscience, New York (1950).
15. D. F. Peppard, G. W. Mason, S. McCarty and F. D. Johnson, *J. Inorg. Nucl. Chem.* 1962, **24**, 321.
16. L. A. Ajawin, J. Demetriou, E. S. Perez de Ortiz and H. Sawistowski, *Extraction '84; Symposium Liquid–Liquid Extraction Science, Int. Chem. Engng Symp. Ser.* No. 88, p. 184.
17. D. F. Peppard, J. R. Ferraro and G. W. Mason, *J. Inorg. Nucl. Chem.* 1959, **12**, 60.
18. J. R. Ferraro, G. W. Mason and D. F. Peppard, *J. Inorg. Nucl. Chem.* 1961, **22**, 285.

Polyhedron Vol. 8, No. 10, pp. 1315–1320, 1989
Printed in Great Britain

0277–5387/89 $3.00+.00
© 1989 Pergamon Press plc

PHOSPHATE COMPLEXATION OF GADOLINIUM(III) IN AQUEOUS SOLUTION

L. S. BINGLER and R. H. BYRNE*

Department of Marine Science, University of South Florida, St. Petersburg, FL 33701, U.S.A.

(*Received* 11 *October* 1988; *accepted* 18 *January* 1989)

Abstract—Examination of the distribution of high specific activity Gd^{153} between tributyl phosphate and a 0.68 M aqueous phase at 25.0°C permits investigation of lanthanide phosphate complexation within rigorous solubility constraints. Our experiments provide the following formation constants with estimated standard errors: $\beta'_1 = [GdHPO_4^+][Gd^{3+}]^{-1}[HPO_4^{2-}]^{-1} = (8.05 \pm 0.7) \times 10^3$; $\beta'_2 = [Gd(HPO_4)_2^-][Gd^{3+}]^{-1}[HPO_4^{2-}]^{-2} = (8.1 \pm 1.9) \times 10^6$; $\beta'_H = [GdH_2PO_4^{2+}][Gd^{3+}]^{-1}[H_2PO_4^-]^{-1} = 50.4 \pm 6.8$. Our results indicate that phosphate complexation of lanthanide ions and trivalent actinides is significant in natural systems, and that the use of phosphate salts as pH buffers in laboratory examinations of metal hydrolysis is generally inadvisable.

Previous investigations of lanthanide ion aqueous equilibria have examined the formation of $LnH_2PO_4^{2+}$,[1,2] but apparently no previous studies have characterized the formation of $LnHPO_4^+$. Lanthanide ion equilibria of the form

$$Ln^{3+} + HPO_4^{2-} \rightleftharpoons LnHPO_4^+, \qquad (1)$$

are of environmental interest because of occasionally high phosphate concentrations (10^{-6}–10^{-4} M) in marine diagenetic systems, and because HPO_4^{2-} is present at much higher concentrations than $H_2PO_4^-$ within the normal pH range of sea water[3] and marine sediments. $LnHPO_4^+$ formation is of direct chemical interest because of the previous use of phosphate as a buffer in chemical systems composed for investigations of lanthanide ion hydrolysis equilibria. Bilal and Kob[4] investigated the hydrolysis of Ce^{3+}, Eu^{3+}, Tb^{3+} and Yb^{3+} in aqueous solutions containing phosphate at high concentrations. The hydrolysis constants reported in their work considerably exceed values[5] obtained in the absence of phosphate.

Examination of Fe^{3+} and Eu^{3+} linear free energy relationships for a variety of ligands (Fig. 1) indicates that rare earth phosphate complexation may be significant at relatively high concentrations of HPO_4^{2-}. The $FeH_2PO_4^{2+}$ formation constant obtained by Galal-Gorchev and Stumm,[13] $\log\beta_1 (H_2PO_4^-) = 3.47$, in conjunction with the plot shown in Fig. 1, provides a $EuH_2PO_4^{2+}$ formation constant estimate of the order 10^2. This is in reason-

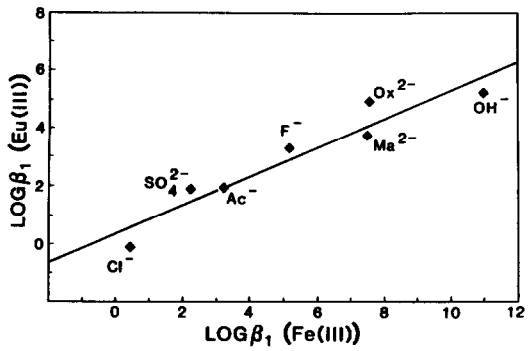

Fig. 1. Formation constants for europium(III) complexes are shown vs iron(III) complexation constants reported for similar conditions. Our thermodynamic data were obtained from the following sources: ($EuCl^{2+}$, 25°C, 1 M);[6] ($FeCl^{2+}$, 25°C, 0.7 M);[7] ($EuSO_4^+$, 25°C, 0.5 M; $FeSO_4^+$, 25°C, 0.5 M);[6] (Eu^{3+} acetate, 20°C, 0.5 M; Fe^{3+} acetate, 20°C, 1 M);[8] (EuF^{2+}, 25°C, 0.7 M);[9] (FeF^{2+}, 25°C, 0.5 M);[6] (europium(III) malonate, 25°C, 1 M);[10] (iron(III) malonate, 25°C, 1 M);[8] (europium(III) oxalate, 25°C, 0.7 M);[11] (iron(III) oxalate, 25°C, 1 M);[10] ($EuOH^{2+}$, 25°C, 1 M; $FeOH^{2+}$, 25°C, 1 M).[12]

* Author to whom correspondence should be addressed.

ably good agreement with the reported values of Borisov *et al.*[1] and Rao *et al.*[2] The $FeHPO_4^+$ formation constant $\log\beta_1(HPO_4^{2-}) = 8.3$, obtained by Galal-Gorchev and Stumm,[13] indicates that $\log\beta_1(EuHPO_4^+)$ should be of the order 10^4. In order to obtain direct information on the significance of lanthanide ion complexation by the ligand HPO_4^{2-}, in both natural and synthetic systems, we have undertaken investigations of lanthanide ion complexation through phase distribution measurements. Gadolinium was used in our investigations because Gd^{153} is available as a high specific activity radionuclide, greatly limiting the total gadolinium concentrations in our experiments [$(Gd^{3+})_T < 10^{-9}$ mol dm^{-3}], and thereby reducing the possibilities of precipitation in our work. The existence of phosphate minerals as important lanthanide bearing ores attests to the low solubility of lanthanide element phosphates. We suspect that the absence of previously reported $LnHPO_4^+$ stability constants is a direct consequence of the substantial stability of lanthanide phosphate minerals.

EXPERIMENTAL

Our experiments examined the influence of HPO_4^{2-} ions on the distribution of Gd^{3+} between 0.68 M $NaClO_4$ and tributyl phosphate (TBP). The procedures used in our phosphate complexation experiments closely follow the procedures used by Lundqvist[5] and Cantrell and Byrne[11] in the examination of lanthanide and actinide complexation by carbonate ions.

Prior to each experiment, concentrated stock solutions of $NaClO_4$ (Aldrich Chemical Co., anhydrous 99$^+$%) were prepared and allowed to stand at pH 8.5–9.5 for approximately 24 h. The solutions were subsequently filtered with a 0.45 μ polycarbonate filter (Nuclepore Corp.) and diluted to 0.68 M. Before use, each filter was rinsed with acid, followed by deionized water. Prior to each experiment, approximately 120 cm^3 of TBP (Fluka, puriss p.a.) and 120 cm^3 of 0.68 M NaOH (Baker, CO_2 free) were combined in a separatory funnel, shaken for 5 min and then allowed to separate for 20 min. The TBP was next transferred into 25 cm^3 plastic tubes and centrifuged at 12,000 rpm, 25°C ± 1°C for 15 min. The TBP in each tube was then carefully removed and returned to a separatory funnel via an Eppendorf pipette. Approximately 120 cm^3 of 0.68 M $NaClO_4$ was added to the separatory funnel, the mixture was shaken for 5 min and then allowed to separate for 20 min. The $NaClO_4$ was then discarded and the process repeated. Subsequent to these pre-equilibration procedures, our Gd^{153} organic–aqueous phase equilibrations were conducted in a 250 cm^3 jacketed beaker maintained at 25°C ± 0.1°C. This beaker contained 100 cm^3 of both TBP and a 0.68 M $NaClO_4$ aqueous phase.

Our phase distribution measurements were conducted over a pH range such that total phosphate was partitioned dominantly between $H_2PO_4^-$ and HPO_4^{2-}. The concentration of each chemical form was determined from total phosphate and pH using the equations

$$(PO_4)_T = M_{HPO_4^{2-}}(1 + (K_2')^{-1}[H^+]) \quad (2)$$

and

$$(PO_4)_T = M_{HPO_4^{2-}} + M_{H_2PO_4^-}, \quad (3)$$

where $(PO_4)_T$ is the total phosphate concentration in the aqueous solution, $M_{HPO_4^{2-}}$ and $M_{H_2PO_4^-}$ indicate the molar concentration of each chemical form, $[H^+] = 10^{-pH}$ is the free hydrogen ion concentration, and K_2' is the $H_2PO_4^-$ dissociation constant:

$$K_2' = \frac{[H^+]M_{HPO_4^{2-}}}{M_{H_2PO_4^-}}. \quad (4)$$

Measurements of pH on the free hydrogen ion concentration scale[14–16] were obtained using a Ross combination pH electrode (Orion No. 810200) and a Corning model 150 pH meter. In titrations of 0.68 M $NaClO_4$ with strong acid, our electrode exhibited Nernstian behaviour. Measurements in perchlorate media required use of a 3 M NaCl filling solution to prevent $KClO_4$ precipitation at the electrode–liquid junction. Titrations of test solutions containing phosphate indicated that, in 0.68 M $NaClO_4$ at 25°C, $\log K_2' = -6.38$.

Aqueous–organic phase distribution measurements were obtained by measuring the net counts (counts above background) of Gd^{153} in each phase. Constant geometry was maintained for each sample. Gamma spectroscopy analyses were performed with a Bicron 2 × 2 inch well type NaI detector (2m WQ/2) and a Tracor Northern Multichannel analyser (TN-1710).

Phase distribution measurements, performed in the absence of phosphate, demonstrated a constant distribution coefficient, of the order 0.09, over the pH range between 4.0 and approximately 8.0. Using spectrophotometric procedures, in the absence of Gd^{153}, no measurable loss of phosphate to the organic phase was observed within the range of pH ($4.0 \leqslant pH \leqslant 7.0$) employed in our phosphate complexation determinations.

Two distinct procedures were used in our phase distribution measurements. (a) In the first case,

prior to the addition of radiotracer, 1 cm^3 of equimolar $NaH_2PO_4 \cdot H_2O$ (J. T. Baker) and Na_2HPO_4 (Fisher Scientific) in 0.68 M $NaClO_4$ was added to 100 cm^3 of 0.68 M $NaClO_4$ in the jacketed beaker, providing a total phosphate concentration equal to 2×10^{-4} M. TBP was added to the beaker and the mixture was subsequently acidified with 0.68 M $HClO_4$ and bubbled with N_2 for 30 min at pH $\simeq$ 4.0. The pH was adjusted to a desired initial value using 0.68 M NaOH and approximately 0.03 cm^3 of Gd^{153} (Isotopes Products Laboratories) was added to the organic–aqueous solution while stirring, providing a 1.3×10^{-10} M solution. Subsequent to bubbling vigorously with N_2 for 30 min, followed by a 30 min period for phase separation, 1 cm^3 samples were taken from each phase for gamma spectroscopy analysis. The solution was then slightly acidified, re-equilibrated while bubbling, and sampled after the 30 min allocated for phase separation. Repetition of this procedure resulted in a total of 19 titration points in two experiments at constant total PO_4 (2×10^{-4} M) within the pH range $4.0 \leqslant pH \leqslant 5.9$. (b) In a second procedure, Gd^{153} was added to the TBP–0.68 M $NaClO_4$ mixture prior to the addition of phosphate. Our phosphate titrant was equimolar $NaH_2PO_4 \cdot H_2O$ and Na_2HPO_4 in 0.68 M $NaClO_4$. Using the previous equilibration procedure (30 min of vigorous bubbling plus 30 min for phase separation) a series of distribution measurements were obtained between 0.0 M total PO_4 and approximately 4×10^{-3} M total PO_4. In two experiments using this procedure, we obtained a total of 22 titration points within the pH range $4.0 \leqslant pH \leqslant 5.4$.

RESULTS

The distribution of Gd^{153} between our tributyl phosphate organic phase and 0.68 M $NaClO_4$ can be described in terms of HPO_4^{2-} and $H_2PO_4^-$ complexation, using an expression identical in form to that used by Cantrell and Byrne[11] in descriptions of Ce^{3+}, Eu^{3+} and Yb^{3+} complexation by CO_3^{2-} and HCO_3^-:

$$D/D^0 = 1 + \beta'_1 M_{HPO_4^{2-}} + \beta'_2 M^2_{HPO_4^{2-}} + \beta'_H M_{H_2PO_4^-}, \quad (5)$$

where D^0 and D are distribution coefficients determined in the absence and presence of phosphate. D and D^0 are expressed as Gd^{153} (aqueous activity/g)/Gd^{153} (organic activity/g), and the parameters β'_1, β'_2 and β'_H are conditional stability constants appropriate to the 0.68 M aqueous medium at 25°C:

$$\beta'_1 = [GdHPO_4^+]/([Gd^{3+}]M_{HPO_4^{2-}})$$

$$\beta'_2 = [Gd(HPO_4)_2^-]/([Gd^{3+}]M^2_{HPO_4^{2-}})$$

$$\beta'_H = [GdH_2PO_4^{2+}]/([Gd^{3+}]M_{H_2PO_4^-}), \quad (6)$$

where $M_{HPO_4^{2-}} = [HPO_4^{2-}] + [NaHPO_4^-]$ and brackets denote the molar concentration of each indicated species.

In the first of our two experimental procedures, no distribution coefficients were obtained prior to the addition of phosphate. Since the total phosphate concentration in the first of our two procedures was only 2×10^{-4} M and β'_H is expected to be on the order of 10^2 or less, the term $\beta'_H M_{H_2PO_4^-}$ was neglected in our data analyses. In these experiments, conducted at constant total phosphate, our distribution data indicated that $[Gd^{3+}]/Gd_T$ was less than 0.60 for only one of 18 data points. Since $Gd(HPO_4)_2^-$ formation should be relatively small compared to $GdHPO_4^+$ under these conditions, our experiments at constant total phosphate were analysed by excluding our highest $M_{HPO_4^{2-}}$ data point and using the following truncated version of eq. (5):

$$D = D^0(1 + \beta'_1 M_{HPO_4^{2-}}). \quad (7)$$

Using eq. (7), our distribution data in the form (D, $M_{HPO_4^{2-}}$) were analysed through least-squares minimization of the residual sum of squares function $RSS = \Sigma_i(D(\text{observed})_i - D(\text{predicted})_i)^2$. The best fit parameters, D^0 and β'_1, obtained in our analyses are shown in Table 1.

Our experiments conducted using variable total phosphate concentrations produced data of the form (D/D^0, $M_{HPO_4^{2-}}$, $M_{H_2PO_4^-}$) where, in contrast to our first two experiments at constant $(PO_4^{3-})_T$, both $M_{HPO_4^{2-}}$ and $M_{H_2PO_4^-}$ varied over wide ranges. Consequently, these data were analysed directly using eq. (5) through minimization of the residual sum of squares function $RSS = \Sigma_i\{D/D^0(\text{observed})_i - D/D^0(\text{predicted})_i\}^2$. Our results obtained in these two experiments are shown in Table 2.

Table 1. Formation constants for $GdHPO_4^+$ at 25°C and 0.68 M ionic strength

D^0	β'_1 (±95% confidence interval)
$(9.28 \pm 0.05) \times 10^{-2}$	$(1.12 \pm 0.05) \times 10^4$
$(8.89 \pm 0.71) \times 10^{-2}$	$(1.22 \pm 0.40) \times 10^4$

Table 2. Formation constants of $GdH_2PO_4^{2+}$, $GdHPO_4^+$ and $Gd(HPO_4)_2^-$ at 25°C and 0.68 M ionic strength. Error estimates encompass the upper and lower 95% confidence limits for each estimated parameter

D^0	β'_H	β'_1	β'_2
8.73×10^{-2}	<57.3	$(8.3\pm1.8)\times10^3$	$(7.5\pm4.7)\times10^6$
8.65×10^{-2}	50.4 ± 15.7	$(7.8\pm1.1)\times10^3$	$(8.7\pm4.1)\times10^6$

DISCUSSION

Our phosphate complexation determinations were designed primarily to provide quantitative characterizations of $GdHPO_4^+$ formation. The average estimate for β'_1 shown in Table 2 is $\log\beta'_1 = 3.91$. We regard the estimates shown in Table 1 as upper bound values due to the possible presence of $Gd(HPO_4)_2^-$ at low concentrations. As such, our Table 1 results indicate that $\log\beta'_1 \leqslant 4.07$. Our Table 1 results can be examined for the influence of $Gd(HPO_4)_2^-$ formation in two ways. In the first case, rather than eliminating the single high data point (D, $M_{HPO_4^{2-}}$) from our analyses, we included this point in an analysis using the following equation:

$$D = D^0(1+\beta'_1 M_{HPO_4^{2-}} + \beta'_2 M^2_{HPO_4^{2-}}). \quad (8)$$

The best fit β'_1 result obtained in this analysis, $\log\beta'_1 = 3.93$, is in very good agreement with our Table 2 results. In a second type of analysis we examined our experiments conducted at constant total phosphate by using eq. (7) and successively eliminating our highest $M_{HPO_4^{2-}}$ data. With one point eliminated from each of our experiments, we obtained the average $\log\beta'_1 = 3.98$ for the two experiments. With two points eliminated from each data set we obtained an identical result, $\log\beta'_1 = 3.98$. Both of these estimates are in good agreement with our Table 2 results.

Our estimates for β'_H, shown in Table 2, are in fair agreement with previous work. Our results indicate that $\beta'_H \leqslant 66$. The single relatively well-defined estimate shown in Table 2, $\log\beta'_H = 1.70$, can be compared with the estimates for $AcH_2PO_4^{2+}$ and $LaH_2PO_4^{2+}$ obtained at 25°C and 0.5 M ionic strength:[2] $\log\beta'_H = 1.59$ and $\log\beta'_H = 1.61$. In addition, at 25°C and 0.5 M ionic strength, Borisov *et al.*[1] obtained the estimates, $\log\beta'_H(Ce^{3+}) = 1.52$, $\log\beta'_H(Pm^{3+}) = 1.69$, $\log\beta'_H(Am^{3+}) = 1.69$ and $\log\beta'_H(Y^{3+}) = 1.89$.

Our β'_2 results are unique in the sense that apparently no other $M(HPO_4)_2^-$ formation constant results have previously been obtained for the lanthanides or any other element. As a check on the internal consistency of our results, it should be noted that for the stepwise stability constants K'_1 and K'_2 (where $K'_1 = \beta'_1$ and $K'_2 = \beta'_2/\beta'_1$), our Table 2 results indicate that $K'_2/K'_1 = \beta'_2/(\beta'_1)^2 \simeq 0.12$. This observation is in good accord with results obtained for lanthanide oxalate complexation: $K'_2/K'_1 = 0.10\pm0.01$ for Ce^{3+}, Eu^{3+} and Yb^{3+} [11] at 25°C and 0.68 M ionic strength.

Activity coefficients appropriate to Gd^{3+} and HPO_4^{2-} at 0.68 M ionic strength and 25°C can be calculated[17] as approximately 0.049 and 0.157. Following our previous activity coefficient choices for $LnCO_3^+$ and $Ln(CO_3)_2^-$,[11] we have chosen $\gamma(LnHPO_4^+) = \gamma Ln(HPO_4)_2^- \simeq 0.5$ for both phosphate complexes. Consequently, our best estimates for β'_1 and β'_2 at zero ionic strength are

$$\log\beta^0_1 = 5.7 \quad \text{and} \quad \log\beta^0_2 = 9.5. \quad (9)$$

The only previous quantitative characterizations obtained for HPO_4^{2-} complexation of trivalent metals are apparently those obtained for $FeHPO_4^+$ [13] and $GaHPO_4^+$.[18] It is noteworthy, however, that the Pm^{3+} distribution data of Borisov *et al.*[1] suggested to these authors "the appearance of appreciable amounts of the complex ions, containing HPO_4^{2-} as addends". While the pH 2.0 and 3.0 data of Borisov *et al.*[1] provided the estimate $\log\beta'_H = 49\pm3$, their pH 4.0 distribution data cannot be interpreted solely in terms of complexation by $H_2PO_4^-$. An appropriate analytical equation for the pH = 4.0 data of Borisov *et al.*[1] can be expressed as

$$D/D^0 = 1+\beta'_H[H_2PO_4^-]+\beta'_1[HPO_4^{2-}]. \quad (10)$$

Consequently,

$$\beta'_H+\beta'_1\left(\frac{[HPO_4^{2-}]}{[H_2PO_4^-]}\right) = (D/D^0-1)[H_2PO_4^-]^{-1} = \Psi_1. \quad (11)$$

Using the Ψ_1 data compilation of Borisov *et al.*[1] for points such that $(PO_4)_T \geqslant 0.005$, plus the estimate $\beta'_H = 49$, we obtain the result $\Psi_1 \simeq 83.7$ and thereby, $\beta'_1 = 34.7$ ($[H_2PO_4^-]/[HPO_4^{2-}]$). Since $-\log K'_2 \simeq 6.5$ at 25°C and $\mu = 0.5$ M, β'_1 can then

be estimated from the data of Borisov *et al.*[1] as

$$\log \beta'_1 \simeq \log 34.7 + 2.5 = 4.05 \pm 0.22, \quad (12)$$

where the listed uncertainty is one half the range of five calculated ${}^1\Psi_1$ estimates. Since Pm^{3+} is a relatively close neighbour of Gd^{3+}, the results obtained in this calculation seem to be in good agreement with the present work.

Due to the similarities noted for trivalent lanthanide and actinide complexation, the results of Rao *et al.*[19] for $AmHPO_4^+$ at 0.5 M ionic strength and 30°C, are of potential interest for direct comparison with the results obtained in the present work. Unfortunately, a variety of features of the Rao *et al.*[19] data analyses renders their reported $AmHPO_4^+$ formation constant result of limited quantitative significance. In order to partition total phosphate among various forms, including HPO_4^{2-} and PO_4^{3-}, Rao *et al.*[19] made use of expressions such as

$$\frac{[PO_4^{3-}]a_H}{[HPO_4^{2-}]} = D_3\left(\frac{\gamma_2}{\gamma_3}\right), \quad (13)$$

where $[PO_4^{3-}]$ and $[HPO_4^{2-}]$ represent species concentrations, a_H is the hydrogen ion activity, D_3 is a dissociation constant at zero ionic strength, and γ_2 and γ_3 are activity coefficients appropriate at 0.50 M ionic strength. In calculating the PO_4^{3-} and HPO_4^{2-} activity coefficients (γ_3 and γ_2), as well as activity coefficients for other species, it is important to note that the parameters γ_2 and γ_3 shown in eq. (13) are individual ion activity coefficients which can be calculated using the Davies equation in the form

$$\log \gamma_i = -AZ_i^2\left(\frac{\sqrt{\mu}}{1+\sqrt{\mu}} - 0.2\mu\right), \quad (14)$$

where μ is the ionic strength, Z_i is ionic charge and $A \simeq 0.5$ at 25°C.[3] Using the Davies equation, γ_3 and γ_2 are calculated as 0.036 and 0.23. Employing a form of the Davies equation appropriate to the calculation of mean ionic activity coefficients,[20] Rao *et al.*[19] calculated $\gamma_3 = 0.34$ and $\gamma_2 = 0.49$. Other problems which have a strong bearing on the reported results of Rao *et al.*[19] include their use of an Am^{3+} hydrolysis constant substantially larger than other reported values,[21,5] and their performance of experiments under conditions ($7.0 \leqslant pH \leqslant 8.0$; $0.005 \leqslant (PO_4^{3-})_T \leqslant 0.03$) which are likely to produce mixed ligand species such as $AmHPO_4(OH)^0$. Due in part to these factors, we regard the apparent agreement between our results and the reported result of Rao *et al.*[19] as fortuitous.

Our lanthanide phosphate complexation results, in conjunction with the carbonate complexation results of Cantrell and Byrne,[11] indicate that environmental phosphate complexation of the trivalent lanthanides and actinides is of modest importance relative to carbonate complexation. Stability constants for lanthanide carbonate complexation are approximately two orders of magnitude greater than for phosphate complexation, and the CO_3^{2-}–HPO_4^{2-} concentration ratio in natural systems is generally between 10 and 1000. Even in the interstitial waters of marine sediments where HPO_4^{2-} concentrations may be as high as 1×10^{-4}, our results indicate that $[Gd^{3+}] \geqslant [GdHPO_4^+]$. In spite of the limited extent of phosphate complexation in most natural systems, our results indicate that phosphate is a poor buffer choice for hydrolysis constant determinations. In the experiments of Bilal and Kob,[4] $Na_xH_{3-x}PO_4$ constituted between 0.2 and 2% of the components used to provide a 1.0 M total ionic strength. This implies, for $pH > 7.5$, the HPO_4^{2-} concentrations in Bilal and Kob's[4] experiments are between 0.0007 and 0.007 M. Rare earth complexation by phosphate is substantial under these conditions and may contribute to substantial hydrolysis constant misestimates. Based on a variety of investigations for the reaction

$$Yb^{3+} + H_2O \overset{\beta_1^*}{\rightleftharpoons} YbOH^{2+} + H^+ \quad (15)$$

at 25°C and 1 M ionic strength, Baes and Mesmer[12] estimate $\log \beta_1^*(Yb^{3+}) = -8.42$. Through direct solubility measurements in the absence of buffers, Kragten and Decnop-Weever[22] obtained the result, $\log \beta_1^* = -7.7$. Bilal and Kob[4] produced the result, $\log \beta_1^*(Yb^{3+}) = -5.30$.

Acknowledgement—This work was supported in part by the National Science Foundation under Grant No. OCE 8400548.

REFERENCES

1. M. S. Borisov, A. A. Elesin, I. A. Lebedev, V. T. Filimonov and G. N. Yakovlev, *Radiokhimiya* 1966, **8**, 1, 42.
2. V. K. Rao, C. J. Shahani and C. L. Rao, *Radiochim. Acta* 1970, **14**, 31.
3. W. Stumm and J. J. Morgan, *Aquatic Chemistry*. Wiley, New York (1981).
4. B. A. Bilal and V. Kob, *J. Inorg. Nucl. Chem.* 1981, **43**, 12, 3393.
5. R. Lundqvist, *Acta Chem. Scand.* 1982, **A36**, 741.
6. A. E. Martell and R. M. Smith, *Critical Stability Constants*, Vol. 4: Inorganic Complexes. Plenum Press, New York (1976).
7. R. H. Byrne and D. R. Kester, *Mar. Chem.* 1975, **4**, 275.
8. A. E. Martell and R. M. Smith, *Critical Stability*

Constants, Vol. 3: Other Organic Ligands. Plenum Press, New York (1977).
9. R. H. Byrne, L. R. Kump and K. J. Cantrell, *Mar. Chem.* 1988, **25**, 163.
10. A. E. Martell and R. M. Smith, *Critical Stability Constants*, Vol. 5: First Supplement. Plenum Press, New York (1982).
11. K. J. Cantrell and R. H. Byrne, *Geochim. Cosmochim. Acta* 1987, **49**, 1837.
12. C. F. Baes and R. E. Mesmer, *The Hydrolysis of Cations*. Wiley-Intersciences, New York (1981).
13. H. Galal-Gorchev and W. Stumm, *J. Inorg. Nucl. Chem.* 1963, **25**, 567.
14. W. A. E. McBryde, *Analyst* 1969, **94**, 337.
15. W. A. E. McBryde, *Analyst* 1971, **96**, 739.
16. R. H. Byrne and D. R. Kester, *J. Sol. Chem.* 1978, **7**, 373.
17. F. J. Millero and D. R. Schreiber, *Am. J. Sci.* 1982, **282**, 1508.
18. Y. I. Mikhailyuk and V. I. Gordienko, *Russ. J. Inorg. Chem.* 1975, **20**, 1617.
19. V. K. Rao, G. R. Mahajan and P. R. Natarajan, *Radiochim. Acta* 1986, **40**, 145.
20. G. N. Lewis and M. Randall, *Thermodynamics*. McGraw-Hill, New York (1961).
21. M. S. Caceci and G. R. Choppin, *Radiochim. Acta* 1983, **33**, 101.
22. J. Kragten and L. G. Decnop-Weever, *Talanta* 1982, **29**, 219.

Polyhedron Vol. 8, No. 10, pp. 1321–1328, 1989
Printed in Great Britain

0277–5387/89 $3.00+.00
© 1989 Pergamon Press plc

THREE COORDINATED COPPER(I) COMPLEXES OF CHELATING LIGANDS DERIVED FROM 2,6-DIACETYLPYRIDINE AND PHENYLALANINE OR TYROSINE

W. L. KWIK* and ALICE W. N. TAY

Department of Chemistry, National University of Singapore, Lower Kent Ridge Road, Singapore 0511

(*Received* 7 *June* 1988; *accepted after revision* 18 *January* 1989)

Abstract—Copper(I) complexes of Schiff-base ligands, L_1 and L_2, derived from condensation of 2,6-diacetylpyridine with phenylalanine methyl ester or tyrosine ethyl ester have been prepared. On the basis of various spectroscopic data, it is proposed that these complexes in the solid-state have mononuclear structures in which the trimethine group acts as tridentate while retaining its planarity. In methanol, spectroscopic properties suggest at least partial dissociation of one-side arm leading to a two-coordinate copper(I) which then interacts with a free imino nitrogen of a second molecule of the copper(I) complex. This results in a more effective overlap of the copper(I) orbital with p_{π^*} of the ligand and hence an increase in absorption intensities.

Interesting examples of copper(I) Schiff-base complexes (Scheme 1) displaying reactivities towards dioxygen have recently been reported.[1–6] The Schiff-base ligands involved (Scheme 1) are those obtained from condensation of 2,6-diacetylpyridine and various amines, and span both the pentadentate types[1–5] (L^1, L^2) as well as those with only three nitrogen donors[6] (L^3, L^4, L^5). It has been noted[6] that some of the chemical behaviours of the five nitrogen and the three nitrogen Schiff bases are distinctly different.

We have previously reported[7] the synthesis and spectral properties of the copper(II) and zinc(II) complexes of the Schiff bases (Scheme 1) derived from condensation of 2,6-diacetylpyridine and phenylalanine methyl ester (L_1), or tyrosine ethyl ester (L_2) containing three nitrogen donor atoms as well as ester carboxylate groups in the side chain. In the following, the isolation and various chemical properties of the corresponding copper(I) complexes [**1** for $CuL_1(BF_4)$ and **2** for $CuL_2(BF_4)$] are presented.

* Author to whom correspondence should be addressed.

EXPERIMENTAL

Synthesis

All solvents were deoxygenated and stored under nitrogen over molecular sieves (4 Å). Methanol, acetonitrile and dichloromethane were treated according to published procedures prior to use. Spectrochemical grade dimethyl sulphoxide (Aldrich, Gold Label) was used for electronic, electrochemical and conductivity measurements. Deuterated dimethyl sulphoxide (Aldrich, Gold Label) used for NMR spectral studies was stored under nitrogen in a dry-box.

2,6-Diacetylpyridine and 2-(2-aminoethyl)pyridine (Aldrich Chemical Company) were used as received. Phenylalanine methyl ester hydrochloride, tyrosine ethyl ester hydrochloride (Sigma Chemical Company) were treated to remove the hydrochloride by the method described by Casella *et al.*[5] Tetra(acetonitrile) copper(I) tetrafluoroborate was prepared by the method of Hemmerich and Sigwart. Electrochemical grade tetraethylammonium perchlorate (Eastman Chemicals) was used without further purification.

The ligand solution was prepared by refluxing 2,6-diacetylpyridine (2 mmol) and the base (4 mmol) (phenylalanine methyl ester/tyrosine ethyl ester) under nitrogen in dry, deoxygenated MeOH (100 cm^3) for about 20 h, whereupon an intense yellow colour developed.

Freshly prepared $[Cu(CH_3CN)_4]BF_4$ (2 mmol) was dissolved in deoxygenated CH_3CN (50 cm^3) and the solution filtered to remove trace amounts of blue copper(II) salt present. The colourless filtrate was warmed before being added to the hot ligand solution. The ensuing blood-red solution was then reduced to near dryness at 85°C by rotary evaporation, to yield a hygroscopic, dark red solid. This was recrystallized twice from deoxygenated MeOH in a dry-box. The final, dark red solid was dried *in vacuo* at 80°C for 6 h prior to elemental analysis.

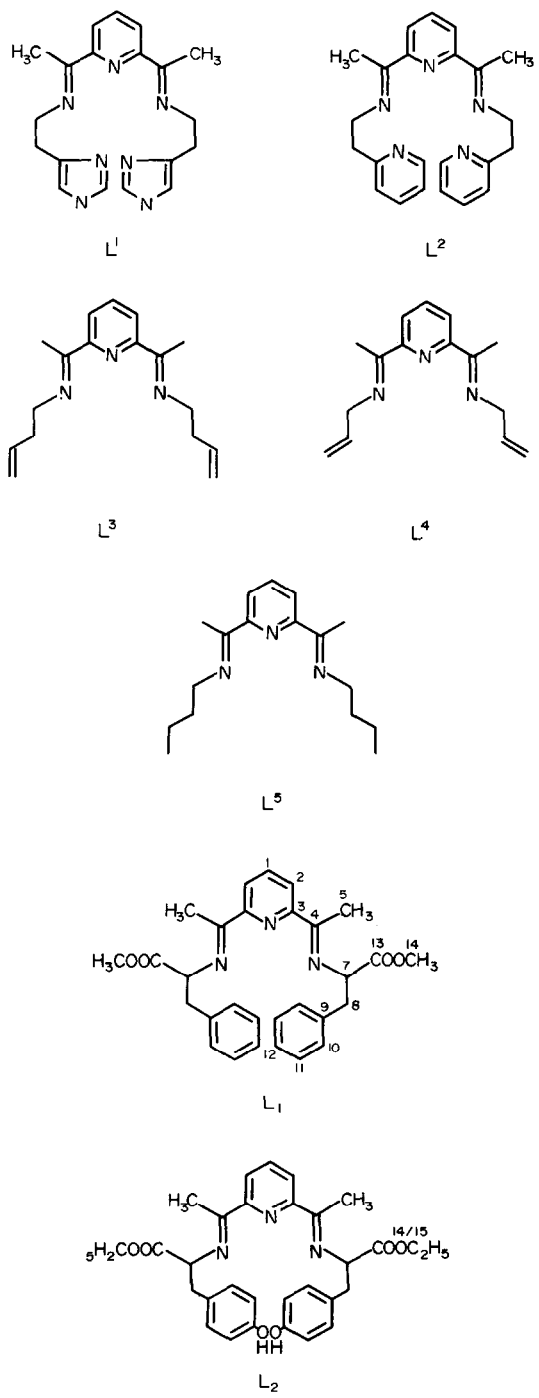

Scheme 1.

Compound **1**. Found: C, 53.4; H, 4.9; N, 6.4; Cu, 9.6. Calc. for $C_{29}H_{33}N_3O_5CuBF_4$: C, 53.2; H, 5.0; N, 6.4; Cu, 9.6%. IR data (KBr, cm^{-1}): 1636 ($\nu_{C=N}$); 1740 ($\nu_{C=O}$); 1267 (ν_{C-OR}); 1636 ($\nu_{COO(as)}$); 1385 ($\nu_{COO(s)}$). Λ_M = 76 (MeOH); 37 (DMSO); 149 (CH_3CN) S cm^2 mol^{-1}.

Compound **2**. Found: C, 50.9; H, 5.0; N, 6.1; Cu. 8.6. Calc. for $C_{31}H_{39}N_3O_8CuBF_4$: C, 50.8; H, 5.3; N, 5.7; Cu, 8.7%. IR data (KBr, cm^{-1}): 1615 ($\nu_{C=N}$); 1734 ($\nu_{C=O}$); 1268 (ν_{C-OR}); 1615 ($\nu_{COO(as)}$); 1373 ($\nu_{COO(s)}$). Λ_M = 87 (MeOH); 36 (DMSO); 151 (CH_3CN) S cm^2 mol^{-1}.

Measurements

IR spectra in the 4000–400 cm^{-1} region were recorded on a Perkin–Elmer Model 1710 Fourier Transform IR spectrometer. Spectra extending into the far-IR region of 200 cm^{-1} were recorded on a Perkin–Elmer Model 567 spectrometer calibrated with polystyrene film. CsI and KBr pellets were employed throughout. Electronic spectra were recorded on a Perkin–Elmer Lambda 9 UV–vis–near-IR spectrophotometer. Conductivities of 10^{-3} M solutions of the complexes were measured at 30°C using a CM-115 conductivity meter (Kyoto Electronics). The ^1H and ^{13}C NMR spectra were obtained for samples in DMSO-d_6 solutions at 90 MHz using a Jeol Fx90 Q FT NMR spectrometer. Cyclic voltammograms were obtained in DMSO solutions at room temperature under a constant flow of N_2, using a Pine Instrument RDE 4 potentiostat. A three-electrode system was employed, with a glassy carbon ring-disc electrode (disc radius = 0.382 cm) serving as the working electrode, a platinum foil as the counter electrode, and a saturated calomel electrode (SCE) as the reference electrode. All solutions were 0.1 mol dm^{-3} in tetraethylammonium perchlorate and 10^{-3} mol dm^{-3} in the complex.

RESULTS AND DISCUSSION

IR spectral study

The IR spectra of **1** and **2** are similar in important aspects to those of the free ligands, though there

Table 1. Chemical shifts (ppm) of ^{1}H NMR signals

Compound/complex	Protons H(1)	H(2)	H(7)	H(10)	H(11)	H(12)	H(14)	H(8)
2,6-diacetylpyridine	8.16	2.73	—	—	—	—	—	—
Phenylalanine methyl ester		—	3.58	7.21	7.21	7.21	3.58	3.58
Tyrosine ethyl ester		—	3.40	6.65	6.95	—	4.00	2.68 2.74
L_1	8.15	2.73	3.70	7.25	7.25	7.25	3.60	3.10
L_2	8.15	2.71	3.50	6.70	7.00	—	4.00	3.00
1	8.14	2.75	4.20	7.30	7.30	7.30	3.60	3.15
2	8.14	2.72	4.20	6.74	7.04	—	4.10	3.00

are distinct shifts of the characteristic bands. Both display strong IR absorptions at: (i) 1740, 1286 and 1240 cm^{-1} of the ester carbonyl (COOR),[8-10] (ii) 1636 cm^{-1} for **1** and 1625 cm^{-1} for **2** of the imino $\nu_{C=N}$[11] and (iii) 1050 cm^{-1} for the BF_4^- ion. As there is no significant difference in the IR absorption characteristics of the two copper(I) complexes, it is tentatively concluded that there is no significant structural difference between the two complexes. The presence of only one distinct absorption band due to the imino stretching ($\nu_{C=N}$) in the 1600–1660 cm^{-1} region, suggests that both complexes assume a structure in which the two imino (C=N) groups are equivalent. It appears that a dinuclear structure in which the two imino (C=N) nitrogen atoms are bonded to different copper centres can be excluded for these two copper(I) complexes.[6] It would seem reasonable to assume that the trimethine group functions as a tridentate chelating group to a single copper(I) ion, thus retaining planarity upon complexation. Moreover, a comparison of the IR spectra of these complexes shows that they closely resemble those of other metal complexes where trimethine group planarity has been proven by X-ray analysis.[5] These considerations lead us to propose that in **1** and **2**, the copper(I) ions are mononuclear and three-coordinate. This is consistent with the presence of uncoordinated ester groups as suggested from the IR absorption characteristics.[8-10] The most probable disposition of the donor atoms in L_1 and L_2 is such that the metal ion has a T-shaped geometry. Such a geometry, though unusual, has been observed in the ligand systems,[6] bis[2-(3′,5′-dimethylpyrazol-1-yl)ethyl]ether (Y = O) and the corresponding sulphide (Y = S) and amine (Y = NH), see Structure 1.

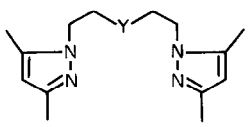

Structure 1.

^{1}H *NMR spectral study*

Both the copper(I) complexes display broad ^{1}H NMR signals at 25°C, most likely due to the presence of trace amounts of copper(II) ions. As the temperature is raised to 100 and 150°C, the spectra became better resolved.

A comparison of the spectra of the free ligands versus those of the complexes and those reported by Nelson,[6] reveals that the effect of complexation on the chemical shift is most significant for H(7) yielding a change in δ_H values of *ca* 0.5–0.7 ppm (Table 1). This is consistent with the proximity of H(7) to the imino nitrogen and similar changes in δ_H values have been observed for the zinc(II) analogues.[7,12] It is also of interest to note that the protons of the carboxylate group of the amino acid components are only marginally affected by condensation and complexation. This observation further points to the absence of any interaction between the carboxylate oxygen and the copper(I) ion in these complexes, in contrast to the case of the analogous zinc(II) complexes.[7,12]

^{13}C *NMR spectral study*

The ^{13}C NMR spectra of **1** and **2**, as well as those of the ligands L_1 and L_2, are generally of well-resolved peaks (Table 2). Assignments were made with the aid of the "off-resonance" technique, whereby the number of protons bound to each unique carbon atom could be determined without loss of the nuclear overhauser enhancement.[13,14] Reference was also made to values of ^{13}C chemical shifts reported for similar complexes.[6]

Comparison of the chemical shifts of L_1 and L_2 and those of the corresponding copper(I) complexes showed that the largest change is observed for the imino carbon, C(4). The shift of C(4) from 198.5 to 166.8–175 ppm upon condensation and complexation is not only supported by reported values

Table 2. Chemical shifts (ppm) of ^{13}C NMR signals

Compound/complex	C(1)	C(2)	C(3)	C(4)	C(7)	C(8)	C(9)	C(10)	C(11)	C(12)	C(13)	C(14)	C(15)
2,6-diacetylpyridine	138.8	124.4	152.1	198.5	—								
Phenylalanine methyl ester					41.0	55.9	137.7	128.6	129.5	126.8	175.5	51.7	
Tyrosine ethyl ester					40.0	55.8	127.5	115.0	130.0	155.6	174.9	59.8	14.0
1	138.5	126.6	152.2	170.0	54.6	55.5	138.5	128.1	128.8	127.9	170	52.1	
2	139.1	124.0	152.2	170.4	53.9	55.1	128.0	115.5	130.3	156	170	65.1	14.0

but also consistent with the lower electronegativity of nitrogen in comparison to that of oxygen.

The proximity of C(7) to the imino nitrogen is expected to induce significant changes in the chemical shifts upon condensation and complexation. Indeed, changes of 13.6–13.9 ppm have been observed for both copper(I) complexes. The larger changes of these three nitrogen systems, in comparison to the five nitrogen complexes (Table 2), would seem to indicate stronger imino nitrogen–metal interactions in the former.

Cyclic voltammetric studies

1 and **2** display a small cathodic wave at 0–40 mV and a larger wave at −450 to −500 mV, but there is only one anodic wave at +300 to +460 mV. The range of values into which these waves fall indicate that they are most likely attributable to the electrode processes of $Cu^{2+} \rightarrow Cu^{+}$ and $Cu^{+} \rightarrow Cu^{0}$ for the cathodic wave, and of $Cu^{+} \rightarrow Cu^{2+}$ for the anodic wave. Moreover, the larger ΔE_p for the first process means that the electron transfer is irreversible in each case.

That the $Cu^{2+} \rightarrow Cu^{+}$ process was detected as a small but distinct wave is not unexpected in view of the ease with which **1** and **2** undergo oxidation. That the anodic process of $Cu^{0} \rightarrow Cu^{+}$ is not detected is probably a manifestation of a coupled chemical reaction which occurs after the electrode reduction steps in the forward cathodic scan.

Electronic spectral study: nature of the complexes in solution

At room temperature, as well as at 80 K, solution and solid-state (KBr/Nujol mull) electronic spectra measured over the range 30,000–10,000 cm^{-1} (Table 3) are found to be solvent dependent. Whereas absorption maxima at ~ 35,700 cm^{-1}, attributable to the ligands $\pi \rightarrow \pi^*$ transition, are observed in MeOH, DMSO and CH_3CN and intense well-defined bands at ~ 22,730 and ~ 22,220 cm^{-1} for **1** and **2**, respectively (Fig. 1), are displayed only in MeOH and DMSO. In CH_3CN, a shoulder of much lower intensity appeared at 25,000 cm^{-1}. The high molar absorptivities of these lower energy bands in MeOH and DMSO (Table 3) clearly indicate that these are due to the charge-transfer transitions (CT) from filled *d*-orbitals of the copper(I) to the vacant π^* orbital of the trimethine group.[11] These bands are further characterized by a steady increase in intensity over a time period of ~ 30 and 60 min in carefully deoxygenated MeOH and DMSO, respectively.

Similar increases in absorbances with time were observed over a five-fold concentration range, 2×10^{-4}–1×10^{-3} M [Fig. 2(a)]. The apparent "ε"s

Table 3. Electronic spectral absorptions

Solvents	$10^{-3}/cm^{-1}$ (ε/$dm^3\ mol^{-1}\ cm^{-1}$) **1**	**2**
KBr pellet	20.8, 35.7	21.0, 35.7
Nujol mull	20.8	21.0
MeOH	22.2(2500), 35.7(16,000)	22.7(2500), 35.7(1500)
5:1 MeOH–ETG[a] (298 K)	22.2(2500), 35.7(16,000)	22.7(2500), 35.7(15,000)
5:1 MeOH–ETG[a] (80 K)	22.2(3800), 33.3(24,000)	22.7(3900), 35.7(23,000)
DMSO	22.7(3000), 35.7(15,000)	22.7(3000), 35.7(15,000)
CH_3CN	25.6(sh), 35.7(16,000)	25.6(sh), 35.7(15,000)

[a] ETG = ethyleneglycol.

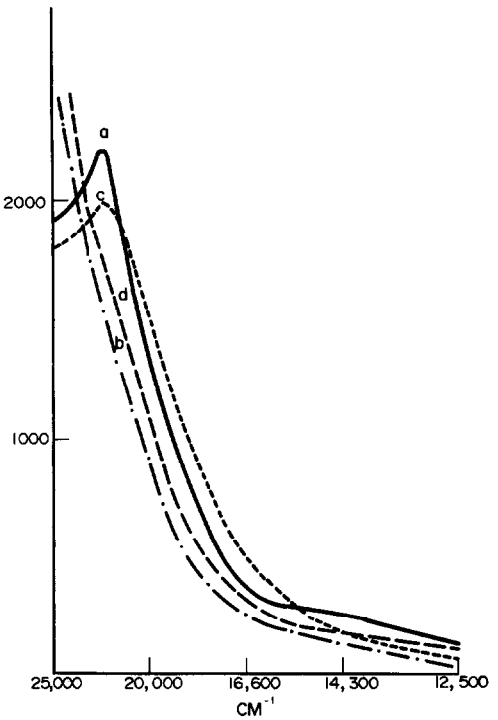

Fig. 1. Electronic spectra of **1** (a ——) in deoxygenated DMSO; (b — · —) solution a after oxygenation for *ca* 1 h; (c -----) solution b after degassing—gentle heating under N_2 for *ca* 1 h; (d – – – –) solution c after oxygenation for *ca* 30 min.

calculated for these absorption maxima are seen to be fairly constant, within some inherent experimental error, due to oxidation/decomposition of the complexes in solution.

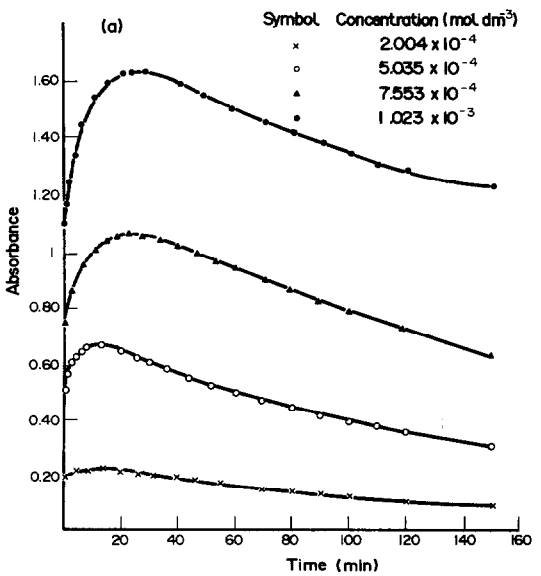

Fig. 2(a). Plot of absorbance of **1** vs *t* (min) at different concentrations in MeOH.

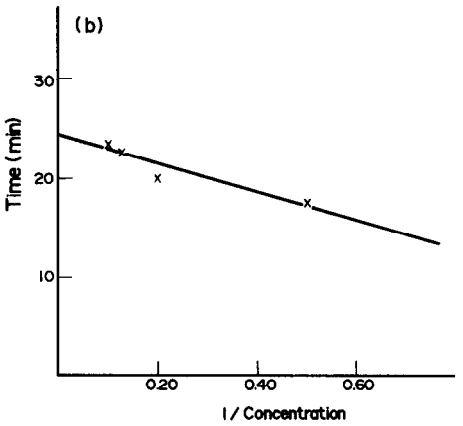

Fig. 2(b). Plot of $1/C$ vs *t* (min).

The plot of $1/C$ (with C being the concentration of the respective complex) vs *t* (the time taken to reach maximum absorbance at each concentration) [Fig. 2(b)], was found to be linear for both complexes in MeOH over the concentration range, 2×10^{-4}–1×10^{-3} M. This is an interesting observation, although no further conclusions could be drawn at this stage because of the complexities of possible decompositions due to the ease of oxidation of these complexes in solution. Moreover, the remarkably similar behaviour of **1** and **2** suggests that the process does not involve the phenolic OH in the tyrosine component to any significant extent.

In the following, an attempt will be made to account for: (i) the markedly different absorption spectra at 25,000–20,000 cm^{-1} in CH_3CN and in MeOH/DMSO; (ii) the remarkable increases in intensities of the absorption maxima at 22,700/22,200 cm^{-1} for **1** and **2**, respectively, in MeOH, as well as in DMSO.

Proposed mechanism for (i)

It must be mentioned that such markedly different absorption behaviour in CH_3CN and MeOH–DMSO are not unique for **1** and **2**. Urbach and coworkers[15,16] reported similar solvent dependence of electronic absorptions for a mononuclear copper(I) complex with the ligand shown in Structure 2.

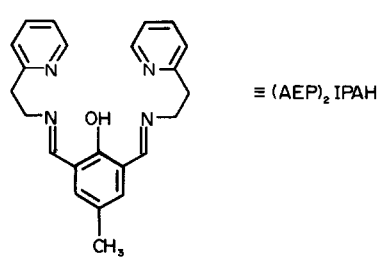

Structure 2.

Thus the copper(I) complex of $(AEP)_2IPAH$ displays only one band at 22,600 cm^{-1} in MeOH and DMSO, but two bands at 22,400 and 28,300 cm^{-1} in MeCN, with the first band being reduced in intensity relative to that in MeOH. This behaviour was interpreted as a competition between the ligand and acetonitrile for coordination of the copper(I) according to the equilibrium:

$$[Cu(AEP)_2IPAH]^+ + CH_3CN\,(excess) \longrightarrow (AEP)_2IPAH + [Cu(CH_3CN)_n]^+.$$

This equilibrium is reasonable in light of the known affinity of copper(I) for acetonitrile.[16] It was also found in this case, that addition of excess $[Cu(CH_3CN)_4]BF_4$ to an acetonitrile solution of the $[Cu(AEP)_2IPAH]^+$ produces a dramatic increase in intensity for the 22,400 cm^{-1} band which was associated with the complex, while the 28,300 cm^{-1} band, due to the free ligand, disappeared.

For **1** and **2** it was found that addition of excess $[Cu(CH_3CN)_4]BF_4$ to a methanolic solution containing 10% CH_3CN brought about a significant increase in absorbances at 22,200–22,700 cm^{-1}. Such behaviour suggests the relatively weaker binding of L_1 and L_2 as compared to $(AEP)_2IPAH$. This is not surprising in view of the binding of copper(I) by two more pyridine rings in the latter.[16]

Proposed mechanism for (ii)

The electronic absorption spectra of the copper(I) complexes of L^3 and similar Schiff-base bands reported by Nelson *et al.*,[6] comprise absorptions at 22,200–22,700 cm^{-1} appearing only as a shoulder of relatively weak intensity. On the other hand, the five-coordinated copper(I) complexes of Schiff-base ligands L^1 and L^2 due to Wilson *et al.*,[4] display well-defined absorptions similar to those of **1** and **2**.

The weaker CT band as observed for complexes of L^4 and L^5, can be rationalized by consideration of the coordination geometry of the copper(I) complexes due to the disposition of donor atoms in these complexes. It was found that the metal ion would in fact have a T-shaped geometry. Such an unusual geometry has been observed in a few copper(I) complexes[17–19] with ligands such as bis[2-(3′,4′-dimethylpyrazol-1-yl)ethyl]ether (pze) (Structure 3).

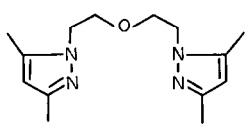

Structure 3.

The X-ray structure of the Cu^I–pze complex shows that the copper(I) is essentially two-coordinate with a weak interaction by the oxygen atom. Thus it is expected that the T-shaped disposition in copper(I) complexes of L^4 and L^5 ensues in poor overlap of the pyridine *p*-orbital with the filled *d*-orbital of copper(I). This, in turn, leads to CT bands of relatively lower intensity. The stronger CT band in the five-coordinated copper(I) complexes reported by Wilson *et al.*[4] is probably due to stronger binding brought about by the two imidazyl/pyridyl nitrogen donors (in addition to the DAP pyridine nitrogen) in these ligands. In fact as shown recently,[4] the trimethine group assumes a highly distorted, non-T-shaped disposition, the bond angle between the two imino to copper(I) bonds being 148° and significantly different from the 180° expected of the T-shaped geometry. Such distortion from T-shaped geometry in turn allows for better overlap between the pyridyl (trimethine) nitrogen *p*-orbital and the filled *d*-orbital of copper(I) and thus the observed intense CT band.

A consideration of electronic spectral behaviour in relation to the structures of the two series of copper(I) complexes mentioned above, leads to a possible explanation of the observed increase in intensities of the CT bands for **1** and **2** with time in MeOH–DMSO. It appears that such an increase must be related to a change in geometry around copper(I), so that more efficient overlap of the respective orbitals of the ligand L_1/L_2 and of copper(I) can be brought about. Taking all experimental data available into consideration, the equilibrium indicated in Scheme 2 appears most favourable.

In the above equilibrium it is proposed that one of the imino nitrogen swings open leaving a two-coordinated copper(I); the driving force for step (i) probably arises from the strong hydrogen bonding ability, particularly of MeOH, with which the free imino nitrogen can form hydrogen bonds, as first suggested by Urbach.[12] Step (ii) is proposed on the basis that the rate of increase in absorbance is inversely proportional to the concentration of the complex. It would seem reasonable that at least two copper(I) centres must be involved. These copper(I) centres may attain four-coordination through bonding with a MeOH molecule; alternatively it may remain three-coordinate but with more efficient overlap of the filled *d*-orbital on copper(I) with pyridyl nitrogen *p*-orbital. Furthermore, as step (ii) is statistically unfavourable, there is a slow increase over a time period of 30–60 min. It should

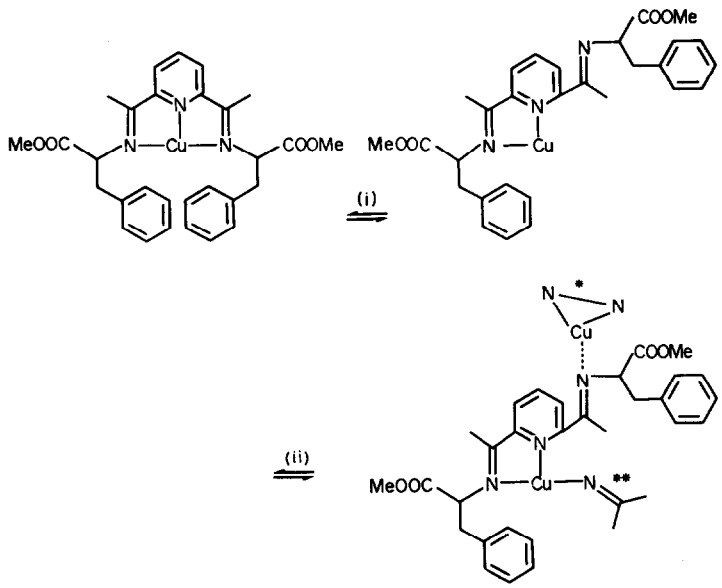

Scheme 2. * N | N only the part of the trimethine group that binds to the two-coordinate copper(I) is shown: ** N< only the bound N donor of the trimethine group is shown.

be emphasized that these time periods are only approximate upper limits, as the processes suggested in steps (i)/(ii) are competing against decomposition of the complexes produced by slow oxidation. Finally, the involvement of hydrogen bonding in step (i) is consistent with the order of observed increases in absorbances at 22,700–22,200 cm^{-1} for MeOH > DMSO > acetone; in the last case the increase lasted for only 7 min.

The proposed equilibrium is also consistent with the observed ^{1}H and ^{13}C NMR spectra described above. Thus the peak due to the methyl protons, C(5), was found to be extremely broadened, probably the result of an average of the two sets of imino methyl protons. Likewise, the imino C(5) appears as a broad peak in the ^{13}C NMR spectra of **1** and **2**. The fact that no separate signals were observed for the protons and carbons associated with the two imino nitrogens could be due to rapid exchange of the bound and unbound imino groups.

In addition, such a change in coordination geometry, brought about by opening up of one of the side arms in solution, is also consistent with the observed differences in spectra of samples dispersed in KBr/Nujol mull and of methanol/DMSO solutions. In KBr/Nujol mull, the absorption at 22,700 cm^{-1} appears only as a broad shoulder (Table 3). In glassed solution the bands at 22,200–22,700 cm^{-1} become better defined. This is in no way contradictory to the proposed equilibrium, as some of the copper(I) is already in the geometry type resulting from step (ii) of the above equilibrium in such a glassed solution.

Finally solvation by MeOH/DMSO to give rise to four-/five-coordinated copper(I), as well as participation of the phenyl ring of the tyrosine/phenylalanine residue in L_1/L_2 have been considered. However, mechanisms involving these processes could not fully account for the observed experimental findings.

Reactions with dioxygen

Both **1** and **2** have reasonable air stabilities over periods of days in the solid-state. The solutions in the presence of air, however, develop green or green–brown colours at rates dependent on the nature of the complex and of the solvent.

As the intensely red coloration was retained in DMSO over a significantly longer time than in MeOH, this was selected to be the solvent used for studying the oxygenation. Upon exposure to dioxygen (1 atm), the red coloration of a solution of **1** and **2** in deoxygenated dry DMSO at room temperature disappears, yielding a green–yellow solution. The change is complete in about 1.5 h and can be partially reversed by gentle heating of the oxygenated solution under a stream of dry nitrogen (Fig. 1). The degree of reversibility of the reaction determined spectrophotometrically is about 70%

and the oxy–deoxy cycle process can be repeated 2–3 times until the solution became brown and did not show any further colour change upon further exposure to dioxygen.

The change of colour of a methanolic solution of **1** or **2** upon exosure to dioxygen was found to be completely irreversible. A similar finding has previously been reported by Ibers and co-workers.[5]

Reactions with carbon monoxide

In view of the similarity in structure of the ligands L_1 and L_2 to those reported by Nelson *et al.*,[6] **1** and **2** are expected to interact with CO. Upon introduction of 1 atm of CO to a degassed DMSO solution of **1** or **2**, the solution changed from a red to yellow–brown colour. The spectral changes were found to be only partially reversible. Similar spectral changes have been reported by Nelson *et al.*[6] in a study of the carbonylation reaction of the copper(I) complex of the Schiff-base ligands, L^3–L^5. However, further investigation of the carbonylation of **1** and **2** was rendered difficult due to the strong IR absorption of DMSO in the region of interest.

REFERENCES

1. M. G. Simmons and L. J. Wilson, *J. Chem. Soc., Chem. Commun.* 1978, 634.
2. M. G. Simmons, C. L. Merrill, L. J. Wilson, L. A. Bottomley and K. M. Kadish, *J. Chem. Soc., Dalton Trans.* 1980, 1827.
3. C. L. Merrill, L. J. Wilson, T. J. Thamann, T. N. Loehr, N. S. Ferres and W. H. Woodruff, *J. Chem. Soc., Dalton Trans.* 1984, 2207.
4. J. A. Goodwin, D. M. Stanbury, L. A. Wilson, C. W. Eigenbrot and W. R. Scheidt, *J. Am. Chem. Soc.* 1987, **109**, 279.
5. L. Casella, M. E. Silver and J. A. Ibers, *Inorg. Chem.* 1984, **23**, 1409.
6. S. M. Nelson, A. Lavery and M. G. B. Drew, *J. Chem. Soc., Dalton Trans.* 1986, 911.
7. W. L. Kwik, K. P. Ang and A. W. N. Tay, *Polyhedron* 1988, **7**, 695.
8. A. D. Cross and R. A. Jones, *An Introduction to Practical Infrared Spectroscopy*. Butterworth, London (1969).
9. L. J. Bellamy, *The Infrared Spectra of Complex Molecules*. Chapman and Hall, London (1975).
10. K. Nakamoto, *Infrared and Raman Spectra of Inorganic and Coordination Compounds*. John Wiley, New York (1987).
11. L. Casella and M. Gullotti, *Inorg. Chem.* 1981, **20**, 1306.
12. R. H. Bible, *Interpretation of NMR Spectra*. Plenum Press, New York (1966).
13. D. H. Busch, D. J. Olzanski, J. C. Stevens, W. P. Schammel, N. Kojima, N. Herron, L. Zimmer, K. A. Holter and J. Mocak, *J. Am. Chem. Soc.* 1981, **103**, 1472.
14. R. J. Abraham and P. Loftus, *Proton and C-13 NMR Spectroscopy*. Heyden, London (1978).
15. J. J. Grzybowski and F. L. Urbach, *Inorg. Chem.* 1980, **19**, 2604.
16. S. E. Manahan and R. T. Iwamoto, *J. Electroanal. Chem.* 1967, **14**, 213.
17. T. N. Sorrell and M. R. Malachowski, *Inorg. Chem.* 1983, **22**, 1883.
18. T. N. Sorrell, C. Shen, C. J. O. O'Connor and C. J. O'Connor, *Inorg. Chem.* 1987, **26**, 1755.
19. M. J. Schilstra, P. J. Birker, G. C. Verschoor and J. Reedijk, *Inorg. Chem.* 1987, **21**, 2637.

Polyhedron Vol. 8, No. 10, pp. 1329–1334, 1989
Printed in Great Britain

0277–5387/89 $3.00+.00
© 1989 Pergamon Press plc

SYNTHESIS, SPECTROSCOPIC AND MAGNETIC PROPERTIES OF NICKEL(II) WITH N-PROTECTED AMINO ACIDS: CRYSTAL AND MOLECULAR STRUCTURE OF BIS(N-ACETYLGLYCINATO)TETRAAQUONICKEL(II)

S. S. SANDHU,* M. S. HUNDAL and GEETA SOOD

Department of Chemistry, Guru Nanak Dev University, Amritsar, India

and

S. S. DHILLON

Department of Chemistry, Khalsa College, Amritsar, India

(*Received* 5 *June* 1988; *accepted after revision* 18 *January* 1989)

Abstract—Nickel(II) complexes of the general formula $NiL_2 \cdot nH_2O$ have been prepared with various N-protected amino acids and characterized by thermogravimetric, magnetic susceptibility, IR and UV spectroscopy. The crystal structure of bis(N-acetylglycinato) tetraaquonickel(II) has been determined. The coordination around nickel is octahedral with two acetylglycine ligands *trans* to each other. Acetylglycine coordinates with nickel through a single oxygen of the carboxylate group, and the remaining four coordination sites are occupied by four water molecules. The structure is held together by strong intermolecular hydrogen bonding. Spectroscopic studies indicate that all complexes are octahedral in structure.

Simple amino acids, having no side chains, coordinate to metal ions through the amino nitrogen and carboxyl oxygen. This results in the formation of five- or six-membered chelate rings with the metal ions in α- and β-amino acids, respectively.[1] If the amino nitrogen is substituted by an acetyl or benzoyl group, the affinity of the amino nitrogen for the metal ion decreases. In such cases, the coordination takes place through the carboxylate group only. The carboxylate group can act as a symmetrical or unsymmetrical bridging bidentate,[2] symmetric or unsymmetric chelating bidentate[2a,3,4] or non-chelating unidentate ligand[5] towards the metal ion. Marcotrigiano and co-workers have prepared nickel (II) complexes with †N-Ac—Gly,[6] N-Bz—Gly,[6] N-Ac—DL-Val,[7] N-Ac—DL-Trp,[8] N-Ac—DL-Ala[9] and N-Ac—DL-Leu[10] and characterized them by magnetic and spectral studies. They have suggested that in the complexes of N-protected amino acids with nickel(II), the coordination occurs through the carboxyl group only. This fact still awaits the confirmation by crystal structure analysis of any of the nickel(II) complexes with N-protected amino acids. The crystal structure of the title compound has been undertaken for this reason. Other related complexes have been synthesized and characterized by electronic, IR and magnetic susceptibility data.

EXPERIMENTAL

All chemicals were reagent grade and used as received. The magnetic susceptibilities of powdered samples of metal complexes were measured by Gouy's method. The diamagnetic corrections for ligands and the metal ions were applied by using appropriate Pascal's constants. The IR spectra were recorded on a SP3-300, Pye Unicam spectrophotometer. The reflectance spectra were recorded in the range 300–1000 nm using magnesium oxide as the standard reflector. The electronic spectra of the solutions of the complexes in methanol were

* Author to whom correspondence should be addressed.
† Expansion of abbreviations given in Table 1.

recorded in the range 300–1500 nm using a VSU2-P Carl Zeiss spectrophotometer.

Freshly prepared nickel hydroxide (approximately 0.0012 mol) was added to hot solutions of N-acetyl amino acids (0.002 mol) dissolved in 25 cm^3 of water. The reaction mixture was heated on a water bath for about 1 h and unreacted nickel hydroxide was removed by filtration. The resulting light green coloured solutions were concentrated to a semi-solid state. The semi-solid residues were kept in a sulphuric acid dessicator for a few days and allowed to solidify. The complexes were powdered and dried *in vacuo* at room temperature. In the case of N-benzoylamino acids a 1 : 3 water–ethanol mixture was used as solvent.

The crystals of $Ni(Ac\text{–}Gly)_2(H_2O)_4$ were obtained by the liquid diffusion method, by layering acetone on top of the water solution of the complex. Small, green coloured, prismatic crystals with well-defined faces were obtained after 24 h.

Crystal data

$C_8H_{20}N_2O_{10}Ni$, $M = 362.96$, monoclinic space group $P2_1/a$, $a = 14.460(2)$, $b = 10.776(4)$, $c = 4.809(5)$ Å, $\beta = 96.95(3)°$, $D_{calc} = 1.625$ g cm^{-3} for $Z = 2$, $D_{meas} = 1.602$ g cm^{-3}, $\mu(Cu\text{-}K_\alpha) = 23.41$ cm^{-1}.

Data were collected by the multiple exposure, multiple film equi-inclination method. A total of 912 reflections were collected by visual methods using integrated Weissenberg photographs. Data were corrected for Lorentz and polarization effects, but not for absorption. The structure was solved by the heavy-atom method and positions of all the non-hydrogen atoms were determined by subsequent Fourier Maps.* Hydrogen atoms were calculated on geometric considerations. Full-matrix least-squares refinements converged to final $R = 0.11$ and $R_w = 0.11$. All the atoms were refined anisotropically and unit weights were used as they gave the best convergence. Hydrogens of the water molecules could not be located from the difference Fourier synthesis. Therefore, the hydrogen bonds were derived from the short intermolecular contacts between the atoms. The high R value is due to the fact that intensity data were measured from photographs and absorption corrections were not applied.

* Programs for structure determination and refinement were written by Dr G. M. Sheldrick. The program for molecular structure interpretation was written by Dr M. Nardelli of Universita di Parma.

RESULTS AND DISCUSSION

Eighteen complexes of nickel(II) with N-protected amino acids have been prepared. Their analytical data are given in Table 1. All of these complexes possess the 1 : 2 metal–ligand stoichiometry. The analytical data corresponds to the general formula $NiL_2 \cdot nH_2O$, where n ranges from 2 to 5. The protecting groups on N(amino) are simple groups (Ac, Bz and Form) and highly electron-withdrawing groups (MCA, TCA and TFA). All complexes are non-electrolytes as expected.

Description of the structure

The coordination around nickel is octahedral with two N-Ac—Gly ligands *trans* to each other. N-Ac—Gly coordinates to the metal ion only through one carboxyl oxygen. The second carboxyl oxygen does not take part in the coordination and remains free. The remaining four positions around the metal ion are occupied by four water molecules. Figure 1 shows the perspective view of the structure and its labelling scheme. Bond lengths and bond angles are given in Table 2. Non-chelating monodentate coordination through the carboxyl group has been found for the first time in the case of nickel(II). A similar type of structure[11] has been found in the case of $[Fe(Gly)_2(H_2O)_4]^{2+}$. The Ni—O(2), Ni—O(10) and Ni—O(11) bond lengths agree well with the bond lengths found in other octahedral complexes of nickel(II) with amino acid ligands.[12–14] Mean Ni—O(carboxyl) and Ni—O(water) bond lengths are 2.13(1) and 2.12(5) Å, respectively, as given by Freeman[15] in the amino acid complexes of nickel(II).

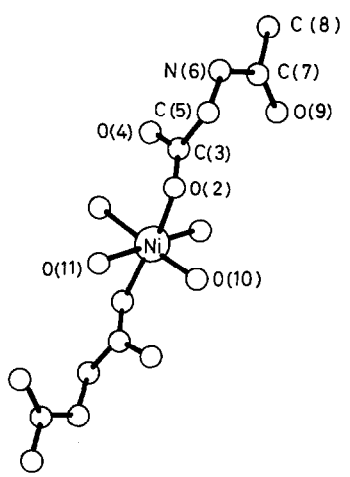

Fig. 1. Perspective view of the molecule showing the atom labelling scheme. Unlabelled atoms are related to the labelled ones centrosymmetrically.

Table 1. Analytical data[a]

Sr. No.	Complexes[b]	C	H	N	Ni
1	$Ni(Ac—Gly)_2 \cdot 4H_2O$	26.7 (26.5)	5.6 (5.5)	8.0 (7.7)	15.9 (16.2)
2	$Ni(Ac—Phe)_2 \cdot 2H_2O$	51.8 (52.1)	4.9 (5.5)	5.6 (5.5)	11.3 (11.6)
3	$Ni(Ac—Leu)_2 \cdot 2H_2O$	43.4 (43.8)	7.6 (7.3)	6.8 (6.4)	13.4 (13.4)
4	$Ni(MCA—Gly)_2 \cdot 4H_2O$	22.3 (22.2)	4.9 (4.2)	6.6 (6.5)	13.3 (13.6)
5	$Ni(MCA—Ala)_2 \cdot 2H_2O$	28.8 (28.3)	3.9 (4.2)	6.9 (6.6)	13.4 (13.9)
6	$Ni(MCA—Phe)_2 \cdot 2H_2O$	45.7 (45.8)	4.6 (4.5)	5.5 (4.9)	10.4 (10.2)
7	$Ni(MCA—Leu)_2 \cdot 2H_2O$	37.6 (37.8)	6.0 (5.9)	5.4 (5.5)	11.3 (11.5)
8	$Ni(TCA—Ala)_2 \cdot 2H_2O$	21.3 (21.4)	2.6 (2.5)	5.0 (5.0)	10.2 (14.4)
9	$Ni(TFA—Gly)_2 \cdot 2H_2O$	21.6 (22.1)	2.0 (2.3)	6.2 (6.4)	13.1 (13.5)
10	$Ni(TFA—Ala)_2 \cdot 2H_2O$	25.7 (25.9)	3.0 (3.0)	6.3 (6.0)	12.4 (12.7)
11	$Ni(TFA—Val)_2 \cdot 2H_2O$	32.1 (32.4)	3.6 (4.2)	5.3 (5.4)	11.8 (11.3)
12	$Ni(Bz—Gly)_2 \cdot 5H_2O$	43.2 (42.8)	5.0 (4.8)	5.6 (5.5)	11.6 (11.6)
13	$Ni(Bz—Ala)_2 \cdot 2H_2O$	50.5 (50.1)	5.5 (5.0)	5.5 (5.8)	11.8 (12.2)
14	$Ni(Bz—Val)_2 \cdot 2H_2O$	53.1 (53.7)	5.7 (5.9)	5.5 (5.2)	10.6 (10.9)
15	$Ni(Bz—Leu)_2 \cdot 2H_2O$	55.4 (55.5)	6.5 (6.7)	5.1 (5.0)	10.1 (10.4)
16	$Ni(Form—Phe)_2 \cdot 3H_2O$	47.8 (48.3)	4.8 (5.2)	5.8 (5.6)	12.1 (11.8)
17	$Ni(Form—Val)_2 \cdot 2H_2O$	37.8 (37.6)	6.4 (6.3)	7.5 (7.3)	15.8 (15.3)
18	$Ni(Form—Leu)_2 \cdot 2H_2O$	40.3 (40.9)	6.3 (6.8)	7.3 (6.8)	14.6 (14.3)

[a] Calculated values are given in parentheses.

[b] AC = acetyl, Bz = benzoyl, Form = formyl, MCA = monochloroacetyl, TCA = trichloroactyl, TFA = trifluoroacetyl, Gly = glycine, Phe = phenylalanine, Leu = leucine, Ala = alanine, Val = valine, Trp = tryptophan.

The dimensions of the N-Ac–Gly residue are not significantly different from those found in the refined crystal structure of N-Ac–Gly,[16] except in the case of the carboxyl group. The C(3)—O(4) bond distance 1.27(2) Å is slightly longer than a normal C=O double bond distance. It may be due to the strong hydrogen bonding in the complex involving O(4). The C(7)—O(9) bond is lengthened and the C(7)—N(6) bond is shortened from their normal values, showing a considerable amount of resonance in the amide group.[17] The atoms O(2)—C(3)—O(4)—C(5) lie in an approximate plane with C(3) deviating from the plane by 0.03 Å. The group of atoms C(5)—N(6)—C(7)—C(8)—O(9) does not deviate significantly from planarity. The deviations of the individual atoms from the respective planes are given in Table 3. The dihedral angle between the two planes is 85.0° compared to 5.2° in (Ac—Gly), 6.6° in* $Cu(Ac—Gly)_2(phen)$,[3b] 79.3° in $Cu(Ac—Gly)_2(H_2O)_4$[3a] and 76.3 and 22.8° in $[Cu(Ac–Gly)_2(H_2O)]_2$. It shows that in the nickel(II)

* phen = 1,10-phenathroline.

Table 2. Bond lengths (Å) and bond angles (°)[a]

Ni—O(2)	2.09(1)	C(3)—C(5)	1.57(2)
Ni—O(10)	2.10(1)	C(5)—N(6)	1.44(2)
Ni—O(11)	2.09(1)	N(6)—C(7)	1.33(2)
C(3)—O(2)	1.24(2)	C(7)—C(8)	1.53(2)
C(3)—O(4)	1.27(2)	C(7)—O(9)	1.23(2)
O(2)—Ni—O(10)	89.8(4)	O(4)—C(3)—C(5)	117(1)
O(2)—Ni—O(11)	91.9(4)	C(3)—C(5)—N(6)	113(1)
O(10)—Ni—O(11)	89.4(4)	C(5)—N(6)—C(7)	103(1)
C(3)—O(2)—Ni	122(1)	N(6)—C(7)—C(8)	113(1)
O(2)—C(3)—O(4)	128(1)	N(6)—C(7)—O(9)	122(1)
O(2)—C(3)—C(5)	114(1)	C(8)—C(7)—O(9)	125(1)

[a] The results have been reported to the last significant figure.

Table 3. Equations of weighted least-squares planes with the deviation (Å) of each atom from the plane in brackets

	Plane	M_1	M_2	M_3	D
1	O(2)—C(3)—O(4)—C(5) [O(2), −0.0074; C(3), 0.0345; O(4), −0.0079; C(5), −0.0128]	0.87134	−0.25368	−0.42002	−0.47647
2	C(5)—N(6)—C(7)—C(8)—O(9) [C(5), −0.0192; N(6), 0.0148; C(7), 0.0136; C(8), −0.0253; O(9), −0.003]	−0.55985	−0.29454	−0.77448	−2.92075

Table 4. Torsion angles (°)

	Ac—Gly	$Ni(Ac—Gly)_2(H_2O)_4$
O(2)—C(3)—C(5)—N(6)	−176.6(4)	167(1)
O(4)—C(3)—C(5)—N(6)	3.6(7)	−18(2)
C(3)—C(5)—N(6)—C(7)	−178.4(5)	−77(1)
C(5)—N(6)—C(7)—C(8)	−178.1(5)	−177(1)
C(5)—N(6)—C(7)—O(9)	1.0(8)	1(2)

complex there is a greater twist around the C(3)—C(5) bond than in the copper(II) complexes.

Table 4 gives the calculated torsion angles for the structures of Ac—Gly and the present complex. All the torsion angles are almost the same except for C(3)—C(5)—N(6)—C(7). In Ac—Gly, N(6)—C(7) is nearly anti to the C(3)—C(5) bond. But in the complex, this angle has reduced by about 100°, showing that during complexation there is a rotation along C(5)—N(6) bond. Therefore the free ligand is in a somewhat expanded form, while during complexation it acquires a folded form.

There is an extensive network of hydrogen bonds involving free carboxyl oxygen O(4), peptide oxygen O(9), peptide nitrogen N(6) and oxygens of both the water molecules O(10) and O(11). The types of hydrogen bonds and their distances are given in Table 5. The main packing interaction is the hydrogen bond $O(4)\cdots H(6)—N(6)^{I}$ of length 2.97(1) Å and $O(4)\cdots H(6)—N(6)^{I} = 151(1)°$ ($I = -x, -y+1, -z$). The O(4) atom is also hydrogen bonded to the water molecules.

Spectroscopic and magnetic studies

The band positions in the electronic absorption spectra of the complexes are given in Table 6. Three

Table 5. Hydrogen bonding distances (Å)

$O(4)\cdots N(6)^{I}$	2.97(1)	$O(9)\cdots O(10)^{III}$	2.65(1)
$O(4)\cdots O(10)^{II}$	2.65(1)	$O(10)\cdots O(11)^{II}$	2.98(1)
$O(4)\cdots O(11)^{II}$	3.18(1)	$O(10)\cdots O(11)^{IV}$	2.75(1)

$I = -x, -y+1, -z$; $II = -x, -y, -z$; $III = -x+0.5, y+0.5, -z$; $IV = -x, -y, -z+1$.

Table 6. Electronic absorption spectra and ligand field parameter (cm^{-1}), molar extinction coefficient ($dm^3\ mol^{-1}\ cm^{-1}$) in parentheses and magnetic susceptibility data

Sr. No.	Complexes	$^3A_{2g} \rightarrow {}^3T_{1g}^{(P)}$	$^3A_{2g} \rightarrow {}^3T_{1g}^{(F)}$	[a]	$^3A_{2g} \rightarrow {}^3T_{2g}^{(F)}$	Dq	B'	β	ν_2(calc)	μ_{eff} (BM)
1	Ni(Ac—Gly)$_2 \cdot 4H_2O$	25000(8.2)	14700(3.0)	13400(2.9)	8700(3.3)	870	906	0.86	14360	3.24
2	Ni(Ac—Phe)$_2 \cdot 2H_2O$	25000(11.4)	14900(3.8)	13400(3.7)	8700(4.0)	870	920	0.87	14360	3.11
3	Ni(Ac—Leu)$_2 \cdot 2H_2O$	25320(12.2)	14800(5.0)	13000(4.7)	8700(5.9)	870	934	0.88	14410	3.21
4	Ni(MCA—Gly)$_2 \cdot 4H_2O$	25320(8.4)	14600(2.9)	13500(2.8)	8770(2.9)	877	921	0.87	14410	3.42
5	Ni(MCA—Ala)$_2 \cdot 2H_2O$	25320(10.6)	14700(3.7)	13510(3.7)	8810(3.7)	881	906	0.86	14550	3.45
6	Ni(MCA—Phe)$_2 \cdot 2H_2O$[b]	—	—	—	—	—	—	—	—	3.40
7	Ni(MCA—Leu)$_2 \cdot 2H_2O$	25000(16.2)	14800(5.9)	13500(5.4)	8890(4.2)	889	875	0.83	14800	3.41
8	Ni(TCA—Ala)$_2 \cdot 2H_2O$	25320(10.3)	14700(3.8)	13700(3.5)	8700(4.1)	870	928	0.88	14400	3.43
9	Ni(TFA—Gly)$_2 \cdot 2H_2O$	25320(7.9)	15150(3.4)	13500(2.9)	9390(3.7)	939	837	0.79	15230	3.49
10	Ni(TFA—Ala)$_2 \cdot 2H_2O$	25320(9.8)	14700(4.1)	13330(3.3)	9302(4.4)	930	807	0.76	15130	3.56
11	Ni(TFA—Val)$_2 \cdot 2H_2O$	25320(12.3)	14710(4.6)	13700(4.4)	8890(4.2)	889	890	0.84	14640	3.56
12	Ni(Bz—Gly)$_2 \cdot 5H_2O$	25320(9.3)	15000(3.5)	13600(3.2)	8800(3.9)	880	928	0.88	14540	3.08
13	Ni(Bz—Ala)$_2 \cdot 2H_2O$	25320(9.8)	15000(3.5)	13400(3.4)	8700(3.9)	870	948	0.90	14410	3.28
14	Ni(Bz—Val)$_2 \cdot 2H_2O$[b]	—	—	—	—	—	—	—	—	3.12
15	Ni(Bz—Leu)$_2 \cdot 2H_2O$[b]	—	—	—	—	—	—	—	—	3.23
16	Ni(Form—Phe)$_2 \cdot 3H_2O$	25320(11.5)	15150(4.4)	13890(3.8)	8810(4.8)	881	936	0.89	14550	3.32
17	Ni(Form—Val)$_2 \cdot 2H_2O$	25000(7.3)	14930(3.3)	14290(3.5)	8700(3.7)	870	922	0.87	14360	3.33
18	Ni(Form—Leu)$_2 \cdot 2H_2O$	25320(9.9)	14930(4.1)	13700(3.7)	8700(4.2)	870	943	0.89	14410	3.25

[a] Triplet–singlet transition.
[b] Not sufficiently soluble.

main absorption bands have been observed. The molar extinction coefficients of these bands lie in the ranges 2.9–5.9, 2.9–5.9 and 7.3–16.2 $dm^3\ mol^{-1}\ cm^{-1}$, respectively. These values support that the complexes have a NiO_6 chromophore.[18] The Dq values of all the complexes fall into the range 800–900 cm^{-1}, which are close to the values found for the NiO_6 chromophore. This indicates that the ligand field strength of N-acyl amino acids are almost equal to that of water ($Dq = 850\ cm^{-1}$). By comparing the Dq values of N-acyl derivatives, the following spectrochemical series can be proposed:

(1) TFA—Gly > Bz—Gly > MCA—Gly = Ac—Gly

(2) TCA—Ala > TFA—Ala > Bz—Ala > MCA—Ala

(3) MCA—Phe > Form—Phe > Ac—Phe

(4) MCA—Leu > Bz—Leu > Form—Leu

(5) TFA—Val > Bz—Val > Form—Val.

It has been observed that the amino acids having stronger electron-withdrawing groups on the terminal amino group are placed higher in the spectrochemical series. The calculated numerical values of the inter-electric repulsion parameter, B', supports partial covalent bonding.

The magnetic moment values were obtained at room temperature and vary in the range 3.11–3.56 BM. Due to the lack of data at variable temperature, diagnostic conclusions cannot be arrived at.

The IR data indicate that in N-protected amino acids the N—H stretching frequencies in these complexes do not show coordination of this group with the metal ion. The shift of the amide I band to higher frequencies in the complexes also supports its non-participation in coordination. The analysis of ν(COO) frequencies indicates that in all compounds, except bis(acetylglycinato)tetraaquonickel(II), the carboxylate group acts as a bidentate group.

Acknowledgement—G. Sood and S. S. Dhillon thank the University Grants Commission, India, for financial support.

REFERENCES

1. H. C. Freeman, *Inorganic Biochemistry* (Edited by G. L. Eichhorn), Vol. 1, p. 121. Elsevier Scientific, Amsterdam (1973).
2. (a) L. P. Battaglia, A. Bonamartini Corradi, G. Marcotrigiano, L. Menabue and G. C. Pellacani, *Inorg. Chem.* 1981, **20**, 1075; (b) M. R. Udupa and B. Krebs, *Inorg. Chim. Acta* 1979, **37**, 1.
3. (a) M. R. Udupa and B. Krebs, *Inorg. Chim. Acta* 1978, **31**, 251; (b) L. P. Battaglia and A. Bonamartini Corradi, *Acta Cryst.* 1977, **B33**, 3886.
4. L. P. Battaglia, *Inorg. Chem.* 1982, **21**, 1391.
5. J. N. Brown and L. M. Trefonas, *Inorg. Chem.* 1973, **12**, 1730.
6. G. Marcotrigiano and G. C. Pellacani, *Inorg. Nucl. Chem. Lett.* 1975, **11**, 643.
7. G. Marcotrigiano, L. Menabue, G. C. Pellacani and M. Saladini, *Inorg. Chim. Acta* 1979, **32**, 149.
8. G. Marcotrigiano, L. Antolini, L. Menabue and G. C. Pellacani, *Inorg. Chim. Acta* 1979, **35**, 177.
9. G. Marcotrigiano, L. Menabue and G. C. Pellacani, *Bull. Chem. Soc. Japan* 1977, **50**, 742.
10. G. Marcotrigiano, P. Morini, L. Menabue and G. C. Pellacani, *Transition Met. Chem.* 1979, **4**, 119.
11. I. Lindqvist and R. Rosenstein, *Acta Chem. Scand.* 1960, **14**, 1228.
12. (a) H. C. Freeman, J. M. Guss and R. L. Sinclair, *J. Chem. Soc., Chem. Commun.* 1968, 485; (b) P. Jose, L. M. Pant and A. B. Biswas, *Acta Cryst.* 1964, **17**, 24.
13. (a) D. Van der Helm and M. B. Hossain, *Acta Cryst.* 1969, **B25**, 457; (b) T. Noguchi, *Bull. Chem. Soc. Japan* 1962, **35**, 99; (c) E. E. Castellano, G. Oliva, J. Zukerman-Schpector and R. Calvo, *Acta Cryst.* 1986, **C42**, 16.
14. (a) K. A. Fraser and M. M. Harding, *J. Chem. Soc. A* 1967, 415; (b) H. C. Freeman and J. M. Guss, *Acta Cryst.* 1972, **B28**, 2090.
15. H. C. Freeman, *Adv. Protein Chem.* 1967, **22**, 257.
16. J. Donohue and R. E. Marsh, *Acta Cryst.* 1962, **15**, 941.
17. A. Caron and J. Donohue, *Acta Cryst.* 1969, **B25**, 404.
18. A. B. P. Lever, *Inorganic Electronic Spectroscopy*. American Elsevier, Amsterdam (1968).

Polyhedron Vol. 8, No. 10, pp. 1335–1338, 1989
Printed in Great Britain

0277–5387/89 $3.00+.00
© 1989 Pergamon Press plc

COMPLEXING PROPERTIES OF SQUARIC ACID WITH IRON IN BUTAN-2-OL

L. A. HALL

Department of Chemistry, The University of the West Indies, St. Augustine, Trinidad, West Indies

(*Received* 11 *August* 1988; *accepted after revision* 18 *January* 1989)

Abstract—The distorted octahedral iron(II) squarate, $[Fe(HC_4O_4)(OH)]_2 \cdot C_4H_9OH$, has been synthesized by reacting solutions of $FeCl_2 \cdot 4H_2O$ and squaric acid in butan-2-ol under anaerobic conditions. The characterization of the complex was achieved by elemental and spectroscopic analyses.

The iron(II) squarates prepared from ethanol and propan-2-ol are five-coordinate.[1,2] However, the complex prepared from butan-2-ol apparently has a layered structure with butan-2-ol molecules loosely held between the layers, such that the iron shows distorted octahedral coordination. So far, this is the only first row transition metal squarate prepared in an alcoholic medium and under anaerobic conditions that is six-coordinate.[1-4]

EXPERIMENTAL

The squaric acid was obtained from Sigma Chemical Company. The butan-2-ol, obtained from BDH (Poole, U.K.), was dried with anhydrous calcium sulphate and distilled prior to use.

Approximately 0.52 g (2.6 mmol) of $FeCl_2 \cdot 4H_2O$ was dissolved in 200 cm^3 of hot deaerated butan-2-ol. A hot deaerated solution (150 cm^3) containing 0.30 g (2.6 mmol) of squaric acid was then added to the iron(II) chloride solution and the mixture allowed to cool in an inert atmosphere. The yellow complex was collected as described elsewhere,[1] except that after the initial evacuation of the drying pistol, the vacuum pump was disconnected from the system. Continuous evacuation resulted in the decomposition of the complex. Yield: 0.21 g (35%). Found: C, 32.6; H, 4.6; Fe, 24.9. Calc. for $C_{12}H_{14}O_{11}Fe_2$: C, 32.3; H, 3.1; Fe, 25.0%.

The IR spectrum between 4000 and 600 cm^{-1} was recorded on a Pye Unicam SP 3-200 spectrophotometer using Nujol as the mulling agent. The spectrum between 600 and 300 cm^{-1} was recorded on a Perkin–Elmer 983 spectrophotometer using a Nujol mull and AgBr as window material. The reflectance spectrum was carried out on a Perkin–Elmer spectrophotometer equipped with a reflectance attachment. The room temperature magnetic moment was determined by the Gouy method using a Newport magnetic balance and $Hg[Co(SCN)_4]$ as standard.

The carbon, hydrogen analyses were carried out by Huffman Laboratories, Colorado, U.S.A., and the iron determination by atomic absorption spectrophotometry using a Pye Unicam SP 9 spectrophotometer.

The Mössbauer spectra were obtained under similar conditions to those described elsewhere.[5]

RESULTS AND DISCUSSION

The O—H stretch in the IR spectrum of the complex, occurs at 3330 cm^{-1} (Table 1). No C=O absorption is observed and this has been attributed to the extent of electron delocalization on the squarate rings. This delocalization is also responsible for the absence of the carbonyl absorption in the IR spectra of the potassium salt of squaric acid[6] and a number of iron(II) squarates synthesized by Wrobleski and Brown.[7] The absorptions at 1500 and 710 cm^{-1} are characteristic squarate absorptions.[8] The bands between 900 and 1150 cm^{-1} have been assigned to the vibrations of the butan-2-ol molecules coordinated to the iron atoms in the complex.[9] The absorption at 1100 cm^{-1} is assumed to be due to the bending O—H vibration in the hydroxyl bridge.[10] The Fe—O bands occur between 400 and 600 cm^{-1}.[10,11] Four of the five peaks attri-

Table 1. IR spectroscopic data for $[Fe(HC_4O_4)(OH)]_2 \cdot C_4H_9OH$

Frequency[a] (cm^{-1})	Assignment
3330 m	O—H stretch
1500 s	C—C and C—O stretching
1150 w, 1060 w, 1020 vw, 990 w, 960 w, 900 w	C—C—O stretching of the butan-2-ol of crystallization
1100 m	O—H bending
720 m	C—O deformation due to squarate
590 m, 550–580 m, 500–530 m, 450–470 m, 417–440 m	Fe—O stretching

[a] s = strong, w = weak, vw = very weak, m = medium.

buted to the Fe—O vibrations are split. The split peaks occur at 417–440 cm^{-1}, 450–470 cm^{-1}, 500–530 cm^{-1} and 550–580 cm^{-1}, while the unsplit peak appears at 590 cm^{-1}. The number of Fe—O bands and the splitting observed, may be due to differences in Fe—O bond distances and the existence of both symmetric and asymmetric stretching Fe—O modes.[11]

The Mössbauer spectra of the complex at 78 and 293 K show chemical shifts of 1.35(1) and 1.23(1) mm s^{-1}, respectively, with corresponding quadrupolar splittings of 2.82(1) (78 K) and 2.22(1) mm s^{-1} (293 K). These chemical shifts and the quadrupole splitting temperature dependence are typical of high spin iron(II) in a tetragonally distorted octahedral environment[12,13] (Figs 1 and 2). The Mössbauer spectra show that the complex has a high recoil-free fraction. This is interpreted to be indicative of the complex being polymeric.

The electronic spectrum of the complex shows a sharp absorption at 10,000 cm^{-1}, a broad band at 6550 cm^{-1}, and two small peaks at 4650 and 4350 cm^{-1}. These absorptions are consistent with high-spin iron(II) in ligand fields of less than O_h symmetry.[14]

Elemental analysis of the complex allows for only one butan-2-ol molecule per iron(II) squarate dimer. Therefore, in order to accommodate a distorted octahedral environment around the iron atoms, a layer structure, in which pairs of dimers share butan-2-ol molecules, is proposed (see Structure 1).

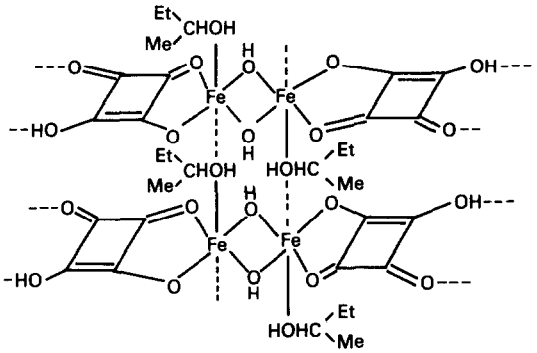

Structure 1.

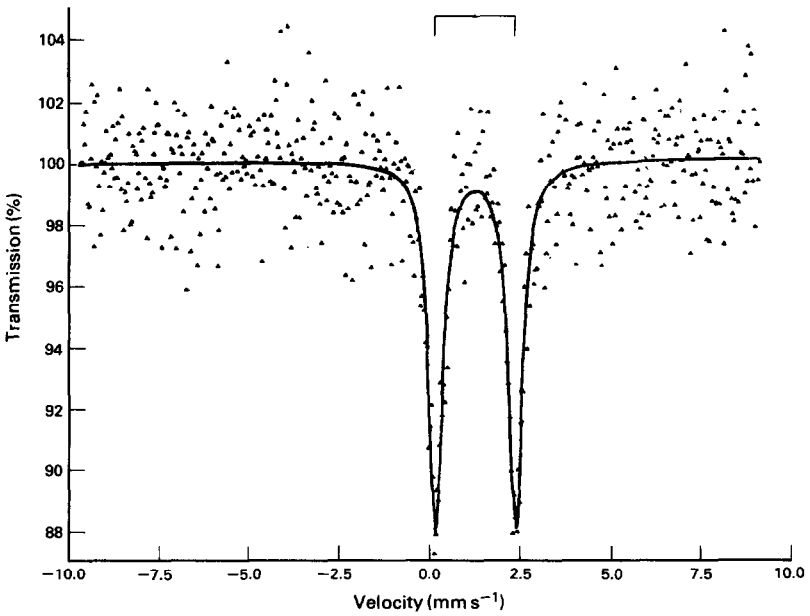

Fig. 1. Mössbauer spectrum of $[Fe(HC_4O_4)(OH)]_2 \cdot C_4H_9OH$ at 293 K.

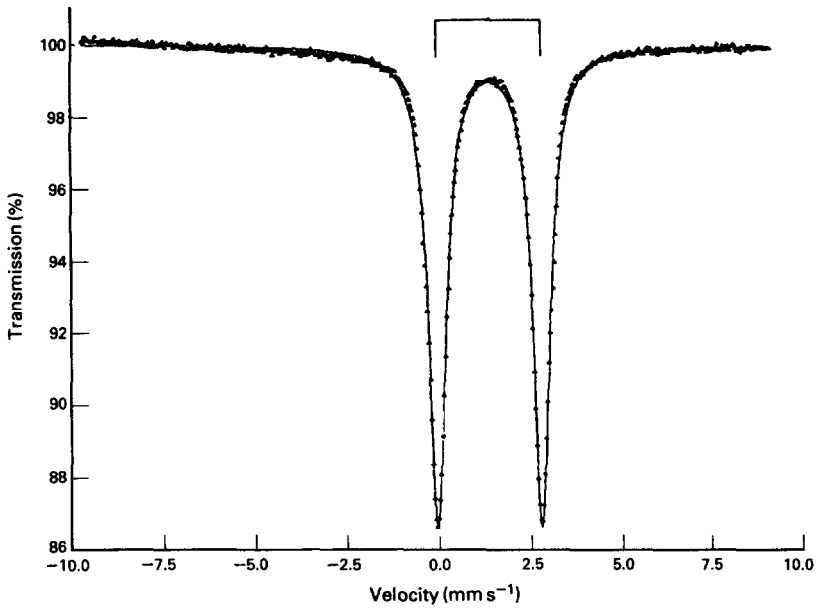

Fig. 2. Mössbauer spectrum of $[Fe(HC_4O_4)(OH)]_2 \cdot C_4H_9OH$ at 78 K.

In such a structure, layers of iron(II) squarate dimers, hydrogen-bonded together, are stacked on each other with butan-2-ol molecules being loosely held between the layers and shared by iron atoms, in accordance with the apparent polymeric nature of the complex suggested by the analysis of the Mössbauer spectra. Drying the complex *in vacuo* at room temperature for more than about 5 min, results in its decomposition which is accompanied by oxidation. This is most likely because the alcohol molecules, being only loosely held between the layers, are easily removed by vacuum drying at room temperature leaving the iron atoms in an unstable square-planar environment. Square-planar iron(II) normally requires macromolecular ligands to achieve stability.[15] Thus, after the removal of the alcohol molecules, the structure collapses and the decomposition/oxidation of the complex occurs. If the complex is simply exposed to the atmosphere at room temperature, decomposition occurs very slowly.

It is possible that the increase in size of the butan-2-ol molecule, compared to the ethanol and propan-2-ol molecules, forces the complex to adopt this structure instead of the five-coordinate ones proposed for the complexes prepared from ethanol and propan-2-ol.

The room temperature magnetic moment (298 K) of the complex is 4.72 BM, which is consistent with high spin octahedral iron(II).

The complex, like other squarates, is insoluble in most common solvents[7] and therefore, recrystallization was not possible. The poor quality of the hydrogen analysis has been attributed to this and solvent contamination which has been observed in other squarates.[1,3,16] A layered structure, like the one proposed for the complex, would be susceptible to solvent contamination between layers.

Acknowledgements—I wish to thank Mr A. Kuperman and Dr W. Tinto for their help in obtaining the reflectance spectrum, and Dr J. Silver for his assistance in obtaining the Mössbauer spectra.

REFERENCES

1. O. St. C. Headley and L. A. Hall, *Polyhedron* 1985, **4**, 1697.
2. D. I. Maharaj and L. A. Hall, *Polyhedron* 1988, **7**, 2155.
3. O. St. C. Headley and L. A. Hall, *Polyhedron* 1986, **5**, 1829.
4. D. I. Maharaj and L. A. Hall, *Inorg. Chim. Acta* 1988, **145**, 235.
5. M. Y. Hamed, R. C. Hider and J. Silver, *Inorg. Chim. Acta* 1982, **66**, 13.
6. S. Cohen, J. Lacher and J. Park, *J. Am. Chem. Soc.* 1959, **81**, 3480.
7. J. Wrobleski and D. Brown, *Inorg. Chem.* 1979, **18**, 2738.
8. F. G. Baglin and C. B. Rose, *Spectrochim. Acta* 1970, **26a**, 2298.
9. G. Socrates, *Infrared Characteristic Group Frequencies*, p. 45. John Wiley, New York (1980).
10. J. Ferraro, R. Driver, W. Walker and W. Wozniak, *Inorg. Chem.* 1967, **6**, 1586.

11. R. Adams, R. L. Martin and G. Winter, *Aust. J. Chem.* 1967, **20**, 773.
12. D. P. Riley, P. H. Merrell, J. A. Stone and D. H. Busch, *Inorg. Chem.* 1975, **14**, 490.
13. B. Y. Enwiya, J. Silver and I. E. G. Morrison, *J. Chem. Soc., Dalton Trans.* 1982, 2231.
14. A. B. P. Lever, *Inorganic Electronic Spectroscopy*, 2nd edn, p. 376. Elsevier, Amsterdam (1984).
15. D. Riley, J. Stone and D. Busch, *J. Am. Chem. Soc.* 1977, **99**, 767.
16. B. Gerstein and M. Habenschuss, *J. Appl. Phys.* 1972, **43**, 5155.

Polyhedron Vol. 8, No. 10, pp. 1339–1344, 1989
Printed in Great Britain

0277–5387/89 $3.00+.00
© 1989 Pergamon Press plc

PREPARATION AND CHARACTERIZATION OF NEW TERDENTATE AMINODIPHOSPHINES AND CORRESPONDING VANADIUM(III) DIALKYLAMIDES

A. A. DANOPOULOS and P. G. EDWARDS*

School of Chemistry, University of Wales College of Cardiff, P.O. Box 912, Cardiff CF1 3TB, U.K.

(*Received* 12 *October* 1988; *accepted* 18 *January* 1989)

Abstract—The new amines, $HN(CH_2CH_2PR_2)_2$ (R = Me, Et), have been prepared by the nucleophilic substitution of halide in $HN(CH_2CH_2Cl)_2 \cdot HCl$ or the free amine by the corresponding dialkylphosphido anions. The new amines are readily deprotonated by the action of alkyl lithium reagents. Action of the amido anion, $^-N(CH_2CH_2PMe_2)_2$, on $VCl_3 \cdot 3THF$ leads to the new ternary amide $Cl_2VN(CH_2CH_2PMe_2)_2$, from which a new class of organovanadium amido complexes can be obtained by reaction with alkyl or aryl lithium reagents.

The use of polyphosphine ligands in coordination and organometallic chemistry is not widespread, but is increasing. Interest in polyphosphines as ligands is encouraged by the recent development of rational synthetic methods for some of them[1] and since the wide variability of the chelate bite, denticity and functionalization available enables rational modification of the metal ion environment.[2] Some interesting results from using terdentate amidophosphines have recently appeared[3] and we have reported on the stabilization of vanadium and titanium amides with similar linear amidoamines.[4] Since partial substitution of halide ligands on metal centres is possible with this amine, without the common event of redistribution to binary amido complexes[5] that occurs with other amido ligands, we now have potential access to a wide variety of tractable derivatives in oxidation states previously rare or unattainable. In view of this, we are interested in studying similar applications of terdentate amidophosphine ligands, as the tertiary phosphine functions may further aid stabilization of low oxidation states. To this end, we report herein the preparation and characterization of the new amines $(R_2PCH_2CH_2)_2NR'$ (R′ = H, R = Me, Et; R′ = $PhCH_2$, R = Me) and vanadium(III) halide, methyl and phenyl derivatives of the corresponding amide (R = Me). To our knowledge, the only similar ligand system that has been used for the stabilization of transition metal amido complexes, although not for vanadium(III), is the series $(R_2PCH_2Si(Me)_2)_2NH$ (R = alkyl or aryl).[3] There are a number of transition metal amino complexes containing neutral ligands of the type $(Ph_2PCH_2CH_2)_2NR$ (R = H, alkyl).[6]

* Author to whom correspondence should be addressed.

RESULTS AND DISCUSSION

Synthesis of $(Me_2PCH_2CH_2)_2NR$ (R = H, CH_2Ph)

Our preparation of bis(dimethylphosphinoethyl)amine is based on the nucleophilic substitution of chloride in bis-2-chloroethylamine [eq. (1)] by the dimethylphosphido anion in liquid ammonia. This method is similar to the preparation of the phenyl analogue, $(Ph_2PCH_2CH_2)_2NH$, reported by Sacconi[6a] in excellent yields.

$$HN(CH_2CH_2Cl_2)_2 + 2NaPMe_2 \longrightarrow HN(CH_2CH_2PMe_2)_2 + 2NaCl. \quad (1)$$

In contrast, our yields are moderate to low (based on amine). The variability in yield may be due to variations in basicity of the nucleophiles. Thus $^-PMe_2$ is a stronger base than $^-PPh_2$, which results in competitive proton abstraction from the secondary amine [eq. (2)] and subsequent intramolecular reactions.

$$Me_2P^- + HNR_2 \longrightarrow Me_2PH + R_2N^- \quad (2)$$
$$(R = CH_2CH_2Cl).$$

Support for this comes from the following observations:

(1) When the reaction is carried out using $NaPMe_2$ and $PhCH_2N(CH_2CH_2Cl)_2$ instead of $HN(CH_2CH_2Cl)_2$, $PhCH_2N(CH_2CH_2PMe_2)_2$ is obtained in almost quantitative yield (> 92% redistilled product) without detection of any side products (NMR). To date, we have been unable to cleave the benzyl–nitrogen bond under reductive conditions ($Na/NH_3(l)$ or $H_2/HCOOH/Pd/C$).

(2) Addition of the amine hydrochloride to solutions of 3 mole equivalents of $NaPMe_2$ in $NH_3(l)$ enable higher (up to 60%), although more variable, yields of $(Me_2PCH_2CH_2)_2NH$ to be isolated. Variation in yield is likely due to difficulties encountered in the careful control of the solid addition. This becomes more difficult as the scale is increased and yields as low as 25% have been obtained. This method is also wasteful in phosphide, since 1 mole equivalent is required to sacrificially neutralize the hydrochloride salt. It appears that substitution of halide competes favourably with neutralization of the ammonium function in liquid ammonia, such that the hydrochloride acts as a somewhat protected secondary amine. This is highlighted by the total failure of the attempted syntheses of the diethylphosphino and di-isopropylphosphino analogues from the free amine in liquid ammonia or THF. The ethyl homologue may be prepared in variable but low yields from the hydrochloride in THF [eq. (3)]

$$ClH_2N(CH_2CH_2Cl)_2 + 3LiPEt_2 \longrightarrow$$
$$HN(CH_2CH_2PEt_2)_2 + HPEt_2 + 3LiCl, \quad (3)$$

in a manner similar to Whiteside and co-workers' preparation[7] of the phenyl analogue, although they use *t*-butoxide rather than phosphide to neutralize the ammonium function. Again this fails for the isopropyl.

The new phosphines are effectively characterized by ^1H and ^{31}P NMR (Table 1). The spectra display patterns consistent with the assigned structures, thus protons adjacent to nitrogen are shifted from 1 to 2 ppm downfield, relative to those adjacent to phosphorus and $^3J_{P—H} > {}^2J_{P—H}$. The IR spectrum of the secondary amine shows the N—H stretch at 3280 cm^{-1}.

Preparation of $LiN(CH_2CH_2PMe_2)_2$

The lithium amide may be prepared by deprotonation of the amine with alkyl lithium reagents such as MeLi in diethyl ether and Bu"Li in hexane. The latter is more convenient since the solubility of the product is considerably less in aliphatic hydrocarbons than in ethers, and pure microcrystalline material is more readily isolated. The white pyrophoric amide is characterized by the absence of ν(N—H) in the IR and by broadened resonances in the ^1H NMR (C_6D_6). These are of the appropriate

Table 1. $^{31}P[^1H]$ and ^1H NMR data for the new diphosphinoamines

Compound	$^{31}P[^1H]$[a]	^1H[b]	Assignment
$PhCN_2N(CH_2CH_2PMe_2)_2$	−53.7	0.90, d, 12H ($^2J_{P—H}$ = 2.6 Hz)	$P(CH_3)_2$
		1.45, d of t, 4H ($^3J_{H—H}$ = 8.4 Hz[c])	$(CH_2)P$
		2.65, m, 4H ($^3J_{P—H}$ = 9 Hz)	$(CH_2)N$
		4.52, s, 2H	$(CH_2)Ph$
		7.2–7.5, m, 5H	$(CH_2)Ph$
$HN(CH_2CH_2PMe_2)_2$	−57.6	0.95, d, 12H ($^2J_{P—H}$ = 2.6 Hz)	$P(CH_3)_2$
		1.49, d of t, 4H ($^3J_{H—H}$ = 7.5 Hz[c])	$(CH_2)P$
		2.75, q, 4H ($^3J_{P—H}$ = 7.8 Hz)	$(CH_2)N$
$HN(CH_2CH_2PEt_2)_2$	−28.2	1.09, d of t, 12H ($^3J_{P—H}$ = 14 Hz, $^3J_{H—H}$ = 6.9 Hz)	CH_2CH_3
		1.38, q, 8H ($^3J_{H—H}$ = 7 Hz[d])	CH_2CH_3
		1.58, m, 4H ($^3J_{H—H}$ = 7.3 Hz, $^2J_{P—H}$ = 1.2 Hz)	$(CH_2)P$
		2.81, q, 4H[e]	$(CH_2)N$

[a] Measured in C_6D_6, in ppm relative to 85% H_3PO_4.
[b] Measured in C_6D_6 and referenced to residual protons (δ = 7.27).
[c] $^2J_{P—H}$ poorly resolved but estimated to be *ca* 2 Hz.
[d] $^2J_{P—H}$ estimated to be *ca* 7 Hz.
[e] $^3J_{P—H}$ estimated to be *ca* 7.5 Hz.

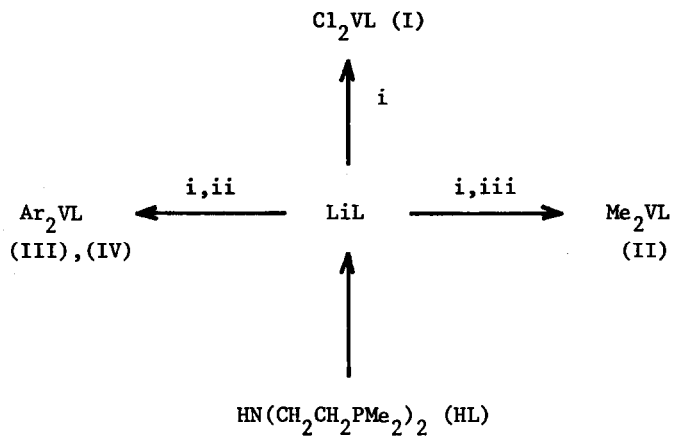

Notes: i) VCl_3.3THF in THF; ii) ArLi (Ar = C_6H_5, 4-MeC_6H_4); iii) MeLi.

Scheme 1.

intensity ratios and not significantly shifted from those of the free amine (Table 1). The broadening is presumably due to fluxionality in solution at ambient temperatures.

Vanadium(III) *derivatives*

Routes to the new complexes described below are collected in Scheme 1. All the following compounds are ESR silent in solid, solution or glass (290 and 99 K) and except for **II** below, analytical data are consistent with the proposed formulations. Magnetic susceptibilities (see Experimental) confirm the d^2 paramagnetic state of the vanadium(III) ions.

Interaction of $Cl_3V \cdot 3THF$ with $LiN(CH_2CH_2PMe_2)_2$ in THF, enables the isolation of the purple crystalline $Cl_2VN(CH_2CH_2PMe_2)_2$ (**I**). An identical material may be isolated from $VCl_3(NMe_3)_2$ by a similar procedure. Attempts to obtain crystals suitable for X-ray crystallography have so far been unsuccessful. It is likely, however, that the stereochemistry about vanadium is similar to that in the analogous amine complex $Cl_2VN(CH_2CH_2NEt_2)_2$,[4a] where the three anionic donors occupy the equatorial sites of a distorted trigonal bipyramid, with the neutral donors in the apical positions.

I may be readily converted to organometallic derivatives by the action of organolithium reagents. Thus with methyl lithium, an oil, $Me_2VN(CH_2CH_2PMe_2)_2$ (**II**), may be obtained from petroleum ether. The compound decomposes upon attempted distillation and is very soluble in apolar solvents. More definitive characterization of this material is difficult since we have been unable to obtain reliable microanalytical data, however in light of the magnetic susceptibility, the absence of chloride in the product ($AgNO_3$ using compound **I** as control) and the similarity of this system with the analogous $Me_2VN(CH_2CH_2NEt_2)_2$,[4b] we believe there is little doubt as to the nature of **II**. We are presently investigating reactions of **II**, as well as other compounds reported herein, in order to shed more light on this and other chemical properties.

With aryl lithium reagents, **I** provides the similar diarylvanadium amides $Ar_2VN(CH_2CH_2PMe_2)_2$ [Ar = Ph (**III**), 2-CH_3-C_6H_4 (**IV**)]. **III** and **IV** are both readily prepared from **I** in THF, and both may be obtained as emerald green crystals in good yield from petroleum ether. Attempts to obtain X-ray crystallographic data have so far failed. The compounds are very air-sensitive, especially in solution, becoming brown and eventually yellowish, presumably due to oxidation to vanadium(V) species. As well as by analytical data, **III** and **IV** are additionally identified by IR spectra that show characteristic aryl absorbancies (ν(C⋯C) at 1558 cm^{-1} for **III** and 1568 cm^{-1} for **IV**).

EXPERIMENTAL

Materials and methods

The following materials were either purchased from Aldrich [$(ClCH_2CH_2)_2NH_2Cl$, $PSCl_3$, Bu^nLi in hexane] or prepared following literature methods (Me_2PPMe_2,[8] $HPEt_2$,[9] $VCl_3 \cdot 3THF$,[10] $VCl_3 \cdot 2NMe_3$[11] and $PhCH_2N(CH_2CH_2Cl)_2 \cdot HCl$[6c]). PBu^n_3 was dried over and distilled from CaH_2 under nitrogen prior to use. Ammonia was condensed onto and distilled from sodium directly into the reaction vessel. Solvents were dried over the appropriate drying agents and distilled under nitrogen immediately prior to use.

Manipulations of all the new compounds reported here, were performed using standard Schlenk-line or dry-box techniques under purified nitrogen atmospheres or *in vacuo*. The quality of the nitrogen used has a significant bearing on the success of the preparation of the metal complexes described herein. Instruments used were: IR, Perkin–Elmer 783; NMR, Bruker WM 360 (^{1}H, 360 MHz; ^{31}P, 145 MHz); magnetic susceptibility, Johnson Matthey magnetic susceptibility balance. Analyses were carried out by Butterworth Laboratories Ltd, Teddington, U.K.

(1) *Preparation of* $PhCH_2N(CH_2CH_2PMe_2)_2$

$PhCH_2N(CH_2CH_2Cl)_2$ was liberated from the hydrochloride (8.6 g, 0.0032 M) by addition of diethyl ether (50 cm^3), followed by aqueous NaOH (2.5 g, 0.046 M, as a 10% w/w solution) and the organic phase dried over $MgSO_4$. This solution was deoxygenated and added dropwise to a solution of $NaPMe_2$ (from Me_2PPMe_2, 3.9 g, 0.032 M and Na, 1.47 g, 0.064 M) in ammonia (100 cm^3) at −60°C, until the orange colour had faded to pale yellow. Care was taken not to over-run the endpoint. The ammonia was allowed to warm and then evaporate. Diethyl ether (100 cm^3) was added to the white residue, followed by deoxygenated water (50 cm^3). The aqueous phase was separated and washed with diethyl ether (3 × 50 cm^3). The combined organic phase was distilled at atmospheric pressure to remove solvent, followed by low pressure. The fraction boiling at 120°C/0.05 mm was collected and was found to be pure by ^{1}H NMR. Yield: 8.5 g, 95% based on $PhCH_2N(CH_2CH_2Cl)_2 \cdot HCl$. IR (neat): 3080 w, 3055 w, 3020 m, 2945 s, 2880 s, 2800 s br, 1650 m, 1600 w, 1490 m, 1449 s, 1414 s br, 1360 m, 1289 m, 1105 m br, 1090 m, 1028 m, 990 m, 933 s, 881 m, 812 w, 727 s, 694 s, 662 w, 610 w, 465 w.

(2) *Preparation of* (a) $(Me_2PCH_2CH_2)_2NH$ *and* (b) $(Et_2PCH_2CH_2)_2NH$

The most reproducible results (best average yields based on phosphorus) were obtained by the following methods.

(a) To a solution of sodium (8.8 g, 0.38 M) in ammonia (500 cm^3) held at −78°C, was added dropwise with efficient mechanical stirring, Me_2PPMe_2 (22 g, 0.18 M) over 15 min. The resultant green solution was stirred for 1 h at −78°C. A solution of $HN(CH_2CH_2Cl)_2$ was prepared in the following way. To a suspension of $ClH_2N(CH_2CH_2Cl)_2$ (32.1 g, 0.18 M) in diethyl ether (100 cm^3), was added dropwise with cooling (0°C), an aqueous solution of NaOH (18 g in 100 cm^3, 2.5-fold mole excess). The two phases were separated, the aqueous phase was washed with ether (3 × 50 cm^3) and the combined ether phase dried over $MgSO_4$. Since the free amine slowly quaternizes in solution, the drying process was limited to approximately 2 h. The efficiency of this drying becomes critical since traces of moisture will destroy $NaPMe_2$ and deplete the resultant yield of the next step. We suggest using generous portions of $MgSO_4$ and stirring or shaking this mixture. The dried filtered solution of $HN(CH_2CH_2Cl)_2$ was degassed by boiling under reduced pressure and was then added dropwise to the ammonia solution of $^-PMe_2$. Addition of amine was stopped when the colour of the ammonia solution became pale yellow. The quantity of amine added was normally less than that expected on a stoichiometric basis. Addition of excess amine seriously depletes the yield. Following this addition, the mixture was allowed to warm to −33°C over 1 h. The ammonia was then allowed to evaporate, ether (200 cm^3) was added and the white slurry hydrolysed by careful addition of deoxygenated water (100 cm^3). The two phases were separated, the aqueous phase washed with ether (3 × 50 cm^3) and the combined organic phase dried over $MgSO_4$. Filtration followed by atmospheric pressure distillation, through a 20 cm Vigreux column, left a high boiling residue that was fractionated at reduced pressure. The fraction boiling at 60–65°C/0.01 mm Hg consists mainly of $(Me_2PCH_2CH_2)_2NH$ and was redistilled providing a fraction boiling at 63–65°C/0.01 mm Hg of pure (NMR) phosphine. Yield: 12.2 g, 35% based on Me_2PPMe_2. IR (neat): 3280 m br, 2955 s, 2920 s, 2895 s, 2815 s, 1630 w br, 1455 m br, 1425 s br, 1360 w, 1332 m, 1291 m, 1277 m, 1118 s, 992 m, 939 s, 889 m, 860 w, 814 w, 785 w, 708 s, 687 m, 676 m.

(b) A solution of Et_2PLi (prepared from Et_2PH and PhLi, 25.4 g, 0.26 M) in THF (300 cm^3) held at −40°C, was treated with small portions of $ClH_2N(CH_2CH_2Cl)_2$ (15.7 g, 0.088 M in total) over 2 h with vigorous stirring. The mixture was allowed to warm to room temperature and was stirred (24 h). After hydrolysis with deoxygenated water (100 cm^3), the two phases were separated and the aqueous phase washed with ether (3 × 50 cm^3). After drying ($MgSO_4$), the combined organic phase was distilled at atmospheric pressure through a 20 cm Vigreux column to remove solvents and the residue was vacuum distilled. The fraction boiling at 100–104°C/0.04 mm Hg was collected. Yield: 4.4 g, 20% based on amine hydrochloride. IR (neat): 3275 m, 2910 s br, 2810 s, 2730 w, 1605 w br, 1455 s, 1415 s, 1375 s, 1330 m, 1290 w, 1275 w, 1230 m br, 1175

w, 1115 s, 1038 s, 755 s br, 690 m, 669 s, 630 w, 613 w.

(3) *Preparation of* $LiN(CH_2CH_2PR_2)_2$

(a) (R = Me). To a solution of $HN(CH_2CH_2PMe_2)_2$ (4.6 g, 0.024 M) in petroleum ether (90 cm^3) cooled to −78°C, was added a solution of Bu^nLi (9 cm^3, 2.5 M in hexane, 5% molar excess) dropwise with stirring. Upon warming to ambient temperature, a white precipitate of the lithium amide appeared. Recooling (−78°C), followed by filtration and washing the precipitate with cold (−78°C) petrol, enables the isolation of a white microcrystalline material after drying *in vacuo*. Yield: 4.18 g, 88% based on $HN(CH_2CH_2PMe_2)_2$. This material may be recrystallized from toluene to give large colourless prisms, although the microcrystalline material is pure enough for the applications described below. The material is very air-sensitive in both the solid and in solution, as are the derivatives below. IR (Nujol): 1292 m, 1277 m, 1156 m, 1125 w, 1097 m, 1070 m, 942 s, 926 m, 916 m, 882 w, 871 w, 842 w, 809 w, 719 s, 708 m, 693 m, 656 w, 628 w, 610 w, 423 w, 370 m br, 318 w br.

(b) (R = Et). The ethyl derivative may be prepared in a manner similar to that described in (a) above, except that after warming to room temperature, the amide was obtained as an oil after removal of solvent *in vacuo*. Yield: 85% based on $HN(CH_2CH_2PEt_2)_2$.

(4) *Preparation of* $Cl_2VN(CH_2CH_2PMe_2)_2$ (I)

(a) To a solution of $VCl_3 \cdot 3THF$ (2.5 g, 6.7 mmol) in THF (70 cm^3), cooled to −78°C, was added with vigorous stirring, a solution of $LiN(CH_2CH_2PMe_2)_2$ (64 cm^3, 0.015 M in toluene) over 15 min. The colour of the solution changed from light orange to deep red–brown. The solution was allowed to warm to ambient temperature when it was stirred for a further 1 h. The volatile materials were removed *in vacuo* and the brown residue extracted into toluene (50 cm^3). The deep red solution was filtered through celite and the filtrate concentrated (to approximately 10 cm^3). Cooling slowly (to −20°C) gave purple needles that were isolated, washed with petrol and dried *in vacuo*. Yield 1.1 g, 48% based on $VCl_3 \cdot 3THF$. The compound is soluble in aromatic hydrocarbons and ethers, and sparingly soluble in aliphatic hydrocarbons.

(b) **I** may alternatively be prepared from $VCl_3 \cdot 2NMe_3$ using a procedure identical to that described in (a) above except for the substitution of $VCl_3 \cdot 3THF$ for the same molar quantity of $VCl_3(NMe_3)_2$. Found (Calc.): C, 31.6 (30.6); H, 6.0 (6.4); N, 4.2 (4.5%). $\mu_{eff} = 2.61$ BM. IR (Nujol): 1278 w, 1180 w, 1075 m, 1055 m, 979 m, 953 s, 927 m, 909 m, 868 w, 839 w, 738 m, 720 m, 663 w, 644 m, 393 m, 328 m, 295 w.

(5) *Preparation of* $(C_6H_5)_2VN(CH_2CH_2PMe_2)_2$ (III)

To a solution of $VCl_3 \cdot 3THF$ (0.27 g, 0.72 mmol) in THF (30 cm^3), was added a solution of $LiN(CH_2CH_2PMe_2)_2$ (9.5 cm^3, 0.076 M in toluene, 0.7 mmol) with stirring at −78°C. The resultant red–brown solution was allowed to warm to ambient temperature and then recooled to −78°C. At this point a solution of C_6H_5Li (1.2 cm^3, 1.25 M in Et_2O, 1.5 mmol) was added dropwise with stirring. The solution was allowed to warm to 0°C and the volatile materials were then removed *in vacuo*. The brown–green residue was extracted into petrol (3×20 cm^3), filtered through celite and concentrated to approximately 5 cm^3. Cooling to −20°C provides bright green plates which were isolated by filtration. Yield: 0.17 g, 60% based on $VCl_3 \cdot 3THF$. The compound is very soluble in hydrocarbons and ethers. Found (Calc.): C, 59.7 (60.5); H, 7.8 (7.5); N, 3.1 (3.5%). $\mu_{eff} = 2.59$ BM. IR (Nujol): 3100 m, 3030 s, 1558 m, 1325 m, 1293 m, 1280 m, 1237 w, 1210 m, 1188 w, 1151 m, 1083 m, 1066 m, 1050 m, 1019 w, 996 m, 975 m, 942 s, 918 m, 857 w, 830 m, 770 w, 739 m, 718 m, 700 s, 519 m, 484 m, 448 m, 345 m, 280 w, 250 w.

(6) *Preparation of* $(2\text{-}CH_3C_6H_4)_2VN(CH_2CH_2PMe_2)_2$ (IV)

The preparation of **IV** is identical to that of **III**, except for the substitution of C_6H_5Li with the equivalent molar quantity of $2\text{-}MeC_6H_4Li$. The product is obtained as green plates from petrol as for **III** and has similar properties to **III**. Yield: 58%. Found (Calc.): C, 62.7 (62.1); H, 8.2 (8.0); N, 3.4 (3.3%). IR (Nujol): 3050 m, 1592 w, 1568 m, 1323 m, 1294 m, 1280 m, 1260 m, 1244 m, 1212 m, 1189 w, 1164 w, 1090 s, 1078 s, 1031 s, 998 m, 979 m, 944 s, 920 m, 861 w, 799 m br, 747 s, 736 s, 720 m, 660 m, 541 m, 519 w, 484 m, 432 m, 399 m, 320 w, 288 w.

(7) *Preparation of* $Me_2VN(CH_2CH_2PMe_2)_2$ (II)

II may be prepared by a similar procedure to that described for **III** above, with $VCl_3 \cdot 3THF$ (0.5 g, 1.34 mmol) in THF (50 cm^3), and a solution of lithium amide in toluene (17.6 cm^3, 1.34 mmol) followed by a solution of MeLi in Et_2O (2.5 cm^3, 2.68 mmol). The product can be obtained as a

green–brown oil by evaporation of the filtered hexane extract. Attempts to distil and crystallize this oil have failed. $\mu_{eff} = 2.55$ BM.

Acknowledgements—We thank the SERC for support and Albright and Wilson Ltd, for a generous gift of Bu^n_3P.

REFERENCES

1. D. W. Meek, in *Homogeneous Catalysis with Metal Phosphine Complexes* (Edited by L. H. Pignolet), Chap. 8, pp. 257–296. Plenum Press, New York (1983).
2. R. Mason and D. W. Meek, *Angew. Chem. Int. Ed. Engl.* 1978, **17**, 183.
3. M. D. Fryzuk and K. Bhangu, *J. Am. Chem. Soc.* 1988, **110**, 961; M. D. Fryzuk, A. Carter and A. Westerhaus, *Inorg. Chem.* 1985, **24**, 642.
4. A. R. Wills, P. G. Edwards, R. L. Short and M. B. Hursthouse, *J. Chem. Soc., Chem. Commun.* 1988, 115; A. R. Wills and P. G. Edwards, *J. Chem. Soc., Dalton Trans.* 1988, in press.
5. M. F. Lappert, P. P. Power, A. R. Sanger and R. C. Shrivastava, in *Metal and Metalloid Amides*. Ellis Horwood, Chichester (1980).
6. (a) L. Sacconi and R. Morassi, *J. Chem. Soc. A* 1968, 2997; (b) M. M. Taqui Khan, V. Vijay Sen Reddy and H. C. Bajaj, *Polyhedron* 1987, **6**, 1727; M. M. Taqui Khan and E. Ramo Rao, *Polyhedron* 1987, **6**, 921; (c) M. M. Taqui Khan and V. Vijay Sen Reddy, *Inorg. Chem.* 1986, **25**, 208.
7. M. E. Wilson, R. G. Nuzzo and G. M. Whitesides, *J. Am. Chem. Soc.* 1978, **100**, 2269.
8. G. Kordosky, B. R. Cook, J. Cloyd and D. W. Meek, *Inorg. Synth.* 1973, **14**, 14.
9. K. Issleib and A. Tzschach, *Chem. Ber.* 1959, **92**, 704.
10. L. E. Manzer, *Inorg. Synth.* 1982, **21**, 135.
11. M. W. Duckworth, G. W. A. Fowles and P. T. Greene, *J. Chem. Soc. A* 1967, 1592.

Polyhedron Vol. 8, No. 10, pp. 1345–1350, 1989
Printed in Great Britain

0277–5387/89 $3.00+.00
© 1989 Pergamon Press plc

CHIRAL HETEROCYCLIC LIGANDS—VI.* (4*S*,7*R*)-7,8,8-TRIMETHYL-4,5,6,7-TETRAHYDRO-4,7-METHANO-1H(2H)-INDAZOLE AND X-RAY STRUCTURE OF A COPPER(II) COMPLEX

ANDREW A. WATSON, DONALD A. HOUSE and PETER J. STEEL†

Chemistry Department, University of Canterbury, Christchurch, New Zealand

(*Received* 17 *October* 1988; *accepted* 19 *January* 1989)

Abstract—Dichlorobis[(4*S*,7*R*)-7,8,8-trimethyl-4,5,6,7-tetrahydro-4,7-methano-2H-indazole]copper(II), $C_{22}H_{32}Cl_2N_4Cu$, crystallizes in the monoclinic space group $C2$ with $a = 23.110(5)$, $b = 7.533(1)$, $c = 7.041(1)$ Å, $\beta = 105.25(2)°$ and $Z = 2$. The structure was refined to $R = 2.9\%$. The copper atom lies on a crystallographic two-fold rotation axis and has coordination geometry intermediate between tetrahedral and square-planar. A system of bifurcated (intra- and intermolecular) N—H···Cl hydrogen bonds connects the molecules in chains. The crystal structure and NMR studies of a palladium(II) complex show that the title ligand complexes through the more sterically hindered N(1) nitrogen. It is proposed that for unsymmetrical pyrazoles, the relative stabilities of the tautomers of the ligand is an important factor in determining the choice of the site of coordination to metal ions.

The coordination chemistry of pyrazoles and of pyrazole-derived ligands has expanded rapidly over the last decade and has been the subject of a recent review.[1] Simple neutral pyrazoles readily coordinate through the unsubstituted (pyridine-like) nitrogen to form complexes (**1**) with various transition metals, while the pyrazolide anion can act as a 1,2-exobidentate ligand (**2**), which bridges two metals or metalloids.[1] Numerous multidentate ligands which contain pyrazole groups have also been synthesized and their coordination chemistry studied.[1,2] Of these, the polypyrazolylmethanes and polypyrazolylborates are the most well studied.[3]

The most commonly used pyrazoles are the commercially available ligands, pyrazole (**3**), 3,5-dimethylpyrazole (**4**) and the unsymmetrical 3(5)-methylpyrazole (**5**), which exists in solution as two tautomers (**5a**, **5b**).[4] Also well studied is the readily available unsymmetrical ligand indazole (**6**) which exists in solution as the 1-H tautomer (**6a**).[4] It is generally accepted[1] that the unsymmetrical ligands **5** and **6** coordinate to metal ions through the less sterically hindered nitrogen. Thus, **5** coordinates as the 5-methyl tautomer (**5b**), and **6** as the 1-H tautomer (**6a**), as has been confirmed by X-ray crystal structure determinations of metal complexes.[5–8]

Despite extensive research into the coordination chemistry of pyrazoles and the importance of chiral ligands in asymmetric catalysis, the coordination chemistry of non-racemic chiral pyrazoles is completely unexplored. We have previously reported[9–13] the synthesis and study of diverse multidentate ligands derived from the chiral ligand (**7**), which is readily available[14,15] in optically pure form from (+)-camphor, a common source of chirality in numerous important chiral auxiliaries.[16,17] We herein describe the first transition metal complexes of **7**. NMR studies of a palladium(II) complex and the X-ray crystal structure of a copper(II) complex reveal the surprising result that **7** coordinates through the more hindered [N(1)] nitrogen, that is as the 2-H tautomer (**7b**).

RESULTS AND DISCUSSION

The ligand **7** was prepared by formylation of camphor and subsequent condensation with hydra-

* For Part V, see ref. 13.

† Author to whom correspondence should be addressed.

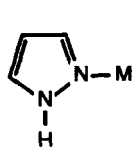

(1)

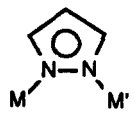

(2)

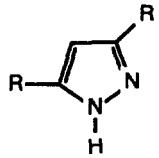

(3) R = H

(4) R = CH_3

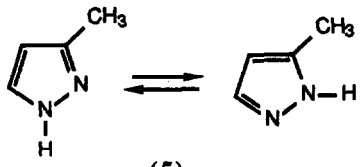

(a) (5) (b)

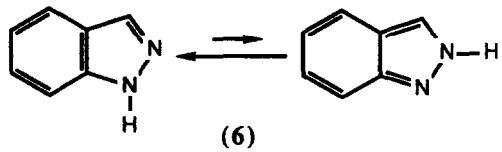

(a) (6) (b)

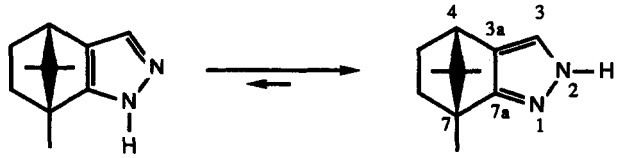

(a) (b)

(7)

zine, as previously reported.[14] Comparison of the ^1H and ^{13}C NMR spectra of **7** with the spectra of substituted derivatives,[10–13] indicates that in solution, **7** exists preferentially as the 2-H tautomer (**7b**). Particularly diagnostic in this respect are the chemical shifts for C(3) and the quaternary carbons C(3a) and C(7a), which are sensitive to the position of N-substitution in tetrahydroindazoles.[18,19] The greater stability of **7b** relative to **7a**, parallels the tautomerisms of other tetrahydroindazoles and the carbocyclic analogue isodicyclopentadiene.[20]

Reaction of **7** with MCl_2 (M = Pd, Cu) led to the isolation of complexes of stoichiometry $M(7)_2Cl_2$. The N—H IR stretching frequencies suggested the existence of N—H···Cl hydrogen bonds in both complexes, as have been observed in related pyrazole complexes of copper(II)[21] and palladium(II).[22] The Pd—Cl stretch at 350 cm^{-1} suggests *trans* coordination at the square-planar palladium as was observed[11] in a related complex of a substituted derivative of **7**. Because of the non-equivalence of the two nitrogens in **7**, two modes of coordination are possible corresponding to whether the ligand complexes as the 1-H tautomer (**7a**) or as the 2-H tautomer (**7b**). By analogy with the accepted tendency for coordination to occur through the less hindered nitrogen,[1] it would be expected that **7** should coordinate through the less hindered N(2) nitrogen, that is as the 1-H tautomer (**7a**). However, this expectation is not supported by the NMR spectra of the palladium complex. In particular, the ^{13}C NMR spectrum showed similar chemical shift values to those of the free ligand which, as stated above, exists as the 2-H tautomer (**7b**). Furthermore, the C(7) methyl protons experience a marked downfield shift in the complex (1.94 ppm) relative to the free ligand (1.33 ppm). This can be attributed to deshielding by an adjacent chlorine atom (as observed in related complexes[10]) only if coordination occurs through the N(1) nitrogen, that is as tautomer (**7b**).

In order to unambiguously determine the mode of coordination of **7**, a single crystal X-ray structure determination of the copper complex was undertaken. This structure was also of interest in order to determine the nature (intra- or intermolecular) of the hydrogen bonding in the complex and to determine the coordination geometry at the copper atom. Related CuN_2X_2 complexes exhibit a variety of coordination geometries at the copper atom, commonly involving expansion of the coordination number by association of square-planar monomeric

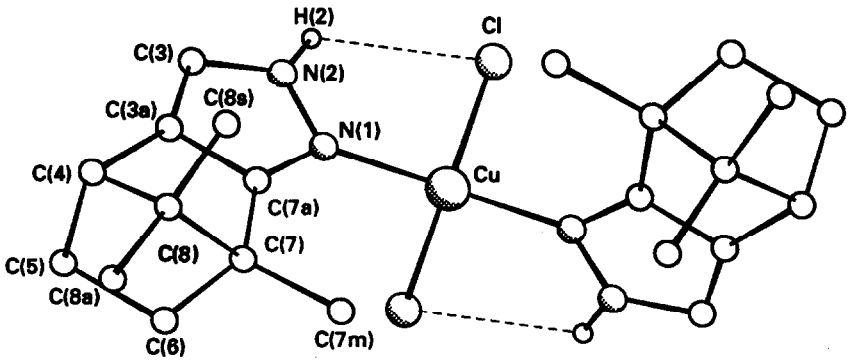

Fig. 1. Perspective view and atom labelling of the crystal structure. C—H hydrogens omitted for clarity.

units through axial interaction to adjacent molecules.[23–27]

Figure 1 shows a perspective view and atom labelling of the complex, which crystallizes in the monoclinic space group $C2$ with the copper atom lying on a crystallographic two-fold rotation axis. Table 1 lists bond lengths and angles for the complex. The geometry at the four-coordinate copper atom is intermediate between tetrahedral and square-planar, with the N(1)—Cu—C(1) mean planes mutually inclined at an angle of 57.0(2)° (cf. tetrahedral, 90°; square-planar, 0°). There is no expansion of the CuN_2Cl_2 core, as has been frequently observed in related structures which have square-planar coordination at the copper and weak axial interactions to atoms in adjacent molecules. The geometry at the copper atom probably results[28] from a combination of steric repulsion between the bulky bornyl groups of the ligand and the constraints imposed by hydrogen bonding. As shown in Fig. 2, H(2) is involved in bifurcated inter- and intramolecular hydrogen bonds, which connect molecules in chains perpendicular to the b axis (N(2)···Cl, 3.174(3) Å; H(2)···Cl, 2.67(2) Å; N(2)—H(2)···Cl, 113(2)°; N(2)···Cl*, 3.256(3) Å; H(2)···Cl*, 2.57(2) Å; N(2)—H(2)···Cl*,

Table 1. Bond lengths (Å) and angles (°) for the copper complex of 7

Cu—Cl	2.250(1)	Cu—N(1)	1.949(2)
N(1)—N(2)	1.362(4)	N(1)—C(7a)	1.336(5)
N(2)—C(3)	1.351(4)	C(3)—C(3a)	1.366(5)
C(3a)—C(4)	1.510(6)	C(3a)—C(7a)	1.395(4)
C(4)—C(5)	1.539(6)	C(4)—C(8)	1.573(5)
C(5)—C(6)	1.559(4)	C(6)—C(7)	1.554(5)
C(7)—C(7a)	1.498(5)	C(7)—C(7m)	1.527(4)
C(7)—C(8)	1.588(5)	C(8)—C(8s)	1.524(6)
C(8)—C(8a)	1.528(7)		

Cl—Cu—N(1)	95.4(1)	Cl—Cu—C(1a)	135.2(1)
N(1)—Cu—N(1a)	142.4(2)	Cl—Cu—N(1a)	98.7(1)
Cu—N(1)—N(2)	123.9(2)	Cu—N(1)—C(7a)	131.6(2)
N(2)—N(1)—C(7a)	104.5(2)	N(1)—N(2)—C(3)	111.8(3)
N(2)—C(3)—C(3a)	106.9(3)	C(3)—C(3a)—C(4)	149.0(3)
C(3)—C(3a)—C(7a)	105.5(3)	C(4)—C(3a)—C(7a)	105.5(3)
C(3a)—C(4)—C(5)	105.7(3)	C(3a)—C(4)—C(8)	99.6(3)
C(5)—C(4)—C(8)	102.1(3)	C(4)—C(5)—C(6)	103.5(3)
C(5)—C(6)—C(7)	104.5(3)	C(6)—C(7)—C(7a)	103.5(3)
C(6)—C(7)—C(7m)	115.4(3)	C(7a)—C(7)—C(7m)	118.6(3)
C(6)—C(7)—C(8)	101.1(3)	C(7a)—C(7)—C(8)	97.7(3)
C(7m)—C(7)—C(8)	117.6(3)	N(1)—C(7a)—C(3a)	111.3(3)
N(1)—C(7a)—C(7)	138.9(3)	C(3a)—C(7a)—C(7)	109.8(3)
C(4)—C(8)—C(7)	93.7(3)	C(4)—C(8)—C(8s)	113.5(3)
C(7)—C(8)—C(8s)	113.3(3)	C(4)—C(8)—C(8a)	113.7(3)
C(7)—C(8)—C(8a)	113.6(3)	C(8s)—C(8)—C(8a)	108.6(4)

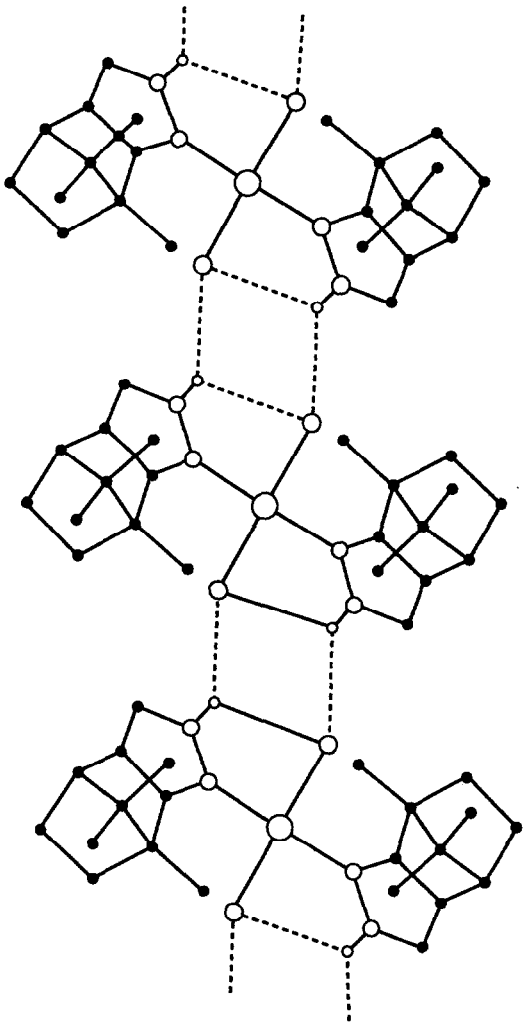

Fig. 2. Molecular packing projected down the *b* axis and showing hydrogen bonds as dashed lines.

128(2)° where Cl* is related to Cl by the transformation $-x, y, 2-z$). Both these forms of hydrogen bonding are common in complexes of pyrazoles.[5,7,29-32] The pyrazole ring is planar (maximum deviation from the mean plane: 0.004(5) Å) and the pyrazole rings are mutually inclined at an angle of 91.8(2)°. The geometry of the bornyl moiety is normal[9,13] and no close intermolecular contacts exist, other than those associated with the hydrogen bonding.

In accord with the conclusions drawn from the NMR studies, the crystal structure determination unambiguously demonstrates that the ligand coordinates through the more hindered N(1) nitrogen and hence as the 2-H tautomer. This is at variance with the generally accepted belief that steric factors control the site of coordination of unsymmetrical pyrazoles. Since we have shown above that the 2-H tautomer (**7b**) is the more stable tautomer, it is possible that this is a controlling factor in determining the mode of coordination of **7**.

For unsymmetrical pyrazoles the relative stabilities of the tautomers depend on a number of factors.[4,33] For **5**, the energy difference between the two tautomers is small,[4,33,34] and although a preference in favour of the 5-methyl tautomer was observed by low temperature ^{1}H NMR spectroscopy[35] and solid state ^{13}C NMR,[36] the fact that this ligand coordinates as the 5-methyl tautomer (**5b**) is probably indeed controlled by steric factors. A similar argument applies to **8**,[36,37] which has been reported to coordinate to gold(I) in both tautomeric forms[38] and to copper(II) as **8a**.[32] Highly significant however, is the report[8] of an X-ray structure of a platinum(II) complex of **9** in which coordination occurs as the 5-methyl tautomer (**9b**), which is expected to be the more stable tautomer.[33] Steric arguments would predict that coordination should occur as the 3-methyl tautomer (**9a**). Indazole (**6**) is well known[4,39] to exist as the 1-H tautomer (**6a**) and hence its preference for N(2) coordination may reflect the greater stability of **6a** rather than to be due to steric factors. Recent calculations[40] on tetrahydroindazoles (**10**) suggest a slight preference for the 2-H tautomer (**10b**). Introduction of the 4,7-methano bridge present in **7** should further stabilize the 2-H tautomer (**7b**), as the NMR studies show. These results lead us to propose that for unsymmetrical pyrazoles, the relative stabilities of the tautomers of the ligand is an important factor in determining the choice of the site of coordination to metal ions.[41]

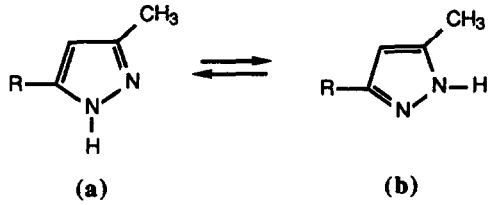

(a) (b)

(5) R = H

(8) R = C_6H_5

(9) R = CF_3

EXPERIMENTAL

Physical methods

IR and UV spectra were recorded with Shimadzu IR27G and Varian DMS100 spectrophotometers, respectively. Optical rotations were recorded with

a JASCO ORD/CD5 spectropolarimeter. ^1H and ^{13}C NMR spectra were recorded with a Varian XL300 spectrometer, operating at 299.930 and 75.426 MHz, respectively, for $CDCl_3$ solutions with Me_4Si as internal standard. Microanalyses were performed by the Chemistry Department, University of Otago.

Syntheses

The ligand **7** was prepared from (+)-camphor as previously described.[14] ^1H NMR: δ 0.66, s, 3H, *syn*-8-CH_3; 0.96, s, 3H, *anti*-8-CH_3; 1.33, s, 3H, 7-CH_3; 2.78, d, 1H, H(4); 7.09, s, 1H, H(3). ^{13}C NMR: δ 10.8, 7-CH_3; 19.2, *anti*-8-CH_3; 20.4, *syn*-8-CH_3; 27.8, C(5); 33.7, C(6); 47.1, C(4); 50.0, C(8); 61.0, C(7); 119.9, C(3); 125.8, C(3a); 166.0, C(7a).

Palladium complex of **7**. A mixture of palladium(II) chloride (0.05 g, 0.29 mmol), dichloromethane (10 cm^3) and **7** (0.10 g, 0.56 mmol) was stirred at room temperature for 5 days. The resulting yellow solution was filtered and concentrated to give a solid which was recrystallized from methanol–dichloromethane to give orange crystals. Yield: 33%. ν_{max} 3200 (NH), 2900, 1460, 1140, 1050, 660, 560, 350 cm^{-1}. λ_{max} ($CHCl_3$) 382 nm ($\varepsilon = 217$ M^{-1} cm^{-1}). λ ($\Delta\varepsilon$) 406 nm (+2.59 M^{-1} cm^{-1}), 380 (0). λ ([M]) 430 nm (+208.3° M^{-1} m^{-1}), 413 (0), 361 (−488), 340 (0). ^1H NMR: δ 0.65, s, 3H, *syn*-8-CH_3; 0.97, s, 3H, *anti*-8-CH_3; 1.94, s, 3H, 7-CH_3; 2.65, d, 1H, H(4); 6.56, s, 1H, H(3). ^{13}C NMR: δ 11.5, 7-CH_3; 19.2, *anti*-8-CH_3; 20.5, *syn*-8-CH_3; 27.9, C(5); 32.4, C(6); 46.8, C(4); 51.8, C(8); 62.0, C(7); 122.0, C(3); 128.3, C(3a); 166.5, C(7a). Found: C, 49.1; H, 6.1; N, 10.5. Calc. for $C_{22}H_{32}Cl_2N_4Pd$: C, 49.9; H, 6.1; N, 10.6%.

Copper complex of **7**. An ethanolic solution of **7** (0.41 g, 2.33 mmol) was added to an ethanolic solution of cupric chloride dihydrate. The resulting yellow crystals were filtered and air-dried. Yield: 60%. M.p. 218–220°C. ν_{max}(KBr) 3375, 2950, 1580, 1430, 1390, 1270, 1160, 1120, 1060, 830, 660, 560, 300 cm^{-1}. λ_{max}($CHCl_3$) 728 nm. Found: C, 53.8; H, 6.8; N, 11.3. Calc. for $C_{22}H_{32}Cl_2N_4Cu \cdot H_2O$: C, 54.3; H, 6.6; N, 11.5%.

Crystallography

Intensity data were collected with a Nicolet R3m four-circle diffractometer using monochromatized Mo-K_α radiation ($\lambda = 0.7107$ Å) and a yellow crystal measuring $0.35 \times 0.16 \times 0.08$ mm. Cell parameters were determined by least-squares refinement, the setting angles of 25 accurately centred reflections ($2\theta > 23°$) being used. Throughout data collection the intensities of three standard reflections were monitored at regular intervals and this indicated no significant crystal decomposition. The intensities were corrected for Lorentz and polarization effects, but no correction for absorption was deemed necessary. Reflections with $I > 3\sigma(I)$ were used for structure solution and refinement.

The structure was solved by conventional Patterson and Fourier methods, and refined by blocked-cascade least-squares procedures. The absolute configuration employed was that consistent with the known[42] absolute configuration of (+)-camphor from which the ligand was synthesized. All non-hydrogen atoms were refined with anisotropic thermal parameters. Hydrogen atoms were included in calculated positions with isotropic thermal parameters equal to the isotropic equivalent of their carrier atoms. The function minimized was $\Sigma w(|F_o| - |F_c|)^2$, with $w = [\sigma^2(F_o) + 0.00026F_o^2]^{-1}$. All calculations (including diagrams) were performed on a Nova 4X computer using SHELXTL.[43] Final atom coordinates, thermal parameters and structure factors have been deposited with the Editor as supplementary data. Atom coordinates have also been deposited with the Cambridge Crystallographic Data Centre.

Crystal data at −120°C: $C_{22}H_{32}Cl_2N_4Cu$, M_r 487.0, monoclinic, space group $C2$, $a = 23.110(5)$, $b = 7.533(1)$, $c = 7.041(1)$ Å, $\beta = 105.25(2)°$, $V = 1182.5(4)$ Å^3, $F(000)$ 510, D_c ($Z = 2$) 1.37 g cm^{-3}, $\mu = 11.7$ cm^{-1}, θ–2θ scans, $2\theta_{max} = 55°$, $N = 1464$, $N_0 = 1330$, 131 parameters, $S = 1.17$, $R = 0.029$, $R_w = 0.033$.

Acknowledgement—We acknowledge grants from the Research Committee of the New Zealand Universities Grants Committee.

REFERENCES

1. S. Trofimenko, *Prog. Inorg. Chem.* 1986, **34**, 115.
2. J. Reedijk, in *Comprehensive Coordination Chemistry* (Edited by G. Wilkinson, R. D. Gillard and J. A. McCleverty), Vol. 2, p. 73. Pergamon Press, Oxford (1987).
3. A. Shaver, in *Comprehensive Coordination Chemistry* (Edited by G. Wilkinson, R. D. Gillard and J. A. McCleverty), Vol. 2, p. 245. Pergamon Press, Oxford (1987).
4. J. Elguero, C. Marzin, A. R. Katritzky and P. Linda, The tautomerism of heterocycles, in *Adv. Heterocycl. Chem.* Suppl. 1 (1976).
5. J. Reedijk, B. A. Stork-Blaisse and G. C. Vershoor, *Inorg. Chem.* 1971, **10**, 2594.
6. P. Dapporto and F. Mani, *J. Chem. Res.* (*S*) 1979, 374.
7. R. W. M. ten Hoedt, J. Reedijk and G. C. Vershoor, *Recl. Trav. Chim. Pays-Bas* 1981, **100**, 400.

8. J. L. Atwood, K. R. Dixon, D. T. Eadie, S. R. Stobart and M. Zaworotko, *Inorg. Chem.* 1983, **22**, 774.
9. P. J. Steel, *Acta Cryst.* 1983, **39C**, 1623.
10. D. A. House, P. J. Steel and A. A. Watson, *Aust. J. Chem.* 1968, **39**, 1525.
11. A. A. Watson, D. A. House and P. J. Steel, *J. Organomet. Chem.* 1986, **311**, 387.
12. A. A. Watson, D. A. House and P. J. Steel, *Inorg. Chim. Acta* 1987, **130**, 167.
13. D. A. House, P. J. Steel and A. A. Watson, *J. Chem. Soc., Chem. Commun.* 1987, 1575.
14. R. Jacquier and G. Maury, *Bull. Soc. Chim. Fr.* 1967, 295.
15. S. Nagai, N. Oda, I. Ito and Y. Kudo, *Chem. Pharm. Bull.* 1979, **27**, 1771.
16. T. Money, *Nat. Prod. Rep.* 1985, **2**, 253.
17. W. Oppolzer, *Tetrahedron* 1987, **43**, 1969.
18. S. Sutthivaiyakit, W. Sucrow, H. Wonnemann and C. Kruger, *Lieb. Ann. Chem.* 1985, 794.
19. J. de Mendoza, P. Prados and J. Elguero, *Heterocycles* 1985, **23**, 2629.
20. P. D. Bartlett and C. Wu, *J. Org. Chem.* 1984, **49**, 1880.
21. J. Reedijk, J. C. A. Windhorst, N. H. M. van Ham and W. L. Groeneveld, *Recl. Trav. Chim. Pays-Bas* 1971, **111**, 234.
22. F. Colleta, R. Ettorre and A. Gambaro, *J. Inorg. Nucl. Chem.* 1975, **37**, 314.
23. B. J. Hathaway, in *Comprehensive Coordination Chemistry* (Edited by G. Wilkinson, R. D. Gillard and J. A. McCleverty), Vol. 5, p. 533. Pergamon Press, Oxford (1987).
24. J. A. C. van Ooijen and J. Reedijk, *J. Chem. Soc., Dalton Trans.* 1978, 1170.
25. R. H. P. Francisco, J. R. Lechat and Y. P. Mascarenhas, *Acta Cryst.* 1979, **35B**, 1468.
26. W. E. Marsh, W. E. Hatfield and D. J. Hodgson, *Inorg. Chem.* 1982, **21**, 2679.
27. M. Biagini Cingi, A. M. Manotti Lanfredi, A. Tiripicchio, J. P. Cornelissen, J. P. Haasnoot and J. Reedijk, *Inorg. Chim. Acta* 1987, **129**, 217.
28. H. H. Murray, R. G. Raptis and J. P. Fackler, *Inorg. Chem.* 1988, **27**, 26.
29. F. S. Keij, R. A. G. de Graff, J. G. Haasnoot, A. J. Oosterling, E. Pedersen and J. Reedijk, *J. Chem. Soc., Chem. Commun.* 1988, 423.
30. S. Gorter, A. D. van Ingen Schenau and G. C. Verschoor, *Acta Cryst.* 1974, **30B**, 1867.
31. J. Reedijk, J. C. Jansen, H. Van Koningsveld and C. G. van Kralingen, *Inorg. Chem.* 1978, **17**, 1990.
32. W. C. Velthuizen, J. G. Haasnoot, A. J. Kinneging, F. J. Rietmeijer and J. Reedijk, *J. Chem. Soc., Chem. Commun.* 1983, 1366.
33. J. Elguero, in *Comprehensive Heterocyclic Chemistry* (Edited by A. R. Katritzky and C. W. Rees), Vol. 5, p. 167. Pergamon Press, Oxford (1984).
34. A crystal structure containing both tautomers of **5** hydrogen bonded to an alcohol hydroxyl group has recently been reported; F. Toda, K. Tanaka, J. Elguero, Z. Stein and I. Goldberg, *Chem. Lett.* 1988, 1061.
35. M. T. Chenon, C. Coupry, D. M. Grant and R. J. Pugmire, *J. Org. Chem.* 1977, **42**, 659.
36. R. Faure, E.-J. Vincent, A. Rousseau, R. M. Claramunt and J. Elguero, *Can. J.Chem.* 1988, **66**, 1141.
37. O. Bensaude, M. Chevrier and J.-E. Dubois, *Tetrahedron* 1978, **34**, 2259.
38. G. Banditelli, A. L. Bandini, G. Minghetti and F. Bonati, *Can. J. Chem.* 1981, **59**, 1241.
39. R. Faure, E.-J. Vincent and J. Elguero, *Heterocycles* 1983, **9**, 1713.
40. D. Kocjan, M. Hodoscek and D. Hadzi, *J. Mol. Struct. Theochem.* 1987, **37**, 331.
41. A dynamic metal-proton interexchange has recently been reported in a copper(I) complex of a symmetrical pyrazole; J. Diez, S. Falagan, P. Gamasa and J. Gimeno, *Polyhedron* 1988, **7**, 37.
42. M. G. Northholt and J. H. Palm, *Recl. Trav. Chim. Pays-Bas* 1966, **85**, 143.
43. G. M. Sheldrick, *SHELXTL User Manual*, Revision 4. Nicolet XRD Corporation, Madison, Wisconsin (1984).

Polyhedron Vol. 8, No. 10, pp. 1351–1355, 1989
Printed in Great Britain

0277–5387/89 $3.00+.00
© 1989 Pergamon Press plc

SYNTHESIS AND ELECTROCHEMICAL OXIDATION OF TETRANUCLEAR NICKEL CARBONYL PHOSPHINE CLUSTERS. THE STRUCTURE OF $Ni_4(CO)_6(PMe_3)_4$

MANFRED BOCHMANN* and IAN HAWKINS

School of Chemical Sciences, University of East Anglia, Norwich NR4 7TJ, U.K.

and

LESLEY J. YELLOWLEES

Department of Chemistry, University of Edinburgh, Edinburgh EH9 3JJ, U.K.

and

MICHAEL B. HURSTHOUSE and RICHARD L. SHORT

Department of Chemistry, Queen Mary College, London E1 4NS, U.K.

(*Received* 1 *November* 1988; *accepted* 19 *January* 1989)

Abstract—Treatment of bis(cyclooctadiene)nickel with carbon monoxide and trialkylphosphines in a 2:3:2 ratio provides a high-yield route to the clusters, $Ni_4(\mu\text{-}CO)_6L_4$ ($L = PMe_3$, PBu^n_3). The clusters are cleaved by PPh_3 and I_2, and are oxidized electrochemically in two successive one-electron steps; only the first oxidation step to a monocation is reversible. The molecular structure of $Ni_4(CO)_6(PMe_3)_4$ consists of a regular Ni_4 tetrahedron with edge-bridging CO and terminally coordinating PMe_3 ligands.

Whereas there are numerous carbonyl phosphine clusters of palladium and platinum,[1,2] related nickel clusters are rare, but examples include $Ni_4(CO)_6[P(CH_2CH_2CN)_3]_4$, isolated in low yield by thermolysis of $Ni(CO)_2[P(CH_2CH_2CN)_3]_2$[3] and $Ni_3(\mu\text{-}CO)_3(CO)_3[HC(PPh_2)_3]$.[4] Our recent serendipitous isolation and structural characterization of the unusual co-crystallization compound, $\{[Ni(PMe_3)_4]\cdot BF_4\cdot[Ni_4(\mu\text{-}CO)_6(PMe_3)_4]\}$, as one of the products formed during the carbonylation of $[NiMe(PMe_3)_4]BF_4$,[5] prompted us to synthesize similar nickel carbonyl phosphine clusters by a more rational route and in a pure form. We report here the preparation of the clusters, $Ni_4(\mu\text{-}CO)_6L_4$ [$L = PMe_3$ (**1**) and $L = PBu^n_3$ (**2**)].

EXPERIMENTAL

General procedures

All experiments were carried out under nitrogen using standard vacuum-line techniques. Solvents were distilled from sodium benzophenone (diethyl ether, THF), sodium (toluene) or calcium hydride (dichloromethane, acetonitrile). Perkin–Elmer 297 and 684 (IR) and Jeol PMX-60 and FX-100 (^1H, ^{31}P NMR) spectrometers were used. Melting points were determined in sealed capillaries under nitrogen and are uncorrected. $Ni(1,5\text{-}COD)_2$ was prepared as described.[6]

Preparation of $Ni_4(\mu\text{-}CO)_6(PMe_3)_4$ (1)

A solution of bis(1,5-cyclooctadiene)nickel (2.75 g, 10.0 mmol) was stirred at room temperature in 200 cm^3 toluene containing trimethylphosphine (1.04 cm^3, 10 mmol) in a partially evacuated flask. Carbon monoxide (400 cm^3, 16 mmol) was admitted from a gas burette. After the initial rapid gas uptake, the solution was stirred until no further carbon monoxide was consumed (*ca* 6 h). During this time, the colour of the solution changed from yellow to orange–brown. Volatiles were then removed *in vacuo* and the residue was washed with 2×20 cm^3 of cold methanol, dissolved in 50 cm^3 toluene, filtered and left to crystallize at $-20°C$.

* Author to whom correspondence should be addressed.

The product was obtained as orange rods (1.06 g, 1.53 mmol, 61%), m.p. 136–137°C.

IR (Nujol mull) 1800 vs, br, 1760 vs, br, 1420 m, 1305 m, 1288 s, 951 vs, br, 735 s, 678 m, 515 vs, br, 385 vs, br cm^{-1}. Found: C, 30.9; H, 5.1. Calc. for $C_{18}H_{36}Ni_4O_6P_4$: C, 30.6; H, 5.1%.

Preparation of $Ni_4(\mu\text{-}CO)_6(PBu^n_3)_4$ **(2)**

This compound was obtained in a fashion similar to **1**. The greenish-orange reaction mixture was filtered through Kieselguhr prior to vacuum removal of volatiles. The product is best recrystrallized from diethyl ether and obtained as orange prisms (1.5 g, 1.25 mmol, 50%), dec. 90°C.

IR (Nujol mull) 1800 vs, 1450 s, 1410 s, 1350, 1309, 1218, 1095, 1050, 970, 792, 730 cm^{-1}. Found: C, 53.6; H, 9.1. Calc. for $C_{54}H_{108}Ni_4O_6P_4$: C, 53.5; H, 9.0%.

Thermolysis of **1**

A solution of **1** in refluxing toluene, darkens to deep brown over a period of 4 h and yields **4** as overgrown black needles as the sole product, dec. > 150°C.

IR (Nujol mull) 2000 m, 1770 vs, 1748 vs, 1690 vs, 1420, 1301, 1285 m, 960 vs, 832, 675, 520 w, br, 470 w, br cm^{-1}; solution spectrum in Et_2O: 2002, 1781, 1755, 1719, 1694 cm^{-1}. Found: C, 29.4; H, 5.0. Calc. for $C_{23}H_{45}Ni_6O_8P_5$: C, 28.9; H, 4.7%.

X-ray crystallography

All X-ray measurements were made on a crystal of dimensions $0.5 \times 0.2 \times 0.2$ mm using an Enraf–Nonius CAD4 diffractometer and graphite monochromated Mo-K_α radiation ($\lambda = 0.71069$ Å), following previously detailed procedures.[7] The structure was solved via the application of direct methods and refined by full-matrix least-squares. Non-hydrogen atoms were refined anisotropically; hydrogens were included in idealized positions and refined as components of rigid groups with group U_{iso} values. Experimental details are as follows.

Crystal data. $C_{18}H_{36}Ni_4O_6P_4$, $M_r = 707.11$, orthorhombic, $a = 10.062(1)$, $b = 16.347(3)$, $c = 18.079(2)$ Å, $V = 2973.7$ Å^3. Space group *Pnma*, $Z = 4$, $D_c = 1.58$ g cm^{-3}, μ(Mo-K_α) = 26.27 cm^{-1}, $F(000) = 1456$.

Data collection. $1.5 \leqslant \theta \leqslant 25°$, $+h$, $+k$, $+l$, ω–2θ scan, data measured: 2978, unique: 2625, observed: 1643 [$I > 1.5\sigma(I)$].

Refinement. 170 parameters, weights = $[\sigma^2(F) + 0.00002F_o^2]^{-1}$, $R = 0.048$, $R_w = 0.043$.

Tables of atomic coordinates and displacement factor coefficients, full lists of bond lengths and angles and lists of F_o/F_c values have been deposited as Supplementary Data with the Editor.

Electrochemistry

Electrochemical measurements were carried out using a Princeton Applied Research 170 electrochemical system. The electrochemical cell contained a 0.002 cm^{-2} platinum disk working electrode, a platinum wire auxiliary electrode and a silver/silver chloride reference electrode (ferrocene/ferrocinium: $E_{1/2} = +0.55$ V vs silver/silver chloride). The variable temperature studies were performed using a Haacke Q thermostated bath.

Spectroelectrochemical data were collected as before[8] using a Metrohm E506 potentiostat and an optically transparent electrode (platinum/rhodium gauze) cell located directly in the beam of a Perkin–Elmer Lambda 9 spectrophotometer.

RESULTS AND DISCUSSION

Treatment of a 1:1 mixture of bis(1,5-cyclooctadiene)nickel and trimethylphosphine in toluene at room temperature with 1.5 equivalents of carbon monoxide gives $Ni_4(\mu\text{-}CO)_6(PMe_3)_4$ **(1)**, together with some $Ni(CO)_2(PMe_3)_2$; the former is obtained as orange crystals in 40–60% yield [eq. (1)].

The IR spectrum of **1** in hexane solution indicates the presence of a single type of bridging CO ligand by a single sharp band at 1796 cm^{-1}. The ^1H and ^{31}P NMR spectra in C_6D_6 consist of singlets at δ 1.1 and 4.6 ppm, respectively. The analogous cluster $Ni_4(\mu\text{-}CO)_6(PBu^n_3)_4$ **(2)** is prepared similarly, as orange air-stable crystals and is characterized by an IR band at 1798 cm^{-1} (hexane solution) and a singlet at δ 27.5 ppm in the ^{31}P NMR spectrum.

$$4Ni(COD)_2 + 4L + 6CO \longrightarrow Ni_4(\mu\text{-}CO)_6L \quad (1)$$

(1) L = PMe_3
(2) L = PBu^n_3.

Attempts to synthesize a similar tricyclohexylphosphine cluster were unsuccessful. The poorly soluble, brown solid which was obtained did contain bridging CO ligands as indicated by several IR bands between 1830 and 1760 cm^{-1}, but could not be separated from the more stable $Ni(CO)_2(PCy_3)_2$. The reaction with PPh_3 gives $Ni(CO)_2(PPh_3)_2$ exclusively.

By contrast to the reactions with nickel, we found recently that the application of this synthetic approach to palladium gives rise to the cluster, $Pd_8(\mu_3\text{-}CO)_2(\mu\text{-}CO)_6(PMe_3)_7$.[2] The analogous reac-

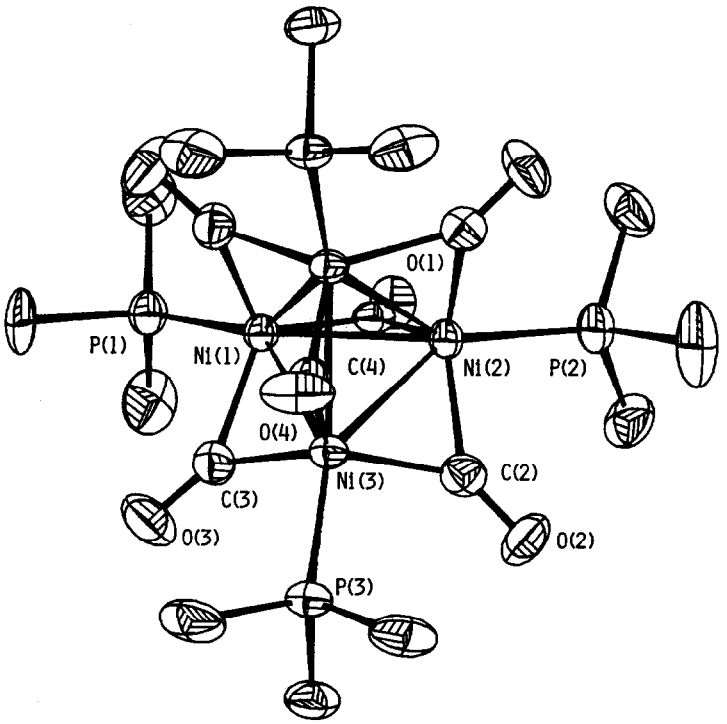

Fig. 1. The molecular structure of **1**, showing the atomic numbering scheme. Ellipsoids correspond to 50% probability.

tion between $Pt(1,5\text{-}COD)_2$, PMe_3 and CO produces a black, insoluble, microcrystalline material which contains both terminal and bridging CO ligands (ν(CO) 2000, 1825, 1775 cm^{-1}), but could not be identified.

The structure of **1** (Fig. 1) is based on a regular Ni_4 tetrahedron and resembles the Ni_4 cluster in $\{[Ni(PMe_3)_4]\cdot BF_4\cdot[Ni_4(CO)_6(PMe_3)_4]\}$ (**3**).[5] Selected bond lengths and angles are given in Table 1. The molecule lies on a crystallographic mirror plane which contains Ni(1), P(1), Ni(2), P(2), C(1), O(1), C(4) and O(4). The average Ni—Ni distance of 2.492(4) Å in **1**, compares well with the Ni—Ni bond length of 2.476(6) Å in **3**. The edges of the Ni_4 tetrahedron are bridged by six CO ligands. The average Ni—C distances in **1** (1.921 Å) are 0.12 Å longer than in **3**, while the C—O distances are shorter by about the same amount, and the Ni—C—Ni angles in **1** (81°) are consequently 6° more acute. These structural differences are reflected in the slightly higher CO stretching frequency of **1** (1796 cm^{-1}), compared to **3** (1780 cm^{-1}). The previously reported $P(CH_2CH_2CN)_3$ analogue of **1** has slightly longer Ni—Ni bonds (2.509 Å) and intermediate average Ni—C distances (1.886 Å) and Ni—C—Ni angles (83.4°).[3b]

Table 1. Selected bond lengths (Å) and angles (°) of **1**

Ni(1)—Ni(2)	2.477(4)	Ni(1)—Ni(3)	2.502(4)
Ni(2)—Ni(3)	2.489(3)	Ni(3)—Ni(3a)	2.498(4)
Ni(1)—P(1)	2.157(5)	Ni(2)—P(2)	2.149(5)
Ni(1)—C(1)	1.903(13)	Ni(2)—C(1)	1.911(13)
Ni(2)—C(2)	1.929(10)	Ni(3)—C(2)	1.896(10)
O(1)—C(1)	1.193(12)		

Ni(3)—Ni(1)—Ni(2)	60.0	C(1)—Ni(1)—P(1)	96.0(4)
C(3)—Ni(1)—P(1)	95.2(4)	C(3)—Ni(1)—C(1)	122.4(3)
C(2)—Ni(2)—P(2)	94.8(3)	C(2)—Ni(2)—C(1)	119.1(4)
Ni(2)—C(1)—Ni(1)	81.0(5)	O(1)—C(1)—Ni(1)	140.6(8)
O(1)—C(1)—Ni(2)	138.4(8)	Ni(3)—C(2)—Ni(2)	81.2(4)
Ni(3)—C(3)—Ni(1)	81.3(4)	Ni(3)—C(4)—Ni(3)	80.5(5)

Compounds **1** and **2** belong to a family of 60-valence electron (VE) clusters with tetrahedral metal frameworks, for example $[Fe_4(\mu_3\text{-}CO)(\mu\text{-}CO)_3(CO)_9]^{2-}$,[9] $M_4(CO)_{12}$ (M = Co, Rh),[10,11] $Ir_4(\mu\text{-}CO)_3(CO)_5(PMe_3)_4$[12] and $Ni_4(\mu\text{-}CO)_6[P(CH_2CH_2CN)_3]_4$.[3] The cobalt, rhodium and iridium clusters all have planar triangular bases $M_3(\mu\text{-}CO)_3L_3$, similar to the basal $Ni_3(\mu\text{-}CO)_3L_3$ unit in **1**, but are capped by ML_3 fragments. Thus the apical–basal M—M distances are longer than the bonds between the basal metal atoms. In $Ir_4(CO)_8(PMe_3)_4$, the steric effect of packing the four PMe_3 and eight CO ligands around the Ir_4 core results in the lengthening of one basal Ir—Ir distance. No such distortions are present in the nickel compounds.

No 60-VE clusters of the $M_4(CO)_6L_4$ structure are known for palladium and platinum, which instead form the 58-VE clusters $M_4(\mu\text{-}CO)_5(PMe_2Ph)_4$, in which the metal core adopts a butterfly structure.[13,14]

No reaction occurs between **1** or **2** and diphenyl acetylene or dimethyl acetylenedicarboxylate, in contrast to the reactivity of the isoelectronic $Co_4(CO)_{12}$ which gives $Co_4(CO)_{10}(C_2R_2)$ or $Co_2(CO)_6(C_2R_2)$, depending on the alkyne used.[15] Treatment of the clusters with triphenylphosphine cleaves the Ni—Ni bonds and gives $Ni(CO)_2(PPh_3)_2$,[16] again in contrast to $Co_4(CO)_{12}$ where ligand substitution takes place.[17] If **1** is reacted with only one equivalent of PPh_3, a mixture of $Ni(CO)_2(PPh_3)_2$ and unreacted **1** is formed. There is no reaction with H_2 or $LiBEt_3H$, or with $AgBF_4$ in THF and trimethylamine N-oxide in acetonitrile. The addition of elemental sulphur or selenium leads to the evolution of CO and the formation of unidentified insoluble products, while **1** reacts with iodine to give the known[18] complex $NiI_2(CO)(PMe_3)_2$.

Electrochemical oxidation of **1** *and* **2**

There is no observable redox process of **1** in THF solution in the reductive range, whereas an irreversible oxidative process is observed at a modest positive potential. The oxidation process is still irreversible at −40°C. In dichloromethane, however, the oxidation is fully reversible with a half-wave potential $E_{1/2} = +0.28$ V vs silver/silver chloride (0.3 M $NBu^n_4BF_4$ as supporting electrolyte). Coulometry confirms that this oxidation is a one-electron process. A further, irreversible oxidation step is observed at +0.78 V. For complex **2**, the reversible oxidation step is found at $E_{1/2} = +0.35$ V. Evidently, removal of one electron from the metal-centred HOMO of the cluster leaves the Ni_4 core intact, while the second oxidation step induces fragmentation:

$$Ni_4(CO)_6L_4 \underset{}{\overset{+0.28\,V}{\rightleftharpoons}} [Ni_4(CO)_6L_4]^+ \xrightarrow{+0.78\,V} \text{Fragmentation.}$$

This interpretation is confirmed by spectroelectrochemistry results in the 5000–30,000 cm^{-1} region. On oxidation of **1** in dichloromethane at −40°C at a constant potential of +0.5 V, the spectrum of **1** is gradually replaced by the spectrum of $\mathbf{1}^+$ (Figs 2 and 3), with the disappearance of the absorption at 21,700 cm^{-1} and an increase in intensity of weak bands at 8600 and 13,600 cm^{-1}. The presence of an isosbestic point (Fig. 3) indicates a clean conversion of **1** into $\mathbf{1}^+$. The first electron-transfer step is totally reversible, since reversal of the electrogeneration potential to 0 V results in the complete recovery of the absorption spectrum of the starting material **1**, that is $\mathbf{1}^+$ is a stable species in dichloromethane.

There is no evidence for intervalence bands in the spectrum, in accord with the assumption that the positive charge in $\mathbf{1}^+$ is delocalized over the Ni_4 core.

Thermolysis of **1**

At prolonged reaction times (24 h) the formation of **1** from $Ni(COD)_2$ is accompanied by small amounts of a dark brown material (**4**) which crys-

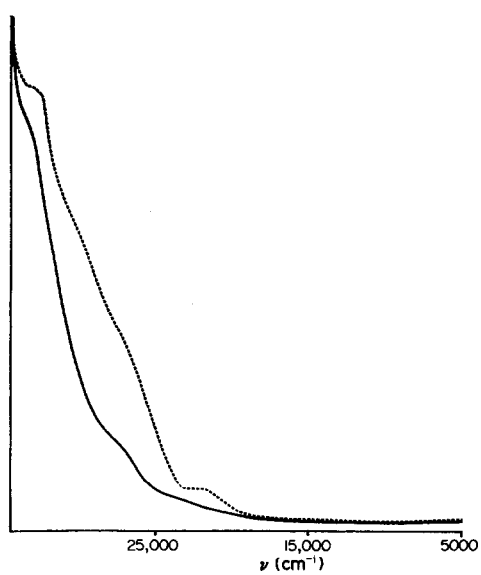

Fig. 2. Electronic spectrum of **1** (···) and of electrochemically generated $\mathbf{1}^+$ (——) in CH_2Cl_2 solution at −40°C, in the range of 5000–30,000 cm^{-1}. Supporting electrolyte: 0.2 M $NBu^n_4BF_4$.

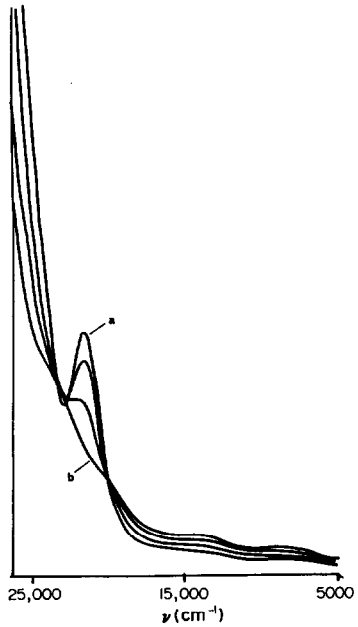

Fig. 3. Electrochemical generation of 1^+ (a) initial spectrum of **1**; (b) spectrum of 1^+. Recording conditions were as for Fig. 2.

tallizes as fine black needles. An identical material is obtained as the sole product by refluxing **1** in toluene for 4 h. The IR spectrum indicates the presence of a terminal CO and several bridging CO ligands. Attempts to grow crystals suitable for X-ray diffraction were unsuccessful. The positive-ion fast atom bombardment mass spectrum (FAB–MS) shows the ion grouping of the highest mass at *m/e* 957. Assuming that this mass corresponds to the parent peak, the result would suggest the presence of the 86-VE cluster $Ni_6(CO)_8(PMe_3)_5$. Four successive losses of CO are seen, in addition to peaks due to $[Ni_6(CO)_5(PMe_3)_4]^+$ (*m/e* 795) and $[Ni_5(CO)_4(PMe_3)_4]^+$ (*m/e* 709). The formulation of **4** as an 86-VE cluster is consistent with the existence of the trigonal-antiprismatic cluster anion $[Ni_6(CO)_{12}]^{2-}$.[19] Other 86-VE clusters are $[M_6(CO)_{18}]^{2-}$ (M = Ru,[20] Os[21]), $M_6(CO)_{16}$ (M = Co,[22] Rh[23]) and $[Re_6C(CO)_{18}H_2]^{2-}$;[24] all have an octahedral M_6 core.

Acknowledgements—We gratefully acknowledge the support by the University of East Anglia (to I.H.) and the provision of FAB–MS and X-ray facilities by the SERC.

REFERENCES

1. P. M. Maitlis, P. Espinet and M. J. H. Russell, in *Comprehensive Organometallic Chemistry* (Edited by E. W. Abel, F. G. A. Stone and G. Wilkinson), Chap. 38.3. Pergamon Press, Oxford (1982); F. R. Hartley, *ibid.*, Chap. 39; R. Goddard, P. W. Jolly, C. Krüger, K. P. Schick and G. Wilke, *Organometallics* 1982, **1**, 1709; E. G. Mednikov, N. K. Eremenko, Y. L. Slovokhotov and Y. T. Struchkov, *J. Organomet. Chem.* 1986, **301**, C35.
2. M. Bochmann, I. Hawkins, M. B. Hursthouse and R. L. Short, *Polyhedron* 1987, **6**, 1987.
3. (a) L. S. Meriwether, E. C. Colthup, M. L. Fiene and F. A. Cotton, *J. Inorg. Nucl. Chem.* 1959, **11**, 181; (b) M. J. Bennet, F. A. Cotton and B. H. C. Winquist, *J. Am. Chem. Soc.* 1967, **89**, 5366.
4. J. A. Osborn and G. G. Stanley, *Angew. Chem. Int. Ed. Engl.* 1980, **19**, 1025.
5. M. Bochmann, I. Hawkins, M. B. Hursthouse and R. L. Short, *J. Organomet. Chem.* 1987, **332**, 361.
6. R. A. Schunn, *Inorg. Synth.* 1974, **15**, 5.
7. R. A. Jones, K. M. A. Malik, M. B. Hursthouse and G. Wilkinson, *J. Am. Chem. Soc.* 1979, **101**, 4128.
8. G. A. Heath, L. J. Yellowlees and P. S. Braterman, *J. Chem. Soc., Chem. Commun.* 1981, 287.
9. R. J. Doedens and L. F. Dahl, *J. Am. Chem. Soc.* 1966, **88**, 4847.
10. F. H. Carré, F. A. Cotton and B. A. Frenz, *Inorg. Chem.* 1976, **15**, 380.
11. C. H. Wei, G. R. Wilkes and L. F. Dahl, *J. Am. Chem. Soc.* 1967, **89**, 4792.
12. D. J. Darensbourg and B. J. Baldwin-Zuschke, *Inorg. Chem.* 1981, **20**, 3846.
13. J. Dubrawski, J. C. Kriege-Simondsen and R. D. Feltham, *J. Am. Chem. Soc.* 1980, **102**, 2089.
14. J. Chatt and P. Chini, *J. Chem. Soc. A* 1970, 1538; R. G. Vranka, L. F. Dahl, P. Chini and J. Chatt, *J. Am. Chem. Soc.* 1969, **91**, 1574.
15. R. S. Dickson and P. J. Frazer, *Adv. Organomet. Chem.* 1974, **12**, 323.
16. P. W. Jolly and G. Wilke, *The Organic Chemistry of Nickel*, Vol. I, p. 57. Academic Press, New York (1974).
17. D. Labrove and R. Poilblanc, *Inorg. Chim. Acta* 1972, **6**, 387.
18. C. Saint-Joly, A. Mari, A. Gleizes, M. Dartiguenave, Y. Dartiguenave and J. Galy, *Inorg. Chem.* 1980, **19**, 2403.
19. J. C. Calabrese, L. F. Dahl, A. Cavalieri, P. Chini, G. Longoni and S. Martinengo, *J. Am. Chem. Soc.* 1974, **96**, 2616.
20. P. F. Jackson, B. F. G. Johnson, J. Lewis, M. McPartlin and W. J. H. Nelson, *J. Chem. Soc., Chem. Commun.* 1979, 735.
21. C. R. Eady, B. F. G. Johnson and J. Lewis, *J. Chem. Soc., Chem. Commun.* 1976, 302.
22. P. Chini, *Inorg. Chem.* 1969, **8**, 1206.
23. E. R. Corey, L. F. Dahl and W. Beck, *J. Am. Chem. Soc.* 1963, **85**, 1202.
24. G. Ciani, G. D'Alfonso, P. Romiti, A. Sironi and M. Freni, *J. Organomet. Chem.* 1983, **244**, C27.

Polyhedron Vol. 8, No. 10, pp. 1357–1360, 1989
Printed in Great Britain

0277–5387/89 $3.00+.00
© 1989 Pergamon Press plc

THE CRYSTAL AND MOLECULAR STRUCTURE OF $UO_2(NO_3)_2[Ph_2P(O)CH_2C(O)Ph]_2$ AND ITS ROLE IN THE SOLVENT EXTRACTION OF THE URANYL ION

RYSZARD BABECKI, ANDREW W. G. PLATT* and JOHN C. TEBBY

Department of Chemistry and Biology, Staffordshire Polytechnic, College Road, Stoke on Trent ST4 2DE, U.K.

and

JOHN FAWCETT and DAVID R. RUSSELL

Department of Chemistry, The University, Leicester LE1 7RH, U.K.

and

ROBERT LITTLE

Department of Ceramic Technology and Geological Sciences, Staffordshire Polytechnic, College Road, Stoke on Trent ST4 2DE, U.K.

(*Received* 16 *November* 1988; *accepted* 19 *January* 1989)

Abstract—The uranyl complexes, $UO_2(NO_3)_2(HL)_2$ (**1**) and the new complexes, $UO_2L_2(HL)_2$ (**2**) and $UO_2(ClO_4)_2(HL)_4 \cdot 2H_2O$ (**3**) (HL = $Ph_2P(O)CH_2C(O)Ph$), have been prepared. Spectroscopic studies of **1** and **3** indicate that the ligand is bound via the phosphoryl oxygen atom and that the carbonyl oxygen is not involved in bonding to the uranium. The crystal structure of the uranyl nitrate complex (**1**) has been determined, and confirms this bonding mode. The coordination about the uranium atom is distorted hexagonal-bipyramidal. The structure is compared with that of the analogous triphenylphosphine oxide complex and the differing U—O—P bond angles discussed. Solvent extraction studies of uranyl nitrate from aqueous media have been carried out using HL in dichloromethane solution as the extractant. Uranium is extracted as **1** from 4 M HNO_3, but as **2** from neutral aqueous solution.

There is considerable interest in the use of β-ketophosphonates as extractants for a variety of metals.[1–4] Coordination of the neutral ligand can occur in a monodentate[4] or bidentate fashion.[5] They also have the capacity to act as acidic ligands and have been shown to bond in a similar manner to β-diketones.[6,7]

In many cases, the exact nature of the complexes responsible for the extraction process is uncertain. Extraction of uranyl ions with $(BuO)_2P(O)CH_2C(O)Ph$ (HL′) has been interpreted in terms of the formation of $UO_2(NO_3)_2(HL')_2$ and $UO_2L'_2HL'$ from nitric and perchloric acid media, respectively,[4] although the complexes were not isolated. Structural studies of a number of uranium complexes of relevance to solvent extraction have been determined, but these were not demonstrated to be involved in any extraction processes.[8] With this in mind, we have studied the solvent extraction reactions of HL with uranyl nitrate to characterize the complexes involved in the extraction process.

RESULTS AND DISCUSSION

Equilibration of a CH_2Cl_2 solution of HL with uranyl nitrate in 4 M HNO_3 imparted a yellow

* Author to whom correspondence should be addressed.

colouration to the organic phase, indicative of uranium extraction. Solution IR spectral characteristics of the extract were identical to those of **1** in the same solvent. Furthermore, the solid complex which can be isolated from the organic phase had spectroscopic properties identical with those of an authentic sample.[9]

The single crystal X-ray structure of **1** was determined to fully characterize the solvent extraction complex and since no structures of β-ketophosphine oxide metal complexes have been reported.

The complex crystallizes with two molecules in the asymmetric unit, the structure of one of these is shown in Fig. 1 and selected bond lengths and angles are collected in Table 1. The coordination of the uranium atom is based on a distorted hexagonal-bipyramid with the oxygens of the uranyl ion occupying the axial positions. The nitrate ion is bidentate, whilst the ketophosphine oxide is clearly monodentate with the carbonyl oxygens situated symmetrically above and below the equatorial plane at distances of over 4 Å from the uranium atom. The six oxygens of the nitrate and phosphine oxide ligands lie within 3° of the equatorial plane through the uranium atom perpendicular to the O=U=O axis. Other bond lengths and angles are essentially the same as those found in the analogous triphenylphosphine oxide complex,[10] except for the U—O—P angle which is 165° compared with 160° in the Ph_3PO complex. The U—O—P angle would be governed by electrostatic repulsion between the positively-charged uranium and phosphorus centres and the steric requirements of the complex, both tending to widen the angle. Simple models show that HL can adopt less sterically demanding positions than Ph_3PO when coordinated to uranium. However in **1**, the carbonyl oxygens are oriented towards the uranium, presumably by weak electrostatic attraction. In this conformation, HL is bulkier than Ph_3PO and this increase in steric requirements is presumably responsible for the widening of the U—O—P angle in **1**.

Table 1. Selected bond lengths (Å) and angles (°) with standard deviations in parentheses for the two molecules in the asymmetric unit of $UO_2(NO_3)_2(HL)_2$

	Molecule 1	Molecule 2
Bond lengths		
U(1)—O(1)	2.369(6)	2.354(7)
U(1)—O(2)	1.755(7)	1.764(7)
U(1)—O(4)	2.529(6)	2.525(7)
U(1)—O(6)	2.514(8)	2.515(7)
O(1)—P(1)	1.508(7)	1.491(7)
P(1)—C(1)	1.797(11)	1.823(8)
C(1)—C(2)	1.471(14)	1.491(13)
C(2)—O(3)	1.230(14)	1.213(14)
N(1)—O(4)	1.275(13)	1.259(13)
N(1)—O(5)	1.205(13)	1.214(11)
Non-bonded distances		
U(1)—O(3)	4.11	4.06
Bond angles		
O(2)—U(1)—O(1)	87.2(3)	90.1(3)
O(2)—U(1)—O(4)	91.4(3)	90.4(3)
O(2)—U(1)—O(6)	92.8(3)	92.6(3)
O(6)—U(1)—P(1)	165.0(4)	166.4(3)
O(1)—U(1)—O(6)	64.9(2)	65.5(2)
O(6)—U(1)—O(4)	50.0(2)	49.9(2)
P(1)—C(1)—C(2)	114.8(7)	112.0(7)
C(1)—P(1)—O(1)	113.4(4)	112.6(4)
C(1)—C(2)—O(3)	124.1(11)	125.8(8)
N(1)—O(4)—U(1)	97.2(5)	97.7(6)
O(5)—N(1)—O(4)	123.2(8)	122.6(10)

Equilibration of neutral aqueous uranyl nitrate

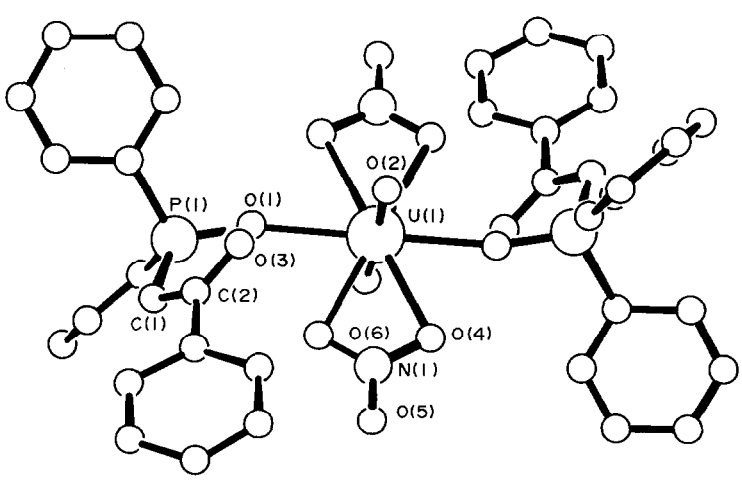

Fig. 1. Structure of $UO_2(NO_3)_2(HL)_2$.

with HL in dichloromethane also leads to the extraction of uranium into the organic phase. In this case, however, **1** is not found in the organic layer as evidenced by the solution IR spectrum which shows no strong bands due to nitrate ions and a shift in the U=O stretch from 935 cm^{-1} in **1** to 920 cm^{-1}. It was not possible to isolate the extraction complex free from HL from this system. It was noted, however, that equilibration of a CH_2Cl_2 solution of **1** with water led to the formation of the same extraction species in the organic layer (solution IR evidence) whilst distributing $UO_2(NO_3)_2$ and HNO_3 into the aqueous layer as shown in eq. (1):

$$2UO_2(NO_3)_2(HL)_{2(Org)} + (Aq) \longrightarrow UO_2L_2(HL)_{2(Org)} + UO_2(NO_3)_{2(Aq)} + 2HNO_{3(Aq)}. \quad (1)$$

Isolation and characterization of the extraction complex was possible in this case due to the absence of excess HL. The elemental analysis for **2** indicates contamination by a small quantity of HL. This is presumably present due to competing equilibria such as that shown in eq. (2):

$$UO_2(NO_3)_2(HL)_{2(Org)} \longrightarrow 2HL_{(Org)} + UO_2(NO_3)_{2(Aq)}. \quad (2)$$

The IR spectrum of the isolated complex shows bands typical of monodentate HL, with an additional absorption at 1510 cm^{-1} consistent with the presence of the anionic ligand L. The position of this band is in the accepted region for the C···O stretch in metal acetylacetonate complexes.[11] Most striking, however, is the absence of any bands due to the nitrate ion. The probable structure of the extraction complex **3** is shown in Fig. 2, where the ligand is acting as a neutral monodentate ligand and as an anionic chelating ligand.

Confirmation of the nature of **2** was obtained by equilibration of a dichloromethane solution of the perchlorate complex **3** with water. Here, the uranium-to-ligand ratio is 1 : 4 and it would be expected that the extraction would proceed predominantly according to eq. (3) with little uranium distributed into the aqueous layer:

$$UO_2(ClO_4)_2(HL)_{4(Org)} \longrightarrow UO_2L_2(HL)_{2(Org)} + 2HClO_{4(Aq)}. \quad (3)$$

The acidity of the aqueous phase increased during the extraction and little uranium was extracted from the organic layer. Solution IR analysis of the CH_2Cl_2 confirmed the presence of **2** and there were no absorptions due to perchlorate ions observable, indicating that the forward reaction of eq. (3) is favoured for the perchlorate complex.

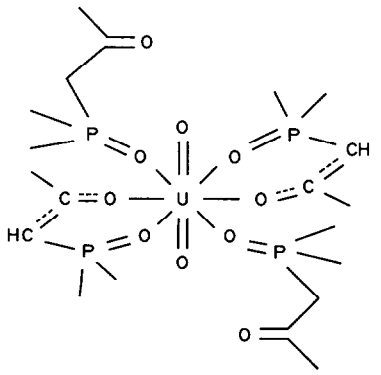

Fig. 2. A possible structure of $UO_2L_2(HL)_2$ (phenyl groups omitted).

EXPERIMENTAL

Preparation of $Ph_2P(O)CH_2C(O)Ph$ (HL)

The ligand was prepared by a literature procedure;[12] spectroscopic and physical properties were identical to the literature values.

Preparation of $UO_2(NO_3)_2(HL)_2$ (**1**)

Uranyl nitrate was dissolved in ethanol and a solution of HL in ethanol added. The mixture was heated under reflux for 2 h and allowed to cool to room temprature. The yellow crystals were filtered and dried to give a quantitative yield. Physical and spectroscopic data were identical to those reported in the literature.[12] Crystals for the structure determination were grown by slow evaporation from a toluene–ethanol solution.

Preparation of $UO_2(ClO_4)_2(HL)_4 \cdot 2H_2O$ (**3**)

Uranyl perchlorate and excess HL were refluxed in ethanol for 2 h. The solvent was evaporated and the resulting oil recrystallized from ethanol–diethyl ether at 0°C, to give the product as a pale yellow powder in 50% yield. Found: C, 53.9; H, 3.9. Calc. for $UO_2(ClO_4)_2(HL)_4 \cdot 2H_2O$: C, 53.8; H, 4.1%. IR data [cm^{-1} (KBr)]: C=O 1680, P=O 1150, 1130 Cl—O 1080, U=O 935.

Preparation of $UO_2L_2(HL)_2$ (**2**)

$UO_2(NO_3)_2(HL)_2$ (0.5 g, 0.48 mmol) in 5 cm^3 of CH_2Cl_2 was equilibrated with 5 cm^3 of water. The organic layer was separated, dried ($MgSO_4$) and evaporated to give 0.32 g (85%) of the product as a yellow–orange solid. Found: C, 63.8; H, 4.3; N,

0. Calc. for $UO_2L_2(HL)_2$: C, 62.0; H, 4.3; N, 0%. IR data [cm^{-1} (KBr)]: C=O 1680, C···O 1510, P=O 1178, 1145, U=O 920.

Extraction of $UO_2(NO_3)_2$ *from* 4 M HNO_3

10 cm^3 of 2M $UO_2(NO_3)_2$ was equilibrated with 10 cm^3 of 2 M HL in CH_2Cl_2. The dichloromethane layer was separated, dried ($MgSO_4$) and evaporated. The resulting solid was recrystallized from ethanol to give 0.66 g of $UO_2(NO_3)_2(HL)_2$; 64% based on HL originally in the organic phase.

Crystal data

$UC_{40}H_{34}N_2O_{12}P_2$, $M = 1034.69$, triclinic space group $P\bar{1}$, $a = 11.877(1)$, $b = 15.999(2)$, $c = 11.362(40)$ Å, $\alpha = 89.78(10)$, $\beta = 94.70(10)$, $\gamma = 110.23(2)°$, $U = 2018.5$ Å^3, $Z = 2$, (Mo-K_α) = 0.7107 Å, $\mu = 39.55$ cm^{-1}, $d_x = 1.702$ g cm^{-3}, $F(000) = 1011.9$.

The unit cell dimensions of the crystal were determined from an oscillation photograph for the rotation axis c, and from the refined data of the zero layer reflections for a, b and γ.

The intensities of 8382 reflections with $2\theta < 54°$ and ($\pm h$, $\pm k$, l) were measured on a Stoe STADI-2-Weissenberg diffractometer with graphite monochromated Mo-K_α radiation using an ω-scan technique. The data were corrected for Lorentz and polarization effects to yield 4701 reflections with $I \geqslant 3\sigma(I)$.

The uranium atoms were located on special positions using the Patt option of SHELXS 84.[13] All subsequent calculations were carried out using the SHELX computer program.[14] An absorption correction was carried out on the data, maximum and minimum transmission factors were 0.730 and 0.228, respectively. All non-hydrogen atoms were refined in the latter stages as anisotropic. Phenyl and methylene hydrogen atoms were included in calculated positions with C—H fixed at 1.08 Å and constrained isotropic thermal parameters.

Final cycles of refinement employed a weighting parameter $g(0.0009)\{w = 1/[\sigma^2(F)+gF^2]\}$ and gave the final residual indices $R\{= \Sigma(|F_o|-|F_c|)/\Sigma|F_o|\} = 0.043$ and $R_w\{[= \Sigma w(|F_o|-|F_c|)^2/\Sigma w|F_o|^2]^{1/2}\} = 0.044$. The final difference Fourier map was featureless, the highest residual peak of 1.4 e at approximately 1 Å from uranium. An analysis of the weighting scheme over $|F_o|$ and $\sin\theta/\lambda$ was satisfactory.

Final atomic positional and thermal parameters and lists of $|F_o|$ and $|F_c|$ values have been deposited as supplementary material with the Editor, from whom copies are available on request. Atomic coordinates have also been deposited with the Cambridge Crystallographic Data Centre.

Acknowledgement—The authors wish to thank Dr M. A. Beckett for many helpful discussions.

REFERENCES

1. M. Burgard and B. Ceccaroll, *J. Phys. Chem.* 1982, **86**, 4817.
2. B. Ceccaroll, J. Alstad and M. J. F. Leroy, *Polyhedron* 1982, **1**, 257.
3. J. B. Brunette, L. Jurdy, M. J. F. Leroy and B. Allard, *Spectrochim. Acta* 1981, **37a**, 991.
4. J. C. Martin and M. J. F. Leroy, *J. Chem. Res. (S)* 1978, **88**, (M) 1113.
5. C. M. Mikullski, W. Henry, L. L. Pytlewski and N. M. Karayannis, *J. Inorg. Nucl. Chem.* 1978, **40**, 769.
6. F. A. Cotton and R. A. Schunn, *J. Am. Chem. Soc.* 1963, **85**, 2394.
7. M. Th. Youinov and J. E. Guerchais, *Inorg. Chim. Acta* 1976, **19**, 257.
8. J. H. Burns, *Inorg. Chem.* 1983, **22**, 1174.
9. A. D. Buss, W. B. Cruse, O. Kennard and S. Warren, *J. Chem. Soc., Perkin Trans. (I)* 1984, 243.
10. N. W. Alcock, M. M. Roberts and D. Brown, *J. Chem. Soc., Dalton Trans.* 1982, 25.
11. K. Nakamonto, *Infrared and Raman Spectra of Inorganic and Coordination Compounds*, 4th edn. Wiley, New York (1986).
12. C. N. Lester and M. R. Truter, *J. Chem. Soc. A* 1971, 738.
13. G. M. Sheldrick, SHELXS, private communication.
14. G. M. Sheldrick, SHELX 76, Program for crystal structure determination. University of Cambridge, U.K. (1976).

Polyhedron Vol. 8, No. 10, p. 1361, 1989
Pergamon Press plc. Printed in Great Britain

BOOK REVIEWS

Organometallic Chemistry: An Overview. John S. Thayer. Published by VCH Publishers, New York, 1988. ISBN 0-89573-121-5, 170 pp., $35.00.

This is an introductory text for those with a good background in chemistry who are interested in this important and industrially relevant topic.

The text itself is easily comprehensible and well indexed. The first chapter deals largely with the historical development of organometallic chemistry but also gives notes on nomenclature. The next chapter indicates general synthetic methods (concentrating on M—C σ-bonds), and following ones deal with more specific types: ionic and radical carbanions; and "electron deficient" compounds, with short sections on specific elements (Li, Mg, Be and Al). At the beginning of Chapter 5 the σ-bonded organometallics are categorized, apparently largely on the basis of reactivity, into (1) reactive metals, (2) heavy metals and (3) metalloids. Although this subdivision has some chemical basis, I found this taxonomy rather clumsy and may obscure some important chemical truths, especially for those unfamiliar with the field, for whom this book was intended. The separation of the "metalloids" (e.g. B, Si, Ge, P, As, Se, Te) is reasonable, but the grouping of Zn, Cd, Be, Mg and Al with transition metals (group (1), the reactive metals) seems strange, as does placing Ga in group (1) and In in group (2). Furthermore, I was not entirely satisfied that the term "reactive" was adequately explained. There is also a tendency to compartmentalize unwisely: for example, Section 5.3 on Grignard reagents; 5.4 on M—C bond lability, a concept perhaps best illustrated by highlighting more specifically the Schlenk reaction in the previous section or by the Ziegler–Natta polymerization reactions referred to in Section 5.5.

Chapters 8–10 concern M—C synergistic bonds: first those with "divalent" carbon, then those involving unsaturated hydrocarbons, and finally polynuclear species both with and without M—M bonds.

Most of the remainder of the book deals with biological aspects of organometallics: in medicine, toxicology, biosynthesis and environmental aspects. There is a short final chapter on more recent advances in the field (covering the literature up to 1986) which arose after earlier chapters had been completed.

In conclusion, despite reservations about the organization of material, this book does give a clear introduction to the field. It could be recommended as an introductory undergraduate text provided that it is read *in toto* (or almost so) rather than as a reference work on specific topics; a task facilitated by it being both readable and relatively brief.

Department of Chemistry
Queen Mary College
Mile End Road
London E1 4NS, U.K.

DARIO M. FRIGO

The Chemistry of the Semiconductor Industry. Edited by S. J. Moss and A. Ledwith. Published by Blackie, Glasgow and London, 1987. ISBN 0-216-92005-1.

This book gives an account of the electronics industry with specific reference to the role played by chemistry.

It begins with an overview of the electronics industry itself, including a general history and a brief indication of where the future probably lies. The next three chapters concern, respectively, the three principal types of material used: silicon, with accounts of extraction and purification of polysilicon and thence conversion to single-crystal wafers; III–V compounds, with concentration on GaAs and InP; and II–VI compounds, which includes a useful section on phase equilibria. The next four chapters deal with the techniques of crystal growth: chemical vapour deposition (CVD), plasma-enhanced CVD, metal–organic vapour phase epitaxy (MOVPE), and liquid phase epitaxy (LPE). Subsequent sections concern processing techniques to produce devices, specifically photoresists, electron beam and X-ray resists, the chemistry of wet etching, and later on (apparently out of sequence) plasma etching and an account of the properties of polymers in plasmas. Sandwiched between these sections are ones on the polyimides, a general view of molecular electronics, and a more theoretical chapter on computer modelling of semiconductor interfaces. Certain aspects of the industry have been omitted on the grounds that chemistry plays only a minor role.

Although the book has been written by some 20 authors, the result is pleasingly free of repetition of material but inevitably, as with any compartmentalized pot-pourri, it suffers from a lack of cross-referencing between chapters which might indicate a greater wholeness of subject. Another inevitable criticism is that in a field that is so fast moving the most up to date expose is substantially old-hat by the publishing date; this book covers the literature up to 1986. On the other hand, the book is (on the whole) well done: most sections are fairly clearly written and authoritative. It can therefore be highly recommended to those who require background reading upon one or more topics covered, or a foundation upon which to read further in the appropriate journals.

Department of Chemistry
Queen Mary College
Mile End Road
London E1 4NS, U.K.

DARIO M. FRIGO

Polyhedron Vol. 8, No. 10, p. 1363
Pergamon Press plc. Printed in Great Britain

CORRIGENDUM

Cluster of clusters: a new series of high nuclearity Au—Ag clusters. Boon K. Teo (*Polyhedron* Vol. 7, No. 22/23, pp. 2317–2320, 1988).

On page 2319 of this paper, the caption of Fig. 4(f) should be $s_7(75)$. Similar changes occur in the Abstract as well as in the text.

Polyhedron Vol. 8, No. 11, pp. 1365–1370, 1989
Printed in Great Britain

0277–5387/89 $3.00+.00
© 1989 Pergamon Press plc

2,5-TOLUENEDIAMINE-N,N′-DISUCCINIC ACID. PREPARATION, DISSOCIATION CONSTANTS AND COORDINATING CAPACITY WITH DIVALENT CATIONS

J. FUENTES,* R. REBOSO and A. RODRIGUEZ

Departamento de Química Inorgánica, Universidad de La Laguna, Tenerife, Canary Islands, Spain

(*Received* 17 *October* 1988; *accepted* 9 *November* 1988)

Abstract—2,5-Toluenediamine-N,N′-disuccinic acid (2,5-TDDS) was obtained for the first time and identified, and a formula is proposed on the basis of the results of analytical, potentiometric, conductimetric and spectrophotometric analyses. Its dissociation constants were determined potentiometrically, in an aqueous solution of 0.5 M NaCl and at 25 ± 0.05°C, by means of the Schwarzenbach criterion and the MINIQUAD program. The values obtained for $\log \beta_i$ are as follows: $\log \beta_1 = 6.52$, $\log \beta_2 = 11.06$, $\log \beta_3 = 14.75$, $\log \beta_4 = 17.75$ and $\log \beta_5 = 19.74$. The stability constants of the complexes formed by 2,5-TDDS with the divalent cations Mg, Ca, Mn, Co, Ni, Zn and Cd were determined potentiometrically, at $\mu = 0.5$ M NaCl and at 25 ± 0.05°C.

From the work reported in the literature[1] on the complexing capacity of aromatic diamines, it is deduced that upon introducing carboxymethyl groups their coordinating action is enhanced by metallic cations. This prompted us to prepare a large number of such derivatives with a view to utilizing them as chelating agents of di- and trivalent metallic ions.[2,3] In this work we report on the preparation, identification and determination of the dissociation constants of the new ligand, 2,5-toluenediamine-N,N′-disuccinic acid (2,5-TDDS), as well as the calculation of its stability constants with divalent metal cations. This ligand possesses two coordination spheres in *para* positions which should facilitate the formation of binuclear complex species of the M_2Y or mixed MM′Y types. This fact, together with the presence of asymmetric chains joined to the benzene ring, making its utilization possible in stereospecific syntheses of metallic complexes, renders it additionally interesting.

EXPERIMENTAL

Preparation of 2,5-*toluenediamine*-N,N′-*disuccinic acid*

To an aqueous solution of 0.75 M of 2,5-toluenediamine sulphate, previously neutralized with NaOH and kept at 90°C, an identical volume of a further solution of 1.5 M sodium bromosuccinate was added. The reaction mixture was kept under an inert atmosphere, continuously stirred and 2 M NaOH was added so that the pH of the solution was maintained between 7 and 8. Once the pH (~ 7) was stabilized, an excess (20%) of sodium bromosuccinate was added and the addition of 2 M NaOH was renewed until stabilization was again attained. The solution was filtered and concentrated hydrochloric acid was added to pH 6.5. Then a saturated aqueous solution of $Cd(NO_3)_2 \cdot 4H_2O$ in excess was added to precipitate a pale pink product whose yield became more copious upon adding methanol to the solution. The product was separated by filtering, washed with water to remove Cl^- and NO_3^- and then suspended in a small amount of water through which a H_2S current was passed. The filtrate, after separation of the CdS precipitate, was concentrated in a rotary evaporator and taken to dryness in a desiccator *in vacuo* over P_4O_{10}. The product is a pale beige solid which is highly soluble in water, and melts at 145°C with decomposition; it may be kept unaltered in a desiccator with P_4O_{10}.

Apparatus and experimental techniques

The experimental device utilized in the potentiometric study of 2,5-TDDS alone and in the pres-

* Author to whom correspondence should be addressed.

ence of metal cations has been described in ref. 2. The titrations were carried out in an aqueous solution of 0.5 M NaCl and at 25 ± 0.05°C, 100 cm^3 being the initial volume and the initial concentration of the acid was of the order 10^{-3} M. The measurements were recorded with a Radiometer potentiometer (the 64pHM type) with an accuracy of the order of 0.1 mV, and using glass and calomel electrodes, G202B and K401, respectively, from the same company. The cell used was of the type: Glass electrode/soln of 2,5-TDDS/M^{II}; ($\mu = 0.5$; $T = 25 \pm 0.05$°C)/Calomel electrode; the standard potential of which and the $[H^+]$ were determined in a similar manner to that described in ref. 4. Conductimetric measurements of the acid alone and in the presence of the cations studied were performed as indicated for the potentiometric determinations, utilizing the same experimental device and temperature and without adjusting the ionic strength. The metal–acid ratios were 1:1, 2:1 and 15:1 for all the cations and the initial concentration of the acid was of the order 10^{-3} M. The measurements were recorded in a Radiometer conductimeter, model CDM 83, equipped with a CDC 304 conductivity cell from the same company.

The high and low resolution mass spectra were performed on a VG Micromass spectrometer, model ZAB-1F, at 15 eV, by direct insertion of the sample. The UV spectrum was taken on a Perkin–Elmer 550S spectrophotometer using quartz cells and thermostated at 25°C. The IR spectrum was taken in the range 4000–600 cm^{-1} on a Beckman 20-AX spectrophotometer, using KBr pellets as support. Elemental analysis was determined with a Carlo Erba 1106 elemental analyser.

The solutions of the metal chlorides were prepared at a concentration of approx. 0.1 M and were calculated as indicated in ref. 4, as were those of EDTA, HCl and carbonate-free NaOH.

RESULTS AND DISCUSSION

Identification of the product

Found: C, 49.9; H, 5.7; N, 7.7. Calc. for $C_{15}H_{18}N_2O_8 \cdot 1/2H_2O$: C, 49.6; H, 5.3; N, 7.7%.

The mean value obtained for the equivalent of the acid was 90.75. The substitution of a hydrogen from each of the two $—NH_2$ groups of the 2,5-toluenediamine by HOOC—CH(COOH)—CH_2—COOH groups would give rise to a molecular mass of 363.32, which is in agreement with the formula $C_{15}H_{18}N_2O_8 \cdot 1/2H_2O$ with four carboxylic groups.

The results of the conductimetric titration of a 10^{-3} M aqueous solution of 2,5-TDDS with 0.1 M NaOH are plotted in Fig. 1 [conductivities, λ, vs values of a (mols of NaOH/mol of acid)]. The presence of four defined points at $a = 1$, 2, 3 and 4 seems to confirm the existence of four acidities in the product obtained.

As also seen in the case of 1,4-phenylenediamine-N,N′-disuccinic acid,[2] the signal corresponding to the molecular ion is not observed in the mass spectrum. However, a peak appearing at m/z 266 was interpreted as corresponding to $M^+ - 2CO_2$. In ref. 2 we discussed the fact that this type of "apparent molecular ion" is presented in molecules with little thermal stability, or in those which readily lose neutral molecules.[5] The fragments at m/z 207 and 161, whose elemental analyses were determined by high resolution, may be interpreted as successive losses of $—CH_2CO_2H$ and HCO_2H from the $M^+ - 2CO_2$ ion.

The UV spectrum of 2,5-TDDS acid in a 2×10^{-5} M aqueous solution shows three absorption bands at 207, 253 and 293 nm which were assigned to the allowed spin transitions (180, 200 and 260 nm) typical of the benzene ring.[6] The bathochromic shifts, observed in the three bands of the acid relative to those of benzene, are caused by substitution in the benzene ring of the two $—NH(C_4H_5O_4)$ auxochromic groups that produce, according to Braude,[7] the π–p conjugation between the non-shared electrons of the substituent and the π-system of the ring.

The IR spectrum shows a 1,2,5-substituted aromatic ring (812 cm^{-1}),[8] secondary aromatic amine groups (3409 cm^{-1}),[9] $—CO_2^-$ (1404, 1620 and 1565 cm^{-1}),[10] $—CO_2H$ in non-monomeric acids (3000–2500 and 1725 cm^{-1})[10,9] and the OH of the crystallization water (3600–3300 cm^{-1}).[11] The similarity of the IR spectrum of this compound with those of 1,3- and 1,4-phenylenediamine-N,N′-disuccinic acids led us to propose a dimerization by the way of intermolecular hydrogen bonds.[2]

Determination of the dissociation constants of 2,5-TDDS *acid*

Since 2,5-TDDS is tetrabasic, we have designated it as H_4Y for simplification purposes. The dissociation equilibria that permit the corresponding constants to be defined are:

$$H_4Y \rightleftharpoons H_3Y^- + H^+ \quad (1)$$

$$H_3Y^- \rightleftharpoons H_2Y^{2-} + H^+ \quad (2)$$

$$H_2Y^{2-} \rightleftharpoons HY^{3-} + H^+ \quad (3)$$

$$HY^{3-} \rightleftharpoons Y^{4-} + H^+. \quad (4)$$

In order to determine these constants, several solu-

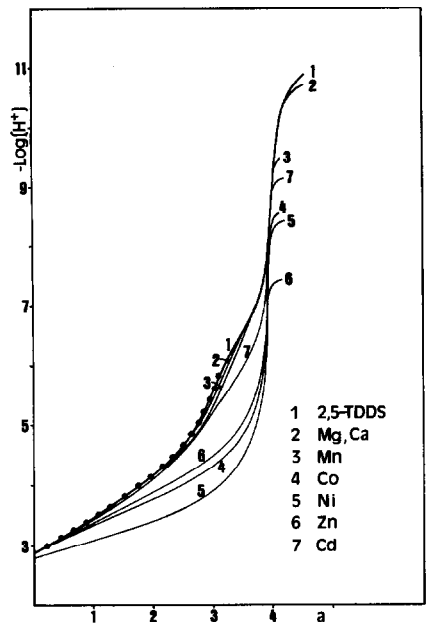

Fig. 1. Potentiometric curves of free acid 2,5-TDDS (—— experimental, ····· calculated) and in the presence of different divalent cations in the ratio $[M^{II}]/[2,5\text{-TDDS}] = 1:1$.

tions of the acid at concentrations of the order of 10^{-3} M, at ionic strength 0.5 M in NaCl and 25 ± 0.05°C, were titrated potentiometrically with NaOH. The values of $-\log[H^+]$ vs a are plotted in Fig. 1, where two potentiometric jumps are observed, one of which is well defined at $a = 4$ and the other less defined and with inflection at $a = 3$. Between $a = 0$ and $a = 3$ the curve does not present inflections, which proves that the first three equilibria are simultaneous and that, consequently, the ΔpK_s must be smaller than two units, whereas the last two equilibria must be successive or at least not totally simultaneous. For the calculation of the dissociation constants the graphical criteria of Bjerrum[12] and Schwarzenbach *et al.*[13] were employed, and refined with the MINIQUAD program.[14,15]

The values found for $\log \beta_i$ and pK_i are presented in Table 1, the standard deviations in the significant number are indicated in parentheses. The Bjerrum values given in Table 1 were refined by means of successive approximations,[16] since the relation between two successive constants was below 10^4. In addition to the four constants defined earlier, the value for a fifth constant appears in Table 1, which has been designated as K_0 and corresponds to the equilibrium:

$$H_5Y^+ \overset{K_0}{\rightleftharpoons} H_4Y + H^+.$$

As indicated in our study of 1,4-phenylenediamine-N-succinic acid,[17] the existence of the H_5Y^+ species can be interpreted as proceeding from the following self-dissociation equilibrium:

$$2H_4Y \rightleftharpoons H_5Y^+ + H_3Y^-.$$

The good fit between the curve of the experimental potentiometric titration and that calculated upon refining the dissociation constants of the acid can be observed in Fig. 1.

Stability constants

The process of formation of a metal complex, in which the ligand is a weak organic acid, can be represented by the equation:

$$H_mY + xM^{q+} \rightleftharpoons M_xH_{m-n}Y^{qx-n} + nH^+. \quad (5)$$

In this type of reaction new species are formed in solution, which can be detected by conductimetric and/or potentiometric techniques.

The conductimetric titration curves of the acid in the presence of the divalent cations under study for the ratio $[M^{II}]/[\text{acid}] = 1:1$ are plotted in Fig. 2. The curve corresponding to the titration of the free acid has been included for comparison purposes. For the cations Mg^{2+} and Ca^{2+} a decrease in the slope is observed only in the interval $3 < a < 4$ (the shift in those of Sr^{2+} and Ba^{2+} is negligible), which can be interpreted if it is assumed that in addition to equilibrium (4) of dissociation of the acid, the fol-

Table 1. Dissociation constants of 2,5-TDDS acid at 25°C and $\mu = 0.5$ M NaCl

	$\log \beta_1$	$\log \beta_2$	$\log \beta_3$	$\log \beta_4$	$\log \beta_5$
MINIQUAD	6.52(1)	11.06(1)	14.75(1)	17.75(1)	19.74(1)
	pK_0	pK_1	pK_2	pK_3	pK_4
Schwarzenbach	—	3.08	3.61	4.60	6.53
Bjerrum	—	3.16	3.59	4.62	6.53
MINIQUAD	1.99	3.00	3.68	4.54	6.52

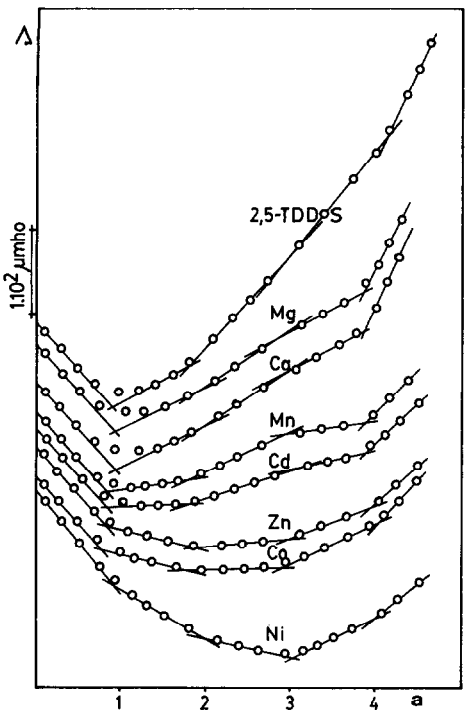

Fig. 2. Conductimetric curves of free acid 2,5-TDDS and in the presence of different divalent cations in the ratio $[M^{II}]/[2,5\text{-TDDS}] = 1:1$.

lowing equilibria come about:

$$\begin{aligned} Y^{4-} + M^{2+} &\overset{K_c}{\rightleftharpoons} MY^{2-} \quad 3 < a < 4 \\ HY^{3-} + M^{2+} &\rightleftharpoons MY^{2-} + H^+. \end{aligned} \tag{6}$$

For the cations Mn^{2+}, Cd^{2+}, Zn^{2+}, Co^{2+} and Ni^{2+} (which deviate the curve of the acid from $a = 1$) these deformations are explained by means of the formation equilibria (7), (8) and (6):

$$H_2Y^{2-} + M^{2+} \overset{K''}{\rightleftharpoons} MH_2Y \quad 1 < a < 2 \tag{7}$$

$$HY^{3-} + M^{2+} \overset{K'}{\rightleftharpoons} MHY^- \quad 2 < a < 3, \tag{8}$$

where K'', K' and K_c are the corresponding stability constants.

The potentiometric curves in the ratio 1 : 1 plotted in Fig. 1 are deformed with respect to that of the acid from $a = 1$, with the exception of those corresponding to Mg^{2+} and Ca^{2+} which are only deformed between $a = 3$ and $a = 4$. The decrease observed in the pH from $a = 1$ is in agreement with the formation of complex species described earlier and which, in accordance with the shift equilibria:

$$H_3Y^- + M^{2+} \rightleftharpoons MH_2Y + H^+ \quad 1 < a < 2$$

$$H_2Y^{2-} + M^{2+} \rightleftharpoons MHY^- + H^+ \quad 2 < a < 3$$

$$HY^{3-} + M^{2+} \rightleftharpoons MY^{2-} + H^+ \quad 3 < a < 4,$$

induce 2,5-TDDS acid to behave like a strong acid.

In the case of the curves with excess of metal a greater deformation is observed, both in the conductimetric and potentiometric curves, with respect to the ratio 1 : 1, due to the fact that the concentration of metal ion shifts the equilibria defined by eq. (5) towards the right. In the interval $3 < a < 4$, the deformation of the curve of the acid is even more marked as a consequence of the additional shift of protons by the metal cation:

$$MHY^- + M^{2+} \rightleftharpoons M_2Y + H^+$$

and formation of the bimetallic particle M_2Y:

$$MY^{2-} + M^{2+} \overset{K_M}{\rightleftharpoons} M_2Y.$$

For the determination of the stability constants, solutions of 2,5-TDDS acid in 0.5 M NaCl were potentiometrically titrated in the presence of a metal cation in the ratios $[M^{II}]/[2,5\text{-TDDS}] = 1:1$, 1 : 2, 2 : 1 and 15 : 1. For the calculation of such constants the graphical criterion of Schwarzenbach[13] was used, and the values obtained were refined by means of the MINIQUAD program.[14,15] The models used in the calculation are in agreement with the results foreseen in the qualitative study and the best fits were achieved, after testing several hypotheses considering the exis-

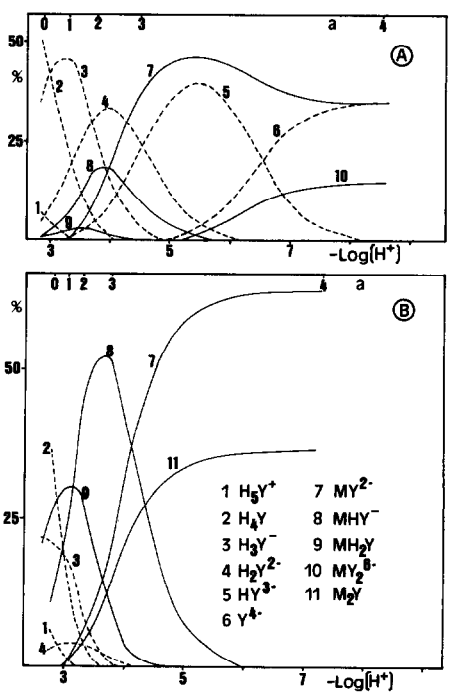

Fig. 3. Distribution diagrams of the species as a function of $-\log[H^+]$ for the system $[Ni^{II}]/[2,5\text{-TDDS}]$ in the ratios: 1 : 2 (A) and 15 : 1 (B).

Table 2. Stability constants of 2,5-TDDS acid with M^{II} at 25°C and $\mu = 0.5$ M NaCl

	Log β_i				
M^{II}	MH_2Y	MHY^-	MY^{2-}	MY_2^{6-}	M_2Y
Ni	13.145(36)	10.417(04)	6.374(04)	8.925(12)	7.808(17)
Co	12.687(23)	9.195(07)	5.231(03)	—	6.395(54)
Zn	12.744(17)	8.993(04)	4.667(02)	—	6.108(22)
Cd	11.798(23)	7.635(37)	2.837(03)	—	3.710(34)
Mn	12.127(54)	7.983(24)	2.487(18)	—	—
Mg	—	—	0.934(60)	—	—
Ca	—	—	0.962(60)	—	—

	log K''		log K'		log K_c		log K_{2c}	log K_M
	(I)	(II)	(I)	(II)	(I)	(II)	(I)	(I)
Ni	2.08	2.16	3.89	3.78	6.37	6.19	2.60	1.43
Co	1.62	1.51	2.67	2.89	5.23	5.07	—	1.16
Zn	1.53	1.48	2.49	2.57	4.66	4.58	—	1.45
Cd	0.73	0.78	1.11	1.37	2.84	2.82	—	0.87
Mn	1.06	0.93	1.46	1.22	2.49	2.33	—	—
Mg	—	—	—	—	0.93	—	—	—
Ca	—	—	—	—	0.96	—	—	—

Calculated values by: (I) MINIQUAD program; (II) Schwarzenbach criterion. The standard deviations in the last significant number are indicated in parentheses.

tence of MH_2Y, MHY^- and MY^{2-} for Mn^{2+}, of the above species plus the bimetallic particle, M_2Y, for the cations Co^{2+}, Zn^{2+} and Cd^{2+} and of all the above mentioned species plus MY_2^{6-} only in the case of Ni^{2+}. The existence of the species MY^{2-} was only taken into account for Mg^{2+} and Ca^{2+}. The calculated values of the logarithms of the stability constants are presented in Table 2.

The species distribution diagrams as a function of $-\log[H^+]$ for the system $[Ni^{II}]/[2,5\text{-TDDS}]$ in the ratios 1:2 and 15:1 are plotted as an example in Fig. 3.

Acknowledgement—This work was supported by the Government of the Canary Islands, for which we are grateful.

REFERENCES

1. A. E. Martell and R. M. Smith, *Critical Stability Constants*, Vol. 2—Amines. Plenum Press, New York (1982); D. Perrin (Ed.), *Stability Constants of Metal–Ion Complexes*, Part B—Organic Ligands. Pergamon Press, Oxford (1979).
2. B. Rodríguez Ríos, J. Fuentes Díaz and R. Reboso Barroso, *An. Quím.* 1984, **80B**, 32; 1984, **80B**, 37; 1984, **80B**, 424.
3. B. Rodríguez Ríos, A. Peralonso and A. Mederos, *An. Quím.* 1963, **59B**, 493; 1963, **59B**, 501; 1965, **61B**, 717; A. Mederos, A. Rodríguez González and B. Rodríguez Ríos, *An. Quím.* 1970, **66B**, 531; 1973, **69B**, 601; 1973, **69B**, 731.
4. B. Rodríguez Ríos and J. Fuentes Díaz, *An. Quím.* 1976, **72**, 420.
5. J. Seibl, *Espectrometría de Masas*. Alhambra, Madrid (1973).
6. H. H. Jaffe and M. Orchin, *Theory and Applications of Ultraviolet Spectroscopy*. John Wiley, New York (1966).
7. K. Bowden and E. A. Braude, *J. Chem. Soc.* 1952, 1068.
8. K. Nakanishi and P. H. Solomon, *Infrared Absorption Spectroscopy*. Holden Day, San Francisco (1977).
9. L. J. Bellamy, *The Infrared Spectra of Complex Molecules*. Methuen, London (1959).
10. R. M. Silverstein and G. C. Bassler, *Identification Spectrométrique des Composés Organiques*. Masson et Cie-Gauthier-Villars, Paris (1968).
11. K. Nakamoto, *Infrared Spectra of Inorganic and Coordination Compounds*. John Wiley, New York (1963); K. Nakamoto, *Infrared and Raman Spectra of Inorganic and Coordination Compounds*, 4th edn. John Wiley, New York (1986).

12. J. Bjerrum, *Metal Ammine Formation in Aqueous Solution*. P. Haase (1957).
13. G. Schwarzenbach, A. Willi and R. O. Bach, *Helv. Chim. Acta* 1947, **30**, 1303.
14. A. Sabatini, A. Vacca and P. Gans, *Inorg. Chim. Acta* 1976, **18**, 237.
15. F. R. Hartley, C. Burgess and R. M. Alcok, *Solution Equilibria*. Ellis Horwood, Chichester (1980).
16. T. M. Sc. D. Beck, *Chemistry of Complex Equilibria*. Van Nostrand Reinhold, London (1970).
17. B. Rodríguez Ríos, J. Fuentes Díaz and R. Reboso Barroso, *An. Quím.* 1984, **80B**, 60.

Polyhedron Vol. 8, No. 11, pp. 1371–1377, 1989
Printed in Great Britain

0277–5387/89 $3.00+.00
© 1989 Pergamon Press plc

STUDIES ON TRANSITION METAL PEROXO COMPLEXES—IX.† CARBOXYLATO PEROXO COMPLEXES OF NIOBIUM(V), TANTALUM(V), ZIRCONIUM(IV) AND HAFNIUM(IV)

ANDREW C. DENGEL and WILLIAM P. GRIFFITH‡

Inorganic Chemistry Laboratories, Imperial College of Science and Technology, London SW7 2AY, U.K.

(*Received* 28 *October* 1988; *accepted* 6 *December* 1988)

Abstract—The new complexes $K_3[M(O_2)_3(tart)]\cdot H_2O$ (M = Nb, Ta; tart = tartrate), $K_3[M(O_2)_3(L)]\cdot 2H_2O$ [M = Nb, Ta; L = glycollate (glyc), citrate (cit)], $K_3[Nb(O_2)_3(mal)]\cdot 2H_2O$ (mal = malate), $K[M(O_2)_2(dipic)(H_2O)]\cdot 2H_2O$ (M = Nb, Ta; dipic = dipicolinate), $K_6[M_2(O_2)_6(tart)]\cdot 2H_2O$ (M = Nb, Ta), $K_2[M(O_2)(ox)_2]\cdot 2H_2O$ (M = Zr, Hf) and $K_2[M(O_2)_2(cit)]\cdot H_2O$ (M = Zr, Hf) have been prepared and characterized on the basis of the Raman and IR spectra of the solids, the Raman spectra of their aqueous solutions and, in some cases, their ^{13}C NMR spectra. They are likely to contain eight-coordinate metal atoms with the peroxo groups side-bonded to the metal atoms.

Transition metal peroxo complexes are of current interest because many of them are efficient stoichiometric or catalytic oxidants for organic substrates;[2] however, they tend, unless stabilized by suitable co-ligands, to be unstable towards heat or impact. Such co-ligands are hard donors such as the oxo (O^{2-}), fluoro (F^-) or hydroxo (OH^-) ligands; we have recently shown[3] that carboxylate anions capable of forming five-membered rings with the metal atom are excellent co-ligands for coordinated O_2^{2-} in molybdenum and tungsten complexes of the form $K_2[MO(O_2)_2L]$ (M = Mo, W; L = citrate, malate, tartrate, tartronate, quinate, glycollate). In this paper we extend our studies on carboxylato peroxo complexes to the Group V and Group IV elements niobium, tantalum, zirconium and hafnium.

RESULTS AND DISCUSSION

Niobium and tantalum complexes

Although salts of the fluoroperoxo complexes $[M(O_2)F_5]^{2-}$ (M = Nb,[4,5] Ta[6]) and $[M(O_2)_2F_4]^{3-}$ (M = Nb,[7] Ta[8]) have received much attention, there are relatively few carboxylato peroxo complexes of niobium and tantalum. The oxalato peroxo complexes $(NH_4)_3[Nb(O_2)(ox)_3]$,[9] $K_3[M(O_2)_2(ox)_2]\cdot H_2O$ (M = Nb, Ta;[10] the X-ray crystal structure of the niobium complex has been determined[11]) and the salts of $[Nb(O_2)_3(ox)]^{3-}$[12] have been prepared. The aminocarboxylato peroxo species $[M(O_2)_3(EDTA)]^{3-}$[13] and $[M(O_2)_2(pic)_2]^-$[14] (M = Nb, Ta; EDTA = ethylenediamine tetraacetate, pic = picolinate) are also known.

(i) *Mononuclear complexes.* We find that reaction of aqueous solutions of the tetraperoxo species $K_3[M(O_2)_4]$ (M = Nb, Ta) with the carboxylic acid in a 1:1 mole ratio in the presence of excess H_2O_2 leads to the new complexes $K_3[M(O_2)_3(tart)]\cdot H_2O$, $K_3[M(O_2)_3(cit)]\cdot 2H_2O$, $K_3[M(O_2)_3(glyc)]\cdot 2H_2O$, $K[M(O_2)_2(dipic)(H_2O)]\cdot 2H_2O$ and $K_3[Nb(O_2)_3(mal)]\cdot 2H_2O$. The presence of excess H_2O_2 in the reaction mixture serves to increase the yield of the product. As was the case with reaction of $[M'O_4]^{2-}$ with H_2O_2 and carboxylic acids H_2L to give the complexes $[M'O(O_2)_2L]^{2-}$ (M' = Mo, W), only those carboxylic acids capable of forming five-membered rings with the metals reacted. Reactions with species such as malonic acid and succinic acid, which would give six-membered rings, were unsuccessful. Mandelic acid gave no isolable product despite its potential ability to form a five-membered ring; presumably the phenyl group is sufficiently electron-

† For Part VIII, see ref. 1.

‡ Author to whom correspondence should be addressed.

withdrawing to prevent formation of a stable complex. The tridentate dipicolinato ligand in coordination can form two five-membered rings (as in $[VO(OO^tBu)(dipic)]$[14]); presumably, in the cases of these diperoxo dipicolinato complexes, a water molecule occupies the eighth coordination site.

Despite many attempts, it was in no instance possible to obtain crystals large or well enough formed for an X-ray crystal structure determination.

In Table 1 we list those Raman and IR bands which can clearly be assigned to the three typical modes of the coordinated (side-bonded) peroxo ligand,[1,3,15] viz. the O—O stretch (ν(O—O) near 880 cm^{-1}, the symmetric metal–peroxo stretch $\nu_{sym}[M(O_2)]$ near 650 cm^{-1} (both giving rise to polarized Raman bands for the aqueous solutions), and the asymmetric metal–peroxo stretch $\nu_{asym}[M(O_2)]$ near 600 cm^{-1}, depolarized for aqueous solutions. As in other peroxo complexes, ν(O—O) is strong and sharp both in the Raman and the IR; $\nu_{sym}[M(O_2)]$ is weak in the Raman and strong in the IR; and $\nu_{asym}[M(O_2)]$ is strong in the Raman and weak in the IR. Thus, the vibrational characteristics of these complexes suggest that the peroxo ligand is side-bonded to the metal atom. The similarity in band profiles of Raman spectra of the solids and of their aqueous solutions suggests that the structures of the species in the solid state are retained in aqueous solution.

The relatively low solubility of the salts in water made measurement of ^{13}C NMR spectra difficult; only in the cases of $[M(O_2)_3(glyc)]^{3-}$ (M = Nb, Ta) and $[Ta(O_2)_3(tart)]^{3-}$ were satisfactory spectra recorded. The niobium glycollato complex shows ^{13}C bands at δ 182.3 and 73.0 ppm, and analogous bands at δ 183.4 and 73.7 ppm were observed for solutions of $K_3[Ta(O_2)_3(glyc)]\cdot 2H_2O$. The resonances near δ 183 ppm are likely to arise from the carboxylic carbon atom (δ 178.8 ppm for free glycollic acid) and those near δ 73 ppm from the hydroxyl-bearing carbon atom (δ 62.0 ppm for the free acid). The downfield shift in resonance, observed also in $[MoO(O_2)_2(glyc)]^{2-}$ (M = Mo, W),[3] is expected since donation of electrons from the oxygen atoms adjacent to these carbon centres will effect deshielding of the latter. The ^{13}C NMR spectrum of $[Ta(O_2)_3(tart)]^{3-}$ shows a group of resonances centred around δ 180 ppm and another centred around δ 80 ppm, likely to arise from the carboxylate- and hydroxyl-bearing carbon atoms, respectively (they are observed in the free acid at δ 176.8 and 74.4 ppm). Again, similar downfield shifts were observed in $[MO(O_2)_2(tart)]^{2-}$ (M = Mo, W),[3] due to complexation as with the glycollate, but the complexity of the resonances suggests that some decomposition to $[Ta_2(O_2)_6(tart)]^{6-}$ may have occurred.

We suggest that all these complexes involve eight-coordinate niobium or tantalum; dodecahedral coordination has been demonstrated by X-ray crystallography for the anion in $KMg[Nb(O_2)_4]\cdot 7H_2O$[16] and $(NH_4)_3[Nb(O_2)_4]$.[9]

(ii) *Binuclear complexes.* We have reported the isolation of unusual binuclear tartrato-bridged peroxo complexes, $K_4[M_2O_2(O_2)_4(C_4H_2O_6)]\cdot 4H_2O$ (M = Mo, W), and established the X-ray crystal structure of the molybdenum salt.[3,17] It is therefore of interest to establish whether niobium and tantalum will form such species. We find that reaction of $[M(O_2)_4]^{3-}$ and (+)-tartaric acid in a 1:2 mole ratio in the presence of excess H_2O_2 gives sparingly soluble salts which analyse as $K_6[M_2(O_2)_6(tart)]\cdot 2H_2O$ (M = Mo, W). They are too insoluble for ^1H or ^{13}C NMR measurements, but the Raman and IR spectra suggest that they contain side-bonded peroxo ligands. The Raman and IR bands assignable to tartrate vibrations are similar in position and profile to those observed for $K_4[M_2O_2(O_2)_4(tart)]\cdot 4H_2O$ (M = Mo, W),[3,17] and we suggest that these new species contain eight-coordinated metal centres, probably having dodecahedral coordination as in other niobium and tantalum peroxo complexes. In this, each metal atom carries three side-bonded peroxo ligands and a bridging tartrate group, as in $K_4[Mo_2O_2(O_2)_4(tart)]\cdot 4H_2O$.[3,17] The deprotonated hydroxo and carboxylato oxygens of one half of the tartrate ligand give a five-membered ring with the metal.

Zirconium and hafnium complexes

Far fewer peroxo complexes of zirconium and hafnium are known than of niobium and tantalum, and X-ray data on only one of these are reported in the literature. Salts of $[Zr(O_2)_4]^{4-}$ (but not $[Hf(O_2)_4]^{4-}$) have been reported[18] and evidence presented for the existence of $[Zr_2(O_2)_3(SO_4)(H_2O)_4]$.[19] The fluoro complex $(NH_4)_3[Zr(O_2)F_5]$ has been made[15] and shown by X-ray structure analysis to contain a pentagonal bipyramidal anion;[20] salts of $[Zr_2(O_2)_2F_7]^{3-}$ are also known.[21] The known carboxylato peroxo complexes are $[Zr(O_2)(ox)(H_2O)_2]\cdot nH_2O$,[22] $[Zr(O_2)L_2]$ and $[Zr(O_2)L'(H_2O)]$ (L = picolinato, 8-hydroxyquinolinato, aniline-2-carboxylato, 2-aminophenoxido; L′ = N-(2-carboxyphenyl)salicylideneaminato).[23]

We have attempted to prepare peroxo complexes of these metals with oxalic, citric, tartaric and glycollic acids, the anions of which have proven complexing ability and the capability of forming five-membered rings with metals.

Reaction of the soluble oxychlorides $ZrOCl_2 \cdot 8H_2O$ and $HfOCl_2 \cdot 8H_2O$ with potassium oxalate (1 : 2 metal–ligand ratio) in the presence of H_2O_2 gave the new complexes $K_2[M(O_2)(ox)_2] \cdot 2H_2O$ as white, sparingly soluble salts; the pHs of formation were 3(Zr) and 2(Hf), values low enough to suppress hydrolysis of the zirconyl and hafnyl reactants. A similar procedure with potassium citrate gave $K_2[M(O_2)_2(cit)] \cdot H_2O$. With potassium tartrate no carboxylato complexes could be isolated, but glycollic acid and $MOCl_2 \cdot 8H_2O$ with KOH (mole ratio 1 : 1 : 2) in the presence of excess H_2O_2 gave white materials with analyses falling midway between the formulations $K_2[M(O_2)(glyc)_2] \cdot 2H_2O$ and $K_2[M(O_2)_2(glyc)] \cdot H_2O$. The IR spectra of these materials showed broad bands in the region 900–1000 cm^{-1}, which may arise from polymeric zirconyl or hafnyl moieties.

The low solubility of the $K_2[M(O_2)(ox)_2] \cdot 2H_2O$ and $K_2[M(O_2)_2(cit)] \cdot H_2O$ salts prevented study of their ^1H or ^{13}C spectra. Their vibrational spectra showed, in addition to bands typical of coordinated oxalate and citrate modes, bands typical of side-bonded peroxo ligands. The stoichiometries suggest six-coordination (assuming side-on coordination for peroxide) or seven-coordination if one molecule of water participates in the coordination sphere. On the basis of the known pentagonal bipyramidal symmetry of the anion in $(NH_4)_3[Zr(O_2)F_5]$[20] we suggest that these salts could also contain pentagonal pyramidal anions, viz. $[M(O_2)(ox)_2(H_2O)]^{2-}$ and $[M(O_2)_2(cit)(H_2O)]^{2-}$. The presence of only one citrate group rather than two is likely to arise from the steric crowding that would occur in a bis citrato complex.

EXPERIMENTAL

Preparation of $K_3[Nb(O_2)_4] \cdot \frac{1}{2}H_2O$

A sample of fresh Nb_2O_5 was obtained by addition of $NbCl_5$ (5.0 g) to a 2 M solution of KOH (50 cm^3) at 0°C. The Nb_2O_5 was filtered off, washed with cold water and dried. It was then fused (2.0 g, 7.52 mmol) with KOH pellets (3.4 g, 60.6 mmol) in a nickel crucible. The cooled melt was taken up in a minimum of water, and treated with 30% H_2O_2 (5 cm^3). The cloudy solution was heated for 15 min at 75°C on a water bath and filtered when hot. On cooling, the filtrate gave yellow–white crystals of $K_3[Nb(O_2)_4] \cdot \frac{1}{2}H_2O$, which are filtered off, washed with ethanol and air-dried. Found: K, 33.6; $(O_2)^{2-}$, 37.4. $HK_3NbO_{8.5}$ requires: K, 33.9; $(O_2)^{2-}$, 37.0%. Infrared (IR) and Raman (R) data (cm^{-1}): IR (Nujol mull): 813vs, 598s, 548s, 463br, 295m; R (solid, KBr disc): 841(10), 815(2), 600(1), 548(8), 521(3), 459(2), 300(2), 271(5).

A similar sample was obtained by the alkali fusion of potassium niobate followed by the same work-up. The sodium salt was prepared by using NaOH instead of KOH.

Preparation of $K_3[Ta(O_2)_4] \cdot \frac{1}{2}H_2O$

Fresh Ta_2O_5 (2.0 g, 4.53 mmol) [prepared by the addition of $TaCl_5$ (5.0 g) to a 2 M solution of potassium hydroxide (50 cm^3)] and potassium hydroxide pellets (2.0 g, 35.6 mmol) were fused in a nickel crucible. The cooled melt was taken up in a minimum of water, treated with 30% H_2O_2 (5 cm^3) and heated to 75°C for 15 min. The cloudy suspension was filtered when hot. On cooling at room temperature, the filtrate gave white crystals of $K_3[Ta(O_2)_4] \cdot \frac{1}{2}H_2O$, which were filtered off, washed with ethanol and air-dried. Found: K, 26.2; $(O_2)^{2-}$, 28.9. $HK_3O_{8.5}Ta$ requires: K, 26.9; $(O_2)^{2-}$, 29.4%. Infrared (IR) and Raman (R) data (cm^{-1}): IR (Nujol mull): 847m, 808vs, 621m, 594m, 560m, 531vs, 441s; R (solid, KBr disc): 836(10), 815(4), 633(2), 577(3), 558(4), 340(2).

A similar sample was obtained by alkali fusion of potassium tantalate. The sodium salt was prepared by using NaOH instead of KOH.

Preparation of $K_3[M(O_2)_3(tart)] \cdot H_2O$ (M = Nb, Ta) *and* $K_3[M(O_2)_3(L)] \cdot 2H_2O$ (M = Nb, L = glyc, cit, mal; M = Ta, L = glyc, cit)

$K_3[M(O_2)_4] \cdot \frac{1}{2}H_2O$ (1.44 mmol) and H_2L (1.44 mmol) were dissolved in water (25 cm^3). The solution was treated with excess 30% H_2O_2 (10 cm^3) with stirring. Addition of ethanol (*ca* 20 cm^3) and storage at 5°C yielded a light yellow (M = Nb) or white (M = Ta) solid, which was filtered off, washed with ethanol and air-dried.

Preparation of $K[M(O_2)_2(dipic)(H_2O)] \cdot 2H_2O$ (M = Nb, Ta)

$K_3[M(O_2)_4] \cdot \frac{1}{2}H_2O$ (1.48 mmol) and dipicolinic acid (pyridine-2,6-dicarboxylic acid) (1.48 mmol) were dissolved in water (15 cm^3) and the solution treated with 30% H_2O_2 (5 cm^3). Addition of ethanol (15 cm^3) and storage at 5°C gave a yellow (M = Nb) or white (M = Ta) solid, which was filtered off, washed with ethanol and air-dried.

Table 1. IR, Raman, ^{13}C NMR and analytical data

Complex		Vibrational data (cm^{-1})[a]			Analytical data (%)[b]				
		ν(O—O)	$\nu_{sym}[M(O_2)]$	$\nu_{asym}[M(O_2)]$	C	H	K	$(O_2)^{2-}$	N
$K_3[Nb(O_2)_3(tart)]\cdot H_2O$	IR	855s	647m	594m	11.0	1.5	24.2	20.1	—
	R	862(10)	638(2)	570(7)	(10.2)	(1.3)	(24.8)	(20.3)	
	R*	860(10)p	634(2)p	582(8)dp					
$K_3[Ta(O_2)_3(tart)]\cdot H_2O$[c]	IR	847s	642m	586m	8.5	0.8	21.2	17.8	—
	R	855(10)	636(3)	593(8)	(8.6)	(1.1)	(20.9)	(17.1)	
	R*	854(10)	640(2)	592(7)					
$K_6[Nb(O_2)_6(tart)]\cdot 2H_2O$	IR	861m	638m	591m	7.0	0.9	29.9	24.5	—
		849s			(6.0)	(0.8)	(29.5)	(24.2)	
	R	867(10)	628(2)	575(8)					
	R*	860(10)p	625(2)p	580(7)dp					
$K_6[Ta(O_2)_6(tart)]\cdot 2H_2O$	IR	850s	641m	575m	4.5	0.4	23.9	19.4	—
	R	843(10)	633(3)	555(7)	(4.9)	(0.6)	(24.2)	(19.8)	
	R*	841(10)p	636(2)p	562(8)dp					
$K_3[Nb(O_2)_3(glyc)]\cdot 2H_2O$[d]	IR	855s	625m	594m	5.2	0.7	29.1	25.1	—
	R	852(10)	618(3)	589(7)	(5.8)	(1.5)	(28.1)	(23.1)	
$K_3[Ta(O_2)_3(glyc)]\cdot 2H_2O$[e]	IR	838s	624m	580m	4.0	0.7	22.9	20.7	—
	R	854(10)	619(2)	569(8)	(4.8)	(1.2)	(23.3)	(19.0)	
$K_3[Nb(O_2)_3(cit)]\cdot 2H_2O$	IR	859s	648m	594m	13.8	1.6	22.7	18.6	—
	R	860(10)	632(3)	586(8)	(14.1)	(2.0)	(22.9)	(18.7)	
$K_3[Ta(O_2)_3(cit)]\cdot 2H_2O$	IR	853s	645m	592m	12.6	1.4	19.2	15.2	—
	R	857(10)	632(3)	597(7)	(12.0)	(1.7)	(19.5)	(16.0)	
$K_3[Nb(O_2)_3(mal)]\cdot 2H_2O$	IR	849s	639m	576m	10.2	1.4	24.2	20.0	—
	R	863(10)	635(3)	577(7)	(10.1)	(1.7)	(24.7)	(20.2)	
$K[Nb(O_2)_2(dipic)(H_2O)]\cdot 2H_2O$	IR	851s	618m	589m	20.2	1.1	10.8	14.9	2.9
		845s		576m	(20.3)	(2.2)	(9.4)	(15.4)	(3.4)
	R	848(10)	611(4)	586(8)					
		836(8)		573(6)					

$K[Ta(O_2)_2(dipic)(H_2O)]\cdot 2H_2O$	IR	848s	616m	566m	16.3	0.9	9.2	12.1	2.4
	R	847(10)	604(3)	561(7)	(16.7)	(1.8)	(7.8)	(12.7)	(2.8)
$K_2[Zr(O_2)(ox)_2]\cdot 2H_2O$	IR	840s	620m	560m	11.6	0.7	18.5	7.5	—
	R	848(10)		565(2)	(11.6)	(1.0)	(18.9)	(7.7)	
	R*	855(10)p							
$K_2[Hf(O_2)(ox)_2]\cdot 2H_2O$	IR	846s	623m	555m	9.1	0.9	15.3	6.1	—
	R	856(10)		572(3)	(9.6)	(0.8)	(15.6)	(6.4)	
	R*	860(10)p							
$K_2[Zr(O_2)_2(cit)]\cdot H_2O$	IR	855s	638w	548m	16.6	1.9	16.4	14.1	—
	R	853(10)br		550(3)	(16.3)	(1.8)	(17.7)	(13.9)	
	R*	862(10)p							
		842(8)p							
$K_2[Hf(O_2)_2(cit)]\cdot H_2O$	IR	858s	635w	552m	14.9	1.6	16.8	11.3	—
	R	868(10)br		554(3)	(13.6)	(1.5)	(14.8)	(12.1)	
	R[d]	872(10)p							
Zr glycollato complex[f]	IR	846s		555br	8.5	2.3	21.3	10.1	—
	R	851(10)							
Hf glycollato complex[f]	IR	849s		530br	7.9	2.2	—	11.2	—
	R[g]	—	—	—					

[a] Data for solids, or * for aqueous solutions (relative Raman intensities in parentheses).
[b] Calculated values in parentheses.
[c] ^{13}C NMR: δ 180 and 80 ppm relative to $(CH_3)_4Si$.
[d] ^{13}C NMR: δ 182.3 and 73.0 ppm.
[e] ^{13}C NMR: δ 183.4 and 73.7 ppm.
[f] Formulation discussed in text; IR and Raman spectra also show broad bands in 940–950 cm^{-1} region.
[g] Sample decomposed in laser beam.
IR = infrared; R = Raman; p = polarized; dp = depolarized; br = broad; s = strong; m = medium; w = weak.

Preparation of $K_6[M_2(O_2)_6(tart)]\cdot 2H_2O$ (M = Nb, Ta)

$K_3[M(O_2)_4]\cdot \frac{1}{2}H_2O$ (2.88 mmol) and (+)-tartaric acid (1.44 mmol) were dissolved in water (30 cm^3) and the solution treated with 30% H_2O_2 (10 cm^3), with stirring. Addition of ethanol and storage at 0°C yielded a light yellow (M = Nb) or white (M = Ta) solid, which was filtered off, washed with ethanol and air-dried.

Attempted preparation of other carboxylato peroxo complexes

The reactions of malonic, salicylic, succinic and mandelic acids with $K_3[M(O_2)_4]\cdot \frac{1}{2}H_2O$ (M = Nb, Ta), in the presence of H_2O_2, each yielded only the unreacted potassium tetraperoxometallate(V) salt upon precipitation with ethanol.

Preparation of $K_2[M(O_2)(ox)_2]\cdot 2H_2O$ (M = Zr, Hf)

Zirconyl chloride, $ZrOCl_2\cdot 8H_2O$ (1.00 g, 3.10 mmol) and potassium oxalate (1.14 g, 6.20 mmol) were dissolved in water (15 cm^3). Addition of 30% H_2O_2 (10 cm^3) with stirring, followed by storage overnight at 0°C, gave a white solid, which was filtered off, washed with cold ethanol (3 × 10 cm^3) and dried in a vacuum desiccator over silica gel. The solid proved to be slightly hygroscopic and was therefore stored in a desiccator permanently.

The analogous hafnium complex was similarly prepared and isolated as a white hygroscopic solid by the reaction of hafnyl chloride, $HfOCl_2\cdot 8H_2O$, with potassium oxalate and excess H_2O_2.

Preparation of $K_2[M(O_2)_2(cit)]\cdot H_2O$ (M = Zr, Hf)

The oxychloride, $MOCl_2\cdot 8H_2O$ (3.10 mmol) and potassium citrate (3.10 mmol) were dissolved in water (25 cm^3), and the solution treated with 30% H_2O_2 (10 cm^3) with stirring. Addition of ethanol and storage at 0°C gave white hygroscopic solids (M = Zr, Hf) which were collected, washed with ethanol and dried in a vacuum desiccator over silica gel. Both compounds were stored in a desiccator.

Preparation of glycollato peroxo complexes of Zr^{IV} *and* Hf^{IV}

Zirconyl chloride (1.00 g, 3.10 mmol) and glycollic acid (0.47 g, 6.2 mmol) were dissolved in water (15 cm^3), and 30% H_2O_2 (5 cm^3) added, followed by a solution of KOH (0.35 g, 6.2 mmol) in water (5 cm^3). A yellow–white solid appeared at 5°C and was collected, washed with cold ethanol and air-dried. (Found: C, 8.5; H, 2.3; K, 21.3; $(O_2)^{2-}$, 10.1%.) A similar compound was obtained using a 1:1:2 zirconium–glycollate–KOH molar ratio. Similarly, the analogous white hafnium compound was prepared using both 1:2:2 and 1:1:2 hafnium–glycollate–KOH ratios. (Found: C, 7.9; H, 2.2; $(O_2)^{2-}$, 11.2%.)

General experimental

Raman spectra were recorded on a Spex Ramalog 5 instrument with a Spex Datamate data acquisition unit, using the exciting lines at 568.2 and 530.9 nm from a Coherent model 52 krypton-ion laser, at 568.2 nm from a Coherent Innova 90 krypton-ion laser and at 514.5 nm from a Coherent Innova 70 argon-ion laser. Spectra of solids were taken as spinning discs on a potassium bromide base and of aqueous solution in spinning cells. IR spectra were measured on a Perkin–Elmer 683 spectrometer as liquid paraffin mulls between potassium bromide plates. The ^{13}C NMR spectra were recorded by Miss Sue Johnson on a Brüker WM250 Fourier transform spectrometer at 62.9 MHz. Carbon, nitrogen and hydrogen analyses were carried out by Mr K. Jones of the Microanalytical Department, Imperial College. Peroxide analyses were performed by iodometric titration and potassium was analysed gravimetrically (as the tetraphenylborate).

Acknowledgements—We thank Interox Chemicals and the SERC for a CASE grant to one of us (A.C.D.), and Diana Anderson for helpful discussions.

REFERENCES

1. N. J. Campbell, A. C. Dengel, C. F. Edwards and W. P. Griffith, *J. Chem. Soc., Dalton Trans.*, submitted for publication.
2. H. Mimoun, *The Chemistry of Peroxides* (Edited by S. Patai), p. 469 and refs therein. Wiley, New York (1983).
3. A. C. Dengel, W. P. Griffith, R. D. Powell and A. C. Skapski, *J. Chem. Soc., Dalton Trans.* 1987, 991.
4. R. Stomberg, *Acta Chem. Scand.* 1983, **37A**, 523.
5. A. C. Dengel and W. P. Griffith, *Spectrochim. Acta* 1987, **43A**, 1173.
6. Z. Ruzic-Toros, B. Kojic-Prodic and M. Sljukic, *Acta Cryst.* 1976, **32B**, 1096.
7. Z. Ruzic-Toros, B. Kojic-Prodic and M. Sljukic, *Inorg. Chim. Acta* 1984, **86**, 205.
8. R. Schmidt, G. Pausewang and W. Massa, *Z. Anorg. Chem.* 1982, **488**, 108.
9. J. E. Guerchais and B. Spinner, *Bull. Soc. Chim. Fr.* 1965, 1122.
10. C. Djordjevic and N. Vuletic, *Inorg. Chem.* 1968, **7**, 1864.

11. G. Mathern and R. Weiss, *Acta Cryst.* 1971, **27B**, 1572.
12. R. N. Shchelekov, E. N. Traggeim, M. A. Michnik and K. I. Petrov, *Russ. J. Inorg. Chem.* 1972, **17**, 1270.
13. N. Vuletic, E. Prcic and C. Djordjevic, *Z. Anorg. Chem.* 1979, **450**, 67.
14. H. Mimoun, *Israel J. Chem.* 1983, **23**, 451.
15. W. P. Griffith and T. D. Wickins, *J. Chem. Soc. A* 1968, 397; W. P. Griffith and T. D. Wickins, *J. Chem. Soc. A* 1967, 590.
16. G. Mathern and R. Weiss, *Acta Cryst.* 1971, **27b**, 1598.
17. A. C. Dengel, W. P. Griffith, R. D. Powell and A. C. Skapski, *J. Chem. Soc., Chem. Commun.* 1986, 555.
18. R. Schwarz and H. Giese, *Z. Anorg. Chem.* 1928, **176**, 209.
19. G. V. Jere and G. D. Gupta, *J. Inorg. Nucl. Chem.* 1970, **32**, 537.
20. R. Schmidt, G. Pausewang and W. Massa, *Z. Anorg. Chem.* 1986, **535**, 135.
21. G. V. Jere and M. T. Santhamma, *Inorg. Chim. Acta* 1977, **24**, 57.
22. G. D. Gupta and G. V. Jere, *Ind. J. Chem.* 1972, **10**, 102; G. D. Gupta and G. V. Jere, *Ind. J. Chem.* 1968, **6**, 54.
23. M. T. H. Taradfer and M. A. L. Miah, *Inorg. Chem.* 1986, **25**, 2265.

Polyhedron Vol. 8, No. 11, pp. 1379–1386, 1989
Printed in Great Britain

0277–5387/89 $3.00+.00
© 1989 Pergamon Press plc

STUDIES ON TRANSITION METAL PEROXO COMPLEXES—X.* THE NATURE OF PEROXOVANADATES IN AQUEOUS SOLUTION

NICHOLAS J. CAMPBELL, ANDREW C. DENGEL and WILLIAM P. GRIFFITH†

Inorganic Chemistry Laboratories, Imperial College of Science and Technology, London SW7 2AY, U.K.

(*Received* 6 *December* 1988; *accepted* 19 *December* 1988)

Abstract—The nature of the species formed in solutions of $[VO_4]^{3-}$, in excess H_2O_2 from pH 14 to acid, has been studied by Raman spectroscopy and ^{51}V NMR; polymerization processes are far simpler in the presence than in the absence of H_2O_2. The principal species present are likely to be $[V(O_2)_4]^{3-}$, $[VO(O_2)_3]^{3-}$, $[V(OH)(O_2)_3]^{2-}$, *cis*-$[VO_2(O_2)_2(H_2O)]^{3-}$, $[V_2O_3(O_2)_4]^{4-}$ or $[V_2(OH)O_2(O_2)_4]^{3-}$, $[VO(O_2)_2(H_2O)]^{-}$ and $[VO(O_2)(H_2O)_4]^{+}$. A brief Raman study is also reported of spectra of $[M(O_2)_4]^{3-}$ (M = Nb, Ta) in excess H_2O_2 from pH 11 to 7.

The nature of the species formed when aqueous solutions of the orthovanadate ion $[VO_4]^{3-}$ are acidified has been studied by a number of techniques,[2–7] including Raman spectroscopy,[4,5] ^{51}V NMR[6,7] and ^{17}O NMR.[6] The reaction sequence is complex, involving monomers, dimers, tetramers and decamers.[2] We have recently shown[8] by the combined use of Raman and NMR (^{95}Mo, ^{183}W) that polymerization processes for molybdate, $[MoO_4]^{2-}$, and tungstate, $[WO_4]^{2-}$, in the presence of aqueous H_2O_2, are far less complex than those in aqueous solution alone. Here, we present similar data for the $[VO_4]^{3-}$–H_2O_2–H_2O system, using as a guide the ^{51}V[9,10] and ^{17}O[9] NMR data of Howarth *et al.* with new ^{51}V NMR results; we have previously reported a very restricted Raman study of peroxovanadates in solution.[4] Although in such systems, NMR can give valuable information on the number of species present in solution, we seek to show here that, as with molybdenum peroxo complexes, the *combined* use of NMR and Raman can give useful information on the nature of such species. The technique of comparing profiles of Raman spectra of species with known structures together with profiles of solute species has been used, so we report first the vibrational spectra of some solid oxoperoxovanadates which have already been structurally characterized, and also attempt an assignment of vibrational modes for the $[V_2(OH)O_2(O_2)_4]^{3-}$ ion using isotopic substitution.

* For Part IX, see ref. 1.

† Author to whom correspondence should be addressed.

RESULTS AND DISCUSSION

(A) *Raman and IR spectra of peroxovanadates of known structures*

The structures of $(NH_4)_4[V_2O_3(O_2)_4]$[11,12] and $(NH_4)_3[V_2(OH)O_2(O_2)_4]$[13] have been studied by X-ray single crystal analysis, and there is a brief mention of the X-ray crystal structure of $(NH_4)_3[V(O_2)_4]$.[12]

For assignments of Raman and IR bands we use commonly accepted mode descriptions: stretching vibrations [ν(V=O)] of terminal V=O bonds in VO and *cis*-VO_2 units will occur near 900 cm^{-1} with their deformations δ(V=O) near 320 cm^{-1}.[14] For the triangular $V(O_2)$ unit, the O—O stretch [ν(O—O)] is expected near 880 cm^{-1}, with the asymmetric and symmetric $V(O_2)$ stretches {ν^{as}[$V(O_2)$] and ν^{s}[$V(O_2)$]} near 600 cm^{-1}.[15,16] For binuclear complexes containing bent 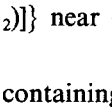 units, the asymmetric and symmetric V—O stretches, $\nu^{as}(V_2O)$ and $\nu^{s}(V_2O)$, might be expected to lie near 700 and 500 cm^{-1}, respectively, by analogy with the corresponding modes in $[Cr_2O_7]^{2-}$[17] and in $[M_2O_3(O_2)_4(H_2O)_2]^{2-}$ (M = Mo, W).[8] The IR

spectra of oxomono- and diperoxovanadates have been discussed by Schwendt.[18]

$K_3[V(O_2)_4]$. The Raman and IR spectra of this unstable purple compound are reported in Table 1; the IR spectrum has already been reported.[18]

The vibrational spectra are very simple, with ν(O—O), $\nu^{as}[V(O_2)]$ and $\nu^{s}[V(O_2)]$ appearing at 859, 623 and 571 cm^{-1} in the Raman. The IR band at 373 cm^{-1} may be a $V(O_2)$ deformation.

$(NH_4)_3[V_2(OH)O_2(O_2)_4]$ *and* $K_4[V_2O_3(O_2)_4]$. Salts containing $[V_2(OH)O_2(O_2)_4]^{3-}$ and $[V_2O_3(O_2)_4]^{4-}$ can be isolated from peroxovanadate solutions using the appropriate pH control.[19] Although our attempts to prepare the claimed $(NH_4)_4[V_2O_3(O_2)_4]$[11,12] gave either the known complexes $(NH_4)_3[V_2(OH)O_2(O_2)_4]$[13] or $(NH_4)[VO(O_2)_2(NH_3)]$,[20] we did succeed in making $K_4[V_2O_3(O_2)_4]\cdot 2H_2O$. By using ^2H_2O or $H_2{}^{18}O$ as solvent we were also able to isolate $K_3[V_2(O^2H)O_2(O_2)_4]$ and $(NH_4)_3[V_2(^{18}OH)^{18}O_2(O_2)_4]$, although partial deuteration only was achieved in the former case. By comparison of the Raman and IR spectra of the normal and isotopically substituted complexes and also by using our previous data[8] on the vibrational spectra of normal and isotopically substituted (^2H, ^{18}O) $K_2[M_2O_3(O_2)_4(H_2O)_2]$ (M = Mo, W), tentative assignments of some of the vibrational modes in $[V_2(OH)O_2(O_2)_4]^{3-}$ and $[V_2O_3(O_2)_4]^{4-}$ can be made. There are reports on the IR spectra of $M_4[V_2O_3(O_2)_4]$ (M = K,[16,18,19] NH_4[18,19]) and of $M_3[V_2(OH)O_2(O_2)_4]$ (M = K, NH_4 and Cs with deuteration data[18,19]), but no Raman spectra have been reported.

There is unlikely to be $^{18}O/^{16}O$ exchange for the peroxo ligands during isolation of $(NH_4)_3[V_2(^{18}OH)^{18}O_2(O_2)_4]$ from $H_2{}^{18}O$, so Raman and IR bands near 880, 610 and 520 cm^{-1} are assigned to ν(O—O), $\nu^{as}[V(O_2)]$ and $\nu^{s}[V(O_2)]$, respectively, since they are unaffected by ^{18}O-substitution. The greater intensity of the 520 cm^{-1} Raman band compared with that near 610 cm^{-1} suggests that the former arises from the symmetric $\nu(O_2)$ stretch (for molybdenum and tungsten peroxo complexes $\nu^{s}[M(O_2)]$ lies at high wavenumbers than $\nu^{as}[M(O_2)]$,[8] but for vanadium peroxo complexes the reverse situation obtains). In $K_3[V_2(OH)O_2(O_2)_4]\cdot 2H_2O$, an IR band at 1055 cm^{-1} shifts to 770 cm^{-1} on deuteration and we assign this to a V—O—H deformation mode, δ[V(OH)]; Wieghardt and Quilitzsch have similarly assigned a band at 996 cm^{-1}, shifting to 730 cm^{-1} on deuteration, for $Cs_3[V_2(OH)O_2(O_2)_4]$.[19] The bands near 970 and 320 cm^{-1} shift by some 50 and 6 cm^{-1}, respectively, on ^{18}O substitution and so are assigned to V=O stretches and deformations ν(V=O) and δ(V=O), respectively; similar bands and shifts were noted for $K_2[M_2O_3(O_2)_4(H_2O)_2]\cdot 2H_2O$ (M = Mo, W).[8] The assignments of $\nu^{as}(V_2O)$ and $\nu^{s}(V_2O)$ (the asymmetric and symmetric stretches of the V(OH)V bridge) are more difficult; we tentatively assign the IR band in $(NH_4)_3[V_2(OH)O_2(O_2)_4]$ at 635 cm^{-1} to $\nu^{as}(V_2O)$, since it shifts to 621 cm^{-1} on ^{18}O substitution, and the weak Raman band at 460 cm^{-1}, shifting on ^{18}O substitution to 446 cm^{-1}, to $\nu^{s}(V_2O)$. Assignments for $M^{I}_4[V_2O_3(O_2)_4]\cdot nH_2O$ (M = K, Cs) then follow. The profiles of their Raman and IR spectra are like those of $K_2[M_2O_3(O_2)_4(H_2O)_2]\cdot 2H_2O$,[8] as might be expected in view of their structural similarities. Raman spectra of these species in solution are discussed below.

(B) *Raman and* ^{51}V *NMR spectra of peroxovanadates in aqueous solutions*

Solutions studied were from 1.0 to 0.1 M in vanadium and $[VO_4]^{3-}$; H_2O_2–V ratios were 5:1, 2:1 and 1:1. Most studies were carried out on solutions of 0.5 M in $[VO_4]^{3-}$ with a five-fold excess of H_2O_2 and, unless otherwise stated, it is on those solutions that the work described below was carried out, since Raman spectra for lower vanadium concentrations are difficult to measure. The pH of solutions was adjusted by the addition of HCl, though the use of $HClO_4$ or H_2SO_4 produced very little change in the positions of ^{51}V NMR resonances. Data for 0.5 M $[VO_4]^{3-}$ in 2.5 M H_2O_2 at different pH are summarized in Table 2.

It seems likely that, with the exception of the dodecahedral[12] $[V(O_2)_4]^{3-}$ ion, all the peroxovanadates involved are seven-coordinated;[11-13] in order to achieve this, the species postulated below have, in some cases, coordinated water molecules in their formulae, though it is not possible using the methods employed here to detect the presence of aqua ligands.

pH > 13.5. At these high pHs it seems likely that the unstable purple $[V(O_2)_4]^{3-}$ is the dominant species.[21] Although Raman spectra of such solutions were very difficult to record owing to the colour and decomposition, polarized bands at 883, 855 and 572 cm^{-1} were observed, likely to be due to ν(O—O) of $[V(O_2)_4]^{3-}$, ν(O—O) of OOH^- and $\nu^{s}[V(O_2)]$, respectively, while a depolarized band at 621 cm^{-1} may be due to $\nu^{as}[V(O_2)]$. These values are reasonably close to those observed for the Raman spectrum of solid $K_3[V(O_2)_4]$. No ^{51}V NMR spectra could be recorded at these high pHs owing to problems of solution decomposition, but Howarth assigned a shift of δ −737.6* to the species.[9] This

* Relative to $VOCl_3$ (δ = 0 ppm). All ^{51}V spectra are quoted relative to this standard.

Table 1. Raman and IR spectra of solid peroxovanadate, peroxoniobate and peroxotantalate complexes

		ν(V=O)	ν(O—O)	$\nu^{as}(V_2O)$	$\nu^{as}[M(O_2)]$	$\nu^{s}[M(O_2)]$	$\nu^{s}[V_2O]$	Other strong bands
$K_3[V(O_2)_4]$	R	—	859(10)	—	623(5)	571(6)	—	
	IR		854s		620s	567vs		807m, 373s, 335s
$(NH_4)_3[V_2(OH)O_2(O_2)_4]$	R	970(4) 943(4)	885(4) 880(4)	644(1)	610(2)	521(10)	460(1)	360(1), 347(1), 323(2), 270(2)
	IR	970vs 950vs	888s 864s	635m	610s	525m	475w	1055m [δV(OH)]
$(NH_4)_3[V_2(^{18}OH)^{18}O_2(^{16}O_2)_4]$	R	928(5) 901(3)	880(3)	627(1)	609(2)	519(10)	446(1)	360(2), 342(2), 314(2), 266(2)
	IR	926vs 904vs	882vs 864vs	621m	610vs	522m	455w	1018m [δV(18OH)]
$K_3[V_2(OH)O_2(O_2)_4]\cdot 2H_2O$	R	976(5) 939(5)	887(5) 881(5)	621(1)	608(2)	526(10)	466(1)	1050(1) [δV(OH)], 365(1)
	IR	974vs 945vs	889vs 868vs		618vs	530s	473w	1055m [δV(OH)] 384m, 345w
$K_4[V_2O_3(O_2)_4]\cdot 2H_2O$	R	953(6)	885(5) 843(10)	649(1)	625(2)	571(4) 525(7)	477(1)	345(4), 330(1), 312(3), 280(1)
	IR	948s	870vs		625vs	557w	485w	
$Cs_3[V_2(OH)O_2(O_2)_4]$	R	954(3) 934(2)	884(3) 877(2)		610(2)	520(10)	491(1)	358(1), 319(2), 245(2)
	IR	958vs 940vs	887vs 872vs	634s	612vs	523m	483w	
$K_3[Nb(O_2)_4]\cdot 1/2H_2O$	R	—	841(10) 815(2)	—	548(8)	521(3)	—	300(2), 271(5)
	IR	—	813vs	—	548s	522m	—	598s, 463br
$K_3[Ta(O_2)_4]\cdot 1/2H_2O$	R	—	836(10) 815(4)	—	558(4)	530sh	—	633(2) 621m, 441s
	IR	—	847m 808vs	—	560m	531s	—	

Table 2. Raman, IR and ^{51}V NMR spectra of 0.5 M $[VO_4]^{3-}$ in 2.5 M H_2O_2 solution

pH	Vibrational data[a]									^{51}V NMR data[b]					
14.0				883(10)	855(2)	621(2) 586(2)	572(4)								
13.5	981(3)	975(4)		891(6)	881(4)		536(10)		316(3)	−838.2w *(200)*	−763.2s *(200)*	−742.4w *(80)*			
12.7	977(3)	968(3)		888(7)		623(1)	535(10)	476(1)	323(4)		−762.8s				
12.0	979(3)	972(3)		889(6)		620(1)	536(10)	471(1)	324(2)		−763.5s				
11.2	973(3)	966(3)		887(7)		624(2)	535(10)	475(2)	322(5)						
10.9	973(3)	962(1)	949(1)	890(5)		620(1)	535(10)	473(1)	326(1)		−764.0s				
10.6	976(3)	962(1)	948(1)	890(4)		623(2)	535(10)	472(2)	302(1)		−764.4s				
	975m*	964m*	940w*	885m*											
10.3	975(5)	962(2)	951(1)	887(4)		615(2)	535(10)	490(2)			−763.5s		−730.2w		
		963m*	950m*		829s*						*(200)*				
10.0	978(3)	972(3)	950(1)	889(6)	879(4)	633(2)	539(10)	429(1)	304(4)			−759.7w	−729.0m		
9.1	976(3)	963(2)	947(1)	899(6)	880(4)	630(1)	537(10)	484(1)	314(3)			−757.3w	−729.1s		
8.9	976(6)	966(4)	948(3)	890(7)		613(2)	526(10)	494(2)	324(3)						
8.4	979(6)	969(3)	948(2)	889(7)		633(2)	539(10)	494(2)	325(3)			−756.8w	−730.1s		
	977m*	960m*	948s*		829s*										
8.1	978(6)	965(4)	949(2)	890(7)		633(2)	538(10)	481(2)	322(5)			−756.8w	−730.1m		
7.8	976(6)	963(2)	952(1)	891(8)	878(4)	632(2)	533(10)	492(2)	322(3)				−730.6s		
7.2	977(4)	964(4)	950(1)	890(8)		634(2)	538(10)	488(1)	320(4)						
7.0	975(4)	970(3)	947(2)	890(7)		627(1)	537(10)	490(1)	314(3)			−756.8w	−730.9s		
	973m*	967m*	950s*												
6.5	976(6)	970(5)	950(3)	884(7)	880(7)	629(2)	535(10)	483(1)	322(6)			−756.4w	−728.5s	−697.8w	
6.0	980(5)	975(4)	952(2)		876(4)	624(3)	535(10)	480(1)	323(5)						
5.5	981(5)	977(4)	949(2)	889(7)		631(1)	537(10)	480(1)	319(4)			−757.7w	−729.5s	−694.9m	
5.3	985(4)	976(4)	950(2)	893(8)		633(1)	536(10)	497(2)	314(4)						
	980m*		950m*												
4.7	984(4)	977(2)	949(1)	893(7)		633(2)	537(10)	500(2)	319(4)			−757.6w	−729.6m	−694.2s	
4.5	984(3)	975(2)	951(5)	887(6)		631(1)	537(10)	480(1)	319(4)			−757.7w *(600)*	−728.0w *(300)*	−694.5s	
4.0	985(4)			890(6)		632(2)	535(10)	476(1)	321(4)					−694.2s	
	982m*														
2.0	987(4)			890(6)		640(1)	538(10)	500(2)	321(3)					−695.4s	
1.5	987(4)			893(7)		640(1)	537(10)	500(2)	321(3)					−695.4s	
0.8	977(7)			890(2)		630(1)	545(10)	340(6)						−693.8s *(300)*	665.1w *(400)*
0.4	976(8)			890(4)		589(2)	542(10)								−542.7s *(300)*
HCl	976(10)			878(4)		593(7)	543(8)		314(2)						

[a] Frequencies in cm^{-1}; Raman data or *IR. Relative Raman intensities in parentheses; polarized bands underlined, otherwise depolarized.
[b] Shifts (δ) in ppm relative to $\delta = 0$ for $VOCl_3$. Line intensities at halfwidth in italicized parentheses.

tetraperoxovanadate is likely to be the most highly peroxidated species present; the existence of the reported bright-red "$NH_4 \cdot VO_3 \cdot 6H_2O_2$"[22] could not be verified.

pH 13.5–10. At pH 13.5 a number of new Raman bands appear: polarized bands at 981 and 975 cm^{-1}, clearly due to ν(V═O), and a depolarized band at 316 cm^{-1} probably arising from δ(V═O). The ν(O—O) band at 883 cm^{-1} shifts to 891 and 881 cm^{-1}, and $\nu^s[V(O_2)]$ to 536 cm^{-1}. Both 0.5 and 0.1 M $[VO_4]^{3-}$ solutions show ^{51}V NMR shifts at −838, −763 and −742 ppm at pH 13, with the −838 and −742 ppm shifts apparent only when excess H_2O_2 is present. Howarth *et al.* have assigned shifts close to these values to $[VO(O_2)_3]^{3-}$, $[VO_2(O_2)_2]^{3-}$ and $[V(O_2)_4]^{3-}$, respectively.[10] Although we have shown that the claimed "triperoxo" species $K_3[V(O_2)_3ox] \cdot H_2O$ and $(NH_4)[V(O_2)_3bipy] \cdot 3H_2O$,[23] are perhydrates containing $[VO(O_2)_2ox]^{3-}$ and $[VO(O_2)_2bipy]^-$ anions,[24] there is an X-ray crystal structure of $(Me_4N)_2[V(OH)(O_2)_3] \cdot 4H_2O$.[25] There is also spectrophotometric evidence for the existence in solution of yellow $[VO(O_2)_3]^{3-}$ and $[V(OH)(O_2)_3]^{2-}$ species.[26] Therefore we agree with Howarth *et al.*[9,10] in assigning the δ −838 ppm resonance to $[VO(O_2)_3]^{3-}$ and suggest that the Raman bands at 981, 891, 536 and 316 cm^{-1} arise from this species. The δ −742 ppm resonance is very narrow, suggesting a very symmetrical environment about the metal, and could arise from the dodecahedral $[V(O_2)_4]^{3-}$.

As the pH drops below 13 these −838 and −742 ppm ^{51}V peaks give way to the resonance centred near −763 ppm, and this persists to pH 8. At these pH the Raman spectra in the ν(V═O) region show two polarized bands at 976 and 963 cm^{-1} (seen also in IR spectra of solutions), together with a new depolarized band near 950 cm^{-1}. For a species containing a VO_2 moiety, a *cis*-arrangement of the oxo ligands is likely, and for such a *cis*-VO_2 unit two Raman active ν(V═O) bands, one polarized and one depolarized, are expected.[14] Although the diperoxo complexes of vanadium so far examined by X-ray crystal structure analysis contain $VO(O_2)_2$ rather than $VO_2(O_2)_2$ units (e.g. the anions in $(NH_4)[VO(O_2)_2(NH_3)]$[20] and $K_3[VO(O_2)_2ox] \cdot H_2O$[27]) there is no intrinsic reason why complexes containing *cis*-$VO_2(O_2)_2$ units should not exist. We suggest that the species responsible for the relatively sharp δ −763 ppm resonance and the Raman bands near 963, 950, 890, 623 and 535 cm^{-1} arise from *cis*-$[VO_2(O_2)_2(H_2O)]^{3-}$, a coordinated water molecule bringing the coordination sphere to the normal seven for vanadium(V) peroxo complexes. IR spectra of solutions at these high pHs are difficult to record owing to decomposition in the beam.

In solutions with an H_2O_2–V ratio of 1 : 1, a ^{51}V shift at −621 ppm is seen, from pH 13 to 8. It disappears if more H_2O_2 is added and so could arise from a monoperoxo species such as $[VO_3(O_2)]^{3-}$ or a protonated form of this.

pH 10–1. Near pH 10 the sharp −764 ppm resonance gives way to a broader shift near −757 ppm and a new feature appears near −730 ppm, both persisting down to pH 4. Peaks in this region were also observed for aqueous solutions of $K_4[V_2O_3(O_2)_4]$ over the pH range 8–4, with a new peak appearing in the latter solution at −695 ppm. The broad −757 ppm feature is concentration-dependent, increasing in relative intensity with increasing vanadium concentration and so may arise from $[V_2O_3(O_2)_4]^{4-}$ or $[V_2(OH)O_2(O_2)_4]^{3-}$ (a resonance near −767 ppm has been assigned to $[V_2(OH)O_2(O_2)_4]^{3-}$[9]). Raman spectra of solutions of 0.5 M $[VO_4]^{3-}$ in 2.5 M H_2O_2, from pH 10 to 4, do not change drastically with pH, but the spectra of solutions of $K_4[V_2O_3(O_2)_4]$ or $(NH_4)_3[V_2(OH)O_2(O_2)_4]$ in water near pH 6 are similar in profile to those of the parent solids; three bands (978, 958 and 948 cm^{-1}) are observed in the ν(V═O) region, and bands at 890, 617 and 530 cm^{-1} are due to ν(O—O), $\nu^{as}[M(O_2)]$ and $\nu^s[M(O_2)]$, respectively, but no bands near 630 and 460 cm^{-1} assignable to $\nu^{as}(V_2O)$ and $\nu^s(V_2O)$ were seen. The −730 ppm peak is difficult to assign, but could perhaps arise from $[VO(OH)(O_2)_2(H_2O)]^{2-}$.

At pH 6.5 a new ^{51}V resonance appears near −697 ppm, persisting until pH 0.8, while the −757 and −729 ppm features become progressively less prominent and disappear near pH 4.5. We propose that this −697 ppm peak arises from $[VO(O_2)_2(H_2O)]^-$ (alkali metal salts of this have been isolated[28]) rather than the $[V(OH)_2(O_2)_2]^-$ suggested by Howarth *et al.*[9,10] (Russian workers have noted a resonance at −710 ppm assigned to $[VO(O_2)_2]^-$).[29] At pH 4, where this species becomes predominant, the Raman spectra become much simpler: there is only one polarized ν(V═O) band near 985 cm^{-1} with no depolarized band in the region, suggesting the absence of *cis*-VO_2 units. The polarized bands near 890 and 535 cm^{-1} may be assigned to ν(O—O) and $\nu^s[V(O_2)]$, respectively, while a depolarized band near 632 cm^{-1} is likely to arise from $\nu^{as}[V(O_2)]$. These bands are close in wavenumber to the IR and Raman bands observed for solid $K_3[VO(O_2)_2ox] \cdot H_2O_2$ and $(NH_4)[VO(O_2)_2bipy] \cdot 4H_2O$,[24] IR bands for solid $M[VO(O_2)_2(H_2O)]$ (M = K,[18,28] Cs,[18] NMe_4[18]), and in the IR spectrum of $K[VO(O_2)_2(H_2O)]$ in aqueous solution.[28] In further support of

our assignment of the −697 ppm peak to $[VO(O_2)_2(H_2O)]^-$, we note that aqueous solutions of another mono-oxodiperoxovanadate, $(NH_4)[VO(O_2)_2(NH_3)]$, show a single ^{51}V resonance at −695 ppm from pH 7 to 1. It has been observed that solutions of $[VO_4]^{3-}$ in excess H_2O_2 will epoxidize maleic and fumaric acids at pH 6;[30] the species responsible could well be $[VO(O_2)_2(H_2O)]^-$.

There is good evidence also from kinetic and mechanistic data for the existence in aqueous solutions of species containing $[VO(O_2)_2]^-$ units;[31,32] such a species may be responsible for the catalytic oxidation of diphenylsulphide by $[VO_4]^{3-}$ in excess H_2O_2.[31]

Below pH 1. As the pH drops below 3, the solutions of 0.5 M $[VO_4]^{3-}$ in 2.5 M H_2O_2 become markedly redder in colour, a change associated with the formation of the red complex containing the $VO(O_2)^+$ unit.[32] The Raman spectra of such solutions show polarized bands near 977, 890 and 542 cm^{-1} assigned to ν(V=O), ν(O—O) and $\nu^s[V(O_2)]$, respectively, and depolarized bands at 589 and 340 cm^{-1} assigned to $\nu^{as}[V(O_2)]$ and δ(V=O). At pH 1, two ^{51}V resonances are observed, at δ −665 and −543 ppm.

The origin of the −665 ppm resonance is not clear; Howarth tentatively assigned a shift at −650 ppm to $[V_2O(O_2)_4(H_2O)_2]$,[10] while Makarov *et al.* assign it to $[VO(O_2)]^+$.[29] It is only observed when excess H_2O_2 is present, disappearing if H_2O_2–V ratios of 2 : 1 or less are used, suggesting that it is a diperoxo species. The second resonance at −543 ppm may be assigned with confidence to a $VO(O_2)^+$ unit.[9,10] A number of oxomonoperoxovanadates containing the unit have been studied by X-rays (e.g. $[VO(O_2)pic(H_2O)_2]$[33] and $[VO(O_2)(pic)bipy]\cdot H_2O$;[34] pic = pyridine-2-carboxylate), and species containing $VO(O_2)^+$ have been implicated in oxidation reactions.[30] It is probably present in our system as $[VO(O_2)(H_2O)_4]^+$, which in concentrated HCl may well give species such as $[VO(O_2)Cl_n]^{1-n}$.

We conclude that several peroxovanadate species are formed when $[VO_4]^{3-}$ (or V_2O_5) are dissolved in excess aq. H_2O_2 over a wide pH range. However, the system is much simpler than that of $[VO_4]^{3-}$ over the same range in the absence of H_2O_2,[2-7] while being more complex than the corresponding $[MoO_4]^{2-}$–H_2O_2 and $[WO_4]^{2-}$–H_2O_2 systems.[8] Our Raman and ^{51}V NMR results are on the whole in agreement with those of Howarth *et al.*,[9,10] the main exception being the species giving a ^{51}V NMR resonance at −697 ppm; this they assign to $[V(OH)_2(O_2)_2]^-$, but we assign it on the strong evidence of the Raman spectra to $[VO(O_2)_2(H_2O)]^-$.

The span of ^{51}V NMR shifts for these peroxo- and oxoperoxovanadates is remarkable; possible reasons for its origin have been discussed.[9,35]

(C) *Raman spectra of peroxoniobates and peroxotantalates in aqueous solution*

Very high concentrations of H_2O_2 are needed to dissolve M_2O_5 or $K_8[M_6O_{19}]\cdot 16H_2O$ (M = Nb, Ta). However, we have prepared the known tetraperoxo salts $K_3[Nb(O_2)_4]\cdot 1/2H_2O$[36-39] and $K_3[Ta(O_2)_4]\cdot 1/2H_2O$,[37,38] repeated our earlier Raman and IR measurements on the solid salts[40] (see Table 1) and measured the Raman spectra of aqueous solutions of the salts from pH 11 to 7 in the presence of excess H_2O_2.

As with $K_3[V(O_2)_4]$, the spectra of the solids are easily assigned. At pH 11 the Raman spectrum profile of the aqueous solution (in the presence of H_2O_2) of $K_3[Nb(O_2)_4]$ is very similar to that of the solid; there is a single polarized band at 845 cm^{-1} assigned to ν(O—O), a polarized band at 540 cm^{-1} from $\nu^s[Nb(O_2)]$ and a depolarized band at 520 cm^{-1} from $\nu^{as}[Nb(O_2)]$. Unlike the vanadium system, though, there is little change in the Raman spectrum of the solution at pH 9 (pH was adjusted using HCl). However, at this pH, a gelatinous pale yellow precipitate starts to form; this precipitation is complete by pH 7. The Raman spectra of the supernatant solution remains essentially unchanged to pH 7, though the intensities of the peaks decrease, finally disappearing at pH 7. The precipitate is likely to be a complex containing the $[NbO_2(O_2)]^-$ moiety.[36-39] With $K_3[Ta(O_2)_4]\cdot 1/2H_2O$ the Raman spectrum of the aqueous solution at pH 10.7 is similar in profile to that of the solid salt, with polarized bands at 850 and 550 cm^{-1} assigned to ν(O—O) and $\nu^s[Ta(O_2)]$, respectively; $\nu^{as}[Ta(O_2)]$ appears at around 525 cm^{-1} as a shoulder. However, precipitation occurs at pH 10, presumably due to a species containing $[TaO_2(O_2)]^-$.[37,38] Thus, at relatively high pH at least, the peroxoniobate and peroxotantalate systems appear to be simpler than the peroxovanadates.

EXPERIMENTAL

$K_3[V(O_2)_4]$

This was prepared by a method based on that of Fergusson *et al.*[41] A solution of $K_3[VO_4]$ (2.0 g) in 30% H_2O_2 (12 cm^3) was cooled to ice-bath temperatures. The purple solution was added dropwise to ice-cold ethanol and the purple precipitate was filtered off, washed with ether and air-dried.

(Found: K, 39.3; O_2^{2-}, 42.8. Calc. for K_3VO_8: K, 39.5; O_2^{2-}, 43.2%.)

$(NH_4)[VO(O_2)_2(NH_3)]$

This was prepared by a method based on that of Drew and Einstein.[20] Divanadium pentoxide, V_2O_5 (1.82 g, 0.01 mol), was dissolved in 30% H_2O_2 (50 cm^3). To the deep red solution obtained, ammonium nitrate (1.60 g, 0.02 mol) was added, followed immediately by concentrated ammonium hydroxide, which was added dropwise until a bright yellow solution was obtained. This solution was allowed to stand for 12 h, after which bright yellow crystals were obtained. (Found: N, 16.6; H, 4.1; O_2^{2-}, 38.5. Calc. for $VO_5N_2H_7$: H, 16.9; H, 4.3; O_2^{2-}, 38.6%.)

$K_4[V_2O_3(O_2)_4]\cdot 2H_2O$

This was prepared by the method of Schwendt and Uskert.[42] Potassium vanadate, $K_3[VO_4]$ (0.69 g, 5 mmol), was dissolved in H_2O (20 cm^3), and 1 M KOH (5 cm^3) and 30% H_2O_2 (3 cm^3) were added. The yellow solution formed was mixed with ethanol (50 cm^3) and the resulting yellow precipitate was washed with ethanol and ether. (Found: K, 32.8; O_2^{2-}, 27.2. Calc. for $K_4V_2O_{13}H_4$: K, 33.2; O_2^{2-}, 27.2%.)

$K_3[V_2(OH)O_2(O_2)_4]\cdot 2H_2O$

This was prepared by the method of Wieghardt and Quilitzsch.[19] Divanadium pentoxide, V_2O_5 (0.91 g, 5 mmol), was dissolved with stirring in 30% H_2O_2 (30 cm^3) and H_2O (30 cm^3) and the solution filtered. The red solution was cooled in an ice bath and 1 M KOH (20 cm^3) slowly added. The yellow solution obtained was allowed to stand at 2°C for 24 h, after which a yellow solid was filtered off, washed with ethanol and ether, and air-dried. (Found: K, 26.8; O_2^{2-}, 29.8. Calc. for $K_3V_2O_{13}H_5$: K, 27.1; O_2^{2-}, 29.6%.)

$K_3[V_2(O^2H)O_2(O_2)_4]\cdot 2H_2O$

$K_3[V_2(OH)O_2(O_2)_4]\cdot 2H_2O$ (0.3 g) was dissolved in ^2H_2O (25 cm^3) with gentle warming and the yellow solution allowed to stand for 24 h. The solution was slowly evaporated to dryness on a vacuum line.

$Cs_3[V_2(OH)O_2(O_2)_4]$

This was prepared by the method of Wieghardt and Quilitzsch.[19] Divanadium pentoxide (0.91 g, 5 mmol) was dissolved, with stirring, in 30% H_2O_2 (30 cm^3). The solution was filtered and 0.5 M Cs_2CO_3 (20 cm^3) and 1 M CsCl (10 cm^3) solutions were added at room temperature. The solution was allowed to stand at 2°C for 24 h, after which a yellow powder was filtered off, washed with ethanol and ether, and air-dried. (Found: Cs, 57.8; O_2^{2-}, 18.8. Calc. for $Cs_3V_2O_{11}H$: Cs, 58.8; O_2^{2-}, 18.8%.)

$(NH_4)_3[V_2(OH)O_2(O_2)_4]\cdot 2H_2O$

This was prepared by the method of Wieghardt and Quilitzsch.[19] Ammonium metavanadate, $NH_4[VO_3]$ (2.35 g, 0.02 mol), was dissolved in concentrated ammonia (10 cm^3) and H_2O (80 cm^3) and cooled in an ice bath. 30% H_2O_2 (10 cm^3) and ethanol (30 cm^3) were added and the solution allowed to stand for 24 h. Yellow crystals were filtered off, washed with ethanol and ether, and air-dried. (Found: N, 11.6; H, 4.2; O_2^{2-}, 34.3. Calc. for $N_3H_{17}V_2O_{13}$: N, 11.4; H, 4.6; O_2^{2-}, 34.7%.)

$(NH_4)_3[V_2(^{18}OH)^{18}O_2(O_2)_4]\cdot 2H_2{}^{18}O$

$(NH_4)_3[V_2(OH)O_2(O_2)_4]\cdot 2H_2O$ (0.07 g) was dissolved under N_2 gas in $H_2{}^{18}O$ (98.4%, 1.0 cm^3) with very gentle warming. The solution was allowed to stand under nitrogen at room temperature for 24 h to facilitate exchange and was then evaporated to dryness *in vacuo*. The solid rapidly decomposed in air.

$K_3[Nb(O_2)_4]\cdot 1/2H_2O$

A sample of fresh Nb_2O_5 was obtained by the careful addition of $NbCl_5$ to an aqueous solution of KOH at 0°C. The Nb_2O_5 was filtered off, washed with cold H_2O and dried. Nb_2O_5 (2.0 g) and KOH pellets (3.4 g) were fused in a nickel crucible. The cooled melt was taken up in a minimum of H_2O and treated with 30% H_2O_2 (5 cm^3). The cloudy solution was heated for 15 min at 75°C on a water bath and filtered when hot. On cooling, the filtrate gave yellow–white crystals of the potassium tetraperoxoniobate, which were filtered off, washed with ethanol and air-dried. (Found: K, 33.6; O_2^{2-}, 37.4. Calc. for $HK_3NbO_{8.5}$: K, 33.9; O_2^{2-}, 37.0%.)

$K_3[Ta(O_2)_4]\cdot 1/2H_2O$

Fresh Ta_2O_5 (prepared by the careful addition of $TaCl_5$ to an aqueous solution of KOH at 0°C; 2.0 g) and KOH pellets (2.0 g) were fused in a nickel crucible. The cooled melt was taken up in minimum H_2O, treated with 30% H_2O_2 (5 cm^3) and heated at 75°C for 15 min. The cloudy suspension was filtered when hot. On cooling, the filtrate yielded

white crystals of potassium tetraperoxotantalate, which were filtered, washed with ethanol and air-dried. (Found: K, 26.2; O_2^{2-}, 28.9. Calc. for $HK_3O_{8.5}Ta$: K, 26.9; O_2^{2-}, 29.4%.)

Raman spectra were measured for solids on a KBr matrix as spinning discs or in solutions in spinning cells using a Spex Ramalog 5 spectrometer and a Coherent Radiation Innova 90 krypton-ion laser, with excitation at 6471 and 5648 Å. IR spectra were measured on a Perkin–Elmer 683 instrument, for solids as liquid paraffin films between caesium iodide plates or as aqueous solutions between calcium fluoride plates. ^{51}V NMR spectra were measured on a Brüker WM250 instrument at 65.7 MHz in 10 mm NMR tubes, with 5 mm inserts containing ^2H_2O for locking purposes.

Acknowledgements—We thank the SERC and Interox Chemicals Ltd for a CASE award to one of us (A.C.D.), and Mr R. Sheppard and Miss Sue Johnson for the NMR measurements.

REFERENCES

1. A. C. Dengel and W. P. Griffith, *Polyhedron* 1989, **8**, 1371.
2. M. T. Pope, *Heteropoly and Isopoly Oxometallates*. Springer, Berlin (1987).
3. M. T. Pope and B. W. Dale, *Quart. Rev.* 1968, **22**, 527.
4. W. P. Griffith and P. J. B. Lesniak, *J. Chem. Soc. A* 1969, 1066.
5. W. P. Griffith and T. D. Wickins, *J. Chem. Soc. A* 1966, 1087.
6. E. Heath and O. W. Howarth, *J. Chem. Soc., Dalton Trans.* 1981, 1105.
7. M. A. Habayeb and O. E. Hileman, *Can. J. Chem.* 1980, **58**, 2255.
8. N. J. Campbell, A. C. Dengel, C. F. Edwards and W. P. Griffith, *J. Chem. Soc., Dalton Trans.*, in press.
9. A. T. Harrison and O. W. Howarth, *J. Chem. Soc., Dalton Trans.* 1985, 1173.
10. O. W. Howarth and J. R. Hunt, *J. Chem. Soc., Dalton Trans.* 1979, 1388.
11. R. Stomberg, S. Olsen and I-B. Svensson, *Acta Chem. Scand.* 1984, **A38**, 653.
12. I-B. Svensson and R. Stomberg, *Acta Chem. Scand.* 1971, **25**, 898.
13. N. J. Campbell, W. P. Griffith and A. C. Skapski, *Transition Met. Chem.* 1985, **10**, 353.
14. W. P. Griffith, *J. Chem. Soc. A* 1969, 211.
15. W. Massa and G. Pausewang, *Z. Anorg. Chem.* 1979, **456**, 169.
16. W. P. Griffith and T. D. Wickins, *J. Chem. Soc. A* 1968, 397.
17. D. V. Luu and M. Abenoza, *Compt. Rend. Acad. Sci. (Paris)* 1969, **269B**, 208.
18. P. Schwendt, *Coll. Czech. Chem. Comm.* 1983, **48**, 248.
19. K. Wieghardt and U. Quilitzsch, *Z. Naturfor.* 1979, **34B**, 242.
20. R. E. Drew and F. W. B. Einstein, *Inorg. Chem.* 1972, **11**, 1079.
21. J. A. Connor and E. A. V. Ebsworth, *Adv. Inorg. Chem. Radiochem.* 1964, **6**, 294.
22. N. E. Khakalina, G. K. Yurchenko, Z. N. Dymova and G. A. Bogdanov, *Russ. J. Inorg. Chem.* 1977, **22**, 301.
23. J. Sala-Pala and J. E. Guerchais, *J. Chem. Soc. A* 1971, 1132.
24. N. J. Campbell, M. V. Capparelli, W. P. Griffith and A. C. Skapski, *Inorg. Chim. Acta* 1983, **77**, L215.
25. R. E. Drew, F. W. B. Einstein, J. S. Field and D. Begin, *Acta Cryst.* 1975, **31A**, 135.
26. F. Chauveau, *Bull. Soc. Chim. France* 1960, 819.
27. D. Begin, F. W. B. Einstein and J. Field, *Inorg. Chem.* 1975, **14**, 1785.
28. P. Schwendt, P. Petrovic and D. Uskert, *Z. Anorg. Chem.* 1980, **466**, 232.
29. A. P. Makarov, A. E. Gekhman, Y. M. Nekidelov, E. P. Talzi, O. Ya. Polotnyuk, K. I. Zamraev and I. I. Moiseev, *Bull. Acad. Sci. USSR Div. Chem. Sci.* 1985, **34**, 1764.
30. M. A. Beg and I. Ahmad, *J. Org. Chem.* 1977, **42**, 1590.
31. Y. Ogata and K. Tanaka, *Can. J. Chem.* 1982, **60**, 848.
32. F. Secco, *Inorg. Chem.* 1980, **19**, 2722.
33. H. Mimoun, L. Saussine, E. Daire, M. Postel, J. Fischer and R. Weiss, *J. Am. Chem. Soc.* 1983, **105**, 3101.
34. H. Szentivanyi and R. Stomberg, *Acta Chem. Scand.* 1983, **37A**, 709.
35. D. Rehder and K. Wieghardt, *Z. Naturfor.* 1983, **36B**, 1251.
36. V. A. Titova and I. G. Slatinskaya, *Russ. J. Inorg. Chem.* 1969, **14**, 1730.
37. A. Sieverts and E. L. Müller, *Z. Anorg. Chem.* 1928, **173**, 297.
38. N. K. Grigor'eva and K. I. Selezneva, *Bull. Acad. Sci. USSR Div. Chem. Sci.* 1962, 1067.
39. B. Spinner, *Rev. Chim. Min.* 1969, **6**, 319.
40. W. P. Griffith, *J. Chem. Soc.* 1964, 5248.
41. J. E. Fergusson, C. J. Wilkins and J. F. Young, *J. Chem. Soc.* 1962, 2136.
42. P. Schwendt and D. Uskert, *Chem. Zvesti* 1981, **35**, 229.

Polyhedron Vol. 8, No. 11, pp. 1387–1389, 1989
Printed in Great Britain

0277–5387/89 $3.00+.00
© 1989 Pergamon Press plc

LINEAR ENTHALPY CORRELATION IN MOLYBDENUM(VI) OCTAHEDRAL SUBSTITUTIONS

D. O. MÁRTIRE, M. R. FÉLIZ* and A. L. CAPPARELLI†‡

Instituto de Investigaciones Fisicoquimicas Teóricas y Aplicadas (INIFTA),
Facultad de Ciencias Exactas, Universidad Nacional de La Plata, Casilla de Correo 16,
Sucursal 4, (1900) La Plata, Argentina

(*Received* 24 *November* 1988; *accepted* 19 *December* 1988)

Abstract—For the complexing reactions: $MoO_4H^- + LH_n^q \rightleftarrows C$; a linear correlation of the form: $\log k = 4.50 + 0.42 \times pK$, is found for all kinetic data available (pK corresponds to the reaction $LH_{n+1}^{q+1} \rightleftarrows LH_n^q + H^+$). This empirical correlation is interpreted on the basis of a linear free energy relation. From the values of the slope, it is possible to infer that these reactions should proceed via I_a mechanisms. Similar results are found for WO_4H^-.

Much attention has been devoted to the investigation of complexing of molybdenum(VI) with different ligands.[1] The kinetics and mechanisms of complex formation between MoO_4^{2-} and several chelating ligands in aqueous solutions have been reported.[2–6] The formation of 1:1 complexes involves two reactive species of molybdenum(VI): MoO_4^{2-} and MoO_4H^-.

It is known[2] that the reaction pathways with no proton transfer do not contribute to reaction rates. This means that the interaction between MoO_4^{2-} and a fully deprotonated ligand, or between MoO_4H^- and a completely protonated ligand, do not take place.

Then all possible reaction pathways can be included in one of the following two groups of reactions:

Group I:

$$MoO_4^{2-} + LH_n^q \rightleftarrows C \quad n > 1 \qquad (1)$$

Group II:

$$MoO_4H^- + LH_n^q \rightleftarrows C \quad m > n > 0. \qquad (2)$$

Here LH_m and L will denote the fully protonated and deprotonated ligand species, respectively.

The experimental rates of complexation with unprotonated oxyanions—group I—decrease with increasing ligand basicity.[2] Empirical correlations between the rate and the ligand basicity can be found in the literature.[2–3] A correlation accounting for this behaviour based on theoretical considerations has been recently proposed by us.[4]

Whenever the comparison is possible, the same species of ligand reacts more rapidly,[7] about two to six orders of magnitude, with the protonated oxyanion than it does with the deprotonated one.

The difference in the orders of magnitude between rate constants for both groups of reactions has been explained as follows: the molybdate ion MoO_4^{2-} has a tetrahedral configuration.[8] Adding ligands to molybdate changes its configuration from tetrahedral to octahedral. Therefore reaction (1) involves an expansion of the coordination sphere. There are several evidences for the octahedral configuration of MoO_4H^- in solution.[9–12] Then it should be expected that reactions belonging to group II would be by a substitution mechanism.

The principal aim of this contribution is to find a correlation between the rate constants for group II reactions with the ligand basicity, through pK, and to propose an interpretation of such a correlation on the basis of linear free energy relations (LFER).

RESULTS AND DISCUSSION

All available experimental rate constants for group II reactions are listed in Table 1. The reacting ligand species LH_n and the pK value for the reaction $LH_{n+1}^{q+1} \rightleftarrows LH_n^q + H^+$ are also shown in this table.

Inspection of the values in Table 1 shows that

* Member of CICPBA.
† Member of CONICET.
‡ Author to whom correspondence should be addressed.

Table 1. Rate constants for the reaction $MoO_4H^- + LH_n^q \rightleftarrows C$

Ligand	Species	pK^a	k_1	log k_1[b]
Pyrogallol	LH_2^-	9.28	2.1×10^8	8.32
Pyrogallol	LH^{2-}	11.43	3.6×10^8	8.56
Epinephrine	LH_2^-	10.0	3.8×10^8	8.59
Epinephrine	LH^{2-}	8.7	3.6×10^7	7.56
Oxine	LH	4.96	4.5×10^6	6.65
Oxine	L^-	9.57	1.5×10^8	8.18
Oxine-5-SO_3^-	LH^-	3.89	3.9×10^6	6.59
Oxine-5-SO_3^-	L^{2-}	8.21	4.0×10^7	7.60
Citric acid	L^{3-}	5.69[c]	1.03×10^6	6.01[d]
Malic acid	L^{2-}	4.71[c]	1.3×10^7	7.11[e]
thb	LH^{2-}	11.82	5.3×10^9	9.72
thb	LH_2^-	9.08	6.6×10^7	7.82
Catechol	LH^-	9.54	4.8×10^7	7.68
Catechol	L^{2-}	12.0	3.0×10^{10}	10.48
edta	LH_2^{2-}	2.0	2.3×10^5	5.35
l-dopa	L^{4-}	9.78	2.1×10^8	8.32
l-dopa	LH^{3-}	8.8	4.0×10^7	7.60
Gallic acid	LH_2^{2-}	8.4	1.0×10^8	8.00[f]

[a] pK values were taken from ref. 3. Otherwise, other sources are cited.

[b] A. E. Martell and R. M. Smith, *Critical Stability Constants*, Vol. 5, First Supplement. Plenum Press, New York (1982).

[c] Rate constants were taken from ref. 2. Otherwise, other sources are cited.

[d] Taken from ref. 5.

[e] Taken from ref. 4.

[f] K. Kustin and S. T. Liu, *J. Am. Chem. Soc.* 1973, **95**, 2487.

the rate increases with increasing ligand basicity. A linear regression fits the following equation:

$$\log k = 0.42\times \mathrm{p}K + 4.50. \quad (3)$$

Figure 1 shows a plot of log k vs pK.

For metal complexes it is well recognized that high thermodynamic stability is not necessarily correlated with kinetic inertness.[13] However, within a series of related reactions proceeding by a common mechanism, it is reasonable to expect a correlation between free energy of activation, $\Delta G^{\ddagger}$, and standard free energy, $\Delta G^{\ominus}$.[14] So, within the LFER approximation, the following expression can be written:

$$\Delta G^{\ddagger} = \alpha \Delta G^{\ominus} + \text{constant}, \quad (4)$$

where α is a parameter from which information regarding the reaction mechanism can be inferred.

For a series of octahedral substitutions, the α parameter of the Brønsted relationship (4), allows us to discriminate I_d or O mechanisms from the I_a mechanism. For the first two, $\alpha = 1$, while for the latter, $\alpha = 0.5$.[15]

Since ΔH makes a far larger contribution to ΔG than does $T\Delta S$, wherever a free energy relationship exists, the following relationship will also hold:[15]

$$\Delta H^{\ddagger} = \alpha \Delta H^{\ominus} + \text{constant}. \quad (5)$$

From the Arrhenius equation, $d\ln k/dT = E_m/RT^2$, with $E_m = \Delta H^{\ddagger} + RT$, and eq. (5), it is possible to obtain

$$d\ln k/dT = (\alpha \Delta H^{\ominus} + \text{constant})/RT^2. \quad (6)$$

A reaction equilibrium constant, K, and $\Delta H^{\ominus}$ are related through the Van't Hoff equation

$$d\ln k/dT = \Delta H^{\ominus}/RT^2. \quad (7)$$

By substituting eq. (7) into eq. (6) and integrating at constant temperature:

$$\log k = A - \alpha \log K. \quad (8)$$

In order to compare eq. (8) with eq. (3), where the ligand pK is involved, it should be assumed that the differences in the rate constant values in Table 1 arise from the enthalpy of ligand protonation, other contributions to $\Delta H^{\ominus}$ remaining constant. Therefore, by taking $\mathrm{p}K = -\log K$, the value of 0.42 is obtained for α.

Moreover, according to the α value, the octahedral substitutions should proceed via an I_a mechanism. This correlation could be accidental, but very similar results can be found for the series of octahedral substitutions in WO_4H^-. By employing

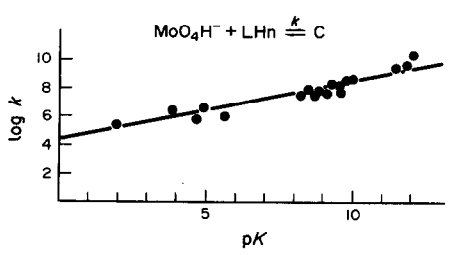

Fig. 1. Linear correlation between log k and pK values for the reaction of MoO_4H^- with different ligands.

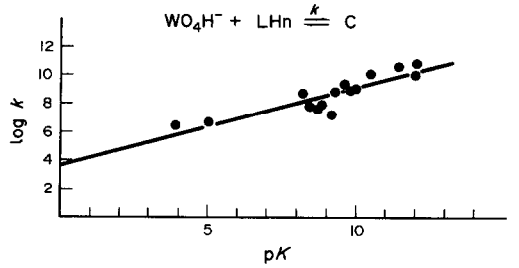

Fig. 2. Linear correlation between log k and pK values for the reaction of WO_4H^- with different ligands.

Kustin's data[2] a linear regression can be obtained with a slope of 0.54. A plot of $\log k$ involving WO_4H^- vs the ligand pK is shown in Fig. 2.

These results support an I_a mechanism for octahedral substitution in reactions of group II for MoO_4H^- and WO_4H^-.

Acknowledgements—This work was supported in part by the Consejo Nacional de Investigaciones Cientificas y Técnicas (CONICET) de la República Argentina and Comision de Investigaciones Cientificas de la Provincia de Buenos Aires (CIC). One of the authors (D.O.M.) wishes to thank the CIC for a research studentship. The authors are grateful to Dr J. Czarnowski for comments on the manuscript.

REFERENCES

1. N. Stolica, in *Standard Potentials in Aqueous Solutions* (Edited by A. Bard, R. Parsons and J. Jordan). IUPAC. Marcel Dekker, New York (1985) and refs cited therein.
2. K. Gilbert and K. Kustin, *J. Am. Chem. Soc.* 1976, **98**, 5502.
3. S. Funahashi, Y. Kato, M. Nakayama and M. Tanaka, *Inorg. Chem.* 1981, **20**, 1752 and refs cited therein.
4. D. O. Mártire, M. R. Féliz and A. L. Capparelli, *Polyhedron* 1988, **7**, 2709.
5. D. O. Mártire, M. R. Féliz and A. L. Capparelli, *An. Asoc. Quím. Argent.* 1987, **76**, 601.
6. D. O. Mártire, M. R. Féliz and A. L. Capparelli, *Polyhedron*, accepted for publication.
7. H. Diebler and R. E. Timms, *J. Chem. Soc. A* 1971, 273.
8. R. H. Busey and O. L. Keller Jr, *J. Chem. Phys.* 1964, **41**, 215.
9. C. Schwarzenbach and J. Muir, *J. Inorg. Nucl. Chem.* 1958, **8**, 302.
10. D. S. Honig and K. J. Kustin, *J. Phys. Chem.* 1972, **76**, 1575.
11. R. R. Vold and R. L. Vold, *J. Magn. Res.* 1975, **19**, 365.
12. M. L. Freeman, *J. Am. Chem. Soc.* 1958, **80**, 2072.
13. F. Basolo and R. G. Pearson, *Mechanisms of Inorganic Reactions*, 2nd edn. John Wiley, New York (1967).
14. J. E. Leffler and E. Grunwald, *Rates and Equilibria of Organic Reactions*. John Wiley, New York (1963)
15. T. W. Swaddle, *Coord. Chem. Rev.* 1974, **14**, 217 (LFER).

Polyhedron Vol. 8, No. 11, pp. 1391–1399, 1989
Printed in Great Britain

0277–5387/89 $3.00+.00
© 1989 Pergamon Press plc

PREPARATION AND CHARACTERIZATION OF RUTHENIUM(II) CLATHROCHELATE COMPLEXES

JAMES G. MULLER and KENNETH J. TAKEUCHI*

Department of Chemistry, State University of New York at Buffalo, Buffalo, NY 14214, U.S.A.

and

JOSEPH J. GRZYBOWSKI

Department of Chemistry, Gettysburg College, Gettysburg, PA 17325, U.S.A.

(*Received* 7 *October* 1988; *accepted* 5 *January* 1989)

Abstract—Synthetic routes were developed for the preparation of clathrochelate complexes of ruthenium(II) utilizing a totally encapsulating ligand derived from dioxime ligands (1,2-cyclohexanedione dioxime, diphenylglyoxime and dimethylglyoxime) and various boron capping agents (boronic acids, borate esters, and boron halides). These complexes were fully characterized by ^{1}H NMR, UV–vis and IR spectroscopies. Cyclic voltammetric electrochemical experiments were performed and indicate that the stability of a ruthenium(III) clathrochelate complex is dependent on the nature of the substituent attached to the boron cap. Specifically, the stability increases with the length of the linear chain alkoxy groups attached to boron, and decreases for bulky alkoxy groups.

There has been extensive research concerning the coordination chemistry of ruthenium,[1–3] especially in the utilization of polydentate nitrogen donors.[4–16] In particular, the development of synthetic conditions for tris-diimine ruthenium(II) complexes, particularly tris-bipyridine ruthenium(II) complexes, has been of great current interest due to their chemical stability,[17] redox stability,[17,19,21,23,26,27] photochemical,[17–21,24,25] photocatalytic [17,20,22] and DNA cleaving properties.[27] Despite this focus on tris-diimine complexes, there are only three reported examples of totally encapsulated complexes of ruthenium(II) derived from polydentate nitrogen donors,[28–30] even though they offer possible increases in thermodynamic and kinetic stability.[31] It has been suggested that the reason for the scarcity of ruthenium(II) caged complexes is the synthetic difficulties encountered when utilizing a substitutionally inert metal centre such as ruthenium.[28–30] We wish to report the synthesis and characterization of a series of clathrochelate complexes of ruthenium(II), which utilize various dioxime ligands (1,2-cyclohexanedione dioxime, diphenylglyoxime and dimethylglyoxime) and boron capping agents containing aryl, halide, alkyl and alkoxy substituents (Fig. 1).

The clathrochelate structures were chosen as the totally encapsulating ligands because of their kinetic and thermodynamic stability,[32] their proven

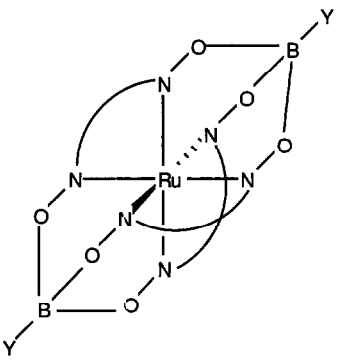

Fig. 1. Structure of ruthenium(II) clathrochelate complexes, where O—N—N—O = 1,2-cyclohexanedione dioxime, diphenylglyoxime, or dimethylglyoxime and Y = phenyl, *n*-butyl, methyl, fluoro, methoxy, ethoxy, *n*-propoxy, *i*-propoxy, *n*-butoxy, *n*-pentoxy or *n*-decoxy.

* Author to whom correspondence should be addressed.

utility in electron transfer reactions[33–36] and because of the variety of structural modifications on dioxime clathrochelates that are possible.[35,37–43] The ability to readily modify these clathrochelate ligands is important, because it allows for the correlation between ligand modification and complex stability.

EXPERIMENTAL

Materials

$Ru^{II}(DMSO)_4Cl_2$ and methylboronic acid were prepared as previously described.[44,25] All other chemicals were obtained commercially: phenylboric acid (Aldrich Chemical Co.), *n*-butylboronic acid (Lancaster Synthesis Ltd), boric acid (Fisher Scientific Co.), sodium borate (Fisher Scientific Co.), boron trifluoride diethyl etherate (Lancaster Synthesis Ltd), 1,2-cyclohexanedione dioxime (Aldrich Chemical Co.), diphenylglyoxime (Aldrich Chemical Co.) and dimethylglyoxime (Lancaster Synthesis Ltd). All solvents were purified by passage through a column of activated basic alumina immediately before use. All syntheses were carried out under nitrogen unless otherwise stated.

Measurements

Elemental analyses were conducted by Atlantic Microlabs. IR spectra in Nujol mulls were measured with a Perkin–Elmer 710 B IR spectrophotometer. Electronic absorption spectra were measured with a Bausch and Lomb Spectronic 2000 spectrophotometer equipped with a Houston Instrument Model 200 recorder, and the ^1H NMR spectra were recorded with a JEOL FX90Q Fourier transform NMR spectrometer. Cyclic voltammetric experiments were performed using methylene chloride as the solvent and tetra-*n*-butylammonium tetrafluoroborate as the supporting electrolyte, which was prepared by standard methods.[46] A platinum working electrode (Bioanalytical Systems), a platinum auxiliary electrode and a saturated sodium chloride calomel reference electrode (SSCE) were used for all electrochemical experiments. Cyclic voltammetry was conducted with an IBM EC/225 polarographic analyser equipped with a Houston Instruments Model 100 recorder.

Preparation of the complexes

Tris(μ - 1,2 - *cyclohexanedione dioximato* - O : O′) *diphenyldiborato*(2−)-N,N′,N″,N‴,N⁗,N⁗′]*ruthenium*(II), $Ru^{II}(NOX)_3(BC_6H_5)_2$ (**1**).* A 100 mg sample of $Ru^{II}(DMSO)_4Cl_2$ (0.206 mmol) and 90 mg of 1,2-cyclohexanedione dioxime ($NOXH_2$) (0.633 mmol) were added to 20 cm^3 of degassed THF, and were heated at reflux for 20 h, yielding a dark brown solution which was cooled to room temperature and reduced to dryness by rotary evaporation. To the brown residue, 10 cm^3 of methanol and 0.50 mg of phenylboric acid (0.410 mmol) were added, and the resulting mixture was stirred at room temperature for 2 h. The mixture was then rotary evaporated to dryness and purified by column chromatography, with neutral alumina as the stationary phase and methylene chloride as the eluent. The first yellow band was collected, reduced to a volume of 1 cm^3 by rotary evaporation and diluted with 2 cm^3 of hexanes to induce precipitation. Orange microcrystals were collected by vacuum filtration and washed with hexanes; yield (65 mg) 45%.

[*Tris*(μ - 1,2 - *cyclohexanedione dioximato* - O : O′) *di*-n-*butylborato*(2−)-N,N′,N″,N‴,N⁗,N⁗′]*ruthenium*(II), $Ru^{II}(NOX)_3(B\text{-}n\text{-}C_4H_9)_2$ (**2**). This complex was prepared and purified as described for **1**, whereby 50 mg of *n*-butylboric acid (0.490 mmol) instead of phenylboric acid were used to yield the complex as orange microcrystals; yield (35 mg) 26%. Found: C, 46.8; H, 6.4. Calc. for $C_{26}H_{42}N_6O_6B_2Ru(0.5H_2O)$: C, 46.9; H, 6.5%.

[*Tris*(μ - 1,2 - *cyclohexanedione dioximato* - O : O′) *dimethyldiborato*(2−)-N,N′,N″,N‴,N⁗,N⁗′]*ruthenium*(II), $Ru^{II}(NOX)_3(BCH_3)_2$ (**3**). This complex was prepared and purified as described for **1**, whereby 25 mg of methylboronic acid (0.417 mmol) instead of phenylboric acid were used to yield the complex as an orange powder; yield (18 mg) 15%. Found: C, 42.0; H, 5.3. Calc. for $C_{20}H_{30}N_6O_6B_2Ru$: C, 41.9; H, 5.3%.

[*Tris*(μ - 1,2 - *cyclohexanedione dioximato*-O : O′) *dimethoxydiborato*(2−)-N,N′,N″,N‴,N⁗,N⁗′] *ruthenium*(II), $Ru^{II}(NOX)_3(BOCH_3)_2$ (**4**). 100 mg of $Ru^{II}(DMSO)_4Cl_2$ (0.206 mmol) and 90 mg of $NOXH_2$ (0.633 mmol) were added to 20 cm^3 of degassed methanol, and heated at reflux for 24 h. The transparent red solution was cooled to room temperature, treated with 25 mg boric acid (0.412 mmol) and heated to reflux for 15 min. While still under reflux, a suspension of 39 mg of sodium borate (0.103 mmol) in 10 cm^3 of methanol was then added dropwise over a period of 1 min through the top of the reflux condenser. Heating was continued for an additional 45 min. The solution was cooled and stirred at room temperature for 8 h. The existing solution was rotary evaporated to dryness and purified as for **1**. Orange microcrystals were collected by vacuum filtration;

* Improvement of synthesis reported in ref. 29.

yield (39 mg) 31%. Found: C, 39.6, H, 5.0. Calc. for $C_{20}H_{30}N_6O_8B_2Ru$: C, 39.7; H, 5.0%.

[*Tris*(μ - 1,2 - *cyclohexanedione dioximato* - O : O′) *diethoxydiborato* (2−) - N, N′, N″, N‴, N⁗, N⁗′] *ruthenium*(II), $Ru^{II}(NOX)_3(BOC_2H_5)_2$ (**5**). This complex was prepared and purified as described for **4**, except a total of 30 cm^3 of ethanol was used instead of methanol, yielding the complex as orange microcrystals; yield (48 mg) 37%. Found: C, 41.8; H, 5.4. Calc. for $C_{22}H_{34}N_6O_8B_2Ru$: C, 41.7; H, 5.4%.

[*Tris*(μ - 1,2 - *cyclohexanedione dioximato* - O : O′) *di* - i - *propoxydiborato*(2−) - N,N′,N″,N‴,N⁗, N⁗′]*ruthenium*(II), $Ru^{II}(NOX)_3(B\text{-}i\text{-}OC_3H_7)_2$ (**6**). A 100 mg sample of $Ru^{II}(DMSO)_4Cl_2$ (0.206 mmol), 90 mg of $NOXH_2$ (0.633 mmol) and 25 cm^3 of 2-propanol were added to a round bottom flask, equipped with a reflux condenser and a Soxhlet extractor filled with activated 4 Å molecular sieves. The solution was heated at reflux for 20 h, cooled to room temperature, treated with 25 mg boric acid (0.412 mmol) and then heated at reflux for 15 min. While still under reflux, a suspension of 39 mg of sodium borate in 5 cm^3 of 2-propanol was rapidly poured directly into the reaction vessel, with continued heating for an additional 45 min. The final orange solution was cooled, and stirred at room temperature for 8 h. The existing suspension was vacuum filtered and the orange solid was purified as for **1**. Orange microcrystals were collected by vacuum filtration; yield (36 mg) 26%. Found: C, 43.5; H, 5.8. Calc. for $C_{24}H_{38}N_6O_8B_2Ru$: C, 43.6; H, 5.8%.

[*Tris*(μ - 1,2 - *cyclohexanedione dioximato* - O : O′) *di* - n - *propoxydiborato*(2−) - N,N′,N″,N‴,N⁗, N⁗′]*ruthenium*(II), $Ru^{II}(NOX)_3(B\text{-}n\text{-}OC_3H_7)_2$ (**7**). A 100 mg sample of $Ru^{II}(DMSO)_4Cl_2$ (0.206 mmol) and a 90 mg sample of $NOXH_2$ were added to 20 cm^3 of degassed THF, and were heated at reflux for 20 h yielding a dark brown solution that was rotary evaporated to dryness. The brown residue was treated with 20 cm^3 of 1-propanol and 25 mg of boric acid (0.412 mmol). The resulting solution was heated at 75°C for 15 min, and then 39 mg of sodium borate suspended in 5 cm^3 of 1-propanol were added dropwise over a period of 1 min directly to the reaction vessel. Heating was then continued for an additional 45 min. After heating, the dark brown solution was stirred at room temperature for 8 h. The solution was then rotary evaporated to dryness and purified as for **1**. The product was collected by vacuum filtration as orange microcrystals; yield (48 mg) 35%. Found: C, 43.7; H, 5.8. Calc. for $C_{24}H_{38}N_6O_8B_2Ru$: C, 43.6; H, 5.8%.

[*Tris*(μ - 1,2 - *cyclohexanedione dioximato* - O : O′) *di* - n - *butoxydiborato*(2−) - N,N′,N″,N‴,N⁗, N⁗′] *ruthenium*(II), $Ru^{II}(NOX)_3(B\text{-}n\text{-}OC_4H_9)_2$ (**8**). This complex was prepared as described for **7**, except a total of 25 cm^3 of 1-butanol was used instead of 1-propanol, and was removed by vacuum distillation instead of rotary evaporation. The product was purified as for **1**. The product was collected by vacuum filtration as dark orange microcrystals: yield (66 mg) 46%. Found: C, 45.2; H, 6.2. Calc. for $C_{26}H_{42}N_6O_8B_2Ru$: C, 45.3; H, 6.1%.

[*Tris*(μ - 1,2 - *cyclohexanedione dioximato* - O : O′) *di* - n - *pentoxydiborato*(2−) - N,N′,N″,N‴,N⁗, N⁗′]*ruthenium*(II), $Ru^{II}(NOX)_3(B\text{-}n\text{-}OC_5H_{11})_2$ (**9**). This complex was prepared as described for **7**, except a total of 25 cm^3 of 1-pentanol was used instead of 1-propanol. The product was collected by vacuum filtration as a yellow powder; yield (42 mg) 28%. Found: C, 46.9; H, 6.5. Calc. for $C_{28}H_{46}N_6O_8B_2Ru$: C, 46.9; H, 6.7.

[*Tris*(μ - 1,2 - *cyclohexanedione dioximato* - O : O′) *di*-n-*decoxydiborato*(2−)-N,N′,N″,N‴,N⁗,N⁗′] *ruthenium*(II), $Ru^{II}(NOX)_3(B\text{-}n\text{-}OC_{10}H_{21})_2$ (**10**). This complex was prepared as described for **7**, except a total of 25 cm^3 of 1-decanol instead of 1-propanol was used. The product was purified as for **1**. The product was collected as an orange powder; yield (45 mg) 25%. Found: C, 53.3; H, 7.8. Calc. for $C_{38}H_{66}N_6O_8B_2Ru$: C, 53.2; H, 7.8%.

[*Tris*(μ - 1,2 - *cyclohexanedione dioximato* - O : O′) *difluorodiborato*(2−) - N,N′,N″,N‴,N⁗,N⁗′] *ruthenium*(II), $Ru^{II}(NOX)_3(BF)_2$ (**11**). A 100 mg sample of $Ru^{II}(DMSO)_4Cl_2$ (0.206 mmol) and 90 mg of $NOXH_2$ (0.633 mmol) were added to 20 cm^3 of degassed THF, and heated at reflux for 20 h. The existing brown solution was cooled to room temperature, treated with 1 cm^3 of distilled boron trifluoride diethyl etherate (25.32 mmol) and heated at reflux for 1 h. The existing suspension was cooled to room temperature and vacuum filtered. The orange solid was purified as for **1**. The product was collected by vacuum filtration as a yellow powder; yield (38 mg) 32%. Found: C, 36.6; H, 4.1. Calc. for $C_{18}H_{24}N_6O_6B_2Ru(0.5H_2O)$: C, 36.6; H, 4.3%.

[*Tris*(μ - 1,2 - *diphenyl* - 1,2 - *ethanedione dioximato* - O : O′)*di* - n - *buryldiborato*(2−) - N,N′,N″, N‴,N⁗,N⁗′]*ruthenium*(II), $Ru^{II}(DPG)_3(B\text{-}n\text{-}C_4H_9)_2$ (**12**). A 100 mg sample of $Ru^{II}(DMSO)_4Cl_2$ (0.206 mmol) and 149 mg of diphenylglyoxime (0.633 mmol) were added to 40 cm^3 of degassed methanol. The solution was heated at reflux for 12 h, cooled to room temperature and treated with 0.50 mg of *n*-butylboronic acid (4.90 mmol). The existing brown solution was stirred at room temperature for 2 h, then rotary evaporated to dryness and purified as for **1**. The product was

collected by vacuum filtration as red microcrystals; yield (17 mg) 8.6%. Found: C, 63.0; H, 5.1. Calc. for $C_{50}H_{48}N_6O_6B_2Ru$: C, 63.1; H, 5.1%.

[*Tris*(μ - 1,2 - *diphenyl* - 1,2 - *ethanedione dioximato* - O:O′)*dimethoxydiborato*(2−) - N,N′,N″,N‴,N⁗,N⁗⁗]*ruthenium*(II), $Ru^{II}(DPG)_3(BOCH_3)_2$ (**13**). This complex was prepared as described for **4**, whereby 149 mg of diphenylglyoxime (0.633 mmol) instead of 1,2-cyclohexanedione dioxime and a total of 50 cm^3 of methanol were used, and the initial reflux time was 12 h. The product was purified as for **1**. The product was collected by vacuum filtration as a red powder; yield (25 mg) 14%. Found: C, 58.6; H, 4.1. Calc. for $C_{44}H_{36}N_6O_8B_2Ru$: C, 58.7; H, 4.0.

[*Tris*(μ - 2,3 - *butanedione dioximato* - O:O′)*di* - n - *butyldiborato*(2−) - N,N′,N″,N‴,N⁗,N⁗⁗] *ruthenium*(II), $Ru^{II}(DMG)_3(B\text{-}n\text{-}C_4H_9)_2$ (**14**). A 100 mg sample of $Ru^{II}(DMSO)_4Cl_2$ (0.206 mmol) and 72 mg of dimethylglyoxime (0.633 mmol) were added to 20 cm^3 of degassed methanol, and heated at reflux for 24 h. The solution was cooled to room temperature and treated with 0.50 mg of *n*-butylboronic acid (4.90 mmol). The existing dark orange solution was stirred at room temperature for 2 h, then rotary evaporated to dryness and purified as for **1**. The product was collected as yellow powder by vacuum filtration; yield (10 mg) 8.5%. Found: C, 41.3; H, 6.3. Calc. for $C_{20}H_{36}N_6O_6B_2Ru$: C, 41.5; H, 6.3%.

[*Tris*(μ - 2,3 - *butanedione dioximato* - O:O′) *dimethoxydiborato*(2−) - N,N′,N″,N‴,N⁗,N⁗⁗] *ruthenium*(II), $Ru^{II}(DMG)_3(BOCH_3)_2$ (**15**). This complex was prepared as described for **6**, whereby 72 mmol of dimethylglyoxime (0.633 mmol) instead of 1,2-cyclohexanedione dioxime and a total of 30 cm^3 of methanol were used, and the initial reflux time was 24 h. The product was purified as for **1**. The product was collected by vacuum filtration as orange microcrystals; yield (24 mg) 22%. Found: C, 32.0; H, 4.6. Calc. for $C_{14}H_{24}N_6O_8B_2Ru$: C, 31.9; H, 4.6%.

RESULTS AND DISCUSSION

Synthesis

The starting material $Ru^{II}(DMSO)_4Cl_2$ was a useful source of ruthenium(II), because of the substitutional lability of the DMSO and Cl^- ligands,[18,44] and because of the ease of $Ru^{II}(DMSO)Cl_2$ synthesis relative to $[Ru^{II}(DMF)_6](CF_3SO_3)_2$, which has been employed in the synthesis of other ruthenium(II) caged complexes.[28]

* Improvement of synthesis reported in ref. 29.

Notably, the use of $Ru^{II}(DMSO)_4Cl_2$ in place of $Ru^{III}Cl_3 \cdot 3H_2O$ in the synthesis of $Ru^{II}(NOX)_3(BC_6H_5)_2$ increased the product yield from 12 to 45%.*

The following equations depict the variety of reaction conditions necessary for the synthesis of ruthenium(II) clathrochelate complexes.

$$Ru^{II}(DMSO)_4Cl_2 + 3NOXH_2 \xrightarrow[THF]{\Delta}$$

$$\xrightarrow[40\,BF_3\cdot(OEt)_2]{} Ru^{II}(NOX)_3(BF)_2 \quad (1)$$

$$\xrightarrow[2n\text{-}C_4H_9B(OH)_2]{MeOH} Ru^{II}(NOX)_3(B\text{-}n\text{-}C_4H_9)_2 \quad (2)$$

$$\xrightarrow[2B(OH)_3,\ 0.5Na_2B_4O_7\cdot 10H_2O\ n\text{-}C_4H_9OH]{\Delta} Ru^{II}(NOX)_3(BO\text{-}n\text{-}C_4H_9)_2. \quad (3)$$

The general synthesis of transition metal clathrochelate complexes involves a template reaction among the transition metal, three dioxime ligands and a Lewis acid which caps the dioxime oxygens.[38] New reaction conditions were developed for some of the alkoxy-boron capped ruthenium(II) clathrochelate complexes (complexes **7**–**10**), since the alkoxide of the boron cap has a large effect on the overall reaction, in contrast to iron(II) clathrochelates.[38–43] These alkoxy-boron capped ruthenium(II) clathrochelates were synthesized in two separate reactions, employing the insertion of the dioxime ligands in THF, and the capping step in the appropriate alcohol. All alkoxy-boron capped ruthenium(II) clathrochelate complexes employed $B(OH)_3$ in combination with an alcohol to produce an alkoxy-borane capping agent. For the synthesis of $Ru^{II}(NOX)_3(BO\text{-}i\text{-}C_3H_7)_2$ (**6**) and $Ru^{II}(DMG)_3(BOCH_3)_2$ (**15**), it was necessary to remove the water liberated in the reaction through the use of a Soxhlet extractor filled with 4 Å molecular sieves, a safer and convenient method of water removal compared to water removal with a benzene–water–alcohol azeotrope.[38] Finally, the synthesis of $Ru^{II}(NOX)_3(BF)_2$ (**11**) involved the reflux of excess boron trifluoride diethyl etherate in THF. Attempts to prepare this complex by the methods employed by Rose[38] and Grzybowski[42] utilizing 1-butanol or methylene chloride, failed to yield the desired boron–halide capped clathrochelate.

^1H *NMR spectroscopy*

The ^1H NMR data for all complexes are reported in Table 1. The proton spectra provide data concerning the dioxime ligand used, and the substituents attached to the boron cap (Fig. 2). Firstly,

Table 1. ^{1}H NMR spectral data for $Ru^{II}(NOX)_3(B—Y)_2$, $Ru^{II}(DPG)_3(B—Y)_2$ and $Ru^{II}(DMG)_3(B—Y)_2$ in $CDCl_3$[a]

Y	1,2-Cyclohexanedione dioxime (NOX)	Y
C_6H_5	1.71 (s, 12 H), 2.88 (s, 12 H)	7.36 (m, 4 H), 7.89 (m, 6 H)
n-C_4H_9	1.67 (s, 12 H), 2.80 (s, 12 H)	0.93 (m, 10 H), 1.48 (m, 8 H)
CH_3	1.70 (s, 12 H), 2.83 (s, 12 H)	0.27 (s, 6 H)
F	1.74 (s, 12 H), 2.83 (s, 12 H)	
OCH_3	1.73 (s, 12 H), 2.86 (s, 12 H)	3.70 (s, 6 H)
OC_2H_5	1.72 (s, 12 H), 2.85 (s, 12 H)	1.36 (t, 6 H), 3.99 (q, 4 H)
O-n-C_3H_7	1.72 (s, 12 H), 2.84 (s, 12 H)	1.00 (m, 6 H), 1.66 (m, 4 H), 3.88 (t, 4 H)
O-i-C_3H_7	1.71 (s, 12 H), 2.84 (s, 12 H)	1.35 (d, 12 H), 4.40 (m, 2 H)
O-n-C_4H_9	1.71 (s, 12 H), 2.84 (s, 12 H)	0.88 (t, 6 H), 1.61 (m, 8 H), 3.92 (t, 4 H)
O-n-C_5H_{11}	1.71 (s, 12 H), 2.84 (s, 12 H)	0.96 (m, 6 H), 1.43 (m, 12 H), 3.79 (m, 4 H)
O-n-$C_{10}H_{21}$	1.72 (s, 12 H), 2.85 (s, 12 H)	0.88 (t, 6 H), 1.28 (m, 32 H), 3.91 (t, 4H)
Y	Diphenylglyoxime (DPG)	Y
n-C_4H_9	7.26 (m, 30 H)	0.72 (m, 10 H), 1.23 (m, 8 H)
OCH_3	7.31 (m, 30 H)	3.40 (s, 6 H)
Y	Dimethylglyoxime (DMG)	Y
n-C_4H_9	2.29 (s, 18 H)	0.96 (m, 10 H), 1.55 (m, 8 H)
OCH_3	2.33 (s, 18 H)	3.73 (s, 6 H)

[a] All shifts are relative to an Me_4Si internal standard. Abbreviations: s = singlet; d = doublet; t = triplet; q = quartet; m = multiplet.

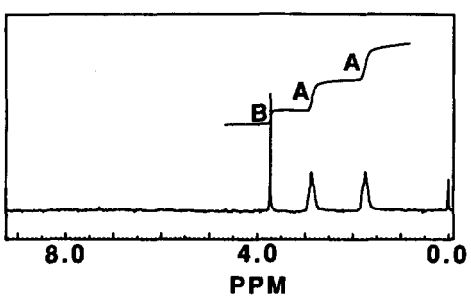

Fig. 2. ^{1}H NMR spectrum of $Ru^{II}(NOX)_3(B—OCH_3)_2$ in $CDCl_3$, where A = methylene protons, B = methyl protons.

the ^{1}H spectra for all ruthenium(II) clathrochelates complexes containing 1,2-cyclohexanedione dioxime complexes show two broad singlets, the first in the range 1.67–1.74 ppm and the other in the range of 2.80–2.88 ppm. These resonances are assigned to the methylene protons of the cyclohexane ring, which is consistent with the spectra of the free ligand and other clathrochelate complexes.[29,38,42] Similarly assigned is the multiplet associated with the diphenylglyoxime ligands ($\approx$ 7.3 ppm) and the singlet associated with dimethylglyoxime ligands ($\approx$ 2.3 ppm). Secondly, the other resonances present are from the aryl, alkyl and alkoxy moieties attached to the boron cap. The protons of the alkyl or aryl substituents show only slight variation in chemical shift compared with the alkyl boronic acid starting materials. The two resonances centred at 7.36 and 7.89 ppm of the ^{1}H spectrum of $Ru^{II}(NOX)_3(BC_6H_5)_2$ have been previously assigned to the phenyl hydrogen atoms.[29] In all ruthenium(II) clathrochelates which contain boron n-butyl substituents, the upfield multiplet can be assigned to the α-methylene and terminal methyl protons, while the downfield multiplet can be assgned to the β- and γ-methylene protons. This assignment is consistent with the ^{1}H NMR spectrum of n-butyl boronic acid, and the assignments made for iron(II) clathrochelate complexes.[42] The ^{1}H spectra of alkoxy-containing complexes show resonances reminiscent of the free alcohol, but with a downfield shift of 0.2–0.4 ppm, which suggests the ruthenium complex is more electron withdrawing than the hydrogen atom. This observation is consistent with that observed for alkoxy-boron capped iron(II) complexes.[38]

Electronic spectroscopy

The UV–vis spectral data for all complexes are given in Table 2. Complexes containing either 1,2-cyclohexanedione dioxime or dimethylglyoxime display similar electronic spectra which are dominated by an intense and complex absorbance

Table 2. UV–vis spectral data of $Ru^{II}(L)_3(B—Y)_2$

Y	L[a]	λ_{max} nm (10^{-4} ε M^{-1} cm^{-1})
C_6H_5	NOX	399 (1.6)
n-C_4H_9	NOX	391 (1.5)
CH_3	NOX	393 (1.8)
F	NOX	394 (1.6)
OCH_3	NOX	385 (1.6)
OC_2H_5	NOX	387 (1.6)
O-n-C_3H_7	NOX	388 (1.3)
O-i-C_3H_7	NOX	386 (1.8)
O-n-C_4H_9	NOX	387 (1.7)
O-n-C_5H_{11}	NOX	387 (1.8)
O-n-$C_{10}H_{21}$	NOX	386 (2.2)
n-C_4H_9	DPG	410 (2.5); 456 (2.5)
OCH_3	DPG	409 (2.3); 459 (2.1)
n-C_4H_9	DMG	390 (1.8)
OCH_3	DMG	382 (1.6)

[a] NOX = 1,2-cyclohexanedione dioxime, DPG = diphenylglyoxime, DMG = dimethylglyoxime.

(ε = 16,000 M^{-1} cm^{-1}) in the region 382–399 nm (Fig. 3). The electronic spectra of ruthenium(II) clathrochelates containing diphenylglyoxime are quite different (Fig. 4), where two distinct, very intense bands ($\varepsilon \approx$ 24,000 and 23,000 M^{-1} cm^{-1}) centred in the ranges 409–410 and 456–459 nm, respectively, are observed. All of the ruthenium(II) clathrochelate complexes reported here display absorption bands in which neither the λ_{max} nor the extinction coefficient show great sensitivity to the various boron substituents. The electronic spectra of other tris-diimine ruthenium(II) complexes, such as $[Ru(bpy)_3]^{2+}$, also show intense complex absorption bands ($\varepsilon \approx$ 15,000 M^{-1} cm^{-1}) centred at 454 nm.[47] These absorbances are attributed to a Ru($d\pi$) → π^* (ligand) MLCT transition,[48] and by analogy, the absorbances present in the electronic

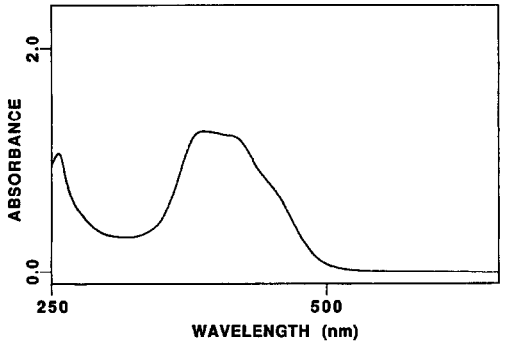

Fig. 3. UV–vis spectrum of $Ru^{II}(NOX)_3(B—OCH_3)_2$ (8.1×10^{-5} M) in CH_2Cl_2.

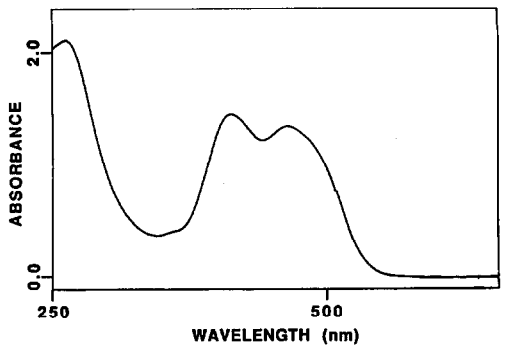

Fig. 4. UV–vis spectrum of $Ru^{II}(DPG)_3(B—OCH_3)_2$ (6.4×10^{-5} M) in CH_2Cl_2.

spectrum of ruthenium(II) clathrochelates can be assigned to charge-transfer bands. This assignment is reminiscent of those made for iron(II) clathrochelates.[38,43] It has also been observed that extinction coefficients of tris-diimine complexes are generally smaller than those of clathrochelate complexes,[49] which is also consistent with our results.

IR spectroscopy

Selected bands and their assignments are presented in Table 3. The assignments of the C=N (1500–1540 cm^{-1}), N—O (1210–1255 and 1060–1100 cm^{-1}) and B—O (1185–1200 cm^{-1}) stretches are consistent with assignments made for cobalt(II), cobalt(III) and iron(II) clathrochelate complexes.[32,38–40,43] The data in Table 3 demonstrate that there is virtually no effect on the frequency or the intensity of the N—O stretches when the substituents attached to the boron atom are varied from alkyl to fluoride or alkoxy groups (Fig. 5). It has also been observed that the absorbance for the C=N stretch appears at approximately the same frequency (1540 cm^{-1}) for the complexes containing either 1,2-cyclohexanedione dioxime or dimethylglyoxime, but for complexes containing diphenylglyoxime there is a slight shift to lower frequencies ($\Delta\nu \approx$ 40 cm^{-1}). All of the above observed trends have also been observed for analogous iron(II) clathrochelate complexes.[38,42,43] The absorbances for the B—O stretches for complexes containing alkyl or fluoride boron substituents could not be assigned because of their weak intensity and their masking by the absorbances for the N—O stretches.

Electrochemistry

The results of all cyclic voltammetric experiments are given in Table 4. The cyclic voltammetric exper-

Table 3. IR spectral data for $Ru^{II}(L)_3(B—Y)_2$[a]

Y	L[b]	ν(C=N) (cm^{-1})	ν(N—O) (cm^{-1})	ν(B—O) (cm^{-1})
C_6H_5	NOX	1540 m	1210 s, 1060 s	
n-C_4H_9	NOX	1530 m	1210 s, 1080 s	
CH_3	NOX	1550 m	1210 s, 1090 s	
F	NOX	1540 m	1230 m, 1070 s	
OCH_3	NOX	1535 m	1240 s, 1060 s	1200 s
OC_2H_5	NOX	1530 m	1230 s, 1070 s	1190 s
O-n-C_3H_7	NOX	1540 m	1255 s, 1075 s	1185 s
O-i-C_3H_7	NOX	1530 m	1240 s, 1070 s	1190 s
O-n-C_4H_9	NOX	1530 m	1240 s, 1070 s	1190 s
O-n-C_5H_{11}	NOX	1530 m	1230 s, 1070 s	1190 s
O-n-$C_{10}H_{21}$	NOX	1530 w	1230 m, 1070 s	1190 s
n-C_4H_9	DPG	1500 m	1220 s, 1100 s	
OCH_3	DPG	1500 m	1230 s, 1080 s	1180 s
n-C_4H_9	DMG	1530 m	1220 s, 1080 s	
OCH_3	DMG	1540 m	1230 s, 1090 s	1200 s

[a] The medium for all IR spectra was Nujol mull. Abbreviations: s = strong; m = medium; w = weak.

[b] NOX = 1,2-cyclohexanedione dioxime, DPG = diphenylglyoxime, DMG = dimethylglyoxime.

iments were conducted to determine purity and as a method to correlate steric and electronic effects to the stability of the ruthenium(II) and ruthenium(III) metal centres associated with the clathrochelate complexes. To measure the stability of the electrochemically generated ruthenium(III) clathrochelates, the ratios of the cathodic current ($i_{p,c}$) and anodic current ($i_{p,a}$) associated with the ruthenium(III/II) quasi reversible couple were determined (Fig. 6). The $i_{p,c}/i_{p,a}$ ratio is a useful technique for determining stability, since this ratio approaches a value of one with increasing reversibility or stability associated with the oxidized species.[46]

From examination of Table 4 it is clear that the 1,2-cyclohexanedione dioxime complexes containing alkyl substituents attached to the boron atom (complexes **2**, **3**) have similar $i_{p,c}/i_{p,a}$ ratios (≈ 0.86) and therefore the ruthenium(III) centres possess similar stability characteristics. In examining the effect of varying the alkoxy-substituted boron cap on ruthenium 1,2-cyclohexanedione

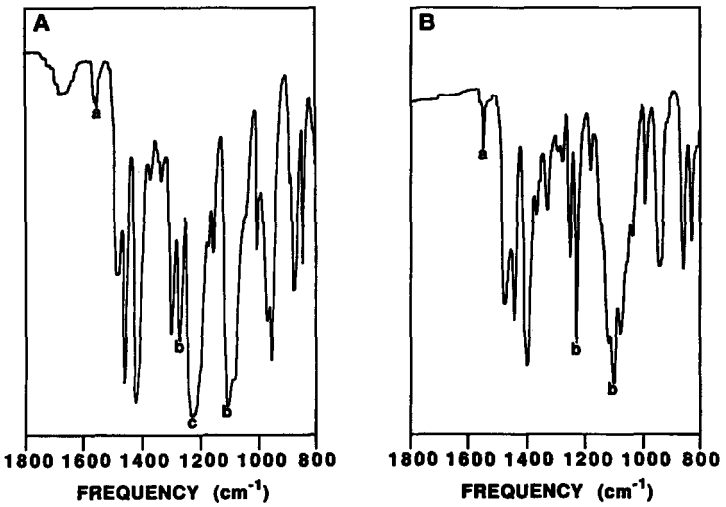

Fig. 5. IR spectra of (A) $Ru^{II}(NOX)_3(B$-n-$OC_4H_9)_2$ and (B) $Ru^{II}(NOX)_3(B$-n-$C_4H_9)_2$, where a = C=N stretch, b = N—O stretches, and c = B—O stretch.

Table 4. $E_{1/2}$ potentials, ΔEp and $i_{p,c}/i_{p,a}$ values for $Ru^{II}(L)_3(B—Y)_2$ complexes in CH_2Cl_2[a]

Y	L[b]	$E_{1/2}$ (V vs SSCE)	ΔEp (mV)	$i_{p,c}/i_{p,a}$
C_6H_5	NOX	+1.22	100	0.86
n-C_4H_9	NOX	+1.17	80	0.84
CH_3	NOX	+1.14	80	0.86
F	NOX	+1.33	110	0.86
OCH_3	NOX	+1.21	110	0.77
OC_2H_5	NOX	+1.20	90	0.84
O-n-C_3H_7	NOX	+1.20	110	0.86
O-i-C_3H_7	NOX	+1.20	140	0.77
O-n-C_4H_9	NOX	+1.21	100	0.88
O-n-C_5H_{11}	NOX	+1.21	100	0.90
O-n-$C_{10}H_{21}$	NOX	+1.22	110	0.93
n-C_4H_9	DPG	+1.34	100	0.85
OCH_3	DPG	+1.43	110	0.76
n-C_4H_9	DMG	+1.15	120	0.85
OCH_3	DMG	+1.23	90	0.78

[a] $E_{1/2} = (E_{p,a}+E_{p,c})/2$; ΔEp = peak separation; $i_{p,c}/i_{p,a}$ = peak current ratio. Conditions: 0.1 M n-Bu_4NBF_4 in CH_2Cl_2; Pt working electrode; SSCE reference electrode; scan rate = 100 mV s^{-1}.

[b] NOX = 1,2-cyclohexanedione dioxime, DPG = diphenylglyoxime, DMG = dimethylglyoxime.

dioxime complexes, the $i_{p,c}/i_{p,a}$ ratio increases in the order: O-n-$C_{10}H_{21}$ > O-n-C_5H_{11} > O-n-C_4H_9 > O-n-C_3H_7 > OC_2H_5 > OCH_3 ≈ O-i-C_3H_7; therefore the electrochemically generated ruthenium(III) clathrochelate complexes containing alkoxy-boron caps increase in stability with increasing length of the linear alkoxy chain. This phenomenon does not appear to be associated with electronic or steric size effects associated with the alkoxy substituents. Electronic effects are similar for the alkoxy substituents, where the $E_{1/2}$ values for the alkoxy-boron capped clathrochelate complexes are within 2 mV of each other. The observation that $Ru^{II}(NOX)_3(BO\text{-}n\text{-}C_3H_7)_2$ has a $i_{p,c}/i_{p,a}$ ratio of 0.86, and $Ru^{II}(NOX)_3(BO\text{-}i\text{-}C_3H_7)_2$ has a value of 0.77, suggests that bulky alkoxy substituents attached to boron decrease the ruthenium(III) stability. The effect of the dioxime ligand on the ruthenium(III) stability is seen upon observing the $E_{1/2}$ and $i_{p,c}/i_{p,a}$ ratios for analogous 1,2-cyclohexanedione dioxime (NOX), diphenylglyoxime (DPG), and dimethylglyoxime (DMG) complexes. The $E_{1/2}$ values increase in the following order: DPG > DMG ≈ NOX, and $i_{p,c}/i_{p,a}$ ratios are essentially identical (complexes **2**, **4**, **12**–**15**). These results demonstrate that the boron substituents have a distinct effect on the stability of the ruthenium(III) centre, while dioxime ligands show little effect.

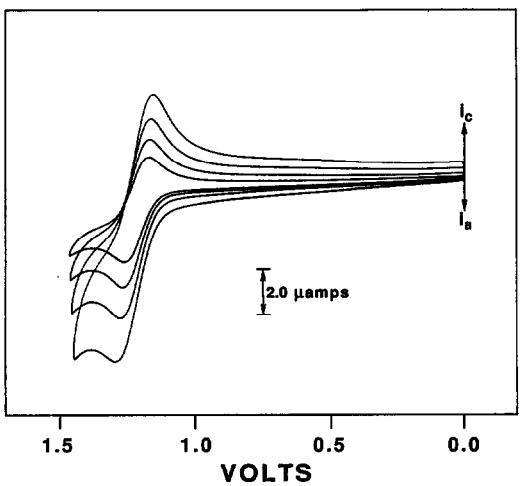

Fig. 6. Cyclic voltammogram of $Ru^{II}(NOX)_3(B\text{-}n\text{-}OC_{10}H_{21})_2$ in 0.1 M n-Bu_4NBF_4 in CH_2Cl_2. Scan rates: 50 mV s^{-1}, 100 mV s^{-1}, 200 mV s^{-1} and 400 mV s^{-1}; Pt working electrode, SSCE reference electrode.

CONCLUSIONS

In order to further investigate the chemistry of ruthenium(II) closed cage diimine complexes, synthesis methods have been developed for the preparation of a series of novel ruthenium(II) clathrochelate complexes. Characterization of these complexes by elemental analysis, ^1H NMR,

UV–vis and IR spectroscopies demonstrate that these complexes are closed cage diimine complexes containing ruthenium(II), three dioxime ligands and two boron capping ligands.

Acknowledgements—This work was supported in part by the donors of the Petroleum Research Fund, administered by the American Chemical Society, the ARCO Chemical Company and the Research Development Fund of the State University of New York at Buffalo. In addition, the authors gratefully acknowledge the contributions of Carol A. Bessel to this paper.

REFERENCES

1. K. R. Seddon, *Coord. Chem. Rev.* 1985, **67**, 171.
2. K. R. Seddon, *Coord. Chem. Rev.* 1982, **41**, 79.
3. E. A. Seddon and K. R. Seddon, *The Chemistry of Ruthenium*. Elsevier, New York (1984).
4. P. Bernhard and A. M. Sargeson, *Inorg. Chem.* 1988, **27**, 2582.
5. D. M. Bryan, S. D. Bell, R. Kumar, M. J. Clarke, V. Rodriguez, M. Sherban and J. Charkoudian, *J. Am. Chem. Soc.* 1988, **27**, 2040.
6. P. A. Lay, R. H. Magnuson and H. Taube, *Inorg. Chem.* 1988, **27**, 2040.
7. M. E. Marmion and K. J. Takeuchi, *J. Am. Chem. Soc.* 1986, **108**, 510.
8. M. E. Marmion and K. J. Takeuchi, *J. Am. Chem. Soc.* 1988, **110**, 1472.
9. S. A. Kubow, M. E. Marmion and K. J. Takeuchi, *Inorg. Chem.* 1988, **27**, 2761.
10. R. A. Leising and K. J. Takeuchi, *Inorg. Chem.* 1987, **26**, 4391.
11. A. R. Chakravarty, A. Chakravorty, F. A. Cotton, L. R. Falvello, B. K. Ghosh and M. Tomas, *Inorg. Chem.* 1983, **22**, 1892.
12. A. R. Chakravarty and A. Chakravorty, *Inorg. Chem.* 1981, **20**, 3138.
13. A. R. Middleton, J. R. Thornback and G. Wilkinson, *J. Chem. Soc., Dalton Trans.* 1980, 174.
14. P. V. Bernhart and G. A. Lawrance, *Polyhedron* 1987, **6**, 1875.
15. D. D. Walker and H. Taube, *Inorg. Chem.* 1981, **20**, 2828.
16. F. R. Keene, M. R. Snow, P. J. Stephenson and E. R. T. Tiekink, *Inorg. Chem.* 1988, **27**, 2040.
17. A. Juris, V. Balzani, F. Barigelletti, S. Campagna, P. Belser and A. von Zelewsky, *Coord. Chem. Rev.* 1988, **84**, 85.
18. R. A. Krause, *Struct. Bond. (Berlin)* 1987, **67**, 1.
19. R. J. Watts, *J. Chem. Educ.* 1983, **60**, 834.
20. K. Kalyanasundaran, *Coord. Chem. Rev.* 1982, **46**, 159.
21. E. C. Constable and T. A. Leese, *Inorg. Chim. Acta* 1988, **146**, 55.
22. A. B. P. Lever, P. Seymour and P. A. Auburn, *Inorg. Chim. Acta* 1988, **145**, 43.
23. M. Inoue and R. Cedeno, *Inorg. Chim. Acta* 1988, **145**, 117.
24. N. P. Ayala, J. N. Demas and B. A. DeGraff, *J. Am. Chem. Soc.* 1988, **110**, 1523.
25. R. P. Thummel, F. Lefoulon and S. Chirayil, *Inorg. Chem.* 1987, **26**, 3072.
26. R. P. Thummel and Y. Decloite, *Inorg. Chim. Acta* 1987, **128**, 245.
27. L. A. Basile and J. K. Barton, *J. Am. Chem. Soc.* 1987, **109**, 7548.
28. P. Bernhard and A. M. Sargeson, *J. Chem. Soc., Chem. Commun.* 1985, 1516.
29. J. G. Muller, J. J. Grzybowski and K. J. Takeuchi, *Inorg. Chem.* 1986, **25**, 2665.
30. P. Belser, L. De Cola and A. von Zelewsky, *J. Chem. Soc., Chem. Commun.* 1988, 1057.
31. A. M. Sargeson, *Pure Appl. Chem.* 1986, **58**, 1511.
32. D. R. Boston and N. J. Rose, *J. Am. Chem. Soc.* 1968, **90**, 6859.
33. D. Borchardt, K. Pool and S. Wherland, *Inorg. Chem.* 1982, **21**, 93.
34. D. Borchardt and S. Wherland, *Inorg. Chem.* 1984, **23**, 2537.
35. D. Borchardt and S. Wherland, *Inorg. Chem.* 1986, **25**, 901.
36. P. Bernhard and A. M. Sargeson, *Inorg. Chem.* 1987, **26**, 4122.
37. D. R. Boston and N. J. Rose, *J. Am. Chem. Soc.* 1973, **95**, 4163.
38. J. N. Johnson and N. J. Rose, *Inorg. Chem.* 1973, **12**, 1232.
39. S. C. Jackels, J. Zektzer and N. J. Rose, *Inorg. Synth.* 1978, **17**, 139.
40. S. C. Jackels and N. J. Rose, *Inorg. Synth.* 1982, **21**, 112.
41. J. J. Grzybowski, *Inorg. Chem.* 1985, **24**, 1125.
42. M. K. Robbins, D. K. Naser, J. L. Heiland and J. J. Grzybowski, *Inorg. Chem.* 1985, **24**, 3381.
43. H. C. Rai, A. K. Jena and B. Sahoo, *Inorg. Chim. Acta* 1979, **35**, 29.
44. I. P. Evans, A. Spencer and G. Wilkinson, *J. Chem. Soc., Dalton Trans.* 1973, 204.
45. P. A. McCusker, E. C. Ashby and H. S. Makowski, *J. Am. Chem. Soc.* 1957, **79**, 5179.
46. P. T. Kissinger and W. Heineman, *Laboratory Techniques in Electroanalytical Chemistry*. Dekker, New York (1984).
47. R. H. Fabian, D. M. Klassen and K. R. Sonntag, *Inorg. Chem.* 1980, **19**, 1977.
48. F. E. Lytle and D. M. Hercules, *J. Am. Chem. Soc.* 1969, **91**, 255.
49. P. Krumholz, *J. Am. Chem. Soc.* 1953, **75**, 2163.

Polyhedron Vol. 8, No. 11, pp. 1401–1406, 1989
Printed in Great Britain

0277–5387/89 $3.00+.00
© 1989 Pergamon Press plc

FORMATION OF PRIMARY AMIDE COMPLEXES OF Fe^+, Co^+ AND Rh^+ IN THE GAS PHASE

STEVEN W. BUCKNER† and BEN S. FREISER‡

Department of Chemistry, Purdue University, West Lafayette, IN 47907, U.S.A.

(*Received* 29 *July* 1988; *accepted after revision* 18 *January* 1989)

Abstract—Primary amide complexes, M^+–NH_2, of Fe^+, Co^+ and Rh^+ are formed in thermal ion–molecule reactions using a Fourier transform mass spectrometer. Contrary to previous belief, these complexes have relatively high M—N bond strengths. These complexes were generated in reactions of various metal–ligand cations with NH_3. Collision-induced dissociation was used to probe the structures of these complexes. Mechanisms for the formation reactions are all proposed to proceed via oxidative addition of N—H bonds in NH_3 to the various metal centres, followed by reductive elimination of either H_2O or H_2.

Amide complexes of later transition metals are rare.[1–8] This has been attributed to the unfavourable interaction between the *p* electron density on the nitrogen atom and the filled *d* orbitals on the metal. However, the weak bond strength in these types of complexes which makes them so rare could be useful for catalytic reactions which involve transferring the NR_2 group. Many recent efforts to prepare amide complexes for later transition metals have involved placing electron-withdrawing substituents on the nitrogen to withdraw $p\pi$ electron density to help stabilize the M—N bond.[9,10] Though these types of complexes are interesting, it is also important to investigate complexes in which R is hydrogen or a hydrocarbon.

Recently, we have been investigating the chemistry of M—N bonds in gas-phase complexes. Initially, bond dissociation energies were obtained for $FeNH_2^+$ and $CoNH_2^+$ using ion–molecule bracketing techniques.[11] Surprisingly, these species were observed to have relatively high M—N bond strengths. In another study, the chemistry of MNH^+ (M = V, Fe) was investigated.[12] As expected, $D(V^+—NH)$ is much higher than $D(Fe^+—NH)$ [which is comparable to $D(Fe^+—NH_2)$]. The reactions of $FeNH^+$ with alkenes proceed by transfer of the NH group, which is the last step in a catalytic cycle for generating organic imines from NH_3, N_2O and alkenes.

Oxidative addition of N—H bonds has been a topic of renewed interest in recent years.[4,12–17] This type of reaction may have use in catalytic activation of NH_3. In the present paper, the preparation of some primary amide complexes of Rh^+, Fe^+ and Co^+ in the gas phase are reported along with mechanisms for their formation. These reactions are proposed to involve oxidative addition of N—H to the metal centres.

EXPERIMENTAL

All experiments were performed on a Nicolet FTMS-1000 Fourier transform mass spectrometer.[18] Briefly, the instrument is equipped with a 5.2 cm cubic trapping cell in a 0.9 T magnetic field produced by a Varian 15 in. electromagnet.

MOH^+,[19] FeH^+,[20] $MC_5H_6^+$[21] and MCH_3^+[22] were synthesized via reactions (1)–(4).

$$M^+ + CH_3NO_2 \longrightarrow MOH^+ + CH_2NO \quad (M = Fe, Co) \quad (1)$$

$$Fe^+ + CH_3NO_2 \xrightarrow{-NO} FeOCH_3^+ \xrightarrow[(Ar)]{CID} FeH^+ + CH_2O. \quad (2)$$

$$M^+ + c\text{-}C_5H_{10} \longrightarrow MC_5H_6^+ + 2H_2 \quad (M = Fe, Co, Ni, Rh) \quad (3)$$

† Present address: Department of Chemistry, University of Arizona, Tucson, AZ 85721, U.S.A.

‡ Author to whom correspondence should be addressed.

$$M^+ + CH_3I \longrightarrow MCH_3^+ + I \quad (M = Fe, Co) \quad (4)$$

Neutral reagents for reactions (1)–(4) were admitted to the cell via a pulsed solenoid valve inlet system[23] and pumped away by a 5 in. diffusion pump in about 400 ms, permitting further interrogation of the selected metal–ligand ion. The product ions from reactions (1)–(4) were isolated by swept double resonance ejection pulses[24] prior to reaction with NH_3. Argon was always present at a static background pressure of $\approx 1 \times 10^{-5}$ torr to serve as a collision gas for collision-induced dissociation (CID) experiments. The FTMS–CID experiment has previously been described in detail.[25] Since it is a multi-collision process, rearrangements can occur prior to dissociation. Therefore, CID, as used in the present study, is only suggestive of likely structures and not conclusive for structural identification.[26a] The uncertainty in ion kinetic energy in the CID experiment is 35% at 1 eV, 10% at 10 eV and 5% at 30 eV.[26b]

Metal ions were produced by laser desorption–ionization of a pure foil of the appropriate metal using the fundamental output of a Quanta Ray Nd:YAG laser (10 ns pulse duration, $\approx$ 100 mJ pulse^{-1}).[27] Metal ions produced by this method have been shown to be kinetically and electronically excited.[28] The high static background pressure of argon used for CID also served to thermalize the ions prior to reaction.

RESULTS AND DISCUSSION

Singly-charged first row groups 6–12 atomic metal ions react at thermal energies with NH_3 only via slow condensation,[12] reaction (5).

$$M^+ + NH_3 \longrightarrow MNH_3^+. \quad (5)$$

However, Cr^+ which has been directly laser desorbed and not collisionally and radiatively cooled, reacts with NH_3 via reactions (6)–(8). After trapping the Cr^+ in $\approx 2 \times 10^{-5}$ torr argon for 1 s, the remaining Cr^+ reacts with NH_3 only via slow condensation.

$$(Cr^+)^* + NH_3 \longrightarrow CrNH_3^+ \quad (6)$$
$$\longrightarrow CrNH_2^+ + H^\cdot \quad (7)$$
$$\longrightarrow CrNH^+ + H_2. \quad (8)$$

Kinetic excitation of the cooled Cr^+ with an R.F. pulse at its cyclotron frequency (up to 140 eV lab energy) results in the reopening of pathways (7) and (8). Kinetic excitation results in formation of less than 0.1% of the bond cleavage products, whereas directly laser desorbed Cr^+ forms 0–4% of these products (depending on day-to-day fluctuations in experimental conditions). The higher reaction efficiency of directly laser desorbed Cr^+, relative to kinetically excited Cr^+, indicates it is reacting through a metastable electronic state. Cr^+ has previously been shown to react through metastable electronic states to dehydrogenate CH_4 in the gas phase.[29,30] Several cases have been documented in which specific electronic states have been observed to be much more effective at promoting endothermic reactions than kinetically excited metal ions.[31,32]

$FeNH_2^+$ and $CoNH_2^+$ can be synthesized by reaction of MOH^+ with NH_3, reaction (9)

$$MOH^+ + NH_3 \longrightarrow MNH_2^+ + H_2O \quad (9)$$
$$(M = Fe, Co).$$

Observation of reaction (9) together with ligand displacement reactions of MNH_2^+ indicate 79 kcal mol^{-1} > $D(Fe^+—NH_2)$ > 55 kcal mol^{-1} and 73 kcal mol^{-1} > $D(Co^+—NH_2)$ > 57 kcal mol^{-1}.[11] Interestingly, CH_3CN displaces $CH_3^\cdot$ from $CoCH_3^+$, but does not displace $NH_2^\cdot$ from $CoNH_2^+$, suggesting $D(Co^+—NH_2)$ is greater than $D(Co^+—CH_3)$, which in turn, is greater than $D(Co^+—H)$.[33] This is in contrast to saturated metal complexes in which M—N bond strengths are weaker than M—H or M—C bonds.[33,34]

FeH^+, which reacts with alkanes by initial C—H insertion followed by elimination of H_2 to form an activated Fe^+–alkyl complex,[20] reacts with NH_3 to form $FeNH_2^+$, reaction (10)

$$FeH^+ + NH_3 \longrightarrow FeNH_2^+ + H_2. \quad (10)$$

However, $FeCH_3^+$ is unreactive with NH_3. $FeCH_3^+$ has also been observed to be unreactive with alkanes.[35] It has been proposed that absence of reactivity of $FeCH_3^+$ with alkanes is due to an energetic barrier to oxidative addition to form an Fe^+–methyl–alkyl–hydride complex. A similar barrier may exist for the reaction of $FeCH_3^+$ with NH_3. Interestingly, $CoCH_3^+$ reacts with NH_3 only via displacement of $CH_3^\cdot$, reaction (11)

$$CoCH_3^+ + NH_3 \longrightarrow CoNH_3^+ + CH_3^\cdot. \quad (11)$$

$CoCH_3^+$ reacts with alkanes larger than ethane by initial insertion into a C—H bond, followed by elimination of CH_4 to form an activated Co^+–alkyl complex. The absence of bond insertion processes in reaction (11) is most likely due to rapid displacement of $CH_3^\cdot$ prior to bond insertion.

The bond activation processes presented in this paper can be rationalized by initial oxidative addition of an N—H bond to the metal centre.

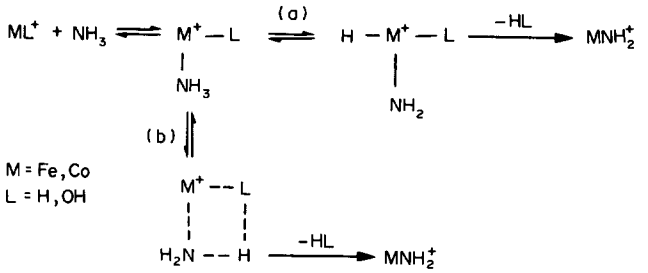

Fig. 1. Mechanism for formation of MNH_2^+ (M = Fe, Co).

Oxidative addition of N—H bonds in NH_3 is rare and has only been reported twice in solution studies, for trinuclear osmium clusters[13] and recently for an iridium(I) complex.[8] Oxidative addition may also be occurring in the reactions of $CpTiC_5H_4TiCp_2$ and Cp_2MH_2 with NH_3.[14] In a recent gas-phase study from our laboratory, groups 3–5 metal ions were observed to exothermically dehydrogenate NH_3 via a mechanism which was proposed to include oxidative addition of N—H bonds.[12] A mechanism for reactions (9) and (10) is shown in Fig. 1. Route (a) proceeds by oxidative addition of an N—H bond, followed by reductive elimination of HL (L = ligand on the reactant). Route (b) involves concerted loss of HL through a four-centred σ-metathesis intermediate.[36] The highly unsaturated electron-rich nature of the metal centres used in the present study would greatly favour reaction pathway (a).

The reactions of $M(c\text{-}C_5H_6)^+$ (M = Fe, Co, Ni, Rh) with NH_3 are shown in eqs (12)–(15). $FeC_5H_6^+$ and $CoC_5H_6^+$ undergo bond insertion, reaction (13), whereas $RhC_5H_6^+$ and $NiC_5H_6^+$ only undergo attachment and ligand displacement reactions. The differences in reactivity can be rationalized by considering the structures of the reactant ions.

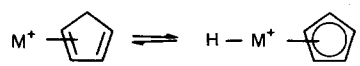

I II

Ion–molecule reaction studies have indicated $Fe(c\text{-}C_5H_6)^+$ and $Co(c\text{-}C_5H_6)^+$ exist in equilibrium between the cyclopentadiene (I) and the hydrido–cyclopentadienyl (II) complexes, while $Ni(c\text{-}C_5H_6)^+$ and $Rh(c\text{-}C_5H_6)^+$ only exist in the cyclopentadiene form.[37,38] Once the complex is in structure II, an incoming NH_3 can displace $H^\cdot$ or, after N—H bond insertion, can reductively eliminate H_2. Figure 2 shows a mechanism for reactions (13) and (14). CID of $Fe(c\text{-}C_5H_5)(NH_2)^+$ proceeds by reactions (16)–(19). Loss of NH_2 and C_5H_5 is consistent with the product ion structures proposed in Fig. 2.

Rh(propene)$^+$, generated in reaction (20), has been observed to undergo five H/D exchanges with D_2.[39]

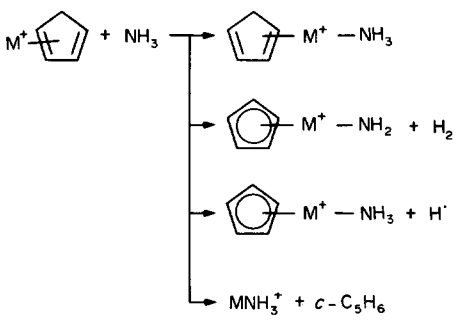

	Fe	Co	Ni	Rh	
	3	34	65	100	(12)
	79	9	0	0	(13)
	15	2	0	0	(14)
	3	55	35	0	(15)

	10 eV	80 eV	
$Fe(C_5H_5)(NH_2)^+ \xrightarrow{Ar} FeC_5H_5^+ + NH_2$	83	38	(16)
$\rightarrow FeC_5H_4^+ + NH_3$	17	26	(17)
$\rightarrow FeNH_2^+ + C_5H_5$	0	15	(18)
$\rightarrow Fe^+ + NH_2 + C_5H_5$	0	21	(19)

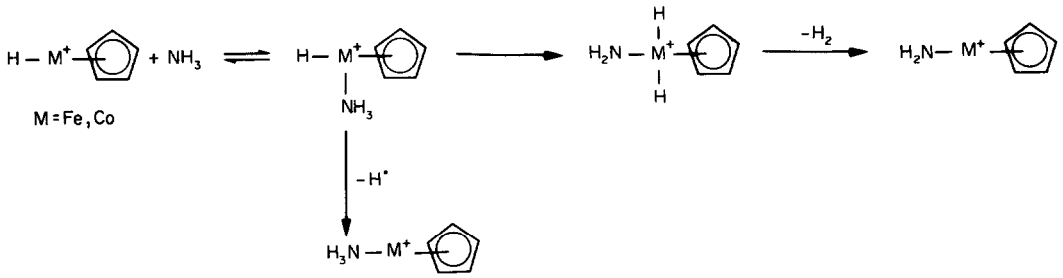

Fig. 2. Mechanism for the reaction of $M(c\text{-}C_5H_6)^+$ with NH_3.

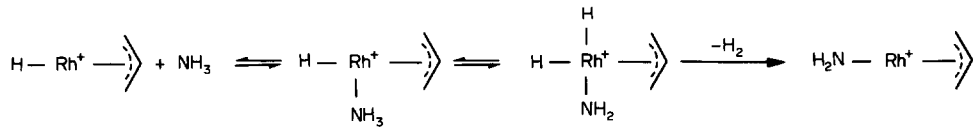

Fig. 3. Mechanism for the reaction of $RhC_3H_6^+$ with NH_3.

$$Rh^+ + C_3H_8 \longrightarrow Rh(C_3H_6)^+ + H_2 \quad (20)$$

This is due to the presence of an equilibrium between the propene (**III**) and hydrido–allyl (**IV**) structures for $Rh(C_3H_6)^+$. The D_2 can dissociate on the Rh^+ centre, and H/D exchange can occur via structure **IV**.

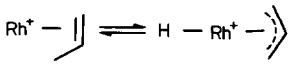

III **IV**

The only non-exchangeable H• is the secondary H atom on the propene ligand. Though Rh^+, Rh(butadiene)$^+$, and Rh(cyclopentadiene)$^+$ only react with NH_3 via slow attachment, Rh(propene)$^+$ reacts rapidly with NH_3 via reactions (21) and (22):

$$RhC_3H_6^+ + NH_3 \longrightarrow RhNH_3^+ + C_3H_6 \quad 75\% \quad (21)$$

$$\longrightarrow RhC_3H_5NH_2^+ + H_2 \quad 25\%. \quad (22)$$

The observation of reaction (21) indicates $D(Rh^+—NH_3) > D(Rh^+—C_3H_6) > 30$ kcal mol^{-1}.[40] The presence of the hydrido–allyl structure makes reaction (22) possible, as shown in Fig. 3. After initial attachment of NH_3 to the metal centre, an N—H bond dissociates on the metal centre. When $Rh(C_3H_6)^+$ is in the hydrido–allyl form, H_2 can be eliminated after dissociation of NH_3 on the metal centre. The final structure in this mechanism is an allyl–amide (**V**).

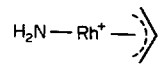

V

CID of the product ion from reaction (22) gives a variety of products, reactions (23)–(27).

	24 eV lab energy	
$RhC_3H_7N^+ \xrightarrow{Ar} Rh^+ + C_3H_7N$	14%	(23)
$\longrightarrow RhNH_3^+ + C_3H_4$	17%	(24)
$\longrightarrow RhHCN^+ + C_2H_6$	9%	(25)
$\longrightarrow RhC_3H_4^+ + NH_3$	30%	(26)
$\longrightarrow RhC_3H_5N^+ + H_2$	30%.	(27)

The fragment ions do not include NH_2 or C_3H_5, which would be diagnostic for an allyl–amide structure. However, $RhC_3H_7N^+$ reacts with D_2 to undergo four H/D exchanges, which is indicative of an allyl–amide structure. A mechanism for the four H/D exchanges is illustrated in reaction (28). After initial dissociative attachment of D_2, a D• can migrate onto the allyl ligand to form propene. A terminal H• can migrate back onto the metal centre followed by elimination of HD. All four of the terminal hydrogen atoms on the allyl ligand are exchangeable.

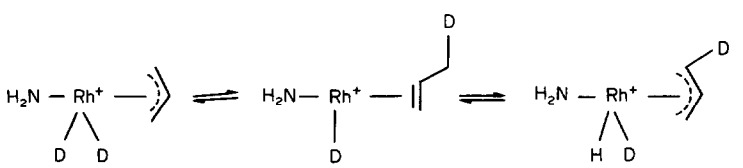

(28)

Absence of direct cleavage in the CID results indicates that isomerization of $Rh(allyl)(NH_2)^+$ occurs prior to dissociation. Reaction (29) shows a rearrangement for the allyl–amide structure which would be expected to have a low barrier. This rearrangement is similar to the equilibrium between the hydrido–allyl and propene structures.

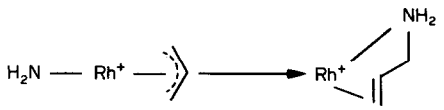

(29)

CONCLUSION

The synthesis of the three primary amide complexes, MNH_2^+ (M = Fe, Co), $M(c\text{-}C_5H_5)(NH_2)^+$ (M = Fe, Co) and $Rh(allyl)(NH_2)^+$, all proceed by reaction of NH_3 with a metal ion complex containing a σ-bound group, either $OH^\bullet$ or $H^\bullet$. CID proceeds by direct cleavage of $NH_2^\bullet$ for MNH_2^+ and $M(c\text{-}C_5H_5)(NH_2)^+$, but $Rh(allyl)(NH_2)^+$ under goes rearrangement prior to dissociation and direct cleavage of NH_2 is not observed.

Acknowledgements—Research in our laboratory is supported by the Division of Chemical Sciences, Office of Basic Energy Sciences, United States Department of Energy (DE-FG02-87ER13766) and the National Science Foundation (CHE-8612234). S.W.B. acknowledges the W. R. Grace Foundation for fellowship support.

REFERENCES

1. For a discussion of transition metal amide complexes, see: M. F. Lappert, P. P. Power, A. R. Sanger and R. C. Srivastava, *Metal and Metalloid Amides*. Ellis Horwood, West Sussex, U.K. (1980).
2. D. A. Edwards and R. T. Ward, *J. Chem. Soc., Dalton Trans.* 1977, 89.
3. B. Cetinyaka, M. F. Lappert and S. Torroni, *J. Chem. Soc., Chem. Commun.* 1979, 843.
4. Y. Yamamoto, H. Yatagai and K. Maruyama, *J. Chem. Soc., Chem. Commun.* 1980, 835.
5. P. A. Lay, A. M. Sargeson, B. W. Skeleton and A. H. White, *J. Am. Chem. Soc.* 1981, **104**, 6161.
6. H. E. Bryndza, W. C. Fultz and W. Tam, *Organometallics* 1985, **4**, 939.
7. P. R. Sharp and Y.-W. Ge, *J. Am. Chem. Soc.* 1987, **109**, 3796.
8. A. L. Casalnuovo, J. C. Calabrese and D. Milstein, *Inorg. Chem.* 1987, **26**, 971.
9. V. V. Mainz and R. A. Anderson, *Organometallics* 1984, **3**, 675.
10. (a) M. D. Fryzuk, P. A. MacNeil and S. J. Rettig, *Organometallics* 1985, **4**, 1145; (b) M. D. Fryzuk, P. A. MacNeil and S. J. Rettig, *Organometallics* 1986, **5**, 2469.
11. S. W. Buckner and B. S. Freiser, *J. Am. Chem. Soc.* 1987, **109**, 4715.
12. S. W. Buckner, J. R. Gord and B. S. Freiser, *J. Am. Chem. Soc.* 1988, **110**, 6606.
13. (a) B. F. G. Johnson, J. Lewis, T. I. Odiaka and P. R. Raithby, *J. Organomet. Chem.* 1981, **216**, c56; (b) E. G. Bryan, B. F. G. Johnson and J. Lewis, *J. Chem. Soc., Dalton Trans.* 1977, 1328.
14. (a) J. N. Armor, *Inorg. Chem.* 1978, **17**, 203; (b) G. L. Hillhouse and J. E. Bercaw, *J. Am. Chem. Soc.* 1984, **106**, 5472.
15. J. Allison and B. D. Radecki, *J. Am. Chem. Soc.* 1984, **106**, 946.
16. D. Hedden, D. M. Roundhill, W. C. Fultz and A. L. Rheingold, *J. Am. Chem. Soc.* 1984, **106**, 5014.
17. (a) C. C. Yin and J. Deeming, *J. Chem. Soc., Dalton Trans.* 1975, 2091; (b) A. A. Kazi, A. J. Deeming, I. P. Rothwell, M. B. Hursthouse and J. D. J. Backer-Dirks, *J. Chem. Soc., Dalton Trans.* 1981, 2039.
18. (a) M. B. Comisarow and A. G. Marshall, *Chem. Phys. Lett.* 1974, **25**, 282; (b) A. G. Marshall, *Accts Chem. Res.* 1985, **18**, 316.
19. C. J. Cassady and B. S. Freiser, *J. Am. Chem. Soc.* 1985, **107**, 1566.
20. T. J. Carlin, L. Sallans, C. J. Cassady, D. B. Jacobson and B. S. Freiser, *J. Am. Chem. Soc.* 1983, **105**, 6320.
21. D. B. Jacobson and B. S. Freiser, *J. Am. Chem. Soc.* 1983, **105**, 7492.
22. J. Allison and D. P. Ridge, *J. Am. Chem. Soc.* 1979, **101**, 4998.
23. T. J. Carlin and B. S. Freiser, *Anal. Chem.* 1983, **55**, 571.
24. M. B. Comisarow, G. Parisod and V. Grassi, *Chem. Phys. Lett.* 1978, **57**, 413.
25. R. B. Cody and B. S. Freiser, *Int. J. Mass Spec. Ion Phys.* 1982, **41**, 199.
26. (a) R. G. Cooks (Ed.), in *Collision Spectroscopy*, p. 357. Plenum Press, New York (1978); (b) W. D. Huntress, M. M. Mosesman and D. D. Elleman, *J. Chem. Phys.* 1971, **54**, 843.
27. R. B. Cody, R. C. Burnier, W. D. Reents, T. J. Carlin, D. A. McCrery, R. K. Lengel and B. S. Freiser, *Int. J. Mass Spect. Ion Phys.* 1980, **33**, 37.
28. H. Kang and J. L. Beauchamp, *J. Phys. Chem.* 1985, **89**, 3364.
29. (a) R. B. Freas and D. P. Ridge, *J. Am. Chem. Soc.* 1980, **102**, 7129; (b) W. D. Reents and D. P. Ridge, *J. Phys. Chem.* 1985, **89**, 5666.
30. J. B. Schilling and J. L. Beauchamp, *Organometallics* 1988, **7**, 194.
31. N. Aristov and P. B. Armentrout, *J. Phys. Chem.* 1987, **91**, 6178.
32. L. Sanders, S. Hanton and J. C. Weisshaar, *J. Phys. Chem.* 1987, **91**, 5145.
33. M. J. Calhorda and J. A. Martinho Simoes, *Organometallics* 1987, **6**, 1188.
34. H. E. Bryndza, L. K. Fong, R. A. Pacielo, W. Tam and J. E. Bercaw, *J. Am. Chem. Soc.* 1987, **109**, 1444.
35. D. B. Jacobson and B. S. Freiser, *J. Am. Chem. Soc.* 1984, **106**, 3891.
36. M. E. Thompson, S. M. Baxter, A. R. Bulls, B. J.

Burger, M. C. Nolan, B. D. Santarsiero, W. P. Schaefer and J. E. Bercaw, *J. Am. Chem. Soc.* 1987, **109**, 203.

37. J. L. Beauchamp, A. E. Stevens and R. R. Cordeman, *Pure Appl. Chem.* 1979, **51**, 967.
38. D. B. Jacobson and B. S. Freiser, *J. Am. Chem. Soc.* 1985, **107**, 72.
39. G. D. Byrd and B. S. Freiser, *J. Am. Chem. Soc.* 1982, **104**, 5944.
40. Observation of $Rh^+ + C_3H_8 \rightarrow RhC_3H_6^+ + H_2$ implies $D(Rh^+—C_3H_6) > 30$ kcal mol^{-1}, with $\Delta H_f(C_3H_8)$ and $\Delta H_f(C_3H_6)$ taken from: H. M. Rosenstock, D. Draxl, B. W. Steiner and J. T. Herron, *J. Phys. Chem. Ref. Data Suppl. 1* 1977, **6**.

Polyhedron Vol. 8, No. 11, pp. 1407–1412, 1989
Printed in Great Britain

0277–5387/89 $3.00+.00
© 1989 Pergamon Press plc

MANGANESE COMPLEXES WITH 2-HYDROXY-3(3-METHYL-2-BUTENYL)-1,4-NAPHTHOQUINONE (LAPACHOL). REDOX CHEMISTRY AND SPECTROSCOPY IN DIMETHYLSULPHOXIDE

MARIO E. BODINI* and VERÓNICA ARANCIBIA

Facultad de Química, Pontificia Universidad Católica de Chile, Casilla 6177, Santiago, Chile

(*Received* 7 *September* 1988; *accepted after revision* 18 *January* 1989)

Abstract—The redox behaviour of the ligand Lapachol has been studied in dimethylsulphoxide, and the conditions for the formation of the corresponding semiquinone have been determined. The combination of this semiquinone with manganese(II) in a 1 : 1 mole ratio forms a green complex which has been characterized by cyclic voltammetry, controlled-potential electrolysis, optical spectroscopy and magnetic susceptibility measurements. The metal centre in this complex has the characteristics of manganese(III), indicating an intramolecular charge-transfer between the metal and the ligand. The formation constant for the [Mn^{III}(TA)] complex (TA represents the trianion of the fully reduced ligand) has been evaluated voltammetrically and turns out to be 1.8×10^{15} M^{-1}. The direct interaction of manganese(III) with semiquinone leads to disproportionation yielding manganese(II) and the free ligand. These results may be relevant to the mechanism of the oxygen evolution reaction in photosystem II of green plant photosynthesis.

For many years it has been known that manganese is an essential co-factor in a number of biological systems,[1] and it is particularly necessary for the catalysis of oxygen evolution in photosystem II.[2–5] In this case, manganese appears to serve as an electron-transfer agent in reactions with molecular oxygen. Because quinones are present in significant quantities in chloroplasts[6] and are thought to be involved in the primary reactions of Photosystem II,[7–9] a mechanism has been proposed in which manganese exists in the oxidation states II, III and IV, and a catechol–semiquinone–*ortho*-quinone system is bound to this metal centre.[1]

Considering that the most abundant naturally occurring quinones are *para*-quinones,[10] we have decided to study the redox chemistry of a series of manganese complexes with these quinones in order to understand the interaction of these ligands with manganese.[11]

In this work, we report our results for the manganese complexes with 2-hydroxy-3(3-methyl-2-butenyl)-1,4-naphthoquinone (Lapachol), a naturally occurring *para*-quinone with a hydroxyl group in position 2, which enhances its binding ability. The manganese(II) complex in its reduced form has been evaluated.

All the studies have been carried out in dimethylsulphoxide, which is a solvent that stabilizes the radical species formed after the reduction of the quinone.

The electron delocalization in the deprotonated form of the ligand may lead to resonant structures corresponding to the *ortho*- and *para*-quinone configurations. Therefore, the redox chemistry of these complexes may correlate with the catechol analogues reported in the literature.[12–15]

EXPERIMENTAL

Equipment

A three-electrode potentiostat (Tacussel Model PRT 20-2X potentiostat/galvanostat with Model GSTP wave generator) was used for the cyclic voltammetric and controlled-potential electrolysis experiments.

* Author to whom correspondence should be addressed.

A current integrator based on operational amplifiers was used as a coulometer in the controlled-potential electrolyses. Cyclic voltammograms were recorded on a Hewlett–Packard Model 7004 A X-Y recorder.

The electrochemical cell was equipped with a Beckman platinum-inlay working electrode (area 0.23 cm^2), a platinum coil auxiliary electrode, and an Ag/AgCl reference electrode filled with an aqueous tetramethylammonium chloride solution and adjusted to 0.000 V vs SCE.[16] The latter was contained in a Pyrex tube with a soft-glass cracked tip; this electrode was placed inside a Luggin capillary. For controlled-potential electrolysis, a platinum mesh working electrode was employed.

A Beckman Model ACTA CV spectrophotometer was used for UV–vis spectrophotometric measurements. The magnetic susceptibility measurements were made with a Varian XL-100 NMR spectrometer using the method of Evans,[17] as modified by Retting.[18] Diamagnetic corrections were made.[19]

Air-sensitive compounds were handled in a glove bag (Aldrich) under a nitrogen atmosphere and the oxygen content was monitored with a Beckman Model Monitor II oxygen analyser.

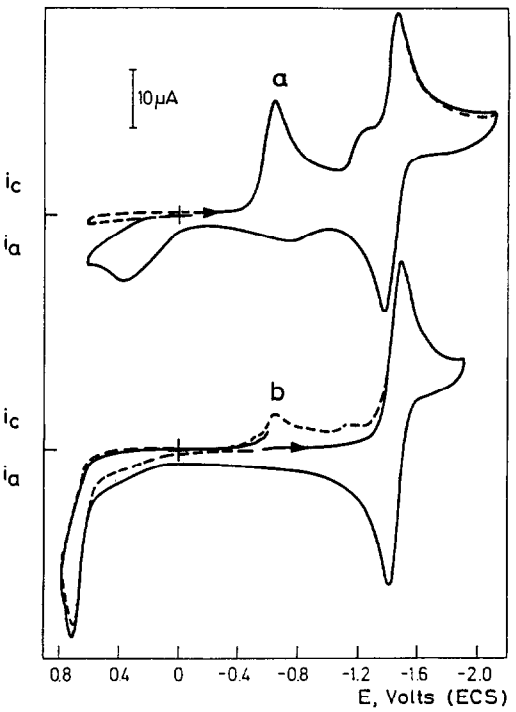

Fig. 1. Cyclic voltammograms in Me_2SO (0.1 M TEAP; $v = 0.1$ V s^{-1}) of solutions that are 1 mM in Lapachol (a); and 1 mM in Lapachol and 1 mM in TEAOH (b).

Reagents

The reagents for the investigation and syntheses included $Mn^{II}(ClO_4)_2 \cdot 6H_2O$ (G. Frederick Smith), 2-hydroxy-3(3-methyl-2-butenyl)-1,4-naphthoquinone (Lapachol) (Aldrich), tetraethylammonium hydroxide (TEAOH) (25% in methanol, Eastman), tetramethylammonium chloride (Aldrich), and tetraethylammonium perchlorate (TEAP) (G. Frederick Smith). Aldrich Gold Label grade solvents were used without further purification for all of the experiments. High purity argon gas was used to deaerate solutions.

Because the solvation water of the $Mn^{II}(ClO_4)_2 \cdot 6H_2O$ salt interfered with the stoichiometric formation of the complexes under study, $[Mn^{II}(DMU)_6][ClO_4]_2$ (DMU = dimethylurea)[20] was used in all the experiments in which the manganese(II) complexes were formed *in situ*. As a source of manganese(III), $[Mn^{III}(Urea)_6][ClO_4]_3$[21] was used in all the experiments.

RESULTS AND DISCUSSION

In DMSO, the cyclic voltammetric behaviour of Lapachol (HONQ), and of its corresponding monoanion (ONQ^-) in the presence of an equimolar amount of TEAOH is illustrated in Fig. 1.

The ligand exhibits an irreversible reduction peak at −0.65 V vs SCE [Fig. 1(a)], a sort of shoulder which can be associated with a second irreversible reduction process at −1.27 V vs SCE, and then a couple with a cathodic peak at −1.47 V vs SCE, and the corresponding anodic peak at −1.38 V vs SCE. The latter couple can be considered as a quasi-reversible system, because the peak separation is not the theoretical value predicted for a one-electron reversible process.

In the cyclic voltammogram, an irreversible anodic peak shows up at +0.36 V vs SCE, which corresponds to the oxidation of the product generated on the surface of the electrode after the reduction at −0.65 V vs SCE. If the potential scan direction is reversed at −1.00 V vs SCE, the anodic peak at 0.36 V vs SCE is observed as well. Upon addition of 1 equivalent of base [Fig. 1(b)], the reduction peak at −0.65 V vs SCE disappears, and so does the small reduction process at −1.27 V vs SCE. The redox process observed appears to be more reversible, with a peak separation of 60 mV ($E_c = 1.48$ V, $E_a = 1.42$ V vs SCE).

On the other hand, an irreversible anodic peak shows up at 0.70 V vs SCE, which is also present when the potential scan is made initially in the positive direction. Therefore, it must be concluded that it corresponds to the oxidation of the

monoanion of Lapachol, leading probably to a radical species which decomposes very readily.

Controlled-potential electrolysis at −0.85 V vs SCE of a solution of the ligand (HONQ) yields partially the monoanion, with 0.7 equivalents of charge transferred. After the electrolysis is complete, the cyclic voltammogram of the solution still shows the small cathodic peak at −1.27 V vs SCE. Further electrolysis of the resulting solution at −1.70 V vs SCE yields a brown solution, with 1.3 equivalents of charge transferred.

From these results we can conclude that the redox chemistry of this ligand can be represented by the following set of equations:

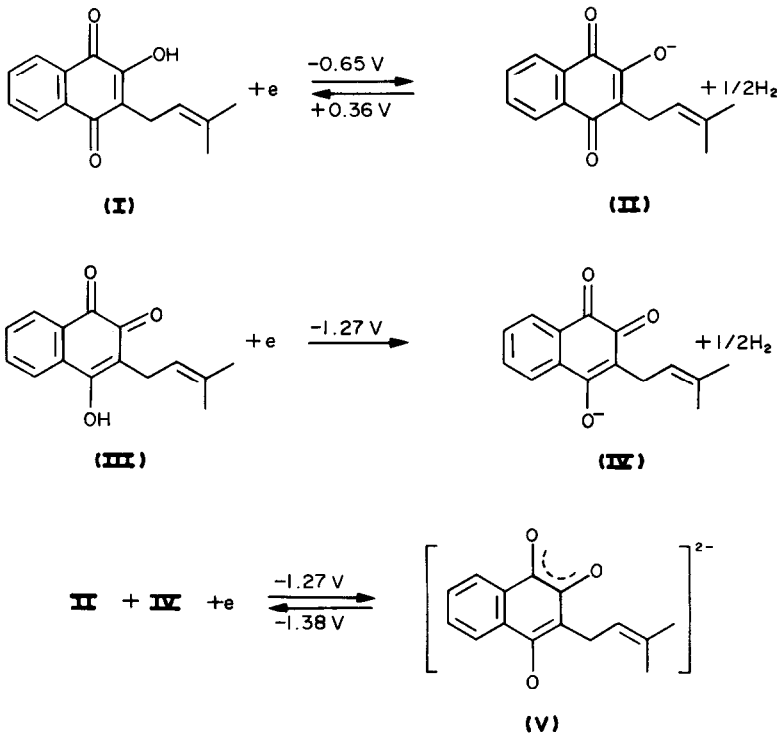

(1)

(2)

(3)

The presence of the *ortho*- and *para*-quinone isomeric forms of the ligand has also been observed in previous work carried out by our group with Lawsone,[11] indicating that in these cases the coexistence of the two isomers is inevitable in the solid compounds. A tautomeric equilibrium is not very likely, because after the complete reduction of the proton of one isomer, the cyclic voltammogram shows only the presence of the other form of the ligand and not a mixture of the two isomers.

When the two isomers are deprotonated, the anions correspond to resonance structures of a singles species, and that is the reason why only one cathodic peak is observed for the reduction to the corresponding semiquinone [Fig. 1(a) and (b)].

Figure 2(a) illustrates the cyclic voltammograms of Lapachol after controlled-potential electrolysis at −0.85 V vs SCE (monoanion), and Figs 2(b)–(d) illustrate the cyclic voltammograms for 1 : 3, 1 : 2 and 1 : 1 combinations of $[Mn^{II}(DMU)_6][ClO_4]_2$ and deprotonated Lapachol in DMSO. The results indicate that reduction of the ligand in the presence of an equimolar quantity of manganese(II) occurs at a peak potential that is 0.76 V (−0.71 V vs SCE) more positive than that for the ligand in a metal-free solution. The corresponding oxidation is observed at −0.48 V vs SCE. Therefore, the peak separation is 0.23 V, which can be considered to correspond to a quasi-reversible process. Controlled-potential electrolysis at −1.1 V vs SCE of a solution containing a 1 : 1 mole ratio of the anion of the quinone and manganese(II) indicates that one equivalent of charge is being transferred. So, a very stable complex of the semiquinone and manganese(II) is being formed. With respect to the stoichiometry, the cyclic voltammograms show that a 1 : 1 complex is formed, because in any other mole ratio the excess of the ligand is observed.

The other peaks in the cyclic voltammograms correspond to the excess of the ligand.

Figure 3 illustrates the UV–vis spectra of the different forms of this ligand. It can be observed that Lapachol presents absorption maxima at 225 nm (ξ = 20,000 cm^{-1} M^{-1}) corresponding to the benzene ring, another maximum at 248 nm (ξ = 13,400 cm^{-1} M^{-1}) associated to the quinonoid

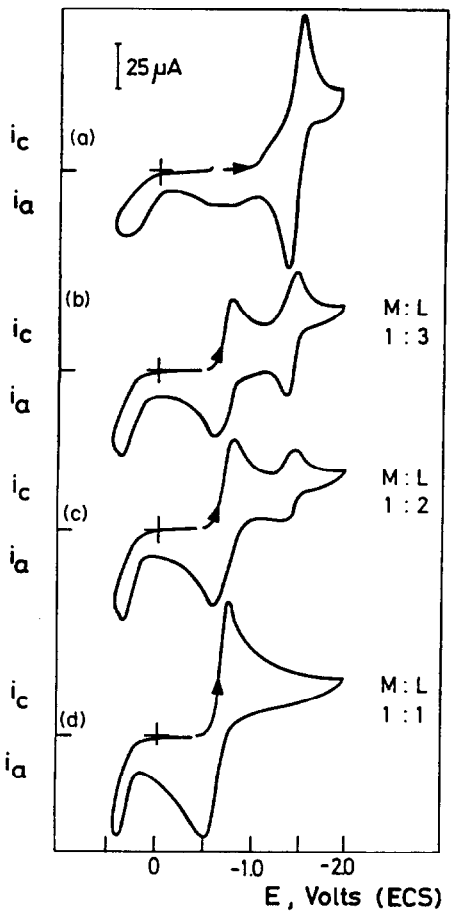

Fig. 2. Cyclic voltammograms in Me_2SO (0.1 M TEAP; $v = 0.1$ V s^{-1}) of a 3 mM solution of Lapachol after complete electrolysis at −0.7 V vs SCE ($n = 0.7$), and after the addition of 1, 1.5 and 3 mM $[Mn^{II}(DMU)_6][ClO_4]_2$.

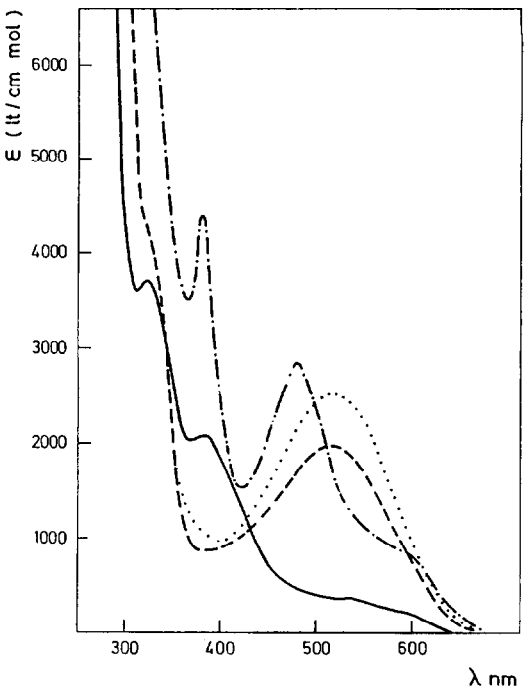

Fig. 3. Absorption spectra in Me_2SO of: (——) 1 mM Lapachol; (– – – –) 1 mM Lapachol after complete electrolysis at −1.1 V vs SCE ($n = 0.7$); (-----) 1 mM Lapachol after complete electrolysis at −1.5 V vs SCE ($n = 1.0$).

system,[22] and two less intense absorption maxima at 325 nm ($\xi = 3700\ cm^{-1}\ M^{-1}$) and at 385 nm ($\xi = 2100\ cm^{-1}\ M^{-1}$). The monoanion shows a well-defined visible absorption band at 515 nm ($\xi = 2500\ cm^{-1}\ M^{-1}$) which is responsible for the red colour of the solution. On the other hand, the semiquinone species shows well-defined absorption maxima at 236 nm ($\xi = 17{,}000\ cm^{-1}\ M^{-1}$), 305 nm ($\xi = 13{,}800\ cm^{-1}\ M^{-1}$), 380 nm ($\xi = 4000\ cm^{-1}\ M^{-1}$) and 480 nm ($\xi = 3000\ cm^{-1}\ M^{-1}$).

In the presence of manganese(II) in a 1 : 1 mole ratio, the UV–vis spectrum of the monoanion of Lapachol looks exactly the same, indicating that there is a very weak or no interaction at all between the metal ion and the ligand under these conditions.

Figures 4 and 5 show the UV–vis spectra of solutions of the semiquinone, and of this form of the ligand in the presence of 1/3, 1/2 and 1 equivalent of the metal ion. It can be observed that in both figures the spectra do not show the absorption maxima

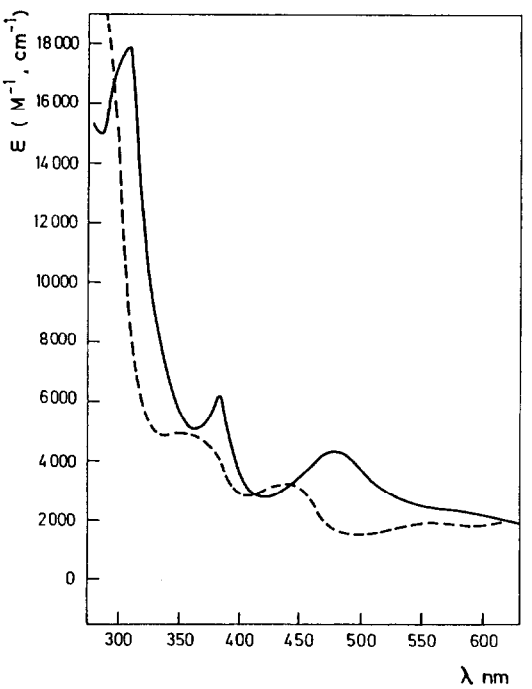

Fig. 4. Absorption spectra in Me_2SO of: (——) 1 mM semiquinone of Lapachol; (– – – –) 1 mM semiquinone of Lapachol + 1 mM $[Mn^{II}(DMU)_6][ClO_4]_2$

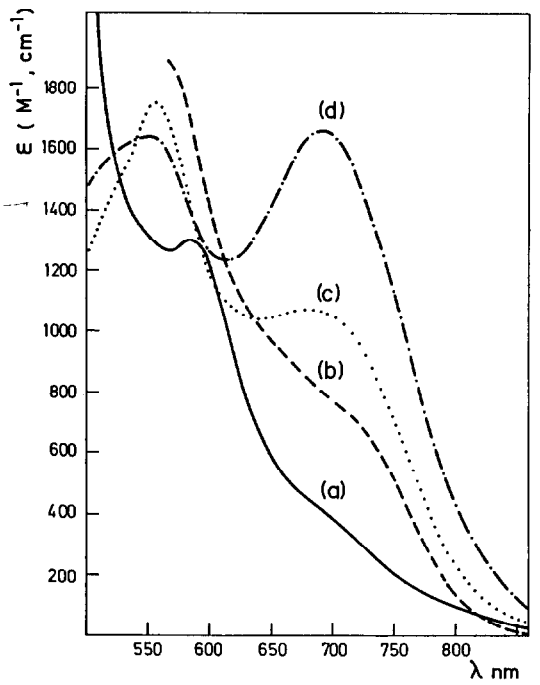

Fig. 5. Visible spectra in Me_2SO of: (a) 1 mM semiquinone of Lapachol; (b) same as a plus 1/3 mM $[Mn^{II}(DMU)_6(ClO_4)_2]$, (c) same as a plus 1/2 mM $[Mn^{II}(DMU)_6(ClO_4)_2]$, (d) same as a plus 1 mM $[Mn^{II}(DMU)_6][ClO_4]_2$.

corresponding to the presence of free semiquinone: 305, 380, 480 nm (Fig. 4) and 590 nm (Fig. 5), but instead present absorption maxima at 360 nm ($\xi = 4800$ cm^{-1} M^{-1}), 440 nm ($\xi = 3300$ cm^{-1} M^{-1}) and 683 nm ($\xi = 2200$ cm^{-1} M^{-1}), which are due to the bound semiquinone.

The magnetic susceptibility measurements for solutions that contain 5 mM $[Mn^{II}(DMU)_6][ClO_4]_2$ in DMSO are 5.9 μB as expected for a high-spin (d^5) manganese(II) ion. For a 5 mM solution of the semiquinone in DMSO (prepared by controlled-potential electrolysis) in the presence of 5 mM of manganese(II), the solution obtained presents a magnetic moment of 5.11 μB which indicates that the species in solution is a high-spin manganese(III) complex.

These results indicate that the metal centre is manganese(III) in the 1 : 1 complex. This is consistent with observations of Sawyer[23] and Pierpont[24] for manganese complexes with 3,5-di-*tert*-butyl-catechol. In these cases, the presence of a counter-ligand is needed to raise the energy of the filled manganese(II) *d* orbitals slightly above the semiquinone partially filled π^* orbitals, and cause electrons localized on the metal ion to move to the lower energy ligand-localized level. In the case of the ligand Lapachol, this effect is observed with no counter-ligand present in the complex, probably due to the lower energy of the semiquinone π^* orbitals as a consequence of the high delocalization of the π-system.

Therefore, the semiquinone binds to manganese(II) forming a 1 : 1 complex (green), which is generated on the surface of the electrode at -0.71 V vs SCE [Fig. 2(d)]:

$$ONQ^- + Mn^{II} + e^- \underset{-0.48\ V}{\overset{-0.71\ V}{\rightleftharpoons}} [Mn^{II}(ONSQ^-)] \downarrow [Mn^{III}(TA)], \quad (4)$$

or in solution when manganese(II) is combined with the semiquinone.

$$Mn^{II} + ONSQ^- \longrightarrow [Mn^{II}(ONSQ^-)] \longrightarrow [Mn^{III}(TA)].$$

Consideration of the voltammetric data for free $ONSQ^{2-}$ and ONQ^- (Fig. 1) and eq. (3), indicates that the thermodynamic redox potential for the $ONSQ^{2-}/ONQ^-$ couple ($E^{0\prime}_{12}$) has a value between $E_{p,a} = -1.38$ V vs SCE and $E_{p,c} = -1.47$ V vs SCE, a reasonable estimate is that:

$$E^{0\prime}_{12} \approx E_{p,a} - (\Delta E_{p/2});$$

$$-1.38 - 0.03 = -1.41 \text{ V vs SCE.}$$

In the case of the $[Mn(ONSQ^{2-})]^0/Mn^{II} + ONQ^-$ couple [Fig. 2(b)–(d)] and eq. (4), the thermodynamic redox potential ($E^{0\prime}_{22}$) must have a value between $E_{p,a} = -0.48$ V vs SCE and $E_{p,c} = -0.71$ V vs SCE. Therefore,

$$E^{0\prime}_{22} \simeq E_{p,a} - (\Delta E_{p/2});$$

$$-0.48 - 0.03 = -0.51 \text{ V vs SCE.}$$

Subtraction of eq. (4) from eq. (3) (with these estimated values for $E^{0\prime}_{12}$ and $E^{0\prime}_{22}$) gives:

$$Mn^{II} + ONSQ^{2-} \longrightarrow [Mn(ONSQ)]^0 \quad K_{f[MnONSQ]}.$$

The difference in formal potentials, $\Delta E^{0\prime}_{12,22}$, provides a direct measure of $K_{f[MnONSQ]}$:

$$\Delta E^{0\prime}_{12,22} = -0.90 = -0.059 \log K_{f[MnONSQ]}$$

and

$$K_{f[MnONSQ]} = 1.8 \times 10^{15} \ (25°C).$$

Cyclic voltammetry and spectroscopy of solutions in which manganese(III) is combined with the semiquinone indicate that there is a direct interaction that leads to the formation of manganese(II) and quinone.

In the cyclic voltammograms of Lapachol in the presence of manganese(III), the reduction of manganese(III) to manganese(II) is observed previously

and from then on the process is analogous to that described for manganese(II) and Lapachol.

The results of this study show that the redox behaviour of manganese complexes with *para*-quinones with a hydroxy group in position 2 is analogous to that found previously with *ortho*-quinone complexes. Manganese(II) binds strongly to the semiquinone, leading to the formation of a 1 : 1 complex in which the electrons in the metal–ligand molecular orbitals are localized closer to the ligand, giving manganese(III) character to the metal centre. This interesting property shown by a naturally occurring quinone such as Lapachol, may be relevant to the mechanism of the water evolution reaction of photosystem II of green plant photosynthesis.

Acknowledgements—This work was supported by a Research Grant from the Pontificia Universidad Católica de Chile, and by CONICYT-Chile through the FONDECYT No. 1128/86 Research Project.

REFERENCES

1. G. L. Lawrence and D. T. Sawyer, *Coord. Chem. Rev.* 1978, **27**, 173.
2. R. Radmer and G. M. Cheniae, *Primary Processes*, Vol. 2. Elsevier North Holland, New York (1977).
3. A. J. Bearden and R. Q. Makin, *Rev. Biophys.* 1975, **7**, 131.
4. R. L. Heath, *Int. Cytol.* 1973, **34**, 49.
5. J. Livorness and T. D. Smith, *Struct. Bond.* 1982, **48**, 1.
6. H. K. Lichtenthater, *Prog. Photosynth. Res., Proc. Int. Congr.* 1969, **1**, 304.
7. H. H. Stichl and H. T. Witt, *Z. Naturfor.* 1969, **24B**, 1588.
8. H. J. van Gorkom, *Biochem. Biophys. Acta* 1974, **347**, 439.
9. D. B. Knaff, R. Malkin, J. C. Myron and M. Stoller, *Biochem. Biophys. Acta* 1977, **459**, 402.
10. S. Patai, *The Chemistry of the Quinonoide Compounds*, Part 2. John Wiley, London (1974).
11. V. Arancibia and M. E. Bodini, *An. Quím.* 1986, **82B**, 309.
12. D. T. Sawyer, M. E. Bodini, L. A. Willis, T. L. Riechel and K. D. Magers, *Adv. Chem. Ser.* 1977, **162**, 330.
13. K. D. Magers, C. G. Smith and D. T. Sawyer, *Inorg. Chem.* 1978, **17**, 515.
14. K. D. Magers, C. G. Smith and D. T. Sawyer, *J. Am. Chem. Soc.* 1978, **100**, 989.
15. K. D. Magers, C. G. Smith and D. T. Sawyer, *Inorg. Chem.* 1980, **19**, 492.
16. D. T. Sawyer and J. L. Roberts, *Experimental Electrochemistry for Chemists*, pp. 144–145. Wiley-Interscience, New York (1974).
17. D. F. Evans, *J. Chem. Soc.* 1959, 2003.
18. M. F. Rettig, private communication. University of California, Riverside, California.
19. B. N. Figgis and J. Lewis, *Modern Coordination Chemistry* (Edited by J. Lewis and R. G. Wilkins). Interscience, New York (1960).
20. P. W. van Loenwen and W. L. Groenwald, *J. Inorg. Nucl. Chem. Lett.* 1967, **3**, 145.
21. H. Oghakozorg and J. Summers, *Inorg. Chem.* 1982, **21**, 3903.
22. J. Singh, T. Ogata, R. E. Moore, W. J. Chend and P. J. Scheuer, *Tetrahedron* 1968, **24**, 6053.
23. S. E. Jones, D. H. Chin and D. T. Sawyer, *Inorg. Chem.* 1981, **20**, 4257.
24. M. W. Lynch, D. N. Hendrickson, B. J. Fitzgerald and C. G. Pierpont, *J. Am. Chem. Soc.* 1984, **106**, 2041.

Polyhedron Vol. 8, No. 11, pp. 1413–1417, 1989
Printed in Great Britain

0277–5387/89 $3.00+.00
© 1989 Pergamon Press plc

SYNTHESIS AND PROPERTIES OF ORGANOTIN(IV) COMPLEXES OF DIMETHYLDITHIOCARBAMATE. THE CRYSTAL STRUCTURE OF $CH_3OOCCH_2CH_2Sn(S_2CNMe_2)Cl_2$

OK-SANG JUNG, JONG HWA JEONG and YOUN SOO SOHN*

Division of Chemistry, Korea Advanced Institute of Science and Technology, Seoul 136-791, Korea

(*Received* 8 *November* 1988; *accepted* 19 *January* 1989)

Abstract—Organotin(IV) complexes, $CH_3OOCCH_2CH_2Sn(S_2CNMe_2)_xCl_{3-x}$ ($x = 1$–3), have been synthesized and characterized. The crystal structure of $CH_3OOCCH_2CH_2Sn(S_2CNMe_2)Cl_2$ (**1**) (monoclinic $P2_1/c$ space group; $a = 8.115(2)$, $b = 17.800(2)$, $c = 10.375(2)$ Å, $\beta = 111.41(2)°$, $Z = 4$, $R = 0.0396$) shows that the tin atom adopts a distorted octahedral geometry via the chelating dithiocarbamate ligand and intramolecular carbonyl oxygen-to-tin coordination. Spectral data (IR, and ^1H, ^{13}C and ^{119}Sn NMR) along with the cryoscopic data indicate that complex **1** has the same molecular structure both in the solid state and in solution. Other complexes, $CH_3OOCCH_2CH_2Sn(S_2CNMe_2)_2Cl$ (**2**) and $CH_3OOCCH_2CH_2Sn(S_2CNMe_2)_3$ (**3**), have also been characterized in terms of their spectroscopic properties. The spectral data suggest that in complexes **2** and **3** the intramolecular carbonyl oxygen-to-tin coordination is not allowed in order to accommodate two or three bidentate dithiocarbamate ligands.

Since the Hutton group [1,2] developed a novel route to "estertin" compounds they have received considerable attention because of the variety of coordination geometries about the tin atom and also their applicability as a PVC stabilizer with low mammalian toxicities.[3–6] The crystal structure of $CH_3OOCCH_2CH_2SnCl_3$[7] revealed that the central tin atom was penta-coordinated with the intramolecular carbonyl oxygen-to-tin coordination. However, the intramolecular coordination can be broken on coordination by external donor molecules, e.g. 2,2′-bipyridyl, 1,10-phenanthroline, etc.[8–10] In an effort to extend this chemistry, we have prepared the organotin(IV) complexes with the dimethyldithiocarbamate ligand (Me_2NCS_2), which is potentially bidentate.[11–14] In this paper, structural features of the isolated complexes both in the solid state and in solution are discussed based on their spectral properties together with the crystal structure of $CH_3OOCCH_2CH_2Sn(S_2CNMe_2)Cl_2$.

EXPERIMENTAL

All manipulations were performed under a dinitrogen atmosphere with the use of the standard Schlenk techniques. All chemicals were of reagent grade and used without further purification. The solvents used were dried by reflux over appropriate reagents and distilled before use. Chemical analyses were carried out by the Chemical Analysis Laboratory at KAIST. The molecular weights were determined cryoscopically in benzene using a Cryette A automatic cryoscope. The IR spectra in the 4000–400 cm^{-1} region were measured on KBr pellets with a Analect Instrument fx 6160 FT–IR spectrometer. All the NMR spectra were measured in chloroform solution. ^1H NMR spectra were recorded on a JEOL JNM–DMX 60 spectrometer, and ^{13}C and ^{119}Sn NMR spectra on a Bruker AM-200 operating at 50.32 MHz (^{13}C) and 74.63 MHz (^{119}Sn) in the pulse mode with Fourier transform at ambient temperature ($23 \pm 2°C$). The chemical shifts determined are relative to external Me_4Si (^{13}C) and Me_4Sn (^{119}Sn) for the indicated nuclei.

Preparation of $CH_3OOCCH_2CH_2SnCl_3$

This compound was prepared by the literature method.[1] Melting point: 69–70°C (ref. 1, 70°C). Found: C, 15.3; H, 2.2; Cl, 34.1. Calc. for $C_4H_7Cl_3O_2Sn$: C, 15.4; H, 2.3; Cl, 34.1%.

* Author to whom correspondence should be addressed.

Preparation of $Na \cdot S_2CNMe_2 \cdot 2H_2O$

To an aqueous solution of $Na \cdot S_2CNMe_2$ prepared in the standard manner,[15,16] was added ethanol (ethanol/water = 3), and the mixture was left overnight. The white crystalline solid thus obtained was recrystallized from a H_2O–EtOH solvent pair (1 : 2) resulting in the dihydrate. Melting point: 108°C (ref. 16, 108°C). Found; C, 20.1; H, 5.6; N, 7.8. Calc. for $C_3H_6NS_2Na \cdot 2H_2O$: C, 20.1; H, 5.6; N, 7.8%.

Preparation of $CH_3OOCCH_2CH_2Sn(S_2CNMe_2)Cl_2$ (**1**)

A solution of $Na \cdot S_2CNMe_2 \cdot 2H_2O$ (0.90 g, 5 mmol) dissolved in 50 cm^3 of ethanol was added dropwise to an equimolar solution of $CH_3OOCCH_2CH_2SnCl_3$ (1.56 g, 5 mmol) in 50 cm^3 of ethanol. The reaction mixture was cooled to about 0°C, and the NaCl formed was removed by filtration. The solvent from the filtrate was removed under reduced pressure at 30°C. The resultant solid was recrystallized from a chloroform–petroleum ether solvent pair (1 : 1). The colourless crystalline solid (m.p. 165–167°C) was obtained in 85% yield. Molecular weight measured: 410.4 (theory: 396.9). Found: C, 21.1; H, 3.3; N, 3.5. Calc. for $C_7H_{13}Cl_2NO_2S_2Sn$: C, 21.2; H, 3.3; N, 3.5%.

Preparation of $CH_3OOCCH_2CH_2Sn(S_2CNMe_2)_2Cl$ (**2**)

$Na \cdot S_2CNMe_2 \cdot 2H_2O$ (1.80 g, 10 mmol) in 100 cm^3 of ethanol was reacted with $CH_3OOCCH_2CH_2SnCl_3$ (1.56 g. 5 mmol) in 50 cm^3 of ethanol, in the same manner as used for the preparation of **1**. The resultant solid was recrystallized from a chloroform–petroleum ether solvent pair (1 : 1). The pale yellow crystalline solid (m.p. 119–120°C) was obtained in 82% yield. Molecular weight measured: 477.5 (theory: 469.6). Found: C, 25.4; H, 4.0; N, 5.9. Calc. for $C_{10}H_{19}ClN_2O_2S_4Sn$: C, 25.6; H, 4.1; N, 6.0%.

Preparation of $CH_3OOCCH_2CH_2Sn(S_2CNMe_2)_3$ (**3**)

Reaction of $CH_3OOCCH_2CH_2SnCl_3$ (1.56 g, 5 mmol) with $Na \cdot S_2CNMe_2 \cdot 2H_2O$ (2.70 g, 15 mmol) in the mole ratio of 1 : 3 according to the same method as used for the preparation of **1**, followed by recrystallization from a chloroform–petroleum ether solvent pair (1 : 1), resulted in an orange crystalline solid (m.p. 169–170°C) in 81% yield. Molecular weight measured: 557.5 (theory: 548.3). Found: C, 28.0; H, 4.4; N, 7.5. Calc. for $C_{13}H_{25}N_3O_2S_6Sn$: C, 28.5; H, 4.6; N, 7.7%.

Crystallographic analysis of $CH_3OOCCH_2CH_2Sn(S_2CNMe_2)Cl_2$

All X-ray crystallographic data were obtained on an Enraf–Nonius CAD4 diffractometer with graphite-monochromated molybdenum radiation ($\lambda(K_{\alpha 1}) = 0.70930$ Å, $\lambda(K_{\alpha 2}) = 0.71359$ Å) at an ambient temperature of 23 ± 2°C. A well-formed crystal was glued to the interior of a thin-walled glass capillary, which was then sealed. Preliminary diffractometric investigations indicated monoclinic symmetry. From the observed extinctions $0k0$, $k = 2n+1$, and $h0l$, $l = 2n+1$, the space group was uniquely determined as $P2_1/c$ (C_{2h}^5 No. 14).[17] The lattice constants were determined by least-squares refinement of the diffraction geometry for 25 intense reflections having $13 \leqslant \theta_{Mo\text{-}K_\alpha} \leqslant 21$. Crystal parameters and procedural information corresponding to data collection and structure refinement for the complex are given in Table 1. The structure of complex **1** was solved by the conventional heavy atom method and difference Fourier techniques. Non-hydrogen atoms were refined by use of full-matrix least-squares procedures using SHELX-76, a system of computer programs for X-ray structure determination by G. M. Scheldrick.[18] All atoms were anisotropically refined. The final R indices were $R = 0.0396$, $R_G = 0.0508$.

RESULTS AND DISCUSSION

Reaction of $CH_3OOCCH_2CH_2SnCl_3$ with the dithiocarbamate ligand in appropriate molar ratios, followed by recrystallization, afforded the solid products, $CH_3OOCCH_2CH_2Sn(S_2CNMe_2)_xCl_{3-x}$ ($x = 1$–3) (as established by chemical analysis, molecular weight determination and spectral data of IR, ^1H, ^{13}C and ^{119}Sn NMR), due to the metathesis reaction represented by the following equation:

$$CH_3OOCCH_2CH_2SnCl_3 + xNa \cdot S_2CNMe_2 \longrightarrow CH_3OOCCH_2CH_2Sn(S_2CNMe_2)_xCl_{3-x} + xNaCl \quad (x = 1\text{–}3).$$

All the products are crystalline solids with sharp melting points, which are soluble in benzene and in polar organic solvents such as chloroform, dichloromethane, acetone, tetrahydrofuran and dimethylsulphoxide, but insoluble in water and in saturated aliphatic hydrocarbons. These complexes have shown to be monomeric in benzene and are fairly air-stable.

Table 1. Crystal parameters and experimental details for CH_3OOC $CH_2CH_2Sn(S_2CNMe_2)Cl_2$

Formula	$C_7H_{13}Cl_2NO_2S_2Sn$
Formula weight	396.92
Crystal system	Monoclinic
Space group	$P2_1/c$
a (Å)	8.115(2)
b (Å)	17.800(2)
c (Å)	10.375(2)
β (°)	111.41(2)
V (Å^3)	1395
Z	4
$d_{calc.}$ (g cm^{-3})	1.890
Crystal size (mm)	$0.26 \times 0.36 \times 0.56$
Crystal shape	Tetragonal
μ (cm^{-1})	23.11
Radiation	Mo-K_α ($\lambda = 0.71073$ Å)
Scan method	ω–2θ
Data collected	$h, k, \pm l$, $1 \leqslant \theta \leqslant 25$
Number of unique observations	2743
Number of unique data with $I > 3\sigma(I)$	2075
Number of parameters refined	136
Over determination ratio	15.26
$R = (\Sigma \|\|F_o\| - \|F_c\|\|/\Sigma \|F_o\|)$	0.0396
$R_G = [\Sigma \|F_o - F_c\|^2/\Sigma F_o^2]^{1/2}$	0.0508

Structure of complex **1**

The molecular geometry and labelling scheme for complex **1** are shown in Fig. 1.

In Table 2, relevant bond distances and angles are tabulated. Complex **1** exists as a discrete molecule which contains a five-membered chelate ring, for-

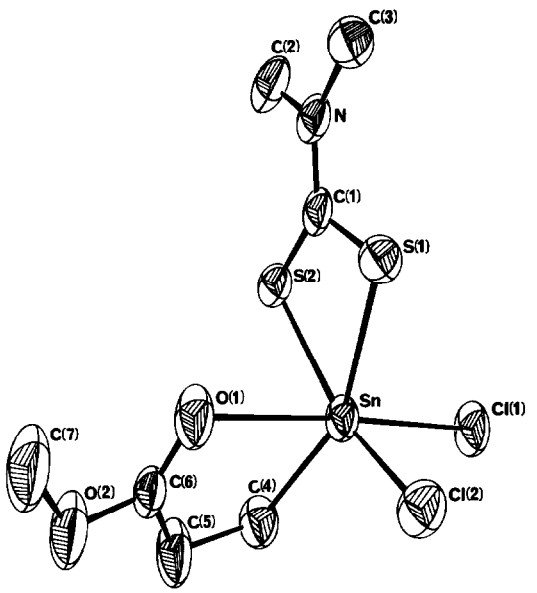

Fig. 1. ORTEP drawing of $CH_3OOCCH_2CH_2Sn(S_2$ $CNMe_2)Cl_2$ (**1**) including the atom labelling scheme.

Table 2. Bond distances (Å) and angles (°) for CH_3 $OOCCH_2CH_2Sn(S_2CNMe_2)Cl_2$

Sn—S(1)	2.462(2)	S(1)—Sn—S(2)	70.1(1)
Sn—S(2)	2.657(2)	S(1)—Sn—Cl(1)	99.1(1)
Sn—Cl(1)	2.413(2)	S(1)—Sn—Cl(2)	88.8(1)
Sn—Cl(2)	2.428(2)	S(2)—Sn—Cl(1)	93.5(1)
Sn—O(1)	2.436(6)	S(2)—Sn—Cl(2)	158.5(1)
Sn—C(4)	2.131(8)	S(1)—Sn—O(1)	83.1(2)
C(1)—S(1)	1.749(9)	S(2)—Sn—O(1)	90.2(2)
C(1)—S(2)	1.694(9)	S(1)—Sn—C(4)	156.7(3)
C(1)—N	1.32(1)	S(2)—Sn—C(4)	98.6(3)
C(2)—N	1.49(1)	Cl(1)—Sn—Cl(2)	94.1(1)
C(3)—N	1.47(1)	Cl(1)—Sn—O(1)	176.2(2)
C(6)—O(1)	1.20(1)	Cl(2)—Sn—O(1)	82.8(2)
C(7)—O(2)	1.48(1)	Cl(1)—Sn—C(4)	102.0(3)
C(6)—O(2)	1.33(1)	Cl(2)—Sn—C(4)	99.5(3)
C(4)—C(5)	1.52(1)	C(4)—Sn—O(1)	76.5(3)
C(6)—C(5)	1.50(1)	S(1)—C(1)—S(2)	117.6(5)
		C(1)—S(1)—Sn	88.7(3)
		C(1)—S(2)—Sn	83.6(3)
		S(1)—C(1)—N	117.7(7)
		S(2)—C(1)—N	124.7(7)
		C(2)—N—C(3)	116.4(8)
		C(2)—N—C(1)	119.8(9)
		C(1)—N—C(3)	123.7(8)
		C(6)—O(1)—Sn	108.2(6)
		C(6)—O(2)—C(7)	116.8(7)
		C(6)—C(5)—C(4)	113.7(8)
		C(5)—C(4)—Sn	113.3(6)
		C(5)—C(6)—O(1)	125.7(8)
		C(5)—C(6)—O(2)	112.4(8)

med via ester carbonyl oxygen-to-tin coordination, and a four-membered chelate ring from the bidentate dithiocarbamate ligand. Thus the tin atom is hexa-coordinate with the coordinating atoms S(1), S(2), C(4), Cl(2), Cl(1) and O(1) in a distorted octahedral arrangement. The small bite angle (70.1(1)°) of the dithiocarbamate ligand is in part responsible for the distortion of the octahedral geometry. The dithiocarbamate ligand is bonded to the tin atom in an anisobidentate fashion: Sn—S(1) and Sn—S(2) distances of 2.462(2) and 2.657(2) Å, respectively, are comparable with those of 2.48(1) and 2.79(1) Å in $Me_2Sn(S_2CNMe_2)Cl$.[13] The bond distances Sn—O(1) (2.436(6) Å), Sn—Cl(1) (2.413(2) Å) and Sn—Cl(2) (2.428(2) Å) are slightly longer than those (2.347(5), 2.357(2) and 2.303(2) Å, respectively) in $CH_3OOCCH_2CH_2SnCl_3$.[7] This indicates weak coordination, presumably due to the low Lewis acidity of the tin atom in the hexa-coordinate, compared with penta-coordinate complexes in the solid-state.

Spectroscopic properties of complexes **1**, **2** *and* **3**

The characteristic IR bands of complexes **1**–**3** relevant to their molecular structures are listed in Table 3.

Among the stretching modes, the ν(C=O) band in the 1650–1750 cm^{-1} region is known to depend on the nature of coordination of the carbonyl oxygen-to-metal.[8–10] The ν(C=O) bands of complexes **2** (1724 cm^{-1}) and **3** (1727 cm^{-1}) are in the same region as that of the free organic ester, CH_3OOCCH_3 (1740 cm^{-1}),[9] in which the carbonyl group is not coordinated, whereas the band of complex **1** (1652 cm^{-1}) exhibits a remarkable red shift from that of the organic ester. Such results clearly indicate that the coordination of the carbonyl oxygen-to-tin is maintained in complex **1** (see its crystal structure), but such a coordination is broken to accommodate two or three potentially bidentate dithiocarbamate ligands. The blue shifts of the ν(C—N) mode of complexes **1** and **2**, compared to that of the complex **3**, may be ascribed to the increase of Lewis acidity of the tin(IV) atom by the presence of the electronegative group (Cl). The appearance of the single band for ν(C—S) in the 950–1050 cm^{-1} region is indicative of the bidentate behaviour of the dithiocarbamate ligand.[19,20]

Table 3. Relevant IR bands for $CH_3OOCCH_2CH_2Sn(S_2CNMe_2)_xCl_{3-x}$[a]

Compound	ν(C=O) (cm^{-1})	ν(C—N) (cm^{-1})	ν(C—S) (cm^{-1})
1	1652(vs)	1541(vs)	972(s)
2	1724(vs)	1556(vs)	972(s)
3	1727(vs)	1517(vs)	979(s)

[a] $x = 1$, **1**; $x = 2$, **2**; $x = 3$, **3**.
vs: very strong.
s: strong.

The ^1H and ^{13}C NMR data listed in Table 4, along with ^{119}Sn NMR data, also support the presence of carbonyl oxygen-to-tin coordination in complex **1**: $\delta(^1H) = 4.0$ ppm for $—OCH_3$ in complex **1** shows a downfield shift by 0.3 ppm compared to that of complexes **2** and **3**, and $\delta(^{13}C)$ values for the C=O and $—OCH_3$ in complex **1** are deshielded by approximately 6 ppm (C=O) and 3 ppm ($—OCH_3$), respectively, relative to those of complexes **2** and **3**.

Table 4. ^1H, ^{13}C and ^{119}Sn NMR data for $CH_3OOCCH_2CH_2Sn(S_2CNMe_2)_xCl_{3-x}$[a]

Compound	^1H NMR (δ, ppm)	^{13}C NMR (δ, ppm)[b]	^{119}Sn NMR (δ, ppm)[c]
1	4.0(s, $—OCH_3$); 3.5(s, $—N(CH_3)_2$); 3.0(t, $—CH_2—$); 1.9 (t, $—CH_2Sn$)	195.8(C—S); 181.0(C=O); 54.7($—OCH_3$); 47.0($—N(CH_3)_2$); 31.9($—CH_2—$); 28.6($—CH_2Sn$)	−386.4
2	3.7(s, $—OCH_3$); 3.4(s, $—N(CH_3)_2$); 2.7(t, $—CH_2—$); 2.3(t, $—CH_2Sn$)	199.0(C—S); 174.3(C=O); 51.8($—OCH_3$); 46.4($—N(CH_3)_2$); 39.4($—CH_2—$); 31.0($—CH_2Sn$)	−605.5
3	3.7(s, $—OCH_3$); 3.4(s, $—N(CH_3)_2$); 2.8(m, $—CH_2—$); 2.6(m, $—CH_2Sn$)	201.9(C—S); 174.5(C=O); 51.6($—OCH_3$); 45.7($—N(CH_3)_2$); 44.2($—CH_2—$); 31.7($—CH_2Sn$)	−804.5

[a] $x = 1$, **1**; $x = 2$, **2**; $x = 3$, **3**.
[b] Pulse width: 3.0 μs; pulse repetition: 3.0 s.
[c] Pulse width: 10.0 μs; pulse repetition: 3.0 s.

^{119}Sn NMR spectroscopy has recently been found to be very useful for the elucidation of the nature of coordination in the dithiocarbamatotin(IV) complexes.[21-26] Even though for each complex with the same coordination number, some wide range of $\delta(^{119}Sn)$ values are observed depending on the different organic and dithiocarbamate groups attached to the tin atom, there is an approximate linear relationship between the $\delta(^{119}Sn)$ values and the coordination numbers of the complexes. Thus for the known dithiocarbamatotin(IV) complexes, $\delta(^{119}Sn)$ have been found to lie between -150 and -250 ppm in penta-coordinate, between -300 and -500 ppm in hexa-coordinate, and between -700 and -800 ppm in hepta-coordinate compounds.[21-27] The relationship $\delta(^{119}Sn) = -386.4$ ppm for complex **1** indicates that the tin atom is hexa-coordinated, implying that both the dithiocarbamate and ester groups act as chelating ligands. Assuming from the above-mentioned spectroscopic data that the ester group acts as monodentate in complexes **2** and **3**, the low $\delta(^{119}Sn)$ values of the complexes (-605.5 and -804.5 ppm, respectively) suggest that all the dithiocarbamate groups are bidentate, resulting in the hexa- and hepta-coordinate complexes, respectively. Although complexes **1** and **2** have the same hexa-coordinated tin atom, the ^{119}Sn chemical shift in complex **2** appears much further upfield than that in complex **1** owing to the partial change of donor atoms coordinated to tin(IV).

In conclusion, the spectroscopic and cryoscopic data in solution are completely in accordance with the crystal structure for complex **1**, and the similar complexes, **2** and **3**, are monomeric in solution and presumably are hexa- and hepta-coordinate, respectively, both in solution and in the solid-state.

Acknowledgement—This research was supported financially by the Ministry of Science and Technology.

REFERENCES

1. R. E. Hutton and V. Oakes, *Organotin Compounds: New Chemistry and Applications* (Edited by J. J. Zuckerman), Advances in Chemistry Series 157, Chap. 8. American Chemical Society, Washington, D.C. (1976).
2. J. W. Burley, R. E. Hutton and V. Oakes, *J. Chem. Soc., Chem. Commun.* 1976, 803.
3. R. E. Hutton and V. Oakes, *Organotin Compounds: New Chemistry and Applications* (Edited by J. J. Zuckerman), Advances in Chemistry Series 157, Chap. 9. American Chemical Society, Washington, D. C. (1976).
4. B. K. Deb and A. K. Ghosh, *Polyhedron* 1986, **5**, 863.
5. T. G. Kugele, U.S. Pat. 4,118,371 (1978).
6. C. J. Evans and S. Karpel, *Organotin Compounds in Modern Technology*. J. Organomet. Chem. Lib. 16, Elsevier, Amsterdam (1985).
7. P. G. Harrison, T. J. King and M. A. Healy, *J. Organomet. Chem.* 1979, **182**, 17.
8. D. Maughan, J. L. Wardell and J. W. Burley, *J. Organomet. Chem.* 1981, **212**. 59.
9. R. A. Howie, E. S. Paterson, J. L. Wardell and J. W. Burley, *J. Organomet.Chem.* 1986, **304**, 301.
10. E. S. Paterson, J. L. Wardell and J. W. Burley, *J. Organomet. Chem.* 1984, **273**, 313.
11. K. Kim, J. A. Ibers, O. S. Jung and Y. S. Sohn, *Acta Cryst.* 1987, **C43**, 2317.
12. V. G. Kumar Das, C. Wei and E. Sinn, *J. Organomet. Chem.* 1985, **290**, 291.
13. K. Furue, T. Kimura, N. Yasuoka, N. Kasai and M. Kakudo, *Bull. Chem. Soc. Jpn* 1970, **43**, 1661.
14. O. S. Jung, Y. S. Sohn and J. A. Ibers, *Inorg. Chem.* 1986, **25**, 2273.
15. D. Coucouvanis, *Prog. Inorg. Chem.* 1970, **2**, 233.
16. R. E. Reid, *Organic Chemistry of Bivalent Sulfur*, Vol. IV. Chemical Publishing Company, New York (1962).
17. *International Tables for X-ray Crystallography*, Vol. 4. Kynoch Press, Birmingham, U.K. (1974).
18. G. M. Scheldrick, SHELEX 76, Program for Crystal Structure Determination. University of Cambridge, U.K. (1976).
19. F. Bonati and R. Ugo, *J. Organomet. Chem.* 1967, **10**, 257.
20. C. P. Sharma, N. Kumar, M. C. Khandpal, S. Chandra and V. G. Bhide, *J. Inorg. Nucl. Chem.* 1981, **43**, 923.
21. J. Otera, T. Hinoishi and R. Okawara, *J. Organomet. Chem.* 1980, **202**, C93.
22. J. Otera, *J. Organomet. Chem.* 1981, **221**, 57.
23. J. Otera, T. Hinoishi, Y. Kawabe and R. Okawara, *Chem. Lett.* 1981, 273.
24. J. Otera, A. Kusaba, T. Hinoishi and Y. Kawasaki, *J. Organomet. Chem.* 1982, **228**, 223.
25. J. Otera, T. Yano and K. Kusakabe, *Bull. Chem. Soc. Jpn* 1983, **56**, 1057.
26. J. Holecek, M. Nadvornik, K. Handlir and A. Lycka, *J. Organomet. Chem.* 1983, **241**, 177.
27. O. S. Jung and Y. S. Sohn, *Bull. Korean Chem. Soc.* 1988, **9**, 365.

Polyhedron Vol. 8, No. 11, pp. 1419–1423, 1989
Printed in Great Britain

0277-5387/89 $3.00+.00
© 1989 Pergamon Press plc

PREPARATION AND CHARACTERIZATION OF MIXED AMIDO–PHOSPHIDO COMPOUNDS OF MOLYBDENUM(IV). A COMPARISON OF π-DONATING LIGANDS IN $Mo(NMe_2)_4$, $Mo(PCy_2)_4$ AND $[Mo(NMe_2)_2(PPh_2)_2]$ BASED ON X-RAY STUDIES

MALCOLM H. CHISHOLM,* CHARLES E. HAMMOND and JOHN C. HUFFMAN

Department of Chemistry and Molecular Structure Center, Indiana University, Bloomington, IN 47405, U.S.A.

(*Received* 23 *August* 1988; *accepted* 25 *January* 1989)

Abstract—Two preparative routes to mixed amido–phosphido complexes $[M(NMe_2)_{4-x}(PR_2)_x]$ have been investigated involving the addition of either R_2PH or $LiPR_2$ to hydrocarbon solutions of $Mo(NMe_2)_4$. The former method has allowed the replacement of two NMe_2 ligands and the isolation of the crystalline compound $[Mo(NMe_2)_2(PPh_2)_2]$. The latter synthetic approach has allowed the isolation of $[Mo(NMe_2)_3P(t\text{-}Bu)_2]$. Both compounds are monomeric in solution and in the solid-state $[Mo(NMe_2)_2(PPh_2)_2]$ adopts a structure closely related to those seen for $Mo(NMe_2)_4$ and $Mo(PCy_2)_4$. Specifically, the Mo—N (1.941(9) and 1.913(9) Å) and the Mo—P distances (2.260(3) and 2.264(3) Å) are (within the criteria of 3σ) identical to those seen in $Mo(NMe_2)_4$ and $Mo(PCy_2)_4$, respectively. Furthermore, the $Mo(NC_2)_4$, $Mo(PC_2)_4$ and $Mo(NC_2)_2(PC_2)_2$ units are all arranged in a common manner allowing the pnictinide-containing ligands to π-donate to the d^2 Mo(4+) centre. In this instance, NMe_2^- and PPh_2^- are both acting as 4-electron donors ($\sigma^2+\pi^2$) and only subtle distinctions based on the angles at nitrogen and phosphorus imply that the relative π-donor ability is $Me_2N^- > Ph_2P^-$. This result is compared to $[1,2\text{-}M_2(PR_2)_2(NMe_2)_4]$ structures where, based on M—P and M—N distances together with the angles subtend at nitrogen and phosphorus, the order is clearly established, $Me_2N^- > Ph_2P^-$. Crystal data for $[Mo(NMe_2)_2(PPh_2)_2]$ at −156°C: $a = 11.151(6)$, $b = 29.156(2)$, $c = 9.682(5)$ Å, $\beta = 119.99(2)°$, $Z = 4$, $d_{calc} = 1.351$ g cm^{-3} and space group $P2_1/c$

We recently reported the preparation and characterization of $[1,2\text{-}M_2(PR_2)_2(NMe_2)_4]$ (M≡M) compounds (M = Mo and W).[1] These exist in *anti*- and *gauche*-rotamers, both in solution and in the solid-state, and based on both considerations of M—P bond lengths and pyramidality at the phosphorus atom we determined that the relative π-donor ability of the ligands was in the order $Me_2N^- > R_2P^-$. In these compounds there are two metal *d* orbitals at each metal atom capable of accepting ligand p_π electrons, namely the d_{xy} and $d_{x^2-y^2}$ orbitals. The M≡M bond utilizes primarily metal d_{z^2} and d_{xz}/d_{yz} to form M—M σ and π_x/π_y orbitals, respectively.

In the case of the monomeric compounds of Mo(4+), $Mo(NMe_2)_4$[2] and $Mo(PCy_2)_4$,[3] the M—N/M—P distances are entirely consistent with formal double bonds and the sum of the angles at N and P are close to 360°. Moreover, the symmetry of the $M(EC_2)_4$ skeleton allows the N/P p_π orbitals to interact with vacant Mo d_{z^2}, d_{xy}, d_{xz} and d_{yz} atomic orbitals giving an effective 18-valence-shell electron-count at the metal centre.

In the compound $Cp_2Hf(PEt_2)_2$, there is only one metal hybrid orbital available for π-bonding and one phosphorus atom is trigonal planar and the other pyramidal with short, 2.488(1) Å, and long, 2.682(1) Å, M—P distances, respectively.[4] It should be noted that in this case the two C_2P planes are aligned such that only one phosphorus p_π orbital can interact with the Hf d_π orbital.

* Author to whom correspondence should be addressed.

We were interested in comparing the metal–ligand bonding in mixed amido–phosphido compounds of formula $[Mo(NMe_2)_{4-x}(PR_2)_x]$. A number of hypothetical scenarios can be envisaged, including dimerization by either phosphido or amido bridge formation giving Mo≡Mo bonds. The latter are seen, for example, in the compounds $Mo_2(OPr^i)_8$[5] and $[Mo_2(NMe_2)_4(OR)_4]$, where R = 4-methylcyclohexyl and diisopropylmethyl, which rather interestingly choose to form NMe_2 bridges rather than OR bridges.[6] We describe here our preparation and characterization of mixed phosphido–amido compounds of Mo(4+).

RESULTS AND DISCUSSION

Synthesis

Two synthetic strategies were attempted. In one, R_2PH and $Mo(NMe_2)_4$ were allowed to react in a hydrocarbon solvent. This proved successful in the case of R = Ph but not R = Bu^t or Cy, presumably reflecting the acidity of the P—H bond.[7] In this way $[Mo(NMe_2)_2(PPh_2)_2]$ was isolated by crystallization. The second method involved the addition of $LiPR_2$ to a hydrocarbon solution of $Mo(NMe_2)_4$. Rather interestingly, and for reasons that are not apparent, this allowed PR_2-for-NMe_2 exchange when R = Bu^t but not when R = Ph. In any event, substitution only occurred once—quite probably for steric reasons—yielding $[Mo(NMe_2)_3P(t\text{-}Bu)_2]$.

Both new compounds are air-sensitive and must be handled in dry and oxygen-free atmospheres and solvents. They are monomeric in solution and may be crystallized from hexane.

Solid-state and molecular structure of $[Mo(NMe_2)_2(PPh_2)_2]$

A ball-and-stick drawing of the molecule is given in Fig. 1 and selected bond distances and bond angles are given in Table 1. The atom numbering scheme used in Table 1 is shown in Fig. 2.

The molecule has a virtual C_2 axis of symmetry and the geometry about molybdenum is similar to that found in $Mo(NMe_2)_4$ and $Mo(PCy_2)_4$. The $M(EC_2)_4$ units in the latter compounds (E = N and P) are oriented in an identical manner and the same arrangement is found for the $Mo(NC_2)_2$ unit in $[Mo(NMe_2)_2(PPh_2)_2]$. The C_2N and C_2P planes face one another in $[Mo(NMe_2)_2(PPh_2)_2]$ and are related by the virtual C_2 axis of symmetry. The M—N and M—P distances are short, indicative of double bonds, and are essentially identical to those found in $Mo(NMe_2)_4$ and $Mo(PCy_2)_4$, respectively. Evidently, since there are four available metal d_π

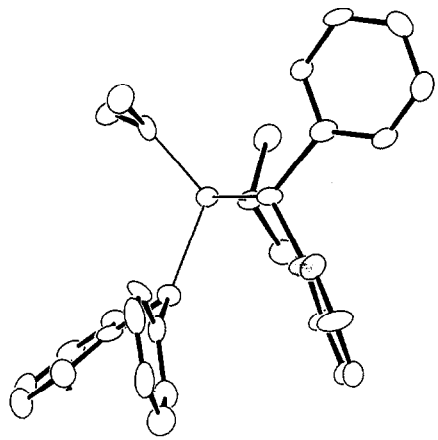

Fig. 1. A ball-and-stick drawing of the $[Mo(NMe_2)_2(PPh_2)_2]$ molecule. Hydrogen atoms are omitted for clarity.

Table 1. Pertinent bond distances (Å) and angles (°) in $[Mo(NMe_2)_2(PPh_2)_2]$

A	B	Distance	
Mo(1)	P(8)	2.260(3)	
Mo(1)	P(21)	2.264(3)	
Mo(1)	N(2)	1.941(9)	
Mo(1)	N(5)	1.914(9)	
P(8)	C(9)	1.836(10)	
P(8)	C(15)	1.829(11)	
P(21)	C(22)	1.837(11)	
P(21)	C(28)	1.852(11)	
N(2)	C(3)	1.442(15)	
N(2)	C(4)	1.473(16)	
N(5)	C(6)	1.477(15)	
N(5)	C(7)	1.475(14)	
A	**B**	**C**	**Angle**
P(8)	Mo(1)	P(21)	93.35(11)
P(8)	Mo(1)	N(2)	108.51(26)
P(8)	Mo(1)	N(5)	115.47(28)
P(21)	Mo(1)	N(2)	115.29(27)
P(21)	Mo(1)	N(5)	108.52(28)
N(2)	Mo(1)	N(5)	114.1(4)

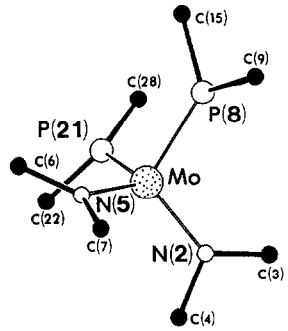

Fig. 2. The central $[Mo(NC_2)_2(PC_2)_2]$ unit of the $[Mo(NMe_2)_2(PPh_2)_2]$ molecule showing the atom numbering scheme used in Table 1.

orbitals, these are used equally well by both NMe_2 and PPh_2 ligands. Only in an examination of the angles at the pnictinide atoms is there any evidence for differences in ligand-to-metal bonding and here the difference is extremely subtle.

A pyramidal (pseudo-tetrahedral) atom has 328.5° as the sum of its three angles, while for a trigonal planar atom the sum is, of course, 360°. These parameters are compared for all the compounds $Mo(NMe_2)_4$, $Mo(PCy_2)_4$ and $[Mo(NMe_2)_2(PPh_2)_2]$ in Table 2 and provide a consistent trend. For the mixed amido–phosphido compound, the sum of the angles at nitrogen (358.2°) is greater than in $Mo(NMe_2)_4$ (357.0°) and at phosphorus the sum (353.9°) is smaller than in $Mo(PCy_2)_4$ (355.5°).

Two other related measures of pyramidality are: (i) the angle between the M—P or M—N line and the respective PC_2 or NC_2 plane and (ii) the P or N atom distance out of the plane containing the MC_2 atoms. These parameters are compared in Table 3. It is worthy of note that even though the P—C bond distances are shorter for the PPh_2 ligand than the PCy_2 ligand, the distance that P deviates from the MoC_2 plane is greater for the $[Mo(NMe_2)_2(PPh_2)_2]$ compound than for $Mo(PCy_2)_4$.

Table 2. Summation of the angles (°) about the pnictinide in selected monomeric compounds of Mo(4+)

$Mo(NMe_2)_4$[a]		$[Mo(NMe_2)_2(PPh_2)_2]$[b]			$Mo(PCy_2)_4$[c]
N(1) 356.7		N(2) 358.5			P(1) 354.7
N(2) 357.0		N(5) 357.9			P(2) 355.5
N(3) 357.2			P(8)	354.5	P(3) 355.9
N(4) 356.9			P(21)	353.3	P(4) 356.0
Average 357.0	vs	358.2		353.9 vs	355.5

[a] Molecule 1 in ref. 2.
[b] This work.
[c] Ref. 3.

Table 3. Comparisons of pyramidality in selected monomeric compounds of Mo(4+)

(a) Angles (°) between Mo—E and the EC_2 planes

$Mo(NMe_2)_4$[a]		$[Mo(NMe_2)_2(PPh_2)_2]$[b]			$Mo(PCy_2)_4$[c]
N(1) 15.6		N(2) 11.0			P(1) 19.9
N(2) 16.2		N(5) 12.9			P(2) 18.2
N(3) 15.4			P(8)	20.4	P(3) 17.4
N(4) 16.9			P(21)	22.8	P(4) 17.0
Average 16.0	vs	12.0		21.6 vs	18.4

(b) Distances (Å) that N/P is out of the MoC_2 plane

$Mo(NMe_2)_4$[a]		$[Mo(NMe_2)_2(PPh_2)_2]$[b]			$Mo(PCy_2)_4$c
N(1) 0.156		N(2) 0.130			P(1) 0.264
N(2) 0.164		N(5) 0.112			P(2) 0.241
N(3) 0.158			P(8)	0.266	P(3) 0.230
N(4) 0.174			P(21)	0.295	P(4) 0.230
Average 0.163	vs	0.121		0.281 vs	0.241

[a] Molecule 1 in ref. 2.
[b] This work.
[c] Reference 3.

Concluding remarks

In the mixed ligand compound $[Mo(NMe_2)_2(PPh_2)_2]$, both the amide and phosphide compete equally well as π-donor ligands, at least as can be judged by M—N or M—P distances. Only the very subtle changes noted in Tables 2 and 3 can be argued to support the view that the π-donating ability is in the order $NMe_2^- > PPh_2^-$. The difference between the bonding at the $(M{\equiv}M)^{6+}$ and Mo(4+) centres reflects the relative number of available metal d_π orbitals.

EXPERIMENTAL

Dry and oxygen-free solvents and atmospheres were used throughout. Manipulations and syntheses were carried out using standard dry-box and Schlenk techniques. NMR spectra were recorded in toluene-d_8 or benzene-d_6 on a Nicolet 360 (^{31}P) and a Varian 300 (^1H and ^{13}C) spectrometer. IR were recorded as Nujol mulls between CsI plates on a Perkin–Elmer 283 spectrophotometer. Elemental analyses were obtained from Alfred Bernhardt Mikroanalytische Laboratorium.

$[Mo(NMe_2)_2(PPh_2)_2]$

A flask was charged with $Mo(NMe_2)_4$ (509 mg), $HPPh_2$ (1.00 cm^3) and pentane (10 cm^3) and a stir bar. The purple solution of $Mo(NMe_2)_4$ in pentane changed colour to a red–brown solution. After 2 days of stirring the pentane was removed *in vacuo*. Aliquot analysis by NMR spectroscopy indicated the presence of $Mo(NMe_2)_4$, $HPPh_2$ and $Mo(NMe_2)_3PPh_2$. Upon standing for 1 day in a nitrogen atmosphere dry-box, crystals of $[Mo(NMe_2)_2(PPh_2)_2]$ had formed. These were coated with $HPPh_2$ and trace amounts of $[Mo(NMe_2)_3PPh_2]$, as identified by NMR spectroscopy. After liberal washings with pentane and benzene, 40 mg of pure crystals were isolated. Found: C, 60.9; H, 5.8; N, 4.8. Calc. for $MoC_{28}H_{32}N_2P_2$: C, 60.6; H, 5.8; N, 5.0%.

IR data (cm^{-1}): 1580(m), 1565(w), 1415(m), 1366(m), 1297(w), 1243(w), 1185(w), 1158(w), 1145(w), 1114(w), 1095(w), 1083(w), 1064(w), 1040(w), 1025(w), 939(w), 737(s), 690(s), 673(w) 661(w), 523(m), 477(w), 462(w), 456(w), 435(w), 320(w).

NMR data: ^1H, 25°C, C_6D_6: δ 3.23 (t), $^4J_{PH} = 2.7$ Hz (NMe_2); δ 7.64 (br), 7.08 (m), 6.99 (d) (Ph); ^{13}C, 25°C, C_6D_6: δ 49.0 (t), $^3J_{C—P} = 5$ Hz, ^{31}P δ 190 vs 85% H_3PO_4 in D_2O external lock.

NMR data for $Mo(NMe_2)_3(PPh_2)$: ^1H, 22°C, C_6D_6: δ 3.31 (d), $^4J_{PH} = 1.8$ Hz (NMe_2); ^{13}C, 25°C, C_6D_6: δ 50.8 (d), $^3J_{PC} = 4$ Hz; ^{31}P δ 154 (s) vs 85% H_3PO_4 in D_2O external lock.

$[Mo(NMe_2)_3P(t\text{-}Bu)_2]$

THF (15 cm^3) was added to the solids, $Mo(NMe_2)_4$ (400 mg) and $LiP(t\text{-}Bu)_2$ (240 mg). Reaction was immediate and the solution had a red–violet colour. The solvent was removed *in vacuo* and the residue extracted with pentane, filtered and the solvent again removed *in vacuo*. (The filtered solid has an identical IR spectrum of $LiNMe_2$.) A second extraction of 367 mg with pentane and crystallization from pentane gave 215 mg of red–violet crystals. Found: C, 44.8; H, 9.5; N, 11.1. Calc. for $MoC_{14}H_{36}N_3P$: C, 45.0; H, 9.7; N, 11.2%.

IR data (cm^{-1}): 1409(s), 1354(s), 1240(m), 1231(m), 1170(m), 1155(m), 1147(s), 1112(m), 1030(m), 1017(w), 943(s), 938(vs), 928(s), 805(m), 565(s).

NMR data: ^1H, 22°C, C_6D_6: δ 3.31 (d), $^4J_{PH} = 1.2$ Hz (NMe_2); δ 1.16 (d), $^3J_{PH} = 12$ Hz (P—*t*-Bu); ^{13}C, C_6D_6: δ 51.6 (d), $^3J_{P—C} = 3$ Hz (NMe); δ 44.8 (d), $^1J_{PC} = 13$ Hz ($PCMe_3$); δ 34.7 (d), $^2J_{P—C} = 5$ Hz ($PCMe_3$); ^{31}P, 22°C, pentane: δ 237 (s) vs 85% H_3PO_4 in D_2O: ^{95}Mo δ 3355 (d), $^1J_{Mo—P} = 322$, $\Delta\nu^{1/2} = 70$ Hz. Sample run in pentane and δ relative to external Na_2MoO_4, 2M in D_2O.

Crystallographic studies

General operating procedures and a listing of programs have been given previously.[8] A summary of crystal data is given in Table 4. A suitable crystal was located and transferred to the goniostat using standard inert atmosphere handling techniques employed by the IUMSC and cooled to −155°C for characterization and data collection.

A systematic search of a limited hemisphere of reciprocal space located a set of diffraction maxima with symmetry and systematic absences corresponding to the unique monoclinic space group $P2_1/c$. Subsequent solution and refinement of the structure confirmed this choice.

Data were collected in the usual manner using a continuous θ–2θ scan with fixed backgrounds. The data were reduced to a unique set of intensities and associated sigmas in the usual manner. The structure was solved by a combination of direct methods (MULTAN78) and Fourier techniques. Refinement progressed smoothly, with a difference Fourier phased on the non-hydrogen atoms revealing the positions of most of the hydrogen atoms. The positions of the latter were fixed in their

Table 4. Summary of crystal data for $[Mo(NMe_2)_2(PPh_2)_2]$

Empirical formula	$MoC_{28}H_{32}N_2P_2$
Colour of crystal	Yellowish-brown
Crystal dimensions (mm)	$0.25 \times 0.25 \times 0.25$
Space group	$P2_1/c$
Cell dimensions	
Temperature (°C)	−156
a (Å)	11.151(6)
b (Å)	29.156(21)
c (Å)	9.682(5)
β (°)	119.99(2)
Z (molecules/cell)	4
Volume (Å^3)	2726.38
Calculated density	1.351
Wavelength	0.71069
Molecular weight	554.46
Linear absorption coefficient (cm^{-1})	6.019
Detector to sample distance (cm)	22.5
Sample to source distance (cm)	23.5
Average omega scan width at half height	0.25
Scan speed (° min^{-1})	6.0
Scan width (deg + dispersion)	1.5
Individual background (s)	6
Aperture size (mm)	3.0×4.0
2θ range (°)	6–45
Total number of reflections collected	3938
Number of unique intensities	3578
Number of $F > 2.33\sigma(F)$	3397
$R(F)$	0.0896
$R_w(F)$	0.0941
Goodness-of-fit for the last cycle	2.989
Maximum δ/σ for last cycle	0.05

idealized positions for the remainder of the refinement. Although a final difference Fourier was featureless (maximum peak = 0.45 e Å^{-3}), the residuals remained quite high (R(F) = 0.0896 and R_w(F) = 0.0941). ψ scans for several reflections indicated no significant absorption problems. It was observed that some decomposition of the sample had occurred during the sample transfer process, and it may be that this decomposition affected the quality of the data. There were no significant voids in the lattice, indicating solvent loss was not a problem.

Atomic positional parameters have been deposited with the Director, Cambridge Crystallographic Centre.

Acknowledgements—We thank the National Science Foundation for support. C.E.H. thanks Professor W. E. Buhro for many helpful discussions.

REFERENCES

1. W. E. Buhro, M. H. Chisholm, K. Folting and J. C. Huffman, *J. Am. Chem. Soc.* 1987, **109**, 4552; W. E. Buhro, M. H. Chisholm, K. Folting, J. C. Huffman and J. D. Martin, manuscript in preparation.
2. M. H. Chisholm, F. A. Cotton and M. W. Extine, *Inorg. Chem.* 1978, **17**, 1329; D. C. Bradley and M. H. Chisholm, *J. Chem. Soc. A* 1971, 2741.
3. R. T. Baker, P. J. Kruisic, T. H. Tulip, J. C. Calabrese and S. S. Wreford, *J. Am. Chem. Soc.* 1983, **105**, 6763.
4. R. T. Baker, J. F. Whitney and S. S. Wreford, *Organometallics* 1983, **2**, 1049.
5. M. H. Chisholm, F. A. Cotton, M. W. Extine and W. W. Reichert, *Inorg. Chem.* 1978, **17**, 2944.
6. M. H. Chisholm, C. E. Hammond and J. C. Huffman, *Polyhedron* 1989, **8**, 129.
7. K. Issleib and R. Kummel, *J. Organomet. Chem.* 1965, **3**, 84.
8. M. H. Chisholm, K. Folting, J. C. Huffman and C. C. Kirkpatrick, *Inorg. Chem.* 1984, **23**, 1021.

Polyhedron Vol. 8, No. 11, pp. 1425–1430, 1989
Printed in Great Britain

0277–5387/89 $3.00+.00
© 1989 Pergamon Press plc

LANTHANIDE–ANION COMPLEXATION OF A NEW POLYAMINOPOLYCARBOXYLATE, DTTAP

DOUGLAS J. SAWYER*

Department of Chemistry, Iowa State University, Ames, IA 50011, U.S.A.

and

JACK E. POWELL

Ames Laboratory, U.S. Department of Energy and Department of Chemistry, Iowa State University, Ames, IA 50011, U.S.A.

(*Received* 11 *January* 1989; *accepted* 25 *January* 1989)

Abstract—The protonation constants (α's) and the stability constants (*K*'s) of diethylenetriamine-N,N,N′,N″-tetraacetic acid-N″-propionic acid (DTTAP) and its anion–lanthanide complexes, respectively, have been determined experimentally, providing information about the nature of chelation across the lanthanide series. The stability constants indicate that DTTAP can participate in a successful separation of Am from the lanthanides.

The safe disposal of high-level wastes from nuclear power plants is a growing concern. Nearly all of the components of the high-level waste can be managed safely.[1,2] The ideal disposal process for the waste will involve the removal of the transuranic actinides. Once these elements are removed, they can be transmuted in a high-flux reactor, or disposed in other ways.

Sufficient methods have been developed for removing the actinides from all the waste components, except the lanthanides. Separation from the lanthanides is necessary for effective transmutation.

The key to a successful An/Ln separation is the existence of a chelating agent that will bind the transuranic An^{III} ions more tightly than any of the trivalent lanthanides.

Two major factors affect the value of a chelating agent for use in Am/Ln separations. It is favourable for the ligand to exhibit maximum Ln–ligand complex stability near Nd. Since Am^{III} and Nd^{III} possess nearly identical radii, all Ln–ligand complex stabilities should be lower than that of Nd^{III} for the maximum Am–Ln separation factor (α_{Ln}^{Am}) to be realized. Secondly, if the overall stabilities of the Ln–ligand complexes could be near $K = 10^{19}$–10^{20}, then the selection of the ligand for actinide ions over lanthanide ions would be enhanced over that of ligands with lower overall stability. Also, in this range the exchange kinetics would be favourable in a cation exchange separation of Am^{III} from the lanthanides using the chelating agent in the mobile phase.

This work describes the experimental determination of the protonation constants (α's) and the stability constants (*K*'s) of diethylenetriamine-N,N,N′,N″-tetraacetic acid-N″-propionic acid (DTTAP) and its anion–Ln complexes, respectively. The values were obtained from pH measurements in a simulated potentiometric titration described below.

The results provide some information about chelation across the lanthanide series. The stability constant values indicate that DTTAP is a candidate for participation in the disposal of high-level radioactive waste.

EXPERIMENTAL

Materials

All chemicals were of reagent-grade. Deionized water in this laboratory was prepared by passing

* Author to whom correspondence should be addressed. Present address: Department of Chemistry, Arizona State University, Tempe, AZ 85287-1604, U.S.A.

condensed steam through a mixed bed of anion- and cation-exchange resins.

Trivalent lanthanide nitrate solutions

Approximately 0.1 M lanthanide nitrate solutions were prepared by the dilution of concentrated stock solutions, which were prepared from Ln_2O_3 samples of 99.999% purity using the method described by Adolphson.[3]

Ligand solution

A 0.01110 M standard solution of DTTAP was prepared by dilution of the pure concentrated solution. The solution was standardized by several potentiometric titrations with standard KOH solution. The synthesis of this ligand is described elsewhere.[4]

pH_c *measurements*

All pH_c measurements were carried out using a Beckman model 1019 research pH meter equipped with a Phoenix Model 5733928 pH electrode. Standard solutions with known hydrogen-ion concentrations were prepared ($\mu = 0.100$ M) so that the pH_c could be measured directly.[5]

Procedure

Determination of protonation constants. The five protonation constants (α's) for DTTAP were determined using two separate sets of DTTAP solutions. Solutions prepared at high pH (8.7–10) were used to determine α_1 and α_2, and solutions prepared at low pH (2.8–6) were used to determine α_3, α_4 and α_5. Nineteen solutions were prepared in all; twelve of which were low pH solutions, and seven of which were high pH solutions.

Each of the nineteen solutions was prepared by combining 4.00 cm^3 of ligand solution, a measured amount of standard KOH solution, and an appropriate amount of KNO_3 solution to produce 0.100 M ionic strength. The required amount of KNO_3 was calculated for each solution using the computer program ALPHA, described elsewhere.[5] The solutions were all diluted to $25.00 \pm .01$ cm^3 with deionized water. The solutions were then equilibrated for 8 h in a constant temperature water bath at 25.00 ± 0.05°C, prior to the measurement of pH_c.

The five α values were calculated from the pH_c data using the computer program OMEGA, developed by Johnson[6] and Miller.[7] The least-squares analysis employed by this program has been described in detail by Tse.[8]

Determination of stability constants

The values of K_{ML} and K_{MHL} were determined for the complexes formed by DTTAP with the trivalent elements La–Lu, excluding Pm, using 8–10 carefully prepared solutions for each metal–DTTAP system.

Each of the solutions was prepared by combining 4.00 cm^3 of ligand solution, a measured amount of KOH solution, a measured amount of metal nitrate solution, and an appropriate amount of KNO_3 solution to produce 0.100 M ionic strength. The required amount of KNO_3 was calculated for each solution using the computer program BETA, described elsewhere.[5] The volume of metal nitrate solution was selected to provide a 1:1 ratio of metal–ligand. The solutions were diluted to 25.00 ± 0.01 cm^3 with deionized water, and then equilibrated for 12–16 h in a constant temperature water bath at 25.00 ± 0.05°C, prior to the measurement of pH_c.

The values of K_{ML} and K_{MHL} for each lanthanide–DTTAP system were calculated from the pH_c data using the computer program HCMPLX, developed by Potter.[9]

RESULTS AND DISCUSSION

Protonation constants

The protonation constants for DTTAP are displayed in Table 1 along with the logarithms of the five stepwise protonation constants (pK_a values).

The values of the fourth and fifth stepwise protonation constants indicate that DTTAP is a weaker acid than DTPA in the lower pH region (see Fig. 1).[10] These results are expected, when con-

Table 1. Protonation constants for the DTTAP anion at 25.00 ± 0.05°C ($\mu = 0.10$)

α_N	$\log K^a$	K
$\alpha_1 = \frac{[HL]}{[H][L]} = 4.35 \times 10^9$	9.64	$\frac{[HL]}{[H][L]}$
$\alpha_2 = \frac{[H_2L]}{[H]^2[L]} = 3.18 \times 10^{18}$	8.86	$\frac{[H_2L]}{[H][HL]}$
$\alpha_3 = \frac{[H_3L]}{[H]^3[L]} = 1.05 \times 10^{23}$	4.52	$\frac{[H_3L]}{[H][H_2L]}$
$\alpha_4 = \frac{[H_4L]}{[H]^4[L]} = 3.69 \times 10^{26}$	3.54	$\frac{[H_4L]}{[H][H_3L]}$
$\alpha_5 = \frac{[H_5L]}{[H]^5[L]} = 2.26 \times 10^{29}$	2.79	$\frac{[H_5L]}{[H][H_4L]}$

[a] ± 0.08.

DTPA:

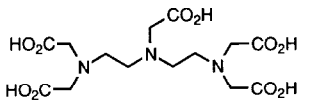

DTTAP:

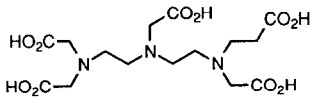

EEDTA:

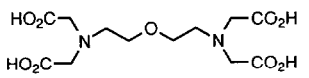

DETAP:

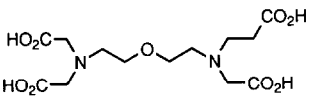

CEDTA:

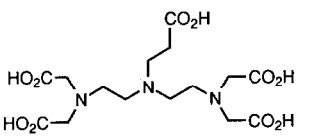

Fig. 1. Key for identifying some polyaminopolylcarboxylate ligands.

sidering that the only difference between the two ligands is that in DTTAP a propionate group has replaced one acetate group on one end of the DTPA ligand. The propionate group, being less acidic, retains a proton at higher pH values than does the acetate group.

It is also observed that three protons are dissociated at low pH and the two remaining protons are dissociated at high pH. These two most tightly bound protons are each stabilized by association with two carboxylate groups and one nitrogen atom, at opposite ends of the molecule.

Metal–anion stability constants

The Ln–DTTAP stability constants are reported in Table 2. A plot of the $\log K_{ML}$ values vs metal cationic radius is shown in Fig. 2 for DTTAP and several other ligands.[10–12] The DTTAP ligand shows an overall stability with the lanthanides of about 10^3 times lower than that of DTPA. The maximum ligand affinity at Eu for DTTAP represents a shift of the maximum relative to DTPA.

The overall magnitude of the Ln–DTTAP complex stability constants is expected. A 10^3-fold attenuation is also observed when comparing the Ln–ligand stabilities of DETAP with EEDTA. The attenuation is explained in both cases by the replacement of an acetate group, capable of forming stable five-membered chelate rings, with a propionate group which will form less stable six-membered rings upon chelation. Furthermore, if the acetate group bonded to the *middle* nitrogen of DTPA is replaced with a propionate group, a more drastic 10^6-fold attenuation in complex stabilities is observed. This attenuation is shown by comparing the DTPA and CEDTA Ln–ligand complex stability constant values. The less drastic attentuation for the DTTAP system is expected because a bulky chelate ring at an end nitrogen is not expected to affect the rest of the molecule as much as a bulky chelate ring in the middle of the molecule.

Table 2. Stability constants of trivalent Ln–DTTAP complexes at $25.00 \pm 0.05°C$ ($\mu = 0.10$)

M	K_{MHL}	$\log K_{MHL}$[a]	K_{ML}	$\log K_{ML}$[a]
La	0.242×10^{12}	11.38	0.243×10^{18}	17.39
Ce	0.177×10^{13}	12.25	0.177×10^{19}	18.25
Pr	0.604×10^{13}	12.78	0.439×10^{19}	18.64
Nd	0.942×10^{13}	12.97	0.862×10^{19}	18.94
Sm	0.251×10^{14}	13.40	0.382×10^{20}	19.58
Eu	0.229×10^{14}	13.36	0.559×10^{20}	19.75
Gd	0.239×10^{14}	13.38	0.552×10^{20}	19.74
Tb	0.353×10^{14}	13.55	0.331×10^{20}	19.52
Dy	0.326×10^{14}	13.51	0.348×10^{20}	19.54
Ho	0.258×10^{14}	13.41	0.281×10^{20}	19.45
Er	0.191×10^{14}	13.28	0.219×10^{20}	19.34
Tm	0.130×10^{14}	13.11	0.255×10^{20}	19.41
Yb	0.146×10^{14}	13.16	0.327×10^{20}	19.51
Lu	0.122×10^{14}	13.09	0.220×10^{20}	19.34

[a] All values ± 0.30.

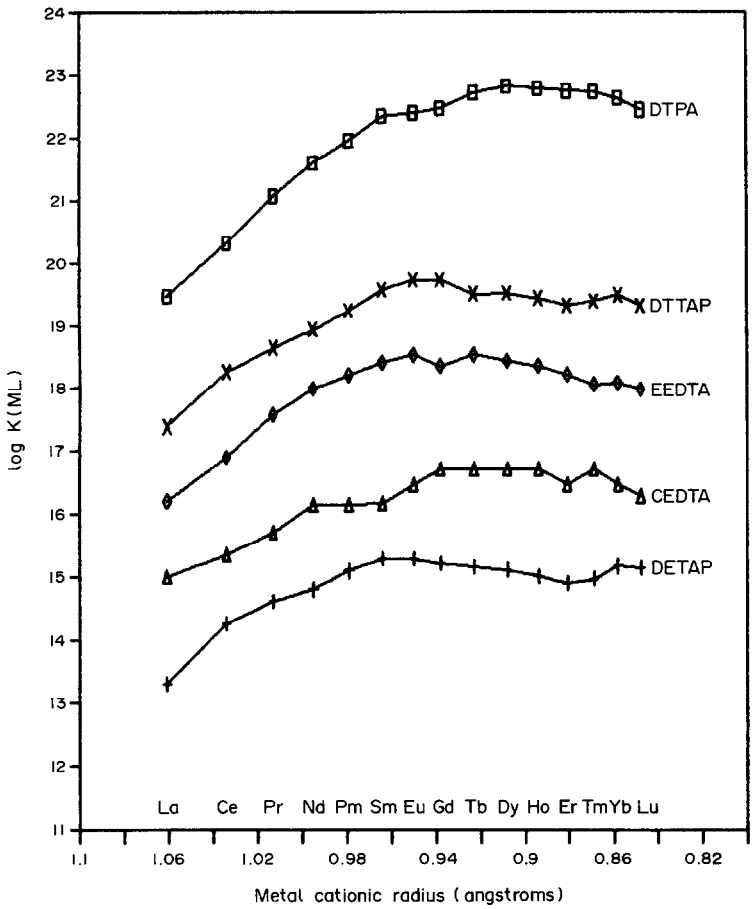

Fig. 2. Stability constants of some Ln–anion complexes as a function of the metal cationic radius.

The shift of the Ln–ligand complex stability maximum from right to left is also expected for the DTTAP function relative to the DTPA function. A similar shift is observed in the DETAP function relative to the EEDTA function. Both shifts are explained by a change in dentate character of the ligand across the lanthanide series. The size of the coordination sphere of the trivalent lanthanides diminishes significantly from La to Lu. It is reasonable to assume that a large ligand such as DTTAP or DPTA would coordinate in an octadentate fashion to the larger lanthanide ions and be forced to coordinate in a lower-dentate fashion to the smaller lanthanide ions.

In progressing from La to Lu, the large polyaminopolycarboxylate ligands most likely experience a breaking of at least one of the chelate rings in order to coordinate the smaller ions with a minimum of steric hindrance. This decrease in coordination number of aqueous lanthanide ions across the series is generally agreed upon by experts in this field.[13–15] By replacement of an acetate with a propionate moiety, a ligand will have a more strained six-membered chelate ring that will be likely to "fail" faster than the more stable five-membered ring offered by the acetate group. DTTAP, therefore, shows an earlier turnover in the $\log K_{ML}$ vs ionic radius function, due to an earlier failure of its octadentate character relative to that of DTPA.

The minimum Am–Ln separation factor (α_{Ln}^{Am}) for DTTAP can be estimated by interpolation, as explained by Powell and Ling.[11] As shown in Fig. 3, the estimated value for $\log \alpha_{Nd}^{Am}$ is 0.98. If one subtracts the difference ($\log K_{EuL} - \log K_{NdL}$) from 0.98, the value for $\log \alpha_{Eu}^{Am}$ is estimated:

$$\log \alpha_{Eu}^{Am} = 0.17$$

$$\alpha_{Eu}^{Am} = 1.48.$$

The estimated minimum separation factor of 1.48 for Am and the strongest complexing lanthanide ion does not represent the largest separation factor known for these systems. EEDTA provides a known value of 1.71,[16] which is the largest known to date.

The value of 1.48 for α_{Eu}^{Am}, estimated in this work, suggests that DTTAP is a chelating agent capable of

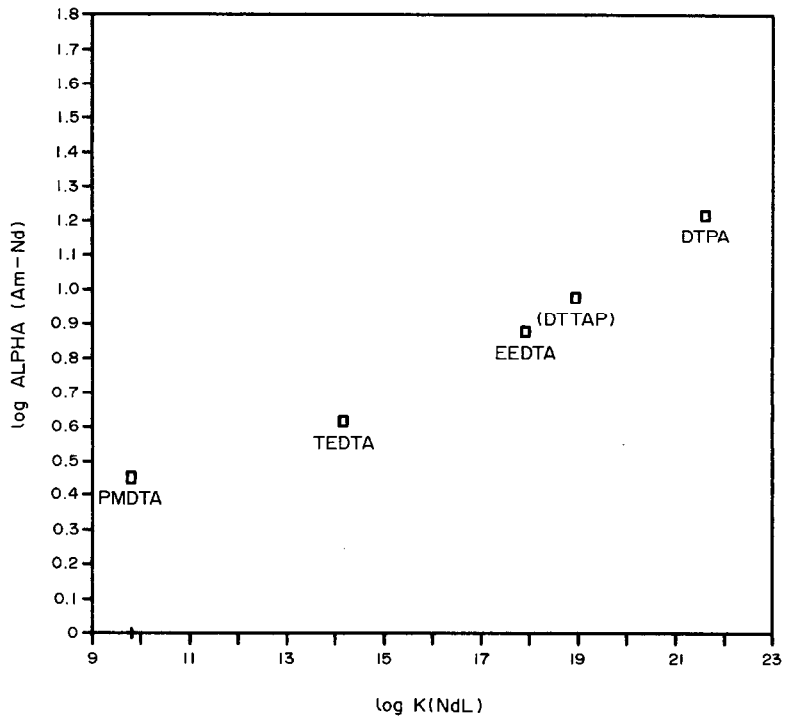

Fig. 3. Am^{3+}–Nd^{3+} separation factors as a function of affinity.[11]

effecting a separation of Am from the lanthanides.

Although the value for α_{Ln}^{Am} estimated here for the DTTAP system is slightly less than the value observed for the EEDTA system, one should keep in mind that 1.48 is the minimum estimated value for α_{Ln}^{Am}, and that the actual value may be larger. The value of $\log \alpha_{Nd}^{Am}$ for DTTAP could be more of the order of 1.22. This would result in a value of 2.57 for α_{Eu}^{Am}.

There is some precedent for considering the higher value of α_{Nd}^{Am} for the DTTAP system. In 1985, Powell and Ling[11] reported a value of 0.73 for $\log \alpha_{Y}^{Ho}$ for the DETAP system. This value is very close to the value observed for $\log \alpha_{Y}^{Ho}$ for the EEDTA system, despite the considerable difference in stabilities of the Ho–EEDTA and the Ho–DETAP complexes. While the replacement of an acetate by a propionate moiety resulted in a decrease in the overall stability of the Ho–L and Y-L complexes, the Ho–Y separation factor was virtually *unchanged.* Since Ho^{III} and Y^{III} have nearly identical radii, the Am^{III} and Nd^{III} system is expected to behave similarly; and it is not unreasonable to consider the possibility of a $\log \alpha_{Nd}^{Am}$ value for the DTTAP system close to that of the DTPA system. This consideration would result in a very attractive value for α_{Ln}^{Am} of 2.57; far superior to any separation factors observed to date for these systems.

Acknowledgements—This work was supported by the Department of Chemistry, Iowa State University and was performed at Ames Laboratory. Ames Laboratory is operated for the U.S. Department of Energy by Iowa State University under contract No. W-7405-ENG-82.

REFERENCES

1. E. J. Wheelwright, W. J. Bjorklund, L. M. Browne, G. H. Bryan, L. K. Holton, E. R. Irish and D. H. Siemens, *Nucl. Technol.* 1982, **58**, 271.
2. G. Persson, S. Wingefors, J. O. Liljenzin and I. Svantesson, *Radiochim. Acta* 1984, **35**, 163.
3. M. L. Adolphson, PhD dissertation. Iowa State University, Ames, Iowa (1969).
4. D. J. Sawyer, J. E. Powell and H. R. Burkholder, *J. Chromatog.* 1988, **455**, 193.
5. D. J. Sawyer, PhD dissertation. Iowa State University, Ames, Iowa (1988).
6. D. A. Johnson, PhD dissertation. Iowa State University, Ames, Iowa (1973).
7. J. H. Miller, PhD dissertation. Iowa State University, Ames, Iowa (1977).
8. P. K. Tse, PhD dissertation. Iowa State University, Ames, Iowa (1983).
9. M. W. Potter, PhD dissertation. Iowa State University, Ames, Iowa (1981).
10. A. E. Smith and R. M. Martell, *Critical Stability Constants*, Vol. 1. Plenum Press, New York (1974).

11. J. E. Powell and D. R. Ling, *Inorg. Chem.* 1985, **24**, 2067.
12. V. F. Vasileva, O. Yu. Lavrova, N. N. Dyatlova and V. G. Yashunskii, *Zh. Obshch. Khim.* 1966, **36**, 674.
13. R. L. Hahn and A. Narten, *J. Less Common Metals* 1986, **122**, 233.
14. A. Habenschuss and F. H. Spedding, *J. Chem. Phys.* 1979, **70**, 3758.
15. H. Kanno and J. Hiraishi, *J. Chem. Phys. Lett.* 1980, **75**, 553.
16. J. E. Powell, M. W. Potter, H. R. Burkholder, E. D. H. Potter and P. K. Tse, *Polyhedron* 1982, **1**, 277.

Polyhedron Vol. 8, No. 11, pp. 1431–1436, 1989
Printed in Great Britain

0277–5387/89 $3.00+.00
Pergamon Press plc

SELECTIVE HOMOGENEOUS HYDROGENATION OF BENZOTHIOPHENE AND QUINOLINE CATALYSED BY RUTHENIUM, OSMIUM, RHODIUM AND IRIDIUM COMPLEXES

ROBERTO A. SÁNCHEZ-DELGADO* and EDGAR GONZÁLEZ

Chemistry Centre, Instituto Venezolano de Investigaciones Científicas, I.V.I.C., Apartado 21827, Caracas 1020-A, Venezuela

(*Received* 4 *January* 1989; *accepted* 25 *January* 1989)

Abstract—The homogeneous selective hydrogenation of benzothiophene to 1,2-dihydrobenzothiophene and of quinoline to 1,2,3,4-tetrahydroquinoline is efficiently achieved by the use of $RuCl_2(PPh_3)_3$, $[RuHCl(CO)(PPh_3)_3]$, $[OsHCl(CO)(PPh_3)_3]$, $RhCl(PPh_3)_3$, $[Rh(cod)(PPh_3)_2]PF_6$, and $[Ir(cod)(PPh_3)_2]PF_6$ (cod = cyclooctadiene) at 170°C and 115 bar and 150°C and 30 bar H_2, respectively.

Homogeneous hydrogenation of organic compounds by transition metal complexes has been an area of continuously growing interest, since it has proved to be of great utility in many practical applications and has played a key role in the fundamental understanding of catalytic reactions in general. Although a great proportion of the published papers have dealt with the hydrogenation of C=C bonds, a wide variety of other substrates have been investigated.[1]

One area which has received little attention is the hydrogenation of sulphur- and nitrogen-containing compounds, which is important in connection with industrially important reactions.

Heavy petroleum, tar sands and coal derived liquids contain organic nitrogen and sulphur in varying levels. Nitrogen and sulphur compounds are poisons for cracking and reforming catalysts, and produce polluting oxides on combustion; therefore they must be removed by hydrodesulphurization (HDS) and hydrodenitrogenation (HDN) processes.[2] HDS and HDN are conventionally carried out over molybdenum or tungsten sulphides supported on alumina and promoted by cobalt or nickel.[2] However, it has been reported that sulphides of ruthenium, rhodium, osmium and iridium show the highest activity of all the *d*-block elements for HDS reactions.[3]

It is thus of considerable interest to study the fundamental aspects of the reactions of model sulphur and nitrogen compounds with hydrogen in the presence of these and other transition metals.

Continuing our research programme on the homogeneous hydrogenation of polar organic molecules,[4] in this paper we report our results on the homogeneous hydrogenation of benzothiophene and quinoline catalysed by a series of transition metal complexes. Related work on quinoline hydrogenation has been previously published by Fish *et al.*,[5] by Lynch *et al.*[6a] and by Laine *et al.*[6b] Hydrogenation of benzothiophene (or any S-heterocycle) has been very little studied; while our work was in progress, Fish mentioned this reduction catalysed by $RhCl(PPh_3)_3$[5b] and $RuCl_2(PPh_3)_3$.[5d] There are, to our knowledge, no other reports on this reaction.

RESULTS

The metal complexes used in this work were chosen on the basis of their known catalytic activity for the hydrogenation of polar and/or aromatic molecules. Benzothiophene and quinoline were selected as substrates since they are generally considered as adequate models of petroleum and coal constituents, and have been frequently used as mechanistics probes in heterogeneous HDS and HDN reactions, respectively.[2]

After proper screening, the reaction conditions were chosen as in Tables 1 and 2. Under these

* Author to whom correspondence should be addressed.

Table 1. Homogeneous hydrogenation of benzothiophene[a]

Catalyst	Initial rate[b]	k_n[c]	Relative activity[d]
$[Rh(cod)(PPh_3)_2]PF_6$[e]	6.23±0.38	81±6	2.1
$RuCl_2(PPh_3)_3$[f]	6.14±0.37	56±2	1.8
$[Ir(cod)(PPh_3)_2]PF_6$[e]	5.02±0.12	48.1±2.2	1.3
$RhCl(PPh_3)_3$[f]	3.79±0.09	38±1	1.0
$[OsHCl(CO)(PPh_3)_2]$[f]	2.56±0.05	25.1±0.9	0.7
$[RuHCl(CO)(PPh_3)_3]$[e,g]	2.21±0.12	19.5±0.9	0.5

[a] 170°C, 110 bar H_2, [BT] = 1.3×10^{-1} M, [cat.] = 2.4×10^{-3} M, $V = 35$ cm^3.
[b] Rates in mmol prod. (mmol cat.)$^{-1}$ h^{-1}.
[c] k_n as defined in the text.
[d] Relative activities from k_n values.
[e] In THF.
[f] In toluene.
[g] [cat.] = 1.2×10^{-3} M.

Table 2. Homogeneous hydrogenation of quinoline[a]

Catalyst	Initial rate[b]	k_n[c]	Relative activity[d]
$[Rh(cod)(PPh_3)_2]PF_6$[e]	199.1±4.9	2392±166	4.1
$RuCl_2(PPh_3)_3$[f]	63.3±2.5	1020±60	1.8
$RhCl(PPh_3)_3$[f]	52.3±1.9	580±27	1.0
$[RuHCl(CO)(PPh_3)_3]$[f]	29.0±0.4	306±11	0.5
$[Ir(cod)(PPh_3)_2]PF_6$[e]	17.0±0.5	178±9	0.3
$[OsHCl(CO)(PPh_3)_3]$[g]	5.4±0.2	78±5	0.1

[a] 150°C, 30 bar H_2, [quinoline] = 1.2×10^{-1} M, $V = 35$ cm^3.
[b] Rates in mmol prod. (mmol cat.)$^{-1}$ h^{-1}.
[c] k_n as defined in the text.
[d] Relative activities from k_n values.
[e] 4.1×10^{-4} M in CH_2Cl_2.
[f] 1.3×10^{-3} M in toluene.
[g] 2.3×10^{-3} M in toluene.

conditions, efficient and regiospecific hydrogenation to 1,2-dihydrobenzothiophene and to 1,2,3,4-tetrahydroquinoline (*ca* 100% selectivity for all the complexes) is achieved [eqs (1) and (2)].

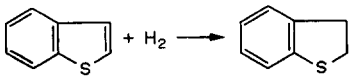

(1)

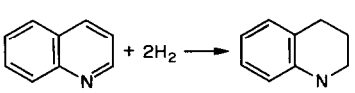

(2)

Representative examples of the catalytic runs are shown in Figs 1 and 2; values of the initial rate (in turnover frequency units) were obtained from the slopes of these straight lines, and are collected in Tables 1 and 2. The observed kinetics in both cases may be expressed by the simple equation $-d[substrate]/dt = k_{obs}[substrate]$, where $k_{obs} = k[H_2][catalyst]$. The integrated form of this equation was plotted as $\log([substrate]_0/[substrate]_t)$ vs t; from the slopes of the straight lines values of $k'_{obs} = k[H_2][catalyst]/2.3$ were obtained. These values were then normalized for comparison purposes by dividing by the concentration of the catalyst, to yield the values of k_n collected in Tables 1 and 2; these values were used to calculate the relative catalytic activities also collected in Tables 1 and 2, where Wilkinson's catalyst, $RhCl(PPh_3)_3$, was arbitrarily assigned a value of 1.0.

Further experiments were carried out in the case of quinoline hydrogenation catalysed by $[RuHCl(CO)(PPh_3)_3]$, in order to gain some insight

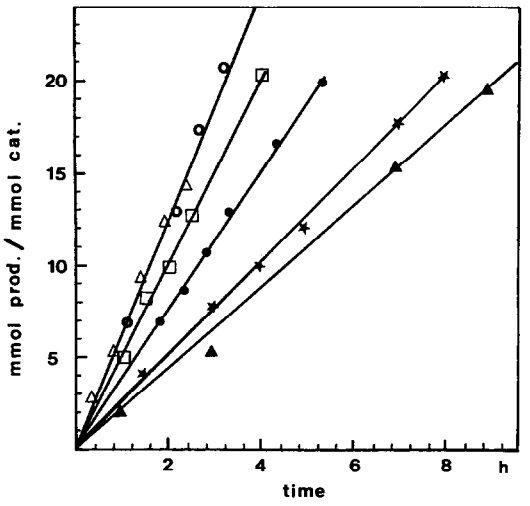

Fig. 1. Homogeneous hydrogenation of benzothiophene catalysed by (○): $[Rh(cod)(PPh_3)_2]PF_6$, (△): $RuCl_2(PPh_3)_3$, (□): $[Ir(cod)(PPh_3)_2]PF_6$, (●): $RhCl(PPh_3)$, (★): $[OsHCl(CO)(PPh_3)_3]$ and (▲): $[RuHCl(CO)(PPh_3)_3]$. Reaction conditions as in Table 1.

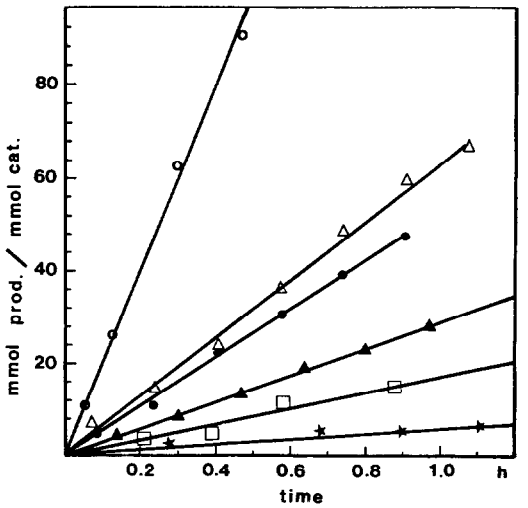

Fig. 2. Homogeneous hydrogenation of quinoline catalysed by (○): $[Rh(cod)(PPh_3)_2]PF_6$, (△): $RuCl_2(PPh_3)_3$, (●): $RhCl(PPh_3)_3$, (▲): $[RuHCl(CO)(PPh_3)_3]$, (□): $[Ir(cod)(PPh_3)_2]PF_6$ and (★): $[OsHCl(CO)(PPh_3)_3]$. Reaction conditions as in Table 2.

into the influence of other reaction parameters such as the nature of the solvent, additives and the reducing gas on the catalytic activity. These data are collected in Table 3.

DISCUSSION

The catalytic precursors used in this work were chosen on the basis of their known activity for other hydrogenation reactions. The $RhCl(PPh_3)_3$ and $RuHCl(PPh_3)_3$ complexes developed by Wilkinson and co-workers have attracted a great deal of attention over the years and are probably the most widely used homogeneous hydrogenation catalysts today.[7]

We have recently shown that complexes of the type $[MHX(CO)(PPh_3)_3]$ (M = Ru, Os) display a rich catalytic chemistry; they are, for instance, amongst the most efficient systems known to hydrogenate C=O bonds.[4]

Finally, the catalytic potential of cationic rhodium and iridium complexes has been successfully exploited by several groups.[1,8] Particularly interesting for our purposes are the kinetic and mechanistic investigations conducted by Halpern and co-workers on the hydrogenation of polynuclear aromatic hydrocarbons.[9]

With these precedents in mind we decided to test these types of compounds as potential catalysts for

Table 3. Hydrogenation of quinoline catalysed by $[RuHCl(CO)(PPh_3)_3]$[a]

Solvent	Additive	%1,2,3,4 THQ	%5,6,7,8 THQ
CH_3CN	—	0	0
CH_3OH	—	7.0	1.0
THF	—	56.0	0
Toluene	—	58.5	1.0
Toluene	H_2O	58.0	0
Toluene	HCl	50.5	0.5
Toluene	Et_3N	44.5	0.5
Toluene	KOH	47.0	0
Toluene	CO[b]	4.0	0
Toluene	CO^b/H_2O	1.0	0
Toluene	CO^b/H_2O/KOH	0	0

[a] 150°C, 30 bar, 2 h, [cat.]–[Q] = 1 : 100; [cat]–[add.] = 5 : 1.
[b] $CO–H_2$ = 1 : 1.

the hydrogenation of heterocyclic aromatic substrates, a subject which has been little developed in the literature.

Analysis of the data collected in Tables 1 and 2 reveals several interesting points: all the ruthenium, osmium, rhodium and iridium complexes tested are indeed very efficient catalysts precursors for the specific hydrogenation of the heterocyclic ring in benzothiophene and quinoline. Fish has previously reported the catalytic activity of $RuCl_2(PPh_3)_3$ and $RhCl(PPh_3)_3$ for these reactions,[5] but to our knowledge, this is the first report on the use of iridium or osmium complexes, or of cationic rhodium derivatives in this type of hydrogenation.

Reduction of the sulphur heterocycle requires more drastic conditions than that of the nitrogen-containing ring. Decomposition of the complexes is not apparent in the time range investigated; prolonged ($\sim$ 24 h) reaction in the hydrogenation of benzothiophene does lead to some decomposition and a consequent loss in catalytic activity. Also, small amounts ($< 1\%$) of ethylbenzene (a product of benzothiophene HDS most likely promoted by metallic particles) are observed in these prolonged reactions.

The relative activities are somewhat different for the two substrates. For benzothiophene (BT) hydrogenation (Fig. 1 and Table 1), the cationic rhodium and iridium diolefin complexes are considerably more active than Wilkinson's catalyst. From the known chemistry of these cationic complexes of rhodium and iridium,[10] we infer that the diene is rapidly hydrogenated and replaced by a substrate molecule, which then enters the catalytic cycle [eq. (3)]:

$$[M(cod)(PPh_3)_3]^+ + BT + 2H_2 \longrightarrow [M(BT)(PPh_3)_2]^+ + \text{cyclooctane.} \quad (3)$$

For chlorophosphine complexes we note that $RuCl_2(PPh_3)_3$ (which generates $RuHCl(PPh_3)_3$ *in situ*) is also more active than $RhCl(PPh_3)_3$. Incorporation of a carbonyl ligand in the coordination sphere as in $[RuHCl(CO)(PPh_3)_3]$ results in a marked drop in the hydrogenation rate. The osmium complex $[OsHCl(CO)(PPh_3)_3]$ is slightly more active than the ruthenium analogue, which is an unusual but not unprecedented observation.[4a]

For quinoline, which is hydrogenated under milder conditions, higher turnover frequencies as well as greater differences in catalytic activities are observed (Fig. 2 and Table 2).

The cationic rhodium complex shows the highest activity also in this case, but the iridium analogue is less active than $RhCl(PPh_3)_3$. Since the mechanism of quinoline reduction is probably very similar to that of benzothiophene, this indicates that iridium requires higher temperatures and H_2 pressures to reach hydrogenation activities comparable to those of rhodium.

$RuCl_2(PPh_3)_3$ is also in this case rapidly transformed into $[RuHCl(PPh_3)_3]$, and hydrogenates quinoline more efficiently than $RhCl(PPh_3)_3$, in agreement with data reported by Fish.[5] As for benzothiophene, incorporation of a CO ligand in the $[RuHCl(CO)(PPh_3)_3]$ complex causes a drop in catalytic activity. The osmium complex, $[OsHCl(CO)(PPh_3)_3]$, is in this case less active than the ruthenium analogue, probably also related to the more forced conditions necessary to activate osmium. It is, however, still a reasonably efficient catalyst, and this adds to the series of homogeneous organic reactions previously reported by us for this type of osmium compound.[4b]

Hydrogenation of the benzene ring does not take place to any detectable extent during hydrogenation of benzothiophene or quinoline, or if pure 1,2-dihydrobenzothiophene or 1,2,3,4-tetrahydroquinoline are used as substrates under the same reaction conditions. Interestingly, isolated heterocycles such as thiophene or pyridine were not hydrogenated by the same metal complexes. This indicates that although the benzene ring is unreactive towards hydrogen under our reaction conditions, its presence is essential in order to activate the heterocyclic rings towards catalytic reduction. This activation may be due to either an electronic effect of the arene making the heterocycle more susceptible to attack by hydrides, or to coordination to the metal centre through the benzene ring, placing the heterocycle in a convenient position to undergo hydrogenation.

On the other hand, the high selectivity for the reduction of the sulphur- and nitrogen-containing rings could be taken as an indication that both benzothiophene and quinoline bind to the metal through the heterocycle and not through the arene ring. We have recently demonstrated that thiophene is π-bonded in the complexes $[M(\eta\text{-thiophene})(PPh_3)_2]PF_6$ (M = Rh, Ir),[10b] and Chaudret and Jalon have shown that both S- and N-heterocycles can be π-bonded to ruthenium in $[C_p^*Ru(arene)]^+$ complexes.[11] Also, Spies and Angelici have reported π-bonded thiophene ruthenium complexes[12] and rhodium and iridium cyclopentadienyl derivatives containing benzothiophene π-coordinated through the arene ring.[13] In the case of quinoline, a further likely coordination mode would be through a metal–nitrogen σ bond, as described recently by Fish in the case of $[Cp^*Rh(quinoline)]^+$ complexes.[14]

For the $[RuHCl(CO)(PPh_3)_3]$-catalysed reduction of quinoline, the data in Table 3 indicate that

strongly coordinating solvents such as CH_3CN totally inhibit the reaction, probably by blocking the coordination sites necessary to activate the substrate. In methanol, a polar, but less strongly coordinating solvent, moderate activity is observed, whilst in THF a much higher conversion is reached. The best solvent seems to be toluene, in terms of activity, solubility and stability.

Addition of water to the reaction mixture causes no effect on the hydrogenation rates, in contrast to other catalytic hydrogenations which are promoted by small amounts of water.[15] On the other hand, addition of acid (HCl) or bases (Et_3N or KOH) produced adverse effects on the catalytic rates. Virtually no hydrogenation was detected if the reactions were carried out under syngas instead of pure hydrogen, or under water gas shift conditions, in opposition with our previous observations that nitro compounds can be efficiently reduced by $[RuHCl(CO)(PPh_3)_3]$, and other metal complexes under H_2, H_2/CO or CO/H_2O.[4d]

EXPERIMENTAL

The complexes $[M(cod)(PPh_3)_2](PF_6)$,[16] $RuCl_2(PPh_3)_3$,[17] $RhCl(PPh_3)_2$,[18] $[RuHCl(CO)(PPh_3)_3]$,[19] and $[OsHCl(CO)(PPh_3)_3]$[20] were prepared by literature procedures. Solvents and quinoline were distilled from appropriate drying agents. Benzothiophene was purified by recrystallization.

A typical hydrogenation run was as follows: the substrate, the catalyst, the solvent and tetrahydronaphthalene (as internal standard) were introduced into a glass-lined stainless steel autoclave fitted with a valve for sampling the solution during the run; the whole operation was carried out inside a nitrogen-filled glove bag or dry box. The sealed autoclave was then taken out and charged to the desired pressure and subsequently introduced into a thermostatted silicone-oil bath. During the run, samples of the reaction mixture were periodically extracted via the sampling valve, and the total pressure of the system was continuously adjusted to a constant value by admitting hydrogen from a high pressure reservoir. Reaction conditions are shown in Tables 1 and 2. The samples were immediately analysed by use of a Varian 3700 gas chromatograph fitted with a flame ionization detector and a Varian CDS-401 Vista data system. A 3 m 20% SP-2100 0.1 CW on 100/200 Supelcoport column at 110°C, and a combination of two columns: 3 m 20% SP-2100 0.1 CW on 100/120 Supelcoport at 55°C for 10 min, then 80°C min^{-1} to 155°C for 28 min, were used for the analysis of benzothiophene and quinoline reactions, respectively.

Each run was repeated at least three times in order to ensure reproducibility. The data were plotted with the aid of conventional graphic computer programs.

Acknowledgements—A Graduate Fellowship from FGMA (to E.G.) and generous financial support from CONICIT (Project S1-1814) are gratefully acknowledged.

REFERENCES

1. B. R. James, *Homogeneous Hydrogenation*. John Wiley, New York (1973); L. H. Pignolet (Ed.), *Homogeneous Catalysis with Metal Phosphine Complexes*. Plenum Press, New York (1983); B. R. James, in *Comprehensive Organometallic Chemistry* (Edited by G. Wilkinson, F. G. A. Stone and E. A. Abel). Pergamon Press, Oxford (1982).
2. J. R. Katzer and R. Sivasubramanian, *Catal. Rev. Sci. Engng* 1979, **20**, 155; R. M. Laine, *Catal. Rev. Sci. Engng* 1983, **25**, 459; S. C. Schuman and H. Shalit, *Catal. Rev.* 1970, **4**, 245; P. C. H. Mitchell, *Catalysis (London)* 1977, **1**, 204; P. C. H. Mitchell, *Catalysis (London)* 1981, **4**, 175; P. Grange, *Catal. Rev. Sci. Engng* 1980, **21**, 135; O. Weisser and S. Landa, *Sulphide Catalysts—Their Properties and Applications*. Pergamon Press, Oxford (1973); H. Topsøe, B. S. Clausen, N.-Y. Topsøe and E. Pedersen, *Ind. Engng Chem. Fundam.* 1986, **25**, 25.
3. T. A. Pecoraro and R. R. Chianelli, *J. Catal.* 1981, **67**, 430; J. P. R. Vissers, C. K. Groot, E. M. van Oers, V. H. J. de Beer and R. Prins, *Bull. Soc. Chim. Belg.* 1984, **93**, 813.
4. (a) R. A. Sánchez-Delgado, N. Valencia, R. L. Márquez-Silva, A. Andriollo and M. Medina, *Inorg. Chem.* 1986, **25**, 1106; (b) R. A. Sánchez-Delgado, A. Andriollo, E. González, N. Valencia, V. León and J. Espidel, *J. Chem. Soc., Dalton Trans.* 1985, 1859; (c) R. A. Sánchez-Delgado and B. A. Oramas, *J. Mol. Catal.* 1986, **36**, 283.
5. (a) R. H. Fish, A. D. Thormodsen and G. A. Cremer, *J. Am. Chem. Soc.* 1982, **104**, 5234; (b) R. H. Fish, J. L. Tan and A. D. Thormodsen, *J. Org. Chem.* 1984, **49**, A500; (c) R. H. Fish, *Ann. N.Y. Acad. Sci.* 1983, **415**, 292; (d) R. H. Fish, J. L. Tan and A. D. Thormodsen, *Organometallics* 1985, **4**, 1743.
6. (a) T. J. Lynch, M. Banah, M. McDougall, H. D. Kaesz and C. R. Porter, *J. Mol. Catal.* 1982, **17**, 109; (b) R. M. Laine, D. W. Thomas and L. W. Cary, *J. Am. Chem. Soc.* 1982, **104**, 1763.
7. F. H. Jardine, *Prog. Inorg. Chem.* 1981, **28**, 63; F. H. Jardine, *Prog. Inorg. Chem.* 1984, **31**, 265.
8. R. R. Schrock and J. A. Osborn, *J. Am. Chem. Soc.* 1976, **98**, 2134, 2143 and 4450; A. S. C. Chan and J. Halpern, *J. Am. Chem. Soc.* 1980, **102**, 838.
9. R. Wilczynski, W. A. Fordyce and J. Halpern, *J. Am. Chem. Soc.* 1983, **105**, 2006.
10. (a) B. R. James, *Adv. Organomet. Chem.* 1979, **17**, 319; (b) R. A. Sánchez-Delgado, R.-L. Márquez-

Silva, J. Puga, A. Tiripicchio and M. Tiripicchio-Camellini, *J. Organomet. Chem.* 1986, **316**, C35.
11. B. Chaudret and F. Jalon, *J. Chem. Soc., Chem. Commun.* 1988, 711.
12. G. H. Spies and R. J. Angelici, *J. Am. Chem. Soc.* 1985, **107**, 5569.
13. S. C. Huckett, L. L. Miller, R. A. Jacobson and R. J. Angelici, *Organometallics* 1988, **7**, 686.
14. R. H. Fish, H.-S. Kim, J. E. Babin and R. D. Adams, *Organometallics* 1988, **7**, 2250.
15. R. A. Sánchez-Delgado and O. L. de Ochoa, *J. Organomet. Chem.* 1980, **202**, 427; R. A. Sánchez-Delgado, A. Andriollo, O. L. de Ochoa, T. Suárez and N. Valencia, *J. Organomet. Chem.* 1981, **209**, 77; R. R. Schrock and J. A. Osborn, *J. Chem. Soc., Chem. Commun.* 1970, 567.
16. R. R. Schrock and J. A. Osborn, *J. Am. Chem. Soc.* 1971, **93**, 2397.
17. T. A. Stephenson and G. Wilkinson, *J. Inorg. Nucl. Chem.* 1966, **28**, 942.
18. J. A. Osborn, F. H. Jardine, J. F. Young and G. Wilkinson, *J. Chem. Soc.* 1966, 1711.
19. N. Ahmad, J. J. Levinson, S. D. Robinson and M. F. Uttley, *Inorg. Synth.* 1974, **15**, 45.
20. L. Vaska, *J. Am. Chem. Soc.* 1964, **86**, 1943.

Polyhedron Vol. 8, No. 11, pp. 1437–1443, 1989
Printed in Great Britain

0277–5387/89 $3.00+.00
© 1989 Pergamon Press plc

CLUSTER CONDENSATIONS. THE DIMERIZATION OF $[Os_3(CO)_9(\mu_3\text{-}CO)(\mu_3\text{-}S)]$

RICHARD D. ADAMS* and JIN-GUU WANG

Department of Chemistry, University of South Carolina, Columbia, SC 29208, U.S.A.

(*Received* 5 *December* 1988; *accepted* 27 *January* 1989)

Abstract—UV irradiation of $[Os_3(CO)_9(\mu_3\text{-}CO)(\mu_3\text{-}S)]$ (**1**) under a CO atmosphere has yielded the new hexaosmium cluster complex $[Os_6(CO)_{20}(\mu_3\text{-}S)(\mu_4\text{-}S)]$ (**2**) in 13% yield (30% based on the amount of **1** consumed). Compound **2** is a dimer of **1** based on its formula, but its structure is considerably different. Compound **2** was characterized by a single-crystal X-ray diffraction analysis. Crystal data: $Os_6S_2O_{20}C_{20}\cdot 1/3CHCl_3\cdot H_2O$, $M = 1759.0$, rhombohedral, $R\bar{3}$ (No. 148), $a = 43.333(9)$, $c = 10.203(1)$ Å, $V = 16592(9)$ Å^3, $D_c = 3.17$ g cm^{-3}, $Z = 18$, λ(Mo-K_α) = 0.71069 Å (graphite monochromator) $\mu = 202.4$ cm^{-1}. Methods: MITHRIL, difference Fourier, full-matrix least-squares. Refinement of 2754 reflections [$F^2 \geqslant 3\sigma(F^2)$], ($1 \leqslant 2\theta \leqslant 43°$), gave R and R_w values of 0.041 and 0.042, respectively. Data/parameters ratio = 11.1, highest peak in final difference Fourier = 1.60 e Å^{-3}. The molecule consists of one cluster of four metal atoms arranged in the form of a planar spiked-triangle, that is linked to a second group of two metal atoms by one quadruply-bridging sulphido ligand and one triply bridging sulphido ligand. The dimerization involved the transfer of one metal atom from one cluster to the second cluster. When **2** is photolysed under an atmosphere of nitrogen, it loses 3 mol of CO and condenses to the known cluster complex $[Os_6(CO)_{17}(\mu_4\text{-}S)_2]$ (**3**).

Sulphido ligands have been shown to promote the formation of cluster compounds by facilitating the aggregation of metal atoms about the sulphur site, and by stabilizing the molecules by serving as bridging ligands.[1–3] We have shown that sulphido ligands can promote the oligomerization of clusters forming both dimers [eqs (1)–(3)][4–6] and cyclotrimers [eq. (4)][7] joined through bridging sulphido ligands. Ligand eliminations from these oligomers can lead to further condensation by the formation of metal–metal bonds. In one case, this was observed to occur by a sequential shift of the metal atoms from one cluster to the other, eq. (5).[6]

We have now investigated the nature of the photo-induced dimerization of $[Os_3(CO)_9(\mu_3\text{-}CO)(\mu_3\text{-}S)]$ (**1**) under a CO atmosphere. The dimeric product $[Os_6(CO)_{20}(\mu_4\text{-}S)(\mu_3\text{-}S)]$ (**2**), was isolated and has been characterized by a single-crystal X-ray diffraction analysis. The results of this study are reported herein.

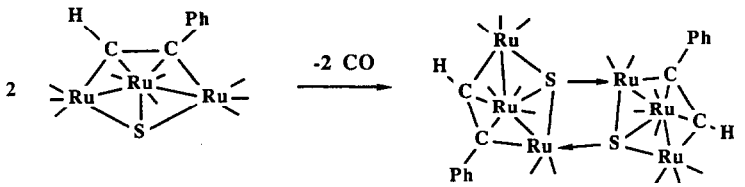

(1)

EXPERIMENTAL

General

$[Os_3(CO)_9(\mu_3\text{-}CO)(\mu_3\text{-}S)]$ (**1**) was prepared as previously reported.[8] CP grade CO was purchased from Linde and was used without further purification. All chromatographic separations were performed in air. TLC separations were performed on silica gel plates (0.25 mm Kieselgel 60 F254, E. Merck, F.R.G.). IR spectra were recorded on a Nicolet 5DXB FT–IR spectrophotometer.

* Author to whom correspondence should be addressed.

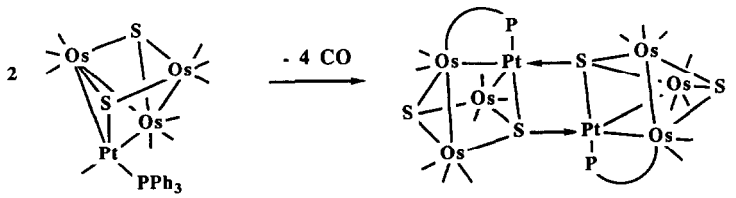

(2)

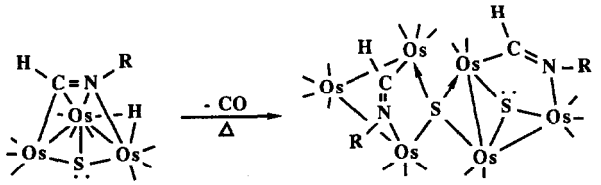

(3)

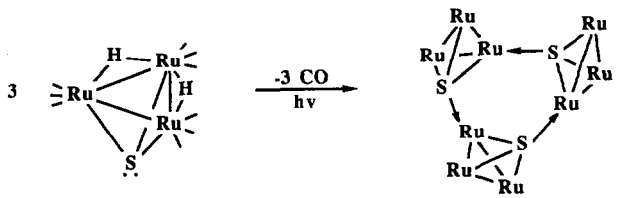

(4)

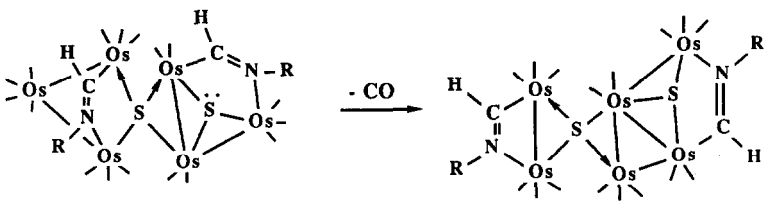

(5)

Preparation of $[Os_6(CO)_{20}(\mu_4\text{-}S)(\mu_3\text{-}S)]$ (**2**)

Compound **1** (80 mg) was dissolved in 30 cm^3 of CH_2Cl_2 and photolysed for 12 h under a CO atmosphere. During this time, the yellow solution turned to a red–brown colour. The solvent was then removed *in vacuo* and the residue was chromatographed by TLC. Elution with a hexane–CH_2Cl_2 (9:1) solvent mixture yielded (in order of elution): yellow $[Os_3(CO)_9(\mu_3\text{-}S)_2]$[9] (1.2 mg), red $[Os_4(CO)_{13}(\mu_3\text{-}S)_2]$[10] (1.7 mg), orange $[Os_4(CO)_{13}(\mu_3\text{-}S)]$[11] (2.7 mg), unreacted **1** (45.5 mg) and red–brown **2** (10.4 mg, 13%). IR for **2**: (ν(CO) in hexane) 2137(w), 2108(s), 2079(s), 2064(vs), 2048(m), 2037(m), 2031(m), 2010(m), 2004(s), 1987(w), 1980(w), 1974(w). Compound **2** can also be obtained, albeit in a lower yield by the UV photolysis of **1** under a N_2 atmosphere for 3.5 h.

Conversion of **2** *to* $[Os_6(CO)_{17}(\mu_4\text{-}S)_2]$ (**3**)

Compound **2** (10.0 mg) was dissolved in 20 cm^3 of CH_2Cl_2 and photolysed for 1 h under a N_2 atmosphere. The red–brown solution turned to a greenish-brown. After removal of the solvent *in vacuo*, the residue was chromatographed by TLC. Elution with a hexane–CH_2Cl_2 (9:1) solvent mixture yielded (in order of elution): $[Os_3(CO)_9(\mu_3\text{-}S)_2]$ (0.7 mg), $[Os_4(CO)_{13}(\mu_3\text{-}S)_3]$ (0.8 mg), $[Os_4(CO)_{13}(\mu_3\text{-}S)]$ (1.5 mg) and green **3** (5.5 mg, 58%).

Crystallographic analysis

Dark brown crystals of **2** were grown from hexane–$CHCl_3$ solutions at −20°C. The data crystal was mounted in a thin-walled glass capillary. Diffraction measurements were made on a Rigaku AFC6 automatic diffractometer using graphite-monochromatized Mo-K_α radiation. The unit cell was determined from 25 randomly selected reflections obtained by using the AFC6 automatic search, centre, index and least-squares routines. Crystal data, data collection parameters and results of the analyses are listed in Table 1. All data processing was performed on a Digital Equipment Corp. MICROVAX II computer by using the TEXSAN structure solving program library (v 2.0), obtained from Molecular Structure Corporation, The Woodlands, Texas. Neutral atom scattering factors were calculated by the standard procedures.[12a] Anomalous dispersion corrections were applied to all atoms.[12b] Full-matrix least-squares refinements minimized

Table 1. Crystallographic data for the structural analysis of **2**

Formula	$Os_6S_2O_{20}C_{20}\cdot 1/3CHCl_3\cdot H_2O$
Formula weight	1759.0
Temperature	23°C
Crystal system	Rhombohedral
Lattice parameters	$a = 43.333(9)$ Å
	$c = 10.203(1)$ Å
	$V = 16592(9)$ Å^3
Space group	$R\bar{3}$ (No. 148)
Z	18
D_{calc} (g cm^{-3})	3.17
μ(Mo-K_α) (cm^{-1})	202.4
Radiation	Mo-K_α
Absorption correction	Empirical
Transmission coefficients (Maximum; Minimum)	1.00; 0.57
2θ maximum (°)	43.0
Number of observations [$I > 3\sigma(I)$]	2754
Number of variables	248
R, R_w	0.041, 0.042
Goodness-of-fit	1.44
Maximum shift on final cycle	0.17
Largest peak in final difference	1.60 (e$^-$ Å^3)

the function:

$$\sum_{hkl} w(|F_{obs}| - |F_{calc}|)^2,$$

where

$$w = 1/\sigma(F)^2, \quad \sigma(F) = (F_{obs}^2)/2F_{obs}$$

and

$$\sigma(F_{obs}^2) = [\sigma(I_{raw})^2 + (PF_{obs}^2)^2]^{1/2}/Lp.$$

Compound **2** crystallized in the rhombohedral crystal system. A statistical analysis of the data indicated a centrosymmetrical space group. The space group, $R\bar{3}$, was selected and confirmed by the successful solution and refinement of the structure. The structure was solved by a combination of direct methods (MITHRIL) and difference Fourier syntheses. All atoms larger than oxygen were refined using anisotropic thermal parameters. In the final stages of the refinement a molecule of $CHCl_3$ from the crystallization solvent was located in the lattice. Its carbon atom was located on a three-fold symmetry site. An additional peak was observed in a general position about 3 Å from the chlorine atoms. It was approximately the size of an oxygen atom, and was suspected to be an H_2O of crystallization. It was satisfactorily refined with this assignment although its hydrogen atoms were not located. Error analyses were calculated from the inverse matrix obtained on the final cycle of refinement.*

RESULTS AND DISCUSSION

The new compound $[Os_6(CO)_{20}(\mu_4\text{-}S)(\mu_3\text{-}S)]$ (**2**), was obtained as the principal product, 13% yield (30% yield based on the amount of reagent consumed), when solutions of $[Os_3(CO)_9(\mu_3\text{-}CO)(\mu_3\text{-}S)]$ (**1**) were irradiated (UV) for 12 h under a CO atmosphere. Small amounts of the known cluster complexes $[Os_3(CO)_9(\mu\text{-}S)_2]$,[9] $[Os_4(CO)_{13}(\mu_3\text{-}S)_2]$[10] and $[Os_4(CO)_{13}(\mu_3\text{-}S)]$[11] were also obtained. The molecular structure of **2** was established by a single-crystal X-ray diffraction analysis. An ORTEP drawing of the structure of **2** is shown in Fig. 1. Selected intramolecular bond distances and angles are listed in Tables 2 and 3, respectively. The six osmium atoms in **2** are arranged in two groups consisting of four and two atoms. The group of four consists of a triangle of three with the fourth bonded only to one of the three and lying in the plane of the triangle. Two of the Os—Os distances within the triangular group are nearly equal in length, Os(1)—Os(3) = 2.955(2) Å and Os(2)—Os(3) = 2.945(2) Å, but are much longer than the third distance, Os(1)—Os(2) = 2.803(2) Å. The Os—Os distances in $Os_3(CO)_{12}$, 2.878(3) Å,[13] lie approximately midway between these limiting

*Complete tables of bond lengths, angles, atomic coordinates, thermal parameters, and observed and calculated structure factors for **2** have been deposited as supplementary material with the Editor, from whom copies are available upon request. Atomic coordinates have also been deposited with the Cambridge Crystallographic Data Centre.

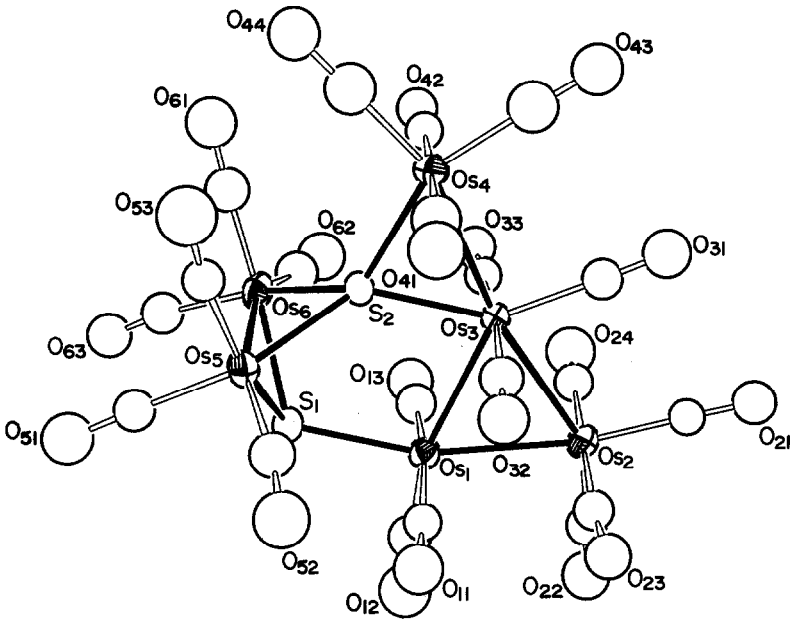

Fig. 1. An ORTEP drawing of $[Os_6(CO)_{20}(\mu_4\text{-}S)(\mu_3\text{-}S)]$ (**2**) showing 50% probability thermal ellipsoids.

values, while the sulphur-bridged bond Os(3)—Os(4) = 2.878(2) Å is identical to that in $Os_3(CO)_{12}$. The metal atoms in the two-atom group are mutually bonded at the short distance of 2.716(2) Å. The shortness of this bond may be due to contraction effects from the two bridging sulphido ligands. Similarly short Os—Os distances have been observed in other doubly-bridged diosmium groupings.[6,14] The two groups of metal atoms are held together by two bridging sulphido ligands. Ligand S(2) is a quadruple bridge that bridges both atoms of the two-atom group and Os(3)—Os(4) of the four-atom group. The Os—S(2) bond distances are normal, 2.360(7)–2.404(7) Å. The Os—S(2)—Os angles between metal atoms that are bonded are small, 74.6(2) and 68.9(2)°, while those between non-bonded metal atoms are very large, range 129.1(3)–132.3(3)°. Similar values were observed for the sulphido ligands in the compound $[Os_6(CO)_{18}(\mu_4\text{-}S)_2(\mu\text{-}HC{=}NPh)_2]$.[14] Ligand S(1) is a triple bridge that bridges both atoms of the two-atom group, but extends only to Os(1) of the four-atom group. The Os—S(1) bond distances are all slightly longer than those to S(2), 2.464(7), 2.423(8) and 2.435(7) Å. The Os(5)—S(1)—Os(6) angle is similar to the Os—S—Os angles between the bonded metal atoms and S(2), but the angles between the non-bonded metal atoms are much smaller than those about S(2), 114.5(3) and 114.3(3)°. The osmium atoms of the four-atom group all lie in a plane within ±0.002 Å, while the vector between Os(5) and Os(6) is nearly perpendicular to this. The molecule contains 20 linear terminal carbonyl ligands distributed among the metal atoms as shown in Fig. 1. Assuming that S(1) serves as a four-electron donor and S(2) serves as a six-electron donor, then all of the metal atoms can achieve 18 electron configurations. The most interesting feature about the formation of **2** is that one

Table 2. Intramolecular distances for **2**

Atom	Atom	Distance	Atom	Atom	Distance
Os(1)	C(12)	1.80(4)	Os(4)	C(43)	1.90(4)
Os(1)	C(13)	1.81(3)	Os(4)	C(42)	1.90(3)
Os(1)	C(11)	1.93(3)	Os(4)	C(41)	1.95(3)
Os(1)	S(1)	2.464(7)	Os(4)	S(2)	2.388(7)
Os(1)	Os(2)	2.803(2)	Os(5)	C(52)	1.86(3)
Os(1)	Os(3)	2.955(2)	Os(5)	C(51)	1.90(3)
Os(2)	C(21)	1.86(3)	Os(5)	C(53)	1.91(3)
Os(2)	C(24)	1.86(3)	Os(5)	S(2)	2.396(7)
Os(2)	C(22)	1.87(3)	Os(5)	S(1)	2.423(8)
Os(2)	C(23)	1.90(3)	Os(5)	Os(6)	2.716(2)
Os(2)	Os(3)	2.945(2)	Os(6)	C(61)	1.85(4)
Os(3)	C(31)	1.88(3)	Os(6)	C(62)	1.88(4)
Os(3)	C(33)	1.91(3)	Os(6)	C(63)	1.89(3)
Os(3)	C(32)	1.93(3)	Os(6)	S(2)	2.404(7)
Os(3)	S(2)	2.360(7)	Os(6)	S(1)	2.435(7)
Os(3)	Os(4)	2.878(2)	O	C(av)	1.15(3)
Os(4)	C(44)	1.87(4)			

Distances are in angstroms. Estimated standard deviations in the least significant figure are given in parentheses.

Table 3. Intramolecular bond angles for **2**

Atom	Atom	Atom	Angle	Atom	Atom	Atom	Angle
C(12)	Os(1)	S(1)	96(1)	C(43)	Os(4)	S(2)	153(1)
C(12)	Os(1)	Os(2)	103(1)	C(43)	Os(4)	Os(3)	100(1)
C(12)	Os(1)	Os(3)	164(1)	C(42)	Os(4)	S(2)	88.6(9)
C(13)	Os(1)	S(1)	87(1)	C(42)	Os(4)	Os(3)	89.8(8)
C(13)	Os(1)	Os(2)	94(1)	C(41)	Os(4)	S(2)	90(1)
C(13)	Os(1)	Os(3)	94(1)	C(41)	Os(4)	Os(3)	90(1)
C(11)	Os(1)	S(1)	88.7(8)	S(2)	Os(4)	Os(3)	52.2(2)
C(11)	Os(1)	Os(2)	92.1(8)	C(52)	Os(5)	S(2)	111(1)
C(11)	Os(1)	Os(3)	93.3(8)	C(52)	Os(5)	S(1)	102(1)
S(1)	Os(1)	Os(2)	161.0(2)	C(52)	Os(5)	Os(6)	155(1)
S(1)	Os(1)	Os(3)	99.5(2)	C(51)	Os(5)	S(2)	152.3(9)
Os(2)	Os(1)	Os(3)	61.46(4)	C(51)	Os(5)	S(1)	90.0(9)
C(21)	Os(2)	Os(1)	167.5(8)	C(51)	Os(5)	Os(6)	96.6(9)
C(21)	Os(2)	Os(3)	106.0(8)	C(53)	Os(5)	S(2)	91.2(9)
C(24)	Os(2)	Os(1)	91(1)	C(53)	Os(5)	S(1)	159.5(9)
C(24)	Os(2)	Os(3)	88(1)	C(53)	Os(5)	Os(6)	103.3(8)
C(22)	Os(2)	Os(1)	91(1)	S(2)	Os(5)	S(1)	76.2(2)
C(22)	Os(2)	Os(3)	153(1)	S(2)	Os(5)	Os(6)	55.7(2)
C(23)	Os(2)	Os(1)	88.8(9)	S(1)	Os(5)	Os(6)	56.2(2)
C(23)	Os(2)	Os(3)	92.6(9)	C(61)	Os(6)	S(2)	92(1)
Os(1)	Os(2)	Os(3)	61.80(4)	C(61)	Os(6)	S(1)	160(1)
C(31)	Os(3)	S(2)	144(1)	C(61)	Os(6)	Os(5)	104(1)
C(31)	Os(3)	Os(4)	90.7(9)	C(62)	Os(6)	S(2)	112(1)
C(31)	Os(3)	Os(2)	78.9(9)	C(62)	Os(6)	S(1)	103(1)
C(31)	Os(3)	Os(1)	135.6(9)	C(62)	Os(6)	Os(5)	156(1)
C(33)	Os(3)	S(2)	88.8(9)	C(63)	Os(6)	S(2)	153(1)
C(33)	Os(3)	Os(4)	92.6(9)	C(63)	Os(6)	S(1)	93(1)
C(33)	Os(3)	Os(2)	88.1(9)	C(63)	Os(6)	Os(5)	98(1)
C(33)	Os(3)	Os(1)	84.8(9)	S(2)	Os(6)	S(1)	75.8(2)
C(32)	Os(3)	S(2)	89(1)	S(2)	Os(6)	Os(5)	55.4(2)
C(32)	Os(3)	Os(4)	91.4(9)	S(1)	Os(6)	Os(5)	55.8(2)
C(32)	Os(3)	Os(2)	89.0(9)	Os(5)	S(1)	Os(6)	68.0(2)
C(32)	Os(3)	Os(1)	88.2(9)	Os(5)	S(1)	Os(1)	114.5(3)
S(2)	Os(3)	Os(4)	53.1(2)	Os(6)	S(1)	Os(1)	114.3(3)
S(2)	Os(3)	Os(2)	137.2(2)	Os(3)	S(2)	Os(4)	74.6(2)
S(2)	Os(3)	Os(1)	80.5(2)	Os(3)	S(2)	Os(5)	132.3(3)
Os(4)	Os(3)	Os(2)	169.66(5)	Os(3)	S(2)	Os(6)	131.1(3)
Os(4)	Os(3)	Os(1)	133.60(5)	Os(4)	S(2)	Os(5)	131.4(3)
Os(2)	Os(3)	Os(1)	56.74(4)	Os(4)	S(2)	Os(6)	129.1(3)
C(44)	Os(4)	S(2)	108(1)	Os(5)	S(2)	Os(6)	68.9(2)
C(44)	Os(4)	Os(3)	160(1)				

Angles are in degrees. Estimated standard deviations in the least significant figure are given in parentheses.

metal atom was shifted from one triosmium cluster to the other to produce the 4 : 2 distribution of metal atoms. Clearly, the sulphido ligands have played a key role in the linking of the two triosmium clusters and in the redistribution of the metal atoms. Since **2** contains 20 CO ligands there was overall no loss of CO, nevertheless, it is believed that the UV irradiation initiates the reaction by the decarbonylation of one of the two clusters of **1** involved in the formation of **2**. This paves the way for the linking of the two clusters through a sulphido bridge by the formation of a donor–acceptor bond, by using the lone pair of electrons on the sulphido ligand of one cluster and the vacant site generated by the loss of CO on the second cluster. Such a complex is represented by the intermediate **A** shown in Scheme 1. Intermediate **A** could reasonably isomerize to **B** by shifting S(2) into a bridging position across Os(5) and Os(6) and shifting the triply bridging CO ligands to terminal positions on Os(2)

and Os(5). Intermediate **B** has a close structural similarity to the compound $[Os_6(CO)_{17}(\mu\text{-}HC{=}NC_6H_4\text{-}p\text{-}F)_2(\mu_3\text{-}S)(\mu_4\text{-}S)(\mu\text{-}H)_2]$ (**4**).[6] Addi-

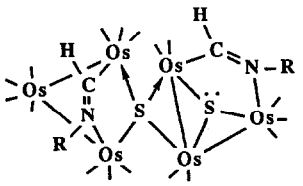

4

tion of CO to **B** at Os(4) could cause cleavage of the Os(4)—S(1) bond, which could then transform to **C** by formation of a donor–acceptor bond between Os(1) and S(2). Intermediate **C** contains two triply-bridging sulphido ligands. The formation of a donor–acceptor bond between S(2) and Os(4) would induce the opening of the Os(4)—Os(5)—Os(6) cluster by cleavage of the Os(4)—Os(5) bond and yield **D**. The formation of **2** would be completed by an isomerization that would involve cleavage of the Os(4)—Os(6) bond and formation of a bond between Os(3) and Os(4). This could be facile, since the Os(4)—Os(6) bond in **D** could be viewed as a donor–acceptor metal–metal bond.

When solutions of **2** were photolysed in the absence of CO, **2** lost three moles of CO and was converted into the known compound $[Os_6(CO)_{17}(\mu_4\text{-}S)_2]$ (**3**) in 58% yield.[14] Small amounts of $[Os_4(CO)_{13}(\mu_4\text{-}S)_2]$, $[Os_4(CO)_{13}(\mu_3\text{-}S)]$ and $[Os_3(CO)_9(\mu_3\text{-}S)_2]$ were also obtained. Compound **3** can be obtained in 44% yield directly by

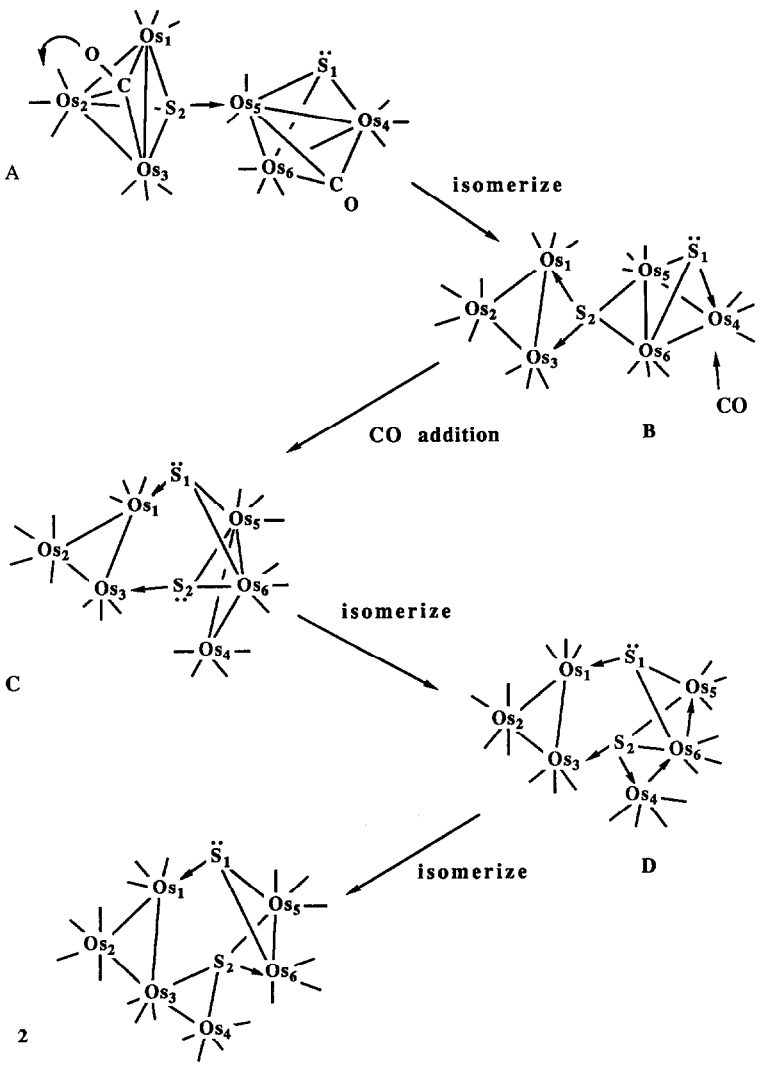

Scheme 1.

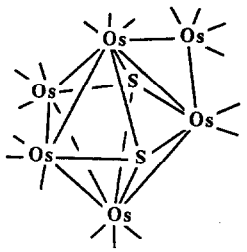

3

UV irradiation of solutions of **1**.[8] The transformation of **2** to **3** has involved a considerable rearrangement of the structure of **2**. We have not observed any of the intermediates that must have been traversed in this process. Thus, we do not, at this time, wish to propose a mechanism for this process.

Acknowledgement—This research was supported by the National Science Foundation under Grant CHE-8612862.

REFERENCES

1. R. D. Adams, *Polyhedron* 1985, **4**, 2003.
2. H. Vahrenkamp, *Angew. Chem. Int. Ed. Engl.* 1975, **14**, 322.
3. K. H. Whitmire, *J. Coord. Chem.* 1988, **17**, 95.
4. R. D. Adams, J. E. Babin and T. A. Wolfe, *Polyhedron* 1989, **8**, 1123.
5. R. D. Adams and T. S. A. Hor, *Organometallics* 1984, **3**, 1915.
6. R. D. Adams, Z. Dawoodii, D. F. Foust and B. E. Segmüller, *J. Am. Chem. Soc.* 1983, **105**, 831.
7. R. D. Adams, D. Mannig and B. E. Segmüller, *Organometallics* 1983, **2**, 149.
8. R. D. Adams, I. T. Horváth and H. S. Kim, *Organometallics* 1984, **3**, 548.
9. (a) B. F. Johnson, J. Lewis, P. G. Lodge, P. R. Raithby, K. Henrick and M. McPartlin, *J. Chem. Soc., Chem. Commun.* 1979, 719; (b) R. D. Adams, I. T. Horváth, B. E. Segmüller and L. W. Yang, *Organometallics* 1983, **2**, 144.
10. R. D. Adams, I. T. Horváth, P. Mathur, B. E. Segmüller and L. W. Wang, *Organometallics* 1983, **2**, 1078.
11. R. D. Adams, I. T. Horváth, B. E. Segmüller and L. W. Yang, *Organometallics* 1983, **2**, 1301.
12. *International Tables for X-ray Crystallography*, Vol. IV. Kynoch Press, Birmingham, U.K. (1975): (a) Table 2.2B, pp. 99–101; (b) Table 2.3.1, pp. 149–150.
13. M. R. Churchill and B. G. DeBoer, *Inorg. Chem.* 1977, **16**, 878.
14. R. D. Adams, I. T. Horváth and L. W. Yang, *J. Am. Chem. Soc.* 1983, **105**, 1533.

Polyhedron Vol. 8, No. 11, pp. 1445–1446, 1989
Printed in Great Britain

0277–5387/89 $3.00+.00
Pergamon Press plc

THE STRUCTURES OF Ph_3PICl AND Ph_3PIBr

KEITH B. DILLON* and JAMES LINCOLN

Chemistry Department, University of Durham, South Road, Durham DH1 3LE, U.K.

(*Received* 5 *July* 1988; *accepted after revision* 27 *January* 1989)

Abstract—The compounds Ph_3PICl and Ph_3PIBr, formed by reaction between Ph_3P and ICl or IBr, respectively, in non-polar solvents, have been shown to have the ionic structures $Ph_3PI^+X^-$ by means of solid state ^{31}P NMR spectroscopy.

Tertiary phosphines react readily with halogens to form phosphorus(V) derivatives, eq. (1):

$$R_3P + X_2 \longrightarrow R_3PX_2. \quad (1)$$

When R = Ph and X = Cl, Br or I, the products have ionic phosphonium salt structures $R_3PX^+X^-$, as has been demonstrated by solid state ^{31}P NMR spectroscopy.[1,2] Conductometric studies in MeCN as solvent have also shown the formation of ionic products at a 1:1 molar ratio of reactants.[3] Previous solution work on reactions of interhalogens with Ph_3P has led to rather confusing results, however. Conductance measurements on the Ph_3P–IBr systems in MeCN showed a break in the plot at a 1:1 molar ratio of reactants, but the yellow solid isolated from the solution analysed as $Ph_3PI_{1.5}Br_{0.5}$.[3] A 1:2 reaction product $Ph_3P(IBr)_2$, could also be isolated, and this, too, was a 1:1 electrolyte. Structures were suggested for these complexes of $[Ph_3PBr]^+[Ph_3PI]^+(I^-)_2$ and $[Ph_3PBr]^+[I_2Br]^-$, respectively. The related compounds Ph_3PI_3Br and Ph_3PIBr_3 were similarly obtained from 1:1 reactions of Ph_3PI_2 with IBr, and of Ph_3PBr_2 with IBr. These, too, were assigned ionic structures, with the cation containing the halogen of lower atomic number. The 1:1 product Ph_3PIBr was not described. More recently, the Ph_3P:ICl system in MeCN has been shown to give breaks in the conductance plot at 3:2 and 3:4 molar ratios of the reactants, and an explanation for this behaviour has been proposed.[4] The compound Ph_3PICl was isolated as a yellow crystalline solid, however, by adding anhydrous diethyl ether to a 1:0.5 mixture of Ph_3P and ICl_3 in MeCN. It gave good elemental analyses, but its structure was not discussed.

We have now prepared the compounds Ph_3PICl and Ph_3PIBr as yellow solids by stoichiometric reactions between Ph_3P and ICl or IBr, respectively, in non-polar solvents. They have been shown to have the ionic structures $Ph_3PI^+X^-$ (X = Cl or Br) by means of solid state ^{31}P NMR spectroscopy.

EXPERIMENTAL

All manipulations including NMR sample preparation were carried out either under an inert atmosphere of dry nitrogen or *in vacuo*. Diethyl ether was dried over sodium, and other solvents were dried over molecular sieve. Triphenylphosphine was recrystallized from toluene. Other reagents were obtained commercially and were used without further purification. The compound Ph_3PICl was prepared by treating a solution of Ph_3P in diethyl ether with an equimolar quantity of ICl dissolved in benzene. The yellow solid which precipitated was separated in an inert atmosphere box. For Ph_3PIBr, which had not been described previously in the literature, equimolar quantities of Ph_3P and IBr were dissolved separately in dichloromethane and the solutions were mixed, with stirring. The bright yellow solid was separated and dried *in vacuo*. (Found: C, 47.5; H, 4.2; P, 6.6; I, 26.9; Br, 16.8. $C_{18}H_{15}BrIP$ requires: C, 46.1; H, 3.2; P, 6.6; I, 27.1; Br, 17.0%.) The NMR results indicate that it should be named and formulated as iodotriphenylphosphonium bromide, $Ph_3PI^+Br^-$.

Elemental analyses and ^{31}P NMR spectra were obtained as described in previous papers.[2,5,6] ^{31}P chemical shifts were measured relative to external 85% H_3PO_4, with the downfield (higher frequency) direction taken as positive.

* Author to whom correspondence should be addressed.

RESULTS AND DISCUSSION

The compounds Ph_3PICl and Ph_3PIBr were both isolated as yellow solids, as described above. Their solid state ^{31}P NMR spectra were recorded and the results are shown in Table 1, together with the previously reported solid state data for Ph_3PCl_2,[2] Ph_3PBr_2[1] and Ph_3PI_2.[1] The results show conclusively that Ph_3PICl has the ionic phosphonium salt structure $Ph_3PI^+Cl^-$ in the solid state. This deduction is consistent with solution state NMR results for the Ph_3PCl^+ cation, which gives shifts of 64.2 ± 2.2 ppm, irrespective of both counter-ion and solvent,[2,7-18] apart from one report of a value of 56.3 ppm in $MeNO_2$.[14]

The results for Ph_3PIBr are less clear-cut, since the shift difference between Ph_3PBr_2 and Ph_3PI_2 in the solid state is quite small. Nevertheless, the value obtained (Table 1) is clearly compatible with the formulation of this compound, too, as a salt of the Ph_3PI^+ cation. This conclusion is again consistent with solution data for the Ph_3PBr^+ cation, for which values of 48.3 ± 0.2 in $PhNO_2$[1] and 49.0 in 25 oleum[18] have been reported. It is also noteworthy that freshly-prepared Ph_3PI_2 is yellow, whereas Ph_3PCl_2 and Ph_3PBr_2 are white. We therefore conclude that the halogen with the higher atomic number is present in the cation in both instances, unlike some of the species deduced to be present from conductance studies in MeCN.[3,4] This discrepancy may be readily rationalized, however, since the compounds isolated in this work are unlikely to be stable in polar solvents. They are stabilized by precipitation as solids from less polar media, but the weakness of the P—I bond makes it susceptible to attack by lighter halide ions if the compound is brought into solution. In keeping with this premise, an attempt to obtain a solution ^{31}P NMR spectrum from Ph_3PICl in $PhNO_2$ resulted in the appearance of three resonances, at 66.0 ± 0.1 (Ph_3PCl^+), 34.7 ± 0.2 (possibly Ph_3PI^+), and -21.8 ± 0.3 ppm, the third peak remaining unassigned. A solution of Ph_3PIBr in $PhNO_2$ showed a single peak only, at 40.5 ± 0.4 ppm, in good agreement with the solid state value and probably due to the Ph_3PI^+ cation. This result suggests that Ph_3PIBr is more stable in solution than Ph_3PICl, which does not seem unreasonable since there will be a much larger difference in bond strength between P—Cl and P—I bonds than between P—Br and P—I bonds. Hence attack by Cl^- ions on the Ph_3PI^+ cation is expected to be more facile than attack by Br^- ions.

Table 1. δ ^{31}P (ppm) for solid Ph_3PXY and Ph_3PX_2 compounds

Compound	δ ^{31}P	Reference
Ph_3PICl	40.5 ± 2	This work
Ph_3PIBr	41.7 ± 2	This work
Ph_3PCl_2	62.0 ± 8	2
Ph_3PBr_2	48.6 ± 0.5	1
Ph_3PI_2	42.5 ± 1.0	1

Acknowledgement—We thank Dr A. Royston for assistance in recording the ^{31}P NMR spectra.

REFERENCES

1. K. B. Dillon and T. C. Waddington, *Nature Phys. Sci.* 1971, **230**, 158.
2. K. B. Dillon, R. J. Lynch, R. N. Reeve and T. C. Waddington, *J. Chem. Soc., Dalton Trans.* 1976, 1243.
3. A. D. Beveridge, G. S. Harris and F. Inglis, *J. Chem. Soc. A* 1966, 520.
4. M. Farhat Ali and G. S. Harris, *J. Chem. Soc., Dalton Trans.* 1980, 1545.
5. K. B. Dillon, R. N. Reeve and T. C. Waddington, *J. Chem. Soc., Dalton Trans.* 1977, 1410.
6. K. B. Dillon, A. W. G. Platt and T. C. Waddington, *J. Chem. Soc., Dalton Trans.* 1980, 1036.
7. G. A. Wiley and W. R. Stine, *Tetrahedron Lett.* 1967, 2321.
8. D. B. Denney, D. Z. Denney and B. C. Chang, *J. Am. Chem. Soc.* 1968, **90**, 6332.
9. H. P. Latscha, *Z. Naturfor.* 1968, **23b**, 139.
10. A. Schmidpeter and H. Brecht, *Angew. Chem. Int. Edn Engl.* 1967, **6**, 564.
11. K. B. Dillon, R. J. Lynch, R. N. Reeve and T. C. Waddington, *J. Inorg. Nucl. Chem.* 1974, **36**, 815.
12. K. B. Dillon, R. N. Reeve and T. C. Waddington, *J. Inorg. Nucl. Chem.* 1976, **38**, 1439.
13. B. V. Timokhin, V. P. Feshin, V. I. Dmitriev, V. I. Glukhikh, G. V. Dolgushin and M. G. Voronkov, *Dokl. Akad. Nauk SSSR (Engl. transl.)* 1977, **236**, 966.
14. B. V. Timokhin, V. I. Dmitriev, V. I. Glukhikh and N. A. Korchevin, *Bull. Acad. Sci. USSR, Div. Chem. Sci.* 1978, **27**, 1160.
15. B. V. Timokhin, V. N. Dudnikova, V. A. Kron and V. I. Glukhikh, *Zh. Org. Khim. (Engl. transl.)* 1979, **15**, 337.
16. K. B. Dillon, N. D. Khabbass and C. J. Ludman, unpublished work; N. D. Khabbass, PhD thesis. Durham (1981).
17. B. V. Timokhin, V. N. Vengel'nikova, A. V. Kalabina and V. I. Donskikh, *J. Gen. Chem. USSR* 1981, **51**, 1307.
18. K. B. Dillon, M. P. Nisbet and T. C. Waddington, *Polyhedron* 1982, **1**, 123.

Polyhedron Vol. 8, No. 11, pp. 1447–1451, 1989
Printed in Great Britain

0277-5387/89 $3.00+.00
© 1989 Pergamon Press plc

SYNTHESIS AND SPECTRAL STUDIES OF METALLOPORPHYRINS OF IRON, COBALT, COPPER AND RHODIUM WITH CARBON, NITROGEN AND SULPHUR DONOR LIGANDS

MORTEZA MASSOUDIPOUR, SHARAD KUMAR TEWARI and KRISHNA KUMAR PANDEY*

Department of Chemistry, Devi Ahilya University Indore, Khandwa Road, Indore 452 001, India

(*Received* 27 *September* 1988; *accepted after revision* 27 *January* 1989)

Abstract—[Rh(TPP)Cl] (TPP = *meso*-tetraphenylporphyrin) was prepared by reaction of [$RhCl_3 \cdot 3H_2O$] with HCHO in the presence of H_2TPP. Reaction of this complex with COS yielded [Rh(TPP)(CO)Cl]. $S_3N_3Cl_3$ reacted with [Fe(TPP)Cl] in THF in the presence of iron powder to give the air-sensitive complex [Fe(TPP)(NS)]. Reaction of $SOCl_2$ with [Fe(TPP)Cl] in the presence of zinc dust yielded [Fe(TPP)(SO_2)]. [Cu(TPP)(COS)] was prepared by interaction of COS with [Cu(TPP)]. Reaction of the blue solution of S_7NH with [M(TPP)] (M = Cu, Co) and [Co(TNPP)] (TNPP = *meso*-tetrakis(2-nitrophenyl)porphyrin) yielded [Cu(TPP)(S_3N)], [Co(TPP)(S_3N)] and [Co(TNPP)(S_3N)] complexes. Reaction of C_5H_6 with [Fe(TPP)Cl] in the presence of zinc dust yielded [Fe(TPP)(C_5H_5)], which reacted with NO to afford [Fe(TPP)(C_5H_5)(NO)]. These complexes have been characterized by elemental analysis, IR and electronic spectroscopy.

The reactions of the diatomic molecules O_2, NO and CO with metalloporphyrins and their relationship to the corresponding haemoprotein complexes have been intensively investigated.[1–8] Synthesis, structure and bonding of the transition metal complexes with ligands such as NS,[9–13] NSO,[14–16] NSO_2,[17] NS_2,[18] NS_3[19–25] and COS[26,27] have been a subject of much current interest. However, the complexes of metalloporphyrins with these ligands have not yet been described. We have recently reported for the first time the synthesis and characterization of a disulphidothionitrato(tetraphenylporphyrinato)iron(III) complex.[21] Herein we wish to report reactions of S_7NH, $S_3N_3Cl_3$, COS, $SOCl_2$, NO and C_5H_6, in the presence of zinc, with metalloporphyrins. A simple synthetic route for [Rh(TPP)Cl] by reaction of [$RhCl_3 \cdot 3H_2O$] with HCHO in the presence of H_2TPP has also been reported.

EXPERIMENTAL

All the reagents used were AnalaR or of chemically pure grade. The solvents were dried by standard procedures and were freshly distilled and degassed before use. Every reaction was carried out under dry nitrogen. H_2(TPP), H_2(TNPP), [Co(TPP)], [Cu(TPP)], S_7NH, $S_3N_3Cl_3$, COS and NO were prepared as previously described.[28–35]

The analyses for sulphur and chloride in the complexes were carried out by using standard methods.[36,37] Carbon and hydrogen in the complexes were analysed by the microanalytical section of the Central Drug Research Institute, Lucknow and the Indian Institute of Technology, Kanpur. The results are reported in Table 1. The IR spectra of samples were recorded with a Perkin–Elmer Model 580 spectrometer using KBr pellets. The electronic spectra of the samples were recorded with a Varian 634S and Simadzu-160 spectrophotometer. Important IR frequencies and the electronic data of the complexes are given in Table 2.

(a) *Chloro*(meso-*tetraphenylporphyrinato*)*rhodium* (III), [Rh(TPP)(Cl)]

To a solution of [$RhCl_3 \cdot 3H_2O$] (0.2 g, 0.76 mmol) in ethylene glycol (20 cm^3), formaldehyde (10 cm^3) was added and the resulting solution was refluxed until the colour of solution changed to pale yellow.

* Author to whom correspondence should be addressed.

Table 1. Analytical data of the metalloporphyrin complexes

Compound	Melting point (°C)	Elemental analysis (%) calculated (found)				
		C	N	H	Cl	S
[Rh(TPP)Cl]	> 300	70.4	7.5	3.6	4.9	—
		(70.3)	(7.4)	(3.7)	(4.7)	
[Rh(TPP)(CO)Cl]	> 300	69.3	7.3	3.7	4.7	—
		(69.4)	(7.2)	(3.6)	(4.5)	—
[Fe(TPP)(NS)]	> 300	73.8	9.7	3.8	—	4.7
		(74.0)	(9.8)	(3.9)	—	(4.5)
[Fe(TPP)(SO_2)]	> 300	72.0	7.8	3.6	—	4.5
		(72.1)	(7.7)	(3.8)	—	(4.4)
[Co(TPP)(S_3N)]	> 300	67.4	8.8	3.5	—	12.5
		(67.6)	(9.0)	(3.6)	—	(12.3)
[Cu(TPP)(S_3N)]	> 300	67.4	8.8	3.4	—	12.3
		(67.2)	(8.9)	(3.6)	—	(12.2)
[Co(TNPP)(S_3N)]	> 300	55.0	12.8	2.3	—	10.2
		(54.9)	(13.0)	(2.5)	—	(10.0)
[Cu(TPP)(COS)]	> 300	73.3	7.5	3.6	—	4.4
		(73.4)	(7.6)	(3.8)		(4.3)
[Fe(TPP)(CO)]	> 300	77.5	8.1	4.1	—	—
		(77.6)	(8.0)	(4.0)		
[Fe(TPP)(C_5H_5)]	> 300	80.4	7.7	4.5		—
		(80.2)	(7.6)	(4.6)	—	—
[Fe(TPP)(C_5H_5)(NO)]	> 300	77.1	9.3	4.2	—	—
		(77.0)	(9.2)	(4.3)		

This was then reduced to 10 cm^3 and was added dropwise over the course of 30 min to a hot, stirred solution of H_2(TPP) (0.204 g, 0.33 mmol) in ethylene glycol (40 cm^3). It was then refluxed for 25 h. On addition of distilled water (100 cm^3), the brown complex [Rh(TPP)Cl] separated out. This was centrifuged, washed several times with water and dried *in vacuo* (yield: 0.14 g, 56%).

(b) *Chloro-carbonyl*(meso-*tetraphenylporphyrinato*) *rhodium*(III), [Rh(TPP)(CO)(Cl)]

To a solution of [Rh(TPP)Cl] (0.1 g, 0.13 mmol) in toluene (30 cm^3), COS was bubbled for 8 h. The solution was kept overnight, then reduced to 5 cm^3 under reduced pressure. On addition of *n*-hexane (30 cm^3), the [Rh(TPP)(CO)Cl] complex separated out. This was centrifuged, washed with *n*-hexane and dried *in vacuo* (yield: 0.09 g, 87%).

(c) *Thionitrosyl*(meso-*tetraphenylporphyrinato*) *iron*(I), [Fe(TPP)(NS)]

A solution of $S_3N_3Cl_3$ (0.04 g, 0.16 mmol) in 25 cm^3 of tetrahydrofuran (THF) was added to a stirred solution of [Fe(TPP)Cl] (0.30 g, 0.43 mmol) in the presence of iron powder (1.0 g) and the reaction mixture was stirred for 3 h. It was then filtered, evaporated to dryness under reduced pressure and extracted with 20 cm^3 of dichloromethane. On the addition of methanol (60 cm^3), the dark blue complex [Fe(TPP)NS] separated out, which was filtered, washed with methanol and dried *in vacuo* (yield: 0.18 g, 58%).

(d) *Sulphur-dioxide*(meso-*tetraphenylporphyrinato*) *iron*(II), [Fe(TPP)(SO_2)]

$SOCl_2$ (2 cm^3) was added to a solution of [Fe(TPP)Cl] (0.2 g, 0.28 mmol) in benzene (40 cm^3) and zinc dust (4.0 g) added. The reaction mixture was stirred for 5 h. It was then filtered and reduced to 5 cm^3 under reduced pressure. On addition of methanol (30 cm^3), a greenish violet complex [Fe(TPP)(SO_2)] separated out, which was centrifuged, washed with methanol and dried *in vacuo* (yield: 0.098 g, 47%).

(e) *Disulphidothionitrato*(meso-*tetraphenylporphyrinato*)*cobalt*(III), [Co(TPP)(S_3N)]

A blue solution of S_7NH (0.12 g, 0.5 mmol) in 5 cm^3 of dimethylformamide (DMF) was added to a stirred solution of [Co(TPP)] (0.33 g, 0.5 mmol) in DMF (15 cm^3). The reaction mixture was further stirred for 8 h. It was then filtered and concentrated

Table 2. Electronic spectral data and important IR frequencies

Compound	Solvents	UV–vis λ_{max} (nm)	UV–vis (ε_{max}) ($M^{-1}\,cm^{-1}$)	IR (cm^{-1})
[Rh(TPP)(CO)Cl]	CH_2Cl_2	415	(1.8×10^5)	
		527	(3.2×10^4)	ν(CO) = 2055
[Fe(TPP)(NS)]	Benzene	410	(2.1×10^5)	
		500	(3.1×10^4)	ν(NS) = 1270
		530	(2.7×10^4)	
		565	(1.6×10^4)	
[Fe(TPP)(SO_2)]	Benzene	408	(9.0×10^4)	
		510	(2.8×10^4)	$\nu(SO_2)$ = 1080, 1235
		580	(1.0×10^4)	
[Cu(TPP)(COS)]	CH_2Cl_2	410	(1.0×10^5)	
		420	(9.8×10^4)	ν(COS) = 1712
		540	(3.5×10^4)	
		575	(1.6×10^4)	
[Co(TPP)(S_3N)]	Benzene	410	(9.0×10^4)	ν(NS) = 749, 725
		532	(1.6×10^4)	ν(S—S) = 620
[Cu(TPP)(S_3N)]	Benzene	412	(1.37×10^5)	ν(NS) = 938, 734, 720
		468	(1.4×10^4)	
		538	(3.5×10^4)	ν(S—S) = 595
		560	(2.8×10^4)	
		608	(7.0×10^3)	
[Co(TNPP)(S_3N)]	Benzene	420	(1.5×10^5)	ν(NS) = 940, 735
		522	(2.5×10^4)	
		553	(2.0×10^4)	ν(S—S) = 605
		598	(9.0×10^3)	
[Fe(TPP)(C_5H_5)]	Benzene	410	(1.1×10^5)	$\nu(C_5H_5)$ = 852, 1405
		570	(9.0×10^3)	
[Fe(TPP)(C_5H_5)(NO)]	Benzene	410	(9.6×10^4)	
		502	(1.0×10^4)	ν(NO) = 1705
		531	(6.4×10^3)	
		572	(8.3×10^3)	

to 5 cm^3 under reduced pressure. On addition of methanol (50 cm^3), a brownish violet complex [Co(TPP)S_3N] separated out, which was filtered, washed with methanol and dried *in vacuo*. It was recrystallized from CH_2Cl_2–CH_3OH (yield: 0.23 g, 60%).

(f) *Disulphidothionitrato*(meso-*tetraphenylporphyrinato*)*copper*(III), [Cu(TPP)(S_3N)]

A blue solution of S_7NH (0.12 g, 0.5 mmol) in 5 cm^3 of dimethylformamide (DMF) was added to a stirred solution of [Cu(TPP)] (0.34 g, 0.5 mmol) in DMF (15 cm^3). The reaction mixture was stirred for 8 h. The reddish violet complex [Cu(TPP)(S_3N)] was isolated by a procedure similar to that given in (e) (yield: 0.2 g, 51%).

(g) *Disulphidothionitrato*[meso-*tetrakis*(2-*nitrophenyl*)*porphyrinato*)]*cobalt*(III), [Co(TNPP)(S_3N)]

To a stirred solution of [Co(TNPP)] (0.212 g, 0.25 mmol) in DMF (15 cm^3), was added a blue solution of S_7NH (0.06 g, 0.25 mmol) in DMF (5 cm^3). The reaction mixture was stirred for 8 h and the brownish violet complex [Co(TNPP)(S_3N)] was isolated by a procedure similar to that given in (e) (yield: 0.124 g, 52%).

(h) *Carbonylsulphide*(meso-*tetraphenylporphyrinato*)*copper*(II), [Cu(TPP)(COS)]

To a solution of [Cu(TPP)] (0.1 g, 0.148 mmol) in toluene (30 cm^3), COS was bubbled for 10 h. It was kept for 50 h, then reduced to 5 cm^3 under reduced pressure. On addition of *n*-hexane, the pinkish brown complex [Cu(TPP)COS] separated

out. This was centrifuged, washed with *n*-hexane and dried *in vacuo* (yield: 0.085 g, 78%).

(i) *Carbonyl*(meso-*tetraphenylporphyrinato*)*iron*(II), [Fe(TPP)(CO)]

To a solution of [Fe(TPP)] (0.1 g, 0.15 mmol) in benzene (30 cm^3), COS was bubbled for 8 h. It was kept for 2 days, then reduced to 5 cm^3 under reduced pressure. On addition of *n*-hexane (30 cm^3), the blue complex [Fe(TPP)(CO)] separated out. This was centrifuged, washed with *n*-hexane and dried *in vacuo* (yield: 0.09 g, 86%).

(j) *Cyclopentadienyl*(meso-*tetraphenylporphyrinato*) *iron*(III), [Fe(TPP)(C_5H_5)]

Freshly distilled monocyclopentadiene (C_5H_6) (1 cm^3) and zinc dust (1.0 g) were added to a stirred solution of [Fe(TPP)Cl] (0.2 g, 0.284 mmol) in benzene (50 cm^3). The reaction mixture was stirred for 5 h. It was then filtered and reduced to 5 cm^3 under reduced pressure. On addition of methanol (25 cm^3), the brown complex [Fe(TPP)(C_5H_5)] separated out. This was centrifuged, washed with methanol and dried *in vacuo*, and the product was recrystallized from dichloromethane and methanol (yield: 0.108 g, 52%).

(k) *Nitrosyl-cyclopentadienyl*(meso-*tetraphenylporphyrinato*)*iron*(II), [Fe(TPP)(NO)(C_5H_5)]

To a solution of [Fe(TPP)(C_5H_5)] (0.1 g, 0.136 mmol) in chloroform (20 cm^3), nitric oxide was bubbled for 30 min. It was reduced to 5 cm^3 under reduced pressure. On addition of methanol (50 cm^3), the brown complex [Fe(TPP)(NO)(C_5H_5)] separated out. This was centrifuged, washed with methanol and dried *in vacuo* (yield: 0.056 g, 54%).

RESULTS AND DISCUSSION

[Rh(TPP)Cl] was prepared by the interaction of the carbonyl complex of rhodium (prepared by refluxing formaldehyde with [$RhCl_3 \cdot 3H_2O$] in ethylene glycol) with H_2TPP. The IR spectrum of [Rh(TPP)Cl] is similar to that reported previously and prepared by other methods.[38] The reaction of COS with [Rh(TPP)Cl] resulted in the formation of [Rh(TPP)(CO)Cl]. The IR spectrum of this complex showed an absorption band at 2055 cm^{-1} due to the carbonyl stretching frequency.

Reaction of a green solution of trithiazyltrichloride in THF with $Fe^{II}TPP$, afforded [Fe^{III}(TPP)Cl]. When the same experiment was carried out in the presence of an excess of iron powder, the dark blue complex [Fe(TPP)(NS)], was isolated. The reaction system and the product [Fe(TPP)(NS)], are highly moisture-sensitive. From the six preparative experiments, only twice was the [Fe(TPP)(NS)] complex isolated.

$$Fe^{II}TPP + (NSCl)_3 \xrightarrow{THF} [Fe(TPP)(NS)] + \cdots.$$

The IR spectrum of [Fe(TPP)(NS)] showed a peak at 1270 cm^{-1} due to the thionitrosyl stretching vibration, which is in the range of thionitrosyl stretching frequencies observed in linearly bonded thionitrosyl complexes.[13,39]

Reaction of $SOCl_2$ with [Fe(TPP)] in the presence of zinc dust in benzene resulted in the formation of a green complex, [Fe(TPP)(SO_2)]. A plausible mechanism involved the prior formation of sulphur monoxide which disproportionated to sulphur dioxide and sulphur, and the resulting sulphur dioxide coordinated to the metal centre,[40,41] The IR spectrum of [Fe(TPP)(SO_2)] showed absorption bands at 1235 and 1080 cm^{-1} due to the η'-planar (sp^2) coordinatd SO_2 group.[42]

Heptasulphurimide reacted with [M^{II}(P)] to afford the disulphidothionitrato complexes [M^{III}(P)(S_3N)].



M = Fe, Cu, CO P = TPP
M = Co P = TNPP.

The IR spectra of the complexes [Cu(TPP)(S_3N)], [Co(TPP)(S_3N)] and [Co(TNPP)(S_3N)] show absorption bands in the regions, 912–940 cm^{-1} and 720–749 cm^{-1} due to ν(NS) and 595–620 cm^{-1} due to ν(S—S), which are in close agreement with the values for the coordinated bidentate S_3N^- ligand.

Reaction of COS with [Cu(TPP)] at room temperature in toluene, yielded a pinkish brown complex [Cu(TPP)(COS)], in which COS was bonded to the metal through carbon and sulphur. This is supported by its IR spectrum which exhibited a band at 1712 cm^{-1}, the characteristic IR frequency of a bidentate COS group.[26] Reaction of COS with [Fe(TPP)] resulted in the formation of [Fe(TPP)(CO)], which in its IR spectrum showed an absorption band at 1972 cm^{-1} due to ν(CO) (cf. literature value, 1973 cm^{-1}).[43,44]

Monocyclopentadiene (C_5H_6) in the presence of zinc dust reacted with [Fe(TPP)] giving a brown complex [Fe(TPP)(C_5H_5)]. The IR spectrum of this complex exhibited absorption bands at 852, 875 and 1405 cm^{-1} due to the cyclopentadienyl ligand. NO

reacted with [Fe(TPP)(C_5H_5)] to give the nitrosyl complex [Fe(TPP)(C_5H_5)(NO)]. The IR spectrum of this complex exhibited an absorption band at 1705 cm^{-1} due to the nitrosyl stretching frequency. The corrected stretching frequency (ν'(NO) 1655 cm^{-1}) of NO, calculated according to Ibers' rules,[45] falls above 1610 cm^{-1}. This is evidence for the presence of a linear nitrosyl group in this complex.

Acknowledgement—This work was supported by the University Grants Commission, New Delhi [Project No. F 12-18/86 (SR-III)].

REFERENCES

1. G. B. Jameson and J. A. Ibers, *Comm. Inorg. Chem.* 1983, **2**, 97.
2. J. P. Collman, *Accts Chem. Res.* 1977, **10**, 265.
3. C. A. Reed, in *Metal Ions in Biological Systems* (Edited by H. Sigel), p. 277. Marcel Decker, New York (1978).
4. T. G. Traylor, *Accts Chem. Res.* 1981, **14**, 102.
5. B. B. Wayland, J. V. Minkiewicz and M. E. Abd-Elmageed, *J. Am. Chem. Soc.* 1974, **96**, 2795.
6. B. B. Wayland and L. W. Olson, *J. Am. Chem. Soc.* 1974, **96**, 6036.
7. J. P. Collman, R. R. Gangne, C. A. Reed, T. R. Halbert, G. Lang and W. T. Robinson, *J. Am. Chem. Soc.* 1975, **97**, 1427.
8. D. L. Anderson, C. J. Weschler and F. Basolo, *J. Am. Chem. Soc.* 1974, **96**, 5599; C. K. Chang and T. G. Traylor, *Proc. Nat. Acad. Sci. U.S.A.* 1973, **70**, 2647; W. S. Brinigar, C. K. Chang, J. Geibel and T. G. Traylor, *J. Am. Chem. Soc.* 1974, **96**, 5597.
9. K. K. Pandey, D. K. M. Raju, H. L. Nigam and U. C. Agrawala, *Ind. Nat. Sci. Acad.* 1982, **A48**, 16.
10. H. W. Roesky, K. K. Pandey, W. Clegge, M. Noltemeyer and G. M. Sheldrick, *J. Chem. Soc., Dalton Trans.* 1984, 719.
11. K. K. Pandey, *Proc. Int. Conf. Coord. Chem.* 1984, **23**, 654.
12. K. K. Pandey, H. W. Roesky, M. Noltemeyer and G. M. Sheldrick, *Z. Naturfor.* 1984, **B39**, 590; J. W. Bats, K. K. Pandey and H. W. Roesky, *J. Chem. Soc., Dalton Trans.* 1984, 2081.
13. H. W. Roesky and K. K. Pandey, *Adv. Inorg. Radiochem.* 1983, **26**, 337.
14. K. K. Pandey and U. C. Agrawala, *Ind. J. Chem.* 1981, **A20**, 906.
15. R. D. Tiwari, K. K. Pandey and U. C. Agrawala, *Inorg. Chem.* 1982, **21**, 845.
16. H. W. Roesky, K. K. Pandey, B. Krebs and M. Dartmann, *J. Chem. Soc., Dalton Trans.* 1984, 2271.
17. K. K. Pandey, *Spectrochim. Acta* 1983, **A39**, 925.
18. K. K. Pandey, *Inorg. Chim. Acta* 1986, **111**, 9.
19. J. Weiss, *Z. Anorg. Allg. Chem.* 1985, **521**, 37.
20. H. W. Roesky, K. K. Pandey, M. Noltemeyer and G. M. Sheldrick, *Acta Cryst.* 1984, **C40**, 1555.
21. K. K. Pandey and M. Massoudipour, *Inorg. Chim. Acta* 1987, **138**, 169.
22. K. K. Pandey, D. T. Nehete and M. Massoudipour, *Inorg. Chim. Acta* 1987, **129**, 253.
23. J. Bojes and T. Chivers, *J. Chem. Soc., Chem. Commun.* 1980, 1023.
24. J. Weiss, *Z. Anorg. Allg. Chem.* 1986, **532**, 184.
25. J. Bojes, T. Chivers and P. W. Codding, *J. Chem. Soc., Chem. Commun.* 1981, 1171.
26. K. K. Pandey and H. L. Nigam, *Rev. Inorg. Chem.* 1984, **6**, 69.
27. T. R. Gaffney and J. A. Ibers, *Inorg. Chem.* 1982, **21**, 2851.
28. A. D. Adler, F. R. Lango, J. D. Finarelli, J. Assour and L. Karsakoff, *J. Org. Chem.* 1967, **32**, 476.
29. A. D. Adler, F. R. Longo, F. Kampas and J. Kim. *J. Inorg. Nucl. Chem.* 1970, **32**, 2443.
30. R. Rothmund and A. R. Menotti, *J. Am. Chem. Soc.* 1948, **70**, 1808.
31. E. B. Fleischer, C. K. Miller and L. E. Webb, *J. Am. Chem. Soc.* 1964, **86**, 2342.
32. J. H. Fuhrhop and K. M. Smith, in *Porphyrins and Metalloporphyrins* (Edited by K. M. Smith), p. 798. Elsevier, Amsterdam (1975).
33. H. G. Heal and J. Kane, *Inorg. Synth.* 1968, **11**, 184.
34. W. L. Jolly and K. D. Maguire, *Inorg. Synth.* 1967, **9**, 102.
35. G. Beaur, *Hand-book of Preparative Inorganic Chemistry*, 2nd edn, Vol. 1. Academic Press, New York (1963).
36. F. P. Treadwell and W. T. Hall, *Analytical Chemistry*, 9th edn, Vol. 2. John Wiley, New York (1958).
37. A. I. Vogel, *A Text-book of Quantitative Inorganic Analysis*, 3rd edn. Longmans, Green and Co., London (1961).
38. B. R. James and D. V. Stynes, *J. Am. Chem. Soc.* 1972, **94**, 6225.
39. T. Chivers and F. Edelmann, *Polyhedron* 1986, **5**, 1661.
40. I. P. Lovenz, W. Hiller and M. Conrad, *Z. Naturfor.* 1985, **40B**, 1383.
41. W. A. Schenk, *Angew. Chem. Int. Ed. Engl.* 1987, **26**, 98 and refs therein.
42. D. M. P. Mingos, *Transition Met. Chem.* 1978, **3**, 1.
43. B. B. Wayland, L. F. Mehne and J. Swartz, *J. Am. Chem. Soc.* 1978, **100**, 2379.
44. G. R. Eaton and S. S. Eaton, *J. Am. Chem. Soc.* 1975, **97**, 235; J. J. Bonnet, S. S. Eaton, G. R. Eaton, R. H. Holm and J. A. Ibers, *J. Am. Chem. Soc.* 1973, **95**, 2141.
45. B. L. Haymore and J. A. Ibers, *Inorg. Chem.* 1975, **14**, 3060.

Polyhedron Vol. 8, No. 11, pp. 1453–1455, 1989
Printed in Great Britain

0277-5387/89 $3.00+.00
Pergamon Press plc

EQUILIBRIA IN COMPLEXES OF N-HETEROCYCLIC MOLECULES—XLVII.* SPECIATION IN AQUEOUS $[Cr(2,2'\text{-BIPYRIDYL})_3]^{3+}$

P. S. CARTWRIGHT and R. D. GILLARD†

Department of Chemistry, University College, P.O. Box 78, Cardiff CF1 1XL, U.K.

(*Received* 13 *June* 1988; *accepted after revision* 15 *February* 1989)

Abstract—Solutions of the salts $[Cr(bipy)_3]X_3$ ($X = Cl^-$ or ClO_4) in water, show reversible pH-dependence of luminescence. The circular dichroism is independent of pH.

The nature of the species actually present in solutions in protic media containing the complex ions $[M(LL)_3]^{n+}$ [e.g. M = Cr, $n = 3$; M = Ru, $n = 2$ or 3; LL = a di-imine like 2,2-bipyridine (bipy) or 1,10-phenanthroline (phen)] and of intermediates in solvolyses, has been hotly debated.[2] For example, the variation of species with pH has been much studied.

We comment here on some simple but illuminating observations on aqueous solutions of $[Cr(LL)_3]X_3$, where LL = 2,2′-bipyridine or 1,10-phenanthroline and X is the conjugate base of a very strong acid like HCl or $HOClO_3$.

The apparent variability or irreproducibility of properties (such as quenching of luminescence) often observed in such compounds, may usually be traced to impurity. (For example, in the photophysics[3] of $[Ir(phen)_2Cl_2]^+$ or the rates of decay of luminescence of $[Cr(phen)_3]^{3+}$, where apparently identical samples behaved differently.)[4] It is, in this field of work, consequently more than ever vital to be sure of the nature of solid compounds.

Figure 1 shows the variations (fully reversible) of luminescence for $[Cr(bipy)_3]^{3+}$ with pH. In a similar experiment, Kane-Maguire and Langford reported[5] the partial quenching of luminescence of $[Cr(phen)_3]^{3+}$ at high concentration of hydroxide. They interpreted this decrease in intensity with no shift of wavelength, as being consistent with attack by hydroxide on an aromatic ring of ground or excited state $[Cr(phen)_3]^{3+}$.

The variation with pH of the rates of several reactions of $[Cr(bipy)_3]^{3+}$ (solvolysis, racemization, photoracemization) follow such a common profile[2,6a] that the intermediacy of a 1 : 1 adduct of the cation with the hydroxide ion is accepted. The vari-

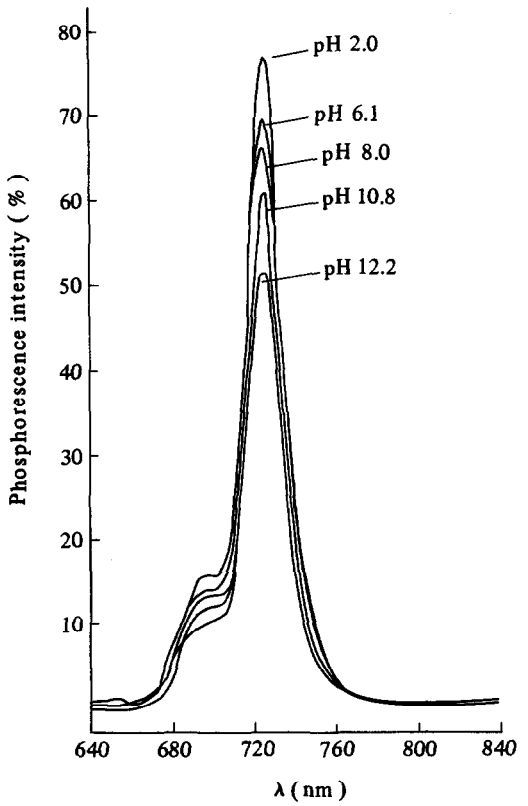

Fig. 1. Change in phosphorescence of $[Cr(bipy)_3]^{3+}$ as a function of pH: experimental details are in "Synthetic and spectroscopic studies of transition metal complexes" by P. S. Cartwright, PhD thesis, University of Wales (1987).

* For Part XLVI, see ref. 1.

† Author to whom correspondence should be addressed.

ation of luminescence intensity (I) varies with pH in the same way (particularly clear from plotting I^{-1}).

Quenching of luminescence (a term used to denote any emission of a photon from any excited state, i.e. fluorescence and/or phosphorescence) can arise[7] in several ways. These are (a) energy transfer, (b) excited donor–quencher chemical reaction, (c) catalysed deactivation without energy transfer or chemical reaction and (d) exciplex formation. The catalytic effects —(c)— are ruled out for the hydroxide ion, since these arise either from a heavy atom affecting spin-orbit coupling or from a paramagnetic quencher. Energy transfer —(a)— is ruled out since hydroxide has no low-lying energy levels. Exciplex formation —(d)— with $[Cr(LL)_3]^{3+}$ requires some other interacting π-system (not present). As pointed out[7] by Demas and Addington, mere ion-pairing between an excited donor and a quencher cannot itself quench (the possibility of energy or electron transfers must still be present for quenching to occur).

Hydroxide [in the related context of quenching photo-aquations of ions of chromium(III)] has been described[8] in a vague phrase as a "non-innocent quencher", i.e. not acting by electronic energy transfer. However, it was also said that "quenching by OH^- . . . has to take place by means of some kind of chemical reaction".

The only possible mechanism for the luminescence of $[Cr(LL)_3]^{3+}$ to be quenched by hydroxide is indeed by chemical reaction, and we (like Kane-Maguire and Langford in relation to $[Cr(phen)_3]^{3+}$) take this to be covalent addition[2] to one ligand, rather than to the metal ion.

From the presently available measurements of electronic spectra, the presence of pH-dependent speciation is obvious only in emission. We agree with Serpone that[6a,9] the electronic absorption spectrum of $[Cr(bipy)_3]^{3+}$ is independent of pH from 0 to 10.7, and we add the independence of the circular dichroism (a property often more sensitive than isotropic absorption) of resolved salts of both ions (bipy and phen) over the pH range from 2 to 11. However, despite the earlier observation[5] by Kane-Maguire and Langford of the pH dependence of luminescence of $[Cr(phen)_3]^{3+}$, Serpone and his associates found[9] no change of the luminescence of $[Cr(bipy)_3]^{3+}$ in the pH range 0–10.7. The change we find, reproducibly (Fig. 1), is about a 25% "quenching" from pH 2.0 to 10.8 and about a third of the intensity of the luminescence arising from "chrome doublet" states is quenched from pH 2.0 to 12.2 (the higher limit in our own study). It is, of course, common enough experience for other chromophores that fluorescence and phosphorescence are much more sensitive to change than are absorption spectra.

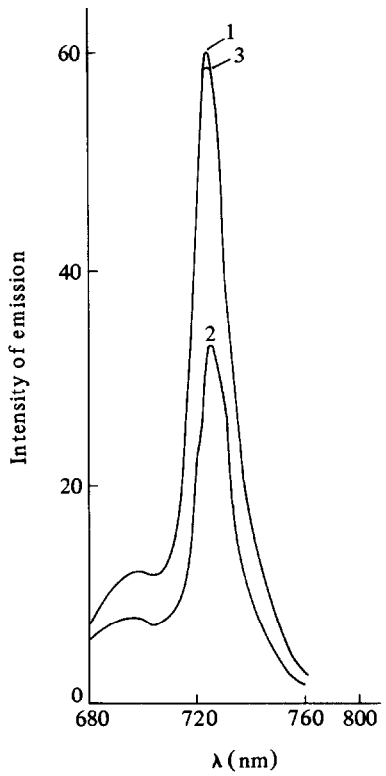

Fig. 2. Quenching of luminescence of $[Cr(phen)_3]^{3+}$ and its reversibility: (1) original solution at pH *ca* 4.5; (2) pH changed to *ca* 12 by conc. NaOH; (3) pH restored to *ca* 2 by conc. $(HO)_2SO_2$.

The yellow colour (absorption spectrum) of $[Cr(LL)_3]^{3+}$ salts in MeCN or DMSO does change (to red–violet) on adding base (Bu_4NOH in H_3COH–toluene) but not with full reversibility—the yellow *colour* reappears with HCl treatment, but the electronic spectrum (and CD for the resolved species) differ from the original. The basic solutions racemize quickly (for LL = bipy faster than for LL = phen). It is not yet clear that this change of species with base is related to those in water.

In conclusion, the notion advanced[10] in 1969 that di-imines coordinated to metal ions behave like quaternized imines, offers a good account of the simple properties of aqueous solutions. It has been taken up recently. Srivatsa and Sawyer invoke[11] exactly such nucleophilic attack of hydroxyl on a bound pyridine as being intermediate in the hydroxide-induced reduction of tetraphenylporphinato-iron(III) in pyridine. Others, studying the thermal and light-induced reductions of aqueous $[Ru(bipy)_3]^{3+}$, have repeated[12] a prior suggestion[13] that a pseudobase is an intermediate.

In the context of the present chromium(III) species, it is worth remarking that a simple theoretical analysis[6c] of whether coordinated N-heterocycles (as opposed to quaternized ones) would ever undergo nucleophilic attack, concluded that if any triply charged ion might polarize the ligands enough to induce this, chromium(III) was the one (although we doubt[14] the conclusion itself: our more extensive calculations point to a clear similarity between the electronic populations of coordinated and of quaternized N-heterocycles).

EXPERIMENTAL

Complex compounds were made, resolved and characterized as previously described.[15] Luminescence measurements used an Aminco–Bowman spectrofluorimeter with excitation at 430 nm. The several classes of experiment were:

(a) Reversibility: a freshly made solution (typically 10^{-3} M) had its luminescence measured (640–800 nm, spectrum 1), was treated with one drop of strong base (pH > 12) giving spectrum 2, quite different from 1 in intensity, then with conc. $(HO)_2SO_2$ back to pH 1–2, giving spectrum 3 coincident with 1, as in Fig. 2.

(b) Detailed pH profiles, as in Fig. 1.

(c) Time course, to establish possible interference from products of solvolysis. An aqueous solution (10^{-3} M) of $[Cr(bipy)_3]^{3+}$ at pH 12 was left and its luminescence (640–780 nm) recorded at times 0, 5, 6, 15 and 19 min. The measured intensities at peak emission 726.5 nm were (arbitrary scale) respectively as: 42.5; 39.4; 38.9, 33.3, 12.1. After acidification, the final solution had intensity 16.5. The sole luminescing species in base is the adduct of hydroxide with $[Cr(bipy)_3]^{3+}$, since the luminescence profile is constant with time. The rate of disappearance of the luminescing species at the particular pH of the time measurement, agrees quite well with the known rate of solvolysis of $[Cr(bipy)_3]^{3+}$. The growth of intensity by about a third on re-acidification of the residual pH 12 solution jibed well with Fig. 1.

Acknowledgements—We wish to thank SERC for a Quota Studentship, Dr E. D. Owen for help with spectrofluorimetry and Dr H. P. J. M. Dekkers (University of Leiden) for some valued comments on emission spectroscopy.

REFERENCES

1. R. D. Gillard and S. H. Mitchell, *Polyhedron* 1988, **7**, 1175.
2. R. D. Gillard, *Coord. Chem. Rev.* 1975, **16**, 67; R. D. Gillard, *Coord. Chem. Rev.* 1983, **50**, 303; R. D. Gillard, *Comm. Inorg. Chem. A* 1986, **5**, 175.
3. R. Ballordini, G. Varani, L. Moggi and V. Balzani, *J. Am. Chem. Soc.* 1977, **99**, 6881 and refs therein.
4. J. Lilie, W. L. Waltz, S. H. Lee and L. L. Gregor, *Inorg. Chem.* 1986, **25**, 4487; the sample supplied by this laboratory gave reproducible results, consistent with those from one other source.
5. N. A. P. Kane-Maguire and C. H. Langford, *Inorg. Chem.* 1976, **15**, 464.
6. (a) N. Serpone, G. Ponterini, M. A. Jamieson, F. Bolletta and M. Maestri, *Coord. Chem. Rev.* 1983, **50**, 209; (b) E. C. Constable, *Polyhedron* 1983, **2**, 551; (c) P. A. Lay, *Inorg. Chem.* 1984, **23**, 4775.
7. J. N. Demas and J. W. Addington, *J. Am. Chem. Soc.* 1976, **98**, 5800.
8. D. Sandrini, M. T. Gandolfi, A. Juris and V. Balzani, *J. Am. Chem. Soc.* 1977, **99**, 4523.
9. M. Maestri, F. Bolletta, N. Serpone, L. Moggi and V. Balzani, *Inorg. Chem.* 1976, **15**, 2048.
10. R. D. Gillard and B. T. Heaton, *J. Chem. Soc. A* 1969, 451; this original suggestion was reproduced in full, with structural formulae of the covalent hydrate, by J. A. Broomhead and W. Grumley, *Inorg. Chem.* 1971, **10**, 2002.
11. G. S. Srivatsa and D. T. Sawyer, *Inorg. Chem.* 1985, **24**, 1732.
12. D. Kotkar, V. Joshi and P. K. Ghosh, *Inorg. Chem.* 1986, **25**, 4334.
13. J. A. A. Sagues, R. D. Gillard, R. J. Lancashire and P. A. Williams, *J. Chem. Soc., Dalton Trans.* 1979, 193.
14. D. W. Clack and R. D. Gillard, *Inorg. Chim. Acta* 1988, **141**, 37.
15. P. S. Cartwright, R. D. Gillard and E. R. J. Sillanpaa, *Polyhedron* 1987, **6**, 105.

Polyhedron Vol. 8, No. 11, pp. 1457–1459, 1989
Printed in Great Britain

0277–5387/89 $3.00+.00
© 1989 Pergamon Press plc

COMMUNICATION

NEW ORGANOMETALLIC DIALKYLAMIDO COMPLEXES. X-RAY CRYSTAL STRUCTURE OF $Ph_2VN(CH_2CH_2NEt_2)_2$

A. R. WILLS and P. G. EDWARDS*

School of Chemistry and Applied Chemistry, University of Wales, College of Cardiff, P.O. Box 912, Cardiff CF1 3TB, U.K.

and

M. HARMAN and M. B. HURSTHOUSE

Department of Chemistry, Queen Mary College, Mile End Road, London E1 4NS, U.K.

(*Received* 26 *January* 1989; *accepted* 15 *February* 1989)

Abstract—New complexes of titanium(III) and vanadium(III) stabilized by a chelating terdentate amido ligand have been prepared, providing access to the study of a rare class of compounds; the crystal structure of the aryl vanadium(III) derivative has also been determined. In addition, preliminary studies indicate that chromium(III) behaves in a different manner when forming complexes with this ligand.

We are currently interested in the study of dialkylamido complexes of *d*-block elements in groups IV and V, containing metal–carbon bonds, since organometallic complexes of these metals are well known to catalyse various organic transformations. Vanadium aryls, for example, are active as alkene polymerization or oligomerization catalysts.[1] There are, however, few well characterized examples of such compounds,[2] especially for vanadium(III), as isolation of products is typically hampered by marked tendencies towards disproportionations and oxidations. Consequently, this area of study for electropositive metals has been largely limited to cyclopentadienyl, neutral phosphino[2a] or bulky ligands.[2b] The few examples of metals in groups IV and V coordinated to both aryl (or alkyl) and dialkylamido ligands,[3] illustrate that these compounds are an important class in terms of their reactivity, and are non-trivial to synthesize in a rational manner. We have recently reported[4] routes to new dialkylamido complexes of these metals that contain halide ligands available for substitutions. We now present preliminary studies of these complexes that demonstrate access to new reactive methyl and phenyl derivatives of titanium and vanadium stabilized by chelating terdentate amido ligands. We also report the X-ray crystal structure of $Ph_2VN(CH_2CH_2NEt_2)_2$, the first organometallic derivative of a vanadium amido complex to be so characterized. The new compounds described here are represented in Scheme 1.

Preparation of these compounds is by interaction of alkyl or aryl lithium reagents with the amido metal dihalide complex in tetrahydrofuran. The new compounds may be prepared more conveniently by a "one pot" procedure where the amido metal dihalide precursor is generated as an intermediate (from $MCl_3 \cdot 3THF$[4]) *in situ* prior to the addition of the organolithium reagent. They may be recrystallized from petroleum ether and are soluble in apolar solvents. The compounds have provided satisfactory elemental analyses (Butterworth Laboratories Ltd, Teddington, U.K.).

Both titanium compounds are d^1 paramagnets that give rise to ESR spectra† and consistent solid-state magnetic susceptibilities;‡ are monomeric in

* Author to whom correspondence should be addressed.

† *g* values observed were typical of those expected for titanium(III) d^1 compounds, superhyperfine coupling was not observed.

‡ Me_2TiL, $\mu_{eff} = 1.719$ BM; Ph_2TiL, $\mu_{eff} = 1.414$ BM; Me_2VL, $\mu_{eff} = 2.613$ BM; Ph_2VL, $\mu_{eff} = 2.579$ BM.

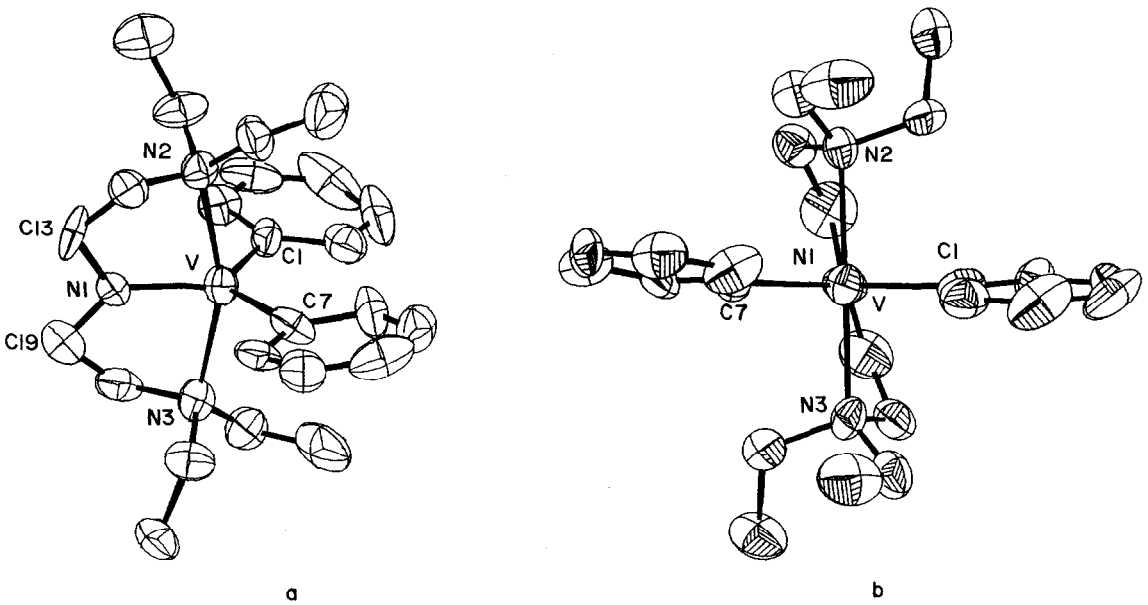

Fig. 1. (a) A view illustrating the distorted trigonal bipyramidal geometry around vanadium. (b) A view illustrating the planar nature of the amido nitrogen atom. Selected bond angles (°):

N(2)—V—N(1)	158.9(2)	C(7)—V—N(3)	97.2(3)
C(1)—V—N(1)	120.3(3)	C(7)—V—C(1)	123.7(3)
C(1)—V—N(2)	98.2(3)	C(13)—N(1)—V	121.6(2)
C(1)—V—N(3)	91.9(3)	C(19)—N(1)—V	121.6(6)
C(7)—V—N(1)	116.0(3)	C(19)—N(1)—V	122.2(6)
C(7)—V—N(2)	92.5(3)	C(13)—N(1)—C(19)	116.2(7)

Selected bond lengths (Å):

N(1)—V	1.874(8)	N(2)—V	2.262(8)
N(3)—V	2.280(8)	C(1)—V	2.162(8)
C(7)—V	2.140(8)	C(13)—N(1)	1.452(10)
C(19)—N(1)	1.441(10)		

benzene solution (cryoscopy) and molecular ions are not observed in the mass-spectrum, although typical ligand fragmentations are.

For vanadium, both the methyl and phenyl derivatives appear to have two unpaired electrons (d^2, magnetic susceptibility) and both compounds are ESR silent in solution, solid or glass at 20 or −110°C. Again both compounds are monomeric in solution (cryoscopy, benzene) and unlike their titanium analogues, both display molecular ions in their mass spectra (295 amu for the dimethyl and 419 amu for the diphenyl).

Crystals of $Ph_2VN(CH_2CH_2NEt_2)_2$ suitable for X-ray crystallography were obtained from petroleum ether. The structure of the molecule is shown in Fig. 1.* The dimensions of comparable parts of the structure are similar to those of the precursor $Cl_2VN(CH_2CH_2NEt_2)_2$.[4] The vanadium–carbon average bond lengths (2.151(8) Å) are somewhat longer (by 0.07 Å) than that

*Crystal data: $C_{24}H_{38}N_3V$, $M_r = 419.52$, orthorhombic, $a = 14.075(1)$, $b = 18.095(5)$, $c = 18.778(3)$ Å, $V = 4782.9$ Å^3. Space group: *Pbca*, $Z = 8$, $D_c = 1.17$ g cm^{-3}, $F(000) = 1808$, μ(Mo-K_α) = 4.13 cm^{-1}, λ(Mo-K_α) = 0.71069 Å. Structure solved via routine procedures, refined by least-squares with non-hydrogens anisotropic, idealized phenyl rings, hydrogen atoms refined but with group U_{iso} values. $R = 0.079$, $R_w = 0.087$ for 269 parameters and 1977 observed [$F_o > 3\sigma(F_o)$] data from 4198 measured.

$$LTiR_2 \longleftarrow LiR \longrightarrow LVR_2$$

R = Me, Ph
L = $-N(CH_2CH_2NEt_2)_2$

Scheme 1. All organometallic derivatives were prepared by the action of 2 mole equivalents of the organolithium reagent on the corresponding $LMCl_2$ in THF. Yields (based on $MCl_3 \cdot 3THF$) after crystallization from hexane are: $LTiR_2$: R = Me, 60%; R = Ph, 83%; LVR_2: R = Me, 70%; R = Ph, 61%.

reported in the only other vanadium(III) aryl for which such data is available.[5]

In the diphenyl complex, the vanadium–amido nitrogen bond is longer (1.874(8) Å) than in the analogous dichloride (1.834(8) Å), but is still considerably shorter than the vanadium–amino nitrogen bonds (acerage 2.271(8) Å), indicating substantial metal–nitrogen multiple bonding. The coordination around vanadium can be described as trigonal bipyramidal with the amino nitrogens axial and distorted towards the equatorial amido nitrogen. Since the structures of the present compound and its precursor are very similar, although the steric demands of phenyl groups are different to those of chloride, the distortion must largely be due to the steric constraints of the chelating nitrogen ligand, especially in view of the fact that purely electronic constraints of stereochemistry appear to provide more regular structures in similar environments, as demonstrated by the regular trigonal-bipyramidal $VCl_3(NMe_3)_2$.[6]

The reaction of $LiN(CH_2CH_2NEt_2)_2$ with $CrCl_3 \cdot 3THF$ in THF provides the dark green crystalline and hydrocarbon soluble complex, $[(Et_2NCH_2CH_2)_2NCrCl_2]_n$. Analytical data are consistent with this compound being empirically analogous to the titanium and vanadium compounds, however, there are significant differences in physical properties. In the mass spectrum, a peak corresponding to the monomeric unit is observed, however peaks at higher m/z values are also present and are consistent with fragments arising from a dimeric unit. All these peaks show an isotope envelope indicative of the presence of both chloride and chromium. In addition to the mass-spectral data, the magnetic susceptibility (20°C, $\mu_{eff} = 3.23$ BM, Gouy method) is lower than would be expected for a monomeric d^3 chromium(III) compound of this nature. It is likely that this compound is not structurally analogous to the titanium and vanadium compounds, probably as a result of the preference of d^3 compounds for six-coordinate rather than five-coordinate stereochemistries. These observations point to it being a dimer, with either two bridging chlorides or bridging amido nitrogens. Further studies into the nature of the chromium compound are in progress. We are currently investigating extensions of this chemistry to the heavier congeners of titanium and vanadium. Indications are that these materials are very reactive with numerous substrates and investigations of chemical properties are being undertaken.

Acknowledgements—We thank the University of Wales for a studentship (A.R.W.) and the SERC for access to the Crystallography and Mass Spectroscopy Services.

REFERENCES

1. G. Heublein, W. Siedd, D. Stadermann, H. Hartung and G. Kreisel, *Ger. (East) Pat.* 12698 (1977); *Chem. Abstr.* 1978, **88**, 106023.
2. (a) M. Bottrill, P. D. Gaverns and J. McMeeking, in *Comprehensive Organometallic Chemistry* (Edited by G. Wilkinson, F. G. A. Stone and E. W. Abel), Vol. 3, Chap. 22. Pergamon Press, Oxford (1982); N. G. Connelly, in *Comprehensive Organometallic Chemistry* (Edited by G. Wilkinson, F. G. A. Stone and E. W. Abel), Vol. 3, Chap. 24. Pergamon Press, Oxford (1982); (b) R. T. Baker and M. F. Lappert, *J. Organomet. Chem.* 1974, **76**, C45.
3. M. F. Lappert, P. P. Power, A. R. Sanger and R. C. Shrivastava, in *Metal and Metalloid Amides*. Ellis Horwood, Chichester (1980).
4. A. R. Wills, P. G. Edwards, R. L. Short and M. B. Hursthouse, *J. Chem. Soc., Chem. Commun.* 1988, 115.
5. S. Ciurli, C. Floriani, A. Chiesi-Villa and C. Guastini, *J. Chem. Soc., Chem. Commun.* 1986, 1401.
6. P. T. Greene and P. L. Orioli, *J. Chem. Soc. A* 1969, 1621.

Polyhedron Vol. 8, No. 11, pp. 1461–1462, 1989
Printed in Great Britain

0277–5387/89 $3.00+.00
© 1989 Pergamon Press plc

COMMUNICATION

SYNTHESIS AND PROPERTIES OF N-BIS(TRIFLUOROMETHYL)NITROXY-IMINOARSINE $(CF_3)_2NON{=}AsH$: THE FIRST TWO-COORDINATE IMINOARSINE CONTAINING AN As=N DOUBLE BOND

H. G. ANG* and F. K. LEE

Department of Chemistry, National University of Singapore, Kent Ridge Road, Singapore 0511, Republic of Singapore

(*Received* 13 *February* 1989; *accepted* 10 *March* 1989)

Abstract—$(CF_3)_2NON{=}AsH$ (**A**), the first example of a two-coordinate iminoarsine, was synthesized by a condensation reaction between $(CF_3)_2NONO$ and AsH_3. It underwent substitution reactions with the $(CF_3)_2NO$ radical to afford $(CF_3)_2NON{=}AsON(CF_3)_2$. Both the iminoarsines, $(CF_3)_2NON{=}AsR$ (where R = H and $ON(CF_3)_2$), underwent addition reactions with HI to give $(CF_3)_2NONHAsRI$.

Although unsaturated compounds containing N=M double bonds (where M = P, Si, and Ge in low coordination) have received increasing attention in recent years, the number of such compounds which are thermodynamically stable is still small.[1–10] The stability of these bonds has been attributed to the presence of bulky groups and also to mesomeric effects.[6,7,10] However, we have recently reported the synthesis of several stable iminophosphines, $(CF_3)_2NON{=}PR$ (where R = H and $ON(CF_3)_2$), whose substituents consist of electronegative groups.[9] We now report the first examples of iminoarsines, namely $(CF_3)_2NON{=}AsR$ (where R = H and $ON(CF_3)_2$), which contains two-coordinate arsenic and whose stability also appeared to be influenced by perfluoro substituents.

The reactions of O-nitrosobis(trifluoromethyl) hydroxylamine with arsine at room temperature in a 1:1 ratio in an evacuated glass ampoule, gave N-bis(trifluoromethyl)nitroxy-iminoarsine, $(CF_3)_2NON{=}AsH$ and water, according to the equation:

$$AsH_3 + (CF_3)_2NONO \longrightarrow (CF_3)_2NON{=}AsH + H_2O. \quad \textbf{(A)}$$

A dark brown intractable solid, which is hygroscopic, was also formed in the reaction ampoule.

The iminoarsine **A**, obtained in about 42% yield, was isolated at the −86°C trap as a white solid on trap-to-trap vacuum fractionation. Its IR spectrum shows the following absorption bands: 2238 cm^{-1} (νAs—H); 1322, 1273, 1245, 1186 cm^{-1} (νC—F); 1070 cm^{-1} (νN—O); 972 cm^{-1} (νC—N); 721 cm^{-1} (δC—F). The band located at 869 cm^{-1} can be attributed to the As=N stretching vibration. The EI MS (70 eV) of iminoarsine (**A**) does not exhibit the parent ion but gave other fragmentation ions at *m/z* 170 $[CF_2NONAsH]^{+\cdot}$, 154 $[CF_2N_2AsH]^{+\cdot}$, 119 $[AsNON]^{+\cdot}$ and 69 $[CF_3]^{+\cdot}$. The molecular weight determined by Regnault's method was 258 g mol^{-1} (compound **A** requires 258 g mol^{-1}).

The presence of the AsH moiety in **A** was chemically confirmed by its reactions with the bis (trifluoromethyl)nitroxy radical, which is a powerful hydrogen abstractor and a radical scavenger.[11] The reactions gave the bis(trifluoromethyl)nitroxy derivative $(CF_3)_2NON{=}AsON(CF_3)_2$ in 52% yield, together with a quantitative amount of bis(trifluoromethyl)hydroxylamine, as shown by the equation:

$$(CF_3)_2NON{=}AsH + 2(CF_3)_2NO \longrightarrow (CF_3)_2NON{=}AsON(CF_3)_2 + (CF_3)_2NOH. \quad \textbf{(B)}$$

* Author to whom correspondence should be addressed.

The iminoarsine **B**, shows typical IR absorptions due to the $(CF_3)_2NO$ group located at 1291, 1244, 1199, 1080, and 722 cm^{-1} and the As=N group at 869 cm^{-1}. Its mass spectrum shows fragmentation ions at *m/z* 344 $[C_2F_9N_3O_2As]^{+\cdot}$, 168 $[C_2F_6NO]^{+\cdot}$ and 75 $[As]^{+\cdot}$. Its molecular weight determined by Regnault's method was 425 g mol^{-1} (compound **B** requires 425 g mol^{-1}).

The presence of the As=N double bond in the $(CF_3)_2NO$-substituted iminoarsines, **A** and **B**, was chemically confirmed by its reactions with anhydrous hydrogen iodide to afford the addition products, according to the equation:

$$(CF_3)_2NON{=}AsR + HI \longrightarrow (CF_3)_2NO\underset{H}{N}\text{—}\underset{I}{As}R$$

(**C**): R = H
(**D**): R = $ON(CF_3)_2$.

Both products, **C** and **D**, were isolated by trap-to-trap vacuum fractionation at the −60°C trap, the former as a pale yellow solid in 75% yield and the latter as a pale yellow liquid in 85% yield. The IR spectra of the products, **C** and **D**, showed the N—H stretching vibrations at 3398 and 3415 cm^{-1}, respectively, suggesting that addition involves the migration of the hydrogen to the nitrogen atom and the iodine to the more electropositive arsenic atom. The IR spectra also showed the presence of the AsH group, **C**: 2271 cm^{-1}; and the $(CF_3)_2NO$ group(s), **C**: 1323, 1271, 1240, 1213, 1184, 1068, 972 and 717 cm^{-1}; **D**: 1312, 1269, 1226, 1046, 972 and 712 cm^{-1}. The EI MS (70 eV) of both products consist of the following fragmentation ions, **C**: *m/z* 218 $[HNAsHI]^{+\cdot}$, 217 $[NAsHI]^{+\cdot}$, 216 $[NAsI]^{+\cdot}$, 168 $[C_2F_6NO]^{+\cdot}$, 149 $[C_2F_5NO]^{+\cdot}$, 130 $[C_2F_4NO]^{+\cdot}$, 127 $[I]^{+\cdot}$ and 69 $[CF_3]^{+\cdot}$; **D**: 257 $[C_2F_6NONAs]^{+\cdot}$, 168 $[C_2F_6NO]^{+\cdot}$, 149 $[C_2F_5NO]^{+\cdot}$ and 69 $[CF_3]^{+\cdot}$. Analysis for iodine in the products **C** and **D** gave 33.02 and 22.07%, respectively; (Calc: **C**, 32.90%; **D**, 22.96%). ^1H NMR of product **C** consists of δNH, 6.13 ppm (multiplet) and δAsH, 0.40 ppm (multiplet) w.r.t TMS; and ^{19}F NMR of product **C** consists of δCF_3, 16.39 ppm (singlet) w.r.t. CF_3COOH.

Acknowledgements—We thank the National University of Singapore for a research grant. One of us (L.F.K.) thanks the University for a Research Scholarship.

REFERENCES

1. E. W. Abel and S. A. Mucklejohn, *Phosphorus and Sulphur* 1981, **9**, 235.
2. E. Niecke and W. Flick, *Angew. Chem. Int. Ed.* 1973, **7**, 585.
3. E. Niecke, R. Ruger and W. W. Schoeller, *Angew. Chem. Int. Ed.* 1981, **20**, 1034.
4. N. Wiberg, K. Schurz and G. Fischer, *Angew. Chem. Int. Ed.* 1985, **24**, 1053.
5. N. Wiberg, G. Wagner and G. Miller, *Angew. Chem. Int. Ed.* 1985, **24**, 229.
6. C. Glidewell, D. Lloyd and K. W. Lambard, *J. Chem. Soc., Dalton Trans.* 1987, 501.
7. C. Glidewell, D. Lloyd, K. W. Lambard and J. S. McKechnie, *Tetrahedron Lett.* 1987, **28**, 343.
8. N. Wiberg, *J. Organometal. Chem.* 1984, **273**, 141.
9. H. G. Ang and F. K. Lee, *Polyhedron* 1989, **8**, 379.
10. N. Wiberg, *J. Organometal. Chem.* 1984, **273**, 141.
11. H. G. Ang, *J. Chem. Soc., Chem. Commun.* 1968, 1320.

Polyhedron Vol. 8, No. 12, pp. 1463–1470, 1989
Printed in Great Britain

0277–5387/89 $3.00+.00
© 1989 Pergamon Press plc

A NEW RADIATION-CATALYTIC ROUTE TO HYDRAZINE AND AMMONIA

J. O. DZIĘGIELEWSKI

Department of Inorganic and Radiation Chemistry, Institute of Chemistry, Silesian University, Katowice, Szkolna 9 Street, Poland

(*Received* 7 *February* 1988; *accepted* 12 *December* 1988)

Abstract—In methanol solution, nitrogen was reduced to H_4N_2 and H_3N using the molybdenum(IV) complex with dppe and γ-radiation. Radiation-catalytic yields of hydrazine and ammonia were determined. These yields increase with increasing concentration of the molybdenum(IV) complex. $[Mo(N_2)_2(dppe)_2]$, H_4N_2 and H_3N were isolated and identified. Other intermediates of the reduction were also observed. The initial form of the catalyst was reproduced by oxidation of molybdenum(0) to molybdenum(IV) with the coordinated nitrogen. The solvent participated in the latter reaction. The process of N_2 fixation and reduction is a chain-reaction (see yields of H_4N_2 and H_3N in Table 1). The mechanism of the radiation-catalytic reduction of N_2 was suggested.

Many investigations on the molecular N_2 fixation and reduction using transition metal compounds have been carried out for over 20 years.[1,2] Molybdenum complexes play an important role in this process.[3–22] It is easy to fix N_2 by using metal ions in a low oxidation state. In most cases reduction of the coordinated N_2 with acids,[1,7,10,11,15,18,19] alcohol solutions[1,5,6,11,12] or other reagents,[1,6,8,9,13,14,16,17,20] was inefficient, which was connected with the oxidation of the central ion and destruction of the complex. The attempts to overcome these difficulties using the hydride complexes[11] were unsuccessful. Application of UV[23] or ionizing radiation,[24,25] in the case of dinitrogen complexes, led to the liberation of N_2. Significant progress was achieved by the use of catalytic systems[26–32] or electrocatalysis.[33,34] Amalgams of alkali metals are also used as reducers.[35] A report on the cyclic reduction of N_2 by electrocatalysis[36,37] and radiation-catalysis[38] has appeared recently.

Very recently, an attempt of N_2 fixation and reduction (to H_4N_2) by the UV irradiation of the hydride complexes of molybdenum and tungsten with phosphine compounds in N_2 saturated cyclohexane was made.[39] H_3N is a typical product of the reduction (sometimes together with H_4N_2). On the basis of our earlier radiation-spectroscopic investigations,[40–44] one can expect that a complex which exhibits a suitable symmetry and a proper spin state of the central ion with the free non-bonding acceptor orbitals localized on ligands, can be used for the N_2 fixation and reduction in the field of ionizing radiation. These conditions are met in the case of $[MoOCl(dppe)_2]Cl$[40,42] (dppe = $Ph_2PCH_2CH_2PPh_2$). The solvent type is also important in processes generated by ionizing radiation. Methanol is a suitable solvent because dppe contains low energetic acceptor orbitals and forms $(dppe)^-$ anions with e_s^-, which react with the $CH_3OH_2^+$ cations giving the neutral dppe molecules without decomposition.[45] Stability of the $Mo(dppe)_2$ group in the irradiated $[MoOCl(dppe)_2]^+$ complex, in methanol solutions, was shown earlier.[40,42]

The main purpose of this work was an attempt to fix and reduce molecular N_2 in the field of radiation by $[MoOCl(dppe)_2]^+$ in a methanol solution.

EXPERIMENTAL

The $[MoOCl(dppe)_2]Cl$ complex was prepared according to the literature.[46] Methanol was distilled after the removal of water. A solution of H_2SO_4 (0.05 mol dm^{-3}) or KOH (about 10^{-7}, 10^{-5} and 1 mol dm^{-3}) in methanol, was saturated for 30 min with N_2 (O_2 was removed with Cu) or with Ar. Then $[MoOCl(dppe)_2]Cl$ was dissolved and the solutions were saturated again (N_2 or Ar, 15 min). The concentration of N_2 was 6.83×10^{-3} mol dm^{-3}.[47] Next, the solutions of Mo^{IV} were irradiated in a Co γ-

Table 1. Radiation yields of hydrazine and ammonia in acidified methanol solutions

Condition of reduction of N_2			The radiation yields (number of molecules per 100 eV)					
Concentration (mol dm^{-3})			$N_2H_4 \cdot H_2SO_4$	$(NH_4)_2SO_4$				
$[MoOCl(dppe)_2]^+$	H_2SO_4	The dose rate (eV cm^{-3} s^{-1})	Evaluated	Evaluated	Calculated on the basis of the disproportionation of $N_2H_4 \cdot H_2SO_4$	Total yield $G_{N_2H_4 \cdot H_2SO_4} + G_{(NH_4)_2SO_4}$	Concentration of $N_2H_4 \cdot H_2SO_4$ and $(NH_4)_2SO_4$ calculated on the basis of total yield (column 7) and the dose rate (column 3) (1 min of irradiation) (mol dm^{-3})	Moles of $N_2H_4 \cdot H_2SO_4$ and $(NH_4)_2SO_4$ per 1 mole $[MoOCl(dppe)_2]^+$ (1 min of irradiation)
1	2	3	4	5	6	7	8	9
5×10^{-3}	5×10^{-2}	3.97×10^{17}	2.8	—	—	—	—	—
1×10^{-2}	5×10^{-2}	3.97×10^{17}	6.0	—	—	—	—	—
4×10^{-2}	5×10^{-2}	3.97×10^{17}	11.3	20.6	15.6	31.9	6.7×10^{-4}	1.7×10^{-2}
1×10^{-1}	5×10^{-2}	3.97×10^{17}	21.0	41.7	28.0	62.7	2.7×10^{-3}	2.7×10^{-2}
2×10^{-1}	2×10^{-5}	2.20×10^{14}	5.5	6.1	7.2	11.6	2.5×10^{-6}	1.25×10^{-5}
2×10^{-1}	5×10^{-2}	2.20×10^{14}	5.5	9.6	7.2	15.1	3.3×10^{-6}	1.65×10^{-5}

source "Issledovatel". The dose rates were 3.97×10^{17} or 2.2×10^{4} eV cm^{-3} s^{-1} (recalculated for the methanol solutions). During the irradiation process, N_2 was bubbled through the solutions (earlier saturated with N_2) in a continuous or periodical way (10 min of saturation after each 30 min of irradiation). A system of methanol washers was used for N_2 or Ar saturation. The concentration of gases was kept constant to maintain the original concentrations of H_2SO_4, KOH and [MoOCl(dppe)$_2$]Cl. H_4N_2 was isolated quantitatively from irradiated alkaline ([KOH] $\approx 10^{-7}$ mol dm^{-3}) solution by adding $CuCl_2$ to a solution of Mo^{IV} before irradiation (see Table 1 for Cu^{II} concentration) or in a coordinated form with Mo and dppe ([KOH] $\approx 10^{-5}$ mol dm^{-3}). The Mo complexes with N_2 in the coordination sphere were isolated (not quantitatively) from the irradiated solutions at [KOH] = 1 mol dm^{-3}. Hydrazine was directly determined in the irradiated solutions or in the form of the Cu^{II} complex from the alkaline solutions by *p*-dimethylaminobenzoic aldehyde (following a previous dissolution in H_2SO_4).[48,49] Ammonia was determined by the indophenol test.[37,50]

The dose was determined with a Fricke dosimeter. The UV and visible spectra were recorded on a Beckman 5240 spectrometer, and IR spectra on a Specord IR 75 Carl Zeiss Jena spectrometer.

RESULTS AND DISCUSSION

Figures 1 and 2 show the numbers of $(N_2H_6)SO_4$ and $(NH_4)_2SO_4$ molecules as a function of dose and concentration of [MoOCl(dppe)$_2$]Cl, for the different rates of dose. Table 1 presents the radiation yields, calculated from Figs 1 and 2. From Figs 1 and 2, it is evident that the numbers of $(N_2H_6)SO_4$ molecules are the non-linear functions of dose and show the distinct maxima, and that the formation of ammonia and hydrazine are not simultaneous. In fact, after the binding of H_4N_2 as a form of the Cu^{II} complex and its removal from the methanol solution as a precipitate, there is no evidence of H_3N in the precipitate or in solution and the numbers of hydrazine molecules are the linear functions of dose (Fig. 3).

In the absence of $Cu^{II}Cl$ in the alkaline solution, formation of H_3N and H_4N_2 is similar to that shown in Figs 1 and 2. Table 2 presents the evaluated yield of H_4N_2 in the alkaline solutions. The shapes of the formation curves for H_4N_2 may originate not only from its conversion, but also from its decomposition.

Participation of Cu^{II} and Mo^{IV} in oxidation or

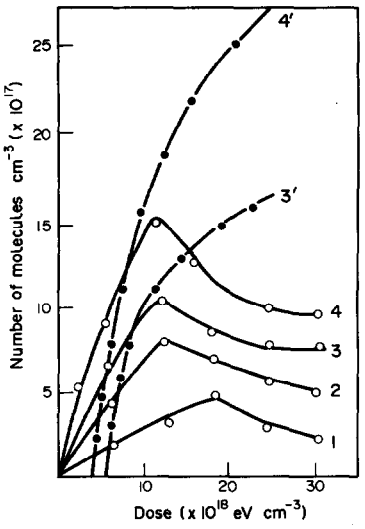

Fig. 1. Numbers of $N_2H_6^{2+}$ (curves 1–4) and NH_4^+ (curves 3′ and 4′) ions as a function of the dose and concentration of [MoOCl(dppe)$_2$]Cl: 1—5×10^{-3} mol dm^{-3}; 2—1×10^{-2} mol dm^{-3}; 3 and 3′—4×10^{-2} mol dm^{-3}; 4 and 4′—1×10^{-1} mol dm^{-3}.

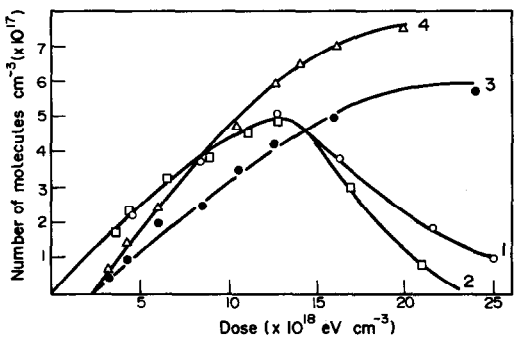

Fig. 2. Numbers of $N_2H_6^{2+}$ (curves 1 and 2) and NH_4^+ (curves 3 and 4) ions as a function of the dose and concentration of H_2SO_4 (concentration of [MoOCl(dppe)$_2$]$^+$ = 2×10^{-1} mol dm^{-3}): 1 and 3—2×10^{-5} mol dm^{-3}; 2 and 4—5×10^{-2} mol dm^{-3}.

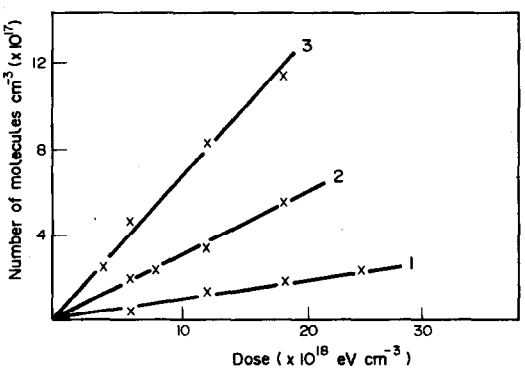

Fig. 3. Numbers of H_4N_2 molecules as function of the dose and concentration of [MoOCl(dppe)$_2$]Cl: 1—1.07×10^{-2} mol dm^{-3} ([$CuCl_2$] = 3.7×10^{-4} and [KOH] = 7.30×10^{-7} M); 2—2.70×10^{-2} mol dm^{-3} ([$CuCl_2$] = 3.7×10^{-4} and [KOH] = 7.40×10^{-7} M); 3—4.20×10^{-2} mol dm^{-3} ([$CuCl_2$] = 4.1×10^{-4} and [KOH] = 8.13×10^{-7} M).

Table 2. Radiation yields of hydrazine in alkalized methanol solutions. The dose rate was 3.97×10^{17} eV cm^{-3} s^{-1} and [KOH] ≈ $7\text{–}8 \times 10^{-7}$ mol dm^{-3}

Concentration of $[MoOCl(dppe)_2]^+$ (mol dm^{-3})	The radiation yield number of molecules per 100 eV solutions		Concentration of Cu^{II} ion (mol dm^{-3})
	Without Cu^{II} ions	With Cu^{II} ions	
1.07×10^{-2}	1.7	2.1	3.70×10^{-4}
2.14×10^{-2}	2.7	—	—
2.70×10^{-2}	—	3.7	3.75×10^{-4}
4.20×10^{-2}	5.0	7.6	4.10×10^{-4}

disproportionation of H_4N_2 was experimentally excluded (see Figs 5 and 6). Formation of H_3N due to disproportionation of H_4N_2 is also in disagreement with the data in Table 1.

Taking into account the values of the rate constants in the reaction of H_4N_2 with e_s^- ($k_{H_4N_2+e_s^-} = 3 \times 10^2$ dm^3 mol^{-1} s^{-1} [51]) and with H atoms ($k_{N_2H_5^++H} = 2.4 \times 10^4$ dm^3 mol^{-1} s^{-1} [52]), one should exclude this interaction with the unstable products of CH_3OH radiolysis. The presence of amines was also not proved and it excludes a reaction of H_4N_2 with (CH_2OH) radicals. Hence, according to the data presented above, the Mo with dppe complex in the field of radiation causes a binding (fixation) and reduction of N_2 to H_3N, and H_4N_2 is an intermediate product. The data in Table 1 indicate that the fixation and reduction of N_2 are chain processes, because the radiation yield of these processes is higher than a few molecules per 100 eV[53] ($G_{H_4N_2} + G_{H_3N} \cong 62$). Taking into account the fact that the value of the negative effective charge on N_β in Mo—N_α—N_β is higher than for N atoms in Mo—NH_2—NH_2, one can expect a greater influence of the H^+ ion concentration on H_3N yield compared to H_4N_2. Figure 2 meets these expectations, which proves the formation of H_3N via H_4N_2 reduction. A non-linear dependence of the number of H_4N_2 molecules as a function of the dose is caused by the hydrogenation of H_4N_2, and a higher rate of hydrogenation (a two-electron process; $G_{H_3N} > G_{H_4N_2}$) compared with the reduction of N_2 to H_4N_2 (a four-electron process) leads to a decreasing number of hydrazine molecules. The significant influence of the rate of dosage on the H_3N and H_4N_2 yields is due to the higher stationary concentration of the Mo^0 and Mo^{II} complexes with H_4N_2. All the processes caused by the irradiation of the methanol solutions of $[MoOCl(dppe)_2]Cl$ saturated with N_2, were followed by testing the changes in the coordination sphere of the central atom. Figure 4 shows a spectrum of a precipitate (dark brown) isolated from the irradiated complex of Mo^{II} in a 1 M methanol solution of KOH, saturated periodically with N_2.

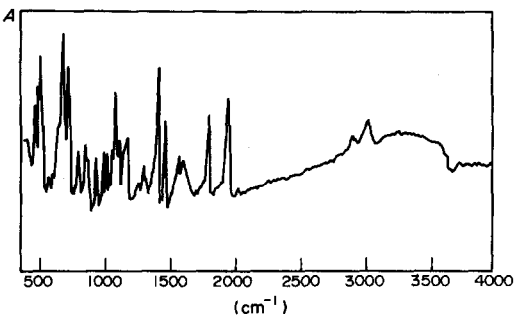

Fig. 4. IR spectrum of precipitate formed as a result of irradiation of $[MoOCl(dppe)_2]Cl$ (concentration = 10^{-2} mol dm^{-3}) in a 1 M methanol solution of KOH, periodically saturated with N_2. Dose = 2.48×10^{19} eV cm^{-3}.

According to Fig. 4, there is a valence vibration of N_2—Mo—N_2 (*trans*) at 1977 cm^{-1}. For the *cis* (C_{2v} symmetry) configuration of N_2 molecules, one can expect two ν_{Mo-N_2} vibrations (A_1 and B_1), while for C_{4v} symmetry 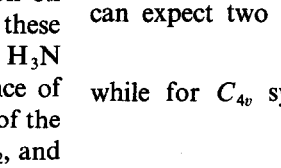 ν_{Mo-N_2} will occur at higher frequency if L is a stronger acceptor, or at lower frequency, if L is a weaker acceptor than N_2, during the formation of π-bonds.[3,54–57] The vibration at 1820 cm^{-1} can be assigned to $\nu_{Mo-CO-Mo}$ or ν_{Mo-CO}.[58] A band at 1820 cm^{-1} also occurs for a precipitate formed after irradiation of $[MoOCl(dppe)_2]Cl$ in a methanol solution of KOH (1 mol dm^{-3}), saturated with Ar. Carbon monoxide is a product of radiation decomposition of CH_3OH, particularly in an alkaline environment and in the presence of acceptors of the charge of the CH_2O^-

anion radicals[25] (see the proposed mechanism). A substance, whose spectrum is shown in Fig. 3, decomposes quickly.

In the light of the above data, one can assume that the unstable substance is a mixture of $[Mo(N_2)_2(dppe)_2]$, $[Mo(CO)(Cl)(dppe)_2]$ and $[MoOCl(dppe)_2]$. A substance with CO groups exchanges carbon monoxide for N_2 in the field of radiation, forming a bis-dinitrogen complex. A solution of $[MoOCl(dppe)_2]Cl$ irradiated in 1 M KOH in methanol, under constant saturation of N_2, forms a yellow–orange precipitate, and its IR spectrum is identical with the earlier interpreted one of $[Mo(N_2)_2(dppe)_2]$.[44] Hence we can assume the radiation route for the formation of the Mo^0 bis-dinitrogen complex.

In irradiated, alkaline ($[KOH] \geqslant 10^{-5}$ mol dm^{-3}) and constantly saturated with N_2 solutions of the Mo^{IV} complex, a chestnut substance is formed (Fig. 5 shows its IR spectrum). It is evident from Fig. 5 that the Mo complex contains dppe in its coordination sphere (ν_{C-H} at 3040 and 2900 cm^{-1}, ν_{P-C} at 1430 and 1480 cm^{-1} and aromatic deformation modes of C—C and C—H in the range 500–1350 cm^{-1}),[40,44] and also the Mo=O group ($\nu_{Mo=O}$ at 943 cm^{-1}). In the region of ν_{NH_2}, four bands at 3220, 3420, 3480 and 3550 cm^{-1} occur. Taking into account the intensities and their frequencies, one can assume that two of them are due to free NH_2 groups and the other two (at the lower frequencies) originate from Mo—NH_2 groups. Such a large number of ν_{NH_2} bands and the large differences in frequencies suggest the assignment of these vibrations to Mo—NH_2—NH_2 groups. An analysis of the deformation mode of NH_2 groups is not possible because of overlapping with dppe bands. A spectrum of the Mo complex does not change with time, indicating the stability of H_4N_2 within the coordination sphere of Mo.

The isolated product of N_2 reduction from an

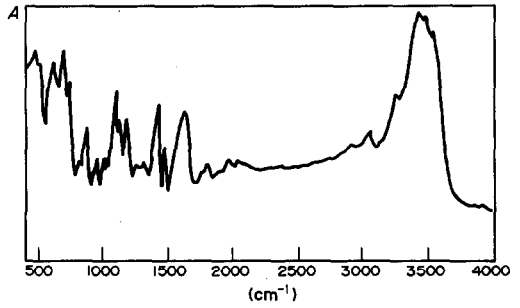

Fig. 5. IR spectrum of precipitate formed as a result of irradiation of $[MoOCl(dppe)_2]Cl$ (concentration = 10^{-2} mol dm^{-3}) in methanol in the presence of KOH ($\approx 10^{-5}$ mol dm^{-3}) saturated with N_2. Dose = 2×10^{21} eV cm^{-3}.

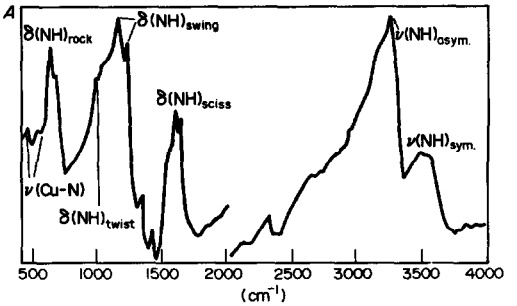

Fig. 6. IR spectrum of precipitate formed as a result of irradiation of $[MoOCl(dppe)_2]Cl$ (concentration = 10^{-2} mol dm^{-3}) in methanol ($[KOH] \approx 10^{-7}$ mol dm^{-3}, $[CuCl_2] = 4 \times 10^{-4}$ mol dm^{-3}) saturated with N_2. Dose = 7.15×10^{20} eV cm^{-3}.

irradiated solution of $[MoOCl(dppe)_2]Cl$ in the presence of $Cu^{II}Cl$ is a dark blue precipitate and its spectrum is shown in Fig. 6. A similar precipitate, having an identical spectrum, is obtained during the reaction of $CuCl_2$ with H_4N_2 in alkaline CH_3OH ($[KOH] \approx 10^{-7}$ mol dm^{-3}). Similar spectra of Cu^{II} complexes with hydrazine and its derivatives (similar to Fig. 1) are known.[59,60] ν_{N-H} and δ_{N-H} present in Fig. 6 prove the reduction of N_2 to H_4N_2. A 2 : 1 molar ratio of H_4N_2 to $CuCl_2$ in the complex has been found. Taking into account the possible symmetries of Cu^{II} complexes[61] and with the aid of analysis of normal modes of NH_2 groups (seen in Fig. 6), one can come to the conclusion that the complex of Cu^{II} with H_4N_2 has a D_{2d} symmetry, because the number of normal vibrations active in the IR for the NH_2 group is six ($3B_2$ and $3E$). Complexes with D_{4h} or C_{2v} symmetry should have four (A_{1u}, $2E_u$ and B_{2u}) and 11 ($4A_1$, $4B_1$ and $3B_2$) vibrations active in the IR, respectively. In Fig. 6 two bands (among four : $2B_2$ and $2E$) were assigned to ν_{Cu-N}. δ_{Cu-N} vibrations occur at a lower frequency than those in Fig. 6. Hence, according to Fig. 6, the Cu^{II} with H_4N_2 complex is the $CuCl_2 \cdot 2H_4N_2$ compound and it is a chain type polymer:

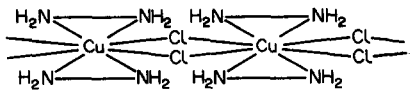

This conclusion is confirmed by magnetochemical data ($\chi_g = 3.2 \times 10^{-6}$ erg G^{-2} g^{-1}, and μ_{eff} calculated for an elementary unit of the chain polymer for a dimer is 0.8 mB) and by stoichiometrical analysis: Cu 23.3% (calc. 32.03%); Cl 35.2% (calc. 35.7%). A spectrum of $CuCl_2 \cdot 2H_4N_2$ did not change.

According to all these facts, the proposed mechanism of radiation-catalytic fixation and reduction of N_2 is as follows:

(0) $CH_3OH \rightsquigarrow e_s^-, CH_3OH_2^+,$

$H, CH_2OH(CH_2O^-)$

(1) $[MoOCl(dppe)_2]Cl \xrightarrow[CH_2O^-]{e_s^-, H}$

$[MoCl_2(dppe)_2] + CO + H_2 + H_2O$

(2) $[MoCl_2(dppe)_2] \xrightarrow[2N_2]{e_s^-, H}$

$[Mo(N_2)_2(dppe)_2] + 2Cl^-(HCl)$

(3) $[Mo(N_2)_2(dppe)_2] \xrightarrow[H_2^+]{CH_3OH_2^+}$

$$\left[\begin{matrix} N{-}NH_2 \\ \| \\ Mo(CH_3O)(dppe)_2 \end{matrix}\right]^+ + N_2$$

(4) $$\left[\begin{matrix} N{-}NH_2 \\ \| \\ Mo(CH_3O)(dppe)_2 \end{matrix}\right]^+ \xrightarrow[CH_3OH_2^+]{e_s^-, H}$$

$$\left[\begin{matrix} N{-}NH_2 \\ \| \\ Mo(dppe)_2 \\ \| \\ O \end{matrix}\right]^+ + CH_4 + CH_3OH$$

(5) $$\left[\begin{matrix} N{-}NH_2 \\ \| \\ Mo(dppe)_2 \\ \| \\ O \end{matrix}\right]^+ \xrightarrow[CH_3OH_2^+, H_2^+]{e_s^-, H, 2Cl^-}$$

$2NH_3 + [MoOCl(dppe)_2]Cl + CH_3OH.$

The reduction of $[MoOCl(dppe)_2]Cl$ and other complexes of Mo by e_s^-, H and CH_2O^- was observed earlier,[40-42] and the formation of $[MoCl_2(dppe)_2]$ was shown.[40] Of course, e_s^- can play some role in non-acidic solutions, while CH_2O^- can only participate when in alkaline solutions. Reaction (2) is confirmed quite well by formation of the Mo^0 bis-dinitrogen complex which is protonated at the very moment of formation [reaction (3)]. Reaction (3) is usually generated by H^+ ions or by molecules of alcohol.[7,62-64] Hydrogen atoms react with N_2 molecules in the gaseous state.[65] Hence, it is likely that the reduction of the N_2 ligand and H_4N_2 by molecular H_2^+ ions [reactions (3) and (5)] formed in acidic methanol ($H^+ + H \rightarrow H_2^+$ [66]), occurs. H_2^+ ions are able to reduce gaseous N_2,[67] so the reduction of coordinated nitrogen should be even easier.

Reaction (4) presents the formation of Mo=O and H_4N_2 (see Fig. 5). A hydrazide (2−) ligand in the Mo^{IV} with dppe complex is not reduced effectively by the central ion.[5,62,68] The unstable products of radiolysis (e_s^-, H, CH_2O^-) reduce the central ions to lower oxidation state ($k_{Mo^V + e_s^-} > 10^9$ $dm^3\ mol^{-1}\ s^{-1}$,[43] $k_{CH_3OH + e_s^-} \approx 10^5$ $dm^3\ mol^{-1}\ s^{-1}$ [72]), the reduced central ion reduces a protonated hydrazide ligand to H_4N_2 and then to H_3N [reactions (4) and (5)]. The poor reducing power of Mo^{IV} was mentioned,[62] therefore protonation of *trans*-$[Mo(N_2)_2(dppe)_2]$ does not lead to H_4N_2 and H_3N.[5,7,62]

The diamagnetic complex of Mo^{IV} with dppe and with =N—NH_2, exhibits C_{4v} symmetry, hence by analogy with $[MoOCl(dppe)_2]^+$ its electron configuration is likely to be $(b_2)^2$. A low Mo^{IV} reduction potential in the hydrazide complex can be explained by the delocalization of $(b_2)^2$ electrons on phosphorus 3*d* orbitals (strong Mo—P bond). Monodentate phosphines form weaker Mo—P bonds, hence the delocalization of the Mo electrons is not so effective; that electrons can more easily reduce the protonated hydrazide group.

Reaction (5) is confirmed by the formation of H_3N and the presence of $[MoOCl(dppe)_2]Cl$ in a product obtained after several irradiations of a solution of the Mo^{IV} complex saturated with N_2. A solution saturated with Ar contains only $[MoCl_2(dppe)_2]$. Multiple irradiation of that same solution of the Mo^{IV} complex with dppe and saturated with N_2 leads to H_4N_2, H_3N and $[MoOCl(dppe)_2]Cl$ in all cases. Hence, the fixation and the reduction of N_2 by the use of the Mo^{IV} complex in the field of radiation are radiation-catalytic processes in which $[MoOCl(dppe)_2]^+$ undergoes the necessary modification to a form which is able to fix N_2, and following a reduction of coordinated nitrogen a reproduction of the original form of catalyst occurs. Due to gradual reduction of N_2 it is possible, in some conditions, to obtain H_3N or H_4N_2, or simultaneously both of these products.

REFERENCES

1. A. D. Allen and C. V. Senoff, *J. Chem. Soc., Chem. Commun.* 1965, 621.
2. J. Chatt, *New Trends in the Chemistry of Nitrogen Fixation*. Academic Press, London (1980).
3. H. M. Colquhoun and R. A. Head, *Inorg. Chim. Acta* 1980, **45**, L123.
4. L. J. Archer and T. A. George, *Inorg. Chim. Acta* 1980, **44**, L129.
5. M. Hidai, T. Takahashi, I. Yokotake and Y. Uchida, *Chem. Lett., Chem. Soc. Jpn* 1980, 645.
6. G. E. Bossard, D. C. Busby, M. Chang and T. A. George, *J. Am. Chem. Soc.* 1980, **102**, 1001.
7. T. Takahashi, Y. Mizobe, Y. Uchida and M. Hidai, *J. Am. Chem. Soc.* 1980, **102**, 7461.
8. A. J. L. Pombeiro, *J. Organomet. Chem.* 1980, **202**, C15.
9. D. C. Busby, T. A. George, S. D. A. Iske Jr and S. D. Wagner, *Inorg. Chem.* 1981, **20**, 22.

10. T. A. George and R. A. Kovar, *Inorg. Chem.* 1981, **20**, 285.
11. S. N. Anderson, M. E. Fakley, R. L. Richards and J. Chatt, *J. Chem. Soc., Dalton Trans.* 1981, 1973.
12. R. A. Henderson, G. Davies, J. R. Dilworth and R. N. F. Thorneley, *J. Chem. Soc., Dalton Trans.* 1981, 40.
13. M. Nardelli, C. Pelizzi, G. Predieri and G. P. Chiusoli, *J. Organomet. Chem.* 1981, **204**, 75.
14. H. M. Colquhoun, *Transition Met. Chem.* 1981, **6**, 57.
15. K. Iwanami, Y. Mizobe, T. Takahashi, T. Kodama, Y. Uchida and M. Hidai, *Bull. Chem. Soc. Jpn* 1981, **54**, 1773.
16. G. E. Bossard and T. A. George, *Inorg. Chim. Acta* 1981, **54**, L239.
17. G. E. Bossard and T. A. George, *Inorg. Chim. Acta* 1981, **54**, L241.
18. G. E. Bossard and T. A. George, *Inorg. Chem.* 1983, **22**, 1968.
19. T. A. George and L. M. Koczon, *J. Am. Chem. Soc.* 1983, **105**, 6334.
20. F. Minzoni, M. Nardelli, C. Pelizzi and G. Predieri, *Gazz. Chim. Ital.* 1984, **114**, 221.
21. A. K. Rappe, *Inorg. Chem.* 1984, **23**, 995.
22. T. Yamabe, K. Hori, T. Minato and K. Fukui, *Inorg. Chem.* 1980, **19**, 2154.
23. R. J. W. Thomas, G. S. Laurence and A. A. Diamantis, *Inorg. Chim. Acta* 1978, **30**, L353.
24. M. Venturi, A. Breccia, Q. G. Mulazzani and M. D. Ward, *Atti. Acad. Naz. Lincei. Rc.* 1974, **56**, 366.
25. A. K. Pikaev, *Sovrem. Radiac. Chim., Nauka, Moskva* 1986.
26. N. T. Denisov, W. F. Schuvalov and N. I. Schuvalova, *Dokl. AN SSSR* 1970, **195**, 897.
27. A. E. Schilov, A. K. Schilova and T. A. Vorontsova, *React. Kinet. Catal. Lett.* 1975, **3**, 143.
28. E. L. Moorehead, B. J. Weathers, E. A. Ufkes, P. R. Robonson and S. N. Schrauzer, *J. Am. Chem. Soc.* 1977, **99**, 6089.
29. G. N. Schrauzer, E. L. Moorehead, J. H. Grate and L. Hughes, *J. Am. Chem. Soc.* 1978, **100**, 4760.
30. N. T. Denisov, N. I. Schuvalova and A. E. Schilov, *Kinetika i Cataliz* 1985, **26**, 1493.
31. N. P. Luneva, A. P. Moravsky, A. E. Schilov and S. N. Anderson, *Nouv. J. Chim.* 1982, **6**, 245.
32. A. K. Schilova, W. D. Machaev and A. E. Schilov, *Dokl. AN SSSR*, 1984, **277**, 1414.
33. G. W. Nikolaeva, S. I. Kulakovskaa, O. N. Efimov and A. E. Schilov, *Kinetika i Kataliz* 1985, **26**, 473.
34. W. W. Strelec, A. B. Gavrilov, W. N. Carev, A. K. Schilova, L. P. Didenko and A. E. Schilov, *Kinetika i Kataliz* 1986, **27**, 332.
35. N. T. Denisov, G. G. Terechina, N. I. Schuvalova and A. E. Schilov, *Kinetika i Kataliz* 1973, **14**, 939.
36. L. P. Didenko, A. K. Schilova and A. E. Schilov, *Dokl. AN SSSR* 1980, **254**, 643.
37. C. J. Pickett, K. S. Ryder and J. Talarmin, *J. Chem. Soc., Dalton Trans.* 1986, 1453.
38. J. O. Dzięgielewski, Materials of Annual Congress of Polish Chemical Society, Report P-66, Kielce 19-22 IX (1984); Materials of Scientific Congress of Polish Society of Radiation Research, Report B-39, Łódź 17–19 IV (1986).
39. A. P. Pivovarov, Yu. W. Gak, Yu. M. Schulga, W. D. Machaev, A. P. Borisov and Yu. G. Borodko, *Izw. AN SSSR* 1979, 2590.
40. H. W. Czarnik-Matusewicz and J. O. Dzięgielewski, *Radiochem. Radioanal. Lett.* 1982, **51**, 352.
41. J. O. Dzięgielewski, R. Gil and P. Głowacki, *Radiochem. Radioanal. Lett.* 1982, **50**, 251.
42. J. O. Dzięgielewski, *Polyhedron* 1984, **3**, 1131.
43. J. O. Dzięgielewski, *Polyhedron* 1985, **4**, 1091.
44. J. O. Dzięgielewski, B. Jeżowska-Trzebiatowska, R. Gil-Bortnowska and R. Grzybek, *Polyhedron* 1986, **5**, 833.
45. J. O. Dzięgielewski, *Tetrahedron* 1986, **42**, 109.
46. A. V. Butcher and J. Chatt, *J. Chem. Soc. A* 1971, 2356.
47. N. A. Kirillin and A. E. Scheinblin, *Termodinamika Roztvorov*. Gosenergoizdat, Moskva (1956).
48. M. Peres and A. Retit, *Bull. Soc. Chim. France* 1947, 122.
49. G. V. Watt and J. D. Chisp, *Anal. Chem.* 1952, **24**, 2006.
50. W. T. Bolleter, C. J. Buskman and P. W. Tidwell, *Anal. Chem.* 1961, **33**, 592.
51. W. A. Seddon, J. W. Fletcher and F. C. Sopchysyn, *Can. J. Chem.* 1976, **54**, 2807.
52. J. Delaire, P. Cordier and J. Belloni, *J. Phys. Chem.* 1976, **80**, 1687. A. K. Pikaev and A. S. Kabachi, *Reakcjonnaja Sposobnost Pervichnych Productov Radioliza Vody*, p. 157. Energoizdat, Moskva (1982).
53. A. K. Pikaev, *Sovremennaa Radiacionnaa Chimia*, p. 92. Nauka, Moskva (1985).
54. M. Sato, T. Tatsumi and M. Hidai, *J. Am. Chem. Soc.* 1978, **100**, 4447.
55. S. Donovan-Mtunzi, R. L. Richards and J. Mason, *J. Chem. Soc., Dalton Trans.* 1984, 2729.
56. W. Hussain, G. F. Leigh, H. Mohd. Ali, C. J. Pickett and D. Rankin, *J. Chem. Soc., Dalton Trans.* 1984, 1703.
57. T. Tatsumi, H. Tominaga, M. Hidai and Y. Uchida, *J. Organomet. Chem.* 1976, **114**, C27.
58. J. G. Bullitt, F. A. Cotton and T. J. Marks, *Inorg. Chem.* 1972, **11**, 671.
59. L. D. Cicishvyly, T. J. Cucunova, P. W. Pogoryvshvyly and Yu. Ya. Carytonov, *Issledovanya v Oblasty Chimii Kompleksnych i Prostych Soyedyneni Nekotorych Perechodnych i Redkych Metallov*, p. 23. Macnereba, Tbylysy (1978).
60. S. S. Bucko, P. J. Schmanko, E. S. Demeter and W. M. Buzash, *Problemy Sovremennoy Bioenerganicheskoy Chimii*, p. 217. Nauka, Novosybirsk (1986).
61. J. O. Dzięgielewski, *Chemia nieorganiczna—Część III. Chemia metali grup pobocznych* (Inorganic Chemistry—Part III. Chemistry of Transition Metals), p. 443. Wydawnictwo Uniwersytetu Śląskiego, Katowice (1987).
62. J. Chatt, A. J. Pearma and R. L. Richards, *J. Chem. Soc., Dalton Trans.* 1977, 1852.

63. J. Chatt, A. J. Pearman and R. L. Richards, *J. Chem. Soc., Dalton Trans.* 1979, 1766.
64. M. Hidai, T. Kadoma, M. Sato, M. Harokava and Y. Uchida, *Inorg. Chem.* 1976, **15**, 2694.
65. M. C. Sauer and J. Mani, *J. Phys. Chem.* 1970, **74**, 59.
66. J. O. Dzięgielewski, *Physical Chemistry of the Irradiated Solutions of Tetracycline, its Derivatives and Complex Compounds of* Co^{II}, Ni^{II} *and* Cu^{II} *Ions with Tetracycline*, pp. 1–78. Prace Naukowe Uniwersytetu Śląskiego No 676, Katowice (1986).
67. S. A. Przeżecky and M. T. Dmitrev, *Radiaconnye fizikochimicheskye Procesy v Vozdushnoy srede*, p. 109. Atomizdat, Moskva (1978).
68. J. Chatt, G. A. Heath and R. L. Richards, *J. Chem. Soc., Dalton Trans.* 1974, 2074.
69. K. M. Idriss-Ali and G. R. Freeman, *Radiat. Phys. Chem.* 1984, **62**, 2217.

Polyhedron Vol. 8, No. 12, pp. 1471–1475, 1989
Printed in Great Britain

0277–5387/89 $3.00+.00
© 1989 Pergamon Press plc

THE INSERTION OF THE [M(CO)$_3$(NN)] FRAGMENTS (M = Mo, W; NN = 2,2′-BIPYRIDINE; 1,10-PHENANTHROLINE; ETHYLENEDIAMINE) INTO THE Hg—X (X = Cl, Br, I, N_3, SCN) BONDS OF THE [η^5-$C_5H_5Fe(CO)_2(HgX)$] COMPLEXES. HETEROTRIMETALLIC COMPOUNDS WITH Fe—Hg—M—X BONDINGS

J. GRANIFO* and M. E. VARGAS

Departamento de Ciencias Químicas, Facultad de Ingeniería y Administración, Universidad de La Frontera, Casilla 54-D, Temuco, Chile

(*Received* 17 *August* 1988; *accepted after revision* 18 *January* 1989)

Abstract—The tricarbonyl complexes [M(CO)$_3$(NN)(CH$_3$CN)] (M = Mo, W; NN = bipy, phen, en) react with the binuclear complexes [η^5-$C_5H_5Fe(CO)_2(HgX)$] (X = Cl, Br, I, SCN, N_3) to generate trinuclear products of the formula [η^5-$C_5H_5Fe(CO)_2HgM(CO)_3(NN)X$]. These complexes were characterized using IR and electronic spectroscopy. The results are interpreted as the insertion of M(CO)$_3$(NN) fragments into the Hg—X bonds to give the Fe—Hg—M—X arrays, with the metallic centre, M, being seven-coordinate. The general properties of the new compounds and their reactivity towards monodentate bases and mercury halide derivatives are discussed.

In previous work,[1] we established that the reaction of the M(CO)$_3$(NN) fragments [M = Mo, W; NN = 2,2′-bipyridine (bipy), 1,10-phenanthroline (phen)] with mercury halides, HgX_2 (X = Cl, Br, I), can be considered as the insertion of the former between the atoms of the Hg—X bonds to give either bimetallic or trimetallic complexes with X—Hg—M—X and X—M—Hg—M′—X (M′ = Mo, W) arrangements, respectively.

In an effort to gain further insight into the factors and conditions determining the insertion behaviour of the M(CO)$_3$(NN) fragments, we have now studied this reaction with the [CpFe(CO)$_2$(HgX)] complexes (Cp = η^5-C_5H_5; X = Cl, Br, I, N_3, SCN).[2] The results of this study show that, in all cases, new trimetallic compounds are obtained, using as the source of the insertion fragments the [*fac*-M(CO)$_3$(NN)(CH$_3$CN)] complexes.[1]

RESULTS AND DISCUSSION

Treatment of the [CpFe(CO)$_2$(HgX)] compounds (X = Cl, Br, I, SCN, N_3) with [M(CO)$_3$(NN)(CH$_3$CN)] (M = Mo, W; NN = bipy, phen, en) in methanol at room temperature, affords the heteronuclear trimetal complexes [CpFe(CO)$_2$HgM(CO)$_3$(NN)X], according to the reaction:

$$[CpFe(CO)_2(HgX)] + [M(CO)_3(NN)(CH_3CN)] \longrightarrow [CpFe(CO)_2HgM(CO)_3(NN)X] + CH_3CN. \quad (1)$$

The new compounds are air-stable, orange coloured microcrystalline solids. On exposure to sunlight they decompose producing mercury. They are soluble in organic solvents such as methylene chloride, chloroform and acetone; less soluble in alcohols and insoluble in light petroleum. Nevertheless, they are not at all stable in solution.

IR spectra

The IR spectra of the [CpFe(CO)$_2$HgM(CO)$_3$(NN)X] complexes in the CO stretching region (Fig. 1, Table 1) show the superimposition of the characteristic patterns of the CpFe(CO)$_2$Hg[2] and [HgM(CO)$_3$(NN)X] moieties. The last one has been characterized in the [M(CO)$_3$(NN)X]$_2$Hg[1] and [M(CO)$_3$(NN)(X)(HgX)] complexes.[1,3] This

* Author to whom correspondence should be addressed.

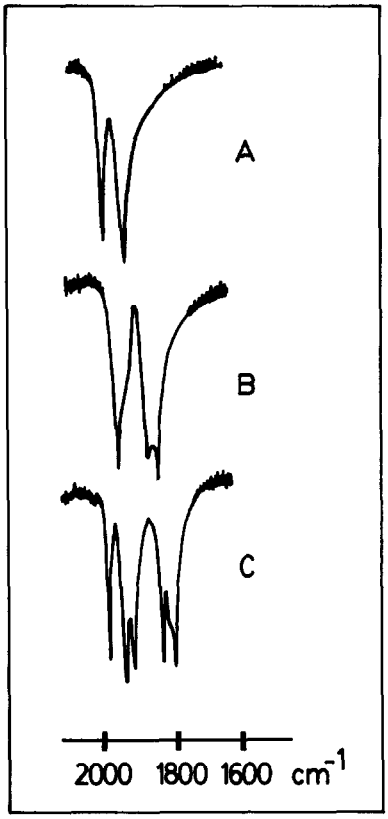

Fig. 1. IR spectra in the ν(CO) region of the complexes: (A) [CpFe(CO)$_2$(HgCl)]. (B) [Mo(CO)$_3$(bipy)(Cl)(HgCl)] and (C) [CpFe(CO)$_2$HgMo(CO)$_3$(bipy)Cl], measured using KBr discs.

fact is consistent with the M(CO)$_3$(NN) fragments having been inserted into the Hg—X bonds, giving rise to the Fe—Hg—M—X arrays.

The reaction products of the [CpFe(CO)$_2$HgSCN] complexes with [M(CO)$_3$(NN)(CH$_3$CN)] present the typical IR bands of the N-bonded thiocyanate ligands.[4] More specifically, the ν(CN) stretching vibrations appear near 2070 cm^{-1} and the patterns of the deformation vibrations, δ(NCS), are multiplets centred at *ca* 480 cm^{-1}. The products containing the azido group are characterized by the absorption ν(NN) at *ca* 2050 cm^{-1}. The other IR absorption regions show the presence of bands assignable to all other coordinated ligands.

Electronic absorption spectra in the visible region

The electronic spectra of the [CpFe(CO)$_2$HgM(CO)$_3$(NN)X] complexes in the visible region have been measured in dichloromethane solution. These consist of only one broad band in the 400–490 nm region when NN = bipy or phen, but it is absent if NN = en

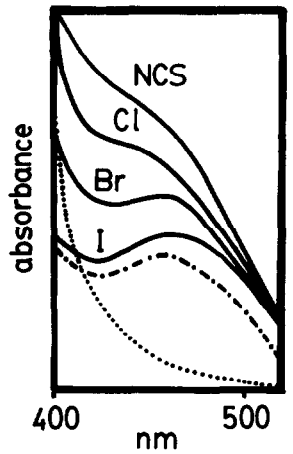

Fig. 2. Visible spectra of [CpFe(CO)$_2$HgMo(CO)$_3$(bipy)X] (——), [CpFe(CO)$_2$HgMo(CO)$_3$(en)Cl] (·····) and [Mo(CO)$_3$(bipy)(Cl)(HgCl)] (—·—·—·) complexes in dichloromethane solution.

(Table 1, Fig. 2). The intensity of this band is difficult to assess, as it generally appears on the tail of a much more intense absorption arising from the UV (Fig. 2). Nevertheless, in the [CpFe(CO)$_2$HgM(CO)$_3$(NN)] moiety, this absorption depends on X which is correlated with the spectrochemical series (Table 1), since it is shifted slightly towards the blue region in the sequence I < Br < Cl < NCS. Likewise, the related tricarbonyl complexes [M(CO)$_3$(NN)(X)(HgX)],[3] show comparable spectra (Fig. 2). For instance, their unique band in the visible ($\varepsilon > 3000$ M^{-1} cm^{-1}) is detected only when the π-delocalized bis-chelate ligands, bipy or phen, are present. These antecedents and the fact that the [CpFe(CO)$_2$(HgX)] complexes do not present absorption maxima in the visible, permit us to associate the band between 440 and 490 nm of the [CpFe(CO)$_2$HgM(CO)$_3$(NN)X] complexes with a NN(π^*) ← M($d\pi$) charge-transfer transition (MLCT).[5]

Reactivity of the [CpFe(CO)$_2$HgM(CO)$_3$(NN)X] *complexes with Lewis bases*

Dissolution of the [CpFe(CO)$_2$HgM(CO)$_3$(NN)X] complexes (M = Mo; NN = bipy, phen; X = Cl, Br, I) in donor solvents such as acetonitrile, produce slow colour changes of the solution from yellow to violet. The MLCT NN(π^*) ← M($d\pi$) absorption in the visible of the trimetallic complexes is displaced by that of the [Mo(CO)$_3$(NN)(CH$_3$CN)] complexes by *ca* 500 nm.[6] In addition, the UV region shows the superimposition of the bands of the [CpFe(CO)$_2$(HgX)] and [Mo(CO)$_3$(NN)(CH$_3$CN)] complexes. In methylene chloride and in the pres-

Table 1. Analytical, IR and visible spectra for the $[CpFe(CO)_2HgM(CO)_3(NN)X]$ complexes

Compound			Analysis (%)[a]			IR data (cm^{-1})[b]	Visible spectra (nm)[c]
M	NN	X	C	H	N	ν(CO)	NN(π^*) ← M($d\pi$)
Mo	bipy	Cl	31.9(32.1)	1.9(1.7)	3.8(3.7)	1991, 1939, 1922, 1842, 1818	450
		Br	30.6(30.3)	1.6(1.7)	3.3(3.5)	1992, 1940, 1918, 1845, 1820	460
		I	28.5(28.6)	1.6(1.6)	3.4(3.3)	1990, 1938, 1915, 1835, 1815	470
		N_3	31.9(31.8)	1.8(1.7)	9.2(9.3)	1990, 1940, 1930, 1840, 1810	[d]
		NCS	32.5(32.7)	1.6(1.7)	5.6(5.4)	1987, 1930, 1925, 1840, 1822	440
	phen	Cl	34.0(34.2)	1.8(1.7)	3.5(3.6)	1990, 1930, 1910, 1838, 1817	445
		Br	32.4(32.3)	1.7(1.6)	3.4(3.4)	1985, 1933, 1916, 1825, 1820	450
		I	30.9(30.6)	1.6(1.5)	3.3(3.2)	1988, 1930, 1918, 1830, 1825	465
		N_3	33.7(33.9)	1.8(1.7)	8.9(9.0)	1988, 1925, 1915, 1830, 1818	[d]
		NCS	34.8(34.7)	1.7(1.6)	5.4(5.3)	1985, 1930, 1920, 1835, 1825	440
	en	Cl	22.0(22.1)	2.1(2.0)	4.2(4.3)	1987, 1930, 1920, 1830, 1815	—
		Br	20.6(20.7)	2.0(1.9)	4.1(4.0)	1985, 1928, 1918, 1833, 1825	—
		I	19.5(19.4)	1.8(1.8)	4.0(3.8)	1986, 1925, 1920, 1830, 1820	—
		N_3	21.7(21.8)	2.1(2.0)	10.5(10.6)	1988, 1926, 1918, 1835, 1822	—
		NCS	23.3(23.1)	1.8(1.9)	6.1(6.2)	1985, 1925, 1916, 1835, 1824	—
W	bipy	Cl	28.8(28.7)	1.7(1.6)	3.5(3.3)	1984, 1920, 1910, 1835, 1815	475
		Br	27.5(27.3)	1.4(1.5)	3.2(3.2)	1984, 1924, 1915, 1833, 1824	485
		I	25.8(25.9)	1.6(1.4)	2.9(3.0)	1987, 1938, 1916, 1834, 1820	495
		N_3	28.6(28.5)	1.5(1.6)	8.5(8.3)	1988, 1933, 1920, 1836, 1824	[d]
		NCS	29.0(29.3)	1.7(1.5)	4.7(4.9)	1990, 1940, 1922, 1834, 1822	465
	phen	Cl	30.7(30.7)	1.6(1.5)	3.4(3.3)	1988, 1938, 1925, 1830, 1810	470
		Br	29.3(29.2)	1.5(1.4)	3.2(3.1)	1985, 1936, 1915, 1830, 1820	480
		I	27.9(27.7)	1.4(1.4)	2.8(2.9)	1987, 1935, 1918, 1835, 1820	490
		N_3	30.7(30.5)	1.6(1.5)	8.3(8.1)	1988, 1938, 1930, 1835, 1810	[d]
		NCS	31.1(31.3)	1.5(1.5)	5.0(4.8)	1987, 1935, 1925, 1822, 1818	460
	en	Cl	19.4(19.5)	1.9(1.8)	3.9(3.8)	1990, 1938, 1925, 1825, 1820	—
		Br	18.5(18.4)	1.6(1.7)	3.7(3.6)	1986, 1933, 1920, 1835, 1820	—
		I	17.2(17.3)	1.7(1.6)	3.4(3.4)	1988, 1937, 1923, 1838, 1822	—
		N_3	19.5(19.3)	1.8(1.8)	9.6(9.4)	1990, 1936, 1920, 1840, 1825	—
		NCS	20.1(20.4)	1.6(1.7)	5.7(5.5)	1990, 1938, 1925, 1835, 1820	—

[a] Required values are given in parentheses.
[b] KBr discs, all bands are strong.
[c] In CH_2Cl_2.
[d] Complex is too unstable in solution.

ence of an excess of monodentate base, such as triphenylphosphine or tetramethylthiourea, the trimetallic complexes react in a similar way to when they are in acetonitrile, giving solutions containing the $[CpFe(CO)_2(HgX)]$ and $[Mo(CO)_3(NN)L]$ complexes. These results suggest the existence of the equilibrium (L = donor solvent or monodentate bases):

$$[CpFe(CO)_2HgMo(CO)_3(NN)X] + L \longrightarrow [CpFe(CO)_2(HgX)] + [Mo(CO)_3(NN)L]. \quad (2)$$

The reaction rate of the $[CpFe(CO)_2HgMo(CO)_3(NN)X]$ complexes with acetonitrile was measured following the absorbance increase at 500 nm. The plots of $\ln(A - A_\infty)$ vs t yield straight lines indicating a first- or pseudo-first-order kinetic law. The rate constants depend on the electronegativity of the halide and increase in the sequence $Cl(k_{obs} = 0.1\ s^{-1}) < Br(k_{obs} = 1\ s^{-1}) < I(k_{obs}$ greater than $1\ s^{-1})$. When X = NCS or N_3 this reaction does not take place. Then, a plausible explanation for these results might be related mainly to the net electronic density upon the hepta-coordinate molybdenum atom.

The inert character of the $[CpFe(CO)_2M(CO)_3(NN)X]$ complexes (M = W) can probably be attributed to the softer character of the tungsten atom.

Exchange reactions with mercuric halides

The $[CpFe(CO)_2HgM(CO)_3(NN)Cl]$ complexes (M = Mo, W; NN = bipy, phen) react in acetone with $HgCl_2$. The characteristics of the reaction depend on the stoichiometric proportions of the reactants. If it is 1 : 1, the colour of the solution changes rapidly from orange to yellow, but if it is 2 : 1, then, besides the colour change, the symmetric trimetallic complexes $[M(CO)_3(NN)Cl]_2Hg$[1] are precipitated, while in solution the presence of the compound $[CpFe(CO)_2(HgCl)]$ is detected. These results suggest the occurrence of the following exchange reactions:

$$[CpFe(CO)_2HgM(CO)_3(NN)Cl] + HgCl_2 \longrightarrow [CpFe(CO)_2HgCl] + [M(CO)_3(NN)(HgCl)Cl] \quad (3)$$

$$[CpFe(CO)_2HgM(CO)_3(NN)Cl] + [M(CO)_3(NN)(HgCl)Cl] \longrightarrow [CpFe(CO)_2(HgCl)] + [M(CO)_3(NN)Cl]_2Hg. \quad (4)$$

In the first step, an exchange process involving the trimetallic complex $[CpFe(CO)_2HgM(CO)_3(NN)Cl]$ and mercuric chloride occurs, giving the soluble complexes $[CpFe(CO)_2(HgCl)]$ and $[M(CO)_3(NN)Cl(HgCl)Cl]$ [eq. (3)]. This last product, in its own time, exchanges with a second molecule of the initial complex yielding a solution containing the $[CpFe(CO)_2(HgCl)]$ complex and the insoluble compound $[M(CO)_3(NN)Cl]_2Hg$ [eq. (4)].

The verification of the above exchange reaction sequence was made by involving the $[CpFe(CO)_2HgM(CO)_3(NN)Cl]$ and $[M(CO)_3(NN)(HgCl)Cl]$ complexes in the reaction. The formation of the products indicated in eq. (4) was observed. Further evidence was gained when by this same process it was possible to isolate the asymmetric trimetallic complexes M′—Hg—M′[1] (M′ = Mo, W; NN = bipy, phen):

$$[CpFe(CO)_2HgM(CO)_3(NN)Cl] + [M'(CO)_3(NN')(HgCl)Cl] \longrightarrow [CpFe(CO)_2(HgCl)] + [Cl(NN)(CO)_3MHgM'(CO)_3(NN')Cl]. \quad (5)$$

The $[CpFe(CO)_2HgM(CO)_3(NN)Cl]$ complexes with NN = en, undergo the same reactions, but no noticeable colour changes of the solutions are observed due to the absence of the $NN(\pi^*) \leftarrow M(d\pi)$ band.

EXPERIMENTAL

The solvents were purified by standard methods and all operations were carried out under a nitrogen atmosphere. The starting materials, $M(CO)_4(NN)$,[7,8] $[M(CO)_3(NN)(CH_3CN)]$,[9] $[M(CO)_3(NN)(X)(HgX)]$[1,3] and $[CpFe(CO)_2(HgX)]$,[2] (M = Mo, W; NN = bipy, phen, en; X = Cl, Br, I), were prepared by similar methods to those described in the literature. The $[CpFe(CO)_2(HgX)]$ complexes ($X = N_3$, SCN) were precipitated by treating an acetonitrile solution of $[CpFe(CO)_2(HgCl)]$ with an excess of the NaX salt dissolved in water; the yellow crystals were filtered off and washed with water. The IR spectra were obtained by means of a Perkin–Elmer 577 spectrophotometer. The electronic spectra were recorded on a Carl–Zeiss DMR 22 instrument.

Synthesis of $[CpFe(CO)_2HgM(CO)_3(NN)X]$ ($Cp = \eta^5\text{-}C_5H_5$; M = Mo, W; NN = bipy, phen, en; X = Cl, Br, I, SCN, N_3)

These compounds were synthesized by reaction of the $[M(CO)_3(NN)(CH_3CN)]$ and $[CpFe(CO)_2(HgX)]$ complexes in methanol. All these substances were orange microcrystalline solids. The following preparation is described as a typical one.

$[CpFe(CO)_2HgMo(CO)_3(en)Cl]$. A mixture of 0.304 g (0.736 mmol) of $[CpFe(CO)_2(HgCl)]$ and 0.207 g (0.736 mmol) of freshly prepared $[Mo(CO)_3(en)(CH_3CN)]$ was vigorously stirred in 10 cm^3 of methanol in the dark for 0.5 h. The bright orange precipitate was filtered and washed 3–4 times with 3 cm^3 portions of methanol. 0.394 g (82% yield) of the microcrystalline compound were obtained. The elemental analyses of these compounds are given in Table 1.

Acknowledgements—Financial support given by the Dirección de Investigación de la Universidad de La Frontera (Project N° 1032126) to carry out this work is gratefully acknowledged. Also, we thank Miss J. Navarro, Miss A. Videla and Miss E. Klein (USACH) for their helpful assistance.

REFERENCES

1. P. Correa, M. E. Vargas and J. Granifo, *Polyhedron* 1987, **6**, 1781.
2. M. J. Mays and J. D. Robb, *J. Chem. Soc. A* 1968, 329; R. Kumar, A. R. Manning and P. T. Murray, *J. Organomet. Chem.* 1987, **323**, 53.
3. K. E. Edgar, B. F. G. Johnson, J. Lewis and S. B. Wild, *J. Chem. Soc. A* 1968, 2851.

4. D. M. Adams, *Metal Ligand and Related Vibrations*, p. 327. E. Arnold, London (1967).
5. H. Saito, J. Fujita and K. Saito, *Bull. Chem. Soc. Jpn* 1968, **41**, 359, 863.
6. J. Granifo, M. E. Vargas, J. Costamagna and M. A. François, *Polyhedron* 1988, **7**, 489.
7. M. H. B. Stiddard, *J. Chem. Soc.* 1962, 4712.
8. C. S. Kraihanzel and F. A. Cotton, *Inorg. Chem.* 1963, **2**, 533.
9. L. W. Houk and G. R. Dobson, *Inorg. Chem.* 1965, **5**, 2119.

Polyhedron Vol. 8, No. 12, pp. 1477–1484, 1989
Printed in Great Britain

0277–5387/89 $3.00+.00
© 1989 Pergamon Press plc

COMPLEXES OF HYDROXAMATES—VII. EQUILIBRIA AND KINETICS OF IRON(III) REACTIONS WITH SALICYLHYDROXAMIC ACID

NADYAH M. SHUAIB,* MOHAMED S. EL-EZABY* and OMNIYA AL-HUSSAINI

Department of Chemistry, Faculty of Science, University of Kuwait, P.O. Box 5969, 13060 Safat, Kuwait

(*Received* 27 *September* 1988; *accepted after revision* 18 *January* 1989)

Abstract—The equilibria involved in the system iron(III)–salicylhydroxamic acid (SAX) has been studied at the ionic strength of 0.15 M Cl^- in the pH range 1.0–5.0, and at the ionic strength of 1.0 M Cl^- in the H^+ concentration range 0.01–1.0 M. Potentiometric as well as spectrophotometric methods have been used to determine the formation constants in aqueous solutions. Potentiometric methods yielded different equilibrium models to the spectrophotometric methods. The difference was rationalized on the basis that the iron(III) ions were easily hydrolysed to yield oligomeric forms when the ligand concentration was not in excess. The rate of the reaction of iron(III) with SAX has been also studied under pseudo-first-order conditions in the pH range 1.0–3.0 at 0.15 M Cl^- ionic strength, as well as in the H^+ concentration range 0.2–1.0 M at 1.0 M Cl^- ionic strength. A reaction mechanism is suggested and is discussed in the light of the spectrophotometric equilibrium results and compared with pertinent literature values.

Salicylhydroxamic acid (SAX) and its halogen derivatives have been reported to act as antitubercular, antifungal agents.[1] They showed strong hypoglycemic action and can lower blood serum cholesterol levels.[1] In addition, it was discovered to be effective against trypanosomiasis.[1]

Salicylhydroxamic acid forms stable complexes with iron(III) in acidic medium ($pH \leqslant 3.5$)[2] and the preparation of a tris-chelate solid has been reported.[3] However, a complete picture of iron(III) complexes with SAX over a wide range of pH has not been investigated. Furthermore, the kinetics of the interaction of iron(III) with SAX has not been studied.

The importance of such a study lies in the fact that simple monohydroxamic acids could be involved in the iron metabolic cycle for mammals. The successful prediction of biological activity for a given iron complex depends on our ability to relate the biological functions to the physicochemical properties of the complex measured *in vitro*. These properties are diverse and include solubility, toxicity, stability and lability under physiological conditions. Due to the tendency of iron(III) to undergo extensive hydrolysis and polymerization in aqueous solution, the prime concern is the selection of the ligand which stabilizes the metal ions at biological pH and secondly, is the lability of the formed complex. This work emphasizes these approaches.

EXPERIMENTAL

The stock solution of iron(III) chloride (Merck) was prepared in acidic media (1:1 at $pH < 1.0$). The concentration of iron(III) was checked by EDTA complexometric titration, as previously described.[5] SAX (Hundhill, 99%) stock solution (0.02 M; the maximum concentration in aqueous solution) was prepared by accurate weighing of the required amount of the solid (used as provided) and dissolving in doubly distilled water.

Measurements of pH were obtained using an Orion Research Ionalyser Model 901 provided with Orion glass (91-01) and calomel (91-02) electrodes, as well as a Radiometer Model PHM 84 Research pH-meter equipped with a Russell combined glass electrode (CNL). The Orion system was used in

* Authors to whom correspondence should be addressed.

the potentiometric titration, while the Radiometer system was used in the spectrophotometric study. The pH-meter was calibrated by using the appropriate Radiometer or Merck buffers (2.00, 4.00 and 6.87).

Kinetic measurements were carried out using the Union Giken Stopped-flow Reaction Analyser (RA-401) provided with an RA-451 data processor, RA-453 monitor scope and RA-452 x–y recorder. The recorded rates are the average of 5–10 replicate determinations. The data were processed using a program written for the Guggenheim kinetic method, followed by matching the calculated rate curves with the experimental curves.

Spectrophotometric measurements were obtained using a Shimadzu spectrophotometer Model 160 provided with thermostatted cuvettes.

The temperature was adjusted to $(25 \pm 0.1)^{\circ}C$ using Julabo and Grant thermostats. The ionic strength was kept at 0.15 M when the pH values were $\geqslant 1.0$ and at 1 M when they were in the H^+ concentration range 0.01–1.0 M.

The computation of formation constants was carried out using the potentiometric program SUPERQUAD (85)[6] and the spectrophotometric program SQUAD(II) (82).[7] The number of absorbing species was determined by making use of the TRIANG program.[8]

RESULTS AND DISCUSSION

Salicylhydroxamic acid interacted with iron(III) to produce different coloured solutions as the pH increased from ~ 1.0 to 7.5. Solution spectra are shown in Fig. 1. The maximum wavelengths are blue shifted as the pH increases. This is usually the case in most iron(III) complexation with chelating ligands. The change in absorbance with pH served as the basis for the determination of formation constants of the iron(III) complexes in solution. Although potentiometric methods are superior to spectrophotometric methods in the determination of the formation constants of the metal ion complexes in solutions, the latter approaches are favourable, in particular, in the case of iron(III) complexes where considerable hydrolysis and/or polymerization are known to occur in solution when an excess concentration of ligands was not used. In this work, the potentiometric method was used as a comparative method to emphasize the effect of variation in experimental conditions on the complex formation in solutions. The SQUAD II and SUPERQUAD programs have been used as previously described[5] to evaluate the formation constants given in Table 1. It was noticed that potentiometric methods yielded sets of constants different from those obtained by spectrophotometric methods. This may be due to the fact that in the latter case the concentration of ligand was at least 20 times that of iron(III), whereas, in the former case it was only three or four times. Higher concentrations of the ligand usually suppress the hydrolysis and/or polymerization of the metal ions in solution. In addition, lower concentrations of iron(III) [$(1.0–5.0) \times 10^{-5}$ M] were used in the spectrophotometric methods than in the potentiometric methods [$(0.05–1.0) \times 10^{-3}$ M].

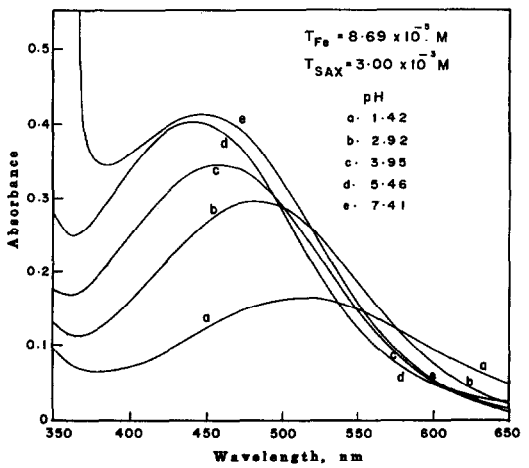

Fig. 1. The UV–vis spectra of iron(III)–SAX systems at different pHs.

Most of the formation constants obtained from the potentiometric results are for hydrolysed and polymerized species, while those obtained from spectrophotometry are mononuclear species with simple stoichiometry. We have not confirmed the presence of the previously reported[2] protonated species of the composition 1 : 1 : 2 (SAX^{-}–Fe^{3+}–H^{+}) at pH lower than 2.0. However, in a separate experiment, the spectra were taken in the H^+ concentration range 0.1–1.0 M at ionic strength 1.0 M Cl^-. One complex species was only determined with the stoichiometry 1 : 1 : 2, which is likely indicating the protonation of an —NH group. The mode of ligation cannot be simply decided from just the information obtained from potentiometric or spectrophotometric calculations. However, by analogy with other monohydroxamic and simple salicylic acids, one can predict the ligation sites involved in the complex formation. In the case of the protonated species 1 : 1 : 2, the ligation is through the oxygen atoms of the hydroxamate and carbonyl groups, and a five-membered chelate complex is probably formed with the protons located on the hydroxamate and phenoxy groups. This situation is usually encountered in most of the monohydroxamates. The chelation through the oxygen atom of the car-

Table 1. The formation constants obtained for the iron(III)–SAX system and other pertinent systems. $(SAX)_LFe_qH_r$ is the complex species (L = ligand), M = iron(III) and H the hydrogen ion, p, q and r are the stoichiometric coefficients of L, M and H, and σ is the standard deviation in the formation constant

L	Stoichiometric coefficients p	q	r	$\log \beta_{pqr}$ ($\pm\sigma$)	Method	pH range	Literature values
SAX	1	0	1	9.91 (0.01)	Potentiometric		
	1	0	2	17.44 (0.01)	Potentiometric		
	1	0	3[a]	18.53[a] (0.007)	Spectrophotometric[a]		$pK_{NH_3^+} = 1.33$[b]
	0	1	−1		—		−3.05[c]
	0	1	−2		—		−6.31
	1	1	0	17.22 (0.04)	Spectrophotometric[d]	1.0–5.0	
	1	1	1	19.36 (0.02)	Spectrophotometric		
	1	1	2[a]	19.23 (0.07)	Spectrophotometric		
	2	1	0	29.55 (0.06)	Spectrophotometric		
	3	1	0	38.80 (0.36)	Spectrophotometric		
	1	1	−1	8.97 (0.06)	Spectrophotometric	5.0–8.0	
	2	1	1	29.17 (0.09)	Spectrophotometric		
	2	1	−2	8.49 (0.10)	Spectrophotometric		
	1	1	−1	10.39 (0.14)	Potentiometric[e]	1.0–3.54	
	2	1	−2	7.41 (0.04)	Potentiometric	6.75–7.75	
	1	2	−2	11.40 (0.11)	Potentiometric		
	2	1	1	31.09 (0.04)	Potentiometric		
	2	2	−3	15.89 (0.16)	Potentiometric		
AX[f]	1	1	0		Spectrophotometric		10.38
	2	1	0		Spectrophotometric		20.28
	3	1	0		Spectrophotometric		27.90
SAL[g]	1	1	0		Spectrophotometric		16.05
	2	1	0		Spectrophotometric		30.38
	3	1	0		Spectrophotometric		39.31

[a] $\mu = 1.0$ M Cl^-.
[b] Reference 10.
[c] Reference 9.
[d] The standard deviation in absorbance was 6.41×10^{-3}, 40 solutions were used and the wavelength range was 400–600 nm.
[e] Xi^2 was 12.85 and $\sigma = 1.825$ for errors in burette volume and pH equal to 0.001. The number of data points was 382. The data points were equally weighted.
[f] Reference 12.
[g] Reference 13.

bonyl group and the nitrogen atom of the hydroxamate is not possible since the less stable four-membered ring will be formed, in addition to the low affinity of iron(III) to the nitrogen atom.

In addition, there may be a possibility of ligation through the oxygen atom of the hydroxyl group and the oxygen atoms of either the carbonyl group or hydroxamate group to form either six- or seven-membered chelates, the latter being less probable. In this case the salicylhydroxamate will resemble the ligation property of salicylic acid (SAL) with iron(III).[11]

On the other hand, the ligation in the 1 : 1 : 1 species may be similar to the regular monohydroxamates where it is possibly through the oxygen atoms of the hydroxamate and carbonyl groups with the proton located on the phenoxy group ($pK_3 = 9.91$). The difference in the magnitudes of the formation constants of the 1 : 1 : 1 and 1 : 1 : 2 species is not significant (Table 1) and may be attributed to the difference in the ionic strength, which renders the value of the formation constant of 1 : 1 : 2 species less than that of the 1 : 1 : 1 species. This conclusion indicates that the 1 : 1 : 2 species is of lower stability than the 1 : 1 : 1 species and the deprotonation of the H_3SAX^+ is greatly facilitated in the presence of iron(III).

The other higher complex species occurs above

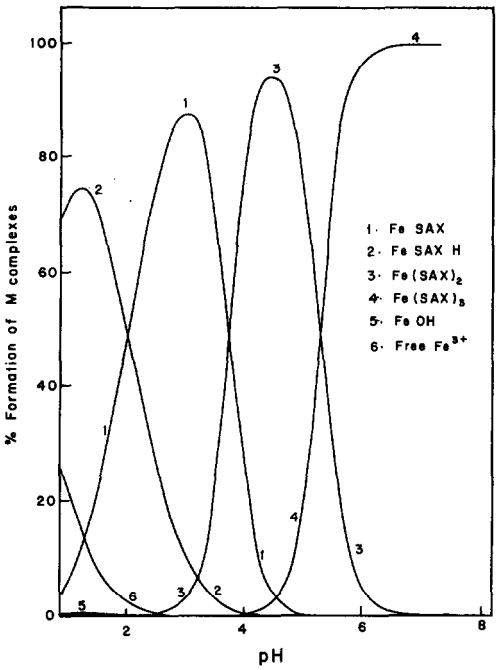

Fig. 2. SPECN program distribution diagram of different species as a function of pH, obtained from spectrophotometric measurements.

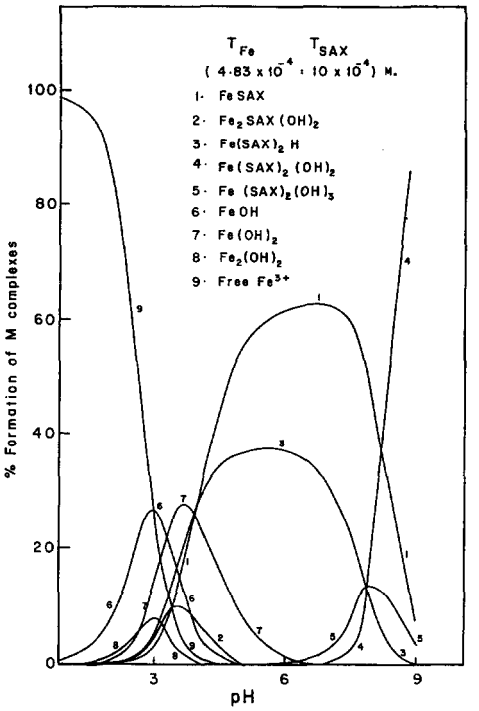

Fig. 3. SPECN program distribution diagram of different species as a function of pH, obtained from potentiometric measurements.

pH 3.0 and the mode of chelation is similar to the 1 : 1 species. The formation constants for all the complex species were obtained in the pH range 1.0–5.0. Figure 2 shows the dependence of the complex formation on pH as obtained from the program SPECN.[12] Unfortunately the spectral data above pH 5.0 did not yield an equilibrium model similar to that obtained from the potentiometric work, although they agree on the presence of three complex species (Table 1) but their formation constants are different.

The distribution of complex species as a function of pH obtained from the potentiometric study is shown in Fig. 3. The $1:1:-1$ or $2:1:-1$ species are just ternary complexes involving SAX and OH^- as ligands. The species involving more than one metal ion are mostly dimers where the OHs are probably acting as bridges between the metal ions.

It is worth mentioning that the complexes obtained from the spectrophotometric study have higher formation constants than those obtained from iron(III) with acetohydroxamic acid (AX),[12] which emphasizes the effect of the resonance of the aromatic ring on the stability of iron(III) complexes with hydroxamates.

The kinetics of the interaction of iron(III) *with* SAX

Two sets of kinetic experiments have been carried out at 0.15 and 1.00 M ionic strengths in the wavelength range 400–530 nm. The one at 0.15 M ionic strength was studied in the pH range 1.0–3.0, and the other at 1.0 M ionic strength was made in the H^+ concentration range 0.01–1.00 M. In both cases, pseudo-first-order conditions were preserved, in the first set the concentration of the ligand was at least 10 times that of iron(III) (T_{Fe} was kept constant) and in the second the concentration of iron(III) was at least 10 times that of the ligand (T_{SAX} was kept constant). Figure 4(a) shows the experimental dependence of k_{obs} on pH for the first set. The rate constants are monotonically increasing as the pH is increasing. A plot of the k_{obs} values as a function of T_{SAX} at interpolated pH values are linear, Fig. 4(b). These linear relations can be represented by the following equation:

$$k_{obs} = AT_{SAX}, \quad (1)$$

where A is a pH-dependent parameter. The mechanism of the reaction may be represented as in Scheme 1, where the aquated Fe^{3+}, $Fe(OH)_2^+$ are the only significant species in the iron(III) solution and H_2SAX is the only species in solution. The chloro complexes of iron(III) have been ignored due to their low formation constant values. The contributions of the iron(III) dimeric species to the mechanism have also been neglected under the experimental conditions used (pH = 1.0–3.0).

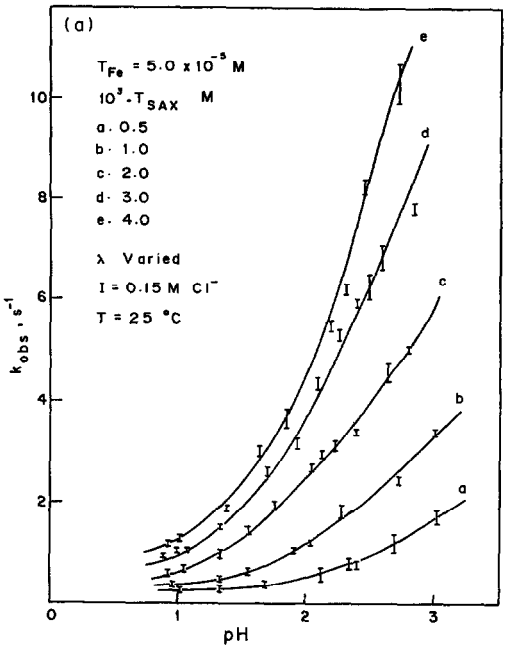

Fig. 4(a). The observed rate constants as a function of pH and T_{SAX}.

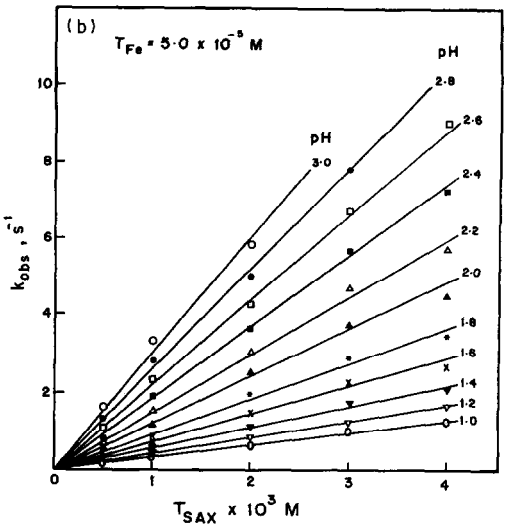

Fig. 4(b). The dependence of the observed rate constants, k, as a function of T_{SAX} at interpolated pH values obtained from Fig. 4(a).

One may ignore the contribution from the backward rate constants in the kinetic equation since the intercept at various values of pH are of negligible magnitudes ($\sim$ zeros), Fig. 4(b). The rate equation is expressed as follows:

$$d(C_1+C_2)/dt = Q_1\,dC_2/dt$$

$$= \alpha_{0SAX}T_{SAX}\left(\frac{T_{Fe-Q_1C_2}}{Q_2}\right)Q_3 \quad (2)$$

where,

$$C_1 = (FeHSAX^{2+}), \quad C_2 = (FeSAX^{+})$$

$$\alpha_{0SAX} = (H^+)^2/\{(H^+)^2+K_{1h}(H^+)+K_{1h}K_{2h}\},$$

where K_{1h} and K_{2h} are the first and the second deprotonation constants.

$$Q_1 = 1+(H^+)/K_{1CH}, \quad [K_{1CH} = (C_2)(H^+)/(C_1)],$$

$$Q_2 = 1+K_{10H}/(H^+)+K_{10H}K_{20H}/(H^+)^2,$$

$$K_{10H} = (FeOH)^{2+}(H^+)/(Fe^{3+}),$$

$$K_{10H}K_{20H} = Fe(OH)_2^+(H^+)^2/(Fe^{3+})$$

and

$$Q_3 = k_1+k_2+[K_{10H}/(H^+)](k_3+k_4)$$

$$+(K_{10H}K_{20H}/(H^+)^2)(k_5+k_6).$$

The integrated form of eq. (1) is:

$$k_{obs} = \frac{\alpha_{0SAX}Q_3}{Q_2}T_{SAX}. \quad (3)$$

On multiplying the slopes (Table 2) by Q_2 and by plotting as a function of $(H^+)^{-1}$, a straight line was obtained with an intercept equal

(a) $Fe_{aq}^{3+}+H_2SAX \underset{k_{-1}}{\overset{k_1}{\rightleftharpoons}} FeHSAX^{2+}+H^+$

K_{1CH}

(b) $Fe_{aq}^{3+}+H_2SAX \underset{k_{-2}}{\overset{k_2}{\rightleftharpoons}} FeSAX^{+}+2H^+$

(c) $Fe(OH)_{aq}^{2+}+H_2SAX \underset{k_{-3}}{\overset{k_3}{\rightleftharpoons}} FeHSAX^{2+}+H_2O$

(d) $Fe(OH)_{2aq}^{+}+H_2SAX \underset{k_{-4}}{\overset{k_4}{\rightleftharpoons}} FeSAX^{+}+H^+ +H_2O$

(e) $Fe(OH)_{2aq}^{+}+H_2SAX \underset{k_{-5}}{\overset{k_5}{\rightleftharpoons}} FeHSAX^{2+}+H^+ +H_2O$

(f) $Fe(OH)_{2aq}^{+}+H_2SAX \underset{k_{-6}}{\overset{k_6}{\rightleftharpoons}} FeSAX^{+}+2H_2O$

Scheme 1. k_i and k_{-i} are the forward and backward rate constants.

Table 2. The values of the parameter A at interpolated values of pH, and the calculated and observed values of AQ_2

pH	$10^{-2}\times A$	$10^{-3}\times(AQ_2)_{obs}$	$10^{-3}\times(AQ_2)_{calc}$
1.0	3.25	0.33	0.57
1.2	4.25	0.43	0.61
1.4	5.50	0.56	0.67
1.6	7.25	0.75	0.77
1.8	9.00	0.95	0.93
2.0	12.00	1.31	1.17
2.2	14.75	1.70	1.56
2.4	18.50	2.33	2.18
2.6	21.75	3.12	3.17
2.8	26.00	4.58	4.72
3.0	30.25	7.23	7.19

$AQ_2 = A(1+K_{10H}/(H^+)+K_{10H}K_{20H}/(H^+)^2)$ where A = slope of eq. (1).

to 4.67×10^2 ($=k_1+k_2$) and slope equal to 6.74 [$=K_{10H}(k_3+k_4)$]. This finding actually indicates that the reactions (a) → (d) in Scheme 1 are significant in the formation of the 1 : 1 metal complex species. There is, however, a slight variation between calculated and observed values of AQ_2 at lower pH values (Table 2). This may be explained as being due to the effect of the greater chloride complexing ability to iron(III) at higher acidity. The value of (k_1+k_2) is less than k_3+k_4 ($=7.56\times10^3$ $mol^{-1}\ dm^3\ s^{-1}$), indicating the higher reactivity of $FeOH^{2+}_{aq}$ over Fe^{3+}_{aq} species when interacting with SAX.

The observed rate constants, k'_{obs}, obtained at the ionic strength 1.0 M Cl^- have a peculiar dependence on the H^+ concentration. At a H^+ concentration lower than 0.2 M, a monotonic increase in k'_{obs} as the pH increased was observed, which is similar to the results obtained for the first set of experiments at 0.15 M ionic strength. However, at values greater than 0.2 M, there was an increase in the values of the k'_{obs} as the H^+ concentration was increased. There was a limited range of H^+ concentration where the k'_{obs} were not affected, Fig. 5(a). When the values of k'_{obs} were plotted as a function of T_{Fe}, at interpolated values of H^+ concentration, linear curves were obtained, Fig. 5(b). This behaviour can be expressed empirically as follows:

$$k'_{obs} = B+CT_{Fe}, \qquad (4)$$

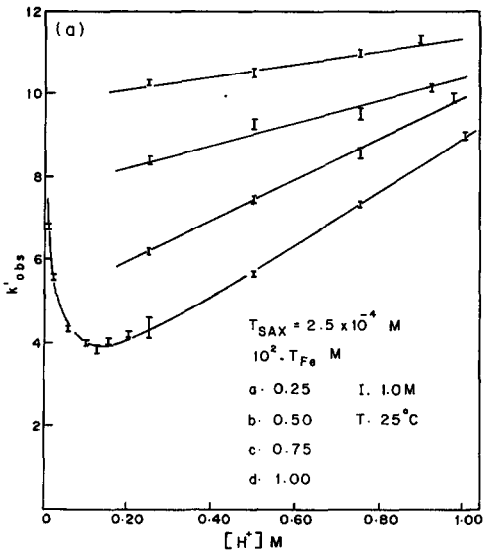

Fig. 5(a). The dependence of the observed rate constant, k', as a function of H^+ concentration at different T_{Fe} values.

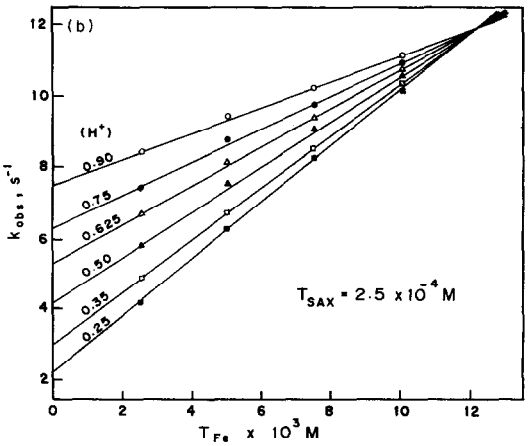

Fig. 5(b). The dependence of the observed rate constants, k', as a function of T_{Fe} at interpolated values of H^+ concentration.

where B and C are parameters which are dependent on H^+ concentration.

The rate data represented by eq. (4) can be described by the mechanism shown in Scheme 2.

The derived k'_{obs} is as follows:

$$k'_{obs} = Q_6+Q_5T_{Fe}/Q_2Q_4, \qquad (5)$$

$$Fe^{3+}_{aq}+H_3SAX^+ \rightleftharpoons FeH_2SAX^{3+}+H^+; \qquad k_1, k_{-1}$$

$$Fe(OH)^{2+}+H_3SAX^+ \rightleftharpoons FeH_2SAX^{3+}+H_2O; \qquad k_2, k_{-2}$$

Scheme 2.

Table 3. The values of the parameters B and C at interpolated values of H^+ concentration

$[H^+]$ (M)	B (s^{-1})	$10^{-2} \times C$ ($mol^{-1}\,dm^3\,s^{-1}$)	$10^{-2} \times (CQ_4Q_2)$
0.25	2.15	8.15	10.8
0.35	2.95	7.45	9.16
0.50	4.15	6.45	7.48
0.625	5.20	5.60	6.27
0.75	6.20	4.80	5.33
0.90	7.40	3.80	4.14

B and C are defined by eq. (4).

where H_3SAX^+ is the protonated species of H_2SAX ($pK_{1h} = 1.09$),

$$Q_4 = [(H^+) + K_{1h}]/(H^+),$$

$$(K_{1h} = [(H_2SAX)(H^+)/(H_3SAX^+)])$$

$$Q_5 = k_1 + k_2K_{10H}/(H^+)$$

and

$$Q_6 = k_{-2} + k_{-1}(H^+).$$

The plot of Q_6 ($= B$) (Table 3) vs (H^+) is linear in the H^+ concentration range $\sim$ 0.2–0.9, with values of the intercept and slope equal to 0.10 ($= k_{-2}$) and 8.11 ($= k_{-1}$), respectively. On the other hand, the plot of the quantity CQ_4Q_2 (Table 3) vs the reciprocal of H^+ concentration yielded a straight line, in the H^+ concentration range $\sim$ 0.3–0.9, with an intercept and slope equal to 0.7×10^2 ($= k_1$) and 3.43×10^2 ($= k_2K_{10H}$, i.e. $k_2 = 3.85 \times 10^5$). This reflects the importance of $Fe(OH)^{2+}$ species on the rate of the formation of FeH_2SAX. The mechanism shown in Scheme 2 has ignored the contribution from the chloro complexes of iron(III), $Fe(OH)_2^+$, and the iron(III) dimer, $[Fe_2(OH)_2]^{4+}$. However, the inclusion of the last two species did not successfully explain the rate data. Besides, the inclusion of the formation of the complex species, FeHSAX, in the mechanism did not interpret the dependence of the rate data on H^+ concentration.

CONCLUSION

The kinetic results of some structurally related systems are summarized in Table 4. It seems that the reactivity of $Fe(OH)^{2+}$ species towards different ligands are mostly similar except that a slight increase would be observed in the combination of the OH group with the hydroxamate group in the *ortho*-position. Although this similarity is clearly defined, the reactivity for Fe^{3+} is larger for ligands containing hydroxamate groups. This may indicate the ligand contribution to reactivity rather than that of the metal ion species. It is probably the first time a rate constant value $\sim$ 100 times greater than the regular value for the reactivity of $Fe(OH)^{2+}$, in the formation of FeH_2SAX species, has been reported. However, this may also indicate the more favourable reactivity of the chloro complexes of iron(III) towards these ligands, although these chloro complexes are not stable complexes.

Table 4. Summary of some SAX structurally related systems at 1.0 M ionic strength

Ligand	Rate constant Fe_{aq}^{3+} ($mol^{-1}\,dm^3\,s^{-1}$)	Rate constant $FeOH^{2+}$ ($mol^{-1}\,dm^3\,s^{-1}$)
Salicylic acid,[a] OHC_6H_4COOHS	$\leqslant 0.10 \times 10^2$	3.5×10^3
Phenol,[a] C_6H_5OH		1.5×10^3
Acetohydroxamic acid,[b] $CH_3CONHOH$	1.50×10^2	4.35×10^3
Glycine hydroxamic acid[c] ($H_2NCH_2CONHOH$)	1.50×10^2	$\sim 2.7 \times 10^4$
Salicylhydroxamic acid[e] ($OHC_6H_4CONHOH$)	4.67×10^2[d]	7.56×10^3[d]
Salicylhydroxamic acid	0.7×10^2	3.85×10^5

[a] Reference 14.
[b] Reference 12.
[c] Reference 5.
[d] At 0.15 M Cl^- ionic strength.
[e] In obtaining these values, k_1 or k_2 was assumed to be negligible, similarly k_3 or k_4 was ignored.

REFERENCES

1. H. Kehl (Ed.), *Chemistry and Biology of Hydroxamic Acid*, S. Karger, Basel, Switzerland (1982).
2. R. G. Deshpande and D. V. Jahagirdar, *Ind. J. Chem.* 1977, **15A**, 753.
3. B. Chatterjee, *Coord. Chem. Rev.* 1978, **26**, 281.
4. D. A. Brown, M. V. Chidambaram, J. J. Clarke and D. M. McAleese, *Bioinorg. Chem.* 1978, **9**, 255.
5. M. S. El-Ezaby and M. M. Hassan, *Polyhedron* 1985, **4**, 429.
6. P. Gans, A. Sabatini and A. Vacca, *J. Chem. Soc., Dalton Trans.* 1985, 1195.
7. D. J. Leggett, S. L. Kelly, L. R. Shiue, Y. T. Wu, D. Chang and K. M. Kadish, *Talanta* 1983, **30**, 579.
8. F. R. Hartley, C. Burgess and R. M. Alcock, *Solution Equilibria*. Ellis Horwood, Chichester (1980).
9. L. N. Mulay and P. W. Selwood, *J. Am. Chem. Soc.* 1954, **77**, 2693.
10. A. S. Bhaduri and N. N. Ghosh, *Z. Anorg. Allg. Chem.* 1960, **303**, 117.
11. G. Saini and E. Mentasti, *Inorg. Chim. Acta* 1970, **4**, 210.
12. N. M. Shuaib, H. M. Marafie, M. M. Hassan and M. S. El-Ezaby, *Inorg. Biochem.* 1987, **31**, 171.
13. L. G. Sillén and A. E. Martell, *Stability Constants of Metal Ion Complexes*, Special Publication 25. The Chemical Society, London (1971).
14. J. Xu and R. B. Jordan, *Inorg. Chem.* 1988, **27**, 1502.

Polyhedron Vol. 8, No. 12, pp. 1485–1496, 1989
Printed in Great Britain

0277–5387/89 $3.00+.00
© 1989 Pergamon Press plc

CYCLOPALLADATED *o*-CARBORANES. PALLADIUM TRANSFER FROM CYCLOPALLADATED N,N-DIMETHYLBENZYLAMINES, 1C-DIPHENYLPHOSPHINO-*o*-CARBORANE AND η^3-ALLYLS IN CARBOXYLIC ACID SOLVENTS*

ALEXANDER D. RYABOV,† ALEXEY V. ELISEEV and EKATERINA S. SERGEYENKO

Department of Chemistry, Moscow State University, 119899, Moscow, U.S.S.R.

and

ALEXANDER V. USATOV, LEONID I. ZAKHARKIN and VALERY N. KALININ

Institute of Organo-element Compounds, Academy of Sciences of the U.S.S.R., 117813, Vavilov str. 28, Moscow, U.S.S.R.

(*Received* 22 *December* 1988; *accepted* 24 *January* 1989)

Abstract—1-Diphenylphosphinomethyl-*o*-carborane, *o*-$HCB_{10}H_{10}CCH_2PPh_2$ (DPMC), reacts with Na_2PdCl_4 (methanol) or $PdCl_2(PhCN)_2$ (benzene) to give the "bis-adduct" *trans*-[$PdCl_2$(DPMC)$_2$], which on thermolysis in *n*-propanol transforms into the five-membered Pd—P—C—C—B palladacycle, di-μ-chlorobis[(1-diphenylphosphinomethyl-*o*-carboranyl-B,P)palladium(II)] (**IIa**), as a mixture of B(3) and B(4) metallated isomers according to ^{1}H and ^{31}P NMR. If the internal palladation is performed in the presence of LiBr or NaI, the corresponding bromo- or iodo-bridged dimers are obtained. Complex **IIa** can also be prepared via ligand exchange in carboxylic acid solvents. In particular, palladium(II) migrates from cyclopalladated chloro-bridged N,N-dimethylbenzylamine or 1C-diphenylphosphino-*o*-carborane, i.e. from complexes with C,N-five- and B,P-four-membered palladacycles, respectively, to 1-diphenylphosphinomethyl-*o*-carborane yielding **IIa**. Migration of palladium(II) is also observed from the compounds with great stability towards acetic acid, namely the [$PdCl(\eta^3$-allyl)]$_2$ dimers. No such processes except with this particular ligand were found in the case of palladium(II) allyls and other entering ligands (azobenzene, 2-phenylpyridine, α-methylstyrene). The exchange processes described clearly show that complex **IIa** is characterized by a remarkable thermodynamic stability in acetic acid which accounts for the course of many exchange reactions.

The σ-bond metathesis for C—H and related bonds in transition metal complexes is an intriguing problem.[1] In general, there are three key mechanisms of such metathetical transformations. The first, involving reductive C—H bond elimination, followed by oxidative addition, is typical, for example, of rhodium(I/III),[2] iridium(I/III),[3] and platinum(0/II)[4] couples; the second observed for scandium(III)[1] and thorium(IV)[5] complexes occurs via a concerted four-centred mechanism; finally, the third, realized in palladium(II) complexes,[6] is induced by the acid cleavage of the metal–carbon bond followed by subsequent metallation of the incoming ligand. The latter pathways were previously exemplified by the ligand exchange reactions of type (1), involving the starting cyclopalladated chloro- or acetato-bridged dimer and incoming ligand.[6]

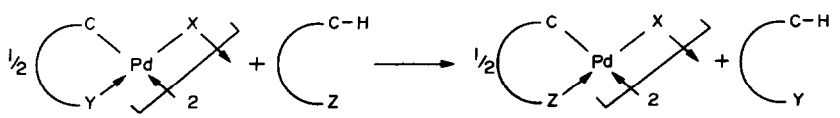

(1)

In the present paper we report on several related reactions which involve not only the C—H bond metathesis but that of B—H and η^3-allyl bonds

* The key compounds used in this study are shown in Fig. 1.

† Author to whom correspondence should be addressed.

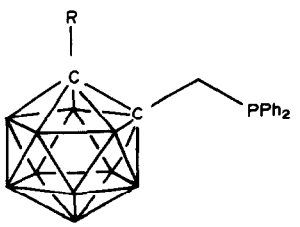

R = H, 1C-diphenylphosphinomethyl-*o*-carborane (DPMC)

R = Me, 1C-diphenylphosphinomethyl-2C-methyl-*o*-carborane (DPMMC)

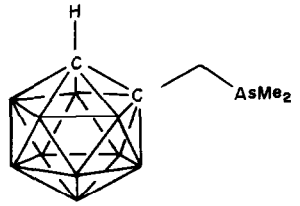

1C-dimethylarsinomethyl-*o*-carborane (DAMC)

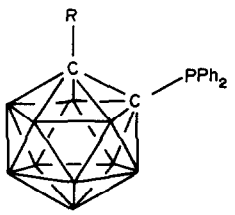

R = H, 1C - diphenylphosphino - *o* - carborane (DPC)

R = Me, 1C - diphenylphosphino - 2C - methyl - *o*-carborane (DP2MC)

R = *i*-Pr, 1C-diphenylphosphino-2C-isopropyl-*o*-carborane (DPIC)

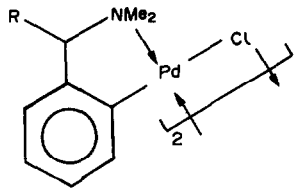

R = H, di-μ-chlorobis[(2-dimethylaminomethylphenyl-C^1,N)palladium(II)] ([PdCl(damp)]$_2$)

R = *S*-Me, di-μ-chlorobis[(*S*-2-dimethylaminoethylphenyl-C^1,N)palladium(II)] ([PdCl(*S*-daep)]$_2$)

R = *R*-Me, di-μ-chlorobis[(*R*-2-dimethylaminoethylphenyl-C^1,N)palladium(II)] ([PdCl(*R*-daep)]$_2$)

Fig. 1. The compounds used in the present study.

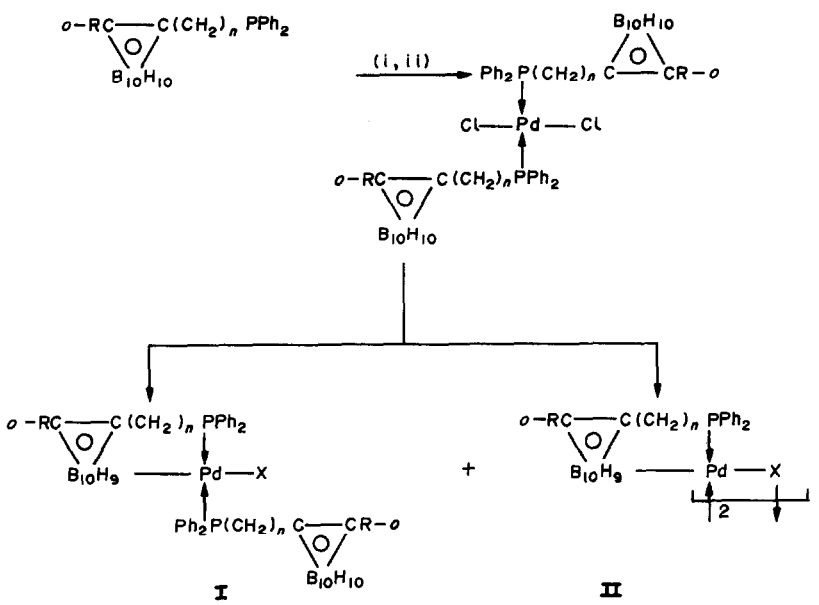

	R	*n*	X
a	H	1	Cl
b	Me	1	Cl
c	H	0	Cl
d	Me	0	Cl
e	*i*-Pr	0	Cl
f	H	1	Br
g	H	1	I
h	Me	0	Br

Scheme 1. (i)—Na_2PdCl_4–MeOH; (ii)—$PdCl_2(PhCN)_2$–C_6H_6.

as well and lead to cyclopalladated *o*-carboranes.[7] Some of the results presented here have been previously communicated.[8]

RESULTS

Interaction of P-*donor* o-*carboranes with simple palladium salts*

The reaction between DPMC, as well as DPMMC, and Na_2PdCl_4 in methanol or $PdCl_2(PhCN)_2$ in benzene, both at 20°C, cleanly affords the simple bis-adducts *trans*-$[PdCl_2(DPMC)_2]$ or *trans*-$[PdCl_2(DPMMC)_2]$ (Scheme 1). The geometry of the former is supported by a single strong IR band at 350 cm^{-1}.[9] As expected, the ligand is coordinated through phosphorus and only one isomer is present as judged from the corresponding $^{31}P\{^1H\}$ NMR singlet resonance of the complexed ligand at δ 10.9. (The free ligand resonates at δ −16.3.) Thermolysis of *trans*-$[PdCl_2(DPMC)_2]$ in different solvents induces the B—H bond palladation to afford a mixture of monomeric and dimeric complexes **Ia** and **IIa**, the relative amounts of which depend on the nature of solvent (Scheme 1). In particular, one obtains a 1 : 1 mixture in toluene, while only the dimer is formed in isopropanol. When thermolysed in isopropanol in the presence of a 10-fold excess of NaBr or NaI, *trans*-$[PdCl_2(DPMC)_2]$ transforms into the corresponding bromo- and iodo-bridged dimers **IIf** and **IIg**, in good yields. Two peaks of bridging chlorides in the IR spectrum are seen at 287 and 248 cm^{-1} and of bromides at 216 and 200 cm^{-1} (cf. with ref. 10). As usual, halide bridges can be cleaved by pyridine or 4-methylpyridine to afford monomers **III**, which are sufficiently soluble in common solvents, and, thus, useful for NMR structural investigations. The corresponding data for **III**, as well as for **I** and **II**, are summarized in Table 1. The formation of the five-membered palladacycle with a Pd—P—C—C—B chain makes the methylene CH_2 protons diastereotopic, giving in the ^1H NMR spectrum two quartet doublets with ^2J(HP) and ^2J(HH). Two sets of signals in **I**–**III** suggests that the complexes are a mixture of B(3) and B(4) palladated carboranes as shown in Fig. 2. The ^{31}P NMR spectra of **III** confirm this, since again two resonances are observed. It should be pointed out that the latter signals are doubled in the parent dimers **II** (Table 1). The reason is that every linkage isomer [B(3) or B(4)] is probably a mixture of *ab–hg* and *ab–gh* (*trans* and *cis*) isomers (see Scheme 1).

Table 1. Parameters of the ^1H and ^{31}P NMR spectra of cyclopalladated *o*-carboranes

Compound (Isomer)		^1H[a]	^{31}P[b]
Ia	[B(3)]	3.40d(2H, PCH_2, ^2J(HP) 9.0), 3.50m(1H, PCH_2, ^2J(HH) 15.0; ^2J(HP) 12.0, ^4J(HP) 4.5), 4.03q(1H, PCH_2, ^2J(HH) 15.0, ^2J(HP) 7.0), 3.28s(1H, $C^{cb}H$), 5.75s(1H, $C^{cb}H$), 7.45m(10H, Ph), 7.78m(10H, Ph) ($CDCl_3$)	19.53d(^2J(PP) 398.0) 46.37d(^2J(PP) 398.0) ($CHCl_3$)
	[B(4)]		19.89d(^2J(PP) 398.0) 56.66d(^2J(PP) 398.0)
IIa	[B(3)] *ab–hg*[c]	3.99q(1H, PCH_2, ^2J(HH) 16.5, ^2J(HP) 6.0), 4.43q(1H, PCH_2, ^2J(HH) 16.5, ^2J(HP) 9.0), 5.24s(1H, $C^{cb}H$), 7.96m(10H, Ph)	54.55s, 55.15s [$(CH_3)_2CO$]
	ab–gh[c]	4.02q(1H, PCH_2, ^2J(HH) 16.5, ^2J(HP) 6.5), 4.49q(1H, PCH_2, ^2J(HH) 16.5, ^2J(HP) 9.0), 5.34s(1H, $C^{cb}H$), 7.96m(10H, Ph), [$(CD_3)_2CO$]	
	[B(4)]		59.67s, 60.07s [$(CH_3)_2CO$]
IIb	[B(3)]		54.61s, 54.82s [$(CH_3)_2CO$]
	[B(4)]		58.74[c] [$(CH_3)_2CO$]
IIc			4.7s ($CHCl_3$)
IId	[B(3)]		−2.3s, −2.7s ($CHCl_3$)
	[B(4)] *ab–hg*[c]	1.76s(3H, CH_3), 7.58m(10H, Ph)	11.8s, 12.0s ($CHCl_3$)
	[B(4)] *ab–gh*[c]	1.78s(3H, CH_3), 8.25m(10H, Ph) ($CDCl_3$)	

continued overleaf

Table 1—*continued*

Compound (Isomer)		^1H[a]	^{31}P[b]
IIe	[B(4)]	0.47d(3H, C*H*$_3$CH, ^3J(HH) 7.0), 1.15d(3H, C*H*$_3$CH, ^3J(HH) 7.0), 2.06m(1H, CH$_3$C*H*, ^3J(HH) 7.0), 7.55m(10H, Ph) ($CDCl_3$)	
	ab–hg[c]		13.2s, 13.4s ($CHCl_3$)
	ab–gh[c]	0.51d(3H, C*H*$_3$CH, ^3J(HH) 7.0), 1.15d(3H, C*H*$_3$CH, ^3J(HH) 7.0), 2.06m(1H, CH$_3$C*H*, ^3J(HH) 7.0), 8.23m(10H, Ph) ($CDCl_3$)	
IIf	[B(3)]		56.34s, 57.16s
	[B(4)]		61.23[c] [$(CH_3)_2CO$]
IIg	[B(3)]		56.3s, 57.2s
	[B(4)]		61.2[c] [$(CH_3)_2CO$]
IIIa[d]	[B(3)]	3.29q(1H, PCH$_2$, ^2J(HH) 16.5, ^2J(HP) 7.8), 3.50q(1H, PCH$_2$, ^2J(HH) 16.5, ^2J(HP) 10.2), 3.65s(1H, C^{cb}H), 7.46m(6H, Ph), 7.84m(4H, Ph) ($CDCl_3$)	51.27s ($CHCl_3$)
	[B(4)]	3.30q(1H, PCH$_2$, ^2J(HH) 16.5, ^2J(HP) 7.8), 3.51q(1H, PCH$_2$, ^2J(HH) 16.5, ^2J(HP) 10.2), 4.03s(1H, C^{cb}H), 7.46m(6H, Ph), 7.84m(4H, Ph) ($CDCl_3$)	58.9s ($CHCl_3$)
IIIb	[B(3)]	2.23s(3H, CH$_3$), 3.07q(1H, PCH$_2$, ^2J(HH) 18.0, ^2J(HP) 6.0), 3.82q(1H, PCH$_2$, ^2J(HH) 18.0, ^2J(HP) 11.0), 7.40m(6H, Ph), 8.0m(4H, Ph) ($CDCl_3$)	53.0s ($CHCl_3$)
	[B(4)]	1.96s(3H, CH$_3$), 3.12q(1H, PCH$_2$, ^2J(HH) 15.0, ^2J(HP) 10.3), 3.36q(1H, PCH$_2$, ^2J(HH) 15.0, ^2J(HP) 9.0), 7.43m(6H, Ph), 7.92m(4H, Ph) ($CDCl_3$)	57.8s ($CHCl_3$)
IIId	[B(3)]	2.08s(3H, CH$_3$), 7.47m(6H, Ph), 8.35m(4H, Ph) ($CDCl_3$)	−1.4s ($CHCl_3$)
	[B(4)]	1.68s(3H, CH$_3$), 7.45m(6H, Ph), 8.30m(4H, Ph) ($CDCl_3$)	13.1s ($CHCl_3$)
IIIe	[B(4)]	0.45d(3H, C*H*$_3$CH, ^3J(HH) 7.0), 1.13d(3H, C*H*$_3$CH, ^3J(HH) 7.0), 2.01m(1H, CH$_3$C*H*, ^3J(HH) 7.0), 7.53m(6H, Ph), 8.25m(4H, Ph) ($CDCl_3$)	14.8s ($CHCl_3$)
IIIf	[B(3)]		52.44s ($CHCl_3$)
	[B(4)]		59.76s ($CHCl_3$)
IIIg	[B(3)]		53.70s ($CHCl_3$)
	[B(4)]		61.17s ($CHCl_3$)
IIIh	[B(4)]		13.05s ($CHCl_3$)
IV	[B(3)]	1.50s(3H, CH$_3$As), 1.54s(3H, CH$_3$As), 2.66d(1H, CH$_2$As, ^2J(HH) 15.0), 2.99d(1H, CH$_2$As, ^2J(HH) 15.0), 3.46s(1H, C^{cb}H), 1.67s(3H, CH$_3$As), 1.73s(3H, CH$_3$As), 2.96d(1H, CH$_2$As, ^2J(HH) 14.0), 3.08d(1H, CH$_2$As, ^2J(HH) 14.0), 5.01s (1H, C^{cb}H) ($CDCl_3$)	—
	[B(4)]	1.43s(3H, CH$_3$As), 1.46s(3H, CH$_3$As), 2.57d(1H, CH$_2$As, ^2J(HH) 13.5), 2.84d(1H, CH$_2$As, ^2J(HH) 13.5), 3.78s(1H, C^{cb}H), 1.69s(3H, CH$_3$As), 1.70s(3H, CH$_3$As), 2.99[e](1H, CH$_2$As), 5.13s(1H, C^{cb}H) ($CDCl_3$)	—
V[f]	[B(3)]	1.69s(3H, CH$_3$As), 1.76s(3H, CH$_3$As), 2.68d(1H, CH$_2$As, ^2J(HH) 14.0), 2.95d(1H, CH$_2$As, ^2J(HH) 14.0), 3.56s(1H, C^{cb}H) ($CDCl_3$)	—
	[B(4)]	1.71s(3H, CH$_3$As), 1.72s(3H, CH$_3$As), 2.61d(1H, CH$_2$As, ^2J(HH) 14.0), 2.80d(1H, CH$_2$As, ^2J(HH) 14.0), 3.76s(1H, C^{cb}H) ($CDCl_3$)	—

[a] Bruker WP-200SY (200 MHz).
[b] Bruker WP-200SY (81.01 MHz).
[c] Arbitrary assignment.
[d] L = d_5-py in all monomeric compounds, **III**.
[e] Unresolved signal.
[f] Recorded in the presence of d_5-py.

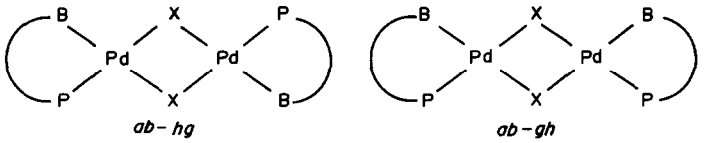

The nature of added metal halide has a remarkable effect on the rate of intramolecular metallation of *trans*-$[PdCl_2(DPMC)_2]$. The hot solution of the latter in *n*-propanol is yellow, and it becomes colourless when intramolecular palladation into **II** occurs. Thus, one can qualitatively estimate the relative rates in the presence of a 10-fold molar excess of MHal. At reflux, the fading occurs in a matter of 18–20, 10–15 and 5–7 min in the presence of LiCl, LiBr and NaI, respectively, the concentration of LiCl having negligible effect on the rate of internal metallation. Thus, the reactivity order Cl < Br < I suggests that this B—H bond palladation has a strong nucleophilic character. In accord with this is the relative amount of B(3) isomer formed (85%), which is independent of the nature of halide in the case of DPMC. In fact, the electron density is the lowest at B(3) of the *o*-carborane backbone,[11] and hence, the nucleophilic reagent would attack this position more readily. There is the same reactivity order in the case of DPMMC, but, contrary to DPMC, the relative amount of the B(4) isomer increases in the order Cl < Br < I (25, 35 and 70%, respectively), and this may reflect the steric effect of the methyl group at C(2), Fig. 2.

Direct palladation of DPC, DP2MC, and DPIC proceeds with such facility that the metallation occurs at 20°C giving four-membered palladacycles **Ic, IId** and **IIe**, respectively, in high yields (Table 2). Dimeric **IIc** is not formed under these conditions. The ratio of B(3) and B(4) isomers is the same as in the exchange reactions (see below). Only in the case of DP2MC is it strongly dependent on the solvent used. In particular, one obtains only the

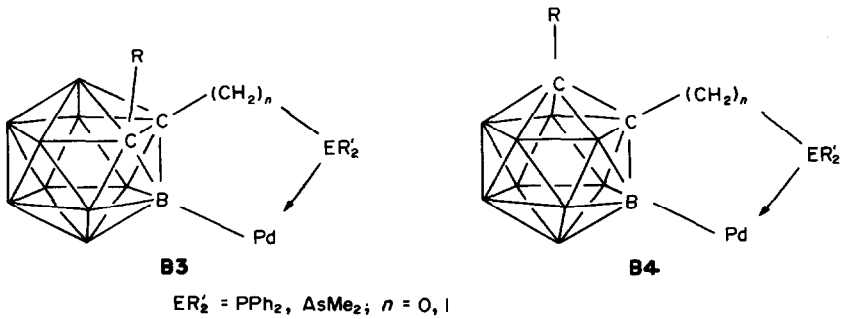

Fig. 2. Two possible isomers of the cyclopalladated *o*-carborane derivatives.

Table 2. Yields of the cyclopalladated *o*-carboranes and the bis-adducts in reactions with simple palladium salts and the corresponding analytical data

Compound	Yield (%)	Brutto-formula	Calc./Found (%) C	H	B	Pd
$[PdCl_2(DPMC)_2]$	90–96	$C_{30}H_{46}B_{20}Cl_2P_2Pd \cdot C_6H_6$	45.9/46.0	5.9/5.6	22.9/23.0	10.8/11.3
$[PdCl_2(DPMMC)_2]$	96	$C_{32}H_{50}B_{20}Cl_2P_2Pd$	43.8/43.2	5.9/5.7	24.0/24.3	12.5/12.0
$[PdCl_2(DAMC)_2]$	93	$C_{10}H_{38}As_2B_{20}Cl_2Pd$	17.3/17.1	5.7/5.5	30.5/30.8	
Ia	90–95	$C_{30}H_{45}B_{20}ClP_2Pd \cdot \frac{1}{2}C_6H_6$	45.6/45.8	5.3/5.6	24.9/25.0	12.3/12.3
Ic	87–93	$C_{28}H_{41}B_{20}ClP_2Pd$	42.3/42.2	5.3/5.2	27.1/27.2	13.3/13.3
IIa	90–95	$C_{30}H_{44}B_{20}Cl_2P_2Pd_2$	37.1/37.3	5.0/4.6	22.1/22.4	21.9/22.0
IIb	99	$C_{32}H_{48}B_{20}Cl_2P_2Pd_2$	39.6/38.4	5.3/4.9	21.0/21.7	21.4/21.4
IIc[a]	13	$C_{28}H_{40}B_{20}Cl_2P_2Pd_2 \cdot \frac{1}{2}C_6H_6$	38.1/38.1	4.8/4.4	22.1/22.1	
IId	80	$C_{30}H_{44}B_{20}Cl_2P_2Pd_2 \cdot C_6H_6$	41.0/41.4	4.9/4.8	20.7/20.7	20.4/20.4
IIe	93–98	$C_{34}H_{52}B_{20}Cl_2P_2Pd_2$	40.1/39.9	5.1/5.1	21.0/21.1	20.6/20.8
IIf	91	$C_{30}H_{44}B_{20}Br_2P_2Pd_2$	34.6/34.1	4.5/4.2	20.4/20.5	20.1/20.2
IIg	95	$C_{30}H_{44}B_{20}I_2P_2Pd_2$	32.1/32.4	4.1/3.9	18.5/18.8	17.9/18.5
IIh	90	$C_{30}H_{44}B_{20}Br_2P_2Pd_2 \cdot \frac{1}{2}C_6H_6$	36.8/36.2	4.8/4.4	19.4/19.8	
IV	82	$C_{10}H_{37}B_{20}As_2ClPd$	18.2/18.1	5.6/5.6	32.4/32.5	
V	13	$C_{10}H_{36}B_{20}As_2Cl_2Pd_2$	14.5/14.9	4.4/4.5		

[a] Table 3, run 5.

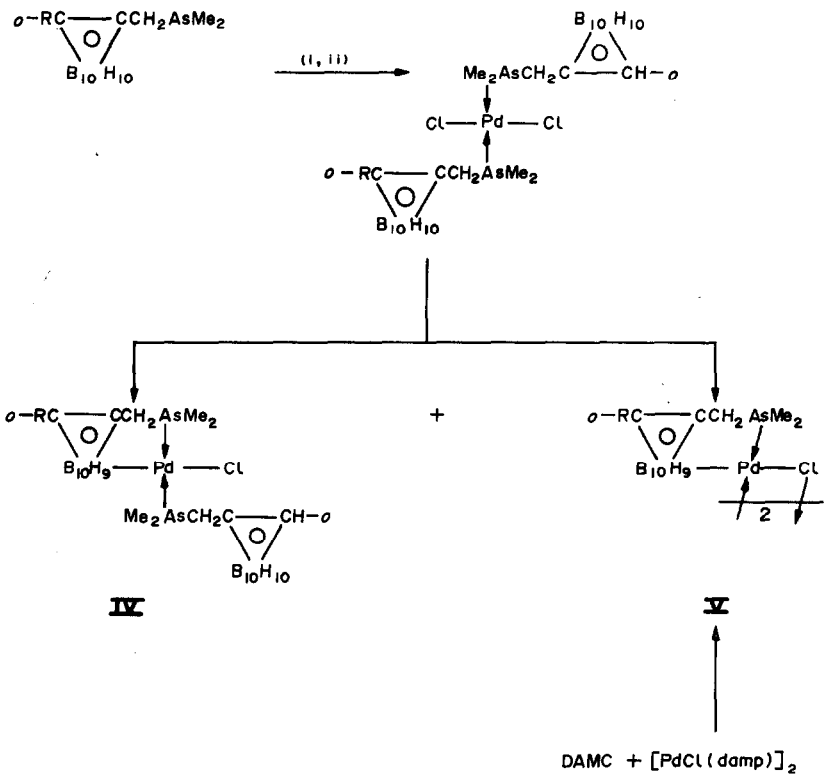

Scheme 2. (i)—Na_2PdCl_4–MeOH; (ii)—$PdCl_2(PhCN)_2$–C_6H_6.

B(4) isomer of **IId** in MeOH, while a mixture of B(3) and B(4) in a ratio of 1 : 4 and 3 : 2 is seen in $CHCl_3$–HOAc (1 : 1) and benzene, respectively.

Interaction of DAMC *with palladium salts*

The transformations of DAMC in the presence of simple palladium complexes (Scheme 2) are much the same as those of the related phosphorus ligands DPMC and DPMMC. Thermal cyclopalladation of *trans*-$[PdCl_2(DAMC)_2]$ in *n*-propanol again gives a 1 : 1 mixture of B(3) and B(4) isomers identical to those in Fig. 2, as judged from the two sets of diastereotopic methyls at As of equal intensity.

Cyclopalladation of DPMC *and related ligands via the exchange of cyclopalladated ligands*

Dimers **II** can be very easily prepared in high yields by the ligand exchange strategy, eq. (2), developed by us previously for C,N-palladacycles.[6] In particular, DPMC and DPMMC react readily with an equimolar amount of chloro-bridged cyclopalladated N,N-dimethylbenzylamine, [PdCl (damp)]$_2$, at 70°C in a HOAc–$CHCl_3$ mixture, to afford five-membered palladacycles, **IIa** and **IIb**, respectively, without detectable amounts of monomers **I**, Table 3. As above, complexes **II** are a mixture of B(3) and B(4) palladated species. The

Table 3. Cyclopalladation of *o*-carborane derivatives via the exchange of cyclopalladated ligands in HOAc–$CHCl_3$ solvent

Run	Starting complex	Incoming ligand	*T*(°C)/Time (h)	Product	Yield (%)	Isomer ratio (%) [B(3)]	[B(4)]
1	$[PdCl(damp)]_2$	$HCB_{10}H_{10}CCH_2PPh_2$	70/25	**IIa**	83	80	20
2	$[PdCl(R\text{-daep})]_2$	$HCB_{10}H_{10}CCH_2PPh_2$	25/172	**IIa**	44		
3	$[PdCl(S\text{-daep})]_2$	$HCB_{10}H_{10}CCH_2PPh_2$	25/172	**IIa**	49		
4	$[PdCl(damp)]_2$	$MeCB_{10}H_{10}CCH_2PPh_2$	70/25	**IIb**	95	70	25
5	$[PdCl(damp)]_2$	$HCB_{10}H_{10}CPPh_2$	50/5	**IIc**	13		
6	$[PdCl(damp)]_2$	$MeCB_{10}H_{10}CPPh_2$	25/74	**IId**	74	20	80
7	$[PdCl(damp)]_2$	*iso*-$PrCB_{10}H_{10}CPPh_2$	25/60	**IIe**	40	0	100
8	$[PdCl(damp)]_2$	$HCB_{10}H_{10}CCH_2AsMe_2$	25/96	**IV**	66	50	50
9	**IIe**	$HCB_{10}H_{10}CCH_2PPh_2$	60/6	**IIa**	65		

relative amounts of these according to ^{31}P NMR of the monomeric d_5-py derivatives, are shown in Table 3. It should be pointed out that the "carborane version" of the exchange reaction is limited by the ligands with phosphorus donor atoms. Ligands with N-donors, namely *o*-$HCB_{10}H_{10}CCH_2NEt_2$ and *o*-$HCB_{10}H_{10}CN{=}NPh$, reduce palladium(II) in acetic acid medium, as carboranes without donor centres do reacting with palladium(II) acetate.[12]

According to ^1H NMR, the interaction between $[PdCl(damp)]_2$ and DPMC begins with the cleavage of chloro-bridges of the palladium dimer by the phosphorus donor. (No such cleavage occurs during the formation of the four-membered palladacycles, see below.) Since mono-substituted *o*-carborane is prochiral,[13] the reaction with optically active cyclopalladated *R* and *S* α-methyl-N,N-dimethylbenzylamine, $[PdCl(daep)]_2$, could afford optically active palladated DPMC. The product **IIa** proved to be racemic, confirming the previous conclusion that the exchange of cyclopalladated ligands proceeds by the dissociative route, i.e. the palladation of C—H and B—H bonds follows the complete departure of the leaving ligand.[6c]

Five-membered palladacycles incorporating the As donor atom are also available via the ligand exchange. In particular, DAMC reacts with $[PdCl(damp)]_2$ to give **V** without **IV**, Scheme 2.

Four-membered cyclopalladated carboranes can also be prepared in the same way even under milder conditions, Table 3. In particular, DPIC and $[PdCl(damp)]_2$ react in a HOAc–$CHCl_3$ mixture at room temperature to give **IIe** in an isolated 40% yield. No pre-equilibrium bridge-cleavage by these incoming ligands takes place, obviously, due to their large cone angles. Remarkably, the ^{31}P NMR spectrum of dimeric **IIe** contains only two signals at δ 13.2 and 13.4 as expected for the mixture of *ab–hg* and *ab–gh* isomers. Addition of d_5-py, which monomerizes the dimer, transforms the two signals into one at δ 14.8, as expected for the one-linkage isomer. We believe that the palladacycle formed is the B(4) isomer, since the B(3) position is sterically hindered by the bulky isopropyl group, Fig. 2. Isopropyl C—H bonds are not metallated, and one can observe two doublets of diastereotopic methyls at δ 0.45 and 1.13 (J = 7 Hz) in the case of **IIIe**. Contrary to five-membered palladacycles **IIa,b,f,g**, the ^{11}B NMR spectroscopy of four-membered species **IIc–e,h** gives direct evidence for the presence of the Pd—B bond. In particular, the ^{11}B NMR spectrum of **IIe** contains a well separated signal shifted

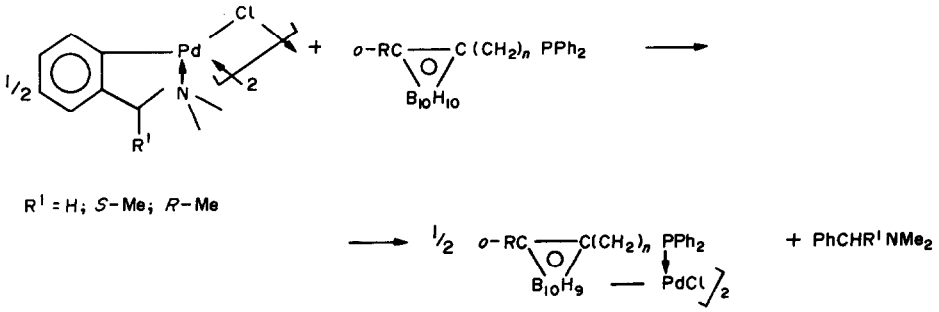

(2)

upfield at δ −19.3, the area under which corresponds to one boron. It should be pointed out that we never observed such separated ^{11}B signals in the related five-membered complexes.

DP2MC reacts with $[PdCl(damp)]_2$ like DPIC giving, however, a mixture of B(3) and B(4) palladated products. There are two corresponding signals both in the ^{31}P (δ −1.4 and 13.1) and ^{11}B (δ −16.6 and −18.9) NMR spectra of the monomeric complex obtained from **IId** and d_5-py. It is clear that the less sterically demanding methyl group allows the palladation of the B^3—H bond as well giving B(3) and B(4) products in a molar ratio of 1 : 4. Under the same conditions DPC also gives **IIc** in a low yield but without monomer **Ic**.

The ligand exchange in P-*donor* B-*palladated complexes*

In the previous section we considered the palladium(II) transfer from an N-donor ligand to a P-donor one. It was interesting to find out whether such an exchange from a P-donor ligand is possible. Reaction (3), between the four-membered cyclopalladated chloro-bridged dimer derived from DPIC (**IIe**) and free DPMC, shows that this is the case yielding the five-membered B-palladated chloro-bridged dimer **IIa** in 65% yield. It should be pointed out that the exchange takes place when only DPMC is the incoming ligand. No migration of palladium(II) from **IIe** was observed when $PhCH_2PPh_2$ or *o*-$PhCB_{10}H_{10}CN{=}NPh$ were tested as palladium(II) scavengers. At the same

time the reaction between $[PdCl(dmap)]_2$ and $PhCH_2PPh_2$ yields the cyclopalladated product $[PdCl(o\text{-}C_6H_4CH_2PPh_2)]_2$ in 21% yield (see Experimental). Note that palladation of $PhCH_2PPh_2$ by $Pd(OAc)_2$ gives the corresponding acetato palladacycle in 19% yield.[14] possibly indicating different mechanisms of the two rearrangements. By measuring the concentration of α-methylstyrene liberated, one could follow the reaction kinetics by GLC (Fig. 3). It is seen that the initial rate of dissociation is practically independent

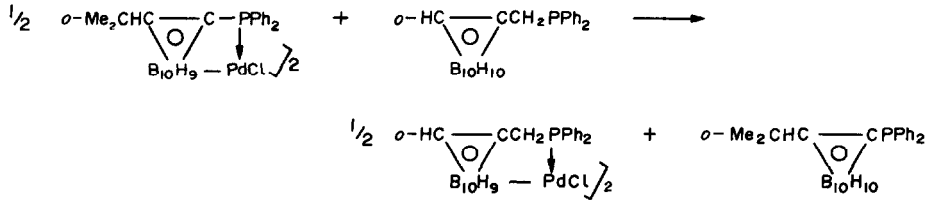

(3)

Palladation of DPMC *by* η^3*-allyl palladium*(II) *dimers*

We have recently presented evidence[15] that $[PdCl(\eta^3\text{-allyl})]_2$ complexes are very resistant to protolytic cleavage, and the departure of the η^3-bonded allyl in acetic acid takes place in the monomeric phosphine complex $[PdCl(\eta^3\text{-}2\text{-}PhC_3H_4)(PPh_3)]$ when the latter is thermolysed at 80°C in the presence of lithium chloride:

$$[PdCl(\eta^3\text{-}2\text{-}PhC_3H_4)(PPh_3)] + HOAc + LiCl \longrightarrow \tfrac{1}{2}[PdCl_2(PPh_3)]_2 + H_2C{=}CMePh + LiOAc. \quad (4)$$

Wishing to carry out the reaction of type (4) with DPMC as a tertiary phosphine, we have found that the compound $[PdCl_2(DPMC)]_2$ does not form, but complex **IIa** is obtained instead [eq. (5)]. The reaction course is independent of whether the η^3-allyl dimer and DPMC or prepared before the monomer $[PdCl(\eta^3\text{-allyl})(DPMC)]$ has been introduced into the reaction (Table 4). The ratio of B(3) and B(4) isomers formed (Table 4) differed from that observed above in reaction (2) in acetic acid solvent, of the nature of added salt. We have also found that reaction (5) occurs even in the absence of added salts and the highest yield of **IIa** (75%) is achieved in this case. It is noteworthy that a palladacycle from the η^3-allylpalladium moiety was obtained by

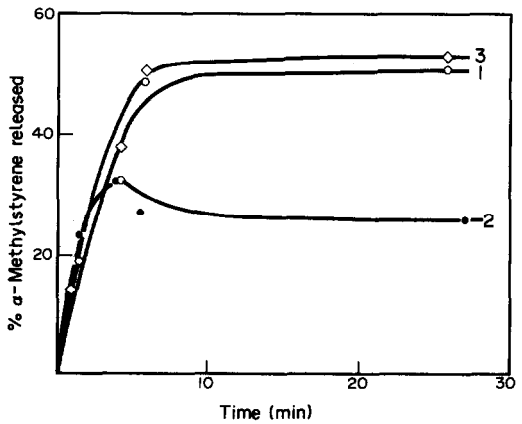

Fig. 3. Kinetic curves of reaction (5), as followed by measuring the liberation of α-methylstyrene from **VIb** by GLC: 1—LiCl, 2—LiBr and 3—LiI; 80°C, HOAc–$CHCl_3$.

Table 4. Cyclopalladation of 1-diphenylphosphinomethyl-*o*-carborane derivatives via the exchange of η^3-allyl ligands in HOAc–$CHCl_3$ solvent at 80°C

Starting complex	Added salt[a]	Time (h)	Product	Yield (%)	Isomer ratio (%) [B(3)]	[B(4)]
VIa	—	24	**IIa**	74.5	50	50
VIa[b]	LiCl	48	**IIa**	48	—	—
VIb	LiCl	48	**IIa**	47	64	36
VIb	LiBr	48	**IIf**	39	72	28
VIb	LiI	48	**IIg**	23	> 90	< 10

[a] Three-fold excess with respect to the starting complex.

[b] The $[PdCl(\eta^3\text{-}C_3H_5)(DPMC)]$ complex was introduced into the reaction mixture.

us only in the case of the carborane with a tertiary phosphine group in a side chain. No migration of palladium(II) from η^3-allyls to azobenzene, 2-phenylpyridine, N,N-dialkylbenzylamines as well as the exchange between dimeric η^3-allyls and corresponding allylic alkenes occurs.



VI [R = H (a), Ph (b)]

DISCUSSION

The cyclopalladated derivative of DPMC can be prepared in several ways as shown in Scheme 3. Of particular interest are pathways 2–3 which occur in acidic media. Our previous mechanistic investigation of the exchange of cyclopalladated C,N ligands[6c] revealed that at equilibrium, palladium(II) is preferably bound to a ligand which is the most resistant to the acidic cleavage, in particular, by acetic acid. The results of the present study clearly show that C,N-palladacycles are less protolytically stable than C,P, B,P and B,As ones; the four-membered B,P-carboranyl palladacycles are less stable than the corresponding five-membered ones. But the most surprising was the migration of palladium(II) from η^3-allyls which are very strongly bound to the central atom. It is clear that the lability of η^3-allyls is profoundly increased by the coordinated tertiary phosphines, since no exchange is observed in the case of 2-phenylpyridine, although the latter readily cleaves chloro-bridges of $[PdCl(\eta^3\text{-}2\text{-}PhC_3H_4)]_2$ to yield $[PdCl(\eta^3\text{-}2\text{-}PhC_3H_4)(2\text{-}Phpy)]$ with an equilibrium constant of 1.8×10^3 M^{-1} in $CHCl_3$ at 25°C. At the same time, one should assume that **IIa** itself must be very unreactive

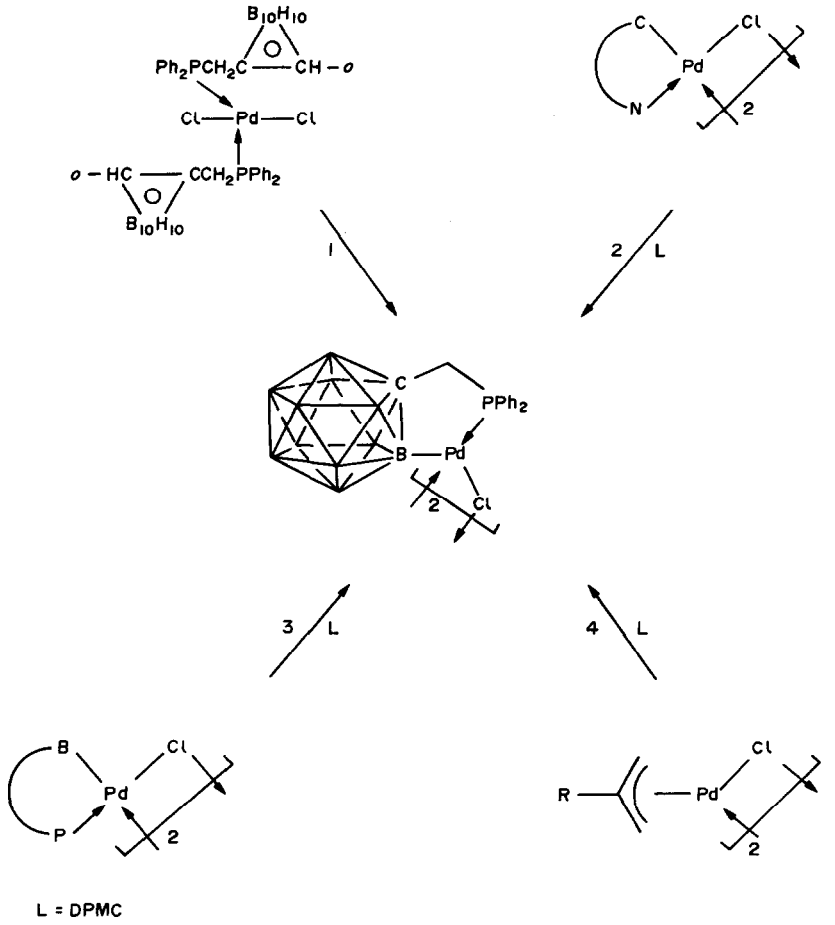

Scheme 3.

towards acidic solvents. This was shown[6c] to be the driving force of the exchange of σ-bound ligands in palladium(II) complexes in protic solvents. Palladacycle **IIa** thus appears to be a deep "potential well" in acidic media, since the σ-bond metathesis leads to this particular compound in all cases studied.

EXPERIMENTAL

Instrumentation

IR spectra in the 400–4000 cm^{-1} region were recorded on a JASCO A-200 spectrophotometer with KBr pellets; those in the far-IR region were obtained on a Bruker JFS-113 instrument in Nujol mulls. ^1H NMR spectra were obtained using Tesla BS-467 (60 MHz) and Bruker WP-200 SY (200 MHz) spectrometers using TMS as internal standard. Chemical shifts are given in the δ scale and J are in Hertz throughout. ^{11}B and ^{31}P spectra were recorded on the Bruker instrument with BF_3–Et_2O and 85% H_3PO_4 as external standards, respectively.

Materials

Palladium(II) cyclopalladated complexes $[PdCl(damp)]_2$ and $[PdCl(daep)]_2$, were prepared as described in refs 16 and 17, respectively. $PhCH_2PPh_2$ was obtained according to ref. 18. Precursors of the four-membered B,P-palladacycles DPC, DPIC and DP2MC were prepared as described in ref. 19. Diphenylphosphinomethyl carborane derivatives and DAMC were synthesized according to the procedures of Zakharkin *et al.*,[19,20] respectively. Preparation of palladium(II) η^3-allyl complexes is described in detail elsewhere.[15]

General procedure for the synthesis of bis-adducts trans-$[PdCl_2L_2]$, *the precursors of five-membered palladacycles*

To a solution of DPMC, DPMMC or DAMC (1.6 mmol) in 5 cm^3 of benzene (or 10 cm^3 of methanol), 0.75 mmol of $PdCl_2(PhCN)_2$ in 10 cm^3 of benzene (or Na_2PdCl_4 in 10 cm^3 of methanol) was added and the mixture was stirred for 3 h at room temperature. The precipitate formed was filtered, washed with hexane and dried *in vacuo*. Yields and analytical data of the compounds formed are summarized in Table 2.

Cyclopalladation of trans-$[PdCl_2(DPMC)_2]$ *in toluene*

The bis-adduct (0.43 g, 0.46 mmol) was refluxed in 15 cm^3 of toluene. In a matter of 20 min the reaction mixture turned colourless from dark yellow; 20–25 cm^3 of heptane was added and the mixture cooled. The crystals formed were filtered, washed with hexane and dried to yield 100 mg (45%) of dimeric compound **IIa**. The mother liquor was evaporated *in vacuo* and the residue was crystallized from benzene–hexane to yield 178 mg (45%) of monomeric compound **Ia**. The corresponding characteristics are given in Tables 1 and 2.

Cyclopalladation of trans-$[PdCl_2(DAMC)_2]$ *in toluene*

This was performed as described above to yield 30 mg (13%) of **V** and 310 mg (82%) of **IV** from 0.40 g (0.57 mmol) of the starting material. For data see Tables 1 and 2.

General procedure for the cyclopalladation of trans-$[PdCl_2(DPMC)_2]$ *and* trans-$[PdCl_2(DPMMC)_2]$ *in* n-*propanol*

A mixture of 0.50 g of the complex and a 10-fold excess of lithium bromide or sodium iodide in 20 cm^3 of *n*-propanol was refluxed until the solution faded. The precipitate formed after cooling was filtered, washed consequently with water, methanol and hexane, and dried to yield **IIa,b**. For data see Tables 1 and 2.

Non-metathetical cyclopalladation of 1-*diphenylphosphino*-o-*carboranes*

To 1.0 mmol of DPC, DPIC or DP2MC dissolved in 5–10 cm^3 of the corresponding solvent (MeOH, C_6H_6), 0.5 mmol of the palladium(II) compound (Li_2PdCl_4, Na_2PdCl_4, $PdCl_2(PhCN)_2$), dissolved in 15–20 cm^3 of the same solvent, was added and the mixture was mixed at room temperature until it became colourless. The precipitate which formed was filtered, washed with hexane and recrystallized from benzene–hexane to yield either monomer **Ic** or dimers **IId,e**. The bromo-bridged dimer can be obtained by performing the reaction in methanol in a 10-fold excess of LiBr. For data see Tables 1 and 2.

Di-μ-chlorobis[(2-*diphenylphosphinomethylphenyl*-C^1,P)*palladium*(II)]

To a mixture of $[PdCl(damp)]_2$ (0.095 g, 0.17 mmol) and $PhCH_2PPh_2$ (0.096 g, 0.34 mmol) in 3 cm^3 of chloroform, acetic acid (3 cm^3) was added. The reaction solution was kept for 4 days at room temperature and then 20:20 cm^3 of $CHCl_3$–H_2O was added. The organic layer was separated, twice

washed with 10 cm^3 water and dried over $MgSO_4$. The solution was then concentrated *in vacuo* and column-chromatographed (SiO_2–$CHCl_3$). The first band was separated, the solvent removed, and the residue recrystallized from hexane–benzene to afford pale yellow crystals of [PdCl(*o*-$C_6H_4CH_2PPh_2$)]$_2$ (0.030 g, 21%). Found: C, 56.0; H, 4.2. Calc. for $C_{19}H_{16}ClPd \cdot 1/6C_6H_6$: C, 55.8; H, 4.0%. Spectral data were as reported in ref. 14.

Metathetical preparation of di-μ-chlorobis[(1-*diphenylphosphinomethyl- and -2-methyl-*o*-carboranyl*-B^{3,4},P)*palladium*(II)] (**IIa** *and* **IIb**)

(a) *From* [PdCl(damp)]$_2$ *or* [PdCl(daep)]$_2$. Acetic acid (4 cm^3) was added to a mixture of [PdCl(damp)]$_2$ (0.0975 g, 0.175 mmol) and DPMC (0.121 g, 0.35 mmol) dissolved in 4 cm^3 of chloroform. The solution was thermostatted at 70°C for 25 h. Cooling to room temperature afforded white scaly crystals which were washed subsequently with $CHCl_3$–HOAc (1:1), HOAc, HOAc–H_2O (1:1) and pure water. Product **IIa** was then dried *in vacuo* over NaOH. Yield 83% (0.142 g). **IIb** was obtained in 95% yield in a similar way.

(b) *From di-μ-chlorobis*[(1C-*diphenylphosphino*-2C-*isopropyl*-*o*-*carboranyl*-B^4,P)*palladium*(II)] (**IIe**). Acetic acid (2 cm^3) was added to a solution of **IIc** (0.078 g, 0.077 mmol) and DPMC (0.060 g, 0.176 mmol) in 2 cm^3 of chloroform. The mixture was thermostatted for 6 h at 60°C to produce fine white crystals of **IIa**. The mixture was cooled to −5°C and after 30 min the crystals were filtered and treated as above. Yield 65% (0.048 g).

(c) *From di-μ-chlorobis*[(η^3-*allyl*)*palladium*(II)]. Acetic acid (4 cm^3) was added to a mixture of [PdCl(η^3-C_3H_5)]$_2$ (0.143 g, 0.39 mmol) and DPMC (0.116 g, 0.34 mmol). The resulting solution was kept at 80°C for 24 h to produce white crystals of **IIa** which were treated as above. The runs with [PdCl(η^3-2-PhC_3H_4)]$_2$ in the absence and in the presence of lithium chloride, bromide and iodide were obtained in a similar way. Data are given in Table 4.

Metathetical preparation of di-μ-chlorobis[(1-*diphenylphosphino*-2-*isopropyl*-*o*-*carboranyl*-B,P)*palladium*(II)] (**IIe**) *from* [PdCl(damp)]$_2$

Acetic acid (9 cm^3) was added to a mixture of DPIC (0.260 g, 0.690 mmol) and [PdCl(damp)]$_2$ (0.190 g, 0.345 mmol). This mixture was kept for 60 h at room temperature and then 20:20 cm^3 $CHCl_3$–H_2O was added. The organic layer was separated, washed twice with water (10 cm^3) and dried over $MgSO_4$. The solvent was removed *in vacuo* and the residue was crystallized from benzene–hexane. White crystals of **IIe** were filtered, washed with hexane and dried. Yield 40% (0.141 g). Data are given in Tables 1 and 2.

Metathetical preparation of di-μ-chlorobis[(1-*diphenylphosphino*-2-*methyl*-*o*-*carboranyl*-B,P)*palladium*(II)] (**IIf**)

A solution of [PdCl(damp)]$_2$ (0.263 g, 0.746 mmol) and DP2MC (0.212 g, 0.746 mmol) in 9 cm^3 of chloroform was mixed with 9 cm^3 of HOAc. The mixture was filtered and allowed to stand for 48 h at room temperature. White crystals which formed were filtered, washed consequently with HOAc–$CHCl_3$ (1:1), HOAc, HOAc–H_2O (1:1), H_2O and air-dried to yield 0.130 g of **IIf** (35%). An additional crop of less pure **IIf** (0.146 g) can be obtained by slow evaporation of chloroform from the initial filtrate, the total yield being 74%. Data are given in Tables 1 and 2.

REFERENCES

1. M. E. Thompson, S. M. Baxter, A. R. Bulls, B. J. Burger, M. C. Nolan, B. D. Santarsiero, W. P. Schaefer and J. C. Bercaw, *J. Am. Chem. Soc.* 1987, **109**, 203.
2. W. D. Jones and F. J. Feher, *J. Am. Chem. Soc.* 1986, **108**, 4814.
3. A. H. Janowicz and R. G. Bergman, *J. Am. Chem. Soc.* 1983, **105**, 3929.
4. M. Hackett and G. M. Whitesides, *J. Am. Chem. Soc.* 1988, **110**, 1449.
5. J. W. Bruno, T. J. Marks and L. R. Morse, *J. Am. Chem. Soc.* 1983, **105**, 6824.
6. (a) A. D. Ryabov and A. K. Yatsimirsky, *Inorg. Chem.* 1984, **23**, 789; (b) A. D. Ryabov and G. M. Kazankov, *J. Organomet. Chem.* 1984, **268**, 85; (c) A. D. Ryabov, *Inorg. Chem.* 1987, **26**, 1252.
7. For a review of cyclometallated carboranes see: V. N. Kalinin, A. V. Usatov and L. I. Zakharkin, *Metalloorganicheskaya Khimia* (*Russ.*) 1989, **2**, 54.
8. V. N. Kalinin, A. V. Usatov and L. I. Zakharkin, *J. Organomet. Chem.* 1984, **254**, 127; A. D. Ryabov, A. V. Usatov, V. N. Kalinin and L. I. Zakharkin, *Izv. AN SSSR Ser. Khim.* 1986, 1212; 2790.
9. K. Nakamoto, *Infrared and Raman Spectra of Inorganic and Coordination Compounds*, 3rd edn. Wiley, New York (1978).
10. J. Dehand, M. Pfeffer and J. Shamir, *Spectrochim. Acta* 1977, **33A**, 1101.
11. R. N. Grimes, *Carboranes*, Chap. 6. Academic Press, New York (1970).
12. A. Ya. Usyatinskii, A. D. Ryabov, T. M. Scherbina, V. I. Bregadze and N. N. Godovikov, *Izv. AN SSSR Ser. Khim.* 1983, 1637.
13. V. I. Sokolov, *Vvedenie v Teoreticheskuyu Stereokhimiyu*, p. 57. Nauka, Moscow (1979).

14. K. Hiraki, Y. Fuchita and T. Uchiyama, *Inorg. Chim. Acta* 1983, **69**, 187.
15. A. D. Ryabov, A. V. Eliseev and A. K. Yatsimirsky, *Appl. Organomet. Chem.* 1988, **2**, 101.
16. A. D. Ryabov, A. V. Polyakov and A. K. Yatsimirsky, *J. Chem. Soc., Perkin Trans. II* 1983, 1503.
17. A. D. Ryabov and G. M. Kazankov, *Vestnik Mosk. Un-ta, Ser. 2, Khimia* 1988, **29**, 220.
18. A. M. Aguiar, J. Beisler and A. Mills, *J. Org. Chem.* 1962, **27**, 1001.
19. L. I. Zakharkin, M. N. Zhubekova and A. V. Kazantsev, *Zh. Obsch. Khim.* 1972, **42**, 1024.
20. L. I. Zakharkin, A. I. Kovredov, I. S. Savel'eva and M. G. Meiramov, *Izv. AN SSSR Ser. Khim.* 1980, 2645.

Polyhedron Vol. 8, No. 12, pp. 1497–1502, 1989
Printed in Great Britain

0277-5387/89 $3.00 + .00
© 1989 Pergamon Press plc

REACTION OF ORGANOALUMINIUM SPECIES WITH BIDENTATE PHOSPHINE LIGANDS. SYNTHESIS AND MOLECULAR STRUCTURE OF $[AlCl_3][(Ph_2P)_2CH_2][AlCl_2(CH_3)]$ AND $[AlCl_3]_2[(Ph_2P(O))_2CH_2]$

SAMUEL A. SANGOKOYA, BAOSHENG LEE, MARK F. SELF, WILLIAM T. PENNINGTON and GREGORY H. ROBINSON*

Department of Chemistry, Clemson University, Clemson, SC 29634-1905, U.S.A.

(*Received* 30 *November* 1988; *accepted* 27 *January* 1989)

Abstract—Reaction of methylaluminium sesquichloride with bis(diphenylphosphino) methane and bis(diphenylphosphinoyl)methane affords $[AlCl_3][(Ph_2P)_2CH_2][AlCl_2(CH_3)]$ (**I**) and $[AlCl_3]_2[(Ph_2P(O))_2CH_2]$ (**II**), respectively. Compound **I** crystallizes in the triclinic space group $P\bar{1}$ with unit cell parameters $a = 10.009(3)$, $b = 10.748(4)$, $c = 14.806(5)$ Å, $\alpha = 90.38(3)$, $\beta = 103.36(2)$, $\gamma = 96.89(3)°$, $V = 1537.5$ Å^3 and $\rho = 1.36$ for $Z = 2$. Compound **II** crystallizes in the monoclinic space group $C2$ with unit cell parameters $a = 12.773(2)$, $b = 13.028(3)$, $c = 9.461(2)$ Å, $\beta = 104.43(2)°$, $V = 1524.60$ Å^3 and $\rho = 1.49$ for $Z = 2$. Full-matrix least-squares refinement based on 3034 observed reflections for **I** converged at $R = 0.047$ ($R_w = 0.066$); full-matrix least-squares refinement based on 1565 observed reflections for **II** converged at $R = 0.043$ ($R_w = 0.050$). Both products result from reaction of the disproportionation products of methylaluminium sesquichloride, $AlCl_3$ and $AlCl_2(CH_3)$.

Principally due to the fact that the close proximity of the two phosphorus atoms can often facilitate interesting behaviour in bimetallic complexes,[1–5] the bidentate phosphine ligand bis(diphenylphosphino)methane has proven to be quite popular in transition metal chemistry. Interestingly, the oxygen analogue of this ligand, bis(diphenylphosphinoyl)methane, has generated substantially less attention in transition metal chemistry. Although there has been sporadic interest in the organo main group chemistry, specifically organoaluminium chemistry, of bis(diphenylphosphino) methane,[6–11] the literature reveals only one study concerning the corresponding chemistry of bis(diphenylphosphinoyl)methane.[12] Herein, we report the synthesis and molecular structure of $[AlCl_3][(Ph_2P)_2CH_2][AlCl_2(CH_3)]$ (**I**) and $[AlCl_3]_2[(Ph_2P(O))_2CH_2]$ (**II**), isolated from reaction of methylalumium sesquichloride with bis(diphenylphosphino)methane and bis(diphenylphosphinoyl) methane, respectively.

* Author to whom correspondence should be addressed.

EXPERIMENTAL

Synthesis

Standard Schlenk techniques were employed in conjunction with an inert atmosphere dry-box (Vacuum Atmospheres HE-43 Dri-Lab). Solvents were purified and degassed prior to use. Methylaluminium sesquichloride was purchased from Aldrich Chemical Company and used as received. Both phosphine ligands were prepared in our laboratory. Single crystal X-ray data were collected on a Nicolet R3m/V diffractometer with graphite-monochromated Mo-K_α radiation. ^{1}H NMR data were recorded on a JEOL-FX90Q NMR spectrometer. ^{31}P NMR data were recorded on an IBM 200-MHz NMR spectrometer.

(1) $[AlCl_3][(Ph_2P)_2CH_2][AlCl_2(CH_3)]$ (I)

Inside the dry-box a reaction vessel was charged with bis(diphenylphosphino)methane (1.0 g, 2.8 mmol) and toluene (25 cm^3). Methylaluminium sesquichloride (1.0 cm^3, 3.0 mmol) was slowly added via syringe. Reaction was immediate and exothermic. The reaction vessel was subsequently removed

from the dry-box and heated in an oil bath for 6 h at 100°C. The solution was filtered and transferred to a 100 cm^3 Schlenk flask. The solution was concentrated and the flask was cooled to −15°C when colourless, extremely air-sensitive crystals were isolated; m.p. = 160–162°C. ^1H NMR (C_6D_6): δ −0.371 (s, 3H, Al(CH_3)), 3.72 (d of d, 2H, P—CH_2—P, $J_{P—CH}$ = 5.5 Hz), 7.36 (m, 20H, $2C_6H_5$). ^{31}P NMR (C_6D_6): δ −25.85 (d, 1P, *P*—Al($(CH_3)Cl_2$), 4.87 (d, 1P, *P*—$AlCl_3$, $J_{P—P}$ = 53.71 Hz).

(2) $[AlCl_3]_2[(Ph_2P(O))_2CH_2]$ (II)

A reaction vessel was charged with bis(diphenylphosphinoyl)methane (0.50 g, 1.2 mmol) and methylaluminium sesquichloride (0.47 cm^3, 2.4 mmol) in a mixture of chlorobenzene–heptane (28 and 2 cm^3, respectively). The reaction vessel was removed from the dry-box and heated in an oil bath (120°C) for 24 h. Upon cooling to room temperature a multitude of small colourless, rectangular, extremely air-sensitive crystals were obtained in quantitative yield; m.p. = 177–179°C. ^1H NMR ($CDCl_3$): δ 3.5 (t, 2H, P—CH_2—P), 7.2 (m, 20H, C_6H_5). ^{31}P NMR ($CDCl_3$): δ 46.33 (s, 2P, *P*—$AlCl_3$).

X-ray structural solution and refinement

Single crystals of both compounds were mounted in thin-walled glass capillaries under an inert atmosphere of argon. Structures of both compounds were solved by direct methods using the SHELXTL[13] package of computer programs. Early in the refinement of **I** the thermal parameters of atoms Cl(5) and C(26) indicated that each of these two positions was occupied by both chloro and methyl groups, alternatively. The occupancy factors of these two atoms, both treated as chlorine, refined to values of 0.77 and 0.58, respectively. These values indicate that the position reported for the Cl(5) atom is occupied 55% by a chlorine atom and 45% by a methyl group, and that the position reported for the C(26) atom is occupied 55% by a methyl group and 45% by a chlorine atom. Hydrogen atoms of the methylene and phenyl groups for both compounds were located by standard difference Fourier techniques and were included in the structure factor calculations at idealized positions ($d_{C—H}$ = 0.95 Å); the methyl hydrogen atoms for compound **I** could not be located. An isotropic group thermal parameter was refined for the phenyl and methylene hydrogen atoms of each compound. As **II** crystallizes in an acentric space group,* refinement was carried out for both enantiomeric conformations of the molecule. Refinement of the model corresponding to the reported coordinates yielded residual values of $R = 0.043$, $R_w = 0.050$, and GOF = 1.15, while an identical refinement of the inverted model yielded final residuals of $R = 0.0436$, $R_w = 0.0502$, and GOF = 1.17. A summary of crystallographic data is given in Table 1.†

RESULTS AND DISCUSSION

For some time now this laboratory has been interested in the interactions of organoaluminium species with various sulphur-[14–16] and nitrogen-based[17–20] macrocyclic ligands. More recently our attention has shifted to the corresponding organoaluminium chemistry of multidentate open chain amines.[21–23] As a logical extension of this work we have endeavoured to examine the organoaluminium chemistry of multidentate phosphorus ligands. The versatile bidentate phosphine ligand bis(diphenylphosphino)methane was chosen to initiate these studies. We have recently reported interesting products resulting from reaction of organoaluminium species with bis(biphenylphosphino)methane,[6] its oxygen derivative,[12] and its sulphur derivative.[24] An interesting study concerning the organo main group chemistry of the bidentate phosphine ligand bis(diphenylphosphino)ethane has recently appeared.[25] Herein, we report the synthesis and molecular structure of $[AlCl_3][(Ph_2P)_2CH_2][AlCl_2CH_3]$ (**I**) and $[AlCl_3]_2[(Ph_2P(O))_2CH_2]$ (**II**).

In that methylaluminium sesquichloride, $(CH_3)_3Al_2Cl_3$, is usually regarded as a mixture of dimethylaluminium chloride and methylaluminium dichloride, it is interesting to note that **I** contains one $AlCl_2(CH_3)$ adduct and one $AlCl_3$ adduct, while **II** contains two $AlCl_3$ units. The presence of these species can be traced to Lewis acidity and basicity. Ziegler[26] reported nearly 30 years ago that an alkylaluminium halide dimer, in the presence of a sufficiently strong Lewis base, will readily disproportionate to favour the strongest available Lewis acid species. Necessarily, Ziegler suggested

* Space group *C*2 was verified as the correct choice by analysis of intensity distribution, packing considerations, and by the successful solution and refinement of the structure.

†Supplementary material available. Tables of crystal data, fractional coordinates, bond distances and angles, and calculated and observed structure factors have been deposited with the Cambridge Crystallographic Data Centre. Complete structural information is available from the Editor.

Table 1. Crystallographic data for $[AlCl_3][(Ph_2P)_2CH_2][AlCl(CH_3)_2]$ (I) and $[AlCl_3][(Ph_2P(O))_2CH_2][AlCl_3]$ (II)

	(I)	(II)
Formula	$Al_2Cl_5P_2C_{26}H_{25}$	$Al_2Cl_6P_2C_{25}H_{22}O_2$
Formula weight	630.66	682.98
Crystal system	Triclinic	Monoclinic
Space group	$P\bar{1}$	$C2$
a (Å)	10.009(3)	12.773(2)
b (Å)	10.748(4)	13.028(3)
c (Å)	14.806(5)	9.461(2)
α (°)	90.38(3)	
β (°)	103.36(2)	104.43(2)
γ (°)	96.89(3)	
Volume (Å^3)	1537.47	1524.61
Z	2	2
ρ	1.36	1.49
μ (cm^{-1})	6.48	7.49
Absorbance transmission factors	0.87–1.00	0.92–1.00
Diffractometer	Nicolet R3m/V	
λ(Mo-K_α) (Å)	0.71073	
Temperature	21°C	
2θ limits (°)	3.50–45.0	
Reflections measured	4295 (4036 unique)	3986 (2003 unique)
Reflections observed	3034	1565
Goodness-of-fit	1.58	1.15
R	0.047	0.043
R_w	0.066	0.050

that this proceeds through the transient formation of a mixed alkyl–halo-bridged dimer (instead of the more commonly preferred di-halo-bridged dimer). Similarly, it is reasonable that the dimer of methylaluminium sesquichloride, capable of producing the reactive aluminium species in I and II, $AlCl_3$ and $AlCl_2(CH_3)$, proceeds through a mixed halo–alkyl- (chloro–methyl-) bridged species. Bridge cleavage of such a dimer would provide both $AlCl_3$ and $AlCl_2(CH_3)$. This situation for methylaluminium sesquichloride is illustrated in Fig. 1. Furthermore, of all the possible dimeric species of methylaluminium sesquichloride, only the mixed bridged species given in Fig. 1 can readily provide the reactive species [$AlCl_3$ and $AlCl_2(CH_3)$]. Indeed, we have recently observed a similar disproportionation of diethylaluminium chloride in its reaction with the nitrogen macrocycle cyclam.[17]

The X-ray crystal structure of $[AlCl_3][(Ph_2P)_2CH_2][AlCl_2(CH_3)]$ (I) is given in Fig. 2. The mean Al—Cl bond distance in I is 2.097(3) Å. The overall conformation of $(Ph_2P)_2CH_2$ in I is easily compared to that of the uncomplexed ligand.[27] The central methylene P—C—P bond angle in the uncomplexed ligand of 108.2(5)° is generally indicative of an atom in a tetrahedral environment. This P—C—P bond angle in I has increased to 122.4(2)°, resulting in C(13) being in a severely distorted tetrahedron. A comparison of I with the recently reported $[Al(CH_3)_3]_2[(Ph_2P)_2CH_2]$[6] complex is warranted. The P—C—P bond angle of 121.4(2)° in this complex is not as great as that observed in I. The Al—P bond distances of 2.585(2) and 2.521(2) Å in $[Al(CH_3)_3]_2[(Ph_2P)_2CH_2]$ compares to 2.451(2) and 2.497(2) Å for I.

While bis(diphenylphosphino)methane has been

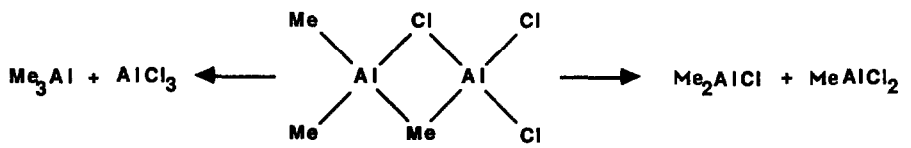

Fig. 1. Organoaluminium products resulting from bridge cleavage of the proposed transient mixed alkyl–halo isomer of methylaluminium sesquichloride, $Me_3Al_2Cl_3$.

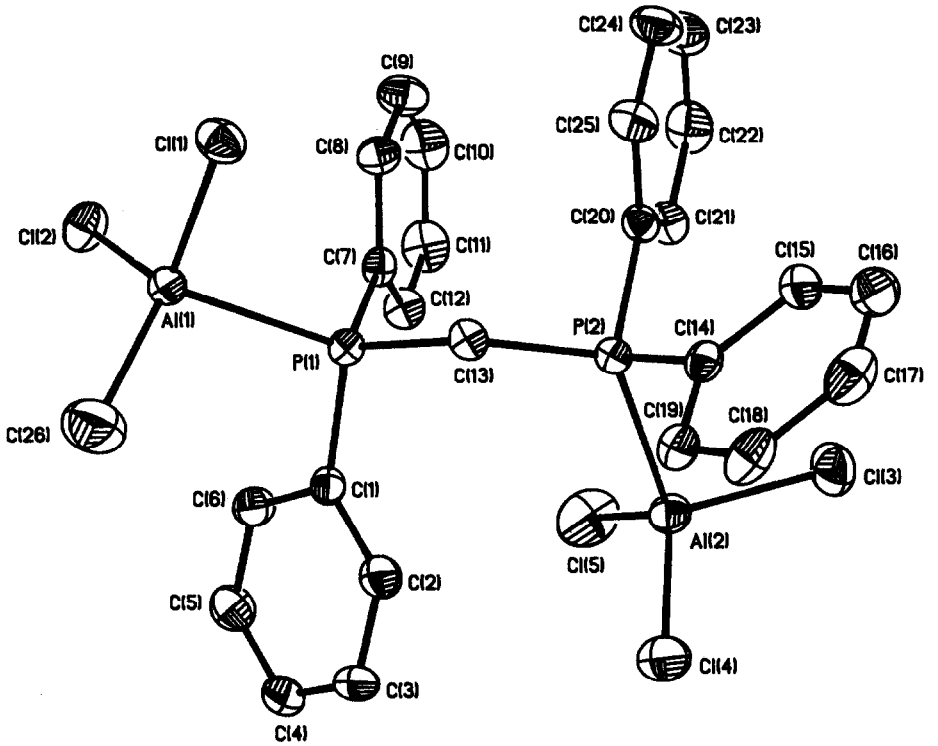

Fig. 2. A view of the $[AlCl_3][(Ph_2P)_2CH_2][AlCl_2(CH_3)]$ (I) molecule showing the atom labelling scheme. Thermal ellipsoids show 35% probability levels; hydrogen atoms have been omitted. Selected bond distances (Å) and angles (°): Al(1)—Cl(1), 2.138(2); Al(1)—Cl(2), 2.122(2); Al(2)—Cl(3), 2.112(2); Al(2)—Cl(4), 2.094(3); Al(2)—Cl(5), 2.020(4); Al(1)—C(26), 1.998(5); Al(1)—P(1), 2.451(2); Al(2)—P(2), 2.497(2); P(1)—C(13)—P(2), 122.4(2); Al(1)—P(1)—C(1), 106.9(2); Al(1)—P(1)—C(7), 112.9(2); Al(1)—P(1)—C(13), 110.7(1); C(1)—P(1)—C(7), 110.3(2); Al(2)—P(2)—C(14), 105.9(2); Al(2)—P(2)—C(20), 114.5(2); C(13)—P(2)—C(14), 100.6(2); C(14)—P(2)—C(20), 106.2(2).

examined in organoaluminium chemistry, the corresponding chemistry of the oxygen analogue, bis(diphenylphosphinoyl)methane, has remained largely unexplored. This ligand was allowed to react with methylaluminium sesquichloride; $[AlCl_3]_2[(Ph_2P(O))_2CH_2]$ (II) was the only product isolated. The X-ray crystal structure of $[AlCl_3]_2[(Ph_2P(O))_2CH_2]$ (II) is given in Fig. 3. Compound II resides about a crystallographic two-fold axis. The independent Al—O bond distance of 1.756(5) Å indicates a relatively strong aluminium–oxygen interaction. The P—O bond distance is 1.512(5) Å. Due to a relaxation of steric constraints, the P—C—P bond angle of 119.5(5)° in II is expectedly less than that observed in I. The mean Al—Cl distance is 2.107(4) Å.

Even though the presence of an oxygen atom on each phosphorus atom serves to sufficiently increase the acidity of the methylene hydrogen atoms so as to facilitate condensation in the presence of trimethylaluminium,[12] condensation is not observed in the present case where an alkylaluminium halide is concerned.

The fact that I contains one $AlCl_3$ adduct and one $AlCl_2(CH_3)$ adduct, while II has two $AlCl_3$ adducts is particularly noteworthy. It is reasonable that the central P—C—P fragment of the ligand plays a predominant role in the isolated reaction products. As mentioned earlier, the P—C—P bond angle in the uncomplexed ligand is 108.2(5)°. To accommodate one $AlCl_3$ and $AlCl_2(CH_3)$ unit, as in I, the P—C—P bond angle increased to 122.4(2)°. It is therefore conceivable that for bis(diphenylphosphino)methane to accept two of the slightly larger $AlCl_3$ units [rather than one of each $AlCl_3$ and $AlCl_2(CH_3)$], the P—C—P would have been forced to undergo still further distortion from its preferred tetrahedron. Thus, it was easier for the ligand to accept one slightly smaller $AlCl_2(CH_3)$ unit and one $AlCl_3$ unit than two $AlCl_3$ units. Conversely, in II the presence of an oxygen atom on either phosphorus atom serves to relieve some of

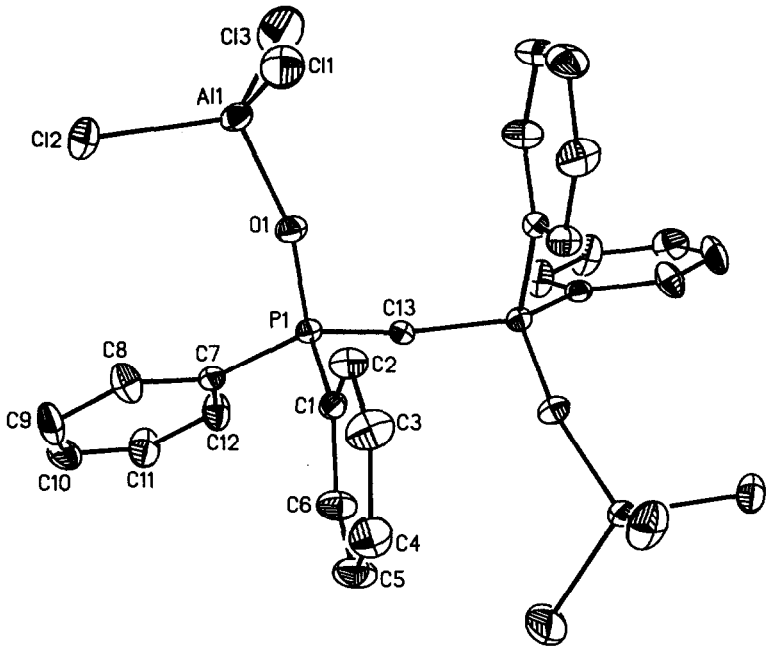

Fig. 3. A view of the $[AlCl_3]_2[(Ph_2P(O))_2CH_2]$ (II) molecule showing the atom labelling scheme. Thermal ellipsoids show 35% probability levels; hydrogen atoms have been omitted. Selected bond distances (Å) and angles (°): Al(1)—Cl(1), 2.133(4); Al(1)—Cl(2), 2.116(3); Al(1)—Cl(3), 2.072(4); Al(1)—O(1), 1.756(5); P(1)—O(1), 1.512(5); P(1)—C(13)—P(1a), 199.5(5); C(7)—P(1)—C(13), 111.9(3); Al(1)—O(1)—P(1), 164.0(3); O(1)—P(1)—C(1), 109.7(3); O(1)—P(1)—C(13), 108.5(2).

the immediate steric strain about the P—C—P (P—C—P = 119.5(5)°) fragment and bis(diphenylphosphinoyl)methane was able to accept two $AlCl_3$ units.

We feel that this study is significant in that it provides further information on the dimeric species of alkylaluminium halides in the presence of strong Lewis bases.

Acknowledgement—We are grateful to the National Science Foundation for support of this work to G.H.R. (RII-8520554).

REFERENCES

1. N. Van Order Jr, *J. Am. Chem. Soc.* 1987, **109**, 5680.
2. M. O. Albers, D. C. Liles, D. J. Robinson and E. Singleton, *Organometallics* 1987, **6**, 2179.
3. B. Delavaux, B. Chaudret, G. Dahan and R. Pollblanc, *Organometallics* 1985, **4**, 935.
4. B. Chaudret, F. Dahan and S. Saba, *Organometallics* 1985, **4**, 1490.
5. J. A. Iggo, D. P. Markham, B. L. Shaw and M. Thornton-Pett, *J. Chem. Soc., Chem. Commun.* 1985, 432.
6. G. H. Robinson, M. F. Self, S. A. Sangokoya and W. T. Pennington, *J. Spect. Cryst. Res.* 1988, **18**, 285.
7. H. Schmidbaur, S. Lauteschläger and G. Müller, *J. Organomet. Chem.* 1985, **281**, 25.
8. Y. Inoue, T. Kagawa, Y. Uchida and H. Hashimoto, *Bull. Chem. Soc. Jpn* 1972, **45**, 1996.
9. T. Kagawa and H. Hashimoto, *Bull. Chem. Soc. Jpn* 1972, **45**, 1739.
10. Y. Inoue, T. Kagawa and H. Hashimoto, *Tetrahedron Lett.* 1970, **13**, 1099.
11. T. Kagawa, Y. Inoue and H. Hashimoto, *Bull. Chem. Soc. Jpn* 1970, **43**, 1250.
12. G. H. Robinson, B. Lee, W. T. Pennington and S. A. Sangokoya, *J. Am. Chem. Soc.* 1988, **110**, 6260.
13. G. M. Sheldrick, SHELXTL, Crystallographic Computing System, Revision 5.1. Nicolet Instruments Division, Madison, Wisconsin (1986).
14. G. H. Robinson and S. A. Sangokoya, *J. Am. Chem. Soc.* 1988, **110**, 1494.
15. S. A. Sangokoya, B. Lee, W. T. Pennington and G. H. Robinson, *J. Coord. Chem.* 1989, **19**, 331.
16. G. H. Robinson, H. Zhang and J. L. Atwood, *Organometallics* 1987, **6**, 887.
17. G. H. Robinson and S. A. Sangokoya, *Organometallics* 1988, **7**, 1453.
18. G. H. Robinson, E. S. Appel, S. A. Sangokoya, H. Zhang and J. L. Atwood, *J. Coord. Chem.* 1988, **17**, 373.
19. G. H. Robinson, A. D. Rae, C. F. Campana and S. K. Byram, *Organometallics* 1987, **6**, 1227.
20. G. H. Robinson, H. Zhang and J. L. Atwood, *J. Organomet. Chem.* 1987, **331**, 153.
21. G. H. Robinson, S. A. Sangokoya, F. Moise and W. T. Pennington, *Organometallics* 1988, **7**, 1887.
22. G. H. Robinson, F. Moise, W. T. Pennington and S.

A. Sangokoya, *J. Cryst. Spect. Res.* 1988, **18**, 387.
23. G. H. Robinson and S. A. Sangokoya, *J. Am. Chem. Soc.* 1987, **109**, 6852.
24. G. H. Robinson, M. F. Self, W. T. Pennington and S. A. Sangokoya, *Organometallics* 1988, **7**, 2424.
25. D. C. Bradley, H. Chudzynska, M. M. Faktor, D. M. Frigo, M. B. Hursthouse, B. Hussain and L. M. Smith, *Polyhedron* 1988, **7**, 1289.
26. K. Ziegler, *Organometallic Chemistry* (Edited by H. Zeiss), p. 194. Reinhold, New York (1960).
27. M. F. Self, R. D. Rogers and G. H. Robinson, unpublished results.

Polyhedron Vol. 8, No. 12, pp. 1503–1507, 1989
Printed in Great Britain

0277–5387/89 $3.00+.00
© 1989 Pergamon Press plc

SYNTHESIS AND X-RAY CRYSTAL STRUCTURE OF $Fe(CO)_2[O_2CCH_2P(C_6H_5)_2]_2$, THE FIRST IRON CARBONYL COMPLEX WITH TWO CARBOXYLATE LIGANDS

JÁNOS TAKÁCS* and LÁSZLÓ MARKÓ†

Research Group for Petrochemistry of the Hungarian Academy of Sciences, Schönherz 10, H-8200 Veszprém, Hungary

and

PAUL KIPROF, EBERHARDT HERDTWECK and WOLFGANG A. HERRMANN†

Anorganisch-chemisches Institut der Technischen Universität München, Lichtenbergstraße 4, D-8046 Garching, Germany

(*Received* 29 *November* 1988; *accepted* 27 *January* 1989)

Abstract—$Fe(CO)_2[O_2CCH_2P(C_6H_5)_2]_2$ (I) was synthesized from $FeSO_4 \cdot 7H_2O$ and $Na[O_2CCH_2P(C_6H_5)_2]$ under CO pressure. The 18-electron compound has an octahedral coordination sphere around Fe^{2+}. Two diphenylphosphinoacetate ligands are bonded to the iron through the phosphorus atoms and one of the oxygen atoms of the carboxylato groups. Two carbonyl groups and two carboxylato oxygen atoms are in *cis* positions to each other, while the phosphorus atoms adopt *trans* positions. The unit cell contains both enantiomers of the chiral octahedral compound.

Due to the possibility of obtaining compounds with interesting structures and increased reactivity, the combination of hard and soft donor atoms in bidentate ligands has recently become more attractive,[1–4] especially since N—P and O—P type bidentate ligands have been used with success in homogeneous catalysis.[5,6] In continuation of our studies on iron(II) carbonyl complexes, prepared by the convenient method of CO absorption at atmospheric pressure,[7,8] we now report the synthesis and X-ray crystal structure of $Fe(CO)_2[O_2CCH_2P(C_6H_5)_2]_2$ (I), which to our knowledge, is the first mononuclear dicarboxylato iron carbonyl.

RESULTS AND DISCUSSION

Synthetic and spectroscopic results

Compound I was synthesized from $FeSO_4 \cdot 7H_2O$ and $Na[O_2CCH_2P(C_6H_5)_2]_2$ under CO pressure according to eq. (1):

$$Fe^{2+} + 2(C_6H_5)_2PCH_2CO_2^- \xrightarrow[MeOH,\ 100°C]{133\ bar\ CO} \underset{(I)}{Fe(CO)_2[O_2CCH_2P(C_6H_5)_2]_2}. \quad (1)$$

Under ambient conditions (1 bar CO, 25°C), there is no CO absorption. This result contrasts the synthesis of the isoelectronic and structurally similar compounds of formulae, $Fe(CO)_2(S—N)_2$ (S—N = *o*-$SC_6H_4NH_2$ or $SCH_2CH_2NH_2$)[7] and $Fe(CO)_2(DPPE)(SR)_2$ (DPPE = $Ph_2PCH_2CH_2PPh_2$; R = C_2H_5, $CH(CH_3)CH_2CH_3$, C_6H_5, etc.).[8] Compound I can also be prepared from $Fe(CO)_4I_2$ and $Na[O_2CCH_2P(C_6H_5)_2]$, but this route is less convenient and yields a less pure product.

The soft and nucleophilic character of the phosphorus atoms is probably one of the major contributors to the formation and thermal stability of I. While compounds of type $Fe(CO)_4(O_2CR)_2$ are not known and also other types of group VIII metal carbonyls containing M—O bonds are rather rare, in I the strong electron-withdrawing effect of the oxygen atoms is compensated by the two phosphorus atoms. Another factor contributing to the

* Currently an Alexander von Humboldt Fellow at the Anorganisch-chemisches Institut der Technischen Universität München.

† Authors to whom correspondence should be addressed.

stability of **I** is the special chelate effect of the ligand. For example, all our efforts to synthesize $Fe(CO)_2(PR_3)_2(O_2CR)_2$ type complexes with monodentate ligands, as well as experiments with P—P and O—O type diphos and dicarboxylato ligands were unsuccessful. In addition, the synthesis of the analogous complex $Fe(CO)_2[O_2CCH_2CH_2P(C_6H_5)_2]_2$ from $FeSO_4 \cdot 7H_2O$ and $Na[O_2CCH_2CH_2P(C_6H_5)_2]$ according to eq. (1) was unsuccessful; this result reflects the importance of the number of atoms in the chelating ligand.

In the solution IR spectrum of **I** (CH_2Cl_2), three well separated CO absorption bands were found. The band at 1660 cm^{-1} is assigned to the carboxylato C=O group, while the two bands of equal intensity in the metal carbonyl region (2048 and 1998 cm^{-1}) are characteristic of a *cis*-dicarbonyl structure. The latter two absorptions are at somewhat higher wave numbers ($\approx$ 20–25 cm^{-1}) than the ν(CO) bands of the $Fe(CO)_2(DPPE)(SR)_2$ complexes, which reflects the stronger electron-withdrawing capability of the carboxylato group as compared to the thiolate ligand.

The ^{31}P NMR ($CDCl_3$) spectrum of **I** shows a single absorption at δ 38.5 ppm due to the equivalent phosphorus nuclei. (The symmetry element is a C_2 axis.) The ^1H NMR spectrum ($CDCl_3$) displays multiplets of the phenyl protons in the range δ 7.4–7.9 ppm and two doublets of virtual triplets at δ 3.44 ppm, as well as 3.65 ppm. These latter resonances can be assigned to the diastereotopic methylene protons (H_AH_B) of the ligands which both couple with the phosphorus atoms ($H_AH_BP_XP_{X'}$ pattern, $^2J(H_AH_B) = 16.5$ Hz and $J(H_AP_XP_{X'}) = J(H_BP_XP_{X'}) = 11.0$ Hz). The following signals were found in the ^{13}C NMR spectrum (CD_2Cl_2): δ 34.8 (CH_2, t, $^1J(CP) = 28.2$ Hz), δ 127.7–134.1 (aromatic carbons), δ 177.2 (CO_2 groups, t, $^{2+3}J(CP) = 21.3$ Hz), δ 209.7 (CO groups, t, $^2J(CP) = 42$ Hz). The investigation of the reactions of **I** is the subject of further studies in the Veszprém laboratory.

X-ray structural results

A single crystal of the title compound, crystallized from CH_2Cl_2–*n*-hexane, was used for diffraction data collection. Data were collected at room temperature on a CAD-4 (Enraf–Nonius) with graphite-monochromated Mo-K_α radiation ($\lambda = 71.07$ pm). Parameters of data collection are summarized in Table 1. Lattice constants were obtained by a least-squares fit of 75 reflections in the range $37.07 \leqslant 2\theta \leqslant 58.8$.[10] Intensities of three standard reflections for decomposition and three orientation control reflections were measured every 60 min and every 200 reflections, respectively, during data collection. No decay or disorientation has been observed. Corrections for Lorentz and polarization effects were applied. No correction was applied on account of a negligible absorption coefficient ($\mu = 6.9\ cm^{-1}$). The structure was solved by direct methods (SHELX-86)[11] and refined by subsequent least-squares and difference Fourier techniques.[12] All hydrogen positional parameters could be obtained from difference Fourier maps and were refined with individual isotropic thermal parameters. All non-hydrogen atoms were refined using anisotropic thermal parameters. Scattering factors were taken from ref. 13, including anomalous scattering.[14] The refinement yielded final R values of $R = 0.047$ and $R_w = 0.035$, with all observed reflections ($I \geqslant 0.0$). With a maximum of 0.16 e $Å^{-3}$ and a minimum of -0.18 e $Å^{-3}$, final difference Fourier maps demonstrated no more significant electron density. All computations were carried out on a VAX 11/730 and a VAX 8200 with the Program System STRUX.[15]

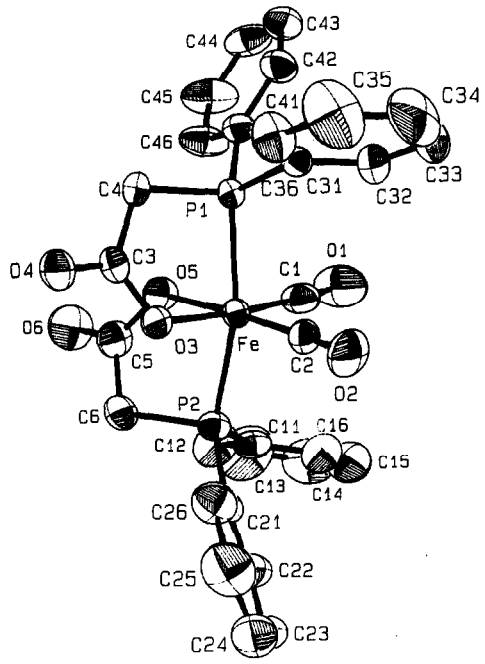

Fig. 1. ORTEP drawing[16] of $Fe(CO)_2[O_2CCH_2P(C_6H_5)_2]_2$, at 50% probability level, showing the labelling scheme. Hydrogen atoms are omitted for clarity.

The structure of the molecule can be best described as a distorted octahedron (see Fig. 1). Two phosphorus atoms (d(Fe—P) 225.24(3) pm and 226.18(3) pm) are in *trans* positions to each other. The remaining coordination sites are occupied by two carboxylato oxygen atoms in *cis* positions [d(Fe—O) 197.80(8) and 198.46(7) pm;

Table 1. Crystallographic data, parameters of data collection and structure refinement for $Fe(CO)_2[O_2CCH_2P(C_6H_5)_2]_2$ (I)

(a)	Crystal parameters	
	Empirical formula	$C_{30}H_{24}FeO_6P_2$
	Formula weight	598.3
	Crystal colour and shape	Yellow, parallelopiped
	Crystal dimensions (mm)	$0.60 \times 0.30 \times 0.60$
	Radiation	Mo-K_α ($\lambda = 71.073$ pm)
	Temperature (°C)	22 ± 1
	Space group	$C2/c$ (Int. Tab. No. 15)
	a (pm)	3629.3(2)
	b (pm)	757.36(5)
	c (pm)	2108.2(1)
	β (°)	104.35(< 1)
	V (pm^3)	5614×10^6
	Z	8
	ρ(calc.) (g cm^{-3})	1.416
	μ(Mo-K_α) (cm^{-1})	6.9
(b)	Data collection	
	Scan type	ω-scan
	Scan time (s)	Maximum 60
	Scan width (°)	$(1.00 \pm 0.35 tg\theta) \pm 25\%$ for corrections
	Maximum 2θ (°)	60
	Number of reflections measured	8556 (0/46; 0/10, −26/26) ($h+k = 2n$)
	Number of independent reflections	6817
	Corrections	Lorentz–Polarization,
	Standard reflections	3 every 3600 s intensity check
		3 every 200 orientation check
(c)	Refinement	
	Solution	Direct methods
	Hydrogen atoms	All found, refined
	Refinement	Full-matrix least-squares
	Minimization function	$\Sigma w(F_o - F_c)^2$
	Weighting scheme	$1/\sigma(F_o)^2$
	Anomalous dispersion	All non-hydrogen atoms
	Number of reflections included *NO*	6817 $I \geqslant 0.0$
	Number of parameters refined *NV*	448
	R	0.047[a]
	R_w	0.035[b]
	Goodness-of-fit	3.300[c]
	Shift/error	< 0.001

[a] $R = \Sigma ||F_o| - |F_c|| / \Sigma |F_o|$.
[b] $R_w = [\Sigma w(|F_o| - |F_c|)^2 / \Sigma w F_o^2]^{1/2}$.
[c] G.O.F. $= \Sigma w(|F_o| - |F_c|)^2 / (NO - NV)]^{1/2}$.

O—Fe—O 87.29(3)°] and two carbonyl ligands also in *cis* positions to each other (d(Fe—C) 175.6(1) and 178.3(1) pm; C—Fe—C 92.59(6)°). This conformation of the compound is the only stable arrangement possible, with respect to the steric bulk of the phenyl groups in the phosphine ligands as well as to the strong synergetic *trans* interaction between the π-donor oxygen atoms and the π-acceptor carbonyl groups. The angle P—Fe—P differs significantly from linearity (P—Fe—P 167.00(1)°). This effect is due to the strain of the five-membered rings formed by the chelate ligands. Selected bond lengths and angles are given in Table 2.

Table 2. Selected bond lengths (pm) and bond angles (°) of the title compound I

Fe—P(1)	225.24(3)	P(1)—Fe—P(2)	167.00(1)
Fe—P(2)	226.18(3)	P(1)—Fe—O(3)	82.75(2)
Fe—O(3)	198.46(7)	P(1)—Fe—O(5)	87.65(3)
Fe—O(5)	197.80(7)	P(1)—Fe—C(1)	92.87(4)
Fe—C(1)	175.6(1)	P(1)—Fe—C(2)	94.37(4)
Fe—C(2)	178.3(1)	P(2)—Fe—O(3)	89.61(2)
P(1)—C(4)	180.8(1)	P(2)—Fe—O(5)	81.48(2)
P(1)—C(31)	180.2(1)	P(2)—Fe—C(1)	94.52(4)
P(1)—C(41)	181.6(1)	P(2)—Fe—C(2)	95.91(4)
P(2)—C(6)	181.9(1)	O(3)—Fe—O(5)	87.29(3)
P(2)—C(11)	180.8(1)	O(3)—Fe—C(1)	175.52(5)
P(2)—C(21)	181.1(1)	O(3)—Fe—C(2)	88.73(4)
O(1)—C(1)	113.5(1)	O(5)—Fe—C(1)	91.60(5)
O(2)—C(2)	112.1(1)	O(5)—Fe—C(2)	175.24(5)
O(3)—C(3)	130.2(1)	C(1)—Fe—C(2)	92.59(6)
O(4)—C(3)	121.4(1)	Fe—P(1)—C(4)	98.49(4)
O(5)—C(5)	128.6(1)	Fe—P(1)—C(31)	114.20(4)
O(6)—C(5)	121.5(1)	Fe—P(1)—C(41)	121.01(4)
C(3)—C(4)	151.8(2)	Fe—P(2)—C(6)	95.89(4)
C(5)—C(6)	153.3(2)		

EXPERIMENTAL

$Na[O_2CCH_2P(C_6H_5)_2]$ was prepared according to ref. 15.

Synthesis of $Fe(CO)_2[O_2CCH_2P(C_6H_5)_2]_2$ (I)

A 100 cm^3 rocking autoclave was charged with 1.0 mmol of $FeSO_4 \cdot 7H_2O$ (278 mg), 2.0 mmol of $Na[O_2CCH_2P(C_6H_5)_2]$ (532 mg) and 55 cm^3 of methanol under an atmosphere of CO. Then the vessel was pressurized to 100 bar CO at 25°C and kept for 4 h at 100°C in a rocking autoclave heater. After 4 h the pressure was released, and the yellow solution as well as the solid was transferred under argon to a Schlenk tube. The solvent was pumped off. The residue was then first washed with a small amount of benzene–*n*-hexane mixture (1 : 2), then extracted with CH_2Cl_2. The CH_2Cl_2 solution was filtered under argon to remove Na_2SO_4. Addition of *n*-hexane and cooling to −20°C yielded yellow crystals of I. After recrystallization from the CH_2Cl_2–*n*-hexane (2 : 1) mixture, analytically pure I was obtained. Yield: 390 mg (65%). Single crystals suitable for X-ray diffractometry were grown by the slow diffusion method from CH_2Cl_2–*n*-hexane. Melting point, 210°C (dec.). Found: C, 60.1; H, 4.1; Fe, 9.5; P, 10.5. Calc. for $C_{30}H_{24}FeP_2O_6$: C, 60.2; H, 4.0; Fe, 9.3; P, 10.3%.

Acknowledgements—One of the authors (J.T.) is grateful to the Alexander von Humboldt-Stiftung for the award of a Research Fellowship. We wish to thank R. A. Paciello and A. C. Filippou for helpful discussions.

REFERENCES

1. P. Braunstein, D. Matt, Y. Dusausoy and J. Fischer, *Organometallics* 1983, **2**, 1417.
2. P. Braunstein, D. Matt and Y. Dusausoy, *Inorg. Chem.* 1983, **22**, 2043.
3. P. Braunstein, D. Matt, D. Nobel, S. E. Bouaoud, B. Carluer, D. Grandjean and P. Lemoine, *J. Chem. Soc., Dalton Trans.* 1986, 415.
4. J. Podlahova and J. Gracias, *Coll. Czechoslovak Chem. Comm.* 1986, **51**, 664.
5. W. Keim, R. Appel, A. Storeck, C. Krüger and R. Goddard, *Angew. Chem. Int. Ed. Engl.* 1981, **20**, 116.
6. M. Peuckert and W. Keim, *Organometallics* 1983, **2**, 594.
7. J. Takács, E. Soós, Z. Nagy-Magos, L. Markó, G. Gervasio and T. Hoffmann, *Inorg. Chem.*, submitted.
8. J. Takács, L. Párkányi and L. Markó, *J. Organomet. Chem.* 1989, **361**, 109.
9. K. Issleib and G. Thomas, *Chem. Ber.* 1960, **93**, 803.
10. "XRAY76-SYSTEM", Program "PARAM", adapted to VAX 11/730 by M. Birkhahn and E. Herdtweck. Universität Marburg (1979) and Technische Universität München (1986).
11. G. M. Sheldrick, "SHELX-86", Universität Göttingen, F.R.G. (1986).
12. B. A. Frenz, The ENRAF Nonius CAD4 SDP SYSTEM, Computing in Crystallography, S. 64-71. Delft University Press, Delft, Holland (1978).
13. D. T. Cromer and J. T. Waber, *International Tables*

of Crystallography, Vol. IV, Table 2.2B. Kynoch Press, Birmingham, U.K. (1974).
14. D. T. Cromer, *International Tables of Crystallography*, Vol. IV, Table 2.3.1. Kynoch Press, Birmingham, U.K. (1974).
15. R. E. Schmidt, M. Birkhahn, W. Massa, P. Kiprof and E. Herdtweck, STRUX-II. Programmsystem zur Verarbeitung von Röntgendaten. Universität Marburg (1980) and Technische Universität München (1985/1987).
16. C. K. Johnson, ORTEP, A Fortran Thermal Ellipsoid Plot Program for Crystal Structure Illustrations. National Laboratories, Oak Ridge/Tennessee, U.S.A. (1965).

Polyhedron Vol. 8, No. 12, pp. 1509–1515, 1989
Printed in Great Britain

0277–5387/89 $3.00+.00
© 1989 Pergamon Press plc

COBALT(II) AND COBALT(III) COMPLEXES WITH HEXADENTATE DIOXIME SCHIFF BASE LIGANDS

M. MOHAPATRA, V. CHAKRAVORTTY and K. C. DASH*

Department of Chemistry, Utkal University, Vani Vihar, Bhubaneswar—751004, India

(*Received* 5 *July* 1988; *accepted after revision* 27 *January* 1989)

Abstract—Cobalt(II) salts interact with the hexadentate dioxime Schiff base ligands derived from triethylenetetramine and isonitroso ethylmethyl ketone (H_2L') or isonitrosopropiophenone (H_2L''), to form two interesting types of complexes. With CoX_2 (X = Cl, NCS), binuclear, four-coordinated cobalt(II) complexes of the type $[Co_2(H_2L)X_2]X_2$ (L = L′, L″; X = Cl, NCS) are formed, which are paramagnetic with low magnetic moments (2.5–3.5 BM). In contrast, under identical conditions, CoX_2 (X = Br, I, NO_3, ClO_4) form mononuclear, six-coordinated and diamagnetic cobalt(III) complexes of the type $[Co(HL)]X_2$.

The vicinal dioximes e.g. dimethylglyoxime (DH_2), form cobalt(III) complexes containing the Co $(DH_2)^+$ group, which closely simulate the reactions of vitamin-B_{12} and are important in its model chemistry.[1–3] Imidazole is a versatile ligand for metal ions in many biologically important molecules.[4,5] Recent work from this laboratory has focussed attention on the interaction of imidazole with cobaloximes.[6–9] As a continuation of our work on cobaloximes[6–9] and with a view to gain more knowledge about the interaction of the dioxime-based Schiff base complexes, we have now synthesized a series of tetra-, penta- and hexadentate ligands in order to study their ligating behaviour with cobalt as such and in the presence of imidazole ligands.

This paper is concerned with the hexadentate dioxime-based Schiff base ligands, N,N′,N″,N‴-triethylenetetramine bis(isonitroso ethylmethylketoneimine) (H_2L') and N,N′,N″,N‴-triethylenetetramine bis(isonitroso propiophenoneimine (H_2L'') (**I**), synthesized by the condensation of triethylenetetramine with isonitroso ethylmethylketone (diacetylmonoxime) and isonitrosopropiophenone, respectively. The formation of $[Co(H_2L')](ClO_4)_3$, $[Co(H_2L')Br_3]\cdot 3H_2O$ and $[Co(L')](ClO_4)$ using the hexadentate ligand H_2L' has been reported.[10] With the same ligand, Chakravorty and co-workers[11] obtained Fe(L′), $[Fe(H_2L')](ClO_4)_2$, $[Ni(H_2L')](ClO_4)_2$ and $[Ni(L')](ClO_4)_2$ complexes, in addition to the above cobalt(III) complexes. Our investigation using a different synthetic approach and a series of coordinating and non-coordinating anions yield two different types of complexes—$[Co_2(H_2L)X_2]X_2$ (L = L′, L″; X = Cl, NCS) (**II**) and $[Co(HL)]X_2$ (L = L′, L″; X = Br, I, NO_3, ClO_4) (**III**). The former series of complexes are paramagnetic and binuclear, where the ligands seem to act as binucleating ligands forming two four-coordinate cobalt(II) centres, and in the latter, the six-coordinating sites of the mono-protonated hexadentate ligands, H_2L' and H_2L'', are bonded to one cobalt(III) centre, yielding diamagnetic, octahedral complexes. While all the complexes were synthesized from cobalt(II) salts, oxidation of cobalt(II) to cobalt(III) occurred in most cases (except for Cl^- and NCS^- salts) even in the absence of any external oxidizing agent.[12] With $CoCl_2$ and $Co(NCS)_2$, dimeric, paramagnetic cobalt(II) compounds were formed.

EXPERIMENTAL

Materials

Hydrated $CoCl_2$, $Co(NO_3)_2$ and $Co(ClO_4)_2$ were from BDH. $CoBr_2\cdot 6H_2O$ was prepared by the reaction of HBr with $CoCO_3$ in H_2O and recrystallization from H_2O. Ethanolic solutions of Co $(NCS)_2$ and CoI_2 were obtained by metathesis of $Co(NO_3)_2\cdot 6H_2O$ and KNCS or KI, respectively.

* Author to whom correspondence should be addressed.

The starting materials, diacetyl monoxime (isonitroso ethylmethylketone) was from Loba-Chemie and isonitrosopropiophenone was synthesized[13] from propiophenone.

The hexadentate Schiff base ligands N,N′,N″,N‴-triethylenetetramine bis(isonitroso ethylmethylketoneimine) (H_2L') and N,N′,N″,N‴-triethylenetetramine bis(isonitroso propiophenoneimine) (H_2L'') were prepared by condensing diacetyl monoxime or isonitrosopropiophenone with triethylenetetramine in Et_2O and *n*-hexane, respectively.

All the complexes were synthesized by a general method, detailed below. However, for $CoCl_2$ and $Co(NCS)_2$, green, dinuclear and four-coordinated cobalt(II) complexes were obtained, and for other cobalt(II) salts, CoX_2 (X = Br, I, NO_3, ClO_4), under identical conditions, orange, mononuclear and six-coordinated cobalt(III) complexes were obtained. The syntheses and analyses of each of these compounds were reproducible, establishing their authenticity.

Synthesis of cobalt perchlorate complex with N,N′,N″,N‴-*triethylenetetramine bis(isonitrosopropiophenoneimine)* $[Co(HL'')](ClO_4)_2$

To a warm solution of $Co(ClO_4)_2 \cdot 6H_2O$ (0.36 g, 1 mmol) in 10 cm^3 of EtOH, the prepared hexadentate ligand, H_2L'' (0.31 g, 1 mmol), was added slowly with constant stirring. Within about 10 min, an orange coloured compound formed and the mixture was stirred for a further 1 h to ensure completion of the reaction. The compound was then collected on a glass frit, washed three times with 3 cm^3 of Et_2O and dried *in vacuo*. Yield 0.36 g (66%).

Cobalt and halogen were determined by standard methods.[6–9] The microanalytical data for carbon, hydrogen and nitrogen were obtained from the Analytical Chemistry Department, Chemical Centre, University of Lund, Sweden.

The magnetic susceptibility, thermogravimetry, cyclic voltammetry, electrolytic conductivity, electronic spectra, mass spectra, and ^1H and ^{13}C NMR spectral measurements were carried out as reported earlier.[6–9] IR spectra in the 4000–400 cm^{-1} region were recorded as KBr pellets on a NICOLET 20 SXC FTIR spectrophotometer fitted with a data station. The diffuse reflectance spectra of complexes were obtained with a Hitachi-330 spectrometer.

RESULTS AND DISCUSSION

The hexadentate dioxime Schiff base ligands (I) derived from the condensation of triethylenetetramine and diacetylmonoxime (isonitroso ethylmethylketone) (H_2L') or isonitrosopropiophenone (H_2L'') interact with $CoCl_2$ and $Co(NCS)_2$ to form the binuclear, four-coordinated cobalt(II) complexes $[Co_2(H_2L)X_2]X_2$ (L = L′, L″; X = Cl, NCS), with a presumable structure **II**, where the neutral ligands, H_2L, seem to act as doubly tridentate. A similar behaviour of these ligands was observed earlier for certain copper(II) salts which formed complexes of the type $(CuX_2)_2 \cdot H_2L \cdot nH_2O$.[14] With CoX_2 (X = Br, I, NO_3 and ClO_4), however, mononuclear and six-coordinated complexes of the type $[Co(HL)]X_2$ (**III**) were obtained. All the complexes reported in this work are presented in Table 1. This difference in behaviour for the chloro and thiocyanato complexes, as compared to bromo, iodo, nitrato and perchlorato complexes, is adequately supported by our ESCA measurements,[15] which favour the binuclear structure for the former complexes. The molar conductivity values for all the complexes in DMF medium (*ca* 10^{-3} M) are in the range of 110–140 Ω^{-1} cm^2 mol^{-1}, suggesting them to be 1:2 electrolytes.[16] The conductance values for the cobalt(III) complexes of the type $[Co(HL)]X_2$ (**III**), were measured over a wide range of concentrations

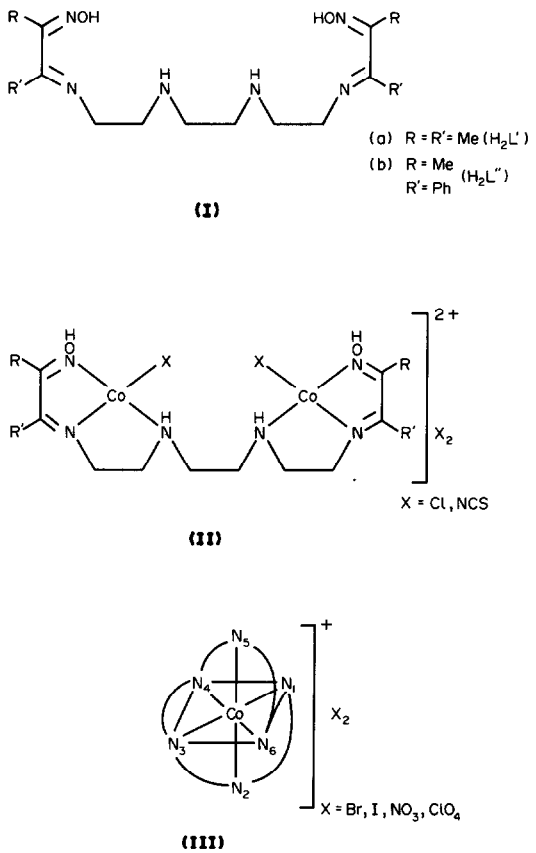

Scheme 1.

Table 1. Colour, melting point, analyses, magnetic moment and conductivity data of cobalt(II) and cobalt(III) complexes

Complex	Formula (Mol. wt)	Colour	Melting point (°C)	Analytical data (%)[a]					μ_{eff}	Λ_M[c]
				Co	X[b]	C	H	N		
$[Co_2(H_2L')Cl_2]Cl_2$	$Co_2C_{14}H_{28}N_6O_2Cl_4$ (571.9)	Parrot green	215	20.8 (20.6)	24.6 (24.9)	29.6 (29.5)	4.5 (4.5)	14.5 (14.7)	3.5	110.2
$[Co_2(H_2L')(NCS)_2](NCS)_2$	$Co_2C_{18}H_{28}N_{10}O_2S_4$ (661.9)	Deep green	205	17.2 (17.8)	—	32.6 (32.6)	4.6 (4.2)	20.9 (21.1)	2.8	119.9
$[Co_2(H_2L'')Cl_2]Cl_2$	$Co_2C_{24}H_{32}N_6O_2Cl_4$ (695.9)	Parrot green	215	16.4 (16.9)	20.2 (20.4)	41.2 (41.3)	4.6 (4.6)	12.3 (12.1)	3.1	116.9
$[Co_2(H_2L'')(NCS)_2](NCS)_2$	$Co_2C_{28}H_{32}N_{10}O_2S_4$ (785.8)	Deep green	188	14.9 (15.0)	—	42.6 (42.7)	3.6 (3.5)	17.7 (17.8)	2.5	146.1
$[Co(HL')]Br_2$	$CoC_{14}H_{27}N_6O_2Br_2$ (529.7)	Yellow–brown	265	10.8 (11.1)	29.8 (30.1)	31.6 (31.7)	5.2 (5.1)	15.1 (15.3)	Diamag.	121.0
$[Co(HL')]I_2$	$CoC_{14}H_{27}N_6O_2I_2$ (623.7)	Yellow–brown	225	9.4 (9.4)	40.5 (40.7)	26.7 (26.9)	4.7 (4.3)	13.6 (13.5)	Diamag.	126.2
$[Co(HL')](NO_3)_2$	$CoC_{14}H_{27}N_8O_8$ (493.9)	Orange–yellow	225	11.7 (11.9)	—	33.8 (34.0)	5.5 (5.5)	22.4 (22.6)	Diamag.	127.5
$[Co(HL')](ClO_4)_2$	$CoC_{14}H_{27}N_6O_2Cl_2$ (568.9)	Orange–yellow	210(d)	10.5 (10.3)	—	29.6 (29.5)	5.0 (4.7)	14.4 (14.7)	Diamag.	112.3
$[Co(HL'')]Br_2$	$CoC_{24}H_{31}N_6O_2Br_2$ (653.7)	Yellow	225	9.4 (9.0)	23.8 (24.4)	43.8 (44.0)	4.3 (4.7)	12.7 (12.8)	Diamag.	121.0
$[Co(HL'')]I_2$	$CoC_{24}H_{31}N_6O_2I_2$ (747.7)	Yellow	220	7.4 (7.8)	33.7 (33.9)	38.2 (38.5)	4.0 (4.1)	11.4 (11.2)	Diamag.	129.2
$[Co(HL'')](NO_3)_2$	$CoC_{24}H_{31}N_8O_8$ (617.9)	Yellow	> 235	9.2 (9.5)	—	46.6 (46.6)	5.2 (5.0)	18.2 (18.1)	Diamag.	125.2
$[Co(HL'')](ClO_4)_2$	$CoC_{24}H_{31}N_6O_{10}Cl_2$ (692.9)	Orange	> 235	8.5 (8.5)	—	41.1 (41.6)	4.3 (4.5)	12.2 (12.1)	Diamag.	120.0

[a] Theoretical values in parentheses.
[b] X = Cl, Br, I.
[c] All values in Ω^{-1} cm^2 mol^{-1} at room temperature in DMF.

using DMF as solvent. A plot of $\Lambda_\infty - \Lambda_e$ vs $\sqrt{C}$ gives a straight line, the slopes of which also indicate them to be 1 : 2 electrolytes.[17]

All the cobalt(III) complexes, $[Co(HL)]X_2$, are diamagnetic, coloured yellow or orange. However, the dimeric cobalt(II) complexes, $[Co_2(H_2L)X_2]X_2$ (X = Cl, NCS), are green and have magnetic moments in the range 2.5–3.5 BM, fairly close to the reported values for the spin-paired, square-planar cobalt(II) complexes.[18] The IR and TG studies do not show the presence of coordinated H_2O and these compounds seem to be dimeric and square-planar with the hexadentate ligand acting as a doubly tridentate ligand coordinating to two cobalt(II) centres, whose fourth position is occupied by either the Cl^- or NCS^-.

Formation of the ligands from the condensation of isonitrosoketones and triethylenetetramine was confirmed from the IR spectra which showed no typical absorption bands assignable to either C=O or NH_2 functions. The sharp bands of weak–medium intensity occurring in the 1600–1700 cm^{-1} region in the ligands, which shift to somewhat lower frequencies in the complexes, are appropriately assigned to coupled C⟷N and C⟷C stretching modes.[11] The ν(N—O) vibration of the complexes in the 1140–1190 cm^{-1} region suggests the oxime groups to be N-coordinated.[19] The ν(OH) vibrations of the ligands, H_2L' and H_2L'', appear at 2600 and 2800 cm^{-1}, respectively, and in the complexes they appear in the 3400 cm^{-1} region. The new bands of the complexes in the 520 cm^{-1} region is assigned to a ν(Co—N) vibration and at 1075 cm^{-1} to a ν'(NO) vibration.[20] The metal-sensitive strong as well as sharp bands occurring at 765–780 cm^{-1} may be attributed to the C=N—O deformation vibration mode. The metal-dependent strong and sharp bands at 990, 920 and 910 cm^{-1} can be ascribed to the deformation vibration modes of the ligand, analogous to the bands of metalloporphyrins.[21,22]

In the two cobalt(II) thiocyanato complexes, $[Co_2(H_2L)(NCS)_2](CNS)_2$ (L = L', L''), the bands at 2060–2080 cm^{-1} and 834–848 cm^{-1} are assigned to the ν(C≡N) and ν(C—S) vibrations of the N-coordinated isothiocyanate group.[23] The δ(NCS) signal is observed at 428 cm^{-1}. The vibration bands for the free thiocyanato groups in these complexes are also appropriately assigned. In the cobalt(III) complexes, $[Co(HL)]X_2$ (X = ClO_4, NO_3), the polyatomic anions are present in the outer-sphere. In the perchlorato complexes, the strong, unsplit absorptions in the 1100 and 620 cm^{-1} regions correspond to ν_3 and ν_4 absorption bands. The ν_1 and ν_2 bands for the uncoordinated ClO_4^- ion (both IR inactive) are not discernible and there is no tendency of ν_3 and ν_4 to split, which is good evidence in favour of non-coordination of the ClO_4^- group.[24] For the nitrato complexes, a strong and unsplit band around 1380 cm^{-1} (ν_3) and two IR active deformation bands at *ca* 830 cm^{-1} (ν_2) and at *ca* 700 cm^{-1} (ν_4) are observed. The absence of the ν_1 band as well as the appearance of the unsplit ν_3 band, suggest that the NO_3^- ion is not involved in covalent bonding to the cobalt(III) centre[25,26] (see Table 2).

The solid-state (diffuse reflectance) spectra and the spectra in DMF solution seem to be identical for the cobalt(III) complexes, with a peak of weak to moderate intensity at ~ 16,000 cm^{-1} assignable to a $^1A_{1g} \rightarrow {}^1E_g$ transition, typical of low-spin six-coordinated cobalt(III) complexes.[12] The more intense band in the 44,000–49,000 cm^{-1} region is attributable to the intra-ligand π–π^* transition of the coordinated oxime group. The band in the 26,000–30,000 cm^{-1} region may be due to the $^1A_{1g} \rightarrow {}^1A_{2g}$ transition,[12] while that at around 38,000 cm^{-1} may be due to the possible $d\pi(Co) \rightarrow \pi^*(HL)$ MLCT transition.[27] The low-spin, square-planar complexes of cobalt(II) invariably exhibit[28,29] a fairly broad but strong band at around 17,000–18,000 cm^{-1} as observed here.

The ^1H and ^{13}C NMR spectra of the hexadentate ligand, H_2L', and its cobalt(III) complexes $[Co(HL')]X_2$ (X = Br, I, NO_3, ClO_4), have been assigned (see Tables 3 and 4). In the ^1H NMR spectra, the two sharp singlet signals observed at 1.90 and 1.98 ppm for the ligand, H_2L', (**Ia**) are shifted downfield in the complexes to 2.40 and 2.48 ppm, respectively. These signals are due to the two magnetically non-equivalent —CH_3 groups. A virtual triplet in the 3.27–3.40 ppm region in the ligand, which shifts downfield to 3.87–4.05 ppm in the complexes, is assigned to the ethylene (—CH_2—CH_2—) protons in the ligand chain.[30] The —OH (oxime) proton of the ligand resonating at 8.31 ppm, undergoes considerable upfield shift on coodination and appears in the complexes in the vicinity of 6.0 ppm.

The ^{13}C NMR spectrum of the ligand and its complexes shows that the two non-equivalent —CH_3 groups give ^{13}C signals at 8.64 and 13.44 ppm in the ligand, which shift downfield in the complexes to *ca* 13.0 ppm and 17.5 ppm, respectively. The ethylene carbons (—CH_2—CH_2—) resonate at 48.96–51.84 ppm in the free ligand and appear as a symmetrical triplet. In the complexes, these signals shift downfield to 50.4–54.72 ppm and appear as a singlet and a doublet. The two other carbons (C^c and C^d) in the diacetylmonoxime skeleton resonate at 156.48 and 164.16 ppm, respectively, in the free ligand. On complexation the observed shift of C^c is either nil or slightly upfield,

Table 2. Prominent IR absorption bands of some cobalt(II) and cobalt(III) complexes (in cm^{-1})

Complex	ν(NH)	ν(OH)	ν(C⋯N)+ν(C⋯C)	ν(N—O)	ν'(N—O)	δ(N—O)	ν(Co—N)	Anion vibration modes
H_2L'	3300	2650	1688 1620					
H_2L''	3340	2800	1640 1620					
$[Co_2(H_2L')Cl_2]Cl_2$	3150	3415	1651 1614	1151	1071	782	524	
$[Co_2(H_2L')(NCS)_2](NCS)_2$	3143	3445	1652 1615	1157	1069	780	523	2057, 834, 428 (N-bonded) 780, 496 (Ionic)
$[Co_2(H_2L'')Cl_2]Cl_2$	3145	3435	1640 1580	1160	1074	775	520	
$[Co_2(H_2L'')(NCS)_2](NCS)_2$	3150	3432	1600	1145	1065	765	521	2080, 848, 430 (N-bonded) 785, 492 (Ionic)
$[Co(HL')]Br_2$	3059	3407	1636 1615	1165	1073	781	517	
$[Co(HL')]I_2$	3078	3405	1635 1612	1163	1071	780	514	
$[Co(HL')](NO_3)_2$	3060	3424	1616	1164	1072	782	517	702, 832, 1384 (Ionic)
$[Co(HL')](ClO_4)_2$	3056	3428	1645 1615	1145		781	517	625, 939, 1089 (Ionic)
$[Co(HL'')]Br_2$	3154	3431	1630 1615	1160	1072	780	523	
$[Co(HL'')]I_2$	3060	3427	1632 1618	1132	1070	783	518	
$[Co(HL'')](NO_3)_2$	3150	3420	1610 1570	1195	1068	770	521	700, 822, 1375 (Ionic)
$[Co(HL'')](ClO_4)_2$	3175	3450	1615 1580	1170	1073	780	520	622, 942, 1070 (Ionic)

Table 3. ^{1}H chemical shifts for some cobalt(III) complexes[a]

Compound	δ(—CH_3)[a]	Δ	δ(—CH_3)[b]	Δ	δ(CH_2—CH_2)	δ(—OH)	Δ
H_2L'	1.90		1.98		3.27 3.36 3.42	8.31	
$[Co(HL')]Br_2$	2.40	0.5	2.48	0.5	3.87 3.97 4.05	6.02	−2.29
$[Co(HL')]I_2$	2.40	0.5	2.48	0.5	3.87 4.01 4.09	5.98	−2.33
$[Co(HL')](NO_3)_2$	2.35	0.45	2.48	0.5	3.87 3.91 4.04	5.90	−2.41
$[Co(HL')](ClO_4)_2$	2.40	0.5	2.48	0.5	3.87 3.96 4.08	5.80	−2.51

[a] All measurements in DMSO-d_6; all values in ppm downfield from TMS as internal standard.

Table 4. ^{13}C chemical shifts for some cobalt(III) complexes[a] at room temperature

Compound	δ(—CH_3)[a]	Δ	δ(—CH_3)[b]	Δ	δ(CH_2—CH_2)	δ(C^c—C^c)	Δ	δ(C^d—C^d)	Δ
H_2L'	8.64		13.44		48.96 49.92 51.84	156.48		164.16	
$[Co(HL')]Br_2$	13.44	4.8	17.76	4.32	50.88 53.76 54.72	156.48	0	177.6	13.44
$[Co(HL')]I_2$	13.44	4.8	17.76	4.32	50.88 53.76 54.72	155.52	−0.96	177.6	13.44
$[Co(HL')](ClO_4)_2$	12.96	4.32	17.28	3.84	50.4 53.76 54.72	153.6	−2.8	175.56	11.4

[a] All measurements in DMSO-d_6; all values in ppm relative to internal DMSO-d_6, exhibiting a heptet centred at 39.6 ppm downfield to TMS.

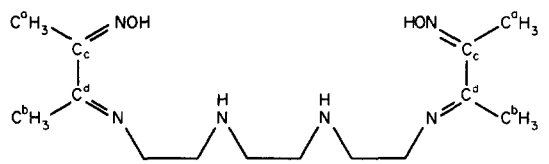

(H_2L')

whereas the shift for C^d is substantially downfield (175.56–177.6 ppm).

The cyclic voltammograms of the samples were run in DMF using platinum as the working electrode and $(Et_4N)ClO_4$ (TEAP) as the supporting electrolyte. All voltammograms are usually characterized by three reductive waves at 0.81–0.92, 1.3 and 1.4–1.5 V corresponding to the reduction of $Co^{III} \rightarrow Co^{II} \rightarrow Co^{I} \rightarrow Co^{0}$, respectively. Often, the first peak, which is ill-defined, is accompanied by another similar peak in the 0.51–0.53 V region. The negative scan for $[Co(HL')](ClO_4)_2$ is shown in Fig. 1. In the positive scan for $[Co(HL')]X_2$ (X = ClO_4, NO_3), the experimental base line obtained indicates

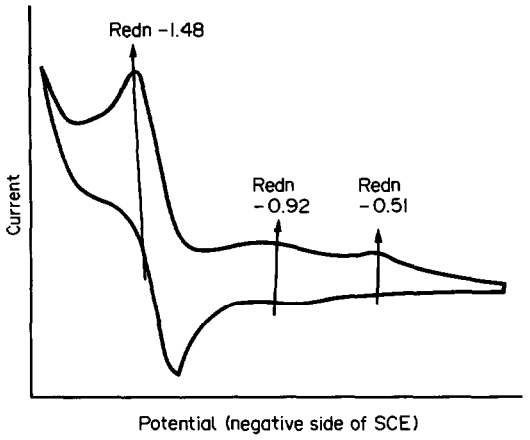

Fig. 1. Cyclic voltammogram of $[CoHL'](ClO_4)_2$ in DMF solution (negative side of SCE).

no effective chemical change. For the $[Co(HL')]Br_2$ complex, peaks at 0.67 and 0.75 V and for the $[Co(HL')]I_2$ complex, peaks at 0.57, 0.76 and 0.39 V are obtained. These are obviously not due to any effective oxidation of the metal[31] and may have arisen due to the oxidation of Br^- and I^- ions.

The mass spectra of the ligand, H_2L', and its complexes were investigated. For the ligand, the molecular ion peak at *m/z* 312, along with other prominent peaks due to the fragmentation products at 295, 254, 213, 185, 156, 142, 113, 99, 58 and 42, are obtained and appropriately assigned. However, for the complexes, no molecular ion peak nor any fragmentation product containing the metal were obtained. The thermogravimetric studies also show that the thermal stability of the complexes is quite high and with an increase in temperature the ligand is lost in steps giving polymeric intermediates, often forming Co_3O_4 as the stable end product at around 600°C.

Acknowledgements—Grateful thanks are due to UGC, New Delhi for a Fellowship to one of the authors (M.M.). The authors are grateful to Dr Ingmar Persson and Dr B. Rebenstorf of Inorganic Chemistry 1, Chemical Centre, University of Lund, Sweden, for the carbon, hydrogen, and nitrogen microanalyses and FTIR (as well as reflectance spectra) measurements, respectively, to Professor A. Chakravorty, Indian Association for Cultivation of Science, Jadavpur, Calcutta, for the cyclic voltammetric results and to Dr P. S. Pandey, I.I.T., Delhi, for the NMR measurements.

REFERENCES

1. G. N. Schrauzer, *Accts Chem. Res.* 1968, **1**, 97.
2. J. M. Pratt and P. J. Craig, *Adv. Organomet. Chem.* 1973, **11**, 331.
3. D. G. Brown, *Prog. Inorg. Chem.* 1973, **18**, 177.
4. H. C. Freeman, *Inorganic Biochemistry* (Edited by G. L. Eichhorn), p. 121. Elsevier, Amsterdam (1973).
5. A. R. Norris, E. Buncel and S. E. Taylor, *J. Inorg. Biochem.* 1982, **16**, 279.
6. J. K. Das and K. C. Dash, *Polyhedron* 1985, **4**, 1109; 1986, **5**, 1857.
7. J. K. Das and K. C. Dash, *Synth. React. Inorg. Met.-Org. Chem.* 1985, **15**, 839.
8. J. K. Das and K. C. Dash, *Ind. J. Chem.* 1985, **24A**, 387, 696.
9. J. K. Das and K. C. Dash, *Transition Met. Chem.* 1985, **10**, 422; 1986, **11**, 170.
10. A. V. Ablov, N. I. Belichuk and V. N. Kaftanat, *Zh. Neorg. Khim.* 1972, **17**, 749; A. V. Ablov, N. I. Belichuk and V. N. Kaftanat, *Russ. J. Inorg. Chem.* 1972, **17**, 392.
11. J. G. Mohanty, R. P. Singh and A. Chakravorty, *Inorg. Chem.* 1975, **14**, 2178.
12. V. V. Ramanujam and V. Alexander, *Inorg. Chem.* 1987, **26**, 3124.
13. W. H. Hartung and F. Crossby, in *Organic Synthesis* (Collect. Vol. II) (Edited by A. H. Blatt), p. 363. Wiley, New York (1943).
14. N. I. Belichuk, A. V. Ablov and V. N. Kaftanat, *Zh. Neorg. Khim.* 1973, **18**, 2283; N. I. Belichuk, A. V. Ablov and V. N. Kaftanat, *Russ. J. Inorg. Chem.* 1973, **18**, 1207.
15. K. C. Dash, M. Mohapatra, B. Folkesson and R. Larsson, *J. Electron Spectrosc. Related Phenom.*, communicated.
16. J. V. Quagliano, J. Fujita, G. Fraz, D. J. Philips and S. Y. Tyree, *J. Am. Chem. Soc.* 1961, **83**, 3770.
17. R. D. Feltham and R. G. Hayter, *J. Chem. Soc.* 1964, 4587.
18. B. N. Figgis and R. S. Nyholm, *J. Chem. Soc.* 1959, 338.
19. K. Burger, I. Ruff and F. Ruff, *J. Inorg. Nucl. Chem.* 1965, **27**, 179.
20. N. Yamazaki and Y. Hohokabe, *Bull. Chem. Soc. Jpn* 1971, **44**, 63.
21. L. J. Boucher and J. J. Katz, *J. Am. Chem. Soc.* 1967, **89**, 1340.
22. H. Ogoshi, N. Masai, Z. Oshida, J. Takemoto and K. Nakamoto, *Bull. Chem. Soc. Jpn* 1971, **49**, 44.
23. R. A. Bailey, S. L. Kozak, T. W. Michelsen and W. N. Mills, *Coord. Chem. Rev.* 1971, **6**, 407.
24. J. W. L. Martin, J. H. Timons, A. E. Martell, P. Rudolf and A. Clearfield, *Inorg. Chem.* 1981, **20**, 814.
25. W. B. Simpson and N. Logan, *Spectrochim. Acta* 1965, **21**, 857.
26. C. C. Addison and D. Sutton, *Prog. Inorg. Chem.* 1967, **8**, 195.
27. Y. Yamano, I. Masuda and K. Shimura, *Bull. Chem. Soc. Jpn* 1967, **44**, 1581.
28. G. W. Everett, Jr. and R. H. Holm, *J. Am. Chem. Soc.* 1965, **87**, 5266.
29. M. Nicolini, C. Pecile and A. Turco, *Coord. Chem. Rev.* 1966, **1**, 133.
30. *Handbook of Proton NMR Spectrum and Data*, Vol. 1, p. 242 and Vol. 2, p. 292. Asahi Research Centre (1985).
31. J. Topich and J. Halpern, *Inorg. Chem.* 1979, **18**, 1339.

Polyhedron Vol. 8, No. 12, pp. 1517–1522, 1989
Printed in Great Britain

0277–5387/89 $3.00+.00
© 1989 Pergamon Press plc

THE SYNTHESIS, CHARACTERIZATION AND REACTION OF (PROPARGYLOXY)CHLOROCYCLOTRIPHOSPHAZENES

Y. W. CHEN-YANG,* W. S. CHIEN and J. R. CHUNG

Department of Chemistry, Chung Yuan Christian University, Chung-Li, Taiwan 32023, R.O.C.

(*Received* 27 *September* 1988; *accepted* 27 *January* 1989)

Abstract—The reaction of the sodium propargyloxide, $NaOCH_2C{\equiv}CH$, with hexachlorocyclotriphosphazene, $N_3P_3Cl_6$, led to a series of (propargyloxy)chlorocyclotriphosphazenes, $N_3P_3Cl_{6-n}(OCH_2C{\equiv}CH)_n$, ($n = 1$–6). All the compounds were characterized by a combination of elemental analysis, IR spectroscopy, mass spectrometry and NMR (^1H, ^{13}C, ^{31}P) spectroscopy. The results indicated that the substitution pattern of propargyloxylation was predominantly non-geminal with comparable amounts of the *cis* and *trans* isomers. However, a significant amount of geminal isomer was observed for the tris compounds from the ^{31}P spectrum. The mono- and bis-substituted derivatives have been converted to their phenoxy derivatives, $N_3P_3(OC_6H_5)_{6-n}(OCH_2C{\equiv}CH)_n$, ($n = 1$, 2), and the phenoxy derivative, $N_3P_3(OC_6H_5)_5(OCH_2C{\equiv}CH)$, underwent an oxidative coupling reaction to produce a phosphazene-containing diacetylene, $[\text{-}N_3P_3(OC_6H_5)_5(OCH_2C{\equiv}C\text{-})]_2$.

Since the phosphazene compounds received renewed attention in 1965,[1] hundreds of organophosphazenes and their polymer analogues have been synthesized.[2,3] Recently, Allen *et al.*[4–9] showed that the range of synthesis of new and useful phosphazene derivatives could be expanded by the incorporation of an organofunctional substituent on the phosphazene ring, and this substitutent could serve as the site for various synthetic transformations leading to new monomeric and polymeric phosphazene moieties. We were interested in preparing C≡C containing phosphazenes and chose propargyl alcohol as the substituent for the following reasons. Nucleophilic substitution on $N_3P_3Cl_6$ occurs via the hydroxy end of propargyl alcohol, leaving the terminal acetylene group. Through the terminal acetylenic unit the phosphazene may polymerize to yield substituted benzenoids or be oxidative coupled to form diacetylene derivatives. The pendant acetylenic units can also function as π-donors for transition metal units such as dicobalt hexacarbonyl residues, to form complexes which may function as catalysts.[10] Furthermore, the acetylene-terminated cyclotriphosphazene compounds may be used as the terminated monomers to co-polymerize with some organic oligomers to form phosphazene-containing acetylene-terminated co-polymers, which are able to be further cured through the terminated acetylene group like some acetylene-terminated organo polymers.[11–13]

Although C≡C containing organocyclotriphosphazenes have previously been prepared,[14–16] none of the particular series of (alkynyloxy)chlorocyclotriphosphazenes were reported in detail. In this paper, we describe the synthesis and the characterization of a series of (propargyloxy)chlorocyclotriphosphazenes, $N_3P_3Cl_{6-n}(OCH_2C{\equiv}CH)_n$ ($n = 1$–6). The preferred substitution pattern of the propargyloxide ions with hexachlorocyclotriphosphazene, $N_3P_3Cl_6$, compounds are discussed. It is anticipated that this information would be valuable for an initial analysis of the related reactions that take place in the high polymeric systems. In addition, a preliminary study concerning the potential of the terminal acetylene group on the phosphazene for synthetic work is also studied.

* Author to whom correspondence should be addressed.

EXPERIMENTAL

Materials and methods

The hexachlorocyclotriphosphazene, $N_3P_3Cl_6$, was kindly supplied by the Nippon Fine Chemical Co., Japan and was used as received. Diethyl ether was distilled from sodium. Propargyl alcohol (Tokyo Chem.) was distilled before use. NMR spectra (in d-acetone) were recorded on a JEOL JNM-FX100 spectrometer. Tetramethylsilane, Me_4Si, was used as internal reference for ^1H and ^{13}C NMR measurements. For ^{31}P NMR, 85% H_3PO_4 was used as external reference. Chemical shifts upfield of the reference were assigned a negative sign. IR spectra were obtained as thin films (KBr discs) on a Perkin–Elmer 710 B spectrometer. Mass spectra were recorded on a JEOL JMS-D100 spectrometer. Elemental analyses were performed by the Instrument Centre of NSC at Tainan, Taiwan.

All reactions were carried out under anhydrous conditions in a three-necked round-bottomed flask fitted with a reflux condenser and a pressure-equalizing dropping funnel. The system was stirred magnetically and proceeded under nitrogen.

Preparation of $N_3P_3Cl_5(OCH_2C{\equiv}CH)$ (**1**) *and* $N_3P_3Cl_4(OCH_2C{\equiv}CH)_2$ (**2**)

A solution of sodium propargyloxide was prepared from sodium (1.40 g, 0.061 mol) and propargyl alcohol (2.52 g, 0.045 mol) in diethyl ether (100 cm^3). To this was slowly added a solution of hexachlorocyclotriphosphazene (10.0 g, 0.029 mol) in diethyl ether (75 cm^3). The solution was then stirred at reflux for 72 h and was then allowed to cool to room temperature. The salt was filtered off and the filtrate was washed with water and dried over anhydrous sodium sulphate. The solvent was removed at reduced pressure to yield 8.2 g of a pale yellow liquid. A 1.0 g sample of this liquid was purified by column chromatography with chloroform–hexane (1 : 9) as the eluant. The first product obtained was 0.18 g (16.8% of theory) of unreacted $N_3P_3Cl_6$. Continued elution from the column yielded 0.39 g (36.7% of theory) of a colourless liquid. Found: C, 71.7; H, 6.7; N, 10.4; *m/z* 365. Calc. for $C_3H_3Cl_5N_3OP_3$ (**1**): C, 71.1; H, 6.7; N, 10.4; *m/z* 365. IR(cm^{-1}): 3295 (s, ≡C—H str), 2130 (w, C≡C str), 1220 (s, PN str), 1040 (s, POC str), 990 (m, POC str), 885 (s, PCl), 760 (m, PCl).

The third compound obtained from the column yielded 0.20 g (17.9% of theory) of a colourless liquid. Found: C, 18.6; H, 1.6; N, 10.4; *m/z* 385. Calc. for $C_6H_6Cl_4N_3O_2P_3$ (**2**): C, 18.6; H, 1.6; N, 10.9; *m/z* 385. IR(cm^{-1}): 3300 (s, ≡C—H str), 2130 (m, C≡C str), 1220 (s, PN str), 1040 (s, POC str), 985 (m, POC str), 885 (s, PCl), 740 (m, PCl).

Preparation of $N_3P_3Cl_3(OCH_2C{\equiv}CH)_3$ (**3**)

The sodium propargyloxide (6.80 g, 0.087 mol) was prepared as above and diethyl ether (100 cm^3) was slowly added to a solution of $N_3P_3Cl_6$ (10.0 g, 0.029 mol) in diethyl ether (175 cm^3) at room temperature. The reaction mixture was stirred for 2 days and worked-up as before to give 6.9 g of a yellow liquid. A 1.0 g sample of this liquid was separated by using column chromatography with chloroform–hexane (2 : 3) as the eluant. The following compounds were obtained in succession: $N_3P_3Cl_5(OCH_2C{\equiv}CH)$ (**1**), 0.14 g (1.3%); $N_3P_3Cl_4(OCH_2C{\equiv}CH)_2$ (**2**), 0.23 g (20.6% of theory).

The third compound eluted was 0.29 g (24.7% of theory) of a colourless liquid. Found: C, 26.5; H, 2.2; N, 10.3; *m/z* 405. Calc. for $C_9H_9Cl_3N_3O_3P_3$ (**3**): C, 26.6; H, 2.2; N, 10.3; *m/z* 405. IR(cm^{-1}): 3300 (s, ≡CH str), 2130 (m, C≡C str), 1240 (s, PN str), 1030 (s, POC str), 985 (m, POC str), 900 (s, PCl), 800 (m, PCl). This compound was further isolated to obtain a small amount of the non-geminal isomer.

Preparation of $N_3P_3Cl_2(OCH_2C{\equiv}CH)_4$ (**4**)

Sodium propargyloxide (11.9 g, 0.15 mol) was prepared as above and diethyl ether (100 cm^3) was slowly added to a solution of $N_3P_3Cl_6$ (10.0 g, 0.029 mol) in diethyl ether (175 cm^3) at room temperature. The reaction mixture was stirred for 2 days and worked-up as before to give 7.30 g of a yellow liquid. A 1.0 g sample of this liquid was separated by column chromatography with hexane–diethyl ether (4 : 1) as the eluant. The following compounds were obtained in succession: $N_3P_3Cl_5(OCH_2C{\equiv}CH)$ (**1**), trace; $N_3P_3Cl_4(OCH_2C{\equiv}CH)_2$ (**2**), trace and $N_3P_3Cl_3(OCH_2C{\equiv}CH)_3$ (**3**), 0.12 g (10.2%).

The fourth compound eluted was 0.51 g (41.4% of theory) of a colourless liquid. Found: C, 33.1; H, 2.9; N, 9.6; *m/z* 425. Calc. for $C_{12}H_{12}Cl_2N_3O_4P_3$ (**4**): C, 33.1; H, 2.8; N, 9.7; *m/z* 425. IR (cm^{-1}): 3300 (s, ≡CH str), 2130 (m, C≡C str), 1230 (s, PN str), 1030 (s, POC str), 990 (s, POC str), 900 (s, PCl str), 790 (m, PCl).

Preparation of $N_3P_3Cl(OCH_2C{\equiv}CH)_5$ (**5**) *and* $N_3P_3(OCH_2C{\equiv}CH)_6$ (**6**)

The reaction of sodium propargyloxide (16.0 g, 0.220 mol) (prepared as above) and $N_3P_3Cl_6$ (10.0 g, 0.029 mol) in diethyl ether (200 cm^3) was carried

out as described above to yield 5.4 g of a pale yellow liquid. A 1.0 g sample of this liquid was separated by using column chromatograhy with chloroform–methanol (100 : 1) as the eluant. The first major product obtained was $N_3P_3Cl_4(OCH_2C{\equiv}CH)_2$ (**4**), 0.027 g (2.20% of theory) as a colourless liquid. The second major compound eluted was 0.19 g (14.7% of theory) of a colourless liquid. Found: C, 40.5; H, 3.4; N, 9.4; *m/z* 445. Calc. for $C_7H_6Cl_4N_3O_2P_3$ (**5**): C, 40.4; H, 3.4; N, 9.4; *m/z* 445. IR(cm^{-1}): 3300 (s, ≡CH str), 2130 (m, C≡C str), 1235 (s, PN str), 1030 (s, POC str), 990 (s, POC str), 900 (m, PCl), 770 (m, PCl).

The third major compound eluted was 0.33 g (24.5% of theory) of a colourless liquid which was solidified in refrigerator (m.p. = 29°C). Found: C, 46.5; H, 3.9; N, 8.9; *m/z* 465. Calc. for $C_{18}H_{18}N_3O_6P_3$ (**6**): C, 46.5; H, 3.9; N, 9.0; *m/z* 465. IR(cm^{-1}): 3300 (s, ≡CH str), 2130 (m, C≡C str), 1230 (s, PN str), 1030 (s, POC str), 995 (s, POC str). By using propargyl alcohol as solvent and reacting for 24 h, the yield of the major compound (**6**) was increased to 70%.

Reaction of $N_3P_3Cl_5(OCH_2C{\equiv}CH)$ (**1**) *and sodium phenoxide*

The reaction of $N_3P_3Cl_5(OCH_2C{\equiv}CH)$ (**1**) (4.8 g, 0.013 mol) with an excess of sodium phenoxide (9.0 g, 0.078 mol), prepared from sodium (1.8 g, 0.078 mol) and phenol (7.3 g, 0.078 mol) in THF (100 cm^3), was allowed to reflux for 2 days. The salt was filtered out. After removing the solvent, the oily residue was dissolved in diethyl ether, washed with water and dried over anhydrous sodium sulphate. The solvent was removed at reduced pressure to yield 8.2 g of a pale yellow syrup. A 1.0 g sample of this syrup was then purified by column chromatography, with dichloromethane–hexane (3 : 2) as the eluant, to produce 6.3 g (74% of theory) of a colourless liquid which was solidified in a refrigerator to a white solid (m.p. = 49°C), $N_3P_3(OC_6H_5)_5(OCH_2C{\equiv}C)$ (**7**). Found: C, 60.5; H, 4.3; N, 6.4; *m/z* 655. Calc. for $C_{33}H_{28}N_3O_6P_3$ (**7**): C, 60.5; H, 4.3; N, 6.4; *m/z* 655. IR (cm^{-1}): 3300 (s, ≡C—H, str), 2120 (w, C≡C str), 1160–1220 (s, P—O—Ar str), 1220–1280 (s, PN str), 1050 (s, P—O—C str).

Reaction of $N_3P_3Cl_4(OCH_2C{\equiv}CH)_2$ (**2**) *and sodium phenoxide*

Sodium phenoxide (7.5 g, 0.065 mol) prepared as above in THF (50 cm^3) was added to a solution of compound **2** (5.0 g, 0.013 mol) in THF (50 cm^3). The reaction mixture was stirred and refluxed for 2 days. It was then worked-up as above for compound **7** to give a pale yellow syrup. The crude product was then purified by column chromatography with dichloromethane–hexane (3 : 2) as eluant. The yield of isolated product, $N_3P_3(OC_6H_5)_4(OCH_2C{\equiv}C)_2$ (**8**), was 5.61 g (70% of theory). Found: C, 58.5; H, 4.2; N, 6.9; *m/z* 617. Calc. for $C_{30}H_{26}N_3O_6P_3$ (**8**): C, 58.4; H, 4.2; N, 6.8; *m/z* 617. IR (cm^{-1}): 3300 (s, ≡C—H str), 2150 (m, C≡C str), 1595, 1495 (s, C=C arom. str), 1200–1280 (s, PN str), 1160–1200 (s, P—O—Ar str), 1050 (s, P—O—C str).

Oxidative coupling reaction of $N_3P_3(OC_6H_5)_5(OCH_2C{\equiv}CH)$ (**7**)

Hay's catalyst was prepared by reaction of equal moles of CuCl and N,N,N′,N′-tetramethylethyl diamine in acetone with the inlet of oxygen. In the solution of the catalyst (0.1 g) in acetone (20 cm^3) with the inlet of oxygen, a solution of compound **7** (3.0 g, 4.9 mmol) in acetone (20 cm^3) was added dropwise and stirred for 4 h. After removing the acetone, the deep green mixture was washed several times with 20 cm^3 of an aqueous solution of hydrochloric acid (5% conc.) to obtain a thick green syrup. The crude product was then purified by column chromatography with chloroform–*n*-hexane (10 : 3) as eluant to obtain 2.3 g (78% of theory) of white solid (m.p. = 112.5°C)—the diacetylene $[-N_3P_3(OC_6H_5)_5(OCH_2C{\equiv}C)-]_2$ (**9**). Found: C, 60.6; H, 4.1; N, 6.4. Calc. for $C_{66}H_{54}N_6O_{12}P_6$ (**9**): C, 60.3; H, 4.1; N, 6.3. IR(cm^{-1}): 2145 (w, C≡C str), 1595, 1495 (s, C=C arom. str), 1200–1270 (s, PN str), 1150–1200 (s, P—O—Ar str), 1050 (s, P—O—C str).

RESULTS AND DISCUSSION

Although there are two acidic protons on the propargyl alcohol, as expected, since the alcoholic proton is more acidic than the acetylenic proton, the alkoxide is quantitatively generated from the reaction of sodium and propargyl alcohol. The sodium alkoxide was then reacted with $N_3P_3Cl_6$ to obtain a series of (propargyloxy)chlorocyclotriphosphazenes, $N_3P_3Cl_{6-n}(OCH_2C{\equiv}CH)_n$ (n = 1–6), according to the ordinary nucleophilic substitution reactions.

Compounds **3**–**6** were only slightly soluble in hexane, pentane and petroleum ether, but the other compounds were soluble in most of the organic solvents but insoluble in water, and these compounds were all stable to air and atmospheric moisture.

The mass spectral data for all the compounds

Table 1. ^{1}H and ^{13}C NMR data[a]

Compound	Type	-O—$C_\alpha H_{b2} C_\beta \equiv C_\gamma$—$H_a$ H_a	H_b	$J_{H_a-H_b}$	J_{P-H}	C_α	C_β	C_γ	J_{C-P}	J_{a-a}	J_{g-b}	J_{g-a}
1		3.51(t)	5.13(d,d)	2.4	14.0	57.0(d)	75.6(d)	78.8	5.9	158.6	255.9	4.4
2	g[b]	3.40(t)	4.91(d,d)	2.4	13.4	55.5	76.1	78.0	—	156.7	254.5	4.4
	n	3.47(t)	5.10(m)	2.4	—	56.5	76.1	78.4	4.4	—	—	—
3	g	3.15(t)	4.66(d,d)	2.4	12.2	55.1(d)	76.8	77.6	4.4	154.4	253.0	4.0
	n	3.22(t)	4.85(m)	2.7	—	56.3	77.3	78.1	4.4	155.9	254.4	—
4	g	3.30(t)	4.84(d,d)	2.4	11.0	54.8	77.0	77.2	4.4	153.7	253.0	—
	n	3.38(t)	5.02(m)	2.4	13.3	55.8	77.0	77.8	4.4	155.1	254.4	—
5	g	3.28(t)	4.83(m)	2.4	—	54.3	78.1	76.8	—	153.0	254.5	—
	n	3.35(t)	5.00(d,d)	2.4	11.6	55.2	78.1	77.3	—	153.0	254.5	—
6		3.25(t)	4.81(m)	2.4	—	54.0	78.4	76.4	3.7	153.0	253.0	—
7		3.23(t)	4.28(d,d)	2.4	8.3	53.7	77.3	75.2	—	—	—	—
8		3.25(t)	4.65(m)	2.4	8.4	54.0	77.4	75.5	—	144.4	235.0	—
		3.00(t)	4.30(m)	2.4	8.4	53.7	77.4	75.3	—	144.4	235.0	—
9		—	4.00(d)	—	9.0	53.9	73.5	70.8	—	154.4	—	—

[a] The data were measured in d-acetone, the chemical shifts are given in ppm relative to TMS and the coupling constants are in Hz.

[b] g: the atoms are in the $P(OR)_2$ environment. n: the atoms are in the $PCl(OCH_2C{\equiv}CH)$ environment.

displayed a parent ion with the characteristic Cl_n ($n = 1$–5) isotope patterns. The fragmentation pathway observed mainly involved the loss of alkynyloxy $-OCH_2C{\equiv}CH$ and alkynyl $-CH_2C{\equiv}CH$ groups as well as chlorine.

The IR spectra of all the compounds were similar and consistent with the proposed structures. In each case, an intense absorbance between 1200 and 1300 cm^{-1} was observed as a characteristic of the PN skeleton in cyclophosphazene compounds. The ≡C—H, C≡C and P—O—C absorbances were observed at 3300, 2100 and 1030 cm^{-1}, respectively.

As listed in Table 1, the ^{1}H and ^{13}C NMR spectra were all as expected and closely resembled one another. The chemical shifts of the atoms in the $P(OCH_2C{\equiv}CH)Cl$ environment were all slightly downfield from that in the $P(OCH_2C{\equiv}CH)_2$ environment.

Evidence for the occurrence of a trace amount of the geminal isomers was obtained for compound **2** from the ^{31}P NMR spectrum. It predominantly showed a second-order AB_2 system and a trace

Table 2. ^{31}P NMR data[a]

Compound	Spectrum	Type	PCl_2	$PCl(OR)$[b]	$P(OR)_2$	$P(OR)(O\Phi)$	$P(O\Phi)_2$	J_{AB}	J_{AC}	J_{BC}
1	AB_2	*gem*	21.6(B)	14.8(A)	—	—	—	63.9	—	—
2	AB_2	*gem*	22.9(B)	—	5.1(A)	—	—	62.9	—	—
	AB_2	non-*gem*	24.2(A)	18.4(B)	—	—	—	68.4	—	—
3	ABC	*gem*	25.3(A)	20.4(B)	8.4(C)	—	—	71.4	72.1	73.6
	A_3	non-*gem*	—	21.5	—	—	—	—	—	—
4	AB_2		—	23.3(B)	11.5(A)	—	—	80.1	—	—
5	AB_2		—	25.7(A)	14.1(B)	—	—	82.6	—	—
6	A_3		—	—	17.0	—	—	—	—	—
7	AB_2		—	—	—	12.5(A)	9.6(B)	88.4	—	—
8	AB_2	*gem*	—	—	16.3(A)	—	9.4(B)	87.9	—	—
		non-*gem*	—	—	—	12.9(B)	9.3(A)	89.7	—	—
9	AB_2		—	—	—	13.5(A)	9.7(B)	88.2	—	—

[a] The data were measured in d-acetone, the chemical shifts are given in ppm (±0.5 ppm) relative to 85% H_3PO_4, and the coupling constants are in Hz.

[b] OR represents the $OCH_2C{\equiv}CH$ group and OΦ represents the OC_6H_5 group.

amount of the AX_2 system and implied the product isolated was predominantly non-geminal isomers. However, the chemical shifts for the *cis* and *trans* forms were so close to each other that only one set of the AB_2 pattern was found for the non-geminal isomers.

The ^{31}P NMR spectra of compound **3** also showed the existence of both geminal and non-geminal isomers. It was found that the estimated percentage of the geminal form might be as high as 35%. This was rationalized by the fact that in the substitution reaction, ignoring the steric effect, the nucleophile had equal opportunity to substitute the chlorine atom at the geminal position or the non-geminal position for the non-geminal bis isomers, therefore, a significant amount of the geminal tris compound was produced. A small amount of the non-geminal isomers was isolated by column chromatography, but attempts to isolate the geminal form were unsuccessful.

For compound **4**, although it was expected to have non-geminal and geminal isomers, the sample isolated was proved to be exclusively the non-geminal form from the ^{31}P NMR spectrum, showing that the substitution in this stage was almost all of the non-geminal pattern.

The data in Table 2 show that the ^{31}P chemical shifts are decreasing (more upfield) in the order of $PCl_2 > P(OCH_2C{\equiv}CH)Cl > P(OCH_2C{\equiv}CH)_2$, implying a more electron-withdrawing effect by the propargyloxy group than by the Cl atom. In addition, the coupling constants also increase with increasing numbers of the propargyloxy substituents.

In order to understand some of the chemical properties of the synthesized (propargyloxy)chlorocyclotriphosphazenes, two reactions were carried out as a preliminary study. One was the further substitution reaction with sodium phenoxide and the other was the oxidative coupling reaction.

The reactions of compounds **1** and **2** with sodium phenoxide proceeded smoothly to give the expected derivatives $N_3P_3(OC_6H_5)_5(OCH_2C{\equiv}CH)$ (**7**) and $N_3P_3(OC_6H_5)_4(OCH_2C{\equiv}CH)_2$ (**8**) in good yields.

The elemental analysis, mass, IR and NMR (^1H, ^{13}C, ^{31}P) spectroscopic properties of compounds **7** and **8** were in accord with the assigned structures. Of particular interest was the ^{31}P NMR spectrum of compound **8**, which also showed the presence of the non-geminal isomers and a trace amount of the geminal isomer like its parent compound **2**. However, the two sets of AB_2 patterns of the *cis* and *trans* non-geminal isomers were separated by approximately 0.3 ppm. Comparison of their peak areas showed that the relative abundances of the two forms was roughly 35 : 65%. On consideration of the steric effect of the substituted groups on the ring, together with the examples studied by others,[6,17,18] it was suggested that the *trans* isomer was more abundant.

For simplicity, derivative **7**, containing only one acetylene group, was further used as an example to carry out the oxidative coupling reaction through the terminal actylene group. The reaction followed Hay's method[18] and is shown in the following scheme:

$$N_3P_3(OC_6H_5)_5(OCH_2C{\equiv}CH) \xrightarrow{O_2,\text{catalyst}} [\text{-}N_3P_3(OC_6H_5)_5(OCH_2C{\equiv}C\text{-})]_2.$$

(9)

Product **9** was obtained as a colourless solid (m.p. = 112°C). The IR and ^1H NMR spectra showed the absence of the terminal proton (≡CH). A typical secondary AB_2 pattern was found in the ^{31}P NMR spectrum, as expected. The elemental analysis and the ^{13}C NMR spectrum confirmed unambiguously that the structure of compound **9** contained all the diacetylene group. This result showed that after all of the chlorine atoms were replaced by the OC_6H_5 groups, the PN skeleton was sufficiently stable to allow organic chemistry to be carried out on the side groups and it is possible to carry out various chemical reactions through the terminal acetylene groups.

CONCLUSIONS

From this study, it has been shown that the reaction of sodium propargyloxide with $N_3P_3Cl_6$ led to a series of compounds of the type $N_3P_3Cl_{6-n}(OCH_2C{\equiv}CH)_n$ (n = 1–6). The reaction was found to predominantly follow a non-geminal pathway, just like the majority of the reactions of alkoxides with hexachlorocyclotriphosphazene.[6,17,18] As observed in the reaction between sodium 2,2,2-trifluoroethoxide and hexachlorophosphazene[18] and that between sodium vinyloxide with hexachlorocyclotriphosphazene, a significant amount of the tris geminal isomer, which could be produced from both the geminal and the non-geminal bis compounds, was found in this study.

The fact that the (propargyloxy)chlorocyclotriphosphazenes (**1**) and (**2**) could be derivatized leaving the terminal acetylene group intact and that compound **7** could be further reacted through the acetylene group, demonstrates that one can prepare the analogous polyphosphazenes with a pendant acetylene group and carry out various synthetic transformations through the acetylene group on the (propargyloxy)chlorocyclotriphosphazenes syn-

thesized in this study. Work along this line, especially those compounds with $n = 1$ or 2, is currently in progress in our laboratory.

Acknowledgement—This work was supported by the National Science Council of R.O.C. through grant No. NSC-71-0204-M033-01.

REFERENCES

1. H. R. Allcock and R. L. Kubel, *J. Am. Chem. Soc.* 1965, **87**, 4216.
2. H. R. Allcock, *Chem. Engng News* 1985, **63**, 22.
3. R. H. Neilson and P. Wilsian-Neilson, *Chem. Rev.* 1988, **88**, 541.
4. C. W. Allen, *J. Polym. Sci. Polym. Sym.* 1983, **70**, 79.
5. C. W. Allen, K. Ramachandran, R. P. Bright and J. C. Shaw, *Inorg. Chim. Acta* 1982, **64**, L109.
6. K. Ramachandran and C. W. Allen, *Inorg. Chem.* 1983, **22**, 1445.
7. C. W. Allen and R. P. Bright, *Inorg. Chim. Acta* 1985, **99**, 107.
8. D. E. Brown and C. W. Allen, *Inorg. Chem.* 1987, **26**, 934.
9. C. W. Allen and J. A. Mackay, *Inorg. Chem.* 1986, **25**, 4628.
10. H. R. Allcock, P. J. Harris and R. A. Nissan, *J. Am. Chem. Soc.* 1985, **103**, 2256.
11. P. M. Hergenrother, *Reactive Oligomers* (Edited by F. W. Harris and H. J. Spinelli), p. 1 and refs cited therein. American Chemical Society, Washington, D.C. (1985).
12. J. S. Wallace, F. E. Arnold and W. A. Feld, *Reactive Oligomers* (Edited by F. W. Harris and H. J. Spinelli), p. 17. American Chemical Society, Washington, D.C. (1985).
13. P. M. Lindley, L. G. Picklesimer, B. Evans, F. E. Arnold and J. J. Kane, *Reactive Oligomers* (Edited by F. W. Harris and H. J. Spinelli), p. 31. American Chemical Society, Washington, D.C. (1985).
14. T. Chivers, *Inorg. Nucl. Chem. Lett.* 1971, **7**, 827.
15. C. W. Allen, J. L. Desorcie and K. Ramachandran, *J. Chem. Soc., Dalton Trans.* 1984, 2843.
16. V. S. Frank, E. E. Stahly and R. G. Rice, *U.S. Patent* 3676311 (1972).
17. J. I. Schmutz and J. R. Allcock, *Inorg. Chem.* 1975, **14**, 2433.
18. E. T. McBee, K. Okuhara and C. Morton, *J. Inorg. Chem.* 1966, **5**, 450.
19. A. S. Hay, *J. Org. Chem.* 1962, **27**, 3320.

Polyhedron Vol. 8, No. 12, pp. 1523–1529, 1989
Printed in Great Britain

0277–5387/89 $3.00 + .00
© 1989 Pergamon Press plc

PSEUDOHALIDE DERIVATIVES OF MANGANESE(II) AND COPPER(II) COMPLEXES WITH MEPIRIZOLE, A BIOLOGICALLY ACTIVE PYRIMIDYL–PYRAZOLE LIGAND

M. BENETÓ, J. GARCÍA* and L. SOTO

Departament de Química Inorgánica, Universitat de València, Facultad de Farmacia, Avda Blasco Ibañez, 13, 46010, València, Spain

and

J. V. FOLGADO and E. ESCRIVÁ

Facultat de Químiques, Avda Dr. Moliner, 50, 46100 Burjassot, València, Spain

(*Received* 24 *October* 1988; *accepted after revision* 27 *January* 1989)

Abstract—The synthesis and characterization of thiocyanate and azide derivatives of mepirizole (4-methoxy-2-(5-methoxy-3-methyl-pyrazol-1-yl)-6-methylpyrimidine, hereinafter L) with manganese(II) and copper(II) is reported. The compounds were characterized by IR, electronic and EPR spectra and analytical data. Spectroscopic results suggest the existence of dimeric neutral entities $[L_2Cu_2(\mu\text{-}X)_2(X)_2]$ (X = NCS or N_3) with unsymmetrical end-to-end bridges and five-coordination geometry around the copper(II) ion. Magnetic susceptibility data show that in the azide derivative the copper atoms are antiferromagnetically coupled ($J = -18$ cm^{-1}), but no magnetic exchange interaction could be detected in the thiocyanate compound up to 4.2 K. With regard to manganese(II) complexes ($MnL_2(NCS)_2 \cdot 2H_2O$ and $MnL(N_3)_2$), an octahedral stereochemistry is proposed for the metal atom in both thiocyanate and azide derivatives, thus implying a polymeric structure in the second one.

In recent years considerable attention has been paid to pyrazoles, pyrimidines and related N-containing heterocyclic derivatives due to the significant role played by this kind of system in several biological processes, often related to their coordinating ability for a trace metal ion.[1–4] We have focussed on the study of pyrimidino–pyrazoles from the coordination chemistry point of view. In our earlier work[5–7] we reported the study of the interaction of several metal ions with mepirizole (4-methoxy-2-(5-methoxy-3-methyl-pyrazol-1-yl)-6-methylpyrimidine, hereinafter L), a biologically active pyrimidino–pyrazole derivative used as an anti-inflammatory agent.[8] In previous structural studies[9–11] we have shown that the mepirizole acts as a bidentate ligand through two nitrogen atoms (which are asterisked in Fig. 1) with significant steric hindrance to the formation of metallic complexes.

The azide ligand has various modes of binding. So, terminal (**A**), μ-1,1 (or end-on) bridging (**B**) and μ-1,3 (or end-to-end) bridging (**C**) are known in azido coordination compounds:[12]

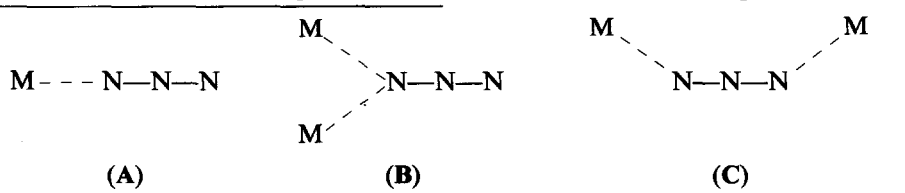

(A) (B) (C)

Because of the importance of azide coordination in protein studies, several authors have examined its coordination properties in relevant model systems.[13] On the other hand, all three coordination modes

* Author to whom correspondence should be addressed.

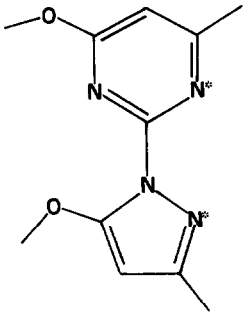

Fig. 1. Schematic view of the mepirizole ligand.

are also exhibited by the thiocyanate group. Moreover, the NCS anion can function as a unidentate ligand (as N_3 in A) in two ways depending on whether the nitrogen atom or the sulphur atom is bonded to the metal.

In this paper we report the synthesis and characterization of azide and thiocyanate derivatives of complexes of mepirizole with manganese(II) and copper(II). The insight gained into the nature and properties of these compounds may be a good basis for studies in related, more complex chelating systems.

EXPERIMENTAL

Preparation of the complexes

A solution of mepirizole (2 mmol for the MLX_2 complexes or 4 mmol for the $MnL_2(NCS)_2 \cdot 2H_2O$ compound) in ethanol (25 cm^3) was added with stirring to an aqueous solution of the metallic nitrate (2 mmol in 25 cm^3). Then a solution of the respective potassium or sodium pseudohalide salt (4 mmol) in H_2O (25 cm^3) was added. The powders which appeared in each case were separated by filtration, washed with a water–ethanol mixture and dried in a desiccator over silica gel.

Analysis

Carbon, hydrogen and nitrogen contents were determined by elemental analysis. Metals were determined by atomic absorption. Analytical data are given in Table 1.

Physical measurements

IR spectra (KBr pellets) were recorded on a Pye–Unicam SP 2000 spectrophotometer. Electronic spectra (diffuse reflectance) were registered using a Perkin-Elmer Lambda 9 UV/VIS/IR spectrophotometer. Polycrystalline powder and frozen solution EPR spectra were obtained on a Bruker ER 200 X-band spectrometer equipped with a variable temperature device. Variable temperature (4.2–298 K) magnetic susceptibility data were obtained on polycrystalline samples with a Faraday-type magnetometer equipped with a continuous flow Oxford Instruments cryostat. $Hg(SCN)_4Co$ was used as the susceptibility standard. Diamagnetic corrections were applied using Pascal's constants.[14] The molar conductances in solution were measured using a Radiometer CDC 304 electrode (cell constant 1.0 cm) in conjunction with a Radiometer CDM 83 conductivity bridge.

RESULTS AND DISCUSSION

As shown in Table 1, the analytical data correspond with the assigned molecular formulae. Attempts to isolate the $MnL(NCS)_2$ compound were unsuccessful, as occurs with the analogous cobalt(II) and nickel(II) complexes.[15]

Assignments of the more relevant IR spectral bands in the complexes are listed in Table 2. Bands due to the mepirizole ligand are not included. As can be expected, characteristic bands of the pyrimidine and pyrazole rings of the free ligand are shifted to lower wavenumbers upon complexation, indicating coordination of the heterocycle N-atoms.[6]

Table 1. Analytical data of the complexes

Compound	%C		%N		%H		%M		
	calc.	found	calc.	found	calc.	found	calc.	found	(Ω^{-1} cm^2 mol^{-1})
$MnL_2(NCS)_2 \cdot 2H_2O$	37.5	37.7	20.2	20.0	4.4	4.2	15.7	15.3	56[a]
$MnL(N_3)_2$	34.6	34.9	36.4	35.5	3.9	3.8	14.4	14.8	i.s.[b]
$CuL(NCS)_2$	37.7	37.9	20.3	20.2	3.4	3.2	15.4	15.5	10[c]
$CuL(N_3)_2$	33.3	34.0	35.0	35.2	4.0	4.1	15.9	15.4	$\simeq 0$[c]

[a] *ca* 10^{-3} M in nitromethane.
[b] i.s.—insufficiently soluble for determination.
[c] In chloroform.

Table 2. Relevant IR (cm^{-1}) data

Compound	$\nu(X)^a$	$\nu'(X)^a$	$\delta(X)^a$
$MnL_2(NCS)_2 \cdot 2H_2O$	2077, 2072	805	478
$CuL(NCS)_2$	2117, 2089	—	475
$CuL(N_3)_2$	2090, 2050	1330	602
$MnL(N_3)_2$	2072, 2070	1332	612

^{a}X = NCS, N_3, $\nu = \nu$(CN) or ν_{as}(NNN); $\nu' = \nu$(CS) or ν_s(NNN).

Manganese(II) *complexes*

The molar conductance value of the thiocyanate derivative (Table 1) is lower than expected for a 1 : 1 electrolyte in nitromethane,[16] indicating the non-ionic character of the complex. The positions of the bands assignable to NCS group vibrations suggest that it acts as a monodentate terminal N-bonded ligand.[17–19] On the other hand, the well-defined splitting of the ν(CN) band may be interpreted as evidence for a *cis*-octahedral arrangement,[20] as could be expected from the steric hindrance imposed by the methyl groups of the mepirizole. A broad band centred at *ca* 3400 cm^{-1} is observed in the IR spectrum, consistent with the existence of water of crystallization.[21] The IR spectrum of the $MnL(N_3)_2$ compound is compatible with the presence of a mono-coordinated and/or bridging μ-1,1 azide.[17,19] This assignment is only tentative since the best defined feature of this spectrum, the absorption centred at *ca* 2070 cm^{-1} (ν_{as}), cannot be used as diagnostic for the coordination mode of the azide group.

The electronic spectra of both manganese compounds display three weak bands at *ca* 18,500, 21,000 and 23,500 cm^{-1} and are assigned[22] to $^6A_{1g} \rightarrow {}^4T_{1g}$, $^6A_{1g} \rightarrow {}^4T_{2g}$ and $^6A_{1g} \rightarrow {}^4B_g, {}^4A_{1g}$ transitions, respectively. The other expected transitions which must occur at higher energies than 25,000 cm^{-1} are masked by a charge-transfer band. The position of the observed *d–d* transition bands are very similar to those reported for MnN_6 chromophores.[23,24] In the spectrum of the thiocyanate derivative, a well-defined splitting of the $^4T_{2g}$ band ($\Delta\nu = 1300$ cm^{-1}) is observed. This fact may be interpreted in terms of a tetragonal splitting of the $^4T_{2g}(^4G)$ state, as has been reported for some *cis*-MnL_4L_2 chromophores,[25] being consistent with the IR and EPR (see below) interpretation. On the other hand, the room temperature magnetic moments (5.91 and 6.12 BM for the $MnL_2(NCS)_2 \cdot 2H_2O$ and $MnL(N_3)_2$ compounds, respectively) are consistent with a d^5 high-spin configuration. Unfortunately, no conclusive information about the manganese stereochemistry can be obtained from these spectral and magnetic data.

The polycrystalline powder, room temperature EPR spectrum of $MnL_2(NCS)_2 \cdot 2H_2O$ shows one very strong line centred at $g = 2.00$. In addition, there are several shoulders both at lower and higher field [Fig. 2(a)], which suggest a low value of the zero-field splitting parameter D. By using the Dowsing and Gibson diagrams[26] it can be estimated that $0.05 \leqslant D \leqslant 0.10$ cm^{-1}. The λ ($= E/D$) parameter cannot be accurately determined, but it might be assumed to be less than 0.1. The small value of both D and λ parameters may be indicative of a *cis*-octahedral arrangement[27] in line with the spectral data. The frozen solution (nitromethane, 100 K) EPR spectrum is analogous to that obtained on a polycrystalline sample, indicating a similar geometry around the manganese(II) ion in both cases. Moreover, in the frozen solution EPR spectrum, the hyperfine coupling with the manganese nucleus ($I = 5/2$), with an averaged value of $|A| = 90 \times 10^{-4}$ cm^{-1}, can be observed. In manganese(II) complexes the ionic character of the metal–ligand bond is proportional to the magnitude of A, with an estimated value of 100×10^{-4} cm^{-1} for a "full-ionic" bond.[28] The value obtained for the compound under consideration falls in the range observed for other MnN_6 chromophores,[23,24] indicating a similar covalent character in the Mn—N bonds.

The EPR spectrum of the $MnL(N_3)_2$ compound shows only an isotropic signal at $g = 2.01$ without any appreciable shoulder either at lower or higher field [Fig. 2(b)]. This suggests a D value close

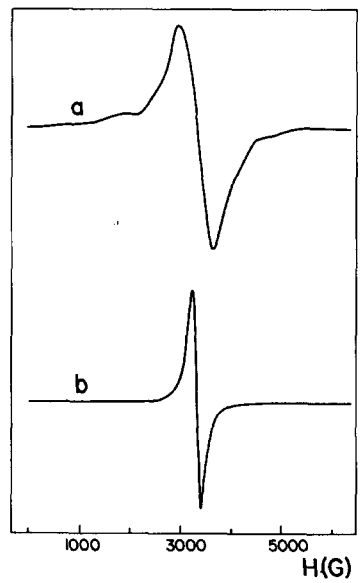

Fig. 2. X-band EPR spectra of polycrystalline samples of (a) $MnL_2(NCS)_2 \cdot 2H_2O$ and (b) $MnL(N_3)_2$.

to zero, but it is not possible to estimate the λ value. Hence, on the basis of the EPR results it cannot be established what the geometry of the metallic environment is. As in the analogous azide derivatives of cobalt(II) and nickel(II),[15] the very poor solubility of the compound in common solvents suggests a polymeric structure for this derivative.

Copper compounds

The IR data of the $CuL(NCS)_2$ compound suggest an end-to-end bridging coordination mode for the NCS^- group. In fact, non-observance of ν(CS) and the shifting of ν(CN) to higher wavenumbers argues in favour of simultaneous coordination of both N and S ends of the thiocyanate to give Cu—NCS—Cu bridged entities.[17,19] On the other hand, from the IR data of the copper(II) azide derivative no conclusive information can be obtained about the azide coordination mode, as has been previously discussed.

The electronic spectra of both compounds exhibit a very broad unresolved band in the visible region (Table 3). The position of the band intensity maximum suggests for the two complexes, a pentacoordinated copper(II) chromophore with an intermediate geometry between the ideal square pyramidal and trigonal bipyramidal,[22,29] although a distorted tetrahedral environment cannot be ruled out.[9] Apart from the *d–d* band, both spectra display a more intense band centred at *ca* 20,000 cm^{-1} assigned to a metal–ligand ($t_{2g} \Rightarrow \pi^*$) charge-transfer band.[30]

The X-band EPR spectrum of a polycrystalline sample of $CuL(NCS)_2$ shows an axial-type signal [Fig. 3(a)] which remains unchanged from room temperature down 90 K. The resulting g and A values (Table 3) are in good agreement with a mainly $d_{x^2-y^2}$ copper(II) ground state.[29,31] The spectrum also shows a weak intensity feature at *ca* 1620 G. This can be assigned to a $\Delta M_s = 2$ forbidden transition, thus suggesting a magnetic coupling interaction between two copper atoms. The G parameter, defined as $G = g_\parallel - 2/g_\perp - 2$ (which is indicative of exchange interactions between copper centres in polycrystalline solids), is close to four, indicating that exchange interactions are weak.[32]

The observed magnetic behaviour of the copper

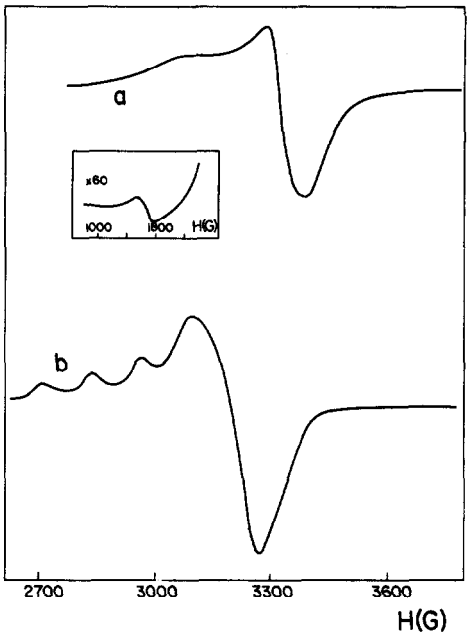

Fig. 3. X-band EPR spectra of $CuL(NCS)_2$: (a) polycrystalline sample and (b) $CHCl_3$ frozen solution at 100 K.

Table 3. Electronic spectral data and EPR parameters for $CuLX_2$ compounds

Compound	Electronic spectral data (cm^{-1})	EPR parameters $g_\parallel$	$g_\perp$	$A_\parallel$ (cm^{-1})	$A_\perp$ (cm^{-1})	$R = g_\parallel/A_\parallel$ (cm)
$CuL(NCS)_2$	soln[a,b] 12,600(125), 19,600(sh), 24,800(1180)	2.33 2.26	2.08 2.07	0.0132	0.0022	177
	solid 13,380, 21,300(sh), 22,100					
$CuL(N_3)_2$	soln[a,b] 13,700(137), 19,800(sh), 23,000(1670)	2.28 2.15[c]	2.06 2.15[c]	0.0145	0.0013	157
	solid 11,900, 21,700					
$CuLCl_2$[d]	soln[a,b] 12,700(94), 22,500(1210)	2.30	2.09	0.0138	0.0018	167
	solid 13,000, 22,200	2.10[c]	2.10[c]			

[a] EPR parameters correspond to frozen solution ($CHCl_3$, 105 K).
[b] ε_{molar} are given in parentheses.
[c] Average value of g in the isotropic signal.
[d] From refs 11 and 41.

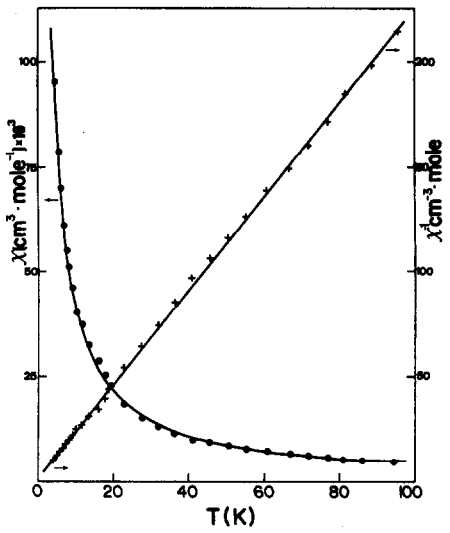

Fig. 4. Temperature dependence of the molar magnetic susceptibility X_M and the inverse susceptibility of $CuL(NCS)_2$. The solid lines were obtained by fitting to the Curie–Weiss formulae (see text).

thiocyanate derivative agrees with the EPR interpretation. In fact, the good fit of the inverse susceptibility to a straight line with temperature in the range 4.2–100 K, adhering closely to the Curie law (Fig. 4), indicates a very small singlet–triplet splitting. The whole susceptibility data were fitted to the Curie–Weiss expression $X = C/(T-\theta)$ affording $C = 0.443\ cm^3\ mol^{-1}\ K$ and $\theta = -0.6\ K$. The small absolute value of the Weiss correction, less than 1 K, reflects a very weak antiferromagnetic coupling ($|J| < 0.5\ cm^{-1}$), which would only be detected unambiguously at temperatures below 4.2 K. From the Curie constant $C = N\beta^2g^2S(S+1)/3k$ with $S = 1/2$, a g value of 2.17 can be obtained, in good agreement with the EPR data. This result indicates that the two copper ions in a pair of $CuL(NCS)_2$ moieties may be considered as essentially magnetically non-coupled. At the present time, all spectroscopic and magnetic data suggest a dimeric structure with a copper(II) ion environment geometry close to square pyramidal with end-to-end asymmetric Cu—NCS---Cu bridges (Fig. 5).

Dealing with the $CuL(N_3)_2$ compound, the EPR

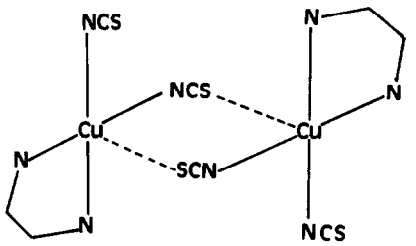

Fig. 5. Schematic view of the proposed approximate geometry for dimeric $[L_2Cu_2(\mu\text{-}NCS)_2(NCS)_2]$ species.

room temperature polycrystalline powder spectrum consists of an extremely broad feature (2200 G peak-to-peak) centred at *ca* 3200 G. Cooling down to 4.2 K does not improve this broad feature, although its intensity decreases and a weak axial signal ($g_\parallel = 2.28$, $g_\perp = 2.06$) due to monomeric impurities, becomes more intense as the temperature is lowered. Even though the poor resolution of this spectrum precludes any qualitative interpretation, it apparently arises from unresolved transitions in a triplet state. In fact, the magnetic behaviour at low temperatures supports this argument. A representation of the magnetic susceptibility vs temperature is shown in Fig. 6. Upon cooling down, the magnetic susceptibility increases until a maximum is reached at *ca* 19 K, after which the susceptibility decreases. The magnetic moment (per Cu^{2+} ion) varies from 1.87 BM at 281 K to 0.28 BM at 4.7 K, being typical of an antiferromagnetic interaction. The experimental data were fitted to the Bleaney–Bowers equation modified according to Khan and co-workers[33] to take into account some paramagnetic impurity (ρ):

$$X = (2N\beta^2g^2)[3+\exp(-J/kT)]^{-1}(1-\rho)/kT + 2N\beta^2g^2\cdot\rho/2kT+2N\alpha,$$

where J (singlet–triplet energy gap), g and ρ were taken as adjustable parameters. The temperature independent paramagnetism was assumed as $N\alpha = 6\times10^{-5}\ cm^3\ mol^{-1}$ of copper(II) ions. The least-squares fitting procedure led to $J = -18\ cm^{-1}$, $g = 2.16$ and $\rho = 0.036$. The agreement factor between the observed and calculated data, defined

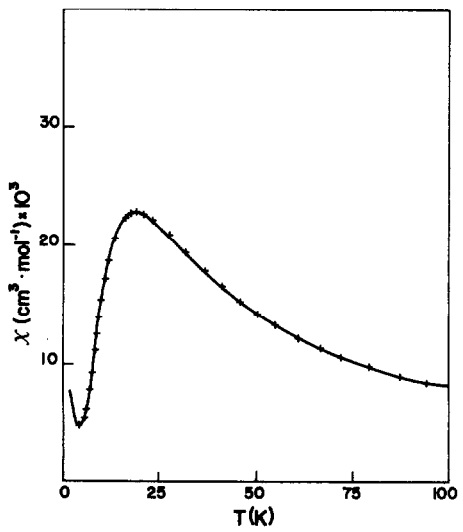

Fig. 6. Experimental (+) and theoretical (—) temperature dependences of the molar magnetic susceptibility of $CuL(N_3)_2$.

as $R = \Sigma(X_{M_{theory}} - X_{M_{exp}})^2/\Sigma X_{M_{theory}}$, is then equal to 1.53×10^{-4}.

The magnetic behaviour of μ-azido copper(II) binuclear complexes has been the subject of several studies in recent years.[34-37] The interaction between two copper(II) ions is ferromagnetic when they are bridged by an azido group in a μ-1,1 fashion or strongly antiferromagnetic in a symmetrical μ-1,3 fashion. On the other hand, when two N_3 groups bridge in an unsymmetrical μ-1,3 fashion (with a short Cu—N bond and a long Cu—N bond) the dimeric copper(II) compound exhibits either negligible interaction when the geometry around the metal atom is square pyramidal or weak antiferromagnetic interaction when this geometry tends toward trigonal bipyrimidal.[36] In the light of the results obtained, the existence of unsymmetrical end-to-end azido bridges, similar to those pointed out for the copper thiocyanate derivative, may be stated, implying dimeric $[Cu_2L_2(\mu\text{-}N_3)_2(N_3)_2]$ entities in the compound. In this sense, the different magnetic behaviour of both $CuL(NCS)_2$ and $CuL(N_3)_2$ compounds could be understood on the basis of: (1) a greater distortion of the copper(II) environment toward the TBP geometry in the azide derivative (supported by the electronic spectral data), with a significant contribution of the d_{z^2}-type orbital to the magnetic orbital and (2) probably, a greater unsymmetrical character in the NCS bridges, as has been argued for the interpretation of the magnetic behaviour in related azido bridged dimers.[34]

Finally, for both copper compounds the electronic spectral and EPR data indicate the non-preservation of the proposed dimeric entities in a non-coordinating solvent such as chloroform. In this solvent, the $CuL(NCS)_2$ and $CuL(N_3)_2$ complexes show an isotropic hyperfine EPR spectra at room temperature. In frozen solution at 100 K, X-band EPR spectra show very similar axial signals for two complexes [the corresponding $CuL(NCS)_2$ compound is shown as the representative in Fig. 3(b)], and do not exhibit any sign of coupling apart from the copper hyperfine structure. The resulting EPR parameters are listed in Table 3, together with those corresponding to the chloride derivative for comparison. The A value has been estimated from the relation $A_0 = (A_\parallel + 2A_\perp)/3$, where the A_0 values were obtained from the room-temperature spectra, assuming that dA/dT is negligible.[38] The whole of the EPR results suggest a flattened tetrahedral copper environment (CuN_4 chromophore) with a d_{xy} ground state,[31,39] being similar to those previously reported[9,10,40] for the $CuL_2(ClO_4)_2$ and $CuLCl_2$ compounds, where the copper atom exhibits a flattened tetrahedral stereochemistry (indeed, the CuN_4 and CuN_2Cl_2 chromophores have formally D_{2d} and C_{2v} symmetry, respectively). With regard to the electronic spectral data, by using the position of the d–d band intensity maximum (Table 3) as criterion for the distortion of the proposed CuN_4 chromophore,[9] the parameter ϕ may be estimated, defined as the dihedral angle between N_L—Cu—N_L and N_x—Cu—N_x planes ($\phi = 0$ for D_{4h} symmetry and $\phi = 90°$ for Td symmetry), affording $\phi = 55°$ for $CuL(N_3)_2$ and $\phi = 62°$ for $CuL(NCS)_2$. These values are consistent with the obtained R factor (Table 3) for both compounds, also related with the ϕ parameter.[39]

In short, the EPR and electronic spectral data, besides the low conductivity of the solutions (Table 1) indicating the non-electrolyte character,[16] support the existence in $CHCl_3$ solution of neutral $[CuL(X)_2]$ species, with a flattened tetrahedral stereochemistry for the copper atoms.

Acknowledgement—We thank Dr J. P. Tuchagues for his assistance with susceptibility measurements.

REFERENCES

1. S. Trofimenko, *Chem. Rev.* 1972, **72**, 497.
2. J. G. Voss and W. L. Groeneveld, *Inorg. Chim. Acta* 1977, **24**, 123.
3. A. R. Katritzky and C. W. Rees (Eds), *Comprehensive Heterocyclic Chemistry*, Vol. 5. Pergamon Press, Oxford (1984).
4. N. Saha and D. Mukherjee, *Transition Met. Chem.* 1987, **12**, 156 and refs therein.
5. J. García, M. Mollá and J. Borrás, *Polyhedron* 1985, **4**, 757.
6. J. García, M. Mollá and J. Borrás, *Synth. React. Inorg. Met.-org. Chem* 1985, **15**, 553.
7. J. Tormo, J. García and M. Mollá, *Synth. React. Inorg. Met.-org. Chem.* 1986, **16**, 821.
8. E. Tabaka, R. Kodama, Y. Tanaka, R. Dohmori, H. Tachizanawa and P. Naito, *Chem. Pharm. Bull.* 1970, **18**, 1900.
9. J. García, M. Mollá, J. Borrás, C. Foces-Foces, F. H. Cano and M. Martínez Ripoll, *Transition Met. Chem.* 1985, **10**, 460.
10. L. Soto, J. P. Legrós, J. García and M. Mollá, *Acta Cryst.* 1987, **C43**, 834.
11. J. Suarez-Varela, L. Soto, J. P. Legrós, C. Esteve and J. García, *Polyhedron* 1988, **7**, 229.
12. Z. Dori and R. F. Ziolo, *Chem. Rev.* 1973, **73**, 247.
13. K. D. Karlin, B. I. Cohen, J. C. Hayes, A. Farooq and J. Zubieta, *Inorg. Chem.* 1987, **26**, 147 and refs therein.
14. P. W. Selwood, *Magnetochemistry*. Wiley, Interscience, New York (1956).
15. M. Benetó, J. García and E. Escrivá, *J. Coord. Chem.*, in press.
16. W. J. Geary, *Coord. Chem. Rev.* 1971, **7**, 81.

17. A. H. Norbury, *Adv. Inorg. Chem. Radiochem.* 1975, **17**, 232.
18. K. Nakamoto, *Infrared and Raman Spectra of Inorganic and Coordination Compounds*, 3rd edn. John Wiley, New York (1978).
19. A. H. Golub, H. Kholer and V. V. Slopenko, *Chemistry of Pseudohalides*. Elsevier, Amsterdam (1986).
20. C. M. Harris and E. D. McKenzie, *J. Inorg. Nucl. Chem.* 1967, **29**, 1047.
21. F. Franks, *Water, a Comprehensive Treatise*, Vol. 2. John Wiley, New York (1977).
22. A. B. P. Lever, *Inorganic Electronic Spectroscopy*, 2nd edn. Elsevier, Amsterdam (1986).
23. R. Singh, J. S. Ahuja and C. L. Yakoava, *Polyhedron* 1982, **1**, 327.
24. R. A. Palmer, M. C. Yang and J. C. Hempel, *Inorg. Chem.* 1978, **17**, 1200.
25. L. L. Lohr Jr, *J. Chem. Phys.* 1966, **45**, 3611.
26. R. D. Dowsing and J. F. Gibson, *J. Chem. Phys.* 1969, **50**, 294.
27. R. D. Dowsing, J. F. Gibson, M. Goodgame and P. J. Hayward, *J. Chem. Soc.* 1970, 1133.
28. G. M. Wolterman and J. R. Wasson, *Chem. Phys. Lett.* 1973, **16**, 92.
29. B. J. Hathaway, *Struct. Bond.* 1984, **57**, 55.
30. A. B. P. Lever, *J. Chem. Educ.* 1974, **51**, 612.
31. M. Massacesi, G. Ponticelli and W. G. Krishnan, *J. Molec. Struct.* 1980, **69**, 165.
32. B. J. Hathaway and D. E. Billing, *Coord. Chem. Rev.* 1970, **5**, 143.
33. C. Chauvel, J. J. Girerd, Y. Jeannin, O. Kahn and G. Lavigne, *Inorg. Chem.* 1979, **18**, 3015.
34. T. R. Felthouse and D. N. Hendrickson, *Inorg. Chem.* 1978, **17**, 444.
35. J. Comarmoond, P. Plumere, J. M. Lehn, Y. Agnus, R. Louis, R. Weiss, O. Kahn and I. Morgenstern-Badarau, *J. Am. Chem. Soc.* 1982, **104**, 6330.
36. M. F. Charlot, O. Kahn, M. Chaillet and C. Larren, *J. Am. Chem. Soc.* 1986, **108**, 2574.
37. P. Chaudhuri, K. Oder, K. Wieghardt, B. Naber and J. Weiss, *Inorg. Chem.* 1986, **25**, 2818.
38. F. G. Herring and R. L. Tapping, *Can. J. Chem.* 1974, **52**, 4016.
39. J. Gouteron, S. Jeannin, J. Livage and C. Sanchez, *Inorg. Chem.* 1984, **23**, 3387.
40. M. C. Mollá, J. García and J. Borrás, *An. Res. Soc. Esp. Fis. Quim.* 1987, **83**, 18.

Polyhedron Vol. 8, No. 12, pp. 1531–1536, 1989
Printed in Great Britain

0277–5387/89 $3.00+.00
© 1989 Pergamon Press plc

BIMETALLIC HEXANUCLEAR COMPOUNDS CONTAINING UNUSUAL COPPER–LANTHANIDE ARRAYS: THE CRYSTAL STRUCTURES OF $Cu_4Ln_2L_8(LH)_4(OH)_2(NO_3)_4(H_2O)_2$ (Ln = Dy OR Gd; LH = 2-(1H)-PYRIDONE, C_5H_5NO)

DAVID M. L. GOODGAME,* DAVID J. WILLIAMS* and RICHARD E. P. WINPENNY

Chemistry Department, Imperial College of Science, Technology and Medicine, London SW7 2AY, U.K.

(*Received* 3 *November* 1988; *accepted* 3 *February* 1989)

Abstract—Reaction of copper hydroxide, 2-(1H)-pyridone (= LH), and dysprosium (or gadolinium) nitrate in methanol results in the formation of the unusual hexanuclear complexes, $Cu_4Ln_2L_8(LH)_4(OH)_2(NO_3)_4(H_2O)_2$ [Ln = Dy(**1**) and Gd(**2**)], which have been characterized by X-ray diffraction. The compounds are isostructural and in each case four copper and two lanthanide ions are bridged by trinucleating 2-pyridone anions to form an essentially octahedral Cu_4Ln_2 core. The lanthanide atoms are each nine-coordinate and the copper atoms five-coordinate. The core is surrounded by an exterior of largely hydrophobic ligand units.

The recent, rapid developments in the synthesis of high-temperature superconductors of the mixed-metal oxide type have been mainly focussed on systems containing combinations of copper and yttrium or lanthanide (= Ln) ions. Attention is also increasingly being paid to the techniques of sample preparation, both in terms of the experimental method[1] and choice of precursor chemicals.[2] Precursors comprising Cu/Ln heterometallic complexes of organic ligands are of potential value in this context because they contain well-defined Cu_x/Ln_y combinations for conversion to oxides by thermal methods. We have extended our recent studies on heterometallic compounds involving lanthanide ions[3] to include Cu/Ln systems. During this work we have obtained two unusual, new hexanuclear complexes: $Cu_4Ln_2L_8(LH)_4(OH)_2(NO_3)_4(H_2O)_2$ (Ln = Dy(**1**) and Gd(**2**) and LH = 2-pyridone) and we report here the structures of these compounds.

* Authors to whom correspondence should be addressed.

EXPERIMENTAL

Preparation

Reaction of copper hydroxide (1 mmol), 2-pyridone (6 mmol) and the appropriate hydrated lanthanide nitrate (2 mmol) in refluxing methanol (100 cm^3) resulted in a dark green solution, which on evaporation at room temperature for 6 weeks with regular filtrations, gave crystals suitable for single-crystal X-ray diffraction analysis.

X-ray study

Crystals of **1** and **2** formed as dark green cubes from methanol. They contained solvent methanol and required coating with epoxy resin to prevent solvent loss and consequent crystal decomposition, during data collection. Despite these precautions, three separate crystals were required for **2**. The crystal data are: $Cu_4Ln_2L_8(LH)_4(OH)_2(NO_3)_4(H_2O)_2 \cdot 3CH_3OH$ (**1**): $C_{63}H_{70}Cu_4Dy_2N_{16}O_{31}$, orthorhombic, $a = 16.751(6)$, $b = 21.463(6)$, $c = 23.471(6)$ Å, $V = 8439$ Å^3, space group *Pbnn*, $Z = 4$ (the complex has crystallographic C_2 sym-

metry), $M_r = 2126.6$, $D_c = 1.67$ g cm^{-3}, μ(Cu-K_α) = 104 cm^{-1}; $Cu_4Ln_2L_8(LH)_4(OH)_2(NO_3)_4(H_2O)_2 \cdot 2CH_3OH$ (**2**): $C_{62}H_{66}Cu_4Gd_2N_{16}O_{30}$, orthorhombic, $a = 16.774(16)$, $b = 21.344(11)$, $c = 23.441(16)$ Å, $V = 8392$ Å^3, space group *Pbnn*, $Z = 4$ (the complex has crystallographic C_2 symmetry), $M_r = 2084.0$, $D_c = 1.65$ g cm^{-3}, μ(Cu-K_α) = 125 cm^{-1}.

Refined unit cell parameters for crystals of approximate dimensions, **1**: 0.6 × 0.3 × 0.34 mm, **2**: 0.5 × 0.3 × 0.32 mm, were obtained by centring 18 reflections on a Nicolet R3m diffractometer. For **1**, 5842 independent reflections were measured ($\theta \leqslant 58°$) with graphite monochromated Cu-K_α radiation using ω-scan measurement routine. Of these, 3899 had $|F_o| > 3\sigma(|F_o|)$ and were considered observed. For **2**, 5946 independent reflections were measured on three crystals (844 on the first, 826 on the second and 4276 on the third; data were collected until the sample had decomposed by ≈ 25%). Of these, 2866 were considered observed. The data were corrected for Lorentz and polarization factors. For **1**, an empirical absorption correction, based upon 398 azimuthal measurements, was applied.

The structure of **2** was solved by the heavy-atom method, which revealed the position of the gadolinium. The remaining non-hydrogen atoms were located from subsequent ΔF maps and were refined anisotropically. Two methanol solvent fragments, each of site occupancy 50%, were also located from ΔF maps and were refined isotropically. The pyridone rings were idealized and refined as rigid bodies. The positions of the hydrogen atoms of the pyridones were idealized, C—H = 0.96 Å, assigned isotropic thermal parameters, $U(H) = 1.2U_{eq}(C)$, and allowed to ride on their parent carbon atoms. Refinement was by block-cascade, full-matrix least-squares to $R = 0.115$, $R_w = 0.107$ [$w^{-1} = \sigma^2(F)$

Table 1. Bond lengths (Å) and angles (°) for **1** with ESDs in parentheses

Dy—O(1)	2.418(10)	Dy—O(2)	2.402(10)
Dy—O(3)	2.307(14)	Dy—O(4)	2.459(11)
Dy—O(5)	2.400(11)	Dy—O(6)	2.291(13)
Dy—O(9)	2.449(13)	Dy—O(71)	2.432(12)
Dy—O(72)	2.652(27)		
Cu(1)—O(1)	1.978(11)	Cu(1)—O(2)	1.983(10)
Cu(1)—O(10)	2.326(13)	Cu(1)—N(1a)	1.955(9)
Cu(1)—N(5a)	1.944(10)	Cu(2)—O(4)	1.948(12)
Cu(2)—O(5)	1.983(11)	Cu(2)—O(81)	2.338(14)
Cu(2)—N(2a)	1.959(10)	Cu(2)—N(4a)	1.940(9)
O(1)—Dy—O(2)	63.6(3)	O(1)—Dy—O(3)	134.5(4)
O(2)—Dy—O(3)	73.3(4)	O(1)—Dy—O(4)	108.7(3)
O(2)—Dy—O(4)	78.2(4)	O(3)—Dy—O(4)	74.7(4)
O(1)—Dy—O(5)	76.3(4)	O(2)—Dy—O(5)	109.5(4)
O(3)—Dy—O(5)	134.9(4)	O(4)—Dy—O(5)	62.7(4)
O(1)—Dy—O(6)	74.9(4)	O(2)—Dy—O(6)	134.9(4)
O(3)—Dy—O(6)	135.9(4)	O(4)—Dy—O(6)	134.4(4)
O(5)—Dy—O(6)	75.0(4)	O(1)—Dy—O(9)	146.8(4)
O(2)—Dy—O(9)	144.7(4)	O(3)—Dy—O(9)	78.7(5)
O(4)—Dy—O(9)	74.0(4)	O(5)—Dy—O(9)	76.2(4)
O(6)—Dy—O(9)	80.3(4)	O(1)—Dy—O(71)	75.2(3)
O(2)—Dy—O(71)	75.6(3)	O(3)—Dy—O(71)	80.6(5)
O(4)—Dy—O(71)	148.2(4)	O(5)—Dy—O(71)	144.5(4)
O(6)—Dy—O(71)	77.5(4)	O(9)—Dy—O(71)	120.6(3)
O(1)—Cu(1)—O(2)	79.9(4)	O(1)—Cu(1)—O(10)	90.7(4)
O(2)—Cu(1)—O(10)	91.7(4)	O(1)—Cu(1)—N(1a)	94.5(4)
O(2)—Cu(1)—N(1a)	170.6(4)	O(10)—Cu(1)—N(1a)	95.9(4)
O(1)—Cu(1)—N(5a)	170.8(4)	O(2)—Cu(1)—N(5a)	96.0(4)
O(10)—Cu(1)—N(5a)	97.6(4)	N(1a)—Cu(1)—N(5a)	88.5(4)
O(4)—Cu(2)—O(5)	80.0(5)	O(4)—Cu(2)—O(81)	86.3(5)
O(5)—Cu(2)—O(81)	86.7(4)	O(4)—Cu(2)—N(2a)	173.6(5)
O(5)—Cu(2)—N(2a)	95.6(5)	O(81)—Cu(2)—N(2a)	98.1(4)
O(4)—Cu(2)—N(4a)	94.0(4)	O(5)—Cu(2)—N(4a)	171.1(5)
O(81)—Cu(2)—N(4a)	99.6(4)	N(2a)—Cu(2)—N(4a)	89.9(4)

$+0.001F^2$]. The maximum and minimum residual electron densities in the final ΔF map were 1.54 and -1.17 e Å^{-3}, respectively.

The structure of **1** was solved by refining the coordinates of **2** using the data for **1** and with dysoprosium replacing gadolinium. Refinement was as for **2**, but ΔF maps showed two methanol fragments, one of site occupancy 50%, the other of full weight, but with two 50% occupancy sites for the oxygen atoms. Refinement was to $R = 0.099$, $R_w = 0.096$ [$w^{-1} = \sigma^2(F) + 0.001F^2$]. The maximum and minimum residual electron densities in the final ΔF map were 2.59 and -2.18 e Å^{-3}, respectively.

In both structures, although the atoms of the central metal core do not exhibit significant thermal anisotropy, as one moves further out the anisotropic vibrations become very pronounced—particularly in the pyridone and nitrate groups. This, coupled with the difficulty in correcting for the absorption effects of an irregular, partially split crystal (hence higher than average ESDs in the cell parameters) coated in epoxy resin, probably explains the high final value of R.

Computations were carried out on an Eclipse S140 computer using the SHELXTL program system.[4] Scattering factors were taken from ref. 5. Important bond lengths and angles are listed in Tables 1 and 2.

RESULTS AND DISCUSSION

The X-ray structural analyses show **1** and **2** to be isostructural. The lanthanide ions are coordinated to nine oxygen atoms (Fig. 1). Four of these oxygens are from deprotonated 2-pyridone units, two from neutral pyridone ligands, two from a bidentate nitrate anion and one from a water molecule. The

Table 2. Bond lengths (Å) and angles (°) for **2** with ESDs in parentheses

Gd—O(1)	2.451(14)	Gd—O(2)	2.427(15)
Gd—O(3)	2.392(20)	Gd—O(4)	2.463(15)
Gd—O(5)	2.453(16)	Gd—O(6)	2.350(20)
Gd—O(9)	2.463(18)	Gd—O(71)	2.518(22)
Gd—O(72)	2.713(27)		
Cu(1)—O(1)	1.927(16)	Cu(1)—O(2)	1.998(15)
Cu(1)—O(10)	2.356(21)	Cu(1)—N(1a)	1.903(15)
Cu(1)—N(5a)	1.945(17)	Cu(2)—O(4)	1.963(15)
Cu(2)—O(5)	1.943(17)	Cu(2)—O(81)	2.373(24)
Cu(2)—N(2a)	1.954(17)	Cu(2)—N(4a)	1.964(14)
O(1)—Gd—O(2)	62.2(5)	O(1)—Gd—O(3)	132.4(6)
O(2)—Gd—O(3)	73.2(6)	O(1)—Gd—O(4)	108.4(5)
O(2)—Gd—O(4)	76.7(5)	O(3)—Gd—O(4)	74.6(6)
O(1)—Gd—O(5)	77.5(5)	O(2)—Gd—O(5)	107.1(5)
O(3)—Gd—O(5)	134.1(6)	O(4)—Gd—O(5)	61.6(5)
O(1)—Gd—O(6)	74.9(6)	O(2)—Gd—O(6)	134.5(6)
O(3)—Gd—O(6)	137.5(6)	O(4)—Gd—O(6)	134.3(6)
O(5)—Gd—O(6)	75.6(6)	O(1)—Gd—O(9)	148.3(6)
O(2)—Gd—O(9)	144.7(6)	O(3)—Gd—O(9)	79.3(6)
O(4)—Gd—O(9)	74.9(5)	O(5)—Gd—O(9)	76.9(5)
O(6)—Gd—O(9)	80.8(6)	O(1)—Gd—O(71)	72.3(5)
O(2)—Gd—O(71)	75.8(5)	O(3)—Gd—O(71)	81.9(7)
O(4)—Gd—O(71)	147.9(6)	O(5)—Gd—O(71)	143.8(6)
O(6)—Gd—O(71)	77.5(7)	O(9)—Gd—O(71)	122.0(5)
O(1)—Cu(1)—O(2)	79.8(6)	O(1)—Cu(1)—O(10)	90.5(7)
O(2)—Cu(1)—O(10)	91.5(7)	O(1)—Cu(1)—N(1a)	96.3(7)
O(2)—Cu(1)—N(1a)	170.4(7)	O(10)—Cu(1)—N(1a)	97.4(7)
O(1)—Cu(1)—N(5a)	171.9(7)	O(2)—Cu(1)—N(5a)	94.9(7)
O(10)—Cu(1)—N(5a)	95.9(7)	N(1a)—Cu(1)—N(5a)	87.9(7)
O(4)—Cu(2)—O(5)	80.3(7)	O(4)—Cu(2)—O(81)	85.3(8)
O(5)—Cu(2)—O(81)	88.4(7)	O(4)—Cu(2)—N(2a)	173.1(7)
O(5)—Cu(2)—N(2a)	95.1(7)	O(81)—Cu(2)—N(2a)	99.7(8)
O(4)—Cu(2)—N(4a)	92.5(7)	O(5)—Cu(2)—N(4a)	170.6(7)
O(81)—Cu(2)—N(4a)	96.9(7)	N(2a)—Cu(2)—N(4a)	91.6(7)

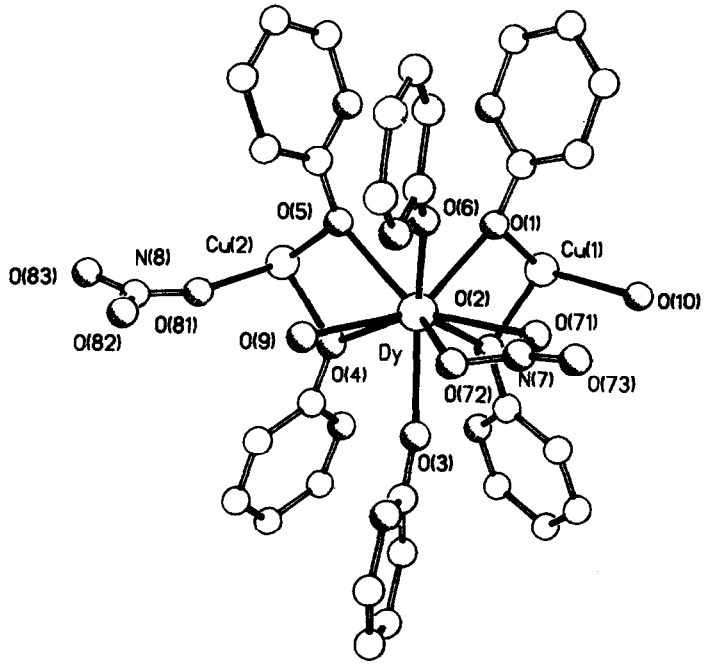

Fig. 1. The lanthanide coordination environment in **1**, showing the numbering scheme.

lanthanide–oxygen bond lengths (Tables 1 and 2) are unexceptional. The coordination geometry in each case is best described as face-capped square antiprismatic. The degree of distortion is small; the angle between the mean planes of the square faces is 1.0° for **1** and 1.3° for **2**. The two faces are rotated out of register by 46° for both compounds. The capping oxygen atom is contributed by one of the oxygen atoms of the bidentate nitrate group. This oxygen atom is at a significantly longer distance (Ln—O $\approx$ 2.68 Å).

There are two types of copper site in the structure. In both, the copper ion is five-coordinate with square-pyramidal geometry (Fig. 2). The principal difference between the two copper sites is the source of the apical oxygen atom. For Cu(1) and Cu(1′) the oxygen is derived from an hydroxide anion, whilst for Cu(2) and Cu(2′) it is from a nitrate anion. In all cases the basal atoms are two pyridone oxygen atoms and two nitrogen atoms in a *cis*-arrangement. The oxygen atoms are shared with the lanthanide ion, and the two nitrogen atoms are derived from different pyridone ligands. The copper–donor atom bond lengths are normal, for the base *ca* 1.97 Å, and for the apical oxygen considerably longer, *ca* 2.35 Å. As might be expected, the copper(II) ions are raised slightly (0.09–0.14 Å) above the basal plane of the pyramid.

Each deprotonated 2-pyridone unit is tri-nucleating, the exocyclic oxygen atom bridging between the lanthanide ion and one copper, and the nitrogen bound to another copper. This appears to be the first example of 2-pyridone binding in this way, although we have recently shown that a related ligand 2-pyrrolidone binds three metal atoms in $[Hg Ag(C_4H_6NO)_2(NO_3)]_2$.[6] The $CuLnO_2$ rings formed in **1** and **2** are nearly planar in all cases. The di-

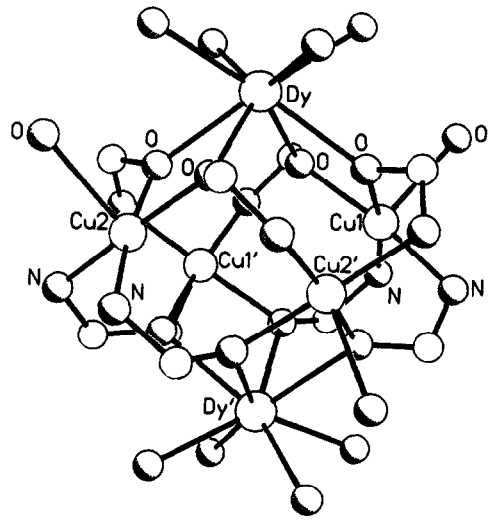

Fig. 2. The ligand-bridged metallic core of **1**, also showing the copper(II) coordination environments. (Atoms not involved in metal atom bridging have been omitted for clarity.)

hedral angles between the LnO_2 and CuO_2 planes within each four-membered ring are within the range 176–178°, and the largest deviation from planarity is for Cu(2) in **1**, which is 0.03 Å out of the plane. The angles at the oxygen atoms are also very similar for all oxygens involved [range 108.0(6)–109.8(6)°].

The result of these several interactions is an unusual spheroidal molecule with four copper and two lanthanide atoms comprising an essentially octahedral core, in which the copper atoms occupy the equatorial region while the lanthanide atoms occupy *trans*-positions (Fig. 3); metal–metal distances in both compounds are within the range 3.57–3.78 Å. This octahedron of metal ions is surrounded by a largely hydrophobic exterior presented by the organic ligands. The exceptions to this are two orthogonal, non-intersecting, hemi-circumferal seams extending from equatorial copper to equatorial copper via a lanthanide atom (Fig. 4). These hydrophilic seams comprise two nitrate anions, one hydroxide anion and a water molecule.

Both structures contain included methanol molecules which are involved in hydrogen bonding interactions with the main molecule. One fragment binds weakly to the hydroxide anion on Cu(1) (O(10)—O(11) = 2.77 Å in **1**, 2.92 Å in **2**) and the other to the water molecule on the lanthanide atom (O(9)—O(21) = 2.73 Å in **1**, 2.68 Å in **2**). This water

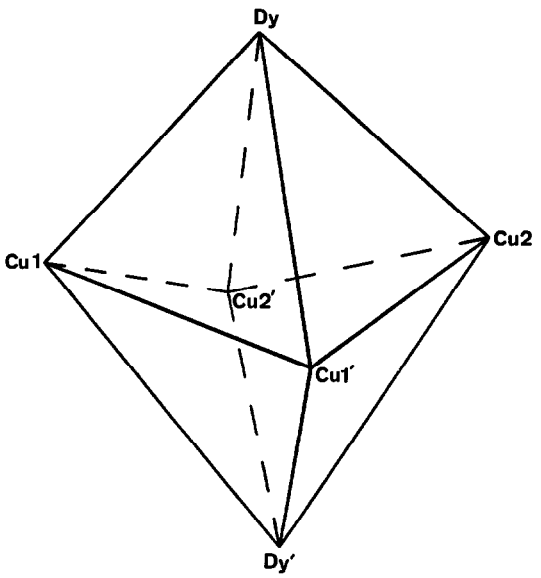

Fig. 3. The distorted octahedron of metal atoms in **1**. Metal–metal distances are, in **1**, Cu(1)—Dy 3.57, Cu(2)—Dy 3.58, Cu(1)—Cu(2′) 3.72, Cu(1)—Cu(1′) 3.77, Cu(2)—Cu(2′) 3.78 Å and in **2**, Cu(1)—Gd 3.59, Cu(2)—Gd 3.60, Cu(1)—Cu(2′) 3.72, Cu(1)—Cu(1′) 3.77, Cu(2)—Cu(2′) 3.77 Å.

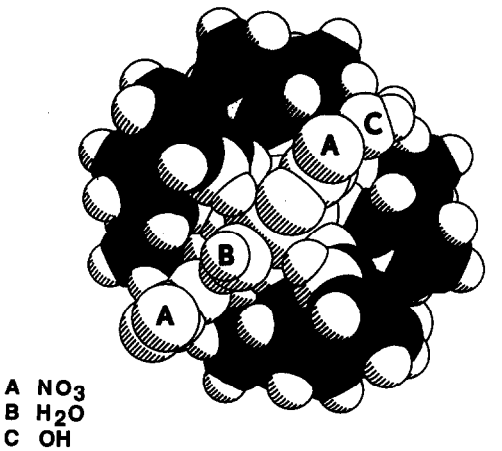

Fig. 4. Space filling representation of **1** viewed down the Ln—Ln axis showing the largely hydrophobic exterior and the central hydrophilic belt.

molecule, in turn, forms a second intramolecular hydrogen bond to the nitrate group attached to Cu(2) (O(9)—O(81) = 2.80 Å in **1**, 2.85 Å in **2**). There are also intramolecular hydrogen bonds between the protonated 2-pyridone ligands and the nitrate anions, in **1** N(3)—O(72) = 3.04, N(6)—O(72) = 2.79 Å, in **2** N(3)—O(72) = 3.12, N(6)—O(72) = 2.97 Å.

Although 2-pyridone and its derivatives have previously been employed to form homobimetallic compounds,[7,8] as far as we are aware they have not, prior to this work, been used to bridge heterometals. That 2-pyridone will do so suggests that a large range of mixed-metal compounds involving this type of organic ligand could be synthesized. The ready availability of many, varied, substituted derivatives of this basic ligand also leads to the possibility of fine tuning such polymetallic systems, not only by choice of metal combinations but also by choice of ligand.

Acknowledgement—We thank the SERC for a Research Studentship (R.E.P.W.) and for funds for the diffractometer.

REFERENCES

1. D. Baghurst, A. M. Chippendale and D. M. P. Mingos, *Nature* 1988, **332**, 311.
2. T. Kumagai, W. Kondo, H. Yokota, H. Minamiue and S. Mizuta, *Chem. Lett.* 1988, 551 and refs therein.
3. D. M. L. Goodgame, D. J. Williams and R. E. P. Winpenny, *J. Chem. Soc., Chem. Commun.* 1988, 437.
4. G. M. Sheldrick, SHELXTL. An Integrated System for Solving, Refining and Displaying Crystal Structures from Diffraction Data, Revision 4.1. University of Göttingen, F.R.G. (1983).

5. *International Tables for X-ray Crystallography*, Vol. IV, pp. 99–143. Kynoch Press, Birmingham, U.K. (1974).
6. D. M. L. Goodgame, D. J. Williams and R. E. P. Winpenny, *Polyhedron* 1988, **7**, 1299.
7. Y. Nishida and S. Kida, *Bull. Chem. Soc. Jpn* 1985, **58**, 383.
8. D. P. Bancroft, F. A. Cotton, L. K. Falvello and W. Schwotzer, *Inorg. Chem.* 1986, **25**, 763 and refs therein.

Polyhedron Vol. 8, No. 12, pp. 1537–1544, 1989
Printed in Great Britain

0277–5387/89 $3.00+.00
© *1989* Pergamon Press plc

BRIDGING RATHER THAN CHELATION IN THE SUBSTITUTION CHEMISTRY OF THE OSMIUM(I) COMPLEX $[Os_2(MeCO_2)_2(CO)_6]$ WITH POTENTIALLY CHELATING PHOSPHINES AND ARSINES

ANTONY J. DEEMING,* DIDIER NUEL, NEIL P. RANDLE and CAROLINE WHITTAKER

Department of Chemistry, University College London, 20 Gordon Street, London WC1H 0AJ, U.K.

(*Received* 18 *January* 1989; *accepted* 3 *February* 1989)

Abstract—Substitution of the osmium(I) dimer $[Os_2(MeCO_2)_2(CO)_6]$ with monophosphines has been previously shown to give mono- and disubstituted products with the introduced ligands exclusively *trans* to the Os—Os bond. This has allowed the preparation of the complexes, $[Os_2(MeCO_2)_2(CO)_4(PPh_3)(\eta^1\text{-L})]$ and $[Os_2(MeCO_2)_2(CO)_4(\eta^1\text{-L})_2]$, in which the ligands L are $Ph_2PCH_2PPh_2$ (dppm), $Ph_2PCH_2CH_2PPh_2$ (dppe) or $1,2\text{-}C_6H_4(AsMe_2)_2$ (diars). These ligands are normally found to be chelating or bridging but here are coordinated through a single heteroatom, but these complexes show no tendency to lose CO ligands *cis* to the metal–metal bonds to allow the ligands L either to chelate or bridge. There is, however, a strong tendency to form oligomers with bridging diphosphine ligands linking separate Os_2 groups, but the designed synthesis of chains of Os_2 units has failed because of slow redistribution reactions involving cleavage of the Os—L—Os bridges.

It is very easy to substitute the axial CO ligands (those *trans* to the Os—Os bond) of the osmium(I) dimer $[Os_2(MeCO_2)_2(CO)_6]$ (**1**), to give the complexes $[Os_2(MeCO_2)_2(CO)_4L_2]$ (L = PPh_3, PMe_2Ph, py, MeCN, MeNC).[1–3] We have been unable to substitute the CO ligands *cis* to the Os—Os bond.[3] This large difference in lability between the different CO sites has allowed us to label the axial CO sites selectively and to observe very slow intramolecular scrambling between axial and equatorial ligands ($t_{1/2}$, *ca* 6 days at 20°C). It is difficult to synthesize anything but the disubstituted species by direct substitution, but the monosubstituted compounds $[Os_2(MeCO_2)_2(CO)_5L]$ may be prepared by using the ligand L under mild conditions to displace the coordinated THF ligand from $[Os_2(MeCO_2)_2(CO)_5(THF)]$ prepared from **1** in refluxing THF.[3]

We report here our attempts to establish how difficult it really is to substitute more than two CO ligands per dimer by introducing readily chelating or bridging bidentate ligands into the axial positions. We have found no evidence that monodentate diphosphine or diarsine ligands, L, in the complexes $[Os_2(MeCO_2)_2(CO)_4(\eta^1\text{-L})_2]$, compound **2** (L = $Ph_2PCH_2PPh_2$, dppm), compound **3** (L = $Ph_2PCH_2CH_2PPh_2$, dppe) and compound **4** (L = $1,2\text{-}(Me_2As)_2C_6H_4$, diars), can become bidentate by displacing an adjacent CO ligand even under rather forcing conditions. In none of our work have we been able to displace the CO *trans* to acetate. However, we have been able to use this property to build compounds with Os_2 units linked by dppm and dppe bridges, and have attempted to construct chain and rings of Os_2 units linked in this way. Although we have evidence for catenation and ring formation in this system, controlled synthesis of such compounds is impaired by slow Os—P bond cleavage leading to mixed products. Ruthenium analogues of some of the osmium compounds reported in this paper have been described recently, in particular $[Ru_2(MeCO_2)_2(CO)_4(\eta^1\text{-dppm})_2]$ and the polymer $[Ru_2(MeCO_2)_2(CO)_4(\mu\text{-dppm})]_n$.[4]

* Author to whom correspondence should be addressed.

RESULTS AND DISCUSSION

Synthesis and studies on η^1-diphosphine and η^1-diarsine compounds

Reaction of $[Os_2(MeCO_2)_2(CO)_6]$ (**1**) with a three-fold excess of the diars ligand in refluxing chloroform gave a 58% yield of the compound $[Os_2(MeCO_2)_2(CO)_4(\eta^1\text{-diars})_2]$ (**2**) (Scheme 1). The IR ν(CO) spectrum is very similar to that of $[Os_2(MeCO_2)_2(CO)_4(PMe_2Ph)_2]$;[3] ν(CO)($CHCl_3$) 2006vs, 1976m, 1925vs and 1907sh cm^{-1} for **2**, compared with 2011vs, 1969m, 1938vs and 1907w cm^{-1} for the PMe_2Ph complex (Table 1). We have been able to use spectra of this characteristic kind to identify di-axially substituted tetracarbonyl Os_2 complexes. On its own this evidence would require each diars ligand to be axially coordinated through one arsenic atom and corroboration of this comes from the ^1H NMR spectrum. Three methyl singlets in the ratio 12 : 12 : 6 are assigned to the coordinated and free $AsMe_2$ groups and the $MeCO_2$ ligands, respectively (Table 1). Compound **2** is rapidly formed in refluxing chloroform, but even in refluxing toluene over 48 h there is no further CO substitution even though the η^1-diars is ideally positioned to chelate. In none of our work on this system have we been able to displace the CO *trans* to acetate.

Likewise, reactions of **1** with an excess of dppm or dppe give the complexes $[Os_2(MeCO_2)_2(CO)_4(\eta^1\text{-L})_2]$ (**3**) (L = dppm) and (**4**) (L = dppe) (Scheme 1), whose IR and NMR spectra are totally consistent with the η^1-modes of coordination of the diphosphines. The clearest evidence for this comes from $^{31}P\{^1H\}$ NMR spectra. For example, free dppm gives a singlet at δ −22.2, whereas **3** gives an AA′XX′ spectrum with the multiplets centred at δ −26.8 and 17.2 for free and coordinated PPh_2 groups, respectively (Table 1 and Fig. 1). The occurrence of an AA′XX′ rather than an AX spectrum results from there being a substantial spin–spin coupling between the dppm ligands across the Os_2 unit. Simulation of this spectrum for **3** gave $^3J_{AA}$ = 60 Hz for the P—Os—Os—P coupling constant, which is close to the corresponding value of 59.3 Hz for $[Os_2(MeCO_2)_2(CO)_4(PMe_2Ph)(PPh_3)]$,[3] but lower than the value of 115 Hz for $[Ru_2(MeCO_2)_2(CO)_4(\mu^1\text{-dppm})_2]$.[4]

As with the η^1-diars compound (**2**), compounds **3** and **4** show no tendency to lose CO ligands. We have not been able to prepare $[Os_2(MeCO_2)_2(CO)_5(\eta^1\text{-dppm})]$ by the direct action of dppm (1 mol/mol dimer), since the first and second substitution reactions have similar rates and this compound reacts further with itself to form chains (see later). To synthesize compounds with one η^1-diphosphine ligand we reacted $[Os_2(MeCO_2)_2(CO)_5(PPh_3)]$ with the diphosphine. Since the pentacarbonyl compounds cannot be formed directly from **1**, compound **1** was heated in refluxing tetrahydrofuran until $[Os_2(MeCO_2)_2(CO)_5(THF)]$ was formed quantitatively. Subsequent treatment of this with PPh_3 yields the corresponding pentacarbonyl compound. Reactions of this PPh_3 complex with the appropriate diphosphine yields the compounds $[Os_2(MeCO_2)_2(CO)_4(PPh_3)(\eta^1\text{-L})]$ (**5**) (L = dppm) and (**7**) (L = dppe). When 1 mol of dppm per mol of $[Os_2(MeCO_2)_2(CO)_5(PPh_3)]$ is used, compound (**5**) is only a minor product (20%); the major product is the dppe-bridged compound $[\{Os_2(MeCO_2)_2(CO)_4(PPh_3)\}_2(\mu\text{-dppm})]$ (**6**) (70%). Likewise, the μ-dppe compound (**8**) is formed in the reaction with dppe (Scheme 2). Even when a two-fold excess of dppe is used, a 21% yield of **8** accompanies the formation of **7** (51%). This implies that the uncoordinated PPh_2 groups of compounds **5** and **7** compete very effectively with the free dppm or dppe for substitution of the starting material $[Os_2(MeCO_2)_2(CO)_5(PPh_3)]$. Compounds **5** and **7** are thermally stable in refluxing xylene over 48 h; again no further CO substitution occurs.

These results led us to explore the possibility of building chains of Os_2 units linked by dppm ligands.

Synthesis of dppm-*bridged compounds*

The reaction of **1** with dppm (0.5 mol/mol Os_2) does not lead specifically to $[\{Os_2(MeCO_2)_2(CO)_5\}_2(\mu\text{-dppm})]$ (**9**) but to a complex mixture. This was expected because our earlier work had

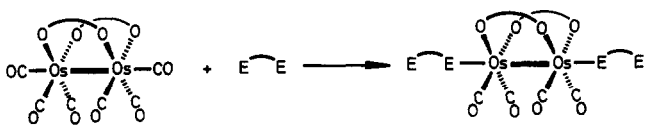

(1)

(2) (E⌒E = diars)
(3) (E⌒E = dppm)
(4) (E⌒E = dppe)

Scheme 1.

Table 1. IR, ^1H and $^{31}P\{^1H\}$ NMR data for new compounds

Compound	$\nu(CO)^a$ (cm^{-1})	$\nu(CO_2)^a$ (cm^{-1})	$\delta(H)^b$	$\delta(P)^c$
2	2006s 1976vs 1925vs 1907m	1600m 1450m	7.68(m,C_6H_4) 1.80(s,$AsMe_2$) 1.78(s,$AsMe_2$) 1.73(s,$MeCO_2$)	
3	2010vs 1967m 1934vs 1900w	1574s 1434m	7.30(m,Ph) 3.35(m, CH_2) 1.39(s,$MeCO_2$)	17.2(m) −26.8(m)
4	2009vs 1966m 1933vs 1900w	1574s 1434m	7.33(m,Ph) 2.54(m,CH_2) 2.05(m,CH_2) 1.52(s,$MeCO_2$)	19.6(m) −11.8(m)
5	2010vs 1967m 1935vs 1902w	1576s 1442m	7.44(m,Ph) 7.19(m,Ph) 3.36(dd,CH_2, J 9.0,11.0) 1.48(s,$MeCO_2$)	19.2(d) 16.6(dd) −27.0(d)
6	2010vs 1968m 1936vs 1902w	1576s 1442m	7.44(m,Ph) 7.15(m,Ph) 4.15(t,CH_2) 1.65(s,$MeCO_2$)	18.4(m) 16.1(m)
7	2010vs 1967m 1935vs 1901w	1575s 1444m	7.44(m,Ph) 7.23(m,Ph) 2.61(m,CH_2) 2.05(m,CH_2) 1.56(s,$MeCO_2$)	19.1(m)[d] −11.5(d)
8	2010vs 1966m 1935vs 1900w	1576s 1444s	7.41(m,Ph) 2.52(m,CH_2) 1.50(s,$MeCO_2$)	19.3(s,br)[e]
9	2071vs 2003m 1978vs 1925m	1568vs 1444m	7.30(m,Ph) 4.18(t,CH_2) 1.98(s,$MeCO_2$)	18.7(s)
10	2071vs 2000vs 1976vs 1924m	1570vs 1444m	7.38(m,Ph) 2.51(m,br,CH_2) 1.75(s,$MeCO_2$)	23.2(s)
12	2011vs 1968m 1937vs 1900w	1576s 1571s 1446s 1442s	7.18(m,Ph) 4.20(m,br,CH_2) 1.88(s,$MeCO_2$) 1.71(s,$MeCO_2$)	17.2(s) 15.5(s)

[a] Recorded in $CHCl_3$.

[b] Recorded in $CDCl_3$ at room temperature at 200 MHz.

[c] Recorded in $CDCl_3$ at 80.98 MHz relative to 80% H_3PO_4; free ligands: PPh_3 δ −5.8, dppm δ −21.0, dppe δ −12.3.

[d] Overlapping doublet and doublet doublet.

[e] Signals overlap.

indicated that substitution of the second CO of **1** is at least as fast as the first, so that monosubstituted species are not formed specifically. However, compound **9** can be formed in a pure state by reaction of dppm with a 10-fold excess of compound **1**, from which it is easily separated by TLC at the end of the reaction. We were able to synthesize the dppm compound (**9**) and the dppe analogue (**10**) in this way (Scheme 3). These compounds are easy to characterize since they each show a single $^{31}P\{^1H\}$ NMR resonance in the region expected for coordinated ligand and the ν(CO) spectrum is characteristic of a pentacarbonyl compound; ν(CO) for **9** in chloroform; 2071vs, 2003vs, 1978vs and 1925m cm^{-1}, compared with 2072vs, 2001vs, 1978s, and 1922m cm^{-1} for $[Os_2(MeCO_2)_2(CO)_5(PPh_3)]$. Thus the pentacarbonyl and tetracarbonyl Os_2 units can be easily distinguished by their IR spectra.

This synthetic method can then be applied to making three Os_2 units linked by two μ-dppm ligands. Using the compound $[Os_2(MeCO_2)_2(CO)_4(\eta^1\text{-dppm})_2]$ (**3**) as the starting "diphosphine ligand", reaction with a large excess of **1** gave a mixture of **1** and the compound $[Os_2(MeCO_2)_2(CO)_5(\mu\text{-dppm})Os_2(MeCO_2)_2(CO)_4(\mu\text{-dppm})Os_2(MeCO_2)_2(CO)_5]$ (**11**), more simply formulated as $[Os_6(MeCO_2)_6(CO)_{14}(dppm)_2]$. The formation of **11** was followed by $^{31}P\{^1H\}$ NMR spectra which demonstrated that this method led to **11**, but over a period, redistribution of the ligands led to its breakdown. Thus a solution of **3** and **1** (1 : 10 mol ratio) in d^6-benzene was prepared and the spectrum recorded immediately and then periodically over 10 days. After 30 min at room temperature the spectrum of **3** had disappeared to be replaced by signals in a 3 : 1 ratio for coordinated and free PPh_2 groups, respectively. The signal at δ −27 is like that

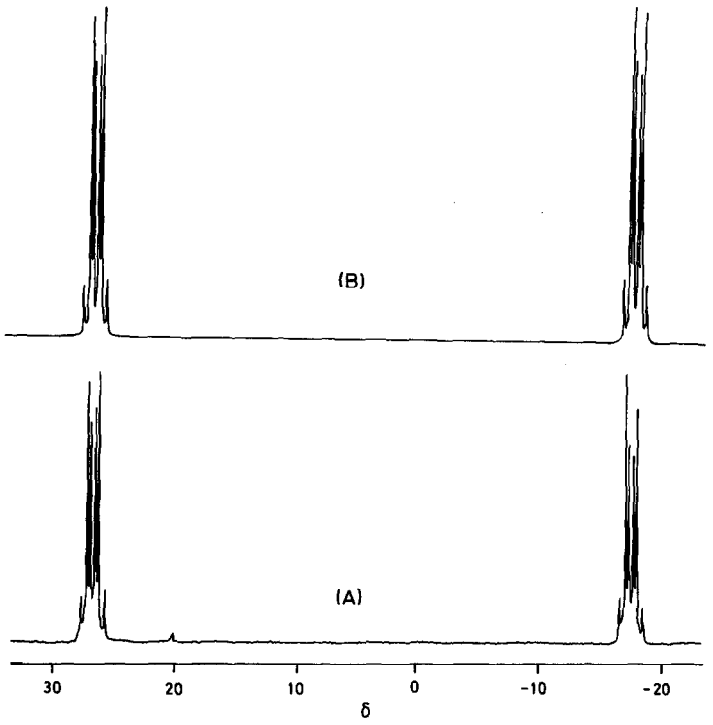

Fig. 1. $^{31}P\{^{1}H\}$ NMR spectra: (A) a $CDCl_3$ solution of $[Os_2(MeCO_2)_2(CO)_4(\eta^1\text{-dppm})_2]$ (3) and (B) the simulated spectrum using $J(PCP) = 70$ Hz and $J(POs_2P) = 60$ Hz.

for free PPh_2 in **3**, but the other signal centred at δ +16 is a complex multiplet (at least 24 lines) consistent with overlapping multiplets of a second-order spectrum and with the formation of $[Os_2(MeCO_2)_2(CO)_5(\mu\text{-dppm})Os_2(MeCO_2)_2(CO)_4(\eta^1\text{-dppm})]$, the species one would expect to be the initial product. After 4 h the spectrum had simplified and was dominated by an AA'BB' pattern (δ 19.0 and 15.8) which we assign to $[Os_6(MeCO_2)_6(CO)_{14}(dppm)_2]$ (**11**) with the complete loss of signals for free PPh_2 around δ −27. (The same spectrum was obtained immediately on mixing the complexes **3** and $[Os_2(MeCO_2)_2(CO)_5(THF)]$ in 1 : 10 mol ratio in C_6H_6. Clearly the THF ligand is more rapidly displaced than CO, but the THF compound in excess is unstable and the solution becomes dark brown in 1 h.) Analysis of the AA'BB' spectrum gave the values $J(POs_2P) = 42$ Hz and $J(PCH_2P) = 32$ Hz, both values smaller than the corresponding values for compound **3**. Bridging will open the PCP angle which is expected to lower the value of $J(PCH_2P)$.

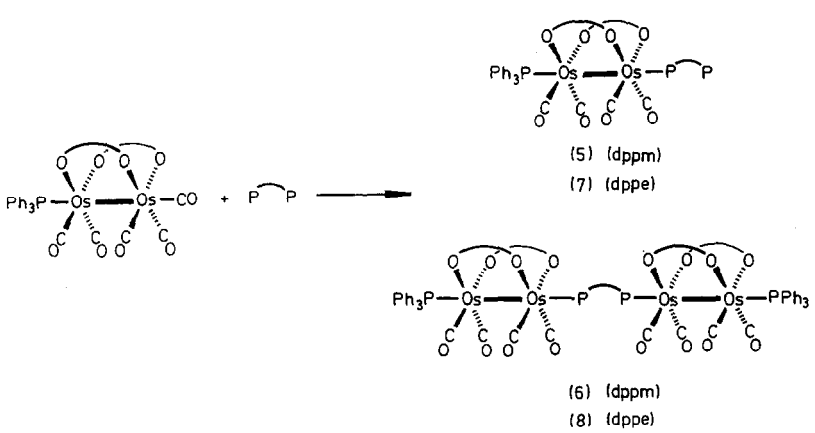

Scheme 2.

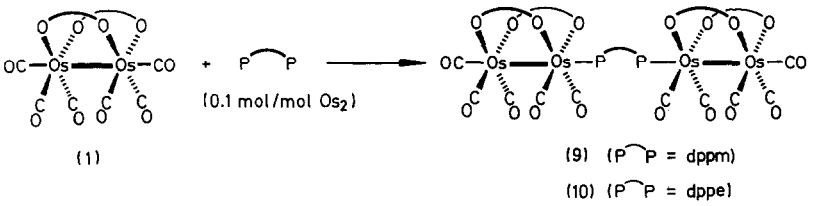

Scheme 3.

If the Os—P bonds were completely inert at room temperature, no further reaction of compound **11** with **1** could occur, but over the next few hours and days the spectrum changed. After 24 h a singlet at δ 18.7 had grown to about the same intensity as that of the AA'BB' signals of **11** and after 10 days the singlet predominated with **11** only in trace amounts. The final product is $[\{Os_2(MeCO_2)_2(CO)_5\}_2(\mu\text{-dppm})]$ (**9**). This is the expected product if cleavage of Os—P bonds of **11** occurred to give transient η^1-dppm compounds, which then reacted with the excess of complex **1** to reform a μ-dppm ligand. Under the conditions of an excess of **1** we would predict that all the dppm ligand would be incorporated into compound **9**. The reaction of **11** with **1** to give two molecules of **9** is stoichiometrically precise and the vacant coordination site created by the cleavage of an Os—P must be filled by the CO subsequently displaced when **1** reacts with the η^1-dppm intermediate. Thus the conversion can only be quantitative if no CO is lost from solution. Attempts to isolate compound **11** by separating the reaction mixture (TLC) when **11** predominated in solution gave only impure samples. We also monitored the reaction by IR. In the early stages absorptions of tetracarbonyl, pentacarbonyl and hexacarbonyl species were apparent but only pentacarbonyl and hexacarbonyl after 10 days, that is compounds **9** and **1**, respectively. These reactions are summarized in Scheme 4.

Further evidence for the cleavage of Os—P bonds in this system came from the reaction of $[\{Os_2(MeCO_2)_2(CO)_5\}_2(\mu\text{-dppm})]$ (**9**) with an excess of dppm, in an attempt to synthesize a complex with two Os_2 units bridged by dppm and with terminal uncoordinated PPh_2 groups. Instead, complete conversion to $[Os_2(MeCO_2)_2(CO)_4(\eta^1\text{-dppm})_2]$ (**3**) occurred. Thus in this Os_2/dppm system, an excess of dppm will always lead to **3** and a deficiency of dppm, that is an excess of $[Os_2(MeCO_2)_2(CO)_6]$ (**1**), will lead to **9**, however the particular components are introduced.

A simple direct way to grow chains of Os_2 units bridged by dppm might be to react precisely equi-

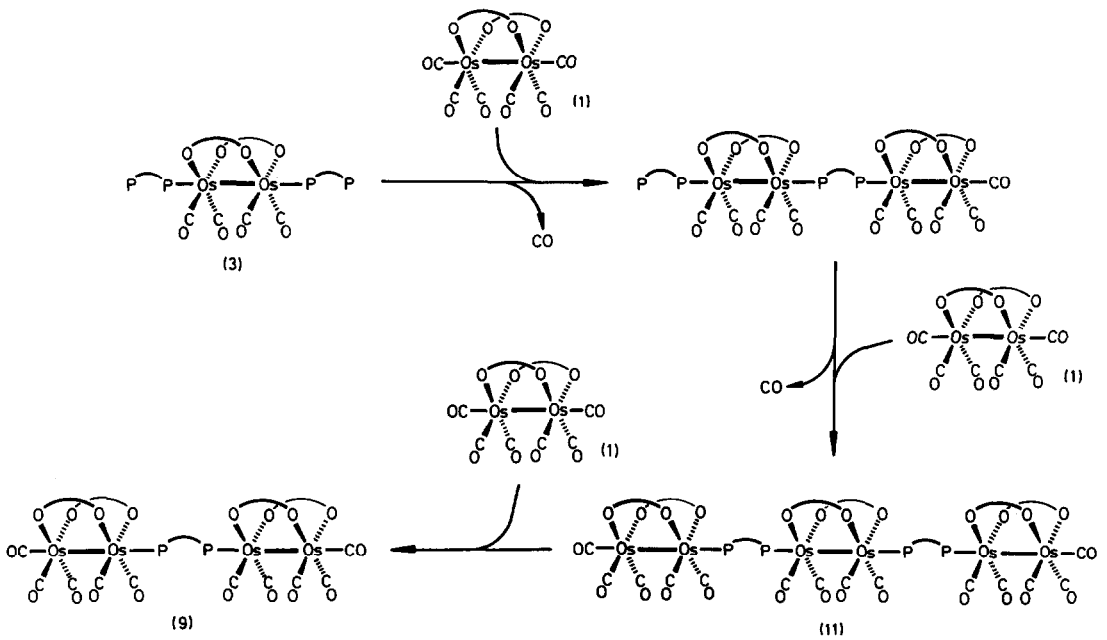

Scheme 4.

molar amounts of $[Os_2(MeCO_2)_2(CO)_6]$ (**1**) and dppm. An accurately equimolar solution of these compounds in $CDCl_3$ was monitored by its $^{31}P\{^1H\}$ NMR spectrum. Changes occur smoothly over 72 h at room temperature, by which time all traces of any signal for uncoordinated PPh_2 had disappeared and the IR spectrum contained only absorptions for a tetracarbonyl species (ν(CO)($CHCl_3$): 2009vs, 1967m, 1933vs and 1907w cm^{-1}). Therefore we assign the product the formula $[Os_2(MeCO_2)_2(CO)_4(\mu\text{-dppm})]_n$. If the compound is a linear chain, it must contain > 50 Os_2 units since $> 2\%$ of chain termini would have been detected spectroscopically. That is the molar mass must be $> 50{,}000$ and yet the compound is still slightly soluble in chloroform. However, the compound is not in a single form since four singlets of non-integral intensities are observed in the $^{31}P\{^1H\}$ NMR spectrum in the coordinated PPh_2 region (δ 17.2, 16.8, 16.3 and 15.5) (Fig. 2), indicating the presence of various forms. TLC gave several broad ill-defined bands; one band of which gave just two phosphorus signals at δ 17.2 and 15.5. Attempts to grow crystals for an X-ray structure determination gave only microcrystals. The compound may be a high molar mass linear polymer since $[Ru_2(MeCO_2)_2(CO)_4(\mu\text{-MeSCH}_2\text{SMe})]$ has been shown to be such a polymer with two crystallographically different Ru_2 units alternating along the chain.[4] The different NMR signals might therefore be for non-equivalent links in the polymer chain. However, because of the significant solubility of **12** we believe that at least one form of the compound might be cyclic. Even though the dppm ligands are coordinated axially there is sufficient flexibility in the system to get cyclic oligomers. In the absence of more information the nature of this material remains uncertain.

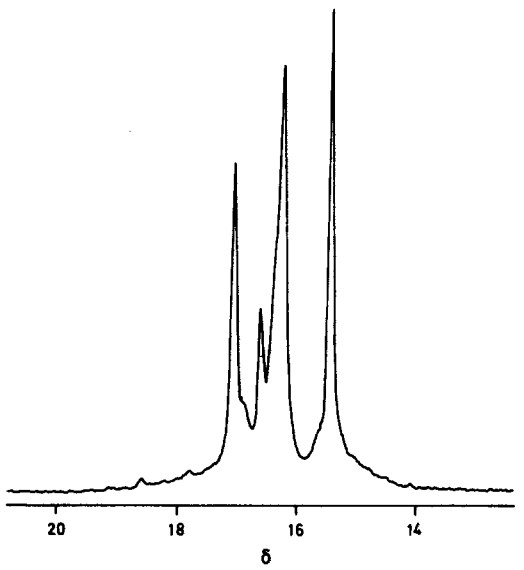

Fig. 2. $^{31}P\{^1H\}$ NMR spectrum of $[Os_2(MeCO_2)_2(CO)_4(\mu\text{-dppm})]_n$ formed from an equimolar mixture of **1** and dppm in $CDCl_3$ over 70 h at room temperature.

EXPERIMENTAL

The compound $[Os_2(MeCO_2)_2(CO)_6]$ (**1**) was prepared from $[Os_3(CO)_{12}]$ and acetic acid[1] and its derivative $[Os_2(MeCO_2)_2(CO)_5(PPh_3)]$[3] from the hexacarbonyl as reported. The ligands dppm and dppe were obtained from Aldrich plc and diars was synthesized by known methods. Reactions but not work-up procedures were carried out under nitrogen. TLC was carried out with Keiselgel HF 254 (Merck) and the petroleum ether used as eluant mixtures had b.p. 30–40°C. NMR spectra were recorded on a Varian XL200 and IR spectra on a Perkin–Elmer PE983 spectrometer.

Substitution of $[Os_2(MeCO_2)_2(CO)_6]$ (**1**) *with an excess of* diars

A lemon-yellow solution of compound **1** (0.050 g) and diars (0.065 cm^3, *ca* 3 mol/mol Os_2) in chloroform (20 cm^3) was refluxed for 1 h. Removal of the solvent gave a yellow oil, which was washed several times with pentane to remove excess of ligand and to leave a residual lemon-yellow solid, which was recrystallized from dichloromethane–hexane mixtures to give $[Os_2(MeCO_2)_2(CO)_4(\eta^1\text{-diars})_2]$ (**2**) as yellow crystals (0.035 g, 58%) (Found: C, 28.9; H, 3.4. $C_{28}H_{38}As_4O_8Os_2$ requires: C, 28.4; H, 3.2%).

Substitution of $[Os_2(MeCO_2)_2(CO)_6]$ (**1**) *with an excess of* dppm

A solution of dppm (0.290 g, 10 mol/mol Os_2) and compound **1** (0.050 g) in benzene (25 cm^3) was refluxed for 1 h. The solvent was removed under reduced pressure and the pale yellow residue separated by TLC (eluant: petroleum ether–CH_2Cl_2, 2:3 v/v). The top, colourless band gave unreacted dppm and the very pale yellow band below it gave $[Os_2(MeCO_2)_2(CO)_4(\eta^1\text{-dppm})_2]\cdot 0.5CH_2Cl_2$ (**3**) as pale yellow crystals (Found: C, 49.1; H, 3.6; Cl, 2.4; P, 9.3. $C_{58.5}H_{51}ClO_8Os_2P_4$ requires: C, 49.4; H, 3.6; Cl, 2.5; P, 8.7%).

Substitution of $[Os_2(MeCO_2)_2(CO)_6]$ (**1**) *with an excess of* dppe

This reaction was carried out similarly, from **1** (0.050 g) and dppe (0.300 g) to give $[Os_2(Me$

$CO_2)_2(CO)_4(\eta^1$-dppe$)_2]$ (**4**) as pale yellow crystals (0.068 g, 64%) (Found: C, 51.6; H, 3.7; P, 8.7. $C_{60}H_{54}O_8Os_2P_4$ requires: C, 51.2; H, 3.8; P, 8.8%).

Reaction of $[Os_2(MeCO_2)_2(CO)_5(PPh_3)]$ *with* dppm

A solution of the PPh_3 compound (0.050 g) and dppm (0.018 g, 1 mol/mol Os_2) in chloroform (20 cm^3) was refluxed for 20 min. Removal of the solvent and TLC work-up (eluant: CH_2Cl_2–petroleum ether–diethyl ether, 13:6:1 v/v/v) gave two pale yellow bands which were extracted with dichloromethane to give two products. Recrystallization of these from CH_2Cl_2–hexane mixtures gave $[Os_2(MeCO_2)_2(CO)_4(PPh_3)(\eta^1$-dppm$)]$ (**5**) (0.018 g, 20%) (Found: C, 48.1; H, 3.3; P, 7.15. $C_{51}H_{43}O_8Os_2P_3$ requires: C, 48.7; H, 3.4; P, 7.4%) and $[\{Os_2(MeCO_2)_2(CO)_4(PPh_3)\}_2(\mu$-dppm$)]$ (**6**) (0.042 g, 70%) (Found: C, 43.6; H, 3.1; P, 5.7. $C_{77}H_{64}O_{16}Os_4P_4$ requires: C, 43.4; H, 3.0; P, 5.8%), each as creamy-yellow crystals.

Reaction of $[Os_2(MeCO_2)_2(CO)_5(PPh_3)]$ *with* dppe

A similar reaction to that above using the PPh_3 complex (0.100 g) and dppe (0.090 g, 2 mol/mol Os_2) gave, after TLC separation (eluant: petroleum ether–CH_2Cl_2, 1:1 v/v), bands yielding two products each as pale yellow–green crystals from CH_2Cl_2–methanol mixtures: $[Os_2(MeCO_2)_2(CO)_4(PPh_3)(\eta^1$-dppe$)]$ (**7**) (0.063 g, 52%) (Found: C, 48.7; H, 3.4; P, 7.1. $C_{52}H_{45}O_8Os_2P_3$ requires; C, 49.1; H, 3.5; P, 7.3%) and $[\{Os_2(MeCO_2)_2(CO)_4(PPh_3)\}_2(\mu$-dppe$)]$ (**8**) (0.025 g, 21%) (Found: C, 43.6; H, 3.1; P, 6.1. $C_{78}H_{66}O_{16}Os_4P_4$ requires: C, 43.7; H, 3.1; P, 5.8%).

Thermolysis of η^1-dppm, η^1-dppe *and* η^1-diars *complexes*

(a) $[Os_2(MeCO_2)_2(CO)_4(PPh_3)(\eta^1$-dppm$)]$ (**5**). A solution of this complex in xylene was heated under reflux for 48 h. Removal of the solvent and TLC work-up (eluant: petroleum ether–CH_2Cl_2, 1:1 v/v) gave the starting material (85–90%) as the only observed carbonyl compound.

(b) $[Os_2(MeCO_2)_2(CO)_4(PPh_3)(\eta^1$-dppe$)]$ (**7**). A similar treatment gave a 90% recovery of compound **7**.

(c) $[Os_2(MeCO_2)_2(CO)_4(\eta^1$-diars$)_2]$ (**2**). The IR spectrum of a solution of this complex in refluxing toluene over 48 h showed no change and chromatographic work-up gave **2** (90%) as the only observed metal carbonyl compound.

Substitution of $[Os_2(MeCO_2)_2(CO)_6]$ (**1**) *with a deficiency of* dppm

A solution of dppm (0.015 g, 0.1 mol/mol Os_2) in benzene (10 cm^3) was added dropwise to a refluxing solution of **1** (0.130 g) in benzene (15 cm^3) over 30 min, and the reflux was continued for a further 30 min to give a lemon-yellow solution. Removal of the solvent under reduced pressure and TLC work-up (eluant: petroleum ether–CH_2Cl_2, 2:3 v/v) gave two main bands yielding compounds **1** and $[\{Os_2(MeCO_2)_2(CO)_5\}_2(\mu$-dppm$)]\cdot 0.5CH_2Cl_2$ (**9**) (0.036 g, 55% based on dppm) (Found: C, 30.7; H, 2.1; Cl, 2.5; P, 3.7. $C_{43.5}H_{35}ClO_{18}Os_4P_2$ requires: C, 30.65; H, 2.0; Cl, 2.1; P, 3.6%).

Substitution of $[Os_2(MeCO_2)_2(CO)_6]$ *with a deficiency of* dppe

This reaction was carried out similarly with dppe (0.010 g) and **1** (0.165 g) to give $[\{Os_2(MeCO_2)_2(CO)_5\}_2(\mu$-dppe$)]$ (**10**) as orange microcrystals (0.022 g, 52% based on dppe) (Found: C, 32.0; H, 2.1; P, 4.0. $C_{44}H_{36}O_{18}Os_4P_2$ requires: C, 31.5; H, 2.1; P, 3.7%).

Reaction of $[Os_2(MeCO_2)_2(CO)_4(\eta^1$-dppm$)_2]$ (**3**) *with a large excess of* **1** *attempting to synthesize* $[Os_6(MeCO_2)_6(CO)_{14}(dppm)_2]$ (**11**)

A mixture of **1** (0.3750 g) and **3** (0.0788 g, 0.1 mol/mol of **1**) in C_6D_6 (3 cm^3) was prepared in a 10 mm diameter NMR tube. Initially not all of **1** dissolved. The $^{31}P\{^1H\}$ NMR spectrum was recorded immediately and then periodically over 24 h and again after 10 days. The spectra showed that after 4 h 90% of the dppm was in the form of compound **11**, but after 10 days this had converted (> 95%) into $[\{Os_2(MeCO_2)_2(CO)_5\}_2(\mu$-dppm$)]$ (**9**), which could be isolated by TLC.

Reaction of **1** *with an equimolar amount of* dppm

$[Os_2(MeCO_2)_2(CO)_6]$ (0.0500 g) and dppm (0.0288 g, 1.00 mol/mol Os_2) were accurately weighed into a 10 mm diameter NMR tube and dissolved in $CDCl_3$ (2.5 cm^3). The tube was kept at about 15°C and the $^{31}P\{^1H\}$ NMR spectrum recorded over 70 h, by which time there was no detectable signal for uncoordinated PPh_2 groups. The solvent was removed under reduced pressure and the residue separated by TLC (eluant: petroleum ether–CH_2Cl_2, 2:3 v/v) to give several very broad, ill-defined bands of which the strongest was extracted with CH_2Cl_2 to give a pale yellow solid (Found: C, 40.0; H, 2.7; Cl, 0.15; P, 6.0.

$C_{33}H_{28}O_8Os_2P_2$ requires: C, 39.8; H, 2.8; Cl, 0.0; P, 6.2%). The low chlorine content indicates a little CH_2Cl_2 in the crystals; $[Os_2(MeCO_2)_2(CO)_4(dppm)]_{50}(CH_2Cl_2)$ requires: C, 39.8; H, 2.85; Cl, 0.14; P, 6.2%. Recrystallization from CH_2Cl_2–methanol mixtures gave yellow–cream microcrystals, none being suitable for a single-crystal X-ray structure determination.

Acknowledgement—We thank the SERC for a research grant and for a studentship (to N.P.R.).

REFERENCES

1. G. R. Crooks, G. Gamlen, B. F. G. Johnson, J. Lewis and I. G. Williams, *J. Chem. Soc. A* 1969, 2761.
2. J. G. Bullitt and F. A. Cotton, *Inorg. Chim. Acta* 1971, **5**, 406.
3. A. J. Deeming, N. P. Randle, M. B. Hursthouse and R. L. Short, *J. Chem. Soc., Dalton Trans.* 1987, 2473.
4. S. J. Sherlock, M. Cowie, E. Singleton and M. M. de V. Steyn, *Organometallics* 1988, **7**, 1663.

Polyhedron Vol. 8, No. 12, pp. 1545–1548, 1989
Printed in Great Britain

0277–5387/89 $3.00+.00
© 1989 Pergamon Press plc

POLYMERIC COORDINATION OF 4,4′-DITHIODIPYRIDINE WITH COBALT(II), NICKEL(II) AND COPPER(II) HALIDES

J. GUILLERMO CONTRERAS* and HERNÁN CORTÉS

Departamento de Química, Universidad de Concepción, Casilla 3-C, Concepción, Chile

(*Received* 8 *November* 1988; *accepted* 3 *February* 1989)

Abstract—A series of complexes of the type MX_2(4,4′-DTDP)$_2$ (**A**) and MX_2(4,4′-DTDP) (**B**), where M = Co^{II}, Ni^{II} or Cu^{II}, X = Cl, Br or I and 4,4-DTDP is 4,4′-dithiodipyridine, have been prepared and spectroscopically characterized. The chloride and bromide complexes are of type **A** and possess a polymeric octahedral structure, whereas the iodide derivatives are polymeric tetrahedral type **B** species. The copper(II) chloride complex is also type **B**, whereas the bromide derivative can be formulated as Cu_2Br_4(4,4′-DTDP) in which the organic ligand is in a *cis* conformation and bridging two copper atoms. The copper atoms are also bridged by bromide ligands in such a way that each metal atom is tetrahedrally coordinated. Although, a structure consisting of a polymer dimer with each ligand molecule bridging two Cu_2Br_4 units is also possible.

In a previous paper we reported the preparation and characterization of a series of complexes of 4,4′-dithiodipyridine (4,4′-DTDP) with group IIB metal halides.[1] The IR spectra showed that the uncoordinated ligand adopts a *trans* conformation and that both pyridine residues are chemically equivalent. In the coordination compounds, the ligand is bridging two metal halide units to produce a polymeric pseudotetrahedral structure.

Ferraro *et al.*[2] have reported the preparation and characterization of $CoCl_2$(4,4′-DTDP)$_2$ and $CoBr_2$(4,4′-DTDP)$_2$ and found that they possess a polymeric octahedral structure, based on some four IR bands.

Since the N,S- or N,N-coordination are precluded for this ligand unless it adopts a *cis* or *gauche* conformation to accommodate the various stereochemical requirements imposed by the metal ions, it seems clear that even in these cases considerable angular strain needs to be introduced. However, a pure S-coordination cannot be completely ruled out. In an attempt to know more about the coordination capability of this ligand we have prepared and characterized complexes of cobalt(II), nickel(II) and copper(II) halides of the type MX_2(4,4′-DTDP)$_2$ or MX_2(4,4′-DTDP). In order to study the influence of the halogen we have also prepared the cobalt(II) and nickel(II) iodide complexes of the title ligand.

EXPERIMENTAL

The coordination compounds of 4,4′-DTDP were prepared by a general method. To a hot ethanolic solution of the ligand the stoichiometric amount of the appropriate metal halide dissolved in the same solvent, was added. The complexes precipitated out and were filtered off, washed with ethanol and dried. All compounds are insoluble in most common solvents precluding conductivity measurements. Table 1 gives the analytical and magnetic data for the compounds reported here.

The IR and Raman spectra were obtained as described previously.[3,4] The electronic spectra were obtained in Nujol mulls in the range of 200–2500 nm and recorded on a Zeiss PMQ II spectrophotometer. The magnetic measurements were carried out at room temperature (20°C) on a Cahn electrobalance coupled to a digital millivoltmeter and to a permanent magnet of *ca* 8000 *g*.

RESULTS AND DISCUSSION

The free 4,4′-DTDP shows four bands in the region 1400–1650 cm^{-1} that are due to the C=C

* Author to whom correspondence should be addressed.

Table 1. Analytical and magnetic data for the 4,4′-DTDP complexes of cobalt(II), nickel(II) and copper(II) halides

	Complex[a]	C (%)	H (%)	X (%)	M (%)	μ_{eff}(BM)
I	$NiCl_2$(4,4′-DTDP)$_2$	42.0 (42.1)	2.9 (2.8)	12.1 (12.4)	10.9 (10.3)	3.40
II	$NiBr_2$(4,4′-DTDP)$_2$	36.1 (36.4)	2.8 (2.4)	24.4 (24.3)	8.7 (8.9)	3.44
III	NiI_2(4,4′-DTDP)	22.7 (22.5)	1.3 (1.5)	47.3 (47.6)	10.3 (11.0)	3.15
IV	$CoBr_2$(4,4′-DTDP)$_2$	12.6 (12.2)	1.4 (1.2)	24.3 (25.0)	8.7 (8.4)	5.20
V	CoI_2(4,4′-DTDP)	22.8 (22.5)	1.8 (1.5)	47.6 (48.2)	11.4 (11.1)	4.54
VI	$CuCl_2$(4,4′-DTDP)	33.1 (33.8)	1.8 (2.2)	20.1 (20.0)	18.1 (17.9)	2.10
VII	Cu_2Br_4(4,4′-DTDP)	18.5 (18.0)	1.4 (1.2)	47.9 (47.9)	19.1 (19.1)	1.04

[a] 4,4′-DTDP = $C_{10}H_8N_2S_2$; Calculated values are given in parentheses.

and C=N stretching modes of the pyridine rings.[5] At 990 cm^{-1}, the A_1 breathing mode occurs and the bands detected at 803, 725 and 698 cm^{-1} can be assigned to the out-of-plane C—H and C—C deformation modes.[6] The band at 414 cm^{-1} corresponds to a ϕ(C—C) out-of-plane deformation mode.[6,7]

In the coordination compounds of cobalt(II), nickel(II) and copper(II) we have also observed four bands in the 1400–1650 cm^{-1} region, implying that the pyridine residues are equivalent[8] and hence the free and coordinated pyridine groups adopt a *trans* conformation about the S—S bond.

Band I (1562 cm^{-1} in free ligand) shifts by *ca* 15–30 cm^{-1} upon coordination, whereas band IV (1402 cm^{-1} in free ligand) moves to higher frequencies by *ca* 5–20 cm^{-1}. Bands II and III remain unchanged or shift slightly (*ca* 5 cm^{-1}) to higher frequencies.

The free ligand shows a weak feature at 1452 cm^{-1} that is absent in the coordination compounds.

Sinha[9] has shown that a shift greater than 10 cm^{-1} of the ring breathing mode is also an indication of pyridine coodination. As in the 2,2′-DTDP ligand, the γ(C—H) mode observed at 803 cm^{-1} in the free ligand, is shifted slightly in the coordination compounds or disappears to be replaced by two or three bands located at variable frequencies. The ϕ(C—C) mode detected at 698 cm^{-1} shifts by *ca* 15–25 cm^{-1}, appearing as a single band. The same situation is observed for the band at 414 cm^{-1}.

It is worth noting that if one pyridine residue was bonded to the metal and the other uncoordinated, two bands due to this mode should be observed. The lower frequency band would be shifted by *ca* 3–6 cm^{-1} with respect to the free ligand. Since in our case a single band is detected (except for compound **VII**), we can conclude that both pyridine groups are coordinated[5,6,10] to produce a polymeric structure. The complex ($CuBr_2$)$_2$(4,4′-DTDP) deserves special mention, in which the band at 445 cm^{-1} is rather broad, presumably containing two components. In fact, it is likely that in this case the ligand is in a *cis* conformation with the two pyridine groups not being fully equivalent. This effect has been observed in [Cu(OAc)$_2$]$_2$LE where LE is the 1,2-bis(2′-pyridyl)ethane.[11] At room temperature a single broad band located at 417 cm^{-1} suggests a *trans* conformation of the ligand, however at low temperature the band splits into two bands lying at 421 cm^{-1}.

The Raman spectra of all the complexes reported here show the metal–halogen, metal–nitrogen and sulphur–sulphur stretching bands. A very intense emission at *ca* 340 cm^{-1} has also been observed in all cases. Table 2 lists some selected Raman bands for these species. The metal–ligand stretching vibrations were assigned by comparison with previously reported data.[12,13] The metal–halogen stretching bands of compounds **I**, **II** and **IV** correspond to typical values for terminal metal–halogen stretching modes in octahedral complexes, whereas for compounds **III**, **V** and **VI** the frequency values of these modes agree well with those observed for tetrahedral species.

Compound **VII** presents terminal copper–bromide (211 and 201 cm^{-1}) as well as bridging copper–bromide (184 and 188 cm^{-1}) stretching bands, confirming the structure proposed above.

The metal–nitrogen stretching bands have weak intensities and hence their assignments must be taken as only tentative. The ν(S—S) is also weak, though in the complexes of zinc(II), cadmium(II) and mercury(II) shows up with "normal" intensities.[1] An interesting feature appears at 340 cm^{-1}. In all complexes a very strong band at *ca* 340 cm^{-1} is observed. This band must be associated with the C—S bond since it is detected in the pyridine-2-thiol and bis(tolyl)disulphide. It cannot be associated

Table 2. Raman bands for the 4,4′-DTDP complexes of nickel(II), cobalt(II) and copper(II)

Complex[a]	ν(M—X)	ν(M—N)	ν(S—S)	Band at *ca* 340 cm^{-1}
I	213 ms 203 m	283 w 242 w	542 vw	371 m 346 vs 332 s
II	173 vs 152 s	287 w 245 w	542 w	362 m 352 s 339 vs 322 s
III	224 mw 187 s	290 w 241 w	541 m	342 vs
IV	270 m	260 mw	539 mw	341 vs 338 vs
V	183 vs 179 vs	266 vw	547 w	340 vs
VI	312 w 268 mw	239 mw	550 vw?	341 vs
VII	211 m 201 mw 184 m 168 m	278 m 268 w	539 w	362 ms 345 vs

[a] Numbering of the compounds according to Table 1.

with a ring vibration since it is not observed in the pyridine, but detected in tetramethylthiuram disulphide, i.e. a compound that contains a S—S bridge linked to two non-aromatic substituents.[1]

An interesting effect has been observed for this very strong emission. In the octahedral species it shows up split into two or more components, whereas in the tetrahedral ones a single band is observed. A single band was also detected for all tetrahedral species of zinc(II), cadmium(II) and mercury(II). In this sense this band seems to be very sensitive to stereochemistry, though no theoretical explanation could be found. Additional work on this effect for some complexes of other dithiodipyridine is being carried out in our laboratory.

The magnetic moments of all complexes are in the range of high spin values for octahedral and tetrahedral structures. The departure of the corresponding spin-only values must be certainly due to some orbital contribution. Unfortunately, magnetic measurement of a single temperature allows only limited discussion of the stereochemistry of complexes, however the fact is known that tetrahedral cobalt(II) complexes show smaller magnetic moments than the corresponding octahedral ones. The nickel(II) complexes (I) and (II) have moments of 3.40 and 3.44 BM, respectively; these values are in agreement with an octahedral structure.[14] The magnetic moments of freshly prepared samples of compounds I and II consistently gave the same values. These values along with the IR data suggest a polymeric structure of type A (see below).

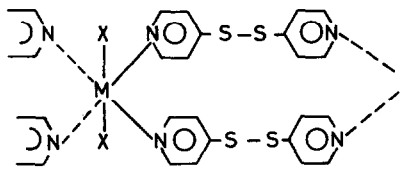

(A)

A similar situation is observed for the $CoBr_2$(4,4′-DTDP)$_2$ (IV) species, for which a magnetic moment of 5.20 BM is observed and hence its A type structure is in agreement with the one proposed by Ferraro and co-workers.[2]

The magnetic moments of complexes III, V and VI are characteristic of a tetrahedral structure.[15] The magnetic moment and the IR data allow us to postulate a polymeric tetrahedral structure for these species:

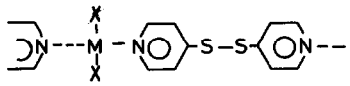

The compound Cu_2Br_4(4,4′-DTDP) (VII) deserves special discussion since its magnetic moment is very low (1.04 BM per copper atom). The IR data suggest that both pyridine residues are coordinated and that the ligand adopts a *cis* configuration. Therefore the structure of this compound is likely to be of type C (see below). Molecular models for this species show that both pyridine groups must be in a face–face configuration and that they are not completely equivalent. The pyridine residues are slightly twisted and not parallel to one another. The angles at the sulphur atoms must be larger than 90°. Alternatively, the structure can consist of a polymer of dimers with each ligand molecule bridging two Cu_2Br_4 units.

The low magnetic moment is probably due to a super-exchange mechanism operating through the bridging bromides and magnetic measurements at several low temperatures are obviously called for.

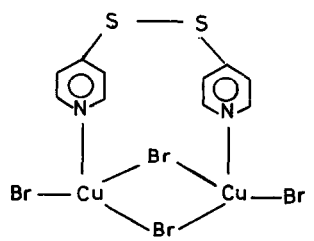

(C)

The electronic spectra of all these species in Nujol mulls show a number of weak absorptions which

are not always easy to assign. Thus, the octahedral nickel(II) complexes show the following bands: 5.26, 9.76, 11.1, 16.3 and 28.6 kK for compound **I** and 4.26, 5.90, 13.5, 16.4 and 22.2 kK for compound **II**. Compound **IV** shows bands at 8.70, 19.7 and 29.4 kK, whereas the tetrahedral complex **V** shows bands at 5.80 and 13.6 kK only. No attempts to assign these bands were made.

Acknowledgement—This work was supported by an operating grant (No. 20.13.55) from the Universidad de Concepción.

REFERENCES

1. J. G. Contreras and H. Cortés, *Spectrochim. Acta A*, in press.
2. J. R. Ferraro, B. B. Murray and N. J. Wieckowicz, *J. Inorg. Nucl. Chem.* 1972, **34**, 231.
3. J. G. Contreras and G. V. Seguel, *Spectrosc. Lett.* 1987, **20**, 591.
4. J. G. Contreras, L. M. Silva-Triviño and M. E. Solís, *Inorg. Chim. Acta* 1988, **142**, 51.
5. M. Keeton and A. B. P. Lever, *Inorg. Chem.* 1971, **10**, 47.
6. J. H. S. Green, W. Kynaston and H. M. Paisley, *Spectrochim. Acta* 1963, **19**, 549.
7. N. S. Grill, R. H. Nuttall, D. E. Scaife and D. W. A. Sharp, *J. Inorg. Nucl. Chem.* 1961, **18**, 79.
8. D. A. Baldwin, A. B. P. Lever and R. V. Parish, *Inorg. Chem.* 1969, **8**, 107.
9. S. P. Sinha, *Spectrochim. Acta* 1964, **20**, 879.
10. R. J. H. Clark and C. S. Williams, *Inorg. Chem.* 1965, **4**, 350.
11. M. Keeton, A. B. P. Lever and B. S. Ramaswamy, *Can. J. Chem.* 1970, **48**, 3185.
12. K. Nakamoto, *Infrared and Raman Spectra of Inorganic and Coordination Compounds*. Wiley, New York (1978).
13. J. R. Ferraro, *Low-Frequency Vibration of Inorganic and Coordination Compounds*. Plenum Press, New York (1971).
14. J. Lewis and R. G. Wilkinson, *Modern Coordination Chemistry*. Interscience, New York (1960).
15. J. Lewis, *Sci. Prog.* 1963, **51**, 452.

Polyhedron Vol. 8, No. 12, pp. 1549–1556, 1989
Printed in Great Britain

0277–5387/89 $3.00+.00
© 1989 Pergamon Press plc

SYNTHESIS AND METAL-COMPLEXING ABILITY OF *m*-XYLYLENEBIS(β-DIKETONES)

ANDREW W. MAVERICK* and DANIEL P. MARTONE

Department of Chemistry, Louisiana State University, Baton Rouge, LA 70803, U.S.A.

and

JULIE R. BRADBURY and JANET E. NELSON

Department of Chemistry, Washington University, St. Louis, MO 63130, U.S.A.

(*Received* 14 *September* 1988; *accepted after revision* 13 *February* 1989)

Abstract—The preparation of the bis(β-diketone) $XBAH_2$ (3,3′-[1,3-phenylenebis(methylene)bis(2,4-pentanedione)]) and five of its derivatives, and a study of their complexation reactions with Cu^{2+}, is reported. Of these ligands (LH_2), only sterically unhindered derivatives of acetylacetone readily yield binuclear copper(II) complexes, Cu_2L_2. The introduction of bulkier groups (Ph, *t*-Bu) into the 2,4-pentanedione portions of the ligands inhibits the complex-forming reaction, resulting in lower yields ($XBBH_2$; see ligand abbreviations in Fig. 1), no reaction ($XBPH_2$) or decomposition ($XBDH_2$). The copper complex of Cl_4XBAH_2 appears to be polymeric; this is probably due to the steric effects of the bulky chlorine atom in the two-position.

We have been interested in the use of new cofacial binuclear transition metal complexes as catalysts for multi-electron redox reactions. The cofacial geometry is attractive in these systems because of the possibility of intramolecular binding and activation of small redox-active substrates. We have concentrated on bis(β-diketones) as ligands for these complexes, because β-diketones form planar complexes with a variety of metal ions and also because the synthetic versatility of the bis(β-diketones) should make the cofacial binuclear complexes accessible for a variety of bridging groups. Our initial report concerned the synthesis of $Cu_2(XBA)_2$ (**1**) (see drawing below; all ligands discussed herein are *meta* isomers),[1] and its structural and spectroscopic properties.

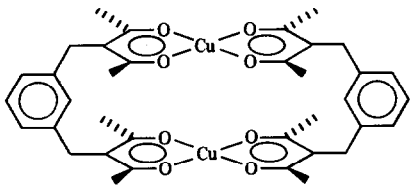

1

More recently we have shown that larger bis(β-diketone) species can undergo selective intramolecular complexation reactions,[2] and we have observed multi-electron redox activity in the bis(β-ketoenamine) complexes, $M_2(BBI)_2$ (**2**), shown below.[3]

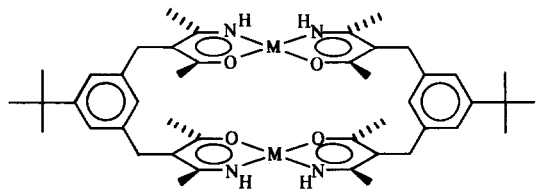

2

We have also been interested in the influence of other substituents in the bis(β-diketone) ligands on the complexation reactions and on the stereochemistry and reactivity of the resulting complexes. Therefore, we have prepared several new *m*-xylylenebis(β-diketones) (**3**) (see Fig. 1); syntheses of these ligands, and a discussion of their ability to form metal complexes, are reported herein.

* Author to whom correspondence should be addressed.

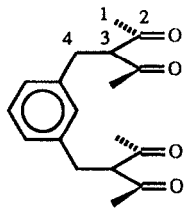

XBAH$_2$, **3a**

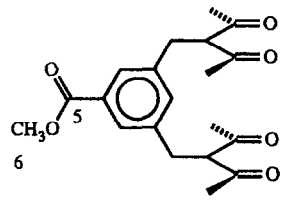

EBAH$_2$, **3b**

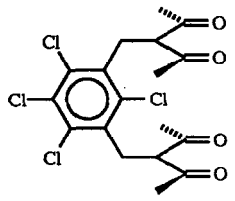

Cl$_4$XBAH$_2$, **3c**

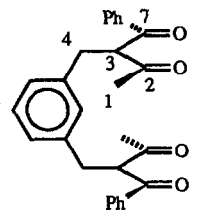

XBBH$_2$, **3d**

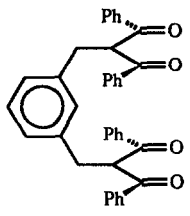

XBDH$_2$, **3e**

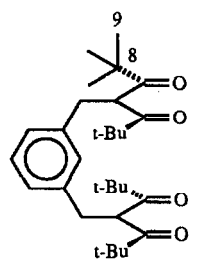

XBPH$_2$, **3f**

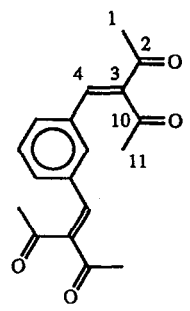

XBE, **4**

Fig. 1. Structures of bis(β-diketones) (**3a–f**) and the unsaturated tetraketone (**4**). Also shown is the numbering scheme used for the NMR spectral data in Table 2.

EXPERIMENTAL

Materials and procedures

The ligand syntheses were carried out under N_2; this led to improved purity of the bis(β-diketone) products. *t*-Butyl alcohol (Mallinckrodt) was purified by treatment with potassium metal and subsequent distillation. Methyl 3,5-bis(bromomethyl)benzoate[4] and 1,3-bis(bromomethyl)-2,4,5,6-tetrachlorobenzene[5] were prepared by literature procedures. Other chemicals and solvents were reagent or spectrophotometric grade and were used as received. Melting points (uncorrected) were measured by using an Electrothermal apparatus. ^{1}H and ^{13}C NMR spectra were recorded on Varian XL300 or Bruker AC100 or AC200 instruments. Microanalyses were performed by Desert Analytics (Tucson, Arizona) or Midwest Laboratories (Indianapolis, Indiana).

*Bis(β-diketones)**

(a) *By nucleophilic substitution*

The general method of Martin and co-workers[6] was used for all six ligands. The appropriate β-

*Abbreviations for β-diketones: acacH = acetylacetone (2,4-pentanedione); bzacH = benzoylacetone (1-phenyl-1,3-butanedione); dbmH = dibenzoylmethane (1,3-diphenyl-1,3-propanedione); dpmH = dipivaloylmethane (2,2,6,6-tetramethyl-3,5-heptanedione); bzacacH = 3-benzylacetylacetone; Cl$_5$bzacacH = 3-(pentachlorobenzyl)acetylacetone. Abbreviations for the new ligands **3** are given in Fig. 1.

Table 1. Synthesis of bis(β-diketones) (**3a–f**) by nucleophilic substitution

Compound	Scale[a]	Reaction time (h)	Yield (%)	Melting point (°C)
$XBAH_2$ (**3a**)	23	20	80	89–92; 105[b]
$EBAH_2$ (**3b**)	17	130	*ca* 60	Oil
Cl_4XBAH_2 (**3c**)	5	15	45	142–144
$XBBH_2$ (**3d**)	30	24	67	87.5–88.5
$XBDH_2$ (**3e**)	15	48	65	130–131
$XBPH_2$ (**3f**)	30	24	*ca* 50	107.5–108.5

[a] Quantity of benzylic dihalide used with 200 cm^3 *t*-butyl alcohol solvent (mmol).

[b] Two different crystal modifications; see Experimental.

diketone (3 mol) was added slowly to a refluxing solution of potassium *t*-butoxide (2 mol) in *t*-butyl alcohol. After 30 min of further refluxing, the appropriate 1,3-bis(bromomethyl)benzene derivative (1 mol) was added in small portions; approximately 1 h later, KI (*ca* 0.25 mol) was added. Variations in reaction time and proportion of solvent are noted in Table 1. After the reaction mixture became acidic to moist litmus, three-fourths of the *t*-butyl alcohol was removed by distillation at atmospheric pressure, and further work-up proceeded as follows.

For $XBAH_2$ (**3a**), $EBAH_2$ (**3b**) and Cl_4XBAH_2 (**3c**), the residue was extracted with H_2O and CH_2Cl_2 and the CH_2Cl_2 layer removed, dried with Na_2SO_4 and evaporated to dryness. Excess acetylacetone was removed from the product under dynamic vacuum at room temperature (24–48 h). $XBAH_2$ (**3a**), when prepared by this method, was obtained as an oil; this material sometimes solidified partially over a period of weeks, and pure solid $XBAH_2$ (m.p. 89–92°C; entirely in the enol form) could be isolated from the mixture by trituration with methanol. $EBAH_2$ (**3b**) was obtained only as an oil; it was further characterized by its mass spectrum (parent ion, *m/e* 360,361) and by NMR (see Tables 2 and 3). Cl_4XBAH_2 (**3c**) was crystallized from toluene.

For $XBBH_2$ (**3d**), the *t*-butyl alcohol was removed completely. Excess benzoylacetone was then removed by dissolving the residue in CH_2Cl_2, extracting with a six-fold excess of 0.4 M

Table 2. ^1H NMR chemical shifts[a]

Atom	$XBAH_2$ (**3a**) (*k*)	$XBAH_2$ (*e*)	$EBAH_2$ (**3b**) (*k*)	$EBAH_2$ (*e*)	Cl_4XBAH_2 (**3c**)	$XBBH_2$ (**3d**)	$XBDH_2$ (**3e**)	$XBPH_2$ (**3f**)	XBE (**4**)
C-1	2.13s	2.19s	2.07s	2.15s	2.18s	2.08s			2.30s
C-3	4.07t		3.94t		3.93t	4.74t	5.47t	4.72t	
C-4	3.18d	3.71s	3.17d	3.68s	3.50d	3.25d	3.37d	3.06d	7.38
C-6			3.90						
C-9								1.10s	
C-11									2.44s
O—H		16.9		16.8					
Aromatic	7.06–7.3		7.1–7.7			7.0–8.0	7.1–8.1	7.01m	7.43

[a] In δ (ppm) vs TMS, in $CDCl_3$; tabulated according to attached carbon atom (see Fig. 1) unless otherwise noted. Resonances attributable to the keto and enol tautomers, where they could be distinguished, are tabulated under the headings *k* and *e*, respectively.

Table 3. ^{13}C NMR chemical shifts[a]

Atom	$XBAH_2$ (**3a**) (*k*)	$XBAH_2$ (*e*)	$EBAH_2$ (**3b**) (*k*)	$EBAH_2$ (*e*)	Cl_4XBAH_2 (**3c**)	$XBBH_2$ (**3d**)	$XBDH_2$ (**3e**)	$XBPH_2$ (**3f**)	XBE (**4**)
C-1	29.6	23.2	29.6	23.3	29.7	28.6			26.6
C-2	203.1	191.6	202.9	192.0	202.5	202.9	195.3	209.3	196.2
C-3	69.6	108.5	69.6	107.8	66.1	64.4	58.8	57.0	143.8
C-4	34.0	32.8	33.6	32.7	31.5	34.5	35.0	35.7	133.8
C-5			167.0						
C-6			52.3						
C-7						195.6			
C-8								44.5	
C-9								27.1	
C-10									204.8
C-11									31.8
Aromatic	127–140		126–141		133–135	127–139	127–139	127–139	130–139

[a] In δ (ppm) vs TMS, in $CDCl_3$. Resonances attributable to the keto and enol tautomers, where they could be distinguished, are tabulated under the headings *k* and *e*, respectively.

NaOH(aq)* and then with $NaHCO_3$(aq) and H_2O, drying with Na_2SO_4 and evaporating to dryness. The amber oily residue was placed in a refrigerator and, when it had largely solidified (several weeks), it was triturated with methanol, collected by filtration, washed with methanol, and air-dried to yield a white powder.

For $XBDH_2$ (**3e**) and $XBPH_2$ (**3f**) the residue was washed with hot water, taken up in benzene, precipitated by addition of hexane, and recrystallized from benzene–hexane.

(b) *Preparation of* $XBAH_2$ (**3a**) *from isophthalaldehyde*

(i) XBE (**4**) (3,3′-[1,3-*phenylenebis*(*methylidene*)]*bis*(2,4-*pentanedione*)). Isophthalaldehyde (13.4 g, 0.1 mol), acetylacetone (20.0 g, 0.2 mol), benzoic acid (12.2 g, 0.1 mol) and triethylamine (10.1 g, 0.1 mol) were dissolved in benzene (100 cm^3) and the solution was brought to reflux, using a Dean–Stark trap to collect the water formed in the condensation. After *ca* 34 h the expected quantity of water had collected and the solvent was removed. The residue was dissolved in CH_2Cl_2 and the solution extracted successively with 5% $NaHCO_3$(aq), H_2O, 5% HCl(aq) and H_2O, dried with $MgSO_4$ and evaporated to dryness. The resulting dark red oil was extracted several times with boiling diethyl ether and the yellow ether extracts were concentrated and cooled to *ca* −15°C to give a pale yellow product (total yield 10–20%).

(ii) $XBAH_2$. XBE (2.70 g, 9.05 mmol) was dissolved in methanol (150 cm^3) and 10% Pd/C (*ca* 0.10 g) added. Catalytic hydrogenation (2–3 atm, RT) required 3–5 h. Filtration and removal of the solvent gave partially solid, colourless $XBAH_2$ in almost quantitative yield. Analytically pure crystalline material was obtained from methanol by slow cooling. The melting point of this product (105°C) was noticeably higher than that for $XBAH_2$ prepared by method (a) above. NMR spectra for solutions of this higher-melting material show that both keto and enol tautomers are present, in contrast to the material prepared by method (a), which is entirely in the keto form. Martin *et al.* observed multiple crystal forms in other bis(β-diketones);[6] we have also shown in a closely related bis(β-diketone)[3] that the ratio of keto and enol tautomers depends on the solvent of crystallization.

Copper(II) *complexes*

(a) *Two-phase method*

A solution of bis(β-diketone) (0.05–0.2 M) in CH_2Cl_2 or $CHCl_3$ was extracted with a 10-fold

* A pH > 13 is probably required for efficient extraction of benzoylacetone into water, as judged from its pK_a [8.7: J. R. Jones, *Ionization of Carbon Acids*. Academic Press, London (1973)] and from its partition coefficient, which strongly favours solution in CH_2Cl_2 (Y. Yoshimura and N. Suzuki, *Anal. Chim. Acta* 1976, **85**, 383). A similar pK_a is expected for $XBBH_2$, but its partition coefficient is likely to favour solution in CH_2Cl_2 much more strongly than that for benzoylacetone.

excess of $Cu(NH_3)_4^{2+}$(aq). The organic layer was dried over Na_2SO_4, filtered and evaporated to dryness. The residue was purified by washing with benzene; alternatively, the complex was crystallized over a period of several days by dissolving the residue in CH_2Cl_2 or $CHCl_3$ and layering the solution with CH_3CN, isopropyl alcohol or diethyl ether.

(b) *One-phase method*

Bis(β-diketone) (1 mmol) was added to a stirred solution of (i) $Cu(NO_3)_2 \cdot 3H_2O$ (0.23 g, 1 mmol) and Et_3N (0.22 g, 2.2 mmol) in *N*,*N*-dimethylformamide (40 cm^3); or (ii) $Cu_2(OAc)_4 \cdot 2H_2O$ (0.20 g, 0.5 mmol) in pyridine (50 cm^3). Formation of a complex was indicated by the appearance of a precipitate ($Cu_2(XBA)_2$, $[Cu(Cl_4XBA)]_n$) or a dark olive-green solution ($Cu_2(XBB)_2$) after 6–8 h. $Cu_2(XBB)_2$ was precipitated by pouring the solution into a large excess of vigorously stirred dil. NaCl(aq).

The crude solid products were collected, washed with fresh solvent where appropriate, and air-dried; some of the complexes could be crystallized from CH_2Cl_2 or $CHCl_3$ as outlined in (a) above. In cases where the complexes could be prepared by more than one method (e.g. $Cu_2(XBA)_2$), the products were identical, as judged by electronic absorption spectra. The binuclear copper complexes are generally soluble only in chlorinated hydrocarbon solvents. Analytical data for the ligands and new copper(II) complexes are presented in Table 4; ^1H and ^{13}C NMR spectral data for the ligands appear in Tables 2 and 3.

Recovery of ligands from copper(II) complexes

A solution of the complex in CH_2Cl_2 or $CHCl_3$ was extracted with excess 0.1 M HCl, which decolorized the CH_2Cl_2 layer; when large amounts of the copper complex were used, the pale blue colour of $Cu(H_2O)_6^{2+}$ could be observed in the aqueous layer. The CH_2Cl_2 layer was then washed with water, dried over Na_2SO_4, filtered and evaporated to dryness. The residue was characterized by its ^1H NMR spectrum in $CDCl_3$ or CD_2Cl_2.

Table 4. Analytical data[a]

	C	H	Cl
$XBAH_2$ (**3a**)	71.5 (71.5)	7.0 (7.3)	
Cl_4XBAH_2 (**3c**)	49.2 (49.1)	4.1 (4.1)	31.3 (32.2)
$XBBH_2$ (**3d**)	78.6 (78.8)	6.1 (6.1)	
$XBDH_2$ (**3e**)	82.6 (82.9)	5.6 (5.5)	
$XBPH_2$ (**3f**)	76.2 (76.5)	9.9 (9.8)	
XBE (**4**)	72.4 (72.5)	6.1 (6.1)	
$Cu_2(EBA)_2$	57.2 (56.9)	5.3 (5.3)	
$Cu_2(XBB)_2$	63.8 (68.9)	4.9 (5.0)	
$[Cu(Cl_4XBA)]_n$	41.3 (43.1)	3.2 (3.2)	26.2 (28.3)

[a] Calculated values in parentheses.

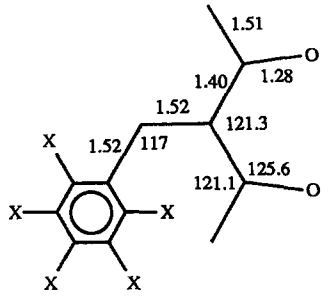

Fig. 2. Geometry utilized in SYBYL[9] molecular-mechanics calculations for 3-benzylacetylacetonato (X = H) and 3-(pentachlorobenzyl)acetylacetonato (X = Cl) metal complexes. Distances (Å) and angles (°) are average values based on crystal structure investigations of $Cu_2(XBA)_2$[1] and $Cu_2(NBA)_2 \cdot 2CHCl_3$.[2]

Molecular-mechanics calculations

For these calculations, the SYBYL program set[7] was utilized. The geometry assumed in the calculations, which was intended to approximate that of the complexes (rather than the free ligands) as closely as possible, is illustrated in Fig. 2. Bond lengths and angles used in the acac and CH_2 moieties were average values from the X-ray crystal structures of $Cu_2(XBA)_2$[1] and $Cu_2(NBA)_2 \cdot 2CHCl_3$;[2] idealized C—H distances and phenyl-ring geometries were assumed. In generating the potential-energy contour diagrams in Figs 2 and 3, only the torsion angles about the acac–CH_2 and CH_2–arene bonds (α and β, respectively) were allowed to vary; therefore, the results reflect only changes in torsional and van der Waals interactions.

RESULTS AND DISCUSSION

Ligand synthesis

All of the bis(β-diketone) ligands could be prepared in satisfactory yield by modifications of the nucleophilic-substitution procedure described by Shamma and co-workers[6] for *p*-$XBAH_2$ (3,3′-[1,4-phenylenebis(methylene)bis(2,4-pentanedione]). Our initial attempts to prepare the *meta*-substituted isomer, $XBAH_2$ (**3a**), by this method led to oily products that were difficult to purify. As an alternative

approach, therefore, we explored Knoevenagel condensation of isophthalaldehyde with acetylacetone to produce the unsaturated tetraketone XBE (**4**), followed by catalytic hydrogenation. (Similar condensations of isophthalaldehyde with diethyl malonate[8] and terephthalaldehyde with acetylacetone[9] have been reported.) Although the yields of $XBAH_2$ were much lower by this method, the product was an analytically pure crystalline solid.

The ligands $XBAH_2$ (**3a**) and $EBAH_2$ (**3b**) show evidence for both keto and enol tautomers in their ^1H and ^{13}C NMR spectra (see Tables 2 and 3) in $CDCl_3$; the other four bis(β-diketones) exist entirely in the keto form.

Copper complexes

Since the copper(II) complexes we have studied previously are easily prepared and purified,[1-3] we investigated the reactions of copper(II) with the new ligands as well. Only the unhindered acetylacetone derivatives $XBAH_2$ (**3a**) and $EBAH_2$ (**3b**) produced copper(II) complexes in good yield. With $XBBH_2$ (**3d**) the copper(II) product, which is probably also binuclear, could be obtained only in low yield by the single-phase method in DMF. Although $Cu_2(XBB)_2$ prepared by this method was not analytically pure, unchanged $XBBH_2$ (identified by ^1H NMR) could be regenerated from it by extraction of a $CHCl_3$ solution with dilute acid. Also, its relatively high solubility in CH_2Cl_2 and $CHCl_3$, and its EPR spectrum,* indicate that it is likely to be a discrete binuclear complex. Cl_4XBAH_2 (**3c**) also reacted with Cu^{2+} only in the single-phase attempts, but the product in this case was a grey powder that was insoluble in common organic solvents. Based on the low solubility of the material, and on a conformational study of Cl_4XBA^{2-} complexes (see below), we believe the complex is polymeric.

No reaction occurred under these conditions between copper(II) and $XBDH_2$ (**3e**) or $XBPH_2$ (**3f**). More vigorous conditions, such as heating the pure ligands with $Cu(acac)_2$, $Cu_2(OAc)_4 \cdot 2H_2O$ or CuO either under vacuum or in high-boiling solvents (e.g. DMF, mesitylene), also gave no binuclear complexes with the latter two ligands. Small amounts of a crystalline olive-green solid were obtained from $XBDH_2$ in some of these reactions, but this was shown to be $Cu(dbm)_2$.† (Partial hydrolysis of $XBDH_2$ is the most likely source of dibenzoylmethane in these reaction mixtures: the ligand is analytically pure and shows no evidence of inhomogeneity.)

Steric congestion in ligands and complexes

Although the bis(β-diketones) derived from benzoylacetone, dibenzoylmethane and dipivaloylmethane ($XBBH_2$, $XBDH_2$, and $XBPH_2$, respectively) are somewhat easier to purify than $XBAH_2$, their bulky substituents inhibit the formation of metal complexes. Of these three ligands, only $XBBH_2$ could be converted to a copper(II) complex. The increasing difficulty in complex formation along this series can be attributed to the large steric bulk of the phenyl and *t*-butyl substituents. Mononuclear complexes with these substituents, $M(bzac)_2$, $M(dbm)_2$ and $M(dpm)_2$, are well known. However, the metal-containing planes in a binuclear complex such as $Cu_2(XBA)_2$ are sufficiently close together (the distance between the two $Cu(acac)_2$ moieties in **1** is *ca* 5.0 Å) that substantial interference can be anticipated between groups attached to adjacent metal atoms. Therefore, even XBB^{2-} can probably form a discrete binuclear complex such as $Cu_2(XBB)_2$ only if the arrangement of Ph and CH_3 groups is *anti* (as shown for $XBBH_2$ in Fig. 1). This geometric restriction may be responsible for the experimental difficulties we experience in preparing $Cu_2(XBB)_2$ We expect that complexes such as $M_2(XBD)_2$ and $M_2(XBP)_2$ will be much more difficult to prepare.

Conformational analysis of XBA^{2-} *and* Cl_4XBA^{2-} *complexes*

Although Cl_4XBAH_2 yields a copper complex on treatment with Cu^{2+} in DMF, the product is insoluble in all common solvents and is therefore likely to be polymeric. In order to examine the role of steric interactions in this behaviour, and to compare it with the facile formation of $Cu_2(XBA)_2$, we undertook a molecular-mechanics study. Since the relative conformational energies of XBA^{2-} and Cl_4XBA^{2-} are likely to be influenced most strongly by adjacent groups on the aromatic rings and not by longer-range interactions between the acac moieties, we utilized the model compounds 3-benzylacetylacetone (bzacacH; see Fig. 2, with X = H) and its pentachloro derivative (Cl_5bzacacH;

* A. W. Maverick and D. F. Church, work in progress. EPR spectra for $Cu_2(XBA)_2$, $Cu_2(EBA)_2$, and $Cu_2(XBB)_2$ in chloroform or trichloroethylene solution are similar, reflecting weak coupling between the two copper atoms; all are substantially more complex than those for mononuclear copper(II) β-diketone complexes.

† Shown by X-ray crystallography; our results were essentially identical to those previously reported for $Cu(dbm)_2$: M. Blackstone, J. Van Thuijl and C. Romers, *Rec. Trav. Chim. Pays-Bas* 1966, **85**, 557.

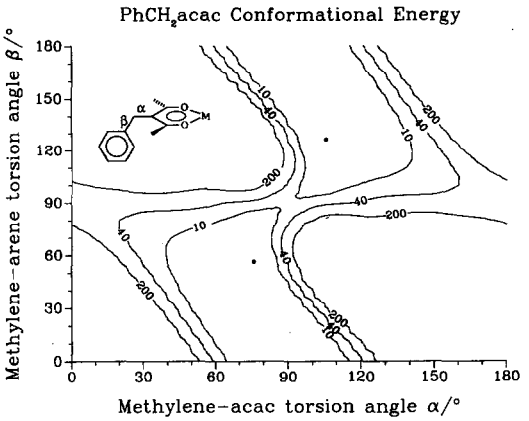

Fig. 3. Calculated potential-energy contour diagram for a 3-benzylacetylacetonato metal complex, based on the geometry in Fig. 2, as a function of torsion angles α and β (see inset structure). Filled circles represent lowest-energy conformations (α = 75, β = 55; α = 105, β = 125°).

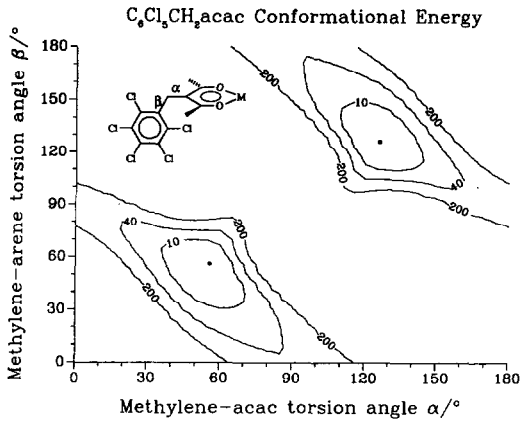

Fig. 4. Calculated potential-energy contour diagram for a 3-(pentachlorobenzyl)acetylacetonato metal complex, based on geometry in Fig. 2, as a function of torsion angles α and β (see inset structure). Filled circles represent lowest-energy conformations (α = β = 55; α = β = 125°).

X = Cl). The bond distances and angles for both of these molecules were taken in part from our previous crystallographic investigations,[1,2] so as to model as closely as possible the interactions that would occur in metal complexes of these ligands.

The geometric features in our ligands that are most important in governing the assembly of binuclear complexes are the torsion angles α and β about the acac–CH_2 and CH_2–arene bonds, respectively. The most symmetrical geometry, with the $M(acac)_2$ and *m*-xylylene moieties perpendicular, is achieved when α = 90° and β = 0°. Experimental values of α and β in the structures of $Cu_2(XBA)_2$ (87.5–88.9° and 2.8–4.3°)[1] and $Cu_2(NBA)_2 \cdot 2CHCl_3$ (81.6–88.4° and 0.3–4.5°, respectively)[2] are close to these ideal values.

Calculated potential-energy contour diagrams are shown in Fig. 3 (for a $bzacac^-$ complex) and Fig. 4 ($Cl_5bzacac^-$). Complexes of benzylacetylacetone show considerable conformational flexibility; we estimate that the conformation corresponding to our assembled binuclear complexes (α ≈ 90°; β ≈ 0°) is no more than 1 kJ mol^{-1} higher in energy than the most stable conformation. In contrast, the set of readily accessible conformations for a $Cl_5bzacac^-$ complex is much smaller; and the barrier for formation of the α = 90°, β = 0° conformation is *ca* 42 kJ mol^{-1}. This unfavourable energy is primarily due to repulsion between the chlorine atom in the two-position and the central carbon atom in the acac moiety. In a hypothetical binuclear $Cu_2(Cl_4XBA)_2$ complex, this repulsion would occur twice in each ligand; therefore, the barrier to formation of a discrete binuclear complex $Cu_2(Cl_4XBA)_2$ may be as high as 160 kJ mol^{-1}.

The strong C---Cl repulsion that accompanies the α = 90°, β = 0° conformation in $Cl_5bzacac^-$ and Cl_4XBA^{2-} could be relieved somewhat by increasing the arene–CH_2–acac bond angle. Even though this distortion introduces additional strain into the molecule, it results in some overall stabilization: calculations suggest that the best compromise is achieved for a bond angle of *ca* 126°. However, this conformation is still *ca* 15 kJ mol^{-1} higher in energy than the optimum conformation in Fig. 4; this would correspond to a 60 kJ mol^{-1} barrier for formation of $Cu_2(Cl_4XBA)_2$. Furthermore, an arene–CH_2–acac bond angle greater than 120° will introduce additional destabilization in a binuclear metal complex (see above) by distorting the metal coordination environment. The proposed polymeric structure, on the other hand, places few restrictions on the conformation of the ligands; in this arrangement, α and β for individual ligands are likely to be close to the minimum-energy values suggested by Fig. 4.

CONCLUSIONS

We have prepared a variety of *m*-xylylenebis(β-diketones). Their capacity for forming cofacial binuclear copper complexes is strongly dependent on steric properties of the substituents, especially those in the β-diketone moieties or in the 2-position of the *m*-xylylene bridge. In general, the binuclear complexes are accessible for a more limited range of substituents than the correspond-

ing mononuclear systems. The hindered ligand Cl_4XBAH_2 (**3c**) is prevented from adopting a conformation suitable for a binuclear complex by unfavourable steric interactions, but a polymeric species is relatively stable. Our experience so far indicates that copper(II) complexes are among the easiest to prepare with these bis(β-diketone) ligands. Therefore, we expect that the steric restrictions outlined here will apply to other metals as well. Work currently in progress in our laboratory includes the conversion of the less hindered new ligands to the corresponding bis(β-ketoenamines) and their complexes, as well as the adaptation of functionalized bis(β-diketones) such as $EBAH_2$ (**3b**) for improving the solubility of the binuclear complexes in more polar solvents.

Acknowledgements—We acknowledge the Donors of the Petroleum Research Fund, administered by the American Chemical Society, for support of this research. We thank Joel T. Fishbain, Yin-Her Li and Jacqueline L. Hampton for experimental assistance. Funds for the Varian XL300 NMR instrument at Washington University were provided in part by NIH Biomedical Research Support Instrument Grant 1 S10 RR02004 and by a gift from the Monsanto Company.

REFERENCES

1. A. W. Maverick and F. E. Klavetter, *Inorg. Chem.* 1984, **23**, 4129.
2. A. W. Maverick, S. C. Buckingham, J. R. Bradbury, Q. Yao and G. G. Stanley, *J. Am. Chem. Soc.* 1986, **108**, 7430.
3. J. R. Bradbury, J. L. Hampton, D. P. Martone and A. W. Maverick, *Inorg. Chem.*, in press.
4. A. Markovac and M. P. LaMontagne, *J. Med. Chem.* 1980, **23**, 1198.
5. J. Peeling, J. B. Rowbotham, L. Ernst and T. Schaefer, *Can. J. Chem.* 1974, **52**, 2414.
6. D. F. Martin, W. C. Fernelius and M. Shamma, *J. Am. Chem. Soc.* 1959, **81**, 130.
7. S. Naruto, I. Motoc, G. R. Marshall, S. B. Daniels, M. J. Sofia and J. A. Katzenellenbogen, *J. Am. Chem. Soc.* 1985, **107**, 5262.
8. R. Ruggli and A. Staub, *Helv. Chim. Acta* 1937, **20**, 918. These authors also hydrogenated the unsaturated product to prepare the tetraethyl ester of *m*-xylylenebis(malonic acid).
9. H. L. Holmes and D. J. Currie, *Can. J. Chem.* 1969, **47**, 4076.

Polyhedron Vol. 8, No. 12, pp. 1557–1560, 1989
Printed in Great Britain

0277-5387/89 $3.00+.00
© 1989 Pergamon Press plc

THE MOLECULAR STRUCTURE OF BIPYRIDINIUM TRIS(BIPYRIDINE)CHROMIUM(III) PERCHLORATE

KYU-WANG LEE and PATRICK E. HOGGARD*

Department of Chemistry, North Dakota State University, Fargo, ND 58105, U.S.A.

(*Received* 17 *January* 1989; *accepted* 15 *February* 1989)

Abstract—$[Cr(bpy)_3](ClO_4)_3$ (bpy = 2,2′-bipyridine) cocrystallizes with bipyridinium perchlorate in the triclinic space group $P\bar{1}$ (No. 2), with $a = 13.532(2)$, $b = 16.596(3)$, $c = 10.324(1)$ Å, $\alpha = 92.16(1)$, $\beta = 100.92(1)$, $\gamma = 102.76(1)°$, $V = 2212.7$ Å^3 and $Z = 2$. The structure was refined to $R = 0.073$ and $R_w = 0.098$. The cocrystallized $HbpyClO_4$ may also have been present in earlier preparations, but could have escaped detection because of the similarity in carbon, hydrogen, nitrogen and chlorine percentages, with and without the cocrystallite.

Hauser *et al.* recently published the crystal structure and low temperature polarized sharp-line absorption spectra for $[Cr(bpy)_3](PF_6)_3$.[1] The space group was reported to be $R32$, in which by necessity the enantiomers must occupy non-equivalent positions. The differences between the two sites, however, appeared extreme. The N—Cr—N bite angle, for example, was reported as 74.8° in one site (equal by symmetry for all three rings) and 84.7° in the other. Large differences in other bond lengths and bond angles were also manifest. If this structure is correct it is unique among transition metal chelate complexes.

Because the geometry of the tris(bipyridine) chromium(III) complex is important to the ligand field analysis of the electronic spectra,[2] we attempted to repeat the solution of the crystal structure of $[Cr(bpy)_3](PF_6)_3$, but failed due to an apparent twinning of the crystals.[3]

We therefore chose another salt, the perchlorate, for crystallographic work. It has been the most commonly used salt of $[Cr(bpy)_3]^{3+}$ for photochemical and spectroscopic studies. A problem surfaced in the course of the elemental analyses of this compound. The carbon, hydrogen and nitrogen analyses were as expected, and in one case so was the chromium analysis. However, another sample from the same batch sent to a different firm produced a chromium percentage about 25% lower than expected. The latter analysis turned out to be correct, however, since refinement of the crystallographic data revealed the presence of cocrystallized bipyridinium perchlorate. This does, however, raise the question of what compound was actually used by previous investigators.

RESULTS AND DISCUSSION

Solution of the X-ray crystal structure showed there to be one chromium complex per asymmetric unit and revealed the presence of the cocrystallized $HbpyClO_4$. The enantiomeric complex is related by inversion symmetry in the $P\bar{1}$ space group. One enantiomer is shown in an ORTEP diagram in Fig. 1. Table 1 contains an abbreviated list of bond lengths and angles.

Table 1 also includes a comparison with the data of Hauser *et al.* for the hexafluorophosphate salt.[1] Although the two sites in the latter compound are characterized by several disparate bond lengths and angles, when they are averaged they agree fairly well with an average of the same quantities from the three rings in the perchlorate salt. For example, the bipyridine bite angle (N—Cr—N) is 79.6, 79.7 and 80.4° in the three rings of $[Cr(bpy)_3](ClO_4)_3 \cdot HbpyClO_4$, as opposed to the 74.8 and 84.7° angles mentioned above for the two sites in the $[Cr(bpy)_3](PF_6)_3$ structure. The inter-ring C—C distance, an important measure of the extent of delocalization, is between 1.46 and 1.49 Å in the perchlorate salt, but stated by Hauser to be 1.39

* Author to whom correspondence should be addressed.

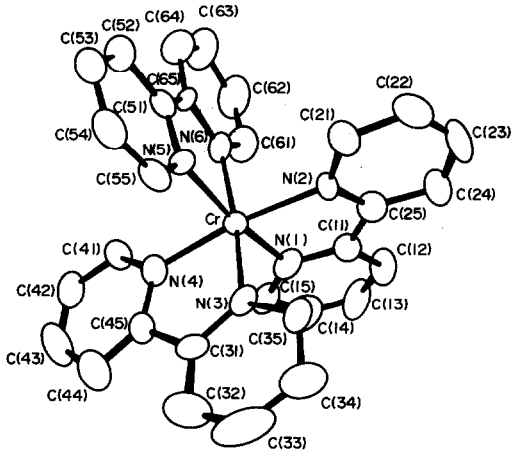

Fig. 1. ORTEP drawing of the $[Cr(bpy)_3]^{3+}$ molecular unit in $[Cr(bpy)_3](ClO_4)_3 \cdot HbpyClO_4$, showing the atom-labelling scheme.

and 1.56 Å in the two sites of the PF_6^- salt. The most likely explanation for the overlarge site differences is that the crystallographic data were refined in the wrong space group.

There are numerous references in the literature to $[Cr(bpy)_3](ClO_4)_3$, and it is impossible to tell which of them are actually cocrystallized with bipyridinium perchlorate. The carbon, hydrogen, nitrogen and chlorine percentages are very similar in $[Cr(bpy)_3](ClO_4)_3$ and $[Cr(bpy)_3](ClO_4)_3 \cdot HbpyClO_4$. There are many reports of the synthesis of $[Cr(bpy)_3](ClO_4)_3$ without the inclusion of analytical data.[4-7] In some cases, one-half of a water of crystallization is included in the formula, either with a (C, H, N, Cl) analysis[8] or without.[9] In one instance, two waters of crystallization are reported,[10] but the supporting analyses were not published. The optimum coincidence in analytical percentages occurs with no additional water molecules, so it may be inferred that bipyridinium perchlorate has not cocrystallized when any water of crystallization is reported.

The bipyridinium ion probably becomes available for cocrystallization through displacement of coordinated bipyridine by water in $[Cr(bpy)_3]^{2+}$. This in turn should be facilitated by higher acid concentrations, and it is likely that the perchloric acid concentration during oxidation is the critical factor in determining whether or not bipyridinium perchlorate is incorporated in the crystal. Porter and Van Houten have also discussed the method and order of addition during the oxidation procedure and how they affect the yield.[6] They found that when $[Cr(bpy)_3]^{2+}$ was first dissolved in acid and then slowly oxidized, the yield was reduced through displacement of bipyridine.

Table 1. Comparison of selected bond lengths (Å) and bond angles (°) for $[Cr(bpy)_3](ClO_4)_3 \cdot HbpyClO_4$ and $[Cr(bpy)_3](PF_6)_3$[a]

		PF_6^- salt	
	ClO_4^- salt	Site 1	Site 2
Cr—N(1)	2.023(9)	2.040	2.053
Cr—N(2)	2.034(8)	2.040	2.053
Cr—N(3)	2.025(8)	2.040	2.053
Cr—N(4)	2.035(7)	2.040	2.053
Cr—N(5)	2.036(9)	2.040	2.053
Cr—N(6)	2.037(9)	2.040	2.053
C(11)—C(25)	1.460(13)	1.55	1.39
C(31)—C(45)	1.490(14)	1.55	1.39
C(51)—C(65)	1.471(14)	1.55	1.39
C(71)—C(85)	1.441(13)		
N(1)—Cr—N(2)	79.7(3)	84.7	74.8
N(1)—Cr—N(3)	93.8(3)	90.8	97.0
N(1)—Cr—N(4)	94.3(3)	94.1	92.3
N(1)—Cr—N(5)	171.4(3)	173.4	168.4
N(1)—Cr—N(6)	92.6(3)		
N(2)—Cr—N(3)	94.1(3)		
N(2)—Cr—N(4)	171.6(4)	173.4	168.4
N(2)—Cr—N(5)	96.6(3)	90.8	97.0
N(2)—Cr—N(6)	89.7(8)	94.1	92.3
N(3)—Cr—N(4)	80.4(3)	84.7	74.8
N(3)—Cr—N(5)	94.2(3)		
N(3)—Cr—N(6)	173.1(4)	173.4	168.4
N(4)—Cr—N(5)	90.2(3)	94.1	92.3
N(4)—Cr—N(6)	96.5(3)	90.8	97.0
N(5)—Cr—N(6)	79.6(3)	84.7	74.8

[a] As reported in ref. 1.

In the procedure we followed,[11] oxidation was not as rapid as in the method advised by Porter and Van Houten. Our "dilute" perchloric acid was approximately 1 M, whereas other workers have often used solutions 10–100 times more dilute. It thus seems that two different products may be formed depending on the perchloric acid concentration and/or the speed of oxidation. The solution characteristics would of course be identical. But without appropriate elemental analyses it is unclear how many of the literature references to this compound do and do not contain cocrystallized $HbpyClO_4$.

EXPERIMENTAL

Tris(2,2′-bipyridine)chromium(III) perchlorate[11] was prepared by air-oxidizing $[Cr(bpy)_3]^{2+}$, made from $CrCl_2$ and bipyridine in stoichiometric ratio,[12] in dilute perchloric acid, and was recrystallized twice from dil. $HClO_4$ solution. Single crystals for

Table 2. Experimental and data processing parameters

(a) Crystal data	
2,2′-Bipyridinium tris(2,2′-bipyridine)chromium(III) perchlorate	
$(C_{10}H_9N_2)(C_{30}H_{24}CrN_6)Cl_4O_{16}$	F_w 1075.55
$F(000) = 834$	
Crystal dimensions (mm)	$0.15 \times 0.25 \times 0.35$
Peak width at half height (°)	0.33
Radiation	Mo-K_α ($\lambda = 0.71069$ Å)
Temperature (°C)	23 ± 1
Space group	Triclinic $P\bar{1}$ No. 2
Lattice parameters	$a = 13.532(2)$ Å
	$b = 16.596(3)$ Å
	$c = 10.324(1)$ Å
	$\alpha = 92.16(1)°$
	$\beta = 100.92(1)°$
	$\gamma = 102.76(1)°$
Unit cell volume	$V = 2212.7(6)$ Å^3
Z value	2
Calculated density (g cm^{-3})	$d = 1.614$
Linear absorption coefficient (cm^{-1})	5.09
(b) Intensity measurements	
Diffractometer	Rigaku AFC6R
Monochromator	Graphite crystal, incident beam
Attenuator	Zr foil, factor 20.7
Take-off angle (°)	6.0
Detector aperture (mm)	6.0 horizontal
	6.0 vertical
Crystal-detector distance (cm)	40
Scan type	ω–2θ
Scan rate (° min^{-1})	16.0 (in omega), 2 re-scans
Scan width (°)	$(1.31 + 0.30 \tan\theta)$
Maximum 2θ (°)	45.1
Number of reflections measured	6123 total; 5827 unique
Corrections	Lorentz-polarization
(c) Structure solution and refinement	
Solution	Direct methods
Minimization function	$\Sigma w(\|F_o\| - \|F_c\|)^2$
Least-squares weight	$4F_o^2/\sigma^2(F_o^2)$
Anomalous dispersion	All non-hydrogen atoms
Reflections included	3624 with $F_o^2 > 3\sigma(F_o^2)$
Parameters refined	618
Unweighted agreement factor	0.073
Weighted agreement factor	0.098
ESD of observation of unit weight	2.39
Maximum e/Å^3 from difference Fourier map	1.03

X-ray analysis were grown by slow evaporation in the dark from dil. $HClO_4$. Solution of the crystal structure revealed the presence of cocrystallized (Hbpy)ClO_4. Found: Cr, 4.9; C, 44.5; N, 10.5; H, 2.8. Calc. for $Cr(C_{10}H_8N_2)_3 \cdot HC_{10}H_8N_2(ClO_4)_4$: Cr, 4.8; C, 44.7; N, 10.4; H, 3.1%. (E & R Microanalytical Laboratories.)

X-ray diffraction data were collected by the Molecular Structure Corporation on a Rigaku AFC6R diffractometer with graphite monochromated Mo-K_α radiation.* Cell constants were determined from 25 centred reflections in the range of $35.90° < 2\theta < 41.29°$. The data were collected at

* *Supplementary material.* Tables of refined atomic coordinates, bond distances, bond angles and anisotropic temperature factors have been deposited at the Cambridge Crystallographic Data Centre.

$23 \pm 1°C$ using the ω–2θ scan technique to a maximum 2θ value of 45.1°. Details are given in Table 2.

The structure was refined at NDSU using direct methods[13] and full-matrix least-squares optimization[14] for 5827 unique reflections to a final R value of 0.073 ($R_w = 0.098$). Because of storage limitations, only the atoms in the $[Cr(bpy)_3]^{3+}$ unit were refined with anisotropic thermal parameters.

Acknowledgements—This material is based upon work supported in part by the National Science Foundation under Grant RII8610675. We also thank the donors of the Petroleum Research Fund, administered by the American Chemical Society, for their support of this research.

REFERENCES

1. A. Hauser, M. Mäder, W. T. Robinson, R. Murugesan and J. Ferguson, *Inorg. Chem.* 1987, **26**, 1331.
2. P. E. Hoggard, *Coord. Chem. Rev.* 1986, **70**, 85.
3. L. J. Radonovich, University of North Dakota, private communication.
4. Y. Saito, J. Takemoto, B. Hutchinson and K. Nakamoto, *Inorg. Chem.* 1972, **11**, 2003.
5. B. Brunschwig and N. Sutin, *J. Am. Chem. Soc.* 1978, **100**, 7568.
6. G. B. Porter and J. Van Houten, *Inorg. Chem.* 1979, **18**, 2053.
7. A. Bakac, K. Zahir and J. H. Espenson, *Inorg. Chem.* 1988, **27**, 315.
8. B. R. Baker and B. D. Mehta, *Inorg. Chem.* 1965, **4**, 848.
9. M. S. Henry and M. Z. Hoffman, *Inorganic and Organometallic Photochemistry* (Edited by M. S. Wrighton), p. 91. American Chemical Society, Washington, DC (1978).
10. T. Ohno, S. Kato, S. Kaizaki and I. Hanazaki, *Inorg. Chem.* 1986, **25**, 3853.
11. S. Herzog, Dissertation, University of Jena, G.D.R. (1952) as cited in *Gmelins Handbuch der Anorganische Chemie*, System 52 (Chromium), Part C, p. 106. Verlag Chemie, Weinheim, F.R.G. (1965).
12. F. Hein and S. Herzog, *Z. Anorg. Allg. Chem.* 1952, **267**, 337.
13. P. Main, S. E. Fiske, G. Germain, J. P. Declerq and M. M. Woolfson, *MULTAN, a System of Computer Programs for Crystal Structure Determination from X-ray Diffraction Data.* Universities of York, U.K. and Louvain, Belgium (1980).
14. B. A. Frenz, *SDP–PLUS Structure Determination Package.* Enraf–Nonius, Delft, Netherlands (1982).

Polyhedron Vol. 8, No. 12, pp. 1561–1565, 1989
Printed in Great Britain

0277-5387/89 $3.00+.00
© 1989 Pergamon Press plc

COMPLEXATION OF LANTHANIDES(III) WITH MACROCYCLIC 18-CROWN-6 IN METHANOL UTILIZING A COLORIMETRIC COMPLEXANT BY SPECTROPHOTOMETRY

EMIKO OHYOSHI* and SUSUMU KOHATA

Yatsushiro National College of Technology, Hirayamashinmachi 2627, Yatsushiro, Kumamoto 866, Japan

(*Received* 27 *June* 1988; *accepted* 15 *February* 1989)

Abstract—A spectrophotometric procedure using a colorimetric complexant has been developed for the study of the complexation between several lanthanides(III) (Ln^{III}) and 18-crown-6 (18C6, A) in methanol. 2-(2-Thiazolylazo)-4-methylphenol (TAC, L) was used as a colorimetric complexant because of its simple structure with which no protonated complexes may be formed. The absorption spectra of the species in the Ln–TAC–18C6 system at various concentrations of 18C6 showed no formation of the ternary complex, LnLA. The conditional stability constants of the Ln(TAC) complexes at constant acidity in the absence ($K_{LnL'}$) and the presence ($K_{Ln'L'}$) of 18C6 were determined by monitoring the absorbance due to the Ln(TAC) complexes. The competition between TAC and 18C6 for the metal ion resulted in a decrease in $K_{Ln'L'}$ with increasing 18C6 concentration. From the dependence of $1/K_{Ln'L'}$ on the concentration of 18C6, the stability constants of the Ln(18C6) complexes could be determined. The stability constants of these complexes were found to decrease with increasing atomic number. The results are compared with those reported previously. On the basis of the complexation trend observed, 18C6 was used as a competitive ligand to increase the selectivity of chelating agents.

Macrocyclic polyethers of the 18-crown-6 type are unique ligands because of their lower complexing-ability with the small lanthanides, despite their higher charge density.[1,2] This trend in the lanthanides is very interesting because a reverse order has been always noted for most chelating agents. It suggests, therefore, that the ligands of the 18C6 type might be used competitively so as to increase the selectivity of the chelating agent. Since 18C6 is soluble both in aprotic and protic (methanol) solvents, it should be suitable for this purpose. Izatt *et al.*[1] studied the lanthanide complexation of 18C6 in methanol by calorimetric titrations and showed no formation of 18C6 complexes with any post-Gd^{III}. However, Almasio *et al.*[3] reported that 18C6 formed very stable complexes with Dy^{III} ($\log K = 7.90$), Er^{III} ($\log K = 7.67$) and Yb^{III} ($\log K = 7.50$) in anhydrous propylene carbonate (aprotic solvent). It thus seemed that further investigations should be made in methanol. Recently, spectrophotometric procedures[4–7] involving the competition of the two ligands have successfully been applied to the study of many complexes.

In the present work, we have developed a similar spectrophotometric procedure to study the complexation of several lanthanides with 18C6 in methanol, and have compared the results with those reported by Izatt *et al.* Also, the competitive effect of 18C6 on the selectivity of chelating agents has been explored.

EXPERIMENTAL

Reagents

All chemicals used were of GR grade. The ligands, TAC (Dojindo Chemical Co.) and 18C6 (Aldrich Chemical Co.) were dissolved in methanol (spectroscopic grade) to prepare 1.0×10^{-3} M and 0.20 M stock solutions, respectively. Seven types of $LnCl_3 \cdot nH_2O$ [Ln = La, Ce, Pr ($n = 7$); Ln = Nd,

* Author to whom correspondence should be addressed.

Eu, Dy, Yb ($n = 6$)] were dissolved in methanol to give concentrations of $5–20 \times 10^{-3}$ M, which were standardized by EDTA titration. Perchloric acid and tetraethylammonium perchlorate were used to adjust the acidity and to control the ionic strength, respectively.

Procedure

(a) The metal solution was added in small steps, 25×10^{-3} cm^3 each time, using a microliter pipet, to 5.0 cm^3 of a methanol solution containing TAC (2.0×10^{-5} M), at a constant acidity and ionic strength, to give concentrations of $2.5–40 \times 10^{-5}$ M. (b) To the same solution, prepared by procedure (a), 18C6 solution was further added in small steps to give concentrations of $1.0–12 \times 10^{-3}$ M. After each addition of the metal and 18C6 solution, the absorbance due to the Ln(TAC) complex (570 nm) was measured using a Shimadzu UV-260 spectrophotometer.

RESULTS AND DISCUSSION

Absorption spectra

Figure 1 shows the variation in absorption spectra of the TAC(L) solutions with varying Yb concentration, C_{Yb}, at $[HClO_4] = 4 \times 10^{-4}$ M and [18C6] = 0 (procedure (a), solid lines 1–4), or varying the 18C6(A) concentration, C_A, at $[HClO_4] = 4 \times 10^{-4}$ M and $C_{Yb} = 1.0 \times 10^{-4}$ M (procedure (b), dotted lines 5–10). In each procedure, (a) or (b), the Yb(TAC) complex formation ($\lambda_{max} = 572$ nm) or its dissociation occurs, respectively. It is seen that the solid and dotted curves have the same isosbestic point (488 nm). Moreover, the two curves, 2 and 8, are identical. These facts indicate that the dissociation of the YbL complex only takes place in procedure (b), i.e. there is no formation of ternary complex, YbLA. Similar results were obtained for other systems of Ln–L and Ln–L–A studied.

Determination of the conditional stability constants of Ln–TAC *complexes*

The absorbance D due to the Ln–TAC complex was used to determine the conditional stability constant at a given acidity, $K_{LnL'}$: D was measured at a constant acidity and various Ln concentrations in the binary Ln–TAC(L) system [procedure (a)]. The constant defined as $K_{LnL'} = [LnL]/([Ln][L'])$, where $[L'] = [L]+[HL]$ (the charges are omitted for simplicity), was determined by the method of Lang[8] [eq. (1)]:

$$C_{Ln}C_L/D = \{C_{Ln}+C_L-(D/\varepsilon_{LnL})\}(1/\varepsilon_{LnL}) + \{1/(K_{LnL'}\varepsilon_{LnL})\}, \quad (1)$$

where C_{Ln} and C_L are the total concentrations of Ln and L, and ε_{LnL} is the molar absorptivity of LnL. Plots of $C_{Ln}C_L/D$ vs $C_{Ln}+C_L-(D/\varepsilon_{LnL})$, where ε_{LnL} is assumed to be D_{max}/C_L (D_{max} is the maximum absorbance), were almost linear and show that only the 1 : 1 complex is formed. The reciprocal of the slope of the line yielded the corrected value of ε_{LnL} which was utilized to replot the above relation. The slope/intercept ratio of the resulting plot gave the $K_{LnL'}$ value. The results obtained for different lanthanides are listed in Table 1. From the values obtained at different acidity for La^{III}, Ce^{III} and Yb^{III}, it is found that $K_{LnL'}$ decreases due to the side reaction, H + L = HL occurring.

In the ternary Ln–TAC(L)–18C6(A) system [procedure (b)], D was observed to decrease with increasing concentration of 18C6 (C_A) (see

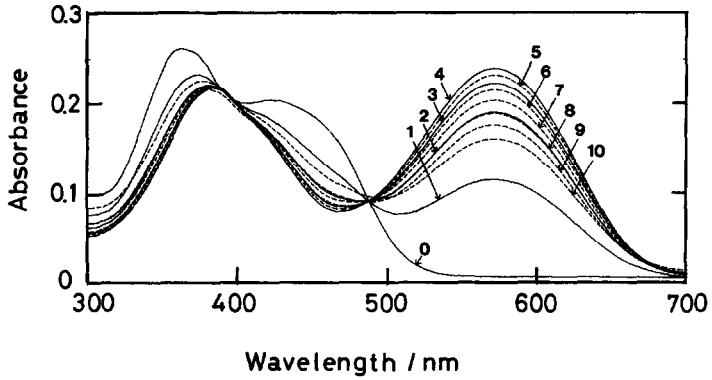

Fig. 1. Spectral changes of Yb–TAC (——) and Yb–TAC–18C6 (– – –) in a 4×10^{-4} M $HClO_4$–methanol solution at $\mu = 0.025$. TAC only: 0, 2.1×10^{-5} M. C_{Yb} in procedure (a): 1, 0.25; 2, 0.5; 3, 0.75; 4, 1.0×10^{-4} M. C_A in procedure (b): 5, 0.2; 6, 0.6; 7, 1.0; 8, 1.4; 9, 1.8; 10, 2.6×10^{-2} M.

Table 1. Conditional stability constants of Ln(TAC) complexes in methanol at 25°C and $\mu = 0.025$

Ln	Ln–TAC $\log K_{LnL'}$ ($[HClO_4]$) $(2\times10^{-4}$ M)	$(4\times10^{-4}$ M)	$(8\times10^{-4}$ M)
La	3.71(11)	3.53(9)	
Ce	4.21(8)	4.06(6)	
Pr		4.22(11)	
Nd		4.28(9)	
Eu		4.30(10)	
Dy		4.21(7)	
Yb		4.73(6)	4.58(7)

The numbers in parentheses are uncertainties of the last decimal place.

curves 5–10 in Fig. 1). The conditional stability constant at a given C_A and at the same acidity as that in the binary system, $K_{Ln'L'}$, which is defined as $K_{Ln'L'} = [LnL]/([Ln'][L'])$, where $[Ln'] = [Ln]+[LnA]+[LnA_2] = C_{Ln}-[LnL]$ and $[L'] = [L]+[HL] = C_L-[LnL]$, was obtained by eq. (2):

$$K_{Ln'L'} = D/[(\varepsilon_{LnL}C_L - D)\{C_{Ln}-(D/\varepsilon_{LnL})\}]. \quad (2)$$

The $K_{Ln'L'}$ values decreased with increasing C_A.

Determination of the stability constants of Ln–18C6 *complexes*

$K_{Ln'L'}$ values obtained at constant acidity and various C_A can be related to the stability constants of the 1:1 and 1:2 Ln–18C6 complexes, K_{LnA} and K_{LnA_2}, where $K_{LnA} = [LnA]/([Ln][A])$ and $K_{LnA_2} = [LnA_2]/([Ln][A]^2)$, as follows:

$$K_{Ln'L'} = [LnL]/([Ln'][L'])$$
$$= [LnL]/\{[Ln](1+K_{LnA}[A]+K_{LnA_2}[A]^2)[L']\}$$
$$= K_{LnL'}/(1+K_{LnA}[A]+K_{LnA_2}[A]^2) \quad (3)$$

$$1/K_{Ln'L'} = (1/K_{LnL'})(1+K_{LnA}[A]+K_{LnA_2}[A]^2), \quad (4)$$

where $[A] = C_A$ since C_A is usually in sufficient excess compared with C_{Ln}. According to eq. (4), a plot of $1/K_{Ln'L'}$ vs [A] (A:18C6) at relatively low values of [A] and constant acidity yields a straight line, and K_{LnA} as the slope/intercept ratio. When formation of LnA_2 occurs with increasing [A], K_{LnA_2} can also be obtained from the slope of the plot according to eq. (5), obtained by rearrangement of eq. (4):

$$\{(1/K_{Ln'L'})-(1/K_{LnL'})\}/[A]$$
$$= (1/K_{LnL'})(K_{LnA}+K_{LnA_2}[A]). \quad (5)$$

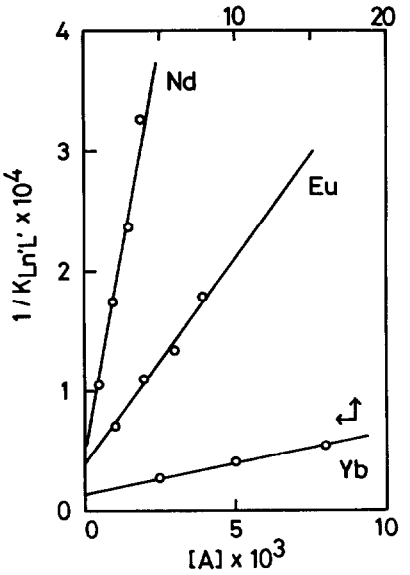

Fig. 2. Plots of the reciprocal conditional stability constants $1/K_{Ln'L'}$ vs [18C6].

Figure 2 shows the results of the plots of eq. (4) for the Ln–TAC–18C6 systems (Ln = Nd^{III}, Eu^{III} and Yb^{III}) at $[HClO_4] = 4\times10^{-4}$ M. Similar linear plots were obtained for Ce^{III}, Pr^{III} and Dy^{III}. However, the acidity was too high for La^{III} to obtain reliable values of $K_{Ln'L'}$. A lower acidity, $[HClO_4] = 2\times10^{-4}$ M, was thus used for La^{III}, and the linear plot of eq. (4) was obtained. At higher acidity, $[HClO_4] = 8\times10^{-4}$ M used for Yb^{III}, or a lower one, $[HClO_4] = 2\times10^{-4}$ M used for Ce^{III}, the plots of eq. (4) were also found to be linear. The facts indicate that these lanthanides only form the 1:1 complex with 18C6 in the range of [18C6] used. The $K_{LnL'}$ values given by the reciprocal intercept of the plots generally agreed with the corresponding values obtained in the binary system (Table 1), but were less accurate than the latter. Thus, we used the latter value for calculation of K_{LnA} which corresponds to the product of the slope and $K_{LnL'}$. The results for different lanthanides are listed in Table 2. By varying the acidity, the K_{LnA} values for Ce^{III} and Yb^{III} remain unchanged, indicating no effect of the hydrogen ion on complexation between Ln and 18C6.

Dependence of the stability of Ln(18C6) *on the atomic number of the lanthanides*

Figure 3 shows the variation in stability constants of Ln–18C6 complexes (K_{LnA}) with atomic number, together with the values reported by Izatt *et al.*,[1] which were obtained by calorimetric titrations

Table 2. Stability constants of Ln(18C6) complexes in methanol at 25°C and $\mu = 0.025$

Ln	Ln–TAC–18C6 $\log K_{LnA}$ ([$HClO_4$]) $(2\times10^{-4}$ M)	$(4\times10^{-4}$ M)	$(8\times10^{-4}$ M)
La	3.89(8)		
Ce	3.67(5)	3.72(6)	
Pr		3.60(8)	
Nd		3.40(6)	
Eu		2.85(10)	
Dy		2.17(6)	
Yb		1.91(8)	1.96(11)

The numbers in parentheses are uncertainties of the last decimal place.

under identical experimental conditions to this work except for the ionic strength. As is expected, the stability constants of the LnA complexes decrease through the lanthanides series despite the increase in charge density.

It is noted that the values of La^{III} to Gd^{III} reported by Izatt *et al.*[1] are about one order of magnitude smaller than ours, and those after Tb^{III} decrease to zero. This difference may arise from the difference in the ionic strength of the solution. The electrolyte $(C_2H_5)_4NClO_4$ (TEAP) was used to adjust the ionic strength to 0.025 in our study, while they performed at $\mu = 0.005$, suggesting no supporting electrolyte being used. As Massaux *et al.*[2] pointed out, the presence of protic solvents such as water or methanol gives rise to a significant reduction of the stability of metal–macrocycle complexes because of solvation effects. It thus seems that the electrolyte TEAP, existing in solution, released the solvent molecules H_2O and/or CH_3OH coordinated to the Ln^{3+} ion and favoured to react the Ln^{3+} ion with 18C6. This effect was confirmed by the fact that the stability of Eu(18C6) increases by increasing the ionic strength, i.e. $\log K_{EuA} = 2.54$, 2.85 and 3.04 at $\mu = 0.013$, 0.025 and 0.05, respectively.

Effect of another ligand on the selectivity of a chelating agent

From eq. (4) simplified by neglecting the last term, the ratio of the conditional stability constants of the chelates for the two lanthanides (Ln_1 and Ln_2), Ln_1L and Ln_2L, at a particular [A] is given by

$$K_{Ln'_1L'}/K_{Ln'_2L'} = K_{Ln_1L'}(1+K_{Ln_2A}[A])/\{K_{Ln_2L'}(1+K_{Ln_1A}[A])\}. \quad (6)$$

It is evident from eq. (6) that when the stability order of LnL for Ln_1 and Ln_2 is opposite to that of LnA, the ratio, $K_{Ln'_1L'}/K_{Ln'_2L'}$, becomes larger than $K_{Ln_1L'}/K_{Ln_2L'}$. This is the case for the present system, L = TAC and A = 18C6. However, the former is smaller than the latter if the stability of LnL and LnA for the two lanthanides varies in the same order.

To make sure of the effect of A on the selectivity of L, we plotted the conditional stability constants of Ln–TAC complexes at $[HClO_4] = 4\times10^{-4}$ M in the absence ($K_{LnL'}$) and in the presence ($K_{Ln'L'}$) of 18C6 ($C_A = 1.0\times10^{-3}$ M) vs atomic number (Fig. 4). The stability of Ln–TAC complexes, either in the absence or presence of 18C6, increases with charge density on the cation, as is characteristic of

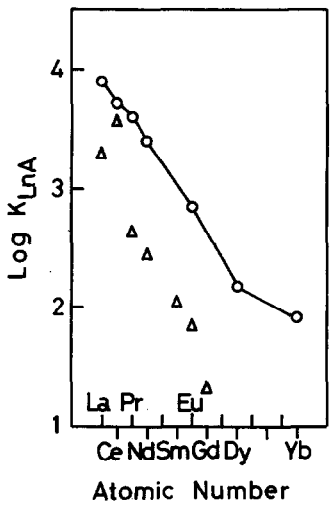

Fig. 3. Plots of stability constants $\log K_{LnA}$ vs the atomic number of lanthanides: this work (○) and ref. 1 (△).

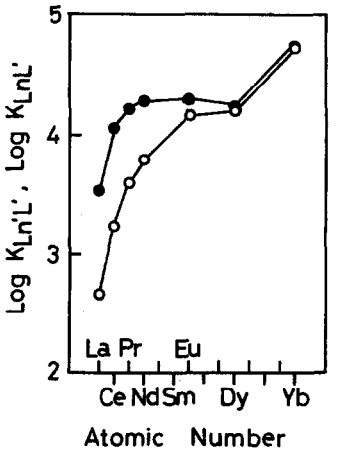

Fig. 4. Plots of conditional stability constants $\log K_{LnL'}$ and $\log K_{Ln'L'}$ vs the atomic number of lanthanides. Ln–TAC (●) and Ln–TAC–18C6(A) ($C_A = 1\times10^{-3}$ M) (○).

usual chelates. However, a comparison of the two curves shows a greater slope in the ternary system than in the binary system. Consequently it is evident that 18C6 reacts competitively with the Ln^{3+} ion to increase the selectivity of TAC. Hence, in order to increase the separation factor of the two lanthanide chelates it is important to choose another ligand which shows an opposite coordinating trend toward lanthanides. This discussion is based on the assumption that no ternary complex, LnLA, is formed.

Acknowledgement—This work was supported by a Grant-in-Aid for Scientific Research from the Ministry of Education, Science and Culture (No. 62540450).

REFERENCES

1. R. M. Izatt, J. D. Lamb and J. J. Christensen, *J. Am. Chem. Soc.* 1977, **99**, 8344.
2. J. Massaux, J. F. Desreux, C. Delchambre and G. Duyckaerts, *Inorg. Chem.* 1980, **19**, 1893.
3. M-C. Almasio, F. Arnaud-Neu and M-J. Schwing-Weill, *Helv. Chim. Acta* 1983, **66**, 1296.
4. V. M. Loyola, R. Pizer and G. Wilkins, *J. Am. Chem. Soc.* 1977, **99**, 7185.
5. E. Ohyoshi, *Analyt. Chem.* 1985, **57**, 446.
6. E. Ohyoshi, *Polyhedron* 1986, **5**, 2101.
7. S. W. Thompson and R. H. Byrne, *Analyt. Chem.* 1988, **60**, 19.
8. R. P. Lang, *J. Am. Chem. Soc.* 1962, **84**, 1185.

Polyhedron Vol. 8, No. 12, pp. 1567–1570, 1989
Printed in Great Britain

0277–5387/89 $3.00+.00
Pergamon Press plc

SYNTHESIS AND STRUCTURAL CHARACTERIZATION OF SOLID SOLUTIONS $Cd_xHg_{1-x}B_4O_7$ ($x = 1$, 0.75, 0.5, 0.25, 0)

Y. LAUREIRO, M. L. VEIGA, A. JEREZ and C. PICO*

Departamento de Química Inorgánica I, Facultad de C.C. Químicas,
Universidad Complutense, 28040 Madrid, Spain

(*Received* 20 *July* 1988; *accepted after revision* 15 *February* 1989)

Abstract—Solid solutions, $Cd_xHg_{1-x}B_4O_7$, were obtained from $Cd(OH)_2$, HgO and $B(OH)_3$ in appropriate stoichiometric amounts, at low temperatures ranging between 523 and 623 K and 10^{-4}–10^{-5} Hg mm. These materials were characterized by X-ray powder diffraction, giving orthorhombic symmetry (space group *Pbca*, No. 61) and the lattice parameters (in Å) are: $a = 8.704$, $b = 14.176$, $c = 8.229$ (for $x = 1$), $a = 8.729$, $b = 14.168$, $c = 8.242$ (for $x = 0.75$), $a = 8.758$, $b = 14.162$, $c = 8.303$ (for $x = 0.5$), $a = 8.769$, $b = 14.147$, $c = 8.348$ (for $x = 0.25$) and $a = 8.792$, $b = 14.107$, $c = 8.382$ (for $x = 0$). IR spectra and TG are discussed on the basis of the stereochemistry of the boron atoms in these structures. The results seem to indicate that this method of synthesis can be applied to the isolation of related metal borates at temperatures that are several hundred degrees below those cited in the literature.

The binary systems MO–B_2O_3 (M = Zn, Cd) have been studied by several workers using calcinated samples.[1–7] The previous literature concerning the HgO–B_2O_3 system is quite limited,[8,9] probably due to the low thermal stability of mercury compounds.

In view of the technical applications of metallic borates and the potential uses of the CdO–B_2O_3 system for recovering materials in devices for nuclear reactors, due to the important cross sections of both elements for slow neutron capture (^{10}B, 3836 and ^{113}Cd, 2000 Barn), we have explored new methods of synthesis in order to obtain solid phases of definite stoichiometry, avoiding the usual ceramic temperature ranges. The experimental conditions are useful to synthesize various metal borates whose characterization is in progress.[10]

The aim of the present paper is to describe the preparation and structural characterization of solid solutions, $Cd_xHg_{1-x}B_4O_7$ with $x = 1, 0.75, 0.5, 0.25$ and 0.

EXPERIMENTAL

Microcrystalline solid solutions were prepared from mixtures of analytical grade $B(OH)_3$ (Merck, F.R.G.), $Cd(OH)_2$ (isolated by hydrolysis of cadmium acetate[2]) and HgO (Merck, F.R.G.), in stoichiometric amounts under a static initial vacuum of 10^{-4}–10^{-5} Hg mm at temperatures between 600 and 673 K over 24 h. An improved crystallinity of the products was obtained when cooling was performed at a rate of 0.5 K h^{-1}. The *d*-spacing measurements were made using a Siemens Kristalloflex D500 powder diffractometer, at a scanning rate of 0.1° 2θ min^{-1}, using Cu-K_α radiation and W ($a = 3.16524$ Å) as internal standard. The unit cell parameters were refined from the 2θ values of the last 14 reflections.[11] X-ray diffraction intensities I'_o were collected by step-scanning from 10 to 120° 2θ with increments of 0.02° 2θ and a counting time of 3 s for each step; the goniometer being controlled by a DACO-MPV2 computer, which carried out the integration of the diffraction peaks and the background correction. The intensities were calculated with the program RIETVELD,[12,13] assuming a unique network $B_4O_7^{2-}$ and statistical distribution of metallic ions in the general positions of the structure (space group, *Pbca*). The discrepancy factors, $R = \Sigma|I_o^{1/2} - I_c^{1/2}|/\Sigma I_o^{1/2}$, between observed and calculated intensities were computed making $I_o = KI'_o$ and $K = \Sigma I_c/\Sigma I'_o$.

Densities were determined by a picnometric method, using CCl_4 as the immersion liquid.

* Author to whom correspondence should be addressed.

Table 1. X-ray diffraction data for $Cd_xHg_{1-x}B_4O_7$ (*d*-spacings in Å)

			$x = 1$			$x = 0.75$			$x = 0.50$			$x = 0.25$			$x = 0$		
h	*k*	*l*	d_{exp}	I_o	I_c	d_{exp}	I_o	I_c	d_{exp}	I_o	I_c	d_{exp}	I_o	I_c	d_{exp}	I_o	I_c
0	2	0	7.09	118	15	7.07	116	115	7.09	118	117	7.09	114	110	—	—	—
1	1	1	5.51	691	690	5.53	628	627	5.54	646	640	5.57	353	350	5.58	252	250
0	2	1	5.37	987	1000	5.38	980	1000	5.39	970	1000	5.40	965	1000	5.41	592	590
1	2	1	4.57	138	348	4.59	392	389	4.60	464	461	4.61	465	461	4.61	171	170
2	1	0	4.160	108	115	4.179	819	815	4.184	917	910	4.195	861	860	4.199	524	520
1	0	2	3.713	296	296	3.733	864	835	3.748	923	919	3.762	781	780	3.788	362	359
1	1	2	3.598	789	781	3.610	859	851	3.635	807	800	—	—	—	3.658	399	400
0	4	0	3.544	444	488	3.545	658	655	3.543	696	694	3.541	791	790	3.529	364	361
2	3	0	3.201	937	930	3.208	930	1000	3.213	928	945	3.215	973	972	3.214	991	1000
2	3	1	2.983	306	302	2.989	467	463	2.995	348	345	2.998	615	614	3.002	285	280
1	3	2	2.923	691	725	2.930	794	791	2.941	746	740	2.948	743	740	2.953	305	304
2	4	0	2.748	197	186	2.750	307	300	2.753	376	374	—	—	—	2.762	143	140
3	1	1	2.687	187	185	2.692	322	312	2.703	272	271	2.710	342	339	2.715	83	80
1	4	2	2.566	737	842	2.565	884	883	2.575	801	800	2.580	733	726	2.580	404	400
1	2	3	2.454	98	86	2.461	349	345	2.479	354	351	2.485	385	376	2.490	224	221
3	0	2	2.371	98	110	2.378	392	390	2.388	337	329	2.396	380	375	2.403	112	110
3	1	2	—	—	—	—	—	—	—	—	—	—	—	—	2.368	149	139
2	1	3	2.290	296	298	—	—	—	2.310	309	307	—	—	—	—	—	—
2	5	1	2.282	404	390	—	—	—	2.288	641	637	2.289	433	430	2.286	83	81
0	6	1	2.271	78	68	2.267	386	384	2.276	575	570	—	—	—	2.265	272	270
4	0	0	2.176	246	235	2.182	312	310	2.192	409	400	2.194	487	473	2.198	206	200
R =				0.029			0.037			0.035			0.034			0.029	

Thermal analyses were carried out on a Mettler TG 50 thermobalance and in a DSC 30 cell attached to a Mettler TA 3000 controller. Sample weights were about 10 mg and thermal runs were performed in air at a rate of 10 K min^{-1}.

IR absorption spectra were recorded on a Perkin–Elmer 1320 spectrophotometer in the range 4000–200 cm^{-1} using KBr pellets.

The boron content was determined by titration with NaOH in the presence of mannitol.[14] Cadmium and mercury contents were measured by complexometric titration with 0.1 M EDTA using eriochrome black T as indicator,[15] and the oxygen content was assigned by difference.

RESULTS AND DISCUSSION

Chemical analyses confirm the stoichiometry $Cd_xHg_{1-x}B_4O_7$ for all the phases ($x = 1$, 0.75, 0.5, 0.25, 0) obtained.

Crystallographic data for these materials are shown in Tables 1 and 2. The discrepancy factors between observed and calculated intensities for the different reflections are in good accordance with the structural data.

The basic structures of CdB_4O_7 ($a = 8.704$, $b = 14.176$, $c = 8.229$ Å) and HgB_4O_7 ($a = 8.79$, $b = 14.10$, $c = 8.39$ Å), which are isomorphous, have been previously determined by other

Table 2. Cell parameters for $Cd_xHg_{1-x}B_4O_7$

		$x = 1$	$x = 0.75$	$x = 0.5$	$x = 0.25$	$x = 0$
a (Å)	=	8.704(1)	8.729(3)	8.758(3)	8.769(0)	8.792(0)
b (Å)	=	14.176(2)	14.168(9)	14.162(0)	14.147(1)	14.107(0)
c (Å)	=	8.229(1)	8.242(0)	8.303(0)	8.348(4)	8.382(4)
V (Å)	=	1015.36	1019.31	1029.82	1035.61	1039.60
d_x (Mg m^{-3})	=	3.51	3.77	4.02	4.28	4.55
d (Mg m^{-3})	=	3.46	3.79	3.98	4.26	4.58
Space group	=	*Pbca*	*Pbca*	*Pbca*	*Pbca*	*Pbca*
Z	=	8	8	8	8	8

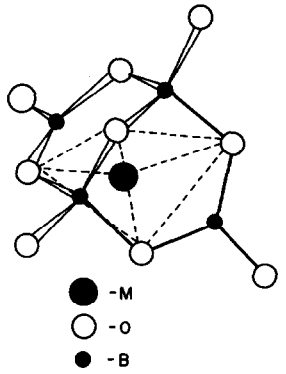

Fig. 1. View of the $B_4O_7^{2-}$ unit showing the cation environment (M = Cd, Hg).

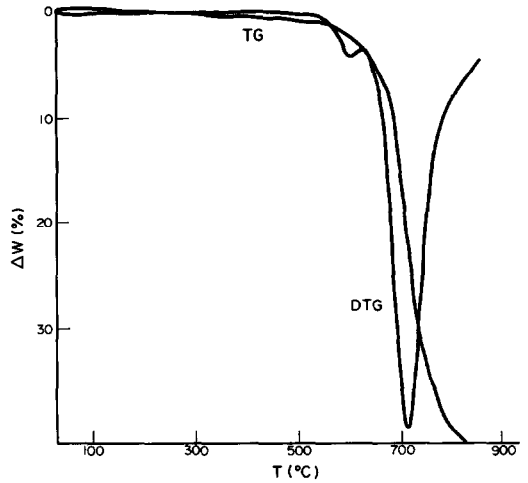

Fig. 3. Thermogravimetric curves for $Cd_{0.5}Hg_{0.5}B_4O_7$.

workers,[5-7] and our crystallographic data are in agreement with those.

Both structures consist of two infinite three-dimensional networks of B—O linkages, connected by two-fold screw axes. The network may be described as composed of borate units containing four boron atoms (two of which are tetrahedrally coordinated and two triangularly coordinated) and five oxygen atoms within the unit, as well as four oxygen atoms shared with four adjacent units. The two tetrahedra and two triangles form a $B_4O_7^{2-}$ unit as shown in Fig. 1, and which is repeated throughout the structure. The cadmium and mercury atoms are surrounded by four close oxygen atoms, arranged in a distorted tetrahedron. These atoms in the solid solutions are randomly distributed in these positions. The metal atoms therefore seems to be mainly covalent tetrahedrally bonded.

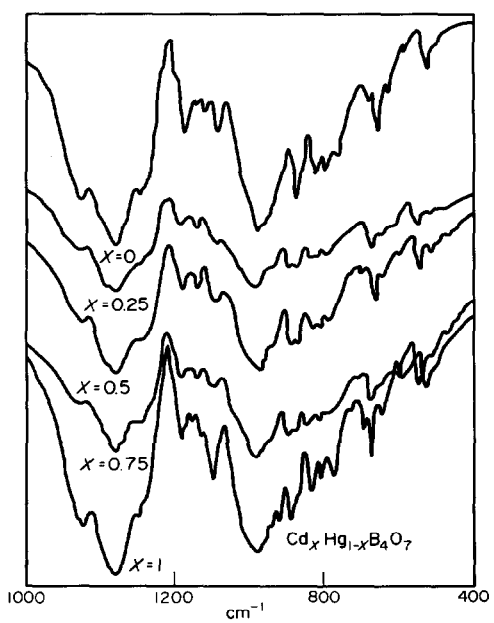

Fig. 2. IR absorption spectra of the solid solutions, $Cd_xHg_{1-x}B_4O_7$.

In Fig. 2 the IR spectra of the synthesized materials are presented. Three well-differentiated zones can be observed:[16] in the 1100–800 cm^{-1} range, strong bands that can be assigned to $\nu(BO_4)$ appear; in the 1500–1100 cm^{-1} region, the observed strong absorptions correspond to $\nu(BO_3)$; the bands in the 700–600 cm^{-1} range can be assigned to the three-fold and four-fold coordinated boron. On the other hand, the frequencies of these vibrations diminish with an increase of the mercury content in the obtained borates.

CdB_4O_7 showed no significant weight loss in this temperature interval. An X-ray diffraction pattern of the residue was identical to the one of the starting material.

TG curves of solid solutions showed weight losses which can be assigned to the mercury elimination according to the process:

$$Cd_xHg_{1-x}B_4O_7 \longrightarrow xCdB_4O_7 + (1-x)Hg + (2-2x)B_2O_3 + 1-x/2O_2.$$

The decomposition residues were characterized by X-ray diffraction and showed the characteristic spacings of CdB_4O_7, broadened as a consequence of the presence of vitreous B_2O_3. Figure 3 shows the thermogravimetric curve for $x = 0.5$.

For $x = 0$ (HgB_4O_7), the decomposition process led to a vitreous residue amorphous to the X-ray. The observed weight loss (59.9%) is concordant with the complete sublimation of mercury and the formation of B_2O_3 (calc. 60.88%).

Acknowledgement—We acknowledge the financial support of CAICYT (Spain), Grant PB85-0057.

REFERENCES

1. E. C. Rao and F. H. Humel, *J. Electrochem. Soc.* 1956, **103**, 29.
2. Y. Laureiro, C. Pico and A. Jerez, *Synth. React. Inorg. Met-Org. Chem.* 1988, **18**, 119.
3. P. B. Hart and E. G. Sheward, *J. Inorg. Nucl. Chem.* 1962, **24**, 633.
4. W. D. Hand and J. Krogh-Moe, *J. Am. Chem. Soc.* 1962, **45**, 197.
5. B. M. Ihara and J. Krogh-Moe, *Acta Cryst.* 1966, **20**, 132.
6. M. Martínez-Ripoll, S. Martínez-Carrera and S. García-Blanco, *Acta Cryst.* 1971, **27B**, 672.
7. E. V. Sokolova and M. A. Simonov, *Dokl. Akad. Nauk. SSSR* 1979, **247**, 603.
8. A. Chretien and R. Priou, *C.R. Acad. Sci. Paris* 1970, **271**, 1310.
9. C. Chang and A. Margrave, *Inorg. Chim. Acta* 1967, **3**, 378.
10. Y. Laureiro, M. L. Veiga, A. Jerez and C. Pico, *Eur. J. Solid State Inorg. Chem.* 1988, **25**, 381.
11. A. Jerez, Programas de Cálculo (Rayos X).
12. P. Thompson and I. G. Wood, *J. Appl. Cryst.* 1983, **16**, 458.
13. M. Martínez-Ripoll and J. Fayos, Inst. Rocasolano (C.S.I.C.), Madrid (1987).
14. N. Howell Furman (Ed.), *Scott's Standard Methods of Chemical Analysis*, 6th edn. Princeton, New Jersey (1962).
15. *Métodos complexométricos de valoración con EDTA*, 3rd edn. Merck, Darmstadt (1987).
16. C. E. Weir and R. A. Schroeder, *J. Res. NBS* 1966, **68A**, 465.

Polyhedron Vol. 8, No. 12, pp. 1571–1573, 1989
Printed in Great Britain

0277–5387/89 $3.00+.00
© 1989 Pergamon Press plc

COMMUNICATION

POLYOXOMOLYBDATE–ALKOXIDE INTERACTIONS. THE CRYSTAL AND MOLECULAR STRUCTURES OF THE ERYTHRITOLATE COMPLEXES $[(n\text{-}C_4H_9)_4N]_2[Mo_2O_5(eryth)]$ AND $[(n\text{-}C_4H_9)_4N][Mo_2O_5(Heryth)]$

LIDUN MA

Center for Measurements and Analysis, Fudan University, Shanghai, P.R.C.

and

SHUNCHENG LIU and JON ZUBIETA*

Department of Chemistry, State University of New York at Albany, Albany, NY 12222, U.S.A.

(*Received* 30 *January* 1989; *accepted* 14 *March* 1989)

Abstract—The reaction of $[(n\text{-}C_4H_9)_4N]_2[Mo_2O_7]$ with *meso*-erythritol in methanol yields $[(n\text{-}C_4H_9)_4N]_2[Mo_2O_5(eryth)]\cdot 0.5C_4H_{10}O_4\cdot H_2O$ (**I**), a complex having the $[Mo_2O_5]^{2+}$ core bound to a single erythritolate tetraanion. Reaction of **I** with chloroacetic acid in methanol results in a single protonation of the coordinated erythritolate ligand to give $[(n\text{-}C_4H_9)_4N][Mo_2O_5(Heryth)]$ (**II**). Crystal data: $C_{40}H_{85}N_2O_{12}Mo_2$ (**I**): orthorhombic, space group *Pbca*, $a = 16.651(3)$, $b = 24.043(5)$, $c = 24.935(5)$ Å, $V = 9982.5(12)$ Å^3, $Z = 8$, $D_{calc} = 1.30$ g cm^{-3}; 3625 reflections to give $R = 0.0522$. $C_{20}H_{43}NO_9Mo_2$ (**II**): monoclinic, space group $P2_1/n$, $a = 21.827(4)$, $b = 18.638(3)$, $c = 29.188(4)$ Å, $\beta = 108.3(1)°$, $V = 11269.9(15)$ Å^3, $Z = 16$, $D_{calc} = 1.49$ g cm^{-3}; 5911 reflections to give $R = 0.0687$.

Coordination complexes of polyoxomolybdates with alkoxy ligands[1–3] have been discussed as models for surface-bound intermediates in heterogeneous catalysis employing solid molybdenum oxides.[4–8] We recently reported the synthesis and structure of $[(n\text{-}C_4H_9)_4N][Mo_2O_5(C_8H_{13}O_5)]\cdot 0.5(C_2H_5)_2O$,[9] a complex containing the $[Mo_2O_5]^{2+}$ core ligated to a tetradentate ligand derived from 2,3,4,5-tetrahydroxy-2,3,4,5-tetramethylfuran, a structure closely related to those of the lyxose dimolybdate, $(NH_4)[Mo_2O_5(C_4H_5O_5)]$,[10] and of the mannitolate derivative $[(n\text{-}C_4H_9)_4N][Mo_2O_5(C_6H_{10}O_6)]$.[11] In the course of our investigations of polyoxomolybdate–polyalkoxide interactions, we have examined the chemistry of *meso*-erythritol with molybdate and have isolated both the tetraanionic and trianionic ligated derivatives, $[(n\text{-}C_4H_9)_4N]_2[Mo_2O_5(eryth)]\cdot 0.5C_4H_{10}O_4\cdot H_2O$ (**I**) and $[(n\text{-}C_4H_9)_4N][Mo_2O_5(Heryth)]$ (**II**), respectively. The conformation of the tetradentate ligand

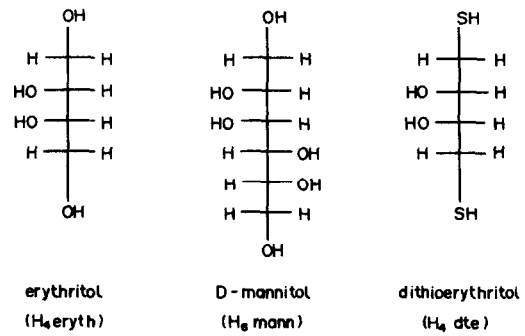

* Author to whom correspondence should be addressed.

is relevant to discussions of dimolybdate binding by dithiothreitol and dithioerythritol, a required component in the synthesis of Fe—Mo cubane clusters by rhodanese.[1,2] Furthermore, the dimolybdate core is shown to be sufficiently flexible in its coordination requirements to accommodate both the $(eryth)^{4-}$ and $(Heryth)^{3-}$ forms of the ligand.

Reaction of $[(n\text{-}C_4H_9)_4N]_2[Mo_2O_7]$ with an equimolar amount of *meso*-erythritol in methanol, followed by addition of ether, gives colourless transparent blocks of a mixture of $[(n\text{-}C_4H_9)_4N]_2[Mo_2O_5(eryth)]\cdot 0.5C_4H_{10}O_4\cdot H_2O$ **(I)** and $[(n\text{-}C_4H_9)_4N][Mo_2O_5(Heryth)]$ **(II)** in 60% yield.* Recrystallization of a portion of the product from methanol–ether, to which triethylamine has been added, yields **I** in pure form, while recrystallization of the remaining portion of the product from methanol, to which several drops of chloroacetic acid have been added, gives **II**. The IR spectrum of **I** is characterized by strong bands at 920 and 905 cm^{-1} associated with $\nu_s(Mo{=}O)$ and $\nu_{as}(Mo{=}O)$, respectively, and a number of features in the 650–900 cm^{-1} range associated with ν(Mo—O—Mo) and ν(Mo—O—alkoxy). Complex **II** exhibits similar IR characteristics with the bands attributed to $\nu_s(Mo{=}O)$ and $\nu_{as}(Mo{=}O)$ appearing at 935 and 905 cm^{-1}, respectively, and a strong, broad absorption at 3410 cm^{-1}, associated with ν(O—H) for the protonated trianionic ligand. The complexes are readily interconverted by the addition of acid or base:

$$\underset{\textbf{(I)}}{[Mo_2O_5(eryth)]^{2-}} \underset{-H^-}{\overset{+H^+}{\rightleftharpoons}} \underset{\textbf{(II)}}{[Mo_2O_5(Heryth)]^-}.$$

Complex **I** crystallizes in the orthorhombic space group *Pcab* with $a = 16.651(3)$, $b = 24.043(5)$, $c = 24.935(5)$ Å, $V = 9982.5(12)$ Å^3, $Z = 8$, $D_{calc} = 1.30$ g cm^{-3}. Structure solution and refinement based on 3625 reflections with $F_o \geq 6\sigma(F_o)$ (Mo-K_α, $\lambda = 0.71073$ Å) converged at $R = 0.0522$. Complex **II** is monoclinic, $P2_1/n$ with $a = 21.827(4)$, $b = 18.638(3)$, $c = 29.188(4)$ Å, $\beta = 108.3(1)°$, $V = 11269.9(15)$ Å^3, $Z = 16$, $D_{calc} = 1.49$ g cm^{-3}. Structure solution and refinement were based on 5911 reflections (conditions as for **I**) and converged at $R = 0.0687$.

The structure of the dinegative anion of **I**, $[Mo_2O_5(eryth)]^{2-}$, is illustrated in Fig. 1, with selected bond lengths and angles presented in the caption. The structure consists of the *syn*-$[Mo_2O_5]^{2+}$ core, bridged and chelated by a single tetradentate tetraanionic erythritolate ligand. The ligand configuration is such that alternate hydroxylate groups bridge the molybdenum centres. This chelation mode requires that the Mo—O_b—Mo angle decreases from the usual range of 112–115° to 104.4(3)°. The Mo—O(bridging alkoxy) distances are inequivalent, such that Mo—O(6) is 2.280(10) Å (av) while Mo—O(8) is 2.203(11) Å (av).†

The structure of one of the four crystallographically-independent monoanions of **II**, $[Mo_2O_5(Heryth)]^-$, shown in Fig. 2, is seen to consist of the same tetradentate ligand configuration about the $[Mo_2O_5]^{2+}$ core as that exhibited by **I**. The most significant structural consequence of pro-

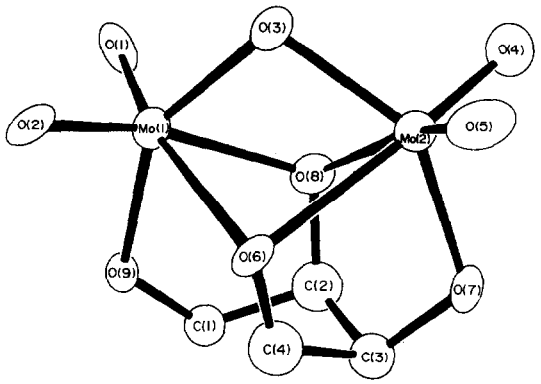

Fig. 1. Perspective view of the complex anion $[Mo_2O_5(C_4H_6O_4)]^{2-}$ **(I)**, showing the atom labelling scheme. Selected bond lengths (Å) and angles (°):

Mo(1)—Mo(2)	3.065(1)	Mo(2)—O(4)	1.658(8)
Mo(1)—O(1)	1.690(6)	Mo(2)—O(5)	1.691(8)
Mo(1)—O(2)	1.661(7)	Mo(2)—O(3)	1.921(6)
Mo(1)—O(3)	1.953(6)	Mo(2)—O(6)	2.271(6)
Mo(1)—O(6)	2.289(6)	Mo(2)—O(7)	1.973(7)
Mo(1)—O(8)	2.208(7)	Mo(2)—O(8)	2.198(7)
Mo(1)—O(9)	1.929(6)		

O(1)—Mo(1)—O(8)	158.8(3)
O(2)—Mo(1)—O(6)	165.5(3)
O(3)—Mo(1)—O(9)	145.1(3)
O(4)—Mo(2)—O(8)	162.8(3)
O(5)—Mo(2)—O(6)	164.9(3)
O(3)—Mo(2)—O(7)	142.8(3)
Mo(1)—O(3)—Mo(2)	104.4(3)
Mo(1)—O(6)—Mo(2)	84.5(2)
Mo(1)—O(8)—Mo(2)	88.2(2)

* Elemental analyses: Found: C, 49.3; H, 8.8; N, 3.1. Calc. for $C_{36}H_{78}N_2O_9Mo_2$ **(I)** (solvent molecules of crystallization are lost upon heating in vacuum): C, 49.4; H, 8.9; N, 3.2%. Found: C, 37.6; H, 6.7; N, 2.0. Calc. for $C_{20}H_{43}NO_9Mo_2$ **(II)**: C, 37.9; H, 6.8; N, 2.2%.

† Final atomic positional and thermal parameters, bond lengths and angles, and F_o/F_c values have been deposited as supplementary material with the Editor, from whom copies are available on request. Atomic coordinates have also been submitted to the Cambridge Crystallographic Data Centre.

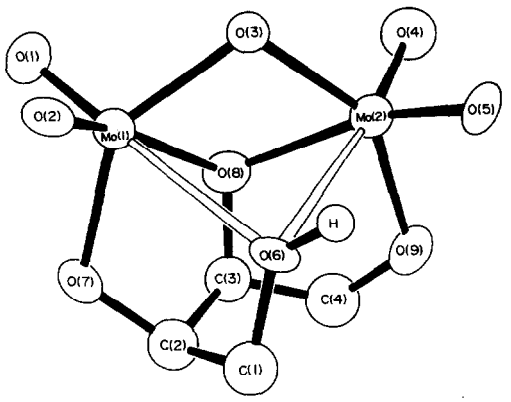

Fig. 2. Perspective view of the complex anion $[Mo_2O_5(C_4H_7O_4)]^-$ (II), showing the atom labelling scheme. Selected bond lengths (Å) and angles (°):

Mo(1)—Mo(2)	3.138(3)	Mo(2)—O(3)	1.92(1)
Mo(1)—O(1)	1.63(1)	Mo(2)—O(4)	1.71(1)
Mo(1)—O(2)	1.74(1)	Mo(2)—O(5)	1.70(2)
Mo(1)—O(3)	1.92(1)	Mo(2)—O(6)	2.53(1)
Mo(1)—O(6)	2.50(1)	Mo(2)—O(8)	2.13(1)
Mo(1)—O(7)	1.93(1)	Mo(2)—O(9)	1.91(1)
Mo(1)—O(8)	2.16(1)		

O(1)—Mo(1)—O(6)	171.3(5)
O(2)—Mo(1)—O(8)	157.5(6)
O(3)—Mo(1)—O(7)	138.4(6)
O(4)—Mo(2)—O(5)	170.9(7)
O(5)—Mo(2)—O(8)	154.3(6)
O(3)—Mo(2)—O(9)	143.2(5)
Mo(1)—O(3)—Mo(2)	109.5(6)
Mo(1)—O(6)—Mo(2)	77.2(4)
Mo(1)—O(8)—Mo(2)	94.1(5)

tonation of the alkoxy group O(6) is the lengthening of the Mo—O(6) bond distances to 2.52(2) Å (av), an unusually long distance when compared to the range of 2.10–2.30 Å, characteristic for bridging alkoxide groups.

The coordination of the $[Mo_2O_5]^{2+}$ core to the tetradentate ligands $(eryth)^{4-}$ and $(Heryth)^{3-}$ in **I** and **II**, respectively, through four consecutive hydroxylate groups with alternate oxygen donors bridging the Mo centres, is also characteristic of the structures of $[Mo_2O_5(C_8H_{13}O_5)]^-$,[9] $[Mo_2O_5(C_4H_5O_5)]^-$[10] and $[Mo_2O_5(mannitolate)]^-$.[11] It is noteworthy that the dithiothreitol structure, $[Mo_2O_5(dtt)]^{2-}$, exhibits bridging through the adjacent alkoxy oxygen donors with the thiolate groups terminal, to provide the only structurally characterized example of binding mode **IV** for such tetradentate ligand types.[12] Although the analogous dithioerythritolate complex, $[Mo_2O_5(dte)]^{2-}$, has not been structurally characterized, it may be argued that the correlation between the configurations of the chelating portion of D-mannitol and *meso*-

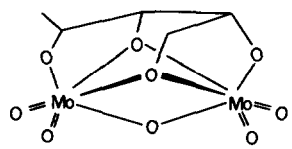

(III)

erythritol to *meso*-dithioerythritol suggests binding mode **III**. The difficulties encountered in the purification and crystallization of the dithioerythritolate complex may reflect the presence of several complex forms as a consequence of variable ligand protonations, $[Mo_2O_5(H_xdte)]^{(2-x)-}$.

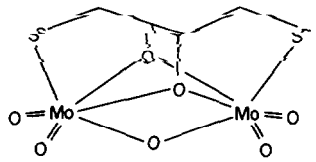

(IV)

The characterization of both $[Mo_2O_5(eryth)]^{2-}$ (**I**) and $[Mo_2O_5(Heryth)]^-$ (**II**) and their ready interconversion, suggest that variations in the degree of ligand deprotonation may be characteristic of complexes containing polyalkoxide and polyalkoxide–thiolate ligands. We are currently investigating the chelation modes of various polyalkoxides and polythiolates with molybdenum–oxo species.

Acknowledgement—This work was supported by NSF grant CHE8514634 to J. Zubieta.

REFERENCES

1. E. M. McCarron III and R. L. Harlow, *J. Am. Chem. Soc.* 1983, **105**, 6179.
2. A. J. Wilson, W. T. Robinson and C. J. Wilkins, *Acta Cryst.* 1983, **C39**, 54.
3. S. Liu, S. N. Shaikh and J. Zubieta, *Inorg. Chem.* 1987, **26**, 4303.
4. R. K. Graselli and J. D. Burrington, *Adv. Catal.* 1981, **30**, 133.
5. H.-F. Liu, R.-S. Liu, K. Y. Liew, R. E. Johnson and J. H. Lunsford, *J. Am. Chem. Soc.* 1984, **106**, 4117.
6. C. J. Machiels, U. Chrowdry, R. H. Staley, F. Ohuchi and A. W. Sleight, in *Catalytic Conversions of Synthetic Gas and Alcohols to Chemicals* (Edited by R. G. Herman). Plenum Press, New York (1984).
7. V. W. Day and W. G. Klemperer, *Science* 1985, **228**, 533.
8. M. T. Pope, *Heteropoly and Isopoly Oxometalates*. Springer, New York (1983).
9. S. Liu and J. Zubieta, *Polyhedron* 1989, **8**, 1213.
10. G. E. Taylor and J. M. Waters, *Tetrahedron Lett.* *1981*, *22*, *1277*.
11. B. Hedman, *Acta Cryst.* 1977, **B33**, 3077.
12. S. J. N. Burgmayer and E. I. Stiefel, *Inorg. Chem.* 1988, **27**, 2518.

Polyhedron Vol. 8, No. 12, pp. 1575–1577, 1989
Printed in Great Britain

0277–5387/89 $3.00+.00
© 1989 Pergamon Press plc

COMMUNICATION

METAL PROMOTED REARRANGEMENT OF $Ph_2PO_2CCH{=}CH_2$; CRYSTAL AND MOLECULAR STRUCTURE OF $[RhCl(Ph_2POPPh_2)(PPh_3)]\cdot THF$, TETRAPHENYLDIPHOSPHOXANE-TRIPHENYLPHOSPHINE CHLORORHODIUM(I) (TETRAHYDROFURAN) 1:1

DEREK J. IRVINE and DAVID J. COLE-HAMILTON*

Chemistry Department, University of St. Andrews, St. Andrews, Fife KY16 9ST, Scotland, U.K.

and

JOHN BARNES

Chemistry Department, University of Dundee, Dundee, Tayside, Scotland, U.K.

and

PHILIP K. G. HODGSON

BP Research Centre, Sunbury-on-Thames, Middlesex, U.K.

(*Received* 30 *January* 1989; *accepted* 15 *March* 1989)

Abstract—Reaction of $[RhCl(PPh_3)_3]$ with two mole equivalents of $Ph_2PO_2CCH{=}CH_2$ produces $[RhCl(Ph_2POPPh_2)(PPh_3)]$, involving a major rearrangement of the ligand to tetraphenyldiphosphoxane, a bidentate diphenyl phosphinous acid anhydride exhibiting a very short P—P separation (2.457 Å).

Ligands of the general form $Ph_2PO_2CCR{=}CR'R''$ are of interest since they promote the binding of highly functionalized alkenes to transition metals and allow such alkenes to take part in catalytic reactions.[1,2] The mechanisms of these reactions are believed to involve both metal and phosphorus centred steps.[2] These complexes also promote regioselective reactions, for example hydrogenation centred on the C(2) double bond of hexa-2,4-dienoic acid.[2]

During studies of the coordination chemistry of this form of ligand, bonding is observed through (i) the phosphorus alone as in $[RhCl(PPh_3)_2(Ph_2PO_2CCH{=}CMe_2)]$, (ii) phosphorus and oxygen, as in $[Rh(PPh_3)_2(Ph_2PO_2CCH{=}CMe_2)][SbF_6]$[3] and (iii) phosphorus and the double bond as in $[RhCl(Ph_2PO_2CCH{=}CMe_2)]_2$.[1] We now report studies of reactions of $Ph_2PO_2CCH{=}CH_2$, which show that disruption of the ligand can occur, producing a rare example of a complex containing tetraphenylphosphoxane, a diphenylphosphinous acid anhydride.

Reaction of $[RhCl(PPh_3)_3]$ with 2 mol equivalents of $Ph_2PO_2CCH{=}CH_2$ prepared from Ph_2PCl, propenoic acid and triethylamine, but not isolated, in tetrahydrofuran (THF) at 3°C produces an orange solution, from which yellow crystals separate on standing at 3°C for several days. The spectroscopic†

* Author to whom correspondence should be addressed.

† ^{31}P NMR δ 106.5 ddd, P_A, $J(RhP_A)$ 170 Hz, $J(P_AP_B)$ 122 Hz, $J(P_AP_C)$ 30 Hz; δ 81.2 ddd, P_B, $J(RhP_B)$ 125 Hz, $J(P_BP_C)$ 382 Hz; δ 25.1 ddd, P_c, $J(RhP_c)$ 132 Hz. FABMS 786 (M^+), 751 ($M—Cl^+$).

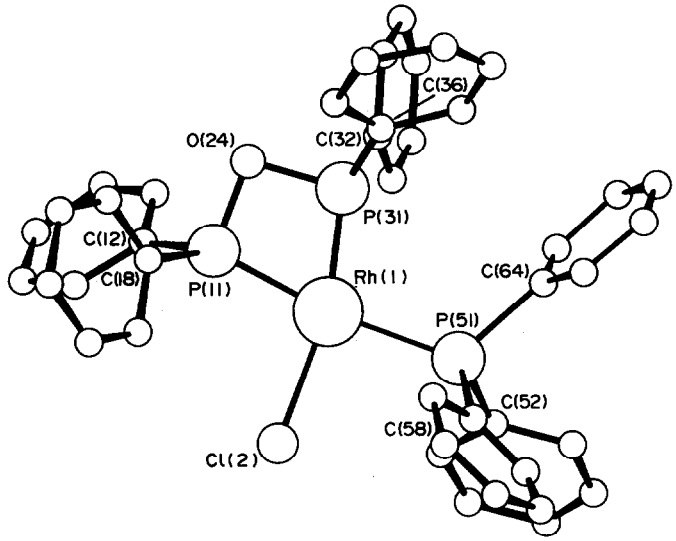

Fig. 1. X-ray structure and numbering scheme for $[RhCl(PPh_3)(Ph_2POPPh_2)]\cdot THF$ (the THF molecule is omitted from the figure).

properties and X-ray crystal* structure show that the compound is $[RhCl(PPh_3)(Ph_2POPPh_2)]\cdot THF$, indicating that a major rearrangement of the $Ph_2PO_2CCH{=}CH_2$ ligand had occurred. Under similar conditions (standing at 3°C for a day), $Ph_2PO_2CCH{=}CH_2$ is stable, with only slight decomposition occurring to give tetraphenyldiphosphine monoxide.[4] The bidentate binding of Ph_2POPPh_2 has only previously been observed in carbonyl complexes of group 6 metals.[5] $[RhCl(PPh_3)(Ph_2POPPh_2)]$ has also been obtained from reaction of 1 mol equivalent of isolated $Ph_2PO_2CCH{=}CHMe$ with isolated $[RhCl(PPh_3)(Ph_2PO_2CCH{=}CHMe)]$, as well as from $[RhCl(PPh_3)_3]$ and isolated $Ph_2PO_2CCH{=}CH{-}CH{=}CHMe$, although in the last case $[RhCl(PPh_3)_2L]$ ($n = 1$ or 2) are also products.[3]

In an attempt to discover the mechanism of the metal promoted rearrangement, we have carried out *in situ* ^{31}P NMR studies. Addition of 1 mol equivalent of $Ph_2PO_2CCH{=}CH_2$ to $[RhCl(PPh_3)_3]$, immediately gives what is thought to be $[RhCl(PPh_3)(Ph_2PO_2CCH{=}CH_2)]$ with *trans* phosphorus atoms and binding of the mixed anhydride through the phosphorus and the double bond.† This compound is stable in solution during the time-scale of the experiment at low temperature, but on addition of a further equivalent of $Ph_2PO_2CCH{=}CH_2$ immediately gives another, as yet unidentified, compound which slowly rearranges to the final product. The observation of $[RhCl(PPh_3)(Ph_2PO_2CCH{=}CH_2)]$ as an intermediate and the failure to produce $[RhCl(PPh_3)(Ph_2POPPh_2)]$ from reaction of $[RhCl(PPh_3)_3]$ with preformed tetraphenyldiphosphine monoxide confirm that the rearrangement to Ph_2POPPh_2 is metal promoted. These reactions are summarized in Scheme 1.

The X-ray structure of $[RhCl(Ph_2POPPh_2)(PPh_3)]$ is shown in Fig. 1, together with important bond lengths and angles in Table 1. The most important are those of the RhPOP ring. The ring angles are all much smaller than the strain free values, most markedly the tight angles at rhodium (68.39°) and oxygen (95.40°), which result in the close approach of the two ring phosphorus atoms (2.457 Å separation). The distance is much less than the sum of the van der Waals radii of phosphorus (3.2 Å), but longer than the largest found P—P single bond distances (2.35 Å in P_4S_7). The usual bonded distances are in the region of 2.10–2.20 Å.

* Crystallographic data: Formula $C_{42}H_{35}ClOP_3Rh\cdot C_4H_8O$, $M = 786.50$, triclinic, space group $P\bar{1}$ $a = 11.294(4)$, $b = 11.475(6)$, $c = 17.144(9)$ Å, $\alpha = 102.31(4)$, $\beta = 102.71(4)$, $\gamma = 74.11(4)°$, $V = 2056.68$ Å^3, $Z = 2$, $D_x = 1.270$ g cm^{-3}, λ (Mo-K_α) = 0.71069 Å, $\mu = 5.60$ cm^{-1}, $F(000) = 878.00$, $T = 293$ K, $R = 0.0718$ for 2329 reflections. Final refinement (minimizing $w||F_o|-|F_c||^2$), 486 refined parameters, $wR = 0.0746$, $w = 1.9641/(\sigma^2(F)+0.000618F^2)$, mean shift/ESD = 0.008, max. shift/ESD = 0.050, max. diff. peak = 0.873, max. neg. peak = 1.427 e Å^{-3}. The atomic coordinates together with complete tables of bond lengths and angles are available on request from the Director of the Cambridge Crystallographic Data Centre, University Chemical Laboratories, Lensfield Road, Cambridge CB2 1EW, U.K. Any request should be accompanied by the full literature citation for this communication.

† ^{31}P δ 113.4 dd, P_D, $J(RhP_D)$ 128 Hz, $J(P_DP_E)$ 439 Hz; δ 28.07 dd, P_E, $J(RhP_E)$ 108 Hz.

Table 1. Selected bond lengths and angles for $[RhCl(PPh_3)(Ph_2POPPh_2)]$

Bond lengths (Å)		Bond angles (°)	
Rh—Cl	2.394(6)	Cl—Rh—P(51)	91.1(2)
Rh—P(31)	2.156(5)	Cl—Rh—P(11)	97.4(2)
Rh—P(11)	2.215(4)	P(11)—Rh—P(31)	68.4(2)
Rh—P(51)	2.356(4)	P(31)—Rh—P(51)	103.1(2)
P(11)—O(24)	1.648(12)	Rh—P(11)—O(24)	97.3(4)
P(31)—O(24)	1.674(10)	Rh—P(31)—O(24)	98.8(4)
		P(11)—O(24)—P(31)	95.4(11)

Table 2. Intra-ring angles for known complexes of Ph_2POPPh_2 with bidentate coordination

	Angles (°)				
Metal	$M—P_1—O$	$M—P_2—O$	P—O—P	P—M—P	Reference
Mo	96.9(1)	96.0(1)	103.3(1)	63.82(3)	5
Cr	97.0(1)	96.1(1)	100.2(1)	66.76(4)	5
Rh	98.8(4)	97.3(4)	95.4(5)	68.4(2)	This work

The P···P distance is less than that in the related $[M(CO)_4(Ph_2POPPh_2)]$ complexes, M = Mo (2.608 Å) or Cr (2.533 Å),[4] and also less than those usually observed in bidentate $Ph_2PCH_2PPh_2$ complexes.[6] MNDO calculations do not indicate any significant P—P bonding.[7] A comparison of the various ring angles in the complexes of Cr, Mo and Rh (Table 2) show that the M—P—O angles are $97.5 \pm 1.5°$ in all cases, suggesting that it is the rigidity of these angles that predetermine the overall ring geometry. Unfortunately, the crystal structure of the isoelectronic $[RhCl(Ph_2PCH_2PPh_2)(PPh_3)]$ has not been reported, although a similar value for $J_{P—P}$ between the $Ph_2PCH_2PPh_2$ phosphorus atoms and that for Ph_2POPPh_2 suggests that it may have similar P—P interactions.[6]

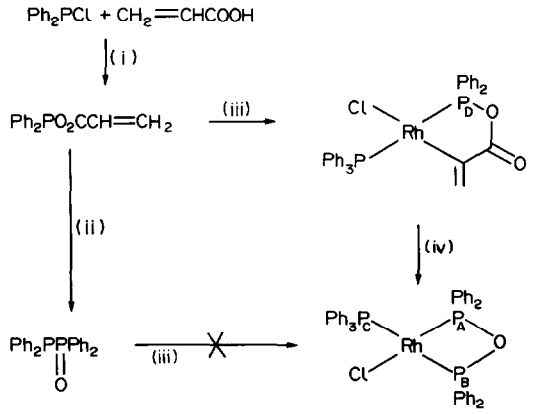

Scheme 1. Preparation and rearrangement of $Ph_2PO_2CCH{=}CH_2$ in the presence or absence of a metal centre: (i) NEt_3, THF, 3°C; (ii) THF, 3°C, 7 days; (iii) $[RhCl(PPh_3)_3]$, 1 : 1, THF, 3°C, 10 min; (iv) $Ph_2PO_2CCH{=}CH_2$, 1 mol equiv, THF, 3°C, 3 days.

The structure, which is distorted square-planar abour rhodium, has an almost planar Rh—P—O—P ring, the oxygen being 0.083 Å out of the P—Rh—P plane. This may be due to the slight difference in angles between the left and right side of the structure, resulting from one ring phosphorus being *trans* to the chlorine atom and the second *trans* to the much bulkier triphenylphosphine group. Hence, the ring geometry is altered slightly to relieve the strain.

Acknowledgements—We thank BP Research International and the SERC for a studentship (D.J.I.), Dr A. Howie (University of Aberdeen) for collection of the X-ray data set and Johnson Matthey plc for generous loans of rhodium salts. The high field NMR machine was purchased mainly with a grant from the SERC.

REFERENCES

1. D. C. Cupertino and D. J. Cole-Hamilton, *J. Chem. Soc., Dalton Trans.* 1987, 443.
2. S. A. Preston, D. C. Cupertino, P. Palma Ramirez and D. J. Cole-Hamilton, *J. Chem. Soc., Chem. Commun.* 1986, 977.
3. D. C. Cupertino, PhD thesis. University of Liverpool, U.K. (1985).
4. K. M. Abraham and J. R. van Wazer, *J. Organomet. Chem.* 1975, **85**, 41.
5. E. H. Wong, L. Prasad, E. J. Gabe and F. C. Bradley, *J. Organomet. Chem.* 1982, **236**, 321 and refs therein.
6. K. W. Chiu, H. S. Rzepa, R. N. Sheppard, G. Wilkinson and W-K. Wong, *Polyhedron* 1982, **1**, 809.
7. C. Glidewell, private communication.

Polyhedron Vol. 8, No. 12, pp. 1579–1580, 1989
Printed in Great Britain

0277–5387/89 $3.00+.00
© 1989 Pergamon Press plc

COMMUNICATION

SYNTHESIS AND X-RAY CRYSTAL STRUCTURE OF A HOMOLEPTIC BISMUTH AMIDE

WILLIAM CLEGG, NEVILLE A. COMPTON, R. JOHN ERRINGTON,* NICHOLAS C. NORMAN* and NEIL WISHART

Department of Chemistry, The University of Newcastle upon Tyne, Newcastle upon Tyne NE1 7RU, U.K.

(*Received* 27 *February* 1989; *accepted* 16 *March* 1989)

Abstract—The reaction between $BiCl_3$ and 3 equivalents of $Li[NPh_2]$ in THF solution affords the bismuth amide complex, $[Bi(NPh_2)_3]$, which has been characterized by X-ray crystallography.

Current interest in the chemistry of bismuth containing compounds is, in part, due to their importance as heterogeneous catalysts[1] and more recently, as superconducting materials with high critical temperatures.[2] Whilst many synthetic routes to such materials are available, any solution based methods are potentially hampered by the apparent lack of suitable precursors reported in the literature. This is particularly evident in the case of bismuth amides and alkoxides, very few reports of which exist. With regard to the former, the only accounts dealing with homoleptic complexes, of which we are aware, describe the syntheses of $[Bi(NR_2)_3]$ (R = Me, Et, *n*-Pr),[3] $[Bi\{N(SiMe_3)_2\}_3]$[4] and $[Bi\{N(Me)SiMe_3\}_3]$,[5] with other examples of molecules containing bismuth bound amides being $[Bi(Me)_2\{N(Me)SiMe_3\}]$,[6] $[BiCl_2(NEt_2)]$,[7] $[BiBr_2(NMe_2)]$,[8] $[BiI(NHR)_2]$ (R = *n*-Pr, *n*-Bu)[9] and $[BiMe_x\{N(Me)SiMe_3\}_y]$ ($x = 1$, $y = 2$; $x = 2$, $y = 1$).[5] As part of a study of bismuth chemistry in general, we have become interested in bismuth amides and report herein some preliminary results including the first crystal structure determination of this class of compound.

A solution of $Li[NPh_2]$ in THF (20 cm^3) was prepared from $HNPh_2$ (1.25 g, 7.42 mmol) and Bu^{n}Li (2.9 cm^3 of a 2.5 M hexane solution, 7.42 mmol) at 0°C. After stirring for 30 min, the solution containing $Li[NPh_2]$ was added to a solution of $BiCl_3$ (0.779 g, 2.47 mmol) in THF (25 cm^3) and the resulting mixture was stirred for 3 h at room temperature. Removal of all volatiles, followed by extraction with toluene (3 × 15 cm^3) and subsequent filtration, afforded an orange solution of $[Bi(NPh_2)_3]$ (**1**), from which an orange solid was obtained upon removal of the toluene under reduced pressure.

Analytically pure crystals of **1** were obtained by solvent diffusion from CH_2Cl_2 (5 cm^3)–hexane (25 cm^3) at −30°C over a period of days (0.53 g, 30%), these being suitable for X-ray diffraction.

Compound **1** is soluble in toluene, THF and CH_2Cl_2, and is very sensitive to traces of moisture.

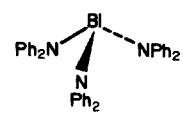

(1)

Characterization was effected by spectroscopic and analytical methods† and confirmed by an X-ray crystallographic study, the results of which are shown in Fig. 1.‡ Compound **1** crystallizes with two

* Authors to whom correspondence should be addressed.

† Spectroscopic data for **1**: NMR in CD_2Cl_2, ^1H, complex multiplets centred at δ 7.2, 6.8 and 6.5, $^{13}C\{^1H\}$ δ 151.7, 144.4, 130.0, 129.9, 124.9, 123.0, 119.0. Found: C, 60.4; H, 4.4; N, 6.0. Calc. for $C_{36}H_{30}BiN_3$: C, 60.6; H, 4.2; N, 5.9%.

‡ Crystal data for **1**: $C_{36}H_{30}BiN_3$, $M = 713.6$, triclinic, $a = 10.314(2)$, $b = 14.670(2)$, $c = 21.292(3)$ Å, $\alpha = 107.97(1)$, $\beta = 95.77(1)$, $\gamma = 99.95(1)°$, $V = 2977.4$ Å^3, $Z = 4$, space group $P\bar{1}$; $R = 0.104$, $R_w = 0.058$ from 4354 unique observed reflections with $2\theta < 45°$, measured with Mo-K_α radiation ($\lambda = 0.71073$ Å) and corrected for absorption. Atomic coordinates, bond lengths and angles, and thermal parameters have been deposited as supplementary data with the Editor from whom copies are available on request. Atomic coordinates have also been deposited with the Cambridge Crystallographic Data Centre.

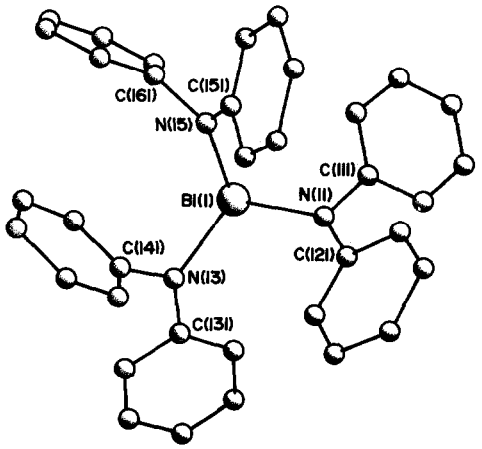

Fig. 1. A diagram of the molecular structure of one of the molecules in the crystal structure of **1**. Important bond length and angle data include:

	Å		Å
Bi(1)—N(11)	2.17(2)	Bi(1)—N(13)	2.28(2)
Bi(1)—N(15)	2.16(3)	Bi(2)—N(21)	2.12(2)
Bi(2)—N(23)	2.26(3)	Bi(2)—N(25)	2.21(4)

	deg.
N(11)—Bi(1)—N(13)	100(1)
N(11)—Bi(1)—N(15)	96(1)
N(13)—Bi(1)—N(15)	100(1)
N(21)—Bi(2)—N(23)	101(1)
N(21)—Bi(2)—N(25)	97(1)
N(23)—Bi(2)—N(25)	99(1)

molecules in the asymmetric unit (one of which is shown in Fig. 1), although the overall molecular geometries of each do not differ significantly and there are no short intermolecular contacts. Each bismuth centre adopts a trigonal pyramidal coordination geometry (sum of angles at Bi(1) = 296°, at Bi(2) = 297°), being bonded to three NPh_2 groups (av. Bi(1)—N = 2.20 Å, Bi(2)—N = 2.20 Å). The amido fragments contain a trigonal planar nitrogen atom with the phenyl groups twisted from coplanarity, the overall spatial arrangement being such as to endow the molecule with approximate C_3 symmetry.

We have also investigated the silylamide complex, $[Bi\{N(SiMe_3)_2\}_3]$ (**2**)[4] which is readily prepared by treatment of $BiCl_3$ with 3 equivalents of $Li[N(SiMe_3)_2]$. Compound **2** can be isolated as a pale yellow powder in good yield by extraction of the crude reaction mixture with hexane followed by filtration and removal of all volatiles. Spectroscopic data* indicate hindered rotation about the Bi—N bonds at low temperature, a feature which would also appear to exist in **1** at room temperature judging by the complexity of the ^1H and ^{13}C NMR spectra when compared with those of $HNPh_2$.

Finally we note that attempted preparations of $[Bi(NPr^i_2)_3]$ and $[Bi\{\overline{NC(Me_2)(CH_2)_3C(Me_2)}\}_3]$, while resulting in transient yellow solutions, have been hindered by the apparent photosensitivity of the Bi—N bonds resulting in facile decomposition.

Further studies are in progress to synthesize a wider range of bismuth amides and to explore their reaction chemistry.

Acknowledgement—We thank SERC and Newcastle University Small Grants Research Sub-Committee for financial support, and BP Research (Sunbury) for a CASE Award (N.A.C.).

REFERENCES

1. Examples are the bismuth molybdate catalysts used in the SOHIO process, see R. K. Grasselli and J. D. Burrington, *Adv. Catal.* 1981, **30**, 133.
2. For a recent overview, see R. Dagani, *Chem. Engng. News* 1988, **66** (No. 20), 24.
3. F. Ando, T. Hayashi, K. Ohashi and J. Koketsu, *J. Inorg. Nucl. Chem.* 1975, **37**, 2011.
4. M. F. Lappert and P. P. Power, unpublished results (1977), taken from *Metal and Metalloid Amides* (Edited by M. F. Lappert, A. R. Sanger, R. C. Srivastava and P. P. Power), p. 459. Ellis Horwood (1979).
5. O. J. Scherer, P. Hornig and M. Schmidt, *J. Organomet. Chem.* 1966, **6**, 259.
6. P. Krommes and J. Lorberth, *J. Organomet. Chem.* 1975, **88**, 329; P. Krommes and J. Lorberth, *J. Organomet. Chem.* 1975, **93**, 339.
7. K. Lal, I. P. Bhatia and R. L. Kaushik, *Curr. Sci. (India)* 1960, **29**, 272; *Chem. Abstr.* 1961, **55**, 3625.
8. K. Moedritzer, J. R. Van Wazer and H. Weingarten, *U.S. Patent* 3,504,005 (1970).
9. D. Hass, *Z. Chem.* 1964, **4**, 185.

* Spectroscopic data for **2**: NMR in $C_6D_5CD_3$, ^1H δ 0.56 (s, $N(SiMe_3)_2$), $^{13}C\{^1H\}$ δ 7.5 (s, $N(SiMe_3)_2$). Both signals are significantly broadened at 190 K, although limiting spectra at lower temperatures have not yet been obtained.

Polyhedron Vol. 8, No. 13/14, p. 1581, 1989
Maxwell Pergamon Macmillan plc. Printed in Great Britain

FOREWORD

This issue contains the papers and posters submitted to the International Conference on the Chemistry of the Early Transition Metals held by the Dalton Division of the Royal Society of Chemistry at the University of Sussex, 10–14 July 1989.

A simple glance through the contents list will reveal the breadth of interests involved in this meeting, with contributions ranging from the solid state properties of refractory materials to studies on metalloproteins.

I have enjoyed reading all of the contributions, and must thank my co-editors Ray Richards and John Dilworth for all their hard work in preparing this issue, which must have been an unpardonable burden to put on top of the conference organization.

E. C. CONSTABLE

Polyhedron Vol. 8, No. 13/14, pp. 1583–1588, 1989
Printed in Great Britain

0277–5387/89 $3.00+.00
© 1989 Maxwell Pergamon Macmillan plc

HYDRIDE TO CARBENE MIGRATIONS

MARK J. WINTER

Department of Chemistry, The University, Sheffield S3 7HF, U.K.

Abstract—Hydrido carbene complexes of the type $CpMH(CO)_2\{=CR^1R^2\}$ (M = Mo, W) are available by the consecutive treatment of $CpMI(CO)_2\{=CR^1R^2\}$ with $NaC_{10}H_8$ and acid. Some of these hydridometal complexes are isolable and fully characterized, while others are too labile to isolate. Most of these compounds [for example, $CpMoH(CO)_2\{=\overline{C(CH_2)_3NMe}\}$ and $CpMH(CO)_2\{=C(NHEt)Ph\}$ (M = Mo, W)] undergo hydride to carbene migration reactions during which an intramolecular source of ligand (a nitrogen donor atom for instance) binds to the metal in order to maintain the 18-electron count. In some cases, the hydride appears to migrate so fast as to prevent its identification. In other cases, the products of hydride to carbene migration rearrange to further products such as η^3-benzyls.

The migration of alkyl to carbonyl to form an acyl group is well known. It is a central process in a number of important catalytic cycles. There are considerably less data, particularly mechanistic, on another fundamental process, the migration of a group R to carbene:



(1)

It is likely that migrations to carbene are central in a number of processes involving carbene complexes, but their facility renders their direct observation infrequent. There are, however, some examples in the literature of very clear hydride,[1,2] alkyl[3] and aryl[4] to carbene migrations. Our interest in this area continues since our first observation of a hydride to carbene migration 3 years ago.[2] This article addresses some of our work on hydride to carbene migrations but we are also working on the migrations of alkyl, aryl and acyl groups to coordinated carbene.

In order to study migrations of a group R to a carbene $\{=CR^1R^2\}$, one needs a source of $L_nM(R)\{=CR^1R^2\}$ complexes. The basic strategy we are currently using to make such complexes is very simple and illustrated in Scheme 1 for the case of hydride. It requires a source of carbene complexes $L_nM(X)(=CR^1R^2)$, where X is a group such as iodide. The next stage is the reduction of the metal halide bond with a reducing agent such as $NaC_{10}H_8$ to form anionic carbene complexes $[L_nM(=CR^1R^2)]^-$. We expected the reaction of acids with these anions to proceed at the metal to form neutral derivatives, $L_nM(H)(=CR^1R^2)$, and that such compounds should be suitable vehicles for studying migrations of hydride to carbene. This turns out to be the case.

SYNTHESIS OF CARBENE COMPLEXES $L_nM(X)(=CR^1R^2)$ (X = HALIDE)

There are many carbene complexes of the general class $L_nM(X)(=CR^1R^2)$ in the literature, but here I shall restrict discussion to the two principle strategies that we use in our laboratories to make carbene complexes of the type $LM(X)(carbene)(CO)_2$ (M = Mo, W; L = Cp or Cp derivative). The first complex we synthesized was the molybdenum complex, **1**[5] (Scheme 2). Addition of $X(CH_2)_3X$ (X = Br or I) to $[CpMo(CO)_3]^-$ results in a straightforward nucleophilic replacement of halide to form $CpMo\{(CH_2)_3X\}(CO)_3$. This undergoes migration of the

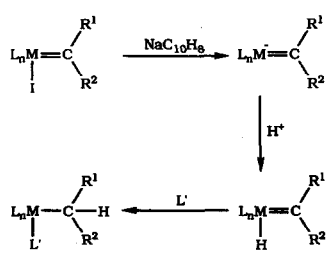

Scheme 1.

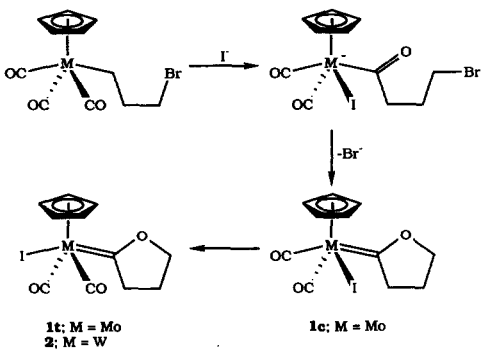

1t; M = Mo
2; M = W

1c; M = Mo

Scheme 2.

$(CH_2)_3X$ (X = Br, I) group to an adjacent carbonyl and coordination of iodide (added as I^- in the case of X = Br) at molybdenum. Ring closure of the resulting acyl anion results in the carbene complex, **1t**, probably by way of the *cis* isomer, **1c**.

The corresponding tungsten reaction also works well to form **2t**, but more forcing conditions are necessary to promote the insertion step. To date, we have not made the analogous chromium compounds.[6] This basic reaction is very adaptable. The most obvious extension is to the corresponding Cp* (η-C_5Me_5)[7] and Ind (η^5-C_9H_7, indenyl) derivatives, and these compounds are known.

As a rule, alkyl groups migrate more readily to isonitrile than carbonyl, even to the extent of multiple migrations being known.[8] This leads to a further extension of the basic synthetic route of Scheme 2. Addition of $I(CH_2)_3I$ to $[LM(CNMe)(CO)_2]^-$ (M = Mo or W; L = Cp, Cp*) results in a one-pot synthesis of the molybdenum and tungsten carbenes, *cis*-$LMI\{=\overline{C(CH_2)_3NMe}\}(CO)_2$ (**3**) and (**4**), from $LMBr(CNMe)(CO)_2$.[9] The fact that these complexes are *cis* whereas the corresponding $\{=\overline{C(CH_2)_3O}\}$ derivatives are *trans* is interesting. We are still examining in detail these differences in structure.

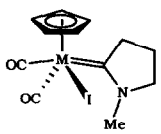

3; M = Mo
4; M = W

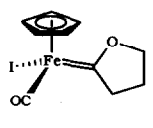

5

The same basic strategy of Scheme 2 also extends to iron. The reaction of $[CpFe(CO)_2]^-$ with $Br(CH_2)_3Br$ followed by I^- results in the new iron carbene complex $CpFeI\{=\overline{C(CH_2)_3O}\}(CO)$ (**5**).[10]

The second main route that we use to make carbene complexes, $L_nM(X)(=CR^1R^2)$, relies upon standard approaches to Fischer-type carbenes. The consecutive additions of PhLi and Et_3O^+ to $CpM(SnPh_3)(CO)_3$ (M = Mo or W) result in the carbenes $CpM(SnPh_3)\{=C(OEt)Ph\}(CO)_2$ (**6**) and (**7**).[11] Under slightly different reaction conditions

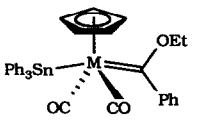

6; M = Mo
7; M = W

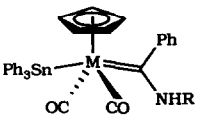

8; M = Mo, R = Me
9; M = W, R = Me
10; M = Mo, R = Et
11; M = W, R = Et

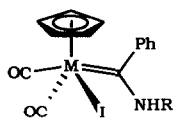

12; M = Mo, R = Me
13; M = W, R = Me
14; M = Mo, R = Et
15; M = W, R = Et

to those published, these reactions proceed in near quantitative yields. The analogous Cp* and Ind derivatives also form in closely related reactions.[12] Aminolysis of these ethoxy carbenes leads to amino carbenes such as $CpM(SnPh_3)\{=C(NHR)Ph\}(CO)_2$ (**8**)–(**11**), in high yield.[11] Again, the Cp* and Ind derivatives are accessible in high yield in analogous reactions.[12]

These M—$SnPh_3$ carbene compounds all react with iodine. In most cases the result is high yield metal–tin bond cleavage to form products such as **12**–**15**, but some of the ethoxy carbene reactions are more complex and the required products are not isolable or are difficult to isolate.[12]

Complexes of non-heteroatom stabilized carbenes are available from these Fischer-type carbenes by application of standard methods. As examples, the reaction of $LiBEt_3H$ with complex **7** followed by protonolysis results in the complex $CpW(SnPh_3)\{=C(H)Ph\}(CO)_2$ (**16**) (Scheme 3); in turn complex **16** reacts with iodine to form the iodotungsten carbene,**17**. Other cases show unexpected behaviour which interfere with these orderly syntheses of halometal carbene complexes, but perhaps it is worth it in some cases. For example, the molybdenum complex, **18**, exists in equilibrium with the η^3-benzyl, **19**, in a remarkable process which involves a $SnPh_3$ to carbene migration. Coordination of the Ph group forming the η^3-benzyl ensures the 18-electron count of the molybdenum atom is maintained.[13]

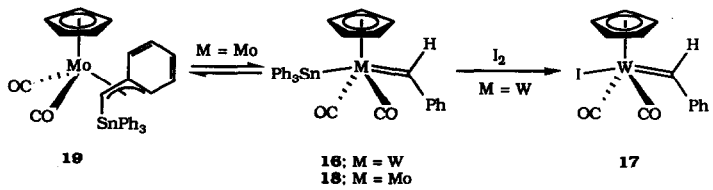

Scheme 3.

FORMATION OF ANIONIC CARBENE COMPLEXES

It is clear that there are many complexes of the type $L_nMI(=CR^1R^2)$ available. Since sodium reduction of halide complexes such as $CpMoI(CO)_3$ results in formation of the anion $[CpMo(CO)_3]^-$, one expects that reduction of $L_nMI(=CR^1R^2)$ complexes would form the anions $[L_nM(=CR^1R^2)]^-$. In our hands, the reagent of choice for reducing these halide complexes is $NaC_{10}H_8$, a common reducing agent for organic chemistry that also finds favour in organotransition metal chemistry. This reduction proves successful in all the molybdenum and tungsten cases that we have examined to date. A small selection of the available anionic metal carbene complexes is shown below.[14]

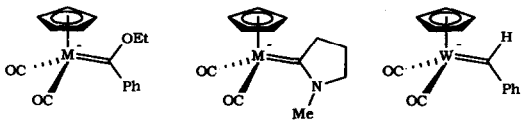

The carbene anions thus produced are a new class of anionic carbene complex. We are aware of one other anion in this class that has been reported by another group.[15] These anions are quite distinct from complexes of the type $L_nM\{=CR^1(CR^2_2Li)\}$[16] which react with electrophiles at the α-carbon atom. This new class of compound is characterized by its reactivity with electrophiles at the metal atom. Most are thermally rather unstable and have to be handled at low temperatures, but are sufficiently stable for their IR spectra to be acquired at ambient temperature, provided this is done reasonably quickly. They show two low frequency ν(CO) bands typically around 1780 and 1660 cm^{-1}. Addition of 15-crown-5 to solutions of a representative example, **22**,[14] results in changes in the IR spectrum, which are about the same in terms of frequency changes as those seen on adding 15-crown-5 to solutions of $[CpMo(CO)_2\{P(OPh)_3\}]^-$.[17] This suggests that the carbene anions exist in solution as tight ion pairs with sodium cations. By way of a chemical derivatization, all the anions made so far react with Ph_3SnCl to form $CpM(SnPh_3)(=CR^1R^2)(CO)_2$; these are all highly crystalline, air-stable materials whose isolation is straightforward.[10]

HYDRIDE TO CARBENE MIGRATIONS

Protonation of solutions of the anion **22** results in formation of the hydride $CpMoH(CO)_2\{=\overline{C(CH_2)_3NMe}\}$ (**25**) (Scheme 4), which exists as a mixture of *cis* (**25c**) and *trans* (**25t**) isomers.[2] The two isomers interconvert quite rapidly on the NMR time scale, with the hydride, Cp and methyl signals coalescing around ambient temperature in the ^1H NMR spectrum. Stirring solutions of the hydride at ambient temperature for several hours results in the new *cis* dicarbonyl $CpMo(CO)_2\{\eta^2\text{-}\overline{CH(CH_2)_3NMe}\}$ (**26**).[2] Compound **26** is also formed in the reaction between $LiBEt_3H$ and *cis*-$CpMoI(CO)_2\{=\overline{C(CH_2)_3NMe}\}$ (**3**).[9]

Early kinetic studies show this hydride to carbene migration is a unimolecular process with an Arrhenius activation barrier of 98 kJ mol^{-1}. The nitrogen atom binds at the metal in order to maintain an 18-electron count. Remarkably, this migration is *reversible* on visible light irradiation.[18] The corresponding tungsten hydride shows no sign of any such hydride to carbene migration. It also exists only as its *trans* isomer. The lack of a *cis* isomer may contribute to its failure to undergo migration, since that is likely to be the isomer which

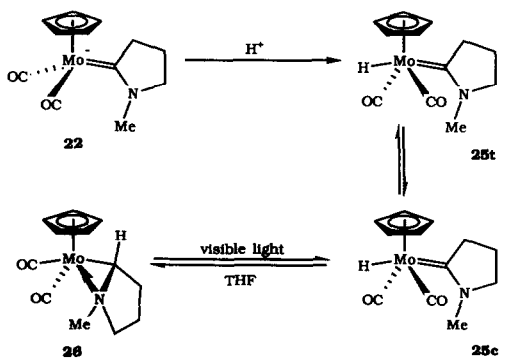

Scheme 4.

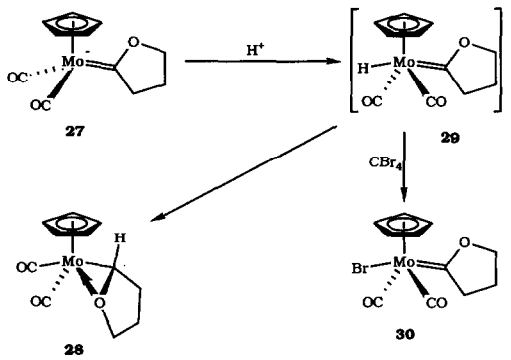

Scheme 5.

undergoes migration, but the strength of the W—H bond is also undoubtedly important.[2]

Protonation of the related anion [CpMo(CO)$_2${=C(CH$_2$)$_3$O}]$^-$ (**27**), results in the rapid formation of CpMo(CO)$_2${η^2-CH(CH$_2$)$_3$O} (**28**) (Scheme 5). This compound is also formed in the reaction of CpMoI(CO)$_2${=C(CH$_2$)$_3$O} (**1t**) with LiBEt$_3$H.[19] Although the hydride, CpMoH(CO)$_2${=C(CH$_2$)$_3$O} (**29**), is not detected at ambient temperature, its existence is implied at low temperatures, since low temperature protonation followed immediately by addition of CBr_4 results in CpMoBr(CO)$_2${=C(CH$_2$)$_3$O} (**30**).[20] This type of reaction is often taken as indicative of the existence of a reactive hydride complex.

Protonation of the anion [CpW(CO)$_2${=C(NHEt)Ph}]$^-$ (**31**) results in the isolable, air-sensitive oil CpWH(CO)$_2${=C(NHEt)Ph} (**32**). This interconverts into the fluxional complex CpW(CO)$_2${η^2-CHPh(NHEt)} (**33**) over 2–3 days by a hydride to carbene migration (Scheme 6). The molybdenum anion, [CpMoH{=C(NHEt)Ph}]$^-$ (**34**), also protonates to form its corresponding hydride, CpMoH(CO)$_2${=C(NHEt)Ph} (**35**). However, although detectable by IR spectroscopy, compound **35** is not isolable since it undergoes a rapid hydride to carbene migration (about 5 min at ambient temperature) to form the complex CpMo(CO)$_2${η^2-CHPh(NHEt)} (**36**). This last migration is complete within a few minutes at ambient temperature.[21]

The corresponding migration reactions of the {=C(OEt)Ph} carbene appear to be very rapid. Protonation of the anions [CpM(CO)$_2${=C(OEt)Ph}]$^-$ (**20**) and (**21**) (Scheme 7) clearly occurs very rapidly, but the corresponding hydrides, CpMH(CO)$_2${=C(OEt)Ph}, are not detectable by IR spectroscopy at ambient temperature. If one assumes that the initial products are these hydrides, then one expects them to undergo hydride to carbene migration to form the compounds CpM(CO)$_2${η^2-CHPh(OEt)} (**37**) and (**38**). These are certainly detectable by IR spectroscopy, but they are too sensitive to isolate and because they also undergo facile isomerizations into the η^3-benzyl derivatives CpM(CO)$_2${η^3-CH(OEt)(C$_6$H$_5$)} (**39**) and (**40**). Both these compounds are fully characterized. This isomerization is driven by the tendency to form the stable η^3-benzyl interaction at the expense of the weak O→M donor bond. The formation of the tungsten derivative is reversible to some extent. Photolysis of a solution of **40** in THF contained in an NMR tube results in a build-up of a small concentration of **38**, detectable by ^{1}H spectroscopy. This soon disappears as it reverts to the η^3-benzyl, **40**.[21]

We have started to examine the corresponding chemistry of non-heteroatom stabilized carbenes. As an example, protonation of anion **24** results in the known η^3-benzyl, **41** (Scheme 8). In this case, there is no sign of any intermediate hydridotungsten complex, nor have we been able to derivatize such an intermediate by reaction with CBr_4 or similar reagents. However, the migration of hydride from

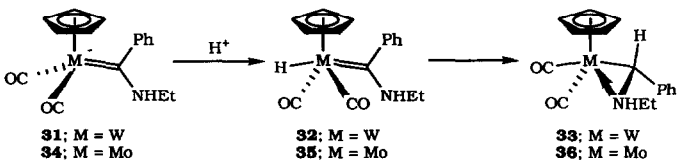

Scheme 6.

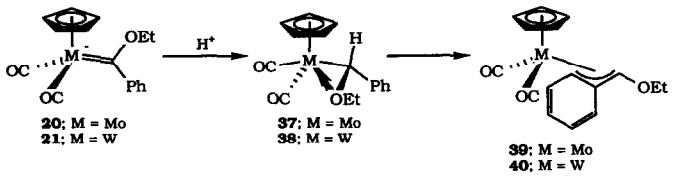

Scheme 7.

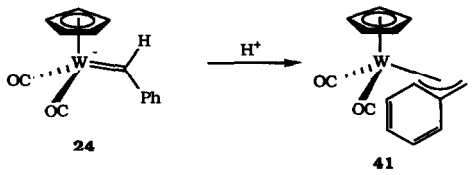

Scheme 8.

such an intermediate hydride and coordination of the phenyl ring would explain the formation of **41** quite neatly.[22] However, we have still to determine in this last example whether protonation occurs at the metal or at the carbene.

What we see from the above survey of results is the gradual emergence of some trends, even though we have yet to quantify them. Clearly hydridotungsten carbene complexes undergo hydride to carbene migration more slowly than the corresponding molybdenum derivatives. Clearly complexes of the carbenes $\{=\overline{C(CH_2)_3NMe}\}$, undergo migration more slowly than the corresponding carbenes $\{=\overline{C(CH_2)_3O}\}$, complexes of carbenes $\{=\overline{C(CH_2)_3NMe}\}$, undergo migration more slowly than the corresponding carbenes {=C(NHEt)Ph}, and complexes of carbenes $\{=\overline{C(CH_2)_3O}\}$, undergo migration more slowly than the corresponding carbenes {=C(OEt)Ph}. In some cases the migrations are sufficiently fast that the intermediate hydrides are not detected. This has to be remedied. Other factors under examination include variation of the metals, ancillary ligands, solvent effects, as well as an examination of a role for external nucleophiles other than the solvent.

Acknowledgements—I should like to acknowledge the skills, dedication and enthusiasm of my co-workers who are listed in the references. I should also like to express my gratitude to the technical staff of the Department of Chemistry at the University of Sheffield, without whose efforts this work could not have taken place.

REFERENCES

1. J. R. Shapley and R. V. Calvert, *J. Am. Chem. Soc.* 1977, **99**, 5225; H. D. Empsall, E. M. Hyde, R. Markham, W. S. McDonald, M. C. Norton, B. L. Shaw and B. Week, *J. Chem. Soc., Chem. Commun.* 1979, 498; R. S. Threlkel and J. E. Bercaw, *J. Am. Chem. Soc.* 1981, **103**, 2650; G. R. Clark, C. E. L. Headford, K. Marsden and W. R. Roper, *J. Organomet. Chem.* 1982, **231**, 335; D. L. Thorn and T. H. Tulip, *Organometallics* 1982, **1**, 1580; A. Van Asselt, B. J. Burger, V. C. Gibson and J. E. Bercaw, *J. Am. Chem. Soc.* 1986, **108**, 5347; H. W. Turner, R. R. Schrock, J. D. Fellmann and S. J. Holmes, *J. Am. Chem. Soc.* 1983, **105**, 4942; P. T. Barger and J. E. Bercaw, *Organometallics* 1984, **3**, 278; J. C. Green, M. L. H. Green and C. P. Morley, *Organometallics* 1985, **4**, 1302; H. Werner and K. Roder, *J. Organomet. Chem.* 1986, **310**, C51; H. Le Bozec, J.-L. Fillaut and P. H. Dixneuf, *J. Chem. Soc., Chem. Commun.* 1986, 1182; G. Parkin, E. Bunel, B. J. Burger, M. S. Trimmer, A. Van Asselt and J. E. Bercaw, *J. Molec. Catal.* 1987, **41**, 21; J. P. Collman, L. S. Hegedus, J. R. Norton and R. G. Finke, in *Principles and Applications of Organotransition Metal Chemistry*, 2nd edn. University Science Books, Mill Valley, California (1987).
2. V. A. Osborn, C. A. Parker and M. J. Winter, *J. Chem. Soc., Chem. Commun.* 1986, 1185.
3. P. R. Sharp and R. R. Schrock, *J. Organomet. Chem.* 1979, **171**, 43; D. L. Thorn and T. H. Tulip, *J. Am. Chem. Soc.* 1981, **103**, 5984; R. S. Threlkel and J. E. Bercaw, *J. Am. Chem. Soc.* 1981, **103**, 2650; J. C. Hayes and N. C. Cooper, *J. Am. Chem. Soc.* 1982, **104**, 5570; H. Kletzin, H. Werner, O. Serhadli and M. L. Ziegler, *Angew. Chem. Int. Edn Engl.* 1983, **22**, 46; H. Werner, H. Kletzin, A. Höhn, W. Paul, W. Knaup, M. L. Ziegler and O. Serhadli, *J. Organomet. Chem.* 1986, **306**, 227.
4. P. Jernakoff and N. J. Cooper, *J. Am. Chem. Soc.* 1981, **103**, 5984; H. Arzoumanian, A. Baldy, R. Lai, J. Metzger, M.-L. N. Peh and Pierrot, *J. Chem. Soc., Chem. Commun.* 1985, 1151.
5. N. A. Bailey, P. L. Chell, C. P. Manuel, A. Mukhopadhyay, D. Rogers, H. E. Tabbron and M. J. Winter, *J. Chem. Soc., Dalton Trans.* 1983, 2397.
6. C. Garland, unpublished results.
7. N. A. Bailey, D. A. Dunn, C. N. Foxcroft, G. R. Harrison, M. J. Winter and S. Woodward, *J. Chem. Soc., Dalton Trans.* 1988, 1449.
8. Y. Yamamoto, K. Aoki and H. Yamazaki, *J. Am. Chem. Soc.* 1976, **96**, 2647.
9. H. Adams, N. A. Bailey, V. A. Osborn and M. J. Winter, *J. Chem. Soc., Dalton Trans.* 1986, 2127.
10. H. Adams, N. A. Bailey, C. E. Housecroft, A. J. Smith, C. Ridgway, P. Taylor and M. J. Winter, manuscript in preparation.
11. W. K. Dean and W. A. G. Graham, *Inorg. Chem.* 1977, **16**, 1061.
12. G. W. Bentley, G. Hough, M. J. Winter and S. Woodward, *Polyhedron* 1989, **8**, 1861.
13. M. J. Winter and S. Woodward, *J. Chem. Soc., Chem. Commun.* 1989, in press.
14. V. A. Osborn and M. J. Winter, *J. Chem. Soc., Chem. Commun.* 1985, 1744; H. Adams, N. A. Bailey, C. E. Davey, V. A. Osborn, C. Ridgway, B. A. Shaw, S. Woodward, M. J. Winter and L. Yellowlees, manuscript in preparation.
15. S.-J. Wang and R. J. Angelici, *J. Organomet. Chem.* 1988, **352**, 151.
16. C. P. Casey, *J. Chem. Soc., Chem. Commun.* 1971, 1220.
17. K. H. Pannell and D. Jackson, *J. Am. Chem. Soc.* 1976, **98**, 4443.
18. C. E. Davey, R. Devonshire and M. J. Winter, *Polyhedron*, 1989, **8**, 1863.

19. H. Adams, N. A. Bailey, P. Cahill, D. Rogers and M. J. Winter, *J. Chem. Soc., Dalton Trans.* 1986, 2119.
20. C. E. Davey, V. A. Osborn and M. J. Winter, unpublished results.
21. M. J. Winter and S. Woodward, manuscript in preparation.
22. M. J. Winter and S. Woodward, *J. Organomet. Chem.* 1989, **361**, C18.

Polyhedron Vol. 8, No. 13/14, pp. 1589–1593, 1989
Printed in Great Britain

0277–5387/89 $3.00+.00
© 1989 Maxwell Pergamon Macmillan plc

FORMATION OF METAL–ELEMENT DOUBLE BONDS BY CHLOROSILANE ELIMINATION

ULRICH SCHUBERT,* UWE KIRCHGÄSSNER, JÜRGEN GRÖNEN and HERMANN PIANA

Institut für Anorganische Chemie der Universität Würzburg, Am Hubland, D-8700 Würzburg, F.R.G.

Abstract—Transition metal complexes, capable of chlorosilane elimination to give metal–element double bonds, are generated as transient species by two novel methods. The first one involves reaction of anionic silyl complexes with geminal dihalides and is exemplified by reactions of $[MeCp(CO)_2Mn\text{-}SiR_3]^-$ with dihalides of carbon and main-group V elements. Formation of carbene complexes and phosphinidene-bridged complexes, $[MeCp(CO)_2Mn]_2PR$, proves that the anionic silyl complex can be used as an equivalent for $[MeCp(CO)_2Mn]^{2-}$ in the synthesis. The second method proceeds by oxidative addition of the C—Cl bond of (α-chlorovinyl)silanes to electronically unsaturated transition-metal complex moieties to give vinylidene complexes, e.g. $(\eta^6\text{-}C_6R'_6)(CO)_2Cr{=}C{=}CR_2$ or $MeCp(CO)(L)Mn{=}C{=}CR_2$. With an excess of (α-chlorovinyl)silane, butatriene complexes are formed instead.

During recent years a large number of reliable preparative methods have been developed to generate metal–element multiple bonds, particularly metal–carbon multiple bonds. Among them, chlorosilane eliminations and related reactions are conspicuously absent, despite their very successful applications in main-group chemistry. One of the reasons is the lack of suitable precursor complexes. In Scheme 1, three routes are shown by which, in principle, formation of metal–element double bonds could be achieved via the intermediates **A** or **B**, which differ by the relative position of the groups R_3Si and X.

In this article, efforts towards the realization of these reactions are described. Discussion is restricted to group VI and VII transition metal compounds. Preliminary results show that the methods can also be applied to earlier or later transition metal compounds.

Anionic silyl (germyl, stannyl) complexes exhibit the typical properties common to negatively-charged metal complexes, like ion pairing or substitution reactions with monohalides,[1,2] but render possible additional preparative applications due to the presence of the silyl ligand, which is not necessarily an innocent bystander in certain reactions.[2] Combination of the substitution chemistry of anionic metal complexes and the reactivity of silyl ligands is a promising onset for reactions according to route (a) in Scheme 1.

Anionic silyl (germyl, stannyl) complexes can be synthesized by several routes, the most versatile one being the deprotonation of hydrido silyl (germyl, stannyl) complexes. The latter complexes are commonly prepared by oxidative addition of $HSiR_3$ to electronically unsaturated metal complexes. Typical representatives involving group VI and VII transition metals are compounds of the type $(\eta^6\text{-}C_6R'_6)(CO)_2Cr(H)SiR_3$ or $(\eta^5\text{-}C_5R'_5)L_2M(H)SiR_3$ (M = Mn, Re), the chemistry of which has recently been reviewed.[3] Addition of $HSiR_3$ to photochemically generated $Cr(CO)_5$ does not result in stable products, but we recently succeeded in preparing phosphine-substituted derivatives **1**, analogously (eq. (1), dppe = $Ph_2PCH_2CH_2PPh_2$), for $SiR_3 = SiCl_3$ or $SiCl_2R$:

$$(dppe)M(CO)_4 + HSiR_3 \xrightarrow[+10°C]{h\nu/\text{toluene}} (dppe)(CO)_3M(H)SiR_3 + CO \quad (1)$$

(M = Cr, Mo, W)

(1) (two isomers)

Two isomers are formed, only one of them having

* Author to whom correspondence should be addressed.

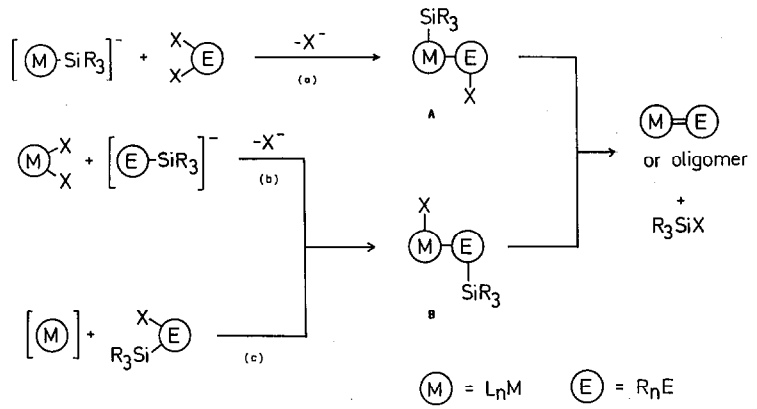

Scheme 1.

a symmetric structure (chemically equivalent phosphorus atoms). The ratio between both isomers (the structures of which still have to be elucidated) depends on the metal, the SiR_3 group and the reaction conditions.[4]

Deprotonation of hydrido silyl complexes was extensively studied for complexes of the type (η^5-C_5R_5)$L_2M(H)SiR_3$ (M = Mn, Re), particularly MeCp- or $Cp(CO)_2Mn(H)SiR_3$ (MeCp = η^5-MeC_5H_4, Cp = η^5-C_5H_5),[5] their acidity strongly depending on the substituents at silicon and the ligands at the metal. Dicarbonyl derivatives are easily deprotonated by a variety of bases, the most convenient being NaH or KH[5b] (as long as there are no substituents at silicon which can be replaced by a hydride ion). The anionic compounds, $[Cp(CO)_2M\text{-}ER_3]^-$ (E = Ge, Sn), were also prepared by displacing a CO ligand of $CpM(CO)_3$ by ER_3^-.[5c,6] There are no reports on attempts to similarly deprotonate hydrido silyl complexes of chromium, molybdenum or tungsten. While preparation of $[(CO)_5M\text{-}SiR_3]^-$ from $[(CO)_5M]^{2-}$ (M = Cr, Mo, W)[7] is not efficient in respect to the formation of metal-element double bonds (*vide infra*), reaction of $[(CO)_5MCl]^-$ with SiR_3^- provides a preparatively interesting access to these particular anionic silyl complexes.[8] Among early transition metal compounds, $[MeCp(CO)_2Mn\text{-}SiR_3]^-$ (**2**) is the only anionic silyl compound which was used to generate metal–element double bonds according to Scheme 1 [route (a)]. Its reactions with geminal dihalides therefore set examples. Reaction with 3,3-dichloro-1,2-diphenylcyclopropene does indeed yield the anticipated carbene complex **3a** [eq. (2a)].[9] Complex **3a** is also obtained by reaction of the corresponding Ph_3Ge- or Ph_3Sn-substituted compounds. We propose that the reaction proceeds by substitution of one chlorine atom to give an intermediate of type **A**, followed by chlorosilane elimination. Similar results were obtained with $[Me_2N{=}CHCl]Cl$ as a dihalide [eq. (2b)]:[10]

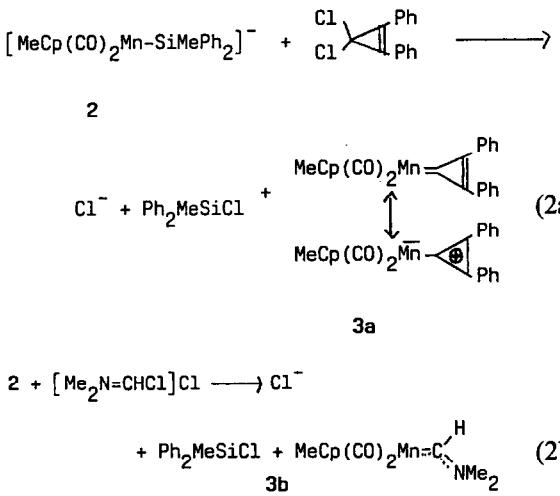

(2a)

(2b)

Complex **2** instantaneously reacts with Ph_3SbBr_2, Ph_3AsCl_2, or R_2TeCl_2 to give $MeCp(CO)_2MnEPh_3$ (E = As, Sb) or $MeCp(CO)_2MnTeR_2$, respectively.[11] Although these complexes are more conveniently prepared by the usual methods, starting from EPh_3 or TeR_2, the outcome of these reactions proves that the substitution/chlorosilane elimination route is more general and not restricted to the formation of carbene complexes. This is corroborated by the formation of the dinuclear, phosphinidene-bridged complex **4**, in the reaction of **2** with $MesPCl_2$ (Mes = 2,4,6-$C_6H_2Me_3$) [eq. (3)].[11] Analogous complexes are also obtained with other dihalides, REX_2 (E = P, As, Sb). Complexes of this type have already been synthesized by other methods and thoroughly investigated by Huttner and co-workers.[12] The question, whether in the reaction of **2** with $MesPCl_2$ a terminal phosphinidene complex is originally formed, as has been postulated for other preparative approaches to these complexes,[12]

remains open.

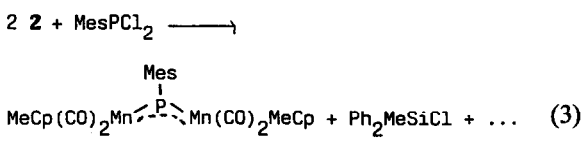

$$2\ \mathbf{2} + MesPCl_2 \longrightarrow MeCp(CO)_2Mn\text{–}P(Mes)\text{–}Mn(CO)_2MeCp + Ph_2MeSiCl + \ldots \quad (3)$$

The same products would be expected if the same geminal dihalides were reacted with the di-anionic complex, $[MeCp(CO)_2Mn]^{2-}$. While this prediction has not yet been verified for $[MeCp(CO)_2Mn]^{2-}$, which was prepared for the first time only very recently,[13] similar reactions of $[(CO)_5Cr]^{2-}$ are known and clearly show the proposed analogy: reactions of $[(CO)_5Cr]^{2-}$ with 3,3-dichloro-1,2-diphenylcyclopropene or $[Me_2N{=}CH_2]^+$ give the corresponding $(CO)_5Cr$(carbene) complexes,[14,15] and complexes of the type $[(CO)_5Cr]_2ER$, *inter alia*, can be synthesized by reaction of $Na_2Cr_2(CO)_{10}$ with REX_2.[12] The anionic silyl compound **2** (and analogously the corresponding germyl and stannyl complex) therefore is an equivalent to $[MeCp(CO)_2Mn]^{2-}$, in respect to preparative applications. This statement can be generalized for other anionic silyl complexes. Compared with di-anionic complexes, anionic silyl complexes offer a number of important advantages: they are easily prepared, they can be handled without particular precautions, and they can be accessed for a greater number of metals in a greater variety of ligand environments. Use of anionic silyl complexes therefore is an interesting preparative alternative to di-anionic complexes, particularly if the latter are inaccessible or difficult to handle.

By reversal of the substitution pattern of the starting compounds, i.e. reaction of transition metal complexes bearing two halogeno ligands with α-silyl-substituted anionic compounds (route (b) in Scheme 1), intermediates of type **B** should be accessible, which would also be suitable precursors for metal–element double bonds. Only very few experiments towards a realization of this approach are known. When Cp_2WCl_2 is reacted with $LiSi(SiMe_3)_3$, the only product is the metal dihydride **5** [eq. (4)], even if an equimolar ratio of the compounds is employed.[16] Mechanistic studies indicate that substitution of a chloro ligand by SiR_3^- is indeed the primary step in this reaction. However, the intermediate complex, $Cp_2W(Cl)Si(SiMe_3)_3$, rearranges instead of eliminating Me_3SiCl.[16b] Reaction of Cp_2MCl_2 (M = Zr, Hf) with $LiSi(SiMe_3)_3$ yields $Cp_2M(Cl)Si(SiMe_3)_3$ as stable compounds.[17]

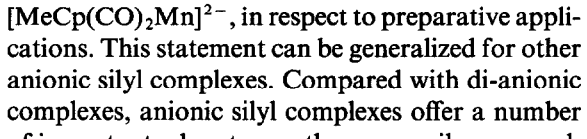

$$Cp_2WCl_2 + 2LiSi(SiMe_3)_3 \longrightarrow 2LiCl + [C_5H_4Si(SiMe_3)_3]_2WH_2 \quad (4)$$

(5)

Reacting the analogous phosphorus compound $LiP(Ar)SiMe_3$ (Ar = 2,4,6-$Bu^t_3C_6H_2$) with Cp_2ZrCl_2 again only gives the substitution product $Cp_2Zr(Cl)P(Ar)SiMe_3$, but two isomers of com-

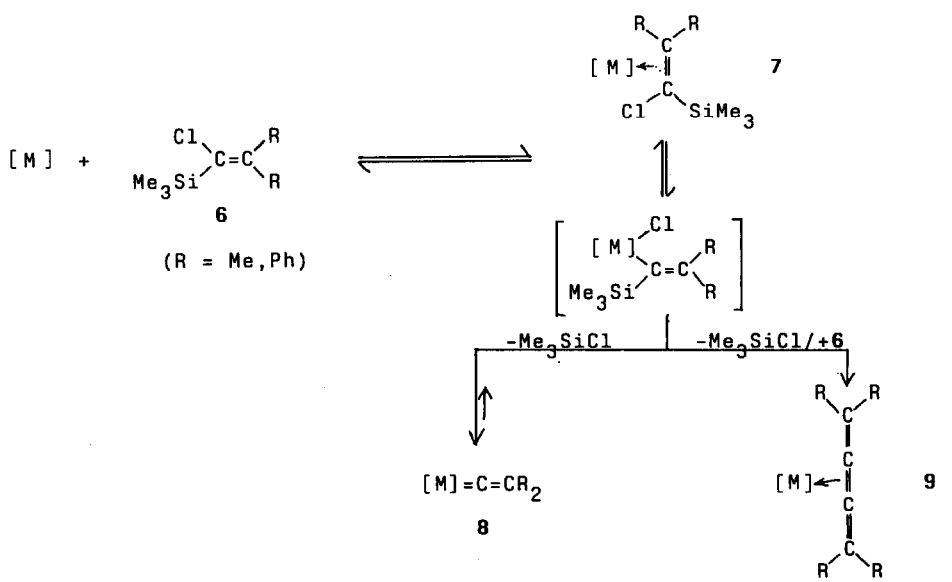

7-9a [M] = MeCp(CO)LMn (L = CO, $P(OPh)_3$, $PMePh_2$)

7-9b: [M] = (π-Ar)$(CO)_2Cr$ (Ar = C_6H_6, C_6Me_6, 1,3,5-$C_6H_3Me_3$)

Scheme 2.

position $MeCpWH[\eta^5\text{-}C_5H_3Me(PAr)]$ are formed with $(MeCp)_2WCl_2$.[18] The isomers are believed to be formed via the anticipated terminal phosphinidene complex; in the light of eq. (4) other mechanisms appear possible.

An alternative approach to type **B** compounds is oxidative addition of a silyl derivative $R_3Si(X)ER'_n$ to a coordinatively unsaturated metal complex (route (c) in Scheme 1). Based on this idea we developed a new method to prepare vinylidene complexes (ER'_n being a vinylidene moiety) using (α-halogenovinyl)silanes (**6**) as precursors. Photochemical reaction of **6** with an equimolar amount of $MeCp(CO)_2LMn$ (L = CO, $P(OPh)_3$, $PMePh_2$ or (π-arene)$(CO)_3Cr$) most likely proceeds by initial oxidative addition of the C—Cl bond to the transition metal fragment, followed by Me_3SiCl elimination to give the vinylidene complexes **8** (Scheme 2).[19] The scope of this new reaction appears to be rather general; it is particularly useful for the synthesis of β-disubstituted vinylidene complexes, which are not so easily prepared by other routes.[20] In the photochemical reaction of the metal carbonyl derivatives with (α-halogenovinyl)silanes, π-olefin complexes, **7**, are sometimes observed as by-products, and in some cases can even be isolated. In the case of $MeCp(CO)_2Mn(\pi\text{-}Me_2C{=}C(Br)SiMe_3)$, we observed slow conversion of the isolated, oily complex to the vinylidene complex $MeCp(CO)_2Mn{=}C{=}CMe_2$.[19b] Presently we are unable to decide whether the π-olefin complexes, **7**, are reversibly formed by-products or precursors to the oxidative addition products.

In the presence of an excess of **6**, the butatriene complexes, **9**, are formed instead of the vinylidene complexes, **8**, but both types of complexes originate from the same precursor, which is the oxidative addition product.[19] To elucidate the mechanism of the butatriene formation, the model reaction shown in Scheme 3 was carried out. Photochemical reaction of $MeCp(CO)_3Mn$ with $Me_2C{=}CHCl$ gives a complex which from spectroscopic data is believed to be the oxidative addition product, **11**. Complex **11** is only stable during irradiation and (reversibly!) converts to the π-olefin complex, **10**, in the dark (Scheme 3). Since elimination of HCl from **11** is less favourable than that of Me_3SiCl in the corresponding reaction of (α-chlorovinyl)silanes, no vinylidene complex is formed. However, the reaction channel leading to a C—C coupled organic ligand is still open. To enable this reaction, $Me_2C{=}C(H)SiMe_3$ is added to a solution of **11**. Formation of the buta*diene* complex, **12**, probably proceeds via a bis-vinyl complex, which reductively eliminates the butadiene.[19b] By extrapolation of the results shown in Scheme 3 one can be certain that the butatriene ligands in **9** do not originate from vinylidene units, but from substituted butadiene ligands ($R_2C{=}C(SiMe_3){-}C(Cl){=}CR_2$), which are formed by coupling of two vinyl units of the (α-

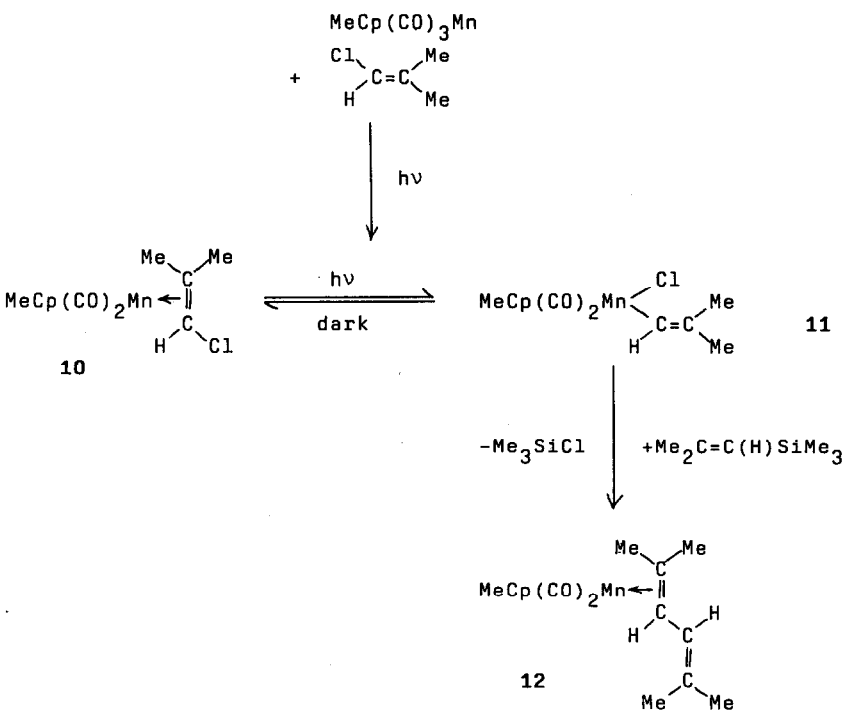

Scheme 3.

chlorovinyl)silanes and then elimination of another Me_3SiCl molecule to give the butatriene unit.

REFERENCES

1. (a) U. Schubert, E. Kunz, M. Knorr and J. Müller, *Chem. Ber.* 1987, **120**, 1079; (b) W. Jetz and W. A. G. Graham, *Inorg. Chem.* 1971, **10**, 1647; (c) E. Colomer, R. J. P. Corriu and A. Vioux, *J. Organomet. Chem.* 1984, **267**, 107; (d) F. Carré, E. Colomer, R. J. P. Corriu and A. Vioux, *Organometallics* 1984, **3**, 970; (e) K. C. Brinkman, A. J. Blakeney, W. Krone-Schmidt and J. A. Gladysz, *Organometallics* 1984, **3**, 1325.
2. (a) E. Kunz, M. Knorr, J. Willnecker and U. Schubert, *New J. Chem.* 1988, **12**, 467; (b) E. Kunz and U. Schubert, *Chem. Ber.* 1989, **122**, 231.
3. U. Schubert, *Adv. Organomet. Chem.* 1989, in press.
4. H. Piana and U. Schubert, unpublished results.
5. (a) W. Jetz and W. A. G. Graham, *Inorg. Chem.* 1971, **10**, 1647; (b) E. Colomer, R. J. P. Corriu, C. Marzin and A. Vioux, *Inorg. Chem.* 1982, **21**, 368; (c) D. F. Dong, J. K. Hoyano and W. A. G. Graham, *Can. J. Chem.* 1981, **59**, 1455.
6. F. Carré, E. Colomer, R. J. P. Corriu and A. Vioux, *Organometallics* 1984, **3**, 1272.
7. D. D. Darensbourg, C. G. Bauch, J. H. Reibenspies and A. L. Rheingold, *Inorg. Chem.* 1988, **27**, 4203.
8. E. E. Isaacs and W. A. G. Graham, *Can. J. Chem.* 1975, **53**, 467.
9. U. Schubert and U. Kirchgässner, *Organometallics* 1988, **7**, 784.
10. U. Kirschgässner and U. Schubert, unpublished results.
11. U. Kirchgässner and U. Schubert, *Chem. Ber.*, submitted.
12. G. Huttner and K. Evertz, *Accts Chem. Res.* 1986, **19**, 406.
13. V. S. Leong and N. J. Cooper, *Organometallics* 1988, **7**, 2080.
14. K. Öfele, *Angew. Chem.* 1968, **80**, 1032; K. Öfele, *Angew. Chem. Int. Ed. Engl.* 1968, **7**, 900.
15. A. J. Hartshorn, M. F. Lappert and K. Turner, *J. Chem. Soc., Dalton Trans.* 1978, 348.
16. (a) U. Schubert, A. Schenkel and J. Müller, *J. Organomet. Chem.* 1985, **292**, C11; (b) U. Schubert and A. Schenkel, *Chem. Ber.* 1988, **121**, 939.
17. B. K. Campion, J. Falk and T. D. Tilley, *J. Am. Chem. Soc.* 1987, **109**, 2049.
18. A. M. Arif, A. H. Cowley, C. M. Nunn and M. Pakulski, *J. Chem. Soc., Chem. Commun.* 1987, 994.
19. (a) U. Schubert and J. Grönen, *Organometallics* 1987, **6**, 2458; (b) U. Schubert and J. Grönen, *Chem. Ber.*, submitted.
20. M. I. Bruce and A. G. Swincer, *Adv. Organomet. Chem.* 1983, **22**, 59.

Polyhedron Vol. 8, No. 13/14, pp. 1595–1600, 1989
Printed in Great Britain

0277–5387/89 $3.00+.00
© 1989 Maxwell Pergamon Macmillan plc

ELECTROPHILIC β-ADDITION TO ISOCYANIDE, CYANIDE AND ALKYNE-DERIVED LIGANDS

ARMANDO J. L. POMBEIRO

Centro de Química Estrutural, Complexo I, Instituto Superior Técnico, Av. Rovisco Pais, 1096 Lisboa Codex, Portugal

Abstract—When binding an electron-rich group VI (Mo or W) or VII (Re) metal site (M), such as $\{M(dppe)_2\}$ (M = Mo or W, dppe = $Ph_2PCH_2CH_2PPh_2$) or $\{ReCl(dppe)_2\}$, isocyanides (M—C≡NR), cyanides (M—N≡CR) or alkyne-derived allene [$M(\eta^2$-H_2C—C=CHR)], vinylidene (M=C=CHR) or alkynyl (M—C≡CR) ligands undergo β-electrophilic attack (commonly by H^+) to give ligating aminocarbyne (M≡C···NHR), methyleneamido (M···N=CHR), η^2-vinyl [M=C(CH_2R)CH_2] or carbyne (M≡C—CH_2R) species, respectively; electronic factors driving the β-electrophilic addition are also discussed.

A number of pathways have been reported[1] for the synthesis of complexes with metal–carbon multiple bonds and usually they are initiated by, or involve, a nucleophilic attack, an α-abstraction process or a scission, elimination or rearrangement reaction at a suitable organic ligand.

Another route, which consists of a *β-electrophilic attack* at an unsaturated C-bonded ligand, is discussed herein and shown to be particularly effective in the case of molecules with unsaturated C—N or C—C bonds when activated by a mononuclear electron-rich metal site with a high π-electron releasing ability, presenting a heavier member of a central transition metal group (Mo, W or Re). Such unsaturated species are well represented by isocyanides and alkyne-derived allene, vinylidene and alkynyl ligands.

Cyanides, at such a type of metal centre, appear to be susceptibile to a similar electrolphilic β-addition reaction.

ELECTROPHILIC β-ADDITION TO ISOCYANIDES AND CYANIDES

Typical isocyanide and cyanide complexes with the above-mentioned electron-rich metal centres are conveniently prepared from parent dinitrogen compounds or, in the case of rhenium, also from benzoyldiazenido precursors. Examples are given in Schemes 1 and 2 which include the preparation of *trans*-$[M(CNR)_2(dppe)_2]$ [M = Mo or W; R = alkyl or aryl; dppe = $Ph_2PCH_2CH_2PPh_2$) [eq. (1)],[2] $[M(CNR)_x(PMe_2Ph)_{6-x}]$ (x = 2 or 3) [eq. (13)],[3] *trans*-$[ReCl(CNR)(dppe)_2]$ {R = H [eqs (7) and (8)],[4] alkyl or aryl [eq. (6)][5]}, *trans*-[ReCl(NCR)$(dppe)_2$] (R = aklyl or aryl) [eq. (9)][6] and $[ReCl(N_2)(CNR)\{P(OMe)_3\}_3]$ [eq. (15)].[7]

These complexes exhibit short metal–carbon (or metal–nitrogen for the cyanide complexes)[6] bond lengths,[7–9] and, in their IR spectra, ν(C≡N) [or ν(N≡C)] occurs at low wavenumbers; a bending of the isocyanide ligand may also occur.[8] These observations are rationalized by some VB considerations, simplified π-MO schemes[10] and theoretical studies,[11] and are in agreement with an extensive π-electron donor character of the metal centres towards the isocyanide or the cyanide ligands; therefore, they are activated to electrophilic attack which was shown to occur at the β-position (relative to the metal) (Schemes 1 and 2).

Hence, *trans*-$[M(CNMe)_2(dppe)_2]$ (M = Mo or W)[12,13] or *trans*-$[ReCl(CNR)(dppe)_2]$ (R = H,[4] alkyl[14] or aryl[14]) react with protic acid to give the aminocarbyne complexes *trans*-$[M(CNHMe)(CNMe)(dppe)_2]^+$ or *trans*-$[ReCl(CNHR)(dppe)_2]^+$ [eqs (2) and (10)], respectively. The molecular structures of the latter (for R = H[4] or Me[14]) have been authenticated by single-crystal X-ray diffraction analyses, which indicate that the aminocarbyne complex should be represented as a hybrid of the following VB forms:

$$\overset{+}{Re}\equiv C-\ddot{N}HR \longleftrightarrow Re=C=\overset{+}{N}HR.$$

Electrophilic β-addition also results from the

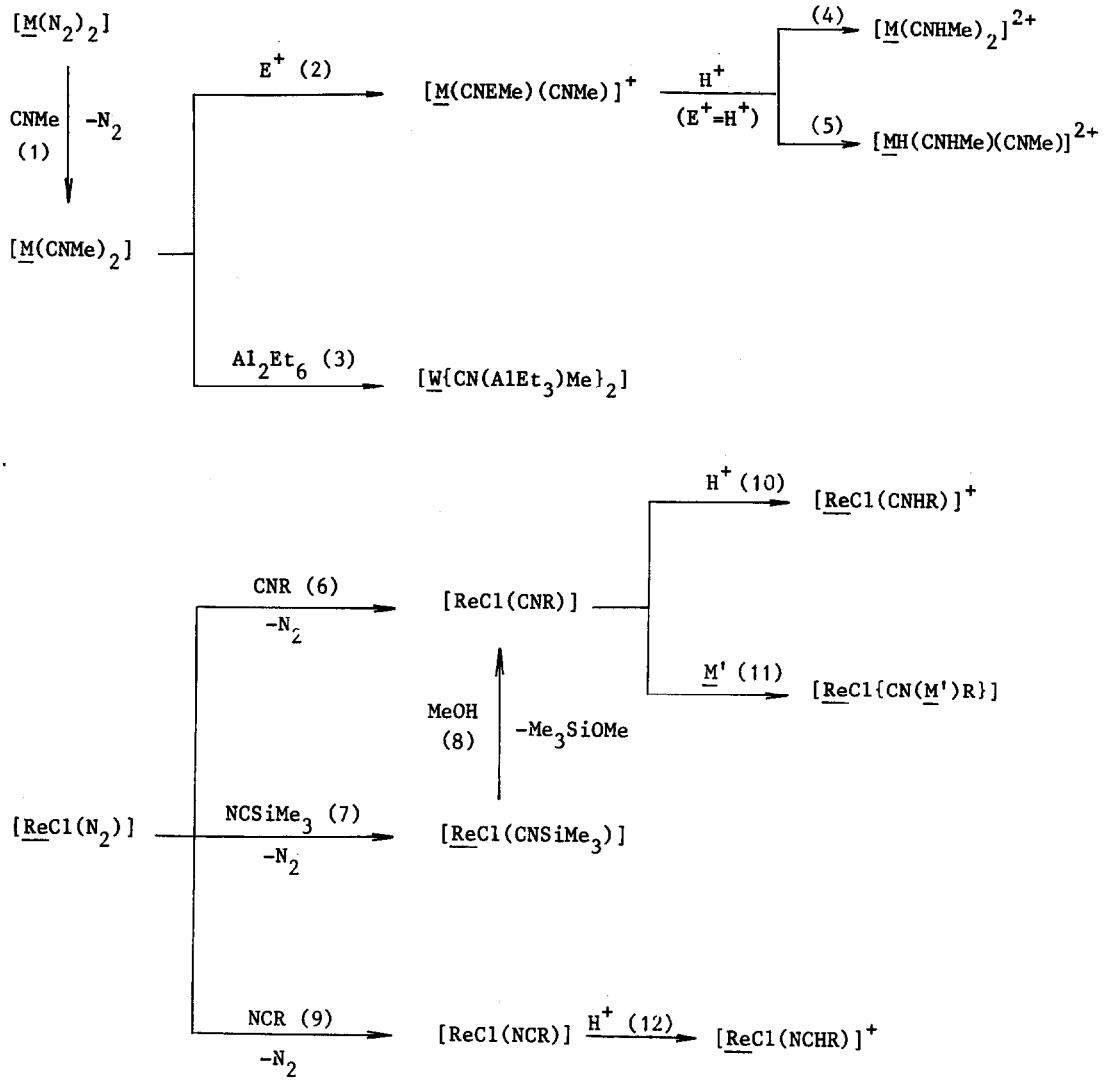

Scheme 1. Syntheses and electrophilic β-addition to electron-rich isocyanide and cyanide complexes with *non*-labile co-ligands. M = *trans*-{M(dppe)$_2$} (M = Mo or W). Re = *trans*-{ReCl(dppe)$_2$}. Equation (2)—$E^+ = H^+$, Me^+ or Et^+. Equation (6)—R = alkyl or aryl. Equation (7)—$NCSiMe_3$ in equilibrium with a small percentage of the isocyanide isomer. Equation (8)—R = H.

reactions of those isocyanide complexes with other electrophiles, particularly a carbocation[15]—from $MeFSO_3$, Me_2SO_4, $[Me_3O][BF_4]$ or $[Et_3O][BF_4]$—or a Lewis acid, such as Al_2Et_6[12] or an unsaturated transition-metal centre (M′) derived, for example, from $CoCl_2(THF)_{1.5}$ or $[ReOCl_3(PPh_3)_2]$.[16]

As products of these reactions, the following types of aminocarbyne complexes have been obtained: $[M(CNEMe)(CNMe)(dppe)_2]^+$ (M = Mo or W, $E^+ = Me^+$ or Et^+) [eq. (2)],[15] $[W\{CN(AlEt_3)_2Me\}_2(dppe)_2]$ [eq. (3)][2] or $[ReCl\{CN(M')R\}(dppe)_2]$ [R = Me or Bu^t, M′ = $CoCl_2(THF)$ or $ReOCl_3(PPh_3)$] [eq. (11)].[16]

The β-electrophilic attack at ligating isocyanide is in agreement with extended Hückel calculations[11] which indicate, e.g. that the nitrogen atom in *trans*-$[ReCl(CNR)(dppe)_2]$ bears a negative charge, whereas both the ligating carbon and the metal exhibit positive net atomic charges.

Cyanides at {ReCl(dppe)$_2$} also appear to be activated towards β-protonation to give methyleneamido species NCHR, as in the formation of $[ReCl\{NC(H)C_6H_4OMe\text{-}4\}(dppe)_2]^+$ by reaction of $[ReCl(NCC_6H_4OMe\text{-}4)(dppe)_2]$ with acid [eq. (12)].[6]

Although the mixed aminocarbyne–isocyanide complexes *trans*-$[M(CNHMe)(CNMe)(dppe)_2]^+$ can undergo protonation which occurs either at the metal or at the isocyanide ligand to give $[MH(CNHMe)(CNMe)(dppe)_2]^{2+}$ [eq. (5)],[13,17]

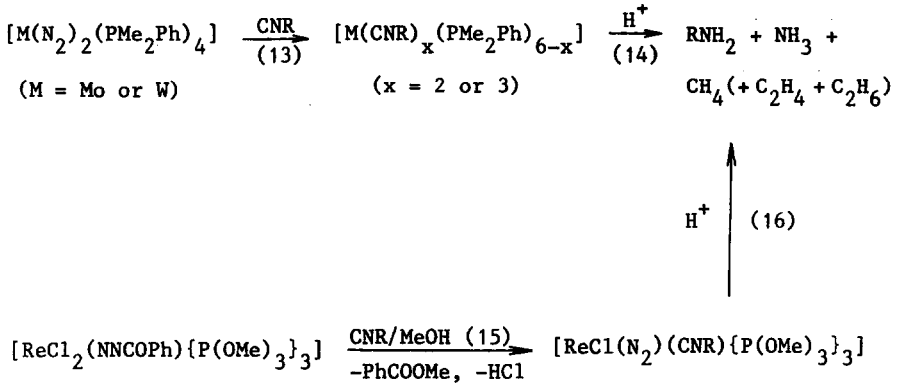

Scheme 2. Syntheses and extensive β-protonation at electron-rich isocyanide complexes with labile co-ligands.

$[M(CNHMe)_2(dppe)_2]^{2+}$ [eq. (4)][12,13] or the unstable species $[M(CNH_2Me)(CNHMe)(dppe)_2]^{3+}$ (which undergoes ready deprotonation),[13] no further electrophilic attack is observed beyond the carbyne stage in these compounds with chelating phosphine ligands.

However, when activated by an electron-rich metal centre with *labile* co-ligands, as in $[M(CNR)_x(PMe_2Ph)_{6-x}]$ (M = Mo or W, $x = 2$ or 3)[18] or in $[ReCl(N_2)(CNR)\{P(OMe)_3\}_3]$,[7] isocyanides can undergo a more extensive protonation with complete reductive cleavage of the unsaturated CN bond (Scheme 2) to give mainly amines (RNH_2) and ammonia apart from hydrocarbons (predominantly methane) in lower yields. The metal behaves as a reducing agent and the facile replacement, during the reaction, of the labile phosphine or phosphite ligand by a stronger electron donor (e.g. the anion from the protic acid or methoxide from the solvent methanol) enhances the π-electron releasing ability of the oxidized metal centre and thus promotes further protonation at intermediate aminocarbyne stages.

ELECTROPHILIC β-ADDITION TO ALKYNE-DERIVED SPECIES

Phenylpropyne ($PhC{\equiv}CCH_3$) and 1-alkynes ($RC{\equiv}CH$) undergo shift reactions with *trans*-$[ReCl(N_2)(dppe)_2]$ or *trans*-$[M(N_2)_2(dppe)_2]$ (M = Mo or W) (Scheme 3): 1,3- and 1,2-hydrogen migrations along the carbon framework of the alkyne occur in the rhenium systems to give the allene and the vinylidene complexes *trans*-$[ReCl(\eta^2\text{-}H_2C{-}C{=}CHPh)(dppe)_2]$ [eq. (17)][19] and *trans*-$[ReCl(=C{=}CHR)(dppe)_2]$ [eq. (18)],[20] respectively, whereas, for the more readily oxidizable molybdenum or tungsten centres, hydrogen shift to the metal is observed to afford for example the alkynyl–hydrido $[MH_2(C{\equiv}CR)_2(dppe)_2]$ [eq. (22)][21] or the derived dialkynyl complexes $[M(C{\equiv}CR)_2(dppe)_2]$.[21,22] The molecular structures of these products have been determined by X-ray analyses.

The metal-centred alkyne rearrangements at the unstable intermediate alkyne complexes have been interpreted[19,20] by considering the destabilizing repulsive interaction between the filled $\pi_\perp$ orbital of the alkyne and a filled d_π orbital of the electron-rich d^6 metal centre.

As observed for isocyanides and cyanides, all those alkyne-derived ligands can undergo β-protonation (Scheme 3). Hence, the η^2-vinyl (metallacyclopropene) complex, *trans*-$[Re\{{=}C(CH_2Ph)CH_2\}(dppe)_2][BF_4]$, whose molecular structure has been determined by an X-ray analysis, is obtained by reaction of the allene compound, *trans*-$[ReCl(\eta^2\text{-}H_2C{-}C{=}CHPh)(dppe)_2]$, with HBF_4 [eq. (19)],[23] and the site of protonation is in agreement with extended Hückel calculations,[23] which indicate that the HOMO of the latter complex has a substantial contribution (36%) to the p_y orbital of the allene carbon in the β-position (relative to rhenium), whereas the α-carbon contributes only 10%. Although the HOMO is mainly metal *d*-centred (54%), protonation occurs at the β-carbon, which offers a highly directional *p* orbital, rather than at the metal with a diffuse electronic density and which is coordinatively saturated.[23]

The vinylidene and the alkynyl species are also protonated at the β-position and e.g. the carbyne complexes *trans*-$[ReCl(\equiv CCH_2R)(dppe)_2][BF_4]$ (R = Bu^t, Ph, etc.) [eq. (20)],[24] *trans*-$[ReF(\equiv CCH_2Bu^t)(dppe)_2][BF_4]$ [eq. (21)][24] (whose molecular structure has been confirmed by X-rays)[24] and $[WF(\equiv CCH_2CO_2Me)(dppe)_2]$ [eq. (23)],[21] as well as the carbene compound $[WF(=CHCH_2Ph)$

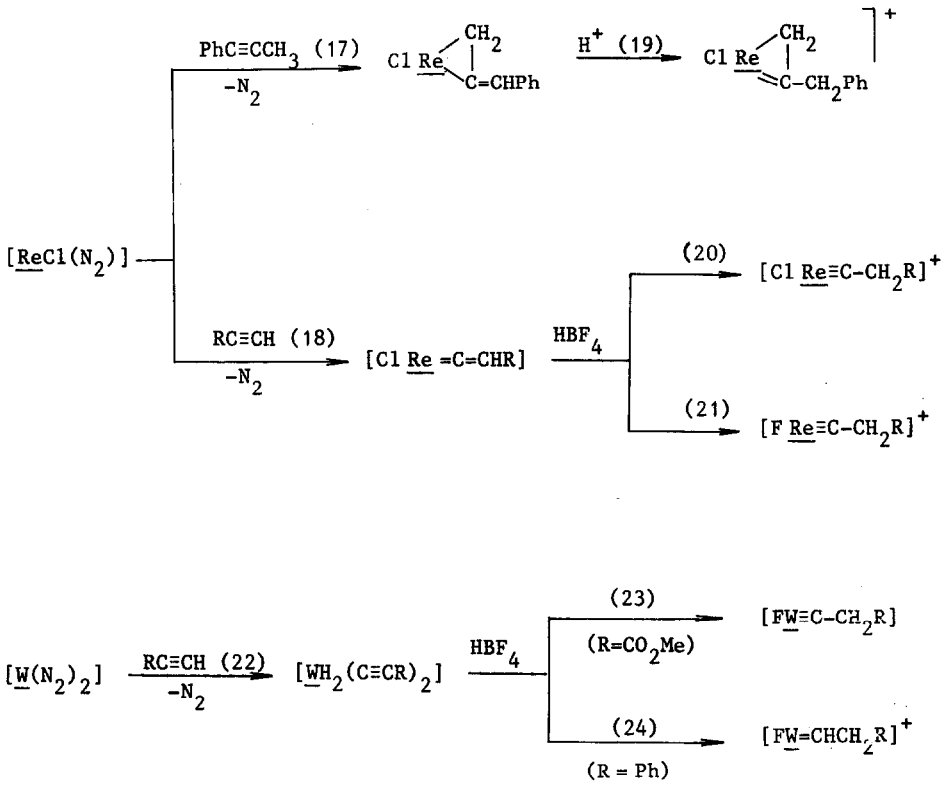

Scheme 3. Syntheses and β-protonation of alkyne-derived electron-rich complexes.

$(dppe)_2][BF_4]$ [eq. (24)],[21] are obtained by reaction of HBF_4 with the appropriate *trans*-[ReCl(=C=CHR)$(dppe)_2$] or [$WH_2(C{\equiv}CR)_2(dppe)_2$] complex, respectively. In these reactions, BF_4^- may behave as a metal fluorinating agent.

The site (β-carbon) of the electrophilic addition to the vinylidene and alkynyl ligands in the complexes mentioned above, is in accord with molecular orbital calculations carried out on other complexes with such substrates (as well as with ligating vinyl);[25] moreover, in the latter systems, the β-electrophilic attack was shown to be charge controlled, whereas the nucleophilic addition, which occurred at the α-carbon, was frontier orbital controlled.[25]

FINAL REMARKS

Electron-rich metal centres with heavier transition metals of central groups (typically Mo-, W- or Re-phosphinic sites), present a high π-electron releasing ability and promote electrophilic attack at unsaturated organic ligands, particularly isocyanides, cyanides and alkyne-derived allene, vinylidene and alkynyl species. Such electrophilic addition appears to be regioselective, occurring at the atom of the substrate in the β-position (relative to the metal), and this has been rationalized by extended Hückel calculations.

This pattern of reactivity contrasts with that commonly observed for isocyanides when ligating an electron-poor metal site; they are then susceptible to activation towards attack by nucleophiles which occurs at the α-position (the ligating atom).[26] This dichotomy of β-electrophilic and α-nucleophilic additions has also been recognized for other related unsaturated species, such as thiocarbonyl,[27] alkynyl,[28] vinylidene[28] and dinitrogen,[29] and has been investigated by MO studies;[30] however, cyanides do not follow this type of regioselectivity and either the electrophilic (mentioned in this work) or the nucleophilic[31] attack occurs at the β-position.

The electrophilic β-additions discussed in this account corresponded to novel types of reactions of isocyanide, organocyanide and allene ligands, and provided novel routes for a variety of species, such as ligating aminocarbynes, methyleneamido or η^2-vinyl ligands; they also allowed the synthesis of novel species, particularly the simplest aminocarbyne group, CNH_2.

As a result of the β-electrophilic addition to isocyanide or to any of the above-mentioned alkyne-derived ligands, a weakening of the unsaturated bond with a concomitant strengthening of the

metal–carbon bond occurs to give species which are stabilized by multiple bond coordination, in accord with a high tendency of the metal (commonly assisted by an electron donor halide ligand) to form multiple bonds to carbon.

As demonstrated by electrochemical studies,[32] these metal–carbon multiple bonded species behave as very strong net electron acceptors (even stronger than carbonyl or isocyanides), according to the following order: carbynes > η^2-vinyl > aminocarbynes.

Although the chemistry of the products of the electrophilic β-additions of this study still remains to be fully explored, they are expected to represent fundamental types of intermediate states in the conversion of isocyanides, cyanides, alkynes and allenes into a variety of organic or organonitrogenated products, namely those formed[33] in their enzymatic reduction.

Acknowledgements—Thanks are due to the co-authors indicated in the citations, particularly Dr R. L. Richards (Nitrogen Fixation Laboratory, University of Sussex), for laboratory and spectroscopic facilities and stimulating discussions; as well as Dr D. L. Hughes (Nitrogen Fixation Laboratory, University of Sussex), Dr P. B. Hitchcock (University of Sussex), Professor U. Schubert (University of Wurzburg), Dr O. Orama (University of Helsinki) and Dr J. C. Jeffery (University of Bristol) for the X-ray diffraction analyses; Dr J. Silvestre (Institut de Recherches sur la Catalyse, Villeurbanne), Professor R. Hoffmann (Cornell University), Dr E. G. Bakalbassis and Professor C. A. Tsipis (Aristotle University, Thessaloniki) for the extended Hückel MO calculations; Dr A. G. Avent (University of Sussex), for running some NMR spectra; and Mr C. Macdonald (Nitrogen Fixation Laboratory, University of Sussex), for recording some NMR spectra and for microanalyses. The author also gratefully acknowledges Professor J. J. R. Fraũsto da Silva (University of Lisbon) for laboratory facilities and guidance. The work has been supported by the INIC, the JNICT, the Calouste Gulbenkian Foundation (Portugal), the British Council, NATO, the Academy of Sciences of Lisbon and the Royal Society.

REFERENCES

1. See, for example, H. P. Kim and R. J. Angelici, *Adv. Organomet. Chem.* 1987, **27**, 51; U. Schubert (Ed.), *Advances in Metal Carbene Chemistry*, NATO ASI Series, D. Reidel, Dordrecht (1989), in press; U. Schubert, in *The Chemistry of the Metal–Carbon Bond* (Edited by F. R. Hartley and S. Patai), Chap. 5. John Wiley, New York (1982).
2. J. Chatt, C. M. Elson, A. J. L. Pombeiro, R. L. Richards and G. H. D. Royston, *J. Chem. Soc., Dalton Trans.* 1978, 165.
3. J. Chatt, A. J. L. Pombeiro and R. L. Richards, *J. Organomet. Chem.* 1980, **190**, 297.
4. A. J. L. Pombeiro, D. L. Hughes, C. J. Pickett and R. L. Richards, *J. Chem. Soc., Chem. Commun.* 1986, 246.
5. A. J. L. Pombeiro, C. J. Pickett and R. L. Richards, *J. Organomet. Chem.* 1982, **224**, 285.
6. A. J. L. Pombeiro, D. L. Hughes and R. L. Richards, *J. Chem. Soc., Chem. Commun.* 1988, 1052.
7. M. F. N. N. Carvalho, A. J. L. Pombeiro, U. Schubert, O. Orama, C. J. Pickett and R. L. Richards, *J. Chem. Soc., Dalton Trans.* 1985, 2079.
8. J. Chatt, A. J. L. Pombeiro, R. L. Richards, G. Royston, K. Muir and R. Walker, *J. Chem. Soc., Chem. Commun.* 1975, 708.
9. M. A. A. F. C. T. Carrondo, A. M. T. S. Domingos and G. A. Jeffrey, *J. Organomet. Chem.* 1985, **289**, 377.
10. A. J. L. Pombeiro, *Rev. Port. Quim.* 1979, **21**, 90.
11. C. A. Tsipis, E. G. Bakalbassis and A. J. L. Pombeiro, *XXVI Int. Conf. Coord. Chem.*, E16. Porton, Portugal (1988).
12. J. Chatt, A. J. L. Pombeiro and R. L. Richards, *J. Chem. Soc., Dalton Trans.* 1980, 492.
13. A. J. L. Pombeiro and R. L. Richards, *Transition Met. Chem.* 1980, **5**, 55.
14. A. J. L. Pombeiro, M. F. N. N. Carvalho, P. B. Hitchcock and R. L. Richards, *J. Chem. Soc., Dalton Trans.* 1981, 1629.
15. J. Chatt, A. J. L. Pombeiro and R. L. Richards, *J. Organomet. Chem.* 1980, **184**, 357.
16. M. F. N. N. Carvalho, A. J. L. Pombeiro, E. G. Bakalbassis and C. A Tsipis, in preparation; M. F. N. N. Carvalho and A. J. L. Pombeiro, *II Meet. Portugal Electrochem. Soc.*, Chap. 8, p. 55. Ofir, Portugal (1986).
17. J. Chatt, A. J. L. Pombeiro and R. L. Richards, *J. Chem. Soc., Dalton Trans.* 1979, 1585.
18. A. J. L. Pombeiro and R. L. Richards, *Transition Met. Chem.* 1980, **5**, 281.
19. D. L. Hughes, A. J. L. Pombeiro, C. J. Pickett and R. L. Richards, *J. Chem. Soc., Chem. Commun.* 1984, 992.
20. A. J. L. Pombeiro, J. C. Jeffery, C. J. Pickett and R. L. Richards, *J. Organomet. Chem.* 1984, **277**, C7.
21. A. Hills, D. L. Hughes, N. Kashef, R. L. Richards, M. A. N. D. A. Lemos and A. J. L. Pombeiro, *J. Organomet. Chem.* 1988, **350**, C4.
22. N. A. Buang, D. L. Hughes, N. Kashef, R. L. Richards and A. J. L. Pombeiro, *J. Organomet. Chem.* 1987, **323**, C47.
23. A. J. L. Pombeiro, D. L. Hughes, R. L. Richards, J. Silvestre and R. Hoffmann, *J. Chem. Soc., Chem. Commun.* 1986, 1125.
24. A. J. L. Pombeiro, A. Hills, D. L. Hughes and R. L. Richards, *J. Organomet. Chem.* 1988, **352**, C5.
25. N. M. Kostic and R. F. Fenske, *Organometallics* 1982, **1**, 974.
26. E. M. Bradley, J. Chatt and R. L. Richards, *J. Chem. Soc. A* 1971, 21; P. M. Treichel, *Adv. Organomet. Chem.* 1973, **11**, 21; F. Bonati and G. Minghetti, *Inorg. Chim. Acta* 1974, **9**, 95; E. Singleton and H. E. Oosthuizen, *Adv. Organomet. Chem.* 1983, **22**, 209.

27. (a) B. D. Dombek and R. J. Angelici, *J. Am. Chem. Soc.* 1975, **97**, 1261; B. D. Dombek and R. J. Algelici, *Inorg. Chem.* 1976, **15**, 2397; J. W. Dunker, J. S. Finer, J. Clardy and R. J. Angelici, *J. Organomet. Chem.* 1976, **114**, C49; W. W. Greaves and R. J. Angelici, *Inorg. Chem.* 1981, **20**, 2983; (b) T. J. Collins and W. R. Roper, *J. Organomet. Chem.* 1978, **159**, 73 and refs therein.
28. A. Davison and J. P. Selegue, *J. Am. Chem. Soc.* 1978, **100**, 7763; A. Davison and J. P. Selegue, *J. Am. Chem. Soc.* 1980, **102**, 2455; M. I. Bruce and A. G. Swincer, *Aust. J. Chem.* 1980, **33**, 1471; M. I. Bruce, *Pure Appl. Chem.* 1986, **58**, 553; K. R. Birdwhistell, T. L. Tonker and J. L. Templeton, *J. Am. Chem. Soc.* 1985, **107**, 4474.
29. J. Chatt, L. M. C. Pina and R. L. Richards (Eds), *New Trends in the Chemistry of Nitrogen Fixation.* Academic Press, London (1980).
30. N. M. Kostic and R. F. Fenske, *Organometallics* 1982, **1**, 974.
31. Yu. N. Kukushkin, *Koordinatsionnaya Khimiya*, 1981, **7**, 323 (Engl. transl., p. 147); B. N. Storhoff and H. C. Lewis Jr, *Coord. Chem. Rev.* 1977, **23**, 1.
32. M. A. N. D. A. Lemos and A. J. L. Pombeiro, *J. Organomet. Chem.* 1988, **356**, C79.
33. B. K. Burgess, in *Molybdenum Enzymes* (Edited by T. G. Spiro), Chap. 4. John Wiley, New York (1985).

Polyhedron Vol. 8, No. 13/14, pp. 1601–1606, 1989
Printed in Great Britain

0277–5387/89 $3.00+.00
Maxwell Pergamon Macmillan plc

SYNTHETIC AND STRUCTURAL STUDIES ON SOME ORGANIC COMPOUNDS OF ZIRCONIUM

ANTONIO ANTIÑOLO, GARRY S. BRISTOW, GRAEME K. CAMPBELL, ALAN W. DUFF, PETER B. HITCHCOCK, ROSE A. KAMARUDIN, MICHAEL F. LAPPERT,* REGINALD J. NORTON, NIGEL SARJUDEEN and DUNCAN J. W. WINTERBORN

School of Chemistry and Molecular Sciences, University of Sussex, Brighton BN1 9QJ, U.K.

and

JERRY L. ATWOOD,* WILLIAM E. HUNTER and HONGMING ZHANG

Department of Chemistry, University of Alabama, University, AL 35486, U.S.A.

Abstract—The synthesis of 11 organozirconium compounds is described, together with their characterization. Nine of them are zirconocene(IV) derivatives bearing cyclopentadienyl (Cp) or related ligands [Cp′ = η-$\bar{C}_5H_5SiMe_3$, $\bar{C}p''$ = η-$\bar{C}_5H_3(SiMe_3)_2$-1,3 or $\bar{C}p'''$ = η-$\bar{C}_5H_2(SiMe_3)_3$-1,2,4]. The remaining two compounds are [$ZrCp''_2$(DMPE)] (**8**) and [$Zr(CH_2Mes)_2Cl_2$]·$2Et_2O$ [DMPE = $(Me_2PCH_2)_2$ and Mes = $C_6H_2Me_3$-2,4,6]. X-ray structural data are presented for seven of these complexes: [$ZrCp_2$(Cl)(OAr)], [$ZrCp_2\{\eta^2$-C(NMe)CHPh$_2\}$(Me)], [$ZrCp_2(NMe_2)$(OAr′)], [$ZrCp'_2(CH_2C_6Me_5)$(Cl)], [$ZrCp''_2(\eta^2$-$BH_4)$(Cl)], (**8**) and [$ZrCp'''(NMe_2)_3$] (Ar = $C_6H_2Bu^t_2$-2,6-Me-4, Ar′ = $C_6H_3Bu^t_2$-2,6). Cyclic voltammetric results are presented for the zirconocene halides of formula [$ZrCp''_2X_2$] (X = F, Cl, or Br) and on some related compounds. The zirconocene(II) complex, **8**, undergoes reversible one-electron oxidation and ESR data are provided on the zirconium(III) product. Some variable temperature NMR results are described on the aryloxides and tetrahydridoborates.

For some years we have been actively pursuing aspects of organozirconium chemistry.[1,2] Among the compounds which we have studied in detail are the metallocene halides [$ZrCp_2Hal_2$] (Cp = η-C_5H_5; Hal = F, Cl, Br, or I). We have recently reported on the synthesis and X-ray structures of [$ZrCp''_2Hal_2$] [Cp″ = η-$C_5H_3(SiMe_3)_2$-1,3].[1] The effect of introducing an alkyl or trimethylsilyl substituent into the cyclopentadienyl ligand on the properties of zirconocene(II, III, or IV) complexes has received some attention.[1–3] The ligand $\bar{C}p''$ was originally introduced into 4*f* element chemistry; *inter alia* we synthesized complexes of formula [{$LnCp''_2(\mu$-Cl)}$_2$] for the early lanthanide metals (Ln = La, Ce, Pr, or Nd);[4] these are not accessible for the $\bar{C}p$ analogues (if formed they disproportionate yielding 2/3$LnCp_3$ + 1/3$LnCl_3$).

A feature of the $\bar{C}p'$ (≡ η-$\bar{C}_5H_4SiMe_3$) and $\bar{C}p''$ ligands is that with increasing trimethylsilyl substitution they generally confer on their metal complexes, increasing lipophilicity and volatility. Furthermore, as a result of their bulk, steric effects may come into play to yield unusual chemistry.

The objectives of this paper are to present some new results on zirconocene derivatives, including a good deal of crystallographic information. Some comparisons will also be made relating to cyclic voltammetry data on the metallocene halides, illustrating the role of (a) trimethylsilyl substituents in the cyclopentadienyl group of [$Zr(\eta$-$C_5H_3RR')_2Cl_2$] (R and R′ = H or $SiMe_3$) and (b) Hal in [$ZrCp''_2Hal_2$]. Because of the bulk of the $\bar{C}p''$ ligand, steric effects may be manifested in various ways. For the tetrahydridoborates this will be shown by the mode of bonding between that ligand and the metal, and for an aryloxide by restriction to rotation about the O—C(Ar) bond; variable temperature

* Authors to whom correspondence should be addressed.

Table 1. Yields and characterization data for the new crystalline organic zirconium complexes

Complex	Data
2	44%, orange crystals; ^{1}H NMR (CD_2Cl_2, 300 K): δ −0.18s (Me), 3.04s ($CHPh_2$), 7.1m (Ph), 5.85 (C_5H_5); $^{13}C\{^1H\}$ NMR (CD_2Cl_2, 300 K): δ 148.6, 129.6, 128.4, and 124.1 (Ph), 112.4 (C_5H_5), 75.6 ($CHPh_2$), 31.8 (Me)
3	47%, yellow crystals, m.p. *ca* 105°C (decomp.); [ν(CN), Nujol] 1628 cm^{-1}; ^{1}H NMR ($CDCl_3$, 300 K): δ 7.36m (Ph), 5.40s (C_5H_5), 4.97s [C(NMe)C*H*], 2.75s (NMe), 0.28s (ZrCH); $^{13}C\{^1H\}$ NMR ($CDCl_3$, 300 K): 239.2 (C=N), 128.6 and 126.8 (Ph), 106.0 (C_5H_5), 56.3 $CHPh_2$, 33.4 (NMe), 9.9 (ZrMe)
4	87%, red–orange crystals, m.p. 157–158°C; ^{1}H NMR ($CDCl_3$, 300 K): δ 5.70–6.62m ($C_5H_4SiMe_3$), 2.38s and 2.34s (CMe), 2.30s (CH_2), 0.43 ($SiMe_3$); $^{13}C\{^1H\}$ NMR (C_6D_6, 300 K): δ 110.7, 117.9, 119.0, and 126.2 ($C_5H_4SiMe_3$), 58.5 (CH_2), 18.3, 17.5, and 17.0 (C*Me*), 0.3 ($SiMe_3$)
5	63%, colourless crystals, m.p. 157–158°C; IR [ν(BH_4), Nujol]: 2500 (s), 2440 (s), 2080 (s), 1340 (s, br), 1140 (s) cm^{-1}; ^{1}H NMR (C_6D_6, 300 K): δ 7.03t and 6.47m (Cp″), 0.29d ($SiMe_3$), −2.0 (BH_4); $^{13}C\{^1H\}$ NMR (C_6D_6, 300 K): δ 142.6, 118.8, and 116.6 (Cp″), 0.1 ($SiMe_3$); ^{11}B NMR (PhMe, 358 K): δ 0.47qui [^1J(BH) 85.5 Hz]
6	62%, colourless crystals, m.p. 150–152°C; IR [ν(BH_4), Nujol]: 2500 (s), 2440 (s), 2080 (s), 1340 (s, br), 1140 (s) cm^{-1}; ^{1}H NMR (C_6D_6, 300 K): δ 7.03t and 6.19m (Cp″) 0.35s ($SiMc_3$), −2.0 (BH_4); $^{13}C\{^1H\}$ (C_6D_6, 300 K): δ 144.9, 119.0, and 116.4 (Cp″), −0.1 ($SiMe_3$); ^{11}B NMR (PhMe, 358 K): δ 0.82qui [J(BH) 87.2 Hz]
8	60%, dark green crystals, m.p. 132°C; ^{1}H NMR (C_6D_6, 300 K); δ 4.68m (Cp″), 1.07t [Me, J(PH) 2Hz], 0.7m (CH_2), 0.39s ($SiMe_3$); ^{13}C (C_6D_6, 300 K): δ 103.1, 102.6 and 97.8 (Cp″), 33.0t [Me, J(PC) 14 Hz], 21.9t [CH_2, J(PC) 5 Hz], 2.5 ($SiMe_3$); $^{31}P\{^1H\}$ (C_6H_6, 300 K) −189.7
10	60%, m.p. 195–200°C, subl. 110°C (10^{-1} Torr); ^{1}H NMR (C_6D_6, 300 K): δ 2.96s (NMe_2) 0.37s ($SiMe_3$-1,2), 0.28s ($SiMe_3$-4); $^{13}C\{^1H\}$ (NMR, 220 K): δ 45.8, 45.1 and 44.3 (NMe_2), 1.1 and −0.35 ($SiMe_3$)
12	29%, white crystals, m.p. 136–138°C; ^{1}H NMR (C_6D_6, 300 K): δ 1.03t (CH_2CH_3), 1.83s (CH_2Mes), 2.54s (*p*-Me), 2.65s (*o*-Me), 3.36q (CH_2CH_3), 6.96s [CH (aromatic)]

NMR data have provided the means of monitoring these effects. Another aspect of ZrCp chemistry relates to steric effects and their influence on thermal stability; this will be demonstrated by reference to the stable compounds [$ZrCp_2\{\eta^2$-C(NMe)$CHPh_2\}$(Me)], [$ZrCp''_2$(DMPE)] and [$ZrCp'''(NMe_2)_3$]. Finally, we draw attention to two new ligands: $\bar{C}H_2$Mes and $\bar{C}H_2C_6Me_5$ (Mes = $C_6H_2Me_3$-2,4,6) which have been developed in the context of zirconium(IV) chemistry.

RESULTS AND DISCUSSION

We report on 11 organozirconium compounds, **1**–**11**, as illustrated in Scheme 1; the synthesis of the aryloxide [$ZrCp_2$(Cl)(OAr)] (Ar = $C_6H_2Bu^t_2$-2,6-Me) (**1**) has already been described,[5] and compounds **2** and **3** have previously been briefly mentioned.[6] Each of the complexes **1**–**8**, **10** and **11** has been obtained in crystalline form and has been fully characterized by microanalytical, IR, and ^{1}H and ^{13}C NMR data. Yields and some spectroscopic information are shown in Table 1. Additionally, single-crystal X-ray crystallographic results are available for complexes **1**, **3**, **4**, **5**, **6**, **8** and **10**, as summarized briefly in Figs 1–7, respectively.

Cyclic voltammetric information has been obtained on a series of zirconocene halides [$ZrCp''_2Hal_2$] (Hal = F, Cl, or Br), as shown in Table 2, which also includes data on related compounds. From Table 2, it is clear that ease of reduction falls

Table 2. Cyclic voltammetry parameters for a range of group 4 metallocene(IV) halides[a]

Compound	E^0(V)[b]	ΔE_{pp}(V)[c]	$i^r : i^f$[d]
[$ZrCp_2Cl_2$]	−1.60	0.22	1.0
[$ZrCp'_2Cl_2$]	−1.56	0.16	1.0
[$TiCp''_2Cl_2$]	−0.70	0.12	0.7
[$ZrCp''_2Cl_2$]	−1.55	0.16	1.0
[$HfCp''_2Cl_2$]	−1.87	0.16	1.0
[$ZrCp''_2F_2$]	−1.71	0.16	1.0
[$ZrBr_2Cp''_2$]	−1.32	0.16	1.0

[a] As 2×10^{-3} mol dm^{-3} solutions in THF, containing 0.2 mol dm^{-3} [NBu^n_4][BF_4] as supporting electrolyte, at a platinum working electrode: potentials were internally referenced to the ferrocene–ferrocinium redox couple (+0.535 V).

[b] E^0 is the potential measured halfway between the potentials of peak cathodic and anodic currents.

[c] ΔE_{pp} is the difference between the potentials at peak anodic and peak cathodic potentials.

[d] ($i^r : i^f$) is the ratio of the peak-forward to peak-reverse currents at 100 MV s^{-1} sweep rate.

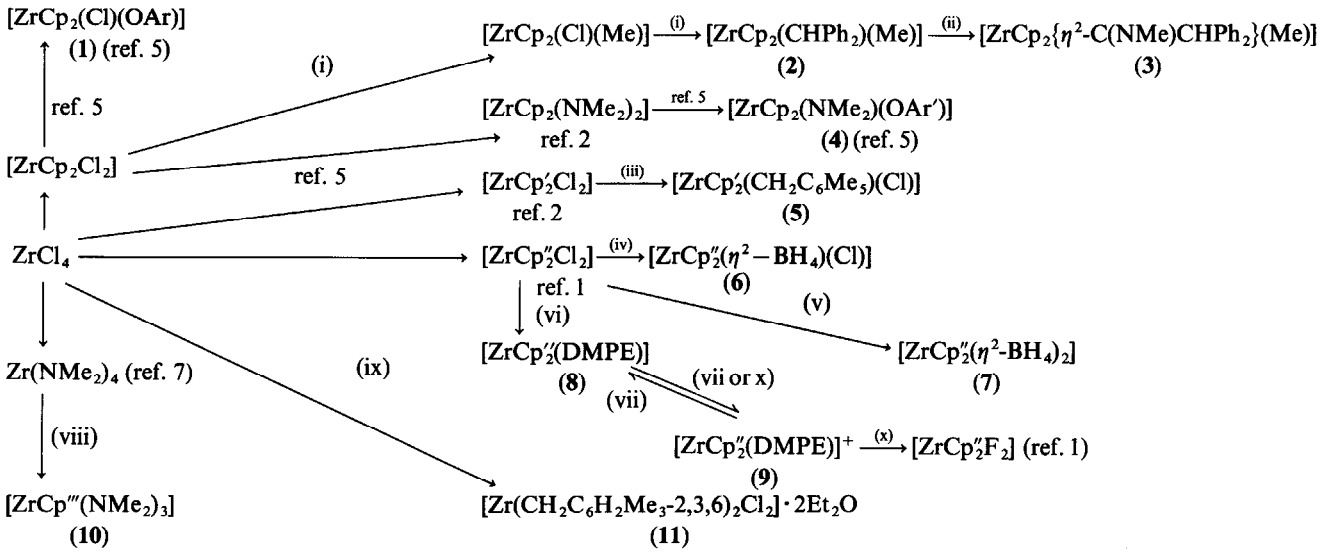

Scheme 1. Reaction conditions: (i) THF solution + MeMgI (1 mol) in Et_2O, 20°C; then $LiCHPh_2$ (1 mol) in THF and TMEDA (1 mol), filtration and cooling of filtrate (−20°C). (ii) MeNC (3 mol), 20°C; then filtration and cooling of filtrate (−20°C). (iii) $Mg(CH_2C_6Me_5)_2(dioxane)_2$ (2 mol) [colourless solid (from $C_6Me_5CH_2MgCl$, dioxane, Mg, THF)], Et_2O, 20°C; then filtration and cooling of filtrate (−30°C). (iv) $Li[BH_4]$ (2 mol), Et_2O, 20°C; then removal of THF, extraction into C_6H_{14}–PhMe, filtration and cooling of filtrate (−30°C). (v) $Na[BH_4]$ (4 mol), THF, 20°C; then removal of THF, extraction into PhMe, filtration and cooling of filtrate (−30°C). (vi) Na—Hg (2 mol Na), DMPE (1 mol), THF, 20°C; then removal of THF, extraction into C_6H_{14}, filtration and cooling of filtrate (−30°C). (vii) CV. (viii) Cp'''H (1 mol), C_6H_6, reflux, 4 h; then concentration and sublimation, *ca* 130°C at 10^{-1} Torr; recrystallized (*n*-C_5H_{12}, −50°C). (ix) $MesCH_2MgCl$ [from $MesCH_2Cl$ (5 mol), Mg (10 mol), $(CH_2Br)_2$ (10 mol), THF], Et_2O, 20°C, 25 h; then filtration, evaporation of filtrate, and extraction into PhMe and cooling (−30°C). (x) $Ag[BF_4]$ (1 mol), THF, 20°C.

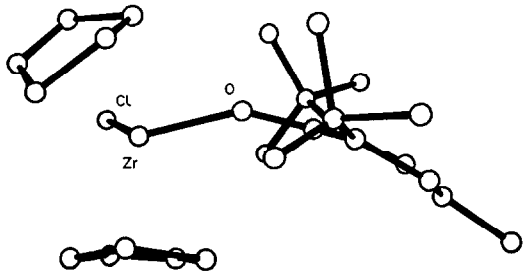

Fig. 1. The X-ray structure of $[ZrCp_2(Cl)(OC_6H_2Bu^t_2\text{-}2,6\text{-}Me\text{-}4)]$ (**1**). Important bond distances and angles: Zr—Cl 2.45(2), Zr—O 1.98(2) Å; O—Zr—Cl 107(1), Zr—O—C 150(1)°.

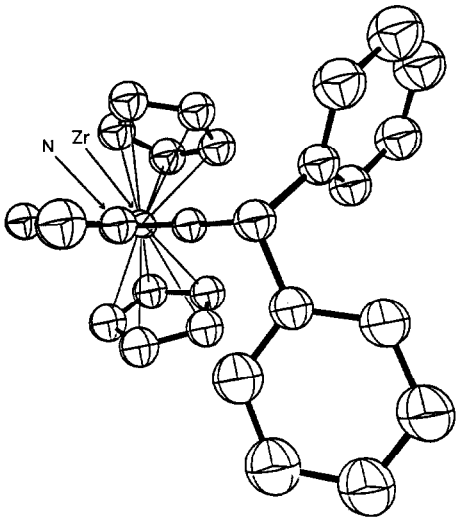

Fig. 2. The X-ray structures of $[ZrCp_2\{\eta\text{-}C(NMe)CHPh_2\}(Me)]$ (**3**). Important bond distances and angles: Zr—CH_3 2.431(5), Zr—N 2.210(4), Zr—η^2-C 2.247(5), C—N 1.260(6) Å; Cen—Zr—Cen 129.8°.

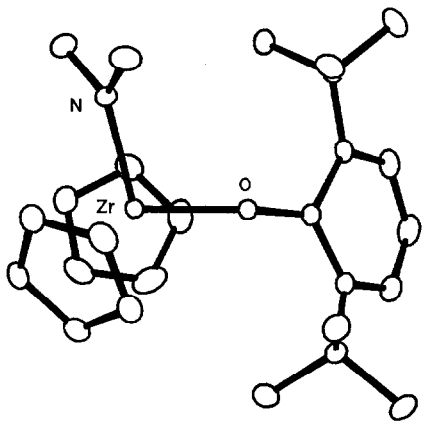

Fig. 3. The X-ray structure of $[ZrCp_2(NMe_2)(OC_6H_3Bu^t_2\text{-}2,6)]$ (**4**). Important bond distances and angles: Zr—N 2.072(2), Zr—O 2.056(1), C—O 2.056(1), Zr—Cen 2.217 Å; O—Zr—N 103.2(1), O—Zr—Cen 106.6 and 109.5, N—Zr—Cen 105.7 and 104.4, Zr—O—C 142.7(1)°.

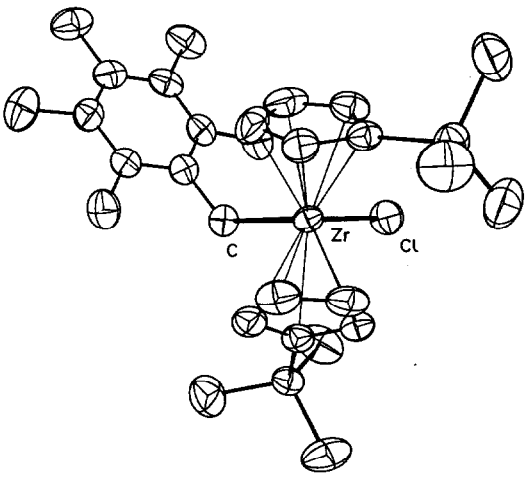

Fig. 4. The X-ray structure of $[ZrCp'_2(CH_2C_6Me_5)(Cl)]$ (**5**). Important bond distances and angles: Zr—C 2.465(1), Zr—CH_2 2.330(5) Å; Zr—CH_2—C 127.2(4), Cl—Zr—CH_2 98.3(1), Cen—Zr—Cen′ 129.4°.

off in the sequence (a) Ti ≫ Zr > Hf, (b) Br > Cl > F, and (c) Cp″ ≥ Cp′ > Cp.

Whereas these results deal with the reduction of zirconium(IV) to zirconium(III), data are also available on the oxidation process zirconium(II) to zirconium(III) in which the substrate was $[ZrCp''_2(DMPE)]$ [DMPE = $(Me_2PCH_2)_2$] (**8**). Thus, there was a reversible one-electron oxidation of $Zr^{II} \rightarrow Zr^{III}$, with $E^{ox} = -0.6$ V followed by an irreversible one-electron $Zr^{III} \rightarrow Zr^{IV}$ oxidation at

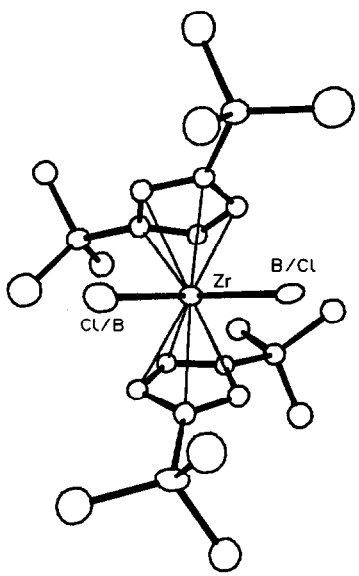

Fig. 5. The X-ray structure of $[ZrCp''_2(\eta^2\text{-}BH_4)(Cl)]$ (**6**). Important bond distances and angles: Zr—B 2.44(1), Zr—Cl 2.410(9), Zr—Cen 2.217 Å; Cl—Zr—B 98.9(4), Cen—Zr—Cen′ 131.9, Cen—Zr—Cl 106.1°.

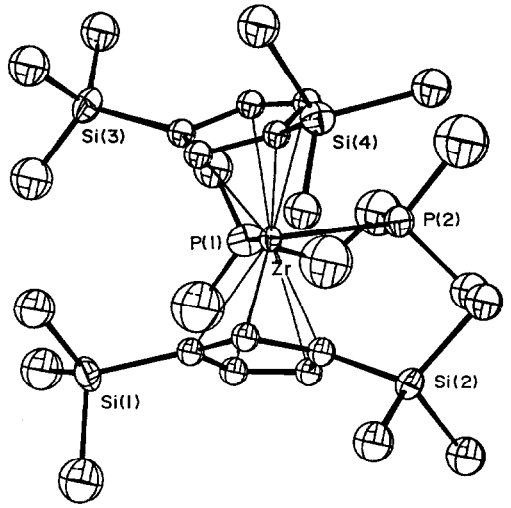

Fig. 6. The X-ray structure of $[ZrCp''_2(DMPE)]$ (**8**). Important bond distances and angles: Zr—P 2.678(3); P(1)—Zr—P(2) 73.7(1), Zr—P—CH_3 126.6(9) and 123.9(5), Zr—P—CH_2 110.7(9)°.

0.49 V (the cell conditions were those of Table 2). The chemical oxidation of complex **8** by $Ag[BF_4]$ (1 mol) in THF, or electrochemically at a potential of −0.6 V, generated a green d^1 complex, showing a triplet ESR signal, $g_{av} = 1.9871$, $a(^{31}P) = 26.7$ G, which decomposed over *ca* 6 h at 20°C to yield the diamagnetic colourless $[ZrCp''_2F_2]$.

The IR spectra of the zirconium(IV) tetrahydridoborato complexes, **6** and **7**, revealed them to have the $Zr(\mu\text{-}H)_2BH_2$ structure, as had been noted for $[ZrCp_2(\eta^2\text{-}BH_4)_2]$.[8] In the prochiral $[ZrCp''_2(Cl)(\eta^2\text{-}BH_4)]$ (**6**), the ^1H NMR signals due to the ring proton H(2) and $SiMe_3$ were each split into doublets. The BH_4 protons were observed as a featureless singlet at 300 K, but this was resolved into a broad 1 : 1 : 1 : 1 quartet at 338 K. Similarly, the ^{11}B NMR spectrum showed fast exchange (a binomial quintet) at 360 K, but a slowing down of the bridge–terminal exchange at lower temperatures, Fig 8; by contrast in $[ZrCp_2(\eta^2\text{-}BH_4)_2]$, this exchange is rapid even at ambient temperature.[8]

As (a) the $\eta\text{-}\bar{C}_5Me_5$ ligand has powerfully extended cyclopentadienylmetal chemistry, and (b) $\bar{C}H_2Ph$ has an important role in zirconium(IV) chemistry,[2] it was considered to be of interest to examine the new ligands $\bar{C}H_2C_6Me_5$ or $\bar{C}H_2C_6H_2Me_3$-2,4,6 (= $\bar{C}H_2Mes$). There was some difficulty in preparing $C_6Me_5CH_2MgCl$ (and attempts to prepare the corresponding lithium benzyl failed), but this was eventually accomplished by using THF as solvent in high dilution (<0.1 mol dm^{-3}), activating the magnesium dust immediately prior to use $[(BrCH_2)_2]$, and slow addition of $C_6Me_5CH_2Cl$. Addition of a 10-fold excess of *p*-dioxane to a THF solution of $C_6Me_5CH_2MgCl$ slowly (several hours at *ca* 25°C) yielded a precipitate of $MgCl_2(THF)_2$ and, from the filtrate, $Mg(CH_2C_6Me_5)_2(p\text{-dioxane})_n$. No doubt due to the bulk of $\bar{C}H_2C_6Me_5$ only one $\bar{C}l$ ligand of $[ZrCp'_2Cl_2]$ was displaced to yield $[ZrCp'_2(CH_2C_6Me_5)(Cl)]$ (**5**) (the Cp analogue and

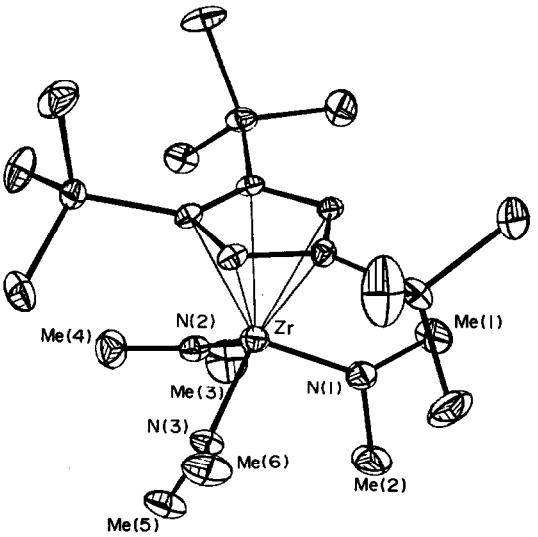

Fig. 7. The X-ray structure of $[ZrCp'''(NMe_2)_3]$ (**10**). Important bond distances and angles: Zr—N(1) 2.051(5), Zr—N(2) 2.047(5), Zr—N(3) 2.067(4) Å; N(1)—Zr—N(2) 97.3(2), N(1)—Zr—N(3) 105.9(2), N(2)—Zr—N(3) 99.5(2)°.

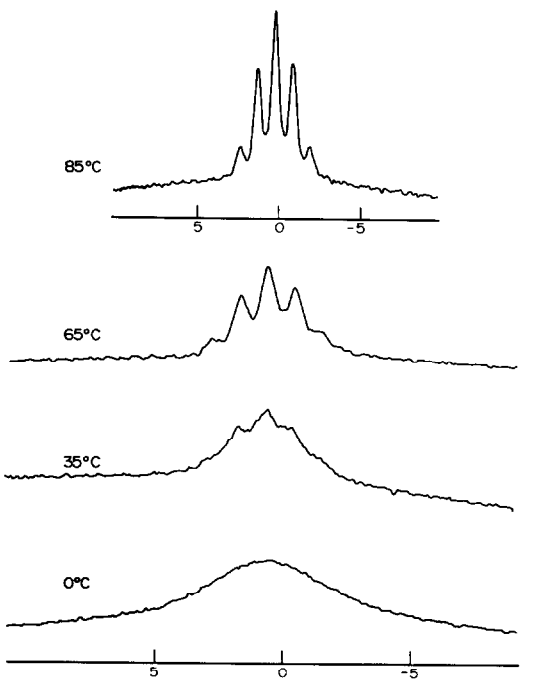

Fig. 8. Variable temperature ^{11}B NMR spectra of $[ZrCp''_2(\eta^2\text{-}BH_4)(Cl)]$ (**6**) in toluene-d_8.

the corresponding Hf complex were also prepared and characterized). The low temperature ^{1}H NMR spectrum of **5** was consistent with the conformation **5a** rather than **5b**, as also evident in the crystal (Fig. 4). From the NMR and the X-ray data, we conclude that the steric demands of the $\bar{C}H_2C_6Me_5$ ligand are not as stringent as those of $\bar{C}H(SiMe_3)_2$ ($\equiv \bar{R}$), cf. corresponding data for [ZrCp$'_2$(R)(Cl)].[9]

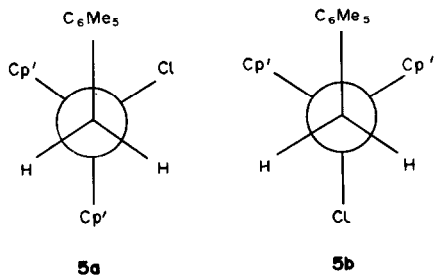

5a **5b**

In the ^{1}H NMR spectrum of [ZrCp$_2$(NMe$_2$)(OAr')] (Ar = C$_6$H$_3$Bu$^t_2$-2,6) (**4**) the 2- and 6-Bu^t groups are distinct and different under ambient conditions, the coalescence temperature (T_c) being 324 K, corresponding to $\Delta G^{\ddagger}_{324K} = 70$ kJ mol^{-1}; as the cyclopentadienyl protons remain equivalent, the effect is attributed to restricted rotation about the O—C(Ar) rather than the Zr—O bond. The T_C value for some analogues [ZrCp$_2$(OAr')(X)] was >343 K for X = OMe (prepared from **4**+MeOH) and >333 K for X = OC(O)NMe$_2$ (prepared from **4**+CO$_2$). The Zr—O bond length and Zr—O—C(Ar) bond angle in **4** (Fig. 3), [ZrCp$_2$(Cl)(OAr')] (**1**) (Fig. 1), and [Zr{η^2-C(NBu^t)CH$_2$Ph}$_2$(OAr)$_2$] (**13**) [2.027(2) Å and 172.7(2)°][10] are available for comparison.

The Zr—CH$_3$ bond length in [ZrCp$_2${η^2-C(NMe)CHPh$_2$}Me] (**3**) (Fig. 2) is remarkably long, cf. 2.287(5) Å in [ZrCp$_2$Me$_2$].[2] There are significant differences in bond lengths relating to the iminoacyl fragment of **13**: Zr—N, 2.221(3); Zr—η^2-C, 2.228(3); C—N, 1.286(4) Å.[10]

The monomeric nature of the monocyclopentadienylzirconium(IV) complex, [ZrCp'''(NMe$_2$)$_3$] [Cp''' = C$_5$H$_2$(SiMe$_3$)$_3$-1,2,4] (**10**), is noteworthy. The steric crowding is evident from the low temperature ^{1}H NMR spectrum (Table 1), which reveals three distinct methyl environments for the NMe$_2$ protons.

Acknowledgements—We thank SERC, the EEC (Stimulation Contract: ST2000335), and NSF (J.L.A.) for support.

REFERENCES

1. A. Antiñolo, M. F. Lappert, A. Singh, D. J. W. Winterborn, L. M. Engelhardt, C. L. Raston, A. H. White, A. J. Carty and N. J. Taylor, *J. Chem. Soc., Dalton Trans.* 1987, 1463 and refs therein.
2. D. J. Cardin, M. F. Lappert and C. L. Raston, *Chemistry of Organo-zirconium and -hafnium Compounds.* Ellist Horwood, Chichester (1986).
3. M. F. Lappert, C. J. Pickett, P. I. Riley and P. I. W. Yarrow, *J. Chem. Soc., Dalton Trans.* 1981, 805.
4. M. F. Lappert, A. Singh, J. L. Atwood and W. E. Hunter, *J. Chem. Soc., Chem. Commun.* 1981, 1190.
5. A. W. Duff, R. A. Kamarudin, M. F. Lappert and R. J. Norton, *J. Chem. Soc., Dalton Trans.* 1986, 489.
6. G. S. Bristow, P. B. Hitchcock and M. F. Lappert, *J. Chem. Soc., Chem. Commun.* 1982, 462.
7. D. C. Bradley and I. M. Thomas, *J. Chem. Soc.* 1960, 3857.
8. T. J. Marks and J. R. Kolb, *Chem. Rev.* 1977, **77**, 263; N. Davies, B. D. James and M. G. H. Wallbridge, *J. Chem. Soc. A* 1969, 2601.
9. M. F. Lappert, P. I. Riley, P. I. W. Yarrow, J. L. Atwood, W. E. Hunter and M. J. Zaworotko, *J. Chem. Soc., Dalton Trans.* 1981, 814.
10. L. R. Chamberlain, L. R. Durfee, P. E. Fanwick, L. Kobriger, S. L. Latesky, A. K. McMullen, I. A. P. Rothwell, K. Folting, J. C. Huffman, W. E. Streib and R. Wang, *J. Am. Chem. Soc.* 1987, **109**, 390.

Polyhedron Vol. 8, No. 13/14, pp. 1607–1610, 1989
Printed in Great Britain

0277–5387/89 $3.00+.00
© 1989 Maxwell Pergamon Macmillan plc

THE METALLATION AND HYDROGENATION OF ARYL RINGS IN EARLY TRANSITION METAL ARYLOXIDE SYSTEMS

ROBERT W. CHESNUT, BRYAN D. STEFFEY and IAN P. ROTHWELL*

Department of Chemistry, Purdue University, West Lafayette, IN 47907, U.S.A.

Abstract—The mixed chloro-aryloxide compounds of stoichiometry $M(OAr\text{-}2,6Ph_2)_2Cl_3$ and $[M(OAr\text{-}2,6Ph_2)_3Cl_2]$ (M = Nb, Ta; $OAr\text{-}2,6Ph_2$ = 2,6-diphenylphenoxide) serve as useful substrates for the synthesis of a series of corresponding tris- and bis-alkyl derivatives. Thermolysis of these alkyl compounds in hydrocarbon solvents leads to the formation of cyclometallated compounds of the type $M(OC_6H_3Ph\text{-}C_6H_4)(OAr\text{-}2,6Ph_2)(R)_2$ and $M(OC_6H_3Ph\text{-}C_6H_4)(OAr\text{-}2,6Ph_2)_2(R)$ (R = CH_3, $CH_2\text{-}C_6H_4\text{-}4Me$). Reduction of the dichlorides $M(OAr\text{–}2,6Ph_2)_3Cl_2$ with sodium amalgam in toluene solution does not yield the corresponding tris-aryloxides. Instead the bis-cyclometallated compounds $M(OC_6H_3Ph\text{-}C_6H_4)_2(OAr\text{-}2,6Ph_2)$ (M = Nb, Ta) are produced in high yield along with H_2. However, in the presence of one atmosphere of H_2 the niobium compound undergoes reduction to produce $Nb(OC_6H_3Ph\text{-}\eta^4\text{-}C_6H_7)(OAr\text{-}2,6Ph_2)_2$. Spectroscopic and structural studies of this latter compound show it to contain an η^4-bound cyclohexadiene ring formed by hydrogenation of an *ortho*-phenyl substituent of an aryloxide ligand. Treatment of the niobium cyclohexadiene complex with H_2 (1000 psi, 25°C) leads to the hydrogenation of the original 2,6-diphenylphenoxide ligands to produce, after hydrolysis, high yields of 2,6-dicyclohexylphenol. The selective side chain hydrogenation of 2,6-diphenylphoxide ligands can also be achieved by reacting alkyl compounds such as $Nb(OAr\text{-}2,6Ph_2)_3Me_2$ with H_2. In this latter case a mono-hydride of stoichiometry $Nb(H)(OAr\text{-}2,6cy_2)_4$ was isolated and structurally characterized.

The high valent early *d*-block, lanthanide and actinide metal–hydride and metal–alkyl bonds have been shown over the last few years to be extremely important functional groups, being implicated in a wide range of stoichiometric and catalytic reactivity.[1–4] Besides their ability to carry out the reduction of unsaturated small molecules and functionalities, a recently demonstrated reactivity of these metal hydrides and alkyls has been their propensity for activating a range of carbon–hydrocarbon bonds both intra- and intermolecularly.[5–8] An intriguing dual reactivity is demonstrated by their reactivity towards olefins.[1,5–7] By careful choice of the metal system and olefin substrate, both migratory insertion into metal–hydride or metal– alkyl bonds can be achieved: reactions of synthetic utility and relevance to catalytic processes. However, it is also possible to obtain metal σ-vinyl products resulting from activation of sp^2-CH bonds and elimination of either alkane or dihydrogen.[5–7] In the case of the related aromatic hydrocarbon substrates, either no reaction is observed or else ring metallation and formation of σ-aryl compounds is found to take place.[5–8] There is little evidence for arene hydrogenation occurring.[9–12] During our studies of the early transition metal chemistry associated with sterically demanding aryloxide ligation[8] we have investigated the behaviour of 2,6-diphenylphenoxide ($OAr\text{-}2,6Ph_2$) as ancillary ligation for supporting organometallic chemistry.[13,14] This work, which is outlined here, has demonstrated that it is possible not only to induce intramolecular metallation of this ligand,[13,14] but that intramolecular hydrogenation of the side chain aryl groups by metal–hydride ligands can also be a directly competing reactivity.[15]

The chloride compounds $M(OAr\text{-}2,6Ph_2)_2Cl_3$ and $M(OAr\text{-}2,6Ph_2)_3Cl_2$ (M = Nb, Ta) prove to be useful substrates for the synthesis of simple alkyl derivatives containing 2,6-diphenylphenoxide ancillary ligation (Scheme 1).[13,14] However, the

* Author to whom correspondence should be addressed.

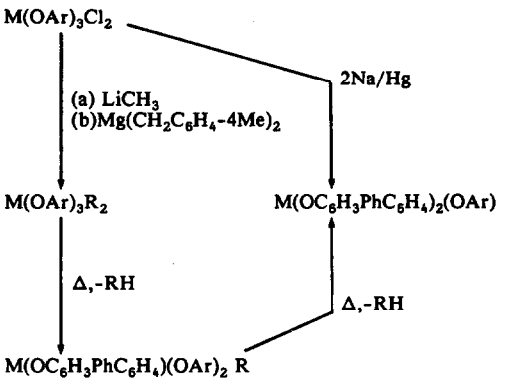

(a) R=CH_3; (b) R=$CH_2C_6H_4(OAr)_2R$
OAr=2,6-diphenylphenoxide
M=Nb, Ta

Scheme 1.

simple methyl and 4-methylbenzyl derivatives are thermally unstable and undergo elimination of methane and *p*-xylene, respectively, to generate cyclometallated compounds. Structural studies[14] confirm the presence of six-membered metallacycle rings formed by the metallation of one of the side chain phenyl groups.[8] The use of labelled compounds such as $Ta(OAr\text{-}2,6Ph_2)_3(CD_3)_2$ clearly shows that the reaction proceeds by loss of CD_3H, indicating the absence of methylidene intermediates.[8] The use of 2,4,6-tri-aryl phenoxides that contain differing substituents attached to the 2- and 6-aryl ring shows that there is only a minor substituent effect on the rate of cyclometallation.[16]

Attempts to form low valent aryloxide compounds of niobium and tantalum by sodium amalgam reduction of $M(OAr\text{-}2,6Ph_2)_3Cl_2$ (M = Nb, Ta) also leads to cyclometallated compounds. In this case, bis-cyclometallated compounds are obtained along with H_2 (Scheme 1).[14,17] A minor component was also observed in the reduction of the niobium compound. It is possible to generate this material in essentially quantitative yields by running the reduction under one atmosphere of H_2. Spectroscopic and structural studies show this compound to be $Nb(OC_6H_3Ph\text{-}\eta^4\text{-}C_6H_7)(OAr\text{-}2,6Ph_2)_2$ in which one of the side chain aryloxide phenyl groups has undergone 1,2-hydrogenation (Scheme 2).[15] The resulting cyclohexadiene ring is then bound to the niobium in an η^4-fashion.[18] Hydrolysis of this material yields two equivalents of $HOAr\text{-}2,6Ph_2$, along with one equivalent of 2-(cyclohex-2-enyl)6-phenylphenol. A combination of 1D and 2D NMR experiments, as well as the use of deuterium labels, conclusively show that the two hydrogen atoms are added in a mutually *cis*-fashion. However, due to the unfavourable stereochemistry at the initial *ipso*-carbon the niobium metal centre has to bind to the *opposite* face of the cyclohexadiene unit to which the hydrogenation took place.[18]

Treatment of toluene solutions of the compound $Nb(OC_6H_3Ph\text{-}\eta^4\text{-}C_6H_7)(OAr\text{-}2,6Ph_2)_2$ with H_2 (1000 psi, 25°C, 6 days or 400 psi, 80°C, 6 h) results in the complete hydrogenation of all of the side chain phenyl rings. Hydrolysis allows the isolation of 2,6-dicyclohexylphenol in 85% isolated yield based on initial 2,6-diphenylphenoxide ligands. Partial hydrogenation followed by hydrolysis yields a mixture of 2,6-diphenylphenol; 2-cyclohexyl-6-phenylphenol and 2,6-dicyclohexylphenol. Com-

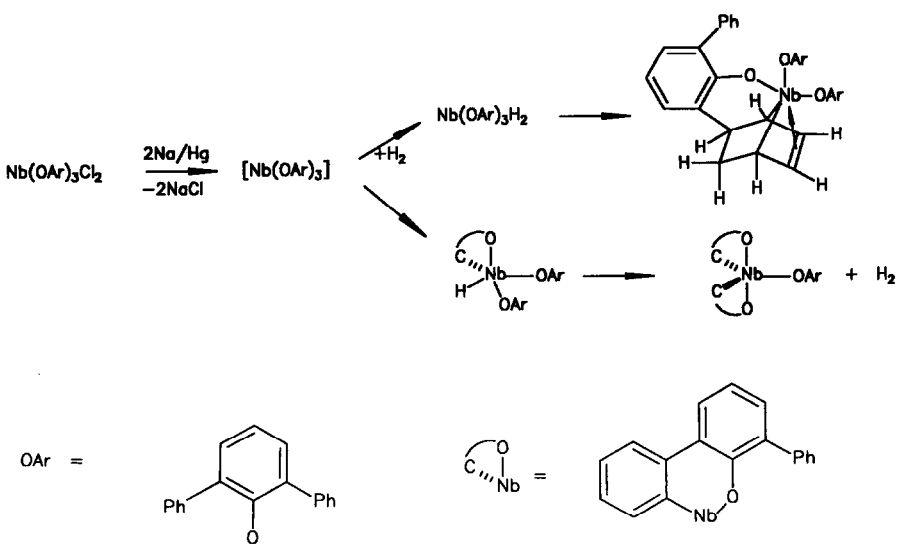

Scheme 2.

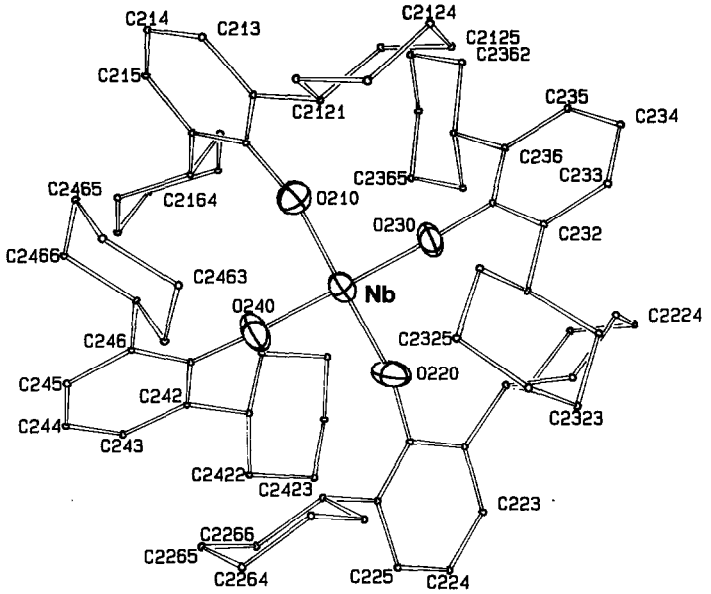

Fig. 1. ORTEP view of Nb(H)(OAr-2,6cy$_2$)$_4$ (molecule 2). Selected bond distances (Å) and angles (°) are

Nb(2)—O(210)	1.901(5)	Nb(2)—O(220)	1.901(5)
Nb(2)—O(230)	1.863(5)	Nb(2)—O(240)	1.875(5)
O(210)—Nb(2)—O(220)	176.2(2)	O(210)—Nb(2)—O(230)	89.8(2)
O(210)—Nb(2)—O(240)	89.8(2)	O(220)—Nb(2)—O(230)	89.9(2)
O(220)—Nb(2)—O(240)	90.3(2)	O(230)—Nb(2)—O(240)	177.5(2)

plete hydrogenation of the substituent phenyl rings can also be achieved by treating the dimethyl substrate, Nb(OAr-2,6Ph$_2$)$_3$Me$_2$, or the bis-cyclometallated compound, Nb(OC$_6$H$_3$Ph-C$_6$H$_4$)$_2$(OAr-2,6Ph$_2$), with H_2. Presumably initial formation of a dihydride intermediate (Scheme 2) takes place by hydrogenolysis of the Nb—C bonds. Analysis of the final reaction mixture by ^{1}H NMR spectroscopy indicates the presence of Nb—*H* functionalities as broad resonances in the δ −10–12 region. In the case of the hydrogenation of Nb(OAr-2,6Ph$_2$)$_3$Me$_2$, large orange blocks of stoichiometry Nb(H)(OAr-2,6cy$_2$)$_4$ (OAr-2,6cy$_2$ = 2,6-dicyclohexylphenoxide) were obtained and structurally characterized (Fig. 1).*

The use of 2,4,6-triphenylphenoxide ligation results in the formation of 2,6-dicyclohexyl-4-phenylphenol, with no evidence for hydrogenation of either the 4-phenyl substituent or the phenoxy ring. The use of deuterium as the reagent gas, as well as the use of asymmetric 2,6-di-arylphenoxide ligation, gives considerable mechanistic insight into these arene hydrogenation processes.

Acknowledgement—We thank the National Science Foundation (Grant CHE-8612063) for financial support of this research.

REFERENCES

1. (a) J. Schwartz and J. Labinger, *Angew. Chem. Int. Ed. Engl.* 1976, **15**, 333; (b) E. I. Negishi, in *Organometallics in Organic Synthesis*. John Wiley, New York (1980); (c) N. M. Doherty and J. E. Bercaw, *J. Am. Chem. Soc.* 1985, **107**, 2670.

* Crystal data for Nb(H)(OAr-2,6cy$_2$)$_4$ at 20°C: a = 39.423(4), b = 22.577(6), c = 22.383(3) Å, β = 99.72(1)°, Z = 12, d_{calc} = 1.165 g cm^{-3} in space group $C2/c$ (No. 15). Of the 13,200 unique reflections collected, $4 \leqslant 2\theta \leqslant 45°$, with Mo-$K_\alpha$ radiation, the 5771 with $I > 3\sigma(I)$ were used in the final refinement to yield R = 0.057, R_w = 0.071. Hydrogen atoms were calculated assuming idealized geometry but were not refined. Two independent molecules were present in the unit cell, one (molecule 1) lying on a two-fold axis, while the other (molecule 2) occupies a general position. The niobium–hydride atom, which presumably lies above or below the square plane, could not be located. Atomic coordinates, bond lengths and angles and thermal parameters have been deposited at the Cambridge Crystallographic Data Centre.

2. P. T. Wolczanski and J. E. Bercaw, *Accts Chem. Res.* 1980, **13**, 121.
3. (a) P. J. Fagan, E. A. Maata and T. J. Marks, in *Catalytic Activation of Carbon Monoxide* (Edited by P. C. Ford), ASC Symp. Series 152. American Chemical Society, Washington, D.C. (1981); (b) K. G. Moloy and T. J. Marks, *J. Am. Chem. Soc.* 1984, **106**, 7051.
4. W. J. Evans, *Adv. Organomet. Chem.* 1985, **24**, 131.
5. P. L. Watson and G. W. Parshall, *Accts Chem. Res.* 1985, **18**, 51 and refs therein.
6. (a) M. E. Thompson and J. E. Bercaw, *Pure Appl. Chem.* 1984, **56**, 1; (b) M. E. Thompson, S. M. Baxter, A. R. Bulls, B. J. Burger, M. C. Nolan, B. D. Santarsiero, W. R. Schaefer and J. E. Bercaw, *J. Am. Chem. Soc.* 1987, **109**, 203.
7. J. W. Bruno, G. M. Smith, T. J. Marks, C. K. Fair, A. J. Schultz and J. M. Williams, *J. Am. Chem. Soc.* 1986, **108**, 40 and refs therein.
8. (a) I. P. Rothwell, *Polyhedron* 1985, **4**, 177; (b) I. P. Rothwell, *Accts Chem. Res.* 1988, **21**, 153; (c) L. D. Durfee and I. P. Rothwell, *Chem. Rev.* 1988, **88**, 1059.
9. (a) E. L. Muetterties and J. R. Bleecke, *Accts Chem. Res.* 1970, **12**, 324; (b) J. W. Johnson and E. L. Muetterties, *J. Am. Chem. Soc.* 1977, **99**, 7395; (c) L. S. Stuhl, M. Rakowski-DuBois, F. J. Kirsekorn, J. R. Bleecke, A. E. Stevens and E. L. Muetterties, *J. Am. Chem. Soc.* 1978, **100**, 2405.
10. (a) H. M. Feder and J. Halpern, *J. Am. Chem. Soc.* 1975, **97**, 7186; (b) R. Wilczynski, W. A. Fordyce and J. Halpern, *J. Am. Chem. Soc.* 1983, **105**, 2066.
11. (a) M. J. Russell, C. White and P. M. Maitlis, *J. Chem. Soc., Chem. Commun.* 1977, 427; (b) M. A. Bennett, T.-N. Huang, A. K. Smith and T. W. Turney, *J. Chem. Soc., Chem. Commun.* 1978, 582; (c) M. A. Bennett, T.-N. Huang and T. W. Turney, *J. Chem. Soc., Chem. Commun.* 1979, 312.
12. R. A. Grey, G. P. Pez and A. Wallo, *J. Am. Chem. Soc.* 1980, **102**, 5948.
13. R. W. Chesnut, L. D. Durfee, P. E. Fanwick, I. P. Rothwell, K. Folting and J. C. Huffman, *Polyhedron* 1987, **6**, 2019.
14. R. W. Chesnut, B. D. Steffey, I. P. Rothwell and J. C. Huffman, *Polyhedron* 1988, **7**, 753.
15. B. D. Steffey, R. W. Chesnut, J. L. Kerschner, P. J. Pellechia, P. E. Fanwick and I. P. Rothwell, *J. Am. Chem. Soc.* 1989, **111**, 378.
16. R. W. Chesnut and I. P. Rothwell, results to be published.
17. B. D. Steffey, L. R. Chamberlain, R. W. Chesnut, D. E. Chebi, P. E. Fanwick and I. P. Rothwell, *Organometallics*, in press.
18. (a) G. Erker, C. Kruger and G. Muller, *Adv. Organomet. Chem.* 1985, **24**, 1; (b) H. Yasuda, K. Tatsumi and A. Nakamura, *Accts Chem. Res.* 1985, **18**, 120; (c) S. Datta, M. B. Fischer and S. C. Wreford, *J. Organomet. Chem.* 1980, **183**, 353.

Polyhedron Vol. 8, No. 13/14, pp. 1611–1614, 1989
Printed in Great Britain

0277–5387/89 $3.00+.00
© 1989 Maxwell Pergamon Macmillan plc

HIGHLY REDUCED CARBONYLS OF THE EARLY TRANSITION METALS

JOHN E. ELLIS

Department of Chemistry, University of Minnesota, Minneapolis, MN 55455, U.S.A.

Abstract—Pioneering ventures in low valent carbonyl and related chemistry of titanium, zirconium, hafnium and other early transition elements have been undertaken to discover new classes of organometallic and inorganic materials. Useful synthetic methodology—involving a two step reductive carbonylation of a variety of group 4 halides by alkali metal naphthalenides at low temperatures—has been developed recently in our laboratory. By this procedure the first carbocyclic and anionic derivatives of the unknown $Ti(CO)_7$, $Zr(CO)_7$ and $Hf(CO)_7$ have been obtained. Also, this method provides the first general route to organophosphine carbonyls of zerovalent titanium, zirconium and hafnium. Very recently the initial stabilized "pure" carbonyl complexes of these elements have been obtained in the form of the hexacarbonylmetallate(2−) ions, $M(CO)_6^{2-}$.

For the past decade most of the research in this laboratory has involved the synthesis, isolation, characterization and study of the general reactivity patterns of novel highly reduced metal carbonyls. These contain *d*-block transition elements in their lowest known formal oxidation states and provide fundamentally new units for chemical synthesis. Examples of these "super-reduced" species include $Na_3[Co(CO)_3]$,[1] $Na_3[Mn(CO)_4]$,[2] $Na_4[Cr(CO)_4]$,[3] $Na_3[V(CO)_5]$[4] and the very recently synthesized $[K(15\text{-Crown-}5)_2]_2[Ti(CO)_6]$[5] of the first row transition elements. Analogous compounds have also been prepared for many of the corresponding second and third row transition metals. Of particular importance in the characterization of $V(CO)_5^{3-}$ and $Ti(CO)_6^{2-}$ were ^{51}V and ^{49}Ti NMR spectra of the 99% ^{13}CO enriched anions.[5,6] These spectra along with the corresponding ^{13}C NMR data provided unequivocal proof for the existence of these anions in solution.

A more recent objective of this research programme has been to examine the reduction of early transition metal halides and related substances by aromatic radical anions at low temperatures as a possible alternative or complement to metal atom vapour syntheses. Chatt, Watson and Davidson were the first to establish the utility of aromatic radical anions (especially of naphthalene) in the synthesis of low valent metal complexes,[7] including $Ru(dmpe)_2(C_{10}H_8)$ where dmpe = $Me_2PCH_2CH_2PMe_2$, and its naphthyl hydride tautomer.[8] Later, in important variations on this theme, Timms'[9] and Wreford's groups[10] employed naphthalenide salts to obtain the first isolated examples of naphthalene and substituted naphthalene complexes of early transition metals directly from their respective halides. Previously, such materials were available only from the interaction of transition metal atoms with naphthalenes.[11,12] Kündig and Timms' pioneering demonstration of the ease with which coordinated naphthalene in $Cr(C_{10}H_8)_2$ and $Mo(C_{10}H_8)_2$ was displaced by carbon monoxide and other small ligands, emphasized the great utility of labile naphthalene complexes in the syntheses of unusual organometallics.[11,13] On the basis of these prior studies, we developed the first useful atmospheric pressure reductive carbonylation synthesis of both $Nb(CO)_6^-$ and $Ta(CO)_6^-$.[14,15] These materials were previously available by only high pressure reactions.[16] It was then proposed that low valent, group 4 carbonyls might be available by similar procedures.[14] At this time we were unaware that the group of Jonas was actively investigating the properties of early transition metal naphthalene complexes obtained via alkali metal naphthalenides.[17] More recently, other groups have appreciated the importance of naphthalenides in the synthesis of unusual early transition metal compounds.[18]

Although early attempts to obtain the previously unknown hexacarbonylmetallates(2−) of titanium, zirconium and hafnium by the same basic procedures used for the niobium and tantalum analogues were totally unsuccessful, in 1984 we were

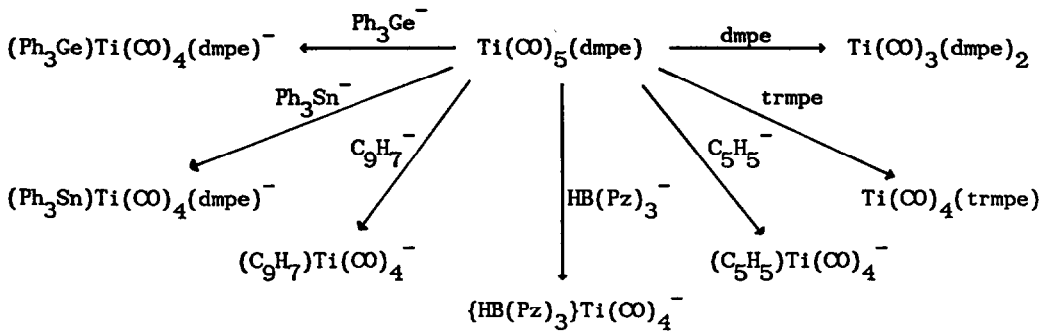

Scheme 1. Reactions of $Ti(CO)_5(dmpe)$ with various main group nucleophiles.

able to obtain zerovalent titanium carbonyls for the first time by this method.[19] For example, reduction of $(C_5Me_5)MCl_3$ (M = Ti, Zr, Hf) by 4 equivalents of $NaC_{10}H_8$ provided brightly coloured reactive intermediates which function as weakly solvated $(C_5Me_5)M^-$ units. Although the actual structure(s) of these and related intermediates are not yet known, we have spectroscopic and other evidence that strongly suggests the presence of coordinated naphthalene in these materials. They readily absorbed carbon monoxide at low temperature and on warming at atmospheric pressure, to provide moderate to excellent yields of $(C_5Me_5)M(CO)_4^-$, the first class of carbonyl anions known for all three groups 4 elements.[19,20] It is especially noteworthy that prior to this work, all hafnium(0) complexes (a grand total of four!) were prepared from atomic hafnium which was generated in a metal atom reactor.[21,22] Studies on the reactions of these intermediates with a variety of small molecules other than carbon monoxide are presently underway in this laboratory and should help to define their general utility in chemical synthesis.

Neutral phosphine carbonyls of group 4 elements have also been obtained in moderate to good yields by similar procedures. Perhaps the most useful of these is $Ti(CO)_5(dmpe)$, the closest "living relative" of the hypothetical $Ti(CO)_7$. This dmpe complex is an extremely valuable precursor to other zerovalent titanium carbonyls, by virtue of its facile reaction with nucleophiles.[23] Some of the reactions of $Ti(CO)_5(dmpe)$ examined are shown in Scheme 1. Due to the thermal instability of $Ti(CO)_5(dmpe)$, this fluxional, seven-coordinate substance was characterized in solution by ^{31}P and ^{13}C NMR spectra of the 99% enriched ^{13}CO derivative (Figs 1 and 2).

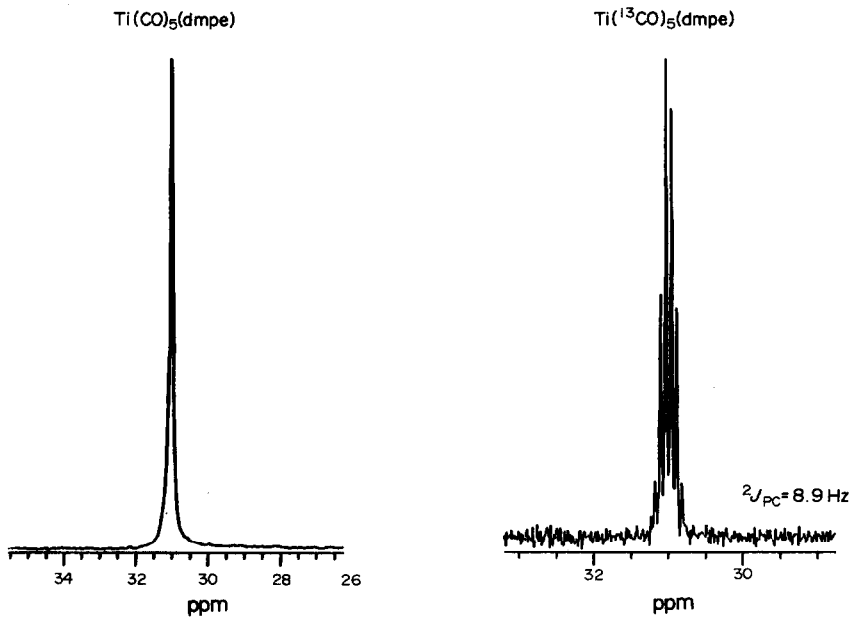

Fig. 1. $^{31}P\{^1H\}$ NMR spectra of $Ti(CO)_5(dmpe)$ and 99% ^{13}C enriched $Ti(^{13}CO)_5(dmpe)$ in THF at room temperature.

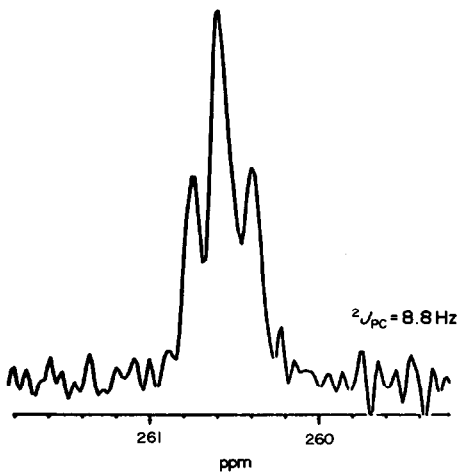

Fig. 2. The $^{31}C\{^1H\}$ NMR spectra of 99% ^{13}C enriched $Ti(^{13}CO)_5(dmpe)$ in THF at room temperature.

While zirconium and hafnium analogues of $Ti(CO)_3(dmpe)_2$ or $Ti(CO)_5(dmpe)$ have not been obtained by this route, phosphine derivatives of the composition $M(CO)_4(trmpe)$, where trmpe is the tripodal ligand 1,1,1-tris(dimethylphosphinomethyl)ethane, have also been prepared by direct reduction of the tetrachlorides of titanium, zirconium and hafnium in the presence of trmpe. These thermally robust materials presently represent the only class of neutral zerovalent metal carbonyls known for all three group 4 elements. Confirmation of the nature of $Zr(CO)_4(trmpe)$ has been provided by an X-ray analysis, the first reported for any Zr(0) carbonyl.[24] The hafnium complex is of particular interest in that is the sole precursor to $Hf(CO)_6^{2-}$ presently known (*vide infra*).

Related research has involved the synthesis and characterization of other new classes of zerovalent titanium carbonyls. For example, seven-coordinate zerovalent titanium carbonyls containing only unidentate ligands, $Ti(CO)_5(EPh_3)_2^{2-}$ (E = Ge, Sn, structurally characterized for Sn), and organoarsine and arylphosphine ligands, $Ti(CO)_3[o\text{-}C_6H_4(AsMe_2)_2]_2$ and $Ti(CO)_4[MeC(CH_2PPh_2)_3]$, respectively, have been prepared for the first time from highly reactive and quite thermally unstable, low valent titanium intermediates, one of which has been characterized as $Ti(CO)_5(PMe_3)_2$ on the basis of ^{13}C and ^{31}P NMR spectra.[25] In other studies, eight-coordinate and formally divalent zirconium and hafnium complexes of the type $M(CO)_4(SnPh_3)_4^{2-}$, $M(CO)_2(dmpe)_2I_2$[26] and $(C_5Me_5)M(CO)_2(dmpe)Cl$ (M = Zr, Hf)[27] have been obtained, where the latter substances are related to $(C_5H_5)Ti(CO)_2(dmpe)H$, the first structurally characterized carbonyl hydride of titanium.[28]

Perhaps, the most significant development in this research on early transition metal carbonyls, however, has been the recent synthesis, isolation and characterization of salts containing $Ti(CO)_6^{2-}$, $Zr(CO)_6^{2-}$ and $Hf(CO)_6^{2-}$.[5,26,29] Noteworthy is the fact that the previously known binary carbonyl dianions of first row transition metals, $Cr(CO)_5^{2-}$ and $Fe(CO)_4^{2-}$, were first prepared over 30 years ago.[30] While no other binary carbonyl of zirconium or hafnium has been reported, the titanium compound may be regarded as a saturated and dianionic derivative of the extremely unstable neutral $Ti(CO)_6$ (dec > −200°C). The latter was prepared by Ozin and co-workers from titanium atoms and observed by matrix isolation spectroscopy.[31] Of crucial importance for the synthesis and isolation of these materials is the the requirement that strong alkali metal ion complexants, such as crown ethers or cryptands, be present during their formation. Weakly solvated alkali metal cations promote decomposition of these dianions to presently uncharacterized substances. By comparison, the isoelectronic anions, $V(CO)_6^-$, $Nb(CO)_6^-$ and $Ta(CO)_6^-$, are thermally stable as unsolvated alkali metal salts at room temperature. Very recently, single crystal, X-ray studies have confirmed the presence of discrete and essentially unperturbed octahedral $Ti(CO)_6^{2-}$, $Zr(CO)_6^{2-}$ and $Hf(CO)_6^{2-}$ units in the $K(cryptand\ 2.2.2)^+$ salts of these materials.[26]

Extensions of this research to the group 3 transition metals, for which no carbonyls are presently known, as well as a general study of the reactivity patterns of these weakly solvated atoms and anions with a variety of small molecules such as dinitrogen, dihydrogen and unsaturated organic species, promises to be a grand adventure. It is also possible that the synthetic methodology developed recently in this group for the synthesis of highly reduced organometallics of the group 4 elements will be of use in the stabilization of unusual materials containing low valent *f*-block elements, an emerging area of chemistry.[32]

Acknowledgements—I wish to express my gratitude and appreciation to all of my co-workers who are listed as joint authors in the references and to the Petroleum Research Fund, administered by the American Chemical Society, and the National Science Foundation for continuing generous support of this research on highly reduced organometallics.

REFERENCES

1. J. E. Ellis, P. T. Barger and M. L. Winzenburg, *J. Chem. Soc., Chem. Commun.* 1977, 686.

2. J. E. Ellis and R. A. Faltynek, *J. Am. Chem. Soc.* 1977, **99**, 1801.
3. J. E. Ellis, C. P. Parnell and G. P. Hagen, *J. Am. Chem. Soc.* 1978, **100**, 3605.
4. J. E. Ellis, K. L. Fjare and T. G. Hayes, *J. Am. Chem. Soc.* 1981, **103**, 6100.
5. K. M. Chi, S. R. Frerichs, S. B. Philson and J. E. Ellis, *J. Am. Chem. Soc.* 1988, **110**, 303.
6. G. F. P. Warnock, S. B. Philson and J. E. Ellis, *J. Chem. Soc., Chem. Commun.* 1984, 843.
7. J. Chatt and H. R. Watson, *J. Chem. Soc.* 1962, 2545.
8. J. Chatt and J. M. Davidson, *J. Chem. Soc.* 1965, 843.
9. P. N. Hawker, E. P. Kündig and P. L. Timms, *J. Chem. Soc., Chem. Commun.* 1978, 730.
10. J. O. Albright, S. Datta, B. Dezube, J. K. Kouba, D. S. Marynick, S. S. Wreford and B. M. Foxman, *J. Am. Chem. Soc.* 1979, **101**, 611.
11. E. P. Kündig and P. L. Timms, *J. Chem. Soc., Chem. Commun.* 1977, 912.
12. Ch. Elsenbroich and R. Mockel, *Angew. Chem. Int. Edn* 1977, **16**, 870.
13. E. P. Kündig and P. L. Timms, *J. Chem. Soc., Dalton Trans.* 1980, 991.
14. C. E. Dewey, J. E. Ellis, K. L. Fjare, K. M. Pfahl and G. F. Warnock, *Organometallics* 1983, **2**, 388.
15. A significantly different atmospheric pressure reductive carbonylation procedure for $Nb(CO)_6^-$ was also developed independently: F. Calderazzo, U. Englert, G. Pampaloni, G. Pelizzi and R. Zamboni, *Inorg. Chem.* 1983, **22**, 1865. This procedure does not work as well for the synthesis of $Ta(CO)_6^-$, however,
16. J. E. Ellis and A. Davison, *Inorg. Synth.* 1976, **16**, 68.
17. K. Jonas and V. Wiskamp, *Z. Naturfor.* 1983, **38b**, 1113.
18. (a) T. G. Gardner and E. S. Girolami, *Organometallics* 1987, **6**, 2551; (b) T. G. Gardner and E. S. Girolami, *Angew. Chem. Int. Edn.* 1988, **27**, 1693; (c) S. Gambarotta and M. Y. Chiang, *J. Chem. Soc., Chem. Commun.* 1987, 698.
19. B. A. Kelsey and J. E. Ellis, *J. Am. Chem. Soc.* 1986, **108**, 1344; B. A. Kelsey and J. E. Ellis, *J. Chem. Soc., Chem. Commun.* 1986, 331.
20. S. R. Frerichs and J. E. Ellis, *J. Organomet. Chem.* 1988, **359**, C41.
21. F. G. N. Cloke, M. F. Lappert, G. A. Lawless and A. C. Swain, *J. Chem. Soc., Chem. Commun.* 1987, 1667 and refs cited therein.
22. The previously known $Hf(\eta\text{-}C_4H_6)_2(dmpe)$ is probably best regarded as containing hafnium in a positive oxidation state: S. S. Wreford and J. F. Whitney, *Inorg. Chem.* 1981, **20**, 3918.
23. K. M. Chi, S. R. Frerichs, B. K. Stein, D. W. Blackburn and J. E. Ellis, *J. Am. Chem. Soc.* 1988, **110**, 163.
24. D. W. Blackburn, K. M. Chi, S. R. Frerichs, M. L. Tinkham and J. E. Ellis, *Angew. Chem. Int. Edn* 1988, **27**, 437.
25. K. M. Chi, S. R. Frerichs and J. E. Ellis, *J. Chem. Soc., Chem. Commun.* 1988, 1013.
26. K. M. Chi and J. Ellis, to be submitted.
27. B. K. Stein, S. R. Frerichs and J. E. Ellis, *Organometallics* 1987, **6**, 2017.
28. S. R. Frerichs, B. K. Stein and J. E. Ellis, *J. Am. Chem. Soc.* 1987, **109**, 5558.
29. K. M. Chi, S. R. Frerichs, S. B. Philson and J. E. Ellis, *Angew. Chem. Int. Edn* 1987, **26**, 1190.
30. H. Behrens, *Adv. Organomet. Chem.* 1980, **18**, 2 and refs cited therein.
31. R. Busby, W. Klotzbucher and G. Ozin, *Inorg. Chem.* 1977, **16**, 822.
32. D. M. Anderson, F. G. N. Cloke, P. A. Cox, N. Edelstein, J. C. Green, T. Pang, A. A. Sameth and G. Shalimoff, *J. Chem. Soc., Chem. Commun.* 1989, 53.

Polyhedron Vol. 8, No. 13/14, pp. 1615–1618, 1989
Printed in Great Britain

0277–5387/89 $3.00+.00
© 1989 Maxwell Pergamon Macmillan plc

GAS SENSORS BASED ON OXIDES OF EARLY TRANSITION METALS

P. T. MOSELEY* and D. E. WILLIAMS

Materials Development Division, Harwell Laboratory, Didcot, Oxon OX11 0RA, U.K.

Abstract—The conductivities of semiconducting oxides are generally influenced by the chemical reactions of any gas molecules that have access to their surfaces. This phenomenon is exploited in the development of gas sensitive resistors that offer a simple route to the monitoring of atmospheric composition. Material properties may be optimized for this application by adjustment of the stoichiometry of the semiconducting oxide. Oxides of early transition metals are particularly useful in this "tuning" process. Examples are given of the development of two oxides with useful gas response characteristics—one for the monitoring of oxygen, the other for ammonia.

There are widespread requirements for gas sensors that are simple and reliable. Two important categories are the monitoring of oxygen partial pressure in a range of background atmospheres and the detection of small concentrations of reducing gases in a background of air.

The special demand in both cases is usually for *specificity*. The oxygen sensor should respond only to changes in p_{O_2} and not to changes in other parameters (e.g. temperature). The reducing gas sensor is required to respond to the presence of one gas and not to others. Sensors based on the measurement of the atmosphere-dependent resistance of a semiconducting oxide ceramics element are of potential interest for both types of application. Specificity is achieved by engineering an optimum stoichiometry within a stable crystal structure.

This paper describes a group of perovskite-structure materials that, when optimally constituted, offer suitable characteristics for oxygen monitoring and a mixed chromium–titanium oxide that responds selectively to the presence of ammonia in air.

OXYGEN SENSING

Processes affecting the bulk conductivity of semiconducting oxides

The resistance of semiconducting oxides is affected by changes in temperature and by changes in stoichiometry. The conductivity of TiO_{2-x} at high temperature follows the prevailing oxygen partial pressure and this has been proposed as the basis of an oxygen sensor,[1] but there is a significant temperature dependence and this is a serious disadvantage.

Temperature. The generation of charge carriers is a thermally-activated process so that, in general, whether a semiconductor is *n*-type or *p*-type, conductivity, σ, increases exponentially with temperature:

$$\sigma = \sigma_0 \exp -E_A/RT, \qquad (1)$$

where E_A is an activation energy.

Stoichiometry. Oxides of transition metals vary in conductivity according to the oxygen partial pressure with which they are in equilibrium.

Generally at the low extreme of the oxygen partial pressure range (left-hand branch of Fig. 1) the material is *n*-type (σ decreasing with increasing p_{O_2}). Above a transition level of oxygen partial pressure that is strongly influenced by the presence of impurities,[2] the material becomes *p*-type (right-hand branch of Fig. 1).

The slopes of the plot in the *n*-type and *p*-type regions reflect the types of crystal defects that are involved in accommodating the change in stoichiometry. For example, if the principal defect is a doubly charged oxygen vacancy, $V_O^{\cdot\cdot}$, replacing an occupied oxygen site, O^x, then the equilibrium can be written

$$O^x \rightleftarrows V_O^{\cdot\cdot} + \tfrac{1}{2}O_2 + 2e^-, \qquad (2)$$

* Author to whom correspondence should be addressed.

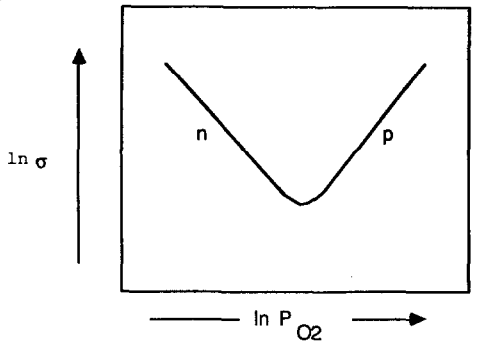

Fig. 1. Isothermal variation of conductivity with oxygen partial pressure for semiconducting oxide.

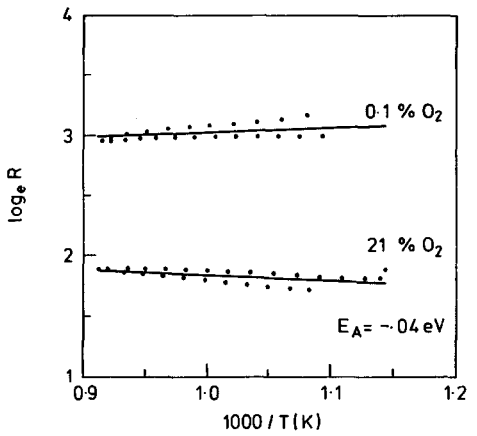

Fig. 2. Conductivity dependence of $BaFe_{0.8}Ta_{0.2}O_3$ on temperature and oxygen partial pressure.

so that the equilibrium constant,

$$K = [V_o^{\cdot\cdot}][e]^2[p_{O_2}]^{1/2}, \quad (3)$$

where [e] is the concentration of electrons.

Now for charge balance $[V_o^{\cdot\cdot}] = 2[e]$, so that eq. (2) becomes

$$K = [2e][e]^2[p_{O_2}]^{1/2} \quad (4)$$

and hence $[e] \propto p_{O_2}^{-1/6}$, defining the slope of the *n*-type part.

Thus the full expression for the conductivity of a transition metal oxide is

$$\sigma = \sigma_o \exp(-E_A/RT)p_{O_2}^{1/N}, \quad (5)$$

where the value of N is -6 for the case of doubly charged oxygen vacancies. Other types of defect lead to other values of slope.[3]

Now in general, as the temperature is raised at a fixed oxygen partial pressure then oxides of transition metals lose oxygen and, if they are *p*-type, their conductivity will tend to decrease. This effect is opposite to the thermal promotion of charge carriers and the possibility arises of doping the transition metal oxide so that the two effects may cancel and the effect of temperature changes will be to leave conductivity unchaged.

Two points should be made. First, if such a balance of thermal effects is achieved it need not alter the effect of changes in oxygen partial pressure at a fixed temperature. Second, such a balance is only possible for *p*-type oxides, where the thermal activation of charge carriers and the stoichiometry effect are opposed.

The combination of an apparent activation energy for conduction of near zero with a significant oxygen partial pressure dependence has been achieved in a group of oxides with the perovskite crystal structure. The materials, which were discovered during a programme of development of vehicle exhaust sensors funded by Lucas Industries plc, are based on barium (or strontium) ferrate doped with certain early transition metals.[4]

Figure 2 clearly shows how the conductivity of $BaFe_{0.8}Ta_{0.2}O_3$ is strongly dependent on oxygen partial pressures but is almost invariant with temperature. The magnitude of the oxygen response and the observed activation energy both vary with the fraction of substitution of tantalum for iron, as shown in Table 1.

The transition to a regime of significant activation energy is not sharp but occurs as the composition moves towards a regime where iron(IV) is no longer required, based on a complete oxygen stoichiometry in the structure.

Very low activation energies are sustained to higher values of x where the ferrate is doped with four-valent ions (Hf^{4+}, Zr^{4+} or Ti^{4+}) rather than tantalum.

REDUCING GASES

Processes affecting the surface conductivity of semiconducting oxides

The oxygen sensitive resistor based on doped barium or strontium ferrates functions due to a

Table 1. Activation energy in air and oxygen sensitivity as a function of composition (the value of x in $BaFe_{1-x}Ta_xO_3$)

	Value of x			
	0.1	0.2	0.3	0.4
Activation energy, E_A[a]	−0.4	−0.4	0.03	0.13
Oxygen sensitivity, N[a]	5.0	5.0	5.9	0.1

[a] Refer to eq. (5).

full equilibration of the stoichiometry of the oxide with the prevailing oxygen partial pressure. This requires an operating temperature in the region of 700–800°C in order to achieve useful response times.

At temperatures of 500°C and below, atmosphere-dependent conductivity changes can be measured that depend solely on surface reactions. The density of charge carriers in the near-surface region of the oxide can be influenced by either direct chemisorption of the target gas or by the interaction of molecules of the target gas with a chemisorbed species (usually an oxygen ion) that is already in place, e.g.

$$2CO + O_2^- \rightarrow 2CO_2 + e^-,$$

where the electron is released by the reaction to return to the conduction band.

Such processes provide a means for detecting reducing gases in air with great sensitivity. The first generation of sensors of this type, based on tin dioxide, can detect methane, carbon monoxide and several other oxidizable gases at concentrations of a few parts per million in air. A disadvantage, however, is that such sensors are inherently non-specific.

In fact, many semiconducting oxides exhibit the facility to catalyse gas reactions at their surfaces and very few of them show the same generality of response to different gases that characterizes the resistance dependence of tin dioxide. Doping of robust crystal structures with suitable cations can often provide the route to an interesting pattern of gas responses by altering electronic and catalytic properties.

Titanium dioxide, like tin dioxide, behaves as an *n*-type semiconductor, offering resistance decreases when reducing gases are introduced to an air ambient. The incorporation of 10% of chromium, which is readily accommodated by the formation of crystallographic shear planes,[5] alters the gas response to that of a *p*-type material. As shown in Fig. 3, $Ti_{0.9}Cr_{0.1}O_{2-x}$ increases in resistance when exposed to small concentrations of carbon monoxide, hydrogen, ethane and ammonia, but does not respond to methane.

A more specific response results from the introduction of 10% of titanium into the robust rhombohedral structure of Cr_2O_3. Figure 4 shows that, when exposed to a sequence of different reducing gases at low concentrations in air, $Cr_{1.8}Ti_{0.2}O_{3-x}$ responds significantly only to ammonia.[6]

Doubtless, further work with other semiconducting oxides will reveal many more materials with specific responses for other gases, and thus we may expect that, in future, the powerful simplicity of the gas sensitive resistor will be exploited far more than it has been with tin dioxide devices.

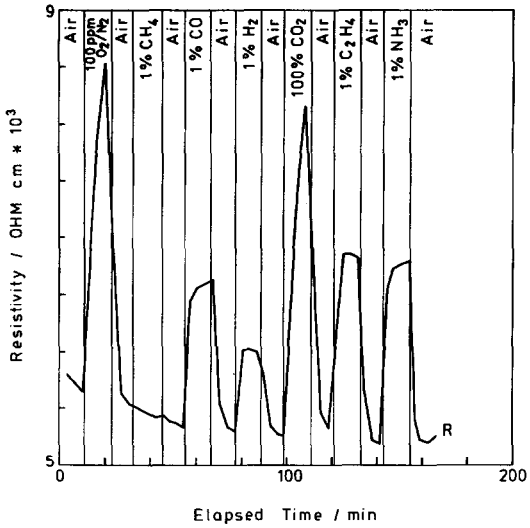

Fig. 3. Resistance responses of $Ti_{0.9}Cr_{0.1}O_{2-x}$ exposed to a sequence of reducing atmospheres and low concentrations of reducing gases in air. An air purge separated the exposures of the material to the different test atmospheres. The resistance increases in the test gases are characteristic of a *p*-type material.

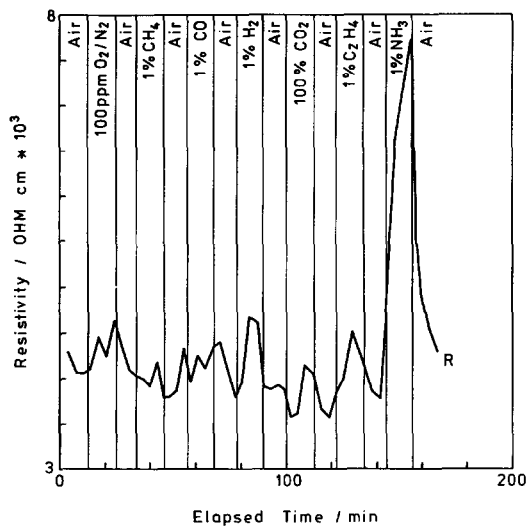

Fig. 4. Resistance responses of $Cr_{1.8}Ti_{0.2}O_{3+x}$ exposed to the same sequence of atmospheres as in the experiment described by Fig. 3.

SUMMARY

We may conclude that adjusting the stoichiometry of semiconducting oxides provides the route to materials with a wide variety of catalytic and electronic properties that will be extremely valuable in the development of specific gas sensors.

Further, the similarity between the mode of operation of such sensors and the mechanisms of heterogeneous catalysis may result in a far wider application of "tailor-made" oxide surfaces.

REFERENCES

1. T. Y. Tien, H. L. Stadler, E. F. Gibbons and P. J. Zacmanidis, *Ceramic Bulletin* 1975, **54**, 280.
2. D. M. Smyth, in *Advanced Ceramics* (Edited by S. Saito), p. 147. Oxford University Press, Oxford (1988).
3. P. Kofstad, *Non-stoichiometry, Diffusion and Electrical Conductivity in Binary Metal Oxides*. Krieger, New York (1983).
4. D. E. Williams, P. McGeehin and B. C. Tofield, *European Patent* EP62-994 and *US Patent* 4,454,494 (1982).
5. R. M. Gibb and J. S. Anderson, *J. Sol. State Chem.* **4**, 379.
6. D. E. Williams, P. T. Moseley, B. C. Tofield and J. O. W. Norris, *UK Patent* 2,202,948 (1987).

Polyhedron Vol. 8, No. 13/14, pp. 1619–1624, 1989
Printed in Great Britain

0277–5387/89 $3.00+.00
© 1989 Maxwell Pergamon Macmillan plc

STRUCTURE AND BONDING IN THE CHALCOGENIDES OF THE EARLY TRANSITION METALS

D. W. BULLETT

School of Physics, University of Bath, Claverton Down, Bath BA2 7AY, U.K.

Abstract—Results of electronic structure calculations are reported for a wide range of chalcogenide compounds of the early transition elements, concentrating on those features relevant to metal–metal bonding and low dimensionality.

In the last 20 years, our knowledge and understanding of the electronic structure and properties of the chalcogenides of transition metals have advanced enormously,[1–3] and any survey of band structure calculations would now require a substantial monograph to do the subject justice. There are a great variety of compositions and structures, even within the binary family of compounds. In order to restrict the discussion here, we will concentrate our considerations on a few examples which display two related phenomena that recur in many of these materials: low-dimensional behaviour and metal–metal bonding.

(1) MX COMPOUNDS

The stoichiometric monochalcogenides exhibit metallic properties and occur most commonly in the two structure types, NaCl (e.g. ScS, YS, LaS and all rare-earth monosulphides, ZrS), or NiAs/MnP (e.g. TiS, Vs, NbS). Excluding MnP, the MX structure types consist of different sequences of alternating metal and non-metal close packed layers: ABCABC . . . for the NaCl type, ABACABAC . . . for the NiAs type (with the metal in the A positions), or ABAB . . . for the WC-type structure of HfS. The occurrence of the NiAs sequence demonstrates the significance of metal–metal interactions between layers: while each X is trigonal-prismatically coordinated by six M atoms, each M is octahedrally coordinated by six X atoms, with an additional pair of M atoms above and below. For example, in TiS the six metal–metal distances within the layer are 3.30 Å, and the two out-of-layer distances are 3.19 Å. Comparing these with the atomic separation in the pure metal (2.95 Å), it is clear that there must be a substantial degree of metal–metal bonding.

In the first column of transition metals the *d*-level lies high relative to the chalcogen *p*-level, ionic contributions predominate, and the Madelung sum favours the rocksalt structure. For more electron-rich transition metals, the competing demands of metal *d*–metal *d* and metal *d*–non-metal *p* covalent interactions act to stabilize some variant of the NiAs structure. The signature of the M—M interactions in the electronic structure near the Fermi level may be seen in band structure calculations reported elsewhere.[4–6] It is perhaps not too surprising that electronic effects drive nearly all "NiAs-type" compounds (even including NiAs itself) into more complicated superstructures as the temperature is lowered, nor that the details of the transition should depend sensitively on composition, especially when this moves off stoichiometry; motion of the metal substructure distorts the lattice of M atoms into a network of criss-crossing zigzag chains, such as those that typify MnP. For higher *d* occupations rocksalt-type structures are again more stable (e.g. the d^5 compounds MnS and MnSe, but not MnTe which prefers a high-spin ground state and the NiAs structure).

(2) MX_2 COMPOUNDS

The dichalcogenides of the early transition elements form a fairly coherent family of quasi-two-dimensional materials. Again the underlying structure is of a sequence of hexagonally-close-packed layers of either metal (M) or non-metal (X) atoms, but now the layer sequence is XMX XMX . . . , and the large separation between the outer X layers of adjacent sandwiches leads to strongly anisotropic properties. A rich variety of stacking sequences occurs in different compounds of the family, and for a detailed survey we refer the

reader to Wilson and Yoffe.[7] Within a single MX_2 sandwich, the coordination of ligands about the central metal atom may be either octahedral (e.g. TiS_2) or trigonal prismatic (e.g. MoS_2). Madelung terms favour the octahedral arrangement, since this avoids anion positions falling one above another, and the more ionic compounds such as the group IV family all occur in this coordination. Figure 1 illustrates the calculated band structure and density of states[8] that typify two of these materials, TiS_2

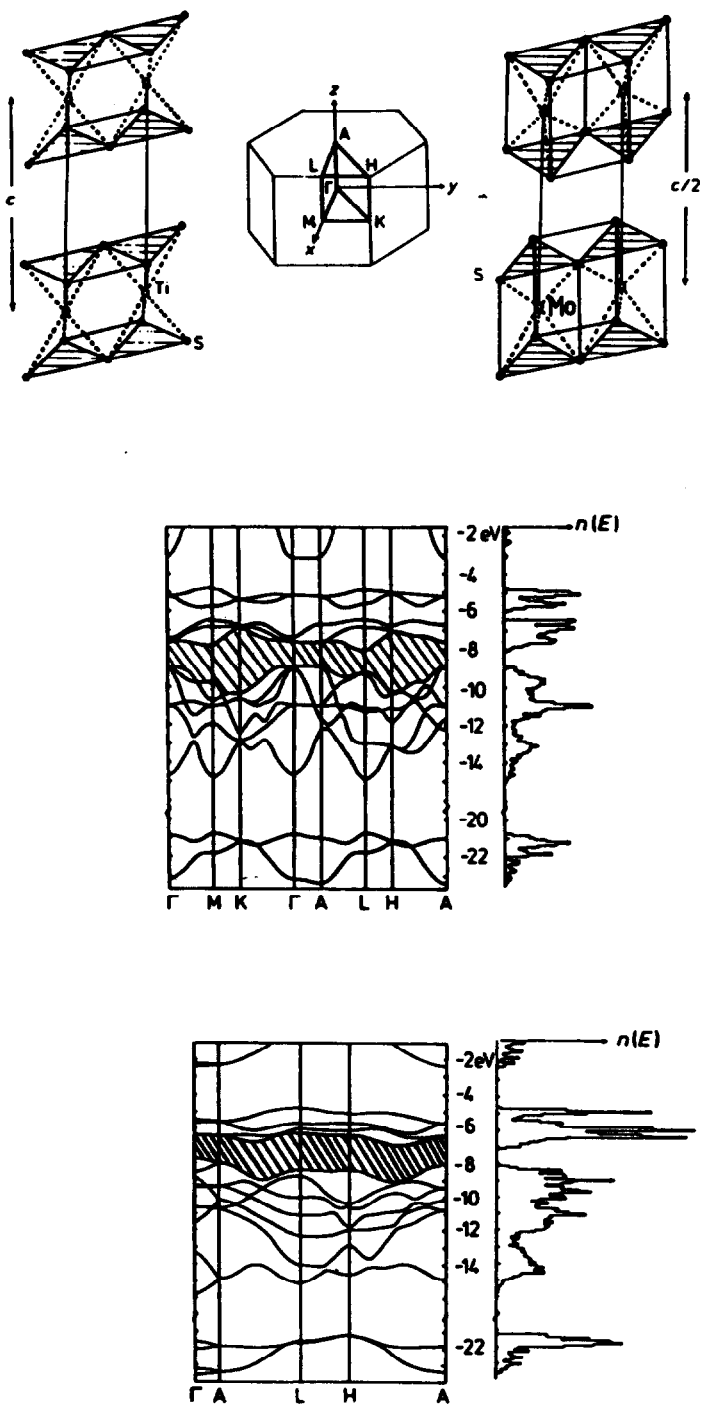

Fig. 1. Coordination of chalcogens around metal atoms in the IT—TiS_2 and 2H—MoS_2 structures, and the resulting electronic structure[8] calculated for these semiconducting compounds. The standard notation for Brillouin zone symmetry points is also shown.

and MoS_2. In TiS_2, as might be anticipated, a semiconducting *p–d* gap separates the six "sulphur *p*-bands" from the five "metal *d*-bands", which themselves split in the octahedral ligand field into t_{2g} and e_g sub-bands; formally these group IV dichalcogenides are d^0 filled *p*-band structures, although because of overlap between *p*- and *d*-bands not all are semiconductors (e.g. $TiTe_2$, $TiSe_2$, $HfTe_2$). The group VI (d^2) dichalcogenides (with the exception of WTe_2 and β-$MoTe_2$) adopt the trigonal prismatic coordination, since in this environment the t_{2g} triplet splits further into a lower singlet (sometimes labelled the "d_{z^2}" band) and upper doublet; complete occupation of the lower band stabilizes the trigonal prismatic coordination in d^2 compounds such as MoS_2 (Fig. 1). Electronic structure investigations of edges and defects in the structure may be particularly significant from the point of view of understanding the active sites for hydrogenation catalysis over MoS_2 and WS_2.

Bridging the two columns of the periodic table, the d^1 dichalcogenides of the group V elements display both coordinations, and some individual members (e.g. TaS_2, $TaSe_2$) can occur in either arrangement, even in successive layers of the same crystal structure. Successive sandwiches are separated by wide van der Waals gaps, and the subtle balance between different contributions to the weak inter-layer interactions lead to a rich variety of different stacking sequences; in some dichalcogenides the repeat distances along the *c*-axis can be many layers. In addition to their interest for the strongly anisotropic elastic, optical, and electrical properties common to all the layer structure dichalcogenides, the group V compounds have been very extensively investigated because of the phase transitions which result from their quasi-two-dimensional metallic nature. Detailed discussions of the subtle features in the electronic structure which drive these charge–density–wave/periodic lattice distortions may be found elsewhere.

Many kinds of atoms and molecules have been inserted into the van der Waals gaps between the MX_2 layers, and this type of intercalation provides an interesting tool for varying structural, magnetic and transport properties. Yamasaki *et al.*[9,10] recently reported some self-consistent (but non-magnetic) band structure calculations for intercalated iron and chromium atoms in TiS_2.

The group VI ditellurides show deviations from the simplest band model, which predicts semiconducting behaviour due to trigonal prismatic crystal-field splitting of the filled non-bonded d_{z^2} orbital, and a detailed interpretation of their electronic structure and crystallography has recently been reported.[11] For WTe_2 and one form of $MoTe_2$, the metal atom is displaced from the centre of an *octahedron* of tellurium atoms, and metal–metal chains with bond lengths only slightly longer than the elemental metals run along the layers. The enhanced Madelung term for this configuration compensates for loss of the lone d_{z^2} band, and results in semi-metallic properties.

(3) MX_3 COMPOUNDS

The crystal structures of the trichalcogenides of groups IV and V transition elements can again be viewed in terms of linked MX_6 trigonal prisms, but this time instead of sharing rectangular side-faces to form two-dimensional layers as in MoS_2, they are linked by sharing triangular end-faces to form MX_3 chains (Fig. 2). Interactions between the chains are weaker in one direction than the other, so that in their properties these compounds display aspects of both one- and two-dimensional behaviour. In all cases there is strong X—X pairing along one side of each triangular face of the prism. This causes the group IV compounds (with the exception of $ZrTe_3$, where there is slight semi-metallic *p–d* band overlap) to be semiconductors: bands formed from antibonding combinations of the paired X σ *p*-orbitals are forced up into the same unoccupied energy range as the metal *d*-bands, giving a formal valence configuration $M^{4+}X^{2-}(X_2)^{2-}$. The group IV trichalcogenides form an isostructural family, from TiS_3 right through to $ThTe_3$, with the slight complication that two variants exist (often denoted **A** and **B**) in the relative orientation of the chains. Their electronic structure,[3,12] and associated optical, electrical transport and vibrational properties have been studied in detail, along with their intercalation reactions with alkali metals such as lithium in connection with applications as solid-state cathodes.

The extra *d*-electron in the group V trichalcogenides, and the consequent tendency for metal–metal pair bonding, causes a variety of structural distortions and phase transitions. The simplest case is NbS_3, where complete metal pairing takes place along the chain axis, to give a doubling of the intrachain lattice parameter.[13] Axial displacements of 0.16 Å from the centres of the coordination prisms give Nb—Nb bonding distances of 3.04 Å. The bridging triangle of sulphur atoms is pushed outwards at one end of the prism and drawn in at the other, in an attempt to conserve M—S bond lengths; anion pairs are fully retained in the structure, with S—S distances of 2.05 Å in NbS_3, compared to 2.09 Å in ZrS_3. As in the group IV structure, unpaired sulphur atoms on neighbouring chains cap two of the rectangular faces of each

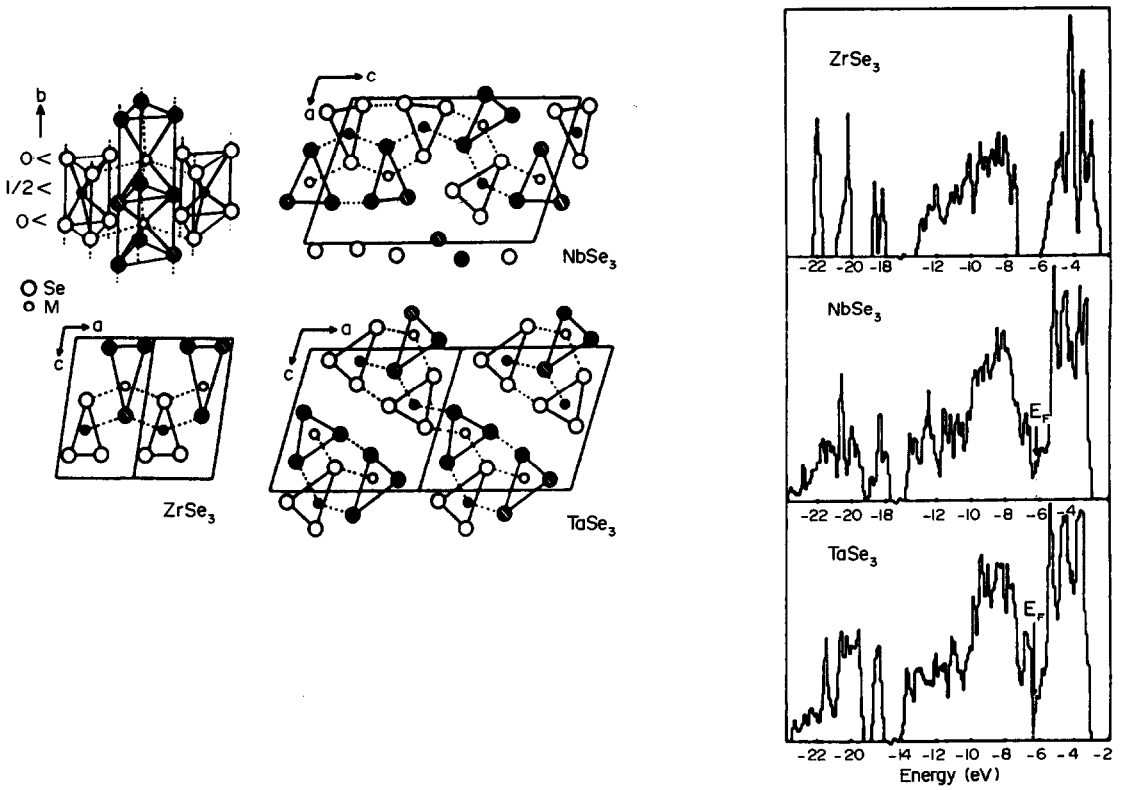

Fig. 2. Atomic arrangements and calculated electron densities of states[15] in some transition metal triselenides MSe_3, showing the stacking of MSe_6 prisms along the b-axis (open atoms at 0, shaded atoms at $\frac{1}{2}b$).

prism to provide a weak bonding of the chains into two-dimensional layers, and overall eight-fold coordination of each metal atom. Figure 3 illustrates the crystal structure and associated density of electron states,[14] with many features reminiscent of $ZrSe_3$, plus the added feature of well-defined Nb—Nb bonding states forming the highest occupied states. The sulphur s-bands again split roughly into three sub-bands—the bonding and anti-bonding s-states of the S_2 pairs, separated by the non-bonding s-state of the third atom in the S_3 triangle—but because of the lower crystal symmetry the distinction is less precise than in $ZrSe_3$, and the non-bonding and antibonding sub-bands of NbS_3 overlap. Eight p-bands per formula unit again form the main valence band, now followed in order of increasing energy by the metal–metal bonding states. A calculated energy gap of 0.5 eV separates

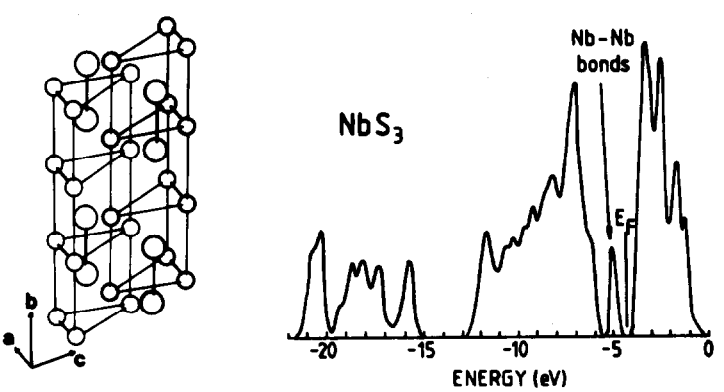

Fig. 3. The NbS_3 structure and the calculated density of states,[14] showing how Nb—Nb pairing along the b-axis leads to metal–metal d-bonding states just below the Fermi level.

these from the unoccupied *d*- and *po**-conduction states; thus the calculated distribution of states accounts naturally for the diamagnetic semiconducting properties and black needle-like appearance of NbS_3 crystals.

In other group V trichalcogenides (and at enhanced pressures and temperatures even in NbS_3), there are different degrees of coupling between the one-dimensional chains and different types of chain within each unit cell. Typical examples are provided by $TaSe_3$ and $NbSe_3$. $TaSe_3$ contains four chains per unit cell, two with strong (2.58 Å) and two with weak (2.90 Å) Se—Se pairing; the weaker Se—Se bonding is compensated by interchain Se—Se distances of only 2.65 Å. The calculated electron density of states for this arrangement of chains[15] shows an energy overlap between *p*- and *d*-bands, with the Fermi energy EF lying in a deep, but non-zero, minimum in the density of states: in $TaSe_3$ some of the states which would otherwise have been Se—Se antibonds within a chain become Se—Se or Ta—Se bonding states between chains, providing the required total of 17 valence bands per pair of MX_3 units (compared to the eight valence *p*-bands per MX_3 unit in $ZrSe_3$). The band structure shows little reason to expect incipient M—M pairing along the chains, nor is there any experimental evidence for a phase transition between 4 and 700 K at atmospheric pressure.

The $NbSe_3$ structure contains six chains per unit cell, in an arrangement most easily recognized as the $TaSe_3$-type blocks of four chains, now interconnected through pairs of tight $ZrSe_3$-type chains. $NbSe_3$ is thus left with two spare electrons per unit cell (six MX_3 units) to place in the bottom of the conduction *d*-band. These lowest *d*-bands rise very rapidly as **k** moves away from the origin along the chain direction (because of a strong d_{z^2} component along this *b*-axis), but are almost dispersionless in directions normal to the chain axis.[15,16] The result is a highly anisotropic metal, showing incommensurate phase transitions and extraordinary non-linear transport properties because of the very weak pinning of these structural distortions to the underlying lattice.[17] At 144 and 59 K, periodic lattice distortions eliminate large properties of the free carriers and the resistivity increases sharply, but even very modest electric fields allow these distortions to slide through the lattice and the resistivity to drop back to its former value. There also exist ternary compounds, such as $FeNb_3Se_{10}$, with a similar kind of one-dimensional metallic band structure but less extreme properties, because the periodic distortions along the chain are now pinned by effects of disorder.

(4) $NbTe_4$, $ZrTe_5$

Further examples of quasi-one-dimensional materials are provided by the group IV transition metal pentatellurides, $ZrTe_5$ and $HfTe_5$, and the group V tetratellurides, $NbTe_4$ and $TaTe_4$, though in none of these materials are the transport properties as spectacularly anomalous as in $NbSe_3$ and TaS_3. The pentatelluride structure preserves the MX_3 trigonal columns characteristic of $ZrSe_3$, but instead of being linked directly into pairs, and then layers, of columns as in the trichalcogenides, the MX_3 columns are now linked through intermediate "Te_2" chains (Fig. 4). This arrangement retains the coordination of eight tellurium atoms around each metal atom: six tellurium neighbours lie at the corners of the triangular prism and two lie outside the rectangular faces. Te—Te pairings are slightly stronger within prisms (2.76 Å) than in the intervening zigzag chains (2.91 Å), the two distances

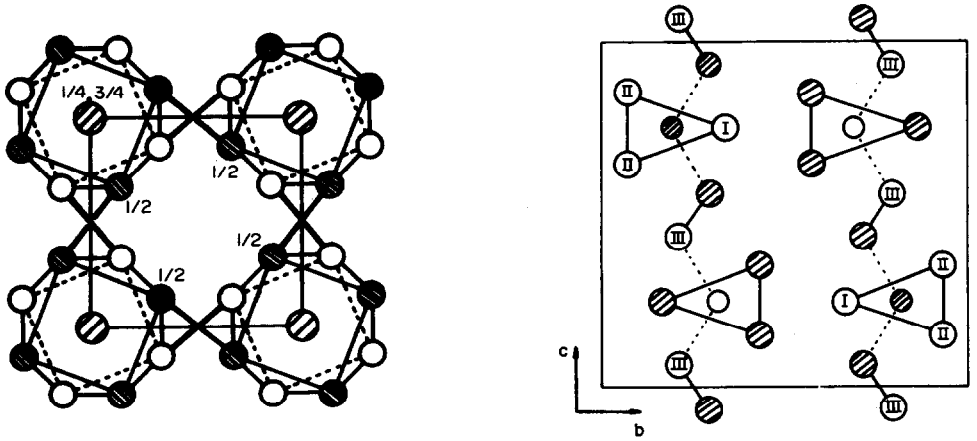

Fig. 4. The MTe_4 and MTe_5 crystal structures.

falling either side of the corresponding single bond distance in elemental tellurium (2.835 Å). Interlayer Te—Te contacts exceeding 4 Å illustrate that interactions between layers are of only the weak van der Waals type. Superficially we might have expected $ZrTe_5$ to be an anisotropic diamagnetic semiconductor: each zirconium donates two electrons to each Te—Te pair and two to each lone tellurium atom, while the zigzag chains of tellurium atoms (bond angle close to 90°) retain the normal p^4 configuration of elemental tellurium. In fact electronic structure calculations[18,19] confirm a semiconducting gap, 1 eV separating the highest occupied from lowest unoccupied bands over most of the Brillouin zone, but interlayer coupling produces a semi-metallic band crossing one edge of the Brillouin zone. In this case there is no intrinsic electron excess, the bands at the Fermi level are not one-dimensional in the sense of $NbSe_3$, and there is much less reason to expect any kind of charge–density–wave instability.

Such instabilities probably do occur in $NbTe_4$ and $TaTe_4$, however. Here again the transition metal atoms lie in one-dimensional columns, but now the repeat units are distorted-square-antiprisms, MX_8. All the telluriums are paired, but the pairing occurs between columns rather than within columns. Thus these are formally d^1 compounds analogous to NbS_3, and one might have expected some form of M—M pairing along the chains, perhaps leading to semiconducting properties. In fact the calculations show that the three-dimensional coupling between MTe_4 columns is too strong to allow an energy gap to open.[20] The superlattice spots seen in X-ray and electron diffraction are probably correctly interpreted in terms of charge–density–wave instabilities, which are unusual in existing even at room temperature.

Space restrictions prevent any more than the briefest mention of other families of metal–metal bonded chalcogenides of the early transition metals. Perhaps the most extensive group that we have omitted are those structures based on the M_6X_8 octahedral unit: the Chevrel series of (primarily ternary) compounds, with their unusual superconducting properties and electronic structures that depend sensitively on the distortions of the Mo_6X_8 unit brought about by the presence of a third component in the lattice and by deviations from stoichiometry.[21,22] Full valence satisfaction of the isolated M_6X_8 cluster would require 42 electrons to be supplied by the six metal atoms (16 are required to fill the chalcogen p-shells, and a further 24 to form M–M bonding states along the 12 edges of the octahedron), and most of the Chevrel compounds conduct only as a result of their intrinsic electron deficit.

The unusual rhenium telluride structure provides an appealing example[23] of a semiconducting compound composed of a quasi-rocksalt array of $[Re_6Te_8]^{2+}$ and $[Te_7]^{2-}$ composite ions, while in $TlMo_3Se_3$ the same Mo_6S_8 octahedral units condense by sharing opposite Mo_3 triangular faces into a one-dimensional metal.[24,25]

REFERENCES

1. J. A. Wilson, *Adv. Phys.* 1972, **21**, 143.
2. J. A. Wilson, *Electronic Structure of Complex Materials* (Edited by P. Phariseau and W. M. Temmerman), p. 657. Plenum Press, New York (1984).
3. D. W. Bullett, *Theoretical Aspects of Band Structures and Electronic Properties of Pseudo-one-dimensional Solids* (Edited by H. Kamimura). Reidel, Dordrecht (1985).
4. W. B. England, S. H. Liu and H. W. Myron, *J. Chem. Phys.* 1974, **60**, 3760.
5. K. Motizuki, K. Katoh and A. Yanase, *J. Phys. C* 1986, **19**, 495.
6. W. Tremel and R. Hoffmann, *J. Am. Chem. Soc.* 1986, **108**, 5174; M. Kertesz and R. Hoffmann, *J. Am. Chem. Soc.* 1986, **106**, 3453.
7. J. A. Wilson and A. D. Yoffe, *Adv. Phys.* 1969, **18**, 193.
8. D. W. Bullett, *J. Phys. C* 1978, **11**, 4501.
9. T. Yamasaki, N. Suzuki and K. Motizuki, *J. Phys. C* 1987, **20**, 395.
10. N. Suzuki, T. Yamasaki and K. Motizuki, *J. Phys. C* 1978, **21**, 6133.
11. W. G. Dawson and D. W. Bullett, *J. Phys. C* 1987, **20**, 6159.
12. D. W. Bullett, *J. Phys. C* 1979, **12**, 277.
13. J. Rijnsdorp and F. Jellinek, *J. Solid-State Chem.* 1978, **25**, 325.
14. D. W. Bullett, *J. Solid-State Chem.* 1980, **33**, 13.
15. D. W. Bullett, *J. Phys. C* 1982, **15**, 3069.
16. N. Shima and H. Kamimura, *Theoretical Aspects of Band Structures and Electronic Properties of Pseudo-one-dimensional Solids* (Edited by H. Kamimura), p. 231. Reidel, Dordrecht (1985).
17. P. Monceau, *Electronic Properties of Inorganic Quasi-one-dimensional Compounds* (Edited by P. Monceau), p. 139. Reidel, Dordrecht (1985).
18. D. W. Bullett, *Solid State Commun.* 1982, **42**, 691.
19. M. H. Whangbo, F. J. DiSalvo and R. M. Fleming, *Phys. Rev.* 1982, **B26**, 687.
20. D. W. Bullett, *J. Phys. C* 1984, **17**, 253.
21. D. W. Bullett, *Phys. Rev. Lett.* 1977, **39**, 664.
22. O. K. Andersen, W. Klose and H. Nohl, *Phys. Rev.* 1977, **B17**, 1760.
23. D. W. Bullett, *Solid State Commun.* 1984, **51**, 51.
24. T. Hughbanks and R. Hoffmann, *Inorg. Chem.* 1982, **21**, 3578; *J. Am. Chem. Soc.* 1983, **105**, 1150.
25. P. J. Kelly and O. K. Andersen, *Superconductivity in d- and f-band metals* (Edited by W. Buckel and W. Webero), p. 137. Kernforschungszentrum Karlsruhe (1982).

Polyhedron Vol. 8, No. 13/14, pp. 1625–1629, 1989
Printed in Great Britain

0277–5387/89 $3.00+.00
© 1989 Maxwell Pergamon Macmillan plc

MOLECULES, CLUSTERS, SOLIDS AND CATALYSTS IN EARLY TRANSITION METAL SULPHIDE SYSTEMS

E. I. STIEFEL,* T. R. HALBERT, C. L. COYLE, L. WEI, W.-H. PAN, T. C. HO, R. R. CHIANELLI and M. DAAGE

Exxon Research and Engineering Company, Clinton Township, Rt. 22E, Annandale, NJ 08801, U.S.A.

Abstract—Inorganic syntheses starting with the tetrathiometallates of molybdenum, tungsten, vanadium and rhenium produce new homonuclear transition metal sulphide (TMS) complexes and clusters by utilizing internal redox processes. The resultant molecular structures often contain features or fragments that resemble those in TMS solids. The homonuclear complexes serve synthetically as excellent ligands, particularly to low-valent organometallic metals. The resulting heteronuclear TMS clusters serve as precursors to TMS solids that are active hydrodesulphurization catalysts. Moreover, the same reactions that lead to the heteronuclear TMS clusters allow decoration of the edges of preformed MoS_2 catalysts, leading to active catalytic materials.

Transition metal sulphide (TMS) solids have remarkable structural and electronic structural characteristics. These are manifested in such interesting phenomena as metallic conductivity,[1] superconductivity,[2] semiconductivity,[3] battery electrode behaviour,[4] photoelectric effects,[5] intercalation reactions,[6] lubrication properties[7] and catalysis.[8–11] Attempts to understand and control these properties have led to significant technological advances. In particular, many studies have shown that variation in synthesis and the resultant structural subtlety of particular TMS systems exerts a profound influence on physical and chemical properties. For catalytic function, significant control of activity and specificity can be achieved by the controlled synthesis of TMS solids. In this paper we discuss how molecular systems, TMS complexes and clusters, can lead either directly as precursors or indirectly through novel methodology, to new TMS solid catalysts.

We first discuss the synthesis of homo- and heteronuclear complexes and clusters and the systematization of methodology for their planned assembly. Many of the TMS complexes and clusters display structural features that resemble those of related solid-state systems. Moreover, these complexes/clusters decompose thermally into active Mo—S and Co—Mo—S catalyst systems. Furthermore, since the molecular reactivity may resemble that of the solid surfaces, reactions of clusters may be used as models for reactions at surfaces of TMS solids. Such reactions lead to interesting new catalytic materials.

MOLECULAR SYNTHESIS AND STRUCTURE

The tetrathiometallate anions have proven to be useful starting points for the preparation of more complex molecular TMS systems.[12–18] We illustrate the reactivity of MoS_4^{2-} in Scheme 1. The reaction of MoS_4^{2-} with RSSR is instructive as it involves the reduction of molybdenum(VI) to molybdenum(V) induced by the external oxidant RSSR.[15,16] Internal redox processes involving electron transfer from sulphur to molybdenum are responsible for this synthetically useful mode of reactivity and illustrate the closeness of sulphur and molybdenum orbital energy levels.

WS_4^{2-} reacts in a similar manner to MoS_4^{2-} but, as tungsten is more difficult than molybdenum to reduce, the internal redox processes are less common and the chemistry to date is less extensive.[17] Although VS_4^{3-} and ReS_4^- have been less investigated than the group VI tetrathiometallates, their chemistry promises to be extensive. When VS_4^{3-} reacts with the organic disulphide of a dithio-

* Author to whom correspondence should be addressed.

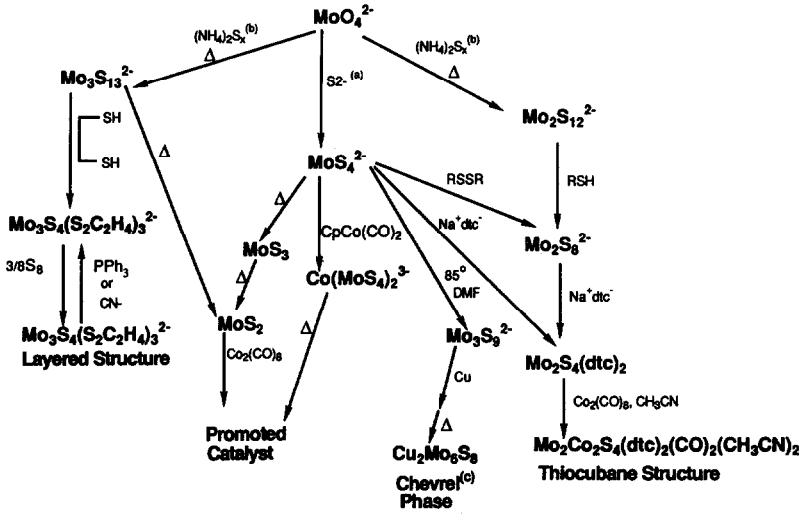

[a] J. J. Berzelius, Poggendorff's Ann. Phys. Chem. 7, 262 (1826).
[b] Ref. 20.
[c] K. S. Nanjundaswamy, N. Y. Vasanthacharya, J. Gopalakrishnan and C. N. R. Rao, Inorg. Chem., 26, 4286 (1987).

Scheme 1. Reactions in the Mo—S system.

carbamate ligand, e.g. the thiuram disulphide, $(^tBu)_2NC(S)S_2(S)CN(^tBu)_2$, the novel structure shown in Fig. 1 occurs.[18] The $V_2(\mu\text{-}S_2)_2^{4+}$ core has dimensions virtually identical to those in the vanadium mineral patronite, VS_4. The reaction of ReS_4^- with thiuram disulphide gives the dinuclear complex $Re_2S_2(dtc)_4$, which in the *meso* stereoisomer has a layered structure with a bis(sulphido)-bridged bioctahedral structure, as shown in Fig. 2. The structure contains a strong Re—Re bond and is reminiscent of the layered distorted octahedral structure of ReS_2.

The ions $Mo_2S_{12}^{2-}$ [19] and $Mo_3S_{13}^{2-}$ [19] have also proven to be useful starting materials (Scheme 1). The trinuclear cluster, $Mo_3S_4(edt)_3^{2-}$ (formed from $Mo_3S(\mu_2\text{-}S_2)_3(S_2)_3^{2-}$) has the layered S—Mo—S structure[20] shown in Fig. 3, which is reminiscent of the layered structure of MoS_2. Clearly, some of the molecular species have *core* structures that are reminiscent of the structures known to be present in TMS solids. A recent spectacular example of this occurrence is the synthesis of the $Mo_6S_8^{4-}$ core structure of the Chevrel phases.[21]

In addition to the structural similarity between the clusters and solids, there may be analogous behaviour in reactivity as well. For example, many layered TMS structures such as MoS_2 can be stoichiometrically inexact, with MoS_{2-x} and MoS_{2+x}

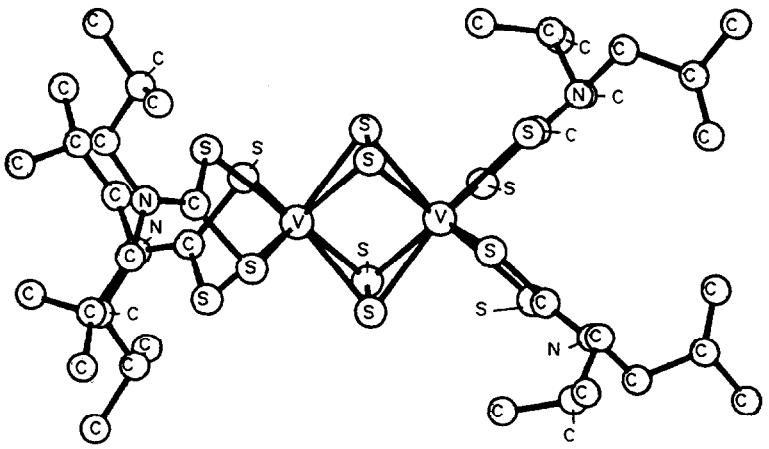

Fig. 1. The structure of $V_2(\mu\text{-}S_2)_2[S_2CN(^tC_4H_9)_2]_4$.

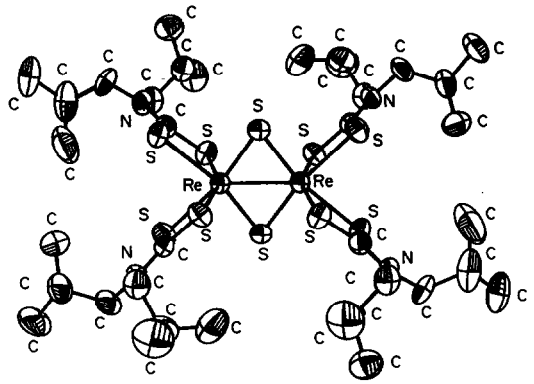

Fig. 2. The structure of $Re_2S_2[S_2CN(^iC_4H_9)_2]_4$.

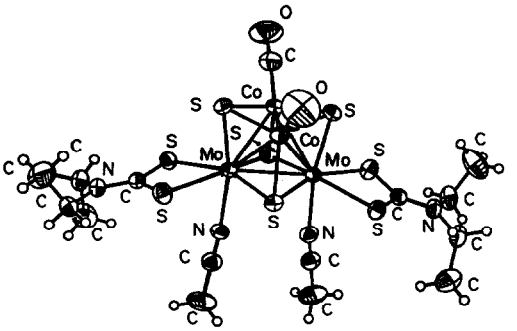

Fig. 4. The structure of $Mo_2Co_2(\mu_3\text{-}S)_4[S_2CN(C_2H_5)_2]_2(CO)_2(CH_3CN)_2$.

stoichiometries both being possible depending upon the mode of preparation and treatment. $Mo_3S_4(edt)_3^{2-}$ displays related behaviour, being easily and reversibly converted to sulphur-rich $Mo_3S_7(edt)_3^{2-}$ by treatment with elemental sulphur.[20] The $Mo_3S_7(edt)_3^{2-}$ species can be converted back to $Mo_3S_4(edt)_3^{2-}$ by sulphur-atom extracting reagents such as CN^- or $P(C_6H_5)_3$.[20] The $Mo_3S_4^+$ core structure can be thought of as sulphur poor, while the $Mo_3S_7^{4+}$ core structure can be viewed as a sulphur-rich analogue of an MoS_2 surface site. The presence of bridging disulphide ligands in the $Mo_3S_7^{4+}$ core suggests that such ligands should be considered as candidate surface species on the edges of MoS_2.

The homonuclear mono-, di- and trinuclear clusters serve as building blocks for the synthesis of heteronuclear clusters. Molecular orbital studies reveal that MoS_4^{2-} and the $Mo_2S_4^{2+}$ core structure should each serve as donor–acceptor ligands, bonding most strongly to low-valent metals.[22,23] MoS_4^{2-} is a versatile bidentate ligand which binds to many transition metals[23] including low valent cobalt where the ion $Co(MoS_4)_2^{3-}$ is formed.[24,25] The $Mo_2Co_2S_4^{2+}$ core cluster, which contains the fully metal–metal bonded thiocubane structure shown in Fig. 4, is formed by reaction of the $Mo_2S_4^{2+}$ core with $Co_2(CO)_8$.[26] This type of reactivity can be exploited in the reactions of solids.

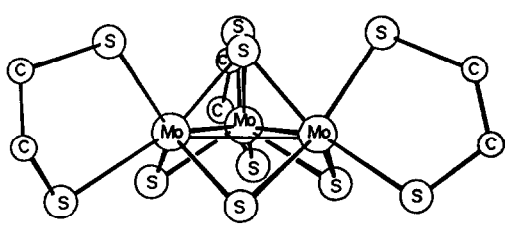

Fig. 3. The structure of $Mo_3(\mu_3\text{-}S)(\mu_2\text{-}S)_3(S_2C_2H_4)_3^{2-}$ in its tetraethyl ammonium salt.

FROM PRECURSORS TO SOLID CATALYSTS

MoS_2 is the TMS phase most closely involved in hydrotreating catalysis, including the industrially important hydrodesulphurization of petroleum feedstocks. In commercial practice, MoS_2 is usually supported on alumina and promoted by nickel or cobalt.[8,9] It has been shown that the properties of MoS_2 formed thermally are dependent on its mode of preparation.[27] Moreover, it is known that incorporation of the usual promotor metals, cobalt or nickel, into the precursor leads to the formation of active catalysts.[28,29]

Discussion of the mechanism of TMS catalysis and of the specific mechanism for promotion is beyond the scope of this article. Suffice it to say that an intimate contact between Mo—S and either Ni—S or Co—S functionalities seem to be implicated. In particular, a so-called Co—Mo—S phase has been suggested as being responsible for the promotion of HDS activity.[30] Mechanistically, this promotion effect could be due to a bridging sulphur in a Co—S—Mo unit, which has a binding energy intermediate between that in Mo—S—Mo and Co—S—Co.[31] This intermediate binding energy for sulphur in the Co—S—Mo structure may be necessary to allow effective binding and facile release of sulphur, thereby maximizing catalytic ability.

Since intimate connection of the promotor metal and molybdenum may be required for optimal catalysis, it seemed appropriate to attempt the use of molecular precursors in which the cobalt and molybdenum are covalently bound in the same precursor molecule. In particular, various salts of $Co(MoS_4)_2^{3-}$ and $Ni(MoS_4)_2^{2-}$ are found to be effective precursors of highly active hydrodesulphurization catalysts.[28,29] Likewise, the $Co_2Mo_2S_4^{2+}$ thiocubane cluster, upon thermal decomposition, forms an active hydrotreating

catalyst.[32] Related clusters have been placed on supports where they show interesting catalytic properties.[33,34]

MOLECULAR APPROACHES TO SURFACE CONTROL

The "surface" of MoS_2 that is important in catalysis is the "edge", rather than the close-packed sulphide basal plane. Unfortunately, the detailed structural nature of the edge is likely complex and is as yet unknown at atomic resolution. Therefore, any rendition of the surface is imprecise and necessarily speculative. A structure showing some of the possible surface species is given in Fig. 5. The presence of terminal or bridging sulphide, disulphide and polysulphide ligands is included to define some of the possibilities. Structures containing S—H or Mo—H links, possible under hydrogenating conditions, are omitted from consideration.

The hypothesized presence of surface terminal and bridging sulphido groups suggests that the surface could react in a manner similar to molecular species containing such units. This appears to be the case. For example, reaction of MoS_2 with $Co_2(CO)_8$ leads to rapid CO evolution and "decoration" of the edge of the layered MoS_2 structure. The use of low-valent, organometallic complexes is suggested by the reactivity of similar low-valent organometallics with molecular complexes containing terminal sulphido ligands.

The "low-valent promotion" (LVP) technique leads to edge-decorated MoS_2 particles, as shown by element specific microscopy. The resultant derivatized surfaces, upon sulphiding with H_2/H_2S, are found to be active in hydrodesulphurization, albeit relatively inactive in hydrodenitrogenation, i.e. selectivity appears to be enhanced by the LVP process.

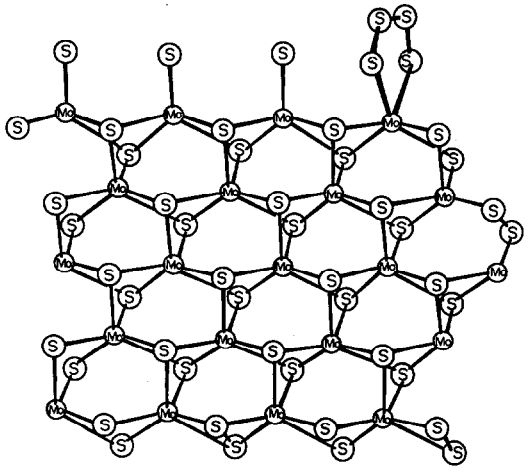

Fig. 5. Possible structures on the edge sites of MoS_2.

The use of LVP, an approach based on analogy with molecular systems, allows the preparation of solid structures wherein the surface species are added on to a pre-existing bulk phase. Such molecular-based grafting approaches carried out at low temperatures offer a distinct alternative to the more conventional thermal methods of catalyst preparation.

REFERENCES

1. J. A. Wilson and A. D. Yoffe, *Adv. Phys.* 1969, **18**, 193.
2. R. Chevrel, M. Hirrien and M. Sergent, *Polyhedron* 1986, **5**, 87.
3. L. F. Schneemeyer and M. S. Wrighton, *J. Am. Chem. Soc.* 1979, **101**, 6496.
4. R. E. Boyas-Severeyn, R. McIntyre and H. Gerischer, *Electrochim. Acta* 1988, **33**, 493.
5. H. Tributsch, *Structure Bonding* 1982, **49**, 128.
6. M. S. Wittingham, *Prog. Solid State Chem.* 1978, **12**, 41.
7. P. C. H. Mitchell, *Wear* 1984, **100**, 281.
8. R. R. Chianelli, *Catal. Rev.-Sci. Engng* 1984, **26**, 361.
9. H. Topsøe and B. S. Clausen, *Catal. Rev.-Sci. Engng* 1984, **26**, 395.
10. T. A. Pecoraro and R. R. Chianelli, *J. Catal.* 1981, **67**, 430.
11. T. C. Ho, *Catal. Rev.-Sci. Engng* 1988, **30**, 117.
12. A. Müller, E. Ahlborn and H. H. Heinsen, *Z. Anorg. Allg. Chem.* 1971, **386**, 102.
13. E. D. Simhon, N. C. Baenziger, M. Kanatzidis, M. Draganjac and D. Coucouvanis, *J. Am. Chem. Soc.* 1981, **103**, 1218.
14. W.-H. Pan, M. E. Leonowicz and E. I. Stiefel, *Inorg. Chem.* 1983, **22**, 672.
15. W.-H. Pan, M. A. Harmer, T. R. Halbert and E. I. Stiefel, *J. Am. Chem. Soc.* 1984, **106**, 459.
16. M. A. Harmer, T. R. Halbert, C. L. Coyle, S. A. Cohen and E. I. Stiefel, *Polyhedron* 1986, **5**, 341.
17. S. A. Cohen and E. I. Stiefel, *Inorg. Chem.* 1985, **24**, 4657.
18. T. R. Halbert, L. L. Hutchings, R. Rhodes and E. I. Stiefel, *J. Am. Chem. Soc.* 1986, **108**, 6437.
19. A. Müller, W. O. Nolte and B. Krebs, *Angew. Chem. Int. Edn Engl.* 1978, **17**, 279.
20. T. R. Halbert, K. McGauley, W.-H. Pan, R. S. Czernuszewicz and E. I. Stiefel, *J. Am. Chem. Soc.* 1984, **106**, 1849.
21. T. Saito, N. Yamamoto, T. Yamagata and H. Imoto, *J. Am. Chem. Soc.* 1988, **110**, 1646.
22. J. Bernholc and E. I. Stiefel, *Inorg. Chem.* 1985, **24**, 1323.
23. A. Müller, E. Diemann, R. Jostes and H. Bögge, *Angew. Chem. Int. Edn. Engl.* 9181, **20**, 934.
24. W.-H. Pan, D. C. Johnston, S. T. McKenna, R. R. Chianelli, T. R. Halbert, L. L. Hitchings and E. I. Stiefel, *Inorg. Chim. Acta* 1985, **97**, L17.
25. A. Müller, R. Jostes, W. Hellmann, C. Römer, H.

Bögge, U. Schimanski, B. Zhuang, L. D. Rosenhein, J. W. McDonald and W. E. Newton, *Z. Anorg. Allg. Chem.* 1986, **533**, 125.
26. T. R. Halbert, S. A. Cohen and E. I. Stiefel, *Organometallics* 1985, **4**, 1689.
27. A. Müller and E. Diemann, *Chimia* 1985, **39**, 312.
28. E. I. Stiefel, W.-H. Pan and R. R. Chianelli, *U.S. Patent* 4,510,260 (9 April 1985); E. I. Stiefel, W.-H. Pan, R. R. Chianelli and T. C. Ho, *U.S. Patent* 4,581,125 (8 April 1988).
29. W. Eltzner, M. Breysse, M. Lacroix and M. Vrinat, *Polyhedron* 1986, **5**, 203.
30. H. Topsøe, in *Surface Properties and Catalysis by Non-metals* (Edited by J. P. Bonelle *et al.*), p. 329. D. Reidel, Dordrecht (1983).
31. R. R. Chianelli, T. A. Pecoraro, T. R. Halbert, W.-H. Pan and E. I. Stiefel, *J. Catal.* 1984, **86**, 226.
32. T. R. Halbert, S. A. Cohen and E. I. Stiefel, *U.S. Patent* 4,730, 064 (8 March 1988).
33. L. T. Thompson Jr, J. Schwank and M. D. Curtis, *AIChE J.* 1989, **35**, 111.
34. M. D. Curtis, J. E. Penner-Hahn, J. Schwank, O. Baralt, D. J. McCabe, L. Thompson and G. Waldo, *Polyhedron* 1989, **8**.

Polyhedron Vol. 8, No. 13/14, pp. 1631–1635, 1989
Printed in Great Britain

0277–5387/89 $3.00+.00
© 1989 Maxwell Pergamon Macmillan plc

THE ELECTROCHROMIC BEHAVIOUR OF ZIRCONIUM DIPHTHALOCYANINE AND MOLYBDENUM PHTHALOCYANINE OXIDE

J. SILVER,* P. J. LUKES, P. K. HEY and J. M. O'CONNOR

Department of Chemistry and Biological Chemistry, University of Essex, Wivenhoe Park, Colchester CO4 3SQ, U.K.

Abstract—The electrochromic behaviour of sublimed, thin films of zirconium and molybdenum phthalocyanines is presented. The electrochromic properties of these M^{IV} phthalocyanines are compared to those of the lanthanide diphthalocyanines. An explanation of the observed electrochromic phenomena in which the reduction and oxidation take place on the phthalocyanine ring rather than on the metals is presented.

The possible applications of electrochromic technology[1] in the areas of "smart" windows and visual display systems has stimulated research interest in a wide range of inorganic,[2,3] organometallic,[4–9] organic[10–11] and graphite insertion compounds.[12] Of these, the lanthanide diphthalocyanines have been shown to possess a wide range of colours, good reversibility and be usable over a reasonable temperature range, 0–90°C. We and others have shown the lanthanide diphthalocyanines can be cycled (colours switched) more than 10^7 times.[8,13]

An electrochromic material is one which shows reversible colour changes under the influence of an applied electric current and/or electric field. The lanthanide diphthalocyanines ($L(pc)_2$) (where L = lanthanide ion, pc = phthalocyanine dianion) possess both ionic and electronic conduction.[14] Such materials can be sublimed as thin green-coloured films onto transparent or non-transparent electrodes.[4b,8,15] The film coated electrode can be placed in a cell containing an electrolyte (e.g. a solution of 5% NaCl) and a counter electrode. Then, when a voltage of around ± 1.5 V is applied, the lanthanide diphthalocyanine layer changes colour. The initial green colour changes as follows for $Lu(pc)_2$ (Lu = Lutetium) and other heavy $L(pc)_2$ materials:[4b,8]

$$\underset{+1.0\text{ V}}{\text{Red}} \longleftarrow \underset{0.0\text{ V}}{\text{Green}} \longrightarrow \underset{-0.8\text{ V}}{\text{Blue}} \longrightarrow \underset{-1.20\text{ V}}{\text{Purple}}$$

(with reference to SCE).

The true formulation of the electrochromic $L(pc)_2$ films has been the subject of much debate in the literature, though we and others favour [L(pc)(p$\dot{c}$)] (where p$\dot{c}$ = the radical monoanion anion of pc) for the green species.[14,16,17]

We have demonstrated that mixed rare-earth element diphthalocyanine material devices exhibit broader absorption bands and enhanced (more pleasing) colours than single element devices. In addition, they display longer lifetimes and the cost of the starting mixed rare-earth element materials (partialy refined ores) is substantially less than that of pure rare-earth elements.[8]

$Sn(pc)_2$ has been found to have a similar structure[18] to the [L(pc)(p$\dot{c}$)] materials,[19,20] although it contains the metal in the IV and not the III oxidation state. It has been shown that turquoise $Sn(pc)_2$ undergoes colour changes through green to red on oxidation, and to blue and purple on reduction.[14] These colours are similar to those of the [L(pc)(p$\dot{c}$)] complexes and like those colours of the latter materials, are said to be due to oxidation and reduction of the pc rings.[14] In the light of these findings we turned our attention to other metal IV phthalocyanines to establish their electrochromic behaviour and structure. We chose zirconium and molybdenum phthalocyanines for this purpose, to compare any electrochromic properties with those of the $L(pc)_2$ materials. We report the results of these studies here.

EXPERIMENTAL

Zirconium diphthalocyanine $[Zr(pc)_2]$[21] (identified from crystal structure) (see Fig. 1) was

* Author to whom correspondence should be addressed.

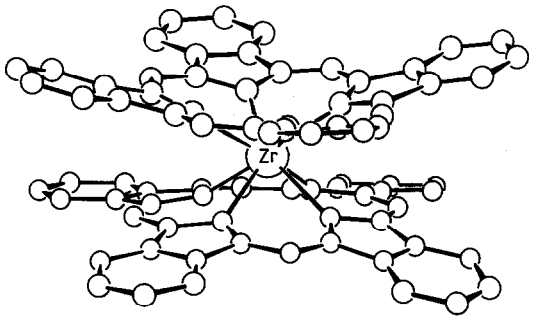

Fig. 1. The structure of $[Zr(pc)_2]$.

prepared by refluxing diaminoisoindoline with $ZrCl_4$ (ratio 8 : 1) in quinoline under an N_2 atmosphere for 2 h. The reaction mixture was filtered hot to avoid the precipitation of tarry by-products. The purple crystalline powder obtained was washed with benzene, methanol and acetone to remove any unreacted starting materials, and then sublimed under vacuum. The product was then resublimed several times under a slow flow of N_2 in a tube furnace until cyan needle-like crystals appeared. The crystals were shown by X-ray diffraction crystal structure analysis to be $[Zr(pc)_2]$.[21]

Molybdenum phthalocyanine oxide [MoO(pc)]

The established procedure to prepare this complex is by the melt reaction of 1,2-dicyanobenzene with ammoniummolybdate.[22] [MoO(pc)] is produced in high yield. This material is cyan–blue in colour, and was identified by its electronic absorption and IR spectra.[22]

Physical measurements

Electronic absorption spectra of the thin films on indium-doped tin oxide covered glass (ITO) (both as sublimed layers and in cell devices) were recorded in a Perkin–Elmer Lambda 5 spectrophotometer.

Thin films on ITO glass were prepared by vacuum sublimation of the powdered metal phthalocyanines using an Edwards E306 vacuum depositing unit. The glass slides were 3 cm × 0.9 cm and had a resistance of 5–20 ohms/□. For cycling tests and for electronic absorption spectroscopy the devices were used as electrodes in 1 cm path length cuvettes, using a platinum wire as a counter electrode. The cuvettes contained approximately 2.5 cm^3 of a 5% NaCl–water solution as electrolyte. A BBC computer interfaced via DAC (digital to analogue converter) was used to change the voltages and cycle the devices in the cuvettes, using a program written in these laboratories.[23] The voltage range used was between +1.2 and −1 V.

RESULTS AND DISCUSSION

$[Zr(pc)_2]$

Examination of the visible spectra of a neutral, sublimed film of $[Zr(pc)_2]$ (Fig. 2) reveals a strong resemblance to that of $[Sn(pc)_2]$.[23] The Q band splits into two with maxima at 702 and 637 nm.

The spectral behaviour on reducing the $[Zr(pc)_2]$ film is shown in Fig. 3. There is a 50% reduction in the Q band intensity, but only a slight change in the position of the main Q bands. However, new bands are seen to develop at 535 and 580 nm and also around 850 nm (close to the limit of the spectrometer). In addition, the Soret band around 350 nm gains in intensity. The absorption at 850 nm in the reduced form is stronger than was seen in $[Sn(pc)_2]$,[23] but otherwise, the two reduced forms are very similar. During the reduction a cyan (neutral colour) to purple–red colour change was observed, though the colour was less intense than that seen for reduced species in the [L(pc)(pc)] complexes.[8] Assuming that the material which sublimed from the $[Zr(pc)_2]$ crystals retained the same stoichiometry as the crystal structure, then the electronic absorption spectra in Figs 2–4 are representative of this material. The reduced form is probably the single-electron reduction product

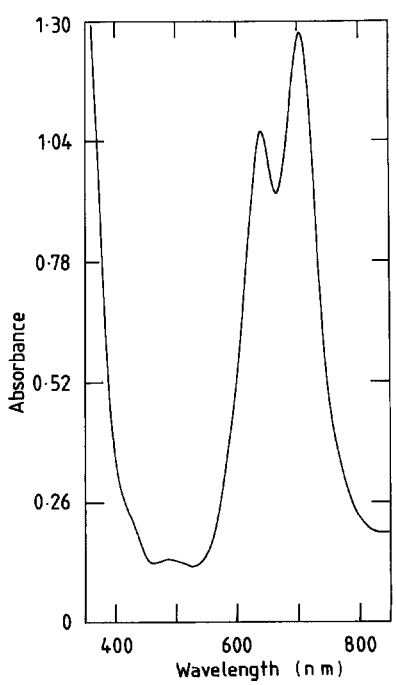

Fig. 2. The electronic absorption spectrum of a neutral sublimed film of $[Zr(pc)_2]$ on an ITO glass slide.

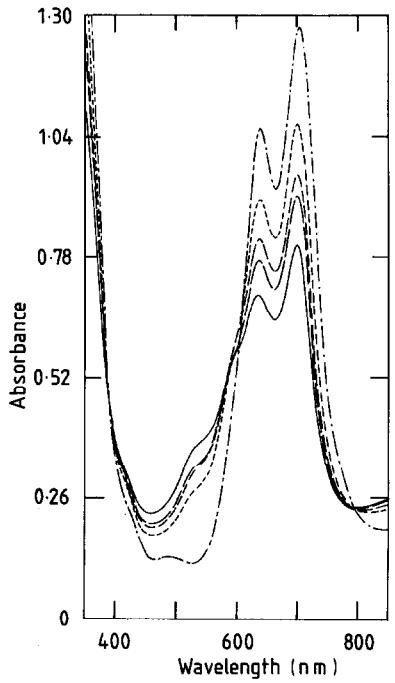

Fig. 3. The electronic absorption spectra of the neutral sublimed film of $[Zr(pc)_2]$ on an ITO glass slide, showing new peaks emerging on reduction at 534.8, 582 and above 850 nm. The successive runs at voltages between 0 and −1.1 V show a decrease in the main absorption bands.

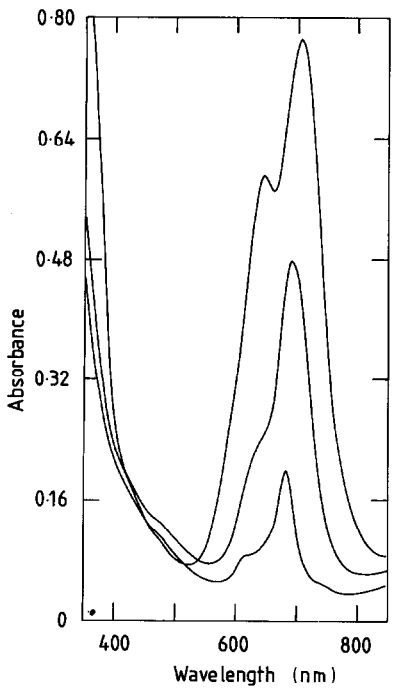

Fig. 4. The electronic absorption spectrum of the neutral sublimed film of $[Zr(pc)_2]$ on an ITO glass slide. Successive runs show both movement and loss of intensity when voltages of +0.5 to +0.1 V are applied. Eventually the slide loses all colour of the $[Zr(pc)_2]$ complex.

from the reaction:

$$[Zr(pc)_2] + e^- \longrightarrow [Zr(pc)_2]^-.$$
cyan purple–red

An explanation of this spectrum could be that the Q band absorption of the neutral phthalocyanine ring is perturbed whilst the second ring (the reduced ring) gives rise to the new bands in the spectra (Fig. 3). The spectral changes on reduction were reversible, and up to 10^3 colour cycles were achieved between the neutral and reduced states, the voltage necessary for reduction was around −1.1 V.

Oxidation of $[Zr(pc)_2]$ films gave rise to an irreversible loss of colour of the film in contrast to the results of others on a gold electrode.[24] The spectra of the oxidized films (Fig. 4) show both an initial movement of the Q bands and a simultaneous loss of intensity. Then a successive spectrum shows further movement and loss of intensity. This change from cyan to colourless was not reversible.

The failure to observe a colour change upon oxidation of the film is surprising, as the [L(pc)(pc)] material series all show colour changes upon oxidation. We found similar difficulties in obtaining an oxidized form for $[Sn(pc)_2]$[25] in contrast to other workers.[14]

[MoO(pc)]

The visible spectrum of a neutral sublimed film of [MoO(pc)] is presented in Fig. 5. A very strong

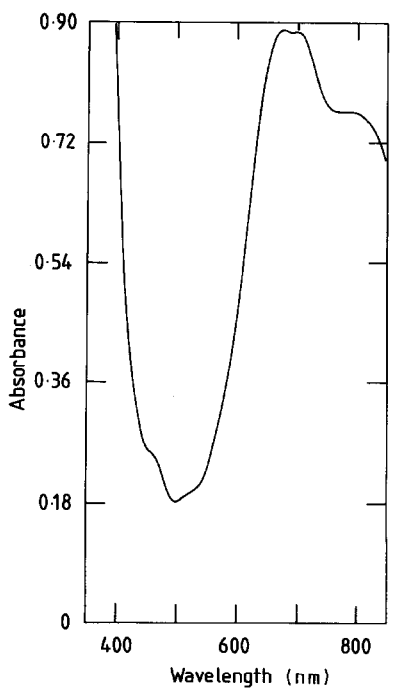

Fig. 5. The electronic absorption spectrum of a neutral sublimed film of [MoO(pc)] on an ITO glass slide.

Table 1. Electronic absorption spectra of [MoO(pc)] film

Neutral		Reduced −0.7 V		Reduced −0.95 V		Cycled	
ν (nm)	I	ν (nm)	I	ν (nm)	I	ν (nm)	I
810	0.95	790	0.75	792	0.60	810	0.74
702	1.00	652	0.90	645	0.58	706	0.92
674	1.00	532	0.57	510	0.53	651	1.00
460	0.31	459	0.47	459	0.41	450	0.51

I = relative intensity normalized on strongest band of the original neutral film.

absorption is present in the 600–850 nm region, but no structure has yet been reported for this material. On the basis of evidence from the similarity of the visible spectra to that of [VO(pc)], it probably resembles the latter material. The data summarizing the electrochromic reduction of [MoO(pc)] are presented in Table 1. The reduction was accompanied by a colour change from cyan–blue (neutral) to purple–violet, in agreement with the results of Collins and Schiffrin.[14]

We suggest that the reduction may be represented as

$$[MoO(pc)] + e^- \longrightarrow [MoO(pc)]^-$$

and that it is pc based, as found in the [L(pc)(pc)] materials and in $[Zr(pc)_2]$, not metal based as suggested by others.[14] This hypothesis is based on the changes in the absorption in the visible region that result from the electronic levels on the pc rings. A change in the metal oxidation state should be expected to move these bands, but not to generate new additional bands.

The reduced to neutral colour change was successfully cycled in several devices 10^4 times. Breakdown of devices was through peeling, possibly caused by films swelling, or induced by mechanical stress, caused by anion incorporation in the lattice.[14] It was noticed that partially peeled devices were still colour cycling on all the peeled film, if they still were in contact with the ITO surface at some point in their periphery. This fact suggests both good conduction properties in the films themselves, and also that the layers are mechanically breaking down, not chemically breaking down.

CONCLUSIONS

$[Zr(pc)_2]$ and [MoO(pc)] both show electrochromic changes, however, neither of these compounds show either the reversibility or the range of colours found in the [L(pc)(pc)] complexes. They are therefore less attractive as potential materials for commercial device applications.

The fact that $[Zr(pc)_2]$ has a similar structure to [L(pc)(pc)] complexes is of great interest as its electrochromic properties are very different. These differences and those of the $[Sn(pc)_2]$ complex[25] must be due to the presence of an M^{IV} species in the complex.

The systems are compared (L = Lanthanide element) and the various identified species listed under their similar colours in Table 2.

It can be seen from this work that the $[Zr(pc)_2]^+$ complex is chemically unstable and degrades, losing its colour. This must mean the the pc rings are chemically broken down (opened) on oxidation. We

Table 2.

Metal oxidation state	Colour of species			
	Red	Green	Blue	Purple
III	$[L(pc)(pc)]^+$	$[L(pc)(pc)]^0$	$[L(pc)_2]^-$	$[L(pc)_2]^{2-}$
IV		$\boxed{[Zr(pc)_2]^+}$	$[Zr(pc)_2]^0$	$[Zr(pc)_2]^-$
IV			$[Sn(pc)_2]^0$	$[Sn(pc)_2]^-$

found that the $[Sn(pc)_2]$ complex behaves similarly. This must be due to the greater polarizing power of the M^{IV} ions destabilizing the oxidized rings. In addition, it can be appreciated that the total electron count is the same in all the blue complexes and in all the purple complexes. It therefore appears that the same number of electrons on the rings cause similar colours in the metal diphthalocyanine complexes irrespective of the charge on the metal, providing the species are chemically stable. This finding is in agreement with the oxidations and reductions being pc ring based.

The [MoO(pc)] material is not a diphthalocyanine and shows a very different spectrum on reduction, with new bands appearing in the visible region. This material turns yellow–grey on oxidation, a colour not found in the metal diphthalocyanines. The fact that the molybdenum(IV) does not form a diphthalocyanine under the conditions tried in this work shows that the stability of the $[MoO]^{2+}$ ion dominates its chemistry. The $[MoO]^{2+}$ ion is able to bind to a single pc ring, presumably the resulting structure is similar to that of [VO(pc)],[26] and the molybdenum atoms sit above the pc plane.

Acknowledgement—Thanks are due to the British Technology Group for support for studentships to P.L., P.H. and J.M.O.

REFERENCES

1. C. M. Lampert, *Solar Energy Mater.* 1984, **11**, 1.
2. (a) M. Green and D. Richman, *Thin Solid Films* 1974, **24**, S45; (b) M. Green and K. Kang, *Solid State Ionics* 1981, **3,4**, 141.
3. (a) E. K. Sichel and J. I. Gittleman, *Appl. Phys. Lett.* 1978, **33**, 564; (b) E. K. Sichel, J. I. Gittleman and J. Zelez, *Appl. Phys. Lett.* 1977, **31**, 109.
4. (a) I. S. Kirin and P. N. Moskalev, *Russ. J. Phys. Chem.* (Engl. Transl) 1967, **41**, 251; (b) P. N. Moskalev and I. S. Kirin, *Russ. J. Phys. Chem.* (Engl. Transl.) 1972, **46**, 1019; (c) P. N. Moskalev and N. I. Alimova, *Russ. J. Inorg. Chem.* (Engl. Transl.) 1975, **20**, 1474.
5. (a) M. M. Nicholson and R. V. Galiardi, Final Report, Contract N62269-76-C-0574, AD-A039596 (May 1977): *Chem. Abstr.* 1977, **87**, 144073V; (b) M. M. Nicholson and F. A. Pizzarello, *J. Electrochem. Soc.* 1979, **126**, 1490; M. M. Nicholson and F. A. Pizzarello, *J. Electrochem. Soc.* 1980, **127**, 821; M. M. Nicholson and F. A. Pizzarello, *J. Electrochem. Soc.* 1981, **128**, 1288.
6. G. A. Corker, B. Grant and N. J. Clecak, *J. Electrochem. Soc.* 1979, **126**, 1336.
7. A. G. Mackay, J. F. Boas and H. J. Troup, *Austr. J. Chem.* 1974, **27**, 955.
8. C. S. Frampton, J. M. O'Connor, J. Peterson and J. Silver, *Displays, Technol. Applications* 1988, **9**, 174.
9. S. A. Song, M. O. O'Connor, D. J. Barber and J. Silver, *J. Crystl. Growth* 1988, **88**, 477.
10. I. F. Chang, B. C. Gilbert and T. J. Sun, *J. Electrochem. Soc.* 1975, **122**, 955.
11. M. Yamana, *Jpn J. Appl. Phys.* 1976, **15**, 2469.
12. P. Pfluger, H. Kunzi and H. Guntherodt, *Appl. Phys. Lett.* 1979, **35**, 771.
13. M. T. Riou and C. Clarisse, *J. Electroanal. Chem. Interfac. Electrochem.* 1988, **249**, 181.
14. G. C. S. Collins and D. J. Schiffrin, *J. Electroanal. Chem.* 1982, **139**, 335.
15. P. N. Moskalev and I. S. Kirin, *Opt. Spectrosc.* 1970, **29**, 220.
16. A. T. Chang and J. Marchon, *Inorg. Chim. Acta* 1983, **53**, L241.
17. C. S. Frampton, J. M. O'Connor and J. Silver, unpublished results.
18. W. R. Bennett, D. E. Broberg and N. C. Bhenziger, *Inorg. Chem.* 1973, **12**, 930.
19. (a) H. De Cian, M. Moussari, J. Fischer and R. Weiss, *Inorg. Chem.* 1985, **24**, 3162; (b) H. De Cian, M. Moussari, J. Fischer and R. Weiss, *Inorg. Chem.* 1988, **27**, 1287; (c) A. D. Darovskikh, O. V. Frank-Kamenetskaya, V. S. Fundamenskii and A. M. Goluber, *Kristallografiya* 1986, **31**, 279.
20. (a) K. Kasuga, M. Tsutsui, R. C. Peterson, K. Tatsumi, M. Van Ordenbosch, G. Pepe and E. F. Mayer Jr, *J. Am. Chem. Soc.* 1980, **102**, 4836; (b) A. M. Darovskikh, A. K. Tsytsenko, O. V. Frank-Kamenetskaya, V. S. Fundamenskii and P. N. Moskalev, *Soc. Phys. Crystallogr.* 1984, **29**, 273.
21. B. Howlin, P. Lukes and J. Silver, unpublished results.
22. S. J. Edmondson and P. C. H. Mitchell, *Polyhedron* 1986, **5**, 317.
23. J. M. O'Connor, unpublished computer program.
24. G. L. Tomliva, N. A. Ovchinnikova and E. A. Luk'yanetc, *Zh. Obshch. Khim.* 1987, **57**, 2100.
25. P. Lukes and J. Silver, unpublished results.
26. R. F. Ziola, C. H. Griffiths and J. M. Troup, *J. Chem. Soc., Dalton Trans.* 1980, **11**, 2300.

Polyhedron Vol. 8, No. 13/14, pp. 1637–1640, 1989
Printed in Great Britain

0277–5387/89 $3.00+.00
© 1989 Maxwell Pergamon Macmillan plc

INFRARED SPECTROSCOPY FROM MEGASECONDS TO PICOSECONDS

JAMES J. TURNER* and MARTYN POLIAKOFF

Department of Chemistry, University of Nottingham, Nottingham NG7 2RD, U.K.

Abstract—The study of the structure and dynamics of chemical intermediates is an important part of the unravelling of reaction mechanisms. Time-resolved UV–vis and resonance Raman spectroscopy play an important role in these investigations. Here we concentrate on the application of IR techniques, including very recent developments, and give examples from organometallic chemistry.

Infrared (IR) spectroscopy is much less "fashionable" than NMR or X-ray crystallography in inorganic or organometallic chemistry. However, IR becomes particularly valuable in probing the structure and dynamics of unstable species where X-ray or NMR are hard to apply. Over the last few years there have been dramatic advances in IR technology which have greatly increased the scope of measurements which can be made. It is the purpose of this paper to illustrate the organometallic possibilities of "state of the art" IR spectroscopy. We show how one can now monitor processes which occur on timescales from 10^6 to 10^{-12} seconds. Our examples include the photochemistry of dinuclear compounds, reaction intermediates, fast reactions in solution and intramolecular rotation.

MEGASECOND IR SPECTROSCOPY

Since we are concerned with unstable species, this title clearly refers to methods of extending the lifetime of such species so that the IR spectra can be obtained at leisure. This implies the technique of matrix isolation which has been applied to a very wide range of organometallics.[1] The most common experimental method is to start by isolating a stable parent molecule at high dilution in a large excess of an inert matrix. The matrix is usually either a frozen rare gas such as argon—in which case the parent must be volatile under high vacuum—or a glass, or cast polymer film. The parent is then photolysed with UV light and the resulting photofragments are trapped in the rigid matrix. In a rare gas matrix at 10 K, there is essentially no limit to the lifetime of the fragments, since reactions at such a low temperature have near zero rate constants: we have in fact kept such species for weeks (1 Ms = 11.57 days!). Particularly when combined with isotopic substitution, the use of IR spectroscopy for structural determination is well known. What is less appreciated is the subtlety of the photochemistry that can be probed with the use of either (or both of) wavelength variation and polarized photolysis/spectroscopy. A recent example[2] that illustrates the former is the photochemistry of $Re_2(CO)_{10}$:

$$Re_2(CO)_{10} \underset{546\,nm}{\overset{313\,nm}{\rightleftharpoons}} eq\text{-}Re_2(CO)_9 \underset{313\,nm}{\overset{546\,nm}{\rightleftharpoons}} ax\text{-}Re_2(CO)_9,$$

where *eq*-$Re_2(CO)_9$ and *ax*-$Re_2(CO)_9$ refer to two different structures of the unbridged $Re_2(CO)_9$ species with empty coordination sites along and perpendicular to the Re—Re axis, respectively.

The second technique[3] depends on the fact that, usually, molecules are held orientationally fixed in the matrix. The UV–vis photolysis is performed with plane-polarized light, and the subsequent IR (and UV–vis) spectroscopy is carried out with light which is plane-polarized in a direction either parallel to, or perpendicular to, the photolysis light. This technique was first used in organometallic chemistry[4] to unravel the primary processes in the photochemistry of $Cr(CO)_6$, a study which has been crucial in understanding very recent IR experi-

* Author to whom correspondence should be addressed.

ments[5] on the picosecond timescale (see later):

$$Cr(CO)_6 \xrightarrow{h\nu} [Cr(CO)_6]^* \longrightarrow \underset{\text{square-pyramidal}}{[Cr(CO)_5]^*}(+CO)$$

$$\longrightarrow \underset{\text{trigonal-bipyramidal}}{[Cr(CO)_5]} \longrightarrow \underset{\text{square-pyramidal}}{[Cr(CO)_5]}.$$

A powerful application of the polarized technique is to dinuclear metal species,[6] where there is a clear distinction between the directions parallel and perpendicular to the metal–metal axis. For instance, it can be shown that the intermediates $Mn_2(CO)_9$[7] and $Cp_2Pt_2(\mu\text{-}CO)$[8] have bridging CO groups at 45 and 90°, respectively, to the M—M axis. Warming up the matrix leads to softening which often allows the trapped fragments to react, with corresponding changes in the IR spectrum. This method has been particularly valuable with frozen hydrocarbon glasses where such changes can be followed right up to room temperature.[9]

"MONOSECOND" IR SPECTROSCOPY

Monosecond simply refers to reactions where the half-life of the important intermediate in solution is of the order of seconds. It is usually possible to increase the lifetime by lowering the temperature. The problem is the solvent; we have shown that liquid rare gases—particularly liquid xenon and krypton—provide an ideal solvent environment for the study of relatively unstable species.[10] For instance, photolysis of the appropriate parent metal carbonyl in liquid xenon under a pressure of hydrogen generates a whole range of "non-classical" H_2 complexes. The nature of the bonding is demonstrated by observation of the appropriate ν(H—H) stretching vibration.[11] It is then possible to use Fourier transform IR to follow changes in the spectrum with photolysis and temperature. This has been a very valuable technique for establishing the mechanism of the $M(CO)_6$ photocatalysed hydrogenation of dienes.[12]

Liquid xenon becomes supercritical at 16.9°C. Chemistry in the supercritical phase is a largely unexplored area. With specially designed cells it is proving possible to use IR spectroscopy to monitor photochemically induced chemical changes; for instance, previously unknown dihydrogen complexes such as (toluene)$Cr(CO)_2(H_2)$ can be observed in supercritical xenon at temperatures up to 80°C.[13]

With a high concentration of compound and large IR extinction coefficients, the time-resolution is limited by the scan time of the FTIR instrument; modern instruments have very short scan times, so that in principle a time resolution of tens of milliseconds with spectral resolution of 8 cm^{-1} can be achieved. With a low concentration it is necessary to generate the species repetitively. Conventional grating spectrometers have much slower scan rates. However their advantage is that the change of intensity at a single wavelength is easily monitored, and this is particularly valuable for kinetic studies.

It must however be noted that most "interesting" kinetics do not occur on such a convenient time scale. Over typical concentration ranges, bimolecular reactions have half-lives from milliseconds to nanoseconds. If we are probing solvent interactions or very fast unimolecular rearrangements, even shorter time resolution will be needed. We consider the techniques in these two stages.

MILLISECOND TO NANOSECOND IR SPECTROSCOPY

There have been spectacular technical advances[14a] in rapid IR spectroscopy since Pimentel's original experiments.[15] Applied to organometallic chemistry, much the most common method is to do "point-by-point" experiments. Here the transient is generated repetitively—invariably these days by a UV laser—and the changing intensity monitored at a series of data points in either the frequency or interferometric domain.

The simplest technique is to utilize a conventional IR dispersive instrument at a series of fixed frequencies, with the slits set wide to make up for the weak IR source, and with a fast IR detector replacing the conventional detector. First used by Siebert,[16] this technique was successfully applied to the organometallic species $M(CO)_6$ (M = Cr, Mo and W) by the Muelheim group.[17] A sophisticated development, employing a combination of a high repetition rate Nd : YAG laser with fast gated detection, has allowed the IR spectrum of the triplet exciton of phthalocyanine to be obtained.[18] The limitation of these experiments is, as implied, the inherent low intensity of the IR source.

Several groups[14] have used a CO laser as source, and examined organometallic transients in both gas phase and solution. A CO laser, operating in the continuous mode, has tunable output between 1600 and 2050 cm^{-1}, a range particularly useful for the detection of ν(C—O) bands of organometallic species. The output consists of a series of very narrow lines approximately 4 cm^{-1} apart; the laser is tuned from one line to the next by rotating a diffraction grating which forms one end of the laser cavity. A CO laser is a much brighter IR source than a globar and, hence, much higher signal/noise is possible.

For instance, using such apparatus recent experiments have followed the recombination kinetics[19] of myoglobin with CO and the reactions[20] of $CpMn(CO)_2$ generated from $CpMn(CO)_3$. The time resolution is limited by a combination of laser power, detector sensitivity/response time, and speed of data handling. However, with appropriate combinations of detectors and digitisers, times over the range of many milliseconds to about 100 nanoseconds can be examined.

Time-resolved IR with a CO laser is limited in its wavenumber range and in its resolution, because the laser lines are 4 cm^{-1} apart. With the increasing reliability of tunable IR diode lasers, both drawbacks can be overcome, in principle at least. These diodes, although much less intense than the CO laser and more difficult to operate, are likely to be applied increasingly to inorganic systems.

In principle, the "point-by-point" technique can also be applied in the interferometric domain by combining fast repetitive transient generation with repetitive scanning of an FTIR instrument. Indeed manufacturers have developed software for re-sorting the data points collected in this way. Thus, following Fourier transformation, it is possible to obtain a set of IR spectra each corresponding to a specific time after the photolytic flash. Although this technique is awash with difficulties,[21] it has proved possible to follow the stretching of polymer films and liquid crystals[22] and, rather more relevant here, the reactions[23] of the intermediate $CpFe(\mu\text{-}CO)_3FeCp$, generated on photolysis of $[CpFe(CO)_2]_2$.

A better way of combining flash photolysis of transients with FTIR is to use "step-scan" rather than "continuous-scan" interferometry. This was originally demonstrated by Murphy *et al.*[24] Very recently, equipment has been developed by Siebert working in association with Bruecker; this has been applied to the photoprocesses of bacteriorhodopsin and very promising preliminary results have been obtained.[25] This is likely to be a significant advance for the study of organometallic intermediates.

PICOSECOND IR SPECTROSCOPY

IR detectors have a time resolution limited to about 100 nanoseconds. Thus to obtain IR spectra in the picosecond range one cannot use the techniques described above. There are broadly speaking two methods of doing it: one is to "cheat" and, via laser mixing techniques, to monitor IR changes in the UV–vis region where much faster detectors are available; the other is to measure the changes in IR bandwidths with temperature.

Laser mixing methods

There have very recently been two interesting applications to metal species. Moore *at al.*[26] have monitored the initial photodissociation step in the myoglobin/CO complex and by using polarized light have even been able to determine the Fe/CO angle! The second application is perhaps more relevant to this meeting. As mentioned above, matrix isolation/polarized photochemistry[4] suggested a particular mechanism for the photolysis of $Cr(CO)_6$. It was long thought, partly on the basis of experiments using picosecond UV–vis detection,[27] that the only important reaction on this time scale, is that between the ground state square-pyramidal $Cr(CO)_5$ fragment and the solvent (e.g. cyclohexane) to give $Cr(CO)_5 \cdots S$. Spears and colleagues,[5] employing picosecond IR detection, have now produced evidence that $Cr(CO)_5$ intermediates with both square-pyramidal and trigonal-bipyramidal structures can be detected in solution and their reactivity towards the solvent is substantially different.

Band width studies

The broadening and coalescence of NMR bands has played a very important role in mechanistic organometallic chemistry.[28] It is frequently said that the IR time scale is much too fast to provide information about kinetics. However there are several examples in the literature where the broadening of IR bands has been correlated with dynamic effects;[29] a simple example[30] is the internal rotation of CH_2ClCH_2Cl. Recently Grevels and colleagues[31] have observed a very striking example in organometallic chemistry. In (diene)$Fe(CO)_3$ complexes where the diene is symmetrical (e.g. norbornadiene), the low temperature solution IR ν(C—O) spectrum shows the three bands expected for C_s symmetry. On warming the solution, however, the two lower frequency bands coalesce into a single band and the overall spectrum is then appropriate to a molecule with three-fold symmetry. Grevels associates this observation with interconversion of the CO groups on a picosecond timescale and applies a modified Bloch equation to estimate the barrier height. In contrast to flash photolysis studies where systems are far from equilibrium, such band coalescence involves a dynamic equilibria on a picosecond timescale.

There is considerable discussion[29a] about the detailed interpretation of such phenomena and in particular whether the modified Bloch equations can be applied. In collaboration with Grevels, we have carefully examined the IR band profiles in liquid rare gas solvents of ^{13}CO substituted diene

molecules and obtained clear evidence of picosecond behaviour.[32] It is possible, particularly when the equations are cast in density matrix form, to draw close analogies between the IR and NMR behaviour. It is our view that careful temperature-dependent IR band analysis, combined with appropriate theoretical analysis, will provide subtle information on very fast dynamics of interest to many transition metal systems. Moreover the experiments are much cheaper than those involving sophisticated laser mixing!

Acknowledgements—We are grateful to many colleagues at Nottingham for help and advice and to SERC, EEC, the Paul Instrument Fund of the Royal Society and the Petroleum Research Fund of the ACS for financial support.

REFERENCES

1. J. K. Burdett, R. N. Perutz, M. Poliakoff and J. J. Turner, *Pure Appl. Chem.* 1977, **49**, 271; J. K. Burdett, *Coord. Chem. Rev.* 1978, **27**, 1; M. S. Wrighton, J. L. Graff, R. J. Kazlauskas, J. C. Michener and C. L. Reichel, *Pure Appl. Chem.* 1982, **54**, 161; R. B. Hitam, K. A. Mahmoud and A. J. Rest, *Coord. Chem. Rev.* 1984, **55**, 1.
2. S. Firth, W. E. Klotzbuecher, M. Poliakoff and J. J. Turner, *Inorg. Chem.* 1987, **26**, 3370.
3. For a detailed description of the use of polarized photochemistry/matrix isolation see M. S. Baird, I. R. Dunkin, N. Hacker, M. Poliakoff and J. J. Turner, *J. Am. Chem. Soc.* 1981, **103**, 5190; also J. Michl and E. W. Thulstrup, *Accts Chem. Res.* 1987, **20**, 192.
4. J. K. Burdett, R. N. Perutz, M. Poliakoff and J. J. Turner, *J. Chem. Soc., Chem. Commun.* 1975, 157; J. K. Burdett, J. M. Grzybowski, R. N. Perutz, M. Poliakoff, J. J. Turner and R. F. Turner, *Inorg. Chem.* 1978, **17**, 147.
5. L. Wang, X. Zhu and K. G. Spears, *J. Am. Chem. Soc.* 1988, **110**, 8695.
6. J. J. Turner, M. Poliakoff and M. A. Healy, *Pure Appl. Chem.* 1989, **61**, 787.
7. I. R. Dunkin, P. Harter and C. S. Shields, *J. Am. Chem. Soc.* 1984, **106**, 7248.
8. A. J. Dixon, S. Firth, A. Haynes, M. Poliakoff, J. J. Turner and N. M. Boag, *J. Chem. Soc., Dalton Trans.* 1988, 1501.
9. K. R. Pope and M. S. Wrighton, *J. Am. Chem. Soc.* 1987, **109**, 4545.
10. J. J. Turner, M. Poliakoff and M. B. Simpson, *J. Molec. Struct.* 1984, **113**, 359.
11. G. E. Gadd, R. K. Upmacis, M. Poliakoff and J. J. Turner, *J. Am. Chem. Soc.* 1986, **108**, 2547.
12. S. A. Jackson, P. M. Hodges, M. Poliakoff, J. J. Turner and F.-W. Grevels, to be published.
13. M. Poliakoff, S. M. Howdle, M. A. Healy and J. M. Whalley, Proc. Int. Symp. Supercrit. Fluids (Edited by M. Perrut), *Chim. Soc. Fr.* 1988, 967.
14. (a) For some relevant references see: M. Poliakoff and E. Weitz, *Adv. Organomet. Chem.* 1986, **25**, 277; (b) chapters in *High Energy Processes in Organometallic Chemistry* (Edited by K. Suslick), ACS Symposium Series 333 (1987), by: T. Seder, A. Ouderkirk, S. P. Church and E. Weutz, p. 81; T. R. Fletcher and R. N. Rosenfeld, p. 99; J. J. Turner, M. A. Healy and M. Poliakoff, p. 110.
15. K. C. Herr and G. C. Pimentel, *Appl. Opt.* 1965, **4**, 25.
16. F. Siebert, W. Mantele and W. Kreutz, *Biophys. Struct. Mech.* 1980, **6**, 139.
17. H. Hermann, F.-W. Grevels, A. Henne and K. Schaffner, *J. Phys. Chem.* 1982, **86**, 5151; and many later papers, e.g. S. P. Church, F.-W. Grevels, H. Hermann and K. Schaffner, *J. Chem. Soc., Chem. Commun.* 1985, 30.
18. K. Iwata, C. Kato and H-o. Hamaguchi, *Appl. Spectrosc.*, in press.
19. A. J. Dixon, P. Glyn, M. A. Healy, P. M. Hodges, T. Jenkins, M. Poliakoff and J. J. Turner, *Spectrochim. Acta* 1988, **44A**, 1309.
20. B. S. Creaven, A. J. Dixon, J. M. Kelly, C. Long and M. Poliakoff, *Organometallics* 1987, **6**, 2600.
21. A. A. Garrison, R. A. Crocombe, G. Mamantov and J. A. deHaseth, *Appl. Spectrosc.* 1980, **34**, 399.
22. (a) W. M. Grim, J. A. Graham, R. M. Hammaker and W. G. Fateley, *International Laboratory* 1984, **April**, 67; S. E. Mollis, W. J. MacKnight and S. L. Hsu, *Appl. Spectrosc.* 1984, **38**, 529; (b) H. Toriumi, H. Sugisawa and H. Watanabe, *Jap. J. Appl. Phys.* 1988, **27**, L935.
23. B. D. Moore, M. Poliakoff, M. B. Simpson and J. J. Turner, *J. Phys. Chem.* 1985, **89**, 850.
24. R. E. Murphy, F. H. Cook and H. Sakai, *J. Opt. Soc. Am.* 1975, **65**, 600.
25. F. Siebert, private communication.
26. J. N. Moore, P. A. Hansen and R. M. Hochstrasser, *Chem. Phys. Lett.* 1987, **138**, 110; *Proc. Natl. Acad. Sci. U.S.A.* 1988, **85**, 5062.
27. J. D. Simon and X. Xie, *J. Phys. Chem.* 1987, **91**, 5538 and refs therein.
28. L. M. Jackman and F. A. Cotton (Eds), *Dynamic Nuclear Magnetic Resonance Spectroscopy*. Academic Press, New York (1975).
29. For some useful reference see (a) R. A. MacPhail and H. L. Strauss, *J. Chem. Phys.* 1985, **82**, 1156; (b) J. J. Turner, M. Poliakoff, S. M. Howdle, S. A. Jackson and J. G. McLaughlin, *Faraday Discuss. Chem. Soc.* 1988, 84.
30. B. Cohen and S. Weiss, *J. Phys. Chem.* 1983, **87**, 3606.
31. F.-W. Grevels, J. Jacke, W. Klotzbuecher, C. Krueger, K. Seevogel and Y.-H. Tsay, *Angew. Chem. Int. Edn Engl.* 1987, **26**, 885; F.-W. Grevels, J. Jacke and K. Seevogel, *J. Molec. Struct.* 1988, **174**, 107.
32. F.-W. Grevels, S. M. Howdle and J. J. Turner, in preparation.

Polyhedron Vol. 8, No. 13/14, pp. 1641–1648, 1989
Printed in Great Britain

0277-5387/89 $3.00+.00
© 1989 Maxwell Pergamon Macmillan plc

BIS(η-ARENE) COMPLEXES OF THE EARLY TRANSITION METALS DERIVED FROM THE 1,3,5-TRI-*t*-BUTYLBENZENE LIGAND

F. GEOFFREY N. CLOKE,* KERRY A. E. COURTNEY, AUSAMA A. SAMEH and ANTHONY C. SWAIN

School of Chemistry and Molecular Sciences, University of Sussex, Brighton BN1 9QJ, U.K.

Abstract—Co-condensation of yttrium, titanium, zirconium, hafnium, niobium, chromium, molybdenum or tungsten atoms with the bulky arene 1,3,5-tri-*t*-butylbenzene, affords the homoleptic sandwich compounds $[M(\eta\text{-}^tBu_3C_6H_3)_2]$, where M = Y, Ti, Zr, Hf, Nb, Cr, or W; in the case of chromium, the reaction also yields the triple-decker sandwich compound $[Cr_2(\eta\text{-}^tBu_3C_6H_3)_2(\mu\text{-}\eta:\eta\text{-}^tBu_3C_6H_3)]$. $[Hf(\eta\text{-}^tBu_3C_6H_3)_2]$ reacts irreversibly with carbon monoxide to give the stable 18-electron carbonyl adduct $[Hf(\eta\text{-}^tBu_3C_6H_3)_2(CO)]$, whereas $[Zr(\eta\text{-}^tBu_3C_6H_3)_2(CO)]$ is unstable in the absence of excess carbon monoxide. Oxidation of $[Nb(\eta\text{-}^tBu_3C_6H_3)_2]$ with silver tetrafluoroborate affords the stable 16-electron cation $[\{Nb(\eta\text{-}^tBu_3C_6H_3)_2\}\{BF_4\}]$.

Starting with its application for the preparation of bis(η-arene)chromium complexes,[1] metal vapour synthesis has developed into a powerful technique for the synthesis of a wide range of homoleptic bis(η-arene)metal complexes, particularly those of the early transition metals where conventional methods have thus far been unsuccessful (Ti, Nb, Ta) or not proved synthetically useful (W).[2] To date however, the homoleptic 16-electron bis(η-arene) complexes of zirconium and hafnium, assumed to be present at low temperature during the co-condensation experiment, have only been isolated as their 18-electron trimethylphosphine adducts $[M(\eta\text{-arene})_2(PMe_3)]$ (M = Zr, Hf),[3] and there has been no definitive evidence for the existence of the analogous 15-electron bis(η-arene)yttrium complex. We were interested to see whether it would be possible to stabilize the electron deficient homoleptic bis(η-arene) complexes of yttrium, zirconium and hafnium by the use of an appropriately bulky arene ligand. Such a strategy has considerable precedent in the use of sterically demanding pentamethylcyclopentadienyl[4,5] and tertiary phosphine[6,7] ligands to stabilize coordinatively unsaturated complexes. We chose 1,3,5-tri-*t*-butylbenzene as the arene ligand because of its high symmetry and size, but also because the combined inductive effect of the *t*-butyl substituents was anticipated to lead to an increase in the metal–arene bond strength. We also felt it possible that such an arene ligand might lead to unusual modifications in the chemistry of other η-arene complexes. Parts of this work have been briefly communicated.[8,9]

EXPERIMENTAL

All manipulations were carried out on a conventional vacuum line using standard Schlenk techniques or in a dry box, under an atmosphere of argon or dinitrogen, and all glassware was flame-dried under vacuum before use. Celite 545 filter aid was dried under vacuum at 300°C. The general design of the metal vapour synthesis apparatus has been described elsewhere.[2] Solvents were dried and purified by prolonged reflux over a suitable drying agent followed by distillation under an atmosphere of dinitrogen. NMR solvents were stored in ampoules containing a freshly prepared potassium mirror under an atmosphere of dinitrogen. Nujol for FAB–mass spectrometry was thoroughly deoxygenated and dried over activated molecular sieves (4 Å). Carbon monoxide was purified by passage through a column containing BASF catalyst and activated molecular sieves (4 Å). Metal samples were vacuum melted in a separate operation prior to their use in the co-condensation experiments

* Author to whom correspondence should be addressed.

(except for chomium, which sublimes under vacuum). 1,3,5-Tri-*t*-butylbenzene was prepared by the literature procedure.[10] NMR spectra were recorded on Bruker WM360 or WP 80 instruments at probe temperature unless otherwise stated, and calibrated by reference to the residual proton chemical shift of the deuterated solvent. ESR spectra were recorded on a Bruker ESP 300 instrument at York and solid-state magnetic susceptibility measurements were made on a SHE905 SQUID magnetometer at Berkeley. IR spectra were recorded on a Perkin–Elmer 1720 FT instrument. Mass spectra were obtaind using the fast atom bombardment (FAB–MS) technique on an MS80RF instrument equipped with a dedicated Kratos ion source and Ion Tech atom gun, using a Nujol matrix, and xenon as the bombarding gas. Microanalyses were performed by Butterworth Laboratories Ltd, London.

Preparation of bis(η-1,3,5-tri-t-butylbenzene)yttrium (1)

Electron beam vapourized yttrium (0.90 g, 10 mmol; power input 400 W) was co-condensed with an excess of 1,3,5-tri-*t*-butylbenzene (25 g, 100 mmol) at 77 K over a 2 h period. After warm-up to room temperature under dinitrogen, the product was extracted from the reactor with *n*-hexane (750 cm^3) and the resultant deep purple solution filtered through a bed of Celite on a frit. The solvent was removed under reduced pressure and excess 1,3,5-tri-*t*-butylbenzene removed by sublimation at 60°C/10^{-4} mbar. The residue was extracted with *n*-pentane (150 cm^3) and the resultant solution again filtered through Celite. Concentration of the solution under reduced pressure and cooling to −30°C afforded deep purple crystals of $[Y(\eta\text{-}^tBu_3C_6H_3)_2]$, which were collected, washed with *n*-pentane (2 × 10 cm^3) at −80°C and dried *in vacuo*. Yield: *ca* 40% based on yttrium (Microanalysis (%) Found: C, 74.41; H, 10.58. Required: C, 74.32; H, 10.40. Mass spectrum: *M/e* 581 [P^+]).

Preparation of bis(η-1,3,5-tri-t-butylbenzene) titanium (2)

Electron beam vapourized titanium (0.35 g, 7 mmol; power input 500 W) was co-condensed with an excess of 1,3,5-tri-*t*-butylbenzene (25 g, 100 mmol) at 77 K over a 2 h period. Identical work-up to **1** above afforded deep red crystals of $[Ti(\eta\text{-}^tBu_3C_6H_3)_2]$ in *ca* 50% yield based on titanium (Microanalysis (%) Found: C, 79.80; H, 10.96. Required: C, 79.90; H, 11.18). ^1H NMR (C_6D_6): δ 5.04 [6H, s, $^tBu_3C_6H_3$], 1.48 [54H, s, $^tBu_3C_6H_3$]. $^{13}C\{^1H\}$ (C_6D_6): δ 111.14 [*ring C*], 7.76 [*ring* CH], 36.27 [$C(CH_3)_3$], 33.07 [$C(CH_3)_3$].

Preparation of bis(η-1,3,5-tri-t-butylbenzene) zirconium (3)

Electron beam vapourized zirconium (0.36 g, 4 mmol; power input 1800 W) was co-condensed with an excess of 1,3,5-tri-*t*-butylbenzene (30 g, 120 mmol) at 77 K over a 3 h period. Identical work-up to **1** above afforded deep green crystals of $[Zr(\eta\text{-}^tBu_3C_6H_3)_2]$ in *ca* 40% yield based on zirconium (Microanalysis (%) Found: C, 74.02; H, 10.32. Required: C, 74.03; H, 10.35. Mass spectrum: *M/e* 582 [P^+]). ^1H NMR (C_6D_6): δ 5.34 [6H, s, $^tBu_3C_6H_3$], 1.33 [54H, s, $^tBu_3C_6H_3$]. $^{13}C\{^1H\}$ (C_6D_6): δ 111.19 [*ring C*], 80.28 [*ring* CH], 35.16 [$C(CH_3)_3$], 32.79 [$C(CH_3)_3$].

Preparation of bis(η-1,3,5-tri-t-butylbenzene) hafnium (4)

Electron beam vapourized hafnium (4.56 g, 25 mmol; power input 2200 W) was co-condensed with an excess of 1,3,5-tri-*t*-butylbenzene (80 g, 325 mmol) at 77 K over a 3 h period. Identical work-up to **1** above afforded purple crystals of $[Hf(\eta\text{-}^tBu_3C_6H_3)_2]$ in *ca* 40% yield based on hafnium (Microanalysis (%) Found: C, 64.15; H, 9.28. Required: C, 64.40; H, 9.00. Mass spectrum: *M/e* 672 [P^+]). ^1H NMR (C_6D_6): δ 5.15 [6H, s, $^tBu_3C_6H_3$], 1.34 [54H, s, $^tBu_3C_6H_3$]. $^{13}C\{^1H\}$ (C_6D_6): δ 107.49 [*ring C*], 76.80 [*ring* CH], 35.57 [$C(CH_3)_3$], 33.39 [$C(CH_3)_3$].

Preparation of bis(η-1,3,5-tri-t-butylbenzene) hafnium(carbonyl) (5)

A solution of $[Hf(\eta\text{-}^tBu_3C_6H_3)_2]$ (200 mg, 0.25 mmol) in *n*-pentane (50 cm^3) was exposed to 1 atm of carbon monoxide for 5 min. The solution was filtered, and concentration under reduced pressure and cooling to −30°C afforded deep green crystals of $[Hf(\eta\text{-}^tBu_3C_6H_3)_2(CO)]$ which were collected, washed with *n*-pentane (2 × 10 cm^3) at −80°C and dried *in vacuo*. Yield: *ca* 80% (Microanalysis (%) Found: C, 62.92; H, 8.55. Required: C, 63.54; H, 8.65). IR (Nujol mull, NaCl plates): 1870 cm^{-1}, strong ν(CO). An identical procedure using ^{13}CO (90% ^{13}C enriched) afforded the ^{13}C labelled carbonyl complex. ^1H NMR (C_6D_6): δ 5.25 [6H, d, $^tBu_3C_6H_3$, J_{CH} 0.98 Hz], 1.47 [54H, s, $^tBu_3C_6H_3$]. $^{13}C\{^1H\}$ (C_6D_6): δ 239.91 [*CO*], 118.62 [*ring C*], 82.90 [*ring* CH], 35.46, [$C(CH_3)_3$], 31.89 [$C(CH_3)_3$]. ^{13}C (gated) (C_6D_6): 239.91 [m, *CO*, J_{CH} 0.98 Hz].

Characterization of bis(η-1,3,5-tri-t-butylbenzene) zirconium (carbonyl) (**6**)

To a 10 mm NMR tube equipped with a greaseless stopcock, was added a solution of [Zr(η-^{t}Bu$_3$C$_6$H$_3$)$_2$] (35 mg, 0.05 mmol) in d_8-toluene. Carbon monoxide (90% ^{13}C enriched) was added via a Toepler pump to a pressure of 1 atm at 77 K. The resultant green solution was allowed to warm to room temperature; ^{13}C{^{1}H} (C_7D_8): δ 234.00 [*C*O], 85.95 [*ring C*H], 31.97 [C(*C*H$_3$)$_3$]. The ^{1}H NMR spectrum was obtained similarly, employing a 5 mm NMR tube and natural abundance carbon monoxide; ^{1}H NMR (C_7D_8): δ 4.88 [6H, s, ^{t}Bu$_3$C$_6$*H*$_3$], 1.37 [54H, s, ^{t}*Bu*$_3$C$_6$H$_3$]. A solution of [Zr(η-^{t}Bu$_3$C$_6$H$_3$)$_2$] in *n*-pentane was exposed to 1 atm of natural abundance carbon monoxide at room temperature, and the resultant solution rapidly transferred to a solution IR cell (1 mm path, NaCl windows) under a carbon monoxide atmosphere; 1890 cm^{-1}, strong, ν(CO).

Preparation of bis(η-1,3,5-tri-t-butylbenzene) niobium (**7**)

Electron beam vapourized niobium (0.87 g, 10 mmol; power input 2000 W) was co-condensed with an excess of 1,3,5-tri-*t*-butylbenzene (80 g, 325 mmol) at 77 K over a 3 h period. Identical work-up to **1** above afforded purple–red crystals of [Nb(η-^{t}Bu$_3$C$_6$H$_3$)$_2$] in *ca* 40% yield based on niobium (Microanalysis (%) Found: C, 72.61; H, 10.49. Required: C, 73.81; H, 10.32. Mass spectrum: *M*/*e* 585 [P$^+$]). ESR (toluene, 25°C): g_{iso} 1.985, decet, A_{iso} 1.7 mT.

Preparation of bis(η-1,3,5-tri-t-butylbenzene) niobium tetrafluoroborate (**8**)

To a stirred solution of [Nb(η-^{t}Bu$_3$C$_6$H$_3$)$_2$] (180 mg, 0.30 mmol) in toluene (30 cm^3), was added a solution of [AgBF$_4$] (60 mg, 0.30 mmol) in toluene (50 cm^3) dropwise at −78°C. A metallic mirror rapidly appeared, and the reaction mixture was allowed to warm to room temperature over 30 min. The resultant red–brown precipitate was collected on a frit, washed with toluene and dried *in vacuo*. The solid on the frit was then extraced with dichloromethane and toluene was carefully layered on the resultant deep orange solution to afford golden orange crystals of [{Nb(η-^{t}Bu$_3$C$_6$H$_3$)$_2$}{BF$_4$}]. The crystals were collected, washed with *n*-pentane (2 × 10 cm^3) and dried under an argon stream. Yield: 80% (Microanalysis (%) Found: C, 62.68; H, 8.31. Required: C, 64.30; H, 8.99).

Reaction of chromium atoms with 1,3,5-tri-t-butylbenzene; preparation of bis(η-1,3,5-tri-t-butylbenzene)chromium (**9**) *and bis(η-1,3,5-tri-t-butylbenzene)(μ-η:η-1,3,5-tri-t-butylbenzene)dichromium* (**10**)

Electron beam vapourized chromium (3.0 g, 50 mmol; power input 400 W) was co-condensed with an excess of 1,3,5-tri-*t*-butylbenzene (80 g, 325 mmol) at 77 K over a 3 h period. Identical work-up to **1** above afforded an orange–green, crystalline product, an approximately equimolar mixture of [Cr(η-^{t}Bu$_3$C$_6$H$_3$)$_2$] and [Cr$_2$(η-^{t}Bu$_3$C$_6$H$_3$)$_2$(μ-η:η-^{t}Bu$_3$C$_6$H$_3$)] in a total *ca* 30% yield based on chromium (Mass spectrum: *M*/*e* 544 [P$^+$] for **9**, 596 [P − 246$^+$] for **10**). Compound **9**, ^{1}H NMR (C_6D_6): δ 4.65 [6H, s, ^{t}Bu$_3$C$_6$*H*$_3$], 1.43 [54H, s, ^{t}Bu$_3$C$_6$H$_3$]; ^{13}C{^{1}H} (C_6D_6): δ 102.20 [*ring C*], 69.13 [*ring C*H], 34.84 [*C*(CH$_3$)$_3$], 33.08 [C(*C*H$_3$)$_3$]. Compound **10**, ^{1}H NMR (C_6D_6): δ 4.71 [3H, s, ^{t}Bu$_3$C$_6$*H*$_3$], 4.43 [6H, s, ^{t}Bu$_3$C$_6$*H*$_3$], 1.29 [27H, s, ^{t}*Bu*$_3$C$_6$H$_3$], 1.26 [54H, s, ^{t}*Bu*$_3$C$_6$H$_3$]; ^{13}C{^{1}H} (C_6D_6): δ 73.43 [outer *ring* C*H*], 70.60 [inner *ring* C*H*], 32.49 and 32.08 [C(*C*H$_3$)$_3$].

Chromatography of a mixture of **9** and **10** on deactivated alumina (4% w/w H_2O, *n*-hexane eluant) yielded a single red band which afforded orange crystals of pure **9** on removal of the solvent *in vacuo*.

Preparation of bis(η-1,3,5-tri-t-butylbenzene) molybdenum (**11**)

Electron beam vapourized molybdenum (0.46 g, 5 mmol; power input 800 W) was co-condensed with an excess of 1,3,5-tri-*t*-butylbenzene (30 g, 120 mmol) at 77 K over a 2½ h period. Identical work-up to **1** above afforded deep green–brown crystals of [Mo(η-^{t}Bu$_3$C$_6$H$_3$)$_2$] in *ca* 30% yield based on molybdenum (Mass spectrum: *M*/*e* 590 [P$^+$]). ^{1}H NMR (C_6D_6): δ 4.87 [6H, s, ^{t}Bu$_3$C$_6$*H*$_3$], 1.34 [54H, s, ^{t}*Bu*$_3$C$_6$H$_3$]. ^{13}C{^{1}H} (C_6D_6): δ 105.56 [*ring C*], 72.88 [*ring C*H], 34.65 [*C*(CH$_3$)$_3$], 32.87 [C(*C*H$_3$)$_3$].

Preparation of bis(η-1,3,5-tri-t-butylbenzene) tungsten (**12**)

Electron beam vapourized tungsten (0.54 g, 3 mmol; power input 1600 W) was co-condensed with an excess of 1,3,5-tri-*t*-butylbenzene (30 g, 120 mmol) at 77 K over a 2½ h period. The work-up was identical to **1** above up to the stage at which all the excess ligand had been removed. Chromatography on deactivated alumina (4% w/w H_2O, *n*-hexane eluant) yielded a single orange band, which on removal of the solvent *in vacuo* afforded orange

crystals of $[W(\eta\text{-}^t Bu_3C_6H_3)_2]$ in *ca* 20% yield based on tungsten (Mass spectrum: *M/e* 676 [P^+]). ^1H NMR (C_6D_6): δ 5.18 [6H, s, $^tBu_3C_6H_3$], 1.33 [54H, s, $^tBu_3C_6H_3$].

RESULTS AND DISCUSSION

The known organometallic chemistry of yttrium is confined to the +3 oxidation state, there being no reported examples of stable unambiguous lower oxidation state complexes of this element. Recently we reported the synthesis of the *formally* yttrium(0) complex [Y('Bu—DAB)$_3$][11] ('Bu—DAB = 'Bu—N=CH—CH=N—'Bu), although the absence of coupling to yttrium (^{89}Y, 100%, $I = \frac{1}{2}$) in the ESR spectrum of the latter strongly suggests that the bulk of the electron density lies in ligand based orbitals. 'Bu—DAB is known to form the stable radical anion 'Bu—DAB$^-$, so that this compound might be best realistically classified as a complex of yttrium(III).

The co-condensation of yttrium atoms with toluene or mesitylene results in deep purple matrices at 77 K, but the colour (presumably due to the formation of a bis(η-arene) complex) is rapidly discharged on warm-up.[12] However, the reaction between yttrium atoms and the bulky 1,3,5-tri-*t*-butylbenzene ligand afforded a thermally stable product, and work-up yielded deep purple crystals of $[Y(\eta\text{-}^t Bu_3C_6H_3)_2]$ (**1**). Compound **1** is highly soluble in hydrocarbon solvents, thermally stable up to 100°C and may be sublimed at 80°C/10^{-4} mbar with partial decomposition. Both the solutions and the solid are highly air-sensitive and must be handled with rigorous exclusion of oxygen and, in particular, water, but may be stored indefinitely under an argon atmosphere.

Compound **1** is paramagnetic with a value for μ_{eff} of 1.74 BM at room temperature in the solid state, but displays no ESR spectrum at room temperature in methylcyclohexane solution. However, cooling the solution to 77 K results in an ESR signal exhibiting coupling to ^{89}Y: $g_\parallel = 2.085$, doublet, $A = 3.0$ mT; $g_\perp = 2.005$. This is consistent with a 15-electron bis(η-arene) complex, predicted to have a ^2E (e_{2g}^3) ground state, in which the large g-value anisotropy would be expected to make an ESR signal hard to detect. The spin-only value for the magnetic moment arising from an unpaired electron in the e_{2g} orbitals presumably results from quenching of any orbital contribution to the magnetic moment by the ligand field. The previously reported X-ray crystallographic results[9] confirm that the molecule possesses the parallel-ring sandwich structure, so that **1** represents the first authentic example of an yttrium(0) complex.

The reaction between titanium atoms and 1,3,5-tri-*t*-butylbenzene gave good yields of deep red $[Ti(\eta\text{-}^t Bu_3C_6H_3)_2]$ (**2**). Compound **2** has similar spectroscopic (see Experimental) and physical properties to previously reported bis(η-arene) titanium complexes,[13] although is somewhat more thermally stable. Of more interest was the potential synthesis of the zirconium and hafnium analogues of **2**: the 16-electron homoleptic bis(η-arene) zirconium and -hafnium complexes are highly thermally unstable for simple arenes such as toluene, but may be trapped as their 18-electron trimethylphosphine adducts $[M(\eta\text{-}MeC_6H_5)_2(PMe_3)]$ (M = Zr, Hf).[3] In the latter, the trimethylphosphine ligand presumably serves not only to give the complex an 18-electron configuration, but also to sterically saturate the metal centre. It therefore was anticipated that the steric bulk and electronic properties of the 1,3,5-tri-*t*-butylbenzene ligand might stabilize the 16-electron bis(η-arene) complexes of these elements.

Co-condensation of zirconium or hafnium atoms with 1,3,5-tri-*t*-butylbenzene afforded deep green $[Zr(\eta\text{-}^t Bu_3C_6H_3)_2]$ (**3**) and purple $[Hf(\eta\text{-}^t Bu_3C_6H_3)_3]$ (**4**), respectively. Compounds **3** and **4** are diamagnetic, thermally stable up to 120°C, and highly air- and water-sensitive. NMR and other characterizing data are given in the Experimental.

It was of interest to see if the 16-electron compounds, **3** and **4**, would undergo simple ligand addition reactions to give 18-electron adducts, despite the bulk of the 1,3,5-tri-*t*-butylbenzene ligands. Treatment with trimethylphosphine gave no observable reaction by ^{31}P NMR (presumably for steric reasons), and reaction with trifluorophosphine led to rapid decomposition. However, exposure of a pentane solution of **4** to carbon monoxide resulted in a rapid irreversible colour change from purple to green, and deep green crystals of $[Hf(\eta\text{-}^t Bu_3C_6H_3)_2(CO)]$ (**5**) could be isolated from the solution in high yield. The carbonyl ligand in **5** is characterized by a low carbonyl stretch at 1870 cm^{-1}, associated with the high electron density on the hafnium(0) centre, and by a ^{13}C NMR resonance (in a sample prepared using ^{13}CO) at δ 240, which is a partially resolved septet in the gated spectrum due to coupling with the ring protons of the two $\eta\text{-}^t Bu_3C_6H_3$ ligands. In contrast, the reaction between CO and the zirconium analogue, **3**, was found to be reversible, so that green $[Zr(\eta\text{-}^t Bu_3C_6H_3)_2(CO)]$ (**6**) could only be characterized spectroscopically in solution in the presence of excess CO; *in vacuo*, the starting bis(η-arene) zirconium complex, **3**, was regenerated quantitatively. The carbonyl ligand in **6** is spectroscopically very similar to that in **5**, showing a

strong carbonyl stretch at 1890 cm^{-1} and a ^{13}C resonance at δ 234, although coupling to the ring protons in the latter was not resolved. The origin of the disparities in the colours of the homoleptic bis(η-arene) complexes, **3** and **4**, and in the relative stabilities of the carbonyl adducts, **5** and **6**, is not clear, but similar differences in the organometallic chemistry of zirconium and hafnium have been previously observed.[14]

Recently we reported on the oxidation of 17-electron bis(η-toluene)niobium: one-electron oxidation of the latter in the presence of a tertiary phosphine gives the stable 18-electron cation $[\{Nb(\eta\text{-}MeC_6H_5)_2(PR_3)\}^+]$, whereas in the absence of the tertiary phosphine the 16-electron $[\{Nb(\eta\text{-}MeC_6H_5)_2\}^+]$ cation is unisolable.[15] This parallels the chemistry of the isoelectronic, neutral $[Zr(\eta\text{-}MeC_6H_5)_2]$, which is also highly unstable, as discussed earlier. Given the stability of the 1,3,5-tri-*t*-butylbenzene derivative $[Zr(\eta\text{-}^tBu_3C_6H_3)_2]$ (**3**), we were encouraged to examine the oxidation of the niobium analogue of **3** in the absence of any additional two-electron ligands.

Red–purple $[Nb(\eta\text{-}^tBu_3C_6H_3)_2]$ (**7**) was obtained in good yield by the co-condensation of niobium atoms with 1,3,5-tri-*t*-butylbenzene. Compound **7** has similar spectroscopic (see Experimental) and physical properties to the bis(η-arene)niobium complexes derived from other arenes (i.e. benzene, toluene and mesitylene) which we reported previously.[16] Oxidation of **7** with one equivalent of silver tetrafluoroborate in toluene solvent at −78°C resulted in the rapid formation of a silver mirror, and orange, crystalline $[\{Nb(\eta\text{-}^tBu_3C_6H_3)_2\}\{BF_4\}]$ (**8**) could be isolated in high yield from dichloromethane–toluene. Compound **8** is very air-sensitive, but stable in dichloromethane solution; tetrahydrofuran (THF) solutions, however, rapidly decompose to regenerate the neutral bis(η-arene) compound, **7** and unidentified by-products (possibly due to ring opening of the THF). Compound **8** is paramagnetic with $\mu_{eff} = 2.2$ BM in solution (Evans' method[17]) at 0°C, but is ESR silent at room temperature; this is in accord with a 16-electron $[Nb(\eta\text{-}^tBu_3C_6H_3)_2]^+$ cation having two unpaired electrons and hence a triplet ground state. This is in marked contrast to the neutral isoelectronic 16-electron zirconium analogue, **3**, which is diamagnetic. Presumably, the positive charge on the niobium centre changes the orbital energies such that the $e_{2g}^3a_{1g}^1$ configuration in the cationic niobium complex is more stable than the e_{2g}^4 configuration in the neutral zirconium compound.

A wide range of bis(η-arene)chromium complexes have been prepared via metal vapour synthesis,[1] and the triple-decker sandwich compound bis(η-mesitylene)(μ-η:η-mesitylene)dichromium can also be obtained in low (2%) yield from the co-condensation of chromium atoms and mesitylene with high metal-to-ligand ratios.[18] The reaction between chromium atoms and 1,3,5-tri-*t*-butylbenzene afforded a green–orange crystalline product after work-up, which ^1H and ^{13}C NMR showed to be an approximately equimolar mixture of the simple sandwich compound $[Cr(\eta\text{-}^tBu_3C_6H_3)_2]$ (**9**), and the triple-decker complex $[Cr_2(\eta\text{-}^tBu_3C_6H_3)_2(\mu\text{-}\eta:\eta\text{-}^tBu_3C_6H_3)]$ (**10**). The ^{13}C NMR spectrum exhibits the characteristic upfield shift for the ring carbons of the bridging arene ligand in **10**, relative to those of the terminal arene ligands (see Experimental);[18] however, the ^1H NMR spectrum shows a corresponding *downfield* shift for the ring *protons*. The origin of this anomaly is not obvious, but may be due to the influence of the substituents—the *t*-butyl groups on the adjacent rings in **10** are almost certainly staggered (see Scheme 1), even in solution, and hence the ring protons of the bridging arene ligand are effectively sandwiched between them. The mass spectrum of the mixture showed strong patterns (with the appropriate chromium isotope distributions) centred at *M/e* 544 for the molecular ion of **9**, and

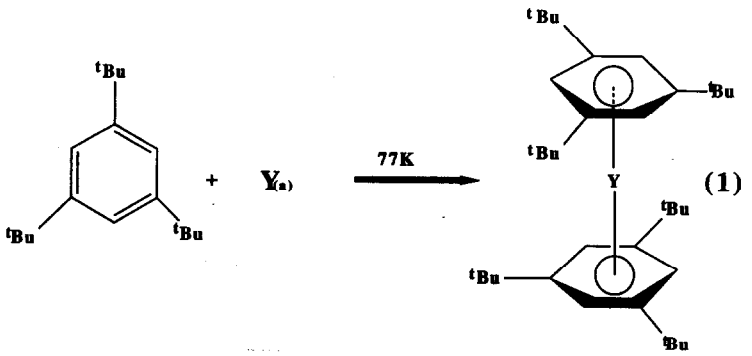

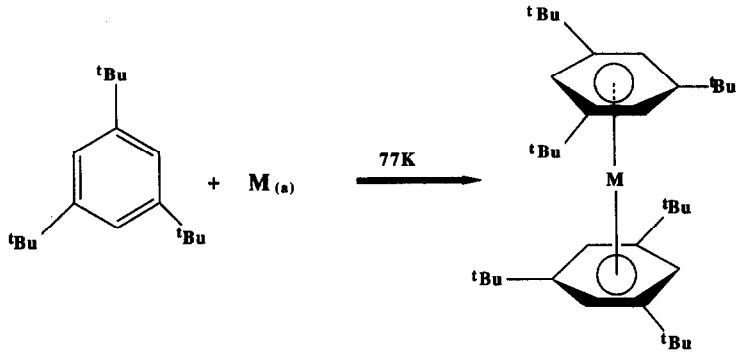

M = Ti, (2); Zr, (3); Hf, (4)

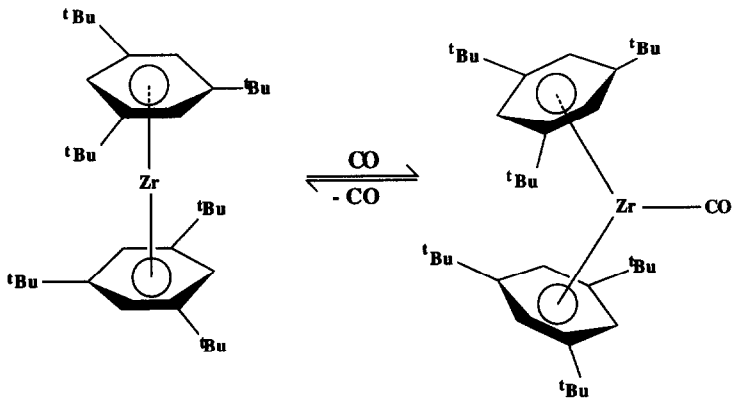

(5)

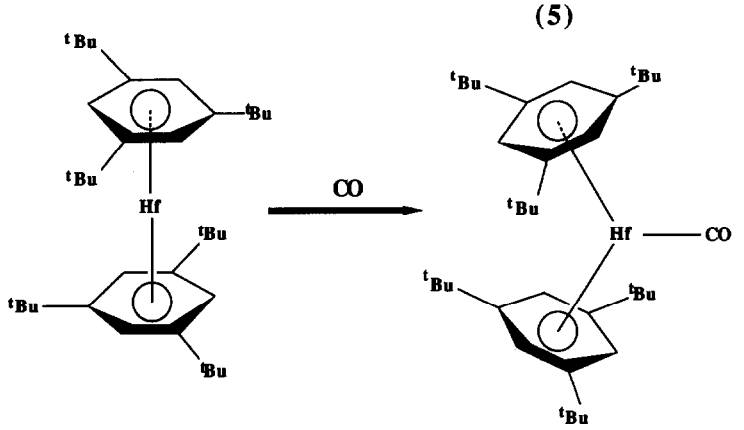

(6)

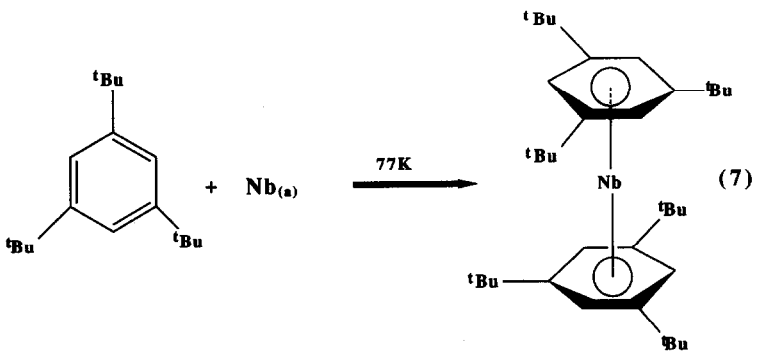

(7)

Scheme 1.

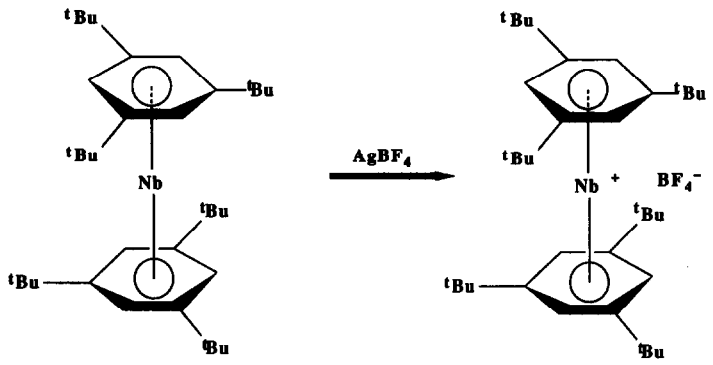

(8)

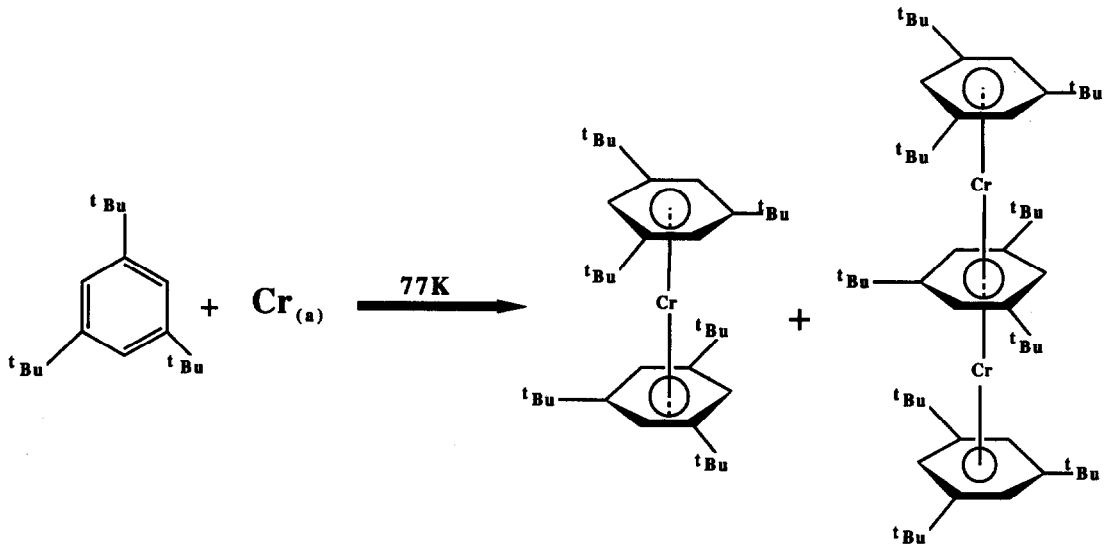

(9) (10)

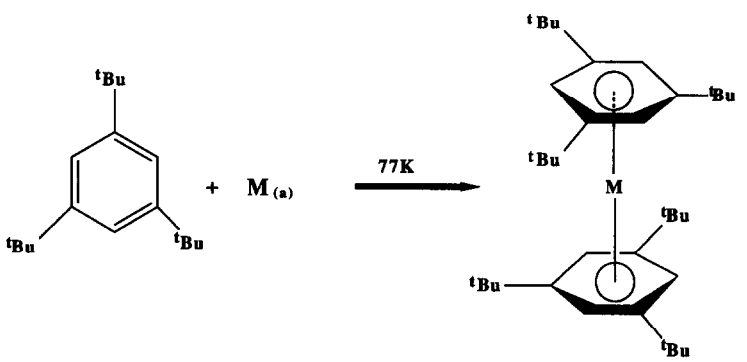

M = Mo, (11); W, (12);

Scheme 1 (*contd*).

at *M/e* 596, the latter ion corresponding to the loss of one arene ring from **10**. Attempts to separate **9** and **10** were unsuccessful; column chromatography on either Sephadex or deactivated alumina resulted in the decomposition of **10**, and only **9** could be eluted from the column; the similar solubilities and volatilities of **9** and **10** also precluded separation by fractional crystallization or sublimation.

The relatively high yield of the triple decker compound, **10**, may be a reflection of the ability of the 1,3,5-tri-*t*-butylbenzene ligand to effectively stabilize the mono(η-arene) fragment [Cr(η-^{t}Bu$_3$C$_6$H$_3$)], which is presumably an intermediate in the formation of **10**. Accordingly, we were encouraged to investigate the reactions of molybdenum and tungsten atoms with 1,3,5-tri-*t*-butylbenzene, there being no known examples of η-arene triple decker complexes of these elements.

The reaction of molybdenum atoms with 1,3,5-tri-*t*-butylbenzene yielded deep green–brown [Mo(η-^{t}Bu$_3$C$_6$H$_3$)$_2$] (**11**) after work-up, there being no evidence for any other (η-arene)molybdenum species by NMR. However, the mass spectrum of the product showed, in addition to the molecular ion of **11**, a very weak pattern corresponding to the ion [Mo$_2$(^{t}Bu$_3$C$_6$H$_3$)$_2^+$]. The latter may arise from trace amounts of the molybdenum analogue of **10**, although its presence as a result of ion recombination reactions in the mass spectrometer cannot be ruled out. The reaction between tungsten atoms and 1,3,5-tri-*t*-butylbenzene gave orange [W(η-^{t}Bu$_3$C$_6$H$_3$)$_2$] (**12**) as the sole product, both by NMR and mass spectrometry. Whether the failure to isolate either molybdenum or tungsten analogues of **10** is due to their intrinsic kinetic/thermodynamic instability and consequent decomposition during matrix warm-up or work-up, or that such species are not formed at all during the co-condensation experiment is not clear, but the former seems more likely.

The results described here (and summarized in Scheme 1) demonstrate the unique ability of the 1,3,5-tri-*t*-butylbenzene ligand to electronically stabilize unsaturated bis(η-arene) complexes of the electropositive early transition metals, and further studies in this area are in progress.

Acknowledgements—We thank SERC for equipment support and a studentship (to A.C.S.), and the Iraqi government for a scholarship (to A.A.S.). We are grateful to Dr R. N. Perutz (York) for recording the ESR spectra, and Dr N. Edelstein (Berkeley) for the solid-state magnetic moment determination. We wish also to thank Dr G. A. Lawless for experimental assistance, and Professor M. F. Lappert for useful discussions.

REFERENCES

1. P. L. Timms, *Adv. Inorg. Radiochem.* 1972, **14**, 121.
2. F. G. N. Cloke and M. L. H. Green, *J. Chem. Soc., Dalton Trans* 1981, 1938.
3. F. G. N. Cloke and M. L. H. Green, *J. Chem. Soc., Chem. Commun.* 1979, 127.
4. F. G. N. Cloke and J. P. Day, *J. Chem. Soc., Chem. Commun.* 1985, 967.
5. J. E. Bercaw, *J. Am. Chem. Soc.* 1974, **96**, 5087.
6. S. Otsuka, *J. Organomet. Chem.* 1980, **200**, 191.
7. B. L. Shaw, *J. Organomet. Chem.* 1980, **200**, 307.
8. F. G. N. Cloke, M. F. Lappert, G. A. Lawless and A. C. Swain, *J. Chem. Soc., Chem. Commun.* 1987, 1667.
9. J. G. Brennan F. G. N. Cloke, A. A. Sameh and A. Zalkin, *J. Chem. Soc., Chem. Commun.* 1987, 1668.
10. S. R. Ditto, *J. Org. Chem.* 1979, **44**, 894.
11. F. G. N. Cloke, H. C. de Lemos and A. A. Sameh, *J. Chem. Soc., Chem. Commun.* 1986, 1344.
12. F. G. N. Cloke and A. A. Sameh, unpublished observations.
13. M. T. Anthony, M. L. H. Green and D. Young, *J. Chem. Soc., Dalton Trans.* 1975, 1419.
14. D. J. Cardin, M. F. Lappert and C. L. Raston, *Chemistry of Organo-zirconium and -hafnium Compounds.* Ellis Horwood, Chichester (1986).
15. J. Bandy, F. G. N. Cloke, H. C. de Lemos, C. K. Prout and J. M. Wallis, *J. Chem. Soc., Dalton Trans.* 1988, 1475.
16. F. G. N. Cloke, M. L. H. Green and D. H. Price, *J. Chem. Soc., Chem. Commun.* 1978, 431.
17. D. F. Evans, *J. Chem. Soc.* 1959, 2005.
18. W. Lamanna, *J. Am. Chem. Soc.* 1986, **108**, 2097.

Polyhedron Vol. 8, No. 13/14, pp. 1649–1652, 1989
Printed in Great Britain

0277–5387/89 $3.00+.00
© 1989 Maxwell Pergamon Macmillan plc

CHARACTERIZATION OF MOLYBDENUM AND VANADIUM CENTRES IN ENZYMES BY X-RAY ABSORPTION SPECTROSCOPY

C. DAVID GARNER,* JUDITH M. ARBER and IAN HARVEY

Chemistry Department, Manchester University, Manchester M13 9PL, U.K.

and

S. SAMAR HASNAIN

The Daresbury Laboratory, Daresbury, Warrington WA4 4AD, U.K.

and

ROBERT R. EADY and BARRY E. SMITH

AFRC, IPSR Nitrogen Fixation Laboratory, University of Sussex, Brighton BN1 9PQ, U.K.

and

EIZE de BOER and RON WEVER

Laboratory of Biochemistry, University of Amsterdam, 1000 HD Amsterdam, The Netherlands

Abstract—Metal K-edge EXAFS studies have provided the only structural evidence so far available for the molybdenum and vanadium centres in enzymes. This paper describes the results of vanadium and iron K-edge EXAFS on the iron–molybdenum and iron–vanadium cofactors of the nitrogenase enzymes for *Klebsiella pneumoniae* and *Azotobacter chroococcum*, respectively, and the vanadium K-edge EXAFS of the bromoperoxidase from *Ascophyllum nodosum*. These and other results suggest that molybdenum and vanadium sites in enzymes may be classified in a similar manner: (a) as part of an Fe_3MS_4 (M = Mo, V) cubane-like cluster which forms a sub-unit of the cofactor of the nitrogenases; (b) bound to one (or more) oxo groups plus sulphur (in the case of molybdenum) or oxygen/nitrogen (in the case of vanadium) ligands to form a catalytic centre for oxygen atom transfer.

Both molybdenum and vanadium are clearly recognized as being essential for the activity of particular enzymes.[1–8] The classification of molybdenum-containing enzymes is clear, to the extent that the nitrogenases are distinct from the oxomolybdo enzymes, not least in respect of the chemical environment of the molybdenum. Thus, the MoFe-protein of the nitrogenases contains an iron–molybdenum cofactor (FeMoco), of approximate composition[9] $MoFe_6S_8$, and oxomolybdo enzymes (such as xanthine oxidase, aldehyde oxidase, sulphite oxidase and nitrate reductase) contain a common molybdenum cofactor (Moco), in which molybdenum is complexed by an organic component known as the molybdopterin (**1**).[10] There is much evidence to support the view that the molybdenum-containing cofactor constitutes the catalytic centre of the corresponding enzyme.

Vanadium is now clearly recognized as an essen-

*Author to whom correspondence should be addressed.

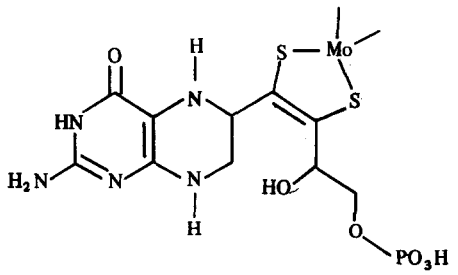

1

tial element for two classes of enzymes. EPR and MCD studies[11] on the VFe-proteins of vanadium nitrogenases indicate that these proteins contain similar redox centres to those of the MoFe-proteins of the molybdenum nitrogenases and a vanadium- and iron-containing cofactor (FeVaco), corresponding to FeMoco, has been extracted from the VFe-protein of *Azotobacter chroococcum*.[12] Also, bromoperoxidases from some marine algae, such as *Ascophyllum nodosum* have been shown to involve vanadium at the catalytically active site.[6-8]

X-ray absorption spectroscopy (XAS), and especially the extended X-ray absorption fine structure (EXAFS) associated with metal absorption edges, has proved to be a powerful and versatile probe of metal centres in proteins.[13] This technique has been widely applied to characterize the molybdenum centres in enzymes and has served to provide chemical details concerning these centres.[2] This paper describes results of XAS studies of vanadium in both nitrogenase and bromoperoxidase, and compares the information obtained to that provided by corresponding studies for molybdenum centres in enzymes.

EXPERIMENTAL

Samples of thionine-oxidized, super-reduced (during enzyme turnover) and dithionite-reduced forms of the VFe-protein of nitrogenase from *A. chroococcum* were prepared and manipulated as described elsewhere.[14,15] Vanadium K-edge XAS were recorded in the fluorescence mode on station 7C at the Photon Factory (Tsukuba-gun, Japan) operating at 2.5 GeV and an average current of 200 mA; *ca* 10 scans were recorded and averaged for each sample. A sagittal focusing, double crystal silicon(111) monochromator was used together with a 200 mm long fused quartz mirror placed at an angle of *ca* 8 mrad to reduce harmonic contamination. Samples were maintained at *ca* 80 K during investigation.

Samples of reduced and native bromoperoxidase from *A. nodosum*, purified as described previously,[7] were studied as the native enzyme, the native enzyme in the presence of hydrogen peroxide, and potassium bromide, and sodium dithionite.[16] XAS were recorded in the fluorescence mode on station 8.1 at the Daresbury Synchrotron Radiation Source operating at 2 GeV and an average current of 130 mA. A slit-less double crystal silicon(111) monochromator was employed, thus minimizing harmonic contamination. Crystal glitches limited the data range to approximately 400 eV beyond the edge. Samples were maintained at *ca* 80 K during data collection. For each bromoperoxidase sample *ca* 15 scans were averaged.

Vanadium K-edge XAS were also collected for a number of compounds considered relevant to these enzyme environments. These data were collected at room temperature in the transmission mode and a single scan was considered sufficient.

Data analysis was accomplished via the curved-wave method for EXAFS calculation and phase-shifts derived from *ab initio* calculations.[17]

RESULTS AND DISCUSSION

The vanadium K-edge XAS studies accomplished for the VFe-protein of *A. chroococcum* nitrogenase and in the bromoperoxidase of *A. nodosum* clearly demonstrate that the vanadium is in a distinctly different chemical environment in the two systems. The difference is clearly apparent from a comparison of Figs 1 and 2, which show the profile of the vanadium K-absorption edge and XANES for the thionine-oxidized and dithionite-reduced VFe-protein, and dithionite-reduced and native bromoperoxidase. This spectral region is very sensitive to the oxidation state of vanadium and its chemical environment.[18]

For the VFe-protein, the vanadium centre changes little as the oxidation level of the protein

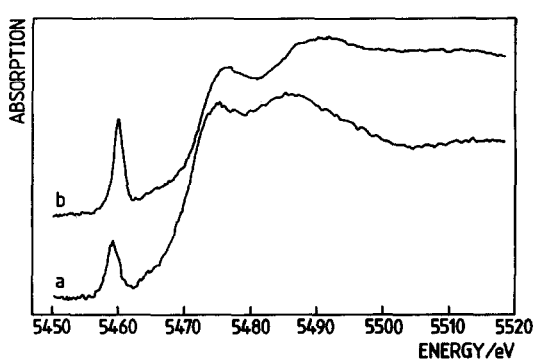

Fig. 1. Vanadium K-edge and XANES of (a) dithionite-reduced and (b) native bromoperoxidase of *Ascophyllum nodosum*.

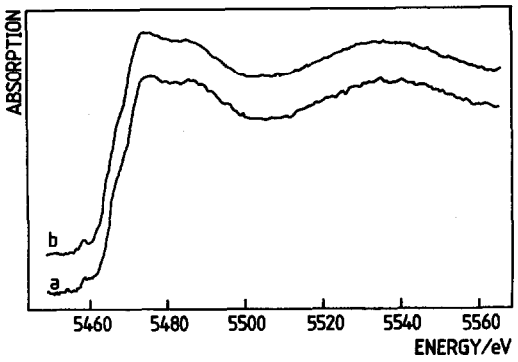

Fig. 2. Vanadium K-edge and XANES of (a) thionine-oxidized and (b) dithionite-reduced VFe-protein of *Azotobacter chroococcum*.

is altered, even when the comparison in Fig. 2 is extended to indicate the super-reduced form of the VFe-protein. The positions of the pre-edge feature (5459 eV) and the edge (5466 eV) indicate an oxidation state of between vanadium(II) and vanadium(IV), and the very weak pre-edge feature implies "octahedral" coordination at the vanadium. Both of these conclusions are consistent with the great similarity of the profiles in Fig. 2 to that recorded[14] for vanadium in $[NMe_4][VFe_3S_4Cl_3(DMF)_3]$.[19]

The comparison provided by Fig. 1 shows that the vanadium environment changes between the dithionite-reduced and native forms of bromoperoxidase, however, in each case the distinct pre-edge feature is typical of compounds with an oxo-vanadium (VO) group. EPR studies[7,20] clearly indicate the presence of vanadium(IV) in dithionite-reduced bromoperoxidase and ^{51}V NMR studies[21] are consistent with the presence of vanadium(V) in the native enzyme. The respective positions of the pre-edge feature (5459 and 5460 eV) and the edge (5469 and 5472 eV) of Fig. 1 are consistent with the assignment of oxidation states by magnetic resonance. Our XAS studies suggest very little change in the vanadium environment upon addition of bromide or peroxide to the native enzyme.

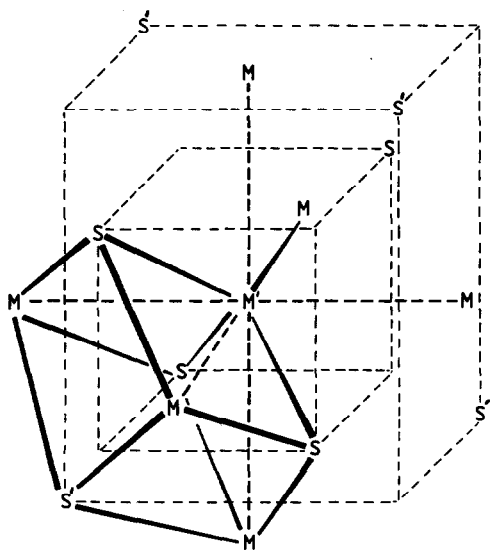

Fig. 3. Metal–sulphur framework, of composition $M'M_6S_8$, proposed for FeMoco and FeVaco, emphasizing one M_4S_4 cubane-like sub-unit.

EXAFS data are readily interpreted to provide the nature, number and distances of atoms immediately adjacent to the primary absorber of the X-rays.[13] The EXAFS associated with the vanadium K-edge for the VFe-protein of nitrogenase is consistent with the vanadium being part of a V—Fe—S cluster,[14,15,22] with 3 ± 1 sulphur atoms at 2.31(3) Å and 3 ± 1 iron atoms at 2.75(3) Å; also, there is evidence for *ca* three light atoms (oxygen, nitrogen) at 2.15(3) Å. These details are consistent with vanadium being octahedrally coordinated in a similar environment to that in the cubane-like cluster anion $[VFe_3S_4Cl_3(DMF)_3]^-$.[19] This situation parallels that for molybdenum in nitrogenase where XAS data[2] are consistent with this element being present in an $MoFe_3S_4$ cubane-like cluster. Iron K-edge EXAFS data recorded for FeMoco[23] and FeVaco show clear evidence for the presence of FeS_2M (M = Mo, V, Fe) rhombs, with Fe---Fe separations of *ca* 2.61 Å, *plus a longer range* Fe---Fe *separation at ca* 3.65 Å. This latter distance has special significance in at least two respects. Firstly, the observation of this relatively long separation implies that the metal–sulphur framework of the cofactors is highly ordered, i.e. the Fe---Fe back-scattered contributions are coherent. Secondly, a geometric relationship appears to exist between the longer and the shorter Fe---Fe separations, viz. $\sqrt{2}\times2.61$ approximates to 3.65. These results are consistent with the structure proposal for FeMoco and FeVaco in Fig. 3. The central M′ is surrounded by an octahedron of six metal atoms (M) and is tetrahedrally coordinated to four sulphur atoms; each of the other four sulphur atoms are also tetrahedrally disposed about M′ and each caps one face of the M_6 octahedron. Molybdenum (or vanadium) is suggested to occupy one M site, thus (Fig. 3) constituting one vertex of an $M_3M'S_4$ cubane-like cluster. Iron atoms are suggested as occupying the M′ and five of the M sites. In this model each M atom is coordinated by *four* sulphur atoms (two S and two S′); for molybdenum (or vanadium), this would permit "octahedral" coordination to be achieved by two ligands external to the cluster, for iron, this is consistent with the iron

EXAFS data[23] which detect only sulphur as the nearest neighbour of this metal in FeMoco.

The EXAFS data for native bromoperoxidase are consistent with the presence of an oxo group (V—O, 1.61(3) Å), together with additional coordination by other light atoms, *ca* three at 1.72(3) Å and *ca* two at 2.11(3) Å. Vanadium in reduced bromoperoxidase is also suggested to be present bound to an oxo group (V—O, 1.63(3) Å) and ligated by similar groups to those found for the native enzyme, *ca* three light atoms at 1.91(3) Å and *ca* two at 2.11(3) Å. The 2.11(3) Å distance is suggested to correspond to coordination by the imidazole group of histidine in each case, the outer carbon and nitrogen shells being clearly apparent for the reduced enzyme. The other ligands are suggested to be the phenols of tyrosines, since the significant reduction in the V—O distance from 1.91(3) to 1.72(3) Å upon oxidation clearly parallels known vanadium chemistry and would correspond to an increase in π-donation from the phenolic oxygen to vanadium upon oxidation.

CONCLUSION

Thus the vanadium centres of the two classes of enzymes presently known to require this metal for catalytic activity are clearly distinguished by XAS. In nitrogenases, vanadium is present as a cubane-like cluster which is part of the larger metal–sulphur cluster cofactor, FeVaco; in bromoperoxidase, vanadium is bound to an oxo group with imidazole and tyrosine suggested as other ligands. This distinction resembles that proposed for molybdenum centres in enzymes.

Acknowledgements—We thank the SERC for financial support and the Directors of the Daresbury Laboratory and the Photon Factory for provision of facilities.

REFERENCES

1. T. G. Spiro (Ed.), *Molybdenum Enzymes*. Wiley-Interscience, New York (1985) and refs therein.
2. S. P. Cramer, *Advances in Inorganic and Bioinorganic Mechanisms* (Edited by A. G. Sykes), Vol. 2, p. 259. Academic Press, London (1983).
3. R. C. Bray, *Quart. Rev. Biophys.* 1988, **21**, 299.
4. B. J. Hales, E. E. Case, J. E. Morningstar, M. F. Dzeda and L. A. Mauterer, *Biochemistry* 1986, **25**, 7251.
5. R. L. Robson, R. R. Eady, T. H. Richardson, R. W. Miller, M. Hawkins, and J. R. Postgate, *Nature* 1986, **322**, 388; R. R. Eady, R. L. Robson, T. H. Richardson, R. W. Miller and M. Hawkins, *Biochem. J.* 1987, **244**, 197.
6. H. Vilter, *Bot. Mar.* 1983, **26**, 1387; H. Vilter, *Phytochemistry* 1984, **23**, 1387.
7. R. Wever, H. Plat and E. de Boer, *Biochim. Biophys. Acta* 1985, **830**, 181; E. de Boer, Y. van Kooyk, M. G. M. Tromp, H. Plat and R. Wever, *Biochim. Biophys. Acta* 1986, **869**, 48.
8. E. de Boer, M. G. M. Tromp, H. Plat, G. E. Krenn and R. Wever, *Biochim. Biophys. Acta* 1986, **872**, 104.
9. M. J. Nelson, M. A. Levy and W. H. Orme-Johnson, *Proc. Natl. Acad. Sci. U.S.A.* 1983, **80**, 147.
10. S. P. Kramer, J. L. Johnson, A. A. Ribeiro, D. S. Millington and K. V. Rajagopalan, *J. Biol. Chem.* 1987, **34**, 16357.
11. J. E. Morningstar and B. J. Hales, *J. Am. Chem. Soc.* 1987, **109**, 6854; J. E. Morningstar, M. K. Johnson, E. E. Case and B. J. Hales, *Biochemistry* 1987, **26**, 1795.
12. B. E. Smith, R. R. Eady, D. J. Lowe and C. Gormal, *Biochem. J.* 1988, **250**, 299.
13. S. S. Hasnain and C. D. Garner, *Prog. Biophys. Molec. Biol.* 1987, **50**, 47.
14. J. M. Arber, B. R. Dobson, R. R. Eady, P. Stevens, S. S. Hasnain, C. D. Garner and B. E. Smith, *Nature* 1987, **325**, 372.
15. J. M. Arber, B. R. Dobson, R. R. Eady, S. S. Hasnain, C. D. Garner, T. Matsushita, M. Nomura and B. E. Smith, *Biochem. J.* 1989, **258**, 733.
16. J. M. Arber, E. de Boer, C. D. Garner, S. S. Hasnain and R. Wever, *Biochemistry*, in press.
17. S. J. Gurman, N. Binsted and I. Ross, *J. Phys. C.* 1984, **17**, 143; S. J. Gurman, N. Binsted and I. Ross, 1986, **19**, 1845.
18. J. Wong, F. W. Lytle, R. P. Messmer and D. H. Maylotte, *Phys. Rev.* 1984, **B30**, 5596.
19. J. A. Kovacs and R. H. Holm, *J. Am. Chem. Soc.* 1986, **108**, 340.
20. E. de Boer, C. P. Keijzers, A. A. K. Klaasen, E. J. Reijerse, D. Collison, C. D. Garner and R. Wever, *FEBS Letts* 1988, **234**, 93.
21. H. Vilter and D. Rehder, *Inorg. Chim. Acta* 1987, **136**, L7.
22. G. N. George, C. L. Coyle, B. J. Hales and S. P. Cramer, *J. Am. Chem. Soc.* 1988, **110**, 4057.
23. J. M. Arber, A. C. Flood, C. D. Garner, C. A. Gormal, S. S. Hasnain and B. E. Smith, *Biochem. J.* 1988, **252**, 421.

Polyhedron Vol. 8, No. 13/14, pp. 1653–1656, 1989
Printed in Great Britain

0277–5387/89 $3.00+.00
© 1989 Maxwell Pergamon Macmillan plc

ELECTROCHEMISTRY OF LIGANDS MULTIPLY BONDED TO MOLYBDENUM AND TUNGSTEN

D. L. HUGHES, D. J. LOWE, M. Y. MOHAMMED, C. J. MacDONALD and C. J. PICKETT*

AFRC Institute of Plant Science Research, Nitrogen Fixation Laboratory, University of Sussex, Brighton BN1 9RQ, U.K.

Abstract—This paper describes some new electrochemically driven reactions of ligands which are multiply bonded to molybdenum or tungsten.

We describe some new electrochemical reactions of ligands which are multiply bonded to molybdenum and tungsten. Our interest was initially focused on the electrochemistry of imide ligands for the following reasons.

First, electron-transfer reactions involving MoNH or WNH groups are plausible steps in electrochemical[1] and biochemical[2] nitrogen fixation pathways, as outlined in Scheme 1 (Box).[3]

Secondly, oxidation reactions involving imide or alkylimide groups might provide a means of diversifying the nitrogen products which can be made from molecular nitrogen, via chemistry at the square-planar $\{M(dppe)_2\}$ assembly (M = Mo or W; dppe = $Ph_2PCH_2CH_2PPh_2$).[4]

However, work with imides has led us to explore the electrochemistry of oxide, methyleneamide, cyanide and aminocarbyne ligating molybdenum or tungsten and has provided some new ligand-centred chemistry.

IMIDE AND OXIDE REDUCTION

Simple imide complexes such as *trans*-$[Mo(NH)Cl(dppe)_2]^+$ are reduced under molecular nitrogen to dinitrogen complexes and ammonia,[3] and this provides some support for a role of the {MNH} group in both electrochemical and biological fixation pathways, Scheme 2.

However, it is also possible to obtain ammonia by hydrolysis of an imide which produces an oxide via a prototropic rearrangement, Scheme 3.[5]

What is rather interesting here is that the primary reversible reduction of the oxides, *trans*-$[MOCl(dppe)_2]^+$, occurs at potentials more than 300 mV positive of those of their imido analogues. Moreover, in the presence of a source of protons, the reduction of the oxide becomes irreversible and, under molecular nitrogen, *trans*-$[M(N_2)_2(dppe)_2]$ is produced in an overall 4F mol^{-1} process. The effect of molecular nitrogen on the voltammetry of the molybdenum oxide is illustrated in Fig. 1; the intermediate detected as peak (i) in the voltammogram is the hydroxide intermediate, *trans*-[Mo(OH)Cl $(dppe)_2$], and that labelled (ii) is of the product, *trans*-$[M(N_2)_2(dppe)_2]$, Scheme 4.[5,6]

The relative ease of the multi-electron reduction of the Mo=O group, compared to that of

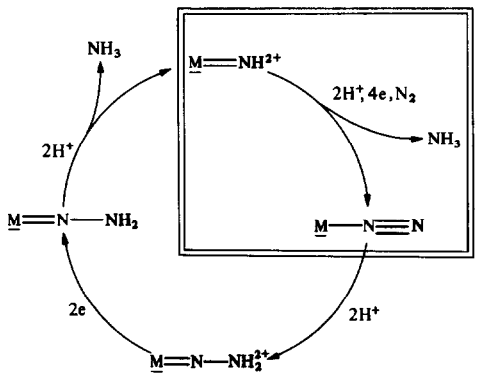

Scheme 1. In this scheme and Scheme 5, M represents a metal centre and conserved co-ligands. Elsewhere it represents the specific assemblies *trans*-{Mo or $W(dppe)_2$}.

* Author to whom correspondence should be addressed.

$$Cl—\underline{Mo}{=}NH^{+} \xrightarrow{2e,H^{+}} Cl—\underline{Mo}—NH_2 \xrightarrow[2N_2,\,-Cl^{-}]{2e,H^{+}} N_2—\underline{Mo}—N_2 + NH_3$$

Scheme 2.

$$MeO—\underline{W}{=}NH^{+} \xrightarrow[-MeOH]{H^{+},H_2O} H_2O—\underline{W}{=}NH^{2+} \longrightarrow O{=}\underline{W}—NH_3^{2+} \xrightarrow{Cl^{-}} O{=}\underline{W}—Cl^{+} + NH_3$$

Prototropic rearrangement

Scheme 3.

$$Cl—\underline{M}{=}O^{+} \xrightarrow{2e,H^{+}} Cl—\underline{M}—OH \xrightarrow[2N_2,\,-Cl^{-}]{2e,H^{+}} N_2—\underline{M}—N_2 + H_2O$$

Scheme 4.

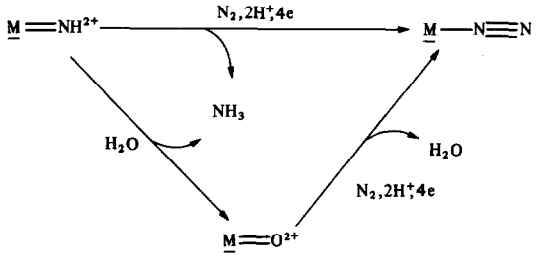

Scheme 5.

Mo=NH, suggests that a sequence involving hydrolysis and oxide reduction might be more favourable in an enzymic nitrogen fixation pathway than direct imide reduction, Scheme 5.[3,5]

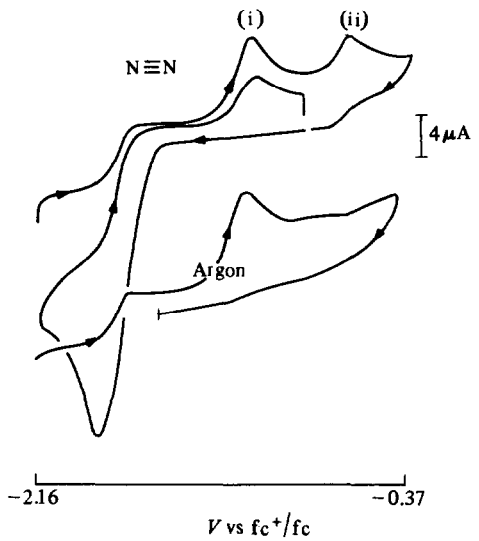

Fig. 1. Clamp voltammograms of *trans*-[MoOCl(dppe)$_2$]$^+$, in a tetrahydrofuran electrolyte containing phenol, showing the detection of the hydroxide (i) and the product (ii), *trans*-[Mo(N$_2$)$_2$(dppe)$_2$]. Potentials are relative to ferrocinium/ferrocene, fc$^+$/fc, here and in Scheme 7. For details see ref. 3.

METHYLIMIDE REDUCTION: GENERATION OF A STRONG BASE

In detail, the electrochemical reduction of *trans*-[Mo(NH)Cl(dppe)$_2$]$^+$ is an irreversible process which initially produces two products viz. the unstable amide, *trans*-[Mo(NH$_2$)Cl(dppe)$_2$], and the nitride, *trans*-[Mo(N)Cl(dppe)$_2$].[2,3] This occurs as an apparent one-electron process, because the primary reduction product removes a proton from the reactant to give the nitride and a cation, the latter is then rapidly reduced to the neutral amide, Scheme 2.[3]

That the primary reduction step involves a single electron-transfer step is suggested by the behaviour of the methylimide analogue, *trans*-[Mo(NMe)Cl(dppe)$_2$]$^+$, which at low temperature displays an electrochemically reversible one-electron reduction, Scheme 6.

We might expect that the reactant, *trans*-[Mo(NMe)Cl(dppe)$_2$]$^+$, would be incapable of furnishing a proton to the neutral one-electron intermediate, but this is not the case. At ambient tem-

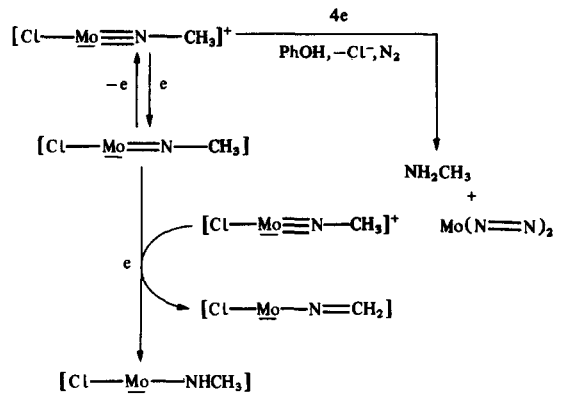

Scheme 6. Oxidation of methylimide and methyleneamide ligands: a radical di-cation and a cyanide.

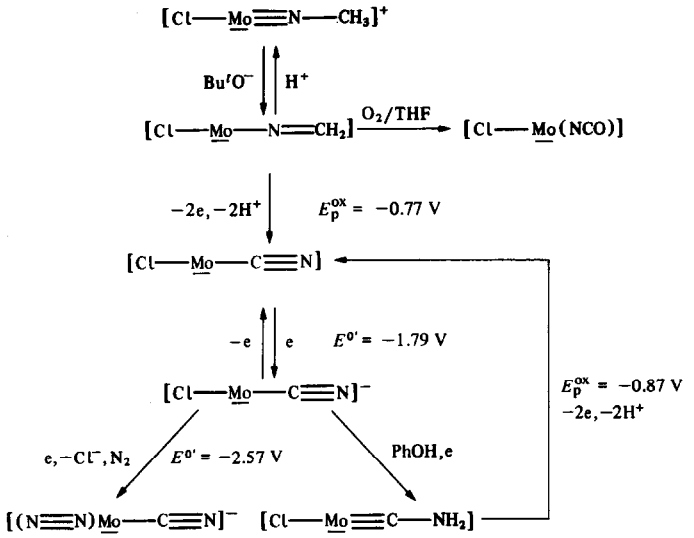

Scheme 7.

peratures, the reduction becomes less reversible and we detect *trans*-[Mo(NHMe)Cl(dppe)$_2$] and the methyleneamide species, *trans*-[Mo(NCH$_2$)Cl(dppe)$_2$], Scheme 6.

Deprotonation of the methylimide by K[OBu^t] affords the methyleneamide by an independent route, and the complex has been isolated and fully characterized.[7] Its formation during electro-reduction is circumvented when phenol is present as a source of protons; a clean four-electron reduction to the amine and *trans*-[Mo(N$_2$)$_2$(dppe)$_2$] is possible on a preparative scale using a mercury cathode and a THF electrolyte, Scheme 6.

Whether the "19-e" primary intermediate adopts a "17-e" bent MoNC configuration remains a matter of speculation, the important message is that we generate a metallo-nitrogen base that is capable of deprotonating the parent carbon acid, the methylimide. Such "father–son" reactions appear to be a common feature of the electrochemistry of imide, alkylimide, hydrazide and diazoalkane cations.[1,3]

Cyclic voltammetry showed that *trans*-[Mo(NMe)Cl(dppe)$_2$]$^+$ undergoes a partially reversible one-electron oxidation in common non-aqueous electrolytes, but our attempts to electrosynthesize clean products in such solvents were unsuccessful.

However, in trifluoroacetic acid containing 0.2 M [NBu$_4$][BF$_4$] and trifluoroacetic anhydride, a medium of low nucleophilicity, the radical di-cation *trans*-[Mo(NMe)Cl(dppe)$_2$]$^{2+}$ is reasonably stable and can be prepared as a solution species by either electro-oxidation at platinum, or by chemical oxidation with [NO][PF$_6$]. We have characterized the di-cation, certain of its isotopically substituted derivatives and a minor co-product, by EPR and ENDOR spectroscopy. This has enabled us to establish that the radical retains the essential structure of the 18-electron parent.[8]

As a means of transforming a methylimide ligand, direct electro-oxidation appeared unpromising, we therefore looked at the oxidation of the de-protonated species, the methyleneamide, *trans*-[Mo(NCH$_2$)Cl(dppe)$_2$].

Electrochemical or iodine oxidation of this complex afforded the cyanide *trans*-[Mo(CN)Cl(dppe)$_2$], which was characterized by an X-ray crystallographic analysis of green prisms isolated in low yield from an anolyte.[7] Labelling studies suggest that the rearrangement of the MoNC framework to MoCN is an intramolecular process, Scheme 7.[7]

THE REDUCTION OF A MOLYBDENUM CYANIDE TO AN AMINOCARBYNE AND TO A DINITROGEN COMPLEX

Cyclic voltammetry shows that *trans*-(Mo(CN)Cl(dppe)$_2$] undergoes two successive one-electron reduction steps in a dry THF electrolyte at a vitreous carbon electrode. The first of these is reversible, the second leads to the irreversible loss of Cl$^-$ and to the formation of the known anionic dinitrogen complex *trans*-[Mo(N$_2$)(CN)(dppe)$_2$]$^-$, Scheme 7. The cyanide also undergoes a reversible one-electron oxidation.

In the presence of a proton source, phenol, the primary reduction of the cyanide becomes an irreversible two-electron process and at a mercury pool cathode the aminocarbyne *trans*-[Mo(CNH$_2$)Cl(dppe)$_2$] is formed in good yield. As far as we

are aware, this is the first example of the partial reduction of a cyanide ligand to aminocarbyne; the complex has an isostructural rhenium analogue, the hitherto unique *trans*-$[Re(CNH_2)Cl(dppe)_2]^+$.[9] In formal terms, the 16-electron Mo^{II}–cyanide is "reduced" to an 18-electron Mo^{IV} product, a process which is chemically reversible, Scheme 7.[7]

The reduction of the cyanide to a molybdo–aminocarbyne provides a chemical precedent for a plausible step in enzymic reduction of CN^- by molybdenum nitrogenase.[10]

CONCLUSIONS

We summarize our conclusions as follows:

(1) In the presence of a proton source, cathode reactions can provide a means of releasing multiply-bonded ligands from $\{M(dppe)_2\}$ assemblies and of exposing a site at which dinitrogen (and other π-acid ligands) can then bind. This is important in the construction of nitrogen fixing pathways and also bears upon possible mechanisms of enzymic fixation.

(2) In the *absence* of a proton source, the primary products of electron-transfer to closed-shell hydrazides, imides or alkylimides can be sufficiently basic to remove a proton from the parent cation. Indeed metallo–nitrogen bases can be electrogenerated which are capable of deprotonating a methylimide ligand.

(3) Electro-oxidation of the methyleneamide to a cyanide and reduction of this cyanide to an aminocarbyne provides a pathway for the isomerization of the $\{MoNCH_2\}$ group to $\{MoCNH_2\}$.

(4) The partial reduction of CN^- at a simple mononuclear molybdenum to a bound aminocarbyne suggests that the generation of a $\{MoCNH_2\}$ group is a plausible stage in cyanide metabolism by molybdenum nitrogenase.

Acknowledgement—We thank Miss Kaye Cate for valuable assistance in the course of this work.

REFERENCES

1. C. J. Pickett and J. Talarmin, *Nature* 1985, **317**, 652; C. J. Pickett, K. S. Ryder and J. Talarmin, *J. Chem. Soc., Dalton Trans.* 1986, 1453.
2. C. J. Pickett, K. S. Ryder and J. Talarmin, *J. Chem.* Mohammed, K. S. Ryder and J. Talarmin, *Nitrogen Fixation: Hundred Years After* (Edited by H. Bothe, F. J. de Bruijn and W. E. Newton), pp. 51–56. G. Fischer, Stuttgart (1988).
3. M. Y. Mohammed and C. J. Pickett, *J. Chem. Soc., Chem. Commun.* 1988, 1119.
4. R. A. Henderson, G. J. Leigh and C. J. Pickett, *Adv. Inorg. Chem. Radiochem.* 1983, **27**, 197.
5. D. L. Hughes, C. J. Pickett and M. Y. Mohammed, *J. Chem. Soc., Chem. Commun.* 1988, 1481.
6. T. I. Al-Salih and C. J. Pickett, *J. Chem. Soc., Dalton Trans.* 1985, 1255.
7. D. L. Hughes, M. Y. Mohammed and C. J. Pickett, unpublished results.
8. D. J. Lowe, M. Y. Mohammed and C. J. Pickett, unpublished results.
9. A. J. Pombeiro, D. L. Hughes, C. J. Pickett and R. L. Richards, *J. Chem. Soc., Chem. Commun.* 1986, 246.
10. J.-G. Li, B. K. Burgess and J. L. Corbin, *Biochemistry* 1982, **21**, 4393.

Polyhedron Vol. 8, No. 13/14, pp. 1657–1668, 1989
Printed in Great Britain

0277–5387/89 $3.00+.00
© 1989 Maxwell Pergamon Macmillan plc

NMR SPECTROSCOPY OF THE EARLY TRANSITION METALS

JOAN MASON

Department of Chemistry, The Open University, Milton Keynes MK7 6AA, U.K.

Abstract—Many early transition metal nuclei have good NMR properties, and the chemical shifts are sensitive to small structural changes. A key role is played in nuclear magnetic shielding, as in electronic spectroscopy, by the ability of transition metals and ligands to split the ligand field and to expand the *d* shell, in coordination complexes and organometallic compounds. Strong periodic trends can be discerned; thus earlier (compared with later) transition metals show the influence of low-lying *d* levels (smaller nephelauxetic influences) in their chemical shifts. The metal shifts correlate with those of ligating atoms, and with substituent effects on the ligands. Quadrupolar linewidths reflect the symmetry of the coordination sphere (as well as the size and mobility of the complex); and spin–spin coupling constants contribute information on bond type and connectivity. The database of NMR spectroscopic information is growing fast as technical problems are solved for less favourable nuclei, and for solid state studies.

With modern NMR instrumentation the chemist can "dial" almost any nucleus and communicate with it in a matter of minutes, according to Laszlo;[1] indeed, the majority of the early transition metals have magnetic nuclei that can yield reasonable spectra by direct observation of many of their (mainly) diamagnetic compounds, with spectrometers that are now standard.[2,3] In favourable cases NMR spectra have also been measured in the solid-state. Connectivity in extended systems, both organometallic and inorganic (notably in polyoxometallates), can be elucidated by 2-D NMR, e.g. COSY for more abundant nuclei (such as ^{51}V), or special pulse sequences such as INADEQUATE for rarer nuclei (such as ^{183}W).[4,5]

Spectroscopy of the metal nucleus has some advantages over work with ligand nuclei (^{1}H, ^{13}C, ^{31}P etc.). Metal nucleus spectra are simpler and easier to interpret, and the chemical shifts (also the relaxation times and coupling constants) probe the coordination sphere directly, and are sensitive to quite small structural changes (as in diastereomers, for example). Because of the recent expansion of this field, mainly key references, and some illustrative ones, will be given. NMR reviews have dealt with the early transition metals,[6] the *d* block as a whole,[7–11] the first transition series only,[12] various selected transition metals,[13–15] organometallic compounds,[16–18] and particular metals (vanadium[19]) or groups (chromium, molybdenum and tungsten[20]). Useful accounts of work carried out with quadrupolar transition metal nuclei are included in reviews of quadrupolar nuclei,[21] and of electrolyte solutions.[22,23] Reviews of NMR results are updated annually.[24]

NMR PROPERTIES OF THE EARLY TRANSITION METALS

Table 1 gives relevant nuclear properties and their definitions.[3] For reasonable accessibility the nucleus must have a large enough receptivity R^C, that is, a large enough natural abundance and magnetogyric ratio (γ). Low-γ nuclei have the further disadvantage of lower working frequencies ($\nu = \gamma B_0/2\pi$), with associated technical problems such as probe ringing, which transforms as a rolling baseline. All of the group 3 and group 5 nuclei in Table 1 have natural abundances in the region of 100%, as compared to 5.5–18.5% in groups 4 and 6. Quadrupolar nuclei ($I > 1/2$) must have, in addition, a sufficiently small (line) width factor WF, and this is uncomfortably large only for ^{177}Hf and ^{181}Ta. A measure of the favourability of a nucleus is the volume of the NMR literature, or database, to date.[6–24]

The most favourable of the early transition metal nuclei is ^{51}V, which has a large receptivity (2170 times that of ^{13}C) and small width factor (0.37). ^{93}Nb has even larger receptivity (2770) but gives broader lines (width factor 7.65), while ^{181}Ta gives very broad lines. ^{95}Mo, also, is well-studied. ^{53}Cr,

Table 1. NMR properties of the early transition metals; the most favourable nucleus is listed in each case

	^{45}Sc	^{47}Ti	^{49}Ti	^{51}V	^{53}Cr	^{55}Mn
I	7/2	5/2	7/2	7/2	3/2	5/2
γ (10^7 rad s^{-1} T^{-1})	6.509	−1.5106	−1.511	2.672	−1.508	24.840
Ξ (MHz)	24.330	5.64276	5.64426	26.350	5.636	6.645
N.A. (%)	100	7.28	5.51	99.76	9.55	100
R^C	1720	0.867	1.18	2170	0.485	1014
Q (10^{-28} m^2)	−0.22	0.29	0.24	0.052	−0.15	0.40
WF (10^{-59} m^4)	6.6	27	7.8	0.37	30	51
	^{89}Y		^{91}Zr	^{93}Nb	^{95}Mo	^{99}Tc
I	1/2		5/2	9/2	5/2	9/2
γ (10^7 rad s^{-1} T^{-1})	−1.316		−2.497	6.567	−1.751	5.050
Ξ (MHz)	44.9220		9.336	24.549	6.547	22.508
N.A. (%)	100		11.23	100	15.72	—
R^C	0.676		6.05	2770	2.92	—
Q (10^{-28} m^2)	—		—0.21	−0.32	−0.015	—
WF (10^{-59} m^4)	—		14	7.6	0.15	−0.13 1.25
	^{139}La		^{177}Hf	^{181}Ta	^{183}W	^{187}Re
I	7/2		7/2	7/2	1/2	5/2
γ (10^7 rad s^{-1} T^{-1})	3.808		1.086	3.244	1.128	6.158
Ξ (MHz)	14.236		4.059	12.128	4.218	23.057
N.A. (%)	99.9		18.50	99.9	14.28	62.93
R^C	343		1.47	213	0.061	011
Q (10^{-28} m^2)	0.22		3.3	3.3	—	—
WF (10^{-59} m^4)	6.6		1000	1480	—	1600

I is the spin quantum number, γ the magnetogyric ratio, and R^C the receptivity (relative to that of ^{13}C in natural abundance, N.A.), which depends on γ^3, I^2, and N.A. Ξ is the resonance frequency of the standard substance in a field of 2.3488 T, at which TMS protons resonate at 100 MHz. WF is a (line)width factor for quadrupolar nuclei which depends on Q^2 and I^{-2} (also called the nuclear IQ).

however, is insensitive and few types of compounds have been measured so far. ^{183}W is a high-resolution nucleus (spin 1/2) but of rather low receptivity, so that indirect methods of detection are often preferable.[5] ^{55}Mn and the radionuclide ^{99}Tc are good NMR nuclei, but ^{189,187}Re give very broad lines.

^{45}Sc, ^{89}Y and ^{139}La have received considerable study, ^{49}Ti and ^{91}Zr rather less, and ^{177}Hf none as yet because of its combination of a low receptivity with a large width factor. ^{49}Ti spectra are complicated by the presence of resonances due to ^{47}Ti, which has rather similar NMR frequency and natural abundance, but gives broader lines (Table 1). ^{175}Lu has not been studied as yet by chemists because of its large width factor (1630), although the receptivity (173) is quite good and its compounds are diamagnetic. One very broad signal has been reported for ^{235}U,[25] which has very low receptivity (0.0054) and large width factor (2820).

NMR TECHNIQUES

Some early transition metal nuclei are sufficiently NMR-receptive that not even a superconducting magnet is needed, as for many vanadium or molybdenum compounds. For less receptive nuclei, sensitivity may be increased by the use of a widebore spectrometer for larger sample volumes, or by higher field working, which increases NMR sensitivity and shift dispersion. Isotopic enrichment was needed to raise a ^{235}U signal,[25] and would be advantageous in bioinorganic studies with ^{95}Mo, for example, since a 6.4-fold enrichment yields a 40-fold advantage in spectrometer time. Multiple resonance or special pulse techniques for sensitivity enhancement (polarization transfer) are of use for spin-1/2 nuclei when there is a resolvable coupling to a high-sensitivity nucleus, usually the proton.[4,5]

Many of the technical problems that arise are related to unfavourable relaxation rates.[4,5] Relax-

ation may be uncomfortably slow, leading to problems of detection or of spectrometer time, for spin-1/2 nuclei with small magnetic moments, such as ^{183}W or ^{89}Y. Depending on the chemical system, relaxation reagents such as $[Cr(pd)_3]$ may be added, or dipole–dipole relaxation may be enhanced by slowing the molecular motions (by cooling the sample, or by use of higher-viscosity solvents). Additional relaxation mechanisms are sometimes advantageous, such as shielding anisotropy (favoured by higher fields) for organometallic compounds of tungsten,[5c] or the spin-rotation mechanism (favoured at higher temperatures).

For quadrupolar nuclei ($I > 1/2$) with large quadrupole moments (Q) relaxation may be uncomfortably fast and lead to (uncertainty) broadening of the lines; although relatively fast quadrupolar relaxation has the advantage that the pulsing can be faster. The linewidth at half-height ($W_{1/2}$) for mobile molecular fluids ($\omega_o\tau_c \ll I$) is given by:[26]

$$W_{1/2} = 1/T_q = \frac{3}{40}\frac{(2I+3)}{I^2(2I-1)}\left\{\frac{e^2qQ}{\hbar}\right\}^2\left\{1+\frac{a^2}{3}\right\}\tau_c, \quad (1)$$

where $T_q(= T_2 = T_1)$ is the relaxation time, e^2qQ the nuclear quadrupole coupling constant (nqcc) as measured by NQR spectroscopy, eq the largest component of the electric field gradient (efg) at the nucleus, with asymmetry parameter a; τ_c is an effective correlation time for the molecular tumbling. On the Stokes–Einstein–Debye frictional model, τ_c is equal to $\eta V/6kT$, where V is the molecular volume, η the viscosity, 1/6 a microviscosity factor as observed for pure liquids, and kT the Boltzmann factor.

Quadrupolar broadening, therefore, is less the smaller the molecule, and the higher the local electronic symmetry (that is, the lower the electric field gradient with which the nuclear electric quadrupole couples). For some transition metal nuclei with large quadrupole moments the main species for which an NMR signal has been reported are relatively small complexes with cubic symmetry, such as tetraoxo, hexafluoro or hexacarbonyl species. An example of the value of a low-viscosity solvent (acetone) is recent pioneer work in ^{53}Cr resonance (with a purpose-built probe), with linewidths ranging from 2–3 Hz for $[Cr(CO)_6]$ to over 3500 Hz for some $[Cr(CO)_5(carbene)]$ compounds.[27] Higher temperatures are often used in ^{95}Mo studies,[20] cf. also the measurement of UF_6 at 380 K (to give a signal 20 kHz wide).[25]

The linewidth can be a useful indicator of the symmetry of the coordination shell, as in studies of the solvation of group 3 ions,[21,22] or of seven- and eight-coordinate complexes formed by lanthanum with small ligands.[28]

In "free" metal ions there may be no permanent efg, if coordination by the solvent is symmetrical, but thermal motions, the buffeting by other ions and dipoles in solution, and fluctuating hydrogen bonds, produce fluctuating efgs, which relax the nuclear electric quadrupole and therefore the nuclear spin.[21–23] These efgs are amplified by distortion of the core electron shells, depending on the Sternheimer antishielding factor γ_∞. This appears as the square in the expression for the linewidth, and increases sharply for heavier ions (cf. the values of ca -40 for Sr^{2+} and -120 for Ba^{2+}).[29]

Fast-relaxing quadrupolar nuclei, also, raise the problem of rolling baselines, arising from contamination of the very short free induction decay by probe ringing. This can be reduced by special pulse sequences (and instrumentation) as the RIDE (Ring-Down Elimination) technique.[30] For heavier elements a degree of quadrupolar broadening is tolerable because of the large shift range.

TRANSITION METAL NUCLEUS SHIELDING

Chemical shifts are given by the paramagnetic term σ_p of Ramsey's perturbation theory,[31–33] which has been reformulated for the transition metals.[34–40] The shift, δ, and nuclear magnetic shielding, σ, are defined with opposite sign, so that increase in δ is given by increase in the absolute magnitude of σ_p. The paramagnetic term is balanced by a diamagnetic term that is comparable in magnitude (each being measured relative to the bare nucleus), but variations in σ_d are small compared with those in σ_p for transition metal nuclei, and can usually be neglected.[33]

For open-shell transition metal compounds the major contribution arises from the mixing into the ground state by the magnetic field of d–d excited states, as these are magnetic dipole allowed (involving circulation of charge). We can therefore visualize circulations of valence d electrons, using ligand field LUMOs (usually $d\pi \rightarrow d\sigma^*$ or $d\sigma \rightarrow d\pi^*$) which reinforce the applied field, deshielding the nucleus. The shielding of main-group nuclei is similarly mediated by $p\sigma \leftrightarrow p\pi$ circulations.[33]

A simple ligand field formulation for a transition metal nucleus in a d^6 octahedral complex is[34]

$$-\sigma_p \approx \left(\frac{\mu_o}{4\pi}\right)\left(\frac{e^2}{m^2}\right)\frac{\langle r^{-3}\rangle_{nd}\langle 0|L^2|0\rangle}{\Delta E}, \quad (2)$$

where μ_o is the permeability of free space, e and m the electronic charge and mass, $\langle r_{nd}\rangle$ the valence

d electron radius, and ΔE the (virtual) excitation energy associated with the angular momentum operator L, with the origin at the metal nucleus. A formulation for main-group or transition elements is[35]

$$-\sigma_p \approx \left(\frac{2\mu_o}{3\pi}\right)(\mu_B^2)\frac{[\langle r^{-3}\rangle_p P_i + \langle r^{-3}\rangle_d D_i]}{\Delta E} \quad (3)$$

where P_i and D_i express the imbalance of charge in the valence p- and d-shells. Fuller expressions sum over the (magnetically allowed) excited states, with appropriate modifications for other symmetries.[35-37] Theoretical studies of nuclear magnetic shielding are reviewed annually.[42]

Most articulations of the theory have centred on cobalt, although studies of earlier transition metal nuclei are increasing. The theory was applied[38] to a range of octahedral cobalt(III) complexes by use of an optical parameter $(h_1/\beta)^{-1}$, where h_1 is the energy of the first spin-allowed absorption band ($^1A_{1g} \rightarrow T_{1g}$) and β the nephelauxetic ratio, discussed below. Deviations were observed for chelate complexes with en, ox (etc.) ligands; more complex optical parameters are required for non-orthoaxial complexes (in which the ligands are not symmetrically disposed on Cartesian axes). Anisotropic nephelauxetism can be used for lower symmetries.[43] The radial term may be modified from the free-atom value by use of an orbital angular momentum reduction factor k, as $k^2\langle r^{-3}\rangle_{nd}$,[43] or as $C_M^2\langle r^{-3}\rangle_{nd}$, where C_M is the coefficient of the d(M) orbital in the LCAO description of the MO;[44] or $\langle r^{-3}\rangle_{nd}$ may be reduced in proportion to a calculated reduction of the central charge by L → M charge-transfer (as in metalate ions)[37] and so on.

Although closed shells make no contribution to the paramagnetic term, the ligand field theory applies also to d^0 and d^{10} complexes because of σ,π-electron delocalization and metal d, s, p orbital mixing. Thus in d^0 complexes ground state nd orbitals may be populated by covalent bonding (including L → M π-bonding).[37,41] In d^{10} compounds back-donation to the ligand (M → L) produces holes in d orbitals, allowing d–d circulations, while L → M donation populates the metal p orbitals.[40] Such effects have been demonstrated by *ab initio* calculations (which are difficult for transition metal nuclei, because of the computing power required).[39,40] In $[Mn(CO)_5L]$ complexes the ^{55}Mn shielding decreases in the sequence H > CN > CH_3 > Cl of the L ligand, as it becomes more π-donating, and also harder, reducing its interaction with the soft acid $Mn(CO)_5^+$.[39] (The deshielding thus correlates with reduction in ΔE, with raising of the $d\pi$ homo and lowering of the $d\sigma^*$ lumo.) In d^{10} complexes of copper, zinc, silver, cadmium, the ^{63}Cu shielding decreases in the sequence CN > NH_3 > Cl of the ligand, as its π-acceptor ability increases, increasing the hole in the d shell. The ^{67}Zn and ^{113}Cd shielding decreases with decrease in ligand electronegativity (with increase in p-contribution to the metal) but in the silver complexes the p and d mechanisms are comparable.[40]

In transition metal nucleus NMR there is usually no *overall* correlation of the chemical shift with the oxidation number of the metal. Thus in Table 2 the more highly shielded complexes of molybdenum and tungsten have (formal) d-electron configurations d^0, d^2, d^4 and d^6. (What they have in common is that all are complexes of strong ligands.) Lower oxidation numbers and negative charges commonly correlate with higher shielding, but the highest ^{95}Mo shielding has been observed[45] for the hydride $[MoCp_2H_3]^+$, in which the metal is formally molybdenum(VI), d^0 (and the complex is positively charged), cf. also the high ^{183}W shielding in $[WCp_2H_2]$.[46] Overall, increase in oxidation number of the metal tends to increase both the energy term (Δ) and the radial factor $\langle r^{-3}\rangle_{nd}$ and these act in opposition, according to eq. (2). There are, however, important regularities.

SHIELDING OF THE EARLY TRANSITION METAL NUCLEI

Table 2 gives approximate ranges of chemical shifts observed for the early transition metals. For the main-group elements the range (or dispersion) of chemical shifts tends to vary periodically, increasing across the row and down the group, reflecting the variation of the radial factor $\langle r^{-3}\rangle_{nd}$,[7,32,35] as seen in the values calculated for the free atoms.[47] Shift ranges are much larger for d block than for main-group elements of similar quantum number (despite smaller $\langle r^{-3}\rangle_d$ than $\langle r^{-3}\rangle_p$ values later in the row). This is attributable in part to the larger range of $\langle 0|L^2|0\rangle$ values [eq. (2)] for d than p orbitals. In eq. (3) the P_i parameter increases (from 0 for spherical symmetry) to 2, for two p orbitals filled and one empty, or vice versa. The D_i parameter, however, can take values up to 12, for three d orbitals filled and two empty (as in low-spin d^6 octahedral complexes), or vice versa (as for d^4 tetrahedral complexes).

For transition elements, also, the energy term may play a larger role. The metal contribution to the ligand field splitting (Δ) increases across the series (with decrease in atomic radius), and increases markedly down the group, by about 50%

from the first series to the second, and 10–25% from the second to the third, with increase in covalent bonding. Very large ranges are observed towards the end of the first transition series (^{59}Co shifts span 19,000 ppm). These can be explained by a large range of ΔE values, and of the angular momentum term; also by relatively large values of the radial terms in the first transition series (as in the second row of the Periodic Table) because of the relatively small number of inner electrons.[7]

In Table 2, the ranges for ^{53}Cr and ^{181}Ta are truncated by the difficulties of observation, due to the low sensitivity and the large quadrupole moment, respectively. For ^{45}Sc and ^{89}Y the small ranges reflect the rather limited chemistry of these elements as well as the relatively small values of $\langle r^{-3}\rangle_{nd}$. The ranges for vanadium, niobium and tantalum are extended by the inclusion of semiconductors[37] (with very small ΔE), and those for molybdenum and tungsten by the quadruply bonded compounds $[M_2(O_2CCF_3)_4]$.[45,48] Metallic solids are not included.

For isostructural compounds, the metal shifts may be scaled, approximately, in proportion to the free atom $\langle r^{-3}\rangle_{nd}$ values. Thus the shift ranges for ^{183}W and ^{181}Ta are in the ratio 1.3, as against 1.2 for the ratio of the free atom $\langle r^{-3}\rangle_{nd}$ values; the corresponding values for the ^{95}Mo/^{93}Nb comparison, are 1.4 and 1.25, respectively. Disparities may be greater in comparisons with heavier elements; thus plotting ^{183}W against ^{95}Mo shifts in corresponding compounds gives lines of slope *ca* 1.7,[49] whereas the ratio of the (free atom) radial terms is two, and the excitation energies are probably similar for the molybdenum and tungsten compounds.[50] Relativistic effects will be identified for heavy atom shifts, but the theory is as yet undeveloped.

THE VARIATION OF METAL NUCLEUS SHIFTS ACCORDING TO THE NATURE OF THE LIGANDS

As shown by eq. (2), the shift (δ) is the greater the closer is the paramagnetic circulation to the resonant nucleus (r small), the smaller its excitation energy (ΔE), and the larger the orbital angular momentum ("unquenched" by the magnetic field) which depends on the imbalance of charge in the $d\pi$ and $d\sigma^*$ (or $d\sigma$ and $d\pi^*$) orbitals. Since ΔE is effectively the ligand field splitting, Δ (or a weighted mean of the splittings for lower symmetries), the shielding tends to increase from weak to strong ligands, following the spectrochemical series. It also increases with increase in d-electron delocalization, or nephelauxetism (cloud expansion), decreasing the radial term $\langle r^{-3}\rangle_{nd}$ from its free-atom value.

INFLUENCE OF THE ENERGY TERM: THE SPECTROCHEMICAL SERIES

Beginning with ^{59}Co shifts,[34] there have been very many δ/λ correlations of transition metal nucleus shifts with the wavelength λ of the long-wavelength UV–vis absorption, according to eqs (2) and (3). In principle, the correlation should be with (spin-allowed) *d–d* excitation energies, but the (relatively weak) bands are often obscured by stronger charge-transfer bands, which may vary in the same sense.[51] Thus ^{53}Cr shifts in carbene complexes $[Cr(CO)_5(CXY)]$ are found to increase as the long-wavelength LMCT (ligand-to-metal charge-transfer) bands go to lower energies.[27] A corresponding relationship is of chemical shifts with the inverse of the binding energies measured by XPES (ESCA), as in ^{49}Ti studies of titanocene dihalides.[52]

If the energy term, ΔE, is dominant, the metal nucleus shielding may be expected to decrease with decrease in the ligand field splitting Δ, following the spectrochemical series in optical spectroscopy. This depends largely on the ligating atom, and may be written as H > C > N > O > F > S > Cl > Br > I, from strong to weak field (an order of decreasing bond strength).[53] Synergic ($\sigma+\pi$) bonding increases Δ, so that O > S > Se > Te, though N > P $\approx$ As.

These regularities are very evident in Table 2. Complexes of strong ligands (H, Cp, CO, RNC, phosphines) show high metal shielding. Low shielding for an M^0 complex (δ ^{95}Mo = 1500) is shown by [Mo(2-PAP)$_3$], with six ligating nitrogens; 2-PAP is 2-(phenylazopyridine).[54] Very low vanadium, niobium and tantalum shielding is observed for the sulvanite type semiconductors A_3BC_4 (with A = Cu, Tl; B = V, Nb, Ta, and C = S, Se, Te).[37] In these the V, Nb, Ta shift increases greatly down the group of the ligand, as S < Se $\ll$ Te, and also as Cu $\ll$ Tl. It is a general observation that very large shifts may be observed when ΔE values are small, since relatively small differences in ΔE bulk large.

The "spectrochemical" pattern is seen also in the vanadates, molybdates and tungstates (O < S < Se). There are usually regular increments in the shift for a given replacement as also in halide and other complexes. In these compounds the metal shielding decreases as the low-energy electronic absorption moves to longer wavelengths, and this was noted also for the ^{17}O shielding, which is

Table 2. Chemical shift comparisons for the early transition metal nuclei[a]

Range (ppm)	δ ^{45}Sc 290		δ ^{49}Ti 2500		δ ^{51}V 6000		δ ^{53}Cr 1800		δ ^{55}Mn 3500
				$[V(CO)_6]^-$	−1952	$[Cr(CO)_6]$	−1795	$[MnH(PF_3)_5]$	−2953
				$[V(PF_3)_6]^-$	−1946	$[Cr(CO)_5(CXY)]$	−1500 to −1750	$[MnH(CO)_5]$	−2578
				$[VCp(CO)_4]$	−1534			$[Mn_2(CO)_{10}]$	−2300
				$[VCp'(CO)_4]$	−1525			$[MnCp(CO)_3]$	−2280
				$[VCp''(CO)_4]$	−1490			$[MnMo(CO)_5]$	−2266
		$[TiF_6]^{2-}$(aq)	0					$[Mn(CO)_5(PPh_3)]^+$	−1630
		$[TiCp_2F_2]$	126					$[MnI(CO)_5]$	−1485
		$[TiCp_2Cl_2]$	391					$[Mn(CO)(NO)_3]$	−1171
		$[TiCp_2Br_2]$	494					$[MnBr(CO)_5]$	−1160
$[Sc(OAc)_3](s)$	−40(5)			$[VOF_3]$	−582			$[MnCl(CO)_3]$	1004
$[Sc]^{3+}$(aq)	0			$[VO_2]^+$(aq, pH 1–2)	−545				
$[ScCp_3]$	13.5			polyoxovanadates	−370 to −700			$[Mn(CO)_5(NCMe)]^+$	−740
				$[VO_4]^{3-}$(aq, pH 10)	−541	$[CrO_4]^{2-}$(aq)	0	MnO_4^-	0
$[Sc(pd)_3]$	85	$[Ti(OP^i)_4]$	305	$[VO(OEt)_3]$	−443			*fac*-$[Mn(CO)_3(NCMe)_3]^+$	490
$[Sc(OH)_4]^-$(aq pH 14)	116			$[VO(NEt_2)_3]$	−365				
$[Sc(THF)_6]^{3+}$	203	$[Ti(NEt_2)_4]$	958	$[VOCl_3]$	0				
				$[VOBr_3]$	432				
				$Cu_3[VS]_4(s)$	635				
				$[VOS_3]^{3-}$ (aq)	758				
$[ScCl_6]^{3-}$	249	$[TiCl_4]$	1163	$[VS_4]^{3-}$(aq)	1392				
		$[TiBr_6]^{2-}$	1176	$Cu_3[VSe_4](s)$	1770				
		$[TiBr_4]$	1675	$Tl_3[VSe_4](s)$	2540				
		$[TiI_4]$	2440	$Cu_3[VTe_4](s)$	3950				

Range (ppm)	δ ^{89}Y 700		δ ^{91}Zr 1000		δ ^{93}Nb 5000		δ ^{95}Mo 1700		δ ^{99}Tc 4500
						$[MoCp_2H_3]Cl$	−2953	$[TcHg]^+$	−3672
$[YCp_3](THF)$	−371					$[MoCp_2H_2]$	−2507	$[Tc(NCMe)_6]^+$	−1908
				$[NbCp(CO)_4]$	−2065	$[MoCp(CO)_3H]$	−2047	$[Tc(dmpe)_3]^+$	−1854
				$[Nb(CO)_6]^-$	−1672	$[Mo(CO)_6]$	−1857		
				$[Nb(PF_3)_6]^-$		$[\{MoCp(CO)_3\}_2]$	−1856		
						$[Mo\{P(OMe)_3\}_6]$	−1358		
						$[MoCp(CO)_3Me]$	−1735		
						$[MoCp(CO)_3I]$	−1248		
						$[MoCp(CO)_3Br]$	−956		
		$[ZrF_6]^{2-}$(aq)	−191.1	$[NbF_6]^-$	−1035				
				$[Nb(NCS)_6]^-$	−882				
				$[Nb(SCN)_6]^-$	−320				
				$[NbCl_5](MeCN)$	−49				
				$[NbOCl_3]$	0				

K[Y(EDTA)](aq, pH 5.5)	−125.9					[MoCp(CO)$_3$Cl]	−836		
[YCp$'_2$Cl](THF)	−103	[ZrCp$_2$Cl$_2$]	−121.9						
[Y(NO$_3$)$_3$]·6H$_2$O(s)	−55	[ZrCp$_2$Br$_2$]	0						
[(YCp$'_2$Cl)$_2$](tol)	−97	[ZrCp$''_2$Cl$_2$]	82						
		[ZrCp$_2$I$_2$]	126.0			polyoxomolybdates	−20 to 150		
[{YCp$'_2$(μ-CH$_3$)}$_2$](tol)	−15					[MoO$_2$(pd)$_2$](dmf)	−4		
YCl$_3$(aq, 3M)	0			Cu$_3$[NbS$_4$](s)	330				
[Y(CH$_3$)CP']THF)	40					[MoO$_4$]$^{2-}$(aq)	0	[TcO$_4$]$^-$	0
[Y(OAc)$_3$](s)	45	[ZrCl$_6$]$^{2-}$(aq, HCl)	601.2	[NbCl$_6$]$^-$	460	[MoO(S$_2$CNEt$_2$)$_3$]$^+$	80	[TcO$_3$F]	44
						[MoO$_2$(S$_2$CNEt$_2$)$_2$]	176	[TcO$_3$]$^+$	161
						[{MoCp'(μ-S)(μ-SH)}$_2$]	389	[TcO$_2$F$_3$]	396
						[MoO$_3$S]$^{2-}$	497		
YCl$_3$·6H$_2$O(s)	58			Cu$_3$[NbSe$_4$](s)	1060	[MoO$_2$S$_2$]$^{2-}$	1067	[TcO$_2$(CN)$_4$]$^{3-}$	806
Y$_2$O$_3$(s)	270, 317[b]			[NbBr$_6$]$^-$	1191	[MoOS$_3$]$^{2-}$	1654		
				Tl$_3$[NbSe$_4$](s)	1200	[MoS$_4$]$^{2-}$	2259		
				Tl$_3$[NbSe$_4$](s)	2030	[Mo$_2$(OCMe$_3$)$_6$]	2645		
				Cu$_3$[NbTe$_4$](s)	2500	[MoSe$_4$]$^{2-}$	3145		
						[Mo$_2$(O$_2$CF$_3$)$_4$]	3874		
Range (ppm)	δ ^{139}La 1700		δ ^{177}Hf —		δ ^{181}Ta 9000		δ ^{183}W 111,500		δ ^{187}Re 7000
[LaCp$_3$(CNCy)$_2$]	−614					[WCp$_2$H$_2$]	−4663		
						[{WCp(CO)$_3$}$_2$]	−4033		
[LaCp$_3$(CNMe)$_2$]	−606					[WCp(CO)$_3$H]	−4010		
				[Ta(CO)$_6$]$^-$	−3450	[W(CO)$_6$]	−3486	[Re(CO)$_6$]$^+$	−3400
[La(NCMe)$_n$]$^{3+}$	−129					[WCp(CO)$_3$I]	−2990		
[LaB$_6$](s)	−128					[WCp(CO)$_3$Br]	−2578		
[La(OAc)$_3$](s)	−30(50)					[WCp(CO)$_3$Cl]	−2400		
La^{3+}(aq)	0			[TaF$_7$]$^{2-}$(HF)	−2295	WF$_6$	−1117		
[La{OP(NMe$_2$)$_3$}$_6$]$^{3+}$	66					polyoxotungstates	−250 to +60		
[La(NCS)$_7$]$^{4-}$	196					[WO$_4$]$^{2-}$(aq)	0	[ReO$_4$]$^-$	0
[La(en)$_4$]$^{3+}$	400					[WO$_3$S]$^{2-}$(aq)	841		
[La(S$_2$CNEt$_2$)$_4$]$^-$	710					[WO$_2$S$_2$]$^{2-}$(aq)	1787		
[LaCl$_6$]$^{3-}$	851			[TaCl$_6$]$^-$(aq)	0	WCl$_6$	2181		
				KTaO$_3$(s)	(0)	[WOS$_3$]$^{2-}$(aq)	2760		
				Cu$_3$[TaS$_4$](s)	(2740)	[WS$_4$]$^{2-}$	3769	[ReS$_4$]$^-$	3500
[LaBr$_6$]$^{3-}$	1090			Cu$_3$[TaSe$_4$](s)	(3730)	[W$_2$(OBu^t)$_6$]	4408		
				Tl$_3$[TaS$_4$](s)	(4070)	[W$_2$(O$_2$CCF$_3$)$_4$]	6760		
				Tl$_3$[TaSe$_4$](s)	(5210)				
				Cu$_3$[TaTe$_4$](s)	(5720)				

[a] The compounds were measured in solution unless the solid state (s) is specified. Cp is η^5-C$_5$H$_5$, Cp' is η^5-C$_5$H$_4$Me, Cp'' is η^5-C$_5$Me$_5$, Cy is cyclohexyl, tol is toluene, pd is 2,4-pentanedionate.

[b] Crystallographically non-equivalent positions.

mediated by the same excitations of oxygen σ- and π-bonding electrons to low-lying d orbitals.[41,51] The chemical shifts of ligating atoms are often found to correlate with those of the metal nucleus, because of the paramagnetic circulations that they have in common.

Dominance of the energy term is evident also in the shifts for halide complexes of Ti, V, Zr, La, Ta, and W. For titanium, the whole shielding range is spanned by the halides, with δ increasing in the sequence F < Cl < Br < I.[12] Other (d^0) complexes of molybdenum and tungsten (containing oxo, nitrido or imido ligands) follow this pattern,[20] as do d^0 arylimido complexes of vanadium, in which the vanadium shift increases with increase in the wavelength of the visible absorption, and with decrease in substituent electronegativity and p-donor ability.[55]

Very low shielding is observed also for the quadruply-bonded carboxylate dimers of molybdenum and tungsten, with low-lying δ orbitals (and considerable electronic asymmetry in the coordination sphere).[45,48] The addition of two axial pyridine ligands to the molybdenum trifluoroacetate dimer lengthens the quadrupole bond, red-shifts the low-energy absorption, and further decreases the ^{95}Mo shielding.[45]

The high metal shielding observed for the cyclopentadienyl compounds, and particularly the hydrides, is clearly related to the strong ligand field, and probably also to nephelauxetism (linked with the back-bonding). The effect of protonation of $[MoCp_2H_2]$ is striking, since it increases the metal shielding by 450 ppm[45] a similar protonation of ferrocene increases the ^{57}Fe shielding by more than twice as much. Such increase (observed also on alkylation) is linked with removal of a relatively low-energy d–d circulation as the d-electron lone pair is stabilized by bonding to hydrogen. An analogue in main-group chemistry is the increase in nitrogen shielding, by 100 ppm or more, with protonation of nitrogen in a delocalized system, pyridine for example.[45]

It is observed for all metal nuclei that alkylation of a polyhapto ligand (as from Cp to Cp′ to Cp″) deshields the metal nucleus, usually incrementally (per alkyl group). This has been attributed to the positive inductive effect of the alkyl groups, and confirmation of this has now been achieved in the XPES measurements on titanocene dihalides, $[TiCp_2X_2]$, $[TiCp''_2X_2]$, etc., since the Ti($2p_{3/2}$) binding energies decrease with methylation of the ligand and deshielding of ^{49}Ti.[52]

^{95}Mo shifts in sandwich complexes with a range of C_5, C_6, and C_7 ring types can be interpreted in terms of the ligand field splittings, with evidence from the (PES) orbital ionization energies. The shielding increases with forward- and back-bonding, and so decreases with an increase in ring size, and from closed to open systems (decreasing, therefore, with increase in reactivity, as observed in other transition metal sandwich complexes).[56]

Bulky substituents are found to deshield a metal (or other) nucleus, usually because of bond-weakening or angle distortion, as may be confirmed by IR spectroscopic or X-ray crystallographic measurements.[27] Deshielding is observed also for a metal nucleus in a four-membered chelate ring, whereas in a five-membered ring the shielding is increased relative to a larger ring or to comparable non-chelating ligands.[49]

In the transition series as a whole (and in main-group compounds) spectrochemical ligand dependence is less common than the nephelauxetic pattern, and is always linked with low-energy magnetically active excitations. Early in the transition series these involve low-lying d orbitals, and often tetrahedral species, in which the ligand field splitting is 4/9 of that for analogous octahedral coordination (and the nephelauxetic effect is smaller for four ligands than for six).

DECREASE IN METAL SHIELDING WITH INCREASE IN METAL–METAL BOND ORDER

In carbon (or nitrogen) resonance, as is well known, higher shielding is observed for triple than double bonds; the carbon shifts are 6, 123 and 72 ppm, respectively, for ethane, ethene and ethyne. In transition metal–metal bonds, however, it is likely that the shielding decreases monotonically with increase in bond order, as observed in ^{95}Mo resonance.[45] This result is not surprising, in view of the decrease in overlap from s to p to d orbitals, and the decrease in electronic symmetry (and increase in quadrupolar broadening) with increase in multiplicity of the M—M bond. It is the high alkyne shielding that is anomalous: the linearity of the bonds at carbon allow free diamagnetic circulation about the bond axis, which is prevented by the higher coordination number in transition metal complexes.[45]

INFLUENCE OF THE RADIAL TERM; THE NEPHELAUXETIC SERIES

The shielding pattern for titanium contrasts dramatically with those observed later in the transition series. For platinum the whole shielding range is spanned by the $[PtX_6]^{2-}$ hexahalides, with δ increasing as I < Br < Cl < I. This nephelauxetic pattern is observed when changes in the radial term

are larger than changes in Δ. For platinum(IV), the Δ and $\langle r^{-3}\rangle_{nd}$ values are both large, at the end of the series. Among the early transition metals, this pattern is evident in d^6 compounds of molybdenum and tungsten, such as $[M(CO)_5X]^-$ or $[Mo(phos)_5X]^-$ halide complexes, in which, again, the Δ and $\langle r^{-3}\rangle_{nd}$ values are large.

The nephelauxetic term, β, obtained from optical spectra,[53] is the ratio of the value of the Racah (interelectron repulsion) parameter B in the complex to that in the gaseous metal ion. The sequence of increase in $(1-\beta)$ and in the d-electron radius is given[53] as $F^- < H_2O <$ urea $< NH_3 <$ en $\approx ox^{2-} < NCS^- < CN^- \approx Cl^- < Br^- < I^- <$ S-ligands < Se-ligands (from hard to soft). For a given metal ion, therefore, the nephelauxetic effect tends to decrease across the row of the table (as C > N > O > F, etc.), but to increase down the group (as F < Cl < Br < I, etc.). The dependence on the ligating atom is weaker in the nephelauxetic compared to the spectrochemical series, and there may be a greater sensitivity to the nature of the metal (strong π-acceptors interacting more strongly with electron-rich metals).

The nephelauxetic effect thus increases with decrease in electronegativity of the ligand, as its reducing power and polarizability increase, also with increase in covalency of the M—L bond. Clearly, there is a difference in periodicity for the spectrochemical and nephelauxetic effects. They reinforce for ligating atoms from the same row, as was found in the early work on cobalt complexes, when linear δ/λ correlations were observed. Down the group of the ligating atom, however, spectrochemical and nephelauxetic effects are usually opposed (with an exception from nitrogen to phosphorus). This explains the multiplicity of δ/λ correlation lines when ligands from different rows of the Periodic Table are compared.[7]

The nephelauxetic pattern has been called "normal ligand (or halogen) dependence" and the spectrochemical pattern, "inverse ligand (or halogen) dependence".[10] The nephelauxetic pattern is normally observed in complexes of the later transition metals, such as cobalt or platinum (which were studied before the early transition metals), and in organic compounds; thus carbon shielding is maximal in CI_4, whereas titanium shielding is minimal in TiI_4.

Curiously, in the quadruply-bonded molybdenum compounds $[Mo_2X_4(PMe_3)_4]$, the metal shift decreases (though rather little) in the sequence Cl > Br > I of the X ligand. This appears to be a relativistic influence of the heavier halogens, since much of the decrease occurs from the bromide to the iodide.[45]

SOLID STATE NMR SPECTROSCOPY OF THE EARLY TRANSITION METAL NUCLEI

With the development of MAS (magic angle sample spinning) NMR instrumentation, solid state spectra are beginning to appear for the early transition metals (many for fairly symmetric species); some solid state shifts are included in Table 2. Spectra and chemical shifts, and some nqcc values, have been reported for ^{45}Sc, ^{89}Y and ^{139}La in inorganic solids,[58] ^{89}Y in aluminate and silicate phases[59] and in bismuth oxide solid solutions,[60] ^{51}V in V_2O_5–Al_2O_3 phases[61] and in vanadyl esters and chlorides,[62] ^{95}Mo in molybdates,[63] and ^{183}W in various tungstates.[64] These include a Keggin compound in which 12 equivalent tungstens, each octahedrally coordinated by oxygen, form a cage with an interstitial phosphorus. The tungsten spinning sidebands give the tensor elements which show an anisotropy of 1357 ppm for the tungsten.[64a] Clearly, the shielding anisotropy relaxation mechanism is likely to be important for ^{183}W compounds, not only polyoxotungstates.[5b,c]

POLYOXOMETALATES

There is a large and important literature of NMR studies of polyoxometalate systems, in resonance of ^{51}V, ^{93}Nb, ^{95}Mo, ^{183}W and many other nuclei (^{31}P, ^{17}O, etc.), as described in the reviews.[64b] Heterocomponents, including paramagnetic substitutions, are usefully studied by NMR.[5b]

BIOINORGANIC STUDIES

Transition metal nucleus NMR is beginning to be used in biological studies, as in recent ^{51}V work on metal ion binding in metalloproteins,[65] and on a vanadate-dependent peroxidase.[66] There have been several studies of the interaction of early transition metals with amino acids, hydroxy acids, etc. and some with polypeptides.

SPIN–SPIN COUPLING TO EARLY TRANSITION METAL NUCLEI

Like metal nucleus chemical shifts, spin–spin coupling constants J(ML) between a metal and a ligand nucleus contain information about the coordination sphere.[67,68] A large number of coupling constants are known from work with the other nucleus: couplings to ^{183}W, for example, from satellites in ^1H, ^{13}C, ^{19}F or ^{31}P spectra. Since J values are proportional to the magnetogyric ratios (γ) of the coupled nuclei, comparisons are made in terms

of the reduced coupling constant K (where J is in Hz and K in N A^{-2} m^{-3}):

$$K(\mathrm{ML}) = \frac{4\pi^2 J(\mathrm{ML})}{h\gamma_{\mathrm{M}}\gamma_{\mathrm{L}}}. \quad (4)$$

Metal nucleus coupling is dominated by the Fermi contact term (J^{Fc}) of Ramsey's second-order perturbation theory.[69] The nuclei interact by way of the s electrons in the bonds between them (since s but not $p, d, \ldots$ electrons can contact the nucleus). Like σ_{p}, J^{Fc} involves a sum over excited states, but can be approximated by use of an effective excitation energy. This now refers to a triplet state ($^3\Delta E$), as the electron spins must be uncoupled. A simple expression is[70]

$$K^{\mathrm{Fc}}(\mathrm{ML}) = \left(\frac{2}{3}\mu_o\mu_B\right)^2 \frac{s_{\mathrm{M}}^2(0)s_{\mathrm{L}}^2(0)P^2}{(^3\Delta E)}, \quad (5)$$

where the $s^2(0)$ terms represent the electron densities at the M and L nuclei, and P is the bond order given by the valence s-orbital coefficients in the MO. Alternatively,[71]

$$K^{\mathrm{Fc}}(\mathrm{ML}) = (\tfrac{2}{3}\mu_o\mu_B)^2 s_{\mathrm{M}}^2(0)s_{\mathrm{L}}^2(0)\pi_{\mathrm{ML}}, \quad (6)$$

where π_{ML} is the mutual polarizability of the orbitals on M and L, involving a sum over excited states. ^1J(VP) values in [VCp(CO)$_3$(PZ$_3$)] complexes have been found to correlate with isotropic ^{31}P hyperfine coupling constants in the ESR spectra of the isoelectronic complexes [FeBr(NO)$_2$(PZ$_3$)],[72] since both couplings are mediated by the Fermi contact.

The $s^2(0)$ terms are strongly periodic, increasing across the row and down the group, so K values vary in this manner.[67] Thus ^1K(WP) parallels ^1K(MoP) in corresponding compounds, with a ratio of 2.76, attributed to the increased electron density at the heavier nucleus.[49] There are strong relativistic increases for heavier elements.[68] Although not allowed for in the simpler theory,[69–71] spin–spin coupling is particularly susceptible to relativistic effects, which involve contraction of s (and p) shells and the consequent expansion of d and f shells, and the spin–orbit splitting of $p, d, \ldots$ shells.[57] These effects become sizeable after the lanthanide series, as for example for tungsten.

Coupling constants commonly decrease in magnitude as $^1K \gg {}^3K > {}^2K > {}^4K$, with alternations of sign. When there are multiple paths for the coupling, as in chelate or other rings, ^1K is the algebraic sum of the contributions. Thus a ^2J(ML) value in a five-membered ring is small (compared with the value for corresponding open-chain ligands) since the ^3J coupling contributes also, and is normally opposite in sign; but a ^2J value in a six-membered ring is increased by the ^4J contribution, for which the sign is the same. One-bond couplings ^1K are usually positive, tending to become negative to the right of the Periodic Table and lower down the groups;[67] a lone pair on a coupled nucleus gives a negative contribution to K^{Fc}. Two-bond couplings ^2K usually correlate with ^1K. ^1K decreases (algebraically) with increase in oxidation number of M. It increases in magnitude (regardless of sign) with increase in electronegativity of substituents on either nucleus (since the bonds to the more electronegative substituents have more p character). Ligands on the metal are less influential than substituents on the ligating atom. Thus the largest ^1J(WP) value observed, 485 Hz, is that for the PF_3 ligand in [W(CO)$_5$(PF$_3$)];[73] and ^1J(VP) values in [VCp(CO)$_3$(PZ$_3$)]$^-$ complexes correlate with the electronegativity (or Taft σ constant) of the substituent Z (e.g. as F > Ph > OMe > $NNMe_2$ > Me).[74]

^1K decreases with increase in coordination number (with decrease in the number of bonds over which the s orbital is distributed). Similarly, magnitudes of ^1K are smaller for bridging than terminal ligands, if monatomic or diatomic (H, N_2, CN etc.). Decrease in a coupling constant in a free ligand is used as a test of complexation (particularly since a negative contribution is lost when a lone pair forms a bond). ^1K increases also with the multiple bonding (with increase in the s component of the σ bond); ^1J(WC) is 80, 120, and 210 Hz, respectively, for W—C, W=C and W≡C bonds in the same complex.[75]

The stereospecificity of coupling constants is well known. ^1K(ML) is greater for equatorial than for axial ligands in trigonal bipyramidal molecules (as the axial bonds are longer, with more p, d character); and greater for ligands which are *trans* to a ligand with a smaller *trans* influence (the tendency to lengthen and weaken a bond *trans* to itself).

In conclusion: many NMR parameters which are measured for analytical purposes have a greater chemical significance than is generally supposed. This may be truer for the transition metal nuclei than for main-group nuclei, for which NMR parameters have been measured for many decades, and for which the theory is better known. The new opportunities provided by the developments in instrumentation ensure that NMR study of the transition metal nuclei, particularly those of the earlier members of the series (^{53}Cr for example) which have only recently come into the spectroscopist's net, offers considerable promise.

REFERENCES

1. P. Laszlo (Ed.), *NMR of Newly Accessible Nuclei*. Academic Press, New York (1983).

2. C. Brévard and P. Granger, *Handbook of High Resolution Multinuclear NMR*. Wiley-Interscience, New York (1981).
3. J. Mason (Ed.), *Multinuclear NMR*. Plenum Press, New York (1987).
4. O. W. Howarth, in *Multinuclear NMR* (Edited by J. Mason), Chap. 5. Plenum Press, New York (1987).
5. (a) J. K. M. Sanders and B. K. Hunter, *Modern NMR Spectroscopy; a Guide for Chemists*, Oxford University Press, Oxford (1987); (b) T. L. Jorris, M. Kozik, N. Casan-Pastor, P. J. Domaille, R. G. Finke, W. K. Miller and L. C. W. Baker, *J. Am. Chem. Soc.* 1987, **109**, 7402; (c) R. Benn, C. Brévard, A. Rufinska and G. Schroth, *Organometallics* 1987, **6**, 938.
6. D. Rehder, in *Multinuclear NMR* (Edited by J. Mason), Chap. 5. Plenum Press, New York (1987).
7. J. Mason, *Chem. Rev.* 1987, **87**, 1299.
8. D. Rehder, *Chimia* 1986, **40**, 186.
9. J. J. Dechter, *Progr. Inorg. Chem.* 1985, **33**, 393.
10. R. G. Kidd, *An. Rep. NMR Spectrosc.* 1980, **10A**, 1.
11. R. G. Kidd and R. J. Goodfellow, in *NMR and the Periodic Table* (Edited by R. K. Harris and B. E. Mann), Chap. 8. Academic Press, London (1978).
12. D. Rehder, *Magn. Res. Rev.* 1984, **9**, 125.
13. P. Granger, in *NMR of Newly Accessible Nuclei* (Edited by P. Laszlo), Chap. 15. Academic Press, New York (1983).
14. R. G. Kidd, in *The Multinuclear Approach to NMR Spectroscopy* (Edited by J. B. Lambert and F. G. Riddell), Chap. 2. NATO ASI Series, Reidel, Dordrecht (1983).
15. P. L. Rinaldi, G. C. Levy and G. R. Choppin, *Rev. Inorg. Chem.* 1980, **2**, 53.
16. W. von Philipsborn, *Pure Appl. Chem.* 1986, **58**, 513.
17. R. Benn and A. Rufinska, *Angew. Chem.* 1986, **24**, 861.
18. J. A. Davies, in *The Chemistry of the Metal–Carbon Bond* (Edited by F. R. Hartley and S. Patai), Chap. 21. Wiley, Chichester (1982).
19. D. Rehder, *Bull. Magn. Reson.* 1982, **4**, 33.
20. M. Minelli, J. H. Enemark, R. T. C. Brownlee, M. J. O'Connor and A. G. Wedd, *Coord. Chem. Rev.* 1985, **68**, 169.
21. T. Drakenberg, *An. Rep. NMR Spectrosc.* 1986, **17**, 231.
22. M. Holz, *Progr. NMR Spectrosc.* 1986, **18**, 327 and refs therein.
23. C. Deverell, *Progr. NMR Spectrosc.* 1969, **4**, 237 and refs therein.
24. *NMR Spec. Per. Rep. R. Soc. Chem.* (various editors) (1972).
25. H. Le Bail, C. Chachary, P. Rigny and R. Bougon, *J. Phys. Lett.* 1983, **44**, 1017.
26. A. Abragam, *The Principles of Nuclear Magnetism*. Oxford University Press, Oxford (1978).
27. A. Hafner, L. S. Hegedus, G. deWeck, B. Hawkins and K. H. Dötz, *J. Am. Chem. Soc.* 1988, **110**, 8413.
28. D. F. Evans and P. H. Missen, *J. Chem. Soc., Dalton Trans.* 1982, 1929.
29. E. A. C. Lucken, *Nuclear Quadrupole Coupling Constants*. Academic Press, London (1969).
30. P. S. Belton, I. J. Cox and R. K. Harris, *J. Chem. Soc., Faraday Trans. 2* 1985, **81**, 63.
31. N. F. Ramsey, *Phys. Rev.* 1950, **78**, 699; 1952, **86**, 243.
32. C. J. Jameson and J. Mason, in *Multinuclear NMR* (Edited by J. Mason), Chap. 3. Plenum Press, New York (1987).
33. J. Mason, *Adv. Inorg. Chem. Radiochem.* 1979, **22**, 199; 1976, **18**, 197.
34. J. S. Griffith and L. E. Orgel, *Trans. Faraday Soc.* 1957, **53**, 601.
35. C. J. Jameson and H. S. Gutowsky, *J. Chem. Phys.* 1964, **40**, 1714.
36. A. D. Buckingham and P. J. Stephens, *J. Chem. Soc.* 1964, 2747, 4583.
37. K. D. Becker and U. Berlage, *J. Magn. Reson.* 1983, **54**, 272.
38. R. Bramley, M. Brorson, A. M. Sargeson and C. E. Schäffer, *J. Am. Chem. Soc.* 1985, **107**, 2780.
39. K. Kanda, H. Nakatsuji and T. Yonezawa, *J. Am. Chem. Soc.* 1984, **106**, 5888.
40. H. Nakatsuji, K. Kanda, K. Endo and T. Yonezawa, *J. Am. Chem. Soc.* 1984, **106**, 4653.
41. B. N. Figgis, R. G. Kidd and R. S. Nyholm, *Proc. R. Soc. A* 1962, **269**, 469; A. Carrington, *Molec. Phys.* 1960, **3**, 271.
42. C. J. Jameson, *NMR Spec. Per. Rep. R. Soc. Chem.*, Chap. 1 (1972).
43. R. Bramley, M. Brorson, A. M. Sargeson and C. E. Schäffer, *Inorg. Chem.* 1987, **26**, 314.
44. T. Nakano, *Bull. Chem. Soc. Jpn* 1977, **50**, 661.
45. R. A. Grieves and J. Mason, *Polyhedron* 1986, **5**, 415.
46. H. C. E. McFarlane, W. McFarlane and D. S. Rycroft, *J. Chem. Soc., Dalton Trans.* 1976, 1616.
47. T. A. Carlson, C. C. Lu, T. C. Tucker, C. W. Nestor and F. B. Malik, *Eigenvalues, Radial Expectation Values, and Potentials for Free Atoms from Z = 2 to 126 as calculated from Relativistic Hartree–Fock–Slater Atomic Wave Functions*. Oak Ridge National Laboratory, Oak Ridge, Tennessee (1970).
48. D. J. Santure, J. C. Huffman and A. P. Sattelberger, *J. Am. Chem. Soc.* 1985, **24**, 371.
49. G. T. Andrews, I. J. Colquhoun and W. McFarlane, *J. Chem. Soc., Dalton Trans.* 1982, 2353.
50. P. S. Braterman, G. W. Milne, E. W. Randall and E. Rosenberg, *J. Chem. Soc., Dalton Trans.* 1973, 1027.
51. A. Müller, E. Diemann and C. K. Jørgensen, *Struct. Bond.* 1973, **14**, 23.
52. P. G. Gassman, W. H. Campbell and D. W. Macomber, *Organometallics* 1984, **3**, 385.
53. C. K. Jørgensen, *Absorption Spectra and Chemical Bonding in Complexes*, Pergamon Press, Oxford (1962); C. K. Jørgensen, *Progr. Inorg. Chem.* 1962, **4**, 73; C. K. Jørgensen, *Modern Aspects of Ligand Field Theory*. North-Holland, Amsterdam (1971).
54. M. N. Ackermann, C. R. Barton, C. J. Deodene, E. M. Specht, S. C. Keill, W. E. Schreiber and H. Kim, *Inorg. Chem.* 1989, **28**, 397.

55. D. D. Devore, J. D. Lichtenhan, F. Takusagawa and E. A. Maatta, *J. Am. Chem. Soc.* 1987, **109**, 7408.
56. J. C. Green, R. A. Grieves and J. Mason, *J. Chem. Soc., Dalton Trans.* 1986, 1313.
57. P. Pyykkö and J. P. Desclaux, *Accts Chem. Res.* 1979, **12**, 276.
58. A. R. Thompson and E. Oldfield, *J. Chem. Soc., Chem. Commun.* 1987, 27.
59. R. Dupree and M. E. Smith, *Chem. Phys. Lett.* 1988, **148**, 41.
60. P. D. Battle, B. Montez and E. Oldfield, *J. Chem. Soc., Chem. Commun.* 1988, 584.
61. L. R. Coustumer, B. Taouk, M. Le Meur, E. Payen, M. Guelton and J. Grimblot, *J. Phys. Chem.* 1988, **92**, 1230.
62. W. Basler, H. Lechert, K. Paulsen and D. Rehder, *J. Magn. Reson.* 1981, **45**, 170.
63. V. M. Mastikhin, O. B. Lipina and R. I. Maximovskaya, *Chem. Phys. Lett.* 1988, **148**, 413.
64. C. T. G. Knight, G. L. Turner, R. Kirkpatrick and E. Oldfield, *J. Am. Chem. Soc.* 1986, **108**, 7426.
65. A. Butler and M. J. Danzitz, *J. Am. Chem. Soc.* 1987, **109**, 1864.
66. H. Vilter and D. Rehder, *Inorg. Chim. Acta* 1987, **136**, L7; D. Rehder, H. Vilter, A. Duch, W. Priebsch and C. Weidemann, *Rec. Trav. Chim.* 1987, **106**, 408.
67. C. J. Jameson, in *Multinuclear NMR* (Edited by J. Mason), Chap. 4. Plenum Press, New York (1987).
68. C. J. Jameson, in *Phosphorus-31 NMR Spectroscopy in Sterochemical Analysis* (Edited by J. G. Verkade and L. D. Quin), Chap. 6. VCH, Deerfield Beach, Florida (1987).
69. N. F. Ramsey, *Phys. Rev.* 1953, **91**, 303.
70. H. M. McConnell, *J. Chem. Phys.* 1956, **24**, 460.
71. J. A. Pople and D. P. Santry, *Molec. Phys.* 1964, **8**, 1.
72. D. Rehder and J. Schmidt, *Transition Met. Chem.* 1977, **2**, 41.
73. R. L. Keiter and J. G. Verkade, *Inorg. Chem.* 1969, **8**, 2115.
74. D. Rehder, W. L. Dorn and J. Schmidt, *Transition Met. Chem.* 1976, **1**, 233.
75. D. N. Clark and R. R. Schrock, *J. Am. Chem. Soc.* 1978, **100**, 6774.

Polyhedron Vol. 8, No. 13/14, pp. 1669–1674, 1989
Printed in Great Britain

0277–5387/89 $3.00+.00
© 1989 Maxwell Pergamon Macmillan plc

REDOX, PHOTOCHEMICAL AND OPTICAL ACTIVITY IN MOLYBDENUM CHEMISTRY: TOWARDS MOLECULAR ELECTRONICS

J. A. McCLEVERTY

School of Chemistry, University of Birmingham, P.O. Box 363,
Birmingham B15 2TT, U.K.

Abstract—Compounds containing the $[Mo(NO)]^{3+}$ group are redox-active. Incorporation into tris(3,5-dimethylpyrazolyl)borato (L*) systems, e.g. [MoL*(NO)XY] where X, Y = halide, alkoxide, aryloxide, amide, anilide, thiolate, etc. affords a variety of species which undergo one-electron reduction. The factors influencing this behaviour are described. Attachment of the molybdenum redox centre to macrocyclic polyethers and the effect of added cation is discussed. The group {MoL*(NO)X} can be attached to the periphery of tetra-aryl porphyrins, and the electrochemistry and photochemistry of the extra-ring metallated species is reported. A series of ferrocenyl compounds, $[(\eta^5\text{-}C_5H_5)Fe(\eta^5\text{-}C_5H_4)C_6H_4E\{ML^*(NO)X\}]$ and *trans*-$[(\eta^5\text{-}C_5H_5)Fe(\eta^5\text{-}C_5H_4)C_6H_4Z{=}ZC_6H_4E\{ML^*(NO)X\}]$ (where Z = CH or H, E = O or NH, M = Mo or W, X = Cl or I) have been prepared, their electrochemistry investigated and several compounds identified as having non-linear optical (Secondary Harmonic Generation) properties.

In general, compounds containing the $[Mo(NO)]^4$ or $[Mo(NO)]^{3+}$ groups are redox-active, readily undergoing one-electron reduction to $[Mo(NO)]^5$ or $[Mo(NO)]^{2+}$ species. This is true of the tris(3,5-dimethylpyrazolyl)borato nitrosyl complexes of molybdenum [MoL*(NO)XY], where X, Y = halide, or pseudo-halide, alkoxide, aryloxide, alkyl- or aryl-amide, alkane or arene thiolate, hydrazide or related species. The most carefully studied of this group of compounds have been the halides, where Y = Cl and I.[1] The dichloride, $[MoL^*(NO)Cl_2]$, is readily reduced electrochemically to the monoanion $[MoL^*(NO)Cl_2]^-$, which is stable in solution and can be isolated by chemical reduction of the neutral precursor using trifluoroethylhydrazine and triethylamine. The diiodide, in contrast, exhibits much more complex behaviour. In scrupulously dry THF, $[MoL^*(NO)I_2]$ is reversibly reduced to the corresponding monoanion at a relatively anodic potential. The ESR spectrum of this species ($\langle g \rangle = 2.027$) is characteristic and consistent with a paramagnetic $[Mo(NO)]^5$ system in which the unique electron is in an orbital predominantly located on the metal. However, if moisture is allowed to enter the system, or if the neutral diodide is exposed to water even in the absence of formally reducing conditions, reduction to $[MoL^*(NO)I_2]^-$ is rapidly superseded by formation of a new reduced species, identified as $[MoL^*(NO)I(solvent)_n]$, resulting from dissociation of I^- from $[MoL^*(NO)I_2]^-$. Iodide ion was readily detected in "wet" solutions of $[MoL^*(NO)I_2]$.

The ESR spectrum of $[MoL^*(NO)I(solvent)_n]$ ($\langle g \rangle = 1.988$) was significantly different to that of $[MoL^*(NO)I_2]^-$ and the two species could be readily identified by this technique. Attempts to isolate $[MoL^*(NO)I_2]^-$ or $[MoL^*(NO)I(solvent)_n]$ were not very successful, although $[MoL^*(NO)I_2Li(OEt_2)_2]$ was obtained on treatment of $[MoL^*(NO)I_2]$ with tolyl lithium in ether. This compound could be regarded either as $[MoL^*(NO)I_2]^-$ stabilized by $[Li(OEt_2)_2]^+$, or as $[MoL^*(NO)I]$ "solvated" by $LiI(OEt_2)_2$. ESR and IR spectral data were most consistent with the former model. Analogues of $[MoL^*(NO)I(solvent)_n]$, where the "solvent" is amine, viz. $[MoL^*(NO)X(NHC_nH_{2n})]$ (X = Cl or I; $n = 4$ or 5) have, however, been isolated and characterized.[2] They too are paramagnetic ($\langle g \rangle = 1.999$) and were very readily oxidized to the diamagnetic $[MoL^*(NO)I(NC_nH_{2n})]$. The electrochemical behaviour was irreversible as expected ($E_p^c = -1.04 \rightarrow 1.68$ V in CH_2Cl_2 vs SCE, depending on X and n).

The compounds [ML*(NO)XQ] (Q = OR, OAr,

NHR, NHAr, SR, SAr), like their dihalide analogues, undergo one-electron reductions, and it is not surprising that when X = Cl, the reduced species are stable to dissociation, whereas [MoL*(NO)IQ]$^-$ readily dissociates with I^- loss. This property can be very important not only for the electrochemical behaviour of this class of molybdenum and related tungsten nitrosyl complexes, but also for the synthetic chemistry of this system.

Substitution of halide in [ML*(NO)X_2] (M = Mo, X = Cl, I; M = W, X = Cl) is facile. Thus, in general, mono-alkoxides and aryloxides are obtained by heating the dihalide with the alcohol or phenol, or by addition of triethylamine or sodium carbonate under milder conditions in the presence of substrate.[3] An alternative is to convert the dihalide to a halide acetate, e.g. [MoL*(NO)X(OCOMe)]; treatment of this with ROH affords the alkoxide with elimination of acetic acid demonstrating neatly the power of acetate as a most effective leaving group.[4] The mono-amido compounds are prepared even more easily by reaction, in many cases at room temperature, of the dihalide with 2 mole equivalents of diluted amine.[3] Formation of [ML*(NO)$(NHR)_2$], however, requires more vigorous conditions.[5] It is also possible to prepare mixed ligand species of the types [ML*(NO)(OR)(NHR)], [ML*(NO)(OR)(SR)] etc.

The structures of representative members of the series [MoL*(NO)XQ] have been determined crystallographically.[6] In all of them, the protective nature of the tris(3,5-dimethylpyrazolyl)borate ligand is evident, the 5-methyl groups hanging down over the metal atom, effectively enforcing six-coordination of these species which normally prefer seven- or eight-coordination. In addition, the bond distances between the metal and the hetero atom of the Q group are short, indicating a substantial amount of p_π–d_π or d_π–d_π bonding between O, N or S and Mo. These factors undoubtedly contribute to the high stability of this class of compounds towards oxidative decomposition and to the facility with which they may be reduced.

The $E_{1/2}$ values of the reduction potentials of [ML*(NO)XQ] are strongly influenced by the nature of M, X and Q.[7] In general, potentials of tungsten compounds are usually between 300 and 500 mV more cathodic than those of their molybdenum analogues. There are insufficient data to state precisely how X influences the redox potential in these species, other than that the $E_{1/2}$ values of iodo complexes are usually significantly more anodic than those of their chloro analogues. However, the value of redox potential is substantially affected by the hetero atom in Q, and by the substituents attached to them. In general, for molybdenum complexes $E_{1/2}$ values fall in the ranges $-0.50 \rightarrow 0.65$ V when Q = OR, $-0.10 \rightarrow -0.42$ V when Q = OAr, $-1.10 \rightarrow -1.22$ V when Q = NHR and $-0.60 \rightarrow -1.10$ V when Q = NHAr. Further fine-tuning of the redox potential can be achieved by using *para-* or *meta*-substitution of aryl rings in species of the type [MoL*(NO)X(ZC_6H_4Y)], where Z = O or NH and Y = H, NH_2, OMe, F, CN, etc., in the *meta* or *para* positions.[8] Thus, in the series [MoL*(NO)I$(NCH_6H_4Z$-*p*)] (Z = NH_2, OH, OMe, H, F, Br, Cl, I, SO_2Ph, N_2Ph) the $E_{1/2}$ value ranged from *ca* -0.5 to -1.0 V and can be correlated very well with Hammett σ constants for these substituents.

MIXED VALENCE SYSTEMS BASED ON MOLYBDENUM AND TUNGSTEN BIMETALLIC COMPLEXES

The facility with which phenolato and anilido complexes could be prepared presented an opportunity to synthesize bimetallic species bridged by $OC_6H_4O^{2-}$, $NHC_6H_4NH^{2-}$ and related groups. A series of compounds, both *meta-* and *para-*, of the type [{ML*(NO)X}$_2$$ZC_6H_4Z$] (Z = O, NH) and [{ML*(NO)X}$_2${$ZC_6H_4EC_6H_4Z$}] (M = Mo or W, X = Cl or I; Z = O or NH, E = nothing, O, S, SO_2, CH_2, CH_2CH_2, CO) were examined electrochemically. All underwent two reduction processes, and the electrochemical behaviour was interpreted in terms of interaction between the two metal centres as follows:[9] (a) very strong where the ligands were *p*-$ZC_6H_4Z^{2-}$; (b) intermediate where the ligands were *m*-$ZC_6H_4Z^{2-}$, $NHC_6H_4OC_6H_4NH^{2-}$ or $OC_6H_4COC_6H_4O^{2-}$; and (c) very weak or negligible where the ligands were $NHC_6H_4QC_6H_4NH^{2-}$ or CH_2CH_2. The extent of coupling was estimated by the separation, ΔE, between the two reduction waves exhibited by the bimetallic species. Systems having ΔE between 500 and 1000 mV revealed strong interaction, those in the range 100–400 mV were regarded as intermediate, whereas those where ΔE was less than 100 mV hardly interacted at all. A careful analysis of the electrochemical data, and comparison with those obtained from "simple" monometallic phenolates and anilides, suggested that interaction between the two redox centres owed much to transmission through the σ-bonding system. Our view was strengthened by the discovery that a number of bimetallic species bridged by *saturated* ligands, e.g. [{MoL*(NO)Cl}$_2${$N(CH_2CH_2)_2N$}], in which the piperidine (2−) ligand is known to adopt the chair configuration, undergo two distinct one-electron reductions (ΔE in this case is 560 mV). Reduction of diamagnetic [{MoL*(NO)Cl}$_2$$(OC_6H_4O$-*p*)] electrochemically

and by cobaltocene afforded the paramagnetic ($S = 1/2$) monoanion.[11] ESR spectral examination of this species at room temperature revealed that the unique electron is hopping between the two metal centres, but that at liquid N_2 temperatures, it is localized on one metal. Similar treatment of the *meta*-isomer revealed that the monoanion exhibits valence-trapped behaviour at room temperature.

PHOTOCHEMICALLY-ACTIVE REDOX SYSTEMS

As a development of our interest in the electrochemical and electronic properties of bimetallic redox systems, we have attempted to prepare biredox centres containing a metal and an organic electron-transfer centre. Porphyrins are well-established redox systems in their own right, and we have succeeded in modifying the periphery of tetraphenylporphyrin to create mono- and tetraphenolic functionality, **IV**.

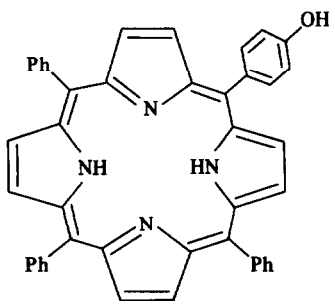

Treatment of $[MoL^*(NO)X_2]$ (X = Cl, I, OH, NHCMePh) with $(HOC_6H_4)Ph_3PorphH_2$ afforded the extra-ring metallated species $[MoL^*(NO)X\{(OC_6H_4)Ph_3PorphH_2\}]$.[12] These species are electrochemically rich, a total of five electron-transfer processes being detected by cyclic voltammetry and differential pulse techniques. However, from the accumulated data, it is quite clear that there is very little interaction between the porphyrin and molybdenum redox centres in the ground state. Thus, the unmetallated porphyrin (i.e. $(HOC_6H_4)Ph_3PorphH_2$) exhibits two oxidation and two reduction processes, all one-electron transfers, and the potentials are virtually unaffected by the nature of the molybdenum species when they are attached. The $E_{1/2}$ values of the molybdenum moiety are influenced only by the nature of X in $[MoL^*(NO)X\{(OC_6H_4)Ph_3PorphH_2\}]$. Similar results have been obtained from related metallophorphyrins, $[MoL^*(NO)X\{(OC_6H_4)Ph_3PorphM'\}]$ (M′ = Zn, Ni, Pt, FeCl).

However, it was noticed that the normal fluorescence of the tetra-arylporphyrins was quenched on attachment of the $\{OMoL^*(NO)X\}$ fragment. Thus the emission at 645 nm (caused by excitation at 510 nm) of $[MoL^*(NO)Cl\{(OC_6H_4)Ph_3PorphH_2\}]$ is reduced to 7% of that in $Ph_4PorphH_2$ and that in the species where X = OH and NHCHMePh to 15 and 25%, respectively. That the observed quenching process is apparently intramolecular has been demonstrated by dilution studies. There is a broad correlation between the efficiency of quenching and the $E_{1/2}$ values for the reduction of the molybdenum fragment in the porphyrin species (X = Cl, $E_{1/2} = -0.29$ V; X = OH, $E_{1/2} = 0.81$ V; X = NHCMePh, $E_{1/2} = -1.12$ V). The energy of the first excited state in the porphyrin fragment is 0.85 eV, and this is sufficient to effect reduction of the molybdenum fragment, at least when X = Cl, and OH. A possible explanation for the quenching effect is that, on photo-excitation of the porphyrin centre, electron-transfer occurs from the macrocycle's first excited state to the LUMO of the $\{MoL^*(NO)X\}$ moiety, thereby preventing normal relaxation processes in the porphyrin which lead to fluorescence. Such behaviour in porphyrins to which quinonoidal groups are attached (the so-called diad, triad and tetrad centres) is well-established and is central to biological photosynthesis.[13]

The extra-ring metallated porphyrins are diamagnetic, at least in the ground state, and thus are ESR "silent". On irradiation (visible light) of dichloromethane–toluene (75:25 v/v) glasses of $[MoL^*(NO)Cl\{(OC_6H_4)Ph_3PorphH_2\}]$, the system is still ESR "silent".[14] It was hoped that signals due to the porphyrin radical cation and $\{OMoL^*(NO)Cl\}^-$ centres would be observed. Reduction of $[MoL^*(NO)Cl\{(OC_6H_4)Ph_3PorphH_2\}]$ with cobaltocene did indeed afford a paramagnetic ($S = 1/2$) species whose ESR spectrum is entirely consistent with a reduced molybdenum phenoxide centre to which a virtually unperturbed porphyrin ring was attached. Interestingly, this system also exhibits extremely efficient fluoroscence quenching.[12]

The behaviour of this system has been further complicated by the observation of apparent photochemically-stimulated intermolecular electron-transfer between $(HOC_6H_4)Ph_3PorphH_2$ and $[MoL^*(NO)Cl_2]$, or species closely related to this dichloride. Solutions of $[MoL^*(NO)Cl_2]$ show weak ESR signals associated with a paramagnetic $\{MoL^*(NO)Cl\}$ ($S = 1/2$) centre. It is not clear whether this is $[MoL^*(NO)Cl_2]^-$, or a closely related species, or a decomposition product. However, when dichloromethane–toluene glasses containing a mixture of $(HOC_6H_4)Ph_3PorphH_2$ and this $[MoL^*(NO)Cl_2]$ are irradiated by visible light,

the weak ESR signal is significantly enhanced. In our view, photo-electron transfer must be occurring between the excited porphyrin and a molybdenum-based acceptor.

TOWARDS MOLECULAR ELECTRONICS: NON-LINEAR OPTICAL PROPERTIES AND SECONDARY HARMONIC GENERATION IN FERROCENYL MOLYBDENUM NITROSYL COMPOUNDS

There is currently great interest in the general field of "molecular electronics". This has stimulated a search for new liquid crystalline compounds, for "organic" metals and semiconductors, for materials exhibiting non-linear optical, photochromic or electrochromic properties and for molecular species exhibiting bulk piezo- or pyro-electric phenomena.

Non-linear optical properties are extremely important in optical information processing, viz. in the switching, amplification and modulation of optical signals. According to the Pockels effect, the refractive index of a material varies with an applied electric field, and this permits the switching or modulation of light signals which are passing through that material in response to the applied field. To a first approximation, the polarization, P, of a material (i.e. the induced dipole per unit volume) is proportional to an applied electric field (produced by the oscillating electric (E) of the radiation) and the linear electrical susceptibility (χ).

However, a more exact description of this relationship includes higher powers of E:

$$\chi = \varepsilon_0(\chi_1 E+\chi_2 E^2+\chi_3 E^3+\chi_4 E^4+\cdots),$$

where χ_2, χ_3, χ_4 are higher order electric susceptibilities and ε_0 is a universal constant. It should be noted that for materials which crystallize in centrosymmetric space groups (which includes the majority of non-chiral coordination and organometallic compounds), the even terms, χ_2 and χ_4, must be zero. In linear optics, the refractive index, η, of a substance is related to the electric susceptibility by the relationship $\eta^2 = 1+\chi_1$. In non-linear optics, if terms beyond second order are ignored, $P = \varepsilon_0(\chi_1 E+\chi_2 E^2)$ which can be simplified to $P = \varepsilon_0\chi_{\text{eff}}E$ where $\chi_{\text{eff}} = (\chi_1+\chi_2 E)$. Thus

$$\eta^2 = 1+\chi_{\text{eff}}.$$

Since χ_{eff} is dependent on the field E, the refractive index is also field dependent. Having established these relationships for materials exhibiting non-linear optical behaviour, similar considerations are needed for molecular species. The molecular dipole moment, μ, which is induced by an applied electric field, E, obeys a relationship very similar to that in solids, viz:

$$\mu = \alpha E+\beta E^2+\gamma E^3+\cdots,$$

where α is the molecular polarizability, and β and γ are the first and second hyperpolarizabilities. To obtain large values for χ_2, large values of β are needed.

The necessary requirements to obtain large values of β in molecules are that they must have (a) excited states close in energy to the ground state, (b) large oscillator strengths for electronic transitions from ground to excited states, and (c) a large difference between ground and excited state dipole moments. This means, in effect, that suitable molecules must be dipolar and highly polarizable. If the molecule as a solid material is to have NLO properties, however, it must crystallize in a non-centrosymmetric space group. This may be achieved adventitiously, but can be guaranteed if a chiral species is isolated as a pure enantiomer or diastereomer. Demonstration of potentially interesting β values is obtained by the Kurtz powder test in which Secondary Harmonic Generation (SHG) is measured by irradiating a powdered or microcrystalline sample with a laser frequency, ν (typically 1907 or 1064 nm), and observation of emission at 2ν. The efficiency of the material as a Secondary Harmonic Generator is referred to that of urea, taken as unity ($\Xi = 1$).

In constructing compounds with potentially non-linear optical properties, design usually requires a powerful donor and separate strong acceptor functions connected by a polarizable bridge. Typical donor groups are NMe_2, OMe or 4-pyridyl and acceptors can be NO_2, CO_2R or 4-pyridinium salts. The bridging group may be a benzene ring or *trans*-$C_6H_4Z{=}ZC_6H_4$—, where Z = CH or N. Some simple organic materials which exhibit SHG are 3-nitroaniline ($\Xi = 8$) and 2-methyl-4-nitroaniline ($\Xi = 22$),[15] and certain types of polyacetylenic compounds have Ξ values in the hundreds. Coordination and organometallic species can have donor or acceptor properties at least as powerful as amines or the cyano group, and the ability of organometallics to exhibit non-linear optical properties was elegantly demonstrated by the ferrocenyl species *trans*-$[(\eta^5\text{-}C_5H_5)Fe\{(\eta^5\text{-}C_5H_4)CH{=}CHC_6H_4NO_2\text{-}p\}]$[16] where the SHG efficiency, Ξ, was 62 (excitation at 1907 nm).

Recognizing that {MoL*(NO)X} is extremely electron-withdrawing (electron "deficient" metal, electronegative X and powerful π-acceptor NO), compounds incorporating this functionality and ferrocenyl residues have been prepared.[17] Three basic types of complex have been prepared: (i) $[(\eta^5\text{-}C_5H_5)Fe(\eta^5\text{-}C_5H_4)C_6H_4E\{ML^*(NO)X\}]$,

(ii) $[(\eta^5\text{-}C_5H_5)Fe(\eta^5\text{-}C_5H_4)C_6H_4N{=}NC_6H_3RE\{ML^*(NO)X\}]$ and (iii) $[(\eta^5\text{-}C_5H_5)Fe(\eta^5\text{-}C_5H_4)C_6H_4CH{=}CHC_6H_4E\{ML^*(NO)X\}]$, where E = O or NH, M = Mo or W, X = Cl or I and R = H or Me. In species (ii) and (iii) the alkene diazo bridges adopt the *trans*-configuration, but as yet no crystallographic data are available. These compounds are, or course, electroactive and the ferrocenyl moiety undergoes a reversible one-electron oxidation at $E_{1/2}$ values in the region of +0.58 V. The oxidation potential is very little influenced by the nature of the attached groups, in contrast to the behaviour of the chelating dithioferrocenyl species $[\{\eta^5\text{-}C_5H_5)Fe(\eta^5\text{-}C_5H_3)S_2\{MoL^*(NO)X\}]$ where there is close contact between the iron and the nitrosyl group on the molybdenum, and $E_{1/2}$ (ferrocenyl) is shifted cathodically by 90 mV relative to dithioferrocene.[18] In a comparable way, the reduction potentials of the {MoL*(NO)X} fragment in the ferrocene-containing systems is little influenced by the metallocene, but follows the normal trends as influenced by M, X and E. In testing these materials for SHG behaviour, we have found that iodides are readily decomposed by laser light at 1064 nm, but this is not too surprising in view of the facile reductive elimination of I^- in solution, referred to above. Many of the compounds investigated exhibit negligible or very low values of Ξ, but a number have been found which give rise to Ξ values up to 125.

In attempting to design compounds' NLO properties, we have resolved the chiral species [ML*(NO)X(OR)] and [ML*(NO)X(HNR)].[19] These species are enantiomeric and resolution was effected by forming alkoxides with optically pure monosaccharides and with resolved $NH_2CHMePh$. It appears that the prochiral $[ML^*(NO)X_2]$ reacts with (+)-sugar or (+)- or (−)-$NH_2CHMePh$ to form two diastereomers, one of which rapidly converts into the thermodynamically stable form. A crystal structure of one diastereomer, $[MoL^*(NO)I(C_{12}H_{19}O_6)]$, where $C_{12}H_{19}O_6H$ is 1,2,5,6-di-O-isopropylidene-D-glucofuranose, has established that the absolute configuration at the metal is *S*. The conformations of all related compounds were then established by CD measurements. The iodoglucofuranose does not exhibit SHG and, so far, incorporation of enantiomerically pure {MoL*(NO)X} fragments into other simnple systems has not yielded compounds with significant Ξ values.

CONCLUSION

The effectiveness and versatility of the redox centres based on {ML*(NO)} has been demonstrated. That these have useful and applicable properties is clear, and the design of molecules which have unusual and even specific electronic properties is already possible. The creation of liquid crystalline species and polymers containing {ML*(NO)} is in progress.

Acknowledgements—I am very grateful to my close colleagues Drs C. J. Jones and P. D. Beer who have provided much of the energy and day-to-day guidance essential to the prosecution of several key developments in the work described above. Those who achieved the results described are mentioned in the references, and to our skilled, dedicated and persevering post-doctoral and post-graduate colleagues must go my particular thanks. We are grateful to Professor M. B. Hursthouse and Drs A. J. Edwards and T. A. Hamor for specific assistance with crystallographic studies, to Professor D. Bloor for carrying out SHG measurements, to Drs F. H. Mabbs and D. Collinson for valuable help with ESR measurements, and to Professor R. D. Gillard and Dr P. Williams for help with CD spectroscopy. Finally, I wish to specially acknowledge the contributions of our Polish colleagues, Drs A. Wlodarczyk and S. S. Kurek, who have reminded us of the value and benefit of a rigorous classical laboratory training. The work described above was generously supported by the SERC and by the University of Birmingham.

REFERENCES

1. T. N. Briggs, C. J. Jones, J. A. McCleverty, B. D. Neaves, N. El. Murr and H. M. Colquhoun, *J. Chem. Soc., Dalton Trans.* 1985, 1249.
2. N. Al-Obaidi, T. A. Hamor, C. J. Jones, J. A. McCleverty, K. Paxton, A. J. Howes and M. B. Hursthouse, *Polyhedron* 1988, **7**, 1931.
3. S. J. Reynolds, C. F. Smith, C. J. Jones and J. A. McCleverty, *Inorg. Synth.* 1985, **23**, 4.
4. A. Wlodarczyk, A. J. Edwards and J. A. McCleverty, *Polyhedron* 1988, **7**, 103.
5. N. Al-Obaidi, T. A. Hamor, C. J. Jones, J. A. McCleverty and K. Paxton, *J. Chem. Soc., Dalton Trans.* 1986, 1525.
6. J. A. McCleverty, *Chem. Soc. Rev.* 1983, **12**, 331.
7. N. Al-Obaidi, M. Chaudhury, D. Clague, C. J. Jones, J. C. Pearson, J. A. McCleverty and S. S. Salam, *J. Chem. Soc., Dalton Trans.* 1987, 1733.
8. N. Al-Obaidi, S. M. Charsley, W. Hussain, C. J. Jones, J. A. McCleverty, B. D. Neaves and S. J. Reynolds, *Transition Met. Chem.* 1987, **12**, 143; C. J. Jones, J. A. McCleverty and P. J. Sidebotham, work to be published.
9. S. M. Charsley, C. J. Jones, J. A. McCleverty, B. D. Neaves, S. J. Reynolds and G. Denti, *J. Chem. Soc., Dalton Trans.* 1988, 293; S. M. Charsley, C. J. Jones, J. A. McCleverty, B. D. Neaves and S. J. Reynolds, *J. Chem. Soc., Dalton Trans.* 1988, 301.
10. N. Al-Obaidi, T. A. Hamor, C. J. Jones, J. A.

McCleverty and K. Paxton, *J. Chem. Soc., Dalton Trans.* 1987, 2653.
11. W. Hussain, C. J. Jones, J. A. McCleverty, G. Sabatino, D. Collinson and F. E. Mabbs, work to be published.
12. S. S. Kurek, P. D. Beer, C. J. Jones, J. A. McCleverty. N. M. Rowley and D. Collinson, work to be published.
13. M. A. Bergkamp, J. Dalton and T. L. Netzel, *J. Am. Chem. Soc.* 1982, **104**, 253; A. Sieniarczuk, A. R. McIntosh, T. Ho, M. J. Stillman, K. J. Roach, A. C. Weedon, J. R. Bolton and J. S. Connally, *J. Am. Chem. Soc.* 1983, **105**, 7224; E. S. Schmidt, T. S. Calderwood and T. C. Bruice, *Inorg. Chem.* 1986, **25**, 971; D. Gust, T. A. Moore, A. L. Moore, D. Barrett, L. O. Harding, L. R. Makings, P. A. Liddell, F. C. De Cshryver, M. van der Auwers, R. V. Bensasson and M. Rougee, *Inorg. Chem.* 1988, **110**, 321.
14. N. M. Rowley, D. Collinson, C. J. Jones and J. A. McCleverty, work to be published.
15. D. J. Williams, *Angew. Chem. Int. Edn. Engl.* 1984, **23**, 690.
16. M. L. H. Green, S. R. Marder, M. E. Thompson, J. A. Bandy, D. Bloor, R. V. Kolinsky and R. J. Jones, *Nature* 1988, **330**, 360.
17. B. Coe, C. J. Jones and J. A. McCleverty, work to be published.
18. P. Sidebotham, P. D. Beer, T. A. Hamor, C. J. Jones and J. A. McCleverty, *J. Organomet. Chem.* 1989, submitted for publication.
19. A. Woldarczyk, S. S. Kurek, J. A. McCleverty, M. A. J. Moss and M. S. Tolley, *Angew. Chem. Int. Edn. Engl.*, submitted for publication.

Polyhedron Vol. 8, No. 13/14, pp. 1675–1682, 1989
Printed in Great Britain

0277–5387/89 $3.00+.00
© 1989 Maxwell Pergamon Macmillan plc

NUCLEOPHILIC BEHAVIOUR OF MONOMERIC *CIS*-TRIOXOTUNGSTEN(VI) COMPLEXES LWO_3 (L = TRIDENTATE N-MACROCYCLE)

PETER SCHREIBER and KARL WIEGHARDT*

Lehrstuhl für Anorganische Chemie I, Ruhr-Universität, D-4630 Bochum, F.R.G.

and

BERNHARD NUBER and JOHANNES WEISS

Anorganisch-Chemisches Institut der Universität, D-6900 Heidelberg, F.R.G.

Abstract—This paper reviews recent work from our laboratory on the nucleophilic behaviour of monomeric complexes of the type LWO_3 and $L'WO_3$ (L = 1,4,7-triazacyclononane and L′ = N,N′,N″-trimethyl-1,4,7-triazacyclononane) which contain a *cis*-trioxometal(VI) unit. The chemistry of oxotungsten(VI) species has received far less attention in the past than the corresponding chemistry of oxomolybdenum(VI) complexes. Crystal structures of $LWO_3 \cdot 3H_2O$, $[L'WO_2(OH)]Br$, $[LWO_2Br]Br$, $[L_2W_2O_5](S_2O_6) \cdot 4H_2O$, $[(LWO_3)_2BPh_2][BPh_4]$, $[LWO_2(\mu\text{-}O)W(O_2)_2O(H_2O)]$, $[(L'MoO_3)_4Co][BPh_4]_2 \cdot C_2H_5OH$ and $[(L'MoO_3)_4Fe^{III}][BPh_4]_3 \cdot Na[BPh_4]$ have been determined and the results are presented here. From this study it is clearly established that the terminal oxo-groups in *cis*-trioxometal(VI) complexes display nucleophilic character. They react readily with electrophiles (H^+, Co^{2+}, Fe^{3+}) or oxophiles, such as the BPh_4^- anion, forming a variety of novel complexes.

A number of oxotungsten(VI) complexes have been characterized by X-ray crystallography in the past.[1] Monomeric compounds containing one or two terminal oxo-groups are quite abundant, whereas the chemistry of the corresponding *cis*-trioxotungsten(VI) complexes has only recently been investigated in more detail. No such complex has been characterized by X-ray crystallography to date;[2] the only example appears to be $(dien)WO_3$ where dien represents diethylenetriamine.[3] This complex is labile in aqueous solution affording uncoordinated amine and WO_4^{2-}. The reaction of WO_3 with oxalate has been reported to give $[WO_3(C_2O_4)]^{2-}$ and $[W_2O_5(C_2O_4)_3]^{4-}$, but again no structural data are available.[4]

We have recently reported the facile synthesis of two *cis*-trioxotungsten(VI) complexes and their molybdenum analogues containing the tridentate macrocycles 1,4,7-triazacyclononane (L) and N,N′,N″-trimethyl-1,4,7-triazacyclononane (L′)

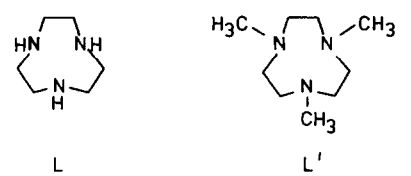

L L′

via exhaustive oxidative decarbonylation of $LM(CO)_3$ species (M = W, Mo) with H_2O_2 in tetrahydrofuran (THF), or via reaction of MO_3 with L and L′ in water according to eqs (1) and (2).[5–7] It was shown that these species are relatively stable in aqueous or alcoholic solutions; they are therefore suited for investigations of the reactivity of the *cis*-trioxotungsten(VI) moiety.

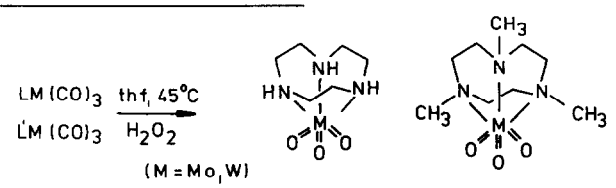

(1)

(2)

* Author to whom correspondence should be addressed.

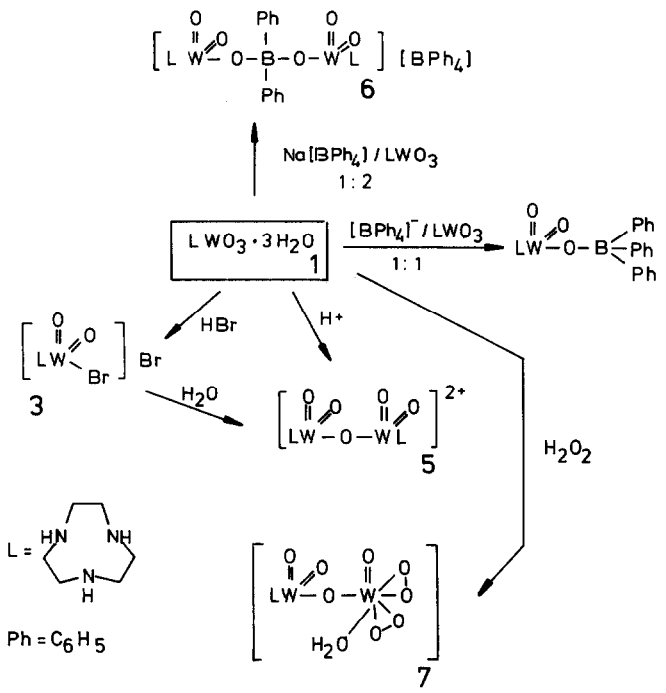

Scheme 1.

From ^{17}O NMR studies of these complexes it was concluded that the terminal oxo-groups of the *cis*-MO_3 unit are quite basic[7] and, consequently, should be susceptible to electrophilic attack by oxophilic reagents such as transition metal cations, protons or suitable silicon and boron compounds. Indeed, we have shown that $Co(ClO_4)_2 \cdot 6H_2O$ reacts in dry methanol with $L'MO_3$ species (M = Mo, W) affording deep blue cations of $[(L'MO_3)_4Co^{II}]^{2+}$ which contain a tetrahedral $Co^{II}O_4$ core. The $L'MO_3$ moieties function as monodentate ligands. A similar species, $[(L'MoO_3)_4Fe^{III}](ClO_4)_3$, with unknown structure, has also been obtained (an $Fe^{III}O_8$ polyhedron has been proposed incorrectly on the basis of IR spectroscopic data).[7] At that time no single crystals suitable for X-ray crystallography were available.

In this report we will review the chemistry of the LWO_3 and $L'WO_3$ species and present crystallographic results of a variety of products. Full details of these investigations will be published subsequently elsewhere.[8]

SYNTHESES

Scheme 1 summarizes the reactions of $LWO_3 \cdot 3H_2O$ investigated. Compounds $LWO_3 \cdot 3H_2O$ (**1**) and $L'WO_3 \cdot 3H_2O$ (**2**) are readily protonated in acidic aqueous solution. Three products have been isolated as colourless, crystalline materials, eqs (3)–(5), depending on the exact reaction conditions:

$$\mathbf{1} + HBr \longrightarrow \underset{(\mathbf{3})}{[LWO_2Br]Br} \quad (3)$$

$$\mathbf{2} + HBr \longrightarrow \underset{(\mathbf{4})}{[L'WO_2(OH)]Br} \quad (4)$$

$$2\,\mathbf{1} + 2H^+ \rightleftharpoons \underset{(\mathbf{5})}{[LWO_2{-}O{-}WO_2L]^{2+}} + H_2O. \quad (5)$$

One terminal oxo-group in **1** or **2** is converted into a coordinated hydroxide generating **4**, which may then undergo substitution reactions with nucleophiles such as Br^- forming **3**. In the absence of coordinating anions, using $HClO_4$ or CH_3SO_3H as the source for protons, **1** dimerizes to produce the μ-oxo-bridged species $[L_2W_2O_5]^{2+}$ (**5**).[9] The corresponding binuclear species, $[L'_2W_2O_5]^{2+}$, has been obtained previously by the reaction of $L'W(CO)_3$ with concentrated nitric acid.[10]

The reaction of **1** with H_2O_2 in aqueous solution affords colourless crystals of an unsymmetrical binuclear complex $[LWO_2(\mu\text{-}O)WO(O_2)_2(H_2O)]$ (**7**), which contains a bis(peroxo)oxoaquatungsten(VI) unit. This reaction demonstrates that the coordinated ligands L and L′ may be cleaved off in solution.

Compounds **1** and **2** were found to react with $[B(C_6H_5)_4]^-$ in acidic aqueous solution. Thus, by using a ratio tungsten–boron of 1 : 1 the neutral

complexes $LWO_3B(C_6H_5)_3$ and $L'WO_3B(C_5H_5)_3$, respectively, precipitated, which contain the W—O—$B(C_6H_5)_3$ structural unit. Goedken and co-workers have recently reported a similar reaction of a vanadyl(IV) complex with $[BPh_4]$.[11] When the tungsten–boron ratio was raised to 2:1 the binuclear complex, $[LO_2W—O—B(C_6H_5)_2—O—WO_2L][B(C_6H_5)_4]$ (**6**), precipitated. These reactions demonstrate convincingly, that the oxo-ligands of the *cis*-trioxotungsten(VI) moiety in **1** and **2** react smoothly with oxophiles; they are good nucleophiles.

The reaction of $L'WO_3$ (or $L'MoO_3$), in weakly coordinating solvents (methanol), with $Co(ClO_4)_2 \cdot 6H_2O$ and $Fe(ClO_4)_3 \cdot 6H_2O$ affords deep blue $[(L'MO_3)_4Co](ClO_4)_2$ and pale yellow $[(L'MO_3)Fe](ClO_4)_3$ (M = Mo, W), respectively.[7] Single crystals suitable for X-ray crystallography have now been obtained with $[BPh_4]^-$ counter-anions: $[(L'MoO_3)_4Co][BPh_4]_2$ (**8**) and $[(L'MoO_3)_4Fe][BPh_4]_3 \cdot Na[BPh_4]$ (**9**).

CRYSTAL STRUCTURES

The structure of the monomeric *cis*-trioxo-molybdenum(VI) complex, (dien)MoO_3, has been reported.[12] Compound **1** represents the first such structurally characterized species of tungsten(VI) (Fig. 1). Surprisingly, there are two significantly different W=O_t bonds in the solid state (Table 1): two short bonds of 1.77(1) Å and one longer W(1)—O(3) bond of 1.851(8) Å. This is in contrast to the structures of (dien)MoO_3,[12] $[LReO_3]Cl$[13] and $[(MoO_3)_2(EDTA)]^{4-}$,[14] where three equivalent short M—O bonds have been found. In **1** each terminal oxo-group is bound via hydrogen bonding to two water molecules of crystallization. The O—W—O bond angles are obtuse (av. 107°). The

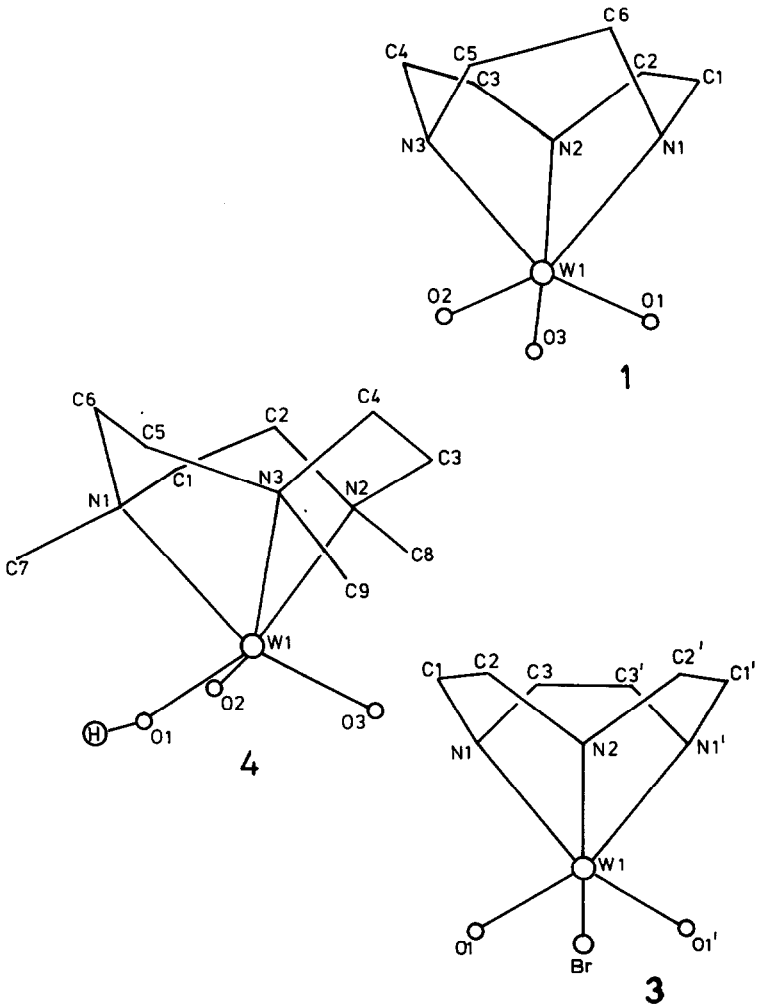

Fig. 1. Perspective view of the neutral molecule and cations in crystals of $LWO_3 \cdot 3H_2O$ (**1**) $[LWO_2Br]Br$ (**3**) and $[L'WO_2(OH)]Br$ (**4**), respectively.

Table 1. Selected bond distances (Å) and angles (°) of the complexes

$LWO_3 \cdot 3H_2O$ (**1**)					
W(1)—O(1)	1.777(9)		W—N(av.)	2.31(1)	
W(1)—O(2)	1.760(9)		N—W—N(av.)	72.2(4)	
W(1)—O(3)	1.851(8)		O—W—O(av.)	107.0(5)	
			N—W—O(av.)	154.8(5); 87.7	
$[LWO_2Br]Br$ (**3**)					
W(1)—Br	2.468(4)		Br—W(1)—O(1)	101.5(5)	
W(1)—O(1)	1.76(2)		O(1)—W(1)—N(1)	161.6(8)	
W(1)—N(1)	2.32(2)		Br—W(1)—N(1)	87.6(6)	
W(1)—N(2)	2.13(3)		N(1)—W(1)—N(2)	74.0(9)	
			O(1)—W(1)—O(1)′	101(1)	
$[L'WO_2(OH)]Br$ (**4**)					
W(1)—O(1)	1.89(1)		O(1)—W(1)—O(2)	100.9(9)	
W(1)—O(2)	1.76(2)		O(1)—W(1)—O(3)	104.5(9)	
W(1)—O(3)	1.79(2)		O(2)—W(1)—O(3)	110.6(9)	
W(1)—N(1)	2.34(2)		N—W(1)—N(av.)	74.2(9)	
W(1)—N(2)	2.30(2)				
W(1)—N(3)	2.36(2)				
$[L_2W_2O_5](S_2O_6) \cdot 4H_2O$ (**5**)					
W(1)—O(1)	1.91(2)	1.88(3)[a]	W(1)—O(1)—W(2)	157.6(9)	
W(1)—O(2)	1.71(1)	1.81(2)	O(1)—W(1)—O(2)	104.4(5)	104(1)[a]
W(1)—O(3)	1.67(1)	1.83(1)	O(1)—W(1)—O(3)	104(1)	108(1)
W(1)—N(1)	2.27(3)	2.13(3)	O(2)—W(1)—O(3)	108.7(7)	106.1(8)
W(1)—N(2)	2.29(1)	2.26(1)			
W(1)—N(3)	2.30(1)	2.35(2)			
$[(LWO_3)_2(\mu\text{-}BPh_2)][BPh_4]$ (**6**)					
W(1)—O(3)	1.729(5)	1.731(4)[a]	O(1)—W(1)—O(2)	105.0(2)	106.6(2)[a]
W(1)—O(2)	1.741(3)	1.725(5)	O(1)—W(1)—O(3)	105.7(2)	105.8(2)
W(1)—O(3)	1.808(4)	1.796(4)	O(2)—W(1)—O(3)	106.4(2)	105.8(2)
B(1)—O(3)	1.513(7)	1.489(10)	B(1)—O(3)—W(1)	152.4(4)	175.7(4)
B(1)—C(13)	1.62(1)		O(6)—B(1)—O(3)	106.2(5)	
B(1)—C(19)	1.62(1)		C(13)—B(1)—C(19)	115.4(5)	
W(1)—N(1)	2.300(6)	2.247(6)	O(6)—B(1)—C(19)	107.7(6)	
W(1)—N(2)	2.317(5)	2.310(6)	O(6)—B(1)—C(13)	109.5(5)	
W(1)—N(3)	2.268(5)	2.339(6)	O(3)—C(1)—C(13)	108.6(6)	
			O(6)—B(1)—C(13)	109.5(5)	
			N—W—N(av.)	72.7	
$[(LWO_2)(\mu\text{-}O)WO(O_2)_2(H_2O)]$ (**7**)					
W(1)—O(1)	1.856(8)		O(1)—W(1)—O(2)	104.9(6)	
W(1)—O(2)	1.755(10)		O(1)—W(1)—O(3)	107.2(6)	
W(1)—O(3)	1.81(1)		O(2)—W(1)—O(3)	106.0(6)	
W(1)—N(1)	2.23(1)		N—W—N(av.)	73.4	
W(1)—N(2)	2.30(1)		W(1)—O(1)—W(2)	152.2(2)	
W(1)—N(3)	2.28(1)		O(1)—W(2)—O(5)	97.8(4)	
W(2)—O(4)	2.411(9)		O(1)—W(2)—O(4)	80.7(3)	
W(2)—O(5)	1.74(1)		O(4)—W(2)—O(5)	177.4(4)	
W(2)—O(6)	1.94(1)		O(1)—W(2)—O(6)	89.3(3)	
W(2)—O(7)	1.92(1)		O(4)—W(2)—O(6)	79.6(4)	
W(2)—O(8)	1.97(1)		O(5)—W(2)—O(6)	102.5(5)	
W(2)—O(9)	1.92(1)		O(1)—W(2)—O(7)	131.8(5)	
W(2)—O(1)	1.966(8)		O(4)—W(2)—O(7)	80.7(4)	
O(8)—O(9)	1.47(2)		O(5)—W(2)—O(7)	101.9(5)	
O(6)—O(7)	1.43(2)		O(6)—W(2)—O(7)	43.6(5)	
			O(1)—W(2)—O(8)	86.8(4)	

Table 1—*continued*

O(6)—W(2)—O(9)	130.1(4)		O(4)—W(2)—O(8)	77.2(4)	
O(7)—W(2)—O(9)	88.7(5)		O(5)—W(2)—O(8)	100.6(5)	
O(8)—W(2)—O(9)	44.4(4)		O(6)—W(2)—O(8)	156.8(4)	
W(2)—O(6)—O(7)	67.4(6)		O(7)—W(2)—O(8)	130.9(4)	
W(2)—O(7)—O(6)	69.0(6)		O(1)—W(2)—O(9)	130.0(4)	
W(2)—O(8)—O(9)	66.0(5)		O(4)—W(2)—O(9)	78.8(4)	
W(2)—O(9)—O(8)	69.7(6)		O(5)—W(2)—O(9)	100.8(5)	
$[(L'MoO_3)_4Co][BPh_4]_2 \cdot C_2H_5OH$ (**8**)					
Co(1)—O(1)	1.914(5)		O(1)—Co(1)—O(4)	109.0(2)	
Co(1)—O(4)	1.926(4)		O(4)—Co(1)—O(1)′	112.9(2)	
Mo(1)—O(1)	1.791(5)	1.783(4)[a]	O(4)—Co(1)—O(4)′	106.6(3)	
Mo(1)—O(2)	1.688(5)	1.719(5)	Co(1)—O(1)—Mo(1)	175.7(3)	
Mo(2)—O(3)	1.711(5)	1.705(5)	Co(1)—O(4)—Mo(2)	175.3(3)	
Mo(1)—N(1)	2.386(6)	2.333(6)	O(1)—Mo(1)—O(2)	107.1(2)	107.0(2)[a]
Mo(1)—N(2)	2.332(9)	2.319(6)	O(1)—Mo(1)—O(3)	106.8(2)	105.7(2)
Mo(1)—N(3)	2.363(6)	2.348(6)	O(2)—Mo(1)—O(3)	105.3(3)	105.5(2)
$[(L'MoO_3)_4Fe][BPh_4]_3 \cdot Na[BPh_4]$ (**9**)					
Fe(1)—O(1)	1.79(2)		Fe(1)—O(1)—Mo(1)	171(1)	
Mo(1)—O(1)	1.85(2)		O(1)—Mo(1)—O(2)	103(1)	
Mo(1)—O(2)	1.64(2)		O(1)—Mo(1)—O(3)	106(1)	
Mo(1)—O(3)	1.67(2)		O(2)—Mo(1)—O(3)	109(1)	
Mo(1)—N(1)	2.38(2)				
Mo(1)—N(2)	2.30(3)				
Mo(1)—N(3)	2.33(3)				

[a] The second column gives distances and angles in the molecule which are related to the first column assuming a non-crystallographic symmetry.

average W—N distance is 2.31(1) Å; the N—W—N bond angles are acute (av. 72.2°) due to the steric constraints of the cyclic triamine.

The structures of the cations in **3** and **4** (Fig. 1) are quite similar, they consist of the *cis*-dioxotungsten(VI) group, a monodentate anion (Br^- or OH), and a tridentate amine ligand. The average $W{=}O_t$ bond length is 1.77 Å and the O=W=O angle is again obtuse in both complexes. Interestingly, the W—N bonds in the *trans* position with

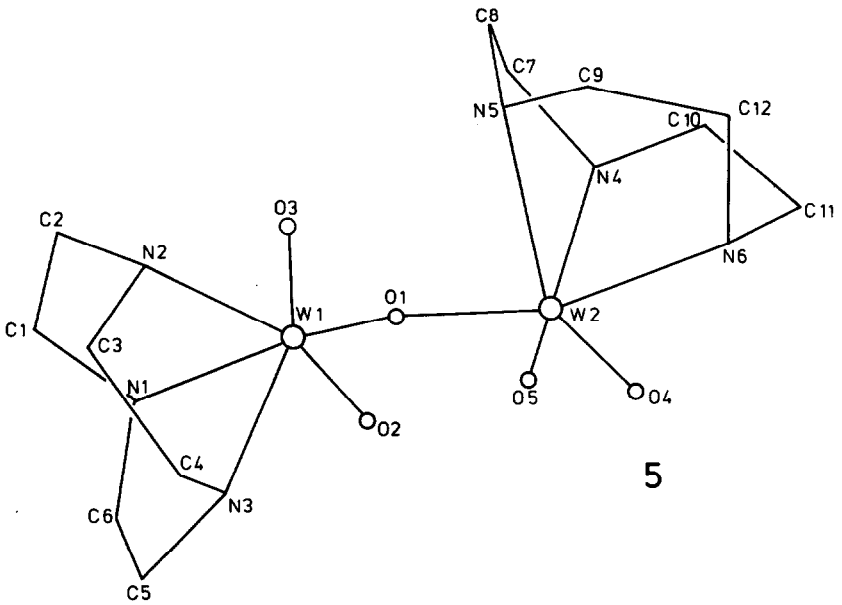

Fig. 2. Perspective view of the dication in $[L_2W_2O_5](S_2O_6) \cdot 4H_2O$ (**5**).

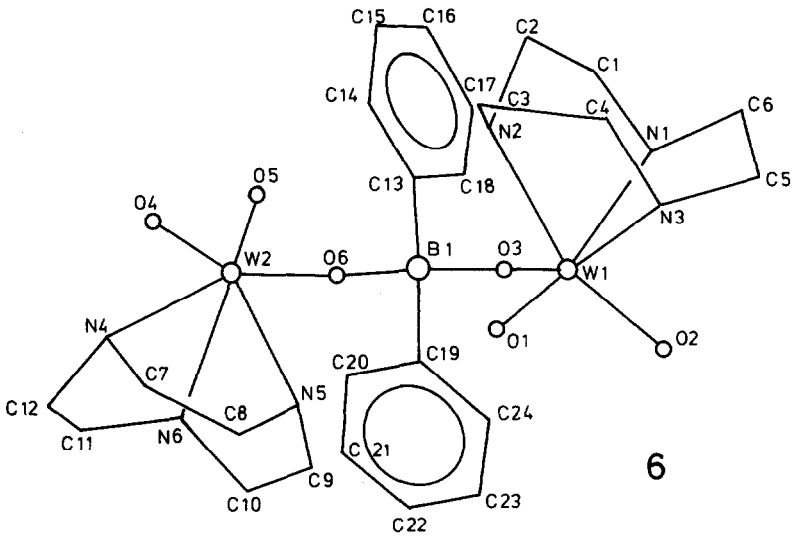

Fig. 3. Perspective view of the cation in $[(LWO_3)_2BPh_2][BPh_4]$ (**6**).

respect to the bromo and hydroxo ligands, are significantly shorter than the corresponding W—N bonds *trans* to the terminal oxo-groups. This reflects a strong structural *trans*-influence of the π-donating oxo-groups. The μ-oxo-bis[*cis*-dioxomolybdenum(VI)]$^{2+}$ unit is known,[1,15] but corresponding complexes of tungsten(VI) have not been structurally characterized previously.[2] $[L_2W_2O_5](S_2O_6)\cdot 4H_2O$ (**5**) has now been characterized by X-ray crystallography (Fig. 2). The overall structure of the dication is very similar to its $[L'_2Mo_2O_5](Br_3)_2$ analogue,[15] except that the μ-oxo bridge is *not* linear (W—O—W 157.6(9)°) as it is in the $[Mo_2O_5]^{2+}$ unit. The terminal W=O_t groups exert again a *trans*-influence on the *trans*-W—N bond lengths (Table 1). The structure of the cation in **6** is shown in Fig. 3. It consists of two LWO_3 units which are connected by a BPh_2-fragment which is bound to one oxo-group of each LWO_3 unit. The boron centre is pseudo-tetrahedrally surrounded by two oxygen and two carbon atoms. The two W—O—B bond angles are obtuse and not equivalent (152.4(4) and 175.7(4)°).

Compound **7** consists of LWO_3 and $WO(O_2)_2(H_2O)$ units connected by an unsymmetrical μ-oxo bridge (Fig. 4). The dimensions of the

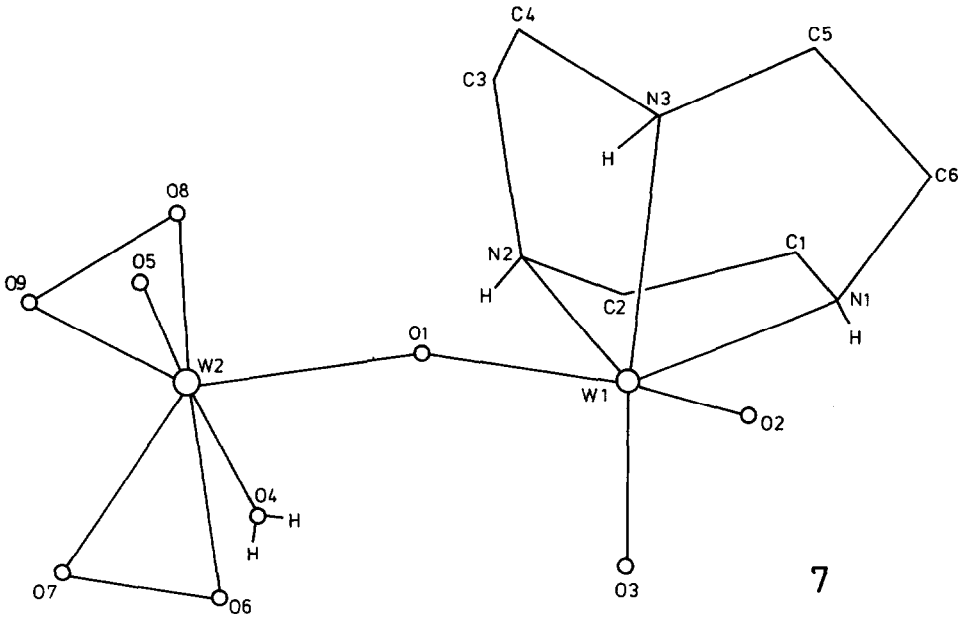

Fig. 4. Perspective view of the molecule in crystals of $[L'WO_2(\mu\text{-}O)WO(O_2)_2(H_2O)]$ (**7**).

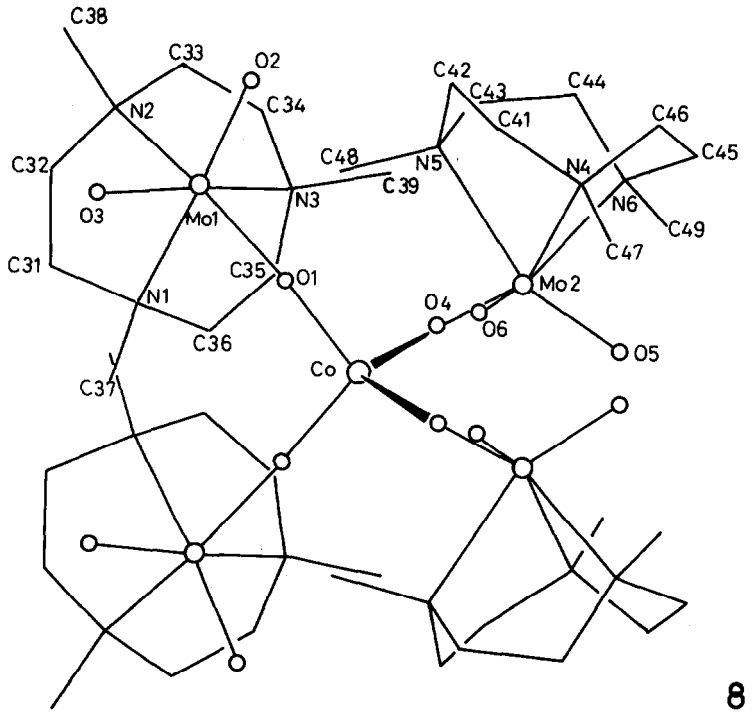

Fig. 5. Perspective view of the dication in $[(L'MoO_3)_4Co][BPh_4]_2 \cdot C_2H_5OH$ (**8**).

$WO(O_2)_2(H_2O)$ unit are very similar to those observed in the binuclear diperoxotungsten(VI) complex, $K_2[\{WO(O_2)_2(H_2O)\}_2O] \cdot 4H_2O$.[16] The LWO_3 unit in **7** is, within experimental error, identical to those in **5**. The W—O—W bridge is again not linear (W—O—W 152.2(2)°).

Figures 5 and 6 show the structures of the cations in **8** and **9**. The cobalt(II) ion in **8** is surrounded

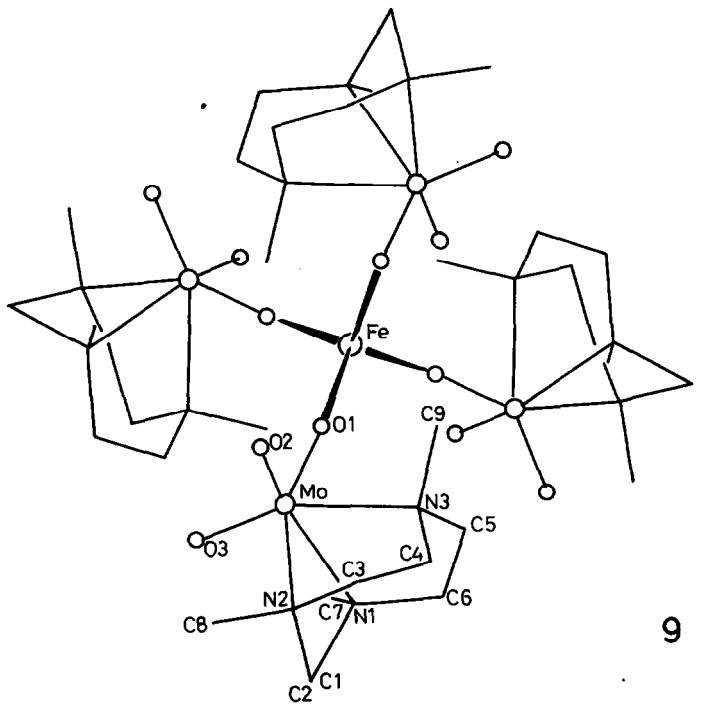

Fig. 6. Perspective view of the trication in $[(L'MoO_3)_4Fe][BPh_4]_3 \cdot Na[BPh_4]$ (**9**).

by four monodentate $L'MoO_3$ ligands forming a slightly distorted tetrahedral CoO_4 central core. Molecular analogues of **8** are $[Co(Me_3PO)_4]^{2+}$ and $[Co(Ph_3PO)_4]^{2+}$ which have not been characterized by X-ray crystallography.[17] The effective magnetic moment of **8** (at 298 K) of 4.2 μ_B is quite typical for tetrahedral cobalt(II).[7] The Co—O bond distance of 1.92 Å is identical to the one found in a heteropolytungstate, $[Co^{II}Mo_{12}O_{40}]^{6-}$.[18] The high-spin iron(III) centre (5.9 μ_B at 298 K) in **9** is in an exact tetrahedral environment of four monodentate $L'MoO_3$ units. Similar $Fe^{III}O_4$ cores have been identified in the compounds $[Fe^{III}W_{12}O_{40}]^{5-}$[19] and $Na_{14}[Fe^{III}_6O_{16}]$.[20]

REFERENCES

1. (a) Z. Dori, *Prog. Inorg. Chem.* 1981, **28**, 245; (b) Z. Dori, in *Comprehensive Coordination Chemistry* (Edited by G. Wilkinson, R. D. Gillard and J. A. McCleverty), Vol. 3, p. 973. Pergamon Press, Oxford (1987).
2. R. H. Holm, *Chem. Rev.* 1987, **87**, 1401.
3. R. S. Taylor, P. Gans, P. F. Knowles and A. G. Sykes, *J. Chem. Soc., Dalton Trans.* 1972, 24.
4. A. K. Sengupta and S. K. Nath, *Ind. J. Chem.* 1981, **20A**, 203.
5. K. Wieghardt, M. Hahn, W. Swiridoff and J. Weiss, *Inorg. Chem.* 1984, **23**, 94.
6. W. Herrmann and K. Wieghardt, *Polyhedron* 1986, **5**, 513.
7. P. S. Roy and K. Wieghardt, *Inorg. Chem.* 1987, **26**, 1885.
8. P. Schreiber, Dissertation, Ruhr-Universität, Bochum (1989).
9. Compound **5** has also been obtained via hydrolysis of **4** in aqueous solution: P. Chaudhuri, K. Wieghardt, W. Gebert, I. Jibril and G. Huttner, *Z. Anorg. Allg. Chem.* 1985, **521**, 23.
10. G. Backes-Dahmann and K. Wieghardt, *Inorg. Chem.* 1985, **24**, 4049.
11. C.-H. Yang, J. A. Ladd and V. L. Goedken, *J. Coord. Chem.* 1988, **18**, 317.
12. F. A. Cotton and R. C. Elder, *Inorg. Chem.* 1964, **3**, 397.
13. K. Wiedhardt, C. Pomp, B. Nuber and J. Weiss, *Inorg. Chem.* 1986, **25**, 1659.
14. J. J. Park, M. D. Glick and J. L. Hoard, *J. Am. Chem. Soc.* 1969, **91**, 301.
15. K. Wieghardt, G. Backes-Dahmann, W. Herrmann and J. Weiss, *Angew. Chem.* 1984, **96**, 890; *Angew. Chem. Int. Edn Engl.* 1984, **23**, 899.
16. F. W. B. Einstein and B. R. Penfold, *Acta Cryst.* 1964, **17**, 1127.
17. R. H. Holm and F. A. Cotton, *J. Chem. Phys.* 1960, **32**, 1168.
18. A. S. Barrett, PhD thesis, Boston University (1972), cited in M. T. Pope, *Inorganic Chemistry Concepts 8: Heteropoly and Isopoly Oxometalates*, p. 24. Springer, Berlin (1983).
19. M. T. Pope and G. M. Varga Jr, *Inorg. Chem.* 1966, **5**, 1249.
20. G. Brachtel and R. Hoppe, *Angew. Chem.* 1977, **89**, 45; G. Brachtel and R. Hoppe, *Angew. Chem. Int. Edn Engl.* 1977, **16**, 43.

Polyhedron Vol. 8, No. 13/14, pp. 1683–1688, 1989
Printed in Great Britain

0277–5387/89 $3.00+.00
© 1989 Maxwell Pergamon Macmillan plc

THE COORDINATION CHEMISTRY OF TECHNETIUM IN ITS INTERMEDIATE OXIDATION STATES

ULDERICO MAZZI

Dipartimento di Scienze Farmaceutiche, Universita di Padova, via Marzolo 5, 35131 Padova, Italy

Abstract—The coordination behaviour of technetium is reviewed with an emphasis placed upon the chemical rather than pharmaceutical properties.

Among the early transition elements technetium is the most recently discovered, but, owing to its considerable use in nuclear medicine as a radiotracer, studies of its chemistry are expanding and its chemical properties are now beginning to be understood.

All technetium coordination chemistry studies to date have been directed towards the synthesis of Tc-99m labelled radiopharmaceuticals. This means that the ligands have been specifically designed to attain this goal, and the range of complexes[1] is limited by the rather special requirements of nuclear medicine. Thus, it is preferred to use only one type of ligand per complex, and from the kinetic point of view, first-order synthetic reactions are preferred. Other possible limitations include the necessary use of pertechnetate as starting material, which may in turn require the use of an external reducing agent if the coordinating ligand is not a suitable reductant for pertechnetate. Finally the reactions must proceed in physiologically relevant solutions. Despite these limitations some important chemical information has been derived and also some pseudo-theoretical studies have been made on the chemical behaviour of technetium.

The electronic configuration of technetium in the ground state is $[Kr]4d^65s^2$ and the element can show formal oxidation states from $+7$ to -1 in its compounds. Technetium complexes can be classified according to the oxidation state of the central metal into two large classes: technetium complexes in intermediate oxidation states and technetium complexes in low oxidation states.

TECHNETIUM(VII), (VI)

Technetium(VII) is exclusively represented by the pertechnetate anion (TcO_4^-). Technetium(VI) usually disproportionates to V and VII, but recently many complexes containing mainly the $Tc{=}N^{3+}$ core have been synthesized and show good stability. Interesting EPR studies on these d^1 systems were performed by Abram *et al.*[3,4]

TECHNETIUM(V)

Technetium(V) complexes can be considered as derived from a two-electron reduction of pertechnetate with the partial elimination of oxygen atoms. Technetium(V) has a d^2 electronic configuration and is diamagnetic or slightly paramagnetic. The magnetic properties arise from the orbital distortion induced by the polar Tc—X group (X = O, N or S), as reported by Chatt *et al.*[5] for rhenium analogues. The presence of at least one oxo group around technetium is a characteristic of technetium(V) cores, while the geometries of the complexes depend on the nature of the ligands. TcO^{3+}, *trans*-TcO_2^+ and $Tc_3O_3^{4+}$ cores are very common in five-, six- or seven-coordinated compounds.

A large group of ligands, mostly symmetrical or unsymmetrical, bidentate, tridentate, tetradentate or pentadentate, can stabilize oxotechnetium(V) and can have O, N, S, As, or P donor atoms. Many complexes have been completely characterized and

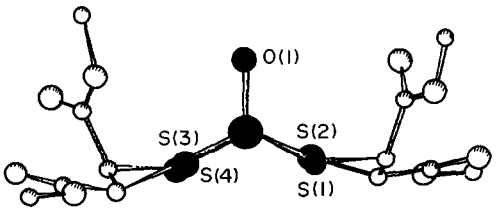

Fig. 1. Structure of (1,2(dicarbomethoxy)ethane-1,2-dithiolato)oxotechnetate(V).[7] An example of the $[TcO(SS)_2]$ configuration.

it is possible to deduce some rules to predict how the type of complex formed depends on the properties of the ligands.

Ligands with exclusively sulphur donor atoms tend to lead to five-coordinate complexes with $Tc{=}O^{3+}$ cores. A general characteristic of these complexes is the "reversed umbrella" shape with the technetium atom displaced above the equatorial plane of the four sulphur atoms[6] (Fig. 1).

Analogous behaviour occurs with OS (e.g. mercaptoethanol)[8] or OO (e.g. ethyleneglycol)[9] donor ligands, where again five-coordination with a $Tc{=}O^{3+}$ core is observed. Occasionally a sixth ligand, *trans* to Tc=O is bound and is preferably a phenolic,[10] alcoholic or hydroxy oxygen,[11] and, sometimes, a halogen or a μ-oxo group bridging two technetium centres.[12] This sixth group is normally weakly bonded if it is a monodentate ligand, whereas it is relatively stable when it is part of a polydentate ligand (Fig. 2).

In all the technetium(V) oxo complexes, the stretching vibration of the Tc=O bond in the IR spectrum is considered a good indicator of its presence. The value ranges from 890 to 1020 cm^{-1}, and the value is related to the electron affinity of the ligands in the equatorial plane and the nature of any sixth ligand *trans* to Tc=O. The Tc=O distance lies in the range 1.61–1.68 Å and correlates in the same way, showing longer distances for six-coordination compared to five-coordinated species with the same type of ligands.[15]

Proceeding towards complexes containing N-donor ligands such as monodentate nitrogen ligands (pyridine, imidazole), diamine (ethylenediamine, 1,2-diaminopropane), cyclam or even diarsine and diphosphine, two *trans*-oxo groups remain in the complex giving the TcO_2^+ core.[6] As a second oxygen is now *trans* to Tc=O, the Tc=O stretching vibration is at 790–834 cm^{-1} for TcO_2^+ complexes and also the Tc—O distance is longer, averaging 1.75 Å for these complexes.

It is possible to conclude that oxygen plays an important role in stabilizing the V oxidation state of technetium. One oxygen is indispensable to alleviate the electron deficiency of the technetium atom and to neutralize its charge. Another oxygen must be located *trans* to Tc=O when the ligands in the equatorial plane do not donate enough electron density to the technetium centre.

The reactivity of the oxotechnetium(V) complexes has also been well studied because it gives information on the kinetic stability of the complexes once injected "*in vivo*". From this point of view, the most stable complexes were with polydentate ligands and with coordinative saturation. In the case of the PnAO complex[16] [PnAO = 3,3′ - (1,3 - propanediyldiimino)bis(3 - methyl - 2 - butanone oximato)], the stabilization is achieved by means of cyclization due to the formation of a hydrogen bridge. Good stabilization was also attained in [TcO(DADS)] (DADS = diaminodisulphur ligand),[17] in which a tetradenate ligand containing a NSSN coordination set forms the square base of the pyramid and the oxo-oxygen is apical (see Fig. 3).

Few detailed studies have been made on the redox properties of technetium(V) owing to the non-reversible nature of the electrode processes. The only study to date deals with the electrochemical behaviour of oxotechnetium complexes containing Schiff's base or 8-quinolinol ligands. The reduction of technetium(V) to technetium(IV) and then to technetium(III) shows the relative stability, or at least the existence of, TcO^{2+} and TcO^+ cores.[18]

Under certain conditions the oxo-oxygen can be replaced by nitrogen or sulphur atoms. Thus, reduction of pertechnetate with hydrazine or substituted hydrazines in the presence of an appropriate ligand, leads to the formation of technetium nitrido complexes (see Fig. 4). $Tc{\equiv}N^{2+}$ is a very stable core and when the first complexes were prepared by Baldas *et al.*[19] it was suggested that its chemistry was less versatile than that of the $Tc{=}O^{3+}$ core. Indeed only five-coordinated products with soft donor atoms in the equatorial plane were initially isolated and characterized.[20] In recent years it has been demonstrated that the $Tc{\equiv}N^{2+}$ core also occurs in a range of six-coordinated complexes with a large variety of ligands,[21,22] including amines, phosphines, cyclam or aminophosphines.

Once formed, the Tc≡N ligand is relatively inert and is not at all readily replaced by oxygen or sulphur. The main characteristic physico-chemical properties of this group reported in the literature are the IR stretching vibration (1050–1070 cm^{-1}) and the Tc—N distance (1.58–1.63 Å). The structures, where available, generally exhibit square-pyramidal configurations with a high displacement of the technetium atom above the equatorial plane

for five-coordinated species and pseudo-octahedral geometries for six-coordinated complexes.

The technetium(V) nitrido complexes exhibit diamagnetic character for analogous reasons to the oxo-compounds. Their reactivity is not yet well studied; but the possibility of their oxidation to technetium(VI) has to be considered because the $Tc{\equiv}N^{3+}$ core is now known to be stabilized by particular ligands such as "salen".[23]

The $Tc{=}S^{3+}$ core is less common and, to date, only one example is known: $[TcS(HBPz_3)Cl_2]$ ($HBPz_3$ = hydrotris(1-pyrazolyl)borato) prepared starting from the known oxo analogue by reaction with B_2S_3.[24] In this complex sulphur is replaced in solution by oxygen from air.

A general theory can rationalize the behaviour of all the technetium(V) complexes reported to date. Duatti *et al.*[25] correlated the Tc=X bond distance (X = O or N) with the magnitude of the displacement of the technetium atom above the equatorial plane in the five- and six-coordinated complexes. The data have been discussed in terms of the basicity of the ligands in the equatorial plane. Soft ligands such as those containing sulphur groups,

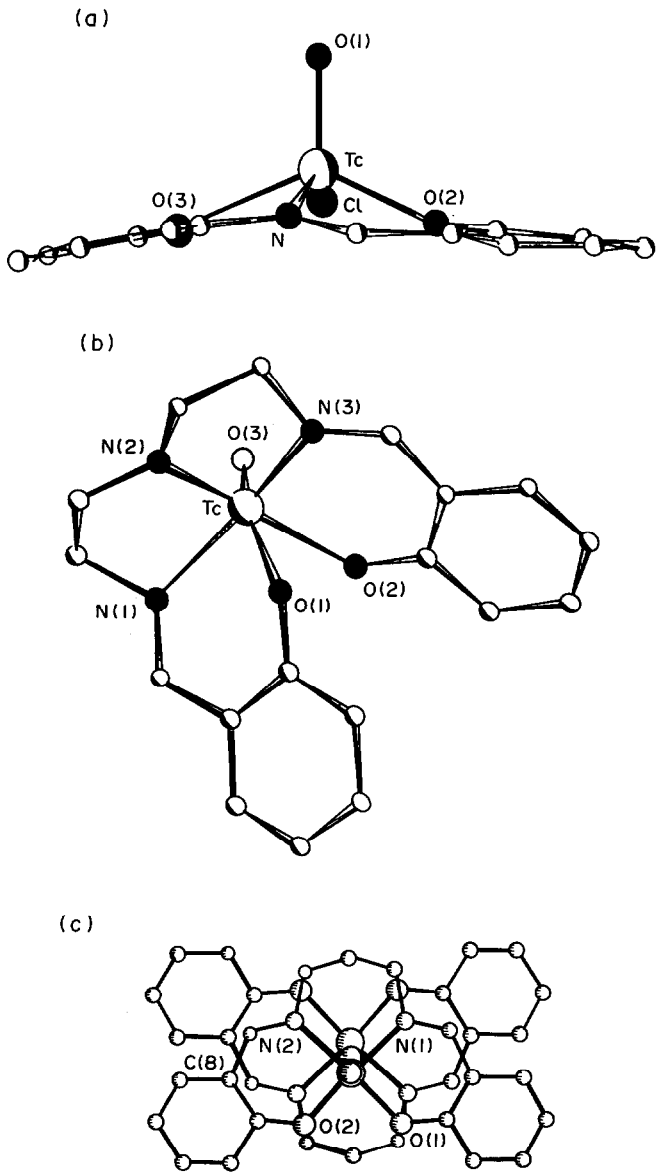

Fig. 2. Examples of structures of technetium(V) complexes with mixed O and N donor atom sets: (a) chloro(N-(2-oxidophenyl)salicylideneiminato)oxotechnetium(V);[13] (b) N,N′-(3-diethyleneaminato)-1,2-diylbis(salicylideneiminato)oxotechnetium(V);[14] (c) oxo-bis(oxo(N,N′-propylenebis(salicylideneiminato)))oxotechnetate(V).[12]

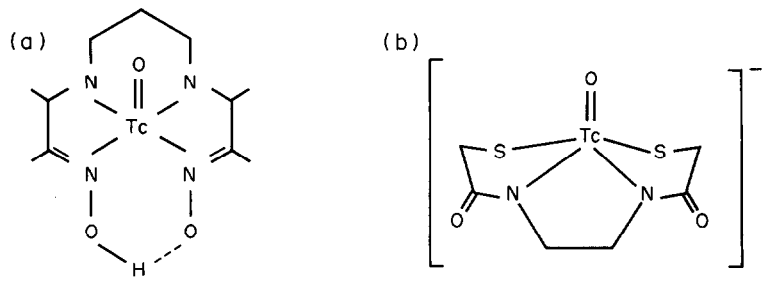

Fig. 3. Structures of (a) [TcO(PnAO)] and (b) [TcO(DADS)].

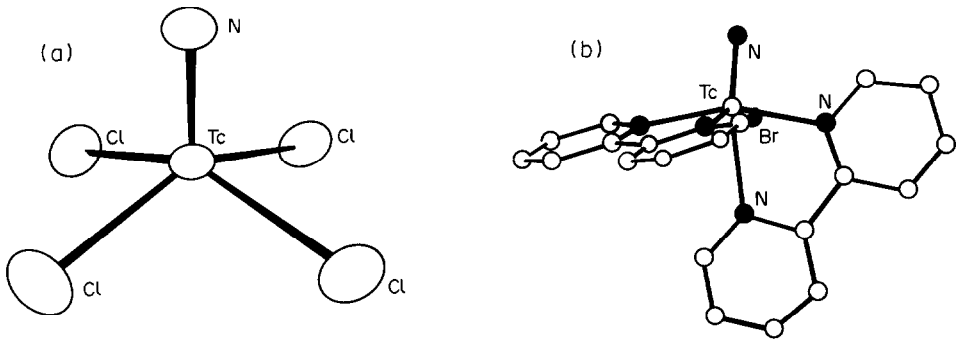

Fig. 4. Technetium nitrido complexes. Structure of: (a) tetrachloronitridotechnetium(VI) anion[19] and (b) bromo-bis(bipyridyl)nitridotechnetium(V).[21]

create high displacement and long Tc—X distances. On decreasing the ligand donating power, the displacement is lower and the Tc=X distance also decreases. The five-coordinate complexes, $[TcXCl_4]^-$, have the lowest displacement and the shortest Tc=X distances. Hard ligands with low basicity stabilize the Tc=X group only by means of a sixth *trans* group. The displacement above the equatorial plane is also related to the basicity of the group *trans* to Tc=X. A pseudo-octahedral geometry is attained only with TcO_2^+ cores.

TECHNETIUM(IV)

The first technetium(IV) product discovered was the very insoluble oxide TcO_2 and this product must be avoided when technetium complexes are prepared. In strong haloacid media, TcO_2 is converted to the hexahalogeno complexes $[Tc^{IV}X_6]^{2-}$.[26] $[TcX_4P_2]$ (X = Cl, Br or I and P = tertiary phosphine) are the first phosphine complexes of technetium synthesized by Fergusson *et al.*[28] and can be produced starting directly from pertechnetate in hydrohalogen acid media (see Fig. 5 for structures).[29] The reactions of these $[TcCl_4P_2]$ complexes with acetylacetone produced complexes of both Tc^{IV} and Tc^{III}[31] revealing the easy interconversion of Tc^{IV} and Tc^{III}.

Relatively few technetium(IV) complexes have been used as radiopharmaceuticals and these include some polymeric phosphate and phosphonate species,[32] and some EDTA complexes such

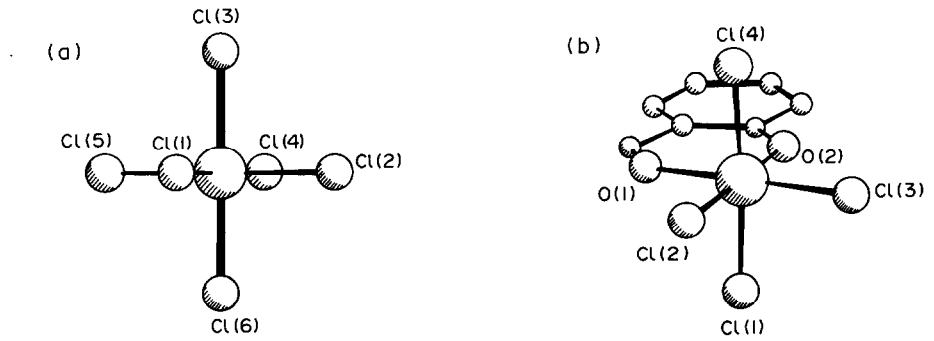

Fig. 5. Examples of technetium(IV) complexes. Structure of: (a) $[TcCl_6]^{2-}$ and (b) $[TcCl_4(sal)]^-$.[30]

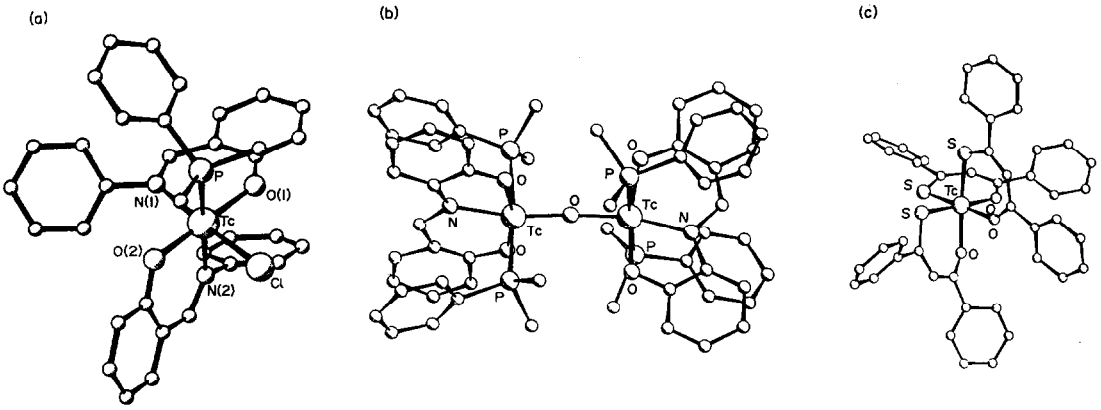

Fig. 6. Examples of technetium(III) complexes: (a) $[TcCl(PMe_2Ph)(Phsal)_2]$; (b) $[\mu\text{-}O(Tc(PMe_2Ph)_2(OPhsal))_2]$;[36] (c) $[Tc(SC(Ph)CHC(Ph)O_3]$.

as $[(H_2EDTA)Tc(\mu\text{-}O)_2Tc(H_2EDTA)]\cdot 5H_2O$.[33] Technetium(IV) is an intermediate oxidation state and is less studied because generally it undergoes kinetically fast reactions so that this oxidation state is by-passed. Thus technetium(V) is reduced by a bielectronic process to technetium(III), and technetium(IV) can be obtained only by oxidation of technetium(III). This bielectronic process could involve the loss of the oxo-oxygen from $Tc{=}O^{3+}$ in the presence of bielectronic reducing agents such as Sn^{II}/Sn^{IV}, P^{III}/P^{V} etc. The Tc^{IV}/Tc^{III} couple is electrochemically reversible and some systems have been studied in detail.[34] Technetium(IV) has a d^3 electronic configuration and usually displays six-coordination. The three unpaired electrons generally lead to high paramagnetic character for the complexes.

TECHNETIUM(III)

The d^4 electronic configuration of technetium(III) provides an electron density high enough to require ligands with back donation capabilities to produce stable complexes. Thus, arsines, carbonyls, acetylacetonate, thiourea, aminopolycarboxylates (EDTA, DTPA, HIDA)[6] or Shiff's base ligands[35–38] will also stabilize technetium(III) (Fig. 6).

Technetium(III) coordination chemistry is not particularly complicated and only six coordination complexes are known which show a two unpaired electron paramagnetism.[6] Favourable complex formation, together with low reactivity, are found when the ligands exhibit π-back bonding capabilities. Interesting examples are $[Tc(NCS)_6]^{3-}$,[39] $Tc(thiourea)_6Cl_3\cdot 4H_2O$[40] and $[Tc(monothiodibenzoylmethanato)_3]$.[41] Also, seven-coordinated technetium(III) complexes are becoming more common following an early report of $[TcCl_3(CO)(PMe_2Ph)_3]$ (Fig. 7).[42] The complex $[TcCl(DMG)_3]$[43] (DMG = dimethylglyoximate) and its derivatives have recently been studied.

Obviously, seven-coordination is only attained easily when the ligands are small enough. However in this situation the seventh possible site has to be occupied in order to prevent nucleophilic destabilizing reactions. The formal charge of technetium(III) complexes is very variable going from 3− in $[Tc(NCS)_6]^{3-}$ to 3+ in $[Tc(thiourea)_6]^{3+}$. Many complexes are monocations e.g. $[TcX_2(DPPE)_2]^{+}$,[44] some are neutral, and some can be monoanionic as in $[Tc(HIDA)_2]^{-}$.[45]

In addition to studies of the chemical reactivity of these complexes, it is important to determine the stability of the technetium complexes. In fact, even though ligand substitution reactions may in general

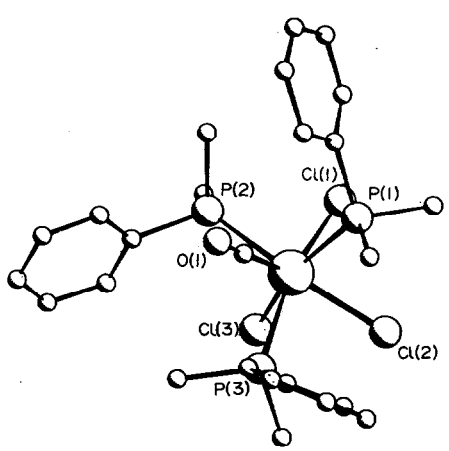

Fig. 7. Heptacoordinated technetium(III) complex: $[TcCl_3(CO)(PMe_2Ph)_3]$.

be slow, the overall charge of the complexes profoundly affects the accessibility or otherwise of redox processes. The properties and stability of the oxidized and reduced forms of the compounds will be different. The redox properties of the technetium(III) complexes $[TcCl_3(PMe_2Ph)_3]$ have been studied in detail,[46] as well as complexes of the type $[TcD_2X_2]^+$ (D = bidentate phosphine).[47]. The Tc^{III}/Tc^{II} couple was found to be electrochemically reversible in several instances, and the reduction potentials are a very useful index of the stability of the complexes *in vivo*.[1]

REFERENCES

1. E. Deutsch and W. Hirth, *J. Nucl. Med.* 1987, **28**, 1491.
2. K. Schwochau, *Radiochim. Acta* 1983, **32**, 139.
3. U. Abram, S. Abram, J. Stach and R. Kirmse, *J. Radioanal. Nucl. Chem.* 1986, **100**, 325.
4. U. Abram, S. Abram, H. Spies, R. Kirmse, J. Stach and K. Kohler, *Z. Anorg. Allg. Chem.* 1987, **544**, 167.
5. J. Chatt, J. D. Garforth, N. P. Johnson and G. A. Rowe, *J. Chem. Soc. A* 1964, 1012.
6. E. Deutsch, K. Libson, S. Jurisson and L. F. Lindoy, *Progr. Inorg. Chem.* 1983, 75.
7. G. Bandoli, M. Nicolini, U. Mazzi, H. Spies and R. Munze, *Transition Met. Chem.* 1984, **9**, 127.
8. A. Davison, A. G. Jones and B. V. DePamphilis, *Inorg. Chem.* 1981, **20**, 1617.
9. A. Davison, B. V. DePamphilis, A. G. Jones, K. J. Franklin and C. J. L. Lock, *Inorg. Chim. Acta* 1987, **128**, 161.
10. G. Bandoli, U. Mazzi, D. A. Clemente and E. Roncari, *J. Chem. Soc., Dalton Trans.* 1982, 2455.
11. S. Jurisson, L. F. Lindoy, K. P. Dancey, M. McPartlin, P. A. Tasker, D. K. Uppal and E. Deutsch, *Inorg. Chem.* 1984, **23**, 227.
12. G. Bandoli, U. Mazzi, M. Nicolini and F. Refosco, *J. Chem. Soc., Dalton Trans.* 1984, 2505.
13. G. Bandoli, U. Mazzi, B. E. Wilcox, S. Jurisson and E. Deutsch, *Inorg. Chim. Acta* 1984, **95**, 217.
14. F. Refosco, F. Tisato, U. Mazzi, G. Bandoli and M. Nicolini, *J. Chem. Soc., Dalton Trans.* 1988, 611.
15. U. Mazzi, F. Refosco, F. Tisato, G. Bandoli and M. Nicolini, *J. Chem. Soc., Dalton Trans.* 1986, 1623.
16. D. E. Troutner, W. A. Volkert, T. J. Hoffman and R. A. Holmes, *Int. J. Appl. Radiat. Isot.* 1984, **35**, 467.
17. A. Davison, A. G. Jones, C. Orvig and M. Sohn, *Inorg. Chem.* 1981, **20**, 1629.
18. F. Refosco, U. Mazzi, E. Deutsch, J. R. Kirchhoff, W. R. Heineman and R. Seeber, *Inorg. Chem.* 1988, **27**, 4121.
19. G. A. Williams, *Technetium in Chemistry and Nuclear Medicine* (Edited by M. Nicolini, G. Bandoli and U. Mazzi), Vol. 2, p. 45. Cortina International, Verona, Italy (1986).
20. J. Baldas, J. Bonnyman, P. M. Pojer, G. A. Williams and M. F. Mackay, *J. Chem. Soc., Dalton Trans.* 1981, 1798.
21. C. M. Archer, J. R. Dilworth, J. D. Kelly and M. McPartlin, *Chem. Comm.*, in press.
22. A. Marchi, B. Garuti, A. Duatti, R. Rossi, L. Magon, V. Ferretti and V. Bertolasi, *Inorg. Chem.*, in press.
23. H. Spies, private communication.
24. A. Duatti and U. Mazzi, private communication.
25. A. Duatti, G. Gilli and V. Bertolasi, private communication.
26. W. Preetz and G. Peters, *Z. Naturfor.* 1980, **35B**, 1355.
27. R. Colton, *Nature* 1962, **193**, 872.
28. E. J. Fergusson and J. H. Hickford, *J. Inorg. Nucl. Chem.* 1966, **28**, 2293.
29. G. Bandoli, D. A. Clemente, U. Mazzi and E. Roncari, *J. Chem. Soc., Dalton Trans.* 1982, **7**, 13381.
30. U. Mazzi, E. Roncari, G. Bandoli and L. Magon, *Transition Met. Chem.* 1979, **4**, 151.
31. U. Mazzi, E. Roncari, G. Bandoli and D. A. Clemente, *Transition Met. Chem.* 1982, **7**, 163.
32. K. Libson, E. Deutsch and B. L. Barnett, *J. Am. Chem. Soc.* 1980, **102**, 2476.
33. H. B. Burgi, G. Anderegg and P. Blauenstein, *Inorg. Chem.* 1981, **20**, 3829.
34. G. A. Mazzocchin, R. Seeber, U. Mazzi and E. Roncari, *Inorg. Chim. Acta* 1978, **29**, 5.
35. A. Duatti, A. Marchi, S. Alvarez Luna, G. Bandoli and U. Mazzi, *J. Chem. Soc., Dalton Trans.* 1987, 867.
36. U. Mazzi, F. Refosco, F. Tisato, G. Bandoli and M. Nicolini, *J. Chem. Soc., Dalton Trans.* 1988, 847.
37. F. Tisato, F. Refosco, U. Mazzi, G. Bandoli and M. Nicolini, *J. Chem. Soc., Dalton Trans.*, in press.
38. S. Jurisson, K. Doncey, P. A. Tasker, M. McPartlin and E. Deutsch, *Inorg. Chem.* 1984, **23**, 4743.
39. H. S. Trop, A. Davison, A. G. Jones, M. A. Davis, D. J. Szaldo and S. J. Lippard, *Inorg. Chem.* 1980, **19**, 1105.
40. M. J. Abrams, A. Davison, R. Faggiani, A. G. Jones and C. J. L. Lock, *Inorg. Chem.* 1984, **23**, 3284.
41. G. Bandoli, U. Mazzi, H. Spies, R. Munze, E. Ludwig, E. Ulhemann and D. Scheller, *Inorg. Chim. Acta* 1987, **132**, 177.
42. G. Bandoli, D. A. Clemente and U. Mazzi, *J. Chem. Soc., Dalton Trans.* 1978, 373.
43. K. Linder, E. N. Treher, P. N. Juri, T. Feld, B. L. Kuczynski, R. K. Narra and A. D. Nunn, *J. Nucl. Med.* 1988, **29**, 800.
44. K. A. Glaval, R. Whillie, J. F. Johnson, R. C. Elder and E. Deutsch, *J. Am. Chem. Soc.* 1980, **102**, 2103.
45. M. P. Loberg and A. T. Fields, *Int. Appl. Radiat. Isotopes* 1978, **29**, 167.
46. G. A. Mazzocchin, R. Seeber, U. Mazzi and E. Roncari, *Inorg. Chim. Acta* 1978, **29**, 1 and 5.
47. R. W. Hurst, W. R. Heineman and E. Deutsch, *Inorg. Chem.* 1981, **20**, 3298.

Polyhedron Vol. 8, No. 13/14, pp. 1689–1693, 1989
Printed in Great Britain

0277–5387/89 $3.00+.00
© 1989 Maxwell Pergamon Macmillan plc

THE TRIPLY-BONDED COMPLEX TETRACHLOROBIS[BIS(DIPHENYLPHOSPHINO)METHANE] DIRHENIUM(II) AND RELATED SPECIES, AND THEIR USE AS REAGENTS IN DIRHENIUM CHEMISTRY

RICHARD A. WALTON

Department of Chemistry, Purdue University, West Lafayette, IN 47907, U.S.A.

Abstract—The complex $Re_2Cl_4(\mu\text{-dppm})_2$ (dppm = $Ph_2PCH_2PPh_2$) and its bromide analogue serve as important precursors to many other dirhenium complexes because of the ability of the bridging dppm ligands to stabilize the dimetal unit. Reactions of these complexes with π-acceptors such as CO and RNC lead to the incorporation of up to three of these ligands, as exemplified by the conversion of $Re_2Cl_4(dppm)_2$ to $Re_2Cl_4(dppm)_2(CO)$, then $Re_2Cl_4(dppm)_2(CO)_2$, and finally $[Re_2Cl_3(dppm)_2(CO)_3]^+$. The redox activity of $Re_2X_4(\mu\text{-dppm})_2$ (X = Cl or Br) has been utilized in the reductive coupling of nitrile ligands (RCN) to give $[Re_2X_3(\mu\text{-}HN_2C_2R_2)(\mu\text{-dppm})_2(NCR)]PF_6$. When a non-bridging phosphine ligand is used, then the reaction course can be quite different. Thus, $\alpha\text{-}Re_2Cl_4(dppbe)_2$ (dppbe = 1,2-bis(diphenylphosphino)benzene) reacts with EtCN in the presence of conc. HCl to give the rhenium(V) imido complex, $Re(NCH_2Et)Cl_3(dppbe)$, in good yield. A different aspect of the redox activity of $Re_2Cl_4(\mu\text{-dppm})_2$ is encountered in its reactions with $LiAlH_4$ in THF to give $Re_2(\mu\text{-H})_2H_6(\mu\text{-dppm})_2$.

The complex $Re_2Cl_4(dppm)_2$ (dppm = bis(diphenylphosphino)methane) is the prototype of an important class of triply-bonded dirhenium complexes of stoichiometry $Re_2X_4[\mu\text{-}R_2A\text{—}X\text{—}AR_2]_2$ which contain a pair of *trans*-bridging $R_2A\text{—}X\text{—}AR_2$ ligands and a staggered rotational geometry (Structure 1). These complexes, which are known in the case of X = Cl or Br for $R_2A\text{—}X\text{—}AR_2$ = dppm,[1–3] $Ph_2AsCH_2AsPh_2$ (dpam)[4,5] or $Ph_2PNHPPh_2$ (dppa),[5] and X = I when $R_2A\text{—}X\text{—}AR_2$ = dppm,[3] are in turn members (or close cousins) of a much more extensive series of multiply-bonded dimetal complexes of stoichiometry $M_2X_4[\mu\text{-}R_2P(CH_2)_nPR_2]_2$, which exist for M = Mo, W or Re, X = Cl, Br or I and n = 1 or 2.[6] X-ray crystal structure determinations of $Re_2Cl_4(dppm)_2$[7] and $Re_2Cl_4(dppa)_2$[5] have confirmed the structure to be as shown in Structure 1.

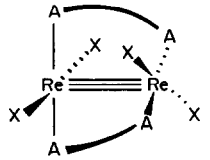

Structure 1.

An important characteristic of $Re_2Cl_4(dppm)_2$, and the other complexes of this type that contain a Re≡Re bond and a $\sigma^2\pi^4\delta^2\delta^{*2}$ ground state electronic configuration,[8,9] is the accessibility of two one-electron oxidations. These correspond to oxidations to $[Re_2Cl_4(dppm)_2]^+$ and $[Re_2Cl_4(dppm)_2]^{2+}$, species which possess Re—Re bond orders of 3.5 ($\sigma^2\pi^4\delta^2\delta^{*1}$ configuration) and 4.0 ($\sigma^2\pi^4\delta^2\delta^{*0}$ configuration), respectively. Cyclic voltammetry on solutions of these complexes in 0.1 M $n\text{-}Bu_4NPF_6$–CH_2Cl_2 show these oxidations to be reversible; oxidation with $[(\eta^5\text{-}C_5H_5)_2Fe]PF_6$ in acetone has been used to prepare the paramagnetic, ESR-active salts $[Re_2X_4(dppm)_2]PF_6$ (X = Cl or Br) and $[Re_2Cl_4(dppa)_2]PF_6$.[5]

The redox activity of $Re_2Cl_4(dppm)_2$ has been used in a sequence of one-electron electrochemical oxidations and coupled chemical reactions which lead to its conversion to $Re_2(\mu\text{-Cl})_2Cl_4(\mu\text{-dppm})_2$, via $Re_2Cl_5(\mu\text{-dppm})_2$, viz.:[2]

$$Re_2Cl_4(dppm)_2 \xrightarrow[+0.6\ V]{CH_2Cl_2} [Re_2Cl_4(dppm)_2]^+$$

$$\xrightarrow[Cl^-]{CH_2Cl_2} Re_2Cl_5(dppm)_2 \xrightarrow[+0.6\ V]{CH_2Cl_2}$$

$$[Re_2Cl_5(dppm)_2]^+ \xrightarrow[Cl^-]{CH_2Cl_2} Re_2Cl_6(dppm)_2.$$

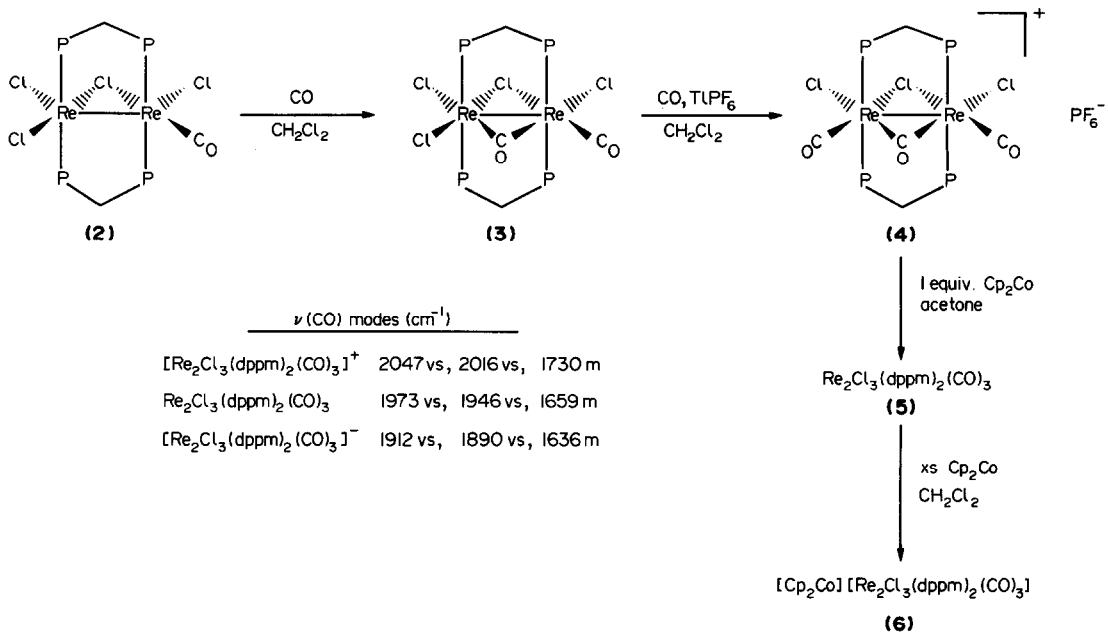

Scheme 1.

This transformation represents a change from a M_2L_8 structure to an edge-sharing bioctahedral M_2L_{10} geometry, with accompanying reduction in the metal–metal bond order from 3.0 ($\sigma^2\pi^4\delta^2\delta^{*2}$ configuration) to 2.0 ($\sigma^2\pi^2\delta^{*2}\delta^2$ configuration).[2] Within the series $Re_2Cl_4(dppm)_2$, $Re_2Cl_5(dppm)_2$ and $Re_2Cl_6(dppm)_2$, the Re—Re distances increase from 2.234(3) to 2.263(1) to 2.616(1) Å.[2,7,10]

In a formal sense, the reaction of $Re_2Cl_4(dppm)_2$ with CO can also be regarded as giving rise to a net two-electron oxidation of the Re_2^{4+} core. The A-frame-like monocarbonyl adduct, **2**, is formed first, and then reacts further to form the carbonyl complexes, **3** and **4** (see Scheme 1), both of which contain a bridging carbonyl ligand.[11–13] Similar complexes have been obtained from $Re_2Br_4(dppm)_2$.[12,13] The structures of all three chloride complexes have been determined by X-ray crystallography,[11–13] and these are represented in Scheme 1. Complex **4** has two reversible one-electron reductions, both of which can be accessed chemically with the use of $(\eta^5\text{-}C_5H_5)_2Co$ as the reducing agent,[13] to give complexes **5** and **6**. The Re—Re distance in **2** (2.338(1) Å)[12] is much shorter than the comparable distances in the edge-shared bioctahedral complexes **3** and **4**, which are 2.584(1)[11] and 2.582(1) Å,[13] respectively. While complex **2** can be regarded as still possessing a Re—Re bond of order three,[14] the distances in **3** and **4** are close to that in $Re_2(\mu\text{-}Cl)_2Cl_4(dppm)_2$,[2] a complex that contains a Re—Re double bond. Formally, a double bond formulation for **3** and **4** arises if we treat the μ-CO ligand as a divalent bridge; this accords with a d^4–d^4 dimetal entity and a $\sigma^2\pi^2\delta^{*2}\delta^2$ configuration, just as in $Re_2(\mu\text{-}Cl)_2Cl_4(dppm)_2$.[2]

A variety of other dirhenium complexes that contain a μ-CO bridge and mixed carbonyl–isocyanide and carbonyl–nitrile ligand sets have also been prepared from $Re_2Cl_4(dppm)_2$.[6,12,15–17] An interesting example is the mixed carbonyl–isocyanide complex $Re_2Cl_4(dppm)_2(CO)(CNxylyl)$ (**7**), which has a structure similar to that of $Re_2Cl_4(dppm)_2(CO)_2$ (**3**), with a bridging CO ligand and a terminal xylyl–NC ligand *cis* to it.[12] In contrast, the *t*-BuNC analogue, $Re_2Cl_4(dppm)_2(CO)(CN\text{-}t\text{-}Bu)$ (**8**), has a structure in which there are no bridging ligands other than the dppm bridges. This conclusion is based upon the X-ray crystal structure determination of $[Re_2Cl_3(dppm)_2(CO)(CN\text{-}t\text{-}Bu)_2]PF_6$ (**9**), a derivative of **8**.[17] A comparison between the structure of **7** and **9** is shown below. The Re—Re

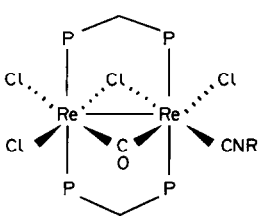

(7)

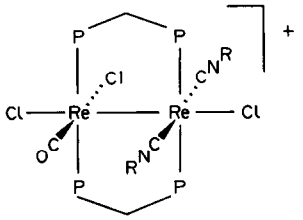

(9)

distances in **7** and **9** are 2.581(1) and 2.379(1) Å, respectively. In view of the close chemical and structural relationships between **8** and **9**, the Re—Re distance in **8** can be expected to be close to 2.38 Å. Since **7** and **8** are both prepared from $Re_2Cl_4(dppm)_2$ by essentially identical procedures,[12] it does not seem reasonable to consider **7** as a derivative of the Re_2^{6+} core (on the assumption of a *divalent* CO bridge), while at the same time maintaining that **8** is a derivative of the triply-bonded Re_2^{4+} core. We would not expect a two-electron redox change to be triggered simply by this switch in isocyanide ligand. Accordingly, any simple bond length/bond order/core charge correlation must be treated with caution since the notion of a Re_2^{6+} core being present in **7** is clearly suspect.

The preceding chemistry, which involves the reactions of $Re_2Cl_4(dppm)_2$ with CO and isocyanide ligands, can be modified to include σ-donors such as PMe_3. Thus, the reactions of $Re_2Cl_4(dppm)_2(CO)$ and $Re_2Cl_4(dppm)_2(CO)_2$ with PMe_3 in CH_2Cl_2 in the presence of $TlPF_6$, yield the complexes $[Re_2Cl_3(dppm)_2(CO)(PMe_3)_2]PF_6$ (**10**) and $[Re_2Cl_3(dppm)_2(CO)_2(PMe_3)]PF_6$ (**11**), respectively, in which the CO and PMe_3 ligands occupy mutually *cis* arrangements in edge-sharing bioctahedral structures.[18] The structure of the cation in **11** is given in Fig. 1 and shows the presence of a semi-bridging CO ligand. The associated Re—C distances are 2.16(1) and 1.96(1) Å; the shorter distance involves the more electron-rich metal centre which contains the PMe_3 ligand. A similar structure is found in the case of the $P(OEt)_3$ analogue of **11**. For both complexes, the Re—Re distances are very similar, being 2.593(1) Å in the case of **11**. The bis(trimethylphosphine) complex, **10**, possesses a symmetric carbonyl bridge and a Re—Re distance (2.602(1) Å) which is similar to that in **11**.[18]

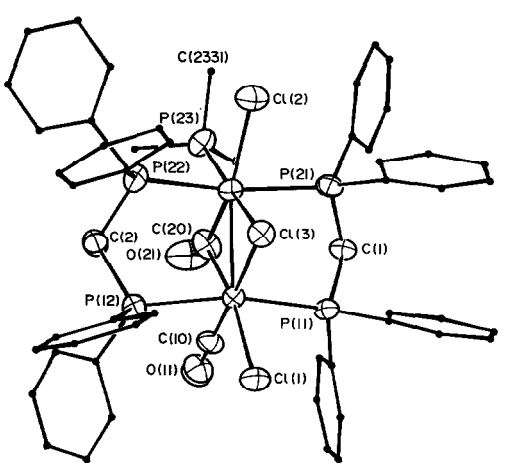

Fig. 1. ORTEP representation of the structure of the $[Re_2Cl_3(dppm)_2(CO)_2(PMe_3)]^+$ cation of **11**.[18] Thermal ellipsoids are drawn at the 50% probability level, except for the carbon atoms of the phenyl rings and PMe_3 ligands where they are shown as circles of arbitrary radius.

An interesting feature in the structure of the carbonyl complex $[Re_2Cl_3(dppm)_2(CO)_3]PF_6$ (**4**), is the surprisingly close C···C contacts between the CO ligands (2.38 Å).[13] However, in spite of the well-defined redox reactivity of the dirhenium unit in **4** (see Scheme 1), we have not yet been able to induce the reductive coupling of the CO ligands in this complex. Accordingly, we suspect that this "steric crowding" of the CO ligands is more a consequence of the non-bonded repulsions between the *all-cis* chloride ligands on the other side of the equatorial plane, rather than an indication of putative C—C bonding. Nonetheless, we have encountered an interesting instance where the redox activity of the complexes $Re_2X_4(dppm)_2$ (X = Cl or Br) can induce the reductive coupling of organic molecules. This involves the reductive coupling of nitriles, in which the dimetal unit is retained and the coupled nitrile ligands exhibit a novel μ_2-η^2 bonding mode.

The reactions of $Re_2X_4(dppm)_2$ with nitriles initially give the bis(nitrile) complexes $[Re_2X_3(\mu\text{-}dppm)_2(NCR)_2]PF_6$.[19] Reaction of these derivatives with further nitrile under reflux conditions affords the green, paramagnetic complexes $[Re_2X_3(\mu\text{-}HN_2C_2R_2)(\mu\text{-}dppm)_2(NCR)]PF_6$ (**12**, X = Cl or Br; R = Me, Et, *i*-Pr, *t*-Bu or Ph). The lability of the nitrile ligands (RCN) in **12** has been demonstrated by carrying out nitrile exchange reactions. The structural identity of these complexes has been confirmed by an X-ray structure analysis of a salt of the $[Re_2Br_3(\mu\text{-}HN_2C_2Me_2)(\mu\text{-}dppm)(NCMe)]^+$ cation.[19,20] The Re—Re distance in this complex is 2.666(1) Å. The geometry is that of an edge-sharing bioctahedron, with *trans*-bridging dppm ligands and three bromide ligands occupying mutually *cis* positions on one side of the equatorial plane. Distances within the five-membered metallacycle ring, formed from the coupled nitrile ligands, can best be rationalized in terms of contributions from a singly deprotonated diimine ligand (as represented in **I**), and a triply deprotonated ene-diamine ligand (as in **II**). Experiments

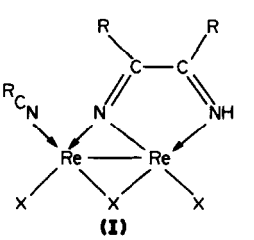

(I)

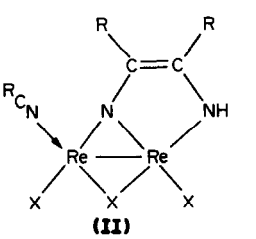

(II)

in which CD_3CN is used in place of CH_3CN in the reaction with $[Re_2Cl_3(dppm)_2(NCMe)_2]PF_6$, have shown that the source of the unique hydrogen in the $HN_2C_2Me_2$ ligand is the acetonitrile ligand itself.[20,21] The treatment of **12** with either $[(\eta^5\text{-}C_5H_5)_2Fe]PF_6$ in acetone, or $NOPF_6$ in CH_2Cl_2, leads to oxidation and the formation of the red, diamagnetic salts $[Re_2X_3(\mu\text{-}HN_2C_2R_2)(\mu\text{-dppm})_2(NCR)](PF_6)_2$ (**13**).[20,21]

These reductive coupling reactions may proceed by the type of carbonyl–carbyne and isocyanide–aminocarbyne coupling mechanism that Lippard and co-workers[22] have provided evidence for in their studies on the reductive coupling of carbonyl and isocyanide ligands. If so, this could involve a nitrile–alkylimido coupling step. Unfortunately, the reactions of $Re_2X_4(dppm)_2$ with nitriles to give **12** require quite forcing conditions, and have not yielded any characterizable reaction intermediates. Accordingly, they do not appear to be ideal from the standpoint of further mechanistic studies. However, we have independent evidence that imido complexes are formed quite readily from the reactions of nitriles with other dirhenium complexes, as shown by our studies of the reactions between $(n\text{-}Bu_4N)_2Re_2X_8$ (X = Cl or Br) and an excess of 1,2-bis(diphenylphosphino)benzene (dppbe) with an alkyl nitrile (RCN) as solvent. Under reflux conditions, and in the presence of a few drops of conc. HX, these reactions afford the mononuclear rhenium(V) imido complexes, $Re(NCH_2R)X_3(dppbe)$.[23,24] The reactions probably proceed via the corresponding dirhenium(II) complex, $\alpha\text{-}Re_2X_4(dppbe)_2$. We have isolated this complex in the case of X = Cl, and find that when it is reacted with EtCN in the presence of conc. HCl, the imido species $Re(NCH_2Et)Cl_3(dppbe)$ can be isolated in 47% yield.[24] One plausible explanation is that the Re_2^{4+} core of $\alpha\text{-}Re_2Cl_4(dppbe)_2$ undergoes disproportionation to rhenium(I) and rhenium(III), and that it is the former mononuclear species which provides the four-electrons necessary to reduce the nitrile.

A different aspect of the redox activity of the dirhenium core of $Re_2Cl_4(dppm)_2$ is encountered in its conversion to the dirhenium octahydride complex, $Re_2H_8(dppm)_2$ (**14**). This octahydride complex is prepared through the reaction of $Re_2Cl_4(dppm)_2$ with $LiAlH_4$ in THF at room temperature, followed by hydrolysis of the reaction mixture. This procedure is adaptable to the synthesis of other octahydride complexes of the type $Re_2H_8(PR_3)_4$ starting from $Re_2Cl_4(PR_3)_4$ (PR_3 = PMe_3, PEt_3, P—*n*-Pr_3, PMe_2Ph, PEt_2Ph, $PMePh_2$ or $Ph_2PCH_2CH_2PPh_2$).[25] The crystal structure and NMR spectral properties of the dppm derivative are consistent with the structue $Re_2(\mu\text{-}H)_2H_6(\mu\text{-dppm})_2$, rather than $Re_2(\mu\text{-}H)_4H_4(\mu\text{-dppm})_2$. The structure of the $Re_2(\mu\text{-dppm})_2$ unit of **14** is shown in Fig. 2. While the tetra-μ-hydrido-bridged structure is preferred in the case of the octahydride complexes with monodentate phosphines,[26] the different structure of **14** is probably a consequence of the constraints imposed by the bridging dppm ligands. This leads to an opening up of the P—Re—P angles (to 164°) and a lengthening of the Re—Re bond (to 2.934(1) Å) compared to the situation in the structurally characterized complex $Re_2(\mu\text{-}H)_4H_4(PEt_2Ph)_4$, where P—Re—P = 102.7(2)° and Re—Re = 2.538(4) Å.[26]

The non-redox substitution chemistry of $Re_2X_4(dppm)_2$ (X = Cl or Br) with carboxylate ligands provides a convenient route to the complexes $Re_2(\mu\text{-}O_2CR)_2X_2(\mu\text{-dppm})_2$; these exist as the *trans* and *cis* isomers, **15** and **16**, respectively.[27] This is a very rare instance where metal–metal bonded dimetal complexes that contain two bridging dppm ligands exist in *trans and cis* isomeric forms. The reactions of $Re_2Cl_4(dppm)_2$ with $(PPN)O_2CR$ (PPN = $[(Ph_3P)_2N]^+$; R = Me, Et or Ph) in CH_2Cl_2 at room temperature for 5 min, afford *trans*-$Re_2(O_2CR)_2X_2(dppm)_2$ in yields of

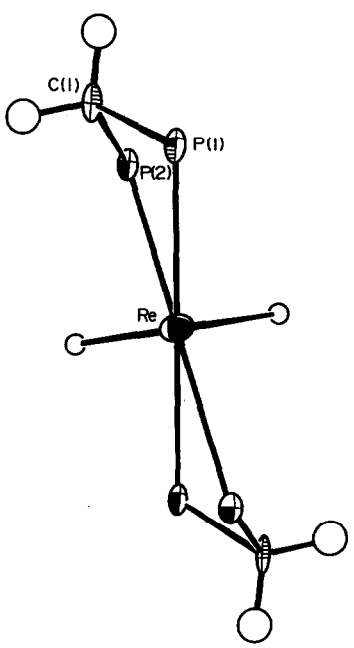

Fig. 2. ORTEP representation of the $Re_2(\mu\text{-}H)_2P_4$ core of $Re_2(\mu\text{-}H)_2H_6(\mu\text{-dppm})_2$ (**14**), as viewed down the Re—Re axis to show the non-zero P_1—Re—Re—P_2 torsional angle (χ = 15.9(1)°).[25] The probable positions of the bridging hydrido ligands are shown as circles of arbitrary radius. Phenyl rings have been omitted but the CH_2 bridgehead groups are included. Thermal ellipsoids for the rhenium, carbon and phosphorus atoms are drawn at the 50% probability level. This structure has $\bar{1}$ symmetry.

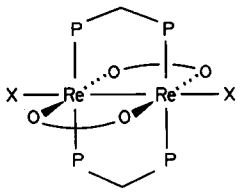

(15)

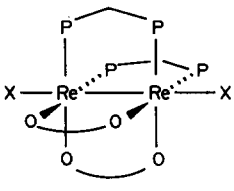

(16)

70% or more. When these *trans* isomers are heated in ethanol for approximately 3 h, they convert to the corresponding *cis* isomers.[27] The *cis* and *trans* isomers are readily oxidized to their corresponding monocationic forms as in the salts *cis*-/*trans*-$[Re_2(\mu\text{-}O_2CR)_2X_2(\mu\text{-dppm})_2]PF_6$; these paramagnetic complexes contain Re—Re bond orders of 3.5 and have structures very similar to those of their parent, neutral dirhenium(II) precursors.[3,27]

Acknowledgements—Support from the National Science Foundation, though Grant Nos CHE85-06702 and CHE88-07444, is gratefully acknowledged. I also wish to acknowledge the research contributions of my talented co-workers that are cited throughout this article.

REFERENCES

1. J. R. Ebner, D. R. Tyler and R. A. Walton, *Inorg. Chem.* 1976, **15**, 833.
2. T. J. Barder, F. A. Cotton, D. Lewis, W. Schwotzer, S. M. Tetrick and R. A. Walton, *J. Am. Chem. Soc.* 1984, **106**, 2882.
3. A. R. Cutler, D. R. Derringer, P. E. Fanwick and R. A. Walton, *J. Am. Chem. Soc.* 1988, **110**, 5024.
4. A. C. Price, PhD thesis, Purdue University (1987).
5. M. T. Costello, D. R. Derringer, A. C. Price, M. I. Rivera, E. M. Scheiber, E. W. Siurek III and R. A. Walton, unpublished results.
6. A. C. Price and R. A. Walton, *Polyhedron* 1987, **6**, 729 and refs cited therein.
7. T. J. Barder, F. A. Cotton, K. R. Dunbar, G. L. Powell, W. Schwotzer and R. A. Walton, *Inorg. Chem.* 1985, **24**, 2550.
8. F. A. Cotton and R. A. Walton, *Multiple Bonds Between Metal Atoms*. John Wiley, New York (1982).
9. F. A. Cotton and R. A. Walton, *Struct. Bond. (Berlin)* 1985, **62**, 1.
10. F. A. Cotton, L. W. Shive and B. R. Stults, *Inorg. Chem.* 1976, **15**, 2239.
11. F. A. Cotton, L. M. Daniels, K. R. Dunbar, L. R. Falvello, S. M. Tetrick and R. A. Walton, *J. Am. Chem. Soc.* 1985, **107**, 3524.
12. F. A. Cotton, K. R. Dunbar, A. C. Price, W. Schwotzer and R. A. Walton, *J. Am. Chem. Soc.* 1986, **108**, 4843.
13. P. E. Fanwick, A. C. Price and R. A. Walton, *Inorg. Chem.* 1987, **26**, 3920.
14. L. B. Anderson, T. J. Barder, D. Esjornson, R. A. Walton and B. E. Bursten, *J. Chem. Soc., Dalton Trans.* 1986, 2607.
15. F. A. Cotton, K. R. Dunbar, L. R. Falvello and R. A. Walton, *Inorg. Chem.* 1985, **24**, 4180.
16. L. B. Anderson, F. A. Cotton, K. R. Dunbar, L. R. Falvello, A. C. Price, A. H. Reid and R. A. Walton, *Inorg. Chem.* 1987, **26**, 2717.
17. P. E. Fanwick, A. C. Price and R. A. Walton, *Inorg. Chem.* 1988, **27**, 2601.
18. J.-S. Qi, P. E. Fanwick and R. A. Walton, unpublished results.
19. T. J. Barder, F. A. Cotton, L. R. Falvello and R. A. Walton, *Inorg. Chem.* 1985, **24**, 1258.
20. D. Esjornson, D. R. Derringer, P. E. Fanwick and R. A. Walton, *Inorg. Chem.*, submitted for publication.
21. D. Esjornson, P. E. Fanwick and R. A. Walton, *Inorg. Chem.* 1988, **27**, 3066.
22. R. N. Vrtis, Ch. P. Rao, S. Warner and S. J. Lippard, *J. Am. Chem. Soc.* 1988, **110**, 2669.
23. M. Bakir, P. E. Fanwick and R. A. Walton, *Inorg. Chem.* 1988, **27**, 2016.
24. M. Bakir, D. Esjornson, P. E. Fanwick, K. S. Jones and R. A. Walton, unpublished results.
25. P. E. Fanwick, D. R. Root and R. A. Walton, *Inorg. Chem.* 1989, **28**, 395.
26. R. Bau, W. E. Carroll, R. G. Teller and T. F. Koetzle, *J. Am. Chem. Soc.* 1977, **99**, 3872.
27. D. R. Derringer, P. E. Fanwick, S. M. V. Osjornson and R. A. Walton, unpublished results.

Polyhedron Vol. 8, No. 13/14, pp. 1695–1700, 1989
Printed in Great Britain

0277–5387/89 $3.00+.00
© 1989 Maxwell Pergamon Macmillan plc

THE VANADIUM NITROGENASE OF *AZOTOBACTER*

ROBERT R. EADY

AFRC Institute of Plant Science Research, Nitrogen Fixation Laboratory,
University of Sussex, Brighton BN1 9RQ, U.K.

Abstract—The properties of the recently characterized vanadium-dependent nitrogenase system of *Azotobacter* are reviewed and compared with the better characterized Mo–nitrogenases. Vanadium is present in V–nitrogenase in a vanadium- and iron-containing protein (VFe protein), analogous in structure and function to the MoFe protein of Mo–nitrogenase. The VFe protein contains vanadium in a polynuclear cluster in an environment with iron, sulphur and oxygen (or nitrogen or carbon) as nearest neighbour atoms, very similar to the environment of molybdenum in the iron and molybdenum cofactor (FeMoco) centre of the MoFe proteins. A vanadium-containing cluster can be extracted from the VFe protein by treatment with N-methylformamide (NMF). The NMF extract contains vanadium, iron and sulphur in a 1:6:5 ratio and activates the inactive MoFe protein synthesized by some mutant organisms unable to synthesize FeMoco. This hybrid protein has the characteristic substrate reduction pattern of a VFe protein, in forming some C_2H_6 from C_2H_2. These data are consistent with the NMF extract containing an iron and vanadium cofactor FeVaco, analogous to FeMoco. Although the hybrid protein is active in nitrogenase assays with H^+ or C_2H_2 as reducible substrates, N_2 is not reduced, suggesting that specific interactions of the cofactor centre with a polypeptide ligand are lacking. Pre-steady-state kinetics of the ATP-dependent electron-transfer from the Fe protein of V–nitrogenase to a VFe protein are very similar to those of Mo–nitrogenase components, consistent with a common mechanism of substrate reduction. However, at low temperatures N_2 is a more effective substrate for V–nitrogenase compared with Mo–nitrogenase.

The role of molybdenum in stimulating biological nitrogen fixation has been known for 50 years,[1] but only in the last 4 years has it been unequivocally established that biological routes for nitrogen fixation exist which do not involve molybdenum.[2–4] The soil bacterium *Azotobacter chroococcum* has a molybdenum-containing nitrogenase,[5] similar to those found in many other organisms, but also has a vanadium-containing nitrogenase which functions under conditions of molybdenum deficiency.[2] A closely-related species, *Azotobacter vinelandii*, has in addition to Mo–nitrogenase and V–nitrogenase,[3] a third nitrogenase system which functions under conditions where both molybdenum and vanadium are deficient.[4,6] When purified, the third system contains only very low levels of molybdenum or vanadium.[4]

All three types of nitrogenase have similar requirements for activity—a low potential electron donor, MgATP and anoxic conditions. They can also be separated into two component proteins. All have a distinctive Fe protein, which together with a MoFe protein or a VFe protein, or a protein which contains neither molybdenum or vanadium, make up the active enzyme. The separate existence of molybdenum-independent nitrogenases was shown by using recombinant DNA techniques to construct strains of *Azotobacter* which lacked the structural genes of the Mo–nitrogenase protein.[6–8] The demonstration of N_2-dependent growth of such strains vindicated the suggestion of Bishop and colleagues that molybdenum-independent routes of N_2 fixation existed in *Azotobacter*.[9,10]

BIOCHEMISTRY OF V–NITROGENASE

Vanadium nitrogenases of *A. chroococcum*[2,11,12] and *A. vinelandii*[3,13] have been purified and characterized, and shown to have very similar properties. Attention has naturally focussed on the role of vanadium in this system, and only an overview of the Fe protein is given here. A schematic view of nitrogenase function is shown in Scheme 1.

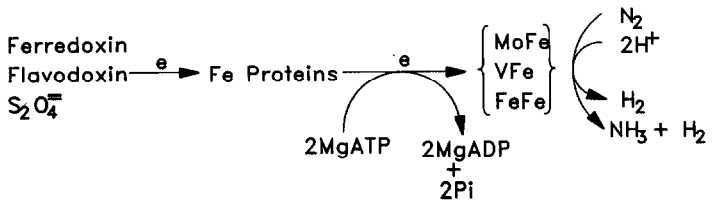

Scheme 1. Function of nitrogenase.

Substrate reduction by V-*nitrogenase*

In addition to N_2, both Mo- and V-nitrogenases will reduce H^+ or C_2H_2 as alternative substrates. A feature of substrate reduction by V-nitrogenase when assayed at 30°C is the decreased effectiveness with which N_2 or C_2H_2 compete with H^+ as a reducible substrate, when compared with Mo-nitrogenase (Table 1). For Mo-nitrogenase functioning under conditions of optimum electron flux, the limiting stoichiometry for N_2 reduction is:

$$N_2 + 8e + 8H^+ + 16MgATP \rightarrow 2NH_3 + H_2 + 16MgADP + 16Pi. \quad (1)$$

The overall reaction requires the sequential MgATP-dependent transfer of eight electrons from the Fe protein to the MoFe protein, and the rate-limiting step is the dissociation of the two proteins following electron transfer (see ref. 14). H_2 evolution concomitant with N_2 reduction, a reaction which utilizes 25% of the electron flux through nitrogenase, has been proposed to arise from a requirement for a reduced site for the binding of N_2, which results in the displacement of H_2. Under conditions where the rate of electron flux is restricted (e.g. by limiting Fe protein or MgATP concentrations), the proportion of electron flux resulting in H_2 evolution increases as partially-reduced MoFe protein species relax to more oxidized forms as H_2 is evolved.[14]

In the case of V-nitrogenase, even when functioning under optimum conditions of electron flux and saturating N_2 levels, approximately half the electron flux results in H_2 evolution. This reaction appears to occur *in vivo*, since cultures of *Azotobacter* evolve considerably more H_2 when fixation occurs by V- rather than Mo-nitrogenase. A study of the kinetics of electron-transfer from the Fe protein to VFe protein by stopped-flow spectrophotometry,[15] has shown that association of the two proteins and the MgATP-dependent electron-transfer occur at rates very similar to those of Mo-nitrogenase and are too fast to be rate-limiting in turnover. The difference in reactivity towards N_2 and H^+ was proposed to reside in the substrate-binding cofactor centre of the VFe protein.

A recent study of the effect of temperature on the reduction of N_2 has shown that as the temperature was decreased from 30°C (the usual assay temperature *in vivo* and *in vitro*) to 5°C, N_2 remained an effective substrate for V-nitrogenase but not Mo-nitrogenase.[16] Over this temperature range, the specific activity for N_2 reduction by Mo-nitrogenase decreased 10-fold more than V-nitrogenase. The lower activity of Mo-nitrogenase at 5°C did not equal that of V-nitrogenase, even under conditions of high electron flux occurring at a 12-fold molar excess of Fe protein. This behaviour which, surprisingly is conferred by the Fe protein of V-nitrogenase, may explain why this apparently less effective nitrogenase has persisted in nature.

Mo-nitrogenase reduces C_2H_2 to give exclusively the two-electron reduced product, C_2H_4. A distinctive difference between Mo- and V-nitrogenase is the formation of C_2H_6 as a minor ($\sim 5\%$) product of C_2H_2 reduction by V-nitrogenase.[17,18] This specificity is conferred by the VFe protein and as discussed below, provided supportive evidence that this protein contains an iron and vanadium cofactor centre at the substrate-binding site.

THE Fe PROTEIN OF V-NITROGENASE

The physicochemical properties of the Fe proteins of V-nitrogenases of *A. chroococcum* and *A. vinelandii* are very similar to those of the Fe protein of Mo-nitrogenase. The four Fe and four acid-labile sulphur atoms that these proteins contain are probably arranged in a single [4Fe–4S] cluster which bridges the two identical subunits.[31] The dithionite-reduced proteins exhibit EPR signals at $g_{av} = 1.95$ and $g = 4$–5, consistent with the presence of both

Table 1. Comparison of the physicochemical properties of VFe protein and MoFe protein

	VFe protein		MoFe protein
	A. chroococcum[2]	*A. vinelandii*[3]	*K. pneumoniae*[3] [1a]
M_r	210,000	200,000	220,000
Subunit structure	$\alpha_2\beta_2\gamma_2$	$\alpha_2\beta_2$	$\alpha_2\beta_2$
Subunit M_r	$2\times 50{,}000$	$2\times 52{,}000$	$2\times 50{,}000$
	$2\times 55{,}000$	$2\times 55{,}000$	$2\times 60{,}000$
	$2\times 13{,}000$		
Metal and S^{2-} content (g atom mol^{-1})			
V	2 ± 0.3	0.7 ± 0.3	ND
Mo	0.06	0.05	2
Fe	19 ± 2	9 ± 2	32 ± 3
S^{2-}	21 ± 1	ND	ND
EPR	5.6, 4.35, 3.77	5.31, 4.34,	
	1.93	2.04, 1.93	4.3, 3.7, 2.015
Specific activity (nmol protein/min/mg of protein)			
NH_4 formation	350	660	990
H_2 under N_2	928	ND	648
H_2 evolution under Ar	1348	1400	2100
C_2H_4 from C_2H_2	608	220	1693
H_2 under C_2H_2	998	ND	304

[a] R. R. Eady and B. E. Smith, unpublished results.

Note that in the presence of N_2 or C_2H_2 the reduction of H^+ to H_2 is not as effectively suppressed with V–nitrogenase as compared with Mo–nitrogenase.

$S = 1/2$ and $S = 3/2$ spin states which together integrate to 1 spin mol. During electron transfer the [4Fe–4S] cluster functions as a 1e donor between the +1 and +2 oxidation levels. MgATP binds to Fe proteins and results in a conformational change which enhances the accessibility of iron in the cluster to chelation by α,α'-bipyridyl, causing the EPR signal at 1.94 to become more axial and lowers the mid-point potential by ~ 100 mV.

In the case of the Fe proteins of V– and Mo–nitrogenases of *A. chroococcum*, the MgADP-bound forms have similar redox mid-point potentials of −463 and −450 mV respectively, and the oxidized proteins are reduced by SO_2^- at very similar rates.[19] The structural genes encoding these proteins have been sequenced and at the amino acid level these proteins show 89% conservation of sequence, including the five invariant cysteine residues which are conserved in all known Fe proteins. A reflection of this high degree of conservation of structure is the ability of both these proteins to form active hybrid nitrogenases with either MoFe or VFe proteins. The Fe proteins associated with V–nitrogenase are clearly typical of the class of Fe proteins associated with Mo–nitrogenases.

THE VFe PROTEIN OF V–NITROGENASE

The overall properties of VFe proteins show strong similarities with MoFe proteins except that vanadium replaces molybdenum (Table 1). This similarity extends to the ability to form active hybrid nitrogenases with the Fe protein from either system. Fully active MoFe proteins are considered to contain two FeMoco centres, the probable site of substrate binding and reduction, and four "P" clusters, Fe/S centres with unusual spectroscopic properties which can be extruded as [4Fe–4S] clusters (see refs 20 and 21). All MoFe proteins have an $\alpha_2\beta_2$ subunit structure and homologous subunits are present in VFe proteins.[2,3] The structural genes encoding these subunits of the VFe protein of *A. chroococcum* have been sequenced,[22] and when compared with the sequences of a number of MoFe proteins, as a group the derived amino acid sequences of VFe protein subunits show only 15–18% conservation with those of MoFe proteins. However, the conserved regions contain five cysteinyl residues in the α subunits, and three in the β subunit, which are conserved in all MoFe protein sequences and are likely candidates for cluster lig-

ation. The VFe of the *A. chroococcum* protein also has an additional small (M_r 13000) subunit and therefore an $\alpha_2\beta_2\delta_2$ subunit structure,[22] and it is probable that the protein of *A. vinelandii* has a similar structure. Despite these differences, together with the probability that the metal content of preparations of the VFe protein so far obtained are not maximal, EPR, MCD and X-ray absorption spectroscopies, together with extrusion experiments, are consistent with the same types of redox centres being present in MoFe and VFe proteins.

EPR spectroscopy

Dithionite-reduced MoFe proteins exhibit an EPR signal with $g = 4.3$, 3.7 and 2.01 arising from the $S = 3/2$ spin system of the FeMoco centre. The EPR spectra of VFe proteins are more complex, since they contain an additional EPR centre. The dithionite-reduced VFe protein of *A. vinelandii*[23] has an EPR spectrum with g values at 5.8, 5.4, 4.34, 2.04 and 1.93. The signals at 5.8 and 5.4 have been assigned to a $S = 3/2$ spin system which integrates to 0.89 spin per vanadium atom. The $g = 4.34$ feature was attributed to adventitious high-spin Fe^{3+} and those at $g = 2.04$ and 1.93 to an $S = 1/2$ spin system associated with a reduced Fe–S centre of low potential. The latter spin integrates to 0.2 spin per vanadium atom.

The EPR spectrum of the VFe protein from *A. chroococcum*[11] has signals at $g = 5.6$, 4.35, 3.77 and 1.94. The first three are consistent with an $S = 3/2$ ground state spin system with the $M_zS = 1/2$ Kramer's doublet being thermally accessible (D. J. Lowe, personal communication). The $g = 1.94$ signal, as with the *A. vinelandii* protein, has been assigned to an $S = 1/2$ spin system associated with a reduced Fe–S centre. The major difference between these proteins is the presence of the feature at $g = 3.77$ in the spectrum of the *A. chroococcum* VFe protein and may reflect differences in the environment of the cofactor centre with a $S = 3/2$ spin state that these spectra suggest is present.

Magnetic circular dichroism spectroscopy

Low temperature MCD spectroscopy has been used to probe the nature of the redox centres of MoFe proteins, since although the room temperature spectra resemble those of [4Fe–4S] clusters, at low temperature the contribution from paramagnetic species predominate and MoFe proteins exhibit distinctive spectra (see ref. 20). A study of the VFe protein of *A. vinelandii*[24] showed the dithionite-reduced protein to have spectra very similar to those shown by the $S = 3/2$ paramagnetic centre of MoFe proteins, with only a small additional contribution from the $S = 1/2$ paramagnetic species. Although VFe protein temperature-dependent MCD transition were consistent with an $S = 3/2$ spin system, it has different electronic and magnetic properties to the cluster in the MoFe protein. By analogy with the MoFe protein, this study provided further spectroscopic data suggesting the presence of a V–Fe–S cluster in VFe proteins.

In the dye-oxidized state, the MCD and magnetization characteristics, although not identical witho those of the "P" clusters of MoFe proteins, are sufficiently similar to be assigned to an $S = 5/2$ spin system associated with clusters analogous to "P" clusters.

X-ray spectroscopic studies

Vanadium–K edge X-ray absorption spectroscopy has been used to provide information about the chemical environment of vanadium in the VFe proteins from both *A. chroococcum*[25,26] (and also Garner *et al. Polyhedron* 1989, **8**, 1649) and *A. vinelandii*.[27] The data for the dithionite-reduced proteins are in good agreement and the absorption edge shows a weak pre-edge feature and an edge inflection. The intensity of the pre-edge feature implies distorted octahedral coordination around the vanadium atom, and the position of these features indicates an oxidation state between vanadium(II) and vanadium(IV). The data closely resemble those for the octahedral VFe_3S_4 complex in $[NMe_3][VFe_3S_4(DMF)_3]^-$ and are different from the complex $[VS_4(FeCl_2)_2][Et_4N]_3$ where vanadium is tetrahedrally complexed to sulphur. These spectral features show no significant change on dye-oxidation of the protein, or under enzyme turnover when the protein is "super-reduced".

The extended X-ray absorption fine structure (EXAFS) spectra have provided information about the distance, type and number of nearest neighbour atoms to the vanadium atom. Fourier transform analysis of the EXAFS region is consistent with vanadium, like molybdenum in MoFe proteins, having iron, sulphur and oxygen (or nitrogen or carbon) atoms as nearest neighbours and at very similar distances (Table 2). No significant changes occur in the EXAFS spectra on dye-oxidation. This insensitivity of the vanadium environment to the oxidation level of the protein is analogous to molybdenum in MoFe proteins, and has been attributed to the unpaired spin being delocalized onto the iron atoms. These data provide strong spectroscopic evidence for the presence of an iron- and

Table 2. The environment of molybdenum in the MoFe protein and vanadium in the VFe protein, deduced from X-ray absorption spectroscopy

	Distance (Å)	Number of atoms	Reference
VFe protein from *A. chroococcum*			
V–S	2.31	3±1	
V–Fe	2.75	3±1	26
V–O (N or C)	2.15	3±1	
VFe protein from *A. vinelandii*			
V–S	2.34	3–4	
V–Fe	2.74	2–4	27
V–O (N or C)	2.15	2–3	
MoFe protein from *Klebsiella pneumoniae*			
Mo–S	2.37	4.5±1	
Mo–Fe	2.67	3.5±1	30
Mo–O (N or C)	2.12	2±1	

vanadium-containing cofactor centre in these VFe proteins.

The iron- and vanadium-containing cofactor

Under the appropriate conditions the molybdenum of the MoFe protein can be extracted by treatment of the protein with N-methyl formamide[28] (NMF). The NMF extract contains FeMoco, which can be assayed by its ability to activate MoFe proteins isolated from mutants unable to synthesize FeMoco. Extraction of the acid-precipitated VFe protein of *A. chroococcum* with NMF[29] resulted in a brown solution containing vanadium, iron and S^{2-} in the ratio 1 : 6 : 5, which exhibited a weak EPR spectrum with g values near 4.5, 3.6 and 2.0, characteristic of a $S = 3/2$ spin system. The NMF extract activated purified FeMoco-less-MoFe protein when recombined with Fe protein in a nitrogenase assay system. The active hybrid protein catalysed the reduction of H^+ to H_2, and the reduction of C_2H_2 to C_2H_4 and C_2H_6. The formation of C_2H_6 from C_2H_2 is a product characteristic of the VFe protein but not the MoFe protein. These data, together with the X-ray absorption data indicate that VFe proteins contain an iron–vanadium cofactor (FeVaco) analogous to FeMoco of the MoFe proteins. The hybrid FeVaco–MoFe protein did not reduce N_2, suggesting that a specific interaction of the polypeptide and cofactor centre is necessary for the reduction of N_2 but not other substrates.

Acknowledgements—I thank the many co-workers who have made significant contributions to the work on V-nitrogenase of *A. chroococcum* discussed above, in particular Professors Barry Smith and Mike Dilworth and Drs David Lowe, Roger Thorneley, Dick Miller, Richard Pau and Rob Robson. I also thank Beryl Scutt for typing.

REFERENCES

1. H. Bortels, *Arch. Microbiol.* 1930, **1**, 333.
2. R. L. Robson, R. R. Eady, T. H. Richardson, R. W. Miller, M. Hawkins and J. R. Postgate, *Nature (Lond.)* 1986, **322**, 388.
3. B. J. Hales, E. E. Case, J. E. Morningstar, M. F. Dzeda and L. A. Mauterer, *Biochemistry* 1986, **25**, 7251.
4. J. R. Chisnell. R. Premakumar and P. E. Bishop, *J. Bacteriol.* 1988, **170**, 27.
5. M. G. Yates and K. Planque, *Eur. J. Biochem.* 1975, **60**, 467.
6. R. N. Pau, L. A. Mitchenall and R. L. Robson, *J. Bacteriol.* 1989, **171**, 124.
7. R. L. Robson, *Arch. Microbiol.* 1986, **146**, 74.
8. P. E. Bishop, R. Premakumar, D. R. Dean, M. R. Jacobson, J. R. Chisnell, T. M. Rizzo and J. Kopzcynski, *Science* 1986, **232**, 92.
9. P. E. Bishop, M. L. Jarlenski and D. R. Hetherington, *Proc. Natl. Acad. Sci. U.S.A.* 1980, **77**, 7342.
10. P. E. Bishop, D. M. L. Jarlenski and D. R. Hetherington, *J. Bacteriol.* 1982, **150**, 1244.
11. R. R. Eady, R. L. Robson, T. H. Richardson, R. W. Miller and M. Hawkins, *Biochem. J.* 1987, **244**, 197.

12. R. R. Eady, T. H. Richardson, R. W. Miller, M. Hawkins and D. L. Lowe, *Biochem. J.* 1988, **256**, 189.
13. B. J. Hales, D. J. Langosch and E. E. Case, *J. Biol. Chem.* 1986, **261**, 15301.
14. D. J. Lowe and R. N. F. Thorneley, *Biochem. J.* 1984, **224**, 877.
15. R. N. F. Thorneley, N. H. J. Bergström, R. R. Eady and D. J. Lowe, *Biochem. J.* 1989, **257**, 789.
16. R. W. Miller and R. R. Eady, *Biochem. J.* 1988, **256**, 429.
17. M. J. Dilworth, R. R. Eady, R. L. Robson and R. W. Miller, *Nature* (*Lond.*) 1987, **327**, 167.
18. M. J. Dilworth, R. R. Eady and M. Eldridge, *Biochem. J.* 1988, **249**, 745.
19. J. Bergström, R. R. Eady and R. N. F. Thorneley, *Biochem. J.* 1988, **251**, 165.
20. P. J. Stephens, in *Molybdenum Enzymes* (Edited by T. G. Spiro), pp. 117–159. Wiley, New York (1985).
21. W. H. Orme-Johnson, *Ann. Rev. Biophys. Biophys. Chem.* 1985, **14**, 419.
22. R. L. Robson, P. R. Woodley, R. N. Pau and R. R. Eady, *EMBO J.* 1989, **8**, in press.
23. J. E. Morningstar and B. J. Hales, *J. Am. Chem. Soc.* 1987, **109**, 6854.
24. J. E. Morningstar, M. K. Johnson, E. E. Case and B. J. Hales, *Biochemistry* 1987, **26**, 1795.
25. J. M. Arber, B. R. Dobson, R. R. Eady, P. Stevens, S. S. Hasnain, C. D. Garner and B. E. Smith, *Nature* (*Lond.*) 1987, **325**, 372.
26. J. M. Arber, B. R. Dobson, R. R. Eady, S. S. Hasnain, C. D. Garner, T. Matsushita, M. Nomura and B. E. Smith, *Biochem. J.* 1989, **258**, 733.
27. G. N. George, C. L. Coyle, B. J. Hales and S. P. Cramer, *J. Am. Chem. Soc.* 1988, **110**, 4057.
28. V. K. Shah and W. J. Brill, *Proc. Natl. Acad. Sci. U.S.A.* 1977, **81**, 232.
29. B. E. Smith, R. R. Eady, D. J. Lowe and C. Gormal, *Biochem. J.* 1988, **250**, 299.
30. M. K. Eidsness, A. M. Flank, B. E. Smith, A. C. Flood, C. D. Garner and S. P. Cramer, *J. Am. Chem. Soc.* 1986, **108**, 2746.
31. R. P. Hausinger and J. B. Howard, *J. Biol. Chem.*, 1983, **258**, 13846.

Polyhedron Vol. 8, No. 13/14, pp. 1701–1704, 1989
Printed in Great Britain

0277–5387/89 $3.00+.00
© 1989 Maxwell Pergamon Macmillan plc

HYDRIDE COMPLEXES OF MOLYBDENUM AND TUNGSTEN IN A SULPHUR ENVIRONMENT

TIMOTHY E. BURROW, NATALIE J. LAZAROWYCH
and ROBERT H. MORRIS*

Department of Chemistry and the Scarborough Campus, University of Toronto, Toronto, Ontario, M5S 1A1, Canada

and

JANETTE LANE and RAYMOND L. RICHARDS*

AFRC IPSR Nitrogen Fixation Laboratory, University of Sussex, Brighton, Sussex BN1 9RQ, U.K.

Abstract—The known methods of preparation of the title complexes are reviewed. The preparation, structure and reactions of new monohydride complexes containing bulky thiolate ligands are then described: $[MH(SR)_3(PMe_2Ph)_2]$ (I) and $[MoH(SR)_3(PR'Ph_2)]$ (II) (M = Mo or W; R = $C_6H_2Me_3$-2,4,6 or $C_6H_2{}^iPr_3$-2,4,6; R′ = Me or Et). Complexes I have an unusual structure with the hydride capping a face of a distorted trigonal bipyramid defined by equatorial thiolates and axial phosphines. A significant discovery is that the hydrides of these complexes of molybdenum(IV) (II) and tungsten(IV) (I and II) undergo $^1H/^2H$ exchange with $^2H_2$. Complexes I react with ligands L = py or $P(OR')_3$ to give $[MH(SR)_3(PMe_2Ph)(L)]$, and with CO to give $[M(SR)_2(CO)_2(PMe_2Ph)_2]$.

Molybdenum compounds coordinated predominantly by sulphur ligands catalyse the transfer of hydrogen to or from a variety of substrates. Catalytic processes include hydrogen transfer to organosulphur compounds by molybdenum disulphide in hydrodesulphurization reactions,[1] and reduction of dinitrogen to ammonia by nitrogenase.[2] Molybdenum hydride intermediates have been suspected but never observed in these reactions.

We have been preparing and studying some simple hydride complexes of molybdenum and tungsten of this type to learn about their reactivity patterns. A significant discovery is that hydrogen gas reacts with our hydride complexes of molybdenum(IV) and tungsten(IV).

ROUTES TO HYDRIDE COMPLEXES OF MOLYBDENUM AND TUNGSTEN IN A SULPHUR ENVIRONMENT

There are only a few reports of hydride complexes of molybdenum with thiolate or other sulphur donor co-ligands e.g. $[MoH(SR)(dppe)_2]$, [dppe = $Ph_2PCH_2CH_2PPh_2$, RS = ^{i}PrS, ^{t}BuS, 2,4,6-$C_6H_2Me_3$ (tmt) or 2,4,6-$C_6H_2(^iPr)_3$ (tipt)],[3] $[MoH_2(C_6H_4S_2)(PMePh_2)_3]$[4,5] and $[MoH(C_6H_4S_2)_3]$.[3–6] Some tungsten hydride complex containing bridging thioethers[7] (Table 1) were the only tungsten complexes of this type before our work [see reactions (4) and (5)]. These four types of complexes were prepared by use of four distinctive sources of hydride (see Table 1). The hydride complexes are reducing as indicated by their reactions listed in the table, but none of the complexes react with dihydrogen.

No syntheses of such molybdenum or tungsten hydrides directly from dihydrogen have been reported. In cases where reaction has been observed, the hydrides result in being bonded to sulphur as in the work of Rakowski-Dubois[8] [reaction (1)]:

$$[Mo(C_5H_4Me)(S)_2]_2 + H_2 \longrightarrow [Mo(C_5H_4Me)(\mu\text{-}SH)(\mu\text{-}S)]_2. \quad (1)$$

Our attempt to react the new complex, *cis*-$[Mo(S_2C_6H_4)_2(PMePh_2)_2]$, with H_2 failed.[5]

* Authors to whom correspondence should be addressed.

Table 1. Group VI metal hydride/sulphur donor complexes

Complex	Source of hydrogen in its preparation	δ(MH) (ppm)	Hydride reacts with:	to give:
$[Cl_3W(\mu\text{-}H)(\mu\text{-}SMe_2)_2WCl_2(SMe_2)]$	Et_3SiH	+3.76	EtSSEt	HSEt
$[Mo(H)(C_6H_4S_2)_3]^{3-}$	BuLi	−10.4	MeOH	H_2
cis-$[Mo(H)(SR)(dppe)_2]$	$HSR/Mo(N_2)_2L_2$	−4 to 5	HSR	H_2
$[Mo(H)_2(S_2C_6H_4)(PMePh_2)_3]$	$[MoH_4L_4]$	−2.3	HSR	H_2

However, this complex does react reversibly with CO (1 atm, 20°C) to give *cis*-$[Mo(S_2C_6H_4)_2(CO)(PMePh_2)]$. The reaction can be driven to the right by use of MeI[5] [reaction (2)]:

$$cis\text{-}[Mo(S_2C_6H_4)_2(PMePh_2)_2]+CO+MeI \longrightarrow cis\text{-}[Mo(S_2C_6H_4)_2(CO)(PMePh_2)]+[PMe_2Ph_2]I. \quad (2)$$

The lack of reaction with H_2 is not surprising considering that the high stretching frequency for the carbonyl complex, 1970 cm^{-1}, signals a very unstable interaction of η^2-H_2 with the d^2-metal binding site of $[Mo(S_2C_6H_4)_2(PMePh_2)]$ (stable η^2-H_2 complexes on d^6-metals are expected when $1840 < \nu(CO) < 1970\ cm^{-1}$).[9]

PREPARATION OF MONOHYDRIDE COMPLEXES OF MOLYBDENUM AND TUNGSTEN CONTAINING BULKY THIOLATE LIGANDS

A route via hydrazido(2−) complexes to some very interesting monohydride complexes of molybdenum and tungsten with the bulky SR^- ligands, 2,4,6-trimethyl or 2,4,6-triisopropylthiophenolate (tmt and tipt, respectively), was recently reported[10] [reactions (3) and (4)]:

$$[M(N_2)_2(PMe_2Ph)_4]+2HBr \longrightarrow [M(NNH_2)(Br)(PMe_2Ph)_3]Br+PMe_2Ph+N_2 \quad (3)$$

$$[M(NNH_2)(Br)(PMe_2Ph)_3]Br+3RSH+2NEt_3 \longrightarrow [M(H)(SR)_3(PMe_2Ph)_2]+N_2+H_2+PMe_2Ph+2HNEt_3Br. \quad (4)$$

The polyhydride route [reaction (5)] is preferred for the synthesis of the analogous tungsten complexes (*ca* 50% yield):[11]

$$[WH_6(PMe_2Ph)_3]+3HSR \longrightarrow [W(H)(SR)_3(PMe_2Ph)_2]. \quad (5)$$

It is the unique route to an unusual 12-electron molybdenum monohydride complex in 40% yield (SR = tipt):[5]

$$[MoH_4(PEtPh_2)_4]+3HSR \longrightarrow [Mo(H)(SR)_3(PEt_2Ph)]+3H_2. \quad (6)$$

STRUCTURES OF THE MONOHYDRIDE COMPLEXES

Preliminary X-ray diffraction work on deep-green crystals of $[M(H)(tipt)_3(PMe_2Ph)_2]$, (M = Mo,[12] W[13]) suggests that they have very similar structures. The stereochemistry can be regarded as capped trigonal bipyramidal with the three bulky thiolates being equatorial, the phosphines being approximately axial and the hydride (not located) capping a PS_2 face (Fig. 1, **I**). The FAB mass spectra of these complexes verify that one hydride is present. Spectroscopic studies show that it is coordinated to the metal and not to a sulphur (e.g. ν(MoH) = 1740 cm^{-1}). This unusual geometry for a six-coordinate complex is explained by a combination of steric and electronic factors. Three large thiolate ligands are always equatorial in complexes like $[Mo(NNPh)(tipt)_3(MeCN)]$[14] and $[Mo(tipt)_3(CO)_2]^-$[15] to minimize inter-ligand repulsions, with one large arene substituent pointing up and two substituents pointing down. Distortion from octahedral geometry gives a favourable diamagnetic, d^2 electronic configuration at the metal.

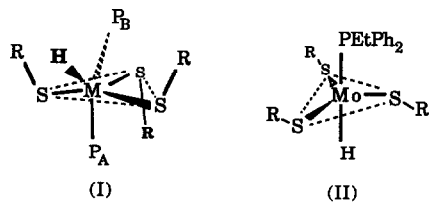

(I) (II)

Fig. 1. The structures of the complexes $[M(H)(SR)_3(PMe_2Ph)_2]$ (**I**) (M = Mo, W; SR = tipt, tmt; P_A and P_B = PMe_2Ph), and $[Mo(H)(tipt)_3(PEtPh_2)]$ (**II**).

The coupling patterns in the ^1H and ^{31}P NMR spectra of the complexes strongly suggest that the capped bipyramidal geometry, structure **I**, is retained in solution. The hydride resonance in the ^1H NMR spectrum of $[W(H)(tipt)_3(PMe_2Ph)_2]$ at δ +9.1 for tungsten shows a large, pseudo-*trans* coupling of 100 Hz to one phosphorus (P_A, Fig. 1) and a small, *cis* coupling of 8 Hz to the other. The resonance has the coupling $^1J(^1H, ^{183}W)$ of 20 Hz expected for a hydrogen bonded to tungsten ($[WH(C_5H_5)(CO)_3]$ has $^1J = 38$ Hz; $[WH_6(PMe_2Ph)_3]$ has $^1J = 37$ Hz) but not to sulphur. A chemical shift of +2 ppm is inferred for the corresponding molybdenum complex by comparison with the ^2H NMR spectrum of the deuterated analogue $[Mo(^2H)(tipt)_3(PMe_2Ph)_2]$ [see reaction (7)]. The hydride chemical shifts are the most positive of those observed so far for chromium group hydrides in a sulphur environment (see Table 1). The $^{31}P\{^1H\}$ NMR spectra indicate that there are two inequivalent phosphorus nuclei with a large coupling constant of 109 Hz for molybdenum and 101 Hz for tungsten, again consistent with a pseudo-*trans* relationship. The ^1H coupled ^{31}P NMR spectra show large $^2J(H, P_A)$ couplings of 100 Hz, as expected.

Related tmt complexes give very similar spectra. Variable temperature ^1H NMR studies indicate that $[W(H)(tmt)_3(PMe_2Ph)_2]$ has more mobile substituents on sulphur than the tipt complex, in keeping with the smaller size of the tmt ligands. Changes in resonances due to the methyl groups on tmt as a function of temperature, indicate that the exchange of arene conformations between the "two up" and "one down" sites is observable, as well as rotation about the S—C bonds.

The FAB mass spectrum and NMR and IR spectra of the green complex $[Mo(H)(tipt)_3(PEtPh_2)]$ [as obtained from reaction (6)] are all consistent with structure **II** of Fig. 1. The hydride has an unusual chemical shift of δ +3.3 and has the large coupling constant, $^2J(H,P)$ 87 Hz, required for a *trans*-disposed phosphine. The IR absorption at 1858 cm^{-1} is in the region expected for ν(MoH). This hydride complex has one of the lowest formal electron counts (12) known for a hydride complex.

REACTIONS OF THE MONOHYDRIDE COMPLEXES

A most interesting property of the complexes **I** (M = W) and **II** is that their hydride ligand undergoes complete H/^2H exchange with 1 atm $^2H_2$ (benzene solution, 20°C, less than 15 h). For example, treatment of a benzene solution of the unsaturated complex **II** with 1 atm $^2H_2$, 22°C, gives 50% conversion to $[Mo(^2H)(tipt)_3(PEtPh_2)]$ in 1.5 h:

$$[MH(SR)_3L_n] + {}^2H_2 \longrightarrow [M{}^2H(SR)_3L_n] + H{}^2H. \quad (7)$$

Presumably, the formation of $[Mo(^2H)(tipt)_3(PEtPh_2)]$ involves the addition of $^2H_2$ to the unsaturated molybdenum, followed by elimination of H^{2}H under the conditions of excess $^2H_2$. There is therefore the possibility of a trihydride, $(\eta^2\text{-}H_2)(H)$,[16,17] or $(H)_2(HSR)$ complex intermediate in these reactions which we have not yet detected. This is to our knowledge the first example of an interaction of molybdenum(IV) with H_2 ($^2H_2$), although reactions with tungsten(IV) are known.[18] Complexes **I** (M = W, SR = tipt) and **II** do not react with $^2HSC_6H_2{}^iPr_3$-2,4,6 (^{2}Htipt) in benzene at 20°C under argon for 48 h and 16 h, respectively; this rules out a mechanism of H_2 interaction which would involve reductive elimination of Htipt from the hydride complex prior to addition of $^2H_2$ (or ^{2}Htipt). There is the possibility that there are $Mo(\eta^2\text{-}H_2)$ or MoH functionalities at the active site of nitrogenase. These would explain why H_2 is released when N_2 reacts, and why there is H^{2}H formation during nitrogen fixation under $^2H_2$ gas. Molybdenum hydrides in the HDS catalyst could explain the hydrogenation of C=C bonds and possibly the hydrogenolysis of S—C bonds.

Despite the positive chemical shift of the hydride, the tungsten complexes are reducing. They react with $CHCl_3$ to give CH_2Cl_2 and unidentified decomposition products.

The molybdenum and tungsten complexes react with pyridine to give $[MH(SR)_3(py)(PMe_2Ph)]$ where P_B in Fig. 1 has been substituted. Complex **I** (W) reacts with $P(OR')_3$ (R' = Me, Et) to give $[MH(SR)_3(P(OMe)_3)(PMe_2Ph)]$, where P_A in Fig. 1 has been replaced. The complexes reductively eliminate RSH under a CO atmosphere to give dicarbonyls $[M(SR)_2(CO)_2(PMe_2Ph)_2]$, which have been shown by X-ray diffraction to have a trigonal prismatic structure.[12]

CONCLUSIONS

Hydrides in a sulphur environment are still fairly rare. We have reported here some new monohydride complexes with several novel features: the chemical shifts of the hydrides are to unusually low field; the geometry and electron count of the complexes is unusual (14-electron, 6-coordinate, but not octahedral for the complexes $[MH(SR)_3(PMe_2Ph)_2]$ and 12-electron, 5-coordinate, trigonal bipyramidal for $[MoH(SR)_3(PEtPh_2)]$). The fact

that these complexes of (formally) molybdenum(IV) and tungsten(IV) react with deuterium is very unusual and significant. As pointed out, the reactivity of these complexes may be of relevance to the hydrodesulphurization reaction and the action of nitrogenase.

Acknowledgements—We acknowledge the support of a NATP collaborative research grant to R.H.M. and R.L.R., and operating grants from NSERC Canada and Imperial Oil Ltd to R.H.M.

REFERENCES

1. F. E. Massoth, *Adv. Catal.* 1978, **27**, 265.
2. R. L. Richards, *Chem. in Britain* 1988, 29.
3. R. A. Henderson, D. L. Hughes, R. L. Richards and C. Shortman, *J. Chem. Soc., Dalton Trans.* 1987, 1115.
4. N. J. Lazarowych and R. H. Morris, *J. Chem. Soc., Chem. Commun.* 1987, 1865.
5. N. J. Lazarowych, PhD thesis, University of Toronto (1989).
6. D. Sellman and L. Zopf, *Z. Naturfor.* 1985, **40B**, 380.
7. P. M. Boorman, K. J. Moynihan, V. D. Patel and J. F. Richardson, *Inorg. Chem.* 1985, **24**, 2989.
8. C. J. Casewit, R. C. Haltiwanger, J. Noordik and M. Rakowski-DuBois, *Organometallics* 1985, **4**, 119.
9. R. H. Morris, K. A. Earl, R. L. Luck, N. J. Lazarowych and A. Sella, *Inorg. Chem.* 1987, **26**, 2674.
10. S. N. Anderson, D. L. Hughes, R. H. Morris and R. L. Richards, *INOR 176*, Third Chemical Congress of North America, Toronto, Canada (1988).
11. T. E. Burrow, MSc thesis, University of Toronto (1989).
12. D. L. Hughes, personal communication.
13. J. F. Sawyer, personal communication.
14. P. T. Bishop, P. J. Blower, J. R. Dilworth and J. A. Zubieta, *Polyhedron* 1986, **5**, 363.
15. J. R. Dilworth, J. Hutchinson and J. A. Zubieta, *J. Chem. Soc., Chem. Commun.* 1983, 1034.
16. R. H. Crabtree, M. Lavin and L. Bonneviot, *J. Am. Chem. Soc.* 1986, **108**, 4032.
17. M. T. Bautista, K. A. Earl, P. A. Maltby and R. H. Morris, *J. Am. Chem. Soc.* 1988, **110**, 4056 and refs therein.
18. M. L. H. Green and G. Parkin, *J. Chem. Soc., Chem. Commun.* 1984, 1467.

Polyhedron Vol. 8, No. 13/14, pp. 1705–1716, 1989
Printed in Great Britain

0277–5387/89 $3.00+.00
© 1989 Maxwell Pergamon Macmillan plc

AN INORGANIC FUNCTIONAL GROUP APPROACH TO THE SYSTEMATIC SYNTHESIS AND REACTIVITY STUDIES OF BINUCLEAR Mo/S AND Mo/S/O COMPLEXES

D. COUCOUVANIS,* A. TOUPADAKIS, SANG-MAN KOO and A. HADJIKYRIACOU

Department of Chemistry, The University of Michigan, Ann Arbor, MI 48109, U.S.A.

Abstract—A number of general reactions, based on molybdenum-coordinated sulphido or polysulphido ligands, can account for the synthesis of many members of the $[Mo_2^V(S)_n(S_2)_{6-n}]^{2-}$, $[Mo_2^V(O)(S)_n(S_2)_{5-n}]^{2-}$ and $[Mo_2^V(O)_2(S)_n(S_2)_{4-n}]^{2-}$ homologous series. These reactions include: (a) sulphur addition and sulphur abstraction reactions; (b) oxidative removal of the S_x^{2-} ligands and their replacement by substitutionally labile ligands; (c) oxidation of coodinated RS^- ligands by S_x^0 fragments, and *in situ* generation of S_x^{2-} ligands; (d) oxidative dimerization reactions of molybdenum(IV) complexes; and (e) reductive elimination of S_x^0 fragments. The synthesis of the new $[(Cp)Mo^V(O)(\mu\text{-}S)_2Mo^V(O)S_4]^-$ and $[(Cp)Mo^V(O)(\mu\text{-}S)_2Mo^V(O)S_2]^-$ anions has alowed the use of ^1H NMR spectroscopy to monitor the solution behaviour and reactivity of the $Mo^V(O)S_2$ group. The existence of the $Mo^V(O)S_2+S_2 \rightleftarrows Mo^V(O)S_4$ equilibrium has been unequivocally established. The $[(Cp)Mo^V(O)(\mu\text{-}S)_2Mo^V(O)S_2]^-$ complex gives a vinyl disulphide derivative by insertion of dicarbomethoxyacetylene, DMA, into the Mo-η^2-S_2 group. Upon prolonged heating to 70°C the vinyl disulphide ligand is converted quantitatively to a dithiolene ligand. The same conversion takes place swiftly at ambient temperatures when catalytic amounts of S_8 are present in the reaction medium. Reaction pathways for both the thermal and catalytic conversions have been suggested by ^1H NMR studies. Preliminary studies of the utility of the $(Et_4N)[Mo_2O_2S_8Cl]$, $[Ni(DMF)_6][Mo_2O_2S_8Cl]_2$, $(Et_4N)_2[Mo_4O_4S_{18}]$ and $(Ph_4P)_2[Mo_2S_6]$ complexes as catalysts for the hydrodesulphurization of thiophene are reported. The Ni/Mo catalyst obtained from $[Ni(DMF)_6][Mo_2O_2S_8Cl]_2$ is at least 10 times more effective than a commercial Co/Mo catalyst.

The binary, Mo/S, or tertiary, Mo/S/O, thiomolybdate complexes[1–4] are characterized by a remarkable complexity in structure and by interesting reactivity characteristics. The vast majority of these complexes are anionic species and can be described in terms of various combinations of the O^{2-}, S^{2-}, S_2^{2-} and S_4^{2-} ligands coordinated to molybdenum(IV), -(V) or -(VI) ions.

At times, the deceivingly simple procedures that are used in the synthesis of some of these compounds result in products with unexpected formal oxidation states for the molybdenum atoms and the appearance of sulphur ligands in various degrees of catenation. The latter phenomena have their origin in facile intramolecular electron transfer processes that derive from a close matching of the S 3*p* and Mo 4*d* orbital energies.† An example of intramolecular electron transfer can be found in the synthesis of the $[(S_4)_2Mo^{IV}{=}S]^{2-}$ and $[(S_4)_2Mo^{IV}{=}O]^{2-}$ anions[6] (Figs 1 and 2). These anions are obtained by the reaction of S_8 with $[Mo^{VI}S_4]^{2-}$ or $[Mo^{VI}S_xO_{4-x}]^{2-}$ under oxidizing conditions! Intramolecular electron transfer also accounts for an apparent diversity in structural isomerism for certain molybdothioanions, where S—S bonds break or form as molybdenum atoms are oxidized or reduced.[2]

Our exploration of the reactivities of the coor-

* Author to whom correspondence should be addressed.

† For the neutral free atoms, a compilation of Roothaan–Hartree–Fock atomic wavefunctions[5] show the sulphur 3*p* orbitals with an energy of −0.43694 a.u. and the molybdenum $4d(s^1d^5)$ with an energy of 0.34811 a.u. The localization of partial positive charge on the molybdenum and partial negative charge on the sulphur is expected to bring these energies even closer together.

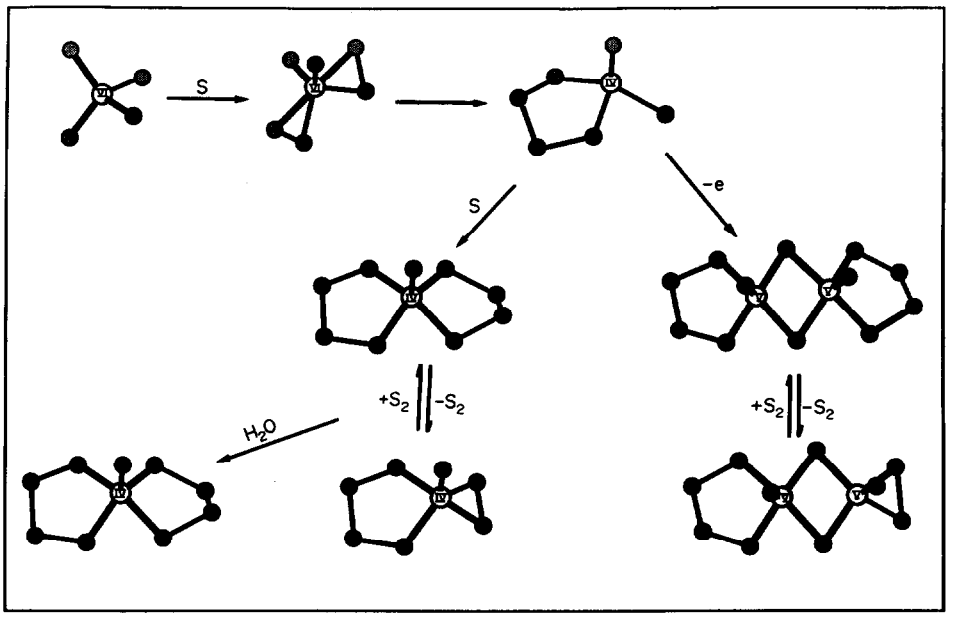

Fig. 1. Possible reaction pathways for the syntheses of the $[(S_4)_2Mo^{IV}{=}S]^{2-}$ and $[(S_4)Mo^{V}{=}S(\mu\text{-}S)]_2^{2-}$ complexes by the reaction of S_8 with the $[MoS_4]^{2-}$ anion.

dinated S^{2-}, S_2^{2-} and S_4^{2-} ligands has revealed a number of reliable general reactions that can be used for the systematic synthesis of certain thiomolybdates. Furthermore, these studies have made it apparent that neighbouring ligands, and the molybdenum oxidation state, have profound influence on reactivity.

In this paper we report on general reactivity patterns of the molybdenum-coordinated S^{2-}, S_2^{2-} and S_4^{2-} ligands. These first attempts in the development of "functional group" chemistry in the Mo/S and Mo/S/O complexes have led to rational syntheses of homologous series of complexes such as $[Mo_2^{V}(S)_n(S_2)_{6-n}]^{2-}$ [2] and $[Mo_2^{V}(O)(S)_n(S_2)_{5-n}]^{2-}$ [7] and a better understanding of the reactions of these complexes with activated alkynes and CS_2.

The synthesis of homologous series of Mo/S and Mo/S/O binary and tertiary complex anions makes it possible to systematically evaluate their activity, and the activity of their Ni^{2+} or Co^{2+} "salts" in the hydrodesulphurization (HDS) reaction of thiophene. In this paper we also report preliminary results on the catalytic properties of certain γ-Al_2O_3 supported, thiomolybdate complexes.

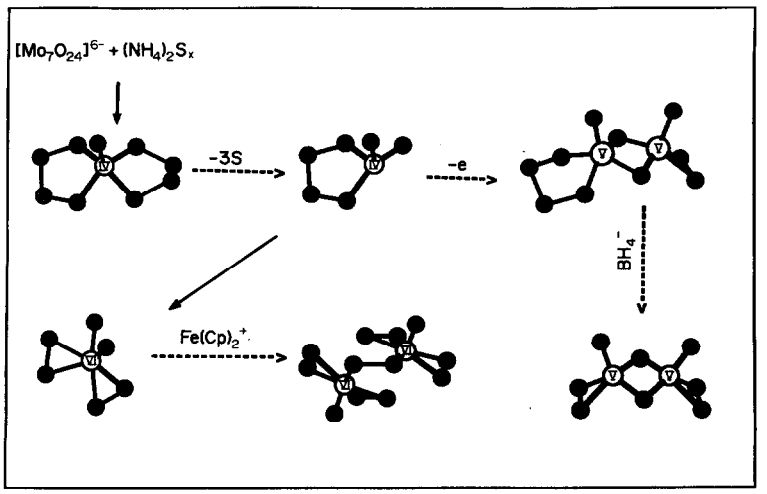

Fig. 2. Possible reaction pathways in the syntheses of the $[(S_4)Mo^{V}{=}O(\mu\text{-}S)]_2^{2-}$; $[(S_2)Mo^{V}{=}O(\mu\text{-}S)]_2^{2-}$ and $[(S_2)_2Mo^{VI}{=}O(S)]_2^{2-}$ complexes.

DISCUSSION

Synthesis of molybdothioanions

A number of general reactions, based on molybdenum-coordinated sulphido or polysulphido ligands, can account for the synthesis of many members of the $[Mo^{V}_{2}(S)_{n}(S_2)_{6-n}]^{2-}$ [2], $[Mo^{V}_{2}(O)(S)_{n}(S_2)_{5-n}]^{2-}$ [7] and $[Mo^{V}_{2}(O)_2(S)_{n}(S_2)_{4-n}]^{2-}$ [8,9] homologous series. Furthermore, these reactions make it possible to design procedures for the synthesis of new thiomolybdate complexes. In the discussion that follows, a detailed account is offered for the synthesis and reactivities of the molybdenum-coordinated sulphido and persulphido functional groups.

The molybdenum-coordinated S^{2-} *ligands*

The reactions of oxomolybdates $[(Mo^{VI}O_4)^{2-}$ or $(Mo^{VI}_{7}O_{24})^{6-}]$ with H_2S or $(NH_4)_2S_x$ under basic conditions give thiomolybdate products that, depending on reaction times or conditions, contain Mo—S_x and Mo=O units in various combinations. The simplest among the S^{2-}_{x} ligands is the S^{2-} ligand that exists mainly as: (a) a terminal ligand in thiomolybdenyl units[1-3] (Mo^{n+}=S, n = IV, V, VI), (b) a μ_2-bridging unit in cores such as $(Mo_2S_2)^{6+}$ [1-4] and (c) a μ_3-bridging unit in $[Mo_3S_{13}]^{2-}$ [10] and in the Mo_4S_4 cores of the $[(L_3Mo)_2S_4]$ complexes[11,12] and in $[Mo_7S_8(H_2O)_{18}]^{8+}$.[13] The nucleophilicity that dominates the chemistry of the S^{2-} ligands depends on the coordination mode [(a), (b) or (c) above] and appears to be stronger for the terminal Mo=S sulphido ligands. In this paper we will direct our attention to the chemistry of the S^{2-} terminal ligands.

The addition of sulphur to terminal sulphido ligands is very likely the end result of electrophilic attack on the Mo^{n+}=S sulphur by the $^{+}S(S)_xS^{-}$ products of heterolytically cleaved S_8 molecules. This general reaction occurs readily with various Mo^{n+}=S groups (n = IV, V, VI) and is encouraged in the synthesis of the $[(S_4)_2Mo^{IV}{=}E]^{2-}$ anions[6] (E = S, O; Fig. 1) and various members of the $[Mo^{V}_{2}(S)_{n}(S_2)_{6-n}]^{2-}$ [2] (Fig. 3) and $[Mo^{V}_{2}(O)(S)_{n}(S_2)_{5-n}]^{2-}$ [7] series. Addition of sulphur atoms to the Mo=S units gives stable Mo-η^2-S_2 units that on occasion may undergo subsequent intramolecular electron transfer on their way to more stable, electron redistribution isomers (Figs 1 and 2). Electrophilic attack on the Mo^{n+}=S sulphur very likely also occurs in the reactions of various thiomolybdates with CS_2[14] and activated alkynes, RC≡CR,[1,15] (*vide infra*).

With transition metal ions, the thiomolybdenyl groups can serve as either electron pair donors, or as a source of sulphide ions for the eventual formation of highly insoluble, thermodynamically stable, transition metal sulphides. The former course of reactivity is aptly represented in the multitude of heterometallic complexes where the MoS_4^{2-} anion serves as a ligand for transition metal ions.[16] The irreversible removal of sulphide ions from Mo=S units by the formation of insoluble transition metal sulphides allows for the introduction of non-sulphur terminal ligands in the thiomolybdate ions by metathetical reactions. An example of this reaction is available in the synthesis of the $[Mo_2O_2S_8X]^{-}$ anions[17] from the reaction

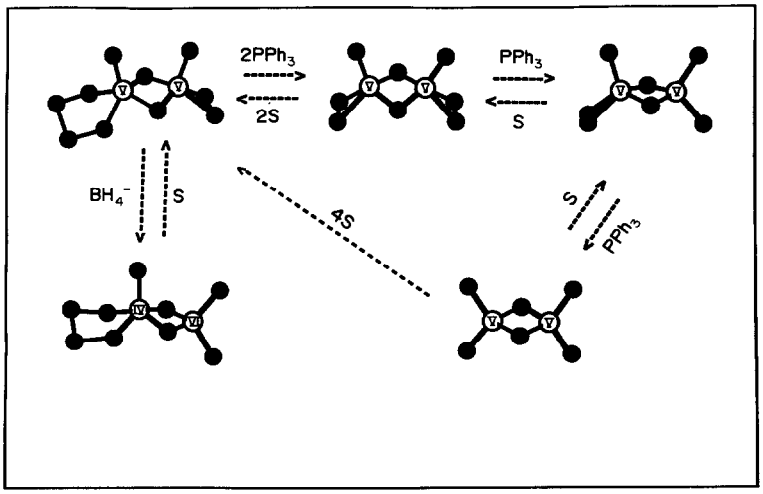

Fig. 3. The syntheses of members in the $[Mo^{V}_{2}(S)_{n}(S_2)_{6-n}]^{2-}$ series by sulphur addition and sulphur-abstraction reactions.

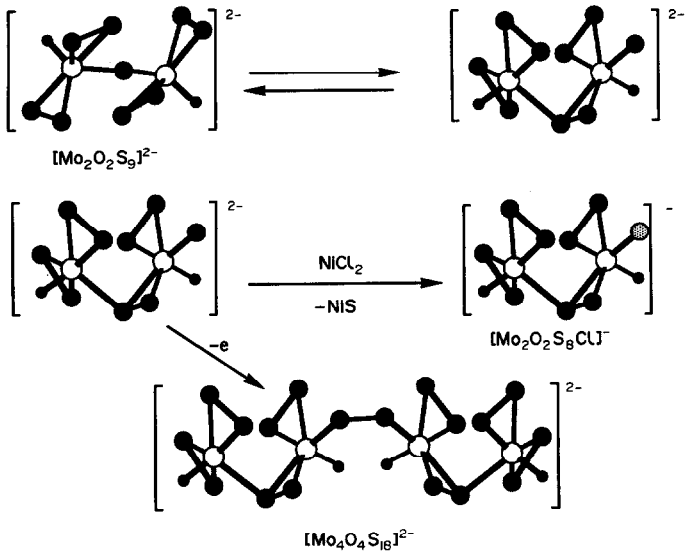

Fig. 4. Reactions and derivatives of the $[[(S_2)_2Mo^{VI}{=}O]_2(S)]^{2-}$ anion.

of NiX_2 (X = Cl, I) with an isomeric form of the $[Mo_2^{VI}O_2S_9]^{2-}$ anion[18] (Fig. 4). The latter is obtained readily by oxidation of the $[(S_4)_2Mo^{IV}{=}O]^{2-}$ anion (Fig. 2).

The oxidation of the thiomolybdenyl group by various oxidizing agents depends on the formal oxidation state of the molybdenum atom and the nature of the neighbouring ligands in the coordination sphere of the molybdenum atom. The dimerization of Mo^V, $4d^1$ complexes to diamagnetic dimeric complexes with a formal Mo—Mo single bond is well documented. Not surprisingly, the one-electron oxidations of $(L)_nMo^{IV}{=}S$ complexes invariably lead to dimerization with formation of the very stable di-μ-sulphido $[(L)_nMo^VS]_2$ products.

Examples of this oxidative dimerization include the formation of $[(S_4)SMo^V{=}E]_2^{2-}$ from the air-oxidation of $[(S_4)_2Mo^{IV}{=}E]^{2-}$ [7] (Figs 1 and 2), and the formation of the $[(L)_2Mo^V{=}S]_2^{2-}$ dimer[1] apparently from the oxidation of an unstable $[(L)_2Mo^{IV}{=}S]^{2-}$ intermediate (L = 1,2-dicarboethoxyethylene-1,2-diethiolate). An unusual oxidation is evident in the reaction of the $[(S_4)_2Mo^{IV}{=}O]^{2-}$ complex with $[(C_5H_5)_2Fe]^+$, and formation of the $[(S_2)_2(O)Mo^{VI}{-}S{-}S{-}Mo^{VI}(O)(S_2)_2]^{2-}$ dimer[17] (Fig. 2). This oxidation may involve the $[(S_2)_2(O)Mo^{VI}{=}S]^{2-}$ intermediate complex that forms as a result of intramolecular electron transfer. The $[(S_2)_2(O)Mo^{VI}(\mu\text{-}S_2)Mo^{VI}(O)(S_2)_2]^{2-}$ dimer (Fig. 2) readily dissociates sulphur to give the apparently more stable $[(S_2)_2(O)Mo^{VI}{-}S{-}Mo^{VI}(O)(S_2)_2]^{2-}$ complex.

The molybdenum-coordinated S_2^{2-} ligands

As discussed previously, the $Mo^{n+}{-}\eta^2\text{-}S_2$ units are obtained by sulphur addition to the $Mo^{n+}{=}S$ units (n = IV, V, VI). The same units also can be obtained by the oxidation of molybdenum-coordinated PhS^- ligands with the dibenzyltrisulphide reagent. This general reaction generates S_x^{2-} ligands *in situ*, from the reduction of S_x^0 fragments by PhS^- ligands, and has been used previously[19] in the synthesis of $[M(S_x)_2]^{2-}$ complexes from the $[M(SPh)_4]^{2-}$ anions. The oxidative removal of the coordinated PhS^- ligands from the $[OMo^V(SPh)_2MoS_4]^{2-}$ derivative[7] of the $[OMo^V(SPh)_4]^-$ complex,[20] with the concomitant introduction of the $\eta^2\text{-}S_2$ ligand, is shown in Fig. 5. This reaction and subsequent sulphur-addition or sulphur-abstraction reactions have made possible the rational synthesis of the new $[Mo_2^V(O)(S)_n(S_2)_{5-n}]^{2-}$ anions (n = 3,4) and derivatives[8] (Figs 5 and 6) based on predictable functional group chemistry.

The $Mo{-}\eta^2\text{-}S_2$ functional groups in the $L_x(S)Mo{-}\eta^2\text{-}S_2$ complexes react with both electrophilic and nucleophilic reagents. Nucleophilic attack by triphenylphosphine, presumably on a highly polarized S_2^{2-} ligand, occurs readily and the ligand undergoes desulphurization with generation of $L_x(S)Mo{=}S$ units. This general sulphur-abstraction reaction has been used effectively for the synthesis of various members of the $[Mo_2^V(S)_n(S_2)_{6-n}]^{2-}$,[2] and $[Mo_2^V(O)(S)_n(S_2)_{5-n}]^{2-}$ [7] series (Figs 3, 5 and 6) from "sulphur-rich" precursors.

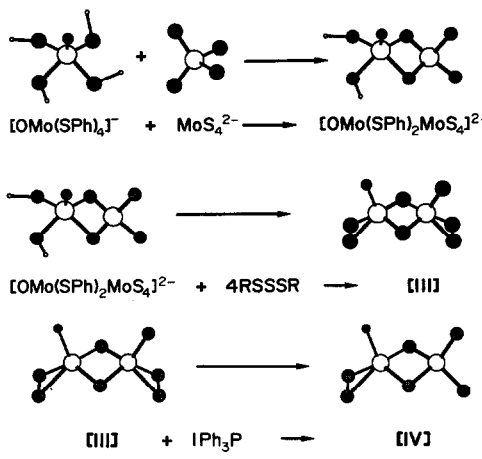

Fig. 5. Syntheses of members of the $[Mo_2^V(O)(S)_n(S_2)_{5-n}]^{2-}$ series ($n = 3, 4$) from $[(PhS)_2Mo^V(O)(Mo^{VI}S_4)]^-$.

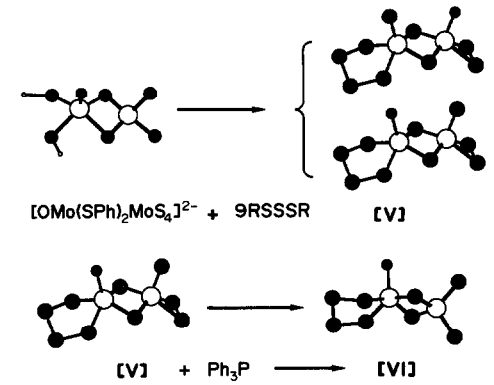

Fig. 6. Synthesis of electron redistribution isomers of the $[Mo_2^V(O)(S)_n(S_2)_{5-n}]^{2-}$ series ($n = 1, 2$) from $[(PhS)_2Mo^V(O)(Mo^{VI}S_4)]^-$.

The reaction of Ph_3P with the $L_x(O)Mo^V$—η^2-S_2 complexes probably proceeds with formation of $L_x(O)Mo^V$=S units that readily dimerize to the $[L_x(O)Mo^V{=}S]_2$ complexes (Fig. 2). The greater tendency of the $L_x(O)Mo^V$=S units to dimerize, by comparison to $L_x(S)Mo^V$=S units, could be attributed in part to steric effects. The molybdenum(V) ions in the four-coordinate $L_x(O)Mo^V$=S units are not only coordinatively unsaturated but considerably less crowded than the molybdenum(V) ions in the $L_x(S)Mo^V$=S units. The importance of this type of steric effect also is apparent in the synthesis of the $[(S_4)Mo^{IV}(O)(Mo^{VI}S_4)]^{2-}$ complex.[7] This anion (but not the isomeric $[(S_4)Mo^{IV}(S)(Mo^{VI}S_3O)]^{2-}$) is obtained exclusively in the reaction of a 50:50 mixture of the $[(S_4)Mo^V(O)(\mu\text{-}S)_2Mo^V(S)(S_2)]^{2-}$ and $[(S_4)Mo^V(S)(\mu\text{-}S)_2Mo^V(O)(S_2)]^{2-}$ isomers with Ph_3P (Fig. 6). A similar preferential sulphur abstraction from a $Mo(S)(\eta^2\text{-}S_2)$ functional group is also apparent in the exclusive synthesis of the $[(S_2)Mo^{IV}(O)(Mo^{VI}S_4)]^{2-}$ anion[7] from $[(S_2)Mo^V(O)(\mu\text{-}S)_2(S)Mo^V(S_2)]^{2-}$ (Fig. 5).

In DMF solution, I_2 oxidation of η^2-S_2^{2-} ligands gives polymeric thiomolybdates when neighbouring terminal S^{2-} ligands are also present on the same molybdenum atom. If instead of S^{2-} a neighbouring O^{2-} ligand is present on the molybdenum atom, the S_2^{2-} ligands are oxidatively removed (as S_8) and are replaced by DMF ligands[8] (Fig. 7). The neutral $[(S_2)Mo^V(O)(\mu\text{-}S)_2Mo^V(O)(DMF)_3]$ complex, and the I^- salt of the $[(DMF)_3Mo^V(O)(\mu\text{-}S)_2Mo^V(O)(DMF)_3]^{2+}$ cation have been obtained in excellent yields in crystalline form.[8] These complexes have made it possible to synthesize a wide

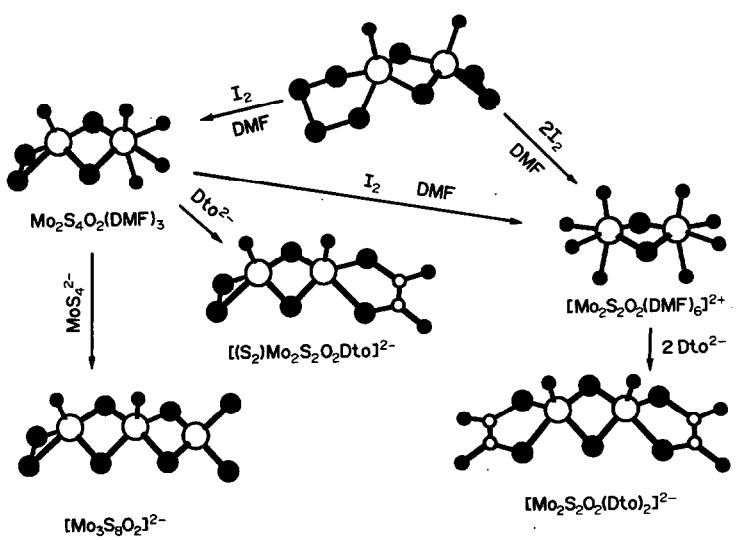

Fig. 7. Iodine oxidation of the S_x^{2-} ligands in the $[(S_4)Mo^V(O)(\mu\text{-}S)_2Mo^V(O)(S_2)]^{2-}$ complex. Synthesis and derivatives of the $[(DMF)_3Mo^V(O)(\mu\text{-}S)_2Mo^V(O)(S_2)]$ and $[(DMF)_3Mo^V(O)(\mu\text{-}S)_2Mo^V(O)(DMF)_3]^{2+}$ complexes.

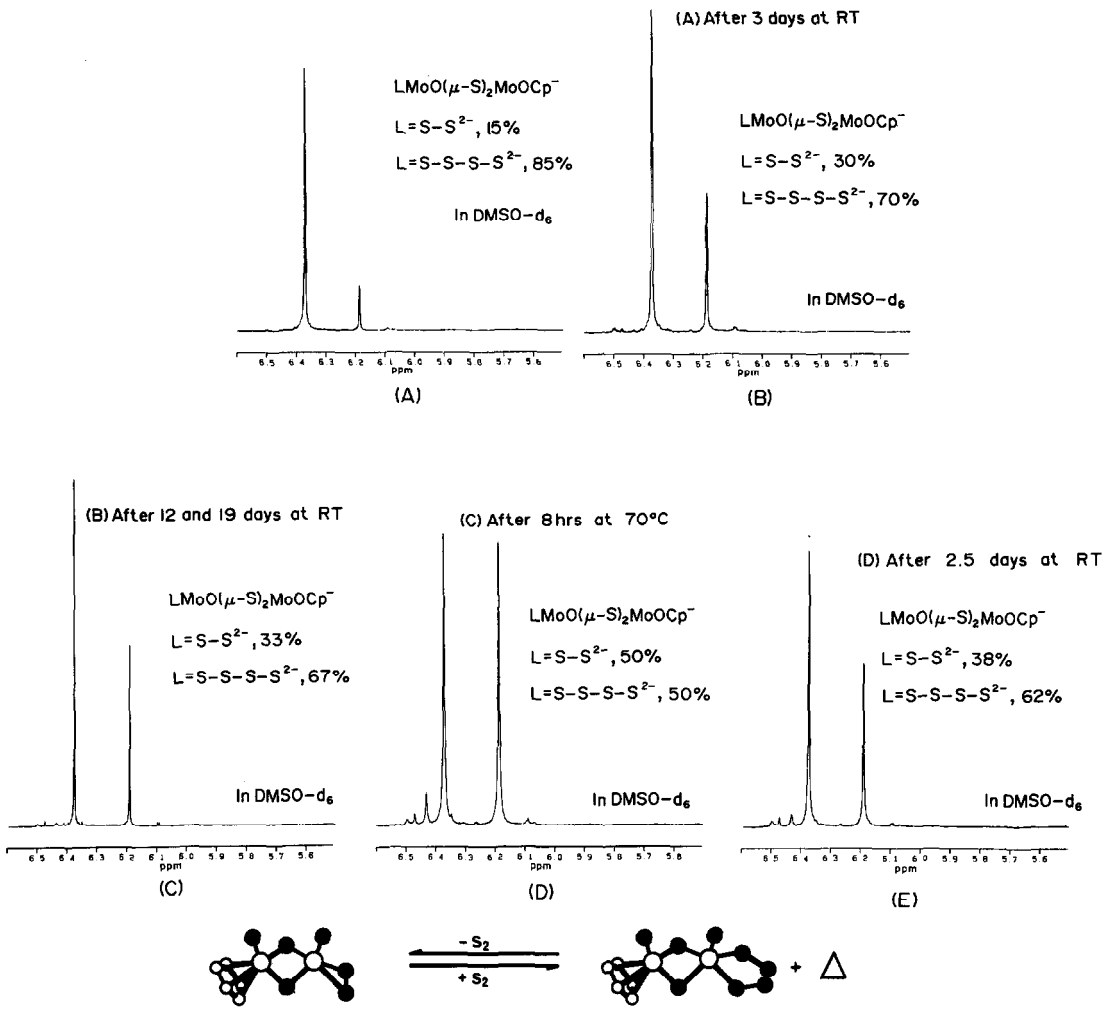

Fig. 8. ^{1}H NMR study of the Cp^- ligand in the $[(Cp)Mo^V(O)(\mu\text{-}S)_2Mo^V(O)(S_2)]^-$ and $[(Cp)Mo^V(O)(\mu\text{-}S)_2Mo^V(O)(S_4)]$ complexes at equilibrium.

variety of complexes containing the $[Mo_2^V(O)_2(\mu\text{-}S)_2]^{2+}$ core by replacement of the labile DMF ligands (Fig. 7).

The molybdenum-coordinated S_4^{2-} ligands

Addition of elemental sulphur to the Mo—η^2-S_2 functional group results in the formation of the Mo—η^2-S_4 unit, in a reaction that could be visualized as an insertion of a polarized $^{\delta+}$S—S$^{\delta-}$ species into the Mo—S_2 bond. This insertion is reversible and in solution the Mo—η^2-S_4 group exists in equilibrium with Mo—η^2-S_2 and elemental sulphur.

This equilibrium has been established unequivocally by an ^{1}H NMR study of mixtures of the $[(Cp)Mo^V(O)(\mu\text{-}S)_2Mo^V(O)S_4]^-$ and $[(Cp)Mo^V(O)(\mu\text{-}S)_2Mo^V(O)S_2]^-$ anions in CH_3CN solution (Fig. 8). Such a mixture, that contains the $[(Cp)Mo^V(O)(\mu\text{-}S)_2Mo^V(O)S_4]^-$ anion as the major component (84%), is obtained[21] in the reaction between $[(Cp)Mo^V(O)(\mu\text{-}S)_2Mo^V(O)(DMF)_3]^+$ and an excess of $(NH_4)_2S_x$. The $[(Cp)Mo^V(O)(\mu\text{-}S)_2Mo^V(O)(DMF)_3]^+$ cation is obtained by I_2 oxidation of the $[(Cp)Mo^V(O)(\mu\text{-}S)_2Mo^V(O)S_2]^-$ complex in DMF solution. It is now apparent that the chemistry of the Mo—η^2-S_4 group is dominated by the presence of the Mo—η^2-S_2 groups. The ready dissociation of S_2 from the coordinated S_4^{2-} ligand is due to a weakening of the S—S bonds proximal to the molybdenum atom. This weakening has been attributed previously to Mo—S $d\pi$–$p\pi$ bonding[1,19,*] and is reflected in unusually long S—S bond lengths in the coordinated ligand.

* See footnote † on p. 1705.

Reactivity of the molybdenum-coordinated S_x^{2-} ligands toward unsaturated electrophilic molecules

The reaction chemistry of the molybdenum thioanions with electrophiles such as CS_2[1,14] and dicarboalcoxyacetylenes[1,15] has been investigated in considerable detail. It appears that both the Mo—η^2-S_x and Mo=S groups are sufficiently nucleophilic to attack by dicarbomethoxyacetylene (DMA). This is clearly established for thiomolybdates that contain both Mo=S and Mo(η^2-S_x) groups. The reactions of the $[(S_4)_2Mo^{IV}{=}S]^{2-}$ and $[(S_4)(S)Mo^{V}(\mu\text{-}S)_2Mo^{V}(S)(S_2)]^{2-}$ complexes with DMA (Fig. 9) proceed until all S_x^{2-} sulphido ligands (with the exception of the μ-S^{2-} ligands) are converted into the dithiolene (DMAD) ligands. The type of DMAD complex obained depends on the synthetic conditions. Thus, the $[(S_4)_2Mo^{IV}{=}S]^{2-}$ complex under anaerobic conditions reacts with DMA to give the $[Mo^{IV}(DMAD)_3]^{2-}$ complex.[15] Under aerobic conditions the same reaction affords the dimeric $[(DMAD)_2Mo^{V}(\mu\text{-}S)_2Mo^{V}(DMAD)_2]^{2-}$.[1] The latter is also obtained from reactions of DMA with either the $[(S_4)(S)Mo^{V}(\mu\text{-}S)_2Mo^{V}(S)(S_2)]^{2-}$ or the $[(S_2)(S)Mo^{V}(\mu\text{-}S)_2Mo^{V}(S)(S_2)]^{2-}$ complex anions. Possible reaction pathways are shown in Fig. 9. The formation of the DMAD ligands in these complexes can be ex-

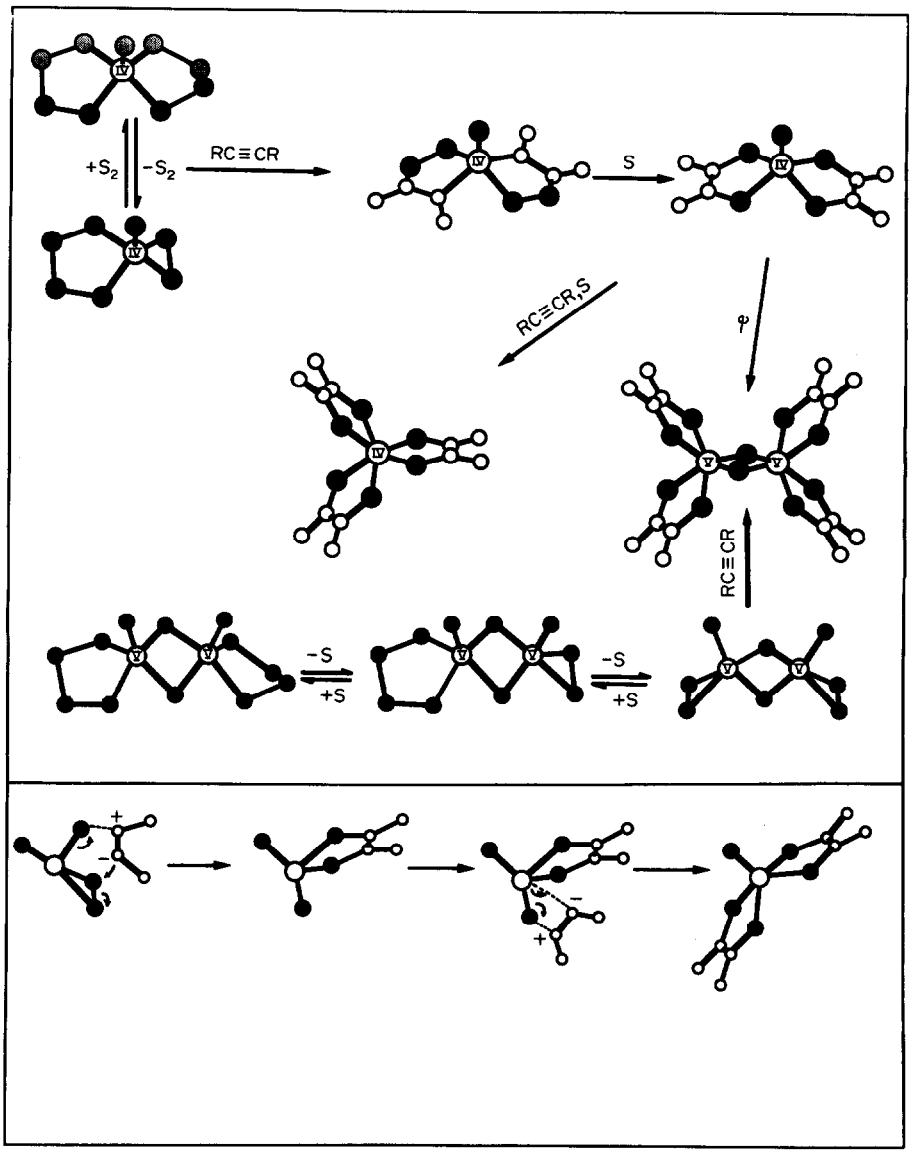

Fig. 9. Reactions of dicarbomethoxyacetylene, DMA, with the $[(S_4)_2Mo^{IV}{=}S]^{2-}$ and $[(S_4)Mo^{V}(S)(\mu\text{-}S)_2Mo^{V}(S)(S_2)]^{2-}$ complexes, under aerobic and anaerobic conditions.

plained in terms of electrophilic attack by DMA on either the Mo=S or the Mo—η^2-S_2 functional groups. The initial step in these reactions is difficult to ascertain, but it could be electrophilic attack by DMA followed by insertion into either the Mo=S or Mo—η^2-S_2 bonds. These insertions lead to the formation of reactive vinyl sulphide or vinyl disulphide ligands, that eventually transform to dithiolenes. This transformation could occur for the vinal sulphide by insertion of sulphur into the Mo—C bond, and for the vinyl disulphide by a thermal or sulphur-catalysed isomerization reaction. Other possible schemes suggested previously[15] for the addition of an alkyne into the Mo—S—S unit include: (a) direct formation of the DMAD dithiolene ligand, by electrophilic attack of DMA on the η^2-S_2 ligand, followed by insertion into the S—S bond and (b) a 4+2 Diels–Alder cycloaddition reaction.

The reactions of oxothiomolybdates with DMA (Fig. 10) have been quite useful from a mechanistic point of view. Replacement of the Mo=S groups by the apparently unreactive Mo=O groups, in otherwise isostructural complexes, simplifies the reactivity patterns and eliminates some of the ambiguities inherent in the reactions of totaly "sulphided" thiomolybdates.

The initial report[22] on the synthesis of the vinyl disulphide complex, $[(L)(O)Mo^{V}(\mu\text{-}S)_2Mo^{V}(O)(L)]^{2-}$ (L = [—(R)C=C(R)—S—S—]^2), from the reaction of DMA with the $[(S_2)(O)Mo^{V}(\mu\text{-}S)_2Mo^{V}(O)(S_2)]^{2-}$ anion, revealed unequivocally that in the $(O)Mo(S_2)$ structural subunits of the thiomolybdate anions, insertion into the Mo—S bond is prevalent. Subsequently, we have observed that the vinyl disulphide complex thermally isomerizes to the $[(DMAD)(O)Mo^{V}(\mu\text{-}S)_2Mo^{V}(O)(DMAD)]^{2-}$ dithiolene complex. The latter and also the $[(DMAD)_2Mo^{IV}{=}O]^{2-}$ complex are obtained directly from the reactions of the $[(S_4)(O)Mo^{V}(\mu\text{-}S)_2Mo^{V}(O)(S_2)]^{2-}$ and $[(S_4)_2Mo^{IV}{=}O]^{2-}$ anions, respectively, with DMA[1] (Fig. 10). Isomerization of vinyl disulphide ligands to dithiolenes also has been reported to proceed via a first-order reaction in the $(Cp)_2Ti$(vinyl disulphide) complex.[23]

The S_4^{2-} ligands play an indirect but important role in promoting the formation of dithiolenes, by supplying dissociated "S_2" that catalyses the vinyl disulphide to dithiolene conversion.

Convincing evidence for the catalytic effects of sulphur in this interconversion has been obtained from ^{1}H NMR studies of the DMA derivatives of the $[(Cp)Mo^{V}(O)(\mu\text{-}S)_2Mo^{V}(O)S_2]^{-}$ complex.[24] This complex initially reacts with DMA to give a vinyl disulphide derivative by insertion of DMA into the Mo—η^2-S_2 group. Upon prolonged heating to 70°C the vinyldisulphide ligand in this complex is converted quantiatively to a dithiolene ligand. The same conversion takes place swiftly at the same temperature when catalytic amounts of S_8 are added to CH_3CN solutions of the vinyl disulphide complex. A plausible reaction pathway for the *thermal*, vinyl disulphide–dithiolene conversion initially

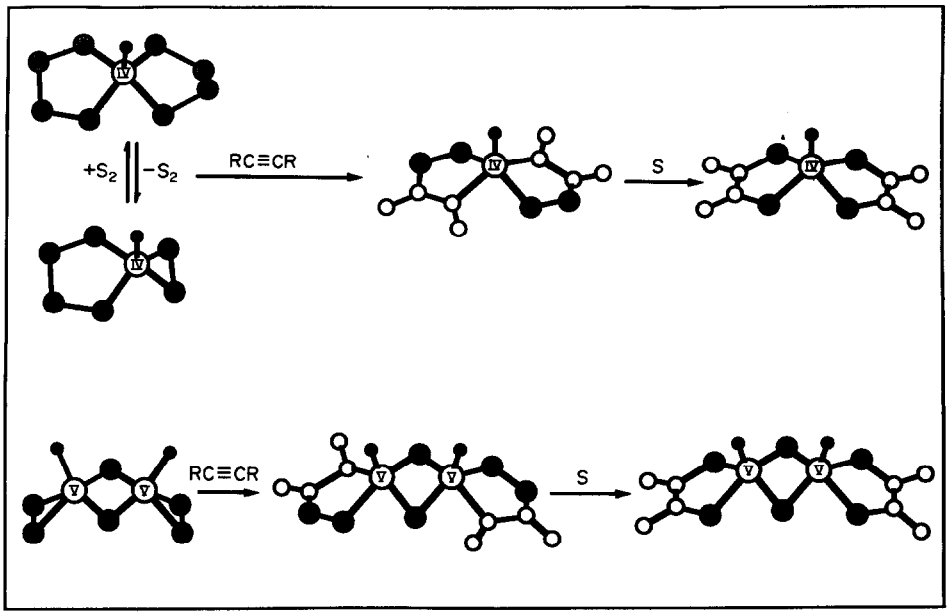

Fig. 10. Reactions of DMA with the $[(S_4)_2Mo^{IV}{=}O]^{2-}$ and $[(S_4)Mo^{V}(O)(\mu\text{-}S)_2Mo^{V}(O)(S_2)]^{2-}$ complexes.

may involve dissociation of a sulphur atom (the one adjacent to the olefinic bond) from the vinyl disulphide complex. The resulting vinyl sulphide complex is expected to be quite reactive and should readily undergo sulphur insertion reactions into the Mo—C bond to give a dithiolene complex. Preliminary results support this proposed sequence of reactions. Thus in the reaction of the $[(Cp)Mo^{V}(O)(\mu\text{-}S)_2Mo^{V}(O)((R)C{=}C(R){-}S{-}S)]^-$ vinyl disulphide complex, with one equivalent of Ph_3P, the two CH_3 resonances of the vinyl disulphide ligand are replaced completely and cleanly by two new resonances that we attribute to the vinyl sulphide complex (Fig. 11). Addition of sulphur to this solution of the vinyl sulphide complex gives a 2 : 1 dithiolene–vinyl disulphide mixture. This experiment suggests that the assumed coordinated vinyl sulphide ligand can undergo sulphur insertion at either the Mo—S or the Mo—C bonds, and that insertion into the Mo—C bond is a more facile process.

The sulphur-catalysed, vinyl disulphide–dithiolene conversion is proposed to proceed via formation of catalytic amounts of the "sulphur-rich" dithiolene complex by sulphur insertion into the Mo—C bond of the vinyl disulphide complex (Fig. 12). Precedence for the insertion of sulphur into a M—C bond exists in the reaction of the $[(\eta^5\text{-}Cp)W(NO)(CH_2SiMe_3)_2]$ complex with S_8 to give $[(\eta^5\text{-}Cp)W(NO)(SCH_2SiMe_3)_2]$.[25] Once formed, the "sulphur-rich" dithiolene complex is expected to undergo nucleophilic attack by the molybdenum-bound carbon atom of the vinyl disulphide ligand. This attack should occur at the electrophilic sulphur atom adjacent to the ethylenic double bond in the "sulphur-rich" dithiolene and will result in sulphur abstraction, formation of dithiolene and regeneration of a sulphur-rich dithiolene that will repeat the cycle. In the scheme shown in Fig. 12 a large excess of sulphur is expected to quench the formation of dithiolene by conversion of most of the vinyl disulphide complex to the "sulphur-rich" dithiolene complex. The latter should be stable in the absence of nucleophilic "sulphur-acceptor" molecules. Indeed, we have observed (by ^1H NMR) a retardation in the rate of formation of dithiolene as larger than catalytic amounts of sulphur are added to the reaction medium.

The importance of alkyne insertion into Mo—S bonds and the formation of vinyl disulphide complexes preceding the formation of dithiolenes, still

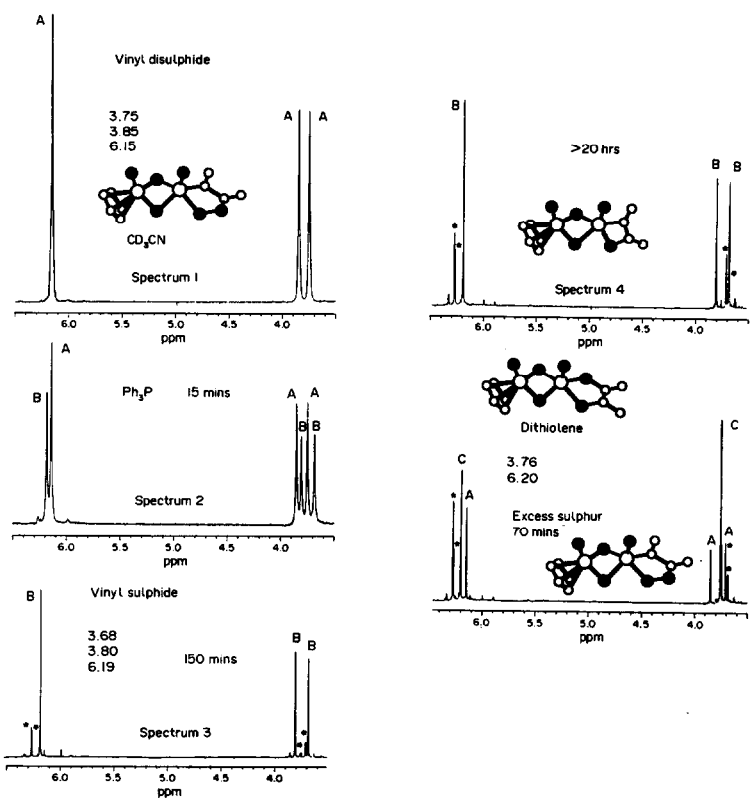

Fig. 11. Addition of triphenyl phosphine to a CH_3CN solution of the $[(Cp)Mo^{V}(O)(\mu\text{-}S)_2Mo^{V}(O)((R)C{=}C(R){-}S{-}S)]^-$ vinyl disulphide complex (**A**) and the proposed generation of a vinyl sulphide analogue (**B**). Addition of elemental sulphur to this solution with the subsequent formation of the vinyl disulphide (**A**) and dithiolene (**C**) complexes.

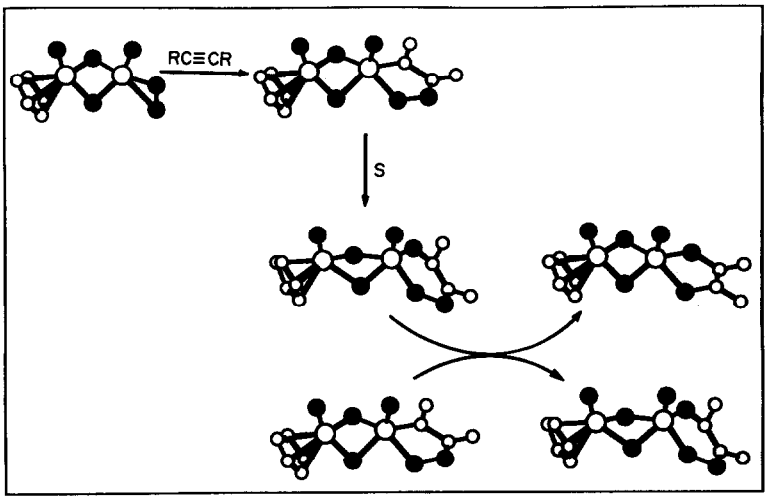

Fig. 12. A proposed reaction pathway, suggested by ^{1}H NMR spectroscopy, for the *sulphur-catalysed transformation* of the vinyl disulphide ligand in the $[(Cp)Mo^{V}(O)(\mu\text{-}S)_2Mo^{V}(O)((R)C{=}C(R)\text{—}S\text{—}S)]^-$ complex to a dithiolene ligand.

remain to be established for certain systems. This is particularly true for the synthesis of diothiolene complexes by the reaction of completely sulphided thiomolybdates with DMA (Fig. 9). To date we have been unable to detect evidence for the formation of a vinyl disulphide ligand in the reactions of DMA with any of the $[Mo_2^{V}(S)_n(S_2)_{6-n}]^{2-}$ complexes. It is entirely conceivable that the nucleophilic Mo—S sulphur atoms in the latter, first react with electrophiles that insert into the Mo=S bond to give short lived vinyl sulphide species. Subsequent intramolecular sulphur transfer from the proximal η^2-S_x^{2-} ligand rapidly results in the formation of dithiolenes.

The importance of the Mo=S group is evident in the relative reactivities of the $[(S_4)_2Mo^{IV}{=}O]^{2-}$ and $[(S_4)_2Mo^{IV}{=}S]^{2-}$ complexes toward CS_2. The latter readily reacts with CS_2 to give both *cis*- and *trans*-$[(CS_4)_2Mo^{IV}{=}S]^{2-}$ complexes.[26] By comparison, the $[(S_4)_2Mo^{IV}{=}O]^{2-}$ complex is totally unreactive toward CS_2. An exception to the facile oxidative dimerization of the $[(L)_2MoS]^{2-}$ complexes is found with the $[(Cs_4)_2Mo^{IV}{=}S]^{2-}$ complex. This anion is quite stable and does not air-oxidize to the $[(CS_4)_2Mo^{V}{=}S]_2^{2-}$ product, at least under mild reaction conditions.

A remarkable characteristic of the Mo—η^2-CS_4 groups is their ability to reversibly release CS_2 (Fig. 13) and revert to Mo—η^2-S_2. On the basis of this observation, we have suggested previously[1] that

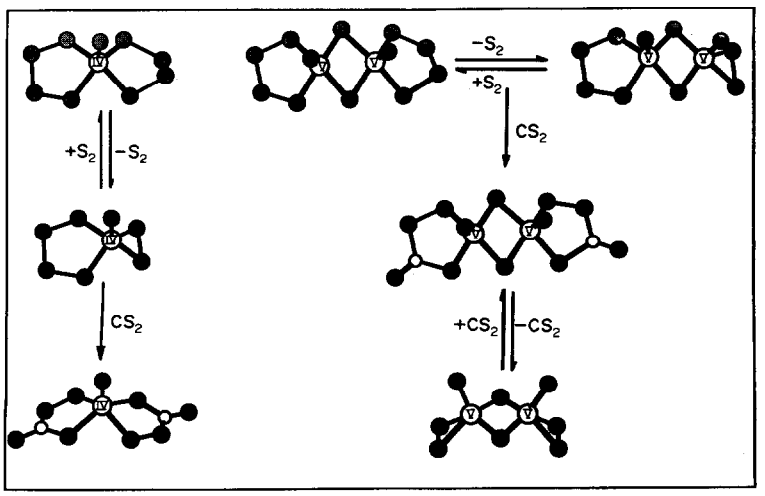

Fig. 13. Reversible addition of CS_2 to the thiomolybdate complexes.

Table 1. Comparison of the thiophene HDS activity[a] over alumina-supported catalysts obtained from thiomolybdate precursors

Catalyst precursor	Per cent molybdenum loading	TOF[b] C_4 (s^{-1})	Per cent conversion,[b,c] C_4
$(Ni(DMF)_6)[Mo_2O_2S_8Cl]_2$	1.7	0.0021–0.0019	54.3–47.5
$(Et_4N)[Mo_2O_2S_8Cl]$	2	0.00028–0.00024	4.2–3.5
$(Et_4N)_2[Mo_4O_4S_{18}]$	2	0.00013–0.00014	1.9–2.1
$(Ph_4P)_2[Mo_2S_6]$	3.2	0.00015–0.00009	8.3–5.2
Commercial Co—Mo—S "Catalco"	[d]	0.0011–0.0009	29.6–25.3

[a] Vapour pressure of thiophene = 20 torr, stream of hydrogen = 20 cm^3 min^{-1}.

[b] The figure of merit "TOF" is defined as the number of moles of desulphurized thiophene, per second, per mole of molybdenum. The first entry gives the TOF number within 30 min of thiophene conversion. The second value gives the TOF number after *ca* 3 h of thiophene conversion.

[c] The major products of thiophene conversion are C_4 hydrocarbons. The ratio of *trans*-/*cis*-butene typically is ~ 1.8; C_3 and C_2 hydrocarbons are minor components.

[d] The commercial catalyst used as reference has a higher per cent metal loading: 12–16% MoO_3 + 2–5% CoO.

under certain conditions the Mo—η^2-S_2 functional group may be directly involved in the activation of C—S bonds in saturated or unsaturated sulphur-containing organic molecules, in the catalysis of the hydrodesulphurization, HDS, reaction.

Supported thiomolybdate complexes as catalysts for the hydrodesulphurization reaction

The removal of sulphur from organosulphur compounds, present in crude petroleum, is carried out catalytically by the HDS reaction[27] [eq. (1)]:

$$RSH + H_2 \longrightarrow H_2S + RH. \qquad (1)$$

The catalyst used industrially consists of "sulphided" molybdates supported on γ-Al_2O_3, although many second- and third-row transition metal sulphides are active catalysts for the HDS reaction, with Ru, Os, Rh and Ir sulphides showing the highest activity.[28] Among the first-row transition metal ions, Ni^{2+} and Co^{2+} ions serve as promoters in the MoS_2 HDS catalysis.[27]

Certain heteromtallic complexes have been used as precursors for the preparation of HDS catalysts. Among them are included: $[(WS_4)_2Ni]^{2-}$[29] and $(MeCp)_2Mo_2Co_2(\mu_3\text{-}S)_2(\mu_4\text{-}S)(CO)_4$.[30] In a preliminary study the thiomolybdate salts $(Et_4N)_2[(S_4)_2Mo^{IV}{=}O]$ and $(Et_4N)_2[(S_4)_2Mo^{IV}{=}S]$ were used as precursors for alumina supported HDS catalysts in the absence of promoter ions.[26] At 205°C, the catalyst obtained from $(Et_4N)_2[(S_4)_2Mo^{IV}{=}O]$ (3.1% loading) approached the activity shown by commercial Co—Mo catalysts, at the same temperature, and showed superior thiophene HDS activity then a similar "catalyst" obtained from $(Et_4N)_2[(S_4)_2Mo^{IV}{=}S]$. These results suggested that the Mo=O groups may be important in HDS catalysis and prompted us to examine other thiomolybdate complex anions. The thiophene–HDS catalytic activities of the $(Et_4N)[Mo_2O_2S_8Cl]$,[31] $[Ni(DMF)_6][Mo_2O_2S_8Cl]_2$,[32] $(Et_4N)_2[Mo_4O_4S_{18}]$[17] and $(Ph_4P)_2[Mo_2S_6]$[2] have been examined* (Table 1).

The $(Et_4N)^+$ cation in $(Et_4N)[Mo_2O_2S_8Cl]$[31] (Fig. 4) can be exchanged conveniently in the reaction of this compound with $NiCl_2 \cdot 6H_2O$ in DMF solution. The black–red $[Ni(DMF)_6][Mo_2O_2S_8Cl]_2$ salt has been isolated in ~ 50% yield.[33] The corresponding iodo complex, $[Ni(DMF)_6][Mo_2O_2S_8I]_2$, has also been obtained by a similar reaction using $NiI_2 \cdot 6H_2O$.[32] The crystal and molecular structure of the latter was determined by X-ray crystallography[32] and the structure of the anion is virtually identical to that of the $[Mo_2O_2S_8Cl]^-$ anion[31] (Fig. 4). An examination of the preliminary results* reported in Table 1 shows that the

* A detailed study of the catalytic properties of the thiomolybdate complexes is currently underway, in collaboration with Professor J. Schwank and Mr J. Lindner in the Department of Chemical Engineering, The University of Michigan. The results of this study will be published in detail elsewhere.

Ni/Mo catalyst obtained from $[Ni(DMF)_6][Mo_2O_2S_8Cl]_2$ is nearly 10 times more effective than a commercial Co/Mo catalyst, on the basis of relative figure of merit values.* At present we are conducting detailed systematic studies of the HDS catalytic properties of the thiomolybdate anions and of the Ni^{2+}, Co^{2+} and Fe^{2+} "salts" of these complexes.

Acknowledgements—The support of this work by a grant (CH-79-0389) from the National Science Foundation is greatefully acknowledged.

REFERENCES

1. D. Coucouvanis, A. I. Hadjikyriacou, M. Draganjac, M. G. Kanatzidis and O. Ileperuma, *Polyhedron* 1986, **5**, 349.
2. A. I. Hadjikyriacou and D. Coucouvanis, *Inorg. Chem.* 1987, **26**, 2400.
3. A. Muller, *Polyhedron* 1986, **5**, 323.
4. M. A. Harmer, T. R. Halbert, W.-H. Pan, C. L. Coyle, S. A. Cohen and E. I. Stiefel, *Polyhedron* 1986, **5**, 341.
5. E. Clementi and C. Roetti, *At. Data Nucl. Data Tables* 1974, **14**, 3.
6. M. Draganjac, E. Simhon, L. T. Chan, M. Kanatzidis, N. C. Baenziger and D. Coucouvanis, *Inorg. Chem.* 1982, **21**, 3321.
7. D. Coucouvanis and Sang-Man Koo, *Inorg. Chem.* 1989, **28**, 2.
8. D. Coucouvanis, A. Toupadakis and A. Hadjikyriacou, *Inorg. Chem.* 1988, **27**, 3272.
9. T. R. Halbert, W. H. Pan and E. I. Stiefel, *J. Am. Chem. Soc.* 1983, **105**, 5476.
10. A. Muller, R. G. Bhattacharyya and B. Pfefferkorn, *Chem. Ber.* 1979, **112**, 778.
11. M. Martinez, B.-L. Ooi and A. G. Sykes, *J. Am. Chem. Soc.* 1987, **109**, 4615.
12. T. Shibahara, H. Kuroya, K. Matsumoto and S. Ooi, *J. Am. Chem. Soc.* 1984, **106**, 789.
13. T. Shibahara, T. Yamamoto, H. Kanadani and H. Kuroya, *J. Am. Chem. Soc.* 1987, **109**, 3495.
14. D. Coucouvanis and M. Draganjac, *J. Am. Chem. Soc.* 1982, **104**, 6820.
15. M. Draganjac and D. Coucouvanis, *J. Am. Chem. Soc.* 1983, **105**, 139.
16. (a) D. Coucouvanis, E. D. Simhon and N. C. Baenziger, *J. Am. Chem. Soc.* 1980, **102**, 6644; (b) J. W. McDonald, G. D. Friesen and W. E. Newton, *Inorg. Chim. Acta* 1980, **46**, L79; (c) A. Muller, W. Hellmann, C. Romer, M. Romer, H. Bogge, R. Jostes and U. Schimanski, *Inorg. Chim. Acta* 1984, **83**, L75; (d) W.-H. Pan, S. T. McKenna, R. R. Chianelli, T. R. Halbert, L. L. Hutchings and E. I. Stiefel, *Inorg. Chim. Acta* 1985, **97**, L17; (e) A. Muller, F. Diemann, R. Jostes and H. Bogge, *Angew. Chem. Int. Edn. Engl.* 1981, **20**, 934; (f) K. P. Callahan and P. A. Piliero, *Inorg. Chem.* 1980, **19**, 2609; (g) D. Coucouvanis, P. Stremple, E. D. Simhon, D. Swenson, N. C. Baenziger, M. Draganjac, L. T. Chan, A. Simopoulos, V. Papaefthymiou, A. Kostikas and V. Petrouleas, *Inorg. Chem.* 1983, **22**, 293; (h) D. Coucouvanis, N. C. Baenziger, E. D. Simhon, P. Stremple, D. Swenson, A. Kostikas, A. Simopoulos, V. Petrouleas and V. Papaefthymiou, *J. Am. Chem. Soc.* 1980, **102**, 1730; (i) D. Coucouvanis, E. D. Simhon, P. Stremple, M. Ryan, D. Swenson, N. C. Baenziger, A. Simopoulos, V. Papaefthymiou, A. Kostikas and V. Petrouleas, *Inorg. Chem.* 1984, **23**, 741–9; (j) D. Coucouvanis, *Accts Chem. Res.* 1981, **14**, 201.
17. A. I. Hadjikyriacou and D. Coucouvanis, *Inorg. Chem.*, in press.
18. D. Coucouvanis and A. I. Hadjikyriacou, *Inorg. Chem.* 1987, **26**, 1.
19. D. Coucouvanis, P. R. Patil, M. G. Kanatzidis, B. Detering and N. C. Baenziger, *Inorg. Chem.* 1985, **24**, 24.
20. (a) I. W. Boyd, I. G. Dance, K. S. Murray and A. G. Wedd, *Aust. J. Chem.* 1978, **31**, 279; (b) J. R. Bradbury, M. F. Mackay and A. G. Wedd, *Aust. J. Chem.* 1978, **31**, 2433.
21. A. Toupadakis and D. Coucouvanis, manuscript in preparation.
22. T. R. Halbert, W.-H. Pan and E. I. Stiefel, *J. Am. Chem. Soc.* 1983, **105**, 5476.
23. M. Draganjac and T. B. Rauchfuss, *Angew. Chem. Int. Edn Engl.* 1985, **24**, 742.
24. A. Toupadakis and D. Coucouvanis, to be published.
25. P. Legzdins and L. Sanches, *J. Am. Chem. Soc.* 1985, **107**, 5525.
26. M. Draganjac, PhD thesis. University of Iowa (1983).
27. (a) F. E. Massoth, *Adv. Catal.* 1978, **27**, 265; (b) J. Topsoe and B. S. Clausen, *Catal. Rev.-Sci. Engng* 1984, **26**, 395; (c) O. Weisser and S. Landa, *Sulfide Catalysts: Their Properties and Applications.* Pergamon Press, London (1973).
28. T. Pecoraro and R. Chianelli, *J. Catal.* 1981, **67**, 430.
29. W. Eltzner, M. Breyse, M. Lacroix, C. Leclerq, M. Vrinat, A. Muller and E. Diemann, *Polyhedron* 1988, **7**, 2405.
30. M. D. Curtis and P. D. Williams, *Inorg. Chem.* 1983, **19**, 2661.
31. A. I. Hadjikyriacou and D. Coucouvanis, *Inorg. Chem.*, in press.
32. A. I. Hadjikyriacou, PhD thesis. University of Michigan (1988).

* This figure of merit is defined as the number of moles of desulphurized thiophene, per second, per mole of molybdenum.

Polyhedron Vol. 8, No. 13/14, pp. 1717–1722, 1989
Printed in Great Britain

0277–5387/89 $3.00+.00
© 1989 Maxwell Pergamon Macmillan plc

EARLY TRANSITION METAL–SCHIFF BASE COMPLEXES: FROM STRUCTURE TO REACTIVITY

CARLO FLORIANI

Institut de Chimie Minérale et Analytique, Université de Lausanne, Place du Château 3, CH-1005 Lausanne, Switzerland

Abstract—A review is given of the chemistry of early transition metal–Schiff base complexes. The emphasis is on the synthetic routes, the structural properties of these complexes, their transformation into organometallic derivatives, and their use for storing and releasing electrons.

The versatile chemistry of late transition metal complexes derived from the use of Schiff base ligands[1a] does not have a counterpart in early transition metals.[1b] Our recent contribution to this area will be reviewed with special emphasis on:

(a) Synthetic methods for functionalizable complexes;
(b) How Schiff base ligands provide new and interesting environments for M—C< functionalities;
(c) Redox reactions which do not involve changes in the oxidation state of the metal.

SYNTHETIC METHODS AND STRUCTURAL PROPERTIES

Schiff base ligands assure a constant coordination geometry and an electronically flexible environment to the metal.

The relative arrangement of the two vacant or functionalizable coordination sites is of a crucial importance for reactivity, but is almost exclusively dependent on the ionic radius of the metal ion. The very versatile method for the synthesis of all these compounds is shown in eqs (1)–(3):[2]

$$MCl_4(THF)_2 + L_4Na_2 \xrightarrow{-NaCl} ML_4Cl_2 \quad (1)$$

$$MCl_4(THF)_2 + 2L'_2Na \xrightarrow{-NaCl} M(L'_2)_2Cl_2 \quad (2)$$

$$M'Cl_3(THF)_3 + L_4Na_2 \xrightarrow{-NaCl} M'L_4(Cl) \quad (3)$$

(M = Ti, Zr, Hf, V, Nb, Mo; M′ = Ti, V).

Reactions (1)–(3) are usually carried out in tetrahydrofuran (THF). A significantly different method is used in case of vanadium(IV) and vanadium(III) derivatives. The availability of oxovanadium(IV) derivatives prompted us to use

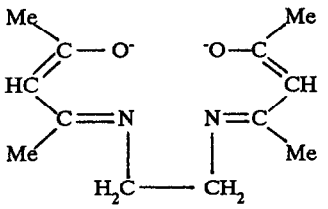

acen = N,N'-ethylenebis-(acetylacetoneiminato) dianion, L_4.

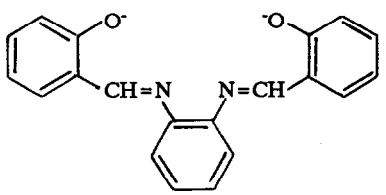

salophen = N,N'-o-phenylenebis-(salicylideneiminato) dianion, L_4.

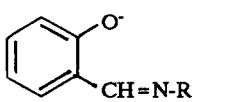

salN-R = N-alkyl-(salicylideneiminato) anion, L'_2.

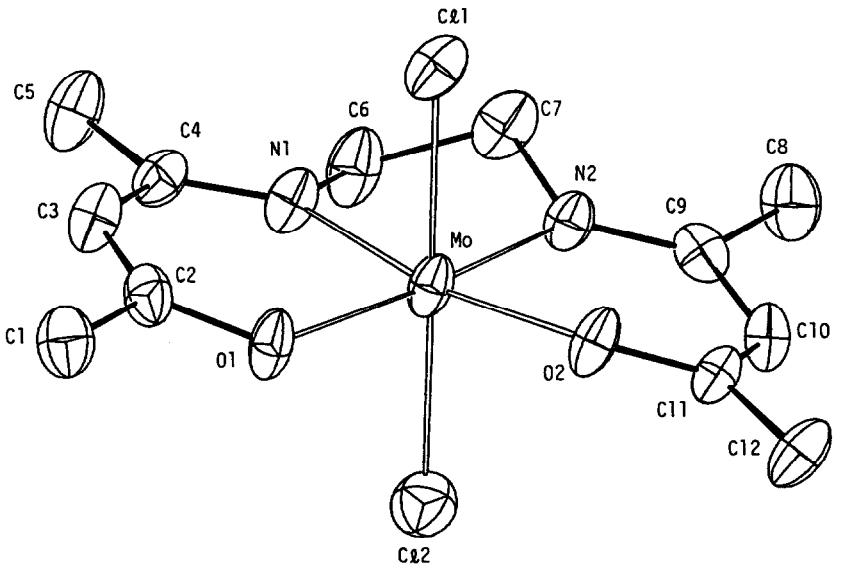

Fig. 1. [Mo(acen)Cl_2]. Bond lengths (Å): Mo—Cl_{av}, 2.394(4); Mo—O_{av}, 2.074(6); Mo—N_{av}, 2.074(6). Bond angles (°): Cl(2)—Mo—Cl(1), 177.9(1); O(1)—Mo—O(2), 103.9(1).

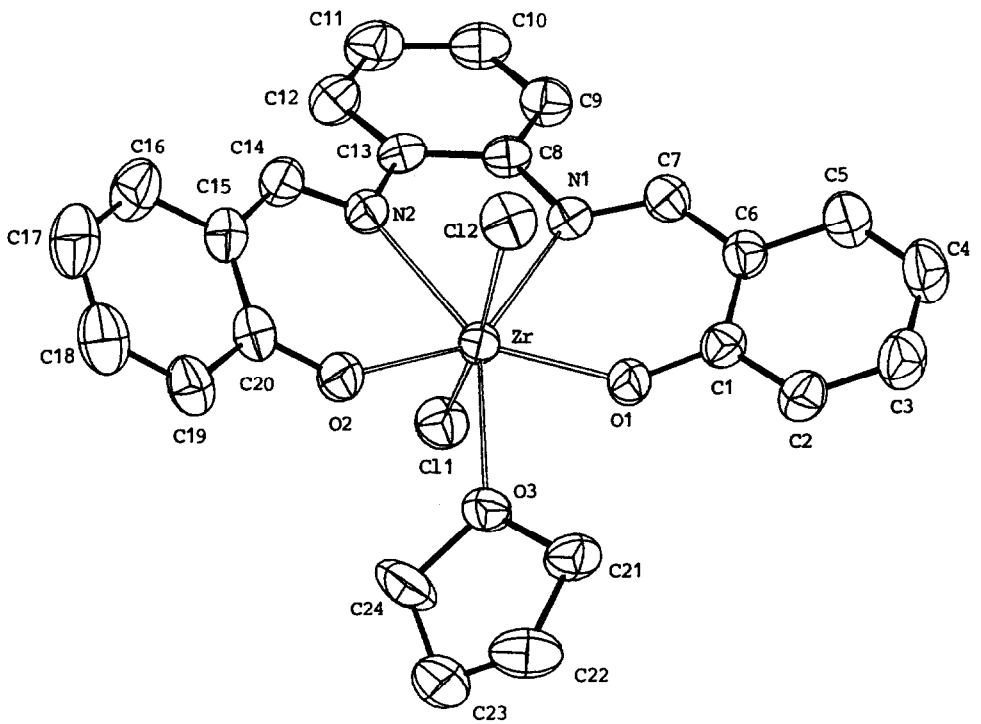

Fig. 2. [Zr(salophen)Cl_2(THF)]. Bond lengths (Å): Zr—Cl(1), 2.447(1); Zr—Cl(2), 2.447(1); Zr—O(1), 2.015(2); Zr—O(2), 2.051(3); Zr—O(3), 2.338(2). Bond angles (°): Cl(1)—Zr—Cl(2), 165.2(1); O(1)—Zr—O(2), 137.6(1).

them as starting materials [see eqs (4) and (5)]:

$$L_4V{=}O + SOCl_2 \xrightarrow[\text{benzene}]{-SO_2} \textit{trans}\text{-}[V(L_4)Cl_2] \quad (4)$$

$$L_4V{=}O + TiCl_3 \xrightarrow[THF]{-TiOCl_2} \textit{trans}\text{-}[V(L_4)(Cl)(THF)]. \quad (5)$$

Structural information is available on the most significant complexes.[2d] Complexes of Ti, V, Nb, Mo containing either a tetradentate or a bidentate Schiff base have a *trans* arrangement of the free or functionalizable coordination sites, as exemplified in Fig. 1 for $[Mo(acen)Cl_2]$ (**1**).[2d] Zirconium and hafnium derivatives are unique complexes showing a *cis–trans* isomerism, the *cis* isomer being the most stable one.[2d] Zirconium complexes containing bidentate ligands have a *cis* configuration, i.e. *cis*-$[Zr(salNMe)_2Cl_2]$ (**2**). In the presence of very rigid tetradentate ligands, the two chlorine atoms are forced to be *trans*, i.e. in $[Zr(salophen)Cl_2(THF)]$ (**3**) (see Fig. 2).[2d] For less rigid tetradentate ligands, i.e. acen, both the *cis*- (**4**) and *trans*- (**5**) isomers have been observed, depending on the ligating ability of the solvent.

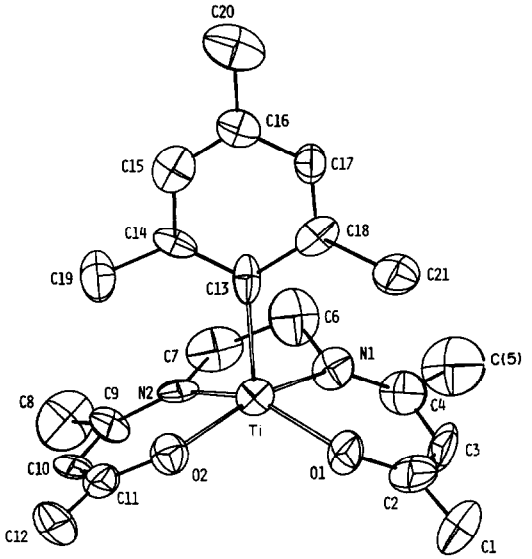

Fig. 3. [Ti(acen)(Mes)]. Bond lengths (Å): Ti—O(1), 1.928(15); Ti—O(2), 1.926(12); Ti—N(1), 2.103(16); Ti—N(2), 2.138(17); Ti—C(13), 2.216(20).

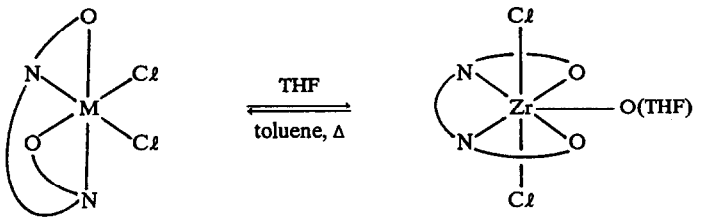

(6)

(4), *cis*-$[Zr(acen)Cℓ_2]$ (5), *trans*-$[Zr(acen)Cℓ_2(THF)]$

Complexes **4** and **5** have been characterized in the solid state by an X-ray analysis, and they maintain their structure in solution, as proven by ^1H NMR spectra in non-coordinating solvents.[2d]

ORGANOMETALLIC DERIVATIVES

The major factor affecting the alkylation reactions of products from reactions (1)–(3) is the oxidation state of the metal. Alkylation and arylation of [M(acen)(Cl)(THF)] ($M = Ti^{III}$, V^{III}) is an extremely clean reaction leading to the corresponding alkyl and aryl derivatives in good yields:[2d,3]

Complexes **7** are isolated in the solid state as monomeric species, usually containing a five-coordinated metal, or in a dimeric form (M = V; R = Me, $PhCH_2$),[3a] with two units sharing an oxygen atom. The structure of the monomeric [Ti(acen)(Mes)] is shown in Fig. 3,[2d] while the structure of the dimer, $[V(acen)(CH_2Ph)]_2$, was reported years ago.[3a]

An interesting synthetic method is the reductive alkylation of oxovanadium(IV) complexes leading to the same vanadium(III) alkyl derivatives shown

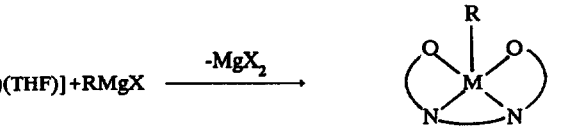

(6) (7), [M(acen)R] (7)

M = Ti, V; R = Me, CH_2Ph, Ph, 2,4,6-$Me_3C_6H_2$.

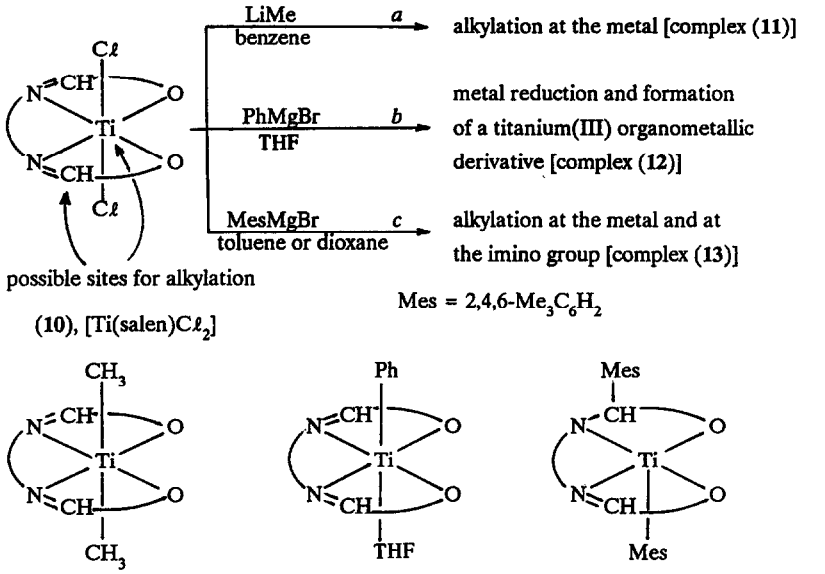

Scheme 1.

in reaction (7). Reaction (8) has to be carried out in THF with an excess of the Grignard reagent:[2d]

$$\underset{\textbf{(8)}}{[VO(salophen)]} \xrightarrow{PhMgBr} \underset{\textbf{(9)},\ M = V;\ R = Ph.}{[V(salophen)(Ph)]} \qquad (8)$$

The alkylation and arylation of compounds in reactions (1)–(3) containing the metal in the IV oxidation state were much more complex than expected because of the presence of electrophilic sites in the ligand,[4] as exemplified by the reactivity of $[Ti(salen)Cl_2]$ (**10**).[5] Depending on the nucleophile and the solvent, the reaction can follow three different pathways (*a*–*c*) (Scheme 1) to form complexes **11**–**13**.[5] The reaction is influenced by a considerable number of variables, of which the polarity of the solvent is probably the major factor determining the reaction pathway.

Among the most plausible mechanisms for explaining the formation of compounds **11**–**13**, we can invoke the intramolecular alkyl migration from the metal to the imino groups of the ligand. The existence, though very thermally labile, of a remarkable *trans*-dimethyltitanium compound should be emphasized. Such a compound is extremely reactive as a consequence of the autolabilization effect of the two methyl groups. Its structure was recently reported and is shown in Fig. 4.[5] The migration of the methyl groups to the ligand was easily followed by ^1H NMR. In order to show that the significant difference in the chemical reactivity of the M—C bond is dependent on the chemical environment, we mention the reaction of [M(acen)(R)] (M = Ti, V) with carbon monoxide.[2d]

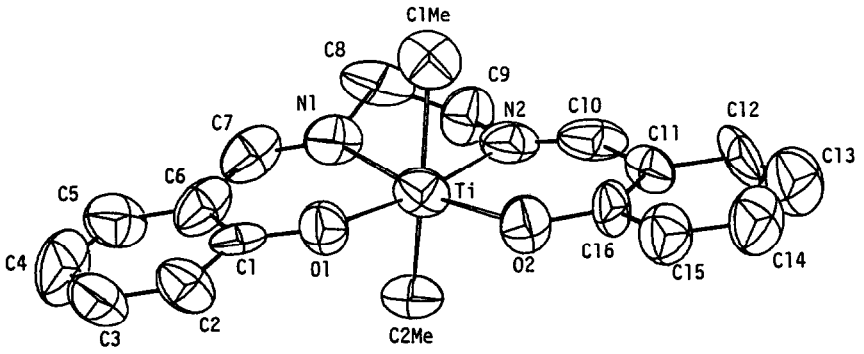

Fig. 4. $[Ti(salen)Me_2]$. Bond lengths (Å): Ti—O(1), 1.83(1); Ti—O(2), 1.86(1); Ti—N(1), 2.14(1); Ti—N(2), 2.15(1); Ti—C(1)Me, 2.15(2); Ti—C(2)Me, 2.15(1). Bond angles (°): O(1)—Ti—O(2), 110.9(4); N(1)—Ti—N(2), 76.5(6); N(1)—Ti—O(1), 86.5(5); N(2)—Ti—O(2), 86.1(5); N(1)—Ti—O(2), 162.6(5); N(2)—Ti—O(1), 162.8(5); C(1)Me—Ti—C(2)Me, 154.9(6).

$2[Ti(acen)(R)] + 2CO \longrightarrow$
(7), R = Mes, CH_2Ph, Me.

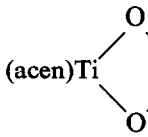

$$(acen)Ti \quad Ti(acen) + \text{organic products} \qquad (9)$$

(13)

$[V(acen)(R)] + CO \longrightarrow$
(7), R = Mes, CH_2Ph, Me.

$$[(acen)V{=}O] + \text{organic products.} \qquad (10)$$

(14)

The probable preliminary insertion of carbon monoxide is followed by the deoxygenation of the resulting acyl, a result very different from that known in cyclopentadienyl chemistry.

REDOX PROPERTIES

Reduction of early transition metals bonded to Schiff base ligands may be rather complex chemistry. The factors affecting the reaction are the nature of the metal, its oxidation state and the nature of the ligand. Reduction of titanium(IV), vanadium(IV) and molybdenum(IV) to titanium(III),[6] vanadium(III) and molybdenum(II)[7] is a rather common and easy reaction. Generation of radical anions at the ligand is quite general in such chemistry,[8] but we found some rare cases in which such a reduction led to the reductive coupling of two imino groups belonging to two different molecules.[9]

Significant examples can be found for different metals, i.e. vanadium(III)[2d] and zirconium(IV),[2d] while the use of the ligand is strictly limited to the rigid and planar "salophen".

The reduction does not affect the degree of oxidation of the metal and the resulting compounds are still vanadium(III) and zirconium(IV) derivatives. In addition to this, these complexes are reducing agents by two and four electrons, respectively. A number of substrates, O_2, I_2, CO_2 and organic functionalities are reduced under very mild conditions.[2d] Reduction occurs with the cleavage of the C—C bond and the restoration of the original imino functionality. The C—C unit is never involved in the interaction with the substrate. Such systems provide a unique example of a molecular rechargeable battery, which is not based on variations of the oxidation state of metals.[2d] The peculiarity of such molecule systems will be discussed in forthcoming papers.

Acknowledgement—We thank the Fonds National Suisse de la Recherche Scientifique for financial support.

REFERENCES

1. (a) G. Wilkinson, R. D. Gillard and J. A. McCleverty (Eds), *Comprehensive Coordination Chemistry*, Vol. 3. Pergamon Press, Oxford (1987); (b) *ibid.*, Vol. 5.
2. (a) M. Mazzanti, C. Floriani, A. Chiesi-Villa and C. Guastini, *Inorg. Chem.* 1986, **25**, 4158; (b) *ibid.*, 1986, **25**, 356; (c) M. Pasquali, F. Marchetti and C. Floriani, *Inorg. Chem.* 1979, **18**, 2401; (d) Unpublished results from our laboratory.
3. (a) S. Gambarotta, M. Mazzanti, C. Floriani, A. Chiesi-Villa and C. Guastini, *J. Chem. Soc., Chem. Commun.* 1985, 829; (b) S. Ciurli, C. Floriani, A. Chiesi-Villa and C. Guastini, *J. Chem. Soc., Chem. Commun.* 1986, 1401.
4. C. Floriani, S. Ciurli, A. Chiesi-Villa and C. Guastini, *Angew. Chem. Int. Edn Engl.* 1987, **26**, 70.

$$2\,[V(salophen)(THF)] + 2\,Na \xrightarrow{-NaCl}$$

(15)

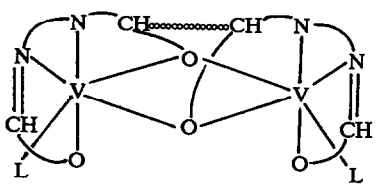

(16) (11)

$$2\,[Zr(salophen)Cl_2(THF)] + 4\,Na \xrightarrow{-NaCl}$$

(17)

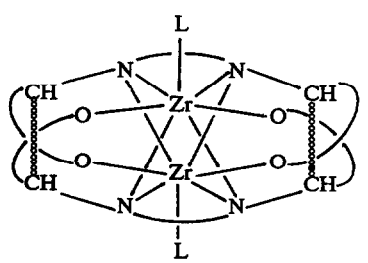

(18) (12)

5. C. Floriani, E. Solari, F. Corazza, A. Chiesi-Villa and C. Guastini, *Angew. Chem. Int. Edn Engl.* 1989, **28**, 64.
6. M. Pasquali, F. Marchetti, A. Landi and C. Floriani, *J. Chem. Soc., Dalton Trans.* 1978, 545.
7. G. Pennesi, C. Floriani, A. Chiesi-Villa and C. Guastini, *J. Chem. Soc., Chem. Commun.* 1988, 350.
8. S. Ciurli, S. Gambarotta, C. Floriani, A. Chiesi-Villa and C. Guastini, *Angew. Chem. Int. Edn Engl.* 1986, **25**, 553; S. Ciurli, E. M. Meyer, C. Floriani, A. Chiesi-Villa and C. Guastini, *J. Chem. Soc., Chem. Commun.* 1987, 281.
9. (a) S. Gambarotta, F. Urso, C. Floriani, A. Chiesi-Villa and C. Guastini, *Inorg. Chem.* 1983, **22**, 3966; (b) S. Gambarotta, M. Mazzanti, C. Floriani and M. Zehnder, *J. Chem. Soc., Chem. Commun.* 1984, 1186.

Polyhedron Vol. 8, No. 13/14, pp. 1723–1727, 1989
Printed in Great Britain

0277–5387/89 $3.00+.00
© 1989 Maxwell Pergamon Macmillan plc

RECENT DEVELOPMENTS IN VANADIUM SULPHUR AND OXYGEN CHEMISTRY

G. CHRISTOU,* D. HEINRICH, J. K. MONEY, J. R. RAMBO, J. C. HUFFMAN and K. FOLTING

Department of Chemistry and the Molecular Structure Center, Indiana University, Bloomington, IN 47405, U.S.A.

Abstract—We survey recent results from our efforts in vanadium sulphur and oxygen chemistry. A unifying theme for most of the discussion is the reactivity characteristics of vanadyl (VO^{2+}) complexes, and it is shown how such complexes are capable of a variety of transformations leading to products with oxidation states in the range III–V and nuclearities in the range 1–5. Also described are mononuclear non-oxo vanadium sulphur complexes, including the structural characterization of both $V(SBu^t)_4$ and $V(SBu^t)_4^-$. The relevance of this work to our understanding of the fate of crude oil vanadyl impurities during hydrotreating processes is discussed.

This paper will survey some of our recent results in vanadium chemistry and will concentrate primarily on the reactivity characteristics of vanadyl ($V{=}O^{2+}$)-containing materials. Our interest in this

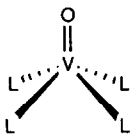

area stems from the presence of large amounts of vanadium impurities in crude oils (as both vanadyl porphyrins and non-porphyrins) and their conversion via currently unknown mechanisms into vanadium(III) sulphides under reducing and sulphide-rich hydrotreating conditions.[1–4] These sulphides contribute to the deactivation of hydrotreating catalysts and thus represent a serious problem in processing the heavy crudes characteristic of the western hemisphere. Our programme is directed towards achieving a greater understanding of the various pathways by which vanadyl impurities are reduced/aggregated/sulphided to vanadium sulphides, an objective which entails the systematic exploration of the reactivity characteristics of model vanadyl complexes. Although such complexes have been prepared in great numbers over many decades, the reactivity chemistry of these very stable materials has been poorly investigated.[5–7] We herein describe the products from the reaction of vanadyl complexes under a variety of conditions.

(1) PRODUCTS CONTAINING ONLY VANADIUM(IV)

A variety of procedures have now been developed that lead to products involving no change in metal oxidation state. These involve both attack at the terminal oxide and attack at the basal ligands. Treatment of $VO(edt)_2^{2-}$ (**1**; edt = ethane-1,2-dithiolate) with $(Me_3Si)_2S$ in MeCN, leads to clean conversion to $VS(edt)_2^{2-}$ (**2**).[8] By rapid addition of a large excess of Et_2O, an intermediate in this transformation can be isolated, viz $V(OSiMe_3)(edt)_2^-$ (**3**),[9] indicating the probable mechanism to be as shown in eq. (1):

$$VO(edt)_2^{2-} + (Me_3Si)_2S \rightarrow V(OSiMe_3)(edt)_2^- + Me_3SiS^- \leftrightarrows V(SSiMe_3)(edt)_2^- + Me_3SiO^- \rightarrow VS(edt)_2^{2-} + (Me_3Si)_2O. \quad (1)$$

Complex **2** may more conveniently be prepared[10] in large quantities by the direct reaction of VCl_3, S and Na_2edt [eq. (2)]:

$$VCL_3 + E + 2.5Na_2edt \rightarrow [VE(edt)_2]^{2-} + 3NaCl + 2Na^+ + \tfrac{1}{2}\text{“}(edt)_2\text{”}. \quad (2)$$

(E = S, Se)

Advantage of this direct synthesis procedure was subsequently taken to prepare an extremely rare

* Author to whom correspondence should be addressed.

example of a selenovanadyl (VSe^{2-}) unit in the complex $VSe(edt)_2^{2-}$ (**4**), which allowed the first structural characterization of this moiety.[10]

In contrast to $(Me_3Si)_2S$, treatment of **1** with equimolar Me_3SiCl leads to attack at the basal edt^{2-} ligands and the formation of dinuclear $V_2O_2(edt)_3^{2-}$ (**5**), shown in Fig. 1.[11] Its formation is rationalized in eq. (3), the aggregation triggered by lowering of the edt–V ratio:

$$2VO(edt)_2^{2-} + 2Me_3SiCl \rightarrow V_2O_2(edt)_3^{2-} + 2Cl^- + Me_3SiSCH_2CH_2SSiMe_3. \quad (3)$$

The VO^{2+} units adopt a *syn*-arrangement. Interestingly, although complex **1** exhibits only irreversible electrochemical processes, the cyclic voltammogram of **5** exhibits a *reversible* one-electron oxidation at −0.83 V vs ferrocene in MeCN; coulometry confirmed the one-electron nature of this process. Reactions employing higher Me_3SiCl–V ratios could lead to a greater degree of aggregation, and such reactions have been under investigation.[11,12]

(2) REACTIONS INVOLVING OXIDATION STATE CHANGES

(a) *Reduction*

To model the reducing conditions that the crude oil vanadyl impurities experience during hydroprocessing, we have treated several model vanadyl complexes with an electron source in the presence of protons; this combination is designed as a low-temperature substitute for hydrogen gas employed at high temperature, and also allows homogeneous single-phase reactions. The electron source chosen is the organic radical anion acenaphthylenide (ACN^-). Treatment of **1** with NaACN in the presence of $HNEt_3Cl$, leads to formation of the V^{III} anion, $V_2(edt)_4^{2-}$ (**6**).[13] In contrast, a similar reaction employing $VO(aet)_2$ (aet = 2-aminoethanethiolate) leads to $V_2O(aet)_4$ (**7**) containing the linear $[V—O—V]^{4+}$ unit.[13] Both **6** and **7** are also

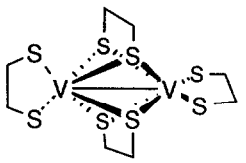

6

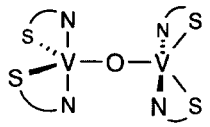

7

available by direct synthesis from VCl_3 and have been structurally characterized.[14,15] In both these transformations, initial reduction of V^{IV} to V^{III} destabilizes the VO multiply-bonded terminal unit and leads to aggregation with either partial or complete loss of the oxide ions, the latter facilitated by H^+. The basic reaction is summarized in eqs (4) and (5):

$$2VO(edt)_2^{2-} + 2e^- + 4H^+ \rightarrow V_2(edt)_4^{2-} + 2H_2O \quad (4)$$

$$2VO(aet)_2 + 2e^- + 4H^+ \rightarrow V_2O(aet)_4 + H_2O + 2H^+. \quad (5)$$

The actual identity of the product (i.e. remaining content of O^{2-}) must be governed by the identity of the basal ligands, since in both reactions sufficient protons were available for complete loss of oxygen as H_2O. That complex **7** is indeed the thermodynamically-preferred product with this ligand is supported by its direct synthesis from VCl_3, Na(aet) and advantitious oxygen (probably H_2O), with no evidence for a non-oxo product.[13]

More recently, we have extended use of this "reductive activation" of the VO^{2+} unit to access additional V^{III} species from simple VO^{2+} complexes. Using $VOCl_4^{2-}$, a convenient source of the VO^{2+} unit, we have investigated reactions with just NaACN or with NaACN/VCl_3; the latter have been investigated in greater detail to date and one example is described here. Reaction of $VOCl_4^{2-}$ with VCl_3 and NaACN in CH_2Cl_2 in the presence of excess pyridine leads to reductive coupling of the VO^{2+} unit with the V^{3+} centre and the formation

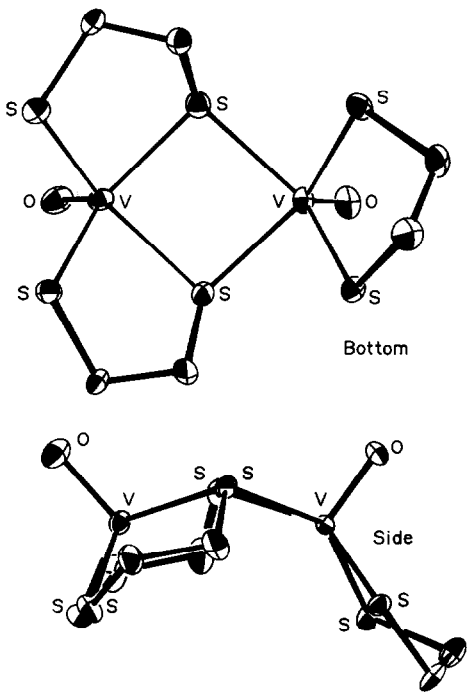

Fig. 1. Two views of the structure of complex **5**, $V_2O_2(edt)_3^{2-}$.

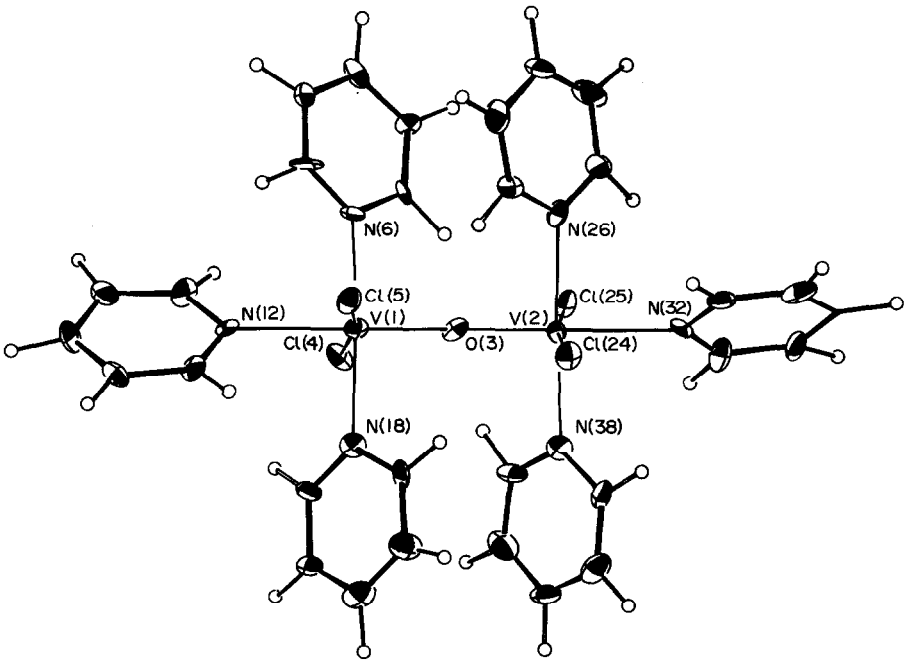

Fig. 2. The structure of complex **8**, $V_2OCl_4(py)_6$.

of $V_2OCl_4(py)_6$ (**8**) (Fig. 2),[12] as summarized in eq. (6):

$$VOCl_4^{2-} + VCl_3 + e^- \xrightarrow{py} V_2OCl_4(py)_6 + 3Cl^- . \quad (6)$$

The complex possesses the same linear $[V—O—V]^{4+}$ unit as **7** but the metals are now six- rather than five-coordinate.

(b) *Oxidation*

An additional ligand type we have been employing is carboxylates, since they have been detected in crude oils and may therefore be involved in metal binding.[1,2,4] Treatment of $VOCl_4^{2-}$ with sodium thiophene-2-carboxylate (Natca) under aerobic conditions leads to formation of deep green $V_5O_9(\mu_4\text{-}Cl)(\mu\text{-tca})_4^{2-}$ (**9**), containing 4 V^{IV}, V^V; its structure is shown in Fig. 3.[16] If the reaction is carried out in the presence of $AgNO_3$ to sequester all available Cl^-, the resulting product is $V_4O_8(tca)_4(NO_3)^{2-}$ (**10**), possessing V^{IV}, 3 V^V. The structure is similar to complex **9** except that the apical VO is absent, leaving a square of four vanadium atoms. In addition, the μ_4-Cl^- is now replaced by a η^1-μ_4-NO_3^-, a single NO_3^- oxygen bridging all four metals. There is no evidence for OH^- instead of O^{2-} in any position of either **9** or **10**. The oxidation state assignments are being confirmed as part of a detailed magnetochemical investigation; results

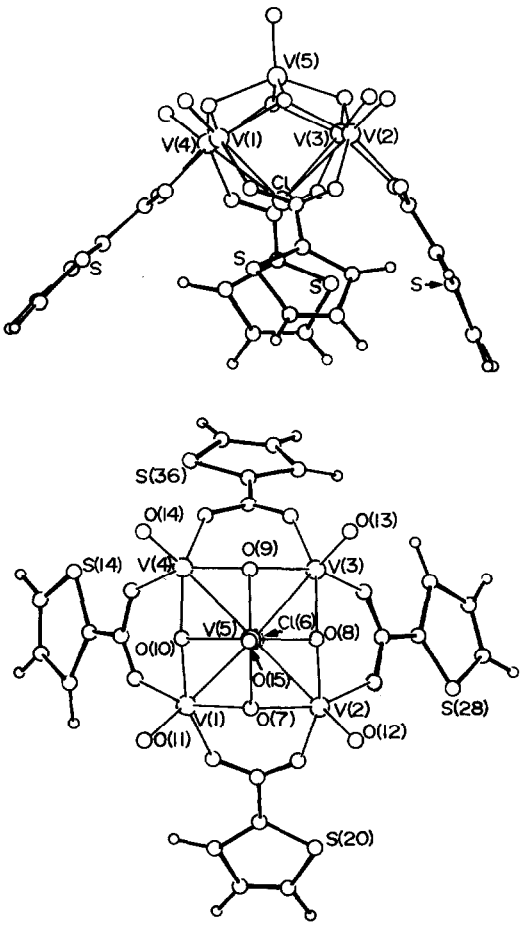

Fig. 3. Two views of the structure of complex **9**, $V_5O_9Cl(tca)_4^{2-}$.

available at the time of writing conclusively establish the V^{IV}, 3 V^{V} nature of **10**, a temperature-independent magnetic moment corresponding to a single unpaired electron per V_4 being observed.

Complexes **9** and **10** can be considered to possess V_xO_y units representing fragments of known iso- or heteropolyvanadates, examples of which include $PV_{14}O_{42}^{9-}$ and $V_{18}O_{42}^{12-}$. The function of the carboxylates is thus to stabilize these "fragments", preventing higher aggregation; it can readily be seen how the RCO_2^- moiety can substitute for an $O_2VO_2^{3-}$ group and terminate higher oligomer formation.

(3) NON-OXO VANADIUM THIOLATE COMPLEXES

We conclude with some recent results in vanadium chemistry not derived from vanadyl starting materials and not possessing any oxygen. Treatment of VCl_3 with 2 NaSBu^t and Bu^{t}SSBu^t leads to formation of V(SBu^t)$_4$ (**11**), whose structure is shown in Fig. 4.[16] This molecule joins the few other known examples of neutral tetrahedral $M(SR)_4$ species, including Ti(SBu^t)$_4$,[17] W(SBu^t)$_4$[19] and Mo(SBu^t)$_4$.[20] The synthetic procedure is summarized in eq. (7):

$$2\,VCl_3 + 6\,NaSBu^t + Bu^tSSBu^t \rightarrow 2\,V(SBu^t)_4 + 6\,NaCl. \quad (7)$$

In the absence of an oxidizing agent, a black intractable solid is obtained, which we believe to be $NaV(SBu^t)_4$ or polymeric $[V(SBu^t)_3]_n$. In a subsequent reaction carried out in the presence of bipy, we hoped to form soluble V(SBu^t)$_3$(bipy), and analytical data on the resulting product certainly supported this formulation:

$$2\,VCl_3 + 6\,NaSBu^t + 2\,bipy \rightarrow [V(SBu^t)_2(bipy)_2][V(SBu^t)_4]. \quad (8)$$

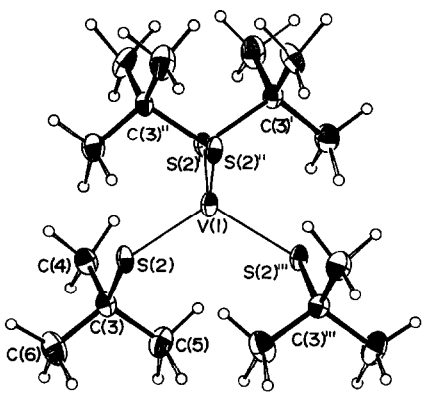

Fig. 4. The structure of complex **11**, V(SBu^t)$_4$.

However, a crystal structure determination showed a ligand redistribution had occurred, for the product was in reality $[V(SBu^t)_2(bipy)_2]^+[V(SBu^t)_4]^-$ (**12**); this would of course yield the analytical formulation "V(SBu^t)$_3$(bipy)". The cation of **12** has an octahedrally-coordinated vanadium and *cis*-Bu^{t}S$^-$ groups, while the anion is essentially identical to the V^{IV} complex, **11**, in Fig. 4, except for the expected slight lenghthening of V—S bond distances.[16]

CONCLUDING COMMENTS

In an attempt to ascertain the possible fate of crude oil vanadyl impurities under reducing and sulphur-rich conditions, we have investigated a variety of reactivity characteristics of model VO^{2+} complexes. Conversion to VS^{2+}, aggregation to $[VO^{2+}]_2$ and reductive coupling to oxo or non-oxo V^{III} aggregates have all been shown to be possible in the initial stages of hydroprocessing, and probably all occur. Interestingly, the complexity of the observed vanadyl carboxylates suggests not all vanadium impurities may be mononuclear if bound to such functionalities; the behaviour of these synthetic clusters under reducing conditions will be interesting to determine.

Continued reaction under reducing and sulphur-rich conditions is known to yield vanadium products with only sulphur ligation which aggregate and deposit on the molybdenum catalyst. To model these species, we have synthesized a variety of V/S species including $V(SBu^t)_4^{0,+}$, $V_2(edt)_4^{2-}$, $V_3S_4(edt)_3^{3-}$ and $V_4S_2(edt)_6^{2-}$ (the latter two from work not described here[15,20]). This kind of progressive build-up of V/S nuclearity may correspond to that occurring for the crude oil vanadium that ultimately leads to $(V/S)_\infty$ polymer formation. The interaction of such synthetic V/S species with synthetic Mo/S species now provides a model system for the initial stages of V/S deposition on the MoS_2 catalyst, which initiates the contribution by the former to the deactivation of the latter. Such investigations are currently in progress.

Acknowledgement—This work was supported by the U.S. Department of Energy, Office of Basic Energy Sciences, Division of Chemical Sciences, under grant DE-FG02-87ER13702.

REFERENCES

1. B. P. Tissot and D. H. Welte, *Petroleum Formation and Occurrence*, 2nd edn. Springer, West Berlin (1984).
2. M. M. Boduszynski, *Energy and Fuels* 1987, **1**, 2.
3. J. G. Reynolds, E. J. Gallegos, R. H. Fish and J. J. Komlenic, *Energy and Fuels* 1987, **1**, 36.

4. *Metal Complexes in Fossil Fuels* (Edited by R. H. Filby and J. N. Branthaver), Vol. 344. *A.C.S. Symp. Ser.* American Chemical Society, Washington D.C. (1987).
5. J. Selbin, *Coord. Chem. Rev.* 1966, **1**, 293.
6. M. Pasquali, F. Marchetti and C. Floriani, *Inorg. Chem.* 1979, **18**, 2401.
7. S. Gambarotta, M. Mazzanti, C. Floriani and M. Zehnder, *J. Chem. Soc., Chem. Commun.* 1984, 116.
8 J. K. Money, J. C. Huffman and G. Christou, *Inorg. Chem.* 1985, **24**, 3297.
9. J. K. Money, K. Folting, J. C. Huffman, D. Collison, J. Temperley, F. E. Mabbs and G. Christou, *Inorg. Chem.* 1986, 25.
10. J. R. Nicholson, J. C. Huffman, D. Ho and G. Christou, *Inorg. Chem.* 1987, **26**, 3030.
11. J. K. Money, J. C. Huffman and G. Christou, unpublished results.
12. J. R. Rambo and G. Christou, unpublished results.
13. J. K. Money, K. Folting, J. C. Huffman and G. Christou, *Inorg. Chem.* 1987, **26**, 944.
14. (a) R. W. Wiggins, J. C. Huffman and G. Christou, *J. Chem. Soc., Chem. Commun.* 1983, 1313; (b) J. R. Dorfman and R. H. Holm, *Inorg. Chem.* 1983, **22**, 3179; (c) D. Szeymies, B. Krebs and G. Henkel, *Angew. Chem. Int. Edn Engl.* 1983, **22**, 885.
15. J. K. Money, J. C. Huffman and G. Christou, *Inorg. Chem.* 1988, **27**, 507.
16. D. Heinrich, J. C. Huffman and G. Christou, unpublished results.
17. M. Bochmann, I. Hawkins and L. M. Wilson, *J. Chem. Soc., Chem. Commun.* 1988, 344.
18. M. L. Listemann, J. C. Dewan and R. R. Schrock, *J. Am. Chem. Soc.* 1985, **107**, 7207.
19. S. Otsuka, M. Kamata, K. Hirotsu and T. Higuchi, *J. Am. Chem. Soc.* 1981, **103**, 3011.
20. J. K. Money, J. C. Huffman and G. Christou, *J. Am. Chem. Soc.* 1987, **109**, 2210.

Polyhedron Vol. 8, No. 13/14, pp. 1729–1731, 1989
Printed in Great Britain

0277–5387/89 $3.00+.00
© 1989 Maxwell Pergamon Macmillan plc

METALLAHETEROCYCLES—PRECURSORS FOR INORGANIC POLYMERS

HERBERT W. ROESKY

Institut für Anorganische Chemie der Universität Göttingen, Tammannstrasse 4, D-3400 Göttingen, F.R.G.

Abstract—Several synthetic routes are described to generate metal-containing heterocycles. Ring systems with one, two or three metal atoms within the skeleton were obtained. At elevated temperatures the heterocycles are converted to polymers via ring opening reactions. The polymers are soluble in organic solvents and were characterized by elemental analysis and molecular weight determinations. Furthermore the synthesis of eight- and nine-membered rings is described.

TITANIUM–NITROGEN COMPOUNDS

Titanium nitride is formed by direct reaction between the elements at 1000–1400°C, by treatment of $TiCl_4$ and ammonia at elevated temperatures, or by the reaction of $TiCl_4$ and nitrogen in the presence of hydrogen. The nitride is a yellow–brown powder, which is isomorphous with TiC and thus has the NaCl structure. The character of bonding within TiN is considered to be more ionic than in TiC. It has many metallic properties, including high melting point (2950°C), high electrical conductance and great hardness. It is unaffected by hot mineral acids but it liberates ammonia with alkalis. Other possible nitrides are TiN_3 and Ti_2N.[1] The properties of the corresponding compounds ZrN and HfN are similar.

Preparation of the first imido and nitrido compounds of titanium

The metallic nitrides of titanium are a challenge to generate new precursors for their preparation which might be soluble or volatile. A synthetic approach is the reaction of organometallic derivatives with ammonia. Treatment of Cp^*TiMe_3 ($Cp^* = C_5Me_5$) with ammonia results in the formation of $[Cp^*Ti(NH)]_3N$ (**1**),[2] eq. (1):

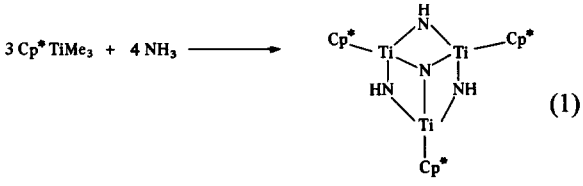

(1)

(1)

Compound **1** is a red, crystalline material. It is soluble in *n*-hexane or pentane. Suitable crystals for an X-ray structural investigation have been obtained from *n*-hexane. The molecule exhibits a six-membered $(TiNH)_3$ ring in a chair form, with tetrahedral coordinated titanium atoms. All three titanium atoms are bridged by a fourth nitrogen atom located on top of the ring. The Ti—N bond lengths (av. 192.4 pm) observed are between those in $CpTiCl_2NPPh_2$ (177.5(13) pm)[3] and $Ph(CNSiMe_3)_2]_2TiCl_2$ (206.6 and 210.1 pm).[4] Compounds of this type might be interesting precursors for the generation of thin films of TiN at low temperatures.

TRIAZATRIMETALLABENZENES—A NEW CLASS OF INORGANIC HETEROCYCLES

In 1983 we reported for the first time[5] the synthesis and structure of $(Cl_2VN_3S_2)_x$, an unsaturated six-membered ring (see Structure 1). This compound has semiconducting properties. We have not been able to generate acyclic polymers from this heterocycle by thermolytic ring opening reactions.

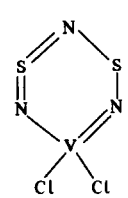

Structure 1.

The reaction of Cp^*TaCl_4 and tris(trimethylstannyl)amine leads to a six-membered ring of composition $[Cp^*TaN(Cl)]_3$ (**2**).[6] The ^1H NMR

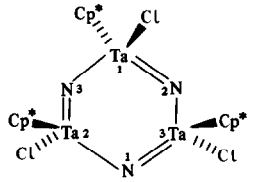

(2)

spectrum indicates two non-equivalent pentamethyl cyclopentadienyl groups ($\delta = 2.08$, 2.12) in a ratio of 1 : 2. From mass spectroscopic investigations we have found the molecular ion (m/z 1905), together with small amounts of the tetramer $[Cp^*TaN(Cl)]_4$. The X-ray structure analysis reveals not a completely planar six-membered ring in the solid state, but instead it exists in a kind of boat conformation, with the atoms Ta(2), N(3), Ta(3) and N(2) lying in the same plane. Ta(1) lies 13 pm and N(1) 39 pm from this plane. The puckered conformation is probably due to steric hindrance. The Ta—N bond lengths (av. 188(2) pm) lie between the values for Ta=NR (175–178 pm) and $TaNR_2$ (195–203 pm) compounds.[7]

TANTALUM–NITROGEN POLYMERS

Thermal ring opening of $[Cp^*TaN(Cl)]_3$ leads to the linear chain polymer, $[Cp^*TaN(Cl)]_n$ (**3**).[8] This polymer is soluble in THF or xylene. The molecular weights of **3** have been determined by viscosity and GPC measurements, with reference to polystyrene standards. GPC measurements supplied molecular masses of about 129, 800, 67,000, 35,800, 11,300 and 3000. From viscosity measurements we have estimated, in reference to the polystyrene calibration curve, the average molecular mass to be 40,000. So far we have not been able to replace the chlorine atoms in the polymer by organic substituents.

POLYMETALLAPHOSPHAZENES

In 1986 we described $[Cl_3MN_3(PPh_2)_2]$ (**4**) (M = Mo, W), the first cyclophosphazenes[9] in which a ring phosphorus atom is replaced by a transition metal in its maximum oxidation state.

Polymetallaphosphazenes have been obtained via a ring-opening reaction upon heating **4** in xylene.

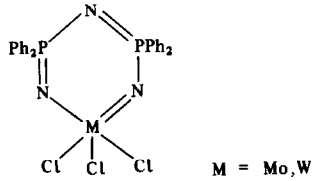

M = Mo,W

(4)

Elemental analyses show that no eliminations occur as side reactions. The molecular weights of the fractions soluble in THF have been determined by HPLC, viscosimetry and GPC measurements. Based on GPC measurements of the THF soluble fractions, we have obtained molecular weights of 35,800, 11,300 and 3500 for the tungsten polymer. The limiting viscosities obtained from the soluble fractions of the molybdenum and tungsten polymer from the viscosity measurements have been compared with those of the polystyrene calibration standards. The results show mean molecular weights of 24,000 (Mo) and 37,000 (W). The different physical methods for the determination of the molecular weights gave comparable results.

EIGHT-MEMBERED METALLACYCLES WITH A $M(NSN)_2M$-FRAME[10] (M = Zr, Hf)

The reactions of Cp_2ZrCl_2, $CpCp^*ZrCl_2$ and $CpCp^*HfCl_2$ with $Me_3SnNSNSnMe_3$ yielded $Cp_2Zr(NSN)_2ZrCp_2$, $CpCp^*Zr(NSN)_2ZrCpCp^*$ and $CpCp^*Hf(NSN)_2HfCpCp^*$:

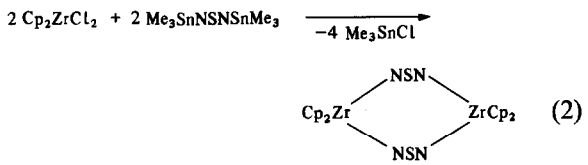

(2)

The compounds are thermally- and air-stable, yellow solids. With Cp and Cp* substituents we observed *cis*- and *trans*-isomers in the product based on ^1H NMR investigations.

HETEROCYCLES CONTAINING TUNGSTEN, PHOSPHORUS, SULPHUR AND NITROGEN IN THE RING SKELETON[11]

Eight-membered rings with tungsten, phosphorus, sulphur and nitrogen atoms as building units for the ring skeleton have been obtained from the new ligand $Me_2S(NPPh_2NSiMe_3)_2$ and WF_6 or WCl_6, respectively, eq. (3):

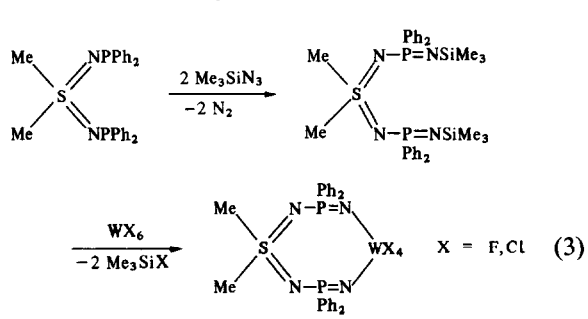

(3)

The X-ray single crystal structure analysis exhibits a puckered eight-membered ring with alternating short and long bond lengths. This is especially characteristic for the P(2)—N(2) and P(1)—N(1) bonds (P(2)—N(2), 165.9(14); P(1)—N(1), 155.4(10) pm).

PREPARATION AND STRUCTURE OF A NINE-MEMBERED NIOBIUM-CONTAINING RING WITH OXYGEN AND NITROGEN ATOMS AS BUILDING BLOCKS

The nine-membered ring, **5**, has been prepared according to the following reaction:

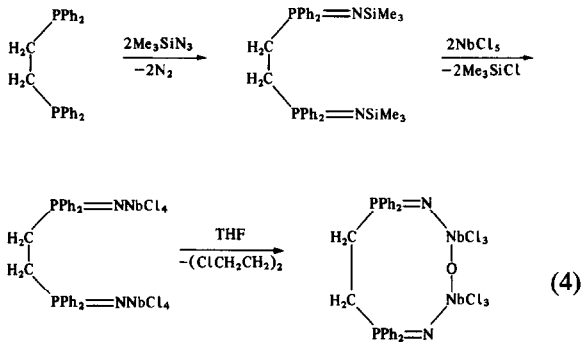

(4)

(5)

Compound **5** crystallizes from acetonitrile with four molecules of solvent. The molecular structure deduced from a single-crystal X-ray study shows a non-planar nine-membered ring with octahedrally coordinated niobium atoms. The sixth coordination site of the metal is occupied by a solvent molecule. The Nb—O—Nb angle is close to linear (176.7(2)°), comparable to that found in $[Nb_2Cl_9O]_2^{2-}$ (174.1(3)°). However, in contrast to $[Nb_2Cl_4O]_2^{2-}$, the Nb—O bond lengths (189.5(1) pm) are equal.

Acknowledgements—I thank Professor J. R. Dilworth for inviting me to Brighton, U.K. I gratefully acknowledge the numerous contributions of my collaborators mentioned in the references. I also thank the VW-Foundation, Deutsche Forschungsgemeinschaft, and Fonds der Chemischen Industrie for financial support of this work.

REFERENCES

1. H. J. Goldschmidt, *Interstitial Alloys*. Butterworths, London (1967); F. A. Cotton and G. Wilkinson, *Advanced Inorganic Chemistry*, Wiley-Interscience, New York (1966); P. Ehrlich, *Z. Anorg. Allg. Chem.* 1949, **259**, 1; A. Brager, *Acta Physiochim. USSR* 1939, **11**, 617; H. Harnisch, G. Heymer and E. Schallas, *Chem.-Ing. Tech.* 1963, **35**, 7; H. Winterhager and K. Hanusch, *Ber. Dtsch. Keram. Ges.* 1969, **46**, 181; F. H. Pollard and G. W. A. Fowles, *J. Chem. Soc.* **152**, 2444.
2. H. W. Roesky, Y. Bai and M. Noltemeyer, *Angew. Chem.*, in press.
3. J. A. Latham, G. J. Leigh, G. Huttner and J. Ibril, *J. Chem. Soc., Dalton Trans.* 1986, 377.
4. H. W. Roesky, B. Meller, M. Noltemeyer, H.-G. Schmidt, U. Scholz and G. M. Sheldrick, *Chem. Ber.* 1988, **121**, 1403.
5. H. W. Roesky, J. Anhaus, H.-G. Schmidt, G. M. Sheldrick and M. Noltemeyer, *J. Chem. Soc., Dalton Trans.* 1983, 1207.
6. H. Plenio, H. W. Roesky, M. Noltemeyer and G. M. Sheldrick, *Angew. Chem.* 1988, **100**, 1377; *Angew. Chem. Int. Edn Engl.* 1988, **27**, 1330.
7. K. P. Frank, J. Strähle and J. Weidlein, *Z. Naturfor.* 1980, **B35**, 300; M. R. Churchill and H. J. Wasserman, *Inorg. Chem.* 1982, **21**, 218; D. C. Bradley, M. B. Hursthouse, K. M. A. Malik, A. J. Nielson and G. B. C. Vuru, *J. Chem. Soc., Dalton Trans.* 1984, 1069; L. R. Chamberlain, I. P. Rothwell and J. C. Huffmann, *J. Chem. Soc., Chem. Commun.* 1986, 1203.
8. H. W. Roesky and M. Lücke, *J. Chem. Soc., Chem. Commun.*, in press.
9. H. W. Roesky, K. V. Katti, U. Seseke, M. Witt, E. Egert, R. Herbst and G. M. Sheldrick, *Angew. Chem.* 1986, **98**, 447; *Angew. Chem. Int. Edn Engl.* 1986, **25**, 477; H. W. Roesky, K. V. Katti, U. Seseke, H.-G. Schmidt, E. Egert, R. Herbst and G. M. Sheldrick, *J. Chem. Soc., Dalton Trans.* 1987, 847; K. V. Katti, H. W. Roesky and M. Rietzel, *Inorg. Chem.* 1987, **26**, 4032.
10. H. Plenio and H. W. Roesky, *Z. Naturfor.* 1988, **B43**, 1575.
11. H. W. Roesky, M. Zimmer and M. Noltemeyer, *Chem. Ber.* 1989, **122**, 63.
12. H. W. Roesky, J. Liebermann, M. Noltemeyer and H.-G. Schmidt, *Chem. Ber.*, in press.

Polyhedron Vol. 8, No. 13/14, pp. 1733–1735, 1989
Printed in Great Britain

0277–5387/89 $3.00+.00
© 1989 Maxwell Pergamon Macmillan plc

THE REACTION OF $[Bu^n_4N]_2[Re_2Cl_8]$ WITH DIPHENYLARSINOETHANE (dpae); EVIDENCE FOR THE FORMATION OF $(dpae)Re_2Cl_6$

JOSEPH FERRY, JOHN GALLAGHER, DESMOND CUNNINGHAM and PATRICK McARDLE*

Department of Chemistry, University College, Galway, Ireland

Abstract—The reaction of dpae with $[Bu^n_4N]_2[Re_2Cl_8]$ yields $[(dpae)_2ReCl]_2[Re_2Cl_8]$ and $(dpae)_2Re_2Cl_4$. The crystal structures of both of these compounds have been determined and the latter contains $(dpae)Re_2Cl_6$ as a minor component.

There have been no successful attempts to synthesize complexes of rhenium(III) which contain a possible quadruple bond and an M—M bridging ligand.[1] The only complex reported to contain an Re—Re quadruple bond and a bidentate ligand, albeit without chelation, was formulated as $(dpae)_2Re_2Cl_6$.[2] This complex was prepared by reaction of dpae with $[Bu^n_4N]_2[Re_2Cl_8]$. This reaction has been re-examined. Using the reaction conditions previously used, refluxing butanol, green and red crystals were isolated. The crystal structures of both of these products have been determined.

The green crystals have the formula $[(dpae)_2ReCl]_2[Re_2Cl_8]\cdot 2BuOH$ (**1**). The crystal data for this compound are given in Table 1 and the structure of the cation is shown in Fig. 1. Final difference maps show what appears to be a coordinated dinitrogen in the vacant coordination site. Dinitrogen coordination is often found in related systems.[3] However, elemental analysis indicated that the nitrogen content was less than measurable, $< 0.5\%$ and $[(dpae)_2Re(N_2)Cl]_2[Re_2Cl_8]$ contains 1.7% of nitrogen. Attempts to refine the apparent N_2 molecule led to N—N and M—N bonds, which were unrealistically long and short, respectively.

The red crystals were formulated as $(dpae)_2Re_2Cl_4$ (**2**), the crystal data are given in Table 1 and the structure is shown in Fig. 2, with the phenyl rings omitted. The Re_2 unit was two-fold disordered within the approximate square antiprism defined by the ligating atoms. The ratio of the major and minor orientations was 0.86:0.14 and only the major orientation is shown in Fig. 2. Two-fold disorder of this type has been observed in all $(L—L)_2Re_2Cl_4$ systems that have been reported.[4] The minor Re_2 configuration, however, did not adopt the expected configuration. In all other cases of two-fold disorder involving $(L—L)_2Re_2Cl_4$ systems the centroids of the M—M bonds of the major and minor components coincide and the bonds are approximately orthogonal. In the present case, the M—M bond centroids are 0.32 Å apart and the M—M bonds deviate from orthogonality (Table 2). The major Re_2 unit, Re(1)—Re(2), shows reasonable bonding

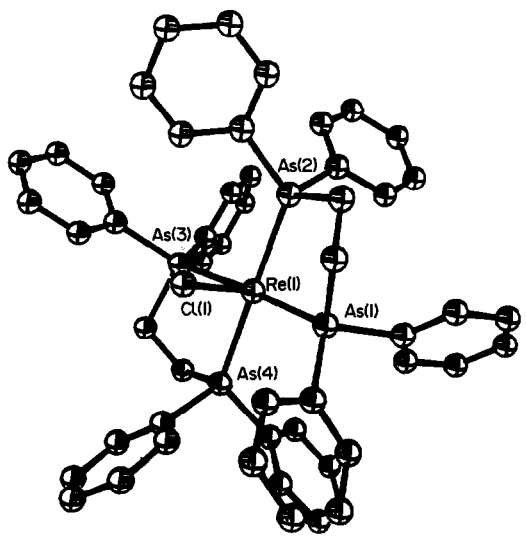

Fig. 1. An ORTEP drawing of $[(dpae)_2ReCl]_2^+$.

* Author to whom correspondence should be addressed.

Table 1. Crystal data for compounds **1** and **2**

	1	**2**
Formula	$C_{112}H_{116}O_2As_8Cl_{10}Re_4$[a]	$C_{52}H_{48}As_4Cl_4Re_2$
Space group	$P2_1/n$	$P2_1/n$
a (Å)	14.924(4)	16.826(4)
b (Å)	21.196(5)	13.334(6)
c (Å)	18.770(5)	23.151(6)
α (°)	90	90
β (°)	98.58(2)	106.31(3)
γ (°)	90	90
U (Å^3)	5870.90	4985.30
μ (cm^{-1})	63.67	75.90
F(000)	3071.51	2839.51
Z	2	4
Radiation, Mo-K_α		
Graphite monochromator	$\lambda = 0.70930$ Å	
Diffractometer	Enraf–Nonius CAD4F	
Orienting reflections,		
Range	25, $13 < \theta < 20°$	
Temperature (°C)	22	
Scan method	ω–2θ	
Data collection range	$2 < 2\theta < 48°$	$2 < 2\theta < 52°$
Number of unique data	8650	8714
Data used	$2326 > 2\sigma I$	$3161 > 3\sigma I$
Number of parameters fitted	321	225
Transmission factors, max./min.	1.0/0.68	1.0/0.507
R[b]	5.87%	5.88%
R_w[c]	5.11%	5.04%
Largest shift/ESD, final cycle	< 0.001	< 0.001
Largest positive peak (e Å^{-3})	1.18	0.74
Largest negative peak (e Å^{-3})	−0.41	−0.61

[a] Contains two Bu^{n}OH molecules per formula unit.
[b] $R = [\Sigma |F_o - F_c|]/\Sigma |F_o|$.
[c] $R_w = [[\Sigma w(|F_o - F_c|)^2]/[\Sigma w(F_o|)^2]]^{1/2}$; $w = 1/[(\sigma F_o)^2]$.

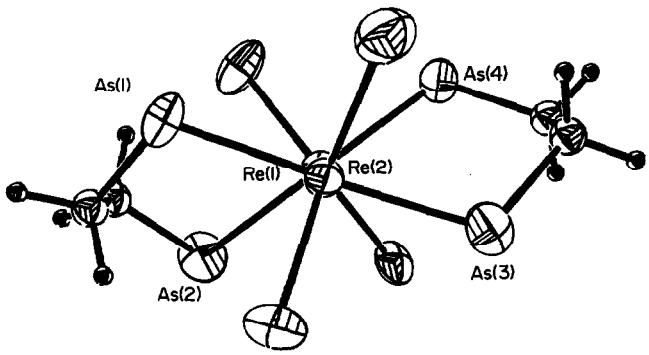

Fig. 2. An ORTEP view down the Re(1)—Re(2) bond of $(dpae)_2Re_2Cl_6$, major component.

Table 2. Selected bond distances (Å) for $(dpae)_2Re^{II}_2Cl_4$ (2)

Re(1)—Re(2)	2.231(2)	Re(3)—Re(4)	2.207(11)
Re(1)—As(1)	2.540(4)	Re(3)—As(1)	2.452(9)
Re(1)—As(3)	2.498(3)	Re(3)—As(4)	2.854(8)
Re(2)—As(4)	2.509(4)	Re(4)—As(3)	2.921(9)
Re(2)—As(2)	2.526(4)	Re(4)—As(2)	2.304(9)
Re(1)—Re(3)	1.574(8)	Re(1)—Re(4)	1.631(8)
Re(2)—Re(3)	1.643(8)	Re(2)—Re(4)	1.554(8)

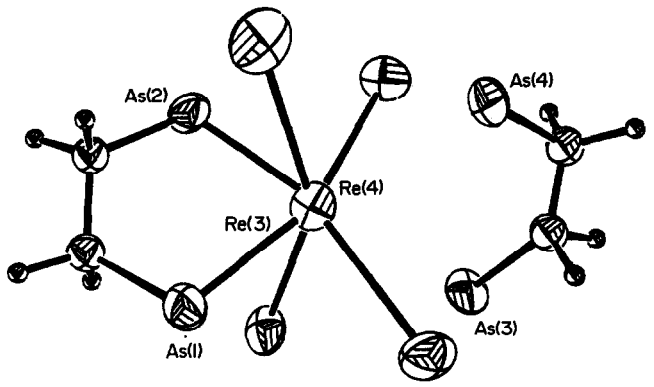

Fig. 3. An ORTEP view down the Re(3)—Re(4) bond of $(dpae)_2Re_2Cl_6$, minor component.

distances to all ligating atoms (Table 2). The minor Re_2 unit, Re(3)—Re(4), is at a bonding distance to only two of the four arsenic atoms (Table 2 and Fig. 3). The most reasonable interpretation of this result is that the minor component is $(dpae)Re^{III}_2Cl_6$ which has co-crystallized with $(dpae)_2Re^{II}_2Cl_4$. Difference maps showed peaks due to the extra chloride ligands in the former, but these were very weak and were not included in the refinement.

Attempts to prepare pure samples of several $(L—L)Re_2Cl_6$ complexes are currently in progress.

REFERENCES

1. (a) F. A. Cotton and L. M. Daniels, *Inorg. Chim. Acta* 1988, **142**, 255; (b) F. A. Cotton, private communication.
2. J. R. Ebner, D. R. Tyler and R. A. Walton, *Inorg. Chem.* 1976, **15**, 833.
3. J. Chatt, J. R. Dilworth and G. J. Leigh, *J. Chem. Soc., Dalton Trans.* 1973, 612.
4. M. Bakir, F. A. Cotton, L. R. Falvello, K. Vidyasagar and R. A. Walton, *Inorg. Chem.* 1988, **27**, 2460.

Polyhedron Vol. 8, No. 13/14, pp. 1736–1741, 1989
Printed in Great Britain

0277–5387/89 $3.00+.00
© 1989 Maxwell Pergamon Macmillan plc

BIFUNCTIONAL PHOSPHAZENES—PRECURSORS FOR THE SYNTHESIS OF CYCLIC AND ACYCLIC METALLAPHOSPHAZENES

M. WITT and H. W. ROESKY*

Institut für Anorganische Chemie der Universität Göttingen, Tammannstraße, D-3400 Göttingen, F.R.G.

Abstract—Several pathways for the synthesis of six-membered metallacyclophosphazenes $Cl_x\overline{MNPR_2NPR_2N}$ with different substituents on phosphorus are reported. Acyclic intermediates are discussed. The reaction of a persilylated aminophosphazene, **7**, with $VOCl_3$ affords the eight-membered ring $(Cl_2VNPPh_2N—)_2$ (**6b**), WCl_6 yields an acyclic compound, **8**, and group IV tetrachlorides lead to the formation of four-membered rings, **9**, with a $\overline{NPNM}$-skeleton. $Me_3SiOPPh_2NSiMe_3$ (**10**) and $TiCl_4$ form an eight-membered ring $(Cl_2TiNPPh_2O—)_2$ (**11**) with the shortest Ti—N bond found so far. The X-ray structures of each type of metallacyclophosphazenes are discussed.

Depending on the nature of the ligands, metal chelates have been found useful catalysts in various aspects of organic chemistry.[1] Thus, we were interested in synthesizing metallaphosphazenes to test their applicability in catalysis. Furthermore, another crucial aspect of our work is the vast area of phosphazene chemistry, namely poly-[2] and cyclophosphazenes.[2,3] Incorporating metal centres in phosphazenes might afford materials with unusual properties depending on the metal atom and the substituents on both the metal and phosphorus centres. In this paper we summarize our present results in building up novel ring systems and open-chain compounds, as well as in attaching new organic groups on phosphorus.

RESULTS AND DISCUSSION

Recently, we have reported the synthesis of metallatriazadiphosphorines, **2a–e**, from the reactions of $[H_2NPPh_2NPPh_2NH_2]^+Cl^-$ (**1a**) with metal halides or metal nitride halides in their highest oxidation state, or by passing chlorine through solutions containing lower metal halides [eq. (1)]:[4]

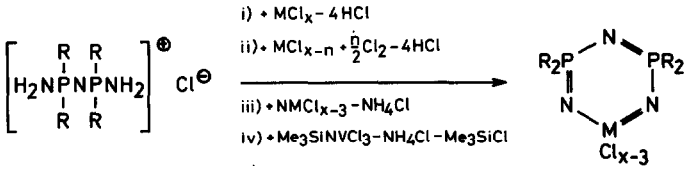

(1)

1 **2**

R		R	M	x	method		R	M	x	method
a	Ph	a Ph	V	2	ii	i	Me	V	2	ii
b	4-ClPh	b Ph	Nb	2	i	j	Me	W	3	ii
c	Me	c Ph	Mo	3	ii	k	Me_2N	W	3	iii
d	Me_2N	d Ph	W	3	ii, iii	l	Mor	V	2	iv
e	O[$(CH_2)_2$]N ≙ Mor	e Ph	Re	4	ii	m	Mor	Mo	3	iii
		f 4-ClPh	Mo	3	ii	n	Mor	W	3	iii
		g 4-ClPh	W	3	ii					
		h 4-ClPh	Re	4	ii					

Starting from the *p*-chlorophenyl-, **1b**, and methyl-substituted, **1c**, precursors, the metallacycles **2f–j** have been synthesized according to method (ii).

* Author to whom correspondence should be addressed.

The phenoxy-substituted phosphazenium salt failed to form the expected rings.[5]

Since aminophosphazenes are known to be affected by both elemental chlorine and hydrogen chloride,[2] these conditions had to be avoided in the reactions of the amino-substituted phosphazenium chlorides, **1d**, **e**. The metallaphosphazenes **2k–n** are accessible only to methods (iii) and (iv).[6]

Monitoring the progress of the reactions by ^{31}P NMR spectroscopy showed the mechanism to be rather complex. The first intermediates identified or isolated were the hexachlorometallates **3**, which on heating, e.g. in $CHCl_3$, subsequently yield two sets of pairs of doublets, indicating unsymmetric acyclic compounds disappearing with the growth of the singlets of **2**.

A second method to avoid acidic conditions, besides the use of metal nitrides, is the reaction in the presence of a tertiary base, e.g. pyridine. While with **1a** and $NbCl_5$, **2b** is formed, $TaCl_5$ yields an inseparable mixture of the hexachlorotantalate, **3a**, and two compounds showing two pairs of doublets in the ^{31}P NMR spectrum.[7] In the reaction of **1e** with $NbCl_5$ and pyridine an open chain compound, **4**, has been isolated as the sole product as shown by ^{31}P NMR, IR and elemental analyses.[6] These facts give rise to the reaction sequence depicted in eq. (2):

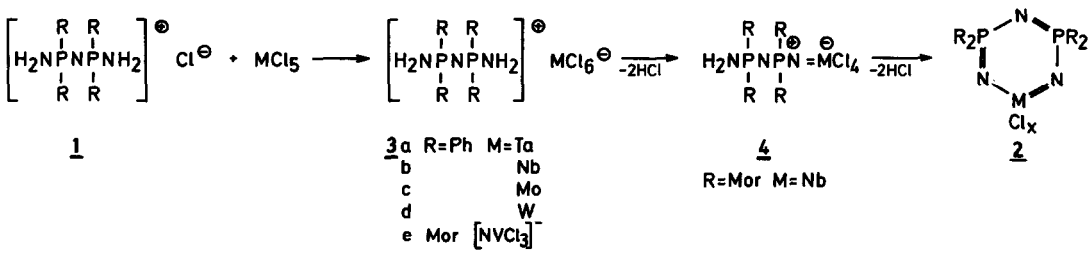

1 2 4

(2)

A somewhat surprising product has been found in the reaction of the CF_3-substituted P-chlorophosphazene, **5a**, and $Cl_3V{=}NSiMe_3$: instead of the expected eight-membered ring system, **6** (*vide infra*), the CF_3-substituted derivative, **2o**, was isolated in low yields as a volatile solid, melting with decomposition at 22.5°C:[8]

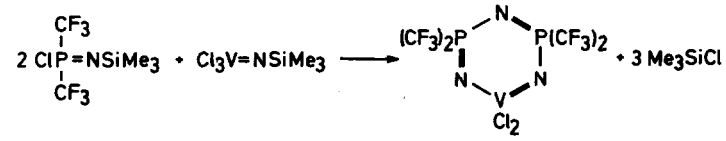

5a 2o

(3)

The expected tetrazadiphosphadivanadocine, **6a**, has been isolated in high yields as a brick-red microcrystalline solid from the reaction according to eq. (4):[9]

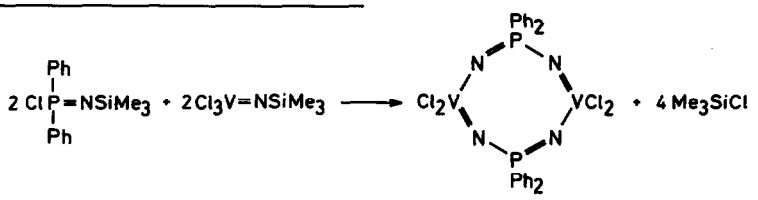

5b 6a

(4)

A derivative, **6b**, is accessible via silyl migration from aminoiminophosphorane, **7**, and $VOCl_3$ in 80% yield, which after recrystallization from CH_2Cl_2–CH_3CN forms translucent brick-red rhombs:[9]

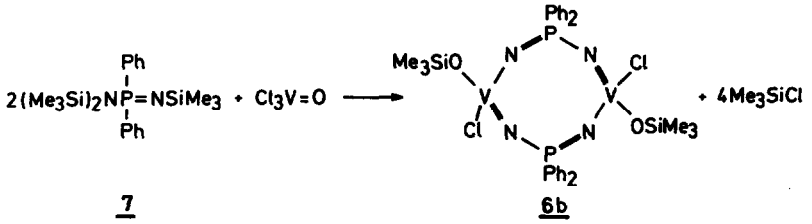

7 6b

(5)

Up until now, attempts to extend this synthetic pathway to other tetrazadiphosphadimetallocines have been unsuccessful. The reaction of **7** with WCl_6 yields an acyclic metal-substituted phosphazene, **8**, characterized by elemental analysis and NMR spectroscopy [eq. (6)]:[6]

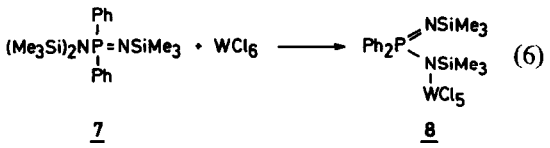

(6)

7 **8**

Since multiple bonds to group IV metals are rather unfavourable, the reactions of **7** with $TiCl_4$[10] and $ZrCl_4$[6] proceed in a different way [eq. (7)]:

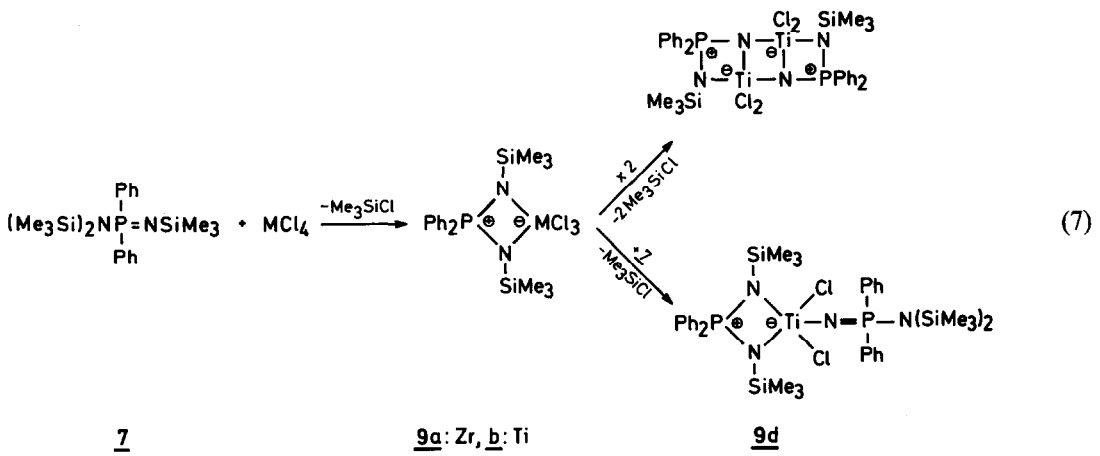

(7)

7 **9a**: Zr, **b**: Ti **9d**

While the reaction of **7** with $ZrCl_4$ proceeds unequivocally, $TiCl_4$ yields a mixture of different products, **9b–d**. By varying the reaction conditions (see Experimental) the yields of the respective compounds could be optimized, the products have been isolated by fractional crystallization from CH_3CN.

The analogous reaction of silyloxyphosphazene, **10**, with $TiCl_4$ leads to the unexpected formation of the eight-membered ring system, **11**, besides several silicon-containing species which have not yet been identified:[11]

Spectroscopical and X-ray investigations

Mass spectroscopical measurements (EI, FI and FD techniques) show the parent ion or $M^+ - Cl$ as the peaks with the highest masses for most of the six-membered rings, **2**. Of the eight-membered rings, only tetrazadiphosphadivanadocine, **6a**, gave the molecular ion, as well as the trichlorosubstituted four-membered rings, **9a**, **b**. The other metallaphosphazenes showed fragmentation and rearrangement patterns, e.g. in the EI mass spectrum of **6b**, $M^+ - Cl$ for **2a** had been detected.[6] Interestingly, the open-chain intermediates $[H_2N(PPh_2N)_2H_2]^+ MCl_6^-$ (**3b–d**) failed to show the signal for the cation. Instead, FI mass spectra consisted of the parent ions of the corresponding six-membered rings, **2b–d**.[6] This is in contrast to the homologous compounds $[H_2N(PPh_2N)_3H_2]^+MC_6^-$, where the cation peak, together with the parent ions of the tetrazatriphosphametallocines with intensities between 0 and 30%, have been observed.[12]

^{31}P NMR studies show downfield shifts for all metallaheterocycles compared to their acyclic phosphazene precursors. The chemical shifts of the six-membered rings, **2**, have been found 20–30 ppm downfield of the corresponding bis(amino-

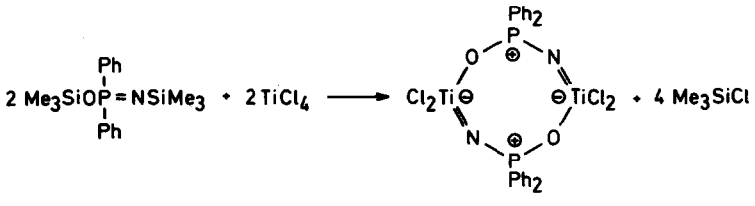

(8)

10 **11**

phosphoranylidene)immonium precursors, **1**.[4,5,8] While the ^{31}P signal of the open-chain compound, **8**, is shifted downfield *ca* 50 ppm, compared to **7**, an upfield shift of 17 ppm and line broadening has been observed for the phosphorus atom in **4** bearing the —N=$NbCl_4$ unit. The other phosphorus atom shows a signal at 14 ppm as does the precursor **2e**.[6] Interestingly, the ^{31}P signals of the vanadium heterocycles **2l**, **2o**, **6a** and **6b** have half-widths of *ca* 1000 c.p.s., which is not due to paramagnetic influence.[13]

X-ray crystallographic work on the four-membered rings, **9a–d**,[10,11] on the six-membered rings, **2c**,[4b] **2d**[4a] and **2o**,[8] and on the eight-membered rings, **6b**,[9] and **11**,[11] has been done. All structures except that of **11** show the ring skeletons to be essentially planar. While donor solvents such as CH_3CN are attached to the metals in the crystal state in **2c**, **d**, **9a–c** and **11** resulting in a distorted octahedral environment, the vanadium compounds, **2o** and **6b**, as well as the titanium heterocycle, **9d**, contain no solvent in the crystals, thus resulting in distorted tetrahedral and trigonal-bipyramidal geometries, respectively. Compounds **9c**, **6b** and **11** are centrosymmetric and **2o** contains a C_2 axis through vanadium and the opposite nitrogen, causing pairwise equal bond lengths and angles. *Trans*-effects due to the CH_3CN and Cl bond in the ring planes of **2c**, **d** make the ring bonds and angles differ slightly. Due to steric effects a somewhat greater deviation from equality is found in the four-membered rings **9a**, **b**, **d**. While bond lengths and angles in the P—N sections of the ring systems do not differ significantly from those of these non-metallated analogues, some unusual features have been found around the metal atoms. While the Ti—N and Zr—N bond lengths in the PN_2M moiety in **9a–d** can be regarded close to single bonds, the Ti—N bonds in the central Ti_2N_2 ring of **9c** are 189.0 pm, in the exocyclic Ti—N—$PPh_2N(SiMe_3)_2$ moiety of **9d** are 179.2 pm, and in **11** are 173.9 pm, which are definitively shorter than single bonds, **11** having the shortest Ti—N distances found so far. The Ti—N—P angles in **9d** (exocyclic) are 170.3° and in **11** are 175.9° and are almost linear. The angles at the ring nitrogen atoms adjacent to the metal atoms are also increased from 158.4° in **6b** to 129.0° in **2o**. The M—N separations in the fully unsaturated rings, **2** and **6b**, have to be regarded as double bonds, the bond angles at the four coordinated vanadium atoms are close to the tetrahedral angle (104.2° in **2o** and 110.8° in **6b**), while the octahedral angles in **2c**, **d** are slightly bigger than 90° and around 75° in the four-membered rings, **9a–d**. The exocyclic Si—O—V angles in **6b** are almost linear.

EXPERIMENTAL

General methods

All manipulations were carried out under an atmosphere of dry argon or nitrogen or *in vacuo*. Solvents were dried and degassed by conventional methods and stored over molecular sieves. If not otherwise noted, solvents and volatile starting materials were transferred into the reaction vessel *in vacuo* at −190°C and the reaction mixtures slowly warmed up to ambient temperatures, solids transferred to the flask in a dry box (prior to condensation) and liquids injected with a syringe. Metal halides and $VOCl_3$ were commercial products, $Cl_3VNSiMe_3$, Cl_3MN (N = Mo, W), and the phosphazene precursors were prepared as described in the papers referred to in this article and the original papers cited therein. The syntheses of the six-membered rings, **2a–e**, have been described elsewhere,[4] the syntheses of **2f–j**[5] closely follow these procedures and are therefore omitted in this article. As a fully characterized example of an amino-substituted metallacyclophosphazene, the synthesis of **2l** together with the CF_3-substituted **2o** are given.

Synthesis of 2,2,4,4-*tetramorpholino*-1,3,5,2λ^5,4λ^5,6λ^6-*triazadiphosphatungstenine*·THF (**21**)[6]

4.9 g (10 mmol) of **1e** and 3.1 g (10 mmol) of $NWCl_3$ were refluxed in 100 cm^3 of $CHCl_3$ for 5 h. The solvent was evaporated and the remainder extracted with hot THF. **2l·THF** precipitates as a microcrystalline, yellow solid in 26% (2.1 g) yield. Found for **2l·THF**: C, 28.9; H, 5.1; Cl, 13.4; N, 11.9. $C_{20}H_{10}Cl_3N_7O_5P_2W$ requires: C, 29.63; H, 4.97; Cl, 13.12; N, 12.09%.

Synthesis of 2,2,4,4-*tetrakis*(*trifluoromethyl*)-1,3,5,2λ^5,4λ^5,6λ^5-*triazadiphosphavanadinine* (**2o**)[8]

2.4 g (10 mmol) of Cl_3V=$NSiMe_3$ and 60 cm^3 of CH_2Cl_2 were cooled to −190°C and 5.8 g (20 mmol) of **5a** were added. After warming up to room temperature the mixture was stirred for 5 h. Volatiles were removed at −10°C *in vacuo* and the crude product was sublimed twice in a cold finger held at −10°C. Compound **2o** was isolated as translucent yellow crystals, which melt at 22.5°C with decomposition, in 28% (1.4 g) yield. Found for **2o**: C, 9.7; Cl, 14.4; N, 8.4. $C_4Cl_2F_{12}N_3P_2V$ requires: C, 9.57; Cl, 14.13; N, 8.37%.

Synthesis of the bis(*aminodiphenylphosphoranylidene*)*immoniumhexachlorometallates* (**3a–d**)[6]

Of the intermediates, **3**, only hexachlorotungstate, **3d**, has been fully characterized.

Equimolar amounts of **1a** and WCl_6 were stirred in CH_2Cl_2 at room temperature for 1 h. Cl_2 evolution was observed. After removal of the solvent, **3d** was recrystallized from CH_3CN. It forms brown blocks melting at 239°C with decomposition. The yield (before recrystallization) was virtually quantitative. Found for **3d**: C, 34.8; H, 3.0; Cl, 27.2; N, 4.7. $C_{24}H_{24}Cl_6N_3P_2W$ requires: C, 35.46; H, 2.98; Cl, 26.16; N, 5.17%.

Synthesis of [(*aminodimorpholinophosphoranylideneimino*) *aminodimorpholinophosphoranylideneimino*] *aminoniobiumtetrachloride* · C_5H_5N (**4**)[6]

4.9 g (10 mmol) of **1e** and 2.35 g (10 mmol) of $NbCl_5$ were refluxed in a mixture of 100 cm^3 of CH_2Cl_2 and 10 cm^3 of pyridine for 6 h. After cooling, pyridine hydrochloride was filtered off, the solution evaporated and the residue extracted with CH_2Cl_2. The compound was isolated as yellow crystals in 15% (1.2 g) yield by slow diffusion of the solvent in an evacuated two legged Schlenk vessel from 21 to 18°C. Found for **4** · C_5H_5N: C, 34.1; H, 5.4; Cl, 19.2; N, 15.1. $C_{21}H_{39}C_{14}N_8NbO_4P_2$ requires: C, 33.0; H, 5.14; Cl, 18.56; N, 14.66%.

Synthesis of 2,2,6,6-*tetraphenyl*-4,4,8,8-*tetrachloro*-1,3,5,7,2λ^5,6λ^5,4λ^5,8λ^5 - *tetrazadiphosphadivanadocine* (**6a**)[9]

2.4 g (10 mmol) of $Cl_3V{=}NSiMe_3$ and 3.1 g (10 mmol) of **5b** in 120 cm^3 CH_3CN were heated for 4 h at 40°C. The solid was filtered off, washed with a little CH_3CN and dried *in vacuo*. The brick-red microcrystalline powder, melting at 225°C with decomposition, was isolated analytically pure in 75% (5 g) yield. Found for **6a**: C, 42.2; H, 3.2; Cl, 21.3; N, 8.4. $C_{24}H_{20}Cl_4N_4P_2N_2$ requires: C, 43.02; H, 3.01; Cl, 21.16; N, 8.36%.

Synthesis of 2,2,6,6-*tetraphenyl*-trans-4,8-*dichloro*-4,8 - *bis*(*trimethylsilyloxy*) - 1,3,5,7,2λ^5,6λ^5,4λ^5,8λ^5-*tetrazadiphosphadivanadocine* (**6b**)[9]

1.7 g (10 mmol) of $VOCl_3$ and 4.3 g (10 mmol) of **7** in 120 cm^3 of CH_3CN were stirred at room temperature for 24 h. The residue was filtered off, washed with a little CH_3CN, and then redissolved in CH_2Cl_2 and a little CH_3CN. At −30°C **6b** crystallizes in brick-red rhombs of m.p. 206°C with decomposition. The yield of crude **6b** was 80% (6.2 g). Found for **6b**: C, 46.1; H, 4.9; Cl, 9.3; N, 7.3. $C_{30}H_{38}C_{12}N_4O_2P_2Si_2V_2$ requires: C, 46.34; H, 4.93; Cl, 9.12; N, 7.4%.

Synthesis of N,N′-*bis*(*trimethylsilyl*)-N-*pentachlorotungstenamino* - P - *diphenyliminophosphorane* (**8**)[6]

7.9 g (20 mmol) of WCl_6 and 8.6 g (20 mmol) of **7** were stirred for 10 h in 150 cm^3 of CH_2Cl_2 at room temperature. The volatiles were evaporated and the tarry dark-brown residue extracted several times with hot PCl_3. An olive–yellow microcrystalline solid residue remained, which was dried thoroughly *in vacuo*. Elemental analysis showed this material to be analytically pure **8** in 55% (8.1 g) yield. Found for **8**: C, 31.3; H, 4.4; Cl, 25.0; N, 3.8. $C_{18}H_{30}C_{15}N_2PSi_2W$ requires: C, 29.92; H, 4.18; Cl, 24.53; N, 3.88%.

Synthesis of 1,3-*bis*(*trimethylsilyl*)-2,2-*diphenyl*-4,4,4 - *trichloro* - 1,3,2λ^5,4λ^4 - *diazaphosphazirconetidine* · CH_3CN (**9a**) *and* -*titanetidine* · CH_3CN (**9b**)[10]

2.4 g (10 mmol) of $ZrCl_4$ or 1.9 g (10 mmol) of $TiCl_4$, respectively, and 4.3 g (10 mmol) of **7** were stirred at 0°C in 100 cm^3 of CH_2Cl_2 for 2 h. Insoluble material was filtered off, volatiles were evaporated and 80 cm^3 of CH_3CN added. After several days at −25°C the products started to crystallize. Additional material has been obtained by partial removal of the solvent. The yields of **9a** (colourless needles melting at 135°C with decomposition) and **9b** (orange cubes melting at 105°C with decomposition) were 48% (2.9 g) and 42% (2.3 g), respectively. Found for **9a** · **CH_3CN**: C, 40.3; H, 5.6; Cl, 17.7; N, 7.1. $C_{20}H_{31}Cl_3N_3PSi_2Zr$ requires: C, 40.17; H, 5.22; Cl, 17.78; N, 7.02%. Found for **9b** · **CH_3CN**: C, 43.8; H, 5.7; Cl, 19.2; N, 7.1. $C_{20}H_{31}Cl_3N_3PSi_2Ti$ requires: C, 43.29; H, 5.63; Cl, 19.17; N, 7.57%.

Synthesis of 3,7-*bis*(*trimethylsilyl*)-2,2,6,6-*tetraphenyl* - 4,4,8,8 - *tetrachloro* - 1,3,5,7,2λ^5,6λ^5,4λ^4,8λ^4-*tetrazadiphosphadititanatricyclo*[2, 2, 0, 0]*octane* · 2CH_3CN (**9c**)[10]

1.1 g (2 mmol) of **9b** · **CH_3CN** were dissolved in 50 cm^3 of CH_3CN and heated to 60°C for 3 h. After several days at −25°C a mixture of crystals of **9b** and **9c** precipitated, which after filtration were separated manually, but were not pure enough for elemental analysis.

Synthesis of 1,3-*bis*(*trimethylsilyl*)-2,2-*diphenyl*-4,4-*dichloro* - 4 - [N,N - *bis*(*trimethylsilyl*)*aminodiphenylphosphoranylideneimino*] - N′ - *amino* - 1,3,2λ^5,4λ^4 - *diazaphosphatitanetidine* · CH_3CN (**9d**)[11]

8.6 g (20 mmol) of **7** and 1.9 g (10 mmol) of $TiCl_4$ were stirred at room temperature for 12 h.

Subsequently all volatiles were evaporated and the solid residue redissolved in 50 cm^3 of CH_3CN. After cooling, **9d · CH_3CN** crystallized in dark yellow blocks melting at 135°C. This was slightly contaminated with **9b · CH_3CN** to give insufficient elemental analyses.

Synthesis of 2,2,6,6-*tetraphenyl*-4,4,8,8-*tetrachloro*-1,5,3,7,2λ^5,6λ^5,4λ^4,8λ^4 - *dioxadiazadiphosphadititanocine* · 4CH_3CN (**11**)[11]

3.8 g (20 mmol) of $TiCl_4$ and 7.2 g (20 mmol) of **10** were stirred in 120 cm^3 of CH_3CN at room temperature for 12 h. Insoluble material was filtered off and volatiles were evaporated. The residue was redissolved in a minimum amount of CH_3CN and kept at −25°C for crystallization. Found for **11 · 4CH_3CN**: C, 46.4; H, 4.2; Cl, 16.2; N, 9.0. $C_{32}H_{22}Cl_4N_6O_2P_2Ti_2$ requires: C, 46.19; H, 3.88; Cl, 17.04; N, 10.10%.

Acknowledgements—We are grateful to the Deutsche Forschungsgemeinschaft, VW-Stiftung and the Fonds der Chemischen Industrie for financial support.

REFERENCES

1. (a) M. T. Reetz, *Organotitanium Reagents in Organic Synthesis*. Springer, Berlin (1986); M. T. Reetz, *Top. Curr. Chem.* 1986, **106**, 1; (b) G. Wilkinson, F. G. A. Stone and E. W. Abel (Eds), *Comprehensive Organometallic Chemistry*, Vols 1–9. Pergamon Press, Oxford (1982).
2. H. R. Allcock, *Phosphorus–Nitrogen Compounds*. Academic Press, New York (1972).
3. J. Haiduc and D. W. Sowerby, *The Chemistry of Inorganic Homo- and Heterocycles*. Academic Press, London (1987).
4. (a) H. W. Roesky, K. V. Katti, U. Seseke, M. Witt, E. Egert, R. Herbst and G. M. Sheldrick, *Angew. Chem.* 1986, **98**, 447; H. W. Roesky, K. V. Katti, U. Seseke, M. Witt, E. Egert, R. Herbst and G. M. Sheldrick, *Angew. Chem. Int. Edn Engl.* 1986, **25**, 477; (b) H. W. Roesky, K. V. Katti, U. Seseke, H.-G. Schmidt, E. Egert, R. Herbst and G. M. Sheldrick, *J. Chem. Soc., Dalton Trans.* 1987, 847; (c) K. V. Katti, H. W. Roesky and M. Rietzel, *Inorg. Chem.* 1987, **26**, 4032; (d) K. V. Katti, U. Seseke, M. Witt and H. W. Roesky, *Phosphorus Sulfur* 1987, **30**, 421.
5. H. W. Roesky and J. Liebermann, unpublished results.
6. M. Witt and H. W. Roesky, unpublished results.
7. H. W. Roesky and M. Rietzel, unpublished results.
8. H. W. Roesky, P. Olms, M. Witt, K. Keller, D. Stalke, T. Henkel and G. M. Sheldrick, *J. Chem. Soc., Chem. Commun.*, in press.
9. M. Witt, H. W. Roesky, M. Noltemeyer and G. M. Sheldrick, *Angew. Chem.* 1988, **100**, 852; M. Witt, H. W. Roesky, M. Noltemeyer and G. M. Sheldrick, *Angew. Chem. Int. Edn Engl.* 1988, **27**, 851.
10. M. Witt, H. W. Roesky, D. Stalke, F. Pauer, T. Henkel and G. M. Sheldrick, *J. Chem. Soc., Dalton Trans.*, in press.
11. M. Witt, H. W. Roesky and D. Stalke, paper in preparation.
12. M. Witt, H. W. Roesky, M. Noltemeyer and A. Schmidpeter, *New. J. Chem.*, in press.
13. D. Marsh, private communication.

Polyhedron Vol. 8, No. 13/14, pp. 1742–1744, 1989
Printed in Great Britain

0277–5387/89 $3.00+.00
© 1989 Maxwell Pergamon Macmillan plc

STRUCTURE AND REACTIVITY OF TRANSITION METAL COMPLEXES: A STEREOCHEMICAL APPROACH

ALISON RODGER

Physical Chemistry Laboratory, South Parks Road, Oxford OX1 3QZ, U.K.

and

BRIAN F. G. JOHNSON*

University Chemical Laboratory, Lensfield Road, Cambridge CB2 1EW, U.K.

Abstract—A novel approach to describing the structure and reactivity of metal complexes, in which steric repulsions and attractive forces are reassessed, is reported.

The structure and reactivity of transition metal complexes have been one of the most intensively pursued areas of inorganic chemistry.[1] X-ray crystallography enables the (solid state) structure of most transition metal complexes to be determined experimentally. Experimental studies of reactivity are, however, of necessity, less direct. For high symmetry systems, symmetry rules for reactants, products and proposed transition states have proved useful complements to experiment, for example see refs 2–6. For lower symmetry systems one can often proceed by analogy with a high symmetry system using a "corresponding" principle.[7] Symmetry analyses have the advantage of giving strict yes/no answers which can be transferred between systems. Their major drawback is that they give no information of the magnitude of an effect for a "yes", nor how much distortion of the system is required to convert a "no" into a "yes, but small". The other theoretical extreme is a detailed calculation of some kind which gives precise information for the system being studied,[8] but usually provides no transferable information to help solve similar problems in other systems.

The stereochemical approach we have developed[7,9] aims to combat the problems inherent in the two types of approach, by coupling symmetry results with a chemically-based electrostatic approximation to the energy of a molecular system, which enables relative stabilities to be determined. When applied to equilibrium structures it enables ground-state geometries to be determined and when applied to proposed transition state geometries it enables the most favourable reaction pathways to be identified. The symmetry results used are those summarized in the classical symmetry selection rule procedure of ref. 3. The energetics follow from partitioning the total energy of a molecule ML_n into three contributions: that due to M—L bonding, that due to L—L interactions and that due to the non-bonding electron density:

$$E_{tot} = \sum M\text{—}L + \sum L\text{—}L + \sum e.$$

The geometry a molecule adopts is then determined by minimizing E_{tot}. The most significant *stabilizing* factor is the M—L bonding interaction. With only a few exceptions,[9] Σ M—L is approximately independent of the orientation of the ligands, as long as the M—L bond length remains the same. Comparison with a wide range of experimental data[8] indicated that Σ L—L is generally dominant over Σe (in contrast to valence-shell electron-pair repulsion theory which assumes a dominant role for the formation of lone *pairs* of spatially localized electrons). Thus, subject to M—L bond length constraints, the geometry adopted by ML_n is determined by L—L interactions. At very short L—L

* Author to whom correspondence should be addressed.

distances, repulsion due to the overlapping of L electron clouds is dominant, at intermediate distances, an attractive r^{-6} dispersion interaction is dominant and at longer range, an r^{-1} repulsive charge–charge interaction is dominant. The short range L—L repulsion is semi-quantitatively accounted for by a hard sphere radius for L. The intermediate range attraction then favours a geometry where L hard spheres are in contact. For uncharged ligands, whose net charges come from polarities of bonds, the r^{-1} repulsion is not important for determining the positions of ligand atoms about a metal. It is, however, crucial for determining the most stable orientations of the next "sphere" of atoms in e.g. $M(OH_2)$. We illustrate this discussion by application to tris-chelate complexes.

GEOMETRY OF TRIS-CHELATE COMPLEXES

The simplest and most successful rationalization of the geometries of a wide range of tris-chelate transition metal complexes is the ligand–ligand repulsion model of Keppert.[10] The previous discussion enables us to understand why this model has been so successful and also to predict where it is likely to be inapplicable and what deviations can be expected.

Let us consider a tris-chelate complex whose ligating atoms are so large that the short range L—L repulsions (most easily viewed as hard sphere repulsions) force M—L bonds to be stretched in order to accommodate three chelates. Keppert's model, where the geometry adopted is that which minimizes repulsion, will then agree with the observed structure. Examples of this are $[Cr(en)_3]^{3+}$ and $Co(S_2COEt)_3$. For complexes with a chelate bite (the distance between ligating atoms of a chelate in units where the M—L bond length is one), b, less than $\sqrt{2}$, the geometry adopted is twisted from octahedral towards a trigonal prism, and conversely for b being greater than $\sqrt{2}$.

The situation is both more complex and more interesting for complexes with smaller ligands, since attractive forces come into play. The short range repulsive forces are still important, since an ML_6 system is crowded, but now the modifying effect of the attractive forces must be taken into account. We consider the attractive force as a perturbation which modifies the repulsion determined geometry. A twist in either direction from the repulsion determined twist angle of Ω_{rep} stabilizes the complex; the question is which direction is more favourable and how much of a twist is expected? The direction and amount of twist depends on b and the L hard sphere radius. The rapid fall off of r^{-6} with distance ensures that the shortest L—L distance is approximately twice the hard sphere radius. Thus, we compare the two twist angles, Ω_+ and Ω_-, at which, respectively, two L not related by a three-fold rotation are closest and two L related by a three-fold rotation are closest. When the energies are calculated it turns out that for larger b, the geometry with the smaller twist angle (i.e. closer to a trigonal prism) is always adopted. The situation is the other way round for small values of b. The change from one type of behaviour to the other occurs for b values of about 1.2. It should, however, be noted that when the energy difference between the two angles is small, other factors such as crystal packing forces can be expected to influence the angle adopted in a crystal. Thus $[Co(en)_3]^{3+}$, for example, is sometimes Ω_+ and sometimes Ω_-.

REARRANGEMENTS OF TRIS-CHELATE COMPLEXES

The only two concerted symmetry allowed mechanisms for a tris-chelate complex are the Ray Dutt and Bailar twist mechanisms. These two mechanisms are usually viewed as quite different, but they are in fact very similar: the Bailar twist involves a totally symmetric twist about the three-fold axis of the complex via a trigonal prismatic transition state, and the Ray Dutt twist is the same twist but about an axis which is a three-fold axis in the octahedral template of the complex, but not in the D_{3h} chelated complex. In order to accommodate the ligating atoms in the trigonal prism, the M—L bonds must stretch during these twists. The most stable transition state will be that with the least M—L bond stretching. It can then be shown that the Bailar twist is more favourable than the Ray Dutt twist if $b > \sqrt{2}$, and conversely though, for $b \approx \sqrt{2}$ the difference is very small. In addition, the smaller the value of b, the less the energy required for a twist mechanism to operate. So as b is usually less than $\sqrt{2}$, a tris-chelate complex will rearrange more readily via a twist mechanism than its octahedral counterpart. Since tris-chelate complexes are usually the more stable, we can conclude that bond breaking mechanisms are usually favoured for tris-chelate mechanisms.

REFERENCES

1. F. A. Cotton and G. Wilkinson, *Advanced Inorganic Chemistry*. Interscience Publishers, New York (1972).
2. R. Willem, M. Gielen, H. Pepermans, J. Brocas, D.

Fastenakel and P. Finocchiaro, *J. Am. Chem. Soc.* 1985, **107**, 1146.
3. A. Rodger and P. E. Schipper, *Inorg. Chem.* 1988, **27**, 458 and refs therein.
4. R. G. Pearson, *Symmetry Rules for Chemical Reactions*. John Wiley, New York (1976).
5. R. E. Stanton and J. W. McIver Jr, *J. Am. Chem. Soc.* 1975, **97**, 3632.
6. A. Metropolous, *J. Phys. Chem.* 1987, **91**, 2233.
7. A. Rodger and B. F. G. Johnson, *Inorg. Chem.* 1989, in press.
8. L. G. Vanquickenborne, M. Hendrickx, I. Hyla-Kryspin and L. Haspeslagh, *Inorg. Chem.* 1986, **25**, 885.
9. A. Rodger and B. F. G. Johnson, *Inorg. Chim. Acta* 1988, **146**, 35.
10. D. L. Keppert, *Prog. Inorg. Chem.* 1977, **23**, 1.

Polyhedron Vol. 8, No. 13/14, pp. 1745–1747, 1989
Printed in Great Britain

0277–5387/89 $3.00+.00
© 1989 Maxwell Pergamon Macmillan plc

THE SYSTEMS L-CYSTEINE AND D-PENICILLAMINE + OXOVANADIUM(IV); A POTENTIOMETRIC AND SPECTROSCOPIC STUDY

J. COSTA PESSOA and L. F. VILAS BOAS

Centro de Química Estrutural, Complexo I, Instituto Superior Técnico, 1096 Lisboa, Portugal

and

R. D. GILLARD*

Department of Chemistry, University of Wales, P.O. Box 912, Cardiff CF1 3TB, Wales, U.K.

Abstract—The equilibria in the systems L-cysteine (and D-penicillamine) + VO^{2+} in aqueous solution for $1.5 \lesssim pH \lesssim 12$ have been studied by a combination of pH-potentiometric and spectroscopic methods (EPR, visible absorption and circular dichroism). For pH > 4, high ligand-to-metal ratios were used. The results of the various methods are made self-consistent, then rationalized assuming an equilibrium model including species MXH_2, MXH, MX_2H_4, MX_2H_3, MX_2H_2, MX_2H, MX_2, M_2X_2 (where H_2X denotes L-cysteine or D-penicillamine, and M denotes VO^{2+}), and several hydrolysis products; their formation constants and individual electronic spectra (isotropic and circular dichroism) are given. Plausible isomeric structures for each of the stoichiometries are discussed.

Although knowledge of the complex equilibria of VO^{2+} in the presence of amino acids is relevant in understanding its possible interaction with likely biological ligands, few reliable data exist.[1–4]

This work involves the study of the L-cysteine and D-penicillamine + VO^{2+} systems in aqueous solution for $1.5 < pH < 12$, by combining the results of potentiometric and spectroscopic techniques [EPR, visible absorption and circular dichroism (CD)].

In the EPR spectra recorded with frozen "solutions" containing VO^{2+} and D-Pen at 77 K with high ligand-to-metal ratios (e.g. 25), the several species that may be detected in the pH range 1.5–4 are of the same type as those found in the pH range 1.5–6 in the L-Ala,[2] L-Ser and L-Thr[3] + VO^{2+} systems. This is also consistent with the visible and CD spectra recorded.

For $pH \gtrsim 4$ ($\gtrsim 4.5$ for L-Cys) all spectroscopic results for the D-Pen (and L-Cys) + VO^{2+} system differ from those found in the other systems. The EPR spectra clearly show that one R—S^- group coordinates for $pH \gtrsim 4$ ($\gtrsim 4.8$ for L-Cys) and two R—S^- groups for $pH \gtrsim 5.5$ ($\gtrsim 6.3$ for L-Cys). In the pH range 7.1–11 only one species is detected in the EPR spectra, corresponding to a N_2S_2 coordination in the equatorial plane.

In Fig. 1 we include some of the CD spectra recorded. In the pH range 8.3–10.3 the CD (and

Table 1. Composition and formation constants of the species in the D-Pen (and L-Cys) + VO^{2+} systems at 25°C and 2.25 M $NaNO_3$. Values for $\log \beta_{xyz}$ of eq. (1) are given

Species	L-Cys + VO^{2+}	D-Pen + VP^{2+}
MLH_2	19.9 (0.2)	19.8 (0.2)
MLH	16.1 (0.3)	16.3 (0.3)
ML_2H_4	~ 39.3 (0.4)	~ 39.5 (0.4)
ML_2H_3	~ 35.8 (0.3)	~ 36.1 (0.3)
ML_2H_2	31.0 (0.3)	31.7 (0.3)
ML_2H	26.0 (0.3)	26.7(0.3)
ML_2	19.2 (0.3)	19.7 (0.3)
M_2L_2	25.2 (0.3)	26.0 (0.3)

* Author to whom correspondence should be addressed.

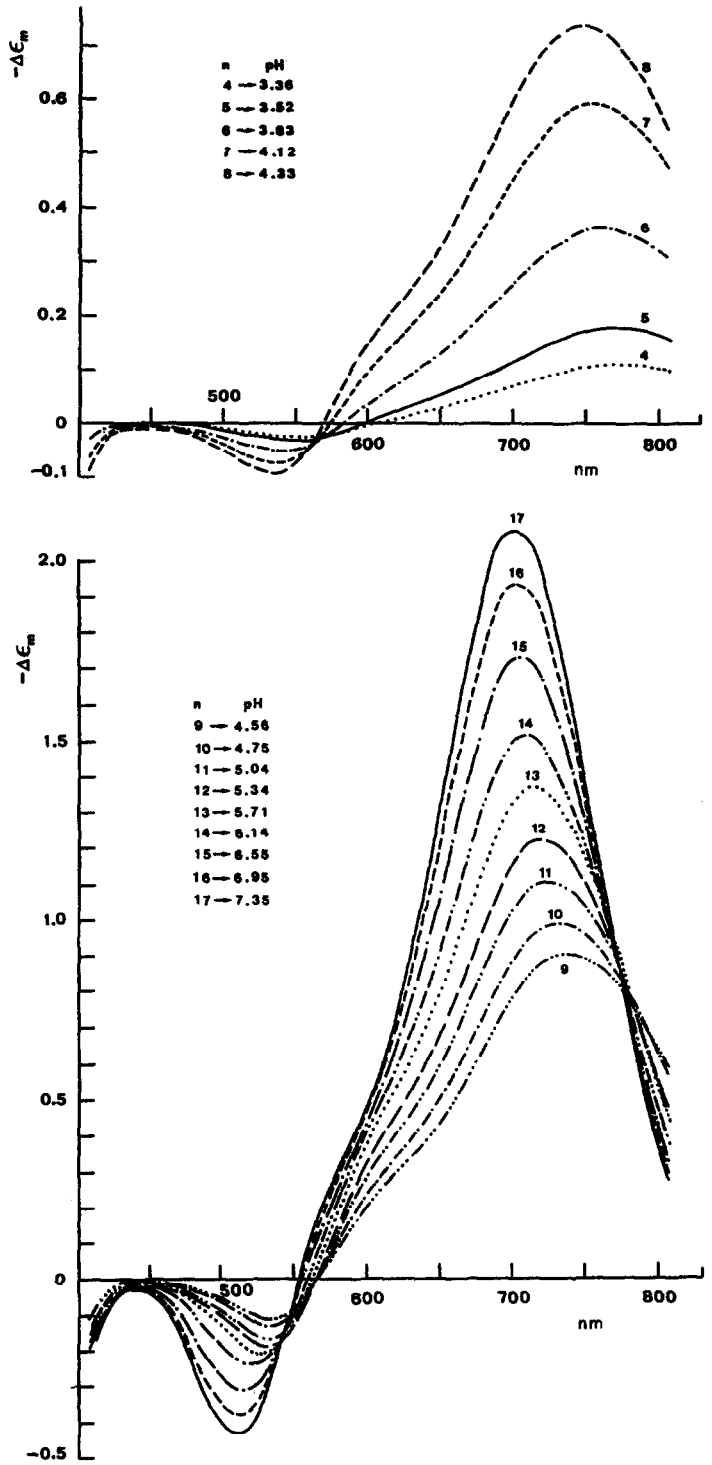

Fig. 1. Circular dichroism spectra of solutions containing L-cys+VO^{2+} with $C_{VO} = 0.01$ M and a ligand-to-metal ratio of 23.7.

visible) spectra practically coincide and are of the same type as those recorded in the system L-cysteine ethyl ester+VO^{2+} for $6 \lesssim pH \lesssim 9$.

The formation constants were calculated using the MINIQUAD,[5] SUPERQUAD[6] and SQUAD[7] programs (the SQUAD program was also used to calculate the individual electronic spectra—isotropic and CD). The calculated $\log \beta_{xyz}$ are summarized in Table 1 and correspond to the general equation:

$$xVO^{2+} + yL^{2-} + zH^{+} \rightleftharpoons (VO)_x(L)_y(H)_z. \quad (1)$$

For each of the log β_{xyz} values, plausible ranges are also given, established by a critical examination of all the calculations.

REFERENCES

1. L. F. Vilas Boas and J. Costa Pessoa, in *Comprehensive Coordination Chemistry* (Edited by G. Wilkinson, R. D. Gillard and J. A. McCleverty), Pergamon Press, Oxford (1987).
2. J. Costa Pessoa, L. F. Vilas Boas, R. D. Gillard and R. J. Lancashire, *Polyhedron* 1988, **7**, 1245.
3. J. Costa Pessoa, L. F. Vilas Boas and R. D. Gillard, *Polyhedron* 1989, **8**, 1173.
4. J. Costa Pessoa, R. L. Marques, L. F. Vilas Boas and R. D. Gillard, *Polyhedron*, submitted for publication.
5. A. Sabatini, A. Vacca and P. Gans, *Talanta* 1974, **21**, 53.
6. P. Gans, A. Sabatini and A. Vacca, *J. Chem. Soc., Dalton Trans.* 1985, 1195.
7. D. J. Legget and W. A. E. McBride, *Analyt. Chem.* 1975, **47**, 1065.

Polyhedron Vol. 8, No. 13/14, pp. 1748–1750, 1989
Printed in Great Britain

0277–5387/89 $3.00+.00
© 1989 Maxwell Pergamon Macmillan plc

ELECTRON SPIN RESONANCE SPECTRAL STUDIES OF VANADYL COMPLEXES WITH SOME SCHIFF BASES

S. S. DODWAD,* R. S. DHAMNASKAR and P. S. PRABHU

Chemistry Department, The Institute of Science, 15 Madam Cama Road, Fort, Bombay 400 032, India

Abstract—Vanadyl complexes with Schiff bases of 2-hydroxy-1-naphthalidene and aryl amines were prepared. The ESR spectra of all the complexes were recorded at room temperature and at liquid nitrogen temperature (177 K), by the method of Kneubuhl, Sands and German. A small polycrystalline sample of the tetracyanoethylene (TCNE) free radical was used as a "g" marker. The spectra were again analysed by the method of Kneubuhl, Sands and Garman. The values $|g|$, $g_{\parallel}$ (parallel), $g_{\perp}$ (perpendicular), $|A|$, $A_{\parallel}$, $A_{\perp}$ were obtained. The expression $h\nu = g\beta H$ was used for evaluating the "g" values. Due to rapid tumbling of the molecules in solution at room temperature the anisotropy is not observed, but it is clearly visible at 177 K. "g" is a function indicating covalency and therefore an order of covalency in the vanadyl complexes has been reported.

The ESR spectra of metal complexes have been studied by various workers.[1-6] Such studies give information regarding the stereochemistry of metal ions in their complexes and the nature of metal–ligand bonding. Detailed ESR studies of metal–oxygen, metal–nitrogen and metal–sulphur bonding have been reported.[7,8] The spectra of vanadyl complexes have been reported by a few authors. The ESR spectra of vanadyl complexes with some Schiff bases have been studied and interpreted by the authors.

EXPERIMENTAL

The vanadyl complexes with Schiff bases of 2-hydroxy-1-naphthalidene-anil and some substituted 2-hydroxy-1-naphthalidene-anils were prepared by refluxing vanadyl sulphate and the corresponding Schiff base in a 1 : 2 ratio in ethanol for 2 h. The complexes were characterized by their electronic and IR spectra, magnetic studies and by conductivity measurements in solution. These properties suggest a square-pyramidal structure for the complexes. The ESR spectra of the vanadyl complexes were recorded on a Varian E-112 spectrometer (X-band) at room temperature (R.T.) and at 177 K in chloroform. A minute polycrystalline sample of the TCNE free radical was used as a "g" marker. All these spectra were run at RSIC, I.I.T., Powai, Bombay. The spectra are represented in Figs 1 and 2.

RESULTS AND DISCUSSION

The ESR spectra were analysed by the method of Kneubuhl,[9] Sands[10] and German *et al.*[11] The "g" values from ESR spectra obtained at R.T. are presented in Table 1. The hyperfine coupling (A) and "g" values at 177 K are presented in Table 2. The ESR spectra (Figs 1 and 2) of the complexes indicate square-pyramidal symmetry. These facts support the observation made on the basis of magnetic and spectral studies. Kivelson and Neiman[3] showed that $g_{\parallel}$ is a moderately sensitive function for indicating covalency. In view of this covalency of the metal–ligand bond in the

Table 1. Room temperature "g" values from ESR spectra of vanadyl complexes

Vanadyl complexes of	$g_{\parallel}$	$g_{\perp}$	$\|g\|$
HNA	1.973	2.008	1.996
HNPCA	1.971	2.001	1.990
HNOCA	1.972	2.000	1.990
HNMCA	1.960	2.005	1.990

* Author to whom correspondence should be addressed.

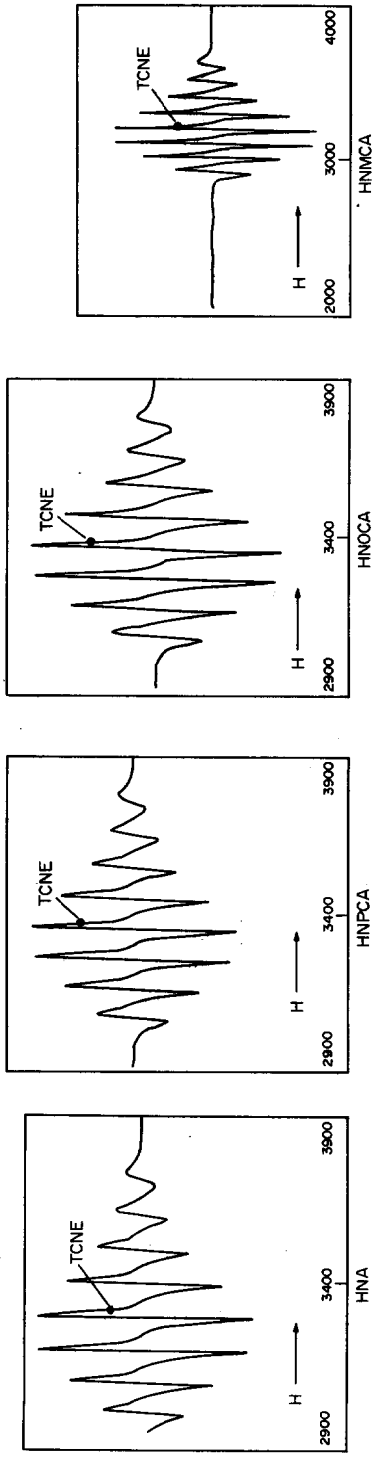

Fig. 1. Room temperature spectra.

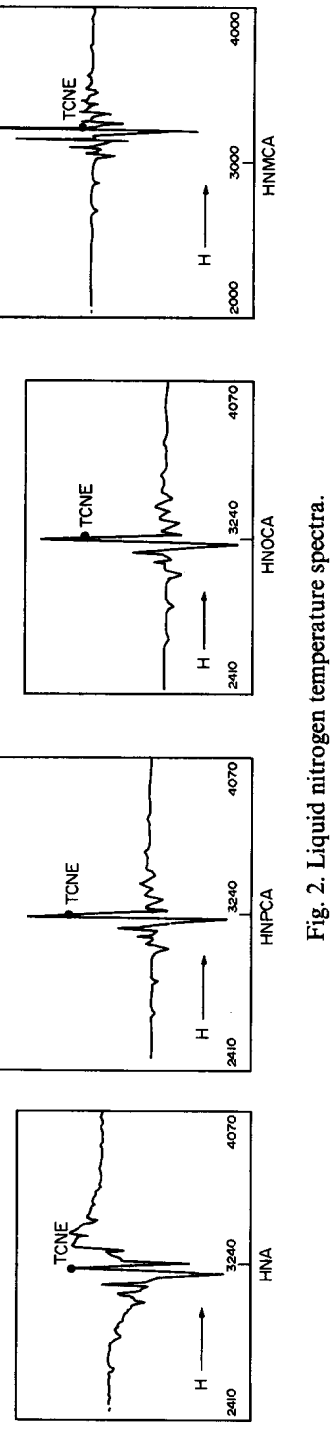

Fig. 2. Liquid nitrogen temperature spectra.

Table 2. Liquid nitrogen temperature "g" values and "A" values of vanadyl complexes

Vanadyl complexes of	$g_\parallel$	$g_\perp$	$\|g\|$	$A_\parallel$	$A_\perp$	$\|A\|$
HNA	1.969	2.005	1.993	158.57	64.28	95.71
HNPCA	1.962	1.991	1.981	171.42	57.85	95.70
HNOCA	1.966	1.993	1.984	171.42	58.57	96.18
HNMCA	1.960	2.005	1.990	174.28	57.14	96.18

present vanadyl complexes the following order is suggested: 2-hydroxy-1-naphthalidene-anil (HNA) > 2-hydroxy-1-naphthalidene-4′-chloro-anil (HNPCA) > 2-hydroxy-1-naphthalidene-2′-chloro-anil (HNOCA) > 2-hydroxy-1-naphthalidene-3′-chloro-anil (HNMCA).

Values for all of the complexes in the polycrystalline state are nearly the same as in chloroform. Therefore it is quite probable that the arrangement of the vanadyl ion in the polycrystalline state and in chloroform may be the same.[8]

There are eight lines in all the spectra taken at room temperature. This is due to hyperfine splitting of ^{51}V whose nuclear spin number $I = 7/2$. This shows that a single vanadium is present in the molecule, i.e. it is a monomer. Since there is rapid tumbling of molecules in solution at room temperature, the anisotropy is not observed and single $|g|$ and $|A|$ values are obtained (Table 1).

The anisotropy is clearly visible in the spectra recorded at 177 K in chloroform. Eight bands each due to $g_\parallel$ and $g_\perp$ are observed separately, the former being fully resolved. $g_\parallel$, $g_\perp$, $A_\parallel$, $A_\perp$, values were measured from the spectra. The values are normal for a square-pyramidal structure.[12–14] From these values, $|A|$ and $|g|$ were calculated using the expressions:

$$|g| = 1/3(g_\parallel + 2g_\perp) \text{ and } |A| = 1/3(A_\parallel + 2A_\perp).$$

The values thus evaluated are shown in Table 2. The values of $|g|$ and $|A|$ calculated from these formulae agree closely with the values measured from room temperature spectra, thus confirming the accuracy of the calculations. The "g" values are all very close to the spin-only value (the free electron value) of 2.0023, suggesting little spin-orbit coupling. The spin Hamiltonian is simple and can be written in terms of "g" and "A" only, as follows:

$$\mathcal{H} = g_\parallel \beta H\zeta S\zeta + g_\perp \beta(HxSx + HySy) + A_\parallel S\zeta I\zeta + A_\perp(SxIx + SyIy).$$

The solution spectra thus agree with the square-pyramidal structure for the vanadyl complexes under study.

REFERENCES

1. M. N. Chary, B. A. Sastry, G. Ponticelli and J. S. Shannon, *Aust. J. Chem.* 1963, **18**, 673.
2. B. J. Hathway and A. A. G. Tomlinson, *Coord. Chem. Rev.* 1970, **5**, 1.
3. D. Kivelson and R. Neiman, *J. Chem. Phys.* 1961, **35**, 149, 158, 162.
4. A. H. Maki and B. R. McGarvey, *J. Chem. Phys.* 1958, **29**, 31, 35.
5. R. P. Singh, K. B. Pandeva and A. Kapahi, *Ind. J. Chem.* 1976, **14A**, 444.
6. D. W. Smith, *J. Chem. Soc. A* 1970, 3108.
7. M. J. Bew, D. E. Billing, R. J. Dudley and B. J. Hathaway, *J. Chem. Soc. A* 1970, 2640.
8. M. N. Chary, K. V. R. Chary, B. A. Sastry and G. Ponticelli, *Ind. J. Pure Appl. Phys.* 1977, **15**, 550.
9. F. K. Kneubuhl, *J. Chem. Phys.* 1960, **33**, 1074.
10. R. H. Sands, *Phys. Rev.* 1955, **99**, 1222.
11. H. R. Garman and J. D. Swalen, *J. Chem. Phys.* 1962, **56**, 3221.
12. A. Syamal and K. S. Kale, *Ind. J. Chem.* 1979, **17A**, 518.
13. L. J. Boucher, E. C. Tynan and T. F. Yen, *Inorg. Chem.* 1968, **7**, 731.
14. L. J. Boucher and T. F. Yen, *Inorg. Chem.* 1969, **8**, 689.

Polyhedron Vol. 8, No. 13/14, pp. 1751–1752, 1989
Printed in Great Britain

0277–5387/89 $3.00+.00
© 1989 Maxwell Pergamon Macmillan plc

REACTIONS OF ALLYLIC COMPOUNDS WITH PHOTO-ACTIVATED MOLYBDENUM HYDRIDE

TAKASHI ITO,* TETSUAKI MATSUBARA, KAZUAKI HAMAMOTO, YOICHIRO YAMASHITA and SUSUMU KURISHIMA

Department of Materials Chemistry, Faculty of Engineering, Yokohama National University, 156 Tokiwadai, Hodogaya-ku, Yokohama 240, Japan

Abstract—$[MoH_4(dppe)_2]$ (**1**) (dppe = $Ph_2PCH_2CH_2PPh_2$) reacted photochemically with allylic esters and carbonates, $RCO_2CH_2CH{=}CH_2$, to give seven-coordinate hydrido-carboxylato complexes, $[MoH(O_2CR)(dppe)_2]$ (**2**), together with H_2 and propene. When the esters with bulky R or carbonates were employed, the yield of propene increased significantly, while that of H_2 remained unchanged. The photoreactions of **1** with N-substituted succinic imides were also investigated.

Transition metal-assisted selective activation of the C—O bond in the unsaturated carboxylic esters and carbonates has been studied in depth for the group 8 transition elements,[1] with reference to their utilization to organic syntheses such as catalytic allyl substitution reactions.[2] In contrast, there have been few such studies with group 6 transition metals,[3] in spite of the recent finding by Trost *et al.* of the metal-dependent chemoselectivity of allylic alkylation.[4]

A yellow suspension of the molybdenum tetrahydride, $[MoH_4(dppe)_2]$ (**1**) (dppe = $Ph_2PCH_2CH_2PPh_2$), in an excess of allyl acetate and benzene as solvent, changed to a deep red solution after irradiation with a 100 W high-pressure mercury lamp *in vacuo* at room temperature. Orange crystals of $[MoH(O_2CCH_3)(dppe)_2]$ (**2**)† were isolated from the solution (yield 45%) and the accompanying formation of H_2 and propene, each in amount corresponding to the yield of **2**, was confirmed by GLC. The reactions of **1** with other allylic esters and carbonates proceeded similarly, affording the corresponding carboxylato and carbonato complexes, respectively [eq. (1)]. The formato complex, **2** (R = H), has been prepared via a different route starting from **1** and carbon dioxide.[5]

$$[MoH_4(dppe)_2] + RCO_2CH_2CH{=}CH_2 \xrightarrow{h\nu} \underset{(1)}{} \underset{(2)}{[MoH(O_2CR)(dppe_2]} + H_2 + CH_3CH{=}CH_2 \quad (1)$$

(R = H, Me, Et, Pr^n, Bu^t, $CH_2{=}C(Me)$, Ph, MeO, EtO).

With the increased bulkiness of R, the yield of propene in the reaction increased significantly, whereas that of H_2 remained unchanged. Thus, when R = Bu^t, 1.01 mol/mol of **1** of propene was evolved together with 0.67 mol of H_2.

The C=C double bond of an allyl group was found to affect the allyl–O bond cleavage, since the C—O bond cleavage did not take place when propyl acetate was employed as the substrate. Considering that **1** has been known to photochemically generate the coordinatively unsaturated intermediate $[MoH_2(dppe)_2]$ (**A** in Scheme 1),[6] we can assume that allyl acetate may coordinate to **A** through its C=C bond to give **B**. Reactions of 1-methylprop-2-enyl acetate and but-2-enyl acetate with **1** under similar conditions, afforded 1-butene and *trans*-2-butene, respectively, as major C_4 products. Absence of the isomerized butenes suggests that the release of olefins occurs directly from the hydrido-σ-allyl intermediate, **C**, without an intervening π-allyl intermediate. The reductive elimination of alkene from **C** yields **2** *via* a monodentate carboxylate, **D**. The less stable carboxylate, **2**, with bulkier R

* Author to whom correspondence should be addressed.

† All new compounds including this complex which were isolated in this study showed satisfactory results in elementary analyses.

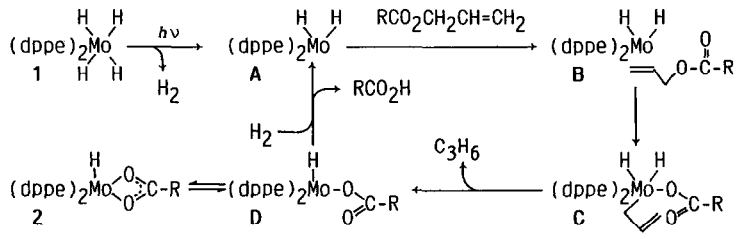

Scheme 1.

groups, may be attacked by H_2 present in the system to regenerate **A**, making the reaction catalytic with respect to the C—O cleavage. The proposed mechanism was supported by the fact that bubbling of H_2 into the reaction system of **1** and allyl pivalate raised the yield of propene to 2.67 mol/mol of **1**, suggesting the possible catalytic hydrogenolysis of allylic esters.

Carboxylato and carbonato complexes, **2**, were moderately air-stable in the solid state and were readily soluble in aromatic hydrocarbons to give reddish-brown air-sensitive solutions. The IR of **2** (R = Me) showed the ν(Mo—H) band at 1870 cm^{-1} and $\nu(CO_2)$ of the bidentate carboxylato ligand at 1540 and 1450 cm^{-1}. The ^1H NMR spectra of **2** (R = Me) in benzene-d_6 at room temperature exhibited a Mo—H signal at δ −6.23 ppm as triplets of triplets (A_2M_2X pattern), suggesting coupling of the hydride with two pairs of magnetically inequivalent ^{31}P nuclei, each consisting of two equivalent ^{31}P (^2J(HP) = 64.8 and 30.7 Hz, respectively). The $^{31}P\{^1H\}$ NMR spectrum of **2** (R = Me) in xylene at room temperature, which showed a pair of triplets at δ 75.4 and 101.0 ppm (with reference to external PPh_3; ^2J(PP) = 17.7 Hz), was consistent with the ^1H NMR results. The spectral characteristics of the other carboxylato and carbonato complexes were very similar to those found for the acetato complex and suggest the pentagonal bipyramidal coordination geometry of the seven-coordinate complex, **2**, at room temperature, which is fluxional in the solution as revealed by the temperature ^1H and $^{31}P\{^1H\}$ NMR spectra.

The preliminary X-ray molecular structural analysis of the single crystal of the carbonato complex, **2** (R = OEt), shows that it possess essentially the same geometry as in solution, although it is considerably distorted from the pentagonal bipyramidal framework.

Reaction of **1** with N-allyloxysuccinic imide in benzene under irradiation resulted in the allyl–O bond cleavage to give a hydrido–oxyimido complex, **3**, together with propene and H_2 [eq. (2)]. Treatment of **3** with CO released N-hydoroxysuccinic imide with the accompanying formation of known $Mo(CO)_2(dppe)_2$:

$$[MoH_4(dppe)_2] \quad \textbf{(1)}$$

$$+\overline{C(O)CH_2CH_2C(O)NO}CH_2CH{=}CH_2 \xrightarrow{h\nu}$$

$$[MoH\{\overline{ONC(O)CH_2CH_2C(O)}\}(dppe)_2] \quad \textbf{(3)}$$

$$+H_2+CH_3CH{=}CH_2. \quad (2)$$

Acknowledgements—This work was supported by a Grant-in-Aid for Scientific Research (No. 63550640) and for Special Project Research (Nos 62215013 and 63106004) from the Ministry of Education, Science and Culture, Japan. T.I. thanks the General Sekiyu Research & Development Encouragement & Assistance Foundation for financial support. The authors thank Dr K. Osakada of Tokyo Institute of Technology, for the single crystal X-ray structural analysis.

REFERENCES

1. See for example, (a) Y. Hayashi, T. Yamamoto, A. Yamamoto, S. Komiya and Y. Kushi, *J. Am. Chem. Soc.* 1986, **108**, 385; (b) T. Yamamoto, M. Akimoto, O. Saito and A. Yamamoto, *Organometallics* 1986, **5**, 1559 and refs cited therein.
2. J. Tsuji, *Organic Synthesis by Means of Transition Metal Complexes*. Springer, Berlin (1975).
3. See for example, B. M. Trost, *Chem. Ber.* 1984, 315.
4. T. Tatsumi, H. Tominaga, M. Hidai and Y. Uchida, *J. Organomet. Chem.* 1981, **215**, 67; T. Tatsumi, H. Tominaga, M. Hidai and Y. Uchida, *J. Organomet. Chem.* 1981, **218**, 177.
5. T. Ito and T. Matsubara, *J. Chem. Soc., Dalton Trans.* 1988, 2241.
6. J. L. Graff, T. J. Sobieralski, M. S. Wrighton and G. L. Geoffroy, *J. Am. Chem. Soc.* 1982, **104**, 7526; M. S. Wrighton, J. L. Graff, R. J. Kazlauskas, J. C. Mitchner and C. L. Reichel, *Pure Appl. Chem.* 1984, **54**, 161.

Polyhedron Vol. 8, No. 13/14, pp. 1753–1755, 1989
Printed in Great Britain

0277–5387/89 $3.00+.00
© 1989 Maxwell Pergamon Macmillan plc

VANADYL AS A DONOR GROUP IN HETEROBIMETALLIC COMPLEXES

B. CASHIN, D. CUNNINGHAM,* J. F. GALLAGHER and P. McARDLE

Department of Chemistry, University College, Galway, Ireland

and

T. HIGGINS

School of Chemical Sciences, Regional Technical College, Galway, Ireland

Abstract—Vanadyl salicylaldimine complexes are capable of forming 1 : 1 adducts with tin Lewis acids, both as a result of ligand oxygen and vanadyl donation to tin; examples of the latter were established by X-ray crystallographic studies.

Despite the very extensive and diverse investigations of vanadyl chemistry, few have addressed one of the fundamental properties of the vanadyl group, viz. its Lewis basicity. Its basic character manifests itself in polymeric structures in which stacking of vanadyl units occurs. Furthermore, there are several reports of vanadyl forming donor bonds to divalent metal ions in heterobimetallic transients, and to ruthenium in a stable vanadium–ruthenium complex, but in no case has this been totally authenticated.[1] This communication describes adduct formation between vanadyl salicylaldimines and tin Lewis acids, in some instances as a result of a ligand oxygen donation, while in others as a result of vanadyl donation to tin; crystallographic studies confirm the latter mode of bonding.

Typical adducts, along with relevant IR data, are in Table 1. Adducts **1**, **5**, **6** and **7** have vanadyl frequencies greater than those of the parent vanadyl complexes, thus consistent with electron drain from vanadium and consequent strengthening of the vanadyl double bond. This observation, coupled with the marked increase of the phenolic C—O stretching frequencies, strongly suggests phenolic oxygen donation to tin.[2] On the other hand, the

Table 1. Vanadyl and phenolic C—O stretching frequency data for the adducts

Compound	ν(V=O) (cm^{-1})	ν(X—O) (cm^{-1})
$SnCl_4 \cdot VO(salen)^a$ (**1**)	1022 (987)[b]	1563 (1532)
$SnPh_2Cl_2 \cdot VO(salen) \cdot H_2O$ (**2**)	928	1539
$SnMe_2Cl_2 \cdot VO(salen)$ (**3**)	943	1537
$SnPh_3Cl \cdot VO(salen)$ (**4**)	940	1538
$SnCl_4 \cdot VO(\alpha,\alpha'\text{-}Me_2\text{-}salen)^c$ (**5**)	1007 (971)	1553 (1538)
$SnPh_2Cl_2 \cdot VO(\alpha,\alpha'\text{-}Me_2\text{-}salen)$ (**6**)	1004	1547
$SnMe_2Cl_2 \cdot VO(\alpha,\alpha'\text{-}Me_2\text{-}salen)$ (**7**)	995	1546
$SnPh_3Cl \cdot VO(\alpha,\alpha'\text{-}Me_2\text{-}salen)$ (**8**)	925	1533
$SnPh_2Cl_2 \cdot VO(3\text{-}MeOsalen) \cdot H_2O^d$ (**9**)	897 (960)	1552 (1554)

[a] salen = N,N′-ethylenebis(salicylideneiminate).
[b] Data in parentheses are for the parent vanadyl salicylaldimine.
[c] α,α'-Me_2-salen = the α,α'-dimethyl analogue of salen.
[d] 3-MeOsalen = the 3,3′-methoxy analogue of salen.

* Author to whom correspondence should be addressed.

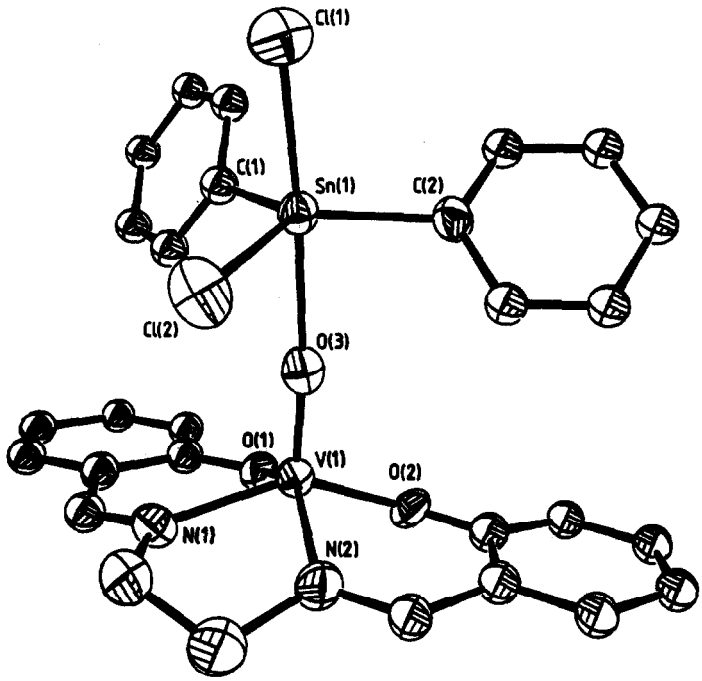

Fig. 1. The asymmetric unit of **2** (the water of crystallization is omitted). Selected parameters: Sn(1)—O(3), 2.335(6); V(1)—O(3), 1.623(6); V(1)—O(1), 1.903(5); V(1)—O(2), 1.902(6); V(1)—N(1), 2.055(7); V(1)—N(2), 2.049(7) Å. Sn(1)—O(3)—V(1) 172.1°.

marked lowering of the vanadyl frequencies (compared to those of the parent vanadyl complexes) coupled with the relatively unperturbed phenolic C—O frequencies for the other adducts of Table 1, suggest vanadyl donation to tin. This was confirmed by X-ray studies for **2** and **9**. Preliminary crystallographic details are shown in Figs 1 and 2, and in Table 2.

There is substantial donation to tin (as indicated by the Sn—O bond lengths[3]) in both adducts,

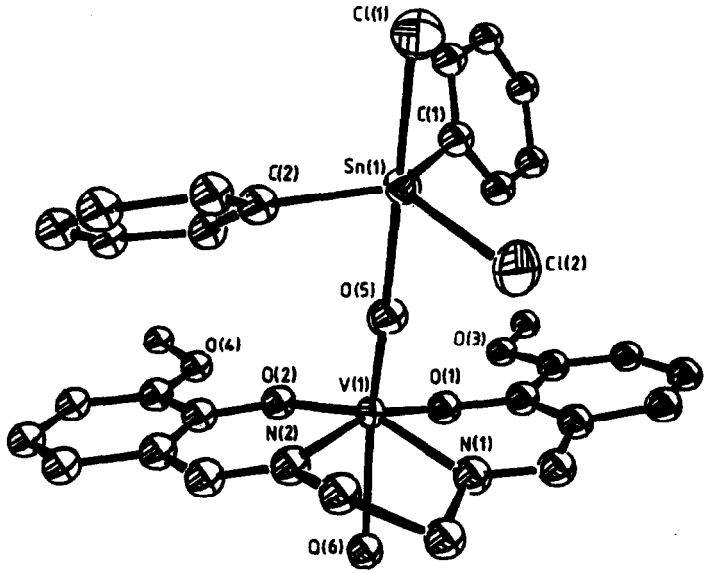

Fig. 2. The asymmetric unit of **9**. Selected parameters: Sn(1)—O(5), 2.307(5); V(1)—O(5), 1.635(5); V(1)—O(1), 1.928(4); V(1)—O(2), 1.919(4); V(1)—O(6), 2.321(5); V(1)—N(1), 2.047(5); V(1)—N(2), 2.054(6) Å. Sn(1)—O(5)—V(1), 163.8(3)°.

Table 2. Preliminary crystallographic details[a]

Compound	2	9
Crystal system	$P\bar{1}$	$P2_1/n$
a (Å)	11.662(2)	13.986(2)
b (Å)	11.757(2)	21.584(3)
c (Å)	12.113(2)	12.098(2)
α (°)	67.09(2)	90
β (°)	82.55(2)	109.80(2)
γ (°)	71.38(2)	90
U (Å^3)	1449.81	3439.51
Z	2	4
D_c (g cm^{-3})	1.59	1.46
F(000)	693.99	2887.95
Crystal dimensions (mm)	$0.35\times0.3\times0.4$	$0.3\times0.4\times0.35$
μ(Mo-K_α) (cm^{-1})	12.94	21.82
Data collected	$+h, \pm k, \pm l$	$\pm h, +k, +l$
Unique reflections	5921	3736
Reflections ($I > 3\sigma I$)(n)	3813	2852
R[b]	0.058	0.045
R_w[c]	0.062	0.053
g	0.00825	0.00484
Goodness-of-fit	0.89	0.90

[a] All measurements performed on an Enraf–Nonius CAD 4 diffractometer with graphite monochromated Mo-K_α radiation ($\lambda = 0.71069$ Å), scan range θ–2θ with $\theta_{max} = 24°$.

[b] $R = \Sigma|F_o - F_c|/\Sigma|F_o|$.

[c] $R_w = \Sigma(|F_o - F_c|\omega^{1/2})/\Sigma(|F_o|\omega^{1/2})$, $\omega = 1/(\sigma^2(F) + gF_o^2)$.

donation being greater in **9** as a result of the *trans* water donation to vanadium. The vanadyl bond lengths are considerably longer than those for either VO(salen) or its sodium adduct (average values 1.588 and 1.584 Å, respectively[4,5]), and there is evidence for a longer V=O bond length in **9** than in **2**; these observations are consistent with the ν(V=O) data of Table 1. Vanadium is 0.6 Å removed from the mean plane defined by the salicylaldimine donor atoms in the case of **2**, and this is essentially as in VO(salen). However, in the case of **9**, vanadium is only 0.334 Å from this plane, a fact which probably reflects the influence of the coordinated water. A most interesting feature of both structures is the close to linear V—O—Sn system which indicates essentially *sp* hybridized oxygen. By contrast, M=O donor moieties, where M is P, As, S, Se, C and N, give M—O—Sn bond angles which are consistent with essentially sp^2 hybridized oxygen.[3]

REFERENCES

1. F. J. Kristine and R. E. Shepherd, *Inorg. Chem.* 1978, **17**, 3145 and refs therein.
2. E. Sinn and C. M. Harris, *Coord. Chem. Rev.* 1969, **4**, 391.
3. J. A. Zubieta and J. J. Zuckerman, *Progr. Inorg. Chem.* 1978, **24**, 251.
4. P. E. Riley, V. L. Pecoraro, C. J. Carrano, J. A. Bonadies and K. N. Raymond, *Inorg. Chem.* 1986, **25**, 154.
5. M. Pasquali, F. Marchetti, C. Floriani and M. Cesari, *Inorg. Chem.* 1980, **19**, 1198.

Polyhedron Vol. 8, No. 13/14, pp. 1756–1757, 1989
Printed in Great Britain

0277-5387/89 $3.00+.00
© 1989 Maxwell Pergamon Macmillan plc

REACTIONS OF MONODINITROGEN COMPLEXES OF MOLYBDENUM. ISOLATION AND CHARACTERIZATION OF HYDRAZIDO(2−) AND MONO- AND DIHYDRIDE COMPLEXES

T. ADRIAN GEORGE* and ROBERT C. TISDALE

Department of Chemistry, University of Nebraska, Lincoln, NE 68588-0304, U.S.A.

Abstract—The mono-N_2 complex *fac*-Mo(N_2)(triphos)(L_2) (**1**), where triphos = $PhP(CH_2CH_2PPh_2)_2$ and L = PMe_2Ph, reacts with HX (X = Br, Cl) to give the hydrazido(2−) complex, [Mo(NNH_2)(η^2-triphos)(PMe_2Ph)$_2$]X (**2**), in which triphos is bidentate. Complex **1** reacts with HBr (1 mol) to give an almost quantitative yield of MoHBr(triphos)(PMe_2Ph) (**3**). With HBr (1 mol), **3** produces MoH_2Br(triphos)(PMe_2Ph).

The bis-N_2 complexes of molybdenum and tungsten occupy a unique position among the N_2 complexes of the transition metal elements, because of their reactivity with (i) acids to afford high yields of ammonia and (ii) alkyl halides to produce organonitrogen ligands.[1-3] Some of these reactions have shown encouraging catalytic behaviour.[4,5] It has been stated that one reason for the unique reactivity behaviour of these complexes is the fact that they contain two rather than the single N_2 ligand found in other metal complexes. Recently we synthesized a series of mono-N_2 complexes of molybdenum and demonstrated that they generate ammonia and hydrazine in an analogous fashion to the bis-N_2 complexes.[6] We now report the isolation and characterization of species formed in the early part of the reactions of acids with *fac*-Mo(N_2)(triphos)(L_2) (**1**).

The reaction of **1** with either 2 mol of HX (X = Br, Cl) in toluene or excess (*ca* 20 mol) of HX in the absence of solvent, afforded a pinkish-yellow hydrazido(2−) complex in moderate yield (eq. 1; X = Br, Cl). Addition of THF to the solid (X = Cl) produced a solution from which **2** (X = Cl) was isolated by the addition of pentane.

$$Mo(N_2)(triphos)(PMe_2Ph)_2 \xrightarrow{HX} [MoX(NNH_2)(\eta^2\text{-triphos})(PMe_2Ph)_2]X \quad (1)$$
(**2**)

Evidence for the formation of a hydrazido(2−) ligand comes from (i) the IR spectrum: ν(NH) 2800–2500 cm^{-1}; 3350 (w) and 3250 (m) cm^{-1} in the BPh_4 salt; (ii) the ^{15}N NMR data: δ −63.34 (m, 1, N_α), −212.30 (m, 1, N_β) which agrees with published data;[7] and (iii) the ^1H NMR spectrum; $\delta(NNH_2)$ 10.6 ppm broad; 5.2 and 5.4 ppm in the BPh_4 and PF_6 salts, respectively.

The ^{31}P NMR spectrum shows the presence of four coordinated phosphorus atoms and with a fifth appearing as a doublet at δ −17.19 ppm, very near to the position for the terminal phosphorus atoms of free triphos. The data suggest that triphos is behaving as a bidentate ligand with P_a and P_b coordinated, and P_c pendant. Therefore, the reaction of **1** is formally analogous to that of the bis-N_2 complexes; a hydrazido(2−) ligand is formed *trans* to the conjugate base of the acid used.[3a,8]

Complex **2** (X = Br) was similarly obtained in greater than 90% yield by thorough extraction of the solid prepared by the reaction of **1** with HBr.

Heating either **6** or **7** in toluene solution resulted in the loss of one PMe_2Ph per mol of complex and the re-coordination of P_c to form *mer*-[MoX(NNH_2)(triphos)(PMe_2Ph)]X.

The reaction of **1** with 1 mol of HBr in benzene at room temperature, rapidly (0.25 h) produced an equimolar mixture of **1** and **2** (X = Br). When the orange solution was allowed to stir for 15 h, a dark green hydride *mer*-Mo(H)Br(triphos)(PMe_2Ph) (**3**) was isolated in quantitative yield. The corresponding chloride, **4**, was obtained in lower yield. Each 16-electron complex exhibited ν(MoH) in the IR spec-

* Author to whom correspondence should be addressed.

trum at 1876 (**3**) and 1874 (**4**) cm^{-1}. The hydride resonance appeared as a split doublet of triplets in the ^1H NMR spectrum at δ −3.60 (**3**) and −3.82 (**4**) ppm, respectively. The ^{31}P NMR spectrum of each complex was interpreted as arising from a coplanar arrangement of *mer*-triphos and PMe_2Ph. Free PMe_2Ph was identified in the ^{31}P NMR spectrum of the reaction mixture and 0.9 mol of N_2 were evolved. The reaction of **3** with HBr (1 mol) resulted in the very rapid formation of the orange eight-coordinate dihydride MoH_2Br_2(triphos)(PMe_2Ph) (**5**). In the IR spectrum ν(MoH) appears at 1878 cm^{-1} and in the ^1H NMR spectrum the hydride resonance occurs as a multiplet at δ −5.90 ppm.

Acknowledgement—We thank the National Science Foundation for their support of this work.

REFERENCES

1. (a) J. Chatt, J. R. Dilworth and R. L. Richards, *Chem. Rev.* 1978, **78**, 589; (b) R. A. Henderson, G. J. Leigh and C. J. Pickett, *Adv. Inorg. Chem. Radiochem.* 1983, **27**, 197; (c) J. Chatt, A. J. Pearman and R. L. Richards, *J. Chem. Soc., Dalton Trans.* 1977, 1852.
2. (a) T. Takahashi, Y. Mizobe, M. Sato, Y. Uchida and M. Hidai, *J. Am. Chem. Soc.* 1980, **102**, 7461; (b) M. Hidai, in *Molybdenum Enzymes* (Edited by T. G. Spiro), Chap. 6. Wiley Interscience, New York (1985).
3. (a) J. A. Baumann, G. E. Bossard, T. A. George, D. B. Howell, L. M. Koczon, R. K. Lester and C. M. Noddings, *Inorg. Chem.* 1985, **24**, 3568; (b) T. A. George, in *Homogeneous Catalysis with Metal Phosphine Complexes* (Edited by L. H. Pignolet), Chap. 13. Plenum Press, New York (1983).
4. (a) W. Hussain, G. J. Leigh and C. J. Pickett, *J. Chem. Soc., Chem. Commun.* 1982, 747; (b) C. J. Pickett, K. S. Ryder and J. Talarmin, *J. Chem. Soc., Dalton Trans.* 1986, 1453; (c) M. Y. Mohammed and C. J. Pickett, *J. Chem. Soc., Chem. Commun.* 1988, 1119.
5. K. Komori, H. Oshita, Y. Mizobe and M. Hidai, *J. Am. Chem. Soc.* 1989, **111**, 1939.
6. T. A. George and R. C. Tisdale, *Inorg. Chem.* 1988, **27**, 2909.
7. (a) J. Chatt, M. E. Fakely, R. L. Richards, J. Mason and I. A. Stenhouse, *J. Chem. Res.* 1979, 322; (b) S. Donovan-Mtunzi, R. L. Richards and J. Mason, *J. Chem. Soc., Dalton Trans.* 1984, 1329.
8. K. Gebreyes, J. Zubieta, T. A. George, L. M. Koczon and R. C. Tisdale, *Inorg. Chem.* 1986, **25**, 405.

Polyhedron Vol. 8, No. 13/14, pp. 1758–1759, 1989
Printed in Great Britain

0277-5387/89 $3.00+.00
© 1989 Maxwell Pergamon Macmillan plc

ZIRCONIUM(III) CHEMISTRY: INFLUENCE OF OLEFINS IN THERMOLYTIC BEHAVIOUR OF $(Cp_2ZrHX)_n$ (X = Cl, CH_2PPh_2)

R. CHOUKROUN,* D. GERVAIS and Y. RAOULT

Laboratoire de Chimie de Coordination du CNRS, 205 route de Narbonne, 31077 Toulouse, France

Abstract—Thermolysis of $(Cp_2ZrHCl)_n$ at 80°C for several weeks results in the formation of the diamagnetic fulvalenide dinuclear zirconium(IV) derivative, $(CpZrCl)_2(C_5H_4—C_5H_4)$, via the intermediate formation of $[CpZrCl(\mu\text{-}\eta^5\text{-}\eta^1\text{-}C_5H_4)]_2$. In the presence of 1,5-COD (COD = cyclooctadiene) the same reaction occurs at room temperature. Under similar conditions, $[Cp_2ZrH(CH_2PPh_2)]_n$ yields paramagnetic zirconium(III) species, $Cp_2Zr(CH_2PPh_2)$; with 1-hexene, at room temperature a labile intermediate, $Cp_2Zr(CH_2PPh_2)$(Hexyl), was observed. These results will be discussed and related to the catalytic activity of both systems for hydrogenation of alkenes.

Improved catalytic performances of $[Cp_2ZrH(CH_2PPh_2)]_n$[1] for hydrogenation of olefins, when compared to the poor result obtained with $(Cp_2ZrHCl)_n$[2] (**1**) under similar experimental conditions (80°C, 40b H_2), led us to study the thermolytic behaviour of both systems in the presence or absence of a substrate.

Thermolysis of $(Cp_2ZrHCl)_n$ (**1**)[1] at 80°C in a sealed tube was followed by ^1H and ^{13}C NMR spectroscopy. The general pathway is reported in Scheme 1. After weeks, the diamagnetic fulvalenide dinuclear zirconium(IV) derivative, $(Cp_2ZrCl)_2(C_5H_4—C_5H_4)$ (**4**),[3] is formed via the intermediate formation of diamagnetic $[CpZrCl(\mu\text{-}\eta^5\text{-}\eta^1\text{-}C_5H_4)]_2$ (**5**). In parallel, diamagnetic $(Cp_2ZrCl)_2$ (**3**)[4] is formed. The same complexes are obtained similarly when thermolytic experiments were carried out in the presence of a stoichiometric amount of $(Cp_2ZrHCl)_n$ and cyclohexene, or starting directly from isolated Cp_2ZrCl (cyclohexyl) (**2b**). In the latter case, evolution of the system occurred after 27 h at 80°C: **2b**: 10%; **3**: 20%; **5**: 50%; **4**: 20%, together with 80% cyclohexane.

In the presence of 1,5-COD, **1** is thermally decomposed at room temperature: **5** is detected after 1 day and is progressively transformed into **4** (quantitatively after 4 weeks). Detection of *ca* 20% of 1,3-COD by C.P.V. (together with cyclooctene, the main organic product of the reaction) may be interpreted by the formation of a labile π-allyl derivative, $Cp_2Zr(\eta^3\text{-}C_8H_{13})Cl$. EPR spectra, registered periodically, show that low intensity signals at the beginning of the reaction become EPR silent after *ca* 1 h of thermolysis.

On the other hand, $[(Cp_2ZrH(CH_2PPh_2)]_n$ (**6**) was previously reported to give rise to zirconium(III) species, Cp_2ZrH and $Cp_2\dot{Z}r(CH_2\dot{P}Ph_2)$,[5] at 80°C (Fig. 1). In the presence of the cyclic

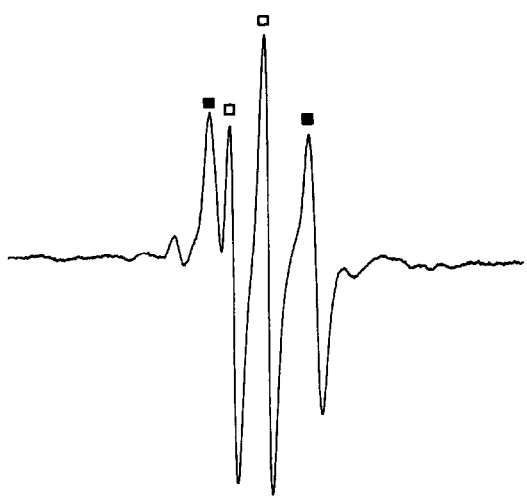

Fig. 1. X band EPR spectrum of $Cp_2ZrH(CH_2\dot{P}Ph_2)$ (**6**) in THF solutions at room temperature, after thermolysis at 80°C: □: Cp_2ZrH (g = 1.987, $a(^1H)$ = 8 G); ■: $Cp_2\dot{Z}r(CH_2\dot{P}Ph_2)$ (g = 1.985, $a(^{31}P)$ = 19.5 G).

* Author to whom correspondence should be addressed.

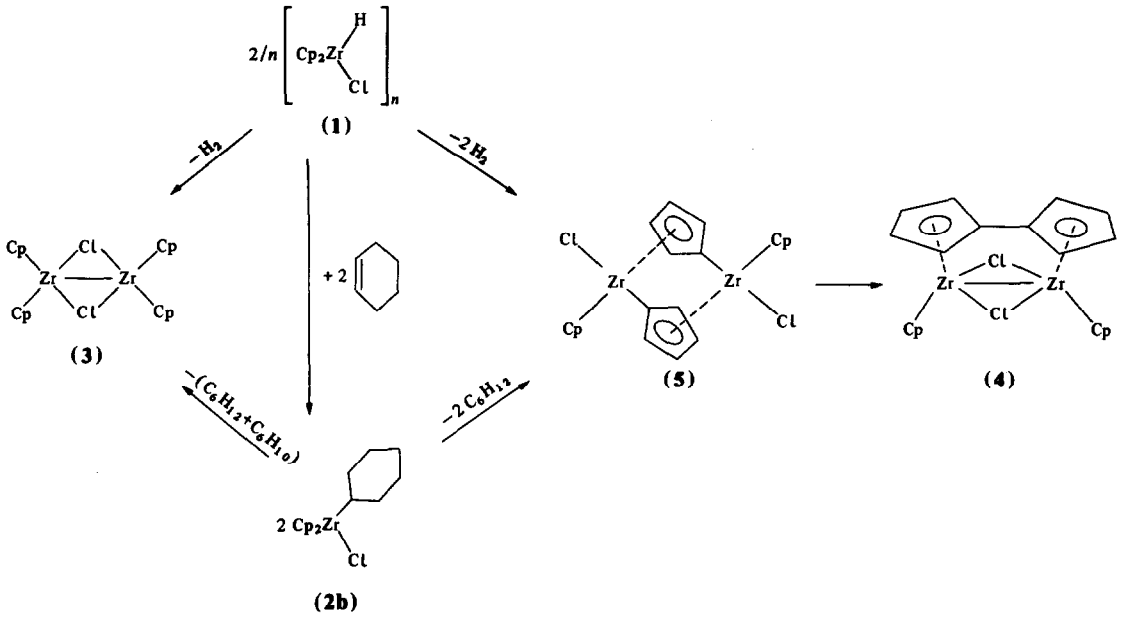

Scheme 1. Pathway of thermolysis of $(Cp_2ZrHCl)_n$ (1).

diene, 1,5-COD, thermolytic decomposition occurs at room temperature to give an intense EPR signal of the chelated zirconium(III) complex, $Cp_2\dot{Z}r(CH_2\dot{P}Ph_2)$,[5,6] and unexploitable ^1H NMR. In the presence of 1-hexene, at room temperature, the course of the reaction, monitored by ^1H and ^{31}P NMR, shows the formation of the zirconium(IV) complex, by insertion of the olefin into the Zr—H bond, which slowly decomposes to give the paramagnetic species, $Cp_2\dot{Z}r(CH_2\dot{P}Ph_2)$, as observed by EPR spectroscopy. At 80°C, the same reaction immediately gives $Cp_2\dot{Z}r(CH_2\dot{P}Ph_2)$.

In summary, thermolytic experiments on **1** give diamagnetic complexes involving C—H activation in the cyclopentadienyl group, whereas **6** gives paramagnetic species stabilized by chelation of the phosphinomethyl group. This may be interpreted as the important role of a paramagnetic zirconium(III) complex in the selective catalytic hydrogenation of cyclodienes.

REFERENCES

1. M. Basso-Bert, R. Choukroun and D. Gervais, *J. Chem. Soc., Chem. Commun.* 1986, 1317.
2. P. C. Wailes, H. Weigold and A. P. Bell, *J. Organomet. Chem.* 1972, **43**, C32.
3. T. Cuenca, W. A. Herrmann and T. V. Ashworth, *Organometallics* 1986, **5**, 2514.
4. T. Cuenca and P. Royo, *J. Organomet. Chem.* 1985, **293**, 61.
5. R. Choukroun and D. Gervais, *J. Chem. Soc., Chem. Commun.* 1985, 224.
6. N. E. Schore, S. J. Young and M. M. Olmstead, *Organometallics* 1983, **2**, 1769.

Polyhedron Vol. 8, No. 13/14, pp. 1760–1761, 1989
Printed in Great Britain

0277–5387/89 $3.00+.00
© 1989 Maxwell Pergamon Macmillan plc

BIMETALLIC COMPLEXES [Zr, Rh]: $Cp'_2Zr(CH_2PPh_2)_2[Rh(\mu\text{-}S\text{-}^tBu)(CO)]_2$ AND $Cp'_2Zr(CH_2PPh_2)_2[Rh(COD)]BPh_4$ ($Cp' = C_5H_4CMe_3$) AND THEIR CATALYTIC BEHAVIOUR AS HYDROFORMYLATION CATALYSTS

R. CHOUKROUN,* D. GERVAIS and C. RIFAÏ

Laboratoire de Chimie de Coordination du CNRS, 205 Route de Narbonne, 31077 Toulouse, France

Abstract—In our strategy, introduction of a substituent into a cyclopentadienyl group could allow new reactivity in the bimetallic system [Zr, Rh], compared with non-substituted cyclopentadienyl analogues [Zr, Rh]. A first step was reached by synthesizing $(C_5H_4CMe_3)_2Zr(CH_2PPh_2)_2$ as a new zirconium-containing diphosphine. The title compounds were isolated and their structural aspects, as well as their catalytic hydroformylation performances, will be presented and compared to previous regular cyclopentadienyl [Zr, Rh] complexes.

The bimetallic d^0–d^8 [Zr, Rh] compounds associating the zirconium-containing diphosphine $Cp_2Zr(CH_2PPh_2)_2$ and various rhodium complexes, present improvements of the catalytic activity for the hydroformylation reaction.[1–3]

In our strategy, introduction of a R substituent in the cyclopentadienyl groups bonded to zirconium in $(C_5H_4R)_2Zr(CH_2PPh_2)_2$ could allow new reactivity and catalytic activity and selectivity of the bimetallic systems [Zr, Rh], compared to the non-substituted cyclopentadienyl analogues. A first step was reached by synthesizing $(C_5H_4CMe_3)_2Zr(CH_2PPh_2)_2$ (**I**) as a new zirconium-containing diphosphine.

Treatment of the binuclear rhodium moiety $[Rh_2(S\text{-}^tBu)_2(CO)_4]$ (**II**) with **I** led to the heterobimetallic complex, **III**, according to the equation:

$$\mathbf{I} + \mathbf{II} \xrightarrow{-2CO} (C_5H_4CMe_3)_2Zr(CH_2PPh_2)_2[Rh_2(S\text{-}^tBu)_2(CO)_2],$$
(III)

which was fully characterized by NMR spectroscopy (^1H, ^{31}P, ^{13}C) and by X-ray structural determination (Fig. 1).

The solid state structure of **III** shows a classical pseudo-tetrahedral arrangement around zirconium (C(11)ZrC(12) = 97.0°) and a classical square-planar coordination geometry around the rhodium atoms, with d(Rh—Rh) = 3.043 Å. This is to be opposed to the analogous system previously reported, $(C_5H_5)_2Zr(CH_2PPh_2)_2[Rh_2(S\text{-}^tBu)_2(CO)_2]$ (**III'**),[4] where the zirconium atom was pentacoordinated (C(11)ZrC(12) = 134.3°) due to interaction with the lone pair of one of the sulphur atoms (Fig. 2).

The catalytic activity in the hydroformylation of 1-hexene of both **III** and **III'** systems has been examined under identical experimental conditions

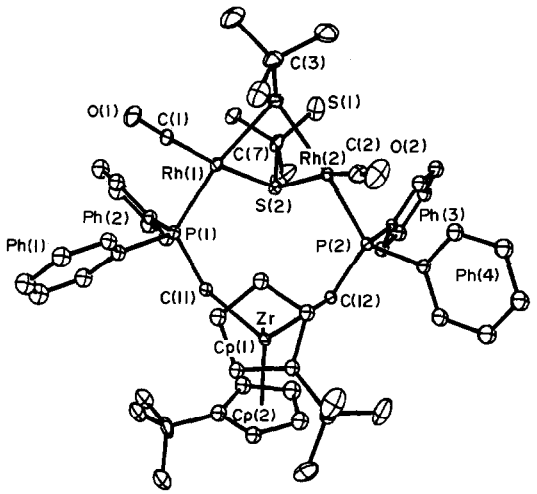

Fig. 1. An ORTEP drawing of $(C_5H_4CMe_3)_2Zr(CH_2PPh_2)_2[Rh_2(CO)_2(S\text{-}^tBu)_2]$ (**III**).

* Author to whom correspondence should be addressed.

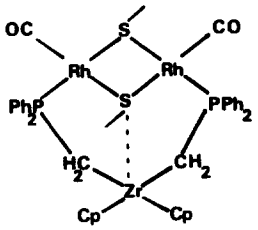

Fig. 2.

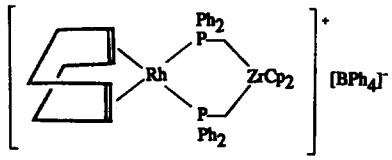

Fig. 4.

(Fig. 3). The catalytic performances are similar (conversion of 1-hexene is nearly quantitative within 2 h and ratio = [heptanal]/[methylhexanal] = 1.9). This may suggest that the donating 'Bu substituent on the cyclopentadienyl groups in **III** counterbalances the donating effect of the sulphur atom on the zirconium centre in **III'** which finally gives the same catalytic results.

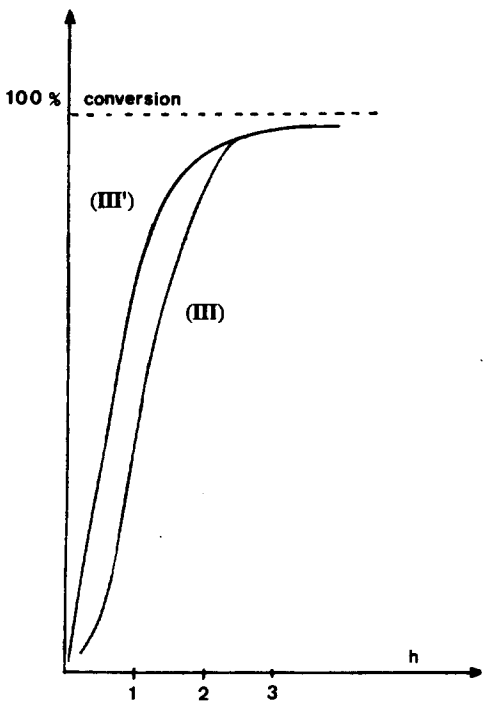

Fig. 3. Hydroformylation of 1-hexene using **III** and **III'** vs time. Conditions: *T*, 80°C; *P*, 20 Bar (1:1 H_2–CO mixture); [1-Hexene]/[Catalyst] = 400; solvent, THF.

Treatment of $Rh(COD)(PPh_3)_2BPh_4$ (**IV**) with **I** led to the crystalline heterobimetallic complex $[(C_5H_4CMe_3)_2Zr(CH_2PPh_2)_2Rh(COD)]^+$ (**V**), fully characterized by NMR spectroscopy (^1H, ^{31}P, ^{13}C). The *cis* position of COD on the rhodium centre forced the *cis* chelation in **V** (Fig. 4) as in **V'**, the homologous complex with regular cyclopentadienyl.[5]

In these cationic systems, in contrast with the non-ionic species previously studied, no improvement of the catalytic performances in the hydroformylation reaction is noted when a zirconium-containing phosphine is added on the rhodium complex.

REFERENCES

1. F. Senocq, C. Randrialiminana, A. Thorez, P. Kalck, R. Choukroun and D. Gervais, *J. Mol. Catal.* 1986, **35**, 213.
2. R. Choukroun, A. Iraqi and D. Gervais, *J. Organomet. Chem.* 1986, **311**, C60.
3. R. Choukroun, D. Gervais, P. Kalck and F. Senocq, *J. Organomet. Chem.* 1987, **335**, C9.
4. R. Choukroun, D. Gervais, J. Jaud, P. Kalck and F. Senocq, *Organometallics* 1986, **5**, 67.
5. R. Choukroun, A. Iraqi, C. Rifaï and D. Gervais, *J. Organomet. Chem.* 1988, **353**, 45.

Polyhedron Vol. 8, No. 13/14, pp. 1762–1764, 1989
Printed in Great Britain

0277–5387/89 $3.00+.00
© 1989 Maxwell Pergamon Macmillan plc

NEW APPROACHES TO PREPARING HETEROBINUCLEAR μ-SULPHIDO COMPLEXES: MODELS FOR STEPS IN HYDRODESULPHURIZATION PROCESSES

P. M. BOORMAN,* J. F. FAIT and G. K. W. FREEMAN

Department of Chemistry, University of Calgary, Calgary, Alberta, Canada T2N 1N4

Abstract—In an attempt to mimic the possible reactions of M—H groups with organosulphur molecules on the surface of hydrodesulphurization catalysts, early transition metal hydrido complexes have been shown to react with thiolato complexes of molybdenum(IV) to eliminate an alkane. The reaction of Cp_2NbH_3 with $Mo(^tBuS)_4$, for example, produces isobutane and a mixture of sulphido-bridged heterobimetallic complexes. The crystal structure of one of these, $Cp_2Nb(\mu\text{-}S)_2Mo(\mu\text{-}S)_2NbCp_2$, confirms that the above type of reaction can generate new cluster molecules.

Reactions in which transition metal centres activate carbon–sulphur bonds are of relevance to the catalytic hydrodesulphurization of fossil fuels.[1] The activation of hydrogen on the surface of the metal sulphide catalysts is now believed to occur via the heterolytic cleavage of the H_2 bond, yielding two types of hydrogen species on the surface, namely protonic —SH and hydridic M—H groups. The activity of the —SH groups has received considerable attention, but the role of the M—H groups has been less studied.[2]

We have been studying systems in which the elimination of an alkane from hydrido(thiolato) or hydrido(thioether) complexes might occur from either one or two metal centres, as per the following equations:

$$H—M—SR \longrightarrow M{=}S + RH \qquad (1a)$$

$$H—M—SR_2 \longrightarrow M—SR + RH \qquad (1b)$$

$$M'—H + M—SR \longrightarrow M{=}S + RH + [M'] \longrightarrow M—S—M' \qquad (2a)$$

$$M'—H + M—SR_2 \longrightarrow M—SR + RH + [M'] \longrightarrow M—(SR)—M'. \qquad (2b)$$

In an earlier paper[3] we reported reactions of type (1b) and we have subsequently turned our attention to the hydride/thiolate reactions. The difficulty of preparing hydrido(thiolato) complexes is well documented,[4] and reactions of type (1a) have been difficult to observe. The twin objectives of activating the C—S bond and having a hydridic M—H group on the same metal centre are, in practice, incompatible and hence we have begun a programme to study heterobimetallic systems which could allow distinct sites for hydride generation and C—S bond activation.[5]

The reaction between the early transition metal hydride Cp_2ZrH_2[6] and $Mo(S^tBu)_4$[7] proceeds via the desired pathway, yielding ^tBuH (isobutane) and an insoluble material containing sulphide ligands. Definitive proof of the hydride's involvement in the production of the isobutane was obtained by using Cp_2ZrD_2, which produced ^tBuD upon reaction with $Mo(^tBuS)_4$. The reaction of Cp_2NbH_3[8] with $Mo(S^tBu)_4$ yields similar results, generating isobutane and an unstable bimetallic species whose ^1H NMR spectrum is consistent with that expected for the compound $Cp_2Nb(\mu\text{-}S)_3Mo(S^tBu)$. Although this species has not been isolated in a crystalline form, from the reaction solution we obtained crystals of the new trinuclear complex, $Cp_2Nb(\mu\text{-}S)_2Mo(\mu\text{-}S)_2NbCp_2$ (**1**). This compound is obtained in relatively low yield and another, polymeric, sulphido-bridged species is also produced. The precise decomposition pathway by which **1** arises from the initial reaction product is not yet known. The structure of **1** is shown in Fig. 1. The (formally) niobium(III) centres might be expected to form metal–metal bonds to the molybdenum(VI) atom. The observed Nb—Mo distances (2.995(9) Å) and the angles subtended at the bridging sulphurs (av. = 79.0(2)°) suggest a weak metal–metal interaction.[9] This compound is intrinsically interesting

* Author to whom correspondence should be addressed.

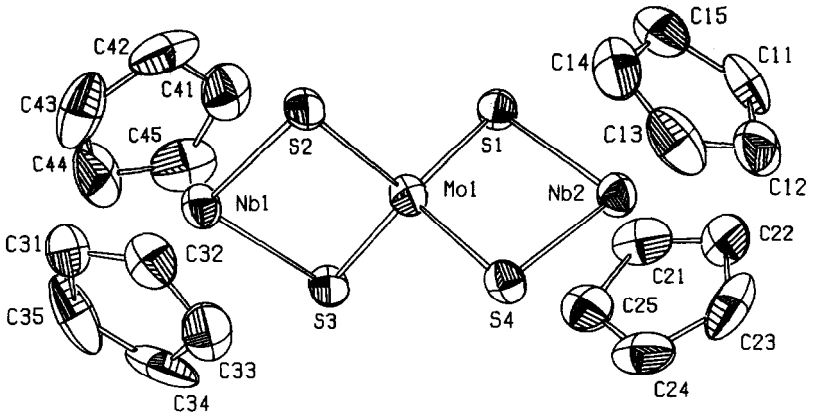

Fig. 1. ORTEP view of the structure of $[(Cp_2Nb)_2MoS_4]$ (**1**), showing the atom labelling scheme. Selected bond lengths (Å) and angles (°):

Mo—Nb(1)	2.9955(9)	Mo—S(4)	2.236(2)	Nb(2)—Cp(1)	2.127(4)
Mo—Nb(2)	2.9959(9)	Nb(1)—S(2)	2.466(2)	Nb(2)—Cp(2)	2.103(4)
Mo—S(1)	2.243(2)	Nb(1)—S(3)	2.462(2)	Nb(1)—Cp(3)	2.101(5)
Mo—S(2)	2.248(2)	Nb(2)—S(1)	2.464(2)	Nb(1)—Cp(4)	2.099(4)
Mo—S(3)	2.243(2)	Nb(2)—S(4)	2.447(2)		

S(1)—Mo—S(4)	107.18(6)	Nb(2)—S(4)—Mo	79.40(5)
S(2)—Mo—S(3)	107.61(6)	S(1)—Mo—S(3)	109.18(7)
S(1)—Nb(2)—S(4)	95.45(6)	S(3)—Mo—S(4)	109.88(6)
S(2)—Nb(1)—S(3)	94.71(6)	S(2)—Mo—S(4)	110.35(6)
Nb(1)—S(2)—Mo	78.73(5)	Cp(1)—Nb(1)—Cp(2)	133.3(4)
Nb(1)—S(3)—Mo	78.93(5)	Cp(3)—Nb(1)—Cp(4)	131.1(4)
Nb(2)—S(1)—Mo	78.89(6)		

in its own right, but more important in the present context, it confirms that the synthetic objective of this work has been realized. The interaction between a strongly hydridic metal hydride and the activated carbon–sulphur bond of a coordinated thiolate has been demonstrated to proceed with C—S bond cleavage, thus illustrating one of the fundamental steps in the HDS process.[1]

The availability of suitable terminal metal thiolate complexes is very limited and hence we proceeded to examine another of the Otsuka[10] molybdenum thiolates, *cis*-$Mo(S^tBu)_2(^tBuNC)_4$. This complex was expected to give more soluble binuclear products, should its thiolates be sufficiently activated to react with hydrido complexes. The following, slow, reaction was observed over a 72 h period:

$$Cp_2NbH_3 + \textit{cis}\text{-}Mo(S^tBu)_2(^tBuNC)_4 \longrightarrow Cp_2Nb(H)(\mu\text{-}S)_2Mo(^tBuNC)_4 + 2\,^tBuH.$$

The possible synthetic value of this type of reaction for making polynuclear sulphido complexes is an obvious secondary benefit of this work. To date, however, we have been unsuccessful in promoting the cleavage of any aryl–sulphur bonds. The additional strength of the C—S bonds in these systems has been noted previously to lead to different reactivity in metal thiolate complexes.[11]

The choice of the metal, as well as its oxidation state, is critically important for both the hydride and the thiolate complex. Thus, for example, the nickel(II) complexes such as [Ni(diphos)(SCH_2CH_2S)] are unreactive towards Cp_2ZrH_2. Similarly, late transition metal hydrides have not been observed to effect cleavage of the S—C bonds in $Mo(S^tBu)_4$. These observations support our earlier hypothesis about factors which control the reactivity of metal thiolates.

EXPERIMENTAL

(1) *Reaction between* Cp_2ZrH_2 *and* $Mo(S^tBu)_4$

A benzene solution of $Mo(S^tBu)_4$ was added to a stirred suspension of the Cp_2ZrH_2 (or Cp_2ZrD_2) in benzene (approx. 1 : 1 molar ratio). Immediate darkening of the solution occurred, accompanied by precipitation of a fine brown precipitate. The insolubility of the precipitate precluded its recrystallization or complete spectroscopic characterization. By carrying out the same reaction in C_6D_6 in

a sealed NMR tube, we were able to confirm the production of isobutane (^{t}BuH and ^{t}BuD), indicating the successful demonstration of the feasibility of the target reaction. ^{1}H NMR, (C_6D_6)^{t}BuH, 0.907 ppm (d, $J = 6.61$ Hz); ^{t}BuD, 0.90 ppm (t, $J = 1.92$ Hz).

(2) *Reaction between* Cp_2NbH_3 *and* $Mo(S^tBu)_4$

The Cp_2NbH_3 reagent has the advantage of being soluble in benzene, hence reaction control and product separation were expected to be easier than for Cp_2ZrH_2, which is polymeric. A 1:1 reaction between Cp_2NbH_3 and $MO(S^tBu)_4$ in benzene appeared to be complete within 1 h, yielding a red–brown precipitate and a dark brown solution. Collection of the precipitate followed by extraction with $CHCl_3$ gave a green–brown solution, from which crystals of $[(Cp_2Nb)_2MoS_4]$ (**1**) were obtained. The residue, after this extraction was completed, was analysed for carbon and hydrogen, and from the *ca* 1:1 ratio obtained appeared to contain only Cp as the organic fragment. Its total insolubility suggested a polymeric sulphido-bridged species.

The dark brown supernatant reaction solution yielded a solid product when treated with hexane, whose elemental analyses and ^{1}H NMR spectrum were consistent with its formulation as $Cp_2Nb(\mu\text{-}S)_3Mo(S^tBu)$. Found: C, 32.70; H, 3.87. Calc: C, 33.33; H, 3.80%. ^{1}H NMR ($CDCl_3$): 1.54 (s, 9H), 5.50 ppm (s, 10H). The instability of this compound in solution suggests that it is the precursor to the μ-sulphido species which precipitate out of solution over a period of time.

(3) *Reaction between* Cp_2NbH_3 *and* $Mo(S^tBuNC)_4$

A benzene solution of Cp_2NbH_3 was added to solution of *cis*-$Mo(S^tBu)_2(^t BuNC)_4$ in the same solvent (1:1). A slow colour change from green to red–brown over *ca* 72 h was accompanied by the precipitation of a red crystalline product. This product is believed to be $Cp_2Nb(H)(\mu\text{-}S)_2Mo(^t BuNC)_4$, the hydride being implied by three inequivalent resonances for coordinated ^{t}BuNC ligands. ^{1}H NMR ($CDCl_3$): 5.68 (s, 10H), 1.64 (s, 9H), 1.63 (s, 9H), 1.38 ppm (s, 18H). Isobutane was observed to be produced in this reaction, as before.

(4) *Crystal structure of* $[(Cp_2Nb)_2MoS_4]\cdot CHCl_3$ (**1**)

A crystal of **1** was mounted on a glass fibre and coated with epoxy resin. Crystal data: $C_{21}H_{21}Cl_3S_4MoNb_2$, $M = 789.75$, orthorhombic, space group $P2_12_12_1$, $a = 11.895(2)$, $b = 12.002(2)$, $c = 18.855(4)$ Å, $V = 2695.614$ Å^3, $D_{calc} = 1.946$ g cm^{-3}, $Z = 4$, λ(Mo-K_α radiation, graphite monochromator) = 0.71069 Å, $2\theta_{max} = 60°$, total number of reflections measured = 8348, number of unique reflections, $[I > 2\sigma(I)] = 4020$, number of variables = 280, $R = 0.043$, $R_w = 0.035$.

Acknowledgements—This work was supported by an operating grant (to P.M.B.) and an infrastructure grant from the Natural Sciences and Engineering Research Council of Canada.

REFERENCES

1. (a) R. R. Chianelli, *Catal. Rev.-Sci. Engng* 1984, **26**, 361; (b) P. Grange, *Catal. Rev.-Sci. Engng* 1980, **22**, 135.
2. (a) S. Harris and R. R. Chianelli, *J. Catal.* 1984, **86**, 400; (b) J. T. Roberts and C. M. Friend, *J. Am. Chem. Soc.* 1986, **108**, 7204; (c) S. C. Huckett, N. N. Sauer and R. J. Angelici, *Organometallics* 1987, **6**, 591; (d) M. Rakowski-Dubois, M. C. VanDerveer, D. L. Dubois, R. C. Haltiwanger and W. K. Miller, *J. Am. Chem. Soc.* 1980, **102**, 7456; (e) S. Vasudevan, J. M. Thomas, C. J. Wright and C. Sampson, *J. Chem. Soc., Chem. Commun.* 1982, 418; (f) D. A. Lesch, J. W. Richardson Jr, R. A. Jacobson and R. J. Angelici, *J. Am. Chem. Soc.* 1984, **106**, 2901; (g) J. W. Hachgenei and R. J. Angelici, *Angew. Chem. Int. Ed. Engl.* 1987, **26**, 909.
3. P. M. Boorman, K. J. Moynihan, V. D. Patel and J. F. Richardson, *Inorg. Chem.* 1985, **24**, 2989.
4. (a) N. J. Lazarowych and R. H. Morris, *J. Chem. Soc., Chem. Commun.* 1987, 1865; (b) C. Shortman and R. L. Richards, *J. Organomet. Chem.* 1985, **C3**, 285; R. A. Henderson, D. L. Hughes, R. L. Richards and C. Shortman, *J. Chem. Soc., Dalton Trans.* 1987, 1115.
5. (a) L. Gelmini and D. W. Stephan, *Organometallics* 1988, **7**, 849; (b) J. H. Sinfelt (Ed.), *Bimetallic Catalysts: Discoveries, Concepts and Applications.* John Wiley, New York (1983).
6. P. C. Wailes and H. Weigold, *J. Organomet. Chem.* 1970, **24**, 405.
7. S. Otsuka, M. Kamata, K. Hirotsku and T. Higuchi, *J. Am. Chem. Soc.* 1981, **103**, 3011.
8. J. A. Labinger and R. Bau (Ed.), *Adv. Chem. Ser.* 1978, **167**, 149.
9. Angles and distances observed for $[Cp_2ZrS]_2$, where no Zr—Zr interaction is proposed, are considerably larger. d(Zr—Zr) = 3.530(2) Å, (Zr—S—Zr) = 90.4°; F. Bottomley, D. F. Drummond, G. O. Egharevba and P. S. White, *Organometallics* 1986, **5**, 1620.
10. M. Kamata, T. Yoshida, S. Otsuka, K. Hirotsku and T. Higuchi, *J. Am. Chem. Soc.* 1981, **103**, 3572.
11. R. D. Adams, D. A. Katachira and L. Yang, *Organometallics* 1982, **1**, 235.

Polyhedron Vol. 8, No. 13/14, pp. 1765–1766, 1989
Printed in Great Britain

0277–5387/89 $3.00+.00
Maxwell Pergamon Macmillan plc

SOLID SOLUTION FORMATION IN ALUMINA–CHROME REFRACTORIES

T. J. DAVIES,* H. G. EMBLEM, C. S. NWOBODO, A. A. OGWU and V. TSANTZALOU

Manchester Materials Science Centre, University of Manchester/UMIST, Manchester, U.K.

Abstract—Preparative procedures, densification, grain growth and change in corundum lattice dimensions in sintered compacts made from chromium(III)oxide/aluminium(III) oxide mixtures were evaluated in a study of alumina–chrome refractories. High energy milling using A-17 "reactive" alumina gave densification at low temperature and the most rapid grain growth, also (by Weibull analysis) the least variability in modulus of rupture, 7% W/W chromium(III)oxide giving minimum strength. XRD confirmed solid solution formation, the corundum lattice dimensions contracting with 7% W/W chromium(III)oxide, other compositions giving lattice expansion. The modulus of rupture at 1150°C for a series of ethyl–silicate-bonded alumina refractories containing 5–12% W/W chromium(III)oxide and fired at 1700°C was also a minimum at 7% W/W chromium(III)oxide.

Resistance to thermal shock and reduction of slag attack can both be achieved by incorporating chromium(III)oxide in alumina or mullite bodies. Examples are the addition of fine chrome to coarse alumina or mullite to reduce slag attack[1] and mullite–chrome systems[2] in which an iron–chromite ore is the source of chrome. Incorporating fine chromium(III)oxide into ethyl–silicate-bonded refractories[3] reduces slag attack and improves resistance to thermal shock. In the present work, preparative procedures, densification, grain growth and change of corundum lattice dimensions in sintered compacts, made from chromium(III)oxide/aluminium(III)oxide mixtures, were evaluated in a study of alumina–chrome refractories.[4–6]

The aluminium(III)oxide materials were MA95 (BA Chemicals Ltd, average particle size 4 μ angular) and A17 "reactive" alumina (Alcoa, average particle size 2μ, round). The chromium(III)oxide (British Chrome and Chemicals Ltd) had an average particle size of 0.4 μ. Materials containing 3, 7 or 14 wt% chromium(III)oxide were prepared by ball-milling, high energy milling, or grinding in a tungsten carbide mill. These mixtures were compacted at 97.5, 120 or 310 MPa and sintered for various times at 1600, 1650 or 1700°C. XRD measurements were used to evaluate changes in the corundum lattice dimensions.

For both aluminium(III)oxide materials, better blending was obtained with increasing chromium(III)oxide content, the highest "green" density being observed with 14 wt% chromium(III) oxide, because the fine chromium(III)oxide particles fill the spaces between the aluminium(III) oxide particles. As expected, high compaction pressure gave high green density. The microstructure observed in the sintered compact depends on (i) composition, (ii) the milling process, (iii) sintering temperature and (iv) sintering time. At a short sintering time, the method of mixing is not important. High energy milling using A17 "reactive" material gave densification at low temperatures and the most rapid grain growth during sintering. For MA95 material the milling process is important, probably because this material has a larger primary particle size. In general, this material gives sintered compacts with lower density.

XRD studies of compacts prepared from A17 "reactive" material with 14 wt% chromium(III) oxide, sintered at 1600°C for 0.5 h, show them to contain free chromium(III)oxide. Other sintered compacts do not contain free chromium(III)oxide. The corundum peak width increases as the chromium(III)oxide content increases. The corundum lattice parameters, a and c, for sintered compacts

* Author to whom correspondence should be addressed.

containing 3 or 14 wt% chromium(III)oxide, increase by 0.02–0.45%, depending on the sintering temperature and the sintering time. However, for sintered compacts containing 7 wt% chromium (III)oxide the parameters decrease, especially in compacts fired at 1650°C, where the *a* parameter decreases by 2.13%. Compacts prepared from MA95 material behave similarly. The results confirm the formation of a chromium(III)oxide/aluminium(III)oxide solid solution. Compacts prepared with MA95 material lose chromium on sintering at high temperature for long periods, suggesting that chromium volatilization is faster than solid solution formation, which would be expected because of the large primary particle size of the MA95 material.

The modulus of rupture of sintered compacts was determined at ambient temperature (three point loading; Instron testing machine). Weibull analysis[7] showed that compacts prepared from high energy milled materials had the highest Weibull modulus (*ca* 17), hence the least variability in strength. Weibull modulus values of 5–20 are common for ceramic materials,[8] the higher values indicating less strength variability. A typical value for the modulus of rupture of a compact prepared from material high energy milled and sintered at 1650°C for 5 h would be 205 MPa.

The modulus of rupture of a series of ethyl–silicate-bonded alumina refractories prepared[9] from coarse alumina grain, and a "fines" fraction comprising fine aluminium(III)oxide plus fine chromium(III)oxide, was determined at 1150°C. The refractories contained from 5 to 12 wt% chromium(III)oxide and were fired at 1700°C prior to determining the modulus of rupture, which was a minimum at 7 wt% chromium(III)oxide. The occurrence of the minimum strength at this level of chromium(III)oxide coincides with the change in aluminium(III)oxide lattice parameters found in aluminium(III)oxide/chromium(III)oxide compositions containing 7 wt% chromium(III)oxide. This change would alter the elasticity of the refractory body, which could reduce the modulus of rupture.

REFERENCES

1. Kyushu Taika-Renga and Kabushiki Kaisha, *British Patent* 1,533,890 (1978).
2. C. Taylor's Sons Company, *British Patent* 1,421,418 (1976).
3. R. D. Shaw and C. Shaw, *British Patent* 1,313,498 (1973).
4. C. S. Nwobodo, MSc dissertation. UMIST, Manchester (1984).
5. A. A. Ogwu, MSc dissertation. UMIST, Manchester (1985).
6. V. Tsantzalou, MSc thesis. UMIST, Manchester (1984).
7. W. A. Weibull, *J. Appl. Mech.* 1951, **18**, 293.
8. R. W. Davidge, *Mechanical Behaviour of Ceramics*, pp. 133–139. Cambridge University Press, London (1980).
9. H. G. Emblem, *Trans. J. Brit. Ceram. Soc.* 1975, **74**, 223.

Polyhedron Vol. 8, No. 13/14, pp. 1767–1769, 1989
Printed in Great Britain

0277–5387/89 $3.00+.00
© 1989 Maxwell Pergamon Macmillan plc

NEW EARLY TRANSITION METAL COMPLEXES STABILIZED BY TERDENTATE ANIONIC P-BLOCK DONOR LIGANDS

A. A. DANOPOULOS, P. G. EDWARDS,* J. S. PARRY and A. R. WILLS

School of Chemistry, University of Wales College of Cardiff, P.O. Box 912, Cardiff CF1 3TB, Wales, U.K.

Abstract—A wide range of new classes of early transition metal and actinide compounds have been isolated with the new amido and phosphido ligands $^{-}E(CH_2CH_2E'R_2)_2$ (where R = alkyl; E = N, E′ = N, P, As and E = P, E′ = P). Structural and chemical properties of metal derivatives are seen to be sensitive to variations in the ligands. Dependent on the nature of the donors, monomeric complexes with pendant bases may be obtained. These may be used as precursors for the preparation of homo- and heterobimetallic compounds.

Our recent studies[1] of complexes with chelating terdentate amido ligands {of the type $HE(CH_2CH_2E'R_2)_2$ (**1**), where E = N, E′ = N, R = Et, **1** = NNN} have shown the potential of these systems to stabilize unusual ternary amido–halide and organometallic compounds. Since partial substitution of halide ligands on metal centres is possible with this amine, without the common event of redistribution to binary amido complexes[2] that occurs with other amido• ligands, we now have potential access to classes of tractable derivatives previously rare or unattainable. In view of this we have exended our study to applications of new terdentate amidophosphine (**1** = PNP, E = N, E′ = P, R = Me, Et, ^{i}Pr) and amidoarsine (**1** = ANA, E = N, E′ = As, R = Me, Et) ligands. To our knowledge, the only similar ligand system that has been used for the stabilization of transition metal amido complexes (for metals in groups IV and VII) is the series $(R_2PCH_2Si(Me)_2)_2NH$ (R = alkyl or aryl).[3]

With PNP ligands, vanadium(III) appears to behave as it does with NNN ligands. Interaction of $Cl_3V \cdot 3THF$ with $LiN(CH_2CH_2PMe_2)_2$ in THF enables the isolation of the purple crystalline $Cl_2VN(CH_2CH_2PMe_2)_2$ (**2**). An identical material may be isolated from $VCl_3(NMe_3)_2$ by a similar procedure. Attempts to obtain crystals suitable for X-ray crystallography have so far been unsuccessful. It is likely, however, that the stereochemistry about vanadium is similar to that in the analogous amine complex $Cl_2VN(CH_2CH_2NEt_2)_2$,[1a] where the three anionic donors occupy the equatorial sites of a distorted trigonal bipyramid, with the neutral donors in the apical positions.

Compound **2** may be readily converted to organometallic derivatives by the action of organolithium reagents. Thus with methyl lithium, an oil, $Me_2VN(CH_2CH_2PMe_2)_2$ (**3**), may be obtained from petroleum ether. The compound decomposes upon attempted distillation and is very soluble in apolar solvents. With aryl lithium reagents, **2** provides the similar diarylvanadium amides, $Ar_2VN(CH_2CH_2PMe_2)_2$ [Ar = Ph (**4**), 2-$CH_3C_6H_4$ (**5**)]. Compounds **4** and **5** are both readily prepared from **2** in THF and both may be obtained as emerald green crystals in good yield from petroleum ether. Attempts to obtain X-ray crystallographic data have so far failed. The compounds are very air-sensitive, especially in solution, becoming brown and eventually yellowish, presumably due to oxidation to vanadium(V) species. As well as by analytical data,† **4** and **5** are additionally identified by IR spectra that show characteristic aryl absorbancies.

For zirconium(IV), the behaviour with PNP ligands differs from that with NNN ligands. For the latter, the only well-characterized amido halide is $(NNN)ZrCl_3$,[1] whereas with the PNP phosphines (**1**, R = Me, Et and ^{i}Pr), compounds formulated as

* Author to whom correspondence should be addressed.

† All new complexes reported here provide satisfactory elemental analyses.

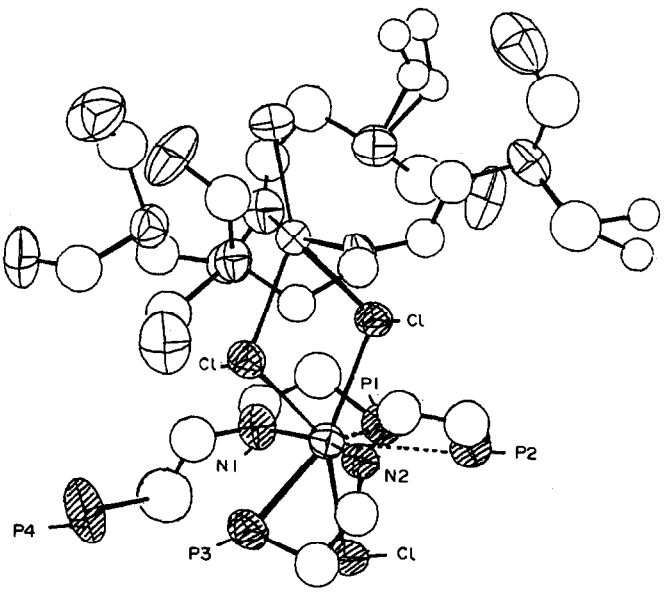

Fig. 1. The structure of $\{[(Et_2PCH_2CH_2)_2N]_2UCl_2\}_2$.

$(PNP)_2ZrCl_2$ (**6**) are the only isolable species. In each case these complexes contain pendant tertiary phosphine donors (by variable temperature ^{31}P NMR). Exchange between free and coordinated phosphine is rapid at room temperature for compounds **5**, where R = Me, Et, and is slow for **6**, where R = ^{i}Pr. With uranium(IV), the compound $[(PNP)_2UCl_2]$ (**7**, R = Et) shows similar behaviour (labile phosphines) and the X-ray crystal structure[4] (Fig. 1) confirms the presence of pendant phosphines in the solid state.

To date we have only a preliminary insight into the properties of ANA ligands. In general with vanadium(III), titanium(III) and zirconium(IV), the products are difficult to isolate. An exception is the well-characterized niobium(IV) dimer, $(ANANbCl_3)_2$ (**8**). This diamagnetic orange crystalline material is far more stable than any other derivatives of this ligand, has magnetically equivalent ligands (NMR) and preliminary X-ray crystallographic studies[5] (Fig. 2) reveal a symmetrical arrangement for the ligands with bridging nitrogen atoms. With NNN ligands under the same conditions, the monomeric, paramagnetic (d^1) $(NNN)_2NbCl_2$[1] is obtained; there is no evidence of a binuclear compound under any conditions.

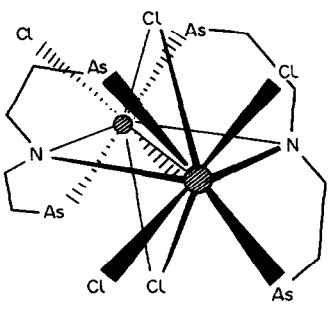

Fig. 2. The structure of $[(Me_2AsCH_2CH_2)_2NNbCl_3]_2$. For clarity, methyl groups have been omitted and ⌒ = —CH_2CH_2—.

As these studies have demonstrated that these ligands may provide compounds with pendant donors, potentially available for coordinating further metal ions and that they may support bimetallic compounds, we have extended this study to the phosphidophosphine ligands (**1** = PPP, E = P, E′ = P, R = Me, Et). As we know that zirconium provides PNP complexes with pendant phosphines, we have attempted the preparation of zirconium PPP complexes. Whereas NNN enables the isolation of only the "mono" ligand derivative and PNP provides only the "bis" ligand derivative despite variations in the stoichiometry of reagents, with PPP both yellow $(PPPZrCl_3)_2$ (**9**) and red $(PPP)_2ZrCl_2$ (**10**) may be prepared by control of stoichiometry and isolated as crystalline solids. The former compound **9** is a dimer (cryoscopy), has magnetically equivalent ligands with bridging phosphido atoms (^{31}P NMR) and is far more stable than **10**. The "bis" ligand derivative (**10**) has pendant phosphines (^{31}P NMR) and reacts with MCl_4 (M = Zr, Hf) and AlX_3 (X = Cl, Br) to give high yields of the 1:1 adducts, each of which contains bridging phosphides (^{31}P NMR).

REFERENCES

1. (a) A. R. Wills, P. G. Edwards, R. L. Short and M. B. Hursthouse, *J. Chem. Soc., Chem. Commun.* 1988, 115; (b) A. R. Wills and P. G. Edwards, *J. Chem. Soc., Dalton Trans.* 1989, in press.
2. M. F. Lappert, P. P. Power, A. R. Sanger and R. C. Shrivastava, in *Metal and Metalloid Amides*. Ellis Horwood, Chichester (1980).
3. M. D. Fryzuk and K. Bhangu, *J. Am. Chem. Soc.* 1988, **110**, 961; M. D. Fryzuk, A. Carter and A. Westerhaus, *Inorg. Chem.* 1985, **24**, 642.
4. A. A. Danopoulos, P. G. Edwards, M. Harman and M. B. Hursthouse, 1989, submitted for publication.
5. P. G. Edwards, A. R. Wills, M. Harman and M. B. Hursthouse, unpublished results.

Polyhedron Vol. 8, No. 13/14, pp. 1770–1773, 1989
Printed in Great Britain

0277–5387/89 $3.00+.00
Maxwell Pergamon Macmillan plc

COORDINATION OF THE MACROCYCLIC THIOETHER 1,4,7-TRITHIACYCLONONANE (TTCN) TO CHROMIUM(3+) AND TO DIMOLYBDENUM(2+) DI-ACETATO BRIDGED MOLECULES

HEINZ-JOSEF KÜPPERS* and KARL WIEGHARDT

Ruhr-Universität Bochum, D4630 Bochum, F.R.G.

Abstract—Although chromium(III) is a hard acid and the macrocyclic thioether 1,4,7-trithiacyclonone (TTCN) a soft base, the following compounds could be synthesized: $[Cr(TTCN)Cl_3]$, $[Cr(TTCN)(SO_3CF_3)_3]$ and $[Cr(TTCN)_2]^{3+}$ (a rare example of a $Cr^{III}(thioether)_6$ coordination sphere). Comparison with the analogous 1,4,7-triazacyclononane (TACN) complexes shows that the bonding is relatively weak and the ligand-field splitting small. This is in contrast to the bonding properties of these ligands in "late" transition metals and results from the lack of π-donor capability of the Cr^{3+} centre. TTCN forms several dimeric di-acetato bridged complexes with the $(Mo_2)^{4+}$ unit. The unique interaction of steric and electronic effects of TTCN causes the unusual coordination of a tridentate ligand to the $[Mo_2(\mu\text{-}OAc)_2]^{2+}$ unit.

The coordination chemistry of the crown thioether 1,4,7-trithiacyclononane (TTCN) has been intensively investigated in the last few years. Although TTCN forms stable complexes with nearly every transition metal,[1] only a few examples of the coordination to early transition metals are known.[2]

We report here the reaction of TTCN with chromium(III) and with the $[Mo_2(\mu\text{-}OAc)_2]^{2+}$ unit.

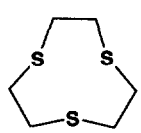

TTCN

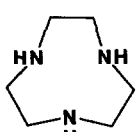

TACN

The strong coordination of TTCN to the "late" transition metals comes from both its steric (*endo*-conformation) and electronic properties (π-acceptor capability). The question arises, whether this soft base can coordinate to a hard acid such as Cr^{3+} (class A metal).

The reaction of $[Cr(H_2O)_6]Cl_3$ (in MeCN) or $[Cr(THF)_3Cl_3]$ (in dioxane) with TTCN yields $[Cr(TTCN)Cl_3]$. This blue–violet complex is inert and sparingly soluble in common solvents. Stirring in trifluoromethanesulphonic acid for some hours, at room temperature, results in the substitution of chloride by triflate to form blue–green $[Cr(TTCN)(SO_3CF_3)_3]$. The IR spectrum confirms monodentate coordination of triflate. In solution, solvent molecules such as CH_3CN, $(CH_3)_2CO$, DMF, THF replace the labile triflate ligands.

All attempts to synthesize the bis-TTCN—Cr^{3+} complex by the reaction of excess TTCN with Cr^{III} salts of $Cr(TTCN)X_3$ ($X = Cl^-$; $CF_3SO_3^-$; solvent) in solution, under various conditions, failed. Only the heating of a mixture of solid $[Cr(H_2O)_6](ClO_4)_3$ and solid TTCN results in the pink, very explosive $[Cr(TTCN)_2](ClO_4)_3$, which decomposes in a few seconds in solution. All compounds gave suitable elemental analyses and IR spectra. The magnetic moments of $\mu_{eff} = 4.1$ BM ($[Cr(TTCN)Cl_3]$) and $\mu_{eff} = 3.9$ BM ($[Cr(TTCN)(SO_3CF_3)_3]$) are in the normal range of octahedral Cr^{3+} compounds.

The electronic spectra allow the discussion of the binding properties in these compounds. For octahedral chromium(III) complexes one expects three bands which correspond to the transitions $^4A_{2g} \rightarrow {}^4T_{2g}(\nu_1)$, $^4A_{2g} \rightarrow {}^4T_{1g}(F)(\nu_2)$ and $^4A_{2g} \rightarrow {}^4T_{1g}(P)(\nu_3)$. In most cases ν_3 is obscured by charge-transfer bands. From the spectra the ligand-field splitting, $10Dq$, can be calculated. The data for the Cr—TTCN complexes and some other Cr^{3+} compounds are summarized in Table 1.

* Author to whom correspondence should be addressed.

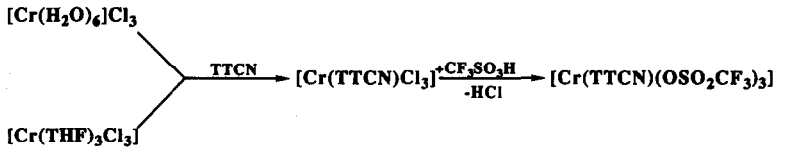

Scheme 1.

Substitution of three Cl^- by TTCN increases $10Dq$ only slightly. Further substitution of Cl^- by a second TTCN molecule does not affect $10Dq$. This can be explained by the loss of charge neutralization, which leads to an increasing positive charge at the chromium centre. This in turn, effects a contraction of the chromium *d*-orbitals and, therefore, decreases their interaction with the ligand orbitals.[8]

The value of $10Dq$ also does not change if one TTCN is replaced by three dimethylsulphide or tetrahydrothiophene ligands. In addition, the open chain ligand $S(CH_2)_3SCH_3$ causes a larger ligand-field splitting than TTCN. Accordingly, the macrocyclic nature of TTCN does not enhance the apparent ligand-field strength (cf. $[Ni(TTCN)_2]^{2+}$). The ring size and the rigidity of the TTCN-macrocycle obviously does not allow optimal interaction between the thioether donor atoms and the relatively large Cr^{3+} centre.

The two pairs, $[Cr(TTCN)_2]^{3+}/[Cr(TACN)_2]^{3+}$ and $[Cr(TTCN)(SO_3CF_3)_3]/[Cr(TACN)(SO_3CF_3)_3]$ (which was synthesized by the reaction of $[Cr(TACN)(Br)_3]$[9] with trifluoromethanesulphonic acid), allow a comparison of the different effect of TTCN and TACN (TACN = 1,4,7-triazacyclononane). Therefore TTCN generates a smaller ligand-field splitting than does TACN for Cr^{3+}; for Fe^{2+}, Co^{3+} or Ni^{2+} the opposite is true.[1a]

The data can be summarized in the following spectrochemical series: $Cl^- < S(CH_3)_2$, TTCN, THT, THF $< H_2O < NH_3 <$ TACN.

In case of Cr^{3+} coordination, TTCN binds weakly. Although the ring size and the rigidity do not allow optimal interaction between the Cr^{3+} and the ligand orbitals, $[Cr(TTCN)_2]^{3+}$ is a rare case of $Cr^{III}(thioether)_6$ coordination. The great difference in the bonding properties of TTCN of chromium(III) and "late" transition metals seems to be the lacking of *p*-donor capability of the metal centre.

Another interesting reaction of TTCN with an early transition metal is the reaction of TTCN with the dimeric molybdenum(II) unit, $[Mo_2(\mu\text{-}OAc)_2]^{2+}$. The chemistry of $(Mo_2)^{4+}$ has been intensively studied in the last 25 years. However, only a few compounds with tridentate coordinated ligand are known.[10] Is TTCN with its unique characteristics[1,2] able to form such a class of coordination compounds?

In 1986, Garner and Clegg described the synthesis of $[(CH_3CN)_3Mo(\mu\text{-}OAc)_2Mo(CH_3CN)_3](BF_4)_2$ (**1**) [see Fig. 1(a)] from $[Mo_2(\mu\text{-}OAc)_4]$ with Me_3OBF_4.[11] This compound proved to be an ideal starting material for the synthesis of several dimeric Mo^{II}—TTCN complexes.

Stirring of **1** with excess TTCN for 12 h at room temperature, in MeCN, leads to the red–violet

Table 1. Absorption maxima and $10Dq$ data of some Cr^{3+} complexes

Compound	ν_1 (nm)	ν_2 (nm)	$10Dq$ (kK)	Reference
$[CrCl_6]^{3-}$	760	535	13.1	3
$[Cr(TTCN)Cl_3]$	690	493	14.5	
$[Cr(S(CH_3)_2)_3Cl_3]$	690	523	14.5	4
fac-$[Cr(THT)_3Cl_3]$	685	480	14.6	5
$[Cr(THF)_3Cl_3]$	675	494	14.8	4
$[Cr(TTCN)(OSO_2CF_3)_3]$	635	475	15.8	
$[Cr(TACN)(OSO_2CF_3)_3]$	523		19.1	
$[Cr(TTCN)_2]^{3+}$	685	509	14.6	
$[Cr(TACN)_2]^{3+}$	439	340	22.7	6
$[Cr(S(CH_2)_3SCH_3)_2]^{3+}$	636	436	15.7	3
$[Cr(H_2O)_6]^{3+}$	575	406	17.4	3
$[Cr(NH_3)_6]^{3+}$	464	350	21.6	7

THT: tetrahydrothiophene.

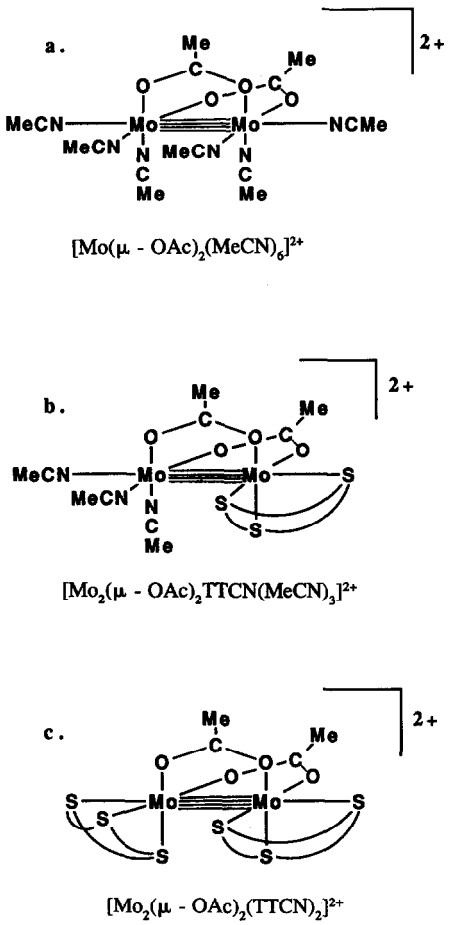

Fig. 1. The structures (b) and (c) are proposed, while (a) has been proved by X-ray analysis.[11]

$[(TTCN)Mo(\mu\text{-}OAc)_2Mo(CH_3CN)_3](BF_4)_2$ (**2**) [see Fig. 1(b)]. Substitution of the last MeCN ligands requires refluxing of **2** in CH_2CCl_2 with excess TTCN. This procedure forms the blue–violet $[(TTCN)Mo(\mu\text{-}OAc)_2Mo(TTCN)](BF_4)_2$ (**3**) [see Fig. 1(c)]. Compound **2** reacts in aqueous solution with KX to form the blue $[(TTCN)Mo(\mu\text{-}OAc)_2Mo(X)_2]$ ($X = Cl^-, Br^-, SCN^-, OCN^-$) (**4**), (**5**), (**6**), (**7**), respectively. The IR spectra of these compounds prove the retention of the bridging $[Mo_2(\mu\text{-}OAc)_2]$ unit. Also, the elemental analyses and the electronic spectra further support this structural suggestion.

In electronic spectra a band at about 500 nm, corresponding to the transition $\delta \rightarrow \delta^*$ in $(Mo_2)^{4+}$ compounds, is expected. The data of these absorption bands are listed in Table 2.

A comparison of the absorption bands of $[Mo_2(\mu\text{-}OAc)_2(CH_3CN_3)_4]^{2+}$ and $[Mo_2(\mu\text{-}OAc)_2(CH_3CN_3)_6]^{2+}$ shows a shift to lower energy. The reason for this is probably the weakening of the metal–metal bond by the coordination of axial MeCN ligands. The bonding of a ligand *trans* to the Mo—Mo axis weakens the metal–metal σ-bonding and therefore increases the metal–metal distance, which causes a smaller overlapping of the π- and δ-orbitals. Substitution of the MeCN ligands by TTCN in **2** and **3** further weakens the metal–metal bonding because of the larger π-acceptor capability of the thioether donor atoms compared to the N-atoms of MeCN. Coordination of ligands with even larger π-acceptor capability, e.g. CO and NO, cleaves the metal–metal bond.[10]

In the solid state the compounds **2**–**7** are stable in air for several weeks. Dissolved in non-coordinating solvents, however, **3**, **6** and **7** rapidly react with air.

The $[Mo_2(\mu\text{-}OAc)_2(TTCN)]$ compounds are an example of the coordination of tridentate ligands to the $[Mo_2(\mu\text{-}OAc)_2]$ unit. This unusual coordination sphere further exemplifies the unique chelating ability of TTCN caused by the interaction of its steric and electronic properties.

Acknowledgements—One of us (H.J.K.) would like to thank Dr S. R. Cooper for helpful discussions and S. Stötzel for synthesizing compounds **4** and **7**.

Table 2. Absorption maxima of $[Mo_2(\mu\text{-}Ac)_2]$ compounds

Compound	λ_{max} (nm) [ε ($dm^3\ mol^{-1}\ cm^{-1}$)]	Reference
$[(CH_3CN)_2Mo(\mu\text{-}OAc)_2Mo(CH_3CN)_2]^{2+}$	526(844)[a]	11
$[(CH_3CN)_3Mo(\mu\text{-}OAc)_2Mo(CH_3CN)_3]^{2+}$	531(925)[a]	11
$[(TTCN)Mo(\mu\text{-}OAc)_2Mo(CH_3CN)_3]^{2+}$	537(1100)[a]	
$[(TTCN)Mo(\mu\text{-}OAc)_2Mo(TTCN)]^{2+}$	550(990)[b]	
$[(TTCN)Mo(\mu\text{-}OAc)_2Mo(SCN)_2]$	586[c]	
$[(TTCN)Mo(\mu\text{-}OAc)_2Mo(OCN)_2]$	600[c]	
$[(TTCN)Mo(\mu\text{-}OAc)_2Mo(Br)_2]$	596[c]	
$[(TTCN)Mo(\mu\text{-}OAc)_2Mo(Cl)_2]$	621[c]	

[a] In MeCN.
[b] In acetone.
[c] Solid state reflectance spectrum.

REFERENCES

1. (a) K. Wieghardt, H.-J. Küppers and J. Weiss, *Inorg. Chem.* 1985, **24**, 3067; (b) H.-J. Küppers, A. Neves, C. Pomp, D. Ventur, K. Wieghardt, B. Nuber and J. Weiss, *Inorg. Chem.* 1986, **25**, 2400; (c) M. N. Bell, A. J. Blake, H.-J. Küppers, M. Schröder and K. Wieghardt, *Angew. Chem. Int. Edn Engl.* 1987, **26**, 250; (d) H.-J. Küppers, K. Wieghardt, B. Nuber and J. Weiss, *Z. Anorg. Allg. Chem.* 1989, in press; (e) S. R. Cooper, *Accts Chem. Res.* 1988, **21**, 141; (f) W. N. Setzer, C. A. Ogle, G. S. Wilson and R. S. Glass, *Inorg. Chem.* 1983, **22**, 266; (g) A. J. Blake, A. J. Holder, T. I. Hyde and M. Schröder, *J. Chem. Soc., Chem. Commun.* 1987, 987.
2. (a) M. T. Ashby and D. L. Lichtenberger, *Inorg. Chem.* 1984, **24**, 636; (b) H. Elias, G. Schmidt, H.-J. Küppers, M. Saher, K. Wieghardt, B. Nuber and J. Weiss, *Inorg. Chem.* 1989, in press.
3. A. L. Hale and W. Levason, *J. Chem. Soc., Dalton Trans.* 1983, 2569.
4. R. J. H. Clark and G. Natile, *Inorg. Chim. Acta* 1970, **4**, 533.
5. J. Hughes and G. R. Willey, *Inorg. Chem. Acta* 1974, **11**, L25.
6. K. Wieghardt, W. Schmidt, W. Herrmann and H.-J. Küppers, *Inorg. Chem.* 1983, **22**, 2953.
7. C. K. Jörgensen, *Adv. Chem. Phys.* 1963, **5**, 33.
8. L. R. Gray, A. L. Hale, W. Levason, F. P. McCullough and M. Webster, *J. Chem. Soc., Dalton Trans.* 1984, 47.
9. P. Chaudhuri, M. Winter, H.-J. Küppers, K. Wieghardt, B. Nuber and J. Weiss, *Inorg. Chem.* 1987, **26**, 3302.
10. F. A. Cotton and R. A. Walton, *Multiple Bonds Between Metal Atoms*. Wiley, New York (1982).
11. G. Pimblett, C. D. Garner and W. Clegg, *J. Chem. Soc., Dalton Trans.* 1986, 1257.

Polyhedron Vol. 8, No. 13/14, pp. 1774–1777, 1989
Printed in Great Britain

0277–5387/89 $3.00+.00
© 1989 Maxwell Pergamon Macmillan plc

TRIPHOSPHANATO ($R_3P_3^{2-}$), PRIMARY PHOSPHIDO (RPH^-) AND DIPHOSPHANATO (DIPHOSPHENE) ($R_2P_2^{2-}$) COMPLEXES OF ZIRCONIUM AND HAFNIUM METALLOCENES

BRIAN L. BENAC and RICHARD A. JONES†

Department of Chemistry, The University of Texas at Austin, Austin, TX 78712-1167, U.S.A.

Abstract—A variety of triphosphanato ($R_3P_3^{2-}$), primary phosphido (RPH^-) and diphosphanato (diphosphene) ($R_2P_2^{2-}$) derivatives of zirconium and hafnium (**I–IV**) have been prepared via reactions of primary phosphides LiPH(R) (R = Ph, *t*-Bu) with Cp_2MCl_2 (Cp = η^5-C_5H_5, C_5Me_5, $C_5H_3(SiMe_3)_2$). The products depend on the steric bulk of the P—R group and the Cp (or substituted Cp) group. When Cp = C_5H_5 or C_5Me_5 and R = Ph, triphosphanato complexes of type **I** are produced (E. Hey, S. G. Bott and J. L. Atwood, *Chem. Ber.* 1988, **121**, 561). When R = *t*-Bu, types **II** and **III** are also formed. For Cp = $C_5H_3(SiMe_3)_2$ diphosphanato complexes **IV** and the diphosphides **III** are formed.

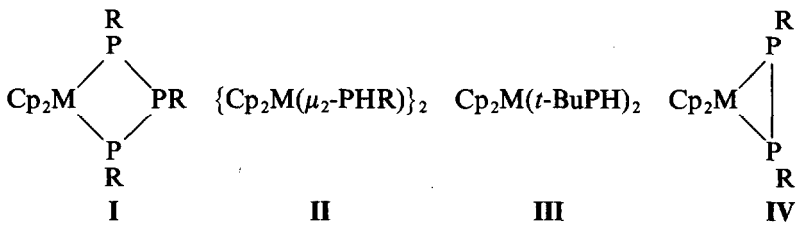

There are several classes of diorganophosphide (R_2P^-) and related complexes of the group 4 metals. Homoleptic complexes such as [Li(DME)][Hf(PCy_2)$_5$] (Cy = *c*-C_6H_{11}) were reported by Baker *et al.*[1] In addition, Bercaw and co-workers have described complexes of mono-pentamethylcyclopentadienyl (Cp*) hafnium such as Cp*HfCl{P(CMe_3)$_2$}$_2$.[2] The largest class of group 4 metal phosphides is comprised of dicyclopentadienyl derivatives of the type $Cp_2M(PRR')_2$ (Cp = C_5H_5; M = Zr, Hf; R, R′ = alkyl, aryl, $SiMe_3$).[3]

The $Cp_2M(PR_2)_2$ compounds have been used primarily as diphosphine ligands in heterobimetallic complexes such as $Cp_2Hf(\mu\text{-}PEt_2)_2Ni(CO)_2$,[4] $Cp_2Zr(\mu\text{-}PEt_2)_2Rh(\eta\text{-indenyl})$[5] and $Cp_2Zr(\mu\text{-}P(C_6H_5)_2)_2Pt\{P(C_6H_5)_3\}$.[6] The heterobimetallics, $Cp_2M(\mu\text{-}PR_2)_2Mo(CO)_4$ (M = Ti, Zr), had been previously prepared by Johannsen and Stelzer[7] and were studied further by others.[8] The only reported primary phosphides of the group 4 metals are the heterobimetallics, $Cp_2M\{\mu\text{-}PH(C_6H_5)\}_2Mo(CO)_4$, made by Johannsen and Stelzer by treating Cp_2MCl_2 (M = Ti, Zr) with *cis*-$Mo(CO)_4(PhPHLi)_2$.[7] We chose to investigate the chemistry of primary phosphido (RPH^-) ligands, since these should possess an additional site of reactivity in the P—H bond which could lead to unusual new phosphinidene (RP^{2-}) complexes.

It has been known for some time that the reaction of Cp_2MCl_2 (Cp = C_5H_5; M = Zr, Hf) with LiPH(Ph) gives the triphosphanato metallocycles $Cp_2M[P(Ph)]_3$ (**Ia**: M = Zr; **Ib**: M = Hf).[9] Even treatment of $Cp_2Zr(CH_3)_2$ and $Cp_2Zr(CH_3)Cl$ with $PhPH_2$ gives only $Cp_2Zr[P(Ph)]_3$ (**Ia**) and no primary phosphido zirconium complexes.[9] These types of compounds **I** were previously made by the reaction of Cp_2MCl_2 with $K_2(PR)_n$ (M = Ti, Zr, Hf).[10]

In our hands, the reaction of Cp_2MCl_2 with LiPH(C_6H_5) also gives the triphosphanato complexes, **Ia** (Cp = C_5H_5; M = Zr; R = C_6H_5) and **Ib** (Cp = C_5H_5; M = Hf; R = C_6H_5). However,

† Author to whom correspondence should be addressed.

Table 1. ^{1}H NMR data for new compounds[a]

Compound	Colour	Signal	^{1}H (δ)	J_{PH} (Hz)
$\{Cp_2Zr(\mu_2$-*t*-BuPH)$\}_2$ (**II**)	Red	C_5H_5	4.99 s	—
		t-BuP*H*	3.00 d	259.22
		*t-Bu*PH	1.45 d	11.71
Cp_2Hf(*t*-BuPH)$_2$ (**IIIa**)	Red	C_5H_5	5.60 t	1.71
		t-BuP*H*	4.10 d	242.28
		*t-Bu*PH	1.43 d	11.76
$Cp^*_2Zr[P(C_6H_5)]_3$ (**Ie**)	Red	$(C_6H_5)P$	6.8–8.25 m	—
		$C_5(CH_3)_5$	1.83 s	—
		$C_5(CH_3)_5$	1.49 s	—
$Cp^*_2Hf[P(C_6H_5)]_3$ (**If**)	Red	$(C_6H_5)P$	6.8–8.25 m	—
		$C_5(CH_3)_5$	1.94 s	—
		$C_5(CH_3)_5$	1.60 s	—
Cp^*_2Zr(*t*-BuPH)$_2$ (**IIIb**)	Purple	*t*-BuP*H*	3.83 d	239.61
		$C_5(CH_3)_5$	1.95 s	—
		*t-Bu*PH	1.53 d	11.20
Cp^*_2Hf(*t*-BuPH)$_2$ (**IIIc**)	Red	*t*-BuP*H*	3.63 d	245.91
		$C_5(CH_3)_5$	2.02 s	—
		*t-Bu*PH	1.56 d	11.10
$Cp''_2Zr[P(Ph)]_2$ (**IVa**)	Orange	$C_5H_3(SiMe_3)_2$	6.2–6.7 br	—
		C_6H_5	6.9–7.5 br	—
		$C_5H_3(SiMe_3)_2$	0.1–0.3 br	—
$Cp''_2Hf[P(Ph)]_2$ (**IVb**)	Green	$C_5H_3(SiMe_3)_2$	6.2–6.7 br	—
		C_6H_5	6.9–7.5 br	—
		$C_5H_3(SiMe_3)_2$	0.1–0.3 br	—
$Cp''_2Zr[P$(*t*-Bu)$]_2$ (**IVc**)	Red–orange	$C_5H_3(SiMe_3)_2$	6.2–6.7	—
		*t-Bu*P	1.62 t	5.5
		$C_5H_3(SiMe_3)_2$	0.1–0.3	—
Cp''_2Zr(*t*-BuPH)$_2$ (**IIId**)	Red	$C_5H_3(SiMe_3)_2$	6.70 br s	—
		$C_5H_3(SiMe_3)_2$	6.26 br s	—
		t-BuP*H*	4.38 d	239.90
		*t-Bu*PH	1.51 d	11.46
		$C_5H_3(SiMe_3)_2$	0.38 s	—
Cp''_2Hf(*t*-BuPH)$_2$ (**IIIe**)	Red	$C_5H_3(SiMe_3)_2$	6.68 br s	—
		$C_5H_3(SiMe_3)_2$	6.23 br s	—
		t-BuP*H*	4.33 d	247.63
		*t-Bu*PH	1.53 d	11.29
		$C_5H_3(SiMe_3)_2$	0.39 s	—

[a] C_6D_6, 25°C, 300.15 MHz.
— Signifies no coupling observed.

the reaction of Cp_2ZrCl_2 with 2 equivalents of the bulkier primary phosphide, LiPH(*t*-Bu), in toluene–ether (70 : 30) at −78°C, results in formation not only of the previously characterized[10b] triphosphanato complex **Ic** (Cp = C_5H_5; M = Zr; R = *t*-Bu) in 15% yield, but also the reduced complex **II** (Cp = C_5H_5; M = Zr; R = *t*-Bu). Compound **II** may be isolated as red crystals in 50% yield after recrystallization from hexane and is very air-sensitive† in the solid-state and in solution. Compound **II** is diamagnetic like other Zr^{III} complexes[12] and NMR data are obtainable. (^{1}H and ^{31}P NMR data for **II** and all other new compounds reported are given in Tables 1 and 2 respectively.) The corresponding reaction of Cp_2HfCl_2[12] with 2

† Since most of all the new complexes were very air-sensitive, all manipulations were performed using either standard Schlenk line or dry-box techniques.

Table 2. $^{31}P\{^1H\}$ data for new compounds[a]

Compound	$^{31}P\{^1H\}$ δ
$\{Cp_2Zr(\mu_2\text{-}t\text{-BuPH})\}_2$ **(II)**	121.85
$Cp_2Hf(t\text{-BuPH})_2$ **(IIIa)**	101.97
$Cp^*_2Zr(t\text{-BuPH})_2$ **(IIIb)**	126.41
$Cp^*_2Hf(t\text{-BuPH})_2$ **(IIIc)**	101.58
$Cp''_2Zr[P(Ph)]_2$ **(IVa)**	228.91
$Cp''_2Hf[P(Ph)]_2$ **(IVb)**	193.22
$Cp''_2Zr[P(t\text{-Bu})]_2$ **(IVc)**	270.56
$Cp''_2Zr(t\text{-BuPH})_2$ **(IIId)**	130.65
$Cp''_2Hf(t\text{-BuPH})_2$ **(IIIe)**	109.06

[a] C_6D_6 solutions, 30°C, 121.51 MHz. Referenced to external 85% H_3PO_4 ($\delta = 0.0$) with high field increasingly negative.

equivalents of LiPH(*t*-Bu) in toluene–THF (60 : 40) also yields the previously characterized[10b] triphosphanato complex **Id** (Cp = C_5H_5; M = Hf; R = *t*-Bu) in 15% yield and the new diphosphido complex **IIIa** (Cp = C_5H_5; M = Hf). Complex **IIIa** can be isolated in 60% yield as red, hexane-soluble, air-sensitive crystals from toluene at −30°C.

Utilizing the bis-pentamethylcyclopentadienyl metal dichlorides, $Cp^*_2ZrCl_2$[13] and $Cp^*_2HfCl_2$,[14] it was hoped that the steric effect of the pentamethylcyclopentadienyl groups would help to stabilize other primary phosphido compounds of zirconium and hafnium. However, reaction of the $Cp^*_2ZrCl_2$ with LiPH(Ph) in toluene–THF (60 : 40) at −78°C, yields upon crystallization from toluene at −30°C, the triphosphanato complex $Cp^*_2Zr\{P(C_6H_5)\}_3$ **(Ie)** in 27% yield. Similarly, for the reaction of $Cp^*_2HfCl_2$ with LiPH(Ph) in THF at room temperature, $Cp^*_2Hf\{P(C_6H_5)\}_3$ **(If)** is isolated in 19% yield from the reaction mixture after recrystallization from toluene at −30°C.

Both compounds **Ie** and **If** are red in solution and the ^1H NMR spectra for both complexes exhibit two distinctly different Cp* resonances. This is due to the orientation of the triphosphanato unit with respect to the Cp* groups. This type of inequivalence of the Cp groups has been extensively studied by Köpf and Voigtländer for the analogous Cp (Cp = C_5H_5) compound.[10b] Table 3 compares the ^{31}P data for the compounds **Ia**, **Ie**, **Ib** and **If**. The ^{31}P resonances for the phosphorus nuclei directly attached to the metal (P_A) for compounds **Ie** and **If** are at higher field than in the normal cyclopentadienyl analogues, compounds **Ia** and **Ib**. This shift to higher field is indicative of less phosphorus lone pair donation to the empty $1a_1$ orbital[15] at the metal centres. Also noticeable is that the resonances for the apical phosphorus nuclei (P_B) shift downfield by ~55 ppm. The other interesting fact from Table 3 is the reduced coupling constant between the phosphorus nuclei (P_A and P_B) in compounds **Ie** and **If** when compared to compounds **Ia** and **Ib**. Nonetheless, despite the steric effect of the pentamethylcyclopentadienyl groups, the driving force of the reaction is the formation of the triphosphanato metallocycle.†

Reaction of $CP^*_2ZrCl_2$ with 2 equivalents of LiPH(*t*-Bu) in toluene–ether (70 : 30) at room temperature for 4 h, affords purple $Cp^*_2Zr(t\text{-BuPH})_2$ **(IIIb)**. Complex **IIIb** can be isolated in 71% yield as purple blocks by crystallization from hexane at −30°C. Similarly, reaction of $Cp^*_2HfCl_2$ with 2 equivalents of LiPH(*t*-Bu) in THF for 2 days affords, after the appropriate work-up, red, crystalline $Cp^*_2Hf(t\text{-BuPH})_2$ **(IIIc)** in 63% yield. Both compounds **IIIb** and **IIIc** are highly air-sensitive in solution and the solid state. In addition, both of these compounds reductively eliminate the diphosphine, (*t*-Bu)PHPH(*t*-Bu), when treated with CO (3 atm) at room temperature in toluene solution, to form the dicarbonyls, $Cp^*_2M(CO)_2$.[17] This reaction demonstrates the weakness of the metal–phosphorus bonds in these complexes and the ease with which the metal centres are reduced.

The reaction of Cp''_2MCl_2[18] (Cp″ = $C_5H_3(SiMe_3)_2$) with 2 equivalents of LiPH(Ph) in toluene–THF (60 : 40) for 2 h, produces the orange crystalline $Cp''_2Zr[P(Ph)]_2$ **(IVa)** and green crystalline $Cp''_2Hf[P(Ph)]_2$ **(IVb)** diphosphanato (diphosphene) complexes in good yield (60–70%), after recrystallization from toluene at −30°C. The ^1H NMR signals at 25°C for **IVa** and **IVb** are very broad and make the assignment and integration of the resonances difficult. The $^{31}P\{^1H\}$ NMR signals for **IVa** and **IVb** are also very broad (**IVa**, $\Delta w_{1/2} = 37$ Hz; **IVb**, $\Delta w_{1/2} = 40$ Hz) at 25°C and indicate that there is some fluctionality of the diphosphanato metallocycle. In contrast to the triphosphanato metallocycles (**I**), complexes **IVa** and **IVb** are easily hydrolysed to $Cp''_2M(OH)_2$ and the *meso* and D,L isomers of diphenyldiphosphine.[19]

Reaction of Cp''_2ZrCl_2 with 2 equivalents of LiPH(*t*-Bu) in toluene at room temperature for 2 days yields, after work-up and crystallization from hexane at −30°C, the red microcrystalline diphos-

† The mechanisms for the formation of the triphosphanato metallacycle are not clear. Professor G. L. Hillhouse and co-workers have synthesized $Cp^*_2HfH(PHPh)$ from the reaction of $Cp^*_2HfH_2$ with $PhPH_2$ and $Cp^*_2Hf(I)(PHPh)$ from the reaction of $Cp^*_2HfI_2$ with LiPH(Ph).[16]

Table 3. ^{31}P data for $(C_5R_5)_2M[P(C_6H_5)]_3$ complexes[a]

Complex	R	M	P_A	P_B	J_{AB} (Hz)
Ia	H	Zr	92.94	−189.78	349.45[b]
Ie	CH_3	Zr	60.87	−134.89	244.95[c]
Ib	H	Hf	67.32	−193.92	330.45[b]
If	CH_3	Hf	36.37	−128.75	215.80[c]

[a] All complexes display an A_2X pattern.
[b] Data from ref. 10b.
[c] Data from this work.

phido compound $Cp''_2Zr(t\text{-BuPH})_2$ (**IIId**) in 11% yield and the red–orange diphosphanato complex $Cp''_2Zr[P(t\text{-Bu})]_2$ (**IVc**) in 48% yield. The $^{31}P\{^1H\}$ NMR resonance for **IVc** at δ 270.56 is much sharper ($\Delta w_{1/2} = 3$ Hz) than in the phenyl analogue **IVa**. The ^1H NMR for **IVc** is also sharper than for **IVa** and **IVb**, and hydrolysis of complex **IVc** yields mainly the D,L isomer of the diphosphine, (*t*-Bu)PHPH(*t*Bu), in addition to $Cp''_2Zr(OH)_2$. In contrast, reaction of Cp''_2HfCl_2 with 2 equivalents of LiPH(*t*-Bu) does not give a diphosphanato complex, but instead only the red diphosphido complex, $Cp''_2Hf(t\text{-BuPH})_2$ (**IIIe**), which is isolated in 55% yield after crystallization from hexane.

From these studies it is evident that the distribution of products depends upon three factors: (1) the metal used and the reducibility of that metal; (2) the steric and electronic nature of the cyclopentadienyl group utilized in stabilizing the complexes and (3) the bulk of the aryl or alkyl group on the phosphorus. In conclusion, primary phosphido complexes of the group 4 metallocenes can be stabilized given the correct conditions and these new complexes should provide a wealth of new and interesting chemistry. Further studies of these and related compounds are in progress.

Acknowledgements—We thank the Robert A. Welch Foundation and the National Science Foundation for support. R.A.J. also thanks the Alfred P. Sloan Foundation for a fellowship (1985–89). We would also like to thank Professor G. L. Hillhouse for helpful discussions and preprints of related work on primary phosphido complexes of bis(pentamethylcyclopentadienyl)zirconium and hafnium.

REFERENCES

1. R. T. Baker, P. J. Krusic, T. H. Tulip, J. C. Calabrese and S. S. Wreford, *J. Am. Chem. Soc.* 1983, **105**, 6763.
2. D. M. Roddick, B. D. Santarsiero and J. E. Bercaw, *J. Am. Chem. Soc.* 1985, **107**, 4670.
3. (a) J. Ellerman and P. Poersch, *Angew. Chem. Int. Ed. Engl.* 1967, **6**, 355; (b) S. R. Wade, M. G. H. Wallbridge and G. R. Willey, *J. Chem. Soc., Dalton Trans.* 1983, 2555; (c) R. T. Baker, J. F. Whitney and S. S. Wreford, *Organometallics* 1983, **2**, 1049; (d) L. Weber, G. Meine, R. Boese and N. Augart, *Organometallics* 1987, **6**, 2484; (e) H. Köpf and V. Richtering, *J. Organomet. Chem.* 1988, **346**, 355.
4. R. T. Baker, T. H. Tulip and S. S. Wreford, *Inorg. Chem.* 1985, **24**, 1379.
5. R. T. Baker and T. H. Tulip, *Organometallics* 1986, **5**, 839.
6. L. Gelmini and D. W. Stephan, *Inorg. Chim. Acta* 1986, **111**, L17.
7. G. Johannsen and O. Stelzer, *Chem. Ber.* 1977, **110**, 3428.
8. T. S. Targos, R. P. Rosen, R. R. Whittle and G. L. Geoffroy, *Inorg. Chem.* 1985, **24**, 1375.
9. E. Hey, S. G. Bott and J. L. Atwood, *Chem. Ber.* 1988, **121**, 561.
10. (a) K. Issleib, G. Wille and F. Krech, *Angew. Chem.* 1972, **84**, 582; (b) H. Köpf and R. Voigtländer, *Chem. Ber.* 1981, **114**, 2731.
11. For example $\{Cp_2Zr(\mu\text{-}PMe_2)\}_2$ in ref. 3b. For other examples see: (a) J. H. Wengrovius, R. R. Schrock and S. C. Day, *Inorg. Chem.* 1981, **20**, 1844; (b) M. Y. Chiang, S. Gambarotta and F. van Bolhuis, *Organometallics* 1988, **7**, 1864.
12. P. M. Druce, B. M. Kingston, M. F. Lappert, T. R. Spalding and R. C. Srivastava, *J. Chem. Soc. A* 1969, 2106.
13. J. M. Manriquez and J. E. Bercaw, *J. Am. Chem. Soc.* 1974, **96**, 6229.
14. D. M. Roddick, M. D. Fryzuk, P. F. Seidler, G. L. Hillhouse and J. E. Bercaw, *Organometallics* 1985, **4**, 1694.
15. J. W. Lauher and R. Hoffmann, *J. Am. Chem. Soc.* 1976, **98**, 1729.
16. G. L. Hillhouse, personal communication.
17. D. J. Sikora, M. D. Rausch, R. D. Rogers and J. L. Atwood, *J. Am. Chem. Soc.* 1981, **103**, 1265.
18. A. Antiñolo, M. F. Lappert, A. Singh, D. J. W. Winterborn, L. M. Engelhardt, C. L. Raston, A. H. White, A. J. Carty and N. J. Taylor, *J. Chem. Soc., Dalton Trans.* 1987, 1463.
19. M. Baudler, B. Carlsohn, D. Koch and P. K. Medda, *Chem. Ber.* 1978, **111**, 1210.

Polyhedron Vol. 8, No. 13/14, pp. 1778–1779, 1989
Printed in Great Britain

0277–5387/89 $3.00+.00
© 1989 Maxwell Pergamon Macmillan plc

DIAZENIDO, DINITROGEN AND TRIISOCYANIDE COMPLEXES OF RHENIUM(I) WITH PHOSPHITE OR PHOSPHONITE CO-LIGANDS

M. FERNANDA, N. N. CARVALHO and ARMANDO J. L. POMBEIRO*

Centro de Química Estrutural, Complexo I, Instituto Superior Técnico, Av. Rovisco Pais, 1096 Lisboa Codex, Portugal

Abstract—Treatment of $[ReCl_2(NNCOPh)(PPh_3)_2]$ with $P(OMe)_3$, $PPh(OEt)_2$ or $PPh(OMe)_2$, in benzene and in the presence of hot methanol, leads to the formation of $[ReCl(N_2)(PPh_3)L_3]$ [L = $P(OMe)_3$ or $PPh(OEt)_2$] or $[ReCl(N_2)\{PPh(OMe)_2\}_4]$, whereas, without hot methanol, intermediate benzoyldiazenido species are obtained. The dinitrogen complexes react with isocyanides to afford $[ReCl(CNR)_3L_2]$ [R = Me, L = $PPh(OMe)_2$; R = C_6H_4Me-4, L = $P(OMe)_3$].

In contrast with the well-documented chemistry of rhenium phosphine complexes, that of phosphite or phosphonite compounds of this metal is relatively underdeveloped and, therefore, is explored in this study.

The chelating benzoyldiazenido complex, $[ReCl_2(NNCOPh)(PPh_3)_2]$, is a known suitable starting material for dinitrogen and benzoyldiazenido complexes of rhenium, commonly with phosphines as co-ligands, such as *trans*-$[ReCl(N_2)L_4]$ [L = PR_3 or $P(OMe)_3$],[1] *mer*-$[Re(\eta^2\text{-}S_2PPh_2)(N_2)(PMe_2Ph)_3]$[2] or $[ReCl_2(NNCOPh)L_3]$,[1–4] from which mono- and diisocyanide complexes, particularly *trans*-$[ReCl(CNR)L_4]$,[5] $[ReCl(N_2)(CNR)L_3]$ or $[Re(\eta^1\text{-}S_2PPh_2)(N_2)(CNR)_2(PMe_2Ph)_2]$,[6] are derived.

We extend now these studies to novel phosphite or phosphonite complexes with dinitrogen, diazenido or isocyanide ligands.

RESULTS AND DISCUSSION

$[ReCl_2(NNCOPh)(PPh_3)_2]$ reacts with a phosphite, $P(OMe)_3$, or a phosphonite, $PPh(OEt)_2$ or $PPh(OMe)_2$, in refluxing benzene, followed by addition of hot methanol, to give the dinitrogen complexes $[ReCl(N_2)(PPh_3)L_3]$ [L = $P(OMe)_3$ or $PPh(OEt)_2$] or $[ReCl(N_2)\{PPh(OMe)_2\}_4]$ (eqs (1) and (2), Scheme 1), isolated as yellow or light brown solids.

However, if the use of hot methanol is avoided, intermediate benzoyldiazenido complexes may be isolated, such as $[ReCl_2(NNCOPh)(PPh_3)_2\{PPh(OMe)_2\}]$ obtained from the reaction of that chelate with $PPh(OMe)_2$. These complexes can undergo NN—C bond cleavage upon nucleophilic attack by methanol, with heating, to give the final dinitrogen compounds, a step which is also involved in the above mentioned and more convenient single-pot synthesis of the dinitrogen complexes.

The IR spectra of the dinitrogen compounds exhibit $\nu(N_2)$ at values (2010–1985 cm^{-1} range) which, by comparison with those known for related compounds, appear to indicate that a phosphonite behaves as a considerably stronger net electron-donor than a related phosphite ligand.

In those complexes, the N_2 and the Cl ligands are believed to be *trans* to each other, thus corresponding to an arrangement which favours the stabilization of the Re—N_2 bond.

They react with isocyanides (added in excess), in THF and at room temperature, to give the triisocyanide complexes $[ReCl(CNR)_3L_2]$ {R = C_6H_4Me-4, L = $P(OMe)_3$ [eq. (3)]; R = Me, L = $PPh(OMe)_2$ [eq. (4)]}, isolated as reddish-brown or brown solids, possibly formed via intermediate mixed dinitrogen–isocyanide compounds of known types,[6] where the Re—N_2 bond (which is usually quite strong in neutral Re^I—N_2 complexes)[5] is labilized by the strong π-electron withdrawing ability of the CNR co-ligand.

Hence, the convenient application of dinitrogen compounds of rhenium to the syntheses of low-valent mono- and diisocyanide complexes with this metal has been extended to triisocyanide species.

* Author to whom correspondence should be addressed.

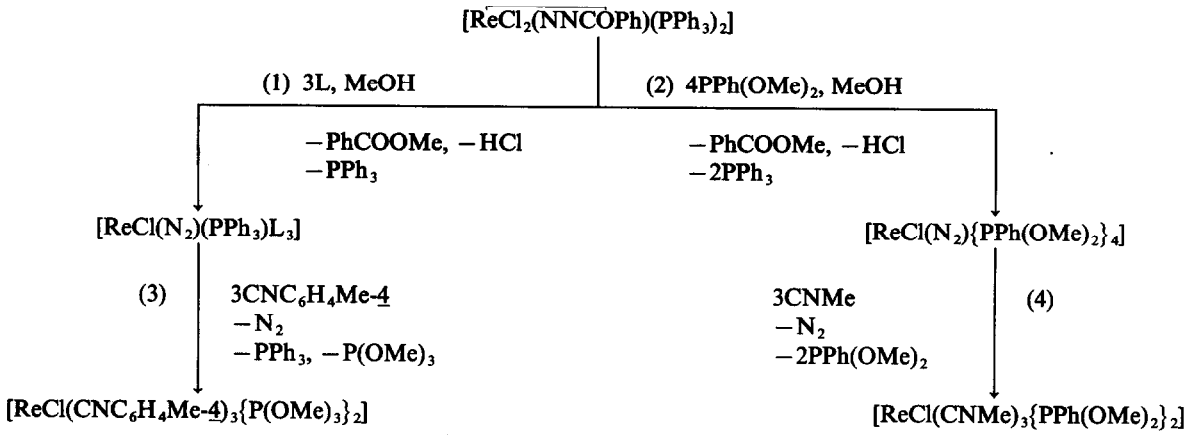

Scheme 1. Syntheses of low-valent dinitrogen and derived triisocyanide complexes of rhenium(I) with phosphites or phosphonites as co-ligands. [Equation (1)—L = $P(OMe)_3$ or $PPh(OEt)_2$. Equation (3)—L = $P(OMe)_3$].

Acknowledgements—This work was partially supported by the National Institute for Scientific Research (I.N.I.C.) and the National Junta for Scientific and Technological Research (J.N.I.C.T.), Portugal. The authors also gratefully acknowledge Dr R. L. Richards (Nitrogen Fixation Laboratory—AFRC, University of Sussex) for stimulating discussions.

REFERENCES

1. G. J. Leigh, R. H. Morris, C. J. Pickett, D. R. Stanley and J. Chatt, *J. Chem. Soc., Dalton Trans.* 1981, 800 and refs therein.
2. J. Chatt, R. H. Crabtree, J. R. Dilworth and R. L. Richards, *J. Chem. Soc., Dalton Trans.* 1974, 2358.
3. J. Chatt, J. R. Dilworth, G. J. Leigh and V. D. Gupta, *J. Chem. Soc. A* 1971, 2631.
4. J. Chatt, W. Hussain, G. J. Leigh, H. M. Ali, C. J. Pickett and D. A. Rankin, *J. Chem. Soc., Dalton Trans.* 1985, 1131.
5. A. J. L. Pombeiro, C. J. Pickett and R. L. Richards, *J. Organomet. Chem.* 1982, **224**, 285.
6. A. J. L. Pombeiro, P. B. Hitchcock and R. L. Richards, *J. Chem. Soc., Dalton Trans.* 1987, 319.

Polyhedron Vol. 8, No. 13/14, pp. 1780–1781, 1989
Printed in Great Britain

0277–5387/89 $3.00+.00
© 1989 Maxwell Pergamon Macmillan plc

SYNTHESIS OF $[Co(\eta^5\text{-}C_5H_5)_2][M(\eta^5\text{-}C_5H_5)Cl_3]$ SALTS (M = Ti OR V): CRYSTAL STRUCTURE OF $[Co(\eta^5\text{-}C_5H_5)_2][Ti(\eta^5\text{-}C_5H_5)Cl_3]$

D. L. HUGHES, M. JIMENEZ-TENORIO and G. J. LEIGH*

AFRC Institute of Plant Science Research, Nitrogen Fixation Laboratory, University of Sussex, Brighton BN1 9RQ, U.K.

Abstract—The salts, $[Co(\eta^5\text{-}C_5H_5)_2][M(\eta^5\text{-}C_5H_5)Cl_3]$ (M = Ti or V), are readily prepared from the reaction between $[Co(\eta^5\text{-}C_5H_5)_2]$ and $[M(\eta^5\text{-}C_5H_5)Cl_3]$ in dichloromethane. The crystal structure of $[Co(\eta^5\text{-}C_5H_5)_2][Ti(\eta^5\text{-}C_5H_5)Cl_3]$ shows well-defined $[Co(\eta^5\text{-}C_5H_5)_2]^+$ and $[Ti(\eta^5\text{-}C_5H_5)Cl_3]^-$ moieties, despite the fact that the anion has been claimed to be unstable above 77 K. IR, NMR and EPR spectroscopic data are also discussed.

The literature suggests that $[Ti(\eta^5\text{-}C_5H_5)Cl_3]^-$ is an unstable species which can be generated by ^{60}Co-γ irradiation of $[Ti(\eta^5\text{-}C_5H_5)Cl_3]$ in methyltetrahydrofuran. It was claimed to be only stable at 77 K, and upon annealing at some higher temperature it produces $[Ti(\eta^5\text{-}C_5H_5)Cl_2]$. Apparently, $[Ti(\eta^5\text{-}C_5H_5)Cl_3]^-$ rapidly loses chloride to give dinuclear or solvated species.[1] Following a report[2] that $[Co(\eta^5\text{-}C_5H_5)_2]$ can reduce $[Ti(\eta^5\text{-}C_5H_4Me)Cl_3]$ to yield a stable paramagnetic product, characterized as $[Ti(\eta^5\text{-}C_5H_4Me)Cl_3]^-$, we have shown that $[M(\eta^5\text{-}C_5H_5)Cl_3]$ (M = Ti or V) and $[Co(\eta^5\text{-}C_5H_5)_2]$ react to give the corresponding salts, $[Co(\eta^5\text{-}C_5H_5)_2][M(\eta^5\text{-}C_5H_5)Cl_3]$. The vanadium salt is diamagnetic, but the titanium one is paramagnetic, giving an axial EPR spectrum with $g_\parallel = 1.743$ and $g_\perp = 1.973$, in good agreement with the reported data for the methylcyclopentadienyl derivatives, although at variance with the earlier report on the existence of $[Ti(\eta^5\text{-}C_5H_5)Cl_3]^-$.[1]

We find that, contrary to the earlier report, $[Ti(\eta^5\text{-}C_5H_5)Cl_3]^-$ is very stable thermally both in the solid state and in solution. Dark green, single crystals of $[Co(\eta^5\text{-}C_5H_5)_2][Ti(\eta^5\text{-}C_5H_5)Cl_3]$ (monoclinic, space group $P2_1/a$, $a = 14.404(1)$, $b = 10.365(1)$, $c = 11.591(1)$ Å, $\beta = 108.256(7)°$ and $Z = 4$) were studied by X-ray crystallography. The structure contains discrete $Ti(\eta^5\text{-}C_5H_5)Cl_3$ and $Co(\eta^5\text{-}C_5H_5)_2$ moieties, separated by van der Waals contacts. The cobalt atom is sandwiched between parallel eclipsed cyclopentadienyl rings, with an average distance (Co—C_5H_5 ring) of 1.631(4) Å,

* Author to whom correspondence should be addressed.

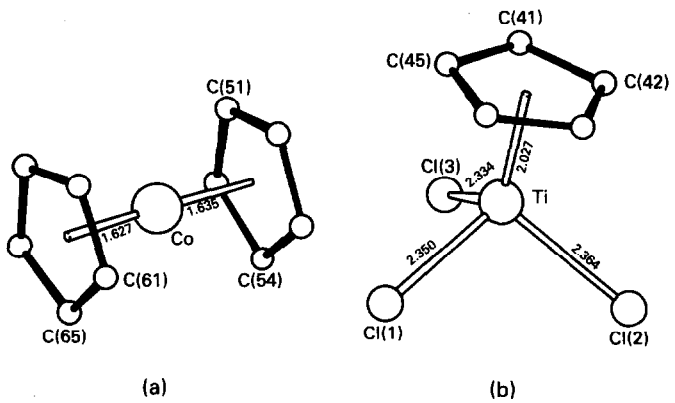

Fig. 1. Diagrammatic representation of the molecular structure of $[Co(C_5H_5)_2]^+$ (a) and $[Ti(C_5H_5)Cl_3]^-$ (b), showing selected bond lengths and atomic numbering.

shorter than the corresponding distance in cobaltocene, 1.726 Å, supporting the formulation as $[Co(\eta^5\text{-}C_5H_5)_2]^+$ rather than the neutral species. The $Ti(\eta^5\text{-}C_5H_5)Cl_3$ moiety has a three-legged piano-stool arrangement, as found for $[Ti(\eta^5\text{-}C_5H_5)Cl_3]$, although all the bond distances are longer than in the titanium(IV) molecule, and fully consistent with our formulation as $[Ti(\eta^5\text{-}C_5H_5)Cl_3]^-$.

The stability in solution of $[Ti(\eta^5\text{-}C_5H_5)Cl_3]^-$ was checked by ^1H NMR spectroscopy. The spectrum of a 1 : 1 mixture of $[Co(C_5H_5)_2]$ and $[Ti(C_5H_5)Cl_3]$ shows a sharp singlet, intensity 10 H, for the cobaltacinium protons and a very broad signal centred at about 27.5 ppm, width of about 4 ppm, of the correct intensity for $[Ti(C_5H_5)Cl_3]^-$.

REFERENCES

1. S. P. Mishra and M. C. R. Symons, *J. Chem. Soc., Dalton Trans.* 1981, 2258.
2. D. B. Morse, D. N. Hendrickson, T. B. Rauchfuss and S. R. Wilson, *Organometallics* 1988, **7**, 496.

Polyhedron Vol. 8, No. 13/14, pp. 1782–1783, 1989
Printed in Great Britain

0277–5387/89 $3.00+.00
© 1989 Maxwell Pergamon Macmillan plc

PREPARATION AND REACTIONS OF A BIS(PHENYLHYDRAZINE) COMPOUND OF VANADIUM(III)

G. JEFFERY LEIGH* and J. ROGER SANDERS

AFRC Institute of Plant Science Research, Nitrogen Fixation Laboratory, University of Sussex, Brighton BN1 9RQ, U.K.

Abstract—Complexes $[VX_2(salen)]$ (X = Cl, Br) are reduced by hydrazines to give either [VX(salen)(ROH)]ROH (R = Me, Et) or $[\{VX(salen)\}_2]$, depending on the solvent. Treatment of [VO(salen)] with I_2 in acetonitrile gives I_5^- or I_7^- salts of the $[\{V(salen)\}_2(\mu\text{-}O)]^+$ cation, which are reduced by diethylaluminium ethoxide in the presence of phenylhydrazine, to give $[V(PhNHNH_2)_2(salen)]I$.

Following the discoveries that vanadium can replace molybdenum in nitrogen-fixing enzymes[1] and that vanadium complexes can reduce dinitrogen to hydrazine in homogeneous protic media,[2] we have been attempting to make vanadium compounds containing partially reduced nitrogen species such as hydrazine. This report describes attempts to use tetradentate Schiff base ligands to bind to four sites on a penta- or hexa-coordinate vanadium atom, leaving sites free for hydrazine or similar ligands; accordingly, the starting materials were $[VX_2(salen)]$ (X = Cl or Br) [salen = N,N′-bis(salicylidene)ethylenediaminate(2−)] and $[VX_2(salophen)]$ [salophen = N,N′-bis(salicylidene) *o*-phenylenediaminate(2−)].

$[VX_2(salen)]$ complexes give [VX(salen)(ROH)] ROH (R = Me or Et) when treated with hydrazines in alcohols. Analyses do not distinguish between this structure and a vanadium(IV) structure containing an alkoxide ligand, but the magnetic moments and EPR spectra of these complexes show them to contain vanadium(III). Treatment of $[VX_2(salen)]$ with hydrazine, phenylhydrazine or silyl-substituted hydrazines in non-protic solvents gives $[\{VX(salen)\}_2]$. These compounds are halide-bridged dimers; the chloride has been prepared[3] from $[VCl_3(THF)]$ (THF = tetrahydrofuran) and Na_2salen. Salophen analogues of all the compounds described above have been made and characterized.

Unlike $[VCl_2(salen)]$ and [VBr(salen)], $[VI_2(salen)]$ is unknown. Treatment of [VO(salen)] with PPh_3I_2 (analogous to the bromide preparation) gives $[VI(OPPh_3)(salen)]I$. Treatment of [VO(salen)] with I_2 in acetonitrile gives dark blue needles, whose composition varies with the relative quantities of starting materials used. Equimolar quantities of [VO(salen)] and I_2 give $[\{V(salen)\}_2(\mu\text{-}O)](I_5)$ with an unsymmetrical oxo-bridged divanadium cation. The colour, elemental analysis, X-ray crystal analysis, magnetic moment and EPR spectrum of this compound are consistent with this structure; in its IR spectrum the band assigned to $\nu_{V=O}$ occurs at 880 cm^{-1} rather than 990 cm^{-1} as in [VO(salen)]. Use of an excess of I_2 in the preparation gives a product whose elemental analysis shows it to be $[\{V(salen)\}_2(\mu\text{-}O)](I_7)$. We have been unable to prepare salophen analogues.

Treatment of $[\{V(salen)\}_2(\mu\text{-}O)]^+$ salts with phenylhydrazine gives [VI(salen)(MeOH)]MeOH or $[\{VI(salen)\}_2]$, depending on the solvent; however, treatment of a suspension of $[\{V(salen)\}_2(\mu\text{-}O)]I_5$ in acetonitrile at 10°C, first with diethylaluminium ethoxide in toluene and then with phenylhydrazine gives $[V(PhNHNH_2)_2(salen)]I$ in good yield. Its magnetic moment and EPR spectrum are normal for a monomeric vanadium(III) compound, and a crystal structure shows that the cation has an octahedral geometry with the phenylhydrazine ligands bound *trans* to one another through the terminal nitrogen atoms (V—N distances, 21.7 nm, V—N—N angles, 111°).

Treatment of the dark blue V^{III}—V^{IV} dimer with trimethylsilyl(trimethyl)hydrazine in acetonitrile, gives $[V(NMeNMe_2)(salen)]I$; attempts to grow X-ray quality crystals of this compound have so far been unsuccessful.

* Author to whom correspondence should be addressed.

Acknowledgements—We thank Mr A. Hills and Dr D. Hughes for X-ray crystal structures, Dr D. Lowe for EPR spectra and Mr C. J. Macdonald for microanalyses.

REFERENCES

1. R. L. Robson, R. R. Eady, T. H. Richardson, R. W. Miller, M. Hawkins and J. R. Postgate, *Nature* 1986, **322**, 388.
2. L. A. Nikonova, A. G. Ovcharenko, O. N. Efimov, V. A. Avilov and A. E. Shilov, *Kinet. Katal.* 1972, **13**, 1602.
3. M. Mazzanti, S. Gambarotta, C. Floriani, A. Chiesi-Villa and C. Guastini, *Inorg. Chem.* 1986, **25**, 2308.

Polyhedron Vol. 8, No. 13/14, pp. 1784–1785, 1989
Printed in Great Britain

0277–5387/89 $3.00+.00
© 1989 Maxwell Pergamon Macmillan plc

THE INTERACTION OF NIOBIUM AND VANADIUM CYCLOPENTADIENYL COMPLEXES WITH SUBSTITUTED HYDRAZINES

M. JIMENEZ-TENORIO and G. J. LEIGH*

AFRC Institute of Plant Science Research, Nitrogen Fixation Laboratory, University of Sussex, Brighton BN1 9RQ, U.K.

Abstract—The hydrazido(1−) complexes $[V(\eta^5\text{-}C_5H_5)Cl_2(NRNR_2)]$ and $[Nb(\eta^5\text{-}C_5H_5)Cl_3(NRNR_2)]$ ($NRNR_2$ = $NMeNMe_2$ or $NPhNH_2$) were synthesized by reaction of $[V(\eta^5\text{-}C_5H_5)Cl_3]$ or $[Nb(\eta^5\text{-}C_5H_5)Cl_4]$ with either the lithium- or trimethylsilyl-substituted hydrazine. The interaction of $[V(\eta^5\text{-}C_5H_5)Cl_3]$ with diphos (diphos = dppe or dmpe) in Et_2O yields the adducts $[V(\eta^5\text{-}C_5H_5)Cl_3(diphos)]$. Complexes such as $[Nb(C_5H_5)(diphos)_2]$ and $[V(C_5H_5)Cl(diphos)]$ are the reaction products of the reduction under N_2 of $[Nb(\eta^5\text{-}C_5H_5)Cl_4]$ and $[V(\eta^5\text{-}C_5H_5)Cl_3]$, either with Na(Hg) or Mg in the presence of phosphines or diphosphines. No stable dinitrogen complexes were isolated.

The reaction of $[Ti(\eta^5\text{-}C_5H_5)Cl_3]$ with trimethylsilyl-substituted hydrazines allows the isolation of hydrazido(1−) complexes, $[Ti(\eta^5\text{-}C_5H_5)Cl_2(NRNR_2)]$ ($NRNR_2$ = $NMeNMe_2$, NH_2NPh, $NHNMe_2$, etc.), which exhibit side-on coordination of the hydrazine fragment.[1,2] We also prepared complexes containing ligands such as RNN^- or R_2NN^{2-}, which correspond to putative intermediates in the process of conversion of dinitrogen to ammonia and/or hydrazine.

The recent discovery of a vanadium-containing nitrogenase[3] prompted us to extend this work to vanadium, and also to niobium.

The starting material, $[V(\eta^5\text{-}C_5H_5)Cl_3]$, is not as easily accessible as $[Ti(\eta^5\text{-}C_5H_5)Cl_3]$.[4] We eventually optimized a three step synthesis pattern for the preparation of $[V(\eta^5\text{-}C_5H_5)Cl_3]$ in reasonable yields.

$[V(\eta^5\text{-}C_5H_5)Cl_3]$ reacts with trimethylsilyl-substituted hydrazines to give the hydrazido(1−) complexes $[V(C_5H_5)Cl_2(NRNR_2)]$, which have been characterized by IR and EPR spectroscopy, and by analyses. The phosphineiminate complex, $[V(C_5H_5)Cl_2(NPPh_3)]$, can be prepared in an analogous fashion from $[V(C_5H_5)Cl_3]$ and Me_3Si $NPPh_3$. Side-on coordination is expected in the hydrazide(1−) complexes, as occurs with titanium compounds, but end-on coordination is likely for $[V(\eta^5\text{-}C_5H_5)Cl_2(NPPh_3)]$, due to the bulk of the $NPPh_3^-$ ligand.

$[Nb(\eta^5\text{-}C_5H_5)Cl_4]$, prepared as described in literature from $NbCl_5$ and $Sn(C_5H_5)Bu^n_3$ in dichloromethane,[5] reacts with $Li(NRNR_2)$ in THF yielding diamagnetic $[Nb(\eta^5\text{-}C_5H_5)Cl_3(NRNR_2)]$ ($NRNR_2$ = $NMeNMe_2$ or $NPhNH_2$). $[Nb(\eta^5\text{-}C_5H_5)Cl_3(NMeNMe_2)]$ is stable in solution, as inferred from its NMR spectrum. However, $[Nb(C_5H_5)Cl_3(NPhNH_2)]$ behaves in a different way, and seems to lose the cyclopentadienyl ligand on standing in THF solution at room temperature.

We also have studied the reactions of $[V(C_5H_5)Cl_3]$ with phosphines and diphosphines. The complexes $[V(C_5H_5)Cl_3(diphos)]$ (diphos = dppe or dmpe) can be prepared in high yields from $[V(C_5H_5)Cl_3]$ and the diphosphine in ether. However, the reaction with PMe_3 is accompanied by decomposition. Presumably reduction of vanadium(IV) to lower oxidation states occurs, and no stable adduct is isolated. The EPR spectra of the $[V(C_5H_5)Cl_3(diphos)]$ complexes show well-defined eight-line patterns with lines broadened due to coupling with phosphorus.

The synthesis of new vanadium and niobium dinitrogen complexes was pursued. Reductions of $[V(C_5H_5)Cl_3]$ and $[Nb(C_5H_5)Cl_4]$ under different conditions yielded no dinitrogen complexes, but

* Author to whom correspondence should be addressed.

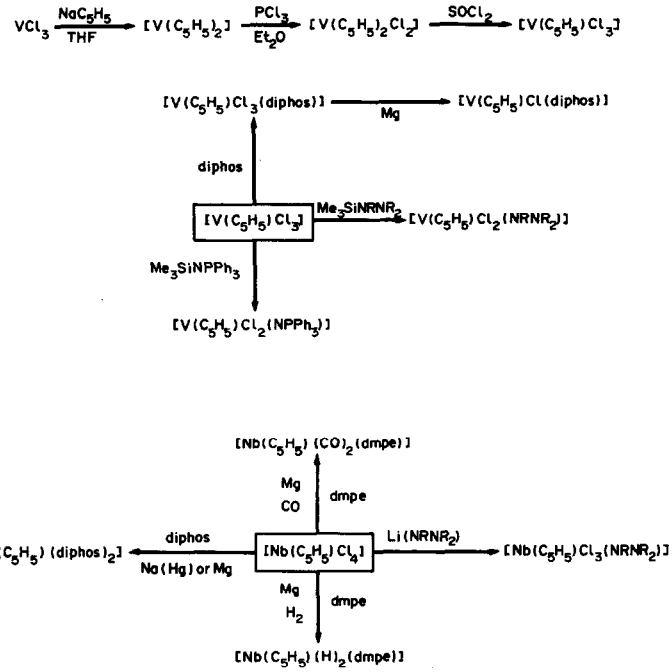

Scheme of reactions.

other low oxidation-state complexes of vanadium and niobium were readily isolated. For example, the reduction of $[V(C_5H_5)Cl_3(dppe)]$ with Mg under N_2, leads to the complex $[V(C_5H_5)Cl(dppe)]$.[6] $[Nb(C_5H_5)Cl_4]$ is reduced either with Na(Hg) or Mg in the presence of a diphosphine yielding $[Nb(C_5H_5)(diphos)_2]$. The reduction of $[Nb(C_5H_5)Cl_4]$ with Mg under CO in the presence of dmpe produces $[Nb(C_5H_5)(CO)_2(dmpe)]$. Reduction under H_2 affords red crystals analysing as $[Nb(C_5H_5)(H)_2(dmpe)]$, which are not yet fully characterized.

REFERENCES

1. I. A. Latham, G. J. Leigh and D. L. Hughes, *J. Chem. Soc., Dalton Trans.* 1986, 393.
2. I. A. Latham, G. J. Leigh, G. Huttner and I. Jibril, *J. Chem. Soc., Dalton Trans.* 1986, 385.
3. R. L. Robson, *Nature* 1985, **322**, 388.
4. R. D. Gorsich, *J. Am. Chem. Soc.* 1958, **80**, 4774.
5. M. J. Bunker, A. de Cian, M. L. H. Green, J. J. E. Moreau and N. Singaporia, *J. Chem. Soc., Dalton Trans.* 1980, 2155.
6. J. Nieman and J. H. Teuben, *Organometallics* 1986, **5**, 1149.

Polyhedron Vol. 8, No. 13/14, pp. 1786–1787, 1989
Printed in Great Britain

0277–5387/89 $3.00+.00
© 1989 Maxwell Pergamon Macmillan plc

REACTIVITY OF SEVEN-COORDINATE MOLYBDENUM(II) AND TUNGSTEN(II) ISOCYANIDE COMPLEXES: THE CRYSTAL STRUCTURE OF $[MoCl(CNBu^t)_4(PMe_3)_2]Cl$

M. J. FERNANDEZ-TRUJILLO, M. JIMENEZ-TENORIO and M. C. PUERTA

Departamento de Quimica Inorganica, Facultad de Ciencias, Universidad de Cadiz, Puerto Real, Cadiz, Spain

and

D. L. HUGHES*

AFRC Institute of Plant Science Research, Nitrogen Fixation Laboratory, University of Sussex, Brighton BN1 9RQ, U.K.

Abstract—The seven-coordinate isocyanide complexes $[MCl_2(CNBu^t)_3(PMe_3)_2]$ (M = Mo or W), react with additional $CNBu^t$ yielding the derivatives $[MCl(CNBu^t)_4(PMe_3)_2]Cl$. The crystal structure of the $[MoCl(CNBu^t)_4(PMe_3)_2]Cl$ complex shows an almost perfect two-fold symmetry for the cation $[MoCl(CNBu^t)_4(PMe_3)_2]^+$ along the Mo—Cl bond, and two different possible orientations for the *t*-butyl groups. The reaction of $[MCl_2(CNBu^t)_3(PMe_3)_2]$ (M = Mo or W) with anhydrous $SnCl_2$ yields complexes containing the $SnCl_3^-$ ligand, derived from the insertion of $SnCl_2$ into the metal–halide bond.

We have been studying the reactivity of 16-electron six-coordinate molybdenum(II) and tungsten(II) species towards organic isocyanides, which allowed us to isolate $[MCl_2(CNBu^t)_3(PMe_3)_2]$ (M = Mo or W).[1] Spectroscopic data for these complexes supported a capped-octahedral structure, with *trans*-phosphines for the molybdenum complex and *cis*-for the tungsten derivative, although fluxional behaviour was also observed.

These complexes react with additional $CNBu^t$ to give $[MCl(CNBu^t)_4(PMe_3)_2]Cl$. Spectroscopic data for these derivatives suggest a capped trigonal prismatic structure, with the chloride ligand in the capping position, as was found for the parent derivatives $[MX(CNR)_6]X$.[2] This has been confirmed by an X-ray structure analysis for the $[MoCl(CNBu^t)_4(PMe_3)_2]Cl$ complex, which crystallizes as $[MoCl(CNBu^t)_4(PMe_3)_2]Cl \cdot 2Me_2CO$ in the monoclinic system, space group $P2_1$, with a = 11.563(6), b = 18.722(2), c = 11.202(2) Å, β = 103.67(1)° and Z = 2.

The crystal is composed of a lattice of molybdenum-complex cations and chloride anions. There are also large regions which, at the time of crystallization, contain acetone(solvent) molecules. There are two distinct solvent sites, each occupied by an acetone molecule, but these solvent molecules do not appear to have any well-defined positions or orientations in these regions.

The molybdenum complex cation $[MoCl(CNBu^t)_4(PMe_3)_2]^+$ has seven-fold coordination in a capped trigonal prismatic pattern. The chloro ligand is the capping atom on the rectangular face formed by two *trans*-phosphines and two *trans*-isocyanides. The opposite edge of the prism has the two remaining isocyanides at its ends. The cation has an almost perfect two-fold symmetry axis along the Mo—Cl bond. As is quite common in related $Mo(CNBu^t)_n$ complexes, there are two possible orientations for each of the *t*-butyl groups, although only one is shown in the figure for clarity.

The reaction of $[MCl_2(CNBu^t)_3(PMe_3)_2]$ with an excess of $SnCl_2$ allows the isolation of yellow–orange $[M(SnCl_3)(CNBu^t)_3(PMe_3)_3](SnCl_3)$ (M = Mo or W). These compounds are formally

* Author to whom correspondence should be addressed.

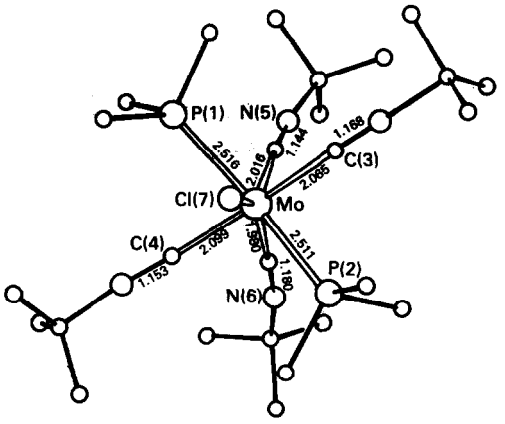

Fig. 1. Diagrammatic representation of the molecular structure of the cation $[MoCl(CNBu^t)_4(PMe_3)_2]^+$, showing selected bond lengths.

derived from the insertion of $SnCl_2$ into the metal–halide bond. ^{119}Sn NMR spectroscopy shows a quartet for coordinated $SnCl_3^-$ coupled with three phosphorus atoms, and a singlet for $SnCl_3^-$ in the external coordination sphere. This, together with ^1H and $^{31}P\{^1H\}$ NMR data, supports a capped-octahedral structure, with $SnCl_3^-$ as the capping ligand, and *fac*-arrangement of phosphines and isocyanides.

REFERENCES

1. M. Jimenez-Tenorio and M. C. Puerta-Vizcaino, *XVIII I.C.C.C.*, B12. Oporto, Portugal (1988).
2. S. J. Lippard, P. A. Bianconi, I. D. Williams and M. P. Engeler, *J. Am. Chem. Soc.* 1986, **108**, 311.

Polyhedron Vol. 8, No. 13/14, pp. 1788–1789, 1989
Printed in Great Britain

0277–5387/89 $3.00+.00
© 1989 Maxwell Pergamon Macmillan plc

POLYTUNGSTATE SELF-ASSEMBLY: STRUCTURES OF THE NEW OXOANIONS, $[W_4(NBu^t)_4O_4Cl_{10}]^{2-}$ AND $[W_6O_{14}Cl_{10}]^{2-}$

WILLIAM CLEGG, R. JOHN ERRINGTON,* DAVID C. R. HOCKLESS and CARL REDSHAW

Department of Chemistry, The University of Newcastle upon Tyne, Newcastle upon Tyne NE1 7RU, U.K.

Abstract—The tetratungstate $[W_4(NBu^t)_4O_4Cl_{10}]^{2-}$ and the hexametalate $[W_6O_{14}Cl_{10}]^{2-}$, isolated from reactions generating organoimidooxo species in solution, have been structurally characterized by X-ray crystallography.

The spontaneous self-assembly of inorganic or metalloorganic fragments in solution to give certain stable, recurring structures has been noted in a variety of systems.[1] During the course of our work with organoimido tungsten compounds, we found that the binuclear complex $[W_2(NBu^t)_2(\mu\text{-}NPh)_2Cl_4(NH_2Bu^t)_2]$,[2] can be converted to the tritungstate $[W_3(NBu^t)_3(\mu\text{-}NPh)_3Cl_7]^-$ (**1**), by treatment with chloride ion [eq. (1)]:[3]

$$3[W_2(NBu^t)_2(NPh)_2Cl_4(NH_2Bu^t)_2] + 2Q^+Cl^- \longrightarrow 2Q[W_3(NBu^t)_3(NPh)_3Cl_7] + 6Bu^tNH_2. \quad (1)$$

The analogy between the structure of the tritungstate (**1**) (Fig. 1) and that of the W_3O_{13} fragment, which is the basic structural unit of many polyoxotungstates,[4] stimulated our interest in polyoxometalate chemistry and we have proceeded to investigate routes to analogous oxo complexes.

Treatment of binuclear $[W_2(NC_6H_4Me\text{-}4)_2Cl_8]$ with $Me_3SiOSiMe_3$ gives the organoimidooxo compound $[W(NC_6H_4Me\text{-}4)(O)Cl_2]$† which, on the basis of its IR spectrum (no terminal W=O stretch and bands at 820 and 720 cm^{-1} due to W—O—W), appears to be polymeric with bridging oxides. Unfortunately, our attempts to break down the polymeric structure to form a trimetalate analogous to **1** have so far been unsuccessful. However, in a reaction designed to produce a *t*-butylimidooxo analogue of **1**, i.e. $[W_3(NBu^t)_3(\mu\text{-}O)_3Cl_7]^-$, we treated $WOCl_4N^+$ with Bu^tNH_2 in the presence of Q^+Cl^- ($Q^+ = Et_4N^+$, $Bu^n_4N^+$, or $Ph_3(PhCH_2)P^+$) and after work-up obtained yellow crystals of the tetrametalate $Q_2[W_4(NBu^t)_4(\mu\text{-}O)_4Cl_{10}]$ (**2**) in high yield.‡ The X-ray crystal structure of the $Ph_3(PhCH_2)P^+$ salt has been determined§ and the anion is shown in Fig. 2 with methyl groups omitted for clarity. The distorted tetrahedron of four tungsten atoms is bridged across two opposite edges by chlorine atoms and across the remaining edges by

* Author to whom correspondence should be addressed.

† Satisfactory microanalytical data have been obtained.

‡ Spectroscopic data for $[W_4(NBu^t)_4O_4Cl_{10}]^{2-}$: δ_H (200 MHz; CD_2Cl_2) 1.34 (s, N*Bu*^{t}). δ_C (50.3 MHz; CD_2Cl_2) 31.98 [C(*C*H_3)$_3$], 71.88 [*C*(CH$_3$)$_3$]. ν(W—O) 900, 840 cm^{-1}; ν(W—Cl) 360, 349, 335 cm^{-1}.

§ Crystal data for $[Ph_3(PhCH_2)P](W_4(NBu^t)_4O_4Cl_{10}]\cdot 2CH_2Cl_2$: $C_{68}H_{84}N_4O_4P_2Cl_{14}W_4$, $M = 4460.4$, triclinic, $a = 12.639(2)$, $b = 12.839(2)$, $c = 27.463(4)$ Å, $\alpha = 79.79(1)$, $\beta = 7997(1)$, $\gamma = 85.67(1)°$, $V = 4314.3$ Å^3, $Z = 2$, space group $P\bar{1}$; $R = 0.061$, $R_w = 0.051$ from 9714 unique observed reflections with $3 < 2\theta < 45°$ measured with Mo-K_α radiation ($\lambda = 0.71073$ Å) and corrected for absorption. Anisotropic thermal parameters were refined for tungsten, phosphorus and chlorine atoms, isotropic for others; hydrogen atoms were included in calculated positions, and phenyl rings were refined as rigid ideal hexagons.

Crystal data for $(Bu^n_4N)_2[W_6O_{14}Cl_{10}]$: $C_{32}H_{72}N_2O_{14}Cl_{10}W_6$, $M = 2166.6$, monoclinic, $a = 18.164(4)$, $b = 19.506(4)$, $c = 18.085(4)$ Å, $\beta = 109.90(2)°$, $V = 6025.0$ Å^3, $Z = 4$, space group $C2/c$; $R = 0.061$, $R_w = 0.049$ from 3243 unique observed reflections with $3 < 2\theta < 50°$ measured with Mo-K_α radiation ($\lambda = 0.71073$ Å) and corrected for absorption. Cations are probably disordered, and were refined with restrained bond lengths and angles, and with isotropic thermal parameters for carbon atoms, and without hydrogen atoms. Atomic coordinates, bond lengths and angles, and thermal parameters have been deposited as supplementary data with the Editor from whom copies are available on request. Atomic coordinates have also been deposited with the Cambridge Crystallographic Data Centre.

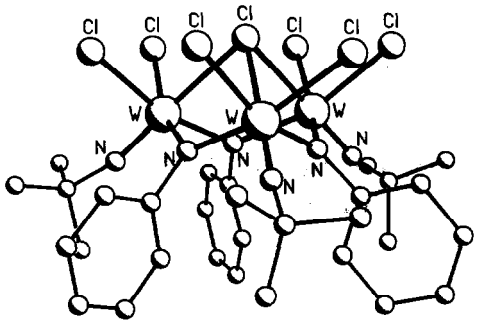

Fig. 1. The molecular structure of **1**.

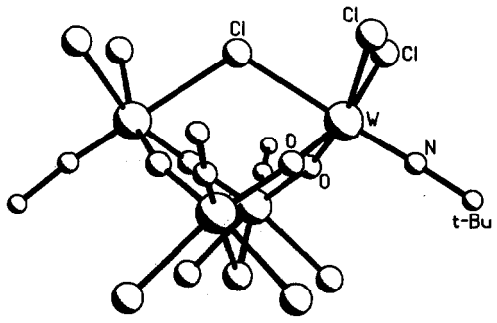

Fig. 2. The molecular structure of **2** without methyl groups. Important mean bond lengths and angles include W—N, 1.697; W—O, 1.879; W—Cl(terminal), 2.407; W—Cl(bridging), 2.657 Å; W—O—W, 159.6; W—Cl—W, 115.6; W—N—C, 174.5°.

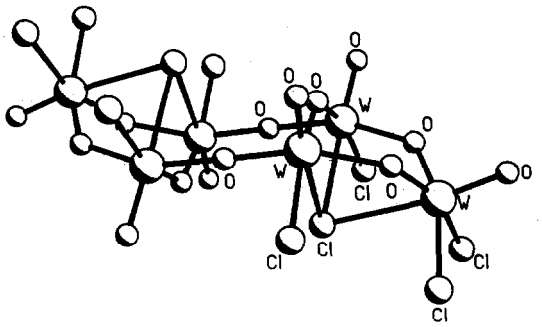

Fig. 3. The molecular structure of **3**. Important mean bond lengths and angles include W—Cl(terminal), 2.311; W—Cl(bridging), 2.803; W—O(terminal), 1.684; W—O(bridging), 1.897 Å; W—Cl—W, 76.8; W—O—W (within W_3 units), 132.4; W—O—W (between W_3 units), 177.9°.

oxygen atoms to give the molecule approximate D_{2d} symmetry. As expected, the stronger π-donor ligands, O and NBu^t, occupy mutually *cis* positions at each tungsten centre. The oxygen bridges are approximately symmetrical with large W—O—W angles (160° av.).

From the reaction between the binuclear tungsten(V) compound $(Bu^n_4N)[W_2O_2Cl_7]$[3] and *p*-tolylazide, designed to introduce a *p*-tolylimido group, we isolated the hexametalate, $[W_6O_{14}Cl_{10}]^{2-}$ (**3**), which has been characterized by X-ray crystallography.* The structure is shown in Fig. 3 and consists of two trinuclear $W_3O_3(\mu\text{-}O)_3Cl_4(\mu_3\text{-}Cl)$ fragments joined by two linear W—O—W linkages about a centre of symmetry. The bent W—O—W bridges are slightly asymmetric with an average angle of 132°. Organomido/oxo exchange is evidently occurring in this reaction and the product which is subsequently isolated depends upon the cation present in solution, since treatment of $[Ph_3(PhCH_2)P][W_2O_2Cl_7]$ with *p*-tolylazide yielded $[Ph_3(PhCH_2)P][W(NC_6H_4Me\text{-}4)Cl_5]$[5] on crystallization. We have observed similar organoimido/oxo exchange during the reaction between tetrametalate (**2**) and 2,2′-bipyridyl in toluene under reflux, which produces $[W(NBu^t)_2Cl_2(bipy)]$, whereas the room-temperature reaction yields the expected product, $[W(NBu^t)(O)Cl_2(bipy)]$. These reactions and other studies of the reactivity of **2** will be discussed in greater detail in a full paper.

Acknowledgement—We thank SERC for a grant (W.C.) and an earmarked studentship (C.R.).

REFERENCES

1. See for example: R. H. Holm, *Chem. Soc. Rev.* 1981, **10**, 455; W. J. Evans and M. S. Sollberger, *J. Am. Chem. Soc.* 1986, **108**, 6095; D. C. Bradley, H. Chudzyunska, D. M. Frigo, M. B. Hursthouse and M. A. Mazid, *J. Chem. Soc., Chem. Commun.* 1988, 1258; F. A. Cotton, P. A. Kibala and W. J. Roth, *J. Am. Chem. Soc.* 1988, **110**, 298.
2. D. C. Bradley, R. J. Errington, M. B. Hursthouse, A. J. Nielson and R. L. Short, *Polyhedron* 1983, **2**, 843; D. C. Bradley, R. J. Errington, M. B. Hursthouse, R. L. Short, B. R. Ashcroft and A. J. Nielson, *J. Chem. Soc., Dalton Trans.* 1987, 2059.
3. D. C. Bradley, R. J. Errington, M. B. Hursthouse and R. L. Short, manuscript in preparation.
4. M. T. Pope, *Heteropoly and Isopoly Oxometalates.* Springer, Berlin (1983).
5. W. Clegg, R. J. Errington and C. Redshaw, *Acta Cryst.* 1989, **C45**, 164.

* See footnote § on previous page.

Polyhedron Vol. 8, No. 13/14, pp. 1790–1791, 1989
Printed in Great Britain

0277-5387/89 $3.00+.00
© 1989 Maxwell Pergamon Macmillan plc

X-RAY CRYSTALLOGRAPHIC STUDIES OF SOME VANADYL COMPLEXES OF SCHIFF BASES

S. S. DODWAD*

Institute of Science, 15 Madam Cama Road, Fort, Bombay—400 032, India

and

D. K. KULKARNI

Institute of Science, Nagpur, India

Abstract—Some vanadyl complexes containing nitrogen and oxygen donors have been synthesized and characterized. They have the general formulae $[VO(C_xH_yNO)_2]$ or $[VO(C_xH_yCl_zNO)_2]$. The molecular structure of these complexes has been reported elsewhere. The present investigation reports the crystal structure determined by the X-ray powder method. All the observed reflections for every sample indicate a single phase with similar crystalline structures. The observed reflections are indexed and the unit cell dimensions are determined within an accuracy of 0.02 Å.

X-ray diffractometry of some metal complexes has been greatly studied and provided information about their crystallization and unit cell dimensions etc. The authors have also studied the vanadyl complexes by X-ray diffractometry.

EXPERIMENTAL AND DISCUSSION

The authors have prepared four vanadyl complexes of Schiff bases by refluxing vanadyl sulphate and the corresponding Schiff base in an ethanolic medium in a 1:2 ratio for 2 h. Their molecular structures are characterized[1] by studying their physical properties. In the present investigation, X-ray studies of these complexes were undertaken. X-ray diffractograms were measured[2] on a PW-1010 Philips diffractometer. The patterns obtained show a concentration of reflection with an abrupt decrease in intensities at higher angles. Similar observations have been reported by Brown and Bngaall.[3] All the observed reflections were indexed by the method described by Henry *et al.*[4] All the complexes crystallized in a primitive tetragonal unit cell with dimensions ranging from 14 to 18 Å. The crystallographic results, e.g. "*d*" in A (calculated and observed) and the "*c*/*a*" ratio, are reported in Tables 1 and 2. The observed "*c*/*a*" ratio is closer to 1.0 on both sides. The calculated and observed "*d*" values agree extremely well with each other, implying that all the reported complexes have similar crystal structures.

* Author to whom correspondence should be addressed.

REFERENCES

1. S. S. Dodwad and P. S. Prabhu, *J. Ind. Chem. Soc.*, accepted.
2. D. K. Kulkarni and A. M. Bhandari, *Curr. Sci.* 1979, **48**, 577.
3. D. Brown, K. W. Bngaall, A. M. Bhandari, P. Lidser and B. Whittaker, *J. Chem. Soc., Dalton Trans.* 1975, 1249.
4. N. F. M. Henry, H. Lipson and A. Wooster, *The Interpretation of X-ray Diffraction Photographs.* Macmillan, London (1961).

Table 1. Structural results of vanadyl complexes of 2-hydroxyl-1-naphthalidene-anil (HNA) and 2-hydroxy-1-naphthalidene-2′-methylanil (HNOMA)

HNA[a]			HNOMA[b]		
"*d*" in A (observed)	"*d*" in A (calculated)	Plane *hkl*	"*d*" in A (observed)	"*d*" in A (calculated)	Plane *hkl*
8.41	8.36	002	9.54	9.54	111
7.92	7.93	200	8.97	8.97	200
7.18	7.09	210	8.00	8.02	210
6.57	6.53	211	7.27	7.25	002
5.59	5.60	220	6.34	6.34	220
4.79	4.80	311	6.01	5.98	300
4.18	4.18	004	4.98	4.97	320
3.95	3.96	400	4.68	4.70	321
3.83	3.84	303	4.38	4.35	410
3.55	3.55	420	4.26	4.23	330
3.18	3.17	500	3.64	3.62	004
2.61	2.61	610	3.41	3.42	511
			3.08	3.08	530

[a] Cell—Primitive tetragonal, $a = 15.86$, $c = 16.72$ Å and $c/a = 1.054$.
[b] Cell—Primitive tetragonal, $a = 17.94$, $c = 14.49$ Å and $c/a = 0.807$.

Table 2. Structural results of vanadyl complexes of 2-hydroxyl-1-naphthalidene-3′-methylanil (HNMMA) and 2-hydroxyl-1-naphthalidene-4′-chloro-anil (HNPCA)

HNMMA[a]			HNPCA[b]		
"*d*" in A (observed)	"*d*" in A (calculated)	Plane *hkl*	"*d*" in A (observed)	"*d*" in A (calculated)	Plane *hkl*
9.80	9.85	111	11.80	11.72	101
9.08	9.11	200	6.60	6.67	211
7.62	7.63	002	5.75	5.75	220
6.44	6.44	220	5.39	5.42	300
4.92	4.92	222	5.03	5.05	113
4.06	4.07	420	4.88	4.91	311
3.82	3.82	004	4.23	4.23	004
2.94	2.93	404	4.06	4.06	400
			3.89	3.84	303
			3.82	3.83	330
			3.64	3.64	420
			3.40	3.40	224
			2.67	2.67	610

[a] Cell—Primitive tetragonal, $a = 18.22$, $c = 15.72$ Å and $c/a = 0.838$.
[b] Cell—Primitive tetragonal, $a = 16.26$, $c = 16.90$ Å and $c/a = 1.039$.

Table 3. Results of X-ray diffraction studies of vanadyl complexes

Complex	Lattice cell dimensions "*a*" in Å	"*c*" in Å	Volume (Å^3)
HNA	15.86	16.72	4205.7
HNOMA	17.94	14.49	4668.5
HNMMA	18.22	15.27	5069.2
HNPCA	16.26	16.90	4468.1

Polyhedron Vol. 8, No. 13/14, pp. 1792–1793, 1989
Printed in Great Britain

0277–5387/89 $3.00+.00
Maxwell Pergamon Macmillan plc

THE PHOTODECOMPOSITION OF THE EARLIER 3*d* METAL–OXALATO COMPLEXES

M. W. ROPHAEL

The National Research Centre, Dokki, Giza, Egypt

and

M. A. MALATI*

Mid-Kent College of Higher and Further Education, Chatham ME5 9UQ, U.K.

Abstract—Under nitrogen, an acidified solution of $[TiO(C_2O_4)_2]^{2-}$ or $[V(C_2O_4)_3]^{3-}$ is photolysed by 254 nm radiation, giving the lower-valent cation and CO_2, trapped as $BaCO_3$. Quantum yields were determined by uranyl–oxalate actinometry, combined with Ti^{3+} titration against iron(III) and vanadium(II) determination by MnO_4^- titration and spectrophotometrically. Values of $\phi_{Ti^{III}}$ and $\phi_{V^{II}}$ in 0.148 M H_2SO_4 were 0.06_8 and 0.04_0, respectively. Both increased with increasing $[H_2SO_4]$. $\phi_{Ti^{III}}$ decreased on reducing the light intensity and was lower than ϕ_{ox}. The results are compared with the published works on the photolysis of the oxalato complexes of chromium(III) and manganese(III).

The photolysis of $[Mn(C_2O_4)_3]^{3-}$ has been extensively studied.[1] We have investigated the photodecomposition of solutions of the oxalato complexes of chromium(III), using a vacuum system[2] and quantum yields were calculated from results of volumetric gas analysis. Recently we reported the photolysis of $[TiO(C_2O_4)_2]^{2-}$ and $[V(C_2O_4)_3]^{3-}$ solutions under a nitrogen atmosphere.[3] In all cases, the metal ion is reduced to a lower oxidation state and oxalate is oxidized to carbon dioxide.

EXPERIMENTAL

$K_3[V(C_2O_4)_3]3H_2O$ was prepared by reducing vanadate(V) by $N_2H_4H_2O$ and CH_3CO_2H, and complexing with oxalate.[4] Titrimetry and gravimetry gave %$(V+C_2O_4)$, 63.5 (calc. 64.8) and %H_2O, 10.8 (calc. 11.1). $K_2[TiO(C_2O_4)_2]\cdot 2H_2O$ (B.D.H.A.R., 98.5% pure) was used as supplied. The absorption spectrum of a solution of the vanadium complex exhibited LMCT at $\lambda < 260$ nm. The corresponding band for the titanium complex had λ_{max} at 210 nm. The spectra agreed with the published data.[5,6]

A solution of either complex (70 cm^3), usually in sulphuric acid, was magnetically stirred and irradiated, under nitrogen, in a cylindrical vessel surrounding the quartz thimble of a Hanovia low pressure mercury lamp (4 W). Carbon dioxide, resulting from the photo-oxidation of oxalate, was trapped in $Ba(OH)_2$/NaOH solution. The titanium(III)–oxalate complex produced was determined by titration with iron(III).[7] Titrations with permanganate before and after irradiation gave the amount of oxalate decomposed. The vanadium(II)–oxalate complex formed on irradiation was estimated from permanganate titrations before and after irradiation, which were repeated after precipitating and filtering off vanadium hydroxides. All titrations were carried out under nitrogen. The effect of light intensity on the photolysis of the titanyl complex was studied by repeating irradiations after surrounding the lamp thimble with a coarse or a fine copper gauze. In one run, a known amount of $TiCl_3$ was added prior to photolysis and two known quantities of oxalate were introduced into the solution, in two experiments, before irradiation. The yield of vanadium(II) was also estimated by measuring the absorbance of the vanadium complex before and after irradiation at the wavelengths of maximum absorption of the original solution and of $[V(C_2O_4)_2(H_2O)_2]^{2-}$, which is believed to be predominant in vanadium(II)–oxalate solutions. The photolysed solution was

* Author to whom correspondence should be addressed.

transferred under nitrogen to a vacuum spectrophotometer cell. For actinometry, a uranyl oxalate solution replaced the photolysed solution. Details of the measurements and quantum yield were as described previously.

RESULTS AND DISCUSSION

Similar to other tris-oxalate complexes of trivalent ions, the following mechanism is suggested for the vanadium complex:

$$[V(C_2O_4)_3]^{3-} \xrightarrow{h\nu} [V(C_2O_4)_2]^{2-} + C_2O_4^-$$

$$[V(C_2O_4)_3]^{3-} + C_2O_4^- \longrightarrow C_2O_4^{2-} + 2CO_2 + [V(C_2O_4)_2]^{2-}.$$

The increase in $\phi_{V^{II}}$ with increasing acid concentration, shown in Table 1, may be ascribed to the higher yield of photolysis of $[V(C_2O_4)(H_2O)_4]^+$, which is believed to predominate at pH < 1. The titration results were in good agreement with the results of spectrophotometry.

The increase in $\phi_{Ti^{III}}$ with increasing acid concentration, indicated in Table 1, suggests that $[TiO(C_2O_4)]$, known to be present at pH < 1,[10] is more readily photolysed than the bis-oxalato ion. This explanation is in agreement with the decrease in the rate of titanium(III) formation from $3.2_0 \times 10^{-3}$ to $1.9_1 \times 10^{-3}$ or $1.6_1 \times 10^{-3}$ mol in the absence or presence of $8.7_5 \times 10^{-2}$ or $1.7_5 \times 10^{-2}$ mol oxalate, respectively. The latter would shift the equilibrium to the left.

$$[TiO(C_2O_4)_2]^{2-} \rightleftharpoons [TiO(C_2O_4)] + C_2O_4^{2-}.$$

At the same acid concentration, the quantum yield of oxalate oxidation, 0.23, was appreciably higher than the yield of titanium(III) formation, 0.06_8. This may be ascribed to photosensitized decomposition of oxalate. Adding titanium(III) to the photolysed titanyl complex had an insignificant effect on the photolysis rate. The amount of photo-produced titanium(III) varied linearly with the irradiation time, as expected.

Table 1. Quantum yields of formation of titanium(III) from titanyl(IV) oxalate and of formation of vanadium(II) from tris-oxalatovanadate(III)

Complex concentration (mol dm^{-3})	[HSO] (mol dm^{-3})	Light intensity quanta ($s^{-1} \times 10^{17}$)	Quantum yield
0.050	0.078	2.06	0.03_8
0.050	0.111	2.06	0.04_2
0.050	0.148	2.06	0.06_8
0.050	0.148	0.94	0.03_9
0.050	0.148	0.71	0.03_4
0.032	None	2.06	0.00_8
0.032	0.148	2.06	0.04_0
0.032	0.295	2.06	0.04_5

The top 5 lines show the yields of titanium(III) and the bottom 3 lines show the yields of vanadium(II).

The higher quantum yield of titanium(III) compared to vanadium(II) can be explained by the apparently lower electron-transfer energy of the titanyl complex compared to the vanadium(III) complex.

The quantum yields of the photolysis of $[Mn(C_2O_4)_3]^{3-}$ are much higher than either of the complexes studied and are appreciable in the visible region. This behaviour is apparently due to the stability of the manganese(II) produced by photolysis. On the other hand, ϕ_{gas} determined for the chromium tris-oxalato ion was lower than that of the titanyl complex, presumably because of the relative instability of chromium(II) compared to the stable chromium(III). The results of the photolysis of the chromium(III) complexes in water and heavy water and at different pH values and temperatures, have been published elsewhere. The interesting feature observed was the production of hydrogen, as well as carbon dioxide, when a solution of *cis*-$[Cr(C_2O_4)_2(H_2O)_2]^-$ was photolysed.

Acknowledgement—M.W.R. thanks the National Research Centre, Egypt for leave of absence, during which the work was carried out.

REFERENCES

1. V. Balzani and V. Carassiti, *Photochemistry of Coordination Compounds*. Academic Press, London (1970).
2. M. W. Rophael and M. A. Malati, *Photochem. Photobiol.* 1973, **17**, 377.
3. M. W. Rophael and M. A. Malati, *Abstr. XIII Int. Conf. Photochem.*, Vol. II, p. 603. Budapest, August 1987.
4. M. A. Malati, *Chemie Labor. Betrieb Supplement* 1988, **39**, 84.
5. H. Hartmann and H. L. Schläfer, *Angew. Chem.* 1954, **66**, 768.
6. A. K. Babko and L. I. Dubovenko, *Russ. J. Inorg. Chem.* 1959, **4**, 165.
7. A. I. Vogel, *A Textbook of Quantitative Inorganic Analysis*, 3rd edn. Longmans, London (1961).
8. M. A. Malati, *Lab. Pract.* 1982, **31**, 1172; S. V. J. Bounds, GRSC Research Project. Mid-Kent College of Higher and Further Education (1984).
9. L. B. Levashova and V. L. Zolotova, *Russ. J. Inorg. Chem.* 1965, **10**, 77.
10. A. A. Grinberg and L. V. Shikheeva, *Russ. J. Inorg. Chem.* 1965, **5**, 287.

Polyhedron Vol. 8, No. 13/14, pp. 1794–1796, 1989
Printed in Great Britain

0277–5387/89 $3.00+.00
© 1989 Maxwell Pergamon Macmillan plc

LOW TEMPERATURE PYROLYSIS PRODUCTS OF CHROMIUM, MOLYBDENUM AND TUNGSTEN HEXACARBONYLS

I. M. WATSON and J. A. CONNOR*

University of Kent, Canterbury, Kent, U.K.

and

R. WHYMAN

ICI Chemicals and Polymers Group, Runcorn, Cheshire, U.K.

Abstract—The Group 6 metal hexacarbonyls have often been investigated as precursors in chemical vapour deposition processes. The solid products, obtained by thermal decomposition of the vapours of the compounds below 300°C, have been re-examined. Under these conditions, all three carbonyls produce a metallic phase with a face-centred cubic structure, distinct from the body-centred cubic structure of the pure metals. Microanalysis shows that the materials contain roughly equimolar amounts of carbon and oxygen. Pyrolysis of ^{18}O-labelled $Mo(CO)_6$ has demonstrated that the oxygen derives from the CO ligand of the precursors. Evidence that the pyrolysis products are insterstial oxycarbides is presented; their response to annealing treatment is described.

The importance of thin films of chromium, molybdenum and tungsten in microelectronics and other technologies has motivated many investigations of chemical vapour deposition processes using the metal carbonyls, $M(CO)_6$, as precursor compounds. In the first such study,[1] it was found that face-centred cubic (fcc) materials formed when $Mo(CO)_6$ and $W(CO)_6$ were pyrolysed below 500°C. Higher temperatures and other precautions were necessary to obtain the body-centred cubic pure metals. The fcc materials were originally formulated as carbides, but chemical analyses carried out on the pyrolysis products of $Mo(CO)_6$[2] and $W(CO)_6$[3] showed the materials contained oxygen. Recently, a similar fcc phase has been prepared by the decomposition of $Cr(CO)_6$ in a corona discharge.[4] The fcc materials, obtained by pyrolysis of the three $M(CO)_6$ complexes below 300°C, have been re-investigated. A fuller appraisal of their chemical nature and probable mechanism of formation than in previous work has been possible.

The pyrolysis products were prepared by subliming the carbonyl up a Pyrex tube under dynamic vacuum, and allowing pyrolysis to occur in a heated portion of the tube. The tubes were 3 mm internal diameter and sealed at their lower end. The carbonyls (Aldrich) were sublimed before use. Each pyrolysis run used roughly 20–30 mg of carbonyl, which was initially placed in the bottom of the tube. The samples of $Cr(CO)_6$ and $Mo(CO)_6$ were held at 50°C, and $W(CO)_6$ at 60°C. The pyrolysis zone was heated by a tubular resistance furnace, 75 mm long. In all cases, the temperature at the centre of the furnace was 300°C. Heavy deposition of solid material from $Cr(CO)_6$ and $Mo(CO)_6$ onto the tube wall began at ~ 150°C, and at ~ 230°C in the case of $W(CO)_6$. The dark, metallic deposits were poorly adherent, and all analyses were performed on loose flakes of material detached from the tubes. The equilibrium vapour pressures of the carbonyls under the conditions used[5] are much higher than the ultimate vacuum of ~ 0.05 torr obtainable in the pyrolysis apparatus. Allowing for the production of CO on decomposition, it is apparent that the pyrolysis products formed under a flux of CO sufficient to eliminate the possibility of oxidation by residual oxygen in the apparatus. The actual CO pressure during pyrolysis was at least 0.2–0.3 torr.

Qualitative analyses of the pyrolysis products

* Author to whom correspondence should be addressed.

were obtained by laser ionization mass analysis (LIMA) using a Cambridge LIMA 2A system. Positive ion LIMA spectra of the pyrolysis products all showed strong M^+, C^+ and O^+ peaks. No polyatomic ions such as CO^+ were detected. These results provided initial evidence that the materials were oxycarbides. Confirmation of the origin of the oxygen was sought by pyrolysing a sample of 50% ^{18}O-labelled $Mo(CO)_6$. This was prepared by reacting cycloheptatriene molybdenum tricarbonyl[6] with $C^{18}O$ (Alfa) in 1,2-dichloroethane solution. LIMA showed that the $^{16}O/^{18}O$ ratio in the pyrolysis product was 1.1 ± 0.1, confirming that 91–100% of the oxygen in the material originated from the CO ligand of the precursor. The mechanism of incorporation of carbon and oxygen into the pyrolysis products will be considered below.

Quantitative analyses were made by conventional chemical methods, and the results are summarized in Table 1. Carbon analyses were performed by combustion with an iron oxide additive in a Carlo Erba 1130 instrument. Samples of Cr_3C_2 (Johnson Matthey), Mo_2C and WC (both Alfa) were used as standards. Oxygen analyses were made by Pascher Laboratories, Remagen, using a Balzers Exhalograph EAO-202 instrument. The results indicated approximately equimolar amounts of oxygen and carbon in each of the pyrolysis products. Very similar analytical data were obtained by Vogt[3] for the low temperature pyrolysis products of $W(CO)_6$.

Scanning electron microscopy (SEM) was used to confirm that the materials had dense, locally uniform microstructures, consisting of grains 50–200 nm in size. These observations helped support the supposition that the products were chemically homogeneous, with bulk compositions reflecting the analytical data.

X-ray powder diffraction patterns were recorded using Cu-K_α radiation. The materials each consisted of a single fcc phase, with the approximate lattice parameters listed in Table 1. Diffuse diffraction peaks, consistent with the particle size broadening expected from 25 nm particles,[7] were observed. Since the actual grain sizes observed by SEM were somewhat larger, disorder in the materials was probably responsible. Pure molybdenum and tungsten have been claimed to crystallize in the fcc structure, but only in the form of extremely thin films, below the thicknesses encountered here.[8] In view of the analytical data, it is likely the pyrolysis products are non-stoichiometric interstitial phases, with the carbon and oxygen atoms occupying octahedral interstices in an fcc lattice of metal atoms, presumably in a random fashion. This suggestion has been made previously,[1,2] but will be briefly reviewed.

Table 1. Analytical data for the pyrolysis products

Precursor	Element weight (%) C	O	Deduced composition	Lattice parameter (Å)
$Cr(CO)_6$	9.55	12.0	$CrC_{0.52}O_{0.49}$	4.14
$Mo(CO)_6$	4.33	5.47	$MoC_{0.38}O_{0.36}$	4.19
$W(CO)_6$	2.44	2.93	$WC_{0.39}O_{0.36}$	4.17

To investigate their thermal stability, samples of the oxycarbides were annealed in evacuated silica ampoules at 600°C for 24 h, and examined by X-ray powder diffraction. The fcc material obtained from $Cr(CO)_6$ was entirely transformed into Cr_3C_2, Cr_2O_3 and an unidentified phase. The $Mo(CO)_6$ pyrolysis product was partially converted into α-Mo_2C, MoO_2 and molybdenum metal, while the $W(CO)_6$ pyrolysis product remained unchanged.

The B1(NaCl) structure described above is one of the types adopted by the so-called Hägg phases, discussed by Toth.[9] The molybdenum and tungsten carbides, α-MoC_{1-x} and α-WC_{1-x}, have this structure. The atomic radius of chromium is slightly too small to allow interstitial carbides to form, and phases such as Cr_3C_2 have more complicated structures. In formulating the pyrolysis products as interstitial phases of this sort, a further novel feature is their relatively large oxygen content. The composition of the $Cr(CO)_6$ pyrolysis product is very close to the idealized composition, $CrC_{0.50}O_{0.50}$, expected for full occupation of the octahedral interstices. In the other two oxycarbides, vacancies must be present. The metal lattices in these materials are rather dilated, particularly in the $Cr(CO)_6$ pyrolysis product. Here, the distance between neighbouring metal atoms is 2.93 Å, which is considerably more than twice the normal radius of a 12-coordinate chromium atom, 1.267 Å.[9] It might be anticipated that the fcc phase would possess limited stability, as shown by the annealing experiments.

In the discussion above, it has been assumed that the pyrolysis products are oxycarbides, containing no undissociated CO. The distance between the carbon and oxygen atoms on adjacent interstitial sites will be ~ 2.95 Å, much too far to allow any direct bonding to be retained. The best evidence that the materials contain no undissociated CO is the lack of any CO^+ or CO^- peaks in their LIMA spectra. Furthermore, their IR spectra, recorded in KBr discs, showed no ν(CO) absorptions. Vogt obtained X-ray photoelectron spectra for the fcc tungsten oxycarbide,[3] but definite conclusions could not be reached about the chemical state of the constituent

atoms. It is known, however, that in the β-state of chemisorbed CO on molybdenum and tungsten surfaces, the C—O bond is greatly weakened, with both atoms involved in bonding to the surface.[10] Desorption of β-CO from tungsten occurs only above $\sim$ 700°C.[11] A recent study of the adsorption of CO on a chromium (110) surface showed that at -150°C CO preferentially bonded in a "side-on" fashion, with ν(CO) appearing in the 1150–1330 cm^{-1} range, and dissociation occurred above -100°C.[12] These findings provide some precedent for the surface dissociation of CO which must occur during synthesis of the oxycarbides. The deposition of carbon in the material could also be accompanied by the production of CO_2, as considered by Kaplan and d'Heurle.[13] This process is clearly not very important here, and it is uncertain whether the slight excess of carbon over oxygen observed in the materials is significant. A study of the gaseous thermal decomposition products of $Mo(CO)_6$ and $W(CO)_6$ by mass spectrometry showed that the CO^+/CO_2^+ ratio was always above 50.[14]

It is likely that the pyrolysis products described closely resemble those obtained in previous work, under somewhat different sets of conditions. Their compositions were not always investigated in great detail, particularly when film deposition rates and electrical properties were of principal interest.[13,15,16] The presence of hydrogen as a background gas clearly did not prevent the incorporation of carbon and oxygen into the pyrolysis products.[2,3] Auger electron spectroscopy (AES) indicated that films produced by the photo-assisted decomposition of $Mo(CO)_6$ had a composition close to the pyrolysis products discussed here.[16] Electron diffraction and AES also showed that similar materials can be obtained by the decomposition of $Cr(CO)_6$[4] and $Mo(CO)_6$[17] in a corona discharge. Hence, the results described are likely to be relevant to a range of low temperature chemical vapour deposition techniques.

Acknowledgements—I.M.W. gratefully acknowledges support from the SERC and ICI Chemical and Polymers, who provided the analyses. Dr M. M. Lee is particularly thanked for her careful LIMA work.

REFERENCES

1. J. J. Lander and L. H. Germer, *Transactions of the American Institute of Mining and Metallurgical Engineers*, 14, Technical Publication 2259 (1947).
2. I. F. Ferguson, J. B. Ainscough, D. Morse and A. W. Miller, *Nature* 1964, **202**, 1327.
3. G. J. Vogt, *J. Vac. Sci. Technol.* 1982, **20**, 1336.
4. F. Okuyama, *J. Appl. Phys.* 1982, **53**, 6226.
5. G. Boxhoorn, J. M. Ernsting, D. J. Stufkens and A. Oskam, *Thermochim. Acta* 1980, **42**, 315.
6. R. B. King, *Organometallic Syntheses*, Vol. 1, pp. 125–126. Academic Press, London (1965).
7. A. R. West, *Solid State Chemistry and its Applications*, pp. 173–175. Wiley, Chichester (1984).
8. K. L. Chopra, *Thin Film Phenomena*, p. 200. McGraw-Hill, London (1969).
9. L. E. Toth, *Transition Metal Carbides and Nitrides*, pp. 31–46 and 79–85. Academic Press, London (1971).
10. M. W. Roberts, *Chem. Soc. Rev.* 1977, **6**, 373.
11. G. Ehrlich, *J. Chem. Phys.* 1961, **34**, 39.
12. N. D. Shinn and T. E. Madey, *J. Chem. Phys.* 1985, **83**, 5928.
13. L. H. Kaplan and F. M. d'Heurle, *J. Electrochem. Soc.* 1970, **117**, 693.
14. A. P. Patokin and V. V. Sagalovich, *Russ. J. Phys. Chem.* 1976, **50**, 370.
15. M. Diem, M. Fisk and J. Goldman, *Thin Solid Films* 1983, **107**, 39.
16. G. A. Kovall, J. C. Matthews and R. Solanki, *J. Vac. Sci. Technol.* 1988, **A6**, 2353.
17. F. Okuyama and Y. Fujimoto, *J. Appl. Phys.* 1984, **56**, 566.

Polyhedron Vol. 8, No. 13/14, pp. 1797–1799, 1989
Printed in Great Britain

0277–5387/89 $3.00+.00
© 1989 Maxwell Pergamon Macmillan plc

PREPARATION AND REACTIONS OF NIOBIUM(V) SULPHIDE COMPLEXES

J. L. SEELA, J. C. HUFFMAN and G. CHRISTOU*

Department of Chemistry and the Molecular Structure Center, Indiana University, Bloomington, IN 47405, U.S.A.

Abstract—An improved synthetic procedure to $(PPh_4)[NbSCl_4]$ (**1**) is described involving the reaction of $NbCl_5$ with two equivalents of $NaSBu^t$. Complex **1** reacts with NaSPh to yield $(PPh_4)[NbS(SPh)_4]$ (**2**), the crystal structure of which confirms a square-pyramidal geometry at the metal with a multiply-bonded sulphur at the apex (Nb—S = 2.171(2) Å).

The sulphur-based chemistry of the group 6 metals, molybdenum and tungsten, has been the subject of intense investigation over many years. In contrast, the corresponding chemistry of the group 5 metals is still only poorly explored. We have a program directed towards the development of group 5 metal–sulphur chemistry and most of our efforts to date have been concentrated in vanadium. However, we herein describe some recent results with niobium involving the +5 oxidation level.

The anion $[NbSCl_4]^-$ was considered an attractive starting point for the synthesis of M—S—SR complexes by metathesis. However, available procedures to this material are less than optimal with respect to yield, purity or convenience of preparation,[1] and we have therefore sought a facile, one-step, high-yield procedure from readily-available starting materials. Given the tendency of Bu^tS^- to act as a sulphide (S^{2-}) source via C—S bond cleavage [eq. (1)]:

$$Bu^tS^- \longrightarrow Bu^{t+} + S^{2-} \qquad (1)$$

the reaction between $NbCl_5$ and equimolar amounts of $NaSBu^t$ in CH_2Cl_2 was investigated. Addition of PPh_4Cl to the reaction mixture led to isolation of approximately equal amounts of green $(PPh_4)[NbSCl_4]$ (**1**) and yellow $(PPh_4)[NbCl_6]$. The formation of two products was rationalized according to eq. (2):

$$2NbCl_5 + 2Bu^tS^- \longrightarrow NbSCl_4^- + NbCl_6^- + Bu^t_2S; \qquad (2)$$

thus, it was suspected that incomplete conversion of $NbCl_5$ to $NbSCl_4^-$ was due to reaction of generated Bu^{t+} with remaining Bu^tS^- [eq. (3)]:

$$Bu^{t+} + Bu^tS^- \longrightarrow Bu^tSBu^t. \qquad (3)$$

If this were really the case, then additional Bu^tS^- should result in clean formation of $NbSCl_4^-$. Treatment of $NbCl_5$ with 2 equivalents of $NaSBu^t$ does indeed produce only $NbSCl_4^-$ [eq. (4)], and isolated yields of pure crystalline $(PPh_4)[NbSCl_4]$ are routinely ~ 60%. The NEt_4^+ salt can be prepared in a similar fashion.

$$NbCl_5 + 2Bu^tS^- \longrightarrow NbSCl_4^- + Bu^t_2S + Cl^-. \qquad (4)$$

Treatment of complex **1** in MeCN with 4 equivalents of NaSPh leads to a rapid colour change from light green to intense red. Removal of solvent and recrystallization from THF–hexanes yields essentially black crystals of $(PPh_4)[NbS(SPh)_4]\cdot$THF (**2**) [eq. (5)]:

$$NbSCl_4^- + 4NaSPh \longrightarrow NbS(SPh)_4^- + 4NaCl. \qquad (5)$$

The structure† of the anion is shown in Fig. 1; the niobium possesses square-pyramidal geometry with a multiply-bonded sulphur atom S(2) at the apex and four terminally-coordinated sulphur atoms from the PhS^- groups in the basal plane. The

* Author to whom correspondence should be addressed.

† Crystal data for $(PPh_4)[NbS(SPh)_4]\cdot$THF at −155°C: triclinic, $P\bar{1}$, $a = 12.442(3)$, $b = 12.154(3)$, $c = 15.887(4)$ Å, $\alpha = 91.73(1)$, $\beta = 92.13(1)$, $\gamma = 102.67(1)°$, $V = 2340.49$ Å^3, $Z = 2$, $d_{calc} = 1.381$ g cm^{-3}, $\mu = 5.297$ cm^{-1}, $\lambda = 0.71069$ Å, 6142 unique reflections ($6 \leqslant 2\theta \leqslant 45°$) collected at 6.0° min^{-1}. The structure was solved by direct methods (MULTAN) and Fourier techniques, and refined by full-matrix least-squares to $R = 5.93$ and $R_w = 5.81\%$ for 4916 reflections with $F > 2.33\sigma(F)$.

Table 1. Selected structural parameters for complex **2**

(a) Bonds			
Nb(1)—S(2)	2.171(2)	Nb(1)—S(17)	2.440(2)
Nb(1)—S(3)	2.443(2)	Nb(1)—S(24)	2.441(2)
Nb(1)—S(10)	2.441(2)		
(b) Angles			
S(2)—Nb(1)—S(3)	108.2(1)	S(10)—Nb(1)—S(17)	82.0(1)
S(2)—Nb(1)—S(10)	110.9(1)	S(10)—Nb(1)—S(24)	138.4(1)
S(2)—Nb(1)—S(17)	109.5(1)	S(17)—Nb(1)—S(24)	84.4(1)
S(2)—Nb(1)—S(24)	110.7(1)	Nb(1)—S(3)—C(4)	112.9(2)
S(3)—Nb(1)—S(10)	83.7(1)	Nb(1)—S(10)—C(11)	113.6(2)
S(3)—Nb(1)—S(17)	142.3(1)	Nb(1)—S(17)—C(18)	113.8(3)
S(3)—Nb(1)—S(24)	83.5(1)	Nb(1)—S(24)—C(25)	113.8(2)

Table 2. Comparison of Nb=S distances and stretching frequencies (ν)

Complex	Nb=S (Å)	ν (cm^{-1})	Reference
$NbS(SPh)_4^-$ (**2**)	2.171(2)[a]	525[b]	[c]
$NbSCl_4^-$	2.085(5)[a]	552	1
$NbSCl_3(SPPh_3)$	2.114(4)[a]	536	2, 3
$NbSBr_3(THT)_2$	2.09(8)[d]	[e]	4
$[NbSCl_2(SPPh_3)(\mu\text{-}Cl)]_2$	2.129(4)[d]	[e]	2, 3
$Nb_6S_{17}^{4-}$	2.196(4)[d]	483	5, 6
$NbS(S_3CNEt_2)_3$	2.122(1), 2.168(1)[d]	493	7
$NbS(SC_2H_4S)(SC_2H_4SC_2H_4S)^-$	2.192[d]	493	8

[a] Site *trans* to Nb=S unoccupied.
[b] NEt_4^+ salt; obscured in the PPh_4^+ salt by cation bands.
[c] This work.
[d] Site *trans* to Nb=S occupied.
[e] Not reported.

important bond lengths and angles are collected in Table 1. It can readily be seen that the NbS_5 core possesses almost perfect C_{4v} symmetry, with the basal Nb—S bonds and S(2)—Nb(1)—S(3,10,17,24) angles lying in the very narrow ranges of 2.440–2.443 Å and 108.2–110.9°, respectively. Of interest is the apical Nb=S distance of 2.171(2) Å, which is at the longer end of the observed Nb=S values; inspection of Table 2 shows a range of 2.085–2.196 Å. We have noted elsewhere in our investigations of V—S chemistry that basal RS^- ligands result in noticeably longer apical $V{=}O^{2+}$ and $V{=}S^{2+}$ distances;[9] we have rationalized this as due to the excellent electron-releasing properties of thiolate ligands. Note that the anionic nature of the PhS^- ligands cannot be the sole explanation, because $NbSCl_4^-$ has the *shortest* distance yet observed. Note also that the distance observed for complex **2** is even longer than those observed for some complexes possessing a sixth ligands *trans* to the sulphide.

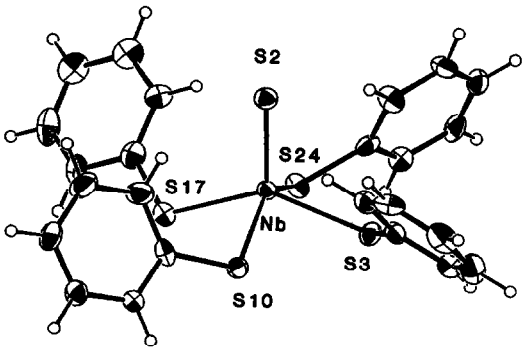

Fig. 1. ORTEP representation of complex **2** at the 50% probability level.

The reactivity characteristics of complex **2** are under investigation. With excess PhCOCl, clean conversion back to complex **1** is observed [eq. (6)]:

$$NbS(SPh)_4^- + 4PhCOCl \longrightarrow NbSCl_4^- + 4PhCOSPh. \quad (6)$$

The products from the reaction of **2** under a variety of other conditions (e.g. reduction, heating, treatment with MeI or I_2, etc.) are currently being investigated.

Acknowledgement—This work was supported by NSF Grant CHE 8808019.

REFERENCES

1. U. Muller and P. Klingelhofer, *Z. Anorg. Allg. Chem.* 1984, **510**, 109.
2. M. G. B. Drew, G. W. A. Fowles, R. J. Hobson and D. A. Rice, *Inorg. Chim. Acta* 1976, **20**, L35.
3. M. G. B. Drew and R. J. Hobson, *Inorg. Chim. Acta* 1983, **72**, 233.
4. M. G. B. Drew, D. A. Rice and D. M. Williams, *J. Chem. Soc., Dalton Trans.* 1983, 2251.
5. J. Sola, Y. Do, J. M. Berg and R. H. Holm, *J. Am. Chem. Soc.* 1983, **105**, 7794.
6. J. Sola, Y. Do, J. M. Berg and R. H. Holm, *Inorg. Chem.* 1985, **24**, 1706.
7. Y. Do and R. H. Holm, *Inorg. Chim. Acta* 1985, **104**, 33.
8. K. Tatsumi, Y. Sekiguchi, A. Nakamura, R. E. Cramer and J. J. Rupp, *J. Am. Chem. Soc.* 1986, **108**, 1358.
9. J. K. Money, J. C. Huffman and G. Christou, *Inorg. Chem.* 1985, **24**, 3297.

Polyhedron Vol. 8, No. 13/14, pp. 1800–1801, 1989
Printed in Great Britain

0277–5387/89 $3.00+.00
© 1989 Maxwell Pergamon Macmillan plc

VANADIUM(V) PROTONATION AND CONDENSATION EQUILIBRIA IN THE pH RANGE 7–10 (NaCl MEDIUM, 25°C); A POTENTIOMETRIC AND SPECTROPHOTOMETRIC STUDY

J. J. CRUYWAGEN,* J. B. B. HEYNS and J. L. VISAGIE

Department of Chemistry, University of Stellenbosch, Stellenbosch, R.S.A.

Abstract—Investigations into the speciation in the vanadium(V)–aqua system are described.

Previous investigations of this system by various methods[1] have shown that several species occur in simultaneous overlapping equilibria in the pH range 7–10. The equilibria can be represented by the following general equation:

$$pH^+ + qHVO_4^{2-} \rightleftharpoons H_p^+(HVO_4^{2-})_q.$$

For brevity, species with overall formation constants $\beta_{p,q}$ are denoted by the coefficients p and q which define their stoichiometry, e.g. (1,1) and (0,2) for $H_2VO_4^-$ and $V_2O_7^{2-}$. The most recent investigations show that the existence of the following ions (−1,0), (0,1), (1,1), (0,2), (1,2), (2,2), (4,4) and (5,5) are fairly well established, but that not all authors agree about the existence of some minor polyanions, e.g. the (2,4), (3,4), (1,3) and (2,3) species.[2–6]

What is now much needed for this system is information about the thermodynamic quantities, ΔH and ΔS, for the various reactions. Such information ought to give a better understanding of the relative stabilities of the different species in terms of the driving forces for the reactions and thereby also provide indirect evidence for the formulation of some of the polyions. The correct interpretation of calorimetric data not only depends on the reaction model chosen, but also relies heavily on the values of the formation constants of the species. With this in mind, we have first conducted a potentiometric investigation supplemented by extensive spectrophotometric measurements in the UV region.

EXPERIMENTAL

Potentiometric measurements were carried out either by a manual titration procedure, as described elsewhere,[7] using a Radiometer PHM 64 Research pH meter and Ross (Orion) electrode, or with a Metrohm 636 Titroprocessor fitted with glass and calomel electrodes. Solutions examined were 0.004000, 0.007985, 0.01500, 0.02823, 0.05853 M in vanadium(V) [all 0.6 M in NaCl], and 0.004000, 0.007998, 0.02992, 0.04250, 0.06000 M in vanadium(V) [all 1.0 M in NaCl]. Spectrophotometric measurements were likewise carried out by a previously reported titration procedure,[7] using a Varian Cary 210 spectrophotometer and Apple II computer for data collection. A total of 62 spectra were collected at 2 nm intervals in the range 220–334 nm, for the following vanadium(V) concentrations: 0.03, 0.015, 0.008, 0.002 and 0.0005 M [all 0.6 M in NaCl]. A flow-through cuvette of variable pathlength[8] was used to facilitate measurements at relatively high concentrations.

RESULTS AND DISCUSSION

The potentiometric data were analysed with the computer program SUPERQUAD.[9] Extensive model testing with the data for 0.6 M NaCl showed that a model (A), comprising the following species, resulted in the lowest s value (1.00): (−1,1), (1,1), (0,2), (1,2), (2,2), (1,3), (2,3), (4,4), (5,5). An alternative model (B) which includes the tetramers (2,4) and (3,4) instead of the trimers (1,3) and (2,3), gave a somewhat higher s value (1.07). In fact, if all four of these species are included the tetramers are rejected and model A is again obtained. On assigning fixed values to the formation constants of the (2,4) and (3,4) species to retain them (in addition to the trimers) in the model (C), a lower s value (1.02) than for model B is obtained, but it is still a little higher than that for model A. Exactly the same pattern of results is obtained using the data for a 1.0 M NaCl medium.

* Author to whom correspondence should be addressed.

Table 1. $\log \beta_{p,q}$ values for various models. Ionic strengths are given in parentheses

Species (p,q)	Model	$\log \beta_{p,q}$ A[a] (0.6)	B[a] (0.6)	C[a] (0.6)	B[a] (1.0)	B[b] (0.6)	Reference 3 (0.6)	Reference 5 (3.0)	Reference 6 (2.0)	Reference 2 (2.0)
$H_2VO_4^-$	(1,1)	7.70	7.56	7.64	7.67	7.98	7.92	8.0	7.91	7.1
$V_2O_7^{4-}$	(0,2)	0.66	0.67	0.67	1.07	0.67	0.67	1.44	1.24	1.39
$HV_3O_7^{3-}$	(1,2)	10.46	10.67	10.63	10.74	10.69	10.59	11.12	10.58	10.3
$H_2V_2O_7^{2-}$	(2,2)	19.01	19.14	19.02	19.17	19.11	18.61	18.8	—	17.5
$V_3O_{10}^{5-}$	(1,3)	12.18	—	11.90	—	—	—	—	12.61	[c]
$HV_3O_{10}^{4-}$	(2,3)	21.57	—	21.01	—	—	—	—	21.94	[c]
$V_4O_{13}^{6-}$	(2,4)	—	23.08	22.80	23.33	23.08	22.80	24.73	22.97	23.5
$HV_4O_{13}^{5-}$	(3,4)	—	31.96	31.98	32.05	31.96	31.9	33.0	32.31	~ 31
$V_4O_{12}^{4-}$	(4,4)	41.60	41.68	41.75	41.77	41.60	41.68	43.24	42.09	40.01
$V_5O_{15}^{5-}$	(5,5)	52.42	51.98	51.98	52.18	51.98	51.98	54.14	52.64	50.05

[a] Models based on potentiometric data.
[b] Spectrophotometric data.
[c] Reported values are inconsistent.

The spectrophotometric data were analysed with the program SPECFIT.[10] Because of the great number of unknowns (constants and molar absorptivities), simultaneous calculation of all spectra and equilibrium constants was not possible. Only the spectrum of the (−1,1) species could be determined experimentally, and was fixed in the calculations. No more than two β-values, in addition to all remaining spectra, could be calculated at one time.

Thus different combinations of two β's were taken in turn as unknowns, after initially assigning their potentiometric values. By following this "iterative" procedure for all species included in the model (C), the model of best fit could be determined. Significantly, only model B, which included the tetramers, yielded acceptable results, while models including trimers yielded either negative molar absorptivities for trimers, or very large uncertainties in their theoretical spectra.

The agreement between the $\log \beta$ values calculated from the potentiometric and spectrophotometric data (model B) and those reported by Pettersson for the same medium, NaCl = 0.6 M, is excellent (Table 1). However, because of the practical limitations on the maximum concentration that can be measured spectrophotometrically, the minor species occurred in relatively low concentrations. The spectrophotometric evidence supporting model B should therefore be accepted with some caution at this stage. The potentiometric measurements are now being extended to still higher concentrations in an attempt to characterize the minor species more conclusively.

An enthalpimetric study of the system has, at the time of writing, been almost completed. Treatment of the data in terms of the above models has just been started. Although it is not expected that the results of the calculations will facilitate a choice between models, the enthalpy and entropy changes should give a clear indication of the driving force responsible for the formation of the major species.

Acknowledgement—We thank SASTECH for financial support.

REFERENCES

1. M. T. Pope, *Heteropoly and Isopoly Oxometalates*, p. 34 and refs cited therein. Springer, Heidelberg (1983).
2. E. Heath and D. W. Howarth, *J. Chem. Soc., Dalton Trans.* 1981, 1105.
3. L. Pettersson, B. Hedman, I. Andersson and N. Ingri, *Chem. Script.* 1983, **22**, 254.
4. L. Pettersson, B. Hedman, A.-M. Nenner and I. Andersson, *Acta Chem. Scand.* 1985, **A39**, 499.
5. L. Pettersson, I. Andersson and B. Hedman, *Chem. Script.* 1985, **25**, 309.
6. A. A. Ivakin, L. D. Kurbatova, M. V. Kruchinina and N. I. Medvedeva, *Russ. J. Inorg. Chem.* (Engl. Transl.) 1986, **31**, 219.
7. J. J. Cruywagen, J. B. Heyns and R. F. Van de Water, *J. Chem. Soc., Dalton Trans.* 1986, 1857.
8. T. Choat, J. J. Cruywagen and J. B. B. Heyns, *Anal. Chem.* 1986, **58**, 2571.
9. P. Gans, A. Sabatini and A. Vacca, *J. Chem. Soc., Dalton Trans.* 1985, 1195.
10. H. Gampp, M. Maeder, C. J. Meyer and A. D. Zuberbühler, *Talanta* 1985, **32**, 95.

Polyhedron Vol. 8, No. 13/14, pp. 1802–1803, 1989
Printed in Great Britain

0277–5387/89 $3.00+.00
© 1989 Maxwell Pergamon Macmillan plc

SOME NEW CYANO AND ISONITRILE COMPLEXES OF $Mo(\eta^5\text{-}C_5H_5)_2$

M. J. CALHORDA,* A. R. DIAS, A. M. MARTINS and C. C. ROMÃO

Centro de Química Estrutural, Instituto Superior Técnico, 1096 Lisboa Codex, Portugal

Abstract—New cyano and isonitrile complexes of molybdenocene, $[MoCp_2(CN)X]$ (X = CN, H, Cl), $[MoCp_2(CNCH_3)X]I$ (X = H, I, CH_3), $[MoCp_2(CNCH_3)_2]I_2$ and $[MoCp_2(CNCH_3)]$, were prepared and characterized. The molybdenocene adduct, $[MoCp_2(CNCH_3)]$, was prepared by reduction of $[MoCp_2Cl_2]$ with Na/Hg or from $[MoCp_2(CNCH_3)H]I$ with NaH. The other complexes were obtained from reaction of $[MoCp_2IX]$ (X = H, I) with the appropriate ligand.

Following our studies on the activation of coordinated nitriles bound to $M(\eta^5\text{-}C_5H_5)_2$ fragments (M = Mo, W; $\eta^5\text{-}C_5H_5$ = Cp),[1] we became interested in studying their isonitrile analogues, as well as their possible cyanide precursors. Although a very large number of molybdenocene derivatives are known for a wide variety of ligands, cyano and isonitrile complexes have not been reported, with the exception of $W(Cp)_2(OR)(CN)$.[2]

Reaction of $Mo(Cp)_2XI$ (X = H, I) with NaCN in acetonitrile, led to the new compounds $Mo(Cp)_2H(CN)$ and $Mo(Cp)_2(CN)_2$, quantitatively, after substitution of iodide by cyanide. The hydride complex reacts with CCl_4 in acetonitrile to give $Mo(Cp)_2Cl(CN)$. The two monocyano derivatives were characterized by elemental analysis, IR spectroscopy (ν(C≡N) at 2080 and 2110 cm^{-1}, for the hydride and the chloride derivatives, respectively) and ^1H NMR spectroscopy (δ_{Cp} = 5.01, δ_H = −9.07 for $Mo(Cp)_2H(CN)$ in d^3-acetonitrile; δ_{Cp} = 5.58 for $Mo(Cp)_2Cl(CN)$ in d^6-acetone). The bis-cyanide complex shows a C≡N stretching frequency at 2100 cm^{-1}, while the chemical shift of the Cp protons is δ 5.49 (D_2O). $Mo(Cp)_2(CN)_2$ can act as a ligand. Reaction with $Cu(BF_4)_2$, for instance, leads to the trinuclear species, $[\{Mo(Cp)_2(CN)_2\}_2Cu][BF_4]$.

Complexes of the neutral CNMe ligand can be obtained in a similar way by reaction of $Mo(Cp)_2XI$ (X = H, I) with the isonitrile in THF or acetonitrile, respectively. $[Mo(Cp)_2H(CNMe)]I$, $[Mo(Cp)_2I(CNMe)]I$ and $[Mo(Cp)_2(CNMe)_2]I_2$ were thus prepared and characterized by elemental analysis and spectroscopy. The C≡N stretching bands are observed at 2190, 2205 cm^{-1}, and 2220, 2240 cm^{-1}, respectively, in the IR spectrum. ^1H NMR spectroscopy gives the following chemical shifts (δ): 5.49 (Cp), 3.60 (Me), −8.84 (H) for the hydride derivative in d^6-acetone; 5.75 (Cp), 3.65 (Me) for the iodide derivative in d^3-acetonitrile; 5.98 (Cp), 3.60 (Me) for the bis-isonitrile complex in d^3-acetonitrile.

The $[Mo(Cp)_2H(CN)]I$ complex reacts with NaH in THF to afford the new molybdenocene derivative $Mo(Cp)_2(CNMe)$. This complex can also be prepared by reduction of $Mo(Cp)_2X_2$ (X = Cl, Br) with Na/Hg in methyl isocyanide. Both elemental analysis (Calc. for $C_{12}H_{16}NMo$: C, 53.54; H, 5.62; N, 5.20. Found: C, 52.86; H, 5.62; N, 4.50%) and ^1H NMR spectroscopy (δ_{Cp} = 4.35, δ_{Me} = 2.76 in d^6-benzene, integrating 10:3) indicate coordination of only one isonitrile ligand, while the bands in the IR spectrum suggest an end-on coordination for this ligand.

Extended Hückel molecular orbital calculations[3] show a preference for this type of coordination, the energy being *ca* 1.5 eV lower than that of a complex containing a bent, side-on coordinated isonitrile. A molecular orbital diagram comparing the two bonding modes is shown in Fig. 1.

The energy of the isonitrile orbitals changes with bending, as studied before.[4] The weaker bonding observed for the side-on coordination mode can be primarily assigned to a smaller overlap between the ligand HOMO and $2a_1$, leading to a less stable bonding molecular orbital.

It is interesting to notice that for the related nitrile complex, $Mo(Cp)_2(NCMe)$,[5] where the nitrile

* Author to whom correspondence should be addressed.

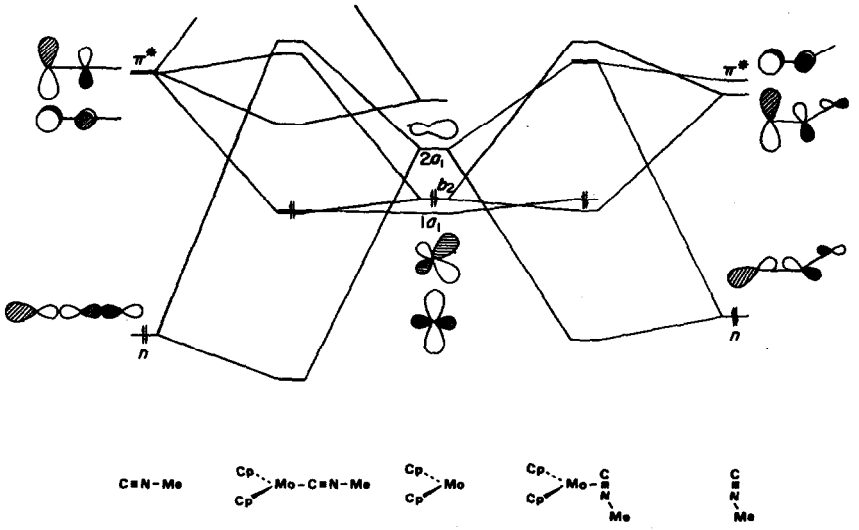

Fig. 1. Interaction between a $MoCp_2$ fragment and end-on (left) or side-on (right) isonitrile.

ligand is known to bind side-on to the molybdenum atom, our calculations give comparable energies for the two coordination geometries.

Reactions between the dication, $[Mo(Cp)_2(CNMe)_2]^{2+}$, and several nucleophiles were studied, but the products have not yet been fully characterized.

REFERENCES

1. M. J. Calhorda, M. A. A. F. de C. T. Carrondo, A. R. Dias, A. M. T. S. Domingos, M. T. L. S. Duarte, M. H. Garcia and C. C. Romão, *J. Organomet. Chem.* 1987, **320**, 63.
2. M. L. H. Green and W. E. Lindsell, *J. Chem. Soc. A* 1969, 2150.
3. R. Hoffmann, *J. Chem. Phys.* 1963, **39**, 1397; R. Hoffmann and W. N. Lipscomb, *J. Chem. Phys.* 1962, **36**, 2179, 3489.
4. J. A. S. Howell, J.-Y. Saillard, A. LeBeuze and G. Jaouen, *J. Chem. Soc., Dalton Trans.* 1982, 2533.
5. T. C. Wright, G. Wilkinson, M. Motevalli and M. B. Hursthouse, *J. Chem. Soc., Dalton Trans.* 1986, 2017.

Polyhedron Vol. 8, No. 13/14, pp. 1804–1806, 1989
Printed in Great Britain

0277–5387/89 $3.00+.00
© 1989 Maxwell Pergamon Macmillan plc

SYNTHESIS OF NOVEL SUBSTITUTED CYCLOPENTADIENES AND THEIR EARLY TRANSITION METAL COMPLEXES

T. JEFFREY CLARK and TERENCE A. NILE*

Department of Chemistry, University of North Carolina at Greensboro, Greensboro, NC 27412, U.S.A.

and

DONALD McPHAIL and ANDREW T. McPHAIL

Department of Chemistry, Paul M. Gross Laboratory, Duke University, Durham, NC 27706, U.S.A.

Abstract—Synthesis of two substituted cyclopentadienes, 1,3-bis(1-methylcyclohexyl) cyclopentadiene, Cp′H and [2-methyl-2-(2-pyridyl)ethyl]cyclopentadiene, Cp″H from fulvene intermediates is reported. These are readily converted to their early transition metal complexes $Cp'W(CO)_3Me$, $Cp''Mo(CO)_3Me$, $Cp''W(CO)_3Me$ and $[Cp''Ti(O)Cl \cdot CH_2Cl_2]_2$. The X-ray crystal structure of the titanium compound shows that the nitrogen of the pyridine cyclopentadienyl substituent is coordinated to the titanium.

The search for synthetic routes to 1,3-cyclopentadienes with a variety of substitution patterns is an area of great current interest. We report here on the synthesis of some novel substituted 1,3-cyclopentadienes (as mixtures of double bond isomers) and their early transition metal complexes.

Regioselective routes to isomeric 1,3-dialkylcyclopentadienes are limited but we have recently developed high yield regioselective syntheses using fulvene intermediates.[1] For example, 1,3-bis(1-methylcyclohexyl)cyclopentadiene (**I**, Cp′H) may be obtained via (1-methylcyclohexyl)-6,6-pentamethylenefulvene (**III**) (Fig. 1). The regio selectivity of the synthesis of **III** is confirmed by isolation of its Diels–Alder adduct with tetracyanoethylene, which yields only **IV**, which is identified by its ^1H NMR spectrum.

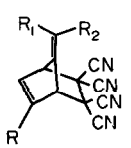

(IV)

The cyclopentadiene, Cp′H, can readily be converted into its transition metal complexes, e.g. $[Cp'W(CO)_3Me]$ (**V**) (Fig. 1). The solution IR spectrum of this compound is solvent dependent. In hexane, for example, it shows three stretches at 2010, 1925 and 1890 cm^{-1}, whereas in chloroform it shows four stretches at 2005, 1920, 1870 and 1820 cm^{-1}. This may be due to varying proportions of rotomers in different solvents, perhaps indicating that the steric bulk of the 1-methylcyclohexyl substituents causes an appreciable barrier to rotation. Similar effects have been observed with other cyclopentadienyl complexes.[2,4] Further studies are underway.

1,3-Cyclopentadienes with substituents containing potential chelating donor atoms should provide organometallic complexes with interesting properties. As an example, [2-methyl-2-(2-pyridyl)ethyl] cyclopentadiene (**VII**, Cp″H) can be obtained in 52% yield from 6-methyl-6-(2-pyridyl)-fulvene (**VI**) eq. (1):

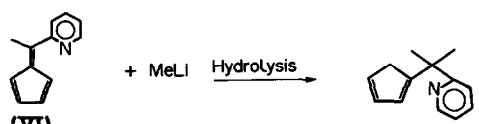

(VI) 52% (VII) (1)

* Author to whom correspondence should be addressed.

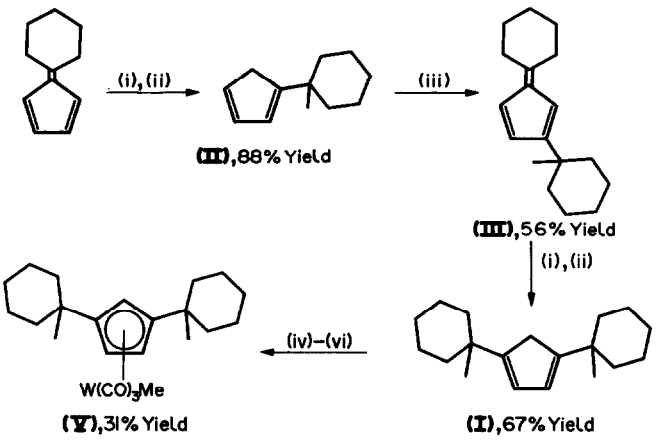

Fig. 1. Synthesis of [1,3-bis(1-methylcyclohexyl)ethylcyclohexyl)cyclopentadienyl]tricarbonylmethyltungsten (V). Reaction conditions (i) MeLi; (ii) H_2O, H^+; (iii) cyclohexanone, pyrrolidine, methanol; (iv) BuLi; (v) $(C_2H_5CN)_3W(CO)_3$; (vi) MeI.

The cyclopentadiene, Cp″H, can be converted to the metal complexes [Cp″M(CO)$_3$Me] (**VIII**, M = Mo; **IX**, M = W). The carbonyl stretches of those complexes are similar to those of the unsubstituted cyclopentadienyl complexes [**VIII**, (CO) 2020, 1940 cm^{-1} (hexane), **IX** (CO) 2020, 1920 cm^{-1} ($CHCl_3$)], indicating no coordination of the nitrogen, as this would be expected to give stretches at lower wavenumbers. Neither thermolysis in refluxing octane or UV irradiation caused changes in the spectra that could be interpreted as chelation of the pyridine moiety or as insertion of carbon monoxide into the metal methyl bond.

However, chelation of the pyridine nitrogen did occur in the [2-methyl-2-(2-pyridyl)ethylcyclopentadienyl]chlorotitanoxane dimer (**X**). This compound was prepared from the reaction between 1,1′-bis(2-methyl-2-(2-pyridyl)ethyl)magnesocene and titanium tetrachloride, followed by recrystallization with wet dichloromethane [eq. (2)].

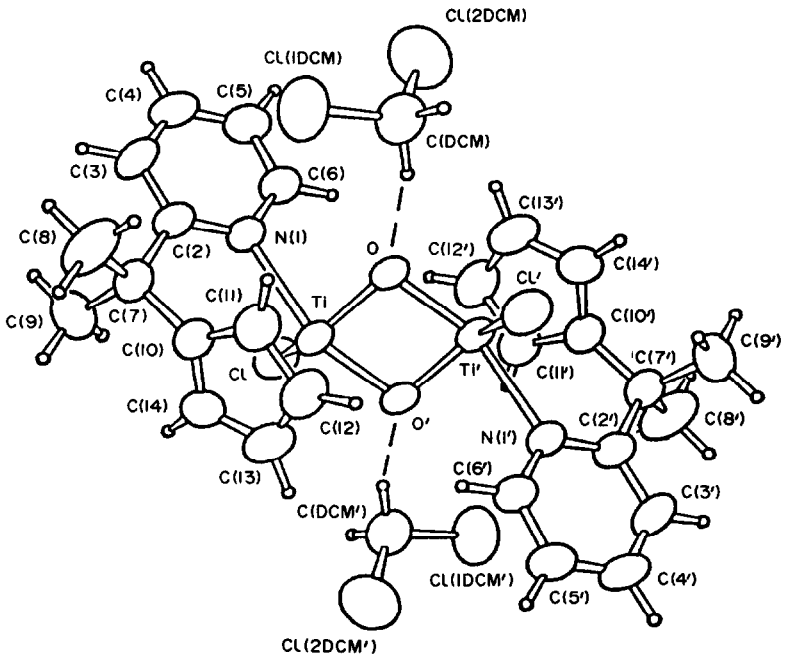

Fig. 2. Structure, solid-state conformation and atom-numbering scheme for **X**: small circles denote hydrogen atoms. Selected bond distances (Å): Ti—N, 2.297(3); Ti—O, 1.791(3); Ti—O′, 1.910(2); Ti—Ti′, 2.801(1).

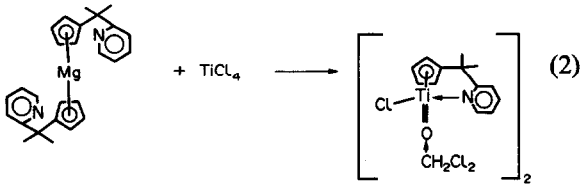

(2)

The X-ray crystal structure confirmed **X** as the product. The crystal structure and ORTEP diagram are shown (Fig. 2).* The titanium centre is coordinated to both the cyclopentadienyl ring, as well as the nitrogen atom, with a Ti—N bond distance of 2.297 Å.

Polytitanoxanes are known,[5] however, this is the first example of a dimeric product. Previous complexes exist as trimers and tetramers. This change in structure is presumed to be due to the internal chelation of the nitrogen atom occupying the coordination site normally used in forming a Ti—O bond in trimeric and tetrameric complexes. The high oxidation state of titanium and electronegative oxygen atoms aid in the internal coordination of the nitrogen atoms in this complex.

*Crystal data of **X**: $[C_{12}H_{11}ClNOTi \cdot CH_2Cl_2]_2$, $M = 737.10$, triclinic space group $P\bar{1}(C_i^1)$, $a = 10.188(3)$, $b = 10.385(2)$, $c = 8.410(3)$ Å, $\alpha = 101.78(2)$, $\beta = 92.76(2)$, $\gamma = 68.51(2)°$, $V = 810.16$ Å^3, $Z = 1$, $D_c = 1.511$ g cm^{-3}, μ(Cu-K_α) = 91.4 cm^{-1}, 2884 non-equivalent reflections, 2014 retained [$I > 3.0\sigma(I)$], $R = 0.046$, $R_w = 0.054$. Atomic coordinates, bond lengths and angles, and thermal parameters have been deposited at the Cambridge Crystallographic Data Centre.

Acknowledgements—We thank the American Chemical Society–Petroleum Research Fund, The University of North Carolina at Greensboro Research Council for support. We would also like to acknowledge the National Science Foundation for a grant to purchase the Varian 3300 Gas–Liquid Chromatograph used to analyse volatile compounds.

REFERENCES

1. T. J. Clark, MS thesis, University of North Carolina at Greensboro (1988).
2. R. D. Adams and F. A. Cotton, *Inorg. Chim. Acta* 1973, **7**, 153.
3. P. Hackett, P. S. O'Neill and A. R. Manning, *J. Chem. Soc., Dalton Trans.* 1974, 1625.
4. S. Luthra, MS thesis, University of North Carolina at Greensboro (1986).
5. P. C. Wailes, R. S. P. Coutts and H. Weigold, *Organometallic Chemistry of Titanium, Zirconium and Hafnium*, 1st edn, p. 43. Academic Press, New York (1974).

Polyhedron Vol. 8, No. 13/14, pp. 1807–1809, 1989
Printed in Great Britain

0277–5387/89 $3.00+.00
© 1989 Maxwell Pergamon Macmillan plc

PHOSPHORUS–CARBON BOND FORMATION IN DITUNGSTEN ALKYNE COMPLEXES INDUCED BY OXIDATIVE ADDITION OF CHLORODIPHENYLPHOSPHINE

MARTIN J. MAYS,* MICHAEL J. MORRIS and PAUL F. REINISCH

University Chemical Laboratory, Lensfield Road, Cambridge CB2 1EW, U.K.

and

MARY McPARTLIN and HAROLD R. POWELL

The Polytechnic of North London, Holloway Road, London N7 8DB, U.K.

Abstract—Thermolysis of $[W_2(CO)_4\{\mu\text{-}(CO_2Me)C_2CO_2Me\}(\eta\text{-}C_5H_5)_2]$ with PPh_2Cl gives $[W_2Cl_2(\mu\text{-}Ph_2PC{\equiv}CHCO_2Me)(\mu\text{-}PPh_2)(\eta\text{-}C_5H_5)_2]$, $[W_2(CO)_2(\mu\text{-}Cl)\{\mu\text{-}Ph_2PC(CO_2Me){=}CCO_2Me\}(\eta\text{-}C_5H_5)_2]$ and $[W_2(CO)C\{\mu\text{-}(CO_2Me)C_2CO_2Me\}(\mu\text{-}PPh_2)(\eta\text{-}C_5H_5)_2]$; further reactions involving these products give $[W_2(CO)O\{\mu\text{-}C(CO_2Me){=}CHCO_2Me\}(\mu\text{-}PPh_2)(\mu\text{-}C_5H_5)_2]$ and the paramagnetic complex $[W_2(CO)Cl(\mu\text{-}Cl)\{M\text{-}Ph_2PC(CO_2Me){=}CCO_2Me\}(\eta\text{-}C_5H_5)_2]$, which has been characterized by an X-ray diffraction study.

We have previously shown that the reaction of $[Mo_2(CO)_4(\mu\text{-}R^1C_2R^2)(\mu\text{-}C_5H_5)_2]$ (R^1,R^2 = H, alkyl or aryl) with PPh_2Cl proceeds via P—Cl bond cleavage and coupling of the diphenylphosphido group with the alkyne in one of three different ways, depending on the nature of R^1 and R^2.[1] In this communication we describe corresponding reactions of ditungsten alkyne complexes. Although these reactions are similar in many respects to those of the dimolybdenum species, additional products are obtained in the ditungsten system, perhaps because of the longer reaction times and higher temperatures (refluxing xylene instead of refluxing toluene) which are needed to induce the reaction to take place.

Prolonged thermolysis (2.5 days) of a xylene solution of $[W_2(CO)_4\{\mu\text{-}(CO_2Me)C_2CO_2Me\}(\eta\text{-}C_5H_5)_2]$ (**1**)[2] with excess PPh_2Cl affords, after chromatographic separation on silica (in order of elution), brown, crystalline $[W_2Cl_2(\mu\text{-}Ph_2PC{=}CHCO_2Me)(\mu\text{-}PPh_2)(\eta\text{-}C_5H_5)_2]$ (**2**)† (CH_2Cl_2–acetone 98:2) (7%), an uncharacterized brown compound, red, crystalline $[W_2(CO)_2(\mu\text{-}Cl)\{\mu\text{-}Ph_2PC(CO_2Me){=}CCO_2Me\}(\eta\text{-}C_5H_5)_2]$ (**3**)† (CH_2Cl_2–acetone 95:5) (42%) and green, crystalline $[W_2(CO)Cl\{\mu\text{-}(CO_2Me)C_2CO_2Me\}(\mu\text{-}PPh_2)(\eta\text{-}C_5H_5)_2]$ (**4**)† (CH_2Cl_2–acetone 92:8) (6%).

The proposed structures of **2**, **3** and **4** (Fig. 1) are based on spectroscopic data and on the results of X-ray diffraction studies of related dimolybdenum complexes.[1] The C—C bond scission involved in the formation of **2** from **1** is, however, a process which was not observed in the dimolybdenum system.

Thermolysis of **3** in xylene for 3.5 days gives **4** and unreacted **3** in approximately equal yields. The phosphorus–carbon bond cleavage necessary for the conversion of **3** to **4** was also not observed in our previous study.[2]

When **4** is absorbed on silica and left to stand

* Author to whom correspondence should be addressed.

† Selected spectroscopic data: (**2**): ^{1}H NMR ($CDCl_3$), δ 4.43 [dd[3], J(PH) 0.8, 0.8, 5H, C_5H_5], 4.39 [dd, ^3J(PH) 1.8, 0.4, 5H, C_5H_5] 3.94 [s, 3H, *Me*], 2.05 [dd, ^3J(PH) 6.1, 1.2, 1H, $CHCO_2Me$]. (**3**): IR ν(CO)(*n*-hexane) (cm^{-1}) 1924s, 1880s, ^{1}H NMR ($CDCl_3$) δ 4.90 [d, ^3J(PH) 1.9, 5H, C_5H_5], 4.86 [s, 5H, C_5H_5], 3.80 [s, 3H, *Me*], 3.61 [s, 3H, *Me*]. (**4**): IR ν(CO)(CH_2Cl_2) (cm^{-1}) 1993s, ^{1}H NMR ($CDCl_3$), δ 5.71 [d, ^3J(PH) 0.7, 5H, C_5H_5], 5.23 [d, ^3J(PH) 1.1, 5H, C_5H_5], 3.98 [d, 3H, Me], 3.76 [s, 3H, *Me*]. (**5**): IR ν(CO)(*n*-hexane) (cm^{-1}) 1916s, ^{1}H NMR ($CDCl_3$), δ 5.64 [d, ^3J(PH) 0.9, 5H, C_5H_5], 5.28 [d, ^3J(PH) 1.2, 5H, C_5H_5], 3.95 [s, 3H, *Me*], 3.68 [s, 3H, *Me*], 2.93 [d, ^3J(PH) 0.3, ^2J(WH) 4.8, 1H, $CHCO_2Me$]. (**6**): IR ν(CO)(CH_2Cl_2) (cm^{-1}) 1912s, ^{1}H NMR ($CDCl_3$) δ 4.88 [m, br, 10H, C_5H_5], 3.82 [s, br, 3H, *Me*], 3.63 [s, br, 3H, *Me*]. Satisfactory microanalytical data were obtained for all the above complexes.

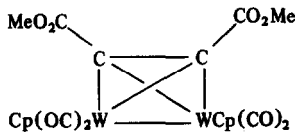

(1)

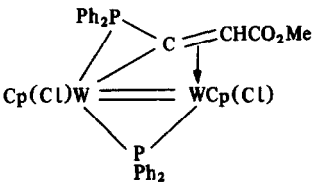

(2)

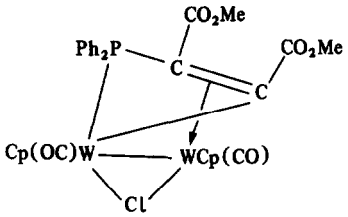

(3)

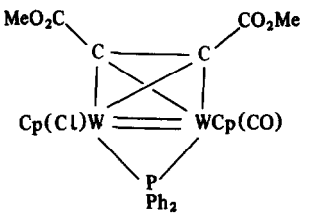

(4)

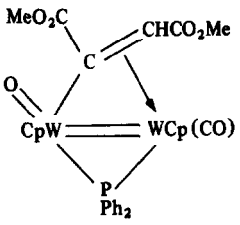

(5)

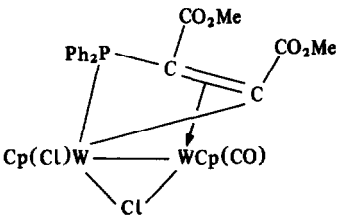

(6)

Fig. 1. Proposed structures of the new complexes.

in air and light for a few days, orange, crystalline $[W_2(CO)O\{\mu\text{-}C(CO_2Me)=CHCO_2Me\}(\mu\text{-}PPh_2)(\mu\text{-}C_5H_5)_2]$ (**5**)† (eluant CH_2Cl_2–acetone 95 : 5) (70%) was the only product isolated. Similar dimolybdenum complexes containing bridging vinyl ligands have been synthesized previously but not by this route.[3]

Photolysis of **3** (toluene solution, 100 W medium pressure UV lamp, 14 h) gave green–brown, crystalline $[W_2(CO)Cl(\mu\text{-}Cl)\{\mu\text{-}Ph_2PC(CO_2Me)=CCO_2Me\}(\eta\text{-}C_5H_5)_2]$ (**6**)† (14%), together with several other products which have not yet been fully characterized. The structure of **6** has been determined by X-ray analysis (Fig. 2).* It is similar to that proposed for **3** except that a terminal CO ligand in **3** is replaced by a Cl ligand in **6**. Two independent molecules were found in the unit cell of **6**. The structures of these molecules are fundamentally the same.

The replacement of a two-electron donor (CO) in the diagmagnetic **3**, by a one-electron donor in

*Crystal data for **6**: $C_{29}H_{26}Cl_2O_5PW_2$, $M = 923.71$, triclinic, space group $P\bar{1}$ (No. 2), $a = 19.768(4)$, $b = 14.143(3)$, $c = 10.915(2)$ Å, $\alpha = 104.74(2)$, $\beta = 99.56(2)$, $\gamma = 99.06(2)°$, $U = 2845.65$ Å^3, $F(000) = 1740$, $\mu(\text{Mo-}K_\alpha) = 82.97$ cm^{-1}, $Z = 4$, $D_c = 2.16$ g cm^{-3}. Data were collected in the θ range 3–25° with a scan width of 0.90°; $R = 0.0475$ for 6153 reflections with $I/\sigma(I) > 3.0$.

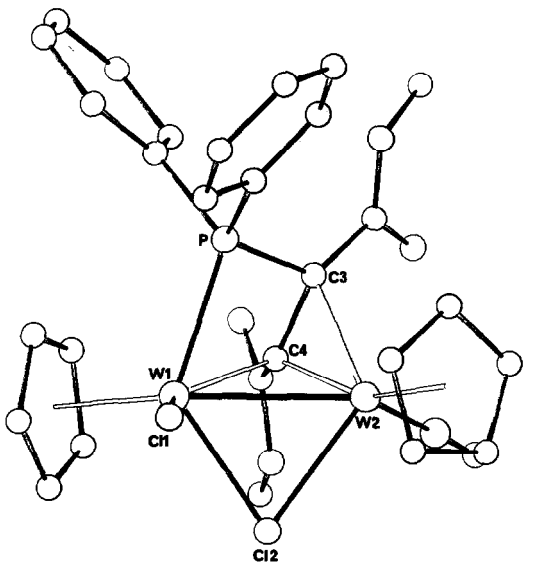

Fig. 2. A diagram of the molecular structure of one of the molecules of **6**. Important mean bond length and angle data for the two molecules include W(1)—W(2), 2.847(1); W(1)—C(4), 2.190(17); W(2)—C(4), 2.098(16); W(2)—C(3), 2.203(15); C(3)—C(4), 1.496(22); C(3)—P, 1.789(17); P—W(1), 2.472(4); W(1)—Cl(1), 2.427(5); W(1)—Cl(2), 2.439(4); W(2)—Cl(2), 2.469(5) Å. Cl(2)—W(1)—W(2), 55.1(1); Cl(1)—W(1)—W(2), 90.4(1); P—W(1)—W(2), 72.4(1); W(2)—C(4)—W(1), 83.1(6); W(1)—P—C(3), 85.6(5)°.

6, implies that **6** should be paramagnetic, and this paramagnetism is revealed both by the broadening of the ^{1}H NMR spectrum of **6** and by an ESR signal which is seen in the temperature range 4–293 K. At 77 K, three g tensors are observed: $g_1 = 1.96$, $g_2 = 1.94$ and $g_3 = 1.89$ which gives $g_{av} = 1.92$. No hyperfine coupling is observed and power saturation measurements show the presence of only one type of radical.[4]

When the CO_2Me groups on the alkyne ligand in **1** are replaced by other substituents some of the reaction products are again different and these are under study.

Acknowledgement—We thank the SERC for financial support.

REFERENCES

1. G. Conole, K. A. Hill, M. McPartlin, M. J. Mays and M. J. Morris, *J. Chem. Soc., Chem. Commun.*, in press.
2. D. S. Ginley, C. R. Bock and M. S. Wrighton, *Inorg. Chim. Acta* 1977, **23**, 85.
3. K. Endrich, R. Korswagen, T. Zahn and M. L. Ziegler, *Angew. Chem. Int. Ed. Engl.* 1982, **21**, 919.
4. C. P. Poule, *Electron Spin Resonance*, 2nd edn. Wiley, New York (1983).

Polyhedron Vol. 8, No. 13/14, pp. 1810–1813, 1989
Printed in Great Britain

0277–5387/89 $3.00+.00
Maxwell Pergamon Macmillan plc

TETRAPHENYLCYCLOPENTADIENONE COMPLEXES OF MOLYBDENUM: X-RAY CRYSTAL STRUCTURE OF $[Mo(CO)_3(C_4Ph_4CO)]_2$

ROY L. BEDDOES, ELIZABETH S. COOK and MICHAEL J. MORRIS*

Department of Chemistry, University of Manchester, Manchester M13 9PL, U.K.

Abstract—The new complex $[Mo(CO)_3(C_4Ph_4CO)]_2$ has been prepared from $[Mo(CO)_6]$ and tetracyclone, and structurally characterized by X-ray diffraction. A high yield synthesis of $[Mo(CO)_2(C_4Ph_4CO)_2]$ is also described; one of the diene ligands of this complex is readily displaced by phosphines or alkynes.

We have recently reported[1] the synthesis and structural characterization of tetraphenylcyclopentadienoneruthenium dicarbonyl dimer (**1**). This complex functions as an effective catalyst precurser for hydrogenation and dehydrogenation reactions, owing to its facile dissociation in solution into two 16e⁻ $Ru(CO)_2(C_4Ph_4CO)$ units, which are thought to be the catalytically active species.[1,2] Since only one other dimer of this type, $[Fe(CO)_2(C_4H_4CO)]_2$, is known,[3] we were interested in preparing further examples. In this communication we report our preliminary studies of molybdenum cyclopentadienone chemistry, including the crystal structure of the dimer $[Mo(CO)_3(C_4Ph_4CO)]_2$.

Overnight reaction of $[Mo(CO)_6]$ with 2 equivalents of tetracyclone in refluxing toluene affords a 95% yield of bright yellow $[Mo(CO)_2(C_4Ph_4CO)_2]$ (**2**), isolated by column chromatography and characterized spectroscopically.† This complex was first prepared in low yield by Weiss and Hübel,[4] and presumably has a structure similar to that of the bis-cyclobutadiene complex, $[Mo(CO)_2(C_4Ph_4)_2]$.[5]

If 1 equivalent of tetracyclone is used with toluene as solvent, the yield of **2** becomes very low and the major product is a brown complex, which as yet we have been unable to characterize, as it decomposes to tetracyclone and insoluble material. However, its IR spectrum shows no peaks due to metal-bound carbonyls, and it therefore seems likely that it contains toluene as a ligand. In support of this view, when a 1:1 mixture of $[Mo(CO)_6]$ and C_4Ph_4CO was refluxed overnight in heptane, the brown material was not obtained; instead a precipitate was deposited consisting of a mixture of the new complex $[Mo(CO)_3(C_4Ph_4CO)]_2$ (**3**) (30% yield following chromatographic separation) and **2** (32% yield).

The nature of complex **3** was suggested by the presence of a peak at 1543 cm^{-1} in its IR spectrum in KBr (cf. 1535 cm^{-1} for **1**), indicative of the ketonic ring carbonyl bonding to a second metal atom; the NMR spectroscopic data† were also consistent with the proposed dimeric formulation, and

* Author to whom correspondence should be addressed. New address: Department of Chemistry, University of Sheffield, Sheffield S3 7HF, U.K.

† Selected spectroscopic data (^1H and ^{13}C NMR spectra in $CDCl_3$ unless otherwise stated; shifts measured in ppm relative to TMS = 0.0 ppm, with coupling constants in Hz; phenyl resonances omitted): (**2**): ν(CO)(KBr) 2008, 1960, 1651, 1634 cm^{-1}; ^{13}C NMR 228.9 (CO), 167.3 (ring CO), 108.9, 95.3 (CPh). (**3**): ν(CO)(KBr) 2020, 1933, 1543 cm^{-1}; ^{13}C NMR (CD_2Cl_2) 242.7 (2CO), 225.3 (4CO), 155.2 (ring CO), 110.3, 104.7 (CPh). (**4a**): ν(CO)(KBr) 1936, 1817, 1603 cm^{-1}; ^1H NMR 4.27 (t, 2H, J(HP) 9.5, CH_2). (**5**): ν(CO)(CH_2Cl_2) 1919, 1608 cm^{-1}; ^1H NMR 5.78 (d, 1H, J 2.4), 4.16 (s, 1H), 4.13 (d, 1H, J 2.4); ^{13}C NMR 237.9 (CO), 166.7 (ring CO), 114.3, 110.9, 109.5, 105.6, 100.9, 93.1, 84.6 (CPh), 100.2, 98.8, 91.5 (CH). (**6**): ν(CO)(CH_2Cl_2) 2000, 1735, 1720 cm^{-1}; ^1H NMR 3.98, 3.62, 3.58, 3.50 (Me); ^{13}C NMR 230.3 (CO), 193.1, 190.0 (CCO_2Me), 170.4, 168.5, 166.5, 156.1 (CO_2Me), 160.9 (ring CO), 155.2, 145.9 (CCO_2Me), 114.4, 102.8, 101.8, 100.5 (CPh), 53.2, 52.7, 52.0, 51.6 (Me). (**7**): ν(CO)(CH_2Cl_2) 1772, 1719 cm^{-1}; ^1H NMR 3.77, 3.75, 3.65, 3.58 (Me); ^{13}C NMR 170.1, 167.6, 165.3, 158.2 (CO_2Me), 167.2 (ring CO), 153.4, 149.8, 149.6, 142.3 (CCO_2Me), 120.3, 115.9, 114.7, 109.9 (CPh), 52.9, 52.6, 52.3, 52.0 (Me). Satisfactory analytical data were obtained for all new complexes.

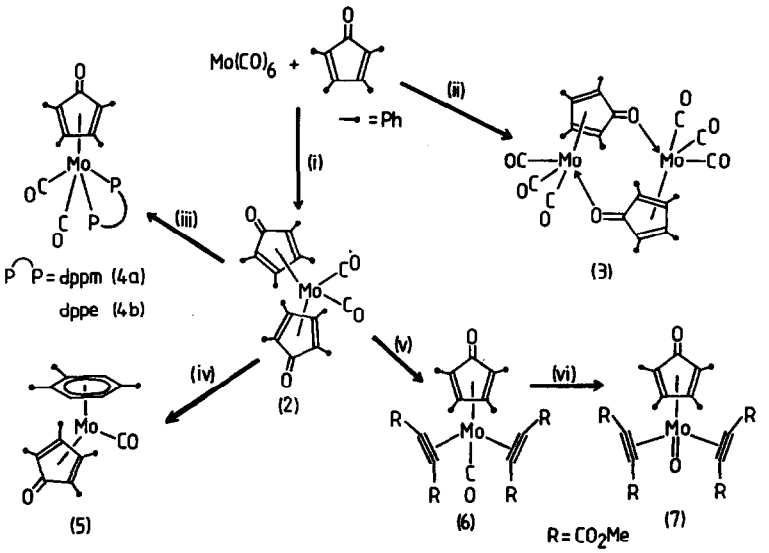

Scheme 1. Reagents and conditions: (i) 1:2 ratio, refluxing toluene, 17 h; (ii) 1:1 ratio, refluxing heptane, 17 h; (iii) dppm or dppe, refluxing toluene, 8 h; (iv) PhC≡CH (5 equivalents), refluxing toluene, 17 h; (v) $C_2(CO_2Me)_2$ (5 equivalents), refluxing toluene, 17 h; (vi) air, or aged THF.

it was confirmed by an X-ray diffraction study.* The structure, shown in Fig. 1, consists of centrosymmetric dimers in which each molybdenum bears three terminal carbonyl ligands and an η^4-bonded tetracyclone ring, the ketonic carbonyl of which is joined to the second molybdenum atom. This carbonyl group is bent back from the diene plane at an angle of 9.6°, in common with other η^4-cyclopentadienone complexes,[1,6] and the C(3)—O(2) bond length of 1.271(8) Å (cf. 1.270 Å in **1**) indicates that this bond is still essentially double in character. These features may be contrasted with those in $[Mo_2(CO)_3(\mu\text{-}C_2Ph_2)(\eta\text{-}C_4Ph_4)(\mu\text{-}C_4Ph_4CO)]$,[7] where the five carbon atoms of the bridging tetracyclone are all coplanar, and the C—O bond length is considerably longer (1.38(2) Å), indicating an η^5-bonded ring.

Preliminary investigations into the reactivity of **2** and **3** indicate that **2** provides a convenient entry into further chemistry. For example, in refluxing toluene one of the tetracyclone ligands is readily replaced by chelating phosphines to give $[Mo(CO)_2(\widehat{P\ P})(C_4Ph_4CO)]$ (**4a**: $\widehat{P\ P}$ = dppm, 92%; **4b**, $\widehat{P\ P}$ = dppe, 90%); further substitution to give the known complexes $[Mo(CO)_2(\widehat{P\ P})_2]$ does not occur. Moreover, under similar conditions, **2** is reactive towards alkynes: thus phenylacetylene gives a red–brown complex, to which we assign the structure $[Mo(CO)(1,2,4\text{-}C_6H_3Ph_3)(C_4Ph_4CO)]$ (**5**) (54%), free 1,2,4-triphenylbenzene, 1,3,5-triphenylbenzene, and pentaphenylbenzene (formed through Diels–Alder condensation of phenylacetylene with the liberated tetracyclone). With dimethyl acetylenedicarboxylate, the sole organometallic product is the green bis-alkyne complex $[Mo(CO)(MeO_2CC{\equiv}CCO_2Me)_2(C_4Ph_4CO)]$ (**6**) (45%), which on standing in the solid state (or immediately on dissolution in THF containing peroxides) undergoes oxidation to the oxo–alkyne species $[MoO(MeO_2CC{\equiv}CCO_2Me)_2(C_4Ph_4CO)]$ (**7**); a strong peak in the IR spectrum at 937 cm^{-1} is assigned to the Mo=O group. These reactions are summarized in Scheme 1.

Further investigations into the reactivity of these complexes are in progress.

Acknowledgements—We thank the Universities of Manchester and Sheffield for support, and Dr B. F. Taylor for helpful NMR experiments.

*The atomic coordinates for this work have been deposited at the Cambridge Crystallographic Data Centre. Crystal data for **3**: $C_{32}H_{20}O_4Mo$, M = 564.4 (for monomer), triclinic, space group $P\bar{1}$ (No. 2), a = 8.980(3), b = 11.332(4), c = 13.516(5) Å; α = 77.55(3), β = 71.94(3), γ = 81.02(3)°, U = 1271 Å^3, D_c = 1.47 g cm^{-3} for Z = 2 (monomer units), $F(000)$ = 636, absorption. coefficient = 6.0 cm^{-1} (λ = 0.71069 Å, Mo-K_α). Final R = 0.0535% for 2194 unique, observed [$F > 3\sigma(F)$] intensity data, collected on an Enraf–Nonius CAD4 diffractometer to a maximum θ of 22°. As $\mu R < 0.11$, no absorption correction was applied, but a linear drift correction for a total intensity drop of 12% was used. The structure was solved by direct methods using the MULTAN 80 program, and eventually refined with anisotropic thermal parameters for all non-hydrogen atoms. A non-unit weighting scheme was used.

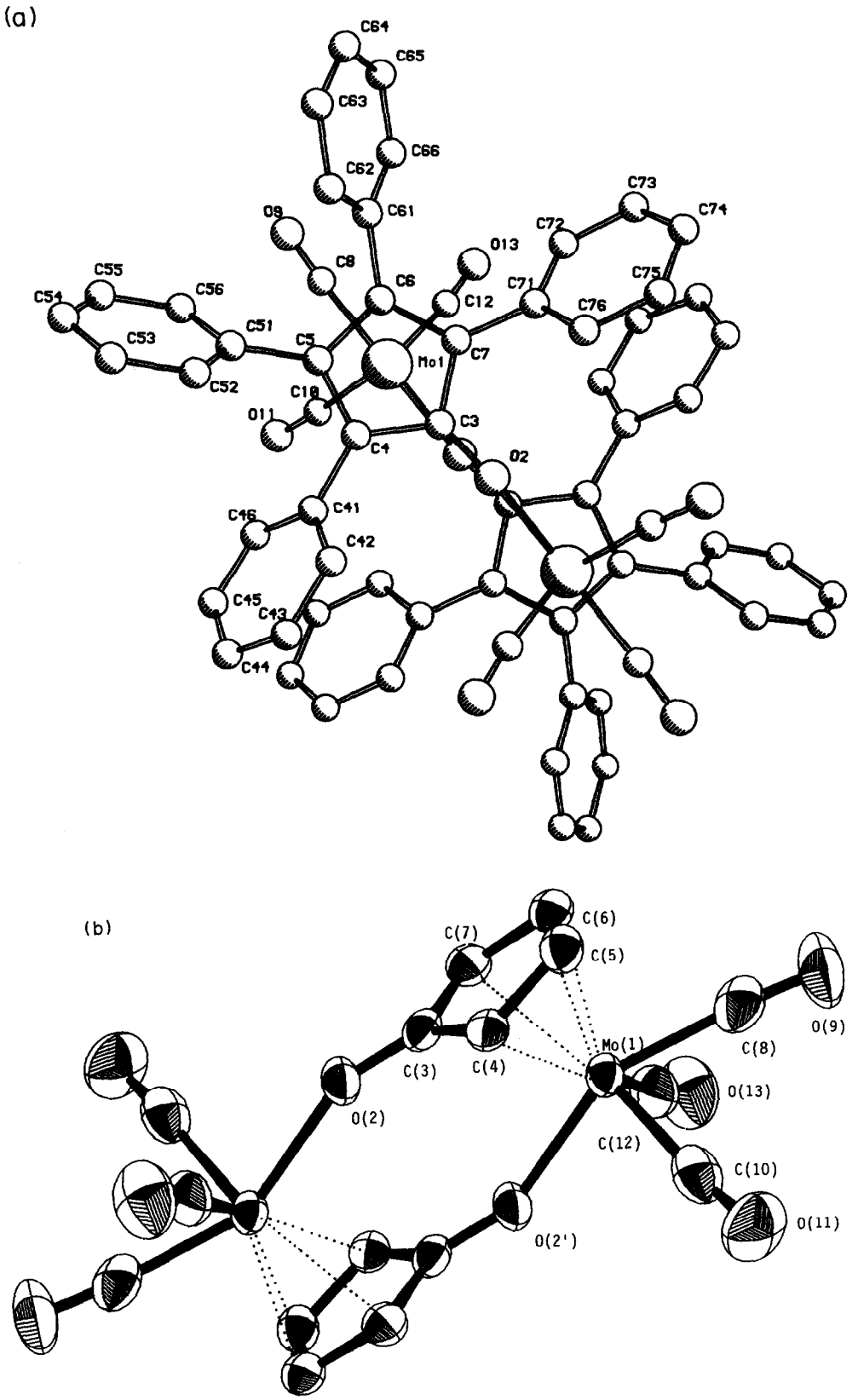

Fig. 1. (a) Molecular structure of **3**. (b) ORTEP plot of **3** with phenyl groups omitted for clarity. Selected interatomic distances and angles: Mo(1)—O(2'), 2.168(5); Mo(1)—C(3), 2.531(7); Mo(1)—C(4), 2.367(7); Mo(1)—C(5), 2.320(8); Mo(1)—C(6), 2.281(8); Mo(1)—C(7), 2.365(8) Å. C(8)—Mo(1)—O(2), 151.1(3)°.

REFERENCES

1. M. J. Mays, M. J. Morris, P. R. Raithby, Y. Shvo and D. Czarkie, *Organometallics*, in press.
2. Y. Blum, D. Czarkie, Y. Rahamim and Y. Shvo, *Organometallics* 1985, **4**, 1459; Y. Shvo, D. Czarkie, Y. Rahamim and D. F. Chodosh, *J. Am. Chem. Soc.* 1986, **108**, 7400.
3. W. Reppe and H. Vetter, *Ann. Chem.* 1953, **582**, 133; E. Weiss, R. G. Merenyi and W. Hübel, *Chem. Ind.* 1960, 407; G. S. D. King, personal communication.
4. E. Weiss and W. Hübel, *J. Inorg. Nucl. Chem.* 1959, **11**, 42.
5. A. Efraty, J. A. Potenza, L. Zyontz, J. Daily, M. H. A. Huang and B. Toby, *J. Organomet. Chem.* 1978, **145**, 315.
6. N. A. Bailey and R. Mason, *Acta Cryst.* 1966, **21**, 652; M. Gerloch and R. Mason, *Proc. R. Soc. A* 1964, **279**, 170; G. C. Cash and R. C. Pettersen, *Inorg. Chem.* 1978, **17**, 650; L. F. Dahl and D. L. Smith, *J. Am. Chem. Soc.* 1961, **83**, 752; K. Hofmann and E. Weiss, *J. Organomet. Chem.* 1977, **128**, 237; T. F. Smith, K. S. Kwan, H. Taube, A. Bino and S. Cohen, *Inorg. Chem.* 1984, **23**, 1943.
7. J. A. Potenza, R. J. Johnson, R. Chirico and A. Efraty, *Inorg. Chem.* 1977, **16**, 2354.

Polyhedron Vol. 8, No. 13/14, pp. 1814–1816, 1989
Printed in Great Britain

0277–5387/89 $3.00+.00
© 1989 Maxwell Pergamon Macmillan plc

COMPUTER MODELLING OF A MOLYBDENUM DISULPHIDE CATALYST

MICHAEL G. B. DREW* and PHILIP C. H. MITCHELL

Department of Chemistry, The University, Whiteknights, Reading RG6 2AD, U.K.

and

SLAVIK KASZTELAN†

Laboratoire de Catalyse Hétérogène et Homogène, U.A. CNRS 402, Université des Sciences et Techniques de Lille Flandres-Artois, F-59655 Villeneuve d'Ascq, Cedex, France

Abstract—Small MoS_2 slabs, which are the active component of hydrotreating catalysts, have been modelled by molecular graphics and molecular mechanics. Active sites at molybdenum are created by removing edge sulphur atoms. The structures and energies of slabs having molybdenum atoms with different degrees of coordinative unsaturation have been investigated. Structures where two molybdenum atoms are *not* linked by at least one sulphur atom are unstable owing to repulsion between the molybdenum atoms. They distort to increase the distance between the molybdenum atoms. Fully saturated slabs (those which terminate with SH groups) are also strained because of repulsions between the SH groups.

We are using computer modelling to investigate fundamental problems of heterogeneous catalysis. Recent work in our laboratory has been concerned with developing molecular graphics and energy calculations to investigate molybdenum disulphide-based catalysts.[1] These catalysts are used for hydrotreating oil feedstocks.[2] A slab model of the active phase of these catalysts has been devised based on the layered structure of MoS_2[3] and on experimental evidence, from transmission electron microscopy, for small single MoS_2 slabs in a hydrodesulphurization catalyst.[4,5] The slab model allows us to consider one slab as representative of the catalytically active phase and is particularly suitable for computer modelling.

In previous work we investigated the interaction of a simple molecule, isoprene, with catalytic sites on the edges of a MoS_2 slab, by molecular graphics and molecular mechanics.[1] In the present work, we consider the process of site generation and investigate the structural and energetic consequences of introducing vacancies at slab edges.

Computer modelling was carried out on an IBM PC–AT with the PC–Chemmod system.[6] The atomic coordinates of MoS_2 were retrieved from the SERC crystallographic database.[7] Molecular mechanics was used to calculate the energies of our structures.[8,9] We start from an ideal model structure and optimize the geometry by minimizing the total steric energy, E, which is approximated by a sum of energy contributions:

$$E = E_s + E_b + E_t + E_{nb},$$

where E_s is the bond stretching energy, E_b, the angle bending energy, E_t, the torsional energy due to rotation about bonds and E_{nb}, the energy of interactions between non-bonded atoms (van der Waals interactions).

The active phase of an alumina-supported molybdenum disulphide catalyst comprises small isolated slabs of MoS_2. In our computer graphics modelling we make a regular MoS_2 single slab by cutting a MoS_2 layer along two different crystallographic edge planes, (10−10) and (−1010).[10,11] We made a series of hexagonal slabs containing from seven up to 61 molybdenum atoms. The 61-atom hexagon is shown in Fig. 1.

The catalytic sites of molybdenum disulphide are edge plane molybdenum atoms exposed by remov-

* Author to whom correspondence should be addressed.

† Present address: Institut Français du Petrole, B.P. 311, 92506 Rueil-Maison, France.

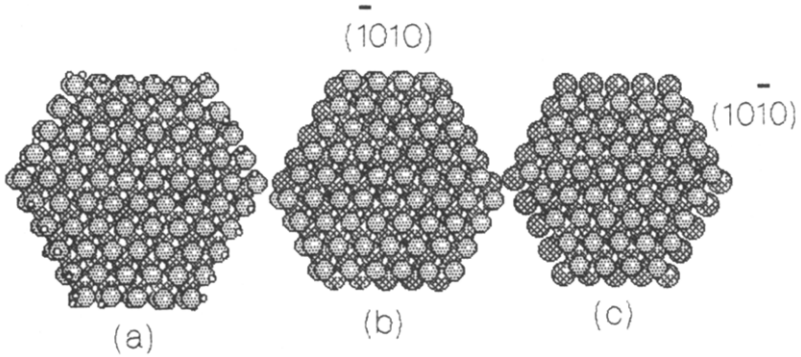

Fig. 1. Computer-drawn representations of hexagonal 61-Mo atom slabs, viewed with their basal plane in the plane of the diagram: (a) fully saturated slab terminated by SH groups; (b) partly unsaturated slab, singly bound SH groups removed from (10−10); (c) fully unsaturated slab, bridging S removed from (−1010). The edge planes are labelled. Note that in our computer graphics representation, the relative atomic sizes are according to their atomic radii: bigger, cross-hatched spheres are molybdenum atoms, small dotted spheres are sulphur atoms. The very small spheres in (a) are hydrogen atoms.

ing edge sulphur atoms.[1,2] The two types of peripheral sulphur atoms are apparent in Fig. 1: the terminal sulphur atoms in the (10−10) edge plane, designated S_I, and the bridging sulphur atoms in the (−1010) edge plane, S_{II}. In recent work the catalytic chemistry of MoS_2 has been associated with the S_{II} edge plane.[12] Various structures can be generated on this plane by removing sulphur atoms from around a pair of adjacent molybdenum atoms. This pair of molybdenum atoms constitutes an elementary ensemble.[13,14]

Molecular mechanics calculations have been carried out on various types of slab, see Fig. 1: (a) saturated, (b) partly unsaturated, singly bound sulphur atoms (S_I) removed, (c) fully unsaturated slabs, bridging sulphur atoms (S_{II}) removed. The saturated slabs are terminated by SH groups, which are necessary for electroneutrality. For the 61-molybdenum atom hexagonal slab, three sides each contain eight S_{II}; therefore, 24 S_{II} can be removed. Successive removal of S_{II} bridging sulphur atoms creates two types of molybdenum ensemble sites: (a) three-fold coordinately-unsaturated molybdenum atoms (designated 3-cus), those linked by one sulphur bridging atom; (b) 4-cus molybdenum atoms, those without bridging sulphur. Up to 12 S_{II} can be removed before 4-cus sites are formed. Our main observations, which refer to the structures *after minimization*, are as follows (final energy, E (kcal mol^{-1}); Mo···Mo nearest neighbour distance, r (Å) in the (−1010) and (10−10) edges):

(a) High energy (or strained) slabs are the ones fully saturated with SH groups [see Fig. 1(a)] (E, 62.9; r, 3.24, 3.48) and the fully unsaturated slab [Fig. 1(c)] (E, 116; r, 4.42, 2.96). The high energies are due to repulsions between the SH groups and pairs of unsaturated molybdenum atoms, respectively. Note how the repulsions open up the Mo···Mo distances (3.18 Å before minimization) along the strained edge [(10−10) in Fig. 1(a) and (−1010) in Fig. 1(c)].

(b) The high strain in the fully saturated slab is consistent with the presence of a type of easily removed sulphur in MoS_2 catalysts,[15] now considered to be the terminal sulphur in the (10−10) edge plane.[12]

(c) The partly unsaturated slab with molybdenum linked by two sulphur atoms is more stable [Fig. 1(b)] (E, 3.55; r, 3.28, 3.25). Unsaturated molybdenum atoms in the (−1010) edge plane are generated by the gradual removal of S_{II} atoms from the 61-Mo slab. The energy of the slab hardly changes as we remove up to 12 S_{II}, four from each S_{II}-type side, provided the molybdenum atoms are kept linked always by one sulphur (after removing 12 S_{II}: E, −2.90; r, 3.35, 3.23). However, successive removal of the last six sulphur atoms leads to large increases in energy because of the strong non-bonded repulsions which then arise between pairs of adjacent unsaturated molybdenum atoms (e.g. after removing three more S_{II}: E, 22.4; r, 4.31, 3.10).

Our calculations clearly show that structures where the two molybdenum atoms are *not* linked by at least one sulphur atom have high energy and are deformed relative to the normal structure. This conclusion is illustrated in Fig. 2. We see that after minimization the distance between the molybdenum atoms has increased; the cavity has opened up. Therefore, in discussing substrate binding at an active site created in the way we have

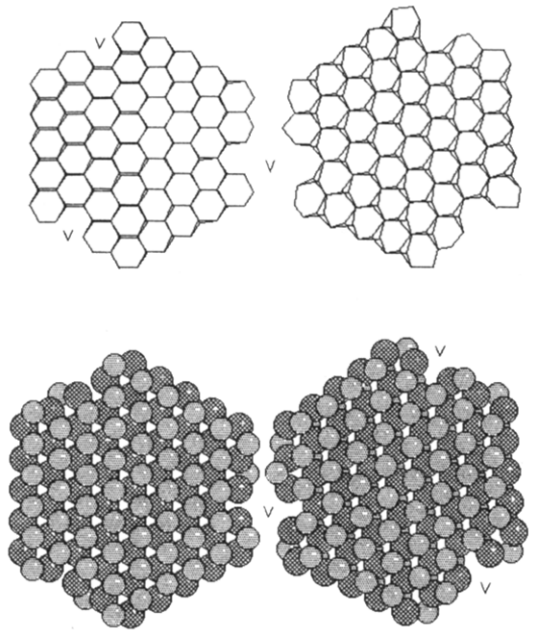

Fig. 2. Vacancies (labelled v) along (−1010), four-fold unsaturated molybdenum atoms, before and after energy minimization showing the expansion of the cavity due to Mo···Mo repulsion.

described we need to consider the final, distorted site. Experimentally, we may relate the deformation to the curved structure of the MoS_2 layers in bulk molybdenum disulphide, which may explain the rag structure of MoS_2.[16]

The active site cavity shown in Fig. 2 is reminiscent of the active centre of an enzyme; moreover, the coordination centre is strained analogously to the entatic-state description of a metalloenzyme.[17] In future work we shall investigate geometric factors in the accommodation and exclusion of a substrate molecule at the site, and electronic factors in binding and activation of the molecule. We shall also be concerned with how the strained site may be stabilized, for example by adsorption of sulphur or a reactant species such as hydrogen or a substrate molecule.

Acknowledgements—S.K. thanks the University of Lille for financial support; M.G.B.D. and P.C.H.M. thank SERC for funds for the purchase of the computer equipment.

REFERENCES

1. M. G. B. Drew, S. J. Edmondson, G. A. Forsyth, R. J. Hobson and P. C. H. Mitchell, *Catal. Today* 1988, **2**, 633.
2. P. C. H. Mitchell, in *Catalysis* (Specialist Periodical Report) (Edited by C. Kemball), Vol. 1, p. 204. The Chemical Society, London (1977); P. C. H. Mitchell, in *Catalysis* (Specialist Periodical Report) (Edited by C. Kemball), Vol. 4, p. 175. The Chemical Society, London (1982).
3. S. Kasztelan, H. Toulhoat, J. Grimblot and J. P. Bonnelle, *Appl. Catal.* 1984, **13**, 127. See also R. Candia, O. Sorensen, J. Villadsen, N. Y. Topsoe, B. S. Clausen and H. Topsoe, *Bull. Soc. Chim. Belg.* 1984, **93**, 783.
4. J. V. Sanders, *Chem. Scr.* 1979, **14**, 141.
5. S. Kasztelan, H. Toulhoat, J. Grimbolt and J. P. Bonnelle, *Bull. Soc. Chem. Belg.* 1984, **93**, 807.
6. PC-Chemmod system, U-Micro Computers, Warrington, U.K.
7. SERC Chemical Databank System, CSSR and ICSD components, Daresbury Laboratory, SERC Daresbury, Warrington, U.K.
8. U. Burkert and N. L. Allinger, *Molecular Mechanics*, ACS monograph 177 (1982).
9. D. N. J. White, Chemmin program, University of Glasgow, private communication.
10. K. Tanaka and T. Okuhara, *J. Catal.* 1982, **78**, 155.
11. P. Ratnasamy and S. Sivasanker, *Catal. Rev.-Sci. Engng* 1980, **22**, 401.
12. A. Wambeke, L. Jalowiecki, S. Kasztelan, J. Grimblot and J. P. Bonnelle, *J. Catal.* 1988, **109**, 320.
13. S. Kasztelan, *C.R. Acad. Sci. Paris Série II* 1988, **307**, 727.
14. H. Toulhoat and S. Kasztelan, in *Proc. 9th Int. Congr. Catal.* (Edited by M. J. Phillips and M. Ternan), Vol. 1, p. 152 (1988).
15. D. G. Kalthod and S. W. Weller, *J. Catal.* 1985, **95**, 455.
16. R. R. Chianelli, T. B. Prestridge, T. A. Pecoraro and J. P. de Neufville, *Science* 1979, **203**, 1107.
17. R. J. P. Williams, *J. Molec. Catal.* 1985, **30**, 1.

Polyhedron Vol. 8, No. 13/14, pp. 1817–1818, 1989
Printed in Great Britain

0277–5387/89 $3.00+.00
© 1989 Maxwell Pergamon Macmillan plc

AN EXPERIMENTAL AND COMPUTATIONAL APPROACH TO MODELLING MOLYBDOENZYMES

M. G. B. DREW,* N. J. JUTSON, P. C. H. MITCHELL and S. A. WASS

Department of Chemistry, The University, Whiteknights, Reading RG6 2AD, U.K.

Abstract—Molybdoenzymes such as xanthine oxidase and nitrate reductase have at their active centre a molybdenum atom coordinated by oxide and sulphur ligands. In these enzymes molybdenum is monomeric; the protein apparently stops the molybdenum from dimerizing. As a first step towards constructing an inorganic analogue of a molybdoenzyme, we have synthesized molybdenum–sulphur complexes in zeolite cages of different sizes. The presence of a monomeric molybdenum(V) complex in the Linde A supercage is shown by its electron spin resonance spectrum. Using our molecular graphics computer system we have constructed accurate models of molybdenum–sulphur complexes in various zeolite cages. We have modelled the minimum energy configuration of the system via molecular mechanics and investigated possible modes of reaction. Our theoretical modelling results account well for our experimental data, and, in particular, suggest that dimerization of the molybdenum complexes cannot occur within the Linde A cage, in agreement with experiment.

Enzymes are remarkable catalysts. They catalyse, under ambient conditions, reactions which over heterogeneous catalysts require elevated temperatures and pressures. They are highly selective. There is an obvious technical interest in exploiting the catalytic chemistry of enzymes.[1]

The key feature of enzyme catalysis which we are modelling is the ability of an enzyme to create a reaction space where the active enzyme groups and the substrate molecule are organized, in order to provide the optimum configuration for the catalysis.[1] The zeolites, as potential biomimetic catalysts, are our particular interest. There are similarities between cavities in the zeolite and those in the protein tertiary structure.[2,3] Also, they can be tailored for shape selectivity and acid/base functionality. Our reaction–space model is a molybdenum centre in a zeolite cage.

Samples of molybdenum dithiocarbamate in the Linde A zeolite were prepared as follows. The zeolite was stirred with an aqueous solution of sodium molybdate for *ca* 3 h; water was removed in a vacuum rotary evaporator; and the molybdenum–zeolite (denoted MoZ) was oven-dried. The reactions of MoZ with sodium diethyldithiocarbamate, $Na[Et_2NCS_2]$ (abbreviated Nadtc), were carried out according to procedures for the preparation of the complexes $MoO_2(dtc)_2$ and $Mo_2O_3(dtc)_4$.[4] For example, MoZ was added to an aqueous solution of sodium diethyldithiocarbamate acidified with dilute hydrochloric acid. The samples were washed with carbon tetrachloride to remove molybdenum dithiocarbamates from the external surface of the zeolite. The products, ModtcZ, with 5 and 10% molybdenum were blue solids. Their strong paramagnetism (ESR, g 1.977) is consistent with the presence of a monomeric molybdenum(V) species. In the absence of the zeolite the molybdenum(V) product was the diamagnetic dimer, $Mo_2O_3(dtc)_4$. Clearly the zeolite stabilizes monomeric molybdenum(V).

Using our molecular graphics computer system we have constructed accurate models of molybdenum dithiocarbamato complexes in various zeolite cages. We report here our calculations with Linde A. Computer modelling was carried out on an IBM PC-AT with the PC-Chemmod system.[5] The atomic coordinates of the zeolites and molybdenum dithiocarbamato complexes were retrieved from the SERC crystallographic database.[6] Molecular mechanics were used to calculate the energies of our structures.[7,8] We start from an ideal model structure and optimize the geometry by

*Author to whom correspondence should be addressed.

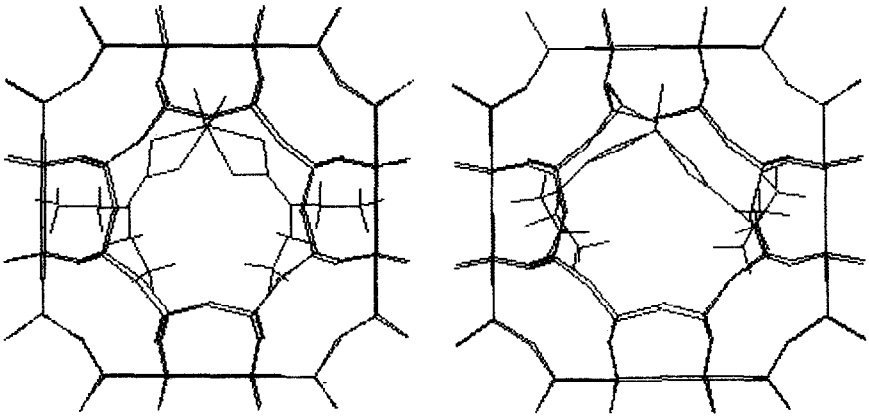

Fig. 1. The molybdenum dithiocarbamato complexes, $MoO_2(dtc)_2$ and $MoO(dtc)_2$, encapsulated in a Linde A cage: computer-drawn representations of the lowest energy structures.

minimizing the total steric energy, E, which is approximated by a sum of energy contributions:

$$E = E_s + E_b + E_t + E_{nb},$$

where E_s is the bond stretching energy, E_b, the angle bending energy, E_t, the torsional energy due to rotation about bonds and E_{nb}, the energy of interactions between non-bonded atoms (van der Waals interactions). The final energies after minimization for molybdenum dithiocarbamates in a Linde A cage were: $MoO_2(dtc)_2$, -17.1; $MoO(dtc)_2$, 50.1; $Mo_2O_3(dtc)_4$, 558 kcal mol^{-1}. The dimer is obviously very strained. The two monomers can, however, fit into the cage; computer-drawn representations of the final structures are shown in Fig. 1. Surprisingly, the monoxo compound, $MoO(dtc)_2$, is more strained than the bigger dioxo compound. The strain is caused by bending of the dithiocarbamates to achieve the best fit in the cage. The observation of a strained coordination centre is of great interest in analogy to the enzyme chemistry, evoking the entatic-state description of a metalloenzyme.[9] Further experimental and computational studies are underway.

Acknowledgement—We thank SERC for a grant for the purchase of computer modelling equipment.

REFERENCES

1. P. C. H. Mitchell, *J. Inorg. Biochem.* 1986, **28**, 107.
2. A. E. Shilov, *J. Molec. Catal.* 1988, **47**, 351.
3. C. A. Tolman and N. Herron, *Catal. Today* 1988, **3**, 235.
4. R. N. Jowitt and P. C. H. Mitchell, *J. Chem. Soc. A* 1970, 1702.
5. PC-Chemmod system, U-Micro Computers, Warrington, U.K.
6. SERC Chemical Databank System, CSSR and ICSD components, Daresbury Laboratory, SERC Daresbury, Warrington, U.K.
7. U. Burkert and N. L. Allinger, *Molecular Mechanics*, ACS monograph 177 (1982).
8. D. N. J. White, Chemmin program, University of Glasgow, private communication.
9. R. J. P. Williams, *J. Molec. Catal.* 1985, **30**, 1.

Polyhedron Vol. 8, No. 13/14, pp. 1819–1820, 1989
Printed in Great Britain

0277–5387/89 $3.00+.00
© 1989 Maxwell Pergamon Macmillan plc

SYNTHESIS, X-RAY STRUCTURE AND REACTIVITY OF THE HALF-SANDWICH IMIDO COMPLEX (η-C_5H_5)$NbCl_2(NCH_3)$

VERNON C. GIBSON† and DAVID N. WILLIAMS

Department of Chemistry, University Science Laboratories, South Road, Durham DH1 3LE, U.K.

and

WILLIAM CLEGG and DAVID C. R. HOCKLESS

Department of Chemistry, The University, Newcastle upon Tyne NE1 7RU, U.K.

Abstract—Room temperature treatment of (η-C_5H_5)$NbCl_4$ with a stoichiometric amount of $(Me_3Si)_2NMe$ in acetonitrile, gives (η-C_5H_5)$NbCl_2(NCH_3)$ in 87% yield. The X-ray structure reveals a three-legged piano stool geometry with a Nb—N bond length of 1.752(2) Å and a Nb—N—C angle of 163.4(3)°.

The reactivity of metal-bound oxygen and nitrogen atoms is of considerable interest due to their role in a variety of important industrial processes.[1] Half-sandwich metal oxides have been the focus of much recent attention[2] due to the stabilizing and solubilizing properties of ancillary C_5R_5 [R = H(Cp), Me(Cp*)] ligands. However, analogous compounds containing the iso-electronic alkylimido ligand (NR) remain rare. For the group 5 metals, we are aware of only two: $CpVCl_2(Ntol)$,[3] which has been prepared from the reaction of $V(Ntol)Cl_3$ with $Me_3SiC_5H_5$, and compounds of the type $Cp^*TaMe_2(NR)$[4] (R = Me, CMe_3, CH_2CMe_3) which are formed upon treatment of Cp^*TaMe_3Cl with LiNHR.

Here, we describe a convenient entry into half-sandwich niobium–imido chemistry through the treatment of $CpNbCl_4$ with heptamethyldisilazane, $(Me_3Si)_2NMe$, according to eq. (1).

$$CpNbCl_4 + (Me_3Si)_2NMe \longrightarrow CpNbCl_2(NMe) + 2Me_3SiCl. \quad (1)$$

(1)

In a typical reaction, $(Me_3Si)_2NMe$ (2.93 g, 16.7 mmol) in acetonitrile (30 cm^3) was added dropwise, with stirring, to a suspension of $CpNbCl_4$ (5.0 g, 16.7 mmol) in acetonitrile (100 cm^3) at room temperature. The red suspension was consumed over a period of 2 h to give a yellow–orange solution, which was stirred for a further 6 h. Removal of the volatile components, followed by washing with light petroleum ether (2×25 cm^3) and drying *in vacuo* gave a yellow powder, which can be recrystallized from toluene to give **1** (3.74 g, 87%) in the form of large orange crystals. Compound **1** has been characterized by ^1H NMR and IR spectroscopies, mass spectrometry and gives satisfactory elemental analyses. The ^1H NMR spectrum (C_6D_6, 250 MHz) reveals singlet resonances at δ 5.72 and 3.21 (ratio 5:3) attributable to equivalent ring hydrogens and the methyl hydrogens of the imido ligand, respectively. Also, a parent ion is observed at m/z 258 (^{35}Cl) in the mass spectrum.

The molecular structure‡ of **1** is shown in Fig. 1, and important bond distances and angles are included in the figure caption. The molecule possesses a three-legged piano stool geometry, with a crystallographic mirror plane which bisects the Cl—Nb—Cl angle and contains the niobium, nitro-

† Author to whom correspondence should be addressed.

‡ Crystal data for **1**: $C_6H_8Cl_2NNb$, $M = 258.0$, monoclinic, $a = 7.1778(6)$, $b = 9.8969(10)$, $c = 7.1994(6)$ Å, $\beta = 118.04(6)°$, $U = 451.41$ Å^3, $Z = 2$, space group $P2_1/m$; $R = 0.016$, $R_w = 0.016$ from 827 unique observed reflections with $2\theta < 50°$, measured with Mo-K_α radiation ($\lambda = 0.71073$ Å) and corrected for absorption. Atomic coordinates, bond lengths and angles, and thermal parameters have been deposited as supplementery data with the Editor, from whom copies are available on request. Atomic coordinates have also been deposited with the Cambridge Crystallographic Data Centre.

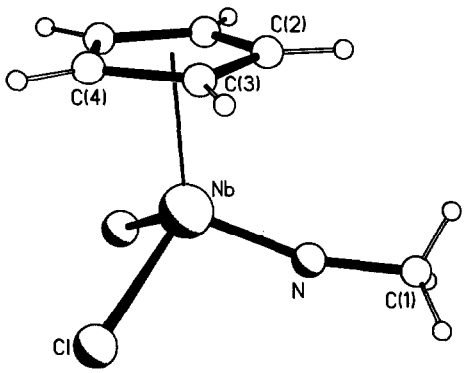

Fig. 1. The molecular structure of **1**. The molecule has crystallographic mirror symmetry. Selected bond lengths and angles are: Nb—Cl, 2.335(1); Nb—N, 1.752(2); Nb—C, 2.380(4), 2.404(3), 2.500(3); N—C(1), 1.432(3) Å. Cl—Nb—Cl, 104.7(1); Cl—Nb—N, 103.3(1); Nb—N—C(1), 163.4(3)°.

gen and carbon atoms C(1) and C(2). The niobium–nitrogen distance of 1.752(2) Å lies within the range expected for a metal–nitrogen triple bond (typically 1.73–1.79 Å for niobium–imido compounds[5–7]), arising by donation of the nitrogen lone pair. The Nb—N—C angle of 163.4(3)° lies at the low end of the range (161–180°)[1] typically observed for a terminal imido ligand containing a *sp*-hybridized nitrogen.

The methyl substituent is bent towards the cyclopentadienyl ring suggesting that the primary interaction of the nitrogen lone pair-containing *p* orbital is with a lobe of a vacant metal orbital projecting *trans* to the Cp ring. Although **1** is formally a 16-electron species (including donation of the lone pair from the imido nitrogen), it does not bind acetonitrile, the reaction solvent. However, it readily reacts with highly basic trimethylphosphine to give colourless, crystalline **2** [eq. (2)] for which a preliminary structural investigation shows a four-legged piano stool geometry, with the trimethylphosphine ligand lying *trans* to one chloro group and *cis* to the methylimido and remaining chloride ligand [as illustrated in eq. (2)]:

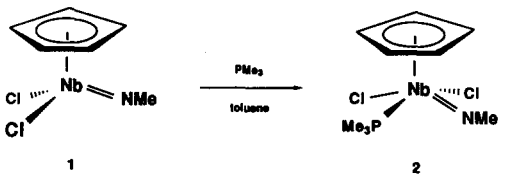

(2)

Further derivatization of **1** may be achieved by exchange of the halide ligands. The compounds $CpNb(OAr)_2(NMe)$ (Ar = 2,6-$Me_2C_6H_3$) and $CpNbMe_2(NMe)$ have been obtained by treatment of **1** with 2 equivalents of LiOAr and MeMgI, respectively. These, and related studies will be described in detail in a future report.

Acknowledgement—V.C.G. and W.C. thank the SERC for grants and a studentship to D.N.W.

REFERENCES

1. See for example, W. A. Nugent and J. M. Mayer, *Metal–Ligand Multiple Bonds*. John Wiley, New York (1988).
2. W. A. Hermann, E. Herdtweck, M. Flöel, J. Kulpe, U. Küsthardt and J. Okuda, *Polyhedron*, 1987, **9**, 1165 and refs therein.
3. D. D. Devore, J. D. Lichtenhan, F. Takusagawa and E. A. Maatta, *J. Am. Chem. Soc.* 1987, **109**, 7408.
4. J. M. Mayer, C. J. Curtis and J. E. Bercaw, *J. Am. Chem. Soc.* 1983, **105**, 2651.
5. F. A. Cotton, S. A. Duraj and W. J. Roth, *J. Am. Chem. Soc.* 1984, **106**, 4749.
6. P. A. Finn, M. S. King, P. A. Kitty and R. E. McCarley, *J. Am. Chem. Soc.* 1975, **97**, 220.
7. L. S. Tan, G. V. Goeden and B. L. Haymore, *Inorg. Chem.* 1983, **22**, 1744.

Polyhedron Vol. 8, No. 13/14, pp. 1821–1822, 1989
Printed in Great Britain

0277–5387/89 $3.00+.00
© 1989 Maxwell Pergamon Macmillan plc

SPIN CROSSOVER IN CHROMIUM(II) COMPLEXES

DOST M. HALEPOTO, DAVID G. L. HOLT, LESLIE F. LARKWORTHY,* DAVID C. POVEY and GALLIENUS W. SMITH

Department of Chemistry, University of Surrey, Guildford GU2 5XH, U.K.

and

G. JEFFERY LEIGH

AFRC Institute of Plant Science Research, Nitrogen Fixation Laboratory, University of Sussex, Brighton BN1 9RQ, U.K.

Abstract—The chromium(II) complex $[CrI_2(depe)_2]$, where depe is 1,2-bis(diethylphosphino)ethane, is unusual in that it is high spin at room temperature, but on cooling undergoes a sharp transition to the low spin form at *ca* 170 K. Other complexes of chromium(II) halides and depe or 1,2-bis(dimethylphosphino)ethene (dmpe) are low spin. The structure of the high spin form of $[CrI_2(depe)_2]$ has been determined.

There are many examples of spin state transitions in complexes with the d^5, d^6 and d^7 configurations,[1] but hardly any with the d^4 configuration. Chromium(II) is an example of a metal ion with the $3d^4$ configuration and it forms many octahedral, high spin complexes, e.g. $[Cr(en)_3]Cl_2$, where en is 1,2-diaminoethane, which have temperature-independent magnetic moments close to the spin-only value for four unpaired electrons ($\mu_{S.O.} = 4.90$ BM, $S = 2$). Complexes containing strong field ligands, e.g. $[Cr(bipy)_3]Cl_2$, where bipy is 2,2′-bipyridyl, are low spin with essentially temperature-independent moments somewhat above the spin-only value for two unpaired electrons ($\mu_{S.O.} = 2.83$ BM, $S = 1$).[2]

The chromium(II) complexes $[CrX_2(depe)_2]$, where X = Cl, Br or I, depe = 1,2-bis(diethylphosphino)ethane, and $[CrX_2(dmpe)_2]$, where X = Br or I, dmpe = 1,2-bis(dimethylphosphine)ethane, have been prepared by the addition of the diphosphine to a solution of the hydrated chromium(II) halide in methanol. The known complex $[CrCl_2(dmpe)_2]$ is low spin in toluene at room temperature ($\mu_{eff} = 2.8$ BM).[3] Magnetic measurements on the solids show that all complexes except $[CrI_2(depe)_2]$ are low spin, with little variation of magnetic moment with temperature. The magnetic behaviour of one low spin complex $[CrI_2(dmpe)_2]$, is depicted in Fig. 1. Rather surprisingly, $[CrI_2(depe)_2]$ is high spin at room temperature, but there is a sharp spin crossover to the low spin form at approximately 170 K (Fig. 2). In accordance with the essentially constant moments of each spin state, the reciprocal susceptibility (χ_{Cr}^{-1}) vs temperature plot follows the Curie law on either side of the discontinuity.

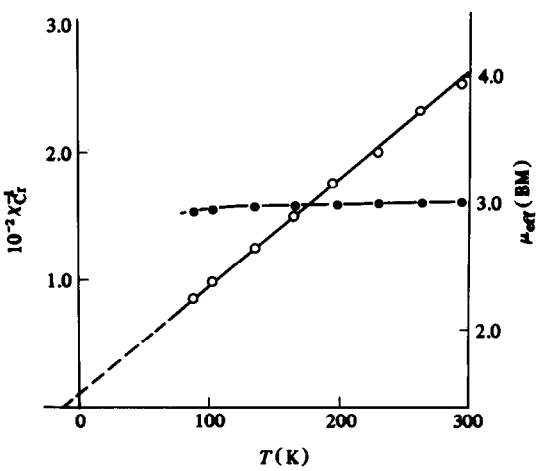

Fig. 1. Variation with temperature of reciprocal molar susceptibility χ_{Cr}^{-1} (○) and effective magnetic moment μ_{eff} (●) of $[CrI_2(dmpe)_2]$.

*Author to whom correspondence should be addressed.

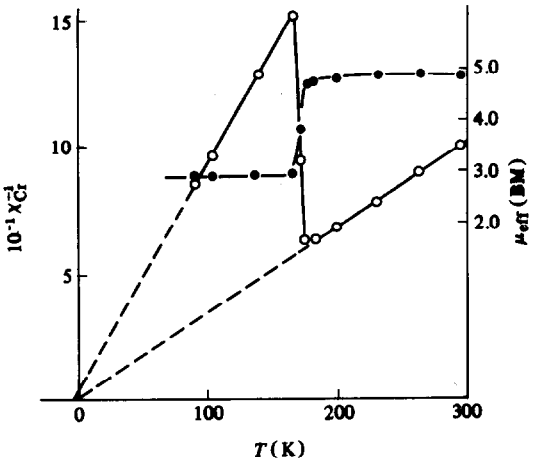

Fig. 2. Variation with temperature of reciprocal molar susceptibility χ_{Cr}^{-1} (○) and effective magnetic moment μ_{eff} (●) of $[CrI_2(depe)_2]$.

The molecular structure of $[CrI_2(depe)_2]$ has been determined at room temperature. It is a *trans* complex; the Cr—P distances are 2.503(1) and 2.533(1) Å, and the Cr—I distance, 3.068(0) Å. Further investigations are in progress.

REFERENCES

1. P. Gütlich, *Struct. Bond.* 1981, **44**, 83; E. König, G. Ritter and S. K. Kulshreshtha, *Chem. Rev.* 1985, **85**, 219.
2. L. F. Larkworthy, K. B. Nolan and P. O'Brien, *Comprehensive Coordination Chemistry*, Vol. 3. Pergamon Press, Oxford (1987).
3. G. S. Girolami, G. Wilkinson, A. M. R. Galas, M. Thornton-Pett and M. B. Hursthouse, *J. Chem. Soc., Dalton Trans.* 1985, 1339.

Polyhedron Vol. 8, No. 13/14, pp. 1823–1824, 1989
Printed in Great Britain

0277–5387/89 $3.00+.00
© 1989 Maxwell Pergamon Macmillan plc

SYNTHESES AND STRUCTURES OF NOVEL VANADIUM(II) COMPLEXES

DAVID G. L. HOLT, LESLIE F. LARKWORTHY,* DAVID C. POVEY and GALLIENUS W. SMITH

Department of Chemistry, University of Surrey, Guildford GU2 5XH, U.K.

and

G. JEFFERY LEIGH

AFRC Institute of Plant Science Research, Nitrogen Fixation Laboratory, University of Sussex, Brighton BN1 9RQ, U.K.

Abstract—The hydrated vanadium(II) compounds $[VCl_2(H_2O)_4]$, $[V(H_2O)_6]Br_2$, $[V(H_2O)_6](BF_4)_2$ and $[V(H_2O)_6](CF_3SO_3)_2$ have been isolated from vanadium and the aqueous acid. From reactions of the hydrogen halide and vanadium immersed in glacial acetic acid, $[VCl_2(CH_3COOH)_4]$ and $[V(CH_3COOH)_6]Br_2$ have been obtained. The structures of $[V(H_2O)_6](CF_3SO_3)_2$, $[VCl_2(CH_3COOH)_4]$ and $[V(CH_3COOH)_6]Br_2$, which are new complexes, have been determined.

Previously, hydrated vanadium(II) salts, e.g. $[V(H_2O)_6]Br_2$, were prepared by electrolytic reduction. There is a brief report[1] that $[V(H_2O)_6]Br_2$ and other hydrates can be prepared from the acid and vanadium, hitherto considered too unreactive towards non-oxidizing acids. We have confirmed this report with the synthesis of $[VCl_2(H_2O)_4]$, $[V(H_2O)_6]Br_2$ and $[V(H_2O)_6](BF_4)_2$, and the new salt $[V(H_2O)_6](CF_3SO_3)_2$ (Scheme 1). Also, the novel complexes $[VCl_2(CH_3COOH)_4]$ and $[V(CH_3COOH)_6]Br_2$ have been prepared from vanadium and glacial acetic acid saturated with HX (X = Cl or Br) (Scheme 2). Satisfactory analytical data have been obtained.

Structure of $[V(H_2O)_6](CF_3SO_3)_2$

In $[V(H_2O)_6](CF_3SO_3)_2$, the VO_6 octahedron has equal V—O distances as expected for a $3d^3$ complex. The mean value of 2.119(1) Å agrees closely with that found for the V—OH_2 distances in $[V(H_2O)_6]SO_4$,[2] (2.131 Å). The triflate anions are extensively hydrogen-bonded to the coordinated water molecules. Eight anions form a cage around each $[V(H_2O)_6]$ octahedron, and the framework of 12 hydrogen bonds consists of two independent contacts from each of the four O(4) water molecules to different triflate anions (O(4)—O(1) = 2.839 Å and O(4)—O(2) = 2.814 Å) and two symmetrical contacts between each water molecule O(3) and the O(2) atoms of two anions (O(3)—O(2) = 2.785 Å). The hydrogen bonding clearly contributes to the stability of the lattice.

Structures of $[VCl_2(CH_3COOH)_4]$ *and* $[V(CH_3COOH)_6]Br_2$

Structural analyses show that these two complexes contain acetic acid coordinated via the carbonyl oxygen, and they also show that in each case the vanadium atom is octahedrally coordinated. In the VCl_2O_4 coordination sphere of $[VCl_2(CH_3COOH)_4]$ the average V—Cl distance is 2.500 Å and the average V—O distance is 2.125 Å (range 2.09–2.15 Å). A bond scan around each chlorine atom shows that six oxygen atoms cluster in a hemisphere around each chlorine atom, with distances of 3.01–3.34 Å, suggesting a weak intramolecular hydrogen bond interaction.

In $[V(CH_3COOH)_6]Br_2$, the VO_6 octahedron is symmetrical with an average V—O distance of 2.11 Å, which is similar to those for the chloro complex

* Author to whom correspondence should be addressed.

$$[V(H_2O)_6]X_2 \xleftarrow[X = Br,\ BF_4\ CF_3SO_3]{HX,\ reflux} V \xrightarrow[reflux]{HCl(aq)} [VCl_2(H_2O)_4]$$

Scheme 1. Compounds isolated from aqueous media.

$$[VCl_2(CH_3COOH)_4] \xleftarrow[CH_3COOH]{HCl(g)} V \xrightarrow[CH_3COOH]{HBr(g)} [V(CH_3COOH)_6]Br_2$$

Scheme 2. Compounds isolated from acetic acid.

and the hydrates above. Each bromide ion is surrounded by three hydroxyl groups with Br—O distances of 3.13–3.19 Å, suggesting that the hydroxyl hydrogen is intermolecularly hydrogen-bonded to the bromide ions. This also occurs in the analogous nickel(II) complex, $[Ni(CH_3COOH)_6](BF_4)_2$.[3]

Vanadium metal is thus a convenient source of vanadium(II) compounds.

REFERENCES

1. A. F. Zueva, O. N. Efimov and A. G. Ovcharenko, *Russ. J. Inorg. Chem.* 1976, **21**, 1075.
2. F. A. Cotton, L. R. Falvello, R. Llusar, E. Libby, C. A. Murillo and W. Schwotzer, *Inorg. Chem.* 1986, **25**, 3423.
3. R. E. Cramer, W. Van Doorne and R. Dubois, *Inorg. Chem.* 1975, **14**, 2462.

Polyhedron Vol. 8, No. 13/14, pp. 1825–1826, 1989
Printed in Great Britain

0277–5387/89 $3.00+.00
© 1989 Maxwell Pergamon Macmillan plc

NEW STRUCTURAL TYPES FOR CHROMIUM(II)

JAYNE JUBB, LESLIE F. LARKWORTHY,* DAVID C. POVEY and GLEN W. SMITH

Department of Chemistry, University of Surrey, Guildford GU2 5XH, U.K.

Abstract—The new compound $Cr(thiourea)_2(NCS)_2$ contains *trans*-planar units stacked along the *a*-axis of the unit cell so that the chromium ions lie in infinite chains. In this first example of chains of directly interacting paramagnetic metal ions, the Cr—Cr separation is 3.97 Å which leads to weak antiferromagnetism but does not provide a conducting pathway. In contrast, the molecules in $Cr(OPD)_2(NCS)_2$, where OPD is *o*-phenylenediamine, prepared during investigations aimed at producing planar Cr^{2+} complexes by template reactions, do not stack and contain thiocyanate bridges. The new complexes $Cr(OPD)Cl_2$ and $[Cr(OPD)_6]Cl_2$ have been prepared. The latter has been used in reactions with acetylacetone aimed at producing planar chromium(II)–tetra-azamacrocyclic complexes, but a new metal-free octa-azamacrocycle has been obtained.

High-spin chromium(II) can exist as tetragonally distorted six-coordinate and planar four-coordinate complexes.[1] The structure of $Cr(thiourea)_2(CNS)_2$ (**A**) revealed *trans*-planar units stacked along the *a*-axis of the unit cell. The chromium ions lie in infinite parallel chains so that the metal ions can directly interact. This suggested that square-planar complexes of chromium(II) could stack and a conducting pathway could arise. In **A** however, the Cr—Cr separation was found to be too large (3.97 Å) and the complex was non-conducting.[2]

An analogous complex, **B**, was prepared using *o*-phenylenediamine (OPD) instead of thiourea. Magnetic measurements showed antiferromagnetic behaviour ($\mu_{eff}^{293} = 4.19$ BM, $\mu_{eff}^{87} = 3.20$ BM) and the structure of **B** revealed a non-stacking system containing thiocyanate bridges.

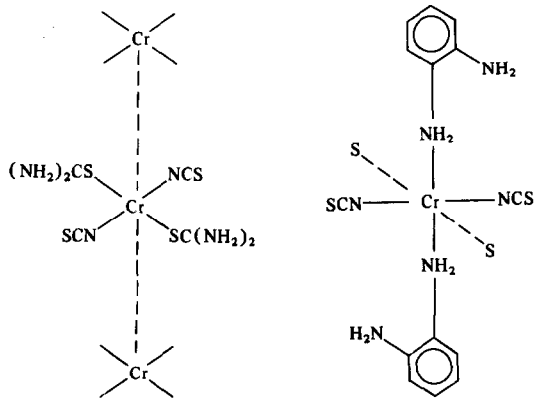

A **B**

Investigations aimed at producing planar chromium(II)–tetra-aza macrocycles were based on the nickel(II) template reactions used by Goedken and Weiss:[3]

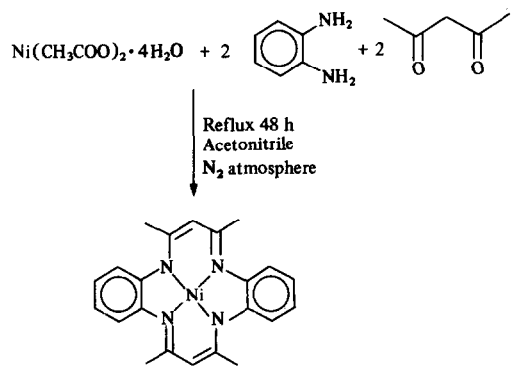

There was no reaction using $Cr_2(CH_3COO)_4 \cdot (H_2O)_2$ due to the thermal stability resulting from its dimeric nature. Since the above route proceeds via the formation of an intermediate OPD complex of nickel(II) which then condenses with acacH, it was decided to synthesis OPD complexes of chromium(II).

Compound **B** was refluxed under nitrogen with acacH in acetonitrile for 48 h. There was no reaction. However, the structure of **B** had shown the presence of monodentate OPD, and the formation of the nickel(II) macrocycle is dependent on the acacH being able to condense with the coordinated $-NH_2$ groups. This possibly requires bidentate OPD.

Efforts were switched to the preparation of a

* Author to whom correspondence should be addressed.

chloride containing an OPD salt of chromium(II), and $[Cr(OPD)_6]Cl_2$ and a polymeric, chloride-bridged compound, $Cr(OPD)Cl_2$, were isolated. In solution, at room temperature, the hexakis(amine) undergoes a series of rapid stepwise equilibria ending with $Cr(OPD)Cl_2$. No $Cr(OPD)_2Cl_2$ could be isolated from this. However, reaction of $[Cr(OPD)_6]Cl_2$ with acacH yielded a highly crystalline, purple–black product, which was believed to be the desired chromium(II) macrocycle. Further characterization, however, revealed it to be the macrocyclic product, **C**.

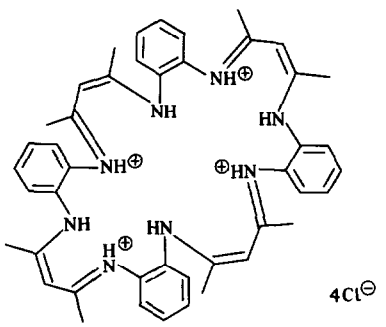

C

Presumably, **C** forms when $[Cr(OPD)_6]Cl_2$ loses two axial ligands, readily in solution, through Jahn–Teller distortion, leaving a square-planar arrangement which condenses with four acacH. The macrocycle is now too bulky to stay coordinated to the chromium ion, so it "relaxes" and the chromium(II) ion is ejected into solution. Other hexakis OPD compounds of nickel(II)[4] and iron(II)[5] have been reported. We repeated the preparation of $[Ni(OPD)_6]Cl_2$ using the method of Marks *et al.*,[4] but this did not undergo the analogous reaction for the formation of **C**.

REFERENCES

1. L. F. Larkworthy, K. B. Nolan and P. O'Brien, *Comprehensive Coordination Chemistry*, Vol. 3. Pergamon Press, Oxford (1987).
2. J. Jubb, L. F. Larkworthy, G. A. Leonard, D. C. Povey and B. J. Tucker, *J. Chem. Soc., Dalton Trans.*, accepted for publication.
3. V. L. Goedken and M. C. Weiss, *Inorg. Synth.* 1980, **20**, 115.
4. D. R. Marks, D. J. Phillips and J. P. Redfern, *J. Chem. Soc. A* 1967, 1464.
5. G. A. Renovitch and W. A. Baker, *J. Chem. Soc. A* 1969, 75.

Polyhedron Vol. 8, No. 13/14, pp. 1827–1829, 1989
Printed in Great Britain

0277–5387/89 $3.00+.00
© 1989 Maxwell Pergamon Macmillan plc

SYNTHESIS AND CHARACTERIZATION OF SOME MIXED LIGAND OXOVANADIUM(IV) COMPLEXES: THE $[LVO]^+$ CHROMOPHORE, WHERE L = HYDROTRIS(3,5-DIMETHYLPYRAZOLYL)BORATE

DAVID COLLISON,* FRANK E. MABBS, MOHAMMAD ALI PASSAND and KEITH RIGBY

Chemistry Department, University of Manchester, Manchester M13 9PL, U.K.

and

WALT E. CLELAND, JR

Chemistry Department, University of Mississippi, MS 38677, U.S.A.

Abstract—The characterization of compounds LVOB, where B = β-diketonate or N,N-diethyldithiocarbamate, is reported. A comparison of their electronic absorption and ESR spectra with those of the corresponding VOB_2 complexes is made. The electronic structures of LVOB are closest to that of a trigonally-distorted octahedron, whilst VOB_2 are closest to that of a square-based pyramid.

We are interested in establishing the relationship between the geometric and electronic structures of oxovanadium(IV) and oxomolybdenum(V) compounds,[1–3] especially when particular constraints are imposed by the ligands. The stabilization of early transition metal oxo compounds by the sterically demanding hydrotris(3,5-dimethylpyrazolyl) borate anion (= L), which has been extensively demonstrated for molybdenum,[3] has now been extended to vanadium(IV) in the form of complexes of formula LVOB, where $B = O^-$ or S-donor uninegative, bidentate ligand. The compounds are most conveniently prepared under non-aqueous conditions according to eq. (1):

$$VOB_2 + KL \xrightarrow[\text{solvent}]{ca\ 50–60°C} LVOB + KB. \quad (1)$$

The complexes show parent-ion peaks for electron impact mass spectrometry. For LVOB, the values of ν(B—H) fall in the range 2510–2539 cm^{-1}, which are comparable with those in a number of LMo(oxy) compounds.[3,4] When B = β-diketonate, the values of ν(V=O) fall in the narrow range 959–967 cm^{-1}, indicative of little variation in the bonding in the V=O fragment. The β-diketonate complexes all exhibit quasi-reversible one-electron oxidations in methyl cyanide as assessed by cyclic voltammetry (e.g. for LVO(acac), acac = 2,4-pentanedionato, $E = 1.45$ V, $\Delta E_p = 80$ mV, $i_{pa}/i_{pc} = 1.04$). There is a small dependence of the potential, E, on the substituents of the β-diketonate ligand.

It is the electronic structure of the LVO (β-diketonate) complexes which are most noteworthy. The electronic absorption spectra of these compounds in toluene solution generally exhibit *four* bands in the range 13,000–26,000 cm^{-1}, which can be assigned to *d–d* transitions based on their extinction coefficients. The energies and extinction coefficients of these bands show only small changes in different solvents, ranging from non-coordinating toluene through dichloromethane to potentially coordinating methyl cyanide. In contrast, the corresponding VO(β-diketonate)$_2$ compounds in non-coordinating solvents usually exhibit only *three d–d* bands[5] [e.g. the band maxima × 10^{-3} cm^{-1} (molar extinction coefficient) are VO(acac)$_2$: 15.44(60), 16.88(67), 25.81(128); LVO(acac): 13.11(54), 17.62(11), 24.22(50), 25.11(50)].

In the VOB_2 compounds, it is generally assumed that the $[VO]^{2+}$ moiety dominates the electronic structure, and hence the *d*-orbital splitting pattern

* Author to whom correspondence should be addressed.

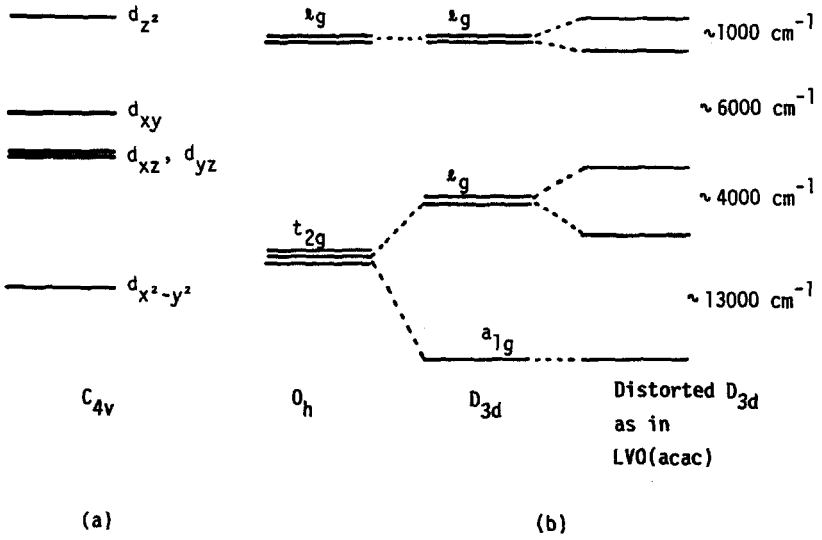

Fig. 1. *d*-Orbital splitting diagram for (a) C_{4v} point symmetry; (b) an octahedron with a predominantly trigonal distortion.

approximates to that expected for a square-based pyramid (C_{4v} point symmetry), see Fig. 1(a). This confines the unpaired electron to an orbital which is perpendicular to V=O. However, in LVOB we propose that the $[VO]^{2+}$ moiety is not so dominant, although it still exerts a *trans*-lengthening effect (V—N(11) = 2.434 Å, V—N(21) = 2.113 Å, V—N(31) = 2.105 Å), and that the tridentate ligand L alters the electronic structure so that it is better regarded as a distorted octahedral complex with the predominant distortion along the three-fold axis of the octahedron. This would lead to an energy level diagram as in Fig. 1(b). This view is reinforced by our single crystal ESR studies on LVO(dtc), where dtc = N,N-diethyldithiocarbamato, diluted in the isomorphous LMoO(dtc).[6] Here, we find that the direction of one principal g and one principal A value approximates to a pseudo-three-fold axis in the complex, see Fig. 2. There are no principal g or A values particularly close to any metal–ligand directions. In contrast to this, compounds which approximate to square-pyramidal geometry have one g and one A tensor axis coincident, or almost coincident, with the V=O direction.[1] Note that it is not possible to obtain the orientations of the g and A tensor axes from frozen solution spectra. However, we must point out that it is not obligatory for the tridentate ligand to impose a three-fold distortion on a compound, since we did not observe it in $LMoOCl_2$.[7]

The principal g and A values for LVO(β-diketonate), obtained from fluid and frozen solution, fall in the range $\bar{g} = 1.970 \pm 0.002$, $\bar{A} = -92.0 \pm 0.9 \times 10^{-4}$ cm^{-1}, $g_1 = 1.948 \pm 0.001$, $g_2 =$

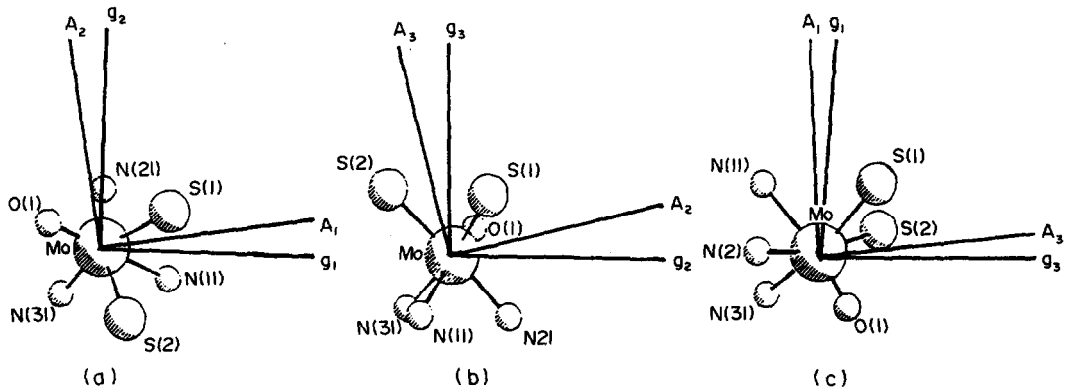

Fig. 2. The relationship of the principal axes of the g and A tensors to the first coordination sphere in LVO(dtc). Views are down: (a) $g_3 = 1.986$ ($A_3 = 50.4 \times 10^{-4}$ cm^{-1}); (b) $g_1 = 1.958$ ($A_1 = -151.7 \times 10^{-4}$ cm^{-1}); (c) $g_2 = 1.983$ ($A_2 = -53.9 \times 10^{-4}$ cm^{-1}).

1.979 ± 0.001, $g_3 = 1.980 \pm 0.002$, $A_1 = -162.3 \pm 1.1 \times 10^{-4}$ cm^{-1}, $A_2 = -57.7 \pm 1.2 \times 10^{-4}$ cm^{-1}, $A_3 = -55.5 \pm 0.9 \times 10^{-4}$ cm^{-1}. From these values (and the appearance of the spectra) alone it would be impossible to deduce that there is any significant difference between the electronic (and hence geometric) structures of LVOB and VOB_2 compounds. The only significant observation from the fluid and frozen ESR spectra is the anticipated increase in the g values and a decrease in the A values as we change from oxygen- to sulphur-donor ligands.

REFERENCES

1. D. Collison, B. Gahan, C. D. Garner and F. E. Mabbs, *J. Chem. Soc., Dalton Trans.* 1980, 667; B. Gahan and F. E. Mabbs, *J. Chem. Soc., Dalton Trans.* 1983, 1695, 1713; D. Collison, B. Gahan and F. E. Mabbs, *J. Chem. Soc., Dalton Trans.* 1983, 1705; J. K. Money, K. Folting, J. C. Huffman, D. Collison, J. Temperley, F. E. Mabbs and G. Christou, *Inorg. Chem.* 1986, **25**, 4583; D. Collison, B. Gahan and F. E. Mabbs, *J. Chem. Soc., Dalton Trans.* 1987, 111; D. Collison, F. E. Mabbs, J. Temperley, G. Christou and J. C. Huffman, *J. Chem. Soc., Dalton Trans.* 1988, 309; F. E. Mabbs and J. Temperley, *Spectrochim. Acta* 1989, **45A**, 285.
2. C. D. Garner, L. H. Hill, F. E. Mabbs, D. L. McFadden and A. T. McPhail, *J. Chem. Soc., Dalton Trans.* 1977, 853, 1202; C. D. Garner, P. Lambert, F. E. Mabbs and T. J. King, *J. Chem. Soc., Dalton Trans.* 1977, 1191; C. D. Garner, H. C. Howlader, F. E. Mabbs, P. M. Boorman and T. J. King, *J. Chem. Soc., Dalton Trans.* 1978, 1350; C. D. Garner, N. C. Howlader, F. E. Mabbs, A. T. McPhail and K. D. Onan, *J. Chem. Soc., Dalton Trans.* 1978, 1848; B. Gahan, N. C. Howlader and F. E. Mabbs, *J. Chem. Soc., Dalton Trans.* 1981, 142; D. Collison, F. E. Mabbs, J. H. Enemark and W. E. Cleland Jr, *Polyhedron* 1986, **5**, 423; C. G. Young, D. Collison, F. E. Mabbs and J. H. Enemark, *Inorg. Chem.* 1987, **26**, 2925.
3. W. E. Cleland Jr, K. M. Barnhart, K. Yamanouchi, D. Collison, F. E. Mabbs, R. B. Ortega and J. H. Enemark, *Inorg. Chem.* 1987, **26**, 1017.
4. C. S. J. Chang, D. Collison, F. E. Mabbs and J. H. Enemark, *Inorg. Chem.*, in press.
5. H. J. Stoklosa and J. R. Wasson, *J. Inorg. Nucl. Chem.* 1976, **38**, 677.
6. C. G. Young, S. A. Roberts, R. B. Ortega and J. H. Enemark, *J. Am. Chem. Soc.* 1987, **109**, 2938.
7. D. Collison, D. R. Eardley, F. E. Mabbs, K. Rigby and J. H. Enemark, *Polyhedron* 1989, **8**, 1833.

Polyhedron Vol. 8, No. 13/14, pp. 1830–1832, 1989
Printed in Great Britain

0277–5387/89 $3.00+.00
© 1989 Maxwell Pergamon Macmillan plc

THE ELECTRONIC STRUCTURES OF "NON-AXIAL" MONO-OXO COMPLEXES OF THE EARLY TRANSITION ELEMENTS

DAVID COLLISON,† FRANK E. MABBS and KEITH RIGBY

Department of Chemistry, University of Manchester, Manchester M13 9PL, U.K.

Abstract—A comparison of the ESR parameters of oxometal complexes of the early transition metals is made. The compounds studied are divided into two groups: (i) those in which the $[MO]^{n+}$ moiety defines the molecular z-direction and constrains the unpaired electron to be in an orbital in the plane perpendicular to M=O and (ii) those in which the $[MO]^{n+}$ moiety does not define the molecular z-direction, necessitating an alternative description for the location of the unpaired electron compared to (i).

The description of the electronic structure of a d-transition metal complex is best determined with recourse to the molecular point symmetry. In the case of the mono-oxo complexes of the early transition metals, the method of descent in symmetry from O_h to C_{4v}, for $[MOX_{4/5}]^{n+}$, has been followed successfully since the early work of Jorgensen,[1] and of Ballhausen and Gray.[2] By using single crystal spectroscopic methods the polarization characteristics of electronic absorption bands or the tensorial relationships of electron spin resonance (ESR) parameters, each with respect to the molecular geometry, have provided the experimental evidence for the electronic description as an axial distortion. It has been demonstrated that the oxo (O^{2-}) group dominates the ligand field and in C_{4v} symmetry the unique elements of the g- and metal A-tensors are coincident and are aligned along the metal–oxo vector.[3a] Similarly, the electronic absorption bands show characteristic parallel and perpendicular polarizations carrying the appropriate vibrational fine structure.[3] For example, in the case of $[Ph_4As][CrOCl_4]$, which crystallizes in the $P_{4/n}$ space group with the anion possessing local C_{4v} symmetry, the ESR parameters are $g_\parallel = 2.006$, $g_\perp = 1.979$; $A_\parallel = 35.1 \times 10^{-4}$ cm^{-1}; $A_\perp = 9.6 \times 10^{-4}$ cm^{-1}, where the parallel direction is found along the Cr—O vector. In the polarized single crystal electronic absorption spectrum three bands are found, centred on 13,000, 18,500 and 22,500 cm^{-1}, carrying vibrational fine structure consistent with ν(Cr—O), ν(Cr—Cl) and ν(Cr—O), respectively. The bands are all more intense in perpendicular than parallel polarization and are assigned as one-electron promotions from $3d^*_{xy}$ to $3d^*_{xz,yz}$, $3d^*_{x^2-y^2}$ and $3d^*_{z^2}$ in order of increasing energy.

In the case of mixed ligand mono-oxo complexes the dominance of the oxo group on the electron structure has previously been demonstrated, or presumed, to be maintained. For the particular examples in oxovanadium(IV) chemistry we select $[VOCl_2(tmu)_2]$,[5] $[VO(mnt)_2]^{2-}$,[6] [VO(salen)][7] and $[VO(meox)_2]$,[8] where tmu = N,N,N′,N′-tetramethylurea, mnt = maleonitriledithiolate, salen = N,N′-bis(salicylidene)ethylenediimine and meox = 2-methylquinolin-8-olate. The relationship between the site symmetry, molecular geometry and "unique" ESR parameters, as obtained from single crystal studies, are given in Table 1 for each of the above complexes. In a similar manner, information for the complexes $[MoOCl_3(hmpa)_2]$,[9] $[LVO(R_2dtc)]$[10] and $[LMoOCl_2]$,[10] where hmpa = hexamethylphosphoramide, L = tris(3,5-dimethylpyrazolyl)hydridoborate and R_2dtc = dialkyldithiocarbamate, are also presented in Table 1.

The information in the table reveals a number of interesting aspects. The symmetry-determined nature of the orientation of the g- and metal A-tensors is demonstrated for those complexes possessing strict C_{4v} or C_2 point symmetry. For the complexes $[VO(mnt)_2]^{2-}$, [VOsalen] and $[MoOCl_3(hmpa)_2]$, the distortion from the highest appropriate symmetry does not require coincidence of a g- and A-tensor element along the metal–oxo

† Author to whom correspondence should be addressed.

Table 1. Selected ESR properties for some d^1-metal–oxo complexes

Complex	Host[a]	Symmetry[b]	"Unique" ESR values		Angle (°) between:[c]			Refs.
			g	$A(10^{-4}\text{cm}^{-1})$	g and A	g and M=O	A and M=O	
High symmetry								
$[CrOCl_4]^-$	$[OsNCl_4]^-$	C_{4v}	1.006	35.1	0	0	0	4(a)
$[MoOCl_4]^-$	$[NbOCl_4]^-$	C_{4v}	1.967	73.3	0	0	0	3
Low symmetry "axial"								
$[VOCl_2(tmu)_2]$	$[InCl_3(tmu)_2]$	C_2	1.938	−172.8	0	0	0	5
$[VO(mnt)_2]^{2-}$	$[MoO(mnt)_2]^{2-}$	$C_1(C_{2v})$	1.970	−136.0	0	0	0	6
[VO(salen)]	[GaCl(salen)]	$C_1(C_s)$	1.956	−175.0	1.7[d]	3.5	4.7	7
$[VO(meox)_2]$	$[GaCl(meox)_2]$	C_2	1.949	−157.3	0[d]	11.7	11.7	8
$[MoOCl_3(hmpa)_2]$(I)	$[NbOCl_3(hmpa)_2]$	$C_1(C_s)$	1.951	75.6	23.0	22.9	0	9
$[MoOCl_3(hmpa)_2]$(II)			1.950	75.6	24.0	23.4	0	9
Low-symmetry "non-axial"								
$[LVO(Et_2dtc)]$	$[LMoO(Et_2dtc)]$	$C_1(C_s)$	1.958	−151.6	3.8	34.3	37.2	10
$[LVO(Pr^n_2dtc)]$	$[LMoO(Pr^n_2dtc)]$	$C_1(C_s)$	1.955	−153.3	4.5	42.0	44.5	10
$[LMoOCl_2]$	$[LSnCl_3]$	C_s	1.969	71.8	35.3[e]	27.4	7.9	10

[a] The (pseudo) isostructural diamagnetic host lattice used to obtain single crystal ESR data.

[b] The point symmetry of the paramagnetic complex is given together with the highest appropriate symmetry in parentheses.

[c] Values of 0 indicate coincidence of direction within experimental error.

[d] Angles with respect to Ga—Cl, the "unique" g value aligns along V=O in the pure compound.

[e] Angles with respect to Sn—Cl.

direction, but for each case at least one of these elements is so defined and therefore behaves as an "axial" complex by comparison with high symmetry. However, when the complexes $[LVO(R_2dtc)]$ (for R = Et or Pr^n) and $[LMoOCl_2]$ are considered, none of the principal axes of the ESR parameters lies along the so-called "unique" molecular direction and so these complexes are classified as "non-axial". An empirical view of these results reveals that the "non-axial" nature of some of these complexes correlates with six-coordination at the metal centre (it should be remembered that six-coordinate, high symmetry complexes, e.g. $[MoOCl_4(H_2O)]^-$, would still be required to have principal ESR parameters coincident with the metal–oxo direction). However, since the ambiguous possibilities for $[MoOCl_3(hmpa)_2]$ both place a principal A-value along the Mo—O vector, then the twist away from the Mo—O direction in the remaining complexes may be a consequence of the strong trigonal field exerted by the facially demanding N-donor ligand, L. The electronic absorption spectra of the complexes labelled "high symmetry" and "axial" in the table all show the expected form, viz. the five-coordinate complexes give three d–d bands (cf. $[CrOCl_4]^-$), which on six-coordination results in the (presumed) shift of the $d^*_{xy} \rightarrow d^*_{z^2}$ transition to higher energy. Whilst the six-coordinate $[LMoOCl_2]$ only shows two broad band envelopes of low extinction coefficient before the onset of charge-transfer transitions, $[LVO(R_2dtc)]$ shows three d–d bands and the related [LVO(acac)] (where acac = acetylacetonate) displays four such bands at 13,110, 17,620, 24,220 and 25,110 cm^{-1}.

CONCLUSIONS

The preliminary data presented for the novel tris(3,5-dimethylpyrazolyl)hydridoborate oxo complexes of molybdenum and vanadium when compared with similar established data has shown some unexpected ESR and optical properties. The currently accepted description for the electronic ground state and electronic properties of d^1-mono-oxo complexes, as depicted in Fig. 1(a), places the unpaired electron in an orbital located in a plane predominantly normal to the metal–oxo vector, and for the principal g- and metal A-values being oriented as indicated by the axis framework. The discovery of vanadium–oxo complexes in which these

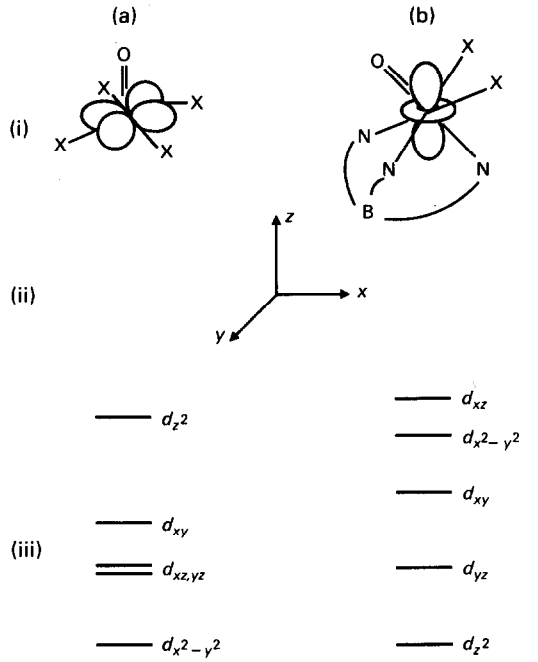

Fig. 1. Description of a metal–oxo complex viewed as (a) axial and (b) trigonal distortions from octahedral symmetry. The predominant ground state orbital (i), molecular and ESR axis framework (ii), and idealized orbital stacking diagram (iii) are shown.

principal directions align near to a pseudo-three-fold axis of an octahedron now implies that a more suitable starting point for the description of the electronic structure of these complexes may be that shown in Fig. 1(b). It should be remembered that the symmetry-determined description of the ground state may intermix the *d*-orbitals. For example,[11] assuming C_s point symmetry we would have

$$\psi_{g.s.} = a_1 d_{x^2-y^2} + b_1 d_{xz} + c_1 d_{z^2}.$$

We are currently investigating the circumstances under which a metal–oxo complex has unusual electronic properties. These effects may also have a profound implication for the reactivity of metal–oxo complexes, especially where the kinetic model requires substrate binding to cause an increase in the coordination number and/or affords a substantial change in the ligand field strength.

REFERENCES

1. C. K. Jorgensen, *Acta Chem. Scand.* 1957, **11**, 73.
2. C. J. Ballhausen and H. B. Gray, *Inorg. Chem.* 1962, **1**, 111.
3. (a) D. Collison, B. Gahan, C. D. Garner and F. E. Mabbs, *J. Chem. Soc., Dalton Trans.* 1980, 667; (b) C. D. Garner, L. H. Hill, F. E. Mabbs, D. L. McFadden and A. T. McPhail, *J. Chem. Soc., Dalton Trans.* 1977, 853.
4. (a) C. D. Garner, I. H. Hillier, F. E. Mabbs, C. Taylor and M. F. Guest, *J. Chem. Soc., Dalton Trans.* 1976, 2257; (b) D. Collison, *J. Chem. Soc., Dalton Trans.* 1989, 1.
5. D. Collison, F. E. Mabbs and J. Temperley, unpublished results.
6. D. Collison, F. E. Mabbs, J. Temperley, G. Christou and J. L. Huffman, *J. Chem. Soc., Dalton Trans.* 1988, 309.
7. D. Collison, F. E. Mabbs and R. Fereday, unpublished results.
8. D. Collison, B. Gahan and F. E. Mabbs, *J. Chem. Soc., Dalton Trans.* 1987, 111.
9. C. D. Garner, P. Lambert, F. E. Mabbs and T. J. King, *J. Chem. Soc., Dalton Trans.* 1977, 1191.
10. D. Collison, F. E. Mabbs and K. Rigby, *Polyhedron* 1989, **8**, 1827, 1833.
11. D. Collison, F. E. Mabbs, J. H. Enemark and W. E. Cleland Jr, *Polyhedron* 1986, **5**, 423.

Polyhedron Vol. 8, No. 13/14, pp. 1833–1834, 1989
Printed in Great Britain

0277–5387/89 $3.00+.00
© 1989 Maxwell Pergamon Macmillan plc

ELECTRON SPIN RESONANCE STUDIES OF LOW SYMMETRY OXOMOLYBDENUM(V) IONS DILUTED IN THE PSEUDO-ISOSTRUCTURAL CHLOROTIN(IV) MOIETY

DAVID COLLISON,* DAVID R. EARDLEY, FRANK E. MABBS and KEITH RIGBY

Chemistry Department, University of Manchester, Manchester M13 9PL, U.K.

and

JOHN H. ENEMARK

Chemistry Department, University of Arizona, Tucson, AZ 85721, U.S.A.

Abstract—The results of a single crystal ESR study of $LMoOCl_2$ diluted in the isostructural host $LSnCl_3$ are reported. These results confirm the monoclinic ESR symmetry deduced previously from frozen solution measurements giving the rotation angle between the tensor axes as 35° compared with 33° in previous study. The single crystal data show that none of the principal g- or A-tensor axes coincide with metal–ligand directions.

Whilst many monomeric oxomolybdenum(V) compounds are known, relatively few detailed single crystal ESR studies have been performed because of the lack of suitable diamagnetic host lattices. In particular, we have been interested in the effects on the spin-Hamiltonian parameters of the ligand hydridotris(3,5-dimethylpyrazolyl)borate (= L), and on systematic changes in the ligands X and Y in molybdenum(V) compounds of formulation LMoOXY.[1] To date we have had to rely on obtaining these parameters from frozen solution spectra, because the chemistry of the preferred diamagnetic isostructural compounds LNbOXY or LMoNXY is not sufficiently well-developed to provide the wide range of required compounds.

Following our successful use[2] of the pseudo-isostructural relationship $[VO]^{2+} \equiv [GaCl]^{2+}$, we now report the use of a similar relationship, viz. $[LMoO]^{2+} \equiv [LSnCl]^{2+}$. We have recently determined the single crystal structure of $LSnCl_3$, and shown it to consist of monomeric six coordinate molecules which have a geometry very similar to that of $LMoOCl_2$. We have grown single crystals of $[LSnCl(MoO)Cl_2]$ containing *ca* 5% molybdenum. An ESR study of these crystals is compatible with the $LMoOCl_2$ molecule occupying the $LSnCl_3$ sites and has yielded values of the metal g- and A-tensors in close agreement with those determined by spectrum simulation of frozen toluene solutions of $[LMoOCl_2]$,[3,4] see Table 1. The simulations assumed monoclinic ESR symmetry, consistent with a mirror plane in $[LMoOCl_2]$. An angle, α, for the rotation of the g- and A-tensor axes in the plane perpendicular to the necessarily coincident g- and A-tensor elements is required in the simulation. The angle α is a variable used in the simulation of the spectra, and its value can only be obtained by systematic variation. The three principal g and A values must also be varied until satisfactory fits of the spectra are obtained at at least two different microwave frequencies (in our case X and Q band). There are no other means of assessing the correctness of values of α or the principal A values from the frozen solution spectra. However, a single crystal study yields the required tensors, and furthermore it provides the orientation of these tensors with respect to the atomic framework. This latter information cannot be obtained from frozen solution spectra. The relationship between the g- and A-tensors and the first coordination sphere is shown in Fig. 1.

The data in Table 1 show that the relative rotation of the g- and A-tensors, derived from the single crystal study, confirm that deduced from simulation of the frozen solution spectra. We have

* Author to whom correspondence should be addressed.

Table 1. Principal values of the g- and A-tensor for $LMoOCl_2$[a,b]

Medium	g_{yy}	g_{zz}	g_{xx}	$\times 10^4$ cm^{-1} A_{YY}	A_{ZZ}	A_{XX}	α°
Frozen toluene	1.941	1.971	1.934	18.1 (20)	71.4 (78)	38.1 (42)	33
$LSnCl_3$ single crystal	1.939[c]	1.969[c]	1.931[c]	33.4 (36.9)	72.2 (78.6)	33.7 (37.4)	35

[a] Values in parentheses are in Gauss.

[b] Lower case letters are used for the principal axes of the g-tensor and upper case letters for those of the A-tensor.

[c] These are the principal values of the g-tensor which become $g_{yy} = 1.939$, $g_{zz} = 1.945$, $g_{xx} = 1.947$ when expressed in the A-tensor axis system ($g_{xz} = 0.017$).

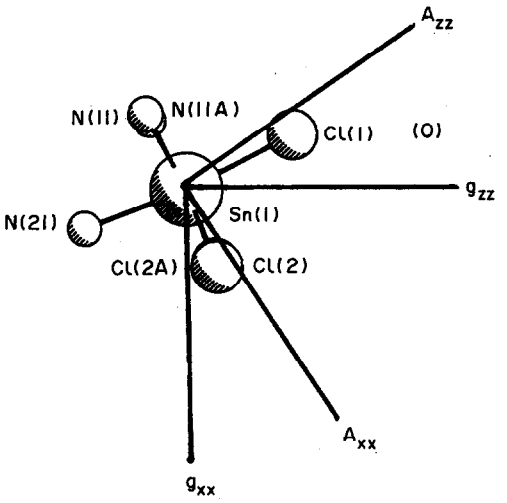

Fig. 1. The orientation of the principal g- and metal A-tensor axes with respect to the first coordination sphere. The view is down the direction perpendicular to the mirror plane in the molecule (g_{YY} and A_{YY} are coincident with this direction and N(21)—Sn(Mo)—C(11)(O) are in the mirror plane).

previously[3,4] assumed that the largest A-tensor element (A_{ZZ}) will be either coincident with or very close to Mo=O. This present single crystal study, whilst in near agreement with this, giving the angle between A_{ZZ} and $SnCl_2$ (Mo=O) as 8°, nevertheless demonstrates the genuine deviation of any principal ESR value away from the metal–oxo direction. However, such a close correspondence between a principal A-tensor element and a metal–oxo direction cannot generally be assumed as we have demonstrated for LVO(dtc).[5]

The single crystal study confirms the monoclinic ESR symmetry previously assumed for $LMoOCl_2$. Recognition of this symmetry has important consequences when trying to relate the ESR parameters to molecular geometry. If we did not know that the ESR symmetry is monoclinic, and merely attempted to interpret the numerical values of the principal g- and A-tensors, we would be tempted to approximate the molecule to be nearly axial, with the implication that the molecular geometry is also nearly axial. Clearly this cannot be true as the only symmetry element that the $LSnCl_3$ molecule has in the crystal structure, and the only one probable for $LMoOCl_2$, is a mirror plane.

REFERENCES

1. W. E. Cleland Jr, K. M. Barnhart, K. Yamanouchi, D. Collison, F. E. Mabbs, R. B. Ortega and J. H. Enemark, *Inorg. Chem.* 1987, **26**, 1017.
2. D. Collison, B. Gahan and F. E. Mabbs, *J. Chem. Soc., Dalton Trans.* 1987, 111; F. E. Mabbs and J. Temperley, unpublished results.
3. D. Collison, F. E. Mabbs, J. H. Enemark and W. E. Cleland Jr, *Polyhedron* 1986, **5**, 423.
4. C. G. Young, J. H. Enemark, D. Collison and F. E. Mabbs, *Inorg. Chem.* 1987, **26**, 2925.
5. D. Collison, F. E. Mabbs, M. A. Passand, K. Rigby and W. E. Cleland Jr, *Polyhedron* 1989, **8**, 1827.

Polyhedron Vol. 8, No. 13/14, pp. 1835–1837, 1989
Printed in Great Britain

0277–5387/89 $3.00+.00
© 1989 Maxwell Pergamon Macmillan plc

IMIDAZOLE AND RELATED HETEROCYCLIC LIGAND COMPLEXES OF OXOVANADIUM(IV)—POTENTIAL MODELS FOR THE REDUCED VANADIUM SITE OF THE SEAWEED BROMOPEROXIDASES

LOUISE J. CALVIOU, DAVID COLLISON,* C. DAVID GARNER, FRANK E. MABBS, MOHAMMAD A. PASSAND and MICHAEL PEARSON

Department of Chemistry, University of Manchester, Manchester M13 9PL, U.K.

Abstract—We have used the model compound approach to comment on the structural hypotheses that in reduced bromoperoxidase (BPO) the vanadium is coordinated by at least one imidazole-type nitrogen donor and possibly a phenolate-type oxygen donor. We report here the synthesis and spectroscopic characterization of representative examples of three classes of oxovanadium(IV)–imidazole complexes

(i) $[VO(acac)_2(imid)]$, where acac = 2,4-pentanedionate and imid = N- or 2-substituted imidazole.
(ii) $[VO(imid)_4Cl]^+$, which is stabilized in solution in the presence of excess imid.
(iii) $[VO(O—N)_2]$, where (O—N) = 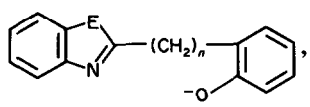 , $n = 0$ or 1, and E = O, S, NH, NMe.

It is the complexes of type (iii) above which most closely resemble the non-axial nature of ESR spectrum of the reduced BPO enzymes.

Vanadium is a trace element, essential for the normal development and growth of plants and animals. In halogen metabolism vanadium finds a role in the marine brown algae *Ascophyllum nodosum* and *Laminaria saccharina* as a component of a bromoperoxidase (BPO)† enzyme.[1] The enzyme appears to operate in nature exclusively with the metal in the +5 oxidation state,[1b,2] and in concert with hydrogen peroxide produces the brominating species tentatively assigned as HOBr.[3] Reduction of the enzyme with sodium dithionite produces an inactive form of BPO, with vanadium now present in the +4 oxidation state.[4] The accessibility of both diamagnetic and paramagnetic levels for this enzyme has meant that a variety of spectroscopic techniques has been applied to elucidate the nature of the metal site, e.g. ^{51}V NMR, EST, EXAFS,[6] ESEEM[7] and FTIR.[8] In particular, the results of X-ray absorption spectroscopy and paramagnetic resonance techniques have suggested that histidine is coordinated to the metal in a distorted electronic environment. There is additional evidence for short V—O interactions to anionic oxygen donor groups, such as those supplied by tyrosine or glutamate residues. We report, here, representative results from the model compound approach to assess the validity of various oxovanadium(IV) imidazole complexes in reproducing the ESR characteristics of the reduced BPO enzymes.

* Author to whom correspondence should be addressed.

† The following abbreviations have been used in this paper: BPO—bromoperoxidase; NMR—nuclear magnetic resonance; ESR—electron spin resonance; EXAFS—extended X-ray absorption fine structure; ESEEM—electron spin echo envelope modulation; FTIR—Fourier transform IR; acac—acetylacetonate; meox—2-methylquinolin-8-olate; imid—imidazole or substituted imidazole; O—M—uninegative bidentate ligand depicted in the abstract.

SYNTHESES OF OXOVANADIUM(IV) IMIDAZOLE COMPLEXES

(i) $[VO(acac)_2(imid)]$ were prepared after the method of Nath and Dash,[9] by treating $[VO(acac)_2]$ with 1 equivalent of imid in diethyl ether. The complexes separated as green powders.

(ii) $[VO(imid)_4Cl]Cl$ were prepared by treating $[VOCl_2(MeCN)_2(H_2O)]$[10] with 5 equivalents of imid in methyl cyanide solution. For N-substituted imidazoles the products formed as purple microcrystals directly from solution.

(iii) $[VO(O—N)_2]$ were prepared from either $VOSO_4 \cdot 5H_2O$ in water by adding a slight stoichiometric excess of the ligand[11] as a solution in ethanol or from $[VO(acac)_2]$ by refluxing in methyl cyanide. The complex where E = O separated as a yellow powder in both cases.

Complexes of each class, (i)–(iii), had satisfactory elemental analyses, consistent with their formulation, for C, H, N, V and Cl, and have characteristic values of $\nu(V{=}O)$ in the IR and Raman spectra. In addition, for class (ii) where imid = 1-vinylimidazole, the complex has been studied by single crystal X-ray diffraction methods. Figure 1 shows a schematic representation of the probable structures about the vanadium atom for each class.

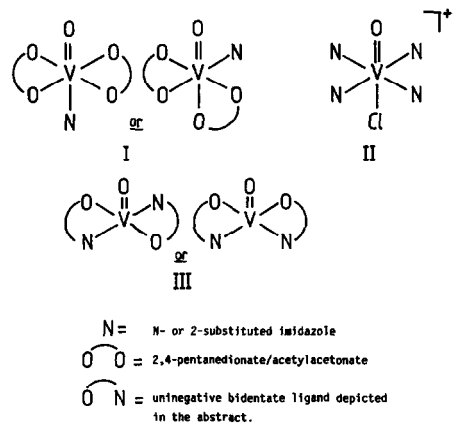

Fig. 1. Schematic representation of oxovanadium(IV) imidazole complexes.

ESR STUDIES

The ESR spectra of the reduced BPO enzyme under a variety of conditions have already been reported[4] and one of these is reproduced in Fig. 2 for comparative purposes. It was deduced from the form of a wide range of enzyme spectra that there is considerable interaction of the unpaired electron with ^1H and ^{17}O nuclei (and with ^{14}N as detected by ESEEM measurements). Thus the optimal resolution obtained in D_2O demonstrates the considerable rhombicity of the ESR parameters, where $g_2 - g_3$ is estimated to be 0.01. This may be compared with the values of $g_2 - g_3$ found for $[VO(meox)_2]$[12] and $[VO(acac)_2]$[13] of 0.005 and 0.004, respectively. Such large distortions away from apparent axial symmetry for oxovanadium(IV) complexes are usually interpreted to be the result of (i) mixed ligand coordination and/or (ii) geometric distortion produced by chelation. There is usually no diagnostic effect in ESR spectroscopy allowing the distinction between five and six coordination in complexes of this type. Visual inspection of Fig. 2 shows the relative extents of rhombicity in the ESR spectra of various model compounds. Class (ii) appears axial, as expected, as does class (i). It is the example from the class (iii) series, in common with $[VO(meox)_2]$, which shows considerable rhombicity; the $g_2 - g_3$ value for the former complex being estimated as 0.012. There is no splitting of the "$g_\perp$" features for class (ii) when spectra are obtained at Q band frequency.

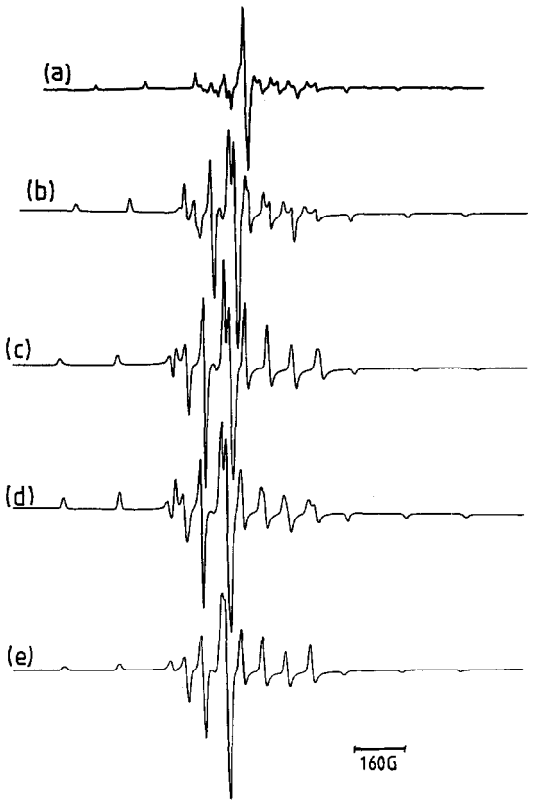

Fig. 2. Frozen solution ESR spectra at X band frequency of BPO and some oxovanadium(IV) complexes. (a) BPO in D_2O; (b) $[VO(meox)_2]$; (c) $[VO(acac)_2(imid)]$; (d) $[V(C—N)_2]$; (e) $[VO(imid)_4Cl]^+$.

CONCLUSIONS

On the basis of the model compound approach to the study of the reduced form of vanadium-containing bromoperoxidase enzymes, the nature of the coordination environment at the metal site may be suggested. The results of EXAFS, ESEEM and now ESR spectroscopy, are consistent with a mono-oxo vanadium(IV) ion coordinated by imidazole-type nitrogen atoms (from histidine), phenolate oxygen (from tyrosine) and weakly bound water in a distorted/strained geometry.

REFERENCES

1. (a) R. Wever, H. Plat and E. de Boer, *Biochim. Biophys. Acta* 1985, **830**, 181; (b) E. de Boer, M. G. M. Tromp, H. Plat, G. E. Krenn and R. Wever, *Biochim. Biophys. Acta* 1986, **872**, 104.
2. E. de Boer, PhD thesis. University of Amsterdam (1988).
3. E. de Boer and R. Wever, *J. Biol. Chem.* 1988, **263**, 12326.
4. E. de Boer, K. Boon and R. Wever, *Biochemistry* 1988, **27**, 1629.
5. H. Vilter and D. Rehder, *Inorg. Chim. Acta* 1987, **136**, L7.
6. J. M. Arber, E. de Boer, C. D. Garner, S. S. Hasnain and R. Wever, *Biochemistry*, in press.
7. E. de Boer, R. Wever, C. P. Keijzers, A. A. Klaassen, E. J. Reijese, D. Collison and C. D. Garner, *FEBS Lett.* 1988, **235**, 93.
8. E. de Boer, C. D. Garner and G. Potter, unpublished results.
9. P. K. Nath and K. C. Dash, *Ind. J. Chem.* 1986, **25A**, 968.
10. S. Bristow, S. C. M. McAvilley, W. Clegg and D. Collison, *Polyhedron* 1989, **8**, 87.
11. (a) L. L.-Y. Wang and M. M. Joullie, *J. Am. Chem. Soc.* 1957, **79**, 5706; (b) C. Rai and J. B. Braunworth, *J. Org. Chem.* 1961, **26**, 3434.
12. D. Collison, B. Gahan and F. E. Mabbs, *J. Chem. Soc., Dalton Trans.* 1987, 111.
13. B. Kirste and H. van Willigen, *J. Phys. Chem.* 1982, **86**, 2743.

Polyhedron Vol. 8, No. 13/14, pp. 1838–1843, 1989
Printed in Great Britain

0277–5387/89 $3.00+.00
© 1989 Maxwell Pergamon Macmillan plc

SYNTHESIS OF CATIONIC ALKYL BIS(CYCLOPENTADIENYL)TITANIUM COMPLEXES BY ONE-ELECTRON OXIDATION OF TITANIUM(III) ALKYLS. THE STRUCTURE OF $[Cp^*_2TiMe(THF)]BPh_4$ AND $[Cp^*_2Ti(OH)(H_2O)]BPh_4 \cdot 2THF$†

MANFRED BOCHMANN,‡ ANDREW J. JAGGAR and LADISLAV M. WILSON

School of Chemical Sciences, University of East Anglia, Norwich NR4 7TJ, U.K.

and

MICHAEL B. HURSTHOUSE‡ and MAJID MOTEVALLI

Department of Chemistry, Queen Mary College, London E1 4NS, U.K.

Abstract—The reaction of Cp^*_2TiMe ($Cp^* = C_5Me_5$) with $AgBPh_4$ in THF gives $[Cp^*_2TiMe(THF)]BPh_4$ (**1**). The sterically congested complex contains a labile THF ligand which is easily displaced by donor molecules. Compound **1** reacts with traces of moisture to give the hydroxo complex $[Cp^*_2Ti(OH)(H_2O)]BPh_4 \cdot 2THF$ (**2**). The structures of both complexes have been determined by X-ray diffraction. The THF ligand in **1** is oriented parallel to the Me—Ti—O plane; the Ti—O (THF) distance is 0.95 Å longer than the titanium–methyl bond. By contrast, the short Ti—OH distance in **2** (1.853 Å) indicates substantial Ti—O double bond character. The more weakly bound water ligand is associated with two THF molecules through strong hydrogen bonds.

The chemistry of cationic alkylbis(cyclopentadienyl) complexes of group IV metals has attracted interest recently because of their possible involvement as intermediates in olefin polymerizations catalysed by homogeneous Cp_2MCl_2/AlR_3 systems.[1–3] Although cationic titanium complexes $[Cp_2TiMe(L)]^+$ ($Cp = \eta^5\text{-}C_5H_5$) are readily accessible, for example by halide displacement from $Cp_2TiMeCl$, in which L is a nitrogen or phosphorus donor ligand,[2] this method does not allow the incorporation of weakly coordinated ligands such as tetrahydrofuran (THF). We report here the synthesis and structure of a THF complex obtained by the oxidation of a titanium(III) alkyl precursor under mild conditions.

EXPERIMENTAL

All operations were carried out under dried argon using standard vacuum-line techniques. Solvents were distilled under nitrogen from sodium benzophenone (THF, diethyl ether, petrol), sodium (toluene) or calcium hydride (dichloromethane). Perkin–Elmer 684 and 1720X (IR) and Jeol PMX-60 spectrometers were used. Cp^*_2TiMe was prepared from Cp^*_2TiCl and LiMe.[4] $AgBPh_4$ was obtained from aqueous $AgNO_3$ and $NaBPh_4$ and dried for several hours at 60°C/10^{-2} mm Hg.

Preparation of $[Cp^*_2TiMe(THF)]BPh_4$ (1)

To a cold (−78°C) solution of Cp^*_2TiMe (0.6 g, 1.8 mmol) in 10 cm^3 of THF was added $AgBPh_4$ (0.77 g, 1.8 mmol) in small portions. The stirred mixture was allowed to warm to room temperature. The colour changed from deep green to brown. Metallic silver was removed by filtration. The filtrate was concentrated *in vacuo* and the residue washed twice with petrol, followed by recrystallization from THF. The addition of a small amount of ether aids crystallization. Compound **1** was obtained as dark red–brown plates (0.8 g, 1.1 mmol, 61%). IR (Nujol mull, cm^{-1}): 3060 (w), 3035 (w), 1580 (m), 1265 (m), 1180 (w), 1143 (m), 1125 (w), 1065 (w), 1030 (w), 1005 (m), 840 (s), 742 (m),

† Dedicated to Professor Sir Geoffrey Wilkinson on the occasion of his retirement from the Sir Edward Frankland Chair of Inorganic Chemistry.

‡ Authors to whom correspondence should be addressed.

730 (s), 703 (s), 625 (w), 615 (m), 605 (m), 490 (w), 465 (w). ^{1}H NMR (pyridine-d_5): 8.05 (m, broad, 8H), 7.45–7.09 (m, 12H, BPh_4^-), 3.65 (m, 4H, THF), 1.71 and 1.65 (34H, THF and Cp* overlapping), 0.61 (s, 3H, Ti—Me). Found: C, 80.7; H, 8.6. Calc. for $C_{49}H_{61}BOTi$: C, 81.2; H, 8.5.

Preparation of $[Cp_2^*Ti(OH)(H_2O)]BPh_4 \cdot 2THF$ (2)

A solution of **1** (0.5 g) in 20 cm^3 of THF was treated with undried CO gas for 1 h. The solution was concentrated and left to crystallize at −15°C. Red–brown rhombic crystals of **2** were recovered in low yield. An identical product was obtained when Cp_2^*TiMe was oxidized with insufficiently dry $AgBPh_4$ in THF. IR (Nujol mull, cm^{-1}): 3620 (s, sharp), 3100–2900 (broad), 3060 (m), 3040 (m), 1670 (w), 1580 (m, BPh_4^-), 1460 (s), 1425 (m), 1265 (m), 1140 (m), 1065 (sh), 1043 (s), 1030 (m), 918 (m), 885 (m), 845 (s), 730 (s), 705 (s), 610 (s), 468 (w), 425 (m). Found: C, 76.1; H. 8.7. Calc. for $C_{52}H_{69}BO_4Ti$: C, 76.5; H, 8.5.

X-ray crystallography

All measurements were made on crystals sealed under argon in glass capillaries, using a CAD4 diffractometer and graphite monochromated Mo-K_α radiation (λ = 0.071069 Å). Unit cell and intensity data were obtained following standard procedures as previously described.[4] In both cases, crystal quality was poor, with variable mosaic spread and low scattering power.

The structures were solved using the heavy-atom procedure and refined via full-matrix least-squares methods. Non-hydrogen atoms were refined anisotropically, hydrogens with idealized positions and group U_{iso} values for all but those on the OH and OH_2 groups in compound **2** which were freely refined isotropically. In the final cycles, a weighting scheme of the type $w = [\sigma^2(F_o) + g(F_o)^2]^{-1}$ was used, with g varied to give flat agreement analogues. Experimental details are as follows:

Crystal data. (a) **1**, $C_{49}H_{61}BOTi$, M_r = 724.73, monoclinic, a = 20.920(6), b = 11.811(2), c = 17.299(7) Å, β = 106.93(4)°, V = 4089.1 Å^3, Z = 4, D_{calc} = 1.18 g cm^{-3}, $F(000)$ = 1560, μ(Mo-K_α) = 2.393 cm^{-1}, space group $P2_1/c$. 8138 intensities measured ($1.5 \leqslant \theta \leqslant 25.0°$), 7171 unique, 3350 observed [$F_o > 3\sigma(F_o)$], corrected for absorption via azimuthal scan data. 577 parameters in least-squares, R = 0.073, R_w = 0.072, g = 0.00023.

(b) **2**, $C_{52}H_{63}BO_4Ti$, M_r = 816.83, triclinic, a = 10.362(5), b = 14.871(6), c = 16.097(5) Å, α = 86.92(2), β = 72.69(3), γ = 85.44(4)°, V = 2359.4 Å^3, Z = 2, $D_{calc.}$ = 1.15 g cm^{-3}, $F(000)$ = 880, μ(Mo-K_α) = 2.18 cm^{-1}, space group $P\bar{1}$. 9090 intensities measured ($1.5 \leqslant \theta \leqslant 25.0°$), 8288 unique, 4920 observed [$F_o > 3\sigma(F_o)$], corrected for absorption via azimuthal scan data. 590 parameters in least-squares, R = 0.071, R_w = 0.067, g = 0.00014.

Atomic coordinates, displacement factor coefficients, full lists of bond lengths and angles and F_o/F_c lists have been deposited as supplementary data with the Editor, from whom copies are available on request. Atomic coordinates have also been deposited with the Cambridge Crystallographic Data Centre.

RESULTS AND DISCUSSION

Titanium(III) alkyls of the general composition Cp_2^*TiR ($Cp^* = C_5Me_5$) are readily prepared by reacting solutions of Cp_2^*TiCl[5] with lithium alkyls in diethyl ether, followed by crystallization of the dark green, paramagnetic complexes at low temperature. Treatment of a THF solution of Cp_2^*TiMe with solid $AgBPh_4$ in the dark, results in an immediate colour change to deep red–brown and a precipitation of metallic silver. Filtration and crystallization at −15°C yields air- and moisture-sensitive $[Cp_2^*TiMe(THF)]BPh_4$ (**1**) as brown crystalline plates [eq. (1)]:[6]

$$Cp_2^*TiMe + AgBPh_4 \xrightarrow{THF,\ RT} [Cp_2^*TiMe(THF)]BPh_4 + Ag^0. \quad (1)$$

(1)

The structure of **1** has been determined by X-ray crystallography. A diagram of the cation is shown in Fig. 1, selected bond lengths and angles are given in Table 1. The titanium centre has pseudo-tetra-

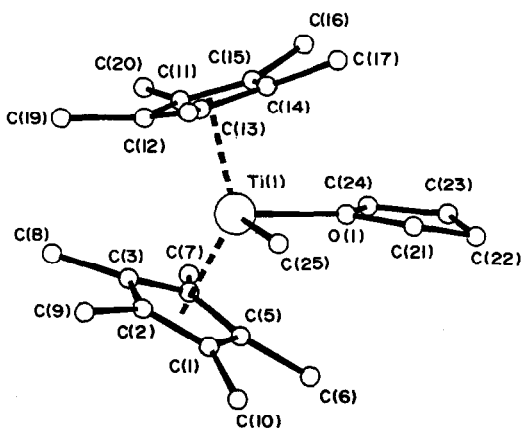

Fig. 1. The structure of $[Cp_2^*TiMe(THF)]^+$, showing the atomic numbering scheme. Ellipsoids correspond to 50% probability.

Table 1. Selected bond lengths and bond angles for **1**

(a) Bond lengths (Å)

O(1)—Ti(1)	2.154(6)	C(1)—Ti(1)	2.439(13)
C(2)—Ti(1)	2.360(10)	C(3)—Ti(1)	2.436(10)
C(4)—Ti(1)	2.422(10)	C(5)—Ti(1)	2.436(12)
C(11)—Ti(1)	2.392(12)	C(12)—Ti(1)	2.393(12)
C(13)—Ti(1)	2.426(10)	C(14)—Ti(1)	2.460(10)
C(15)—Ti(1)	2.468(12)	C(25)—Ti(1)	1.988(10)
C(21)—O(1)	1.444(12)	C(24)—O(1)	1.449(11)
C(2)—C(1)	1.376(15)	C(5)—C(1)	1.398(14)
C(10)—C(1)	1.529(15)	C(3)—C(2)	1.344(13)
C(9)—C(2)	1.565(15)	C(4)—C(3)	1.400(11)
C(8)—C(3)	1.476(14)	C(5)—C(4)	1.387(13)
C(7)—C(4)	1.492(14)	C(6)—C(5)	1.492(17)
C(12)—C(11)	1.405(13)	C(15)—C(11)	1.348(14)
C(20)—C(11)	1.526(16)	C(13)—C(12)	1.434(14)
C(19)—C(12)	1.473(15)	C(14)—C(13)	1.388(10)
C(18)—C(13)	1.510(14)	C(15)—C(14)	1.374(13)
C(17)—C(14)	1.478(14)	C(16)—C(15)	1.525(14)
O(1)—C(21)	1.444(12)	C(22)—C(21)	1.385(14)
C(22)—C(23)	1.530(16)	C(24)—C(23)	1.405(14)
Cp(1)—Ti(1)	2.114(12)	Cp(2)—Ti(1)	2.121(12)

(b) Bond angles (°)

C(25)—Ti(1)—O(1)	88.9(3)	C(5)—C(1)—C(1)	105.3(9)
C(10)—C(1)—C(2)	125.3(11)	C(10)—C(1)—C(5)	128.9(12)
C(3)—C(2)—C(1)	111.5(9)	C(9)—C(2)—C(1)	122.5(10)
C(9)—C(2)—C(3)	124.8(10)	C(4)—C(3)—C(2)	107.1(8)
C(8)—C(3)—C(2)	126.4(8)	C(8)—C(3)—C(4)	124.3(9)
C(5)—C(4)—C(3)	107.1(7)	C(7)—C(4)—C(3)	123.4(8)
C(7)—C(4)—C(5)	128.1(9)	C(4)—C(5)—C(1)	108.8(9)
C(6)—C(5)—C(1)	119.2(10)	C(6)—C(5)—C(4)	131.3(9)
C(15)—C(11)—C(12)	109.8(9)	C(20)—C(11)—C(12)	128.3(10)
C(20)—C(11)—C(15)	120.6(10)	C(13)—C(12)—C(11)	105.4(8)
C(19)—C(12)—C(11)	128.1(10)	C(19)—C(12)—C(13)	122.8(9)
C(14)—C(13)—C(12)	107.1(8)	C(18)—C(13)—C(12)	127.1(8)
C(18)—C(13)—C(14)	125.3(9)	C(15)—C(14)—C(13)	108.8(8)
C(17)—C(14)—C(13)	125.6(8)	C(17)—C(14)—C(15)	124.9(8)
C(14)—C(15)—C(11)	108.9(8)	C(16)—C(15)—C(11)	125.2(10)
C(16)—C(15)—C(14)	125.0(10)	C(22)—C(21)—O(1)	112.0(9)
C(23)—C(22)—C(21)	105.0(9)	C(24)—C(23)—C(22)	106.5(8)
Cp(1)—Ti(1)—Cp(2)	137.81(9)	Cp(1)—Ti(1)—O(1)	106.49(8)
Cp(2)—Ti(1)—O(1)	104.80(8)	Cp(1)—Ti(1)—C(25)	104.13(9)
Cp(2)—Ti(1)—C(25)	104.05(7)		

Cp(1)—defined as centre point of C(1), C(2), C(3), C(4) and C(5).
Cp(2)—defined as centre point of C(11), C(12), C(13), C(14) and C(15).

hedral coordination. The coordinated THF ligand is oriented parallel to the O(1)—Ti—C(25) plane, and the Ti—O distance (2.165 Å) is 0.095 Å longer than the Ti—CH_3 bond. The orientation of the THF ligand and the bond length distribution provide an interesting contrast to the sterically less congested zirconium complex, $[Cp_2ZrMe(THF)]BPh_4$;[7] here, the THF ligand is perpendicular to the O—Zr—CH_3 plane and the Zr—O bond is 0.13 Å shorter than the Zr—CH_3 bond, indicating an effective p_π–d_π interaction between an oxygen lone electron pair and zirconium. In **1**, repulsive interactions between the bulky Cp* ligands and THF override such an electronic stabilization.

Table 2. Selected bond lengths and bond angles for **2**

(a) Bond lengths (Å)

O(1)—Ti(1)	1.853(5)	O(2)—Ti(1)	2.080(5)
C(1)—Ti(1)	2.397(7)	C(2)—Ti(1)	2.437(7)
C(3)—Ti(1)	2.464(8)	C(4)—Ti(1)	2.419(7)
C(5)—Ti(1)	2.430(7)	C(11)—Ti(1)	2.425(8)
C(12)—Ti(1)	2.429(8)	C(13)—Ti(1)	2.421(7)
C(14)—Ti(1)	2.441(7)	C(15)—Ti(1)	2.404(8)
C(21)—O(3)	1.388(8)	C(24)—O(3)	1.395(8)
C(25)—O(4)	1.368(9)	C(28)—O(4)	1.381(10)
C(2)—C(1)	1.403(8)	C(5)—C(1)	1.414(7)
C(6)—C(1)	1.505(9)	C(3)—C(2)	1.411(7)
C(7)—C(2)	1.488(8)	C(4)—C(3)	1.410(8)
C(8)—C(3)	1.502(11)	C(5)—C(4)	1.421(8)
C(9)—C(4)	1.502(8)	C(10)—C(5)	1.491(9)
C(12)—C(11)	1.410(9)	C(15)—C(11)	1.385(9)
C(16)—C(11)	1.506(9)	C(13)—C(12)	1.408(8)
C(17)—C(12)	1.474(9)	C(14)—C(13)	1.379(8)
C(18)—C(13)	1.507(10)	C(15)—C(14)	1.423(8)
C(19)—C(14)	1.492(8)	C(20)—C(15)	1.502(11)
C(22)—C(21)	1.484(9)	C(23)—C(22)	1.449(10)
C(24)—C(23)	1.431(10)	C(26)—C(25)	1.401(11)
C(27)—C(26)	1.491(11)	C(28)—C(27)	1.427(11)
C(31)—B(1)	1.681(9)	C(41)—B(1)	1.680(9)
C(51)—B(1)	1.677(8)	C(61)—B(1)	1.677(9)
H(01)—O(1)	0.789(38)	H(021)—O(2)	1.096(30)
H(022)—O(2)	0.663(27)		
Cp(1)—Ti(1)	2.112(7)	Cp(2)—Ti(1)	2.111(7)

(b) Bond angles (°)

O(2)—Ti(1)—O(1)	90.1(2)	C(24)—O(3)—C(21)	109.8(5)
C(28)—O(4)—C(25)	105.5(6)	C(5)—C(1)—C(2)	108.5(5)
C(6)—C(1)—C(2)	125.2(5)	C(6)—C(1)—C(5)	126.0(6)
C(3)—C(2)—C(1)	107.7(5)	C(7)—C(2)—C(1)	126.2(5)
C(7)—C(2)—C(3)	125.7(6)	C(4)—C(3)—C(2)	108.5(6)
C(8)—C(3)—C(2)	124.9(6)	C(8)—C(3)—C(4)	126.4(5)
C(5)—C(4)—C(3)	107.6(5)	C(9)—C(4)—C(3)	124.9(6)
C(9)—C(4)—C(5)	126.6(6)	C(4)—C(5)—C(1)	107.5(5)
C(10)—C(5)—C(1)	125.3(5)	C(10)—C(5)—C(4)	125.0(5)
C(15)—C(11)—C(12)	108.5(5)	C(16)—C(11)—C(12)	123.5(7)
C(16)—C(11)—C(15)	127.9(7)	C(13)—C(12)—C(11)	106.9(6)
C(17)—C(12)—C(11)	126.6(6)	C(17)—C(12)—C(13)	126.4(6)
C(14)—C(13)—C(12)	109.1(5)	C(18)—C(13)—C(12)	125.2(6)
C(18)—C(13)—C(14)	125.1(5)	C(15)—C(14)—C(13)	107.5(5)
C(19)—C(14)—C(13)	125.7(5)	C(19)—C(14)—C(15)	125.1(6)
C(14)—C(15)—C(11)	107.9(6)	C(20)—C(15)—C(11)	122.8(6)
C(20)—C(15)—C(14)	127.9(6)	C(22)—C(21)—O(3)	108.1(6)
C(23)—C(22)—C(21)	105.4(6)	C(24)—C(23)—C(22)	107.6(6)
C(23)—C(24)—O(3)	109.1(6)	C(26)—C(25)—O(4)	111.8(7)
C(27)—C(26)—C(25)	102.5(7)	C(28)—C(27)—C(26)	104.5(7)
C(27)—C(28)—O(4)	110.5(7)	C(61)—B(1)—C(51)	114.0(4)
C(51)—B(1)—C(31)	105.9(4)	C(51)—B(1)—C(41)	109.1(5)
C(61)—B(1)—C(31)	110.8(5)	C(61)—B(1)—C(41)	104.8(4)
H(01)—O(1)—Ti(1)	125.7(23)	H(021)—O(2)—Ti(1)	119.5(16)
H(022)—O(2)—Ti(1)	133.4(27)	H(022)—O(2)—H(021)	101.9(33)
Cp(1)—Ti(1)—Cp(2)	139.06(6)	O(1)—Ti(1)—Cp(1)	106.92(6)
O(2)—Ti(1)—Cp(1)	104.58(5)	O(1)—Ti(1)—Cp(2)	102.77(6)
O(2)—Ti(1)—Cp(2)	102.87(6)		

Cp(1)—defined as centre point of C(1), C(2), C(3), C(4) and C(5).
Cp(2)—defined as centre point of C(11), C(12), C(13), C(14) and C(15).

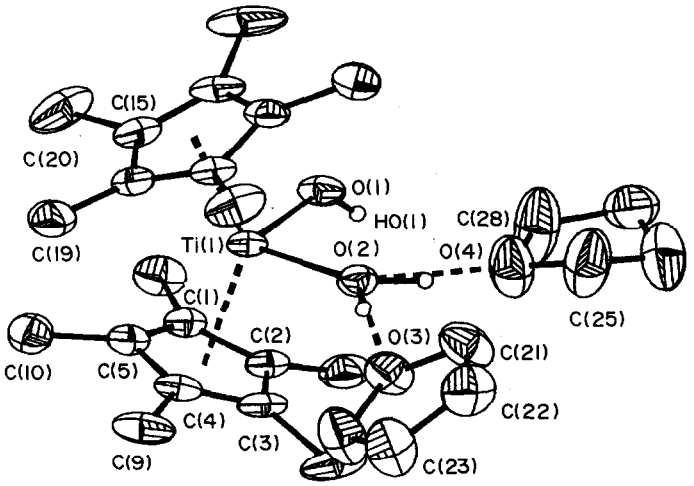

Fig. 2. The structure of $[Cp^*_2Ti(OH)(H_2O)]^+ \cdot 2THF$, including the atomic numbering scheme.

A similar "in-plane" orientation of THF is found in the neutral complexes $Cp_2YbMe(THF)$[8] and $Cp^*_2YbMe(THF)$.[9]

Under ambient conditions, **1** does not polymerize ethylene. It decomposes slowly in non-coordinating solvents such as dichloromethane. Although the THF ligand is labile and easily displaced by donor molecules such as nitriles, isocyanides or pyridine,[10] **1** is less reactive than C_5H_5 and indenyl analogues. For example, whereas $[Cp_2TiMe(MeCN)]^+$ reacts with Bu^{t}NC instantaneously under insertion to give an iminoacyl complex,[2b] the addition of Bu^{t}NC to cold solutions of **1** allows the spectroscopic observation of a relatively stable adduct (ν_{CN} 2202 cm^{-1}; presumably $[Cp^*_2TiMe(Bu^tNC)]^+$), which is converted to the corresponding iminoacyl complex on attempted isolation.

If the oxidation of Cp^*_2TiMe is carried out with $AgBPh_4$ containing traces of moisture, or if a THF solution of **1** is stirred under an atmosphere of CO which has not been rigorously dried, red–brown crystals of the aquo complex, $[Cp^*_2Ti(OH)(H_2O)]BPh_4 \cdot 2THF$ (**3**), are isolated in low yield. The IR spectrum of the complex shows a distinct and very sharp band at 3620 cm^{-1}, typical for an OH ligand free of hydrogen bonding,[7] and a very broad feature at *ca* 3300–2800 cm^{-1}, indicative of hydrogen-bonded OH.

The existence of both OH bonding modes was confirmed by X-ray crystallography. The structure of the complex cation of **3** is shown in Fig. 2, selected bond lengths and angles are given in Table 2. A noticeable feature is the short Ti—OH bond (1.866 Å) which is 0.23 Å shorter than the Ti—OH_2 bond. Similarly short metal–oxygen distances indicative of metal–oxygen double bond character have previously been observed in $Cp^*_2Zr(OH)_2$ and $Cp^*_2Zr(OH)Cl$.[11] The OH ligand does not interact with any of the solvent molecules. The O—H bond is oriented out of the O(1)—Ti—O(2) plane, with a Ti—O(1)—H angle of 125.7°. By contrast, each hydrogen of the H_2O ligand is closely associated with a THF molecule. The strength of this hydrogen bonding is confirmed by the short O—O distances between the H_2O and THF oxygens of 2.55 and 2.70 Å.

While this work was in progress, the independent preparation of trifluoromethylsulphonate complexes, $[Cp^*_2Ti(OH)(H_2O)]CF_3SO_3 \cdot nH_2O$ ($n = 1$, 2), has been reported.[12] The structures of the cations in these complexes strongly resemble that found in **2**; differences arise, however, in the pattern of hydrogen bonding which, in the case of the trifluoromethylsulphonates, includes interactions with the anion and the water of crystallization, and involves both the water and the hydroxo ligand.

Acknowledgement—We are grateful to the SERC for support (to A.J.J. and L.M.W.) and for the provision of X-ray facilities through its National Crystallographic Service.

REFERENCES

1. (a) F. S. Dyachkovski, A. K. Shilova and A. E. Shilov, *J. Polymer Sci.* 1967, **16C**, 2333; (b) J. J. Eisch, A. M. Piotrowski, S. K. Brownstein, E. J. Gabe and F. L. Lee, *J. Am. Chem. Soc.* 1985, **107**, 7219; (c) R. F. Jordan, C. S. Bajgur, R. Willett and B. Scott, *J. Am. Chem. Soc.* 1986, **108**, 7410; (d) R. F. Jordan, R. E. LaPointe, C. S. Bajgur and S. F. Echols, *J. Am. Chem. Soc.* 1987, **109**, 4111.
2. (a) M. Bochmann and L. M. Wilson, *J. Chem. Soc.*,

Chem. Commun. 1986, 1610; (b) M. Bochmann, L. M. Wilson, M. B. Hursthouse and R. L. Short, *Organometallics* 1987, **6**, 2556.
3. M. Bochmann, L. M. Wilson, M. B. Hursthouse and M. Motevalli, *Organometallics* 1988, **7**, 1148.
4. M. B. Hursthouse, R. A. Jones, K. M. A. Malik and G. Wilkinson, *J. Am. Chem. Soc.* 1979, **101**, 4128.
5. J. W. Pattiasina, H. J. Heeres, F. van Bolhuis, A. Meetsma and J. H. Teuben, *Organometallics* 1987, **6**, 1004; A. R. Dias, M. S. Salema, J. A. Martinho Simões, J. W. Pattiasina and J. H. Teuben, *J. Organomet. Chem.* 1988, **346**, C4.
6. M. Bochmann and A. J. Jaggar, *Abstr. XIIIth Int. Conf. Organomet. Chem.*, p. 257, Turin (1988).
7. Polymeric $(Me_3SnOH)_n$ also shows a sharp ν(OH) band at 3620 cm^{-1}: J. M. Brown, A. C. Chapman, R. Harper, D. J. Mowthorpe, A. G. Davies and P. J. Smith, *J. Chem. Soc., Dalton Trans.* 1972, 338.
8. W. J. Evans, R. Dominguez and T. P. Hanusa, *Organometallics* 1986, **5**, 263.
9. K. H. den Haan, J. de Boer, J. H. Teuben, W. J. J. Smeets and A. L. Spek, *J. Organomet. Chem.* 1987, **327**, 31.
10. M. Bochmann and A. J. Jaggar, manuscript in preparation.
11. R. Bortolin, V. Patel, I. Munday, N. J. Taylor and A. J. Carty, *J. Chem. Soc., Chem. Commun.* 1985, 456.
12. U. Thewalt and B. Honold, *J. Organomet. Chem.* 1988, **348**, 291.

Polyhedron Vol. 8, No. 13/14, pp. 1844–1845, 1989
Printed in Great Britain

0277–5387/89 $3.00+.00
© 1989 Maxwell Pergamon Macmillan plc

BIS(SUBSTITUTED BENZOATO) COMPLEXES OF BIS(η-CYCLOPENTADIENYL)TITANIUM(IV). SYNTHESIS, MASS, ^{1}H, ^{13}C NMR AND IR SPECTROSCOPY

Y. DANG and H. J. GEISE*

Department of Chemistry, University of Antwerp (UIA), B-2610 Wilrijk, Belgium

and

R. DOMMISSE and E. ESMANS

Department of Organic Chemistry, University of Antwerp (RUCA), Groenenborgerlaan 171, B-2020 Antwerp, Belgium

and

H. O. DESSEYN

Department of Inorganic Chemistry, University of Antwerp (RUCA), Groenenborgerlaan 171, B-2020 Antwerp, Belgium

Abstract—The synthesis of 31 complexes of the type $Cp_2Ti(OCOPhX)_2$ (X = substituent, Cp = η-C_5H_5) is reported together with their mass, ^{1}H NMR, ^{13}C NMR, mid- and far-IR spectra. The data are consistent with a model in which the Ti—OOC bond strength—weaker than Ti—Cp and Ti—Hal—is stabilized by electron-withdrawing groups, X, on the phenyl ring. The influence of the electronic properties of X also extends into the cyclopentadienyl rings.

In recent years, much research has been devoted to titanium(IV) complexes of the type $Cp_2Ti(OCOR)_2$, which may be attributed to their unique structures[1–4] and to their anticancer activity.[5,6] In the present communication, we are concerned with those complexes where R is a (substituted) phenyl ring or furan ring.

All complexes were obtained by reaction of Cp_2TiCl_2 with the sodium salt of the appropriately substituted benzoic acid, except for two nitro substituted complexes which were made from Cp_2TiCl_2 and nitrobenzoic acid in THF in the presence of triethylamine. Thus, 31 complexes were prepared, which included 13 *para*- (NH_2, OMe, OEt, Me, Et, *t*-Bu, Ph, F, Cl, Br, I, CN, NO_2), eight *meta*- (OMe, Me, F, Cl, Br, I, CN, NO_2), six *ortho*- (Me, Ph, F, Cl, I, CH_3COO^-), two bis- (2,4-Cl, Cl, 3,4-Cl, Cl) and one unsubstituted (H) benzoato complex, as well as one 2-furyl carboxylato complex. They were characterized by MS, ^{1}H NMR, ^{13}C NMR, mid- and far-IR spectra.

EIMS spectra show the ligands L (L = $ArCO_2$) and Cp_2Ti moieties, as well as structurally informative ions, e.g. $(Cp_2TiL)^+$, $(CpTiL)^+$, $(CpTiL—CO_2)^+$, $(Cp_2Ti)^+$ and $(CpTi)^+$. Further numerous ions characteristic of the ligands occur, including the molecular ion of the free substituted benzoic acid, HL. We observe the preferred loss of a benzoic acid ligand, L, over the loss of Cp from the title complexes. This suggests a greater strength of the Ti—Cp bond compared to the Ti—OOC bond. Exceptions are observed in the 4-NO_2 and 3-NO_2 complexes, where the intensity of the $(Cp_2TiL)^+$ ion is low (~ 5%) and that of the $(CpTiL_2)^+$ ion is high (~ 100%), suggesting a strengthening of the Ti—OOC bond due to a decreasing influence of resonance hybrid **b** in Fig. 1. We also note the preferential loss of CO_2 from $(CpTiLi)^+$ and rearrangement processes to $CpTiX^+$ ions when X = hal, with fluorine showing the strongest tendency to coordinate titanium.

* Author to whom correspondence should be addressed.

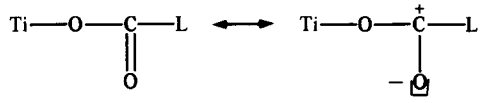

(a) (b)

Fig. 1. Some resonance hybrids of Cp_2TiL_2.

NMR SPECTRA

Signals of the phenyl protons and carbons are easily assigned by applying standard corrections of substituents[7] to the known chemical shifts of the unsubstituted complex.[2] The 10 protons of the two Cp rings absorb in the range 6.57–6.76 ppm (singlet) and the 10 carbons between 118.25 and 119.22 ppm (singlet). The chemical shifts can be correlated with the electronic properties of the substituents on the phenyl rings. As expected, electron-donating groups cause an upfield shift, while electron-withdrawing groups cause a downfield shift. On the other hand, the carboxylate carbons, resonating between 166.92 and 174.84 ppm, show the opposite trend. It may reflect the greater impact of resonance hybrid **a** (Fig. 1) with an electron-withdrawing substituent and of hybrid **b** with a donating one. A quantitative correlation between chemical shifts and substituent parameters is currently under way.

IR SPECTRA

Strong bands are observed near 1640 and 1330 cm^{-1} which are ascribed to the asymmetric COO stretch and the symmetric COO stretch, respectively. The difference $\Delta\nu(\nu_{asym}(COO)-\nu_{sym}(COO))$ is in the range of 300–370 cm^{-1} in all cases. It is clear evidence of monodentate coordination of the benzoate ligand in the complexes. A qualitative IR analysis for all the complexes indicates an increase of $\Delta\nu$ with electron-withdrawing properties of substituents as measured by Hammett $\sigma m/\sigma p$ values. In the far-IR region (500–50 cm^{-1}) tentative assignments include titanium–cyclopentadienyl (420 ± 10 cm^{-1}, 370–335 cm^{-1} and ~ 300 cm^{-1}), titanium–oxygen (~ 400 cm^{-1}), cyclopentadienyl–titanium–cyclopentadienyl (~ 240 cm^{-1}), oxygen–titanium–oxygen (140–110 cm^{-1}) and ligand (500–400 cm^{-1}) vibrations.

REFERENCES

1. D. M. Hoffman, N. D. Chester and R. C. Fay, *Organometallics* 1983, **2**, 48.
2. K. Döppert, H.-P. Klein and U. Thewalt, *J. Organomet. Chem.* 1986, **303**, 205.
3. C. R. Lucas, E. J. Gabe and F. L. Lee, *Can. J. Chem.* 1988, **66**, 429.
4. T. Güthner and U. Thewatt, *J. Organomet. Chem.* 1988, **350**, 235.
5. P. Köpf-Maier and H. Köpf, *J. Organomet. Chem.* 1988, **342**, 167 and refs therein.
6. J. H. Toney and T. J. Marks, *J. Am. Chem. Soc.* 1985, **107**, 847.
7. E. Pretsch, T. Clerc, J. Seill and W. Simon, in *Tabellen zur Strukturaufklärung Organischer Verbindungen mit Spektroskopische Methoden.* Springer, Berlin (1976).

Polyhedron Vol. 8, No. 13/14, pp. 1846–1847, 1989
Printed in Great Britain

0277–5387/89 $3.00+.00
Maxwell Pergamon Macmillan plc

PREPARATION AND REACTIONS OF SOME TITANIUM(IV) CARBOXYLATE SPECIES

N. W. ALCOCK, D. A. BROWN, T. F. ILLSON, S. M. ROE and M. G. H. WALLBRIDGE*

Department of Chemistry, University of Warwick, Coventry CV4 7AL, U.K.

Abstract—A series of compounds of general formula $TiCl_x(RCO_2)_{4-x}$ have been prepared and structurally characterized.

Prior to work carried out here, there were few halo titanium carboxylate compounds known.[1,2] No definitive structural evidence exists in the literature on these compounds. A series of compounds of type $TiCl_x(RCO_2)_{4-x}$ ($x = 2, 3$), have therefore been prepared and fully characterized.

In previous studies[1] a series of trischloromonocarboxylates have been obtained at room temperature by reaction of titanium tetrachloride with carboxylic acids, RCO_2H ($R = CH_3CH_2CH_2$, $(CH_3)_3C$, CH_2Cl, $CHCl_2$, CCl_3) [eq. (1)]:

$$TiCl_4 + RCO_2H \longrightarrow TiCl_3(RCO_2) + HCl \quad (1)$$

$$TiCl_4 + 2RCO_2H \longrightarrow TiCl_2(RCO_2)_2 + 2HCl. \quad (2)$$

The corresponding biscarboxylates were also prepared [eq. (2)]. The biscarboxylate, $TiCl_2(CH_3CH_2CO_2)_2$, was shown by X-ray powder diffraction[3] to exist in two forms. We have extended the range of trischloromonocarboxylates prepared. Thus, in eq. (1), $R = C_6H_5$, $CH_3C(C_6H_5)_2$, $(CH_3)_2CH$, $(CH_3)_3C$, *o*-$CH_3C_6H_4$, *p*-$CH_3C_6H_4$, $C_6H_2(CH_3)_3$, $CH_3CH{=}CH$, $C_6H_5CH{=}CH$. The trichloro-monopivalate derivative, $TiCl_3[(CH_3)_3CCO_2]$, has been structurally characterized by X-ray diffraction study, which shows that the compound is trimeric in the solid state (Fig. 1).

The titanium atoms form an approximate isosceles triangle and are joined by chlorine and carboxylate bridges, an interesting feature is the triply bridging chlorine atom (Cl_3) which bonds to the three titanium atoms. This chlorine atom is located 0.961 Å above the Ti_3 plane. Its bond to Ti(3) is long (2.839 Å) and its bonds to Ti(1) and Ti(2) (2.577, 2.565 Å) show some lengthening relative to the Ti—Cl bonds of the bridging chlorine Cl(2) (2.49, 2.476 Å). The Ti—Cl bridge has elongated (Ti—Cl—Ti angle > 90°), and the angle between the terminal chlorines has opened up from the ideal 90°. The carboxylate O—C—O angles are all between 121 and 123°.

All the compounds prepared were air- and moisture-sensitive. However, some surprisingly stable intermediates in the hydrolysis reaction of titanium(IV) carboxylates, $TiCl_x(RCO_2)_{4-x}$ (R = Me, Ph, $x = 3$; R = Me, $x = 2$) in the solvents, ethylacetate and tetrahydrofuran (EtOAc, THF), have been isolated.[4] The yellow crystalline binuclear complexes, $Ti_2(\mu\text{-}O)(\mu\text{-}O_2CR)_2Cl_4 \cdot 2L$ (L = EtOAc, THF), were obtained in high yield (~ 80%) by the addition of 1 molar equivalent of water to $TiCl_x(RCO_2)_{4-x}$ (R = Me, Ph, $x = 3$; R = Me, $x = 2$) in a solution of the appropriate ligand. It is noteworthy that the μ-oxo species are formed by the hydrolysis of a Ti—Cl bond in

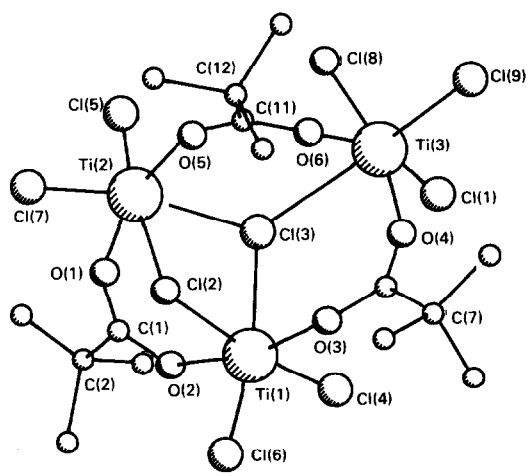

Fig. 1. Structure of $TiCl_3((CH_3)_3CCO_2)$.

* Author to whom correspondence should be addressed.

$TiCl_3(RCO_2)$ (R = Me, Ph), or by hydrolysis of a titanium-carboxylate bond in $TiCl_2(RCO_2)_2$ (R = Me), indicating the stability of the μ-oxo-carboxylate unit formed. The X-ray structure of the adducts (Fig. 2, R = Ph), show near octahedral coordination of the metal atoms, with the ligand *trans* to the bridging oxygen.

The presence of the two carboxylate bridges causes a deviation in the Ti—O—Ti angle (137.4°) from the ideal 180°. The μ-oxo atom arises from water added, since when $H_2{}^{17}O$ is used for the hydrolysis, the ^{17}O NMR of the crystalline product shows a sharp singlet at +810 ppm (relative to H_2O), which is in the region expected for μ-oxo bridges with octahedrally coordinated metal centres.

Preliminary evidence has been obtained for a further product of hydrolysis, namely, $Ti_2Cl_7(CH_3CHCHCO_2)(CH_3CHCHCO_2H)$. This compound forms as yellow–green brick-shaped crystals and X-ray diffraction studies show (Fig. 3) that the compound is dimeric with the two titanium centres linked by two bridging chlorine atoms and one bridging carboxylate group.

The titanium atoms are in pseudo-octahedral environments. The Ti—$Cl_{(bridge)}$ distance (average 2.5 Å) is very similar to the average distance reported for Ti—$Cl_{(bridge)}$ in $TiCl_4$ adducts of 2.49 Å. The Ti—$O_{(carboxylate)}$ distances of 1.896 and 2.008 Å may be compared with the Ti—O distance of 1.966 Å in $TiMgCl_5(ClCH_2CO_2)Cl$ $CH_2COOC_2H_5$),[5] of 2.029 Å in $[TiCl_4MeCO_2Et]_2$,[5] and of 2.014 Å in $[Ti_2(\mu\text{-}O)(\mu\text{-}O_2CR)_2Cl_4\cdot 2L]$; the distance in the latter compound being the Ti—$O_{(carboxylate)}$ distance. Compared with the above, the Ti(1)—O(1) distance of 1.896 Å seems rather short. The C(21)—O(3) bond length of 1.222 Å compared with the C(21)—O(4) bond length of 1.334 Å indicates the presence of a proton on O(4).

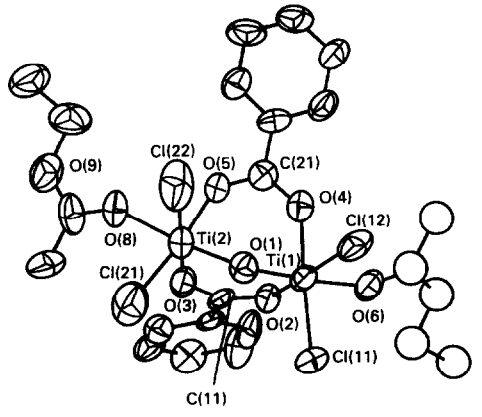

Fig. 2. Structure of $Ti_2(\mu\text{-}O)(\mu\text{-}O_2CPh)_2Cl_4\cdot 2EtOAc$.

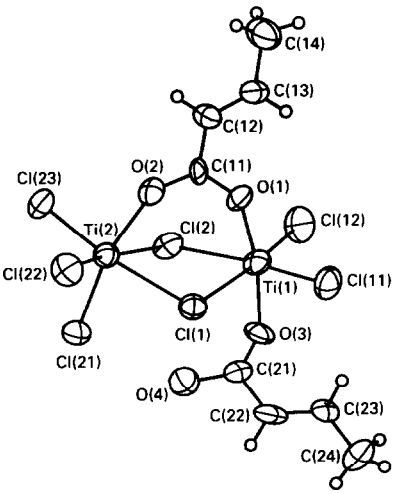

Fig. 3. Molecular structure of $Ti_2Cl_7(CH_3CHCHCO_2)(CH_3CHCHCO_2H)$.

The presence of small amounts of water in the solvents used for recrystallization would have caused the formation of oxo species and liberated HCl. The HCl is then proposed to react with a $Ti_2Cl_6(CH_3CHCHCO_2)_2$ fragment as in eq. (3):

$$Ti_2Cl_6(CCH_3CHCHCO_2)_2 + HCl \longrightarrow Ti_2Cl_7(CH_3CHCHCO_2)(CH_3CHCHCO_2H). \quad (3)$$

The $Ti_2Cl_6(CH_3CHCHCO_2)_2$ species may form by dissociation of the hypothetical trimeric species (cf. Fig. 1) in solution. Attempts to prepare $Ti_2Cl_7(CH_3CHCHCO_2)(CH_3CHCHCO_2H)$ on a large scale are currently in progress.

Acknowledgements—We thank the SERC and ICI C&P for their continuing support.

REFERENCES

1. J. Amaudrut and C. Devin, *CR Acad. Sci. Paris* 1967, **264C**, 2156.
2. R. Kapoor, P. Kapoor and B. K. Bahl, *Ind. J. Chem.* 1986, **25A**, 271.
3. J. Amaudrut, *Bull. Soc. Chim. Fr.* 1977, 624.
4. N. Alcock, P. N. Bartlett, D. Gordon, T. F. Illson and M. G. H. Wallbridge, *J. Chem. Soc., Chem. Commun.* 1986, 614.
5. J. C. J. Bart, I. W. Bass, M. Calcaterra, E. Albiazzati, U. Giannini and S. Parodi, *Z. Anorg. Allg. Chem.* 1983, **496**, 205.

Polyhedron Vol. 8, No. 13/14, pp. 1848–1849, 1989
Printed in Great Britain

0277–5387/89 $3.00+.00
© 1989 Maxwell Pergamon Macmillan plc

SYNTHESIS OF BIS-SILYLATED CYCLOPENTADIENYL NIOBIUM(IV) AND (V) NEUTRAL AND CATIONIC COMPLEXES

A. ANTIÑOLO, M. FAJARDO, F. A. JALÓN, A. OTERO* and M. C. PUERTA

Departamento de Química Inorgánica, Campus Universitario,
Universidad de Alcalá de Henares, Spain

and

Y. MUGNIER

Laboratoire de Synthèse et d'Electrosynthèse Organométalliques, Faculté des Sciences,
6 bd Gabriel, 21000 Dijon, France

Abstract—New niobium(IV) complexes, $Nb(\eta\text{-}C_5H_3RR')_2X_2$, R = H, R′ = $SiMe_3$, X = Br (**1**), X = I (**3**); R = R′ = $SiMe_3$, X = Br (**2**), X = I (**4**), have been isolated in high yields from the reactions of $Nb(\eta\text{-}C_5H_3RR')_2H_3$ and $Nb(\eta\text{-}C_5H_3RR')_2X$ with EtBr and MeI. Both chemical and electrochemical oxidation processes of these niobium(IV) complexes produce the cationic niobium(V) compounds, $[Nb(\eta\text{-}C_5H_4SiMe_3)_2X_2]^+$, X = Cl (**5**), Br (**6**), I (**7**), which exhibit an acidic character towards nucleophilic reagents, such as Me_2SiOR, to give new niobium(V) alkoxo complexes, $[Nb(\eta\text{-}C_5H_4SiMe_3)_2Cl(OR)]^+$, R = CH_3 (**8**), CH_2CH_3 (**9**), $CH(CH_3)_2$ (**10**). Spectroscopic IR, ESR and NMR data are available for these compounds.

During our studies of the electronic and steric influence of trimethylsilyl substituted cyclopentadienyl ligands on the properties of niobocene complexes, we have found that the reactions [eq. (1)] of complexes $Nb(\eta\text{-}C_5H_3RR')_2H_3$ and $Nb(\eta\text{-}C_5H_3RR')_2X$ with an excess of EtBr and MeI represent a new and easy method to isolate quantitatively niobium(IV) complexes, $Nb(\eta\text{-}C_5H_3RR')_2X_2$:

$$Nb(\eta\text{-}C_5H_3RR')_2X + R''\text{—}X \longrightarrow Nb(\eta\text{-}C_5H_3RR')_2X_2. \quad (1)$$

In the case of the trihydride complexes the reaction takes place with the initial formation of $Nb(\eta\text{-}C_5H_3RR')_2X$ and H_2.[1]

A GLC analysis of the gaseous phase allows us to obtain information on the reaction mechanisms and it rules out a pathway via radicals, because C—C coupling has never been observed.

The ESR spectra of d^1 paramagnetic complexes, **1**, **2**, **3** and **4**, were run. (The g_{av} values ranged over 2.0018–2.0806, in keeping with reported data on related compounds.[2])

Complexes $Nb(\eta\text{-}C_5H_4SiMe_3)_2X_2$ can be oxidized both chemically[3] [eq. (2)] and electrochemically to give niobocene d^0 cationic complexes:

$$Nb(\eta\text{-}C_5H_4SiMe_3)_2X_2 + Fc^+PF_6^- \longrightarrow Nb(\eta\text{-}C_5H_4SiMe_3)_2X_2^+ + Fc. \quad (2)$$

Fc = ferrocene

The new air stable d^0 niobium complexes were isolated in high yield as red crystals, X = Cl (**5**), Br (**6**), I (**7**), which have been spectroscopically characterized.†

These complexes can be easily obtained by one-electron oxidation of niobium(IV) complexes in dichloromethane, but when the solvent was THF or DMF the results by cyclic voltammetry show the existence of some interaction between the solvent and the resultant $[Nb(\eta\text{-}C_5H_4SiMe_3)_2X_2]^+$ complex obtained in the electrochemical oxidation process, which was unstable. Thus, when the solvent was THF the oxidation of $Nb(\eta\text{-}C_5H_4SiMe_3)_2Cl_2$ consumed more than one fluorine. Work to identify all of these resultant cationic species is in progress.

* Author to whom correspondence should be addressed.

† ^1H NMR data (solvent $CDCl_3$, δ in ppm relative to TMS) **5**: $C_5H_4SiMe_3$: 6.90 (m; 4); $C_5H_4SiMe_3$: 0.33 (s; 9). **6**: $C_5H_4(SiMe_3$: 7.10 (m; 4); $C_5H_4SiMe_3$: 0.34 (s; 9).

Complex **5** reacts with several nucleophilic reagents, such as H_2O, ROH, Me_3SiOR [eq. (3)]:

$$Nb(\eta\text{-}C_5H_4SiMe_3)_2Cl_2^+PF_6^- + Me_3SiOR \longrightarrow [Nb(\eta\text{-}C_5H_4SiMe_3)_2ClOR]^+PF_6^- + Me_3SiCl. \quad (3)$$

While it has been possible to isolate the corresponding organoalkoxo niobium(V) complexes, R = CH_3 (**8**), CH_2CH_3 (**9**), $CH(CH_3)_2$ (**10**), with Me_3SiOR as yellow crystalline solids which have been spectroscopically characterized,* the reactions with ROH give solutions which probably contain the corresponding adducts, but all attempts to isolate these compounds as solids were unsuccessful and the starting complexes were obtained. Now we are trying to isolate the reaction products using a basic medium and we have also started the electrochemical synthesis of the related compounds.

Finally, preliminary studies show the oxidizing character of the d^0 cationic species. For example [eq. (4)], they may be involved in the catalytic electrochemical oxidation of phosphines:

$$Nb(\eta\text{-}C_5H_4SiMe_3)_2I_2^+ + PR_3 + H_2O \longrightarrow Nb(\eta\text{-}C_5H_4SiMe_3)_2I_2 + OPPh_3 + 2H^+ + e^-. \quad (4)$$

We are now investigating the reactivity of cationic d^0 complexes, through both chemical and electrochemical ways, towards other organic substrates.

* ^1H NMR data (solvent $CDCl_3$, δ in ppm relative to TMS) **8**: $C_5H_4SiMe_3$: 7.01 (m; 6); 7.43 (m; 2); $C_5H_4SiMe_3$: 0.40 (s; 18); OR: 4.61 (s; 3). **9**: $C_5H_4SiMe_3$: 7.11 (m; 6); 7.45 (m; 2); $C_5H_4SiMe_3$: 0.55 (s; 18); OR: 1.55 (t; 3) J_{H-H} = 6.9 Hz, 4.96 (q; 2) J_{H-H} = 6.9 Hz. **10**: $C_5H_4SiMe_3$: 7.10 (m; 4); 7.36 (m; 2); 7.44 (m; 2); $C_5H_4SiMe_3$: 0.61 (s; 18); OR: 1.60 (d; 6) J_{H-H} = 5.5 Hz, 5.26 (m; 1) J_{H-H} = 5.5 Hz.

REFERENCES

1. A. Antiñolo, M. Fajardo, F. A. Jalón, C. López Mardomingo, A. Otero and C. Sanz Bernabé, *J. Organomet. Chem.*, accepted for publication.
2. P. B. Hitchcock, M. F. Lappert and C. R. C. Milne, *J. Chem. Soc., Dalton Trans.* 1981, 180 and refs therein.
3. J. Arnold, T. D. Tilley, A. L. Rheingold and S. J. Geib, *Organometallics* 1987, 473.

Polyhedron Vol. 8, No. 13/14, pp. 1850–1852, 1989
Printed in Great Britain

0277–5387/89 $3.00+.00
© 1989 Maxwell Pergamon Macmillan plc

MONOCYCLOPENTADIENYL LANTHANIDE CHEMISTRY: TOWARDS THE LIMITS OF STERIC UNSATURATION

COLIN J. SCHAVERIEN* and HARRY VAN DER HEIJDEN

Koninklijke/Shell-Laboratorium Amsterdam (Shell Research B.V.), Postbus 3003, 1003 AA Amsterdam, The Netherlands

and

A. GUY ORPEN

Department of Inorganic Chemistry, University of Bristol, Bristol BS8 1TS, U.K.

Abstract—The synthesis and single-crystal X-ray structure determinations of salt- and solvent-free $La(\eta^5\text{-}C_5Me_5)[CH(SiMe_3)_2]_2$, and of its THF precursor, are described. These complexes contain unusual agostic Si—Me bonds that facilitate stabilization of the unsaturated lanthanum centre. The first neutral "mixed" dialkyl organolanthanide complex, $Lu(\eta^5\text{-}C_5Me_5)(CH_2SiMe_3)[CH(SiMe_3)_2](THF)$, has been prepared.

The recent growth in organolanthanide chemistry has produced a wealth of fascinating reactions including propylene oligomerization,[1] methane transmetallation[2] and β-methyl elimination[3] by $Lu(\eta^5\text{-}C_5Me_5)_2Me$. Furthermore, $[M(\eta^5\text{-}C_5Me_5)_2H]_2$ (M = La, Nd, Lu) have been shown to be excellent olefin hydrogenation and ethylene oligomerization catalysts.[4]

Despite this recent increase of interest in organolanthanide chemistry, few mono-ligand supported lanthanide complexes have been prepared. Limitations to the potential scope of bis(pentamethylcylopentadienyl)lanthanide species may exist, however, in that they possess only one reactive metal–carbon or metal–hydride bond. In seeking new catalytic hydrocarbon and alkene transformations we rationalized that neutral, salt- and solvent-free organolanthanide alkyl complexes containing only *one* supporting cyclopentadienyl ligand would allow greater flexibility in this reactivity.

Reaction of $LuCl_3(THF)_3$ with NaC_5Me_5 (1 equiv.) in refluxing THF, under homogeneous conditions, afforded the useful precursor $[Na(THF\cdot OEt_2)]Lu(\eta^5\text{-}C_5Me_5)Cl_3$ (**1**)† in 70% yield:

$$LuCl_3(THF)_3 + NaC_5Me_5 \longrightarrow [Na(THF\cdot OEt_2)]Lu(\eta^5\text{-}C_5Me_5)Cl_3. \quad (1)$$

Compound **1** reacts cleanly with $LiCH(SiMe_3)_2$ in diethyl ether, in the presence of THF (5 equiv.), to afford the monoalkyl complex $[Li(THF)_2]Lu(\eta^5\text{-}C_5Me_5)CH(SiMe_3)_2Cl_2$ (**2**), which after treatment with tetramethylethylenediamine (TMEDA) affords $[Li(TMEDA)]Lu(\eta^5\text{-}C_5Me_5)[CH(SiMe_3)_2]Cl_2$ (**3**).

A LiCl-free, mixed alkyl, complex **5**, can be prepared from reaction of **2** with $LiCH_2SiMe_3$ to give a mixture of $[Li(THF)_3]Lu(\eta^5\text{-}C_5Me_5)(CH_2SiMe_3)[CH(SiMe_3)_2]Cl$ (**4**) and $Lu(\eta^5\text{-}C_5Me_5)(CH_2SiMe_3)[CH(SiMe_3)_2](THF)$ (**5**). Compound **4** loses LiCl on dissolution in non-coordinating solvents, thus recrystallization of this mixture (once) from hexane gave neutral, LiCl-free **5**. This represents the first reported neutral "mixed" alkyl organolanthanide complex.

* Author to whom correspondence should be addressed.

† All compounds have been fully characterized and satisfactory analytical data obtained.

$$[Li(THF)_2]Lu(\eta^5\text{-}C_5Me_5)[CH(SiMe_3)_2]Cl_2 + LiCH_2SiMe_3 \longrightarrow$$
(2)

$$[Li(THF)_3]Lu(\eta^5\text{-}C_5Me_5)(CH_2SiMe_3)[CH(SiMe_3)_2]Cl$$
(4)

Hexane

$$Lu(\eta^5\text{-}C_5Me_5)(CH_2SiMe_3)[CH(SiMe_3)_2](THF).$$
(5)

Complexes **3** and **4** have been structurally characterized.[5]

Attempts at stabilizing the sterically unsaturated lutetium centre with two bis(trimethylsilyl)methyl groups were unsuccessful, presumably due to steric limitations.

Salt-free **5**, especially, has limited thermal stability, with rapid decomposition in solution above 40°C. Use of the 1,3-diphenyl-2,4,5-trimethylcyclopentadienyl ligand gave greater thermal stability to the lutetium alkyl complexes, $[K(OEt_2)]Lu(\eta^5\text{-}C_5Me_3Ph_2)\{CH(SiMe_3)_2\}Cl_2$ (**6**) and $Lu(\eta^5\text{-}C_5Me_3Ph_2)(CH_2SiMe_3)_2(THF)$ (**7**).

Investigation of this chemistry was severely hampered by salt coordination and the poor thermal stability of the salt-free compounds, so we decided to explore similar goals with lanthanum.

Reaction of $La(\eta^5\text{-}C_5Me_5)I_2(THF)_3$[6] (**8**) with two equivalents of $LiCH(SiMe_3)_2$ in hexane–diethyl ether affords thermally unstable, salt-free $La(\eta^5\text{-}C_5Me_5)[CH(SiMe_3)_2]_2(THF)$ (**9**):

$$La(\eta^5\text{-}C_5Me_5)I_2(THF)_3 + 2LiCH(SiMe_3)_2 \longrightarrow$$
(8)

$$La(\eta^5\text{-}C_5Me_5)[CH(SiMe_3)_2]_2(THF).$$
(9)

The removal of coordinated THF is achieved by a novel and potentially general, yet simple chemical method which leaves the highly reactive, electrophilic organolanthanide complex intact. Trimethylsilyl iodide is known to ring-open cyclic ethers such as THF to afford trimethylsilyl ethers. We postulated that this would provide a simple method to *cleanly* remove coordinated THF from highly reactive and sensitive **9**. To our knowledge, this method of THF removal has never been utilized in organometallic chemistry. Treatment of **9** with Me_3SiI affords salt- and solvent-free $La(\eta^5\text{-}C_5Me_5)[CH(SiMe_3)_2]_2$ (**10**), with concomitant formation of $Me_3SiO(CH_2)_4I$. Because of the inherent instability of **9** (half life is *ca* 2 h at 25°C and 40 mM concentration), a more practically useful synthetic approach was needed and discovered. Reaction of **8** with Me_3SiI afforded THF-free $[La(\eta^5\text{-}C_5Me_5)I_2]_n$ (**11**). Treatment of isolated **11** with $KCH(SiMe_3)_2$ (2 equiv.), in ether, gave $La(\eta^5\text{-}C_5Me_5)[CH(SiMe_3)_2]_2$ (**10**) directly in 75% yield.

The X-ray crystal structures of compounds **9** and **10** (Fig. 1) have been determined and reported by us.[7] They show unique β-Si—Me agostic interactions with the lanthanum centre, as opposed to the C—H—M interactions previously observed

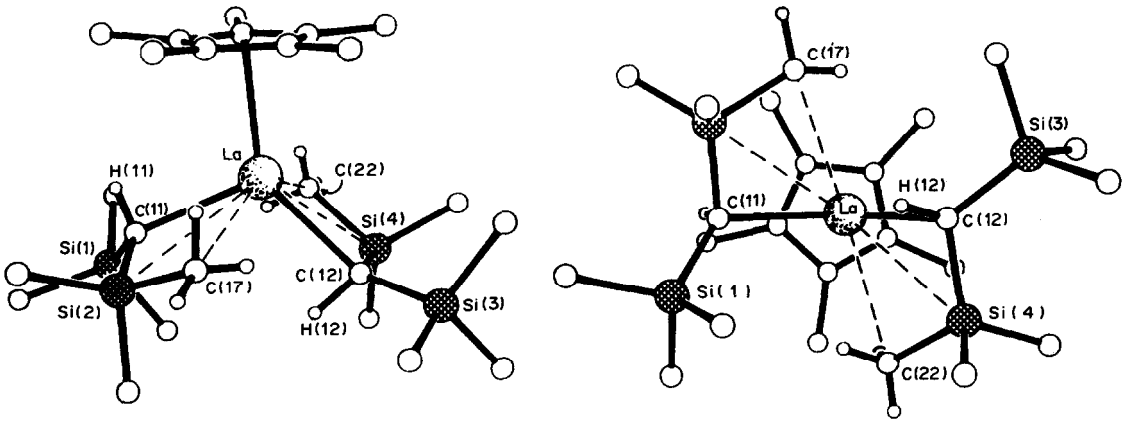

Fig. 1. Alternative views of the molecular structure of $La(\eta^5\text{-}C_5Me_5)[CH(SiMe_3)_2]_2$ (**10**). Methyl group hydrogens have been omitted except for those on C(17) and C(22).

La···C(17)	2.988(6)	La···Si(2)	3,353(2)	La···H(11)	2.64(5)
La···C(22)	3.353(2)	La···Si(4)	3.400(2)	La···H(12)	2.75(5)

La—C(11)—Si(1)	126.4(4)	La—C(12)—Si(3)	129.6(3)
La—C(11)—Si(2)	99.6(3)	La—C(12)—Si(4)	98.8(3)

with the $CH(SiMe_3)_2$ ligand. There appears to be only a marginal lengthening of the interacting Si—Me bond compared to the other Si—Me bonds in the same molecule. Although we were able to locate the hydrogen atoms on the interacting carbon in **10**, and they are not pointing towards the lanthanum, we are in the process of carrying out a single-crystal neutron structure determination on **10** to elucidate exactly the nature of this interaction. Furthermore, variable temperature solid state ^{13}C studies are in progress, and will be reported elsewhere, to determine the dynamic processes available to these rather flexible alkyl groups.

The near-planarity of the La—C—Si—Me system is reminiscent of the planar four-centre intermediates postulated and observed[8] in β-hydride elimination. These species may be viewed as models for the early stages of the β-methyl elimination reaction,[9] analogous to β-C—H agostic species which model the β-hydride elimination reaction.

REFERENCES

1. P. L. Watson, *J. Am. Chem. Soc.* 1982, **104**, 337.
2. P. L. Watson, *J. Am. Chem. Soc.* 1983, **105**, 6491.
3. P. L. Watson and D. C. Roe, *J. Am. Chem. Soc.* 1982, **104**, 6471.
4. G. Leske, H. Lauke, H. Mauermann, H. Schumann and T. J. Marks, *J. Am. Chem. Soc.* 1985, **107**, 8111.
5. H. van der Heijden, P. Pasman, E. J. M. de Boer, C. J. Schaverien and A. G. Orpen, *Organometallics*, in press.
6. P. N. Hazin, J. C. Huffman and J. W. Bruno, *Organometallics* 1987, **6**, 23.
7. H. van der Heijden, C. J. Schaverien and A. G. Orpen, *Organometallics* 1989, **8**, 255.
8. R. B. Cracknell, A. G. Orpen and J. L. Spencer, *J. Chem. Soc., Chem. Commun.* 1984, 326.
9. P. L. Watson, *J. Am. Chem. Soc.* 1982, **104**, 6471.

Polyhedron Vol. 8, No. 13/14, pp. 1853–1854, 1989
Printed in Great Britain

0277–5387/89 $3.00+.00
© 1989 Maxwell Pergamon Macmillan plc

NEW NITROGEN BASE ADDUCTS OF MANGANESE(II) DIALKYLDITHIOPHOSPHATES AND THE X-RAY STRUCTURE OF $[Mn(phen)_3]^{2+}[S_2P(OC_2H_5)_2^-]_2$

MICHAEL G. B. DREW, MASIHUL HASAN* and YANN HELLO†

Department of Chemistry, The University, Whiteknights, Reading RG6 2AD, U.K.

Abstract—A number of manganese(II) complexes with $[(RO)_2PS_2]^-$ ligands have been prepared and structurally characterized.

A review of the literature[1,2] shows that the chemistry of $Mn^{II}[Rdtp]_2$ ($Rdtp = S_2P(OR)_2^-$) and its adducts with N-bases has been neglected. There are however two papers which refer to $Mn^{I}[Rdtp(CO)_4]$ ($R = C_6H_5$,[3] CH_3[4]) and their substituted adducts with N-bases and Lewis bases, but these were published over 20 years ago.

Here we report the characterization for a range of complexes of the type $Mn[Rdtp]_2 \cdot L$, [$R = C_2H_5$, i-C_3H_7, n-C_4H_9; L = bipy (2,2′-bipyridyl), phen (1,10-phenanthroline), dmphen (2,9-dimethyl,1,10-phenanthroline)] and $[Mn(phen)_3]^{2+}$ $[Rdtp^-]_2$ ($R = C_2H_5$, i-C_3H_7). It is surprising that although the $[Mn(phen)_3]^{2+}$ cation has long been known to possess anti-fungal[5] and more recently anti-venereal and contraceptive properties,[6] its single crystal X-ray structure has not been reported,[2] and so we have carried out such a study on $[Mn(phen)_3]^{2+}[Rdtp^-]_2$ ($R = C_2H_5$), and this is described below.

The $Mn[Rdtp]_2 \cdot L$ complexes were prepared by mixing solutions of $[NH_4][Rdtp]$ in H_2O and the appropriate N-base in ethyl alcohol with aqueous $Mn(NO_3)_2 \cdot 6H_2O$ in a stoichiometric ratio. All the complexes described here have been characterized by elemental analysis and IR spectra. Yields are generally in excess of 60%.

The nature of the products [shown in eqs (1)–(3)] is dependent upon L, substituent R and the solvent. When the ratio of metal salt–Rdtp–phen is 1:2:1, then $Mn(Rdtp)_2 \cdot L$ is precipitated in H_2O for $R = C_2H_5$ and n-C_4H_9, but not when $R = i$-C_3H_7. On increasing the relative ratio of phen from 1 to 3, no change in product was observed. When L = bipy, only when $R = n$-C_4H_9 is the compound $Mn[Rdtp]_2 \cdot L$ formed. But on extraction with CH_2Cl_2 from a mixture of solutions of Mn^{II}, $Rdtp^-$ and L in the ratio 1:2:1, a larger range of complexes of this type are obtaind ($R = C_2H_5$, i-C_3H_7; L = phen, bipy, dmphen; and $R = n$-C_4H_9, L = dmphen). In the case of $R = C_2H_5$, L = phen, the major product was yellow crystals of $Mn[Rdtp]_2$(phen). However, small traces of red crystals were also observed, which were separated by repeated recrystallization and characterized as $[Mn(phen)_3]^{2+}[Rdtp^-]_2$.

On the other hand, treatment of $Mn(Rdtp)_2 \cdot L$ ($R = C_2H_5$; L = phen) with 2 mol equivalent of phen gave a yellow complex in quantitative yield, which was identified as $[Mn(phen)_3]^{2+}[Rdtp^-]_2$. This is in marked contrast to the reaction with bipy, where $Mn(Rdtp)_2 \cdot L$ undergoes oxidation to give MnO_2, the disulphide[7] $[(RO)_2P(S)S^-]_2$ (^{31}P NMR, 83.7 ppm) and bipy. Holah and Murphy isolated $[Mn(phen)_3]^{2+}$ with a similar ligand, e.g. $S_2COC_2H_5^-$, by mixing Mn^{II}, $S_2COC_2H_5^-$, and phen (1:2:3) in water, but found that with bipy,

$$Mn^{II} + 2Rdtp^- + L \xrightarrow[H_2O]{} Mn[Rdtp]_2 \cdot L \quad (1)$$

$$Mn[Rdtp]_2 \cdot L + 2L \xrightarrow[C_2H_5OH]{} \begin{cases} \rightarrow [MnL_3]^{2+}[Rdtp^-]_2 \\ \quad (R = C_2H_5,\ L = \text{phen})\ 90\%\ \text{yield} \end{cases} \quad (2)$$

$$\rightarrow MnO_2 + L + \{(RO)_2P(S)S^-\}_2 \quad (R = C_2H_5,\ L = \text{bipy}) \quad (3)$$

* Author to whom correspondence should be addressed.
† Permanent address: Institut des Sciences de l'Ingénieur en Thermique–Enérgetique et Matériaux (ISITEM), Nantes, France.

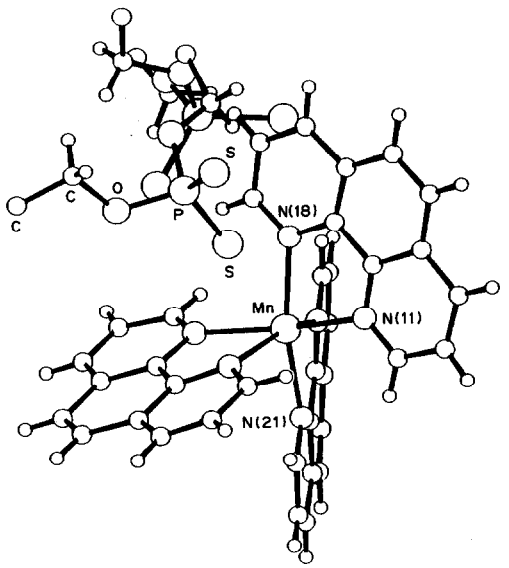

Fig. 1

intractable oils were obtained which could not be characterized.[8]

The above results are not unexpected since complexes of phen with other transition metals are generally more stable[9] than with bipy.

A crystal structure determination was carried out on the yellow crystals of $[Mn(phen)_3]^{2+}[Rdtp^-]_2$ ($R = C_2H_5$).* Preliminary investigations show that the red crystals isolated from the preparation of $Mn[dtp]_2(phen)$ are isomorphous, so we have no immediate explanation for the variation in the colour. Spectral measurements on the two compounds are similar.

The structure is shown in Fig. 1; there are only van der Waals contacts between the ions. In the cation the independent Mn—N distances are 2.224(18), 2.285(13) and 2.263(12) Å. The geometry of the metal atom coordination sphere can be described as distorted octahedral. The main features of the distortion arise from the N—Mn—N chelate angle, for which the mean value is 73.4°. It is noteworthy that of the three *trans* N—Mn—N angles, one at 153.4(5)°, is significantly shorter than the other two [163.6(5)°]. Dimensions in the $Rdtp^-$ anion are compatible with previous studies.[7] Further X-ray and spectroscopic studies on compounds in this series are in progress.

* Crystal data: $[Mn(phen)_3]^{2+}[Rdtp^-]_2$ (**1**), $C_{44}H_{44}N_6S_4O_4P_2Mn$, $M = 965.47$, monoclinic, $a = 16.55(1)$, $b = 17.50(1)$, $c = 17.46(1)$, $\beta = 93.0(1)$, $U = 4680.0$ Å^3, $F(000) = 2004$, $d_m = 1.37(2)$ g cm^{-3}, $d_c = 1.37$ g cm^{-3}, $Z = 4$, $F(000) = 506$, Mo-K_α radiation, $I = 0.7107$ Å, $\mu = 5.85$ cm^{-1}, space group $I2/c$ (No. 15). The structure was determined by statistical methods. The structure consists of $[Mn(phen)_3]^{2+}$ cations with crystallographically imposed C_2 symmetry and discrete $dedtp^-$ anions in general positions. All non-hydrogen atoms were refined anisotropically. Hydrogen atoms were included in calculated positions, although the methyl hydrogen atoms were refined as rigid groups. The final R was 0.098 ($R_w = 0.097$) for 1565 independent data with $I > 2\sigma(I)$. Atomic coordinates, displacement factor coefficients, full lists of bond lengths and angles have been deposited as supplementary data with the Editor, from whom copies are available on request. Atomic coordinates have also been deposited with the Cambridge Crystallographic Data Centre.

REFERENCES

1. J. R. Wasson, G. M. Woltermann and H. Stoklosa, *Fortschr. Chem. Forsch.* 1973, **35**, 65.
2. Cambridge Crystallographic Database, University of Cambridge (1989).
3. R. L. Lambert and T. A. Manuel, *Inorg. Chem.* 1966, **5**, 1287.
4. F. A. Hartman and A. Wojcicki, *Inorg. Nucl. Chem. Lett.* 1966, **2**, 303.
5. A. Shulman and F. P. Dwyer, in *Chelating Agents and Metal Chelates* (Edited by F. P. Dwyer and D. P. Mellor), p. 383. Academic Press, New York (1964).
6. A. Shulman and G. M. Shulman, *Australian Patent*, 498, 201 (1979).
7. M. G. B. Drew, G. A. Forsyth, M. Hasan, R. J. Hobson and D. A. Rice, *J. Chem. Soc., Dalton Trans.* 1987, 1027.
8. D. G. Holah and C. N. Murphy, *Inorg. Nucl. Chem. Lett.* 1972, **8**, 1069.
9. G. B. Deacon, *Inorg. Nucl. Chem. Lett.* 1966, **2**, 299.

Polyhedron Vol. 8, No. 13/14, pp. 1855–1856, 1989
Printed in Great Britain

0277–5387/89 $3.00+.00
© 1989 Maxwell Pergamon Macmillan plc

NEW SYNTHETIC APPROACHES TO $Mn_2(CO)_{10-n}L_n$ DERIVATIVES (L = PHOSPHINES): THEIR CATALYTIC ACTIVITY IN THE HOMOGENEOUS HYDROGENATION OF DIPHENYLACETYLENE AND THE CRYSTAL STRUCTURE OF $Mn_2(CO)_9(PPh_2H)$

ROBERTO GIORDANO and ENRICO SAPPA*

Dipartimento di Chimica Inorganica, Chimica Fisica e Chimica dei Materiali, Università di Torino, Via P. Giuria 7, 10125 Torino, Italy

and

ANTONIO TIRIPICCHIO* and MARISA TIRIPICCHIO CAMELLINI

Istituto di Chimica Generale e Inorganica, Università di Parma, Centro di Studio per la Strutturistica Diffractometrica del CNR, Viale delle Scienze, 43100 Parma, Italy

and

MARTIN J. MAYS

University Chemical Laboratory, Lensfield Road, Cambridge CB2 1EW, U.K.

and

MICHAEL P. BROWN

Donnan Laboratory, University of Liverpool, Grove Street, Liverpool LS9 3BX, U.K.

Abstract—Novel $Mn_2(CO)_{10-n}L_n$ complexes have been investigated as hydrogenation catalysts and a representative member has been structurally characterized.

We are investigating the behaviour of carbonyl clusters, and in particular that of phosphine-substituted and phosphido-bridged derivatives as homogeneous hydrogenation catalysis.[1] We have studied the behaviour of $Mn_2(CO)_{10}$ (**1**), $Mn_2(CO)_9(PPh_2H)$ (**2**), $Mn_2(\mu\text{-}H)(\mu\text{-}PPhH)(CO)_8$ (**3**), $Mn_2(\mu\text{-}H)(\mu\text{-}PPh_2)(CO)$ (**4**) and $Mn_2(\mu\text{-}PPh_2)_2(CO)_8$ (**5**) in the hydrogenation of diphenylacetylene.

Phosphine-substituted dimanganese derivatives are generally obtained by thermal or photochemical activation of the CO's, generally in non-selective processes; indeed it is believed that Mn—Mn bond cleavage occurs and that the phosphine-substituted fragments recombine in a random fashion.[3]

We have attempted the synthesis of $Mn_2(CO)_{10-n}L_n$ derivatives by labilization of CO's with Me_3NO[4] in relatively mild conditions (L = PPh_3, PPh_2H, $PPh_2CH{=}CH_2$, $PPh_2PC{\equiv}CPPh_2$). Heating $Mn_2(CO)_{10}$ with a 1–5 molar excess of ligand in hexane or heptane, in the presence of dry Me_3NO for 2 min, leads to mixtures containing 30–40% of $Mn_2(CO)_9L$, about 5–10% of $Mn_2(CO)_8L_2$ (one or two isomers) and about 50% of unreacted carbonyl (which was re-used).

The complexes were identified by spectroscopy and, in particular, by ^{31}P NMR; for **2** a sharp singlet at δ 51.12 was observed. However, for the other monosubstituted complexes sharp singlets centred at δ 50–60 and a broad peak at δ 20–30 was found (but for PPh_3, a sharp singlet at δ 29.52, a broad peak at δ 74.62 ppm). This should indicate

* Authors to whom correspondence should be addressed.

Table 1

Complex	Reaction time[a]	Conversion[a]	Selectivity to: *cis*-stilbene	Selectivity to: *trans*-stilbene	*trans–cis* ratio[b]
1	1–27	5.0–12.5	24.0–22.4	76.0–77.6	3.2–3.5
2	1–48	5.1–11.9	15.7–21.0	84.3–79.0	5.4–3.8
3	1–76	14.2–21.3	28.9–27.2	71.1–72.8	2.5–2.7
4[c]	48	50.4	20.2	79.8	3.9
5	1–48	5.8–15.4	25.9–27.3	74.1–72.7	2.9–2.7

[a] Minimum and maximum value; 1 atm H_2.
[b] Initial and final valuc.
[c] Under 34 atm pressure of H_2.

that mostly equatorial, monosubstituted complexes are obtained.

Thus, apparently, the use of Me_3NO gives, in most cases, stereospecific substitution of one equatorial CO, a statistically favoured process. In order to confirm the structure of **2**, a suitable crystal of **2** was selected for an X-ray diffraction study. Crystal data: $C_{21}H_{11}Mn_2O_9P$, $M = 548.16$, monoclinic space group, $C2/c$, $a = 24.038(8)$, $b = 14.645(6)$, $c = 16.328(6)$ Å, $\beta = 125.58(2)°$, $Z = 8$, $d_{calc} = 1.559$ g cm^{-3}, μ(Mo-K_α) = 11.50 cm^{-1}. Of 4409 reflections collected on an Enraf–Nonius CAD-4 diffractometer (Mo-K_α) ($3 < \theta < 24°$), 1548, having $I > 2\sigma(I)$, were used in the refinement. All non-hydrogen atoms were refined anisotropically. Hydrogen atoms were clearly located and refined isotropically. Final R and R_w values were 0.0363 and 0.0436, respectively. Atomic coordinates have been deposited with the Director, Cambridge Crystallographic Data Centre. The structure of **2** is shown in Fig. 1. The Mn—Mn distance of 2.910(2) Å, is practically identical to that found in $Mn_2(CO)_{10}$.[5]

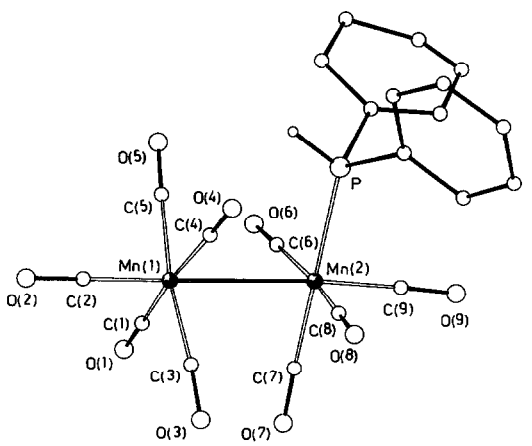

Fig. 1. View of the molecular structure of $Mn_2(CO)_9(PPh_2H)$.

Monosubstituted derivatives, characterized as axial, were obtained with PPh_3, PBu_3, $P(OPh)_3$, $AsPh_3$, $PPhMe_2$ (X-ray structure),[6] $AsPhMe_2$, PPh_2Me and PF_3; only with PH_3 was an equatorial derivative observed.[7] A few X-ray structures for axial,[6] diaxial[8] and diequatorial[8] complexes have been reported; thus **2** is the first confirmed example of equatorial substitution.

Some preliminary results in homogeneous hydrogenation of diphenylacetylene are given in Table 1.

Worthy of note are the high *trans–cis* stilbene ratios observed; identification of the organometallic species in the hydrogenation solutions is in progress in order to gain better insight into the reaction mechanisms.

REFERENCES

1. M. Castiglioni, R. Giordano, E. Sappa, A. Tiripicchio and M. Tiripicchio Camellini, *J. Chem. Soc., Dalton Trans.* 1986, 23; M. Castiglioni, R. Giordano and E. Sappa, *J. Organomet. Chem.* 1988, **342**, 111.
2. J. A. Iggo, M. J. Mays, P. R. Raithby and K. Henrick, *J. Chem. Soc., Dalton Trans.* 1983, 205.
3. P. M. Treichel, in *Comprehensive Organometallic Chemistry* (Edited by G. Wilkinson, F. G. A. Stone and E. W. Abel), Vol. 4, Ch. 29, p. 1. Pergamon Press, Oxford (1982).
4. G. A. Foulds, B. F. G. Johnson and J. Lewis, *J. Organomet. Chem.* 1985, **296**, 147.
5. M. R. Churchill, K. N. Amoh and H. J. Wasserman, *Inorg. Chem.* 1981, **20**, 1609; M. Martin, B. Rees and A. Mitschler, *Acta Cryst.* 1982, **38B**, 6.
6. M. Laing, E. Singleton and R. Reinmann, *J. Organomet. Chem.* 1973, **56**, C21.
7. E. O. Fischer and W. A. Hermann, *Chem. Ber.* 1972, **105**, 186.
8. M. Laing, T. Ashworth, P. Sommerville, E. Singleton and R. Reinmann, *J. Chem. Soc., Chem. Commun.* 1972, 1251.

Polyhedron Vol. 8, No. 13/14, pp. 1857–1858, 1989
Printed in Great Britain

0277–5387/89 $3.00+.00
© 1989 Maxwell Pergamon Macmillan plc

THE INTERACTION OF ORGANOTRANSITION METAL FRAGMENTS WITH OXAAZAMACROCYCLES. SYNTHESIS AND X-RAY CRYSTAL STRUCTURE OF $Mo(CO)_3$[O-en-N-pyn-H_4]·CH_2Cl_2

HARRY ADAMS, NEIL A. BAILEY,* DAVID E. FENTON,* PAUL D. HEMPSTEAD, BRIAN A. HEWES, SIMON J. KITCHEN and MARK J. WINTER*

Department of Chemistry, The University, Sheffield S3 7HF, U.K.

Abstract—The reaction of *fac*-$Mo(NCMe)_3(CO)_3$ with [O-en-N-pyn-H_4] in CH_2Cl_2 gives *fac*-$Mo(CO)_3$[O-en-N-pyn-H_4]·CH_2Cl_2, whose X-ray crystal structure is monoclinic, $a = 10.448(20)$, $b = 14.975(23)$, $c = 16.598(27)$ Å, $\beta = 100.57(14)°$. The macrocycle is bonded confacially to a trigonally elongated octahedral molybdenum through one pyridinyl nitrogen, one amino nitrogen and one oxygen donor.

There is small but burgeoning literature concerning chemistry at the interface between macrocyclic coordination chemistry and organotransition metal chemistry. Much of this work concerns macrocycles bearing homodonor sets (polyaza-, polythia, etc.)[1–7] with relatively little concerning ligands with mixed donor sets (oxaaza-,[8] azathia,[9] etc).[10,11] A constraining factor is the ability to synthesize the free macrocycle in adequate yields. We recently devised a useful route to oxaazamacrocycles based on the template cyclocondensation of the diamino and dicarbonyl containing precursors, followed by reductive demetallation of the macrocyclic Schiff base metal complex so formed.[12] Using this approach, a wide range of macrocycles is accessible and it is of interest to examine their comparative complexing capabilities. We therefore report on the reaction between the macrocycle [O-en-N-pyn-H_4]† with *fac*-$Mo(NCMe)_3(CO)_3$, a source of the $Mo(CO)_3$ fragment.[14]

Addition of a CH_2Cl_2 solution of [O-en-N-pyn-H_4] to a suspension of *fac*-$Mo(NCMe)_3(CO)_3$ in CH_2Cl_2 immediately resulted in a green solution that deposited small brown crystals of complex **1** on standing.‡ The mass spectrum (positive ion FAB) shows a molecular ion [m/z 529; (^{98}Mo)], successive losses of three carbonyl groups from that ion, and the free macrocycle ion (m/z 348; $[M+H]^+$). The compound is insoluble in most common organic solvents and dissolution in donor solvents such as MeCN, pyridine, acetone, etc, results in ligand decomplexation. This phenomenon precludes NMR studies and solution IR studies, but the solid phase IR spectrum shows carbonyl stretches (ν_{CO}(KBr); 1910s, 1775s, and 1740s cm^{-1}) consistent with an asymmetric *fac*-$Mo(CO)_3(L_3)$ structure.

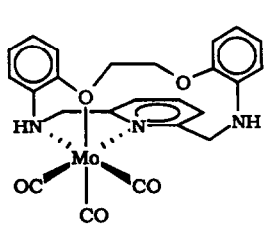

1

* Authors to whom correspondence should be addressed.

† The nomenclature adopted is that of Lindoy (ref. 13); e.g. the macrocycle named as [O-en-N-pyn-H_4] with O-en defining the ethylenic bridge between the two oxygen atoms, N-pyn defining the pyridyl bridge between the two amino nitrogen atoms, and -H_4 indicating that the system is fully reduced. The Chemical Abstracts name is 5,6,12,13,19,20-hexahydro-7,11-nitrilo-7H-dibenzo [e,p]-[1,4,7,15]di-oxadiazacycloheptadecane.

‡ Crystal data for $(C_{21}H_{21}O_2N_3)Mo(CO)_3 \cdot CH_2Cl_2$ (**1**); $C_{25}H_{23}Cl_2MoN_3O_5$; $M = 612.28$; crystallizes from dichloromethane as small yellow needles; monoclinic, $a = 10.448(20)$, $b = 14.975(23)$, $c = 16.598(27)$ Å, $\beta = 100.57(16)°$, $U = 2553(8)$ Å^3; $D_c = 1.594$ g cm^{-3}, $Z = 4$; space group $P2_1/n$ (a non-standard setting of $P2_1/c$, C_5^{2h}, No. 14); Mo-K_α radiation ($\lambda = 0.71069$ Å), μ(Mo-K_α) = 7.51 cm^{-1}, $F(000) = 1239.67$. R converged to 0.097.

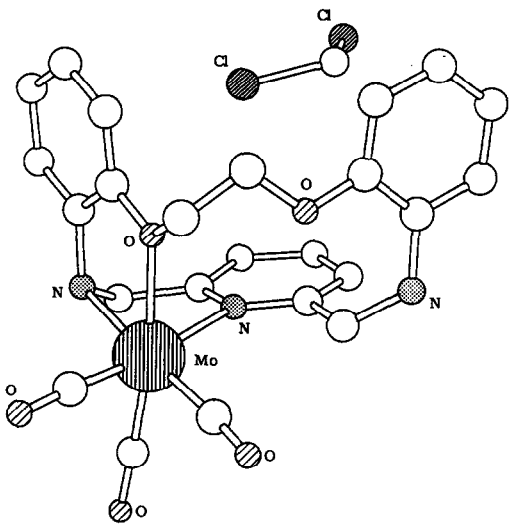

Fig. 1. Molecular structure of $Mo(CO)_3[O\text{-en-}N\text{-pyn-}H_4]\cdot CH_2Cl_2$.

The molecular structure of **1** is illustrated in Fig. 1. The macrocycle adopts a "boat" conformation. The donor set is particularly interesting in that the $Mo(CO)_3$ fragment binds to the pyridinyl nitrogen, one amino nitrogen and one oxygen atom. The angles within the tricarbonyl donor set and the macrocycle donor set are all less than 90°, and so the coordination geometry at the molybdenum atom is a trigonally elongated octahedron. Facial bonding of the N_3 donor set from the macrocycle appears to be sterically disallowed. A feature of the N_2O donor set is that the macrocycle, or its derivatives, might bridge appropriate bimetallic fragments.

Acknowledgements—We thank the SERC and the Royal Society for support.

REFERENCES

1. P. Chaudhuri and K. Wieghardt, *Prog. Inorg. Chem.* 1987, **35**, 329.
2. A. J. Blake, T. J. Hyde, R. S. E. Smith and M. Schroder, *J. Chem. Soc., Chem. Commun.* 1986, 334.
3. M. N. Bell, A. J. Blake, M. Schroder and T. A. Stephenson, *J. Chem. Soc., Chem. Commun.* 1986, 471.
4. R. W. Hay, J. Fraser and G. Ferguson, *J. Chem. Soc., Chem. Commun.* 1987, 1715.
5. D. Sellman and L. Zapf, *Angew. Chem. Int. Edn Engl.* 1984, **23**, 807.
6. T. Yoshida, T. Adachi, T. Ueda, M. Watanabe, M. Kaminaka and T. Higuchi, *Angew. Chem. Int. Edn Engl.* 1987, **26**, 636.
7. M. T. Ashby and D. L. Lichtenberger, *Inorg. Chem.* 1985, **24**, 636.
8. D. Parker, *J. Chem. Soc., Chem. Commun.* 1985, 1129.
9. J. M. Lehn and D. Parker, *J. Chem. Soc., Dalton Trans.* 1985, 1517.
10. G. Ferguson, K. E. Matthes and D. Parker, *Angew. Chem. Int. Edn Engl.* 1987, **26**, 1162.
11. G. Ferguson, K. E. Matthes and D. Parker, *J. Chem. Soc., Chem. Commun.* 1987, 1350.
12. D. E. Fenton, B. P. Murphy, A. J. Leong, L. F. Lindoy, A. Bashall and M. McPartlin, *J. Chem. Soc., Dalton Trans.* 1987, 2543.
13. L. G. Armstrong, L. F. Lindoy, M. McPartlin, G. M. Mockler and P. A. Tasker, *Inorg. Chem.* 1977, **16**, 1665.
14. D. P. Tate, W. R. Knipple and J. M. Augl, *Inorg. Chem.* 1962, **1**, 433.

Polyhedron Vol. 8, No. 13/14, pp. 1859–1860, 1989
Printed in Great Britain

0277–5387/89 $3.00+.00
© 1989 Maxwell Pergamon Macmillan plc

VINYL TO CARBONYL MIGRATION AT MOLYBDENUM

CHRISTOPHER RIDGWAY, MARK J. WINTER* and SIMON WOODWARD

Department of Chemistry, The University, Sheffield S3 7HF, U.K.

Abstract—The methoxy alkyls, $CpM\{CHMe(OMe)\}(CO)_2(PPh_3)$ (M = Mo, W), undergo proton catalysed MeOH loss to give the vinyl, $CpW(\eta^2\text{-}CH{=}CH_2)(CO)_2(PPh_3)$ (for M = W) and the η^3-propenoyl, $CpMo(CO)(PPh_3)(\eta^3\text{-}CH_2CH{=}O)$ (for M = Mo); the formation of the latter is interpreted by a mechanism involving a vinyl to carbonyl migration.

Examples of vinyl to carbonyl migrations are rare.[1–3] We describe here, proton induced MeOH loss from methoxy alkyl derivatives $CpM\{CHMe(OMe)\}(CO)_2(PPh_3)$ (M = Mo, W), a process which results in a molybdenum η^3-propenoyl complex. We suggest this is best rationalized as proceeding by a mechanism involving a vinyl to carbonyl migration.

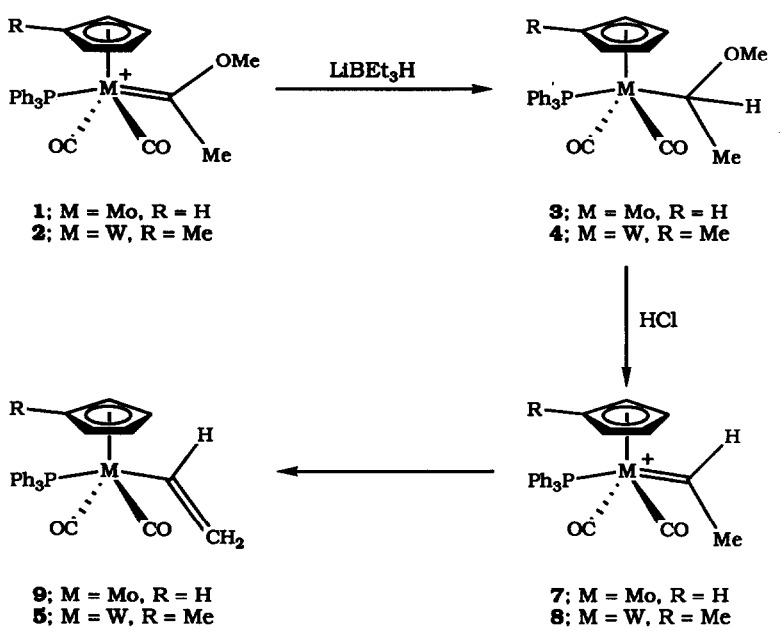

1; M = Mo, R = H
2; M = W, R = Me

3; M = Mo, R = H
4; M = W, R = Me

7; M = Mo, R = H
8; M = W, R = Me

9; M = Mo, R = H
5; M = W, R = Me

6

Additions of $LiBEt_3H$ to suspensions of the cationic carbenes **1**[4] or **2** result in attack at the carbene by H^- and formation of the methoxy alkyl derivatives, **3**[5] and **4**, respectively. The tungsten compound, **4**, undergoes MeOH loss on treatment with traces of HCl dissolved in $CHCl_3$, resulting in the vinyl, **5**. The molybdenum species, **3**, also undergoes proton induced loss of MeOH, but in this case the product is the η^3-propenoyl, **6**. Compound **6** is fluxional by a process not yet fully elucidated, but probably related to the known fluxionality of the η^3-allyls, $CpM(CO)_2(\eta^3\text{-}C_3H_5)$.[6]

* Author to whom correspondence should be addressed.

Deuterium labelled complexes M{CDMe(OMe)}$(CO)_2(PPh_3)(\eta$-$C_5H_4R)$ (**3**-D_1) (R = H) and (**4**-D_1) (R = Me) are accessible by treatment of **1** or **2** with $LiBDEt_3$. Treatment of **3**-D_1 and **4**-D_1 with traces of HCl gives $CpMo(\eta^3$-$CH_2CDC{=}O)(CO)(PPh_3)$ (**6**-D_1) and $Cp'W(\eta^2$-$CD{=}CH_2)(CO)_2(PPh_3)$ (**5**-D_1), respectively. The labelled methyl CpMo$(CD_3)(CO)_3$ is a good precursor for CpM{CH(CD_3)(OMe)}$(CO)_2(PPh_3)$ (**1**-D_3). Treatment of **1**-D_3 with $LiBEt_3H$ followed by acid, results in the sequential formation of CpMo{CH(CD_3)(OMe)}$(CO)_2(PPh_3)$ (**3**-D_3) and $CpMo(\eta^3$-$CD_2CHC{=}O)(CO)(PPh_3)$ (**6**-D_2). In all cases, these isotopomers are exclusive products within the limits of NMR detection.

These results are best interpreted as follows. Protons attack the OMe groups within **3** or **4** causing MeOH loss, resulting in the non-heteroatom stabilized carbene (alkylidene) intermediates, **7** or **8**, respectively. The related cations $[CpM(CO)_2(CHR)(PPh_3)]^+$ (M = Mo or W, R = H; M = W, R = Ph) have a brief existence at low temperatures.[7] Proton loss from the methyl group of **8** gives the tungsten vinyl, **5**. A similar proton loss from the methyl group of the molybdenum intermediate, **7**, would give the currently undetected vinyl, **9**. The formation of **6** from **9** then proceeds by a rapid vinyl to carbonyl migration and double bond coordination. The isotope labelling studies are consistent with these interpretations. In particular, the formation of **6**-D_2 confirms the loss of protons from the methyl group of the intermediate, **7**.

We consider an alternative mechanism in which the alkylidene =CHMe group of **7** links with a carbonyl ligand to form an intermediate ketene complex, from which protons are subsequently lost, as less likely. The rearrangements of the related alkylidenes, $[CpMo(CO)_2(=CHR)(L)]^+$ (L = CO, R = Me; L = PPh_3, R = H), show no sign of comparable coupling reactions;[7,8] indeed, such couplings generally involve direct addition of external CO and require more forcing conditions than those employed here.[9]

The vinyls, $CpFe(\eta^1$-$CH{=}CH_2)(CO)(L)$ (L = CO, PPh_3), $CpW(\eta^1$-$CH{=}CH_2)(CO)_3$, and complex **9** appear not to undergo facile vinyl to carbonyl migrations.[10] The related dicarbonyls, $CpM\{\eta^1$-C$(NR^1_2){=}CHR^2\}(CO)_2\{P(OMe)_3\}$ (R^1 = Et, R^2 = Me; M = Mo, W), convert into η^2-keteneimmonium complexes, but the corresponding tricarbonyls display complex behaviour depending on the metal, R^1 and R^2, to form products including η^3-propenoyl complexes.[2]

That compound **9** undergoes vinyl to carbonyl migration, whereas **5** and $CpFe(\eta^1$-$CH{=}CH_2)(CO)(PPh_3)$ do not, parallels the sluggish tendencies of many iron and tungsten compounds to undergo alkyl to carbonyl migrations relative to those of molybdenum.[11]

Acknowledgements—We are pleased to acknowledge support from the Royal Society and the SERC. S.W. and C.R. are grateful to the SERC for the awards of postgraduate studentships.

REFERENCES

1. L. Cassar and A. Giaruss, *Gazz. Chim. Ital.* 1973, **103**, 793.
2. W. Beck, H. Brix and F. H. Kohler, *J. Organomet. Chem.* 1976, **121**, 211.
3. T. Mitsudo, Y. Watanabe, H. Nakanishi, I. Morishama, T. Inubushi and Y. Takegami, *J. Chem. Soc., Dalton Trans.* 1978, 1298; K. Nakatsu, Y. Inai, T. Mitsudo, Y. Watanabe, H. Nakanishi and Y. Takegami, *J. Organomet. Chem.* 1978, **159**, 111; T. Mitsudo, H. Watanabe, Y. Watanabe, N. Nitani and Y. Takegami, *J. Chem. Soc., Dalton Trans.* 1979, 395.
4. P. M. Treichel and K. P. Wagner, *J. Organomet. Chem.* 1975, **88**, 199.
5. J. T. Gauntlett and M. J. Winter, *Polyhedron* 1986, **5**, 451.
6. J. Y. Merour, C. Charrier, J. Benaim, J. L. Roustan and D. Commereuc, *J. Organomet. Chem.* 1972, **39**, 321; J. W. Faller, C.-C. Chen, M. J. Mattina and A. Jakubowski, *J. Organomet. Chem.* 1973, **52**, 361.
7. S. E. Kegley, M. Brookhart and G. R. Husk, *Organometallics* 1982, **1**, 760.
8. M. L. H. Green, M. Ishaq and R. N. Whiteley, *J. Chem. Soc. A* 1967, 1508.
9. W. A. Herrmann and J. Plank, *Angew. Chem. Int. Edn Engl.* 1978, **17**, 525; G. L. Geoffroy and S. L. Bassner, *Adv. Organomet. Chem.* 1988, **28**, 1.
10. K. A. M. Kremer, G.-H. Kuo, E. J. O'Connor, P. Helquist and R. C. Kerber, *J. Am. Chem. Soc.* 1982, **104**, 6119; T. Bodnar and A. R. Cutler, *J. Organomet. Chem.* 1981, **213**, C31; R. B. King and B. M. Bisnette, *J. Organomet. Chem.* 1964, **2**, 15; S. Quinn and A. Shaver, *Inorg. Chim. Acta* 1980, **38**, 243.
11. K. W. Barnett, D. L. Beach, S. P. Gaydos and T. G. Pollmann, *J. Organomet. Chem.* 1974, **69**, 121; J. P. Collman, L. S. Hegedus, J. R. Norton and R. G. Finke, in *Principles and Applications of Organotransition Metal Chemistry*. University Science Books, Mill Valley, California (1987); J. P. Bibler and A. Wojcicki, *Inorg. Chem.* 1966, **5**, 889.

Polyhedron Vol. 8, No. 13/14, pp. 1861–1862, 1989
Printed in Great Britain

0277–5387/89 $3.00+.00
© 1989 Maxwell Pergamon Macmillan plc

SYNTHESES AND REACTIONS OF $LM(SnPh_3)(CO)_2\{=C(OEt)Ph\}$ ($L = C_5Me_5$ OR η^5-C_9H_7; M = Mo OR W)

GARY W. BENTLEY, GORDON HOUGH, MARK J. WINTER† and SIMON WOODWARD

Department of Chemistry, The University, Sheffield S3 7HF, U.K.

Abstract—Successive treatment of $LM(SnPh_3)(CO)_3$ (M = Mo or W; L = Cp(η-C_5H_5), Cp*(η-C_5Me_5), or Ind(η^5-C_9H_7), indenyl) with PhLi and Et_3O^+ results in the carbene complexes *trans*-$LM(SnPh_3)(CO)_2\{=C(OEt)Ph\}$. These undergo aminolysis with RNH_2 (R = Me, Et) to form the carbenes, *trans*-$LM(SnPh_3)(CO)_2\{=C(NHR)Ph\}$. Most of these compounds react with I_2 to form the new carbenes $LMI(CO)_2\{=C(X)Ph\}$ (X = OEt, NHMe, or NHEt) that exist in *cis*, *trans* or *cis* + *trans* conformations.

We are interested in systems $L_nMR\{=CR^1R^2\}$ that undergo migrations of a ligand R such as hydride, alkyl, acyl and aryl to the coordinated carbene to form new C—H and C—C bonds.[1] The synthetic strategy to form $L_nMR\{=CR^1R^2\}$ complexes relies on $NaC_{10}H_8$ reduction of compounds $L_nMI\{=CR^1R^2\}$, followed by protonation or alkylation. These reactions proceed through the intermediacy of anionic carbene complexes[2] $[L_nM\{=CR^1R^2\}]^-$. We are therefore interested in general syntheses of complexes of the type $L_nMI\{=CR^1R^2\}$ as precursor molecules to further study such migrations. We therefore report syntheses of Cp* (Cp* = η^5-C_5Me_5) and Ind (Ind = η^5-C_9H_7, indenyl) molybdenum and tungsten carbene complexes.

One might expect that Fischer type carbenes, $LMI(CO)_2\{=C(OR)Ph\}$ (M = Mo, W; L = Cp, Cp*, Ind), would arise by treatment of $LMI(CO)_3$ with PhLi followed by alkylation. In fact, this approach fails. For example, the reaction of $CpMI(CO)_3$ with PhLi results in $[CpM(CO)_3]^-$ rather than $[CpMI(COPh)(CO)_2]^-$. It is therefore necessary to synthesize the iodides by an indirect route.

It is already known that consecutive treatment of $CpM(SnPh_3)(CO)_3$ (M = Mo or W) with PhLi in THF and Et_3O^+ in water results in the carbene complexes $CpM(SnPh_3)(CO)_2\{=C(OEt)Ph\}$ in moderate yields.[3] We find these yields increase to nearly quantitative in some cases if the first step is executed in Et_2O. We further find that the related compounds $Cp^*M(SnPh_3)(CO)_2\{=C(OEt)Ph\}$ and $IndM(SnPh_3)(CO)_2\{=C(OEt)Ph\}$ are formed in good yields starting from $Cp^*M(SnPh_3)(CO)_3$ or $IndM(SnPh_3)(CO)_3$ (M = Mo or W), respectively (Scheme 1).

All these compounds are fully characterized. The spectroscopic properties of all are, not unexpectedly, closely related and all are *trans* dicarbonyls. The cyclopentadienyl[3] and indenyl complexes $LM(SnPh_3)(CO)_2\{=C(OEt)Ph\}$ (L = Cp, Ind) are interesting in that their IR spectra show four bands

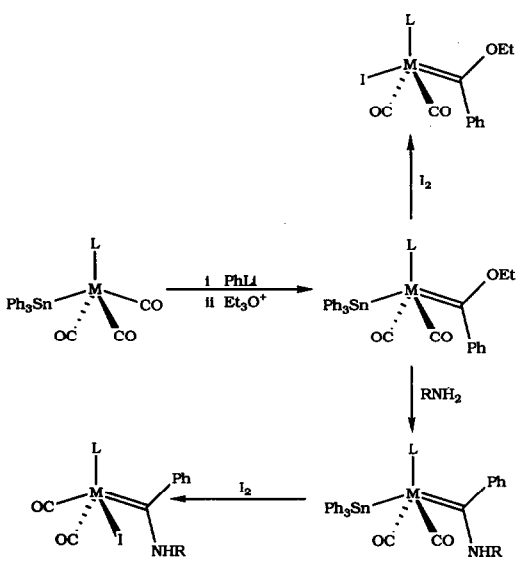

Scheme 1. M = Mo or W; L = Cp, Cp*, or Ind; R = Me, Et.

† Author to whom correspondence should be addressed.

(for instance, $IndMo(SnPh_3)(CO)_2\{=C(OEt)Ph\}$: $\nu_{CO}(Et_2O)$; 1943m, 1929m, 1877s, and 1863s cm^{-1}) rather than the anticipated two. This multiplicity was ascribed earlier[3] to carbene rotamers in the Cp case. Clearly the same phenomenon which produces the four IR bands in the Cp base will account for the band multiplicity in the indenyl case. Notably the Cp* complexes show only two bands in their IR spectrum, a manifestation of the steric influence of the Cp* ligand which is still under investigation.

In common with many other Fischer type carbenes, reactions with aqueous solutions of amines RNH_2 (R = Me, Et) results in aminolysis to form carbenes such as $LM(SnPh_3)(CO)_2\{=C(NHR)Ph\}$ (M = Mo or W; L = Cp or Cp*, Ind; R = Me or Et). These compounds are all *trans* dicarbonyls.

Iodine cleaves the M—$SnPh_3$ bond of all the aminocarbenes cleanly to form the corresponding iodides $LMI(CO)_2\{=C(NHR)Ph\}$ (L = Cp, Cp*, Ind; R = Me, Et) and $SnIPh_3$. The corresponding reactions of the alkoxy carbenes are sometimes less successful. For instance, while iodine reacts with $Cp^*Mo(SnPh_3)(CO)_2\{=C(OEt)Ph\}$ to form $Cp^*MoI(CO)_2\{=C(OEt)Ph\}$ (IR evidence only), the product is not isolable since it undergoes facile loss of EtI to form the η^1-phenyl $Cp^*MoPh(CO)_3$. This is interesting because the corresponding $CpMoPh(CO)_3$ appears to be unstable.[4] On the other hand, formation of $CpWI(CO)_2\{=C(OEt)Ph\}$ is clean and the product isolable in good yield.

Some of these iodometal complexes show interesting isomerism. For instance, the IR spectrum of the tungsten complex $CpWI(CO)_2\{=C(OEt)Ph\}$ in cyclohexane shows eight bands corresponding to three *trans* isomers and one *cis* isomer while the molybdenum analogue just shows two *trans* isomers together with one *cis* isomer in the same solvent. In both cases, the *trans* components of the mixture predominate. The proportions of the isomers are solvent dependent and the NMR spectra show these

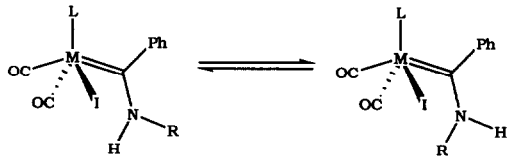

Scheme 2. M = Mo or W; L = Cp, Cp*, or Ind; R = Me, Et.

compounds are fluxional. The multiplicity of the IR bands is a consequence of carbene rotations (but in this case both M=C and C—OEt rotations are involved) and also *cis–trans* isomerism.

The complexes $LMI(CO)_2\{=C(NHR)Ph\}$ exist purely in the *cis* form, but here also these is isomerism since the NMR spectra show that there are two isomers of each complex. We ascribe the presence of two sets of signals to rotamers related by rotation about the carbene-N bond (Scheme 2).

Acknowledgements—We are pleased to acknowledge the award of SERC research studentships to G.W.B. and S.W.

REFERENCES

1. M. J. Winter, *Polyhedron*, 1989, submitted for publication; V. A. Osborn, C. A. Parker and M. J. Winter, *J. Chem. Soc., Chem. Commun.* 1986, 1185; M. J. Winter and S. Woodward, *J. Organomet. Chem.* 1989, **361**, C18.
2. V. A. Osborn and M. J. Winter, *J. Chem. Soc., Chem. Commun.* 1985, 1744.
3. W. K. Dean and W. A. G. Graham, *Inorg. Chem.* 1977, **16**, 1061.
4. A. N. Nesmeyanov, L. G. Makarova, N. A. Ustynyuk and L. V. Bogatyreva, *J. Organomet. Chem.* 1972, **46**, 105; A. N. Nesmeyanov, Y. A. Chapovskii, B. V. Lokshin, A. V. Kisin and L. G. Makarova, *Dokl. Chem. (Engl. Trans.)*, 1966, **171**, 1122.

Polyhedron Vol. 8, No. 13/14, pp. 1863–1864, 1989
Printed in Great Britain

0277–5387/89 $3.00+.00
© 1989 Maxwell Pergamon Macmillan plc

VISIBLE LIGHT PHOTOCHEMICAL REVERSAL OF HYDRIDE TO CARBENE MIGRATION

CARIN E. DAVEY, ROBIN DEVONSHIRE and MARK J. WINTER*

Department of Chemistry, The University, Sheffield S3 7HF, U.K.

Abstract—Visible light photolysis of the complex $CpMo(CO)_2\{\eta^2\text{-}CH(CH_2)_3NMe\}$, which is made by utilizing a hydride to carbene migration within the complex $CpMoH(CO)_2\{=C(CH_2)_3NMe\}$, results in reversal of the hydride to carbene migration to reform $CpMoH(CO)_2\{=C(CH_2)_3NMe\}$.

Migrations of hydride to carbene are important in the context of C—H bond forming reactions at metal centres and in the sense that they are a fundamental reaction step.[1] While frequently postulated in reaction sequences involving carbenes, there are comparatively few well-defined direct observations[2,3] and little mechanistic information on this process. The reverse of hydride to carbene migration is α-elimination.[4] In eq. (1) it is assumed the metal is one whose electron count must be maintained, hence the incoming L′ two electron ligand:



We recently established that the hydride, $CpMoH(CO)_2\{=C(CH_2)_3NMe\}$ (**1**), which exists as a mixture of *cis* and *trans* isomers, undergoes a hydride to carbene migration reaction in forming $CpMo(CO)_2\{\eta^2\text{-}CH(CH_2)_3NMe\}$ (**2**) (Scheme 1). The 18 electron count at the metal is maintained through coordination of the nitrogen atom (an intramolecular source of L′). The conversion of **1** into **2** is a first-order reaction and takes place over several hours at ambient temperature in THF. The Arrhenius activation energy is 98 kJ mol^{-1} in THF.

We report, here, the observation that irradiation by bright, Sheffield, February sunlight (or by light from a fluorescent tube) of solutions containing $CpMo(CO)_2\{\eta^2\text{-}CH(CH_2)_3NMe\}$ (**2**) in THF, or at a slower rate in toluene, results in the reformation of the hydride $CpMoH(CO)_2\{=C(CH_2)_3NMe\}$ (**1**). In effect, this is a light induced α-elimination.

This photoreaction is apparently linked to a UV absorption maximum at 412 nm. Comparison with some related molecules such as $Mo(CO)_4(Ph_2PCH_2CH_2NEt_2)$[5] suggests this is associated with the N → Mo bond. The measured quantum

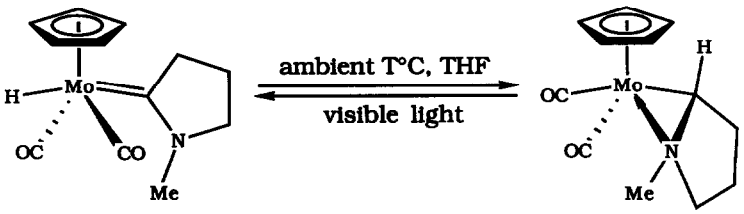

1 **2**

Scheme 1.

*Author to whom correspondence should be addressed.

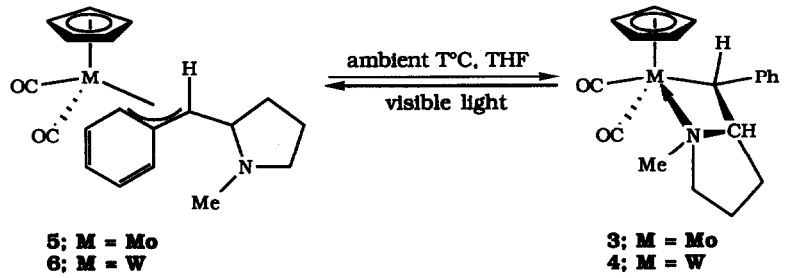

Scheme 2.

yields for the reaction are 0.07 and 0.09 molecules photon^{-1} at 436 and 405 nm in THF, but 0.03 and 0.05 molecules photon^{-1} in toluene. The system shows no sign of phosphorescence or fluorescence.

We currently envisage that irradiation cleaves the N → Mo bond of **2** to leave a vacant coordination site, which in principle can be stabilized by the solvent. From here, the intermediate can revert to starting material or proceed to the hydride, **1**.

We also observe related N → M cleavage in visible light photoreactions of complexes **3** and **4**.[6] In these cases, the α-hydrogen does not migrate to the metal, rather, the phenyl ring enters into the metal coordination sphere producing the fully characterized η^3-benzyl complexes, **5** and **6** (Scheme 2).

We plan to investigate the mechanism of these and related photoreactions using time resolved UV–vis and Raman spectroscopies.

Acknowledgements—C.E.D. is grateful to the SERC for the award of a research studentship. We are also grateful to the SERC for financial support.

REFERENCES

1. J. P. Collman, L. S. Hegedus, J. R. Norton and R. G. Finke, in *Principles and Applications of Organotransition Metal Chemistry*, 2nd edn, pp. 379–82 and refs therein. University Science Books, Mill Valley, California (1987).
2. A. Van Asselt, B. J. Burger, V. C. Gibson and J. E. Bercaw, *J. Am. Chem. Soc.* 1986, **108**, 5347; J. C. Green, M. L. H. Green and C. P. Morley, *Organometallics* 1985, **4**, 1302; H. Werner and K. Roder, *J. Organomet. Chem.* 1986, **310**, C51; H. Le Bozec, J.-L. Fillaut and P. H. Dixneuf, *J. Chem. Soc., Chem. Commun.* 1986, 1182; G. Parkin, E. Bunel, B. J. Burger, M. S. Trimmer, A. Van Asselt and J. E. Bercaw, *J. Molec. Catal.* 1987, **41**, 21.
3. V. A. Osborn, C. A. Parker and M. J. Winter, *J. Chem. Soc., Chem. Commun.* 1986, 1185.
4. R. R. Schrock, *Accts Chem. Res.* 1979, **12**, 98; R. J. Cross, in *The Chemistry of the Metal–Carbon Bond* (Edited by F. R. Hartley and S. Patai), Vol. 2, Chap. 8. Wiley, New York (1985).
5. G. R. Dobson, I. Bernal, G. M. Reisner, C. B. Dobson and S. E. Mansour, *J. Am. Chem. Soc.* 1985, **104**, 525.
6. M. J. Winter, *Polyhedron*, submitted for publication; C. E. Davey and M. J. Winter, unpublished results.

Polyhedron Vol. 8, No. 13/14, pp. 1865–1866, 1989
Printed in Great Britain

0277–5387/89 $3.00+.00
© 1989 Maxwell Pergamon Macmillan plc

THE BINDING OF A $MoFe_3S_4$ DOUBLE-CUBANE CLUSTER BY CYSTEINE ETHYL ESTER

D. J. EVANS,* G. J. LEIGH and J. B. PARRA-SOTO

AFRC Institute of Plant Science Research, Nitrogen Fixation Laboratory, University of Sussex, Brighton BN1 9RQ, U.K.

Abstract—The $MoFe_3S_4$ double-cubane cluster, $[Mo_2Fe_7S_8(\mu\text{-SEt})_6(SEt)_6]^{3-}$ (**1**), is shown by ^1H NMR spectroscopy to react with cysteine ethyl ester hydrochloride, initially to form the terminal chloride substituted cluster $[Mo_2Fe_7S_8(\mu\text{-SEt})_6Cl_6]^{3-}$ (**2**) and this then reacts further to form a novel terminal cysteinate substituted cluster, **3**. The temperature-dependence of the isotropically shifted ^1H NMR signals of **3** is reported.

Cysteinyl residues in proteins are the principal ligands to iron–sulphur clusters in biological systems, as in ferredoxins.[1] The residues which bind ferredoxin and rubredoxin cores to the protein backbone are cysteines, generally in the sequence cys—X—X—cys—X—X—cys, where X is some other non-binding amino acid residue. We have recently demonstrated that a range of other amino acids, including serine and tyrosine, are capable of binding to the model cluster core $\{Fe_4S_4\}^{2+}$.[2,3] Here we describe the first reported interaction between cysteine and a heterometallic double-cubane complex as observed by ^1H NMR spectroscopy.

RESULTS AND DISCUSSION

The iron–sulphur cluster $[Fe_4S_4(SBu^t)_4]^{2-}$ has been shown to react with a range of amino acid ester hydrochlorides, AAHCl, to form $[Fe_4S_4(AAH)_4]^{2+}$.[2,3] The initial reaction produces $[Fe_4S_4Cl_4]^{2-}$, which then reacts further to form the amino acid derivative. The chloride cluster can be prepared independently by reaction of $[Fe_4S_4(SBu^t)_4]^{2-}$ with acetyl chloride[4] or with butyl-2-amine hydrochloride,[3] the liberated amine and thiol being removed from solution by pumping.

We have now extended our studies to the interaction of amino acid esters with $MoFe_3S_4$ double-cubane clusters. We first confirmed that 6 equivalents of acetyl chloride convert the double-cubane cluster, $[NEt_4]_3[Mo_2Fe_7S_8(\mu\text{-SEt})_6(SEt)_6]$ (**1**), in acetonitrile to the terminal chloride substituted cluster, $[NEt_4]_3[Mo_2Fe_7S_8(\mu\text{-SEt})_6Cl_6]$ (**2**),[5,6] and have characterized this product in solution by ^1H NMR spectroscopy (Table 1). The same cluster can be prepared by addition of 6 equivalents of butyl-2-amine hydrochloride to **1**. The terminally coordinated thiolate groups are labile. This behaviour parallels that of the single cluster $[Fe_4S_4(SBu^t)_4]^{2-}$.[3]

Addition of 6 molar equivalents of cysteine ethyl ester hydrochloride to **1** (2×10^{-3} mol dm^{-3}, CD_3CN, ambient temperature) initially generates **2**. Over a period of 3 h the isotropically shifted signals characteristic of the chloride substituted cluster are lost and signals generated by a new species appear (Table 1). The signals at 27.1 and 13.5 ppm are typical of bridging thiolate methylene groups, and that at −1.9 ppm is assigned to the bridging thiolate methyl group. These shifts are similar to those found for a range of $MoFe_3S_4$ double-cubane complexes.[5,6] The signal at low field, 81.8 ppm, is assigned to the β-CH_2 of terminally bound ethyl cysteinate. The relative shifts of the signals arising from terminally coordinated groups and from bridging groups are consistent with other literature data. Addition of 9 or 12 molar equivalents of cysteine ethyl ester hydrochloride to **1** showed the same reactions, except that they were completed quicker. There is no evidence for bridge cleavage, even when a large excess of amino acid ester hydrochloride is employed. Replacement of all six chloro ligands should require 6 equivalents of cysteine ethyl ester hydrochloride, and when only 3 were employed a complex spectrum was obtained, probably resulting from mixed ligand clusters. By analogy with previously reported $[Mo_2Fe_7S_8(\mu\text{-SEt})_6(SR)_6]^{3-}$

* Author to whom correspondence should be addressed.

Table 1. Chemical shifts (ppm) for bridging and terminal groups in $MoFe_3S_4$ double-cubane complexes, 2×10^{-2} mol dm^{-3}, in CD_3CN at ~20°C

	Bridging		Terminal	
	CH_2	CH_3	CH_2	CH_3
$[Mo_2Fe_7S_8(\mu\text{-SEt})_6(SEt)_6]^{3-}$ (1)	24.4, 17.5	0.8	55.9	4.5
$[Mo_2Fe_7S_8(\mu\text{-SEt})_6Cl_6]^{3-}$ (2)	38.2, 26.7	−1.2	—	—
$[Mo_2Fe_7S_8(\mu\text{-SEt})_6(\text{cysteinate})_6]^{3-}$ (3)	27.1, 13.5	−1.9	81.8[a]	—[b]

[a] β-CH_2 of cysteinate.
[b] α-CH of cysteinate concealed under cation/solvent peaks.

clusters,[5,6] we propose that in solution the novel $[Mo_2Fe_7S_8(\mu\text{-SEt})_6(\text{cysteinate})_6]^{3-}$ (3) cluster is generated.

Variable-temperature ^1H NMR data for 3 are listed in Table 2. As the temperature decreases the isotropically shifted bridging methylene groups move to higher field. This change is in the opposite sense, but has similar degree to that observed in the parent cluster. However, the bridging methyl signal moves away from the diamagnetic on decreasing the temperature. The terminal cysteinate β-CH_2 also moves away from the diamagnetic with decrease in temperature. The magnitude of change in shift is large, being 25 ppm over a 105°C range, consistent with binding at an iron site on the cluster. These observations are not consistent with a simple contact shift mechanism.

We are currently investigating the metathesis reaction between 2 and cysteine ethyl ester hydrochloride, cysteine ethyl ester and sodium cysteinate ethyl ester. Also attempts are being made to isolate the novel cluster 3, in order to characterize it definitively.

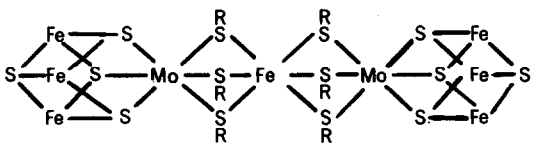

Fig. 1. The cluster core $\{Mo_2Fe_7S_8(\mu\text{-SEt})_6\}^{3+}$.

Table 2. Variable-temperature ^1H NMR results for $[Mo_2Fe_7S_8(\mu\text{-SEt})_6(\text{cysteinate})_6]^{3-}$ (3), 2×10^{-2} mol dm^{-3} in CD_3CN

Temperature (°C)	μ-SCH_2CH_3	μ-SCH_2CH_3	Cysteinate β-CH_2
70	32.6, 18.9	−0.7	71.0
40	29.8, 16.0	−1.3	76.9
10	26.0, 12.6	−2.2	83.8
−5	23.5, 10.8	−2.7	87.4

REFERENCES

1. J. M. Berg and R. H. Holm, in *Iron–Sulphur Proteins* (Edited by T. G. Spiro). Wiley-Interscience, New York (1982).
2. D. J. Evans and G. J. Leigh, *J. Chem. Soc., Chem. Commun.* 1988, 395.
3. D. J. Evans and G. J. Leigh, unpublished results.
4. R. W. Johnson and R. H. Holm, *J. Am. Chem. Soc.* 1978, **100**, 5338.
5. T. E. Wolff, P. P. Power, R. B. Frankel and R. H. Holm, *J. Am. Chem. Soc.* 1980, **102**, 4694.
6. R. E. Palermo, P. P. Power and R. H. Holm, *Inorg. Chem.* 1982, **21**, 173.

Polyhedron Vol. 8, No. 13/14, pp. 1867–1869, 1989
Printed in Great Britain

0277–5387/89 $3.00+.00
© 1989 Maxwell Pergamon Macmillan plc

THE EFFECTS OF THE ARCHITECTURE OF THE ZIEGLER–NATTA CATALYST ON THE MORPHOLOGY OF POLYPROPYLENE

PAULA PUTANOV* and ERNE KIŠ

Institute for Petrochemistry, Gas, Oil and Chemical Engineering, Faculty of Technology, Veljka Vlahovića 2, Novi Sad, Yugoslavia

and

LADISLAV FEKETE and EVA DINGOVA

Naftagas–HIPOL, Gračački put b.b., Odžaci, Yugoslavia

Abstract—The study of replication effects in propylene polymerization by $TiCl_3$ Ziegler–Natta catalysts is made by comparison of optical microscope (OM) and scanning electron microscope (SEM) pictures of the catalyst and the polymer, obtained either in standard conditions or in absence of hydrogen, with corresponding values of "calculated" replication factor (Rc) and "found" replication factor (Rf). It has been shown that under given conditions replication is evident both in structure and substructure details; it is not influenced noticeably by polymerization pressure, but may depend on the time of polymerization in a way dependent on the architecture of the catalyst.

Recent studies have shown that the morphology of polyolefin particles is determined by the size, shape and porosity of the particles of the applied Ziegler–Natta catalyst.[1–5] For the evaluation of replication effects two experimental criteria have been proposed: the found replication factor which represents the ratio of average particles sizes (APS), $Rf = APS_{pol}/APS_{cat}$ and the calculated replication factor which is a function of isotactic polymer yield (Y) and catalyst and polymer densities (δ), $Rc = (Y\delta_{cat}/\delta_{pol})^{1/3}$. Both criteria are based on macroscopic properties closely related to the structure of particles. Detailed study of replication mechanisms including their dependence on polymerization conditions is of interest for remote control of polymerization processes.

Such an approach represents the comparison of microscopic properties of the polymer and the catalyst connected with the analysis of parameters included in Rc and Rf definitions.

EXPERIMENTAL

Propylene polymerization was performed on a laboratory scale at 70°C, 0.6 and 0.9 MPa, in standard conditions and in the absence of hydrogen. A slurry reactor (3 dm^3) was used, with industrial heptane (1.5 dm^3) containing 0.33 g of $TiCl_3$ catalyst and 1.65 g of $Al(C_5H_5)_2Cl$. Commercial catalysts were A and B of irregular shape and C microspherical. Ti–Al ratios were 0.187, 0.173 and 0.0178, respectively. Average particle sizes were determined by sieving and by optical microscopy. OM and SEM were performed by OM Carl Zeiss Lab 2 and SEM JEOL JSM-35.

RESULTS AND DISCUSSION

Data given in Table 1 confirm that under standard testing conditions all three catalysts are able to control the replica phenomena; shape regularity and size distribution of polymer particles correspond to the catalyst used. This similarity of macroscopic properties means that their structures and substructures should coincide.

As has been shown,[2] the structure of $TiCl_3$

* Author to whom correspondence should be addressed.

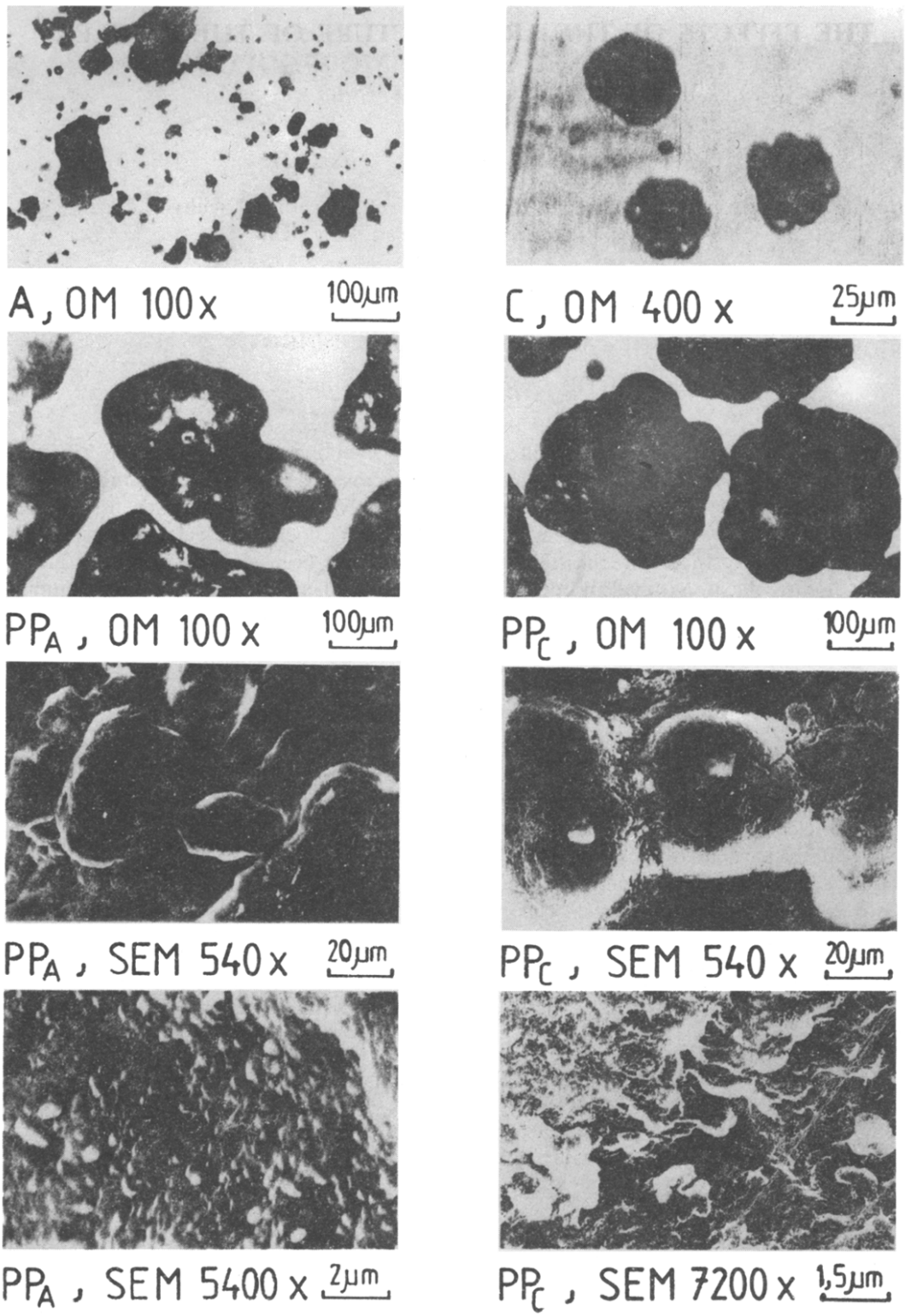

Fig. 1. OM pictures of catalysts A and C; OM and SEM pictures of polypropylene PP produced by catalyst A (PP_A) and by catalyst C (PP_C).

Table 1. Catalyst testing under standard conditions; 0.9 MPa, 4 h (A, B); 0.6 MPa, 2 h (C); 70°C, H_2 = 2 vol %

Catalyst	Shape of the particle	APS_{cat} (μm)	Activity (kgPP/gTi)	II (%)	APS_{pol} (μm)
A	Irregular	31	6.79	98.6	500
B	Irregular	13	13.50	98.4	260
C	Spherical	22	6.41	98.5	380

Table 2. Catalyst testing at 70°C, 0.6 and 0.9 MPa

Catalyst	Time of polymerization (min)	0.6 MPa			0.9 MPa		
		APS_{pol} (μm)	Rf	Rc	APS_{pol} (μm)	Rf	Rc
A	30	270	7.17	8.71	280	8.25	9.03
	60	—	—	—	330	9.48	10.66
	120	360	10.81	11.61	350	12.21	11.29
	180	—	—	—	410	13.31	13.23
	240	380	12.96	12.26	460	14.46	14.84
B	30	125	8.42	9.62	155	10.43	11.92
	60	—	—	—	160	12.07	12.31
	120	185	12.64	14.23	175	14.74	13.46
	180	—	—	—	210	16.41	16.15
	240	195	14.82	15.00	215	17.64	16.54
C	30	220	10.53	10.00	275	12.75	12.50
	60	280	12.64	12.73	290	13.84	13.18
	90	315	13.67	14.32	—	—	—
	120	320	14.56	14.55	—	—	—
	180	350	15.90	15.91	—	—	—

Ziegler–Natta catalyst consists of primary particles, 2–12 nm, which are responsible for catalytic activity and are combined in globules, 15–200 nm, which determine the porosity of the catalyst and are built into coarser particles.

Figure 1 shows the OM and SEM pictures of catalyst samples and of polymers (PP) obtained when hydrogen effects were excluded. Conspicuous analogy in structures and substructures illustrates the mechanism of replication. The data given in Table 2 show that the changes of polymerization pressure do not seem to influence replication to a high extent. The time of polymerization might be of importance when an irregularly shaped catalyst is used, particularly in the first period of polymerization. This method of catalyst particle disintegration unavoidably modifies replication. It can be seen (Table 2) that when a microspherical catalyst is used, Rf and Rc values are very similar during the whole observed period of polymerization. However, with irregularly shaped catalysts, Rf and Rc values differ until a stationary polymerization rate is reached. In such a case, APS_{pol} values experimentally determined at a given yield of isotactic polypropylene will be about 15% higher than those suggested by Rf values.

REFERENCES

1. J. Boor, *Ziegler–Natta Catalysts and Polymerization*. Academic Press, New York (1979).
2. E. Vermelj, V. A. Zaharov, V. B. Fenelonov, V. I. Zalkovskii, R. F. Zagrafskaya, E. M. Moroz and G. D. Bukatov, *Kinet. Katal.* 1981, **XXII 2**, 480.
3. T. DallOcco, U. Zucchini and I. Cuffani, *Int. Symp. Trans. Met. Organomet. Cat. Olef. Polym.*, Hamburg (1987).
4. P. Putanov, E. Kiš, G. Bošković, L. Fekete and E. Dingova, *EURETEC 88, Le Polypropylene*, Paris (1988).
5. P. Putanov, L. Fekete, E. Dingova, E. Kiš and G. Bošković, *EURETEC 88, Le Polypropylene*, Paris (1988).

Polyhedron Vol. 8, No. 13/14, pp. 1870–1871, 1989
Printed in Great Britain

0277–5387/89 $3.00+.00
Maxwell Pergamon Macmillan plc

THE PROTONATION OF METAL HYDRIDES

DAVID DAWSON, RICHARD A. HENDERSON,* ADRIAN HILLS and DAVID L. HUGHES

AFRC Institute of Plant Science Research, Nitrogen Fixation Laboratory, University of Sussex, Brighton BN1 9RQ, U.K.

Abstract—The rôle of acids in the rapid binding (and sometimes transformation) of small molecules at a metal–hydride site is discussed for the systems, $[MoH_4(Ph_2PCH_2CH_2PPh_2)_2]$ and $[WH_6(PMe_2Ph)_3]$.

Although much is known about the binding of small molecules at a metal–hydride site by displacement of dihydrogen, relatively little is known about how such reactions are augmented by the presence of an acid. That such reactions may involve dihydrogen complexes[1–3] as intermediates is a distinct possibility and mechanistic studies on such reactions may elucidate the chemistry of this species, both in simple metal complexes and in biological processes such as nitrogen fixation and hydrogenase activity.[4,5]

We have aleady shown[6] that in the presence of $HBF_4 \cdot OEt_2$, a variety of small molecules can be bound (and sometimes transformed) by $[MoH_4(dppe)_2]$ (dppe = $Ph_2PCH_2CH_2PPh_2$), as illustrated by the selected examples in Fig. 1.

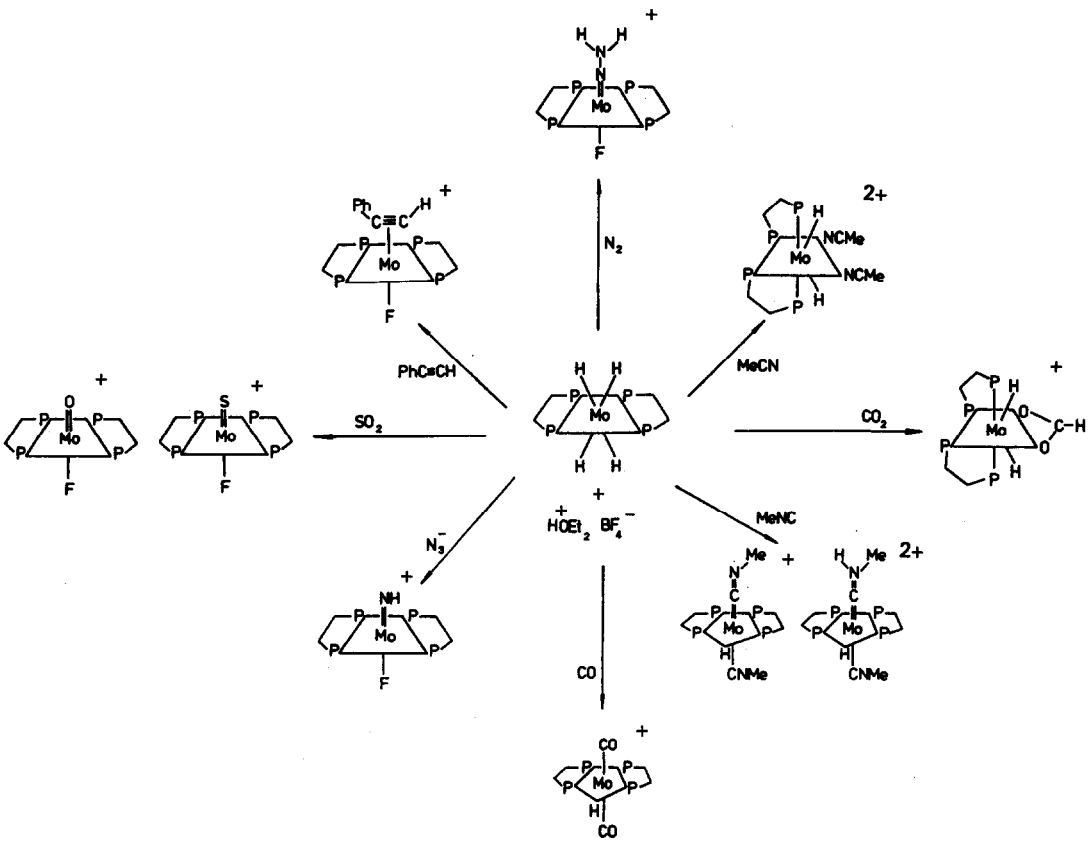

Fig. 1.

* Author to whom correspondence should be addressed.

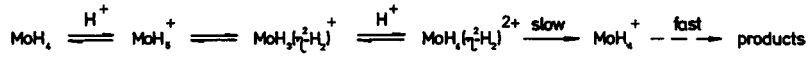

Fig. 2.

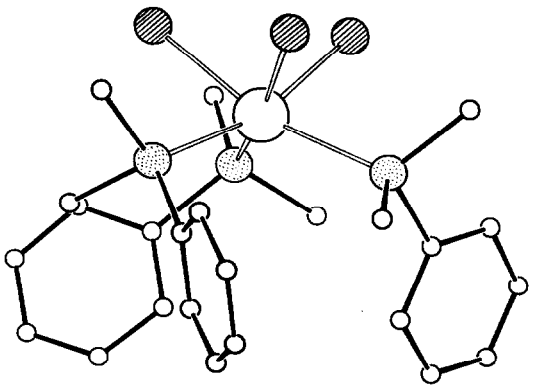

Fig. 3.

Probably the most important feature of this diverse range of reactions is their rapidity: all the reactions are complete within a few seconds under ambient conditions. The mechanism of all these reactions[5] involves the initial rapid diprotonation of the parent tetrahydride, to generate the spectrophotometrically detected $[MoH_4(\eta^2\text{-}H_2)(dppe)_2]^{2+}$. Subsequent rate-limiting loss of dihydrogen generates a coordinatively-unsaturated species capable of binding the substrate, as shown in Fig. 2.

In order to establish whether or not the reactivity pattern shown in Fig. 2 can be generalized, the reactions of other polyhydrido complexes with acids are being studied. In particular, we are investigating the protonation of $[WH_6(PMe_2Ph)_3]$; a system in which direct protonation at the tungsten(VI) centre is precluded since the metal is in its highest formal oxidation state. This system is not so versatile in its reactions with small molecules such as $[MoH_4(dppe)_2]$ in part, at least, because of competitive phosphine loss. However, we have isolated the complexes $[WH_3X_3(PMe_2Ph)_3]$ (X = Cl or Br), $[WH_2(CO)_2(PMe_2Ph)_3](BF_4)_2$ and $[WH_2(NCMe)_3(PMe_2Ph)_3](BF_4)_2$.[7] The structure of the chloro complex has been determined (except for the positions of the hydrides) by X-ray crystallography, as shown in Fig. 3.

Detailed kinetic studies are currently being pursued to establish the mechanism of the rapid protonation of $[WH_6(PMe_2Ph)_3]$.

REFERENCES

1. G. J. Kubas, *Accts Chem. Res.* 1988, **21**, 120.
2. R. H. Crabtree and D. G. Hamilton, *Adv. Organomet. Chem.* 1988, **28**, 299.
3. R. A. Henderson, *Transition Met. Chem.*, in press.
4. R. H. Crabtree, *Inorg. Chim. Acta* 1986, **125**, L7.
5. R. A. Henderson, *J. Chem. Soc., Chem. Commun.* 1987, 1670.
6. R. Ellis, R. A. Henderson, A. Hills and D. L. Hughes, *J. Organomet. Chem.* 1987, **333**, C6.
7. R. H. Crabtree, G. G. Htalky, C. P. Parnell, B. E. Segmüller and R. J. Uriarte, *Inorg. Chem.* 1984, **23**, 354.

Polyhedron Vol. 8, No. 13/14, pp. 1872–1873, 1989
Printed in Great Britain

0277–5387/89 $3.00+.00
© 1989 Maxwell Pergamon Macmillan plc

PREPARATION AND PROPERTIES OF THE NITRILE COMPLEXES *TRANS*-[ReCl(NCR)(dppe)$_2$] (R = ALKYL OR ARYL)

ARMANDO J. L. POMBEIRO* and M. FÁTIMA C. G. SILVA

Centro de Química Estrutural, Complexo I, Instituto Superior Técnico, Av. Rovisco Pais, 1096 Lisboa Codex, Portugal

and

DAVID L. HUGHES and RAYMOND L. RICHARDS

AFRC Nitrogen Fixation Laboratory, University of Sussex, Falmer, Brighton BN1 9RQ, U.K.

Abstract—The series of nitrile complexes *trans*-[ReCl(NCR)(dppe)$_2$] (R = methyl, phenyl or *p*-substituted phenyl; dppe = $Ph_2PCH_2CH_2PPh_2$) has been prepared by reaction of *trans*-[ReCl(N_2)(dppe)$_2$] with the appropriate nitrile, in toluene or tetrahydrofuran under tungsten-filament irradiation. IR properties of these complexes are reported, as well as the molecular structure of *trans*-[ReCl(NCMe)(dppe)$_2$], which presents an unusually short Re—N bond (1.978(5) Å).

Within our interest on the study of the activation of nitrogenase substrates[1] by electron-rich transition metal centres, we have prepared series of isocyanide and alkyne-derived complexes with the rhenium(I) site {ReCl(dppe)$_2$} (dppe = $Ph_2PCH_2CH_2PPh_2$), by reaction of the appropriate substrate with the dinitrogen compound *trans*-[ReCl(N_2)(dppe)$_2$].

The isocyanide complexes *trans*-[ReCl(CNR)(dppe)$_2$] (R = alkyl or aryl)[2] and the vinylidene compounds *trans*-[ReCl(=C=CHR)(dppe)$_2$],[3] as well as the phenylallene species *trans*-[ReCl(H_2C—C=CHPh)(dppe)$_2$],[4] have been obtained by such a route, from the corresponding isocyanides, 1-alkynes (RC≡CH) or phenylpropyne (PhC≡CCH_3), respectively.

We now report our preliminary studies on the reactions of nitriles (which constitute another type of nitrogenase substrates) with *trans*-[ReCl(N_2)(dppe)$_2$].

RESULTS AND DISCUSSION

Treatment of a THF or toluene solution of *trans*-[ReCl(N_2)(dppe)$_2$] by an organonitrile, under tungsten-filament irradiation, affords the corresponding nitrile complexes *trans*-[ReCl(NCR)(dppe)$_2$] [**1**, R = Me or C_6H_4X-4 (X = H, OMe, Me, Cl or F)] [eq. (1)]:

$$\textit{trans}\text{-}[ReCl(N_2)(dppe)_2] + NCR \xrightarrow{h\nu} \textit{trans}\text{-}[ReCl(NCR)(dppe)_2] + N_2 \quad (1)$$

The molecular structure (Fig. 1) of the acetonitrile complex has been authenticated by a single-crystal X-ray diffraction analysis, which indicates an unusually short Re—N bond (1.978(5) Å) as a result of the high π-electron releasing ability of the rhenium centre.

This is consistent with the IR spectra of these complexes which exhibit ν(NC) at values which lie below those observed for the corresponding free nitrile molecules.

However, nitriles are expected to behave as weaker π-acceptors than dinitrogen or isocyanides and, in complexes **1**, the nitrile ligand (for R = alkyl) is rather labile, in contrast with the strong

* Author to whom correspondence should be addressed.

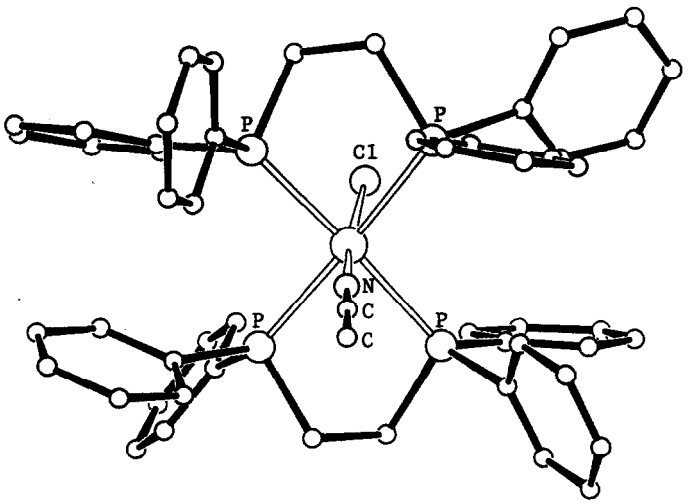

Fig. 1. Molecular structure of *trans*-[ReCl(NCMe)(dppe)$_2$].

coordination[2] of N_2 and CNR to the electron-rich {ReCl(dppe)$_2$} centre.

In agreement with this interpretation, the aryl cyanide complexes are commonly more stable than the alkyl ones. Moreover, for the aromatic series, an inverse correlation appears to be observed between ν(NC) and the Hammett's σ_p constant for the substituent (X) of the aromatic ring: an increase in the electron-withdrawing ability of the latter promotes the net electron acceptor character of the ligand and thus leads to a decrease of ν(NC). A similar trend has been reported[5] for [Mo(N_2)(NCR)(dppe)$_2$].

As a result of the strong π-electron donor character of the metal centre in this study, nitrile ligands appear to be susceptible to activation towards protonation to give ligating methyleneamido-type species, such as NC(H)C_6H_4OMe-4.[6]

Acknowledgements—This work has been partially supported by the National Institute for Scientific Research (I.N.I.C.) and the National Junta for Scientific and Technological Research (J.N.I.C.T.), Portugal.

REFERENCES

1. A. J. L. Pombeiro, in *Coordination Chemistry and Catalysis* (Edited by J. J. Ziólkowski), pp. 100–124. World Scientific, Singapore (1988); A. J. L. Pombeiro, *J. Organomet. Chem.* 1988, **358**, 273.
2. A. J. L. Pombeiro, C. J. Pickett and R. L. Richards, *J. Organomet. Chem.* 1982, **224**, 285.
3. A. J. L. Pombeiro, J. C. Jeffery, C. J. Pickett and R. L. Richards, *J. Organomet. Chem.* 1984, **277**, C7.
4. D. L. Hughes, A. J. L. Pombeiro, C. J. Pickett and R. L. Richards, *J. Chem. Soc., Chem. Commun.* 1984, 992.
5. T. Tatsumi, M. Hidai and Y. Uchida, *Inorg. Chem.* 1975, **14**, 2530.
6. A. J. L. Pombeiro, D. L. Hughes and R. L. Richards, *J. Chem. Soc., Chem. Commun.* 1988, 1052.

Polyhedron Vol. 8, No. 13/14, pp. 1874–1875, 1989
Printed in Great Britain

0277–5387/89 $3.00+.00
Maxwell Pergamon Macmillan plc

OXIDATIONS BY MANGANESE(III)—II. OXIDATION OF CHROMIUM(III)

M. A. MALATI* and A. SEAR

Mid-Kent College of Higher and Further Education, Chatham ME5 9UQ, U.K.

Abstract—The oxidation of chromium(III) by manganese(III) in sulphuric acid solution was followed by extracting aliquots of the quenched reaction mixture with a dibutyl phosphate–xylene solution. The absorbance of the manganese(III) dibutyl phosphate complex gave the concentration of manganese(III) as the reaction proceeded. The reaction followed second-order kinetics. Applying the Eyring equation to the rate constants at different temperatures, gave an activation enthalpy of 129 kJ mol^{-1} and entropy of 140 J K^{-1} mol^{-1}. The suggested mechanism includes a bimolecular slow oxidation of chromium(III) to chromium(IV) by manganese(III), followed by faster oxidations of chromium(IV) and chromium(V) by manganese(III), which is reduced in each stage to manganese(II). Spectral examination proved that $Cr_2O_7^{2-}$ ions are ultimately produced.

Qualitatively, the oxidation of acidified chromium(III) solutions to dichromate by manganese(III) has been reported earlier. An investigation of the oxidation of chromium(III) by various manganese oxides indicated that manganese(III) ions from the solid oxides may be responsible for the oxidation. Later, kinetic studies of the reaction between manganese(III) and chromium(III) showed that it followed second-order kinetics. However, the spectrophotometric technique used encountered a problem of overlapping of the spectra of the reactants and products. A suggested procedure for the separation of manganese(III), based on its extraction with dibutyl phosphate solution, has been developed in the present investigation. The coloured compound extracted was found to be the dibutyl phosphate of manganese(III).

EXPERIMENTAL

Manganese(III) sulphate solutions were freshly prepared by the oxidation of manganese(II) sulphate, in sulphuric acid, by potassium permanganate solutions. The resulting solution was standardized against standard iron(II) or ascorbic acid solution, prepared using boiled-out distilled water. Measured volumes of A.R. chrome alum solution in sulphuric acid were heated in the flash of a reaction vessel at a temperature above that planned for the kinetic run, and then thoroughly mixed with the manganese(III) solution kept at room temperature. A constant ionic strength was maintained by adding sodium sulphate to the reaction mixture. The reaction mixture was placed in a thermostat and aliquots were withdrawn at intervals into bulbs cooled in salt and ice. A quenched aliquot was extracted with an equal volume of Fluka dibutyl phosphate in A.R. xylene (1 : 5 by volume). The absorbance of the organic layer, dried with anhydrous sodium sulphate, was measured at the maximum wavelength of absorption (537 nm). Beer's law was found to be applicable to the coloured solutions. This was established by extracting standardized manganese(III) solutions and measuring the absorbance of the organic layer at the above wavelength.

RESULTS AND DISCUSSION

Figure 1 depicts the results of duplicate runs in which equal concentrations of reactants were mixed at four different temperatures. The reciprocal of the manganese(III) concentration is plotted against time. The rate constants, k_r, calculated from the plots, were used to calculate the activation enthalpy $\Delta H^{\ddagger}$ and entropy $\Delta S^{\ddagger}$ using the Eyring equation:

$$\ln (k_r h/KT) = \Delta H^{\ddagger}/RT + \Delta S^{\ddagger}/R.$$

* Author to whom correspondence should be addressed.

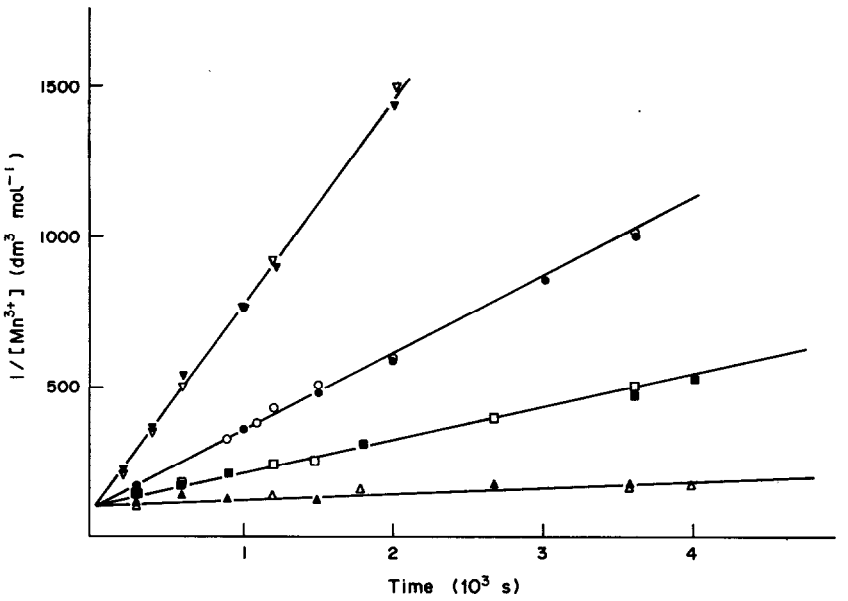

Fig. 1. Variation of the reciprocal of the concentration of manganese(III) with the reaction time at 36°C (△, ▲), 44°C (□, ■), 50°C (○, ●) and 58°C (▽, ▼).

The activation enthalpy estimated from the slope of the plot in Fig. 2 was 129 kJ mol^{-1} and the activation entropy was 140 J K^{-1} mol^{-1}. The mechanism suggested is:

$$Cr^{3+} + Mn^{3+} \xrightarrow{k_1} Cr^{IV} + Mn^{2+}$$

$$Cr^{IV} + Mn^{3+} \xrightarrow{k_2} Cr^{V} + Mn^{2+}$$

$$Cr^{V} + Mn^{3+} \xrightarrow{k_3} Cr^{IV} + Mn^{2+}.$$

If $k_1 \ll k_2$ and k_3, the bimolecular reaction becomes rate-determining. Both chromium(IV) and chromium(V) have been postulated in the reactions involving oxidations by dichromate. The latter ions were identified in the spectra of reaction mixtures near the end of the reaction.

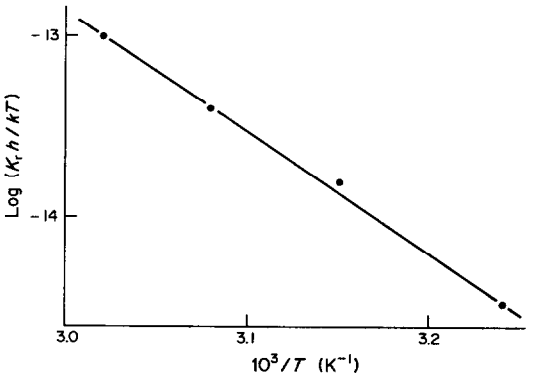

Fig. 2. Variation of $\log(k_r h/kT)$ with the reciprocal of the thermodynamic temperature.

Polyhedron Vol. 8, No. 13/14, pp. 1876–1878, 1989
Printed in Great Britain

0277–5387/89 $3.00+.00
© 1989 Maxwell Pergamon Macmillan plc

BIMETALLIC COMPLEXES OF MOLYBDENUM AND TUNGSTEN WITH FUNCTIONALIZED DIPHOSPHINES: X-RAY CRYSTAL STRUCTURE OF [{W(CO)$_3$}(μ-mtppe)]

MOHAMMED F. M. AL-DULAYMMI, PETER B. HITCHCOCK and RAYMOND L. RICHARDS*

School of Chemistry and Molecular Sciences, University of Sussex, Brighton BN1 9QJ, U.K.

Abstract—The binuclear complexes [{M(CO)$_3$}$_2$(μ-diphos)] (M = Mo or W; diphos = mtppm, mtppe or iptppe) (X-ray structure for M = W, diphos = mtppe), [{M(CO)$_4$}$_2$(μ-dppmpe)] and [{MBr$_2$(CO)$_2$}$_2$(μ-mtppe)], and the mononuclear compounds [M(CO)$_4$(dbtpe)] and [MoBr$_2$(CO)$_2$(mtppe)] have been prepared.

We have recently reported the preparation of diphosphines substituted at phosphorus by potentially ligating groups and we have described some of their complexes with rhodium.[1] Here, we describe the preparation of new binuclear complexes of molybdenum and tungsten with mtppm (**Ia**), mtppe (**Ib**), iptppe (**Ic**), dppmpe (**II**) and mononuclear complexes with dbtpe (**III**). (See Fig. 1 for phosphine nomenclature.)

The reaction of mtppm, mtppe and iptppe with [M(CO)$_3$(MeCN)$_3$] (M = Mo or W) in a 1:2 molar ratio in refluxing THF, produced yellow, crystalline bimetallic complexes of general formula [{M(CO)$_3$}$_2$(μ-diphos)] (diphos = mtppm, mtppe or iptppe) [eq. (1)]:

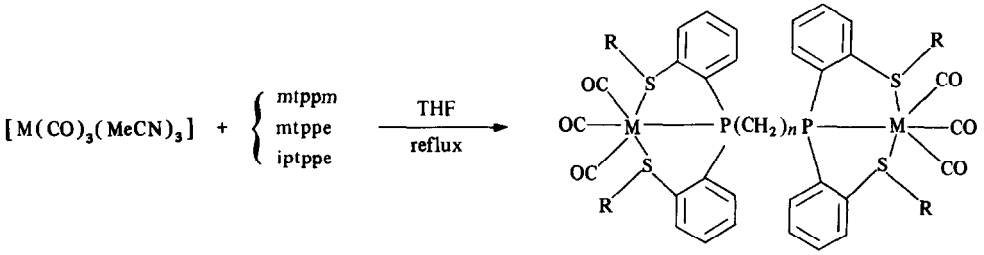

All complexes show a singlet in their ^{31}P{H} NMR spectra, and characteristic (CO) bands in their IR spectra, as expected for tricarbonyl complexes.[2,3]

The X-ray structure of [{W(CO)$_3$}$_2$(μ-mtppe)] (Fig. 2) confirms the above formulation and shows it to be binuclear, with the mtppe ligand coordinated to each metal through one phosphorus and two sulphur atoms in an almost octahedral environment.

In a similar way, dppmpe reacted with [M(CO)$_3$(MeCN)$_3$] (M = Mo or W) to form pale yellow bimetallic tetracarbonyl complexes [eq. (2)]:

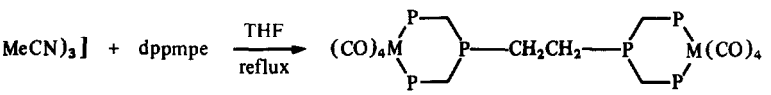

Their structure has been assigned on the basis of elemental analysis and spectroscopic measurements. The mechanism of formation of the tetracarbonyl species is unclear, but presumably they are formed to avoid the highly strained four-membered ring which coordination of the third phosphorus atom would produce. Reactions of the products of eq. (2) with [PdCl$_2$(COD)] (COD = cyclooctadiene) and [{RhCl(CO)$_2$}$_2$] appear to form trinuclear complexes.

The dbtpe ligand reacted with [M(CO)$_3$(MeCN)$_3$] as an ordinary diphosphine, without involvement of the functional groups, to give mononuclear, tetracarbonyl complexes [M(CO)$_4$(dbtpe)].

Two seven-coordinated complexes have been sep-

* Author to whom correspondence should be addressed.

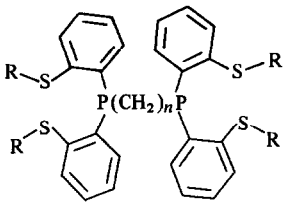

(**Ia**) $n = 1$, R = Me (mtppm)

(**Ib**) $n = 2$, R = Me (mtppe)

(**Ic**) $n = 2$, R = Pr^i (iptppe)

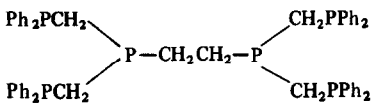

(II) (dppmpe)

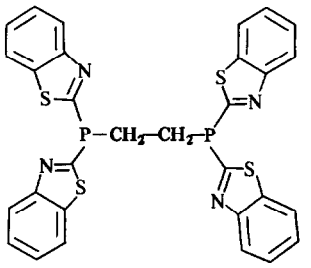

(III) (dbtpe)

Fig. 1. Functionalized diphosphines.

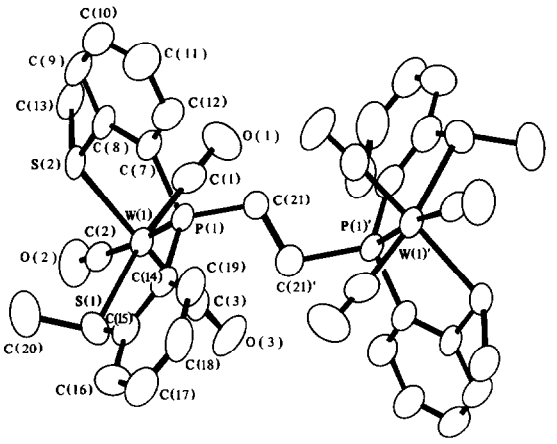

Fig. 2. Structure of [{W(CO)$_3$}$_2$(μ-mtppe)]. Selected bond distances (Å) and angles (°) are:

W(1)—P(1)	2.426(2)	W(1)—C(1)	1.950(11)
W(1)—S(1)	2.515(3)	W(1)—C(2)	1.974(10)
W(1)—S(1)	2.509(2)	W(1)—C(3)	1.971(7)
S(1)—W(1)—S(2)	91.03(8)	S(2)—W(1)—C(1)	93.5(2)
S(1)—W(1)—P(1)	80.27(9)	S(2)—W(1)—C(2)	91.4(2)
S(1)—W(1)—C(1)	169.9(3)	S(2)—W(1)—C(3)	179.2(3)
S(1)—W(1)—P(1)	97.0(3)	P(1)—W(1)—C(1)	91.7(3)
S(1)—W(1)—C(3)	88.9(3)	P(1)—W(1)—C(2)	170.9(2)
S(2)—W(1)—P(1)	80.0(7)	P(1)—W(1)—C(3)	99.2(3)

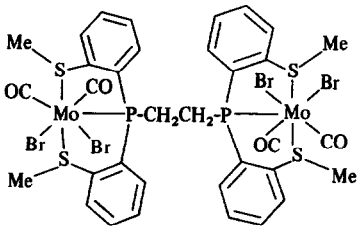

(A)

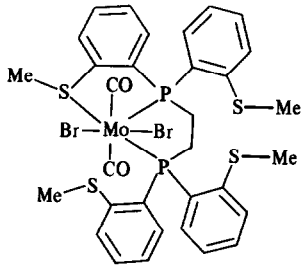

(B)

arated from the reaction of mtppe with the metal halocarbonyls $[MBr_2(CO)_4]$, the binuclear red complex (**A**) and a yellow–orange mononuclear complex (**B**).

The diphosphine (dbtpe) reacted in a similar way with $[MBr_2(CO)_4]$ (M = Mo or W) to give a salmon–pink complex identified as $[MBr_2(CO)_2$ (dbtpe)].

REFERENCES

1. M. F. Al-Dulaymmi, P. B. Hitchcock and R. L. Richards, *J. Organomet. Chem.* 1988, **C31**, 338.
2. J. Chatt and H. R. Watson, *J. Chem. Soc.* 1981, 4980.
3. P. N. Kapoor and P. C. Mercykutty, *J. Organomet. Chem.* 1988, **339**, 97.

Polyhedron Vol. 8, No. 13/14, pp. 1879–1881, 1989
Printed in Great Britain

0277–5387/89 $3.00+.00
© 1989 Maxwell Pergamon Macmillan plc

NEW TECHNETIUM COMPLEXES WITH METAL–NITROGEN BONDS

C. M. ARCHER and J. R. DILWORTH*

Department of Chemistry and Biological Chemistry, University of Essex, Colchester, Essex CO4 3SQ, U.K.

and

J. D. KELLY

Amersham International, White Lion Road, Amersham, Buckinghamshire HP7 9LL, U.K.

and

M. McPARTLIN

North London Polytechnic, London N7 8DB, U.K.

Abstract—The optimal nuclear characteristics of technetium make it an ideal radionuclide for diagnostic medical imaging. However, the development of new imaging agents requires the prior development of technetium coordination chemistry to generate appropriate new complexes and their precursors. Here we report the synthesis of some new technetium complexes containing metal–nitrogen bonds and their coordination chemistry.

TECHNETIUM NITRIDO COMPLEXES

Deutsch *et al.* have synthesized cationic complexes of the type $[TcX_2(dmpe)_2]^+$ (X = halide, dmpe = $Me_2PCH_2CH_2PMe_2$) and showed that their ^{99m}Tc analogues exhibited promise as myocardial imaging agents in rats.[1,2] However, in humans, there was significant "washout" from the heart which was attributed to facile reduction to the neutral $[TcX_2(dmpe)_2]$ species. Earlier we had synthesized $[ReNCl(dppe)_2]^+$ and showed that this required a reduction potential of -1.8 V vs SCE to be reduced irreversibly. We therefore anticipated that complexes of the type $[TcNX(dmpe)_2]^+$ should be significantly harder to reduce than the technetium(III) species $[TcCl_2(dmpe)_2]^+$.

We here report that the nitride precursor $[TcNCl_4]^-$[3] reacts with excess dmpe in methanol under reflux to give orange $[TcNCl(dmpe)_2]^+$ in good yield, isolated as the tetraphenylborate salt. The structure of the complex is shown in Fig. 1. The Tc—N bond length is considerably longer at 1.854(6) Å than in other nitrides such as $[TcNCl_4]^-$ (1.581(5) Å).[3] Such lengthening has been observed before and attributed to steric interactions between the nitride nitrogen and the four co-planar phosphorus atoms.[4]

The ^{99m}Tc analogue of $[TcNCl(dmpe)_2]^+$ was synthesized in high RCP and its biodistribution

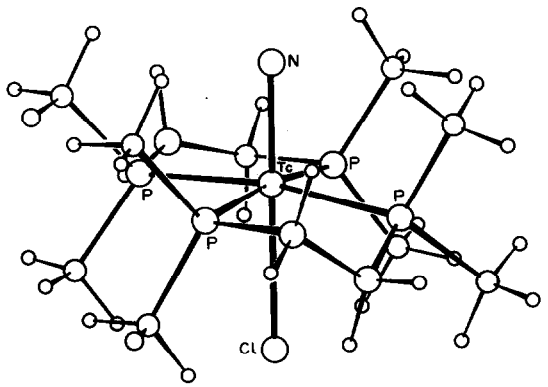

Fig. 1. Structure of $[TcCl(N)(dmpe)_2]^+$.

* Author to whom correspondence should be addressed.

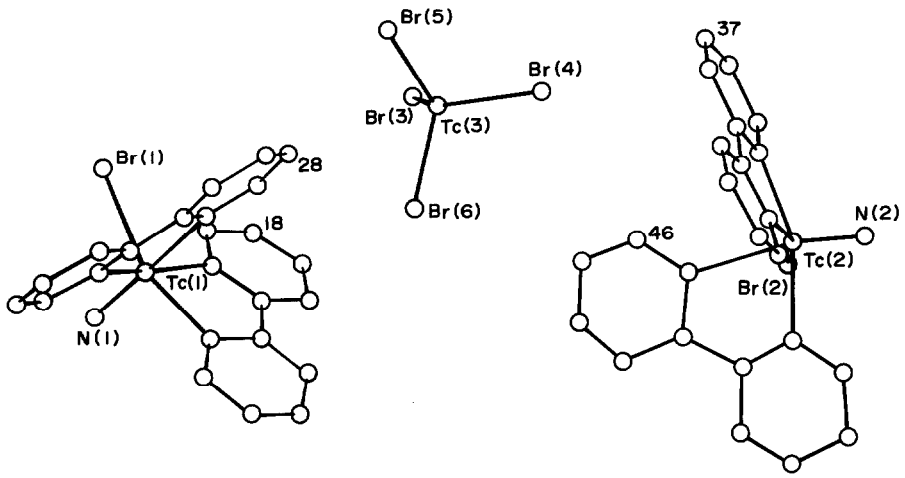

Fig. 2. Structure of $[TcBr(N)(bipy)_2]_2[TcBr_4]$ showing both cation and anion.

studied. Significant heart uptake was observed but there was rapid "washout" of ^{99m}Tc, suggesting reduction to the technetium(IV) species. Cyclic voltammetry was consistent with this, with a reversible reduction process occurring at −0.02 V vs SCE. The unexpected ease of reduction is ascribed to the rapid formation of $[TcN(dmpe)_2]^{2+}$ in solution by loss of the *trans*-chloride ligand labilized by the *trans*-effect.

By contrast, the analogous reaction of $[TcNBr_4]^-$ with 2,2′-dipyridyl in ethanol gives the complex *cis*-$[TcBr(N)(dipy)_2]_2[TcBr_4]$ (see Fig. 2), containing the novel technetium(II) tetrabromotechnetate anion. This represents the first reported example of a tetrahalidometallate complex of a second row transition metal. In contrast to $[TcCl(N)(dmpe)_2]^+$, the nitride and chloride ions are *cis* in $[TcBr(N)(bipy)_2]^+$. This reflects the steric difficulties imposed by arranging the two bipyridyl ligands in a plane and their relatively small bite angle.

Access to technetium(III) chemistry has in the past been restricted by a lack of suitable precursors. We have now synthesized the technetium analogue of $[ReCl_3(MeCN)(PPh_3)_2]$[4] by reduction of $[TcCl_4(PPh_3)_2]$ with zinc in dichloromethane–acetonitrile. The complex is an air-stable, readily soluble, orange, crystalline material which reacts rapidly with a wide range of ligands. Thus, reaction of $[TcCl_3(MeCN)(PPh_3)_2]$ with excess dipyridyl in refluxing methanol gives $[Tc(bipy)_3]^{2+}$ rather than the expected $[TcCl_2(bipy)_2]^+$. The structure of the dication is shown in Fig. 3. The overall geometry about the technetium is, as expected, distorted octahedral and general bond distances and angles are similar to those found in $[Ru(bipy)_3]^{2+}$.[5] Reaction of $[TcCl_3(MeCN)(PPh_3)_2]$ with 2 equivalents of tridentate ligand L^1 gives the purple cationic technetium(III) complex $[TcL^1_2]^+$, whereas the more reducing phosphine ligand L^2 gives, under analogous conditions, the red neutral technetium(II) complex, $[TcL^2_2]$.

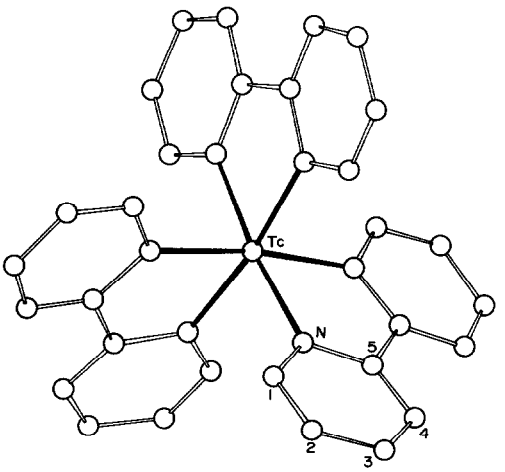

Fig. 3. Structure of $[Tc(bipy)_3]^{2+}$.

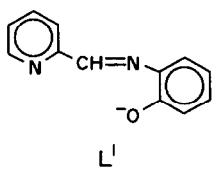

L^1

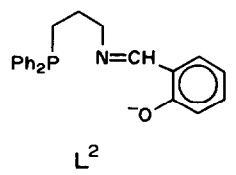

L^2

Acknowledgement—We are grateful to Amersham International plc for financial support of the above work.

REFERENCES

1. J-L. Vanderheyden, M. J. Heeg and E. Deutsch, *Inorg. Chem.* 1985, **24**, 1666.
2. E. Deutsch, W. Bushong, K. A. Glavan, R. C. Elder, V. J. Sodd, K. L. Scholtz, D. L. Fortman and S. J. Lukes, *Science* 1981, **214**, 85.
3. J. Baldas, J. Boas, J. Bonnyman and G. Williams, *J. Chem. Soc., Dalton Trans.* 1984, 2395.
4. J. R. Dilworth, P. L. Dahlstrom, J. R. Hyde and J. Zubieta, *Inorg. Chim. Acta* 1982, **71**, 21.
5. D. P. Rillema, D. S. Jones and H. A. Levy, *J. Chem. Soc., Chem. Commun.* 1979, 849.

Polyhedron Vol. 8, No. 13/14, p. 1882, 1989
Printed in Great Britain

0277–5387/89 $3.00+.00
© 1989 Maxwell Pergamon Macmillan plc

ASPECTS OF THE CHEMISTRY OF A BULKY ZIRCONOCENE(III) CHLORIDE

ANTONIO ANTIÑOLO, MICHAEL F. LAPPERT,* GERARD A. LAWLESS and HELÉNE OLIVIER

School of Chemistry and Molecular Sciences, University of Sussex, Brighton BN1 9QJ, U.K.

We report the synthesis of the zirconium(III) complex $[\{ZrCp''_2(\mu\text{-}Cl)\}_2]$ [Cp'' = η-$C_5H_3(SiMe_3)_2$-1,3] (**1**) and of the 1:1 adduct of its monomeric equivalent with THF (**2**) or PMe_3 (**3**), as shown in Scheme 1. The adducts **2** and **3** are indefinitely stable in solution under ambient conditions, as evident from their ESR spectra.

The NMR spectra of the zirconocene(III) complex, **1**, demonstrates that the compound is essentially diamagnetic (although it showed a weak ESR signal), consistent with the structure shown in Scheme 1; the slight paramagnetism in PhMe is attributed to a small equilibrium concentration of monomer in solution. Support for this formulation also comes from the analogy with the corresponding compound $[\{ZrCp_2(\mu\text{-}Cl)\}_2]$ (Zr, Zr) which has been crystallographically characterized and which shows no ESR signal in solution.[1]

Details of the ESR solution spectra of complexes **2** and **3** are shown in Scheme 1. Both the g_{av} and the $a(^{91}Zr)$ values are consistent with a metal-centred d^1 complex.[2]

Each of the complexes **2** and **3** readily loses the neutral ligand when the volatiles are removed from the solution at 10^{-1} torr. It is clear, therefore, that the donor–acceptor bond in these complexes is quite weak. Nevertheless, the stability of complexes **2** and **3** in solution is directly attributed to the steric effect of the trimethylsilyl substituents in cyclopentadienyl rings.

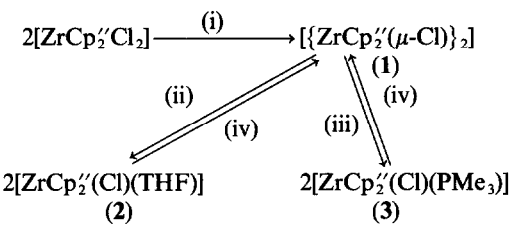

Scheme 1. *Reaction conditions* (25°C): (i) Na–Hg (1 mol), PhMe; (ii) THF; (iii) PMe_3 (1 mol), PhMe; (iv) 25°C at 10^{-1} torr. *Characterization of compounds*: **1**, very pale blue–green crystals, m.p. 137°C; **2**, red solution, g_{av} = 1.9775, $a(^{91}Zr)$ = 23 G; **3**, red solution in PhMe, g_{av} = 1.9780; $a(^{91}Zr)$ = 6 G, $a(^{31}P)$ = 14.5 G.

We are investigating various reactions of complex **1**, including nucleophilic displacement of the $\bar{Cl}$ ligand. Attempts are also being made to obtain X-ray data on crystalline materials.

Acknowledgement—We thank the E.E.C. (Stimulation Contract: ST2000335) for support.

REFERENCES

1. G. Fochi, G. Guidi and C. Floriani, *J. Chem. Soc., Dalton Trans.* 1984, 1253.
2. D. J. Cardin, M. F. Lappert and C. L. Raston, *Chemistry of Organo-zirconium and -hafnium Compounds*, pp. 274–275. Ellis Horwood, Chichester (1986).

* Author to whom correspondence should be addressed.

Polyhedron Vol. 8, No. 13/14, p. 1883, 1989
Printed in Great Britain

0277–5387/89 $3.00+.00
© 1989 Maxwell Pergamon Macmillan plc

SYNTHESIS OF SOME LOW OXIDATION STATE ORGANOTITANIUM COMPOUNDS

MICHAEL F. LAPPERT* and WING-POR LEUNG

School of Chemistry and Molecular Sciences, University of Sussex, Brighton BN1 9QJ, U.K.

and

RUTH A. BARTLETT and PHILIP P. POWER

Department of Chemistry, University of California, Davis, CA 95616, U.S.A.

We have used the ligand $^{-}Cp''$ ($= \eta\text{-}^{-}C_5H_3(SiMe_3)_2\text{-}1,3$) to examine a number of organotitanium compounds in oxidation state +3. The starting materials were either $[TiCl_4]$ or $TiCl_3$; details of the reactions are shown in Scheme 1.

Each of the crystalline compounds $[TiCp''_2Cl]$ (**1**), $[TiCp''_2(CO)_2]$ (**2**) and $[TiCp''_2(\mu\text{-}H)_2BH_2]$ (**3**) has been characterized by microanalytical and spectroscopic data. The paramagnetic compound **1**, like $[Ti(\eta\text{-}C_5Me_5)_2Cl]$,[1] is unusual in being a monomer even in the crystalline state; by contrast, the corresponding unsubstituted cyclopentadienyl is a metal–metal-bonded antiferromagnetic dimer $[\{TiCp_2(\mu\text{-}Cl)\}_2]$.[2] Some important bond lengths and angles for complex **1** are as follows: ($Cp'' = \eta\text{-}C_5H_3(SiMe_3)_2\text{-}1,3$), Ti—Cl 2.346(2), ⟨Ti—C⟩ 2.368 Å (ranging from 2.349(6) to 2.403(5) Å); Cl—Ti—C [Cp''(1)]: 107.6(2), 82.2(2), 92.1(3), 126.9(2), 139.4(2)°; Cl—Ti—C [Cp''(2)]: 110.0(2), 82.5(2), 89.0(2), 122.7(2), 139.9(2)°. The corresponding tetrahydridoborate **3**, like $[TiCp_2(\mu\text{-}H)_2BH_2]$,[3] is also a monomer and on the basis of IR data is formulated as being η^2-bonded.

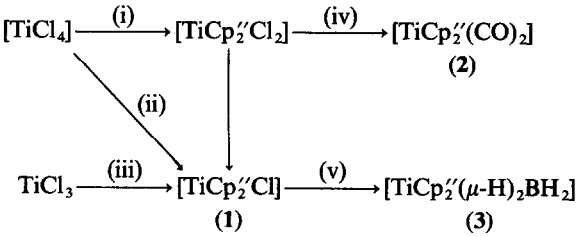

Scheme 1. *Reaction conditions*: (i) LiCp'', C_6H_6, 30°C; (ii) LiCp'', THF, −78°C; (iii) $MgCp''_2$, THF, 30°C; (iv) Na/Hg, CO/1 atm, THF, −78°C; (v) $Na[BH_4]$, THF, 30°C.

REFERENCES

1. J. W. Pattiasina, H. J. Heeres, F. van Bolhuis, A. Meetsma and J. H. Teuben, *Organometallics* 1987, **6**, 1004.
2. R. Jungst, D. Sekutowski, J. Davis, M. Luly and G. D. Stucky, *Inorg. Chem.* 1977, **16**, 1645.
3. K. M. Melmed, D. Coucouvanis and S. J. Lippard, *Inorg. Chem.* 1973, **12**, 232.

* Author to whom correspondence should be addressed.

Polyhedron Vol. 8, No. 13/14, p. 1884, 1989
Printed in Great Britain

0277–5387/89 $3.00+.00
© 1989 Maxwell Pergamon Macmillan plc

SYNTHETIC AND STRUCTURAL STUDIES ON SOME BIS(CYCLOPENTADIENYL)MOLYBDENUM AND -TUNGSTEN COMPLEXES CONTAINING DOUBLY BONDED TIN OR PHOSPHORUS

RAKESH BOHRA, PETER B. HITCHCOCK, MICHAEL F. LAPPERT* and WING-POR LEUNG

School of Chemistry and Molecular Sciences, University of Sussex, Brighton BN1 9QJ, U.K.

We have recently shown that the phosphorus equivalents of arylimides are accessible for certain derivatives of molybdenum and tungsten, as shown in **1** and **2** of Scheme 1.[1]

The X-ray structure of one of the compounds, **1** (M = Mo, Ar = $C_6H_2Bu^t_3$-2,4,6), has been published.[1] We now have the corresponding data on the isomorphous tungsten analogue; some important bond lengths and angles are: W—P 2.349(5), P—C 1.84(2), W—Cen(1) 1.98, W—Cen(2) 1.93 Å; W—P—C(Ar) 114.8(5), P—W—Cen(1) 113.4, P—W—Cen(2) 102.7, Cen(1)—W—Cen(2) 143.7°.

Scheme 1 also reveals some related reactions which were designed to yield analogues in which molybdenum or tungsten bonded to tin rather than phosphorus. We believe that such a tin compound has been isolated, [Mo(Cp_2(SnR$_2$)] (**3**) (R = CH(SiMe$_3$)$_2$). However, along the reaction pathway some further compounds, **4**–**6**, have been identified, for one of which, [WCp$_2$(H){Sn(R)Cl$_2$}] (**4**), there is an X-ray structure. Some important bond lengths and angles in **4** are: W—Sn 2.706(1), W—Cen(1) 1.948, W—Cen(2) 1.938, Sn—Cl 2.442(3) and 2.405(3), Sn—C 2.180(8) Å; W—Sn—C 123.7(2),

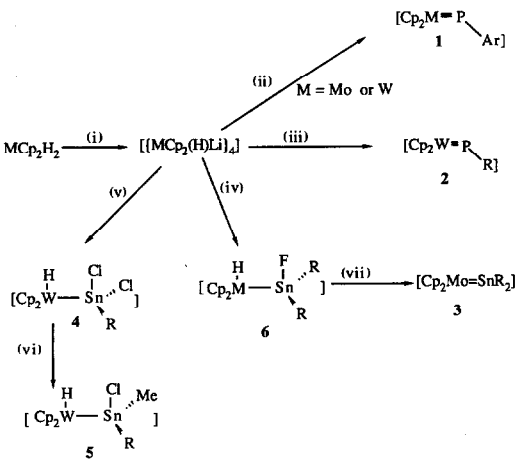

Scheme 1. *Reagents*: (i) LiBu^n, PhMe; (ii) ArPCl$_2$; (iii) RPCl$_2$; (iv) R$_2$SnX$_2$, X = Cl or F; (v) RSnCl$_3$; (vi) LiMe; (vii) LiBu^t, C_6H_{14}.

W—Sn—Cl 117.6 and 109.1, Cen—W—Cen 144.7°.

REFERENCES

1. P. B. Hitchcock, M. F. Lappert and W.-P. Leung, *J. Chem. Soc., Chem. Commun.* 1987, 1282.

* Author to whom correspondence should be addressed.

Polyhedron Vol. 8, No. 15, pp. 1885–1890, 1989
Printed in Great Britain

0277–5387/89 $3.00+.00
© 1989 Maxwell Pergamon Macmillan plc

CLUSTER SYNTHESIS—XXIII. THE SYNTHESIS, STRUCTURE AND BONDING OF $Fe_4(CO)_{10}(\mu\text{-}CO)(\mu_4\text{-}S)_2$

RICHARD D. ADAMS,* JAMES E. BABIN, JAVIER ESTRADA and JIN-GUU WANG

Departments of Chemistry and Physics, University of South Carolina, Columbia, SC 29208, U.S.A.

and

MICHAEL B. HALL* and ARTHUR A. LOW

Department of Chemistry, Texas A&M University, College Station, TX 77843, U.S.A.

(*Received* 15 *December* 1988; *accepted* 13 *February* 1989)

Abstract—The compound $Fe_4(CO)_{10}(\mu\text{-}CO)(\mu_4\text{-}S)_2$ (**1**) was synthesized in 38% yield by the UV induced decarbonylation of $Fe(CO)_5$ in the presence of $Fe_3(CO)_9(\mu_3\text{-}S)_2$. Compound **1** was characterized by a single-crystal X-ray diffraction analysis. Space group: *Pccn*, $a = 6.603(1)$, $b = 15.429(3)$, $c = 17.292(4)$ Å, $Z = 4$. The structure was solved by direct methods and was refined (807 reflections) to the final values of the residuals $R = 0.043$ and $R_w = 0.054$. The molecule consists of a planar array of four iron atoms with a quadruply bridging sulphido ligand on each side of the plane. The shortest metal–metal bond, 2.489(3) Å, contains a bridging carbonyl ligand. Semi-bridging carbonyl ligands bridge the two adjacent metal–metal bonds, 2.532(2) Å. The longest metal–metal bond, 2.605(2) Å, has no carbonyl bridge. Compound **1** is unsaturated (by EAN rule) by the amount of two electrons. The two semi-bridged carbonyl–metal bonds in **1** are significantly shorter than those in the saturated cluster $Fe_2Co_2(CO)_{11}(\mu_4\text{-}S)_2$. A molecular orbital description which explains the differences in bonding between the two compounds is proposed.

Recently, we have demonstrated the value of $Ru(CO)_5$ and $Os(CO)_5$ as reagents for the enlargement of metal carbonyl clusters of ruthenium and osmium that contain sulphido ligands.[1–5] We have now begun investigations into the iron system. This report describes the synthesis and structural characterization of the new iron cluster, $Fe_4(CO)_{10}(\mu\text{-}CO)(\mu_4\text{-}S)_2$ (**1**). The structure of compound **1** was compared with that of $Fe_2Co_2(CO)_{10}(\mu\text{-}CO)(\mu\text{-}S)_2$ (**2**), which has an analogous structure, but has two additional valence electrons.[6] A molecular orbital description that explains differences in the metal–metal bonding of the two structures is proposed.

EXPERIMENTAL

General procedures

Compound **1** is slightly air-sensitive. Thus, all reactions were performed under a dry nitrogen atmosphere. Reagent grade solvents were dried over molecular sieves and were deoxygenated by purging with nitrogen prior to use. $Fe(CO)_5$ was purchased from Alfa. $Fe_3(CO)_9(\mu_3\text{-}S)_2$ was prepared as previously reported.[7] IR spectra were recorded on a Nicolet 5-DXB FT-IR spectrometer. Elemental analysis was performed by Desert Analytics, Tucson, Arizona.

Synthesis of $Fe_4(CO)_{10}(\mu\text{-}CO)(\mu_4\text{-}S)_2$ (**1**)

$Fe_3(CO)_9(\mu_3\text{-}S)_2$ (50 mg, 0.103 mmol) and $Fe(CO)_5$ (0.136 cm^3, 1.03 mmol) were dissolved in 50 cm^3

* Authors to whom correspondence should be addressed.

of cyclohexane solvent in a Pyrex flask. The solution was irradiated (UV external) in the presence of a continuous nitrogen purge for 4.5 h. The solvent was removed *in vacuo* and the residue was chromatographed by TLC on silica gel with hexane solvent. This yielded the following compounds in order of elution: yellow $Fe_2(CO)_6(S)_2$, 3 mg; red $Fe_3(CO)_9(\mu_3\text{-}S)_2$, 21.8 mg, and green **1**, 13.1 mg (38% based on the amount of $Fe_3(CO)_9(\mu_3\text{-}S)_2$ consumed). Found: C, 21.57. Calc: C, 22.18%. IR(νCO in hexane): 2063(w), 2044(s), 2022(m), 2011(m), 1856(w).

Reaction of **1** *with carbon monoxide*

15 mg of **1** were dissolved in 30 cm^3 of hexane. The solution was refluxed under a slow purge of carbon monoxide for 18 h. During this time the green solution turned to a greenish-red colour. The solvent was then removed *in vacuo*, and the residue was chromatographed by TLC. This yielded (in order of elution): yellow $Fe_2(CO)_6(\mu\text{-}S_2)$ (0.5 mg), red $Fe_3(CO)_9(\mu_3\text{-}S)_2$ (6.5 mg) and unreacted **1** (6.4 mg).

Molecular orbital calculations

Fenske–Hall molecular orbital calculations[8] were performed on a VAX 11/780 computer. The iron basis functions were taken from Richardson *et al.*[9] The carbon, oxygen and sulphur functions were taken from the double-ζ functions of Clementi[10] and reduced to a single-ζ function,[11] except for the *p*-valence functions which were retained as the double-ζ function. The atomic functions were made orthogonal by the Schmidt procedure. The Mulliken population analysis[12] was used to determine both the individual atomic charges and the atomic orbital populations.

Calculations were performed on **1** in its crystal structure geometry. Additional calculations were performed on **2** in its crystal structure geometry[6]* and the 2^+ cation of **2** (hereafter designated as **2a**), in order to compare the effect of adding two electrons to the fixed cluster framework. The calculations were performed with 3*d*-orbitals included on the capping sulphur atoms (exponents equal to that of the best atom single-ζ 3*p*-function).

Crystallographic analyses

Very dark green crystals of **1** suitable for X-ray diffraction measurements were grown by slow evaporation of solvent from solutions in a CH_2Cl_2–C_6H_{14} solvent mixture at 5°C. The data crystal was mounted in a thin-walled glass capillary. Diffraction measurements were made on a Rigaku AFC6 fully automated four-circle diffractometer, using graphite monochromatized Mo-K_α radiation. The unit cell was determined and refined from 25 randomly selected reflections obtained by using the diffractometer automatic search, centre, index and least-squares routines. Crystal data and results of the analysis are listed in Table 1. All data processing was performed on a Digital Equipment Corporation MICROVAX II computer by using the TEXSAN structure solving program library obtained from the Molecular Structure Corporation, College Station, Texas. Neutral atom scattering factors were calculated by the standard procedures.[13a] Anomalous dispersion corrections were applied to all non-hydrogen atoms.[13b] Full-matrix least-squares refinements minimized the function

$$\sum_{hkl} w(|F_{obs}| - |F_{calc}|)^2$$

where

$$w = 1/\sigma(F)^2, \quad \sigma(F) = \sigma(F_{obs}^2)/2F_{obs}$$

and

$$\sigma(F_{obs}^2) = [\sigma(I_{raw})^2 + (PF_{obs}^2)^2]^{1/2}/Lp.$$

All non-hydrogen atoms were refined anisotropically. The unit cell and systematic absences indicated that the crystals belonged to the orthorhombic crystal system and the space group, *Pccn*. The structure was solved by a combination of direct methods (MITHRIL) and difference Fourier syntheses.

RESULTS AND DISCUSSION

When purged with nitrogen, solutions of $Fe_3(CO)_9(\mu_3\text{-}S)_2$ and $Fe(CO)_5$ exposed to UV irradiation yield the new compound $Fe_4(CO)_{10}(\mu\text{-}CO)(\mu_4\text{-}S)_2$ (**1**) (38% yield based on the amount of $Fe_3(CO)_9(\mu_3\text{-}S)_2$ consumed in the reaction). When treated with carbon monoxide (1 atm) in refluxing hexane solvent (18 h), compound **1** was converted back to $Fe_3(CO)_9(\mu_3\text{-}S)_2$ (53% yield) by removal of one iron grouping, presumably as $Fe(CO)_5$. Compound **1** was characterized by a single-crystal X-ray diffraction analysis. An ORTEP diagram of the molecular structure of **1** is shown in Fig. 1. Intramolecular bond distances and angles are listed in Tables 2 and 3. The molecule contains a C_2 rotation axis that is crystallographically imposed. The bridging ligand C(11)—O(11) lies on this axis. The cluster consists of a trapezoidal arrangement of four iron

* Additional details concerning the structure of **2** were provided by Professor H. Vahrenkamp.

Table 1. Crystallographic data for X-ray diffraction study

(a)	Formula	$Fe_4S_2O_{11}C_{11}$
	Temperature (±3°C)	23
	Space group	*Pccn*
	a (Å)	6.603(1)
	b (Å)	15.429(3)
	c (Å)	17.292(4)
	V (Å^3)	1761.6(7)
	M_r	595.6
	Z	4
	ρ_{calc} (g cm^{-3})	2.25
(b)	Measurement of intensity data	
	Radiation	
	Monochromator	Mo-K_α (0.71069 Å)
	Detector aperture (mm)	Graphite
	Horizontal	2.0
	Max 2θ	45.0°
	Scan type	Moving crystal–stationary counter
	ω-Scan width:	$A = 1.10°$
	$(A+0.347\tan\theta)°$	
	Background (count time at each end of scan):	$\frac{1}{4}$ additional scan
	ω-Scan rate[a] (° min^{-1})	4.0
	Data used ($F^2 \geqslant 3.0\sigma(F^2)$)	807
	Data measured	1379
(c)	Treatment of data	
	Absorption correction:	Analytical
	Coefficient (cm^{-1}):	35.1
	Transmission coefficient:	
	Maximum	0.83
	Minimum	0.46
	Number of variables	128
	Vertical	2.0
	Crystal faces:	010, 0$\bar{1}$0, 00$\bar{1}$
		0$\bar{1}$1, $\bar{1}$10, 1$\bar{1}$0
	Crystal size (mm):	0.08 × 0.18 × 0.24
	Crystal orientation:	
	Direction; ° from ϕ-axis	a,[a] 3.5
	Reflections measured	$+h, +k, +l$
	P-factor	0.02
	Final residuals R_F	0.043
	R_{wF}	0.054
	Goodness-of-fit	1.87
	Largest shift-error	
	Value of final cycle	0.00
	Largest peak in final difference Fourier (e$^-$ Å^{-3})	0.70

[a] Rigaku software uses a multiple scan technique. If the $I/\sigma(I)$ ratio is less than 10.0, a second scan is made and the results are added to the first scan, etc. A maximum of three scans was permitted per reflection.

atoms which is bridged on each side by a quadruply bridging sulphido ligand. It is structurally very similar to $Fe_2Co_2(CO)_{10}(\mu\text{-}CO)(\mu_4\text{-}S)_2$ (**2**),[6*] and the structures of both compounds will be compared and contrasted. The shortest metal–metal bond in **1** contains a bridging carbonyl ligand, Fe(1)—Fe(1′) = 2.489(3) Å. The corresponding bond in **2** is the cobalt–cobalt bond, which is essentially equal in length, 2.495(2) Å. Fe(2)—Fe(2′) is the longest metal–metal bond in **1**, 2.605(2) Å, and compares favourably with the corresponding Fe—Fe bond in **2**, 2.604(2) Å. The sides of the trapezoid in **1**, Fe(1)—Fe(2), are equal in length, 2.532(2) Å, but are significantly shorter, 0.045–

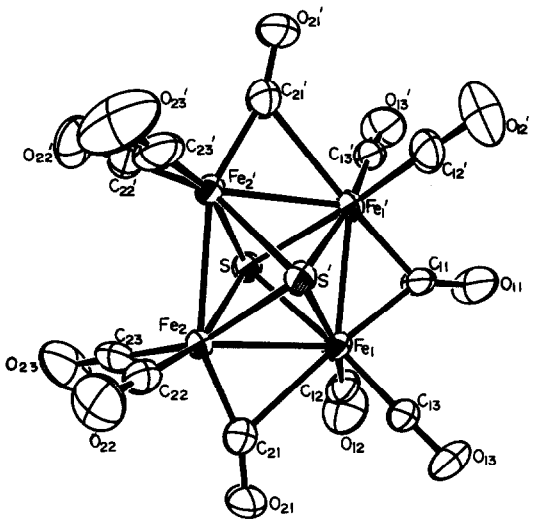

Fig. 1. An ORTEP diagram of $Fe_4(CO)_{10}(\mu\text{-}CO)(\mu_4\text{-}S)_2$ (1) showing 50% probability thermal ellipsoids.

0.048 Å, than the corresponding bonds in **2**, Fe—Co, 2.580(2) and 2.577(2) Å.[9] In both **1** and **2**, these metal–metal bonds contain semi-bridging carbonyl ligands, but the semi-bridging effect is slightly stronger in **1**, Fe(2)—C(21)—O(21) = 161.2(8)°, than in **2**, Fe—C—O = 167(1) and 169(1)°. The metal–sulphur bonds in **1** and **2** are very similar, Fe(1)—S = 2.332(2) Å, Fe(1′)—S = 2.347(2) Å, Fe(2)—S = 2.278(2) Å and Fe(2′)—S = 2.294(2) Å in **1**, and Fe—S = 2.262(3)–2.277(2) Å and Co—S = 2.303(2)–2.329(2) Å in **2**. The non-bonding S···S′ distance in **1** is 2.911(4) Å.

One of the products obtained from the reaction of $Ru(CO)_5$ with $Ru_3(CO)_9(\mu_3\text{-}S)_2$ was $Ru_4(CO)_9(\mu\text{-}CO)_2(\mu_4\text{-}S)_2$.[4] The structure of this compound was determined in the form of the bis-phosphine substituted derivative, $Ru_4(CO)_7(PMe_2Ph)_2(\mu\text{-}CO)_2(\mu_4\text{-}S)_2$ (**3**). The cluster of **3** is similar to that of **1** and **2**, but **3** contains two bridging carbonyl ligands. The Ru—Ru bonds associated with the bridging carbonyl ligands are significantly shorter than the unbridged Ru—Ru bonds.

Compound **1** contains a total of 62 valence electrons. According to the Effective Atomic Number (EAN) rule, it is electron deficient by two electrons, although it does obey the Skeletal Electron Pair (SEP) theory.[14] Compound **2** on the other hand, contains 64 valence electrons and obeys the EAN rule. It was of interest to examine the possibility that the comparative shortness of the Fe(1)—Fe(2) bonds in **1** could be related to its intrinsic unsaturation. These results are described in the following section and are compared with those of Halet *et al.*, who investigated the cluster bonding in the molecules $M_4(CO)_n(\mu_4\text{-}L)_2$ (n = 11, 12) by the extended Hückel method.[15]

In Fig. 2 is shown the coordinate systems used in the calculations. In the coordinate systems about the iron atoms, the z-axis points towards the centre of the Fe_4 trapezoid, the y-axis is tangential to the trapezoid and the x-axis is perpendicular to the Fe_4 plane. The HOMO of compound **1** is primarily of Fe x^2-y^2 character of all four iron atoms with the major portion on the unbridged Fe(2) and Fe(4) atoms (13.5% Fe(2) and Fe(4) x^2-y^2 vs 2.8% Fe(1) and Fe(3) x^2-y^2). It possesses a node through the semi-bridged Fe(1)—Fe(2) and Fe(3)—Fe(4) bonds. The LUMO, 1.88 eV above the HOMO, is very similar to the HOMO of b_u symmetry in Halet's calculations on the cluster $Fe_4(CO)_{12}(\mu\text{-}PH)_2$ (**4**), which contains two more electrons.[15] This orbital is mainly of Fe xz character on all the iron atoms and is antibonding around the Fe_4 ring. It contains slightly more xz character on the bridged Fe(1) and Fe(3) atoms than on the unbridged Fe(2) and Fe(4) atoms (12.3 vs 7.5%). In his calculations on **4**, Halet[15] noted that the HOMO would be stabilized

Table 2. Intramolecular distances for $Fe_4(CO)_{10}(\mu\text{-}CO)(\mu_4\text{-}S)_2$ (1)

Atom	Atom	Distance (Å)	Atom	Atom	Distance (Å)
Fe(1)	C(12)	1.77(1)	Fe(2)	S	2.278(2)
Fe(1)	C(13)	1.79(1)	Fe(2′)	S	2.294(2)
Fe(1)	C(11)	1.93(1)	Fe(2)	Fe(2′)	2.605(2)
Fe(1)	S	2.332(2)	O(11)	C(11)	1.15(2)
Fe(1′)	S	2.347(2)	O(12)	C(12)	1.14(1)
Fe(1)	Fe(1′)	2.489(3)	O(13)	C(13)	1.12(1)
Fe(1)	Fe(2)	2.532(2)	O(21)	C(21)	1.16(1)
Fe(2)	C(23)	1.76(1)	O(22)	C(22)	1.14(1)
Fe(2)	C(22)	1.77(1)	O(23)	C(23)	1.14(1)
Fe(2)	C(21)	1.79(1)	S	S′	2.911(4)

Table 3. Intramolecular bond angles for $Fe_4(CO)_{10}(\mu\text{-}CO)(\mu_4\text{-}S)_2$ (1)

Atom	Atom	Atom	Angle (°)	Atom	Atom	Atom	Angle (°)
C(12)	Fe(1)	C(13)	90.6(4)	C(23)	Fe(2)	Fe(2′)	104.3(3)
C(12)	Fe(1)	C(11)	92.0(4)	C(22)	Fe(2)	C(21)	94.8(4)
C(12)	Fe(1)	S	94.1(3)	C(22)	Fe(2)	S′	92.4(3)
C(12)	Fe(1)	S′	169.1(3)	C(22)	Fe(2)	S	158.2(3)
C(12)	Fe(1)	Fe(1′)	123.0(3)	C(22)	Fe(2)	Fe(1)	133.6(3)
C(12)	Fe(1)	Fe(2)	114.2(3)	C(22)	Fe(2)	Fe(2′)	103.7(3)
C(13)	Fe(1)	C(11)	90.6(3)	C(21)	Fe(2)	S′	104.1(3)
C(13)	Fe(1)	S′	172.0(3)	C(21)	Fe(2)	S	106.7(3)
C(13)	Fe(1)	S	97.5(3)	C(21)	Fe(2)	Fe(1)	63.8(3)
C(13)	Fe(1)	Fe(1′)	123.8(3)	C(21)	Fe(2)	Fe(2′)	152.4(3)
C(13)	Fe(1)	Fe(2)	116.0(3)	S	Fe(2)	S′	79.1(1)
C(11)	Fe(1)	S	95.7(2)	S′	Fe(2)	Fe(1)	58.11(7)
C(11)	Fe(1)	S′	95.2(2)	S′	Fe(2)	Fe(2′)	55.55(7)
C(11)	Fe(1)	Fe(1′)	49.8(3)	S	Fe(2)	Fe(1)	57.53(6)
C(11)	Fe(1)	Fe(2)	141.1(3)	S	Fe(2)	Fe(2′)	54.99(6)
S	Fe(1)	S′	77.0(1)	Fe(1)	Fe(2)	Fe(2′)	88.69(4)
S	Fe(1)	Fe(1′)	58.15(7)	Fe(2)	S	Fe(2′)	69.46(8)
S	Fe(1)	Fe(2)	56.09(6)	Fe(2)	S	Fe(1′)	102.31(9)
S′	Fe(1)	Fe(1′)	57.56(7)	Fe(2)	S	Fe(1)	66.36(7)
S′	Fe(1)	Fe(2)	55.52(6)	Fe(2′)	S	Fe(1′)	66.37(7)
Fe(1′)	Fe(1)	Fe(2)	91.30(4)	Fe(2′)	S	Fe(1)	101.39(9)
C(23)	Fe(2)	C(22)	89.1(4)	Fe(1)	S	Fe(1′)	64.29(8)
C(23)	Fe(2)	C(21)	96.1(4)	O(11)	C(11)	Fe(1)	139.8(3)
C(23)	Fe(2)	S′	159.6(3)	O(11)	C(11)	Fe(1′)	139.8(3)
C(23)	Fe(2)	S	92.1(3)	Fe(1)	C(11)	Fe(1′)	80.4(6)
C(23)	Fe(2)	Fe(1)	131.4(4)	O(12)	C(12)	Fe(1)	178(1)
O(13)	C(13)	Fe(1)	177.3(8)				
O(21)	C(21)	Fe(2)	161.2(8)				
O(22)	C(22)	Fe(2)	179(1)				
O(23)	C(23)	Fe(2)	179(1)				

in the calculations by the addition of *d*-orbitals on the capping phosphorus atom and indeed this is the case for **1**. Our LUMO contains a substantial amount of sulphur *xy* character (7.5%) from each capping sulphur atom.

The calculation on compounds **2** and **2a** (the 2^+ cation of **2**) gave similar orbitals for the HOMO and LUMO of **2a** and the SHOMO and HOMO of **2**, respectively. The HOMO–LUMO gap has shrunk considerably to 0.13 eV for **2a**. Comparing the overlap population between the metal atoms for the three types of metal–metal bonds in the cluster, one can observe the effect of adding two electrons to the M_4 framework. The overlap populations are shown in Table 4. As two electrons are added to **2a** to form **2**, the overlap populations for all three types of metal–metal bonds decrease in value. This is not too surprising since the LUMO of **2a** is antibonding along each metal–metal bond axis. However, the total overlap goes from bonding to antibonding for the semi-bridged Fe—Co bond and the bridged Co—Co bond. The largest decrease in overlap population (0.038) occurs for the bridged Co—Co bond. However, *the metal atoms could be restrained from moving further apart by the bridging carbonyl ligand.* The semi-bridged Fe—Co bonds show a decrease in overlap of 0.026 upon the addition of two electrons. Since semi-bridging ligands are presumably not as supportive as a full bridge, the Fe—Co bonds might be lengthened as a result. The

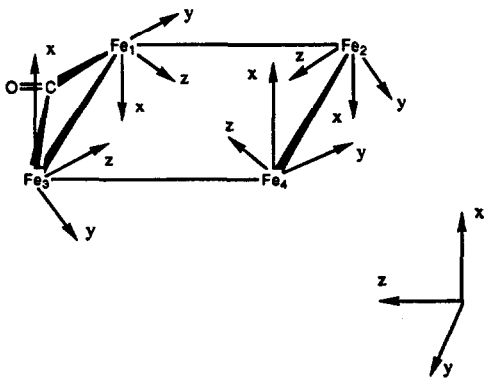

Fig. 2. Molecular and local coordinate systems used in Fenske–Hall calculations on compound **1**.

Table 4. Mulliken overlap populations along the metal–metal bonds of $[Fe_2M_2(CO)_{10}(\mu\text{-}CO)(\mu_4\text{-}S)_2]$ (M = Fe or Co)

Compound	Fe—Fe unbridged	Fe—M semi-bridged	M—M bridged
1 (M = Fe)	0.036	0.016	0.018
2 (M = Co)	0.026	0.017	0.013
2a (M = Co)	0.016	−0.009	−0.025

unbridged Fe—Fe bond shows the smallest decrease in overlap population (0.010) and the overlap is positive for **1**, **2** and **2a**. Thus, bond lengthening effects might remain small on the Fe—Fe bond. We expect that the structural differences between **1** and **2** would be similar to those between **2a** and **2**. This is fully consistent with our observations.

Acknowledgements—This research was supported by the National Science Foundation under Grant No. CHE-8612862 to R.D.A. and by the Robert A. Welch Foundation under Grant No. A-648 to M.B.H. Funds to purchase the VAX 11/780 at Texas A&M University were provided by the National Science Foundation. We wish to thank Professor H. Vahrenkamp for providing us with additional details concerning the structure of **2**.

Supplementary material. Atomic coordinates have been deposited with the Director, Cambridge Crystallographic Data Centre.

REFERENCES

1. R. D. Adams, J. E. Babin and M. Tasi, *Organometallics* 1988, **7**, 503.
2. R. D. Adams, J. E. Babin, M. Tasi and T. Wolfe, *Organometallics* 1987, **6**, 2228.
3. R. D. Adams, J. E. Babin and M. Tasi, *Organometallics* 1987, **6**, 1717.
4. R. D. Adams, J. E. Babin and M. Tasi, *Inorg. Chem.* 1986, **25**, 4514.
5. R. D. Adams, *Polyhedron* 1985, **4**, 2003 and refs therein.
6. H. Vahrenkamp and E. J. Wucherer, *Angew. Chem. Int. Ed. Engl.* 1981, **20**, 680.
7. R. D. Adams and J. E. Babin, *Inorg. Chem.* 1986, **25**, 3418.
8. M. B. Hall and R. F. Fenske, *Inorg. Chem.* 1972, **11**, 768.
9. J. W. Richardson, M. J. Blackman and J. E. Ranochak, *J. Chem. Phys.* 1973, **58**, 3010.
10. (a) E. J. Clementi, *J. Chem. Phys.* 1964, **40**, 1944; (b) E. J. Clementi, *IBM J. Res. Dev.* 1965, **9**, 2.
11. R. F. Fenske and D. D. Radtke, *Inorg. Chem.* 1968, **7**, 479.
12. R. S. Mulliken, *J. Chem. Phys.* 1955, **23**, 1833, 1841.
13. *International Tables for X-ray Crystallography*, Vol. IV. Kynoch Press, Birmingham, U.K. (1975). (a) Table 2.2B, pp. 99–101; (b) Table 2.3.1, pp. 149–150.
14. (a) D. M. P. Mingos, *Acct. Chem. Res.* 1984, **17**, 311; (b) K. Wade, in *Transition Metal Clusters* (Edited by B. F. G. Johnson), Chap. 3. Wiley, Chichester (1980).
15. J. F. Halet, R. Hoffmann and J.-Y. Saillard, *Inorg. Chem.* 1985, **24**, 1695.

Polyhedron Vol. 8, No. 15, pp. 1891–1896, 1989
Printed in Great Britain

0277–5387/89 $3.00 + .00
©1989 Maxwell Pergamon Macmillan plc

PREPARATION OF NOVEL METAL DITHIOCARBAMATE COMPLEXES CONTAINING ω-OH GROUP. STABILIZATION EFFECT OF THE OH GROUP ON THE $HNCS_2$–Mt LINKAGE

RYOKI NOMURA,* SATORU FUJII, AKIHISA TAKABE and HARUO MATSUDA

Department of Applied Chemistry, Faculty of Engineering, Osaka University, Yamada-Oka, Suita, Osaka 565, Japan

(*Received* 1 *September* 1988; *accepted after revision* 20 *February* 1989)

Abstract—The direct condensation between metal oxide powders (Zn^{II}, In^{III}, Sb^{III} and Bi^{III}) and dithiocarbamic acids, prepared by the reaction of ethanolamine or 1,3-propanolamine with CS_2, gave corresponding metal dithiocarbamate complexes in good yields. Although antimony and bismuth dithiocarbamates decomposed up to 80°C to give elimination products such as oxazolidine-2-thione, thiazolidine-2-thione or bis(3-hydroxypropyl)thiourea, the zinc and indium derivatives were recovered after heating in benzene at 80°C for 6 h. In the reactions of organometallic oxides such as Bu_2SnO, $BuSnO_2H$ and Ph_3SbO with the dithiocarbamic acids, the elimination products were directly obtained even at 20°C.

Metal dithiocarbamate complexes are an important class of compounds, especially in analytical and coordination chemistry, and the dithiocarbamates are generally prepared by metathesis or insertion reactions.[1,2] Recently, some newer methods of preparation using metal powders,[3] rods or foils[4] instead of metal salts have been developed. However, these routes, together with the conventional methods, are still limited to the preparation of simple dialkyldithiocarbamates.

Recently, we have proposed a facile synthesis of antimony dithiocarbamate complexes.[5–7] The reaction consisted of direct condensation between the metal oxide and dithiocarbamic acids, without the use of alkaline and/or acidic conditions. Thus, dithiocarbamates which have labile functional groups can now be prepared. In this paper, we describe attempts to extend the direct condensation method to metal derivatives other than antimony, especially for the hydroxyl-substituted dithiocarbamate complexes of main group elements.

EXPERIMENTAL

General

Melting points are uncorrected. IR and NMR spectra were recorded on a Hitachi 260-30 spectrophotometer and a Hitachi R90H FT spectrometer, respectively. Metal oxides (ZnO, In_2O_3, SnO, SnO_2, $(Bu_3Sn)_2O$, Bu_2SnO, $BuSnO_2H$, Sb_2O_3, Bi_2O_3 and TeO_2) were from commercial sources and used without further purification. Amorphous triphenylstibine oxide was prepared by means of the H_2O_2 oxidation method[8] (m.p. 285°C, ref. 9 285–290°C).

Reaction of metal oxides with (ω-hydroxyalkyl) dithiocarbamic acids

Into a suspension of metal oxides (5 mmol) in methanol (20 cm^3), prescribed amounts of aminoalcohols and CS_2 were added dropwise in this order at 0°C. The mixture was then stirred for 5 h at room temperature, filtered off and the filtrate was evaporated *in vacuo* to dryness. The residue was dissolved in MeOH–acetonitrile and the metal dithiocarbamates were crystallized by cooling. Certain metal oxides as well as organometallic oxides directly gave elimination products such as 1,3-thiazolidine-2-thiones (**I**), 1,3-oxazolidine-2-thiones (**II**), or 1,3-bis(3-hydroxypropyl)thiourea (**III**) (Scheme 1).

1,3-*Thiazolidine*-2-*thione* (**Ia**)

Recrystallized from chloroform. Melting point 104.5–106°C (ref. 10 105.5–107°C). ^{13}C NMR

* Author to whom correspondence should be addressed.

($CDCl_3$): δ 33.6(t, SCH_2), 51.3 (t, NCH_2), 201.5 (s, C=S).

1,3-*Oxazolidine-2-thione* (**IIa**)

Recrystallized from chloroform. Melting point 97.5–98.9°C (ref. 11 97–99°C). ^{13}C NMR (DMSO-d_6): δ 43.7 (t, NCH_2), 69.7 (t, OCH_2), 188.4 (s, C=S).

3-*Methyl*-1,3-*thiazolidine*-2-*thione* (**IIb**)

Recrystallized from EtOH–hexane.[5] Melting point 66–68°C (ref. 12 69.5–70.5°C).

3-*Methyl*-1,3-*oxazolidine*-2-*thione* (**IIb**)

Recrystallized from benzene–hexane.[5] Melting point 29–30°C (ref. 13 27–28.5°C).

1,3-*Bis*(3-*hydroxypropyl*)*thiourea* (**III**)

Recrystallized from MeOH–ethyl acetate. Melting point 94–94.5°C (ref. 14 90.4–91°C). ^{13}C NMR (CD_3OD): δ 33.0 (qn, $CH_2CH_2CH_2$), 42.2 (t, CH_2N), 60.3 (t, CH_2OH), 182.6 (S, C=S).

Thermal decompositions

Dithiocarbamates (10 mmol) and methanol (20 cm^3) were placed in a 20 cm^3 glass tube which was set into a 30 cm^3 stainless steel autoclave (SUS 304, Taiatsu Garasu Kogyo Co., Tokyo, TVS-1 type). The reactor was then heated at 80°C for 6 h. After cooling, the mixtures were filtered off. The filtrates were evaporated and chromatographed on silica gel (Wako C-200, eluted by chloroform). Metal sulphide residues were washed several times with MeOH and benzene and dried *in vacuo*.



I **II**

$HO(CH_2)_3NHCNH(CH_2)_3OH$ (S)

III

n	R	
2	H	**a**
2	Me	**b**
3	H	**c**

Scheme 1.

RESULTS AND DISCUSSION

First of all, we investigated the direct condensation using dithiocarbamic acids prepared from N-methylethanolamine and CS_2, and the results obtained are summarized in Table 1. Thus, it was found that N-hydroxyethyl-N-methyldithiocarbamate could be obtained from the oxides of zinc, indium, antimony and bismuth, and two organotin oxides, similarly to dialkyldithiocarbamates.[6] However, tin(II and IV) and tellurium oxides did not react with the dithiocarbamic acids and they were quantitatively recovered. Melting points and analytical and selected spectral data of the isolated dithiocarbamates are shown in Table 2. It should be pointed out that melting points of these hydroxy-substituted dithiocarbamate complexes were lower than those of dialkyl derivatives. For example, melting points of diethyldithiocarbamates of zinc(II), antimony(III) and bismuth(III) are reported as follows: 181.5–182.0,[15] 133–135[6] and 193–195°C,[16] respectively.

The introduction of a β-hydroxyl group could form weak hydrogen bonding with the CS_2 moiety and greatly affect the ν(C—N) and $\delta(N^{13}CS_2)$ as reported previously.[7] Namely, $\delta(N^{13}CS_2)$ of these hydroxyl-substituted dithiocarbamates lie at lower fields than those of diethyl derivatives by 1–5 ppm. In addition, their ν(C—N) bands split into a doublet or showed a slightly higher wave number shift.

Table 1. Reaction of metal oxides with ω-hydroxyalkyldithiocarbamic acids[a]

MtO	Mole ratio[b] n	Yields of Mt(dtc)$_n$[c] EA	MEA	PA
ZnO	2	55	68	41
In_2O_3	3	93	92	nr[d]
Bu_2SnO	2	(99)[e]	93	94
$BuSnO_2H$	3	(69)[e]	72	(41)[f]
Sb_2O_3	3	77	99	82
Ph_3SbO	2	(32)[e]	(92)[g]	(31)[f]
Bi_2O_3	3	94	82	62
TeO_2	4	(42)[e]	nr[d]	(33)[f]

[a] Metal oxides (5 mmol), aminoalcohols (5 × n mmol), methanol (20 cm^3), room temperature, 6 h.

[b] Dithiocarbamic acids–MtO.

[c] EA, $HNCH_2CH_2OH$; MEA, $N(CH_3)CH_2CH_2OH$; PA, $HNCH_2CH_2CH_2OH$.

[d] Ammonium dithiocarbamates were recovered.

[e] **IIa** was obtained.

[f] **III** was obtained.

[g] **IIb** was obtained.

Table 2. Analytical and spectral data of metal dithiocarbamate complexes

$Mt(dtc)_n$[a]	Melting point (°C)	Found C	Found H	Found N	Calculated C	Calculated H	Calculated N	Formula	IR[b] ν(C—N)	$\delta(N^{13}CS_2)$[b,c]
$Zn(EAdtc)_2$	128–131	21.0	4.1	8.3	21.3	3.6	8.3	$C_6H_{12}N_2O_2S_4Zn$	1515	205.0
$Zn(MEAdtc)_2$	126–127.5	26.6	4.7	7.4	26.3	4.4	7.7	$C_8H_{16}N_2O_2S_4Zn$	1510	203.7
$Zn(PAdtc)_2$	Oil	26.8	4.7	7.4	26.3	4.4	7.7	$C_8H_{16}N_2O_2S_4Zn$	1500	204.9
$In(EAdtc)_3$	110	20.1	3.7	7.7	20.7	3.5	8.0	$C_9H_{18}N_3O_3S_6In$	1520	201.4
$In(MEAdtc)_3$	145	24.7	4.2	7.1	25.5	4.3	7.4	$C_{12}H_{24}N_3O_3O_6In$	1505	—[d]
$Bu_2Sn(MEAdtc)_2$	94.0–94.5	35.9	6.4	5.1	36.0	6.4	5.3	$C_{16}H_{34}N_2O_2S_4Sn$	1490	201.8[e]
$BuSn(MEAdtc)_3$	145–147.5	30.6	5.4	6.7	30.7	5.3	6.7	$C_{16}H_{33}N_3O_3S_6Sn$	1485	198.4
$Sb(EAdtc)_3$	Oil	20.3	3.4	7.9	20.4	3.4	7.9	$C_9H_{18}N_3O_3S_6Sb$	1500	210.6
$Sb(MEAdtc)_3$	136–139	24.8	4.3	7.2	25.3	4.2	7.3	$C_{12}H_{24}N_3O_3S_6Sb$	1492, 1486	198.2
$Sb(PAdtc)_3$	Oil	25.4	4.7	7.4	25.3	4.2	7.3	$C_{12}H_{24}N_3O_3S_6Sb$	1510	203.6
$Bi(EAdtc)_3$	85–88	17.6	3.0	6.8	17.5	2.9	6.8	$C_9H_{18}N_3O_3S_6Bi$	1515, 1485	207.6
$Bi(MEAdtc)_3$	Oil	20.9	3.6	6.5	21.8	3.7	6.4	$C_{12}H_{24}N_3O_3S_6Bi$	1485	205.4
$Bi(PAdtc)_3$	Oil	21.3	3.6	6.6	21.8	3.7	6.4	$C_{12}H_{24}N_3O_3S_6Bi$	1490	209.4

[a] See footnote *c* in Table 1.

[b] Values of ν(C—N) and $\delta(N^{13}CS_2)$ for ammonium dithiocarbamates were as follows: EA (1490, 213.3), MEA (1460, 212.0), PA (1480, 213.0); (cm^{-1}, ppm).

[c] In Me_2SO-d_6 unless otherwise noted, concentration, *ca* 10 wt%.

[d] Not detected.

[e] In $CDCl_3$.

These phenomena could be explained by an increase of unequivalency in the two C—S bonds, in other words, an increase in the anisobidenticity.[17]

Generally, it is known that monoalkyldithiocarbamate complexes of heavy metals are thermally labile and are frequently converted into the corresponding alkyl isothiocyanates and metal sulphides *in situ*.[18,19] In our preliminary investigations, the reactions of metal oxides (Zn, In, Sn, Sb, Bi, and Te) with dithiocarbamic acids prepared from monoalkylamines such as ethyl- and butylamine, gave isothiocyanate as the sole product even at −15 to −10°C and no dithiocarbamate was obtained. However, the introduction of a hydroxyl group at the end of the alkyl chains stabilizes such labile mono-substituted dithiocarbamate complexes and they could be isolated from several metal oxides such as zinc, indium, antimony and bismuth in moderate to good yields. Their yields and physical properties are also shown in Tables 1 and 2. In our consideration, the success of isolation of the monosubstituted dithiocarbamate complexes was due to hydrogen bonding between the NCS_2 fragment and the hydroxyl group at the β- or γ-positions.

$$Mt^nO_{n/2} + nHS_2CNHR \longrightarrow Mt(S_2CNHR)_n + n/2H_2O$$

$$R = CH_2CH_2OH,\ CH_2CH_2CH_2OH.$$

The mono-substituted dithiocarbamates obtained were characterized by their ν(C—N) and $\delta(N^{13}CS_2)$ values, which were slightly higher than 1500 cm^{-1} and 200 ppm, respectively. Based on the empirical correlation between δ and ν applied to the NCS_2 fragment reported by van der Linden *et al.*,[17] the high values of δ could be explained by an increase of π-bond order in the whole NCS_2 fragment. Namely, an interaction between the end hydroxyl and one of two sulphur atoms in the CS_2 moiety promoted the delocalization of the unshared electron pair in the nitrogen atoms without a decrease in the anisobidenticity of the CS_2 moiety; namely a slight decrease of their chelation abilities. Then ν(C—N) and $\delta(N^{13}CS_2)$ values appeared at higher positions. Thus, hydrogen bonding by a hydroxyl group can be said to stabilize the NCS_2 fragment. If the intramolecular hydrogen bonding was absent, intermolecular hydrogen bonding using N—H might accelerate the elimination of isothiocyanates.[1]

The effect of chelation was also justified by the observation of ^{119}Sn NMR spectra of two organotin dithiocarbamates as shown in Table 3. In general, it is well known that δ^{119}Sn can be used to estimate the coordination number of the tin atoms. Namely, the δ^{119}Sn value lies at higher fields with an increase of coordination number. For example, δ^{119}Sn lies between −125 and −515 ppm for six-coordinated complexes[20] and between −340 and −790 ppm for seven-coordinated ones.[21] Thus, it could be found that $Bu_2Sn(S_2CN(CH_3)CH_2CH_2OH)_2$ (δ^{119}Sn = −333.6) and $BuSn(S_2CN(CH_3)CH_2CH_2OH)_3$ (δ^{119}Sn = −767.7) existed as six- and seven-coordinated complexes, respectively, like their dialkyl dithiocarbamate analogues.[20-22] However, the values of their δ^{119}Sn were slightly smaller than those of dialkyldithiocarbamates, in the range of 6 and 19 ppm, respectively. These shifts were considered to result from a decrease in the coordination number around the tin atoms to a small extent by the interaction from the end hydroxyl moieties.

Dithiocarbamates as a precursor for heterocycles

The heterocycles containing thione groups such as oxazolidinethiones and oxazinethiones are useful as pharmaceutics and their synthetic precursors.[23-25] Usually, they are prepared from aminoalcohols and CS_2, however, it is known that strong basic and/or reflux conditions are necessary.[26-28] Some modifications were made by using

Table 3. ^{13}C and ^{119}Sn NMR data

Compounds[a]	$\delta(^{13}C)$Bu ($^1J_{^{119}Sn-^{13}C}$, Hz)			$\delta(^{119}Sn)$ ($^2J_{^{119}Sn-^{13}C}$, Hz)[b]
	α	β	γ	
$Bu_2Sn(MEAdtc)_2$[c]	34.0 (608)	28.3 (40)	26.1 (120)	−333.6 (85.2)
$BuSn(MEAdtc)_3$[d]	49.0	26.9 (39)	22.9 (124)	−767.7 (135.2)

[a] See footnote *c* in Table 1.
[b] Me_4Sn as an external standard was used ($\delta(Me_4Sn) = 0$).
[c] $CDCl_3$ solution, 21 wt%.
[e] Me_2SO-d_6 solution, 18 wt%.

organotin aminoalkoxides[12,13] or thiophosgene[29] in place of aminoalcohols and CS_2, respectively.

Organometallic oxides such as Bu_2SnO, $BuSnO_2H$ and Ph_3SbO and tellurium oxide, selectively gave **IIa** in the reactions of ethanolamine and CS_2 under mild conditions, in spite of the formation of corresponding thiazolidine ring. Thus, it can be said that these metallic oxides are useful accelerators for the ring closure into **IIa**. The cyclization was considered to occur through the formation of the dithiocarbamates and successive elimination of **IIa** *in situ*.

In contrast, the isolated dithiocarbamate complexes seemed to be stable. Although thermal decomposition of them in methanol solution at 80°C was carried out, the breakdown of the dithiocarbamate linkage did not occur in the zinc and indium dithiocarbamates. The antimony and bismuth derivatives decomposed but gave complex mixtures of products. The pyrolysates isolated are summarized in Table 4.

In general, dithiocarbamates of primary amines are known to be easily converted into isothiocyanates and are sometimes unable to be isolated.[18,19] However, in these cyclizations, no isothiocyanate was detected by NMR, IR and GLC analyses of the reaction mixture. Thus, we considered that the cyclization proceeded via nucleophilic attack of the end hydroxyl group at the centre carbon of CS_2 moieties, by a concerted mechanism with elimination. Thus, it can be said that these dithiocarbamates should resist the elimination of hydroxyethyl isothiocyanate. In contrast, the reaction of propanolamine gave the symmetrical thiourea. Although it is reported that the formation of hydroxypropyl isothiocyanate must be followed by the cyclization into tetrahydro-1,3-oxazine-2-thione,[14] the formation of thiourea in our reactions preceded by the elimination of the corresponding 3-hydroxypropyl isothiocyanate, because similar formation of a symmetrical thiourea via aryl isothiocyanates was reported in the pyrolysis of the organometallic aryldithiocarbamates.[30]

In conclusion, attributable to the stabilization of the labile $HNCS_2$ fragment by the hydrogen bonding from β- or γ-hydroxyl, dithiocarbamate complexes possessing the NH moiety could be isolated. The chelation also significantly affected the course of succeeding eliminations from the dithiocarbamate complexes. Thus, chelation of the hydroxyl at the β-position was preferable to cyclization–elimination, while chelation of the γ-hydroxyl disturbed the cyclization and promoted the formation of the isothiocyanate.

Table 4. Thermal decomposition of isolated metal dithiocarbamate complexes[a]

$Mt(dtc)_n$[b]	Product (%)
$Zn(EAdtc)_2$	[c]
$In(EAdtc)_3$	[c]
$Sb(EAdtc)_3$	**Ia** (26), **IIa** (31)
$Bi(EAdtc)_3$	**Ia** (24), **IIa** (20)
$Zn(EAdtc)_2$	[c]
$In(EAdtc)_3$	[c]
$Bu_2Sn(MEAdtc)_2$[d]	[c]
$Sb(MEAdtc)_3$	**Ib** (80), **IIb** (14)[e]
$Bi(MEAdtc)_3$	**Ib** (69)
$Zn(PAdtc)_2$	**III** (37)
$Bu_2Sn(PAdtc)_2$	**III** (42)
$Sb(PAdtc)_3$	**III** (21)
$Bi(PAdtc)_3$	**III** (44)

[a] Conditions; $Mt(dtc)_n$ (10 mmol), MeOH (20 cm^3), 80°C, 6 h in a stainless steel autoclave.

[b] See footnote *c* in Table 1.

[c] No reaction occurred and starting dithiocarbamates were recovered.

[d] Crude dithiocarbamate was employed.

REFERENCES

1. G. D. Thorn and R. A. Ludwig, *The Dithiocarbamates and Related Compounds*, pp. 7–56. Elsevier, Amsterdam (1962).
2. P. Coucouvanis, *Prog. Inorg. Chem.* 1979, **22**, 301.
3. T. Tetsumi, M. Sumi, M. Tanaka and T. Shono, *Polyhedron* 1986, **5**, 707.
4. C. Geloso, R. Kumar, J. R. Lopez-Grado and D. G. Tuck, *Can. J. Chem.* 1987, **65**, 928.
5. R. Nomura, M. Kori and H. Matsuda, *Chem. Lett.* 1985, 580.
6. R. Nomura, A. Takabe and H. Matsuda, *Chem. Express.* 1986, **1**, 375.
7. R. Nomura, A. Takabe and H. Matsuda, *Polyhedron* 1987, **6**, 411.
8. D. L. Venezky, C. W. Sink, B. A. Nevett and W. F. Fortescue, *J. Organomet. Chem.* 1972, **35**, 131.
9. J. Burdoner, G. O. Doak and T. S. Evett, *J. Am. Chem. Soc.* 1986, **108**, 4206.
10. A. A. Rosen, *J. Am. Chem. Soc.* 1952, **74**, 2994.
11. F. Feuloyp, G. Csiriny and G. Benath, *Synthesis* 1985, 1149.
12. S. Sakai, T. Fujinami and Y. Ishii, *J. Oganomet. Chem.* 1973, **50**, 113.
13. S. Sakai, Y. Asai, Y. Kiyohara, K. Itoh and Y. Ishii, *Organomet. Chem. Synth.* 1970/1971, **1**, 45.
14. A. F. McKay and M. E. Kreling, *Can. J. Chem.* 1962, **40**, 205.
15. M. Yamashita, M. Teranishi, R. Igarashi and J. Niwa, *Nippon Kagaku Kai-Shi* 1980, 1723.
16. G. E. Manoussakis and P. Karayannidis, *Inorg. Nucl. Chem. Lett.* 1970, **6**, 71.

17. H. L. M. van Gaal, J. W. Diesveld, F. W. Pljpers and J. G. M. van der Linden, *Inorg. Chem.* 1979, **18**, 3251.
18. F. B. Davis, R. Q. Brewster and C. P. Olander, *Org. Synth. Coll.* 1948, **1**, 447.
19. T. Yamashita, I. Okuda and H. Sugiyama, *J. Synth. Org. Chem. Jpn* 1978, **36**, 12.
20. J. Otera, *J. Organomet. Chem.* 1981, **221**, 273.
21. J. Otera, A. Kusaba, T. Hinoishi and Y. Kawasaki, *J. Oganomet. Chem.* 1982, **228**, 223.
22. T. Mitchell, *J. Organomet. Chem.* 1973, **59**, 189.
23. E. Belgodere, R. Bossio, R. Ceucioni, S. Marcaccini and R. Pepino, *J. Heterocycl. Chem.* 1984, **21**, 1241.
24. D. Hoppe and R. Follmann, *Chem. Ber.* 1976, **109**, 3047.
25. A. K. Agrawal, S. S. Parmar, C. Dwivedi and R. D. Harbison, *J. Pharm. Sci.* 1977, **66**, 887.
26. M. Chanon, F. Chanon and J. Metzger, *J. Chem. Soc., Chem. Commun.* 1974, 425.
27. M. G. Etllinger, *J. Am. Chem. Soc.* 1950, **72**, 4792.
28. A. Kjaer and R. B. Jensen, *Acta. Chem. Scand.* 1958, **12**, 1746.
29. T. Mukaiyama, I. Kuwajima and K. Mizui, *J. Org. Chem.* 1966, **31**, 32.
30. E. J. Kupchik and C. T. Theisen, *J. Organomet. Chem.* 1968, **11**, 627.

Polyhedron Vol. 8, No. 15, pp. 1897–1901, 1989
Printed in Great Britain

0277–5387/89 $3.00+.00
© 1989 Maxwell Pergamon Macmillan plc

LIGAND-PAIR FORMATION IN THE PSEUDO-COMPLEX OF 1-(SALICYLIDENEIMINO)-2-METHOXYBENZENE AND TRIPHENYLTIN ISOTHIOCYANATE

J-P. CHARLAND and E. J. GABE

Chemistry Division, N.R.C., Ottawa, Ontario K1A 0R6, Canada

and

L. E. KHOO

School of Chemical Sciences, Universiti Sains Malaysia, Penang, Malaysia

and

F. E. SMITH*

Chemistry Department, Laurentian University, Sudbury, Ontario P3E 2C6, Canada

(*Received* 14 *December* 1988; *accepted* 20 *February* 1989)

Abstract—Triphenyltin isothiocyanate and 1-(salicylideneimino)-2-methoxybenzene (L) form a pseudo-complex of formula $L_2Ph_3SnNCS \cdot HNCS$. The crystal and molecular structures of this compound are reported. The crystals are monoclinic, space group $I2/a$, $a = 10.9050(10)$, $b = 24.6527(16)$, $c = 16.2251(10)$ Å, $\beta = 95.208(7)°$, $V = 4343.91$ Å^3, $Z = 4$, $D_{calc} = 1.409$ Mg m^{-3}, $\mu = 0.70$ mm^{-1}, $F(000) = 1172$, final $R = 0.041$ for 2858 unique observed reflections. The X-ray crystal structure shows the compound to consist of protonated ligand pairs $[L_2H]^+$ co-crystallizing with a five-coordinate organotin moiety of formula $[Ph_3Sn(NCS)_2]^-$. The ligand dimers are held together by hydrogen bonds. The organotin anion is trigonal bipyramidal, with the phenyl groups arranged equatorially and the thiocyanato groups occupying the axial positions.

In our studies of the triorganotin complexes of some potentially bidentate Schiff bases, we have recently published[1,2] the structures of complexes having stoichiometric ratios of ligand–triorganotin of 1 : 1 and 3 : 2.

We now wish to report the crystal and molecular structure of the triphenyltin isothiocyanate complex of 1-(salicylideneimino)-2-methoxybenzene (L) (see Structure 1) in which the ligand–triphenyltin ratio is 2 : 1.

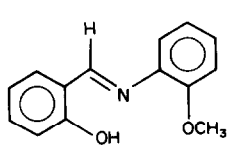

Structure 1. 1-(Salicylideneimino)-2-methoxybenzene (L).

* Author to whom correspondence should be addressed.

EXPERIMENTAL

The reagents triphenyltin chloride, salicylaldehyde and 2-methoxyaniline were obtained commercially and used without further purification. Triphenyltin isothiocyanate (m.p. 168–170°C) was prepared by the literature method[3] and recrystallized from benzene before use. The Schiff base was prepared by the condensation of salicylaldehyde and 2-methoxyaniline in refluxing benzene, the water formed being removed azeotropically. The ligand was purified by recrystallization from 95% ethanol. The complex was prepared by refluxing the calculated amount (for 2 : 1 complex formation) of ligand and triphenyltin isothiocyanate in 95% ethanol for 30 min. The complex crystallized when the solution was cooled in a freezer overnight. It was filtered off and recrystallized from ethanol (m.p. 170–172°C).

X-ray studies

A summary of the crystal data for $[L_2H]^+[Ph_3Sn(NCS)_2]^-$ is given in Table 1. Intensity data were collected at 295 K using graphite monochromatized Mo-K_α radiation on an automated Picker 4-circle diffractometer using the θ–2θ scanning mode with profile analysis[4] at a scan speed of 4° min^{-1}. Three standards were measured after every 100 reflections and no significant decay was detected. The intensity data showed systematic absences consistent with the space groups *Ia* and *I2/a*. The structure was solved and refined successfully in the centrosymmetric space group *I2/a*. The unit cell parameters listed in Table 1 were obtained by a least-squares refinement of the setting angles for 44 reflections ($25° \leqslant 2\theta \leqslant 35°$). The intensity data were corrected for Lorentz and polarization factors, but not for absorption.

The structure was solved with MULTAN[5] plus a difference Fourier map and refined by full-matrix least-squares with the weighting scheme: $w^{-1} = o(F_o)^2 + (0.0002(F_o)^2$.

All heavier atoms were refined anisotropically and hydrogen atoms isotropically. All calculations were performed with the NRCVAX crystal structure programs.[6] Scattering factors were taken from the *International Tables for X-ray crystallography*.[7] The bond lengths and angles are given in Table 2.

RESULTS AND DISCUSSION

It appears to be extremely difficult to coax the triorganotin halides and pseudo-halides to take up six-coordinate configurations on complex formation, regardless of the nature of the ligand involved. The 1 : 1 complexes are trigonal bipyramidal, even with potentially bi- and tridentate ligands, as a result of the adoption of some fascinating stereochemical alternatives.[1,8–12] The recently-reported isolation of a 3 : 2 triorganotin complex with a

Table 1. Crystal data for $[L_2H]^+[Ph_3Sn(NCS)_2]^-$

Parameter	Value
Empirical formula	$C_{48}H_{42}N_4O_4S_2Sn$
Formula weight	921.69
Crystal dimensions (mm)	$0.05 \times 0.10 \times 0.35$
Space group	Monoclinic, *I* 2/*a*
a (Å)	10.905(1)
b (Å)	24.6527(16)
c (Å)	16.225(1)
β (°)	95.21(1)
Z(molecules/cell)	4
F(000)	1171.81
Cell volume (Å^3)	4343.9
D_{calc} (g cm^{-3})	1.409
μ (mm^{-1})	0.70
λ(Mo-K_α) (Å)	0.70930
$2\theta_{max}$	44.9
Number of reflections measured	2913
Number of unique reflections	2858
Number of reflections with $I_{net} > 2.5\sigma(I_{net})$	1844
Last least-squares cycle calculated with	53 atoms 351 parameters 1844 reflections
R_f (significant reflections)	0.041
R_w (significant reflections)	0.040
R_f (all reflections)	0.088
R_w (all reflections)	0.046
Goodness-of-fit	1.288
Maximum Δ/σ	0.252
Last *D*-map	
deepest hole (e Å^{-3})	−0.480
highest peak (e Å^{-3})	0.370

Table 2. Bond lengths (Å) and angles (°) (non-hydrogen atoms only)

Sn—N(1)	2.290(5)	C(5)—C(6)	1.343(14)
Sn—N(1)′	2.290(5)	C(8)—C(9)	1.371(12)
Sn—C(15)	2.123(9)	C(8)—C(13)	1.383(12)
Sn—C(19)	2.127(6)	C(9)—C(10)	1.378(13)
Sn—C(19)′	2.127(6)	C(10)—C(11)	1.360(16)
S—C(25)	1.619(7)	C(11)—C(12)	1.341(19)
O(1)—O(1)″	2.446(9)	C(12)—C(13)	1.386(14)
O(1)—C(1)	1.314(10)	C(15)—C(16)	1.361(10)
O(2)—C(9)	1.352(10)	C(15)—C(16)′	1.361(10)
O(2)—C(14)	1.427(13)	C(16)—C(17)	1.358(14)
N(1)—C(25)	1.140(9)	C(17)—C(18)	1.361(13)
N(2)—C(7)	1.296(13)	C(18)—C(17)′	1.361(13)
N(2)—C(8)	1.419(10)	C(19)—C(20)	1.367(11)
C(1)—C(2)	1.407(11)	C(19)—C(24)	1.398(10)
C(1)—C(6)	1.403(13)	C(20)—C(21)	1.378(14)
C(2)—C(3)	1.401(13)	C(21)—C(22)	1.367(16)
C(2)—C(7)	1.396(12)	C(22)—C(23)	1.366(15)
C(3)—C(4)	1.343(18)	C(23)—C(24)	1.387(12)
C(4)—C(5)	1.389(17)		

N(1)—Sn—N(1)′	176.83(24)	N(2)—C(8)—C(9)	118.4(7)
N(1)—Sn—C(15)	91.58(17)	N(2)—C(8)—C(13)	120.9(8)
N(1)—Sn—C(19)	88.86(23)	C(9)—C(8)—C(13)	120.7(8)
N(1)—Sn—C(19)′	89.67(23)	O(2)—C(9)—C(8)	115.7(7)
N(1)′—Sn—C(15)	91.78(17)	O(2)—C(9)—C(10)	125.9(8)
N(1)′—Sn—C(19)	89.67(23)	C(8)—C(9)—C(10)	118.5(8)
N(1)′—Sn—C(19)′	88.86(23)	C(9)—C(10)—C(11)	120.8(10)
C(15)—Sn—C(19)	117.71(17)	C(10)—C(11)—C(12)	120.9(9)
C(15)—Sn—C(19)′	117.71(17)	C(11)—C(12)—C(13)	120.1(10)
C(19)—Sn—C(19)′	124.59(24)	C(8)—C(13)—C(12)	119.0(10)
O(1)″—O(1)—C(1)	115.0(4)	Sn—C(15)—C(16)	121.3(5)
C(9)—O(2)—C(14)	117.3(7)	Sn—C(15)—C(16)′	121.3(5)
Sn—N(1)—C(15)	150.9(5)	C(16)—C(15)—C(16)′	117.4(9)
C(7)—N(2)—C(8)	129.1(7)	C(15)—C(16)—C(17)	122.1(9)
O(1)—C(1)—C(2)	119.7(7)	C(16)—C(17)—C(18)	118.9(10)
O(1)—C(1)—C(6)	123.1(7)	C(17)—C(18)—C(17)′	120.6(12)
C(2)—C(1)—C(6)	117.2(8)	Sn—C(19)—C(20)	122.8(6)
C(1)—C(2)—C(3)	118.9(8)	Sn—C(19)—C(24)	119.9(5)
C(1)—C(2)—C(7)	123.5(8)	C(20)—C(19)—C(24)	117.2(7)
C(3)—C(2)—C(7)	117.5(8)	C(19)—C(20)—C(21)	121.5(8)
C(2)—C(3)—C(4)	123.1(10)	C(20)—C(21)—C(22)	121.3(9)
C(3)—C(4)—C(5)	116.8(10)	C(21)—C(22)—C(23)	118.4(9)
C(4)—C(5)—C(6)	123.0(11)	C(22)—C(23)—C(24)	120.8(9)
C(1)—C(6)—C(5)	120.8(10)	C(19)—C(24)—C(23)	120.8(8)
N(2)—C(7)—C(2)	125.7(8)	S—C(25)—N(1)	179.5(6)

′ $3/2-x, y, -z$.
″ $3-x, 1-y, 1-z$.

potentially bidentate ligand held promise of an increase in the coordination number of the tin, but the structure[2] showed that this complex too, was five-coordinate, with the ligand behaving as unidentate and the excess ligand co-crystallizing with the complex in the ratio of one free ligand molecule to every two of the organotin complex units. The isolation of the title compound, which has a 2:1 (ligand–triphenyltin) ratio, led us to hope that this time the coordination around the tin might be different. In fact, in a previous report[13] of some 2:1 (ligand–triphenyltin pseudo-halide) complexes, it has indeed been suggested that the tin atom displays an octahedral geometry. However, in the present instance, the results of the X-ray study show that the tin atom once again adopts a five-coordinate

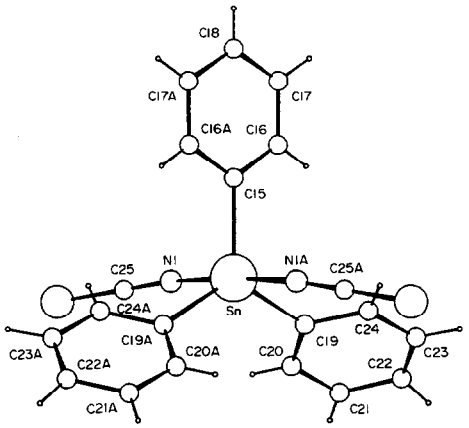

Fig. 1. The five-coordinate organotin anion.

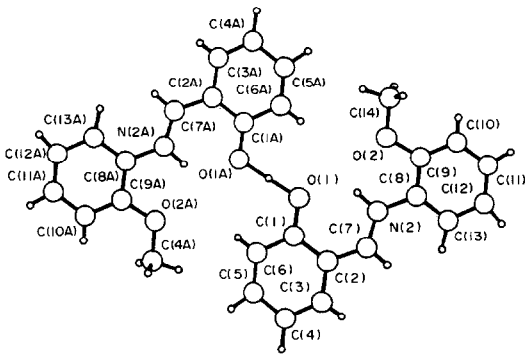

Fig. 2. Cationic ligand dimer.

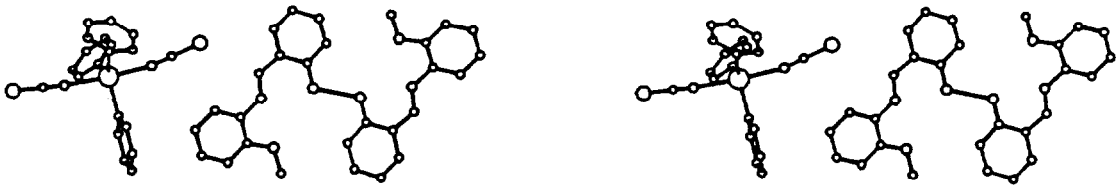

Fig. 3. Stereo pair showing the alignment of the organotin anion and the cationic ligand dimer.

configuration, but with an unusual ionic structure for the complex, consisting of cationic protonated ligand pairs $[L_2H]^+$ co-crystallizing with five-coordinate organotin anions with formula $[Ph_3Sn(NCS)_2]^-$. The ligand dimers are held together by hydrogen bonds between the phenolic oxygen atoms. The organotin anion is trigonal bipyramidal, with the phenyl groups arranged equatorially and the thiocyanato groups occupying the axial positions. The atomic numbering scheme and the structures of the organotin anion and the cationic ligand pair are shown in Figs 1 and 2, respectively. Figure 3 shows the relative alignment of the organotin and ligand-pair species.

In the five-coordinate organotin anion, there is a two-fold symmetry axis passing through Sn, C(15), C(18) and H(18). In this anion, the C—Sn—C angles between the three phenyl rings are 117.9, 117.9 and 124.3°, while the N—Sn—N angle is 176.8°, showing only very slight deviation from trigonal bipyramidal geometry around the tin atom. The average Sn—C(Ph) distance of 2.12 Å is within the range of Sn—C(Ph) distances (2.105–2.16 Å) reported in the literature.[14] The C—C bond lengths in the phenyl groups are all normal. The NCS groups are virtually linear, with NCS angles of 179.7°. The Sn—N distances of 2.307 Å, the C—S bond lengths of 1.606 Å and the N—C bond lengths of 1.137 Å are all similar to those found in isothiocyanatotriphenyl(pyridinium-2-carboxylato)-tin(IV) monohydrate[15] and other metal isothiocyanato complexes.[16–18]

The Schiff base molecules dimerize to form cationic ligand pairs, with an effectively planar structure. In these dimers, which contain one extra proton, both imine nitrogen atoms are protonated. The additional hydrogen atom is situated between the two phenolic oxygen atoms, where the very short O(1)—O(1′) distance of 2.444(9) Å indicates the presence of a hydrogen bond.[19]

This most unusual structure once again demonstrates the reluctance of triorganotin isothiocyanato complexes to adopt a six-coordinate configuration.*

Acknowledgements—Financial assistance from the Natural Sciences and Engineering Research Council Canada, Laurentian University and Universiti Sains Malaysia, is gratefully acknowledged.

* *Supplementary material.* Atomic coordinates, anisotropic temperature factors, a full list of bond lengths and bond angles, and final structure factors have been deposited as supplementary material and are available from the Editor-in-Chief.

REFERENCES

1. L. E. Khoo, J-P. Charland, E. H. Gabe and F. E. Smith, *Inorg. Chim. Acta* 1987, **128**, 139.
2. J-P. Charland, F. L. Lee, E. J. Gabe, L. E. Khoo and F. E. Smith, *Inorg. Chim. Acta* 1987, **130**, 55.

3. R. Seltzer, *J. Org. Chem.* 1968, **33**, 3896.
4. D. F. Grant and E. J. Gabe, *J. Appl. Cryst.* 1978, **11**, 114.
5. G. Germain, P. Main and M. M. Woolfson, *Acta Cryst.* 1971, **A27**, 368.
6. E. J. Gabe, F. L. Lee and Y. Le Page, *Crystallographic Computing 3* (Edited by G. Sheldrick, C. Kruger and R. Goddard), pp. 167–174. Clarendon Press, Oxford (1985).
7. *International Tables for X-ray Crystallography*, Vol. 4, 2nd edn. Kynoch Press, Birmingham (1974).
8. E. J. Gabe, F. L. Lee and F. E. Smith, *Inorg. Chim. Acta* 1984, **90**, L11.
9. L. Prasad, F. L. Lee, Y. Le Page and F. E. Smith, *Acta Cryst.* 1982, **B38**, 259.
10. L. Prasad and F. E. Smith, *Acta Cryst.* 1981, **B38**, 1815.
11. F. E. Smith, L. Prasad, D. C. Povey and M. F. C. Ladd, *Experientia* 1983, **39**, 719.
12. M. F. C. Ladd, D. C. Povey and F. E. Smith, *J. Cryst. Spect. Rec.* 1984, **14**, 249.
13. T. N. Srivastava, A. K. S. Chauhan and P. C. Kamboj, *J. Ind. Chem. Soc.* 1983, **60**, 625.
14. P. G. Harrison, T. J. King and J. A. Richards, *J. Chem. Soc., Dalton Trans.* 1974, 1723.
15. E. J. Gabe, F. L. Lee, L. E. Khoo and F. E. Smith, *Inorg. Chim. Acta* 1986, **112**, 41.
16. A. M. Domingos and G. M. Sheldrick, *J. Organomet. Chem.* 1974, **67**, 257.
17. Y. M. Chow, *Inorg. Chem.* 1970, **9**, 794.
18. E. A. Forder and G. M. Sheldrick, *J. Organomet. Chem.* 1970, **21**, 115.
19. H. L. Carell and J. Donohue, *Isr. J. Chem.* 1972, **10**, 195.

Polyhedron Vol. 8, No. 15, pp. 1903–1908, 1989
Printed in Great Britain

0277–5387/89 $3.00+.00
© 1989 Maxwell Pergamon Macmillan plc

THE PREPARATION AND NMR CHARACTERIZATION OF A HYDRIDO-BRIDGED GOLD–IRIDIUM BINUCLEAR COMPLEX CONTAINING THE CHELATING TRITERTIARY PHOSPHINE LIGAND Cyttp*

STEVEN M. SOCOL and DEVON W. MEEK†

Department of Chemistry, The Ohio State University, Columbus, OH 43210, U.S.A.

and

ROBERT GLASER‡

Department of Chemistry, Ben Gurion University of the Negev, Beersheva 84105, Israel

(*Received* 12 *December* 1988; *accepted* 21 *February* 1989)

Abstract—*Apical*(H,Cl)-*anti-mer*-{IrHCl(Cyttp)(μ-H)[AuPPh$_3$]}BF$_4$, where Cyttp = $C_6H_5P(CH_2CH_2CH_2P(C_6H_{11})_2)_2$, was prepared in THF solution by mixing equimolar quantities of *cis-anti-mer*-[IrH$_2$Cl(Cyttp)] and [AuCl(PPh$_3$)] in the presence of TlBF$_4$. The ^{1}H NMR spectrum (acetone-d$_6$) showed resonances of an apical terminal hydrido proton at −19.68 ppm and a meridional bridging hydrido proton at −5.45 ppm. The assignment of meridional stereochemistry to the bridging hydride indicates that the [Au(THF)PPh$_3$]$^+$ cation attacked the diastereotopic proton that was located *trans* to the higher *trans*-influence ligand in the starting complex. Nuclear Overhauser Effect experiments confirm the apical assignment for the terminal hydride and show that it is spatially close to the *ortho*-protons of the phenyl group (i.e. an anti-configuration diastereomer in which phenyl and chlorine are located on opposite sides of the meridional reference place). Geminal heteronuclear $^2J_{AuP—(\mu\text{-}H)}$ coupling constants for the spin–spin interactions between the μ-hydrido proton and the Cyttp internal phosphorus atom (65.9(3) Hz) or the phosphorus atom bonded to gold (71.1(3) Hz) indicate *trans* linear-type P—Ir—(μ-H) and (μ-H)—Au—P relationships.

Numerous reports on the characterization and preparation of gold-containing mixed-metal complexes and clusters have recently appeared in the literature.[1–11] The structures of some of these mixed-metal compounds illustrate the isolobal analogy between the hydrido ligand and the AuPR$_3$ moiety.[1,5,6,10,11]

Hydrido complexes of gold are relatively rare and those few that have been isolated and unambiguously characterized have bridging hydrido ligands between gold and another transition metal atom in an M—(μ-H)—Au—PR$_3$ sequence.[2,3] These complexes include {M(CO)$_5$(μ-H)[AuPPh$_3$]}BF$_4$ where M = Cr, Mo and W;[2] *mer*-[IrH$_2$(PPh$_3$)$_3$(μ-H)[AuPR$_3$]}BF$_4$ where R = Ph, Et;[3] and *trans*-{Pt(C$_6$Cl$_5$)(PPh$_3$)(μ-H)[AuPPh$_3$]}BF$_4$,[3] {Ru(dppm)$_2$(μ-H)$_2$[AuPPh$_3$]$_2$}(NO$_3$)$_2$ [dppm = bis(1,2-(diphenylphosphino)methane)][6e] and {Ru(dppm)$_2$(μ-H)$_2$[AuPPh$_3$]}PF$_6$.[6i] In the case of {Ir(μ-H)$_2$(bipy)(PPh$_3$)$_2$[AuPPh$_3$]}(BF$_4$)$_2$,[6e] the hydrido ligands were not located by X-ray crystallography, but the X-ray structure and NMR data are consistent with bridging hydrides. However, it is noted that a terminal hydride for {IrH(PPh$_3$)$_3$[AuPPh$_3$]}$^+$ and {IrH(CO)(PPh$_3$)$_3$[AuPPh$_3$]}PF$_6$

* R.G. and S.M.S. dedicate this paper to the memory of their teacher, colleague and friend, Professor Devon W. Meek (died 7 December 1988).

† Deceased.

‡ Author to whom correspondence should be addressed.

have been assigned based on NMR and IR spectroscopic evidence.[6e] Transition metal–gold clusters $\{IrH(PPh_3)_2(NO_3)[AuPPh_3]_2\}BF_4$,[6b] $\{IrH_2(PPh_3)_2[AuPPh_3]_4\}BF_4$,[6d] $\{ReH_4(PPh_3)_2[AuPPh_3]_5\}(PF_6)_2$,[6f] $\{RhH(CO)(PPh_3)_2[AuPPh_3]_3\}PF_6$[6f] and $\{ReH_4[P(p\text{-tol})_3]_2[AuPPh_3]_4\}BPh_4$[6h] have been isolated and partially characterized by NMR spectroscopy and X-ray diffraction analysis. An unambiguous assignment regarding bridging versus terminal hydrido ligands in these clusters was not possible, and in the case of $\{IrH(PPh_3)_2(NO_3)[AuPPh_3]_2\}BF_4$, a terminal Ir—H assignment was most consistent with the NMR data. In addition to the stable binuclear complexes noted above, three unstable intermediates (*trans*-phosphine complexes: $\{Ir(PPh_3)_2(acetone)(\mu\text{-}H)_2[AuPPh_3]\}^{2+}$; $\{Ir(NO_3)(PPh_3)_2(\mu\text{-}H)_2[AuPPh_3]\}^{+}$; and $\{IrH(NO_3)(PPh_3)_2(\mu\text{-}H)[AuPPh_3]\}^{+}$) show M—($\mu$-H)—Au—$PPh_3$ moieties according to NMR spectroscopy.[6b]

Earlier, we[12] reported on the syntheses, reactivities and stereochemistries of six coordinate iridium(III) dihydrido $[IrH_2Z(Cyttp)]^{(0\text{ or }1+)}$ complexes containing the chelating tritertiary phosphine ligand Cyttp[13] [Cyttp = bis((3-dicyclohexylphosphino) propyl)phenylphosphine, $C_6H_5P(CH_2CH_2CH_2P(C_6H_{11})_2)_2$]. This paper reports the preparation and NMR spectroscopy of a stable iridium–gold complex containing a bridging hydrido ligand and the chelating Cyttp ligand.

RESULTS AND DISCUSSION

Cis-anti-mer-$[IrH_2Cl(Cyttp)]$ (**1**) was mixed with $[AuCl(PPh_3)]$ in a 1 : 1 mole ratio in THF, and then an equimolar quantity of $TlBF_4 \cdot 6H_2O$ was added to yield *apical*(H,Cl)-*anti-mer*-$\{IrHCl(Cyttp)(\mu\text{-}H)[AuPPh_3]\}BF_4$ (**2**).

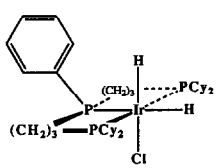

1

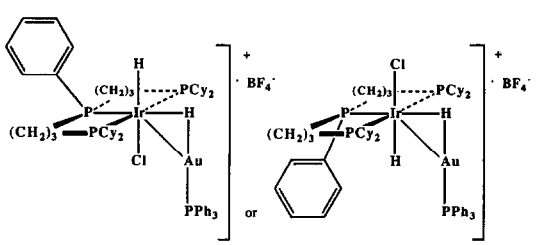

2(a) or 2(b)

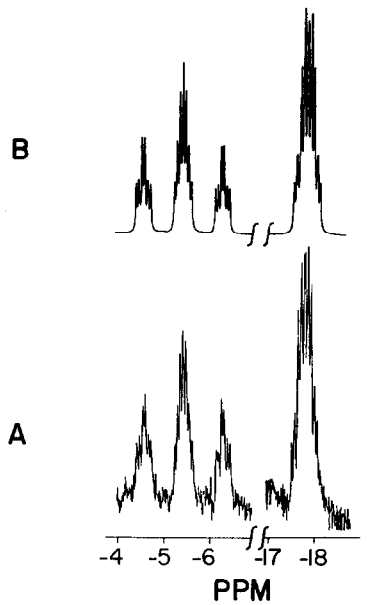

Fig. 1. (A) Hydrido region of the ^1H NMR spectrum (80 MHz, acetone-d_6, 298°K) of *apical*(H,Cl)-*anti-mer*-$\{IrHCl(\mu\text{-}H)(Cyttp)[Au(PPh_3)]\}BF_4$(**2**); (B) hydrido region of the simulated spectrum.

In the preparation of the previously described *mer*-$\{IrH_2(PPh_3)_3(\mu\text{-}H)[AuPPh_3]\}BF_4$ complex, the solvated cation $[Au(THF)PPh_3]^+$ was first prepared (via reaction of $[AuCl(PPh_3)]$ with $AgBF_4$ in THF), and then added to a THF solution of *mer*-$[IrH_3(PPh_3)_3]$.[3]

^1H *NMR spectroscopic studies*

Analysis. The six-spin system for **2** is shown in structures **3(a,b)**. The ^1H NMR partial spectrum (80 MHz, acetone-d_6, 298 K) of **2** in the hydride region is shown in Fig. 1. Two hydrido absorbances were found: a 19-line pattern for H(4) (−5.45 ppm) (three subgroups with relative intensities of 1 : 1 : 2 : 2 : 1 : 1, 1 : 2 : 3 : 4 : 3 : 2 : 1 and 1 : 1 : 2 : 2 : 1 : 1) and a 10-line pattern for H(3) (−17.68 ppm) with relative intensities of 1 : 2 : 4 : 6 : 3 : 3 : 6 : 4 : 2 : 1. These relative intensities show that each proton exhibits 32 transitions as expected for a six-spin system (five coupling constants are involved).

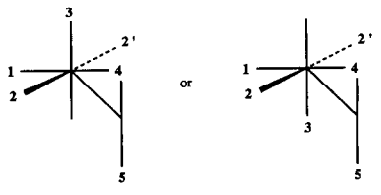

3(a) 3(b)

Mer-H(4) *absorbance*: the multiplicity of 1:1:2:2:1:1 seen for the first and last eight H(4) transitions arises from three coupling constants, of which two are of similar magnitude (homonuclear $^2J_{H(3)—H(4)}$ 4.5(3) Hz and two heteronuclear $^2J_{P(2)—H(4)}/^2J_{P(2')—H(4)}$ both 9.9(3) Hz). The observation of two equal magnitude coupling constants indicate that the enantiotopic symmetry equivalence of the terminal Cyttp phosphorus nuclei in $[IrH_2Cl(Cyttp)]$ (**1**) is also preserved in the binuclear cationic product **2**. Enantiotopic symmetry equivalence for a six-spin system results in the 32 transitions of each nucleus being arranged in a 24-line pattern. Our observation of a 19-line pattern is explicable in terms of five sets of overlapping transitions which result from the fact that $^2J_{P(5)—H(4)} \approx (^2J_{H(3)—H(4)} + {}^2J_{P(1)—H(4)})$ (i.e. 71.1 Hz $\approx$ 4.5(3)+65.9(3) Hz). This explains the intensities of 1:2:3:4:3:2:1 found for the middle subgroups of seven lines. Selective heteronuclear decoupling experiments $\{\underline{P}Ph_3\}$ and $\{P_{internal}$ of Cyttp$\}$ provided the assignment of the respective $^2J_{P(1)—H(4)}$ and $^2J_{P(5)—H(4)}$ coupling constants.

Apical-H(3) *absorbance*: the relative intensities of the 10 lines observed for this absorbance are in the ratio of *ca* 1:2:4:6:3:3:6:4:2:1. The frequency differences between these lines point to a "quartet of triplets" pattern involving two similar magnitude smaller coupling constants (mean value of 5.6(3) Hz) and three similar magnitude larger coupling constants (mean value of 11.7(3) Hz) whose magnitude is approximately twice that of the smaller counterparts. The terminal lines of the H(3) nucleus absorbance are observed as having one unit-transition intensity, while the second and penultimate lines are each two unit-transition intensities. Since the average value of the three larger coupling constants is about double that of the two smaller ones, there is an overlap between each of the smaller triplet patterns and the corresponding adjacent larger triplet pattern, so that the relative intensities are actually 1:2:[1+3]:6:3:3:6:[3+1]:2:1. The very small frequency difference between the two middle three-unit intensity lines of the multiplet, results in their appearance at approximately equal height relative to their six-unit intensity neighbours. The values of the five coupling constants were hand calculated from the spectrum and then refined by iteration calculations and spectrum simulation using the "PANIC"[14] program. The simulated hydrido multiplets are shown in Fig. 1. From the *mer*-H(4) multiplet one can measure the value of the homonuclear $^2J_{H(3)—H(4)}$ coupling constant (4.5(3) Hz) common to both hydride multiplets. Thus, the 5.6(3) Hz value for the two smaller coupling constants represents an average value for $^2J_{H(3)—H(4)}$ and one of the heteronuclear coupling constants assigned as $J_{P(5)—H(3)}$. The signs of the coupling constants have not been determined. The summation of the five H(3) coupling constants is 45.2(3) Hz compared to the observed frequency difference between the terminal lines of 45.4 Hz.

Stereochemical interpretation

^1H and ^{31}P NMR spectral parameters for **2** are listed in Table 1. Hydride H(3) shows two het-

Table 1. ^1H and $^{31}P\{^1H\}$ NMR spectral parameters for *apical*(H,Cl)-*anti-mer*-$\{IrHCl(\mu\text{-}H)(Cyttp)[Au(PPh_3)]\}BF_4$ (**2**)

X	δ_X[a]	X—X	$J_{X—X}$[b]
P(1) (Cyttp internal-P)	−19.18	P(1)—P(2)	27
P(2) (Cyttp terminal-P)	−12.81	P(1)—H(3)	11.7(3)
H(3) (*apical*-H)	−17.68	P(1)—H(4)	65.9(3)
H(4) (*mer*-μ-H)	−5.45	P(1)—P(5)	35
P(5)	46.21	P(2)—H(3)	11.7(3)
		P(2)—H(4)	9.9(3)
		P(2)—P(5)	[c]
		H(3)—H(4)	4.5(3)
		H(3)—P(5)	5.6(3)
		H(4)—P(5)	71.1

[a] ^1H NMR (acetone-d_6) and $^{31}P\{^1H\}$ NMR (THF) δ-values in ppm relative to tetrahydrosilane and 85% H_3PO_4, respectively. Negative values are upfield from the reference standard.

[b] Hz, standard deviation given in parentheses.

[c] Not observed.

eronuclear geminal coupling constants ($^2J_{P(1)—H(3)}$ and $^2J_{P(2)—H(3)}$) each with 11.7(3) Hz magnitudes typical of that expected for a *cis* $^2J_{PH}$ coupling constant in an octahedral complex.[15] The magnitude of the geminal homonuclear 4.5(3) Hz $^2J_{H(3)—H(4)}$ coupling constant is also consistent with a *cis* orientation of the diastereotopic protons.[12] In complex **1** this value is 6 Hz.[12] These three *cis* coupling constants characterize the H(3) proton as one that is apical to the meridional reference plane of the three Cyttp phosphorus atoms. The 5.6(3) Hz magnitude of the heteronuclear $J_{P(5)—H(3)}$ coupling constant is consistent with a terminal hydride which undergoes a longer range splitting interaction with a phosphorus atom ligated to gold. A Nuclear Overhauser Effect experiment (NOE) was performed in which *ortho*-protons of the Cyttp phenyl ring were irradiated, and an intensity enhancement for the H(3) signal was observed. This result simultaneously confirmed the apical assignment for H(3) and enabled the anti configuration of the product to be determined. (The phenyl and Cl are on opposite sides of the three Cyttp phosphorus atom reference plane.) An NOE for H(3) upon $\{H_{phenyl(ortho)}\}$ testifies to a close spatial relationship between these two moieties. Such a close spatial relationship was also found for the analogous case in the starting complex **1**.[12] A similar NOE enhancement of the apical hydride was also observed for compound **1**, whose structure is known from X-ray studies.[12] A single crystal X-ray diffraction analysis of *cis-anti-mer*-[IrH_2Cl(Cyttp)] (**1**), showed that the apical hydrido proton and one of the phenyl *ortho*-protons to have a non-bonded distance of 2.25 Å (within the range of distances commensurate with NOE phenomena).[16]

Hydrido proton H(4) shows two heteronuclear geminal constants $^2J_{P(1)—H(4)}$ and $^2J_{P(5)—H(4)}$ of similar magnitude (65.9(3) and 71.1(3) Hz, respectively). The magnitude of the $^2J_{P(1)—H(4)}$ coupling constant is reduced from the 130 Hz value observed for the analogous coupling in compound **1**. This reduction is similar to that found for the bridging hydrido proton H(b) *trans* to an iridium-bound phosphorus atom ($J_{P(b)—H(b)}$ 72 Hz) in the iridium–gold cluster $\{Ir_3H_3(dppe)_3(\mu\text{-}H)_3[\mu_3\text{-}Au(NO_3)]\}BF_4$ (**4**) (dppe = $Ph_2PCH_2CH_2PPh_2$), whose solid state structure

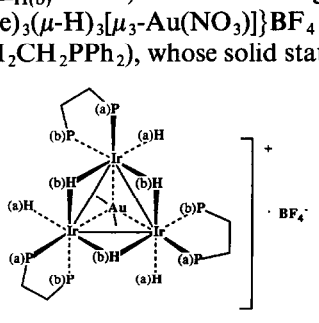

4

was determined by single crystal X-ray crystallography.[6a]

The 71.1(3) Hz magnitude of $^2J_{P(5)—H(4)}$ in **2** is consistent with a linear (μ-H)—Au—P disposition. This stereochemical arrangement is noted in the solid state structure of *mer*-$\{IrH_2(PPh_3)_3(\mu\text{-}H)[AuPPh_3]\}BF_4$ (**5**), and the corresponding coupling constant between the bridging hydrido proton and the phosphorus atom ligated to gold is 79.4 Hz.[3]

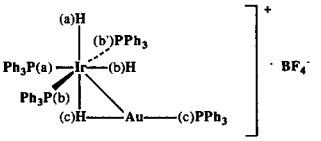

5

The remaining heteronuclear 9.9(3) Hz coupling constant for $^2J_{P(2)—H(4)}$ is reasonable for a hydride *cis* to an iridium-bound phosphorus atom. Thus, the four heteronuclear geminal coupling constants $^2J_{P(1)—H(4)}$, $^2J_{P(2)—H(4)}$, $^2J_{P(2')—H(4)}$ and $^2J_{P(5)—H(4)}$ indicate that H(4) is a bridging hydride close to or in the meridional plane, and having a linear (μ-H)—Au—P orientation to both P(1,5).

While there is literature precedent for the *trans*-(μ-H)—Au—P linear arrangement postulated for **2** on the basis of the 71.1 Hz $^2J_{AuP—(\mu\text{-}H)}$ coupling constant, this does not imply that other angular relationships for this moiety have not been found. NMR evidence has recently been presented which suggested a linear Ir—Au—P relationship (and concomitant reduced (μ-H)—Au—P angle) in some transition metal–[$AuPPh_3$] hydrido complexes, see structure **6**.[6b,e] Based on $^2J_{AuP—(\mu\text{-}H)}$ coupling con-

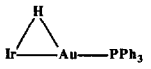

6

stants of *ca* 30 Hz, the M—(μ-H)—[$AuPPh_3$] moiety and a linear Ir—Au—P relationship was proposed for three unstable intermediates having *trans*-$\underline{P}Ph_3$—Ir—$\underline{P}Ph_3$ geometry: $\{Ir(PPh_3)_2$(acetone)$(\mu\text{-}H)_2[AuPPh_3]\}^{2+}$; $\{Ir(NO_3)(PPh_3)_2(\mu\text{-}H)_2[AuPPh_3]\}^{+}$; and $\{IrH(NO_3)(PPh_3)_2(\mu\text{-}H)[AuPPh_3]\}^{+}$.[6b] Subsequent single crystal X-ray crystallography of $\{Ir(\mu\text{-}H)_2$(bipy)$(PPh_3)_2[AuPPh_3]\}(BF_4)_2$ (**7**) proved an approximately linear Ir—Au—P relationship.[6e] Although the hydrido ligands in **7** were not located in the X-ray analysis, the solid-state structure was consistent with a bridging hydrido ligand located *trans* to each nitrogen.[6e] The 31 Hz $^2J_{AuP—(\mu\text{-}H)}$ coupling constant suggested that the above-mentioned stereochemistry for crystalline **7** was maintained in solution.[6e]

In solid state $\{Ru(dppm)_2(\mu\text{-}H)_2[AuPPh_3]_2\}(NO_3)_2$ (**8**) and $\{Ru(dppm)_2(\mu\text{-}H)_2[AuPPh_3]\}PF_6$ (**9**), the positions of the bridging hydrido ligands were now located by single crystal X-ray crystallography.[6e,i] These complexes showed approximately linear Ir—Au—P relationships.[6e,i] However, the observation of a 74.8 Hz $^1J_{AuP-(\mu\text{-}H)}$ coupling constant for **8** has been interpreted as showing a change to *trans*-(μ-H)—Au—PPh_3 stereochemistry in solution.[6e] A change from the solid-state geometry has also been indicated for solutions of **9**.[6i] The 54.0 Hz $^2J_{AuP-(\mu\text{-}H)}$ coupling constant has been interpreted as pointing to a rapid equilibrium between *trans*- and *cis*-(μ-H)—Au—PPh_3 stereochemistries.[6i] For these reasons we believe that the 65.9 Hz $^2J_{P(1)-H(4)}$ and 71.1 Hz $^2J_{P(5)-H(4)}$ coupling constants for **2** indicate *trans* dispositions for the relevant (μ-H)—M—P moieties.

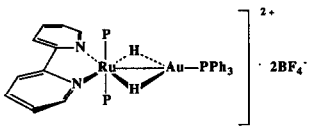

7

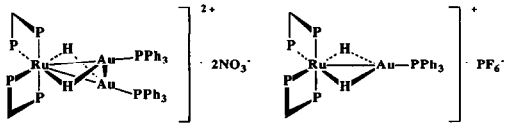

8 9

It is noted that the *mer*-bridging hydride proton H(4) in **2** is *trans* to the stronger *trans*-influence phosphorus (as opposed to being an apical bridging hydride which would have placed it *trans* to the weaker chloro ligand). From the structure of complex **5**, it appears that the cationic $[Au(THF)PPh_3]^+$ species has also attacked the hydrido ligand that is *trans* to a hydride in *mer*-$[IrH_3(PPh_3)_3]$ (as opposed to a proton *trans* to the relatively weaker *trans*-influence phosphorus ligand).

Finally, the position of the putative iridium–gold bond in **2** (postulated by analogy to the solid state structures of **5**, $\{Ir(H)(PPh_3)_2(NO_3)[AuPPh_3]_2\}BF_4$, $\{Ir(H)_2(PPh_3)_2[AuPPh_3]_4\}BF_4$)[3,6b,d] can not be determined from the NMR spectroscopic data without equivocation. Two models [**2(a)** or **2(b)**] are possible, and differ in the orientation of the gold atom *vis-a-vis* the apical hydrido or the apical chloro ligands. The *syn*-periplanar relationship between H(3) and P(5) in model **2(b)** is very similar to that found between H(b) and H(c) in the binuclear complex **5**. Note that $J_{P(c)-H(b)}$ (13 Hz) in **5** is greater than $J_{P(5)-H(3)}$ (5.6(3) Hz) in **2**, although this by itself does not disprove one model over the other. On the other hand, there is a *syn*-periplanar homonuclear P(1)—P(5) relationship in **2** versus an *anti*-periplanar P(a)—P(c) relationship in **5**, and the $^{31}P\{^1H\}$ NMR *syn*-periplanar $J_{P(1)-P(5)}$ (35 Hz) in **2** is markedly larger than the corresponding *anti*-periplanar $J_{P(a)-P(c)}$ (19.5 Hz)[3] coupling constant in **5**. Since models **2(a)** and **2(b)** differ primarily in the *syn*- or *anti*-periplanar H(3)—P(5) relationship, the finding that $J_{P(5)-H(3)} < J_{P(c)-H(b)}$ is a point in favour of model **2(a)**. Unfortunately, several efforts to prepare suitable crystals of **2** for single crystal X-ray diffraction analysis have so far proven unsuccessful.

EXPERIMENTAL

Elemental analysis was performed by MHW Laboratories, Phoenix, Arizona. IR spectra were recorded on a Perkin–Elmer 283B spectrophotometer. ^1H NMR spectra (1.9 T) were recorded in acetone-d_6 solution at 80 MHz on an IBM NR-80 Fourier transform spectrometer. The $^1H\{^{31}P\}$ selective decoupling experiments were performed at 300 MHz on a Bruker WM-300 Fourier transform spectrometer (equipped with an Aspect 3000 data system). Nuclear Overhauser Effect experiments were performed at 500 MHz on a Bruker AM-500 Fourier transform spectrometer (equipped with an Aspect 3000 data system) at The Ohio State University Chemical Instrument Center. Deuterated solvents were used as an internal lock, and the residual protio absorbances were used as internal secondary references (relative to TMS). $^{31}P\{^1H\}$ NMR spectra (2.1 T) were recorded in THF solution at 36.43 MHz on a Bruker HX-90 Fourier transform spectrometer. For ^{31}P NMR spectra, an acetone-d_6 solution of trimethyl phosphate $[(CH_3O)_3P{=}O]$ in a co-axial insert tube was used as an external lock and an external secondary reference (1.594 ppm relative to 85% H_3PO_4), respectively. For all NMR spectra, negative chemical shifts are upfield from the respective reference standards. Protons were decoupled from the phosphorus nuclei by broad-band irradiation. Iteration calculations and simulated NMR spectra were calculated with the use of the "PANIC"[14] program on a Bruker WP-200-SY Fourier transform spectrometer. "PANIC" is a microcomputer version of the "LAOCOON"[17] program.

All reactions were carried out under an atmosphere of high purity nitrogen by using standard Schlenck techniques. Solutions of air-sensitive reagents were transferred between reaction vessels with syringes flushed with nitrogen, stainless steel needles, or a glass transfer tube with a Teflon stopcock.

Cis-anti-mer-$[IrH_2Cl(Cyttp)]$[12] and $[AuCl(PPh_3)]$[18] were prepared by literature methods.

Apical(H,Cl) - *anti* - *mer* - {IrHCl(μ - H)(Cyttp)[Au(PPh_3)]}BF_4 (**2**)

To a solution of *cis-anti-mer*-[IrH_2Cl(Cyttp)] (**1**) (300 mg, 0.37 mmol) and [$AuCl(PPh_3)$] (170 mg, 0.37 mmol) in THF (25 cm^3) was added $TlBF_4 \cdot 6H_2O$ (137 mg, 0.37 mmol). The mixture was stirred for 4 h during which time TlCl precipitated. The solvent was removed under reduced pressure after which the product was extracted with acetone. After removing the acetone solvent, the product was washed with water, and then benzene and recrystallized (acetone–ether) to yield 310 mg (62%) of the title compound **2**. Product **2** was stable indefinitely in the solid state, but decomposes in solution within hours, if not protected from the atmosphere. IR (KBr) cm^{-1}: 2239 [$\nu_{Ir—H(apical)}$].

Found: C, 47.45; H, 5.84; P, 9.31. Calc. for $C_{54}H_{78}AuBClF_4IrP_4$: C, 47.60; H, 5.77; P, 9.09%.

Acknowledgements—Thanks are expressed to Dr Charles Cottrell of The Ohio State University Campus Chemical Instrument Center for performing the NOE experiment. Gratitude is also expressed to the Kreitman Family Endowment Fund, Ben Gurion University of the Negev, for the purchase of a Bruker WP-200-SY FT-NMR spectrometer.

REFERENCES

1. J. W. Lauher and K. Wald, *J. Am. Chem. Soc.* 1981, **103**, 7648.
2. M. Green, A. G. Orpen, I. D. Salter and F. G. A. Stone, *J. Chem. Soc., Chem. Commun.* 1982, 813.
3. (a) H. Lehner, D. Matt, P. S. Pregosin, L. M. Venanzi and A. Albinati, *J. Am. Chem., Soc.* 1982, **104**, 6825; (b) A. Albinati, F. Desmartin, P. Janser, L. F. Rhodes and L. M. Venanzi, *J. Am. Chem. Soc.* 1989, **111**, 2115.
4. (a) J. J. Steggerda, J. J. Bour and J. W. A. van der Velden, *Recl. Trav. Chim. Pays-Bas* 1982, **101**, 164; (b) J. J. Bour, R. P. F. Kanters, P. P. J. Schlebos, W. P. Bosman, H. Behm, P. T. Beurskens and J. J. Steggerda, *Recl. Trav. Chim. Pays-Bas* 1987, **106**, 157; (c) J. J. Bour, R. P. F. Kanters, P. P. J. Schlebos and J. J. Steggerda, *Recl. Trav. Chim. Pays-Bas* 1988, **107**, 211.
5. (a) D. M. P. Mingos, *Phil. Trans. R. Soc. London* 1982, **308A**, 75; (b) D. G. Evans and D. M. P. Mingos, *J. Organomet. Chem.* 1982, **232**, 171; (c) K. P. Hall and D. M. P. Mingos, *Prog. Inorg. Chem.* 1984, **23**, 237.
6. (a) A. L. Casalnuovo, L. H. Pignolet, J. W. A. van der Velden, J. J. Bour and J. J. Steggerda, *J. Am. Chem. Soc.* 1983, **105**, 5957; (b) A. L. Casalnuovo, T. Laska, P. V. Nilsson, J. Olofson, L. H. Pignolet, W. Bos, J. J. Bour and J. J. Steggerda, *Inorg. Chem.* 1985, **24**, 182; (c) A. L. Casalnuovo, T. Laska, P. V. Nilsson, J. Olofson and L. H. Pignolet, *Inorg. Chem.* 1985, **24**, 233; (d) A. L. Casalnuovo, J. A. Casalnuovo, P. V. Nilsson and L. H. Pignolet, *Inorg. Chem.* 1985, **24**, 2554; (e) B. D. Alexander, B. J. Johnson, S. M. Johnson, J. A. Casalnuovo and L. H. Pignolet, *J. Am. Chem. Soc.* 1986, **108**, 4409; (f) P. D. Boyle, B. J. Johnson, A. Buehler and L. H. Pignolet, *Inorg. Chem.* 1986, **25**, 5; (g) P. D. Boyle, B. J. Johnson, B. D. Alexander, J. A. Casalnuovo, P. R. Gannon, S. M. Johnson, E. M. Larka, A. M. Mueting and L. H. Pignolet, *Inorg. Chem.* 1987, **26**, 1346; (h) B. D. Alexander, P. D. Boyle, B. J. Johnson, J. A. Casalnuovo, S. M. Johnson, A. M. Mueting and L. H. Pignolet, *Inorg. Chem.* 1987, **26**, 2547; (i) B. D. Alexander, B. J. Johnson, S. M. Johnson, P. D. Boyle, N. C. Kann, A. M. Mueting and L. H. Pignolet, *Inorg. Chem.* 1987, **26**, 3506.
7. B. F. G. Johnson, J. Lewis, J. N. Nicholls, J. Puga and K. H. Whitmire, *J. Chem. Soc., Dalton Trans.* 1983, 787.
8. A. T. Hutton, P. G. Pringle and B. L. Shaw, *Organometallics* 1983, **2**, 1889.
9. B. K. Teo and K. Keating, *J. Am. Chem. Soc.* 1984, **106**, 2224.
10. G. Lavigne, F. Papageorgiou and J. J. Bonnet, *Inorg. Chem.* 1984, **23**, 609.
11. P. Braunstein, H. Lehner, D. Matt, A. Tiripicchio and M. Titipicchio-Camellini, *Angew. Chem. Int. Ed. Engl.* 1984, **23**, 304.
12. C. Yang, S. M. Socol, D. J. Kountz, D. W. Meek and R. Glaser, *Inorg. Chim. Acta* 1986, **114**, 119.
13. (a) J. B. Letts, PhD dissertation. The Ohio State University, Columbus, Ohio (1982); (b) R. J. Uriarte, T. J. Mazanec, K. D. Tau and D. W. Meek, *Inorg. Chem.* 1980, **19**, 79; (c) J. B. Letts, T. J. Mazanec and D. W. Meek, *Organometallics* 1983, **2**, 695.
14. PANIC. *P*arameter *A*djustment in *N*MR by *I*teration *C*alculation Program. Bruker Analytische Messtechnik, Karlsruhe (1982).
15. H. D. Kaesz and R. B. Saillant, *Chem. Rev.* 1972, **72**, 231.
16. J. H. Noggle and R. E. Schirmer, *The Nuclear Overhauser Effect—Chemical Applications.* Academic Press, New York (1971).
17. S. Castellano and A. R. Bothner-By, *J. Chem. Phys.* 1963, **41**, 3863.
18. (a) J. L. Peterson, PhD dissertation. The Ohio State University, Columbus, Ohio (1973); (b) C. A. McAuliffe, R. V. Parish and P. D. Randall, *J. Chem. Soc., Dalton Trans.* 1979, 1730.

Polyhedron Vol. 8, No. 15, pp. 1909–1912, 1989
Printed in Great Britain

0277-5387/89 $3.00+.00
© 1989 Maxwell Pergamon Macmillan plc

SYNTHESIS OF 1,3-DIPHENYLTRIAZENIDE COMPLEXES OF ALUMINIUM, GALLIUM AND INDIUM: CRYSTAL STRUCTURE OF TRIS(1,3-DIPHENYLTRIAZENIDO)ALUMINIUM(III)

JOHN T. LEMAN and ANDREW R. BARRON*

Chemical Laboratories, Harvard University, Cambridge, MA 02138, U.S.A.

and

JOSEPH W. ZILLER

Department of Chemistry, University of California, Irvine, CA 92717, U.S.A.

and

ROBERT M. KREN

Department of Chemistry, University of Michigan-Flint, Flint, MI 48502, U.S.A.

(*Received* 26 *January* 1989; *accepted* 21 *February* 1989)

Abstract—The reaction of $AlMe_3$ with 1,3-diphenyltriazene [Hdpt] in toluene gives $Al(dpt)_3$, even when $AlMe_3$ is in large excess. The monomeric structure has been established by X-ray diffraction. Crystals of $Al(dpt)_3$ are monoclinic, space group $C2/c$ with $a = 20.587(3)$, $b = 16.005(3)$, $c = 13.236(3)$ Å and $\beta = 119.172(12)°$, $Z = 4$, $R = 0.067$ and $R_w = 0.083$. The aluminium(III) is coordinated by three chelating triazenido ligands to give a trigonally distorted octahedral geometry. The gallium and indium analogues are also reported.

The triazenide anion, RN=N—NR^-, might be expected to display a variety of coordination modes. Transition metal complexes containing monodentate (**1**), chelate (**2**) and bridging (**3**) triazenide ligands have been reported,[1] suggesting a formal analogy to the carboxylate anion, O=C(R)—O^-. Despite this analogy and the wide range of Group III carboxylates reported in the literature,[2] the only examples of Group III triazenides are $Tl(dpt)_3$ (Hdpt = 1,3-diphenyltriazene) and $Tl(ppt)_3$ (Hppt = 1-phenyl-3-(2′-pyridyl)triazene), which were characterized as tris-chelate complexes by IR spectroscopy,[3] and the dimeric $[Tl(dpt)]_2$ whose structure was determined by X-ray crystallography.[4]

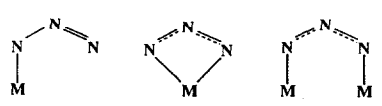

(1) (2) (3)

We now report the synthesis and characterization of the tris(1,3-diphenyltriazenido)aluminium(III), gallium(III) and indium(III) complexes.

RESULTS AND DISCUSSION

The complex $Al(dpt)_3$ (Hdpt = 1,3-diphenyltriazene) was first obtained in low yield from the reaction of $AlCl_3$ with Li(dpt). An improved procedure, however, is the direct reaction of Hdpt with $AlMe_3$ in toluene.

The compound $Al(dpt)_3$ has been fully characterized by elemental analysis and spectral data. The ^1H NMR spectrum, in $CDCl_3$, shows an A_2B_2C pattern for the monosubstituted phenyl groups, indicating that the triazenides are either fluxional on an NMR time scale, or in a symmetrical environment. The ^{27}Al NMR spectrum consists of a broad peak whose shift ($\delta = 25$ ppm) is indicative of a six-coordinate aluminium centre,[5] but is extremely broad ($w_{1/2} = 1160$ Hz), possibly exacerbated by coupling to the quadrupolar ^{14}N nuclei. The IR

* Author to whom correspondence should be addressed.

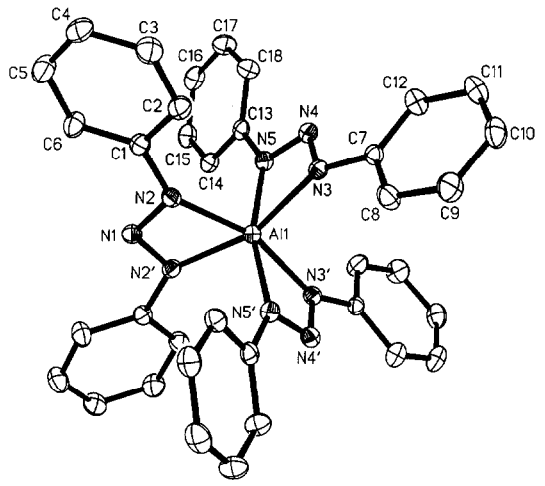

Fig. 1. Molecular structure of $Al(dpt)_3$ showing the atom numbering; hydrogen atoms are omitted for clarity.

spectrum shows bands at 1320 and 1295 cm^{-1}, which are characteristic of chelating triazenide groups.[1] The chelating coordination mode has been confirmed by X-ray crystallography.

The structure of $Al(dpt)_3$ is shown in Fig. 1; selected bond lengths and angles are given in Table 1. One disordered molecule of toluene per $Al(dpt)_3$ is present in the lattice as a solvent of crystallization (see Experimental). The molecule of $Al(dpt)_3$ has a two-fold crystallographic axis passing through Al(1) and N(1). The aluminium is in a trigonally distorted octahedral environment, which is consistent with the ^{27}Al NMR spectrum.

The average Al—N distance (1.972(5) Å) is within the range previously observed for Al—N bonds (1.88–2.09 Å),[6] however, the small N—Al—N angles (64.1(2)-64.2(2)°) suggest that the chelate ring is under considerable strain. The simi-

Table 1. Selected bond lengths (Å) and angles (°) of $Al(dpt)_3$

Al(1)—N(2)	1.972(4)	Al(1)—N(3)	1.977(4)
Al(1)—N(5)	1.968(5)	N(1)—N(2)	1.316(4)
N(2)—C(1)	1.411(5)	N(3)—N(4)	1.315(6)
N(3)—C(7)	1.413(5)	N(4)—N(5)	1.314(4)
N(5)—C(13)	1.407(7)	C(1)—C(2)	1.398(6)
C(1)—C(6)	1.375(7)	C(2)—C(3)	1.389(6)
C(3)—C(4)	1.380(8)	C(4)—C(5)	1.378(7)
C(5)—C(6)	1.375(7)	C(7)—C(8)	1.380(9)
C(7)—C(12)	1.379(8)	C(8)—C(9)	1.379(7)
C(9)—C(10)	1..378(9)	C(10)—C(11)	1.377(10)
C(11)—C(12)	1.381(7)	C(13)—C(14)	1.398(5)
C(13)—C(18)	1.383(8)	C(14)—C(15)	1.384(9)
C(13)—C(16)	1.381(10)	C(16)—C(17)	1.379(6)
C(17)—C(18)	1.385(9)		

N(2)—Al(1)—N(3)	101.1(1)	N(2)—Al(1)—N(5)	93.3(2)
N(3)—Al(1)—N(5)	64.2(2)	N(2)—Al(1)—N(2′)	64.1(2)
N(3)—Al(1)—N(2′)	160.3(2)	N(5)—Al(1)—N(2′)	102.2(2)
N(3)—Al(1)—N(3′)	96.1(2)	N(5)—Al(1)—N(3′)	103.0(2)
N(5)—Al(1)—N(5′)	161.8(2)	N(2)—N(1)—N(2′)	105.2(4)
Al(1)—N(2)—N(1)	95.4(2)	Al(1)—N(2)—C(1)	147.0(3)
N(1)—N(2)—C(1)	116.4(3)	Al(1)—N(3)—N(4)	94.9(2)
Al(1)—N(3)—C(7)	146.5(4)	N(4)—N(3)—C(7)	117.8(4)
N(3)—N(4)—N(5)	105.6(4)	Al(1)—N(5)—N(4)	95.3(3)
Al(1)—N(5)—C(13)	145.8(3)	N(4)—N(5)—C(13)	117.8(4)
N(2)—C(1)—C(2)	117.9(4)	N(2)—C(1)—C(6)	122.9(4)
C(2)—C(1)—C(6)	119.1(4)	C(1)—C(2)—C(3)	119.5(5)
C(2)—C(3)—C(4)	120.5(4)	C(3)—C(4)—C(5)	119.6(5)
C(4)—C(5)—C(6)	120.2(5)	C(1)—C(6)—C(5)	121.1(4)
N(3)—C(7)—C(8)	118.1(5)	N(3)—C(7)—C(12)	122.9(5)
C(8)—C(7)—C(12)	118.9(4)	C(7)—C(8)—C(9)	120.7(6)
C(8)—C(9)—C(10)	120.1(7)	C(9)—C(10)—C(11)	119.5(5)
C(10)—C(11)—C(12)	120.3(6)	C(7)—C(12)—C(11)	120.5(6)
N(5)—C(13)—C(14)	117.2(5)	N(5)—C(13)—C(18)	123.0(4)
C(14)—C(13)—C(18)	119.8(5)	C(13)—C(14)—C(15)	120.2(5)
C(14)—C(15)—C(16)	119.5(4)	C(15)—C(16)—C(17)	120.4(6)
C(16)—C(17)—C(18)	120.5(6)	C(13)—C(18)—C(17)	119.6(4)

larity between the N—N distances within each ligand implies a delocalization of the π-electron in the N_3 portion of the ligand. As with the cobalt analogue, $Co(dpt)_3$,[7] the delocalization could, however, extend to the phenyl rings because the average N—C distance (1.410(6) Å) is significantly shorter than the N—C single bond length of 1.472 Å.[8]

It is interesting to note that $Al(dpt)_3$ is the only product to be isolated from the reaction of Hdpt and $AlMe_3$, even when a large excess of $AlMe_3$ is employed. This suggests that the tris-chelate complex is thermodynamically favoured over $AlMe_2(dpt)$ and $AlMe(dpt)_2$.

The gallium and indium analogues can be obtained in a similar manner to the aluminium complex, and are spectroscopically equivalent (see Experimental). All three complexes are bright yellow–orange crystalline solids with only limited solubility in non-polar organic solvents, are stable under dry nitrogen at room temperature, but decompose slowly in air, both in solution and the solid state.

EXPERIMENTAL

Microanalyses were obtained by Oneida Research Services Inc., Whitesboro, New York. Melting points were determined in sealed capillaries and are uncorrected. IR spectra were recorded in the 4000–600 cm^{-1} region on a Perkin–Elmer 137 grating spectrometer in Nujol mulls. NMR spectra were recorded (in $CDCl_3$) on Bruker AM-250 (^1H) and WM-300 (^{27}Al) spectrometers [δ in ppm relative to $SiMe_4$ (^1H) and external $Al(H_2O)_6^{3+}$ (^{27}Al)]. 1,3-Diphenyltriazene was prepared according to published procedures.[1] All manipulations were carried out under nitrogen. Solvents were distilled and degassed before use.

(1) *Tris*(1,3-*diphenyltriazenido*)*aluminium*(III)

To a solution of Hdpt (5.0 g, 25.0 mmol) in toluene (100 cm^3) at room temperature, was added $AlMe_3$ (4.15 cm^3, 2 M solution in hexane, 8.3 mmol). Immediately following addition, gas was evolved and the solution changed from yellow to orange. After refluxing for 12 h the solvent was reduced in volume and cooled to give orange crystals. The crystals contained toluene of solvation, which was eliminated by dissolving in pentane and removing the volatiles under vacuum. Yield: 4.04 g, 79%. Melting point: 263° dec. Found: C, 69.3; H, 4.14; N, 20.1. Calc. for $Al(dpt)_3$: C, 70.2; H, 4.91; N, 20.4%.

^1H NMR: 7.49 [2H, d, J(H—H) = 9.9 Hz, *o*-H], 7.34 [2H, "t", J(H—H) = 9.3 Hz, *m*-H], 7.19 [1H, t, J(H—H) = 8.6 Hz, *p*-H]. ^{27}Al-{^1H} NMR: +25 (br s, $W_{1/2}$ = 1160 Hz). IR: 1590s, 1480s, 1320m, 1295s, 1275s, 1205s, 1170w, 1070w, 900w, 845w, 755s, 680s, 670s.

(2) *Tris*(1,3-*diphenyltriazenido*)*gallium*(III)

This complex was prepared as for $Al(dpt)_3$ but using $GaMe_3$ to give a yellow solid. Yield: 45%. Melting point: 243°C dec. Found: C, 65.2; H, 4.42; N, 18.7. Calc. for $Ga(dpt)_3$: C, 65.6; H, 4.59; N, 19.1%.

^1H NMR: [2H, d, J(H—H) = 8.9 Hz, *o*-H], 7.35 [2H, "t", J(H—H) = 9.1 Hz, *m*-H], 7.21 [1H, t, J(H—H) = 8.6 Hz, *p*-H]. IR: 1590m, 1480m, 1330sh, 1300s, 1280s, 1205m, 1155m, 1070m, 1020m, 900w, 795w, 755m, 685w, 660w.

(3) *Tris*(1,3-*diphenyltriazenido*)*indium*(III)

This complex was prepared as for $Al(dpt)_3$ but using $InMe_3$ to give an orange solid. Yield: 62%. Melting point: 244–246°C dec. Found: C, 61.5; H, 4.42; N, 17.8. Calc. for $In(dpt)_3$: C, 61.4; H, 4.31; N, 17.9%.

^1H NMR: 7.51 [2H, d, J(H—H) = 10.3 Hz, *o*-H], 7.37 [2H, "t", J(H—H) = 9.2 Hz, *m*-H], 7.22 [1H, t, J(H—H) = 8.4 Hz, *p*-H]. IR: 1590m, 1480s, 1325s, 1310s, 1280s, 1210w, 1070w, 900w, 765m, 690m, 660m.

X-ray crystallography

Collection of X-ray diffraction data. A light orange crystal of approximate dimensions 0.10 × 0.23 × 0.47 mm was immersed in Paratone-N (lube oil additive), mounted on a glass fiber and transferred to the Syntex $P2_1$ diffractometer, which was equipped with a modified LT-1 apparatus. Subsequent set-up operations (determination of accurate unit cell dimensions and orientation matrix) and collection of low temperature (213 K) intensity data were carried out using standard techniques similar to those of Churchill *et al.*[9] Details are given in Table 2.

All 2587 data were corrected for Lorentz and polarization effects and placed on an approximately absolute scale by means of a Wilson plot. A careful survey of a preliminary data set revealed the systematic extinctions hkl for $h-k = 2n+1$ and $h0l$ for $l = 2n+1$; the diffraction symmetry was $2/m$. Possible space groups are the non-centrosymmetric Cc [C_s^4: No. 9] or the centrosymmetric $C2/c$ [C_{2h}^6; No. 15]. Successful solution and refinement of the structure using the centrosymmetric monoclinic space group $C2/c$ later proved it to be the correct choice.

Table 2. Experimental data for the X-ray diffraction study

Formula: $C_{36}H_{30}N_9Al \cdot C_7H_8$
Fw: 707.8
Crystal system: Monoclinic
Space group: $C2/c$
$a = 20.587(3)$ Å
$b = 16.005(3)$ Å
$c = 13.236(3)$ Å
$\beta = 119.172(12)°$
$V = 3808.1(11)$ Å^3
$Z = 4$
$D_{calc.}$ (Mg m^{-3}) = 1.235
Diffractometer: Syntex $P2_1$
Radiation: Mo-K_α ($\lambda = 0.710730$ Å)
Monochromator: Highly oriented graphite
Data collected: $+h$, $+k$, $\pm l$
Scan type: 2θ–θ
Scan width: 1.10° plus K-separation
Scan speed: 2.5° min^{-1} (in ω)
$2\theta_{max}$ (°): 45.0
μ(Mo-K_α) (mm^{-1}) = 0.092
Reflections collected: 2587
Reflections with $\|F_o\| > 3.0\sigma(\|F_o\|)$: 2020
Number of variables: 298
$R_F = 6.7\%$
$R_{wF} = 8.3\%$
Goodness-of-Fit: 2.37

Solution and refinement of the crystal structure. All crystallographic calculations were carried out using either our locally modified version of the UCLA Crystallographic Computing Package[10] or the SHELXTL PLUS program set.[11] The analysis,[12a] both the real ($\Delta f'$) and imaginary ($i\Delta f''$) components of anomalous dispersion[12b] were included. The quantity minimized during least-squares analysis was $\Sigma w(|F_o|-|F_c|)^2$ where $w^{-1} = \sigma^2(|F_o|)+0.00046(|F_o|)^2$.

The structure was solved by direct methods (SHELXTL PLUS); and refined by full-matrix least-squares techniques. Hydrogen atom contributions from the disordered toluene molecule were not included. Refinement of positional and thermal parameters (isotropic for hydrogen atoms and for the carbon atoms of the disordered toluene) led to convergence with $R_F = 6.7\%$, $R_{wF} = 8.3\%$ and G-O-F = 2.37 for 298 variables refined against those 2020 data with $|F_o| > 3.0\sigma(|F_o|)$. A final difference-Fourier map was "clean", ρ(max) = 1.01 e Å^{-3}. Atomic coordinates have been deposited with the Cambridge Crystallographic Data Centre.

Acknowledgements—Funds for the purchase of the Nicolet R3m/V diffractometer system were made available from the National Science Foundation under Grant CHE-85-14495. J.T.L. is a Joshiah Parsons Cooke Fellow, 1988–1989.

REFERENCES

1. D. S. Moore and S. D. Robinson, *Adv. Inorg. Chem. Radio. Chem.* 1986, **30**, 1.
2. M. J. Taylor, in *Comprehensive Coordination Chemistry* (Edited by G. Wilkinson, R. D. Gillard and J. A. McCleverty), Vol. 3. Pergamon Press, Oxford (1988).
3. D. St. C. Black, V. C. Davis, G. B. Deacon and R. J. Schultze, *Inorg. Chim. Acta* 1979, **37**, L528.
4. J. Beck and J. Strahle, *Z. Naturfor.* 1986, **41B**, 1381.
5. R. K. Harris and B. E. Mann, *NMR and the Periodic Table*. Academic Press, London (1978).
6. G. H. Robinson, H. Zhang and J. L. Atwood, *J. Organomet. Chem.* 1987, **331**, 153, and refs therein.
7. (a) M. Corbett and B. F. Hoskins, *J. Am. Chem. Soc.* 1967, **89**, 1530; (b) W. R. Krigbaum and B. Rubin, *Acta Cryst.* 1973, **B29**, 749.
8. L. E. Sulton, *Interatomic Distances and Configuration in Molecules and Ions*, Special Publications No. 18. The Chemical Society, London (1965).
9. M. R. Churchill, R. A. Lashewycz and F. J. Rotella, *Inorg. Chem.* 1977, **16**, 265.
10. UCLA Crystallographic Computing Package. University of California, Los Angeles (1981); C. Strouse, personal communication.
11. Nicolet Instrument Corporation, Madison, Wisconsin (1988).
12. *International Tables for X-Ray Crystallography*, (a) pp. 99–101; (b) pp. 149–150. Kynoch Press, Birmingham, U.K. (1974).

Polyhedron Vol. 8, No. 15, pp. 1913–1921, 1989
Printed in Great Britain

0277–5387/89 $3.00+.00
© 1989 Maxwell Pergamon Macmillan plc

DIVERSITY OF STRUCTURAL TYPES IN POLYMERIC, HETEROMETALLIC COMPLEXES FORMED BY THE REACTION OF BIS(2-PYRROLIDONATO)MERCURY(II) WITH Zn^{2+}, Cd^{2+} AND Hg^{2+} IONS; X-RAY CRYSTAL STRUCTURES OF $[Hg_3Zn_2(C_4H_6NO)_6(NO_3)_{3.33}(CH_3O)_{0.67}]_n$ AND $[Hg_2(C_4H_6NO)_2Cl_2]_n$ (WHERE C_4H_6NO IS THE ANION OF 2-PYRROLIDONE)

DAVID M. L. GOODGAME,* DAVID J. WILLIAMS
and RICHARD E. P. WINPENNY

Chemistry Department, Imperial College of Science, Technology and Medicine, London SW7 2AY, U.K.

(*Received* 28 *November* 1988; *accepted* 21 *February* 1989)

Abstract—Reaction of bis(2-pyrrolidonato)mercury(II) (**1**) with zinc nitrate, cadmium nitrate, or mercury(II) chloride in methanol, yields the compounds $[Hg_3Zn_2(C_4H_6NO)_6(NO_3)_{3.33}(CH_3O)_{0.67}]_n$ (**2**), $[Hg_3Cd(C_4H_6NO)_6(NO_3)_2]_n$ (**3**), and $[Hg_2(C_4H_6NO)_2Cl_2]_n$ (**4**), respectively. Compound **2** is cubic $P4_132$ with $a = 16.370(5)$ Å, $Z = 4$. The structure was refined on 565 reflections to $R = 0.060$. The compound forms a three-dimensional polymer made up of interleaving macrobicyclic units, each macrocycle being 80-membered and containing 10 mercury, 10 zinc, 20 carbon, 20 nitrogen and 20 oxygen atoms. One-third of the zinc atoms are tetrahedrally coordinated by three pyrrolidone oxygen atoms and a methoxide ion; the methoxide groups are replaced by bidentate nitrates on the other zinc atoms. A further nitrate ion symmetrically links a triad of mercury atoms lying within each macrobicycle. Compound **4** is monoclinic $P2_1/c$ with $a = 8.563(2)$, $b = 15.887(2)$, $c = 10.533(2)$ Å, $\beta = 113.55(1)°$, $Z = 4$. The structure was refined on 1513 reflections to $R = 0.051$. The compound forms a loosely linked chain polymer in which units of **1** chelate via the oxygen atoms to the mercury atoms of $HgCl_2$ molecules, with a resultant bending (*ca* 167°) of the Cl—Hg—Cl angle. X-ray powder diffraction photographs show that compound **3** is isostructural with its previously reported cobalt(II) analogue and further information about the cadmium site in **3** was obtained from the EPR spectra of manganese(II)-doped samples.

We have recently demonstrated that bis(2-pyrrolidonato)mercury(II) (**1**) obtained[1] by reaction of 2-pyrrolidone with mercuric acetate, functions as a very versatile ligand system towards other metal ions capable of binding to the oxygen atoms of the pyrrolidone units. The resulting heterometallic, Hg/M, polymeric complexes display a diversity of structural types. Chain polymers involving 16-membered macrocycles were formed when the nitrates of cobalt,[1] lanthanides[2] or thorium[3] were used as the source of the heterometal ions, layer polymers containing contiguous 32-membered macrocycles were obtained[4] with CuX_2 (X = NO_3, ClO_4 or ReO_4). With silver(I) nitrate, however, a simpler, dimeric complex $[HgAg(C_4H_6NO)_2(NO_3)]_2$ was obtained,[5] in which 2-pyrrolidone functions as a trinucleating ligand.

In all these compounds, an important factor influencing the nature of the resulting structure appears to be the preferred coordination number and geometry of the heterometal ion binding to the oxygen atoms of the $Hg(C_4H_6NO)_2$ unit, supplemented by the ability of the two oxygen atoms of that unit to adopt a range of different conformational modes by ligand rotation about the N—Hg—N bonds. These considerations have led us to explore the reactions of **1** with the Group IIB

* Author to whom correspondence should be addressed.

(12) metal ions, Zn^{2+}, Cd^{2+} and Hg^{2+}. These metal ions commonly present a variety of coordination geometries, including, for zinc and mercury(II), the distinct possibility of tetrahedral coordination—a geometry not so far observed in the heterometallic complexes formed by **1**. During these studies we have isolated the compounds $[Hg_3Zn_2(C_4H_6NO)_6(NO_3)_{3.33}(CH_3O)_{0.67}]_n$ (**2**), $\{[Hg_3Cd(C_4H_6NO)_6](NO_3)_2\}_n$ (**3**) and $[Hg_2(C_4H_6NO)_2X_2]_n$ where X = Cl (**4**) or Br (**5**). We report here the results of single crystal X-ray diffraction studies on **2** and **4**, and characterization of **3** by powder diffraction and spectroscopic measurements.

EXPERIMENTAL

Preparations

Compound **2**, $[Hg_3Zn_2(C_4H_6NO)_6(NO_3)_{3.33}(CH_3O)_{0.67}]_n$. Zinc nitrate (1 mmol) in methanol (5 cm^3) was added to a methanolic solution of **1** (2 mmol in 20 cm^3), prepared as described previously.[1] The resulting colourless solution was allowed to evaporate at 3°C. After 2 days, colourless, multi-faceted crystals of suitable quality for X-ray analysis were obtained, and were collected, washed with cold methanol (2×5 cm^3) and dried at the pump. Yield: 64%. Found: C, 20.0; H, 2.7; N, 8.8. Calc. for **2**: C, 20.2; H, 2.6; N, 8.9%.

Compound **3**, $\{[Hg_3Cd(C_4H_5NO)_6](NO_3)_2\}_n$. This was obtained by the method described previously[1] for the cobalt(II) analogue. Yield: 84%. Found: C, 21.9; H, 2.7; N, 8.4. Calc. for **3**: C, 21.5; H, 2.7; N, 8.4%.

The compound could not be obtained in suitable crystalline quality for single crystal X-ray analysis. The manganese(II)-doped samples were obtained using solutions of cadmium nitrate mixed with 1% manganese(II) nitrate.

Compounds **4**, $[Hg_2(C_4H_6NO)_2Cl_2]_n$ *and* **5**, $[Hg_2(C_4H_6NO)_2Br_2]_n$. These were obtained as for **2** but using the appropriate mercury(II) halide in place of zinc nitrate and with evaporation at room temperature.

For **4**, white needles of X-ray quality formed after a day. Yield: 66%. Found: C, 15.0; H, 1.7; N, 4.2. Calc. for **4**: C, 15.0; H, 1.9; N, 4.2%. Raman: ν_1 (Hg—Cl) 300 cm^{-1}. IR: ν_3 (Hg—Cl) 351 cm^{-1}.

For **5**, a cream powder formed after 2 days. Yield: 34%. Found: C, 12.7; H, 1.6; N, 3.3. Calc. for **5**: C, 13.2; H, 1.7; N, 3.8%. Raman: ν_1 (Hg—Br) 187 cm^{-1}. IR: ν_3 (Hg—Br) 249 cm^{-1}.

Attempts to make analogous compounds with mercury(II) iodide, cyanide, or thiocyanate were unsuccessful.

X-ray studies

A summary of the crystal data and of the data collection and refinement parameters for compounds **2** and **4** is given in Table 1. Intensity data were measured with graphite monochromated Cu-K_α radiation using ω-scans on a Nicolet R3m/Eclipse S140 diffractometer system. The data were

Table 1. Summary of crystal data and intensity collection

	2	**4**
Formula	$C_{24.7}H_{38}Hg_3N_{9.3}O_{16.7}Zn_2$	$C_8H_{12}Cl_2Hg_2N_2O_2$
M_r	1464.5	640.3
Crystal system	Cubic	Monoclinic
Space group	$P4_132$	$P2_1/c$
a (Å)	16.370(4)	8.563(2)
b (Å)		15.887(2)
c (Å)		10.533(2)
β (°)		113.55(1)
Cell volume (Å^3)	4387	1314
Molecules/unit cell	4	4
ρ (calc) (g cm^{-3})	2.23	3.24
μ(Cu-K_α) (calc) (cm^{-1})	217	483
Crystal dimensions (mm)	$0.1 \times 0.1 \times 0.1$	$0.04 \times 0.04 \times 0.2$
Unique reflections measured	643	1992
2θ range (°)	100	116
Reflections considered observed $\lvert F_o\rvert > 3\sigma(\lvert F_o\rvert)$	565	1513
R	0.060	0.051
R_w	0.064	0.053
Weight (G)[a]	0.0027	0.0012
Absorption correction	Empirical	Numerical

[a] $w^{-1} = \sigma^2(F) + GF^2$.

Table 2. Selected bond lengths (Å) and angles (°) for **2**

Hg—N(1)	2.026(19)	Zn—O(1)	1.939(16)
Zn—O(6)	2.263(54)	Zn—O(5)	2.565(33)
N(1)—Hg—N(1a)	171.4(10)	O(1)—Zn—O(1a)	104.2(6)
O(6)—Zn—O(1)	99.8(12)	O(6)—Zn—O(1a)	142.9(10)
O(6)—Zn—O(1b)	96.8(15)	O(6)—Zn—O(6a)	49.1(16)
O(5)—Zn—O(1)	114.3(16)		

corrected for Lorentz, polarization and absorption factors.

Both structures were solved by the heavy-atom method and their non-hydrogen atoms refined anisotropically, except for atoms O(5), C(6), N(4), O(7), O(6), O(3), N(3) and O(4) in **2**, which had partial site occupancies and were refined isotropically. The hydrogen atom positions were idealized, C—H = 0.96 Å, assigned isotropic thermal parameters, $U(H) = 1.2\ U_{eq}(C)$ and allowed to ride on their parent carbon atoms. Due to high thermal anisotropy, the methyl protons in **2** were not included in the refinement process. Refinements were by block-cascade, full-matrix least-squares. The chirality and space group of **2** were established by an *R* factor test. Computations were carried out using the SHELXTL program system.[6]

Tables 2 and 3 list selected bond lengths and angles.

Spectroscopy

IR spectra were recorded on a Perkin–Elmer 1720 FTIR spectrometer as Nujol mulls (CsI). Raman spectra of compounds **4** and **5** were obtained on solid samples using a Spex Ramalog V instrument with a Coherent model 52 Krypton ion laser (514.5 nm line), and data collection with a Spex Datamate computer controller. EPR spectra were obtained for polycrystalline samples at room temperature using Varian E12 X-band (*ca* 9.5 GHz) and Bruker ER200 Q-band (*ca* 34 GHz) spectrometers. The Q-band results were used to determine the zero-field splitting parameters *D* and *E* in the Spin Hamiltonian:

$$\mathcal{H} = g\beta B \cdot S + D(S_z^2 - 35/12) + E(S_x^2 - S_y^2).$$

These values were then used to calculate resonance fields using the ESRS program.[7]

RESULTS

We shall first consider compounds **2** and **4**, for which single crystal X-ray structural information is available.

$Hg_3Zn_2(C_4H_6NO)_6(NO_3)_{3.33}(CH_3O)_{0.67}$ (**2**)

The X-ray analysis shows that **2** has the stoichiometry shown above, in which there is partial replacement of the nitrate ions, derived from the zinc nitrate, by methoxide ions from an incomplete solvolysis reaction with the methanol used as solvent. The compound has a complex, polymeric structure with some disorder.

In discussing the details of the structure it is convenient first to consider the coordination environment at the zinc sites (Fig. 1). The zinc atoms are on three-fold rotation axes. The crystal structure represents the average of two superimposed coordination environments, **A** and **B**. In two-thirds of the zinc sites (the **A** sites) the metal ions are coor-

Table 3. Selected bond lengths (Å) and angles (°) for **4**

Hg(1)—Cl(1)	2.320(5)	Hg(1)—Cl(2)	2.314(5)
Hg(1)—O(1)	2.561(16)	Hg(1)—O(2)	2.580(14)
Hg(2)—N(1)	2.036(18)	Hg(2)—N(2)	2.004(18)
Hg(2)—O(2a)	2.625(12)		
Cl(1)—Hg(1)—Cl(2)	166.8(2)	Cl(1)—Hg(1)—O(1)	95.4(3)
Cl(2)—Hg(1)—O(1)	93.4(3)	Cl(1)—Hg(1)—O(2)	89.7(3)
Cl(2)—Hg(1)—O(2)	97.7(3)	O(1)—Hg(1)—O(2)	104.0(5)
N(1)—Hg(2)—N(2)	173.3(6)	N(1)—Hg(2)—O(2a)	93.7(5)
N(2)—Hg(2)—O(2a)	92.8(5)		

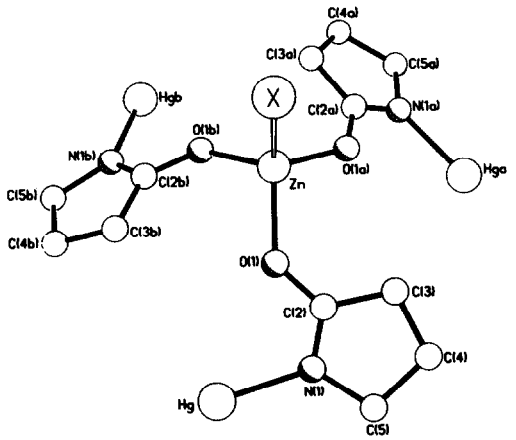

Fig. 1. The zinc environment in **2** showing the crystallographic numbering scheme. X represents the position occupied by the bidentate nitrate, N(4), O(6), O(6a), O(7) (**A** sites), or by the methoxide group, O(5), C(6) (**B** sites).

dinated to five oxygen atoms derived from three symmetry-related 2-pyrrolidone ligands and one bidentate nitrate. The nitrate group is disordered as a consequence of satisfying the crystallographic three-fold site symmetry requirements. In the remaining one-third of the zinc sites (the **B** sites) the nitrate group is replaced by a methoxide ion. If one regards the bidentate nitrate groups in the **A** sites as occupying one coordination position, then the coordination geometry about zinc is best described as distorted tetrahedral in both cases. The distortions are not severe; the angles between the Zn—O(pyrrolidone) bonds are slightly compressed [104.2(6)°] and there is a concomitant increase in the angles to the nitrate/methoxide site [114.3(16)°]. Bond lengths (Table 2) are unexceptional.

The mercury atoms are on two-fold rotation axes and are bound to the nitrogen atoms of two symmetry-related 2-pyrrolidone ligands [Hg—N(1) 2.03(2) Å]. The N—Hg—N unit is slightly distorted from linearity [N(1)—Hg—N(1a) 171(1)°] by interaction of the mercury with oxygen atoms from the second nitrate anion in the asymmetric unit: [Hg—O(2) 2.79(2) Å].

The combination of these zinc and mercury coordination environments leads to the formation of a three-dimensional polymer. A major feature of this array is the presence of a series of 80-membered macrocycles containing 10 mercury, 10 zinc, 20 carbon, 20 nitrogen and 20 oxygen atoms. These intersect at zinc atoms to form three-fold symmetric, interleaving, macrobicyclic units (Fig. 2). The zinc atom at the apex of each such unit is linked by three molecular strands, each spiralling through 120°, to the zinc atom at the base. The base–apex Zn—Zn separation is 18.6 Å.

Each macrobicycle is "waisted" at the intersection of the crystallographic three-fold and two-fold axes, coincident with the position of one of the nitrate ions which lies at the centre of each macrobicycle. By adopting such a position these nitrates serve weakly to link a mercury atom from each of the three strands (Fig. 3). The gross structural arrangement is illustrated schematically in Fig. 4. As far as we are aware, the symmetrical bridging role of the nitrate ion to these three metal ions is unique, though a similar, but asymmetric, linking of three copper atoms has been reported.[8]

The 80-membered macrocyclic rings in this compound are by far the largest we have observed for the heterometallic compounds formed by 2-pyrrolidone. Previously the largest was 32-membered.[4]

There are three independent nitrate anions in the structure; the first is coordinated to the zinc atoms; the second is loosely bound to the mercury atoms; the third is uncoordinated and disordered.

$Hg_2(C_4H_6NO)_2X_2$ [X = Cl (**4**), Br (**5**)]

Crystals suitable for single crystal X-ray study were obtaind for **4** but not for **5**. Compound **4** has a loosely linked polymeric structure, the repeat unit of which is shown in Fig. 5. Each such unit contains two chemically distinct mercury atoms. One of them, Hg(1), is bound to two chloride ions [Hg(1)—Cl(1) 2.320(5), Hg(1)—Cl(2) 2.314(5) Å] and also to two pyrrolidone oxygen atoms [Hg(1)—O(1) 2.56(2), Hg(1)—O(2) 2.58(1) Å]. In compounds containing the $HgCl_2O_2$ unit a wide range of O—Hg—O angles is observed, though with retention of an approximately linear Cl—Hg—Cl moiety. In bis(imidazolidinone)dichloromercury(II)[9] the geometry is square-planar, whilst in bis(testosterone)dichloromercury(II)[10] the O—Hg—O and Cl—Hg—Cl angles are 87 and 164°, respectively. In **4**, O(1)—Hg—O(2) = 104.0(5)° and Cl(1)—Hg—Cl(2) = 166.8(2)°.

The second mercury atom, Hg(2), is strongly bound to two pyrrolidone nitrogen atoms [Hg(2)—N(1) 2.04(2), Hg(2)—N(2) 2.00(2) Å] in an essentially linear fashion [N(1)—Hg(2)—N(2) 173.3(6)°]. The observed distortion from linearity may be ascribed to an Hg(2) interaction with an oxygen atom, O(2′), from a 2-pyrrolidone ligand in the next asymmetric unit [Hg(2)—O(2′) 2.62(1) Å]. This linking of adjacent units results in polymeric strands propagated along the *c*-direction (Fig. 6).

Chelation by **1** results in the formation of an eight-membered ring comprising two mercury, two carbon, two nitrogen and two oxygen atoms. The

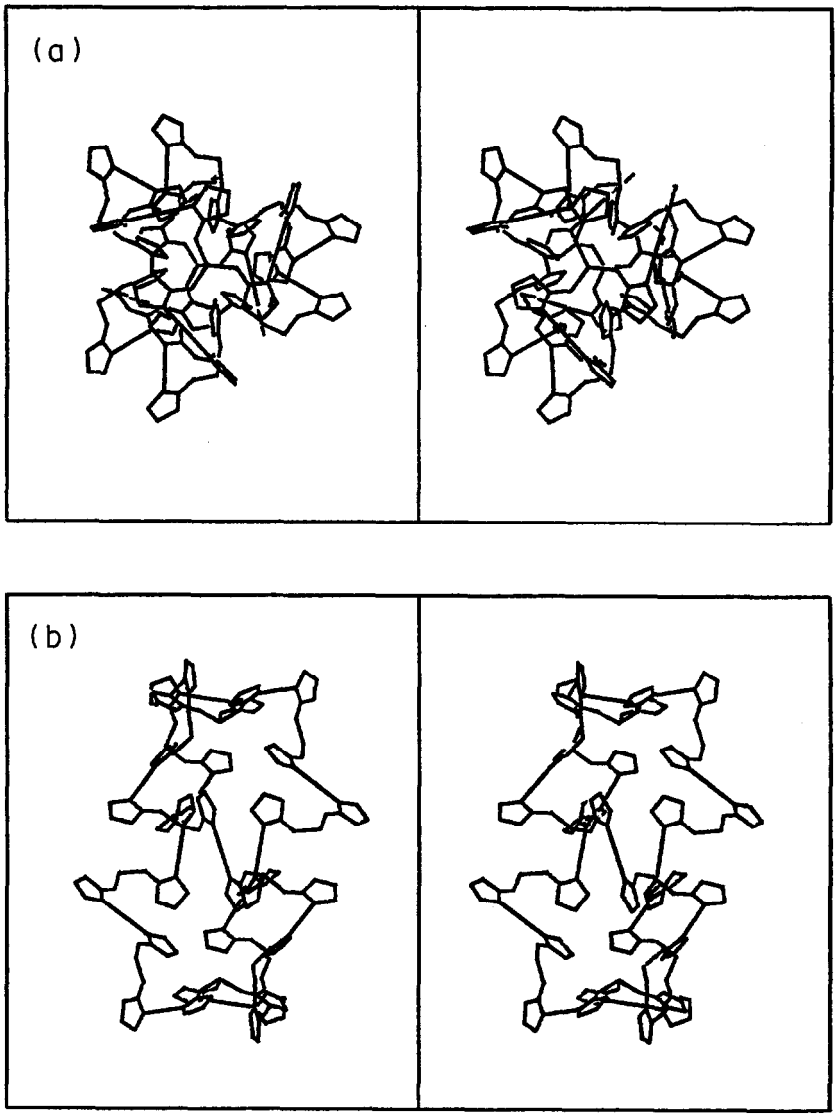

Fig. 2. Stereoscopic view of the packing in **2** showing the macrobicyclic units: (a) plan (viewed down three-fold axis); (b) elevation (viewed down two-fold axis). The anions have been omitted for clarity.

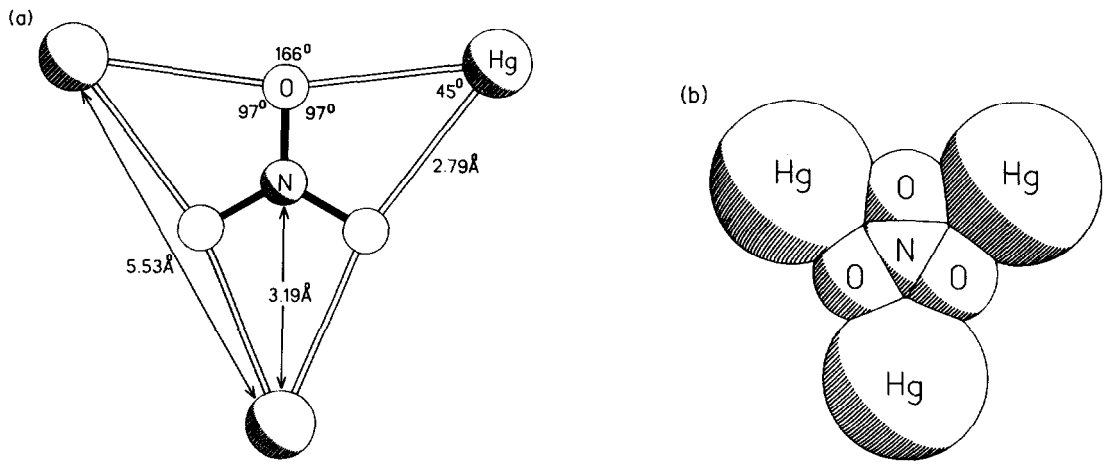

Fig. 3. (a) Skeletal and (b) space-filling representations of the central nitrate environment in **2**.

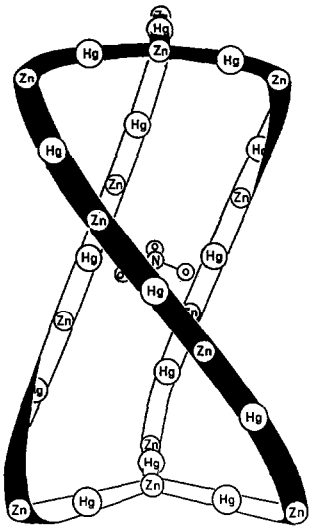

Fig. 4. Schematic representation of the twisted 80-membered macrobicyclic, heterometallic arrays in **2**, also showing the central nitrate ion linking the mercury atoms of each strand.

ring is essentially planar, with the only major deviation from planarity being Hg(1) which lies 0.6 Å below the ring plane, a very similar situation to that in the related Hg/Ag complex.[5] The transannular Hg—Hg distance (3.53 Å) is too long to be considered bonding. This is also true for the Hg(2)—Cl(2) contact (3.33 Å).

In view of the distortion from linearity of the Cl—Hg—Cl unit in **4**, we have studied the effect this has on the metal–halogen stretching bands in the vibrational spectra. For **4** we observed ν_1 (Hg—Cl) at 300 cm^{-1} and ν_3 (Hg—Cl) at 351 cm^{-1}, which are lower than the values reported[11] for linear $HgCl_2$ (ν_1 348, ν_3 405 cm^{-1}). As the analogous bromide, **5**, shows a similar decrease in ν(Hg—Br): ν_1 187, ν_3 249 cm^{-1} (cf. 219 and 294 cm^{-1}, respectively for $HgBr_2$[11]), the Br—Hg—Br unit in **5** is probably also non-linear.

$Hg_3Cd(C_4H_6NO)_6(NO_3)_2$ (3)

Elemental analysis of **3** showed that it had an analogous stoichiometry to the complex $[Hg_3Co(C_4H_6NO)_6(NO_3)_2]_n$ (**6**). Although suitable single crystals of **3** could not be obtained, X-ray powder diffraction photographs confirmed that **3** and **6** are isostructural.

The cobalt atom in **6** is known[1] to be in a slightly *trans*-compressed octahedral CoO_6 coordination geometry (four Co—O bonds of 2.12 Å and two of 2.05 Å). In order to obtain some information about any distortion of the analogous CdO_6 unit, we have used manganese(II) ions as probes for the cobalt and cadmium sites in **3** and **6**, by examining the zero-field splitting (ZFS) in the X- and Q-band EPR spectra of manganese(II) ions doped into these lattices (e.g. Fig. 7). From the Q-band spectrum of **3** the ZFS parameters were calculated to be: $D = -0.037\ cm^{-1}$ and $\lambda (= E/D) = 0.18$. A similar analysis of the spectrum of manganese-doped **6** yielded: $D = -0.034\ cm^{-1}$ and $\lambda = 0.25$. For the latter compound the small value of D and its negative sign (determined as in ref. 12), are in very good agreement with the small axial compression

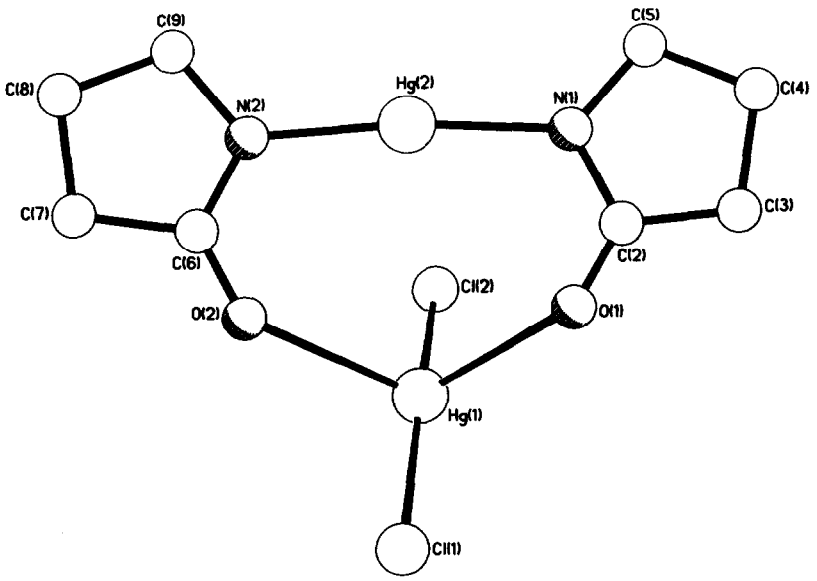

Fig. 5. The molecular structure of **4** showing the crystallographic numbering scheme.

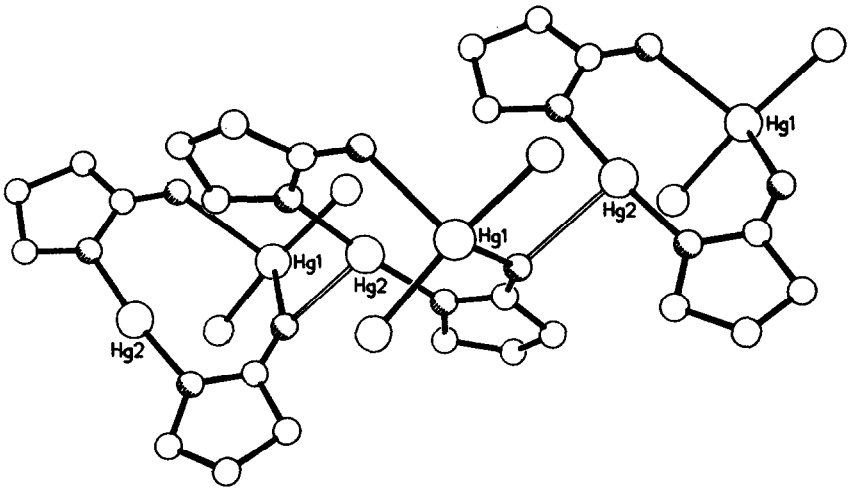

Fig. 6. Part of the polymeric strands in **4**.

observed for the cobalt site in the host lattice. The close similarity of the *D* value found for manganese-doped **3**, both in magnitude and sign, suggests that the cadmium site is also close to octahedral geometry, but with a small axial compression.

DISCUSSION

The two new structural types reported here for compounds **2** and **4** add yet further examples to the novel polymeric heterometallic structures generated by use of **1** as a ligand system. As in the other M/Hg heterometallic compounds formed by **1**, the actual structures adopted, though complex, can be understood by considering both the adoption of a "normal", or near normal, coordination geometry by the metal, M, and the various possible arrangements of **1** as a ligand. The diversity of the ligand behaviour of **1** merits discussion.

The first point to be made is that, from all the structural results we have obtained so far, there is little or no flexibility arising from bending of the N—Hg—N unit. The largest departure from N—Hg—N linearity is 9° in **2**.

That limitation is more than offset by two other factors: (a) the free rotation of the pyrrolidone rings

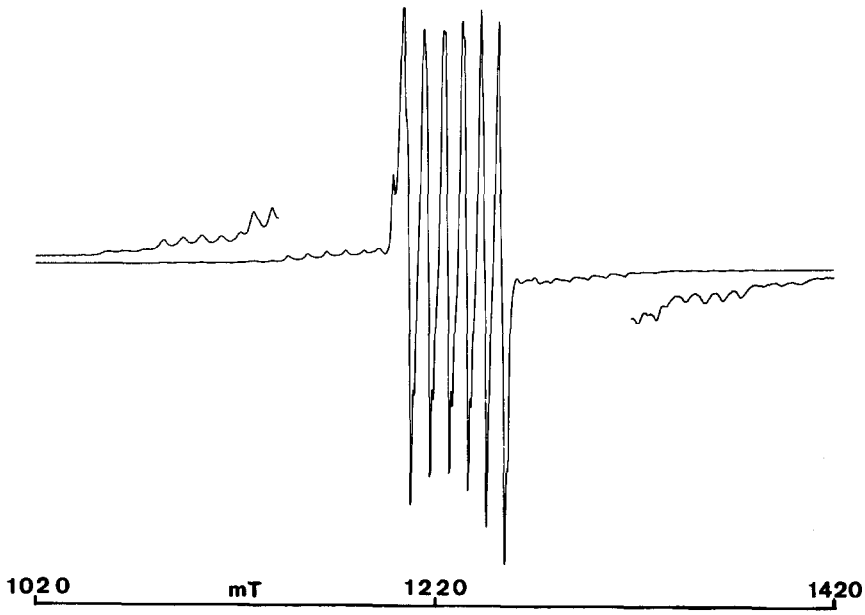

Fig. 7. Q-band EPR spectrum of a manganese(II)-doped sample of **3**.

Table 4. Angle between the mean planes of the pyrrolidone rings in HgL_2 ($L = C_4H_6NO$) in various heterometallic complexes

Complex	Mercury atom	Angle (°)[a]	Reference
$[Hg_2L_2Cl_2]$	Hg(2)	7.0	This work
$[HgAgL_2(NO_3)_2]$	Hg(1)	15.0	5
	Hg(2)	16.9	
$[Hg_3CoL_6(NO_3)_2]_n$	Hg(1)	52.4	1
	Hg(2)	180.0	
$[Hg_3Zn_2L_6(NO_3)_{3.33}(CH_3O)_{0.67}]_n$	Hg	55.7	This work
$[Hg_2EuL_4(NO_3)_3]_n$	Hg(2)	70.8	2
	Hg(1)	107.4	
$[Hg_2ThL_4(NO_3)_6]_n$	Hg(2)	81.0	3
	Hg(1)	133.3	
$[Hg_2CuL_4(ClO_4)_2]_n$	Hg	82.8	4
$[Hg_2CuL_4(NO_3)_2]_n$	Hg	86.1	4
$[Hg_3Tb_2L_6(NO_3)_6]_n$	Hg(1)	110.8	2
	Hg(2)	180.0	

[a] 0° represents *cis*-coplanar, 180° represents *trans*-coplanar.

about the Hg—N bonds and (b) the directionality of the oxygen atom lone pairs of electrons, permitting coordination to other metals in *syn*- or *anti*-dispositions with respect to the mercury atom.

As may be seen from the data collected in Table 4, the mutual free rotation of the pyrrolidone rings about the Hg—N bonds results in a wide range of observed conformations for the HgL_2 unit (where $L = C_4H_6NO$). At the extremes of ring co-planarity, or near co-planarity, the oxygen atoms may be *cis*-disposed (I), O—N—N—O torsion angle *ca* 0° (as in Hg(2) of $Hg_2L_2Cl_2$; torsion angle of 7°) or *trans*-disposed (II), O—N—N—O torsion angle 180° (as in Hg(2) of $[Hg_3CoL_6(NO_3)_2]_n$[1]), but there is also a wide range of intermediate conformations.

Various possible *syn*- and/or *anti*-arrangements for one or two metal ions, M, to bind to **1** are shown in III–VIII (in which, for simplicity, only the NCO fragments of the pyrrolidone rings are shown). Binding modes III and IV are found[5] in $[HgAgL_2(NO_3)]_2$, III is also found in **4**, VI in $[Hg_3CoL_6(NO_3)_2]_n$[1] and VII in $[Hg_3Tb_2L_6(NO_3)_6]_n$.[2] The remaining compounds listed in Table 4 have binding modes related to either V or VII. Clearly it is this capacity of the oxygen atoms to bind in any of these several ways, combined with the possible

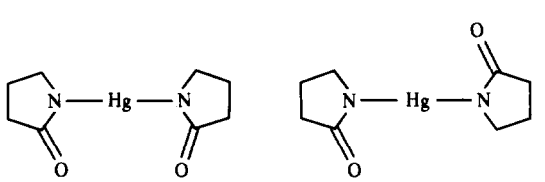

I II

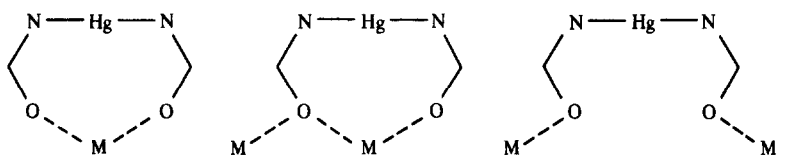

III IV V

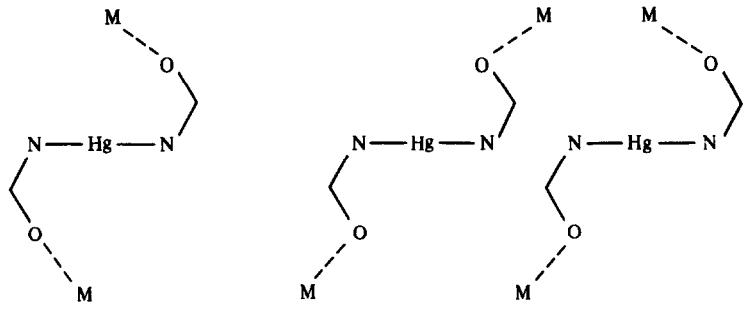

VI VII VIII

rotation of the two pyrrolidone rings about the mercury atom, which accounts for the versatility of the system.

Acknowledgement—We thank the SERC for the X-ray diffractometer, the EPR spectrometers and for a Research Studentship (to R.E.P.W.).

REFERENCES

1. D. M. L. Goodgame, D. J. Williams and R. E. P. Winpenny, *Angew. Chem. Int. Ed. Engl.* 1988, **27**, 261.
2. (a) D. M. L. Goodgame, D. J. Williams and R. E. P. Winpenny, *J. Chem. Soc., Chem. Commun.* 1988, 437; (b) D. M. L. Goodgame, D. J. Williams and R. E. P. Winpenny, *J. Chem. Soc., Dalton Trans.*, in press.
3. D. M. L. Goodgame, D. J. Williams and R. E. P. Winpenny, *Polyhedron* 1988, 7, 1807.
4. D. M. L. Goodgame, D. J. Williams and R. E. P. Winpenny, *Angew. Chem. Int. Ed. Engl.* 1987, **26**, 1044.
5. D. M. L. Goodgame, D. J. Williams and R. E. P. Winpenny, *Polyhedron* 1988, **7**, 1299.
6. G. M. Sheldrick, SHELXTL, An integrated system for solving, refining and displaying crystal structures from diffraction data, Revision 4.1. University of Gottingen, F.R.G. (1983).
7. D. Vivien and J. F. Gibson, *J. Chem. Soc., Faraday Trans.* 1975, **2**, 1640.
8. W. H. Knoth, P. J. Domaille and R. L. Harlow, *Inorg. Chem.* 1986, **25**, 1577.
9. R. J. Majeste and L. M. Trefonas, *Inorg. Chem.* 1972, **11**, 1834.
10. A. Cooper, E. M. Gopalakrishna and D. A. Norton, *Acta Cryst.* 1968, **24B**, 935.
11. K. Nakamoto, *Infrared and Raman Spectra of Inorganic and Coordination Compounds*, 3rd edn, p. 144. Wiley, New York (1977).
12. M. Goodgame and J. N. Okey, *J. Chem. Soc., Dalton Trans.* 1985, 75.

Polyhedron Vol. 8, No. 15, pp. 1923–1931, 1989
Printed in Great Britain

0277–5387/89 $3.00+.00
© 1989 Maxwell Pergamon Macmillan plc

SYNTHESIS, CHARACTERIZATION AND X-RAY CRYSTAL STRUCTURE OF YTTRIUM(III) MACROCYCLIC COMPLEXES WITH A SIX-NITROGEN-DONOR CAVITY

G. BOMBIERI

Istituto di Chimica Farmaceutica, Universita di Milano, Milano, Italy

and

F. BENETOLLO*

Istituto di Chimica e Tecnologia dei Radioelementi, Area de Ricerca CNR, Corso Stati Uniti 4, Padova, Italy

and

W. T. HAWKINS, A. POLO and L. M. VALLARINO

Department of Chemistry, Virginia Commonwealth University, Richmond, VA 23284, U.S.A.

(*Received* 4 *January* 1989; *accepted* 21 *February* 1989)

Abstract—Two novel six-nitrogen-donor macrocyclic complex cations of yttrium(III) were obtained from the metal-templated Schiff-base condensation of 1,2-diaminoethane with either 2,6-diacetylpyridine or 2,6-diformylpyridine. The complex cations were isolated as salts of coordinating as well as non-coordinating anions. Single crystal X-ray analysis was carried out for the mixed acetate perchlorate salt of composition $Y(C_{22}H_{26}N_6)(CH_3COO)_2(H_2O)_{0.5}ClO_4$, which crystallized in the triclinic system, space group $P\bar{1}$ with $Z = 2$, in a unit cell having $a = 13.052(2)$, $b = 11.362(2)$, $c = 11.426(2)$ Å, $\alpha = 108.87(4)$, $\beta = 104.73(4)$ and $\gamma = 100.26(4)°$. The structure was characterized by the presence of two slightly different coordination entities, statistically distributed in the crystal lattice in a 1 : 1 ratio. Both entities contained a yttrium(III) ion linked to the six-nitrogen-donor atoms of the macrocycle, which was slightly folded into a butterfly configuration. A bidentate chelating acetate on the convex side of the macrocycle and either a monodentate acetate or a molecular of water on the opposite side, completed the coordination sphere, resulting in coordination number nine. Ionic acetate and perchlorate balanced the residual charges of the complex cations. The yttrium(III) macrocyclic cations remained undissociated in solution, as shown by the chemical behaviour and NMR spectra.

The complexes of the lanthanide(III) ions with six-donor monomacrocyclic ligands have been extensively studied in regard to synthesis, structure and solution properties. The complexes of crown ethers were the first to be obtained and studied;[1] more recently, a number of six-nitrogen as well as mixed nitrogen–oxygen and nitrogen–sulphur six-donor systems have been reported.[2–18] In contrast, very little is so far known on the macrocyclic chemistry of yttrium(III), despite its close similarity to the lanthanide(III) ions in both size and chemical behaviour. A potentially useful series of lanthanide macrocycles is that containing the six-nitrogen cations L_I and L_{II} (Fig. 1), obtained from the metal-templated cyclic Schiff-base condensation of 1,2-

* Author to whom correspondence should be addressed.

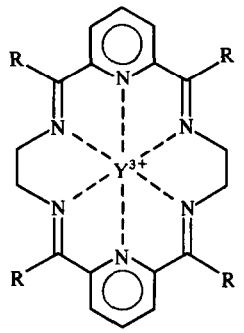

Fig. 1. Schematic formula of macrocyclic complex cations; L_I (R = CH_3), L_{II} (R = H).

diaminoethane with either 2,6-diacetylpyridine (L_I) or 2,6-diformylpyridine (L_{II}). The salts of these macrocyclic cations with appropriate counterions are unique among the lanthanide complexes in that they are very soluble in water as well as in a variety of organic solvents: furthermore, they are inert towards metal release in solution, even in the presence of acids, bases or competing ligands. We were interested in developing a parallel series of macrocyclic complexes of yttrium(III), in the anticipation that these might similarly exhibit a high degree of kinetic stabilization and thus offer a viable alternative to the use of functionalized aminocarboxylic acids[19] for the attachment of the ^{89}Y isotope to biological substrates.

EXPERIMENTAL

Starting materials and procedures

Yttrium salts, 2,6-diacetylpyridine, 2,6-diformylpyridine and the acids (benzoic, 4-hydroxybenzoic, 4-aminobenzoic, 2-furancarboxylic) were purchased from Aldrich Chemical Co. A solution of 1,2- diaminoethane in anhydrous methanol (0.40 M) was prepared as described.[9] All solvents were reagent grade and anhydrous unless specified otherwise. Microanalysis (C, H, N) were performed by Atlantic Microlab, Atlanta, Georgia and Galbraith Laboratories, Knoxville, Tennessee. IR absorption spectra were obtained with a Perkin–Elmer 283 spectrophotometer (4000–200 cm^{-1}) using both KBr pellets and a combination of Nujol and hexachlorobutadiene mulls.

Template synthesis of $YL_I(CH_3COO)_2Cl \cdot 4H_2O$ ($L_I = C_{22}H_{26}N_6$)

Hydrated yttrium(III) acetate and 2,6-diacetylpyridine were dissolved separately in methanol and mixed with a methanol solution of 1,2-diaminoethane (1:2:2 mole ratio) to produce an approximately 2×10^{-2} M solution with respect to yttrium(III). (Best results were obtained with a freshly prepared solution of 1,2-diaminoethane.) The mixture was heated to reflux for 4 h, during which time the colour changed from bright yellow to light amber. After evaporation of the solution to dryness under reduced pressure, the amber-coloured pasty residue was worked up several times with diethyl ether and the resulting solid was filtered and dissolved in the minimum volume of chloroform. The turbid chloroform solution was clarified with charcoal, filtered and evaporated again to dryness under reduced pressure. The residue was crystallized several times from methanol–diethyl ether, affording small off-white crystals which were dried at room temperature over Drierite (yields: 60–70%). Found: C, 44.6; H, 5.6; N, 11.4. Calc. for $YC_{22}H_{26}N_6(CH_3COO)_2Cl \cdot CH_3OH \cdot 4H_2O$: C, 45.0; H, 6.1; N, 11.7%. The compound gradually lost the methanol when exposed to the atmosphere.

The compound was very soluble in water (*ca* 35 mg cm^3) as well as in most organic solvents, except low boiling ethers and aliphatic hydrocarbons. An intense purple colour developed when benzene–chloroform solutions of the complex were heated to boiling for several minutes; the colour faded gradually when the solution cooled down to room temperature in the presence of air.

The IR spectrum of the complex showed the typical pattern of the macrocycle (see below for bromide complex), together with a very strong, broad absorption centred at 3440–3200 cm^{-1} (ν_{OH}). The major carboxylate absorptions appeared as two very strong and rather narrow bands at 1550 cm^{-1} ($\nu_{COO_{asym}}$) and 1440 cm^{-1} ($\nu_{COO_{sym}}$), and a strong sharp band at 655 cm^{-1} [δ(OCO)].

^1H NMR chemical shifts at 89.56 MHz (δ, ppm relative to TMS): 8.31, 6H, py; 3.95, 8H, CH_2; 3.36, 8H, H_2O; 2.53, 12H, CH_3 of macrocycle; 1.35, 6H, CH_3 of acetate.

Metathesis reactions of the bis-acetate-chloride complex of the yttrium(III)–L_I *cation*

(1) Exchange of all anions of the diacetate–chloride with bromide was achieved by warming a methanol solution of the original complex with a two-fold molar excess of conc. hydrobromic acid diluted in methanol at 40°C for 1 h. The resulting solution was chilled at 0°C and diluted with diethyl ether; the nearly colourless crystals that formed (yield: 55%) were filtered, washed with methanol–ether (1:10) and dried over Drierite. Found: C, 33.4; H,

4.6; N, 10.5. Calc. for $Y(C_{22}H_{26}N_6)Br_3 \cdot 5H_2O$: C, 33.3; H, 4.6; N, 10.6%.

The IR spectrum showed the following absorptions (cm^{-1}): 3500–3000 vs, vbr (ν_{OH}), 1660 and 1605, vs, sharp ($\nu_{C=N}$), 1430 m, 1385 vs, 1330 vw, 1303 w, 1268 s, 1230 sh, 1190 s, 1155 vw, 1125 vw, 1065 vw, 1003 m, 975 vw, 930 vw, 880 vw, 808 s, 735 m, 710 vs, 640 vw, 600–400 w,vbr, with peak at 580 m (ρ_{H_2O}). Except for the presence of the water absorptions, this spectrum may serve as an identifying fingerprint for the $C_{22}H_{26}N_6$ macrocycle free of interference from anion absorptions.

(2) Partial exchange of the acetates by chloride was accomplished by dissolving the diacetate–chloride complex in a small volume of methanol, adding conc. hydrochloric acid diluted with methanol (HCl–complex mole ratio, approximately 5:1), and warming the mixture for 1 h at 40°C. Dilution of the resulting chilled solution with diethyl ether gave nearly colourless microcrystals that were filtered, washed with methanol–ether (1:10) and dried over Drierite (yields: 60%). Found: C, 41.1; H, 5.5; N, 12.5. Calc. for $Y(C_{22}H_{26}N_6)(CH_3COO)_{0.5}Cl_{2.5} \cdot 5H_2O$: C, 41.1; H, 5.6; N, 12.5%. The IR spectrum showed the typical macrocycle pattern (see bromide complex) as well as water and acetate absorptions: 1530 cm^{-1} ($\nu_{COO_{asym}}$) and 1460 cm^{-1} ($\nu_{COO_{sym}}$).

(3) Exchange of chloride by perchlorate was accomplished by dissolving the diacetate–chloride complex in a small volume of methanol, adding a five-fold molar excess of solid $LiClO_4$, filtering the resulting cloudy solution and allowing it to stand loosely covered for 1 week at room temperature. The transparent, light amber crystals that formed became cloudy and crumbled upon exposure to the atmosphere; those used for X-ray analysis were stored and handled in their mother liquor.

(4) Reaction of the diacetate–chloride complex with a two-fold excess of $LiBF_4$ in methanol gave nearly colourless microcrystals of the tris-tetrafluoroborate (yield: 75%). Found: C, 29.1; H, 5.7; N, 11.3. Calc. for $Y(C_{22}H_{26}N_6)(BF_4)_3 \cdot 2H_2O$: C, 29.0; H, 5.7; N, 11.3%. The IR spectrum showed, in addition to the typical macrocycle absorptions, a band centred at 1050 cm^{-1} (vs,br) and one at 510 cm^{-1} (m) arising from the ν_3 and ν_4 modes of ionic BF_4^-.

(5) Exchange of the acetates by other carboxylates (benzoate, 4-hydroxybenzoate, 4-aminobenzoate, 2-furancarboxylate) was accomplished by mixing methanol solutions of the diacetate–chloride complex and of the substituent acid (mole ratio, 1:2), warming the mixture at 40°C for 1 h and cooling for 1–2 days in a refrigerator. The nearly colourless crystalline solids that formed were filtered, washed with a small volume of methanol and dried *in vacuo* over Drierite (yields ranged from 50 to 85%). Found: C, 49.7; H, 5.3; N, 10.1. Calc. for $Y(C_{22}H_{26}N_6)(C_6H_4COO)_2Cl \cdot 4H_2O$. C, 49.7; H, 5.2; N, 10.1%. Found: C, 50.6; H, 5.3; N, 10.3. Calc. for $Y(C_{22}H_{26}N_6)(OHC_6H_4(COO)_{1.75}Cl_{1.25} \cdot 4H_2O$: C, 50.2; H, 5.3; N, 10.3%. Found: C, 51.1; H, 5.4; N, 13.2. Calc. for $Y(C_{22}H_{26}N_6)(NH_2C_6H_4COO)_2Cl \cdot 4H_2O$: C, 51.3; H, 5.7; N, 13.3%. Found: C, 46.8; H, 5.3; N, 10.2. Calc. for $Y(C_{22}H_{26}N_6)(C_4H_3OCOO)_2Cl \cdot 5.5H_2O$: C, 46.9; H, 5.3; N, 10.3%. The IR spectra of all these complexes showed the pattern of the macrocycle together with the absorptions of water and of the respective carboxylate.

Template synthesis of $YL_{II}(CH_3COO)_2Cl \cdot 4H_2O$ ($L_{II} = C_{18}H_{18}N_6$)

This compound was obtained from hydrated yttrium(III) acetate, 2,6-diformylpyridine and 1,2-diaminoethane as described for the 2,6-diacetylpyridine analogue, except that the handling of the aldehyde precursor and the template synthesis were carried out in a nitrogen atmosphere. The product (off-white crystals) was obtained in *ca* 70% yields after two recrystallizations from methanol–diethyl ether. Found: C, 41.7; H, 4.9. Calc. for $Y(C_{18}H_{18}N_6)(CH_3COO)_2Cl \cdot 4H_2O$: C, 41.8; H, 5.1%. IR absorptions (cm^{-1}): 3480–3200 vs, vbr (ν_{OH}), 3068 vw, 2922 vw, 2862 vw, 1662 and 1594 vs, sharp ($\nu_{C=N}$), 1540 vs ($\nu_{COO_{asym}}$), 1456 ($\nu_{COO_{sym}}$), 1424 sh, 1385 w, 1338 w, 1277 m, 1253 sh, 1162 m, 1103 w, 1077w, 1045 m–s, 1006 m–s, 983 vw, 956 vw, 936 vw, 824 m, 810 m, 748 w, 680 s (δ_{OCO}), 645 w, 617 vw, 602 vw.

Thermogravimetric measurements

A computer driven Perkin–Elmer TGS System 4 Thermogravimetric Analyser was used, with a dry helium flow of 60 cm^3 min^{-1}. It was observed that some samples underwent a variable-rate mass loss at room temperature when placed under the helium flow; exposure to the atmosphere immediately regenerated the original mass, thus ruling out the possibility that some of the sample had been blown off the balance pan. For this reason, heating of the samples was started after the mass had reached an approximately constant value under helium flow at 25°C. All experiments gave the same general pattern: a first mass loss (4–10%) occurred in either one or two steps at a temperature lower than 120°C, a second mass loss occurred above 180°C and gradual decomposition set in at about 250°C. Samples heated up to 250°C rehydrated instantly upon

cooling and exposure to the atmosphere; their masses and IR spectra were than identical to those of the original samples. Samples heated above 250°C had a slightly charred appearance and less sharp IR spectra. It was observed that samples heated in a helium atmosphere or *in vacuo* above 150°C changed from colourless to deep blue–purple; the colour faded rapidly upon cooling in air but persisted for hours *in vacuo* at room temperature. Representative thermogravimetric results follow: $Y(C_{22}H_{26}N_6)Br_3 \cdot 5H_2O$: mass loss of 9.3% in a step centred at *ca* 110°C (calc. for four H_2O, 9.35%); 2.1% loss between 200 and 250°C (calc. for one H_2O, 2.3%). $Y(C_{22}H_{26}N_6)(C_4H_3COO)_2Cl \cdot 5.5H_2O$: mass loss of 4.49% in a step centred at *ca* 35°C and 1.42% in a step centred at *ca* 105°C, corresponding respectively to two H_2O (calc. 4.39%) and less than one H_2O (calc. for one H_2O, 2.20%). Partial loss of water occurred during equilibration in dry helium flow.

X-ray measurements and structure determination of the yttrium(III)–L_I diacetate perchlorate complex

A transparent, pale yellow, prismatic single crystal of dimensions 0.16 × 0.20 × 0.30 mm was centred on a four-circle Philips PW 1100 diffractometer with graphite-monochromated Mo-K_α radiation. A total of 4771 reflections ($2\theta_{max} = 50°$) were measured, which when merged gave 2959 unique reflections with $I \geqslant 3\sigma(I)$. The intensity data were corrected for Lorentz polarization effects and for absorption, following the method of North *et al.*[20] The structure was solved using three-dimensional Patterson and Fourier techniques and refined with full-matrix least-squares. Hydrogen atoms were introduced at calculated positions and were allowed to ride on associated carbon atoms during the least-squares refinement ($d_{C-H} = 0.98$ Å and $U_{iso} = 0.07$ Å^2). Atomic scattering factors were taken from ref. 21. Data processing and computations were carried out by using the SHELX 76 program package.[22]

In the last stages of refinement, difficulties were encountered in identifying either the species in the ninth coordination position or the positions of the counter ions. While the O(41) position was well identified, the final difference Fourier map showed electron density residuals of the order of 3 e Å^{-3}. These could be best interpreted by considering the O(41) position to be occupied by the oxygen atom of either a water molecule or a monodentate acetate, each with 50% occupancy. Other residuals were accounted for by a statistical distribution of the ionic acetates [0.5 mol/yttrium(III)], together with the disordered perchlorate, as required for complete charge balance. Another minor residual, 0.8 e Å^{-3}, suggested that an even more complicated statistical distribution of the anions might occur; the presence of traces of methanol and water molecules could not be excluded. The best refinement was achieved for the molecular composition $[YL_I(CH_3COO)(H_2O)_{0.5}(CH_3COO)_{0.5}](CH_3COO)_{0.5}(ClO_4)$, which is consistent with IR spectral properties.

Crystal data

$C_{26}H_{33}N_6O_{8.5}ClY$, $M = 689.94$, triclinic space groups $P1$ or $P\bar{1}$ ($P\bar{1}$ was confirmed after structure solution). $a = 13.052(2)$, $b = 11.362(2)$, $c = 11.426(2)$ Å, $\alpha = 108.87(4)$, $\beta = 104.73(4)$, $\gamma = 100.26(4)°$, $U = 1486.60$ Å^3, $Z = 2$, $D_c = 1.54$ Mg m^{-3}, $F(000) = 710$, μ(Mo-K_α) = 20.50 cm^{-1}. Supplementary material (tables of atomic coordinates, atomic vibrations and calculated structure amplitudes) have been deposited with the Editor. Atomic coordinates have been deposited at the Cambridge Crystallographic Data Centre.

RESULTS AND DISCUSSION

Synthesis and spectral properties

The metal-templated synthesis and general properties of the yttrium(III) six-nitrogen macrocyclic complexes, L_I and L_{II}, closely resembled those of the previously reported corresponding complexes of the lanthanide(III) ions.[2,7,9,12] The yttrium(III) macrocyclic entitites had a very high thermal stability, as shown by their thermogravimetric behaviour. In the example of $YL_IBr_3 \cdot 5H_2O$, four of the water molecules were lost below 120°C but the yttrium(III) macrocyclic cation remained essentially undecomposed up to 250°C, this was confirmed by the IR spectrum of samples isolated after the thermobalance experiment. The yttrium(III) macrocycles were also inert with respect to metal release in solution. Their very simple NMR spectra were consistent with the highly symmetrical structures shown in Fig. 1,[10] and no change was observed over a period of time, even in a strongly coordinating solvent such as dimethylsulphoxide.

Treatment with a variety of coordinating and non-coordinating counterions, as well as with strong acids, resulted in anion metathesis without disruption of the macrocyclic entities. Thus, reaction with the stoichiometric quantity of aromatic monocarboxylic acids resulted in exchange of the acet-

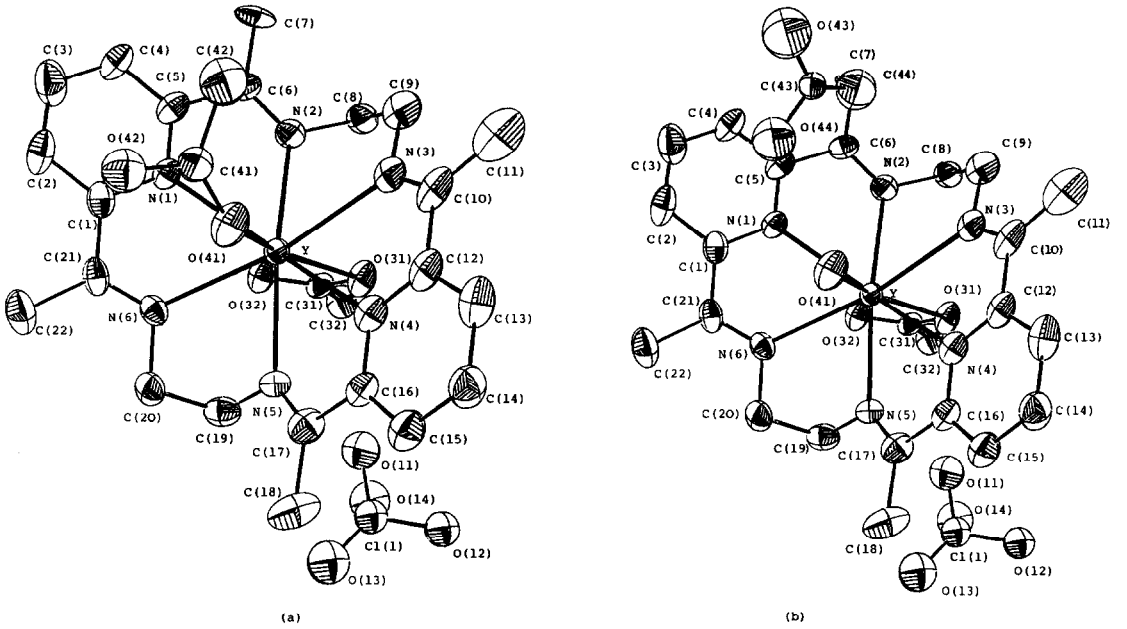

Fig. 2. ORTEP perspective views: (a) $[YL(CH_3COO)_2](ClO_4)$; (b) $[YL(H_2O)(CH_3COO)](CH_3COO)(ClO_4)$. The thermal ellipsoids are at 40% probability.

ates by other monocarboxylates and formation of complexes with the general formula $YL_IX_2Cl \cdot nH_2O$ (X = benzoate, 2-furancarboxylate, 2-hydroxobenzoate, 2-aminobenzoate). Treatment of the diacetate chloride with an excess of $LiClO_4$ resulted in exchange of chloride by perchlorate, yielding a complex of stoichiometry $YL_I(CH_3COO)_2ClO_4 \cdot 0.5H_2O$, the structure of which is discussed in the following section. Finally, substitution of both acetates and chloride was obtained by treatment with a two-fold excess of concentrated hydrobromic or a five-fold excess of $LiBF_4$, resulting in complexes of the formula $YL_IX_3 \cdot nH_2O$ ($X = Br^-$ or BF_4^-).

The IR spectrum of the tribromide complex, being free from anion absorptions, provided a useful "fingerprint" pattern for the identification of the absorptions of the macrocyclic moiety as well as of the anions in other complexes. Especially characteristic were the two intense and sharp absorptions near 1650 and 1600 cm^{-1}, arising from the C=N stretching vibrations. A comparison of the spectrum of the diacetate chloride of the Y—L_I complex with that of the tribromide allowed the unambiguous identification of the carboxylate stretching absorptions as the two very strong and relatively narrow bands at 1550 and 1460 cm^{-1}. The frequency difference between the two bands, $\Delta\nu = 90$ cm^{-1}, suggests that the two acetates present in this complex are both coordinated as bidentate chelating ligands.[23]

Crystal structure of the YL_I *diacetate perchlorate complex*

This compound contains two different complex cations, $[YL_I(CH_3COO)_2]^+$ and $[YL_I(H_2O)(CH_3COO)]^{2+}$, present in a 1:1 ratio in the crystal lattice. The charge of the 1+ cation is balanced by a disordered ionic perchlorate, that of the 2+ cation is balanced by a disordered ionic perchlorate and an ionic acetate. The bonding and conformation of the two Y—L_I complex cations are illustrated in Fig. 2, which also shows the atomic numbering scheme. In each case, the yttrium(III) is nine-coordinate and is bonded to the six nitrogen atoms of the macrocycle, which is slightly folded in a butterfly configuration. In addition, the yttrium(III) is bonded to the two oxygen atoms of a bidentate acetate on the convex side of the macrocycle, and to either a monodentate acetate [Fig. 2(a)] or a water molecule [Fig. 2(b)] on the opposite side. The coordination geometry is the same for both complex cations and is best described, despite the distortion imposed by the presence of a short-span bidentate acetate, as a monocapped square antiprism in which the two bases are defined by [N(1), N(2), O(32), N(6)] and [N(3), O(31), N(5), O(41)], respectively, and the capping position is occupied by N(4).

The bond distances and angles for the two complex cations (a) and (b) are reported in Table 1; significant torsion angles are given in Table 2. The

Table 1. Bond lengths (Å) and angles (°) with ESDs in parentheses

(a) Yttrium environment

Y—N(1)	2.579(8)	N(1)—Y—N(2)	61.2(3)
Y—N(2)	2.551(8)	N(1)—Y—N(6)	61.0(3)
Y—N(3)	2.623(8)	N(2)—Y—N(3)	62.7(3)
Y—N(4)	2.584(8)	N(3)—Y—N(4)	61.3(3)
Y—N(5)	2.498(8)	N(4)—Y—N(5)	61.6(3)
Y—N(6)	2.597(8)	N(5)—Y—N(6)	63.8(3)
Y—O(31)	2.355(6)	O(31)—Y—O(32)	54.9(3)
Y—O(32)	2.415(6)		
Y—O(41)	2.274(7)		

(b) Ligands

N—C(py)$_{av}$	1.35(1)	C—C(py)$_{av}$	1.37(1)
Cl—O$_{av}$	1.44(2)	C—C(aliphatic)$_{av}$	1.50(1)
C(31)—O(31)bidentate	1.27(1)	C(41)—O(41)monodentate	1.26(2)
C(31)—O(32)bidentate	1.27(1)	C(41)—O(42)	1.28(2)
C(31)—C(32)	1.49(2)	C(41)—C(42)	1.44(4)
C(43)—O(43)	1.14(5)		
C(43)—O(44)	1.21(5)		
C(43)—C(44)	1.40(5)		
Y—N(1)—C(1)	119.6(7)	Y—N(1)—C(5)	121.7(7)
N(1)—C(1)—C(2)	119(1)	C(2)—C(1)—C(21)	125(1)
C(1)—C(2)—C(3)	121(1)	C(2)—C(3)—C(4)	119(1)
C(3)—C(4)—C(5)	120(1)	N(1)—C(5)—C(4)	123(1)
C(4)—C(5)—C(6)	122.3(9)	C(5)—C(6)—C(7)	119(1)
C(7)—C(6)—N(2)	126(1)	Y—N(2)—C(6)	124.6(8)
Y—N(2)—C(8)	111.3(6)	C(16)—C(17)—C(18)	117(1)
Y—N(3)—C(9)	118.9(7)	Y—N(5)—C(17)	124.9(8)
Y—N(3)—C(10)	121.6(8)	Y—N(5)—C(19)	112.1(6)
N(3)—C(10)—C(11)	126(1)	Y—N(6)—C(20)	118.7(7)
C(11)—C(10)—C(12)	118(1)	Y—N(6)—C(21)	121.4(7)
C(10)—C(12)—C(13)	123(1)	N(6)—C(21)—C(22)	124(1)
C(12)—C(13)—C(14)	120(1)	C(18)—C(17)—N(5)	125(1)
C(13)—C(12)—N(4)	122(1)	C(1)—C(21)—C(22)	120(1)
C(13)—C(14)—C(15)	118(1)	O(31)—C(31)—O(32)	120(1)
C(14)—C(15)—C(16)	120(1)	O(32)—C(31)—C(32)	120(1)
C(15)—C(16)—C(17)	124(1)	O(31)—C(31)—C(32)	120(1)
C(15)—C(16)—N(4)	122(1)	Y—O(31)—C(31)	93.5(5)
Y—N(4)—C(16)	119.7(7)	Y—O(32)—C(31)	91.2(6)
Y—N(4)—C(12)	120.6(7)		
O—Cl—O$_{av}$	108(1)		

macrocyclic moieties, identical in (a) and (b), consist of two nearly planar sections, C(8)—N(2)···N(6)—C(20) and C(19)—N(5)···N(3)—C(9), with deviations from their best mean planes ranging from −0.17 to 0.20 Å. The macrocycle is folded in the direction of a singly coordinated ligand (water or acetate), with a dihedral angle of 115.7(1)°; the torsion angles N(2)—C(6)—C(9)—N(3) and N(5)—C(19)—C(20)—N(6) are 54(1) and 55(1)°, respectively. The metal coordination sphere is characterized by three slightly different pairs of yttrium–nitrogen bond lengths, the bonds of each pair being *trans* to each other. The Y—N$_{py}$ distance is 2.582 Å (averaged value), the Y—N$_{imine}$ distance for the Y—N(3) and Y—N(6) pair is 2.610 Å, and that for the Y—N(2) and Y—N(5) pair is 2.524 Å. In the organic part of the macrocycle, the average bond distances and angles have the expected values: C=N = 1.27 Å, C—N$_{py}$ = 1.35 Å and C—C$_{py}$ = 1.37 Å.

The presence of two complex species of different stoichiometries statistically distributed in the crystal lattice and accompanied by disordered solvent molecules and disordered anions is unusual but

Table 2. Torsion angles

Atoms	Distances 2–3 (Å)	Angles 1–2–3 (°)	Torsion angles 1–2–3–4 (°)
C(1)—N(1)—C(5)—C(6)	1.33(1)	118(1)	−177(1)
N(1)—C(5)—C(6)—N(2)	1.51(2)	115(1)	0(1)
C(5)—C(6)—N(2)—C(8)	1.28(1)	115(1)	−174(1)
C(6)—N(2)—C(8)—C(9)	1.48(1)	122(1)	100(1)
N(2)—C(8)—C(9)—N(3)	1.52(2)	105(1)	54(1)
C(8)—C(9)—N(3)—C(10)	1.44(2)	109(1)	167(1)
C(9)—N(3)—C(10)—C(12)	1.29(1)	119(1)	−173(1)
N(3)—C(10)—C(12)—N(4)	1.49(1)	116(1)	1(2)
C(10)—C(12)—N(4)—C(16)	1.36(1)	116(1)	175(1)
C(12)—N(4)—C(16)—C(17)	1.34(1)	119(1)	−179(1)
N(4)—C(16)—C(17)—N(5)	1.48(2)	114(1)	−3(2)
C(16)—C(17)—N(5)—C(19)	1.25(1)	118(1)	−176(1)
C(17)—N(5)—C(19)—C(20)	1.49(1)	122(1)	103(1)
N(5)—C(19)—C(20)—N(6)	1.53(1)	106(1)	55(1)
C(19)—C(20)—N(6)—C(21)	1.50(1)	106(1)	173(1)
C(20)—N(6)—C(21)—C(1)	1.27(1)	118(1)	−175(1)
N(6)—C(21)—C(1)—N(1)	1.47(2)	116(1)	−4(2)
C(21)—C(1)—N(1)—C(5)	1.35(1)	116(1)	174(1)

not unique. A somewhat similar situation has been reported for a complex of lanthanium(III) chloride with a bicyclic polyether,[24] in which the presence of (often disordered) solvent molecules promotes crystallization, most likely through the formation of hydrogen bonds. An even closer similarity exists with the lutetium(III) complex of the L_I macrocycle having the formula $[LuL_I(CH_3COO)(H_2O\ 50\%, CH_3OH\ 50\%)](CH_3COO)(ClO_4)(H_2O)_{0.5}$.[10] The structure of this lutetium(III) complex is actually very similar to that of the yttrium(III) complex described in the present work. In both compounds the metal ion is nine-coordinate and bound to the six nitrogen atoms of the macrocyclic ligand, to a bidentate acetate on one side of the macrocycle and to a single O-donor ligand on the other side. In both compounds the macrocycle is hinged at the flexible ethylenediamine segments, resulting in a "butterfly" configuration that relieves steric strain and allows the metal ion to best fit into the ligand cavity. The yttrium(III) and lutetium(III) complexes thus differ only in the identity of the single ligands [50% monodentate acetate and 50% water for yttrium(III), 50% methanol and 50% water for lutetium(III)] that occupy the axial coordination position on the concave side of the macrocycle. This facile interchange of neutral as well as anionic axial ligands within the crystal structure is consistent with the high lability of the exocyclic ligands observed in solution. It should be pointed out that the lutetium(III) and yttrium(III) complexes, even though not strictly isostructural, have very similar cell parameters; also, bond lengths and angles follow a parallel trend, differing in magnitude only to the extent expected from the different sizes of the metal ions.[25] These similarities are illustrated by the representative values reported in Table 3. It is instructive to further compare the structure of the Y—L_I macrocycle with that of the complex cation $[YCl(H_2O)_2(18\text{-crown-}6)]^{2+}$, present in the complex of formula $[Y(H_2O)_7(CH_3OH)][YCl(H_2O)_2(18\text{-crown-}6)]Cl_7 \cdot 2H_2O$.[26] In the 18-crown-6 complex the yttrium(III) is again nine-coordinate and the crown ether ligand is folded in the direction of the single chlorine ligand, with the two water molecules bound on the opposite side. The resulting coordination geometry is described as a tricapped trigonal prism distorted towards a capped square antiprism, and thus approaches that observed in the Y—L_I cation. In the crown complex, the Y—O_{crown} bond distances average 2.44(5) Å vs an average value of 2.572(8) Å for the Y—N_{cycle} bonds of the Y—L_I complex. Conversely, the average of the Y—O_{water} bonds (2.36(3) Å) in the crown complex is shorter than the Y—$O_{water\ or\ monodentate\ acetate}$ (2.274 Å) in the Y—L_I complex. These variations are consistent with the usual trends in M—O and M—N bond lengths for neutral and anionic ligands.

CONCLUSIONS

The results reported here show that yttrium(III) acetate is an effective template for the cyclic Schiff-base condensation of suitable diamine and dicar-

Table 3. Structural similarities of lutetium(III) and yttrium(III) complexes

Structural feature[a]	$[YL_I(O_2CCH_3)(OCOCH_3)]^{+}$ [b] $[YL_I(O_2CCH_3)(H_2O)]^{2+}$	$[LuL_I(O_2CCH_3)(CH_3OH)]^{2+}$ [c] $[LuL_I(O_2CCH_3)(H_2O)]^{2+}$
M^{III} ionic radius (nine-coordination)	1.215	1.172
Macrocyclic dihedral angle	115.7(1)	114.4(1)
M—N(pyridine)	2.582	2.544
M—N′(imine)	2.610	2.594
M—N″(imine)	2.524	2.488
M—O(bidentate acetate)	2.355(6) 2.415(6)	2.325(6) 2.368(5)
M—O(monodentate acetate, water or methanol)	2.274(7)	2.232(6)

[a] Bond lengths in Å, angles in degrees.
[b] This work.
[c] Reference 10.

bonyl precursors, producing complex cations in which the yttrium(III) ion is linked to the six-nitrogen-donor atoms of an 18-atom macrocyclic cavity and to the O-donor atoms of exocyclic ligands (anions or solvent molecules). In solution, the exocyclic ligands are labile and easily undergo metathesis, whereas the macrocyclic cations are inert and retain their identity even in very dilute aqueous solution and in the presence of acids and competing ligands. Coupling of these macrocyclic complexes to a substrate via a functional group present in the periphery of the organic moiety should, therefore, result in attachment of the yttrium(III) to a substrate, in a manner unaffected by dilution and pH changes. Work is in progress to achieve peripheral functionalization of the yttrium macrocycles and their coupling to representative substrates.

Acknowledgements—This work has been supported in part by Virginia Commonwealth University and by NATO Bilateral Project No. 184/85.

REFERENCES

1. J. C. G. Bunzli, in *Handbook on the Physics and Chemistry of Rare Earths* (Edited by K. A. Gshneidner Jr and L. Eyring). Elsevier, Amsterdam (1987); J. C. G. Bunzli and D. Wessner, *Coord. Chem. Rev.* 1984, **60**, 191.
2. J. D. J. Backer-Dirks, C. J. Gray, F. A. Hart, M. B. Hursthouse and B. C. Schoop, *J. Chem. Soc., Chem. Commun.* 1979, 774.
3. W. Radecka-Paryzek, *Inorg. Chim. Acta* 1980, **45**, L147.
4. W. Radecka-Paryzek, *Inorg. Chim. Acta* 1981, **52**, 261.
5. K. K. Abid and D. E. Fenton, *Inorg. Chim. Acta* 1984, **95**, 119.
6. K. K. Abid, D. E. Fenton, U. Casellato, P. A. Vigato and R. Graziani, *J. Chem. Soc., Dalton Trans.* 1984, 351.
7. K. K. Abid and D. E. Fenton, *Inorg. Chim. Acta* 1984, **82**, 223.
8. W. Radecka-Paryzek, *Inorg. Chim. Acta* 1985, **109**, L21.
9. L. De Cola, D. L. Smailes and L. M. Vallarino, *Inorg. Chem.* 1986, **25**, 1729.
10. G. Bombieri, F. Benetollo, A. Polo, L. De Cola, D. L. Smailes and L. M. Vallarino, *Inorg. Chem.* 1986, **25**, 1127.
11. T. W. Bell and F. Guzzo, *J. Chem. Soc., Chem. Commun.* 1986, 769.
12. A. M. Arif, J. D. J. Backer-Dirks, C. J. Gray, F. A. Hart and M. B. Hursthouse, *J. Chem. Soc., Dalton Trans.* 1987, 1665.
13. G. Bombieri, *Inorg. Chim. Acta* 1987, **139**, 21.
14. P. A. Vigato and D. E. Fenton, *Inorg. Chim. Acta* 1987, **139**, 39.
15. A. Polo, J. R. Quagliano and L. M. Vallarino, *66th Ann. Meet., Virginia Academy of Science, 1988.*
16. F. Benetollo, G. Bombieri, L. De Cola, A. Polo, D. L. Smailes and L. M. Vallarino, *39th Am. Chem. Soc. Southeastern Reg. Meet., 1987, Abstr.* No. 476.
17. L. De Cola, D. L. Smailes and L. M. Vallarino, *10th Nat. Conf. Photochemistry.* Ravenna, Italy (1985).
18. N. Sabbatini, L. De Cola, L. M. Vallarino and G. Blasse, *Phys. Chem.* 1987, **91**, 4681.
19. M. K. Moi, C. F. Meares, W. C. Cole and S. J. De Nardo, *189th Am. Chem. Soc. Nat. Meet., 1985, Abstr.* No. 30.
20. A. C. T. North, D. C. Philips and F. Mathews, *Acta Cryst.* 1968, **A24**, 351.
21. *International Tables for X-Ray Crystallography*, Vol. IV. Kynoch Press, Birmingham (1974).

22. G. M. Sheldrick, SHELX, A System of Computer Programs for X-ray Structure Determination (1976).
23. K. Nakamoto, in *Infrared and Raman Spectra of Inorganic and Coordination Compounds*, p. 232. J. Wiley, New York (1986).
24. F. Benetollo, G. Bombieri, G. De Paoli, D. L. Hughes, D. G. Parson and M. R. Truter, *Acta Cryst.* 1985, **C41**, 34.
25. R. D. Shannon, *Acta Cryst.* 1976, **A32**, 751.
26. R. G. Rogers, L. K. Kurihara and E. J. Voss, *Inorg. Chem.* 1987, **26**, 2360.

Polyhedron Vol. 8, No. 15, pp. 1933–1938, 1989
Printed in Great Britain

0277–5387/89 $3.00+.00
© 1989 Maxwell Pergamon Macmillan plc

SKELETAL REARRANGEMENTS IN CLUSTERS—III.* APPLICATION OF VIBRATIONAL SYMMETRY ANALYSES

DAVID J. WALES†

University of Chicago, Department of Chemistry, 5735 South Ellis Avenue, Chicago, IL 60637, U.S.A.

and

D. MICHAEL P. MINGOS

Inorganic Chemistry Laboratory, University of Oxford, South Parks Road, Oxford OX1 3QR, U.K.

(*Received* 19 *October* 1988; *accepted* 10 *March* 1989)

Abstract—We show how geometrical selection rules (such as those due to McIvor and Stanton) may be applied to cluster rearrangements to provide further insight into the types of process which may occur. We also demonstrate how a second-order Jahn–Teller vibrational analysis fits in with the orbital symmetry selection rules for diamond–square–diamond processes.

The theoretical study of rearrangements in cluster compounds has recently been elegantly analysed using Stone's Tensor Surface Harmonic (TSH) theory.[1,2] The new approach, discussed in Parts I and II in this series, enables some cluster rearrangement processes which have an orbital crossing, and are therefore "forbidden" in the Woodward–Hoffmann sense,[3] to be identified very simply. In Part I we also explained, in terms of TSH theory, why Lipscomb's diamond–square–diamond (DSD) process[4] (illustrated in Fig. 1) should generally be energetically favourable.

The conclusion of Part I was that transition states between *closo* boranes or carboranes with a single atom on a principal rotation axis of order three or more will generally have an orbital crossing, and hence be high energy processes. The effect of lower symmetry environments, for example, when there is a single atom on a two-fold axis, was also considered. In Part II this result was extended to show that an orbital crossing will generally result if a mirror plane through the critical face is retained throughout the process. If a C_2 axis is retained, however, then there is an avoided crossing and the process is "allowed".

Using the above rules, and the additional criterion that multiple DSD processes are likely to be less favourable than the single DSD process, it is possible to rationalize the whole range of rearrangement rates of the *closo* boranes and carboranes. In Part II we also discussed the application of the rules to rearrangements of transition metal clusters, and suggested some new mechanisms for these species.

Recently, Rodger and Johnson have considered the geometrical symmetry selection rules for the rearrangement of transition metal clusters with between five and 12 atoms.[5] This approach is not concerned with the conservation of *orbital* symmetry, but with the fact that any reaction mechanism must follow a vibrational normal mode of the cluster at every point. These authors consider single edge-cleavage processes only, on the grounds that these are expected to be most favourable. Some of these mechanisms correspond to the diamond–square–diamond processes considered previously,[1] except that they are considered to be stepwise if more than one edge must be broken. In fact all of the processes considered in Part I are geometrically allowed because they all follow normal modes. The purpose of this paper is to eliminate some candidate

* For Parts I and II, see refs 1 and 2, respectively.

† Author to whom correspondence should be addressed.

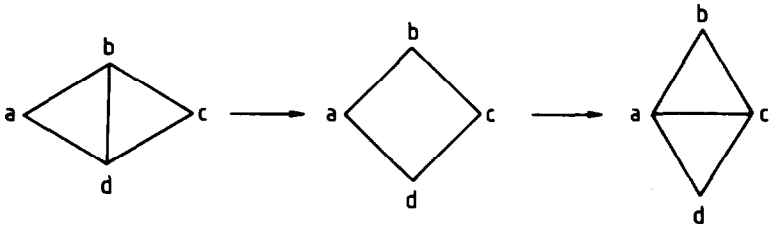

Fig. 1. The diamond–square–diamond process.

structures as transition states using the McIvor–Stanton theorems[6] or the classical selection rules as formulated by Rodger and Schipper.[7] Furthermore, considering the symmetry properties of the transition vector for the DSD process in the point groups C_s and C_2 shows that the orbital symmetry rules developed in Parts I and II are consistent with a vibrational symmetry analysis.

GEOMETRICAL SELECTION RULES

Murrell and Laidler[8] first emphasized the requirement that a true transition state must have precisely one negative "force constant"; that is one normal mode with an associated imaginary frequency. This follows from a straightforward consideration of the multidimensional potential energy surface; if there were two normal modes with negative force constants then the "transition state" would be a hill rather than a saddle point, and there would be a lower energy pathway connecting reactants and products. McIvor and Stanton extended this group theoretical analysis and derived several theorems concerning the transformation of the transition vector and the effect of transition state symmetry operations on the reactants and products.

Their method may be applied as follows. First we assume that the transition state has some specific geometry and find its point group. Then we sketch the displacements of the atoms to their equilibrium positions in the products and reactants. These unlabelled displacement vectors can be regarded as the objects acted upon by the symmetry operations of the transition state point group. If it happens that a symmetry operation of the putative transition state converts the product displacements into reactant displacements, then the transition vector must be antisymmetric under this operation. (The transition vector lies in the direction of the critical normal mode with the negative force constant.) There are various other restrictions on the transformation properties of the transition vector which apply if a symmetry operation maps a reactant onto an equivalent structure.[6] Furthermore, the transition vector must belong to a non-degenerate irreducible representation of the transition state point group by the Murrell–Laidler theorem.

For our purposes the most important result of Stanton and McIvor's work is the antisymmetric nature of the transition vector under operations which interconvert reactant and product displacements. This has an important corollary that a transition state cannot have an odd degree symmetry element linking the product and reactant displacements.[6] (A symmetry element has odd degree if it must be repeated an odd number of times to achieve the identity operation.) The most important examples in this paper will involve structures with a C_3 symmetry axis. Note, however, that this method can only rule out a candidate structure as a transition state for a particular process. It cannot determine whether the structure may be a true transition state for a different reaction, or indeed an intermediate with no negative force constants.

In Rodger and Schipper's approach, the stationary permutation–inversion operations of the product and reactant molecules are considered.[7] With the assumption that all the common stationary operations are preserved throughout the reaction path, it is possible to deduce the symmetry of the transition state, if there is one, for concerted processes which involve only permutations of identical atoms (homoconversions). In fact we can summarize their results for such cases as follows: a transition state for a concerted homoconversion along a maximal symmetry path must have an even-order operation which is not present in the product or reactant. This is a necessary but not a sufficient condition because the operation in question must also be a product generator operation.[7] However, it provides a simple first criterion for examining possible transition state geometries.

For heteroconversions, in which the product is not simply related to the reactant by a permutation of identical nuclei, the geometrical selection rules for concerted processes are much less restrictive. Rodger and Schipper have tabulated the vibrational modes which relate particular point groups, and the presence or absence of modes of the required type is

now the determining factor. In fact their tabulation shows that there is very often a mode (usually E-type) which breaks all the symmetry, and this may help to explain why so many transition states are calculated to have C_1 symmetry.[9] Exceptions arise for point groups with no E modes such as C_{2v}.

APPLICATION TO CLUSTER REARRANGEMENTS

We will consider three specific examples using the McIver–Stanton approach. In each case two DSD processes result in a permutation of the vertices of the starting geometry. First consider the single DSD process leading from the pentagonal bipyramid to the capped octahedron (Fig. 2). The capped octahedron has C_{3v} symmetry and the reactant displacements are clearly mapped onto the product displacement by a C_3 rotation. Since this operation has odd degree, we conclude that the capped octahedron cannot be a transition state for the stepwise double DSD process. It is easy to see that it would be impossible to find a transition vector antisymmetric to this operation: such a species would also have to be antisymmetric under C_3^3, which is the identity operation. This does not preclude the possibility that this structure may be a metastable intermediate, although orbital symmetry considerations suggest that this mechanism probably represents a high-energy process.[2]

The second example is the single DSD process for the bicapped square antiprism (Fig. 3). Again this

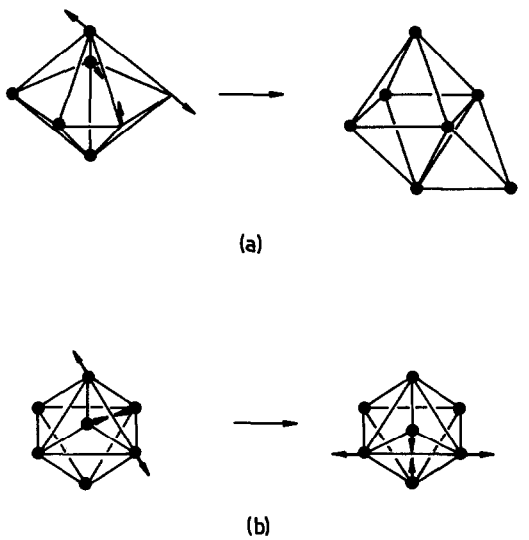

Fig. 2. (a) The single DSD process leading from the pentagonal bipyramid to the capped octahedron, for which (b) the reactant and product displacements are related by a C_3 rotation.

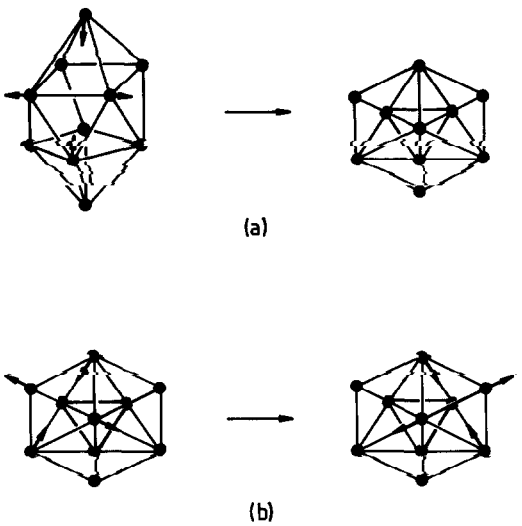

Fig. 3. (a) A single DSD process leading from the bicapped square antiprism to the C_{3v} deltahedron for which (b) the reactant and product displacements are related by a C_3 rotation of the transition state point group.

leads to a C_{3v} intermediate structure for which the reactant and product displacements are related by a C_3 rotation. Hence, we can again conclude that this geometry cannot be a true transition state for the non-concerted double DSD process. There is no such prohibition on the concerted double DSD, however. Furthermore, in this and the previous example a mirror plane through the critical face is considered during each single DSD process. However, this does not necessarily lead to an orbital crossing because the steps do not lead back immediately to the starting geometry. Instead, each intermediate structure has a non-bonding e pair of orbitals at the HOMO–LUMO level, arising from the single atom on the three-fold rotation axis.[1] There is bound to be a significant rise in the total orbital energy for this open shell configuration because the doubly occupied e pair is non-bonding. We conclude that these structures cannot be true transition states and furthermore that they entail significant rises in the electronic energy.

In contrast, consider the single DSD process illustrated in Fig. 4 for the tricapped trigonal prism which leads to a C_{2v} symmetry deltahedron. In this case the point group of the possible transition state contains no odd-order operations. The reactant and product displacements are related by a C_2 operation and one of the reflections, while both sets of displacements are mapped onto themselves under reflection in the other mirror plane. Hence, the transition vector must be antisymmetric under the former operations and symmetric under the

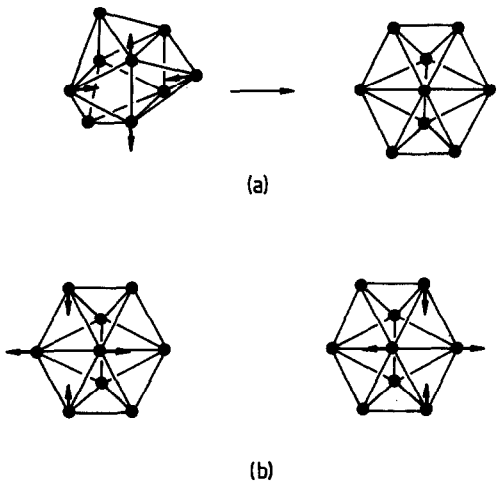

Fig. 4. (a) A single DSD process leading from the tricapped trigonal prism to a C_{2v} symmetry deltahedron and (b) the reactant and product displacements.

latter. It must therefore transform as either B_1 or B_2, depending upon the choice of axes.

The reader may verify that the same conclusions can be reached using the general principle for concerted maximal symmetry homoconversions deduced from Rodger and Schipper's results at the end of the previous section.

THE SECOND-ORDER JAHN–TELLER EFFECT

In this section we will examine the DSD mechanism using the symmetry properties of the terms arising in a perturbation theory analysis of the energy of a distorted molecule.[10] Consider distortion along a normal mode of symmetry species S_i. Using first- and second-order perturbation theory the energy of the distorted system may be written as[10]

$$E(S_i) = E_0 + S_i \int \psi_0 \hat{H}_i \psi_0 \, d\tau + \tfrac{1}{2} S_i^2 \left[\int \psi_0 \hat{H}_{ii} \psi_0 \, d\tau - 2 \sum_m{}' \frac{|\int \psi_0 \hat{H}_i \psi_m \, d\tau|^2}{\Delta E_{m0}} \right].$$

Where ψ_0 is the ground-state wavefunction of the undistorted geometry, ΔE_{m0} is the zeroth-order energy separation between the states ψ_0 and ψ_m of the undistorted geometry, $\hat{H}_i = (\partial \hat{H}/\partial S_i)_0$ and $\hat{H}_{ii} = (\partial^2 \hat{H}/\partial S_i^2)_0$. E_0 is the unperturbed energy of the system and $S_i \int \psi_0 \hat{H}_i \psi_0 \, d\tau$ is the first-order Jahn–Teller term which is not important for non-degenerate electronic states because it vanishes. The term in square brackets can be identified with the "force constant" for distortion along the normal mode in question and can be divided into two parts. The first part, involving the second derivative, represents the nuclear motion in a fixed electron distribution, while the second term represents the "relaxation" of the electron distribution in respect to the nuclear displacement. If this "force constant" is negative then the energy of the system is lowered on distortion and we have a second-order Jahn–Teller effect.

It is often productive to proceed in a non-rigorous manner and consider only the contribution of the HOMO–LUMO mixing to the second part of this term.[10] In this case one simply seeks a normal mode whose symmetry species is contained in the direct product of the symmetry species of the HOMO and the LUMO (and recall that the term $(\partial \hat{H}/\partial S_i)_0$ transforms like S_i). Distortion along such a mode results in the HOMO and LUMO splitting further apart through their mutual admixture, and we will now consider when this occurs for possible single DSD "transition states" of different symmetry.

Consider the product and reactant displacements for the single DSD process sketched in Fig. 5. If the cluster has C_{4v} symmetry it follows from the McIvor–Stanton rules[6] that the transition vector must be antisymmetric under C_4, C_4^3 and σ_d, i.e. it must transform like x^2-y^2. This, in fact, simply corresponds to the displacements as sketched. Now consider descent in symmetry to the point group C_2. The HOMO and the LUMO of the hypothetical *nido* cluster both transform as B in this point group,[2] and the DSD transition vector transforms as A. Since $B \otimes B = A$, we conclude that the contribution of the particular energy term considered above would be non-zero and therefore negative. In C_s, on the other hand, when a diagonal mirror plane is retained, the DSD transition vector transforms as A', while the HOMO and LUMO transform as A' and A''. Since $A' \times A'' = A''$, the DSD mode cannot lead to mixing of the HOMO and LUMO in this case. This fundamental difference between the C_s and C_2 point groups results from the properties of the Tensor Surface Harmonic theory parity operator, $\hat{P}$, which relates L^π and $\bar{L}^\pi$ cluster orbitals.[2] $\hat{P}$ is symmetric to rotations and antisymmetric to reflections, and hence in C_2 the parity

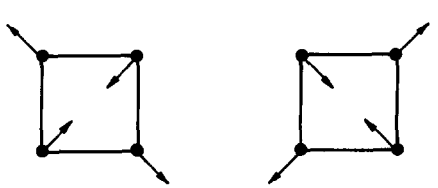

Fig. 5. Displacements to products and reactants in the DSD process. Only the critical face is sketched for clarity.

related HOMO and LUMO belong to the same irreducible representation. In fact, the critical matrix element will have a non-zero component (and lead to a lowering of the energy) for vibrations which transform in the same way as $\hat{P}$. The DSD vibration clearly does transform in this way in C_2, but not in C_s, and this kind of argument could also be applied to predict "mode-softening" in an equilibrium geometry.

This analysis fits in perfectly with the alternative approach of Part II,[2] where we show that a crossing occurs if a mirror plane is retained throughout, and an avoided crossing if a C_2 axis is conserved. Furthermore, if C_{2v} symmetry is conserved throughout a McIvor–Stanton analysis, this leads to the conclusion that the only possible symmetry species for the transition vector is A_1, which does not allow HOMO–LUMO mixing. This analysis, which pertains to the single DSD process in an icosahedron, is again in agreement with the orbital symmetry conclusion, because two mirror planes are retained throughout.

CONCLUSIONS

In this paper we have illustrated how geometrical selection rules may be used to disqualify structures as transition states for skeletal rearrangements in clusters. As examples, we have demonstrated that the stepwise double DSD processes for the pentagonal bipyramid and the bicapped square antiprism have intermediate structures which cannot be true transition states for this mechanism. This does not exclude the possibility that they could be transition states for some other process, or indeed metastable intermediates with no negative force constants. For concerted homoconversions, in which only identical atoms are permuted, the most restrictive conditions are found for paths of maximal symmetry.[7] It is interesting to note that the appearance of a new even-order operation in the "transition state" will lead to an orbital crossing if the symmetry element in question is a C_4 or higher even-order rotation axis.[1]

We have also considered a second-order Jahn–Teller analysis of the diamond–square–diamond mechanism. This alternative approach results in the same conclusion as the orbital symmetry analyses of Parts I and II: single DSD processes, in which a mirror plane is conserved throughout, are expected to be less favourable than those in which a C_2 rotation axis is retained. This is reassuring, since the orbital symmetry arguments generally appear to be the most powerful means for determining the favourability of a proposed reaction path. However, the geometrical rules can be applied to, say, argon clusters just as well as to borohydrides, and the orbital symmetry rules obviously cannot. In fact there is an interesting relation between the single DSD mechanism for $B_8H_8^{2-}$ and a similar process for the Ar_7 skew structure.[11] *Ab initio* calculations for the former structure reveal that the potential energy surface around the transition state is rather flat,[12] and that the barrier to rearrangement is small, in agreement with experiment. A geometrical analysis reveals that the single DSD process, in which a C_2 axis is preserved, is allowed for the Ar_7 skew structure,[12] yet Berry *et al.* could not locate the corresponding saddle point.[12] We conjecture that this region of the Ar_7 potential energy surface is also very flat, making the saddle point difficult to locate. Geometrical analyses of possible "transition states" for the homoconversions of the other Ar_7 geometries which correspond to local minima are in good agreement with the calculations.

Bürgi and Dunitz[13] have demonstrated that reaction pathways can sometimes be traced using X-ray crystallographic analysis of a range of compounds whose distortions from idealized geometries appear to follow a "reaction coordinate". This can lead to a mistaken impression that if a structure is observed in the solid-state it is a good candidate for a transition state. The geometrical selection rules clearly indicate the limitations of this thinking and show how some high symmetry geometries are forbidden as transition states. In the context of the present work, although a capped octahedral geometry has been observed for $Os_7(CO)_{21}$, this structure is forbidden as a transition state for the non-concerted double DSD rearrangement of a pentagonal bipyramid.

Acknowledgements—D.J.W. thanks Downing College, Cambridge, for financial support for his visit to Oxford during which this work was performed. We also thank Dr A. Rodger and Dr P. Schipper for some helpful discussions.

REFERENCES

1. D. J. Wales and A. J. Stone, *Inorg. Chem.* 1987, **26**, 3845.
2. D. J. Wales, D. M. P. Mingos and L. Zhenyang, *Inorg. Chem.*, in press.
3. R. B. Woodward and R. Hoffmann, *Angew. Chem. Int. Ed.* 1969, **8**, 781.
4. W. N. Lipscomb, *Science (Washington DC)* 1966, **153**, 373.
5. A. Rodger and B. F. G. Johnson, *Polyhedron* 1988, **7**, 1107.
6. J. W. McIvor and R. E. Stanton, *J. Am. Chem. Soc.* 1972, **94**, 8618; R. E. Stanton and J. W. McIvor, *J. Am. Chem. Soc.* 1975, **97**, 3632.

7. A. Rodger and P. E. Schipper, *Chem. Phys.* 1986, **107**, 329; A. Rodger and P. E. Schipper, *J. Phys. Chem.* 1987, **91**, 189; A. Rodger and P. E. Schipper, *Inorg. Chem.* 1988, **27**, 458.
8. J. H. Murrell and K. J. Laidler, *Trans. Faraday Soc.* 1968, **64**, 371.
9. M. J. S. Dewar, *Faraday Discuss. Chem. Soc.* 1976, **62**, 197.
10. R. F. W. Bader, *Molec. Phys.* 1960, **3**, 137; R. F. W. Bader, *Can. J. Chem.* 1962, **40**, 1164; R. G. Pearson, *J. Am. Chem. Soc.* 1969, **91**, 1252; R. G. Pearson, *Accts Chem. Res.* 1971, **4**, 152.
11. R. S. Berry, H. L. Davis and T. L. Beck, *Chem. Phys. Lett.* 1988, **147**, 13.
12. D. J. Wales, unpublished work.
13. H. B. Bürgi, *Angew. Chem. Int. Ed.* 1975, **14**, 460.

Polyhedron Vol. 8, No. 15, pp. 1939–1944, 1989
Printed in Great Britain

0277–5387/89 $3.00+.00
© 1989 Maxwell Pergamon Macmillan plc

(CpCo)(ALKYLIDYNE) CLUSTERS FROM HYDROGENATION OF $CpCo(C_2H_4)_2$: SOLID-STATE STRUCTURES AND SOLUTION DYNAMICS OF $(CpCo)_3(CCH_3)_2$ AND $H(CpCo)_4(CCH_3)$

HUBERT WADEPOHL† and HANS PRITZKOW

Anorganisch-Chemisches Institut der Universität, Im Neuenheimer Feld 270, D-6900 Heidelberg, F.R.G.

(*Received* 6 *December* 1988; *accepted* 10 *March* 1989)

Abstract—$CpCo(C_2H_4)_2$ (**1a**) and $Cp'Co(C_2H_4)_2$ (**1b**) (Cp′ = methylcyclopentadienyl) react with dihydrogen to give mixtures of μ_3-alkylidyne clusters, namely $(CpCo)_3(CCH_3)_2$ (**2a**), $(Cp'Co)_3(CCH_3)_2$ (**2b**), $H(CpCo)_4(CCH_3)$ (**3a**), $H(Cp'Co)_4(CCH_3)$ (**3b**), $(CpCo)_4(CCH_3)_2$ (**4a**) and $H(CpCo)_5(CCH_3)$ (**5a**). Compounds **2a**, **3a** and **3b** were separated, and **2a** and **3a** were structurally characterized by single-crystal X-ray crystallography. In solution, **3a** and **3b** show temperature dependent hydride fluxionality.

Stepwise replacement of BH in the (unknown) series of *n*-vertex *closo*-boranes $(BH)_nH_2$ by the isolobal[1] CpCo moiety, formally leads to the metallaboranes $(CpCo)_k(BH)_{n-k}H_2$ and finally to the series of cobalt hydrido clusters, $(CpCo)_kH_2$. Likewise, starting from the *closo*-carboranes, $(BH)_{n-m}(CR)_mH_{2-m}$ ($m = 1$, 2), the metallacarboranes, $(CpCo)_k(BH)_{n-m-k}(CR)_mH_{2-m}$ and cobalt alkylidyne clusters, $(CpCo)_k(CR)_mH_{2-m}$, are obtained. There are numerous examples of cobaltaboranes and cobaltacarboranes, e.g. $(CpCo)_4(BH)_2H_2$,[2] $(CpCo)_3(BH)_3H_2$[3] and $(CpCo)_2(BH)_3(CH)_2$,[4] to name just a few of the more metal-rich examples.[5,6]

The tetranuclear $(CpCo)_4H_4$ (although electron precise, as a tetrahedral molecule it does not comply with the general formula given above) has been prepared by $LiAlH_4$ reduction of $[CpCo(NO)]_2$.[7a] Tricobalt bis(alkylidyne) clusters, $(CpCo)_3(CR)_2$, are formed via cleavage of alkynes with $CpCo(CO)_2$ or $CpCo(C_2H_4)_2$ (**1a**).[8] Thermal decomposition of **1a** and Cp* $Co(C_2H_4)_2$ (**1c**) (Cp* = pentamethylcyclopentadienyl) was reported to yield as the only products, tetrametallic $H(CpCo)_4(CCH_3)$ (**3a**)[9] and trimetallic $(Cp^*Co)_3(CCH_3)_2$ (**2c**),[10] respectively.

RESULTS AND DISCUSSION

We have been looking for a general route into the series of cluster hydrides $(CpM)_kH_2$ (M = Co, Rh). Hydrogenation of unsaturated ligands in metal complexes has opened low energy pathways to polynuclear hydrides. Examples include $[Co(CO)_2(PR_3)]_3H$ from $(\eta^3$-allyl$)Co(CO)_2(PR_3)$ and H_2,[11] and a series of hydrides $[(R_3P)Pt]_xH_y$ ($x = 3$, $y = 6$, R = ^{t}Bu; $x = 4$, $y = 8$, $R_3 = {}^iPr_2Ph$; $x = 5$, $y = 8$, $R_3 = {}^tBu_2Ph$) from $(R_3P)Pt(C_2H_4)_2$ and H_2.[12] In the latter, the steric requirements of the phosphine ligands appear crucial in dictating the cluster nuclearity.[12] Indeed, reaction of **1a** with 1 bar of H_2 in ether or alkane solvents smoothly proceeds, even below room temperature, to yield a dark brown solution. However, analysis by field desorption mass spectroscopy (FD–MS) indicated the presence of the CpCo(alkylidyne) clusters $(CpCo)_3(CCH_3)_2$ (**2a**) (*m/z* 426), $H(CpCo)_4(CCH_3)$ (**3a**) (*m/z* 524), $(CpCo)_4(CCH_3)_2$ (**4a**) (*m/z* 550) and $H(CpCo)_5(CCH_3)$ (**5a**) (*m/z* 648) in appreciable quantities. No traces of $(CpCo)_4H_4$[7] or its higher homologues $(CpCo)_kH_2$ were found in the spectra. Under identical conditions, but in the absence of H_2, pure **1a** proved to be stable in solution for several weeks. Careful low temperature chromatography of the products resulted in the isolation of red **2a** (18% yield) and dark brown **3a** (47% yield). The hexanuclear clusters **4a** and **5a** could not be completely separated from residual **3a**.

By increasing the steric bulk of the Cp ligands we hoped to increase the relative yield of some of the clusters, presumably those with lower nuclearity. Low temperature chromatography of the mixture

† Author to whom correspondence should be addressed.

Table 1. Selected bond lengths (Å) and angles (°) for complex **2a** (standard deviations in parentheses)

Co(1)—Co(2)	2.371(3)	Co(2)—Co(3)	2.389(2)	Co(3)—C(3)	1.897(9)
Co(1)—Co(3)	2.354(1)	Co(2)—C(1)	1.838(4)	Co(3)—C(1c)	2.049(5)
Co(1)—C(1)	1.861(8)	Co(2)—C(3)	1.846(5)	Co(3)—C(2c)	2.027(5)
Co(1)—C(3)	1.812(9)	Co(2)—C(1b)	2.022(4)	Co(3)—C(3c)	2.042(4)
Co(1)—C(1a)	2.079(5)	Co(2)—C(2b)	2.028(3)	Co(3)—C(4c)	2.073(5)
Co(1)—C(2a)	2.090(5)	Co(2)—C(3b)	2.110(3)	Co(3)—C(5c)	2.077(5)
Co(1)—C(3a)	2.110(5)	Co(2)—C(4b)	2.153(4)	C(1)—C(2)	1.518(7)
Co(1)—C(4a)	2.111(5)	Co(2)—C(5b)	2.100(3)	C(3)—C(4)	1.536(8)
Co(1)—C(5a)	2.091(6)	Co(3)—C(1)	1.847(9)		
Co(3)—Co(1)—Co(2)	60.7(1)	Co(3)—C(1)—Co(2)	80.8(2)	Co(3)—C(3)—Co(1)	78.8(1)
Co(3)—Co(2)—Co(1)	59.3(1)	C(2)—C(1)—Co(1)	126.9(7)	Co(3)—C(3)—Co(2)	79.3(3)
Co(2)—Co(3)—Co(1)	60.0(1)	C(2)—C(1)—Co(2)	130.9(3)	C(4)—C(3)—Co(1)	125.0(7)
Co(2)—C(1)—Co(1)	79.7(2)	C(2)—C(1)—Co(3)	138.2(6)	C(4)—C(3)—Co(2)	130.7(3)
Co(3)—C(1)—Co(1)	78.8(1)	Co(2)—C(3)—Co(1)	80.8(2)	C(4)—C(3)—Co(3)	140.5(6)

obtained from hydrogenation (room temperature, 1 bar H_2) of $Cp'Co(C_2H_4)_2$ (**1b**) indeed indicated a higher yield of the trimetallic $(Cp'Co)_3(CCH_3)_2$ (**2b**), compared to the tetrametallic $H(Cp'Co)_4(CCH_3)$ (**3b**). Clusters with higher nuclearity could not be detected in the reaction mixture by FD–MS. However, only **3b** was obtained as a pure solid (11% yield); separation of **2b** from **3b** and other impurities was not possible either by chromatography or crystallization.

In contrast to **1**, a solution of $CpRh(C_2H_4)_2$ was stable under 1 bar of H_2 at room temperature for several days. Addition of a small amount of palladium on charcoal to this solution resulted in the quantitative precipitation of a rhodium mirror.

We have determined the crystal structures of **2a** and **3a**. Compound **2a** has the expected trigonal bipyramidal geometry, with the cobalt atoms occupying equatorial sites and both faces of the Co_3 triangle capped by ethylidyne groups (Fig. 1). The 1,4-C_2Co_3 core has very nearly D_{3h} symmetry. The planes of the Cp rings intersect the Co_3 triangle at dihedral angles close to 90°. Both CoCo and CoC(1/3) bond lengths (Table 1) are similar to the mean values found in $(CpCo)_3(\mu_3\text{-}CSiMe_3)(\mu_3\text{-}CC_2SiMe_3)$ (d(Co—Co) = 2.38 Å, d(Co—C) = 1.873 Å).[8a] The corresponding values for **2c** and **3a** are d(Co—Co) = 2.369 Å, d(Co—C) = 1.94 Å[10] and $d(\text{Co—Co})_{\text{mean}}$ = 2.415 Å, $d(\text{Co—C})_{\text{mean}}$ = 1.85 Å, respectively.

Compound **3a** has a trigonal bipyramidal (or monocapped tetrahedral) Co_4C core (Fig. 2). Since the structure of **3a** was published by others[9] while our work was under way, we shall discuss it here in less detail. Our findings (obtained from two different crystals) are in reasonable accord with those of ref. 9. Although the hydride could not be located in the X-ray diffraction studies, for geometric reasons we believe it to occupy a μ_3-(Co_3) face-bridging position in the solid state. This proposal is substantiated by semi-quantitative potential energy calculations,[13] which give much higher potential energies for all possible μ_2-bridging sites. Application of a modified† topological electron book-keeping treatment[14] gives balanced equations for both poss-

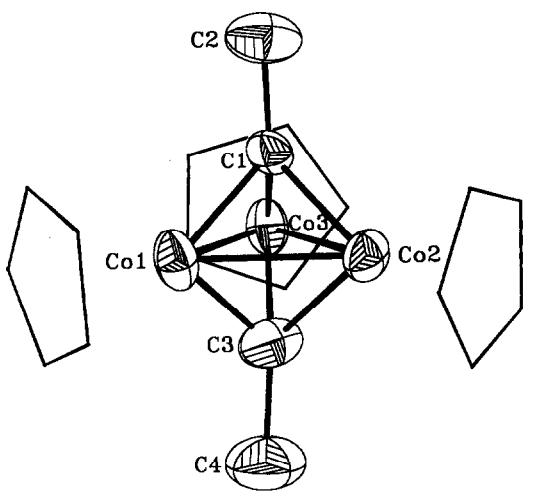

Fig. 1. Molecular structure of complex **2a**.

† To account for the CR groups, the original equations of balance[14] were extended as follows: for $\{(ML_3)_{p-1}(CR)_1H_q\}^{(z+1)+}$ (ML_3 = $Fe(CO)_3$, CoCp), $x = q-s$, $t = (3-n)p+z-q-x$, $2y = (np-z)-q-2t$ (where n, s, t, x, y are defined in analogy to ref. [15]). Hence, $(CpCo)_4(CCH_3)H$ gives $(styx) = (0231)$ [μ_3-H] and (1320) [μ_2-H].

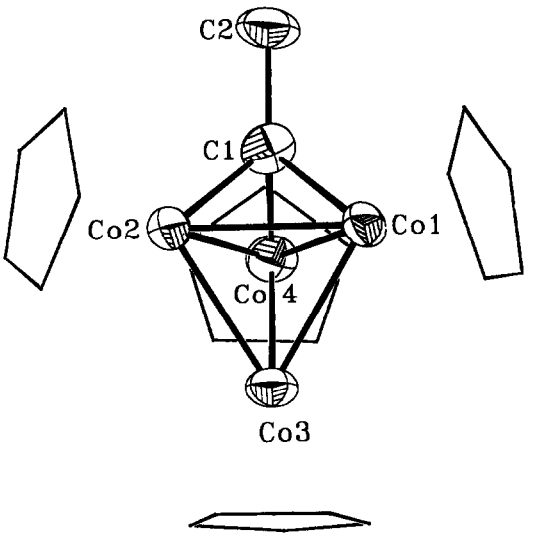

Fig. 2. Molecular structure of complex **3a**.

ible isomers (μ_2-H and μ_3-H). It is tempting to compare these findings with the available data for the closely related isoelectronic $H[Fe(CO)_3]_4(CCH_3)$,[15] which has the same polyhedral structure as **3a**. In the X-ray crystallographic study[15] the hydride was assumed to bridge an equatorial to axial iron–iron edge, based on the lengthening of this bond by 1.5% and the coordination geometry of the adjacent CO groups. Since the CpCo group is a lot more rigid than its isoelectronic and isolobal $Fe(CO)_3$ equivalent, and since the ligand environment in **3a** as a whole is much more crowded, the edge-bridging site is not available to the hydride in the latter molecule.

Table 2. NMR data for complex **2a** (δ in $[D_6]$-benzene)

	^1H	$^{13}C\{^1H\}$
CH_3	4.83 (s, 6H)	50.86
Cp	4.30 (s, 15H)	83.83

In the ^1H NMR spectra of **2a**, **3a** and **3b** (Tables 2 and 3), the ethylidyne groups appear as singlets in the range δ 4.8–5.0. Likewise, the resonances due to the ethylidyne methyl carbons are shifted to low field (δ 50–55) (Tables 2 and 4). Owing to relaxation effects of the quadrupolar ^{59}Co nuclei, no resonances were observed for the carbon atoms capping the Co_3 faces. The hydride resonances appear at δ −19.6 and −19.23 for **3a** and **3b**, respectively, strongly suggesting bridging (either μ_2 or μ_3) sites.[16]

Table 3. ^1H NMR data for complexes **3a** and **3b** (δ in $[D_8]$-toluene)

		3a	
		293 K	190 K
CCH_3		4.92 (s, 3H)	4.87 (s, 3H)
Cp_{ax}[a]		4.81 (s, 5H)	4.82 (s, 5H)
Cp_{eq}[a]		4.56 (s, 15H)	4.63 (s, 10H)
Cp_{eq}[a]			4.48 (s, 5H)
Hydride		−19.6 (s, 1H)	−19.7 (s, 1H)
		3b	
		298 K	200 K
CCH_3		5.01 (s, 3H)	4.94 (s, 3H)
Cp'_{ax}[a]	CH	4.83 (m)[b]	4.88 (m, 2H)
	CH	4.66 (m, 2H)	4.63 (m, 2H)
	CH_3	2.09 (s, 3H)	2.09 (s, 3H)
Cp'_{eq}[a]	CH	4.83 (m)[b]	5.35 (m, 2H)
		4.21 (m, 6H)	4.72 (m, 2H)
			4.59 (m, 2H)
			4.32 (m, 4H)
			3.93 (m, 2H)
	CH_3	1.33 (s, 9H)	1.40 (s, 6H)
			1.10 (s, 3H)
Hydride		−19.23 (s, 1H)	−19.22 (s, 1H)

[a] Subscripts ax and eq denotes "axial" and "equatorial" sites in the trigonal bipyramid.

[b] Integrates to a total of eight hydrogens.

Table 4. ^{13}C NMR data for complexes **3a** and **3b** (δ in [D_8]-toluene at 298 K)

3a		**3b**		
Co_3CCH_3	54.71 (q)	Co_3CCH_3		53.52
Cp_{ax}	74.89 (d)	Cp'_{ax}	*C*H	76.07, 73.58
			CCH_3	87.94
			CH_3	15.24
Cp_{eq}	82.17 (d)	Cp'_{eq}	*C*H	84.67, 79.89
			CCH_3	96.14
			CH_3	14.44

In solution, **3a** and **3b** show dynamic behaviour. In the ^1H NMR spectra of **3a** at room temperature, only resonances for two sets of equivalent cyclopentadienyl protons are observed (intensity ratio 3 : 1) (Table 3). On lowering the temperature, the signal at δ 4.56 (intensity 3) collapses and eventually splits into two singlets (intensity 2 : 1) at 190 K. The spectra can be explained in terms of a dynamic process which involves rapid migration of the hydride across the three "open" Co_3 faces of the Co_4C bipyramid at the higher temperatures, effectively equilibrating the resonances of the two sets of "equatorial" CpCo groups. At low temperature, the structure is static on the NMR time scale, with the hydride most likely capping one of the triangular Co_3 faces. The same dynamic process operates in the methylcyclopentadienyl derivative, **3b**. However, due to the inherently lower symmetry, the low temperature spectra are more complicated (Table 3). Assuming free rotation of the Cp′ ligands, the molecular symmetry of a structure with the hydride localized on a Co_3 face (Fig. 3) approximates to C_s on the NMR timescale. Rings **A** and **A′** are related by symmetry; rings **B** and **C** are effectively bisected by the mirror plane. Therefore the methyl groups of the four Cp′ ligands appear as three signals with an intensity ratio of 2(**A**+**A′**) : 1(**B**) : 1(**C**). All four CH protons in ring **A** (and, by symmetry, also ring **A′**) are non-equivalent, giving a total of four sets of two CH protons each. Each of the rings, **B** and **C**, give rise to two sets of two CH protons, making a total of eight CH multiplets in the spectrum (two of which coincidentally overlap).

Cyclic voltammetry reveals reversible one-electron reduction and oxidation waves for both **2a** and **3a** (Table 5). As expected, reduction and oxidation of the clusters become easier going from the tricobalt Co_3C_2 polyhedron, **2a**, to the tetrametallic Co_4C polyhedron, **3a**. Further electrochemically irreversible one-electron oxidation of the monocations occurs at $E_0 = +1.17$ V (vs SCE) (**2a**) and $E_0 = +0.52$ V (**3a**). A stable monocation and a monoanion of $(CpCo)_3(CPh)_2$ have been prepared in solution.[17] Electrochemical data were given only for the 0/+1 couple; the value of $E_0 = 0.34$ V[17] compares well with $E_0 = 0.23$ V for **2a**.

Both **2a** and **3a** proved to be thermally and chemically very stable. Both compounds can be sublimed *in vacuo* at temperatures above 140°C without decomposition. Attempts to expand the Co_4C polyhedron of **3a** with either $Fe_2(CO)_9$, $Fe_3(CO)_{12}$ or $Co_2(CO)_8$, were not successful. Space filling models show the hydride in **3a** to be completely buried inside the ligand shell of the cluster. Consequently, no sign of deprotonation was apparent after prolonged contact with strong bases like NaH and $Na(HBEt_3)$.

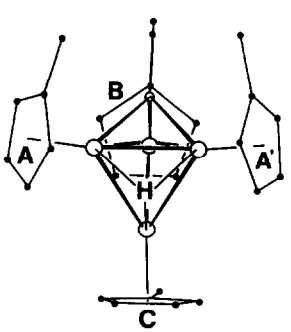

Fig. 3.

Table 5. Electrochemical data for complexes **2a** and **3a** (in V vs SCE)

Couple	**2a**[a]	**3a**[b]
−1/0	−1.95 (rev.)	−1.68 (rev.)
0/+1	0.23 (rev.)	−0.28 (rev.)
+1/+2	1.17 (irrev.)	0.52 (irrev.)

Supporting electrolyte, Bu_4NPF_6.
[a] In propionitrile.
[b] In acetonitrile.

In conclusion, we were able to show that a whole range of CpCo-containing clusters is formed via hydrogenation of $CpCo(C_2H_4)_2$ (**1a**) and $Cp'Co(C_2H_4)_2$ (**1b**) under very mild conditions. Under our reaction conditions (that is, under low pressure of H_2 and consequently with a relatively low concentration of H_2 in the solution), one or more ethylene molecules are always incorporated into the new formed clusters as μ_3-alkylidyne moieties. From our experiments we cannot tell whether the hydride ligands in **3** and **5** originate from gaseous H_2 or from coordinated ethylene. At higher temperatures, and in the absence of dihydrogen, the latter was shown to be the case.[9,10] Conversion of surface bound ethylene to μ_3-ethylidyne is a process which is quite common on metal surfaces,[18] but much less so in molecular systems. Most significantly, a layer of alkylidyne fragments is present on certain metal surfaces during and after the catalytic hydrogenation of ethylene and plays an active role in the catalytic cycle.[19] Hence, the formation and stability of molecular alkylidyne clusters in the hydrogenation reaction of olefin complexes serves as yet another example of the conceptual similarity of molecular and surface organometallic chemistry.[20]

EXPERIMENTAL

All operations were performed under purified N_2. Solvents were dried by conventional methods and stored under N_2. The alumina used for chromatographic separations was Brockmann activity II.

Compound **1a** (1.56 g, 8.7 mmol) in 150 cm^3 of light petroleum was shaken in an atmosphere of H_2 (1 bar) for 48 h. The resulting brown suspension was chromatographed on an alumina column at −30°C. Elution with light petroleum afforded a red solution of $(CpCo)_3(CCH_3)_2$ (**2a**). Further elution with toluene resulted in a brown eluate. Removal of solvent *in vacuo*, followed by crystallization of the residue from a large volume of light petroleum, gave dark brown crystals of $H(CpCo)_4(CCH_3)$ (**3a**) (530 mg, 47%). With ethanol, a mixture (290 mg) of **3a**, $(CpCo)_4(CCH_3)_2$ (**4a**) and $H(CpCo)_5(CCH_3)$ (**5a**) could be obtained from the alumina column. The red solution of **2a** was re-chromatographed with light petroleum on alumina. The solvent was removed from the first red fraction and the residue recrystallized from light petroleum at −78°C to give deep red platelets of **2a** (220 mg, 18%).

Compound **2a**: EI–MS *m/z*(%) 426 (100, M^+), 370 (85, $\{(CpCo)_3-2H\}^+$), 247 (38, $\{(CpCo)_2-H\}^+$), 189 (84, $\{Cp_2Co\}^+$), 124 (20, $\{CpCo\}^+$), 59 (7, Co^+). Compound **3a**: EI—MS *m/z*(%) 524 (67, M^+), 456 (79, $\{M-Cp-3H\}^+$), 370 (34, $\{(CpCo)_3-2H\}^+$), 247 (25, $\{(CpCo)_2-H\}^+$), 189 (69, $\{Cp_2Co\}^+$), 124 (13, $\{CpCo\}^+$).

In a similar way, 250 mg (11%) of pure $H(Cp'Co)_4(CCH_3)$ (**3b**) was obtained from 3.00 g (15.5 mmol) of **1b**. Compound **3b**: FD–MS *m/z*(%) 580 (100, M^+).

X-ray crystallographic data

Red crystals of **2a** were grown from light petrol by slow evaporation of solvent over a period of several weeks. Diffraction data were collected on a two-circle STOE STADI2 diffractometer at ambient temperature. Of the 2621 intensities measured (ω-scans, Mo-K_α X-radiation, $\lambda = 0.71069$ Å, graphite monochromator), 1797 unique reflections had $I \geqslant \sigma(I)$ and only these were used in the solution and refinement of the structure. Intensity data were corrected for Lorentz, polarization and X-ray absorption effects.

Crystal data for **2a**. $C_{19}H_{21}Co_3$, $M = 426.2$, orthorhombic, space group $Pbn2_1$, $a = 9.185(8)$, $b = 13.94(1)$, $c = 13.96(1)$ Å, $V = 1787$ Å^3, $Z = 4$, $D_c = 1.58$ g cm^{-3}, $F(000) = 864$, μ(Mo-K_α) = 26.4 cm^{-1}.

Systematic absences indicated space group *Pbnm* or $Pbn2_1$. The structure was solved, and all non-hydrogen atoms were located by conventional heavy-atom and difference Fourier methods. Hydrogen atoms were included in calculated positions. All remaining atoms were given anisotropic thermal parameters. Refinement by full-matrix least-squares was carried out in both possible space groups. In the centrosymmetric *Pbnm* (crystallographic molecular symmetry *m*) some carbon atoms showed very large anisotropic temperature factors perpendicular to the mirror plane. Therefore refinement was completed in the non-centrosymmetric $Pbn2_1$ with the Cp rings as rigid groups, and converged at $R = 0.057$ ($R_w = 0.043$, with a weighting scheme of the form $w^{-1} = [\sigma^2(F)]$). Scattering factors were taken from ref. 21. All calculations were carried out with the SHELX-76 system of programs.[22]

Acknowledgements—This work was supported by the Land Baden-Württemberg under the auspices of the Forschungsschwerpunkt Nr. 31. We thank Dr K. Steinbach (Universität Marburg) for the FD–MS analyses.

REFERENCES

1. (a) M. Elian, M. M. L. Chen, R. Hoffmann and D. M. P. Mingos, *Inorg. Chem.* 1976, **15**, 1148; (b) R. Hoffmann, *Angew. Chem.* 1982, **94**, 725.

2. T. P. Fehlner, J. Feilong and A. L. Rheingold, *J. Am. Chem. Soc.* 1987, **109**, 1860.
3. J. R. Pipal and R. N. Grimes, *Inorg. Chem.* 1977, **16**, 3255.
4. D. C. Beer, V. R. Miller, L. G. Sneddon, R. N. Grimes, M. Mathew and G. J. Palenik, *J. Am. Chem. Soc.* 1973, **95**, 3046.
5. R. N. Grimes, *Comprehensive Organometallic Chemistry* (Edited by E. W. Abel, F. G. A. Stone and G. Wilkinson), Vol. 1. Pergamon Press, Oxford (1982).
6. (a) K. G. Gilbert, S. K. Boocock and S. G. Shore, *Comprehensive Organometallic Chemistry* (Edited by E. W. Abel, F. G. A. Stone and G. Wilkinson), Vol. 6. Pergamon Press, Oxford (1982); (b) C. E. Housecroft, *Polyhedron* 1987, **6**, 1935.
7. (a) J. Müller and H. Dorner, *Angew. Chem.* 1973, **85**, 867; (b) G. Huttner and H. Lorenz, *Chem. Ber.* 1975, **108**, 973.
8. (a) J. R. Fritch, K. P. C. Vollhardt, M. R. Thompson and V. W. Day, *J. Am. Chem. Soc.* 1979, **101**, 2768; (b) J. R. Fritch and K. P. C. Vollhardt, *Angew. Chem.* 1980, **92**, 570; (c) B. Eaton, J. M. O'Connor and K. P. C. Vollhardt, *Organometallics* 1986, **5**, 394.
9. S. Stella, C. Floriani, A. Chiesi-Villa and C. Guastini, *New J. Chem.* 1988, **12**, 621.
10. R. B. A. Pardy, G. W. Smith and M. E. Vickers, *J. Organomet. Chem.* 1983, **252**, 341.
11. (a) G. Pregaglia, A. Andreetta, G. F. Ferrari and R. Ugo, *J. Chem. Soc., Chem. Commun.* 1969, 590; (b) G. Pregaglia, A. Andreetta, G. F. Ferrari, G. Montrasi and R. Ugo, *J. Organomet. Chem.* 1971, **33**, 73; (c) P. Bradamante, P. Pino, A. Stefani, G. Fachinetti and P. F. Zanazzi, *J. Organomet. Chem.* 1983, **251**, C47.
12. (a) D. Gregson, J. A. K. Howard, M. Murray and J. L. Spencer, *J. Chem. Soc., Chem. Commun.* 1981, 716; (b) P. W. Frost, J. A. K. Howard, J. L. Spencer and D. G. Turner, *J. Chem. Soc., Chem. Commun.* 1981, 1104; (c) J. A. K. Howard, J. L. Spencer and D. G. Turner, *J. Chem. Soc., Dalton Trans.* 1987, 259.
13. A. G. Orpen, *J. Chem. Soc., Dalton Trans.* 1980, 2509.
14. D. M. P. Mingos, *Pure Appl. Chem.* 1980, **52**, 705.
15. P. L. Bogdan, K. H. Whitmire, J. W. Kolis, D. F. Shriver and E. M. Holt, *J. Organomet. Chem.* 1984, **272**, 169.
16. A. P. Humphries and H. D. Kaesz, *Prog. Inorg. Chem.* 1979, **25**, 145.
17. S. Enoki, T. Kawamura and T. Yonezawa, *Inorg. Chem.* 1983, **22**, 3821.
18. (a) G. A. Somorjai and M. A. Van Hove, *Struct. Bonding (Berlin)* 1979, **38**, 1; (b) G. A. Somorjai and S. M. Davies, *Platinum Met. Rev.* 1983, **27**, 54 *cit. lit.*; (c) G. A. Somorjai, *Chem. Soc. Rev.* 1984, **13**, 321 *cit. lit.*
19. A. Wieckowski, S. D. Rosasco, G. N. Salaita, A. Hubbard, B. E. Bent, F. Zaera, D. Godbey and G. A. Somorjai, *J. Am. Chem. Soc.* 1985, **107**, 5910.
20. (a) H. F. Schaefer III, *Accts Chem. Res.* 1977, **10**, 287 *cit. lit.*; (b) E. L. Muetterties, *Pure Appl. Chem.* 1982, **54**, 83 *cit. lit.*
21. D. T. Cromer and J. B. Mann, *Acta Cryst.* 1968, **A24**, 321.
22. G. M. Sheldrick, SHELX-76, Program for crystal structure determination. Cambridge (1976).

Polyhedron Vol. 8, No. 15, pp. 1945–1948, 1989
Printed in Great Britain

0277-5387/89 $3.00+.00
© 1989 Maxwell Pergamon Macmillan plc

SYNTHESIS AND SPECTROSCOPIC CHARACTERIZATION OF A NOVEL IRIDIUM POLYHYDRIDE $[Ir_2(\mu\text{-}H)_3H_2(dippe)_2]PF_6$; dippe = 1,2 BIS(DIISOPROPYLPHOSPHINO)ETHANE

H. EL-AMOURI* and A. BOUAYAD†

Institut de Chimie des Substances Naturelles, CNRS, 91190 Gif-sur-Yvette, France

(*Received* 23 *January* 1989; *accepted* 10 *March* 1989)

Abstract—Treatment of $[Ir(cod)(dippe)]PF_6$ (**1**) (dippe = 1,2 bis(diisopropylphosphino) ethane, $PPr^i_2(CH_2)_2PPr^i_2$) with molecular hydrogen at room temperature, in benzene and in the presence of 10 equivalents of NEt_3, affords the binuclear polyhydride complex $[Ir_2(\mu\text{-}H)_3H_2(dippe)_2]PF_6$ (**2**) and not $[IrH_5(dippe)]$. The complex $[Ir_2(\mu\text{-}H)_3H_2(dippe)_2]PF_6$ (**2**) is shown to be fluxional in solution, whereby the hydrides and the phosphorus ligands exchange rapidly at room temperature with respect to the NMR time scale.

Polyhydrides of the type $[Ir_2(\mu\text{-}H)_3H_2L_4]PF_6$ (L = PPh_3, PPh_2Me) can be conveniently prepared by hydrogenation of the respective complexes, $[Ir(cod)L_2]PF_6$ (L = PPh_3, PPh_2Me).[1-3] However, a second method, concerning the hydrogenation of $[Ir(cod)LL']PF_6$, (L = L′ = PPh_3) (L = PPr^i_3, Pcy_3; L′ = Py) but in the presence of an excess of NEt_3, yields the mononuclear pentahydride complexes of the type IrH_5L_2. The latter compounds are well known, particularly due to their use as precursors in the mild catalytic activation of C—H bonds of saturated hydrocarbons.[4] A notable example is the complex $[IrH_5(PPr^i_3)_2]$.[5] Nevertheless, these monodendate phosphine derivatives tend to be rather labile in solution.[6] Hence we were interested in preparing the hypothetical bidendate species $IrH_5(dippe)$ from $[Ir(cod)(dippe)]PF_6$ (**1**), thus following the second procedure. However, the new polyhydride dimer $[Ir_2(\mu\text{-}H)_3H_2(dippe)_2]PF_6$ (**2**) is formed under these conditions and in this paper we describe its detailed synthesis and fluxional behaviour in solution at ambient temperature.

* Author to whom correspondence should be addressed. New address: Ecole Nationale Supérieure de Chimie de Paris, U.A. 403, 11 Rue Pierre et Marie Curie, 75231 Paris Cédex 05, France.

† Present address: Laboratoire de Chimie Organique et Organométallique, U.A. CNRS No. 35, Université de Bordeaux I, 33405 Talence Cédex, France.

RESULTS AND DISCUSSION

Previous studies carried out by Crabtree *et al.* have shown that hydrogenation of $[Ir(cod)LL']PF_6$ (L = L′ = PPh_3) (L = PPr^i_3, Pcy_3; L′ = Py) in the presence of Lewis base NEt_3 and excess of L, affords the pentahydride complexes IrH_5L_2 [eq. (1)][2]

$$[Ir(cod)LL']PF_6 + 5H_2 \xrightarrow[NEt_3, L]{CH_2Cl_2} IrH_5L_2 + NEt_3HPF_6 + \text{Cyclo-octane} \quad (1)$$

(L = Pcy_3, PPr^i_3).

Following the same procedure, using $[Ir(cod)(dippe)]PF_6$ (**1**) as starting material, we isolated and characterized the polyhydride complex, $[Ir_2(\mu\text{-}H)_3H_2(dippe)_2]PF_6$ (**2**). The complex $[Ir(cod)(dippe)]PF_6$ (**1**) was prepared by treatment of $[Ir(cod)(py)_2]PF_6$[7] with one equivalent of dippe in dichloromethane. The $^{31}P\{^1H\}/CDCl_3$ shows a singlet at 66 ppm (2P), indicating that in solution two equivalent phosphorus nuclei are coordinated to iridium(I). In addition, a septet centred at −140 ppm (1P) corresponding to free PF_6^- was observed. The ^1H NMR/$CDCl_3$ shows by integration, the presence of one equivalent of dippe to that of cod (cod = 1.5-cyclo-octadiene). Satisfactory microanalyses were obtained for carbon, hydrogen and phosphorus. Hydrogenation of a suspension of $[Ir(cod)(dippe)]PF_6$ (**1**) in benzene using one atmosphere of molecular hydrogen at room temperature

and in the presence or absence of NEt_3, yielded the complex $[Ir_2(\mu\text{-}H)_3H_2(dippe)_2]PF_6$ (**2**).

The IR spectrum of complex **2** prepared in Nujol, exhibits a strong band at 830 cm^{-1} assigned to ν(P—F) of free PF_6^- and a medium band at 2200 cm^{-1} assigned to the terminal hydrides ν(Ir—H), which is similar to that observed for the analogous compound, $[Ir_2(\mu\text{-}H)_3H_2(PPh_3)_4]PF_6$.[2] The $^{31}P\{^1H\}$ NMR spectrum of complex **2** recorded at 185 K in CD_2Cl_2, shows a doublet of doublets with some likely second-order contribution corresponding to $(P_a+P_{a'})$ and $(P_b+P_{b'})$ centred at 87 and 89.2 ppm, respectively, with $^2J(P_a—P_b) = {}^2J(P_{a'}—P_{b'}) = 15$ Hz. This suggests two non-equivalent phosphorus atoms P_a (or $P_{a'}$), P_b (or $P_{b'}$) of dippe chelating to iridium(III) (see Fig. 1). However, the coupling value reported for the $[Ir_2(\mu\text{-}H)_3H_2(PPh_3)_4]PF_6$ complex is $^2J(P_a—P_b) = 95$ Hz.[1] This difference is probably due to the chelating effect in complex **2** which forces the two phosphorus atoms P_a, P_b, of dippe to remain in a *cis* geometry. In addition, the $^{31}P\{^1H\}$ NMR of compound **2** shows a septet at −140 ppm, corresponding to free PF_6^- (0.9P) $^1J(P—F) = 712$ Hz. The ^1H NMR of this complex recorded at 180 K in CD_2Cl_2 shows three sets of hydrides at high field: a doublet centred at −8.16 ppm ($^2J(P_a—H_a) = {}^2J(P_{a'}—H_{a'}) = 73$ Hz) corresponding to $(H_a+H_{a'})$ bridging hydrides, where each hydride H_a (or $H_{a'}$) is *trans* to one phosphorus nucleus P_a (or $P_{a'}$); a multiplet centred at −8.35 ppm corresponding to one bridging hydride H_b which is *trans* to P_b and $P_{b'}$ and *cis* to P_a and $P_{a'}$ with the coupling constants ($^2J(P_b—H_b) = {}^2J(P_{b'}—H_b) = 122$ Hz, $^2J(P_a—H_b) = {}^2J(P_{a'}—H_b) = 62$ Hz); and finally a doublet of doublets centred at −21.9 ppm ($^2J(P_a—H_c) = {}^2J(P_{a'}—H_{c'}) = 16$ Hz, $^2J(P_b—H_c) = {}^2J(P_{b'}—H_{c'}) = 20$ Hz) corresponding to $(H_c+H_{c'})$ terminal hydrides, where each H_c (or $H_{c'}$) is *cis* to two phosphorus nuclei P_a (or $P_{a'}$), P_b (or $P_{b'}$). The ^1H NMR of the $[Ir_2(\mu\text{-}H)_3H_2(PPh_3)_4]PF_6$ compound recorded at 193 K shows similar results concerning the bridging hydrides H_a, however the hydrides H_b and H_c were reported to be a broad triplet and a broad singlet, respectively. This is probably due to the high fluxionality in $[Ir_2(\mu\text{-}H)_3H_2(PPh_3)_4]PF_6$ even at this temperature.

Upon warming to room temperature, the signals corresponding to $(H_a+H_{a'})$, H_b and $(H_c+H_{c'})$ in the ^1H NMR spectrum coalesce to give two broad peaks centred at −8.25 and −22.1 ppm, respectively. Furthermore, the signals corresponding to $(P_a+P_{a'})$, $(P_b+P_{b'})$ in the $^{31}P\{^1H\}$ NMR coalesce gradually to give a broad peak centred at 87.3 ppm (Fig. 2). Two mechanisms are proposed for this exchange process: (i) a rapid rotation of the outer part of the octahedron constructed by H_c, P_a and P_b or $H_{c'}$, $P_{a'}$ and $P_{b'}$ around an axis of order three passing through the iridium centres and thus keeping the other part of the molecule fixed, which eventually will lead to the equilibration of these nuclei on the NMR time scale, or (ii) dissociation of one phosphorus atom of the chelated ligand dippe, followed by a rotation of 180° before coordination to iridium(III) which also causes $P_a = P_b$, or $P_{a'} = P_{b'}$, however this may lead to an exchange between the terminal and the bridging hydrides and thus would appear less likely.

Attempts to prepare the target compound IrH_5(dippe) from $[Ir_2(cod)(dippe)]PF_6$ (**1**) under alternative conditions (10 atm H_2, 30 equivalents $HN(Pr^i)_2$, $pK_b = 1.95$, NEt_3, $pK_b = 3.25$)[8] have proven to be unsuccessful, providing also $[Ir_2(\mu\text{-}H)_3H_2(dippe)_2]PF_6$ (**2**) in 40% yield. It is possible that the enforced *cis* arrangement of the phosphorus donor atoms in the chelate phosphine complex disfavours the formation of the mononuclear species "IrH_5(dippe)", for which a *trans* phosphine geometry is preferred. However, another argument could be proposed, the neutral intermediate hydrido species either "IrH(dippe)" or "IrH_3(dippe)" is intercepted by the cationic species, either

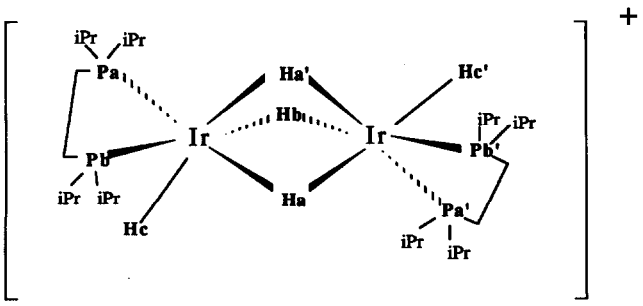

Fig. 1. Structure of $[Ir_2(\mu\text{-}H)_3H_2(dippe)_2]^+$.

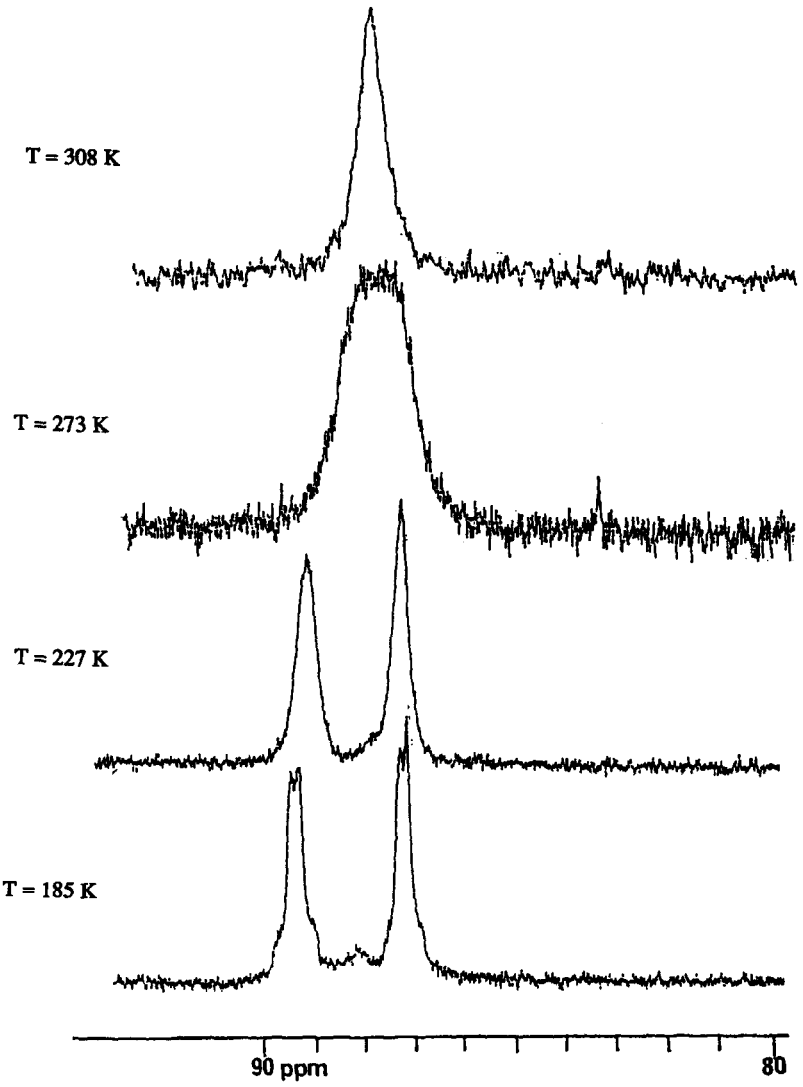

Fig. 2. Variable temperature $^{31}P\{^1H\}$ spectra for the polyhydride cationic complex $[Ir_2(\mu\text{-}H)_3H_2(dippe)_2]^+$, CD_2Cl_2 solution, 101 MHz.

"$IrH_4(dippe)^+$" or "$IrH_2(dippe)^+$", to form the product **2** more rapidly than reacting with H_2 [see Scheme 1 below, path (a) and path (b)]:

Indeed, hydrogenation of $[Ir(cod)(dippe)]PF_6$ (**1**) in benzene employing *t*-BuOK (stronger base than NEt_3 and $HN(Pr^i)_2$), affords a white microcrystalline species after extraction with hexane and passing through an alumina column under hydrogen (yield *ca* 10%). The IR spectrum does not show the characteristic strong absorption at 830 cm^{-1}

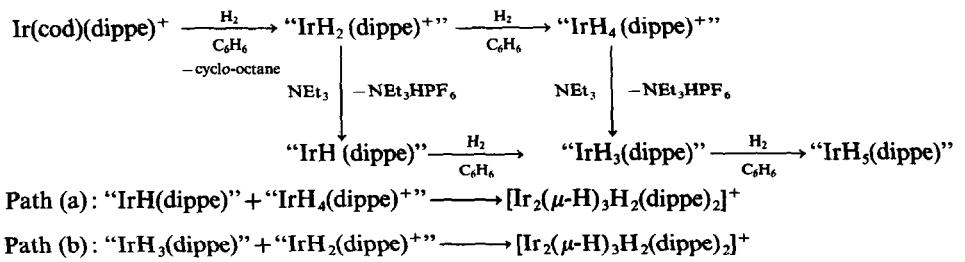

Scheme 1.

for ν(P—F) of free PF_6^-, but investigations are in progress to identify this new complex, the results of which will be presented in due course.

EXPERIMENTAL

Manipulations were carried out using a vacuum line under argon and employing standard Schlenk techniques. In the case of the hydrogenation reaction, argon was replaced by hydrogen.Solvents were purified and dried prior to use by conventional distillation techniques under nitrogen. IR spectra were recorded on a Perkin–Elmer 297 IR spectrometer as Nujol mulls. NMR spectra were recorded on a Bruker AM-250 instrument and chemical shifts are relative to Me_4Si or 85% H_3PO_4 (^{31}P). Data are presented as proton decoupled with down field chemical shifts as positive.

Elemental analyses were performed by the service of microanalyses, CNRS, Gif-sur-Yvette, France. The ligand, 1,2 bis(diisopropylphosphino)ethane (dippe), was synthesized from bis(1,2 dichlorophosphino)ethane ($Cl_2P(CH_2)_2PCl_2$) and the Grignard reagent $(CH_3)_2CHMgBr$, following the procedure of Chatt and co-workers.[9]

Synthesis of $[Ir(cod)(dippe)]PF_6$ **(1)**

A solution of dippe (269 mg, 1.03 mmol) in C_6H_6 (5 cm^3) was transferred via canula to a well-stirred solution of $[Ir(cod)Py_2]PF_6$ (530 mg, 0.87 mmol) in CH_2Cl_2 (15 cm^3), causing a rapid colour change from yellow to deep red. The solution was concentrated under vacuum and addition of diethyl ether provided a deep red product. The solid was filtered and washed successively with benzene and diethyl ether to yield a deep red microcrystalline product (581 mg, 94%. Found: C, 37.2 H, 6.1; P, 13.5 Calc. for $C_{22}H_{44}P_3F_6Ir$: C, 37.2; H, 6.2; P, 13.1%. ^1H NMR ($CDCl_3$) 5 ppm (s, 4H—CH=CH—); 2.5 ppm (sep, 4H—$CH(CH_3)_2$; 2.15 ppm (s, 8H—CH_2—CH_2—); 1.97 ppm (dd, second-order 4H P—$(CH_2)_2$—P); 1.29 ppm (m, 24H $(CH_3)_2CH$—). $^{31}P\{^1H\}/CDCl_3$ 66 ppm (s, 2P); −140 ppm (sep, PF_6^- ^1J(P—F) = 718 Hz).

Synthesis of $[Ir_2(\mu\text{-}H)_3H_2(dippe)_2]PF_6$ **(2)**

Hydrogen was bubbled through a suspension of $[Ir(cod)(dippe)]PF_6$ (250 mg, 0.35 mmol) in C_6H_6 (20 cm^3) in the presence of NEt_3 (0.483 cm^3, 3.5 mmol). The colour of the reaction mixture changed from red to light yellow. After 1 h the solvent was evaporated and the residue was extracted with ethanol (10 cm^3). The light yellow solution of ethanol was concentrated under vacuum until a creamy-yellow microcrystalline product started to precipitate. The product was filtered and washed with cold hexane. Recrystallization from dichloromethane–diethyl ether yielded cream coloured crystals (80 mg, 43%). Found: C, 31.8; H, 6.5. Calc. for $C_{24}H_{61}P_5F_6Ir_2$ C, 31.7; H, 6.5%. ^1H NMR (CD_2Cl_2) $T = 180$ K: 2.1 ppm (m, 16H P—$(CH_2)_2$—P, $CH(CH_3)_2$); 1.1 ppm (m, 48H $(CH_3)_2CH$—); −8.16 ppm (d, $H_{a'}$, H_a, $^2J(P_a—H_a) = {}^2J(P_{a'}—H_{a'}) = 73$ Hz); −8.35 ppm (m, Hb $^2J(P_b—H_b) = {}^2J(P_{b'}—H_b) = 122$ Hz, $^2J(P_a—H_b) = {}^2J(P_{a'}—H_b) = 62$ Hz); −21.9 ppm (dd, $H_{c'}$, H_c, $^2J(P_a—H_c) = {}^2J(P_{a'}—H_{c'}) = 16$ Hz, $^2J(P_b—H_c) = {}^2J(P_{b'}—H_{c'}) = 20$ Hz). $^{31}P\{^1H\}$ NMR/CD_2Cl_2 $T = 185$ K: 87 ppm (d, $P_b+P_{b'}$); 89.1 ppm (d, $P_a+P_{a'}$) $^2J(P_a—P_b) = {}^2J(P_{a'}—P_{b'}) = 15$ Hz; −140 ppm (sep, PF_6^- ^1J(P—F) = 718 Hz). IR/Nujol ν(Ir—H) = 2200 cm^{-1} (s); ν(P—F) = 830 cm^{-1} (*vs*).

Acknowledgements—We thank Dr H. Felkin and Professor J. A. Osborn for many helpful discussions, Claude Mérienne (Ingénieur CNRS I.C.M.O. service de RMN, Faculté des Sciences d'Orsay 91405 Orsay) for the VTNMR spectra, Gaz de France for supporting this work and the Comptoir Lyon-Alemand-Louyot (Paris) for a generous loan of iridium.

REFERENCES

1. R. H. Crabtree, H. Felkin, G. E. Morris, T. J. King and J. A. Richards, *J. Organomet. Chem.* 1976, **113**, C7.
2. R. H. Crabtree, H. Felkin and G. E. Morris, *J. Organomet. Chem.* 1977, **141**, 205.
3. J. R. Shapley, R. R. Shrock and J. A. Osborn, *J. Am. Chem. Soc.* 1969, **91**, 2816.
4. H. Felkin, T. Fillebeen-Khan, Y. Gault, R. Holmes-Smith and J. Zakrewski, *Tetrahedron Lett.* 1984, **25**, 1279.
5. C. J. Cameron, H. Felkin, T. Fillebeen-Khan, N. J. Forrow and E. Guittet, *J. Chem. Soc., Chem. Commun.* 1986, 801.
6. E. K. Barefield, G. W. Parshall and F. N. Tebbe, *J. Am. Chem. Soc.* 1970, **92**, 5234.
7. R. H. Crabtree and G. E. Morris, *J. Organomet. Chem.* 1977, **135**, 395.
8. J. E. Huheey, *Inorganic Chemistry*, p. 267. Harper International, New York (1978).
9. R. J. Burt, J. Chatt, W. Hussain and G. L. Leigh, *J. Organomet. Chem.* 1979, **182**, 203.

Polyhedron Vol. 8, No. 15, pp. 1949–1951, 1989
Printed in Great Britain

0277–5387/89 $3.00+.00
© 1989 Maxwell Pergamon Macmillan plc

DIFFERENCE IN THE POLAROGRAPHIC CATALYTIC CURRENTS OF VANADIUM(III)–EDTA AND VANADIUM(IV)–EDTA WITH THE NITRATE ION

NAKAHIDE KATO

Department of Chemistry, College of Science, Rikkyo University, 3-34 Nishi-Ikebukuro, Toshimaku, Tokyo 171, Japan

(*Received* 13 *June* 1988; *accepted* 10 *March* 1989)

Abstract—Addition of the nitrate ion to V^{III}–EDTA or V^{IV}–EDTA solutions increases the reduction current of vanadium(III) to vanadium(II), and the mechanisms of both cases are considered to be similar. However, the catalytic current of V^{IV}–EDTA was smaller than the V^{III}–EDTA due to the presence of the reaction of vanadium(II) with vanadium(IV).

The polarographic behaviour of V^{III}–EDTA* and its analogous complexes, and the mechanisms of their catalytic waves, have been previously investigated.[1–4] However, the vanadium(III) complex is not stable and undergoes slow oxidation to vanadium(IV) in air, whereas the vanadium(IV) complex is very stable under many conditions.[5] Therefore, V^{IV}–EDTA was used instead of V^{III}–EDTA in the study of the catalytic wave in the present work. Although one would expect[5–7] that the mechanism of the catalytic current of V^{IV}–EDTA is the same as that of V^{III}–EDTA, the observed catalytic current of V^{IV}–EDTA was smaller than that of V^{III}–EDTA. This phenomenon had not been considered hitherto and its mechanism is studied in the present work.

EXPERIMENTAL

The vanadium(IV) stock solution was prepared by dissolving vanadium(IV) oxide sulphate in 1.0 mol dm^{-3} sulphuric acid solution, and its concentration was determined by titration with potassium permanganate. The vanadium(III) stock solution was prepared by air-oxidizing a vanadium(II) solution obtained by electrolysis of the vanadium(IV) stock solution at −1.6 V vs SCE.

An oxygen-free solution containing 0.25 mol dm^{-3} of sodium acetate, 0.35 mol dm^{-3} of potassium chloride and 0.01 mol dm^{-3} of EDTA was poured into an H-type cell. After bubbling nitrogen gas for 10 min, the required amount of vanadium stock solution was added to the solution and the electrochemical measurements were carried out at pH 5.5.

RESULTS AND DISCUSSION

The polarogram of V^{III}–EDTA in the acetate buffer solution contained one wave which corresponded to the reduction of V^{III} to V^{II}.[1/2] When the nitrate ion was added to the V^{III}–EDTA solution, the wave height of V^{III}–EDTA was increased, that is, a catalytic wave appeared. The apparent rate constant k_{app} of the catalytic reaction between V^{II}–EDTA and the nitrate ion was calculated from the ratio of i_c/i_d,[8] where i_d is a diffusion current and i_c is a catalytic current. According to the literature,[7,8] the greater the k_{app}, the greater the catalytic current. The experimental relationship between k_{app} and the concentration of the nitrate ion is shown in Fig. 1, curve (1). As the value of k_{app} decreases with increasing concentration of nitrate ion, it is proposed that the mechanism of the catalytic reaction varies with concentration of

* Ethylenediaminetetraacetatovanadium(III): V^{III}–EDTA.

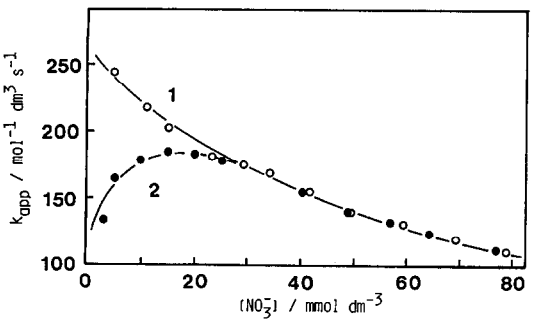

Fig. 1. Relation between k_{app} and the concentration of nitrate ion at pH 5.7. ○ : V^{III}–EDTA and ● : V^{IV}–EDTA.

nitrate ion.[3]* This mechanism was proposed as follows:

$$V^{III}\text{–EDTA} \xrightarrow{e^-} V^{II}\text{–EDTA (diffusion current: } i_d) \quad (1)$$

$$\nu V^{II}\text{–EDTA} + NO_3^- \xrightarrow[k_{app}]{} \nu V^{III}\text{–EDTA} \xrightarrow{\nu e^-} \nu V^{II}\text{–EDTA} \quad (2)$$

(catalytic current: i_c),

where ν represents the stoichiometric factor of the catalytic reaction.

Vanadium(IV)–EDTA produced two polarographic waves of the same height, which correspond to the stepwise reduction to V^{III} and then to V^{II}. When nitrate ion was added to the V^{IV}–EDTA solution, the height of the second wave was enhanced, whereas the height of the first wave remained constant. Therefore, the mechanism of the catalytic wave of V^{IV}–EDTA was considered to be similar to that of V^{III}–EDTA. However, the apparent rate constant, k_{app}, in eq. (2), calculated from the current of the second wave of V^{IV}–EDTA, is smaller than that in the case of V^{III}–EDTA in a low concentration of nitrate ion, as shown in curves (1) and (2) of Fig. 1; although the difference between the rate constants of them becomes smaller with increasing concentration of nitrate ion. That is, the observed catalytic current of V^{IV}–EDTA is smaller than that of V^{III}–EDTA.

When V^{IV}–EDTA was electrolysed at a constant potential corresponding to the reduction of V^{IV} to V^{II} in the acetate buffer solution [eq. (3)], not only V^{II}, but also V^{III} complexes, were found in the bulk solution. This showed that the reaction between V^{II} and V^{IV} (comproportionation)[9,10] occurred after electrolysis [see eq. (4)]:

$$V^{IV}\text{–EDTA} \xrightarrow{2e^-} V^{II}\text{–EDTA (diffusion current)} \quad (3)$$

$$V^{IV}\text{–EDTA} + V^{II}\text{–EDTA} \xrightarrow[\text{comproportionation}]{} 2V^{III}\text{–EDTA} \xrightarrow{2e^-} 2V^{II}\text{–EDTA}. \quad (4)$$

Multi-sweep cyclic voltammetry of V^{IV}–EDTA was carried out with a slow scan rate and a cyclic voltammogram was obtained as shown in Fig. 2. At first sweep, one cathodic shoulder (A) and a peak (B) due to the stepwise one-electron reduction of V^{IV} to V^{II} and an anodic wave (C) due to the oxidation of V^{II} to V^{III} were observed. However, the shape of the voltammogram changed in the direction of the arrows shown in Fig. 2 after repeating the sweeps, and shoulder (A) corresponding to

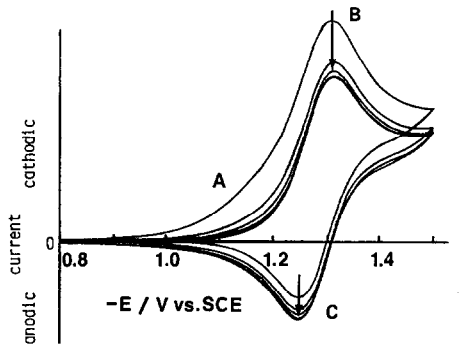

Fig. 2. Multi-sweep cyclic voltammogram of V^{IV}–EDTA at pH 5.7 [V^{IV}–EDTA] = 1.0 mmol dm^{-3}. Scan rate: 0.05 V s^{-1}.

* As the apparent second-order rate constant k_{app} is represented by the product of stoichiometric factor ν and the second-order rate constant k_c,[8] the reaction rate is described as follows:

$$\text{Reaction rate} = \nu k_c[V^{II}\text{–EDTA}][NO_3^-] = k_{app}[V^{II}\text{–EDTA}][NO_3^-].$$

When the concentration of nitrate ion was slightly higher than that of V–EDTA, stoichiometric factor ν was equal to 8. Therefore, the catalytic reaction was considered as follows:

$$8V^{II}\text{–EDTA} + NO_3^- + 10H^+ \rightarrow 8V^{III}\text{–EDTA} + NH_4^+ + 3H_2O.$$

However, when the concentration of nitrate ion was increased, the reaction products of nitrate ion were varied. Therefore, it is considered that the variation of k_{app} is due to that of the stoichiometric factor ν and the concentration of nitrate ion (Fig. 1).

the reduction of V^{IV} to V^{III} disappeared. Then, the steady state cyclic voltammogram of V^{IV}–EDTA became similar to that of V^{III}–EDTA. Therefore, also in the vicinity of electrode surface, the same reaction occurs between V^{II} and V^{IV} as in the bulk solution and the V^{III}–EDTA produced is reduced to V^{II} [see eq. (4)].

In the case of the polarographic behaviour of V^{IV}–EDTA, however, as two electrons should be consumed in both cases [see eqs (3) and (4)], the diffusion current of V^{IV}–EDTA cannot be affected by the reaction represented in eq. (4). The observed total wave height of V^{IV}–EDTA corresponds to a two-electron reduction. Therefore, the validity of eq. (4) cannot be elucidated from the diffusion current of V^{IV}–EDTA.

It has been proposed that the reaction between vanadium(II) and vanadium(IV) complexes produced the monomer and dimer of the vanadium(III) complexes in the bulk solution.[11] However, if the decrease in k_{app}, obtained from the catalytic wave of V^{IV}–EDTA, was caused by the formation of dimer, the height of the second wave of V^{IV}–EDTA should be smaller than that of the first wave in the absence of nitrate ion, because a dimer is generally reduced at more negative potentials than the monomer.[1,12,13] But in the present case, since the difference in the wave heights between the first and second waves of V^{IV}–EDTA has not been observed, it is assumed that the dimer is not formed.

Therefore, the reason for the difference in the catalytic currents of V^{III}–EDTA and V^{IV}–EDTA may be concluded as follows: in the case of V^{IV}–EDTA, two competitive reactions [see eqs (2) and (4)], that is, the reactions of V^{II}–EDTA with nitrate ion and with V^{IV}–EDTA occur in the vicinity of the electrode surface. Namely, V^{II}–EDTA produced by electrolysis, reacts not only with the nitrate ion but also with V^{IV}–EDTA. As the comproportionation does not contribute to the increase of the limiting current, the decrease of the apparent catalytic current can be observed when the concentration of the nitrate ion is low. On the other hand, the catalytic current of V^{III}–EDTA does not decrease due to the absence of V^{IV}–EDTA in the bulk solution.

REFERENCES

1. N. Kato, K. Tanaka and K. Nakano, *J. Electroanal. Chem.* 1983, **149**, 83.
2. T. Kimura, K. Nakano and K. Morinaga, *Nippon Kagaku Zasshi* 1971, **92**, 880.
3. N. Kato, K. Tanaka and K. Nakano, *Rev. Polarography* 1974, **20**, 73; N. Kato, K. Tanaka and K. Nakano, *Rev. Polarography* 1976, **22**, 73.
4. N. Kato, H. Matsui and K. Nakano, *Nippon Kagaku Kaishi* 1985, 131.
5. Y. Israel and L. Meites, *Vanadium*(VII-2) *in Encyclopedia of Electrochemistry of the Element* (Edited by A. J. Bard), Vol. VII, pp. 312–349. Marcel Dekker, New York (1976).
6. Stal' G. Mairanovskii, *Catalytic and Kinetic Waves in Polarography*, pp. 1–55. Plenum Press, New York (1968).
7. R. Guidelli, Chemical reactions in polarography, in *Electroanalytical Chemistry* (Edited by A. J. Bard), Vol. 5. Marcel Dekker, New York (1971).
8. J. Koutecky and J. Cizek, *Coll. Czech. Chem. Commun.* 1956, **21**, 1063.
9. Y. Israel and L. Meites, *J. Electroanal. Chem.* 1964, **8**, 99.
10. J. W. Oliver and J. W. Ross, *J. Phys. Chem.* 1962, **66**, 1699.
11. F. J. Kristine, D. Gard and R. E. Shepherd, *J. Chem. Soc., Chem. Commun.* 1976, 994.
12. C. W. Manning and W. C. Purdy, *Anal. Chim. Acta* 1970, **51**, 483.
13. N. Kato, Y. Narusawa and K. Nakano, *Denki Kagaku* 1986, **54**, 818.

Polyhedron Vol. 8, No. 15, pp. 1953–1956, 1989
Printed in Great Britain

0277–5387/89 $3.00+.00
© 1989 Maxwell Pergamon Macmillan plc

STUDY ON THE COORDINATION OF VITAMIN D_3 TO CALCIUM(II) AND CADMIUM(II) IN SOLUTION

LIU QITAO,* LIU YI and ZHANG FENG

Department of Chemistry, Liaoning University, Shenyang, P.R.C.

(*Received* 25 *January* 1989; *accepted* 10 *March* 1989)

Abstract—The coordination of vitamin D_3 to calcium(II) and cadmium(II) has been studied by potentiometric pH titrations in a 70% (v/v) ethanol–water solution at 37 ± 0.1°C and at 0.10 (KNO_3) ionic strength. The results show that both of the metal ions form 1 : 1 and 1 : 2 complexes with vitamin D_3 and the coordinating tendency of the second ligand to the 1 : 1 complex is unusually strong. This anomalous situation has been explained by intramolecular hydrophobic ligand–ligand interactions in these complexes. The inter-promoting or inter-restraining absorption between these metals and vitamin D_3 in organisms has also been discussed.

It is well known that the absorption of calcium in organisms can be effectively promoted by vitamin D.[1] The inter-restraint of calcium and cadmium when absorbed by organisms has also been published by many authors.[2–4] Again, it has been reported in some papers[4] that the metabolism of vitamin D_3 in animals can partially be affected by calcium and cadmium. According to recent research,[5] the accumulation of cadmium in rats' liver can be effectively reduced if the rats are fed with cadmium, and with calcium or vitamin D_3 at the same time (compared with rats that were fed with cadmium only). These facts show that there must be some complicated interaction between calcium, cadmium, vitamin D and other bioligands existing in the organisms. From the viewpoint of coordination chemistry, it is expected that some useful information can be obtained for explaining the above physiological phenomena by studying the coordination of calcium(II) and cadmium(II) with vitamin D_3, inspecting the species of the complexes, and determining their stabilities in solution. In this paper, the coordination equilibria of Ca^{II}–VD_3 and Cd^{II}–VD_3 systems have been studied by potentiometric pH titrations in 70% (v/v) ethanol–water solution, and some interesting results have been obtained.

EXPERIMENTAL

Apparatus and chemicals

A Radiometer pHM-84 pH meter (Denmark, accuracy ± 0.001) and a 2401B compound glass electrode (U.S.A.) were used for all pH measurements. The temperature of the determining solution system was kept at 37 ± 0.1°C, using a jacketed beaker which permits the circulation of water through it. Calcium(II) and cadmium(II) solutions were prepared, respectively, from A.R. grade pure calcium carbonate (dissolved in 1 : 1 hydrochloric acid and heated slowly to eliminate the extra hydrochloric acid) and high purity cadmium (content is above 99.99%, dissolved in 1 : 3 nitric acid). Vitamin D_3 was of food grade purity (Merck, content >99%). Other chemicals used were all A.R. or G.R. grade pure reagents and not purified further. The water used in all the experiments was double distilled.

Method

The potentiometric pH titrations were carried out in a 70% (v/v) ethanol–water solution at 37 ± 0.1°C and 0.10 ionic strength (maintained with KNO_3) under a high purity N_2 flow. The acidic formation constant of vitamin D_3 was determined by preparing solutions (0.01920 g of vitamin D_3, 35.00 cm^3 of ethanol, 2.00 cm^3 of 0.04454 M nitric acid

* Author to whom correspondence should be addressed.

Table 1. The acidic formation constant of vitamin D_3 and the stability constants of Ca^{II}–VD_3 and Cd^{II}–VD_3 complexes in a 70% (v/v) ethanol–water solution [$t = 37 \pm 0.1$°C, $I = 0.10$ (KNO_3)]

System	Log β_1	Log β_2
H^+–vitamin D_3	12.36 ± 0.04	—
Ca^{II}–vitamin D_3	3.37 ± 0.04(3.43)[a]	7.33 ± 0.02(7.27)
Cd^{II}–vitamin D_3	6.46 ± 0.04(6.45)	13.64 ± 0.01(13.61)

[a] The values in parentheses were obtained by a graphical method.[8]

and 5.00 cm^3 of 1.0 M KNO_3, finally, diluted with water to 50.00 cm^3) and carrying out pH titrations with 0.08829 M carbonate-free sodium hydroxide solution (the details were as described before[6]). The same procedure was used in the determination of the stability constants of the metal complexes, except 5.00 cm^3 of a Ca^{II} or Cd^{II} solution were added to 50 cm^3 of determining solution system (5×10^{-4} M). The concentration ratio of metal to ligand was 1 : 2 in each solution.

Calculation

The TITFIT Basic program[7] (APPLE II HKC8800A computer) has been used for calculating the acidic formation constants of the ligand and the stability constants of the metal complexes. The activity coefficient of the H^+ ion was determined by titrating 50 cm^3 of standard nitric acid solution (the conditions were the same as above) and evaluated using the above program ($\gamma_{H^+} = 0.289 \pm 0.001$ were obtained). The ionic production of water in this mixed solvent was also evaluated in the calculation process of the acidic formation constants of vitamin D_3 to be $pK_w = 15.60 \pm 0.02$ (37°C).

RESULTS AND DISCUSSION

The calculation values, along with the values obtained by graphical methods,[8] are given in Table 1. The results agree quite well. It is evident that each calcium(II) and cadmium(II) can coordinate with vitamin D_3 and form 1 : 1 and 1 : 2 complexes. The stability of the cadmium(II) complex is much higher than that of calcium(II). It is interesting that the stepwise stability constants of a 1 : 2 binary complex of either calcium(II) or cadmium(II) are even higher than the first one. In Table 2, the stepwise stability constants of these complexes, log K_i, and the values of Δ log K are listed. Both of the Δ log K values are positive. This is very unexpected, because the stepwise stability constants of complexes should successively decrease on consideration of either the electrostatic or stereo effects. For the systems in which only the 1 : 1 and 1 : 2 binary complexes are formed, the ratio of the stepwise stability constants, K_2/K_1, should be *ca* 0.25, or the Δ log K value should be *ca* -0.6 on the grounds of statistical considerations.[9] The experimental values of Δ log K listed in Table 2 are much higher than this statistically expected value. This shows that some special process must exist that stabilizes the 1 : 2 binary complexes.

Calcium (alkaline earth metal) is very different from cadmium (d^{10} metal) in electronic structure, but the difference in Δ log K values is rather small, therefore the factors that stabilize the 1 : 2 binary complexes are assumed to be mainly due to the ligand, vitamin D_3. The molecular structure of vitamin D_3 is shown in Fig. 1. The phenolic hydroxyl is the only group that can be coordinated to the metal. In addition, the other side of the molecule consists of a huge hydrophobic group. Therefore, it is possible that if two molecules of vitamin D_3 coordinate simultaneously to the metal ion, the two

Table 2. The stepwise stability constants of calcium(II) and cadmium(II) complexes and the Δ log K values in a 70% (v/v) ethanol–water solution (37°C, $I = 0.10$)

System	log K_1	log K_2	Δ log K = log K_2 − log K_1
Ca^{II}–vitamin D_3	3.37	3.96	+0.59
Cd^{II}–vitamin D_3	6.46	7.18	+0.72

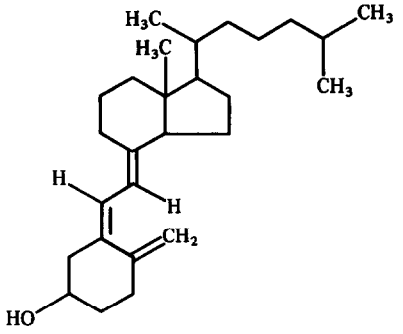

Fig. 1. The structure of the vitamin D_3 molecule.

hydrophobic groups of the vitamin D_3 molecules will close in on each other to form a hydrophobic bond[10] in terms of bridging by the metal ion. The formation of this hydrophobic bond will greatly enhance the stability of the complexes. The possible intramolecular hydrophobic ligand–ligand interaction is illustrated in Fig. 2.

Hydrophobic interactions, as a type of important non-covalent interaction, are significant in the determination of the configuration of some biomolecules, e.g. protein, nucleic, etc., and many other important biological phenomena.[11] It has often been reported in some papers[12–14] that the stability of binary and ternary metal complexes can be enhanced by intramolecular hydrophobic ligand–ligand interactions, however, it is rare that the binary 1 : 2 complexes, like the ones reported in this paper, have such large $\Delta \log K$ values as shown in Table 2. This is probably because most of the research previously reported is about mini-molecule amino acid ligands such as leucine, isoleucine, tryptophan etc., of which the hydrophobic groups are all much smaller than those in vitamin D_3. It can be assumed that a more effective hydrophobic bond could be formed by vitamin D_3. Meanwhile, research into the influence of solvent on the hydrophobic interactions between ligands in complex molecules[15] shows that the addition of an organic solvent (such as dioxane, ethanol, etc.) to an aqueous solution is favourable for the intramolecular hydrophobic interactions in metal complexes in a definite range. Therefore, it is possible that the hydrophobic interactions lead to the positive values of $\Delta \log K$ for the two metal–vitamin D_3 complexes studied in this paper. As the hydrophobic interactions exist not only between vitamin D_3 molecules in the complexes, but also between the vitamin D_3 molecules (that have coordinated to metal) and other biomolecules carrying hydrophobic groups, this should exert a significant influence on the physiological functions of some metal complexes of vitamin D_3. It is known that the best approach for the promotion of vitamin D_3 to calcium absorption is promoting the combination of calcium with the protein of the intestine mucous cell.[1] In addition to the possibility that the calcium which has coordinated with vitamin D_3 further combines with an amino acid residue of a protein (usually with aspartic acid or glutamic acid residues) to form ternary complexes, the hydrophobic interactions existing between the huge hydrophobic group of the vitamin D_3 molecule (coordinated to calcium) and other hydrophobic groups that exist in many biomolecules, will inevitably promote this approach for carrying the calcium through the cell membrane and bridging it closer to the protein molecules. Cadmium is the second two-valent metal ion which can easily coordinate with the calcium-binding proteins (only weaker than calcium),[1] and it should be expected that they restrain each other in the absorption by organisms. On the other hand, for the restraint of vitamin D_3 to cadmium absorption, in addition to indirectly restraining cadmium absorption in terms of promoting calcium absorption and increasing the content of calcium in body, it is also possible that the vitamin D_3 molecules stably coordinate to cadmium (the stability constants of the first complex is larger by three orders than that of calcium, and the second complex is larger by six orders than that of calcium) to restrain the combination of cadmium with biomolecules in the body, and to be excreted directly.

REFERENCES

1. E. Ochiai, *Bioinorganic Chemistry. An Introduction*, pp. 435–449, 475–476. Allyn and Bacon, Boston (1977).
2. N. Sugawara, *Arch. Environm. Contamin. Tox.* 1977, **5**, 167.

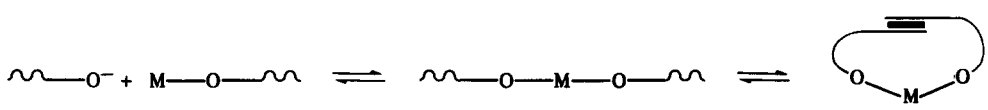

Fig. 2. Schematic diagram of the intramolecular hydrophobic ligand–ligand interaction of VD_3–metal complexes.

3. R. J. Chertok, L. B. Sasser, M. F. Callaham and G. E. Jarboe, *J. Nutr.* 1981, **111**, 631.
4. R. Lorentzon and S. E. Larsson, *Clin. Sci. Mol. Med.* 1977, **53**, 439.
5. Tang Datong, Liu Yonghui and Wang Deqing, *Acta Zool. Sinica* (Chinese Edn) 1984, **30**, 50.
6. Zhang Feng and Liu Qitao, *Chem. J. Chinese Universities* (Chinese Edn) 1987, **8**, 306.
7. A. D. Zuberbuhler and T. A. Kaden, *Talanta* 1982, **29**, 201.
8. F. C. Rossotti and H. S. Rossotti, *The Determination of Stability Constants*. McGraw-Hill, New York (1961).
9. Liu Qitao, *Coordination Chemistry* (Chinese Edn), pp. 173–174. Liaoning University Press, Shenyang (1986).
10. H. A. Scheraga, *Accts. Chem. Res.* 1979, **12**, 7.
11. E. Frieden, *J. Chem. Ed.* 1975, **52**, 754.
12. V. Zelano, E. Roletto and A. Vanni, *Ann. Chim. (Roma)* 1983, **73**, 113.
13. K. Prasad and M. S. Mohan, *J. Coord. Chem.* 1987, **1**, 16.
14. H. Sigel, *Angew. Chem. Int. Edn* 1982, **21**, 389.
15. H. Sigel, R. Tribolet and K. H. Scheller, *Inorg. Chim. Acta* 1985, **100**, 151.

Polyhedron Vol. 8, No. 15, pp. 1957–1963, 1989
Printed in Great Britain

0277–5387/89 $3.00+.00
© 1989 Maxwell Pergamon Macmillan plc

SOLVENT EXTRACTION OF N-ETHYL-GLYOXYLANILIDE OXIME AND OF ITS COPPER(II) AND NICKEL(II) COMPLEXES INTO CHLOROFORM

A. IZQUIERDO,* R. COMPAÑÓ, M. GRANADOS and X. DUARRI

Departament de Química Analítica, Universitat de Barcelona, Diagonal 647, 08028 Barcelona, Spain

(*Received* 13 *January* 1989; *accepted* 10 *March* 1989)

Abstract—The distribution equilibria of N-ethyl-glyoxylanilide oxime (NEG) and of the Cu^{II}–NEG and Ni^{II}–NEG complexes in the water–chloroform system have been studied at 25°C. From the graphical treatment of the equilibrium data it has been deduced that NEG dimerizes in the organic phase, copper is extracted as the CuL_2 complex and nickel as NiL_2 or $NiL_2(HL)$ depending on the NEG concentration. These models have been checked by treating the data with the program LETAGROP–DISTR and the following equilibrium constants have been obtained: NEG, $pK_a = 9.32 \pm 0.03$, $\log K_{DR} = 0.99 \pm 0.04$, $\log K_2 = 1.78 \pm 0.07$; CuL_2, $\log \beta_2 = 7.24 \pm 0.10$, $\log \beta_2 = 12.83 \pm 0.06$, $\log K_{DC} = 2.54 \pm 0.04$; NiL_2, $\log K_{ex} = -8.7 \pm 0.2$; $NiL_2(HL)$, $\log K_{ex} = -6.20 \pm 0.08$.

Mono-oximes formed by the condensation of aromatic amines with chloral and hydroxylamine, with the —NR—CO—CH=N—OH grouping (R = H or alkyl radical), have been widely studied as analytical reagents for metal ions, especially for copper(II), nickel(II), cobalt(II) and palladium(II).[1–4]

These ligands act as bidentate agents, via CO and oximic nitrogen, forming chelating five-membered rings.

The complexes are sparingly soluble in water, but they can be extracted into organic solvents, chloroform being the one that produces the higher values of the recovery factor. While there appear to be analytical applications of these ligands, there have been no solvent extraction studies using this class of reagents. In this work, the distribution equilibria of NEG and of its copper(II) and nickel(II) complexes in the water–chloroform system have been studied. From the effects of the different experimental variables on the distibution ratio, and by means of graphical and numerical methods, the nature of the species which participate in the distribution equilibria has been determined, as well as the constants which control these equilibria.

* Author to whom correspondence should be addressed.

EXPERIMENTAL

Reagents

N-Ethyl-glyoxylanilide oxime (NEG) was synthesized following the procedure of Sandmeyer,[5] modified by Marvel and Hiers.[6] By double recrystallization from water, NEG was obtained as light yellow crystals with a melting point of 171°C.

A stock solution of copper (1 g dm^{-3}) was prepared by dissolving $Cu(NO_3)_2 \cdot 3H_2O$ (analytical reagent grade) in water, and was standardized by iodometry.[7]

A stock solution of nickel (1 g dm^{-3}) was prepared by dissolving $Ni(NO_3)_2 \cdot 6H_2O$, and was standardized gravimetrically as dimethylglyoximate.[7]

All other chemicals were of analytical grade and used without further purification.

Apparatus

A Beckman Acta MVII spectrophotometer, with 1 cm quartz cells, and an atomic absorption spectrophotometer (Perkin–Elmer 4000) with an air–acetylene flame or a graphite furnace (Perkin–Elmer HGA 500), were used. The samples were manually injected into the graphite furnace using a 0.02 cm^3 Eppendorf pipette. A Radiometer pH-meter PHM64, equipped with a Ross combination

pH electrode, standardized with buffer solutions at pH 4.008 and 6.865 (25°C) prepared from Merck salts according to DIN 19266, was also used.

PROCEDURE

Distribution of NEG

10 cm^3 of an aqueous buffer solution with an ionic strength of 0.1 M and saturated with chloroform, and 10 cm^3 of chloroform, saturated with water, containing NEG (10^{-3}–10^{-1} M), were shaken together at 25.0 ± 0.1°C in 30 cm^3 glass stoppered vials for 10 min. After phase separation, an aliquot of the aqueous phase was transferred to a volumetric flask and diluted to the mark with NaOH (0.1 M), and its absorbance was measured at 265 nm against a blank. Finally the pH of the aqueous phase was measured at 25.0 ± 0.1°C.

Distribution of copper(II) *and nickel*(II) *complexes*

10 cm^3 of the aqueous phase saturated with chloroform, containing appropriate concentrations of metal ion, and 10 cm^3 of chloroform saturated with water, containing NEG, were shaken until equilibrium was attained [15 min for copper(II), 30 min for nickel(II)]. The pH of the aqueous phase was adjusted with an acetic acid–sodium acetate buffer when the distribution of copper(II) was studied, and with a potassium dihydrogen phosphate–potassium hydroxide buffer in the case of the nickel(II) study. Potassium nitrate was added to give a constant ionic strength of 0.1 M. After phase separation, the equilibrium concentration of copper(II) or nickel(II) in the aqueous phase was determined by flame AAS or graphite furnace AAS, depending on the concentration level, under the usual conditions. The metal concentration in the organic phase was calculated by difference. The pH of the aqueous phase was measured at 25.0 ± 0.1°C.

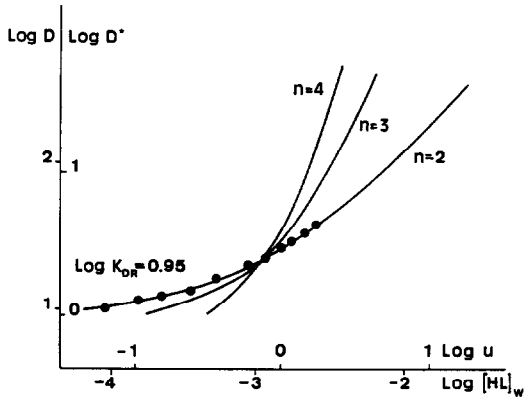

Fig. 1. Influence of reagent concentration on the distribution ratio of NEG. The full lines are the normalized curves log D^* vs log u; $D^* = 1 + nu^{(n-1)}$.

RESULTS AND DISCUSSION

Distribution of NEG *in the water–chloroform system*

The distribution ratio values obtained at pH 4.65 and 9.97, with shaking times between 5 and 60 min, show that 5 min of shaking is enough to attain the distribution equilibrium. In subsequent experiments, an extraction time of 15 min was adopted. The influence of the reagent concentration on the distribution ratio values (Fig. 1) points out that, in the concentration range studied, molecular association in the organic phase must be taken into account. Figure 2 shows the plots of log D vs pH obtained with 10^{-2} and 10^{-3} M NEG solutions in chloroform.

Calculation of the equilibrium constants. Assuming that only the monomeric NEG is capable of distributing into the aqueous phase, and that only one polymeric species exists in the organic

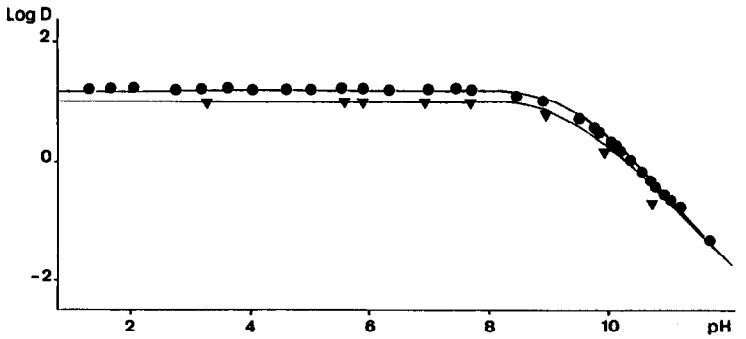

Fig. 2. Influence of pH on the distribution ratio of NEG. ● $C_{HL} = 10^{-2}$ M; ▼ $C_{HL} = 10^{-3}$ M. The full curves are calculated with the program HALTAFALL using the constants given in Table 1.

Table 1. Dissociation constant of NEG and its distribution and dimerization constants in the water–chloroform system

Method	pK_a	$\log K_{DR}$	$\log K_2$	$\sigma(\log D)$
Graphical	9.25	0.95	1.89	
LETAGROP–DISTR[a]	9.32±0.03	0.99±0.04	1.78±0.07	0.03
Spectrophotometric[b]	9.32±0.02			

[a] The limits given for the constants correspond to $\log[K \pm 3\sigma(K)]$; $\sigma(\log D) = [\Sigma(\log D_{exp} - \log D_{calc})^2/N]^{1/2}$.

[b] The limits given for the constant correspond to $-\log[K_a \pm 3\sigma(K_a)]$ obtained by the SQUAD treatment.

phase, the distribution ratio of NEG is given as:

$$D = \frac{[HL]_o + [(HL)_n]_o}{[HL]_w + [L^-]} = \frac{K_{DR}[HL]_w + nK_nK_{DR}^n[HL]_w^n}{[HL]_w + K_a[H^+]^{-1}} \quad (1)$$

where HL represents NEG, and K_{DR}, K_a and K_n are, respectively, the distribution, dissociation and polymerization constants of the reagent. The subscripts o and w denote the organic and the aqueous phase respectively. When $[H^+] \gg K_a$ the following equation is obtained:

$$D = K_{DR} + nK_nK_{DR}[HL]_w^{n-1}. \quad (2)$$

A curve-fitting method[8,9] was applied to the data plotted in Fig. 1 to determine n, K_n and K_{DR}. By introducing $D^* = D/K_{DR}$ and $u = K_n^{1/(n-1)} K_{DR}[HL]_w$ in eq. (2), a family of normalized curves $D^* = 1 + nu^{(n-1)}$ is obtained. In Fig. 1, these curves are plotted superimposed onto the experimental points, log D vs log $[HL]_w$, under the conditions of best fit. The experimental points fit the curve corresponding to $n = 2$, which means that the polymeric species is a dimer. The values obtained for $\log K_{DR}$ and $\log K_2$ are shown in Table 1.

In order to determine K_a and because there is an increase in D due to the formation of dimers in the organic phase, corrected values of D have been calculated $\{D_{corr} = [HL]_o/([HL]_w + [L^-])\}$ and another curve-fitting method was used. In Fig. 3, the experimental curve, log D_{corr} vs pH, and the normalized curve, log D^* vs log u, under the conditions of best fit are shown. The normalized variables are defined by $D^* = D_{corr}/K_{DR}$ and $u = [H^+]/K_a$, and the normalized curve by $D^* = 1/(1+u)$. The pK_a value obtained is shown in Table 1.

The values of the constants obtained graphically were refined by means of the program LETAGROP–DISTR;[10] the final values and their standard deviations are given in Table 1. There is good agreement between the constants obtained by the two methods, as well as between the pK_a obtained spectrophotometrically[11] and refined with the program SQUAD.[12]

The distribution of NEG among the various species, as well as the theoretical log D values, were calculated by HALTAFALL.[13] The calculated log D values are plotted in Fig. 2, superimposed on the experimental points. The good agreement between them confirms the proposed model. The species distribution diagram is shown in Fig. 4.

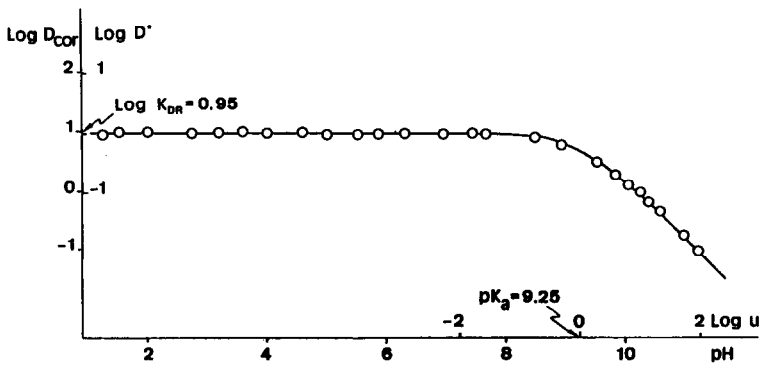

Fig. 3. Log D_{corr} vs pH superimposed on the normalized curve, log D^* vs log u; $D^* = 1/(1+u)$.

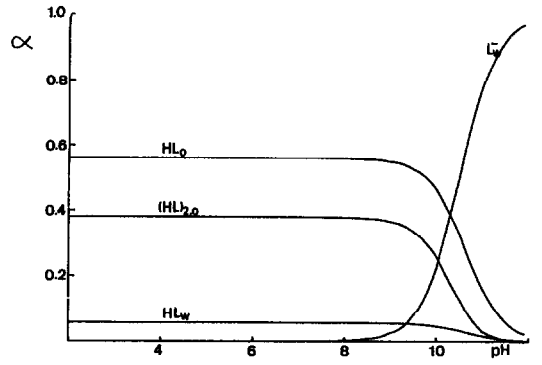

Fig. 4. Distribution diagram of species, $C_{NEG} = 10^{-2}$ M.

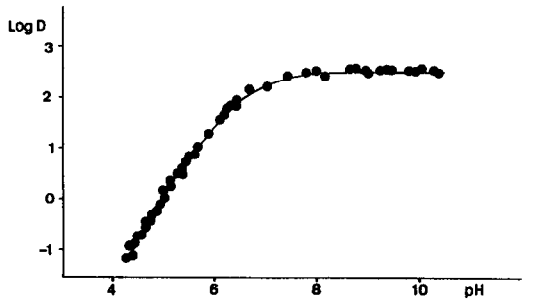

Fig. 5. Influence of pH on the distribution ratio of copper(II). $C_{NEG} = 10^{-2}$ M; $C_{Cu} = 6.3 \times 10^{-5}$ M. The full curve is calculated with the program HALTAFALL using the constants given in Tables 1 and 2.

Distribution of the copper complex

The distribution ratio values obtained with shaking times between 5 min and 3 h, show that the distribution equilibria is attained after 5 min of shaking. In subsequent experiments an extraction time of 15 min was adopted. In order to ascertain the influence of salts used to adjust the ionic strength, series of extractions varying the concentration of ClO_4^-, SO_4^{2-} and NO_3^- at constant pH and NEG concentration were carried out. The distribution ratio increases with the ClO_4^- concentration, for concentrations higher than 10^{-2} M, suggesting that perchlorate is involved in the distribution equilibria. Concentrations above 4×10^{-3} M SO_4^{2-} cause a decrease in the distribution ratio, that can be attributed to the formation of non-extractable Cu^{II}–SO_4^{2-} complexes in the aqueous phase. On the other hand, any influence of nitrate concentration was observed in the range studied (2×10^{-2}–4×10^{-1} M). In subsequent experiments the ionic strength was adjusted to 0.1 M with KNO_3.

Because the pH of the aqueous phases was adjusted with an acetic acid–sodium acetate buffer, the influence of acetate on the distribution equilibrium was studied by varying its concentration over the 10^{-3}–10^{-1} M range. The distribution ratio is independent of the acetate concentration up to 10^{-2} M. At higher acetate concentration, a slight decrease in the log D values was observed. In subsequent experiments the buffer concentration was 5×10^{-3} M.

The influence of metal concentration was studied at pH 4.65 with a NEG concentration of 10^{-2} M. The copper concentration was varied between 6.3×10^{-6} and 1.57×10^{-4} M. The distribution ratio is independent of the metal concentration for concentrations lower than 10^{-4} M. At higher concentrations the distribution ratio increases with the metal concentration, suggesting that polynuclear species are extracted under these conditions. In subsequent experiments a copper concentration of 6.3×10^{-5} M was used.

The influence of pH on the distribution ratio was studied for 10^{-2} M NEG. Figure 5 shows the variation of log D with pH. To determine the effect of the ligand concentration on the distribution ratio, a series of extractions with NEG concentrations between 10^{-3} and 10^{-1} M was performed. In Fig. 6 the values of log D are plotted vs log $[HL]_o$.

Composition of the extracted species and calculation of the equilibrium constants. Since under the experimental conditions only mononuclear species are extracted, and complexes with nitrate, acetate and hydroxide ions[14] can be neglected in the aqueous phase, the metal distribution ratio is given by:

$$D = \frac{\Sigma_n \Sigma_m [ML_n(HL)_m]_o}{[M]_w + \Sigma_p [ML_p]_w}, \qquad (3)$$

where M represents the metal and HL the extracting agent. The subscripts o and w denote the organic and the aqueous phase, respectively. Charges have been omitted for simplicity. If only the $ML_n(HL)_m$

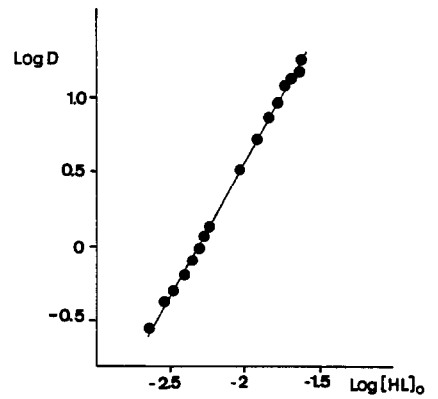

Fig. 6. Influence of reagent concentration on the distribution ratio of copper(II). pH = 5.03; $C_{Cu} = 6.3 \times 10^{-5}$ M.

Table 2. Survey of the equilibrium constants for the extraction of copper(II) with NEG into chloroform

Method	$\log \beta_1$	$\log \beta_2$	$\log K_{DC}$	$\sigma(\log D)$
Graphical	7.04	12.40	2.52	
LETAGROP–DISTR	7.24±0.10	12.83±0.06	2.54±0.04	0.05

species is extracted and the metal is present in the aqueous phase predominantly as the cation M^{n+}, the following equation can be obtained:

$$\log D = \log K_{ex} + n\mathrm{pH} + (n+m)\log[\mathrm{HL}]_o, \quad (4)$$

where K_{ex}, the extraction constant of $ML_n(HL)_m$, is $K_m K_{DC} \beta_n K_a^n / K_{DR}^m$ (β_n: formation constant of ML_n; K_{DC}: distribution constant of ML_n; K_m: adduct formation constant in the organic phase; K_a and K_{DR}: dissociation and distribution constants of the reagent, respectively).

In these conditions, if $\log D$ is plotted vs pH, at constant $[HL]_o$, or vs $\log [HL]_o$ at constant pH, straight lines with slopes n and $n+m$ will be obtained.

When species other than ML_n can be neglected in the organic phase, a plot of $\log D$ vs pH will give a straight line with a slope of zero; in this case the following equation is valid:

$$\log D = \log(K_m K_{DC}) + m \log[\mathrm{HL}]_o. \quad (5)$$

Graphical treatment: the slope of the curve in Fig. 5 ($\log D$ vs pH) varies progressively from a value near to 2, at the lowest pH studied, to zero at pH above 7.3. On the other hand, the values of $\log D$ vs $\log [HL]_o$ give a straight line of slope 1.9 (Fig. 6). According to eqs (4) and (5) this suggests that the simple chelate CuL_2 is the extracted species. The distribution constant of CuL_2 evaluated as the average of the distribution ratios obtained at pH values above 7.3, is $\log K_{DC} = 2.52$ ($s = 2 \times 10^{-2}$).

To calculate K_{DC} and the stability constants of CuL^+ and CuL_2 in the aqueous phase, Sillén's curve-fitting method was applied to the data. The normalized curves are given by $D^* = u^2/(1+pu+u^2)$, where the normalized variables and the parameter p are defined by $D^* = D/K_{DC}$, $u = \beta_2^{1/2}[L^-]$ and $p = \beta_1/\beta_2^{1/2}$. The values of the constants calculated by this method are given in Table 2.

Numerical treatment: the values of the constants obtained graphically were refined by means of the LETAGROP–DISTR program. The results are given in Table 2. The distribution of copper amongst the various species, as well as the theoretical $\log D$ values, were calculated by HALTAFALL. The calculated $\log D$ values have been plotted in Fig. 5 superimposed on the experimental points; the good agreement between them confirms the proposed model. The distribution diagram of species is shown in Fig. 7.

Distribution of the nickel complex

The distribution ratio values obtained with shaking times between 10 min and 3 h, show that the distribution equilibrium is attained after 10 min of shaking. In subsequent experiments an extraction time of 30 min was adopted.

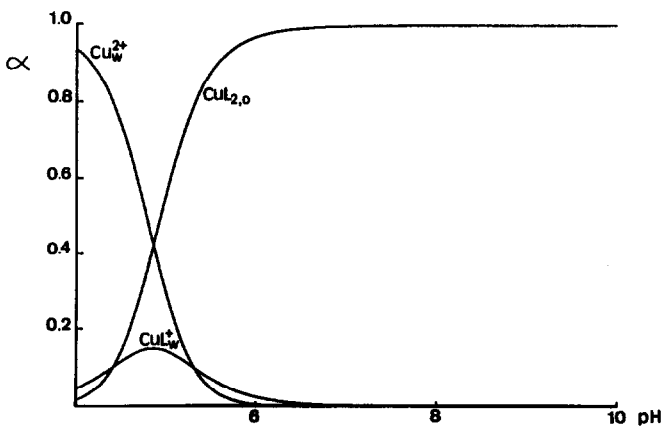

Fig. 7. Distribution diagram of species, $C_{HL} = 10^{-2}$ M; $C_{Cu} = 6.3 \times 10^{-5}$ M.

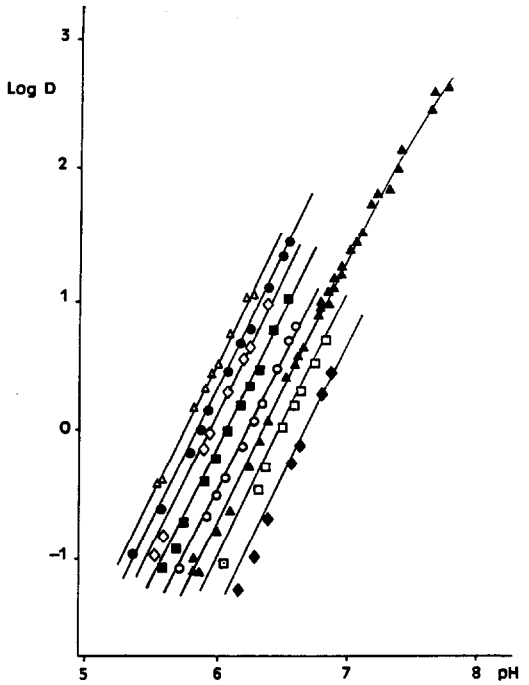

Fig. 8. Influence of pH on the distribution ratio of nickel(II). $C_{Ni} = 6.8 \times 10^{-5}$. C_{HL}: ◆ = 0.005 M; □ = 0.008 M; ▲ = 0.010 M; ○ = 0.015 M; ■ = 0.020 M; ◇ = 0.030 M; ● = 0.040 M; △ = 0.050 M. The full curves are calculated with the program HALTAFALL using the constants given in Tables 1 and 3.

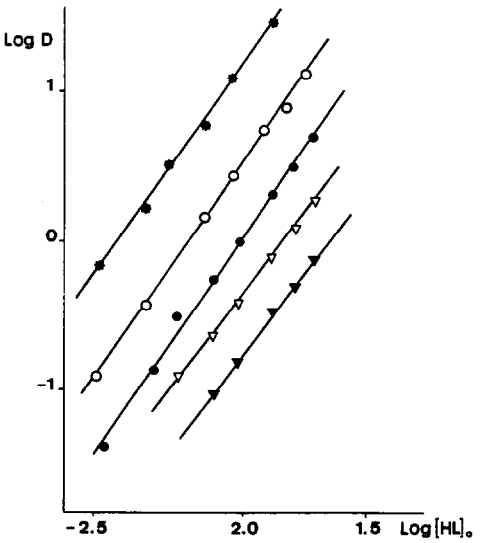

Fig. 9. Influence of the reagent concentration on the distribution of nickel(II). $C_{Ni} = 6.8 \times 10^{-5}$ M. pH: * = 6.6; ○ = 6.3; ● = 6.1; ▽ = 5.9; ▼ = 5.7.

The influence of nitrate was studied by varying its concentration over the range 4×10^{-2}–4×10^{-1} M. The distribution ratio, at constant pH and NEG concentration, was independent of the nitrate concentration. In the rest of the work the ionic strength was adjusted to 0.1 M with KNO_3.

In order to study the influence of the phosphate ion, used to adjust the pH of the aqueous phase, on the distribution equilibrium, the concentration of this substance was varied over the range 5×10^{-3}–1.25×10^{-3} M. The distribution ratio is independent of the phosphate concentration in the range studied. In subsequent experiments the buffer concentration was 1.25×10^{-3} M.

At nickel concentrations below 9×10^{-5} M the metal concentration has no effect on the distribution. For nickel concentrations greater than 9×10^{-5} M the distribution ratio increases with the metal concentration, suggesting that polynuclear species are extracted under these conditions. In subsequent experiments a nickel concentration of 6.8×10^{-5} M was used.

The influence of pH on the distribution ratio was studied for eight different ligand concentrations, ranging between 5×10^{-3} and 5×10^{-2} M. The results of these experiments are plotted in Fig. 8.

To examine the influence of NEG concentration on the distribution ratio, at constant pH, the values of log D corresponding to each reagent concentration were calculated from the curves in Fig. 8 at pH 5.7, 5.9, 6.1, 6.3 and 6.6. These values, plotted against log $[HL]_o$, are given in Fig. 9.

Composition of the extracted species and calculation of the equilibrium constants. Graphical treatment: the curves log D vs pH (Fig. 9) are straight lines with slopes between 2.0 and 2.2. In accordance with eq. (4), this suggests that $n = 2$. The values of log D plotted vs log $[HL]_o$ give straight lines with slopes between 2.8 and 2.9, a fact that, according to eq. (4) suggest that $m = 1$, although the presence of a mixture of NiL_2 and $NiL_2(HL)$ in the organic phase must be considered, $NiL_2(HL)$ being the predominant species.

Table 3. Survey of the equilibrium constants for the extraction of nickel(II) with NEG into chloroform

Method	log $K_{1,2}$	log $K_{1,3}$	σ(log D)
Graphical	−8.72	−6.21	
LETAGROP–DISTR	−8.7±0.2	−6.20±0.08	0.07

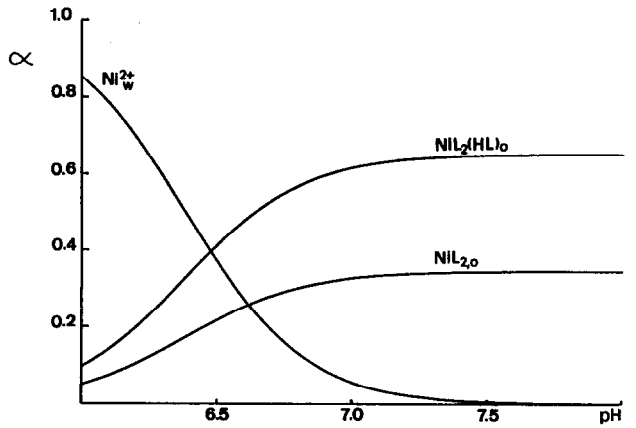

Fig. 10. Distribution diagram of species, $C_{HL} = 10^{-2}$ M; $C_{Ni} = 6.8 \times 10^{-5}$ M.

To calculate the extraction constants of the species NiL_2 ($K_{1,2}$) and $NiL_2(HL)$ ($K_{1,3}$), a curve-fitting method has been used. Superimposing the curve log $D-2$pH vs 2 log $[HL]_o$ on the normalized curve, log Y vs log u, in the conditions of best fit, the values shown in Table 3 are obtained. The normalized variables are defined by $u = (K_{1,3}[HL]_o/K_{1,2})^2$ and $Y = D[H^+]^2K^2_{1,3}/K^3_{1,2}$, and the normalized curve by $Y = u(1+u^{1/2})$.

Numerical treatment: the values obtained graphically were refined by means of the program LETAGROP–DISTR. The results obtained are given in Table 3. The value obtained for $K_{1,3}$ is better defined than that obtained for $K_{1,2}$, because NiL_2, under the experimental conditions, is always a minority species in the organic phase, as can be seen in the species distribution diagram (Fig. 10) calculated by means of the HALTAFALL program. Theoretical log D values have been calculated with HALTAFALL and have been plotted in Fig. 8, superimposed onto the experimental points; good agreement between them confirms the proposed model.

The high percentage of extraction of copper and nickel N-ethyl-glyoxylanilide oximates into chloroform (Fig. 11) means that this reagent can be used for the concentration of micro amounts of these elements.

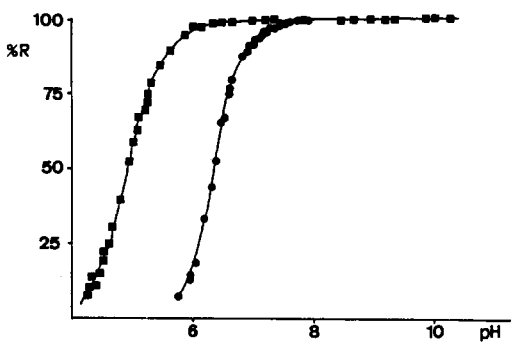

Fig. 11. Effect of pH on the extraction percentage of the N-ethyl-glyoxylanilide oximates of copper(II) (■) and nickel(II) (●). $C_{HL} = 10^{-2}$ M; $C_{Cu} = 6.3 \times 10^{-5}$ M; $C_{Ni} = 6.8 \times 10^{-5}$ M.

REFERENCES

1. F. Buscarons and F. Buscarons Jr, *Anal. Chim. Acta* 1965, **32**, 568.
2. F. Buscarons and A. Izquierdo, *Anal. Real. Soc. Esp. Fis. Quim.* 1962, **LVII(B)**, 601.
3. F. Buscarons and G. Rauret, *Quim. e Ind.* 1968, **15**, 151.
4. J. Duñach and F. Buscarons, *Analysis* 1973, **2**, 510.
5. T. Sandmeyer, *Helv. Chim. Acta* 1919, **2**, 237.
6. C. S. Marvel and G. S. Hiers, *Org. Synth.* 1925, **5**, 71.
7. A. I. Vogel, *A Textbook of Quantitative Inorganic Analysis*. Longman, London (1978).
8. L. G. Sillén, *Acta Chem. Scand.* 1956, **10**, 186.
9. D. Dyrssen and L. G. Sillén, *Acta Chem. Scand.* 1953, **7**, 663.
10. D. Hay Liem, *Acta Chem. Scand.* 1971, **25**, 1521.
11. M. Granados, unpublished data.
12. D. J. Legget, *Anal. Chem.* 1977, **49**, 276.
13. N. Ingri, W. Kakolowicz, L. G. Sillén and B. Warnquist, *Talanta* 1967, **14**, 1261.
14. A. E. Martell and R. M. Smith, *Critical Stability Constants*, Vol. 4. Plenum Press, New York (1976).

Polyhedron Vol. 8, No. 15, pp. 1965–1970, 1989
Printed in Great Britain

0277–5387/89 $3.00+.00
© 1989 Maxwell Pergamon Macmillan plc

COORDINATION COMPOUNDS WITH A BIOMIMETIC N_2S_2 LIGAND, RESULTING IN LONG METAL–THIOETHER BONDS. THE CRYSTAL AND MOLECULAR STRUCTURE OF [1,7-BIS(5-METHYL-4-IMIDAZOLYL)-2,6-DITHIAHEPTANE]BIS(THIOCYANATO-N)COBALT(II)

JACOBUS VAN RIJN, ELISABETH BOUWMAN, JIM R. EMPFIELD, WILLEM L. DRIESSEN* and JAN REEDIJK

Department of Chemistry, Gorlaeus Laboratories, Leiden University, P.O. Box 9502, 2300 RA Leiden, The Netherlands

(*Received* 12 *December* 1988; *accepted* 10 *March* 1989)

Abstract—The biomimetic N_2S_2 ligand, 1,7-bis(5-methyl-4-imidazolyl)-2,6-dithiaheptane (abbreviated bidhp) forms coordination compounds M(bidhp)X_2, with M = Mn, Co, Ni, Cu and X = Br, Cl, NCS. In all compounds, the metal ions are hexacoordinated by both anions and the tetradentate ligand. The ligand-field spectra agree with a distorted octahedral coordination. However, the distortion from octahedral, as indicated by the ligand-field spectrum, is so large in the case of the cobalt chloride and bromide compounds, that the sulphur atoms of the ligand must be at a very large distance from the metal ion. The crystal structure of Co(bidhp)$(NCS)_2$ was determined at room temperature: monoclinic, space group $P2_1/n$, $a = 15.034(3)$, $b = 8.544(3)$, $c = 18.289(4)$ Å, $\beta = 113.24(2)°$, $Z = 4$. The structure was solved by heavy-atom methods and refined by least-squares methods to a residual R value of 0.045 for 1498 significant reflections. The coordination geometry of the cobalt ion is distorted octahedral, with the two thiocyanate nitrogens and the two thioether sulphurs in *cis* positions, and the two imidazole nitrogens in *trans* positions. The cobalt–nitrogen distances are 2.043(7), 2.054(6), 2.058(6) and 2.067(7) Å, and the cobalt–sulphur distances are 2.656(2) and 2.618(2) Å. The cobalt–sulphur distances are significantly longer than in related compounds.

The crystal structure determinations of the Type I or blue copper proteins, plastocyanin[1] and azurin,[2] initiated the design of biomimetic ligands with two heterocyclic nitrogen and two aliphatic sulphur donor atoms.[3] Copper(I) and copper(II) compounds with such ligands, including the title ligand, have been studied intensively.[4] It is also important to investigate the ligating properties of the ligands in a wider sense, that is to investigate the coordination behaviour with respect to other transition metals. Improved insight into the coordinating properties of the ligand will be of use in the study of the copper compounds, and hence the copper proteins. For instance: some spectroscopic techniques offer more characterization possibilities with other metal ions than with copper(II), like NMR (zinc, silver), and ligand-field spectroscopy (nickel, cobalt). This so called substitution technique has also been applied in metal-substituted copper proteins.[5,6]

Furthermore, the coordination chemistry of the other transition metals with this special ligand system may also be of interest in itself because of the greater preference for a certain coordination geometry, especially for cobalt(II) and nickel(II), whereas copper(II) is flexible or shows plasticity, often resulting in isomers or temperature-dependent structures.[7–9]

The N_2S_2 ligand, 1,7-bis(5-methyl-4-imidazolyl)-2,6-dithaheptane (bidhp), which contains two imidazole groups and two thioether atoms, yielded a copper(II) chloride compound with very long copper(II)–thioether bonds. In fact these bonds are comparable in length with the Cu—S bond in plastocyanin and azurin.[10] Whether the copper(II)

* Author to whom correspondence should be addressed.

properties or the ligand constraints are responsible for the occurrence of these long metal–sulphur bonds is not clear. Comparison with related coordination compounds, differing in metal ion and with a different chelate skeleton, should show the particular influence of the propylene bridge in the case of bidhp.[11–15] In this paper we report the synthesis and spectroscopic properties of a number of coordination compounds with bidhp and the crystal structure determination of $Co(bidhp)(NCS)_2$.

EXPERIMENTAL

Most chemicals were commercially available, of reagent quality and used as received.

The synthesis of the bidhp ligand from 4(5)-hydroxymethyl-5(4)-methylimidazole and 1,3-propanedithiol, was described earlier.[4,16]

Synthesis of $M(bidhp)X_2$ (M = Mn, Co, Ni or Cu; X = Cl, Br or NCS)

A solution of 1.1 mmol of the appropriate metal(II) salt (hydrate) in 10 cm^3 of absolute ethanol was added to a warm solution of the ligand (1 mmol) in 10 cm^3 of absolute ethanol (25 cm^3 in case of copper). The colour changed immediately. Most products precipitated after addition of small amounts (5–10 cm^3) of diethyl ether and subsequent cooling to −15°C. They were filtered and dried at ambient temperature and pressure. With copper(II), the products precipitated immediately. Some products were recrystallized from a hot solution after the addition of 10 cm^3 of water. With $NiCl_2$, concentrating the solution to 5 cm^3 was necessary to induce precipitation. The manganese(II) halides precipitated immediately and appeared to be insoluble. As most metal(II) thiocyanates are not commercially available, a solution of 2–2.5 mmol NH_4NCS and 1 mmol of the ligand in absolute ethanol was added to a solution of a metal(II) nitrate or perchlorate. With freshly prepared copper(II) and nickel(II) thiocyanate the same products were obtained.

Single crystals of $Co(bidhp)(NCS)_2$, suitable for X-ray diffraction, were obtained by slow diffusion of solutions of the ligand and the metal salt [as $Co(NO_3)_2 \cdot 6H_2O$ and NH_4NCS (1 : 2)].

Elemental analyses and spectroscopic measurements

Metal contents were determined complexometrically by indirect complexometrical titration with Na_2H_2edta and zinc acetate after destruction of the sample in a boiling mixture of sulphuric acid and hydrogen peroxide (in a volume ratio 2 : 1).[17] Halogen contents were determined by potentiometric titration after combustion of the sample according to Schoeniger.[18] Other elements (C, H, N, S) were analysed at Pascher's Microanalytical laboratory (Bonn, F.R.G.) or the Microanalytical Laboratory of University College (Dublin). IR spectra were recorded on a Perkin–Elmer 580 spectrometer. Samples were prepared as alkali halide pellets (KBr, CsCl, CsI) and as Nujol mulls. Ligand-field spectra were recorded on a Perkin–Elmer 330 spectrophotometer in the diffuse reflectance mode with MgO as the reference. EPR spectra were recorded on a Varian E-3 X-band spectrometer at room temperature for powdered solids. X-ray powder diffractograms were recorded on a Guinier–De Wolff camera.

X-ray diffraction and structure determination

Crystal data. $C_{15}H_{20}CoN_6S_4$, MW = 471.54 g mol^{-1}, monoclinic, $P2_1/n$, $a = 15.034(3)$, $b = 8.544(3)$, $c = 18.289(4)$ Å, $\beta = 113.24(2)°$, $V = 2159(1)$ $Å^3$, $Z = 4$, $D_{calc} = 1.45$ g cm^{-3}, $\mu = 11.76$ cm^{-1}, $F(000) = 975$.

Data collection and structure refinement. A violet plate-shaped crystal of $Co(bidhp)(NCS)_2$ was mounted on a Nonius CAD-4 diffractometer. Cell dimensions were determined by least-squares refinement from the setting angles of 24 reflections ($9 < \theta < 13$). X-ray intensities, using graphite monochromated Mo-K_α radiation ($\lambda = 0.71073$ Å) were collected at room temperature by the ω–θ scan technique for $2 < \theta < 22$, with $-15 < h < 15$, $0 < k < 9$, $-19 < l < 19$. The number of measured reflections was 5706, of which 2856 were independent; from these reflections 1498 were considered as significant [$I > 2\sigma(I)$]. The data were corrected for Lorentz and polarization effects in the usual way and for absorption by using de Graaff's method.[19] This correction was considered necessary as the transmission coefficients varied from 0.90 to 1.06. $R_{int} = 0.029$.

The position of the cobalt ion was determined from a Patterson map. All other non-hydrogen atoms were determined using the Autofour program.[20] The structure was refined by least-squares calculations with anisotropic thermal parameters for the non-hydrogen atoms, using a weighting scheme with factors proportional to $[\sigma(I)]^{-2}$. Scattering factors were taken from ref. 21 for the non-hydrogen atoms and ref. 22 for the hydrogen atoms. The carbon atoms in the bridge between the sulphur atoms showed disorder. Attempts to determine these positions more accurately were unsuccessful. Some hydrogen atoms were found in difference-Fourier maps, others were

placed at 1.00 Å from the parent atoms. The hydrogen atoms were kept at fixed distances to the parent atoms, their isotropic thermal parameters were coupled to one another with a final value of 12.8 Å^2. The refinement converged to R values of $R_f = 0.045$ and $R_w = 0.051$. The final shifts were less than 0.2 times the standard deviations. The highest and lowest remaining peaks in the final difference-Fourier map were +0.47 and −0.42 e Å^{-3}. The atomic coordinates and thermal parameters are available as supplementary material, together with a table of observed and calculated structure factors and analytical data. Atomic coordinates have also been deposited with the Cambridge Crystallographic Data Centre.

RESULTS AND DISCUSSION

Description of the structure of Co(bidhp)(NCS)$_2$

An ORTEP[23] drawing of the structure, also showing the atomic numbering scheme, is depicted in Fig. 1. In Table 1 the relevant bonding distances and bond angles are listed; full tables are available as supplementary material. The asymmetric unit consists of one molecule of Co(bidhp)(NCS)$_2$. There appears to be a pseudo two-fold rotation axis within the molecule through the atoms Co(1) and C(5), with the largest deviations in the orientations of the methyl groups, thiocyanate ions and the dithiaheptane bridge. The cobalt ion is coordinated by two imidazole nitrogen atoms, two thioether sulphur atoms and two thiocyanate nitrogen atoms in a *cis*-distorted octahedral geometry, with the imidazole groups *trans* to each other and the sulphur atoms and thiocyanate anions on mutual *cis* positions. The four, more or less equal, Co—N distances are comparable to those found in related compounds.[24,25] The Co—S distances are quite large, thereby constituting the main (*cis*-)distortion factor. The other distortions from an ideal octahedral geometry, like the small S—Co—N coordination angle of about 78°, originate from steric constraints imposed by the quadridentate ligand.

The ligand bond distances and angles are within the expected range, except for the apparently too short C(4)—C(5) bond and deviating bond angles around C(5). This is obviously the result of the disorder in the aliphatic chain, which is most notably for C(5). The imidazole rings are planar with deviations less than 0.005 Å. The angle between the aromatic rings amounts to 49.9(3)°. Both NCS anions are linear. The bend coordination at N(31) is remarkable, compared to the almost

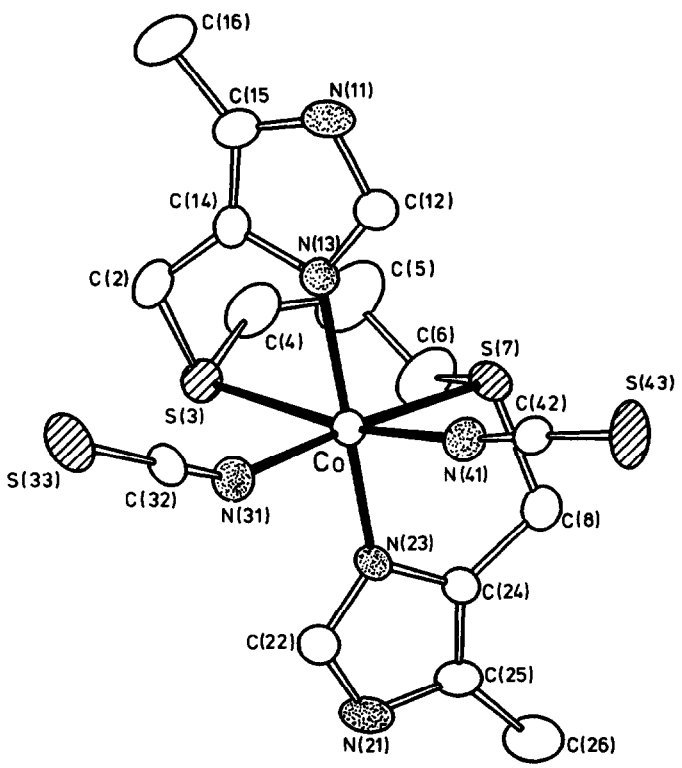

Fig. 1. ORTEP projection[23] and atomic labelling of Co(bidhp)(NCS)$_2$. The hydrogen atoms are omitted for clarity.

Table 1. Selected bond and interatomic distances (Å) and bond angles (°) in Co(bidhp)$(NCS)_2$, with ESDs in parentheses[a]

Co(1)—S(3)	2.656(2)	N(31)—C(32)	1.120(8)
Co(1)—S(7)	2.618(2)	C(32)—S(33)	1.620(8)
Co(1)—N(13)	2.058(6)		
Co(1)—N(23)	2.054(6)	N(41)—C(42)	1.136(8)
Co(1)—N(31)	2.067(7)	C(42)—S(43)	1.606(8)
Co(1)—N(41)	2.043(7)		
		N(11)—H(111)	0.85
S(3)—Co(1)—S(7)	92.16(8)	N(11)—S(33)′	3.350(7)
S(3)—Co(1)—N(13)	77.6(2)	S(33)′—H(111)	2.554(7)
S(3)—Co(1)—N(23)	91.0(2)		
S(3)—Co(1)—N(31)	85.2(2)	N(21)—H(211)	0.85
S(3)—Co(1)—N(41)	170.8(2)	N(21)—S(43)″	3.401(7)
S(7)—Co(1)—N(13)	92.1(2)	S(43)″—H(211)	2.643(7)
S(7)—Co(1)—N(23)	77.9(2)		
S(7)—Co(1)—N(31)	172.6(2)	S(33)′—H(111)—N(11)	156.4
S(7)—Co(1)—N(41)	84.9(2)	S(43)″—H(211)—N(21)	148.9
N(13)—Co(1)—N(23)	164.6(2)		
N(13)—Co(1)—N(31)	94.0(2)	Co(1)—N(31)—C(32)	150.7(7)
N(13)—Co(1)—N(41)	93.8(3)	Co(1)—N(41)—C(42)	172.9(7)
N(23)—Co(1)—N(31)	95.3(3)		
N(23)—Co(1)—N(41)	96.9(2)	N(31)—C(32)—S(33)	177.7(8)
N(31)—Co(1)—N(41)	98.8(3)	N(41)—C(42)—S(43)	177.6(7)

[a] ′ at $-x, -y-1, -z+1$; ″ at $-x+1/2, y+1/2, -z+1/2$.

linear coordination at N(41). This may be caused by stronger intermolecular hydrogen bonding (*vide infra*) and crystal packing.

Each molecule of Co(bidhp)$(NCS)_2$ contains four hydrogen bridges, between the N(1) atoms of the imidazole groups and the sulphur atoms of the thiocyanate anions connecting three neighbouring molecules: viz. between N(11) and S(22) and *vice versa* through a crystallographic centre of inversion, and between N(21) and S(43) to the ones below and above it through the crystallographic screw axis parallel to *b*. Stacking between the aromatic rings is not as complete as in Cu(bidhp)Cl_2;[10] the smallest intermolecular distance between some aromatic atoms is 3.82 Å. The other intermolecular distances are larger than, or close to, the sum of the van der Waals radii.

Spectroscopic properties

The coordination compounds all analyse as M(bidhp)X_2; the analysis data are available as supplementary material. The crystal structure determinations show a distorted octahedral geometry for Co(bidhp)$(NCS)_2$ and for Cu(bidhp)Cl_2.[10] The IR spectra of all compounds show the presence of ligand bands, some of which have shifted due to coordination, but do not yield detailed information. In fact, the IR spectra of all compounds reported here resemble each other quite well, the spectra of the chloride and bromide compounds are even identical. These compounds also appear to have the same X-ray powder pattern; the manganese, cobalt and nickel chlorides and bromides are isomorphous, while the X-ray patterns of the copper chloride and bromide compounds are only slightly different, probably as a result of a slight Jahn–Teller adaption. In Table 2 the colours, X-ray and IR type, and the ligand field and EPR data are summarized. The powder EPR spectrum of the copper halide compounds is typical for a compressed geometry with a d_{z^2} ground state. The equally intensive, ligand-field maxima agree with such a coordination geometry, and have been assigned to the $d_{xz}, d_{yz} \rightarrow d_{z^2}$ and $d_{xy}, d_{x^2-y^2} \rightarrow d_{z^2}$ transitions, respectively, on the basis of a C_2 (distorted octahedral) symmetry. The charge-transfer bands around 26×10^3 cm^{-1} are presumably due to a $\pi_{\text{N-imidazole}}$–d_{Cu} transition. In the thiocyanate series more variation is encountered. The compounds are not X-ray isomorphous; but their IR spectra are quite similar. The EPR spectrum of the copper thiocyanate compound is definitely rhombic, but still indicates a d_{z^2} ground state.

The ligand-field spectra of the cobalt compounds show a distortion from octahedral towards tetrahedral symmetry. This phenomenon has also been observed with other (benz)imidazole-thioether

Table 2. Colours, X-ray and IR type, LF and EPR data of the bidhp compounds

Compound	Colour	X-ray type	IR type	LF ($\times 10^3$ cm^{-1}) and EPR (solid)
$Mn(L)Cl_2$	White	A	I	
$Co(L)Cl_2$	Purple	A	I	18.8; 15.0; 9.3; 5.0(br)
$Ni(L)Cl_2$	Green	A	I	24.3; 14.4; 8.1
$Cu(L)Cl_2$	Brown	A′	I	26.7 (CT); 13.2; 9.2; $g_\perp = 2.19$; $g_\parallel = 2.02$
$Mn(L)Br_2$	White	A	I	
$Co(L)Br_2$	Purple	A	I	18.8; 14.4; 9.5; 5.0(br)
$Ni(L)Br_2$	Green	A	I	23.8; 14.3; 8.1
$Cu(L)Br_2$	Brown	A′	I	26.0 (CT); 13.2; 8.8; $g_\perp = 2.18$; $g_\parallel = 2.03$
$Mn(L)(NCS)_2$	White	B	II	
$Co(L)(NCS)_2$	Purple	C	II′	20.3; 16.9; 9.4–7.8 (br)
$Ni(L)(NCS)_2$	Blue	D	II′	26.5; 16.9; 10.0
$Cu(L)(NCS)_2$	Green	E	III	26.0 (CT); 13.5; 9.5 (sh); $g_1 = 2.24$; $g_2 = 2.17$; $g_3 = 2.03$

ligands.[14,15] This can be understood by assuming pseudo-tetrahedral $N_2N'_2$, N_2Cl_2 and N_2Br_2 ligand fields, as a consequence of the very long Cu—S bonds. In $Co(bidhp)(NCS)_2$, the $N_{imidazole}$—Co—$N_{imidazole}$ coordination angle is 164.6°, significantly smaller than the ideal of 180° for an octahedron, whereas the $N_{thiocyanate}$—Co—$N_{thiocyanate}$ angle is larger than 90°, namely 98.8°. These deviations from octahedral, together with the weak interaction of the sulphur atoms, must be the origin of the "tetrahedral-like" ligand-field spectra of the cobalt compounds.

Comparison with related structures

The structure of $Co(bidhp)(NCS)_2$ is *cis*-distorted octahedral (*vide supra*), with four more or less equal Co—N distances and two long Co—S distances. The distortion from octahedral is less than would be expected from the ligand-field data. In the compound $Co(memi)_2(NCS)_2$[25] (where memi = 5-methyl-4-ethylmercaptomethylimidazole, a bidentate NS ligand) all like donor atoms are in *trans* positions, resulting in a less distorted octahedral geometry. Although in the memi compound the sulphur atoms are on "loose ends" (that is, are more flexible), they are coordinated at shorter distances (2.55 Å).[25] It appears that the propylene bridge between the sulphur atoms gives rise to a more constrained ligand, resulting in longer coordination distances.

In $Ni(bidhx)(NCS)_2$[24] (where bidhx = 1,6-bis(5-methyl-4-imidazolyl)-2,5-dithiahexane, the ethylene N_2S_2 analogue of bidhp) the Ni—S distances are 2.52 Å. The occurrence of these shorter distances may originate from:

(1) the strong preference of nickel for an octahedral geometry, or

(2) the shorter bridge in the ligand bidhx, which forces the sulphur atoms closer to the metal ion.

Both arguments could be valid in the case of Ni $(bidhx)(NCS)_2$. With copper(II), only the second argument may play a role. A comparison of the copper chloride compounds of the two ligands, bidhp[4] and bidhx,[15] shows that both compounds indeed have a comparable coordination geometry (compressed octahedral, which also results in similar EPR signals). However, in $Cu(bidhp)Cl_2$[4] the Cu—S distances are very long (2.8–2.9 Å), whereas in $Cu(bidhx)Cl_2$[15] the sulphur coordination distances are considerably shorter (2.6–2.8 Å). This clearly indicates the effect of the "bridges" in these ligands, whereby the longer bridge maintains the sulphur atoms at a longer distance from the central metal ion.

CONCLUDING REMARKS

The compounds described in this paper clearly indicate that the bis(imidazole)thioether ligand, bidhp, is a very good chelating ligand for the transition metals, manganese(II), cobalt(II), nickel(II) and copper(II). Isomorphous products, all having a distorted octahedral geometry, are formed with these metal halides. The degree of distortion is strongly dependent on the metal ion; in the case of copper, a compressed geometry is obtained, whereas in the case of cobalt, a *cis*-distorted geometry is observed, which results in tetrahedral-type ligand-field spectra.

Acknowledgements—We thank Mr S. Gorter, Dr R. A. G. de Graaff and Mr J. Turkenburg for assistance with the data collection and the structure determination. Participation of one of us (J.R.E.) was enabled by a grant in the Summer Undergraduate Exchange Programme between Leiden University and Bucknell University.

REFERENCES

1. P. M. Colman, H. C. Freeman, J. M. Guss, M. Murata, V. A. Norris, J. A. M. Ranshaw and M. P. Ventakappa, *Nature* 1978, **272**, 319.
2. E. T. Adman, R. E. Stenkamp, L. C. Sieker and L. H. Jensen, *J. Molec. Biol.* 1978, **123**, 35.
3. K. D. Karlin and J. Zubieta, Copper Coordination Chemistry: *Biochemical and Inorganic Perspectives* (1983) and *Biological Copper Chemistry* (1986), Adenine Press, New York and refs cited therein.
4. J. van Rijn, PhD Thesis. Leiden University, The Netherlands (1985).
5. M. Vasak, *J. Am. Chem. Soc.* 1980, **102**, 3953.
6. M. Good and M. Vasak, *Biochemistry* 1986, **25**, 8353.
7. J. Gazo, I. B. Bersuker, L. Garaj, M. Kabesova, J. Kohout, H. Langfelderova, M. Melnik, M. Serator and F. Valach, *Coord. Chem. Rev.* 1976, **19**, 253.
8. B. J. Hathaway, *Struct. Bond. (Berlin)* 1984, **57**, 55.
9. F. Paap, W. L. Driessen, J. Reedijk, M. Dartmann and B. Krebs, *Inorg. Chim. Acta* 1986, **121**, 185.
10. J. van Rijn, W. L. Driessen, J. Reedijk and J.-M. Lehn, *Inorg. Chem.* 1984, **23**, 3584.
11. P. J. M. W. L. Birker, J. Helder, G. Henkel, B. Krebs and J. Reedijk, *Inorg. Chem.* 1982, **21**, 357.
12. M. J. Schilstra, P. J. M. W. L. Birker, G. C. Vershoor and J. Reedijk, *Inorg. Chem.* 1982, **21**, 2637.
13. A. W. Addison, T. N. Rao, J. Reedijk, J. van Rijn and G. C. Verschoor, *J. Chem. Soc., Dalton Trans.* 1984, 1349.
14. J. M. M. Smits, R. Janssen, P. T. Beurskens, J. van Rijn and J. Reedijk, *Polyhedron* 1987, **6**, 1843.
15. E. Bouwman, A. Burik, J. C. ten Hove, W. L. Driessen and J. Reedijk, *Inorg. Chim. Acta* 1988, **150**, 125.
16. E. Bouwman and W. L. Driessen, *Synth. Commun.* 1988, **18**, 1581.
17. G. Schwarzenbach and H. Flaschka, *Die Komplexometrische Titration.* Enke Verlag, Stuttgart (1965).
18. T. S. Ma and R. C. Rittner, *Modern Organic Elemental Analysis.* Marcel Dekker, New York (1979).
19. R. A. G. de Graaff, *Acta Cryst.* 1973, **A29**, 298.
20. A. J. Kinneging and R. A. G. de Graaff, *J. Appl. Cryst.* 1984, **17**, 364.
21. *International Tables for X-ray Crystallography*, Vol. IV. Kynoch Press, Birmingham (1968).
22. R. F. Stewart, E. R. Davidson and W. T. Simpson, *J. Chem. Phys.* 1965, **42**, 3175.
23. C. K. Johnson, ORTEP—Report ORNL-3794. Oak Ridge National Laboratory, Tennessee (1965).
24. E. Bouwman, R. de Gelder, R. A. G. de Graaff, W. L. Driessen and J. Reedijk, *Recl. Trav. Chim., Pays Bas* 1988, **107**, 163.
25. E. Bouwman, C. E. Westheide, W. L. Driessen and J. Reedijk, *Inorg. Chim. Acta*, submitted.

Polyhedron Vol. 8, No. 15, pp. 1971–1977, 1989
Printed in Great Britain

0277–5387/89 $3.00+.00
© 1989 Maxwell Pergamon Macmillan plc

SYNTHESIS, STRUCTURE AND SPECTROSCOPIC PROPERTIES OF SOME 2-PHENYLPHENOXIDE DERIVATIVES OF MOLYBDENUM

MICHAEL J. BARTOS, CHARLES E. KRILEY, JOYCE S. YU, JUDITH L. KERSCHNER, PHILLIP E. FANWICK and IAN P. ROTHWELL*†

Department of Chemistry, Purdue University, West Lafayette, IN 47907, U.S.A.

(*Received* 9 *February* 1989; *accepted* 14 *March* 1989)

Abstract—Treatment of the molybdenum dimethylamido compounds, $Mo(NMe_2)_4$ and $Mo_2(NMe_2)_6$ (Mo≡Mo), with 2-phenylphenol (HOAr-2Ph), leads to formation of the aryloxide compounds, $Mo(OAr\text{-}2Ph)_4(HNMe_2)_2$ (**1**) and $Mo_2(OAr\text{-}2Ph)_6(HNMe_2)_2$ (**2**), respectively. A single crystal X-ray diffraction analysis of **1** shows a *trans* arrangement of dimethylamine ligands about the octahedral MoO_4N_2 core, while in **2** an unbridged $O_3NMo{\equiv}MoNO_3$ central coordination environment is present. Spectroscopic studies on **2** indicate a significant barrier to rotation about the unbridged molybdenum–molybdenum triple bond, presumably due to the steric demands of the OAr-2Ph ligands. Crystal data for $MoO_4N_2C_{52}H_{50}$ (**1**) at 21°C: $a = 9.617(6)$, $b = 10.199(1)$, $c = 12.315(7)$ Å, $\alpha = 107.04(2)$, $\beta = 106.29(5)$, $\gamma = 95.46(2)°$, $Z = 1$, $d_{calc} = 1.317$ g cm^{-3} in space group $P\bar{1}$; for $Mo_2O_6N_2C_{83}H_{70}$ (**2**) at 19°C: $a = 22.890(2)$, $b = 13.854(4)$, $c = 24.337(2)$ Å, $\beta = 113.969(8)°$, $Z = 4$, $d_{calc} = 1.303$ g cm^{-3} in space group $P2_1/c$.

A considerable amount of research effort has been focused over the last few years on exploring the transition metal chemistry that can be supported by alkoxide,[1–3] siloxide[4] or aryloxide[5–9] ligation. A particularly important development has been the use of sterically demanding oxygen-donor ligands attached to early transition metal centres to generate both novel and complementary organometallic chemistry. In this context, our group has recently demonstrated a diverse spectrum of reactivity that can be supported by 2,6-diphenylphenoxide ligands.[7–9] Besides simple σ-coordination through the oxygen atom, this phenoxide can undergo chelation to metal centres via formation of a σ-aryl bond (cyclometallation) or via an η^6-arene interaction.[8,9] Furthermore, the activation and hydrogenation of the side arene rings by niobium hydride groups has been shown to be possible.[10] For the Group 6 metal, molybdenum, both types of chelation have been identified, as well as simple mononuclear and dinuclear derivatives of OAr-2,6Ph$_2$ ligation.[9,11] In this paper we wish to report the synthesis and characterization of some simple molybdenum derivatives of 2-phenylphenoxide (OAr-2Ph). Unlike its more bulky counterpart, OAr-2,6Ph$_2$, more extensive substitution by this ligand is found possible and there is a definite decrease in its tendency to undergo intramolecular CH bond activation.

RESULTS AND DISCUSSION

Both of the molybdenum dimethylamido substrates, $Mo(NMe_2)_4$[12] and $Mo_2(NMe_2)_6$ (Mo≡Mo),[13] react rapidly with 2-phenylphenol (HOAr-2Ph) in hydrocarbon solvents. In the case of the mononuclear compound, reaction with 4 equivalents of HOAr-2Ph causes a rapid loss of the deep-purple colour of $Mo(NMe_2)_4$ and the formation of a deep-red solution. Work-up of the reaction mixture allows the isolation of deep-red crystals of stoichiometry $Mo(OAr\text{-}2Ph)_4(HNMe_2)_2$ (**1**) in good yield. The routine spectroscopic data on **1** is inconclusive as regards its actual structure and whether or not cyclometallation has occurred. The d^2-nature of the Mo^{IV} centre in **1** results in very broad, contact shifted ^{1}H NMR spectra which are

* Author to whom correspondence should be addressed.
† Camille and Henry Dreyfus Teacher–Scholar, 1985–1990; Fellow of the Alfred P. Sloan Foundation, 1986–1990.

difficult to interpret, while the only significant absorption in the IR spectrum is the presence of a band assignable to a $\bar{\nu}$(N—H) stretch of a dimethylamine ligand. A single crystal X-ray diffraction analysis of **1** was carried out in order to accurately determine its molecular structure (Fig. 1). Some selected bond distances and angles are collected together in Table 1. It can be seen that the ligands adopt an almost perfect octahedral environment about the metal centre with *trans*-dimethylamine groups. A crystallographically-imposed inversion centre is present and the unmetallated 2-phenylphenoxide groups are solely oxygen bound. The molecular structure of **1** is closely related to that previously reported for the siloxide compound, $Mo(OSiMe_3)_4(HNMe_2)_2$.[14] The Mo—O distances in **1**, 1.963(3) and 1.972(3) Å, compare favourably with the distances of 1.950(4) and 1.951(4) Å in $Mo(OSiMe_3)_4(HNMe_2)_2$ and 1.919(2)–1.976(2) Å in the cyclometallated compound $Mo(OC_6H_3Ph\text{-}C_6H_4)(OAr\text{-}2,6Ph_2)_2(HNMe_2)$.[7] The Mo—N distances in these three compounds are also very similar, but much longer than found for molybdenum–dialkylamido ligands.[15] The Mo—O—Ar angles in **1** have values of 138.7(3) and 139.6(3)°. These angles are smaller than the almost linear values found in the related siloxide compound, and smaller than typically found for 2,6-diphenylphenoxide ligands bound to related metal centres. Previous work on aryloxide derivatives of early transition metals has shown this structural parameter to be extremely flexible,[5,16] and the smaller angles observed in **1** may be a consequence of packing effects for the asymmetric aryloxide within the coordination sphere.

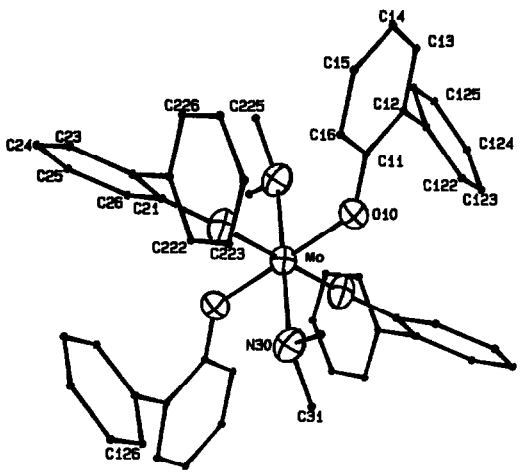

Fig. 1. ORTEP view of $Mo(OAr\text{-}2Ph)_4(HNMe_2)_2$ (**1**), emphasizing the central coordination sphere.

Closely related reactivity is seen between the dinuclear compound $Mo_2(NMe_2)_6$ and HOAr-2Ph. Hence, treatment of bright yellow solutions of the dimethylamido compound with HOAr-2Ph (6 equiv) leads to the formation of reddish-brown solutions from which the hexa-aryloxide $Mo_2(OAr\text{-}2Ph)_6(HNMe_2)_2$ (**2**) can be obtained in almost quantitative yields. Compound **2** belongs to a large and well-characterized class of dimolybdenum and ditungsten compounds of stoichiometry $M_2(OR)_6(L)_2$, that contain an unbridged $\sigma^2\pi^4$ metal–metal triple bond.[17,18] The formation of the amine adduct, **2**, contrasts with the only partial substitution observed on reacting $Mo_2(NMe_2)_6$ with 2,6-diphenylphenol,[11] and the reduction to quadruply bonded $Mo_2(OAr)_4(HNMe_2)_4$ (Mo≡Mo) compounds observed for non-bulky phenoxides.[19] The ^{1}H NMR of diagmagnetic **2** is shown in Fig. 2. The presence of two doublets due to the diastereotopic methyl groups of a Me_2NH ligand, as well as a broad septet due to the N*H* proton, are clearly evident. However, also of particular interest is the presence in the ^{1}H NMR spectrum of two doublets well separated from the aromatic region at $\sim\delta$ 9 and 4 ppm (Fig. 2). Integration of these doublets shows them to be of the same intensity as the N*H* proton signals. Hence, it would appear that they are due to protons on the central, phenolic ring of two different OAr-2Ph ligands. Previous work on dimolybdenum aryloxide anions of the type $[(L)(ArO)_2Mo(\mu\text{-}OAr)_3Mo(OAr)_2(L)]^-$ containing confacial bi-octahedral coordination environments, has shown the presence of contact shifted ^{1}H NMR signals.[19]

Table 1. Selected bond distances (Å) and angles (°) for $Mo(OC_6H_4\text{-}2Ph)_4(HNMe_2)_2$ (**1**)

Mo—O(10)	1.972(3)	Mo—O(20)	1.963(3)
Mo—N(30)	2.239(4)		
O(10)—Mo—O(20)	90.6(1)	O(20)—Mo—N(30)	96.0(1)
O(10)—Mo—O(20)	89.4(1)	O(20)—Mo—N(30)	84.0(1)
O(10)—Mo—N(30)	93.8(1)	Mo—O(10)—C(11)	138.7(3)
O(10)—Mo—N(30)	86.2(1)	Mo—O(20)—C(21)	139.6(3)

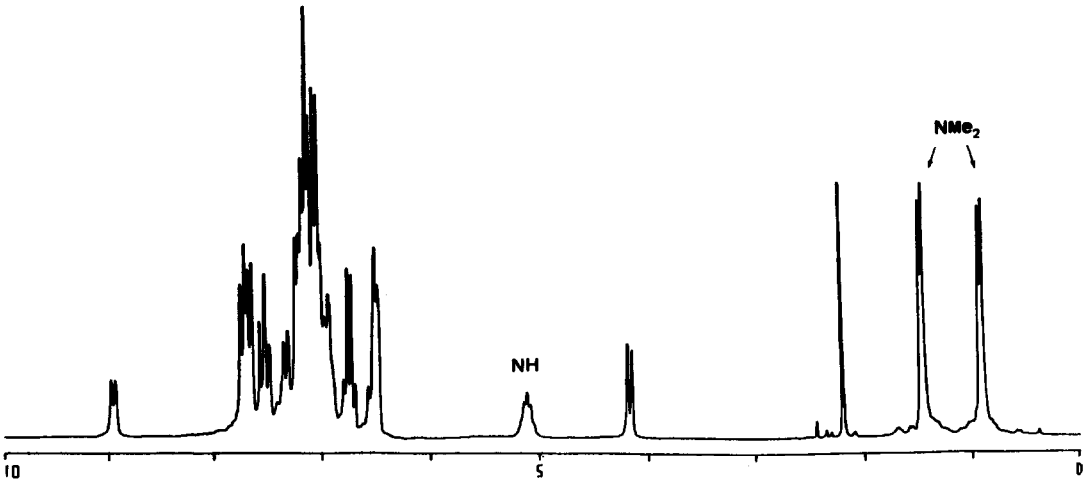

Fig. 2. ^{1}H NMR spectrum (300 MHz, C_6D_6) of $Mo_2(OAr\text{-}2Ph)_6(HNMe_2)_2$ (**2**).

These arise due to the fact that this geometry does not allow strong metal–metal bonding to occur between these particular d^3-metal centres. Hence, low-lying paramagnetic states are available for thermal population, causing temperature dependent, contact-shifted ^{1}H NMR spectra.[19] In order to conclusively characterize the coordination environment in **2**, a single crystal X-ray diffraction analysis was undertaken. An ORTEP representation of the molecular structure of **2** is given in Fig. 3. It can be seen that the structure of **2** consists of two four-coordinate, approximately square-planar molybdenum atoms bound together by an unbridged metal–metal bond. The Mo—Mo distance of 2.247(1) Å compares very favourably with distances typically associated with $\sigma^2\pi^4$ triple bonds between

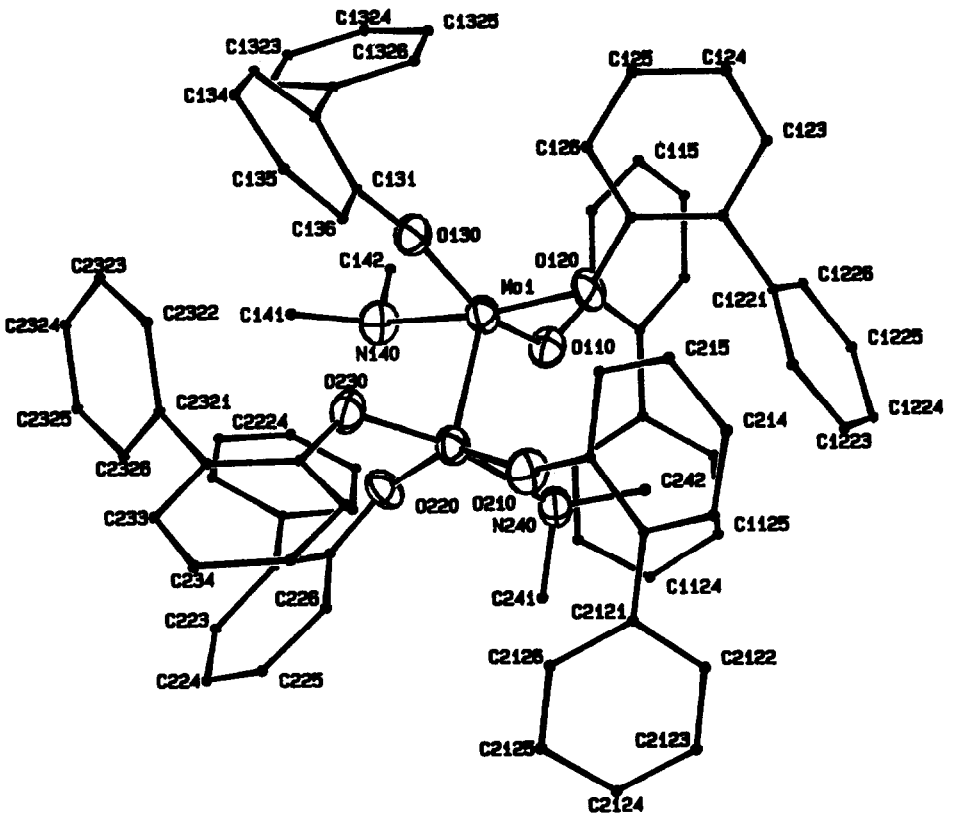

Fig. 3. ORTEP view of $Mo_2(OAr\text{-}2Ph)_6(HNMe_2)_2$ (**2**).

molybdenum atoms.[17,18] The arrangement of the donor atoms about the central dimetal core is of some interest. Newman projections down the metal–metal bond of a generalized 1,2-$Mo_2O_6N_2$ core show that there are two staggered and three eclipsed possible ideal conformations. Previous studies on base adducts of dimolybdenum and ditungsten hexa-alkoxides have shown that the arrangement of the donor atoms is not very regular.[18] However, nearly all of the compounds can be grouped into two classes, those with N—Mo—Mo—N torsion angles of 45–60°, and those with angles of 110–130°. These correspond most closely to the two staggered rotamers. However, in one previous case, that of $W_2(OPr^i_6)(HNMe_2)_2$, a torsion angle of 95° was observed with a structure approaching that of an eclipsed conformer.[18c] It can be seen (Fig. 4) that the solid-state structure of **2** also more closely approximates to an eclipsed geometry, although the N—Mo—Mo—N torsion angle of 97.6(3)° shows a definite distortion towards a staggered structure. The ^1H NMR spectrum of **2** at ambient temperatures clearly shows the presence of two, diastereotopic methyl groups for the $HNMe_2$ ligands. We can hence conclude that dissociation of these ligands is not rapid, and furthermore that rotation about the Mo≡Mo triple bond is not facile on the NMR time scale.[20]

Another interesting structural feature of compound **2** concerns the bonding and orientations of the 2-phenylphenoxide ligands. As a general rule the alkoxide ligands in $M_2(OR)_6L_2$ type compounds can be separated into two types, the four *cis* to the neutral donor atom and the two that are located *trans* in this group. Typically the oxygen atom *trans* to the nitrogen donor has a slightly shorter bond distance, typically of the order of 0.1 Å, than the distances to the two mutually *trans* alkoxide oxygen atoms.[18] This particular manifestation of the *trans* influence appears to be completely lacking in compound **2**. Instead, two of the aryloxide ligands *cis* to the amine ligand, O(130) and O(210), have much shorter contacts with the molybdenum atom than the other aryloxide oxygen atoms (Table 2). Furthermore, these aryloxide ligands contain very large Mo—O—Ar angles of 158.2(6) and 167.9(7)°; 30–40° wider than found for the other groups. These two parameters, shorter Mo—O distance and larger M—O—Ar angles, imply the presence of more oxygen-*p* to metal-*d* π-bonding taking place from these two aryloxide ligands compared to their longer bound counterparts. However, we believe that the ability of these aryloxide ligands to π-donate to the metal is controlled not so much by the position of the oxygen atom in the coordination sphere, but by the packing of their substituent aryl groups. It can be seen from Fig. 3 that the stronger bound aryloxide ligands differ from the other 2-phenylphenoxide groups in that they are oriented so that their phenyl substituents are pointing away from, or *distal* to, the metal–metal bond. The other ligands adopt the exact opposite orientation with their phenyl substituents pointed towards, or *proximal* to, the metal–metal bond. The consequence of the resulting steric crowding over the dimetal centre is that the *proximal* aryloxide ligands have to bend back at their oxygen atom linkage in order to relieve steric

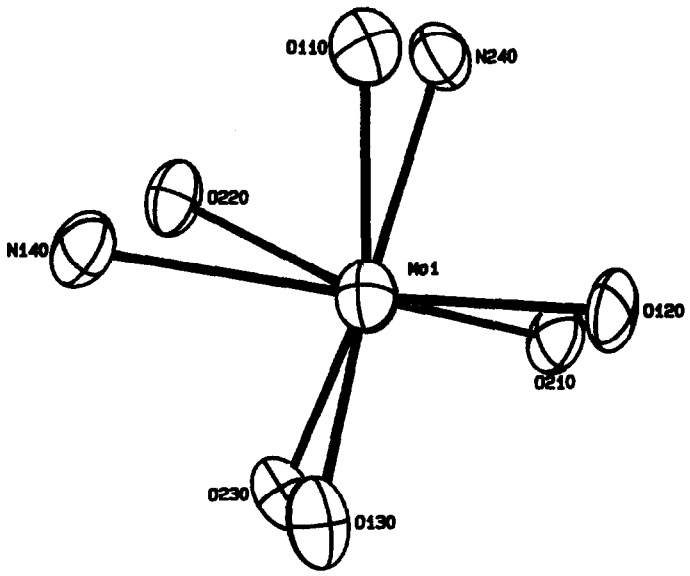

Fig. 4. ORTEP view of the central core of $Mo_2(OAr\text{-}2Ph)_6(HNMe_2)_2$ (**2**), looking down the metal–metal axis.

Table 2. Selected bond distances (Å) and angles (°) for $Mo_2(OC_6H_4\text{-}2Ph)_6(HNMe_2)_2$ (2)

Mo(1)—Mo(2)	2.247(1)		
Mo(1)—O(110)	1.979(6)	Mo(2)—O(210)	1.900(4)
Mo(1)—O(120)	1.961(7)	Mo(2)—O(220)	1.997(7)
Mo(1)—O(130)	1.886(5)	Mo(2)—O(220)	1.970(6)
Mo(1)—N(140)	2.281(9)	Mo(2)—N(240)	2.265(6)
Mo(1)—Mo(2)—O(210)	109.2(2)	Mo(2)—Mo(1)—O(110)	100.2(2)
Mo(1)—Mo(2)—O(220)	100.2(2)	Mo(2)—Mo(1)—O(120)	99.1(2)
Mo(1)—Mo(2)—O(230)	96.7(2)	Mo(2)—Mo(1)—O(130)	106.4(2)
Mo(1)—Mo(2)—N(240)	93.2(2)	Mo(2)—Mo(1)—N(140)	92.8(2)
Mo(1)—O(110)—C(111)	125.3(5)	Mo(2)—O(210)—C(211)	158.2(6)
Mo(1)—O(120)—C(121)	136.1(6)	Mo(2)—O(220)—C(221)	123.3(6)
Mo(1)—O(130)—C(131)	167.9(7)	Mo(2)—O(230)—C(231)	128.4(5)

pressure. However, for the distal aryloxide, the lack of any steric crowding in the position *trans* to the metal–metal bond means that the ligand is free to adopt a more linear Mo—O—Ar angle, thus allowing more π-donation to the metal centre to take place. The other aryloxides which are held by steric constraints to Mo—O—Ar angles of 120–135°, cannot be as effective at π-donation even when they are located *trans* to a weakly bound amine ligand.

A further consequence of the packing of the 2-phenylphenoxide ligands about the dimetal centre is the presence of restricted rotation about the Mo≡Mo triple bond.[20] Furthermore, the ^1H NMR spectrum of **2** (Fig. 2) shows non-equivalent aryloxide ligation, consistent with restricted rotation about the Mo—O—Ar bonds. Unequivalent assignment of the two, well separated aryloxide doublets at δ +9 and +4 ppm is not easy. However, we believe they arise from the two-position hydrogens of two of the non-equivalent aryloxide ligands. The dramatic chemical shift separation between these signals can be ascribed to the strong diamagnetic anisotropy associated with the $\sigma^2\pi^4$ triple bond in **2**.[17] It can be seen (Fig. 3) that the aryloxide ligands bound through O(130) and O(210) are oriented so that the hydrogen atoms in the two-position of the phenoxy ring lie above the metal–metal bond. This should have the effect of deshielding these protons. Hence the doublet at δ 9.0 ppm can tentatively be assigned as being due to these hydrogen atoms. The doublet at δ 4.1 ppm presumably arises from the hydrogen atoms in the two-position of two of the other aryloxide ligands. Both of the other types of aryloxide groups are oriented so that this particular proton is brought into a position distal to the Mo≡Mo bond. Hence, shielding of these protons should occur. However, it is impossible on the basis of the existing data to accurately assign this resonance.

EXPERIMENTAL

All operations were carried out under a dry N_2 atmosphere or *in vacuo*, either in a Vacuum Atmospheres Dri-Lab or by Standard Schlenk techniques. Hydrocarbon solvents were dried by distillation from sodium benzophenone. $Mo_2(NMe_2)_6$[13] and $Mo(NMe_2)_4$[12] were obtained by previously reported procedures. ^1H and ^{13}C NMR spectra were recorded on Varian Associates XL-200 and Varian Associates Gemini 200 spectrometers, and were referenced to Me_4Si using proton impurities of commercial benzene-d_6 or toluene-d_8 as internal standards. Microanalytical data were obtained from the Purdue Microanalytical Laboratory.

$Mo(OAr\text{-}2Ph)_4(NHMe_2)_2$ (1)

To a solution of $Mo(NMe_2)_4$ (0.20 g, 0.74 mmol) in benzene (15 cm^3), was added HOAr-2Ph (0.506 g, 2.98 mmol). The solution was stirred at room temperature for 12 h. Concentration of the benzene solution followed by addition of hexane, produced well-formed red crystals of the product. Yield: 0.37 g (58%). Found: C, 72.7; H, 5.9; N, 3.5. Calc. for $MoC_{52}H_{50}N_2O_4$: C, 72.4; H, 5.8; N, 3.2%. IR (Nujol mull): $\tilde{\nu}$(N—H) = 3233 cm^{-1}.

$Mo_2(OAr\text{-}2Ph)_6(HNMe_2)_2$ (2)

To a solution of $Mo_2(NMe_2)_6$ (1.0 g, 2.2 mmol) in toluene (20 cm^3), was added HOAr-2Ph (2.28 g, 13.4 mmol). An immediate colour change from yellow to red was noted. After being stirred for 3 h, the solvent was removed *in vacuo* and the crude product was recrystallized from toluene by addition of hexane. Yield: 70%. Found: C, 70.6; H, 5.3; N, 2.3. Calc. for $Mo_2O_6N_2C_{76}H_{68}$: C, 70.4; H, 5.3;

N, 2.2%. ^{1}H NMR (C_6D_6, 30°C) δ 9.2 (d), 1.47 (d, HN*Me*$_2$); 5.12 (m, *H*NMe$_2$) 4.18 (d), 8.95 (d, 6.48–7.75 aryl H's).

CRYSTALLOGRAPHIC STUDIES

Selected crystal data and data collection parameters are collected together in Table 3.

A suitable crystal for each of the two compounds was mounted in a glass capillary in a random orientation. Cell constants and an orientation matrix for data collection were obtained from least-squares refinement using the scattering angle of 25 reflections in the range $14.6 < \theta < 20.2°$ for **1** and $14.8 < \theta < 18.9°$ for **2**, as measured by the computer controlled diagonal slit method of centring. Systematic absences and subsequent least-squares refinement indicated the space group $P\bar{1}$ for **1** and $P2_1/c$ for **2**. The data were collected at room temperature in both cases using the ω–θ scan technique. The scan rate varied from 2 to 20° min^{-1} in ω, and data were collected to a maximum 2θ of 45°. Moving crystal, moving counter background counts were made by scanning an additional 25% above and below the scan width. The counter aperture was adjusted as a function of θ. For intense reflections, an attenuator (factor 12.9) was automatically inserted in front of the detector. As a check on crystal and electronic stability, three standard reflections were remeasured every 5000 s of beam time. No decay in standards was observed

Table 3. Crystal data and data collection parameters

	(1)	(2)
Formula	$MoO_4N_2C_{52}H_{50}$	$Mo_2O_6N_2C_{83}H_{70}$
Formula weight	862.93	1383.37
Space group	$P\bar{1}$ (No. 2)	$P2_1/c$ (No. 14)
a (Å)	9.617(6)	22.890(2)
b (Å)	10.199(1)	13.854(3)
c (Å)	12.315(7)	24.337(2)
α (°)	107.04(2)	—
β (°)	106.29(5)	113.969(8)
γ (°)	95.46(2)	—
V (Å^3)	1087(2)	1087(2)
Z	1	4
d_{calc} (g cm^{-3})	1.317	1.303
Crystal dimensions (mm)	0.35 × 0.26 × 0.14	0.56 × 0.35 × 0.31
Temperature (°C)	21	19
Radiation (wavelength)	Mo-K_α (0.70930 Å)	Mo-K_α (0.70930 Å)
Monochromater	Graphite	Graphite
Linear absorption coefficient (cm^{-1})	3.38	3.98
Absorption correction applied	Empirical[a]	None
Transmission factors: min, max	0.50, 1.00	—
Diffractometer	Enraf–Nonius CAD4	Enraf–Nonius CAD4
Scan method	ω–2θ	θ–2θ
h, k, l limits	−10 to 9 −10 to 10 0 to 13	−24 to 22 0 to 24 0 to 26
2θ range (°)	4.00–45.00	4.00–45.00
Scan width (°)	0.90 + 0.35 tan (θ)	0.95 + 0.35 tan (θ)
Take-off angle (°)	1.90	1.90
Programs used	Enraf–Nonius SDP	Enraf–Nonius SDP
F_{000}	450.0	2856.0
p-Factor used in weighting	0.040	0.040
Data collected	2814	9590
Unique data	2814	9590
Data with $I > 3.0\sigma(I)$	2207	4963
Number of variables	268	803
Largest shift/ESD in final cycle	0.00	0.21
R	0.047	0.062
R_w	0.053	0.071
Goodness-of-fit	1.237	1.637

[a] N. Walker and D. Stuart, *Acta Cryst.* 1983, **A39**, 158.

for **1**, while for **2**, a decay correction was applied (overall decay of 12%).

The structures were solved using the Patterson heavy-atom method to reveal the position of molybdenum atoms. The remaining heavy atoms were located in succeeding difference Fourier syntheses. Hydrogen atoms were located and added to the structures, but their positions were not refined. All calculations including the full-matrix least-squares refinement were performed using Enraf–Nonius SDP on a VAX computer.

Acknowledgements—We thank the National Science Foundation (Grant CHE-8612063) for support of the research. NSF support for the Crystallographic Unit at Purdue (Grant CHE-8615556) is also gratefully acknowledged.

Supplementary material—Atomic coordinates have been deposited with the Director, Cambridge Crystallographic Data Centre.

REFERENCES

1. (a) M. H. Chisholm, *Angew. Chem.* 1986, **98**, 21; (b) M. H. Chisholm, *Polyhedron* 1986, **5**, 25; (c) M. H. Chisholm, *J. Sol. State Chem.* 1985, **57**, 120.
2. The chemistry of sterically demanding alkoxides has simultaneously been developed, see T. V. Lubben and P. T. Wolczanski, *J. Am. Chem. Soc.* 1987, **109**, 424 and refs therein.
3. B. D. Murray, H. Hope and P. P. Power, *J. Am. Chem. Soc.* 1985, **107**, 169 and refs therein.
4. (a) D. R. Neithamer, L. Parkanyi, J. F. Mitchell and P. T. Wolczanski, *J. Am. Chem. Soc.* 1988, **110**, 4421; (b) R. E. Lapointe, P. T. Wolczanski and J. F. Mitchell, *J. Am. Chem. Soc.* 1986, **108**, 6832.
5. (a) P. B. Hitchcock, M. F. Lappert and A. Singh, *J. Chem. Soc., Chem. Commun.* 1983, 1499; (b) A. W. Duff, R. A. Kamarudin, M. F. Lappert and J. R. Norton, *J. Chem. Soc., Dalton Trans.* 1986, 489 and refs therein.
6. (a) L. R. Chamberlain, L. D. Durfee, P. E. Fanwick, L. Kobriger, S. L. Latesky, A. K. McMullen, I. P. Rothwell, K. Folting, J. C. Huffman, W. E. Streib and R. Wang, *J. Am. Chem. Soc.* 1987, **109**, 390; (b) L. R. Chamberlain, I. P. Rothwell, K. Folting and J. C. Huffman, *J. Chem. Soc., Dalton Trans.* 1987, 155; (c) L. R. Chamberlain and I. P. Rothwell, *J. Chem. Soc., Dalton Trans.* 1987, 163; (d) S. L. Latesky, A. K. McMullen, I. P. Rothwell and J. C. Huffman, *Organometallics* 1986, **4**, 902; (e) L. R. Chamberlain, I. P. Rothwell and J. C. Huffman, *Inorg. Chem.* 1984, **23**, 2575.
7. (a) C. J. Schaverien, J. C. Dewan and R. R. Schrock, *J. Am. Chem. Soc.* 1986, **108**, 2771; (b) I. A. Latham, L. R. Sita and R. R. Schrock, *Organometallics* 1986, **5**, 1508; (c) K. C. Wallace, J. C. Dewan and R. R. Schrock, *Organometallics* 1986, **5**, 2161; (d) M. R. Churchill, J. W. Ziller, J. H. Freudenberger and R. R. Schrock, *Organometallics* 1984, **3**, 1554.
8. (a) A. E. Ogilvy, P. E. Fanwick and I. P. Rothwell, *Organometalics* 1987, **6**, 72; (b) T. W. Coffindaffer, W. M. Westler and I. P. Rothwell, *Inorg. Chem.* 1985, **24**, 4565; (c) R. W. Chesnut, L. D. Durfee, I. P. Rothwell and J. C. Huffman, *Polyhedron* 1987, **6**.
9. (a) J. L. Kerschner, P. E. Fanwick and I. P. Rothwell, *J. Am. Chem. Soc.* 1987, **109**, 5840; (b) J. L. Kerschner, P. E. Fanwick and I. P. Rothwell, *J. Am. Chem. Soc.* 1988, **110**.
10. B. D. Steffey, R. W. Chesnut, P. S. Pelechia, P. E. Fanwick and I. P. Rothwell, *J. Am. Chem. Soc.*, in press.
11. J. L. Kerschner, J. S. Yu, P. E. Fanwick and I. P. Rothwell, *Organometallics*, in press.
12. D. C. Bradley and M. H. Chisholm, *J. Chem. Soc. A* 1971, 1511.
13. M. H. Chisholm, F. A. Cotton, B. A. Frenz, W. W. Reichert, L. W. Shire and B. R. Stultz, *J. Am. Chem. Soc.* 1976, **98**, 4469.
14. (a) M. H. Chisholm, W. W. Reichert and P. Thornton, *J. Am. Chem. Soc.* 1978, **100**, 2744; (b) Addition of 2,6-dialkylphenols to both $Mo(NMe_2)_4$ and $MoH_4(PMe_2Ph)_4$ has been shown to yield simple substitution products, see S. M. Beshouri, T. W. Coffindaffer, S. Pirzad and I. P. Rothwell, *Inorg. Chim. Acta* 1985, **103**, 111.
15. M. H. Chisholm and I. P. Rothwell, *Comprehensive Coordination Chemistry* (Edited by G. Wilkinson), Vol. 2, Chap. 13.4. Pergamon Press, Oxford (1987).
16. (a) I. P. Rothwell, *Acc. Chem. Res.* 1988, **21**, 153; (b) T. W. Coffindaffer, I. P. Rothwell and J. C. Huffman, *Inorg. Chem.* 1983, **22**, 2906.
17. F. A. Cotton and R. A. Walton, *Multiple Bonds Between Metal Atoms*. John Wiley, New York (1982).
18. (a) M. Akiyama, M. H. Chisholm, F. A. Cotton, M. W. Extine, D. A. Haitko, D. Little and P. E. Fanwick, *Inorg. Chem.* 1979, **18**, 2266; (b) M. H. Chisholm, F. A. Cotton, M. W. Extine and W. W. Reichert, *J. Am. Chem. Soc.* 1978, **100**, 153; (c) J. Leonelli, PhD thesis, Indiana University (1982).
19. T. W. Coffindaffer, G. Niccolai, D. Powell, I. P. Rothwell and J. C. Huffman, *J. Am. Chem. Soc.* 1985, **107**, 3572.
20. M. H. Chisholm, J. C. Huffman and I. P. Rothwell, *Organometallics* 1982, **1**, 251.

Polyhedron Vol. 8, No. 15, pp. 1979–1981, 1989
Printed in Great Britain

0277–5387/89 $3.00+.00
© 1989 Maxwell Pergamon Macmillan plc

BRIDGING AMIDO COMPLEXES FROM REACTIONS IN LIQUID AMMONIA. X-RAY CRYSTAL STRUCTURE OF $[Pt(PMe_2Ph)_2(\mu\text{-}NH_2)_2Pt(PMe_2Ph)_2](BF_4)_2$

CAROLINE A. O'MAHONEY, IVAN P. PARKIN, DAVID J. WILLIAMS and J. DEREK WOOLLINS*

Department of Chemistry, Imperial College of Science, Technology and Medicine, South Kensington, London SW7 2AY, U.K.

(*Received* 24 *February* 1989; *accepted* 15 *March* 1989)

Abstract—Treatment of HBF_4 and a slight excess of sodium in liquid ammonia with $PtCl_2(PR_3)_2$ produces $[M(PR_3)_2(\mu\text{-}NH_2)_2M(PR_3)_2](BF_4)_2$ (**2**) (M = Pt, $PR_3 = PMe_3$, PMe_2Ph, $PMePh_2$, PEt_3, $1/2Ph_2PCH_2CH_2PPh_2$; M = Pd, $PR_3 = 1/2Ph_2PCH_2CH_2PPh_2$) in >80% isolated yield. The products were characterized by ^{31}P and ^1H NMR, IR and microanalysis, and in the case of $PR_3 = PMe_2Ph$ (**2a**), by X-ray crystallography. In **2a**, the cation contains a butterfly Pt_2N_2 ring with a dihedral angle of 32°.

We are involved in the study of the reactivity of sulphur–nitrogen compounds with transition metal centres in liquid ammonia.[1,2] For example, addition of $SOCl_2$ to liquid ammonia, followed by *cis*-$PtCl_2(PR_3)_2$ (**1**), gives *cis*-$Pt(NSO)_2(PR_3)_2$.[3] During the course of the reaction between a NH_3(liq) solution of $[S_3N_2NH_2]BF_4$ and **1**, we obtained the title complex **2** containing μ-NH_2 bridges. However, further investigations led us to the conclusion that this was a product of the reaction of **1** with NH_3(liq). Here, we report on the preparation and characterization of **2**.

EXPERIMENTAL

All solvents were dried prior to use and reactions were performed under an inert atmosphere (N_2, Ar). The bis-phosphineplatinum (palladium) dichlorides were made as previously described.[4] Ammonia (BOC) and $HBF_4 \cdot 2Et_2O$ (Aldrich) were used as supplied. Sodium (BDH) was washed free of oil with hexane prior to use. ^{31}P-{^1H} and ^1H NMR spectra were obtained using a JEOL FX90Q spectrometer operating at 36.21 and 89.55 MHz and are referred to external 85% H_3PO_4 and internal TMS, respectively. IR spectra were recorded as pressed KBr discs using a Perkin–Elmer 1720X instrument. Elemental analysis were performed by the microanalytical service at Imperial College.

Preparation of $[M(PR_3)_2(\mu\text{-}NH_2)_2M(PR_3)_2](BF_4)_2$ (M = Pt, $PR_3 = PMe_3$, PMe_2Ph, $PMePh_2$, PEt_3, $1/2Ph_2PCH_2CH_2PPh_2$; M = Pd, $PR_3 = 1/2Ph_2PCH_2CH_2PPh_2$)

In a typical reaction, $HBF_4 \cdot 2Et_2O$ (0.11 mmol) was added cautiously, dropwise to NH_3 (liq) (5 cm^3) at −78°C, followed by sodium (0.13 mmol) to generate a dark blue solution. $MCl_2(PR_3)_2$ (0.08 mmol) was added and the resultant brown–blue suspension was stirred for 0.5 h at −78°C. The ammonia was then allowed to evaporate slowly under nitrogen as the reaction warmed to room temperature, leaving a white solid. Extraction with CH_2Cl_2 (5 cm^3) and removal of solvent *in vacuo* gave $[M(PR_3)_2(\mu\text{-}NH_2)_2M(PR_3)_2](BF_4)_2$ (0.03 mmol, *ca* 80%). Crystals suitable for X-ray analysis were grown by hexane diffusion into a CH_2Cl_2 solution of **3**. ^{31}P NMR, NH IR vibrational frequencies, microanalyses and yields are given in Table 1.

Crystal data

$C_{52}H_{56}B_2F_8N_2P_4Pt_2$, $M = 1396.7$, monoclinic, $a = 23.084(5)$, $b = 15.420(3)$, $c = 15.466(4)$ Å, $\beta = 106.54(2)°$, $U = 5277$ Å^3, space group $C2/c$,

* Author to whom correspondence should be addressed.

Table 1. Spectroscopic and microanalytical data for the new compounds. Calculated values are in parentheses, for **2a** and **2d** the theoretical values include a $CHCl_3$ and CH_2Cl_2 of crystallization, respectively

Phosphine	δ	J	ν(NH)		C	H	N	Yield (%)
(2a) PMe_3	−13.9	2685	3342	3287	14.7 (14.7)	3.9 (3.9)	2.5 (2.7)	54
(2b) PMe_2Ph	−17.1	2981	3368	3287	34.0 (33.5)	4.2 (4.2)	2.4 (2.3)	75
(2c) $PMePh_2$	−5.6	3053	3358	3263	41.6 (41.4)	3.7 (3.7)	1.8 (1.8)	80
(2d) PEt_3	3.3	2934	3346	3284	24.7 (25.2)	5.4 (5.4)	2.5 (2.4)	68
(2e) dppe	38.4	3044	3357	3265	45.3 (44.9)	3.5 (3.7)	1.6 (2.0)	65
(2f) Pd dppe	64.4	—	3373	3297				

$Z = 4$ (the molecule is disposed about a two-fold axis), $D_c = 1.76$ g cm^{-3}. μ(Cu-K_α) = 116 cm^{-1}, $\lambda = 1.54178$ Å, $F(000) = 2719$.

Data collection and processing

Nicolet $R3m$ diffractometer, ω-scan method, ($2\theta \leqslant 116°$), graphite monochromated Cu-K_α radiation; 3555 independent measured reflections, 3359 observed [$|F_o| > 3\sigma(|F_o|)$], corrected for Lorentz and polarization factors; empirical absorption correction (ellipsoidal) based on 360 azimuthal measurements. Maximum and minimum transmission factors 0.128 and 0.041 respectively.

Structure analysis and refinement

The structure was solved by the heavy atom method and all the non-hydrogen atoms refined anisotropically. The hydrogen atoms were idealized (C—H = 0.96 Å), assigned isotropic thermal parameters $U(H) = 1.2U$ eq(C) and allowed to ride on their parent carbons. The methyl groups were refined as rigid bodies. One of the BF_4^- groups is disorded about a two-fold axis and was refined in two orientations. Refinement was by block-cascade full-matrix least-squares to $R = 0.031$ ($R = \Sigma[|F_o| - |F_c|]/\Sigma(|F_o|)$, $R_w = 0.033$ ($w^{-1} = \sigma^2(F) + 0.00028F^2$). The maximum and minimum residual electron densities in the final ΔF map were 1.53 and −0.56 e Å^{-3}, respectively. The mean and maximum shifts/error in the final refinement cycle were 0.003 and 0.011, respectively.* Computations were carried out on an Eclipse S140 computer using the SHELXTL program system.[5]

RESULTS AND DISCUSSION

There have been surprisingly few reports of binuclear amido-bridged platinum complexes.[6–8] It was claimed in 1967[6] that reaction of *cis*-$PtCl_2(PPh_3)_2$ with hydrazine gives crystals which are a mixture of $[(Ph_3P)_2Pt(NNH)_2Pt(PPh_3)_2]^{2+}$ and $[(Ph_3P)_2Pt(NH_2)_2Pt(PPh_3)_2]^{2+}$ (from X-ray studies), but no ^{31}P NMR data was given. More recently,[7] a neutral NH_2-bridged species, [(Ph_2MeP)(Ph_2PO)Pt(NH_2)$_2$Pt(P(O)Ph_2)(PMePh_2)] (**3**), was obtained from the reaction between $PtCl_2$(dppm) (dppm = $Ph_2PCH_2PPh_2$), NaOH and liquid ammonia. Finally,[8] $[(Ph_3P)MePt(NH_2)_2PtMe(PPh_3)]^{2+}$ (**4**) was obtained by deprotonation of *trans*-$[PtMe(NH_3)(PPh_3)_2]^+$. After observing the formation of **2** from reactions in liquid ammonia containing $[S_3N_2NH_2]BF_4$, we investigated whether the sulphur–nitrogen molecule was the source of the NH_2 bridges or was simply affecting the pH of the solution. Thus, if HBF_4 is added to liquid ammonia and then titrated with sodium until there is a slight excess of sodium (as evinced by a pale blue colouration), addition of **1** results in formation of **2** in high yield. The reaction can be represented by eq. (1) (note that only a slight excess of sodium is required). Attempts to prepare **2** by direct reaction of $NaBF_4$ in liquid ammonia were unsuccessful, suggesting that the pH of the solution is very important:

$$2cis\text{-}PtCl_2(PR_3)_2 + NaNH_2(\text{trace}) + 2NaBF_4 \xrightarrow{NH_3(liq)} [(R_3P)_2Pt(NH_2)_2Pt(PR_3)_2](BF_4)_2, \quad (1)$$

Compounds **2** have been characterized spectro-

* Final atomic positional and thermal parameters, bond lengths and angles and F_o/F_c values have been deposited as supplementary material with the Editor, from whom copies are available on request. Atomic coordinates have also been submitted to the Cambridge Crystallographic Data Centre.

Table 2. Selected bond lengths and angles in **2a**

Pt—P(1)	2.246(1)	Pt—P(2)	2.254(2)
Pt—N(1)	2.091(5)	Pt—N(1′)	2.081(4)
Pt—Pt′	3.134		
P(1)—Pt—P(2)	98.3(1)	P(1)—Pt—N(1)	93.1(1)
P(2)—Pt—N(1)	167.0(1)	P(1)—Pt—N(1′)	169.9(1)
P(2)—Pt—N(1′)	91.7(1)	N(1)—Pt—N(1′)	77.2(2)

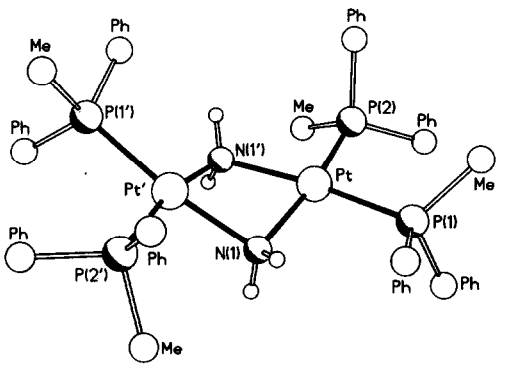

Fig. 1. The X-ray structure of the core of the cation in **2a** showing the atom numbering. Phenyl rings and BF_4^- anions are omitted for clarity.

scopically (Table 1) and in the case of PR_3 = $PMePh_2$ (**2b**) by X-ray crystallography. The ^{31}P NMR spectra are as expected with $^1J\{^{31}P-^{195}Pt\}$ couplings which are appropriate for platinum(II) compounds. In the IR spectra, each compound exhibits two ν(NH) vibrations. The unambiguous location (from a ΔF map) of the protons on the bridging nitrogen atoms in the crystal structure of **2a** (Table 2, Fig. 1) confirms the cation to be a *bis*-amido-bridged species. The molecule has crystallographic C_2 symmetry with the geometry about each platinum being distorted square planar; the P(1)—Pt—P(2) plane is rotated by *ca* 7° relative to that of the N(1)—Pt—N(1′) plane. The Pt—N distance in **2a** is slightly reduced compared to those in the neutral analogues, **3** and **4**, whilst the Pt—Pt′ separation (3.134(1) Å in **2**) is significantly longer (3.087(1) and 3.106(1) Å for **3** and **4**, respectively). The N—Pt—N′ angle (77.2(2)°) does not differ significantly from those previously reported. As in both **3** and **4**, the Pt_2N_2 ring in **2a** is also folded, although in this instance by significantly less (32° in **2** vs *ca* 45° in **3** and **4**). There are no hydrogen bonding interactions between the amido groups and the BF_4^- counterions.

Acknowledgement—We are grateful to Johnson Matthey plc for loans of precious metals.

REFERENCES

1. P. S. Belton, I. P. Parkin, D. J. Williams and J. D. Woollins, *J. Chem. Soc., Chem. Commun.* 1988, 1479.
2. C. A. O'Mahoney, I. P. Parkin, D. J. Williams and J. D. Woollins, *J. Chem. Soc., Dalton Trans.*, accepted for publication.
3. P. F. Kelly, I. P. Parkin and J. D. Woollins, *Phosphurus and Sulphur*, in press.
4. R. Jones, P. F. Kelly, D. J. Williams and J. D. Woollins, *J. Chem. Soc., Dalton Trans.* 1988, 1569.
5. G. M. Sheldrick, *SHELXTL, An Integrated System for Solving, Refining and Displaying Crystal Structures from Diffraction Data.* University of Göttingen, Göttingen, FRG (1978). Revision 5.1 (1985).
6. G. C. Dobinson, R. Mason and G. B. Robertson, *J. Chem. Soc., Chem. Commun.* 1967, 741.
7. N. W. Alcock, P. Bergamini, T. J. Kemp and P. G. Pringle, *J. Chem. Soc., Chem. Commun.* 1987, 235.
8. S. Park, D. M. Roundhill and A. L. Rheingold, *Inorg. Chem.* 1987, **26**, 3974.

Polyhedron Vol. 8, No. 15, pp. 1983–1987, 1989
Printed in Great Britain

0277–5387/89 $3.00+.00
© 1989 Maxwell Pergamon Macmillan plc

ORGANOLANTHANIDES—XIV.* PREPARATION AND STRUCTURE OF BIS(η^5-CYCLOPENTADIENYL)BIS(TRIPHENYLPHOSPHINE OXIDE)YTTERBIUM(II)—THE FIRST X-RAY CRYSTAL STRUCTURE OF A PHOSPHINE OXIDE–ORGANOLANTHANIDE(II) COMPLEX

G. B. DEACON,† B. M. GATEHOUSE and P. A. WHITE

Chemistry Department, Monash University, Clayton, Victoria 3168, Australia

(*Received* 17 *January* 1989; *accepted* 16 *March* 1989)

Abstract—Reaction of $Cp_2Yb(DME)$ (Cp = cyclopentadienyl; DME = 1,2-dimethoxyethane) with triphenylphosphine oxide yields $Cp_2Yb(OPPh_3)_2$. The X-ray crystal structure shows eight-coordinate ytterbium with a pseudo-tetrahedral arrangement of two oxygen donor atoms and the centroids of two eclipsed η^5-cyclopentadienyl rings. Surprisingly short Yb—O distances (2.30(2); 2.33(2) Å) and the absence of major inter-ligand contacts indicate an uncrowded arrangement.

Triphenylphosphine oxide complexes of the oxophilic lanthanide(III) ions are well-known,[2] and phosphine oxides have been used in solvent extraction of lanthanides.[3] Thus, it is surprising that few triphenylphosphine oxide (or other phosphine oxide) complexes of organolanthanides have been prepared.[4–8] The sole crystal structures are those of *cis*- and *trans*-$[(C_5Me_5)_2Sm^{III}OPPh_3]_2(\mu\text{-}OCH{=}CHO)$ (**I** and **II**), where the presence of the phosphine oxide results from attempts to crystallize the novel product(s) of the redox reaction between bis(η^5-pentamethylcyclopentadienyl)samarium(II) and carbon monoxide.[6] There are only two known organolanthanide(II) complexes with triphenylphosphine oxide, viz. $(C_5Me_5)_2M(THF)(OPPh_3)$ (M = Sm[7] or Yb;[8] THF = tetrahydrofuran), and these have been characterized spectroscopically. We now report the preparation and crystal structure of $Cp_2Yb(OPPh_3)_2$ (Cp = cyclopentadienyl). The sole previous X-ray structure of an *un*substituted cyclopentadienyllanthanide(II) complex is that of $Cp_2Yb(DME)$ (DME = 1,2-dimethoxyethane), in which the sites of the cyclopentadienyl ligands are disordered.[9] Organolanthanide(II) X-ray structures are dominated by those of bis(η^5-pentamethylcyclopentadienyl)- derivatives,[5] probably owing to their ease of crystallization.

RESULTS AND DISCUSSION

Preparation and spectroscopic data

Reaction of bis(η^5-cyclopentadienyl)(1,2-dimethoxyethane)ytterbium(II) with triphenylphosphine oxide (mole ratio, 1:2) in DME, gave a black precipitate of bis(η^5-cyclopentadienyl)bis(triphenylphosphine oxide)ytterbium(II) in good yield:

$$Cp_2Yb(DME) + 2Ph_3PO \longrightarrow Cp_2Yb(OPPh_3)_2\downarrow + DME. \quad (1)$$

Although oxidation of $Cp_2Yb(DME)$ by trimethylamine oxide giving $(Cp_2Yb)_2O$ has been observed,[10] a similar reaction was not expected with triphenylphosphine oxide, since $(C_5Me_5)_2Sm(THF)(OPPh_3)$ has been prepared[7] and $(C_5Me_5)_2Sm$ is a much more powerful reductant[5,11] than Cp_2Yb.[12] However, an attempt to prepare an analogous triphenylarsine oxide complex resulted in oxidation presumably in accordance with reaction (2):

$$2CpYb(DME) + Ph_3AsO \longrightarrow Ph_3As + (Cp_2Yb)_2O + 2DME. \quad (2)$$

* For Part XIII, see ref. 1.

† Author to whom correspondence should be addressed.

Table 1. IR absorption frequencies and assignments for $Cp_2Yb(OPPh_3)_2$

Frequency (cm^{-1})	Assignment[a]
1570w	*l*, ν(CC) (a_1), Ph
1435s	*n*, ν(CC) (b_2), Ph
1195s	ν(P=O)
1175s	ν(P=O)
1125s	*q*, X-sensitive (a_1), Ph
1070w	*d*, β(CH), (b_2), Ph
1010m	β(CH) Cp
745(sh), 740s	γ(CH) Cp+*f*, γ(CH) (b_1), Ph
725s	*r*, X-sensitive (a_1)
695s	*v*, ϕ(CC) (b_1)

[a] Based on those for coordinated triphenylphosphine oxide[13] (terminology is that of Whiffen[14]) and η^5-cyclopentadienyl ligands.[15]

^{1}H NMR and mass spectra confirmed the presence of both ligands in $Cp_2Yb(OPPh_3)_2$. The IR spectrum (Table 1) was of considerable interest, showing two ν(P=O) frequencies. One corresponds to that (1193 cm^{-1})[13] of free triphenylphosphine oxide, whilst the other is lowered from the free ligand value, as expected[16] on coordination. This suggests either that solid $Cp_2Yb(OPPh_3)_2$ contains seven-coordinate $Cp_2Yb(OPPh_3)$ and a molecule of uncoordinated triphenylphosphine oxide,* or the two ν(P=O) bands are the antisymmetric and symmetric stretching modes of an eight-coordinate complex with only a small average shift (8 cm^{-1}) from the free ligand value. A crystal structure was needed to resolve the structural alternatives.

The black crystals dissolve in THF to give a purple–brown solution with the visible maximum shifted only 9 nm from that of Cp_2Yb in THF.[18] This result and the insolubility of the complex in DME suggest that dissolution in THF involves at least partial dissociation of triphenylphosphine oxide:

$$Cp_2Yb(OPPh_3)_2 + THF \rightleftharpoons Cp_2Yb(THF)(OPPh_3) + Ph_3PO.$$

X-ray crystal structure

Single crystals of $Cp_2Yb(OPPh_3)_2$ were obtained on partial evaporation of a solution in THF. The crystal structure (Fig. 1) is the first of an organolanthanide(II)–phosphine oxide complex or any Ph_3PO–lanthanide(II) ion complex. It shows eight-coordinate ytterbium with a distorted pseudo-tetrahedral arrangement of two oxygen donor atoms and the centroids (CT) of two eclipsed cyclopentadienyl rings. Selected bond lengths and angles are given with Fig. 1. All O—Yb—CT angles are near 109°, but CT(1)—Yb—CT(2) and O(1)—Yb—O(2) are markedly larger and smaller than tetrahedral, respectively, as is observed in $Cp'_2M(THF)_2$ ($Cp' = Me_3SiC_5H_4$, M = Yb; $Cp' = C_5Me_5$, M = Sm).[5] However, O—M—O and CT—M—CT angles of the present complex are larger and smaller, respectively, than those[5] of $Cp'_2M(THF)_2$, owing to greater steric repulsion between the substituted cyclopentadienyl groups.

The presence of η^5-cyclopentadienyl groups in $Cp_2Yb(OPPh_3)_2$ is indicated by the small variation in Yb—C bond lengths. Greater bond length differences are observed for the η^5-bonded $Cp'_2M(THF)_2$ complexes[5] and $Cp_2Yb(DME)$.[9] Further support for η^5-bonding is provided by the 90° Yb—CT—C angles. Predominantly ionic cyclopentadienyl–metal bonding is indicated[9,19] by the value (1.62 Å) for the effective ionic cyclopentadienyl radius[19] (the average Yb—C distance minus the ionic radius of eight-coordinate Yb^{2+} (1.14 Å)[20]). The Yb—O distances (Fig. 1) are markedly shorter (by 0.16 $Å_{av}$) than those of $Cp_2Yb(DME)$,[9] the only other crystallographically-determined structure of a Cp_2Yb complex. In **I** and **II** (see Introduction), the Sm^{III}—$OPPh_3$ distances are *ca* 0.08 Å shorter than average Sm^{III}—O(THF) bond lengths.[6] The distance (*d*), obtained by subtraction of the appropriate lanthanide ionic radii[20] from lanthanide–oxygen bond distances, also illustrates the shortness of the Yb—O bonds. For most Ph_3PO—M^{3+} (M = lanthanide) complexes[2] and the organometallics **I** and **II**,[6] $d = 1.29 \pm 0.03$ Å (cf. 1.34 ± 0.06 Å for most organolanthanide(II or III) complexes with ethers[9]). Exceptions are two highly hindered tris(bis(trimethylsilyl)amido)lanthanum (III) complexes,[21] for which $d = 1.50$ and 1.52 Å, and the uncrowded $Ce(NO_3)_4(OPPh_3)_2$,[22] for which $d = 1.15$ Å. Values for $Cp_2Yb(OPPh_3)_2$ (1.19, 1.16 Å) approach the last, indicating a relatively uncrowded structure and/or some covalency in the Yb—O bonds.

The sum of the solid cone angle factors (Σc.a.f.) for $Cp_2Yb(OPPh_3)_2$ (0.61), calculated from the X-ray structure parameters using the first-order cone angle model,[23] is within the stable region (0.57–0.77) for organolanthanide(II) complexes.[24] Although significant second-order repulsion[23] involving Ph_3PO molecules may be expected, the

* See, e.g. $LiI(OPPh_3)_5$ which contains $[Li(OPPh_3)_4]^+$ and a molecule of uncoordinated Ph_3PO.[17]

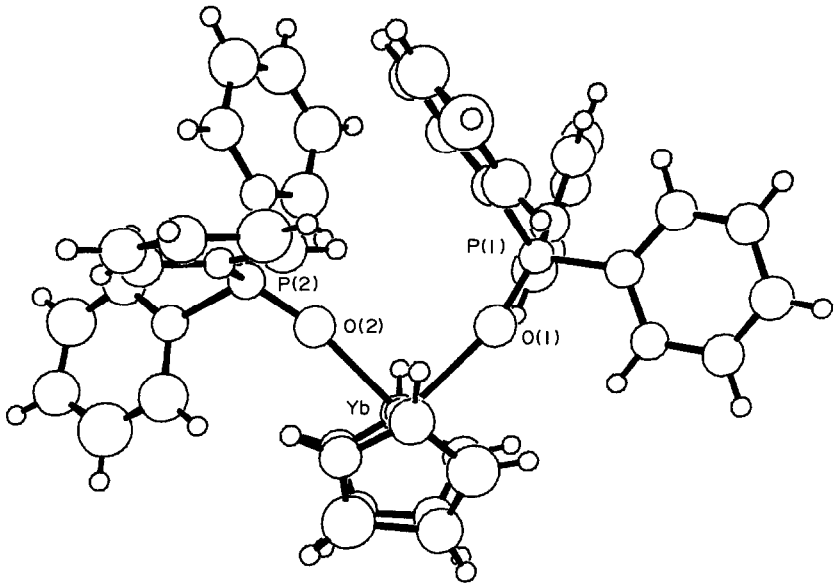

Fig. 1. Crystal structure of $Cp_2Yb(OPPh_3)_2$. Selected bond lengths (Å) and angles (°):

Yb—O(1)	2.30(2)	Yb—C	2.72(2)–2.79(3)
Yb—O(2)	2.33(2)	$(Yb—C)_{av}$	2.76(2)
Yb—CT(1)	2.48(3)	P—O(1)	1.47(2)
Yb—CT(2)	2.49(3)	P—O(2)	1.48(2)

O(1)—Yb—O(2)	90.4(6)	CT(2)—Yb—O(2)	108.9(8)
CT(1)—Yb—CT(2)	128.3(10)	P(1)—O(1)—Yb	163.9(11)
CT(1)—Yb—O(1)	108.0(7)	P(2)—O(2)—Yb	165.9(10)
CT(1)—Yb—O(2)	105.9(7)	$(Yb—CT—C)_{av}$	90.0(12)
CT(2)—Yb—O(1)	108.7(8)		

location is well displaced from the metal ion and the donor atom owing to the spear-like nature of the ligand. There are no significant inter-ligand contacts (cf. $La(N(SiMe_3)_2)_3(OPPh_3)$[21]), and the phenyl rings are well separated from the cyclopentadienyl groups (Fig. 1). Since Σc.a.f. for $Cp_2Yb(OPPh_3)_2$ is at the low end of the stable range, second-order effects are not expected to lead to overcrowding. A meaningful value for the second-order cone angle factor cannot be calculated owing to the substantial variation in O—Yb—*o*-H angles (23–61°).

Despite the short Yb—O bonds, the P—O distances (Fig. 1) are close to the free ligand value (1.46(1) Å)[25] and correlate with the very small shift of ν(P=O) from that of free Ph_3PO. This contrasts with $Ce(NO_3)_4(OPPh_3)_2$,[22] for which the short Ce—O distances are (more expectedly) associated with a large shift in ν(P=O) and larger P—O distances (1.531(8), 1.526(8) Å). In fact, the present P—O distances are shorter than those of all crystallographically characterized Ph_3PO–lanthanide complexes.[2,6] Although many of the differences are within experimental error, the overall trend is clear. Metal–O—P angles in triphenylphosphine oxide complexes are generally near 150°,[26] which is midway between the value (120°) for full covalent bonding and that (180°) for electrostatic bonding and minimum steric repulsion.[26] In lanthanide–$OPPh_3$ complexes, larger angles are usually observed[2] and approach linear in the highly hindered $La(N(SiMe_3)_2)_3(OPPh_3)$.[21] The values for $Cp_2Yb(OPPh_3)_2$ (Fig. 1) are relatively small for lanthanide complexes, and contrast with the larger values[22] for $Ce(NO_3)_4(OPPh_3)_2$ [169.2(5), 173.2(4)°].

EXPERIMENTAL

General

Syntheses were carried out in greaseless Schlenk apparatus under purified (BASF R3/11 oxygen-removal catalyst and molecular sieves) nitrogen. Solids were handled under purified nitrogen or argon in a recirculating atmosphere drybox

(Vacuum Atmospheres HE43-2 Drilab or Miller-Howe 100). Details of solvent purification, handling procedures and spectroscopic methods have been given in previous papers.[18,27-29] The IR spectrum (Table 1) was recorded on a mull of the compound in dry degassed Nujol. For mass spectrometry, the complex was briefly exposed to the atmosphere (with resulting decomposition), before insertion into the spectrometer. For ^{1}H NMR spectroscopy, perdeuterotetrahydrofuran was degassed and distilled from sodium–benzophenone. It contained an aromatic impurity, probably benzene from decomposition of Ph_2CO, hence meaningful integration could not be obtained. Chemical shifts are in ppm downfield from internal TMS.

When $Cp_2Yb(OPPh_3)_2$ was analysed for ytterbium by the reported method (H_2SO_4/HNO_3 digestion, followed by titration with disodium dihydrogen ethylenediaminetetraacetate),[27-29] a satisfactory titrimetric end point could not be obtained. Accordingly, accurately weighed samples (*ca* 0.2 g) were dissolved in pure THF (5 cm^3) and were decomposed with dilute sulphuric acid (2 M, 5 cm^3). The solution was extracted with dichloromethane and the organic layer separated and washed with water. The aqueous layer and washings were heated under a stream of nitrogen. Aliquots of this solution were than buffered to pH 4.5 with hexamethylenetetraamine, and titrated by the standard methods.[27-29] The method was validated by analysis of $Cp_2Yb(DME)$.

Reagents

Triphenylphosphine oxide (K&K) was sublimed under vacuum to decompose any hydrate[26] present, and triphenylarsine oxide (from a modification of the reported preparation[30]) was dehydrated by azeotropic distillation. Both compounds were shown to be anhydrous by IR spectroscopy. $Cp_2Yb(DME)$ was obtained by the reported method.[18]

Preparation of bis(η^5-cyclopentadienyl)bis(triphenylphosphine oxide)ytterbium(II)

Bis(η^5-cyclopentadienyl)(1,2-dimethoxyethane) ytterbium(II) (0.15 g, 0.38 mmol) and triphenylphosphine oxide (0.22 g, 0.79 mmol) reacted immediately on addition of 1,2-dimethoxyethane (5 cm^3) to give a black, highly air- and water-sensitive crystalline precipitate of the title complex, which was filtered off and washed with the solvent (yield, 0.20 g, 61%) (Found: Yb, 20.7. $C_{46}H_{40}O_2P_2Yb$ requires: Yb, 20.1%). ^{1}H NMR: 5.60, s, Cp; 7.4–7.7, m, Ph. Mass spectrum: *m/z* 277 [100%, $C_{18}H_{14}OP^+$], 201 [19, Ph_2PO^+], 185 [10, Ph_2P^+], 183 [15, $C_{12}H_8P^+$], 152 [10, $C_{12}H_8^+$], 77 [24, Ph^+], 66 [12, $C_5H_6^+$], 51 [16, $C_4H_3^+$]. UV–vis–near-IR(300–1100 nm): $\lambda_{max}(\varepsilon)$ 382(sh), 516(130)nm. The filtrate from the synthesis was virtually colourless, suggesting near quantitative precipitation. A similar preparation in THF (25 cm^3) yielded a purple solution, which, on partial evaporation of the solvent, gave black crystals of the title complex (yield, 24%) (Found: Yb, 20.7%), with spectroscopic properties identical with those of the product from the first preparation.

Reaction between $Cp_2Yb(DME)$ *and triphenylarsine oxide*

Dissolution of triphenylarsine oxide (0.82 g, 2.5 mmol) and $Cp_2Yb(DME)$ (0.50 g, 1.3 mmol) in THF (20 cm^3) gave an immediate yellow solution, followed (after *ca* 1 min) by formation of a white precipitate, which redissolved on further stirring. After 12 h, the solution had turned brown, and the vis–near-IR spectrum: λ_{max} 870, 916, 925, 950, 986, 1021, 1032 nm, was indicative[31] of ytterbium(III).

X-ray crystallography

Crystals of $Cp_2Yb(OPPh_3)_2$ were grown by slow distillation of solvent from a solution in THF in a sealed double Schlenk tube, and were stored under dry, degassed Nujol. Selected crystals were mounted under purified argon in 0.8 mm Lindemann capillaries and held in place by high vacuum grease. Crystal data $YbC_{46}H_{40}O_2P_2$: monoclinic, space group $P2_1/c$, $a = 10.925(8)$, $b = 21.942(12)$, $c = 16.839(10)$ Å, $\beta = 99.83(15)°$, $V = 3977.32$ Å^3, $Z = 4$, D_m (air-sensitive material, density not measured), D_c 1.44 g cm^{-3}; Mo-K_α radiation (0.7107 Å), $\mu = 24.8$ cm^{-1}; Philips PW 1100 diffractometer, graphite monochromator, ω–2θ scans at a scan speed of 0.25° s^{-1} (the relatively high speed was used due to a high decomposition rate of several crystals in the X-ray beam) with $6 \leqslant 2\theta \leqslant 40°$ and scan width $(1.20+0.2\tan\theta)°$ at 22°C. 3698 unique reflections, 1656 observed [$F_o \geqslant 6\sigma(F_o)$], absorption correction based on indexed crystal faces (min-max transmission = 0.478/0.673). Solution by Patterson method and subsequent difference Fourier techniques, refinement by full-matrix least-squares methods. Hydrogen atoms inserted in geometrically calculated positions and refinement of position and thermal parameters (anisotropic for ytterbium, phosphorus and oxygen and a single isotropic parameter for hydrogen atoms) resulted in $R = 0.057$,

and $R_w = 0.051$. All calculations were carried out with SHELX76.[32] Atomic scattering factors for neutral atoms[33] were corrected for anomalous dispersion. Full details of the crystal structure results are available on request from the Editor. Atomic coordinates have also been deposited at the Cambridge Crystallographic Data Centre.

Acknowledgement—We are grateful to the Australian Research Council for support.

REFERENCES

1. G. B. Deacon and D. L. Wilkinson, *Inorg. Chim. Acta* 1988, **142**, 329.
2. F. A. Hart, Scandium, yttrium and the lanthanides, Chap. 39 in *Comprehensive Coordination Chemistry* (Edited by G. Wilkinson, R. D. Gillard and J. A. McCleverty), Vol. 3. Pergamon Press, Oxford (1987).
3. *Gmelin Handbook of Inorganic Chemistry*; System No. 39, Part D6, pp. 121–123. Springer, Berlin (1983).
4. H. Schumann and W. Genthe, Organometallic compounds of the rare earths, Chap. 53 in *Handbook of the Physics and Chemistry of Rare Earths* (Edited by K. A. Gschneidner and L. Eyring), Vol. 7. Elsevier, Amsterdam (1984).
5. W. J. Evans, *Polyhedron* 1987, **6**, 803.
6. W. J. Evans, J. W. Grate and R. J. Doedens, *J. Am. Chem. Soc.* 1985, **107**, 1671.
7. W. J. Evans, J. W. Grate, I. Bloom, W. E. Hunter and J. L. Atwood, *J. Am. Chem. Soc.* 1985, **107**, 405.
8. T. D. Tilley, PhD thesis. University of California, Berkeley (1982).
9. G. B. Deacon, P. I. MacKinnon, T. W. Hambley and J. C. Taylor, *J. Organomet. Chem.* 1983, **259**, 91.
10. D. L. Wilkinson, PhD thesis. Monash (1987); G. B. Deacon and D. L. Wilkinson, unpublished results.
11. P. L. Watson, unpublished results in footnote 5 of R. G. Finke, S. R. Keenan, D. A. Schiraldi and P. L. Watson, *Organometallics* 1986, **5**, 598.
12. A. M. Bond, G. B. Deacon and R. H. Newnham, *Organometallics* 1986, **5**, 2312.
13. G. B. Deacon and J. H. S. Green, *Spectrochim. Acta* 1968, **24A**, 845.
14. D. H. Whiffen, *J. Chem. Soc.* 1956, 1350.
15. R. T. Bailey and A. H. Curran, *J. Mol. Struct.* 1970, **6**, 391.
16. F. A. Cotton, R. D. Barnes and E. Bannister, *J. Chem. Soc.* 1960, 2199.
17. A. R. Hands and A. J. H. Mercer, *J. Chem. Soc. A* 1968, 449.
18. G. B. Deacon, A. J. Koplick and T. D. Tuong, *Aust. J. Chem.* 1984, **37**, 517.
19. K. N. Raymond and C. W. Eigenbrot Jr, *Accts Chem. Res.* 1980, **13**, 276.
20. R. D. Shannon, *Acta Cryst.* 1976, **A32**, 751.
21. D. C. Bradley, J. S. Ghotra, F. A. Hart, M. B. Hursthouse and P. R. Raithby, *J. Chem. Soc., Dalton Trans.* 1977, 1166.
22. M-UL-Haque, C. N. Caughlan, F. A. Hart and R. VanNice, *Inorg. Chem.* 1971, **10**, 115.
23. R. D. Fischer and Li Xing-Fu, *J. Less Common Metals* 1985, **112**, 303.
24. P. I. MacKinnon, PhD thesis. Monash (1985).
25. G. Bandoli, G. Bortolozzo, D. A. Clemente, U. Croatto and C. Panattoni, *J. Chem. Soc. A* 1970, 2778.
26. P. L. Goggin, Sulfoxides, amides, amine oxides and related ligands, Section 15.8 in *Comprehensive Coordination Chemistry* (Edited by G. Wilkinson, R. D. Gillard and J. A. McCleverty), Vol. 2. Pergamon Press, Oxford (1987).
27. G. B. Deacon, C. M. Forsyth, R. H. Newnham and T. D. Tuong, *Aust. J. Chem.* 1987, **40**, 895.
28. G. B. Deacon, W. D. Raverty and D. G. Vince, *J. Organomet. Chem.* 1977, **135**, 103.
29. G. B. Deacon, A. J. Koplick, W. D. Raverty and D. G. Vince, *J. Organomet. Chem.* 1979, **182**, 121.
30. R. L. Shriner and C. N. Wolf, *Org. Synth.* 1963, **4**, 911.
31. F. Calderazzo, R. Pappalardo and S. Losi, *J. Inorg. Nucl. Chem.* 1966, **28**, 987.
32. G. M. Sheldrick, SHELX76, Program for Crystal Structure Determination. University of Cambridge, U.K. (1976).
33. *International Tables for X-ray Crystallography*, Vol. IV. Kynoch Press, Birmingham (Present distributor, D. Reidel, Dordrecht) (1974).

Polyhedron Vol. 8, No. 15, pp. 1989–1993, 1989
Printed in Great Britain

0277–5387/89 $3.00+.00
© 1989 Maxwell Pergamon Macmillan plc

CRYSTAL AND MOLECULAR STRUCTURE OF A FIVE-COORDINATE PALLADIUM(II) COMPLEX CONTAINING THE BIDENTATE AZAHETEROCYCLIC LIGAND: TRIS(DIMETHYLPHENYLPHOSPHINE)-2,9-DIMETHYL-1,10-PHENANTHROLINE PALLADIUM(II) TETRAFLUOROBORATE

TOORU SAKAI*

Faculty of Science, Kobe University, Kobe 657, Japan

and

ZENEI TAIRA

Department of Pharmaceutical Science, Tokushima Bunri University, Tokushima 770, Japan

and

SHINSAKU YAMAZAKI

Chemistry Laboratory, Gakuen College Kochi, Kochi, 780, Japan

and

TOMOHARU AMA

Faculty of Science, Kochi University, Kochi, 780, Japan

(*Received* 3 *November* 1988; *accepted* 16 *March* 1989)

Abstract—The determination of the crystal and the molecular structure of a five-coordinate palladium(II) complex and its ^1H and ^{31}P NMR studies are described. The crystals of $[Pd(PMe_2Ph)_3(2,9\text{-}Me_2\text{-phen})][BF_4]_2$ ($C_{38}H_{45}N_2P_3PdB_2F_8$) are monoclinic, space group $P2_1/n$, with $Z = 4$ and unit cell dimensions: $a = 23.346(6)$, $b = 13.429(2)$, $c = 12.929(2)$ Å, $\beta = 91.96(2)°$. The structure was determined by a heavy-atom method from diffractometer data and refined to an R value of 0.048 for 4601 unique observed reflections. Three phosphorus atoms from the three dimethylphenylphosphines, and a nitrogen atom from the 2,9-dimethyl-1,10-phenanthroline (2,9-Me_2-phen), form an approximately square-planar configuration about the palladium atom; Pd—P(1) 2.283(1), Pd—P(2) 2.395(2), Pd—P(3) 2.407(2) and Pd—N(1) 2.164(5) Å. The remaining nitrogen atom is at the apex of a distorted square pyramid, Pd—N(10) 2.588(5) Å. The ^1H NMR spectrum shows fluxional motion which averages the two halves of the 2,9-Me_2-phen.

We have previously described five-coordinate palladium(II) and platinum(II) complexes containing azaheterocyclic ligands[1–3] which are undergoing coordination site exchange of their two nitrogen atoms. From variable temperature ^1H NMR of $[ML(2,9\text{-}R_2\text{-}4,7\text{-}R'_2\text{-phen})_2][X]_n$ (M = Pt, L = PPh_3, R = R′ = H, X = BF_4^-, $n = 2$; M = Pd, L = PPh_3, R = H, R′ = Me or Ph, X = BF_4^-, $n = 2$; M = Pd, L = Cl, R = Me, R′ = H, X = PF_6^-, $n = 1$), the averaging process of the two halves of aza-

* Author to whom correspondence should be addressed.

heterocyclic ligands has best been explained by two synchronous rearrangement systems: one, the twist motion from a trigonal bipyramid to a tetragonal pyramid, and the other, the concurrent oscillation.[3] The crystal structure of $[PdCl(PPh_3)_2(phen)][BF_4]$[2] is a distorted square pyramid with elongation of the apical bond length Pd—N(10) 2.68 Å (2.09 Å for Pd—N(1) at the basal plane). Such elongation of the apical M—L bond length is relatively common in a square-pyramidal structure.[5-8] In the analogous platinum(II) complexes, $[PtCl(PEt_3)_2(phen)]^+$ (two phosphines are mutually *cis* at the basal plane)[6] and $[Pt(CN)(phen)_2]^+$,[4] the corresponding apical bond lengths are 2.84 (2.14) and 2.76 Å (2.05 Å), respectively. Their fluxional behaviour in solution, however, does not seem to proceed via dissociation of the azaheterocyclic ligand, since the observance of ^{195}Pt satellites in the ^1H and ^{13}C NMR spectra shows no such indication. Therefore, the apical bond length M—L, crystallographically determined in the five-coordinate complex, does not seem to be a main factor in determining its fluxional motion. However, the solution structure of $[PdCl(PPh_3)_2(phen)]^+$ is close to a square-planar conformation with an unusual unidentate phen ligand. Fluxional motion of $[PdL_1L_2L_3(2,9\text{-}R_2\text{-}phen)][BF_4]_n$ (L_1 = Cl, $L_2 = L_3 = PPh_3$, R = Me or H, $n = 1$; L_1 = Cl, L_2 or $L_3 = PPh_3$, or $P(OMe)_3$, $n = 1$; L_1 = Cl, $L_2 = L_3 = P(OMe)_3$, $n = 1$; $L_1 = L_2 = L_3 = PMe_2Ph$, R = H or Me, $n = 2$) is thus still ambiguous as to whether it corresponds to an oscillation (intramolecular) or to a dissociation process taking place via an intermolecular pathway.

This paper deals with the crystal structure of $[Pd(PMe_2Ph)_3(2,9\text{-}Me_2\text{-}phen)][BF_4]_2$ in comparison with the solution structure by ^{31}P and ^1H NMR.

EXPERIMENTAL

Yellow crystals of $[Pd(PMe_2Ph)_3(2,9\text{-}Me_2\text{-}phen)][BF_4]_2$ were grown from an acetone–ethanol mixed solution under isothermal vaporization. A crystal of approximate dimensions $0.10 \times 0.13 \times 0.20$ mm was used during the measurements, made using Mo-K_α radiation with a graphite crystal monochromator, on a Rigaku AFC-5 four circle diffractometer ($\lambda = 0.71069$ Å).

Crystal data: $M_r = 453.61$, monoclinic, $a = 23.346(6)$, $b = 13.429(2)$, $c = 12.929(2)$ Å, $\beta = 91.96(2)°$, $U = 4051.3(16)$ Å^3, space group $P2_1/n$, $Z = 4$, $D_x = 1.40$ g cm^{-3}, $F(000) = 1840$, μ(Mo-K_α) = 6.060 cm^{-1}. The cell parameters were refined by least-squares methods on the basis of 25 2θ values with $33 < 2\theta < 38°$. The space group was determined from the systematic absences of reflections ($0k0$; k odd, $h0l$; $h+l$ odd). The intensity data were measured using the ω–2θ scan technique, with a scan speed of 2° s^{-1}. The intensity of the incident beam was monitored throughout the data correction by measuring three reference reflections, and these showed no significant change in intensities ($0.98 < F_o < 1.04$). 7643 reflections were measured ($0 \leqslant h \leqslant 27$, $0 \leqslant k \leqslant 15$, $-15 \leqslant l \leqslant 15$), among those, 1224 were zero intensities, and 1818 were weak [$|F_o| \leqslant 3\sigma(|F_o|)$] and were classified as unobserved. 4601 non-zero unique reflections were corrected for Lorentz and polarization effects, but not for absorption. The position of the palladium atom was obtained from a Patterson synthesis. All other atoms were located by Fourier difference syntheses. The structure was refined by full-matrix least-squares methods with anisotropic thermal parameters for non-hydrogen atoms and isotropic for hydrogen atoms. The R values for the final refinement were $R = 0.048$ and $R_w = 0.051$. The function minimized was $\Sigma\omega||F_o|-|F_c||^2$, with $\omega = 1/[\sigma^2(F_o)]$. Goodness-of-fit, S, was 2.58. The maximum shift over error ratio Δ/σ in the last cycle was less than 0.3 for non-hydrogen atoms and 0.9 for hydrogen atoms. The maximum and minimum heights in a final difference Fourier map were ± 0.2 eÅ^{-3}. A FACOM-M782 computer at the Data Processing Center, Kyoto University, and the UNICSII computation programs system[9] were used for all calculations in the data reduction and the structure analysis. The atom scattering factors were taken from the *International Tables for X-ray Crystallography*.[10]*

RESULTS AND DISCUSSION

Crystal structure of $[Pd(PMe_2Ph)_3(2,9\text{-}Me_2\text{-}phen)][BF_4]_2$

The bond lengths and bond angles are given in Table 1 and the least-squares planes around the palladium atom are given in Table 2. A perspective view of the complex cation with the numbering scheme is given in Fig. 1, whilst the palladium atom and the coordinate atoms are given in Fig. 2.[11]

The crystal structure of $[Pd(PMe_2Ph)_3(2,9\text{-}Me_2\text{-}phen)][BF_4]_2$ consists of separate $[Pd(PMe_2Ph)_3(2,9\text{-}Me_2\text{-}phen)]^{2+}$ cations and two crystallographically independent $[BF_4]^-$ anions. In the co-

*Tables of atomic coordinates, displacement factor coefficients, full lists of bond lengths and angles and F_o/F_c values have been deposited as Supplementary Material with the Editor, from whom copies are available on request. Atomic coordinates have also been deposited with the Cambridge Crystallographic Data Centre.

Table 1. Intramolecular bond distances (Å) and bond angles (°) (ESDs are in parentheses and are in the units of the least significant digit)

(a) Bond distances (Å)			
Pd—P(1)	2.283(1)	Pd—N(1)	2.164(5)
Pd—P(2)	2.395(2)	Pd—N(10)	2.588(5)
Pd—P(3)	2.407(2)		
Pd···C(15)	3.845(7)	Pd···C(16)	3.145(7)
(b) Bond angles (°)			
P(1)—Pd—P(2)	95.0(1)	P(2)—Pd—N(1)	87.7(1)
P(1)—Pd—P(3)	92.1(1)	P(2)—Pd—N(10)	85.3(1)
P(1)—Pd—N(1)	164.5(1)	P(3)—Pd—N(1)	85.6(1)
P(1)—Pd—N(10)	123.5(1)	P(3)—Pd—N(10)	90.3(1)
P(2)—Pd—P(3)	172.9(1)	N(1)—Pd—N(10)	71.9(1)
Pd—N(1)—C(12)	120.1(4)	C(4)—C(13)—C(12)	119.2(6)
N(1)—Pd···C(15)	110.0(2)	N(1)—Pd···C(16)	50.6(2)

ordination sphere around the palladium atom, the interatomic distances of the two nitrogen atoms in 2,9-Me_2-phen from the palladium atom are unequal (Pd—N(1), 2.164(5) and Pd—N(10), 2.588(5) Å). This is not uncommon in square-pyramidal structures studied so far in palladium(II) and platinum(II) complexes. One nitrogen atom with a longer distance [N(10)] is at the apex of a distorted square-pyramidal structure (Fig. 2), in which three phosphorus atoms of $(PMe_2Ph)_3$ occupy three corners of the square basal plane, while the N(1) atom occupies the remaining corner. The angle N(1)—Pd—N(10) is 71.90°. This angle is larger than 68.2° in $[PtCl(PEt_3)_2(phen)]^+$,[6] 70.2° in $[PdCl(PPh_3)_2(phen)]^+$[2] and 69.7° in $[Pt(CN)(phen)_2]^+$.[4]

Table 2. Least-squares planes and deviations (Å) of individual atoms

Basal plane of tetragonal pyramid

$$0.28688X+0.94693Y+0.14498Z = 3.81896$$

P(1)	0.0017(56)	N(1)	0.0101(52)
P(2)	0.0112(60)	Pd*	0.0022(56)
P(3)	−0.0170(67)	N(10)*	−1.4116(62)

Basal plane of trigonal bipyramid

$$0.82481X-0.37552Y+0.42270Z = 1.09412$$

P(1)	0.0097(9)	Pd	−0.0211(2)
N(1)	0.0090(31)	P(2)*	−2.4052(10)
N(10)	0.0024(30)	P(3)*	2.3800(9)

The equations of the planes are in the form $AX+BY+CZ = D$, where $X = ax+cz\cos\beta$, $Y = by$ and $Z = cz\sin\beta$ are coordinates in orthogonal angstrom space. Asterisks indicate the atoms not included in the calculation of the planes. ESDs in parentheses are in the units of the least significant digit.

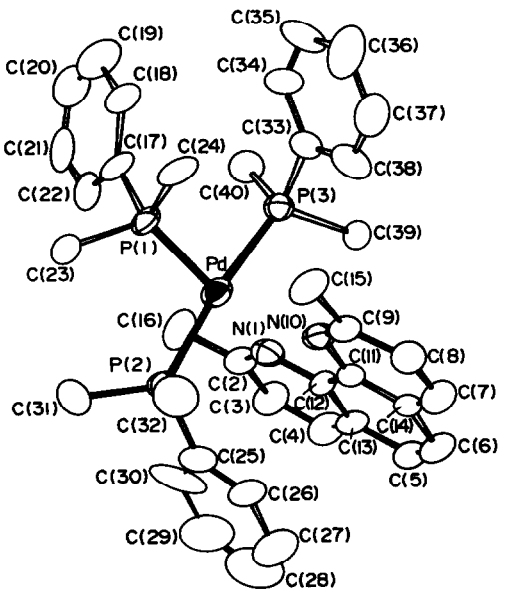

Fig. 1. A perspective view of the complex cation $[Pd(PMe_2Ph)_3(2,9\text{-}Me_2\text{-}phen)]^{2+}$ and the numbering schemes.

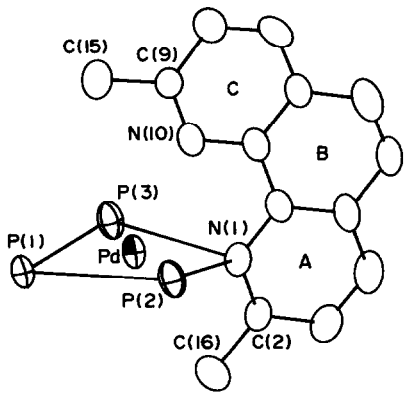

Fig. 2. The palladium atom and the coordinate atoms.

The Pd—N(1) bond length of 2.164(5) Å in $[Pd(PMe_2Ph)_3(2,9\text{-}Me_2\text{-}phen)]^{2+}$ [N(1) is *trans* to P(1)] is slightly longer than the bond length of 2.094(5) Å found in $[PdCl(PPh_3)_2(phen)]^+$ [N(1) is *trans* to Cl]. This may be explained by the larger *trans* influence of phosphorus than chlorine. In fact, this observation in $[Pd(PMe_2Ph)_3(2,9\text{-}Me_2\text{-}phen)]^{2+}$ is comparable with the Pt—N(1) bond length of 2.137(19) Å found in $[PtCl(PEt_3)_2(phen)]^+$ [N(1) is *trans* to P], which is larger than 2.053(5) Å found in $[Pt(CN)(phen)_2]$ [N(1) is *trans* to N(3)]. The Pd—P bond lengths in $[Pd(PMe_2Ph)_3(2,9\text{-}Me_2\text{-}phen)]^{2+}$ are 2.395(2) and 2.407(2) Å for Pd—P(2) and Pd—P(3), respectively, and 2.283(1) Å for Pd—P(1). The P(1), P(2), P(3) and N(1) atoms deviated markedly from the plane (Table 2). The N(1) atom occupies a position slightly displaced from the tetragonal plane in the opposite direction to the N(10) atom. The bond angles around the palladium atom, with the four atoms in the basal plane, deviate a few degrees from 90° (Table 1). The P(2) and P(3) atoms are displaced towards the N(1) atom and away from the P(1) atom. This distortion is due to ligand–ligand repulsion and is in fact in the opposite direction to that found in $[PdCl(PPh_3)_2(phen)]^+$, in which the size of the Cl atom (*trans* to N) is very small in comparison with that of the (PMe_2Ph) group.

The distance, 2.81(2) Å, of the non-bonding N(1)···N(10) is slightly longer than those observed in the bidentate phenanthrolines[12] (2.63–2.73 Å), in the phenanthroline crystal (2.724 Å)[13] and in the free phenanthroline in $[Cu\{SC(NH_2)_2\}(phen)]I(phen)$ (2.767 Å).[14] The least-squares mean plane calculated for the three rings of the phen group shows that the maximum deviation of the atoms from the mean plane is 0.046(7) Å at C(15). This least-squares mean plane contains the Pd and P(1) atoms. The deviation of the Pd and P(1) atoms, though not included in the calculation of the plane, are 0.0271(3) and 0.0950(13) Å, respectively. The structure is so distorted from an ideal square pyramid that it approaches a trigonal bipyramidal structure, which resembles $[PdCl(PPh_3)_2(phen)]^+$. The dihedral angles between three phenyl rings *A*, *B* and *C* (Fig. 2) are 0.69(15), 1.80(16) and 1.68(4)° for *A* and *B*, *A* and *C*, and *B* and *C*, respectively. For the methyl C(15), which is near the apex of the pyramid, the distance between the Pd atom and the C(15) atom is 3.845(7) Å and the angle N(1)—Pd—C(15) is 110.0(2)°. For the other methyl C(16) which is attached to atom C(2) and is at the reverse side of the apex with respect to the basal plane, the distance between the Pd and C(16) atoms is 3.145(7) Å and the angle N(1)—Pd—C(16) is 50.6(2)°. Frenz and Ibers[12] have shown for a series of phen complexes, that an increase of the N—M—N bond angle is correlated with a decrease of the N—M bond distance. This propensity is also observed in the corresponding bond angle and bond length between $[Pd(PMe_2Ph)_3(2,9\text{-}Me_2\text{-}phen)]^{2+}$ and $[PdCl(PPh_3)_2(phen)]^+$. Although the $[PdCl_2(PMe_2Ph)_3]$ molecule possesses pseudo-symmetry of roughly a mirror plane, $[Pd(PMe_2Ph)_3(2,9\text{-}Me_2\text{-}phen)]^{2+}$ has no symmetry element. The reason for this difference may be that 2,9-Me_2-phen has a larger rigid skeleton than the two chlorine atoms.

The two BF_4 anion groups occupy the cavities surrounded by the cation groups. The thermal factors of the component atoms are large. The shortest distance between a palladium atom and a fluorine atom among the BF_4 groups is 4.617(8) Å in Pd···F(23).

The solution structure by ^1H *and* ^{31}P *NMR*[1]

In the solid state, the 2,9-Me_2-phen molecule of the complex has no symmetry element. ^1H NMR exhibits, however, an equivalency of the two nitrogen atoms. This ^1H NMR spectrum corresponds either to fluxional motion or to symmetrical environments around the two halves of the azaheterocyclic ligand. The conductivity data show that the complex has a tight ion-pair and the anion does not interact with palladium(II).[1] As the crystal structures show, the elongation of the apical M—N distance in $[Pd(PMe_2Ph)_3(2,9\text{-}Me_2\text{-}phen)]^{2+}$ is not so pronounced as those observed in $[PdCl(PPh_3)_2(phen)]^+$,[2] $[PtCl(PEt_3)_2(phen)]^+$,[6] and $[Pt(CN)(phen)_2]^+$.[4] Yet, this elongation of the apical M—N distance still raises a question as to whether the nitrogen atom is in the inner sphere or not. The latter two platinum(II) complexes in solution exhibiting fluxional motion do not display any dissociation, as the observance of ^{195}Pt satellites in resonances arising from the azaheterocyclic ligand [^1H, ^{13}C NMR] indicate. It should be noted that the present d^8 system, by allowing five-coordination, becomes coordinatively saturated. This condition slightly differs from $[PdCl(PPh_3)_2(phen)]^+$, in which dissociation of one nitrogen atom may make the d^8 species coordinately unsaturated. Such a distinction has in fact been observed in the visible absorption spectra. The visible spectrum of $[PdCl(PPh_3)_2(phen)]^+$ shows absorption maxima at 335–355 nm, which resemble those of the seldomly ion-paired complexes $[Pt(PEt_3)_2(phen)]^{2+}$ and $[PdCl(PPh_3)(phen)]^+$.[1] On the other hand, the absorption maximum of $[Pd(PMe_2Ph)_3(2,9\text{-}Me_2\text{-}phen)]^{2+}$ is observed at 412 nm ($\varepsilon = 1060$), which resembles that of $[PdCl_2(PMe_2Ph)_3]$ at 410 nm ($\varepsilon = 1020$).[5] The transition may be due to the charge-

transfer bands ($M \rightarrow L$, $L \rightarrow M$). The *d–d* band was probably not resolved owing to its combination with the intense charge-transfer bands at the higher wave number. Therefore, the visible absorption of the present complex is most likely to be characteristic of five-coordination (a bidentate 2,9-Me_2-phen). A fluxional motion which averages two halves of the 2,9-Me_2-phen in $[Pd(PMe_2Ph)_3(2,9\text{-}Me_2\text{-}phen)]^{2+}$ may be explained by oscillation. We have observed a relatively large ^1H NMR downfield shift for 2,9-Me- and 3,8-protons of the azaheterocyclic rings upon coordination. Such a coordination shift is due to paramagnetic anisotropy.[15] Another possible explanation may be the trigonal bipyramidal structure with stereochemical rigidity. This, however, can be excluded by comparing its ^{31}P NMR spectrum with that of an analogous 1,10-phen complex, $[Pd(PMe_2Ph)_3(phen)][BF_4]_2$ (*vide infra*).[1] The ^{31}P NMR spectrum of $[Pd(PMe_2Ph)_3(2,9\text{-}Me_2\text{-}phen)]^{2+}$ indicates an AB_2-spin system with $J_{AB} = 20$ Hz: the ^{31}P triplet appears at higher field than the ^{31}P doublet. Its $^{31}P—^{31}P$ coupling constant is close to the value of 26 Hz for $[PdCl(PMe_3)_3]^+$,[16] and 21 Hz for $[PdCl_2(PMe_3)_3]^+$,[16] which both have a square-pyramidal structure in which three phosphorus atoms are arranged at the coordination plane. These coupling constants are quite different from those observed in a trigonal bipyramidal structure, which have coupling constants equal to 10 Hz for $[PdBr_2(PMe_3)_3]$,[16] and 4 Hz for $[PdI_2(PMe_3)_3]$.[16] Therefore, three phosphines in $[Pd(PMe_2Ph)_3(2,9\text{-}Me_2\text{-}phen)][BF_4]_2$ are, as consistent with the solid state, coplanar including the palladium(II) atom. Any differences in $J(^{31}P—^{31}P)$ between the PMe_2Ph complex and its PMe_3 analogues may not be significant because the corresponding coupling constant of $[PtCl(PMe_2Ph)_3][BF_4]$[17] is 22 Hz, which is in agreement with that observed in $[PtCl(PMe_3)_3]^+$.[18] On the other hand, the ^{31}P NMR spectrum of the analogous phen complex, $[Pd(PMe_2Ph)_3(phen)][BF_4]_2$, shows a reversed pattern of chemical shifts: the ^{31}P doublet appears at higher field than the ^{31}P triplet. The $J(^{31}P—^{31}P)$ value of 23 Hz is close to that of the 2,9-Me_2-phen complex. This means that the environment around the three phosphines in the phen complex is similar to that of the 2,9-Me_2-phen complex. In the five-coordinate palladium(II) and platinium(II) complexes so far studied, axial phosphines or phosphites appear at higher field regions than the equatorial ones.[18–20] Thus, the structure of $[Pd(PMe_2Ph)_3(phen)]^{2+}$ is most likely to be trigonal bipyramidal with two axial phosphines, in which two equatorial bonds, Pd—N, may be arranged at equal distances.[21]

The coordination of $[Pd(PMe_2Ph)_3(2,9\text{-}Me_2\text{-}phen)][BF_4]_2$ in the solid state may be described as the five-coordinate distorted square pyramid, involving a bidentate 2,9-Me_2-phen, one nitrogen atom of which is at the apex of the square pyramid with a weaker interaction between the nitrogen and palladium atoms, rather than the four-coordinate square-planar structure, in which the second nitrogen atom is on the outside of the coordination sphere of the palladium atom.

Acknowledgements—One author (S.Y.) thanks Dr K. Hata (JEOL Ltd, Akishima, Tokyo) for obtaining ^{31}P NMR spectra, and also the Ministry of Education, Science and Culture, for the Grant-in-Aid for Scientific Research (Grant No. 540402).

REFERENCES

1. S. Yamazaki, *Polyhedron* 1985, **4**, 1915.
2. Z. Taira and S. Yamazaki, *Bull. Chem. Soc. Jpn* 1986, **59**, 649.
3. S. Yamazaki, *Bull. Chem. Soc. Jpn* 1987, **60**, 1155.
4. O. Wernberg and A. Hazell, *J. Chem. Soc., Dalton Trans.* 1980, 973.
5. W. J. Louw, D. J. A. de Waal and G. J. Kruger, *J. Chem. Soc., Dalton Trans.* 1976, 2364.
6. G. W. Bushnell, K. R. Dixon and M. A. Khan, *Can. J. Chem.* 1974, **52**, 1367.
7. S. Okeya, T. Miyamoto, S. Ooi and S. Kawaguchi, *Bull. Chem. Soc. Jpn* 1984, **57**, 395.
8. P. Overbosch, G. Koten, D. M. Grove, A. L. Spek and A. J. M. Duisenberg, *Inorg. Chem.* 1982, **21**, 3253.
9. UNICSII. Universal Crystallographic Computation Program System (Edited by T. Sakurai). The Crystallographic Society of Japan, Tokyo (1967).
10. *International Tables for X-ray Crystallography*, Vol. IV. Kynoch Press, Birmingham (1974).
11. C. K. Johnson, Report ORNL-3794. Oak Ridge National Laboratory, Tennessee, U.S.A. (1965).
12. B. A. Frenz and J. A. Ibers, *Inorg. Chem.* 1972, **11**, 1109.
13. S. Nishigaki, H. Yoshioka and K. Nakatsu, *Acta Cryst.* 1978, **B34**, 875.
14. S. R. Hall, D. L. Kepert, C. L. Raston and A. H. White, *Austral. J. Chem.* 1977, **30**, 1955.
15. R. G. Miller, R. D. Stauffer, D. R. Fahey and D. R. Parnell, *J. Am. Chem. Soc.* 1970, **92**, 1511.
16. R. Favez and R. Roulet, *Inorg. Chem.* 1981, **20**, 1598.
17. S. Yamazaki, unpublished result.
18. R. Favez, R. Roulet, A. A. Pinkerton and D. Schwarzenbach, *Inorg. Chem.* 1980, **19**, 1356.
19. P. F. Meier, A. E. Merbach, M. Dartiguena and Y. Dartiguenava, *Inorg. Chem.* 1979, **18**, 610.
20. P. Meakin and J. P. Jesson, *J. Am. Chem. Soc.* 1974, **96**, 5751.
21. R. Gillespie, *J. Chem. Soc.* 1963, 4679.

Polyhedron Vol. 8, No. 15, pp. 1995–1998, 1989
Printed in Great Britain

0277–5387/89 $3.00+.00
© 1989 Maxwell Pergamon Macmillan plc

COMMUNICATION

SYNTHESES AND X-RAY STRUCTURES OF MOLECULAR METAL POLYSELENIDE COMPLEXES $[M(Se_4)_2]^{2-}$ M = Zn, Cd, Hg, Ni, Pb

R. M. HERATH BANDA, JOHN CUSICK, MARCIA L. SCUDDER, DON C. CRAIG and IAN G. DANCE*

School of Chemistry, University of New South Wales, PO Box 1, Kensington, NSW 2033, Australia

(*Received* 4 *January* 1989; *accepted* 21 *February* 1989)

Abstract—Bis-tetraselenide complexes $[M(Se_4)_2]^{2-}$ M = Zn (**1**), Cd (**2**), Hg (**3**), Ni (**4**) and Pb (**5**) are readily prepared by the reaction of Se, Na and MCl_2 in DMF, and crystallized with Ph_4P^+. Crystal structure determinations reveal pseudo-tetrahedral coordination in **1**, **2** and **3**, slightly distorted square-planar coordination in **4**, and in **5** a four coordinate stereochemistry interpreted as primary trigonal orthogonal, plus one secondary bond. There is no evidence of variable size in the metallapolyselenane chelate rings, in contrast with data for comparable polysulphide complexes.

Although aqueous polysulphide reagents are long known, the use of non-aqueous solvents in the preparations of metal complexes has enabled the crystallization and structural characterization of molecular homoleptic metal polysulphides with wide structural variety, containing from one to six metal atoms.[1,2] We expected that many other molecular structures would exist in metal polysulphide solutions, and have deployed metal NMR to confirm that sulphur atom redistribution reactions are facile, and that metal complexes with different metallapolysulphane ring sizes are in equilibrium. Thus, in cadmium polysulphide solutions, the complexes $[Cd(S_x)(S_y)]^{2-}$, $(x,y) = (5,5); (5,6); (6,6); (6,7)$ are in equilibrium, interchanging slowly on the ^{113}Cd NMR time scale at 300 K, with $\Delta\delta_{Cd} \sim 50$ ppm for Δx or $\Delta y = 1$.[3] Comparable results are obtained for complexes $[Hg(S_x)(S_y)]^{2-}$.[4] Metallapolysulphane ring conformations in these compounds occur on a relatively flat potential energy surface, as indicated by the frequent conformational disorder in crystals, and by the absence of Cd or Hg NMR evidence for conformers even at low temperatures.

We are extending these investigations to metal polyselenides and polytellurides, and communicate here preparative and structural results for five $[M(Se_4)_2]^{2-}$ complexes.

Reactions of metal halide, selenium and sodium in DMF generate solutions of metal polyselenide complexes. When the metal precursor is MCl_2, M = Zn, Cd, Hg, Ni, Pb, and the solutions are treated with Ph_4PBr,† brown–black crystals of the compounds $(Ph_4P)_2[M(Se_4)_2]$, M = Zn (**1**), Cd (**2**), Hg (**3**), Ni (**4**), Pb (**5**), are obtained. Compounds

* Author to whom correspondence should be addressed.

† The general preparative procedure involves MCl_2, Se, Na in molar ratios 1 : 8 : 4 in DMF under dinitrogen, with Ph_4PBr slowly diffused into the filtered reaction solution. The cadmium complex (**2**) was prepared with $Cd(NO_3)_2 \cdot 4H_2O$ as precursor.

2–5 have been characterized by crystal structure determination: **1** is isostructural with **2**.*

The $[M(Se_4)_2]^{2-}$ complexes in **2** (M = Cd) and **3** (M = Hg) possess unexceptional tetrahedral coordination, as shown for **2** in Fig. 1. The $CdSe_4$ rings in **2** are fully ordered, while three of the four crystallographically independent $HgSe_4$ rings in **3** are conformationally disordered. Average dimensions in **2** and **3**, respectively, are:† M—Se = 2.643(9), 2.65(2) Å; Se—Se = 2.35(4), 2.32(2) Å; intrachelate Se—M—Se = 104(2), 102(3)°.

The $[Ni(Se_4)_2]^{2-}$ ion in **4** has approximately square-planar coordination, with a slight tetrahedral distortion: the donor selenium atoms lie 0.33 Å to either side and the nickel atom lies within the least-squares plane through the $NiSe_4$ set. Mean dimensions are Ni—Se = 2.297(7) Å; intrachelate Se—M—Se = 102.0(4)°; and interchelate Se—M—Se = 80.0(1)°. Unlike the homologous $[Ni(S_4)_2]^{2-}$ ion crystallized with Et_4N^+,[5,6] and Ph_4P^+,[6] the Se_4^{2-} rings in $[Ni(Se_4)_2]^{2-}$ are not conformationally disordered.

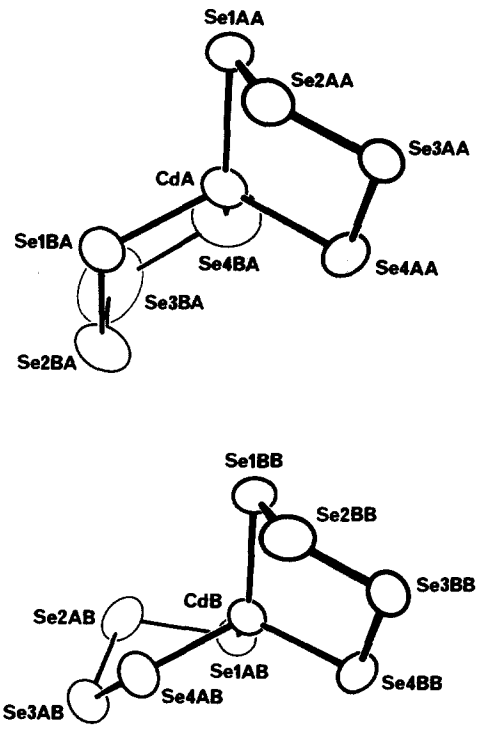

Fig. 1. The two independent $[Cd(Se_4)_2]^{2-}$ complexes in **2**, with atoms outlined at the 50% probability level.

Figure 2 shows the irregular coordination stereochemistry of the molecular complex $[Pb(Se_4)_2]^{2-}$ in **5**. Although the Pb—Se bond lengths are distinctly different, three Pb—Se bonds [to Se(1B), Se(4B) and Se(1A)] are 0.3–0.4 Å shorter than the fourth, and subtend Se—Pb—Se angles that are close to orthogonal. Therefore we interpret the geometry in terms of *trigonal orthogonal* primary coordination, with a longer secondary connection [to Se(4A)] also in a pseudo-orthogonal location, and with two vacant orthogonal positions [*trans* to Se(1A), Se(1B)]. An alternative but less realistic interpretation of the coordination stereochemistry in **5** involves a trigonal bipyramid with one vacant equatorial position.

Complexes **1–4** have polysulphide analogues. However, molecular lead polysulphides have not yet been reported, and **5** is a unique lead polychalcogenide. The trigonal orthogonal primary coordination in **5**, with secondary connections also part of the orthogonal array, is analogous to that

* Crystal data (Enraf–Nonius CAD4 diffractometer); least squares refinement included rigid phenyl groups (**2** and **3**) and slack constraints on disordered MSe_x rings in **3**: **1**, $C_{48}H_{40}ZnP_2Se_8$, $M = 1375.86$, $a = 10.159(5)$, $b = 14.020(4)$, $c = 34.26(1)$ Å, $\beta = 92.11(2)°$, $V = 4875(3)$ Å^3, space group $P2_1$; **2**, $C_{48}H_{40}CdP_2Se_8$, $M = 1422.89$, monoclinic, $a = 10.185(5)$, $b = 14.137(4)$, $c = 34.39(2)$ Å, $\beta = 92.22(2)°$, $V = 4948(4)$ Å^3, space group $P2_1$, $D_{calc} = 1.91$ g cm^{-3}, $Z = 4$, $\mu = 63.6$ cm^{-1}, max/min transmission coefficients 0.70/0.45, 3459 independent observed ($I/\sigma(I) > 3$) reflections (Mo-K_α), $R = 0.046$, $R_w = 0.055$; **3**, $C_{48}H_{40}HgP_2Se_8$, $M = 1511.07$, monoclinic, $a = 23.128(7)$, $b = 20.311(5)$, $c = 23.956(8)$ Å, $\beta = 119.43(1)°$, $V = 9801(5)$ Å^3, space group $P2_1/c$, $D_{calc} = 2.05$ g cm^{-3}, $Z = 8$, $\mu = 91.2$ cm^{-1}, max/min transmission coefficients 0.28/0.16, 4609 independent observed ($I/\sigma(I) > 3$) reflections (Mo-K_α), $R = 0.041$, $R_w = 0.047$; atom labels for the two independent $[Hg(Se_4)_2]^{2-}$ complexes in the asymmetric unit, in the principal conformations are Hg(A), Se(*n*AA) (*n* = 1–4), Se(*n*BA) (*n* = 1–4), Hg(B), Se(*n*AB) (*n* = 1–4), Se(*n*BB) (*n* = 1–4); Se(2AA′) and Se(3AA′) occur in 9% of the unit cells, Se(3AB′) and Se(4AB′) in 13%, and Se(1BA′), Se(2BA′) and Se(3BA′) in 46%; **4**, $C_{48}H_{40}NiP_2Se_8$, $M = 1369.18$, monoclinic, $a = 10.934(6)$, $b = 15.531(3)$, $c = 14.313(7)$ Å, $\beta = 92.54(2)°$, $V = 2428(2)$ Å^3, space group $P2_1$, $D_{calc} = 1.87$ g cm^{-3}, $Z = 2$, $\mu = 64.3$ cm^{-1}, max/min transmission coefficients 0.83/0.71, 2557 independent observed ($I/\sigma(I) > 3$) reflections (Mo-K_α), $R = 0.037$, $R_w = 0.041$; **5**, $C_{48}H_{40}PbP_2Se_8$, $M = 1517.68$, triclinic, $a = 10.349(3)$, $b = 10.759(4)$, $c = 23.034(9)$ Å, $\alpha = 77.03(3)$, $\beta = 83.52(3)$, $\gamma = 78.78(3)°$, $V = 2445(2)$ Å^3, space group $P\bar{1}$, $D_{calc} = 2.06$ g cm^{-3}, $Z = 2$, $\mu = 94.7$ cm^{-1}, max/min transmission coefficients 0.58/0.28, 4354 independent observed ($I/\sigma(I) > 3$) reflections (Mo-K_α), $R = 0.037$, $R_w = 0.044$. Tables of atomic positional and thermal parameters, and lists of observed and calculated structure factors have been deposited as supplementary material with the Editor, and atomic coordinates have been deposited with the Cambridge Crystallographic Data Centre.

† Standard deviations of the sample in parentheses.

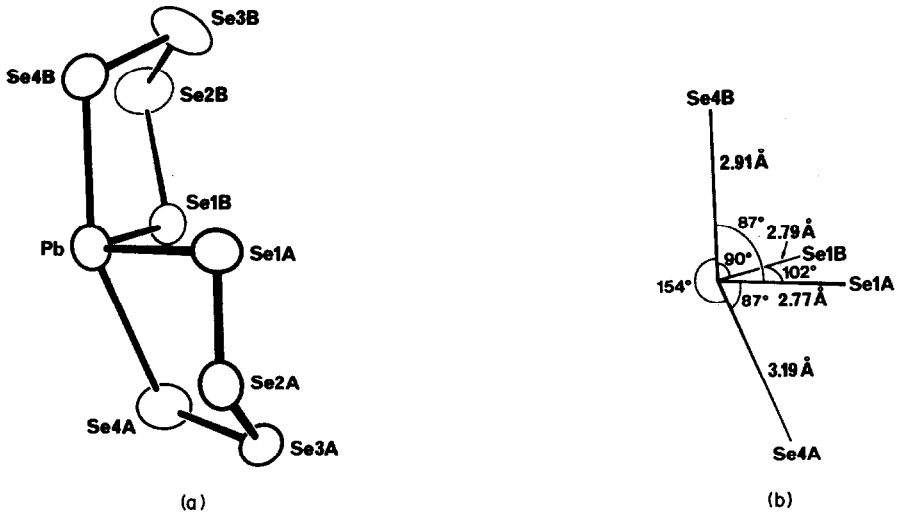

Fig. 2. The $[Pb(Se_4)_2]^{2-}$ complex in **5**, (a) with the atoms drawn as 50% probability ellipsoids and (b) with the principal coordination bond lengths and angles.

which occurs in $[Pb_2(SCH_2CH_2NMe_3)_5](PF_6)_4$[7] and is regarded as characteristic of lead chalcogenide coordination.

There are patterns in the conformations of the MSe_4 rings in **2**–**5**. These conformations are expressed in terms of the five torsional angles within the ring, ϕ_1, ϕ_2, ϕ_3, ϕ_4, ϕ_5 (see Table 1), defined in **I**

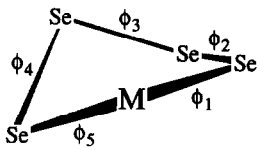

I

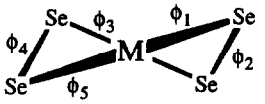

II

and **II** with reference to the two idealized conformations, namely the envelope (symmetry C_s, torsional angles 0, +, −, +, −, or the inverse) and the half-chair (symmetry C_2, torsional angles +, −, +, −, +, or the inverse). The MSe_4 rings in **2** and **3** adopt distorted envelope conformations as in **I**, with the "flap" opposite one of the M—Se bonds, and with the distortion towards the half-chair con-

Table 1. Torsional angles (°) in MSe_4 rings[a]

Compound, ring	ϕ_1	ϕ_2	ϕ_3	ϕ_4	ϕ_5
2, AA	9.2	27.8	−63.8	61.0	−41.5
2, BB	12.9	23.6	−60.0	60.9	−43.4
2, BA	0.9	−32.3	60.0	−52.8	32.0
2, AB	−5.2	−30.9	63.3	−59.3	38.0
3, AA[b]	−5.1	37.6	−63.1	53.3	−28.7
3, BB	4.8	−37.4	62.7	−53.3	28.5
3, BA[b]	8.8	−37.5	59.0	−48.4	23.1
3, AB[b]	7.9	−37.5	57.0	−47.3	23.8
4, A	14.0	−43.7	53.3	−48.2	20.9
4, B	14.5	−41.9	49.8	−44.9	18.9
5, A	−10.4	−24.4	59.6	−67.5	41.6
5, B	18.3	−50.4	66.3	−51.8	18.9

[a] See **I** and **II** for definition of the torsional angles ϕ (which is unambiguous in all cases): ϕ_1 is assigned to be the smallest (ideally 0° in the envelope conformation), while in the half-chair conformation $\phi_1 = \phi_5$, $\phi_2 = \phi_3$.

[b] For the principal conformations.

formation in which the metal lies on the two-fold axis. Apart from conformational inversion, the four rings in **3** are almost identical. Details of the conformations are metal dependent: in **2**, ϕ_1 and ϕ_5 are of opposite sign, while in **3** they have the same sign, which is a manifestation of the fact that the $HgSe_4$ rings are closer to the half-chair conformation. In **4**, both $NiSe_4$ ring conformations are half-chair as in **II**, while in **5** one $PbSe_4$ ring (B) is also half-chair (but more angular than the $NiSe_4$ ring), while the other has the distorted envelope conformation which occurs in **2**.

Full details of the crystal structures will be published separately. We are exploring extensions of the preparative method to other metals and to different polyselenide chain lengths: preliminary ^{113}Cd and ^{199}Hg measurements indicate that metallapolyselenane ring sizes are less variable than metallapolysulphane analogues.

Acknowledgements—The Australian Development Assistance Bureau (R.M.H.B.), the Australian Postgraduate Award Scheme (J.C.) and the Australian Research Grants Scheme are gratefully acknowledged for support of this research. We thank Professor A.D. Rae for the use of the program RAELS, and Professor A. Müller for sending us a copy of ref. 1 prior to publication.

REFERENCES

1. A. Müller and E. Diemann, *Adv. Inorg. Chem. Radiochem.* 1987, **31**, 89.
2. M. Draganjac and T. B. Rauchfuss, *Angew. Chem. Int. Ed. Engl.* 1985, **24**, 742.
3. R. M. Herath Banda, I. G. Dance, T. D. Bailey, D. C. Craig and M. L. Scudder, *Inorg. Chem.* 1989, in press.
4. R. M. Herath Banda, I. G. Dance, T. D. Bailey, D. C. Craig and M. L. Scudder, *Inorg. Chem.*, in preparation.
5. D. Coucouvanis, P. R. Patil, M. G. Kanatzidis, B. Detering and N. C. Baenziger, *Inorg. Chem.* 1985, **24**, 24.
6. A. Müller, E. Krickemeyer, H. Bögge, W. Clegg and G. M. Sheldrick, *Angew. Chem. Int. Ed. Engl.* 1983, **22**, 1006.
7. I. G. Dance, P. J. Guerney, A. D. Rae, M. L. Scudder and A. T. Baker, *Aust. J. Chem.* 1986, **39**, 383.

Polyhedron Vol. 8, No. 15, pp. 1999–2001, 1989
Printed in Great Britain

0277–5387/89 $3.00+.00
© 1989 Maxwell Pergamon Macmillan plc

COMMUNICATION

SYNTHESES AND STRUCTURES OF ANIONIC METAL POLYSELENIDE COMPLEXES $[(C_5H_5)Mo(Se_4)_2]^-$ AND $[Sn(Se_4)_3]^{2-}$, CRYSTALLIZED WITH Ph_4P^+

R. M. HERATH BANDA, JOHN CUSICK, MARCIA L. SCUDDER, DON C. CRAIG and IAN G. DANCE*

School of Chemistry, University of New South Wales, PO Box 1, Kensington, NSW 2033, Australia

(*Received* 22 *February* 1989; *accepted* 16 *March* 1989)

Abstract—Reaction of $(\eta^5\text{-}C_5H_5)_2Mo_2(CO)_6$ with selenium and sodium in DMF yields $[(\eta^5\text{-}C_5H_5)Mo(Se_4)_2]^-$ (**1**), which was crystallized with Ph_4P^+ and characterized by crystal structure determination. With two chelating tetraselenide ligands, **1** is the first member of a new class of mono(cyclopentadienyl)-bis(polychalcogenide) metallates, distinct from existing compounds which are formulated $[(\eta^5\text{-}C_5R_5)_2M(E_x)]$ (E = S, Se; x = 3, 4, 5). $(Ph_4P)_2[Sn(Se_4)_3]$ (**2**), from reaction of selenium, sodium, $SnCl_2$ and Ph_4PBr in DMF, shows no evidence in its crystal structure of the disordered ring size and conformation found in polysulphide homologues.

We have previously communicated the preparations and crystal and molecular structures of the metal polyselenide complexes, $(Ph_4P)_2[Cu_4(Se_4)_{2.4}(Se_5)_{0.6}]$ and $(Ph_4P)_2[Ag_4(Se_4)_{2.1}(Se_5)_{0.9}]$,[1] and $(Ph_4P)_2[M(Se_4)_2]$ (M = Zn, Cd, Hg, Ni and Pb).[2] These compounds were synthesized in a direct procedure involving *in situ* reduction of selenium in the presence of a suitable metal precursor. This preparative method has now been applied to a cyclopentadienyl metal carbonyl, $(\eta^5\text{-}C_5H_5)_2Mo_2(CO)_6$, yielding $(Ph_4P)[(\eta^5\text{-}C_5H_5)Mo(Se_4)_2]$ (**1**). We also report here the preparation of $(Ph_4P)_2[Sn(Se_4)_3]$ (**2**) from $SnCl_2$, and the structures of **1** and **2**.

A mixture of $(\eta^5\text{-}C_5H_5)_2Mo_2(CO)_6$ (3.8 mmol) and selenium (29.1 mmol Se) in DMF was treated with sodium (14.8 mmol) and stirred at 60°C under dinitrogen, and the colour changed from deep red to dark green after 90 min. After cooling and addition of Ph_4PBr in acetonitrile, black needles of **1** were collected and characterized by crystal structure determination.†

The molecular structure of the $[(\eta^5\text{-}C_5H_5)Mo(Se_4)_2]^-$ ion is shown in Fig. 1. There is a small but significant asymmetry in the chelation of both Se_4^{2-} ligands: Mo—Se(1A) = 2.463(1), Mo—Se(4A) = 2.533(1); Mo—Se(1B) = 2.474(1) and Mo—Se(4B) = 2.542(1) Å. The intrachelate Se—Mo—Se angles are both 88°, and the interchelate angles Se(1A)—Mo—Se(4B) and Se(4A)—Mo—Se(1B) are 74.8 and 72.4°, respectively.

Despite a large volume of research on cyclopentadienyl metal polysulphide compounds,[3,4]

* Author to whom correspondence should be addressed.

† Crystal data (Enraf–Nonius CAD4 diffractometer, Mo-K_α radiation): **1**, $C_{29}H_{25}MoPSe_8$, M = 1132.12, triclinic, a = 8.778(3), b = 11.500(4), c = 16.710(6) Å, α = 104.56(2), β = 97.02(2), γ = 93.77(2)°, V = 1612.3(9) Å^3, space group $P\bar{1}$; D_{calc} = 2.33 g cm^{-3}, Z = 2, μ = 94.1 cm^{-1}, max./min. transmission coefficients 0.56/0.30, 3757 independent observed ($I/\sigma(I) > 3$) reflections (Mo-K_α), R = 0.030, R_w = 0.036; ligand atom labels are CpC_n (n = 1–5), Se(nA) (n = 1–4), Se(nB) (n = 1–4); the Se_4^{2-}, ligand A, is disordered with a minor conformation involving atoms Se(2A′) (9%) and Se(3A′) (7%). The largest peak on the final difference electron density map was 0.63 e Å^{-3}. Tables of atomic positional and thermal parameters, and lists of observed and calculated structure factors have been deposited as supplementary material with the Editor, and atomic coordinates have been deposited with the Cambridge Crystallographic Data Centre.

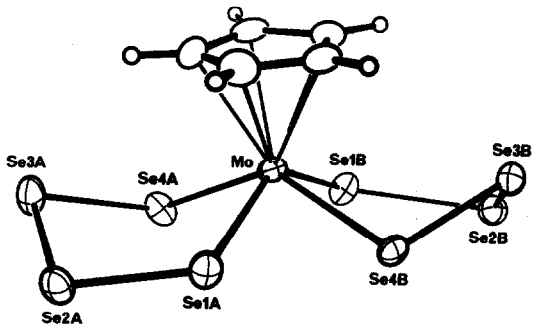

Fig. 1. The $[(\eta^5\text{-}C_5H_5)Mo(Se_4)_2]^-$ ion in **1**, with atoms outlined at the 20% probability level. Se—Se bond lengths are 2.399, 2.310, 2.381 Å and 2.419, 2.343, 2.365 Å in numerical sequence around ligands A and B, respectively. See text for other dimensions.

there is no report of a polysulphide analogue of **1**, or of any mono(cyclopentadienyl)-bis(polychalcogenide)metallate in the general class $[(\eta^5\text{-}C_5R_5)M(E_x)_2]^z$ (E = S, Se). Reactions of a variety of cyclopentadienyl metal carbonyls with elemental sulphur or selenium yield instead, uncharged compounds, usually dimetallic, with bridging E atoms or E_x groups,[4] for example $(\eta^5\text{-}C_5Me_5)Rh(\mu\text{-}S_4)_2Rh(\eta^5\text{-}C_5Me_5)$[5] and $(\eta^5\text{-}C_5Me_5)Rh(\mu\text{-}Se)(\mu,\eta^2\text{-}Se_4)Rh(\eta^5\text{-}C_5Me_5)$.[6] Reactions of $(\eta^5\text{-}C_5R_5)_2MX_n$ precursors with polychalcogenide ions in solution yield the bis-cyclopentadienyl derivatives $[(\eta^5\text{-}C_5R_5)_2M(E_x)]$, such as $[(\eta^5\text{-}C_5H_5)_2M(E_5)]$ (M = Ti, Zr, Hf; E = S, Se),[7-11] $[(\eta^5\text{-}C_5Me_5)_2Ti(S_3)]$,[12] $[(\eta^5\text{-}C_5H_5)_2V(E_5)]$[9,13] and $[(\eta^5\text{-}C_5H_5)_2M(E_4)]$ (M = Mo, W; E = S, Se).[14-17] There is one recent report of a reaction that (like that described here) generates an anionic complex: that is the reaction of $(\eta^5\text{-}C_5H_5)_2Mo_2(CO)_6$ and $(Et_4N)_2Se_6$ in ethanol to form the molybdenum(II) product, $[(\eta^5\text{-}C_5H_5)Mo(CO)_2(\mu,\eta^2\text{-}Se_2)]^-$.[18] Thus **1** is unique as an anionic cyclopentadienyl metal bis-polychalcogenide. It does, however, bear comparison with the molybdenum(IV) compounds, $[XMo(E_4)_2]^{2-}$ (X = O, S, Se; E = S, Se).[19-21]

Table 1. Torsion angles (°) in MSe_4 rings

Compound, ring	Bond M—Se(1)	Se(1)—Se(2)	Se(2)—Se(3)	Se(3)—Se(4)	Se(4)—M
1, A	−30.2	+0.3	+32.3	−56.6	+50.3
1, B	−24.6	−9.5	+41.8	−63.4	+51.1
2, A	−3.9	+37.5	−62.8	+58.0	−31.0
2, B	+13.5	−45.0	+63.5	−50.8	+21.7
2, C	−17.9	+48.4	−62.9	+47.2	−17.4

When a solution of $SnCl_2 \cdot 2H_2O$ in DMF was added to a solution of Na_2Se_6 similarly generated in DMF, followed (after filtration) by a solution of Ph_4PBr in acetonitrile, dark red crystalline $(Ph_4P)_2[Sn(Se_4)_3]$ (**2**) separated and was characterized by X-ray structure determination.* Unlike the homologous polysulphide complexes[22,23] which are heavily disordered in length (S_4, S_5, S_6) and conformation of the polysulphide chain, there is no disorder in **2**. The mean Sn—Se bond length is 2.706(14) Å,† the mean intrachelate Se—Sn—Se angle is 95.9(9)°† and the mean Se—Se distance 2.320(10) Å.†

The torsional angles in the MSe_4 chelate rings, listed in Table 1, show that in **1** ring A adopts the envelope conformation with the flap at Se(4A), ring B is between an envelope [flap at Se(4B)] and half-chair [two-fold axis through Se(1B)], while in **2**, ring A is approximately an envelope [flap at Se(3A)] and rings B and C are close to half-chairs (two-fold axes through tin).

Acknowledgements—The Australian Development Assistance Bureau (R.M.H.B.), the Australian Postgraduate Award Scheme (J.C.) and the Australian Research Council are gratefully acknowledged for support of this research. We thank Marram Kassis for a sample of $Cp_2Mo_2(CO)_6$.

REFERENCES

1. J. Cusick, M. L. Scudder, D. C. Craig and I. G. Dance, *Polyhedron* 1989, **8**, 1139.
2. R. M. Herath Banda, J. Cusick, M. L. Scudder, D. C. Craig and I. G. Dance, *Polyhedron* 1989, **8**, 1995.
3. M. Draganjac and T. B. Rauchfuss, *Angew. Chem. Int. Ed. Engl.* 1985, **24**, 742.
4. J. Wachter, *J. Coord. Chem.* 1987, **15**, 219.
5. H. Brunner, N. Janietz, W. Meier, B. Nuber, J. Wachter and M. L. Ziegler, *Angew. Chem. Int. Ed. Engl.* 1988, **27**, 708.
6. H. Brunner, W. Meier, B. Nuber, J. Wachter and M. L. Ziegler, *Angew. Chem. Int. Ed. Engl.* 1986, **25**, 907.

*Crystal data (Enraf–Nonius CAD4 diffractometer, Mo-K_α radiation): **2**, $C_{48}H_{40}SnP_2Se_{12}$, M = 1745.01, monoclinic, a = 13.307(3), b = 11.696(2), c = 34.699(9) Å, β = 98.82(1)°, V = 5337(2) Å^3, space group $P2_1/c$, D_{calc} = 2.17 g cm^{-3}, Z = 4, μ = 86.8 cm^{-1}, max./min. transmission coefficients 0.37/0.21, 4112 independent observed ($I/\sigma(I) > 3$) reflections (Mo-K_α), R = 0.029, R_w = 0.035; atom labels for the three chelate rings are Se(nA), Se(nB), Se(nC) (n = 1–4). The largest peak on the final difference electron density map was 0.86 e Å^{-3}.

† The standard deviation of the *sample* is given in parentheses.

7. H. Köpf, B. Block and M. Schmid, *Chem. Ber.* 1968, **101**, 272.
8. E. F. Epstein, I. Bernal and H. Köpf, *J. Organomet. Chem.* 1971, **26**, 229.
9. E. G. Muller, J. L. Peterson and L. F. Dahl, *J. Organomet. Chem.* 1976, **111**, 91.
10. (a) J. M. McCall and A. Shaver, *J. Organomet. Chem.* 1980, **193**, C37; (b) A. Shaver and J. M. McCall, *Organometallics* 1984, **3**, 1823.
11. D. Fenske, J. Adel and K. Dehnicke, *Z. Naturfor.* 1987, **42b**, 931.
12. P. H. Bird, J. M. McCall, A. Shaver and U. Siriwardane, *Angew. Chem. Int. Ed. Engl.* 1982, **21**, 384.
13. H. Köpf, A. Wirl and W. Kahl, *Angew. Chem. Int. Ed. Engl.* 1971, **10**, 137.
14. H. Köpf, *Angew. Chem. Int. Ed. Engl.* 1969, **8**, 375.
15. H. Köpf, W. Kahl and A. Wirl, *Angew. Chem. Int. Ed. Engl.* 1970, **9**, 801.
16. B. R. Davis, I. Bernal and H. Köpf, *Angew. Chem. Int. Ed. Engl.* 1971, **10**, 921.
17. H. D. Block and R. Allmann, *Cryst. Struct. Comm.* 1975, **4**, 53.
18. J. Adel, F. Weller and K. Dehnicke, *J. Organomet. Chem.* 1988, **347**, 343.
19. M. Draganjac, E. Simhon, L. T. Chan, M. Kanatzidis, N. C. Baenziger and D. Coucouvanis, *Inorg. Chem.* 1982, **21**, 3321.
20. A. Müller, E. Urichmeyer, H. Bögge, M. Penk and D. Rehder, *Chimia* 1986, **40**, 50.
21. R. W. M. Wardle, C. H. Mahler, C-N. Chau and J. A. Ibers, *Inorg. Chem.* 1988, **27**, 2790.
22. A. Müller, J. Schimanski, M. Römer, H. Bögge, F-W. Baumann, W. Eltzner, E. Krickemeyer and U. Billerbeck, *Chimia* 1985, **39**, 25.
23. I. G. Dance, R. M. Herath Banda, T. D. Bailey, D. C. Craig, I. N. L. Ma and M. L. Scudder, in preparation.

Polyhedron Vol. 8, No. 15, pp. 2003–2006, 1989
Printed in Great Britain

0277–5387/89 $3.00+.00
© 1989 Maxwell Pergamon Macmillan plc

COMMUNICATION

ROTATION OF THE ACETYLIDE LIGAND ON THE TRIANGULAR FACE OF TUNGSTEN–DIRUTHENIUM CLUSTERS. CRYSTAL STRUCTURE AND SOLUTION DYNAMICS OF $LWM_2(CO)_8(CCPh)$, L = C_5H_5, C_5Me_5 AND M = Os, Ru

YUN CHI* and BANG-JI LIU

Department of Chemistry, National Tsing Hua University, Hsinchu 30043, Taiwan, R.O.C.

and

GEN-HSIANG LEE and SHIE-MING PENG†

Department of Chemistry, National Taiwan University, Taipei 10764, Taiwan, R.O.C.

(*Received* 31 *January* 1989; *accepted* 31 *March* 1989)

Abstract—Reaction of $CpW(CO)_3$—C≡CPh with $Os_3(CO)_{10}(CH_3CN)_2$ or $Ru_3(CO)_{12}$ in refluxing toluene gives trinuclear mixed-metal acetylide clusters, $CpWOs_2(CO)_8(C{\equiv}CPh)$ (**1**) and $CpWRu_2(CO)_8(C{\equiv}CPh)$ (**3**); the acetylide ligands of these two complexes are related to each other by a 120° rotation as indicated by X-ray diffraction studies. In solution, the variable temperature ^1H and ^{13}C NMR spectra suggest that the acetylide ligand of **3** undergoes a 360° rotation on the face of the WRu_2 triangle.

The C_2 hydrocarbyl ligands hold a key position in the development of dinuclear, trinuclear and polynuclear organometallic chemistry. This position is in part due to a belief that the chemistry of the C_2 hydrocarbyl ligands in the organometallic complexes is analogous to those adsorbed on metal surfaces. Among the many interesting properties of the C_2 ligands is their fluxionality and mobility on the coordination sphere of the transition metal complexes. Related studies on the C_2 hydrocarbyl ligands have attracted the attention of many theoretical and synthetic chemists. Schilling and Hoffmann[1] have reported the extended Hückel calculation of some hydrocarbyl ligands on the triangular face of homonuclear transition metal complexes. For the C_2 vinylidene complex, $Co_3(CO)_9(CCHR)^+$, Norton and co-workers[2] have reported the disrotatory correlated rotation about the $Co_3(CO)_9$—C vector and C—CHR bond by variable-temperature ^{13}C NMR studies. Stone and co-workers[3] and Shapley and co-workers[4] have both described the so-called "windscreen-wiper" type of motion of a coordinated alkyne ligand on a W_2Os triangular face. For the closely related C_2 acetylide ligand, although the syntheses of many transition metal acetylide clusters have been reported in the literature,[5] no paper has ever focused on the subject of site selectivity and solution fluxionality. We now report the structural and NMR studies of a series of acetylide complexes, which permit an analysis of the solution dynamics of the acetylide ligand.

* Author to whom correspondence should be addressed.
† Author to whom enquiries concerning the X-ray crystallographic work should be addressed.

$LWM_2(CO)_8(\mu_3\text{-}\eta^2\text{-}C{\equiv}CPh)$	M	L	Yield
(1)	Os	C_5H_5	9%
(2)	Os	C_5Me_5	2%
(3)	Ru	C_5H_5	50%
(4)	Ru	C_5Me_5	57%

Treatment of $LW(CO)_3C{\equiv}CPh$[6] with the substance $Os_3(CO)_{10}(CH_3CN)_2$ in refluxing toluene (110°C, 30 min) provided, in addition to a red tetranuclear complex $LWOs_3(CO)_{11}(C{\equiv}CPh)$,[7] a pale yellow trinuclear complex (L = C_5H_5, **1**; L = C_5Me_5, **2**)* in low yield. The $^{13}C\text{-}\{^1H\}$ NMR spectrum of **1** showed two signals at δ 137.5 and 73.8, reminiscent of those reported for the two acetylide carbon nuclei (δ 172.9 and 112.7) in the analogous $CpWFe_2(CO)_8(C{\equiv}CTol)$.[8] The latter is a mixed-metal cluster in which the acetylide ligand functions as a five-electron donor, σ-bonded to the tungsten atom, while employing its two orthogonal alkyne π-bonds to bridge the unique Fe—Fe edge. However, since the colour, as well as the IR spectra of these osmium complexes in the region of CO absorption are substantially different from the complex of iron triads, an X-ray diffraction study was carried out on **1**.†

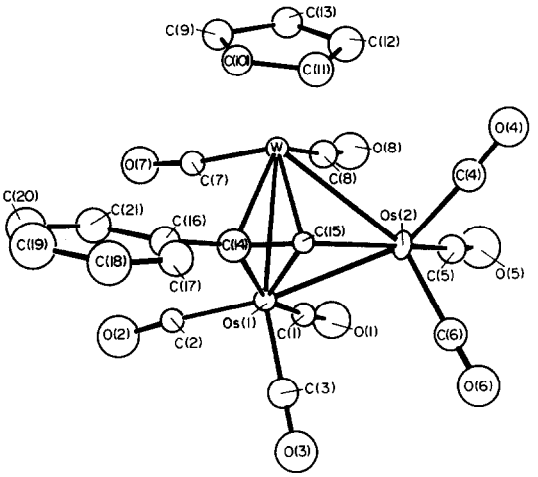

Fig. 1. The ORTEP diagram of **1**. Bond lengths (Å): W—Os(1), 2.8294(19); W—Os(2), 2.9160(18); Os(1)—Os(2), 2.8114(18); W—C(15), 2.20(3); Os(1)—C(15), 2.16(3); Os(2)—C(15), 1.96(3); Os(1)—C(14), 2.17(4); W—C(14), 2.36(4); C(14)—C(15), 1.23(5); C(16)—C(14), 1.47(5). Bond angles (°): Os(2)—C(15)—C(14), 159(3); C(15)—C(14)—C(16), 148(4).

The molecular structure of **1** is shown in Fig. 1, together with some important bond parameters. The molecule has a triangular WOs_2 core structure in which the tungsten atom is coordinated to a Cp ring and two CO ligands, while each of the osmium atoms is linked to three, mutually orthogonal, terminal CO ligands. The most important feature is the orientation of the phenyl acetylide moiety, which is σ-bonded to an osmium atom and at the same time forms a transverse bridge across the second W—Os bond. Therefore, the structure of **1** is related to $CpWFe_2(CO)_8(C{\equiv}CTol)$ by a 120° rotation of the acetylide ligand.

In order to further study the preferred orientation of the acetylide ligand over the triangular face of the trinuclear mixed-metal complexes, we have carried out the syntheses and structural determination of the tungsten–diruthenium analogues. Complexes **3** and **4**‡ were similarly obtained in good yield using $Ru_3(CO)_{12}$ as reagent. Crystals of **3** suitable for X-ray structural determination were obtained by recrystallization from CH_2Cl_2–hexane at room temperature. The structure of **3** is shown in Fig. 2

* Selected spectroscopic data **1**: IR (C_6H_{12}) ν(CO) 2077(s), 2043(vs), 2005(vs), 1995(s), 1965(s), 1924(m); ^1H NMR (CD_2Cl_2, RT): δ 7.68 (d, 2H), 7.37 (t, 2H), 7.20 (t, 1H), 5.29 (s, 5H); $^{13}C\text{-}\{^1H\}$ NMR (CD_2Cl_2, RT): δ 208.3 (J_{W-C} = 165 Hz, W—CO), 204.1 (J_{W-C} = 157 Hz, W—CO), 179.4 (Os—CO), 137.5 (*C*CPh), 73.8 (C*C*Ph, J_{W-C} = 16 Hz). **2**: IR (C_6H_{12}) ν(CO) 2076(s), 2041(vs), 2004(vs), 1991(s), 1963(m), 1905(w); ^1H NMR ($CDCl_3$): δ 7.62 (d, 2H), 7.31 (t, 2H), 7.20 (t, 1H), 1.93 (s, 15H).

† Crystal data for **1**: $C_{21}H_{10}O_8W_1Os_2$, M = 1104.27, monoclinic, space group $P2_1/c$, a = 8.332(3), b = 14.543(4), c = 17.819(5) Å, β = 94.46(3)°, V = 2152.71 Å^3, Z = 4, D_c = 2.945 g cm^{-3}, F(000) = 1703.33, Nonius diffractometer with graphite-monochromated Mo-K_α radiation, λ = 0.70930 Å, μ(Mo-K_α) = 17.28 mm^{-1}. ψ scan absorption correction made, 3777 unique reflections were measured and 2980 reflections with $I > 2\sigma(I)$ were used in refinement. Refinement of 42 atoms and 145 parameters converged to R_F = 0.068 and R_w = 0.090, G.O.F. = 1.768.

‡ Selected spectroscopic data. **3**: IR (C_6H_{12}) ν(CO) 2076(s), 2069(m), 2044(vs), 2033(vs), 2010(vs), 2003(m), 1994(m), 1975(m), 1966(w), 1952(vw), 1930(vw), 1918(vw) cm^{-1}; ^1H NMR ($CDCl_3$, RT): δ7.64–7.24 (m, Ph), 5.56 (s, Cp, **3b**), 5.25 (s, Cp, **3a**); $^{13}C\text{-}\{^1H\}$ NMR (d_8-THF, RT): δ 210.8 (J_{W-C} = 160 Hz, W—CO, **3a**), 210.7 (J_{W-C} = 165 Hz, W—CO, **3a**), 207.6 (J_{W-C} = 169 Hz, W—CO, **3b**), 197.0 (Ru—CO, **3b**), 196.6 (Ru—CO, **3a**), 168.9 (*C*CPh, J_{W-C} = 139 Hz, **3b**), 168.6 (*C*CPh, **3a**), 98.3 (C*C*Ph, J_{W-C} = 22 Hz, **3b**), 85.6 (C*C*Ph, J_{W-C} = 21 Hz, **3a**). **4**: IR (C_6H_{12}) ν(CO) 2071(m), 2064(vs), 2038(s), 2024(vs), 2005(s), 2001(vs), 1986(m), 1970(w), 1965(w), 1955(w), 1936(vw), 1913(vw) cm^{-1}; ^1H NMR (CD_2Cl_2, 273 K): δ 7.65–7.27 (m, Ph), 2.30 (s, Me, **4b**), 1.93 (s, Me, **4a**); $^{13}C\text{-}\{^1H\}$ NMR (d_8-THF, 226 K): δ 218.5 (W—CO, **4a**), 217.3 (W—CO, **4a**), 214.5 (J_{W-C} = 169 Hz, W—CO, **4b**), 175.3 (*C*CPh, **4b**), 173.0 (*C*CPh, J_{W-C} = 141 Hz, **4a**), 100.1 (C*C*Ph, J_{W-C} = 23 Hz, **4b**), 90.2 (C*C*Ph, **4a**).

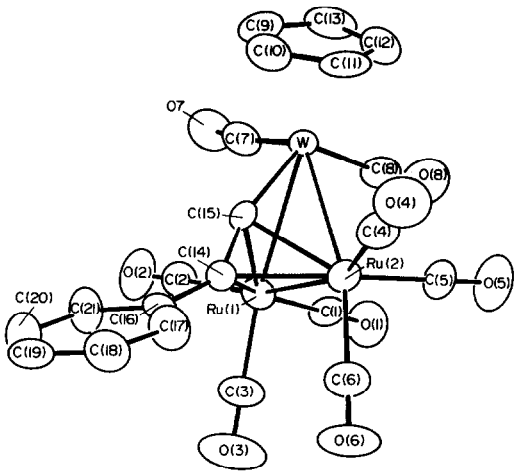

Fig. 2. The ORTEP diagram of **3**. Bond lengths (Å): W—Ru(1), 2.9976(10); W—Ru(2), 2.9651(10); Ru(1)—Ru(2), 2.6612(11); W—C(15), 1.976(8); Ru(1)—C(15), 2.128(8); Ru(2)—C(15), 2.195(7); Ru(1)—C(14), 2.297(8); Ru(2)—C(14), 2.188(8); C(14)—C(15), 1.314(11); C(16)—C(14), 1.470(11). Bond angles (°): W—C(15)—C(14), 162.5(6); C(15)—C(14)—C(16), 142.5(8).

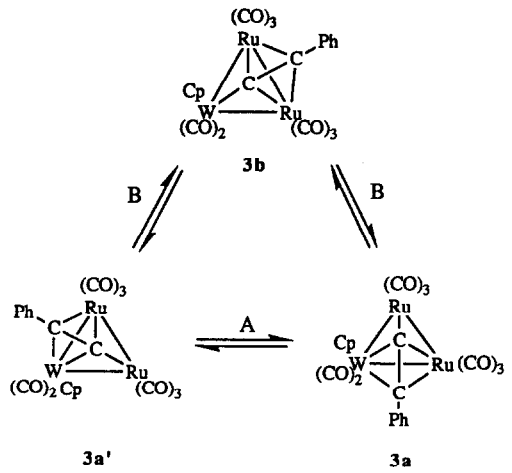

Scheme 1.

with selected structural parameters.* The WRu_2 triangle is near-isosceles and the phenyl acetylide moiety is now σ-bonded to the W atom and, quasi-symmetrically, π-bonded to the two ruthenium atoms. Therefore, we conclude that complex **3** is not isostructural with **1** but rather with the iron-containing complexes.

The solution dynamics of these WRu_2 complexes is of particular interest. Both the ^1H NMR and IR spectra in the region of CO absorption suggest the presence of two isomers. Based on the structural information, we proposed that the isomerization is due to a 360° rotation of the acetylide ligand over (**3a** : **3b** = 1 : 1.2) the WRu_2 triangle (Scheme 1). The assignment of each individual isomer is identified by its characteristic ^{13}C NMR data.

The ^{13}C NMR spectrum of **3** at 205 K exhibits three W—CO signals at δ 210.8, 210.5 and 207.3 in the ratio of 1 : 1 : 2.4. Therefore, the first two resonance lines are assigned to the "asymmetric" isomer (**3a**, acetylide C—C bond is orthogonal to the W—Ru bond) and the third one to the "symmetric" isomer (**3b**, acetylide C—C bond is orthogonal to the Ru—Ru bond). This assignment is not unreasonable because the free rotation of the $CpW(CO)_2$ unit in the asymmetric isomer would be expected to encounter the steric interaction of the phenyl group, whereas in isomer **3b** this process should have a smaller activation energy. Furthermore, five signals at δ 202.5, 200.8, 196.0, 194.2 and 192.4 with an intensity ratio of 1 : 1 : 1 : 1 : 2 can be assigned to the Ru—CO resonances of **3a** to support the assignment; the signal at δ 192.4 is double the intensity of the other four signals and therefore corresponds to two coincident signals.

The Ru—CO signals of **3b** were not observed in this spectrum. However, while the temperature was decreasing to 190 K, its W—CO signal broadened and collapsed, suggesting the slow-down of the $CpW(CO)_2$ rotation, and three very broad Ru—CO signals at δ 203, 198.5 and 189 appeared in the spectrum, consistent with the symmetric nature of **3b**, as suggested by the solid-state structural studies. Interpretation of the ^{13}C NMR data for **4** followed similar studies. From the relative intensities of the methyl signals in the ^1H NMR spectrum at room temperature, it is deduced that an isomer ratio **4a** : **4b** of 1 : 5.5 prevails.

The kinetic parameters of the acetylide ligand rotation have also been calculated from the data of the variable-temperature ^{13}C and ^1H NMR spectroscopies. The racemization process of **3a** consists of a simultaneous correlated rotation of the $CpW(CO)_2$ moiety around an axis through tungsten and a 120° rotation of the acetylide ligand over the tungsten atom (step A, **3a** ↔ **3a'**, Scheme 1). Therefore, the coalescence of the two W—CO resonances, as well as the coalescence of the six

* Crystal data for **3**: $C_{21}H_{10}O_8W_1Ru_2$, $M = 776.29$, monoclinic, space group $P2_1/n$, $a = 12.4756(13)$, $b = 13.216(4)$, $c = 13.395(4)$ Å, $\beta = 97.993(17)°$, $V = 2186.95$ Å^3, $Z = 4$, $D_c = 2.358$ g cm^{-3}, $F(000) = 1447.68$, Nonius diffractometer with graphite-monochromated Mo-K_α radiation, $\lambda = 0.70930$ Å, μ(Mo-K_α) = 6.74 mm^{-1}. ψ scan absorption correction made, 3840 unique reflections were measured and 2851 reflections with $I > 2\sigma(I)$ were used in refinement. Refinement of 42 atoms and 290 parameters converged to $R_F = 0.029$ and $R_w = 0.027$, G.O.F. = 1.583.

Ru—CO resonances in **3a**, would provide the appropriate kinetic data for step A. In fact, both the W—CO and the Ru—CO resonance lines have broadened and merged into single lines during the temperature rise to 300 K. A free energy of activation ($\Delta G^{\ddagger}$), calculated from the dynamic behaviour of the W—CO resonance lines, is estimated to be 62 kJ mol^{-1}.*

In contrast to the racemization of **3a**, isomerization between **3a** and **3b** is consistent with a 120° rotation from a W—Ru edge to the Ru—Ru edge (steps B, **3a** ↔ **3b** or **3a'** ↔ **3b**). Because only two Cp signals were observed in the ^1H NMR spectrum at 300 K, we conclude that the energy barrier of rotation of the $CpW(CO)_2$ unit is much too small to affect the energy barrier of steps B. The free energy of activation ($\Delta G^{\ddagger}$), calculated from the coalescence of the Cp signals, is 67 kJ mol^{-1} at 338 K, providing an estimate of the energy barrier of steps B.

Interestingly, the acetylide ligand of the WOs_2 complexes is static on the time scale of ^{13}C NMR spectroscopy. THe ^{13}C NMR spectrum of **1** at 295 K (d_8-toluene) exhibits two W—CO signals at δ 208.6 and 204.0, a sharp $Os(CO)_3$ line at δ 179.7, and two very broad Os—CO signals at δ 178.8 and 173.4. The exchange of the Os—CO resonances is not due to the rotation of the acetylide ligand, but to a localized $Os(CO)_3$ rotation around an axis through the two different osmium atoms. When the temperature is increased to 350 K, the sharp $Os(CO)_3$ signal remained unchanged and the broad Os—CO signals became a relatively sharp signal at δ 176.5, confirming that the racemization of **1** has not occurred at this temperature.

*The free energy of activation $\Delta G^{\ddagger}$ calculated from the ^{13}C NMR data recorded on d_8-toluene solution is 70 KJ mol^{-1}. This data suggests that the rotation of the acetylide ligand possibly involves a transition state in which the acetylide C—C bond is perpendicular to the WRu_2 triangle.

Acknowledgement—We thank the National Science Council of the Republic of China for generous financial support of this research.

REFERENCES

1. B. E. R. Schilling and R. Hoffmann, *J. Am. Chem. Soc.* 1979, **101**, 4687.
2. R. D. Edidan, J. R. Norton and K. Mislow, *Organometallics* 1982, **1**, 561.
3. L. Busetto, M. Green, B. Hesser, J. A. K. Howard, J. C. Jeffery and F. G. A. Stone, *J. Chem. Soc., Dalton Trans.* 1983, 519.
4. J. R. Shapley, J. T. Park, M. R. Churchill, C. Bueno and H. J. Wasserman, *J. Am. Chem. Soc.* 1981, **103**, 7385.
5. (a) A. J. Carty, *Pure Appl. Chem.* 1982, **54**, 113; (b) Z. Dawoodi, M. J. Mays and K. Henrick, *J. Chem. Soc., Dalton Trans.* 1984, 1769; (c) A. J. Deeming, S. Donovan-Mtunzi and K. Hardcastle, *J. Chem. Soc., Dalton Trans.* 1986, 543; (d) E. Boyar, A. J. Deeming and S. E. Kabir, *J. Chem. Soc., Chem. Commun.* 1986, 577; (e) S. Aime, D. Osella, A. J. Deeming, A. M. M. Lanfredi and A. Tiripicchio, *J. Organomet. Chem.* 1983, **244**, C47; (f) D. Nucciarone, S. A. MacLaughlin, N. J. Taylor and A. J. Carty, *Organometallics* 1988, **7**, 106; (g) A. Galindo, R. Mathieu, A.-M. Caminade and J.-P. Majoral, *Organometallics* 1988, **7**, 2198.
6. M. I. Bruce, M. G. Humphrey, J. G. Matisons, S. K. Roy and A. G. Swincer, *Aust. J. Chem.* 1984, **37**, 1955.
7. Y. Chi, C. H. Wu, S. M. Peng and G. H. Lee, *Organometallics*, in press.
8. M. Green, K. Marsden, I. D. Salter, F. G. A. Stone and P. Woodward, *J. Chem. Soc., Chem. Commun.* 1983, 446.

Polyhedron Vol. 8, No. 15, pp. 2007–2009, 1989
Printed in Great Britain

0277–5387/89 $3.00+.00
© 1989 Maxwell Pergamon Macmillan plc

COMMUNICATION

A COBALT(III)–COPPER(II) BINUCLEAR COMPLEX

BRIAN V. CROOK, HIDEO DOINE, FRANK F. STEPHENS, MARTHA J. CANNON and RODERICK D. CANNON*

School of Chemical Sciences, University of East Anglia, Norwich NR4 7TJ, U.K.

(*Received* 30 *January* 1989; *accepted* 11 *April* 1989)

Abstract—The mixed-metal macrocyclic complex $[Co^{III}Cu^{II}LCl_3]$, where L is the 2:2 condensation product of 2,6-diformyl-4-methyl phenol and 1,3-diaminopropane, has been prepared and characterized spectroscopically and electrochemically. Cyclic voltammetry (in DMF) indicates reversible reduction at the copper(II) centre and a relatively slow intramolecular copper(I) to cobalt(III) electron transfer.

Mixed-metal complexes are important in studies of magnetic and electronic coupling.[1] Complexes of the type $[MM'L]^{2+}$, where M and M′ are divalent metals and L is the binucleating ligand shown in Fig. 1, have been extensively used in such work. Our interest is in the electron-transfer behaviour of the complexes containing potentially oxidizing and reducing metal centres in the same molecule. Here we report the first example of a mixed-metal complex of this class containing a trivalent metal, namely $[Co^{III}Cu^{II}CuLCl_3]$.

First, the complex $[Co^{II}Cu^{II}L]^{2+}$ was generated, by two routes. (1) Following the previous template syntheses of homobinuclear complexes,[2] the organic components $CH_3C_6H_2(OH)(CHO)_2$ (**I**) and 1,3-diaminopropane (**II**) were reacted in the presence of equimolar quantities of $CoCl_2$ and $CuCl_2$, and the mixture of CoCo, CoCu and CuCu complexes was separated by fractional crystallization. (2) Following Okawa and Kida,[3,4] the mononuclear complex $[CH_2(CH_2N:CHC_6H_2(CH_3)(CHO)O)_2Co]$ was obtained from **I**, **II** and $CoCl_2$, then successively reacted with $CuCl_2$ and with **II**. Both products analysed well as $CoCuLCl_2 \cdot H_2O$, and their identity was confirmed by IR and UV spectra. A useful feature is the narrow band which occurs at 372 and 356 cm^{-1} in CoCo and CuCu complexes, and at 365 cm^{-1} in the CoCu complex (molar extinction coefficients $\varepsilon_{max} = 10.7$, 12.1 and 15.9×10^3 M^{-1} cm^{-1}). The mixed-metal spectrum is not an average of the two homonuclear spectra (Fig. 2).

Spectrophotometric titration of the homonuclear cobalt complex, $[CoCoL]^{2+}$, with bromine, indicated successive oxidation to $Co^{III}Co^{II}$ and $Co^{III}Co^{III}$ species. A similar titration of the mixed complex $[CoCuL]^{2+}$ proceeded in one stage to $Co^{III}Cu^{II}$. Controlled oxidation of $[CoCuL]^{2+}$ with chlorine in methanol, yielded the new complex $[CoCuLCl_3]$, a brown solid. Composition was determined by total elemental analysis (nitrogen by Kjeldahl method, cobalt and copper by atomic absorption) and the oxidation state of cobalt(III) was confirmed

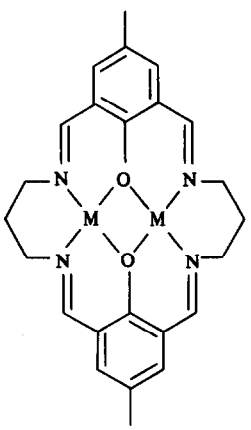

Fig. 1. Structural unit of complexes $[MM'L]^{n+}$.

* Author to whom correspondence should be addressed.

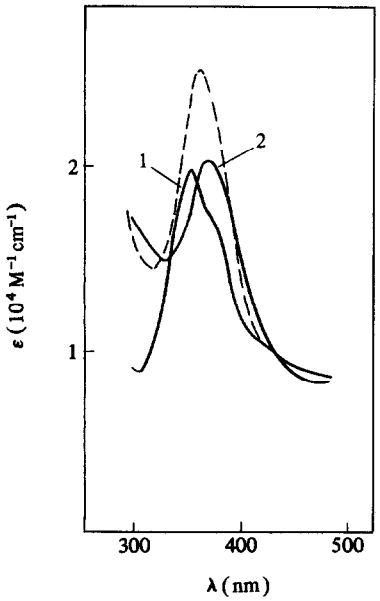

Fig. 2. Near-UV absorption spectra of complexes $[MM'L]^{2+}$. Full-line spectra: **1**, MM′ = CuCu; **2**, CoCo. Broken line, MM′ = CuCo. Chloride salts in methanol, 2.2×10^{-5} M.

by reaction with Fe^{2+} and back-titration. Analysis and Ir spectra showed that there are no solvent molecules of crystallization. The visible band at 675 nm (Fig. 3) is consistent with a *d–d* transition of the $Co^{III}O_2N_2Cl_2$ chromophore (cf. *trans*-$[Co(en)_2Cl_2]^+$, 618 nm[5]).

In agreement with previous reports,[2c,4,6] cyclic voltammetry of the dicopper complex, $[Cu_2L]^{2+}$, showed two nearly reversible one-electron redox processes, assigned as $Cu^{II}Cu^{II}/Cu^{II}Cu^{I}$ and $Cu^{II}Cu^{I}/Cu^{I}Cu^{I}$. The homovalent dicobalt complex $[Co_2L]^{2+}$ gave three waves. One at $E_{mid} = -1.04$ V is assigned as cobalt reduction, $Co^{II}Co^{II}/Co^{II}Co^{I}$, by comparison with the reported potential for [Co^{II}(salen)], $E^{\theta} = -1.19$ V.†[7] The two overlapping waves at 0.41 and 0.52 V are assigned as $Co^{III}Co^{II}/Co^{II}Co^{II}$ and $Co^{III}Co^{III}/Co^{III}Co^{II}$, respectively. The mixed-metal complex $[Co^{II}Cu^{II}L]^{2+}$ showed a reversible wave corresponding to the one-electron process Cu^{II}/Cu^{I}, at $E_{mid} = -0.625$ V, and in addition, a very broad oxidation wave, *ca* +0.4 V, which we assign to a highly irreversible couple Co^{III}/Co^{II} [Fig. 4(a)]. The absence of an oxidation wave corresponding to Co^{II}/Co^{I} may imply a rapid internal electron transfer process, $Co^{II}Cu^{II} + e^- \rightarrow Co^{I}Cu^{II} \rightarrow Co^{II}Cu^{I}$.

For the oxidized mixed-metal complex [$Co^{III}Cu^{II}LCl_3$], a typical voltammogram is shown in Fig. 4(b). In contrast to the Co^{II} Cu^{II} complex, the Cu^{II}/Cu^{I} wave varies with scan rate, from highly irreversible, with a reduction wave only, at the slowest scan, to a nearly symmetrical, quasi-reversible wave at rapid scan, with $E_{mid} = -0.625$ V. At the fastest scan rates only, the irreversible oxidation of the Co^{III}/Co^{II} couple appears. These observations are consistent with a mechanism in which the electron is initially accepted at the copper centre, but is transferred to the cobalt at a relatively rapid rate:

$$Co^{III}Cu^{II} + e^- \longrightarrow Co^{III}Cu^{I} \quad (1)$$

$$Co^{III}Cu^{I} \xrightarrow{k_{et}} Co^{II}Cu^{II}. \quad (2)$$

The alternative initial step in which the electron is accepted at the cobalt centre apparently does not occur in spite of the fact that the cobalt centre is thermodynamically more oxidizing than the copper

† All quoted potentials are relative to $E^{\theta}(Fe(C_5H_5)_2^{+/0}) = 0.400$ V.

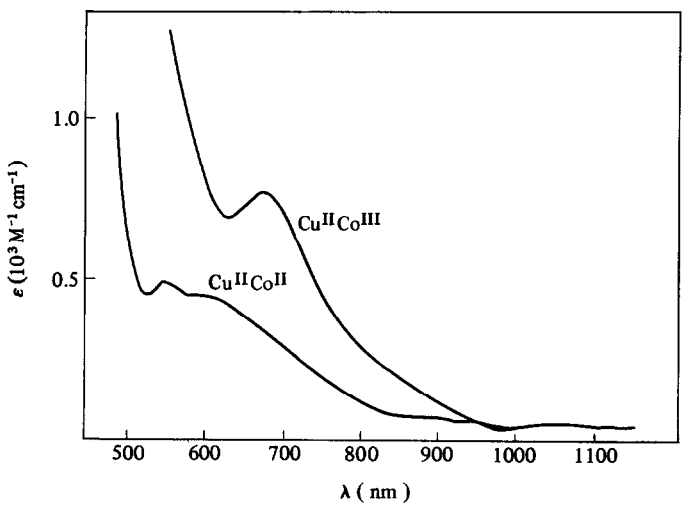

Fig. 3. Visible spectra of $[Co^{II}Cu^{II}L]Cl_2$ and $[Co^{III}Cu^{II}LCl_3]$, in methanol, 5.6×10^{-4} M.

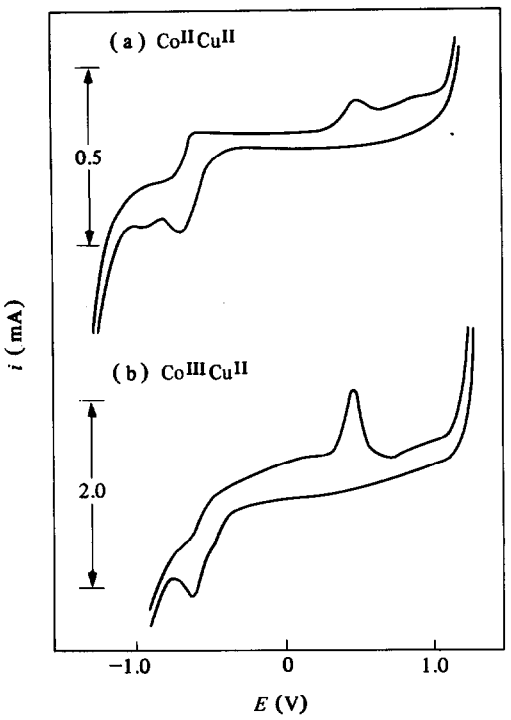

Fig. 4. Cyclic voltammograms of $[Cu^{II}Co^{II}L]^{2+}$ (2.6×10^{-3} M, scan rate 100 mV s^{-1}) and $[Cu^{II}Co^{II}LCl_3]$ (1.8×10^{-3} M, scan rate 50 mV s^{-1}). Both in DMF, 1.0 M $[n\text{-}Bu_4N]BF_4$, 20°C, under N_2 atmosphere. Voltage scale is relative to $E^{\theta}(Fe(C_5H_5)^{2+/0}) = 0.400$ V under the same conditions.

(compare for example the E^{θ} values, $Co^{II}Cu^{II}/Co^{II}Cu^{I}$ and $Co^{III}Co^{II}/Co^{II}Co^{II}$, -0.625 and $+0.61$ V, respectively). Evidently in this complex, as in other complexes of the Schiff base type, the Co^{III}/Co^{II} couple is less reversible than the Cu^{II}/Cu^{I} couple. Following arguments of Nicholson and Shain,[8] the change of the latter couple, from irreversible to reversible, with cycle time, leads to a value of the order 0.5 s^{-1} for k_{et}, the rate constant of the intramolecular electron-transfer reaction (2).

Acknowledgements—We thank the Science and Engineering Research Council, the Royal Society and the Japanese Ministry of Education for financial support.

REFERENCES

1. R. D. Willett, D. Gatteschi and O. Khan (Eds), *Magneto-structural Correlations in Exchange-coupled Systems* (Proc. NATO-ASI). D. Reidel, Dordrecht (1983).
2. (a) N. H. Pilkington and R. Robson, *Aust. J. Chem.* 1970, **23**, 2225; (b) B. F. Hoskins, R. Robson and G. A. Williams, *Inorg. Chim. Acta* 1976, **16**, 121; (c) R. R. Gagné, C. A. Koval, T. G. Smith and M. C. Cimolino, *J. Am. Chem. Soc.* 1979, **101**, 4572; (d) S. L. Lambert and D. N. Hendrickson, *Inorg. Chem.* 1979, **18**, 2683; (e) C. L. Spiro, S. L. Lambert, T. J. Smith, E. N. Duesler, R. R. Gagné and D. N. Hendrickson, *Inorg. Chem.* 1981, **20**, 1229.
3. A. Okawa and S. Kida, *Bull. Chem. Soc. Jpn* 1972, **45**, 1759.
4. (a) R. R. Gagné and C. L. Spiro, *J. Am. Chem. Soc.* 1980, **102**, 1443; (b) R. R. Gagné, C. L. Spiro, T. J. Smith, C. A. Hamann, W. R. Thies and A. K. Shiemke, *J. Am. Chem. Soc.* 1981, **103**, 4073.
5. C. K. Jørgensen, *Absorption Spectra and Chemical Bonding in Complexes*, p. 293. Pergamon Press, Oxford (1962).
6. S. K. Mandal and K. Nag, *J. Chem. Soc., Dalton Trans.* 1983, 2429.
7. D. F. Rohrbach, W. R. Heineman and E. Deutsch, *Inorg. Chem.* 1979, **18**, 2536.
8. R. S. Nicholson and I. Shain, *Analyt. Chem.* 1964, **36**, 706.

Polyhedron Vol. 8, No. 15, p. 2011, 1989
Maxwell Pergamon Macmillan plc. Printed in Great Britain

BOOK REVIEW

Gmelin Handbook of Inorganic Chemistry—Boron—3rd Supplement. Vol. 4. G. Heller, A. Meller, T. Onak. Boron and Cl, Br, I, S, Se, Te, carboranes. Edited by K.-Ch. Buschbeck and K. Niedenzk. Springer, Berlin, 1988. ISBN 3-540-93567-3, 19 figs. xviii, 256pp.

The volume of 256 pages concludes the third supplement issue on boron compounds, and covers the compounds with Cl, Br, I, S, Se, Te and Po. The final chapter of just over 100 pages deals with carboranes and some of their metalla-derivatives, with a useful listing of carborane-containing polymers. The references cover the literature up to the end of 1984.

The first section deals with the boron–chlorine system, starting with some properties of the transient species BCl and the BCl_2 radical, before considering BCl_3. The chemical behaviour of BCl includes sections on chemical vapour deposition of materials (B, BN, metal borides) using BCl_3, dry etching processes, various adducts, substituted derivatives R_xBCl_{3-x} (R = H, organyl, alkyl, aryl, etc; $x = 1, 2$), $Cl_xB(NR_2)_{3-x}$, ClBO, and various heterocyclic compounds. The description of the boron–bromine and –iodine compounds follows a similar pattern, and these three sections account for the first 100 pages of this volume.

The next 50 pages are concerned with compounds with S, Se, Te and Po, although only six pages are devoted to the Se, Te and Po compounds. The comprehensive section on B—S derivatives includes an initial discussion of the interesting B_8S_{16} and $[B_{10}S_{18}]^{6-}$ ion, and the little-investigated thioborates. This is followed by a discussion of species containing H or an organic moiety $[R_xB(SR)_{3-x}$, $x = 0, 1, 2]$; B—S heterocycles, compounds with B—S—O and B—S—N bonds, together with various derivatives of these systems, including heterocyclic compounds.

The last major section is devoted to the carboranes and metalla-carboranes, and deals with the compounds containing from one up to 42 boron atoms. While the maximum number of boron atoms in a single cage is 11, as in $1\text{-}CB_{11}H_{11}\text{-}1\text{-}Me_2NH$, there are several examples of compounds containing cages linked together. Thus, in the carborane containing 20 boron atoms, $(1,2\text{-}C_2B_{10}H_{11}\text{-}9\text{-}S\text{-})_2CH_2$, two carborane icosahedra are linked by a —S—CH_2—S— group. The presentation contains useful tables of NMR data, and synthetic reagents used to prepare the carboranes, in conjunction with the appropriate references.

Since only three authors are involved (G. Heller, A. Meller and T. Onak), there is a good continuity of style in the volume, and each article is well written. The volume as whole continues the high standard set by its predecessors, and will serve as an invaluable source book, both to those already working in the area, and to those who require a convenient source of references as an introduction to the topics discussed.

Department of Chemistry **M. G. H. WALLBRIDGE**
University of Warwick
Coventry CV4 7AL, U.K.

Polyhedron Vol. 8, No. 16, pp. 2013–2016, 1989
Printed in Great Britain

0277–5387/89 $3.00+.00
© 1989 Maxwell Pergamon Macmillan plc

REACTION BETWEEN THE $[MgCl_4]^{2-}$ ANION AND TITANIUM CHLORIDES. THE CRYSTAL STRUCTURE OF $[NBu_4][trans\text{-}TiCl_4(THF)_2]\cdot THF$*

PIOTR SOBOTA,† MUHI O. MUSTAFA and TADEUSZ LIS

Institute of Chemistry, University of Wrocław, 14 Joliot-Curie Str., 50-383 Wrocław, Poland

(*Received* 23 *November* 1988; *accepted* 10 *March* 1989)

Abstract—The reaction between $[TiCl_4(THF)_2]$ and $[NBu_4]_2[MgCl_4]$ in tetrahydrofuran (THF) gave the compound $[NBu_4]_2[TiCl_6]$ (**I**). Under the influence of light in THF solution, the compound undergoes reduction to $[NBu_4][trans\text{-}TiCl_4(THF)_2]\cdot THF$ (**II**). Compound **II** was also obtained by the direct reaction between $[TiCl_3(THF)_3]$ and $[MgCl_4]^{2-}$ ions. Crystals of **II** are orthorhombic, space group $P2_12_12_1$ with $a = 12.18(1)$, $b = 17.09(1)$ and $c = 18.57(2)$ Å; $Z = 4$. The structure was refined by full-matrix least-squares methods to $R = 0.064$ for 1569 independent non-zero reflections.

Reactions between $MgCl_2$ and $TiCl_4$ in THF, depending on molar ratio, produce the following compounds:[1,2] $[Mg(THF)_6][TiCl_5(THF)]_2$, $[(THF)_4Mg(\mu\text{-}Cl)_2TiCl_4]$ and $[Mg_2(\mu\text{-}Cl)_3(THF)_6][TiCl_5(THF)]$. These compounds are used in the ethylene polymerization process.[3] However, $MgCl_2$ and $TiCl_3$ in THF do not react mutually, because, in the simplest sense, the acid–base properties of $MgCl_2$ and $TiCl_3$ are similar. Instead, $MgCl_2$ on reaction with $[NBu_4][BF_4]$ yields $[MgCl_4]^{2-}$ and $[MgCl(THF)_5]^+$ ions:[4,5]

$$3[MgCl_2(THF)_2] + 2[NBu_4][BF_4] \xrightarrow{THF} [NBu_4]_2[MgCl_4]\cdot 2THF + 2[MgCl(THF)_5][BF_4]. \quad (1)$$

The reactivity of the $[MgCl_4]^{2-}$ anion was unknown until now. It was expected that $[MgCl_4]^{2-}$ and $TiCl_4$ or $TiCl_3$ would react mutually to produce new products which should bear useful relations between the structure and mechanism involved in some Ziegler–Natta polymerization systems.

EXPERIMENTAL

All reactions were carried out under N_2 using dried solvents and Schlenk-tube techniques. $[TiCl_4(THF)_2]$, $[TiCl_3(THF)_3]$ and $[NBu_4]_2[MgCl_4]\cdot 2THF$ were obtained by literature methods.[4,6] The crystalline $[NBu_4]_2[MgCl_4]\cdot 2THF$ under vacuum, liberates two THF molecules from the crystal lattice and yields $[NBu_4]_2[MgCl_4]$. Microanalyses were performed at the University of Wrocław. ESR spectra were obtained on a Varian E9 spectrometer and solid-state magnetic moments were determined by the Gouy method. IR spectra were obtained using a Perkin–Elmer 180 spectrometer.

*Bis(tetra-*n*-butylammonium)hexachlorotitanate*(IV) (**I**)

$[TiCl_4(THF)_2]$ (1.5 g, 4.5 mmol) and $[NBu_4]_2[MgCl_4]$ (1.8 g, 2.76 mmol) were dissolved separately in 30 and 40 cm^3 of THF, respectively. The solutions were mixed and the stirring was continued until the compounds dissolved. The solution was filtered off and the volume was reduced *in vacuo* to *ca* 20 cm^3. After 24 h, the yellow compound was filtered off, washed with *n*-pentane (3 × 10 cm^3) and dried *in vacuo*. Yield *ca* 1.9 g; 57%. Found: N, 3.7; Cl, 31.1; Ti, 6.6. $C_{32}H_{72}N_2Cl_6Ti$ requires N, 3.8; Cl, 28.5; Ti, 6.4%. Density 1.28 g cm^{-3}.

*Tetra-*n*-butylammonium tetrachlorobis(tetrahydrofuran)titanate*(III) *tetrahydrofuran* (**II**)

(a) $[NBu_4]_2[TiCl_6]$ (1.5 g, 2 mmol) was dissolved in 50 cm^3 of THF and during slow diffusion of *n*-pentane, yellow crystals appeared. The yellow crys-

* Tetra-*n*-butylammonium tetrachlorobis(tetrahydrofuran)titanate(III) tetrahydrofuran.

† Author to whom correspondence should be addressed.

tals, in the same solution, under the influence of light (near a window), very slowly (1 month) changed colour to blue and simultaneously a white $[NBu_4][Cl]$ salt precipitated. The compound was separated mechanically. The blue crystals were identified by X-ray crystallography as the ionic salt $[NBu_4][trans\text{-}TiCl_4(THF)_2]\cdot THF$. The formation of $[NBu_4][Cl]$ was proved by elementary analysis.

(b) $[TiCl_3(THF)_3]$ (3.2 g, 8.7 mmol) and $[NBu_4]_2[MgCl_4]$ (3.4 g, 5.2 mmol) were suspended in 75 and 65 cm^3 of THF, respectively, and stirred until the solution became light-blue. The solution was filtered off and its volume was reduced to 25 cm^3 and this was left in a refrigerator until crystallization occurred. After 12 h, the crystals were filtered off, washed with THF (2×5 cm^3) and dried *in vacuo*. Yield 3.1 g; 55%. Found: N, 2.3; Cl, 23.5; Ti, 6.7. Calc. for $C_{28}H_{60}Cl_4NO_3Ti$: N, 2.2; Cl, 21.9; Ti, 7.4%.

The good quality, multi-faced crystals for X-ray examination were taken directly from the post-reaction mixture obtained by method (a). The same crystals may be obtained by slow diffusion of *n*-pentane into the compound obtained by method (b) dissolved in THF. The density was measured by flotation in a mixture of $n\text{-}C_4H_9Cl$ and 1,1-dichloroethane. Crystal data. $[N(C_4H_9)_4]^+[(C_4H_8O)_2Cl_4Ti]^-\cdot C_4H_8O$; $M = 648.5$, orthorhombic, $a = 12.18(1)$, $b = 17.09(1)$, $c = 18.57(2)$ Å; $U = 3865(6)$ Å^3, $Z = 4$, $D_c = 1.114(2)$ g cm^{-3}, $D_m = 1.084$ g cm^{-3}, space group $P2_12_12_1$, Mo-K_α radiation $\lambda = 0.71069$ Å, $\mu = 5.3$ cm^{-1}.

A specimen, $0.8\times0.7\times0.6$ mm, was cut from a large crystal and sealed in a capillary. A Syntex $P2_1$ diffractometer, Mo-K_α radiation and a graphite monochromator were used for lattice parameters and intensity measurements at $T = 300(2)$ K. Intensities were measured by the 2θ–ω scan technique up to $2\theta = 48°$. From 3425 measured reflections, 1569 with $I > 3\sigma(I)$ were used for structure determination. The structure was solved by the heavy-atom method and refined using SHELX-76.[7] The thermal parameters of the atoms in the non-bonded THF molecules and some of the carbon atoms in the $[NBu_4]^+$ cations were very high and some of the interatomic distances were rather unrealistic. For that reason, calculations were continued with constraints for non-bonded THF molecules and methyl carbon atoms of the $[NBu_4]^+$ cations. All methylene hydrogen atoms were introduced in calculated positions with d(C—H) = 1.08 Å and were not refined. The refinement was completed by using anisotropic thermal parameters for all non-hydrogen atoms and gave final $R = 0.064$ and $R_w = 0.058$ (the refinement of the parameters for the inverted structure gave $R = 0.065$ and $R_w = 0.059$). Residual electron density in the final difference Fourier map was within -0.25 and 0.25 e Å^{-3}. Attempts to measure data at liquid nitrogen temperature failed because the crystal probably undergoes a phase transition.

Atomic coordinates, displacement factor coefficients and a list of F_o/F_c values have been deposited as supplementary data with the Editor, from whom copies are available on request. Atomic coordinates have also been deposited with the Cambridge Crystallographic Data Centre.

RESULTS AND DISCUSSION

The addition of the $[NBu_4]_2[MgCl_4]$ salt to $[TiCl_4(THF)_2]$ (1:1 molar ratio) in THF, gave a yellow precipitate of $[NBu_4]_2[TiCl_6]$ (I):

$$[TiCl_4(THF)_2]+[NBu_4]_2[MgCl_4]\longrightarrow [NBu_4]_2[TiCl_6]+[MgCl_2(THF)_2]. \quad (2)$$
(I)

The IR spectrum of compound I presents the ν(Ti—Cl) stretching mode at 385 cm^{-1}, which is typical for $[TiCl_6]^{2-}$ anions e.g. in M_2TiCl_6 (M = K, Rb or Cs).[8]

The yellow crystals in THF solution in light under N_2, slowly (1 month) changed their colour from yellow to blue, and simultaneously a white $[NBu_4][Cl]$ salt precipitated:

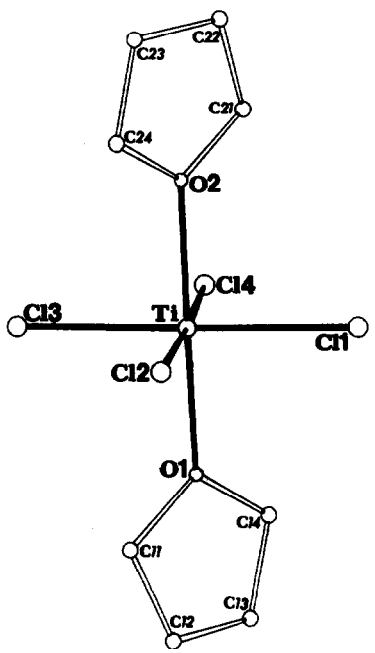

Fig. 1. The overall view of the $[trans\text{-}TiCl_4(THF)_2]^-$ anion.

Table 1. Principal bond lengths (Å) and angles (°) in the [*trans*-$TiCl_4(THF)_2$]$^-$ anion

Bond lengths			
Ti—Cl(1)	2.387(5)	Ti—Cl(2)	2.408(4)
Ti—Cl(3)	2.392(5)	Ti—Cl(4)	2.392(4)
Ti—O(1)	2.083(10)	Ti—O(2)	2.115(10)
Interbond angles			
Cl(1)—Ti—Cl(2)	91.2(2)	Cl(1)—Ti—Cl(3)	178.8(2)
Cl(1)—Ti—Cl(4)	91.7(2)	Cl(2)—Ti—Cl(3)	89.8(2)
Cl(2)—Ti—Cl(4)	177.1(2)	Cl(3)—Ti—Cl(4)	87.3(2)
Cl(1)—Ti—O(1)	89.5(3)	Cl(1)—Ti—O(2)	90.0(3)
Cl(2)—Ti—O(1)	90.8(3)	Cl(2)—Ti—O(2)	88.8(3)
Cl(3)—Ti—O(1)	91.2(3)	Cl(3)—Ti—O(2)	89.3(3)
Cl(4)—Ti—O(1)	89.0(3)	Cl(4)—Ti—O(2)	91.5(3)
O(1)—Ti—O(2)	179.3(4)		

$$[NBu_4]_2[TiCl_6] \xrightarrow[THF]{h\nu} [NBu_4][\textit{trans}\text{-}TiCl_4(THF)_2]\cdot THF \quad \textbf{(II)} + [NBu_4][Cl] + 1/2HCl + C_4H_7OCl. \quad (3)$$

Blue $[NBu_4][\textit{trans}\text{-}TiCl_4(THF)_2]\cdot THF$ **(II)** is also formed in the direct reaction between $[TiCl_3(THF)_3]$ and $[MgCl_4]^{2-}$ ions:

$$2[TiCl_3(THF)_3] + [NBu_4]_2[MgCl_4] \longrightarrow 2[NBu_4][\textit{trans}\text{-}TiCl_4(THF)_2]\cdot THF \quad \textbf{(II)} + [MgCl_2(THF)_2]. \quad (4)$$

Compound **II** is paramagnetic, with $\mu_{eff} = 1.6$ at room temperature. The ESR spectra in the solid state and in CH_2Cl_2 are broad and typical for Ti^{3+}. In $[NBu_4][\textit{trans}\text{-}TiCl_4(THF)_2]\cdot THF$, the titanium atom exists as Ti^{3+}, and the reduction of Ti^{4+} (in **I**) to Ti^{3+} (in **II**) is caused by the influence of light in THF. The post-reaction mixture revealed (MS–GL) the presence of HCl and C_4H_7OCl. The mechanism of these reactions has not yet been explained.

The geometry of the [*trans*-$TiCl_4(THF)_2$]$^-$ anion is presented in Fig. 1. Selected bond lengths and angles are summarized in Table 1. The titanium atom is six-coordinate with four square-planar chlorine atoms and two *trans*-THF molecules.

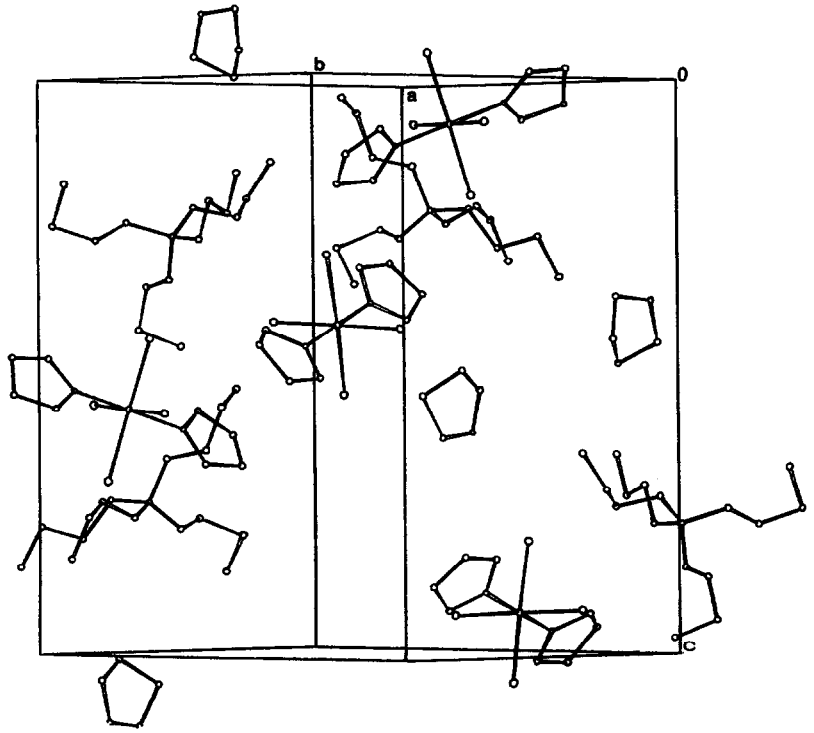

Fig. 2. The packing of the $[NBu_4][\textit{trans}\text{-}TiCl_4(THF)_2]\cdot THF$ crystal. The hydrogen atoms are omitted for clarity.

The $TiCl_4O_2$ unit forms a distorted octahedron. The average Ti—Cl and Ti—O bond lengths are equal, 2.395(9) and 2.10(1) Å, and are similar to 2.352(3) and 2.118(7) Å in $[TiCl_3(THF)_3]$.[10] The structure of [*trans*-$TiCl_4(THF)_2$]$^-$ is similar to that of the [*trans*-$MoCl_4(THF)_2$]$^-$ anion.[11] The parameters presented for the coordinated THF are close to those in $[TiCl_3(THF)_3]$ and the [*trans*-$TiCl_2(THF)_4$]$^+$ cation.[9] The $[NBu_4]^+$ cation has the *cis*-carbon-chain configuration and differs from the *trans* conformation observed earlier[4,12] (see Fig. 2).

The $[MgCl_4]^{2-}$ anion was shown to react easily with $TiCl_4$ and $TiCl_3$, to form the anions $[TiCl_6]^{2-}$ and [*trans*-$TiCl_4(THF)_2$]$^-$, respectively. In our opinion, $MgCl_2$ as a support could react directly with $TiCl_4$ to form the ionic or molecular compounds presented at the beginning of the paper, or undergo ionization under the influence of polar solvents (THF, esters, etc.) to form $[Mg(solvent)_6]^{2+}$, $[MgCl(solvent)_5]^+$ cations and $[MgCl_4]^{2-}$ anions, which would react further with titanium compounds to form the pre-catalyst.

REFERENCES

1. P. Sobota, J. Utko and T. Lis, *J. Chem. Soc., Dalton Trans.* 1984, 2077.
2. P. Sobota and Z. Janas, *J. Organomet. Chem.* 1984, **276**, 171.
3. F. J. Karol, *Catal. Rev. Sci. Engng* 1984, **26**, 557; US Pat 4 302 567 or 4 302 566.
4. P. Sobota, T. Płuziński and T. Lis, *Bull. Pol. Acad. Sci. Chem.* 1985, **33**, 491.
5. P. Sobota, T. Płuziński, J. Utko and T. Lis, *Inorg. Chem.*, in press.
6. L. E. Mazner, *Inorg. Synth.* 1982, **21**, 135; K. H. Thiele and W. Schafer, *Z. Anorg. Allg. Chem.* 1971, **381**, 205.
7. G. M. Sheldrick, SHELX-76, Program for crystal structure determination. University of Cambridge, U.K. (1976).
8. J. A. Bland and S. N. Flengas, *Can. J. Phys.* 1961, **39**, 941.
9. K. Folting, J. C. Huffman, R. L. Bansemer and K. G. Caulton, *Inorg. Chem.* 1984, **23**, 3289.
10. M. Handlovic, D. Miklos and M. Zikmund, *Acta Cryst.* 1981, **B37**, 811.
11. A. Hills and G. J. Leigh, *J. Chem. Soc., Dalton Trans.* 1985, 1069.
12. M. R. Snow and J. A. Ibers, *Inorg. Chem.* 1973, **12**, 249.

Polyhedron Vol. 8, No. 16, pp. 2017–2022, 1989
Printed in Great Britain

0277–5387/89 $3.00 + .00
© 1989 Maxwell Pergamon Macmillan plc

EQUILIBRIA IN AQUEOUS SOLUTION BETWEEN BERYLLIUM(II) AND D,L-ASPARTIC ACID AND D,L-METHIONINE

A. MEDEROS,* E. MEDINA and J. J. ALVAREZ COLOMER

Departamento de Química Inorgánica, Universidad de La Laguna, Tenerife, Canary Islands, Spain

and

F. BRITO

Laboratorio de Equilibrios en Solución, Escuela de Química, Facultad de Ciencias, Universidad Central de Venezuela, Caracas, Venezuela

(*Received* 6 *December* 1988; *accepted* 10 *March* 1989)

Abstract—The complex species formed in aqueous solution between beryllium(II) and D,L-aspartic acid (ASP) and D,L-methionine (MET) were studied at 25°C and 0.5 M ionic strength in $NaClO_4$. The application of the least-squares computer program LETAGROP to the experimental potentiometric data, taking into account hydrolysis of the beryllium(II) ion, upon varying the ligand–metal ratios 4 : 1, 1 : 1 and 1 : 2, at beryllium(II) concentrations of 1, 3 and 6 mM, indicates that only the dihydroxide complexes ($[Be(OH)_2L']^{2-}$ for ASP, H_2L' ligand; $[Be(OH)_2L]^-$ for MET, HL ligand) are formed in significant amounts. The complex species begins to form at pH > 5.5. The formation constants β_{pqr} were determined.

Beryllium(II) is perhaps the most toxic of metallic cations.[1] The most dangerous mode of entry into the body is by the respiratory tract, and the effects are predominantly pulmonary.[2] Animal experiments and blood investigations on beryllium-exposed persons support the supposition that beryllium is bound to a protein as a hapten to form beryllium–protein complexes. *In vitro*, the beryllium ion inhibits numerous enzymes which are competitive towards magnesium or potassium and non-competitive in the form of beryllium binding to the enzymes. Chelating agents for the removal of deposited tissue beryllium have been explored.[2] We have confirmed that six-membered ring chelates are the most stable for beryllium(II), in a similar manner to other elements of the first short period, such as boron and carbon, while copper(II), nickel(II), lanthanides and other heavier elements prefer five-membered ring chelates,[3] and ligands containing propionic groups may be better sequestering agents.

The coordinating properties of beryllium(II) in aqueous solution with aminoacids or polyaminocarboxylic acids have, in general, been very little studied,[4–6] probably because of the strong tendency of the small beryllium(II) cation to hydrolyse.[7] In our studies, in aqueous solutions of the IDA–Be^{II}[8] (IDA = iminodiacetic acid), NTA–Be^{II}[3] (NTA = nitrilotriacetic acid) and EDTA–Be^{II}[9,10] (EDTA = ethylenediaminetetraacetic acid) systems, we have found upon analysing the experimental potentiometric data by means of the NERNST/LETA/GRAFICA version[11] of the LETAGROP program,[12] that the species resulting from the hydrolysis of beryllium(II) must be taken into consideration in the calculations, in order to determine the complex species present in the solution and to obtain correct values of the stability constants.

Beryllium(II) tends towards tetracoordination.[13] EDTA,[9,10] a potentially hexadentate ligand, forms the complexes $[BeHL''']^-$ and $[BeL''']^{2-}$ (H_4L''' ligand). NTA and NTP[3] (NTP = nitrilotripropionic acid), potentially tetradentate ligands, fulfill the coordination requirements of beryl-

* Author to whom correspondence should be addressed.

lium(II) and form the complex $[BeL'']^-$ (H_3L'' ligand). IDA and its analogues,[8] potentially tridentate ligands, only form the monohydroxide complex $[Be(OH)L']^-$ (H_2L' ligand) in significant amounts. The OH^- group will occupy the fourth place in the tetrahedron of coordination.

The present work is a continuation of our studies on the coordinating capacity in aqueous solution of aminoacids with beryllium(II), of D,L-aspartic acid (ASP), a potentially tridentate ligand, and D,L-methionine (MET), a potentially bidentate ligand. No references to the ASP–Be^{II} and MET–Be^{II} systems were found in the tables of stability constants.[4,5] However, Singh and Srivastava[6,14] for the ASP–Be^{II} system, and Perkins[15] for both systems, have determined from potentiometric measurements the stability constants of the complexes BeL' and BeL'_2 (ASP, H_2L' ligand; MET, HL ligand; charges being omitted for simplicity), with contradictory results. But these authors have not taken into consideration the hydrolysis of beryllium(II) in their calculations.

EXPERIMENTAL

Reagents

ASP and MET were prepared by recrystallization of ASP (BDH biochemicals, chromatographically homogeneous) and MET (Flucka puriss.), respectively.

The solution of $Be(ClO_4)_2$ was prepared by reacting metallic beryllium (Spex Industries Inc.) with an excess of $HClO_4$ (Merck, analytical grade), its free acidity[16] being determined, as well as the concentration of beryllium(II), in aqueous solution which was evaluated gravimetrically.[17,18] A carbonate-free sodium hydroxide solution was prepared according to the School of Sillén[19] and standardized against potassium hydrogen phthalate. $NaClO_4$ was prepared by recrystallization of $NaClO_4$ (Merck, analytical grade).

Apparatus and titration procedures

The potentiometric titrations were carried out in an inert argon atmosphere, at 25 ± 0.05°C, $I = 0.5$ M in $NaClO_4$, using a Radiometer Type PHM-64 potentiometer, a Radiometer G 202 B glass electrode and a K 401 calomel electrode. The cell constants were determined according to the method of Biedermann and Sillén,[20] the liquid junction potentials were found to be negligible within the margins of $[H^+]$ studied. It was found that $pK_w = 13.72$, in excellent agreement with reported data.[21] Measurements of the ligands alone were taken at the following concentrations: ASP, $C_L = 3.4$ and 1.2 mM (titration with NaOH) and $C_L = 1.2$ mM (titration with $HClO_4$); MET, $C_L = 4.4$ and 1.6 mM (titration with NaOH) and $C_L = 4.4$ mM (titration with $HClO_4$). Measurements of the ligands in the presence of beryllium(II) at the following concentrations and ligand:metal ratios were also taken: $C_M = 1$, 3 and 6 mM, ratios 4:1 and 1:1 for ASP; $C_M = 1$, 3 and 6 mM; ratios 4:1, 1:1 and 1:2 for MET.

Data treatment

The experimental potentiometric data were analysed by means of the NERNST/LETA/GRAFICA version[11] of the LETAGROP program,[12] based on a generalized form of the least-squares method that establishes the best model and best values of the β_{pqr} constants, minimizing the function $U = \Sigma(Z_{exp} - Z_{calc})^2$, Z being the average number of dissociated protons for the concentration of ligand (Z_c) or for the total concentration of metal (Z_B). The LETAGROP calculations also give standard deviations, $\sigma(Z)$ and $\sigma(\log \beta_{pqr})$.[22] The computations were performed on a Burroughs 6700 computer (Facultad de Ciencias, Universidad Central de Venezuela, Caracas).

Hydrolysis of beryllium(II) was previously studied under the same experimental conditions.[8] The $Be(OH)_2$ species is also found to be present in dilute solutions ($C_M < 10$ mM)[23,24] and at pH > 4.5. This species should also be taken into account since it competes with the hydroxy complexes. For equilibrium (1):

$$Be^{2+} + 2H_2O \rightleftharpoons Be(OH)_2 + 2H^+, \qquad (1)$$

it has been found that $-\log \beta_{-21} = 11.60 \pm 0.10$, which is in good agreement with the literature.[23,24]

RESULTS AND DISCUSSION

Ionization constants of the acids

From the values obtained for the β_{pr} constants corresponding to equilibria (2) and (3):

$$\text{ASP}, pH^+ + rH_2L' \rightleftharpoons [H_p(H_2L')_r]^{p+} \qquad (2)$$

$$\text{MET}, pH^+ + rHL \rightleftharpoons [H_p(HL)_r]^{p+}, \qquad (3)$$

the ionization constants of the acids (K_i) could readily be determined (see Table 1).

The values found for the pK_i are in good agreement with those previously found for the two ligands at the same ionic strength and temperature,[5] unless pK_0 (equilibrium H_2L^+/HL) for MET. The diagrams of the species distribution as a function of $-\log [H^+]$ (Fig. 1(a), ASP; Fig. 1(b), MET), calculated in accordance with the values of $-\log$

Table 1. Ionization constants of ASP and MET (25°C, $I = 0.5$ M in $NaClO_4$)

	No. of titrations/ No. of exptl points	$-\log [H]^+$ range	$\sigma(Z)^a$	pr	$-\log \beta_{pr}$	Equilibrium	pK_i	pK_i^b
				11	-2.03 ± 0.01	$H_3L'^+/H_2L'$	2.03	1.86
ASP	3/125	1.86–10.17	0.023	−11	3.73 ± 0.03	H_2L'/HL'^-	3.73	3.64
				−21	13.32 ± 0.07	HL'^-/L'^{2-}	9.58	9.50
				11	-2.84 ± 0.02	H_2L^+/HL	2.84	2.10
MET	3/70	2.55–10.01	0.016	−11	9.13 ± 0.02	HL/L^-	9.13	9.07

[a] Standard deviation.
[b] Reference 5.

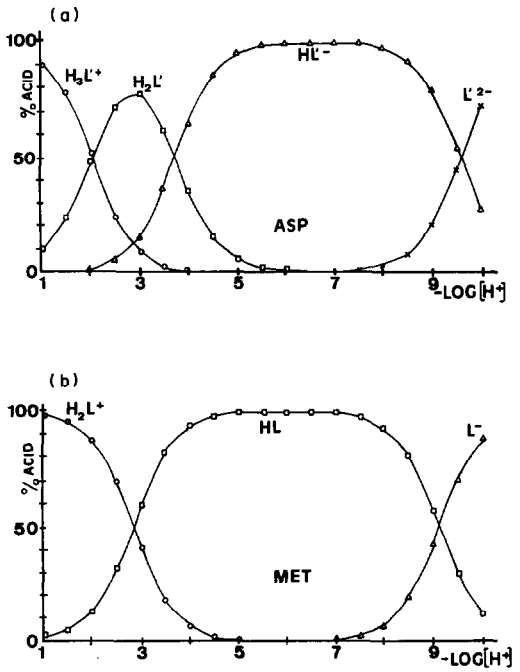

Fig. 1. Species distribution as a function of $-\log [H^+]$: (a) ASP and (b) MET.

β_{pr} given in Table 1, show that the monoprotonated species (HL'^- for ASP; HL for MET), with a fundamentally betainic structure,[25] is practically alone at $-\log [H]$ 5.5–7.5 for ASP and 5–7 for MET.

Formation constants of the complexes formed

The formation constants, β_{pqr}, are defined by means of equilibria (4) and (5)

$$\text{ASP}, pH^+ + qBe^{2+} + rH_2L' \rightleftharpoons [H_pBe_q(H_2L')_r]^{(p+2q)+} \quad (4)$$

$$\text{MET}, pH^+ + qBe^{2+} + rHL \rightleftharpoons [H_pBe_q(HL)_r]^{(p+2q)+}. \quad (5)$$

Taking into account the presence of the hydrolytic species $[Be_2(OH)]^{3+}$, $[Be_3(OH)_3]^{3+}$ and $Be(OH)_2$, an analysis is carried out first of the possible presence of the complex species supposed by Sing and Srivastava[6,14] and Perkins,[15] −211, BeL′, and −421, $[BeL'_2]^{2-}$, for ASP, and −111, $[BeL]^+$, and −212, BeL_2, for MET. For these species, $p/r = 2$ (ASP) and $p/r = 1$ (MET). These species were rejected ($\beta_{pqr} = 0$).

Figure 2(a) shows for ASP, that in the ligand–metal ratio 1:1, $Z_C > 2$, and in the ratio 4:1, $Z_C > 1.25$, at pH > 5.9. This is qualitative proof of the presence of hydroxo complexes with $p/r > 2$. Analogously, Fig. 2(b) shows for MET, that in the ratio 1:1, $Z_c > 1$, and in the ratio 4:1, $Z_C > 0.25$, at pH > 5.9, indicating the presence of hydroxo complexes with $p/r > 1$. In this pH zone, these complexes will, of course, compete with the formation of the $Be(OH)_2$ species [equilibria (1) and (8)] (Fig. 3). The existence of these complexes is short, since at pH ≈ 6.5 the turbidity of the solutions begins.

Thomas and co-workers[26–28] have shown that the trimer species, $[Be_3(OH)_3(H_2O)_6]^{3+}$, is not destroyed if the ligands are mono- or bidentate, since tetracoordination of beryllium(II) is then maintained, displacing one or two molecules of water for each atom of beryllium(II). The possible presence of bi- and trinuclear hydroxo complexes is therefore analysed as: −522, $[Be_2(OH)L'_2]^-$, and −933, $[Be_3(OH)_3L'_3]^{3-}$, for ASP; and −322, $[Be_2(OH)L_2]^+$, and −633, $Be_3(OH)_3L_3$, for MET.

These complexes were accepted, but their β_{pqr} constants are not well-defined, indicating that either the bi- and trinuclear hydroxo complexes are present in the solution in very negligible amounts, or that other hydroxo complexes are present, there being the monomer −311, $[Be(OH)L']^-$ and/or −411, $[Be(OH)_2L']^{2-}$, for ASP, and −211, Be(OH)L, and/or −311, $[Be(OH)_2L]^-$, for MET. Finally, the joint presence of the complexes −522, −933, −311 and −411 for ASP is tested, the simultaneous fit of the six potentiometric titrations studied being verified. The LETAGROP program

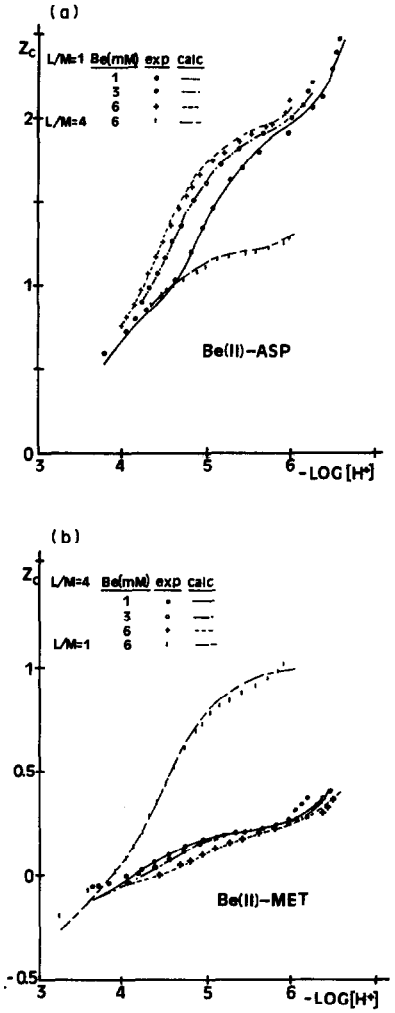

Fig. 2. Z_C vs $-\log [H^+]$ curves: (a) ASP–Be^{II} system and (b) MET–Be^{II} system. The curves have been calculated using the β_{pr} (Table 1), β_{pqr} (Table 2) and β_{pq} constants.

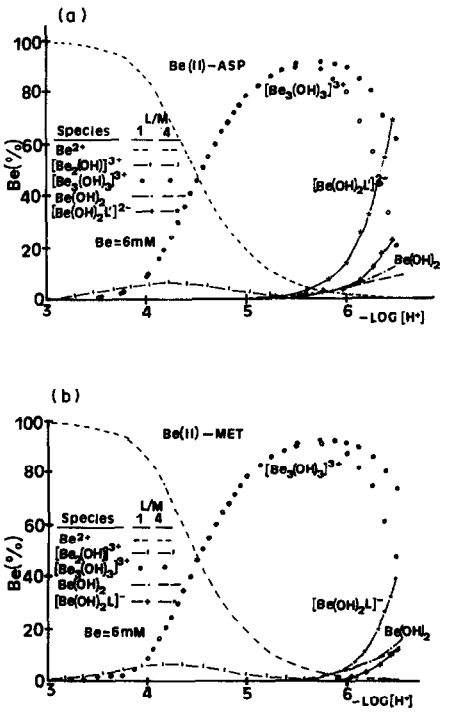

Fig. 3. Species distribution as a function of $-\log [H^+]$: (a) ASP–Be^{II} system and (b) MET–Be^{II} system.

only accepts complex -411, $[Be(OH)_2L']^{2-}$, with the value of β_{-411} indicated in Table 2. The remaining complexes are not present in significant amounts ($\beta_{pqr} \approx 0$). Similarly for MET, the joint presence of the complexes -322, -633, -211 and -311 is proven. The simultaneous fit of the nine potentiometric titrations studied, shows the sole presence, in significant amounts, of complex -311, $[Be(OH)_2L]^-$, with the value of β_{-311} indicated in Table 2. The remaining complexes are not present in significant amounts ($\beta_{pqr} \approx 0$).

The diagram of species distribution presented in Fig. 3(a) for ASP and Fig. 3(b) for MET, shows that the dihydroxo complexes begin to form at pH > 5.5. The limiting margin of existence of the species, $[Be(OH)_2L']^{2-}$ for ASP and $[Be(OH)_2L]^-$ for MET, is conditioned by the greater stability of the hydrolytic species, $[Be_3(OH)_3]^{3+}$. In Fig. 3, it

Table 2. Formation constants (β_{pqr}) and stability constants (K) of the ASP and MET complexes with beryllium(II) (25°C, $I = 0.5$ M in $NaClO_4$)

	No. of titrations/ No. of exptl points	$-\log [H^+]$ range	$\sigma(Z)^a$	pqr	$-\log \beta_{pqr}$	Equilibrium	$\log K$
ASP	6/160	3.79–6.57	0.038	−411	19.23±0.07	[b]	21.52
				−311	≈0		
				−933	≈0		
MET	9/164	3.08–6.50	0.046	−311	15.92±0.15	[c]	20.65
				−211	≈0		
				−633	≈0		

[a] Standard deviation.
[b] Equilibrium: $Be^{2+} + 2\,OH^- + L'^{2-}/[Be(OH)_2L']^{2-}$.
[c] Equilibrium: $Be^{2+} + 2\,OH^- + L^-/[Be(OH)_2L]^-$.

is shown that as the concentration of the ligand increases, the proportion of the dihydroxide complexes increases, and that of the species $[Be_3(OH)_3]^{3+}$ decreases. Since at pH $\approx$ 6 (Fig. 1), the ligands are present in the betainic form, HL'^- (ASP), HL (MET), the complexes are formed fundamentally by means of equilibria (6) and (7):

$$\text{ASP, } 1/3\,[Be_3(OH)_3]^{3+} + HL'^- \rightleftharpoons [Be(OH)_2L']^{2-} + 2H^+ \quad (6)$$

$$\text{MET, } 1/3\,[Be_3(OH)_3]^{3+} + HL \rightleftharpoons [Be(OH)_2L]^- + 2H^+. \quad (7)$$

The formation of these dihydroxo complexes explains the values of Z_C observed in Fig. 2 at pH > 5.9.

The hydrolytic species $Be(OH)_2$ is also formed from $[Be_3(OH)_3]^{3+}$ [equilibrium (8)]:

$$1/3\,[Be_3(OH)_3]^{3+} + OH^- \rightleftharpoons Be(OH)_2, \quad (8)$$

and competes with the dihydroxo complexes, but is present in a smaller proportion than these (Fig. 3).

The ASP and MET ligands behave, therefore, like bidentate ligands. The OH^- will occupy the third and fourth place in the tetrahedron of coordination as observed in the structures proposed for the complexes, $[Be(OH)_2L']^{2-}$ (Fig. 4, ASP) and $[Be(OH)_2L]^-$ (Fig. 5, MET).

The ligands form the complexes from the betainic structure, with loss of the betainic acidity [Figs 1–3, equilibria (6) and (7)], which involves the coordination of the nitrogen atom and an oxygen atom of the carboxylate group. The ASP behaves like a bidentate ligand forming a six-membered chelate ring, these being the most stable for beryllium(II)[3] (Fig. 4). MET forms the five-membered chelate ring as expected (Fig. 5).

These results are in agreement with the stability constants, K, of both dihydroxo complexes (presented in Table 2), which are readily calculated from β_{pqr} (Table 2), β_{pr} (Table 1) and K_w, the ionic product of water. The ASP complex is somewhat more stable than that of MET, since for beryllium(II) the six-membered chelate rings[3] are more stable than the five-membered ones.

ASP behaves like a tridentate chelating agent towards divalent transition cations such as cobalt(II), copper(II) and nickel(II).[29] Its isomer, iminodiacetic acid (IDA) behaves, moreover, as a tridentate chelating agent towards beryllium(II),[8] stabilizing the monohydroxo complex $[Be(OH)L']^-$ and forming five-membered chelate rings. ASP behaves differently towards beryllium(II): it should potentially form a more stable six-membered ring with beryllium(II) and another five-membered one, but this additional ring would be submitted to strong tensions in the tetrahedric coordination with a small cation such as beryllium(II) and would be unstable. The monohydroxo complex of ASP, $[Be(OH)(H_2O)L']^-$, would therefore be formed initially from $[Be_3(OH)_3]^{3+}$ [Fig. 3(a)], a molecule of water occupying the fourth coordination site, and quickly hydrolysing, finally stabilizing the dihydroxo complex $[Be(OH)_2L']^{2-}$. MET, a bidentate ligand, would also initially form the monohydroxo complex $[Be(OH)(H_2O)L]$, the coordinated molecule of water hydrolysing rapidly, and finally stabilizing the dihydroxo complex $[Be(OH)_2L]^-$.

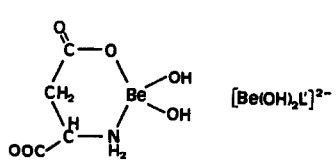

Fig. 4. For ASP: structure proposed for the $[Be(OH)_2L']^{2-}$ complex.

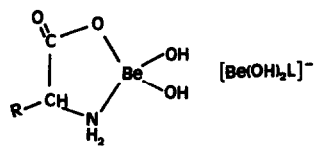

Fig. 5. For MET: structure proposed for the $[Be(OH)_2L]^-$ complex.

Acknowledgements—This work has been carried out under the Agreement of Scientific and Academic Cooperation signed in 1984 between the Faculty of Chemistry of the University of La Laguna (ULL) and the Faculty of Science of the Central University of Venezuela (UCV). We wish to thank the Computer Center of the Faculty of Science (UVC) for computer time at Burroughs 6700; CONICIT, (Caracas, Grant No. 51.78.31.S1-1228), CDCH (UCV, Grant No. C-03.12/83) and the Education Council of the Canary Islands Government (Grant No. 86/22.04.85) for financial support.

REFERENCES

1. E. Ochiai, *Bioinorganic Chemistry*. Allyn and Bacon, Boston (1977).
2. H. G. Seiler and H. Sigel (Eds), *Handbook on Toxicity of Inorganic Compounds*, Chap. 10. Marcel Dekker, New York (1988).
3. A. Mederos, S. Domínguez, A. M. Medina, F. Brito, E. Chinea and K. Bazdikian, *Polyhedron* 1986, **6**, 1365.
4. A. E. Martell and R. M. Smith, *Critical Stability Constants*, Vol. 1, *Amino Acids*. Plenum Press, New York (1974).
5. A. E. Martell and R. M. Smith, *Critical Stability*

Constants, Vol. 5, *First Supplement*. Plenum Press, New York (1982).
6. D. D. Perrin, *Stability Constants of Metal–Ion Complexes. Part B: Organic Ligands*. Pergamon Press, Oxford (1979).
7. C. F. Baes Jr and R. E. Mesmer, *The Hydrolysis of Cations*. John Wiley, New York (1976).
8. A. Mederos, S. Domínguez, M. J. Morales, F. Brito and E. Chinea, *Polyhedron* 1987, **6**, 303.
9. A. Mederos, S. Domínguez, M. Hernández-Padilla, F. Brito and E. Chinea, *Bol. Soc. Quím. Perú* 1984, **50**, 277.
10. A. Mederos, J. M. Felipe, M. Hernández-Padilla, F. Brito, E. Chinea and K. Bazdikian, *J. Coord. Chem.* 1986, **14**, 277.
11. F. Brito and J. M. Gonçalves, Project No. 51.78.31-S1-1228. CONICIT, Caracas, Venezuela (1981).
12. R. Arnek, L. G. Sillén and O. Wahlberg, *Ark. Kemi* 1969, **31**, 353.
13. J. Burgess, *Metal Ions in Solution*. Ellis Horwood, Chichester (1978).
14. M. K. Singh and M. N. Srivastava, *J. Inorg. Nucl. Chem.* 1972, **34**, 567.
15. D. J. Perkins, *Biochem. J.* 1952, **51**, 487; 1953, **55**, 649.
16. G. Gran, *Analyst* 1952, **77**, 661.
17. J. Huré, M. Kremer and F. Bequer, *Anal. Chim. Acta* 1952, **7**, 37.
18. R. Pribil, *Analytical Applications of* EDTA *and Related Compounds*. Pergamon Press, Braunschweig (1972).
19. F. Brito and N. Ingri, *An. Quím.* 1960, **56B**, 165.
20. G. Biedermann and L. G. Sillén, *Ark. Kemi* 1953, **5**, 425.
21. G. Lagerström, *Acta Chem. Scand.* 1959, **13**, 722.
22. L. G. Sillén, *Acta Chem. Scand.* 1962, **16**, 159; L. G. Sillén and B. Warnqvist, *Ark. Kemi* 1969, **31**, 341.
23. F. Bertin, G. Thomas and J. C. Merlin, *Bull. Soc. Chim. Fr.* 1967, 2393.
24. P. L. Brown, J. Ellis and R. N. Sylva, *J. Chem. Soc., Dalton Trans.* 1983, 2001.
25. T. W. G. Solomons, *Organic Chemistry* (Revised printing). John Wiley, New York (1985).
26. F. Bertin and G. Thomas, *Bull. Soc. Chim. Fr.* 1968, 1225.
27. G. Duc, F. Bertin and G. Thomas, *Bull. Soc. Chim. Fr.* 1974, 793; 1975, 495; 1976, 414; 1977, 196 and 645.
28. G. Duc and G. Thomas, *Bull. Soc. Chim. Fr.* 1979, 163; 1980, 169.
29. S. Chabereck Jr and A. E. Martell, *J. Am. Chem. Soc.* 1952, **74**, 6021.

Polyhedron Vol. 8, No. 16, pp. 2023–2028, 1989
Printed in Great Britain

0277–5387/89 $3.00+.00
© 1989 Maxwell Pergamon Macmillan plc

OPTICAL ACTIVITY OF COMPOUNDS FORMED BY AMMINO COMPLEXES OF COBALT(III) AND CARBOHYDRATES—II. D-ARABINOSE COMPLEXES

S. BUNEL,* C. IBARRA, V. CALVO and E. MORAGA

Departamento de Química Inorgánica y Analítica, Facultad de Ciencias Químicas y Farmacéuticas, Universidad de Chile, Casilla 233, Santiago, Chile

(*Received* 20 *January* 1989; *accepted* 10 *March* 1989)

Abstract—Two sugar-containing chiral complexes are formed by the reaction of *cis*-$[Co(NH_3)_4(H_2O)_2]^{3+}$ and D-arabinose at pH 6. Complex **I** is a mixed valence cobalt(II)/cobalt(III) paramagnetic species, whereas complex **II** is a mononuclear cobalt(III) complex. Their syntheses and characterization are described. Visible absorption spectra and IR spectra were recorded. Optical activity was measured via circular dichroism spectra and optical rotatory dispersion. Complex **I** undergoes anomerization in aqueous solution, the rate of this process being pH and chiral complex dependent. Complex **II** does not retain its optical activity in aqueous solution as a result of decomposition. Spectral data support the coordination scheme proposed for each complex.

In previous work we reported the preparation and optical activity of ammino complexes of cobalt(III) containing D-ribose, L-sorbose and D-glucosamine as the second ligand.[1] We also reported the optical rotatory dispersion (ORD) curves of ammino complexes of cobalt(III) and L- or D-arabinose in aqueous solutions.

This work was initialy aimed at isolating D-arabinose complexes which we assumed would have a composition similar to that of the complexes previously mentioned. However, two kinds of chiral compounds containing the sugar were obtained in the same reaction: one of them unexpectedly turned out to be the salt of a mixed valence binuclear cobalt(II)/cobalt(III) complex, **I**; whereas the other was a mononuclear complex salt, **II**.

This paper reports the optical, spectral, magnetic and chemical characteristics of these complexes and we relate these properties to structural models.

EXPERIMENTAL

Materials

Most of the carbohydrates were from Merck. All were used without further purification.

Methods

Visible absorption spectra were measured on a Zeiss PMQ-2 spectrophotometer in 10^{-2}–10^{-3} M aqueous solutions. Optical rotatory dispersion measurements were run on a Perkin–Elmer 141 polarimeter modified with a Baush & Lomb monochromator, with 10^{-2} M aqueous solutions, using a 2 cm pathlength cell, connected to a thermostated bath.

The circular dichroism spectra were recorded on a Cary 60 spectropolarimeter using 10^{-2} M aqueous solutions in 1 cm pathlength cells. IR spectra of complexes were recorded on a DIGILAB FTIR with a spectral resolution of 2 cm^{-1} and KBr pellets, and also on a Leitz Wetzlar IIIG IR spectrometer. The chloride forms of complexes **I** and **II** were employed to avoid the strong sulphate bands.

Carbon, hydrogen and nitrogen were analysed with a Perkin–Elmer 240-C analyser. The Co content was determined by atomic absorption spectroscopy with a Perkin–Elmer 305 spectrometer. The sulphate content was determined by conductimetric titration with a standard $BaCl_2$ solution[2] in a YSI model 32 conductivity meter.

Magnetic susceptibility measurements at 298 K were carried out by the Gouy method. The susceptibility was also determined in the 2.5–300 K

* Author to whom correspondence should be addressed.

range with an SHE magnetometer connected to an SQUID sensor.

Kinetic measurements

The anomerization process developed by the binuclear complex was studied at 15°C in buffered (acetic acid (1M)/sodium acetate) solutions. Optical activity changes were followed on 8.5×10^{-3} M solutions at 550 nm, using 2 cm pathlength thermostated cells and a modified Perkin–Elmer 141 polarimeter, until constant rotations were achieved.

Preparation of the binuclear compound, complex I

Cis-$[Co(NH_3)_4(H_2O)_2]_2(SO_4)_3 \cdot 3H_2O$ (1.685 g, 2.5 mmol) and D-arabinose (3.750 g, 25 mmol) were dissolved in 50 cm^3 of water, and the pH was adjusted to 6 with ammonia. The mixture was maintained at 25°C and the reaction was complete after 3 h. The products were then isolated. Methanol (60 cm^3) was added dropwise to the solution with constant stirring and a well-known tetranuclear ammino complex, $[Co\{(OH)_2Co(NH_3)_4\}_3](SO_4)_3 \cdot nH_2O$, ($n$ = 2–9),[3] was first precipitated, which was separated by filtration. Methanol (100 cm^3) was then added to the stirred solution and a red microcrystalline solid precipitated on the walls of the beaker. This product was collected by vacuum filtration, washed with methanol and ethanol, and dried in a vacuum desiccator. The yield was approximately 300 mg. The residual solution was a deep pink colour and was optically active.

Purification of the binuclear complex

Freshly-prepared binuclear complex was dissolved in 10 cm^3 of water and was poured dropwise into 80 cm^3 of methanol containing 100 mg $NaClO_4$, which prevented formation of a colloidal suspension. Constant stirring was maintained during this process and a pink solid precipitated, which was isolated by vacuum filtration, washed with methanol and ethanol, and dried in a vacuum desiccator. This procedure was repeated until the amplitude of the Cotton-effect, centred at 545 and 475 nm, levelled off. The yield of pure binuclear complex was *ca* 150 mg.

The product is very soluble in water, but insoluble in most organic solvents. It is stable as a solid and retains its optical activity when stored in a dry atmosphere. The compound is also paramagnetic. Optical activity of the aqueous solution of this compound drops slowly until the sign of the Cotton-effect, centred at 500 nm, reverses (see Fig. 1), while the absorption spectrum suffers no variation.

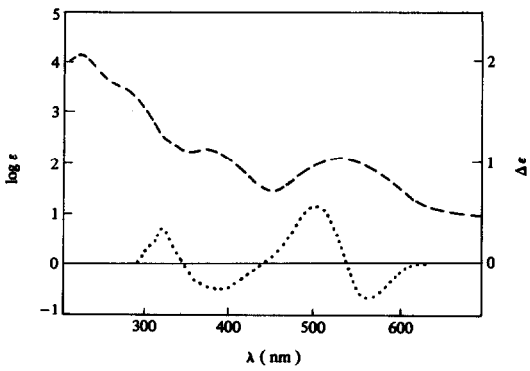

Fig. 1. Visible absorption spectrum (———) and circular dichroism (·····) of aqueous solutions of Complex I.

Analysis for $[Co_2(NH_3)_4(OH)_2(H_2O)_2$ D-arabinose$]_2(SO_4)_3 \cdot 4H_2O$: Found: Co, 20.5; SO_4, 24.8; C, 10.4; H, 4.8; N, 9.5. Calc: Co, 20.8; SO_4, 25.3, C, 10.6; H, 5.3; N, 9.9%.

Preparation of the mononuclear compound, complex II

400 cm^3 of the methanolic residual solution from the previous preparation were concentrated to 120 cm^3 on a 2 dm^3 evaporating dish under a cool air stream. The aqueous solution obtained was precipitated by dropwise addition of 200 cm^3 of absolute ethanol, under vigorous stirring for 30 min. Once pink crystals appeared, the resulting solution was kept at 4°C in the dark for a further 1/2 h before the next stage.

Precipitation was continued by adding another 500 cm^3 of absolute ethanol dropwise to the cold solution. A hygroscopic purple solid appeared, which covered the walls of the beaker. The resulting pink supernatant was discarded and the purple solid was redissolved in 5 cm^3 of distilled water. This concentrated solution was added dropwise to 120 cm^3 of a cold methanol–propanone (1 : 2) mixture, with vigorous stirring. The purple solid quickly covered the bottom of the beaker and a pink suspension developed. Once again the pink supernatant was discarded and the purple solid was easily washed off using 80 cm^3 of cold propanone with vigorous magnetic stirring. The purple solid obtained was quickly transferred to a dark container and dried *in vacuo* overnight. The yield of the purple solid was 230 mg.

Elemental analysis for $[Co(NH_3)_4$ D-arabinose$](NH_4)(SO_4)_2 \cdot 3H_2O$: Found: Co, 10.6; SO_4, 35.5; C, 11.8; H, 5.9; N, 12.5. Calc: Co, 10.9; SO_4, 35.5; C, 11.1; H, 5.2; N, 12.9%.

The resulting mononuclear compound is heat- and light-sensitive, so it was kept in the refrigerator

in a dry container. Under these conditions the compound lasted for at least 3 months without loss of optical activity. Optical activity of the aqueous solutions of this complex decreases very slowly at room temperature in the dark. However, this process speeds up in dim light or acidic media. Cobalt(II) was identified as one of the decomposition products.

The chloride form of complexes I and II were obtained either by anion exchange on Dowex 1X8 or by precipitation with $BaCl_2$ solution. Aqueous solutions so obtained were evaporated and dried in a desiccator.

Regarding the synthesis of the chiral complexes, it must be remembered that the reacting complex *cis*-$[Co(NH_3)_4(H_2O)_2]^{3+}$ in aqueous solution at pH 6 and 25°C, spontaneously forms the tetranuclear ammino complex of cobalt(III) previously mentioned. The formation of this product is enhanced as the pH and temperature increase. The same chiral products containing arabinose were even obtained from a reaction with a 1:1 mole ratio of the reagents, although poorer yields were achieved. The large excess of carbohydrate employed in the present synthesis shifts the course of the reaction with formation of the sugar-containing chiral complexes.

RESULTS AND DISCUSSION

Magnetic susceptibility measurements of the binuclear complex at 298 K and 1 kG gave a magnetic moment, $\mu = 4.49$ BM. The data were corrected to compensate for the diamagnetism of the constituent atoms (Pascal constants). Susceptibilities measured over the range 2–300 K showed a linear dependence of the reciprocal susceptibility on temperature, confirming the presence of one cobalt(II) in the complex. The calculated value of the magnetic moment is higher than the spin only moment for three unpaired electrons (3.89 BM). This is the normal situation for high-spin octahedral cobalt(II) complexes, since they have a very high orbital contribution.[4]

Conductimetric titrations of the binuclear complex with hydrochloric acid showed two inflections due to non-bridged OH groups.[5] This agrees with the Co–SO_4 molar ratio, thus indicating the coordination of two OH ligands.

Table 1 shows that the visible absorption spectrum of the binuclear complex consists of two bands: the first one has $\lambda_{max} = 527$ nm, ($\varepsilon = 109$), whereas the second one is a shoulder at 370 nm, which corresponds to a *d–d* absorption overlapped by a charge-transfer absorption, Fig. 1. This spectrum is similar to that found for ammino complexes

Table 1. Visible absorption and circular dichroism data

	Absorption		CD	
	λ(nm)	$\varepsilon(M^{-1}cm^{-1})$	λ(nm)	$\Delta\varepsilon(M^{-1}cm^{-1})$
Complex I	527	109	562	−0.568
			497	0.994
	370(s)	129	380	−0.419
			318	0.426
Complex II	530	46.38	560	0.38
			495	−0.65
	373	80	375	0.31
			310	−0.567

of cobalt(III) containing ribose, sorbose and glucosamine,[1] where cobalt(III) is surrounded by four nitrogen and two oxygen atoms.

Two circular dichroism signals of opposite sign appear under the first absorption band, detected at 562 and 497 nm. Of the two CD signals, the one with the lower energy corresponds to the $^1A_2$ state, and the other to the ^1E state, both of them derived from the first $^1T_{1g}$ excited state of cobalt(III) in octahedral symmetry, see Fig. 2. These CD signals exhibit the same signs sequence as that of the chiral compounds formed by an ammino complex of cobalt(III) with D-glucosamine, L-sorbose and D-ribose.

The CD spectrum of the binuclear complex also has two signals at 380 and 318 nm, corresponding to the low wavelength visible absorption spectrum. The lower energy signal should correspond to an ^1E state derived from the magnetically forbidden $^1T_{2g}$ state of cobalt(III).[6] The higher energy signal could correspond to a ligand-to-metal charge-transfer state (see Table 1).

The visible spectra of the mononuclear and binuclear complexes are similar, Table 1. In the mononuclear complex, the first band appears at

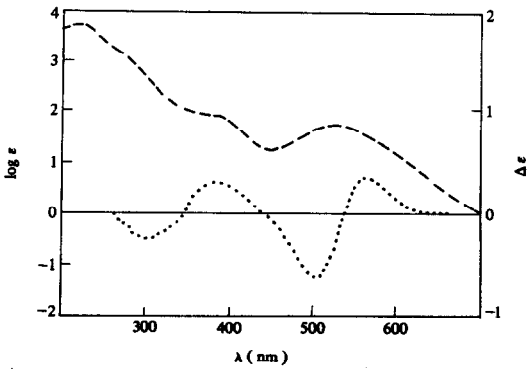

Fig. 2. Visible absorption spectrum (———) and circular dichrosim (·····) of aqueous solutions of Complex II.

530 nm ($\varepsilon = 46$) and there is a shoulder at 373 nm ($\varepsilon = 180$), which is better resolved than that of the binuclear species. There are two circular dichroism signals under the first visible absorption band, Fig. 2. Their signs are opposite to those of the corresponding band of the binuclear complex: one is at 565 nm and the other one at 505 nm.

Circular dichroism signals under the second visible absorption band of cobalt(III) are detected at 385 and 310 nm. The lower energy signal has *d–d* character, corresponding to a transition derived from the $^1T_{2g}$ state. The positive circular dichroism signal at 218 nm in the binuclear complex and the negative one at 310 nm in the mononuclear complex have similar $\Delta\varepsilon$ values. Considering their energies we think that both signals correspond to a ligand-to-metal charge-transfer transition.[7]

The different rotation signs for the same kind of transition in the mono- and the binuclear complexes might originate from an opposite helical distribution of the chelate ring around the cobalt(III) ion in each species.

Solutions of the binuclear complex suffer an inversion of the Cotton-effect signs in the visible spectral region (Fig. 3). This process follows first-order kinetics with complex concentration. It is also first order regarding proton concentration. The specific rate constant at 15°C (288 K), measured under pseudo-first-order conditions at pH 5.4 (buffered solution) is 1.5×10^{-3} min^{-1}. We ascribe this behaviour to anomerization. It is slower than that of D-arabinose solutions at the same pH and temperature, ($k = 1.99 \times 10^{-2}$ min^{-1}).

D-Arabinose is known to exist in the alternative form, with an anomeric composition, 68% α- and 34% β-anomers.[8,9] The cobalt(III) ion can coordinate to this carbohydrate forming five-membered chelate rings through the O(1)H—O(2)H, or O(2)H—O(3)H or O(3)H—O(4)H positions.

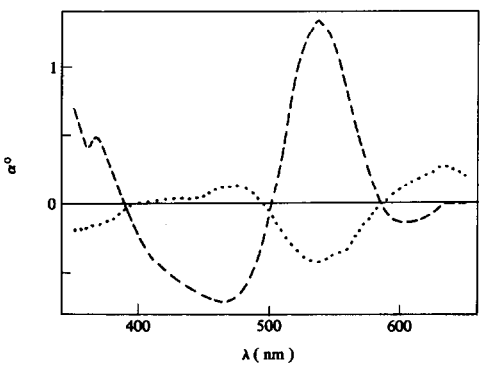

Fig. 3. Optical rotatory dispersion change of a 0.0055 M solution of Complex **I**, pH 5.4, 15°C, 1 cm pathlength cell. Starting solution (–––); same solution after 100 min. (·····).

Chirality is the same, λ, for each one of these in the case of the β-anomer [Fig. 4(a)]. In the case of the α-anomer, chirality originating by bonding through the O(1)H—O(2)H positions is opposite, δ, to that resulting from bonding through the two other coordination positions [Fig. 4(b)].

The Cotton-effect signs under the first visible absorption band and the phenomenon of complex anomerization led us to think that the cobalt(III) ion bonds to the O(1)H group of the β-D-arabinose, in which case the other site of coordination would be O(2)H. Bonding to the ring oxygen atom O(5) is sterically hindered for the alternative conformation of D-arabinose.

Coordination of D-arabinose to the cobalt(II) ion in the binuclear complex has not been discussed yet. Scale models show that simultaneous bonding of O(3)H and O(4)H, or O(4)H and ring oxygen O(5) atoms of the sugar to the metal are feasible.

The FTIR spectrum of the chloride form of complex **I** is not as well-resolved as that of complex **II** in the 3500–3200 cm^{-1} range. However, a clear shift of the CO group ring vibrations of the carbohydrate to lower frequencies can be observed. In this way, the bands in the neighbourhood of 1136, 1093, 1052, 1000 and 943 cm^{-1}, assigned as ν(CO)+

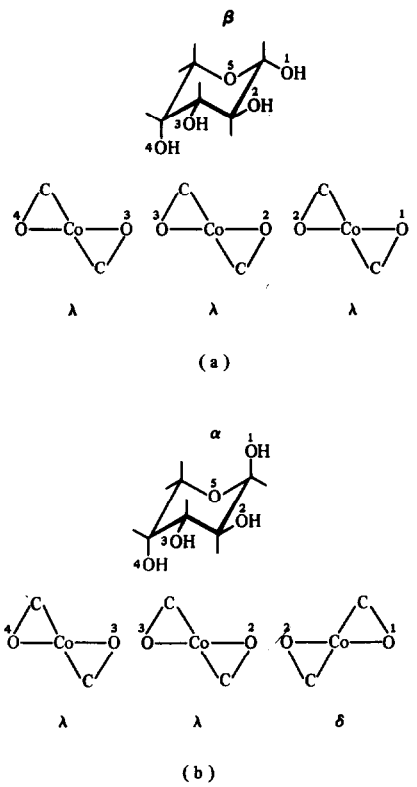

Fig. 4. (a) β-D-Arabinose; (b) α-D-arabinose, alternative form, and their corresponding five-membered ring conformations around cobalt(III).

Table 2. FT–IR transmitance bands (cm^{-1}) with possible assignments

Arabinose	Assignments	Reference	$[Co(NH_3)_4$D-arabinose$]Cl_3$
3536 s	ν(O(4)—H···O(2)H)	10(a)	3530 shoulder 3500 strong
3340 vs	ν(O(1)—H···O(5))	10(a)	3370 sharp–medium 3330 sharp–weak
3321 sh	ν(O(3)—H···O(2)H)	10(a)	3320 sharp–strong 3295 sharp–strong 3280 sharp–strong
3235 b	ν(O(2)—H···O(3)H)	10(a)	3239 shoulder 3195 sharp–strong 3175 sharp–strong 3159 sharp–strong
3000 w	ν(C(5)—H)	10(a)	3000 sharp–weak
2970 sh	ν(C(4)—H)	10(a)	— shoulder
2953 sh	ν(C(3)—H)	10(a)	— no band
2940 m	ν(C(2)—H)	10(a)	2945 medium
—	δ(O—H(2))		1635 strong
—	δ(N—H(3))	11	1595 strong
1402 vw	δ(CH(2))+δ(COH)	10(a)	1415 strong
—	δ(N—H(3))	11	1308 medium
1134 vs	ν(CO)+ν(CC)	10(a)	1145 sharp–weak 1115 sharp–weak
1002 s	ν(CC)+ν(CO)	10(a)	1080 broad–medium 1045 sharp–weak
893 s	δ(COH)α	10(b)	855 broad–weak

ν(CC), ν(CO), ν(CO)+δ(CCO) and ν(CO)+δ(CCH), respectively,[10] are broadened and shifted towards 1108, 1075, 1030 and 983 cm^{-1}, thus suggesting that the CO group could be involved in bonding to the cobalt(II) ion.

In the mononuclear complex, under the same pH and temperature conditions, the optical activity drops to zero. At the same time, the intensity of the first visible absorption band decreases as a result of decomposition of the complex species.

The FT–IR spectra of complex **II** in the chloride form show three major frequency ranges (3500–3200, 1415 and 1145–1045 cm^{-1}), as shown in Table 2. From 3500 to 3200 cm^{-1} the OH···O stretching bands are shifted towards lower frequencies compared with free sugar, thus showing shorter OH···O bridging between O(3)H and O(2)H. However, O(4)H and O(1)H were almost unperturbed compared to UO_2–sugar complexes obtained by Tajmir-Riahi.[10a] In addition, no CH stretching bands were observed for C(4)H and C(3)H, but they were observed for C(1)H, C(2)H and C(5)H. COH and CCH deformation modes of sugar complexes appeared as a strong band at 1415 cm^{-1}. This, together with a set of four unresolved bands (ν(CO)+ν(CC) 1145–1045 cm^{-1}), are indicative of metal–sugar coordination.[10a]

Complex **II** Cotton-effect signs under the first absorption band, which are opposite to those of **I**, might arise from coordination of cobalt(III) to O(1)H and O(2)H atoms of the α-anomer of D-arabinose in its alternative form. This possibility looks more attractive to us, although it cannot be forgotten that the same sequence of Cotton-effect signs could arise from bonding of the metal ion to the O(1)H—O(2)H or O(3)H—O(4)H positions of normal β-D-arabinose. Data provided by the FT–IR spectrum seem to point towards the third proposal.

Acknowledgements—This research was supported by Fondo Nacional de Ciencias (FONDECYT) proyecto 230 and by Departamento Tecnico de Investigacion, Universidad de Chile proyecto Q 2741-8823. We are deeply indebted to Dr Clifford A. Bunton, Department of Chemistry, University of California, Santa Barbara, for many helpful discussions and for performing the FT–IR measurements. We also thank Dr Octavio Peña, CNRS researcher, at Laboratoire de Chimie Minerale B, Universite de Rennes I, France, who performed the magnetic susceptibility measurements.

REFERENCES

1. S. Bunel and C. Ibarra, *Polyhedron* 1985, **4**, 1537.
2. B. J. Heinrich, M. D. Grimes and J. E. Puckett in

Treatise on Analytical Chemistry, (Edited by I. M. Kolthoff and P. J. Elving), Vol. 7, p. 67. Interscience, New York (1961).
3. G. Blyholder and N. Ford, *J. Phys. Chem.* 1964, **68**, 1496.
4. F. A. Cotton and G. Wilkinson, *Advanced Inorganic Chemistry*, 4th Edn, Chap. 21. John Wiley, New York (1980).
5. J. Brigando and D. Colaitis, *Bull. Soc. Chim. Fr.* 1969, **10**, 3440.
6. C. J. Hawkins, J. A. Stark and C. L. Wong, *Austr. J. Chem.* 1972, **25**, 273.
7. T. Ama, H. Kawaguchi and T. Jasui, *Bull. Chem. Soc. Jpn* 1988, **61**, 1141.
8. R. U. Lemieux and J. D. Stevens, *Can. J. Chem.* 1966, **44**, 249.
9. B. Capon, *Chem. Rev.* 1969, **69**, 407.
10. (a) H. Tajmir-Riahi, *Monatsh. Chem.* 1987, **118**, 245; (b) H. Tajmir-Riahi, *Carbohydrate Res.* 1984, **127**, 1.
11. K. Nakamoto, *Infrared and Raman Spectra of Inorganic and Coordination Compounds*, 3rd Edn. Wiley Interscience, New York (1978).

Polyhedron Vol. 8, No. 16, pp. 2029–2033, 1989
Printed in Great Britain

0277–5387/89 $3.00+.00
© 1989 Maxwell Pergamon Macmillan plc

CHARACTERIZATION OF THE 18-CROWN-6–LANTHANUM(III) COMPLEX IN METHANOL USING ^{139}La NUCLEAR MAGNETIC RESONANCE

ZHIGANG CHEN, HEATHER DETTMAN and CHRISTIAN DETELLIER*

Ottawa-Carleton Chemistry Institute, University of Ottawa Campus, Ottawa, Ontario K1N 9B4, Canada

(*Received* 2 *November* 1988; *accepted* 14 *March* 1989)

Abstract—The complex formed between $LaCl_3 \cdot 7H_2O$ and the macrocyclic ligand 18-crown-6 (18C6) in methanol has been characterized by ^{139}La NMR. Two sites in very slow exchange on the ^{139}La NMR chemical shift time scale coexist in methanolic solutions: solvated and 1 : 1 complexed $^{139}La^{III}$. Both chemical shift and relaxation rate data point to the participation of the chloride counteranion and of the crown ether in the first coordination sphere of lanthanum(III). The equilibrium constant of formation of the complex, determined from the populations of the two ^{139}La NMR sites, is in excellent agreement with previously determined data from the literature.

Complexes of lanthanide cations with macrocyclic ligands have attracted considerable interest in the past decade.[1] A large variety of macrocyclic ligands have been involved in the design, synthesis and isolation of these complexes, which are characterized by various stoichiometries.[1–3] The crown ethers[4] have been shown to be very versatile in the nature and the structure of the complexes that they form with lanthanide cations.[1] Numerous reports on the crystal structure determination of such complexes have appeared.[5] However, the studies of their properties in solution are rather scarce.[1,6]

NMR of metallic nuclei is a very useful tool for investigating the properties of the alkali metal cation complexes with crown ethers in solution.[7] More particularly, the stoichiometry of such complexes present in small amounts in solution could be determined.[8] Since ^{139}La with its natural abundance of 99.91% and its receptivity relative to ^{13}C of 342 ($I = 7/2$, $Q = 0.21 \times 10^{-28}$ m^2) is one of the most promising nuclei among the early transition elements,[9] ^{139}La NMR is a good candidate for becoming a useful probe in the study of the La^{III} solution chemistry.

The first ^{139}La NMR experiment was performed as early as 1949.[10] Since, a number of ^{139}La NMR studies have been reported.[11] Most of these investigations focussed on the nature of outer- and inner-sphere lanthanum complexes formed by various anions in aqueous solutions.[11a–c]

This communication is the first report of a ^{139}La NMR study of a La^{III}–crown ether complex in solution.

EXPERIMENTAL

18-Crown-6 (Aldrich, 99%) was purified and vacuum-dried as described previously.[12] $LaCl_3 \cdot 7H_2O$ (Aldrich, 99.9%) and methanol (BDH, Assured) were used as received. All the spectra were recorded within 48 h after the preparation of the sample.

^{139}La NMR spectra were obtained at 42.37 MHz on a Varian XL-300 spectrometer using a 10 mm probe. A 0.1 M solution of $LaNO_3 \cdot 6H_2O$ in D_2O–H_2O (20 : 80) was used as an external reference for the chemical shifts. The 90° pulse width was 16 μs. Typically, pulse widths between 10 and 16 μs were used, without any significant alteration of the spectral region of interest. The delay between the end of the 90° pulse and the beginning of the acquisition was chosen as short as possible, and was always $\leqslant 5$ μs. In the case of Lorentzian lineshapes, the transverse relaxation rates, T_2^{-1}, were obtained directly from the linewidths. The temperature in the probe was measured as described previously.[13] All

* Author to whom correspondence should be addressed.

the experiments reported in Fig. 1 and Table 1 were performed at 300.0 ± 0.5 K.

Analyses of the ^{139}La spectral lineshapes were carried out on an Amdahl mainframe computer using a non-linear least-squares regression.[14] The adjustable parameters were C, p_A, T_{2A}, T_{2B} and ϕ (defined below). ν_A and ν_B were obtained directly from the spectra at $\rho = [18C6]/[La^{III}] = 0$ and $\rho = 1.4$, respectively, and were fixed during the regression. Data were transferred to the mainframe from the spectrometer using an IBM-clone PC intermediate and Kermit software. A program was

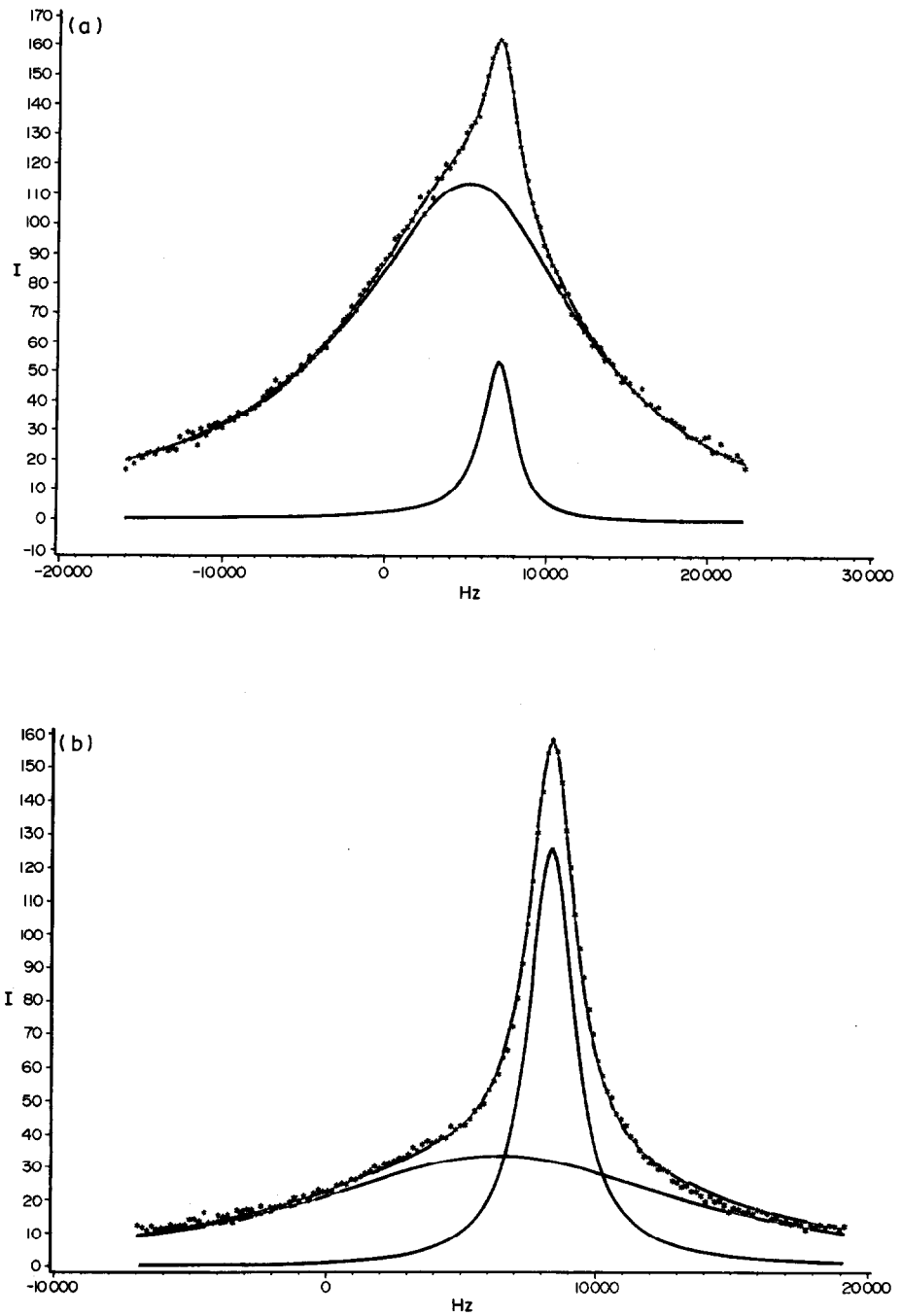

Fig. 1. ^{139}La NMR spectra, at 42.37 MHz, of $LaCl_3 \cdot 7H_2O$ in methanol in the presence of 18-crown-6 ($T = 300.0 \pm 0.5$ K). The points (*) have been obtained from the original spectra, and the solid lines result from a non-linear regression on eq. (1). (a) $[La^{III}]_0 = 0.200$ M; $\rho = [18C6]_0/[La^{III}]_0 = 1.00$ and (b) $[La^{III}]_0 = 0.050$ M; $\rho = 0.50$.

Table 1. ^{139}La NMR parameters of La^{III} and La^{III}–18C6 in methanol solution

$[La^{III}]_0$[a] (M)	ρ[b]	p_A[c]	T_{2A}^{-1}[d] (kHz)	δ_A[e] (ppm)	δ_B[f] (ppm)
0.200	0	1	6.1±0.3	165	
0.200	0.50	0.43±0.07	6.5±0.5		
0.200	0.70	0.33±0.02	6.7±0.5		
0.200	0.90	0.19±0.01	7±1		
0.200	1.00	0.06±0.01	7±1		
0.200	1.40				130
0.100	0	1	6.1±0.3	194	
0.100	0.50	0.46±0.09	6.4±0.5		
0.100	0.70	0.31±0.02	6.4±0.5		
0.100	1.00	0.07±0.01	7±1		
0.100	1.40				150
0.050	0	1	4.8±0.3	230	
0.050	0.50	0.45±0.01	4.8±0.5		
0.050	0.70	0.34±0.01	4.8±0.5		
0.050	0.90	0.16±0.01	5.0±0.5		
0.050	1.00	0.12±0.01	6±1		
0.050	1.40				167

[a] $[LaCl_3 \cdot 7H_2O]_0$ in methanol.

[b] $[18C6]_0/[La^{III}]_0$.

[c] Normalized population of uncomplexed La^{III}, determined from the spectral deconvolution [eq. (1)].

[d] ^{139}La transverse relaxation rate of uncomplexed La^{III} (site A). Due to its very large value, only an estimate could be obtained for T_{2B}^{-1}: 65, 54 and 28 kHz, respectively, for $[La^{III}]_0$ = 200, 100 and 50 mM.

[e] ^{139}La chemical shift of uncomplexed La^{III}.

[f] ^{139}La chemical shift of La^{III}–18C6.

written using Varian "magical" software to digitize and send the data to the PC (*Varian Magnetic Moments* 1987, **3**, 12). The data files were transferred to the mainframe through a Sytek line.

RESULTS AND DISCUSSION

The ^{139}La NMR spectrum of a 0.2 M solution of $LaCl_3 \cdot 7H_2O$ in methanol consists of a single, broad, Lorentzian line, characterized by a chemical shift of 165 ppm, and a linewidth of 1.90 kHz. The addition of 18C6 to the solution resulted in the appearance of a much broader line resonating at lower frequency. The lineshapes were also invariant with temperature variations (300 K < T < 330 K). This is an indication of two species in very slow exchange on the chemical shift time scale. Figure 1 shows the ^{139}La NMR spectra of two solutions of hydrated lanthanum chloride in methanol in the presence of 18C6. Since the crown ether is known to form a 1:1 complex with La^{III} in methanol,[15] the simplest interpretation for the observed ^{139}La spectra is that they result from the superposition of two Lorentzian absorption lines corresponding to the uncomplexed La^{III} solvated cation, and to the 1:1 La^{III}–18C6 complex.

The spectrum resulting from the superposition of two Lorentzian signals can be described by eq. (1),[16,17] which is the two-site slow exchange case ($k \to 0$) of the general equation given by Gold and Zdunek[17] for an imperfectly phase-corrected spectrum:

$$I(\nu) = C[(M+N)\cos\phi + (P+Q)\sin\phi] + B, \quad (1)$$

$$M = T_{2A}P_A/(1+4\pi^2T_{2A}^2(\nu_A-\nu)^2)$$

$$N = (1-P_A)T_{2B}/(1+4\pi^2T_{2B}^2(\nu_B-\nu)^2)$$

$$P = T_{2A}^2P_A(\nu_A-\nu)/(1+4\pi^2T_{2A}^2(\nu_A-\nu)^2)$$

$$Q = (1-P_A)T_{2B}^2(\nu_B-\nu)/(1+4\pi^2T_{2B}^2(\nu_B-\nu)^2).$$

T_{2A}, T_{2B} and ν_A, ν_B correspond to the transverse relaxation times and the chemical shifts of the solvated (A) and complexed (B) sites, respectively; C is a scaling factor; and P_A is the population of site A (here, uncomplexed $^{139}La^{III}$). It was difficult to adequately adjust the phase and baseline of the broad, overlapping peaks. Consequently, the simulation of these spectra required phase (ϕ) and baseline (B) parameters to be included in the lineshape equation.

Table 1 gives the results of the deconvolution of the observed spectra on the basis of eq. (1), for three La^{III} total concentrations and several values of the ratio $\rho = [18C6]_0/[La^{III}]_0$. The transverse relaxation rate characterizing the solvated site, T_{2A}^{-1}, was found to be constant, within experimental error, for a given total La^{III} concentration: 6.8 kHz (0.2 M), 6.3 kHz (0.1 M) and 5.1 kHz (0.05 M). The decrease of the relaxation rate as the concentration decreases is an indication of ionic association. This is further confirmed by the variation of the chemical shift for the solvated La^{III}: 165, 194 and 230 ppm, respectively, for $[La^{III}]$ = 0.2, 0.1, and 0.05 M. The same trend is observed, but to a lesser extent, for the chemical shifts of the complex species: 130, 150 and 167 ppm. All these observations point to the evidence of the participation of the chloride anion in the first coordination sphere of the lanthanum cation, both in the solvated and complexed species. This has recently been shown to be the case in the solid state for a hydrated gadolinium chloride complex with 18C6.[5b] McCain[18] has studied concentrated solutions of $LaCl_3$ in methanol, water and binary mixtures of methanol and water, by ^{139}La and ^{35}Cl NMR. The ^{139}La chemical shift of a 1.45 M $LaCl_3$ solution in methanol was found to be 293 ppm, and the linewidth was 3800 Hz. These values

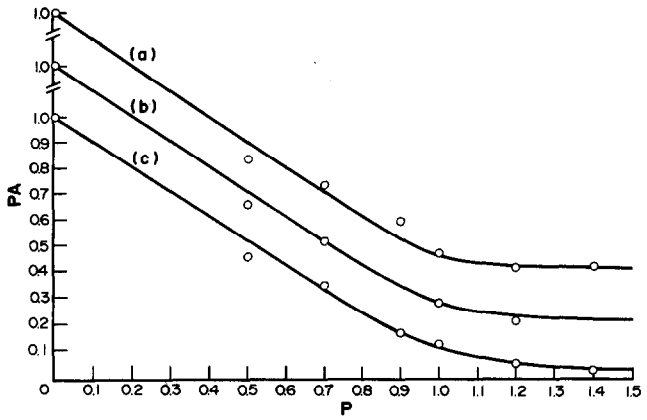

Fig. 2. Normalized populations of uncomplexed La^{III} as a function of $\rho = [18C6]_0/[La^{III}]_0$. $T = 300.0 \pm 0.5$ K. The data points have been obtained from the non-linear regression analysis on eq. (1) shown in Fig. 1 and the solid lines have been calculated on the basis of $\log K_f = 3.2$. $[La^{III}]_0$ = (a) 0.200, (b) 0.100 and (c) 0.050 M.

are of the same order of magnitude as reported in this study. In the binary mixtures, there was evidence for the formation of an La—Cl inner-sphere complex when the precentage of methanol was greater than 66%.

Despite the fact that the nature of the coordinating atoms (oxygens) is the same in the solvent and in the macrocyclic ligand, substantial chemical shift differences between the solvated and the complexed cations can be observed. This could be an indication that, in methanol solution, the crown ether occupies the first coordination sphere of the La^{III} cation. However, due to the paucity of ^{139}La data in the literature, and the lack of possible comparison with similar systems, this point will have to be checked in further studies. Only an estimate could be obtained for the value of the transverse relaxation rate of the complexed $^{139}La^{III}$, which is in the range 28–65 kHz. This very large value reflects a large quadrupolar coupling constant resulting from a strong dissymmetry of the electric charges in the first coordination shell of the La^{III} cation. Again, this is in good agreement with a direct coordination of the crown ether on La^{III}.

From the populations of the solvated (see Table 1) and of the complexed lanthanum cation, it was possible to calculate an equilibrium constant of formation for the 1:1 La^{III}–18C6 complex. A mean value of $\log K_f = 3.2 \pm 0.5$ was obtained. This value is in excellent agreement with the result obtained by Izatt *et al.* on the same system,[15] using titration calorimetry ($\log K_f = 3.29$). Figure 2 shows the population of the solvated La^{III} as a function of the ratio $[18C6]_0/[La^{III}]_0$. The data points are experimental and the solid lines have been calculated from the value of $\log K_f = 3.2$.

In conclusion, the present work demonstrates the potential of ^{139}La NMR to become a very useful technique for probing the structure of lanthanum cations in solution. In the particular case studied here, of hydrated $LaCl_3$ in the presence of 18C6 in methanol, both chemical shift and relaxation rate data point to the participation of the chloride counteranion and of the crown ether in the first coordination sphere of La^{III} in methanolic solutions. Further work is in progress in our laboratory to collect ^{139}La NMR data on other systems, and to access the kinetic parameters of the exchange between the various species in equilibrium in solution.

Acknowledgement—The Natural Science and Engineering Research Council of Canada (NSERCC) is acknowledged for financial support.

REFERENCES

1. J.-C. G. Bünzli and D. Wessner, *Coord. Chem. Rev.* 1984, **60**, 191.
2. J.-C. G. Bünzli and D. Wessner, *Helv. Chim. Acta* 1981, **64**, 582.
3. J.-C. G. Bünzli, W. D. Harrison, A. Giorgetti, G.-O. Pradervand and N. W. Alcock, *Inorg. Chim. Acta* 1985, **109**, 59.
4. C. J. Pedersen, *J. Am. Chem. Soc.* 1967, **89**, 7017.
5. (a) F. Nicolo, D. Plancherel, J.-C. G. Bünzli and G. Chapuis, *Helv. Chim. Acta* 1987, **70**, 1798; (b) R. D. Rogers and L. K. Kurihara, *Inorg. Chem.* 1987, **26**, 1498; (c) R. D. Rogers and L. K. Kurihara, *Inorg. Chim. Acta* 1987, **130**, 131.
6. (a) J. D. Simon, W. R. Moomaw and T. M. Ceckler, *J. Phys. Chem.* 1985, **89**, 5659; (b) D. H. Metcalf, R. C. Carter, R. G. Ghirardelli and R. A. Palmer, *Inorg. Chem.* 1986, **25**, 2175.

7. C. Detellier, in *NMR of Newly Accessible Nuclei* (Edited by P. Laszlo), Vol. 2, Chap. 5. Wiley, New York (1983).
8. (a) H. D. H. Stöver, A. Delville and C. Detellier, *J. Am. Chem. Soc.* 1985, **107**, 4167; (b) H. D. H. Stöver, L. J. Maurice, A. Delville and C. Detellier, *Polyhedron* 1985, **4**, 1091; (c) H. D. H. Stöver, M. Robillard and C. Detellier, *Polyhedron* 1987, **6**, 577.
9. D. Rehder, in *Multinuclear NMR* (Edited by J. Mason), Chap. 19. Plenum Press, New York (1987).
10. (a) W. H. Chambers and D. Williams, *Phys. Rev.* 1949, **76**, 461; (b) W. Dickinson, *Phys. Rev.* 1949, **76**, 1414.
11. (a) S. H. Eggers, M. Adam, E. T. K. Haupt and R. D. Fisher, *Inorg. Chim. Acta* 1987, **139**, 315; (b) J.-C. G. Bünzli, A. F. Merbach and R. M. Nielson, *Inorg. Chim. Acta* 1987, **139**, 151; (c) D. F. Evans and P. H. Missen, *J. Chem. Soc., Dalton Trans.* 1982, 1929; (d) P. L. Rinaldi, S. A. Khan, G. R. Choppin and G. C. Levy, *J. Am. Chem. Soc.* 1979, **101**, 1350; (e) O. Lutz and H. Oehler, *J. Mag. Res.* 1980, **37**, 261.
12. H. P. Graves and C. Detellier, *J. Am. Chem. Soc.* 1988, **110**, 6019.
13. K. M. Brière and C. Detellier, *J. Phys. Chem.* 1987, **91**, 6097.
14. *SAS User's Guide: Statistics*, Version 5, 198X, Chap. 25, p. 575.
15. R. M. Izatt, J. D. Lamb, J. J. Christensen and B. L. Haymore, *J. Am. Chem. Soc.* 1977, **99**, 8344.
16. (a) S. F. Lincoln, *Prog. React. Kinet.* 1979, **9**, 1; (b) J. Sandström, *Dynamic NMR Spectroscopy*. Academic Press, New York (1982).
17. V. Gold and L. Z. Zdunek, *J. Chem. Soc., Faraday Trans. II* 1982, **78**, 1835.
18. D. C. McCain, *J. Inorg. Nucl. Chem.* 1980, **42**, 1185.

Polyhedron Vol. 8, No. 16, pp. 2035–2040, 1989
Printed in Great Britain

0277–5387/89 $3.00+.00
© 1989 Maxwell Pergamon Macmillan plc

SYNTHESIS OF UNSATURATED METHYL(ALKYLIDYNE)DITUNGSTEN COMPLEXES, $[W_2(\mu\text{-CR})(Me)(CO)_3(\eta\text{-}C_5H_5)_2]$ (R = C_6H_4Me-4 OR C_6H_4OMe-2); CRYSTAL STRUCTURE OF THE COMPOUND WITH R = C_6H_4OMe-2

IAN J. HART, JUDITH A. K. HOWARD, RACHEL M. LOWRY, THOMAS P. SPANIOL and F. GORDON A. STONE*

Department of Inorganic Chemistry, The University of Bristol, Bristol BS8 1TS, U.K.

(*Received* 30 *January* 1989; *accepted* 15 *March* 1989)

Abstract—In light petroleum at reflux temperatures, the compounds $[W(Me)(\eta\text{-}C_2H_4)(CO)_2(\eta\text{-}C_5H_5)]$ and $[W(\equiv CR)(CO)_2(\eta\text{-}C_5H_5)]$ (R = C_6H_4Me-4 or C_6H_4OMe-2) afford the ditungsten complexes $[W_2(\mu\text{-CR})(Me)(CO)_3(\eta\text{-}C_5H_5)_2]$. The structure of the product with R = C_6H_4OMe-2 has been established by X-ray diffraction. The W—W bond (2.761(1) Å) is spanned symmetrically by the CC_6H_4OMe-2 group (μ-C—W, 2.01(1) Å). One tungsten atom carries a cyclopentadienyl ligand and two carbonyl groups, one of which weakly semi-bridges the metal–metal bond (W—C—O, 168.3(9)°). The other tungsten atom is ligated by a cyclopentadienyl ring, and by a carbonyl and a methyl group (W—CH_3, 2.24(2) Å).

We have previously reported[1] that UV irradiation of mixtures of the compounds $[M(Me)(CO)_3(\eta\text{-}C_5H_5)]$ (M = Mo or W) and $[W(\equiv CR)(CO)_2(\eta\text{-}C_5H_5)]$ (R = C_6H_4Me-4 or C_6H_4OMe-2) in light petroleum affords the complexes $[MW\{\mu\text{-}C(R)C(O)Me\}(CO)_4(\eta\text{-}C_5H_5)_2]$ (**1**). This reaction involves a coupling of methyl, carbonyl and alkylidyne groups at a dimetal centre. However, the pathway by which these products were formed was by no means clear. Herein we describe related reactions between the ethylene complex $[W(Me)(CO)_2(\eta\text{-}C_2H_4)(\eta\text{-}C_5H_5)]$ and the alkylidine–tungsten species $[W(\equiv CR)(CO)_2(\eta\text{-}C_5H_5)]$, which yield products relevant to the formation of compounds **1**.

RESULTS AND DISCUSSION

The complex $[W(Me)(CO)_2(\eta\text{-}C_2H_4)(\eta\text{-}C_5H_5)]$ was generated by irradiating $[W(Me)(CO)_3(\eta\text{-}C_5H_5)]$ with UV light in the presence of ethylene.[2] It was then treated with $[W(\equiv CC_6H_4Me\text{-}4)(CO)_2(\eta\text{-}C_5H_5)]$; the mixture being refluxed in light petroleum. Separation of products by column chromatography on alumina gave purple crystals of the ditungsten compound $[W_2(\mu\text{-}CC_6H_4Me\text{-}4)(Me)(CO)_3(\eta\text{-}C_5H_5)_2]$ (**2a**), a trace of the previously characterized complex $[W_2\{\mu\text{-}C(C_6H_4Me\text{-}4)C(O)Me\}(CO)_4(\eta\text{-}C_5H_5)_2]$ (**1b**)[1] and an unidentified exceedingly insoluble green material. In a similar reaction, the compounds $[W(Me)(CO)_2(\eta\text{-}C_2H_4)(\eta\text{-}C_5H_5)]$ and $[W(\equiv CC_6H_4OMe\text{-}2)(CO)_2(\eta\text{-}C_5H_5)]$ gave a chromatographical separable mixture of $[W_2(\mu\text{-}CC_6H_4OMe\text{-}2)(Me)(CO)_3(\eta\text{-}C_5H_5)_2]$ (**2b**), a trace of **1d** and the μ-alkyne complex $[W_2\{\mu\text{-}C_2(C_6H_4OMe\text{-}2)_2\}(CO)_4(\eta\text{-}C_5H_5)_2]$ (**3**).

The IR and NMR data for the compounds **2** and **3** were in accord with the formulations proposed. Moreover, as described below, the structure of **2b** was confirmed by an X-ray diffraction study. The IR spectrum of **2a** in the carbonyl region shows three bands at 1941, 1908 and 1835 cm^{-1}, as expected. The absorption at 1835 cm^{-1} may be attributed to a semi-bridging carbonyl group. The ^1H NMR spectrum showed all the expected peaks, including a resonance for the WMe group at −0.40 ppm (J(WH) 7 Hz). The $^{13}C\text{-}\{^1H\}$ NMR spectrum displayed a diagnostic resonance for the μ-C nucleus at δ 360.7 ppm, with two sets of $^{183}W\text{–}^{13}C$ satellite peaks [J(WC) 120 and 101 Hz]. This pattern is in agreement with the $\mu\text{-}CC_6H_4Me$-4 ligand being attached to non-equivalent tungsten

* Author to whom correspondence should be addressed.

Table 1. Selected bond distances (Å) and angles (°) for $[W_2(\mu\text{-}CC_6H_4OMe\text{-}2)(Me)(CO)_3(\eta\text{-}C_5H_5)_2]$ (**2b**)

W(1)—W(2)	2.761(1)	W(2)—C(1)	2.01(1)	O(02)—C(02)	1.44(2)
W(1)—C(1)	2.01(1)	W(2)—C(2)	1.94(1)	C(2)—O(2)	1.16(2)
W(1)—C(4)	1.92(1)	W(2)—C(3)	1.99(1)	C(3)—O(3)	1.14(2)
W(1)—C(5)	2.24(2)	C(1)—C(11)	1.47(1)	C(4)—O(4)	1.17(1)
		C(12)—O(02)	1.39(1)		
C(1)—W(1)—W(2)	46.6(3)	C(1)—W(2)—W(1)	46.5(2)	W(1)—C(1)—W(2)	86.9(4)
C(1)—W(1)—C(4)	71.6(4)	C(1)—W(2)—C(2)	107.3(4)	W(2)—C(1)—C(11)	143.9(6)
C(1)—W(1)—C(5)	97.6(4)	C(1)—W(2)—C(3)	108.0(4)	W(2)—C(1)—C(11)	129.2(6)
C(4)—W(1)—W(2)	118.2(3)	C(2)—W(2)—W(1)	68.1(3)	C(11)—C(12)—O(02)	113.4(8)
C(4)—W(1)—C(5)	86.3(5)	C(3)—W(2)—W(1)	82.7(3)	C(12)—O(02)—C(02)	118.1(9)
C(5)—W(1)—W(2)	100.3(3)	C(2)—W(2)—C(3)	88.2(5)		
W(1)—C(4)—O(4)	173.8(10)	W(2)—C(2)—O(2)	168.3(9)	W(2)—C(3)—O(3)	175.7(9)

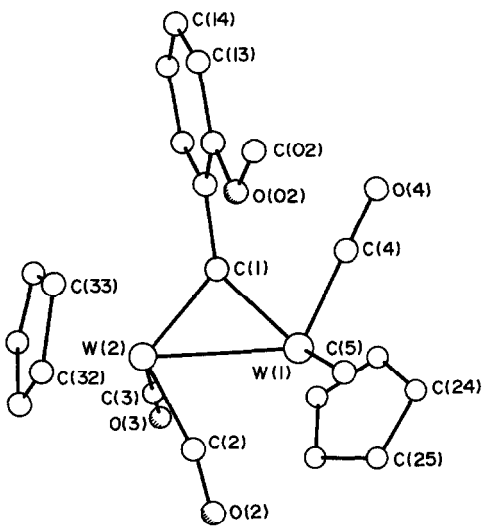

Fig. 1. The molecular structure of $[W_2(\mu\text{-}CC_6H_4OMe\text{-}2)(Me)(CO)_3(\eta\text{-}C_5H_5)_2]$ (**2b**) showing the atom-numbering scheme.

atoms. Moreover, the observed chemical shift is relatively deshielded. This is in accord with a structure in which the C≡W fragment is functioning formally as a four-electron donor,[3] thereby leading to a stable but electronically unsaturated 32 valence-electron species. The three carbonyl groups in **2a** give rise to resonances at δ 238.3, 223.2 and 221.9 ppm. There are two signals (δ 97.7 and 94.1 ppm) for the non-equivalent C_5H_5 ligands, and a characteristic[4] peak for the WMe fragment at δ −15.9 ppm [J(WC) 88 Hz].

Examination of the NMR spectra of **2b** showed that peaks were present corresponding to the presence of two isomers, but discussion is deferred until the results of the X-ray diffraction study are described. The structure is shown in Fig. 1, and selected bond distances and angles are listed in Table 1. The W—W bond (2.761(1) Å) is spanned symmetrically by the alkylidyne group (μ-C—W, 2.01(1) Å). The metal–metal distance is perceptibly shorter than the W—W single bond distances $[W_2(\mu\text{-}HC_2H)(CO)_4(\eta\text{-}C_5H_5)_2]$ (2.987 (1) Å),[5] $[W_2(\mu\text{-}EtC_2Et)(CO)_4(\eta^5\text{-}C_5Et_4C_6H_4Me\text{-}4)(\eta\text{-}C_5H_5)]$ (3.003(1) Å)[6] and $[N(PPh_3)_2][W_2\{\mu\text{-}C(H)C_6H_4Me\text{-}4\}(CO)_7(\eta\text{-}C_5H_5)]$ (3.111(1) Å).[7] However, the W—W separations in the electronically unsaturated 32 valence-electron ditungsten complexes, $[W_2(\mu\text{-}CC_6H_4Me\text{-}4)(CO)_2(L)(\eta^5\text{-}C_9H_7)(\eta^5\text{-}C_2B_9H_9Me_2)]$ [L = $N_2C(C_6H_4Me\text{-}4)_2$ (2.777(1) Å) or O (2.761(1) Å), C_9H_7 = indenyl],[8] are very similar to the metal–metal bond distance in **2b**. Moreover, the fact that C(1) symmetrically spans the W(1)—W(2) bond is also in accord with the electronic unsaturation of **2b** and with electron delocalization within the μ-CW_2 ring. In structures in which an alkylidyne ligand edge-bridges a W—W bond, and the two metal centres have 18 electron shells, the two μ-C—W separations are perceptibly different,[9] indicating the presence of more localized C—W and C=W bonds within the ring. It is noteworthy that the μ-C—W distances in **2b** (2.01(1) Å) are shorter than W=C separation

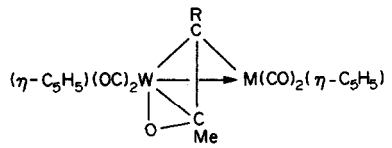

	M	R
(1a)	Mo	C_6H_4Me-4
(1b)	W	C_6H_4Me-4
(1c)	Mo	C_6H_4OMe-2
(1d)	W	C_6H_4OMe-2

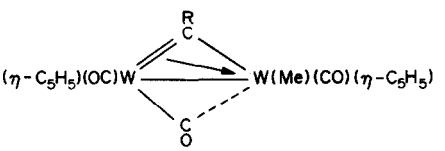

	R
(2a)	C_6H_4Me-4
(2b)	C_6H_4OMe-2

(2.14(2) Å) in $[W(=CPh_2)(CO)_5]$,[10] a molecule in which tungsten has an 18 electron shell.

The W(2) atom in **2b** carries a C_5H_5 ring and two CO groups. However, whereas C(3)O(3) has an essentially linear attachment to the tungsten, the ligand C(2)O(2) weakly semi-bridges the metal–metal bond (W(2)—C(2)—O(2), 168.3(9)°). This is in agreement with the appearance of an IR band at 1835 cm^{-1}, mentioned above. The W(1) atom is ligated by a C_5H_5 ring, a terminal CO ligand and a methyl group. The W(1)—C(5) separation (2.24(2) Å) is within the range expected (2.1–2.3 Å)[11] for σ bonds between tungsten and sp^3 carbon atoms. The *o*-anisol ring in **2b** lies at 99.0° to the plane defined by C(1)W(1)W(2), but with the OMe group and the Me substituent on W(1) on the same side of the μ-CW_2 ring.

The compounds **2** are isolobally mapped with the complex $[W(Me)(CO)(\eta\text{-}C_2H_2)(\eta\text{-}C_5H_5)]$, in which the ethyne molecule functions as a four-electron donor.[12] As mentioned above, complex **2b** is formed as a mixture of two diastereoisomers, a property revealed by the ^1H and $^{13}C\text{-}\{^1H\}$ NMR spectra (see Experimental). The relative intensity of peaks in the spectra indicate that in $CDCl_3$ solution the proportion of the two isomers was *ca* 3 : 1. We suggest that the isomerism arises as a result of the Me and OMe groups being either cisoid (on the same side), or transoid (on the opposite sides) of the μ-CW_2 ring. In the reaction between $[W(\equiv CC_6H_4OMe\text{-}2)(CO)_2(\eta\text{-}C_5H_5)]$ and $[WMe(CO)_2(\eta\text{-}C_2H_4)(\eta\text{-}C_5H_5)]$, the formation of the μ-alkyne complex **3** was unexpected, because in the corresponding reaction involving $[W(\equiv CC_6H_4Me\text{-}4)(CO)_2(\eta\text{-}C_5H_5)]$, the compound $[W_2\{\mu\text{-}C_2(C_6H_4Me\text{-}4)_2\}(CO)_4(\eta\text{-}C_5H_5)_2]$ was not formed. The latter complex is, however, often produced in reactions of $[W(\equiv CC_6H_4Me\text{-}4)(CO)_2(\eta\text{-}C_5H_5)]$ with low-valent metal species.[9,13] Compounds of the type $[M_2(\mu\text{-alkyne})(CO)_4(\eta\text{-}C_5H_5)_2]$ (M = Mo or W) in solution show dynamic behaviour on the NMR timescale,[14,15] and **3** is no exception. Although good quality spectra were not obtained, at −40°C, peaks corresponding to the presence of two isomers were observed, including four CO resonances in the $^{13}C\text{-}\{^1H\}$ NMR spectrum. At room temperature no CO resonances were seen in the spectrum.

In spite of its electronic unsaturation, compound **2a** was unreactive towards PMe_3 or PPh_3 in refluxing tetrahydrofuran (THF), and UV irradiation of **2a** in the presence of PMe_3 was equally fruitless. However, irradiation of **2a** in THF with a stream of CO gas passing through the solution, resulted in the disappearance of the IR bands due to **2a** and the appearance of new carbonyl absorptions at 2018vs, 1972s, 1926s, 1864m, 1678w and 1671w cm^{-1}. On removing the UV source and replacing the CO atmosphere with N_2, these bands gradually disappear, and are replaced by those due to **1b**. Column chromatography of the mixture led to the isolation of **1b** in yields greater than 70%.

Possible pathways to compounds **1b** and **2a** are shown in the Scheme 1, and similar processes can be invoked to account for the formation of the other species, **1** and **2**. The synthesis of **1b** from $[W(Me)(CO)_3(\eta\text{-}C_5H_5)]$ and $[W(\equiv CC_6H_4Me\text{-}4)(CO)_2(\eta\text{-}C_5H_5)]$ proceeds upon UV irradiation of solutions containing a mixture of the two reagents.[1] It is likely that the methyltungsten compound is activated with release of a molecule of CO to give the coordinatively unsaturated species $[W(Me)(CO)_2(\eta\text{-}C_5H_5)]$.[16] The latter could then capture a molecule of $[W(\equiv CC_6H_4Me\text{-}4)(CO)_2(\eta\text{-}C_5H_5)]$ to give intermediate **A**. Reaction of **A** with CO, present in the solutions or scavenged from one of the reactants, might yield the acyl–dimetal complex, **B**, which could collapse to give **1b**. The formation of **2a** from $[W(Me(CO)_2(\eta\text{-}C_2H_4)(\eta\text{-}C_5H_5)]$ and $[W(\equiv CC_6H_4Me\text{-}4)(CO)_2(\eta\text{-}C_5H_5)]$ proceeds in hydrocarbon solvents but only under reflux conditions. Presumably intermediate **A** is again formed, but in the absence of appreciable amounts of free CO in the mixture it releases CO to afford primarily **2a**. The observation that traces of **1b** are formed in the reaction demonstrates the relationship between **2a** and **1b** with the probability of a common intermediate. As mentioned above, UV irradiation of **2a** in the presence of CO gives **1b** in high yield. However, during this conversion the IR spectrum of the mixture shows bands due to a transient species at 1678 and 1671 cm^{-1}, characteristic of an acyl group, as invoked for **B**. The presence of two absorptions near 1675 cm^{-1} may be due to the existence of more than one isomer of **B**. It is noteworthy that **2a** does not react with CO in the absence of UV irradiation. This suggests that **2a** requires initial activation, perhaps to give an intermediate $[W_2(\mu\text{-}CC_6H_4Me\text{-}4)(Me)(CO)_3(\eta\text{-}C_5H_5)_2]$ in which the $(\eta\text{-}C_5H_5)(OC)_2W\equiv CC_6H_4Me\text{-}4$ moiety acts as a two-electron donor to the $W(Me)(CO)(\eta\text{-}C_5H_5)$ fragment. The latter would then possess a 16 electron tungsten centre which would capture a CO molecule to give **A**; which via additional CO could yield **1b**, through the intermediacy of **B**. The conversion of **B** into the product **1b** may involve more than one step. Thus, transfer of the acyl group to the μ-$CC_6H_4Me\text{-}4$ fragment might produce a μ-$C(C_6H_4Me\text{-}4)C(O)Me$ ligand in a species containing a W=W bond. This intermediate (not shown), with the bridging group functioning as a two-electron donor, could transform into **1b**, in which the organic group contributes

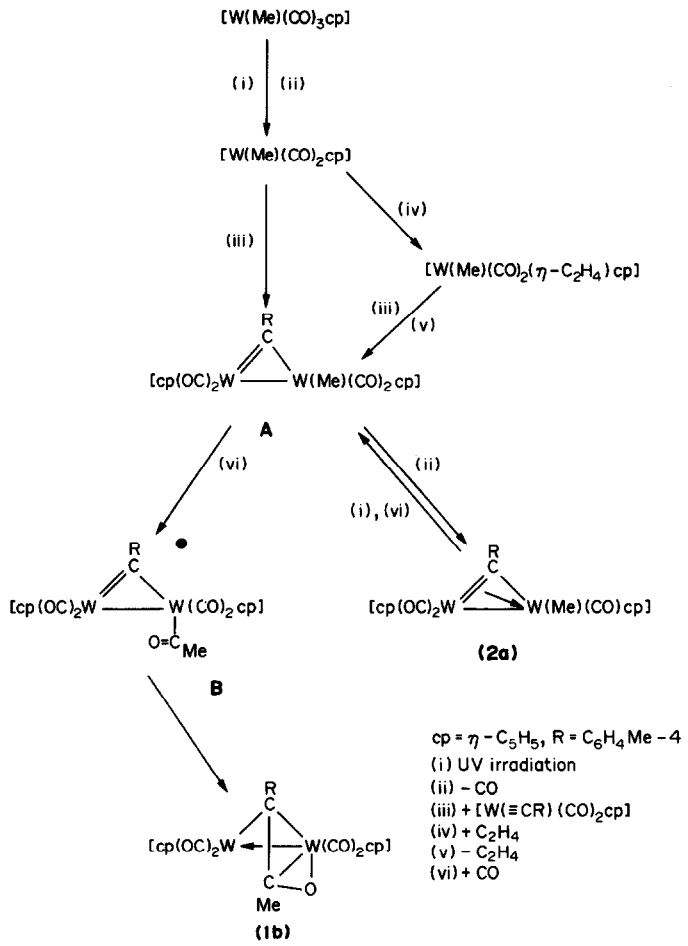

Scheme 1.

four electrons to the ditungsten system. The process would be similar to the transfer of a terminally bound formyl group to a μ-thio-alkylidyne ligand, as in the formation of the complexes $[Fe_2\{\mu\text{-}C(SMe)C(H)O\}(\mu\text{-}CO)(CO)(\eta\text{-}C_5H_5)_2]$.[17] We have attempted to isolate intermediates such as **A** or **B** by UV irradiation of CO saturated solutions of **1b**, but no reaction was observed.

EXPERIMENTAL

Light petroleum refers to that fraction of bp 40–60°C. All reactions were carried out under N_2, using Schlenk tube techniques. Chromatography columns employed BDH alumina (Brockman activity II). The compounds $[W(\equiv CR)(CO)_2(\eta\text{-}C_5H_5)]$ (R = C_6H_4Me-4 or C_6H_4OMe-2) were prepared by procedures described elsewhere,[3,18] while $[W(Me)(CO)_2(\eta\text{-}C_2H_4)(\eta\text{-}C_5H_5)]$[2] was obtained by irradiating $[W(Me)(CO)_3(\eta\text{-}C_5H_5)]$ in light petroleum with UV light (Hanovia medium pressure mercury vapour lamp) under a stream of C_2H_4, the reagent thus prepared being used *in situ*. IR spectra were measured (in CH_2Cl_2) with Nicolet MX-1 and 5ZDX FT spectrophotometers. The NMR spectra were recorded in $CDCl_3$ using JNM JEOL FX90Q, GX270 and GX400 FT spectrometers. The $^{13}C\{^1H\}$ chemical shifts are to high frequency of $SiMe_4$ (0.0 ppm).

Synthesis of the compounds $[W_2(\mu\text{-}CR)(Me)(CO)_3(\eta\text{-}C_5H_5)_2]$

(i) The complex $[W(Me)(CO)_3(\eta\text{-}C_5H_5)]$ (1.75 g, 5.0 mmol) in light petroleum (300 cm^3) was irradiated with UV light at −20°C for *ca* 4 h; the conversion to $[W(Me)(CO)_2(\eta\text{-}C_2H_4)(\eta\text{-}C_5H_5)]$ being monitored periodically by IR. The compound $[W(\equiv CC_6H_4Me\text{-}4)(CO)_2(\eta\text{-}C_5H_5)]$ (1.43 g, 3.5 mmol) was added, and the mixture was refluxed for 6 h. Removal of solvent *in vacuo* gave a brown residue which was dissolved in CH_2Cl_2 (10 cm^3) and chromatographed (3 × 20 cm column). Elution with light petroleum removed traces of $[W(Me)(CO)_3(\eta\text{-}C_5H_5)]$. Elution with CH_2Cl_2–light petroleum (2 : 1) gave a purple fraction and a red

fraction. Removal of solvent *in vacuo* from the purple eluate, and crystallization of the residue from CH_2Cl_2–light petroleum (15 cm^3, 1:10) at −78°C gave purple *microcrystals* of $[W_2(\mu\text{-}CC_6H_4Me\text{-}4)(Me)(CO)_3(\eta\text{-}C_5H_5)_2]$ (**2a**) (0.51 g, 21%), ν_{max}(CO) at 1941m, 1908vs and 1835m cm^{-1}. (Found: C, 35.3; H, 3.0. $C_{22}H_{20}O_3W_2 \cdot CH_2Cl_2$ requires: C, 35.2; H, 2.8%). NMR: ^1H, δ −0.40 [s, 3H, WMe, J(WH) 7 Hz], 2.43 (s, 3H, Me-4), 5.34, 5.36 (s × 2, 10H, C_5H_5), 6.29–7.16 (m, 4H, C_6H_4). $^{13}C\text{-}\{^1H\}$, δ 360.7 [μ-C, J(WC) 120 and 101], 238.3 [CO, J(WC) 156], 223.2 [CO, J(WC) 170], 221.9 [CO, J(WC) 168], 165.5 [$C^1(C_6H_4)$], 134.2, 127.7, 127.4, 122.4, 119.0 (C_6H_4), 97.7, 94.1 (C_5H_5), 21.1 (Me-4), and −15.9 ppm [MeW, J(WC) 88 Hz].

The red eluate from the column was identified by IR as containing a trace of **1b**. A final elution of the column with THF recovered a green eluate, which after removal of solvent *in vacuo* gave green microcrystals (*ca* 0.2 g), as yet unidentified.

(ii) In a similar experiment, the compound $[W(Me)(CO)_2(\eta\text{-}C_2H_4)(\eta\text{-}C_5H_5)]$ (prepared from $[W(Me)(CO)_3(\eta\text{-}C_5H_5)]$ (1.75 g, 5.0 mmol) and C_2H_4) was treated with $[W(\equiv CC_6H_4OMe\text{-}2)(CO)_2(\eta\text{-}C_5H_5)]$ (1.48 g, 3.5 mmol). Separation of products, as described above, afforded purple *microcrystals* of $[W_2(\mu\text{-}CC_6H_4OMe\text{-}2)(Me)(CO)_3(\eta\text{-}C_5H_5)_2]$ (**2b**) (0.45 g, 18%), red *microcrystals* of $[W_2\{\mu\text{-}C_2(C_6H_4OMe\text{-}2)_2\}(CO)_4(\eta\text{-}C_5H_5)_2]$ (0.30 g) and a trace of red **1d**.

For **2b**, ν_{max}(CO) at 1939m, 1907vs and 1830m cm^{-1}. NMR (peaks with asterisk due to minor isomer), ^1H, δ −0.41*, −0.25 [s × 2, 3H, MeW, J(WH) 7], 3.55*, 3.58 (s × 2, 3H, OMe), 5.30, 5.32*, 5.33, 5.36* (s × 4, 10H, C_5H_5), 6.22–6.95 (m, 4H, C_6H_4). $^{13}C\text{-}\{^1H\}$ (measured at −40°C), δ 359.9, 357.3* (μ-C), 237.9 (CO, both isomers), 225.7, 224.0*, 223.2*, 222.2 (CO), 157.9, 157.8* [$C^1(C_6H_4)$], 150.4*, 150.0, 127.3, 127.1*, 125.2, 121.4*, 120.5*, 120.2, 112.1*, 111.2 (C_6H_4), 98.4*, 98.0, 95.0*, 94.6 (C_5H_5), 56.8*, 56.4 (OMe), −12.3, and −15.7* [MeW, J(WC) 87 Hz]. For $[W_2\{C_2(C_6H_4OMe\text{-}2)_2\}(CO)_4(\eta\text{-}C_5H_5)_2]$ (**3**), ν_{max}(CO) at 1969vs, 1937s and 1845m cm^{-1}. NMR (at −40°C); ^1H, δ 3.46*, 3.66 (s × 2, br, 6H, OMe), 5.56 (sbr, 10H, C_5H_5), 6.82–7.32 (m, 8H, C_6H_4). $^{13}C\text{-}\{^1H\}$, δ 231.1, 225.6, 221.4, 213.2 (CO), 164.2*, 157.0, 146.1, 144.3, 134.4*, 131.9*, 127.5, 124.5*, 122.2, 120.2, 112.6*, 110.6 (C_6H_4), 94.3, 91.7* (C_5H_5), 55.6* and 54.5 (OMe).

Crystal structure determination of $[W_2(\mu\text{-}CC_6H_4OMe\text{-}2)(Me)(CO)_3(\eta\text{-}C_5H_5)_2]$ (**2b**)

Crystals of **2b** were grown as dark purple prisms from Et_2O–light petroleum. Diffracted intensities were recorded at 298 K on a crystal of dimensions *ca* 0.2 × 0.2 × 0.4 mm. Of the 3624 reflections ($2\theta \leqslant 50°$), measured on a Nicolet R3m/μ four-circle diffractometer (θ–2θ scans), 2690 had $F \geqslant 3.0\sigma(F)$, and only these were used in the solution and refinement of the structure. Intensity data were corrected for Lorentz, polarization and X-ray absorption effects, the latter by an empirical method based on azimuthal scan data.[19]

Crystal data. $C_{22}H_{20}O_4W_2$, M = 716.1, monoclinic, a = 15.462(2), b = 16.354(2), c = 8.406(1) Å, β = 105.31(1)°, U = 2050(1) $Å^3$, D_c = 2.32 g cm^{-3}, Z = 4, $F(000)$ = 1328, space group $P2_1/a$ (No. 14), Mo-K_α X-radiation (graphite monochromator, $\bar{\lambda}$ = 0.71073 Å), μ(Mo-K_α) = 114.8 cm^{-1}.

The structure was solved, and all non-hydrogen atoms were located, by conventional heavy-atom and difference-Fourier methods. Hydrogen atoms were included in calculated positions (C—H 0.96 Å) with common refined isotropic thermal parameters for groups of related hydrogen atoms. All remaining atoms were given anisotropic thermal parameters. Refinement by full-matrix least-squares, with a weighting scheme of the form $w^{-1} = [\sigma^2(F) + 0.0009|F|^2]$, converged at R = 0.034 (R' = 0.036).* The final electron-density difference synthesis showed no peaks $\geqslant$1.5 or $\leqslant$−1.1 e $Å^{-3}$. Scattering factors, with corrections for anomalous dispersion, were from ref. 20. All calculations were carried out on a DEC micro-Vax II computer with the SHELXTL PLUS system of programs.[19]

REFERENCES

1. I. J. Hart, J. C. Jeffery, R. M. Lowry and F. G. A. Stone, *Angew. Chem. Int. Ed. Engl.* 1988, **27**, 1703.
2. C. G. Kreiter, K. Nist and H. G. Alt, *Chem. Ber.* 1981, **114**, 1845; H. G. Alt, J. A. Schwärzle and C. G. Kreiter, *J. Organomet. Chem.* 1976, **153**, C7.
3. S. J. Dossett, A. F. Hill, J. C. Jeffery, F. Marken, P. Sherwood and F. G. A. Stone, *J. Chem. Soc., Dalton Trans.* 1988, 2453.
4. B. E. Mann and B. F. Taylor, ^{13}C *NMR Data for Organometallic Compounds.* Academic Press, New York (1981).
5. D. S. Ginley, C. R. Bock, M. S. Wrighton, B. E. Fischer, D. L. Tipton and R. Bau, *J. Organomet. Chem.* 1978, **157**, 41.

* Tables of atomic positional and thermal parameters and F_o/F_c values have been deposited as Supplementary Data with the Editor, from whom copies are available on request. Atomic coordinates have also been deposited with the Cambridge Crystallographic Data Centre.

6. G. A. Carriedo, J. A. K. Howard, D. B. Lewis, G. E. Lewis and F. G. A. Stone, *J. Chem. Soc., Dalton Trans.* 1985, 905.
7. D. Hodgson, J. A. K. Howard, F. G. A. Stone and M. J. Went, *J. Chem. Soc., Dalton Trans.* 1985, 1331.
8. J. A. K. Howard, A. P. James, A. N. de M. Jelfs, C. M. Nunn and F. G. A. Stone, *J. Chem. Soc., Dalton Trans.* 1987, 1221.
9. L. J. Farrugia, J. C. Jeffery, C. Marsden, P. Sherwood and F. G. A. Stone, *J. Chem. Soc., Dalton Trans.* 1987, 51.
10. C. P. Casey, T. J. Burkhardt, C. A. Bunnell and J. C. Calabrese, *J. Am. Chem. Soc.* 1977, **99**, 2127.
11. D. M. Collins, F. A. Cotton, S. Koch, M. Millar and C. A. Murillo, *J. Am. Chem. Soc.* 1977, **99**, 1259; M. H. Chisholm, F. A. Cotton, M. W. Extine and B. R. Stults, *Inorg. Chem.* 1976, **15**, 2252; 1977, **16**, 603.
12. H. G. Alt, *J. Organomet. Chem.* 1977, **127**, 349.
13. M. Green, J. C. Jeffery, S. J. Porter, H. Razay and F. G. A. Stone, *J. Chem. Soc., Dalton Trans.* 1982, 2475; M. Green, S. J. Porter and F. G. A. Stone, *J. Chem. Soc., Dalton Trans.* 1983, 513; M. Green, J. A. K. Howard, S. J. Porter, F. G. A. Stone and D. C. Tyler, *J. Chem. Soc., Dalton Trans.* 1984, 2553.
14. W. I. Bailey, M. H. Chisholm, F. A. Cotton and L. A. Rankel, *J. Am. Chem. Soc.* 1978, **100**, 5764.
15. J. A. Beck, S. A. R. Knox, R. F. D. Stansfield, F. G. A. Stone, M. J. Winter and P. Woodward, *J. Chem. Soc., Dalton Trans.* 1982, 195.
16. B. Klein, R. J. Kazlavskas and M. S. Wrighton, *Organometallics* 1982, **1**, 1338.
17. L. Busetto, personal communication.
18. E. O. Fischer, T. L. Lindner, G. Huttner, P. Friedrich, F. R. Kreissl and J. O. Besenhard, *Chem. Ber.* 1977, **110**, 3397.
19. G. M. Sheldrick, SHELXTL programs for use with the Nicolet X-ray system, revision 5-1 (1986).
20. *International Tables for X-ray Crystallography*, Vol. 4. Kynoch Press, Birmingham (1974).

Polyhedron Vol. 8, No. 16, pp. 2041–2045, 1989
Printed in Great Britain

0277–5387/89 $3.00+.00
© 1989 Maxwell Pergamon Macmillan plc

MERCURY THIOETHER CHEMISTRY: THE SYNTHESIS AND STRUCTURE OF $[Hg([9]aneS_3)_2](PF_6)_2$ ([9]aneS$_3$ = 1,4,7-TRITHIACYCLONONANE)

ALEXANDER J. BLAKE, ALAN J. HOLDER, TIMOTHY I. HYDE, GILLIAN REID and MARTIN SCHRÖDER*

Department of Chemistry, University of Edinburgh, West Mains Road, Edinburgh EH9 3JJ, Scotland, U.K.

(*Received* 27 *January* 1989; *accepted* 15 *March* 1989)

Abstract—Reaction of $HgSO_4$ with 2 molar equivalents of [9]aneS$_3$ in refluxing H_2O–MeOH (1:1 v/v) for 1 h affords a colourless solution from which the complex $[Hg([9]aneS_3)_2](PF_6)_2$ can be isolated by addition of NH_4PF_6. $[Hg([9]aneS_3)_2](PF_6)_2 \cdot \frac{1}{3}H_2O$ crystallizes in the monoclinic space group $I2/a$, with $a = 11.8667(10)$, $b = 15.1631(23)$, $c = 14.454(4)$ Å, $\beta = 90.224(19)°$, $V = 2600.7$ Å^3, $D_c = 2.18$ g cm^{-3}, $Z = 4$. The single crystal X-ray structure of the complex shows a crystallographically centrosymmetric cation with hexathia coordination at mercury(II), with Hg—S(1) = 2.728(3), Hg—S(4) = 2.638(3) and Hg—S(7) = 2.712(3) Å. This structure closely resembles that of the silver(I) analogue, $[Ag([9]aneS_3)_2]^+$, which also shows hexathia coordination. Cyclic voltammetry of $[Hg([9]aneS_3)_2]^{2+}$ shows a chemically reversible reduction at $E_{1/2} = -0.15$ V ($\Delta E_p = 80$ mV) vs Fc/Fc^+ at a scan rate of 90 mV s^{-1}.

The chemistry of macrocyclic thioether complexes is of intense current interest.[1,2] We have concentrated our studies on the coordinative properties of tri-, tetra-, penta- and hexathia crowns with the platinum group metal ions,[1] and have found a correspondence between the structures of these complexes and their redox behaviour. The coordinative ambivalence of [9]aneS$_3$ towards metal ions has been central to these studies and had led to the isolation of a range of metal oxidation state species.[3–6]

Few non-porphyrinoid macrocyclic complexes of third-row metal ions have been reported.[7] This is primarily due to the kinetic inertness of these metal ions and the stability of metal complex intermediates leading to full metal insertion. The trithia crown, [9]aneS$_3$, is a particularly attractive ligand for the complexation of third-row metal ions since it incorporates three soft sulphur donors which are pre-organized for facial coordination.[8,9] Binding of [9]aneS$_3$ to a large, inert metal ion, therefore, does not involve metal insertion into a macrocyclic cavity as such, since the formal hole size of [9]aneS$_3$ is too small. We have studied the binding of [9]aneS$_3$ with a range of third row transition metal ions with d^n-configurations from d^5 to d^{10}, e.g. $Os^{II/III}$,[1,3] $Ir^{I/II/III}$,[1] $Pt^{II/III/IV}$,[1,4] $Au^{I/II/III}$.[5] As a continuation of this work, we report herein the synthesis and structure of the d^{10} mercury(II) complex, $[Hg([9]aneS_3)_2]^{2+}$.

The coordination chemistry of [9]aneS$_3$ and related crown ligands with d^{10} metal ions such as zinc(II),[10] cadmium(II),[10] silver(I),[11–14] and gold(I)[5] has been studied. Hexathia coordination at zinc(II)[10] and silver(I)[10–14] has been confirmed. However, the gold(I) species, $[Au([9]aneS_3)_2]^+$, is anomalous, since it adopts a stereochemistry intermediate between that of tetrahedral and linear coordination, with two long and two short Au—S bond lengths i.e. [2+2] coordination.[5] The binding of [14]aneS$_4$ to mercury(II) to afford the dimeric complex $[Hg_2([14]aneS_4)Cl_4]$ has been described previously.[15] This species involves *exo* coordination of two thioether donors of [14]aneS$_4$ to each tetrahedral $HgCl_2$ moiety.[15] Hence, binding of macrocyclic thioether donors to mercury(II) has precedents in the literature,[14,15] and suggested that binding of mercury(II) with [9]aneS$_3$ would be a viable target.

* Author to whom correspondence should be addressed.

RESULTS AND DISCUSSION

Reaction of $HgSO_4$ with 2 molar equivalents of [9]aneS$_3$ in refluxing H_2O–MeOH (1 : 1 v/v) for 1 h gave a colourless solution. Addition of NH_4PF_6 afforded a white product which was recrystallized from H_2O. On the basis of elemental analysis and spectroscopic data the complex was assigned as $[Hg([9]aneS_3)_2](PF_6)_2$. The ^1H NMR spectrum of $[Hg([9]aneS_3)_2](PF_6)_2$ showed a characteristic ABCD pattern for the methylene protons of the macrocyclic ligands (Fig. 1). The ^{13}C NMR spectrum of $[Hg([9]aneS_3)_2]^{2+}$ showed a single resonance at $\delta = 26.6$ ppm assigned to the methylene carbon atoms of [9]aneS$_3$. These data indicated the presence of a single product in solution, with two equivalent [9]aneS$_3$ ligands bound facially to the mercury(II) centre. A single crystal X-ray structure determination was undertaken to confirm the stereochemistry of the complex cation.

Crystals of $[Hg([9]aneS_3)_2](PF_6)_2$ were obtained from H_2O. A view of the cation is shown in Fig. 2. The single crystal X-ray structure of the complex shows a centrosymmetric complex cation: the mercury(II) cation occupies a crystallographic inversion centre with all six thioether donors coordinated to it. Interestingly, the Hg—S distances are not identical: two are significantly shorter (Hg—S(4) = 2.638(3) Å) than the remaining four (Hg—S(1) = 2.728(3), Hg—S(7) = 2.712(3) Å, ∠S(1)HgS(4) = 82.64(9), ∠S(1)HgS(7) = 81.01(8), ∠S(4)HgS(7) = 82.86(9)°), indicating a small but significant

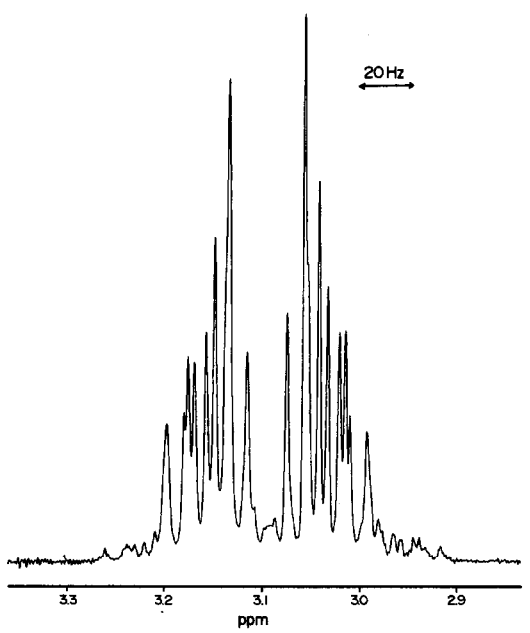

Fig. 1. ^1H NMR spectrum (360 MHz, CD_3CN, 298 K) of $[Hg([9]aneS_3)_2]^{2+}$.

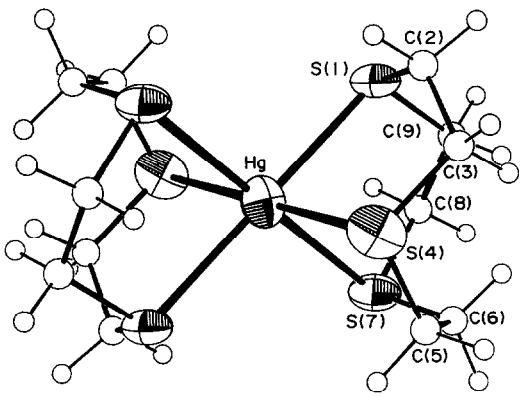

Fig. 2. Single crystal X-ray structure of $[Hg([9]aneS_3)_2]^{2+}$ with numbering scheme adopted.

tetragonal compression for the cation. The related d^{10} complex, $[Ag([9]aneS_3)]^+$, also shows hexathia coordination, with Ag—S bond lengths varying from 2.6665(12) to 2.7813(10) Å, ∠SAgS = 80.35(3), 77.43(3)°.[11] The mercury(II) and silver(I) complexes, therefore, show similar structural features, with the silver(I) species incorporating slightly longer M—S bond lengths reflecting the larger ionic radius of silver(I) over mercury(II) (1.15 vs 1.02 Å[16]). The structural features for these silver(I) and mercury(II) complexes may be interpreted as a compromise between the tendency of second- and particularly third-row d^{10} metal ions to adopt linear coordination, and the preference of [9]aneS$_3$ for facial binding: in the case of mercury(II) and silver(I) the latter appears to dominate.

Interestingly, d^{10} gold(I), which has a particularly strong preference for linear coordination, only binds four thioether donors in $[Au([9]aneS_3)_2]^+$, (Au—S = 2.302(6), 2.350(7), 2.733(8), 2.825(8) Å) to give a structure that is a combination of linear and tetrahedral coordination at gold(I).[5] This contrasts with the recently reported structure of $[Zn([9]aneS_3)_2]^{2+}$ where there is no significant variation in Zn—S bond lengths:[10] these occupy a narrow range (2.491(3)–2.497(3) Å) consistent with the tight coordinative fit of octahedral zinc(II) with facially binding [9]aneS$_3$.

Cyclic voltammetry of $[Hg([9]aneS_3)_2]^{2+}$ shows a chemically reversible reduction at $E_{1/2} = -0.15$ V ($\Delta E_p = 80$ mV) vs Fc/Fc^+ at a scan rate of 90 mV s^{-1} (Fig. 3). Coulometry at 298 K in CH_3CN (0.1 M $^nBuN_4PF_6$) at platinum electrodes shows the reduction to be a two-electron process. However, no stable mercury(I) or mercury(0) species could be isolated under these conditions, with decomposition of the reduction products occurring in solution. The parent mercury(II) complex could not be regenerated from the reduced solution.

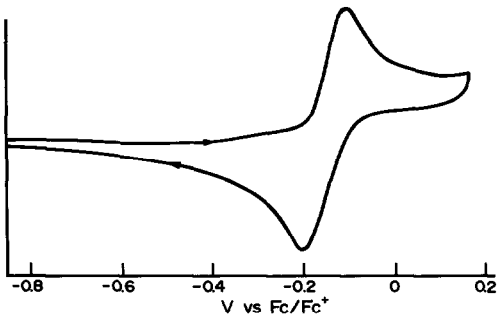

Fig. 3. Cyclic voltammogram of $[Hg([9]aneS_3)_2](PF_6)_2$ in CH_3CN (0.1 M $^nBu_4NPF_6$) at platinum electrodes. Scan rate = 90 mV s^{-1}, 298 K.

We can only speculate at the binding characteristics of [9]aneS$_3$ with $d^{10}s^1$ mercury(I) and/or $d^{10}s^2$ mercury(0). Our previous work has shown that [9]aneS$_3$ binds to gold(I) rather weakly, with the complex $[Au([9]aneS_3)_2]^+$ being highly labile and reactive in solution. Binding of [9]aneS$_3$ to mercury(I) and mercury(0) would be expected to be weaker than with gold(I), explaining the ready decomposition of these low valent mercury complexes in solution. Work is underway to try to stabilize these species at lower temperatures and in alternative solvents.

EXPERIMENTAL

IR spectra were measured as Nujol mulls, KBr and CsI discs using a Perkin–Elmer 598 spectrometer over the range 200–4000 cm^{-1}. UV–vis spectra were measured in quartz cells using Perkin–Elmer Lambda 9 and Pye Unicam SP8-400 spectrophotometers. Microanalyses were performed by the Edinburgh University Chemistry Department microanalytical service. ESR spectra were recorded as solids or as frozen glasses down to 77 K using a Bruker ER200D X-band spectrometer. Electrochemical measurements were performed on a Bruker E310 Universal Modular Polarograph. All readings were taken using a three-electrode potentiostatic system in acetonitrile containing 0.1 M $^nBu_4NPF_6$ or $^nBu_4NBF_4$ as the supporting electrolyte. Cyclic voltammetric measurements were carried out using a double platinum electrode and an Ag/AgCl reference electrode. All potentials are quoted versus ferrocene/ferrocinium (Fc/Fc$^+$). Mass spectra were obtained by electron impact on a Kratos MS 902 and by fast atom bombardment on a Kratos MS 50TC spectrometer. ^{1}H NMR spectra were recorded at 200 and 360 MHz on Bruker WP200 and WH360 spectrometers respectively. ^{13}C NMR spectra were recorded at 50.32 MHz on a Bruker WP200 spectrometer.

Synthesis of $[Hg([9]aneS_3)_2](PF_6)_2$

$HgSO_4$ (0.1 g, 0.34 mmol) was treated with [9]aneS$_3$ (0.13 g, 0.72 mmol) in H_2O–MeOH (30 cm^3, 1:1 v/v) under reflux for 1 h. Addition of excess NH_4PF_6 to the resulting solution afforded a white precipitate, which was collected and recrystallized from water to give $[Hg([9]aneS_3)_2](PF_6)_2$ (0.18 g, 62% yield). Found: C, 16.7; H, 2.91. Calc. for $[Hg([9]aneS_3)_2](PF_6)_2$: C, 16.8; H, 2.90%. ^{1}H NMR spectrum (360 MHz, CD_3CN, 293 K): $\delta = 3.06$ ppm (CH_2, m). ^{13}C NMR spectrum (50.32 MHz, CD_3CN, 293 K): $\delta = 26.6$ ppm (CH_2).

X-ray structure determination of $[Hg([9]aneS_3)_2](PF_6)_2 \cdot \frac{1}{3}H_2O$

A colourless lath (1.00 × 0.173 × 0.078 mm) suitable for X-ray analysis was obtained by recrystallization from hot water.

Crystal data. $C_{12}H_{24}S_6Hg^{2+} \cdot 2PF_6^- \cdot \frac{1}{3}H_2O$, monoclinic, space group $I2/a$ (a non-standard setting of $C2/c$, No. 15), $M = 857.2$, with $a = 11.8667(10)$, $b = 15.1631(23)$, $c = 14.454(4)$ Å, $\beta = 90.224(19)°$, $V = 2600.7$ Å^3, $D_c = 2.18$ g cm^{-3}, [from 2θ values of 20 reflections measured at $\pm\omega$ ($2\theta = 30 \rightarrow 32°$, $\bar{\lambda} = 0.71073$ Å)], $Z = 4$; $F(000) = 1647$, μ(Mo-K_α) = 65.37 cm^{-1}.

Data collection and processing. Stoë STADI-4 four-circle diffractometer, ω–2θ scans with ω scan width $(1.40 + 0.347 \tan\theta)°$, 1722 unique reflections measured ($2\theta_{max} = 45°$, h $-12 \rightarrow 12$, k $0 \rightarrow 14$, l $0 \rightarrow 15$) giving 1236 with $F \geqslant 6\sigma(F)$. Initial absorption correction based on 72Ψ scans (minimum and maximum transmission factors: 0.1036 and 0.1644, respectively). Correction for linear, isotropic crystal decay (*ca* 25%) applied during data reduction.

Structure analysis and refinement. The mercury atom was located from a Patterson synthesis. Iterative rounds of least-squares refinement and difference Fourier synthesis[17] located all other non-hydrogen atoms. At isotropic convergence, final corrections for absorption were made using DIFABS.[18] Anisotropic thermal parameters were refined for mercury, sulphur, phosphorus and the carbon atoms of the cation, and for the two fully occupied fluorine atoms of the disordered PF_6^- ions. Partial occupancies were refined for all other fluorine atoms using fixed isotropic thermal parameters ($U_{iso} = 0.10/0.15$). Hydrogen atoms were included in fixed, calculated positions.[17] The weighting scheme $w^{-1} = \sigma^2(F) + 0.000331F^2$ gave satisfactory agreement analyses. At convergence, R, $R_w = 0.0421$ and 0.0539, respectively, for 156

Table 1. Bond lengths (Å) with standard deviations

Hg—S(1)	2.728(3)	C(3)—S(4)	1.821(13)
Hg—S(4)	2.638(3)	S(4)—C(5)	1.814(12)
Hg—S(7)	2.712(3)	C(5)—C(6)	1.516(16)
S(1)—C(2)	1.790(12)	C(6)—S(7)	1.792(11)
S(1)—C(9)	1.815(11)	S(7)—C(8)	1.799(11)
C(2)—C(3)	1.523(17)	C(8)—C(9)	1.533(15)

Table 2. Angles (°) with standard deviations

S(1)—Hg—S(4)	82.64(9)	Hg—S(4)—C(5)	102.4(4)
S(1)—Hg—S(7)	81.01(8)	C(3)—S(4)—C(5)	104.6(6)
S(4)—Hg—S(7)	82.86(9)	S(4)—C(5)—C(6)	115.5(8)
Hg—S(1)—C(2)	101.0(4)	C(5)—C(6)—S(7)	118.4(8)
Hg—S(1)—C(9)	97.1(4)	Hg—S(7)—C(6)	95.1(4)
C(2)—S(1)—C(9)	103.9(5)	Hg—S(7)—C(8)	104.1(4)
S(1)—C(2)—C(3)	116.7(8)	C(6)—S(7)—C(8)	104.0(5)
C(2)—C(3)—S(4)	117.5(9)	S(7)—C(8)—C(9)	113.5(7)
Hg—S(4)—C(3)	97.6(4)	S(1)—C(9)—C(8)	118.8(8)

Table 3. Selected torsion angles (°) with standard deviations

C(9)—S(1)—C(2)—C(3)	128.4(9)	S(4)—C(5)—C(6)—S(7)	−60.4(11)
C(2)—S(1)—C(9)—C(8)	−51.7(9)	C(5)—C(6)—S(7)—C(8)	−53.0(10)
S(1)—C(2)—C(3)—S(4)	−59.3(11)	C(6)—S(7)—C(8)—C(9)	129.6(18)
C(2)—C(3)—S(4)—C(5)	−53.7(10)	S(7)—C(8)—C(9)—S(1)	−61.1(10)
C(3)—S(4)—C(5)—C(6)	128.2(9)		

parameters, $S = 1.191$. The maximum and minimum residues in the final ΔF syntheses were 0.80 and -0.80 eÅ^{-3}, respectively. The illustration was prepared using ORTEP,[19] molecular geometry calculations utilized CALC,[20] and scattering factor data were taken from ref. 21. Bond lengths and angles are given in Tables 1–3. Atomic positional and thermal parameters, together with F_o/F_c values have been deposited as supplementary data with the Editor, from whom copies are available on request. Atomic coordinates have also been deposited with the Cambridge Crystallographic Data Centre.

Acknowledgement—We thank the SERC for support.

REFERENCES

1. M. Schröder, *Pure Appl. Chem.* 1988, **60**, 517.
2. S. R. Cooper, *Accts Chem. Res.* 1988, **21**, 141.
3. M. N. Bell, A. J. Blake, H-J. Küppers, M. Schröder and K. Wieghardt, *Angew. Chem.* 1987, **99**, 253; *Angew. Chem. Int. Ed. Engl.* 1987, **26**, 250.
4. A. J. Blake, R. O. Gould, A. J. Holder, T. I. Hyde, M. O. Odulate, A. J. Lavery and M. Schröder, *J. Chem. Soc., Chem. Commun.* 1987, 118.
5. A. J. Blake, R. O. Gould, J. A. Greig, A. J. Holder, T. I. Hyde and M. Schröder, *J. Chem. Soc., Chem. Commun.* 1989, in press.
6. M. N. Bell, A. J. Blake, A. J. Holder, T. I. Hyde, A. J. Lavery, G. Reid and M. Schröder, *J. Incl. Phenom.* 1987, **5**, 169; A. J. Blake, A. J. Holder, T. I. Hyde and M. Schröder, *J. Chem. Soc., Chem. Commun.* 1987, 987; A. J. Blake, A. J. Holder, T. I. Hyde, Y. V. Roberts, A. J. Lavery and M. Schröder, *J. Organomet. Chem.* 1987, **323**, 261; A. J. Holder, M. Schröder and T. A. Stephenson, *Polyhedron* 1987, **6**, 461; A. J. Blake, R. O. Gould, A. J. Holder, T. I. Hyde and M. Schröder, *J. Chem. Soc., Dalton Trans.* 1988, 1861.
7. For example see: C-K. Poon, T-W. Tang and C-M. Che, *J. Chem. Soc., Dalton Trans.* 1981, 1697; *J. Chem. Soc., Dalton Trans.* 1983, 1647: J. MacB. Harrowfield, A. J. Herit, P. A. Lay, A. M. Sargeson, A. M. Bond, W. A. Mulac and J. C. Sullivan, *J. Am. Chem. Soc.* 1983, **105**, 5503; A. J. Blake, T. I. Hyde, R. S. E. Smith and M. Schröder, *J. Chem. Soc., Chem. Commun.* 1986, 334; E. Kimura, Y. Lin, R. Machida and H. Zenda, *J. Chem. Soc., Chem. Commun.* 1986, 1020; A. J. Blake, J. A. Greig and M. Schröder, *J. Chem. Soc., Dalton Trans.* 1988, 2645; C. Pomp, S. Drueke, H-J. Küppers, K. Wieg-

hardt, C. Krüger, B. Nuber and J. Weiss, *Z. Naturfor.* 1988, **43B**, 299 and refs therein.
8. R. S. Glass, G. S. Wilson and W. N. Setzer, *J. Am. Chem. Soc.* 1980, **102**, 5068.
9. R. S. Glass, W. N. Setzer, C. A. Ogle and G. S. Wilson, *Inorg. Chem.* 1983, **22**, 266; W. N. Setzer, B. R. Coleman, G. S. Wilson and R. S. Glass, *Tetrahedron Lett.* 1981, **37**, 2743.
10. H-J. Küppers, K. Wieghardt, B. Nuber and J. Weiss, *Z. Anorg. Allg. Chem.*, in press.
11. H-J. Küppers, K. Wieghardt, Y-H. Tsay, C. Krüger, B. Nuber and J. Weiss, *Angew. Chem.* 1987, **99**, 583; *Angew. Chem. Int. Ed. Engl.* 1987, **26**, 575.
12. J. Clarkson, R. Yagbasan, P. J. Blower, S. C. Rawle and S. R. Cooper, *J. Chem. Soc., Chem. Commun.* 1987, 950.
13. A. J. Blake, R. O. Gould, A. J. Holder, T. I. Hyde and M. Schröder, *Polyhedron* 1989, **8**, 513.
14. D. Sevdic and H. Meider, *J. Inorg. Nucl. Chem.* 1977, **39**, 1403 and 1409; D. Sevdic, L. Fekete and H. Meider, *J. Inorg. Nucl. Chem.* 1980, **42**, 885; D. Sevdic and H. Meider, *J. Inorg. Nucl. Chem.* 1981, **43**, 153 and refs therein.
15. N. W. Alcock, N. Herron and P. Moore, *J. Chem. Soc., Chem. Commun.* 1976, 886.
16. R. D. Shannon, *Acta Cryst.* 1976, **A32**, 751.
17. G. M. Sheldrick, SHELX76, Program for crystal structure determination. University of Cambridge, U.K. (1976).
18. N. Walker and D. Stuart, DIFABS, Program for empirical absorption corrections, *Acta Cryst.* 1983, **A39**, 158.
19. P. D. Mallinson and K. W. Muir, ORTEPII, interactive version, *J. Appl. Cryst.* 1985, **18**, 51.
20. R. O. Gould and P. Taylor, CALC, Fortran77 version. University of Edinburgh, Scotland (1985).
21. D. T. Cromer and J. L. Mann, *Acta Cryst.* 1968, **A24**, 321.

Polyhedron Vol. 8, No. 16, pp. 2047–2050, 1989
Printed in Great Britain

0277–5387/89 $3.00+.00
© 1989 Maxwell Pergamon Macmillan plc

TIN–PHOSPHORUS NUCLEAR-SPIN COUPLING IN OCTAHEDRAL COMPLEXES OF TIN(IV)

WILLIAM McFARLANE* and NICHOLAS H. REES

Department of Chemistry, City of London Polytechnic, Jewry Street, London EC3N 2EY, U.K.

(*Received* 21 *February* 1989; *accepted* 15 *March* 1989)

Abstract—Heteronuclear magnetic multiple resonance experiments are used to show that the large values of $^1J(^{119}Sn^{31}P)$ found in tertiary phosphine complexes of tin tetrahalides are negative [corresponding to a positive $^1K(SnP)$], suggesting that the mean excitation energy approximation can provide a valid description of the Fermi contact contribution to this spin coupling interaction, in contrast to the situation for other types of Sn—P interaction over one bond.

Nuclear-spin scalar (J) coupling over one bond has been reported for four main types of tin–phosphorus interaction: (a) tetrahedral Sn^{IV}—P^{III};[1–4] (b) tetrahedral Sn^{IV}—P^V;[2,4] (c) octahedral Sn^{IV}—P^V;[5–7] and (d) trigonal Sn^{II}—P^V,[8] typical ranges for $^1J(^{119}Sn^{31}P)$ being +530–+840, +50–+430, 1400–3000 and 1280–1670 Hz, respectively, with the last two of unknown sign. Note that as $\gamma(^{119}Sn)$ is negative, the corresponding reduced coupling constants $^1K(SnP)$ [defined[9] as $4\pi^2J(^{119}Sn^{31}P)/h\gamma(^{119}Sn)\gamma(^{31}P)$] are negative in cases (a) and (b). This has been attributed[4] to a small s-overlap integral for the tin–phosphorus bond which leads to a breakdown of the mean excitation energy approximation used in certain[10] calculations of the Fermi contact contribution to the coupling constant. However, the *algrebraic increase* in $^1K(SnP)$ between (a) and (b) closely parallels that found[11] in $^1K(PC)$ accompanying the transformation $P^{III} \rightarrow P^V$ for many organophosphorus compounds, although $^1K(PC)$ itself is usually positive in the latter instance. For any discussion[8,12] of the remaining cases it is therefore essential to know the sign of $^1K(SnP)$, and we report here such a determination for species of type (c).

Sign-determining magnetic multiple resonance experiments were performed upon the species $(Et_3P)_2SnCl_4$ and $(Et_3P)(Bu_3P)SnCl_4$. These can be expected to have a *trans* configuration on the basis of X-ray diffraction,[12] IR,[13] Raman[13] and Mössbauer[12,14] spectroscopic studies of related species, and this was confirmed by certain of the NMR spectra as mentioned below.

(i) A 2D $^{13}C/^1H$ chemical shift correlation experiment on $(Et_3P)_2SnCl_4$, using the Bax[15] sequence to achieve simultaneous homonuclear proton decoupling, related carbon and proton transitions associated with particular spin states of the two ^{31}P nuclei, and hence showed for the CH_3 groups $N(^{31}P^{13}C)$ [i.e. $^2J(^{31}P^{13}C)+{}^4J(^{31}P^{13}C)$] to be of opposite sign to $N(^{31}PH)$ [i.e. $^3J(^{31}PH)+{}^5J(^{31}PH)$]. Since $^3J(^{31}PH)$ is generally positive[11] and $^5J(^{31}PH)$ will be negligible, it follows that $N(^{31}P^{13}C)$ is negative.

(ii) Owing to the low natural abundance of ^{13}C, the CH_3 groups and ^{31}P nuclei in $(Et_3P)_2SnCl_4$ form a AA′X spin system [A,A′ = ^{31}P, X = ^{13}C] under conditions of broad band proton decoupling. The ^{31}P spectrum of this system contains weak outer lines whose positions depend upon $^2J(^{31}P^{31}P)$ and they were located by the ^{13}C–{^{31}P} spin tickling experiments[16] shown in Fig. 1. These experiments also showed $^2J(^{31}P^{31}P)$ and $N(^{31}P^{13}C)$ to be of like sign, i.e. negative.

(iii) If attention is confined to magnetically active tin and phosphorus nuclei then the symmetry of $(Et_3P)_2SnCl_4$ precludes relating $^2J(^{31}P^{31}P)$ to $^1J(^{119}Sn^{31}P)$. However, a mixture of $(Et_3P)_2SnCl_4$ and $(Bu_3P)SnCl_4$ was found to contain *ca* 50% of the unsymmetrical species $(Et_3P)(Bu_3P)SnCl_4$, for which $^2J(^{31}P^{31}P)$ is directly measurable at 44.7 Hz. This is almost

* Author to whom correspondence should be addressed.

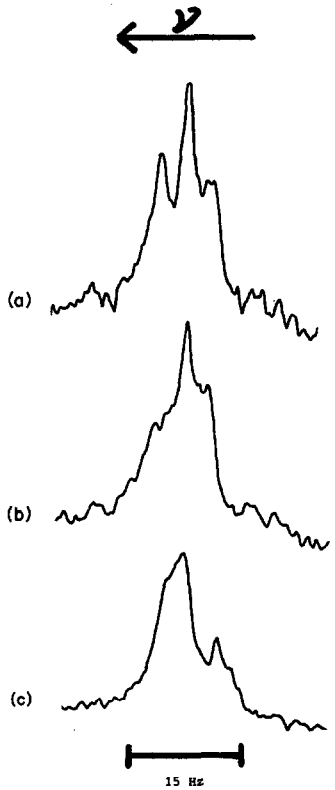

Fig. 1. Proton-decoupled ^{13}C resonance at 22.5 MHz of the methyl groups of *trans*-$(Et_3P)_2SnCl_4$: (a) normal spectrum; (b) with simultaneous irradiation of a weak outer line in the ^{31}P spectrum to high frequency of the central resonance; (c) with simultaneous irradiation of a weak outer line in the ^{31}P spectrum to low frequency of the central resonance.

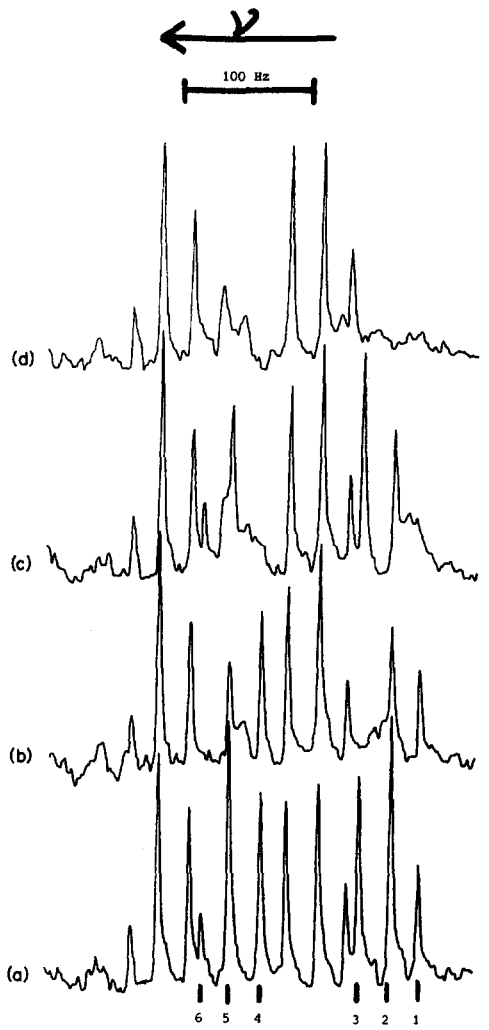

Fig. 2. Low-frequency tin satellites in the proton-decoupled ^{31}P spectrum at 36.2 MHz of a mixture of *trans*-$(Et_3P)_2SnCl_4$ and *trans*-$(Bu_3P)_2SnCl_4$: (a) normal spectrum: lines 5 and 2 are the ^{119}Sn satellites of the Et_3P and Bu_3P resonances, respectively, in the symmetrical species, and lines 6 and 4, and 3 and 1 are the corresponding signals in the mixed species *trans*-$(Et_3P)(Bu_3P)SnCl_4$. The separations 6–4 and 3–1 are equal to $^2J(^{31}P^{31}P)$ in this species. Un-numbered lines are ^{117}Sn satellites; (b) with simultaneous irradiation at $\nu(^{119}Sn)-\frac{1}{2}J(^{119}Sn^{31}P_{Bu})-\frac{1}{2}J(^{119}Sn^{31}P_{Et})$, lines 3 and 6 are removed and lines 2 and 5 lose intensity; (c) with simultaneous irradiation at $\nu(^{119}Sn)+\frac{1}{2}J(^{119}Sn^{31}P_{Bu})+\frac{1}{2}J(^{119}Sn^{31}P_{Et})$, lines 1 and 4 are removed and lines 2 and 5 lose intensity; (d) with simultaneous irradiation at $\nu(^{119}Sn)$, lines 1–6 are removed. Note that as the differences in $\nu(^{119}Sn)$ for the three species are small, some lines from each species are perturbed in each experiment.

identical with its magnitude determined indirectly in $(Et_3P)_2SnCl_4$ and it is therefore reasonable to assume it too is negative. Figure 2 shows expansions of the ^{117}Sn and ^{119}Sn satellites at low frequency in the proton-decoupled ^{31}P spectrum of the mixture. The $^{31}P-\{^{119}Sn\}$ experiments illustrated then show the signs of $^1J(^{119}Sn^{31}P)$ and $^2J(^{31}P^{31}P)$ to be the same (after allowing for the negative γ of ^{119}Sn), and hence $^1J(^{119}Sn^{31}P)$ is negative, and $^1K(SnP)$ is positive.

(iv) Experiments similar to (i) and (ii), but involving the CH_2 groups, were also performed to confirm some of the above signs and to give the results summarized in Table 1.

Table 2 gives a selection of known and newly measured values of $^1J(^{119}Sn^{31}P)$ for species of type (c). From their pattern it is clear that all are of the same negative sign, corresponding to a positive $^1K(SnP)$. This positive sign of the reduced coupling constant and its relatively large magnitude (*ca* 13 nm^{-3}) indicate that the Fermi contact interaction is dominant, and that there is a substantial *s*-overlap integral for the tin–phosphorus bond, so that the mean excitation energy approximation[10] can

Table 1. NMR parameters for *trans*-$(Et_3P)_2SnCl_4$[a]

$\delta(^{31}P)$	$+20.9\pm0.1$ ppm[b]	$\delta(^{119}Sn)$	-572 ± 1 ppm[b,f]
$\delta(^{1}H)_{CH_2}$	$+2.11\pm0.02$ ppm[c]	$\delta(^{1}H)_{CH_3}$	1.20 ± 0.02 ppm[c]
$\delta(^{13}C)_{CH_2}$	$+13.5\pm0.1$ ppm[c]	$\delta(^{13}C)_{CH_3}$	$+7.0\pm0.1$ ppm[c]
$^{1}J(^{119}Sn^{31}P)$	-2391 ± 10 Hz[d]	$^{2}J(^{31}P^{31}P)$	-45.0 ± 2 Hz[e]
$^{1}J(^{31}P^{13}C)_{CH_2}$	$+22.3\pm0.5$ Hz[e]	$^{3}J(^{31}P^{13}C)_{CH_2}$	1.0 ± 0.5 Hz[e]
$^{2}J(^{31}P^{13}C)_{CH_3}$	-6.2 ± 0.2 Hz[e]	$^{4}J(^{31}P^{13}C)_{CH_3}$	0 ± 0.3 Hz[e]
$^{2}J(^{31}PH)+{}^{4}J(^{31}PH)$	-11.8 ± 0.2 Hz	$^{3}J(^{31}PH)+{}^{5}J(^{31}PH)$	$+15.8\pm0.2$ Hz

[a] CH_2Cl_2 solution at 22°C.
[b] To high frequency of external 85% H_3PO_4.
[c] To high frequency of internal Me_4Si.
[d] Solvent-dependent.
[e] Based on computer simulation.
[f] To high frequency of external Me_4Sn.

Table 2. NMR parameters for tertiary phosphine adducts of tin tetrahalides[a]

Species	$\delta(^{119}Sn)$	$\delta(^{31}P)$	$^{1}J(^{119}Sn^{31}P)$	Footnotes
$(Et_3P)_2SnCl_4$	−572	+20.9	−2391	[b]
$(Bu_3P)_2SnCl_4$	−578	+16.7	−2437	[b]
$(Et_3P)(Bu_3P)SnCl_4$	−575	+20.5, +16.0	−2419, −2430	[b]
$(Et_3P)_2SnCl_3Br$	−671	+17.5	−2278	[b]
$(Et_3P)_2SnCl_2Br_2$	−771	+14.0	−2170	[b,c]
$(Et_3P)_2SnCl_2Br_2$	[d]	+13.0	−2164	[b,e]
$(Et_3P)_2SnClBr_3$	−867	+8.3	−2056	[b]
$(Et_3P)_2SnBr_4$	−910	+2.4	−1947	[b]
$(Bu_3P)_2SnClBr_3$	−837	+1.9	(−)2065	[f]
$[(Bu_3P)SnClBr_4]^-$	−1225	+4.8	(−)1405	[f]
$[(Bu_3P)SnBr_5]^-$	−1470	−6.9	(−)1415	[f]
$(Me_2PhP)_2SnCl_3Me$	−462	+16.7,[g] +3[h]	(−)1046,[g](−)2973[h]	[i,j]

[a] With *trans* phosphine ligands unless otherwise stated. Measured in CH_2Cl_2 solution.
[b] This work.
[c] P *trans* to P, Cl *trans* to Cl.
[d] Too weak to detect ^{119}Sn resonance.
[e] P *trans* to P, Cl *trans* to Br.
[f] Reference 6.
[g] P *trans* to CH_3
[h] P *trans* to Cl.
[i] Reference 7.
[j] With *cis* phosphine ligands.

be used, as an earlier treatment has *assumed*.[12] It should then follow that the *magnitude* of $^{1}J(^{119}Sn^{31}P)$ will increase with increasing effective nuclear charge on tin, and this is borne out by the values in Table 2, where stepwise replacement of chloride by bromide brings about a systematic stepwise reduction in the coupling constant. This implies that the energies of the bonding *s*-orbitals of tin(IV) and phosphorus(V) do not differ greatly for case (c), whereas for case (b) there is a substantial difference in these energies. It is also of interest that in the mixed Cl/Br solutions the number of species formed and their ^{31}P and ^{119}Sn spectral types are fully consistent with the proposed *trans* configuration, there being no signals that could be attributed to *cis* species.

Malone and Mann[5] have pointed out that the correlation of a large $^{2}J(^{31}P^{31}P)$ with a *trans* configuration for many transition metal complexes does not extend to derivatives of octahedral tin; we note here further that for complexed tin, the *trans* coupling is also of opposite sign to that usually found in the transition metal case. In addition, for transition metal complexes, $^{1}J(M^{31}P)$ is determined

by the *trans* influence of groups *trans* to phosphorus, whereas for the octahedral tin(IV) complexes, the nature of the groups *cis* to phosphorus has the dominant effect.

EXPERIMENTAL

Samples were prepared and examined in 10 mm o.d. NMR tubes, by the addition of equimolar amounts of the tertiary phosphine and the appropriate tin tetrahalide to dried CH_2Cl_2 under nitrogen at 0°C. The spectra were recorded at 22°C on a JEOL FX 90Q multinuclear spectrometer operating at 89.6, 22.5, 36.2, and 33.3 MHz for ^1H, ^{13}C, ^{31}P and ^{119}Sn, respectively. The 2-D $^{13}C/^1H$ chemical shift correlation spectrum was acquired into a 1024×256 data matrix using a sequence due to Bax,[15] and was manipulated using standard JEOL software. $^{31}C-\{^{31}P\}$ and $^{31}P-\{^{119}Sn\}$ heteronuclear multiple resonance experiments were conducted under conditions of complete proton decoupling and with time-sharing of the irradiation and receiver channels, by applying r.f. power from a GenRad model 1061 frequency synthesizer to the normal proton decoupler coils of the spectrometer.

Acknowledgements—We thank the Royal Society and the SERC for equipment grants, and Dr J. L. Bookham for discussions.

REFERENCES

1. J. P. van Lindhoudt, E. V. van den Berghe and G. P. van der Kelen, *Spectrochim. Chim. Acta* 1980, **36A**, 17.
2. M. Meissner, H. J. Kroth, K.-H. Köhricht and H. Schumann, *Z. Naturfor.* 1981, **36B**, 904.
3. P. G. Harrison, S. E. Ulrich and J. J. Zuckerman, *Inorg. Nucl. Chem. Lett.* 1971, **7**, 865.
4. W. McFarlane and D. S. Rycroft, *J. Chem. Soc., Dalton Trans.* 1974, 1977.
5. J. F. Malone and B. E. Mann, *Inorg. Nucl. Chem. Lett.* 1972, **8**, 819.
6. R. Colton, D. Dakternieks and C.-A. Harvey, *Inorg. Chem. Acta* 1982, **61**, 1.
7. V. S. Petrosyan, N. S. Yashina and E. J. Gefel, *Silicon, Germanium, Tin and Lead Compounds* 1986, **9**, 213.
8. P. A. W. Dean, *Can. J. Chem.* 1982, **61**, 1795; P. A. W. Dean, D. D. Phillips and L. Polensek, *Can. J. Chem.* 1981, **59**, 50.
9. J. A. Pople and D. P. Santry, *Molec. Phys.* 1964, **8**, 1.
10. H. M. McConnell, *J. Chem. Phys.* 1965, **24**, 460.
11. W. McFarlane, *Proc. R. Soc. A* 1968, **306**, 183.
12. G. G. Mather, G. M. McLaughlin and A. Pidcock, *J. Chem. Soc., Dalton Trans.* 1973, 1823.
13. I. R. Beattie and G. A. Ozin, *J. Chem. Soc. A* 1970, 370; R. Rivest, S. Singh and C. Abraham, *Can. J. Chem.* 1967, **45**, 3138; D. Cunningham, M. J. Frazer and J. D. Donaldson, *J. Chem. Soc. A* 1971, 2049.
14. D. Cunningham, M. J. Frazer and J. D. Donaldson, *J. Chem. Soc., Dalton Trans.* 1972, 1647; T. Hinsperger, L. Mihichuk and H. D. Sharma, *Inorg. Chem.* 1970, **9**, 2573.
15. A. Bax, *J. Magn. Reson.* 1983, **52**, 517.
16. I. J. Colquhoun and W. McFarlane, *J. Magn. Reson.* 1978, **31**, 63.

Polyhedron Vol. 8, No. 16, pp. 2051–2056, 1989
Printed in Great Britain

0277–5387/89 $3.00+.00
© 1989 Maxwell Pergamon Macmillan plc

BIS CROWN ETHERS—VI. THE FIRST SINGLE CRYSTAL STRUCTURE OF THE COMPLEX OF SCHIFF BASE TYPE BIS BENZO-15-CROWN-5 AND POTASSIUM PICRATE

DEFEN WANG,* XIAOQIANG SUN and HONGWEN HU

Department of Chemistry, Nanjing University, Nanjing, China

and

YUMING LIU and BENMING CHEN

Institute of Chemistry, Academia Sinica, Beijing, China

and

ZHONGYUAN ZHOU and KAIBEI YU

Chengdu Center of Analysis and Determination, Academia Sinica, Chengdu, China

(*Received* 3 *August* 1988; *accepted after revision* 15 *March* 1989)

Abstract—The first single crystal structure of a complex of potassium picrate and Schiff base type bis-benzo-15-crown-5 with a rigid *meta*-phenylene bridge is reported. Experimental results show that an intermolecular 2:2 (bis crown ether: potassium ion) sandwich complex is formed. The crystals are monoclonic, space group $P2_1/n$, with $a = 19.0924(35)$, $b = 20.4413(30)$, $c = 25.5996(56)$ Å, $\beta = 108.472(15)°$, $V = 9476.07$ Å^3, $D_c = 1.403$ g cm^{-3}. All the structure parameters were refined with the 10,485 observed reflections to give a final $R = 0.089$. The bridging (*meta*-phenylene) units essentially retain their flat rigid structure in the complex. Each potassium ion coordinates with the 10 oxygen atoms of two crown rings. The K—O bond lengths are in the range of 2.799–3.070 Å. The shortest distance between the oxygen atoms of the picrate anion and the K^+ ion is 6.050 Å. The picrate anion is linked to the large cation by ionic bonding. The $CHCl_3$ and H_2O solvent molecules in the crystal are distributed at random.

There has been rapid growth in the research on bis crown ethers in recent years. The commonly used aliphatic chains linking the two crown units are of the ester,[1,2] ether,[3,4] amide[5] and Schiff base types[6] etc. All these crown ethers may exhibit highly selective alkali metal cation complexation by formation of intramolecular complexes in which the cation is sandwiched between the two adjacent crown ether rings. Fan, Hu *et al.* first reported that the complex of potassium thiocyanate and N,N-(4,6-dinitro-1,3-phenylene)-bis(4′-amino benzo-15-crown-5) has a 2:1 intramolecular sandwich crystal structure.[7]

In the previous paper, we reported that the PVC membrane potassium electrode with aromatic ring bridged Schiff base bis(benzo-15-crown-5) as a neutral carrier shows very high selectivity toward K^+ ions.[8] However, because of the rigidity arising from the aromatic ring in the bridge, the two crown units are in a *trans* position and when complexing with the K^+ ion cannot act cooperatively. In order to establish the mode of complexation we therefore prepared single crystals of the complex of potassium picrate and N,N′-(*m*-phenylene dimethylidyne)di-3,4-(1,4,7,10,13-pentaoxacyclopentadeceno)aniline and determined its crystal structure. The result reveals that intermolecular 2:2 (bis crown ether: potassium ion) sandwich type complexes were formed instead of the intramolecular sandwich complexes. This type of complex has not been reported before.

* Author to whom correspondence should be addressed.

EXPERIMENTAL

Synthesis of the complex

Bis crown ether (0.1 g, 0.15 mmol) and potassium picrate (0.04 g, 0.15 mmol) were dissolved in chloroform and methanol respectively and then mixed together. The mixture was refluxed for 2 h, cooled and then filtered. The solvents were allowed to evaporate at room temperature, and the product filtered off, washed with ethanol–chloroform to give light yellow crystals, m.p. 166–168°C (decomp.). Found: C, 51.5; H, 4.6; N, 7.4; K, 3.8. Calc. for $(C_{42}H_{46}N_5O_{17}K)_2 \cdot CHCl_3 \cdot H_2O$: C, 51.0; H, 5.0; N, 7.0; K, 3.9%. IR (KBr disc) 1123, 1227, 1046 cm^{-1}. The characteristic absorption bands of the bis crown ether were found at 1130, 1263, 1054 cm^{-1}. The corresponding absorptions in the complex all moved to lower frequencies, indicating that the oxygen atoms on the ether rings have taken part in complexing with K^+ ion.

Collection of the X-ray diffraction data

A transparent yellow single crystal of dimensions $0.25 \times 0.24 \times 0.30$ mm^3 was mounted on a R3M/E four circle X-ray diffractometer and monochromic CuK_α radiation was used with a θ–2θ scan to collect data in the range $3° \leqslant 2\theta \leqslant 100°$. 12,278 independent reflections were measured of which the observable reflection data with $I > 2.5\sigma(I)$ number 10,485. The crystal has monoclinic symmetry, space group $P2_1/n$, with cell parameters $a = 19.0924(35)$ Å, $b = 20.4413(30)$ Å, $c = 25.5996(56)$ Å, $\beta = 108.472(15)°$; $V = 9476.07$ Å^3. The cell contains four $[C_{36}H_{44}N_2O_{10}K]_2^+$ $[C_6H_2(NO_2)_3O^-] \cdot CHCl_3 \cdot H_2O$ units with the chloroform and water coming from the solvents; $F_{000} = 4175.41$ and $D_c = 1.403$ g cm^{-3}.

Structure determination

The crystal structure was solved by the heavy atom method and developed from electron density syntheses. The coordinates of non-hydrogen atoms and isotropic thermal vibration parameters were then refined by least squares. Anisotropic thermal vibration parameters were then introduced to give $R = 0.0888$ (unit weighting factor).

All the above calculations were performed on an Eclipse/S140 computer with SHELXTL program. The least square method used was the block diagonal matrix approximation. Selected bond lengths, bond angles and least square plane data are listed in Tables 1–4 respectively. The molecular configuration of the bis crown ether complex, in two views, is shown in Figs 1 and 2.

RESULTS AND DISCUSSION

For the convenience of discussion, the two crown ether molecules are designated by A and B respectively and shown in Fig. 1. The corresponding crown rings are represented as C (C_1–C_{10}), D (C_{29}–C_{38}), E (C_{15}–C_{24}), F (C_{43}–C_{52}) respectively. The results of the structure determination revealed that when forming the complex, the crown rings C and D, E and F in bis crown A and B have different space orientations. The crown ring C in molecule A and crown ring F in molecule B share the same space orientations and the same situation occurs in crown ring D in A and crown ring E in B. When the two bis crown molecules A and B form the complex with two potassium ions K_1^+ and K_2^+, two pairs of crown rings with different space orientations C and E, D and F coordinate with each other, forming a bimolecular sandwich complex, with the potassium ion having a coordination number of 10.

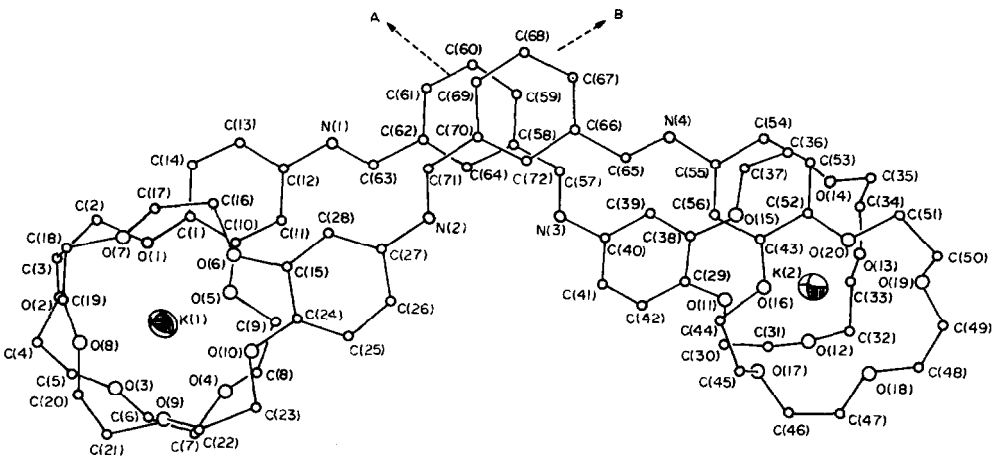

Fig. 1. The molecular configuration of the complex of bis crown ether with potassium ion.

Table 1. Bond lengths (Å) for the complex (standard deviations in parentheses)

K(1)—O(1)	3.037(5)	K(2)—O(11)	2.951(4)	N(1)—C(12)	1.436(8)
K(1)—O(2)	2.947(4)	K(2)—O(12)	2.823(5)	N(2)—C(27)	1.432(9)
K(1)—O(3)	2.799(5)	K(2)—O(13)	2.829(6)	N(3)—C(40)	1.445(9)
K(1)—O(4)	2.871(5)	K(2)—O(14)	2.978(5)	N(4)—C(55)	1.429(8)
K(1)—O(5)	2.861(6)	K(2)—O(15)	3.002(4)	N(1)—C(63)	1.266(9)
K(1)—O(6)	2.910(5)	K(2)—O(16)	2.853(6)	N(2)—C(71)	1.266(9)
K(1)—O(7)	2.846(6)	K(2)—O(17)	2.961(5)	N(3)—C(57)	1.236(8)
K(1)—O(8)	2.805(7)	K(2)—O(18)	2.883(5)	N(4)—C(65)	1.250(8)
K(1)—O(9)	2.834(5)	K(2)—O(19)	2.887(4)	C(62)—C(63)	1.484(9)
K(1)—O(10)	3.042(5)	K(2)—O(20)	2.928(5)	C(70)—C(71)	1.481(9)
K(1)—O(1–10)	2.899	K(2)—O(11–20)	2.910	C(57)—C(58)	1.476(9)
	average		average	C(65)—C(66)	1.474(9)

Table 2. The main bond angles (°) for the complex (standard deviations in parentheses)

O(1)—K(1)—O(2)	54.5(1)	O(15)—C(37)—C(36)	106.6(6)
O(2)—K(1)—O(3)	60.4(1)	O(16)—C(44)—C(45)	104.6(5)
O(3)—K(1)—O(4)	60.5(1)	O(17)—C(45)—C(44)	108.8(6)
O(4)—K(1)—O(5)	58.0(1)	O(17)—C(46)—C(47)	113.7(6)
O(5)—K(1)—O(1)	50.5(1)	O(18)—C(47)—C(46)	108.8(7)
O(6)—K(1)—O(7)	57.1(1)	O(18)—C(48)—C(49)	108.6(7)
O(7)—K(1)—O(8)	62.3(2)	O(19)—C(49)—C(48)	112.7(7)
O(8)—K(1)—O(9)	60.9(2)	O(19)—C(50)—C(51)	108.1(5)
O(9)—K(1)—O(10)	56.6(1)	O(20)—C(51)—C(50)	105.3(6)
O(10)—K(1)—O(6)	50.6(1)	C(1)—O(1)—C(2)	117.5(5)
O(11)—K(2)—O(12)	56.7(1)	C(3)—O(2)—C(4)	114.7(5)
O(12)—K(2)—O(13)	61.5(1)	C(5)—O(3)—C(6)	108.1(6)
O(13)—K(2)—O(14)	60.2(1)	C(7)—O(4)—C(8)	114.5(6)
O(14)—K(2)—O(15)	54.9(1)	C(9)—O(5)—C(10)	117.5(5)
O(15)—K(2)—O(11)	50.8(1)	C(15)—O(6)—C(16)	119.8(5)
O(16)—K(2)—O(17)	56.4(1)	C(17)—O(7)—C(18)	115.1(7)
O(17)—K(2)—O(18)	59.4(1)	C(19)—O(8)—C(20)	112.5(7)
O(18)—K(2)—O(19)	60.5(1)	C(21)—O(9)—C(22)	112.8(7)
O(19)—K(2)—O(20)	56.4(1)	C(23)—O(10)—C(24)	118.2(5)
O(20)—K(2)—O(16)	51.5(1)	C(29)—O(11)—C(30)	117.7(5)
O(1)—C(2)—C(3)	104.6(6)	C(31)—O(12)—C(32)	113.7(6)
O(2)—C(3)—C(2)	109.3(5)	C(33)—O(13)—C(34)	111.7(6)
O(2)—C(4)—C(5)	112.9(7)	C(35)—O(14)—C(36)	112.0(6)
O(3)—C(5)—C(4)	106.7(6)	C(37)—O(15)—C(38)	117.5(5)
O(3)—C(6)—C(7)	108.2(8)	C(43)—O(16)—C(44)	118.2(5)
O(4)—C(7)—C(5)	114.0(6)	C(45)—O(17)—C(46)	113.5(6)
O(4)—C(8)—C(9)	107.3(7)	C(47)—O(18)—C(48)	110.7(6)
O(5)—C(9)—C(8)	105.4(5)	C(49)—O(19)—C(50)	112.8(5)
O(6)—C(16)—C(17)	108.6(6)	C(51)—O(20)—C(52)	118.5(5)
O(7)—C(17)—C(16)	109.3(8)	C(12)—N(1)—C(63)	120.4(6)
O(7)—C(18)—C(19)	112.5(7)	C(27)—N(2)—C(71)	120.9(6)
O(8)—C(19)—C(18)	108.6(8)	C(40)—N(3)—C(57)	120.0(6)
O(8)—C(20)—C(21)	108.4(9)	C(55)—N(4)—C(65)	121.3(5)
O(9)—C(21)—C(20)	112.0(7)	N(1)—C(63)—C(62)	122.2(6)
O(9)—C(22)—C(23)	108.3(8)	N(2)—C(71)—C(70)	120.0(6)
O(10)—C(23)—C(22)	105.9(6)	N(3)—C(57)—C(58)	123.1(6)
O(11)—C(30)—C(31)	104.3(5)	N(4)—C(65)—C(66)	124.1(6)
O(12)—C(31)—C(30)	109.9(6)		
O(12)—C(32)—C(33)	112.3(6)		
O(13)—C(33)—C(32)	107.2(8)		
O(13)—C(34)—C(35)	108.8(7)		
O(14)—C(35)—C(34)	111.6(6)		
O(14)—C(36)—C(37)	109.7(6)		

Table 3. The geometrical relation between the oxygen atoms and the planes of benzene in the complex

Plane	The equation of least square planes	Atom	The distance toward the planes (Å)
		K(1)	1.7358
	0.9489(0.1772)XO−0.3134(0.0183)YO−0.0374(0.0079)	O(1)	−0.1398
	ZO+1.1702(0.1406) = 0	O(2)	0.2973
I		O(3)	−0.3526
	17.409(3.209)X−6.407(0.374)Y−0.957(0.204)	O(4)	0.2473
	Z+1.172(0.1406) = 0	O(5)	−0.0522
		K(1)	−1.6842
	0.9525(0.0361)XO−0.2472(0.0205)YO−0.1779(0.0079)	O(6)	−0.1406
	ZO−5.2369(0.1427) = 0	O(7)	−0.0962
II		O(8)	0.2558
	18.324(0.654)X−5.054(0.419)Y−4.553(0.219)	O(9)	−0.3339
	Z−5.2369(0.1427) = 0	O(10)	0.3149
		K(2)	1.7459
	0.9546(0.0565)XO−0.2175(0.0263)YO−0.2036(0.1044)	O(11)	−0.1035
	ZO−4.0286(0.1606) = 0	O(12)	0.3124
III		O(13)	−0.4054
	18.518(1.023)X+4.446(0.538)Y−5.212(2.513)	O(14)	0.3155
	Z−4.0286(0.1606) = 0	O(15)	−0.1191
		K(2)	−1.7321
	0.9614(0.0221)XO+0.2480(0.0200)YO−0.1194(0.0729)	O(16)	0.0584
	ZO−7.6778(0.1365) = 0	O(17)	−0.2449
IV		O(18)	0.3378
	18.131(0.400)X+5.059(0.408)Y−3.055(1.671)	O(19)	−0.2880
	Z−7.6778(0.1365) = 0	O(20)	0.1367
		C(1)	0.0272
	0.9641(0.0204)XO−0.0254(0.0021)YO−0.2643(0.0006)	C(10)	0.0086
	ZO−4.2638(0.0085) = 0	C(11)	−0.0048
V		C(12)	−0.0079
	19.058(0.370)X−0.520(0.043)Y−6.766(0.014)	C(13)	0.0165
	Z−4.2638(0.0085) = 0	C(14)	−0.0125
		C(15)	−0.0014
	0.8793(0.0018)XO−0.3603(0.0015)YO−0.3114(0.0006)	C(24)	0.0189
	ZO−6.4781(0.0086) = 0	C(25)	−0.0207
VI		C(26)	0.0051
	17.807(0.032)X−7.366(0.030)Y−7.971(0.018)	C(27)	0.0123
	Z−6.4781(0.0086) = 0	C(28)	−0.0142
		C(29)	−0.0100
	0.9765(0.0040)XO+0.1926(0.0014)YO−0.0967(0.0018)	C(38)	−0.0079
	ZO−3.6184(0.0083) = 0	C(39)	0.0207
VII		C(40)	−0.0161
	18.268(0.072)X+3.937(0.029)Y−2.474(0.053)	C(41)	−0.0015
	Z−3.6184(0.0083) = 0	C(42)	0.0148
		C(43)	−0.0021
	0.9611(0.0010)XO+0.1231(0.0019)YO−0.2471(0.0019)	C(52)	0.0069
	ZO−7.3529(0.0063) = 0	C(53)	−0.0017
VIII		C(54)	−0.0084
	18.900(0.018)X+2.517(0.038)Y−6.326(0.105)	C(55)	0.0131
	Z−7.3529(0.0063) = 0	C(56)	−0.0079
		C(58)	−0.0140
	0.9818(0.0042)XO+0.0025(0.0033)YO−0.1899(0.0007)	C(59)	0.0031
	ZO−3.4432(0.0069) = 0	C(60)	0.0081

Table 3.—*continued*

Plane	The equation of least square planes	Atom	The distance toward the planes (Å)
IX		C(61)	−0.0086
	18.928(0.075)X+0.052(0.066)Y−4.862(0.019)	C(62)	−0.0023
	Z−3.4432(0.0069) = 0	C(64)	0.0136
		C(66)	0.0135
	0.9872(0.0012)XO+0.0612(0.0042)YO−0.1475(0.0007)	C(67)	−0.0054
	ZO−6.6910(0.0065) = 0	C(68)	−0.0057
X		C(69)	0.0085
	18.769(0.022)X+1.251(0.085)Y−3.776(0.022)	C(70)	−0.0003
	Z−6.6910(0.0065) = 0	C(72)	−0.0106

Table 4. The angles (°) between the plane normals

I–II	8.9	VIII–VIII	9.5	VII–IX	12.2
III–IV	5.1	IX–X	4.2	VI–X	26.9
V–VI	23.2	V–IX	4.7	VIII–X	6.9

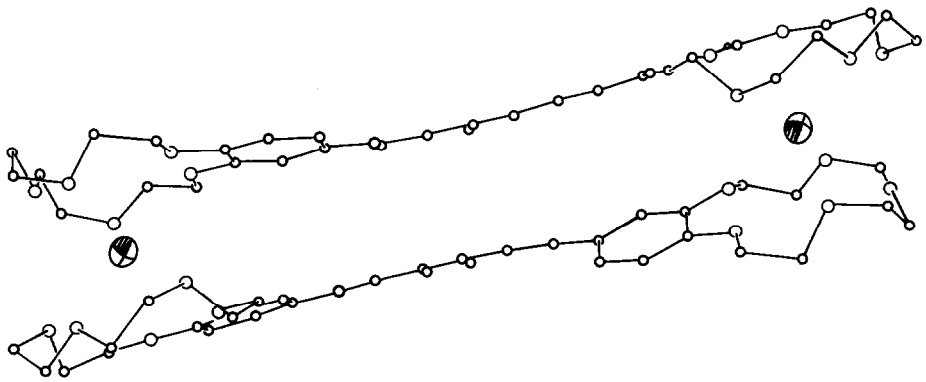

Fig. 2. A perspective view of the molecular framework of the complex.

It is usually thought that bis crown ethers form 1 : 2 intramolecular sandwich complexes with metal ions with a large diameter. The average K—O bond length is 2.906 Å.[7] The Schiff base type bis crown ethers, however, due to their molecular rigidity, form intermolecular sandwich complexes instead. The K—O bond lengths are in the range of 2.799–3.070 Å, the average values are 2.899 Å and 2.910 Å respectively (Table 1), similar to that in the above mentioned 1 : 2 complexes. The values are larger than the sum (2.73 Å) of the ion radius of K^+ (1.33 Å) and the van der Waals radius of oxygen atom (1.40 Å), thus proving that the coordination interaction between K^+ ion and oxygen atoms in our structure is mainly of ion–dipole interaction.

The oxygen atoms in each crown ring are not in good coplanarity (Table 3), showing that the crown rings are largely distorted to satisfy the requirement of lower energy coordination. The two crown rings which form a sandwich structure have their least square planes principally parallel, e.g. the least square planes I and II, and III and IV have dihedral angles 8.9 and 5.1° respectively. The distances of the K_1^+ from the plane of the two crown rings are 1.736 and 1.684 Å respectively, and that of K_2^+ are 1.746 and 1.732 Å. The coordination situation for

the two potassium ions are slightly different due to the different packing environment. It is noteworthy that the two picrate anions do not take part in coordination. The shortest distance between the O^- on the picrate anion and the K^+ ion is 6.050 Å. The picrate anions interact with the large cation only through electrostatic attraction.

The crystal also contains disordered chloroform solvent molecules and a water molecule situated close to the two picrate ions respectively. The results of elemental analysis are consistant with this conclusion.

The angles between the normals to the benzene planes V–VI and VI–X are rather large (23.2 and 26.9° respectively), but all the other benzene planes have relatively small dihedral angles with each other (13°). (Table 4). This indicates that the bridging chains in the two bis crown ethers retain their flat rigid structures in the complexes and this is probably favourable considering the energy and the symmetry of the complexes.

It can be concluded that the good performance of the PVC membrane potassium ion selective electrode based on the Schiff base type bis benzo 15-crown-5 is most probably due to the formation of intermolecular complexes.

Acknowledgement—The National Science Foundation of the People's Republic of China is acknowledged for financial support.

REFERENCES

1. M. Bourgoin, K. H. Wong, J. Y. Hui and J. Smid, *J. Am. Chem. Soc.* 1975, **97**, 3462.
2. K. Kimura, T. Tsuchida, T. Maeda and T. Shono, *Talanta* 1980, **27**, 801.
3. F. Wada, R. Arata, T. Goto, K. Kikukawa and T. Matsude, *Bull. Chem. Soc. Jpn* 1980, **53**, 2061.
4. K. H. Wong and H. L. Ng, *Tetrahedron Lett.* 1979, 4295.
5. K. Kimura, T. Maeda and T. Shono, *Anal. Lett.* 1978, **11**, S21.
6. T. M. Handyside, J. C. Lockhart, M. B. Mcdonnell and P. V. S. Rao, *J. Chem. Soc., Dalton Trans.* 1982, 2331.
7. Yuguo Fan, Guangdi Yang, Jiadong Huang, Xiaozeng You, Hongwen Hu and Cun Li, *Sci. Sinica B* 1987, **12**, 1247.
8. Defen Wang, Xiaoqiang Sun, Jiadong Huang and Hongwen Hu, *Acta Chim. Sinica* 1987, **45**, 92.

Polyhedron Vol. 8, No. 16, pp. 2057–2064, 1989
Printed in Great Britain

0277–5387/89 $3.00+.00
© 1989 Maxwell Pergamon Macmillan plc

EQUILIBRIUM STUDIES ON THE Al^{III}-, Ga^{III}-, In^{III}- AND Tl^{III}-ETHYLENEDIAMINETETRAACETATE-HALIDE AND -SULPHIDE SYSTEMS

IMRE TÓTH* and ERNŐ BRÜCHER

Department of Inorganic and Analytical Chemistry, L. Kossuth University, H-4010 Debrecen, Hungary

and

LÁSZLÓ ZÉKÁNY

Computer Centre, L. Kossuth University, Debrecen, Hungary

and

VLADIMIR VEKSIN

Udmurt State University, Izhewsk, U.S.S.R.

(*Received* 31 *October* 1988; *accepted after revision* 15 *March* 1989)

Abstract—The formation of mixed ligand complexes was studied in the $Al(edta)^-$, $Ga(edta)^-$, $In(edta)^-$ and $Tl(edta)^-$-halide and -sulphide ion systems by potentiometry, using glass and anion-selective electrodes. The stability constants (log K^F_{ML}) of the mixed ligand complexes $M(edta)F^{2-}$ were found to be 4.8 ± 0.2, 1.9 ± 0.1 and 0.9 ± 0.1 for Al^{3+}, Ga^{3+} and In^{3+}, respectively. Values of log $K^X_{ML} = 2.3\pm0.2$, 3.5 ± 0.15 and 5.9 ± 0.2 were measured for $Tl(edta)X^{2-}$, X = Cl^-, Br^- and I^-, respectively. Complexes $M(edta)S^{3-}$ are described. The values of log K^S_{ML} were calculated to be 10.3, 10.6 and 9.4 for Al^{3+}, Ga^{3+} and In^{3+}, respectively. Ionic–covalent interactions in the mixed complexes are discussed. The stability constant of $Tl(edta)^-$ was reinvestigated via spectrophotometric study of the competition reaction in the Tl^{3+}–H^+–$(edta)^{4-}$–X^- system.

The complex-forming properties of the III/B elements change drastically from Al^{3+} to Tl^{III}. Al^{3+}, Ga^{3+} and In^{3+} are considered to be "hard" cations, while Tl^{III} is classified as a typical "soft" cation.[1] However, all these elements form hydroxo complexes of high stability, which must be taken into account in the study of their complexes in aqueous solution.

Formation of the ethylenediaminetetraacetate [$(edta)^{4-}$] complexes of Al^{3+}, Ga^{3+} and In^{3+} has been studied by several authors. The stability constants are well known and increase with increasing atomic number.[2] However, extremely different stability constants have been obtained for $Tl(edta)^-$, the reported log K values ranging between 22.6 and 37.8.[3–7]

Formation of the mixed ligand complexes M(edta)X (X is a secondary ligand) has been observed for a number of metal ions.[8–12] This can be a result of the pentadentate nature of the coordinated $(edta)^{4-}$ or of a higher coordination number of the metal ion. Al^{3+}, Ga^{3+}, In^{3+} and Tl^{III} ions complexed with $(edta)^{4-}$ do not form polynuclear hydroxocomplexes, but the formation of mixed ligand complexes $M(edta)(OH)^{2-}$ is known.[2]

The complex-forming properties of the metal ions can be changed by the presence of a coordinated multidentate ligand, e.g. a change in the "hard" character of the Zn^{2+} ion was reported when it was surrounded by the hydrophobic carbonic anhydrase

* Author to whom correspondence should be addressed.

(CA) in the Zn^{2+}–Ca–halide ion system.[13] "Hard" cations such as Ga^{3+} and In^{3+} can also interact with "soft" ligands containing charged sulphur donor atoms.[14–16] In studies of the formation of the mixed ligand complexes of Al^{3+}-, Ga^{3+}-, In^{3+}- and Tl^{III}-edta with halide and sulphide ions, the trend of the stability constants indicates whether any alteration takes place in the properties of metals.

The formation of mixed ligand complexes may also be of practical importance. The determination of fluoride with an ion-selective electrode can be disturbed in the presence of Al^{3+} when $(edta)^{4-}$ is used as a masking agent,[17–19] due to the formation of mixed ligand complexes $Al(edta)F^{2-}$.

The stability constants of the mixed complexes $M(edta)X^-$ have been obtained via simultaneous pH and pX measurements using glass and ion-selective electrodes. Under the conditions applied, assumption of the dissociation of the complexes $M(edta)^-$ was not necessary, but formation of the complexes $M(edta)(OH)^{2-}$ was taken into account. In the $Tl(edta)^-$–X^- systems, the halide ions can compete with the $(edta)^{4-}$. From studies of the competition reactions by means of spectrophotometry, the stability constant of $Tl(edta)^-$ has been obtained.

EXPERIMENTAL

Chemicals and analysis

Stock solutions of $Al(NO_3)_3$, $Ga(NO_3)_3$ and $In(NO_3)_3$ were prepared by dissolving 5 N gallium (Timföldgyár és Aluminiumkohó, Ajka, Hungary), aluminium and indium (p.a., Reanal) in nitric acid. Freshly prepared Tl_2O_3 was dissolved in perchloric acid to obtain $Tl(ClO_4)_3$ solution. Tl_2O_3 was prepared by oxidation of Tl_2SO_4 (p.a. Schuchardt) with $K_3[Fe(CN)_6]$.[20] Metal ion concentrations were determined by complexometric titration with $Na_2H_2(edta)$ (Reanal). The acid content of the stock solution was measured by pH-potentiometry.[21] Solutions with appropriate $M(edta)^-$/$M(edta)(OH)^{2-}$ ratio were prepared by mixing calculated volumes of metal stock solution, $Na_2H_2(edta)$ and KOH or NaOH solutions. The metal to ligand ratio was 1:1 in all potentiometric experiments. The ratio of $M(edta)^-$ and $M(edta)(OH)^{2-}$ was checked by pH-potentiometric titration with the addition of KOH/NaOH or HNO_3 titrant. These titration curves were used to evaluate the protonation constant (K^{H}_{ML}) and the hydrolysis constant (K^{OH}_{ML}).

KOH and NaOH solutions were kept in argon atmosphere. Their concentrations were analysed pH-potentiometrically using potassium hydrogen phthalate (Merck).

The Na_2S stock solution was prepared by dissolution of recrystallized $Na_2S \cdot 9H_2O$ (Merck) in deaerated distilled water and was stored under argon gas. Sulphide concentration was analysed by oxidation with KIO_3[22] and by precipitation titration with $AgNO_3$.[23] The results coincided well.

NaF, NaCl, NaBr, NaI, KCl, KBr and KI (Reanal) were weighed and dissolved in distilled water for halide titrant solutions.

Procedure

Potentiometric measurements were carried out in argon atmosphere using Radelkis OP 208/1 and Radiometer PHM 84 pH-meters. GK2401B combined, G202B glass (Radiometer), OP-F-0711, OP-Cl-0711P, OP-Br-0711P, OP-I-0711P, OP-SCN-0711, OP-S-0711P anion-selective and OP-8202 Ag/AgCl double junction reference electrodes (Radelkis) were used. Sodium chloride and nitrate solutions were used in the combined electrode and the salt bridge of the reference electrode, respectively, in the case of $NaClO_4$ ionic medium for Tl^{III} systems.

Halide-selective electrodes were calibrated in the range $2 < pH < 8$ for $X = Cl^-$, Br^- and I^-, and $5.5 < pH < 8$ for $X = F^-$. The total concentration of halide varied in the range: $2 \cdot 10^{-4}$ mol $dm^{-3} < C_x < 5 \cdot 10^{-2}$ mol dm^{-3} for $X = Cl^-$, Br^- and I^-, and $2 \cdot 10^{-3}$ mol $dm^{-3} < C_x < 5 \cdot 10^{-2}$ mol dm^{-3} for $X = F^-$. The calibration of the sulphide electrode was described earlier.[16]

Spectrophotometric measurements were made with a Beckman-DB-GT spectrophotometer using 0.1 and 0.2 cm cells.

Constant ionic medium was maintained at $25 \pm 0.2°C$: $I = 0.5$ mol dm^{-3} KNO_3 except for Tl^{III} systems, where $I = 1.0$ mol dm^{-3} $NaClO_4$ ($HClO_4$). The total concentration of metal ions was 0.01 mol dm^{-3} for M = Al, Ga and In, and $2.5 \cdot 10^{-3}$ mol dm^{-3} and $2.5 \cdot 10^{-4}$–$2 \cdot 10^{-5}$ mol dm^{-3} for M = Tl in potentiometric and spectrophotometric experiments, respectively.

The stoichiometric equilibrium constants were calculated from the measured pH values with the method by Irving *et al.*[24] The stoichiometric ionic product of water was found to be $pK_w = 13.83 \pm 0.01$ and $pK_w = 13.70 \pm 0.02$ for $I = 0.5$ mol dm^{-3} KNO_3 and $I = 1.0$ mol dm^{-3} $NaClO_4$, respectively.

Stability constants were calculated from the titration curves and UV spectra with the PSEQUAD program.[25]

RESULTS AND DISCUSSION

The formation of mixed ligand complexes was followed by potentiometric titration using anion-selective and pH electrodes simultaneously. The starting pH of the solutions differed, depending on the optimal selectivity range of the ion-selective electrodes or the required pH limit of the calibration procedure.[16] Typical experimental curves are shown in Figs 1–3.

The stability constants of the complexes

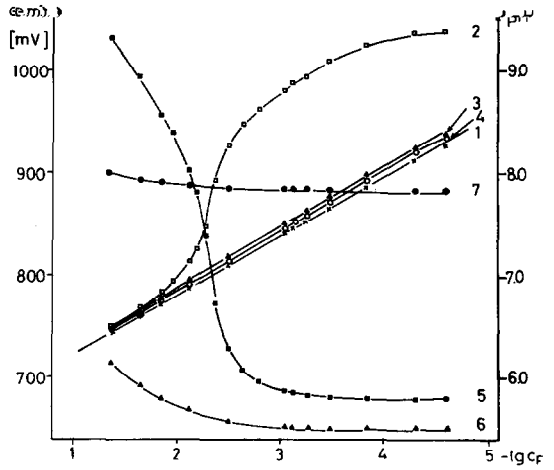

Fig. 1. Formation of M(edta)F^{2-}. EMF and pH vs C_F- (C_{ML} = 0.01 mol dm^{-3}): (1) EMF calibration curve of fluoride-selective electrode (0.5 mol dm^{-3} KNO_3); (2) and (5) Al(edta)$^-$, (3) and (6) Ga(edta)$^-$, (4) and (7) In(edta)$^-$, EMF and pH, respectively.

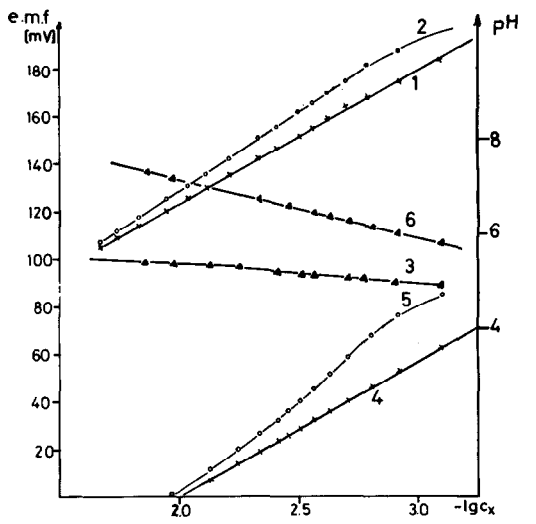

Fig. 2. Formation of Tl(edta)X^{2-}. EMF and pH vs C_X- (C_{TlL} = 0.0025 mol dm^{-3}): EMF calibration curves of chloride-selective (1) and bromide-selective (4) electrodes (1.0 mol dm^{-3} $NaClO_4$); EMF (2) and pH (3), X = Cl^-; EMF (5) and pH (6), X = Br^-.

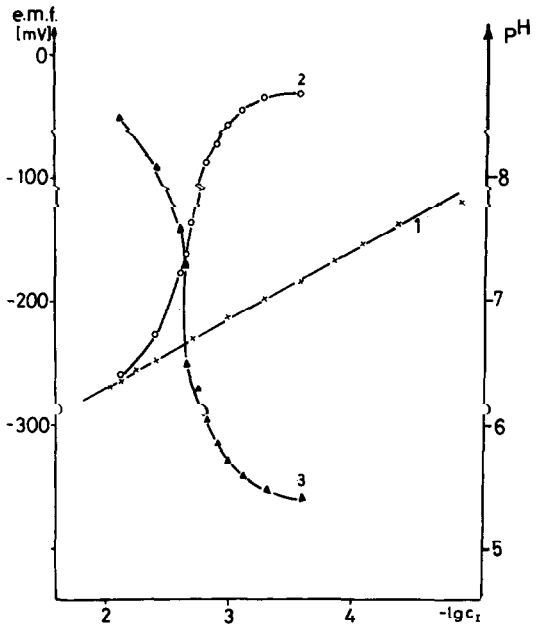

Fig. 3. Formation of Tl(edta)I^{2-}. EMF and pH vs C_{I^-}: (1) EMF calibration of iodide-selective electrode (1.0 mol dm^{-3} $NaClO_4$). EMF (2) and pH (3) in the presence of 0.0025 mol dm^{-3} Tl(edta)$^-$.

M(edta)$^-$ are high enough for dissociation not to occur at a moderate concentration of the halide ion and in a suitable pH range. Thus, only simple equilibrium reactions were taken into account, as follows:

Protonation of complexes:

$$M(edta)^- + H^+ \rightleftharpoons MH(edta) \quad (1)$$

$$K_{ML}^{H} = \frac{[MH(edta)]}{[M(edta)^-]\cdot[H^+]}. \quad (2)$$

Formation of mixed hydroxocomplexes at higher pH:

$$M(edta)\cdot aq^- + H_2O \rightleftharpoons M(edta)(OH)^{2-} + H_3O^+ \quad (3)$$

$$K_{ML}^{OH} = \frac{[M(edta)(OH)^{2-}\cdot[H_3O^+]}{[M(edta)^-]}. \quad (4)$$

Formation of mixed halide (X^-) or sulphide complexes:

$$M(edta)^- + X^- \rightleftharpoons M(edta)X^{2-} \quad (5)$$

$$K_{ML}^{X} = \frac{[M(edta)X^{2-}]}{[M(edta)^-]\cdot[X^-]} \quad (6)$$

$$M(edta)^- + S^{2-} \rightleftharpoons M(edta)S^{3-} \quad (7)$$

$$K_{ML}^{S} = \frac{[M(edta)S^{3-}]}{[M(edta)^-]\cdot[S^{2-}]}. \quad (8)$$

The calculated stability constants,[25] together

Table 1. Stability constants for $M(edta)^{-}$–X^{-} systems

Complex	log K Al[a]	Ga[a]	In[a]	Tl[a]
$MH(edta)^{b}$	2.41 ± 0.03	1.69 ± 0.01	0.66 ± 0.06	—
$M(edta)(OH)^{2-b}$	−5.81 ± 0.01	−5.55 ± 0.005	−8.22 ± 0.01	−6.0 ± 0.2
$M(edta)F^{2-c}$	4.8 ± 0.2	1.9 ± 0.1	0.9 ± 0.1	—
$M(edta)Cl^{2-}$	—[e]	—[e]	—[e]	2.3 ± 0.2[c]
$M(edta)Br^{2-}$	—[e]	—[e]	—[e]	3.5 ± 0.15[c]
$M(edta)I^{2-}$	—[e]	—[e]	—[e]	5.9 ± 0.2[c]
$M(edta)S^{3-d}$	10.3	10.6	9.4	—[f]

[a] $I = 0.5$ mol dm^{-3} KNO_3 for M = Al, Ga and In, and $I = 1$ mol dm^{-3} $NaClO_4$ for M = Tl.

[b] Three titration curves, about 120 points, $\overline{\delta v} = 0.008$ cm^3.

[c] Three titration curves, about 60 points, C_{AlL} and $C_{GaL} = 0.01$ and $5 \cdot 10^{-3}$ mol dm^{-3}, $C_{InL} = 0.01$ mol dm^{-3}, $C_{TlL} = 2.5 \cdot 10^{-3}$ mol dm^{-3}, $\overline{\delta v} = 0.02$ cm^3 or $\overline{\delta U} \leqslant 1$ mV.

[d] Values calculated with the use of eq. (14).

[e] No interaction was found at $C_{ML} = 0.01$ mol dm^{-3}, $C_x = 0$–0.5 mol dm^{-3}, pH = 3.8–7.0.

[f] Probably Tl_2S_5 [Tl(I)polysulphide, red] was formed.

with the standard deviations, are listed in Table 1. EMF and pH values of the titration curves were simultaneously used for the calculations. Optimization of $\delta\bar{v}$ (cm^3) or $\overline{\delta U}$ (mV) was carried out independently, which resulted in practically the same stability constant values (see footnotes to Table 1).

The stability constants of MH(edta) and $M(edta)(OH)^{2-}$ agree well with the literature data except for that of InH(edta). Both repeated experiments using different In^{3+} stock solutions and calculations with refined values of the acid content of the stock solution resulted in a much lower protonation constant as compared to log $K^{H}_{ML} = 1.5$ ($I = 0.1$ mol dm^{-3} $NaClO_4^2$). No $Al(edta)(OH)_2^{3-}$ could be identified below pH = 11, and precipitation occurred at pH > 11.

Formation of mixed ligand halide complexes

The titration curves in Fig. 1 indicate the formation of $M(edta)F^{2-}$. It can be seen that the largest effect of the free F^- concentration was caused by $Al(edta)^-$ (curve 2), but the titration curves of $Ga(edta)^-$ (curve 3) and $In(edta)^-$ (curve 4) did not coincide with the calibration curves (curve 1) either. The increase in pH values (curves 5–7) can be explained by the shift of equilibrium reactions (eq. 3) to the left because of the formation of $M(edta)F^{2-}$. At a higher excess of F^- (pH > 8), at least partial replacement of $(edta)^{4-}$ from $Al(edta)^-$ by F^- should be presumed. The equilibrium system was very complicated: constant potentials could not be observed and the solution became very viscous. In agreement with the literature[17] a value log $K^{F}_{ML} = 4.8 \pm 0.2$ was calculated for the range of pH = 5.8–8.0. A similar effect was not observed in the $Ga(edta)^-$ and $In(edta)^-$–F^- systems.

The high stability of the mixed complex $Al(edta)F^-$ and the formation of complexes $AlF_x^{(3-x)+}$ via the competition reaction explain why the complexones do not have an optimal masking effect for the determination of F^- with an ion-selective electrode in the presence of Al^{3+}.[18,19]

The trend of the stability constants of $M(edta)F^{2-}$ is the same as the trend for the parent complexes of Al^{3+}, Ga^{3+} and In^{3+}.[12] Space for the "second" F^- in the inner sphere is the smallest in $Al(edta)^-$, but, in contrast with the results obtained with bulky ligands, steric effects have no role in the case of F^-; thus, the interaction between $M(edta)^-$ and F^- is dominated by electrostatic forces.

No interaction can be detected between $Al(edta)^-$, $Ga(edta)^-$ or $In(edta)^-$ and Cl^-, Br^-, I^- or SCN^-. This result is not surprising, because the stability constants of the parent complexes in aqueous solution are known to be quite low.[12] Titrations were carried out at pH ≈ 3–4, where the formation of $M(edta)(OH)^{2-}$ can be neglected, and at pH ≈ 7, where this complex exists, but neither the change in potential of the ion-selective electrode nor the pH change revealed any interaction between $M(edta)^-$ and X^- up to $C_x = 0.5$ mol dm^{-3}. Values of $K^{X}_{ML} \approx 1$ were measured by Friedman *et al.*[26] for $In(edta)X^{2-}$ (X = Cl^-, Br^-, I^-, S^{2-} and SCN^-) using an In-amalgam electrode at very high concentrations of X. (The ionic strength was not kept constant.) Supposing $K \approx 1$ under our experimental conditions, δ EMF < 0.3 mV can be

estimated, which is about the same as the uncertainty in the measured EMF.

However, the formation of mixed ligand complexes is found for $Tl(edta)^-$. Typical titration curves obtained in the $Tl(edta)^- - X^-$ ($X^- = Cl^-$, Br^- and I^-) systems are shown in Figs 2 and 3. The trend of the calculated mixed stability constants (Table 1) follows the stability sequence of the Tl^{III}–halide parent complexes: $I^- > Br^- > Cl^-$. The values of the stability constants $\log K^X_{ML}$ are similar to those of $\log K^X_4$ for $TlCl_4^-$ and $TlBr_4^-$.[27-34] There is good agreement for the estimated $\log K_4$ of TlI_4^-,[35] too.

The stability constant of $Tl(edta)^-$

The equilibria in the $Tl(edta)^- - X^-$ systems at high excess of halide ions were studied by means of spectrophotometry. $TlCl_4^-$, $TlBr_4^-$ and TlI_4^- have an absorption maximum at 244, 270 and 292 nm, respectively, while $Tl^{3+}\cdot aq$, $Tl(OH)^{2+}$, $Tl(edta)^-$, $Tl(edta)Cl^{2-}$, $Tl(edta)Br^{2-}$ and $Tl(edta)I^{2-}$ absorb at $\lambda < 230$ nm. Spectra recorded at different pH, different edta concentrations and a high excess of halide ions are plotted in Figs 4–6.

The absorbance of $TlCl_4^-$ decreases with increasing pH, and at pH > 2 the spectrum of $Tl(edta)Cl^{2-}$ can already be seen (Fig. 4a). At lower pH, Cl^- ions

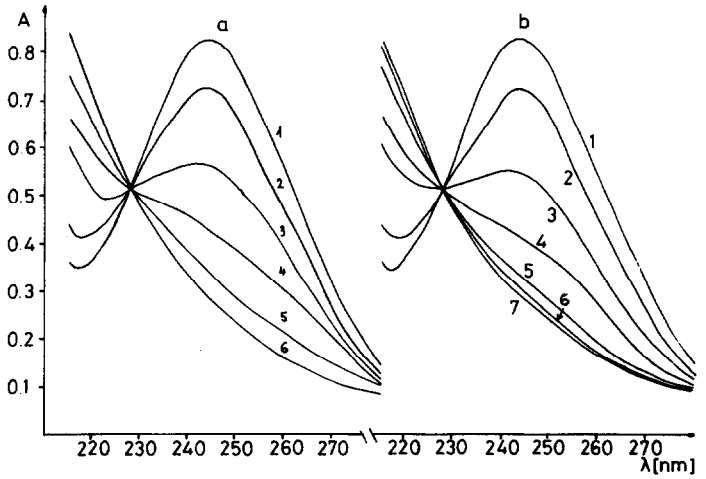

Fig. 4. UV spectra of Tl^{III}–$(edta)^{4-}$–H^+–Cl^- system (a) $C_{TlL} = 5\cdot10^{-4}$ mol dm^{-3}, $C_{Cl^-} = 0.78$ mol dm^{-3}: pH = 0.286 (1), 0.840 (2), 1.100 (3), 1.298 (4), 1.535 (5), 1.987 (6). (b) pH = 1.33, $C_{Cl} = 0.893$ mol dm^{-3}, $C_{Tl} = 5\cdot10^{-4}$ mol dm^{-3}; C_{edta} [mol dm^{-3}] = 0 (1), $1\cdot10^{-4}$ (2), $3\cdot10^{-4}$ (3), $5\cdot10^{-4}$ (4), $1\cdot10^{-3}$ (5), $1.5\cdot10^{-3}$ (6) and $2\cdot10^{-3}$ (7).

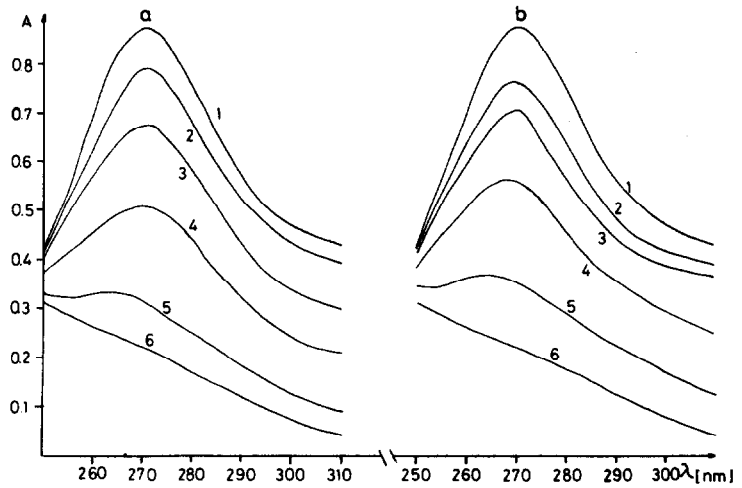

Fig. 5. UV spectra of Tl^{III}–$(edta)^{4-}$–H^+–Br^- system. $C_{Br} = 0.5$ mol dm^{-3}, (a) $C_{Tl(edta)} = 5\cdot10^{-4}$ mol dm^{-3}, pH = 1.230 (1), 1.89 (2), 2.127 (3), 2.411 (4), 2.915 (5), 4.648 (6). (b) pH = 2.07, $C_{Tl} = 5\cdot10^{-4}$ mol dm^{-3}, C_{edta}[mol dm^{-3}] = 0 (1), $3\cdot10^{-4}$ (2), $5\cdot10^{-4}$ (3), $1\cdot10^{-3}$ (4), $2.5\cdot10^{-3}$ (5), $5\cdot10^{-3}$ (6).

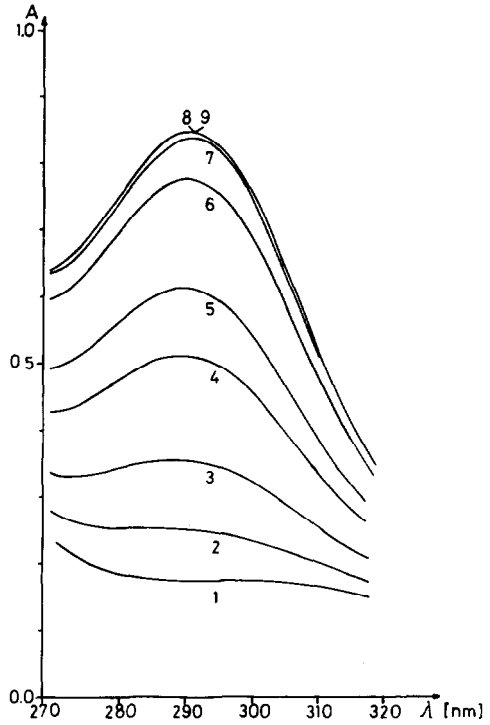

Fig. 6. UV spectra of Tl^{III}–(edta)$^{4-}$–H^+–I^- system. $C_{TIL} = 2.5 \cdot 10^{-4}$ mol dm^{-3}, $C_{I^-} = 5 \cdot 10^{-3}$ mol dm^{-3}: pH = 6.190 (1), 3.845 (2), 3.383 (3), 2.955 (4), 2.717 (5), 3.356 (6), 2.050 (7), 1.813 (8) and 1.592 (9).

replace the ligand edta$^-$ and $TlCl_4^-$ is formed; at higher pH, the apparent stability constant of Tl(edta)$^-$ is high enough to prevent the dissociation of the complex. The isosbestic point at 228 nm suggests the presence of two species only, $TlCl_4^-$ and Tl(edta)Cl^{2-}. The same isosbestic point can be seen in Fig. 4b, which shows the spectra of equilibrium systems at constant pH and Cl^- concentration at different concentrations of edta.

The spectra in Figs 5 and 6 can be explained in the same way for the Tl(edta)$^-$–Br^- and Tl(edta)$^-$–I^- systems. The stability constants of $TlBr_4^-$ and TlI_4^- are higher than that of $TlCl_4^-$; thus, Tl(edta)X^{2-} (X = Br^- and I^-) is formed only at pH > 3.5 and pH > 5, respectively. There are no isosbestic points, because of the higher absorbance of Br^- and I^-.

The equation of the competition reaction can be written as follows:

$$Tl(edta)X^{2-} + 3X^- + nH^+ \rightleftharpoons TlX_4^- + H_n(edta)^{(4-n)-} \quad (9)$$

where $n = 4$, 5 or 6. The equilibrium constant K_x of eq. (9) for $n = 5$ is as follows:

$$K_x = \frac{[TlX_4^-] \cdot [H_5(edta)^+]}{[Tl(edta)X^{2-}] \cdot [X^-]^3 \cdot [H^+]^5}. \quad (10)$$

Values of K_x were evaluated with the program PSEQUAD[25] from the spectra recorded at constant concentration of Tl(edta)$^-$ at different pH, or at constant pH and Tl^{III} concentration with different concentrations of edta. Known protonation constants log K_{H_5L} and log K_{H_6L}[36] were used for the calculation. The following log K_x values were obtained: log $K_{Cl} = 2.83 \pm 0.15$, log $K_{Br} = 7.72 \pm 0.20$ and log $K_I = 17.7 \pm 0.2$. If the concentrations in eq. (10) are expressed with the known constants, the following equation can be obtained:

$$\log K_{TIL} = \log \beta_{TlX_4} + \log \beta_{H_5L} - \log K_x - \log K_{TIL}^X. \quad (11)$$

The calculated values of log K_{TIL} are shown in Table 2, together with the literature data for log β_{TlX_4}. Unfortunately, the constants for log β_{TlX_4} are referred to $I = 3$ mol dm^{-3} $NaClO_4$ or $LiClO_4$, while the determination of log K_{H_5L} and log K_{H_6L} and our experiments were carried out at $I = 1$ mol dm^{-3} $NaClO_4$. The values of log K_{TIL} calculated from eq. (11) are different, but these differences are acceptable with regard to the very large stability constant. It seems from the data in Table 2 that the log K_{TIL} data published by Anderegg *et al.*[6] and Gorelov *et al.*[7] are acceptable.

There are much lower values of log K_{TIL} in the literature: 22.5[4] and 24.0.[5] These are due to the

Table 2. Values calculated for log K_{TIL} with the use of different values of log β_{TlX_4}

	$TlCl_4^-$			$TlBr_4^-$		TlI_4^-
log β_{TlX_4}	17.36[a]	18.5[b]	19.45[c]	26.43[c]	25.7[d]	35.7[e]
log K_{TIL}	34.4	36.6	36.6	37.5	36.8	34.4

[a] 3 mol dm^{-3} $NaClO_4$, $HClO_4$.[27,30]
[b] 3 mol dm^{-3} $LiClO_4$.[28]
[c] 1 mol dm^{-3} $NaClO_4$, 3 mol dm^{-3} $HClO_4$.[29]
[d] 3 mol dm^{-3} $LiClO_4$.[33]
[e] 1 mol dm^{-3} $NaClO_4$, 3 mol dm^{-3} $HClO_4$.[35]

inadequate experimental conditions. Busev *et al.* investigated the competition reaction of Cl^- and $(edta)^{4-}$, but the experiments were carried out at pH ≈ 3.5, where the concentration of TlX_4^- is very low, and the formation of $Tl(edta)X^{2-}$ was not taken into account either.

Log K_{TlL} was evaluated by Kornev *et al.* using the Tl^{III}–Fe^{III} competition at pH ≈ 2, in the presence of Cl^-, but neither the hydrolysis of Tl^{III} [37] nor the formation of $Tl(edta)X^{2-}$ was presumed.

$Tl(edta)^-$ was found to be sensitive to UV light in solution. Investigation of the photochemical reaction of oxidative decarboxylation is in progress.[38]

Formation of mixed ligand sulphide complexes

Titration curves of the $M(edta)(OH)^{2-}$–HS^- systems are shown in Fig. 7. The titration curve (3) of $In(edta)(OH)^{2-}$ differs considerably from the calibration curve, but the interactions of $Al(edta)(OH)^{2-}$ (curve 1) and $Ga(edta)(OH)^{2-}$ (curve 2) with HS^- are also clearly demonstrated. The equilibrium reaction can be described as follows:

$$M(edta)(OH)^{2-} + HS^- \rightleftharpoons M(edta)S^{3-} + H_2O \quad (12)$$

$$K_{ML}^{HS} = \frac{[M(edta)S^{3-}]}{[M(edta)(OH)^{2-}]\cdot[HS^-]}. \quad (13)$$

The values of log K_{ML}^{HS} calculated for M = Al, Ga and In are 2.2±0.1, 2.4±0.1 and 3.7±0.1, respectively. It should be mentioned that reaction (12) is equivalent to the reaction $M(edta)(OH)^{2-} + HS^- \rightleftharpoons M(edta)(OH)(HS)^{3-}$, but the presence of OH^- and HS^- in the inner sphere is not probable. However, there is no reason to suppose a simple substitution of OH^- by HS^-, i.e. $M(edta)(OH)^{2-} + HS^- \rightleftharpoons M(edta)(HS)^{2-} + OH^-$, because of the experimental fact that the formation of mixed sulphido complexes was not suppressed by the increased pH (i.e. higher values of pH–p[HS^-] in Fig. 3). The substitution reaction $Ga(OH)_4^- + HS^- \rightleftharpoons Ga(OH)_2S^{4-} + OH^- + H_2O$ should be proposed for the $Ga(OH)_4^-$–HS^- system, as indicated by the pH-dependence of the equilibrium reaction.[35]

The stability constants log K_{ML}^{S} shown in Table 1 can be calculated by using log K_{ML}^{OH} and the protonation constant of S^{2-} ($K_1^H = [HS^-]/[H^+]\cdot[S^{2-}]$) log $K_1^H = 13.9$[39] as follows:

$$\log K_{ML}^{S} = \log K_{ML}^{HS} + \log K_1^H + \log K_{ML}^{OH}. \quad (14)$$

The stability constants log K_{ML}^{S} are surprisingly high as compared with the only published stability constant of $In(HS)^{2+}$.[40,41] It can be stated that the differences between the titration curves in Fig. 3 can be explained mainly by the different stabilities of the mixed hydroxo complexes $M(edta)(OH)^{2-}$, and only slight effects are exerted by the stability of $M(edta)(S)^{3-}$. This means that even the typically "hard" Al^{3+} can interact with the typically "soft" S^{2-} if the metal ion is "protected" against hydrolysis by forming a complex with a multidentate ligand. The interaction is predominantly electrostatic, particularly for Al^{3+} but the values of log K_{ML}^{S} (Table 1) do not decrease with increasing ionic size (from Al^{3+} to In^{3+}) as was observed for the mixed complexes $M(edta)F^{2-}$. To explain the relatively strong interaction between the complexed Ga^{3+} or In^{3+} and the sulphide ion, resulting in the high log K_{ML}^{S} values for $Ga(edta)S^{3-}$ and $In(edta)S^{3-}$, the importance of covalent interactions must be assumed. Some of the electronic density of the filled orbitals of Ga^{3+} and In^{3+} can be transferred to the empty *d*-orbitals of the sulphide ion, which contributes to the electronic interaction between the metal ion and the charged sulphide ligand.

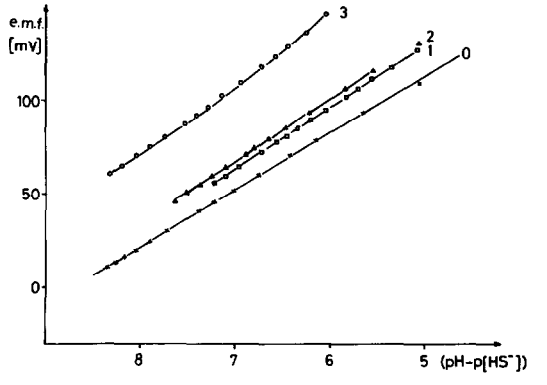

Fig. 7. Formation of $M(edta)S^{3-}$. EMF vs (pH–p[HS^-]) (C_{ML} = 0.01 mol dm^{-3}): (0) calibration curve of sulphide-selective electrode (0.5 mol dm^{-3} KNO_3); (1) $Al(edta)^-$; (2) $Ga(edta)^-$ and (3) $In(edta)^-$.

REFERENCES

1. S. Ahrland, *Struct. Bond* 1966, **1**, 207.
2. G. Anderegg, IUPAC Chemical Data Series, No. 14. *Critical Survey of Stability Constants of EDTA Complexes*. Pergamon Press, Oxford (1977).
3. K. Saito and H. Terry, *J. Chem. Soc.* 1956, 4701.
4. A. I. Busev, V. O. Tipcova and T. A. Sokolova, *Zh. Neorg. Khim.* 1960, **5**, 2749.
5. V. I. Kornev, K. V. Astahkov and V. I. Ribina, *Zh. Neorg. Khim.* 1966, **11**, 1851.
6. G. Anderegg and E. Bottari, *Helv. Chim. Acta* 1967, **50**, 2341.
7. I. P. Gorelov and M. K. Kolosova, *Zh. Neorg. Khim.* 1973, **90**, 18.

8. *Ustoitsivost smeshannich kompleksnih soedinenii v rastvorach.* Ja. D. Fridman i dr. Izd. Ilim, Frunze (1971).
9. D. W. Margerum, T. J. Bydalek and J. J. Bishop, *J. Am. Chem. Soc.* 1061, **83**, 1791.
10. R. Király, I. Tóth and E. Brücher, *J. Inorg. Nucl. Chem.* 1981, **43**, 345.
11. A. Yuchi, H. Hotta, H. Wada and G. Nakagawa, *Bull. Chem. Soc. Jpn* 1987, **60**, 1379.
12. R. E. Smith and A. E. Martell, *Critical Stability Constants* Vol. 4. p. 101. Plenum Press, New York (1976).
13. S. Ahrland, *Inorg. Chim. Acta* 1983, **79**, 94.
14. R. Sarin and K. N. Munshi, *J. Inorg. Nucl. Chem.* 1973, **35**, 201.
15. Y. Sigiura, N. Kojima and H. Tanaka, *Chem. Pharm. Bull.* 1977, **25**, 2263.
16. (a) I. Tóth, L. Zékány and E. Brücher, *Polyhedron* 1984, **3**, 871; (b) 1985, **4**, 279.
17. V. M. Masalovits and T. A. Puskareva, *Zh. Neorg. Khim.* 1980, **25**, 695.
18. J. Vesely, D. Weiss and K. Stulik, *Analysis with Ion-selective Electrodes* p. 131. Ellis Harwood, Chichester (1978).
19. A. Yuchi, K. Ueda, H. Wada and G. Nakagawa, *Anal. Chim. Acta* 1986, **186**, 313.
20. G. Bauer, *Handbook of Preparative Inorganic Chemistry*, Vol. 1. p. 879. Academic Press, New York (1963).
21. W. R. Harris and A. E. Martell, *Inorg. Chem.* 1976, **15**, 713.
22. P. O. Bethge, *Anal. Chim. Acta* 1954, **10**, 4310.
23. I. Tóth, Z. Szabó and P. Solymosi, *Talanta* 1988, **35**, 783.
24. H. M. Irving, M. G. Miles and L. P. Pettit, *Anal. Chim. Acta* 1967, **38**, 475.
25. L. Zékány and I. Nagypál, PSEQUAD: A comprehensive program for the evaluation of potentiometric and/or spectrophotometric equilibrium data, in *Computational Methods for Determination of Formation Constants* (Edited by D. J. Leggett), p. 291. Plenum Press, New York (1985).
26. A. Ya. Fridman, S. D. Ershova and N. M. Dyatlova, *Coord. Khim.* 1978, **4**, 1894.
27. G. Biedermann and T. G. Spiro, *Chim. Scrip.* 1971, **1**, 155.
28. F. Ja. Kulba, V. E. Mironov and J. F. Marvin, *Zh. Fiz. Khim.* 1965, **38**, 2595.
29. S. Ahrland and L. Johansson, *Acta Chem. Scand.* 1964, **18**, 2125.
30. J. M. Woods, R. K. Gallagher, Z. Z. Hugus and E. L. King, *Inorg. Chem.* 1964, **1**, 1313.
31. M. D. Peschanski and S. Velladas-Dubois, *Bull. Soc. Chim. Fr.* 1956, **16**, 1170.
32. A. I. Busev, V. G. Tipcova and T. A. Sokolova, *Vestnik Mosk. Un.-ta, Ser. Khim.* 1960, **6**, 42.
33. Ju. B. Jakovlev, F. Ja. Kulba and V. E. Mironov, *Zh. Neorg. Khim.* 1967, **12**, 3283.
34. S. Ahrland, I. Grente, L. Johansson and B. Noren, *Acta. Chem. Scand.* 1963, **17**, 1567.
35. L. Johansson, *Acta Chem. Scand.* 1966, **20**, 2156.
36. G. Anderegg, *Helv. Chim. Acta* 1967, **50**, 2333.
37. C. F. Baes, Jr. and R. E. Mesmer, *The Hydrolysis of Cations.* Wiley-Interscience, New York (1976).
38. I. Tóth, I. Reiter, E. Brücher and L. Vincze, *Abstract of XIX ICSC, p. 109. Lund, Sweden, Aug. 15–18,* (1988).
39. A. J. Ellis and R. M. Golding, *J. Chem. Soc.* 1959, 127.
40. D. G. Tuck, *Pure Appl. Chem.* 1983, **55**, 1477.
41. K. Tunaboylu and G. Schwarzenbach, *Chimia* 1970, **24**, 424.

Polyhedron Vol. 8, No. 16, pp. 2065–2070, 1989
Printed in Great Britain

0277–5387/89 $3.00+.00
© 1989 Maxwell Pergamon Macmillan plc

PROTONATION AND ZINC COMPLEX FORMATION OF INSULIN

F. GAIZER

Department of Inorganic and Analytical Chemistry, A. József University, Szeged, P.O. Box 440, Hungary

(*Received* 30 *January* 1989; *accepted* 15 *March* 1989)

Abstract—The protonation and zinc complex formation of insulin were studied by pH-metry. Computer evaluation of the experimental data was applied to describe the titration curves by assuming 12 protonation equilibria out of the possible 16. In solutions containing zinc and insulin in a ratio of 1:1, the presence of 11 zinc complexes was substantiated, while in solutions with a Zn:insulin ratio of 2:1, five dizinc complexes were assumed besides the monozinc complexes. A probable assignment of the protonation constants to the functional groups is given and the confidence level of the stability constants is discussed.

The insulin molecule contains 16 functional groups capable of protonation or deprotonation in the pH range 2–12. To determine the values of the protonation constants of the individual functional groups, Tanford and Epstein[1] performed pH-metric titration. From their experimental data, they were able to calculate the values of six protonation constants. On the basis of our previous results,[2,3] it was possible to presume that a computerized evaluation would result in more than six constants. The primary aim of the present work was of a chemical nature: to determine as many protonation constants of insulin as possible; to obtain information about the behaviour of the functional groups of the amino acids in the molecule in comparison with that of the free amino acids and, if there is any difference between them, to try to explain this. The secondary aim of our experiments was to examine the possibility of evaluating such complicated systems, i.e. how many models can describe our data; if there is more than one, what the difference between them is, further, how the individual protonation steps are separated from each other, and what the reliability of the assignment of the individual protonation constants to the individual functional groups is.

To obtain information about the compositions and stabilities of the zinc–insulin complexes, we made pH-metric measurements on solutions containing insulin and zinc ions in different ratios.

EXPERIMENTAL

Chemicals

The beef insulin examined was a product of NOVA. All other chemicals used were of analytical grade.

pH-Metric measurements

These were carried out in solutions with an ionic strength of 0.3 M using sodium chloride as swamping salt, and at 25 ± 0.1°C. An ORION 701/A digital potentiometer (with an accuracy of 0.1 mV) was used. As measuring electrode, a Radiometer G 22 B glass electrode was used. The reference electrode was a Radelkis OP 820 Ag/AgCl electrode with 0.3 M sodium perchlorate as separating electrolyte solution. During the experiments 10.0 cm^3 solutions containing 0.01 M hydrochloric acid were titrated with 0.1 M sodium hydroxide in a nitrogen atmosphere. In the sequence insulin, zinc, the composition of the solutions (expressed in mmol) were as follows: A: 0.9932, 0; B: 1.0041, 1.0027; and C: 0.99998, 2.0053.

The evaluation of the experimental data was carried out with the developed version[4] of the previously published[5] least-squares program. As protonating and complex-forming species, the totally unprotonated insulin molecule was considered. In

the course of refinements, that log β values of the protonating and/or complex forming species resulted in the minimum of the squares of the residuals of electromotive forces $[\Sigma(\Delta E)^2]$ were sought. As a measure of fit, the standard deviations of the residuals, $\sqrt{\Sigma(\Delta E)^2/(NMP-NP-1)}$, are given in Tables 1 and 2 (NMP and NP are the number of experimental points and parameters refined).

RESULTS

The pH-metric titration curves and the Z_H (the average number of protons bound by the insulin) vs a (the number of base equivalents added to the titrant) curves derived from the E vs cm^3 data are plotted in Fig. 1.

The data on the solution containing insulin only were evaluated by considering the peptide as both a monomer and a dimer. The optimum log β values, their errors expressed in hundredths, and the stepwise protonation constants are listed in Table 1.

In the case of solution B, which contained insulin and zinc ions in a ratio of 1 : 1, the evaluation was carried out as follows: insulin was taken as a monomer, the 12 log β's were kept constant, and the composition and stability constants of the zinc–insulin complexes improving the fit were searched for. As a result of the refinements, all the species free of zinc were practically completely transformed to zinc–insulin complexes, and a good fit could be achieved without the protonation constants. The best fit was obtained with the complexes and constants listed in Table 2.

When the data on solution C (ins : Zn = 1 : 2) were evaluated, only the monozinc complexes were taken into consideration and the dizinc–insulin complexes improving the fit were searched for. The compositions of the species and the stability constant values resulting in the optimum fit can also be seen in Table 2.

DISCUSSION

Numerous examinations have been carried out to establish the state of insulin in solution. On the basis of the results obtained by different methods (in spite of a few opposite findings), it may be concluded that insulin is not a monomer in solution, but mainly a dimer, and probably a tetramer and hexamer, too. In conformity, the authors presume an equilibrium of associates and a predominance of the dimer. The association constants of the monomer–dimer equilibrium have been determined by several authors and different methods, and found to

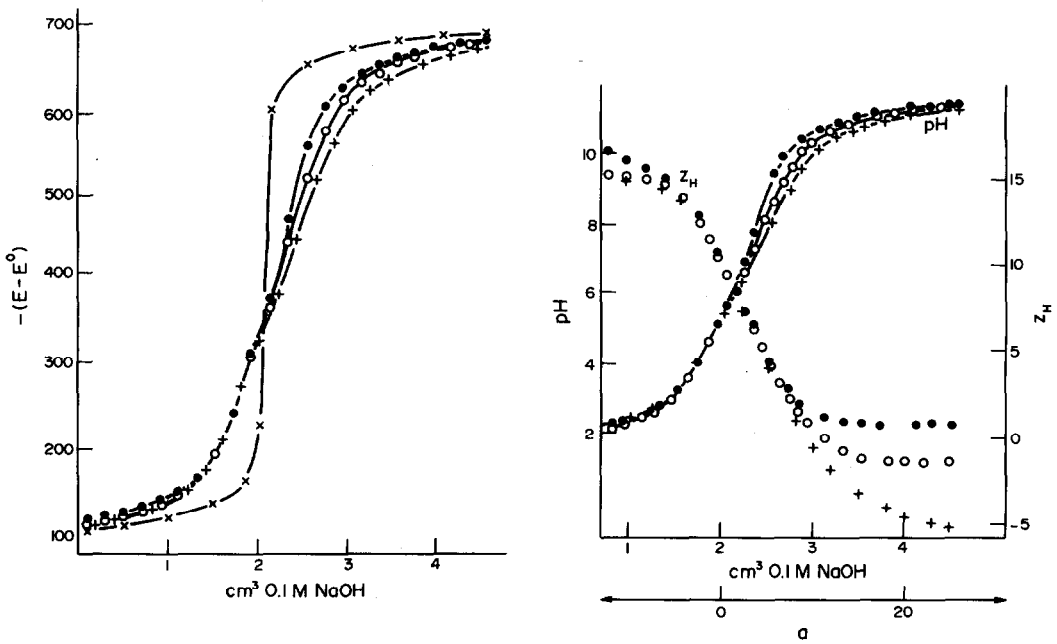

Fig. 1. pH-metric titration of insulin with 0.1 mol dm^{-3} NaOH. Concentrations in mmol dm^{-3} in the sequence T_{Ins}, T_{Zn}: ●: 0.9932, ϕ; ○: 1.0041, 1.0027; and +: 0.99998, 2.0053. × denotes the blank curve; Z_H: average number of protons bound/split off; a: number of base equivalents.

Table 1. Protonation constants of insulin

n	Protonating group	log K of free amino acid	As monomer log β_n	As monomer log K_n present work	As monomer log K_n Tanford *et al.*[1]	As dimer log β_{2n}	As dimer log K_{2n}
1	—NH_2, Arg	12.48	11.62_{13}	11.62	11.90_{20}	23.16	11.58 11.58
2	—NH_2, Lys	10.70		10.50			10.54 10.54
3			32.62_5	10.50		65.32	10.54 10.54
4	—OH, Tyr	10.40	42.47_5	9.85	9.60_{10}	85.06	9.87 9.87
5			51.92_{14}	9.85		103.92	9.43 9.43
6			60.24_{10}	8.32		120.72	8.40 8.40
7	—NH_2, Gly term	9.84	67.61_{16}	7.37	7.45	135.66	7.47 7.47
8	Phe	9.18	74.51_{26}	6.90		149.00	6.67 6.67
9	=N, His	6.08	80.31_{19}	5.80	6.40	161.0	6.0 6.0
10			86.18_{21}	5.87		172.42	5.71 5.71
11				4.87		182.58	5.08 5.08
12			95.92_{15}				
	—COOH, Glu	4.28		4.87	4.73_{10}	191.82	4.62 4.62
13				3.69		199.48	3.83 3.83
14			103.30_{16}	3.69		206.72	3.62 3.62
15	—COOH, Asn term	3.63		2.67			2.69 2.69
16	—COOH, Ala	2.30	108.64_{20}	2.67	3.60_{30}	217.48	2.69 2.69
No. of msd. points					85		
σ, mv				1.53		1.37	

be 10^4–10^5 dm^3 mol^{-1} (e.g. Jeffrey and Coates:[6] 1.2×10^4, UC, pH = 2; Lord *et al.*:[7] 4×10^4, UV, pH = 2; Pekar and Frank:[8] 1.4×10^5, equil. sediment., pH = 7; Goldman and Carpenter:[9] 2.2×10^5, UC, pH = 8 and Jeffrey *et al.*:[10] 1.1×10^5, UV, pH = 7).

Our calculations showed that when insulin was treated as a monomer or dimer the experimental data could be fitted by 12 or 14 log β's, respectively. The fit was somewhat better with the dimer model. However, when the experimental circumstances were taken into consideration, the difference between the two fits was not enough to substantiate the dimeric state of insulin. Therefore, the present data were explained by regarding insulin as a monomer.

It can be seen from the distribution curves in Fig. 2 that all the species relating to the 12 protonation constants are important. The individual protonation steps are not separated in the flat part

Table 2. Formation constants of zinc–insulin complexes

T_{Ins}/T_{Zn}	1:1		1:2	
n	$\log \beta_{H_nZnL}$	$\log K^{H_nZnL}_{H_nL}$	$\log \beta_{H_nZn_2L}$	$\log K^{H_nZn_2L}_{H_nZnL}$
−2			4.35_{12}	
−1	4.94_{50}			
0		~15.58	25.22_{6}	~9.70
1	26.02_{10}	14.40		
2	36.09_{17}		43.98_{14}	7.89
3	45.67_{18}	12.97		
4	54.79_{25}	12.37	61.02_{12}	6.23
5	62.76_{26}	10.77	67.76_{35}	5.20
6	71.20_{23}	10.90	75.45_{10}	4.25
7	77.15_{35}	9.43		
8	84.48_{18}	9.89	87.86_{15}	3.38
9				
10	95.80_{14}	9.47		
11				
12	105.31_{13}	9.26		
13				
14	112.52_{15}	9.09		
15				
16	116.75_{25}	7.98		
No. of msd points	85		88	
σ, mV	1.74		1.64	

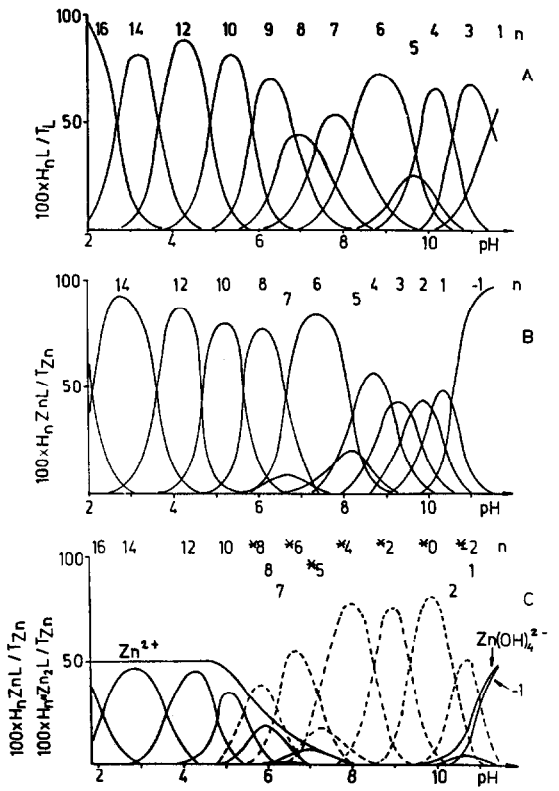

Fig. 2. Distribution of species calculated with constants of Table 2. $T_{Ins} = 1$ mmol dm^{-3}. A: insulin only, B: insulin : Zn = 1 : 1, and C: insulin : Zn = 1 : 2. Numbers are numbers of protons bound by unprotonated insulin.

of the titration curve, which corresponds to our expectations.

From the log β values obtained, we calculated the stepwise protonation constants. It may be concluded that with the exception of carboxyl groups the values of all the protonation constants are smaller than those of free amino acids.[11,12] The reason for this might be the formation of hydrogen bonds between the individual functional groups. It is easy to see that if a hydrogen bond is formed between, for example the guanidine group of arginine and an amino group, their protonation will be hindered. On the other hand, when a hydrogen bond is formed between phenolate and amino groups, the uptake of the first proton proceeds much more easily, and consequently, the values of the protonation constants will be larger than those in the free amino acids. For the formation of hydrogen bonds, insulin has a highly favourable structure. Due to the three disulphide bonds in the molecule, about 30 amino acids (i.e. more than half of the groups capable of protonation) are situated near to each other. Moreover, as the other amino acids are in three chains consisting of 5–11 units, association can easily take place between the chains, and also between the chains and the central part of the molecule. This results in a very complicated situation, even if the molecule is a monomer. With regard to all these effects, it is not probable that the first eight

protonation constants can be correctly assigned to the proper functional groups. Of course, it cannot be excluded, that the assignment in Table 1 is the correct assignment; the arrangement there followed the sequence of the protonation constants of the free amino acids.

When the experimental data on the interaction of insulin and zinc ions were evaluated, the peptide was considered to be a monomer. From the data on the 1 : 1 solution, it was possible to calculate the stability constants of 13 zinc–insulin complexes. As concerns the composition of these species, however, it must be stressed that they are only formal ones, because some of them, and especially those that form in the alkaline region, might be hydroxo complexes. This seems to be substantiated by the fact that it was necessary to assume the presence not only of the species H_2ZnL, but also of ZnL and $H_{-1}ZnL$. Naturally, we tried to substantiate the presence of $Zn(OH)_4^{2-}$ too, but this did not improve the fit.

On the basis of our results, the stability of the monozinc–insulin complexes is definitely high and, as can be seen in Fig. 2, the formation of these complexes even occurs in the pH range where all the potential donor atoms with the exception of carboxylate groups are protonated. This suggests that zinc ions are bound by one of the carboxylates first. The considerable stability of the hydroxo complexes formed in the alkaline region appears from the fact that they do not decompose up to pH 11.5, because there is no precipitate formation in the solution and the presence of the possible product $Zn(OH)_4^{2-}$ cannot be proved.

The experimental data on the insulin : Zn = 1 : 2 solution could be fitted with seven dizinc–insulin complexes, besides the 13 monozinc species. As can be seen from the data in Table 2, the binding of the second zinc to the peptide is much weaker than that of the first one. Another unexpected phenomenon is that the formation of dizinc complexes occurs only above pH 5–6. The weak binding of the second zinc ion is substantiated by the fact that, to achieve an acceptable fit, formation of the tetrahydroxozincate ion had to be assumed, through splitting-off of the second zinc ion.

It must be mentioned finally that, like Tanford and Epstein,[1] we too observed a weak opalescence in the solution at pH 3–3.5. The zinc-free and zinc-containing solutions clarified at pH 7–8 and 9–10, respectively. Our repeated measurements and those carried out in perchlorate medium resulted in constants spreading within the limits of experimental errors. These results, together with the fair agreement between the stability constants calculated from the present measurements and those of Tanford and Epstein[1] suggest that no irreversible precipitate formation takes place in the solutions.

CONCLUSIONS

As a result of the computerized simulation of the pH-metric titration curves, we succeeded in obtaining more information about the protonation equilibria of insulin than could be obtained with non-computerized calculation methods. It seems that the protonation and complex formation steps are well separated in the steep part of the titration curve, and the errors in the log β values of the individual equilibria are realistic. In spite of all this, in our view the acceptance of the data obtained requires much greater caution than could be expected from, e.g. the errors in the stability constants. As mentioned previously, on the basis of our measurements the monomer–dimer question cannot be settled; the reason for this may be that our experimental data contain information that can be described, depending on the model, only with polynomials of order 12–14. The dimeric treatment of insulin results in rather uncertain equilibrium constants, but the monomer assumption is probably a simplification, involving several further questions. On this basis the protonation constants presented here may be regarded only as good semiquantitative data.

Some uncertainty might arise about the monozinc complexes, due to the fact that there is not a large difference between the Z_H values obtained in the solutions containing insulin only or insulin + zinc ions. However, these are independent measurements and it may be assumed that the main conclusions (i.e. the strong binding of the first zinc ion and the weak binding of the second zinc, the compositions of most of the species formed, the relation of the stability constants, etc.) are acceptable.

On the basis of the experience acquired in the course of the evaluation, and the reliability of the information obtained, it may be concluded that peptides containing as many functional groups as insulin can be regarded as the limit of the possibility of evaluation by means of computerized simulation. In our view, stability constants acceptable in every respect result only when the number of functional groups in a molecule is not more than 8–12.

Acknowledgement—The author expresses his gratitude to Professor K. Burger for valuable discussions.

REFERENCES

1. C. Tanford and J. Epstein, *J. Am. Chem. Soc.* 1954, **76**, 2163.

2. K. Burger, F. Gaizer, B. Noszál, M. Pékli and G. Takácsi-Nagy, *Bioinorg. Chem.* 1977, **7**, 355.
3. K. Burger, I. Zay, F. Gaizer and B. Noszál, *Inorg. Chim. Acta* 1979, **34**, L239.
4. F. Gaizer: to be published.
5. F. Gaizer, *Acta Chim. Acad. Sci. Hung.* 1980, **103**, 397.
6. P. D. Jeffrey and J. H. Coates, *Biochemistry* 1966, **5**, 489.
7. R. S. Lord, F. Gubensek and J. A. Rupley, *Biochemistry* 1973, **12**, 4385.
8. A. H. Pekar and B. H. Frank, *Biochemistry* 1972, **11**, 4013.
9. J. Goldman and F. H. Carpenter, *Biochemistry* 1974, **13**, 4566.
10. P. D. Jeffrey, B. K. Milthorps and L. W. Nichol, *Biochemistry* 1976, **15**, 4660.
11. L. G. Sillén and A. E. Martell, *Stability Constants of Metal-ion Complexes*, Spec. Publ. No 17 (1964) and Suppl. No. 1. Spec. Publ. No. 25 (1971). Chem. Soc. London.
12. D. D. Perrin, *Stability of Metal-ion Complexes, Part B., Organic Ligands*, IUPAC Chem. Data Ser. No. 22. Pergamon Press, Oxford (1979).

Polyhedron Vol. 8, No. 16, pp. 2071–2076, 1989
Printed in Great Britain

0277–5387/89 $3.00+.00
© 1989 Maxwell Pergamon Macmillan plc

HYDROLYSIS OF ACTINIDES AND LANTHANIDES: HYDROLYSIS OF SOME TRIVALENT ACTINIDE AND LANTHANIDE IONS STUDIED BY EXTRACTION WITH THENOYLTRIFLUOROACETONE

P. K. MOHAPATRA* and P. K. KHOPKAR

Radiochemistry Division, Bhabha Atomic Research Centre, Trombay, Bombay 400 085, India

(*Received* 24 *October* 1988; *accepted after revision* 22 *March* 1989)

Abstract—In the solvent extraction studies of trivalent Am, Cm, La, Eu and Lu using thenoyltrifluoroacetone (HTTA) in xylene as the extractant, the pH variation experiments at a fixed extractant concentration revealed a reduction in slope from three to two when log D was plotted vs pH. While the plots of log D vs log $[HTTA]_{org}$ gave slopes of three at lower pH values, those at higher pH values showed a slope of two, thus suggesting the extraction of hydroxo chelates $MOH(TTA)_2$ in the higher pH region. The points of intersection of the lines of slopes three and two in the log D vs pH plots are not affected significantly by the nature and concentration of the extractant, and these are shown to be numerically equal to the negative logarithm of the first hydrolysis constants K_h, whose values increase with decreasing ionic radii of the metal ions. The changes in the K_h values on varying ionic strength are as expected from a known empirical relation.

Hydrolysis of trivalent actinides and lanthanides has been extensively studied over the last few decades using different methods such as solvent extraction,[1–5] pH titration,[6–10] electrophoresis,[11] electromigration,[12] solubility[13] and several other methods.[14–18] It is observed from the published data (Table 1) that the values of the first hydrolysis constant for the same metal ion differ widely—in some cases by even five orders of magnitude—and further work in this field is highly desirable in view of the basic importance of the problem by itself, as well as for understanding the chemical behaviour of these metal ions (especially actinides) in various natural environments. Many of the published values of the first hydrolysis constants (K_h) for the trivalent actinides and lanthanides (log $K_h = -6$ to -10) indicate that there is negligible hydrolysis of the ions (e.g. Am^{3+} and Cm^{3+}) below pH 6.[1–5,8,13] However, it is observed[19] that in aqueous solutions of these metal ions which do not contain any complexing agents, serious adsorption problems on the walls of containers are encountered at pH values even lower than 6 but, are negligible at pH < 4. As hydrolysis should be the most likely precursor to adsorption[19] of these ions at the higher pH values, this would indicate that they are probably hydrolysed at pH values lower than 6. Preliminary work carried out earlier[20] in this laboratory with Am^{III} using solvent extraction with thenoyltrifluoroacetone (HTTA), showed that hydrolysis of Am^{III} may be appreciable near pH ~ 3.6. In the present work, hydrolytic behaviour of Am^{III}, Cm^{III}, La^{III}, Eu^{III} and Lu^{III} has been investigated using solvent extraction with HTTA in xylene.

EXPERIMENTAL

Materials

Tracer solutions of the actinides ^{241}Am, ^{244}Cm and the lanthanides ^{140}La, $^{152,154}Eu$ and ^{177}Lu were prepared as described previously.[21] Specific activity of the lanthanide tracers was high enough to maintain the final concentration of all the metal ions $\leqslant 10^{-6}$ M in order to minimize the possibility of polymeric species formation at higher pH. Radioassay of the tracers was carried out by γ-scintillation

* Author to whom correspondence should be addressed.

Table 1. First hydrolysis constants of Am^{III}, Cm^{III}, La^{III}, Eu^{III} and Lu^{III}

Metal ion	Method	Temp. (°C)	Ionic strength (M)	$-\log K_h$	Ref.
Am^{III}	Solvent extraction	20–25	0.1–1.0	5.9–7.6	1, 3, 4, 5
	Solvent extraction	30±0.1	0.01	3.65±0.1	Present work
	pH titration	25	1.0	7.03	8
	Solubility	20	—	⩾8.2	13
	Electrophoresis	15	5×10^{-3}	3.05	11
	Electromigration	25	5×10^{-3}	3.30	12
	—	25	0	0.5–4.0	14, 15
Eu^{III}	Solvent extraction	20–25	0.1–1.0	4.8–7.3	2–4
	Solvent extraction	30±0.1	0.01	3.30±0.1	Present work
	pH titration	25	1.0	8.12	8
	Conductivity	25	$\leqslant10^{-4}$	8.7	16
	Electrophoresis	15	5×10^{-3}	3.15	11
	Electromigration	25	1	8.1	3
Cm^{III}	Solvent extraction	23	0.1	6.05	1
	Electromigration	25	1	3.4	12
	Solvent extraction	30±0.1	0.01	3.30±0.1	Present work
La^{III}	Solvent extraction	25	0.1	7.4	2
	pH titration	21.5	1.0	5.4	9
	pH titration	25	3.0	>10.0	7, 17
	Solvent extraction	30±0.1	0.01	3.85±0.1	Present work
	EMF	20, 25	0.1, 0[a]	8.4, 5.27	18, 19
Lu^{III}	Solvent extraction	25	0.1	3.5	2
	Polarography	20	0.1	7.4	18
	EMF	25	0[a]	6.67	19
	Solvent extraction	30±0.1	0.01	3.10±0.1	Present work

[a] Normalized to 0 ionic strength.

counting, using a well-type NaI(Tl) counter with appropriate settings, except for ^{244}Cm where liquid scintillation counting was used. HTTA (E. Merck Pro analysi, m.p. 43.4°C) and HBTA (Penn. Chem. Res. Inc., m.p. 39.4°C) were of AR grade and were used after recrystallization. HPMBP (1-phenyl-3-methyl-4-benzoyl pyrazolone-5) was synthesized in the laboratory.[22] All other reagents are of AR quality. All HTTA, HBTA and HPMBP solutions prepared for the experiments were initially equilibrated for 6 h with 0.1 M $HClO_4$ in order to establish keto–enol equilibrium. All studies are carried out at 30±0.1°C due to the prevailing higher ambient temperatures (~27°C).

pH variation experiments

pH measurements were made with an EMCO (India) pH meter, with an accuracy of ±0.01 pH units, after standardizing with three standard buffers of pH values 4.01, 3.56 and 6.86.[23] 2 cm^3 of the aqueous phase containing the required tracer and pre-adjusted to different pH values [pH adjustment was carried out with 0.01 M acetate or chloroacetate buffer (Table 2)] were equilibrated with 1 cm^3 of 0.1 M HTTA in xylene, in a thermostated bath maintained at 30±0.1°C, for 1 h. Equilibrium was attained well within this time. After settling for 30 min, aliquots of both the phases were removed for radio-assay. Mass balance was strictly checked to ensure that no adsorption is taking place in the aqueous phase. Equilibrium pH of the aqueous phase was also recorded. In order to study the effect of ionic strength on the hydrolytic behaviour of Am^{III}, pH variation experiments were also carried out without using any buffer ($\mu \leqslant 10^{-3}$ M) and with aqueous solutions containing 0.1 M $NaClO_4$. Also additional experiments, using 0.1 M HTTA in xylene (no buffer was used) as well as 0.2 M HBTA and 0.2 M HPMBP, were carried out for determining the effect of the concentration and nature of the extractant on the values obtained for hydrolysis constants.

HTTA variation experiments

2 cm^3 of 0.01 M acetate buffer solutions containing required tracer and adjusted to constant pH values (3.80 for Am, Cm and Eu and 4.60 for La) were equilibrated with 1 cm^3 of HTTA solutions of

Table 2. Slopes of log D vs pH plots in the lower and higher pH regions using different extractants in xylene

Metal ion	Ionic strength	Extractant	Slope[e]		pH at the intersection point
			Lower pH region	Higher pH region	
Am^{III}	$\leqslant 10^{-3}$ M[a]	0.1 M HTTA	3.21±0.05	2.06±0.05	3.57
	$\leqslant 10^{-3}$ M[a]	0.2 M HTTA	2.84±0.02	1.97±0.06	3.60
	$\leqslant 3\times10^{-3}$ M[b]	0.2 M HTTA	3.12±0.06	2.10±0.06	3.73
	≃0.1 M[c]	0.2 M HTTA	2.80±0.08	1.94±0.06	3.75
	$\leqslant 3\times10^{-3}$ M[b]	0.2 M HBTA	2.88±0.06	2.02±0.07	3.75
	$\leqslant 3\times10^{-3}$ M[b]	0.2 M HPMBP	3.18±0.05	1.89±0.04	3.55
Eu^{III}	$\leqslant 4\times10^{-3}$ M[a]	0.2 M HTTA	2.94±0.07	2.10±0.06	3.25
	$\leqslant$0.01 M[d]	0.2 M HTTA	2.87±0.06	2.11±0.09	3.38
Cm^{III}	$\leqslant$0.01 M[d]	0.2 M HTTA	2.80±0.09	1.92±0.09	3.33
La^{III}	$\leqslant$0.006 M[b]	0.2 M HTTA	2.84±0.07	2.13±0.04	3.85
Lu^{III}	$\leqslant$0.009 M[d]	0.2 M HTTA	2.98±0.02	2.10±0.06	3.10

[a] Dilute HCl solutions.
[b] 0.01 M acetate buffer.
[c] 0.1 M $NaClO_4$+0.01 M acetate buffer.
[d] 0.01 M chloroacetate buffer.
[e] From log D vs pH plots.

different concentrations in the range 0.12–0.40 M for 1 h and later assayed as described earlier.

RESULTS AND DISCUSSION

The extraction of trivalent actinides by HTTA from aqueous solutions is usually represented by the equilibrium

$$M^{3+}_{aq} + 3HTTA_{org} \rightleftharpoons M(TTA)_{3_{org}} + 3H^{+}_{aq} \quad (1)$$

where a binary species, namely $M(TTA)_3$ is extracted. Thus, while plotting log D (where $D = \Sigma[M]_{org}/\Sigma[M]_{aq}$) vs pH a slope of 3 is expected. However, as Fig. 1 indicates, for Am^{III} (as will be shown later for Cm^{III}, Eu^{III}, La^{III} and Lu^{III} also) a deviation from the slope 3 is observed at pH ~ 3.5 and above which the slope is reduced from 3 to 2. This observation was confirmed by repeating this experiment several times. The results shown in Fig. 1 are those obtained by pH variation experiments done by using 0.1 and 0.2 M HTTA in xylene from aqueous solutions containing 10^{-4} to 10^{-3} M HCl. Two distinctly different slopes are observed. The actual values of the slopes are obtained by a least square program and the fitted lines are plotted by the computer, using a x–y plotter (Table 2). Now, even though the slope of 3 at the lower pH region can be accounted for by eq. (1), the slope of 2 obtained at higher pH values is quite intriguing. One of the explanations could be the existence of a precursor such as $MTTA^{2+}$ (which has probably a very fast formation rate) which subsequently gives $M(TTA)_3$ by eq. (2). The other possibilities are given by eqs (3) and (4) which presuppose the formation of a hydroxo species (due to partial hydrolysis of the metal ion) which can subsequently react with 3 and 2 molecules of HTTA respectively

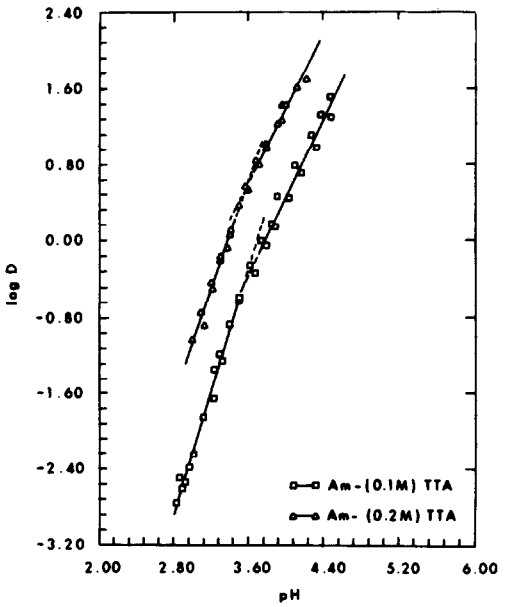

Fig. 1. Variation of log D with pH using 0.1 and 0.2 M HTTA in xylene.

$$MTTA^{2+}_{aq} + 2HTTA_{org} \rightleftharpoons M(TTA)_{3_{org}} + 2H^{+}_{aq} \quad (2)$$

$$MOH^{2+}_{aq} + 3HTTA_{org} \rightleftharpoons M(TTA)_{3_{org}} + H_2O + 2H^+_{aq} \quad (3)$$

$$MOH^{2+}_{aq} + 2HTTA_{org} \rightleftharpoons MOH(TTA)_{2_{org}} + 2H^+_{aq}. \quad (4)$$

Using the values of stability constants for the Am^{III}—TTA complex as reported by Keller and Schreck[24] it can be easily shown that under the present experimental conditions (using the partition coefficient of HTTA as 33.73 ± 0.84[25] and its pKa as 6.23[24] in the aqueous phase) negligible proportion of Am^{III} exists in the form of Am TTA^{2+}, hence ruling out the possibility of the extraction of $M(TTA)_3$ complex, by eq. (2). As will be discussed later, a similar behaviour is also observed when other extractants are used, thus eliminating complexing of the metal ion by the extractant anions in the aqueous phase as the reason for the decrease in the slope from 3 to 2.

In order to ensure which one of the equilibria, eqs (3) or (4), is occurring, variation of HTTA at a constant pH was done in the pH region where a slope of 2 was observed. Figure 2 shows such plots, which are plotted by using a least square program, the fitted slope values with errors being given in Table 3. For americium the pH was kept constant at 3.80 and the results show a straight line with a slope very much closer to 2 than to 3 (Table 3). Thus, the species extracted is certainly not $Am(TTA)_3$ as reported by several workers[1,4] and is probably $Am(OH)(TTA)_2$. A similar species being extracted was reported by Keller and Schreck[24] in the extraction of Ac^{III}. Similarly, the HTTA variation experiments, done for Cm^{III}, La^{III}, Eu^{III} at constant pH, confirm this aspect showing a HTTA dependency of 2 (Fig. 2 and Table 3). HTTA variation experiments were also carried out at a constant pH value in the lower pH region (slope 3 region of Fig. 3) for these metal ions and a dependency of 3 was observed which indicates that different species are extracted before and after the intersection point (Fig. 3) and the extraction of the hydroxo species at higher pH values implies the occurrence of probable hydrolysis.

Table 3. Variation of log D with log $[HTTA]_{org}$ at constant pH values

Metal ion	pH[a]	Slope[b]
Am^{III}	3.80	2.28 ± 0.03
Eu^{III}	3.80	2.16 ± 0.03
Cm^{III}	3.80	2.07 ± 0.09
La^{III}	4.60	1.97 ± 0.08

[a] 0.01 M acetate buffer.
[b] From log D vs log $[HTTA]_{org}$ plots (Fig. 3).

Referring to Fig. 1 the pH regions where slopes of 3 and 2 are observed can be taken as the regions where the species Am^{3+} and $AmOH^{2+}$ respectively exist, and it can be concluded that the pH value at which the above mentioned lines intersect could be

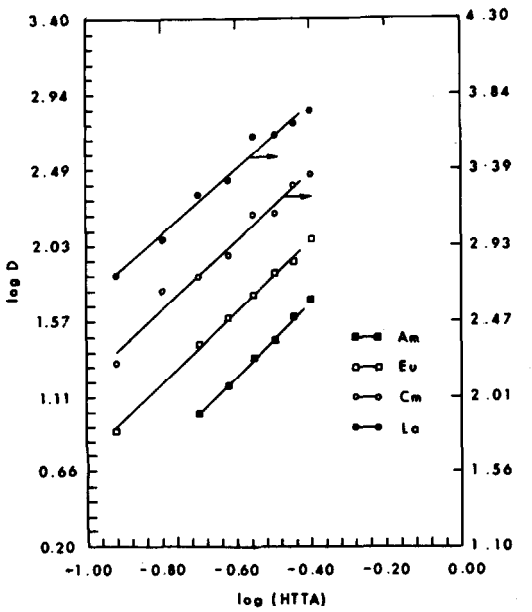

Fig. 2. Variation of log D with log $[HTTA]_{org}$ for Am^{III}, Cm^{III}, Eu^{III} and La^{III}, pH = 3.80 (Am, Cm, Eu) and 4.60 (La).

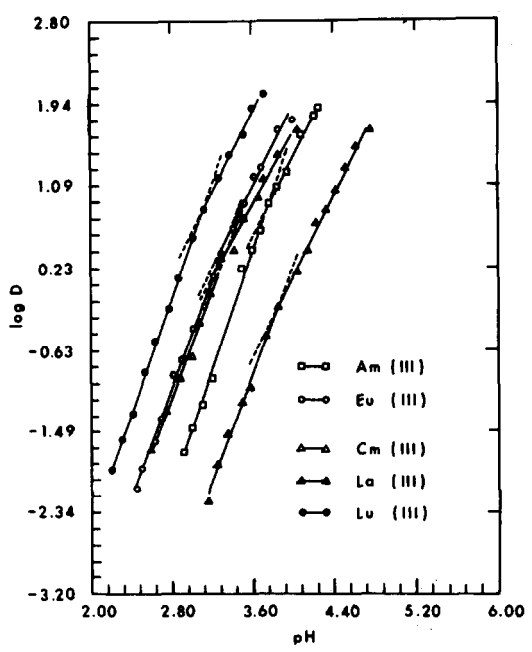

Fig. 3. Variation of log D with pH for some trivalent actinides and lanthanides, 0.01 M acetate buffer (Am, La); 0.01 M chloroacetate buffer (Cm, Eu, Lu).

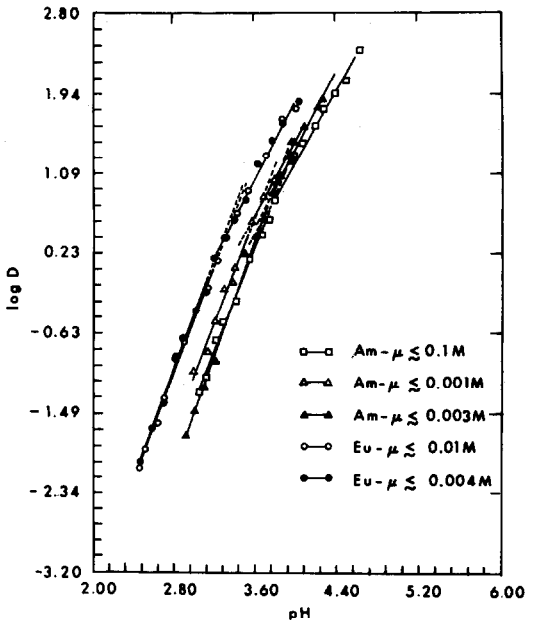

Fig. 4. Variation of log D with pH for Am^{III} and Eu^{III} at different ionic strengths.

the pH where both Am^{3+} and $AmOH^{2+}$ exist with equal concentrations. It can easily be shown that this pH equals the negative logarithm of the first hydrolysis constant, K_h, which pertains to eq. (5)

$$Am^{3+} + H_2O \overset{K_h}{\rightleftharpoons} AmOH^{2+} + H^+. \qquad (5)$$

Figure 4 gives plots of log D vs pH for the extraction of Am^{III} from aqueous solutions of various ionic strengths while Fig. 5 shows similar plots for

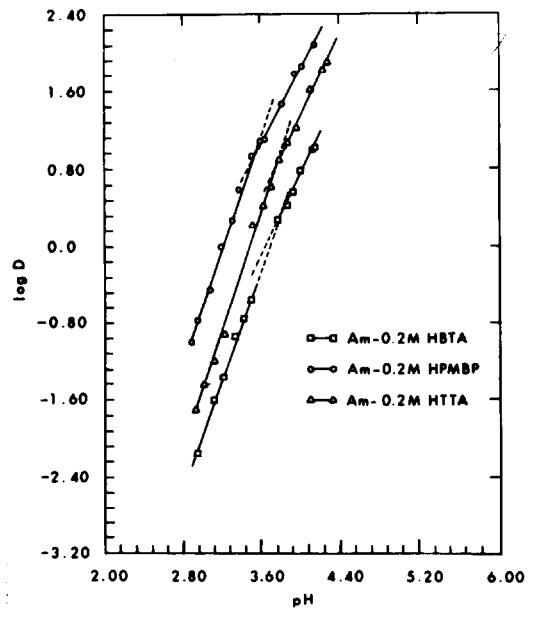

Fig. 5. Variation of log D with pH for Am^{III} using 0.2 M HTTA, HBTA and HPMBP in xylene as extractants.

Am^{III} using three different extractants, namely HTTA, HBTA and HPMBP of the same concentration in xylene. The plots in both figures are similar to those given in Fig. 1, in the sense that they consist of two intersecting lines of slopes ~ 3 and ~ 2 whose exact slopes with errors are given in Table 2 along with the pH values at the points of intersection of these corresponding pair of lines. From Table 2 it is clear that with different extractants the observed behaviour is also similar, the intersection points being centred around pH 3.65 and well within experimental errors. Thus, from a series of experiments the mean value of the first hydrolysis constant for Am^{III} is $10^{-3.65\pm0.1}$.

The low concentration of Am ($\lesssim 10^{-6}$ M) employed, ensures the probable non-occurrence of polymeric species which, as discussed later, can be a source of error in methods such as pH titration and solubility for which use of macro-concentration is mandatory.

The values of hydrolysis constants reported at different ionic strengths can be correlated with each other by an empirical relation[26] which states that the log K_h values decrease with increasing ionic strength by 0.37 units for 0.1 M $NaClO_4$, 0.6 units for 0.5 M $NaClO_4$ and 0.7 units for 1 M $NaClO_4$ at 25°C. In the present study a decrease of ~ 0.2 units is observed for a two order increase in ionic strength (Table 2) which closely follows the relation.[26] The values reported by us at 0.01 M ionic strength (Tables 1 and 4) are obtained from the experimental values using the empirical relation. However, it is seen from Table 1 that values of hydrolysis constants reported by several authors, obtained at different ionic strengths, even after correction (following the empirical relation) are widely different, which will be discussed shortly.

Figure 3 presents plots of log D vs pH for Am^{III},

Table 4. First hydrolysis constants for the reaction $M^{3+} + H_2O \rightleftharpoons MOH^{2+} + H^+$ ($\mu \simeq 0.01$ M; temp. = 30±0.1°C)

Metal ion	Estimated first hydrolysis constants[a] ($-\log K_h$)	$\log \beta^{OH}$ [b]	Effective ionic radii (Å)[c]
La^{3+}	3.85±0.1	10.15±0.1	1.160
Am^{3+}	3.65±0.1	10.35±0.1	1.090
Cm^{3+}	3.30±0.1	10.70±0.1	1.085
Eu^{3+}	3.30±0.1	10.70±0.1	1.086
Lu^{3+}	3.10±0.1	10.90±0.1	0.977

[a] Normalized to 0.01 M ionic strength.
[b] $\log \beta^{OH} = p K_w + \log K_h = [AmOH^{2+}]/[Am^{3+}][OH^-]$.
[c] Ref. 27.

Cm^{III}, La^{III}, Eu^{III} and Lu^{III} using 0.2 M HTTA in xylene as the extractant and the aqueous phase containing 0.01 M acetate or chloroacetate buffer as the case may be (acetate buffer for Am^{III} and La^{III} and chloroacetate buffer for Eu^{III}, Cm^{III} and Lu^{III}). As seen from Table 2, the plots for La^{III}, Eu^{III}, Cm^{III} and Lu^{III} clearly show two different slopes which are close to 3 and 2. Thus, following the arguments as given for Am^{III}, the K_h values can be obtained from the points of intersection. The first hydrolysis constant values of these ions show an interesting decreasing trend as the ionic radii of them increase (Table 4). The lower value for Eu^{III} than expected, is not surprising. The anomalously low value of the stability of Eu^{III} complexes in comparison with that of the other lanthanides has been observed in other systems earlier.[21]

The increasing stabilities of the first hydroxo complexes of the metal ions with decreasing ionic radii, irrespective of the nature of metal ions, indicate that these are essentially ionic inner complexes. Participation of 5*f*-orbitals in the hydroxo complexes of Pu^{III} and Am^{III} suggested by Nair *et al.*[8] is not compatible with the values obtained in the present work. The monotonic increase in the K_h values (or β_{OH} values) obtained with decrease in ionic radii is very similar to the behaviour of the first fluoride complexes of lanthanides as seen from the values reported in the literature.[28] As both fluoride and hydroxide ions are small hard donors which are expected to form essentially ionic complexes, the similarity of their complexing behaviour is hardly surprising. The decrease in the values of K_h from Sm^{III} to Er^{III} as well as the lower K_h values for Am^{III} and Cm^{III} as observed by Guillaumont *et al.*[2] (who have also used solvent extraction with HTTA) probably arises from their assumption of extraction of $M(TTA)_3$ in the organic phase throughout the pH range employed in their extraction studies which is contrary to that observed in the present work.

The values of K_h obtained in the present work for Am^{III} and Eu^{III} are close to those obtained by Marin and Kikindai[11] (electrophoresis method) and by Shalinets and Stepanov[12] (electromigration method). Caceci and Choppin[4] and Rao *et al.*[5] have used a competitive complexing anion in their solvent extraction methods for the determination of K_h and have assumed *a priori* that no hydrolysis occurs below pH 6 and 4 respectively. The values of K_h for Am^{III} obtained by them ($-\log K_h = 7.54$ and 6.80 respectively) are much lower than those obtained in this study. The lower values obtained in the pH titration[9,7,17] and solubility[13] methods are probably affected due to the existence of polymeric species in the macro concentrations of the metal ions necessarily used in these methods.

Acknowledgements—The authors thank Dr P. R. Natarajan, Head, Radiochemistry Division, B.A.R.C., for his keen interest in the work. They also thank Dr V. K. Manchanda for valuable discussions and suggestions.

REFERENCES

1. B. Desire, M. Hussonois and R. Guillaumont, *C.R. Acad. Sc. Series C* 1969, **269**, 448.
2. R. Guillaumont, B. Desire and M. Galin, *Radiochem. Radioanal. Lett.* 1971, **8**, 189.
3. R. Lundquist, *Acta Chem. Scand.* (*A*) 1982, **36**, 741.
4. M. S. Caceci and G. R. Choppin, *Radiochim. Acta* 1983, **33**, 101.
5. V. K. Rao, G. R. Mahajan and P. R. Natarajan, *Inorg. Chim. Acta* 1987, **128**, 131.
6. K. A. Kraus and J. R. Dam, *Natl. Nucl. Energy Series IV* 1949, **148**, 446.
7. G. Biederman and L. Ciavatta, *Acta Chem. Scand.* 1961, **15**, 1347.
8. G. M. Nair, Keshav Chander and J. K. Joshi, *Radiochim. Acta* 1982, **30**, 37.
9. J. Kragten and L. G. D. Weever, *Talanta* 1987, **34**, 861.
10. T. Amaya, H. Kakihana and M. Maeda, *Bull. Chem. Soc. Jpn* 1973, **46**, 1720.
11. B. Marin and T. Kikindai, *C.R. Acad. Sc. Series C* 1969, **268**, 1.
12. A. B. Shalinets and A. V. Stepanov, *Radiokhimiya* 1972, **14**, 280.
13. D. Rai, R. G. Stickert, D. A. Moore and J. L. Ryan, *Radiochim. Acta* 1983, **33**, 201.
14. A. G. Samartseva, *Radiokhimiya* 1969, **11**, 502.
15. Yu. S. Korotkin, *Sov. Radiochem.* 1973, **15**, 682.
16. K. H. Schmidt, J. C. Sullivan, S. Gordon and R. C. Thompson, *Inorg. Nucl. Chem. Lett.* 1978, **14**, 429.
17. E. J. Wheelright, F. H. Spedding and G. Schwarzenbach, *J. Am. Chem. Soc.* 1953, **75**, 4196.
18. L. M. Usherenko and N. A. Skorik, *Zhur. Neorg. Khim.* 1972, **17**, 2918.
19. P. K. Khopkar (unpublished work).
20. H. D. Sharma and P. K. Khopkar, *Report AEET/Radiochemistry/7* India (1959).
21. P. K. Khopkar and J. N. Mathur, *J. Inorg. Nucl. Chem.* 1977, **39**, 2063.
22. J. N. Mathur and P. K. Khopkar, *Sep. Sci. Techn.* 1982, **17**, 985.
23. A. I. Vogel, *A Text-book of Quantitative Inorganic Analysis Including Elementary Instrumental Analysis*, p. 910. Longman's, London (1961).
24. C. Keller and H. Schreck, *J. Inorg. Nucl. Chem.* 1969, **31**, 1121.
25. V. K. Manchanda, (private communication).
26. C. F. Baes and R. E. Mesmer, *The Hydrolysis of Cations*. Wiley, New York (1967).
27. R. D. Shanon, *Acta Cryst.* 1976, **A32**, 751.
28. R. M. Smith and A. E. Martell (Editors), *Critical Stability Constants*, Vol. 4. Plenum Press, New York (1976).

Polyhedron Vol. 8, No. 16, pp. 2077–2086, 1989
Printed in Great Britain

0277–5387/89 $3.00+.00
© 1989 Maxwell Pergamon Macmillan plc

SPECIATION IN AQUEOUS SOLUTIONS OF DI-ETHYLENETRIAMINE-N,N,N′,N″,N″-PENTAMETHYLENEPHOSPHONIC ACID AND SOME METAL COMPLEXES

R. D. GILLARD*† and P. D. NEWMAN†

Department of Chemistry, University College, P.O. Box 78, Cardiff CF1 1XL, U.K.

and

J. D. COLLINS

Research Laboratory, Albright and Wilson Ltd., P.O. Box 80, Trinity Street, Oldbury, Warley, West Midlands B69 4LN, U.K.

(*Received* 15 *August* 1988; *accepted* 19 *April* 1989)

Abstract—Results of magnetic resonance spectra (^1H and ^{31}P) and potentiometry for aqueous solutions of the title acid, H_{10}DTPMP, and for its cadmium and lead complexes, are correlated to give information about the species present. The central nitrogen atom is an anomalously weak base.

Since the discovery[1] by Schwarzenbach, Ackermann and Ruchstuhl of the calcium binding by nitrilodiaceticmethylenephosphonic acid, a whole new class of chelating agents containing aminophosphonate groups has surfaced. Initial studies by Martell's group of the stability of their metal complexes[2–6] were fuelled by their close analogy to the successful oligo-amino-oligo-carboxylates such as H_4EDTA. The mutual repulsion between two or more negative phosphonate groups[2] tends to lower the coordinating ability and denticity of the aminophosphonates with respect to their carboxylate analogues, and also makes them more selective for cations with an enhanced capacity for coordination.[7,8]

The aminocarboxylates (such as nitrilotriacetic acid (NTA), EDTA and DTPA) have been used for decades as scavenging agents for unwanted metal ions in textile and paper processing, e.g. preventing precipitation of insoluble salts. Over the last 15 years, emphasis has swung towards the use of organophosphonates including DNTMP‡ and DTPMP, under various trade names, those for the latter including BRIQUEST 543-45AS and DEQUEST 2060. Their advantage is that they not only form stable complexes, but also act as detergents by dispersing and suspending soil in solution, preventing its redeposition on goods, an ability not shown by aminocarboxylates. In addition, the organophosphonates but not the aminocarboxylates show a so-called threshold effect. Rizkalla studied[9] retardation of $BaSO_4$ precipitation by DTPMP and other organophosphonates, although the "active acid content" of H_{10}DTPMP was determined by titration with NaOH, and the purity calculated on the basis of base compound per equivalent of acid.

When bleaching paper pulp with H_2O_2, the major cost is due to consumption of peroxide, and any loss through decomposition leads to decreased efficiency and increased cost. Trace amounts of metal ions (manganese, iron, copper, chromium and nickel are all present in woodpulp) in bleaching baths can lead to considerable loss of peroxide. $H_nDTPMP^{(10-n)-}$ has recently been shown[10] to be very effective in the prevention of H_2O_2 decomposition in the presence of metal ions.

Detailed assessment of the efficacy of H_{10}DTPMP in such applications requires knowledge of the micro-equilibria in aqueous solution, and we report here our initial work on this.

* Author to whom correspondence should be addressed.
† Now at: School of Chemistry and Applied Chemistry, University of Wales, P.O. Box 912, Cardiff CF1 3TB, U.K.

‡ Often called ENTMP, especially in technological literature.

The structures of the polyaminopolycarboxylate chelates and their metal complexes in solution have been extensively studied by the use of electronic (including circular dichroism[11]), infrared and nuclear magnetic resonance (NMR) spectroscopy.[12,13] The solution structures of the polyaminopolyphosphonates have not been so extensively examined, apart from NMR work on ethylenediamine - N,N,N′,N′ - tetrakis(methylenephosphonic) acid (ENTMP) and di-ethylenetriamine-N,N,N′,N″,N″-pentamethylenephosphonic acid (DTPMP).[14–16] Simple structural spectroscopy on solid metal derivatives of $H_nDTPMP^{(10-n)-}$ has also been published.[17]

RESULTS AND DISCUSSION

The acid, $H_{10}DTPMP$

The titration curve for the free ligand shows three buffer regions with inflections at $\alpha \simeq 2.5$ and 7.0 (α is the number of moles of NaOH added per mole of ligand). The shape of the curve suggests that dissociation occurs in three steps, as shown in Scheme 1. The assumption that all phosphonates are deprotonated prior to nitrogen deprotonation is an over-simplification (*vide infra*).

Reported protonation constants[18,19] of DTPMP are shown in Table 1. The intermediate values of pK are in reasonable agreement, although the extreme values differ considerably. In the medium of ionic strength 3 M which we have employed, the log K values would be depressed as shown[20,21] previously for ENTMP. The first three protonation constants are all greater for DTPMP than for DTPA, implying that nitrogens bonded to methylene-phosphonates are more basic, an effect attributed[2] to the double negative charges of the phosphonate groups, shifting negative charge toward the nitrogen atoms.

Table 1. Protonation constants ($\log_{10} K$) of $DTPMP^{10-}$ at 25°C in an ionic medium of 0.1 M KCl

	From ref. 18	From ref. 19
K_1	12.04	11.12
K_2	10.10	9.36
K_3	8.15	7.74
K_4	7.17	7.07
K_5	6.38	6.28
K_6	5.50	5.38
K_7	4.45	3.82
K_8	2.80	3.10
K_9	—	2.64
K_{10}	—	1.52

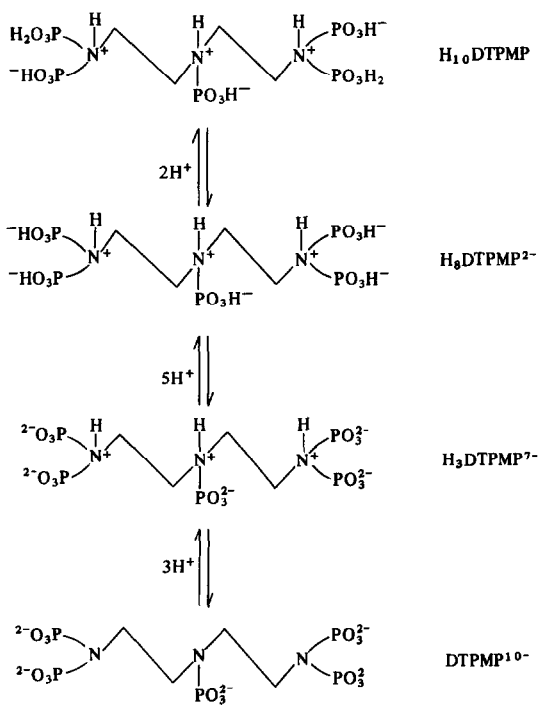

Scheme 1.

As an aside, relating to our main objective of surveying structures of metal complexes, which we shall address in later papers, it is evident from inspection of the titration curves in the presence of equimolar concentrations of metal ions that the stability sequence of the complexes under these conditions is Sr < Mg < Ca ~ Fe < Mn < Co ~ Ni ~ Pb < Cd < Zn < Cu, as expected from the Irving–Williams series.[22] Copper(II) forms by far the most stable chelate, its titration curve starting at a significantly lower pH than those of the other doubly charged metal ions

Insight into protonation schemes of aminocarboxylates[23–26] and aminophosphonates[15] has been obtained largely through the use of ^{1}H NMR based on the observation of chemical shift changes of non-labile protons (protons attached to carbon) as a function of pH. Chapman *et al.*[27] and Kula *et al.*[24] first investigated the protonation of the EDTA tetra-anion using ^{1}H NMR.

^{13}C NMR has been of more limited use in the study of polyaminopolycarboxylate[28–30] and polyaminopolyphosphonate[31] ligands. ^{31}P NMR has been used in the study of metal complexes of polyaminopolyphosphonate ligands,[15,31,32] and, for example, revealed[29] chemical shifts of 5.8 ppm downfield on complexation of cadmium(II) by ENTMP. Coupling constants for carboxylate ^{13}C and phosphonate ^{31}P with spin-1/2 metal nuclides have also been reported.[31,32]

We recorded the ^{1}H, ^{13}C and ^{31}P spectra of DTPMP at various pH values and temperatures. The solutions for NMR were adjusted to the required pH/pD with NaOH/NaOD, and although Na^{+} may complex weakly with $H_nDTPMP^{(10-n)-}$, the spectra have been interpreted as, and will be referred to as, free ligand spectra.

A typical ^{1}H NMR spectrum of $H_nDTPMP^{(10-n)-}$ with assignments is shown in Fig. 1. The two doublets are assigned to the methylenic protons adjacent to the phosphonate groups, and the two triplets to the protons of the non-equivalent carbons of the ethylenic groups. The geminal phosphonate protons are equivalent and couple with the ^{31}P nuclei to give the expected AX doublet. A typical value of J_{H-P} is 12 Hz, with little dependence on pH or temperature. The ethylenic proton resonances are A_2X_2 triplets resulting from coupling between neighbouring methylenes. At neutral values of pH, the difference in chemical shift ($\Delta\delta_{bc}$) is large and much greater than the coupling between them (J_{bc}), so a first order pattern is observed (a partial second order nature is suggested by the slight enhancement in the intensity of the inner lines of the triplets, although this effect is very small). $\Delta\delta_{bc}$ is about 190 Hz at pH = 8.0, reduced to 79 Hz at pH = 1.0, with convergence of peaks at pH = 14.0 ($\delta_b = \delta_c$). The second order nature increases as these limits of pH are approached, as shown by the increased intensities of the inner lines of the triplets. J_{bc} is typically 6.5 Hz. The clarity of the triplet varies from an obvious triplet at pH = 8–10, to a single peak with flanking shoulders at other values of pH.

The pH dependence of the non-labile proton resonances is shown in Fig. 2. Addition of a proton to a basic site produces the greatest change in the signals of the CH_2 groups linked directly to the electron-donating atom. The large change of chemical shift (0.66 and 0.85 ppm downfield) for the (a) and (b) proton resonances on lowering the pD from 14 to 9 reflects extensive protonation of terminal nitrogens in this pD range. This conclusion is based on the size of the shifts relative to those in the pD range from 9 to 1 (shifts of 0.29 and 0.17 ppm downfield), and the similarity between the curves for the (a) and (b) proton resonances in the pD range from 9 to 14 (protonation on O^{-} of phosphonate would cause a shift only of the (a) resonance). In addition, the signal due to the (c) protons is shifted by 0.35 ppm downfield on lowering the pD from 14 to 9. This agrees with published shifts for protons situated two bonds away from a nitrogen site undergoing protonation. The (d) proton signal is less shifted (0.14 ppm), indicating only partial protonation of the central nitrogen. On lowering the pD from 10 to 8, a slight upfield movement of the (d) proton resonance is observed. This coincides with an increased downfield shift for the (a) and (b) protons, and may reflect slight deprotonation of the central nitrogen, and increased protonation of the terminal nitrogens (increased protonation at the terminal nitrogens may lead

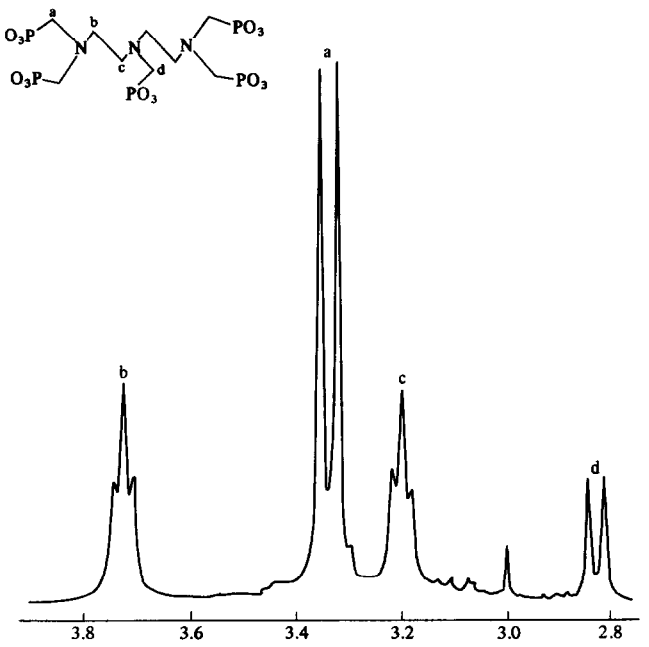

Fig. 1. 360 MHz ^{1}H NMR spectrum of $H_{10}DTPMP$ solution at pD *ca* 8.0 (using a Bruker WM-360 spectrometer).

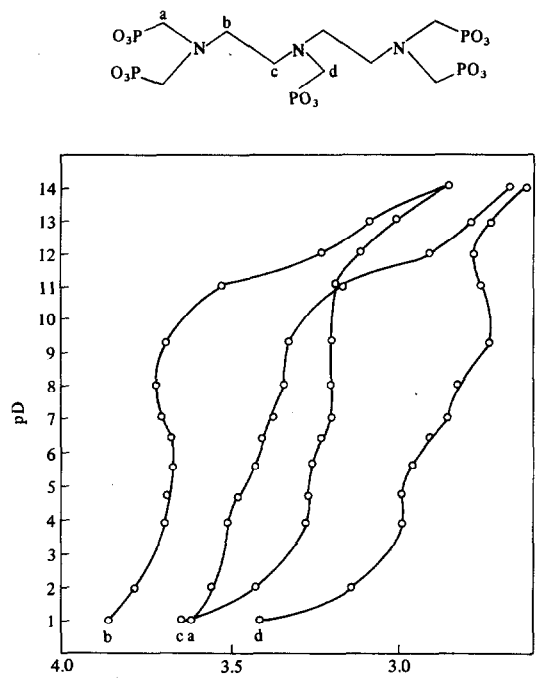

Fig. 2. Variation of the chemical shifts (δ in ppm versus DSS reference) of the non-labile protons of H_{10}DTPMP with pD.

to deprotonation of the central nitrogen as a result of a coulombic repulsion effect as seen[33] with aminopolycarboxylates). Alternatively, the central nitrogen may deprotonate slightly because of partial protonation of the phosphonate groups.

The largest change in δ for the (c) and (d) proton resonances of DTPMP occurs in the pD range from 1 to 4, suggesting enhanced protonation at the central nitrogen. The shift of the resonance due to the (c) protons approximates that for the (d) protons, so the possibility of phosphonate protonation producing these changes is dismissed. The downfield shift of δ for the (c) and (d) signals is greater in the pD range from 4 to 1 than in the range from 14 to 9 (allowance being made for the shift induced in the (c) proton signals as a result of terminal nitrogen protonation of 0.35 ppm). This suggests that the central nitrogen cannot be protonated more than 50% of the time at values of pD > 4. Since the average number n of labile hydrogens attached to each $H_nDTPMP^{(10-n)-}$ moiety is at least six at pD = 4, phosphonate groups must be protonated to a substantial degree before complete protonation of the central nitrogen. In this case, the assumption that nitrogen protonation is complete before phosphonate protonation starts does not apply, and equations of the type often used (e.g. for DTPA[34] and for ENTMP[15]) to deduce variation of percentage times of protonation of labile sites from the observed variance of chemical shift with pD outlined earlier are inapplicable.

At pD = 8.5–9.0, the terminal nitrogens are protonated *ca* 100% of the time. The average number of protons, n, attached to each $H_nDTPMP^{(10-n)-}$ ligand at this pD is 2.0–2.5. Assuming that the terminal nitrogens are deprotonated at pD = 14, and fully protonated at pD = 9, a downfield shift of 0.66 ppm for the (a) proton resonance and 0.65 ppm for the (b) proton resonance is associated with protonation of the adjacent terminal nitrogen. These values are in good agreement with those for oligo-amino-oligocarboxylates[23] and ENTMP.[15] In the pD range from 1 to 9, the δ change for the (a) protons is 0.29 ppm downfield. If the ligand is fully protonated (in the zwitterionic form) at pD = 1, each terminal phosphonate group is doubly protonated approximately 75% of the time: thus, this degree of phosphonate protonation produces a change in δ of 0.29 ppm. Of this shift, 0.15 ppm occurs in the pD range from 4 to 9, and is evidence for monoprotonation of terminal phosphonates before pD = 4. Based on the close analysis of the pD–δ curves, the dominant microspecies and microequilibria associated with the di-, tetra-, and hexaprotonated DTPMP moieties are shown in Figs 3 and 4.

In H_6DTPMP^{4-}, the terminal nitrogens are protonated 100% of the time, the terminal phosphonates are monoprotonated *ca* 75% of the time, and the central nitrogen is protonated not more than 50% of the time. All representations are based solely on the ^1H NMR δ changes with pD (and conformers are ignored). All microspecies interchange rapidly, so that an average distribution only is observed in the NMR spectrum.

Structure 1 in H_4DTPMP^{6-} suggests an increasing basicity of phosphonate groups on protonation at their adjacent nitrogens, contrary to the situation for carboxylate groups.[39] This may be a consequence of the inherent differences between the PO_3^{2-} and COO^- groups. Protonation at PO_3^{2-} is expected to minimize repulsion between neighbouring phosphonates.

The ^{31}P NMR spectra of DTPMP consist of two triplets of relative intensity 4:1, which collapse to singlets on decoupling from the methylene protons. A typical value of J_{P-H} is 11.6 Hz, in agreement with the coupling constant obtained from the ^1H spectra. The larger signal is assigned to the four equivalent phosphorus atoms of the terminal phosphonates, and the smaller peak to the unique phosphorus of the central phosphonate. The variation of the ^{31}P chemical shifts with pH is shown in Fig. 5. The variations observed are in good agreement with the scheme described for the variation of pro-

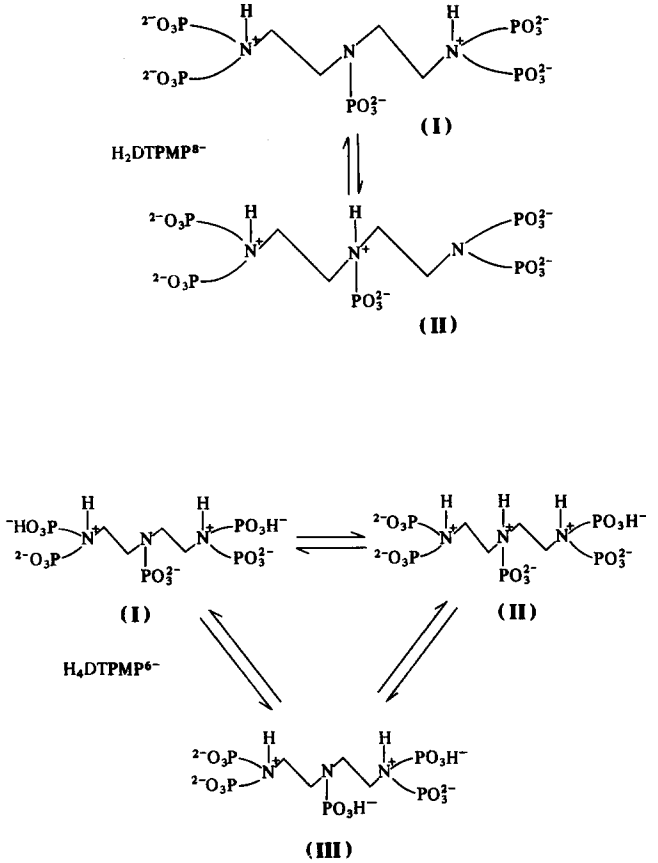

Fig. 3. Dominant diprotonated and tetraprotonated microspecies, $(H_2DTPMP)^{8-}$ and $(H_4DTPMP)^{6-}$.

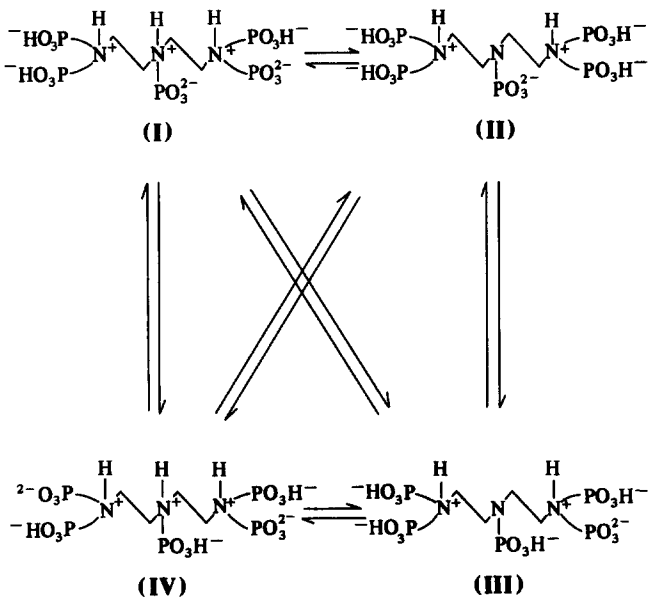

Fig. 4. Dominant hexaprotonated microspecies $(H_6DTPMP)^{4-}$.

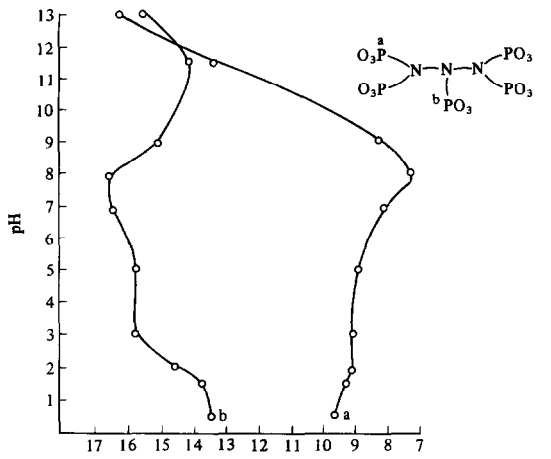

Fig. 5. Variation of ^{31}P NMR chemical shifts for DTPMP as a function of pH.

ton-δ with pD, although the presence of valence *p*-electrons on phosphorus produces a downfield shift on increasing the electron density around the ^{31}P nuclei, i.e. on deprotonating DTPMP (the opposite is true for ^{1}H where only valence *s*-electrons are present). The large downfield shift (7.8 ppm) observed for the terminal ^{31}P phosphonate resonance in the pH range from 9 to 13 indicates that nitrogen protonation has a greater effect on the ^{31}P signal than does protonation of phosphonate oxygens. This is somewhat surprising, because the nitrogen site is more distant with respect to the phosphorus atom than the oxygen site. However, protonation of adjacent oxygens has been shown to produce relatively small δ shifts, e.g. protonation of PO_4^{3-} to give $(HO)_3PO(H_3PO_4)$ produces[35] an upfield shift of only 5.7 ppm.

No great dependence on pH of the carbon-13 resonance signals of DTPMP is observed. (All peaks are coupled to the methylene protons to give triplets in the decoupled spectra: a typical J_{C-H} value is 54 Hz). Such insensitivity of these resonances to pH changes accords with[28,29] aminopolycarboxylate ligands.

Complexes of DTPMP with diamagnetic metal ions

The Cd^{2+}–DTPMP and Pb^{2+}–DTPMP systems were studied at various temperatures and values of pD. Typical spectra are shown in Figs 6 (Cd) and 7 (Pb). Spectral characteristics of the free ligand evidently persist for the lead complex at lower values of pD, but not for cadmium, reflecting its stronger complexing.

The Cd–DTPMP spectrum at pD = 11.0 shows some interesting features. The doublet of the central phosphonate protons is retained, but the terminal

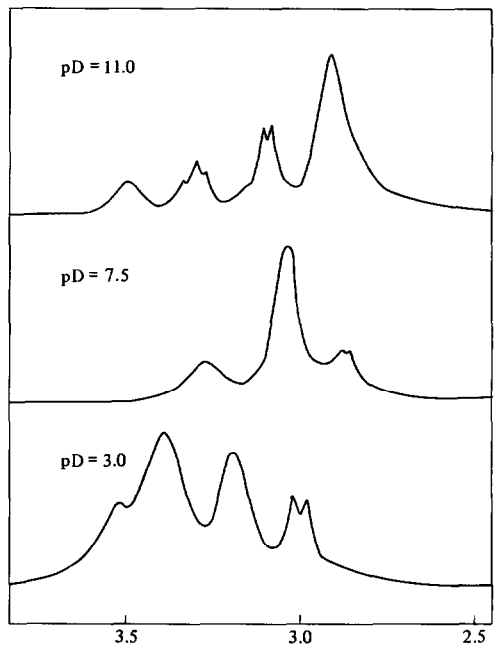

Fig. 6. 360 MHz ^{1}H NMR spectra of Cd^{2+}–DTPMP at selected pD values.

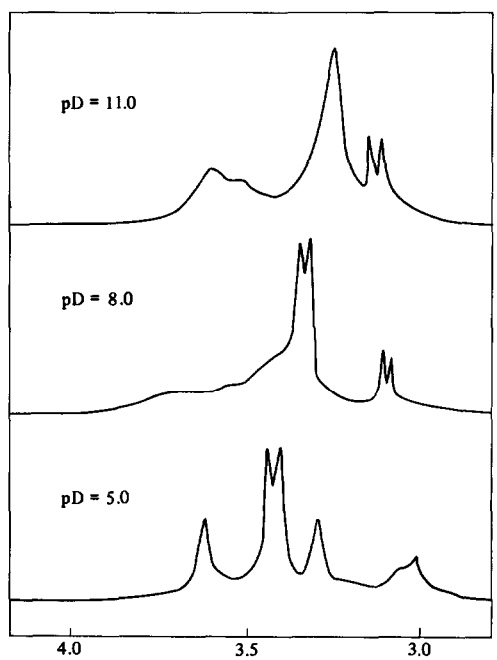

Fig. 7. 360 MHz ^{1}H NMR spectra of Pb^{2+}–DTPMP at selected pD values.

phosphonate doublet is replaced by a large asymmetrical singlet, whose broadness and asymmetry suggest that it may be an unresolved multiplet. Such splitting would arise if the geminal protons of the terminal methylenephosphonate groups became inequivalent as a result of relatively long-lived Cd—N bonds (Fig. 8). In the free ligand spectra,

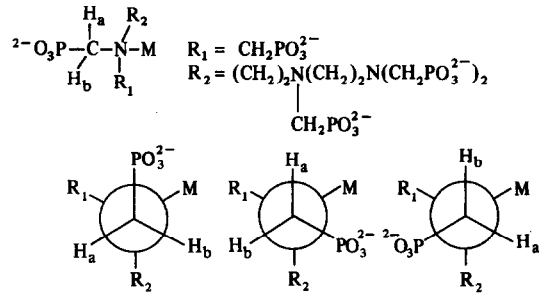

Fig. 8. Non-equivalence in geminal protons produced by long-lived M—N bonds. The non-equivalence of the phosphonate protons is caused by the inherent dissymmetry of the situation and/or the different amounts of time each proton spends in the various rotational conformations.

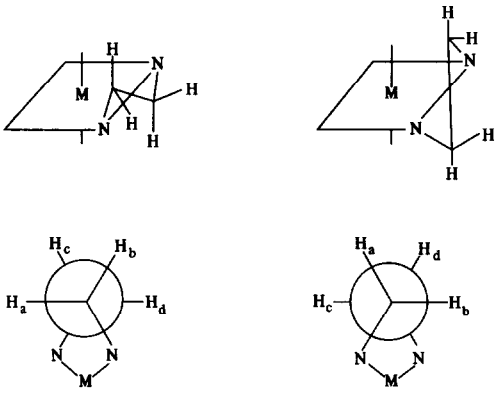

Fig. 9. Conformations of one ethylenic group of DTPMP in a complex with long-lived metal–ligand bonds. If the rate of interconversion of these two forms is slow, the geminal ethylenic protons become inequivalent.

the geminal (a) protons are made equivalent by the rapid umbrella inversion of the nitrogen atom, split only by coupling to ^{31}P, giving a simple doublet. Where such inversion is prevented by the formation of M—N bonds long-lived on the NMR time scale, these geminal protons are no longer equivalent and mutually couple to give an AB quartet (Fig. 8). This pattern would be further complicated in DTPMP by coupling with the ^{31}P nuclei. The observation of an asymmetrical singlet as opposed to a multiplet in the Cd–DTPMP spectrum may suggest that J_{X-Y} approximates to $\Delta\delta_{XY}$ (X and Y are the geminal phosphonate protons). Alternatively, the poor resolution may be associated with bond lifetimes only slightly longer than or comparable to the NMR time scale. The simple doublet for the (d) protons may reflect a shorter Cd—$N_{central}$ bond lifetime, or a non-interacting central phosphonate group. The former situation reflects a reduced basicity of N_{cent} relative to N_{term} as for the free ligand, where the proton affinity of $N_{term} > N_{cent}$. In the case where the phosphonate is non-interacting, a simple doublet would occur if rotational motion produced a time averaged plane of symmetry through the central methylene–phosphonate group.

The spectral appearance and peak integrals indicate that the ethylenic protons are represented by four separate resonances (two clearly visible, one underlying the central phosphonate doublet, and a further one lost beneath the large singlet) in the Cd–DTPMP spectrum at pD = 11.0. This may be associated with a non-equivalence in the geminal ethylenic protons produced by increased rigidity of the chelate, and hindrance of the "wagging" motion of the ethylenic backbone. This situation is summarized in Fig. 9.

The pD dependence of the proton resonances of Cd–DTPMP is shown in Fig. 10. The downfield shift of the (d) proton signal at high pD may reflect

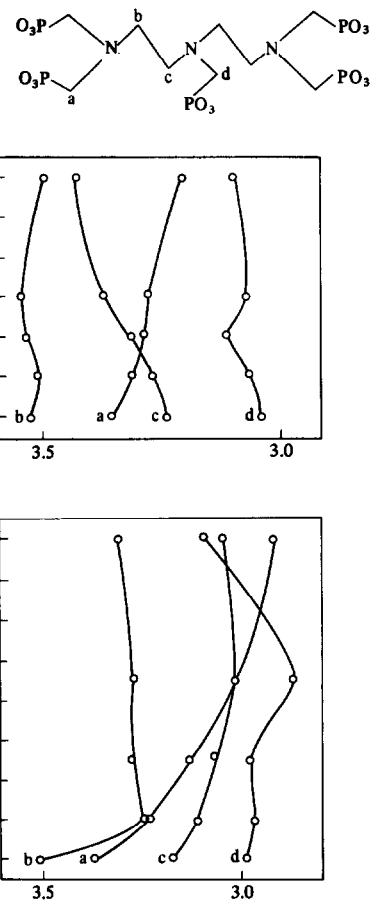

Fig. 10. Variation of ^1H NMR chemical shifts for the Cd^{2+} (lower) and Pb^{2+} (upper) complexes of DTPMP as a function of pD.

an increased degree of protonation at the central phosphonate. This would coincide with an increased interaction between the ligand and cadmium, and is further evidence for a non-interacting central phosphonate group.

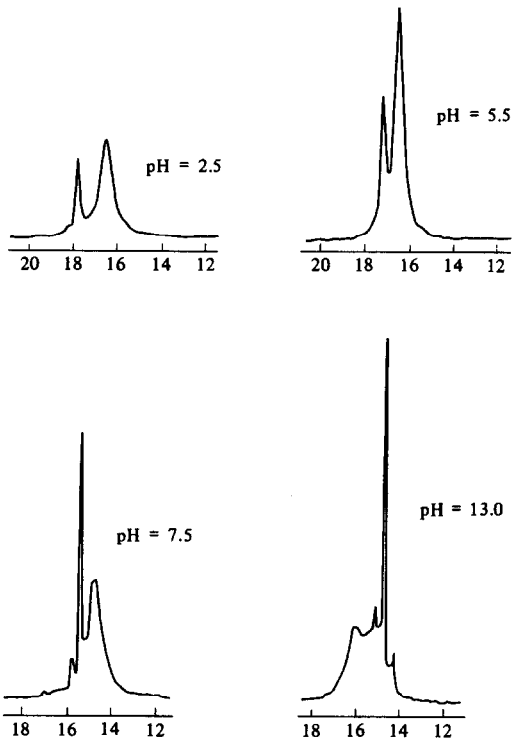

Fig. 11. ^{31}P NMR spectra of Cd^{2+}–DTPMP at selected pH values. Chemical shift values (in ppm) relative to 85% H_3PO_4.

The results of ^{31}P (proton decoupled) NMR studies of Cd–DTPMP at variable pH are summarized in Fig. 11. The peaks are broad at lower pHs, like those[31] of Cd–ENTMP. The central phosphonate peak converts to a sharp singlet at higher pH, but the terminal phosphonate resonance remains broad (26 Hz at peak half-width compared with 3.6 Hz for free DTPMP at pH = 7.5). This broadening increases as the solution becomes more alkaline (Fig. 11), and is indicative of Cd—O_{term} bond lifetimes comparable to the NMR time scale, i.e. the intramolecular exchange of phosphonate donor groups between positions in-plane and out-of-plane with respect to the nitrogen donors is not sufficiently rapid for the terminal phosphonates to allow the observation of a single sharp ^{31}P resonance. The sharp singlet for the central phosphonate may be the result of its restriction to one type of position only, or because[34] the central phosphonate is non-interacting as in Cd–DTPA. At pH = 13.0, the ^{31}P spectrum consists of a broad mound with a sharp singlet flanked by two smaller peaks (Fig. 11). The sharp singlet is assigned to the central phosphonate. The flanking peaks, equidistant from the sharp singlet, may be satellites from coupling between the central phosphorus and the spin-1/2 nuclides of cadmium (^{111}Cd and ^{113}Cd total 25% natural abundance), a phenomenon already observed[32] with Cd–ENTMP. The ^{31}P-$\{^{111/113}Cd\}$ coupling may be mediated through the M—N—C—P or M—O—P linkages. The latter was thought more likely for Cd–ENTMP, although the central phosphonate group is thought not to coordinate in Cd–DTPMP, suggesting coupling through the nitrogen and carbon to phosphorus. This is also supported by the lower J_{P-Cd} value for Cd–DTPMP; only 14.5 Hz compared with 45.9 Hz in[32] Cd–ENTMP. Six peaks are present in the ^{13}C spectrum at pH = 13, supporting the idea of non-equivalent ethylenic and/or methylene–phosphonate groups in Cd–DTPMP.

The ^{1}H spectra for Pb–DTPMP are simpler than those of the cadmium complex (Fig. 7), reflecting more labile Pb—O and Pb—N bonds. This observation arises because all protons equivalent in the free ligand are made equivalent in the lead complex by internal averaging. At pD = 12 and 5°C, three singlets are observed of relative intensity 6:2:1. The large peak contains 12 protons and is assigned to the terminal phosphonates and a coinciding ethylenic resonance. The two smaller peaks then comprise one ethylenic resonance representing four protons, and the (d) proton signal of the central phosphonate. Some line broadening is evident and is associated with a decreased lability of the Pb—L bonds. At 60°C, the large doublet is resolved and only two peaks are observed. The pD–δ curves shown in Fig. 10 reveal only slight shifts in the resonances from pD = 5 to 11.

The proton decoupled ^{31}P spectra for Pb–DTPMP are broad at lower pHs but sharpen as the pH is raised, until only one peak is observed at pH = 13. This singlet reflects equivalence of all phosphonate groups produced by rapid internal exchange of these groups and/or a negligible non-equivalence for ^{31}P in the in-plane and out-of-plane positions. No coupling with ^{207}Pb (21% naturally abundant spin-1/2 isotope) is observed.

CONCLUSIONS

Addition of H^+ to the DTPMP deca-anion induces protonation at the terminal nitrogens initially, then protonation of phosphonate groups. The central nitrogen is not protonated extensively until the pH is below 4. This is contrary to the situation encountered with DTPA, where all three nitrogens are appreciably more basic than the carboxylate groups.

The ^{1}H and ^{31}P NMR spectra of the complexes of DTPMP depend on the strength of the individual metal–ligand bonds, and the structure of the complexed ligand. The ^{13}C spectra are less variable.

The most complicated spectra (discussed elsewhere) occur with the trivalent metal ions, where all M—L bonds may be long-lived, and the coordination number of the metal commonly exceeds six. The M^{2+}–DTPMP (here M = Cd or Pb) complexes give simpler spectra indicative of shorter bond lifetimes and less asymmetrical complexes, and some features permit us to comment on structures in complex ions.

EXPERIMENTAL

Materials

H_{10}DTPMP (purity not less than 93%) in the full acid form was a white powder from Albright and Wilson Ltd., Oldbury. It had as sole impurity a methyl group in place of one of the terminal methylene-phosphonate groups. Thermogravimetric analysis showed the acid to contain 5% water by wt, corresponding to a composition of H_{10}DTPMP · $1.5H_2O$. All metal nitrates and chlorides were of BDH Analar grade (or equivalent), and were used as supplied. Solutions were prepared in distilled or doubly distilled water (potentiometric work) using grade A or precalibrated grade B glassware.

Measurements[36]; *Potentiometric*

Accurately prepared 1.71×10^{-3} M solutions of DTPMP (50 ml) were measured potentiometrically in the absence and presence of the metal ion as a function of added CO_2-free NaOH solution. The solutions were titrated in a sealed jacketed glass cell thermostatted at 25 ± 0.05°C. Dilution effects were minimized by the use of strong base (*ca* 3.5 M) as the titrant, added through two microsyringes of maximum capacity 250 and 25 μl, respectively. The total volume change after addition of base was 0.55%. Activity coefficients were held constant by the use of $NaNO_3$ as a supporting electrolyte (ionic strength was 3 M). The pH of the solutions was monitored using a Radiometer pHM85 pH meter with a GK2401B (or GK2401C) combined electrode, and the expression,[37] for magnetic resonance experiments, true pD = 0.40 + pH measured in D_2O.

^{31}P *NMR*

Solutions (0.06 M) of DTPMP (with and without an equivalent amount of metal ion) for ^{31}P NMR were prepared in 10 ml of H_2O with sufficient D_2O to obtain a lock signal. The ionic strength was maintained at 3 M by the use of $NaNO_3$. The pH was adjusted with 8.4 M NaOH and measured with comparator indicator papers. The ^{31}P spectra were recorded using 10 mm tubes with a Jeol FX-90-Q spectrometer (specifically tuned for ^{31}P) at a working frequency of 36.21 MHz. Measurements were usually made at ambient temperature (*ca* 27°C). The chemical shift values were measured with respect to 85% H_3PO_4 as an external reference.

REFERENCES

1. G. Schwarzenbach, H. Ackermann and P. Ruchstuhl, *Helv. Chim. Acta* 1949, **32**, 1175.
2. R. J. Motekaitis, I. Murase and A. E. Martell, *J. Inorg. Nucl. Chem.* 1971, **33**, 3353.
3. S. Westerback and A. E. Martell, *Nature* 1956, **178**, 321.
4. S. Westerback, K. S. Rajan and A. E. Martell, *J. Am. Chem. Soc.* 1965, **87**, 2567.
5. K. S. Rajan, I. Murase and A. E. Martell, *J. Am. Chem. Soc.* 1969, **91**, 4408.
6. N. Ockerbloom and A. E. Martell, *J. Am. Chem. Soc.* 1958, **80**, 2352.
7. M. I. Kabachnik, T. Ya. Medved, N. M. Dyatlova, O. G. Arkhipova and M. V. Rudomino, *Russ. Chem. Rev.* 1968, **37**, 503.
8. M. I. Kabachnik, T. Ya. Medved, N. M. Dyatlova and M. V. Rudomino, *Russ. Chem. Rev.* 1974, **43**, 733.
9. E. N. Rizkalla, *J. Chem. Soc. Faraday Trans.* I 1983, **79**, 1857.
10. D. F. Evans and M. W. Upton, *J. Chem. Soc., Dalton Trans.* 1985, 2525.
11. R. D. Gillard, *Spectrochim. Acta* 1964, **20**, 1431.
12. A. A. McConnell, R. H. Nutall and D. M. Stalker, *Talanta* 1978, **25**, 425.
13. N. A. Kostromina, *Russ. Chem. Rev.* 1973, **42**, 261.
14. I. N. Marov, L. V. Ruzaikina, V. A. Ryabukhin, P. A. Korovaikov and N. M. Dyatlova, *Koord. Khim.* 1977, **3**, 1333 (English Trans.).
15. E. N. Rizkalla and G. R. Choppin, *Inorg. Chem.* 1983, **22**, 1478.
16. J. Oakes and E. G. Smith, *J. Chem. Soc., Dalton Trans.* 1983, 601.
17. N. Palta, B. V. Rao, S. N. Dubey and D. M. Puri, *Polyhedron* 1984, **3**, 527.
18. M. I. Kabachnik, I. M. Dyatlova, T. Ya. Medved, Yu. F. Belugin and V. V. Sidorenko, *Proc. Acad. Sci. (USSR)* 1967, **175**, 621.
19. L. I. Tikhonova, *Russ. J. Inorg. Chem.* 1968, **13**, 1384.
20. R. J. Motekaitis, I. Murase and A. E. Martell, *Inorg. Nucl. Chem. Lett.* 1971, **7**, 1103.
21. R. J. Motekaitis, I. Murase and A. E. Martell, *Inorg. Chem.* 1976, **15**, 2303.
22. H. Irving and R. J. P. Williams, *J. Chem. Soc.* 1953, 3192.

23. J. L. Sudmeier and C. N. Reilley, *Analyt. Chem.* 1964, **36**, 1698.
24. R. J. Kula, D. T. Sawyer, S. I. Chan and C. M. Finley, *J. Am. Chem. Soc.* 1963, **85**, 2930.
25. J. L. Sudmeier and C. N. Reilley, *Analyt. Chem.* 1964, **36**, 1707.
26. R. J. Kula and D. T. Sawyer, *Inorg. Chem.* 1964, **3**, 458.
27. D. Chapman, D. R. Lloyd and R. H. Prince, *J. Chem. Soc.* 1963, 3645.
28. O. W. Howarth, P. Moore and N. Winterton, *J. Chem. Soc., Dalton Trans.* 1974, 2271.
29. R. Hagen, J. P. Warren, D. H. Hunter and J. D. Roberts, *J. Am. Chem. Soc.* 1973, **95**, 5712.
30. G. R. Choppin, S. A. Khan and G. C. Levy, *Spect. Lett.* 1980, **13**, 205.
31. A. D. Keller, T. Drakenberg, R. W. Briggs and I. M. Armitage, *Inorg. Chem.* 1985, **24**, 1170.
32. G. H. Reed and J. L. Bock, *Biochem. Biophys. Res. Commun.* 1979, **86**, 460.
33. R. J. Day and C. N. Reilley, *Analyt. Chem.* 1964, **36**, 1073.
34. P. Letkeman and J. B. Westmore, *Can. J. Chem.* 1971, **49**, 2073.
35. M. M. Crutchfield, C. F. Callis, R. R. Irani and G. C. Roth, *Inorg. Chem.* 1963, **1**, 813.
36. Further details are in the M.Sc. thesis of P. D. Newman, Univ. of Wales (Univ. College, Cardiff) 1987.
37. P. K. Glasoe and F. A. Long, *J. Phys. Chem.* 1960, **64**, 188.

Polyhedron Vol. 8, No. 16, pp. 2087–2088, 1989
Printed in Great Britain

0277–5387/89 $3.00+.00
© 1989 Maxwell Pergamon Macmillan plc

COMMUNICATION

ONE-STEP SYNTHESIS OF A C-FUNCTIONALIZED PHOSPHA-ALKENE: X-RAY CRYSTAL STRUCTURE OF 2,4,6-^{t}Bu$_3$C$_6$H$_2$P=C(H)CN

ALAN H. COWLEY,* CHRISTINE M. NUNN and MAREK PAKULSKI

Department of Chemistry, The University of Texas at Austin, Austin, TX 78712, U.S.A.

(*Received* 7 *March* 1989; *accepted* 31 *March* 1989)

Abstract—The reaction of 2,4,6-^{t}Bu$_3$C$_6$H$_2$PCl$_2$ with two equivalents of LiCH$_2$CN results in the exclusive formation of the *cis* (i.e. *Z*) isomer of the C-functionalized phospha-alkene, 2,4,6-^{t}Bu$_3$C$_6$H$_2$P=C(H)CN (**1**). The structure of **1** was established by X-ray crystallography.

Sterically protected phospha-alkenes provide the opportunity of studying the phosphorus–carbon double bond free of resonance effects or transition metal fragments. Following the report of PhP=C(^{t}Bu)(OSiMe$_3$) by Becker,[1] acyclic phospha-alkenes with localized P=C bonds have been prepared in large numbers.[2] The most general strategy for the construction of the P=C functionality involves at least a two-step process, the salient features of which are the attachment of an appropriately substituted carbon fragment to phosphorus followed by a 1,2-elimination.

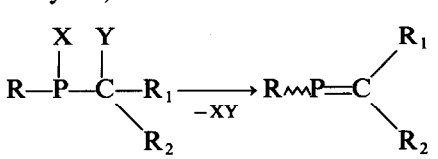

Alternative synthetic procedures, such as metathesis[3] or the reaction of lithiated silylphosphines with aldehydes or ketones,[4] are also multistep in character. We report a convenient one-step synthesis of a functionalized phospha-alkene starting with the readily available[5] dichlorophosphine, ArPCl$_2$ (Ar = 2,4,6-^{t}Bu$_3$C$_6$H$_2$).

EXPERIMENTAL

Dry, powdered LiCH$_2$CN[6] (0.9 g, 19.0 mmol) was added over a 30 min period to a stirred solution of 2,4,6-^{t}Bu$_3$C$_6$H$_2$PCl$_2$ (3.47 g, 10.0 mmol) in 60 cm^3 of THF at −78°C. The resulting deep red reaction mixture was allowed to warm slowly to room temperature. A ^{31}P{^{1}H} NMR assay of the reaction mixture revealed the presence of **1** (359 ppm), traces of 2,4,6-^{t}Bu$_3$C$_6$H$_2$PCl$_2$ (155 ppm) and several very low intensity peaks in the range +60 to −10 ppm. After removing the solvent and volatiles *in vacuo*, the crude product was purified by column chromatography (silica gel/2:1 hexane–toluene eluant) and recrystallized from hexane at −20°C. The yield of colourless crystalline **1** was 67.2%.

NMR (C$_6$D$_6$, 25°C): ^{1}H (300 MHz) 1.21 ppm (s, 9H, *para*-^{t}Bu), 1.23 ppm (s, 18H, *ortho*-^{t}Bu), 5.88 ppm (d, 1H, PCH, $^2J_{PH}$ = 21 Hz), 7.37 ppm (s, 2H, C$_6$H$_2$); ^{13}C{^{1}H} (75.4 MHz): 31.3 ppm (s, *para*-C(*C*H$_3$)$_3$), 34.0, 34.1 ppm (s, *ortho*-C(*C*H$_3$)$_3$), 38.0 ppm (s, *C*(CH$_3$)$_3$), 122.4 ppm (s, *meta*-C$_{arom}$), 134.8 ppm (d, *ortho*-C$_{arom}$, $^2J_{PC}$ = 37 Hz), 153.0 ppm (d, CH, $^1J_{PC}$ = 200 Hz); ^{31}P{^{1}H} (121.5 MHz): 359 ppm (d, $^2J_{PH}$ = 21 Hz). IR (C$_6$D$_6$): ν_{CN} = 2268, 2279 cm^{-1}. Electron-impact MS (70 eV): *m/e* 315 (M$^+$, 30%).

The structure of **1** was determined by X-ray crystallography: C$_{20}$H$_{30}$NP, M_r = 315.44, monoclinic, $P2_1/c$, a = 10.898(5), b = 10.338(1), c = 18.164(3) Å, β = 102.95(2)°, V = 1994.4 Å^3, Z = 4, D_c = 1.050 g cm^{-3}, μ = 1.31 cm^{-1} for Mo-K_α radiation (λ = 0.71073 Å). Intensity data: Enraf–Nonius diffractometer, θ–2θ scan mode, 3924 unique reflections in the range $3.0 \leqslant 2\theta \leqslant 52.0°$. The structure of **1** was solved by direct methods and refined

* Author to whom correspondence should be addressed.

(full-matrix, least-squares) by using 1780 reflections with $I > 3.0\sigma(I)$. The final residuals were $R = 0.0956$ and $R_w = 0.1041$.*

RESULTS AND DISCUSSION

The reaction of $ArPCl_2$ (Ar = 2,4,6-$^tBu_3C_6H_2$) with $LiCH_2CN$ in THF proceeds in one step to afford the phospha-alkene, **1**. We were not able to detect the presumed intermediate monochlorophosphine, **2**.

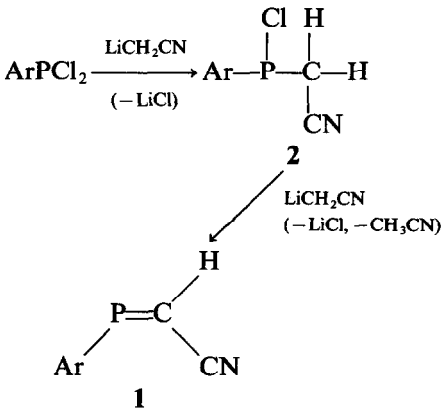

The presence of the phosphorus–carbon double bond in **1** was evident from the $^{31}P\{^1H\}$ NMR chemical shift of +359 ppm; moreover, the presence of C—H, Ar and CN moieties was established by ^1H, $^{13}C\{^1H\}$ NMR or IR spectroscopy. However, use of these data did not permit unequivocal assignment of the isomeric preference, hence an X-ray crystal structure was undertaken. Compound **1** adopts a *cis* (i.e. *Z*) structure in the solid state (Fig. 1). This represents an interesting contrast with ArP=C(H)Ph (**2**), a phospha-alkene with somewhat similar substituents.[4] In this case, the *E* isomer is the ground state and photolysis is necessary to effect conversion to the more sterically hindered *Z* isomer. The P—C—C and C—P—C bond angles in **1** [126.4(7) and 103.4(4)°] lie between those found for **2*E*** [125.4(4) and 100.5(3)°] and **2*Z*** [139.1(2) and 105.8(1)°], suggesting that **1** is less sterically congested than **2*Z***. This view is supported by the fact that the P=C bond length in **1** [1.660(9) Å] is towards the low end of the range observed for acyclic phospha-alkenes. Subtle electronic effects may also be operative.

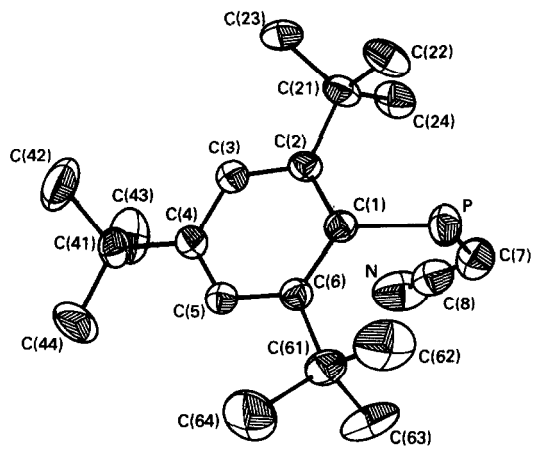

Fig. 1. View of 2,4,6-$^tBu_3C_6H_2P$=C(H)CN (**1**) showing the atom numbering scheme. Important bond lengths (Å) and angles (°): P—C(1) 1.834(7), P—C(7) 1.660(9), N—C(8) 1.140(14), C(1)—P—C(7) 103.4(4), P—C(7)—C(8) 126.4(7), C(7)—C(8)—N 179(1).

Acknowledgements—We are grateful to the National Science Foundation and the Robert A. Welch Foundation for financial support.

REFERENCES

1. G. Becker, *Z. Anorg. Allg. Chem.* 1970, **423**, 242.
2. For a review, see R. Appel, F. Knoll and I. Ruppert, *Angew. Chem. Int. Ed. Engl.* 1981, **20**, 731.
3. A. H. Cowley, R. A. Jones, J. G. Lasch, N. C. Norman, C. A. Stewart, A. L. Stuart, J. L. Atwood, W. E. Hunter and H.-M. Zhang, *J. Am. Chem. Soc.* 1984, **106**, 7015.
4. M. Yoshifuji, K. Toyota, I. Matsuda, T. Niitsu and N. Inamoto, *Tetrahedron* 1988, **44**, 1363 and refs therein.
5. M. Yoshifuji, I. Shima, N. Inamoto, K. Hirotsu and T. Higuchi, *J. Am. Chem. Soc.* 1981, **103**, 4587; A. H. Cowley, N. C. Norman and M. Pakulski, *Inorg. Synth.*, in press.
6. R. Das and C. A. Wilkie, *J. Am. Chem. Soc.* 1972, **94**, 4555.

*Supplementary material available: Atomic coordinates have been deposited with the Director, Cambridge Crystallographic Data Centre.

Polyhedron Vol. 8, No. 16, pp. 2089–2090, 1989
Printed in Great Britain

0277–5387/89 $3.00+.00
© 1989 Maxwell Pergamon Macmillan plc

COMMUNICATION

THE HIGH-YIELD PREPARATION OF *ARACHNO*-THIABORANES 4-SB_8H_{12} AND 4-$SB_8H_{11}^-$

KAREL BAŠE† and MALCOLM G. H. WALLBRIDGE

Department of Chemistry, University of Warwick, Coventry CV4 7AL, U.K.

and

XAVIER L. R. FONTAINE, NORMAN N. GREENWOOD,* JANE H. JONES, JOHN D. KENNEDY and BOHUMIL ŠTÍBR†

School of Chemistry, University of Leeds, Leeds LS2 9JT, U.K.

(*Received* 13 *April* 1989; *accepted* 28 *April* 1989)

Abstract—The oxidative degradation of *arachno*-6-$SB_9H_{12}^-$, using formaldehyde as an oxidizing agent, affords *arachno*-4-SB_8H_{12} in practically quantitative yield; the deprotonation of 4-SB_8H_{12} with NaH produces the new *arachno*-4-$SB_8H_{11}^-$ anion, in quantitative yield.

There is a current resurgence of interest in polyhedral heteroboranes of the chalcogens, and we have long had some interest in this area. A recent report[1] by Kang and Sneddon improves (to 20%) our original reported yield (14%)[2] for the preparation of *arachno*-4-SB_8H_{12}. So that exploration of this area of chemistry can be better facilitated, we now report details of a straightforward procedure that readily affords this compound in practically quantitative yield. The procedure makes use of formaldehyde as an oxidizing agent [formal stoichiometry as in eq. (1)], rather than $FeCl_3$ as used by Kang and Sneddon, and the thiaborane starting material, $Cs[SB_9H_{12}]$, is easily obtained from $B_{10}H_{14}$ in *ca* 90% yield[3] by well-tried procedures. We describe a typical procedure.

$$[SB_9H_{12}]^- + HCHO + H_3O^+ + 2H_2O \longrightarrow SB_8H_{12} + CH_3OH + B(OH)_3 + H_2. \quad (1)$$

To a suspension of $Cs[SB_9H_{12}]$ (2.563 g, 9.34 mmol; prepared as in ref. 3) in H_2O (20 cm^3), was added CH_2Cl_2 (20 cm^3), an aqueous solution of formaldehyde (*ca* 38% solution; 5 cm^3) and aqueous hydrochloric acid (*ca* 18% solution; 3 cm^3). The mixture was stirred for 20 min at ambient temperature, and the CH_2Cl_2 layer separated and dried over $CaCl_2$. Evaporation to dryness gave the crude product in approximately quantitative yield. NMR spectroscopy (CD_2Cl_2 solution)‡ showed that the product was pure and, in particular, free from *nido*-SB_9H_{11}.[4] Careful sublimation (25°C; 1.3 Pa; cold surface at −70°C) gave 4-SB_8H_{12} as a colourless, stinking, volatile solid (0.987 g; 81% yield based on $Cs[SB_9H_{12}]$ consumed).

The yield can be improved by very careful sublimation, but *ca* 80% is perhaps a more realistic target for normal laboratory preparation of the compound as starting material for further investigation. Alternatively, for synthetic purposes, it is often convenient to use the $CaCl_2$-dried CH_2Cl_2 solution directly, with the presumption that the

* Author to whom correspondence should be addressed.

† Permanent address: Institute of Inorganic Chemistry, Czechoslovak Academy of Sciences, 250 68 Řež near Prague, Czechoslovakia.

‡ NMR data for 4-SB_8H_{12} are as follows {ordered as: assignment $\delta(^{11}B)$/ppm [$\delta(^1H)$/ppm]}: BH(7) +14.5 [+3.96], BH(5,9) −3.4 [+3.12], BH(1) −12.4 [+2.76], BH(6,8) −13.5 [+1.24 (*exo*) and −0.68 (*endo*)-type], BH(2,3) −13.3 [+0.73], and H(μ-5,6; μ-8,9) −[−1.87]; CD_2Cl_2 solution at 294 K.

$SB_9H_{12}^- \rightarrow SB_8H_{12}$ conversion has occurred quantitatively. Thus, for example, with $[Pt(PPh_3)_4]$ we have obtained [9,9-$(PPh_3)_2$-*arachno*-6,9-$SPtB_8H_{10}$] in 95% yield based on $Cs[SB_9H_{12}]$.

Pure 4-SB_8H_{12} itself appears to be unstable to storage, and is best prepared freshly; it appears to be more stable under certain acid conditions (e.g. in CH_2Cl_2 in the presence of CF_3COOH). It can be simply and quantitatively deprotonated, using the standard borane/NaH/OEt_2 technique, to give the new *arachno*-[4-SB_8H_{11}]$^-$ anion;* this is stable for weeks as its Na^+ salt, which may be prepared by removing the OEt_2 *in vacuo* and drying the residue at 25°C and 1.3 Pa. Quantitative reprotonation to give neutral SB_8H_{12} can be simply effected with stoichiometric quantities of acids such as CF_3COOH, in solvents such as CH_2Cl_2.

Acknowledgements—We thank the SERC, the Royal Society, and the British Council for support, and the Czechoslovak Academy of Sciences for granting leave to K.B. and B.Š.

REFERENCES

1. S. O. Kang and L. G. Sneddon, *Inorg. Chem.* 1988, **27**, 3298.
2. K. Baše, *Collect. Czech. Chem. Commun.* 1983, **48**, 2593.
3. R. W. Rudolph and W. R. Pretzer, *Inorg. Synth.* 1983, **22**, 226.
4. M. Bown, X. L. R. Fontaine and J. D. Kennedy, *J. Chem. Soc., Dalton Trans.* 1988, 1467.

*NMR data for [4-SB_8H_{11}]$^-$ as follows {ordered as: assignment $\delta(^{11}B)$/ppm [$\delta(^1H)$/ppm]}: BH(7) −5.7 [+2.20], BH(5,9) +3.9 [+3.32], BH(1) −29.5 [+1.48], BH(6,8) −38.0 [0.54 (*exo*) and −0.78 (*endo*-type)], BH(2,3) −27.5 [+1.17], and H(μ-5,6; μ-8,9) −[−2.82]; $[NHEt_3]^+$ salt, CD_2Cl_2 solution at 294 K.

Polyhedron Vol. 8, No. 17, pp. 2091–2097, 1989
Printed in Great Britain

0277–5387/89 $3.00+.00
Pergamon Press plc

SUBSTITUTION KINETICS IN THE COMPLEXES OF PENTACYANORUTHENATE(II) WITH ETHYLENEDIAMINE

A. L. TOKMAN and L. A. GENTIL

Departamentos de Química y de Ingeniería Química, Universidad Nacional de Mar del Plata, 7600 Mar del Plata, Argentina

and

J. A. OLABE*

Departamento de Química Inorgánica, Analítica y Química Física, Facultad de Ciencias Exactas y Naturales, Universidad de Buenos Aires, Pabellón 2, Ciudad Universitaria, 1428 Capital Federal, Argentina

(*Received* 23 *December* 1987; *accepted after revision* 10 *March* 1989)

Abstract—The salt $Na_3[Ru(CN)_5(en)]\cdot 2H_2O$ (en = ethylenediamine) has been prepared and characterized by its IR and electronic spectral properties. The dissociation rate constant, k_{-L}, was found to be dependent on pH, as expected from the protonation of the unbound N-site of the en ligand. From the values of $k_{-en} = 6.2\times10^{-5}\ s^{-1}$ and $k_{-Hen^+} = 1.07\times10^{-4}\ s^{-1}$ (25°C) and activation parameter data, as well as considering the dependence of the rate on the concentration of reactants, a dissociative mechanism was postulated. The pK_a of the Hen^+ ligand was shown to be 9.7 (25°C), only slightly lower than for free (aqueous) Hen^+ (9.98). The formation rate constants, k_L, were determined for L = en (0.89 $M^{-1}\ s^{-1}$) and L = Hen^+ (0.83 $M^{-1}\ s^{-1}$); the kinetic analysis suggests an ion pair–dissociative interchange mechanism, as well as the action of solvation effects. From k_{-L} and k_L, values of the stability constants, K_{st} (M^{-1}), were calculated. A comparative discussion is made with the aid of data from related complexes of the $[Ru(CN)_5L]^{n-}$ and $[Fe(CN)_5L]^{n-}$ series.

Among the cyano complexes of the transition metals,[1] the pentacyanoruthenates are presently being intensively studied, as they offer a possibility for developing a systematic work on structure and reactivity.[2–6] The interest is enhanced by the rich chemistry presented by the $[Fe(CN)_5L]^{n-}$ system;[7] a wide availability of L ligands (which may bind through σ-only or σ–π interactions) has allowed the latter complexes to be employed in substitutional[7–12] and electron-transfer reactivity studies.[13,14] When L is potentially biphilic, bridged species may be generated and mixed-valence systems may be constructed when attaching, for instance, some other $M'X_5$ moiety (e.g. $Fe(CN)_5^{2-}$, $Ru(NH_3)_5^{3+}$) to the unbound L site in the $M(CN)_5L^{n-}$ complex.[15,16]

A particular group of ligands L is formed by oxidizable species such as hydrazine or ethylenediamine (en); these molecules form stable, unidentate complexes with $Fe(CN)_5^{3-}$;[17–19] for hydrazine, an autoxidation process is set up when the $[Fe(CN)_5(N_2H_4)]^{3-}$ ion is placed in contact with dissolved oxygen;[20] also, ligand dehydrogenation processes have been found to occur in the bidentate ion, $[Fe(CN)_4(en)]^{2-}$.[21]

According to the above-mentioned picture, the case of L = en merits special concern among the complexes of the $[Ru(CN)_5L]^{n-}$ series; ligand dehydrogenation reactions have been observed in some ruthenium(II) complexes,[22] and they could be seemingly also operative in the pentacyanoruthenate system, as suggested by the highly oxidizing properties expected for the $[Ru(CN)_5L]$ (II,III) couple.[16] As a previous step to studies concerning the reactions of coordinated en, the basic structural and substitution kinetic features of the latter ligand are needed; this is the subject of the present work.

* Author to whom correspondence should be addressed.

EXPERIMENTAL

(a) *Preparation of* $Na_3[Ru(CN)_5(en)] \cdot 2H_2O$

In a preliminary step, $Na_4[Ru(CN)_6] \cdot 10H_2O$ was obtained by a double decomposition reaction: an aqueous solution [0.050 g in 10 cm^3 of potassium hexacyanoruthenate (Ventron)] was treated with a slight excess of $AgNO_3$ and the resulting precipitate was filtered off; then, aqueous sodium iodide in stoichiometric proportions was added to the solid and the mixture was filtered again. The resulting solution was concentrated at 25°C until the volume was 2 cm^3, and crystals of the desired salt were obtained by adding cold acetone. To a solution of 0.1 mmol of $Na_4[Ru(CN)_6] \cdot 10H_2O$ in 5 cm^3 of water, 1 mmol of en was added and then, slowly, 1.7 cm^3 of aqueous bromine solution (0.0117 M in Br_2 and 0.0117 M in NaBr). The mixture was left for 30 min at room temperature and then more en was added (1 mmol). After 24 h, the solution was concentrated in a rotavap at 25°C, until the volume was 1 cm^3; a precipitate was obtained by adding 5 cm^3 of acetone to the solution, at 0°C. The solid was highly hygroscopic and was stored under $CaCl_2$. Found: C, 19.5*; H, 3.2; N, 24.4; Na, 16.7. Calc.: C, 21.2; H, 3.0; N, 24.7; Na, 17.4%. Water was determined by thermal loss (100°C): Found: 9.4. Calc.: 9.1%.*

(b) *Electronic and IR spectra*

The visible-near UV spectrum was obtained in a Shimadzu UV 210A double-beam spectrophotometer. The IR spectrum was run on a Perkin–Elmer 580B spectrophotometer, with the solid sample pressed into KBr discs.

(c) *Kinetic measurements*

A single-beam Metrolab 325 spectrometer, interfaced with a recorder was used. The temperature was controlled in a thermostatted optical cell with the aid of a circulating bath (Lauda MGW).

(i) *Dissociation kinetics.* The starting solutions were prepared by dissolution of the solid complex or, alternatively, by the *in situ* generation of the $[Ru(CN)_5(en)]^{3-}$ complex from sodium pentacyano(nitrosyl)ruthenate(II) dihydrate,† by the reaction with aqueous hydrazine in a molar ratio 1:0.75, at pH 8.5 and in the presence of a 50-fold excess of en. The solutions contained $[Ru(CN)_5(en)]^{3-}$ (5×10^{-5} M) and free en (2×10^{-3} M); the concentration of the entering ligand, pyrazine (pyz), was 0.1 M in most of the experiments (saturation kinetics conditions, see below) and the ionic strength was 1 M (NaCl). The experiments at 25°C were performed at different pHs, covering the range 6–13. The temperature was varied in the range 25–45°C, for the extreme values, 6.0 and 13.0, i.e. for conditions where the predominant complex ions were $[Ru(CN)_5(Hen)]^{2-}$ (Hen^+ = monoprotonated unidentate en) and $[Ru(CN)_5(en)]^{3-}$, respectively. The kinetic runs were monitored by following the increase of absorbance at 370 nm, the maximum of the $[Ru(CN)_5(pyz)]^{3-}$ ion.[2,‡] Pseudo-first-order rate constants, k_{exp}, were obtained by plotting $\ln(A_\infty - A_t)$ vs time; a linear behaviour was observed for a period always higher than two half-lives. Activation parameters were calculated by least-squares fitting from Eyring plots; errors were obtained by an analysis of variance about regression, employing Student's t values for 90% confidence limits.

A set of experiments was performed for variable concentrations of pyz, from 2×10^{-3} to 0.1 M (T = 25°C, pH 7.0 and 13.0); k_{exp} increased with the concentration of pyz, attaining limiting values for concentrations higher than 0.05 M. This rate saturation behaviour has also been found in the kinetics of the dissociation reactions for other $[Ru(CN)_5L]^{n-}$ ions.[4–6]

(ii) *Formation kinetics.* The $[Ru(CN)_5(H_2O)]^{3-}$ ion was generated in solution through the reaction of aqueous bromine with $[Ru(CN)_6]^{4-}$.[2,5] As the $[Ru(CN)_5(en)]^{3-}$ and $[Ru(CN)_5(Hen)]^{2-}$ complexes do not show a sufficiently high absorption in the visible-near UV region, a direct method could not be used, as with other $[Ru(CN)_5L]^{n-}$ complexes

---

* Low values for carbon are currently found with the cyano complexes; better values could not be obtained through extended heating. Nevertheless, the quoted results for the other elements, as well as the stoichiometric experiment with isonicotianamide (see below), strongly suggests that the solid material is the title compound. The presence of binuclear impurities can be reasonably discarded on the grounds of the synthetic procedure employed (a high excess of en was used), as well as considering the consistency of the kinetic results.

† A low yield of $Na_2[Ru(CN)_5(NO)] \cdot 2H_2O$ is obtained by the published procedure;[3] well behaved solutions of the $Ru(CN)_5(NO)^{2-}$ ion could be prepared by mixing solutions of $Ru(CN)_6^{4-}$ (1×10^{-3} M) with equimolar aqueous bromine and adding solid $NaNO_2$ (final concentration 2×10^{-3} M), at pH 6.

‡ A consistent final value for the absorbance of the $[Ru(CN)_5(pyz)]^{3-}$ ion was obtained when starting with either of the described procedures for generating the $[Ru(CN)_5(en)]^{3-}$ ion; a complementary check was also done by using isonicotinamide (ison) as a scavenger (a reliable value of the molar absorbance for the $[Ru(CN)_5(ison)]^{3-}$ ion has been recently obtained from pure solid samples).[4]

with L being a *N*-heterocyclic ligand. Thus, we used a competitive technique under similar conditions as employed for the study of formation reactions in related complexes.[23] To a solution of the $[Ru(CN)_5(H_2O)]^{3-}$ ion (5×10^{-5} M), mixtures with a variable content of en ($0.5–3 \times 10^{-3}$ M) and a fixed concentration of pyz (1×10^{-3} M) were added (pseudo-first-order conditions) with $I = 0.1$ M (NaCl). The rate of the reaction was followed by measuring the increase of absorbance of the $[Ru(CN)_5(pyz)]^{3-}$ ion, and k_{exp} values were calculated as mentioned above for the dissociation process. Activation parameters were obtained from experiments at pH 7 and 13 (range 25–43°C) for a fixed value of en concentration (1×10^{-3} M); values of k_{en} and k_{Hen^+} were calculated from k_{exp} and previously quoted values of k_{pyz} for the different temperatures.[5]

RESULTS AND DISCUSSION

The IR spectrum

The results for $Na_3[Ru(CN)_5(en)] \cdot 2H_2O$ are presented in Table 1. A tentative assignment is made by comparison with related complexes and free en.[19] The intense band at 2045 cm^{-1} is typical of the stretching mode of cyanide coordinated to a ruthenium(II) centre.[2,24] The bands at 580 and 380 cm^{-1} may be assigned to bending ($\delta_{C—Ru—C}$) and stretching ($\nu_{Ru—C}$) modes, by comparison with similar bands observed for $K_4[Ru(CN)_6]$.[24] An additional band at 465 cm^{-1} is probably related to a $\delta_{C—Ru—N}$ vibration. The other bands correspond to vibrations associated to coodinated en or bound water. The spectrum is rather complex and we are not presently attempting a detailed analysis of the latter bands.

Table 1. IR absorption bands (cm^{-1}) and assignments for $Na_3[Ru(CN)_5(en)] \cdot 2H_2O$

3410 m	ν(NH)	1280 m	ω(CN,en)
3350 s,br	ν(OH)	1240 w	ω(CN,en)
2950 w	ν(CH)	1220 m	ω(CN,en)
2870 w	ν(CH)	1145 m	δ(CN,en)
2045 vs	ν(CN)	870 w	$\omega(NH_2,en)$
1620 sh	$\delta(H_2O)$	820 m	$\omega(NH_2,en)$
1590 s	$\delta(NH_2)$	580 m	δ(C—Ru—C)
1490 s	$\delta(CH_2)$	465 m	δ(C—Ru—N)
1455 sh	$\delta(CH_2)$	380 w	ν(Ru—C)
1395 m	$\omega(CH_2)$		
1360 m	$\omega(CH_2)$		

m: medium; s: strong; vs: very strong; w: weak; br: broad; sh: shoulder. ν: stretching; δ: bending; ω: wagging.

The electronic spectrum

A single absorption maximum was found at 280 nm ($\varepsilon = 550$ M^{-1} cm^{-1}); the energy and intensity were independent of pH in the range 7–12. As will be shown later, the $[Ru(CN)_5(Hen)]^{2-}$ ion is predominantly found at pH 7, while the deprotonated complex, $[Ru(CN)_5(en)]^{3-}$, is formed at pHs higher than 12; thus we conclude that the influence of the state of protonation of the en ligand on the relevant energy levels of the electronic transition is undetectable. The assignment of the band may be readily performed on comparing with results recently reported for other $[Ru(CN)_5L]^{n-}$ complexes (L = H_2O, NH_3, pyz, dimethylsulphoxide, CN^-);[6] in the latter series, the energy of the transition was found to increase in the above-mentioned order. The presently reported value for L = en is in fact very close to that for L = NH_3 (285 nm), as expected from the similar nature of the coordinating atoms. The results are consistent with a ligand-field model for tetragonally distorted low-spin d^6 complexes, which has also been applied to $[Co(CN)_5L]^{n-}$ [25] and $[Fe(CN)_5L]^{n-}$ [8,9] complexes. According to this model, the observed band is assigned to the orbitally allowed $^1A_1 \rightarrow {}^1E_1(1)$ transition; other possible transitions should be either of lower intensity or be buried in the tail of the growing absorption observed for wavelengths lower than 250 nm. The model predicts a dependence of the energy on the type of ligand L; thus, the relative position of the excited state, $^1E_1(1)$ (which is mainly d_{z^2}, antibonding), is influenced by the σ-bonding properties of L; as L becomes stronger, the $^1E_1(1)$ state becomes higher in energy, as found in the $[Ru(CN)_5L]^{n-}$ series.

When comparing with the $[Fe(CN)_5L]^{n-}$ series, it is found that the energies for corresponding bands are shifted to higher values (about 0.12–0.14 μm^{-1}) for the ruthenium(II) complexes;[6] (cf. the value of the $^1A_1 \rightarrow {}^1E_1(1)$ transition in the $[Fe(CN)_5(Hen)]^{2-}$ ion, 402 nm).[19] The degree of back-bonding interaction with $\pi^*(CN^-)$ orbitals is lower in iron(II) compared to ruthenium(II); thus, the value of 10 *Dq* increases when going from the first to the second transition series for a given $[M(CN)_5L]^{n-}$ type of complex; the old assertion proposing similar values of 10 *Dq* for $[Ru(CN)_6]^{4-}$ and $[Fe(CN)_6]^{4-}$ has been recently revised on the grounds of new experimental evidence and alternative assignments for the ligand-field bands in the $[Ru(CN)_6]^{4-}$ ion.[6]

Kinetics of the dissociation and formation reactions

The previously discussed structural features are nicely reflected in the kinetic behaviour of

$[Ru(CN)_5(en)]^{3-}$ and $[Ru(CN)_5(Hen)]^{2-}$ complexes toward the interchange of the L ligand; a dissociative loss of (H)en is accomplished when the complexes are placed in contact with a ligand such as pyz, which binds strongly to $Ru(CN)_5^{3-}$ [eq. (1)]

$$[Ru(CN)_5(H)en]^{n-} + pyz \longrightarrow [Ru(CN)_5(pyz)]^{3-} + (H)en. \quad (1)$$

The pseudo-first-order rate constant, k_{exp}, showed a dependence on the concentration of pyz. The results are shown in Table 2, for two extreme values of pH, 6 and 13. The following conclusions can be drawn from these results: (1) a saturation value is obtained for k_{exp} at high concentrations of pyz; (2) as the concentration of pyz falls to zero, k_{exp} tends towards a value close to k_{-pyz}, the rate dissociation constant for the loss of pyz from the $[Ru(CN)_5(pyz)]^{3-}$ ion;[5] (3) a plot of $1/k_{exp}$ vs 1/[pyz] shows a linear behaviour for low values of 1/[pyz], with a downward curvature for the higher values of 1/[pyz]. All of the latter results are consistent with a dissociative mechanism, as has been fully demonstrated in the behaviour of $[Fe(CN)_5L]^{n-}$ and $[Ru(CN)_5L]^{n-}$ complexes.[4-6] Within the latter framework, the saturation value of k_{exp} is shown to be equal to k_{-L}, the rate dissociation constant for the loss of ligand L.

A particular fact is shown by the dependence of the limiting value of k_{exp} with pH (Fig. 1), which is characteristic of systems where a protonation of the L ligand is feasible (cf. the case of L = en,[27] N_2H_4[18] and some aminoacids[11] coordinated to $Fe(CN)_5^{3-}$).

Table 2. Pseudo-first-order rate constants for the dissociation of $L = Hen^+$ and L = en from the $[Ru(CN)_5L]^{n-}$ ions, at different concentrations of the scavenger ligand, pyrazine[a]

$[Ru(CN)_5(Hen)]^{2-}$[b]		$[Ru(CN)_5(en)]^{3-}$[c]	
10^2[pyz] (M)	$10^5 k_{exp}$ (s^{-1})	10^2[pyz] (M)	$10^5 k_{exp}$ (s^{-1})
15.0	11.4	15.0	6.3
10.0	11.4	10.0	6.3
5.0	11.0	7.5	6.2
2.5	9.1	5.0	6.0
1.25	7.1	2.5	5.0
0.60	5.7	1.25	4.2
0.30	4.4	0.60	3.8
0.15	3.5	0.30	3.6
		0.15	3.4

[a] $[Ru] = 5 \times 10^{-5}$ M; $[en] = 2 \times 10^{-3}$ M; $I = 1$ M (NaCl); $T = 25°C$.
[b] pH 6.0.
[c] pH 13.0.

The pH dependence may be accounted for by the following reaction sequence [eqs. (2–4)]:

$$[Ru(CN)_5(Hen)]^{2-} \underset{}{\overset{k_{-Hen^+}}{\rightleftharpoons}} Ru(CN)_5^{3-} + Hen^+ \quad (2)$$

$$[Ru(CN)_5(Hen)]^{2-} \overset{K_a}{\rightleftharpoons} [Ru(CN)_5(en)]^{3-} + H^+ \quad (3)$$

$$[Ru(CN)_5(en)]^{3-} \overset{k_{-en}}{\rightleftharpoons} Ru(CN)_5^{3-} + en, \quad (4)$$

followed by

$$Ru(CN)_5^{3-} + pyz \longrightarrow [Ru(CN)_5(pyz)]^{3-}. \quad (5)$$

In this scheme, the dependence of k_{exp} (saturation value) on pH should be as in eq. (6):

$$k_{exp} = (k_{-Hen^+}[H^+] + k_{-en}K_a)/([H^+] + K_a). \quad (6)$$

A good fit of eq. (6) to the data in Fig. 1 was obtained by taking $k_{-Hen^+} = 1.07 \times 10^{-4}$ s^{-1}, $k_{-en} = 6.20 \times 10^{-5}$ s^{-1} and $pK_a = 9.7$. When comparing with k_{-Hen^+} and k_{-en} for the $[Fe(CN)_5L]^{n-}$ system (1.04×10^{-2} s^{-1}, 5.6×10^{-3} s^{-1}, respectively), the presently reported values are shown to be considerably lower. The result may be explained by taking into account the higher Ru—N σ-interaction. The rate quotient, $k_{-Hen^+}/k_{-en} = 1.8$, is very close to the one found for the pentacyanoferrate system (1.9). An analysis of the significance of changes in this reactivity quotient, related to the influence of solvation effects in the dissociation reactions of several $[Fe(CN)_5(diamine)]^{3-}$ complexes, may be found elsewhere.[26]

It is a well-known fact that the rate dissociation

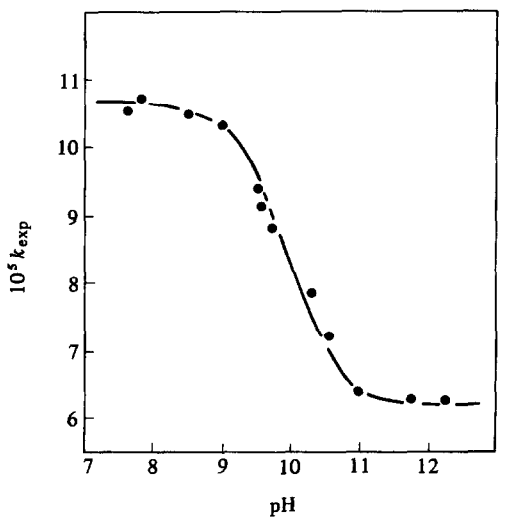

Fig. 1. Plot of k_{exp}, the pseudo-first-order rate dissociation constant, against pH. $[Ru] = 5 \times 10^{-5}$ M; $[en] = 2 \times 10^{-3}$ M; [pyz] = 0.1 M (saturation conditions); $T = 25°C$; $I = 1$ M (NaCl).

constant values, k_{-L}, are strongly dependent on the nature and type of bonding of L. The presently reported values for L = en and L = Hen$^+$ are close but slightly lower than $k_{-NH_3} = 3.7 \times 10^{-4}$ s^{-1} (25°C); [6] this is in keeping with the "σ-only" bonding character of the ligands and with the fact that en is slightly more basic than NH_3. The k_{-L} values for other $[Ru(CN)_5L]^{n-}$ complexes with π-acceptor ligands (L = pyz, dimethylsulphoxide, CN^-) were shown to be substantially lower (range 10^{-5}–10^{-8} s^{-1}). [6] It is also remarkable that the k_{-L} values for the complexes with (H)en can be adequately fit to the linear correlation between $\log k_{-L}$ and the energy of the $^1A_1 \rightarrow {}^1E_1(1)$ transition, which was shown to hold for several $[Ru(CN)_5L]^{n-}$ complexes. [6]

The value found for $pK_a = 9.7$ is 0.3 units lower than pK_a for aqueous Hen$^+$. [28] The shift is only modest but seems to be significant and merits discussion. The lowering of pK_a for a ligand upon coordination should be considered as a normal fact; however, no shift could be detected with the $[Fe(CN)_5(Hen)]^{2-}$ ion, [27] while a lowering of two pK_a units was found with the $[Fe(CN)_5(N_2H_5)]^{2-}$ ion. [18] These results were interpreted as being due to the influence of the different distances of the positive charge to the metal centre in both iron(II) complexes. [18] In the present case, the lowering for $[Ru(CN)_5(Hen)]^{2-}$, in contrast to $[Fe(CN)_5(Hen)]^{2-}$, may be interpreted as additional evidence for the higher σ-interaction in the ruthenium(II) complex compared to the iron(II) one.

From k_{-L} values at different temperatures (Table 3), activation parameters for the dissociation reactions were calculated: $\Delta H_d^{\ddagger} = 111 \pm 3$ kJ mol^{-1}, $\Delta S_d^{\ddagger} = 55 \pm 5$ J mol^{-1} deg^{-1} for L = Hen$^+$, and $\Delta H_d^{\ddagger} = 122 \pm 5$ kJ mol^{-1}, $\Delta S_d^{\ddagger} = 49 \pm 7$ J mol^{-1} deg^{-1} for L = en. The $\Delta H_d^{\ddagger}$ and $\Delta S_d^{\ddagger}$ values for both complexes fall within the range found for other members of the $[Ru(CN)_5L]^{n-}$ series. Although the values are consistent with the proposed dissociative mechanism, the interpretation of activation parameter data should be carefully considered, in view of the influence of solvent effects (cf. ref. 26 for the $[Fe(CN)_5(H)(en)]^{n-}$ system).

The rate of formation of the $Ru(CN)_5^{3-}$ complexes with Hen$^+$ and en, starting from the $[Ru(CN)_5(H_2O)]^{3-}$ ion and en at the appropriate pH, were found to be first order in each of the reagents. Under competitive conditions with pyrazine (see Experimental), eq. (7) holds:

$$k_{exp} = k_{en}[en] + k_{pyz}[pyz]. \quad (7)$$

A similar relation holds for L = Hen$^+$. The specific second-order rate constants, k_{Hen^+} and k_{en}, were obtained by plotting k_{exp} (25°C) against the concentration of (H)en, as shown in Fig. 2; thus, $k_{Hen^+} = 0.83$ M^{-1} s^{-1} and $k_{en} = 0.89$ M^{-1} s^{-1}. These values are of the same order as previously found for other $[Ru(CN)_5L]^{n-}$ complexes. [5] The results may be interpreted in terms of an ion pair–dissociative interchange mechanism [eqs (8) and (9)]:

$$[Ru(CN)_5(H_2O)]^{3-} + L \overset{K_{ip}}{\rightleftharpoons} \{[Ru(CN)_5(H_2O)]^{3-}, L\} \quad (8)$$

$$\{[Ru(CN)_5(H_2O)]^{3-}, L\} \overset{k_{-H_2O}}{\rightleftharpoons} [Ru(CN)_5L]^{n-} + H_2O. \quad (9)$$

In this mechanism, $k_L = K_{ip} k_{-H_2O}$; the rate-determining loss of water in the outer-sphere complex, k_{-H_2O}, should be little influenced by the type of ligand L. This should also be the case with K_{ip}, if the charge on L is not varied. On the above grounds, we should expect higher values for k_{Hen^+} than for k_{en}; both values are, however, nearly equal and the reason is probably associated to the remote distance

Table 3. Specific rates of dissociation and formation of pentacyanoruthenate(II) complexes of Hen$^+$ and en, at different temperatures

Dissociation reactions[a]				Formation reactions[b]			
pH 6.0		pH 13.0		pH 7.0		pH 13.0	
T (°C)	$10^5 k_{-Hen^+}$ (s^{-1})	T (°C)	$10^5 k_{-en}$ (s^{-1})	T (°C)	k_{Hen^+} (M^{-1} s^{-1})	T (°C)	k_{en} (M^{-1} s^{-1})
25	11.4	25	6.3	25	0.83	25	0.89
31	32.1	30	16.4	29	1.39	29	1.46
35	55.8	35	31.1	33.5	2.31	32.5	2.43
39.5	98.6	39.5	63	39	3.67	39	4.60
43	173	43	126	43	5.18	44	7.53

[a] [Ru] = 5×10^{-5} M; [en] = 2×10^{-3} M; [pyz] = 0.1 M (saturation conditions); I = 1 M (NaCl).

[b] [Ru] = 5×10^{-5} M; [en] = 1×10^{-3} M; [pyz] = 1×10^{-3} M; I = 0.1 M (NaCl). Values of k_{en} and k_{Hen^+} were obtained from eq. (9), taking k_{pyz} at the different temperatures from ref. 5.

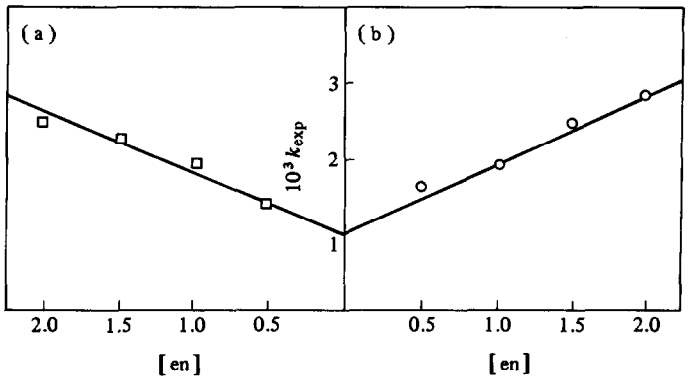

Fig. 2. Plot of k_{exp}, the pseudo-first-order rate formation constant, against the concentration of ethylenediamine [eq. (7)]. (a) pH 7.0; (b) pH = 13.0 [Ru] = 5×10^{-5} M; [pyz] = 1×10^{-3} M; $T = 25°C$; $I = 0.1$ M (NaCl).

of the positive charge to the coordinating site (the rate of coordination of en should also be favoured on statistical grounds). Deviations from the expected k_L values have also been observed in the formation reactions of some pentacyano(amino acid)ferrate(II) complexes.[11]

From data presented in Table 3, the activation parameters for the formation reactions were: $\Delta H_f^{\ddagger} = 85 \pm 3$ kJ mol^{-1}, $\Delta S_f^{\ddagger} = 42 \pm 6$ J mol^{-1} deg^{-1} for L = Hen$^+$, and $\Delta H_f^{\ddagger} = 83 \pm 2$ kJ mol^{-1}, $\Delta S_f^{\ddagger} = 33 \pm 5$ J mol^{-1} deg^{-1} for L = en. The $\Delta H_f^{\ddagger}$ values are about 15 kJ higher than the values found for the entry of N-heterocyclic ligands into the $[Ru(CN)_5(H_2O)]^{3-}$ ion.[5] The positive $\Delta S_f^{\ddagger}$ values, in turn, contrast with the negative values found in the same system (cf. however, ref. 4). It is likely that an "isokinetic" relation, leading to mutually compensatory $\Delta H^{\ddagger}$ and $T\Delta S^{\ddagger}$ values is operative in the formation reactions of $[Ru(CN)_5L]^{n-}$ systems. This type of behaviour is usually found in a series of related reactions governed by a common mechanism and seems to be characteristic of the influence of solvation effects.[29]

From k_{-L} and k_L values, the stability constants, K_{st} (M^{-1}), corresponding to reaction (10) may be calculated:

$$[Ru(CN)_5(H_2O)]^{3-} + L \underset{k_{-L}}{\overset{k_L}{\rightleftharpoons}} [Ru(CN)_5L]^{n-} + H_2O. \quad (10)$$

Values of K_{st} of 7.5×10^3 and 1.4×10^4 M^{-1} were found for L = Hen$^+$ and L = en, respectively. Although the complexes are shown to be moderately stable, it is likely that aquation and dimerization processes could be set up in aqueous solutions, in the absence of excess ethylenediamine. In the above-mentioned conditions, and provided that ethylenediamine is the bridging ligand, favourable conditions could be found for auto-oxidation processes leading to coordinated di-imine products.

Acknowledgements—To CONICET and CICPBA for partial financial support. A.L.T. was a fellow from CONICET and J.A.O. is a member of the scientific staff from CONICET.

REFERENCES

1. A. G. Sharpe, *The Chemistry of Cyano Complexes of the Transition Metals*. Academic Press, New York (1976).
2. C. R. Johnson and R. E. Shepherd, *Inorg. Chem.* 1983, **22**, 1117, 2439.
3. J. A. Olabe, L. A. Gentil, G. Rigotti and A. Navaza, *Inorg. Chem.* 1984, **23**, 4297.
4. J. M. A. Hoddenbagh and D. H. Macartney, *Inorg. Chem.* 1986, **25**, 380, 2099.
5. L. A. Gentil, H. O. Zerga and J. A. Olabe, *J. Chem. Soc., Dalton Trans.* 1986, 2731.
6. J. A. Olabe, H. O. Zerga and L. A. Gentil, *J. Chem. Soc., Dalton Trans.* 1987, 1267.
7. H. E. Toma and J. M. Malin, *Inorg. Chem.* 1973, **12**, 1039, 2080.
8. H. E. Toma, E. Giesbrecht, J. M. Malin and E. Fluck, *Inorg. Chim. Acta* 1975, **14**, 11.
9. H. E. Toma, A. A. Batista and H. B. Gray, *J. Am. Chem. Soc.* 1982, **104**, 7509.
10. N. E. Katz, P. J. Aymonino, M. A. Blesa and J. A. Olabe, *Inorg. Chem.* 1978, **17**, 556.
11. D. H. Macartney and A. McAuley, *J. Chem. Soc., Dalton Trans.* 1981, 1780.
12. M. J. Blandamer, J. Burgess, K. W. Morcom and R. Sherry, *Transition Met. Chem.* 1983, **8**, 354.
13. A. Haim, *Comments Inorg. Chem.* 1985, **4**, 113.
14. A. Haim, *Prog. Inorg. Chem.* 1983, **30**, 273.
15. C. Creutz, *Prog. Inorg. Chem.* 1983, **30**, 1.
16. W. W. Henderson and R. E. Shepherd, *Inorg. Chem.* 1985, **24**, 2398.
17. N. E. Katz, J. A. Olabe and P. J. Aymonino, *J. Inorg. Nucl. Chem.* 1977, **39**, 908.

18. J. A. Olabe and L. A. Gentil, *Transition Met. Chem.* 1983, **8**, 65.
19. J. A. Olabe and P. J. Aymonino, *J. Inorg. Nucl. Chem.* 1974, **36**, 1221.
20. I. A. Funai, M. A. Blesa and J. A. Olabe, *Polyhedron* 1989, **8**, 419.
21. A. M. da Costa Ferreira and H. E. Toma, *J. Chem. Soc., Dalton Trans.* 1983, 2051.
22. P. A. Adcock, F. R. Keene, R. S. Smythe and M. R. Snow, *J. Am. Chem. Soc.* 1984, **23**, 2336.
23. R. E. Shepherd and H. Taube, *Inorg. Chem.* 1973, **12**, 1392.
24. W. P. Griffith and G. T. Turner, *J. Chem. Soc. A* 1970, 958.
25. V. M. Miskowski and H. B. Gray, *Inorg. Chem.* 1975, **14**, 401.
26. N. E. Katz, M. A. Blesa, J. A. Olabe and P. J. Aymonino, *J. Chem. Soc., Dalton Trans.* 1978, 1603.
27. M. A. Blesa, J. A. Olabe and P. J. Aymonino, *J. Chem. Soc., Dalton Trans.* 1976, 1196.
28. A. Vacca and D. Arenave, *J. Phys. Chem.* 1967, **71**, 1495.
29. T. W. Swaddle, *Coord. Chem. Rev.* 1974, **14**, 242.

Polyhedron Vol. 8, No. 17, pp. 2099–2103, 1989
Printed in Great Britain

0277–5387/89 $3.00+.00
© 1989 Pergamon Press plc

THE DISTRIBUTION OF Fe^{3+} BETWEEN AQUEOUS NITRATE AND ORGANIC DI(2-ETHYLHEXYL)PHOSPHORIC ACID (DEHPA)–HEXANE SOLUTIONS

V. SALVADÓ, X. RIBAS and A. MASANA

Departament de Química, Col. legi Universitari de Girona (U.A.B.), 17071 Girona, Spain

and

M. MUHAMMED* and M. VALIENTE†

Química Analítica, Universitat Autonoma de Barcelona, 08193 Bellaterra, Spain

(*Received* 18 *January* 1989; *accepted* 10 *March* 1989)

Abstract—The extraction of iron(III) from aqueous solutions by di(2-ethylhexyl)phosphoric acid (DEHPA, HA) in hexane at constant ionic strength (0.5 M $NaNO_3$), has been investigated under acidic conditions by means of metal distribution measurements. Iron(III) was extracted by ion-exchange reactions via the species: $FeA_3(HA)_3$, $Fe_2A_3(HA)_5$ and $Fe_3A_3(HA)_3$ in the organic phase. The corresponding stability constants were determined as: $\log \beta_1 = 16.87$, $\log \beta_2 = 25.02$ and $\log \beta_3 = 18.39$, respectively.

Iron(III) often co-exists with other metal ions and its separation e.g. by solvent extraction, is of practical significance. Investigations on the extraction of iron by di(2-ethylhexyl)phosphoric acid (DEHPA, HA) have been reported by several authors.[1–6] In some of these studies the stability constants of the extracted species were determined. In other cases only the stoichiometric relationship of metal–extractant in the organic phases is given. The information on the species responsible for the extraction of iron(III) by DEHPA is not well established. Baes[1,2] suggests the formation of the $FeA_3(HA)_3$ and $Fe_3A_8ClO_4$ species when the Fe^{III}/DEHPA ratio is higher than 0.1. Sato and co-workers[3,4] studied the extraction of iron(III) from two different aqueous solutions; in hydrochloric acid solutions, the $FeA_3(HA)_3$[3,4] and $Fe_2A_{10}H_4$[3] species were obtained, while in highly concentrated nitric acid solutions, only the $Fe(NO_3)_3 \cdot 3HA$ species were reported to be formed.

A related study of the kinetics of the extraction of iron(III) by DEHPA was performed by Coleman and Roddy,[5] who suggested that the $FeA_3(HA)_3$ species existed in the organic phase. Table 1 summarizes the various studies performed using different aqueous media and diluents at 25°C.

On the other hand, the extraction of iron(II) by DEHPA has been recently reported by Sastre and Muhammed,[7] who explain the process by the formation of the $FeA_2(HA)_2$ and $FeA_2(HA)_4$ species in the organic phase. Such species are found to be independent of the aqueous ionic media.

In the present work we report a systematic study of the extraction of iron(III) from acidic solutions in 0.5 M $NaNO_3$ by di(2-ethylhexyl)phosphoric acid (DEHPA) in hexane.

EXPERIMENTAL

Reagents and solutions

Ferric nitrate (Merck, AR) was used to prepare stock solutions in 0.5 M NO_3^-. The iron(III) content and free acid were determined by standard procedures.[8,9] Pure $NaNO_3$ (Probus, AR), purified as described in ref. 10, was used as the ionic media. A $^{59}Fe(NO_3)_3$ radioactive stock solution was prepared from the corresponding ferric citrate (General Radioquimica S.A., Paris), 0.2 mCi cm^{-3}

* On leave from the Department of Inorganic Chemistry, The Royal Institute of Technology (KTH), S-100 44 Stockholm, Sweden.

† Author to whom correspondence should be addressed.

Table 1. Summary of literature data on the extraction of iron(III) by di(2-ethylhexyl) phosphoric acid (DEHPA, HA)

Model	Media	Reference
$FeA_3(HA)_3$	ClO_4^-	1
$FeA_3(HA)_3 + Fe_3A_8ClO_4$	ClO_4^-	2
$FeA_3(HA)_3 + FeA_{10}H_4$	HCl, H_2SO_4, HNO_3	3
$Fe(NO_3)_3 \cdot 3(HA)$	Concentrated HNO_3	4
$FeA_3(HA)_3$	ClO_4^-	5
$Fe(OH)A_2$	H_2SO_4	6
$FeA_3(HA)_3 + Fe_2A_3(HA)_5 + Fe_3A_3(HA)_3$	NO_3^- 0.5 M	This work

activity, and used in the radiometric analysis. Solutions of HNO_3 in 0.5 M NO_3^- were employed to adjust the pH of the aqueous solutions. The pH of the aqueous solutions was measured by a CRISON Model DIGILAB 517 pH meter, provided with a combined INGOLD glass electrode. Solutions of di(2-ethylhexyl)phosphoric acid (DEHPA, HA) were prepared from DEHPA (BDH) in hexane (Probus, AR). The γ-activity of radioactive solutions was measured with a well-type NaI scintillation counter (Berthold Model LB 6628 U).

Method of investigation

The distribution of iron(III) has been studied as a function of both the metal concentration in the aqueous phase and the ligand concentration in the organic phase. The general composition of the aqueous phase (AS) was:

$$AS = B \text{ mM } Fe^{3+};\ H \text{ mM } H^+;$$

$$(500 - H - 3B) \text{ mM } Na^+;\ 500 \text{ mM } NO_3^-.$$

A few drops of $^{59}Fe(NO_3)_3$ solution were added to the aqueous phase and the pH was kept constant at 0.7 in all aqueous solutions. The composition of the organic phase was C mol dm^{-3} of DEHPA in hexane, where C varies from 0.075 to 0.0075 M.

The experimental procedure was as follows: equal volumes (10 cm^3) of organic and aqueous solutions were placed in stoppered glass tubes and were shaken mechanically with a rotary rack for 12 h. The phases were centrifuged, separated and measurement of the γ-radiation of each phase was then performed to determine the distribution coefficient, D, of iron(III) for each experiment. D is obtained by:

$$D = I_o/I_a, \tag{1}$$

where I_o represents the number of cpm in the organic phase and I_a the cpm in the aqueous phase. Some examples of the experimental data are collected in Fig. 1 in the form of log D vs log [HA].

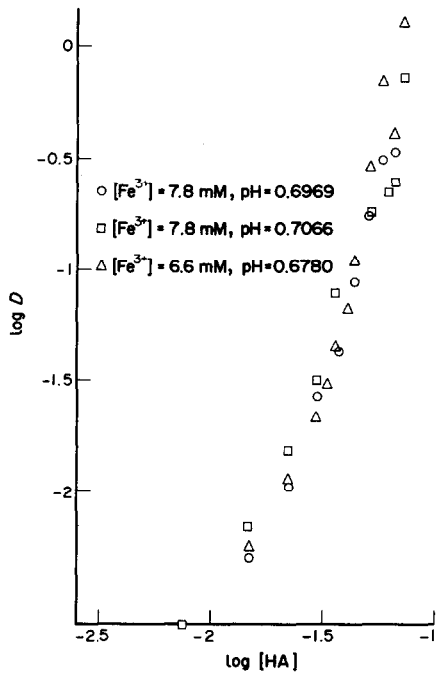

Fig. 1. Experimental data for the extraction of iron(III) from aqueous NO_3^- 0.5 M by DEHPA.

RESULTS

The extraction of iron(III) by DEHPA in hexane may be represented by:

$$nFe^{3+} + m(HA)_{2\,org} \rightleftarrows Fe_nA_3(HA)_{2m-3\,org} + 3H^+;\quad \beta_n, \tag{2}$$

where:

$$\beta_n = \frac{[Fe_nA_3(HA)_{2m-3\,org}][H^+]^3}{[Fe^{3+}]^n[(HA)_{2\,org}]^m}. \tag{3}$$

DEHPA is known to exist as dimers in aliphatic diluents:[11]

$$2(HA)_{org} \rightleftarrows (HA)_{2\,org};\quad K_d = \frac{[(HA)_{2\,org}]}{[(HA)_{org}]^2}. \tag{4}$$

The distribution coefficient, D, is defined by:

$$D = \frac{[Fe^{III}_{org}]}{[Fe^{III}_{aq}]} = \frac{\Sigma n[Fe_nA_3(HA)_{2m-3\,org}]}{[Fe^{3+}]}, \quad (5)$$

where $[Fe^{III}_{org}]$ and $[Fe^{III}_{aq}]$ are the total concentration of iron(III) in the organic and aqueous phases, respectively. In the acidity range used in the aqueous solution, we have assumed that the hydrolysis of iron(III) is practically suppressed. Using eqs (2) and (3), the distribution coefficient, D [eq. (5)], can be expressed in a logarithmic form:

$$\log D = \log K_{n,m} + m \log[(HA)_2] + 3pH. \quad (6)$$

Further, by taking into account the high K_d value of eq. (4), it is possible to rewrite eq. (6) as follows:

$$\log D - 3pH = \log K_{n,m} + m \log(C/2). \quad (7)$$

The experimental data were plotted in the form $\log D - 3pH$ vs $\log(C/2)$ (Fig. 2). An average slope, m, of this representation is found to be approximately three, which indicates that three molecules of DEHPA dimers may be associated with iron(III) in the organic phase.

Computer calculations

The distribution data were analysed numerically using the computer program LETAGROP–DISTR[12] on the basis of eq. (2). In these calculations a set of species is assumed to exist and their formation constants are determined by minimization of the error-square sum defined by:

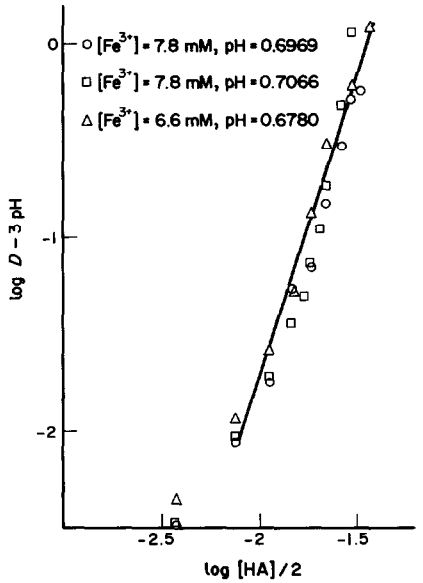

Fig. 2. Graphical treatment of experimental data. The average slope is equal to three.

$$U = \Sigma_{Np}(\log D_{calc} - \log D_{exp})^2, \quad (8)$$

where D_{exp} are the experimental values of the distribution coefficient and D_{calc} is a corresponding value calculated by the program. Np is the number of experimental points.

As a starting point in this treatment, we have considered the speciation and stability constants for this system that are reported in the literature.[1–6] Table 2 summarizes the results from the numerical

Table 2. Results of the numerical treatment of experimental data in the extraction of iron(III) by DEHPA

Model	U	σ	$\log\beta_n$	Remarks
$FeA_3(HA)_3$ + Fe_3A_8	0.30×10^2	1.06	19.2 Max. 19.6 22.0 Max. 22.3	
$FeA_3(HA)_3$ + $Fe_2A_{10}H_4$ + Fe_3A_8	0.98	0.20	18.45±0.260 29.15±0.259	Rejected
$FeA_3(HA)_3$ + $Fe_2A_3(HA)_5$	0.32	0.10	18.2 Max. 18.4 24.80±0.055	
$FeA_3(HA)_3$ + $Fe_2A_3(HA)_5$ + $Fe_3A_3(HA)_3$	0.019	0.03	17.5 Max. 17.1 25.0 Max. 25.2 18.3 Max. 18.5	G.K.[a]

[a] G.K.: the U value has an absolute minimum.

treatment. As seen, the best fit for our experimental data is accomplished by the model including the $FeA_3(HA)_3$, $Fe_2A_3(HA)_5$ and $Fe_3A_3(HA)_3$ species in the organic phase.

These results are expressed by the following reaction equations and corresponding formation constants:

$$Fe^{3+} + 3(HA)_{2\,org} \rightleftarrows FeA_3(HA)_{3\,org} + 3H^+; \quad \log\beta_1 = 16.87 \quad (9)$$

$$2Fe^{3+} + 4(HA)_{2\,org} \rightleftarrows Fe_2A_3(HA)^{3+}_{5\,org} + 3H^+; \quad \log\beta_2 = 25.02 \quad (10)$$

$$3Fe^{3+} + 3(HA)_{2\,org} \rightleftarrows Fe_3A_3(HA)^{6+}_{3\,org} + 3H^+; \quad \log\beta_3 = 18.39. \quad (11)$$

DISCUSSION

The extraction of iron(III) from acidic solutions in 0.5 M NO_3^- by DEHPA in hexane, is found to proceed via the formation of the species, in the organic phase, represented by eqs (9)–(11). This seems to follow the general behaviour of the extraction of metals by alkylphosphoric acids.[13]

Two of these species, $Fe_2A_3(HA)_5$ and $Fe_3A_3(HA)_3$, appear to be electrically charged and it is assumed that they form ion pairs with nitrate ions. From these considerations the results obtained will be conditional on the media employed in this study.

Our results generally agree with the data reported in Table 1. The $FeA_3(HA)_3$ species have been suggested by several authors,[1–5] however, the species of the type $FeA_{10}H_4$ proposed by Sato,[3,4] was rejected in our calculations (cf. Table 2). In this case it is observed that such stoichiometry does not follow the general equation (2). For the sake of comparison, Fig. 3 represents experimental points in the form log $D-3$pH vs log [HA], the various solid lines represent calculated values based on different literature models. As seen in this representation, the model proposed in this work is the most consistent with the experimental data.

The distribution of species in the organic phase, as function of extractant concentration, is represented in Fig. 4. As can be seen in this figure, predominance of the $FeA_3(HA)_3$ and $Fe_2A_3(HA)_5$ species is found, whereas the $Fe_3A_3(HA)_3$ species is only slightly relevant (less than 1%) in the iron(III) and DEHPA iron(III) concentration ranges studied.

The model obtained in this study shows a general tendency to form polynuclear species in the organic phase, on the other hand, it seems to be logical that nucleation of species is a successive process which,

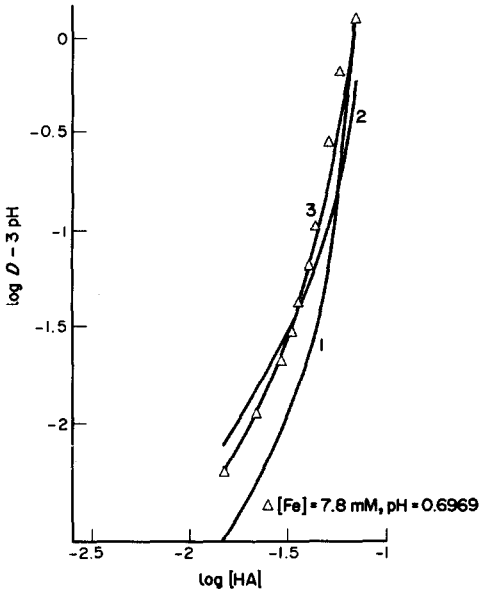

Fig. 3. Correlation of experimental and calculated points from different models. Model 1 corresponds to ref. 3, model 2 to ref. 2 and model 3 to this work.

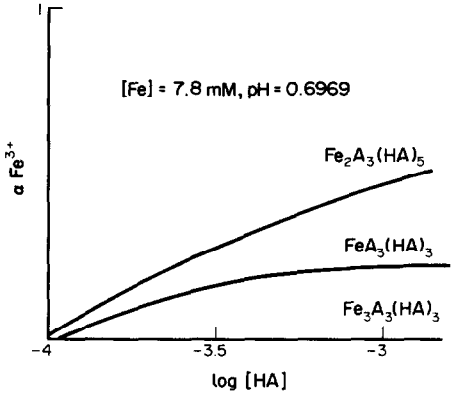

Fig. 4. Distribution of species in the organic phase as a function of the extractant concentration.

in our case, is represented by the $Fe_2A_3(HA)_5$ and $FeA_3(HA)_3$ species. Comparison of these results with those reported for Fe^{II}–DEHPA[7] extraction shows a fundamental difference which is related to the nucleation of the metal species in the organic phase. Thus, iron(II) does not present polynuclear species, while iron(III), in the organic phase, confirms its tendency to form polynuclear complexes in aqueous solutions.

REFERENCES

1. C. F. Baes and H. T. Baker, *J. Phys. Chem.* 1960, **64**, 89.
2. C. F. Baes, *J. Inorg. Nucl. Chem.* 1962, **24**, 89.
3. T. Sato and T. Nakamura, *Proc. Int. Solvent Extraction Conf.* 1971, 238.

4. T. Sato, T. Nakamura and M. Ikeno, *Hydrometallurgy* 1985, **15**, 209.
5. C. F. Coleman and J. W. Roddy, *Solvent Extraction Revs* 1971, **1**, 63.
6. F. Islam and H. Rahman, *J. Inorg. Nucl. Chem.* 1979, **41**, 417.
7. A. Sastre and M. Muhammed, *Chem. Script.* 1987, **27**, 385.
8. A. I. Vogel, *Quantitative Inorganic Analysis*. Longmans, London (1973).
9. G. Charlot, *Quimica Analitica General*, Vol. 1. Toray-Masson (Ed.), Barcelona (1971).
10. *Some Laboratory Methods*. Mimeograph, Department of Inorganic Chemistry, The Royal Institute of Technology, Stockholm (1958).
11. J. R. Ferraro, G. W. Mason and D. F. Peppard, *J. Inorg. Nucl. Chem.* 1961, **22**, 285.
12. D. H. Liem, *Acta Chem. Scand.* 1971, **25**, 1521.
13. T. Sekine and Y. Hasegawa, *Solvent Extraction Chemistry*. Marcel Dekker, New York (1977).

Polyhedron Vol. 8, No. 17, pp. 2105–2108, 1989
Printed in Great Britain

0277–5387/89 $3.00+.00
© 1989 Pergamon Press plc

COORDINATION COMPLEXES OF FORMYLFERROCENE BENZOYLHYDRAZONE WITH LANTHANIDES

MA YONGXIANG,* MA ZHONGQIAN and ZHAO GANG

Department of Chemistry, Lanzhou University, Lanzhou 730000, China

and

MA YUN and YANG MIN

Light Industrial College of Northwest, Xianyang, Shanxi Province, China

(*Received* 4 *January* 1989; *accepted* 15 *March* 1989)

Abstract—The coordination complexes of formylferrocene benzoylhydrazone (HL) with lanthanide elements, $LnL_3 \cdot nH_2O$ (where Ln = lanthanide and Y, n = 1–3), have been prepared by the reaction of HL with the metal(III) chlorides in acetonitrile. The elemental analyses, IR and UV spectra, molar conductance and thermal analyses show that the ligand coordinates to the metals in the enolic form with a molar ratio of 3:1. We propose a plausible structure and discuss the thermal properties for the complexes.

Due to their biological activities and variable bonding when forming complexes with metal ions, the coordination chemistry of acid hydrazones have attracted the attention of many investigators.[1–6] Acid hydrazones can coordinate to metal ions in (a) the enolic form or (b) the keto form:

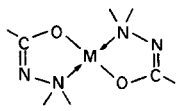

(a)

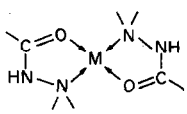

(b)

In general, they coordinate to central ions in the keto form when complexing with metal chlorides, nitrates, sulphates and thiocyanates etc., but in the enolic form with metal acetates in ethanol.

We have previously reported on the lanthanide complexes of some aroylhydrazones coordinated in the keto form which have not been studied so far by other investigators.[7–9] The present work describes Y^{III} and lanthanide(III) complexes with formylferrocene benzoylhydrazone coordinated in the enolic form, which were prepared by the reaction of the hydrazone with metal chlorides in acetonitrile rather than with acetates.

EXPERIMENTAL

Materials

The lanthanide(III) chlorides were prepared from their oxide and hydrochloric acid. Formylferrocene was prepared according to the literature method.[10] The other chemicals were analytic reagent grade.

Preparation of formylferrocene benzoylhydrazone (HL)

The HL was prepared by refluxing equimolar quantities of formylferrocene and benzoylhydrazine in ethanol until the appearance of some precipitate, concentrating the solution to one-third of its original volume and collecting the reddish-orange crystals obtained on a Büchner funnel, washed several times with cold ethanol and dried. Yield 85.2%, m.p. 186–187°C. Found: C, 65.0; H, 4.9; N, 8.4. Calc. for $C_{18}H_{16}FeN_2O$: C, 65.1; H, 4.8; N, 8.4%. ^{1}H NMR: δ(DMSO), 4.23 (s, 5H)

* Author to whom correspondence should be addressed.

(C_5H_5Fe); 4.46 (t, 2H) (protons on 3,4-positions of C_5H_5Fe); 4.65 (t, 2H) (protons on 2,5-positions of C_5H_5Fe); 7.45–7.95 (m, 5H) (phenyl); 8.30 (s, 1H) (azomethine); 11.58 (s, 1H) (—NH which disappears on deuteration) ppm.

Preparation of complexes

Lanthanide(III) or yttrium(III) chlorides (0.20 mmol) were dissolved in 20 cm^3 of acetonitrile and 2 cm^3 of triethyl orthoformate under heating. 0.8 mmol of HL in 20 cm^3 of acetonitrile was added dropwise into the above solution and maintained for 7–10 h under heating and stirring until the reddish-orange solution changed to brown. After cooling, the precipitate was filtered and washed several times with cold acetonitrile and ether. Yield > 76%. The elemental analyses of these complexes along with their formulae are listed in Table 1.

Physical measurements

IR spectra were made on KBr pellets using a Nicolet 5DX spectrophotometer in the 400–4000 cm^{-1} region. UV spectra were measured with a DU-7B ultraviolet–visible spectrometer in the 190–700 nm region using a solution in DMF. Electrolytic conductance measurements were carried out by a DDS-IIA molar conductometer and DMF as solvent at 25°C. Thermal characterization studies were made with a Du Pont 1090 thermal analyzer in a nitrogen atmosphere.

Table 1. The elemental analyses of the complexes

Complex	Formula	Elemental analysis (%) C	H	N
I	$YL_3 \cdot 3H_2O$	56.4(57.1)[a]	4.1(4.5)	7.4(7.4)
II	$LaL_3 \cdot 3H_2O$	54.5(54.7)	4.2(4.3)	6.8(7.1)
III	$CeL_3 \cdot 3H_2O$	54.1(54.6)	4.1(4.3)	6.8(7.1)
IV	$PrL_3 \cdot 3H_2O$	54.1(54.6)	4.2(4.3)	7.5(7.1)
V	$NdL_3 \cdot 2H_2O$	54.8(55.1)	4.0(4.2)	7.3(7.1)
VI	$SmL_3 \cdot 2H_2O$	54.8(55.0)	4.0(4.2)	7.2(7.1)
VII	$EuL_3 \cdot 2H_2O$	54.2(54.8)	4.3(4.2)	7.2(7.1)
VIII	$GdL_3 \cdot H_2O$	56.0(55.5)	4.0(4.1)	7.8(7.2)
IX	$TbL_3 \cdot H_2O$	55.8(55.4)	4.0(4.1)	7.5(7.2)
X	$DyL_3 \cdot H_2O$	55.2(55.2)	4.0(4.0)	7.3(7.2)
XI	$HoL_3 \cdot H_2O$	54.8(55.1)	4.0(4.0)	7.3(7.1)
XII	$ErL_3 \cdot H_2O$	54.9(55.0)	4.0(4.0)	7.6(7.2)
XIII	$TmL_3 \cdot H_2O$	55.4(54.9)	4.1(4.0)	7.2(7.1)
XIV	$YbL_3 \cdot H_2O$	55.6(54.8)	4.1(4.0)	7.2(7.1)
XV	$LuL_3 \cdot H_2O$	55.4(54.7)	4.0(4.0)	7.1(7.1)

[a] Calculated values are given in parentheses.

RESULTS AND DISCUSSION

The complexes of lanthanide elements with formylferrocene benzoylhydrazone are amorphous brown powders. They are insoluble in water and petroleum ether, sparingly soluble in diethyl ether, benzene and methylene chloride, but soluble in methanol, ethanol, DMSO and DMF. Their elemental analyses show that $LnCl_3 \cdot nH_2O$ form complexes with loss of chloride ions and they conform to the formula $LnL_3 \cdot 1\text{–}3H_2O$.

IR spectra

The IR spectra (Table 2) show that the characteristic frequencies of these complexes exhibit significant changes as compared with those of the parent ligand. The bands at 3213, 1648, 1557 and 1287 cm^{-1} attributed to ν(N—H), ν(C=O)(amide I), amide II and ν(C—N)(amide III) have disappeared, whereas three new bands at around 1595, 1360 and 1237 cm^{-1} due to ν(C=N—N=C), ν(N=CO^-) and ν(C—O) are observed. The strong and broad bands at 3376–3395 cm^{-1} indicate the presence of water molecules associated in the complexes. It is clear that the ligand undergoes enolization in acetonitrile and then coordinates to lanthanide ions in enolic form, accompanied by the release of all chloride ions. In addition, the characteristic frequencies of the ferrocenyl appear at *ca* 1440, 1150, 820 and 480 cm^{-1}, and those of phenyl at *ca* 1600 and 1490 cm^{-1} in the ligand and all complexes.

UV spectra

The UV spectra of the ligand and its complexes are shown in Table 3. It can be seen that the UV spectra of all complexes are similar, but different from that of the ligand. The characteristic bands of the complexes at 295–297 nm arising from π–π^* transition (B band) of the cyclopentadienyl ring hardly shift as compared with their ligand. The band at 316 nm in the ligand is attributed to the *K* band (π–π^* transition), which is shifted to a longer wavelength by 30–43 nm in complexes. It is possible that the metal *f*-orbital overlap with the *p*-orbital of the ligand makes the whole molecule form a large conjugate system after enolizing and coordinating, and the formation of which decreases the transition energy required between π and π^* orbitals. Thus, this leads to a more bathochromic shift of the *K* band of the complexes. Band 3 at 455 nm of the ligand is weak and broad due to a charge-transfer transition between cyclopentadienyl ring and iron, which vanishes in the complexes, perhaps by virtue of a bathochromic shift of the *K* band and a hyp-

Table 2. Important IR absorption frequencies (in cm^{-1}) of the ligand and its complexes

Complex	Ln^{3+}	ν(O—H)	ν(N—H)	Amide I ν(C=O)	ν(C=N—N=C)	Amide II	ν(N=CO$^-$)	Amide III ν(C—N)	ν(C—O)	ν(N—N)
HL	—	—	3213ms	1648vs	—	1557s	—	1287s	—	920m
I	Y	3376br.m	—	—	1595s	—	1358s	—	1237m	920m
II	La	3395br.m	—	—	1595s	—	1358s	—	1237m	927m
V	Nd	3395br.m	—	—	1589s	—	1363s	—	1240m	927m
VI	Sm	3386br.m	—	—	1595s	—	1359s	—	1237m	920m
VII	Eu	3396br.m	—	—	1595s	—	1366s	—	1237m	927m
VIII	Gd	3396br.m	—	—	1595s	—	1358s	—	1237m	921m
IX	Tb	3396br.m	—	—	1595s	—	1361s	—	1237m	921m
X	Dy	3396br.m	—	—	1595s	—	1366s	—	1237m	927m
XII	Er	3376br.m	—	—	1595s	—	1365s	—	1237m	920m
XIV	Yb	3396br.m	—	—	1595s	—	1364s	—	1237m	927m
XV	Lu	3396br.m	—	—	1595s	—	1365s	—	1237m	927m

br = broad, s = strong, vs = very strong, m = medium.

Table 3. Important UV spectra of the ligand and some complexes

Complex	Ln^{3+}	Absorption bands (nm, λ_{max}) (1)	(2)	(3)
HL	—	295	316	455
I	Y	295	353	—
II	La	297	346	—
V	Nd	295	346	—
VI	Sm	296	345	—
VII	Eu	297	350	—
VIII	Gd	296	351	—
IX	Tb	295	358	—
X	Dy	296	359	—
XII	Er	297	356	—
XIV	Yb	297	357	—
XV	Lu	295	346	—

sochromic shift of band 3 after forming complexes. It is possible that a bathochromic shift of the *K* band and a hypsochromic shift of band 3 are due to the formation of a large conjugate system in the molecule.

Molar conductance

Dissolving the lanthanide complexes in DMF afforded a brown solution. The molar conductance values (Table 4) of the complexes in DMF lie in the range 20–41 $ohm^{-1}\ cm^2\ mol^{-1}$. A comparison of these values with those previously reported in the literature[11] for 1:1 electrolytes in DMF (65–90 $ohm^{-1}\ cm^2\ mol^{-1}$) shows the non-electrolytic nature of the complexes in DMF.

Table 4. Molar conductances of the complexes in DMF at 25°C

Complex	Ln^{3+}	Conc. (10^{-3} mol)	λ_{max} $ohm^{-1}\ cm^2\ mol^{-1}$
I	Y	1.11	28
II	La	1.14	42
V	Nd	1.15	39
VI	Sm	0.98	30
VIII	Gd	0.99	22
IX	Tb	1.00	25
X	Dy	0.88	34
XII	Er	1.05	20
XIV	Yb	1.03	23
XV	Lu	1.10	40

Table 5. Data of thermal analyses of some complexes

Complex	Ln^{3+}	D.t. (°C)	Leaving group	Weight loss
II	La	60	$3H_2O$	3.8(4.5)[a]
		283–310	$3C_6H_5CO^+$	26(26.6)
		317–606	remainder organic group	41(43.0)
		> 607	residue, 3Fe+La	29(26)
VI	Sm	60	$2H_2O$	2.3(3.1)
		290–309	$3C_6H_5CO^+$	30.6(26.7)
		307–830	remainder organic group	41.0(43.3)
		> 830	residue, 3Fe+Sm	26.1(26.9)
XV	Lu	66	H_2O	2.5(1.5)
		290–313	$3C_6H_5CO^+$	26.7(26.6)
		740–794	remainder organic group	42.4(43.0)
		> 794	residue, 3Fe+Lu	28.4(28.9)

[a] Calculated values are given in parentheses.

Thermal analysis

Thermal analysis data of the complexes, $LaL_3 \cdot 3H_2O$, $SmL_3 \cdot 2H_2O$ and $LuL_3 \cdot H_2O$, are shown in Table 5. It can be seen that the thermal properties of these complexes are analogous. First of all, they lose their water molecules at about 60°C showing that the water molecules are not coordinated to the metal ions. The anhydrous complexes decompose and lose three $C_6H_5CO^+$ groups at about 290–310°, and the remaining organic groups at 310°C. The residues decompose completely at 606–830°C leaving Fe_3Ln.

Summarizing our results, three molecules of the ligand coordinate to a lanthanide(III) ion through their nitrogen atom in azomethine and oxygen atom (in enolic form) in acetonitrile, accompanied by the release of three chloride ions, their coordination numbers are equal to six. Thus, we propose a plausible structure for our complexes as shown in Fig. 1.

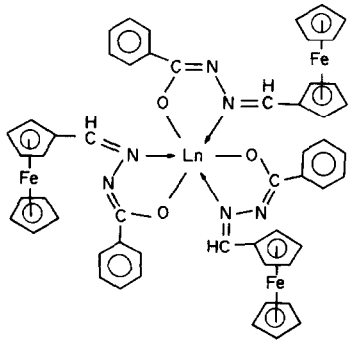

Fig. 1.

REFERENCES

1. A. Albert, *Nature* 1953, **9**, 370.
2. H. H. Fox and J. T. Gibas, *J. Org. Chem.* 1956, **21**, 356.
3. R. M. Issa, M. F. El-Shazly and M. F. Iskander, *Z. Anorg. Allg. Chem.* 1967, **354**, 90.
4. L. El Sayed and M. F. Iskander, *J. Inorg. Nucl. Chem.* 1971, **33**, 435.
5. M. F. Iskander and L. El Sayed, *Inorg. Chim. Acta* 1976, **16**, 147.
6. S. R. Patil, U. N. Kantank and D. N. Sen, *Inorg. Chim. Acta* 1982, **63**, 261; 1983, **68**, 1.
7. M. Yongxiang and Z. Gang, *Polyhedron* 1988, **7**, 1101.
8. M. Yongxiang and Z. Gang, *Inorg. Chim. Acta* 1988, **144**, 265.
9. M. Yongxiang, Z. Tongjun and Z. Gang, *Lanthanide Actinide Res.* 1988, **2**, 235.
10. P. J. Graham, R. V. Lindsey, G. W. Parshall, M. L. Peterson and G. M. Whitman, *J. Am. Chem. Soc.* 1957, **79**, 3416.
11. W. J. Geary, *Coord. Chem. Rev.* 1971, **7**, 81.

Polyhedron Vol. 8, No. 17, pp. 2109–2113, 1989
Printed in Great Britain

0277–5387/89 $3.00+.00
© 1989 Pergamon Press plc

SYNTHESIS AND THERMAL STABILITY OF CYCLOPENTADIENYL LANTHANIDE COMPLEXES CONTAINING *o*-ALDEHYDOPHENOLATO OR FURFURALCOHOLATO LIGAND

ZHONGZHI WU,* ZHONGWEN YE and ZHENNAN ZHOU

Institute of Organic Chemistry, Anhui Normal University, Wuhu, Anhui Province, P.R.C.

(*Received* 26 *January* 1989; *accepted* 15 *March* 1989)

Abstract—Eight new complexes of the type $Cp_nLn(sal)_{3-n}$ or $Cp_nLn(fur)_{3-n}$ ($n = 1, 2$; $Cp = C_5H_5$, Ln = Nd, Yb; sal = *o*-aldehydophenolato, fur = furfuralcoholato) have been synthesized and characterized. These complexes are not very stable to heat and tend to disproportionate at moderately high temperatures. Their relative stability has been determined and discussed. The disproportionation reactions are reversible.

It is well known that the labile behaviour of η^5-cyclopentadienyl complexes of *f*-transition metals might (under certain condition) lead to a mixture of disproportionation products.[1] Up to now, however, the published articles dealing with the disproportionation reaction of η^5-cyclopentadienyl lanthanide complexes are rare. Recently, we have reported that either dicyclopentadienyl samarium acetate and halides or lanthanide organometallics involving both cyclopentadienyl and β-diketonato chelate ligands are not very stable to heat and tend to disporportionate at moderately high temperatures.[2,3] The purpose of this paper is to extend the investigation of thermal stability and disproportionation reactions to the cyclopentadienyl lanthanide complexes involving *o*-aldehydophenolato or furfuralcoholato chelate ligands.

RESULTS AND DISCUSSION

By adopting the very versatile method of liberating cyclopentadiene from a Cp_3Ln moiety by the action of acids stronger than C_5H_6, we have synthesized eight complexes by the reaction of Cp_3Nd or Cp_3Yb with salicylaldehyde (Hsal) or furfuralcohol (Hfur). They are:

1 : 1 ratio of reactants		1 : 2 ratio of reactants	
$Cp_2Nd(sal)$	(I)	$CpNd(sal)_2$	(II)
$Cp_2Nd(fur)$	(III)	$CpNd(fur)_2$	(IV)
$Cp_2Yb(sal)$	(V)	$CpYb(sal)_2$	(VI)
$Cp_2Yb(fur)$	(VII)	$CpYb(fur)_2$	(VIII)

All these complexes were characterized by elemental analysis, IR (Table 1), XPS (Table 2) and MS (Table 3) spectroscopy.

The IR spectra of all the complexes show absorptions at about 750, 780, 1010, 1440, 3100 cm^{-1}, characteristic of η^5-cyclopentadienyl ligand.[4] The band of C=O stretching vibration for the free CHO in complexes I, II, V and VI is shifted from 1695 cm^{-1} to a lower frequency 1595–1632 cm^{-1}.[5] The band of C—O—C stretching vibration for the epoxy ring in complexes III, IV, VII and VIII is shifted from 1050 cm^{-1} to a lower frequency 1005–1011 cm^{-1}. So, in these complexes one could postulate the O → M dative bond.

As both *o*-aldehydophenolato and furfuralcoholato are bidentate ligands, the cryoscopic method for molecular weight determination in benzene of all the complexes has been made. It appears that all eight complexes are present as monomers. From the data of XPS (Table 2), it is revealed that in each complex the binding energy of the metal is decreased, as compared with the corresponding substances for reference. Thus, it is confirmed that all the eight complexes are chelates. This is in agreement with the fact that the greatest tendency to form chelate complexes is found in polyfunctional ligands whose donor atoms are separated by two or three carbon atoms. The ring produced by chelate formation will be five- or six-membered. The structure proposed for these complexes may be:

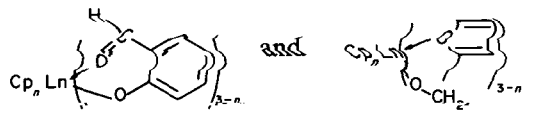

$n = 1, 2$; Ln = Nd, Yb

* Author to whom correspondence should be addressed.

Table 1. Analytical and part of IR data for the complexes I–VIII

Complex	Formula	Colour	Yield (%)	D.t. (°C)[b]	Elemental analysis (%)[a] Ln	C	H	IR (cm^{-1}) ν(C=O)	ν(C—O—C)
I	$C_{17}H_{15}O_2Nd$	Yellow	85	175	37.1 (36.5)	51.8 (51.6)	3.6 (3.8)	1632	
II	$C_{19}H_{15}O_4Nd$	Yellow	92	165	31.3 (31.9)	50.6 (50.5)	3.4 (3.3)	1625	
III	$C_{15}H_{15}O_2Nd$	Blue	78	300	38.8 (38.8)	48.2 (48.5)	4.0 (4.1)		1005
IV	$C_{15}H_{15}O_4Nd$	Blue	90	280	35.9 (35.7)	44.4 (44.6)	3.4 (3.7)		1009
V	$C_{17}H_{15}O_2Yb$	Yellow	35	200	40.7 (40.8)	48.7 (48.1)	3.1 (3.6)	1595	
VI	$C_{19}H_{15}O_4Yb$	Yellow	68	190	35.8 (36.0)	47.6 (47.5)	3.0 (3.1)	1630	
VII	$C_{15}H_{15}O_2Yb$	Yellow	90	350	43.4 (43.6)	45.4 (45.0)	3.6 (3.8)		1009
VIII	$C_{15}H_{15}O_4Yb$	Yellow	54	360	40.0 (40.0)	42.0 (41.7)	3.5 (3.5)		1011

[a] Calculated values are given in parentheses.
[b] D.t. = decomposition temperature.

Table 2. XPS data of complexes I–VIII and complexes for references

	Complex	XPS (eV) $Nd_{3d_{5/2}}$ or $Yb_{4d_{5/2}}$	ΔE[a]
I	$Cp_2Nd(OC_6H_4CHO)$	984.0	
	$Cp_2Nd(OC_6H_5)$	984.7	−0.7
II	$CpNd(OC_6H_4CHO)_2$	984.5	
	$CpNd(OC_6H_5)_2$	985.3	−0.8
III	$Cp_2Nd(OCH_2CCHCHCH)$ (O)	984.0	
	$Cp_2Nd(OCH_3)$	984.5	−0.5
IV	$CpNd(OCH_2CCHCHCH)_2$ (O)	984.3	
	$CpNd(OCH_3)_2$	985.0	−0.7
V	$Cp_2Yb(OC_6H_4CHO)$	185.9	
	$Cp_2Yb(OC_6H_5)$	186.5	−0.6
VI	$CpYb(OC_6H_4CHO)_2$	186.3	
	$CpYb(OC_6H_5)_2$	186.9	−0.6
VII	$Cp_2Yb(OCH_2CCHCHCH)$ (O)	186.0	
	$Cp_2Yb(OCH_3)$	186.5	−0.5
VIII	$CpYb(OCH_2CCHCHCH_2)$ (O)	186.2	
	$CpYb(OCH_3)_2$	186.8	−0.6

[a] ΔE is the binding energy difference.

Table 3. MS data for complexes I–VIII at different temperatures of vaporization

Complexes Cp_nLnL_{3-n} (Cp = C_5H_5, L = sal or fur) and mol. species	Temp. of vaporization (°C)	Main peaks, m/z[a]
I $n = 2$, sal = OC_6H_4CHO.	80, 100, 150	393(M), 328(M-Cp), 272(M-sal), 207(M-Cp-sal), 142(Nd).
M = $Cp_2Nd(sal)$, M″ = Cp_3Nd.	170, 200, 250	337(M″), 272(M″-Cp), 207(M′-2Cp), 142(Nd).
II $n = 1$, sal = OC_6H_4CHO.	50, 70, 90	449(M), 384(M-Cp), 328(M-sal), 207(M-2sal), 142(Nd).
M = $CpNd(sal)_2$, M′ = $Cp_2Nd(sal)$,	100, 120, 150	393(M′), 328(M′-Cp), 272(M′-sal), 263(M′-2Cp), 142(Nd).
M″ = Cp_3Nd.	170, 200, 250	337(M″), 272(M″-Cp), 207(M″-2Cp), 142(Nd).
III $n = 2$, fur = $OCH_2CCHCHCH$. (O)	80, 100, 150	369(M), 304(M-Cp), 272(M-fur), 207(M-Cp-fur), 142(Nd).
M = $Cp_2Nd(fur)$, M″ = Cp_3Nd, M‴ = $Nd(fur)_3$.	170, 200, 250	433(M‴), 337(M″), 272(M″-Cp), 207(M″-2Cp), 142(Nd).
IV $n = 1$, fur = $OCH_2CCHCHCH$. (O)	50, 80, 90	401(M), 336(M-Cp), 304(M-fur), 239(M-Cp-fur), 142(Nd).
M = $CpNd(fur)_2$, M′ = $Cp_2Nd(fur)$,	100, 120, 150	369(M′), 304(M′-Cp), 272(M′-fur), 207(M′-Cp-fur), 142(Nd).
M″ = Cp_3Nd, M‴ = $Nd(fur)_3$.	170, 200, 250	433(M‴), 337(M″), 272(M″-Cp), 207(M″-2Cp), 142(Nd).
V $n = 2$, sal = OC_6H_4CHO.	100, 150, 200	425(M), 360(M-Cp), 304(M-sal), 295(M-2Cp), 174(Yb).
M = $Cp_2Yb(sal)$, M″ = Cp_3Yb.	220, 250	425(M), 369(M″), 304(M″-sal), 295(M-2Cp), 239(M″-2Cp), 174(Yb).
VI $n = 1$, sal = OC_6H_4CHO.	80, 100, 120	481(M), 416(M-Cp), 295(M-Cp-sal), 239(M-2sal), 174(Yb).
M = $CpYb(sal)_2$, M′ = $Cp_2Yb(sal)$,	150, 200	425(M′), 304(M′-sal), 295(M′-2Cp), 174(Yb).
M″ = Cp_3Yb.	220, 250	425(M′), 369(M″), 304(M″-Cp), 295(M′-2Cp), 239(M″-2Cp), 174(Yb).
VII $n = 2$, fur = $OCH_2CCHCHCH$. (O)	100, 150, 170	401(M), 336(M-Cp), 239(M-Cp-fur), 174(Yb).
M = $Cp_2Yb(fur)$, M″ = Cp_3Yb.	200, 220, 250	401(M), 369(M″), 336(M-Cp), 304(M″-Cp), 174(Yb).
VIII $n = 1$, fur = $OCH_2CCHCHCH$. (O)	80, 100, 120	433(M), 368(M-Cp), 336(M-fur), 239(M-2fur), 174(Yb).
M = $CpYb(fur)_2$, M′ = $Cp_2Yb(fur)$,	150, 170	401(M′), 336(M′-Cp), 304(M′-fur), 239(M′-Cp-fur), 174(Yb).
M″ = Cp_3Yb.	200, 220, 250	401(M′), 369(M″), 336(M′-Cp), 304(M″-Cp), 174(Yb).

[a] MS data are given for the isotopes ^{142}Nd, ^{174}Yb, ^{16}O, the peak patterns correspond to theoretical values based on the natural abundance of isotopes.

For the purpose of studying the thermal stability of these complexes, the mass spectra of them were recorded at different temperatures of vaporization. We found that complexes of the type Cp_2LnL (L = *o*-aldehydophenolato or furfuralcoholato) are thermally more stable than those of the type $CpLnL_2$. During the course of raising the temperature, $CpLnL_2$ first disproportionates into Cp_2LnL and LnL_3, and then into Cp_3Ln and LnL_3. The disproportionation reaction presumably involves the following equilibria:

$$2CpLnL_2 \rightleftharpoons Cp_2LnL + LnL_3$$

$$3Cp_2LnL \rightleftharpoons 2Cp_3Ln + LnL_3.$$

The reversibilities of the above disproportionation have been verified by their reverse reactions. The purified products of the reverse reactions, $CpLnL_2$ and Cp_2LnL, are all characterized by elemental analysis and MS.

We suggest that lability of η^5-Cp ligands is the cause of the disproportionation reactions. It is also possible that the disproportionation reaction takes place via an intermediate bimolecular complex in which the Cp groups are bonded in an η^5-fashion to one molecule and in an η^1-fashion to the second molecule of the complex. The transfer of one Cp group from one molecule to another may initiate the disproportionation. Since the transfer of one Cp group is more facile than the transfer of two groups at the same time, $CpLnL_2$ is thermally less stable than Cp_2LnL.

In view of the MS data, complexes of Yb, either of the type Cp_2LnL or $CpLnL_2$, are thermally more stable than the analogues of Nd. At about 160°C, the disproportionations of four Nd complexes (I–IV) are apparently complete. But even at 250°C, all four Yb complexes (V–VIII) are only partially disproportionated. We suppose that the greater thermal stability of Yb complexes compared with their Nd analogues is due to the lanthanide contraction. Compared with Nd^{3+}, the radius of Yb^{3+} is smaller and the attraction of the Ln—L bond formed by Yb^{3+} and an anionic ligand will be stronger. Another reason for the superior thermal stability of the Yb complexes may be due to the greater steric saturation present around the smaller metal centre.[6,7]

Probably due to the large radii and coordination unsaturation of lighter lanthanides, their organometallics involving both Cp and Cl ligands, such as Cp_2LnCl and $CpLnCl_2$ (Ln = La, Ce, Pr and Nd) have not been synthesized. Here, the facile preparation of the unsolvated and room-temperature stable Cp_nNdL_{3-n} ($n = 1$, 2; L = *o*-aldehydophelato, furfuralcoholato) is obviously due to stabilization of the species by the chelation effect.

EXPERIMENTAL

All operations on these organolanthanide complexes were performed under prepurified argon using Schlenk techniques or in a glovebox. All solvents were refluxed and distilled over finely divided $LiAlH_4$ or blue sodium benzophenone under argon immediately before use. Salicylaldehyde and furfuralcohol were dried and distilled under argon. Cp_3Nd and Cp_3Yb were prepared by a published procedure.[8]

Metal analyses of lanthanides were accomplished by using the direct complexometric procedure with disodium EDTA. The elemental analysis data for C and H were obtained on a Yanaco MT-2 analyzer. IR were recorded on a Perkin–Elmer 983(G) (CsI crystal plate, Nujol and Fluorolube mulls) instrument. XPS data were obtained on a VG MK-II X-ray photoelectron spectrometer. MS were recorded on a VG ZAB-HS organic mass spectrometer.

Preparation of complexes I, II, V and VI

A 20 cm^3 THF solution of salicylaldehyde (1.5 or 3.0 mmol) was added dropwise with stirring to a 30 cm^3 THF solution of Cp_3Nd or Cp_3Yb (1.5 mmol). The reaction mixture was allowed to stir for 24 h at room temperature. The resulting solution was concentrated *in vacuo* to about 15 cm^3. By addition of 30 cm^3 of *n*-hexane, a solid precipitated out which was recrystallized from THF/*n*-hexane and washed with *n*-hexane to afford the product. Yields, analyses and physical properties of all four complexes are listed in Table 1.

Preparation of complexes III, IV, VII and VIII

A 20 cm^3 THF solution of furfuralcohol (1.5 or 3.0 mmol) was added dropwise with stirring to a 30 cm^3 THF solution of Cp_3Nd or Cp_3Yb (1.5 mmol), and gradually a precipitate was produced. After stirring for 24 h at room temperature, the reaction mixture was centrifuged. The precipitate was separated from the solution, washed twice with THF and dried under vacuum. Yields, analyses and physical properties of all four complexes are listed in Table 1.

Preparation of $Ln(sal)_3$

A THF solution of three equivalents of salicylaldehyde and one equivalent of Cp_3Nd or Cp_3Yb

was stirred at room temperature for 24 h. The resulting solution was concentrated *in vacuo*. By addition of equi-volume *n*-hexane, an orange product precipitated out, which was recrystallized from THF/*n*-hexane and dried *in vacuo* to afford $Ln(sal)_3$. Their analytical data are as follows: $Nd(sal)_3$: Yield 90%. Found: Nd, 28.5; C, 50.3; H, 3.0. Calc. for $C_{21}H_{15}O_6Nd$: Nd, 28.4; C, 49.7; H, 3.0%. $Yb(sal)_3$: Yield 92%. Found: Yb, 32.4; C, 46.8; H, 2.8. Calc. for $C_{21}H_{15}O_6Yb$: Yb, 32.3; C, 47.2; H, 2.8%.

Preparation of $Ln(fur)_3$

A mixture of three equivalents of furfuralcohol and one equivalent of Cp_3Nd or Cp_3Yb in THF was allowed to react at room temperature. After stirring for 24 h, the resulting solution was concentrated *in vacuo*. Upon addition of *n*-hexane brown precipitates were formed, filtered off, recrystallized from THF/*n*-hexane and dried *in vacuo*. $Nd(fur)_3$: Yield 53%. Found: Nd, 33.3; C, 40.7; H, 3.3. Calc. for $C_{15}H_{15}O_6Nd$: Nd, 33.1; C, 41.4; H, 3.5%. $Yb(fur)_3$: Yield 70%. Found: Yb, 37.4; C, 38.5; H, 3.2. Calc. for $C_{15}H_{15}O_6Yb$: Yb, 37.3; C, 38.8; H, 3.5%.

Reaction of $Nd(sal)_3$ *and* $Cp_2Nd(sal)$

A mixture of $Nd(sal)_3$ (1 mmol) and $Cp_2Nd(sal)$ (1 mmol) in 20 cm^3 THF was stirred for 24 h at room temperature. The resulting solution was centrifuged and concentrated to about 10 cm^3 *in vacuo*. By addition of 20 cm^3 *n*-hexane a yellow solid precipitated out which was recrystallized from THF/*n*-hexane twice. The product, $CpNd(sal)_2$ (II), was characterized by elemental analyses and MS.

According to a similar procedure, the reaction of $Nd(sal)_3$ with Cp_3Nd (mol ratio, 1:2) gave $Cp_2Nd(sal)$ (I), the reaction of $Yb(fur)_3$ with $Cp_2Yb(fur)$ (mol ratio, 1:1) gave $CpYb(fur)_2$ (VIII) and the reaction of $Yb(fur)_3$ with Cp_3Yb (mol ratio, 1:2) gave $Cp_2Yb(fur)$ (VII). All the three products were also characterized by elemental analyses and MS.

Acknowledgements—We wish to express our cordial thanks to the mass spectra group of the University of Science and Technology of China for measurement of mass spectra. We also thank Mr Baohui Du and Mrs Jipin Hu for assistance.

REFERENCES

1. K. W. Bagnall, in *Organometallics of the f-Elements* (Edited by T. J. Marks and R. D. Fischer), pp. 221–247. Riedel, Dordrecht (1979).
2. Zhongwen Ye, Huaizhu Ma and Yongfei Yu, *J. Less-Common Met.* 1986, **125**, 405.
3. Zhongwen Ye, Yongfei Yu and Huaizhu Ma, *Polyhedron* 1988, 7, 1095.
4. Changtao Qian, Changqin Ye, Hanzhang Lu, Yuqin Li, Jialie Zhou, Yuanwen Ge and M. Tsutsui, *J. Organomet. Chem.* 1983, **247**, 161.
5. W. W. Simons (Editor), *The Sadtler Handbook of Infrared Spectra*, pp. 403, 605. Sadtler Research Laboratories (1978).
6. W. J. Evans, *Polyhedron* 1987, **6**, 803.
7. R. D. Fischer and L. Xing-Fu,. *J. Less-Common Met.* 1985, **112**, 303.
8. J. M. Birmingham and G. Wilkinson, *J. Am. Chem. Soc.* 1965, **78**, 42.

Polyhedron Vol. 8, No. 17, pp. 2115–2117, 1989
Printed in Great Britain

0277–5387/89 $3.00+.00
© 1989 Pergamon Press plc

STABILITY CONSTANTS OF THALLIUM(I)-BENZO-15-CROWN-5 COMPLEX IN ALCOHOLS

EWA LADA and MAREK K. KALINOWSKI*

Department of Chemistry, University of Warsaw, Pasteura 1, 02-093 Warszawa, Poland

(*Received* 7 *February* 1989; *accepted* 15 *March* 1989)

Abstract—The complexation of thallium(I) by benzo-15-crown-5 was studied in methanol, ethanol, propanol-1, butanol-1,2-methylpropanol, 4-hydroxy-4-methyl-2-pentanone, pentanol-1, ethylene glycol and 2-aminoethanol by employing polarographic techniques.

The stability constants of the complexes, K_s, were found to vary with the nature of solvent; it has been observed that linear correlation between the $\log K_s$ values and the Kirkwood term, $(\varepsilon-1)/(2\varepsilon+1)$, of the solvents exists. The results are discussed in the frame of the changes of the Tl^I ion solvation.

It is well known that macrocyclic polyethers, viz. crown ethers, are capable of forming stable complexes with many cations; most of the results can be found in a compilation given by Izatt *et al.*[1] Interest in this phenomenon was stimulated when it was found that these synthetic ligands are similar in their structures and reactivity to many naturally occurring compounds of the macrocyclic type which are known to exhibit selective cation complexation. There are at least three factors that make a significant contribution to the binding of cations by the crowns: (i) the cation radius–hole size relation, (ii) the number of the donor sites participating in the binding and (iii) the properties of a solvent. Of these factors, the third will be considered in the present article.

The solvent effect on K_s, the stability constant of complexation

$$M^+_{solv} + crown_{solv} \rightleftharpoons (crown, M^+)_{solv} \quad (1)$$

$$K_s = (c_{crown,M^+})/c_M + c_{crown} \quad (2)$$

remains largely unknown (note that the subscript, "solv" marks the species in a solvated form). Complexation [eq. (1)] can be formally analysed as a phenomenon accompanied by desolvation (or at least partial desolvation) of the M^+ ion and the ligand, and then by solvation of a newly formed species, viz. the (crown, M^+) complex. Thus in order to form this complex in solution the following inequality must be fulfilled[2]

$$\Delta G^0_{compl} + \Delta G^0_{solv}(crown, M^+) < \Delta G^0_{solv}(M^+) + \Delta G^0_{solv}(crown) \quad (3)$$

where ΔG^0_{compl} is the free energy of binding of M^+ by a given ligand. Obviously, all ΔG^0_{solv} terms are influenced upon changing the solvent. Thus, it is clear from eq. (3) that in addition to the free energy of solvation of the cations, the free energies of solvation for the complexed cation and the ligand should be considered.

We wish to report here the complexation of thallium(I) by benzo-15-crown-5 in the solvents: methanol, ethanol, propanol-1, butanol-1, 2-methylpropanol, pentanol-1, 4-hydroxy-4-methyl-2-pentanone, ethylene glycol, and 2-aminoethanol. The stability constants were calculated from polarographic data; 0.05 M tetrabutylammonium perchlorate was used as the supporting electrolyte.

EXPERIMENTAL

Polarographic and cyclic voltammetric curves were determined in a three electrode system; a Radelkis OH 105 apparatus being used. The working electrode was either a mercury drop electrode with a mechanically controlled drop time of 2.0 s or a hanging mercury drop electrode.[3] The potentials were measured against an aqueous SCE, a two part salt bridge being used. In one arm of this bridge was solvent and electrolyte exactly as in the polarographic vessel. All solutions were deaerated by pure argon which was passed through molecular sieves, 0.4 nm, and presaturated by bubbling through the

* Author to whom correspondence should be addressed.

solvent. The measurements were performed at a temperature of 23 ± 0.1°C.

Methanol, ethanol and propanol-1 of spectral grade were used without purification. All remaining alcohols were rectified at reduced pressure under an argon atmosphere. Tetrabutylammonium perchlorate was prepared by conversion of $(n\text{-}C_4H_9)_4NI$; it was recrystallized several times from water and dried *in vacuo* at 60°C. Benzo-15-crown-5 and $TlClO_4$ (Merck) were used without further purification.

RESULTS AND DISCUSSION

Thallium(I) reduces at a dropping mercury electrode forming a single diffusion-controlled one electron wave in all the solvents under investigation (see also ref. 4 and references therein). The wave is reversible; this follows clearly from the shape of cyclovoltammograms and from the slope of polarographic curves. We have registered the cyclic voltammetric curves with the difference $E_{pa} - E_{pc}$ about 60 mV and with equal peak currents in the cathodic and anodic sweep (scan rate 0.05 V s^{-1}). Semilogarithmic analysis gives $\Delta E/\Delta \log[(i/i_0 - i)]$ values close to the 60 mV/log unit. Thus, the cathodic reduction of Tl^+ can be considered as the process:

$$Tl^+ + e \rightleftharpoons Tl(Hg) \qquad (4)$$

and, consequently, corresponding half-wave potentials may be assumed as equal to the formal potentials ($E^0_{1/2}$) for eq. (4). Addition of benzo-15-crown-5 shifts these potentials in a negative direction in all the solvents under study. Cyclic voltammetric curves indicate that the reversibility of the electrochemical processes is preserved as before, so the polarographic method may be used for the calculation of K_s, the stability constants. For this purpose we have examined the effect of the crown concentration (c_{crown}) on the half-wave potential and the limiting current of Tl^+. It should be pointed out that the measurements were carried out at fixed ionic strength; it was kept approximately constant by the electrolyte used in the experiments.

It can be shown that for 1 : 1 complexation[5]

$$\Delta E_{1/2} = (RT/F) \ln (K_s c_{crown}) + (RT/F) \ln (i_{crown,Tl^+}/i_{Tl^+}) \qquad (5)$$

$\Delta E_{1/2}$ is defined as $E_{1/2} - E^0_{1/2}$ where $E_{1/2}$ stands for the potential determined at a given c_{crown} value; the ratio of the limiting currents, $i_{crown,Tl^+}/i_{Tl^+}$, is attributed to a change in the diffusion coefficient of Tl^+ on complexation. The assumption made in deriving eq. (5) is that the crown concentration is much larger than the concentration of the thallium(I) ions, so that the ligand concentration at the electrode surface may be assumed equal to the concentration in the bulk. Table 1 indicates that this condition has been fulfilled in our experiments.

The K_s values calculated according to eq. (5) are collected also in Table 1. The data indicate that complexation is visibly dependent on the nature of the solvent. We have considered this finding using correlation analysis.

Earlier results for dibenzo-18-crown-6, K^+ binding in aprotic solvents show that some interaction exists between the solvent and the complex.[7] However, the effect is not large and stabilization of the complex may be primarily considered in terms of the potassium cation desolvation. Since solvent donicities correlate reasonably well with $\Delta G_{solv}(M^+)$, the donor numbers[8] and the K_s values were compared in some papers.[2,9-11] Let us add here

Table 1. Stability constants, K_s ($dm^3\ mol^{-1}$), for benzo-15-crown-5,Tl^+ complex in alcohols

Solvent	$(\varepsilon-1)/(2\varepsilon-1)$	c_{Tl} (mM)	c_{crown} (mM)	log K_s
Methanol	0.4773	0.125	2–10	3.05 3.00[a]
Ethanol	0.4698	0.187	1.7–4.3	3.30
Propanol	0.4629	0.025	1.6–4.5	3.44
Butanol-1	0.4574	0.017	2–4.6	3.63
2-Methylpropanol	0.4588	0.019	1.7–5.7	3.60
4-Hydroxy-4-methyl-2-pentanone	0.4599	0.164	1.5–7.5	3.54
Pentanol-1	0.4479	0.015	1.2–3.7	3.95
Ethylene glycol	0.4804	0.030	0.5–8	2.86
2-Aminoethanol	0.4808	0.035	0.4–11	2.95

[a] Determined polarographically.[6]

Errors in the determination of K_s do not exceed ±20%.

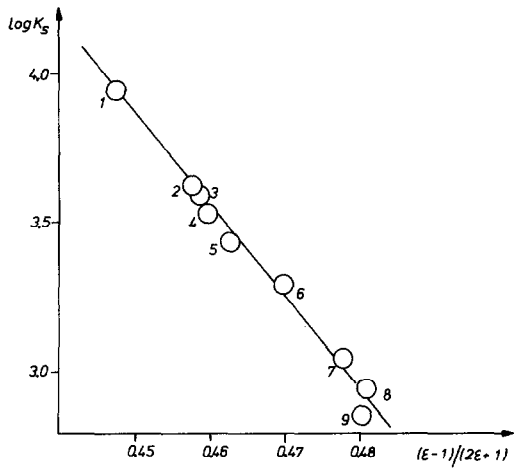

Fig. 1. Dependence of log K_s values of thallium (I)-benzo-15-crown-5 complex in alcohols on Kirkwood term $(\varepsilon-1)/(2\varepsilon+1)$. (1) pentanol-1, (2) butanol-1, (3) 2-methylpropanol, (4) 4-hydroxy-4-methyl-2-pentanone, (5) propanol, (6) ethanol, (7) methanol, (8) 2-aminoethanol, (9) ethylene glycol.

that it is not known yet whether crown complexes show the effect of ligand solvation; although this phenomenon was widely demonstrated for the [2,2,2]-cryptand, Na^+ complex.[12]

The variation in the K_s values for benzo-15-crown-5,Tl^+ complex with the solvent (Table 1) cannot be discussed in terms of the Lewis basicity of alcohols. On the basis of our results one can prove a greater contribution to solvation from non-specific, long-range interactions. The function $(\varepsilon-1)/(2\varepsilon+1)$ from the Kirkwood model was chosen as the parameter describing those interactions (ε is the electric permittivity). Indeed, the following relationship can be obtained for the log K_s values in nine solvents.

$$\log K_s = (-30.96 \pm 1.16) * (\varepsilon-1)/(2\varepsilon+1) + (17.80 \pm 0.54) \quad (6)$$

(errors are standard deviations).

The correlation coefficient of the regression is $r = 0.995$ and F test yields 705.5 which means that the measurement errors can explain the deviations from the assumed model completely. Thus, the solvent change of the log K_s values should be treated as limited by the ΔG^0_{solv} terms of the ionic species, viz. $\Delta G^0_{solv}(Tl^+)$ and ΔG^0_{solv}(crown, Tl^+). Of course, the relative contribution due to the energetics of complexation seems to be much greater for the thallium(I) ions (cf. text above).

As can be seen from eq. (6), solvent effects on the K_s values are manifested in the changes of long-range intermolecular forces. In other words, we may conclude that this relation does not reflect any specific viz. short-range solvation effects. A reasonable explanation seems to be that we have the solvents characterized by approximately the same Lewis basicities. These are the reasons why the present study was restricted to alcohols as the solvents.

Acknowledgements—The authors are grateful to Prof. Ulrich Mayer (Vienna, Austria) for samples of the crown ether. This work was sponsored as a part of Problem CPBP 01.15.

REFERENCES

1. R. M. Izatt, J. S. Bradshaw, S. A. Nielsen, J. D. Lamb, J. J. Christensen and D. Serv, *Chem. Rev.* 1985, **85**, 271.
2. E. Lada, S. Filipek and M. K. Kalinowski, *Austr. J. Chem.* 1988, **41**, 437.
3. W. Kemula and J. Zawadowska, *Fresenius Z. Anal. Chem.* 1980, **39**, 300.
4. M. I. Bellavance and B. Miller, in *Encyclopedia of Electrochemistry of the Elements* (Edited by A. J. Bard), Vol. 4. Ch. 4. Marcel Dekker, New York (1975).
5. D. D. De Ford and D. N. Hume, *J. Am. Chem. Soc.* 1951, **73**, 5321.
6. A. Hoffmanova, J. Koryta, M. Brezina and L. Mittal, *Inorg. Chim. Acta* 1978, **28**, 73.
7. F. de Jong and N. D. Reinhoudt, *Adv. Phys. Chem.* 1980, **17**, 279.
8. V. Gutmann, *The Donor–Acceptor Approach to Molecular Interactions*. Plenum, New York (1978).
9. A. I. Popov, in *Solute–Solvent Interactions* (Edited by J. F. Coetzee and C. D. Ritchie), Vol. 2, p. 271. Marcel Dekker, New York (1976).
10. Y. C. Lee, J. Allison and A. I. Popov, *Polyhedron* 1985, **4**, 441.
11. M. Shamispur, G. Rounaghi and A. I. Popov, *J. Soln Chem.* 1980, **9**, 701.
12. M. H. Abraham, A. F. Danil de Namor and W. H. Lee, *J. Chem. Soc., Chem. Commun.* 1977, 893.

Polyhedron Vol. 8, No. 17, pp. 2119–2124, 1989
Printed in Great Britain

0277–5387/89 $3.00+.00
© 1989 Pergamon Press plc

SYNTHESIS AND STRUCTURE OF A TRIPLY-CHLORO-BRIDGED DIMER OF A HOMOBINUCLEAR Rh^I COMPLEX: $[\{Rh_2(CO)(HC(PPh_2)_3)\}_2(\mu\text{-}Cl)_3]^+[Rh(CO)_2Cl_2]^-$

H. EL-AMOURI, A. A. BAHSOUN, J. A. OSBORN,* M. T. YOUINOU and J. FISCHER

Laboratoire de Chimie des Métaux de Transition et de Catalyse, UA au CNRS n° 424, Université Louis Pasteur, Institut Le Bel, 4, rue Blaise Pascal, 67000 Strasbourg, France

(*Received* 10 *February* 1989; *accepted* 15 *March* 1989)

Abstract—The tripod ligand $HC(PPh_2)_3$ reacts with $Mo(CO)_3(CH_3CN)_3$ yielding $Mo(CO)_3(CH_3CN)(HC(PPh_2)_3)$. Reaction of this Mo^0 complex with $[Rh(CO)_2Cl]_2$ gives unexpectedly the tetranuclear species $[Rh_2(CO)(HC(PPh_2)_3)]_2(\mu\text{-}Cl)_3^+$ (**3**) which crystallizes as the $Rh(CO)_2Cl_2^-$ salt (**3a**). This complex crystallizes in the monoclinic space group $P2_{1/c}$ with $Z = 4$, with all dimensions $a = 19.685(3)$, $b = 19.524(3)$, $c = 22.657(4)$ Å, and $\beta = 96.96(2)°$. A direct route to the PF_6^- salt of **3** (**3b**) is also presented. The ^{31}P NMR data show **3a** and **3b** to be identical and that the tetranuclear structure is retained in solution, i.e. two units of binuclear Rh^I species bridged by three chlorine atoms. In each binuclear unit, the tripod ligand spans two Rh^I which are linked directly by a metal–metal bond (Rh—Rh = 2.696 Å).

The assembling ligand $HC(PPh_2)_3$ (**1**) has been used with some success for the synthesis of bimetallic[1] and trimetallic[2] species. One of our more recent objectives has been the synthesis of heterobimetallic complexes capable of activating small molecules by means of their simultaneous interaction with two different metals.[3] The strategy involves, firstly the synthesis of a precursor complex in which a single metal centre is chelated by two phosphorus atoms of **1**, followed by a second reaction in which the pendant non-coordinated phosphorus atom reacts with a second labile metal complex. This approach depends implicitly on the stability of the precursor complex under the reaction conditions of the second reaction. Here we illustrate a constraint of its use where an attempt to synthesize a Mo—Rh complex resulted unexpectedly in the isolation of a tetranuclear rhodium species.

EXPERIMENTAL

All experiments were carried out on a high vacuum line or in a nitrogen filled glove box. Solvents were dried prior to use by conventional distillation under nitrogen and the appropriate reagent, e.g. THF (sodium benzophenone), acetone ($CaSO_4$), and MeOH, CH_2Cl_2 and acetonitrile (CaH_2).

Infrared spectra were recorded on a Perkin Elmer 597 spectrophotometer as Nujol mulls and/or in solution (0.1 mm KBr cells). NMR spectra were acquired on a Bruker SY-200 (^1H, ^{13}C, ^{31}P) and a AM-400 (^{31}P) instrument; chemical shifts are relative to Me_4Si (^1H, ^{13}C) or 85% H_3PO_4 (^{31}P). Data are presented as proton decoupled with downfield chemical shifts as positive. Elemental analyses were performed by the Service Central d'Analyses of the CNRS.

Materials

$RhCl_3, nH_2O$ was purchased from Johnson Matthey Chimie, the ligand[4] $HC(PPh_2)_3$ (tripod), the complexes $[Rh(CO)_2Cl]_2$,[5] and $Mo(CO)_3(MeCN)_3$[6] were prepared as previously described.

Preparations

$Mo(CO)_3(CH_3CN)[HC(PPh_2)_3]$, (**2**). A yellow solution of $Mo(CO)_3(MeCN)_3$ (1.07 g, *ca* 3.50

* Author to whom correspondence should be addressed.

mmol) in 60 cm^3 of CH_2Cl_2/MeCN (10:1) was added dropwise under nitrogen for 30 min at room temperature to a well stirred solution of tripod (2.06 g, 3.64 mmol) in CH_2Cl_2. The solution darkened to deep yellow and the microcrystalline, pure $Mo(CO)_3(MeCN)[HC(PPh_2)_3]$ precipitated, and was separated, washed twice with hexane and dried *in vacuo* (yield 65%). IR (cm^{-1}, in Nujol) ν (CO) 1925 (s), 1840 (ms), 1780 (s); ^{31}P NMR [$(CD_3)_2CO/CH_2Cl_2$ (+1 drop CH_3CN)]: δ (ppm) 24.9 (d, 2P), −21.9 (t, 1P), J(P–P) = 25 Hz. Found: C, 63.9; H, 4.3; N, 1.8; P, 11.5. Calc for $C_{42}H_{34}O_3NP_3Mo$ (mol. wt 789): C, 63.9; H, 4.3; N, 1.8; P, 11.8%.

$[\{Rh_2(CO)(HC(PPh_2)_3)\}_2(\mu\text{-}Cl)_3]^+[Rh(CO)_2Cl_2]^-$, (**3a**). A solution of $[Rh(CO)_2Cl]_2$ (0.287 g, 0.737 mmol) in 4 cm^3 of THF was added to a rapidly stirred yellow slurry of **2** (0.38 g, 0.48 mmol) in 9 cm^3 of THF. The mixture changed from yellow to give a deep red solution. Stirring was continued for 20 h during which a yellow orange compound precipitated. Purification was achieved by recrystallization from an acetone–ether mixture yielding pure yellow orange crystals of **3a** · $2CH_3COCH_3$ (**3a′**) which were suitable for X-ray determination. IR (cm^{-1}, Nujol mull) ν(CO) 2065 (ms), 1995 (s), 1970 (s), 1960 (vs); ^{31}P NMR (see text).

$[\{Rh_2(CO)(HC(PPh_2)_3)\}_2(\mu\text{-}Cl)_3]^+(PF_6)^-$ (**3b**). Method 1. **3a** (0.300 g, *ca* 0.155 mmol) was added to NH_4PF_6 (0.100 g, 0.60 mmol) in THF. The mixture was stirred for 24 h, then the yellow slurry filtered and the product **3b** washed several times with THF. Method 2. A tripod $HC(PPh_2)_3$ solution in 40 cm^3 (0.381 g, *ca* 0.67 mmol) was added in a dropwise fashion for 10–15 min to a well-stirred solution of $[Rh(CO)_2Cl]_2$ (0.236 g, *ca* 0.61 mmol) and NH_4PF_6 (0.493 g, ca 3.0 mmol) in 60 cm^3 of THF. Stirring the solution at room temperature under a slow flow of argon for three days yielded an orange coloured solution which was taken to dryness *in vacuo*. The orange product was washed successively with MeOH (2 × 15 cm^3) and with Et_2O (2 × 30 cm^3) and then dried *in vacuo*. Pure complex **3b** was recovered in 70% yield. IR (cm^{-1}, Nujol mull) ν(CO) 1985 (sh), 1975 (s), 1965 (s). Found: C, 48.6; H, 3.6; Cl, 5.7; F, 6.0; P, 11.0. Calc for $C_{76}H_{62}O_2Cl_3F_6P_7Rh_4$ (mol. wt 1855.5): C, 49.1; H, 3.4; Cl, 5.7; F, 6.1; P, 11.6%.

X-ray experiments. All data for **3a′** were collected on a Philips PW 1100/16 diffractometer equipped with a low temperature device using graphite monochromated Mo-K_α radiation (λ 0.71063 Å). The crystal data and data collection parameters are summarized in Table 1. No significant intensity changes were observed for three standard reflections monitored every hour during the data collection period. The Enraf-Nonius SDP package was used[7] on a PDP 11/60 computer for the computations, except that a local data reduction program was employed. The initial step-scan data were converted to intensities by the Lehmann–Larson method[8] and then corrected for Lorentz, polarization and absorption factors, the latter computed by the empirical method of Wacker and Stuart.[9]

Table 1. Crystal data, intensity collections, and structure refinement parameters for **3a′**

Formula	$C_{84}H_{74}O_6P_6Cl_5Rh_5$
Mol. weight	2057.16
Cryst. syst.	monoclinic
a (Å)	19.685(3)
b (Å)	19.524(3)
c (Å)	22.657(4)
β (deg)	96.96(2)
V (Å^3)	8643.6
Z	4
d (calcd), (g cm^{-3})	1.581
F(000)	4104
Abs. coeff. (μ, cm^{-1})	12.34
Space group	$P2_1/c$
Crystal dimen. (mm)	0.32 × 0.14 × 0.10
Temperature	−100°C
Scan mode	$\theta/2\theta$ flying step-scan
Scan speed (deg s^{-1})	0.026
Scan width (deg)	1.0 + 0.34 tan θ
2θ range	6–50
Octants	$+h$, $+k$, $\pm l$
Unique total data	16261
Unique obsd data	8005
Criterion for observ.	$I > 3\sigma(I)$
No. of variables	905
Transmiss. factors (max/min)	1.13/0.76
R_F/R_{wF}, (%)	6.9/8.8
GOF	1.32

The structure was solved by using direct methods which revealed positions of the metals and some of the phosphorus and chloride atoms. The remaining non-hydrogen atoms were located from difference Fourier maps computed after blocked-cascade least-squares refinement. After refinement of the heavy atoms, a difference Fourier map revealed maxima of residual electron density close to the positions expected for hydrogen atoms; they were introduced into the structure factor calculations at their calculated positions (C—H 0.95 Å) and with isotropic temperature factors defined as B(H) = 1 + B eq(C) Å^2 but were not refined (hydrogens of the solvates not included). Full least-squares refinements minimizing $\Sigma w(|F_o| - |F_c|^2)$ with $\sigma^2(F^2) = \sigma^2_{counts} + (0.08\ F^2)^2$ converged to the

conventional R factors shown in Table 1. Final difference maps revealed no significant maxima. The scattering factor coefficients and anomalous dispersion coefficients come respectively from references 10a and 10b.*

RESULTS AND DISCUSSION

Complex formation

The tripod ligand $HC(PPh_2)_3$ reacts with $Mo(CO)_3(CH_3CN)_3$ in CH_2Cl_2 at room temperature under an argon atmosphere to form yellow $Mo(CO)_3(CH_3CN)HC(PPh_2)_3$ (**2**) displacing two CH_3CN molecules. The complex **2** was characterized by elemental analysis, IR, and NMR spectroscopy. The IR spectrum of **2** shows strong carbonyl absorptions at 1925, 1840 and 1780 cm^{-1} which can be compared with the IR of fac-$Mo(CO)_3(CH_3CN)_3$ which exhibits terminal carbonyl bands at 1913 and 1790 cm^{-1}. The $^{31}P\{^1H\}$ NMR sprectrum of **2** displays a doublet in the downfield region at 25.0 ppm $J(P_1—P_2) = 25$ Hz assigned to two P atoms of the ligands chelating the Mo centre, while a triplet centred at −21.9 ppm $J(P_1—P_2) = 25$ Hz results from the P atom of the uncoordinated arm of tripod. These observations are consistent with a mononuclear Mo^0 complex, with the CO ligands bonded in a fac-configuration. The spectroscopic features do not allow a distinction between the two possible isomers (Scheme 1). In either case, **2** or **2′** possesses a P_2 atom available for the formation of a binuclear complex although **2′** would seemingly more easily form a metal–metal-bonded species. Thus in order to investigate the construction of heterobinuclear complexes combining early and late transition metals by this approach the reaction of $Mo(CO)_3(CH_3CN)HC(PPh_2)_3$ with the labile Rh^{I} species, $[Rh(CO)_2Cl]_2$, was studied.

When $[Rh(CO)_2Cl]_2$ was added to $Mo(CO)_3(CH_3CN)HC(PPh_2)_3$ (molar ratio 1.5 : 1) a yellow-orange microcrystalline compound **3a** precipitated. IR spectrum of **3a** shows four absorptions resulting from terminal carbonyl ligands at 2065, 1995, 1970 and 1960 cm^{-1}, and the $^{31}P\{^1H\}$ NMR spectrum

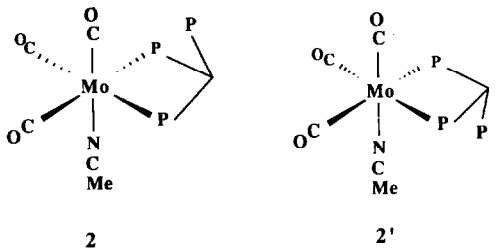

Scheme 1.

of the complex exhibits several resonances, all of which showed large P—Rh couplings namely a doublet of triplets of doublets centred at 31.5 ppm and two somewhat overlapping quartets of broad doublets at 3.5 ppm (*vide infra* the spectroscopic features of **3b**). The elemental analysis and the above spectroscopic data did not allow us to determine a detailed structure for **3a**. Accordingly, an X-ray diffraction analysis was carried out on a single crystal of this complex.

Crystallographic study of $[\{Rh_2(CO)(HC(PPh_2)_3)\}_2(\mu\text{-}Cl)_3]^+[Rh(CO)_2Cl_2]^- \cdot 2\,CH_3COCH_3$, **3a′**. The ORTEP view of the cation of **3a′** with the labelling scheme used is given in Fig. 1 and appropriate bond distances and angles are listed in Table 2. The crystal structure of **3a′** consists of four discrete molecules of $[\{Rh_2(CO)(HC(PPh_2)_3)\}_2(\mu\text{-}Cl)_3]^+$ with $[Rh(CO)_2Cl_2]^-$ as the counter anion. Each tetrameric core consists of two sets of binuclear units linked by three bridging chloride atoms in a slightly asymmetric fashion [Rh(1)—Cl(3) = 2.391(3) Å; Rh(4)—Cl(3) = 2.404(3) Å; Rh(2)—Cl(1) = 2.405(3) Å; Rh(4)—Cl(1) = 2.403 (3) Å; Rh(2)—Cl(2) = 2.419(3) Å; Rh(3)—Cl(2) =

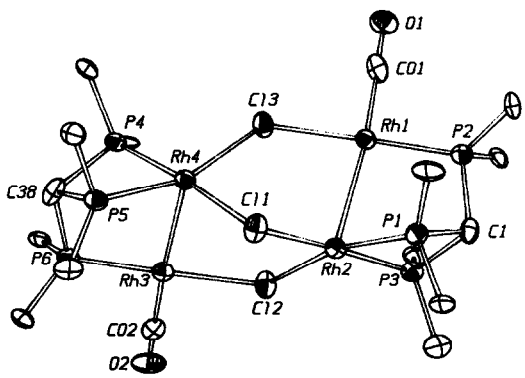

Fig. 1. ORTEP view of the cation of complex **3a′**; each phenyl group is reduced to its *ipso* carbon atom (50% probability thermal ellipsoids). Hydrogen atoms are omitted.

*Complete tables of final fractional coordinates (Tables 3 and 4), anisotropic temperature factors (Table 5), observed and calculated structure factor amplitudes (× 10) for all observed reflections for **3a′** (34 pages) have been deposited with the Editor, from whom copies are available on request. Atomic coordinates have also been deposited with the Cambridge Crystallographic Data Centre.

Table 2. Selected bond lengths and angles for **3a'**

Bond lengths (Å)			
Rh(1)—Rh(2)	2.704(1)	Rh(3)—Rh(4)	2.688(1)
Rh(1)—Cl(3)	2.391(3)	Rh(3)—Cl(2)	2.417(3)
Rh(1)—CO(1)	1.80(1)	Rh(3)—CO(2)	1.82(1)
Rh(1)—P(2)	2.216(3)	Rh(3)—P(6)	2.220(3)
Rh(1)—Cl(2)	2.405(1)	Rh(4)—Cl(1)	2.403(3)
Rh(2)—Cl(2)	2.419(3)	Rh(4)—Cl(3)	2.404(3)
Rh(2)—P(1)	2.188(3)	Rh(4)—P(4)	2.208(3)
Rh(2)—P(3)	2.193(3)	Rh(4)—P(5)	2.192(3)
Bond angles (°)			
Rh(2)—Rh(1)—Cl(3)	82.98(8)	Rh(4)—Rh(3)—Cl(2)	85.41(8)
Rh(2)—Rh(1)—CO(1)	174.2(4)	Rh(4)—Rh(3)—CO(2)	176.8(4)
Rh(2)—Rh(1)—P(2)	95.80(9)	Rh(4)—Rh(3)—P(6)	94.44(9)
Cl(3)—Rh(1)—CO(1)	91.2(4)	Cl(2)—Rh(3)—CO(2)	91.5(4)
Cl(3)—Rh(1)—P(2)	178.6(1)	Cl(2)—Rh(3)—P(6)	177.8(1)
CO(1)—Rh(1)—P(2)	90.0(4)	CO(2)—Rh(3)—P(6)	88.7(4)
Rh(1)—Rh(2)—Cl(1)	102.68(8)	Rh(3)—Rh(4)—Cl(1)	98.04(8)
Rh(1)—Rh(2)—Cl(2)	108.99(9)	Rh(3)—Rh(4)—Cl(3)	109.54(9)
Rh(1)—Rh(2)—P(1)	80.36(9)	Rh(3)—Rh(4)—P(4)	81.63(9)
Rh(1)—Rh(2)—P(3)	82.25(9)	Rh(3)—Rh(4)—P(5)	84.70(9)
Cl(1)—Rh(2)—Cl(2)	91.1(1)	Cl(1)—Rh(4)—Cl(3)	91.6(1)
Cl(1)—Rh(2)—P(1)	97.9(1)	Cl(1)—Rh(4)—P(4)	172.2(1)
Cl(1)—Rh(2)—P(3)	168.9(1)	Cl(1)—Rh(4)—P(5)	100.0(1)
Cl(2)—Rh(2)—P(1)	165.3(1)	Cl(3)—Rh(4)—P(4)	95.9(1)
Cl(2)—Rh(2)—P(3)	96.6(1)	Cl(3)—Rh(4)—P(5)	160.3(1)
P(1)—RH(2)—P(3)	72.9(1)	P(4)—Rh(4)—P(5)	72.2(1)
Rh(2)—Cl(1)—Rh(4)	100.3(1)		
Rh(2)—Cl(2)—Rh(3)	123.2(1)		
Rh(1)—Cl(3)—Rh(4)	127.6(1)		

2.417(3) Å]. The rhodium atoms in each binuclear unit are clasped together by the tripod ligand, each rhodium possessing a different geometry. One rhodium is surrounded by two chloride atoms and two phosphorus atoms [Rh(2)—P(1) = 2.188(3) Å and Rh(2)—P(3) = 2.193(3) Å] forming the basal plane of a distorted square pyramid, with the apical position occupied by the second rhodium at a distance 2.704(1) Å corresponding to a single metal–metal bond between Rh(1)—Rh(2). The second rhodium centre displays an approximate square planar arrangement and is bound to one carbonyl group [Rh(1)—CO(1) = 1.80(1) Å] *trans* to Rh(2), to one chloride and to one phosphorus atom of the tripod ligand [Rh(1)—P(2) = 2.216(3) Å]. The planes defined by Cl(1), Cl(2), P(1), P(3) and Cl(3), CO(1), Rh(1), P(2) are nearly perpendicular (93°8). The bond distances from the phosphorus atoms of the tripod ligand to the rhodium atoms range from 2.188 to 2.220 Å and are slightly shorter than those recently reported[11] in a binuclear rhodium(I) complex containing the same ligand. These observations as well as the shortening of the Rh—Rh bond (mean 2.696 Å) in **3a'** compared to 2.745 Å may[11] result from the constraint due to the existence of the stable tetranuclear unit. The array of the four rhodiums held together by three bridging chloride atoms is thus best described as two binuclear units, assuming a pseudo two-fold axis of symmetry perpendicular to the $(Rh)_4$ core and passing through the Cl(1) atom. Such a frame of four Rh atoms has however a precedent, thus the structure[12] of $[\{Rh_4(\mu\text{-}Cl)_2(\mu\text{-}L)_2(\mu\text{-}CO)_2(CO_2)(nbd)_2\}]$, [L = pyrrolo-(2,3-b)pyridine anion, nbd = norbornadiene] shows analogously two binuclear units of Rh^I, (Rh—Rh = 2.686 Å) bridged together through two chloride atoms forming a quasi-planar Rh_4Cl_2 core.

Synthesis and spectroscopic features of $[\{Rh_2(CO)(HC(PPh_2)_3)\}_2(\mu\text{-}Cl)_3]^+(PF_6)^-$, **3b**. Although an anion exchange reaction of **3a** with NH_4PF_6 occurs in THF to yield $[\{Rh_2(CO)(HC(PPh_2)_3)\}_2(\mu\text{-}Cl)_3]^+(PF_6)^-$, **3b**, a more convenient route to prepare the latter was investigated. When tripod (1 eq) was added in a dropwise fashion to a mixture of $[Rh(CO)_2Cl]_2$ with excess NH_4PF_6 in

THF, **3b** could be isolated from the orange-red solution as the major product in good yield. We have found that the use of a large volume of THF is necessary for this purpose otherwise precipitation of the complexes **3a** and **3b** will occur simultaneously. The IR spectrum of **3b** shows typical stretching frequencies for terminal bonded carbonyls at 1985 (sh), 1975 (s), and 1965 (s) cm^{-1} and the vibrations characteristic of the PF_6^- anion. At room temperature, the 81 MHz $^{31}P\{^1H\}$ NMR spectrum of **3b** shows essentially an identical pattern of shifts and couplings in the low field region to that of **3a**; an additional resonance (septet) due to PF_6^- is observed at −145 ppm in the spectrum of **3b**.

The $^{31}P\{^1H\}$ spectrum was also carried out at 161.9 MHz to permit unambiguous assignments of the chemical shift and coupling constant data (Fig. 2). The complex pattern suggests that the solid state structure is maintained in solution. A schematic diagram of the structure of **3** derived from the X-ray structure (Scheme 2) shows that all four Rh as well as all six P environments should be magnetically distinct. The spectrum however can be analysed in terms of a ABMXY system (A, B, M = P; X, Y = Rh) indicating that the couplings between the two halves of the molecule do not significantly affect the spectrum or are zero, as we have supposed for this simulation. The essential features of this analysis are: (i) The occurrence of a pair of triplets of doublets centred at δ 53.0 that arises from spin coupling of the phosphorus nucleus P_M directly linked to Rh_Y [$^1J(P_M—Rh_Y) = 175$ Hz] and

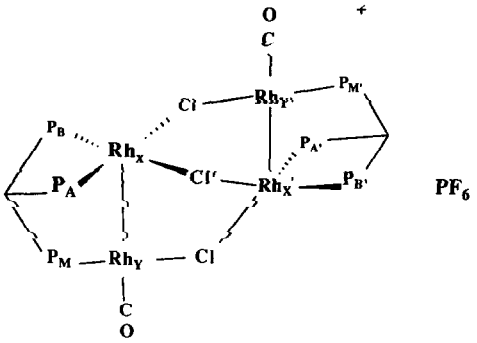

Scheme 2.

through the methine carbon to the two other P nuclei P_A and P_B of the tripod ligand, $^2J(P_M—P_A) = 10$ Hz and $^2J(P_M—P_B) = 9$ Hz; each line of the triplets is further split into a doublet by a two bond coupling [$^2J(P_M—Rh_X) = 3.5$ Hz]. Such weak interaction between P and Rh nuclei through a metal–metal bond was previously observed for the heterobinuclear[1] complex $[(CO)_5FeRh(HC(PPh_2)_3)]^+$, ($^2J_{P—Fe—Rh} = 1.8$ Hz). (ii) Two partially overlapping sets of complex quartets chemically well shifted from the P_M signals. In this case each quartet can be regarded as the AB pattern expected for a pair of mutually coupled non-equivalent phosphorus nuclei P_A and P_B $^2J(P_A—P_B) = 98$ Hz, two sets of quartets arising from phosphorus–rhodium coupling $^1J(P_A—Rh_X) = {}^1J(P_B—Rh_X) = 144$ Hz. However the two lowest field resonances (A part of the AB pattern) of each quartet appear as a doublet of doublets whereas the highest field resonances (B

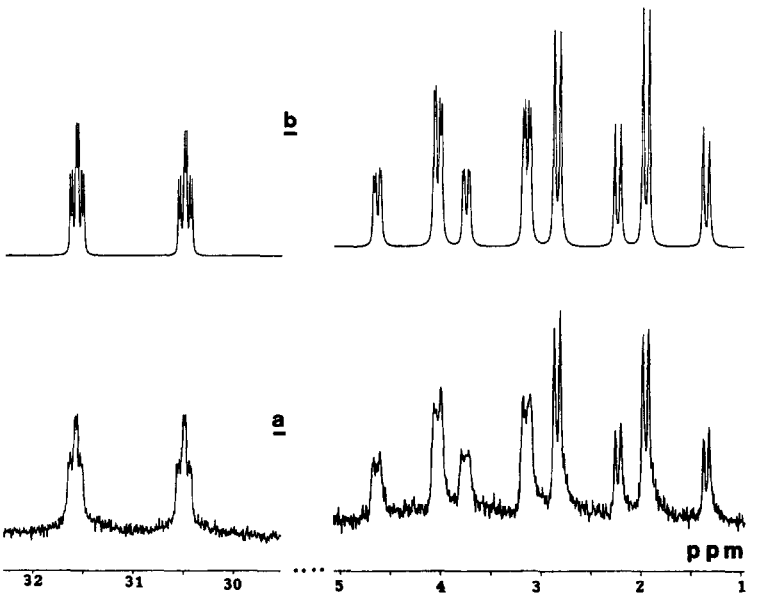

Fig. 2. $^{31}P\{^1H\}$ NMR spectrum of **3b**, $[\{Rh_2(CO)(HC(PPh_2)_3)\}_2(\mu\text{-}Cl)_3]^+(PF_6)^-$ at 25°C, 161.9 MHz. (a) Experimental spectrum; (b) simulated spectrum using the Bruker's PANIC computer program.

part) arise clearly as an unperturbed doublet. The perturbations within each quartet are associated with the different couplings of the phosphorus nuclei P_A and P_B respectively with the Rh_Y centre through a metal–metal bond. The most feasible interpretation is to assume that the splitting as a doublet of doublet in one case is due to P_A—P_M coupling [$^2J(P_A—P_M) = 10$ Hz] with a further very small splitting of each line from P_A—Rh_Y coupling [$^2J(P_A—Rh_Y = 3$ Hz]. In contrast the phosphorus P_B arises as a proper doublet $^2J(P_B—P_M) = 9$ Hz and $^2J(P_B—Rh_Y) = 0$ at highest field. The computer simulation reproduces the experimental spectrum accurately (see Fig. 2) with δ P_B 2.15 and δ P_A 3.85 and using the various coupling constants cited above. We note the one bond coupling $^1J(P_M—Rh_Y) = 175$ Hz for square planar phosphine P_M is *ca* 20% larger than for the phosphines P_A and P_B, $^1J(P_A—Rh_X) = {}^1J(P_B—Rh_X) = 144$ Hz chelated to a Rh^I in a square pyramidal configuration. The rather high values of such ^1J(P—Rh) couplings are consistent with the P nucleus lying *trans* to halogen atoms.[13]

In conclusion, although our objectives to synthesize mixed bimetallic systems have not been successful in this case, the isolation and characterization of the tetranuclear Rh^I complex enabled us to envisage and synthesize other bimetallic complexes of this type such as $[Rh_2(CO)_2(CH_3CN)_2$ (tripod)$]^{2+}$.[11] Further, the synthesis of mixed bimetallic systems involving Rh^I have been achieved using for example [Rh(tripod)(diene)]$^+$ as precursor.[14]

REFERENCES

1. A. A. Bahsoun, J. A. Osborn, P. H. Bird, D. Nucciarone and A. V. Peters, *J. Chem. Soc., Chem. Commun.* 1984, 72.
2. (a) J. A. Osborn and G. G. Stanley, *Angew. Chem. Int. Ed. Engl.* 1980, **19**, 1025; (b) J. A. Osborn, G. G. Stanley and P. H. Bird, *J. Am. Chem. Soc.* 1988, **110**, 2217.
3. (a) C. P. Casey, R. M. Bullock and F. Nief, *J. Am. Chem. Soc.* 1983, **105**, 7574; (b) M. J. Breen, P. H. Shulman, G. L. Geoffroy, A. L. Rheingold and W. C. Fultz, *Organometallics* 1984, **3**, 782; (c) G. S. White and D. W. Stephan, *Inorg. Chem.* 1985, **24**, 1499; (d) G. S. Fergusson and P. T. Wolczanski, *Organometallics* 1984, **4**, 1601; (e) S. W. Carr, B. L. Shaw and M. Thornton-Pett, *J. Chem. Soc., Dalton Trans.* **1985**, 2131; (f) S. W. Carr and B. L. Shaw, *Polyhedron* 1987, **6**, 11.
4. A. A. Bahsoun, J. A. Osborn, C. Voelker, J. J. Bonnet and G. Lavigne, *Organometallics* 1982, **1**, 1114.
5. J. A. McCleverty and G. Wilkinson, *Inorg. Synth.* 1966, **8**, 211.
6. D. P. Tate, W. R. Knipple and J. M. Angl, *Inorg. Chem.* 1962, **1**, 433.
7. B. A. Frenz, *The Enraf-Nonius CAD4-SDP*, in *Computing in Crystallography* (Edited by H. Schenk, R. Olthof-Hazekamp, H. von Koningsveld and G. C. Bassi), pp. 64–71. Delft University: Delft (1978).
8. M. S. Lehmann and F. K. Larson, *Acta Cryst.* 1974, **A30**, 580.
9. N. Walker and D. Stuart, *Acta Cryst.* 1983, **A398**, 158.
10. (a) D. T. Cromer and J. T. Waber, *International Tables for X-Ray Crystallography*; Table 2.2.b. Kynoch Press, Birmingham, England (1974); (b) *ibid.* Table 2.3.1.
11. H. El-Amouri, A. A. Bahsoun, J. Fischer and J. A. Osborn, *Ang. Chem. Int. Ed. Engl.* 1987, **11**, 1169.
12. L. A. Oro, M. A. Ciriano and B. E. Villarroya, *J. Chem. Soc., Dalton Trans.* 1985, 1891.
13. P. S. Pregosin and R. W. Kunz, ^{31}P *and* ^{13}C *NMR of Transition Metal Phosphine Complexes*, pp. 26 and 39. Springer; New York (1979).
14. H. El-Amouri, A. A. Bahsoun and J. A. Osborn, *Polyhedron* (to be submitted).

Polyhedron Vol. 8, No. 17, pp. 2125–2129, 1989
Printed in Great Britain

0277–5387/89 $3.00+.00
© 1989 Pergamon Press plc

INTRAMOLECULAR ISOMERIZATION OF CHROMIUM AND TUNGSTEN BIS(TRIFLUOROPHOSPHINE)CARBONYLS

LEIGH DENHAM BOTTOMLEY,* RONALD J. CLARK† and TOMAS G. BERGER

Department of Chemistry, Florida State University, Tallahassee, FL 32306-3006, U.S.A.

(*Received* 10 *September* 1988; *accepted after revision* 31 *March* 1989)

Abstract—The thermally induced isomerization of chromium and tungsten bis(trifluorophosphine) carbonyl compounds was analysed by gas chromatography. These hexacoordinate chromium and tungsten compounds were found to isomerize intramolecularly without bond breakage. Rates of the isomerization were calculated from the Simplex optimized fit of first-order decay to the data. Activation parameters were also calculated. This example of intramolecular isomerization was concluded to be under steric control.

The intramolecular isomerization of hexacoordinate zero-valent d^6 metal complexes is not common. Muetterties discussed the possibility of octahedral isomerization using his topological representations as early as 1968.[1] He concluded that the activation barriers would be too large to accommodate a non-bond-breaking mechanism. However, soon he and co-workers found the first case of intramolecular isomerization.[2] That example concerned the isomerization of dihydrido complexes, H_2ML_4, where M = Fe or Ru, L = phosphine or phosphite. It was concluded that the isomerization occurred via hydrogen transversal of the tetrahedral face of the phosphorus atoms for a variety of ligands. Later, Pomeroy and Graham[3] observed the *cis–trans* isomerization of $M(CO)_4(SiCl_3)_2$, where M = Ru or Os. The stereochemical non-rigidity of $W(CO)_5P(OMe)_3$ was unambiguously established by Darensbourg and Baldwin.[4] They employed a double labelling experiment and incorporated ^{13}C and ^{18}O, and then monitored the ^{13}C NMR shift induced by ^{18}O to delineate stereospecific sites. Ligand rearrangements were observed to occur with bonds intact.

Examples of intramolecular isomerization of substituted six-coordinate carbonyls are on the increase. The first full kinetics study of this phenomenon was by Darensbourg,[5] concerning the *cis–trans* isomerization of $Mo(CO)_4(P—n\text{-}Bu_3)_2$. Another more recent illustration[6] is the study of the *cis–trans* isomerization of labelled $Mo(CO)_4(^{13}CO)PR_3$. Finally, recent work by Howell[7] on chromium, molybdenum and tungsten compounds of the type $Mo(CO)_4L_2$ illustrates the same process. Related intramolecular processes have been found by Angelici in thiocarbonyl complexes.[8] While there are examples in the literature of hexacoordinate stereochemical non-rigidity, there have been very few kinetic studies of the metal carbonyls substituted with phosphines. We undertook this study with trifluorophosphine ligands to see if the small size of the ligand would affect the rate of the isomerization or the equilibrium concentration of the two species.

EXPERIMENTAL

Compounds

Cis- and *trans*-bis(trifluorophosphine)metal carbonyls were synthesized by the photochemical techniques previously published.[9] They were separated by preparative gas chromatography and purity was checked by GC prior to thermal induction.

Apparatus

Sealed liquid samples were equilibrated at various temperatures in a silicone oil bath that was capable of maintaining temperatures to two-tenths of a degree.[10] Analysis was carried out on a Varian Autoprep A-700 gas chromatograph. The column

* Present address: Department of Chemistry, Agnes Scott College, Decatur, GA 30030, U.S.A.

† Author to whom correspondence should be addressed.

was a 7 m, 1/4 in. copper tube packed with 35% DC 702 on Chromosorb P (30/60 mesh). The GC was equipped with a thermal conductivity detector.

Procedure

Pure samples of either *cis*- or *trans*-$M(PF_3)_2(CO)_4$, (M = Cr or W) were dried by vacuum sublimation through granular P_4O_{10} (Baker Chemicals). Samples (0.01 cm^3) were then sealed in 3 mm i.d. glass tubing of approximately 10 cm length under vacuum, after several freeze–pump–thaw cycles to remove oxygen. Samples were placed in a constant temperature bath and were removed at various time intervals. Samples were kept at −196°C until they were analysed by GC. The GC conditions were set so that the *cis* and *trans* peaks were baseline resolved. The column temperatures used were the lowest temperatures consistent with reasonably rapid analysis. *Cis–trans* peaks eluted within 10 min. Pure compounds were often trapped and re-analysed to check if decomposition or isomerization occurred due to the separation process, but none was found. The column temperatures used were 80°C for chromium complexes and 100°C for tungsten complexes. The thermal conductivity detector was calibrated with known amounts of all compounds and small correction factors applied to area measurements accordingly. Area measurements were made by cut and weigh. Labelling experiments were carried out on both the chromium and tungsten *trans* compounds. A several-fold molar excess of 90% ^{13}CO (Monsanto) was sealed in a 30 cm^3 tube with the pure *trans* compound. After heating, the *cis*- and *trans*-$M(PF_3)_2(CO)_4$ were separated from each other and examined carefully by IR spectroscopy.

RESULTS AND DISCUSSION

Upon heating neat *cis*-$Cr(PF_3)_2(CO)_4$ at elevated temperatures (100–140°C), isomerization to a *cis–trans* mixture was observed. No decomposition occurs and 100% of the starting material can be accounted for. Similar behaviour is seen starting with *trans*-$Cr(PF_3)_2(CO)_4$. The samples are in such small volume tubes that the carbonyl should be predominantly in the liquid phase. The phase of the reactant seems to be of little significance to the rates of reaction. Preliminary work done in the gas phase shows similar rates of transformation. The kinetic behaviour of *cis*-$Cr(PF_3)_2(CO)_4$ at 100°C is illustrated in Fig. 1. The same *cis–trans* ratio is reached from either pure compound. No other components are detected by GC, except at the highest temperature and longest times. Scrambling products comprise no more than 1% of the total peak area under these conditions. Analysis by GC is capable of detecting all mononuclear six-coordinate species and the isomeric distribution of di- and tri-substituted metal carbonyls. Tungsten exhibits the same kinetic behaviour as chromium, giving a clean *cis–trans* isomerization but at slower rates. The reactions appear to proceed via a non-bond breaking mechanism because no other scrambling products are detected. Photochemical activation of the same compounds, which is known to be a bond-breaking process, results in a full array of $M(PF_3)_x(CO)_{6-x}$ species.

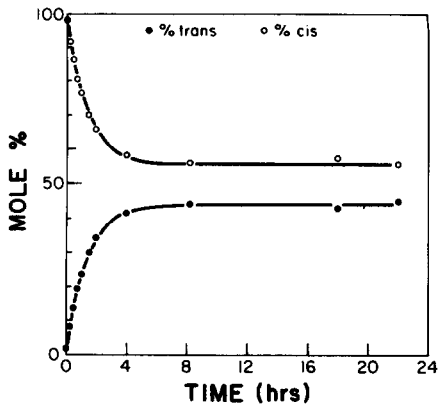

Fig. 1. Isomerization of *cis*-$Cr(PF_3)_2(CO)_4$ at 100°C.

The assumption that the thermal isomerization occurs by an intramolecular process is confirmed by ^{13}C studies. The *trans*-diphosphines of both chromium and tungsten isomerize to the *cis* isomer in the presence of 90% labelled ^{13}CO, without any incorporation of the label into the product. The size of the ^{13}CO peaks in the IR spectrum of the isolated isomer did not increase above natural abundance, indicating no bond breakage. The samples for the ^{13}C exchange were placed in containers of larger volume than the regular samples and existed primarily in the gas phase. Therefore, the solubility of CO in the liquid phase is not of concern. However, the same systems in the presence of UV light yield both isomerization and substitution products, all containing extensive ^{13}CO incorporation.

The rates of isomerization for chromium and tungsten were analysed as opposing first-order reactions, as in eq. (1), in which $K_{eq} = k_1/k_{-1} = [trans]/[cis]$.

$$cis\text{-}M(PF_3)_2(CO)_4 \underset{k_{-1}}{\overset{k_1}{\rightleftharpoons}} trans\text{-}M(PF_3)_2(CO)_4. \quad (1)$$

The integrated rate equation[11] is:

$$\ln \frac{C_e}{C_e - C} = (k_1 + k_{-1})t, \quad (2)$$

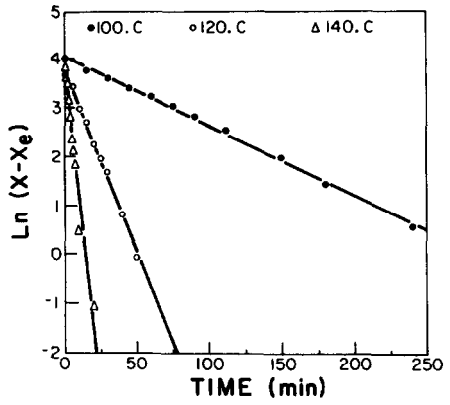

Fig. 2. Natural log of $C - C_e$ vs t for *trans*-$Cr(PF_3)_2(CO)_4$.

where C_e is the concentration of *cis* or *trans* at equilibrium and C is the concentration of *cis* or *trans* at any time t. A plot of $\ln(C - C_e)$ vs t should be linear, the slope being equal to the sum of the rate constants. Figure 2 illustrates these plots for *trans* to *cis* isomerization of $Cr(PF_3)_2(CO)_4$ at 100°C. This plot is shown to illustrate that the reactions are first-order and reversible. A model, $C = C_e \exp[-(k_1 + k_{-1})t] + C_e$ [exponential form of eq. (2)], was fitted to the kinetic data for *cis*- and *trans*-$M(PF_3)_2(CO)_4$ for the chromium and tungsten compounds. The model was fit to the data using a BASIC Simplex iterative routine. Simplex is known to be an excellent method of curve fitting. The BASIC program used was an adaptation of the PASCAL version by Cacerci and Cacheris.[12] The equilibrium concentration, C_e, and the sum of the rate constants were the adjustable parameters. The results of the program were used to calculate k_1 and k_{-1} from the known K_{eq}. The results are listed in Table 1.

Table 1 gives the sum of the rate constants, the equilibrium ratio of *cis–trans*, and the forward and reverse rate constants for chromium and tungsten disubstituted metal carbonyls at three temperatures. The rates increase smoothly with increasing temperature. The rate for the *cis–trans* isomerization (k_1) is 1.5–2 times faster than the reverse *trans–cis* isomerization (k_{-1}) for a given metal. For example, the ratio of k_1/k_{-1} for tungsten is 2.0, 2.1 and 2.2 at 100, 120, 140°C, respectively. This is also equal to K_{eq}. The equilibrium constant increases only slightly with increasing temperature. The equilibrium constant, and therefore the relative *cis* concentrations, increases from chromium to tungsten reflecting the relative sizes of the metals. The average K_{eq} for chromium is 1.36 and for tungsten is 2.09.

Activation parameters of chromium and tungsten were calculated from the plots of $\ln k$ vs $1/t$ illustrated in Fig. 3 and are reported in Table 2. The entropies for chromium and tungsten are negative, indicating that the transition state is more ordered than the ground state. These data are similar to those of Darensbourg for the intramolecular isomerization of $Mo((PBu)_3)_2(CO)_4$.[5] He observed negative entropies and a $\Delta H^{\ddagger}$ of ~ 24 kcal mol^{-1} for this complex.

The thermodynamic equilibrium concentrations

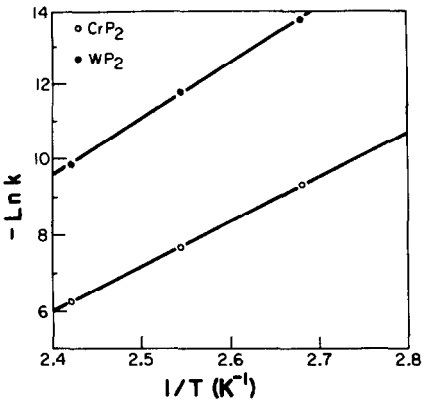

Fig. 3. Natural log of the rate constant vs reciprocal time for *trans–cis* isomerization.

Table 1. Rate constants and K_{eq} for isomerization of $M(PF_3)_2(CO)_4$, where M = Cr and W

	Temperature (°C)	$(k_1 + k_{-1}) \pm \sigma$ (h^{-1})	K_{eq} *cis–trans*	$k_1 \pm \sigma$ ($\times 10^6\ s^{-1}$)	$k_{-1} \pm \sigma$ ($\times 10^6\ s^{-1}$)
CrP_2	100	0.739±0.047	1.29	115±7	89±6
	120	3.795±0.064	1.38	610±9	442±9
	140	16.60±0.738	1.41	2697±120	1912±85
WP_2	100	0.011±0.001	1.95	2±1	1±1
	120	0.081±0.002	2.10	15±1	7±1
	140	0.569±0.020	2.23	109±4	49±2

Table 2. Activation parameters[a] for isomerization of $M(PF_3)_3(CO)_4$, where M = Cr and W

	cis–trans		*trans–cis*	
Compound	$\Delta H^{\ddagger}$	$\Delta S^{\ddagger}$	$\Delta H^{\ddagger}$	$\Delta S^{\ddagger}$
CrP_2	23.3±0.1	−14.5±0.1	22.6±0.1	−16.8±0.3
WP_2	29.9±0.6	−5.0±1.6	28.6±0.8	−9.8±2.1

[a] Enthalpy in kcal mol^{-1}; entropy in eu.

of the *cis* and *trans* isomers appear to be a combination of steric and electronic contributions. Metal carbonyls disubstituted with phosphine prefer the *trans* configuration when steric effects alone are considered. Indeed, many of the bulkier phosphine ligands are known to yield complexes that exist only in the *trans* form.[7,13] If the electronic effects are considered alone then the complex prefers the *cis* configuration due to a *trans* effect. Rather than one CO competing with another CO for electron density from the metal *d* orbitals, CO prefers to reside *trans* to a poorer π-bonding acceptor making the carbonyls *cis* to one another. The experimental findings which result from those two effects can be seen in Table 3. The table combines our data with those of Howell.[7] Listed in that table are the K_{eq} values for the *cis–trans* isomerization of several chromium and tungsten phosphine and phosphite complexes. The smaller the ligand cone angle, the larger the proportion of *cis* at equilibrium. Further, the larger the metal atom (W > Cr), the larger the concentration of *cis*. For chromium and a ligand having a cone angle of 130°, there is very little *cis* isomer present. As the cone angle decreases to 104° for PF_3, the *cis* form becomes the preferred isomer, with a K_{eq} of 1.36 at 100°C. The *cis–trans* ratios for the larger tungsten are 2.09. Strictly random isomerization would yield a K_{eq} of 4 (12 *cis* combinations, compared to three *trans*) if no electronic or steric effects were present.

Table 3. K_{eq} for *cis–trans* isomerization for some phosphines and phosphites of $M(PF_3)_2(CO)_4$, where M = Cr or W

	K_{eq} (*cis–trans*)		
Ligand	Cr	W	Cone angle[a]
P(*n*-Bu)$_3$	0.02[b]	0.11[b]	130
$P(OPh)_3$	0.07[b]	0.29[b]	121
$P(OCH_3)_3$	0.2[b]	0.98[b]	107
PF_3	1.36±0.06[c]	2.09±0.14[c]	104

[a] Data from ref. 10.
[b] Data from ref. 7.
[c] This work.

This study supports the previous findings of Darensbourg,[5] Howell[7] and others, proving that intramolecular processes offer the lowest energy pathway for isomerization of chromium and tungsten carbonyls disubstituted with phosphine ligands. This work adds to the small but growing body of literature on intramolecular octahedral isomerizations. It is clear that the coordination sphere of d^6 metals is not rigid. The reaction of the bis(trifluorophosphine) molybdenum carbonyls is not as straightforward as the chromium and tungsten compounds. Isomerization and substitution/ligand scrambling reactions occur simultaneously under identical reaction conditions. While the ligand scrambling must occur via an intermolecular route, the isomerization products appear to occur via both inter- and intramolecular routes. The different reaction chemistry for molybdenum bis(trifluorophosphine) carbonyl compounds is being studied.[14]

The disubstituted carbonyl complexes are not the only compounds thought to be fluxional. Experiments on scrambling of ^{13}CO in *cis*-$M(CO)_4(^{13}CO)(P(OMe)_3)$ (M = Cr, Mo and W) indicate that site exchange occurs for the $M(CO)_5PR_3$ species as well.[4,15] The exchange was intramolecular for chromium and tungsten and dissociative for molybdenum, similar to our results. Preliminary studies on the meridional and facial isomers of the triphosphines, $M(PF_3)_3(CO)_3$, show the same type of thermal reactions as found with the diphosphines.[14]

REFERENCES

1. (a) E. L. Muetterties, *J. Am. Chem. Soc.* 1968, **90**, 5097; (b) E. L. Muetterties, *Accts Chem. Res.* 1970, **3**, 266.
2. (a) F. N. Tebbe, P. Meakin, J. P. Jesson and E. L. Muetterties, *J. Am. Chem. Soc.* 1970, **92**, 1068; (b) P. Meakin, L. J. Guggenberger, J. P. Jesson, D. H. Gerlach, F. N. Tebbe, W. G. Peet and E. L. Meut-

terties, *J. Am. Chem. Soc.* 1970, **92**, 3482; (c) P. Meakin, E. L. Meutterties, F. N. Tebbe and J. P. Jesson, *J. Am. Chem. Soc.* 1971, **93**, 4701.
3. R. K. Pomeroy and W. A. G. Graham, *J. Am. Chem. Soc.* 1972, **94**, 274 and other papers.
4. D. J. Darensbourg and B. J. Baldwin, *J. Am. Chem. Soc.* 1979, **101**, 6447.
5. D. J. Darensbourg, *Inorg. Chem.* 1979, **18**, 14.
6. D. J. Darensbourg and R. L. Gray, *Inorg. Chem.* 1984, **23**, 2993.
7. D. T. Dixon, J. C. Kola and J. A. S. Howell, *J. Chem. Soc., Dalton Trans.* 1984, 1307.
8. B. D. Dombek and R. J. Angelici, *J. Am. Chem. Soc.* 1976, **98**, 4110.
9. (a) E. L. Denham, PhD Dissertation. Florida State University, Tallahassee (1985); (b) E. L. Denham and R. J. Clark, *J. Chromatogr.* 1984, **301**, 253.
10. W. D. Scott, *Electronics World* 1964, Nov., 46.
11. J. W. Moore and R. G. Pearson, *Kinetics and Mechanism*, 3rd edn, p. 304. Wiley-Interscience, New York (1981).
12. M. S. Caceci and W. P. Cacheris, *Byte* 1984, May, 340.
13. J. A. S. Howell and P. M. Burkinshaw, *Chem. Rev.* 1983, **83**, 557.
14. T. G. Berger, R. J. Clark and L. D. Bottomley, manuscript in preparation.
15. D. J. Darensbourg, B. J. Baldwin and J. A. Froelich, *J. Am. Chem. Soc.* 1980, **102**, 4688.

Polyhedron Vol. 8, No. 17, pp. 2131–2137, 1989
Printed in Great Britain

0277–5387/89 $3.00+.00
© 1989 Pergamon Press plc

EXCHANGE INTERACTIONS IN CARBOXYLATE-BRIDGED ALTERNATING CHAINS OF COPPER(II). SYNTHESIS, CRYSTAL STRUCTURE, SPECTROSCOPIC AND MAGNETIC PROPERTIES OF CATENA-BIS(N-SALICYLIDENE-L-METHIONINATO)AQUADICOPPER(II)

M. S. PALACIOS,‡ E. MEDINA and F. G. MANRIQUE

Departamento de Química Inorgánica, Universidad de La Laguna, 38200 La Laguna, Tenerife, Spain

and

M. T. do P. GAMBARDELLA and R. H. de A. SANTOS

Instituto de Física e Química de São Carlos, Universidade de São Paulo, São Paulo, Brazil

and

M. L. RODRIGUEZ

Instituto Universitario de Química Orgánica, Universidad de La Laguna, Tenerife, Spain

and

J. M. DANCE

Laboratoire de Chimie du Solide du CNRS, Université de Bordeaux I, France

(*Received* 15 *July* 1988; *accepted after revision* 5 *April* 1989)

Abstract—The synthesis, crystal structure, spectroscopic and magnetic properties are reported for catena-bis(N-salicylidene-L-methioninato)aquadicopper(II), Cu-SALENMET. The compound crystallizes in the orthorhombic space group $P2_12_12_1$, with $Z = 4$. Lattice constants: $a = 5.077(1)$, $b = 13.229(1)$, $c = 37.602(2)$ Å, and $V = 2525(8)$ Å^3. Least-squares refinement of 171 parameters led to a final $R = 0.052$ for 1208 independent reflections having $I > 3\sigma(I)$. The asymmetric unit consists of two copper atoms and two SALENMET (N-salicylidene-L-methioninato) groups. Each metal atom is directly attached to a single SALENMET group. The first of the two copper atoms has a (4+2) tetragonally elongated coordination geometry. The SALENMET group directly attached to it and the oxygen atom of a coordinated water molecule occupy four of the coordination sites. The coordination sphere is completed by two carboxylic oxygen atoms, one belongs to a SALENMET group of an adjacent ($x-1$, y, z translation) asymmetric unit and the other belongs to the SALENMET group which is directly attached to the other copper atom within the asymmetric unit. This second copper atom has a (4+1) tetragonally elongated square pyramidal coordination geometry. Three of the coordination sites are occupied by the SALENMET group directly attached to it, one of them by the last above mentioned carboxylic oxygen atom. In this way, this oxygen atom is coordinated to both copper atoms within the asymmetric unit and the two SALENMET groups become linked through a Cu—O—Cu bridge. The coordination sphere is completed by two carboxylic

‡ Author to whom correspondence should be addressed.

oxygen atoms which belong to SALENMET groups of an adjacent asymmetric unit ($x-1$, y, z translation). The crystal structure consists of discrete polymeric units generated only by translation along the crystallographic a axis. The polymeric units are built by bonds through adjacent asymmetric units as described above. Magnetic susceptibility data reveal antiferromagnetic interactions that may be described by the Heisenberg alternating-chain theory. The best fit of the magnetic susceptibility data yields values for the exchange coupling constant and alternation parameter (J, α) of -62.9 cm^{-1} and 0.58, respectively.

A previous report[1] described the synthesis and spectroscopic properties of an anhydrous Cu^{II} compound with a Schiff base derived from salicylaldehyde and L-methionine having the empirical formula $CuSNO_3C_{12}H_{13}$ which exhibits magnetic susceptibility data that may be described by the Heisenberg dimer model.[2] Starting from this anhydrous compound, we have prepared the hydrated catena-bis(N-salicylidene-L-methioninato)aquadicopper(II), Cu-SALENMET, which is a good example of alternating Heisenberg exchange coupled S = 1/2 chains. The synthesis, crystal structure, spectroscopic properties and results of magnetic measurements are discussed in this article.

EXPERIMENTAL

Synthesis

All chemicals were reagent grade and used as received. Cu-SALENMET was prepared by the following general method: salicylaldehyde (0.05 mol) was dissolved in 400 cm^3 of ethanol; the amino acid (0.05 mol) was dissolved in a minimum quantity of water and added dropwise, with stirring, to the salicylaldehyde solution. Copper(II) acetate monohydrate (0.05 mol) was then dissolved in 200 cm^3 of water and added dropwise to the Schiff base solution. After the mixture was refluxed at 80°C overnight, a bright green precipitate was collected and dried *in vacuo*. Successive recrystallizations from aqueous ethanolic solutions of the bright green powder, characterized as the anhydrous $CuSNO_3C_{12}H_{13}$ complex, produced fine dark green needles. The compound was collected by filtration and dried in air. Cu-SALENMET is soluble in most common organic solvents. Found: C, 44.5; H, 4.3; N, 4.3; Cu, 19.6. Calc. for $CuSNO_{3.5}C_{12}H_{14}$: C, 44.5; H, 4.4; N, 4.3; Cu, 19.6%.

Chemical analyses of C, H and N were determined with a Carlo Erba 1106 elemental analyser. Copper analyses were carried out by atomic absorption with a Perkin–Elmer 305 apparatus.

Crystallographic data collection and refinement of the structure

An examination of the crystal by precession methods established that the compound crystallizes in the orthorhombic system. The space group $P2_12_12_1$ was confirmed by the structure solution. The dark green crystal used for intensity measurements with approximate dimensions $0.6\times0.35\times0.05$ mm was mounted on a glass fibre approximately along the crystallographic a axis. The six faces were identified as belonging to {100}, {001} and {010}. The lattice constants, determined by least-squares calculation based on the setting angles of 25 automatic centred reflections on an CAD-4 Enraf Nonius diffractometer, equipped with graphite monochromated Mo-K_α radiation ($\lambda = 0.71073$ Å), are: $a = 5.077(1)$, $b = 13.229(1)$, $c = 37.602(2)$ Å; $V = 2525(8)$ Å^3; $Z = 4$. The calculated density for four formula units of $Cu_2N_2S_2O_7C_{24}H_{28}$ (mol wt = 647.71) in the unit cell is 1.772 g cm^{-3}. The intensity data were collected in the range $0° < 2\theta < 50°$; the ω-2θ scan technique was employed, with a take-off angle of 1.2°. The reflections were scanned at 1° min^{-1} in zig-zag mode. The intensities of three standards reflections were measured every hour and showed no significant variations during data collection. A total of 2598 independent reflections were measured (at 22°C); of these, 1208 were found having $I > 3\sigma(I)$ and used in the solution and refinement of the structure. Data were corrected for Lorentz and polarization effects but not for absorption ($\mu = 18.35$ cm^{-1} for Mo-K_α).

The copper and sulphur atoms were located from a Patterson synthesis. Least-squares of these four atoms followed by a difference Fourier synthesis revealed the position of the oxygen and nitrogen atoms. The remaining non-hydrogen atom coordinates were obtained on a subsequent difference Fourier map. The hydrogen atoms were included in the final refinement model at their calculated positions (C—H = 1.08 Å) with overall isotropic parameter $U = 0.06$ Å^2.

The final full-matrix least-squares refinement with anisotropic thermal parameters for non-

Table 1. Fractional atomic coordinates and equivalent isotropic temperature factors,[4] with ESDs in parentheses for Cu-SALENMET

Atom	x/a	y/b	z/c	B_{eq} (Å^2)
Cu(1′)	−0.2283(5)	0.2778(1)	0.6093(1)	1.42(7)
O(1′)	0.102(2)	0.2669(8)	0.6405(3)	2.3(4)
O(2′)	0.460(2)	0.3576(8)	0.6545(3)	3.4(4)
O(3′)	−0.493(2)	0.2848(9)	0.5742(3)	3.1(4)
S(1′)	−0.107(1)	0.7041(4)	0.6683(2)	5.1(2)
N(1′)	−0.069(3)	0.4034(9)	0.5959(4)	2.6(2)
Cu(1)	0.2659(6)	0.1334(1)	0.6566(1)	1.66(7)
O(1)	0.590(3)	0.1550(7)	0.6282(3)	2.8(4)
O(2)	0.945(3)	0.0771(9)	0.6045(3)	4.0(5)
O(3)	−0.007(3)	0.1063(9)	0.6896(3)	3.6(5)
N(1)	0.404(3)	−0.005(1)	0.6574(4)	2.5(5)
S(1)	0.209(2)	−0.2246(4)	0.5632(1)	5.5(2)
O(W)	0.536(4)	0.210(1)	0.7033(4)	7.9(8)
C(1′)	0.245(5)	0.347(1)	0.6385(5)	2.8(6)
C(2′)	0.138(4)	0.439(1)	0.6200(5)	3.0(7)
C(3′)	0.025(4)	0.509(1)	0.6497(5)	3.8(8)
C(4′)	−0.099(5)	0.604(1)	0.6349(5)	4.5(8)
C(5′)	−0.307(5)	0.652(2)	0.7028(6)	6.0(1)
C(6′)	−0.124(4)	0.452(1)	0.5660(5)	2.3(6)
C(7′)	−0.311(4)	0.425(1)	0.5406(5)	3.2(7)
C(8′)	−0.336(4)	0.486(1)	0.5100(5)	3.2(7)
C(9′)	−0.518(5)	0.468(2)	0.4849(5)	3.5(8)
C(10′)	−0.700(4)	0.386(2)	0.4896(5)	4.0(8)
C(11′)	−0.681(4)	0.328(1)	0.5198(4)	3.0(7)
C(12′)	−0.493(4)	0.343(1)	0.5467(4)	2.9(7)
C(1)	0.728(5)	0.075(1)	0.6198(4)	3.0(7)
C(2)	0.601(4)	−0.024(1)	0.6309(4)	2.5(6)
C(3)	0.487(4)	−0.071(1)	0.5957(4)	2.3(6)
C(4)	0.343(4)	−0.169(1)	0.6030(5)	4.3(8)
C(5)	0.498(5)	−0.254(2)	0.5376(6)	8.0(1)
C(6)	0.365(4)	−0.069(1)	0.6831(5)	3.2(7)
C(7)	0.160(3)	−0.055(1)	0.7088(5)	2.3(6)
C(8)	0.140(4)	−0.133(1)	0.7352(4)	3.3(7)
C(9)	−0.042(5)	−0.137(2)	0.7604(6)	5.1(9)
C(10)	−0.225(5)	−0.056(2)	0.7622(5)	4.2(8)
C(11)	−0.206(4)	0.025(2)	0.7387(5)	4.0(8)
C(12)	−0.019(4)	0.027(1)	0.7125(5)	3.0(7)

hydrogen atoms and fixed isotropic hydrogen contribution converged to $R = 0.052$ and $R_w = 0.049$ (for 171 parameters and 1208 observed reflections). The function minimized was $\Sigma_w(|F_o|-|F_c|)^2$, and $w = [\sigma^2(F_o)+0.00073F_o^2]^{-1}$. Anomalous dispersion terms and atomic scattering factors were taken from ref. 3. The final atomic positional parameters and equivalent isotropic temperature factors[4] for the non-hydrogen atoms are listed in Table 1. All calculations were performed with the SHELX-76 package of programs.[5]‡

‡ Listings of observed and calculated structure factors, anisotropic thermal parameters, hydrogen atom coordinates, and bond lengths and angles pertaining to the ligand are available as supplementary material.

Electronic, infrared and EPR spectroscopies

The diffuse reflectance spectrum in the 300–900 nm region was carried out on a Beckman DU-2 spectrophotometer after dilution of the sample in $BaSO_4$. The IR spectrum was recorded with a Perkin–Elmer 681 spectrophotometer in KBr pellets as support, in the 625–4000 cm^{-1} spectral range. The room and low temperature EPR spectra were recorded on a Bruker X-band ER 200D spectrometer using a 100 kHz modulation.

Magnetic susceptibility measurements

The magnetic susceptibility data were measured on powdered samples on a Faraday type micro-

balance between 4.2–308 K. The data were corrected for the diamagnetism of the ligand system and for the temperature independent paramagnetism (taken to be 60×10^{-6} emu mol^{-1}). The correction for the diamagnetism was estimated by use of Pascal's constants[6] and found to be -180×10^{-6} emu mol^{-1}.

RESULTS AND DISCUSSION

Description of the structure

Tables 2 and 3 contain the interatomic distances and angles relevant to the copper coordination spheres, respectively. The asymmetric unit, shown in Fig. 1, consists of a dimeric part which includes two copper atoms and two SALENMET groups (where SALENMET is the N-salicylidene-L-methioninato group). Each copper atom is directly attached to a single SALENMET group and linked through a carboxylic oxygen atom O(1′). Both copper centres have four relatively short bonding interactions and additional longer contacts. The Cu(1) atom is bonded to O(1), O(3) and N(1) of the SALENMET group directly attached to it and to an oxygen atom O(W) from a water molecule. The coordination sphere is completed by two carboxylic oxygen atoms, one [O(2)] belonging to an adjacent ($x-1$, y, z translation) asymmetric dimeric unit, and the remaining [O(1′)] belonging to the SALENMET group which is directly attached to the second copper atom within the asymmetric unit. The equa-

Table 2. Interatomic distances (Å) relevant to the copper coordination spheres, with ESDs in parentheses for Cu-SALENMET

Cu(1′)—O(1′)	2.05(1)	Cu(1)—O(1′)	2.04(1)
Cu(1′)—O(3′)	1.89(1)	Cu(1)—O(3)	1.89(1)
Cu(1′)—N(1′)	1.92(1)	Cu(1)—N(1)	1.96(1)
Cu(1′)—O(1)*	2.00(1)	Cu(1)—O(1)	1.98(1)
Cu(1′)—O(2′)*	2.55(1)	Cu(1)—O(2)	2.65(1)
Cu(1′)—Cu(1)	3.621(4)	Cu(1)—O(W)	2.45(2)
Cu(1′)—O(2)*	2.80(1)	Cu(1′)—Cu(1)*	3.662(3)

* $x-1$, y, z symmetry.

Table 3. Interatomic angles (deg) relevant to the copper coordination spheres, with ESDs in parentheses for Cu-SALENMET

O(1′)—Cu(1′)—O(2′)*	98.9(4)	O(1′)—Cu(1)—O(1)	93.1(5)
O(1′)—Cu(1′)—O(3′)	170.4(5)	O(1′)—Cu(1)—O(2)*	76.9(4)
O(1′)—Cu(1′)—N(1′)	82.3(5)	O(1)—Cu(1)—O(3)	170.9(5)
O(1′)—Cu(1′)—O(1)*	96.7(4)	O(1′)—Cu(1)—O(3)	93.4(5)
O(2′)*—Cu(1′)—O(3′)	90.2(4)	O(1′)—Cu(1)—N(1)	163.1(5)
O(2′)*—Cu(1′)—O(1)*	79.2(4)	O(1′)—Cu(1)—O(W)	94.8(5)
O(3′)—Cu(1′)—N(1′)	94.3(5)	O(1)—Cu(1)—O(2)*	98.8(4)
O(3′)—Cu(1′)—O(1)*	87.7(5)	O(1)—Cu(1)—N(1)	81.1(5)
N(1′)—Cu(1′)—O(1)*	173.4(5)	O(1)—Cu(1)—O(W)	82.1(5)
O(2′)*—Cu(1′)—N(1′)	94.5(5)	O(2)*—Cu(1)—O(3)	88.9(5)
O(1′)—Cu(1′)—O(2)*	73.4(4)	O(2)*—Cu(1)—N(1)	88.2(5)
O(2′)*—Cu(1′)—O(2)*	129.0(4)	O(2)*—Cu(1)—O(W)	171.7(5)
O(3′)—Cu(1′)—O(2)*	103.0(4)	O(3)—Cu(1)—N(1)	94.3(6)
N(1′)—Cu(1′)—O(2)*	132.2(5)	O(3)—Cu(1)—O(W)	91.0(5)
O(1)*—Cu(1′)—O(2)*	53.0(4)	N(1)—Cu(1)—O(W)	100.1(6)
Cu(1′)—O(1′)—Cu(1)	124.3(5)	Cu(1′)†—O(1)—Cu(1)	133.8(6)
Cu(1′)—N(1′)—C(2′)	115(1)	Cu(1)—N(1)—C(2)	114(1)
Cu(1′)—N(1′)—C(6′)	124(1)	Cu(1)—N(1)—C(6)	124(1)
Cu(1′)—O(1′)—O(2′)	139.4(6)	Cu(1)—O(1)—O(2)	144.0(7)
Cu(1′)—O(1′)—C(1′)	112(1)	Cu(1)—O(1)—C(1)	117(1)
Cu(1′)—O(3′)—C(12′)	126(1)	Cu(1)—O(3)—C(12)	126(1)
Cu(1′)†—O(1)—C(1)	109(1)		

* $x-1$, y, z symmetry; † $1+x$, y, z symmetry.

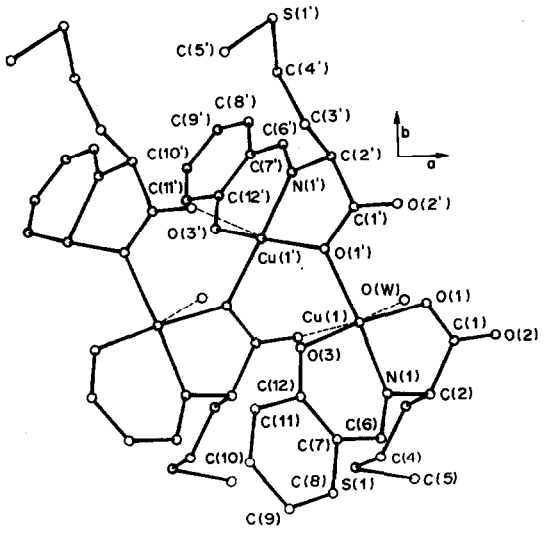

Fig. 1. ORTEP drawing of the molecular packing arrangement in Cu-SALENMET, showing the contacts between adjacent asymmetric dimeric units related through the symmetry operation $x-1, y, z$. Unlabelled atoms are related to the labelled atoms by the symmetry operation.

torial plane of this tetragonally elongated octahedron is made up of atoms O(1), O(3), N(1) and O(1′). As shown in Table 4, the deviation of these atoms from the mean plane is −0.203, −0.186, 0.209 and 0.180 Å, respectively. The displacement of Cu(1) with respect to the mean plane of the O(1)O(3)N(1)O(1′) entity is −0.074 Å, being less than those of the plane determining atoms. In the equatorial plane the coordination bond lengths vary for Cu(1)—O bonds from 1.89(1) to 2.04(1) Å, while the Cu(1)—N bond length is 1.96(1) Å. The axial Cu(1)—O(W) and Cu(1)—O(2)* (* = $x-1, y, z$ translation) bond lengths are 2.45(2) and 2.65(1) Å, respectively.

The second copper atom in the asymmetric unit, Cu(1′), is bonded to O(1′), O(3′) and N(1′) of the SALENMET group directly attached to it. The O(1′) atom is coordinated to both copper atoms within the asymmetric unit in such a way that the two SALENMET groups become linked through a Cu(1)—O(1′)—Cu(1′) bridge. The coordination sphere around Cu(1′) is completed by two carboxylic oxygen atoms belonging to SALENMET groups of an adjacent ($x-1, y, z$ translation) asymmetric dimeric unit, O(1)* and O(2)*. The equatorial plane of this tetragonally elongated square pyramid is made up by the atoms O(1′), O(3′), N(1′) and O(1)*, with the deviations of these atoms from the mean plane being 0.126, 0.132, −0.136 and −0.122 Å, respectively (Table 4). The displacement of Cu(1′) from the mean plane of the O(1′)O(3′)N(1′)O(1)* entity is only −0.020 Å. The equatorial coordination bond lengths vary for Cu(1′)—O bonds from 1.89(1) to 2.05(1) Å, whilst

Table 4. Least-squares planes through selected atoms and deviations of atoms from the planes for Cu-SALENMET

(a) Deviations (Å) from the planes

Plane 1	O(1′) [0.126], O(3′) [0.132], N(1′) [−0.136], O(1)* [−0.122], ‡Cu(1′) [−0.020], ‡O(2)* [1.952]
Plane 2	O(1) [−0.203], O(3) [−0.186], N(1) [0.209], O(1′) [0.180], ‡Cu(1) [−0.074], ‡O(W) [−2.512], ‡O(2)* [2.557]
Plane 3	O(2)* [0.000], O(W) [0.000], O(1) [0.000]; ‡Cu(1) [−0.182], ‡N(1) [−2.064], ‡O(1′) [1.821]
Plane 4	O(W) [−0.065], O(2)* [−0.073], N(1) [0.064], O(1′) [0.074], ‡Cu(1) [−0.070], ‡O(1) [1.881], ‡O(3) [−1.964]

(* $x-1, y, z$ symmetry; ‡ atoms not included in the plane calculation)

(b) Equation of the planes

Plane	A	B	C	D
1	0.5150	−0.5260	−0.6768	−18.0161
2	−0.5173	−0.3652	−0.7740	−20.3778
3	−0.2236	0.9384	−0.2635	−4.9697
4	0.7187	0.1912	−0.6686	−15.1287

(The equation of the planes is of the form $Ax+By+Cz-D=0$)

(c) Dihedral angles (deg) between selected planes

Planes	
2–3	−88.7
2–4	85.6
3–4	78.8

the Cu(1′)—N bond length is 1.92(1) Å. The axial Cu(1′)—O(2′)* distance is 2.55(1) Å. The O(2) atom from a SALENMET group of an adjacent ($x-1$, y, z translation) asymmetric dimeric unit located at 2.80(1) Å gives a severely distorted octahedron, with interatomic angles N(1′)—Cu(1′)—O(2)* and O(1)*—Cu(1′)—O(2)* of 132.2(5) and 53.0(4)°, respectively. The contacts between adjacent asymmetric dimeric units are shown in Fig. 1.

Defining the coordination numbers of each copper atom may be a matter for personal choice, but rigorously in terms of strongly bound ligands, four-coordination would be appropriate.

The bond lengths and angles around the metal atoms are in fairly good agreement with the values given for Cu^{II} complexes with Schiff bases derived from salicylaldehyde and L-glycine,[7] L-tyrosine[8] and L-phenylalanine.[9]

The crystal structure of Cu-SALENMET consists of discrete polymeric units generated only by translation along the crystallographic a axis. The polymeric units are built by the bonds through adjacent asymmetric dimeric units as described above. As shown in Fig. 1, adjacent asymmetric dimeric units are connected via the carboxylic oxygen atoms O(2′), O(1) and O(2), through Cu(1)—O(2)*—C(1)*—O(1)*—Cu(1)*, Cu(1′)—O(1)*—Cu(1)* and Cu(1′)—O(2′)*—C(1′)*—O(1′)*—Cu(1′)* bridges.

The Cu(1)—Cu(1′) distance within the asymmetric unit is 3.621(4) Å, whilst the Cu(1′)—Cu(1)* separation between adjacent asymmetric units is 3.662(3) Å. The Cu(1)—O(1′)—Cu(1′) bridge angle is 124.3(5)°, whilst the bridge angle between adjacent asymmetric units Cu(1′)†—O(1)—Cu(1) († = $1+x$, y, z translation) is 133.8(6)°.

Other structural features of the asymmetric dimeric unit are the O(1)—C(1)—O(2) and O(1′)—C(1′)—O(2′) angles of 124(1) and 125(1)°, respectively, and the C(1′)—O(1′)—Cu(1′) and C(1)—O(1)—Cu(1) angles involving equatorial oxygen atoms of 112(1) and 117(1)°, respectively. The Cu(1)—O(1′)—C(1′)—O(2′)—Cu(1′)† and Cu(1)—O(1)—C(1)—O(2)—Cu(1)† bridge adjacent asymmetric units lengths are 7.13 and 7.38 Å, respectively.

All the intramolecular bond distances and angles in the SALENMET groups fall in the normal range. All the interpolymeric separations are greater than 4 Å.

Electronic, infrared and EPR spectroscopies

The room temperature diffuse reflectance spectrum exhibits a maximum centred around 680 nm; its shape and *d–d* band position agree with those reported for octahedral and square pyramidal Cu^{II} stereochemistries. A shoulder at 480 nm, of similar intensity to the former, has been previously associated with tetragonally distorted octahedral Cu^{II} environments.[10] In agreement with the structural data, the IR spectrum of Cu-SALENMET shows a broad band around 3400 cm^{-1} which is assignable to ν(O—H) vibrations of the coordinated water molecule. A broad and strong band around 1660–1595 cm^{-1} may be attributed to ν(C=N), asymmetric ν(OCO) and phenyl ring stretching vibrations. The ν(C—O) band must be that appearing at 1520 cm^{-1}.

The room temperature X-band EPR spectrum of a powdered sample of the compound shows only one broad (peak to peak separation *ca* 500 G) signal centred at $g = 2.12$. Lowering the temperature of the sample to 4.2 K has no effect on the shape of the signal which decreases in intensity.

Magnetic properties

The experimental corrected magnetic susceptibilities are shown graphically in Fig. 2. The rounded maximum around 116 K indicates the presence of antiferromagnetic interactions. An attempt to fit the susceptibility curve to the classical Heisenberg dimer model was unsuccessful as well as a fitting using the Bonner and Fisher chain model.[11] The structure of Cu-SALENMET and the possibility of various exchange pathways led us to use the alternating linear chain model studied by Duffy

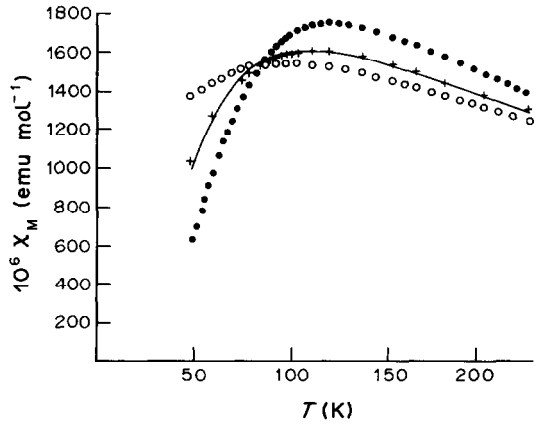

Fig. 2. Magnetic susceptibility data versus temperature for Cu-SALENMET. The solid line through the data was generated by the expression given in the text for Heisenberg exchange in an alternating chain with an exchange coupling of -62.9 cm^{-1}, and an alternation parameter of 0.58. The "best fit" to the data obtained for (●) $\alpha = 0$ ($2J = -73.4$ cm^{-1}, $g = 2.22$ and $\theta = -96$ K) and (○) $\alpha = 1$ ($J = -54.8$ cm^{-1} and $g = 2.13$) are also shown.

and Barr[12] and more recently by Hatfield.[13] The Hamiltonian for the Heisenberg alternating linear chain may be written as:

$$H = -2J \sum_{i=1}^{n/2} (\hat{S}_{2i}\hat{S}_{2i} + \alpha \hat{S}_{2i}\hat{S}_{2i+1}),$$

where J is the exchange integral between a spin and one of its nearest neighbours, and αJ is the exchange integral between that spin and its other nearest neighbour.

The temperature dependence of the magnetic susceptibility of Heisenberg alternating chains with $J < 0$ and $1 \geqslant \alpha \geqslant 0$ is given through an expression:[14]

$$\chi_M = Ng^2\mu_B^2/kT(A + Bx + Cx^2) \times (1 + Dx + Ex^2 + Fx^3)^{-1},$$

where $x = |J|/kT$, α is the alternation parameter, and the coefficients A to F are power series in terms of α.[13,14] The agreement factor $[\Sigma(\chi_{cal} - \chi_{obs})^2/\Sigma(\chi_{obs})^2]^2$ could be lowered down to 0.016 by using an alternation parameter $\alpha = 0.58$, an exchange integral $J = -62.9$ cm^{-1}, and a g-value equal to the EPR experimentally determined 2.12. The best agreement factors which could be reached for the dimer and uniform Heisenberg chain models were 0.034 and 0.070, respectively. Figure 2 shows the experimental points and the three calculated curves for $\alpha = 0$, $\alpha = 0.58$ and $\alpha = 1$.

The ability of the alternating linear chain model to describe the magnetic behaviour of Cu-SALENMET may be interpreted in terms of the different super-exchange pathways created by the crystallographic translation along the a axis. Between the Cu^{II} ions, the magnetic exchange can only occur via the $d_{x^2-y^2}$ orbitals which contain in the case of the elongated octahedral and square pyramidal stereochemistries the single electron, and the appropriate bridging atoms' orbitals. The different magnitude of the exchange integrals may be related to the structural data which implies not only the possibility of different super-exchange pathways (Cu—O—Cu or Cu—O—C—O—Cu) but also significant differences in the bonding distances and angles.

Finally, the comparison of the antiferromegnatic $|J|$ value for Cu-SALENMET with that observed for the anhydrous Cu^{II} compound which served as the starting material in the preparation of Cu-SALENMET, for which a presumable Cu^{II} acetate binuclear structure has been suggested,[1,2] with $2J = -339.2$ cm^{-1}, clearly indicates that the Cu^{II} ions within a pair are less coupled in the hydrated complex. Changes in the magnetic behaviour must be associated with the structural rearrangement during the hydration. It is unfortunate that it has not been possible to grow single crystals of the anhydrous species for an X-ray structural analysis.

Acknowledgement–M. S. Palacios thanks Professor P. Hagenmuller for his hospitality during her stay at the Laboratoire de Chimie du Solide du CNRS at Bordeaux.

REFERENCES

1. A. Mederos, F. G. Manrique and A. Medina, *An. Quim.* 1981, **77B**, 206.
2. M. S. Palacios, Doctoral Thesis, 1986, Departamento Química Inorgánica, Universidad de La Laguna, Tenerife, Spain.
3. D. T. Cromer and J. T. Waber, *International Tables for X-ray Crystalloraphy*. Kynoch Press, Birmingham (1974).
4. W. C. Hamilton, *Acta Cryst.* 1959, **12**, 609.
5. G. M. Sheldrick, SHELX-76, *Program for Crystallography Structure Determination*. University of Cambridge (1976).
6. P. W. Selwood, *Magneto Chemistry*. Interscience, New York (1956).
7. T. Ueky, T. Ashida, Y. Sasada and M. Kakudo, *Acta Cryst.* 1967, **B22**, 870.
8. R. Hämäläinen, M. Ahlgren, U. Turpeinen and M. Rantala, *Acta Chem. Scand.* 1978, **A32**, 235.
9. R. Hämäläinen, U. Turpeinen, M. Ahlgren and M. Rantala, *Acta Chem. Scand.* 1978, **A32**, 549.
10. D. E. Fenton, R. S. Nyholm and M. R. Truter, *J. Chem. Soc.* 1971, 1577.
11. J. C. Bonner and M. E. Fisher, *Phys. Rev.* 1964, **135**, 640.
12. W. Duffy and K. P. Barr, *Phys. Rev.* 1968, **165**, 647.
13. W. E. Hatfield, *J. Appl. Phys.* 1981, **52**, 1987.
14. J. W. Hall, W. E. Marsh, R. R. Weller and W. E. Hatfield, *Inorg. Chem.* 1981, **20**, 1033.

Polyhedron Vol. 8, No. 17, pp. 2139–2146, 1989
Printed in Great Britain

0277–5387/89 $3.00+.00
© 1989 Pergamon Press plc

CRYSTAL STRUCTURES AND SPECTROSCOPY STUDIES OF LANTHANIDE COMPLEXES WITH L-PROLINE $[Ln(L\text{-}proH)_2(H_2O)_5]Cl_3$ (Ln = Ho, Dy)

J. LEGENDZIEWICZ,* T. GŁOWIAK and E. HUSKOWSKA

Institute of Chemistry, University of Wrocław, 50 383 Wrocław, Poland

and

DAO CONG-NGOAN

Department of Chemistry, University of Hanoi, Hanoi, Vietnam

(*Received* 31 *October* 1988; *accepted after revision* 5 *April* 1989)

Abstract—The isomorphic crystals of dysprosium(III) and holmium(III) complexes with proline of formula $[Ln(C_5H_9NO_2)_2(H_2O)_5]Cl_3$ (compound **I** holmium; compound **II**, dysprosium) were synthesized and characterized by crystal structures and spectroscopic properties.

The space group is $P2_1$ with lattice parameters: **I** $a = 11.968(2)$, $b = 11.030(2)$, $c = 8.309(2)$ Å, $\beta = 106.97(3)°$; **II** $a = 11.968(4)$, $b = 11.038(4)$, $c = 8.302(2)$ Å, $\beta = 107.00(3)°$. The structures of the title compounds differ significantly from that of $[Nd(proH)_3(H_2O)_2](ClO_4)_3$, with different bonding modes for the proline ligands. The holmium and dysprosium structure contains one-dimensional polymers with the chains lying along the *y*-axis. Absorption spectra of the holmium monocrystal were measured along the *a*-axis at room temperature. Intensities of *f–f* transitions were analysed on the basis of Judd theory.

The influence of the bonding mode of the carboxyl group on the intensity of the $^5I_8 \rightarrow {}^5G_6$ hypersensitive transition of the Ho^{3+} ion was considered and confronted for all spectroscopy data available for holmium carboxylate monocrystals.

Spectroscopic properties of the lanthanides are widely used in the study of biomolecular structure. Applications include the different aspects of absorption and luminescence spectroscopy leading to determination of discrete equilibrium structures, binding of ligands by metal ions to molecular systems, and other structural factors as well. For that reason the study of the model systems of lanthanide ions with amino acids, simple peptides, is important for the understanding of more complicated systems.

In order to study the Ln^{3+} ion interaction with amino acids, the series of crystal structures of lanthanide(III) complexes were investigated.[1–8]

All the determined structures are in dimeric or polymeric form. The kind of polymer in these complexes depends significantly on the stoichiometric relations of Ln^{3+}–amino acid (Ln–A).[2,4,6] The bonding mode of carboxyl groups in lanthanide carboxylate seems to depend on the stoichiometric relations in complexes as well.[9,10] But even for the same bonding mode of the carboxyl group *syn–syn*, *syn–anti* and *anti–anti* forms can exist giving many significant, structural possibilities in bonding to the metal ions. The whole series of lanthanide ions are able to form isomorphic compounds[1,2] with amino acids; however these rules can be broken.[5,6]

Recently in our laboratory, crystals of a neodymium complex of formula $[Nd(C_5H_9NO_2)_3(H_2O)_2](ClO_4)_3$ were synthesized, where the proline molecules were bound with lanthanide ions by simple bridges of the Nd—O—C—O—Nd type and the structure consisted of linear polymers lying along the *z*-axis, similar to those in the neodymium(III) complex with glycine.[2,4]

* Author to whom correspondence should be addressed.

To investigate the problem of ion size dependence on the structure of complexes as well as on the kind of polymers, the studies were extended to the holmium(III) and dysprosium(III) complexes with proline.

EXPERIMENTAL

The crystals of dysprosium and holmium complexes were grown from the concentrated aqueous solutions of $HoCl_3$ and $DyCl_3$ at pH ~ 4, 0; the amino acid concentration was maintained well below the lanthanide concentration.

Monocrystals of dimension $\sim 0.20 \times 0.25 \times 0.45$ mm were selected for the data collections. A Syntex $P2_1$ diffractometer and Mo-K_α radiation with a graphite monochromator were used for lattice-parameter and intensity measurements. The intensities of reflections were measured by the $\theta/2\theta$ scan technique up to $2\theta_{max} = 55.0°$. The scan rate varied from 2.0 to 29.3° min^{-1}. The data were corrected for Lorentz, polarization and absorption effects; 2525 reflections (for **I**) and 2440 reflections (for **II**) with $I > 4.0\sigma(I)$ were used for the structure determinations. All calculations were performed using Syntex XTL programs[11] and scattering factors for neutral atoms were taken from the *International Tables for X-ray Crystallography* (1974).[12]

The structure of the holmium complex was solved by the heavy-atom method, whereas the structure analysis of the dysprosium complex was commenced using the position parameters of atoms in the holmium complex. Full-matrix least-squares refinements were terminated at $R = 0.033$ ($R_w = 0.050$) for **I** and at $R = 0.032$ ($R_w = 0.048$) for **II**.*

Absorption spectra of the $[Ho(L\text{-}proH)_2(H_2O)_5]Cl_5$ single crystal along the *a*-axis were recorded at room temperature in the region of 8000–40,000 cm^{-1} on the Cary 14 spectrophotometer. Oscillator strengths of *f–f* transitions were estimated by means of the integrating program ICH 30.

Based on the Judd–Ofelt theory,[13,14] the intensities of *f–f* transitions were analysed and values of Ω_λ parameters were calculated from the following relation:

$$P_{JJ'} = \chi(8\pi^2 mc/3h) \sum_{\lambda=2,4,6} \Omega_\lambda \times \langle f^N\psi J \| U^{(\lambda)} \| f^N\psi' J' \rangle^2 \times (2J+1)^{-1},$$

where $\langle f^N\psi J \| U^{(\lambda)} \| f^N\psi' J' \rangle$ is the reduced matrix element of the unit tensor operator of $U^{(\lambda)}$, Ω_λ are treated as phenomenological parameters that may be derived from the experimental oscillator strengths by the least-squares method, and $\Omega_\lambda = (1.086 \times 10^{11}\chi)^{-1} \times \tau_\lambda$.

RESULTS AND DISCUSSION

The crystals of $[Ln(L\text{-}proH)_2(H_2O)_5]Cl_3$ (Ln = Ho, Dy) are not isomorphic with the crystal of the neodymium complex with L-proline.[4] There are two independent proline molecules (zwitterion form) in the title structures. Each of them has a different coordination mode to lanthanide ions. The proline 1 coordinates to one cation by only one carboxyl oxygen, whereas the proline 2 coordinates by both carboxyl oxygens to form a carboxylate bridge of the Ln—OCO—Ln type. In this way, the lanthanide ions are bridged to each other by single carboxyl bridges and the structures are different from the structure of the europium complex with L-α-alanine, which has the same stoichiometric ratio, lanthanide–amino acid = 1 : 2.[1,5] The structure of the title compounds differs significantly from the structure of $[Nd(proH)_3(H_2O)_2](ClO_4)_3$ as well. The zigzag chains of one-dimensional polymers are formed along the *y*-axis (see Fig. 1). The Ln—Ln distances in every chain are equal to 5.959(2) Å for **I** and

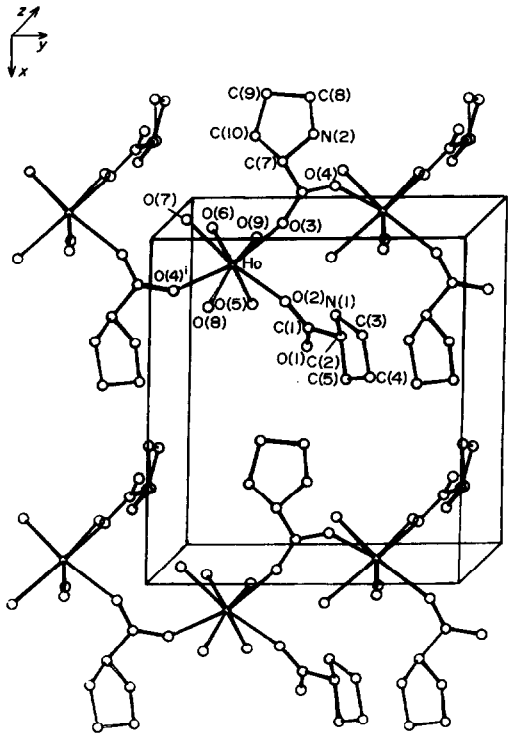

Fig. 1. An ORTEP (Johnson, 1976) view of the $[Ho(L\text{-}proH)_2(H_2O)_5]Cl_3$ structure.

* The final atomic, positional and thermal parameters, lists of F_o/F_c values, have been deposited as supplementary material with the Editor, from whom copies are available on request.

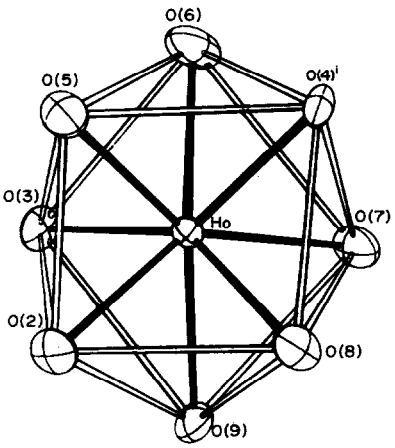

Fig. 2. The coordination polyhedron of $[Ho(L\text{-}proH)_2(H_2O)_5]Cl_3$.

5.963(4) Å for **II**. The average Ln—O distances in the coordination sphere of **I** and **II** are 2.365(9) and 2.373(9) Å, respectively.

The eight coordinating oxygen atoms (in which three derive from the carboxyl group of prolines and five derive from the water molecules) form a polyhedron which can be described as an intermediate between a dodecahedron and a square antiprism (Fig. 2). The atoms O(2), O(9), O(6), O(4^i) take positions A and the atoms O(3), O(8), O(5), O(7)—positions B in the dodecahedron. The parameter Δ is defined as $\Sigma d_i^2/8$, $i = 1$–8, d_i being the distance between the observed position of the i-th atom (vertex) and the relevant one in the ideal, least-squares-fitted[15] is 0.039 for both structures. When the coordination polyhedron is described as a square antiprism, the "square" faces are made up by atoms O(2), O(5), O(4^i), O(8) and O(3), O(6), O(7), O(9). In this case, $\Delta = 0.050$ for both structures, and the dihedral angles between these "square" planes are 1.9° and 2.6° for **I** and **II**, respectively. The interatomic distances and angles within the polyhedra are given in Table 1.

The ring conformations of proline molecules determined according to Ashida and Kakudo[16] and Cremer and Pople[17] exhibit E, C_s–C_α-endo type for proline 1 and T, C_2-C_γ-exo type for proline 2. The interatomic distances and angles for proline molecules are given in Table 2. The parameters determining conformations of the rings are given in Table 3. The torsion angles are given in Table 4.

The crystal structures are stabilized by the hydrogen bonds of O—H···O, O—H···Cl and N—H···Cl types (see Table 5).

The absorption spectra of the $[Ho(proH)_2(H_2O)_5]Cl_3$ monocrystal along the a-axis are shown in Fig. 3. It shows sets of lines in the range

Table 1. Selected interatomic distances (Å) and angles (°) within coordination polyhedrons

	I	II
Ln—O(2)	2.318(10)	2.318(10)
Ln—O(3)	2.333(8)	2.343(8)
Ln—O(4^i)	2.367(8)	2.367(7)
Ln—O(5)	2.336(10)	2.354(10)
Ln—O(6)	2.398(8)	2.402(8)
Ln—O(7)	2.386(10)	2.408(9)
Ln—O(8)	2.351(9)	2.362(9)
Ln—O(9)	2.426(7)	2.432(7)
O(5)—O(3)	3.18(1)	3.22(1)
O(5)—O(6)	2.97(2)	2.95(1)
O(2)—O(3)	2.99(1)	3.02(1)
O(2)—O(9)	2.78(1)	2.80(1)
O(8)—O(9)	2.94(1)	2.95(1)
O(8)—O(7)	3.17(1)	3.18(1)
O(4^i)—O(7)	3.00(1)	3.01(1)
O(4^i)—O(6)	2.78(1)	2.77(1)
O(8)—O(2)	2.83(1)	2.83(1)
O(8)—O(4^i)	2.79(1)	2.81(1)
O(4^i)—O(5)	2.93(1)	2.92(1)
O(5)—O(2)	2.73(1)	2.75(1)
O(3)—O(9)	2.89(1)	2.89(1)
O(3)—O(6)	2.76(1)	2.77(1)
O(6)—O(7)	2.95(1)	2.99(1)
O(7)—O(9)	2.76(1)	2.76(1)
O(8)—Ln—O(5)	107.1(3)	107.0(3)
O(9)—Ln—O(6)	124.9(3)	125.1(3)
O(4^i)—Ln—O(2)	125.0(3)	124.7(3)
O(7)—Ln—O(3)	101.6(3)	101.6(3)

$i = -x, -1/2+y, -z$.

8000–40,000 cm^{-1} owing to transitions from the $^5I_8$-ground state multiplet to various excited states.

The absorption bands are complex and correspond mainly to the electric dipole transitions. Only in a few cases are the intensities of magnetic transitions included.

The oscillator strength values were determined for all bands in the measured spectral range and are tabulated in Table 6. The values of P_{exp} and P_{calc} show satisfactory agreement. Among the f–f transitions in lanthanide ions, some satisfying the selection rule $|\Delta J\| \leqslant 2$ manifest an extraordinary sensitivity to the variation of ion environment. These transitions are termed the hypersensitive ones. The intensities of all f–f transitions do not differ significantly from these of other systems, but the intensity of the hypersensitive transition is essentially different from the intensity observed for the aquo ion, $HoCl_3$[18] and carboxylate monocrystal. The differences in intensity observed for the hypersensitive transition can be given by symmetry change, polarizability of the ligands,[19] or by some other effects. So it is reasonable to consider all of the

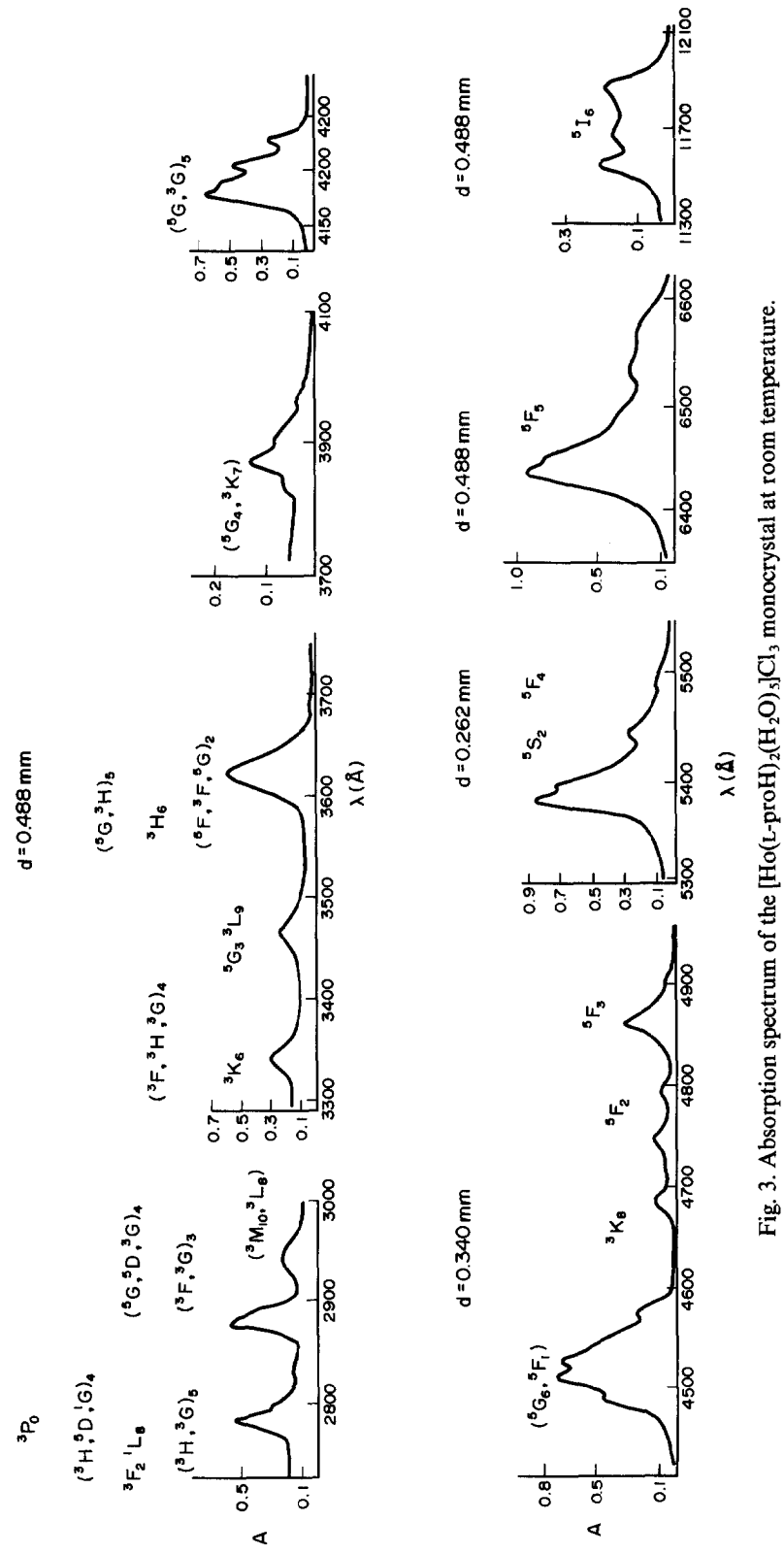

Fig. 3. Absorption spectrum of the $[Ho(L\text{-}proH)_2(H_2O)_5]Cl_3$ monocrystal at room temperature.

Table 2. Interatomic distances (Å) and angles (°) for proline molecule

	I	II
C(1)—O(1)	1.23(2)	1.26(2)
C(1)—O(2)	1.26(2)	1.25(2)
C(1)—C(2)	1.51(2)	1.51(2)
C(2)—C(5)	1.54(2)	1.56(2)
C(2)—N(1)	1.49(2)	1.50(2)
C(5)—C(4)	1.49(3)	1.55(2)
C(4)—C(3)	1.55(3)	1.48(3)
C(3)—N(1)	1.52(2)	1.51(2)
C(6)—O(3)	1.27(1)	1.27(1)
C(6)—O(4)	1.26(1)	1.26(1)
C(6)—C(7)	1.51(2)	1.51(2)
C(7)—C(10)	1.51(2)	1.52(2)
C(7)—N(2)	1.51(1)	1.49(1)
C(10)—C(9)	1.57(2)	1.54(2)
C(9)—C(8)	1.53(3)	1.53(3)
C(8)—N(2)	1.49(2)	1.49(2)
O(1)—C(1)—O(2)	126.1(13)	127.9(12)
O(1)—C(1)—C(2)	118.6(12)	117.4(11)
O(2)—C(1)—C(2)	115.3(11)	114.7(10)
C(1)—C(2)—C(5)	118.1(12)	116.6(11)
C(1)—C(2)—N(1)	111.2(10)	111.7(10)
C(2)—C(5)—C(4)	106.2(15)	102.0(13)
C(5)—C(4)—C(3)	104.1(16)	105.9(15)
C(4)—C(3)—N(1)	106.9(14)	107.5(13)
C(3)—N(1)—C(2)	105.0(10)	105.4(10)
N(1)—C(2)—C(5)	101.9(11)	100.9(10)
O(3)—C(6)—O(4)	123.3(10)	122.6(10)
O(3)—C(6)—C(7)	117.9(9)	118.4(9)
O(4)—C(6)—C(7)	118.6(9)	118.8(9)
C(6)—C(7)—C(10)	112.2(10)	112.6(9)
C(6)—C(7)—N(2)	109.1(9)	109.3(8)
N(2)—C(7)—C(10)	107.3(10)	106.3(9)
C(7)—C(10)—C(9)	105.0(12)	106.5(12)
C(10)—C(9)—C(8)	102.9(14)	102.5(14)
C(9)—C(8)—N(2)	104.5(14)	104.9(13)
C(8)—N(2)—C(7)	107.3(10)	107.7(10)

Table 3. The parameter determined conformations of the proline rings

	I	II
Proline 1	*E*, C_s-C_α-endo	*E*, C_s-C_α-endo
	N(1), C(3), C(4), C(5)	N(1), C(3), C(4), C(5)
	$\delta_{max} = 0.02(3)$	0.04(2)
	$\delta_{C(2)} = 0.58(1)$	0.63(1)
	$Q = 0.39(2)$	0.42(2)
	$\phi = 3.4(30)$	7.5(25)
Proline 2	*T*, C_2-C_γ-exo	*T*, C_2-C_γ-exo
	C(8), N(2), C(7)	C(8), N(2), C(7)
	$\delta_{C(9)} = -0.75(2)$	−0.72(7)
	$\delta_{C(6)} = 1.35(1)$	1.34(1)
	$Q = 0.35(2)$	0.34(2)
	$\phi = 90.1(23)$	89.7(23)

Parameter values are in order: type of conformation, atoms defining the plane in the ring, δ_{max} = maximum atom deviation from the plane (Å); δ_C = individual atom deviation from the plane (Å); Q = total puckering amplitude (Å) and ϕ = phase angle (°).

spectroscopic data of the carboxylate monocrystal with a well known structure, and consider which factor plays an important rôle in the intensity changes. Up to now we have the spectroscopic data for $[Ho_2(L\text{-}\alpha\text{-alanine})_4(H_2O)_8]Cl_6$ with the C_{2v} point symmetry for the Ho^{3+} ion,[1,5] and for some other holmium carboxylates, as follows:

			CN	P_{exp} $^5I_8 \rightarrow {}^5G_6{}^5F_1$	τ_2
(1) $[Ho_2(L\text{-}\alpha\text{-alanine})_4(H_2O)_8]Cl_6$	dimer	C_{2v}	8	896.2	1.53 ± 0.29
(2) $[Ho_2(L\text{-}\alpha\text{-alanine})_4(H_2O)_8](ClO_4)_6$	dimer	C_{2v}	8	1012.41	2.09 ± 0.24
(3) $[Ho(proH)_2(H_2O)_5]Cl_3$	polymer	D_2 or C_2	8	1116.3	2.19 ± 0.37
(4) $[Ho(Gly)_3(H_2O)_3](ClO_4)_3$	polymer	C_{2v}	9	1024.58 1013.6 975.8	2.69 ± 0.46
(5) $[Ho_2(Glu)_2(H_2O)_9](ClO_4)_6$	polymer	C_{2v}	9	1137.0	3.07 ± 0.48

Table 4. Torsion angles (°)

O(1)—C(1)—C(2)—N(1)	−173.0(11)	−172.2(10)
O(2)—C(1)—C(2)—N(1)	7.1(12)	6.2(12)
O(1)—C(1)—C(2)—C(5)	−55.9(16)	−56.9(15)
O(2)—C(1)—C(2)—C(5)	124.2(15)	121.5(14)
C(1)—C(2)—C(5)—C(4)	−161.7(20)	−162.6(17)
C(2)—C(5)—C(4)—C(3)	25.6(18)	29.2(17)
C(5)—C(4)—C(3)—N(1)	−2.5(19)	−5.4(17)
C(4)—C(3)—N(1)—C(2)	−22.3(15)	−21.6(15)
C(3)—N(1)—C(2)—C(1)	168.7(12)	163.6(12)
C(3)—N(1)—C(2)—C(5)	37.0(14)	39.1(14)
N(1)—C(2)—C(5)—C(4)	−39.7(19)	−41.5(17)
O(3)—C(6)—C(7)—N(2)	161.5(12)	161.9(11)
O(4)—C(6)—C(7)—N(2)	−23.4(11)	−23.1(11)
O(3)—C(6)—C(7)—C(10)	−79.7(13)	−80.2(12)
O(4)—C(6)—C(7)—C(10)	95.5(13)	94.8(12)
C(6)—C(7)—N(2)—C(8)	109.8(13)	110.5(12)
C(7)—N(2)—C(8)—C(9)	30.6(16)	29.2(15)
N(2)—C(8)—C(9)—C(10)	−36.4(17)	−34.8(16)
C(8)—C(9)—C(10)—C(7)	28.9(16)	28.0(16)
C(9)—C(10)—C(7)—C(6)	−130.7(14)	−130.5(14)
C(9)—C(10)—C(7)—N(2)	−10.9(13)	−10.9(13)
C(10)—C(7)—N(2)—C(8)	−12.0(13)	−11.3(12)

For the first two single crystals, the coordination mode of the carboxyl group is the same (simple bridge —O—C(=O)—O—) and in such a coordination of the carboxyl group, almost always the CN = 8 and the coordination polyhedra are distorted antiprism (SAP) or bicapped trigonal prism (BCTP).[1,4,5,20]

In the last two single crystal structures the coordination mode of the carboxyl group changed (there are two types of carboxyl group bonding mode[2,8] and CN = 9) however, the symmetry seems to be probably the same, C_{2v} for **4** and **5**.

If the Judd static model of intensity plays the main rôle we must observe the same intensity for four (**1**, **2**, **4** and **5**) monocrystals. However, if the polarizability mechanism takes part including the covalency effect one can expect the increase of intensity for the last three monocrystals. The bonding mode of the carboxyl group allows us to expect high covalency in **4** and **5** monocrystals, although the increase of intensity was observed for the glutamic acid monocrystal only.

In the case of complex **3** with proline the situation

Table 5. Distances (Å) and angles (°) of hydrogen bonds

D—H···A	D···A		H···A		< D—H···A	
	I	II	I	II	I	II
O(5)—H(19)···O(1)	2.63(2)	2.60(2)	1.83(1)	1.81(1)	144.4(7)	143.2(7)
O(5)—H(20)···Cl(2^{ii})	3.08(1)	3.11(1)	2.332(3)	2.325(3)	143.8(6)	144.9(6)
O(6)—H(21)···Cl(3^{iii})	3.12(1)	3.14(1)	2.459(3)	2.405(3)	129.3(5)	129.3(6)
O(6)—H(22)···Cl(1^{iii})	3.19(1)	3.19(1)	2.333(3)	2.167(3)	158.3(5)	156.0(5)
O(7)—H(24)···Cl(3^{iv})	3.18(1)	3.19(1)	2.320(2)	2.321(3)	152.9(5)	152.0(6)
O(8)—H(25)···Cl(1)	3.14(1)	3.14(1)	2.337(3)	2.331(3)	165.8(7)	166.9(7)
O(8)—H(26)···Cl(2^{v})	3.09(1)	3.11(1)	2.433(3)	2.332(3)	128.3(6)	125.6(5)
O(9)—H(27)···Cl(3^{vi})	3.11(1)	3.12(1)	2.273(3)	2.276(3)	149.4(5)	149.3(5)
O(9)—H(28)···Cl(3^{iv})	3.12(1)	3.12(1)	2.274(3)	2.269(3)	151.5(5)	151.3(5)
N(1)—H(2)···Cl(2)	3.15(1)	3.16(1)	2.211(5)	2.192(5)	159.4(6)	160.1(6)
N(1)—H(3)···Cl(3^{vi})	3.16(1)	3.17(1)	2.186(3)	2.192(3)	165.3(6)	167.5(6)
N(2)—H(11)···Cl(2^{vii})	3.24(1)	3.25(1)	2.538(5)	2.545(5)	126.8(6)	126.6(6)
N(2)—H(12)···Cl(1^{iv})	3.13(1)	3.14(1)	2.146(3)	2.150(3)	171.8(6)	171.6(6)

Table 6. Oscillator strengths of f–f transitions of monocrystals of $[Ho(L\text{-}proH)_2(H_2O)_5]Cl_3$ (τ_λ parameter values calculated from Judd's relation)

Spectral region (Å)	$S'L'J'$	$P_{exp} \times 10^8$	$P_{calc} \times 10^8$
11,100–12,300	$^5I_6$	154.6	212.7
6200–6700	$^5F_5$	524.9	509.7
5200–5600	$^5S_2$, $^5F_4$	769.9	732.0
4820–4960	$^5F_3$	226.0	242.2
4710–4820	$^5F_2$	139.1	137.6
4630–4710	$^3K_8$	67.7	143.1
4380–4630	$^5G_6$, $^5F_1$	1116.3	1130.4
4090–4320	$(^5G, ^3G)_5$	474.6	406.8
3800–4050	$^5G_4$, $^3K_7$	124.5	92.0
3530–3780	$(^5G, ^3H)_5$, $^3H_6$, $(^5F, ^3F, ^5G)_2$	497.5	407.0
3410–3530	$^5G_3$, $^3L_9$	128.1	175.6
3305–3410	$(^3F, ^3H, ^3G)_4$, $^3K_6$	103.3	128.6
2910–3020	$^3M_{10}$, $^3L_8$	134.1	182.0
2855–2910	$(^5G, ^5D, ^3G)_4$, $(^3F, ^3G)_3$	327.5	398.5
2750–2825	$^3P_0$, $(^3H, ^5D, ^1G)_4$, $^3F_2$, $^1L_8$, $(^3H, ^3G)_5$	273.1	310.5
		RMS = 5.52×10^{-7}	

$\tau_2 = 2.19 \pm 0.37$; $\tau_4 = 5.41 \pm 0.47$; $\tau_6 = 5.79 \pm 0.43$.

is somewhat different. It is the first case among the complexes with amino acids where the carboxyl group is bonded with the Ln^{3+} ion not only by a simple bridge but also via only one oxygen of the carboxyl group of the second proline molecule (see Fig. 1). This type of coordination is very rarely represented in complexes of lanthanide carboxylates. The Ln—O bonding length for this type of coordination in the title compound is the shortest (Ln—O(2) = 2.318 Å). All Ln—O distances are even shorter than those observed in the complex with glutamic acid. The intensity of the hypersensitive transition is significantly higher for the title monocrystal in comparison with the data presented for the holmium complex with alanine and almost equal with that for glutamic acid.

In the presented data the lanthanide ions occupy C_{2v} point symmetry. Since the coordination polyhedron for the complex with proline can be described as an intermediate between dodecahedron and square antiprism, so the symmetry can change. In both cases distortion provides the reason why the symmetry becomes lower than in ideal polyhedra. In fact, we cannot observe the D_{2d} or D_{4d} symmetry, but only the lower one, i.e. D_2 or C_2. However, it is clear from the shape characteristics that the structure of the title compound is closer to the dodecahedron, so the D_2 point symmetry seems to be reasonable and higher than C_{2v}. We were not able to synthesize the europium complex with proline and we cannot confirm the point symmetry of the Ln^{3+} ion on the basis of luminescence spectra.

The intensity results of the hypersensitive transition indicate the increase of the oscillator strength value, which is similar for glutamic acid. Such a phenomenon can be explained by the covalency effect and/or by vibronic mechanism, which is similar to the case of the $[Nd(proH)_3(H_2O)_2](ClO_4)_3$ monocrystal.

CONCLUSIONS

(1) The new type of Ho^{3+} and Dy^{3+} compounds with proline were obtained which differ in the structure and coordination of proline molecules from those in the monocrystal of $[Nd(proH)_3(H_2O)_2](ClO_4)_3$.

(2) The linear polymer in the structure is formed in a different way when compared with the polymer in the $[Nd(proH)_3(H_2O)_2](ClO_4)_3$ structure.

(3) Analysis of spectroscopic data of monocrystal Ho^{3+} carboxylates led us to the conclusion that the covalency effect and vibronic mechanism can affect the intensity changes of hypersensitive transitions.

(4) The differences in the spectroscopic properties for the series of lanthanide carboxylates have been found.

REFERENCES

1. J. Legendziewicz, T. Głowiak, E. Huskowska and C. N. Dao, *Rare Earths Spectroscopy*, p. 146. World Scientific, Singapore (1985).
2. J. Legendziewicz, E. Huskowska, A. Waśkowska and

Gy. Argay, *Inorg. Chim. Acta* 1984, **95**, 57; 1984, **94**, 89.
3. J. Legendziewicz, E. Huskowska, C. N. Dao and T. Głowiak, *Abstracts of the 10th European Crystallography Meeting*, p. 162. Science Publishing House, Wrocław (1986).
4. T. Głowiak, E. Huskowska, C. N. Dao and J. Legendziewicz, *Polyhedron* 1988, **7**, 2495.
5. C. N. Dao, T. Głowiak, E. Huskowska and J. Legendziewicz, *J. Less-common Met.* 1988, **136**, 339.
6. J. Legendziewicz, T. Głowiak, C. N. Dao and E. Huskowska, *J. Less-common Met.* (in press).
7. I. Csóregh, P. Kierkegaard, J. Legendziewicz and E. Huskowska, *Acta Chim. Scand.* 1987, **41**, 453.
8. I. Csóregh, P. Kierkegaard, J. Legendziewicz and E. Huskowska, *Inorg. Chem.* (in press).
9. T. Głowiak, C. N. Dao and J. Legendziewicz, *Acta Cryst.* 1986, **C42**, 1494.
10. T. Głowiak, J. Legendziewicz, C. N. Dao and E. Huskowska, *J. Less-common Met.* 1987, **134**, 153.
11. *Syntex (1976). XTL/XTLE. Structure Determination System.* Syntex Analytical Instrument, Cupertino, California (1976).
12. *International Tables for X-ray Crystallography*, Vol IV. Kynoch Press, Birmingham (1974).
13. B. R. Judd, *Phys. Rev.* 1962, **127**, 750.
14. G. S. Ofelt, *J. Chem. Phys.* 1962, **37**, 511.
15. M. G. B. Drew, *Coord. Chem. Rev.* 1977, **24**, 179.
16. T. Ashida and M. Kakudo, *Bull. Chem. Soc. Japan* 1974, **45**, 1129.
17. D. Cremer and J. A. Pople, *J. Am. Chem. Soc.* 1975, **97**, 1354.
18. W. T. Carnall, P. R. Fields and K. Rajnak, *J. Chem. Phys.* 1968, **49**, 4412.
19. S. F. Mason, R. D. Peacock and B. Stewart, *Chem. Phys. Lett.* 1974, **29**, 149; S. F. Mason, R. D. Peacock and B. Stewart, *Mol. Phys.* 1975, 1829; S. F. Mason, *J. Less-common Met.* 1983, **93**, 45.
20. J. Legendziewicz, T. Głowiak, G. Oczko and C. N. Dao, *J. Less-common Met.* 1986, **125**, 45.

Polyhedron Vol. 8, No. 17, pp. 2147–2150, 1989
Printed in Great Britain

0277–5387/89 $3.00+.00
© 1989 Pergamon Press plc

METAL–(PHENYLTHIO)ALKANOIC ACID INTERACTIONS—XII* THE CRYSTAL STRUCTURE OF POTASSIUM (4-CHLORO-2,5-DIMETHYLPHENYLTHIO)-ACETATE-(4-CHLORO-2,5-DIMETHYLPHENYLTHIO)ACETIC ACID ADDUCT

COLIN H. L. KENNARD†

Department of Chemistry, University of Queensland, Brisbane 4067, Australia

and

GRAHAM SMITH

Department of Chemistry, Queensland University of Technology, Brisbane 4000, Australia

and

THOMAS C. W. MAK and WAI-HING YIP

Department of Chemistry, The Chinese University of Hong Kong, Shatin, New Territories, Hong Kong

and

WING-HONG CHAN

Department of Chemistry, Hong Kong Baptist College, Kowloon, Hong Kong

(*Received* 6 *January* 1989; *accepted* 14 *April* 1989)

Abstract—The crystal structure of a potassium adduct with a substituted (phenylthio)acetic acid has been determined using X-ray diffraction, and refined to a residual $R = 0.043$ for 1932 observed reflections. The adduct, $[(KL)(LH)]_n$, where LH = (4-chloro-2,5-dimethylphenylthio)acetic acid, is triclinic, space group $P\bar{1}$, $Z = 2$, $a = 7.313(2)$, $b = 9.386(2)$, $c = 17.371(5)$ Å, $\alpha = 77.53(2)$, $\beta = 79.28(2)$, $\gamma = 84.95(2)°$. The K atom is surrounded by a distorted octahedron comprising five oxygens [K—O, 2.691–2.777(3) Å] and one sulphur atom [K—S, 3.349(2) Å], with oxygens also bridging in a polymer structure. There are two hydrogen atoms at special positions contributing to the one H^+. The compound is an example of a type A, $[(M^+)_2(HX_2^-)_2]$ system, with one hydrogen atom being shared by two crystallographically related X groups. There are two conformationally different (HX_2^-) groups in the structure.

This is an extension to the investigation of a group of disordered compounds $[M^+X^- \cdot HX]$ found for metal complexes of (phenylthio)alkanoic acids.[2] Speakman[3,4] classified two fundamental types of acid–salt $[M^+X^- \cdot HX]$ structures: type A, where the two X-units are crystallographically equivalent, and type B, where the two X-units are crystallographically non-equivalent, and occur as an anion and neutral molecule. In all of Speakman's type A cases, the intercarboxyl hydrogen bond occurs about either an inversion centre or a two-fold axis. In the present example, with formula (KL)(LH), where LH = (4-chloro-2,5-dimethylphenylthio)acetic acid, an unusual variation of the type A structure is found.

* For part XI see ref. 1.

† Author to whom correspondence should be addressed.

EXPERIMENTAL

Preparation

The complex was prepared by reaction for *ca* 1 h at 90°C, of a 2:1 stoichiometric quantity of (4-chloro-2,5-dimethylphenylthio)acetic acid (as a 50% aqueous ethanolic solution) with potassium carbonate.[5] The filtered solution, on standing, gave crystals suitable for X-ray examination.

Elemental analysis

Found: C, 48.2; H, 4.3. Calc. for $C_{20}H_{21}Cl_2KO_4S_2$: C, 48.1; H, 4.2%.

Crystal data

$C_{20}H_{21}Cl_2KO_4S_2$, $M_r = 499.5$, triclinic, space group $P\bar{1}$, $a = 7.313(2)$, $b = 9.386(2)$, $c = 17.371(5)$ Å, $\alpha = 77.53(2)$, $\beta = 79.28(2)$, $\gamma = 84.95(2)°$, $V = 1142.5(5)$ Å^3, $Z = 2$, $D_c = 1.451$, $D_m = 1.457$ g cm^{-3}, $F(000) = 516$, μ(Mo-K_α) = 6.65 cm^{-1}, $t = 293$ K.

X-ray data collection and structure refinement

Data were collected from a single crystal (0.42 × 0.40 × 0.20 mm) on a Nicolet R3m four-circle diffractometer using monochromatic Mo-K_α radiation ($\lambda = 0.71069$ Å). 4526 reflections were collected up to $2\theta_{max} = 56°$. Data were processed using the profile fitting procedure of Diamond[6] and corrected for absorption (maximum, minimum transmission factors, 0.827 and 0.782, respectively). Of these, 1932 with $I > 2.5\sigma(I)$ were considered observed and used in structure analysis. The structure was solved by the Patterson method (SHELXS-86[7]) and refined using SHELX-76[8] on the University of Queensland's IBM 3081 computer. Blocked-matrix anisotropic refinement (100 variable parameters maximum) was used for all non-hydrogen atoms. All hydrogens were located from a difference-Fourier synthesis and their positional and thermal parameters refined. Residuals R, R_w and w were 0.043, 0.051 and $[0.74/(\sigma^2 F_o + 3.5 \times 10^{-3} F_o^2)]$, respectively. $\{R = [\Sigma||F_o| - |F_c||]/\Sigma|F_o|]$ and $R_w = [\Sigma w(||F_o| - |F_c||]^2/\Sigma w|F_o|^2)^{0.5}]\}$. Neutral atom scattering factors were used.[9]

Bond distances and angles about the coordination sphere are given in Table 1. Final atomic coordinates, anisotropic thermal parameters, intramolecular bond distances and angles, and observed and calculated structure factors have been deposited with the Editor as supplementary material and are available on request.

DISCUSSION

The structure of the compound is polymeric, based on a repeating centrosymmetric dimeric unit (Fig. 1). The irregular six-coordination about each

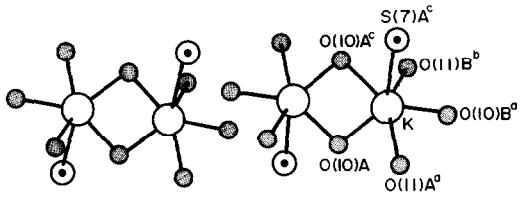

Fig. 1. Stereoview of the coordination sphere about potassium.

Table 1. Bond distances (Å) and angles (°) about the coordination polyhedron

(a)	Distances			
	K—O(10)B^a	2.691(3)	K—O(10)A	2.737(2)
	K—O(11)B^b	2.749(3)	K—O(10)A^c	2.754(2)
	K—S(7)A^c	3.349(2)	K—O(11)A^a	2.777(3)
(b)	Angles			
	O(10)B^a—K—O(11)B^b	70.4(2)	O(11)B^b—K—O(11)A^a	139.1(2)
	O(10)B^a—K—S(7)A^c	92.8(1)	S(7)A^c—K—O(10)A	135.2(1)
	O(10)B^a—K—O(10)A	130.6(2)	S(7)A^c—K—O(10)A^c	55.6(1)
	O(10)B^a—K—O(10)A^c	143.3(2)	S(7)A^c—K—O(11)A^a	120.0(1)
	O(10)B^a—K—O(11)A^a	74.3(2)	O(10)A—K—O(10)A^c	85.1(2)
	O(11)B^b—K—S(7)A^c	82.1(1)	O(10)A—K—O(11)A^a	71.3(2)
	O(11)B^b—K—O(10)A	118.9(2)	O(10)A^c—K—O(11)A^a	135.1(2)
	O(11)B^b—K—O(10)A^c	85.7(7)		

[a] $-x, 1-y, -z$.
[b] $1+x, -1+y, z$.
[c] $1-x, 1-y, -z$.

Table 2. Comparative features of Group 1A metal–(phenylthio)alkanoates

Example	Coordination number	M—O range (Å)	Type[3,4]	Reference
$[K(PTA)(PTAH)]_n$	7	2.729–3.034(3)	B	5
$[Cs(PTA)(PTAH)]_n$	8	3.03–3.45(1)	B	2
$[Cs(DCMPTA)(DCMPTAH)]_n$	6	3.123–3.237(8)	A	2
$[Cs(PTPA)(H_2O)]_n$	6	3.02–3.33(1)	Conventional	2
$[K_2(LHL)_2]_n$	6	2.691–2.777(3)	A	This work

PTAH = (phenylthio)acetic acid.
DCMPTAH = (2,4-dichloro-5-methylphenylthio)acetic acid.
PTPA = 2-(phenylthio)propionic acid.
LH = (4-chloro-2,5-dimethylphenylthio)acetic acid.

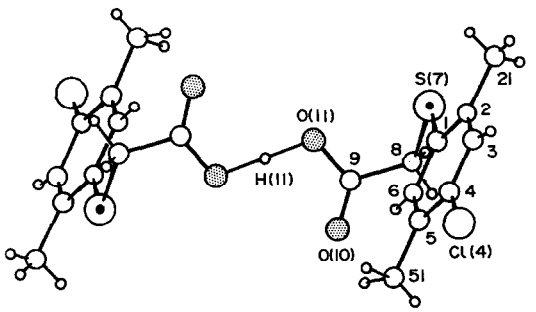

Fig. 2. Molecular conformation and atom number scheme for ligands. Only Ligand B is shown.

potassium comprises one sulphur atom [K—S, 3.349(2) Å] and five oxygens from four different carboxyl oxygens [K—O, 2.691(3), 2.777(3) Å; mean 2.742(3) Å], involving two different ligands. These ligands (A and B), are conformationally different, being either extended (A) or convoluted (B), and are related to their equivalent halves through inversion centres at (0, $\frac{1}{2}$, 0) and ($\frac{1}{2}$, 0, 0). The unusual feature of each of the ligand pairs is the location of protons at these inversion sites (Figs 2 and 3). Since each must have half-occupancy, the pair shares half a proton, making the formula of the complex $[(K^+)_2(LHL^-)_2]_n$. The protons are at intermediate positions between the two carboxyl oxygens with the O(11)—H(11) distances 1.224(2) Å (A) and 1.231(3) Å (B). Although this example represents a type B, $[M^+(L)(LH)]$ adduct[3,4] it has crystallographically different ligand and acid species both with protons at special positions with inversion-related ligands having shared half-protons. This has no precedent among the Group 1A carboxylates. However, an analogous example is found in the Group 1B metal complex adduct, silver(I) picolinate picolinic acid.[10] This present example is

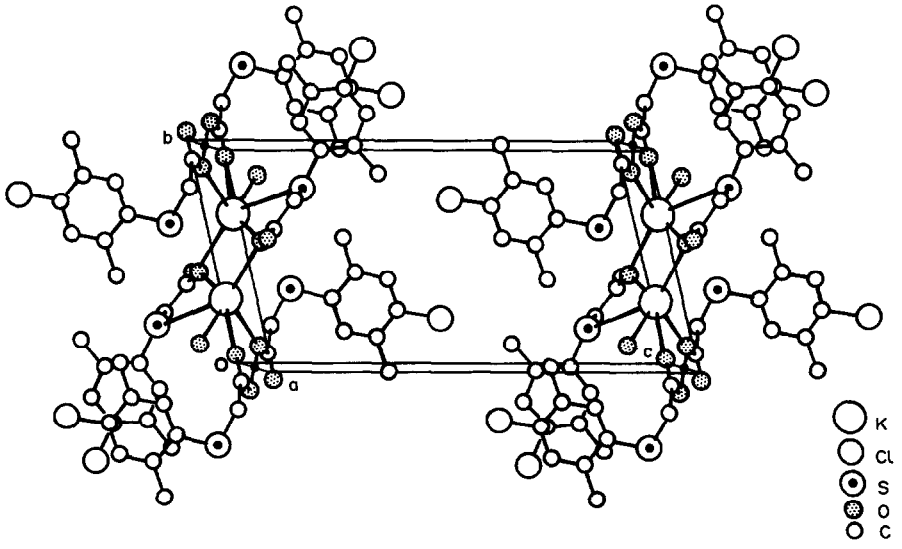

Fig. 3. Packing of the polymer molecules in the unit cell.

also the first among the structures of the Group 1A metal–(phenylthio)alkanoate complexes in which any metal to sulphur bonding is found. The result is a closure of a five-membered chelate ring such as is found in silver(I) (phenylthio)acetate.[11] All these complexes are polymeric (Table 2) with irregular coordination, while only one has a conventional "salt" structure [caesium 2-(phenylthio)propionate hydrate].[2] Among the others, both Type A and Type B examples are found, but the types of co-ordinating and bridging systems vary. With [Cs(PTA)(PTAH)]$_n$, [PTAH = (phenylthio)acetic acid], analogous bifurcated bridging oxygens are found but, in addition, bidentate (O, O′) carboxylates also bridge. In [Cs(DCMPTA)-(DCMPTAH)]$_n$ [DCMPTAH = 2,4-dichloro-5-methylphenylthio) acetic acid], the bridging is through carboxylato (O, O′) groups, while in [Cs(PTPA)(H_2O)]$_n$, [PTPAH = 2-(phenylthio)propionic acid], which is a conventional compound, there is an additional bridging water molecule.

Acknowledgements—The authors thank the Chinese University of Hong Kong for provision of data collection services, and the University of Queensland for computing facilities.

REFERENCES

1. G. Smith, E. J. O'Reilly, C. H. L. Kennard, T. C. W. Mak, W.-H. Yip and W.-H. Chan, *Aust. J. Chem.* 1988, **41**, 1769.
2. T. C. W. Mak, W.-H. Yip, W.-H. Chan, C. H. L. Kennard, G. Smith and E. J. O'Reilly, *Polyhedron* 1989, **8**, 793.
3. J. C. Speakman, *Struct. Bond.* 1972, **12**, 141.
4. H. N. Shrivastava and J. C. Speakman, *J. Chem. Soc.* 1961, 1151.
5. T. C. W. Mak, W.-H. Yip, G. Smith, E. J. O'Reilly and C. H. L. Kennard, *Inorg. Chim. Acta* 1984, **88**, 35.
6. R. Diamond, *Acta Cryst. A* 1969 **24**, 43.
7. G. M. Sheldrick, SHELXS-86, Program for Solution of Crystal Structures, University of Gottingen (1986).
8. G. M. Sheldrick, SHELX-76, Program for Crystal Structure Determination, University of Cambridge, England (1976).
9. *International Tables for X-ray Crystallography*, Vol. 4 (Edited by J. A. Ibers and W. C. Hamilton). Kynoch Press, Birmingham (1974).
10. J. P. Deloume, R. Faure and H. Loiseleur, *Acta Cryst. B* 1977, **33**, 2709.
11. W.-H. Chan, T. C. W. Mak, W.-H. Yip, C. H. L. Kennard, G. Smith and E. J. O'Reilly, *Aust. J. Chem.* 1987, **40**, 981.

Polyhedron Vol. 8, No. 17, pp. 2151–2155, 1989
Printed in Great Britain

0277–5387/89 $3.00+.00
© 1989 Pergamon Press plc

DINUCLEAR PALLADIUM(II) COMPLEXES WITH BRIDGING MERCAPTO GROUP: X-RAY CRYSTAL STRUCTURE OF A CHLORO/MERCAPTO BRIDGED DIMER

V. K. JAIN† and R. P. PATEL

Chemistry Division, Bhabha Atomic Research Centre, Bombay 400 085, India

and

K. V. MURALIDHARAN

Water Chemistry Division, Bhabha Atomic Research Centre, Bombay 400 085, India

and

R. BOHRA

Department of Chemistry, University of Rajasthan, Jaipur 302 004, India

(*Received* 16 *January* 1989; *accepted* 14 *April* 1989)

Abstract—Dinuclear palladium(II) complexes of the type $[Pd_2Cl_2(\mu\text{-}X)(\mu\text{-}SR)(PMe_2Ph)_2]$ (X = Cl or SR; R = Et or Pr^i) have been prepared and characterized. All these complexes adopt a *cis*-configuration. The structure of $[Pd_2Cl_2(\mu\text{-}Cl)(\mu\text{-}SEt)(PMe_2Ph)_2]$ was established by X-ray crystallography: the crystals are triclinic, space group $P\bar{1}$ with $a = 9.273(3)$, $b = 10.412(3)$, $c = 13.767(6)$ Å, $\alpha = 80.84(3)$, $\beta = 81.62(3)$, $\gamma = 68.04(3)°$ and $Z = 2$. The geometry around one palladium is slightly distorted while the other one is almost square-planar.

Recently, we have reported mercapto bridged dinuclear platinum(II) and palladium(II) complexes.[1–3] For the palladium complexes[1,4] containing both chloro and mercapto bridges, an unambiguous differentiation between *sym cis–trans*-μ-chloro and *trans*-μ-mercapto could not be made in the absence of valuable couplings, although the former geometry was suggested. Here, we report the synthesis of $[Pd_2Cl_2(\mu\text{-}X)(\mu\text{-}SR)(PMe_2Ph)_2]$ (X = Cl, SR; R = Et, Pr^i) and the crystal and molecular structure of $[Pd_2Cl_2(\mu\text{-}Cl)(\mu\text{-}SEt)(PMe_2Ph)_2]$.

RESULTS AND DISCUSSION

The complex $[Pd_2Cl_2(\mu\text{-}Cl)_2(PMe_2Ph)_2]$ reacts with mercaptans RSH (R = Et, Pr^i), in acetone to yield dimercapto bridged palladium complexes which on treatment with the former complex in chloroform affords $[Pd_2Cl_2(\mu\text{-}Cl)(\mu\text{-}SR)(PMe_2Ph)_2]$. The dinuclear products have been characterized by elemental analysis (Table 1) and by NMR spectroscopy. All the complexes display single resonances in their ^{31}P NMR spectra in $CDCl_3$. The replacement of the bridging chloride by the SR group results in shielding of the ^{31}P resonance. The ^1H NMR spectra of dimercapto bridged complexes showed two sets of SR proton resonances as expected for *sym cis* configuration. The chloro–mercapto bridged complexes exhibited only one set of SR proton resonances. The ^1H NMR spectra displayed two doublets for the P—Me protons indicating non-equivalence of the methyl group on each phosphine due to the absence of a plane of symmetry containing the Pd—P axis as revealed from X-ray analysis.

† Author to whom correspondence should be addressed.

Table 1. Physical, analytical and $^{31}P\{^1H\}$ NMR data for $[Pd_2Cl_2(\mu\text{-}X)(\mu\text{-}SR)(PMe_2Ph)_2]$

Complex	Solvent of recrystallization (% yield)	M.p.	Analysis found (calc.) C	H	S	$^{31}P\{^1H\}$ δ in ppm
$[Pd_2Cl_2(\mu\text{-}Cl)_2(PMe_2Ph)_2]$	—	—	—	—	—	14.7
$[Pd_2Cl_2(\mu\text{-}SEt)_2(PMe_2Ph)_2]$	$CHCl_3$/EtOH (88)	166	34.9 (35.2)	4.6 (4.7)	9.9 (9.4)	−1.6
$[Pd_2Cl_2(\mu\text{-}Cl)(\mu\text{-}SEt)(PMe_2Ph)_2]$	$CHCl_3$/MeOH (65)	208	33.5 (32.9)	4.8 (4.1)	5.2 (4.9)	10.2
$[Pd_2Cl_2(\mu\text{-}SPr^i)_2(PMe_2Ph)_2]$	Acetone/MeOH (53)	163–164	37.9 (37.2)	5.1 (5.0)	9.3 (9.0)	−2.8
$[Pd_2Cl_2(\mu\text{-}Cl)(\mu\text{-}SPr^i)(PMe_2Ph)_2]$	$CHCl_3$/MeOH (90)	237–240 (dec.)	33.3 (34.0)	4.3 (4.4)	5.2 (4.8)	9.9

Molecular structure of $[Pd_2Cl_2(\mu\text{-}Cl)(\mu\text{-}SEt)(PMe_2Ph)_2]$

The bond lengths and bond angles are listed in Table 2. A PLUTO[5] plot of the molecule is shown in Fig. 1, while Fig. 2 depicts a stereoscopic pair of molecules. The coordination around one of the palladium sites [Pd(1)] is slightly distorted relative to the other. The deviations of the atoms from the least-squares plane are: Pd(1) = 0.0011(2), P(1) = −0.032(2), Cl(1) = −0.083(3), Cl(2) = −0.110(4) and S(1) = −0.019(2) Å which suggest a pyramidization at Pd(1). The corresponding values at the other palladium site are: Pd(2) = −0.001(1), P(2) = 0.001(2), Cl(3) = 0.001(3), Cl(2) = −0.001(3) and S(1) = 0.001(3). The Pd—S—Cl—Pd bridge is not planar and the two coordination planes are inclined to each other at 134.26(5)°. The Pd—P bond length [⟨2.227(2)⟩ Å] is, as usual, less than the radius sum. The bond distances Pd—Cl(terminal) [⟨2.334(2)⟩ Å], Pd—Cl(bridging) [⟨2.445(2)⟩ Å] and Pd—S [⟨2.280(2)⟩ Å] are in good agreement with the values reported in the literature.[6,7] These are also in keeping with the known *trans*-influence order P ≫ S > Cl. The average P—C distance [1.81(1) Å] is normal. The average C—C distance

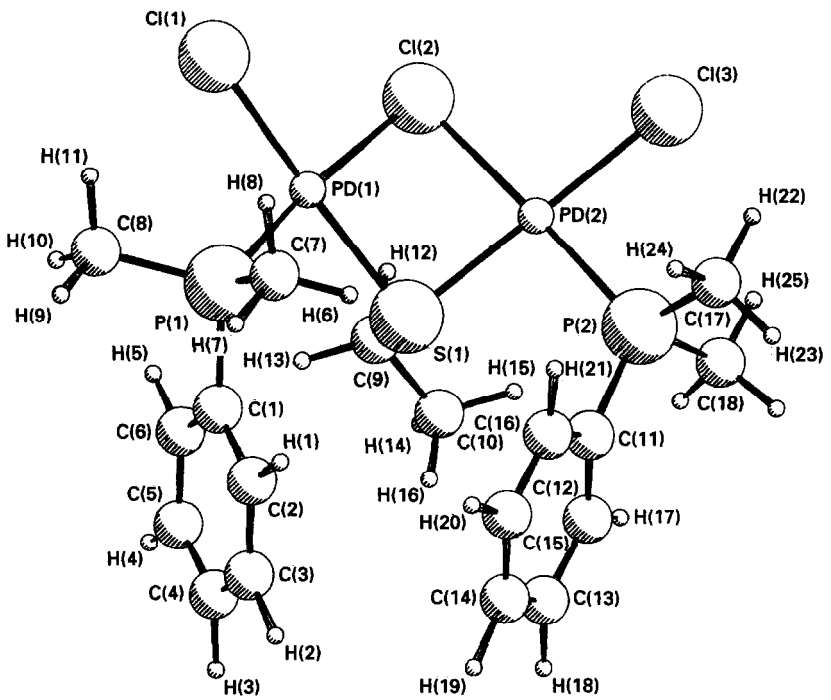

Fig. 1. PLUTO plot of the molecule $[Pd_2Cl_2(\mu\text{-}Cl)(\mu\text{-}SEt)(PMe_2Ph)_2]$.

Table 2. Bond lengths (Å) and angles (°)

Pd(1)—Pd(2)	3.234(1)	P(2)—C(18)	1.812(10)
Pd(1)—Cl(1)	2.331(2)	C(1)—C(2)	1.380(10)
Pd(1)—Cl(2)	2.443(2)	C(2)—C(3)	1.402(11)
Pd(1)—P(1)	2.228(2)	C(3)—C(4)	1.359(14)
Pd(1)—S(1)	2.231(2)	C(4)—C(5)	1.367(12)
Pd(2)—Cl(2)	2.438(2)	C(5)—C(6)	1.384(11)
Pd(2)—Cl(3)	2.337(2)	C(6)—C(1)	1.385(11)
Pd(2)—S(1)	2.279(2)	C(9)—C(10)	1.484(14)
Pd(2)—P(2)	2.226(2)	C(11)—C(12)	1.395(10)
S(1)—C(9)	1.831(8)	C(12)—C(13)	1.392(13)
P(1)—C(1)	1.813(7)	C(13)—C(14)	1.357(16)
P(1)—C(7)	1.809(8)	C(14)—C(15)	1.387(12)
P(1)—C(8)	1.820(10)	C(15)—C(16)	1.366(12)
P(2)—C(11)	1.795(7)	C(16)—C(11)	1.394(12)
P(2)—C(17)	1.801(8)		

Cl(2)—Pd(1)—Cl(1)	94.3(1)	C(18)—P(2)—Pd(2)	110.4(3)
S(1)—Pd(1)—Cl(2)	84.6(1)	C(18)—P(2)—C(17)	105.4(5)
P(1)—Pd(1)—Cl(1)	91.2(1)	C(2)—C(1)—P(1)	122.2(6)
P(1)—Pd(1)—S(1)	89.8(1)	C(6)—C(1)—P(1)	118.1(5)
Cl(3)—Pd(2)—Cl(2)	94.5(1)	C(6)—C(1)—C(2)	119.6(6)
S(1)—Pd(2)—Cl(2)	84.8(1)	C(3)—C(2)—C(1)	119.7(8)
P(2)—Pd(2)—Cl(3)	87.3(1)	C(4)—C(3)—C(2)	119.1(8)
P(2)—Pd(2)—S(1)	93.5(1)	C(5)—C(4)—C(3)	122.2(8)
Pd(2)—Cl(2)—Pd(1)	82.9(1)	C(6)—C(5)—C(4)	118.8(8)
Pd(2)—S(1)—Pd(1)	90.3(1)	C(5)—C(6)—C(1)	120.6(7)
C(9)—S(1)—Pd(2)	102.8(3)	C(10)—C(9)—S(1)	111.6(6)
C(1)—P(1)—Pd(1)	114.5(3)	C(12)—C(11)—P(2)	122.2(6)
C(7)—P(1)—Pd(1)	108.1(3)	C(16)—C(11)—P(2)	118.9(5)
C(7)—P(1)—C(1)	108.4(3)	C(16)—C(11)—C(12)	118.9(7)
C(8)—P(1)—Pd(1)	116.3(3)	C(13)—C(12)—C(11)	119.4(9)
C(8)—P(1)—C(1)	103.7(4)	C(14)—C(13)—C(12)	121.4(8)
C(8)—P(1)—C(7)	105.3(4)	C(15)—C(14)—C(13)	119.0(9)
C(11)—P(2)—Pd(2)	117.1(3)	C(16)—C(15)—C(14)	121.1(9)
C(17)—P(2)—Pd(2)	113.0(3)	C(15)—C(16)—C(11)	120.2(7)
C(17)—P(2)—C(11)	104.2(3)		

in the two phenyl rings is 1.38 Å. The complex, as expected with bridging thiolato ligands, has a *sym cis–trans*-μ-chloro configuration.

The P—Pd—S bond angles at the two palladium atoms are significantly different. The angle at Pd(1) is very close to the ideal value 90° being 89.8(1)°, whereas at Pd(2) it is 93.5(1)°. In an earlier reported[8] platinum structure involving a dithiolato bridge, this angle is larger than 90° in order to minimize the steric crowding of the alkyl and aryl groups on the S and P atoms. The Cl—Pd—Cl bond angle [⟨94.4(1)°⟩] is normal, whilst the Cl(2)—Pd—S(1) angle [⟨84.7(1)°⟩] is considerably < 90° indicating the strain in the four-membered

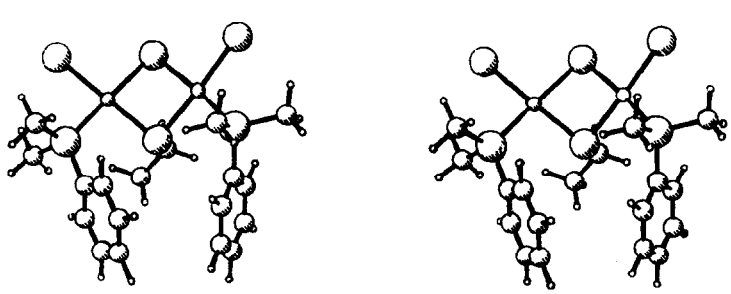

Fig. 2. Stereoview of the molecule.

Table 3. Comparison of bond lengths and angles in Pd and Pt complexes

Bond	Pd	Pt[a]
Average bond distances in angstroms		
M—Cl	2.334(1)	2.34(1)
M—μ-Cl	2.447(1)	2.45(1)
M—P	2.227(1)	2.22(1)
M—S	2.280(1)	2.24(1)
M—M′	3.234(1)	3.263(5)
Average bond angles in degrees		
Cl(1)—M—P(1)	91.2(1)	91.0(11)
Cl(3)—M′—P(2)	87.3(1)	89.1(11)
Cl(1)—M—Cl(2)	94.3(1)	94.0(11)
Cl(2)—M′—Cl(3)	94.5(1)	92.8(11)
P(1)—M—S	89.8(1)	93.0(11)
P(2)—M′—S	93.5(1)	95.1(11)
Cl(2)—M—S	84.6(1)	81.9(11)
Cl(2)—M′—S	84.8(1)	83.1(11)
M—Cl(2)—M′	82.9(1)	83.4(11)
M—S—M′	90.3(1)	93.5(11)

[a] Ref. 13.

ring. The Pd—S—Pd bond angle of 90.3(1)° lies within the wide range of values (83–92°) reported.[9,10] The angle at the bridging chlorine Pd—Cl(2)—Pd [⟨82.9(1)°⟩] is significantly smaller than that reported[11,12] in chloro bridged dinuclear palladium and platinum complexes but, agrees well with that observed in the analogous platinum derivative (Table 3). The two dimethyphenylphosphine ligands adopt different conformations. The methyl group C(7) on one of the P atoms [P(1)], lies very nearly in the plane of the phenyl ring attached to the same P atom. This is not seen at the other P atom. The mercaptoethyl group is in an axial configuration, with respect to the mean plane, through the Pd—Cl—S—Pd bridge atoms (Fig. 2). The two phenyl rings are inclined to each other at 128.0(3)° and make angles of 74.4(3)° and 89.8(2)° with their respective coordination planes. The Pd—Pd distance, as in the platinum derivative,[13] is 3.234(3) Å which is significantly shorter than hitherto reported[11,12] in halogen bridged dinuclear palladium(II) complexes. The structure, as seen from Table 3, seems to be isomorphous to the platinum derivative with the only significant difference being the angles P(1)—Pd(1)—S(1) and Pd(1)—S(1)—Pd(2), which are not as large as those observed in the platinum analogue. A comparison of the bond lengths and angles of the two homologous Pd and Pt complexes is given in Table 3. Figure 3 shows a packing of the two molecules in the unit cell.

EXPERIMENTAL

$[Pd_2Cl_2(\mu\text{-}Cl)_2(PMe_2Ph)_2]$ was prepared according to the literature method.[14] Analytical grade solvents were used throughout. General methods and spectroscopic techniques have been described previously.[1,2]

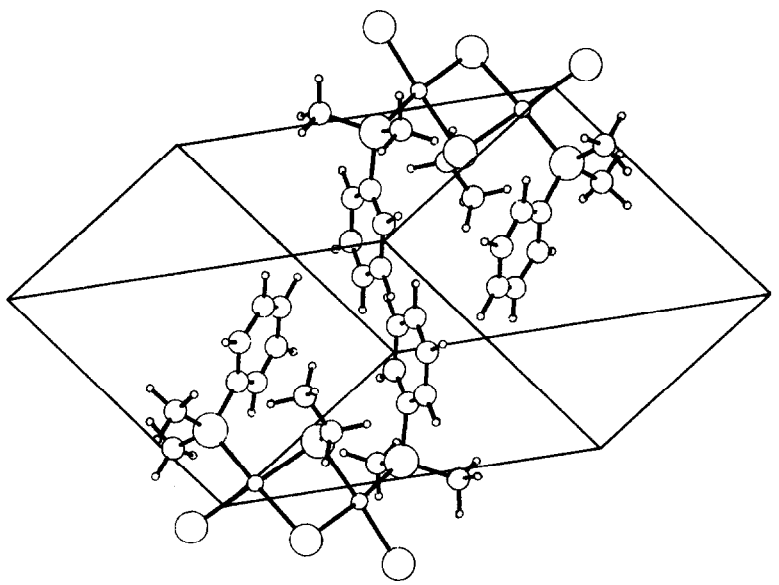

Fig. 3. Packing of two molecules in the unit cell.

Preparation of $[Pd_2Cl_2(\mu\text{-}SEt)_2(PMe_2Ph)_2]$

To an acetone suspension of $[Pd_2Cl_2(\mu\text{-}Cl)_2(PMe_2Ph)_2]$ (406 mg, 0.64 mmol) excess of ethyl mercaptan (0.5 cm^3) was added and the reaction mixture stirred at room temperature for 3 h. The solvent was stripped off and the residue was recrystallized from chloroform–methanol mixture to give yellow crystals in 88% (388 mg) yield. ^1H NMR data in $CDCl_3$ S—CH_2 δ 2.20 (Q, 7 Hz), 2.98 (m)*; S—C—CH_3 δ 0.92 (t, 7 Hz), 1.44 (t, 7 Hz)*; P—Me δ 1.66 (d, 11 Hz), 1.76 (d, 11 Hz); P—Ph δ 7.38–7.69 (m) (**trans* to phosphine ligand). Similar reaction with excess Pr^iSH, however, gave a mixture of products as revealed by ^{31}P NMR spectroscopy, but when carried out in 1:4 stoichiometry in acetone, yielded the dimercapto complex which was recrystallized thrice from acetone–methanol mixture. [^1H NMR in $CDCl_3$ —S—CH< δ 3.75(m), 3.05(m); —CMe_2 δ 1.70 (d, 6 Hz), 1.09 (d, 6 Hz); PMe_2 δ 1.67 (d, 11 Hz), 1.74 (d, 11 Hz); P—Ph δ 7.35–7.72 ppm.] The chloro–mercapto bridged complexes were obtained by heating an equimolar mixture of $[Pd_2Cl_2(\mu\text{-}Cl)_2(PMe_2Ph)_2]$ and $[Pd_2Cl_2(\mu\text{-}SEt)_2(PMe_2Ph)_2]$ in chloroform and recrystallizing them from chloroform–methanol. [^1H NMR in $CDCl_3$: $[Pd_2Cl_2(\mu\text{-}SEt)(\mu\text{-}Cl)(PMe_2Ph)_2]$: —$SCH_2$ δ 2.45 (q, 7 Hz, ^4J(P—H) 1.3 Hz); C—CH_3 δ 1.03 (t, 7 Hz); PMe_2 δ 1.92 (d, 12 Hz), 1.82 (d, 12 Hz); P—Ph δ 7.42–7.68 (m). $[Pd_2Cl_2(\mu\text{-}SPr^i)(\mu\text{-}Cl)(PMe_2Ph)_2]$: —SCH< δ 3.55 (m); —CMe_2 δ 1.15 (d, 6 Hz); PMe_2 δ 1.80 (d, 12 Hz), 1.91 (d, 12 Hz); PPh δ 7.33–7.81 (m).]

Crystallographic studies

(i) *Crystal data.* $C_{18}H_{27}P_2SCl_3Pd_2$, mol.wt. = 656.3, triclinic, $P\bar{1}$, $a = 9.273(3)$, $b = 10.412(3)$, $c = 13.767(6)$ Å, $\alpha = 80.84(3)$, $\beta = 81.62(3)$, $\gamma = 68.04(3)°$, volume = 1211.67 $Å^3$, $Z = 2$, $D_c = 1.80$ g cm^{-3}, $D_m = 1.78$ g cm^{-3}, $F(000) = 648$, $\mu = 18.68$ cm^{-1}.

(ii) *Data collection.* Intensity data for 4243 reflections were collected on an Enraf–Nonius CAD-4 diffractometer with graphite monochromator using Mo-K_α radiation ($\lambda = 0.7107$ Å) employing ω-2θ step scan in the range $2 \leqslant \theta \leqslant 25°$ with $0 \leqslant h \leqslant 11$, $-11 \leqslant k \leqslant 12$ and $-15 \leqslant l \leqslant 16$. Data were corrected for Lorentz and polarization effects. No absorption correction was applied.

(iii) *Structure determination.* The structure was solved by Patterson and successive Fourier methods. All hydrogen atoms were fixed at calculated positions. The non-hydrogen atoms were refined isotropically (five cycles) and anisotropically (three cycles) by the least-squares method. The final R for 3950 unique reflections [$I \geqslant 2.5\sigma(I)$] was 0.032 and wR = 0.049 with $[\Delta/ESD]_{max} = 0.709$. $\Delta\rho$ in the final difference map was 0.45 and -1.02 e $Å^{-3}$. Program SHELX76[15] and the ND-500 computer were used for all calculations, and the scattering factor for palladium was taken from *International Tables for X-ray Crystallography*, Vol. IV (1974).

Acknowledgements—The authors are thankful to the Analytical Chemistry Division for providing micro analysis of the compounds and, to Dr J. P. Mittal and Dr K. S. Venkateswarlu for their interest in this work.

N.B. Anisotropic temperature factors, hydrogen atom coordinates and F_o, F_c listings have been deposited with the Editor.

REFERENCES

1. V. K. Jain, *Inorg. Chim. Acta* 1987, **133**, 261.
2. V. K. Jain and G. S. Rao, *Inorg. Chim. Acta* 1987, **127**, 161.
3. H. C. Clark, V. K. Jain and G. S. Rao, *J. Organomet. Chem.* 1985, **279**, 181.
4. J. Chatt and F. A. Hart, *J. Chem. Soc.* 1953, 2363; P. L. Goggin, R. J. Goodfellow and F. J. S. Reed, *J. Chem. Soc.* 1971, 2031.
5. W. D. S. Motherwell and W. Clegg, *PLUTO Program for Plotting Molecules and Crystal Structures.* Univ. of Cambridge, England (1978).
6. H. C. Clark, G. Ferguson, V. K. Jain and M. Pervez, *Inorg. Chem.* 1985, **24**, 1477.
7. H. C. Clark, G. Ferguson, P. N. Kapoor and M. Pervez, *Inorg. Chem.* 1985, **24**, 3924.
8. M. C. Hall, A. J. Jarvis, B. T. Kilbourn and P. G. Owston, *J. Chem. Soc., Dalton Trans.* 1972, 1544.
9. R. O. Gould and M. M. Harding, *J. Chem. Soc.* (*A*) 1970, 875.
10. R. H. Fenn and G. R. Segrott, *J. Chem. Soc.* (*A*) 1979, 3197.
11. A. B. Goel, S. Goel and D. Van der Veer, *Inorg. Chim. Acta* 1981, **54**, L267.
12. J. R. Holden and N. C. Baenziger, *J. Am. Chem. Soc.* 1955, **77**, 4987.
13. V. K. Jain, R. P. Patel and V. M. Padmanabhan, unpublished results.
14. F. R. Hartley, *The Chemistry of Platinum and Palladium.* Wiley, New York (1973).
15. G. M. Sheldrick, *SHELX76. Program for Crystal Structure Determination.* Univ. of Cambridge, England (1976).

Polyhedron Vol. 8, No. 17, pp. 2157–2167, 1989
Printed in Great Britain

0277–5387/89 $3.00+.00
© 1989 Pergamon Press plc

SYNTHESIS, CHARACTERIZATION, AND X-RAY CRYSTAL STRUCTURE OF TRIS-ISOTHIOCYANATO COMPLEXES OF THE YTTRIUM(III) AND EUROPIUM(III) IONS WITH A SIX-NITROGEN-DONOR MACROCYCLIC LIGAND

G. BOMBIERI

Instituto di Chimica Farmaceutica, Universita di Milano, Milano, Italy

and

F. BENETOLLO* and A. POLO

Instituto di Chimica e Tecnologia dei Radioelementi, Area di Ricerca C.N.R., Corso Stati Uniti 4, Padova, Italy

and

L. DE COLA, W. T. HAWKINS and L. M. VALLARINO

Department of Chemistry, Virginia Commonwealth University, Richmond, VA 23284, U.S.A.

(*Received* 2 *February* 1989; *accepted* 14 *April* 1989)

Abstract—Tris-isothiocyanato complexes of the general formula $[M(NCS)_3L]$ have been synthesized and characterized, in which M is yttrium(III) or europium(III) and L is an 18-member macrocyclic ligand with a six-nitrogen-donor cavity ($L_I = C_{22}H_{26}N_6$, $L_{II} = C_{18}H_{18}N_6$). X-ray analysis of the yttrium(III) and europium(III) complexes of ligand L_I showed the coexistence in the same crystal of two kinds of nine-coordinate molecules with different macrocycle conformations. The two complexes were isostructural and crystallized in the monoclinic *Cc* space group, with cell parameters $a = 33.244(3)$, $b = 11.976(2)$, $c = 14.164(2)$ Å, $\beta = 92.72(5)°$ for europium and $a = 33.226(3)$, $b = 11.986(2)$, $c = 14.102(2)$ Å, $\beta = 92.84(5)°$ for yttrium. The structure of the europium(III) complex, refined by block matrix least-squares, gave the final values $R = 0.0236$ and $R_w = 0.0244$; the structure of the yttrium(III) complex, refined by full matrix, resulted in $R = 0.042$ and $R_w = 0.039$.

A considerable number of lanthanide(III) complexes with the six-nitrogen-donor macrocyclic ligands L_I and L_{II} (Fig. 1) have been synthesized by metal-templated, Schiff-base cyclic condensation of appropriate diamine and diketone precursors.[1–9] A representative selection of these compounds has been characterized by single-crystal X-ray diffraction analysis,[1,4,6–9] as well as infrared (IR) and nuclear magnetic resonance (NMR) spectra.[1–7] A detailed luminescence study has been carried out for a europium(III) derivative.[10,11] Yttrium(III) complexes of the same six-nitrogen macrocycles have also been reported.[12] All these complexes shared as a common feature the presence of a highly inert macrocyclic entity accompanied by two or three labile oxygen-donor exocyclic ligands, linked to the central metal ion on opposite sides of the macrocycle. The presence of coordinating oxygen-donor counterions, such as acetate or nitrate, was

* Author to whom correspondence should be addressed.

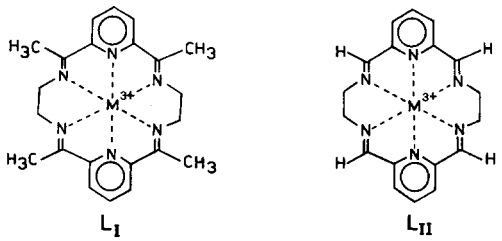

L_I L_{II}

Fig. 1. Schematic formulae of complexes of M^{3+} ions with the $L_I = C_{22}H_{26}N_6$ and $L_{II} = C_{18}H_{18}N_6$ macrocyclic ligands.

observed greatly to facilitate the metal-template synthesis of these macrocycles; however, substitution by non-coordinating counterions, or by counterions with different donor atoms, was shown to be feasible once the macrocyclic cations had been formed. In the present work, we set out to prepare and characterize a representative number of complexes of the L_I and L_{II} macrocycles with NCS^- counterions. The metals chosen were europium(III), for its potential as a monochromatic luminscent material, and yttrium(III), which being diamagnetic offers the opportunity for NMR studies.

EXPERIMENTAL

Starting materials and procedures

Sodium thiocyanate (Aldrich Chemical Co.) was dehydrated *in vacuo* over phosphorus pentoxide. The macrocyclic complexes of the general formula $ML(CH_3COO)_2Cl \cdot nH_2O$ (M = yttrium(III) and europium(III); L = $C_{22}H_{26}N_6$ (L_I) or $C_{18}H_{18}N_6$ (L_{II}); n = 3–6) were prepared as previously described.[5,12] All solvents were reagent grade and anhydrous unless stated otherwise. Thermogravimetric measurements were carried out on Perkin–Elmer TGS-2 thermogravimetric system, under a dry helium flow of 60 $cm^3\,min^{-1}$. IR spectra were taken with a Perkin–Elmer Model 160 FTIR spectrophotometer. Fluorescence spectra were taken with an SLM-Model 800 photon-counting spectrofluorometer. ^1H NMR spectra were obtained with a JEOL FX90 Q spectrometer. Microanalyses (C, H, N) were performed by Atlantic Microlabs, Atlanta, Georgia.

Preparation of the $[M(NCS)_3L]$ *complexes* (M = *yttrium*(III) *or europium*(III); L = L_I *or* L_{II})

All complexes were obtained by metathesis from the corresponding diacetate-chloride salts, following the procedure outlined here for the Y—L_I species. A filtered solution of $YL_I(CH_3COO)_2Cl \cdot 4H_2O$ in methanol (1 mmol in 75 cm^3) and a filtered solution of NaNCS in methanol (4 mmol in 35 cm^3) were each warmed to approximately 60°C and mixed. The resulting solution was stoppered lightly and allowed to stand at room temperature for several days. The off-white crystalline solid that formed was filtered, washed first with cold methanol and then with diethylether, and dried *in vacuo* over phosphorus pentoxide. Yields, *ca* 60%. Found: C, 47.1; H, 4.3; N, 19.8. Calc. for $Y(NCS)_3(C_{22}H_{26}N_6)$: C, 47.1; H, 4.1; N, 19.8%.

The other complexes of this series also had analyses corresponding to the anhydrous $[M(NCS)]_3L$ species.

X-ray measurements and structure determination

A single crystal of $[Eu(NCS)_3L_I]$, having approximate dimensions $0.41 \times 0.28 \times 0.40$ mm, was used for data collection on a Philips PW1100 diffractometer. Final lattice parameters, as determined from a least-squares refinement of $(\sin\theta)/\lambda^2$ values for 18 reflections ($2\theta < 25°$) accurately centred on the diffractometer, are given in Table 1 together with the details of data collection. The intensities were corrected for Lorentz, polarization and absorption following North and Phillips method.[13]

The structure of the Eu—L_I complex was solved via Patterson function and refined first in the space group $C2/c$, with a molecule of $[Eu(NCS)_3L_I]$ as the asymmetric unit. In this space group the refinement stopped at $R = 15\%$, with unrealistic values of bond distances and angles. Attempts to interpret the ligand structure with a statistical distribution of the atoms of the macrocyclic ligand were unsuccessful. Starting from two europium(III) positions of the $C2/c$ space group, and moving them out of the symmetry-related positions of $C2/c$ to partly eliminate the centrosymmetric solution for the rest of the molecule, we were able to interpretate the electron density residuals in terms of two independent $[Eu(NCS)_3L_I]$ units in the non-centrosymmetric Cc space group. Refinement was accomplished in blocks, refining alternatively the $[Eu(1)(NCS)_3L_I]$ and $[Eu(2)(NCS)_3L_I]$ units, with anisotropic thermal parameters for all non-hydrogen atoms. The hydrogens were introduced at calculated positions (C—H = 0.98 Å), with fixed unique isotropic thermal parameter ($U = 0.07$ Å^2), and allowed to ride on associated carbon atoms. The refinement converged to $R = 0.0236$, $R_w = 0.0244$. The function minimized was $\Sigma w(|F_o| - |F_c|)^2$. The number of parameters for each block was 348. In the final difference map, $\Delta\rho$ was

Table 1. Crystal data

Formula	$EuC_{25}H_{26}N_9S_3$	$YC_{25}H_{26}N_9S_3$
W	700.70	637.64
Crystal system	Monoclinic	Monoclinic
a (Å)	33.244(3)	33.226(3)
b (Å)	11.976(2)	11.986(2)
c (Å)	14.164(2)	14.102(2)
β (°)	92.72(5)	92.84(5)
U (Å^3)	5632.8	5609.2
Space group	Cc	Cc
D_c (g cm^{-3})	1.65	1.51
Z	8	8
$F(000)$	2800	2608
Radiation	Mo-K_α	Mo-K_α
μ (cm^{-1})	23.3	22.7
Reflection measured	5425	4377
Scan method	$\theta/2\theta$	$\theta/2\theta$
Scan speed (° min^{-1})	1.8	1.8
Scan width (°)	1.20	1.20
Background counts (s)	20	20
$2\theta_{max}$ (°)	50°	50°
σ limit [$I \geqslant n\sigma(I)$]	$n = 3$	$n = 3$
Unique observed data with [$I \geqslant 3\sigma(I)$]	3337	1672
No. of parameters	348 (For each of the two blocks)	398
Weighting scheme w	$1[\sigma^2(F_o)+0.000320(F_o)^2]^{-1}$	$1.5364[\sigma^2(F_o)+0.000431(F_o)^2]^{-1}$
$R = \Sigma[\|F_o\|-\|F_c\|]/\Sigma\|F_o\|$	0.0236	0.042
$R_w = [\Sigma w(\|F_o\|-\|F_c\|)^2/\Sigma w\|F_o\|^2]^{1/2}$	0.0244	0.039
Max Δ/σ	0.1	0.6
GOF	1.0	1.6
Standard reflections	121–151	−311 6–22 55–3
Min–max trans. coeff.	0.78–0.82	0.79–0.81

$< |0.3|$ e Å^{-3}. Scattering factors and anomalous dispersion corrections were taken from the *International Tables for X-ray Crystallography*.[14] The programs used were SHELX 76[15] for the structure solution and refinement, ORTEP[16] and PLUTO[17] for drawing, and PARST[18] for geometrical calculations.

Data collection and treatment for the yttrium(III) compound were carried out as described for the europium(III) analogue. A single crystal of the yttrium(III) complex, having approximate dimensions 0.10 × 0.24 × 0.32 mm, was used for the analysis and crystallographic parameters are reported in Table 1. The $[Y(NCS)_3L_I]$ compound was isostructral with the europium(III) analogue and its structure was solved in a similar manner. (In this case, too, no reasonable results were obtained from a $C2/c$ centrosymmetric solution.) However, owing to the poor quality of the crystal, and consequently to the limited number of reflections observed (see Table 1), only the yttrium(III) and NCS groups were refined anisotropically, while the other non-hydrogen atoms were refined isotropically. The hydrogens were included in calculated positions, as described for the europium(III) complex. The number of parameters refined by full matrix least-squares was 398, and the refinement converged to $R = 0.042$ and $R_w = 0.039$. In the final difference Fourier map, $\Delta\rho$ was $< |0.35|$ e Å^{-3}.

Bond lengths and angles are given in Tables 2 and 3, and torsion angles are given in Tables 4 and 5. Supplementary material (tables of atomic coordinates, atomic vibrations and calculated structure amplitudes) has been deposited at the Cambridge Crystallographic Data Centre.

RESULTS AND DISCUSSION

General characteristics of the complexes

The $[M(NCS)_3L]$ complexes synthesized and investigated in this work were nearly colourless crystalline solids, stable to air and moisture and

Table 2. Bond lengths (Å) and angles (°) for $[Eu(NCS)_3L_I]$, with ESDs in parentheses

(a) Europium environment

Eu(1)—N(1)	2.656(8)	Eu(2)—N(11)	2.719(8)
Eu(1)—N(2)	2.668(9)	Eu(2)—N(12)	2.625(7)
Eu(1)—N(3)	2.538(8)	Eu(2)—N(13)	2.578(8)
Eu(1)—N(4)	2.542(7)	Eu(2)—N(14)	2.569(8)
Eu(1)—N(5)	2.592(8)	Eu(2)—N(15)	2.639(7)
Eu(1)—N(6)	2.489(8)	Eu(2)—N(16)	2.560(8)
Eu(1)—N(60)	2.475(8)	Eu(2)—N(10)	2.429(9)
Eu(1)—N(70)	2.527(8)	Eu(2)—N(20)	2.439(8)
Eu(1)—N(80)	2.514(7)	Eu(2)—N(30)	2.411(9)
N(60)—C(60)	1.19(1)	N(10)—C(101)	1.08(1)
N(70)—C(70)	1.26(1)	N(20)—C(102)	1.16(1)
N(80)—C(80)	1.14(1)	N(30)—C(103)	1.16(1)
C(60)—S(60)	1.56(1)	C(101)—S(1)	1.69(1)
C(70)—S(70)	1.55(1)	C(102)—S(2)	1.656(8)
C(80)—S(80)	1.58(1)	C(103)—S(3)	1.680(9)

N(1)—Eu(1)—N(2)	61.3(3)	N(11)—Eu(2)—N(12)	58.7(3)
N(1)—Eu(1)—N(6)	61.7(3)	N(11)—Eu(2)—N(16)	63.3(3)
N(2)—Eu(1)—N(3)	61.7(3)	N(12)—Eu(2)—N(13)	62.4(3)
N(3)—Eu(1)—N(4)	60.5(3)	N(13)—Eu(2)—N(14)	60.3(3)
N(4)—Eu(1)—N(5)	61.1(3)	N(14)—Eu(2)—N(15)	60.3(3)
N(5)—Eu(1)—N(6)	62.8(3)	N(15)—Eu(2)—N(16)	62.2(3)
N(60)—Eu(1)—N(70)	145.5(4)	N(10)—Eu(2)—N(20)	137.8(4)
N(60)—Eu(1)—N(80)	143.3(5)	N(10)—Eu(2)—N(30)	75.1(5)
N(70)—Eu(1)—N(80)	70.0(4)	N(20)—Eu(2)—N(30)	146.6(5)
Eu(1)—N(60)—C(60)	145.8(9)	Eu(2)—N(20)—C(102)	139.7(9)
N(60)—C(60)—S(60)	168(1)	N(20)—C(102)—S(2)	164.9(9)
Eu(1)—N(70)—C(70)	127.0(9)	Eu(2)—N(10)—C(101)	136(1)
N(70)—C(70)—S(70)	174(1)	N(10)—C(101)—S(1)	171(1)
Eu(1)—N(80)—C(80)	151.7(9)	Eu(2)—N(30)—C(103)	149(1)
N(80)—C(80)—S(80)	175(1)	N(30)—C(103)—S(3)	176(1)

(b) Macrocycle

Eu—N(py)—C	119.9(8)	Eu—N(aliphatic)—C	119.4(8)
N—C(py) 1.34(1)	C—C(py) 1.38(1)	C—C(aliphatic)	1.51(1)

extremely stable to heat; their thermogravimetric analysis showed only a gradual mass loss of < 1% up to 250°C. The IR absorption spectra of the yttrium(III) and europium(III) complexes of each macrocycle were identical to one another and those of complexes of the L_I and L_{II} macrocycles were extremely similar. Each spectrum showed the very strong characteristic ν(C≡N) absorptions at *ca* 1640 and 1590 cm^{-1}, together with the "fingerprint pattern" of the respective macrocycle[12] and the absorptions arising from the N-bonded NCS^- ligands. For the Y—L_I complex, the latter had the following values (cm^{-1}): ν(C≡N), 2062 sh, 2049 vs; ν(C—S), 813 m-w, partly overlaid by macrocycle absorption; ν(M—N), 488 sh, 474 w; similar values were observed for the other complexes. The splitting of the ν(C≡N) and the ν(M—N) absorptions was consistent with the low symmetry of the $M(NCS)_3$ moiety as determined by X-ray crystallography.

The $[M(NCS)_3L]$ complexes were insoluble in water and either insoluble or sparingly soluble in most organic solvents. This prevented the measurement of carbon-13 NMR spectra under the conditions of our experiment; however, the proton spectrum of the Y—L_I complex in deuterodimethylsulphoxide gave results consistent with the presence in solution of a highly symmetrical macrocyclic entity which did not undergo degradation over a period of several days. (^{1}H chemical

Table 3. Bond lengths (Å) and angles (°) for $[Y(NCS)_3L_I]$, with ESDs in parentheses

(a) Yttrium environment

Y(1)—N(1)	2.58(4)		Y(2)—N(11)	2.65(4)	
Y(1)—N(2)	2.57(3)		Y(2)—N(12)	2.54(3)	
Y(1)—N(3)	2.50(4)		Y(2)—N(13)	2.46(2)	
Y(1)—N(4)	2.57(3)		Y(2)—N(14)	2.55(3)	
Y(1)—N(5)	2.63(3)		Y(2)—N(15)	2.72(3)	
Y(1)—N(6)	2.56(3)		Y(2)—N(16)	2.51(4)	
Y(1)—N(60)	2.40(3)		Y(2)—N(10)	2.53(4)	
Y(1)—N(70)	2.39(3)		Y(2)—N(20)	2.40(3)	
Y(1)—N(80)	2.49(4)		Y(2)—N(30)	2.35(3)	
N—C(NCS)$_{av.}$	1.20(5)		N—C(NCS)$_{av.}$	1.12(6)	
C—S(NCS)$_{av.}$	1.53(4)		C—S(NCS)$_{av.}$	1.69(4)	
N(1)—Y(1)—N(2)		61(1)	N(11)—Y(2)—N(12)		61(1)
N(1)—Y(1)—N(6)		66(1)	N(11)—Y(2)—N(16)		61(1)
N(2)—Y(1)—N(3)		60(1)	N(12)—Y(2)—N(13)		63.9(9)
N(3)—Y(1)—N(4)		63(1)	N(13)—Y(2)—N(14)		58.3(8)
N(4)—Y(1)—N(5)		60(1)	N(14)—Y(2)—N(15)		60.2(9)
N(5)—Y(1)—N(6)		60(1)	N(15)—Y(2)—N(16)		64(1)
N(60)—Y(1)—N(70)		143(1)	N(10)—Y(2)—N(20)		141(1)
N(60)—Y(1)—N(80)		146(1)	N(10)—Y(2)—N(30)		76(1)
N(70)—Y(1)—N(80)		69(1)	N(20)—Y(2)—N(30)		143(1)
Y(1)—N(60)—C(60)		155(2)	Y(2)—N(20)—C(102)		140(2)
Y(1)—N(70)—C(70)		141(2)	Y(2)—N(10)—C(101)		118(4)
Y(1)—N(80)—C(80)		155(3)	Y(2)—N(30)—C(103)		145(2)
N—C—S$_{av.}$		169(3)	N—C—S$_{av.}$		170(3)

(b) Macrocycle

Y—N(py)—C$_{av.}$		120.9(2)	Y—N(aliphatic)—C$_{av.}$		119.5(2)
N—C(py)$_{av.}$	1.35(5)	C—C(py)$_{av.}$	1.39(5)	C—C(aliphatic)$_{av.}$	1.52(5)

shifts, δ, ppm vs. TMS: 8.40–8.35, complex pattern, 6H, py; 3.95, 8H, CH_2; 2.55, 12H, CH_3.) These values were very similar to those previously reported for complexes of the same ligand with other diamagnetic metal ions and/or other counterions.[6,12] In the solid state, the tris-isothiocyanato complexes of europium(III) showed the modest ligand-mediated luminescence (most intense emissions: *ca* 615 nm) that has been observed for these same macrocycles in the presence of acetates as counterions.[11] In solution, the luminescence was almost completely quenched.

Crystal structure of the europium(III)—L_I *and yttrium*(III)—L_I *tris-isothiocyanato complexes*

The crystal of the europium complex was found to contain two distinct molecules, having the same formula, $[Eu(NCS)_3L_I]$, as well as the same metal coordination environment, but differing in the conformation of the L_I macrocyclic ligand. The structures of the two complex molecules are illustrated as ORTEP drawings in Figs 2a and 2b. In each molecule the Eu^{III} ion is linked to the six nitrogen atoms of the macrocyclic ligand, which consists of two approximately planar sections hinged at the —CH_2—CH_2— side chains to give a "folded butterfly" configuration. In addition, the Eu^{III} is linked to the three nitrogen atoms of the isothiocyanato ligands, two on the convex side of the macrocycle and the third on the opposite side. However, the two complex molecules differ in the conformations of the macrocyclic ligands, and two "planar" sections of which exhibit different foldings (111.3° for molecule *a* and 102.1° for molecule *b*). The torsion angles about the —CH_2—CH_2— side chains are also different: for molecule *a*, N(2)—C(8)—C(9)—N(3) is 55(1)° and N(5)—C(19)—C(20)—N(6) is 48(1)°; for molecule *b*, N(15)—C(49)—C(50)—N(16) is 50(1)° and

Table 4. Torsion angles (°) for $[Eu(NCS)_3L_I]$

C(1)—N(1)—C(5)—C(6)	179(1)	C(31)—N(11)—C(35)—C(36)	−173(1)
N(1)—C(5)—C(6)—N(2)	−5(2)	N(11)—C(35)—C(36)—N(12)	−12(2)
C(5)—C(6)—N(2)—C(8)	−178(1)	C(35)—C(36)—N(12)—C(38)	176(1)
C(6)—N(2)—C(8)—C(9)	177(1)	C(36)—N(12)—C(38)—C(39)	−174(1)
N(2)—C(8)—C(9)—N(3)	55(1)	N(12)—C(38)—C(39)—N(13)	−49(1)
C(8)—C(9)—N(3)—C(10)	104(1)	C(38)—C(39)—N(13)—C(40)	−109(2)
C(9)—N(3)—C(10)—C(12)	−172(1)	C(39)—N(13)—C(40)—C(42)	176(1)
N(3)—C(10)—C(12)—N(4)	−11(2)	N(13)—C(40)—C(42)—N(14)	5(2)
C(10)—C(12)—N(4)—C(16)	−178(1)	C(40)—C(42)—N(14)—C(46)	−5(1)
C(12)—N(4)—C(16)—C(17)	−5(1)	C(42)—N(14)—C(46)—C(47)	−169(1)
N(4)—C(16)—C(17)—N(5)	10(1)	N(14)—C(46)—C(47)—N(15)	−8(2)
C(16)—C(17)—N(5)—C(19)	−178(1)	C(46)—C(47)—N(15)—C(49)	172(1)
C(17)—N(5)—C(19)—C(20)	172(1)	C(47)—N(15)—C(49)—C(50)	−168(1)
N(5)—C(19)—C(20)—N(6)	48(1)	N(15)—C(49)—C(50)—N(16)	−50(1)
C(19)—C(20)—N(6)—C(21)	113(1)	C(49)—C(50)—N(16)—C(51)	−104(2)
C(20)—N(6)—C(21)—C(1)	−173(1)	C(50)—N(16)—C(51)—C(31)	171(1)
N(6)—C(21)—C(1)—N(1)	166(2)	N(16)—C(51)—C(31)—N(11)	−168(2)
C(21)—C(1)—N(1)—C(5)	2(1)	C(51)—C(31)—N(11)—C(35)	2(1)

N(12)—C(38)—C(39)—N(13) is 43(1)°. Thus, even though the Eu^{III} ions are located close to the *C2/c* general positions, the conformations of the macrocyclic ligands cause the space group symmetry to be lowered to *Cc*. The coexistence of two species with different stoichiometries and/or slightly different conformations appears to be a common feature in macrocyclic complexes of the lanthanides.[6,12,19,20]

Examination of the europium(III) coordination sphere in molecules *a* and *b* shows some interesting features. In molecule *a*, where the folding of the macrocycle is smaller (111.3° for *a* vs 102.1° for *b*), each of the Eu—N_L bond distances is shorter than the corresponding distance in *b*, even though the same trends are observed for the Eu—N_{py} and Eu—$N_{aliphatic}$ distances. Conversely, the average Eu—NCS bond distance is longer for Eu(1) in *a* (2.505 Å) than for Eu(2) in *b* (2.427 Å). The NCS^- ligands themselves are all appreciably different from one another, even though each shows the same structural pattern. In each case the NCS group is linear but the Eu—NCS linkage is bent at the N atoms, with an average M—N—C angle of 142° in

Table 5. Torsion angles (°) for $[Y(NCS)_3L_I]$

C(1)—N(1)—C(5)—C(6)	169(3)	C(31)—N(11)—C(35)—C(36)	−175(4)
N(1)—C(5)—C(6)—N(2)	−2(5)	N(11)—C(35)—C(36)—N(12)	−7(5)
C(5)—C(6)—N(2)—C(8)	−172(3)	C(35)—C(36)—N(12)—C(38)	173(3)
C(6)—N(2)—C(8)—C(9)	177(3)	C(36)—N(12)—C(38)—C(39)	−174(3)
N(2)—C(8)—C(9)—N(3)	44(4)	N(12)—C(38)—C(39)—N(13)	−47(4)
C(8)—C(9)—N(3)—C(10)	104(4)	C(38)—C(39)—N(13)—C(40)	−103(4)
C(9)—N(3)—C(10)—C(12)	−172(3)	C(39)—N(13)—C(40)—C(42)	162(3)
N(3)—C(10)—C(12)—N(4)	−3(5)	N(13)—C(40)—C(42)—N(14)	14(4)
C(10)—C(12)—N(4)—C(16)	173(3)	C(40)—C(42)—N(14)—C(46)	7(3)
C(12)—N(4)—C(16)—C(17)	6(3)	C(42)—N(14)—C(46)—C(47)	−178(3)
N(4)—C(16)—C(17)—N(5)	12(4)	N(14)—C(46)—C(47)—N(15)	−3(5)
C(16)—C(17)—N(5)—C(19)	−176(3)	C(46)—C(47)—N(15)—C(49)	173(4)
C(17)—N(5)—C(19)—C(20)	170(3)	C(47)—N(15)—C(49)—C(50)	−163(4)
N(5)—C(19)—C(20)—N(6)	49(3)	N(15)—C(49)—C(50)—N(16)	−61(4)
C(19)—C(20)—N(6)—C(21)	120(3)	C(49)—C(50)—N(16)—C(51)	−105(4)
C(20)—N(6)—C(21)—C(1)	171(3)	C(50)—N(16)—C(51)—C(31)	174(3)
N(6)—C(21)—C(1)—N(1)	178(4)	N(16)—C(51)—C(31)—N(11)	−158(5)
C(21)—C(1)—N(1)—C(5)	0(3)	C(51)—C(31)—N(11)—C(35)	−10(4)

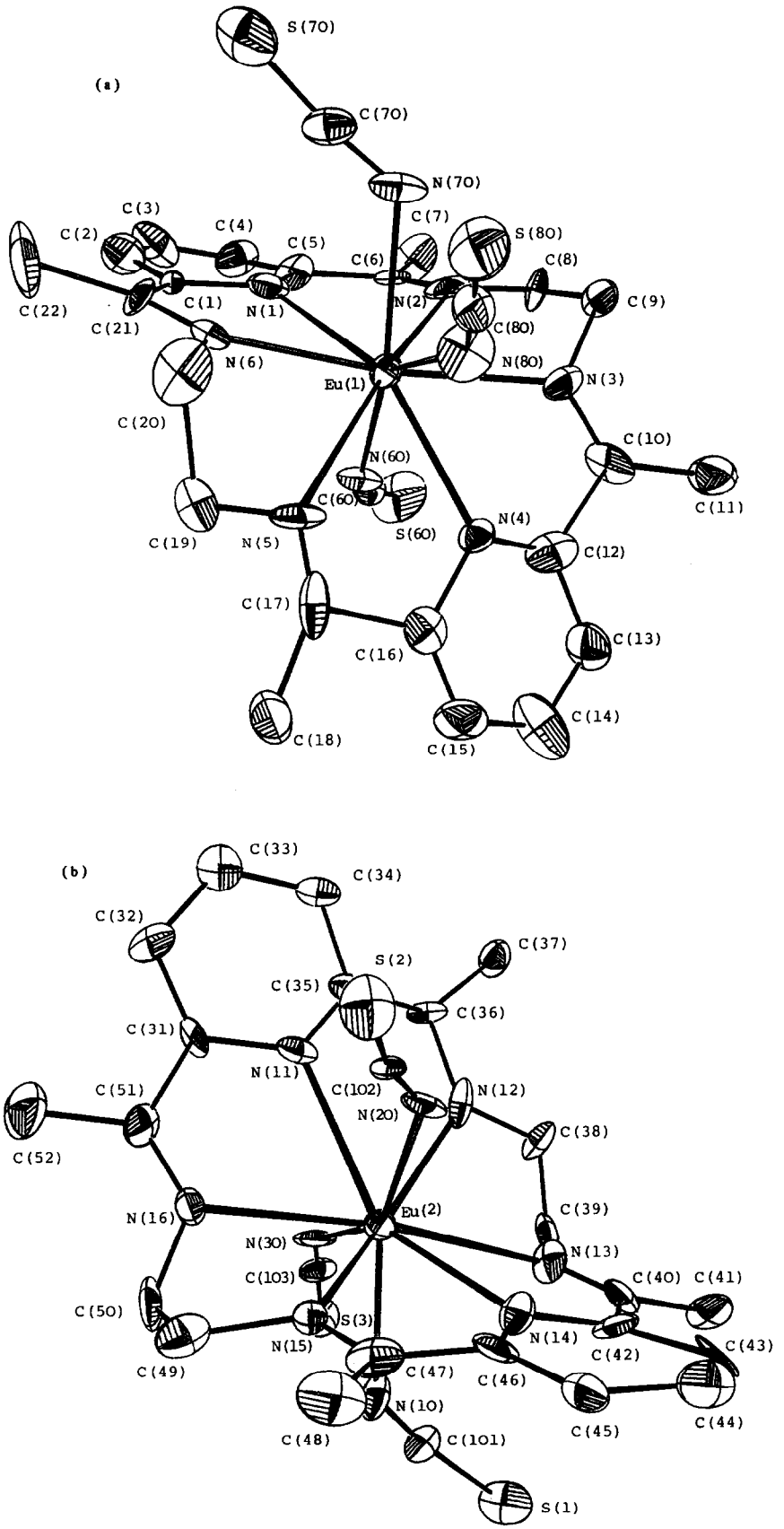

Fig. 2. ORTEP view of the two independent molecules present in the crystal of $[Eu(NCS)_3L_1]$. (Ellipsoids are at 40% probability; hydrogen atoms are omitted for clarity.)

both *a* and *b*; individual M—N—C angles range from 127.0 to 151.7°. A considerable variation is also observed in the bond lengths of the isothiocyanato ligands; the C—N distances range from 1.08 to 1.26 Å, whilst the C—S distances range from 1.55 to 1.69 Å. Considering that the two main resonance forms for a coordinated isothiocyanato ligand are M—N≡C—S (M—N—C angle, 180°; Pauling bond lengths: N≡C, 1.15 Å, C—S, 1.81 Å) and M—N=C=S (M—N—C angle, 120°; Pauling bond lengths:[21] N=C, 1.29 Å, C=S, 1.61 Å), the observed bond angles and distances suggest that both forms contribute, to only slightly different extents, to the Eu—NCS bonding in these molecules. Thus, the metal–NCS linkage in $[Eu(NCS)_3L_I]$ differs appreciably from that present in the salt $[(C_4H_9)_4N]_3[Er(NCS)_6]$, the only other isothiocyanato lanthanide(III) complex for which the structure is known.[22] In the octahedral $[Er(NCS)_6]^{3-}$ ion, the Er—N—C—S groups are nearly linear, with the N—C bond [1.10(3) Å] and the S—C bond [1.61(3) Å] just slightly shorter than expected for the linear resonance form above.[21]

A comparison among the bond angles and distances of the Eu(1)—NCS groups further reveals that, as the M—N—C angle decreases and approaches 120°, the corresponding C—N bond length increases while the C—S bond length decreases, each approaching its typical double bonded value; whilst the Eu(2)—NCS groups do fit into this pattern for that concerning the C—N bond distances and the M—N—C angles, also if the C—N average fits better into a triple bond value and the C—S into a single bond value. Inconsistencies of this kind have been observed for other metal–isothiocyanate complexes,[22] as steric factors and packing requirements can also play an important rôle in determining the NCS ligand geometries. The molecule packing of $[Eu(NCS)_3L_I]$, viewed down the *b* axis, is shown in Fig. 3. The structure is rather compact and shows a number of intermolecular contacts among sulphur atoms and also between sulphur atoms and macrocycle atoms; these contacts might be responsible for the peculiarities in bond angles and distances observed for the isothiocyanate ligands. Two rather short interactions are S(80)···S(3)′ ('$1/2+x$, $1/2-y$, z) of 3.718(9) Å and S(2)···S(60)″ ("x, $1-y$, $3/2+z$) of 3.592(7) Å. The S(70) atom is involved also in numerous contacts of the order of 3.5 Å with the carbon atoms of the adjacent molecules at x, $-y$, $1/2+z$ (for Eu(1)—L), and x, $1-y$, $-1/2+z$ (for Eu(2)—L). This could account for the highest bending for Eu(1)—N(70)—C(70) angle 127.0(9)°.

The structure of the yttrium(III) complex $[Y(NCS)_3L_I]$, was studied to obtain information on the effect of the metal ionic radius on the conformation of the macrocycle. The yttrium complex was found to be isostructural with the europium analogue and, similar to it, was characterized by the presence in the crystal lattice of two molecules of identical formula but different ligand conformations. The two "planar" halves of the L_I ligand formed an angle of 111.1(4)° for Y(1) and 103.2(4)° for Y(2), maintaining the trend observed for the europium analogue. The isothiocyanate ligands were again coordinated to the metal ion in an angular fashion, and their bond distances followed the general trend previously discussed for the europium species, the average values being N—C = 1.21(5) Å, C—S = 1.54(4) Å for Y(1), and N—C = 1.13(6) Å, C—S = 1.70(5) Å for Y(2). Unfortunately, the poor quality of the yttrium crystal, and consequently the high values of the ESDs, did not allow the observation of subtle differences in the bond lengths of Y(1) and Y(2). For example, the Y(1)—NCS average distance, 2.44(5) Å, was indistinguishable from the Y(2)—NCS average distance, 2.43(5) Å. Similarly, Y(1)—N_L and Y(2)—N_L had the same average value, 2.57(4) Å, coincident with the value of 2.570(8) Å reported for the nine-coordinated yttrium(III) complex $[Y(CH_3COO)_{1.5}(H_2O)_{0.5}L](CH_3COO)_{0.5}ClO_4$.[12] These yttrium(III)–ligand bond lengths, when compared to the corresponding values of the europium(III) species, reflect exactly the difference in ionic radii of the two metal ions for C.N. = 9, as given by Shannon.[23]

Attempts to describe the coordination polyhedron of the Eu^{III} and Y^{III} ions in the $[M(NCS)_3L_I]$ complexes in terms of their preferred nine-coordinate geometries, tricapped trigonal prism or monocapped square antiprism, were unsuccessful. We then attempted to describe the coordination of the macrocycle through the geometrical arrangement of the nitrogen atoms around the metal centre. The puckering analysis[24] on these six-nitrogen moieties gave the following results: with the smaller Y^{3+} ion, the puckering constants were $Q = 1.16(4)$, $\theta = 93(2)°$ and $\phi = 137(2)°$ for Y(1), and $Q = 1.16(4)$, $\theta = 85(2)°$ and $\phi = -42(2)°$ for Y(2) species; in each case the six-nitrogen ring was not planar but had a slightly twisted half-chair conformation. For the europium(III) analogue, the puckering constants were $Q = 1.10(1)$, $\theta = 90.5(6)°$, $\phi = 139.5(7)°$ in the Eu(1) species and $Q = 1.12(1)$, $\theta = 87.7(7)°$, and $\phi = -39.5(6)°$ in the Eu(2) species; the six-nitrogen ring had approximately the same half-chair conformation as in the yttrium(III) species. The only possible geometrical description of the coordination polyhedron is based on an approxi-

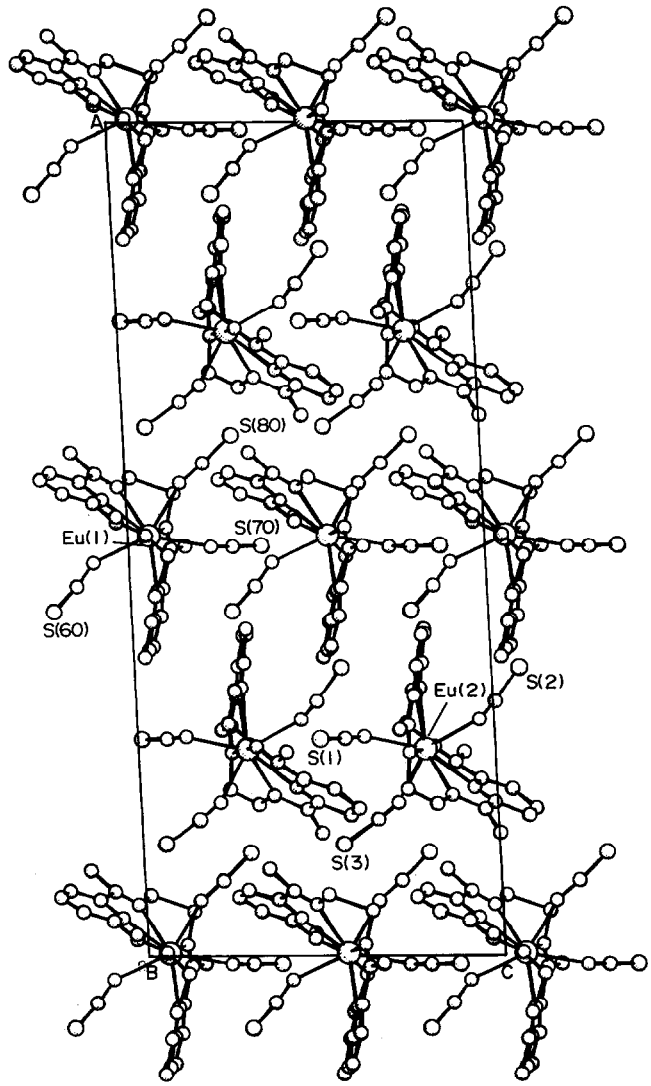

Fig. 3. Unit cell of $[Eu(NCS)_3L_I]$ viewed down the *b* axis.

mately planar pentagon defined by the two nitrogens of the pyridine rings, N(1) and N(4), and the three nitrogens of the NCS moieties N(60), N(70) and N(80), with deviations from the best mean plane ranging from −0.476(10) to 0.376(9) Å. The two nitrogens of one diamine moiety, N(2) and N(3), are below this five-nitrogen plane (−2.16(1) and −2.17(1) Å); those of the other diimine moiety, N(5) and N(6), are above it (2.23(1) and 2.22(1) Å). The values for Eu(1) do not differ appreciably from those for Eu(2), Y(1) and Y(2); they are reported as examples of this unusual geometrical situation.

Finally, it is instructive to compare the bending of the L_I macrocycle in the complexes reported here with that observed in complexes of the same ligand with other lanthanides and/or other negative ligands. The values of the macrocycle foldings are shown in Table 6, together with the coordination numbers and ionic radii of the central metals. For the nitrato-complexes, the progressive departure from planarity from lanthanum(III) to neodymium(III) was explained as a requirement to maintain six-coordination as the radius of the central metal decreased.[7] A similar trend was observed for the yttrium(III)[12] and lutetium(III)[6] with acetates as anionic ligands. In contrast, for the isothiocyanato complexes described in the present study, the folding of the macrocycle does not match the values of the ionic radii. Furthermore, the presence within the same crystal of two complex entities with the same formula but different foldings suggests that the NCS^- ligands, being less bulky than either nitrates or acetates, allow a greater flexibility of the macrocycle, so that the con-

Table 6. Dihedral angles for six-nitrogen macrocycles of the lanthanides

Macrocyclic complex[a]	Coordination number of metal ion	Ionic radius (Å)[b]	Macrocycle folding (°)	Ref.
$[La(NO_3)_3L_I]$	12	1.216	153.3	7
$[Ce(NO_3)_2(H_2O)L_I]^+$	11	1.196	121.0	7
$[Nd(NO_3)(H_2O)_2L_I]^{2+}$	10	1.163	116.1	7
$[Lu(CH_3COO)(H_2O)L_I]^{2+}$	9	1.032	114.4	6
$[Lu(CH_3COO)(CH_3OH)L_I]^{2+}$	9	1.032	114.4	6
$[Y(CH_3COO)(H_2O)L_I]^{2+}$	9	1.075	115.7	12
$[Y(CH_3COO)(CH_3COO)L_I]^+$	9	1.075	115.7	12
$[Eu(NCS)_3L_I]$	9	1.120	111.3 102.1	This work
$[Y(NCS)_3L_I]$	9	1.075	111.1 103.2	This work

[a] In all these species, the macrocycle is bent towards the less hindering single ligand.
[b] According to Shannon for IX coordination.[23]

formation is influenced to a rather significant extent also by crystal packing requirements.

CONCLUSIONS

This work has shown that the trivalent yttrium and europium cations, when coordinated to the six-nitrogen cavity of the 18-member macrocyclic systems L_I and L_{II}, display an unusual preference for the N-donor atoms of the NCS ligands, compared to either the O-donor atoms of polar solvents (water, methanol) or those of negatively charged ligands such as acetates. The molecular tris-isothiocyanato complexes, $[M(NCS)_3L]$, are insoluble in water and either insoluble or sparingly soluble in most organic solvents; also, unlike most other salts of these macrocycle systems, they show no tendency to include solvent molecules in either the metal coordination sphere or the crystal lattice. The electronic and steric requirements of the central Y^{III} and Eu^{III} ion appear to be fully satisfied by coordination to nine nitrogen atoms—six from the macrocycle cavity and three from the isothiocyanato groups. The remarkable stability of this nine-nitrogen coordination sphere, not previously observed in compounds of yttrium(III) or the lanthanide(III) ions, is further emphasized by the nearly identical folding of the macrocycle in the yttrium(III) and europium(III) species, despite the difference in the ionic radii of these two elements. The coexistence of different macrocycle conformations within the same crystal, in the absence of external influences due to chlathrated solvent molecules, suggests that the conformation of the macrocycle is the result of several cooperative factors that include not only the ionic radius of the encapsulated metal ion but also crystal packing forces and steric requirements of the exocyclic ligands.

Acknowledgements—This work was supported in part by Virginia Commonwealth University and by NATO Bilateral Project No. 184/85.

REFERENCES

1. J. D. J. Backer-Dirks, C. J. Gray, F. A. Hart, M. B. Hursthouse and B. C. Schoop, *J. Chem. Soc., Chem. Commun.* 1979, 774.
2. W. Radeck-Paryzek, *Inorg. Chim. Acta* 1980, **45**, L147; W. Radecka-Paryzek, *Inorg. Chim. Acta* 1981, **52**, 261.
3. K. K. Abid and D. E. Fenton, *Inorg. Chim. Acta* 1984, **95**, 119.
4. K. K. Abid, D. E. Fenton, U. Casellato, P. A. Vigato and R. Graziani, *J. Chem. Soc., Dalton Trans.* 1984, 351.
5. L. De Cola, D. L. Smailes and L. M. Vallarino, *Inorg. Chem.* 1986, 1729.
6. G. Bombieri, F. Benetollo, A. Polo, L. De Cola, D. L. Smailes and L. M. Vallarino, *Inorg. Chim.* 1986, **25**, 1127.
7. A. M. Ariff, J. D. J. Backer-Dirks, C. J. Gray, F. A. Hart and M. B. Hursthouse, *J. Chem. Soc., Dalton Trans.* 1987, 1665.
8. G. Bombieri, *Inorg. Chim. Acta* 1987, **21**, 139.
9. P. A. Vigato and D. E. Fenton, *Inorg. Chim. Acta* 1987, **139**, 21.
10. L. De Cola, D. L. Smailes and L. M. Vallarino, 10th National Conference of Photochemistry, Ravenna, Italy, 1985.

11. N. Sabbatini, L. De Cola, L. M. Vallarino and G. Blasse, *Phys. Chem.* 1987, **91**, 4681.
12. G. Bombieri, F. Benetollo, W. T. Hawkins, A. Polo and L. M. Vallarino, *Polyhedron* 1989, **8**, 1923.
13. A. C. T. North, D. C. Phillips and F. S. Mathews, *Acta Cryst.* 1968, **A24**, 351.
14. *International Tables for X-Ray Crystallography* (Present distributor Kluxer Academic Publishers, Dordrecht), Vol. IV. Kynoch Press, Birmingham (1974).
15. G. M. Sheldrick, SHELX, *A System of Computer Programs for X-Ray Structure Determination* (1976).
16. C. K. Johnson, *ORTEP II*, Report ORNL-5138, Oak Ridge National Laboratory, Tennessee (1976).
17. W. D. S. Motherwell and W. Clegg, *PLUTO, Program for Plotting Molecular and Crystal Structures.* Univ. of Cambridge, England (1978).
18. M. Nardelli, *Comput. Chem.* 1983, **7**, 95.
19. J. C. G. Bünzli, B. Klein, D. Wessner, K. J. Schenk, G. Chapuis, G. Bombieri and G. De Paoli, *Inorg. Chim. Acta* 1981, **54**, L43.
20. F. Nicolo', D. Plancherel, G. Chapuis and J. C. G. Bunzli, *Inorg. Chem.* 1988, **27**, 3518.
21. L. Pauling, *Nature of the Chemical Bond*, 3rd edn. Cornell University Press, Ithaca, New York (1960).
22. J. L. Martin, L. C. Thompson, L. J. Rodanovich and M. D. Glick, *J. Am. Chem. Soc.* 1968, **90**, 4493.
23. R. D. Shannon, *Acta Cryst. Sect. A: Cryst. Phys., Diffraction Theor. Gen. Cryst.* 1976, **A32**, 751.
24. D. Cremer and J. A. Pople, *J. Am. Chem. Soc.* 1975, **97**, 1354.

Polyhedron Vol. 8, No. 17, pp. 2169–2177, 1989
Printed in Great Britain

0277–5387/89 $3.00+.00
© 1989 Pergamon Press plc

STRUCTURE, SYNTHESIS AND CHARACTERIZATION OF CHIRAL, PHOSPHIDO-PHOSPHINE, DIPHOSPHINE PLATINUM(II) MONO- AND DIMERIC COMPLEXES: THE MOLECULAR STRUCTURE OF BOTH $[Pt_2Cl_3\{(R^*)\text{-}\mu\text{-}^iPrPCH_2P^iPr_2\}\{(R^*)\text{-}H^iPrPCH_2P^iPr_2\}]$ AND $[Pt_2Cl_3\{(R^*)\text{-}\mu\text{-}^iPrPCH_2P^iPr_2\}\{(S^*,S^*)\text{-}\mu\text{-}H^iPrPCH_2P^iPrH\}]$

JOHN C. HUFFMAN, BRIAN R. LLOYD† and WILLIAM E. STREIB

Department of Chemistry, Indiana University, Bloomington, IN 47405, U.S.A.

(*Received* 1 *February* 1989; *accepted* 14 *April* 1989)

Abstract—The preparation and spectroscopic characterization of the chiral phosphido-phosphine, diphosphine dimeric complex $[Pt_2Cl_3\{(R^*)\text{-}\mu\text{-}^iPrPCH_2P^iPr_2\}\{(R^*)\text{-}\mu\text{-}H^iPrPCH_2P^iPr_2\}]$ (**3a**) is reported. The further isolation of $[PtCl_2(H^iPrPCH_2P^iPr_2)]$ (**1**) and $[Pt_2Cl_3\{(R^*)\text{-}\mu\text{-}^iPrPCH_2P^iPr_2\}\{(R^*)\text{-}H^iPrPCH_2P^iPr_2\}]$ (**2b**) has led to a rationalization of the racemate's, **3a**, predomination, over other potential isomers, e.g. $[Pt_2Cl_3\{(R^*)\text{-}\mu\text{-}^iPrPCH_2P^iPr_2\}\{(S^*)\text{-}\mu\text{-}H^iPrPCH_2P^iPr_2\}]$ (**3b**), in terms of its mechanism of formation. The mixed ligand dimer, $[Pt_2Cl_3\{(R^*)\text{-}\mu\text{-}^iPrPCH_2P^iPr_2\}\{(S^*,S^*)\text{-}\mu\text{-}H^iPrPCH_2P^iPrH\}]$ (**4**), has also been prepared and characterized spectroscopically. The structures of **2b** and **4** have been elucidated via X-ray diffraction studies.

The use of diphosphine ligands of the type $R_2PCH_2PR_2$ in the stabilization of dimers against their degradation to mononuclear fragments has received significant attention.[1] The question as to when these ligands will bridge forming dimers, as opposed to coordinating in a chelate fashion generating mononuclear fragments, has been interpreted with regard to the steric bulk of the "R" substituents of the diphosphine.[2]

Unlike their tertiary analogues, secondary diphosphines of the type $HRPCH_2PR_2$ and $HRPCH_2PRH$ have received little attention, though they possess the same ability to stabilize multinuclear centres through bridging coordination modes.[2a,3] Further, these systems are of interest due to the potential of increasing nuclearity through phosphorus–hydrogen bond activation.

We now report the generation of complexes of the type $[Pt_2Cl_3(\mu\text{-}RPCH_2PR_2)(HRPCH_2PR'_2)]$ (R = ^{i}Pr, R′ = ^{i}Pr, H), which are formed through the chelating or bridging interactions of the ligands $H^iPrPCH_2P^iPr_2$ and $H^iPrPCH_2P^iPrH$ with platinum(II) centres.

RESULTS

Stoichiometric reaction of $[PtCl_2(SMe_2)_2]$ and $H^iPrPCH_2P^iPr_2$ affords the isolation of $[Pt_2Cl_3\{(R^*)\text{-}\mu\text{-}^iPrPCH_2P^iPr_2\}\{(R^*)\text{-}\mu\text{-}H^iPrPCH_2P^iPr_2\}]$ (**3a**) in good yield. However, when the same reaction was carried out for shorter time periods, significant quantities of $[PtCl_2(H^iPrPCH_2P^iPr_2)]$ (**1**) were isolated. Further, small quantities of another complex, $[Pt_2Cl_3\{(R^*)\text{-}\mu\text{-}^iPrPCH_2P^iPr_2\}\{(R^*)\text{-}H^iPrPCH_2P^iPr_2\}]$ (**2b**), were also isolated from these reaction systems (see Experimental).

The mononuclear complex, **1**, is readily characterized by the use of ^{31}P and ^1H NMR spectra. The ^{31}P NMR spectrum reveals two resonances at δ −27.6 and −80.0, a doublet and doublet of doublets, respectively. The shifts are to high field of the free ligand, as expected for chelating diphosphines, $\delta_{complex} - \delta_{free\ ligand}$: ΔP^a, −33.2, ΔP^b, −35.4.[4] The higher field resonance shows a $^1J(PH) = 404$ Hz due to the presence of the phosphorus–hydrogen bond. The ^1H NMR posseses a resonance at δ 4.33,

† Author to whom correspondence should be addressed. Present address: Department of Chemistry, University of British Columbia, 2036 Main Mall, Vancouver, B.C. Canada V6T 1Y6.

^1J(PH) = 404 Hz, ^3J(HH) = 7 Hz, ^3J(HH) = 4 Hz due to the PH group of the diphosphine ligand. The two protons of the bridging methylene unit are observed as two independent resonances, δ 3.46 and 2.87, due to the non-equivalency induced by molecular asymmetry arising from the PH group of the diphosphine.

Complex **2b**, characterized by an X-ray diffraction study on its chloroform solvate as $[Pt_2Cl_3\{(R^*)\text{-}\mu\text{-}{}^iPrPCH_2P^iPr_2\}\{(R^*)\text{-}H^iPrPCH_2P^iPr_2\}]\cdot 2CHCl_3$ (Fig. 1), consists of two distorted square-planar platinum(II) centres linked through a bridging phosphido-unit of a phosphido-phosphine ligand, $-P(^iPr)CH_2P^iPr_2$. The distortions arise from the steric strain involved in the generation of the four-membered heterocyclic rings. These distorted ring angles, P(6)Pt(1)P(8), 74.24(8)°; P(15)Pt(2)P(17), 73.57(8)°, are formed by the chelating diphosphine and phosphido-phosphine ligands.[3c,5] The phosphido-bridge in this complex is asymmetrically bound to the two platinum centres; Pt(1)P(6), 2.250(2) Å, Pt(2)P(6), 2.348(2) Å.

The ^{31}P NMR of complex **2b** possesses four non-equivalent phosphorus resonances each to high field of the corresponding free ligand shifts; P^a, δ −24.9; P^b, δ −68.8; P^c, δ −53.9 and P^d, δ −32.6. The high field shift of the resonances for P^a and P^b confirms the chelation of the diphosphine ligand within this complex; $\delta_{complex} - \delta_{free\ ligand}$: ΔP^a, −30.5; ΔP^b, −23.2.[4] The resonance for P^b possesses a large doublet splitting in the proton coupled spectrum, $^1J(P^bH)$ = 445 Hz. The resonance for P^c has two large one bond platinum couplings, $^1J(Pt^AP^c)$ = 2385 Hz, $^1J(Pt^BP^c)$ = 1926 Hz, indicating the presence of a phosphido-bridge. A large doublet splitting, $^2J(P^aP^c)$ = 367 Hz confirms that P^a and P^c are mutually *trans* to each other.

The ^{1}H NMR spectrum of complex **2b** reveals a resonance attributable to a PH functional unit; δ 5.08, $^1J(P^bH)$ = 443 Hz, $^2J(Pt^BH)$ = 45 Hz. Two resonances at δ 4.35 and 2.57 are assigned to the bridging methylene protons of the phosphido-phosphine ligand. This assignment is based on the observed chemical shifts and couplings of phosphido-phosphine ligands observed in related complexes **3a** and **4**. Resonances at δ 3.47 and 2.95 are therefore assigned to the bridging methylene protons of the diphosphine chelate. These chemical shifts are very similar to those observed in the mononuclear chelate, complex **1**.

The ^{31}P NMR of complex **3a**, as in complex **2b**, possesses four non-equivalent phosphorus resonances; P^a, δ 34.0; P^b, δ −5.0; P^c, δ −54.6; P^d, δ −27.8. However, two of the resonances are shifted to much lower field than the corresponding resonances in complex **2b**. Such relative chemical shifts confirm the presence of a bridging diphosphine; $\delta_{complex} - \delta_{free\ ligand}$: ΔP^a, +28.6; ΔP^b, +40.6. Resonances for P^a and P^d possess a large two-bond coupling, $^2J(P^aP^d)$ = 411 Hz, due to their mutual *trans* orientation. The resonance for P^c has two large one bond platinum–phosphorus coupling constants, $^1J(Pt^AP^c)$ = 2279 Hz and $^1J(Pt^BP^c)$ = 2978 Hz, due to the bridging phosphido-group of the phosphido-phosphine ligand. Only the resonance for P^b possesses a large one bond phosphorus–hydrogen coupling, $^1J(P^bH)$ = 411 Hz.

In the ^{195}Pt NMR spectra, two non-equivalent resonances are observed; Pt^A, δ −2539; Pt^B, δ −2801. The Pt^A resonance consists of three large one bond platinum–phosphorus couplings while the resonance for Pt^B possesses only two.

In the ^{1}H NMR spectra of complex **3a** the resonance attributed to the proton of the PH functional unit is readily observable at δ 4.62, $^1J(P^bH)$ = 410 Hz, ^3J(HH) = 12 Hz. Resonances at δ 5.23 and 2.81 are due to the bridging methylene protons of the chelating phosphido-phosphine ligand based on the results of selective phosphorus decoupling experiments.

A 1:1 reaction of $[PtCl_2(SMe_2)_2]$ with an equimolar mixture of $H^iPrPCH_2P^iPr_2$ and $H^iPrPCH_2P^iPrH$ yields a mixture of complex **3a** and $[Pt_2Cl_3\{(R^*)\text{-}\mu\text{-}{}^iPrPCH_2P^iPr_2\}\{(S^*,S^*)\text{-}\mu\text{-}H^iPrPCH_2P^iPrH\}]$ (**4**). Complex **4** was isolated in low yields as a pure white crystalline solid via fractional crystallization.

A sample of complex **4**, recrystallized from benzene, was found to contain 3/2 equivalents of solvated benzene through an X-ray diffraction study, Fig. 2. Structurally, it consists of a bridging chelate phosphido-phosphine ligand which forms a four-membered heterocyclic ring at the Pt^BCl metal centre. The Pt^ACl_2 and Pt^BCl centres are bridged by a disecondary diphosphine, thereby completing a six-membered heterocyclic ring in a twist boat configuration. This conformation minimizes the steric interactions of the isopropyl groups of P(10) and P(18). The four-membered ring possesses the typical strain of a chelating ligand system with a distorted ring angle, P(18)Pt(2)P(20), 73.3(1)°. The phosphido-bridge, unlike complex **2b**, is symmetrically bound to both metal centres.

As in the previously discussed dimers, complex **4** possesses four non-equivalent phosphorus resonances; P^a, δ −1.5; P^b, δ 5.5; P^c, δ −64.7; P^d, δ −24.1. Due to their lower field shifts the resonances for P^a and P^b are assigned to a bridging diphosphine. These two resonances are also observed to possess one bond phosphorus–hydrogen couplings; $^1J(P^aH)$ = 376 Hz, $^1J(P^bH)$ = 415 Hz. The resonance for P^c is assignable to that of the bridging

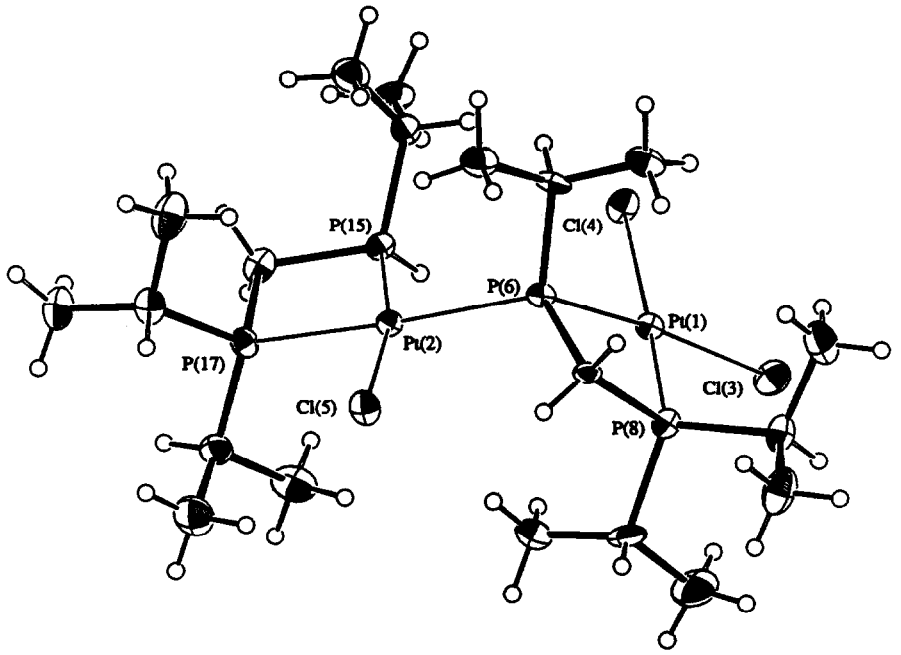

Fig. 1. The molecular structure of $[Pt_2Cl_3\{(R^*)\text{-}\mu\text{-}^iPrPCH_2P^iPr_2\}\{(R^*)\text{-}H^iPrPCH_2P^iPr_2\}]\cdot 2CHCl_3$. Selected bond distances (Å) and angles (°) are:

Pt(1)Cl(3)	2.395(2)	Pt(1)P(6)	2.250(2)	Pt(2)P(17)	2.298(2)
Pt(1)Cl(4)	2.388(2)	Pt(2)Cl(5)	2.362(2)	Pt(2)P(6)	2.348(2)
Pt(1)P(8)	2.200(2)	Pt(2)P(15)	2.228(2)		

Cl(3)Pt(1)Cl(4)	90.18(8)	P(6)Pt(1)P(8)	74.24(8)	P(6)Pt(2)P(15)	98.29(8)
Cl(3)Pt(1)P(6)	171.28(8)	Cl(5)Pt(2)P(6)	94.03(8)	P(6)Pt(2)P(17)	171.71(8)
Cl(3)Pt(1)P(8)	97.04(8)	Cl(5)Pt(2)P(15)	167.58(8)	P(15)Pt(2)P(17)	73.57(8)
Cl(4)Pt(1)P(6)	97.89(8)	Cl(5)Pt(2)P(17)	94.15(8)	Pt(1)P(6)Pt(2)	120.12(9)
Cl(4)Pt(1)P(8)	170.99(8)				

Selected non-bonding distances (Å) are: Pt(1)Pt(2) 3.985(1)

phosphido-group due to the presence of two large one bond platinum–phosphorus coupling constants; $^1J(Pt^AP^c) = 2103$ Hz, $^1J(Pt^BP^c) = 2965$ Hz. The two bond phosphorus–phosphorus coupling observable in the resonances for P^a and P^d, $^2J(P^aP^d) = 388$ Hz, confirms their mutual *trans* orientation.

The ^{195}Pt NMR spectra show two resonances; Pt^A, δ −2613; Pt^B, δ −2800. As for complex **3a**, the Pt^A resonance consists of three large one bond platinum–phosphorus couplings, while the Pt^B resonance possesses only two.

The ^1H NMR reveals the presence of two PH functional units; P^aH, δ 4.36, $^1J(P^aH) = 370$ Hz; P^bH, δ 5.02, $^1J(P^bH) = 415$ Hz. Selective phosphorus decoupling experiments confirm that resonances at δ 4.63 and 3.14 are due to the bridging methylene protons of the phosphido-phosphine ligand.

DISCUSSION

All of the observed complexes possess a sufficient number of chiral centres so as to generate a complicated isomeric mixture. The dinuclear platinum systems formed exclusively from the $H^iPrPCH_2P^iPr_2$ ligand possess two chiral centres which generate four stereochemical isomers. The asymmetry of the phosphine centres of the ligand and the two platinum centres of the dimer introduce the possibility of geometrical isomerism increasing the number of possible isomers to eight.[3c] In the mixed ligand system, from which complex **4** is generated, the bridging diphosphine is symmetrical eliminating the geometrical isomerism; however, the presence of a third chiral centre allows the possible generation of eight stereochemical isomers.

The mixed ligand product, complex **4**, was characterized as $[Pt_2Cl_3\{(R^*)\text{-}\mu\text{-}^iPrPCH_2P^iPr_2\}$

{(S*,S*)-μ-H^{i}PrPCH$_2$P^{i}PrH}] by an X-ray diffraction study, Fig. 2. The bridging diphosphine, in this structure, has an isopropyl group on one of the phosphorus atoms in an axial position with the axial site of the other phosphorus atom occupied by a proton. This reduces steric strain within the system which results from diaxial interactions within bridging diphoshines, Fig. 2. Substitution of the proton on P(10) with an isopropyl group leads to the structural framework proposed for complexes **3a** and **3b**. However, two axial isopropyl groups on the bridging diphosphine would be expected to increase the steric interactions sufficiently so as to cause this structure to be that of a minor isomer, complex **3b**. Therefore the major isomer within this reaction system, complex **3a**, was proposed to be [Pt$_2$Cl$_3${(R*)-μ-^{i}PrPCH$_2$P^{i}Pr$_2$}{(R*)-H^{i}PrPCH$_2$P^{i}Pr$_2$}]. This parallels observations in the related palladium system reported earlier.[3c] These assignments are further supported by the observed ^{31}P NMR chemical shifts for the P^b resonances of complexes **4**, **3b** and **3a**. The chemical shift of the resonance for P^b would be expected to reflect greater variations in changes of chirality at P^b rather than structural changes at P^a (i.e. exchanging a proton for an isopropyl group). In Table 1 the chemical shifts for the P^b resonance in complexes 4, **3b** and **3a** are 5.5, 6.6 and −5.0, respectively. The similar chemical shifts of the resonance for P^b in complexes **4** and **3b** suggest that these complexes possess a common chirality at this specific phosphorus atom.

Complex **2b** was characterized as [Pt$_2$Cl$_3${(R*)-μ-^{i}PrPCH$_2$P^{i}Pr$_2$}{(R*)-H^{i}PrPCH$_2$P^{i}Pr$_2$}] by an X-ray diffraction study, Fig. 1. Structurally, it represents the product of a condensation reaction between two monomeric chelates, complex **1**, which release a molecule of HCl. The phosphido-bridge in this complex is much more asymmetrically bound, than in complex **4**, due to the differing *trans* influences of phosphorus and chlorine. The loss of only one proton in the generation of a single phosphido-bridge

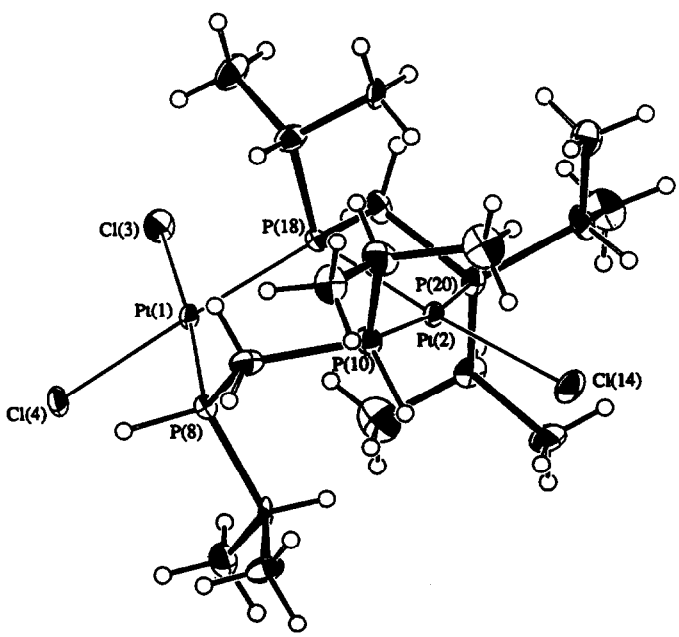

Fig. 2. The molecular structure of [Pt$_2$Cl$_3${(R*)-μ-^{i}PrPCH$_2$P^{i}Pr$_2$}{(S*,S*)-μ-H^{i}PrPCH$_2$P^{i}PrH}] · 3/2C$_6$H$_6$. Selected bond distances (A) and angles (°) are:

Pt(1)Cl(3)	2.362(4)	Pt(1)P(18)	2.257(4)	Pt(2)P(20)	2.278(4)
Pt(1)Cl(4)	2.382(4)	Pt(2)Cl(14)	2.383(4)	Pt(2)P(18)	2.258(4)
Pt(1)P(8)	2.228(4)	Pt(2)P(10)	2.300(4)		

Cl(3)Pt(1)Cl(4)	89.6(1)	P(8)Pt(1)P(18)	94.0(1)	P(10)Pt(2)P(18)	97.1(1)
Cl(3)Pt(1)P(8)	175.2(1)	Cl(14)Pt(2)P(10)	91.8(1)	P(10)Pt(2)P(20)	170.0(1)
Cl(3)Pt(1)P(18)	90.7(1)	Cl(14)Pt(2)P(18)	171.1(1)	P(18)Pt(2)P(20)	73.3(1)
Cl(4)Pt(1)P(8)	85.8(1)	Cl(14)Pt(2)P(20)	97.9(1)	Pt(1)P(18)Pt(2)	117.7(5)
Cl(4)Pt(1)P(18)	178.1(1)				

Selected non-bonding distances (Å) are: Pt(1)Pt(2) 3.869(2)

Table 1. ^{31}P NMR platinum–phosphorus coupling constant (Hz) and chemical shift data (ppm) for dimeric platinum(II) complexes

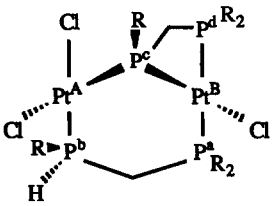

3a

	δP^a	δP^b	δP^c	δP^d
	34.0	−5.0	−54.6	−27.8
$^1J(Pt^APa)$	2541			
$^3J(Pt^BPa)$	99.9			
$^1J(Pt^BPb)$		3747		
$^3J(Pt^APb)$		162		
$^1J(Pt^APc)$			2279	
$^1J(Pt^BPc)$			2978	
$^1J(Pt^APd)$				2169
$^3J(Pt^BPd)$				44.4

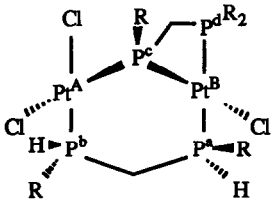

4

	δP^a	δP^b	δP^c	δP^d
	−1.5	5.5	−64.7	−24.1
$^1J(Pt^APa)$	2303			
$^3J(Pt^BPa)$	44			
$^1J(Pt^BPb)$		3747		
$^3J(Pt^APb)$		249		
$^1J(Pt^APc)$			2103	
$^1J(Pt^BPc)$			2965	
$^1J(Pt^APd)$				2297
$^3J(Pt^BPd)$				41

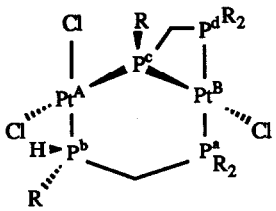

3b

	δP^a	δP^b	δP^c	δP^d
	32.9	6.6	−64.1	−31.9
$^1J(Pt^APa)$	2500			
$^3J(Pt^BPa)$	108			
$^1J(Pt^BPb)$		3835		
$^3J(Pt^APb)$		188		
$^1J(Pt^APc)$			2250	
$^1J(Pt^BPc)$			2800	
$^1J(Pt^APd)$				2182

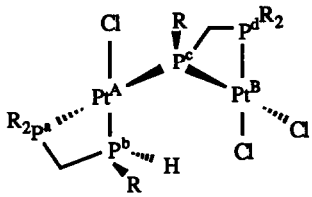

2b

	δP^a	δP^b	δP^c	δP^d
	−24.9	−68.8	−53.9	−32.6
$^1J(Pt^BPa)$	1700			
$^1J(Pt^BPb)$		3075		
$^3J(Pt^APb)$		115		
$^1J(Pt^APc)$			2385	
$^1J(Pt^BPc)$			1926	
$^1J(Pt^APd)$				2317

is totally attributable to the smaller backbone of the diphosphine ligands and the resultant steric strain that would result in further PH activation. This is not the case for diphosphines with longer carbon backbones, as shown by Meek and co-workers.[6] Complex **2b** represents a model of the likely intermediate species that would be formed enroute to bis-phosphido-phosphine dimers, $[Pt_2Cl_2\{\mu\text{-}RP(CH_2)_nPR_2\}]$. The steric strain induced by the distorted ring angles, P(6)Pt(1)P(8), 74.24(8)°; P(15)Pt(2)P(17), 73.57(8)°, of the four membered rings in complex **2b** presumably contributes to the observed instability of this complex in solution over long periods of time. Observation of complex **2b** by ^{31}P NMR over a 3-week period showed that 25% of this complex disproportionates into mononuclear chelates, complex **3a** and an unidentified monomer possibly formed from reaction of the free phosphido fragment and the chloroform solvent. Another 25% was observed to rearrange into complex **3b**. This rearrangement to complex **3b** may involve disproportionation; however, since the conversion is stereospecific, any intermediates formed by disproportionation would have to be sufficiently short-

lived as to prevent inversion at the phosphido-bridge. The stereospecific formation of complex **3b** is attributable to an exchange of Cl(4) and P(17) via the breaking of the P(17)Pt(2) bond, rotation about the P(15)Pt(2) bond, migration of Cl(4) and formation of the P(17)Pt(1) bond. The slow rate of this interconversion is probably due to the formation of a bridging diphosphine ligand which possess diaxial interactions between two sterically demanding isopropyl groups.

The isolation of these complexes suggests a mechanistic pathway for the formation of the diastereotopically related platinum dimers as shown in Scheme 1. It involves the condensation of two mononuclear chelates inducing the loss of HCl and the formation of a dinuclear dichelate. This system undergoes subsequent rearrangement to form the stereospecific dinuclear complex possessing the bridging diphosphine, either complex **3a** or complex **3b**. Observation of the reaction system by ^{31}P NMR spectroscopy confirms the formation of complex **1** within the reaction mixture followed by its disappearance over time. However, there is no evidence of the formation of a dinuclear dichelate intermediate to complex **3a**, complex **2a**. Therefore if this proposed mechanism is correct the conversion of the intermediate dichelate into complex **3a** must be sufficiently fast so as to account for its absence in the ^{31}P NMR spectra. The slow rate of conversion of complex **2b** to complex **3b** was attributed to the steric crowding of two isopropyl groups in the diaxial positions of the bridging diphosphine. However, complex **3a** has a proton and isopropyl group occupying the diaxial positions of the bridging diphosphine, a much less sterically demanding situation. Since complex **3a** lacks the steric demands of complex **3b**, complex **2a** might be expected to undergo this interconversion much more rapidly, thereby relieving the ring strain within its diphosphine chelate ring.

The products isolated from these systems are consistent with the formation of a dinuclear dichelate in which the phosphido linkage binds *cis* to the phosphorus atom of the diphosphine ligand bearing the proton and one isopropyl group, as opposed to the diisopropylphosphine end. This is presumably due to the reduced steric interaction at this site. This rationalizes the absence of the geometric isomer to

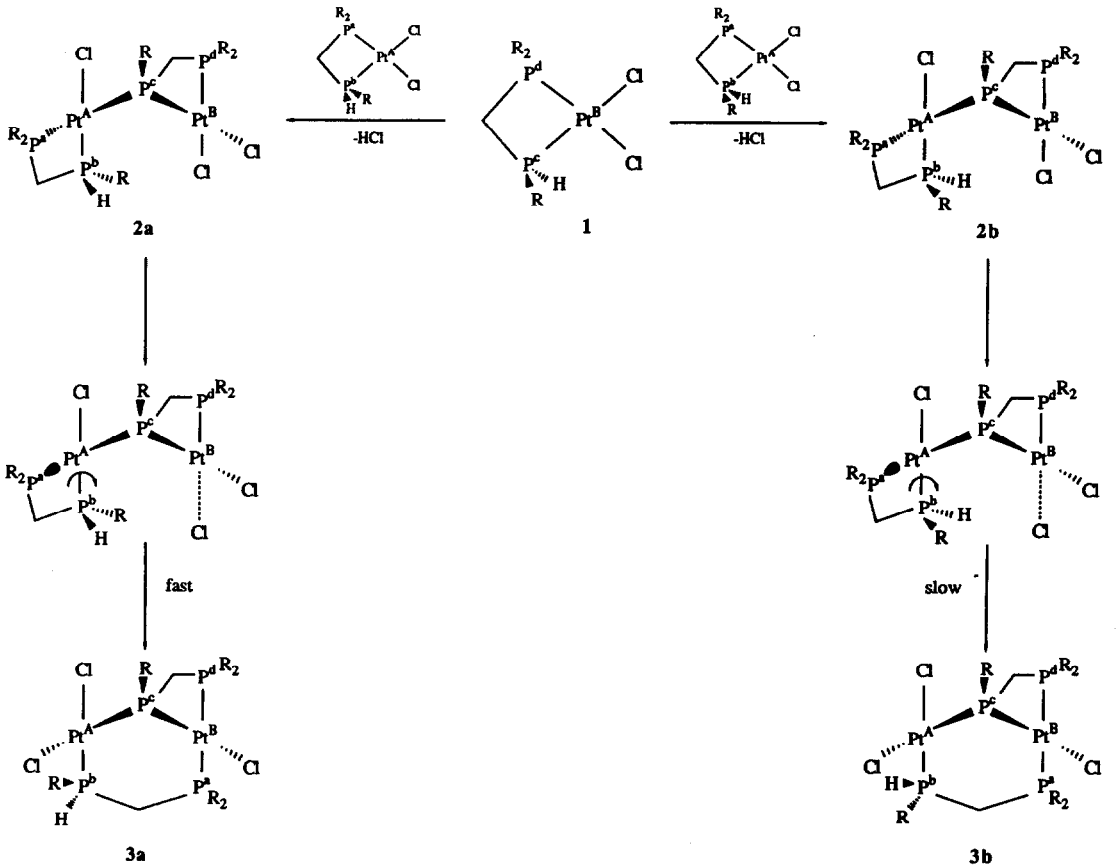

Scheme 1.

complex **3a**, in which the proton bearing phosphorus of the bridging diphosphine is bound to the $Pt^{B}ClP_3$ centre. Without the formation of the dichelate there is no obvious reason why both geometric isomers should not be formed in identical yield; however, steric effects controlling the conformation of the dichelate indirectly dictate which dimer is formed. The presence of the phosphido-bridge *cis* to the secondary phosphine end of the diphosphine leads to the coordination of the tertiary phosphine end to the $Pt^{B}Cl$ metal centre, after rearrangement. This steric effect is further evidenced by mixed ligand reactions of $H^iPrPCH_2P^iPr_2$ and $Ph_2PCH_2PPh_2$ or $^iPr_2PCH_2P^iPr_2$ with $[PtCl_2(SMe_2)_2]$ in which no mixed ligand products could be isolated, only $[PtCl_2(Ph_2PCH_2PPh_2)]$, $[PtCl_2(^iPr_2PCH_2P^iPr_2)]$ and complex **3a**. The steric bulk of the alkyl and aryl substituents on the phosphorus prohibit coordination of the phosphido-bridge fragment and therefore formation of the mixed ligand dimers.

EXPERIMENTAL

^1H NMR spectra were recorded on Nicolet NT 360, Varian XL 300 and Bruker WP 500 spectrometers. ^{31}P and ^{195}Pt spectra[7] were recorded on Nicolet NT 360 spectrometer. Chemical shifts are quoted with respect to Me_4Si (^1H), 85% H_3PO_4 (^{31}P), and K_2PtCl_4/D_2O (^{195}Pt).

$[PtCl_2(SMe_2)_2]$ was prepared by the literature method. The ligands $H^iPrPCH_2P^iPr_2$ and $H^iPrPCH_2P^iPrH$ were prepared by the literature method.[3b] All syntheses and reactions involving the phosphine ligands were carried out under N_2(g).

$[Pt_2Cl_3\{(R^*)\text{-}\mu\text{-}^iPrPCH_2P^iPr_2\}\{(R^*)\text{-}\mu\text{-}H^iPrPCH_2P^iPr_2\}]$ (**3a**)

In a typical reaction $H^iPrPCH_2P^iPr_2$ (3.4 g) was added dropwise to a stirring solution of $[PtCl_2(SMe_2)_2]$ (6.1 g) in ~ 200 cm^3 of CH_2Cl_2. After 24 h, the solvent was removed and the resultant yellow oil was redissolved in a minimum of hot methanol. This was allowed to cool slowly to room temperature after which it was stored at ~ -10°C over a 40 h period. A white solid was isolated and dried *in vacuo*, yield 5.7 g. From this sample crystals could be obtained by dissolution in $CHCl_3$ followed by slow evaporation of the solvent. The crystalline product could be isolated in nearly quantitative yields > 90%. NMR ($CDCl_3$): ^1H: 4.62 [dd, ^1J(PH) = 410 Hz, ^3J(HH) = 12 Hz, *H*P]; 5.23 [m, ^2J(HH) = 16.2 Hz, ^4J(PH) = 2.4 Hz, ^2J(PH) = 9.1. Hz, ^2J(PH) = 9.7 Hz, ^3J(PtH) ~ 85 Hz, $CH^aH^bP_2{}^iPr_3$]; 2.81 [dt, ^2J(HH) = 16.2 Hz, ^2J(PH) = 10.7 Hz, ^2J(PH) = 10.7 Hz, $CH^aH^bP_2{}^iPr_3$]; 3.20 [d septet, ^3J(HH) = 7.3 Hz, ^2J(PH) = 7.7 Hz, C*H*Me$_2$]; 2.63 [m, 2 C*H*Me$_2$]; 2.47 [dd septet, ^3J(HH) = 7.3 Hz, ^4J(HH) = 2.4 Hz, ^2J(PH) = 7.4 Hz, C*H*Me$_2$]; 2.05 [septet, ^3J(HH) = 7.0 Hz, C*H*Me$_2$]; 1.81 [m, C*H*Me$_2$]; 2.56 [m, $^2J(H^{a'}H^{b'})$ = 13.9 Hz, ^2J(PH) = 6.9 Hz, ^2J(PH) = 6.9 Hz, ^4J(PH) = 2.5 Hz, ^4J(PH) = 2.5 Hz, $CH^{a'}H^{b'}P_2{}^iPr_3H$]; 1.55–1.23 [complex multiplet, $CH^{a'}H^{b'}P_2{}^iPr_3H$ and CH*Me*$_2$]; ^{31}P: 34.0 [m, $^2J(P^aP^b)$ = 7.4 Hz, $^2J(P^aP^c)$ = 11.1 Hz, $^2J(P^aP^d)$ = 381 Hz, $^1J(Pt^AP^a)$ = 2541 Hz, $^3J(Pt^BP^a)$ = 99.9 Hz, P^a]; −5.0 [m, $^2J(P^bP^a)$ = 7.4 Hz, $^2J(P^bP^c)$ = 14.8 Hz, $^1J(Pt^BP^b)$ = 3747 Hz, $^3J(Pt^AP^b)$ = 162 Hz, $^1J(P^bH)$ = 411 Hz, P^b]; −54.6 [m, $^2J(P^cP^a)$ = 11.1 Hz, $^2J(P^cP^b)$ = 14.8 Hz, $^2J(P^cP^d)$ = 40.7 Hz, $^1J(Pt^AP^c)$ = 2279 Hz, $^1J(Pt^BP^c)$ = 2978 Hz, P^c]; −27.8 [m, $^2J(P^dP^a)$ = 381 Hz, $^2J(P^dP^c)$ = 40.7 Hz, $^1J(Pt^AP^d)$ = 2169 Hz, $^3J(Pt^BP^d)$ = 44.4 Hz, P^d]; ^{195}Pt: −2539 [m, $^1J(Pt^AP^a)$ = 2542 Hz, $^1J(Pt^AP^c)$ = 2288 Hz, $^1J(Pt^AP^d)$ = 2169 Hz, $^3J(Pt^AP^b)$ = 163 Hz, Pt^A]; −2801 [m, $^1J(Pt^BP^b)$ = 3754 Hz, $^1J(Pt^BP^c)$ = 2982 Hz, $^3J(Pt^BP^a)$ = 98 Hz, Pt^B]. Found: C, 24.0; H, 4.5; Cl, 24.5. Calc. for $C_{20}H_{47}P_4Cl_3Pt_2 \cdot 1.5CHCl_3$: C, 23.7; H, 4.5; Cl, 24.5%.

$[Pt_2Cl_3\{(R^*)\text{-}\mu\text{-}^iPrPCH_2P^iPr_2\}\{(R^*)\text{-}H^iPrPCH_2P^iPr_2\}]$ (**2b**)

Redissolving the white solid (1.23 g) of the previous reaction in a minimum of $CHCl_3$, followed by filtration, allows the isolation of a less soluble white solid in extremely low yield. This product was washed three times with a minimum of $CHCl_3$ and then dried *in vacuo*, yield 0.0266 g. NMR: ^1H (CD_2Cl_2): 5.08 [m, $^1J(P^bH)$ = 443 Hz, $^2J(Pt^BH)$ = 45 Hz, *H*P]; 4.35 [m, ^2J(HH) = 15.6 Hz, ^2J(PH) = 9.5 Hz, ^2J(PH) = 5.6 Hz, ^4J(PH) = 4.3 Hz, ^3J(PtH) ~ 135 Hz, $CH^aH^bP_2{}^iPr_3$]; 2.57 [m, ^2J(HH) = 15.6 Hz, ^2J(PH) = 7.0 Hz, ^2J(PH) = 7.0 Hz, ^4J(PH) 2.0 Hz, ^3J(PtH) ~ 20 Hz, $CH^aH^bP_2{}^iPr_3$]; 3.47 [m, $CH^{a'}H^{b'}P_2{}^iPr_3H$]; 2.95 [m, ^2J(HH) = 16.7 Hz, ^2J(PH) = 11.4 Hz, ^2J(PH) = 10.0 Hz, ^4J(PH) = 5.5 Hz, $CH^{a'}H^{b'}P_2{}^iPr_3H$]; 3.68 [d septet, ^3J(HH) = 7.3 Hz, ^2J(PH) = 7.3 Hz, C*H*Me$_2$]; 2.55–2.34 [complex multiplet 4C*H*Me$_3$]; 2.15 [m, ^3J(HH) = 7.0 Hz, ^2J(PH) = 9.7 Hz, C*H*Me$_2$]; 1.54–1.17 [complex multiplet, CH*Me*$_2$]; ^{31}P ($CDCl_3$): −24.9 [m, $^2J(P^aP^b)$ = 64.3 Hz, $^2J(P^aP^c)$ = 367 Hz, $^1J(Pt^BP^a)$ = 1700 Hz, P^a]; −68.8 [m, $^2J(P^bP^a)$ = 64.3 Hz, $^2J(P^bP^c)$ = 13.8 Hz, $^1J(Pt^BP^b)$ = 3075 Hz, $^3J(Pt^AP^b)$ = 115 Hz, $^1J(P^bH)$ = 445 Hz, P^b]; −53.9 [m, $^2J(P^cP^a)$ = 367 Hz,

$^2J(P^cP^b)$ = 13.8 Hz, $^2J(P^cP^d)$ = 42.9 Hz, $^1J(Pt^AP^c)$ = 2385 Hz, $^1J(Pt^BP^c)$ = 1926 Hz, P^c]; −32.6 [m, $^2J(P^dP^c)$ = 42.9 Hz, $^1J(Pt^AP^d)$ = 2317 Hz, P^d]. Found: C, 25.3; H, 5.1. Calc. for $C_{20}H_{47}P_4Cl_3Pt_2 \cdot 0.5CHCl_3$: C, 25.4; H, 4.9%.

$[Pt_2Cl_3\{(R^*)\text{-}\mu\text{-}^i PrPCH_2P^iPr_2\}\{(S^*)\text{-}\mu\text{-}H^iPrPCH_2P^iPr_2\}]$ (**3b**)

Complex **3b** could be observed in a sample of complex **2b** in CD_2Cl_2 which had been left standing at room temperature for an excess of 3 weeks when observed by ^{31}P NMR spectroscopy. NMR ($CDCl_3$): ^{31}P: 32.9 [m, $^2J(P^aP^b)$ = 12 Hz, $^2J(P^aP^c)$ = 10 Hz, $^2J(P^aP^d)$ = 379 Hz, $^1J(Pt^AP^a)$ = 2500 Hz, $^3J(Pt^BP^a)$ = 108 Hz, P^a]; 6.6 [m, $^2J(P^bP^a)$ = 12 Hz, $^2J(P^bP^c)$ = 19 Hz, $^1J(Pt^BP^b)$ = 3835 Hz, $^3J(Pt^AP^b)$ = 188 Hz, P^b]; −64.1 [m, $^2J(P^cP^a)$ = 10 Hz, $^2J(P^cP^b)$ = 19 Hz, $^2J(P^cP^d)$ = 45 Hz, $^1J(Pt^AP^c)$ = 2250 Hz, $^1J(Pt^BP^c)$ = 2800 Hz, P^c]; −31.9 [m, $^2J(P^dP^a)$ = 379 Hz, $^2J(P^dP^c)$ = 45 Hz, $^1J(Pt^AP^d)$ = 2182 Hz, P^d].

$[PtCl_2(H^iPrPCH_2P^iPr_2)]$ (**1**)

Halting the synthesis of complex **3a** after 3 h of reaction time allows the isolation of a white crystalline solid. The solvent is removed under vacuum and the resultant oil is redissolved in a minimum of acetone. The first fraction of crystals are generated by slow evaporation of the solvent acetone system, yield < 20%. NMR ($CDCl_3$): ^1H: 4.33 [m, $^3J(HH)$ = 7 Hz, $^3J(HH)$ = 4 Hz, $^1J(P^bH)$ = 404 Hz, $^3J(P^aH)$ = 6 Hz, HP]; 3.46 [m, $^2J(HH)$ = 16 Hz, $^3J(HH)$ = 7 Hz, $^2J(PH)$ = 11 Hz, $^2J(PH)$ = 9 Hz, $^3J(PtH)$ = 125 Hz, $CH^aH^bP_2$]; 2.87 [m, $^2J(HH)$ = 16 Hz, $^3J(HH)$ = 4 Hz, $^2J(PH)$ = 11 Hz, $^2J(PH)$ = 11 Hz, $CH^aH^bP_2$]; 2.60 [m, $^2J(HH)$ = 7 Hz, $2CHMe_2$]; 2.35 [m, $^3J(HH)$ = 7 Hz, $^2J(PH)$ = 9 Hz, $CHMe_2$]; 1.6–1.2 [complex multiplet, $CHMe_2$]; ^{31}P: −27.6 [m, $^2J(P^aP^b)$ = 64 Hz, $^1J(PtP^a)$ = 2930 Hz, P^a]; −80.0 [m, $^2J(P^bP^a)$ = 64 Hz, $^1J(PtP^b)$ = 3003 Hz, $^1J(P^bH)$ = 404 Hz, P^b].

$[Pt_2Cl_3\{(R^*)\text{-}\mu\text{-}^iPrPCH_2P^iPr_2\}\{(S^*,S^*)\text{-}\mu\text{-}H^iPrPCH_2P^iPrH\}]$ (**4**)

A mixture (1.37 g) ~1:1 of $H^iPrPCH_2P^iPr_2$ and $H^iPrPCH_2P^iPrH$ was added dropwise to a stirring solution of $[PtCl_2(SMe_2)_2]$ (2.52 g) in acetone. The solution was allowed to stir for ~ 1 h at 45°C and then cooled to ambient temperature. The solvent was then removed under vacuum and the residue oil dissolved in a minimum of hot methanol. The solution was pipetted off a very small quantity of insoluble precipitate and was allowed to cool slowly to room temperature. The system was then stored at ~ −10°C over a 24 h period. A white crystalline solid was then isolated and dried *in vacuo*, yield 0.923 g. This product was identified by ^{31}P NMR as a mixture of complexes **3a** and **4**. Pure **4** was isolated by washing these crystals in a minimum of $CHCl_3$ three consecutive times and isolating the insoluble fraction, yield 0.117 g. NMR ($CDCl_3$): ^1H: 5.02 [m, $^3J(HH)$ = 2.6 Hz, $^1J(P^bH)$ = 415 Hz, $^3J(PH)$ = 26.9 Hz, $^3J(PH)$ = 8.3 Hz, HP^b]; 4.36 [m, $^1J(P^aH)$ = 370 Hz, $^3J(PH)$ = 12.2 Hz, $^3J(PH)$ = 12.2 Hz, $^3J(PH)$ = 5.4 Hz, HP^a]; 4.63 [m, $^2J(HH)$ = 16.6 Hz, $^2J(PH)$ = 8.8 Hz, $^2J(PH)$ = 8.8 Hz, $^4J(PH)$ = 2.0 Hz, $^3J(PtH)$ ~ 84 Hz, $CH^aH^bP_2{}^iPr_3$]; 3.14 [m, $^2J(HH)$ = 16.6 Hz, $^2J(PH)$ = 11.2 Hz, $^2J(PH)$ = 11.2 Hz, $CH^aH^bP_2{}^iPr_3$]; 2.66 [m, $^2J(HH)$ = 14 Hz, $^2J(PH)$ = 7 Hz, $^2J(PH)$ = 7 Hz, $CH^{a'}H^{b'}P_2{}^iPr_2$]; 2.19 [m, $^2J(HH)$ = 14 Hz, $^2J(PH)$ = 11 Hz, $^2J(PH)$ = 11 Hz, $CH^{a'}H^{b'}P_2{}^iPr_2$]; 2.69 [septet, $^3J(HH)$ = 7.5 Hz, 2 $CHMe_2$]; 2.49 [septet, $^3J(HH)$ = 7.1 Hz, $CHMe_2$]; 2.48 [septet, $^3J(HH)$ = 7.2 Hz, $CHMe_2$]; 2.38 [septet, $^3J(HH)$ = 6.8 Hz, $CHMe_2$]; 2.31 [m, $^3J(HH)$ = 7.1 Hz, $CHMe_2$]; 2.30 [m, $^3J(HH)$ = 7.1 Hz, $CHMe_2$]; 1.53–1.22 [complex multiplet, $CHMe_2$]; ^{31}P: −1.5 [m, $^2J(P^aP^b)$ = 18.5 Hz, $^2J(P^aP^c)$ = 11.1 Hz, $^2J(P^aP^d)$ = 388 Hz, $^1J(Pt^AP^a)$ = 2303 Hz, $^3J(Pt^BP^a)$ = 44 Hz, $^1J(P^aH)$ = 376 Hz, P^a]; 5.5 [m, $^2J(P^bP^a)$ = 18.5 Hz, $^2J(P^bP^c)$ = 14.8 Hz, $^1J(Pt^BP^b)$ = 3832 Hz, $^3J(Pt^AP^b)$ = 249 Hz, $^1J(P^bH)$ = 415 Hz, P^b]; −64.7 [m, $^2J(P^cP^a)$ = 11.1 Hz, $^2J(P^cP^b)$ = 14.8 Hz, $^2J(P^cP^d)$ = 40.7 Hz, $^1J(Pt^AP^c)$ = 2103 Hz, $^1J(Pt^BP^c)$ = 2965 Hz, P^c]; −24.1 [m, $^2J(P^dP^a)$ = 388 Hz, $^2J(P^dP^c)$ = 40.7 Hz, $^1J(Pt^AP^d)$ = 2297 Hz, $^3J(Pt^BP^d)$ = 41 Hz, P^d]; ^{195}Pt: −2613 [m, $^1J(Pt^AP^a)$ = 2300 Hz, $^1J(Pt^AP^c)$ = 2103 Hz, $^1J(Pt^AP^d)$ = 2300 Hz, $^3J(Pt^AP^b)$ = 246 Hz, $^3J(PtPt)$ ~ 330 Hz, Pt^A]; −2800 [m, $^1J(Pt^BP^b)$ = 3830 Hz, $^1J(Pt^BP^c)$ = 2970 Hz, $^3J(PtPt)$ ~ 330 Hz, Pt^B]. Found: C, 23.6; H, 4.7. Calc. for $C_{17}H_{41}P_4Cl_3Pt_2$: C, 23.6; H, 4.8%.

X-ray crystallographic study of $[Pt_2Cl_3\{(R^*)\text{-}\mu\text{-}^iPrPCH_2P^iPr_2\}\{(R^*)\text{-}H^iPrPCH_2P^iPr_2\}]$ (**2b**) *and* $[Pt_2Cl_3\{(R^*)\text{-}\mu\text{-}^iPrPCH_2P^iPr_2\}\{(S^*,S^*)\text{-}\mu\text{-}H^iPrPCH_2P^iPrH\}]$ (**4**)

A locally modified Picker four-circle diffractometer system was used in a moving crystal-moving detector mode for both studies. A molybdenum source and oriented graphite monochromator were utilized. Cooling was provided by a liquid nitrogen boil-off cooling system. The diffractometer system, cooling system and techniques used have been described in detail previously.[8] Both structures were

solved by a combination of direct methods (MULTAN78) and Fourier Techniques, and refined by full-matrix least-squares. In both cases hydrogen atoms were placed in fixed idealized geometries.

$[Pt_2Cl_3\{(R^*)\text{-}\mu\text{-}{}^iPrPCH_2P^iPr_2\}\{(R^*)\text{-}H^iPrPCH_2P^iPr_2\}]\cdot 2CHCl_3$. Space group $P2_1/n$; cell parameters (at $-146°C$) $a = 15.668(1)$, $b = 15.300(1)$, $c = 17.930(1)$ Å, $\beta = 115.52(1)°$; $D_{calc} = 1.964$ g cm^{-1} for $Z = 4$; crystal dimensions $0.40 \times 0.30 \times 0.30$ mm; linear absorption coefficient = 80.867 cm^{-1}; min/max absorption correction = 0.151/0.240. Data collection for $h, k, +/-l$ in the range $6 \geqslant 2\theta \geqslant 50°$; 6° min^{-1}; 6 s stationary backgrounds; 1.8° scan width. Total unique reflections = 6843; 6308 with $F > 3.0\sigma(F)$. R_{av} for 500 reflections measured more than once = 0.031. Final residuals are $R(F) = 0.0432$ and $R_w(F) = 0.0426$.

$[Pt_2Cl_3\{(R^*)\text{-}\mu\text{-}{}^iPrPCH_2P^iPr_2\}\{(S^*,S^*)\text{-}\mu\text{-}H^iPrPCH_2P^iPrH\}]\cdot 3/2C_6H_6$. Space group $P1$; cell parameters (at $-155°C$) $a = 12.944(2)$, $b = 13.442(3)$, $c = 10.289(2)$, $\alpha = 105.38(1)$, $\beta = 98.19(1)$, $\gamma = 86.15(1)°$; $D_{calc} = 1.912$ g cm^{-1} for $Z = 2$; crystal dimensions $0.07 \times 0.06 \times 0.05$ mm; linear absorption coefficient = 87.077 cm^{-1}; min/max absorption correction = 0.581/0.647. Data collection for $+/-h, k, +/-l$ in the range $6 \geqslant 2\theta \geqslant 45°$; 4° min^{-1}; 6 s stationary backgrounds; 2.0° scan width. Total unique reflections = 4486; 3810 with $F > 3.0\sigma(F)$. R_{av} for 265 reflections measured more than once = 0.053. Final residuals are $R(F) = 0.0518$ and $R_w(F) = 0.0506$.

Final positional and equivalent isotropic thermal parameters, bond distances, bond angles, calculated hydrogen atom parameters, anisotropic thermal parameters and observed and calculated structure factors have been deposited with Cambridge Crystallographic Data Centre.

Acknowledgements—We would like to thank IU Foundation and the Department of Chemistry for the award of a Chester Davis Fellowship (B.R.L.) and Professor M. H. Chisholm for both the supply of research facilities and useful discussions (B.R.L.).

REFERENCES

1. R. J. Puddephatt, *Chem. Soc. Rev.* 1983, **12**, 99.
2. (a) K. A. Azam, G. Ferguson, S. S. M. Ling, M. Parvez, R. J. Puddephatt and D. Srokowski, *Inorg. Chem.* 1985, **24**, 2799; (b) Lj. Manojlovic-Muir, K. W. Muir, A. A. Frew, S. S. M. Ling, M. A. Thompson and R. J. Puddephatt, *Organometallics* 1984, **3**, 1637 and refs 4, 5, 6 and 7 therein.
3. (a) D. J. Brauer, S. Hietkamp, H. Sommer and O. Stelzer, *Angew. Chem. Int. Edn Engl.* 1984, **23**, 734; (b) W. Radeck-Paryzek, A. H. McLennan and R. J. Puddephatt, *Inorg. Chem.* 1986, **25**, 3097; (c) Lj. Manojlovic-Muir, B. R. Lloyd and R. J. Puddephatt, *J. Chem. Soc., Dalton Trans.* 1987, 201; (d) D. J. Brauer, P. C. Knuppel and O. Stelzer, *Chem. Ber.* 1987, **120**, 81.
4. P. E. Garrou, *Chem. Rev.* 1981, **81**, 229.
5. B. Delavaux, B. Chaudret, F. Dahan and R. Poilblanc, *Organometallics* 1985, **4**, 935.
6. (a) D. W. Meek, R. Waid, K. D. Tau, R. M. Kirchner and C. M. Morimoto, *Inorg. Chim. Acta.* 1982, **64**, L221; (b) R. Glaser, D. J. Kountz, J. C. Gallucci and D. W. Meek, *Inorg. Chim. Acta* 1983, **77**, L207; (c) R. Glaser, D. J. Kountz, R. D. Waid, J. C. Gallucci and D. W. Meek, *J. Am. Chem. Soc.* 1984, **106**, 6324.
7. Differences in the platinum–phosphorus couplings in the observed ^{31}P and ^{195}Pt NMR spectra are due to the poorer resolution and signal to noise of the ^{195}Pt NMR spectra. The values determined from the ^{31}P NMR spectra should be considered of greater accuracy.
8. M. H. Chisholm, K. Folting, J. C. Huffman and C. C. Kirkpatrick, *Inorg. Chem.* 1984, **23**, 1021.

Polyhedron Vol. 8, No. 17, pp. 2179–2182, 1989
Printed in Great Britain

0277–5387/89 $3.00+.00
© 1989 Pergamon Press plc

COMPLEXES OF THE PLATINUM METALS—XXXVI.* OXIDATIVE SUBSTITUTION REACTIONS OF RUTHENIUM(II) AND OSMIUM(II) COMPLEXES $MCl_2(PPh_3)_3$—NEW β-DIKETONATE DERIVATIVES, MCl_2(β-DIKETONATE)$(PPh_3)_2$

STEPHEN F. COLSON and STEPHEN D. ROBINSON†

Department of Chemistry, King's College London, Strand, London WC2R 2LS, U.K.

(*Received* 31 *March* 1989; *accepted* 17 *April* 1989)

Abstract—The ruthenium(II) and osmium(II) complexes $MCl_2(PPh_3)_3$, undergo oxidative substitution reactions with β-diketones under aerobic conditions in warm benzene to afford ruthenium(III) and osmium(III) β-diketonate complexes, MCl_2(β-diketonate)$(PPh_3)_2$. Generally these products appear to adopt the less sterically hindered *trans*-phosphine stereochemistry, but one example, $RuCl_2\{CF_3C(O)CHC(O)CF_3\}(PPh_3)_2$, deposits from hot and cold reactions as yellow (*trans*-phosphines) and red (*cis*-phosphines) isomers, respectively.

The ruthenium(II) complexes $RuCl_2(PPh_3)_n$ ($n = 3$ or 4) and their osmium analogues $OsCl_2(PPh_3)_n$, have been extensively employed as precursors in ligand (L) substitution reactions leading to a wide variety of ruthenium(II) and osmium(II) species, $MCl_2L(PPh_3)_3$ or $MCl_2L_2(PPh_3)_2$.[2] They are also susceptible to aerobic oxidation in solution yielding ill-characterized ruthenium(III) or osmium(III) products. The combination of these two processes—substitution and oxidation—was first achieved some 9 years ago in this laboratory, when a series of carboxylates, $MX_2(O_2CR)(PPh_3)_2$, were obtained by treatment of the complexes $MX_2(PPh_3)_3$ with carboxylic acids in benzene solution under aerobic conditions.[3] We have subsequently shown that a parallel reaction involving 1,3-diaryltriazene affords a range of ruthenium(III) and osmium(III) triazenide derivatives, MX_2(ArNNNAr)$(PPh_3)_2$.[4] The extension of our oxidative-substitution technique to the synthesis of ruthenium(III) and osmium(III) β-diketonate complexes, MCl_2(β-diketonate)$(PPh_3)_2$, is now reported.

* For part XXXV, see ref. 1.

† Author to whom correspondence should be addressed.

EXPERIMENTAL

For general experimental details see ref. 4. β-Diketones were used as purchased without further purification. Melting points, analytical data and selected IR data are given in Tables 1 and 2.

Synthesis of dichloro(2,4-pentanedionato)bis(triphenylphosphine)ruthenium(III)

Dichlorotris(triphenylphosphine)ruthenium (0.3 g, 0.31 mmol) was added to a solution of 2,4-pentanedione (0.1 g, 1 mmol) in benzene (10 cm^3) and the mixture stirred at 70°C for 1 h under aerobic conditions. Upon cooling, the dark green solution was diluted with light petroleum and allowed to stand for 12 h, over which time the product precipitated. Recrystallization from dichloromethane–ethanol, followed by washing the precipitate with ethanol and light petroleum and drying *in vacuo*, afforded green crystals (0.21 g, 81.0%).

The following were prepared by the same method:

Dichloro(3-methyl-2,4-pentanedionato)bis(triphenylphosphine)ruthenium(III) as green needle crystals (52.0%).

Dichloro(3-ethyl-2,4-pentanedionato)bis(triphenylphosphine)ruthenium(III) as green needle crystals (29.0%).

Table 1. Melting points[a] and analytical data[b]

Complex	Melting point (°C)	Analysis (%) C	H	N	Cl
$RuCl_2\{MeC(O)CHC(O)Me\}(PPh_3)_2$	184–186	61.8(61.9)	4.5(4.7)		9.1(8.9)
$RuCl_2\{MeC(O)CMeC(O)Me\}(PPh_3)_2$	194–198	61.9(62.3)	4.7(4.8)		
$RuCl_2\{MeC(O)CEtC(O)Me\}(PPh_3)_2$	206–210	62.3(62.7)	4.9(5.0)		
$RuCl_2\{PhC(O)CHC(O)Ph\}(PPh_3)_2$	266–270	65.5(66.6)	4.4(4.5)		
$RuCl_2\{CF_3C(O)CHC(O)Me\}(PPh_3)_2$	157–160	57.7(58.0)	3.9(4.0)		
$RuCl_2\{CF_3C(O)CHC(O)CF_3\}(PPh_3)_2$[c]	162–163	54.6(54.5)	3.4(3.4)		8.1(7.8)
$RuCl_2\{CF_3C(O)CHC(O)CF_3\}(PPh_3)_2$[d]	141–144	54.6(54.5)	3.4(3.4)		8.1(7.8)
$RuBr_2\{MeC(O)CHC(O)Me\}(PPh_3)_2$	225–228	54.8(55.6)	4.1(4.2)		
$RuCl_2\{MeC(O)CHC(O)Me\}py(PPh_3)$	234–236	54.3(54.8)	4.3(4.5)	2.0(2.3)	
$RuCl_2\{CF_3C(O)CHC(O)Me\}py(PPh_3)$	245–248	50.5(50.4)	3.4(3.6)	2.1(2.1)	
$RuCl_2\{CF_3C(O)CHC(O)CF_3\}py(PPh_3)$	253–257	46.5(46.7)	2.8(2.9)	1.9(1.9)	
$RuCl\{CF_3C(O)CHC(O)CF_3\}(CO)(PPh_3)_2$	207–210	55.7(56.2)	3.3(3.5)		
$OsCl_2\{MeC(O)CHC(O)Me\}(PPh_3)_2$	276–280	55.3(55.7)	4.2(4.2)		
$OsCl_2\{CF_3C(O)CHC(O)Me\}(PPh_3)_2$	219–222	52.6(52.4)	3.4(3.6)		
$OsCl_2\{CF_3C(O)CHC(O)CF_3\}(PPh_3)_2$	226–230	49.3(49.6)	3.1(3.2)		

[a] Melting points taken in sealed tubes under nitrogen.
[b] Calculated figures in parentheses.
[c] "Red" isomer.
[d] "Yellow" isomer.

Dichloro(1,3 - diphenyl - 1,3 - propanedionato) bis(triphenylphosphine)ruthenium(III) as yellow–green microcrystals (68.0%).

Dichloro(1,1,1 - trifluoro - 2,4 - pentanedionato) bis(triphenylphosphine)ruthenium(III) as green needle clusters (38.0%).

Dichloro(1,1,1,5,5,5 - hexafluoro - 2,4 - pentanedionato)bis(triphenylphosphine)ruthenium(III) (yellow isomer) as shiny black needles, which on grinding gave a yellow microcrystalline powder (54.0%).

Dichloro(1,1,1,5,5,5 - hexafluoro - 2,4 - pentanedio-

Table 2. Selected IR data[a]

Complex	$\nu(\beta$-diketonate) (cm^{-1})			ν(M—Cl) (cm^{-1})	
$RuCl_2\{MeC(O)CHC(O)Me\}(PPh_3)_2$	1551(s)	1514(s)		330(m)	323(m)
$RuCl_2\{MeC(O)CMeC(O)Me\}(PPh_3)_2$	1562(s)	1513(m)		335(m)	322(m)
$RuCl_2\{MeC(O)CEtC(O)Me\}(PPh_3)_2$	1552(s)	1511(m)		332(m)	322(m)
$RuCl_2\{PhC(O)CHC(O)Ph\}(PPh_3)_2$	1525(s)	1513(s)		332(m, sh)	
$RuCl_2\{CF_3C(O)CHC(O)Me\}(PPh_3)_2$	1601(s)	1571(m)	1511(m)	337(m)	320(m)
$RuCl_2\{CF_3C(O)CHC(O)CF_3\}(PPh_3)_2$[b]	1619(s)	1599(s)		347(m)	328(w)
$RuCl_2\{CF_3C(O)CHC(O)CF_3\}(PPh_3)_2$[c]	1608(s)	1570(m)	1540(m)	345(m, sh)	
$RuBr_2\{MeC(O)CHC(O)Me\}(PPh_3)_2$	1551(s)	1520(s)			
$RuCl_2\{MeC(O)CHC(O)Me\}py(PPh_3)$	1562(s)	1515(s)		326(m)	276(w)
$RuCl_2\{CF_3C(O)CHC(O)Me\}py(PPh_3)$	1594(s)	1567(m)	1516(m)	359(w)	336(m)
$RuCl_2\{CF_3C(O)CHC(O)CF_3\}py(PPh_3)$	1607(s)	1588(s)	1550(m)	349(m)	339(m)
$RuCl\{CF_3C(O)CHC(O)CF_3\}(CO)(PPh_3)_2$[d]	1616(s)	1539(m)		328(w)	
$OsCl_2\{MeC(O)CHC(O)Me\}(PPh_3)_2$	1556(s)	1516(s)		323(sh)	
$OsCl_2\{CF_3C(O)CHC(O)Me\}(PPh_3)_2$	1600(s)	1582(s)	1520(m)	324(sh)	
$OsCl_2\{CF_3C(O)CHC(O)CF_3\}(PPh_3)_2$	1618(m)	1596(s)	1550(m)	339(w)	324(m)

[a] KBr disc, s = strong, m = medium, w = weak, sh = shoulder.
[b] "Red" isomer.
[c] "Yellow" isomer.
[d] ν(CO), 1958 cm^{-1}.

nato)bis(triphenylphosphine)ruthenium(III) (red isomer) as red platelets (71.5%) from reactions conducted at room temperature.

Dibromo(2,4 - pentanedionato)bis(triphenylphosphine)ruthenium(III) was similarly prepared from dibromotris(triphenylphosphine)ruthenium as orange–brown needles (45.0%).

Synthesis of dichloro(2,4-pentanedionato)(pyridine)(triphenylphosphine)ruthenium(III)

Dichloro(2,4 - pentanedionato)bis(triphenylphosphine)ruthenium(III) (0.15 g, 0.2 mmol) was added to a solution of pyridine (0.5 g, 6 mmol) in benzene (10 cm^3) and the mixture refluxed for 10 min. The green solution rapidly turned orange, accompanied by precipitation of the product which was collected by filtration. Recrystallization from dichloromethane–ethanol, followed by washing the precipitate with ethanol and light petroleum and drying *in vacuo*, afforded pink crystals (0.1 g, 86.5%).

The following were prepared by the same method:

Dichloro(1,1,1 - trifluoro - 2,4 - pentanedionato)(pyridine)(triphenylphosphine)ruthenium(III) as red–orange platelets (64.0%).

Dichloro(1,1,1,5,5,5 - hexafluoro - 2,4 - pentanedionato)(pyridine)(triphenylphosphine)ruthenium (III) as orange needle clusters (63.0%), using the "yellow isomer" precursor.

Synthesis of chloro(carbonyl)(1,1,1,5,5,5 - *hexafluoro* - 2,4 - *pentanedionato)bis(triphenylphosphine)ruthenium*(II)

A solution of dichloro(1,1,1,5,5,5-hexafluoro-2,4-pentanedionato)bis(triphenylphosphine)ruthenium (III) ("red isomer") (0.15 g, 0.17 mmol) in benzene (15 cm^3) was refluxed under a carbon monoxide atmosphere for 6 h. After cooling, the orange solution was evaporated to dryness under reduced pressure. The resulting oil was recrystallized from dichloromethane–ethanol. Washing the precipitate with ethanol and light petroleum, followed by drying *in vacuo*, afforded orange crystals (0.07 g, 45.0%).

The same compound can also be prepared from the "yellow isomer" under identical reaction conditions.

Synthesis of dichloro(2,4-pentanedionato)bis(triphenylphosphine)osmium(III)

Dichlorotris(triphenylphosphine)osmium (0.3 g, 0.3 mmol) was added to a solution of 2,4-pentanedione (0.15 g, 1.5 mmol) in benzene (10 cm^3) and the mixture stirred at 70°C for 1 h. Upon cooling, the solution was diluted with light petroleum and allowed to stand for 12 h, over which time the product precipitated. Filtration of the solution, followed by washing of the precipitate with ethanol and light petroleum and drying *in vacuo*, afforded red–brown microcrystals (0.15 g, 59.0%).

The following were prepared by the same method:

Dichloro(1,1,1 - trifluoro - 2,4 - pentanedionato)bis(triphenylphosphine)osmium(III) as red–brown platelets (31.5%).

Dichloro(1,1,1,5,5,5 - hexafluoro - 2,4 - pentanedionato)bis(triphenylphosphine)osmium(III) as orange–brown platelets (53.0%).

RESULTS AND DISCUSSION

The "oxidative substitution" reactions:

$$MX_2(PPh_3)_3 + RCO_2H \xrightarrow{O_2} MX_2(O_2CR)(PPh_3)_2$$

(M = Ru, Os; X = Cl, Br)

first reported from this laboratory in 1979,[3] and subsequently extended to cover other weak organic acids—1,3-diaryltriazenes[4] and selected Schiff bases[5]—have now been shown to provide a convenient route to new ruthenium(III) and osmium(III) β-diketonate complexes, MCl_2(β-diketonate)$(PPh_3)_2$. The new β-diketone derivatives, which with one exception appear to exist in a single isomeric form, are obtained as green (M = Ru) or red–orange–brown (M = Os), air-stable, crystalline solids by addition of the complexes $MCl_2(PPh_3)_3$ to solutions of β-diketones in warm (or cold) benzene under aerobic conditions. In contrast, the exception, $RuCl_2\{CF_3C(O)CHC(O)CF_3\}(PPh_3)_2$, deposits in red and yellow isomeric forms from cold and warm benzene, respectively. All the complexes are paramagnetic with magnetic moments (*ca* 1.8 BM) corresponding to low spin d^5 systems with one unpaired electron. Because of their magnetic properties the complexes do not give narrow line NMR spectra. Furthermore, their IR spectra (Table 2), while confirming the presence of β-diketonate ligands, do not permit unambiguous distinction between the three possible geometric isomers **I**, **II** and **III**. Consequently, stereochemical assignments were confirmed by a combination of X-ray and chemical methods. X-ray diffraction studies on the red and yellow isomers, $RuCl_2\{CF_3C(O)CHC(O)CF_3\}(PPh_3)_2$, reported elsewhere[6] reveal *cis*- and *trans*-phosphine arrangements (**I** and **II**), respectively. Attempts to differ-

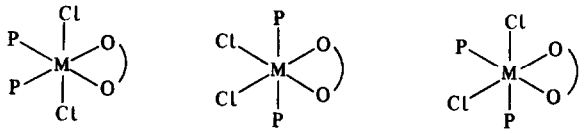

(M = Ru, Os; P = PPh_3)

(I) **(II)** **(III)**

entiate isomers **I** and **II** by chemical means centred on ligand substitution reactions. Carbonylation (CO, 1 atm, benzene, 6h) reduced *both* isomers to the known[7] ruthenium(II) carbonyl complex $RuCl\{CF_3C(O)CHC(O)CF_3\}(CO)(PPh_3)_2$, although the product from the red isomer was contaminated with $RuCl_2(CO)_2(PPh_3)_2$ [ν(CO 2060, 1995 cm^{-1} $CHCl_3$ solution]. However, substitution with pyridine (solution in refluxing benzene, 10 min) occurred only for the yellow isomer (**II**). Reactions of the other ruthenium(III) complexes with pyridine gave similar pyridine substitution products, $RuCl_2$(β-diketonate)py(PPh_3), thus suggesting, that like the "yellow" isomer, they possess the less sterically congested *trans*-phosphine geometry. Failure of the corresponding osmium complexes to undergo pyridine substitution may indicate that they adopt the *cis*-phosphine structure (**I**), but seems more likely to reflect the greater kinetic inertness of the osmium(III) centre relative to ruthenium(III), particularly since the related osmium(III) carboxylate, $OsBr_2(O_2CMe)(PPh_3)_2$, has already been shown[8] by diffraction methods to possess *trans*-phosphine stereochemistry.

Only hexafluoroacetylacetone gave "red" and "green" isomers, other β-diketones investigated gave a single isomer irrespective of reaction temperatures (70 and 25°C) employed. Attempts to convert the "red" isomer to the "green" form by heating in benzene alone or the presence of added hexafluoroacetylacetone, triphenylphosphine or pyridine were unsuccessful. Finally, attempts to perform the reaction under anaerobic conditions gave unchanged starting materials.

Acknowledgements—We thank Johnson Matthey plc for a generous loan of ruthenium trichloride, and King's College for a studentship awarded to S.F.C.

REFERENCES

1. B. G. Olby and S. D. Robinson, *Inorg. Chim. Acta*, submitted for publication.
2. F. H. Jardine, *Prog. Inorg. Chem.* 1984, **31**, 265.
3. D. S. Moore and S. D. Robinson, *Inorg. Chem.* 1979, **18**, 2307.
4. S. F. Colson and S. D. Robinson, *Inorg. Chim. Acta* 1988, **149**, 13.
5. V. Alteparmakian and S. D. Robinson, *Inorg. Chim. Acta* 1986, **116**, L37.
6. S. F. Colson, S. D. Robinson, P. D. Robinson and C. C. Hinckley, *Acta Cryst.* 1989, **C45**, 715.
7. M. A. M. Queirós and S. D. Robinson, *Inorg. Chem.* 1978, **17**, 310.
8. C. C. Hinckley, M. Matusz, P. A. Kibala and P. D. Robinson, *Acta Cryst.* 1987, **C43**, 1880.

Polyhedron Vol. 8, No. 17, pp. 2183–2188, 1989
Printed in Great Britain

0277–5387/89 $3.00+.00
© 1989 Pergamon Press plc

REACTIVITY OF NEODYMIUM(III) ISOPROPOXIDE DERIVATIVES: SYNTHESIS, CHARACTERIZATION AND CRYSTAL STRUCTURE OF $[Nd_4(\mu_3\text{-}OH)_2(\mu_2,\mu_1\text{-}acac)_6(acac)_4]$

OLIVIER PONCELET and LILIANE G. HUBERT-PFALZGRAF*

Laboratoire de Chimie Moléculaire, Unité Associée au CNRS, Université de Nice, Parc Valrose, 06034 Nice, France

(*Received* 21 *February* 1989; *accepted* 21 *April* 1989)

Abstract—Reaction between neodymium chips and isopropanol led to the isolation of $[Nd(O^iPr)_3]_4 \cdot 4^iPrOH$. Its desolvation results in a soluble polynuclear neodymium(III) oxoisopropoxide, whose reactivity has been investigated. Reaction with acetylacetone produced a compound analysing as $Nd_2(OH)(acac)_5$, which has been characterized by IR and ESR spectroscopy, as well as by X-ray diffraction. It crystallizes in the monoclinic $P2_1/n$ system with unit cell dimensions $a = 14.52(5)$, $b = 14.20(4)$, $c = 15.25(5)$ Å, $\beta = 101.4°$ and $Z = 4$. Least-squares refinement converged to a final $R_w = 0.050$. The molecule is a centrosymmetric, tetranuclear neodymium(III) hydroxo acetylacetonate cluster, $[Nd_4(\mu_3\text{-}OH)_2(\mu_2,\mu_1\text{-}acac)_6(acac)_4]$. Two dinuclear $Nd_2(OH)(acac)_5$ units are linked by two triply bridging pyramidal μ-hydroxo ligands and by two bridging-chelating β-diketonate ligands. The metal atoms are eight-coordinated with a distorted square antiprism geometry.

High purity neodymium derivatives are of interest for optical fibers,[1] various non-linear optic materials[2] and high temperature superconductors.[3] Moreover, neodymium alkoxide, β-diketonates and related derivatives often display the highest activity among rare earth catalysts for polymerization reactions.[4] The commonest neodymium alkoxide, the trisisopropoxide, was reported to be obtained by oxidation of the metal by isopropanol,[5] as well as by a metathesis reaction between neodymium chloride and sodium isopropoxide.[6] However, this latter reaction appears complex, as it also forms $[Nd_6(\mu_6\text{-}Cl)(\mu_3\text{-}OR)_2(\mu_2\text{-}OR)_9(OR)_6]$ (R = ^{i}Pr), which has been structurally characterized.[7] Contamination of alkoxides by chloride residues might preclude their use as molecular precursors for high-tech oxide-based materials[8] via sol-gel or chemical vapour decomposition techniques.

Thus, the simple and direct synthetic approach, starting from the metal and isopropanol, appeared more attractive for obtaining pure neodymium(III) isopropoxide. This led to the isolation in high yields of a soluble, non-volatile polynuclear oxoisopropoxide. Investigation of its reactivity led to the isolation of a neodymium(III) hydroxo-acetylacetonate, which was characterized by X-ray diffraction. It corresponds to a tetranuclear cluster, $[Nd_4(\mu_3\text{-}OH)_2(\mu_2,\mu_1\text{-}acac)_6(acac)_4]$ (acacH = $C_5H_8O_2$, acetylacetone).

EXPERIMENTAL

All reactions were routinely performed under dry, oxygen-free argon, using Schlenk tubes and vacuum-line techniques. Solvents were purified by standard methods. ESR and IR spectra were registered on Bruker ER-200D and IR S45 spectrometers, respectively. Microanalytical data were obtained from the Centre de Microanalyse du CNRS.

$Nd_4(O^iPr)_{12} \cdot 4^iPrOH$ (1)

Neodymium chips (23.4 g, 0.164 mol) were allowed to react with isopropanol in toluene (300 cm^3, 1:1 in volume). The catalyst ($HgCl_2$ + $Hg(OAc)_2$ 1:1, 15 mg) was added after heating at 80°C for 1 h and refluxing was maintained for

* Author to whom correspondence should be addressed.

a further 48 h. The hot reaction medium was filtered and light blue–pink crystals were obtained by cooling (46.9 g, 75.6%). Found: C, 37.4; H, 6.9. Calc. for $C_{48}H_{116}O_{16}Nd_4$: C, 37.7; H, 7.7%.

X-ray quality crystals were obtained directly from the reaction medium. Their structure could only be partially solved so far as a result of disorder problems due to the presence of coordinated isopropanol. Cell parameters: $a = 20.604(8)$, $b = 20.724(10)$, $c = 14.660(5)$ Å, orthorhombic.

Drying of **1** under vacuum at room temperature led to a progressive loss of alcohol and isopropylether with the formation of a compound analysing as $[Nd_6O_5(O^iPr)_8]$ (**2**) (30.9 g, 80%) after 48 h. Complex **2** is soluble in common organic solvents, including pentane (although dissolution is slow in this case). Found: C, 19.8; H, 4.0. Calc. for $C_{24}H_{56}O_{13}Nd_6$: C, 20.3; H, 4.0%.

By contrast with yttrium, no attack of the neodymium chips was observed in the absence of a mercury catalyst. No reaction occurs between neodymium and methanol or *t*-butanol in conditions similar to that of the synthesis of the isopropoxide derivative.

$Nd_2(OH)(acac)_5$ (**3**)

A solution of acetylacetone (6.3 cm^3, 60.3 mmol) in 15 cm^3 of toluene was added over 1 h to a solution of **2** (2.07 g, 1.46 mmol). After 24 h, the light blue solution was evaporated to dryness, and after recrystallization in acetone 1.9 g (88%) of $Nd_2(OH)(acac)_5$, only slightly air-sensitive, soluble in the common organic solvents (toluene, THF, $CHCl_3$ . . .) was obtained. Found: C, 37.6; H, 4.6. Calc. for $C_{25}H_{96}O_{11}Nd_2$: C, 37.5; H, 4.5%. IR (Nujol, cm^{-1}): 1607 [ν(C=O)], 1520 [ν(C=C)], 1258 [π_{as}(C—O)], 1016, 916, 650; 523, 449 [ν(Nd—O)]. MS (m/e^+, %): Nd(acac)$_3$ (40%), Nd(acac)$_2$ (23%), Nd(OH)(acac) (5%), NdO (5%), acacH (25%), C_3H_7O (100%).

X-ray crystallography of $Nd_2(OH)(acac)_5$ (**3**)

A light blue–pink parallelepiped crystal, grown from acetone solution at room temperature, was introduced into a Lindemann capillary and mounted onto an Enraf–Nonius CAD-4 automatic diffractometer. The Laue symmetry and systematic absences, $h0l$ for $h+1 = 2n+1$ and $0k0$ for $k = 2n+1$, indicate monoclinic symmetry and space group $P2_1/n$. The lattice parameters were determined from 25 computer-centred reflections. The unit cell parameters and basic information about data collection and structure refinement are given in Table 1. Corrections for Lorentz and polarization effects were applied, but not for absorption. The atomic scattering factors were taken from Cromer and Waber.[9]

The structure was solved on a PDP 11/44 computer using the Enraf–Nonius SPP program.[10] The atomic positions were obtained by direct methods and subsequent Fourier differences series. Complex **3** is a dimer with a centre of symmetry at $\frac{1}{2},0,\frac{1}{2}$. Refinement of coordinates and thermal parameters, first isotropic and then anisotropic, of the 38 independent non-hydrogen atoms led to final values of 0.043 for R and 0.050 for R_w. The function minimized was $w = (|F_o| - |F_c|)^2$, where $w = 1/\sigma^2(F_o)$. Hydrogen parameters were not introduced in the refinement.

Positional parameters and equivalent isotropic thermal parameters are given as supplementary material.*

RESULTS AND DISCUSSION

Reactions between isopropanol and neodymium have been reported to lead to the isolation of $Nd(O^iPr)_3$.[5] Indeed, crystals, solvated by isopropanol (ν(OH): 3348 cm^{-1} in the IR) and analysing as $[Nd(O^iPr)_3]\cdot{}^iPrOH$ (**1**) were obtained from the reaction medium in high yields ($\simeq$ 75%). Their structure could only partially be solved so far, as a result of disorder problems and loss of the alcohol molecules, but appears to correspond to a tetranuclear species, $Nd_4(\mu_3\text{-}O^iPr)_2(\mu\text{-}O^iPr)_4(O^iPr)_6(^iPrOH)_4$.[11] The analytical data of these light blue–pink crystals showed, after removal of the alcohol (drying *in vacuo* at room temperature for 48 h), a too-low carbon and hydrogen content with respect to a $Nd(O^iPr)_3$ composition, but were found to be in agreement with an oxoalkoxide of empirical formula $Nd_6O_5(O^iPr)_8$ (**2**). Complex **2** is highly soluble in common solvents including hydrocarbons, but its paramagnetic character precluded the obtaining of structural information by NMR techniques.

We have previously shown with yttrium, that although $Y(O^iPr)_3$ species solvated by alcohol are predominant in solutions, their isolation is achieved as a complex structural unit: $Y_5O(O^iPr)_{13}$.[12] Stabilization of other *f* element isopropoxides $Ln(O^iPr)_3$ as similar polymetallic oxoisopropoxides has also been observed for ytterbium[13] or lan-

* Supplementary material. Tables of final fractional coordinates, anisotropic thermal parameters, complete bond lengths and angles (4 pp.), tables of calculated and observed structure factors (18 pp.) have been deposited with the Cambridge Structural Data File.

Table 1. X-ray crystal data and data collection of $[Nd_4(OH)_2(acac)_{10}]$ at room temperature

Compound	$C_{25}H_{40}O_{11}Nd_2$
Colour	Light blue–pink
Molecular weight	805.07
Crystal system	Monoclinic
a (Å)	14.52(5)
b (Å)	14.20(4)
c (Å)	15.25(5)
α (°)	90
β (°)	101.4(1)
γ (°)	90
V (Å^3)	3085(3)
Z	4
Density (calc.) (g cm^{-3})	1.733
Crystal dimension (mm)	$0.5 \times 0.15 \times 10.15$
Space group	$P2_1/n$
$F(000)$ (e$^-$)	1592
Diffractometer	Enraf–Nonius CAD-4
Radiation	Mo-K_α ($\lambda = 0.71069$ Å)
Linear absorption coefficient (cm^{-1})	33.92
Scan type	θ–2θ
Scan range (°)	20–40
hkl limits	$-13 \leqslant h \leqslant +13$, $-13 \leqslant k \leqslant +13$, $l \leqslant 14$
Data collected	6032
Unique data used ($F_o^2 > 3\sigma(F_o^2)$)	5124
Number of parameters refined	342
$R = \Sigma(\|F_o\| - \|F_c\|)/\Sigma\|F_o\|$	0.043
$R_w = (\Sigma w(\|F_o\| - \|F_c\|)^2/w\|F_o\|^2)^{1/2}$	0.050
Quality-of-fit indicator	2.1
Largest shift/ESD final cycle	0.7

thanum.[14] Although the origin of the oxo ligands may be multiple, we have established in the case of yttrium, that aggregation of metals into a closed polyhedral moiety represents an alternative for a trivalent metal to achieve high coordination numbers despite the loss of the labile isopropanol molecules. Thermal gravimetric analyses have shown that desolvation and condensation by elimination of diisopropyl ether occur simultaneously.[14]

Similar results are obtained in the case of neodymium. Although the structure of the polynuclear oxoalkoxide could not be established by X-ray diffraction so far, its formation in reproducible and high yields excludes accidental hydrolysis. Comparison of the reactions between the reaction medium and **2** with an excess of $Al(O^iPr)_3$ was made in a refluxing toluene–alcohol medium. No reaction was observed when starting from **2**, while that with the reaction medium offered, by fractional distillation, the heterometallic alkoxide[15] $Nd[Al(O^iPr)_4]_3$ in high yield (70%). These results are also supported by the behaviour of the yttrium isopropoxide derivatives: the reactivity of the species formed *in situ* and the isolated oxoalkoxide $Y_5O(O^iPr)_{13}$ are definitely different.[12]

In order to achieve the characterization of **2**, its reactivity was investigated, especially towards other potential oxygen mono- or bidentate ligands, which could also lead to molecular precursors of oxides.

No reaction occurred between **2** and *t*-butanol, in refluxing toluene; alkoxo exchange reactions and/or reactions involving the oxo ligands could however be achieved with acetic acid or acetylacetone, offering compounds analysing as $Nd_6O_3(OAc)_4(O^iPr)_8$ and $Nd_2(OH)(acac)_5$ (**3**), respectively. The solubility of **3** is attractive, by contrast with the poor solubility of the carboxylate derivative. Its IR spectra confirmed the obtaining of a species different from $Nd(acac)_3$, previously obtained by reaction between $[Nd(O^iPr)_3]_n$ and acetylacetone,[16,17] the main spectral differences being the presence of an additional absorption band at 725 cm^{-1} and a notable shift to higher frequencies (40 cm^{-1}) for the stretching ν_s(C=O) mode. By contrast with the isopropoxides derivatives **1** and **2**, which were ESR silent down to 100 K (probably due to very short relaxation times,



Fig. 1. ESR spectrum of $[Nd_4(\mu_3\text{-}OH)_2(\mu_2,\mu_1\text{-}acac)_6(acac)_4]$ in toluene solution at 298 K.

as often observed for lanthanide compounds), **3** displays a spectrum at room temperature (Fig. 1). However, since ESR spectra of *f* elements are mainly an illustration of spin–orbit effects,[18] an X-ray structure determination of **3** was undertaken.

The crystal structure of $[Nd_4(OH)_2(acac)_{10}]$ consists of a centrosymmetric tetranuclear cluster (Figs 2 and 3). Relevant interatomic distances and angles are collected in Table 2.

Two dinuclear $Nd_2(OH)(acac)_5$ units are linked by two triply bridging hydroxo and two bridging-chelating β-diketonate ligands. Although the hydrogen atoms were not crystallographically located, an unambiguous assignment as μ_3-hydroxo was made on the basis of several criteria. The sum of the Nd—O—Nd angles is 326.5 around O(1), close to the value (328.4) expected for pure sp^3 hybridized atoms.[19] Moreover, an oxo ligand would lead to mixed valency Nd^{III}–Nd^{IV} species. Although the stabilization of neodymium(IV) is possible with some ligands,[20] no molecular neodymium(IV) compounds have been reported so far. Finally, an O—H stretching mode is observed at 3450 cm^{-1} in the IR spectrum, confirming the presence of hydroxo ligands in the aggregate. Although both the metal atoms are eight-coordinated, with Nd—O bond lengths ranging from 2.370(7) to 2.654(6) Å, Nd(1) and Nd(2) have slightly different environments. The coordination polyhedra around the two metals are distorted square antiprisms (Fig. 4), but Nd(2) is surrounded by two hydroxo ligands, one chelating and three bridging-chelating acetylacetonato groups, while Nd(1) is linked to only one hydroxo group.

The Nd—O bond distances fall in the range of the values previously reported in the literature for neodymium oxide derivatives or Nd—O coordination bonds,[21,22] but are much longer than the values observed for terminal Nd—O^{i}Pr linkages.[7] The longest Nd—O bond distances correspond to β-diketonate oxygen atoms in bridging positions. The Nd—O bond lengths involving chelating acac ligands are significantly different (2.38, 2.44 Å), but close to the values determined in $Nd(acac)_3 \cdot 2H_2O$.

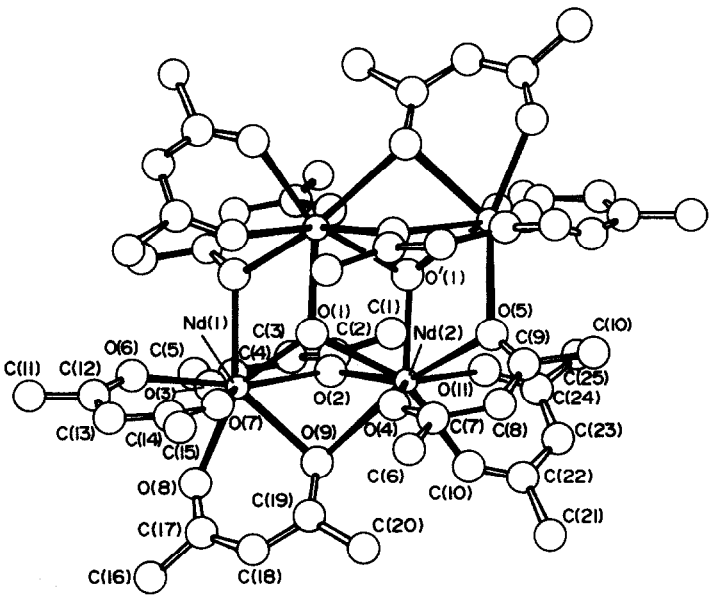

Fig. 2. ORTEP view of $[Nd_4(\mu_3\text{-}OH)_2(\mu_2,\mu_1\text{-}acac)_6(acac)_4]$, showing the atom numbering scheme.

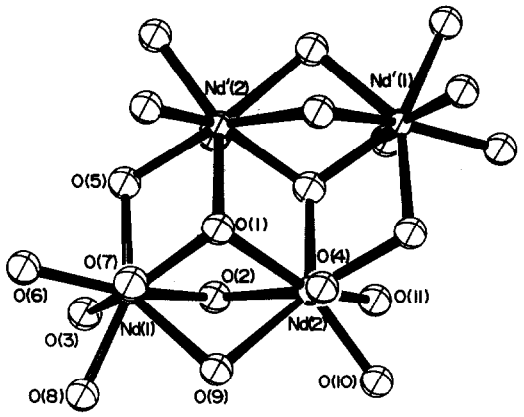

Fig. 3. Neodymium oxygen core of **3**.

The Nd(μ_3-OH) linkages are in agreement with the value observed for other triply bridged metal–hydroxo bonds.[19]

The rest of the bonding in the acac ligands appears normal, with C—O and C—C bond lengths ranging from 1.25(1) to 1.31(2) Å and from 1.38(1) to 1.52(2) Å, respectively. Close intermolecular contacts between most oxygen atoms are noted, as commonly observed for β-diketonate derivatives. The bridging-chelating ligands, especially those of the $Nd_2(OH)(acac)_5$ unit, display a larger bite and more deviation towards planarity of the cycle than the simple chelating ones. The shortest metal–metal distances correspond to those of the dinuclear $Nd_2(OH)(acac)_5$ unit with a value of 3.833 Å.

The synthesis of $[Nd_4(\mu_3\text{-}OH)_2(acac)_{10}]$ from the oxoalkoxide in nearly quantitative yield implies that the oxo ligands, or at least some of them, are reactive towards acetylacetone, as also previously observed for oxo species of various elements.[23] The hydroxo ligand can thus result from direct reactivity with the β-diketone or from further hydrolysis of an $Nd(acac)_3$ species, since water appears as a byproduct. Hydroxo species formulated as $Ln(acac)_2OH$ have been previously suggested to form by hydrolysis of $Ln(acac)_3$ or by thermal decomposition of their hydrates, but were not characterized.[23,24] Complex **3** belongs to the very few hydroxide lanthanide derivatives structurally characterized[25] and is the first one for neodymium.

Table 2. Selected bond lengths and angles for $[Nd_4(\mu_3\text{-}OH)_2(acac)_{10}]$

Bond lengths (Å)

Nd(1)—O(1)	2.428(6)	Nd(1)—O(8)	2.374(6)	Nd(2)—O'(1)	2.418(6)
Nd(1)—O(2)	2.594(5)	Nd(1)—O(9)	2.542(6)	Nd(2)—O(9)	2.654(6)
Nd(1)—O(3)	2.370(7)	Nd(2)—O(1)	2.459(5)	Nd(2)—O(10)	2.371(6)
Nd(1)—O(5)	2.564(6)	Nd(2)—O(2)	2.625(6)	Nd(2)—O(11)	2.420(6)
Nd(1)—O(6)	2.384(6)	Nd(2)—O(4)	2.417(5)		
Nd(1)—O(7)	2.445(6)	Nd(2)—O(5)	2.485(6)		

Angles (coordination polyhedron) (°)

O(1)—Nd(1)—O(2)	70.4(2)	O(5)—Nd(1)—O(9)	135.0(2)	O(2)—Nd(2)—O(4)	133.4(2)
O(1)—Nd(1)—O(3)	134.9(3)	O(6)—Nd(1)—O(7)	70.9(2)	O(2)—Nd(2)—O'(1)	78.0(2)
O(1)—Nd(1)—O(5)	69.3(2)	O(6)—Nd(1)—O(8)	76.2(3)	O(2)—Nd(2)—O'(5)	147.5(2)
O(1)—Nd(1)—O(6)	120.0(2)	O(6)—Nd(1)—O(9)	136.5(2)	O(9)—Nd(2)—O(4)	77.5(2)
O(1)—Nd(1)—O(7)	68.6(2)	O(7)—Nd(1)—O(8)	85.2(2)	O(9)—Nd(2)—O'(1)	133.1(2)
O(1)—Nd(1)—O(8)	139.4(2)	O(7)—Nd(1)—O(9)	77.7(2)	O(9)—Nd(2)—O'(5)	145.5(2)
O(1)—Nd(1)—O(9)	72.6(2)	O(8)—Nd(1)—O(9)	71.9(3)	O(10)—Nd(2)—O(4)	82.6(2)
O(2)—Nd(1)—O(3)	71.9(3)	O(1)—Nd(2)—O(2)	69.4(2)	O(10)—Nd(2)—O'(1)	140.9(2)
O(2)—Nd(1)—O(5)	77.7(2)	O(1)—Nd(2)—O(9)	70.1(2)	O(10)—Nd(2)—O'(5)	82.1(2)
O(2)—Nd(1)—O(6)	154.3(3)	O(1)—Nd(2)—O(10)	147.2(2)	O(11)—Nd(2)—O(4)	137.9(2)
O(2)—Nd(1)—O(7)	132.3(3)	O(1)—Nd(2)—O(11)	142.6(2)	O(11)—Nd(2)—O'(1)	76.3(2)
O(2)—Nd(1)—O(8)	112.2(2)	O(2)—Nd(2)—O(9)	65.5(2)	O(11)—Nd(2)—O'(5)	75.6(2)
O(2)—Nd(1)—O(9)	67.6(2)	O(2)—Nd(2)—O(10)	119.2(2)	O(4)—Nd(2)—O'(5)	69.4(2)
O(3)—Nd(1)—O(6)	87.0(2)	O(2)—Nd(2)—O(11)	88.5(2)	O(4)—Nd(2)—O'(1)	111.9(2)
O(3)—Nd(1)—O(7)	155.1(2)	O(9)—Nd(2)—O(10)	84.6(2)	O(5')—Nd(2)—O'(5)	70.8(2)
O(3)—Nd(1)—O(8)	78.3(2)	O(9)—Nd(2)—O(11)	128.4(2)	Nd(1)—O(1)—Nd(2)	103.3(2)
O(3)—Nd(1)—O(9)	114.0(2)	O(10)—Nd(2)—O(11)	69.9(3)	Nd(1)—O(1)—Nd'(2)	113.2(2)
O(5)—Nd(1)—O(6)	84.4(2)	O(1)—Nd(2)—O(4)	72.0(2)	Nd(2)—O(1)—Nd'(2)	110.0(2)
O(5)—Nd(1)—O(7)	108.8(2)	O(1)—Nd(2)—O'(1)	70.0(2)	Nd(1)—O(2)—Nd(2)	94.5(2)
O(5)—Nd(1)—O(8)	150.9(2)	O(1)—Nd(2)—O'(5)	107.0(2)	Nd(1)—O(9)—Nd(2)	95.1(2)
				Nd(1)—O(5)—Nd'(2)	106.5(2)

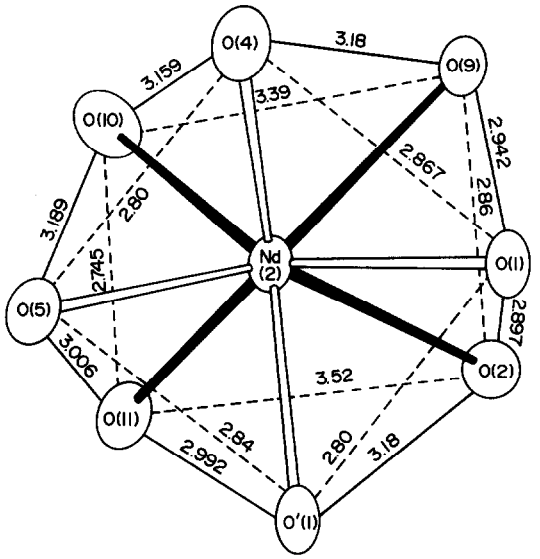

Fig. 4. Coordination polyhedron around Nd(2), showing the extent to which the faces are distorted from the ideal square.

Octacoordination appears to be favoured for the lanthanides in β-diketonate derivatives, as illustrated by the structural data of $Ln(acac)_3 \cdot nH_2O$ (Ln = Y, La, Nd, Eu; $n = 2$ or 3) and $[Ln(dpm)_3]_2$ (Ln = Pr, Er; dpmH = dipivaloylmethane).[20,23] Thus formation of a tetranuclear cluster for $[Nd_4(\mu_3\text{-}OH)_2(acac)_{10}]$, the first example of such a structural unit for neodymium, allows the metal to attain this coordination number.

These results, as well as those obtained on yttrium with the formation of $Y_5O(O^iPr)_{13}$,[12] suggest extensive and promising oxopolymetallic chemistry for lanthanides with anionic oxygen donor ligands.

Acknowledgements—Support by the CNRS (AIR and GRECO 93 "Précurseurs Moléculaires de Matériaux Inorganiques") is acknowledged. We wish to thank Dr M. Pierrot (University of Aix-Marseille) and Dr J. C. Daran (Paris) for the X-ray studies.

REFERENCES

1. S. H. Wang and L. L. Hench, *Science of Ceramic Chemical Processing* (Edited by L. L. Hench and D. R. Ulrich), p. 201. Wiley, New York (1986).
2. P. Maestro, *J. Less-Common Met.* 1985, **111**, 43.
3. R. J. Cava, B. Batlogg, J. J. Krajewski, L. W. Rupp, L. F. Schneemeyer, T. Siegrist, R. B. Van Dover, P. Marsh, W. F. Peck Jr, P. K. Gallagher, S. H. Glarum, J. H. Marshall, R. C. Farrow, J. V. Waszcak, R. Hull and P. Trevor, *Nature* 1988, **336**, 211.
4. Z. Shen, *Inorg. Chim. Acta* 1987, **140**, 7.
5. L. M. Brown and K. S. Mazdiyasni, *Inorg. Chem.* 1970, **9**, 2783.
6. S. N. Misra, T. N. Misra and R. C. Mehrotra, *Aust. J. Chem.* 1968, **21**, 797.
7. R. A. Andersen, D. H. Templeton and A. Zalkin, *Inorg. Chem.* 1978, **17**, 1962.
8. L. G. Hubert-Pfalzgraf, *New J. Chem.* 1987, 662.
9. D. T. Cromer and J. T. Waber, *Acta Cryst.* 1965, **18**, 17.
10. B. Frenz, *Computing in Crystallography* (Edited by H. Schenk, R. Olthof-Hazekamp, H. Van Koningsveld and G. C. Bass), p. 4. Delft University Press, Holland (1978).
11. S. Jagner, G. Helgesson, O. Poncelet and L. G. Hubert-Pfalzgraf, unpublished results.
12. O. Poncelet, O. W. J. Sartain, L. G. Hubert-Pfalzgraf, K. Folting and K. G. Caulton, *Inorg. Chem.* 1989, **28**, 263.
13. D. C. Bradley, H. Chudzynska, D. M. Frigo, M. B. Hursthouse and M. A. Mazid, *J. Chem. Soc., Chem. Commun.* 1988, 1258.
14. N. El Khokh and L. G. Hubert-Pfalzgraf, unpublished results.
15. R. C. Mehrotra, M. M. Agrawal and A. Mehrotra, *Synth. Inorg. Metal-Org. Chem.* 1973, **3**, 181.
16. R. C. Mehrotra, T. N. Misra and S. M. Misra, *Ind. J. Chem.* 1965, **3**, 525.
17. S. Misumi and N. Iwasaki, *Bull. Chem. Soc. Jpn* 1967, **40**, 550.
18. A. Abragam and B. Bleaney, *Electron Paramagnetic Resonance of Transition Metal Ions*. Clarendon Press, Oxford (1970).
19. S. M. Gorun, G. C. Papaefthymiou, R. B. Frankel and S. J. Lippard, *J. Am. Chem. Soc.* 1987, **109**, 3337; L. M. Babcock, V. W. Day and W. G. Klemperer, *J. Chem. Soc., Chem. Commun.* 1988, 519.
20. F. A. Hart, *Comprehensive Coordination Chemistry* (Edited by G. Wilkinson), Vol. 3. Pergamon Press, Oxford (1987).
21. C. Wenqi, J. Zhongsheng, X. Yan, F. Yuguo and Y. Guangdi, *Inorg. Chim. Acta* 1987, **130**, 125; K. J. Range, M. Stadler, F. Rau and U. Klement, *Angew. Chem. Int. Edn Engl.* 1987, **26**, 1174.
22. L. A. Aslanov, M. A. Porai Koshits and M. O. Dekaprilevich, *J. Struct. Chem.* 1971, **12**, 431.
23. R. C. Mehrotra, R. Bohra and D. P. Gaur, *Metal β-diketonates and Allied Derivatives*. Academic Press, New York (1978); R. C. Mehrotra, P. N. Kapoor and J. M. Botwara, *Coord. Chem. Rev.* 1980, **312**, 67.
24. J. K. Przystal, W. G. Bos and I. B. Liss, *J. Inorg. Nucl. Chem.* 1971, **33**, 679.
25. W. J. Evans, M. A. Hozbar, S. G. Bott, G. H. Robinson and J. L. Atwood, *Inorg. Chem.* 1988, **27**, 1990.

Polyhedron Vol. 8, No. 17, pp. 2189–2191, 1989
Printed in Great Britain

0277–5387/89 $3.00+.00
Pergamon Press plc

REDUCTION OF METAL ACYL COMPLEXES PROMOTED BY MONOHYDRIDES, $Cp_2M(CO)H$ (M = Nb, Ta)

A. DORMOND and C. MOISE*

Laboratoire de Synthèse et d'Electrosynthèse Organométalliques associé au CNRS (UA 33), Faculté des Sciences, 6 bd Gabriel 21000 Dijon, France

(*Received* 7 *March* 1989; *accepted* 24 *April* 1989)

Abstract—Niobium or tantalum monohydrides reduce η^2-acyl zirconium and hafnium complexes and provide models for the CO stoichiometric conversion in ethylene. A plausible reduction mechanism implies a proton transfer to the carbon atom of the acetyl unit.

The reduction of carbon monoxide by transition metal hydrides is of great economic and fundamental interest. Studies of stoichiometric "model" reactions between hydride complexes and "activated" carbon monoxide might help to improve known catalyst systems or to discover new effective types. Stoichiometric reductions of CO[1] and of methyl carbonyl derivatives[2,3] have been achieved by the hydrido zirconium complex, $Cp_2^*ZrH_2$; moreover, products arising from hydrogen transfer to a η^2-acetyl unit have been obtained with the group 6 transition metal hydrides, Cp_2MoH_2 and Cp_2WH_2.[4] We have recently shown that the d^2 hydrido carbonyl complexes, $Cp_2M'(CO)H$ (M' = Nb, Ta), are able to function as hydrogen transfer reagents, when opposed to organic substrates.[5,6] We report here that these monohydrides are also capable of hydrogenating metal acyl complexes, a reaction which is viewed as a fundamental step in CO hydrogenation reactions.

RESULTS AND DISCUSSION

The reaction of the zirconium or hafnium acyl complexes, $Cp_2M(COMe)Me$ (**1**) or (**2**), with the monohydrides, $Cp_2M'(CO)H$ (**3a**, M' = Nb) or (**3b**, M' = Ta), proceeded rapidly in toluene solution as evidenced by a fast colour change from purple to green; the binuclear complexes, **4** or **5**, can be isolated as green crystals in high yield, eq. (1):

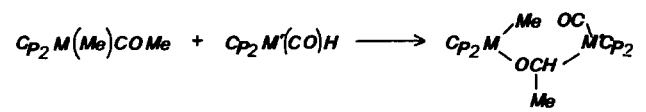

(1)

1 M = Zr; **2** M = Hf; **3**(a,b); **4**(a,b) M = Zr; **5**(a,b) M = Hf

a = M' = Nb ; b = M' = Ta

Using the acetyl titanium derivatives $Cp_2Ti(COCH_3)Cl$, the monochlorides $Cp_2M'(CO)Cl$ were formed by a metathetical reaction, but the titanium component was not identified.

The structure of the binuclear complexes, **4** and **5**, is easily established by their elemental analyses and spectroscopic data (Table 1).

The IR spectra show one intense absorption near 1890 cm^{-1} due to the M' bonded carbonyl stretching. The ^1H NMR spectra show for both the Cp_2Zr (or Cp_2Hf) and Cp_2Nb (or Cp_2Ta) units non-equivalence of the Cp ligands due to the chiral centre of the —OCHMe— bridge.

The monohydrides, $Cp_2M'(CO)H$ **3a** or **3b**, are thus able to reduce zirconium or hafnium acyl complexes. A reaction involving a simple hydride addition seems unlikely in view of the poor hydridic character of these monohydrides which do not react with methanol or acetone. The basic properties of the d^2 complexes (**3a** or **3b**)[6,7] and the well-known carbenic character of the carbon in the η^2-acetyl ligand suggest a mechanism with the initial

* Author to whom correspondence should be addressed.

Table 1. ^{1}H NMR (C_6D_6) and IR (toluene) data for **4** and **5**

	Cp_2M	Cp_2M'	CH	CMe	MMe	CO (cm^{-1})
4a (M = Zr, M′ = Nb)	5.83(s)	4.66(s)	5.13(q)	1.63(d)	0.11(s)	1900
4b (M = Zr, M′ = Ta)	5.82(s) 5.78(s)	4.57(s) 4.55(s)	5.08(q)	1.73(d)	0.09(s)	1884
5a (M = Hf, M′ = Nb)	5.78(s) 5.75(s)	4.64(s) 4.60(s)	5.14(q)	1.62(d)	0.01(s)	1895
5b (M = Hf, M′ = Ta)	5.78(s) 5.75(s)	4.57(s) 4.55(s)	5.11(q)	1.72(d)	0.00(s)	1883

formation of an acid–base adduct A, followed by a H^+ internal migration from the niobium or tantalum atom [eq. (2)]. We have postulated a similar prototropy to account for the reduction of acylchlorides into aldehydes.[5]

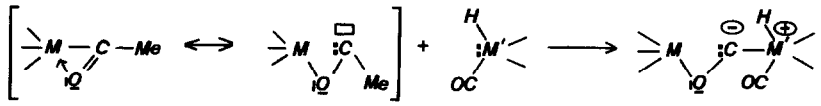

(2)

A

The lifetime in solution of the zirconium complexes **4** is limited (about 2 days). As shown by periodic ^{1}H NMR monitoring, the resonance signals of **4a** or **4b** slowly disappear with a concomitant growth of two sets of signals. The former includes two singlets at 5.74 and 0.26 ppm and is attributed, by comparison with an authentic sample, to $(Cp_2ZrMe)_2O$.[8] The latter set shows one singlet for the Cp ligands and one AMX system in the olefinic region (Table 2).

These resonances are assigned to the ethylenic derivatives $Cp_2M'(CO)CH{=}CH_2$ (**6**) and the evolution of the complexes **4** can be summarized as follows:

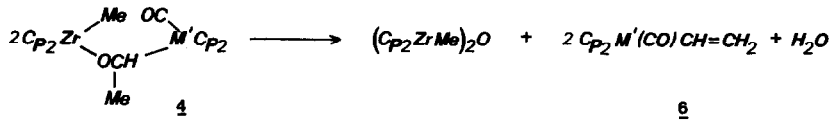

4 6

By treating complexes **6** with HCl, evolving ethylene is detected and the chlorocarbonyl derivatives $Cp_2M'(CO)Cl$[5] are formed in quantitative yields.

The results described above are an example of a stoichiometric synthesis of ethylene incorporating carbon from CO. According to the hypotheses previously postulated by Caulton,[4] a cleavage of the C—O bond in **4**, leading to $Cp_2Zr(Me)O^-$ and $Cp_2M'(CO)CHMe^{\oplus}$ could be assumed as a preliminary step in the formation of $(Cp_2ZrMe)_2O$ and ethylenic complexes, **6**.

It is noteworthy, however, that such an evolution does not occur with the hafnium complexes, **5**, but the reasons why are not clear.

These studies possess features reminiscent of those reported by Caulton and co-workers using Cp_2MoH_2 and Cp_2WH_2 and illustrate the closely related properties of the group 5 monohydrido complexes $Cp_2M'(CO)H$. In both series, the reduction of the dihapto acyl group could be achieved by

Table 2. ^{1}H NMR (C_6D_6) and IR (toluene) data for **6**

	Cp	$CH{=}CH_2$	CO (cm^{-1})
6a (M′ = Nb)	4.55(s)	6.75(m), 6.25(m) 6.05(m)	1930
6b (M′ = Ta)	4.52(s)	6.65(m), 6.40(m) 6.15(m)	1907

a H^+ donation from an early transition metal complex.

EXPERIMENTAL

All operations were carried out under an argon atmosphere by standard Schlenk techniques. All solvents were dried and distilled from sodium benzophenone. The IR data were obtained using a Perkin–Elmer 580B spectrophotometer and the ^1H NMR spectra (references to Me_4Si) were recorded with a JEOL FX100 apparatus. The monohydrido carbonyl complexes, $Cp_2M'(CO)H$, were obtained according to ref. 9 (M′ = Nb) and ref. 6 (M′ = Ta); the dimethyl derivatives Cp_2MMe_2 (M = Zr, Hf) were prepared from Cp_2MCl_2 and MeLi and purified by sublimation.[10]

Satisfactory elemental analyses have been obtained for complexes **4** and **5**.

Complexes **4** *and* **5**

These are obtained by the following general procedure.

$Cp_2M(CH_3)_2$ (1 mmol) and $Cp_2M'(CO)H$ (1 mmol) were mixed in toluene (25 cm^3) under CO (1 atm) and the solution was stirred for 2 h at room temperature. The solvent was removed and the green solid was recrystallized from a mixture of toluene–heptane on fast cooling. Yield 70%.

Acknowledgement—We thank Mrs D. Perrey for her technical assistance.

REFERENCES

1. J. Manriquez, D. R. McAlister, R. D. Sanner and J. E. Bercaw, *J. Am. Chem. Soc.* 1978, **100**, 2716.
2. P. T. Wolczanski, R. S. Threlkel and J. E. Bercaw, *J. Am. Chem. Soc.* 1979, **101**, 218.
3. P. T. Barger and J. E. Bercaw, *Organometallics* 1984, **3**, 278.
4. J. A. Marsella and K. G. Caulton, *J. Am. Chem. Soc.* 1980, **102**, 1747; J. A. Marsella, K. Folting, J. C. Huffman and K. G. Caulton, *J. Am. Chem. Soc.* 1981, **103**, 5596.
5. J. C. Leblanc, C. Moise and J. Tirouflet, *J. Organomet. Chem.* 1985, **292**, 225.
6. J. F. Reynoud, J. F. Leboeuf, J. C. Leblanc and C. Moise, *Organometallics* 1986, **5**, 1863.
7. J. D. Labinger, in *Comprehensive Organometallic Chemistry* (Edited by G. Wilkinson, F. G. A. Stone and E. W. Abel), Vol. 3, p. 705. Pergamon Press, Oxford (1982).
8. W. E. Hunter, D. C. Hrncir, R. V. Bynum, R. A. Penttila and J. L. Atwood, *Organometallics* 1983, **2**, 750.
9. J. A. Labinger, *Adv. Chem. Ser.* 1978, **167**, 149.
10. E. Samuel and M. D. Rausch, *J. Am. Chem. Soc.* 1973, **95**, 6253.

Polyhedron Vol. 8, No. 17, pp. 2193–2198, 1989
Printed in Great Britain

0277–5387/89 $3.00+.00
© 1989 Pergamon Press plc

HYDROGEN TRANSFER FROM METHANOL TO THE DOUBLE BONDS OF AN OLEFINIC TERTIARY PHOSPHINE COMPLEX OF RHODIUM(I)*

MARTIN A. BENNETT† and LEE L. WELLING

Research School of Chemistry, Australian National University, G.P.O. Box 4, Canberra, A.C.T. 2601, Australia

(*Received* 4 *April* 1989; *accepted* 28 *April* 1989)

Abstract—On heating with anhydrous sodium carbonate in methanol, the five-coordinate rhodium(I) complex [RhCl(*o*-CH_2=$CHC_6H_4PPh_2$)$_2$], containing (2-vinylphenyl)diphenylphosphine, is converted into the planar rhodium(I) carbonyl complex, *trans*-[RhCl(CO)(*o*-$CH_3CH_2C_6H_4PPh_2$)$_2$], containing (2-ethylphenyl)diphenylphosphine. The added hydrogen and CO are derived from methanol, probably via an intermediate formaldehyde complex.

The ligand (2-vinylphenyl)diphenylphosphine, *o*-CH_2=$CHC_6H_4PPh_2$ (**1**) (sometimes referred to as *o*-styryldiphenylphosphine and abbreviated SP), forms a five-coordinate rhodium(I) complex $RhCl(SP)_2$ (**2**) in which both vinyl groups are coordinated.[1–3] Complex **2** reacts with CO to give a salt, $[Rh(CO)(SP)_2]Cl$ (**3**) (ν(CO) *ca* 2040 cm^{-1}), which readily reverts to **2** in the absence of CO; in the presence of $NaBF_4$, NH_4PF_6 or $NaBPh_4$, stable salts of the five-coordinate cation $[Rh(CO)(SP)_2]^+$ can be isolated. Treatment of **2** with $AgBF_4$ generates a four-coordinate, presumably planar cation, $[Rh(SP)_2]^+$ (**4**), which takes up ligands (L) such as CO, C_2H_4, SO_2, CS_2, pyridine and tertiary phosphines to give five-coordinate species $[RhL(SP)_2]^+$.[4,5]

Brookes[2] reported that reaction of $RhCl(SP)_2$ with a suspension of anhydrous Na_2CO_3 in methanol gave a complex **5** of empirical formula $RhCl(CO)(SP)_2$. This compound, unlike its apparent isomer **3**, did not seem to lose CO readily, was a non-electrolyte in nitromethane, and had a C≡O stretching frequency of only 1964 cm^{-1} in its IR spectrum. The poor solubility of **5** in organic solvents prevented NMR studies, so Brookes was unable to determine whether the vinyl groups, which he assumed to be present, were coordinated or free. We report here our reinvestigation of the nature of complex **5**.

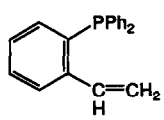

1

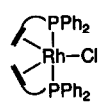

2

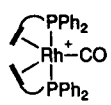

3

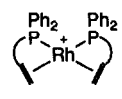

4

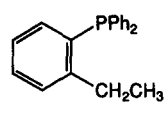

6

RESULTS AND DISCUSSION

In order to obtain a more soluble cationic derivative, **5** was treated with $AgBF_4$ in CD_3CN, cf. the formation of $[Ir(CO)(CH_3CN)(PPh_3)_2]BF_4$ from $IrCl(CO)(PPh_3)_2$ and $AgBF_4$ in acetonitrile.[6] The

* Dedicated to Professor Sir Geoffrey Wilkinson on the occasion of his "retirement".

† Author to whom correspondence should be addressed.

^{1}H NMR spectrum of the yellow solution obtained after removal of precipitated AgCl showed no resonances attributable to vinyl protons; instead there was a triplet at δ 0.95 and a quartet at δ 3.05 (J_{HH} = 7.5 Hz) typical of an ethyl group. This observation immediately suggested that the ligand present in **5** was (2-ethylphenyl)diphenylphosphine, *o*-$EtC_6H_4PPh_2$ (**6**), and that **5** was its planar rhodium(I) carbonyl complex, [RhCl(CO)(*o*-$EtC_6H_4PPh_2)_2$]. The cationic acetonitrile complex was isolated as an uncrystallizable yellow oil from the reaction of **5** with $AgBF_4$ in CH_3CN. It analysed fairly satisfactorily for [Rh(CO)(CH_3CN)(*o*-$EtC_6H_4PPh_2)_2$]BF_4, and showed a strong band at 2000 cm^{-1} due to ν(CO) and a weak band at *ca* 2300 cm^{-1} due to ν(CN) in its IR spectrum.

Treatment of **5** with sodium cyanide, in hot aqueous 2-methoxyethanol, gave free (2-ethylphenyl)diphenylphosphine (**6**) as an oil, which showed a parent ion peak in its mass spectrum. The ^{1}H NMR spectrum of **6** showed a triplet at δ 1.12 (J_{HH} = 7 Hz) and a doublet of quartets at δ 2.88 (J_{HH} = 7 Hz, J_{PH} = 2 Hz) due to the CH_3 and CH_2 protons, respectively, and was identical with that of the tertiary phosphine isolated from the reaction of [Rh(SP)$_2$]BPh_4 with hydrogen, which gives Rh(η-$C_6H_5BPh_3$)(SP) and *o*-$EtC_6H_4PPh_2$.[5]

Compound **6** was also synthesized independently in two steps from 2-ethylaniline [eq. (1)]. It reacted immdiately at room temperature with [$RhCl(CO)_2]_2$ in benzene to give a lemon–yellow precipitate whose spectroscopic properties were identical with those of complex **5** prepared from $RhCl(SP)_2$ (**2**) and sodium carbonate in methanol [eq. (2)].

The ^{31}P{^{1}H} NMR spectrum of **5** consisted of a doublet due to equivalent phosphorus atoms, the magnitude of J_{RhP} (125.5 Hz) being typical of planar rhodium(I) complexes of the type *trans*-$RhCl(CO)L_2$.[7] The reported ν(CO) and ν(RhCl) data,[2] which we confirm, are also typical of this class of compound.[7,8] The ^{1}H NMR spectrum of **5**, measured on a more sensitive instrument than was available either to us or to Brookes in the earlier work, was initially ambiguous because the sample prepared according to the original procedure contained ethanol of solvation; this was not removed completely even on heating *in vacuo*. The ^{1}H NMR spectrum (in CD_2Cl_2) of a sample that had been washed with methanol instead of ethanol showed a pattern typical of an ethyl group, consisting of a triplet at δ 1.05 and a quartet at δ 3.19 (J_{HH} = 7.4 Hz), in addition to aromatic resonances in the region δ 6.9–7.8.

To confirm that methanol was the source of the hydrogen added to **2**, a sample of complex **2** was heated with sodium carbonate suspended in [D_4]-methanol, and the resulting complex (**5a**) was treated with sodium cyanide. The ^{1}H NMR spectrum of the liberated tertiary phosphine (**6a**) contained a pair of complex multiplets centred at δ 1.15 and 2.9 with an intensity ratio of 2 : 1, and the ^{2}H NMR spectrum showed two poorly resolved multiplets at δ 1.1 and 2.9 with an intensity ratio of *ca* 1 : 1. These observations suggest that dideuterated compounds such as *o*-$CH_2DCHDC_6H_4PPh_2$ are the main species present. In agreement, the mass spectrum

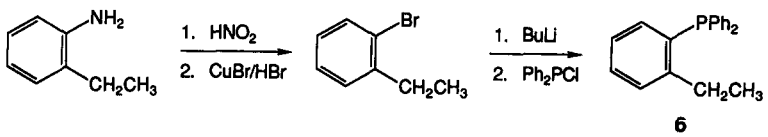

(1)

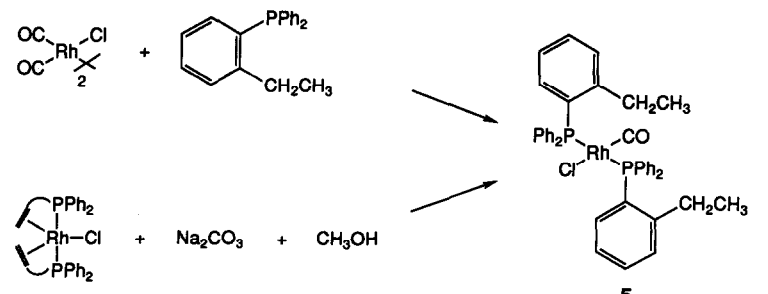

(2)

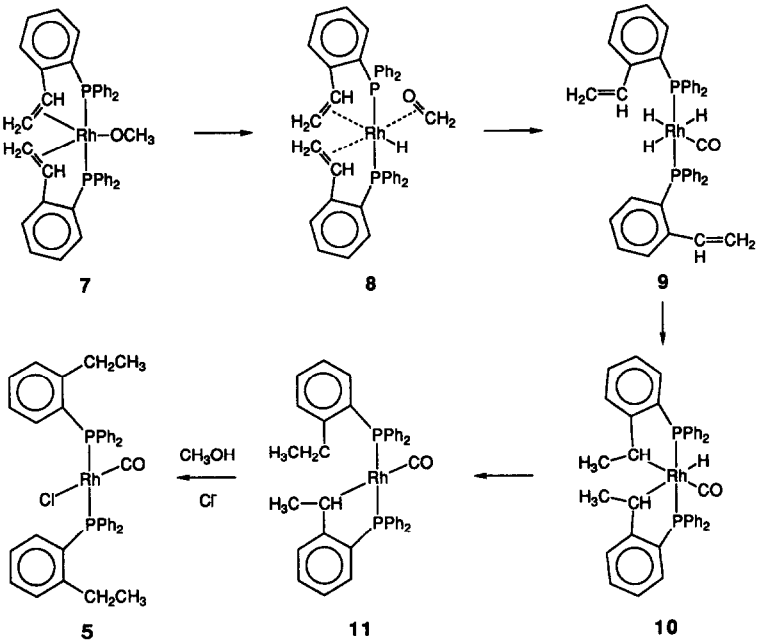

Scheme 1. Generation of (2-ethylphenyl)diphenylphosphine from (2-vinylphenyl)diphenylphosphine on rhodium.

showed intense peaks due to [*M*] and [*M*—H] at *m/z* 292 and 291 (cf. 290 and 289 in the mass spectrum of **6**), but there was also a peak at *m/z* 293 suggestive of the presence of some trideuterated compounds; these could be formed by base-catalysed H/D exchange at the benzylic carbon atom.

The stoichiometry of the reaction of **2** with methanolic Na_2CO_3 is presumed to be as shown in eq. (3):

$$RhCl(o\text{-}CH_2{=}CHC_6H_4PPh_2)_2 + CH_3OH \longrightarrow RhCl(CO)(o\text{-}CH_3CH_2C_6H_4PPh_2)_2 \quad (3)$$
(**5**)

When tertiary phosphine halide complexes of the *d*-block elements are heated with alcohols under basic conditions, hydrido or hydrido (carbonyl) complexes are often formed.[9,10] In these reactions the hydride ligand probably arises by β-elimination of aldehyde or ketone from an intermediate alkoxide. A plausible mechanism based on this premise for the formation of **5** from **2** is shown in Scheme 1. In the first step, the chloride ligand of **2** is replaced by methoxide, and the resulting methoxo complex **7** undergoes β-elimination to give a rhodium–hydride and formaldehyde; the latter probably remains in the coordination sphere as complex **8**. In the next step, formaldehyde undergoes oxidative addition to rhodium to give the hydrido (carbonyl) complex **9**, a process in which a hydrido(formyl) complex is a likely intermediate.[11,12] Two of the three hydride ligands of **9** then add to the pendant vinyl groups to give the bis(alkyl)rhodium(III) chelate complex **10**, and reductive elimination of the remaining hydride ligand with one of the rhodium(III)–carbon σ-bonds forms the five-coordinate rhodium(I) chelate alkyl **11**, which contains one (2-ethylphenyl)diphenylphosphine ligand. Finally, protonolysis of the remaining rhodium–carbon σ-bond in the presence of chloride ion forms the second (2-ethylphenyl)diphenylphosphine ligand, thus giving complex **5**.

We suggest in Scheme 1 that intermediates **9**–**11** contain a five-membered chelate ring, Rh{*o*-CH(CH$_3$)C$_6$H$_4$PPh$_2$}. An octahedral ruthenium(II) compound, **12**, containing such a ring is formed when $RuCl_2(CO)_2(SP)_2$ is heated in 2-methoxyethanol,[13] a reaction that is closely related to that described here. Also, complexes of this type have been obtained by the protonation of SP coordinated to low-valent metals such as iron(0),[14] ruthenium(0),[14] palladium(0),[15] platinum(0)[16] and rhodium(I),[17] and by the reaction of metal hydrides, such as $MnH(CO)_5$[18] and $PtHCl(PPh_3)_2$,[19] with SP. The reaction of $ReH(CO)_5$ with SP, however, gives the alternative six-membered ring compound [Re(*o*-CH$_2$CH$_2$C$_6$H$_4$PPh$_2$)(CO)$_4$],[18] and the possibility that compounds **9**–**11** contain six-membered rings cannot be excluded.

The suggestion that free or coordinated formaldehyde is an intermediate in the conversion of **2** to **5** is supported by the observation that

$[Rh(SP)_2]BF_4$ (**4**) reacted on heating with paraformaldehyde to give a yellow solid which had a strong ν(CO) band at 1990 cm^{-1}. Although this compound

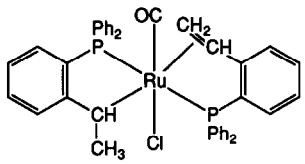

12

could not be isolated in a pure state, it probably contained *trans*-$[Rh(CO)_2(o\text{-}EtC_6H_4PPh_2)_2]BF_4$, because, on treatment with lithium chloride, it gave a poorly soluble yellow solid that was identical in its spectroscopic features with **5**. Moreover, of the simple monohydric alcohols, only methanol can supply the units of CO and four H required to convert **2** into **5**, thus accounting for the observation[2] that the reaction does not proceed in ethanol.

There are several examples in the literature of the addition of dihydrogen to the double bonds of olefinic tertiary phosphines when these ligands are coordinated to rhodium(I). Treatment of $[Rh(SP)_2]BPh_4$ with dihydrogen gives the η^6-tetraphenylborate complex, $Rh(SP)(\eta^6\text{-}C_6H_5BPh_3)$, and free (2-ethylphenyl)diphenylphosphine.[5] But-3-enyldiphenylphosphine, $CH_2{=}CHCH_2CH_2PPh_2$ (mbp), which is a more flexible ligand than SP, is converted into coordinated *n*-butyldiphenylphosphine by the addition of dihydrogen to methanolic solutions of $RhCl(mbp)_2$ and $RhCl(CO)(mbp)_2$.[20] In these cases, however, the methanol is not a source of H_2, but only serves to promote ionization of the chloride ion in the coordination sphere. This favours oxidative addition of H_2 to the cationic rhodium centre and permits transfer of the hydride ligands to the adjacent double bonds.

EXPERIMENTAL

The following instruments were used for spectroscopic measurements: Jeol PMX 60 and Varian HA 100 (^{1}H NMR), Varian XL 200 (^{1}H NMR, ^{31}P NMR at 80.98 MHz), Bruker B-KR-322S (^{31}P NMR at 24.3 MHz), Bruker CXP 200 (^{31}P NMR at 80.96 MHz), Bruker HFX 270 (^{2}H NMR at 41.45 MHz), PE 683 (IR, 4000–400 cm^{-1}), PE 225 (IR, 4000–200 cm^{-1}), Hitachi FIS-3 (IR, 400–50 cm^{-1}), VG Micromass 7070 (mass spectra at 70 ev). Analyses were carried out in the Microanalytical Laboratory of this School.

(2-Vinylphenyl)diphenylphosphine[21] and $[RhCl(CO)_2]_2$[22] were prepared by literature procedures. 2-(Bromo)ethylbenzene was made from redistilled commercial 2-ethylaniline by the usual method of diazotization and treatment with CuBr, although the yield of product after steam distillation was only 20%.

All operations requiring tertiary phosphines and their metal complexes were carried out under purified nitrogen or argon by the use of standard Schlenk procedures.

Preparation of (2-ethylphenyl)diphenylphosphine, o-$EtC_6H_4PPh_2$ **(6)**

A solution of 2-(bromo)ethylbenzene (16 g, 0.088 mol) in ether (10 cm^3) was added to a solution of 1.6 M butyllithium (55 cm^3) in ether (50 cm^3) and the mixture was stirred at 0°C. The clear, colourless solution was cooled to −40°C and treated dropwise with a solution of chlorodiphenylphosphine (15.9 g, 0.072 mol) in ether (20 cm^3). The mixture was allowed to warm to room temperature, stirred for 0.5 h and then cooled again to 0°C. Saturated aq. NH_4Cl was added, the ether layer was separated and washed with water, and the aqueous layer was extracted with ether. The combined ether extracts were dried over magnesium sulphate and evaporated to give the product as a thick, colourless oil. Yield: 22.7 g (90%). The crude product contained some phosphine oxide, as shown by a strong band at *ca* 1190 cm^{-1} in the IR spectrum and by the ^{31}P NMR spectrum. No attempt was made to remove the impurity. ^{1}H NMR ($CDCl_3$, 60 MHz) δ 1.1 (t, $J = 7$ Hz, CH_3), 2.9 (q, CH_2), 6.8–7.4 (m, Ar). $^{31}P\{^1H\}$ NMR ($CHCl_3$, 24.3 MHz) δ −15.3(s) due to **6**, +31.8(s) probably due to phosphine oxide, intensity ratio *ca* 8 : 1.

Preparations of carbonylchlorobis{(2-ethylphenyl)-diphenylphosphine}rhodium(I), $[RhCl(CO)(o\text{-}EtC_6H_4PPh_2)_2]$ **(5)**.

(1) *From* $[RhCl(o\text{-}CH_2{=}CHC_6H_4PPh_2)_2]$ **(2)**. The procedure was as described by Brookes.[2] Complex **2** (800 mg, 1.12 mmol) and finely divided anhydrous Na_2CO_3 (552 mg, 5.21 mmol) were suspended in methanol (40 cm^3) and heated under reflux for 3 h. At *ca* 60°C the bright yellow suspension turned orange and at *ca* 80°C it became dark yellow. The yellow precipitate was washed first with water, then with ethanol or methanol, and dried *in vacuo*. Yield: 622 mg (74%). IR (cm^{-1}, Nujol) 1955 [ν(CO)], 309 [ν(RhCl)]. ^{1}H NMR (CD_2Cl_2, 200 MHz) δ 1.05 (t,

J = 7.4 Hz, CH_3), 3.19 (q, CH_2), 6.9–7.8 (m, Ar). $^{31}P\{^1H\}$ NMR (CD_2Cl_2) δ 25.6 (d, J_{RhP} = 125.5 Hz). Found: C, 65.8; H, 5.2; Cl, 4.2; P, 7.75. Calc. for $C_{41}H_{38}ClOP_2Rh$: C, 65.9; H, 5.1; Cl, 4.75; P, 8.3%.

The deuterated complex, [RhCl(CO)(*o*-[D$_2$]EtC$_6$H$_4$PPh$_2$)$_2$] (**5a**), was prepared similarly from complex **2** and anhydrous Na_2CO_3 in [D_4]-methanol.

(2) *From* [RhCl(CO)$_2$]$_2$ *and* *o*-EtC$_6$H$_4$PPh$_2$ (**6**). A solution of [RhCl(CO)$_2$]$_2$ (374 mg, 0.96 mmol) in benzene (20 cm^3) was treated dropwise with a solution of *o*-EtC$_6$H$_4$PPh$_2$ (**6**) (1.12 g, 3.85 mmol) in benzene (15 cm^3). Gas came off immediately and a lemon–yellow solid precipitated. The IR spectrum of this solid was identical with that of the compound prepared from complex **2** and methanolic Na_2CO_3.

(3) *From* [Rh(*o*-CH$_2$=CHC$_6$H$_4$PPh$_2$)$_2$]BF$_4$ *and formaldehyde*. A suspension of [RhCl(*o*-CH$_2$=CHC$_6$H$_4$PPh$_2$)$_2$] (**2**) (0.50 g, 0.70 mmol) in dichloromethane (10 cm^3) was treated with a suspension of $AgBF_4$ (0.137 g, 0.70 mmol) in dichloromethane (10 cm^3), and the mixture was stirred for 1 h. The precipitated AgCl was removed by centrifuging and the resulting red solution was evaporated to dryness under reduced pressure to give [Rh(*o*-CH$_2$=CHC$_6$H$_4$PPh$_2$)$_2$]BF$_4$ (**4**) as a reddish-yellow solid. Yield: 0.58 g, quantitative. This solid was taken up in THF and the yellow solution was treated with paraformaldehyde (420 mg, *ca* 10-fold excess). The mixture was heated under reflux for 1 h to give a yellow–brown solid, which showed a strong ν(CO) band at 1990 cm^{-1} and a broad strong band at *ca* 1100 cm^{-1} characteristic of BF_4^-. On treatment with lithium chloride in methanol, this compound gave an immediate dark yellow precipitate whose IR spectrum matched that of [RhCl(CO)(*o*-EtC$_6$H$_4$PPh$_2$)$_2$] (**5**).

Preparation of [Rh(CO)(CH$_3$CN)(*o*-EtC$_6$H$_4$PPh$_2$)$_2$]BF$_4$

A suspension of [RhCl(CO)(*o*-EtC$_6$H$_4$PPh$_2$)$_2$] (**5**) (80 mg, 0.11 mmol) in acetonitrile or [D_3]-acetonitrile (3 cm^3) was treated with a solution of $AgBF_4$ (18 mg, 0.09 mmol) in the same solvent (0.5 cm^3). The precipitated AgCl was removed by centrifugation and solvent was evaporated from the supernatant liquid to leave a yellow oil, which could not be induced to crystallize. The yield was almost quantitative. ^1H NMR (CD_3CN, 100 MHz) δ 0.95 (t, J = 7 Hz, CH_3), 3.05 (q, CH_2), 7.0–7.7 (m, Ar). IR (cm^{-1}, Nujol) 2033 w [ν(CN)], 2000 vs [ν(CO)], *ca* 1050 vs, br [BF_4]. Found: C, 59.7; H, 4.8; N, 1.8; P, 7.3. Calc. for $C_{43}H_{41}NOP_2Rh$: C, 61.5; H, 5.0; N, 1.7; P, 7.35%.

Displacement of (2-*ethylphenyl*)*diphenylphosphine* (**6**) *from* [RhCl(CO)(*o*-EtC$_6$H$_4$PPh$_2$)$_2$] (**5**)

A suspension of complex **5** (514 mg, 0.69 mmol) in 2-methoxyethanol (30 cm^3) was treated with a solution of sodium cyanide (648 mg, excess) in water (30 cm^3). The mixture was stirred at 100°C overnight to give a light brown oil and a clear, colourless mother liquor. The latter was removed by decantation, and the oil was washed with water and dried *in vacuo*. It was identified as *o*-EtC$_6$H$_4$PPh$_2$ (**6**) by comparison of its spectroscopic properties with those of a sample of **6** prepared independently. ^1H NMR (100 MHz, $CDCl_3$) δ 1.12 (t, J_{HH} = 7 Hz, CH_3), 2.88 (dq, J_{HH} = 7 Hz, J_{PH} = 2 Hz, CH_2), 6.8–7.3 (m, Ar). $^{31}P\{^1H\}$ NMR (24.3 MHz, $CHCl_3$) δ −15.6(s). Mass spectrum: m/z 290.1224 (M, most intense peak), calc. for $C_{20}H_{19}P$: 290.344; 289(M−H).

The deuterated ligand *o*-[D$_2$]EtC$_6$H$_4$PPh$_2$ (**6a**) was obtained from complex **5a** by a similar procedure. ^1H NMR (100 MHz, $CDCl_3$) δ 1.0—1.2 (m, 2*H*, CH_2D), 2.7–3.0 (m, 1*H*, CHD). ^2D NMR (41.45 MHz, $CDCl_3$) δ 1.1 (br s, 1*D*, CH_2D), 2.9 (br s, 1*D*, CHD). Mass spectrum: m/z 293, 292(M), 291(M−H), 290(M−D).

REFERENCES

1. M. A. Bennett and E. J. Hann, *J. Organomet. Chem.* 1971, **29**, C15.
2. P. R. Brookes, *J. Organomet. Chem.* 1972, **42**, 459.
3. M. A. Bennett, E. J. Hann and R. N. Johnson, *J. Organomet. Chem.* 1977, **124**, 189.
4. P. R. Brookes, *J. Organomet. Chem.* 1972, **43**, 415.
5. M. A. Bennett and E. J. Hann, *J. Organomet. Chem.* 1977, **124**, 213.
6. C. A. Reed and W. R. Roper, *J. Chem. Soc., Dalton Trans.* 1973, 1365.
7. R. S. Dickson, *Organometallic Chemistry of Rhodium and Iridium*, pp. 63–64 and refs cited therein. Academic Press, London (1983).
8. R. P. Hughes, in *Comprehensive Organometallic Chemistry* (Edited by G. Wilkinson, F. G. A. Stone and E. W. Abel), Vol. 5, pp. 302–306 and refs cited therein. Pergamon Press, Oxford (1982).
9. R. A. Schunn, in *Transition Metal Hydrides* (Edited by E. L. Muetterties), p. 203, Marcel Dekker, New York (1971).
10. H. D. Kaesz and R. B. Saillant, *Chem. Rev.* 1972, **72**, 231 and refs cited therein.
11. D. L. Thorn, *Organometallics* 1982, **1**, 197.
12. K. L. Brown, G. R. Clark, C. E. L. Headford, K. Marsden and W. R. Roper, *J. Am. Chem. Soc.* 1979, **101**, 503.
13. M. A. Bennett, R. N. Johnson and I. B. Tomkins, *Inorg. Chem.* 1975, **14**, 1908.
14. M. A. Bennett, G. B. Robertson, I. B. Tomkins and P. O. Whimp, *J. Organomet. Chem.* 1971, **32**, C19.

15. M. A. Bennett, C. Chiraratvatana, G. B. Robertson and U. Tooptakong, *Organometallics* 1988, **7**, 1403.
16. M. A. Bennett, C. Chiraratvatana, G. B. Robertson and U. Tooptakong, *Organometallics* 1988, **7**, 1394.
17. M. A. Bennett, S. J. Gruber, E. J. Hann and R. S. Nyholm, *J. Organomet. Chem.* 1971, **2**, C12.
18. M. A. Bennett and R. Watt, *Chem. Comm.* 1971, 94.
19. (a) P. R. Brookes, *J. Organomet. Chem.* 1973, **47**, 179; (b) C. Chiraratvatana, PhD thesis. Australian National University, 1984.
20. P. W. Clark and G. E. Hartwell, *J. Organomet. Chem.* 1975, **102**, 387; 1977, **139**, 385.
21. M. A. Bennett, W. R. Kneen and R. S. Nyholm, *J. Organomet. Chem.* 1971, **26**, 293.
22. J. A. McCleverty and G. Wilkinson, *Inorg. Synth.* 1966, **8**, 211.

Polyhedron Vol. 8, No. 17, pp. 2199–2207, 1989
Printed in Great Britain

0277–5387/89 $3.00+.00
© 1989 Pergamon Press plc

EQUILIBRIUM AND KINETIC STUDIES OF THE INTERACTION OF $[Ru^{III}(EDTAH)(H_2O)]$ WITH CO

M. M. TAQUI KHAN,* AMJAD HUSSAIN, M. A. MOIZ and R. M. NAIK

Discipline of Coordination Chemistry and Homogeneous Catalysis, Central Salt & Marine Chemicals Research Institute, Bhavnagar—364 002, India

(*Received* 31 *October* 1988; *accepted* 26 *April* 1989)

Abstract—Interaction of $[Ru(EDTAH)(H_2O)]$ (**1**), $MHL(H_2O)$, with CO in aqueous solution was investigated by potentiometry, spectrophotometry and electrochemistry. Complex **1** reacted with CO in the pH range 2–3.5 to form the protonated and the normal carbonyl complexes, MHLCO (**2**) and MLCO (**3**), respectively (L = EDTA, HL = EDTAH). Complex **3** combined with **1** to form the μ-CO—μ-OH dimer, [ML(CO)(OH)ML] (**4**). The log of the stability constants, determined spectrophotometrically, for the formation of complexes **2**, **3** and **4** at 25°C (μ = 0.1 M) are 2.4, 4.9 and 3.72, respectively. The kinetics of the formation of complexes **2**–**4** were studied spectrophotometrically. The complexes constitute the first series of ruthenium(III)–carbonyls in aqueous solution, by the direct interaction of a soluble aquo Ru^{III}–EDTA complex with CO.

Carbonylation and hydroformylation reactions of olefins offer efficient routes for the manufacture of valuable chemicals.[1–5] Necessary feed stocks for industrial processes can also be produced by utilization of these reactions.[6] Carbonyl complexes are formed as intermediates[1–5] in hydroformylation with cobalt, rhodium, palladium and ruthenium complexes in the course of these reactions. Apart from their importance as homogeneous catalysts in carbonylation and oxo reactions, carbonyl complexes are important in their own right due to the types of bonding and structures exhibited by these complexes.[7] Much of the understanding about carbonyl complexes comes from the study of metal complexes in lower oxidation states,[7] partly due to the stabilization of these oxidation states by CO and cluster formation in the case of the carbonyls of ruthenium, osmium, rhodium and iridium.[8] Except for the kinetics of some of these complexes[9] in non-aqueous media, very few equilibrium or kinetic studies have been carried out on the metal carbonyls of these metal ions in aqueous solution.[10–14] The reason may be the instability of the lower oxidation states and the hydrolytic tendency of the higher oxidation states of these metal ions in aqueous solution. For instance, chloro complexes of ruthenium(III) become aquated in acidic medium[15] and complexes such as ruthenium(III)–aminopolycarboxylates are hydrolysed[16] at pH between 4 and 5. This may be the reason why no serious attempts seem to have been made to study the carbonyl complexes in aqueous solution. With interest now being directed to water-soluble catalysts,[17] there is a need to develop the aqueous solution chemistry of ruthenium, rhodium and osmium carbonyl complexes in general and that of ruthenium complexes in particular, since these complexes have been found to be excellent catalysts in certain carbonylation reactions.[18]

Except for ruthenium(III)–aminopolycarboxylates[11,16,19–21] and to a certain extent chlororuthenium complexes,[15] no systematic equilibrium studies on ruthenium(III) complexes in aqueous solution have been attempted. Equilibrium data for the replacement of H_2O by various ligands in the aquo ruthenium(II) amine complex have been reported.[12] Enthalpy for interaction of CO with $[Ru(NH_3)_5H_2O]^{2+}$ was evaluated calorimetrically.[13] Reaction of $RuCl_3 \cdot xH_2O$ with CO, in acidic medium, was studied in solution by IR techniques.[10] Kinetics of the formation of carbonyl complexes by the interaction of CO and HCOOH and their conversion to other species was reported.[22]

* Author to whom correspondence should be addressed.

In this paper, we report the solution equilibria and kinetic studies of the interaction of [Ru(EDTAH)(H_2O)] with CO in aqueous medium.

EXPERIMENTAL

Materials

Ruthenium trichloride, $RuCl_3 \cdot xH_2O$, was purchased from Johnson Mathey (U.K.). A.R. grade Na_2EDTA, purchased from BDH, was used as obtained. The nitrogen used was of analar grade (4 ppm O_2) and was purified by passing it through vanadous sulphate and alkaline pyrogallate solution. Carbon monoxide was prepared by the reaction of sodium formate and H_2SO_4, and purified by passing through a tower of KOH pellets.[23] K[Ru(EDTAH)Cl] was prepared by the known procedure.[24]

Potentiometry

Potentiometric titrations were carried out under nitrogen as described previously.[20] For the titration under CO, the solution was saturated with the gas by bubbling CO for an hour and the titrations were carried out under an atmosphere of CO until the titration was complete. All titrations were carried out at 5, 15, 25 and 35°C and $\mu = 0.10$ (KCl). Protonation constants were computed by a curve fitting method using PROGRAM PKAS.[25]

Spectrophotometry

For recording electronic absorption spectra and carrying out spectrophotometric experiments, a Shimadzu UV-160 spectrophotometer equipped with a temperature controller TCC-240A was used. Matched 10 or 2 mm cells were used to record the spectra. All measurements were taken at 5, 15, 25 and 35°C and $\mu = 0.10$ (KCl).

The wavelength of the maximum absorbance (λ_{max}) for the carbonyl complexes was found by passing CO through the solution of [Ru(EDTAH)(H_2O)] (**1**) and recording the spectra.

All spectrophotometric experiments were carried out at the λ_{max} (390 nm) corresponding to the formation of the carbonyl complexes. The ε_{max}^{390} value was found by noting the absorbance of the 390 nm peak in the presence of a 10-fold excess of CO at the pH of maximum absorbance, as obtained from the pH–absorbance profile (Fig. 3). The ε_{max}^{390} value was then calculated using Beer's law.

In order to study the effect of $[H^+]$, the pH of complex **1** was adjusted to the required value and then CO was passed through the solution and the $[H^+]$ noted. The absorbance was taken for solutions ranging in pH from 0.0 to 4.0.

For determination of the formula of the carbonyl complexes, two sets of experiments were performed. In the first set, the concentration of complex **1** or CO was of the order of 10^{-5} M and in the second set, the concentrations were of the order of 10^{-4} M. In each of these sets two sets of experiments were carried out: (1) in the first set the concentration of CO was kept constant and that of complex **1** varied; (2) in the second set the concentration of complex **1** was kept constant and that of CO varied. The formula of the complexes formed was determined by plotting absorbance vs concentration of the variant.

Stability constants of the carbonyl complexes were determined by carrying out the experiments at two different concentrations of complex (10^{-5} and 10^{-4} M). The λ_{max} and ε_{max} values at the lower concentration correspond only to the formation of **3**. For the solution of higher concentration (set 2), the species present at pH 3–4 were complexes **3** and **4**. The concentration of species **3** and **4** were determined by the application of Beer's law and their formation constants were calculated by setting up and solving algebraic equations.[27]

Electrochemistry

DPP and CV were recorded on a PAR electrochemical system 174, equipped with a precision X–Y recorded and Model 173 galvanostat, as described previously.[20] For recording CV and DPP at different pH the same procedure as for absorption spectra was followed.

Kinetics

A freshly prepared saturated solution of CO in doubly distilled water was used in all kinetic measurements. The concentration of CO in the saturated solution was calculated from its solubility at a given temperature and 1 atm. The CO concentration in the experiment was varied by diluting the saturated solution to the desired concentration. The concentrations of CO and complex **1** were varied over a wide range (10^{-5}–10^{-3} M). The reactants were equilibrated at 35°C for 1/2 h before mixing, and the pH of the solution was adjusted to a desired value with HCl or NaOH solutions using a pH meter calibrated with HCl and NaOH.[20]

The change in the absorption of the 390 nm band was used to monitor the reaction as a function of time under pseudo first-order conditions of [complexes] and [CO]. The required quantity of complex **1** solution was taken in a cuvette and the necessary

volume of saturated CO solution was added. The spectra were then recorded as a function of time. The total volume of the solution in each experiment was kept constant.

For studying the effects of varying the complex concentration, on the rate of reaction, different quantities of complex **1** solution were used, while maintaining a constant CO concentration in the solution. All kinetic runs were carried out at 5, 15, 25 and 35°C and $\mu = 0.1$ M (KCl).

RESULTS AND DISCUSSION

Equilibrium studies

Equilibrium studies were carried out using potentiometric, spectrophotometric and electrochemical techniques.

The potentiometric titration curve of complex **1** under CO exhibited an inflection at $a = 1.5$ (Fig. 1), indicating the release of $1\frac{1}{2}$ equivalents of proton per metal ion. The pH at $a = 0$ showed that $1\frac{1}{2}$ equivalents of proton are completely liberated. Thus, the equilibrium was completely shifted to the right and the potentiometric data between $a = 0$ and 1.5 could not be utilized for the calculation of stability constants.

Beyond $a = 1.5$, however, the dimeric, carbonyl complex becomes further hydrolysed as follows:

$$(ML)_2CO(OH) \overset{K_D^{OH}}{\rightleftharpoons} (ML)_2CO(OH)_3 + 2H^+ \quad (1)$$

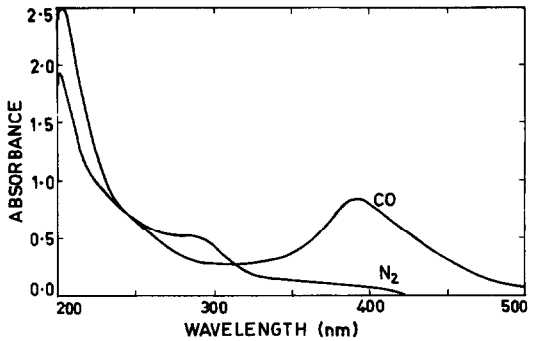

Fig. 2. Absorption spectra of [Ru(EDTAH)(H$_2$O)] solution (1×10^{-3} M) under N_2 and CO at 35°C, $\mu = 0.1$ M KCl.

$$K_D^{OH} = [(ML)_2CO(OH)_3][H^+]^2/[(ML)_2CO(OH)].$$

The value of K_D^{OH} was found to be $10^{-8.22}$ at 35°C ($\mu = 0.1$ M KCl).

Since there was a large drift in the pH after $a = 2.5$, the data was not used for any stability constant calculations.

For the equilibrium studies under CO between $a = 0$ and 1.5, the spectrophotometric method was used. The absorption spectra of complex **1** under N_2 and CO are given in Fig. 2 and the data are tabulated in Table 1. The spectrophotometric results indicate that at low metal ion concentrations (of the order of 10^{-5} M) a monomer exists, while at higher concentrations (of the order of 10^{-4} M) a

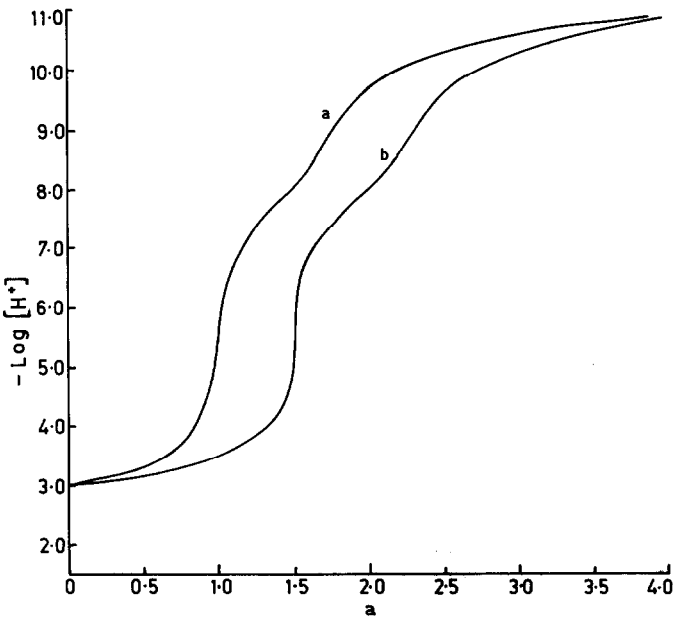

Fig. 1. Potentiometric titration curves of [Ru(EDTAH)(H$_2$O)] solution (1×10^{-3} M) at 35°C and $\mu = 0.1$ M KCl in presence of (a) N_2 (b) CO.

Table 1. Electronic absorption spectrum of complex **1** under N_2 and CO, at 35°C and $\mu = 0.1$ M (KCl)

Condition	λ (ε)	Assignment
Under N_2	203(9700) vs	CT band of EDTA
	283(2790) sh	CT band of EDTA
Under CO	203(12,500) vs	CT band of EDTA
	264.5(2730) wsh	CT band of EDTA
	390(5280) s	$O{\equiv}C \rightarrow Ru^{III}$ charge-transfer

vs—very strong; s—strong; sh—shoulder; wsh—weak shoulder.

dimer exists in solution. This was further supported by plotting the change in absorbance vs the concentration of the variant ([ML] or [CO]) and noting the break in the graph.

From the above observations it is evident that the reactions taking place between $a = 0$ and 1.5 can be written as:

$$\underset{\textbf{(1a)}}{ML} + CO \overset{K_{CO}}{\rightleftharpoons} \underset{\textbf{(2)}}{MLCO} \qquad (2)$$

$$K_{CO} = [MLCO]/[ML][CO]$$

$$MLCO + ML \overset{K_D}{\rightleftharpoons} \underset{\textbf{(3)}}{(ML)_2CO(OH)} + H^+ \qquad (3)$$

$$K_D = [(ML)_2CO(OH)][H^+]/[MLCO][ML].$$

The stability constant K_{CO} was determined by using low concentrations (10^{-5} M) of complex **1** and CO. Since at this concentration complex **2** is the only absorbing species at λ_{max}. The value of K_{CO} was found to be $10^{4.90}$. At higher concentrations of complex **1** (10^{-4} M) a dimer, **3**, also exists. The overall stability constant for the formation of the dimer, β_{CO}^{OH}, was found to be $10^{8.62}$:

$$2ML + CO \overset{\beta_{CO}^{OH}}{\rightleftharpoons} \underset{\textbf{(3)}}{(ML)_2CO(OH)} + H^+ \qquad (4)$$

$$\beta_{CO}^{OH} = [(ML)_2CO(OH)][H^+]/[ML]^2[CO].$$

The constant for reaction (3) was calculated from the expression:

$$K_D = \beta_{CO}^{OH}/K_{CO} \qquad (5)$$

and has the value $10^{3.72}$.

At very low pH (around 1.0) a protonated carbonyl species, MLHCO, is formed, as expressed by the equilibria:

$$MLH + CO \overset{K_{CO}^{H}}{\rightleftharpoons} MLHCO \qquad (6)$$

$$K_{CO}^{H} = [MLHCO]/[MLH][CO]$$

$$MLCO + H^+ \overset{K_H^2}{\rightleftharpoons} MLHCO \qquad (7)$$

$$K_H^2 = [MLHCO]/[MLCO][H^+].$$

K_H^2 can be determined as follows: a plot of absorbance at 264.5 nm against pH shows an inflection between pH 1.15 and 1.35.

At the minimum of the inflection, equilibrium (7) completely shifts to the right and only the MLHCO species is present in solution, while at the maximum only the MLCO species is present. At the midpoint of the inflection, [MLHCO] = [MLCO] and thus

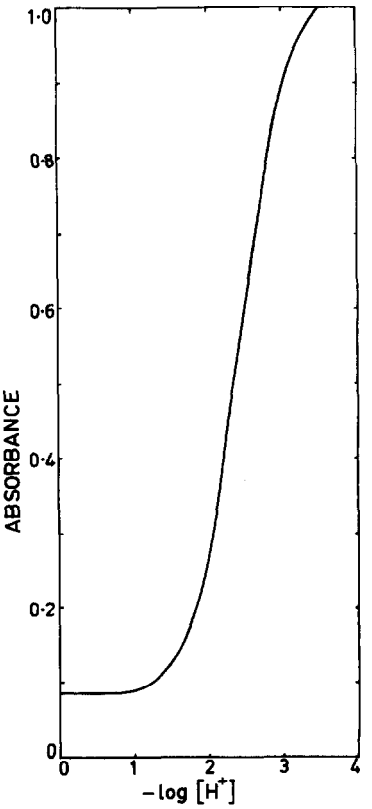

Fig. 3. Change in absorbance of 390 nm peak with $-\log[H^+]$ at 35°C, $\mu = 0.1$ M KCl.

$K_H^2 = [H^+]^{-1}$. The value thus obtained is $10^{1.24}$. K_{CO}^H is given by the expression:

$$K_{CO}^H = K_{CO}/K_H^1 K_H^2,$$

where K_H^1 is the protonation constant for ML under N_2

$$ML + H \overset{K_H^1}{\rightleftharpoons} MLH \qquad (8)$$

$$K_H^1 = [MLH]/[ML][H^+] = 10^{2.36}.$$

Since the errors involved in the calculation of the thermodynamic parameters associated with the constants K_{CO}^H, K_{CO} and K_D do not justify their separate calculations, the thermodynamic parameters ΔH^0, ΔS^0 for the overall reaction (4), as represented by the constant β_{CO}^{OH} for **4**, were calculated. The value of ΔH^0 for reaction (4) calculated in the temperature range 5–35°C is −14.2 kcal mol^{-1} and ΔS^0 at 35°C is −3.2 e.u. The enthalpy of formation of $[Ru(NH_3)_5CO]^{2+}$ from $[Ru(NH_3)_5H_2O]^{2+}$ and CO was reported[16] to be −38.0 kcal mol^{-1}.

The lower endothermic value of ΔH^0 for **4**, as compared to $[Ru(NH_3)_5CO]^{2+}$, reflects the lower stability of the M—CO bond in the ruthenium(III) complex **4**, as compared to ruthenium(II) complexes. As expected, the entropy for the formation of the dimer **4** is more negative compared to the mononuclear carbonyl species.

Electrochemical studies were carried out to confirm the oxidation state of ruthenium in the carbonyl complexes **2**–**4**. The DPP and CV of complex **1** in the absence and presence of CO are presented in Figs 4(a) and (b), respectively. In the absence of CO, DPP of **1** [Fig. 4(a)] exhibits peaks at −0.350, −0.800, −1.110 V, corresponding to Ru^{3+}/Ru^{2+}, Ru^{2+}/Ru^{+}, $H^+/\frac{1}{2}H_2$ couples, respectively[20] (Table 2). The Ru^{3+}/Ru^{2+} couple of **1** shifts to more negative potentials on increasing the pH, which is due to hydrolysis of **1**. In the absence of CO, the CV of complex **1** [Fig. 4(b)] exhibits two reversible peaks (Table 2). Cathodic (Ep_c) and anodic (Ep_a) peaks with $ipc/ipa = 1$ were observed for the reversible

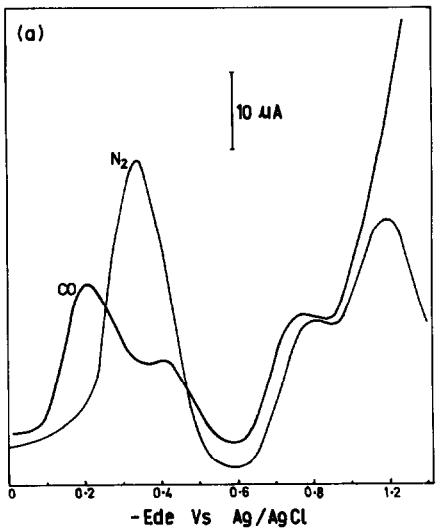

Fig. 4(a). Differential pulse polarograms of [Ru(EDTAH) Ru^{3+}/Ru^{2+} couple, with an $E_{1/2}$ value of 0.350 pH = 3.0, T = 25°C, μ = 0.1 M KCl.

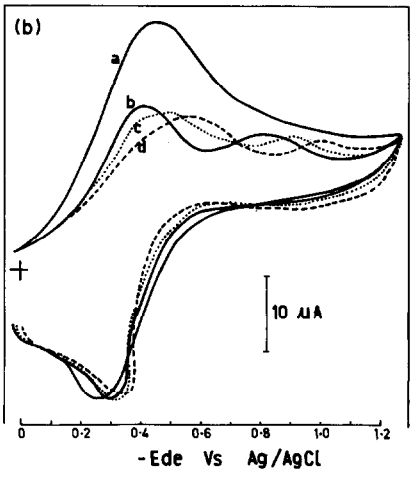

Fig. 4(b). Cyclic voltammograms of [Ru(EDTAH)(H$_2$O)] solution (1×10^{-3} M) at 25°C, μ = 0.1 M KCl, (a) under N_2 at "a" ([NaOH]/[ML]) = 0.0; (b)–(d) under CO at a = 0.0, 0.5, 1.0, respectively.

Table 2. DPP and CV data of complex formed by interaction of K[Ru (EDTAH)(H$_2$O)] with CO at 35°C and μ = 0.10 M (KCl)

	DPP	CV	
Complex	$-E_{1/2}$ (V) (vs Ag/AgCl)	$-Ep_c$ (V)	$-Ep_a$ (V)
1 under N_2	0.350, 0.800, 1.110	0.400, 0.795	0.300
1 under CO	0.220, 0.420, 0.765	0.220, 0.490, 0.780	0.180

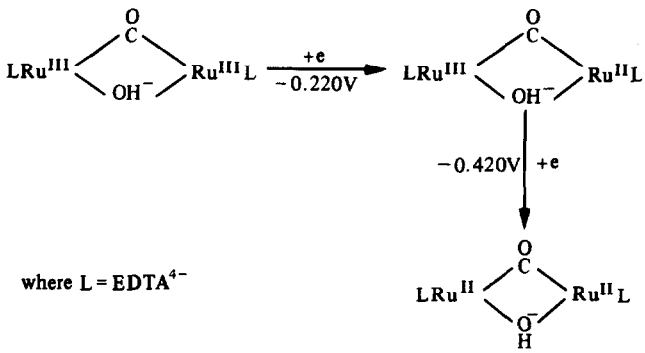

Scheme 1.

Ru^{3+}/Ru^{2+} couple, with an $E_{1/2}$ value of 0.350 V, the same as observed in DPP.[20] The other two couples, viz. Ru^{2+}/Ru^{+} and $H^{+}/\frac{1}{2}H_2$, are irreversible.

On passing CO into the solution of **1**, the peak due to the Ru^{3+}/Ru^{2+} couple splits and two peaks are exhibited at -0.220 and -0.420 V (see Scheme 1) in DPP and -0.220 and -0.490 V in CV. Such split peaks are characteristic of dimers[20,26] and result from the stepwise reduction of metal ions in dimer **4**. This further confirms the formation of dimer complex **4**, as was discussed in the potentiometric results. The peak due to Ru^{2+}/Ru^{+} appears at -0.765 V, but no peak appears for $H^{+}/\frac{1}{2}H_2$ in the dimer.

The peaks due to the Ru^{3+}/Ru^{2+} couple in complex **4** is pH dependent and shifts to more negative potentials on increasing the pH. This is due to further hydrolysis of the dimer [reaction (5)] to the hydroxo species. In the CV of **4** the potential due to the Ru^{3+}/Ru^{2+} couple shifts to more negative values until $a = 2.5$, beyond which, new peaks are exhibited due to the decomposition of complex **4** to unidentified species. No study was, therefore, carried out above $a = 2.5$.

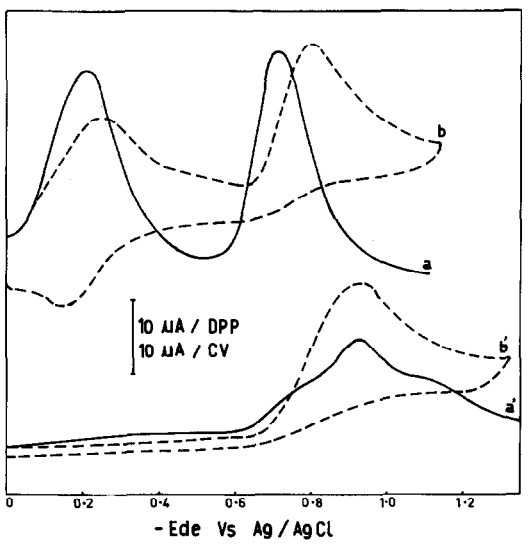

Fig. 5. Differential pulse and cyclic voltammograms at 25°C, $\mu = 0.1$ M KCl. (a) and (b) DPP and CV of [Ru^{III}(EDTAH)(H_2O)] solution (1×10^{-3} M) refluxed under a CO atmosphere. (a′) and (b′) DPP and CV of [Ru^{II}–EDTA–CO] solution (1×10^{-3} M).

In order to confirm the oxidation state of the metal ion in complexes **2–4**, a solution of **1** was refluxed under a CO atmosphere for 3 h. The DPP and CV of such a solution are shown in Figs 5(a) and (b). It may be seen that the Ru^{3+}/Ru^{2+} peak is still seen even under refluxing conditions. As a further check, an authentic sample of Ru^{II}–EDTA–CO was prepared by the reduction of MLH with H_2/Pt under CO.[27] DPP and CV of such a solution did not exhibit any peak due to Ru^{3+}/Ru^{2+} [Fig. 5(a′) and (b′)]. Thus complexes **2–4**, formed in solution on reaction of **1** with CO, are stable ruthenium(III) carbonyl species.

Kinetics of the formation of complexes **2**, **3** *and* **4**

The kinetics of the carbonylation reaction were followed spectrophotometrically by recording repetitive scans (Fig. 6) of the reaction between complex **1** and CO by monitoring the growth of the peak at 390 nm with the formation of CO complexes. The peaks due to complex **1** at 203, 283 and 365 nm (Fig. 6) decrease with the formation of complexes **2**, **3** and **4**. An isobestic point (Fig. 6) was observed at 310 nm, which showed the existence of two species in equilibrium.

The kinetics of complex formation were found to follow first-order dependence in the concentration of complex **1**, as well as in [CO], over a wide range of concentration (10^{-5}–10^{-3} M) of either reactant. The values of the pseudo first-order rate constants, K_{obs}, were obtained from the slopes of a plot of $\log(A_\infty - A_t)$ vs time. The values of A_∞ were

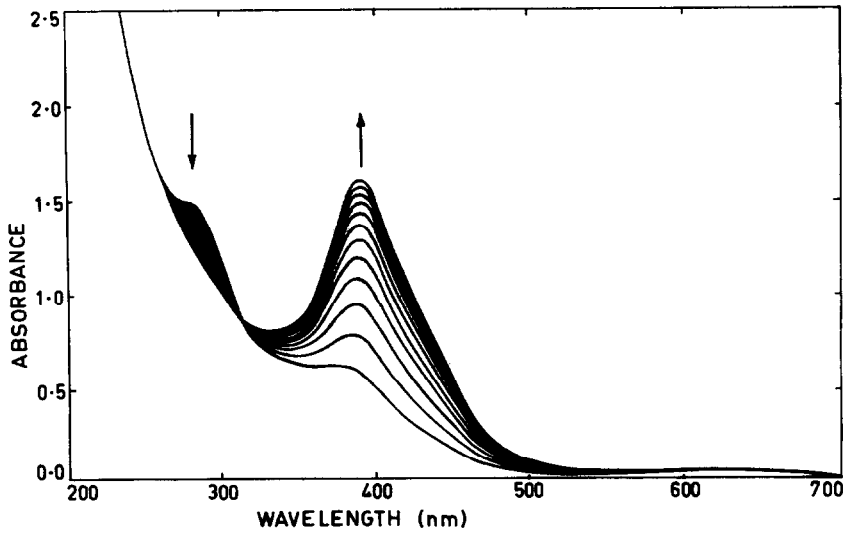

Fig. 6. Repetitive scan at 2 min intervals of the reaction between [Ru(EDTAH)(H$_2$O)] (1×10^{-5} M) and [CO] (4.64×10^{-4} M) at 25°C, $\mu = 0.1$ M KCl.

obtained by allowing the reaction to proceed to more than five times the half-life of the reaction. The first-order dependence plot of k_{obs} vs [CO] is given in Fig. 7.

The reaction between **1** and CO was studied in the pH range 2.5–3.8. The rate was found to increase with pH in the range 2.5–3.2, while it remained constant in the pH range 3.2–3.8 (Fig. 8). In the pH range investigated, complex **1** exists in two forms: [Ru(EDTAH)(H$_2$O)] (**1**) and the "normal" form [Ru(EDTA)(H$_2$O)]$^-$ (**1a**).

Our experimental observations on the complexation of **1** with CO enabled us to suggest the most plausible mechanism for the present reaction system using eqs (9)–(11):

$$\underset{\textbf{(1)}}{[Ru(EDTAH)(H_2O)]} + CO \underset{k_{-a}}{\overset{k_a}{\rightleftharpoons}} \underset{\textbf{(2)}}{[Ru(EDTAH)CO]} + H_2O \quad (9)$$

$$\underset{\textbf{(1a)}}{[Ru(EDTA)(H_2O)]^-} + CO \underset{k_{-b}}{\overset{k_b}{\rightleftharpoons}} \underset{\textbf{(3)}}{[Ru(EDTA)(CO)]^-} + H_2O \quad (10)$$

$$\underset{\textbf{(3)}}{[Ru(EDTA)(CO)]^-} + \underset{\textbf{(1a)}}{[Ru(EDTA)H_2O]^-} \underset{k_{-c}}{\overset{k_c}{\rightleftharpoons}} \underset{\textbf{(4)}}{[(RuEDTA)_2(CO)(OH)]^{3-}} + H^+. \quad (11)$$

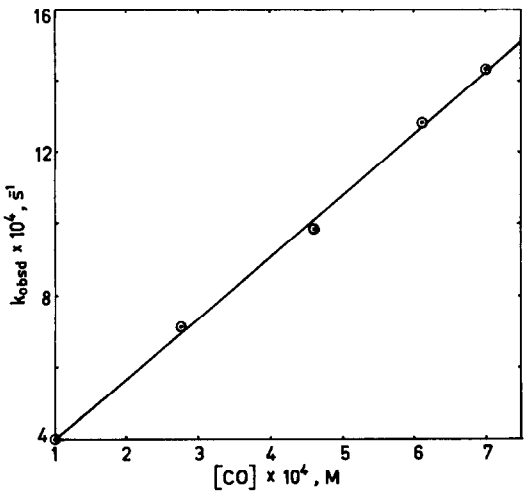

Fig. 7. First-order dependence kinetic plot in [CO] at pH = 3.0, $T = 25$°C, $\mu = 0.1$ M KCl.

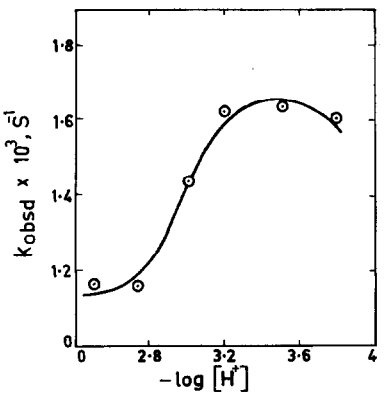

Fig. 8. pH dependence of observed rate constants for the reaction of [Ru(EDTAH)(H$_2$O)] (5×10^{-5} M) with [CO] (7×10^{-4} M) at 25°C, $\mu = 0.1$ M KCl.

In the proposed mechanism both the protonated and normal complexes, **1** and **1a**, combine with CO to form complexes **2** and **3**, respectively. Complex **3** further reacts with **1a** to give complex **4**.

The rate expression for reactions (9)–(11) can be written in terms of the specific rate constants, k_1, k_a, k_b, k_c and by expressing the concentrations of complex **1** in terms of **1** and **1a**.

$$k_1\left(1+\frac{K_{1a}}{[H^+]}\right)=k_a+\frac{k_bK_{1a}}{[H^+]}+\frac{k_c(K_{1a})^2K_{CO}[1a]}{[H^+]^2}, \quad (12)$$

where

$$k_1=\frac{\text{rate}}{[1]_T[CO]}; \quad K_{1a}=\frac{1}{K_H^1}.$$

At pH < 3.8 the last term on the RHS of eq. (12) drops out and a plot of the LHS of the expression vs $1/[H^+]$ yields a straight line. The intercept and slope of which give k_1 and k_2 as 1.02 and 2.42 M^{-1} s^{-1}, respectively (see Fig. 9).

At pH 3.8 all the constants in eq. (12) except k_c are known. By substituting the values of the known quantities into eq. (12), k_c was found to be 1.45×10^{-3} M^{-1} s^{-1}, which is about three orders of magnitude lower than k_a and k_b and hence is the rate-determining step.

From the values of the equilibrium constants for reactions (1), (2) and (3), the values of the "off rates" k_{-a}, k_{-b} and k_{-c} are 4.06×10^{-3} s^{-1}, 3.05×10^{-5} s^{-1}, 2.76×10^{-7} M^{-1} s^{-1}. The off rates are much slower than the "on rates" and decrease in the order $k_{-a} > k_{-b} > k_{-c}$. In fact for reactions (1)–(3), the rate of formation "on rates" are therefore the equilibrium controlling rates. The most unstable complex, **2**, is readily deprotonated to form **3**. The formation of **2** is, therefore, promoted in acidic solution.

The values of the activation parameters, $\Delta H^\ddagger$ and $\Delta S^\ddagger$, corresponding to the slow step, k_c, in the temperature range 15–45°C are $\Delta H^\ddagger = 9.5$ kcal mol^{-1} and $\Delta S^\ddagger = -25.5$ e.u. The values of $\Delta H^\ddagger$ and $\Delta S^\ddagger$ reported[10] for the ruthenium(III) carbonyl, $[Ru^{III}Cl_5(H_2O)]^{2-}$, are 24.0 kcal mol^{-1} and 7.0 e.u., respectively. The value of $\Delta H^\ddagger$ is more exothermic by about 16.0 kcal mol^{-1} for the carbonylation of complex **1** than for the pentachloro ruthenium(III) species. Since the overall reaction involves a displacement of the H_2O molecule by CO the enthalpies should depend on the labilization of the H_2O molecule in the complexes. The lability of the H_2O molecule in these complexes depends[14] on the extent of σ-donation and π-back-bonding of the ligands present in the coordination sphere of the metal ion. A good σ-donor increases[14] the electron density on ruthenium(III) and assists in the labilization of the H_2O molecule in a nucleophilic displacement reaction. The presence of a strong σ-donor in the coordination sphere of ruthenium(III) in **1** makes the H_2O molecule much more labile than in the pentachloro complex, reflecting on the favourable enthalpy of activation. The entropy of activation, $\Delta S^\ddagger$, for the formation of dimer **4** is much more negative than the monomeric chloro ruthenium(III) complex.

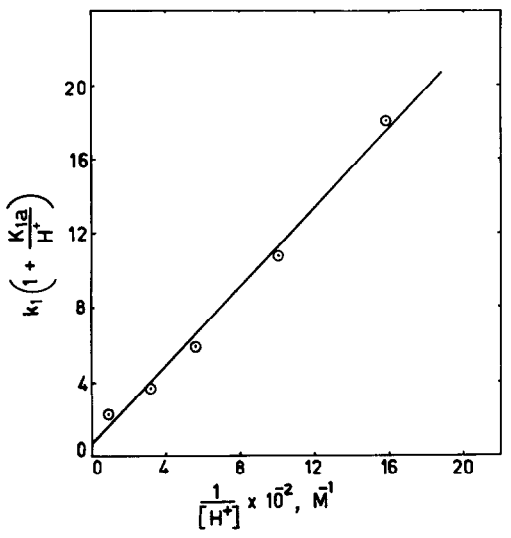

Fig. 9. Plot of $k_1(1+(K_{1a}/[H^+]))$ vs $[H^+]^{-1}$; [Ru (EDTAH)(H_2O)] = 5×10^{-5} M, [CO] = 7×10^{-4} M at 25°C, μ = 0.1 M KCl.

REFERENCES

1. I. Wender and P. Pino (Ed.), *Organic Synthesis via Metal Carbonyls*, Vols 1 and 2. Interscience, New York (1968); I. Wender, *Catal. Rev. Sci. Engng* 1976, **14**, 97.
2. J. Falbe, *Synthesis mit kohlen monoxyd.*, Springer, Berlin (1967); J. Falbe (Ed.), *New Synthesis with* CO, Springer, Berlin (1980).
3. R. L. Prent, *Adv. Organomet. Chem.* 1979, **17**, 1; R. F. Heck, *Adv. Organomet. Chem.* 1966, **4**, 283.
4. M. Orchim, *Accts Chem. Res.* 1981, **14**, 259.
5. I. Tkatchenko, in *Comprehensive Organometallic Chemistry* (Edited by G. Wilkinson, F. G. A. Stone and E. W. Abel), Vol. 8, pp. 110–224. Pergamon Press, Oxford (1982).
6. C. Bolleghi, R. Ganzerla, M. Lenarda and G. Moretli, *J. Molec. Catal.* 1987, **40**, 129.
7. N. Yu Kukushkin, *Koord. Khim.* 1986, **12**, 147; M. Schroder and T. A. Stephenson, *Comprehensive Coordination Chemistry* (Edited by G. Wilkinson), Vol. 4, Chap. 45, p. 277. Pergamon Press, Oxford (1987).
8. A. A. Bhatacharya, C. C. Nagel and S. G. Shore,

Organometallics 1983, **2**, 1187 and refs therein; E. R. Corey and L. F. Dahl, *J. Am. Chem. Soc.* 1961, **83**, 2203; C. H. Wei, G. R. Wilkes and L. F. Dahl, *J. Am. Chem. Soc.* 1967, **89**, 4792; M. R. Churchill and J. P. Hutchinson, *Inorg. Chem.* 1978, **17**, 3528.

9. R. Colton and R. H. Farthing, *Aust. J. Chem.* 1971, **24**, 903; 1967, **20**, 283; 1969, **22**, 2011.
10. J. Halpern, B. R. James and A. L. W. Kemp, *J. Am. Chem. Soc.* 1966, **88**, 5142.
11. T. Matsubara and C. Creutz, *Inorg. Chem.* 1979, **18**, 1956.
12. A. Yeh and H. Taube, *Inorg. Chem.* 1980, **19**, 3740.
13. J. F. Wishart, H. Taube, K. J. Breslauer and S. S. Isied, *Inorg. Chem.* 1984, **23**, 2997.
14. S. S. Isied and H. Taube, *Inorg. Chem.* 1976, **15**, 3070.
15. M. M. Taqui Khan, G. Ramachandraiah and A. Prakash Rao, *Inorg. Chem.* 1986, **25**, 665; M. M. Taqui Khan, G. Ramachandraiah and A. Prakash Rao, *Inorg. Chem.* 1988, **27**, in press.
16. M. M. Taqui Khan, A. Hussain, K. Venakatasubramanian, G. Ramachandraiah and V. Oommen, *J. Molec. Catal.* 1988, **44**, 117.
17. M. K. Markiewicz and M. C. Baird, *Inorg. Chim. Acta.* 1986, **113**, 95; F. J. Waller, *J. Molec. Catal.* 1985, **31**, 123.
18. M. M. Taqui Khan, S. B. Halligudi and S. H. R. Abdi, *J. Molec. Catal.* 1988, **44**, 179; M. M. Taqui Khan, S. B. Halligudi and S. H. R. Abdi, *J. Molec. Catal.* 1988, **45**, 215; M. M. Taqui Khan, S. B. Halligudi and S. Shukla, *Angew. Chem. Int. Edn.* 1988, **27**, 1735.
19. N. A. Ezerskaya and T. P. Solovykh, *Zh. Neorg. Khim.* 1966, **11**, 1462, 1855; 2196, **12**, 2922.
20. M. M. Taqui Khan, A. Hussain, G. Ramachandraiah and M. A. Moiz, *Inorg. Chem.* 1986, **25**, 3023.
21. K. Shimizu, T. Matsubara and G. P. Sato, *Bull. Chem. Soc. Jpn* 1974, **47**, 1615.
22. J. Halpern and A. L. W. Kemp, *J. Am. Chem. Soc.* 1966, **88**, 5147.
23. A. I. Vogel, *Text Book of Practical Organic Chemistry*. Orient Longmans (1976).
24. A. A. Diamantis and J. V. Dubrawski, *Inorg. Chem.* 1981, **20**, 1142.
25. R. J. Motekaitis and A. E. Martell, *Can. J. Chem.* 1982, **60**, 168.
26. P. S. Bhattacharya, A. Chakravorty, F. A. Cotton, R. Mukherjee and W. Schwartzu, *Inorg. Chem.* 1984, **23**, 1709.
27. M. M. Taqui Khan and A. Hussain, *Ind. J. Chem.* 1980, **20A**, 50.

Polyhedron Vol. 8, No. 17, pp. 2209–2211, 1989
Printed in Great Britain

0277–5387/89 $3.00+.00
© 1989 Pergamon Press plc

COMMUNICATION

THE FIRST STRUCTURALLY CHARACTERIZED COMPLEX CONTAINING BRIDGING 2,2′-BIPYRIDINE. SYNTHESIS AND X-RAY CRYSTAL STRUCTURE OF $(PPN)_2[Pt(C_6F_5)_3(\mu\text{-}2,2'\text{-bipy})Pt(C_6F_5)_3]$

RAFAEL USON,* JUAN FORNIES, MILAGROS TOMAS, JOSE M. CASAS and CONSUELO FORTUÑO

Departamento de Química Inorgánica, Instituto de Ciencia de Materiales de Aragón, Universidad de Zaragoza-C.S.I.C., 50009 Zaragoza, Spain

(*Received* 7 *February* 1989; *accepted* 31 *March* 1989)

Abstract—The reactions between $Q_2[Pt_2(\mu\text{-}C_6F_5)_2(C_6F_5)_4]$ (Q = NBu_4, PPN) and 2,2′-bipy (molar ratio 1:1) in CH_2Cl_2 afford the binuclear $Q_2[(C_6F_5)_3Pt(\mu\text{-}2,2'\text{-bipy})Pt(C_6F_5)_3]$ complex, which contains the 2,2′-bipy acting as a bridging ligand. A similar reaction with 1,10-phen renders *cis*-$Pt(C_6F_5)_2$phen and $Q_2[Pt(C_6F_5)_4]$ (Q = NBu_4). On the other hand, $(NBu_4)_2[Pd_2(\mu\text{-}C_6F_5)_2(C_6F_5)_4]$ reacts in CH_2Cl_2 with either bipy or phen (N—N) (1:1), yielding in both cases *cis*-$Pt(C_6F_5)_2$(N—N) and $(NBu_4)_2[Pd(C_6F_5)_4]$. The structure of the binuclear platinum complex (Q = PPN) which contains for the first time a 2,2′-bipy bridging ligand has been determined by X-ray crystallography.

2,2′-Bipyridine (bipy) and 1,10-phenanthroline (phen) have been much used[1] in coordination chemistry as powerful chelating ligands. The rigid geometry of phen forces the two donor nitrogen atoms into a *cis*-position, but since the bipy molecule is not rigid and the free ligand adopts a *trans*-configuration in the solid state,[2] it should be expected that the formation of binuclear complexes containing bridging *trans*-bipy might be feasible. Only a few complexes have been reported[3–8] for which such a bridging structure has been invoked, always on indirect evidence; to the best of our knowledge, no definite structural evidence based on X-ray studies has been given, so far.† Here, we report the synthesis of the first well-authenticated binuclear complex with a bridging *trans*-bipy ligand, as demonstrated by single crystal X-ray crystallography.

Addition of 2,2′-bipy to a yellow dichloromethane solution of $(NBu_4)_2[Pt_2(\mu\text{-}C_6F_5)_2(C_6F_5)_4]$[9] (1:1 molar ratio, room temperature) gives, after 1 h stirring, a colourless solution from which after evaporation to dryness and washing the residue with ^{i}PrOH, the binuclear $(NBu_4)_2[Pt_2(\mu\text{-}2,2'\text{-bipy})(C_6F_5)_6]$ (1) [eq. (1)] in 74% yield, as a consequence of the symmetric cleavage of the bridge in the binuclear precursor.

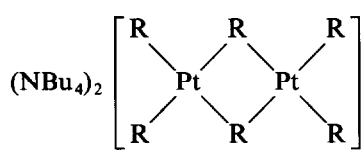

$(NBu_4)_2[R_3Pt(\mu\text{-}2,2'\text{-bipy})PtR_3]$. (1)

As expected, substitution of the 1,10-phen for 2,2′-bipy [in eq. (1)] causes the unsymmetric cleavage of the bridge system in the precursor to afford *cis*-$Pt(C_6F_5)_2$phen[10] (insoluble in the CH_2Cl_2 solution) and $(NBu_4)_2[Pt(C_6F_5)_4]$,[11] thereby illustrating the constraint imposed by the structural rigidity of the phen molecule.

Notwithstanding, the analogous binuclear palladium complex $(NBu_4)_2[Pd_2(\mu\text{-}C_6F_5)_2(C_6F_5)_4]$[12] reacts with both bipy or phen under unsymmetric

* Author to whom correspondence should be addressed.

† Search in the Cambridge Crystallographic Data Centre.

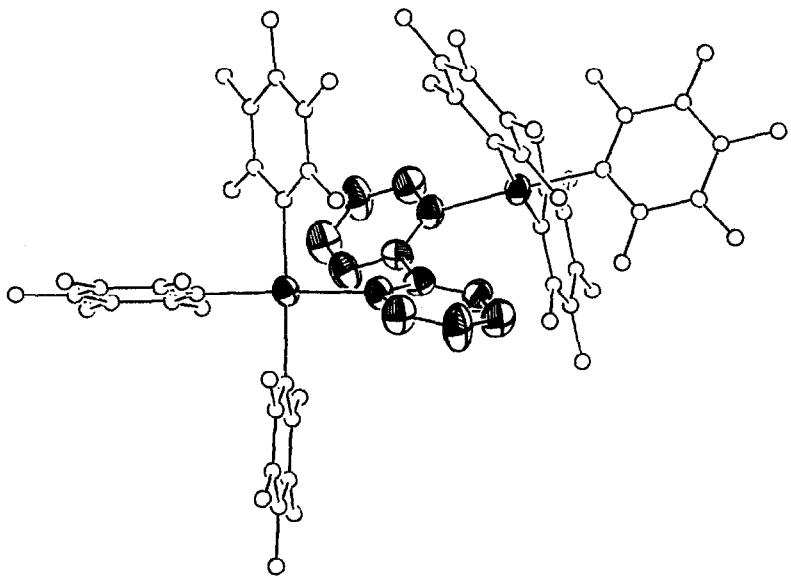

Fig. 1. An ORTEP view of the $[(C_6F_5)_3Pt(\mu\text{-bipy})Ph(C_6F_5)]^{2-}$ anion. The carbon and fluorine atoms of the C_6F_5 groups are drawn with arbitrary radii for clarity.

Distances:

Pt—C(6)	2.117(7)	Pt—C(18)	2.039(4)	C(1)—C(1′)	1.501(25)
Pt—C(12)	2.107(6)	Pt—N(1)	2.115(7)		

Angles:

C(12)—Pt—C(18)	90.4(2)	C(6)—Pt—N(1)	89.4(3)
C(18)—Pt—C(6)	88.1(2)	N(1)—Pt—C(12)	92.2(3)

cleavage of the bridge to give *cis*-$Pd(C_6F_5)_2(bipy)$[10] and $(NBu_4)_2[Pd(C_6F_5)_4]$[11] or, respectively, *cis*-$Pd(C_6F_5)_2(phen)$[10] and $(NBu_4)_2[Pd(C_6F_5)_4]$.[11]

Complex **1** gives microanalytical and spectroscopic data which are in accordance with the proposed formulae,* but all attempts to grow suitable crystals for X-ray studies failed since only thin filiform specimens were obtained. Thereafter, the similar $(PPN)_2[Pt_2(\mu\text{-}2,2'\text{-bipy})(C_6F_5)_6]$ (**2**) was prepared and suitable crystals were grown by slow diffusion (*ca* 2 weeks, −30°C) of *n*-hexane into a CH_2Cl_2 solution of **2**.†

The structure of the anion, $[Pt_2(\mu\text{-}2,2'\text{-bipy})(C_6F_5)_6]^{2-}$, is shown in Fig. 1, it lies on a crystallographic C_2 axis and comprises two fragments "$Pt(C_6F_5)_3$" bridged by the bipy ligand. Each platinum atom is in a nearly regular square-planar environment, formed by three carbon atoms of the C_6F_5 groups and a nitrogen atom of the bridging bipy. The Pt—C distances are in the range 2.039(4)–2.117(7), similar to Pt—C distances found in other pentafluorophenyl platinum complexes,[15–18] the shortest Pt—C distance being that corresponding to carbon *trans* to the nitrogen atom of the bipy, in accordance with the low *trans*-influence of the amine donor ligand.

The C—C and C—N distances and bond angles within the pyridine rings, are similar to those found in the free ligand.[2] Each pyridine ring is practically planar, and the largest deviation of any atom from the least-squares best plane is 0.019 Å,[19] however the entire coordinated bipy is not planar; both pyridine rings are rotated around the C(1)—C(1′) bond, the dihedral angle formed by the least-squares pyridine planes is 41.89°, the nitrogen atoms being in *trans*-positions.

Acknowledgement—We thank the Dirección General de Investigación Científica y Técnica (Spain) for financial support (project PB85-0128) and for a research grant (to J.M.C.).

* Spectroscopic data for **1**: IR: C_6F_5 X-sensitive[13] (Nujol) cm^{-1}: 802s, 707m, 763s; NMR in CD_2Cl_2, ^1H (bipy signals): δ 7.21 (m, 2H), 8.09 (m, 2H), 9.40 (m, 2H), 11.14 (m, 2H).[14]

† Crystal data for **2**: $Pt_2P_4F_{30}N_4C_{118}H_{68}$. Monoclinic, space group $C_{2/c}$, $a = 41.673(8)$, $b = 15.534(5)$, $c = 19.522(3)$ Å, $\beta = 116.42(2)°$, $U = 11313$ Å^3, $Z = 4$. $\mu(M_0\text{-}K_\alpha) = 25$ cm^{-1}. Empirical absorption correction[20] (transmission factors 0.314–0.545). Phenyl rings were refined as rigid groups with C—C, 1.395 Å. 4508 unique reflections with $F_o \geq 6\sigma(F_o)$, NP = 605. Refinement converged at $R = 0.039$, $R_w = 0.042$.

REFERENCES

1. J. Reedijk, in *Comprehensive Coordination Chemistry* (Edited by G. Wilkinson, R. D. Gillard and J. A. McCleverty), Vol. 2, p. 73 and refs therein. Pergamon Press, New York (1987).
2. L. L. Merryt Jr and E. D. Schroeder, *Acta Cryst.* 1956, **9**, 801.
3. D. N. Lawson and G. Wilkinson, *J. Chem. Soc.* 1965, 1900.
4. A. S. Mufti and R. C. Poller, *J. Organomet. Chem.* 1965, **3**, 99.
5. M. Komura, Y. Kawasaki, T. Tanaka and R. Okawara, *J. Organomet. Chem.* 1965, **4**, 308.
6. G. Matsubayashi, *J. Inorg. Nucl. Chem.* 1966, **28**, 2937.
7. G. W. A. Fowles and G. R. Willey, *J. Chem. Soc.* 1968, 1435.
8. T. Cuenca and P. Royo, *J. Organomet. Chem.* 1985, **293**, 61.
9. R. Usón, J. Forniés, M. Tomás, J. M. Casas, F. A. Cotton, L. R. Falvello and R. Llusar, *Organometallics* 1988, **7**, 2279.
10. R. Usón, J. Forniés, J. Gimeno, P. Espinet and R. Navarro, *J. Organomet. Chem.* 1974, **81**, 115.
11. R. Usón, J. Forniés,. F. Martínez and M. Tomás, *J. Chem. Soc., Dalton Trans.* 1980, 888.
12. R. Usón, J. Forniés, M. Tomás, J. M. Casas and R. Navarro, *J. Chem. Soc., Dalton Trans.* 1989, 169.
13. R. Usón and J. Forniés, in *Advances in Organometallic Chemistry* (Edited by F. G. A. Stone and R. West), Vol. 28, p. 219 and refs therein. Academic Press, San Diego (1988).
14. F. A. Kramer Jr and R. West, *J. Phys. Chem.* 1965, **69**, 673.
15. R. Usón, J. Forniés, M. A. Usón, J. F. Yagüe, P. G. Jones and K. Meyer-Bässe, *J. Chem. Soc., Dalton Trans* 1986, 947.
16. R. Usón, J. Forniés, M. Tomás, B. Menjón and A. J. Welch, *J. Organomet. Chem.* 1986, **304**, C24.
17. J. Forniés, M. A. Usón, J. I. Gil and P. G. Jones, *J. Organomet. Chem.* 1986, **311**, 243.
18. F. A. Cotton, L. R. Falvello, R. Usón, J. Forniés, M. Tomás, J. M. Casas and I. Ara, *Inorg. Chem.* 1987, **26**, 1366.
19. M. Nardelli, *Comput. Chem.* 1983, **7**, 95.
20. A. C. T. Noth, D. C. Phillips and F. S. Mathews, *Acta Cryst.* 1968, **A24**, 351.

Note added in proof: After submission of the present manuscript, a letter giving some structural information on the compound [(μ-4,4′-dimethyl-2,2′-bipyridyl)bis (pentacarbonyl chromium(0)] has been published [C. Long, *et al.*, *Inorg. Chim. Acta* 1989, **157**, 151]. Neither bond distances nor bond angles are given, probably owing to the "very small crystals of marginal quality for X-ray work" obtained by the authors.

Polyhedron Vol. 8, No. 17, pp. 2213–2214, 1989
Printed in Great Britain

0277–5387/89 $3.00+.00
© 1989 Pergamon Press plc

COMMUNICATION

SPECTROPHOTOMETRIC DETERMINATION OF THE REACTION STOICHIOMETRY OF THE REDUCTION OF OCTACYANOTUNGSTATE(V) BY HYDROXYLAMINE IN ACIDIC AND BASIC MEDIA

J. H. POTGIETER

Department of Chemistry, University of Pretoria, Pretoria 0002, Republic of South Africa

(*Received* 3 *April* 1989; *accepted* 4 *May* 1989)

Abstract—The stoichiometry of the reduction of octacyanotungstate(V) by hydroxylamine in basic and acidic media has been studied by a spectrophotometric technique. It was found that the stoichiometric ratio between $W(CN)_8^{3-}$ and hydroxylamine was 2:1 in a basic medium and 1:1 in an acidic medium, in agreement with previously proposed values.

The reaction of hydroxylamine with a variety of oxidizing agents has been studied[1] and various oxidation products, i.e. NH_3, $H_2N_2O_2$, N_2 and N_2O have been reported. These investigations were performed in acidic solutions of pH 0.4–5.6. Jindal *et al.*[2] found that the oxidation of hydroxylamine by $Fe(CN)_6^{3-}$ in a weak acidic medium produced N_2 as the main reaction product.

Although the oxidation of hydroxylamine in acidic solution has been extensively investigated, very little is known about the reaction in alkaline media. Van Wyk *et al.*[3] have conducted a kinetic study of the oxidation of hydroxylamine by octacyanotungstate(V) over a wide pH range and have found that the reaction occurred quickly in alkaline media, but was slow in acidic media. It was also observed that N_2 was generated by the reaction between $W(CN)_8^{3-}$ and hydroxylamine at pH values of ~ 6. The present investigation is a continuation of the work by Van Wyk *et al.* and is also part of a research project on the redox properties of the cyano complexes of molybdenum, tungsten and iron.

EXPERIMENTAL

$Cs_3W(CN)_8 \cdot 2H_2O$ was prepared as described by Leipoldt and co-workers,[4,5] and was used as a primary standard[6] after recrystallization. Hydroxylammonium chloride (Merck *pro analisi*) was used as a source of hydroxylamine. The hydroxylammonium chloride solution was neutralized with sodium hydroxide. This solution was renewed daily. All other reagents used were analytical-grade, and redistilled water was used throughout.

Spectrophotometric measurements were made in both alkaline and acidic media using buffer mixtures made with KH_2PO_4 or sodium hydroxide solutions at constant ionic strength. Stoichiometric data were obtained by monitoring the decrease in $[W(CN)_8^{3-}]$ after reaction with various hydroxylamine concentrations on a Pye-Unicam SP 1700 spectrophotometer at 357 nm. All measurements were taken at 25°C.

In the alkaline medium the absorbance of the $W(CN)_8^{3-}$ solution was measured immediately after mixing with the hydroxylamine, while 3 h waiting time was allowed in the acidic medium before any measurements were made.

RESULTS AND DISCUSSION

The absorbance of different, partly reduced $W(CN)_8^{3-}$ solutions in basic and acidic media by increasing amounts of hydroxylamine are summarized in Table 1.

The absorbance of a 5.0×10^{-4} mol dm^{-3} $W(CN)_8^{4-}$ solution was 0.110. The graphical representation shown in Fig. 1 allows calculation of

Table 1. Observed absorbance values of partly reduced $W(CN)_8^{3-}$ in different media, $T = 25°C$

$10^4[W(CN)_8^{3-}]$ (mol dm^{-3})	Amount of $W(CN)_8^{3-}$ (mmol)	Acidic medium (pH ≃ 4, 6) Amount of hydroxylamine (mmol)	Absorbance	Basic medium (pH ≃ 13) Amount of hydroxylamine (mmol)	Absorbance
5.0	0.0100	0.0000	0.896	0.0000	0.900
5.0	0.0100	0.0005	0.873	0.0005	0.800
5.0	0.0100	0.0010	0.798	0.0010	0.725
5.0	0.0100	0.0015	0.770	0.0015	0.625
5.0	0.0100	0.0020	0.696	0.0020	0.558
5.0	0.0100	0.0025	0.635	0.0025	0.478
5.0	0.0100	0.0030	0.646	0.0030	0.383
5.0	0.0100	0.0035	0.582	0.0035	0.301
5.0	0.0100	0.0040	0.512	0.0040	0.225
		0.0050	0.504		
		0.0055	0.420		
		0.0060	0.384		
		0.0065	0.366		

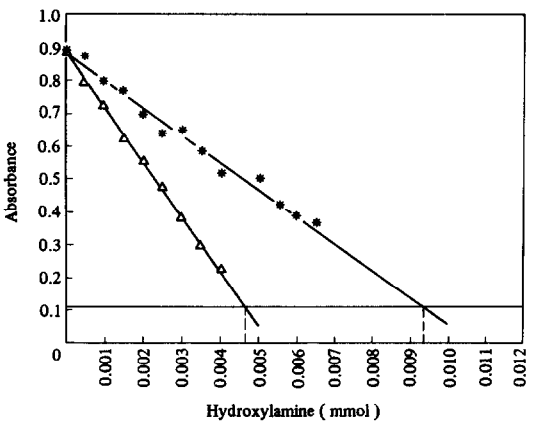

Fig. 1. Absorbance of different, partly reduced $W(CN)_8^{3-}$ solutions as a function of the amount of hydroxylamine added.

the stoichiometric relationship for the reaction between $W(CN)_8^{3-}$ and hydroxylamine in both media.

From the two intersection values of the curves in Fig. 1 the stoichiometric ratio between $W(CN)_8^{3-}$ and hydroxylamine is calculated to be ≃ 2 : 1 in the basic medium and ≃ 1 : 1 in the acidic medium. The reaction between $W(CN)_8^{3-}$ and hydroxylamine can therefore by represented by the following balanced equations:

Basic medium:

$$4W(CN)_8^{3-} + 2NH_2OH + 4OH^- \longrightarrow 4W(CN)_8^{4-} + N_2O + 5H_2O$$

Acidic medium:

$$2W(CN)_8^{3-} + 2NH_2OH \longrightarrow 2W(CN)_8^{4-} + 2H^+ + N_2 + 2H_2O.$$

These results are in agreement with the proposed stoichiometric values used in the reaction scheme for the kinetic study of the oxidation of hydroxylamine by octacyanotungstate(V) by Van Wyk *et al.*[3]

Acknowledgements—The author is grateful to the Department of Chemistry, University of the Orange Free State and the research fund of this university (UOFS) for the use of their apparatus and financial assistance.

REFERENCES

1. W. C. Bray, M. E. Simpson and A. A. Mackenzie, *J. Am. Chem. Soc.* 1919, **41**, 1363; A. Kurtenacker and R. Neusser, *Z. Anorg. Allg. Chem.* 1923, **131**, 27; T. H. James, *J. Am. Chem. Soc.* 1939, **61**, 2379; 1940, **62**, 536; 1942, **64**, 731; J. H. Anderson, *Analyst* 1964, **89**, 357; 1966, **91**, 532; W. A. Waters and I. R. Wilson, *J. Chem. Soc. A* 1966, 534; B. J. Thakuria and Y. K. Gupta, *J. Chem. Soc., Dalton Trans.* 1975, 77; G. Bengtsson, *Acta Chem. Scand.* 1973, **27**, 1717; 1973, **27**, 3053; G. S. Barney, *J. Inorg. Nucl. Chem.* 1976, **38**, 1677; G. J. Bridgart, W. A. Waters and I. R. Wilson, *J. Chem. Soc., Dalton Trans.* 1973, 1582; R. Tomat and A. Rigo, *J. Inorg. Nucl. Chem.* 1974, **36**, 611; N, Rajasekar, R. Subramaniam and E. S. Gould, *Inorg. Chem.* 1983, **22**, 971.
2. V. K. Jindal, M. C. Agrawal and S. P. Mushran, *J. Chem. Soc. A* 1970, 2060.
3. A. J. Van Wyk, C. R. Dennis, J. G. Leipoldt and S. S. Basson, *Polyhedron* 1987, **6**, 641.
4. J. G. Leipoldt, L. D. C. Bok and P. J. Cilliers, *Z. Anorg. Allg. Chem.* 1974, **407**, 350.
5. L. D. C. Bok, J. G. Leipoldt and S. S. Basson, *Z. Anorg. Allg. Chem.* 1975, **415**, 81.
6. S. S. Basson, L. D. C. Bok and S. R. Grobler, *Z. Anal. Chem.* 1974, **268**, 287.

Polyhedron Vol. 8, No. 17, pp. 2215–2217, 1989
Printed in Great Britain

0277–5387/89 $3.00+.00
© 1989 Pergamon Press plc

COMMUNICATION

THE PREPARATION AND X-RAY STRUCTURES OF $Pt(SeSN_2)(PMe_2Ph)_2$ AND $[Pt(SeSN_2H)(PMe_2Ph)_2]BF_4$

CAROLINE A. O'MAHONEY, IVAN P. PARKIN, DAVID J. WILLIAMS and J. DEREK WOOLLINS*

Department of Chemistry, Imperial College of Science, Technology and Medicine, South Kensington, London SW7 2AY, U.K.

(*Received* 4 *April* 1989; *accepted* 17 *May* 1989)

Abstract—Reaction of $[Se_2SN_2]_2Cl_2$ with $PtCl_2(PMe_2Ph)_2$ in liquid ammonia gives $Pt(SeSN_2)(PMe_2Ph)_2$ (**4**), which may be protonated with HBF_4 to form $[Pt(SeSN_2H)(PMe_2Ph)_2]BF_4$ (**5**); the new compounds being characterized by IR, NMR and X-ray crystallography.

Recently, we have described the synthesis of metalla–sulphur–nitrogen complexes containing $S_2N_2^{2-}$, $S_2N_2H^-$ or S_3N^- ligands.[1–4] Complexes of the type $[Pt(S_2N_2H)(PR_3)_2]X$ (**1**) are of particular interest since they form one dimensional stacked structures with channels of cations and anions. Clearly, it would be advantageous to replace the sulphur atoms by seleniums in the PtSN rings to enhance the electronic interactions between the layered cations, a strategy that has been found to be useful for organic metals. However, the synthesis of selenium substituted analogues of **1** is non-trivial since there is a paucity of suitable starting materials, although we have been able to prepare $Pt(Se_3N)Cl(PMe_2Ph)$ in low yield from a high temperature reaction involving Se_4N_4.[5] One very successful strategy for the preparation of M—S—N complexes has been to perform the reaction in liquid ammonia using cations such as $[S_3N_2Cl]^+$ or $[S_4N_3]^+$.[6] Here, we report on the reaction of $[Se_2SN_2]_2Cl_2$ (**2**) with *cis*-$PtCl_2(PMe_2Ph)_2$ (**3**) in liquid ammonia to give $Pt(SeSN_2)(PMe_2Ph)_2$ (**4**) [eq. (1)], which can be protonated using HBF_4 to give $[Pt(SeSN_2H)(PMe_2Ph)_2]BF_4$ (**5**) [eq. (2)]. Compounds **4** and **5** are the first examples of complexes containing S—Se—N anions as ligands.

$$cis\text{-}PtCl_2(PMe_2Ph)_2 + 1/2[Se_2SN_2]_2Cl_2 \xrightarrow{\text{liq. } NH_3} Pt(SeSN_2)(PMe_2Ph)_2 + SeCl_2 + NH_4Cl \quad (1)$$

$$Pt(SeSN_2)(PMe_2Ph)_2 + HBF_4 \longrightarrow [Pt(SeSN_2H)(PMe_2Ph)_2]BF_4. \quad (2)$$

In a typical reaction, **2** (1 mmol) was dissolved in liquid ammonia (5 cm^3) at −78°C and **3** (1 mmol) was added. After stirring for 1 h the reaction was allowed to warm to room temperature and the ammonia allowed to evaporate off. The product, **4**, was obtained by extraction into CH_2Cl_2 and crystallized from CH_2Cl_2–petrol ether (yield *ca* 0.7 mmol, 70%). Protonation of **4** to form **5** was carried out in THF–benzene, the isolated yield being 70%.†

The spectroscopic properties of **4** and **5** are as expected.‡ The ^{31}P NMR spectra are of the AX type with ^{195}Pt and ^{77}Se satellites; the chemical

* Author to whom correspondence should be addressed.

† Microanalyses (calculated values in parentheses): $Pt(SeSN_2)(PMe_2Ph)_2$ (**4**) C, 31.0(31.4); H, 3.5(3.5); N, 4.8(4.6). $[Pt(SeSN_2H)(PMe_2Ph)_2]BF_4$ (**5**) C, 27.2(27.5); H, 3.1(3.3); N, 3.9(4.0).

‡ For **4**: ^{31}P δ_A −6.7, δ_B −27.1 ppm ^1J_A 2837, ^1J_B 2799 Hz; for (**5**): δ_A −12.4, δ_B −30.1, ^1J_A 2687. ^1J_B 3227, $^2J\{^{31}P–^{31}P\}$ 24 Hz. Poorly resolved shoulders suggesting $^2J–\{^{31}P–^{77}Se\}$ couplings of *ca* 30 Hz are also observed. IR (**4**): 1071(vs) [ν(SN)], 642(s) [ν(SN)], 546(m) [ν(SeN)], 401(m), 356(m) [δ(SN)]; **5**: 3299(s) [ν(NH)], band at *ca* 1070 obscured by BF_4^- vibrations, 645(m) [ν(SN)], 519(m), [ν(SeN)], 447(m), 331(m) cm^{-1}, 323(sh) [δ(SN)].

shifts and coupling constants being similar to the M—S—N analogues. The mass spectra show the parent ion with the appropriate isotopic substitution pattern for compounds containing one selenium and one platinum atom.

Despite the significantly larger covalent radius of selenium relative to sulphur, the X-ray structures* of **4** and **5** are isostructural with their PtS_2N_2 analogues.[2] In the neutral compounds both the $PtS_2N_2/PtSeSN_2$ rings display similar rotational disorder. Figure 1 shows a schematic representation of the disorder in **4**. Despite the disorder, the analysis shows unequivocally that the selenium atom is bound to platinum. Because of the inevitably poor accuracy of the bond lengths and angles in the $PtSeSN_2$ ring in the structure of **4** we determined the structure of the protonated compound **5**. In **5**, as a consequence of the synthetic route employed, the selenium atom is again bound to platinum and furthermore, the structure still displays the characteristic stacking seen previously

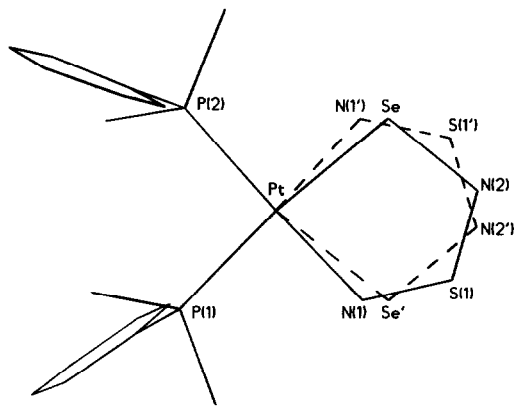

Fig. 1. A schematic representation of the disordered structure of $Pt(SeSN_2)(PMe_2Ph)_2$ (**4**).

for $[Pt(S_2N_2H)(PR_3)_2]X$ compounds.[3] The bond lengths for atoms not connected to selenium in **5** are the same as in $[Pt(S_2N_2H)(PMe_2Ph)_2]BF_4$ (**6**), there being a characteristic shortening of the Pt—P(2) bond length (*trans* to nitrogen) relative to Pt—P(1). With the exception of the angle at platinum (85.5(2) in **5**, cf. 84.6(2)° in **6**), the angles within the metallacycle are contracted in **5** compared to **6** as a result of the longer bonds around the selenium atom. There is a hydrogen bond (3.19 Å) between N(1)—H in the cation and F(1) in the anion. (The X-ray structure of **5** is shown in Fig. 2.) As mentioned above, the

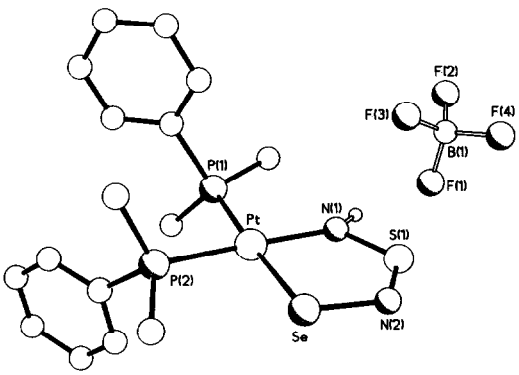

Fig. 2. The X-ray structure of $[Pt(SeSN_2H)(PMe_2Ph)_2]BF_4$ (**5**), showing the cation–anion hydrogen bonding. Selected bond lengths (Å) and angles (°):

Pt—P(1)	2.301(2)	N(1)—S(1)	1.602(7)
Pt—P(2)	2.262(2)	S(1)—N(2)	1.514(9)
Pt—Se	2.401(1)	N(2)—Se	1.833(9)
Pt—N(1)	2.030(7)		

P(1)—Pt—P(2)	94.3(1)
N(1)—Pt—Se	85.5(2)
Pt—N(1)—S(1)	122.8(4)
N(1)—S(1)—N(2)	111.4(4)
S(1)—N(2)—Se	120.1(4)
N(2)—Se—Pt	100.2(2)

* *Crystal data* **4**, $C_{16}H_{22}N_2P_2PtSSe$, monoclinic, $a = 17.170(3)$, $b = 13.879(3)$, $c = 17.921(4)$ Å, $\beta = 109.46(2)°$, $U = 4027$ Å^3, space group $C2/c$, $Z = 8$, $M = 610.4$, $D_c = 2.01$ g cm^{-3}, μ(Cu-K_α) = 178 cm^{-1}. Data were measured on a Nicolet R3m diffractometer with graphite monochromated Cu-K_α radiation using ω-scans. The structure was solved by the heavy-atom method. The structure displays partial two-fold disorder in the $PtSeSN_2$ ring about an axis bisecting the P—Pt—P angle. The occupancies of the two orientations refined to 0.85 and 0.15, respectively. The non-hydrogen atoms were refined anisotropically with the exception of the 0.15 occupancy atoms which were refined isotropically using absorption corrected data (empirical absorption correction, maximum and minimum transmission factors: 0.59 and 0.23, respectively) to give $R = 0.052$, $R_w = 0.054$ for 2439 independent observed reflections [$|F_o| > 3\sigma(|F_o|)$, $\theta \leqslant 58°$].

5, $C_{16}H_{23}BF_4N_2P_2PtSSe$, monoclinic, $a = 8.514(2)$, $b = 17.179(7)$, $c = 16.119(1)$ Å, $\beta = 104.41(4)°$, $U = 2283$ Å^3, space group $P2_1/n$, $Z = 4$, $M = 698.2$, $D_c = 2.03$ g cm^{-3}, μ(Cu-K_α) = 161 cm^{-1}. Data were measured on a Nicolet R3m diffractometer with graphite monochromated Cu-K_α radiation using ω-scans. The structure was solved by the heavy-atom method and refined anisotropically using absorption corrected data (numerical absorption correction based on faced indexed crystal, maximum and minimum transmission factors: 0.246 and 0.054, respectively) to give $R = 0.043$, $R_w = 0.047$ for 2921 independent observed reflections [$|F_o| > 3\sigma(|F_o|)$, $\theta \leqslant 58°$]. The atomic coordinates are available on request from the Director of the Cambridge Crystallographic Data Centre, University Chemical Laboratory, Lensfield Road, Cambridge CB2 1EW, U.K. Any request should be accompanied by a full literature citation for this communication.

monoselenated cations and anions in **5** form infinite stacks of dimer pairs, without any significant increase in the interlayer separations relative to **6** (intra-dimer separation: 3.54 Å; inter-dimer separation: 4.55 Å in **5**). The interaction between adjacent metallacycles has not been influenced by the introduction of a selenium atom as the synthesis resulted in the selenium being bound to the platinum in a site which does not overlap with adjacent rings.[3] Work on the preparation of the fully substituted $PtSe_2N_2$ analogues and on the use of **4** and **5** in the synthesis of new heterocycles is in progress.

Acknowledgement—We are grateful to Johnson Matthey plc for loans of K_2PtCl_4.

REFERENCES

1. R. Jones, P. F. Kelly, C. P. Warrens, D. J. Williams and J. D. Woollins, *J. Chem. Soc., Chem. Commun.* 1986, 711.
2. R. Jones, C. P. Warrens, D. J. Williams and J. D. Woollins, *J. Chem. Soc., Dalton Trans.* 1987, 907.
3. R. Jones, P. F. Kelly, D. J. Williams and J. D. Woollins, *J. Chem. Soc., Dalton Trans.* 1988, 803.
4. R. Jones, T. G. Purcell, D. J. Williams and J. D. Woollins, *Polyhedron* 1987, **6**, 2165.
5. P. F. Kelly, A. M. Z. Slawin, D. J. Williams and J. D. Woollins, *J. Chem. Soc., Chem. Commun.*, accepted for publication.
6. P. S. Belton, I. P. Parkin, D. J. Williams and J. D. Woollins, *J. Chem. Soc., Chem. Commun.* 1988, 1479.

Polyhedron Vol. 8, No. 17, pp. 2219–2221, 1989
Printed in Great Britain

0277–5387/89 $3.00+.00
© 1989 Pergamon Press plc

COMMUNICATION

COPPER(II) PROMOTED DESULPHURIZATION OF *N*-PHENYLTHIOUREA. THE SYNTHESIS AND X-RAY STRUCTURE OF [{Cu(bipy)(pc)$_2$}$_2$] (bipy = 2,2′-BIPYRIDINE, pc = PHENYLCYANAMIDE)

MARK L. BRADER, ERIC W. AINSCOUGH,* EDWARD N. BAKER and ANDREW M. BRODIE*

Department of Chemistry and Biochemistry, Massey University, Palmerston North, New Zealand

(*Received* 19 *April* 1989; *accepted* 17 *May* 1989)

Abstract—The reaction of *N*-phenylthiourea with a copper(II) acetate/2,2′-bipyridine ethanol solution affords the phenylcyanamide complex, [{Cu(bipy)(pc)$_2$}$_2$] (bipy = 2,2′-bipyridine, pc = phenylcyanamide), and elemental sulphur. An X-ray structure of the phenylcyanamide complex shows it to be a centrosymmetric dimer with each copper having a distorted tetragonal pyramidal geometry. The pc anions exhibit two different coordination modes: (a) monodentate, coordinating through the cyano nitrogen and (b) bidentate, bridging two copper atoms via the cyano and amido nitrogens.

The interaction of thiones, such as heterocyclic thioamides[1] and thioureas,[2] with copper(II) salts normally results in the reduction of the metal and the formation of complexes of copper(I) in which the ligand remains intact. Occasionally copper(II) complexes are obtained.[1–6] However, some exceptions to this reactivity pattern have been reported. For example, the reaction of benzothiazoline-2-thione in chloroform with solid copper(II) perchlorate hexahydrate yields a copper(I) complex containing the trisulphide of the reactant thioamide,[7] and 1-methylimidazoline-2(3*H*)-thione reacts with a variety of copper(II) salts in methanol[8,9] or nitromethane[10,11] to afford copper(II) complexes of the monosulphide, bis(1-methylimidazol-2-yl)sulphide, coordinated as an N-donor chelate. In contrast to these latter results, we have found that while thioazolidine-2-thione in nitromethane is also desulphurized by copper(II), the products are copper(I) or copper(II) complexes of the N,S-chelate, 3-(2-thiazolin-2-yl)thiazolidine-2-thione.[12] As an extension to this work we have examined the reactivity of *N*-phenylthioureas with the copper(II) acetate/2,2′-bipyridine system in ethanol, and report in this paper that the copper(II) promoted desulphurization of the thiourea occurs to afford coordinated phenylcyanamide, as for example in the complex [{Cu(bipy)(pc)$_2$}$_2$] (bipy = 2,2′-bipyridine, pc = phenylcyanamide).

Addition of a solution of *N*-phenylthiourea (0.30 g, 2 mmol) in ethanol (10 cm^3) to a solution of copper(II) acetate monohydrate (0.20 g, 1 mmol) and 2,2′-bipyridine (0.16 g, 1 mmol) in the same solvent (30 cm^3) gave an intense green solution. This was filtered and allowed to stand for a few days whereupon a yellow solid (*ca* 0.02 g), identified as sulphur, on the basis of its IR spectrum and m.p. 111–112°C (ref. 13, 113°C), was deposited. The sulphur was removed by filtration and after a further few days, dark red crystals (0.27 g) were obtained.

The IR spectrum showed the compound did not contain *N*-phenylthiourea since ν(N—H) absorptions in the 3000–3500 cm^{-1} range were absent. Instead, intense bands at 2175, 2147 and 2103 cm^{-1}, characteristic of ν(C≡N) frequencies were observed. The IR spectrum gave no evidence for the presence of the acetate ion, indicating it had been replaced by a new anionic species. Spectroscopic and magnetic data were typical for a

* Authors to whom correspondence should be addressed.

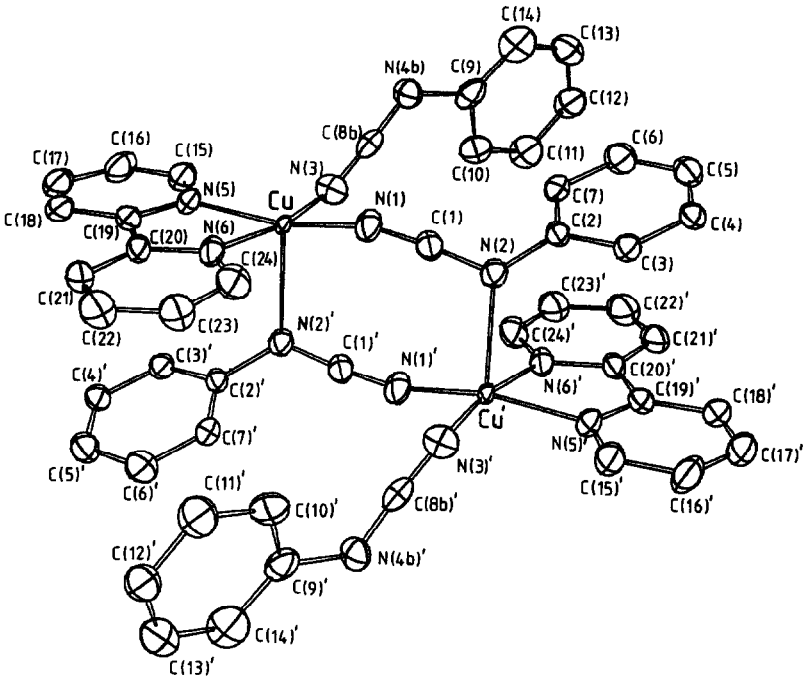

Fig. 1. Structure of $[\{Cu(bipy)(pc)_2\}_2]$. Selected bond lengths (Å) and angles (°) are:

Cu—N(1)	1.938(5)	Cu—N(5)	2.012(5)
Cu—N(2′)	2.355(6)	Cu—N(6)	2.052(5)
Cu—N(3)	1.942(6)		
N(1)—Cu—N(3)	94.3(2)	N(3)—Cu—N(2′)	98.5(2)
N(1)—Cu—N(2′)	99.7(2)	N(3)—Cu—N(5)	92.0(2)
N(1)—Cu—N(6)	92.4(2)		

copper(II) complex (λ_{max}(dimethylsulphoxide) 496 (1900), 658 (400) nm (ε/dm^3 mol^{-1} cm^{-1}); ESR (ethanol, 110 K) g_{11} 2.28, A_{11} 181 × 10^{-4} cm^{-1}, $g_\perp$ 2.07; μ_{eff} 1.98 BM). Microanalytical data* indicated the loss of sulphur. On the basis of these results the dark red compound was formulated as a copper(II)–phenylcyanamide complex with 2,2′-bipyridine as a co-ligand, and this was confirmed in a preparation using phenylcyanamide itself as a starting reagent. The dimeric nature of the complex, *viz.* $[\{Cu(bipy)(pc)_2\}_2]$, and the mode of phenylcyanamide to copper binding were determined from a single-crystal X-ray structure.†

The complex consists of a centrosymmetric dimer (see Fig. 1) with dimerization being achieved via the end-to-end NCN bridging of two phenylcyanamide ligands to the two copper atoms. The two phenylcyanamide ligands in the asymmetric unit exhibit different coordination modes. One is monodentate, coordinating through the terminal cyano nitrogen, N(3), and the other is bidentate, binding to two different copper atoms through the cyano, N(1), and amido, N(2), nitrogen atoms. Each copper atom has a distorted tetragonal geometry. The disorder associated with the N(4) and C(8) atoms of the monodentate phenylcyanamide ligand prevents accurate comparison of its bond parameters with those of the bridging phenylcyanamide. The bond lengths for this latter ligand [N(1)—C(1) 1.169(7), C(1)—N(2) 1.293(7), N(2)—C(2) 1.409(7) Å] suggest, however, that both resonance structures are important, although **A** predominates.

* Found: C, 63.3; H, 4.1; N, 18.4. $C_{24}H_{18}CuN_6$ requires: C, 63.5; H, 4.0; N, 18.5%.

† Crystal data at 153 K for $[\{Cu(bipy)(pc)_2\}_2]$: $C_{48}H_{36}Cu_2N_{12}$, M = 907.0, monoclinic, space group $P2_1/c$, a = 9.625(3), b = 20.945(5), c = 9.956(3) Å, β = 97.10(2)°, V = 1992(1) Å^3, D_c = 1.51 g cm^{-3}, D_o = 1.53 g cm^{-3}, Z = 2, $F(000)$ = 932, λ(Mo-K_α) = 0.71069 Å, μ(Mo-K_α) = 10.63 cm^{-1}; 2702 measured intensities ($5 \leqslant 2\theta \leqslant 45°$), 1689 unique with $I > 3\sigma(I)$. Structure solved by heavy-atom methods and refined by full-matrix least-squares to R = 0.0429 and R_w = 0.0432. The refinement included equally occupied disorder sites for the N(4) and C(8) atoms of the terminal phenylcyanamide ligand, with C(10) as an alternative site for bonding to the phenyl.

Atomic coordinates, bond lengths and angles, and thermal parameters have been deposited at the Cambridge Crystallographic Data Centre.

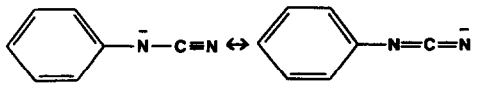

(A) (B)

The desulphurization reaction of *N*-phenylthiourea can be attributed to the redox activity of copper(II). The initial interaction of the thiourea with the copper(II)–bipy system would be expected to lead to an unstable copper(II)–*N*-phenylthiourea complex. The observation of highly coloured transient copper(II)–thiourea species has been noted previously[2,14] and thiourea (tu) itself forms the complex $[Cu(bipy)_2(tu)]ClO_4$ which has been characterized by X-ray crystallography,[4] although the interaction of thioureas with copper(II) normally results in copper(I) compounds.[2] The most likely initial oxidation product of *N*-phenylthiourea is the formamidinium disulphide cation, $[(PhNH)(NH_2)CS—SC(NH_2)(NHPh)]^{2+}$. Disulphide salts of this type have been shown to arise from the oxidation of substituted thioureas with copper(II) perchlorate[14] and are known to decompose in neutral or acidic solution with the precipitation of sulphur.[15] The subsequent re-oxidation of copper(I) to copper(II), in the presence of the formed phenylcyanamide and 2,2′-bipyridine, would yield the characterized complex $[\{Cu(bipy)(pc)_2\}_2]$. A number of halogen-substituted phenyl thioureas also give rise to phenylcyanamide complexes,[16] and it has recently been shown that a similar reaction occurs when unsubstituted thiourea itself reacts with the $[Cu(C_9H_{21}N_3)(H_2O)_2]^{2+}$ ($C_9H_{21}N_3$ = *N*,*N*′,*N*″-trimethyl-1,4,7-triazacyclononane) cation.[17] It would appear, therefore, that the desulphurization of thioureas by copper(II) in the presence of a Lewis base has the potential to provide a convenient route into copper–cyanamide chemistry.

Acknowledgements—We thank the New Zealand University Grants Committee for support and the award of a postgraduate scholarship (to M.L.B.) and Dr W. T. Robinson (University of Canterbury) for the collection of X-ray crystallographic data.

REFERENCES

1. E. S. Raper, *Coord. Chem. Rev.* 1985, **61**, 115.
2. E. A. H. Griffith, W. A. Spofford and E. L. Amma, *Inorg. Chem.* 1978, **17**, 1913.
3. A. Montenero and C. Pelizzi, *Inorg. Chim. Acta* 1972, **6**, 644.
4. M. B. Ferrari, A. B. Corradi, G. G. Fava, C. G. Palmieri, M. Nardelli and C. Pelizzi, *Acta Cryst.* 1973, **B29**, 1808.
5. F. Pavelcik, J. Kratsmar-Smogrovic, O. Svajlenova and J. Majer, *Collect. Czech. Chem. Commun.* 1981, **46**, 3186.
6. M. B. Ferrari, G. G. Fava and A. Montenero, *Cryst. Struct. Commun.* 1975, **4**, 577.
7. S. Jeannin, Y. Jeannin and G. Lavigne, *Inorg. Chem.* 1979, **18**, 3528.
8. D. A. Baldwin, J. C. A. Boeyens, R. G. Copperthwaite, J. H. N. Loubser and A. J. Markwell, *J. Cryst. Spect. Res.* 1984, **14**, 157.
9. D. A. Baldwin, J. C. A. Boeyens, L. Denner and A. J. Markwell, *J. Cryst. Spect. Res.* 1986, **16**, 763.
10. E. W. Ainscough, E. N. Baker, A. G. Bingham and A. M. Brodie, *J. Chem. Soc., Dalton Trans.* 1989, 39.
11. E. W. Ainscough, M. L. Brader, A. M. Brodie and G. J. Gainsford, unpublished results.
12. E. W. Ainscough, B. F. Anderson, E. N. Baker, A. G. Bingham, M. L. Brader, A. M. Brodie and G. J. Gainsford, *Inorg. Chim. Acta* 1985, **105**, L5.
13. R. C. Weast (Ed.), *CRC Handbook of Chemistry and Physics*, 69th edn, p. B-135. CRC Press, Boca Raton, Florida (1988).
14. D. A. Zatko and B. Kratochvil, *Analyt. Chem.* 1968, **40**, 2120.
15. M. Hoffmann and J. O. Edwards, *Inorg. Chem.* 1977, **16**, 3333.
16. M. L. Brader, PhD thesis, Massey University, New Zealand (1988).
17. P. Chaudhuri, K. Weighardt, B. Nuber and J. Weiss, *J. Chem. Soc., Chem. Commun.* 1985, 265.

Polyhedron Vol. 8, No. 17, pp. 2223–2224. 1989
Pergamon Press plc. Printed in Great Britain.

BOOK REVIEW

Advances in Boron and the Boranes. Edited by J. F. Liebman, A. Greenberg and R. E. Williams. VCH Publishers, Weinheim, F.R.G., 1988, 547 pp., $84.00.

A book containing 22 articles on boron chemistry is to be welcomed. This is especially true when it has been compiled in honour of Professor Anton B. Burg, who with H. I. Schlesinger in the 1930s at Chicago University carried out seminal researches on the chemistry of diborane. Indeed, from these early studies stemmed the multifacet chemistry of the boranes and their derivatives as we know it today. For almost 60 years Anton Burg has continued to make significant contributions to our knowledge of the boranes, and in the first chapter of the book he presents an overview of his research and the philosophy behind his endeavours. He omits, however, to refer to his seemingly inexhaustible supply of energy, allowing him to work very long hours with great dedication, and his ability to "inspire" his co-workers to do the same. This Reviewer looks back with amusement to his arrival in sunny Southern California in 1951, an area almost smog free at the time; joining Burg's group, and being told not to allow the climate to interfere with daily attendance in the laboratory.

Among the Contributors to the book are many who have made important contributions to boron chemistry over a long period. The subject matter reviewed and the authors for Chapters 2–22 are as follows:

2. Classical Pentaborane(9) Chemistry Applied to the Preparation of Higher Boron Hydride Systems and Some Newer Aspects of the Chemistry of Pentaborane(9) and Decaborane(14).
   James R. Wermer and Sheldon G. Shore
3. Syntheses and Reactions of 9- and 10-Atom Carboranes and Heteroboranes
   Bohumil Štibr, Jaromír Plešek and Stanislav Heřmánek
4. Palladium- and Platinum-promoted Reactions of Polyhedral Boranes and Carboranes
   Edward W. Corcoran, Jr and Larry G. Sneddon
5. The Elucidation of Cluster Rearrangement Mechanisms Using Isotopically Labeled Boron Hydrides
   Donald F. Gaines, Darrell E. Coons and Joseph A. Heppert
6. Chemistry of Lower Boranes Involving Trimethylphosphine
   Goji Kodama
7. Some Chemistry of the Small Carboranes
   Thomas Onak
8. The Polyhedral Boron Monohalides: Prototypical Electron-deficient Cluster Compounds
   John A. Morrison
9. The Polyborane–Carborane-Carbocation Analogy Extended: New B—H—C Bridge Hydrogen Containing Cations, C—Me—$C_2BH_7^+$ (cf. *arachno*-$B_3H_8^-$), C,C(—Me)$_2$$CBH_4^+$ (cf. *nido*-B_2H_6) and B—Me—C,C′(—t-Bu)$_2$$C_2B$ (cf. $C_3H_3^+$) Confirmed as Carboranes
   Robert E. Williams, G. K. Surya Prakash, Leslie D. Field and George A. Olah
10. Search for Cluster Catalysis with Metallacarboranes
    M. Frederick Hawthorne
11. Synthetic Strategies in Boron Cage Chemistry
    Russell N. Grimes
12. Borane (BH_3) in Unusual Environments
    Thomas D. Fehlner
13. Recent Studies of Thiaboranes and Azaboranes
    Lee J. Todd, Aheda Arafat, Jeff Baer and John C. Huffman
14. Recent Advances in the Chemistry of Main Group Heterocarboranes
    Narayan S. Hosmane and John A. Maguire
15. Pharmacologically Active Boron Analogues of Amino Acids
    Bernard F. Spielvogel
16. Asymmetric Synthesis with Boronic Esters
    Donald S. Matteson
17. The Pyrazaboles
    Kurt Niedenzu
18. Organometallic Chemistry of Strong Acids: From Boron to Carbon
    Allen R. Siedle
19. The Gas Phase Kinetics of Boron and Borane
    S. H. Bauer
20. The Molecular Structures of Boranes and Carboranes
    Robert A. Beaudet
21. Aspects of the Estimation of Physical Properties of Boron Compounds by the Use of Isoelectronic and Plemeioelectronic Analogies
    Joel F. Liebman, James S. Chickos and Jack Simons
22. The Unsynchronized–Resonating–Covalent–Bond

Theory of the Structure and Properties of Boron and the Boranes
Linus Pauling and Zelek S. Herman

Most of the articles focus on the research results of their Authors. In this context, Chapters 2–7, 11, 12, 14 and 20 are essential reading for anyone wishing to keep up with progress at the frontiers of boron chemistry. The Editors are to be congratulated for arranging for the inclusion of such a wealth of material within one book. Moreover, there is a very useful General Index, largely based on compound formulae, which enables a reader to locate subject matter. The book should be available in all libraries claiming to have a modicum of coverage of the chemical "litterature".*

F. GORDON A. STONE
Department of Inorganic Chemistry
The University
Bristol BS8 1TS, U.K.

* As pointed out by A. B. Burg in Chapter 1, the word "litterature" is from the fourth paragraph of the preface to the long novel "Sylvie and Bruno" by Lewis Carroll. It describes the piles of scraps which make up that novel.

Polyhedron Vol. 8, No. 18, pp. 2225–2232, 1989
Printed in Great Britain

0277–5387/89 $3.00+.00
© 1989 Pergamon Press plc

KINETIC STUDY OF THE MOLYBDENUM(VI)–L-HISTIDINE AND MOLYBDENUM(VI)–IMIDAZOLE SYSTEMS

D. O. MÁRTIRE, M. R. FÉLIZ* and A. L. CAPPARELLI†‡

Instituto de Investigaciones Fisicoquimicas Teóricas y Aplicadas (INIFTA), Facultad de Ciencias Exactas, Universidad Nacional de La Plata, Casilla de Correo 16, Sucursal Nro. 4, (1900) La Plata, República Argentina

(*Received* 21 *September* 1988; *accepted after revision* 20 *February* 1989)

Abstract—Using the temperature-jump technique, the study of the kinetics of the complexation of the oxomolybdate anion with l-histidine has been carried out in aqueous solutions at pH 5.0–7.0, ionic strength 0.1 M ($NaClO_4$) and 25°C. A reaction scheme for the formation of the 1 : 1 complex is proposed, which accounts for the observed relaxation rates. This investigation included the study of the polymerization of molybdenum(VI) in the same pH range. The molybdenum(VI)–imidazole system was also studied in order to determine the possible participation of the imidazole nitrogen of histidine in its coordination to molybdenum(VI).

Molybdenum is present in cofactors of several enzymes. Some of them are involved in important biochemical processes such as nitrogen fixation.[1–3] As a result, structural,[4–14] thermodynamic[15–25] and kinetic[26–34] studies of the complexation between molybdate and different chelating ligands have been the subject of several investigations.

The specific reaction between molybdenum(VI) and histidine is of special biochemical interest.[35–37] In the present paper, the kinetics of complex formation between molybdate and histidine at 25°C and ionic strength 0.1 M ($NaClO_4$) was studied. The equilibria of molybdenum(VI) in slightly acid solutions are complex since various polynuclear species are formed. Different sets of species have been proposed in order to assign the equilibria in molybdate solutions.[38–42]

Sasaki and Sillén[39] and Aveston *et al.*[38] proposed the presence of heptameric and octameric species in these solutions. The data of Sasaki and Sillén (μ = 3 M $NaClO_4$, 25°C) and those of Aveston *et al.* (1 M NaCl, 25°C) were more recently re-interpreted.[41,42]

Since the formation of a 1 : 1 complex between molybdate and histidine takes place in the same pH region,[43,44] a kinetic study of this reaction requires the knowledge of the rate constants of the polymerization reactions involved. Honig and Kustin[45] investigated the relaxation kinetics of polymer formation of molybdate using the temperature-jump technique at 25°C and 1.0 M ionic strength. However, since the equilibria involved are strongly dependent on ionic strength,[38,39,42] it is necessary to study the kinetics of the polymerization processes at 0.1 M ionic strength.

Furthermore, the interpretation of Kustin's data was based on the results of Aveston *et al.*[39] According to the new interpretation of Aveston's data,[42] octameric species of molybdenum(VI) should not be considered under the experimental conditions of Kustin's investigation. Such considerations have motivated a kinetic study of molybdenum(VI) polymerization in this work.

The molybdenum(VI)–imidazole system was also studied, in order to determine whether the imidazole nitrogen of this histidine participates in its coordination to molybdate.

EXPERIMENTAL

All the chemicals used were of a reagent grade. Solutions were prepared with de-ionized distilled water.

The ionic strength was maintained at 0.1 M with sodium perchlorate. The pH was adjusted to within pH ±0.02, as read on a Metrohm AG-pH-meter.

* Member of CICPBA.
† Member of CONICET.
‡ Author to whom correspondence should be addressed.

The hydrogen ion concentrations were obtained from pH readings, assuming the activity coefficients of the hydrogen ion to be 0.73 under all experimental conditions of this work.

To obtain unambiguous data, the study of the systems, molybdenum(VI)–histidine and molybdenum(VI)–imidazole, was performed in the presence of excess metal. The reaction was followed by measuring the absorbance change of a pH indicator. The indicators used were phenol red, chlorophenol red and tymol blue.

The temperature-jump equipment consisted of the SBA-7 model from Studientgesellschaft mbH Gottingen, F.R.G., with spectrophotometric detection. The temperature jump was 5°C and the final temperature 25°C. The temperature of the reaction solution was controlled to ± 0.2°C using a thermoelectric circulating bath.

The relaxation times, obtained from an average of at least four relaxation curves, are affected by a maximum uncertainty of $\pm 10\%$.

RESULTS

The results obtained with the three systems will be discussed separately in the following sections.

(I) *Polymerization of molybdenum*(VI)

The traces obtained in these experiments showed the presence of only one relaxation process. The experimentally determined relaxation time for the reaction is summarized in Table 1. Above pH 6 no relaxation processes were detected. The equilibria involved in the polymerization of molybdate have not been studied at 0.1 M ionic strength.

According to the re-interpretation of the data of Aveston *et al.*[42] ($\mu = 3$ M) and those of Sasaki and Sillén[41] ($\mu = 1$ M), only monomeric and heptameric species of molybdate should be present within the molybdate concentration and pH ranges of the present work.

It is known that the stability of polymeric species increases with increasing ionic strength. The effect of the ionic medium on condensation equilibria was ascribed by several authors to the complexation between medium cations and highly charged polymetalate anions[38,46,47] or to decreased water activity.[42]

The dependence of these equilibria on the medium leads us to assume that under the conditions of the present investigation ($\mu = 0.1$ M), the only polymeric species are those postulated at ionic strength 1 M.[41] In this way, the molybdate equilibria can be written as shown:

Table 1. Study of condensation reactions of molybdate at 25°C and 0.1 M ionic strength. Experimental and calculated relaxation times

pH	InH	$[Mo]_0 \times 10^2$ (M)	τ_{exp} (ms)	$(1/\tau)$ $(s^{-1})^a$
5.20	CR	1	8.18	122 (113)
5.33	CR	1	8.92	112 (112)
5.37	CR	1.5	6.67	150 (141)
5.38	CR	0.8	17.6	56.8 (62.1)
5.45	CR	1	12.6	79.4 (67.9)
5.50	CR	1.5	7.80	128 (122)
5.51	CR	2	6.64	151 (164)
5.57	PR	1	25.0	40.0 (36.3)
5.60	CR	1.5	19.7	50.8 (69.8)
5.65	PR	2	9.84	102 (107)
5.67	CR	2	10.2	97.9 (92.8)
5.82	CR	1.5	38.8	25.7 (30.1)
5.88	PR	2	28.8	34.7 (31.8)
5.88	PR	3	16.6	60.1 (60.7)

τ_{exp}—experimental relaxation times. PR—phenol red, CR—chlorophenol red, $[Mo]_0$ is the analytic concentration of molybdenum(VI)

[a] The quantities in parentheses are reciprocal calculated relaxation times.

$$MoO_4^{2-} + H^+ \rightleftharpoons MoO_4H^- \quad (K_1) \qquad (1)$$

$$7MoO_4^{2-} + 8H^+ \rightleftharpoons Mo_7O_{24}^{6-} + 4H_2O \quad (K_6) \qquad (2)$$

$$Mo_7O_{24}^{6-} + H^+ \rightleftharpoons Mo_7O_{24}H^{5-} \quad (K_3). \qquad (3)$$

Scheme 1.

The protolytic reactions are very rapid, so that they may be assumed to be equilibrated at all times compared with reaction (2).

The relaxation time derived for this mechanism is

$$1/\tau = k_6 X + k_{-6} \qquad (4)$$

where:

$$X = 8[M]^7[H]^7(-\delta H/\delta Hept) + 7[H]^8[M]^6(-\delta M/\delta Hept), \qquad (5)$$

with $Hept = Mo_7O_{24}^{6-}$.

The expressions for $(-\delta H/\delta Hept)$ and $(-\delta M/\delta Hept)$ were derived as in ref. 45 and are given in Appendix 1.

The equilibrium constants used in the analysis of the experimental data are presented in Table 2. Concentrations were calculated on a computer using a Newton Raphson iteration.

The values of K_6 and K_3 are not known under the present experimental conditions. They were handled as parameters, taking as entry values those at $\mu = 1$ M.[42]

Table 2. Equilibrium constants used in this work

Reaction	log K
$MoO_4^{2-} + H^+ \rightleftharpoons MoO_4H^-$	3.74[a]
$MoO_4H^- + H^+ \rightleftharpoons MoO_4H_2$	3.77[a]
$7MoO_4^{2-} + 8H^+ \rightleftharpoons Mo_7O_{24}^{6-} + 4H_2O$	52.03[a]
$Mo_7O_{24}^{6-} + H^+ \rightleftharpoons Mo_7O_{24}H^{5-}$	4.78[b]
$hist^- + H^+ \rightleftharpoons histH$	8.87[c]
$histH + H^+ \rightleftharpoons histH_2$	14.90[c]
$histH_2 + H^+ \rightleftharpoons histH_3$	16.61[c]
$MoO_4^{2-} + hist^- + 2H^+ \rightleftharpoons MoO_3hist^- + H_2O$	16.76[c]
$PR^- + H^+ \rightleftharpoons PRH$	7.95[d]
$CR^- + H^+ \rightleftharpoons CRH$	9.0[e]
$TB^- + H^+ \rightleftharpoons TBH$	5.9[e]

hist—histidinate, RF^-, CR^- and TB^-—the basic forms of the indicators phenol red, chlorophenol red and tymol blue, respectively.

[a] A. E. Martell and R. M. Smith, *Critical Stability Constants*, Vol. 5, Supplement. Plenum Press, New York (1982).

[b] Values which best fit the experimental kinetic data.

[c] Reference 44.

[d] H. Ushio, H. Trimm, R. Patel and M. Zemany, *J. Chem. Sol.* 1981, **10**, 39.

[e] H. Strehlow and W. Knoche, *Relaxation Chemical Kinetics*. Springer, Berlin (1977).

As was expected, the value of K_6 which best fitted the experimental data was lower than that at $\mu = 1.0$ M. A least-squares analysis has been carried out on the data shown in Table 1 to determine the best values of the rate parameters in eq. (5). The values thus obtained are $k_6 = (6.09 \pm 0.37) \times 10^{52}$ and $k_{-6} = 28.7 \pm 4.2$. The correlation coefficient was 0.98.

Honig and Kustin's data[45] could be re-analysed on the basis of the set of monomeric and heptameric species proposed by Cruywagen and co-workers[42] for this system under the same experimental conditions. These are the species shown in Scheme 1. Thus the reaction shown in Scheme 1 could also describe the behaviour of these data.

Honig and Kustin[45] observed two relaxation times in some experiments, the relative error being $\pm 25\%$ for the longer and $\pm 50\%$ for the shorter one, but both being of the same order of magnitude. This implies that the existence of the shorter relaxation time is indeed doubtful. In this case, we could re-interpret Kustin's data on the basis of Scheme 1 by considering the longer relaxation time for those experiments where two relaxation times were reported.

A least-squares analysis on Kustin's $1/\tau$ against X determined the following values for k_6 and k_{-6}:

$$k_6 = 9.8 \times 10^{52} \quad (6)$$

$$k_{-6} = 16.4, \quad (7)$$

with a correlation coeffcient of 0.99.

(II) *Molybdenum*(VI)–*histidine system*

Histidine-indicator blanks were run at each pH. The results were negative. The extension of the pH range above 6 suggests the molybdenum(VI)–histidine interaction. Since polymerization reactions are not observed above pH 6, experiments will be separated into two groups: (a) pH > 6 and (b) pH < 6.

(a) pH > 6. Experimental relaxation rates belonging to this pH zone are summarized in Table 3. The magnitude of the relaxation amplitudes increases with increasing molybdate concentration and with decreasing pH. Above pH 6.8, the amplitude of relaxation curves is very small.

Johansen and Jones[44] found the following stoichiometry for complex formation:

$$MoO_4^{2-} + L^- + 2H^+ \rightleftharpoons MoO_3L^- + H_2O, \quad (8)$$

where L^- denotes histidinate.

The stoichiometry allows at least two possible reaction pathways which are shown in the following scheme:

$$MoO_4^{2-} + LH_2^+ \underset{k_{-1}}{\overset{k_1}{\rightleftharpoons}} MoO_3L^- + H_2O \quad \text{(a)} \quad (9)$$

$$MoO_4H^- + LH \underset{k_{-2}}{\overset{k_2}{\rightleftharpoons}} MoO_3L^- + H_2O \quad \text{(b)}, \quad (10)$$

Table 3. Study of the complexation of molybdenum(VI) with histidine (pH > 6)

pH	InH	[Mo] × 10^2 (M)	τ_{exp} (ms)	$1/\tau$ (s^{-1})[a]
6.00	PR	3	29.7	33.6 (35.1)
6.10	TB	2	45.6	21.9 (24.8)
6.11	CR	3	33.0	30.3 (30.5)
6.15	CR	2	42.7	23.4 (23.8)
6.20	PR	2	45.3	22.1 (22.6)
6.22	CR	3	32.1	31.1 (26.7)
6.23	PR	1	70.0	14.3 (18.0)
6.35	TB	0.8	65.1	15.4 (17.4)
6.35	PR	3	41.3	24.2 (23.1)
6.37	CR	1	56.2	17.8 (17.9)
6.41	CR	2	48.5	20.6 (19.7)
6.47	CR	3	45.1	22.2 (21.1)
6.55	PR	2	45.0	22.2 (18.4)

[a] The quantities in parentheses are reciprocal calculated relaxation times. For abbreviations see Table 1. In the pH range 6.6–7.00, the measured relaxation amplitudes are too small to obtain reliable relaxation times. At higher pH, no relaxation processes are detected.

where only the reactant species present at major concentrations were included. Reactions (a) and (b) are indistinguishable.

Assuming protolytic reactions to be equilibrated, the following expression for $1/\tau$ can be obtained:

$$1/\tau = k_F([M](-\delta LH_2/\delta C)+[LH_2](-\delta M/\delta C)) + k_R = k_F Y + k_R, \quad (11)$$

where

$$k_F = k_1 + k_2 K_3/K_4 \quad (12)$$

$$k_R = k_{-1} + k_{-2} \quad (13)$$

and

$$K_3 = [LH][H]/[LH_2] \quad (14)$$

$$K_4 = [M][H]/[MH]. \quad (15)$$

Application of mass balance and equilibrium conditions for the protolytic reactions leads to the following expressions for $\delta M/\delta C$ and $\delta LH_2/\delta C$.

$$\delta LH_2/\delta C = (-1+(d_1+[H][LH])/\Delta) \quad (16)$$

$$\delta M/\delta C = -(1+\delta MH/\delta C), \quad (17)$$

with

$$\Delta = d_1 - [H]d_2 \quad (18)$$

$$d_1 = K_3(\beta K_4+[M])+[LH]K_4+[H]([LH]+\beta K_3) \quad (19)$$

$$d_2 = [M]+\beta(K_4+[H]) \quad (20)$$

$$\beta = (K_5+[H]+[I])/(K_5+[H]) \quad (21)$$

and

$$\delta MH/\delta C = [H]([LH]-[M]) + \beta[H](K_3+[H])/\Delta. \quad (22)$$

Experimental $1/\tau$ against Y are plotted in Fig. 1. The experimental $1/\tau$ values were treated with a linear least-squares routine to obtain the best fit rate constants. These constants are

$$k_F = (1.4\pm0.2)\times10^3 M^{-1}s^{-1} \quad (23)$$

$$k_R = (15.8\pm1.2)s^{-1}. \quad (24)$$

From these experimental rate constants, the following limit values for k_1, k_2, k_{-1} and k_{-2} can be obtained

$$k_1 \leqslant 1.4\times10^3 \quad (25)$$

$$k_2 \leqslant 7.2\times10^5 \quad (26)$$

$$k_{-1} \leqslant 15.8 \quad (27)$$

$$k_{-2} \leqslant 15.8. \quad (28)$$

(b) pH < 6. Experimental relaxation times belonging to this pH zone are summarized in Table 4. Despite the presence of heptamers below pH 6, according to Johansen and Jones, a 1 : 1 complex between molybdate and histidine is formed. Then, monomeric molybdate should be the active species of molybdenum(VI). Since the polymerization mechanism is known (see above), the complete mechanism should be given by the following scheme:

$$M+LH_2 \rightleftharpoons C+H_2O \quad (K_2) \quad (29)$$

$$MH+LH \rightleftharpoons C+H_2O \quad (30)$$

$$MH \rightleftharpoons M+H \quad (K_I^{-1}) \quad (31)$$

$$7M+8H^+ \rightleftharpoons Hept+4H_2O \quad (K_6) \quad (32)$$

$$HeptH \rightleftharpoons Hept+H \quad (K_d), \quad (33)$$

where only the specis of higher concentrations were included.

The assumption of rapid protolytic reactions allows the system to be described by two rate equa-

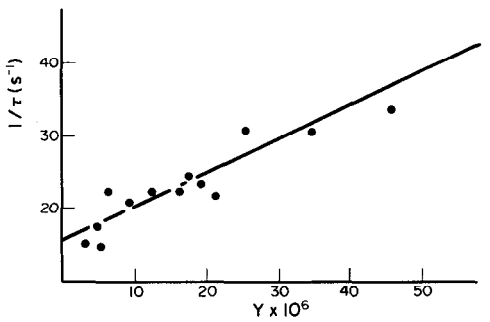

Fig. 1. Molybdenum(VI)–L-histidine system: experimental relaxation rate ($1/\tau$) vs Y, as given by eq. (11).

Table 4. Study of complexation of molybdenum(VI) with histidine: experimental and calculated relaxation times (pH < 6)

pH	InH	$[M]_0\times10^2$ (M)	τ_1 (ms)	τ_2 (ms)	τ_{exp} (ms)
5.39	CR	2	48	5.3	6.1
5.55	CR	2	45	6.7	6.5
5.60	PR	1	79	30	30
5.75	CR	2	62	26	12
5.85	CR	3	47	24	18
5.86	CR	1	120	32	20
5.88	TB	2	130	32	34
5.92	PR	2	150	32	35
6.00	PR	3	220	32	30

τ_1 and τ_2—calculated relaxation times, τ_{exp}—experimental relaxation time. For other abbreviations see Table 1.

tions,

$$d\delta C/dt = k_F([M]\delta LH_2 + [LH_2]\delta M) - k_R\delta C \quad (34)$$

$$d\delta Hept/dt = k_6(8[M]^7[H]^7\delta H + 7[H]^8[M]^6\delta M) - k_{-6}\delta Hept. \quad (35)$$

The reciprocal relaxation times[48] are given by

$$1/\tau_{+,-} = 1/2\left(-(a_{11}+a_{22}) \pm \sqrt{(a_{11}+a_{22})^2 - 4(a_{11}a_{22}-a_{12}a_{21})}\right). \quad (36)$$

The expressions for the a_{ij} terms are given in Appendix 2.

Even though a system of coupled reactions can give rise to two relaxation times, only one may be observed.[48,49]

The values for τ_+ and τ_- are also summarized in Table 4. As can be seen in Table 4, we are observing τ_-, whose main contribution arises from the polymerization steps.

This observation does not necessarily mean that the complexation between molybdate and histidine is unimportant; it only means that the observed response is only sensitive to the polymerization pathway. The fit of τ_{exp} to τ_- is reasonably good.

(III) *Molybdenum*(VI)–*imidazole system*

Experimental relaxation times are summarized in Table 5. As can be seen in Table 5, relaxation processes are observed in the same pH region in which the polymerization of molybdenum(VI) occurs. Above pH 6, no relaxation curves were detected. This behaviour suggests that in both systems the process which is responsible for the relaxation may be the same. Then, eq. (5) should be valid for the experimental data.

The experimental $1/\tau$ values are plotted against X in Fig. 2. The following values for k_6 and k_{-6} were calculated by a least-squares treatment of the data

$$k_6 = (6.12 \pm 0.52) \times 10^{52} \quad (37)$$

$$k_{-6} = (37.8 \pm 5.3). \quad (38)$$

Table 5. Kinetic study of the molybdenum(VI)–imidazole system: experimental and calculated relaxation times

pH	InH	$[M]_0 \times 10^2$ (M)	τ_{exp} (ms)	$1/\tau$
5.15	CR	1	8.36	120 (133)
5.20	CR	1	7.75	129 (134)
5.27	CR	1	7.33	136 (131)
5.33	CR	1	8.33	120 (120)
5.45	PR	1	9.47	105 (73.6)
5.48	CR	1	12.4	80.5 (62.5)
5.50	PR	1	13.3	75.3 (56.9)
5.51	CR	1.5	7.93	126 (124)
5.55	CR	2	6.11	164 (167)
5.60	PR	1	40.8	24.5 (42.0)
5.62	CR	1.5	12.8	78.4 (67.3)
5.67	CR	2	10.7	93.5 (98.4)
5.80	CR	2	27.9	35.8 (48.1)
5.82	CR	1.5	38.8	25.8 (39.1)
5.88	PR	2	28.8	34.7 (40.7)
5.00	PR	3	16.6	60.1 (60.3)
5.89	PR	3	16.7	59.7 (64.2)

For abbreviations see Table 1.

Although polymerization is the process responsible for relaxation, the existence of a complex between molybdenum(VI) and imidazole could be possible. To discard this possibility, the quantity X was recalculated assuming a 1 : 1 complex between both reactives. However, the best fit of the experimental data was found when the equilibrium constant for the complex formation tended to zero. This behaviour shows that under these experimental conditions, there is no complexation between molybdenum(VI) and imidazole. Furthermore, to our knowledge, no complexes of this ligand with molybdenum(VI) have been reported.

DISCUSSION

The histidine molecule presents three potential coordination sites in aqueous solution. The carboxyl group, the imidazole nitrogen and the amino

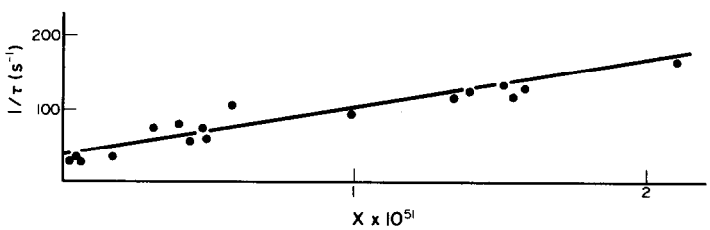

Fig. 2. Molybdenum(VI)–imidazole system: experimental relaxation rate ($1/\tau$) vs X, as given by eq. (5).

nitrogen become available for complexation as the pH increases.

Spence and Lee[43] found no evidence of complex formation between molybdenum(VI) and the compounds L-alanine or N-acetyl-L-histidine. But, for the L-histidine methyl ether,[43] they obtained very similar results to those of histidine. According to their observations, these authors propose that histidine acts as a bidentate ligand and uses the amino group and the 1-nitrogen of the imidazole ring for complex formation with molybdenum(VI).

The lack of imidazole reactivity which was found in the present paper, can also be attributed to the need of both the amino and imidazole nitrogens to be present in the ligand to form the complex.

Wilkins and co-workers[10] proposed that histidine behaves as a tridentate ligand towards molybdenum(VI) in the solid phase.

The complexation of molybdate with L-histidine shows the following features:

—two protons are required according to reaction (8). To account for this stoichiometry, reaction pathways (a) and (b) are proposed. Both reactions are indistinguishable.

—thermodynamic as well kinetic results show that no complexation takes place above pH 7. The postulation of MoO_4H^- as a reactive species has been considered in the literature, even at higher pH.[27,28,33] If the contribution of reaction pathway (b) was significant, complexation should take place in basic solutions. However, as stated, no complex is formed above pH 7. Therefore, it can be inferred that reaction (b) should not significantly contribute to the reaction rate.

The previous considerations leave LH_2^+ as the ligand reactive species and $k_F = k_1$. The complete ionization scheme for histidine is shown in Fig. 3.

According to this scheme, there are three LH_2^+

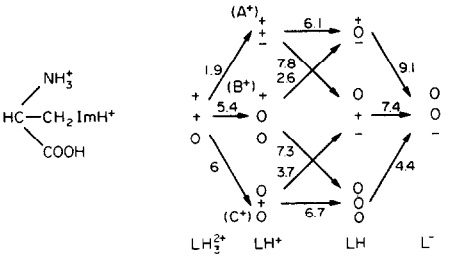

Fig. 3. Ionization scheme for histidine. The microscopic pK values were taken from ref. 50.

Table 6. Experimental kinetic values for 1 : 1 molybdate complex formation

Ligand	Species	pK	k_1	log k_1
Pyrogallol	LH_2^-	11.43[a]	130[c]	2.11
Pyrogallol	LH_3	9.28[a]	1.1×10^3[c]	3.04
Epinephrine	LH_2^-	10.0[a]	3.8×10^2[c]	2.58
Epinephrine	LH_3	8.7[a]	7.2×10^2[c]	2.86
Oxine	LH	9.57[a]	4.1×10^2[c]	2.61
Oxine	LH_2^+	4.96[a]	5.0×10^5[c]	5.70
Oxine-5-SO_3	LH^-	8.21[a]	2.5×10^3[c]	3.40
Oxine-5-SO_3	LH_2	3.89[a]	5.0×10^6[c]	6.70
as	LH_2^-	5.32[a]	7.1×10^4[a]	4.85
Citric acid	LH^{2-}	5.69[b]	1.03×10^4[f]	4.01
Malic acid	LH^-	4.71[b]	8.3×10^5[g]	5.92
thb	LH_2^-	11.82[a]	79[c]	1.82
thb	LH_3	9.08[a]	5.5×10^2[c]	2.74
Catechol	LH_2	9.54[a]	300[h]	2.48
L-dopa	LH^{3-}	9.78[a]	330[c]	2.52

as—alizarinsulphonic acid. thb—1,2,4-trihydroxybenzene.

[a] Reference 29.

[b] A. E. Martell and R. M. Smith, *Critical Stability Constants*, Vol. 5, 1st Supplement. Plenum press, New York (1982).

[c] Reference 26.

[d] Reference 27.

[e] Reference 28.

[f] Reference 33.

[g] Reference 34.

[h] Reference 31.

species (A, B and C). However, the concentration of A is at least 10^3 times higher than those of B and C.[50] Then, the limit value of the rate constant k_1, should be assigned to the following reaction:

$$MoO_4^{2-} + H_3N{-}\underset{\displaystyle COO^-}{\underset{|}{CH}}{-}CH_2{-}ImH^+ \underset{k_{-1}}{\overset{k_1}{\rightleftharpoons}} C + H_2O, \quad (39)$$

where Im denotes the imidazole ring. This means that the active species of the ligand has protonated both amino and imidazole nitrogens.

Until recently, only two empirical correlations between the rate constants of molybdenum(VI) complex formation and basicity of ligands were discussed in the literature.[26,29]

We recently predicted, [34] on theoretical grounds, a correlation between $\log k_1$ (k_1 is the rate constant of the reaction between MoO_4^{2-} and the monoprotonated ligand) and the pK of the ligand. This correlation is based on an associative mechanism, where a chelating group attacks at one of the faces of the tetrahedral molybdate.[29–34] Another chelating group, which is protonated, interacts with an oxo group, the reaction being controlled by the proton transfer from the ligand to an oxo group. This process weakens the Mo—O bond, thus allowing the coordination sphere expansion.

If the determining step is the deprotonation of one of the sites of the ligand, the reaction rate should be dependent on the ligand nature and, to some extent, independent of the degree of protonation of other chelating sites of the ligand. Therefore, the correlation found in the literature,[34] could be extended to include all active species, LH_n, for a given ligand. The available values of experimental kinetic rate constant values (k) for 1 : 1 molybdate complex formation are presented in Table 6. The correlation equation found is shown below

$$\log k = -0.57\text{p}K + 8.23, \quad (40)$$

where the pK vaues are those corresponding to the deprotonation of the chelating group involved in the limiting reaction step.[34]

This correlation enables us to predict the value of $\log k$ for the molybdenum(VI)–histidine complex. If we attribute the rate-determining step to the deprotonation of the imidazole nitrogen (pK = 6.03), the expected value of $\log k$ is 4.79. On the other hand, if the determining step is attributed to deprotonation of amino nitrogen (pK = 8.87), the value of $\log k$ predicted by the correlation is 3.17. Since the upper limit value determined in the present paper is 3.14, we propose the deprotonation of the amino nitrogen as the rate-determining step.

Acknowledgements—This work was supported in part by the Consejo Nacional de Investigaciones Cientificas y Técnicas de la República Argentina (CONICET) and Comisión de Investigaciones Cientificas de la Provincia de Buenos Aires (CICPBA). Some of the equipment and drugs used in the present work were provided by the cooperation agreement between the University of Mainz and the Universidad Nacional de La Plata. One of the authors (D.O.M.) wishes to thank the CICPBA for a Research Studentship. The authors are grateful to Dr J. Czarnowski for comments on the manuscript.

REFERENCES

1. E. Ochiai, *Química Bioinorgànica* Reverté, Madrid (1985).
2. R. A. D. Wentworth, in *Progress in Inorganic Chemistry* (Edited by J. Lippard), Vol. 22, p. 1. John Wiley, New York (1980) and refs cited therein.
3. V. K. Shah, R. Ugalde, J. Imperial and E. Brill, *Ann. Rev. Biochem.* 1984, **53**, 231.
4. R. J. Kula, *An. Chem.* 1966, **38**, 1383.
5. M. M. Caldeira, M. L. Ramos and V. M. S. Gill, *Can. J. Chem.* 1987, **65**, 827.
6. M. M. Caldeira and V. M. S. Gil, *Polyhedron* 1986, **5**, 381.
7. M. M. Caldiera, M. E. Saraiva and V. M. S. Gil, *Inorg. Nucl. Chem. Lett.* 1981, **17**, 295.
8. M. M. Caldeira and V. M. S. Gil, *Can. J. Chem.* 1984, **62**, 2094.
9. I. I. Somova, Y. E. Tselinskii, M. V. Mokhosoev and O. P. Karpov, *Russ. J. Inorg. Chem.* 1974, **19**, 41.
10. R. J. Butcher, H. K. J. Powell, C. J. Wilkins and S. H. Yong, *J. Chem. Soc., Dalton Trans.* 1976, 356.
11. Y. A. Buslaev and R. L. Davidovich, *Russ. J. Inorg. Chem.* 1968, **13**, 656.
12. O. A. Rajan and A. Chakravorty, *Inorg. Chem.* 1981, **20**, 660.
13. W. P. Griffith, *J. Chem. Soc. A* 1969, 211.
14. D. O. Mártire, M. R. Féliz and A. L. Capparelli, *Z. Physik Chem.*, in press.
15. M. Cadiot and B. Viossat, *Rev. Chem. Miner.* 1969, **6**, 727.
16. R. A. Chalmers and A. G. Sinclair, *J. Inorg. Nucl. Chem.* 1967, **29**, 2065.
17. A. A. Fedorov, *Zh. Anal. Khim.* 1974, **29**, 891.
18. A. A. Fedorov, *Zh. Obshch. Khim.* 1975, **45**, 1072.
19. J. J. Cruywagen and R. F. Van der Water, *Polyhedron* 1986, **5**, 521.
20. M. Bartusek, J. Havel and D. Matula, *Coll. Czech. Chem. Commun.* 1986, **51**, 2702.
21. A. Beltrán, *J. Inorg. Nucl. Chem.* 1981, **43**, 1337.
22. N. Stolica, in *Standard Potentials in Aqueous Solution* (Edited by A. Bard, R. Parsons and J. Jordan). IUPAC, M. Dekker, New York (1985).
23. E. R. Clark, *J. Inorg. Nucl. Chem.* 1962, **24**, 1381.
24. M. J. Baillie and D. H. Brown, *J. Chem. Soc.* 1961, 3691.
25. A. A. Fedorov and A. V. Pavlinova, *Zh. Obshch. Khim.* 1972, **42**, 238.

26. K. Kustin and K. Gilbert, *J. Am. Chem. Soc.* 1976, **98**, 5502.
27. P. F. Knowles and H. Diebler, *Trans. Faraday Soc.* 1968, **64**, 977.
28. H. Diebler and R. Timms, *J. Chem. Soc. A* 1971, 273.
29. S. Funahashi, Y. Kato, M. Nakayama and M. Tanaka, *Inorg. Chem.* 1981, **20**, 1752.
30. D. S. Honig and K. Kustin, *J. Phys. Chem.* 1972, **41**, 215.
31. K. Kustin and S. T. Liu, *J. Am. Chem. Soc.* 1973, **95**, 2487.
32. D. S. Honig and K. Kustin, *J. Am. Chem. Soc.* 1973, 5525.
33. D. Mártire, M. Féliz and A. Capparelli, *An. Asoc. Quim. Arg.* 1987, **76**, 601.
34. D. Mártire, M. Féliz and A. Capparelli, *Polyhedron* 1988, **7**, 2709.
35. J. T. Spence, in *Reactivity of Coordination Compounds* (Edited by H. Sigel), Vol. 5 (Metal Ions in Biological System Series). M. Dekker, New York (1976).
36. O. M. Aguilar, H. Remlaender, W. Arnold and A. Peuhler, *J. Bacteriol.* 1987, **169**, 5393.
37. R. Ugalde, J. Imperial, U. K. Shah and W. Brill, *J. Bacteriol.* 1984, **159**, 888.
38. J. Aveston, E. W. Anacker and J. S. Johnson, *Inorg. Chem.* 1964, **3**, 735.
39. Y. Sasaki and L. G. Sillén, *Ark. Kemi* 1968, 253.
40. Y. Sasaki, L. Lindquist and L. G. Sillén, *J. Inorg. Nucl. Chem.* 1959, **9**, 93.
41. K. H. Tytko, G. Baethe, E. R. Hirschfelder, M. Mehmke and D. Stellhorn, *Z. Anorg. Allg. Chem.* 1983, **503**, 43.
42. K. H. Tytko, G. Beathe and J. J. Cruywagen, *Inorg. Chem.* 1985, **24**, 3132.
43. J. T. Spence and J. Y. Lee, *Inorg. Chem.* 1965, **4**, 385.
44. E. S. Johansen and O. Jons, *Acta Chem. Scand.* 1981, **A35**, 233.
45. D. S. Honig and K. Kustin, *Inorg. Chem.* 1972, **11**, 65.
46. W. G. Baldwin and G. Wiesc, *Ark. Kemi* 1968, **31**, 419.
47. G. Wiese and D. Bose, *Z. Naturforsch. B, Anorg. Chem. Org. Chem.* 1974, **29B**, 630.
48. M. Eigen and L. De Maeyer, *Theoretical Basis of Relaxation Spectrometry in Techniques of Chemistry* (Edited by G. G. Hammes), Vol. VI, Part II. Wiley-Interscience, New York (1974).
49. G. Schwarz, *Rev. Mod. Phys.* 1968, **40**, 206.
50. R. J. Sundberg and R. Bruce Martin, *Chem. Rev.* 1974, **74**, 471.

APPENDIX I

From conservation conditions of metal, protons and indicator, the following equations can be written:

$$\delta M/\delta Hept = (X_2X_6 - X_3X_5)/\Delta \quad (A1.1)$$

$$\delta H/\delta Hept = (X_3X_4 - X_1X_6)/\Delta, \quad (A1.2)$$

where

$$X_1 = 1 + K_1[H] \quad (A1.3)$$

$$X_2 = K_1[M] + 7K_3[Hept] \quad (A1.4)$$

$$X_3 = 7(1 + K_3[H]) \quad (A1.5)$$

$$X_4 = K_1[H] \quad (A1.6)$$

$$X_5 = \beta + K_1[M] + 9K_3[Hept] \quad (A1.7)$$

$$X_6 = 8 + 9K_3[H], \quad (A1.8)$$

with

$$\Delta = 1 + K_1[H] + K_1[M] + 9K_3[Hept] + 2K_1K_3[H][Hept] \quad (A1.9)$$

$$\beta = (K_5 + [H] + [I])/(K_5 + [H]) \quad (A1.10)$$

and

$$K_5 = [I][H]/[IH]. \quad (A1.11)$$

APPENDIX II

From conservation relations for the molybdate, hydrogen and indicator, and assuming rapid protolytic equilibra, the following relations can be written:

$$a_{11} = k_F([M]T_1 + [LH_2]Z_1) - k_R \quad (A2.1)$$

$$a_{12} = k_F([M]T_2 + [LH_2]Z_2) \quad (A2.2)$$

$$a_{21} = k_6(8[M]^7[H]^7Y_1 + 7[H]^8[M]^6Z_1) \quad (A2.3)$$

$$a_{22} = k_6(8[M]^7[H]^7Y_2 + 7[H]^8[M]^6Z_2) - k_{-6}, \quad (A2.4)$$

where

$$T_1 = R_1K_6[H] + 2[L][H]K_6Y_1 \quad (A2.5)$$

$$T_2 = R_2K_6[H] + 2[L][H]K_6Y_2 \quad (A2.6)$$

and

$$Z_1 = (X_3X_9 + X_1X_6 - X_2X_9)/\Delta \quad (A2.7)$$

$$Z_2 = (X_5(X_1X_6 - X_2X_9) - X_1X_3X_8)/\Delta \quad (A2.8)$$

$$Y_1 = -(X_4X_9 + X_1X_7)/\Delta \quad (A2.9)$$

$$Y_2 = X_1(X_4X_8 - X_5X_7)/\Delta \quad (A2.10)$$

$$R_1 = (-X_3X_7 + X_4X_6 + X_2X_7)/\Delta \quad (A2.11)$$

$$R_2 = X_2(X_5X_7 - X_4X_8)/\Delta \quad (A2.12)$$

$$\Delta = X_1(X_3X_7 - X_4X_6) + X_2X_4X_9 \quad (A2.13)$$

with

$$X_1 = 1 + K_d[H] + K_6[H]^2 \quad (A2.14)$$

$$X_2 = [L](K_d + 2K_6[H]) \quad (A2.15)$$

$$X_3 = K_1[M] + 7K_3[Hept] \quad (A2.16)$$

$$X_4 = 1 + K_1[H] \quad (A2.17)$$

$$X_5 = 7(1 + K_3[H]) \quad (A2.18)$$

$$X_6 = 1 + \alpha + K_1[M] + 9[Hept]K_3 + K_d[L] + 4[L][H]K_6 \quad (A2.19)$$

$$X_7 = K_1[H] \quad (A2.20)$$

$$X_8 = 8 + 9K_3[H] \quad (A2.21)$$

$$X_9 = K_d[H] + 2K_6[H]^2 \quad (A2.22)$$

$$\alpha = ([IH] + [I])K_5/([H] + K_5)^2. \quad (A2.23)$$

Polyhedron Vol. 8, No. 18, pp. 2233–2236, 1989
Printed in Great Britain

0277–5387/89 $3.00+.00
© 1989 Pergamon Press plc

THERMODYNAMIC PROPERTIES OF ACTINIDE COMPLEXES. URANYL(VI)– AND THORIUM(IV)–ASPARTATE SYSTEMS

ARTURO BISMONDO* and LUIGI RIZZO

Istituto di Chimica e Tecnologia dei Radioelementi, Area della Ricerca del CNR, Corso Stati Uniti 4, 35020 Padova, Italy

(*Received* 29 *September* 1988; *accepted after revision* 22 *March* 1989)

Abstract—Stability constants, enthalpies and entropies in the formation of uranyl(VI) and thorium(IV) with aspartic acid have been determined at 25.0°C in a 1.0 mol dm^{-3} aqueous solution of sodium perchlorate by means of the potentiometric and calorimetric techniques. Because of precipitation of solid compounds, only two complexes of 1 : 1 and 1 : 2 stoichiometry were observed in the uranyl(VI)–asparate system and only one complex of 1 : 1 stoichiometry in the thorium(IV)–aspartate system. Comparison of values of stability constants and enthalpy and entropy changes with the corresponding values of some mono- and di-carboxylate ligands suggests that the binding of both metal ions involves one carboxylate group only, the one furthest from the positive amino group.

In previous works we have reported the changes in the thermodynamic functions for the uranyl(VI) and thorium(IV) complex formation with some aminomonocarboxylate ligands.[1–3] From the values of the stability constants and enthalpy and entropy changes, it was deduced that those ligands bind to metal ion through the carboxylate group only, whereas the amino group, in the experimental conditions used, is protonated. We have examined the coordination behaviour of some amino acids, which have two carboxylic groups in the chain, in order to evaluate the influence of another group on the capacity of amino acids to form stable bonds to actinide ions. For this purpose, we have chosen initially aspartic acid, an α-amino acid with an additional carboxylic acid group in the side chain.

Complexation of the uranyl(VI) ion with aspartate in solution below pH 3.5 was studied by potentiometry,[4] where it was reported that the uranyl(VI) was bound to one of the carboxylic groups only, and by NMR spectroscopy[5] where it appears that the aspartate is bound via two carboxylic groups with the uranyl ion. A more recent study of uranyl(VI) ion by means of the solvent extraction technique[6] suggests that, at pH 8, the binding of aspartate involves both the carboxylate groups, but there is no uranyl–amino group interaction.

In order to clarify the question whether aspartic acid coordinates via one or two carboxylate groups to uranyl(VI) and thorium(IV) ions, in the range of pH below 3, we have examined these systems by carrying out potentiometric and calorimetric measurements.

EXPERIMENTAL

Stock solutions of uranyl(VI) and thorium(IV) perchlorate, containing an excess of perchloric acid, were prepared and standardized as reported before.[1] Aspartic acid (Baker product) was recrystallized from water and dried at 100°C, before weighing to prepare the appropriate buffer solution. For each system several potentiometric and calorimetric titrations were carried out by adding a known amount of buffer solutions of ligand to a known volume of a solution containing the metal ion (C_M^0 = 10–30 mmol dm^{-3}) and perchloric acid (C_H^0 = 10–20 mmol dm^{-3}).

Potentiometric measurements were carried out with a Radiometer pH 64; the titration vessel was equipped with a glass electrode (Metrohm EA-157) and a double junction Ag/AgCl reference electrode (Metrohm EA-440). The reaction heats were determined by a Tronac model 450 calorimeter; the reaction vessel was a rapid response, silvered glass vacuum Dewar of 25 cm^3 capacity. The burette capacity was 5 cm^3 and the titrant delivery rate was

* Author to whom correspondence should be addressed.

0.2119 cm^3 min^{-1}. The precision and accuracy of the equipment were checked by standard methods. The procedures and titration techniques have been described earlier.[1] The calculations were performed by a CDC computer 6700.

RESULTS AND DISCUSSION

Proton–ligand system

Under the experimental conditions of this work, the ligand exists as zwitterion form and thus the pK_a value of the amino group was not determined, because it is not needed for the calculations. The values calculated for the equilibrium constants and the enthalpy changes relative to the protonation of two carboxylic groups were determined by adding known volumes of $HClO_4$ or NaOH standard solutions to solutions containing different concentrations of the ligand. The values obtained (see Table 1) are sufficiently in agreement with the data available in the literature taking into account the different experimental conditions[9] ($\log \beta_{011} = 3.66\ M^{-1}$, $\Delta H_{011} = -4.6$ kJ mol^{-1}, $\log \beta_{021} = 5.56\ M^{-1}$, $\Delta H_{021} = -10.5$ kJ mol^{-1}).

Metal–ligand systems

For the uranyl(VI)–aspartate system the potentiometric measurements were limited to small concentrations of ligand in relation to the small solubility in aqueous solution of the acidic form and to the limitation of using the salt of the ligand because of the high tendency of free uranyl ion to hydrolyse. In addition, precipitation of uranyl(VI) compounds occurred at low pH values and for this reason the measurements were limited to the pH range up to about 3.4. The elemental analysis of precipitates indicated the formation of hydrolysis products. As a result, the $\bar{n}$ range of complex formation was limited to values of 1.6 and calculations were made for complexes with no more than two ligands. This is shown in Fig. 1, where the complex formation curves are plotted. The data show that $\bar{n}$ values are not dependent on C_M, therefore no polynuclear complexes are formed and, in the pH range used, hydrolytic reaction of the uranyl(VI) is negligible.

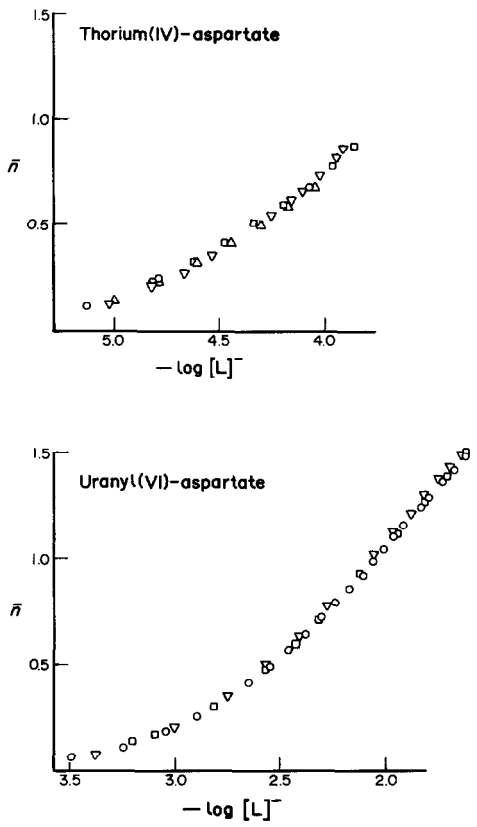

Fig. 1. The complex formation curves of uranyl(VI)– and thorium(IV)–aspartate systems. Concentrations in 10^{-3} mol dm^{-3}; $\delta = HL/L^-$. For uranyl(VI) system: ○, □, ▽ denote $C_M^0 = 20.59$, $C_H^0 = 14.67$, $C_M^0 = 30.89$, $C_H^0 = 15.50$ and $C_M^0 = 10.30$, $C_H^0 = 13.97$ titrated with $\delta = 0.12$ buffer; for thorium(IV) system: ○, □, △, ▽ denote $C_M^0 = 30.24$, $C_H^0 = 22.50$, $C_M^0 = 20.16$, $C_H^0 = 22.55$, $C_M^0 = 27.21$, $C_H^0 = 20.25$ and $C_M^0 = 10.08$, $C_H^0 = 10.86$ titrated with $\delta = 0.15$ buffer.

Table 1. The stability constants and changes in enthalpy and entropy for the formation of proton–, uranyl(VI)–, and thorium(IV)–aspartate complexes at 25.0°C in 1.0 mol dm^{-3} sodium perchlorate medium

p	q	r	Reaction	$\log \beta_{pqr}$	ΔH (kJ mol^{-1})	ΔS (J mol^{-1} K^{-1})
0	1	1	$H+L \rightleftarrows HL$	3.72±0.02	−5.9±0.2	51
0	2	1	$2H+L \rightleftarrows H_2L$	5.77±0.03	−10.3±0.2	76
1	0	1	$UO_2+L \rightleftarrows UO_2L$	2.41±0.03	8.9±0.4	76
1	0	2	$UO_2+2L \rightleftarrows UO_2L_2$	4.14±0.04	10.5±0.6	114
1	0	1	$Th+L \rightleftarrows ThL$	4.21±0.03	10.9±0.4	117

For the thorium(IV)–aspartate system, the experimental conditions were more restrictive. For this system, because of precipitation at low pH values (pH < 2.3), the $\bar{n}$ range of complex formation ($\bar{n} < 0.7$) was too low to allow any reliable calculation of complex formation with more than one ligand. As can be seen in Fig. 1, the complex formation curves for this system too, indicate that both polynuclear and hydrolytic reactions are negligible. The calorimetric measurements for both systems were limited by the above mentioned experimental conditions and by relatively small amounts of complexation heat in the titrations. Hence, no very accurate information could be obtained about the ΔH values of both systems.

The obtained values of the thermodynamic functions log β_{pqr}, ΔH and ΔS for the examined systems are reported in Table 1. The limits of error refer to three standard deviations as obtained from the computer programs Miniquad 75 and Letagrop Kalle. In order to perform a comparison, the available data on the complex formation of uranyl(VI) and thorium(IV) with some mono- and di-carboxylate ligands are reported in Table 2.

The value of the stability constant for the uranyl(VI)–monoaspartate system, obtained by us, is in fairly good agreement with that reported in the literature,[4] i.e. log $\beta_{101} = 2.63$, taking into account the different experimental conditions. In that work it was reported that uranyl(VI) ion is bound to aspartate ligand by one of the carboxylate groups only, the one furthest from the positive amino group. Our data confirm that hypothesis. In fact we can notice that the value of the stability constant for the first complex of the uranyl(VI) with aspartate is relatively smaller than that for the 1 : 1 uranyl(VI)–monosuccinate system (see Table 2). These values would indicate that there is a possible loss of the chelate effect with respect to succinate system (the succinate behaves as a bidentate chelating agent through the two carboxylate groups coordinated to the metal ion). Moreover, the value of the 1 : 1 stability constant for the uranyl(VI)–aspartate complex is comparable with that for the succinic monoprotonated acid log $K_{111} = 2.28$. This analogous behaviour is confirmed by the enthalpy changes, as their values are relatively low and both close to the value for the uranyl(VI)–acetate system (see Table 2). As the value of the stability constant of the 1 : 1 uranyl(VI)–glycine complex is smaller than that of the aspartate complex, it should be possible to show that the β-carboxylate group is bound to the metal ion. The values of the entropy changes suggest this hypothesis. In Table 2, the value for the succinate system ($\Delta S = 146$) shows that this ligand binds through both carboxylate groups, having a value comparable with that for the diacetate system,[8] while the values for acetate, succinate monoprotonate and aspartate ($\Delta S = 87, 79, 76$ respectively) show that these ligands bind through one carboxylate group only. Moreover, as the ΔS value of the glycine system ($\Delta S = 35$) is smaller than that of the aspartate system ($\Delta S = 76$), it is reasonable to assume that the uranyl(VI) ion is bound to the β-carboxylate group, while the α-carboxylate group is deprotonated in correspondence with the protonation of the amino group.

Similar results seem to hold for the thorium(IV)–aspartate system. Comparing the values of the 1 : 1 stability constant for the aspartate complex (log $\beta_{101} = 4.21$) with that for the succinate complex (log $\beta_{101} = 6.44$) it would seem that there is no interaction of thorium with both of the carboxylate groups. By analogy with uranyl(VI), the values of enthalpy and entropy changes for the thorium(IV)–aspartate system are comparable in magnitude with those of the complex with the succinic monoprotonated acid. In fact the values of ΔH and ΔS for the thorium–succinate complex, where the ligand binds via both carboxylate groups, are higher than the values for aspartate complex, while the last values ($\Delta H = 10.9$, $\Delta S = 117$) are comparable to

Table 2. The stability constants and the changes in enthalpy and entropy for the formation of uranyl(VI) and thorium(IV) 1 : 1 complexes at 25.0°C in 1.0 mol dm^{-3} sodium perchlorate medium

	Uranyl(VI)				Thorium(IV)			
Ligands	log β	ΔH (kJ mol^{-1})	ΔS (J mol^{-1} K^{-1})	Ref.	log β	ΔH (kJ mol^{-1})	ΔS (J mol^{-1} K^{-1})	Ref.
Acetate	2.46	11.8	87	9	3.86	11.3	112	10
Diacetate	4.38	17.9	144	9	6.97	15.8	186	10
Succinate	3.85	21.7	146	11	6.44	18.6	186	12
H-Succinate	2.28	10.0	79	11	3.60	8.5	97	12
Glycine	1.16	3.9	35	1	2.55	4.2	63	1
Aspartate	2.41	8.9	76	—	4.21	10.9	117	—

the values for the thorium monoacetate complex ($\Delta H = 11.3$, $\Delta S = 112$). Therefore it is reasonable to presume that, for the aspartate, one carboxylate group only binds to the metal ion. The fact that the values of thermodynamic functions for the thorium glycine system are all smaller than those for the aspartate system and, on the other hand, the last values are comparable to the acetate system, can show that the aspartate ligand binds through the furthest carboxylate group from the amino group.

REFERENCES

1. A. Bismondo, L. Rizzo, G. Tomat, D. Curto, P. Di Bernardo and A. Cassol, *Inorg. Chim. Acta* 1983, **74**, 21.
2. A. Bismondo, L. Rizzo, P. Di Bernardo and P. L. Zanonato, *J. Chem. Soc., Dalton Trans.* 1987, 695.
3. A. Bismondo and L. Rizzo, *Radiochim. Acta* 1989, **47**, 47.
4. I. Feldmann and L. Koval, *Inorg. Chem.* 1963, **2**, 145.
5. H. Wieczorek and H. Kozlowski, *Inorg. Nucl. Chem. Lett.* 1980, **16**, 401.
6. A. Sarto and G. R. Choppin, *Radiochim. Acta* 1984, **36**, 135.
7. A. E. Martell and R. M. Smith, *Critical Stability Constants*, Vol. 5. Plenum Press, New York (1982).
8. Y. Hasegava and G. R. Choppin, *Inorg. Chem.* 1977, **16**, 2931.
9. R. Portanova, P. Di Bernardo, A. Cassol, E. Tondello and L. Magon, *Inorg. Nucl. Chem.* 1974, **8**, 233.
10. R. Portanova, P. Di Bernardo, O. Traverso, G. A. Mazzocchin and L. Magon, *J. Inorg. Nucl. Chem.* 1975, **37**, 2177.
11. A. Bismondo, A. Cassol, P. Di Bernardo, L. Magon and G. Tomat, *Inorg. Nucl. Chem. Lett.* 1981, **17**, 79.
12. P. Di Bernardo, A. Cassol, G. Tomat, A. Bismondo and L. Magon, *J. Chem. Soc., Dalton Trans.* 1983, 733.

Polyhedron Vol. 8, No. 18, pp. 2237–2243, 1989
Printed in Great Britain

0277–5387/89 $3.00+.00
© 1989 Pergamon Press plc

MOLECULAR REORIENTATION IN CRYSTALS OF NEUTRAL METAL CARBONYL CLUSTERS: A POTENTIAL ENERGY APPROACH

DARIO BRAGA* and FABRIZIA GREPIONI

Dipartimento di Chimica "G. Ciamician", Universita' di Bologna, Via F. Selmi 2, 40126 Bologna, Italy

(*Received* 24 *November* 1988; *accepted* 24 *April* 1989)

Abstract—The occurrence of reorientational motions of parts or of entire molecules of neutral metal carbonyl clusters in the solid state is explored by means of the pairwise potential energy method developed to study analogous phenomena in organic crystals. The method is applied, here, mainly to species which show dynamic behaviour in the solid on the basis of MAS NMR experiments. The nature (whether static or dynamic) of the disorder observed in crystals of $[Fe_3(CO)_{12}]$ and $[Co_4(CO)_{12}]$ is also discussed.

There is increasing interest in the solid-state behaviour of neutral metal carbonyl clusters now that spectroscopic techniques (mainly ^{13}C MAS NMR) are providing information on the occurrence of dynamic processes for these species also in the condensed state of matter.[1] In fact, ^{13}C MAS NMR has afforded remarkable results in the metal cluster field, showing that the phenomenon of "fluxionality" (in the broad sense of CO ligand migrational processes around the metal cores) must be invoked to explain the spectral patterns recorded at different temperatures for a number of solid binary metal carbonyl clusters. The averaging mechanism implied by the solid-state NMR experiments is essentially of two kinds: (i) reorientation of the metal polyhedron within the carbonyl envelope and (ii) migration of the CO ligands around the metal frame usually through a bridge–terminal exchange. Mechanism (i) has been invoked in the cases of $[Fe_3(CO)_{12}]$[2] and $[Co_4(CO)_{12}]$,[3] while (ii) has been found to occur for $[Co_2(CO)_8]$.[4] In the former case the migrational motion has also been related to the well-known disorder present in crystals of $[Fe_3(CO)_{12}]$ and $[Co_4(CO)_{12}]$.[5,6]

Recently, a different interpretation of the dynamic behaviours shown by these species in the solid state has been proposed in terms of small amplitude librations involving both the inner metal frames and the surrounding CO ligands.[7] These motions do not imply extensive molecular reorientation but only displacements of the metal and CO nuclei around equilibrium positions, which are frozen out as the temperature is decreased, in agreement with the appearance of static structures on the NMR time scale.[8]

In general, molecular motions in crystals can be distinguished in two broad classes (with no clear borderline, however) on the basis of their amplitudes.[9a] Small amplitude displacements are usually related to rigid-body librations and/or translations or to intramolecular motions (bond bending, torsions, etc.) along the normal coordinates of the systems,[9b] and are characterized by weak restoring forces (compared with those implied by bond stretchings). Displacements of this kind are associated with "potential energy wells" having steep walls, but more or less flat bottoms. Large amplitude molecular motions are otherwise related to the presence of rather smooth potential energy surfaces, along which large displacements and reorientational jumps can easily occur. The forces opposing such motions are mainly, if not entirely, intermolecular. In this context, jumps between energy minima are often related to the occurrence of "dynamic" disorder in the crystal structures.[10,11] Molecular crystals of organic substances are known to show both kinds of phenomena, which are the subject of continuing investigations.

We now intend to apply some concepts and procedures developed in this neighbouring field to the investigation of molecular motions of some "fundamental" metal carbonyl clusters in the solid state.

*Author to whom correspondence should be addressed.

Although molecular motions of these latter species present essentially the same features as those of organic molecules, there are significant differences arising from the peculiar nature of the bonding interactions between the CO groups and the metal frame, the availability of substantially different coordination modes of almost equivalent energy for the ligands which can bound in terminal and various bridging fashions, the nature of the atomic species involved (transition metal atoms), let alone the very special structural non-rigidity implied by the phenomenon of fluxionality.[12] Nonetheless, the goal of this paper is to show that, in spite of the substantial simplifications required in dealing with transition metal clusters, the study of the potential energy terms associated with molecular motions of these species can afford relevant information in this rather unexplored area of the solid-state chemistry. Recently, the same approach, combined with an analysis of the observed mean square displacement parameters, has been applied to study the reorientational motion of the C_5H_5 ligands in *cis*- and *trans*-$[(C_5H_5)_2Fe_2(CO)_4]$, showing that a correlation is possible between the dynamic behaviours observed by MAS NMR, the height of the potential energy barriers in the solid and the orientation of the mean square displacement parameters.[13]

The following discussion will be devoted to the examination of species for which ^{13}C MAS NMR spectroscopy information is available, and whose solid-state structures are well studied. In particular $[Ru_3(CO)_{12}]$, which is "static",[14] and the "dynamic" species $[Fe_3(CO)_{12}]$, $[Co_4(CO)_{12}]$ and $[Co_2(CO)_8]$ mentioned above, will be studied. In the cases of $[Fe_3(CO)_{12}]$ and $[Co_4(CO)_{12}]$, a discrimination between "dynamic" disorder, arising from rigid-body reorientation of the entire molecules, and "static" disorder, generated either by random occupation of the crystal sites by the molecules in two alternative orientations or by differently oriented domains in the crystals, will also be attempted.

METHOD

The potential energy of a crystal made up of discrete molecular units, interacting by Van der Waals interactions and with no contribution of ionic nature, can be calculated as follows.[15] The potential energy (p.e.) is obtained as a simple function of the intermolecular atomic separations by using "conventional" repulsion–attraction potential energy terms of the kind

$$\text{p.e.} = \sum_i \sum_j Ae^{-BR_{ij}} - CR_{ij}^{-6}$$

acting between a central reference molecule and the surrounding ones, which are distributed according to the crystal symmetry. No coulombic interactions between permanent atomic charges or bond polarities are taken into account at the present stage of the investigation. The coefficients A, B and C are taken from the literature.[9a,16] No such coefficients are available for transition metal atoms and this constitutes an *a priori* drawback for these kind of calculations. However, it should be stressed that the aim of this work is not the exact evaluation of packing energies associated with a given crystal structure, but a comparison of the energy barriers associated with molecular reorientational processes. The peculiar features of the species under examination (a metal core encapsulated within a CO shell) simplify the problem: the potential energy barriers opposing the motion are largely dominated by outer CO···CO intermolecular interactions with little contribution (if any at all) coming from the inner metal core. We have proved this assumption by attributing to the metal atoms the values of A, B and C of the corresponding noble gases and of several main group elements whose values are available,[16] showing that neither the shape of the energy profiles, nor the height of the energy barriers, are significantly different from the ones obtained without metal contribution, while the absolute "depth" of the potential wells shows more marked changes. The comparison of the potential energy curves obtained for $[Ru_3(CO)_{12}]$ with different choices of A, B and C for the metal atoms and without metal contribution is shown in Fig. 1 for a complete rotation between -180 and $180°$ around an axis perpendicular to the Ru_3 triangle (also see below). All other curves were then obtained by taking into account only carbon and oxygen atom contributions. It should be pointed out that all molecular reorientations, whether of entire molecules or of parts of them, were performed by considering a static molecular environment, with no cooperation by the molecule surrounding the reorienting one. This limitation is known to cause overestimation of the potential energy barriers.[17] Although a detailed analysis of the intermolecular cooperation ("gear-like" motion of the molecules surrounding the reference one) requires further work and will be the subject of a future report,[18] it can be anticipated that the effect is never such as to "flatten" down the very high energy barriers (usually hundreds of kcal mol^{-1}) experienced by the reorienting molecule during the rigid-body motion. It is also important to note, at this stage, that the absolute minima for all the species under examination are invariably observed at 0° rotations, thus showing that the method correctly

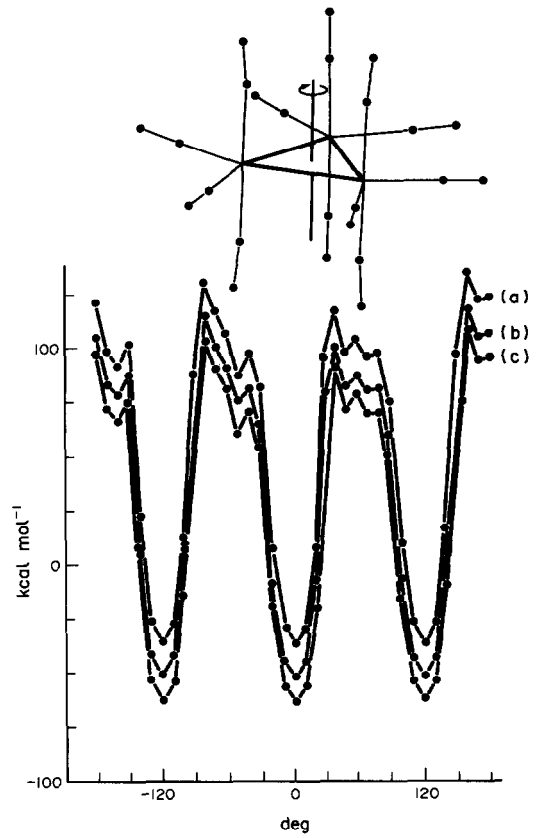

Fig. 1. $[Ru_3(CO)_{12}]$: Potential energy profiles for a rotation around the molecular three-fold axis, obtained without metal contribution (a) and by treating ruthenium as argon (b) and xenon (c).

attributes the lowest energy to the observed crystal structure.

Atomic coordinates and space groups were taken from the original papers. All calculations were performed by using a slightly modified version of the program OPEC, Organic Packing Energy Calculations and Volume Analysis.[19] References 16 and 19 give more details on the computational procedures.

RESULTS AND DISCUSSION

Reorientation and disorder in $[Fe_3(CO)_{12}]$

$[Fe_3(CO)_{12}]$ has been shown to be disordered in its crystal structure,[5] having the molecule lying around an inversion centre in the $P2_1/n$ space group, which generates a second image of the Fe_3 triangle and of the 12 CO groups. The molecule possesses idealized C_2 symmetry with the pseudo two-fold axis passing through the Fe—Fe bond, which bears the two asymmetric bridging COs, and the opposite Fe atom (see top of Fig. 2).

In order to perform the potential energy calculations, a model crystal was built in the acentric space group $P2_1$ with only one independent ordered molecule in the asymmetric unit. The molecule was then allowed to rotate from -180 to 180°, and the p.e. calculated every 10° step around an axis perpendicular to the Fe_3 plane and corresponding to the largest moment of inertia of the molecule. The p.e. profile is reported in Fig. 3. There are three interesting features which should be pointed out: (i) the molecule lies in a rather deep potential well (-34.65 kcal mol^{-1} if no iron contribution is taken into account), with steep walls which lead to rapidly increasing p.e. barriers on both sides; (ii) "sub-minima" are observed after 60 and -120° rotations, although associated with much higher p.e. values; (iii) a negative minimum, almost equivalent to the one at 0°, is observed after a 180° (or -180°) rotation from the original orientation. Analogous behaviour, but without sub-minima, is observed if the rotation is carried out around the minor inertia axes, which are coplanar with the Fe_3 triangle.

These facts indicate that the rotation around the

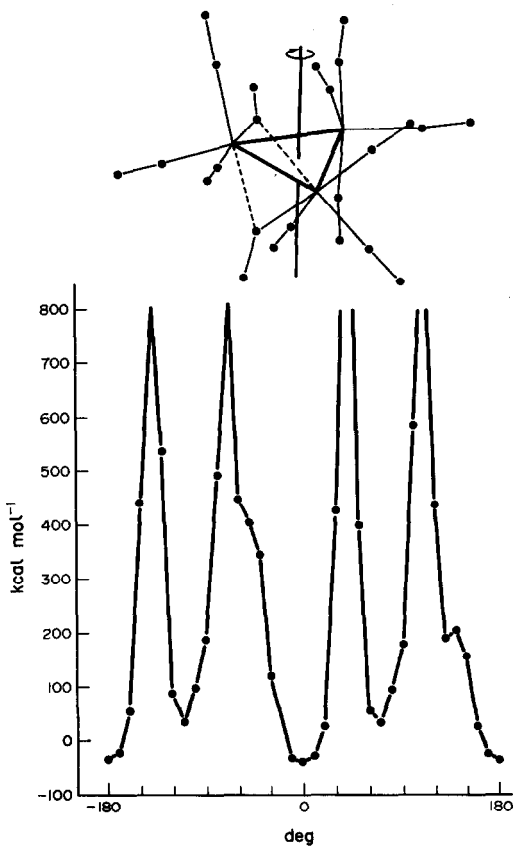

Fig. 2. $[Fe_3(CO)_{12}]$: Potential energy profile for a rotation around the molecular two-fold axis.

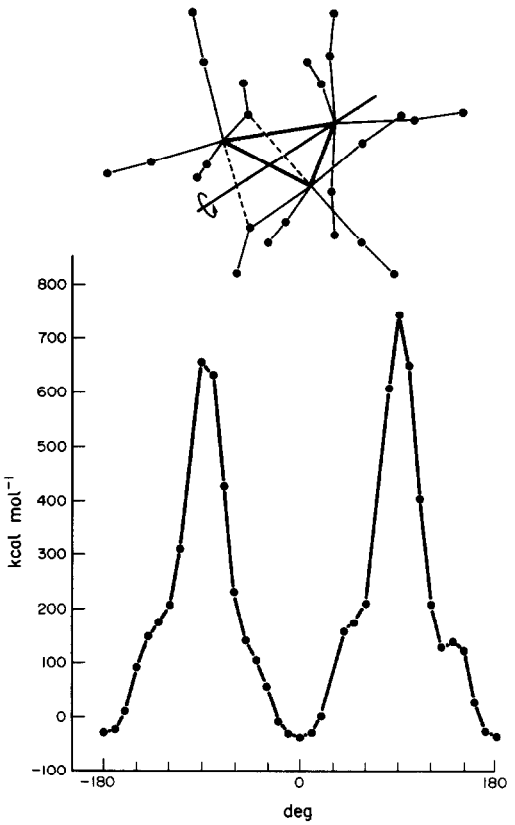

Fig. 3. $[Fe_3(CO)_{12}]$: Potential energy profile for a rotation around the major inertia axis.

inertia axis is prevented by the upsurge of very high p.e. barriers, thus ruling out the possibility of a full-scale rotational motion of the molecule as a rigid body. Furthermore, the crystal environment does not discriminate between the molecule in one orientation or in the reverse one. This latter observation is in keeping with a model of static disorder arising from random occupation of the crystal sites by the molecule in two "packing-equivalent" orientations, determined by the quasi-icosahedral peripheral polyhedron described by the 12 CO ligands. The possibility of a domain disorder generated by short-range order (say of a few hundred Å) within domains having different orientations in the crystal, can be ruled out.

Concerning the ^{13}C MAS NMR evidence for the occurrence of dynamic processes in solid $[Fe_3(CO)_{12}]$,[2] it must be stressed that there are no means, beside quantum-mechanical calculations, of evaluating the energy barriers associated with the proposed rotation of the Fe_3 triangle *within* the CO shell. It is otherwise possible to explore the displacement of the Fe_3 triangle and of the surrounding ligands around the molecular two-fold axis. As illustrated elsewhere,[7] such motion is enough to bring about the change of the molecular symmetry from C_2 to D_3 in the solid, so accounting for the equilibration of the carbon atom nuclei observed on the NMR time scale. The librational motion can be simulated by allowing displacement of the terminal and bridging ligands around an axis passing through the middle of the bridged Fe—Fe bond and the opposite iron atom as illustrated in Fig. 2. The p.e. associated with this motion remains negative within a fairly large angular range ($\pm 20°$) and is constant at about the value of the minimum between $\pm 10°$. All this may be taken as a qualitative indication that the crystal packing does not hinder a limited swinging of the ligands around their equilibrium positions, which causes, *inter alia*, increased degree of asymmetry of the bridging ligands and, ultimately, the adoption of quasi-terminal positions. Such a dynamic process is the only one which can explain the solid-state NMR spectral pattern without requiring large jumps of the metal core between the crystallographic observed positions.[2] Obviously, additional potential energy terms that couple CO group deformation with the librational modes would be required for a better assessment of the fundamental modes that could lead to exchange on the NMR time scale.

Reorientational motion and disorder in $[Co_4(CO)_{12}]$

Similar reasoning may be applied to $[Co_4(CO)_{12}]$, which also shows disorder and dynamic behaviour in the solid state.[3,6] $[Co_4(CO)_{12}]$ crystallizes in the orthorhombic space group *Pccn*, with the molecule lying around a crystallographic two-fold axis which generates a second orientation of the cluster at 180°.[6] A model crystal containing only ordered molecules was built in the monoclinic space group $P2_1/c$ (with $\beta = 90°$). The molecule was allowed to rotate from -180 to 180°, first around the two-fold axis of the disorder model and then around each of the tetrahedron three-fold axes. In the former case the p.e. pattern is very much modulated (see Fig. 4) showing sub-minima every 60° and two minima of energy almost identical to that calculated at 0° after a 180 or $-180°$ rotation. If the same rotation is carried out around one of the other two axes comprising an atom of the bridged base, similar patterns are observed. If the molecule is instead allowed to rotate around the idealized molecular three-fold axis (the one comprising the apical cobalt atom bearing three terminal COs and passing through the centre of the opposite triangular face, see Fig. 5), the minimum at 180° disappears, while p.e. minima are observed every 120°. These latter minima correspond to swapping the sites occupied by the basal ligands and by the terminal COs of the apical atom.

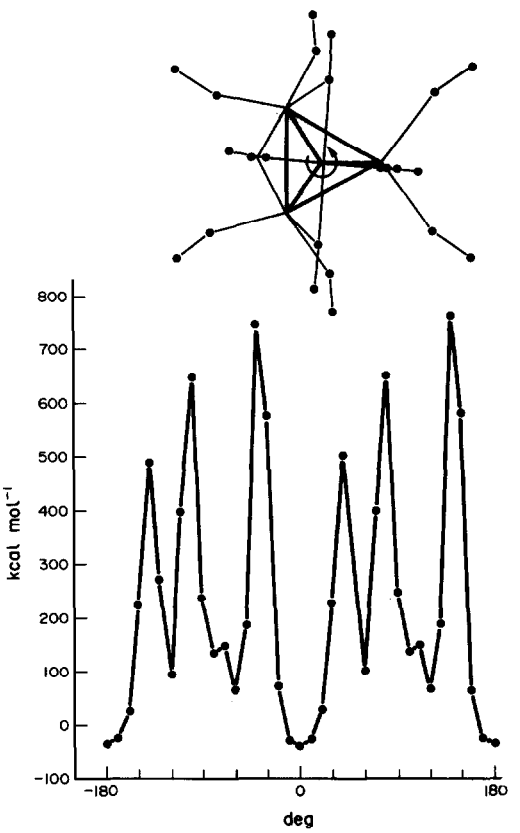

Fig. 4. $[Co_4(CO)_{12}]$: Potential energy profile for a rotation around the crystallographic two-fold axis of the disordered crystal.

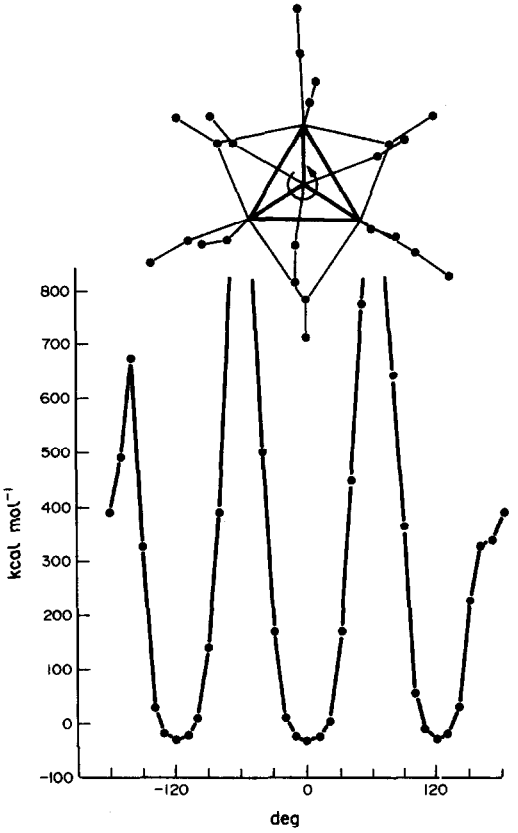

Fig. 5. $[Co_4(CO)_{12}]$: Potential energy profile for a rotation around the molecular three-fold axis.

From the above results it can be concluded that, as observed for $[Fe_3(CO)_{12}]$, the disorder has random rather than domain nature.

Molecular reorientation in $[Ru_3(CO)_{12}]$

$[Ru_3(CO)_{12}]$ has been reported to be static in the solid state,[14] so that it is well suited as a test case for the method. The p.e. profiles reported in Fig. 1 have been calculated, analogously to $[Fe_3(CO)_{12}]$, by allowing rotation of the molecule around its major inertia axis, which corresponds to the molecular three-fold axis passing through the middle of the Ru_3 triangle. It is worth recalling that the crystal structure of $[Ru_3(CO)_{12}]$ does not show disorder.[21] The p.e. profile shows three—almost identical—minima centred at 0, −120 and 120°, which correspond to site-swapping between the three $Ru(CO)_4$ units constituting the cluster. These minima are separated by fairly large energy barriers, though somewhat less pronounced than in the previous cases. It should be pointed out, however, that the height of the barriers is not necessarily related to the overall packing "efficiency",[20] but rather reflects the nature of the obstacles encountered by the molecule during the hypothetical motion through the crystal. On the other hand, the p.e. value corresponding to the crystal structure (0° rotation) is the lowest obtained for the species discussed herein, even if no metal atom contribution is taken into account (−36.6 kcal mol^{-1}). This fact is in strict accord with the existence of a tight molecular packing for $[Ru_3(CO)_{12}]$, evidenced by the value of its packing coefficient (0.72), as discussed elsewhere.[20]

Molecular reorientation and libration in $[Co_2(CO)_8]$

$[Co_2(CO)_8]$ is the only species for which the occurrence of a CO scrambling process in the solid (of the kind commonly observed in solution) has been invoked in order to account for the features and temperature dependence of the ^{13}C MAS NMR spectra.[4] The structure of $[Co_2(CO)_8]$ also has been subjected to independent studies,[22] which have shown that two independent "half" molecules are related to the other "halves" by a crystallographic mirror plane bisecting the Co—Co bond and con-

taining the two bridging CO ligands. In order to approach the ligand motion around the molecule, the crystal of $[Co_2(CO)_8]$ (space group $P2_1/m$) has been described in the isomorphous subgroup $P2_1$ with two independent entire molecules in the asymmetric unit.

It should be emphasized that there is no simple reorientational motion which can describe the cyclic CO exchange between crystallographic independent sites able to equilibrate bridging and terminal ligands on the NMR time scale. It is only possible to simulate some components of the motion by allowing rotations around appropriately selected axes. The effect of a rotation around the Co—Co axis of the terminal COs bound to one or both cobalt atoms, which is probably one of the possible intermediate stages of the fluxionality process in solution, is shown in Fig. 6. Minima, separated by high potential barriers, are observed every 120°. More interesting appears to be the effect of slightly rotating three terminal and one bridging CO belonging to one of the CO atoms around an axis perpendicular to the Co—Co bond and parallel to the vector joining the bridging COs (see Fig. 7). This motion may simulate the "opening up" of a CO bridge to lead from the bridged structure to an intermediate stage with all terminal ligands. The p.e. profile associated with this motion, although

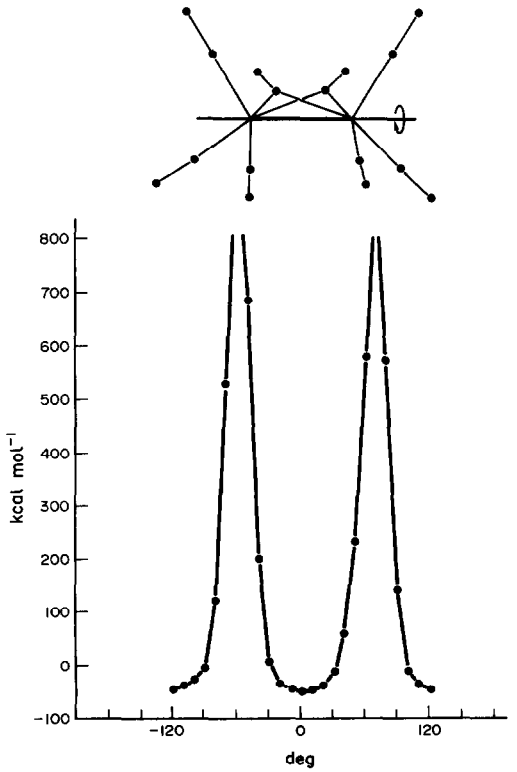

Fig. 6. $[Co_2(CO)_8]$: Potential energy profile for a rotation of the terminal CO ligands around the Co—Co axis.

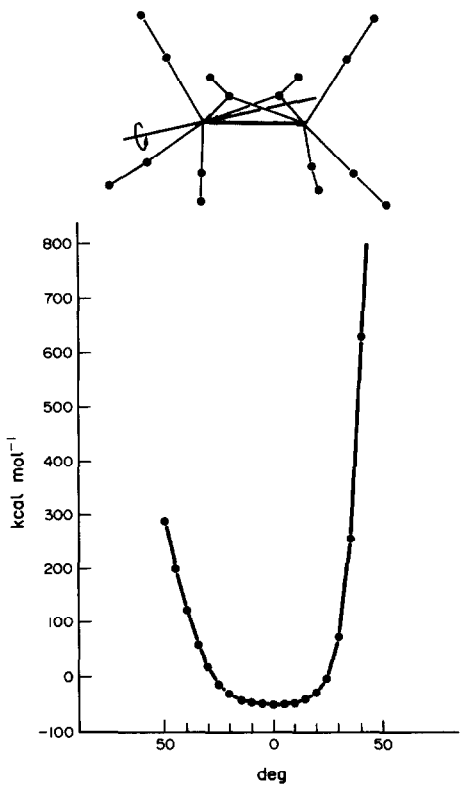

Fig. 7. $[Co_2(CO)_8]$: Potential energy profile for a libration of three terminal and one bridging CO around an axis perpendicular to the Co—Co bond and passing through one cobalt atom.

obtained without contributions of intramolecular nature, is rather flat (p.e. values remain negative between −28 and 24°), indicating that the ligands can be displaced to a fairly large extent without encountering excessive steric hindrance by the neighbouring molecules. This observation is important because it offers the possibility to envisage a swinging motion of the ligands around the cobalt centres, possibly accompanied by slight tilting of the Co—Co axis around its centre of mass, which can suffice in equilibrating the carbon nuclei of terminal and bridging ligands as required by the MAS NMR experiments. This all occurs with no need for site exchange among the ligands.

CONCLUSIONS

We have shown that potential energy studies, though confined to atom-pair non-bonded interactions, are a useful tool for the investigation of dynamic processes in the solid state even for transition metal complexes, and also offer a discriminating criterion to distinguish between static and dynamic disorder and between random and domain disorder. The results obtained are very much qualitative and admittedly based on large

(and sometimes simplistic) assumptions and approximations of various kinds. Although no "absolute" energy values can be obtained, the present analysis correctly recognizes the possible relationship between the different phenomena taken into account: effect of crystal packing, occurrence of disorder, dynamic behaviour as evidenced by spectroscopic techniques. The main outcomes of this work can be summarized as follows:

(1) There is no evidence for facile reorientational processes of molecules regarded as rigid-bodies in crystals of transition metal clusters. The energy barriers associated with these motions are enormous when compared with those calculated for "dynamic" organic molecules such as benzene and naphthalene derivatives[16] or adamantanes,[23] although, at first sight, the molecules' shapes (spheres, cylinders, etc.) would seem very similar. It should be pointed out, however, that most carbonyl clusters of low nuclearity are better described as "lumpy" objects with the oxygen atoms sticking out of the surfaces and fitting in the interstices of the surrounding molecules. Thus it is not surprising that the energy barriers associated with the reorientations should be generally higher than for other more globular molecules, where the problem of atoms pushing past the surrounding ones can be less dramatic.

(2) The salient symmetry features of the molecules are recognized by the crystal packing during the motions, showing minima for orientations made equivalent by the idealized molecular symmetries.

(3) In this context, the appearance of energy minima corresponding to genuinely alternative orientations of molecules such as $[Fe_3(CO)_{12}]$ or $[Co_4(CO)_{12}]$, but in contrast with the molecular symmetry, even in model crystals built up of ordered units, is an indication that the whole crystal is modulated around an average object generated by the superposition of the two orientations. Therefore the possibility of a mosaic crystal made up of differently oriented domains being the cause of disorder can be ruled out. It should be mentioned, in passing, that MAS NMR should be affected differently by a sample showing random or domain disorder.

(4) The alternative interpretation of the dynamic behaviour observed for $[Fe_3(CO)_{12}]$, $[Co_4(CO)_{12}]$ and $[Co_2(CO)_8]$, based on concerted small-amplitude librations of the metal frames and of the CO ligands, appears to be somewhat substantiated by the presence of broad potential energy minima associated with limited displacements of the ligands whose motion is involved in the equilibration process.

Acknowledgements—It is a pleasure to thank Professor A. Gavezzotti for many useful discussions and for his careful review of the manuscript. Financial support by CNR is acknowledged.

REFERENCES

1. C. A. Fyfe and R. E. Wasylishen, *Solid State Chemistry Techniques* (Edited by A. K. Cheetham and P. Day), Chap. 6, p. 190. Clarendon Press, Oxford (1987).
2. (a) H. Dorn, B. E. Hanson and E. Motell, *Inorg. Chim. Acta* 1981, **54**, L71; (b) B. E. Hanson, C. E. Lisic, J. T. Petty and G. Iannacone, *Inorg. Chem.* 1984, **25**, 4062.
3. B. E. Hanson and E. C. Lisic, *Inorg. Chem.* 1986, **25**, 716.
4. B. E. Hanson, M. J. Sullivan and R. J. Davis, *J. Am. Chem. Soc.* 1984, **106**, 251.
5. (a) C. H. Wei and L. F. Dahl, *J. Am. Chem. Soc.* 1969, **91**, 1351; (b) F. A. Cotton and J. M. Troup, *J. Am. Chem. Soc.* 1974, **96**, 4155.
6. (a) C. H. Wei, *Inorg. Chem.* 1969, **8**, 2384; (b) F. H. Carrè, F. A. Cotton and B. A. Frenz, *Inorg. Chem.* 1976, **15**, 380.
7. C. E. Anson, R. E. Benfield, A. W. Bott, B. F. G. Johnson, D. Braga and E. A. Marseglia, *J. Chem. Soc., Chem. Commun.* 1988, 889.
8. R. E. Benfield, D. Braga and B. F. G. Johnson, *Polyhedron* 1988, 7, 2549.
9. (a) A. Gavezzotti and M. Simonetta, *Chem. Rev.* 1981, **82**, 1; (b) J. D. Dunitz, V. Schomaker and K. N. Trueblood, *J. Phys. Chem.* 1988, **92**, 856.
10. A. Gavezzotti and M. Simonetta, *Organic Solid State Chemistry* (Edited by G. R. Desiraju), pp. 391–430. Elsevier, New York (1987).
11. J. L. Amoros and M. Amoros, *Molecular Crystals.* John Wiley, New York (1968).
12. For a general survey of the field see B. F. G. Johnson (Ed.), *Transition Metal Clusters.* John Wiley, New York (1980).
13. D. Braga, F. Grepioni and C. Gradella, *J. Chem. Soc., Dalton Trans.*, in press.
14. S. Aime, M. Botta, R. Gobetto, D. Osella and L. Milone, *Inorg. Chim. Acta* 1988, **146**, 151.
15. A. J. Pertsin and A. I. Kitaigorodski, *The Atom–Atom Potential Method.* Springer, Berlin (1987).
16. A. Gavezzotti and M. Simonetta, *Acta Cryst.* 1975, **A31**, 165 and refs therein.
17. A. Gavezzotti and M. Simonetta, *Acta Cryst.* 1986, **A32**, 997.
18. D. Braga and F. Grepioni, unpublished.
19. A. Gavezzotti, *J. Am. Chem. Soc.* 1983, **105**, 5220.
20. D. Braga and F. Grepioni, *Acta Cryst.*, in press.
21. M. R. Churchill, F. J. Hollander and J. P. Hutchinson, *Inorg. Chem.* 1977, **16**, 2655.
22. (a) G. G. Summer, H. P. Klug and L. E. Alexander, *Acta Cryst.* 1964, **17**, 732; (b) P. C. Leung and P. Coppens, *Acta Cryst.* 1983, **B39**, 535.
23. C. A. Fyfe and D. Harold-Smith, *Can. J. Chem.* 1976, **54**, 783.

Polyhedron Vol. 8, No. 18, pp. 2245–2249, 1989
Printed in Great Britain

0277–5387/89 $3.00+.00
© 1989 Pergamon Press plc

EQUILIBRIA IN COMPLEXES OF N-HETEROCYCLIC MOLECULES—XLVIII.* DIMORPHS OF *FACIAL*-TRICHLORO-TRIS-PYRIDINE-IRIDIUM(III)

R. D. GILLARD† and S. H. MITCHELL

School of Chemistry and Applied Chemistry, University of Wales College of Cardiff, P.O. Box 912, Cardiff CF1 3TB, Wales, U.K.

(*Received* 30 *January* 1989; *accepted* 26 *April* 1989)

Abstract—Crystalline dimorphs of *fac*-$[Ir(py)_3Cl_3]$ are described and characterized. They give identical solutions and one converts irreversibly to the other.

Even in single solid phases containing individual uncharged molecules (including octahedral compounds—for example,[2] *fac*-$Ir(CH_3)_3(PMe_2Ph)_3$—there are many examples of differing geometry for such molecules at inequivalent positions within the unit cell.

The existence of distinct crystalline forms of such molecular structures seems likely to be common. Though not so commonly noticed, there are in fact plenty of cases. For example,[3] $[Pt(bipy)Cl_2]$ molecules may pack in the common yellow form and a less common red form.

We describe here a new case, that of *fac*-$[Ir(py)_3Cl_3]$, ostensibly a well known compound, in the sense that many properties have been reported (such as far-IR and Raman, and its electronic spectrum). However, all such reports seem (so far as we can see) to relate to measurements on samples actually provided by Delepine or his associates, so we describe our preparations in detail.

Delepine first synthesized[4] *fac*- and *mer*-$[Ir(py)_3Cl_3]$, both via extensive heating of chloro- or pyridinechloro-precursors ($IrCl_3 \cdot 3H_2O$, K_3IrCl_6, *cis*- or *trans*-$[Ir(py)_2Cl_4]^-$ and others) with pyridine. Some picoline (i.e. methylpyridine) analogues have also been described, by his students: *fac*- and[5] *mer*-$[Ir(3\text{-pic})_3Cl_3]$, and[6] $[Ir(2\text{-pic})_3Cl_3]$ (probably the *mer*-isomer).

The *fac*-isomer was isolated here as a by-product in the synthesis of the *trans*-$[Ir(py)_4Cl_2]^+$ cation: we recently reported[7] the structure of one dimorph of the chloride hexahydrate of this. A more recent report[8] of the analogous dibromorhodium compound is of an isostructural lattice.

* For part XLIX, see ref. 1.

† Author to whom correspondence should be addressed.

EXPERIMENTAL

fac-$[Ir(py)_3Cl_3]$ (*Form* A)

$K_3IrCl_6 \cdot 3H_2O$ (0.521 g) dissolved in water (18 cm^3) and heated (steam bath) was treated with a mixture of pyridine (6.5 cm^3) and ethanol (3 cm^3). Reaction to a yellow solution was complete after ~ 15 min; the solution was evaporated to ~ 20 cm^3 (to remove ethanol and some pyridine), and allowed to cool. Yellow crystals (Form **A**) slowly formed; these were collected. The filtrate was concentrated to ~ 10 cm^3 giving a second crop. Contaminating *trans*-$[Ir(py)_4Cl_2]Cl \cdot nH_2O$ in this second crop was extracted with hot water. Total yield of **A** = 0.065 g (13.5%). Other similar preparations, and one using $IrCl_3 \cdot 3H_2O$ gave yields in the range 12–18%. With propan-2-ol (instead of ethanol) as catalyst/solvent the yield improved to 29%.

Form B

$K_3IrCl_6 \cdot 3H_2O$ (0.104 g) dissolved in water (1.5 cm^3), pyridine (0.1 cm^3), propan-2-ol (0.5 cm^3) and chloroform (2.0 cm^3) was set to reflux very slowly in a 5 cm^3 foil-covered flask. After 8 h, yellow crystals had formed in the chloroform layer. The reflux was continued overnight, then the yellow crystals were removed by filtration and washed with chloroform. Yield = 0.026 g (27%).

Properties

Form **B** differs from Form **A** in the vibrational spectrum, X-ray diffraction and thermogravimetric analysis, although both show the same solubility properties: they dissolve (giving

identical solutions) only very slowly in cold solvents: CH_2Cl_2, $CHCl_3$, pyridine, H_3CCN and 50 : 50 H_2O–pyridine; although both are insoluble in water. Both are slightly soluble in propan-2-one (acetone) and hardly soluble (if at all) in CS_2.

Form **A** was dissolved in 50% v/v aqueous pyridine, passed through an anion exchange resin (Sephadex A25) and recovered by steam distilling pyridine (i.e. evaporating the solution to remove pyridine vapour but keeping the volume constant by adding water): 95% of the original mass of complex was recovered as long needles entirely of Form **B**.

Form **A** can be recrystallized from 20–50% v/v aqueous pyridine with varying degrees of success (0–100%). However, in no instance was it possible to obtain Form **A** from Form **B**.

Both forms were neutral, since (dissolved in 50% v/v aqueous pyridine) they pass through anion and cation (Sephadex A25 and C25, respectively) exchange resins; if the solutions are allowed to age, then the *anion* exchange resin retains some complex, suggesting slow base hydrolysis to $[Ir(py)_2Cl_3(OH)]^-$. Analyses are given in Table 1.

The solution electronic spectra from both forms indicate that the basic structural unit is the same (Table 2): the band positions of Jorgensen are in good agreement with ours; the figures[10] of Rio and Lareze for absorption wavelengths of the *fac*-isomer differ slightly; they included extinction coefficients.

Vibrational spectra are presented in Table 3, and in Figs 1 and 2. IR spectra were measured using Perkin–Elmer 557 and Pye Unicam SP3-200 spectrometers (calibrated with polystyrene) on NaCl or CsI plates for mulls in Nujol or fluorolube.

X-ray diffraction: there is a small difference

Table 1. Analytical results for solid *fac*-$[Ir(py)_3Cl_3]$

	Form **A**	Form **B**	Calc. for $[Ir(C_5H_5N)_3Cl_3]$
C (%)	33.8	32.7	33.6
H (%)	3.1	3.1	2.8
N(%)	8.4	8.6	7.8
Cl (%)	20.0	21.9	19.9
Ir (%)	36.1	35.9	35.9
Total	101.4	102.2	
T (°C)[a]	275	280	
Loss (% mass)	3.7	3.4	3.7 ($\frac{1}{4}$py)
T	340	330	
Loss	24.5	25.3	25.8 ($1\frac{3}{4}$py)
T	630	460 and 610	
Loss	36.6	35.1	34.6 (py+3Cl)

[a] Thermogravimetric analysis with a Stanton Redcroft TG750 thermobalance in nitrogen flowing at 25 $cm^3\ min^{-1}$: heating rate was 2°C min^{-1}.

Table 2. Electronic spectra of the various forms of monomeric $[Ir(py)_3Cl_3]$

	λ (nm)	ε (mol dm^{-2} $\times 10^{-2}$)	λ	ε	λ	ε	λ	ε	λ	ε	Reference
Form **A**	325	822	275.5	1248	265.5	1200					This work
Form **B**	325	825	276	1248	266.5	1200					This work
fac	330	600	282	920	267	970					10
	326.5		276		265						9(a)
fac	324										9(b)
mer	319	~ 547	274		267	1319	262		250		This work
	319[a]	1600			265						9(a)
mer	314										[a]

[a] Reference 9(a) also describes a weak singlet–triplet band at 432 nm.

Table 3. IR and Raman (R) spectra for solid monomeric $[Ir(py)_3Cl_3]$

	fac-A		*fac*-B		*mer*-	
ν	IR	R[a]	IR	R[a]	IR	R[a]
4	1600m		1607m		1611m	
5	1482m		1485m		1486m	
	1471m		1473m		1478m	
14	1450s		1452m		1452s	
			1447s			
15	1338w		1340w		1347w	
16	1236m		1236vw		1237m	
6	1217m		1220m		1215s	
	1210s		1211s			
17			1153m		1157w	
7	1072w		1069m[b]		1076sh	
	1064m				1067m	
8	1052w				1050w	
9		1026vs		1024vs		1030vs
						1021vs
	1015m		1015m		1016w	
	983w		985w		982w	
	974w		973w		970w	
23 or	953w		848w		953w	
24	944w					
	878w		871w		871w	
					857w	
					785s	
25	771s		768s[b]		767s	
	763s				760s	
26	700s		703s		699s	
	696s		692w		693s	
10	656w		647w		648w	
	653w					
	644m					
27	465w		471w		481w	
					477w	
					471w	
[c]	325m	328m,sh	329m	328s	331s	
		322s	324sh	323m		
	316s	318m,sh		317m	320m	318s
	313w,sh		313m	312w,sh	310sh	310s
	302sh		304sh		307sh	
	270m	274w	270m	273w	273w	276w
	265sh				263m	266w
					256sh	
		242w		241w	246sh	
		225w,br		223w,br		232w,br

[a] Selected bands only (see text).
[b] Bands with structure.
[c] Bands arising from Mpy and M—Cl vibrations.

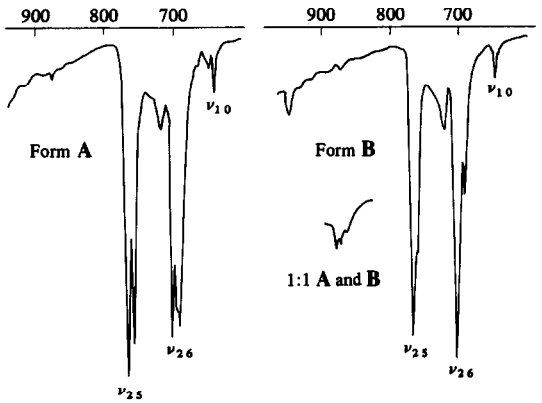

Fig. 1. IR spectra of ligand modes (600–950 cm^{-1}) in the forms of *fac*-$[Ir(py)_3Cl_3]$.

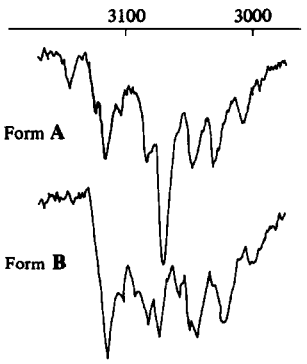

Fig. 2. Patterns of C—H stretching modes in the IR spectra of the forms of *fac*-$[Ir(py)_3Cl_3]$.

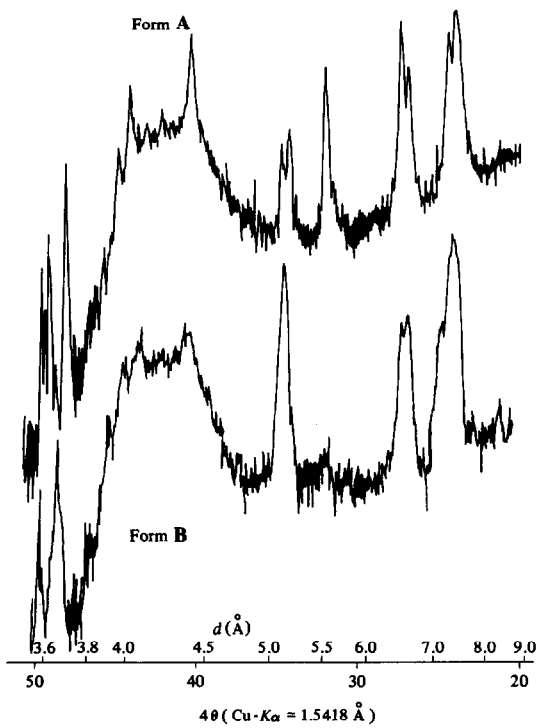

Fig. 3. X-ray diffraction patterns for the powdered dimorphic forms of *fac*-$[Ir(py)_3Cl_3]$.

between the two powder patterns, illustrated in Fig. 3. The diffraction patterns have not been previously reported, nor are any crystallographic details yet known: crystal morphology is so far poor.

RESULTS AND DISCUSSION

The distinguishing differences between the spectra of the two *fac* forms are: a slight difference in a number of band positions, especially M—L/M—Cl bands; the change in activity of two bands (ligand modes): ν_{16} has medium intensity in Form **A**, but is almost absent in Form **B**, and vice versa for ν_{17}; a distinctive difference in the splitting of ligand modes ν_{10}, ν_{25} and ν_{26} (Fig. 1) and a different structure in the C—H stretching region (Fig. 2: **A** at *3144, 3116, 3084, 3071, 3048, 3032 and 3009; **B** at 3115, 3083, 3074, *3058, *3045, 3023 and 2001 cm^{-1}. The bands marked * have no counterpart in the spectrum of the other dimorph).

There are two published studies[11,12] of the IR spectra of *fac*-$[Ir(py)_3Cl_3]$, both on samples supplied by Delepine. The spectrum of Clark and Williams is limited to the far-IR, and agrees closely with the present Form **A**. Harbelin *et al.* record more of the spectrum (4000–1000 cm^{-1}). While their spectrum agrees better with that of Form **A**, the detail is poor: it appears to be a hybrid, containing some peaks of Form **A** and others of Form **B**. It probably represents chiefly Form **A** since the authors describe ν_{16} as a prominent band (it is almost undetectable in our Form **B**).

The splitting of the ligand modes in the *fac* form **B** is most similar to that reported for *fac*-$[Rh(py)_3Cl_3]$.

The IR spectra and corresponding Raman spectra (Table 3) are very similar in the M—L/M—Cl stretching region.

Isolated molecules of *fac*-$[Ir(py)_3Cl_3]$ have a three-fold axis of symmetry only if the pyridine ligands are equivalent, i.e. (i) freely rotating with a period less than that of the detection method, (ii) fixed in an orientation where all three planes make equal angles with the axis which passes through the iridium ion and the centre of the triangle defined by the three chloride ligands or (iii) all three rotating in phase through successive conformations like those in (ii). Evidently, the molecules actually possess no such C_3 symmetry in either Form **A** or **B**, since some pyridine ring vibrations are no longer equivalent and splitting occurs. This probably arises from the site symmetry(ies) of the complex molecules. While this inequivalence is much less pronounced for Form **B**, there is fine structure on many bands.

The earlier suggestion[13] that the Raman vibration ν_9 is insensitive to environment but sen-

sitive to the configuration of the complex molecules seems to be borne out, in that the *mer*-isomer shows two bands of relative intensity, approximately 1 : 2, corresponding to *cis*- and *trans*-ligands, respectively, while the *fac*-isomer gives only a single band at 1025 cm^{-1} (Table 3).

Form **A** seems metastable with respect to **B**, at least in 50% v/v aqueous pyridine as solvent, so may be viewed as a metastable intermediate in the sense of Ostwald's law. The kinetic conditions necessary to produce Form **A** depend subtly on the original reaction conditions (e.g. temperature or concentration of aqueous pyridine) or on the presence of a trace of some other complex, e.g. *trans*-$[Ir(py)_4Cl_2]^+$, which determines the form by its presence when nucleation begins, or by being incorporated in trace amounts into the crystal lattice.

The present example again demonstrates the frequency of occurrence of various distinct solid forms of individual coordination compounds, and the care needed to identify the particular phase in hand.

REFERENCES

1. J. A. Arce Sagues, R. D. Gillard and P. A. Williams, *Transition Met. Chem.* 1989, **14**, 110.
2. E. G. Lundquist, K. Folting, J. C. Huffman and K. G. Caulton, *Polyhedron* 1988, **7**, 2171.
3. E. Bielli, P. M. Gidney, R. D. Gillard and B. T. Heaton, *J. Chem. Soc., Dalton Trans.* 1974, 2133.
4. M. Delepine, *Ann. Chim.* 1923, **9**, 145 : a later detailed study (H.-H. Schmidtke and A. Wolf, *Inorg. Chim. Acta* 1978, **29**, 11) of the luminescence spectra of mixed complex compounds containing chloride and pyridine as ligands on iridium(III) was concerned only with ionic species, including only those isomers of composition $[Ir(py)_3Cl_3]$ which were *cis*- or *trans*-$[Ir(py)_4Cl_2]^+$ salts of *cis*- or *trans*-$[Ir(py)_2Cl_4]^-$ ions.
5. F. Lareze, *Compt. Rend.* 1964, **259**, 3789.
6. M. Guillot, *Compt. Rend.* 1962, **182**, 1090; M. Guillot, *Bull. Soc. Chim. Fr.* 1962, **39**, 852.
7. R. D. Gillard, S. H. Mitchell, P. A. Williams and R. S. Vagg, *J. Coord. Chem.* 1984, **13**, 325.
8. M. M. Muir, G. M. Gomez, J. A. Muir and S. Sanchez, *Acta Cryst.* 1987, **C43**, 839.
9. C. K. Jorgensen, *Acta Chem. Scand.* 1957, **11**, 151; C. K. Jorgensen, *Absorption Spectra and Chemical Bonding in Complexes*. p. 191. Pergamon Press, Oxford (1962).
10. F. Lareze and G. Rio, *Bull. Soc. Chim. Fr.* 1975, 2393.
11. R. J. H. Clark and C. S. Williams, *J. Chem. Soc.* 1965, 350.
12. F. Herbelin, J. D. Herbelin, J. P. Mathieu and H. Poulet, *Spectrochim. Acta* 1966, **22**, 1515.
13. A. W. Addison and R. D. Gillard, *J. Chem. Soc., Dalton Trans.* 1973, 2002.

Polyhedron Vol. 8, No. 18, pp. 2251–2254, 1989
Printed in Great Britain

0277-5387/89 $3.00+.00
© 1989 Pergamon Press plc

COMPLEXATION OF THE URANYL ION BY CROWN ETHERS, DIAZA-CROWN ETHERS AND ANALOGOUS ACYCLIC LIGANDS IN SOLUTION

J. LAGRANGE, J. P. METABANZOULOU, P. FUX and P. LAGRANGE*

URA 405 au CNRS, EHICS, 1 rue Blaise Pascal, 67000 Strasbourg, France

(*Received* 1 *March* 1989; *accepted* 26 *April* 1989)

Abstract—The complexation of uranyl ion, UO_2^{2+}, with several crown ethers (15C5; 18C6; 21C7; 24C8; 30C10) substituted or not by benzo or carboxylic groups and with several diaza-crown ethers (21; 22; 23 coronands) substituted or not by alkyl chains have been investigated in propylene carbonate and in acetonitrile (in the presence of 0.1 M tetraethylammonium perchlorate). The results are compared with those obtained for the complexation of UO_2^{2+} by analogous acyclic ligands. The inclusion of UO_2^{2+} in the cavity of the 18C6 ligand family is demonstrated. The substitutions of the ligands have, in general, only small effects on the complexation.

The inclusion of the uranyl ion in a crown ether (or a diaza-crown ether) of the appropriate size has been demonstrated in the solid state, by structural determinations.[1–5] In solution, the uranium inclusion is in competition with the solvation of the ligand cavity, and the complexation of uranium itself is also in competition with the solvation. Only weak complexes are observed with crown ethers in water: the coordination between the uranyl ion and the complexing groups of the ligand occurs with hydrogen bond formation between the hydrogen atoms of the water molecules solvating the uranium and the oxygen atoms of the crown ether.[6] In water, the uranyl ion is only stable in acidic medium. Thus, the polyaza-crown ethers are not useful, because the amino functions of the ligand are protonated[7] in this acidic medium.

In this work, we have determined the nature and the stability constants of the complexes formed between the uranyl ion and the ligands mentioned below (Fig. 1), in propylene carbonate, principally, and in acetonitrile. These two organic solvents have been chosen for their solvating properties. They both have sufficiently high dielectric constants to provide good dissociation of the strong electrolytes, but the metallic cations are less solvated by these organic solvents than by water. Thus, the complexation and inclusion of the uranyl ion in a macrocyclic ligand must be more facile in propylene carbonate or in acetonitrile than in water.

The ligands are: 1,4,7,10,13-pentaoxacyclopentadecane (15C5); 1,4,7,10,13,16-hexaoxacyclooctadecane (18C6); 1,4,7,10,13,16,19-heptaoxacycloheneicosane (21C7); 2,3,11,13,-dibenzo-1,4,7,10,13,16-hexaoxacyclooctadeca-2,11-diene (DB18C6); 2,3,14,15-dibenzo-1,4,7,10,13,16,19,22-octaoxacyclotetracosa-2,14-diene (DB24C8); 1,4,7,10,13,16-hexaoxacyclooctadeca-2,3,11,12-tetracarboxylic acid (18C6TCA); 1,4,10-trioxa-7,13-diazacyclopentadecane (21); 1,7,10,16-tetraoxa-4,13-diazacyclooctadecane (22); 1,7,10,13,19-pentaoxa-4,16-diazacycloheneicosane (23); 4,13-dimethyl-1,7,10,16-tetraoxa-4,13-diazacyclooctadecane (22DM); 4,13-didecyl-1,7,10,16-tetraoxa-4,13-diazacyclooctadecane (22DD); 4,13-dihydroxyethyl-1,7,10,16-tetraoxa-4,13-diazacyclooctadecane (22DETOH); diethylamine (DEA); diethyl ether (DEE); 2,5,8,11,14-pentaoxapentadecane (TeEG); 1,8-diaminooctane (DAO); 1,8-diamino-3,6-dioxaoctane (DAOO); tris[2-(2-methoxyethoxy)-ethyl]-amine (TDA).

EXPERIMENTAL

Reagents

Uranium(VI) perchlorate was obtained from Ventron and tetraethylammonium perchlorate

* Author to whom correspondence should be addressed.

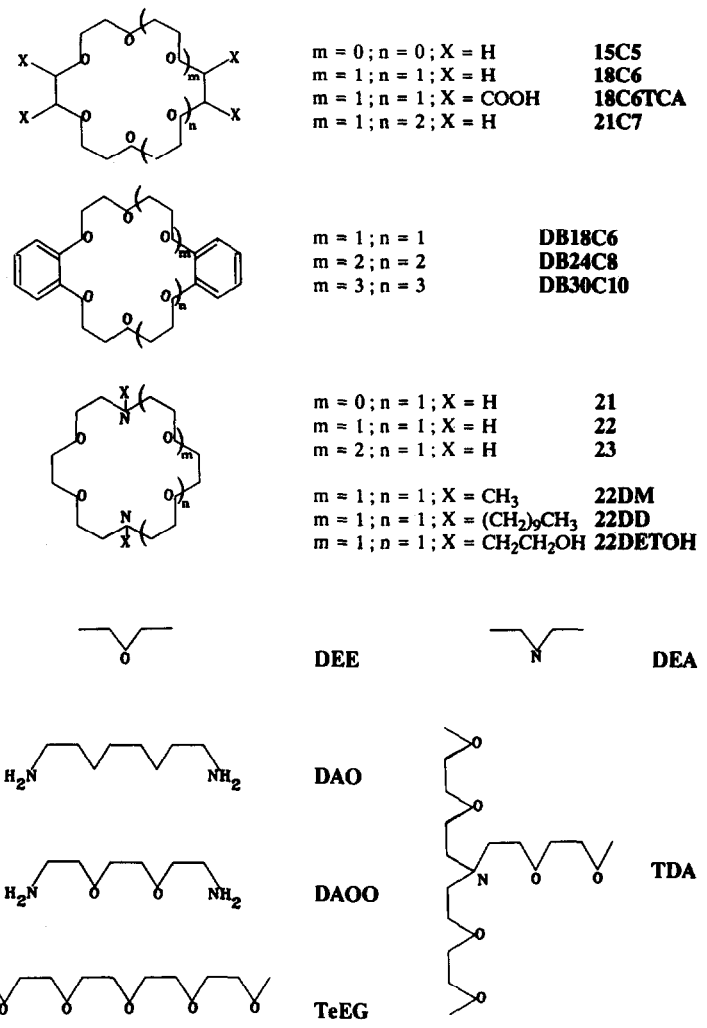

Fig. 1. The ligands.

(Fluka) was recrystallized twice from water and carefully dried *in vacuo*. The ligands were obtained from Merck, except for 21C7 (from Parish), 22DM and 22DETOH (synthesized by Gramain *et al.*[8] Propylene carbonate (Fluka) was purified according to Gosse.[9] Acetonitrile, Uvasol, was purchased from Merck.

The ionic strength was maintained at 0.1 M by the addition of tetraethylammonium perchlorate, $(TEA)ClO_4$.

The residual water content was determined by a Karl Fischer titration. All test solutions contained less than 150 ppm of water.

Spectrophotometric measurements

Spectrophotometric measurements were performed with a Kontron Uvikon 860 spectrophotometer between 230 and 350 nm, in quartz cells, at 25 ± 0.1°C. The absorbances of the solutions containing between 10^{-4} and 10^{-6} M of uranyl ion and between 10^{-3} and 10^{-6} M of a given ligand were recorded at 5 nm intervals. Data treatments were conducted using the Sillen's generalized least-squares method LETAGROP–SPEFO.[10] (The computer was an IBM 3081.) The calculation allows us to choose the stoichiometry and stability constant of the formed complexes which gives the most appropriate model.

RESULTS

Each formed complex, $(UO_2)_xL_y^{2x+}$, is characterized by its stoichiometry, $(x:y)$. The logarithms of the stability constants, β, of the equilibria:

$$xUO_2^{2+} + yL \rightleftharpoons (UO_2)_xL_y^{2x+},$$

Table 1. Complexation by crown ethers in propylene carbonate (— indicates that no complex was observed)

Ligand	Complex	log β
15C5	—	—
18C6	1:1	5.29±0.01
21C7	1:1	3.09±0.01
DB18C6	1:1	5.51±0.31
DB24C8	1:1	3.63±0.16
DB30C10	1:1	2.95±0.12
18C6TCA	1:1	5.61±0.21

with

$$\beta = \frac{[(UO_2)_x L_y^{2x+}]}{[UO_2^{2+}]^x [L]^y}$$

are tabulated in Table 1 for the complexation of UO_2^{2+} by crown ethers in propylene carbonate, in Table 2 by diaza-crown ethers in propylene carbonate, in Table 3 by acyclic ligands in propylene carbonate, and in Table 4 for the complexation in acetonitrile. In acetonitrile, the low solubility of the aza ligands did not allow us to carry out measurements using these aza complexing agents. The uncertainty limits quoted are twice the computed standard deviations.

DISCUSSION

The discussion will take into account the following points: the possibility of the uranyl ion inclusion in crown ethers and in diaza-crown ethers, the influence of the presence of substituting groups on the ligands, and the influence of the solvent.

Table 2. Complexation by diaza-crown ethers in propylene carbonate

Ligand	Complex	log β
21	1:1	4.96±0.20
	1:2	8.56±0.25
22	1:1	7.45±0.05
	1:2	12.40±0.04
23	1:1	6.79±0.10
	1:2	12.96±0.10
22DM	1:1	6.90±0.10
	1:2	14.28±0.19
22DD	1:1	3.88±0.19
	1:2	7.74±0.20
22DETOH	1:1	7.08±0.20
	1:2	14.50±0.25

Table 3. Complexation by acyclic ligands in propylene carbonate (— indicates that no complex was observed)

Ligand	Complex	log β
DEE	—	—
TeEG	1:1	2.99±0.20
DEA	1:1	< 1
	1:2	7.03±0.01
DAO	1:1	3.08±0.20
DAOO	1:1	3.81±0.20
TDA	1:1	4.41±0.20
	1:2	8.19±0.20

Complexation by crown ethers and analogous linear ligands

The uranyl ion complexation by crown ethers shows only the formation of 1:1 complexes, when they are observed. The inclusion in the ligand hole is only possible if this cavity has a diameter greater than the ionic diameter of the uranyl ion (2.8 Å),[11] measured in the equatorial plane. Thus, 15C5 which has a cavity diameter of *ca* 1.8 Å[12] does not complex the uranyl ion. Furthermore, the ether function is a weak complexing group and the uranyl ion is being complexed only by poly-coordinating ligands having more than one ether group. Diethyl ether does not provide observable complexation with the uranyl ion, but TeEG gives a stable 1:1 chelate. The complexation by 18C6 shows a complex 200 times more stable than those formed with TeEG in propylene carbonate and in acetonitrile. This effect must be due to the inclusion of the cation in the ligand cavity (macrocyclic effect), but the stability increase is limited by the difficulty encountered by UO_2^{2+} to penetrate into the hole of the crown ether.[13] The best crown ether seems to be 18C6 with its adapted cavity (diameter around 2.9 Å).[12]

Table 4. Complexation in acetonitrile (— indicates that no complex was observed)

Ligand	Complex	log β
DEE	—	—
TeEG	1:1	1.47±0.12
15C5	—	—
18C6	1:1	3.80±0.30
DB18C6	1:1	6.00±0.40
DB24C8	1:1	5.16±0.35

Complexation by diaza-crown ethers and analogous ligands

Amines are better complexing agents than ether and a complexation by diethylamine is observed in propylene carbonate: formation of a stable 1:2 complex. The metals have a greater affinity for nitrogen atoms than for oxygen atoms. Thus, we can conclude that "exclusive" or "inclusive" complexes can be observed with the diaza-crown ethers. The inclusion of the uranyl ion in the ligand cavity is more complicated with the diaza-crown ethers than with the crown ethers, because 1:1 and 1:2 complexes are observed with the "diaza" ligands. However, the 1:1 complexes with 21 or 22 or 23 ligands are 100–1000 times more stable than the analogous complexes formed with the acyclic ligands: DAO, DAOO and TDA. Thus, this macrocyclic effect allows us to conclude that, at least, a partial inclusion of the uranyl ion in the diaza-crown ether must be probable. The best ligand is the 22 coronand which is analogous to 18C6.

Influence of the substituting groups of the ligands

With the crown ethers, the benzo groups increase the complexing power of the ligands. These substitutions maintain the ligand cavity open and entry for the cation is easier. The carboxylic acid substituents can also assist the entry of the cation into the ligand cavity. In conclusion, these substitutions only have a small effect on the complexation in propylene carbonate, but a more important effect for "benzo" groups in acetonitrile.

With the diaza-crown ethers, the complexation is inhibited by the alkyl chains bonded to the ligand 22. This effect increases with the length of the chains. The decyl groups could be inside the coronand cavity and the possibility of inclusion of the uranyl ion in the crown ether decreases strongly. The presence of two methyl groups or two alcohol groups has a very weak influence on the complexation. These observations present limitations in the use of alkyl chains which can immobilize these macrocyclic ligands on a polymer matrix.

Influence of the solvent

Only the complexation of uranyl ion by crown ethers and analogous linear ether ligands has been carried out in propylene carbonate and in acetonitrile. The "aza" ligands are not soluble enough in acetonitrile. We notice that the ligands without "benzo" groups are better complexing agents of the uranyl ion in propylene carbonate than in acetonitrile. A decrease in the stability constants is observed when the solvent has a greater solvating property of the metallic cation, as we can see in Table 5 for the complexation of the uranyl ion by 18C6. The structure of the complexes changes from "inclusive" in propylene carbonate to "outer sphere" in water.

Table 5. Logarithm of the stability constant of the 1:1 complexes formed between UO_2^{2+} and 18C6 in different solvents

Propylene carbonate	Acetonitrile	MeOH–H_2O (90:10%)	H_2O
5.29	3.80	3.15[a]	2.0[b]

[a] Reference 14. [b] Reference 6.

The influence of the "benzo" substituting groups of the crown ethers is greater in acetonitrile than in propylene carbonate because they hinder the solvation of the hole in the coronands, which is easier for acetonitrile than for propylene carbonate. A similar effect has been previously observed by Kolthoff *et al.*[15] for the complexation of K^+ and Na^+. The crown ether cavities are probably more strongly solvated by the acetonitrile molecules than by the larger propylene carbonate molecules.

REFERENCES

1. R. M. Costes, G. Folcher, N. Keller, P. Plurien and P. Rigny, *Inorg. Nucl. Chem. Lett.* 1975, **11**, 469.
2. R. M. Costes, G. Folcher, P. Plurien and P. Rigny, *Inorg. Nucl. Chem. Lett.* 1976, **12**, 13.
3. R. M. Costes, G. Folcher, P. Plurien and P. Rigny, *Inorg. Nucl. Chem. Lett.* 1976, **12**, 491.
4. A. Navaza, F. Villain and P. Charpin, *Polyhedron* 1984, **3**, 143.
5. A. Dejean, P. Charpin, G. Folcher, P. Rigny, A. Navaza and G. Tsoocaris, *Polyhedron* 1987, **6**, 189.
6. M. Brighli, P. Fux, J. Lagrange and P. Lagrange, *Inorg. Chem.* 1985, **24**, 80.
7. B. Spiess, F. Arnaud and M. J. Schwing-Weill, *J. Inorg. Nucl. Chem.* 1979, **15**, 13.
8. P. Gramain and Y. Frere, *New J. Chim.* 1979, **3**, 53.
9. B. Gosse and A. Denat, *J. Electroanal. Chem. Interfac. Electrochem.* 1974, **56**, 129.
10. L. G. Sillen and V. Warnqvist, *Arkiv. Kemi* 1968, **31**, 377.
11. L. Cattalini, U. Croatto, S. Degetto and E. Tondello, *Inorg. Chim. Acta* 1971, **5**, 19.
12. N. K. Dalley, in *Synthetic Multidentate Macrocyclic Compounds* (Edited by R. M. Izatt and J. J. Christensen), Academic Press, New York (1978).
13. P. Fux, J. Lagrange and P. Lagrange, *J. Am. Chem. Soc.* 1985, **107**, 5927.
14. C. Luca and H. A. Azab, *Analyt. Lett.* 1984, **17**, 1937.
15. I. M. Kolthoff and M. K. Chantooni, *Analyt. Chem.* 1980, **52**, 1039.

Polyhedron Vol. 8, No. 18, pp. 2255–2263, 1989
Printed in Great Britain

0277–5387/89 $3.00+.00
© 1989 Pergamon Press plc

THEORETICAL STUDY OF HYDROXAMIC ACIDS

N. J. FITZPATRICK*

Department of Chemistry, University College, Belfield, Dublin 4, Ireland

and

R. MAGESWARAN

Department of Chemistry, University of Jaffna, Jaffna, Sri Lanka

(*Received* 7 *March* 1989; *accepted* 26 *April* 1989)

Abstract—*Ab initio* molecular orbital calculations on formohydroxamic and acetohydroxamic acids give stabilities in the order: *E*-keto > *Z*-keto > *Z*-enol > *E*-enol. However, on hydration the *E*-keto and *Z*-keto order is reversed, in agreement with NMR results. Methyl substituted forms are also considered, and the importance of hydrogen bonding is noted.

Hydroxamic acids can occur as many isomers and conformers. Recently *cis–trans* isomerism in monoalkylhydroxamic acids has been studied by ^{1}H, ^{13}C and ^{15}N NMR spectroscopy,[1] where it was predicted that, in the keto form, *Z*- and *E*-isomers can exist, if restricted rotation about the C—N bond occurs.

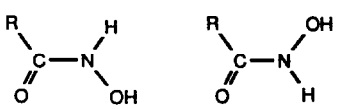

Z E

Also tautomerism would lead to enolic hydroxamic acid, RC(OH)NOH, forms. The experimental NMR spectra show that both the *Z* and *E* forms exist in solution, as do the enol forms. However the X-ray crystal structure of acetohydroxamic acid hemihydrates indicates that in the crystal the *Z*-keto form is found,[2] which is similar to propionohydroxamic acid.[3] Also, ^{1}H and ^{13}C NMR studies on N-substituted hydroxamic acids have shown that the *Z*–*E*-isomer ratio is solvent dependent; the *Z*-isomer predominates in polar solvents like DMSO-d_6. The predominance of the *Z*-isomer in DMSO-d_6 may be due to the preferential stabilization of the *Z*-isomer by solvation/hydrogen bonding with some residual water present.[4]

The stabilities of different forms of the isolated and hydrated hydroxamic acids in this study were examined using *ab initio* molecular orbital calculations. Previously, the geometry of formohydroxamic acid was studied using the INDO–MO formalism.[5] In the present study the Gaussian 82 program[6] with 3–21*g* basis sets[7] was used to consider formohydroxamic and acetohydroxamic acids and their hydrated forms, as well as methyl substituted species.

RESULTS AND DISCUSSION

(a) *Formohydroxamic acid*

It has been shown that formohydroxamic acid[4] occurs in different isomers and conformers. Figure 1 shows the optimized geometries for the structures considered. The global minimum is the non-planar *E*-keto structure, with an energy of −242.35827 au. This is 32.9 kJ mol^{-1} more stable than the form with a planar geometry. The energies of the other optimized structures, relative to the global minimum, are also shown in Fig. 1. All the structures in the figure do not correspond to a critical point of order zero; however the four lowest energy forms (*E*- and *Z*-keto and enol) had order zero critical points.

It is noteworthy that the nitroso structure, the highest energy form considered, is 189.2 kJ mol^{-1} above the global minimum. The second lowest

* Author to whom correspondence should be addressed.

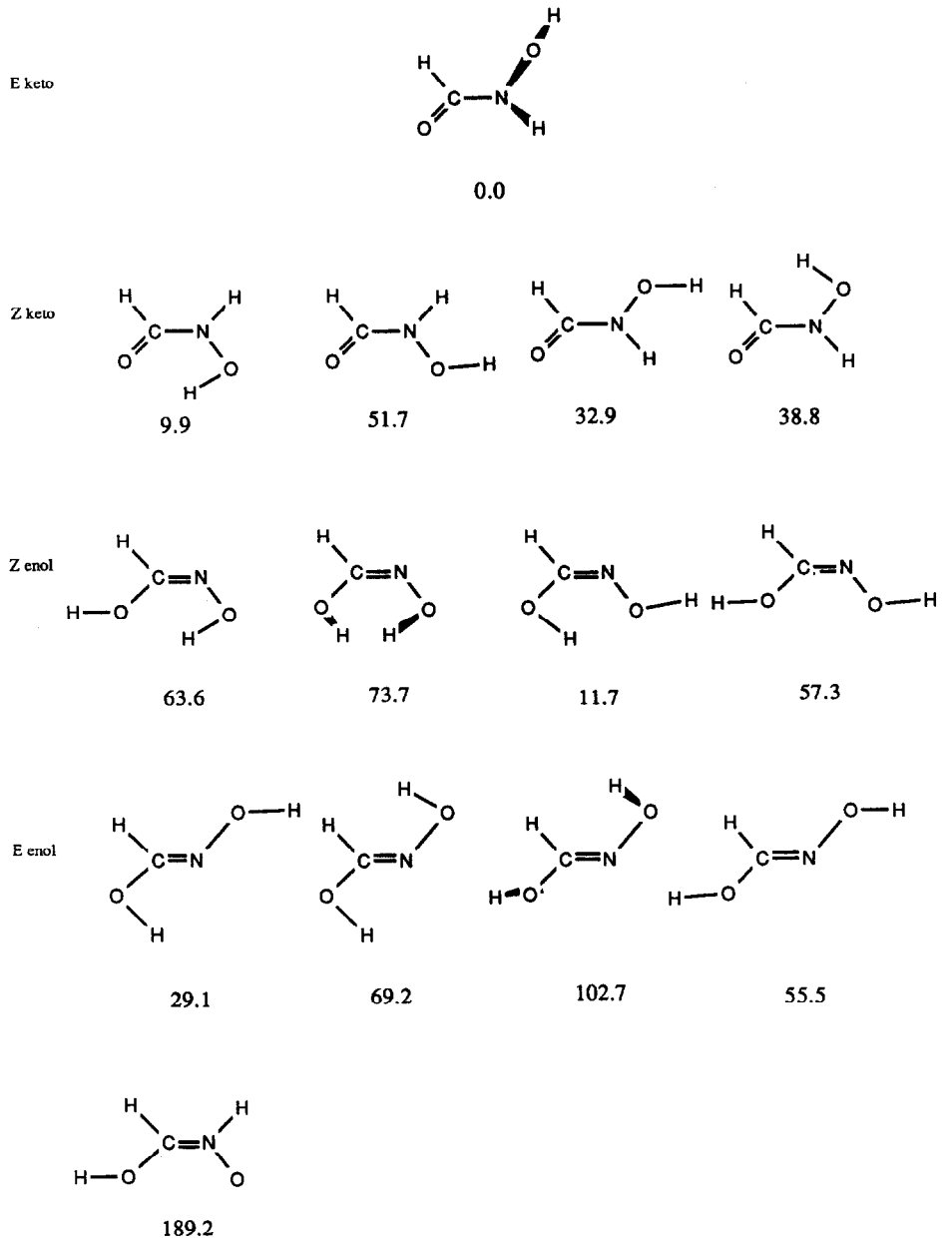

Fig. 1. Optimized structures and relative energies (kJ mol^{-1}) of formohydroxamic acid.

energy form is the *Z*-keto form, which is 9.9 kJ mol^{-1} above the global minimum. The next most stable structure is the *Z*-enol form (11.7 kJ mol^{-1} above the global minimum), and next in stability to this is the *E*-enol form at 29.1 kJ mol^{-1} above the minimum. Both the most stable *Z*- and *E*-enol forms have HOCN dihedral angles of 0° and CNOH dihedral angles of 180°, indicating the stabilizing effect of having the C(OH) group closer to the C=N double bond and the N(OH) group further away. The *Z*-enol form is more stable than the *E*-enol one, illustrating the influence of intramolecular hydrogen bonding in the isolated molecules.

Figure 2 shows the geometries, charge distributions and overlap populations between appropriate atoms of the most stable structures. In both the keto and enol *Z* forms, the intramolecular hydrogen bonding is indicated by the overlap populations, which are 0.049 for the keto and 0.046 for the enol form. The charge on the carbonyl oxygen in the *Z*-keto form is −0.632, while the charge on the other oxygen is −0.479; the strong electronic repulsion between these two oxygens outweighs the intramolecular hydrogen bonding in the *Z*-keto form, thus the *E*-keto form is energetically favoured. Again in the *Z*-enol form, the hydrogen bonding and the oxygen–oxygen repulsion act in

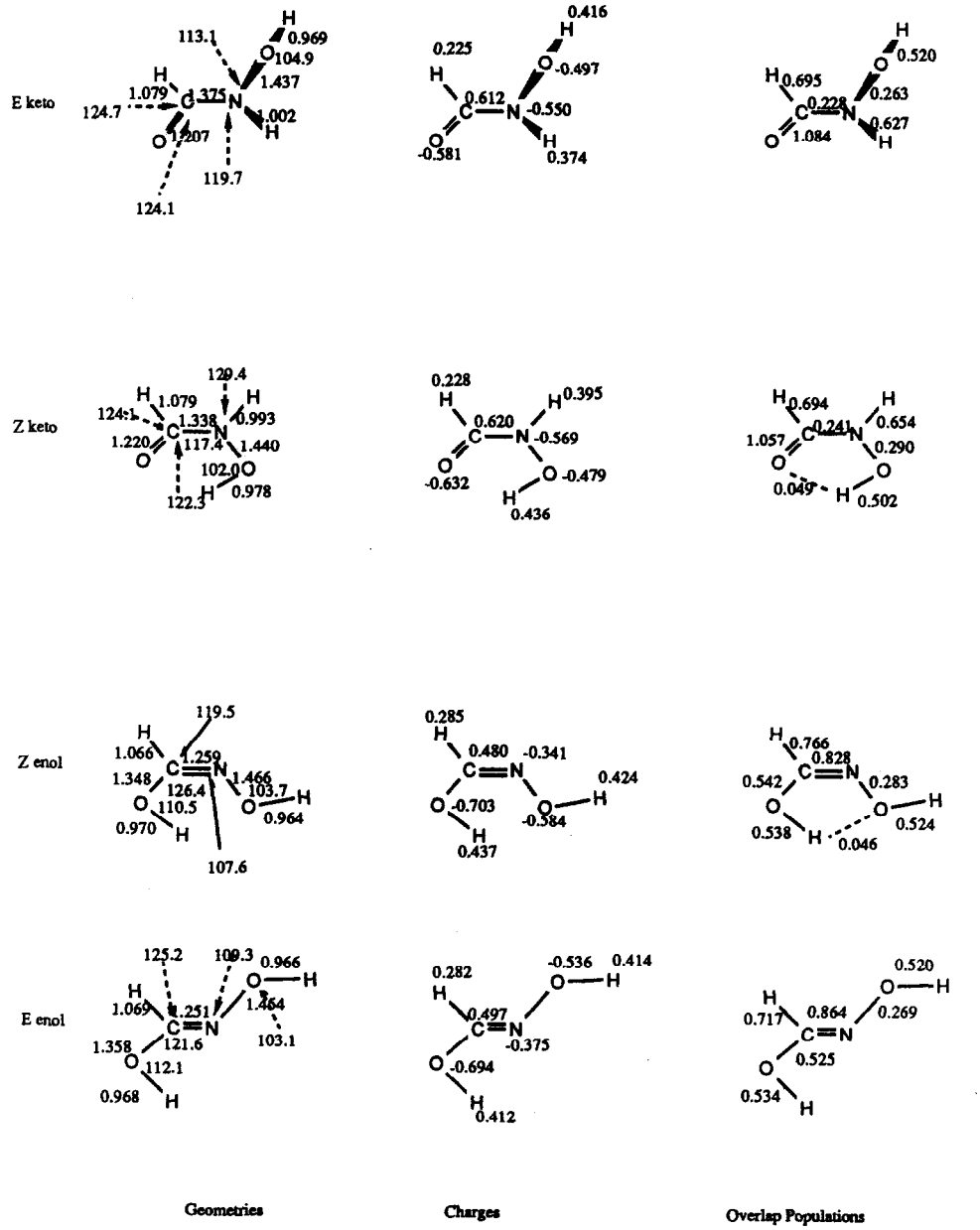

Fig. 2. Geometries, charges and overlap populations for the most stable forms of formohydroxamic acid. Bond lengths in Å, bond angles in degrees. In the *E*-keto form the dihedral angles are: HNCH = 157.0°; ONCH = 21.0°; HONC = 116.2°.

opposite directions. However, in this case the hydrogen bonding is more important and the *Z*-enol form is more stable than the corresponding *E*-enol one. The C—H bond lengths in the four most stable structures vary little, from 1.079 to 1.066 Å. Also the NH (from 1.002 to 0.993 Å) and OH (from 0.978 to 0.964 Å) bond lengths show little variation. However, the NO bond lengths vary by a reasonable amount in changing from the keto to the enol forms as expected, 1.437–1.454 Å (*E* forms) and 1.440–1.466 Å (*Z* forms). The C=O bond lengths are 1.207 Å (*E*) and 1.220 Å (*Z*), while the corresponding C—O distances in the enol forms are 1.358 Å (*E*) and 1.348 Å (*Z*). Thus the C=O bond lengthening in the *Z*-keto form, where there is hydrogen bonding, relative to the *E*-keto form, is noted. The C—N lengths are 1.375 Å (*E*) and 1.338 Å (*Z*), while the corresponding C=N distances are 1.251 and 1.259 Å. Thus the C=N bond distance differs little in the *E*- and *Z*-enol forms, but the C—N single bond distance is smaller in the *Z*-keto form, showing the effect of delocalization of the nitrogen lone pair in the planar *Z* form. The calculated XH (X = C, O, N) bond lengths are close

to the standard values of Pople and Beveridge.[8] However, the calculated N—O bond lengths are found to be greater than the standard value, as are the C—N bond lengths (the standard C—N bond length in the N—C=O groups is 1.32 Å), particularly in the *E*-keto form, where the nitrogen lone pair is not delocalized, due to non-planarity of the molecule, to the extent that it is in the *Z*-keto form. Most of the angles around carbon are close to 120°, while the NOH angle varies little (102.0–104.9°).

The charges on the oxygen atoms are large and negative in all of the four most stable structures. In the keto forms, carbons have large positive and nitrogen large negative charges; the absolute values of these are smaller (Fig. 2) in the enol forms due to the drift of electrons towards oxygen [N—C=O].

The overlap populations (Fig. 2) clearly show the bond order differences. The C—N bond orders are low, indicating ease of rotation about the C—N bond, even though hydrogen bonding may hinder rotation from the *Z* form. It is noteworthy that the *Z*-keto form has higher C—N and lower C=O overlap populations, showing more delocalization than the *E*-keto form. In the enol forms, the *Z* structure has lower C=N and higher C—O overlap populations, again showing the effects of delocalization. The extent of intramolecular hydrogen bonding in the *Z*-keto and -enol forms is also shown by the appreciative O···H overlap populations (0.049 in the keto, 0.046 in the enol; Fig. 2).

(b) *Hydrated formohydroxamic acids*

X-ray crystallographic studies have shown that in the solid state, acetohydroxamic acid exists in the *Z* form with a water molecule hydrogen bonded to two molecules of acetohydroxamic acid.[2] Preliminary NMR studies indicate that the *Z*-keto isomer predominates in DMSO-d_6, where there is the possibility of hydrogen bonding with the trace amount of water present, stabilizing the *Z* form.[4] Therefore it was decided to consider the four most stable forms of formohydroxamic acid (*E*- and *Z*-keto and enol forms) with varying amounts of water coordinated. Figure 3 shows the structures of the hydrated forms of formohydroxamic acid with varying amounts of coordinated water and their relative energies (kJ mol^{-1}).

From Fig. 3 it is seen that the most stable form, with one molecule of water coordinated, is now the *Z*-keto form, followed by the *E*-keto form. The enol forms with one molecule of water are at higher energy than the keto forms, while within the enol forms the *Z* structure has the lower energy.

In summary, with one molecule of coordinated water the stability order is *Z*-keto > *E*-keto > *Z*-enol > *E*-enol, while for the isolated species the order is *E*-keto > *Z*-keto > *Z*-enol > *E*-enol. In the most stable form with one molecule of water coordinated, there is appreciable hydrogen bonding; the (HO)H···O(=C) overlap population is 0.106 and the $(H_2)O\cdots H(ON)$ value is 0.164. The corresponding hydrogen–oxygen distances are 1.776 and 1.623 Å, respectively. In the *E*-keto form the hydrogen bonding is less; the (HO)H···O(=C) overlap population is 0.088 and the $(H_2)O\cdots H(N)$ value is 0.126. In this case the corresponding hydrogen–oxygen distances are 1.912 and 1.870 Å, respectively. Also, in the *Z*-keto form with one molecule of water, compared with the unhydrated form, the ONC angle is increased from 117.4 to 121.3°, and the O···O distance is increased from 2.666 to 2.824 Å, thus the oxygen–oxygen repulsion descreases.

In the enol forms, there are two possibilities. The oxygen atom of the water can be hydrogen bonded to either (CO)H or (NO)H. In both the *Z* and *E* forms, the former has the lower energies. In the enol form, as in the isolated molecules, the *Z* form has a lower energy than the *E* form. The hydrogen bonding is stronger in the *Z* form, where the $(H_2)O\cdots H(O)$ and (HO)H···O(N) overlap populations are 0.182 and 0.098, and the corresponding hydrogen–oxygen distances are 1.581 and 1.759 Å. In the *E*-enol form the corresponding overlap populations are less, $(H_2)O\cdots H(O) = 0.150$, $(HO)H\cdots N(O) = 0.073$; the corresponding distances are greater, 1.662 and 2.045 Å, respectively. The H···O overlap populations are greater than the H···N values and the corresponding hydrogen bond distances are in the reverse order.

The charge distributions in the hydrated molecules are of interest. The absolute value of the charge on the oxygen and hydrogen atoms involved in hydrogen bonding in both the *Z*-keto and -enol forms are larger than in the unhydrated form. In general, the addition of a molecule of water increases the absolute values of the negative charges on the oxygen attached to carbon and the nitrogen due to a drift of electrons: O → N → C → O.

The study was extended to formohydroxamic acid with two molecules of water. As seen from Fig. 3, the trend is the same as with one molecule of coordinated water. The order of stability in both cases is *Z*-keto > *E*-keto > *Z*-enol > *E*-enol. It is of interest to note that the spread of energies for the *Z*-keto, *E*-keto and *Z*-enol forms is small, only 12.8 kJ mol^{-1}, while the *E*-enol form is much higher in energy (58.8 kJ mol^{-1}) than the lowest energy *Z*-keto form. In the *E*-enol form with two water molecules the second water molecule, close to H(ON), pushes the first water molecule away from this group, reducing the hydrogen bonding between

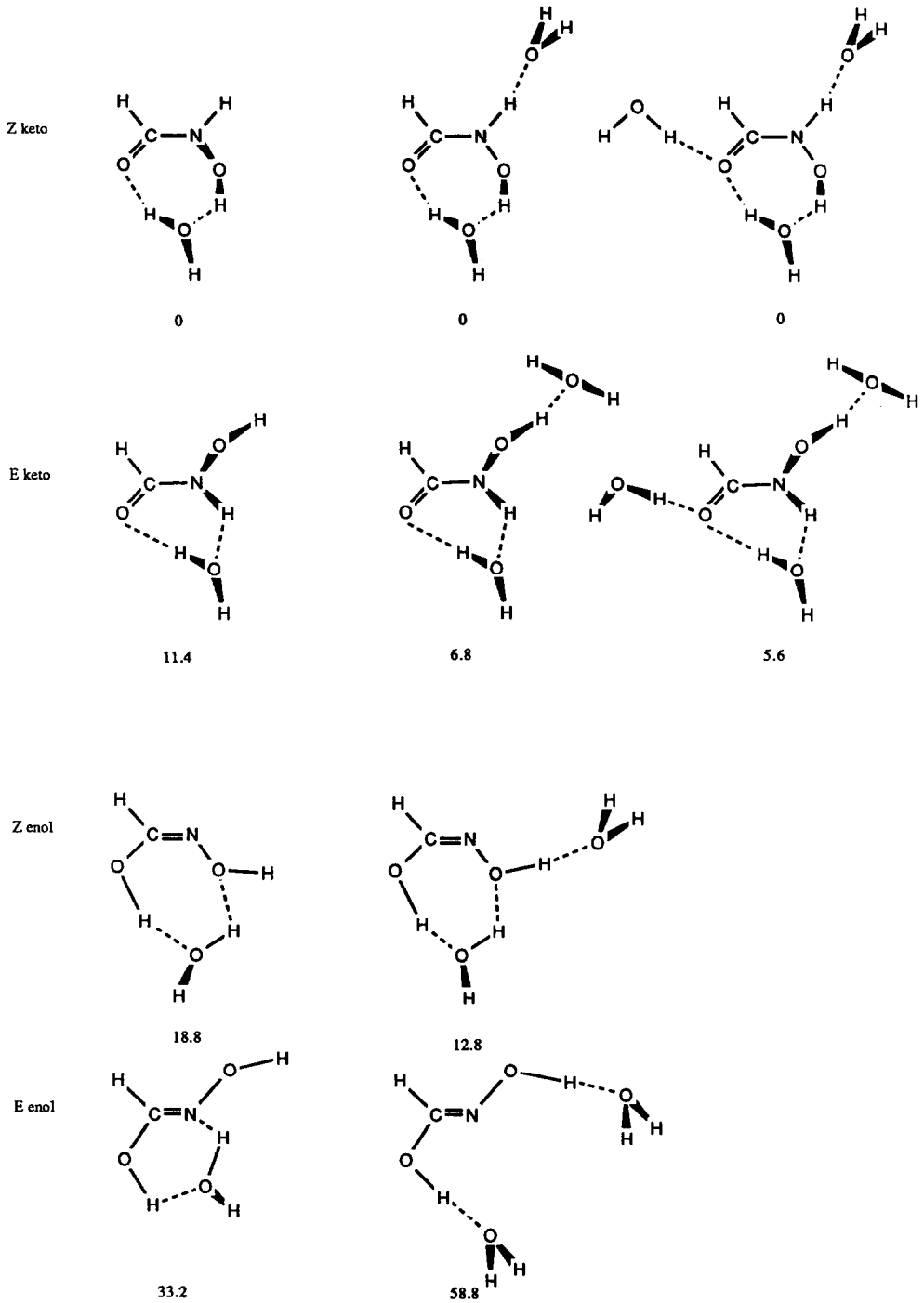

Fig. 3. Optimized structures and relative energies (kJ mol^{-1}) of formohydroxamic acid water complexes.

the hydrogen in the first water molecule and the nitrogen atom. The addition of a second molecule of water closer to H(N) in the *Z*-keto form, has a tendency to push the electron density $H \rightarrow O \rightarrow N \rightarrow C \rightarrow O$. In all forms the C–O distances are longer and the C–N distances shorter, with two water molecules coordinated than with one and the CO bond orders are decreased and the CN bond order increased by adding the second water molecule.

In the crystal structure of acetohydroxamic acid, the carbonyl oxygen is hydrogen bonded to two hydrogen atoms. Therefore the influence of a third molecule of water closer to the carbonyl oxygen was considered for the *Z*- and *E*-keto forms. Again the *Z* form was found to have the lower energy.

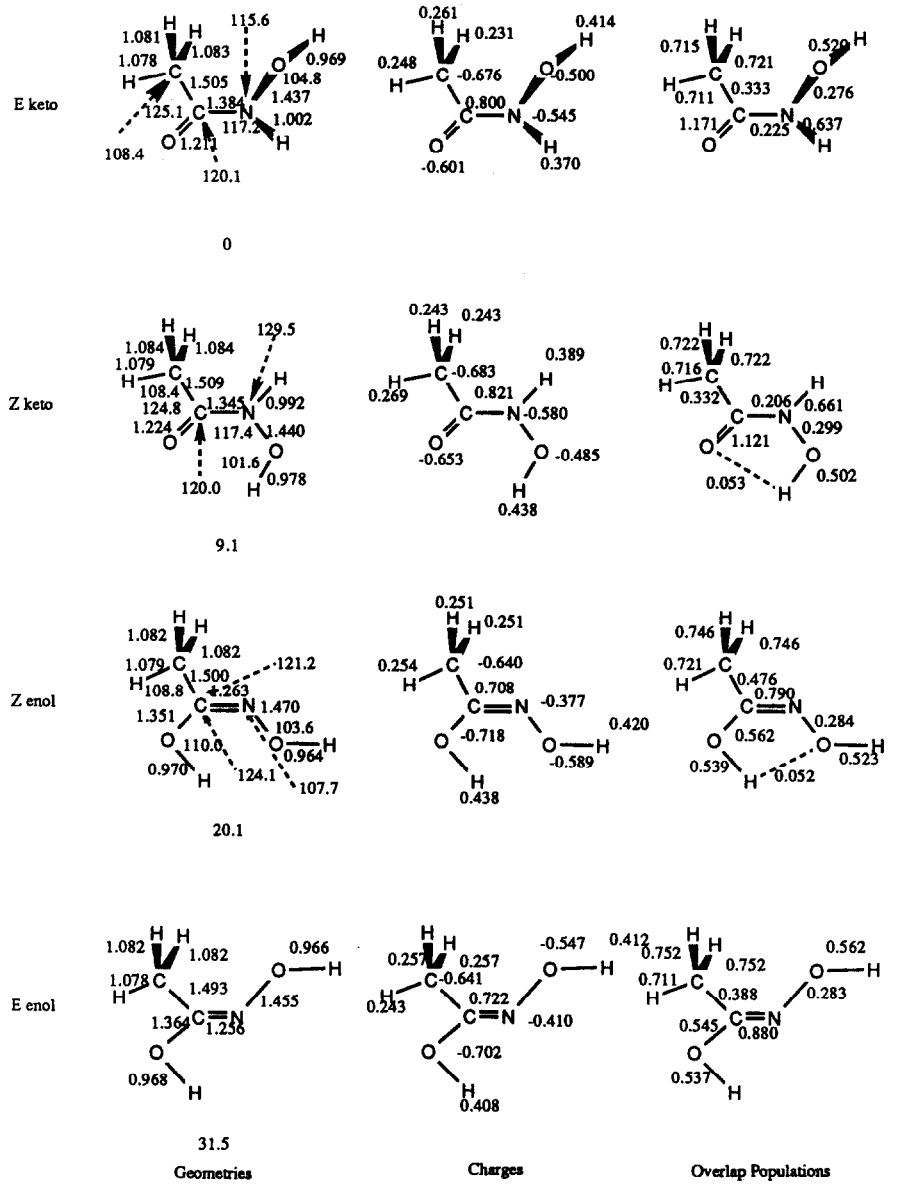

Fig. 4. Geometries, charges and overlap populations for the most stable forms of acetohydroxamic acid. Bond lengths in Å, bond angles in degrees. In the *E*-keto form the dihedral angles are: $HNCC(H_3) = 159.1°$; $ONCC(H_3) = 24.3°$.

The addition of a third molecule of water decreases the CN bond length and increases the corresponding CO value.

The energy of the *Z*-keto forms of HC(O)NH(OH) is −242.35451 au. The successive addition of water molecules lowers the energy by 75.62226, 75.60740 and 75.60167 au; thus the addition of the first water molecule to the isolated formohydroxamic acid has the greatest effect.

(c) *Acetohydroxamic acid*

The theoretical studies were extended to acetohydroxamic acid; the optimized structures are summarized in Fig. 4. As in the case of formohydroxamic acid, the lowest energy form is *E*-keto (−281.19064 au). The next lowest is *Z*-keto, followed by *Z*-enol and then *E*-enol; the same trend was calculated for formohydroxamic acid. The *Z*-keto, *Z*-enol and *E*-enol forms are 9.1, 20.1 and 31.5 kJ mol^{-1} above the *E*-keto structure, which are close to the values obtained for formohydroxamic acid. Thus the methyl substituent does not appreciably change the order or values of the relative energies. The CC(O)NH(OH) portion of the *Z*-keto and the CC(OH)=N(OH) portions of the *Z*- and *E*-enol forms are planar, which is analogous to the formohydroxamic results. The $ONCC(H_3)$ and

$HNCC(H_3)$ angles of the non-planar and stable *E* (keto) form are 24.3 and 159.1°, respectively. The carbonyl group charges show that replacement of a hydrogen by a methyl group increases the absolute values of the oxygen and carbon charges, but the remaining charges differ little in the two molecules. In the *Z*-keto form the importance of hydrogen bonding is indicated by the C=O···H overlap population (0.053), which is slightly greater than the corresponding value in formohydroxamic acid. Other changes in going from the *E*- to *Z*-keto forms of acetohydroxamic acid parallel those of the formohydroxamic acid.

Comparing the enol forms, it is noted that the (CO)H···O(N) overlap population (0.052) in *Z*-enol acetohydroxamic acid is slightly greater than the corresponding value in formohydroxamic acid (0.046). The absolute values of the O, N and C(O) charges in both the *Z*- and *E*-enol forms of acetohydroxamic acid are greater than those in the corresponding formohydroxamic acid. The changes in going from the *Z*- to *E*-enol forms parallel those of formohydroxamic acid. In the *Z*-enol form the C=N overlap population is appreciably less than that in the *E*-enol form, supporting the delocalization of electron density around the five-membered ring, as was found in the corresponding formohydroxamic acid.

Unlike formohydroxamic acid, it is possible to get methylene analogues by enolization of acetohydroxamic acid. Figure 5 shows the optimized geometries and relative energies of the different conformers considered. Of these, the lowest energy form, with energy of −281.15488 au is 93.9 kJ mol^{-1} above that of the most stable *E*-keto isomer of acetohydroxamic acid.

It is interesting to note that:

(i) not all, but most, of the conformers in Fig. 5 are planar;
(ii) in both the lower energy *E* and *Z* forms the H(OC) atom is on the same side of the OC bond as the methylene group;
(iii) in the most stable form, the geometry of the CNH(OH) group has not changed appreciably from the geometry in *E*-keto acetohydroxamic acid.

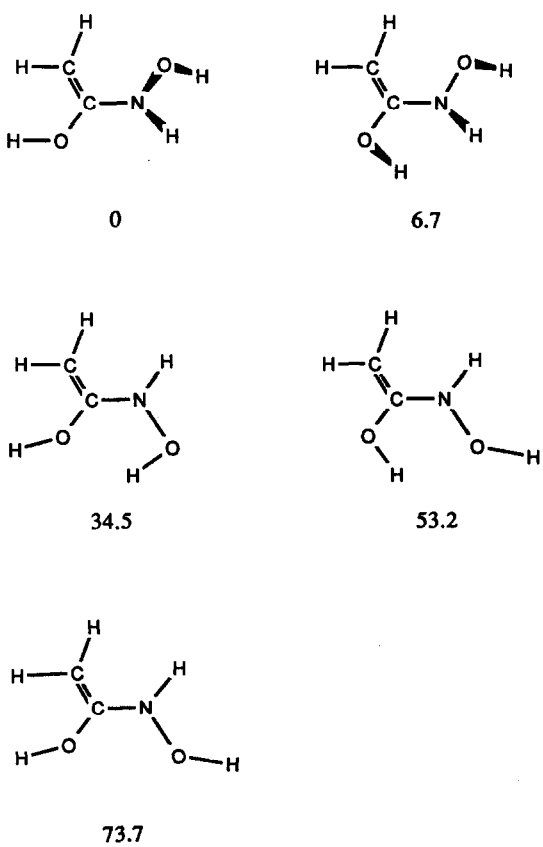

Fig. 5. Optimized structures and relative energies (kJ mol^{-1}) of CH_2=C(OH)NH(OH). The most stable form is 93.9 kJ mol^{-1} above the *E*-keto form of acetohydroxamic acid.

(d) *Hydrated acetohydroxamic acid*

Since the ^1H NMR indicated that in DMSO-d_6 $CH_3CONH(OH)$ may exist mainly in the *Z* form, it was decided to consider the two most stable forms of acetohydroxamic acid with one molecule of coordinated water. The optimized structures are shown in Fig. 6. As is the case of formohydroxamic acid,

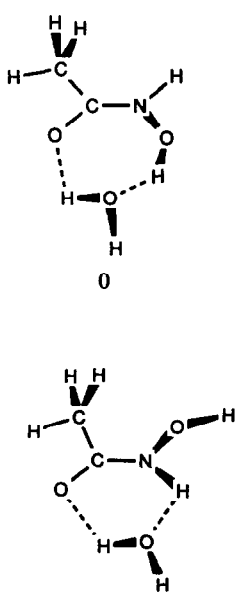

Fig. 6. Optimized structures and relative energies (kJ mol^{-1}) of acetohydroxamic acid water complexes.

the *Z*-keto form (−356.80822 au) was calculated to be more stable than the *E*-keto form; the energy difference is 8.9 kJ mol^{-1}. Thus, as in the case of formohydroxamic acid, hydration reverses the stability order of the keto forms. The difference in energy between the isolated *Z*-keto acetohydroxamic acid and its hydrated form (75.62103 au) is similar to the corresponding formohydroxamic value (75.62226 au).

N-*methyl and* O-*methyl acetohydroxamic acids*

Since it is possible that the *Z*–*E* ratios of N- and O-methylacetohydroxamic acids may vary in different solvents,[4] it was decided to consider the stabilities of these substituted acetohydroxamic acids. The results are shown in Figs 7 and 8, respectively. The N- or O-methyl substitution did not change the order of stability, since in both cases the *E*-keto forms are the most stable ones. The C(O)···H(ON) overlap population in the *Z*-keto form of N-methylacetohydroxamic acids (0.056) is slightly greater than that in acetohydroxamic acid (0.053), and the energy difference between the *Z*- and *E*-keto forms of $CH_3C(O)N(CH_3)OH$ (14.5 kJ mol^{-1}) is slightly greater than that in acetohydroxamic acid (9.1 kJ mol^{-1}). It is noteworthy, that in the N-methyl species, the two forms considered differ little in energy, indicating the importance of hydrogen bonding in the *Z*-keto form.

In O-methylacetohydroxamic acid, there is no NOH group to participate in hydrogen bonding, the *Z*-keto form is 39.8 kJ mol^{-1} above the *E*-keto form. Thus the importance of hydrogen bonding in

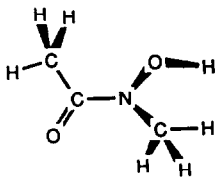

0

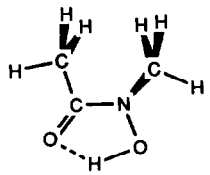

14.5

Fig. 7. Optimized structures and relative energies (kJ mol^{-1}) of N-methylacetohydroxamic acid.

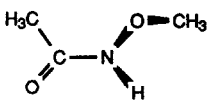

0

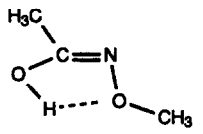

20.1

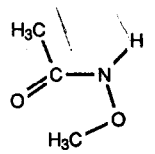

39.8

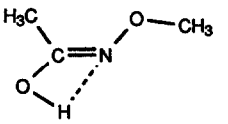

31.1

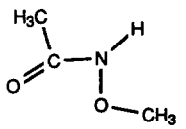

47.8

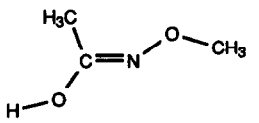

61.9

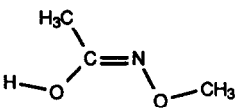

75.7

Fig. 8. Optimized structures and relative energies (kJ mol^{-1}) of O-methylacetohydroxamic acid. The most stable form is 11.5 kJ mol^{-1} above the corresponding form of the N-methyl analogue.

stabilizing structures in this series is noted. The calculations show that the *Z*- and *E*-enol forms, which have hydrogen bonds, are more stable than the *Z*-keto form. The order of stability is: *E*-keto > *Z*-enol > *E*-enol > *Z*-keto. The *Z*-enol form is 19.7 kJ mol^{-1} more stable than the *Z*-keto form, whereas the energy difference between the *E*-enol and *Z*-keto forms is smaller (8.7 kJ mol^{-1}). The other structures with the OH and OCH_3 groups rotated by 180° were considered and their energies are appreciably higher (Fig. 8). Figure 9 shows conformers of $CH_2{=}C(OH)NH(OCH_3)$. In all cases the energies are higher than the species in Fig. 8.

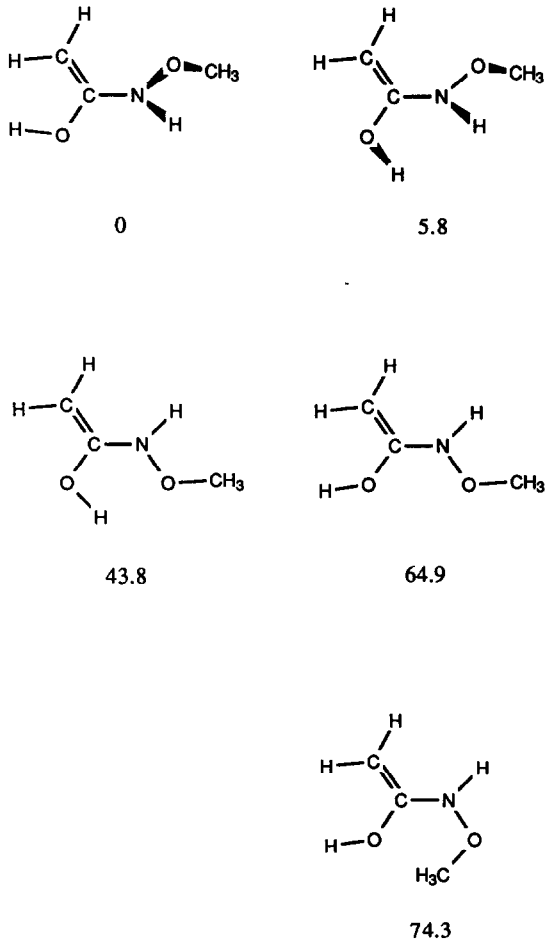

Fig. 9. Optimized structures and relative energies (kJ mol^{-1}) of CH_2=C(OH)NH(OCH_3). The most stable structure is 106.2 kJ mol^{-1} above the *E*-keto form of O-methylacetohydroxamic acid.

CONCLUSION

Ab initio molecular orbital calculations show that the isolated *E*-keto forms of formohydroxamic and acetohydroxamic acids have the lowest energy and that they are non-planar. Even though hydrogen bonding in the planar *Z*-keto species can occur, the *Z*-keto forms are less stable. However on hydration, oxygen–oxygen interactions decrease and hydrogen bonding increases, thus the *Z*-keto forms become the most stable. The importance of hydrogen bonding is noted in the *Z*-keto and in the enol forms. In the case of O-methylacetohydroxamic acid, where there is no possibility of hydrogen bonding the *Z*-keto form, the *Z*- and *E*-enol forms become more stable than the *Z*-keto form.

REFERENCES

1. D. A. Brown, W. K. Glass, R. Mageswaran and, in Part, B. Girmay, *Mag. Res. Chem.* 1988, **26**, 970.
2. B. H. Brecher and R. W. H. Small, *Acta Cryst.* 1970, **B26**, 1705.
3. G. Ferguson, private communication.
4. D. A. Brown, W. K. Glass and R. Mageswaran, preliminary results.
5. R. Hilal and H. Moustafa, *Int. J. Quant. Chem.* 1984, **26**, 183.
6. J. S. Binkley, M. J. Frisch, D. J. DeFrees, K. Raghavachari, R. A. Whiteside, H. B. Schelgel, E. M. Fluder and J. A. Pople, Gaussian 82. Carnegie-Mellon University, Pittsburgh, Pennsylvania (1983).
7. J. S. Binkley, J. A. Pople and W. J. Hehre, *J. Am. Chem. Soc.* 1980, **102**, 939.
8. J. A. Pople and D. L. Beveridge, *Approximate Molecular Orbital Theory*. McGraw Hill, New York (1970).

Polyhedron Vol. 8, No. 18, pp. 2265–2270, 1989
Printed in Great Britain

0277–5387/89 $3.00+.00
Pergamon Press plc

SYNTHESIS AND CRYSTAL STRUCTURE OF $[Mo_2FePt(\mu\text{-}\sigma,\sigma',\sigma'':\eta^5\text{-}CC_5H_4)_2(CO)_4\{HB(pz)_3\}_2]$ [$HB(pz)_3$ = HYDROTRIS(PYRAZOL-1-YL)BORATE]; A COMPLEX DERIVED FROM A 1,1′-FERROCENE DERIVATIVE WITH $C{\equiv}Mo(CO)_2\{HB(pz)_3\}$ SUBSTITUENTS

SIMON J. DAVIES, ANTHONY F. HILL, MASSIMINO U. PILOTTI and F. GORDON A. STONE*

Department of Inorganic Chemistry, The University of Bristol, Bristol BS8 1TS, U.K.

(*Received* 30 *March* 1989; *accepted* 4 *May* 1989)

Abstract—Treatment of $[Mo(CO)_6]$ in tetrahydrofuran, with 1,1′-dilithioferrocene in light petroleum, followed by $(CF_3CO)_2O$ and tmeda ($Me_2NCH_2CH_2NMe_2$) affords the ferrocene-substituted bis(alkylidynemolybdenum) complex $[Mo_2Fe(\mu\text{-}\sigma,\sigma':\eta^5\text{-}CC_5H_4)_2(O_2CCF_3)_2(CO)_4(tmeda)_2]$. The latter with $K[HB(pz)_3]$ [$HB(pz)_3$ = hydrotris(pyrazol-1-yl)borate] in CH_2Cl_2 gives $[Mo_2Fe(\mu\text{-}\sigma,\sigma':\eta^5\text{-}CC_5H_4)_2(CO)_4\{HB(pz)_3\}_2]$, which with $[Pt(cod)_2]$ (cod = cyclo-octa-1,5-diene), in light petroleum saturated with ethylene, yields the tetranuclear metal complex $[Mo_2FePt(\mu\text{-}\sigma,\sigma',\sigma'':\eta^5\text{-}CC_5H_4)_2(CO)_4\{HB(pz)_3\}_2]$. The structure of this product was established by *X*-ray diffraction, and the results of this study are compared with those obtained for related compounds in which the two metal–metal bonds of an acyclic trimetal system, in this case Mo—Pt—Mo, are each spanned by an alkylidyne group and semi-bridged by a carbonyl ligand.

The complexes $[M(\equiv CR)(CO)_2L]$ (M = W, Mo or Cr; R = alkyl or aryl; L = η-C_5H_5, η-C_5Me_5, or $HB(pz)_3$) have been widely employed as precursors for the synthesis of compounds containing heteronuclear metal–metal bonds.[1,2] The methodology involves addition of coordinatively unsaturated metal–ligand fragments to the C≡M triple bonds of the alkylidyne–metal reagents. This process can be carried out sequentially in some circumstances to construct molecular arrays in which chains or rings of metal atoms are held together by bridging alkylidyne ligands.[3]

The trimetal compounds $[M_2M'(\mu\text{-}CR)_2(CO)_4L_2]$ (**1**), obtained by treating the species $[M(\equiv CR)(CO)_2L]$ with zero-valent metal–alkene complexes $[M'(alkene)_n]$ (M′ = Ni, Pd or Pt; n = 3 or 4),[4] are important intermediates in many syntheses. This is because they are unsaturated, and metal–ligand fragments can be added to the dimetallacyclopropene ring systems present in **1**. The structures of three compounds of this class, **1a**,[4a] **1c**[4a] and **1q**,[4c] have been firmly established by *X*-ray diffraction studies. The molecules have essentially linear M—M′—M spines, with the two metal–metal bonds each bridged by an alkylidyne ligand and semi-bridged by a carbonyl group. The two alkylidyne fragments lie on the same side of the M—M′—M axis.

In this paper we describe the synthesis and structure of the novel tetranuclear metal complex $[Mo_2FePt(\mu\text{-}\sigma,\sigma',\sigma'':\eta^5\text{-}CC_5H_4)_2(CO)_4\{HB(pz)_3\}_2]$ (**2**), a species related to the compounds **1** but with the bridging alkylidyne carbon atoms linked by a ferrocene moiety. It was hoped that **2** might be a starting point for further syntheses based on addition of metal–ligand fragments to the C≡Mo bonds. Moreover, the structure of **2** was of interest, since the ferrocene group would constrain the positions of the ligated alkylidyne–carbon atoms. The possibility of a donor Fe→Pt bond also arises, since were such a linkage present it would provide a mechanism for relieving the electronic unsaturation at the platinum atom. In the compounds **1** the d^{10} metal atoms have formally 14-

* Author to whom correspondence should be addressed.

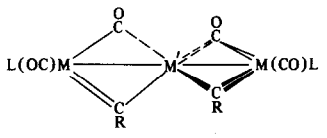

	M′	M	R	L
(1a)	Ni	W	C_6H_4Me-4	η-C_5H_5
(1b)	Pd	W	C_6H_4Me-4	η-C_5H_5
(1c)	Pt	W	C_6H_4Me-4	η-C_5H_5
(1d)	Ni	W	Me	η-C_5H_5
(1e)	Ni	W	Ph	η-C_5H_5
(1f)	Ni	W	Me	η-C_5Me_5
(1g)	Ni	W	Ph	η-C_5Me_5
(1h)	Ni	W	C_6H_4Me-4	η-C_5Me_5
(1i)	Ni	Mo	C_6H_4Me-4	η-C_5H_5
(1j)	Pt	W	Me	η-C_5H_5
(1k)	Pt	W	Ph	η-C_5H_5
(1l)	Pt	W	Me	η-C_5Me_5
(1m)	Pt	W	Ph	η-C_5Me_5
(1n)	Pt	W	C_6H_4Me-4	η-C_5Me_5
(1o)	Pt	Mo	C_6H_4Me-4	η-C_5H_5
(1p)	Ni	W	Me	HB(pz)
(1q)	Pt	W	Me	$HB(pz)_3$
(1r)	Pt	W	C_6H_4Me-4	$HB(pz)_3$
(1s)	Pt	Cr	C_6H_4Me-4	$HB(pz)_3$
(1t)	Pt	Mo	C_6H_4Me-4	$HB(pz)_3$
(1u)	Ni	W	$C_6H_4(OMe\text{-}2)Cr(CO)_3$	η-C_5H_5
(1v)	Ni	Mo	$C_6H_4(OMe\text{-}2)Cr(CO)_3$	η-C_5H_5
(1w)	Pt	Mo	$C_6H_4(OMe\text{-}2)Cr(CO)_3$	η-C_5H_5

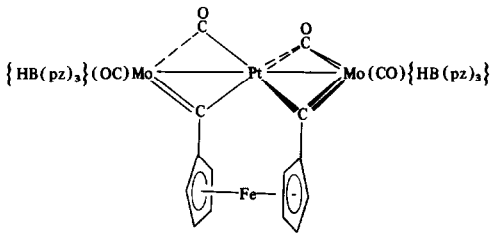

(2)

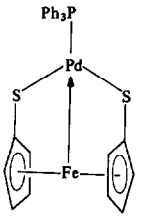

(3)

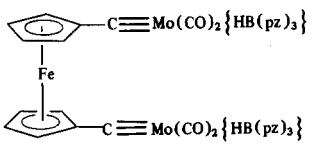

(4)

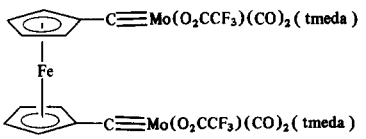

(5)

electron shells, unless it is assumed that the RC≡ $M(CO)_2L$ ligands are each contributing either three or four electrons to the M′ centres rather than two.[5] If an Fe→Pt electron-pair donor bond was a feature of the structure of **2** the situation would be somewhat akin to that in the compound $[FePd(\mu\text{-}\sigma,\sigma':\eta^5\text{-}SC_5H_4)_2(PPh_3)]$ (**3**) which has an Fe→Pd linkage.[6]

RESULTS AND DISCUSSION

Compound **2** was prepared by treating a THF (tetrahydrofuran) solution of the bis(alkylidyne-molybdenum) compounds $[Mo_2Fe(\mu\text{-}\sigma,\sigma':\eta^5\text{-}CC_5H_4)_2(CO)_4\{HB(pz)_3\}_2]$ (**4**) with an ethylene-saturated THF solution of $[Pt(cod)_2]$ (cod = cycloocta-1,5-diene). Complex **4**, required for this synthesis, was obtained from the reaction between $K[HB(pz)_3]$ and $[Mo_2Fe(\mu\text{-}\sigma,\sigma':\eta^5\text{-}CC_5H_4)_2(O_2CCF_3)_2(CO)_4(tmeda)_2]$ (**5**). The latter, the starting point for the sequence of reactions leading to **2**, was prepared via a procedure developed by Mayr and co-workers[7] for the synthesis of alkylidyne–metal compounds. For **5**, this involved treating a THF suspension of $[Mo(CO)_6]$ with 1,1′-dilithioferrocene, followed by addition of trifluoroacetic anhydride and tmeda.

Spectroscopic data characterizing compounds **4** and **5** are given in the Experimental. The IR spectra of both complexes show two terminal CO bands. For **4** these absorptions are at 1987 and 1904 cm^{-1}, and for **5** they are at 1992 and 1909 cm^{-1}. In addition, the IR spectrum of **5** shows a C=O absorption for the O_2CCF_3 group at 1735 cm^{-1}. In the $^{13}C\{^1H\}$ NMR spectra of **4** and **5** diagnostic peaks for alkylidyne–carbon nuclei occur at δ 293.2 and 286.9 ppm, respectively. Although it was possible to prepare **4** from **5** in virtually quantitative yield, the latter was obtained only in low and variable yield (*ca* 3–15%).

The synthesis of **2** proceeded smoothly in high yield (*ca* 80%). The IR spectrum displayed three CO stretching bands at 1970, 1941 and 1821 cm^{-1}. Although the two C_5H_4 groups in **2** are equivalent, each has two pairs of non-equivalent CH groups. Consequently, the ^1H NMR spectrum shows two signals for these groups at δ 4.22 and 4.72. In the

$^{13}C\text{-}\{^1H\}$ NMR spectrum the μ-C nuclei resonate at δ 300.6 ppm. This may be compared with the signal for the μ-C atoms in the spectrum of **1t** at δ 310.7 ppm.[4c] Interestingly, the CO ligands of **2** give rise to only a single peak at δ 231.1 ppm, in contrast with the related "bow-tie" type compounds (**1**), all of which show two peaks for the carbonyl groups in their $^{13}C\text{-}\{^1H\}$ NMR spectra.[4] To explain this observation a dynamic process is invoked for **1**, involving an oscillatory or rocking motion of the $Mo(CO)_2\{HB(pz)_3\}$ fragments so that exchange of CO ligands between terminal and semi-bridging sites occurs. This proposal is consistent with the rest of the spectrum which shows only three peaks for the carbon atoms of the $HB(pz)_3$ groups (δ 143.5, 134.5 and 104.6 ppm), when nine would be expected for a static structure. Similarly, there are only three resonances for the carbon atoms of the ferrocene group, that at δ 99.6 ppm being assigned to C^1 of the C_5H_4 rings and the peaks at δ 72.5 and 71.0 arising from the $C^{2,5}$ and $C^{3,4}$ carbons of the rings. Of particular interest is the $^{195}Pt\text{-}\{^1H\}$ NMR spectrum which shows a single peak at δ 76.8 ppm. This is in contrast with the platinum-containing trimetallic species, **1**, which show resonances in the range δ 1340–1750 ppm.[4b,c] It was thought initially that this large difference in chemical shift was due to the presence of a direct iron–platinum interaction in **2**, of the kind mentioned in the Introduction. However, this was disproved by an *X*-ray crystallographic study, the results of which are summarized by the data given in Table 1. The molecular structure is shown in Fig. 1.

Several features of the structure are of interest. Each molybdenum atom carries one terminal and one semi-bridging carbonyl group [Mo(1)—C(3)—O(3) 166.0(8) and Mo(2)—C(1)—O(1) 167.4(8)°]. The Mo—Pt separations (2.716 Å) are the same as those found (mean 2.716 Å) for the W—Pt distances in **1q**.[4c] Moreover, the μ-C—Mo and μ-C—Pt separations in **2** are also very similar to the μ-C—W and μ-C—Pt distances in **1q**. The Mo(1)—Pt—Mo(2) angle (167.9(1)°) in **2** may be compared with the corresponding W—Pt—W angle (172.8(1)°) in **1q**.

The Fe—Pt separation (3.715 Å) in **2** is clearly non-bonding, in contrast with the Fe—Pd distance (2.878 Å) in **3**.[6] Moreover, the C_5H_4 rings of the ferrocene moiety are not tilted, as would occur if a weak Fe—Pt interaction were to develop. It seems likely that the constraints imposed by the geometry around the sp^2 carbon atoms, C(10) and C(20), in **2** inhibit a closer approach of the iron and platinum atoms. In contrast, in **3** the sulphur atoms would be able to adjust to the more acute angle required to accommodate an Fe—Pd bond. Another important difference between **2** and **3**, however, relates to the respective oxidation states of the platinum and palladium atoms. The former in the zero oxidation state would seek to have a tetrahedral arrangement of ligating groups, whereas the latter in the oxidation state +II would have a preference for a square-planar arrangement of the coordinating groups.

In compound **2** the dihedral angle between the two dimetallacyclopropene rings (131°) is appreciably larger than those found previously (Table 2) for these rings in the structures of **1a**,[4a] **1c**[4a]

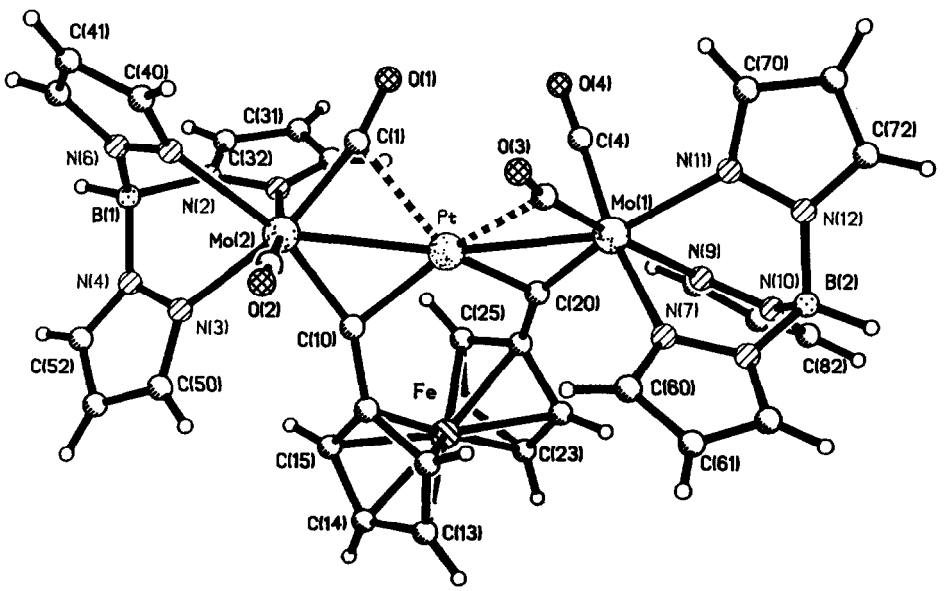

Fig. 1.

Table 1. Selected internuclear distances (Å) and angles (°) for $[Mo_2FePt(\mu\text{-}\sigma,\sigma',\sigma'':\eta^5\text{-}CC_5H_4)_2(CO)_4\{HB(pz)_3\}_2]$ (**2**)

Mo(1)—Pt	2.716(2)	Mo(2)—Pt	2.717(2)	Mo(1)—C(20)	1.90(1)
Pt—C(20)	2.01(1)	Mo(2)—C(10)	1.93(1)	Pt—C(10)	2.01(1)
Mo(1)—C(3)	2.00(1)	Pt—C(3)	2.31(1)	C(3)—O(3)	1.16(1)
Mo(2)—C(1)	1.99(1)	Pt—C(1)	2.33(1)	C(1)—O(1)	1.14(1)
Mo(1)—C(4)	1.99(1)	C(4)—O(4)	1.15(1)	Mo(2)—C(2)	1.99(1)
C(2)—O(2)	1.15(1)	C(10)—C(11)	1.43(1)	C(20)—C(21)	1.44(1)
Mo(1)—N(7)	2.21(1)	Mo(1)—N(9)	2.23(1)	Mo(1)—N(11)	2.25(1)
Mo(2)—N(1)	2.21(1)	Mo(2)—N(3)	2.22(1)	Mo(1)—N(5)	2.25(1)
Fe—C(cp)	2.04 av.				

Mo(1)—Pt—Mo(2)	167.9(1)	Mo(1)—C(20)—Pt	87.8(4)	Mo(1)—Pt—C(20)	44.3(3)
Pt—Mo(1)—C(20)	47.8(3)	Mo(2)—C(10)—Pt	87.1(4)	Mo(2)—Pt—C(10)	45.3(3)
Pt—Mo(2)—C(10)	47.6(3)	Mo(1)—C(3)—O(3)	166.0(8)	Mo(1)—C(4)—O(4)	177(1)
Pt—C(3)—O(3)	115.9(8)	Mo(2)—C(1)—O(1)	167.4(8)	Mo(2)—C(2)—O(2)	179(1)
Pt—C(1)—O(1)	114.7(8)	Fe—C(11)—C(10)	119.6(7)	Fe—C(21)—C(20)	120.0(7)
C(11)—C(10)—Mo(2)	152.3(8)	C(11)—C(10)—Pt	120.3(7)	C(21)—C(20)—Mo(1)	151.3(8)
C(21)—C(20)—Pt	120.8(7)				

Table 2.

Complex	M—M′—M angle (°)	Dihedral angle (°)[a]	M μ-C
$[Mo_2FePt(\mu\text{-}\sigma,\sigma',\sigma'':\eta^5\text{-}CC_5H_4)_2(CO)_4\{HB(pz)_3\}_2]$ (**2**)	167.9	131	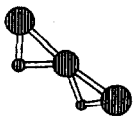
$[W_2Pt(\mu\text{-}CC_6H_4Me\text{-}4)_2(CO)_4(\eta\text{-}C_5H_5)_2]$ (**1c**)	165.5	97	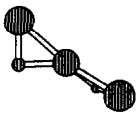
$[W_2Ni(\mu\text{-}CC_6H_4Me\text{-}4)_2(CO)_4(\eta\text{-}C_5H_5)_2]$ (**1a**)	174.5	93	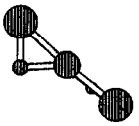
$[W_2Pt(\mu\text{-}CMe)_2(CO)_4\{HB(pz)_3\}_2]$ (**1q**)	172.8	79	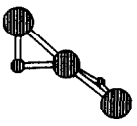
$[W_2Au(\mu\text{-}CC_6H_4Me\text{-}4)_2(CO)_4(\eta\text{-}C_5H_5)_2]^+$ (**6**)	162.8	62	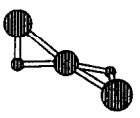

[a] Dihedral angle between the two dimetallacyclopropene rings. Angles greater than 90° reflect a distortion towards a square-planar geometry with a *cis*-C_2M' fragment. Conversely, angles less than 90° reflect a distortion towards a square-planar geometry with a *trans*-C_2M' fragment. The constraints of the two dimetallacyclopropene rings lead to μ-C—M′—M angles which are significantly less than those expected for idealized tetrahedral (or square-planar) geometries.[4a]

and **1q**,[4c] and in the salt $[W_2Au(\mu\text{-}CC_6H_4Me\text{-}4)_2(CO)_4(\eta\text{-}C_5H_5)_2][PF_6]$ (**6**).[8] The latter has the smallest inter-planar dihedral angle, but the structure differs from those of the other compounds by the absence of semi-bridging carbonyl groups. The large dihedral angle between the two dimetallacyclopropene rings in **2** may be attributed to the constraint imposed by the ferrocene fragment, resulting in C(10) and C(20) (Fig. 1) becoming distorted away from a pseudo-tetrahedral coordination around the platinum. However, the geometries of the metallacyclopropene rings in all these compounds, with their μ-C—M′—M angles of *ca* 45°, result in angles at the central metal atom, M′, which are far from tetrahedral.[4a]

The synthesis of complex **2** represents a novel addition to the class of compounds of type **1**. Unfortunately the use of **2** in the preparation of polynuclear metal species is currently inhibited by the poor yields in the synthesis of its precursor, **5**.

EXPERIMENTAL

All experiments were carried out under nitrogen, using Schlenk tube techniques. Solvents were rigorously dried before use. Light petroleum refers to that fraction of b.p. 40–60°C. Alumina used for chromatograhy columns was BDH aluminium oxide (Brockman activity II). The instrumentation employed for the spectroscopic measurements has been reported previously.[9] NMR chemical shifts (δ) are in ppm, and coupling constants are in Hz. The reagents $[Pt(cod)_2]$[10] and 1,1′-dilithioferrocene[11] were prepared by the methods described earlier.

Preparation of ferrocene-substituted alkylidyne molybdenum compounds

(i) A THF (50 cm^3) suspension of $[Mo(CO)_6]$ (5.3 g, 20.0 mmol) was treated with a hexane (100 cm^3) suspension of the tmeda complex of 1,1′-dilithioferrocene (0.10 mol dm^{-3}, 10 mmol). Sufficient light petroleum (*ca* 50 cm^3) was then added to the red–brown solution to complete the separation of a dark oil. The supernatant liquid was discarded, and the residual oil was washed twice with light petroleum (100 cm^3) and once with Et_2O (100 cm^3); ultrasonic irradiation being used each time to agitate the mixtures. The oily solid was then dried *in vacuo*, dissolved in THF (100 cm^3), and cooled to *ca* −80°C. Trifluoroacetic anhydride (3.0 cm^3, 25 mmol) was added, followed by tmeda (3.5 cm^3, 20 mmol). The mixture was warmed to room temperature, stirred for 30 min, and then filtered through an alumina plug (5 × 5 cm). Solvent was removed *in vacuo*, and the residue was dissolved in a minimum of CH_2Cl_2 (*ca* 15 cm^3) and chromatographed on alumina (4 × 30 cm column). Elution with CH_2Cl_2 removed a yellow uncharacterized side product. Subsequent elution with CH_2Cl_2–THF (3:2) gave a red fraction. Removal of solvent *in vacuo*, followed by crystallization of the residue from a mixture of CH_2Cl_2 (10 cm^3) and hexane (30 cm^3) at −78°C, gave pink–red *microcrystals* of $[Mo_2Fe(\mu\text{-}\sigma,\sigma':\eta^5\text{-}CC_5H_4)_2(O_2CCF_3)_2(CO)_4(tmeda)_2]$ (**5**) (1.0 g, 10%). IR: ν_{max} (in THF) at 1992s, 1909vs(CO) and 1735m cm^{-1} (C=O). NMR ($CDCl_3$): ^1H, δ 2.60, 2.72, 2.95 (s × 3, 32 H, tmeda), 4.43 and 4.56 [s(br) × 2, 8 H, C_5H_4]; $^{13}C\text{-}\{^1H\}$, δ 286.9 (C≡Mo), 225.0 (CO), 160.6 [q, C=O, J(FC) 19.5], 116.3 [q, CF_3, J(FC) 291], 90.5 [$C_{ipso}(C_5H_4)$], 70.9, 70.4 [$C^{2-5}(C_5H_4)$], 59.8, 55.7 and 50.0 (tmeda).

(ii) A CH_2Cl_2 (50 cm^3) suspension of **5** (0.42 g, 0.43 mmol) and $K[HB(pz)_3]$ (0.25 g, 0.86 mmol) was stirred for 5 h. Solvent was removed *in vacuo*, and the residue was dissolved in a mixture of CH_2Cl_2 (5 cm^3) and toluene (10 cm^3), and chromatographed on a water-cooled alumina column (5 × 20 cm). Elution with the same solvent mixture removed a red band. Solvent was evaporated *in vacuo*, and the residue was crystallized at −78°C from a mixture of CH_2Cl_2 (3 cm^3) and hexane (20 cm^3) to afford pink *microcrystals* of $[Mo_2Fe(\mu\text{-}\sigma,\sigma':\eta^5\text{-}CC_5H_4)_2(CO)_4\{HB(pz)_3\}_2]$ (**4**) (0.40 g, 94%). (Found: C, 43.8; H, 3.0; N, 17.0. $C_{34}H_{28}B_2FeMo_2N_{12}O_4$ requires: C, 43.5; H, 3.0; N, 17.9%.) IR: ν_{max} (in CH_2Cl_2) at 1987s and 1904vs cm^{-1} (CO). NMR (in $CDCl_3$): ^1H, δ 4.50, 4.76 [s(br) × 2, 8 H, C_5H_4], 6.17, 7.65, 7.91 (m × 3, 18 H, $C_3H_3N_2$); $^{13}C\text{-}\{^1H\}$, δ 293.2 (C≡Mo), 225.4 (CO), 143.4, 142.2, 134.6, 104.6 ($C_3H_3N_2$), 89.9 [$C_{ipso}(C_5H_4)$], 71.2 and 70.9 [$C^{2-5}(C_5H_4)$].

Preparation of $[Mo_2FePt(\mu\text{-}\sigma,\sigma',\sigma'':\eta^5\text{-}CC_5H_4)_2(CO)_4\{HB(pz)_3\}_2]$

The compound $[Pt(cod)_2]$ (0.17 g, 0.41 mmol) was dissolved portion-wise in cold (0°C) ethylene-saturated THF (25 cm^3). This mixture was then transferred (ethylene pressure) via a flexible steel cannula to a THF (25 cm^3) solution of **4** (0.38 g, 0.41 mmol), and the reactants were stirred for 3 h. Solvent was removed *in vacuo*, and the residue was dissolved in CH_2Cl_2–light petroleum (10 cm^3, 2:1) and chromatographed. Elution with the same solvent mixture removed a dark red fraction from which solvent was removed *in vacuo*. The residue was crystallized from CH_2Cl_2–EtOH (10 cm^3, 1:5) to give red *crystals* of $[Mo_2FePt(\mu\text{-}\sigma,\sigma',\sigma'':\eta^5\text{-}CC_5H_4)_2(CO)_4\{HB(pz)_3\}_2]$ (**2**) (0.37 g, 82%). [Found: C, 30.2; H, 2.0. $C_{34}H_{28}B_2FeMo_2N_{12}O_4Pt$

requires: C, 29.7; H, 1.8%.] IR: ν_{max} (in CH_2Cl_2) at 1970s, 1941vs and 1821m(br) cm^{-1} (CO). NMR (in CD_2Cl_2): ^1H, 4.22, 4.72 (s × 2, 8 H, C_5H_4), 6.17, 7.68 and 8.15 (s × 3, 18 H, $C_3H_3N_2$); ^{13}C-{^1H}, δ 300.6 (μ-C), 231.3 (CO), 143.5, 134.5, 104.6 ($C_3H_3N_2$), 99.6 [$C_{ipso}(C_5H_4)$], 72.5 and 71.0 [$C^{2-5}(C_5H_4)$]; ^{195}Pt-{^1H}, δ 76.8 (to high frequency of Ξ (^{195}Pt) $\simeq$ 21.4 MHz).

Crystal structure determination

Dark red prisms of **2** were grown from CH_2Cl_2–light petroleum. That chosen for data collection (*ca* 0.56 × 0.56 × 0.60 mm) was sealed under nitrogen in a Lindemann glass capillary. Diffracted intensities were collected (θ–2θ scans) at 298 K in the range $3.0 \leqslant 2\theta \leqslant 50°$, on a Nicolet *P3m* four-circle diffractometer. Of 5190 unique reflections, 3929 had $F \geqslant 4\sigma(F)$, and only these data were used in the solution and refinement of the structure. Corrections were applied for Lorentz, polarization and *X*-ray absorption effects; the latter by a procedure based on azimuthal scan data.[12]

Crystal data for **2**. $C_{34}H_{28}B_2FeMo_2N_{12}O_4Pt \cdot 1.5CH_2Cl_2$, $M = 1260.5$, monoclinic, $a = 16.188(4)$, $b = 13.585(6)$, $c = 20.820(8)$ Å, $\beta = 103.67(3)°$, $U = 4449(2)$ Å^3, $Z = 4$, $D_c = 1.89$ g cm^{-3}, $F(000) = 2520$, space group $P2_1/a$, Mo-K_α *X*-radiation ($\bar{\lambda} = 0.71069$ Å, graphite monochromator), μ(Mo-K_α) = 43.2 cm^{-1}.

The structure was solved, and all non-hydrogen atoms located, by conventional heavy-atom and difference Fourier methods. Hydrogen atoms were included in calculated positions (C—H, 0.96 Å) with fixed isotropic thermal parameters. The metal atoms and carbon atoms of the C_5H_4 and CO groups were refined anisotropically; the remaining atoms were refined isotropically. Refinement by blocked-cascade least-squares converged at $R = 0.048$ ($R_w = 0.047$) with a weighting scheme of the form $w^{-1} = [\sigma^2(F) + 0.000325|F|^2]$.* The final electron-density difference synthesis showed no residual peaks $\geqslant 0.99$ or $\leqslant -0.85$ eÅ^{-3}. Scattering factors and corrections for anomalous dispersion were taken from ref. 13. All calculations were carried out using a DEC micro-Vax II computer with the SHELXTL PLUS system of programs.[12]

*Atomic positional and thermal parameters, bond lengths and angles, and structure factor values have been deposited as supplementary material with the Editor. Atomic coordinates have also been submitted to the Cambridge Crystallographic Data Centre.

Acknowledgements—We thank Dr J. C. Jeffery for helpful discussions, the SERC for research studentships (to S.J.D. and M.U.P.), and the U.S. Air Force Office of Scientific Research for partial support (Grant 86-0215).

REFERENCES

1. F. G. A. Stone, *Am. Chem. Soc., Symp. Ser.* 1983, **211**, 383; F. G. A. Stone, *Pure Appl. Chem.* 1986, **58**, 529; F. G. A. Stone, in *Organometallic Compounds, Synthesis, Structure and Theory* (Edited by B. L. Shapiro), pp. 1–28. Texas A&M University Press, U.S.A. (1983); F. G. A. Stone, *Angew. Chem., Int. Ed. Engl.* 1984, **23**, 89.
2. F. G. A. Stone and M. L. Williams, *J. Chem. Soc., Dalton Trans.* 1988, 2467 and refs to previous papers cited therein.
3. S. J. Davies, J. A. K. Howard, R. J. Musgrove and F. G. A. Stone, *Angew. Chem., Int. Ed. Engl.* 1989, **28**, 624; S. J. Davies, J. A. K. Howard, M. U. Pilotti and F. G. A. Stone, *J. Chem. Soc., Chem. Commun.* 1989, 190.
4. (a) T. V. Ashworth, M. J. Chetcuti, J. A. K. Howard, F. G. A. Stone, S. J. Wisbey and P. Woodward, *J. Chem. Soc., Dalton Trans.* 1981, 763; (b) G. P. Elliott, J. A. K. Howard, T. Mise, I. Moore, C. M. Nunn and F. G. A. Stone, *J. Chem. Soc., Dalton Trans.* 1986, 2091; (c) S. H. F. Becke, M. D. Bermúdez, N. H. Tran-Huy, J. A. K. Howard, O. Johnson and F. G. A. Stone, *J. Chem. Soc., Dalton Trans.* 1987, 1229; (d) S. J. Davies and F. G. A. Stone, *J. Chem. Soc., Dalton Trans.* 1989, 785.
5. S. J. Dossett, A. F. Hill, J. C. Jeffery, F. Marken, P. Sherwood and F. G. A. Stone, *J. Chem. Soc., Dalton Trans.* 1988, 2453; S. J. Dossett, A. F. Hill, J. A. K. Howard, B. A. Nasir, T. P. Spaniol, P. Sherwood and F. G. A. Stone, *J. Chem. Soc., Dalton Trans.* 1989, in press.
6. D. Seyferth, B. W. Hames, T. G. Rucker, M. Cowie and R. S. Dickson, *Organometallics* 1983, **2**, 472.
7. G. A. McDermott, A. M. Dorries and A. Mayr, *Organometallics* 1987, **6**, 925.
8. G. A. Carriedo, J. A. K. Howard, K. Marsden, F. G. A. Stone and P. Woodward, *J. Chem. Soc., Dalton Trans.* 1984, 1589.
9. A. F. Hill, B. A. Nasir and F. G. A. Stone, *Polyhedron* 1989, **8**, 179.
10. J. L. Spenser, *Inorg. Synth.* 1979, **19**, 213.
11. A. G. Osborne, R. E. Hollands, J. A. K. Howard and R. F. Bryan, *J. Organomet. Chem.* 1981, **205**, 395.
12. G. M. Sheldrick, *SHELXTL programs for use with the Nicolet X-ray system.* Revision 5.1 (1986).
13. *International Tables for X-ray Crystallography*, Vol. 4. Kynoch Press, Birmingham (1974).

Polyhedron Vol. 8, No. 18, pp. 2271–2281, 1989
Printed in Great Britain

0277–5387/89 $3.00+.00
© 1989 Pergamon Press plc

COMPOUNDS WITH PLATINUM–MOLYBDENUM OR –TUNGSTEN BONDS DERIVED FROM THE ALKYLIDYNE METAL COMPLEXES $[M(\equiv CR)(CO)_2(\eta\text{-}C_5H_5)]$ (M = Mo OR W; R = C_6H_4Me-4 OR $C_6H_3Me_2$-2,6)

THOMAS P. SPANIOL and F. GORDON A. STONE*

Department of Inorganic Chemistry, The University of Bristol, Bristol BS8 1TS, U.K.

(*Received* 12 *April* 1989; *accepted* 28 *April* 1989)

Abstract—The compound $[Pt(C_2H_4)_2(PPr^i_3)]$ in light petroleum reacts with the reagents $[M(\equiv CC_6H_3Me_2\text{-}2,6)(CO)_2(\eta\text{-}C_5H_5)]$ (M = W or Mo) to afford the electronically unsaturated 30 valence electron dimetal complexes $[MPt(\mu\text{-}CC_6H_3Me_2\text{-}2,6)(\mu\text{-}CO)(CO)(PPr^i_3)(\eta\text{-}C_5H_5)]$. The latter readily add a molecule of CO or CNR (R = Bu^t or $C_6H_3Me_2$-2,6) to give the compounds $[MPt(\mu\text{-}CC_6H_3Me_2\text{-}2,6)(CO)_2(PPr^i_3)(L)(\eta\text{-}C_5H_5)]$ (M = W, L = CO or CNR; M = Mo, L = CO). Protonation of these species with $HBF_4\cdot OEt_2$ affords the salts $[WPt(\mu\text{-}H)(\mu\text{-}CC_6H_3Me_2\text{-}2,6)(CO)_2(PPr^i_3)(L)(\eta\text{-}C_5H_5)][BF_4]$ (L = CO or CNR) and $[MPt\{\mu\text{-}\sigma:\eta^3\text{-}C(H)C_6H_3Me_2\text{-}2,6\}(CO)_3(PPr^i_3)(\eta\text{-}C_5H_5)][BF_4]$ (M = Mo or W). Whereas the xylylidyne compounds $[M(\equiv CC_6H_3Me_2\text{-}2,6)(CO)_2(\eta\text{-}C_5H_5)]$ react with the complexes $[Pt_3(CNR)_6]$ to yield the dimetal species $[MPt(\mu\text{-}CC_6H_3Me_2\text{-}2,6)(CO)_2(CNR)_2(\eta\text{-}C_5H_5)]$, the *p*-tolylmethylidyne analogues $[M(\equiv CC_6H_4Me\text{-}4)(CO)_2(\eta\text{-}C_5H_5)]$ on treatment with the platinum isocyanide reagents give the trimetal complexes $[MPt_2(\mu_3\text{-}CC_6H_4Me\text{-}4)(CO)_2(CNR)_4(\eta\text{-}C_5H_5)]$. NMR data for the new compounds are reported and discussed.

The carbon–metal triple bonds of the alkylidyne complexes $[M(\equiv CR)(CO)_2L]$ [M = W, Mo or Cr; R = alkyl or aryl; L = η-C_5H_5, η-C_5Me_5 or $HB(pz)_3$ {hydrotris(pyrazol-1-yl)borate}] readily add low-valent metal–ligand fragments, thereby providing a versatile route to compounds having heteronuclear metal–metal bonds:[1]

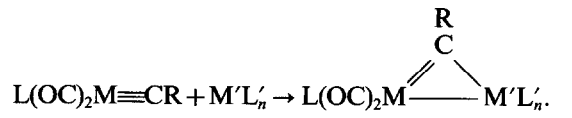

By this procedure, dimetal species involving most of the transition elements have been obtained.[2] Among the first reactions of this type to be studied were those between the tungsten compound, $[W(\equiv CC_6H_4Me\text{-}4)(CO)_2(\eta\text{-}C_5H_5)]$, and the zero-valent platinum species, $[Pt(C_2H_4)(PR_3)_2]$ (R = Me or Ph). In this manner the compounds $[WPt(\mu\text{-}CC_6H_4Me\text{-}4)(CO)_2(PR_3)_2(\eta\text{-}C_5H_5)]$ (**1**) were prepared.[3] As a consequence of the success of this early work, the *p*-tolylmethylidyne tungsten complex became the reagent of choice for testing the general applicability of this method of synthesizing dimetal compounds.[1c] However, later studies with other alkylidyne metal complexes $[M(\equiv CR)(CO)_2L]$ [M = Cr, Mo or W, R = $C_6H_3Me_2$-2,6, L = η-C_5H_5;[2a] M = Mo, R = C_6H_4Me-4, L = η-C_5H_5;[2d] M = W, R = C_6H_4Me-4, L = $HB(pz)_3$ or η-C_5Me_5;[2e,f] M = W, R = $SiPh_3$, L = C_5H_5[4a]] revealed that the nature of the products obtained depends on the metal M, the group L, and the substituent R on the ligated carbon atom of the C≡M bond. Thus, for example, by varying L or R the C≡M moiety can function formally towards an $M'L'_n$ fragment as either a two- or a four-electron donor.[2a,f] Moreover, changing the ligands L′ present in the $M'L'_n$ moiety can also influence the structure of the heteronuclear dimetal compounds isolated.

Further extending the scope of this area of heteronuclear metal–metal bond chemistry, we report herein reactions of the compounds $[M(\equiv CC_6H_3Me_2\text{-}2,6)(CO)_2(\eta\text{-}C_5H_5)]$ (M = Mo or W) with the zero-valent platinum reagents $[Pt(C_2H_4)_2(PPr^i_3)]$[4] and $[Pt_3(CNR)_6]$ (R = Bu^t or $C_6H_3Me_2$-2,6).[5] The platinum species function as

* Author to whom correspondence should be addressed.

sources of the 12-electron $Pt(PPr^i_3)$ and 14-electron $Pt(CNR)_2$ fragments, respectively. A comparison can thus be made with the earlier results involving $Pt(PR_3)_2$ groups,[3] mentioned above. Moreover, an extension of studies[2a,6] with the reagents $[M(\equiv CC_6H_3Me_2\text{-}2,6)(CO)_2(\eta\text{-}C_5H_5)]$ was of particular interest, since the presence of the bulky xylyl group on the alkylidyne-carbon atom has been shown to influence the nature of the products obtained, compared with analogous reactions employing the species $[M(\equiv CC_6H_4Me\text{-}4)(CO)_2(\eta\text{-}C_5H_5)]$. Indeed, as described below, a further example of the differing patterns of behaviour is revealed in the reactions involving the triplatinum isocyanide complexes.

RESULTS AND DISCUSSION

In light petroleum at 0°C, the compound $[Pt(C_2H_4)_2(PPr^i_3)]$, generated *in situ* from $[Pt(cod)_2]$ (cod = cyclo-octa-1,5-diene), PPr^i_3 and C_2H_4, reacts with the species $[M(\equiv CC_6H_3Me_2\text{-}2,6)(CO)_2(\eta\text{-}C_5H_5)]$ (M = W or Mo) to give the dimetal complexes $[MPt(\mu\text{-}CC_6H_3Me_2\text{-}2,6)(\mu\text{-}CO)(CO)(PPr^i_3)(\eta\text{-}C_5H_5)]$ [M = W (**2a**) or Mo (**2b**)], characterized by the data given in Tables 1–3. In their IR spectra both compounds show a band at *ca* 1750 cm^{-1}, suggesting the presence of a bridging carbonyl ligand. The $^{13}C\text{–}\{^1H\}$ NMR spectra were informative (Table 2). For both compounds only one CO resonance was observed, indicating that the two carbonyl groups undergo rapid site-exchange on the NMR time scale. The carbonyl signals are doublets due to $^{31}P\text{–}^{13}C$ coupling, and these signals also show ^{195}Pt satellite peaks. These couplings support the IR evidence for a bridging CO ligand. Resonances for the ligated carbon nuclei of the xylylidyne ligands were observed at δ 290.4 (**2a**) and 307.9 ppm (**2b**). These chemical shifts are little different from those found for the terminally bound xylylidyne groups in the spectra of the precursors $[M(\equiv CC_6H_3Me_2\text{-}2,6)(CO)_2(\eta\text{-}C_5H_5)]$ (M = W, δ 297.4 ppm; M = Mo, δ 310.5 ppm).[2a] Moreover, although the resonances for the alkylidyne μ-C nuclei in compounds **2a** and **2b** show $^{31}P\text{—}^{13}C$ and $^{195}Pt\text{–}^{13}C$ couplings, the values observed (Table 2) are about half those associated with the corresponding signals in the $^{13}C\text{–}\{^1H\}$ NMR spectra of the complexes **1** [J(PC) *ca* 60; J(PtC) *ca* 750 Hz].[3] Also in the spectra of the latter, the chemical shifts of the μ-C nuclei (*ca* δ 340 ppm) are appreciably more deshielded than those in the spectra of **2a** and **2b**. As discussed previously,[7] these data provide strong evidence that in **2a** and **2b** the xylylidyne ligands asymmetrically bridge the metal–metal bonds, being much closer to the tungsten or molybdenum atoms than to the platinum. In the complex $[WPt(\mu\text{-}CC_6H_3Me_2\text{-}2,6)(CO)_2(PEt_3)(\mu\text{-}\sigma:\eta^5\text{-}$

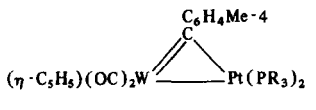

	PR_3
(1a)	PMe_3
(1b)	PMe_2Ph
(1c)	$PMePh_2$
(1d)	PPh_3

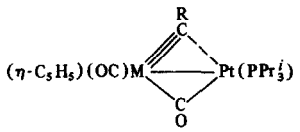

	M	R
(2a)	W	$C_6H_3Me_2$-2,6
(2b)	Mo	$C_6H_3Me_2$-2,6
(2c)	W	$SiPh_3$

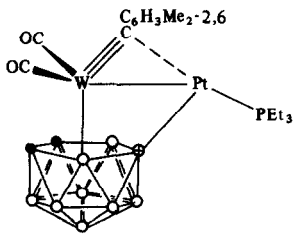

● CMe ○ BH ⊕ B

(3)

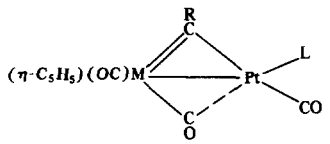

	M	R	L
(4a)	W	$C_6H_3Me_2$-2,6	PPr^i_3
(4b)	Mo	$C_6H_3Me_2$-2,6	PPr^i_3
(4c)	W	C_6H_4Me-4	PMe_3
(4d)	W	C_6H_4Me-4	PMe_2Ph
(4e)	W	C_6H_4Me-4	$PMePh_2$
(4f)	W	C_6H_4Me-4	PPh_3

Table 1. Analytical[a] and physical data for the complexes

Compound[b]	Colour	Yield (%)	ν(CO) or (NC)[c] (cm^{-1})	Analysis (%) C	H	N
$[WPt(\mu\text{-CR})(\mu\text{-CO})(CO)(PPr^i_3)(\eta\text{-}C_5H_5)]$ (**2a**)	Brown	89	1 918vs, 1 742m(br)	38.2(38.6)	4.8(4.5)	
$[MoPt(\mu\text{-CR})(\mu\text{-CO})(CO)(PPr^i_3)(\eta\text{-}C_5H_5)]$ (**2b**)	Brown	85	1 932vs, 1 755m(br)	43.3(43.6)	5.3(5.1)	
$[WPt(\mu\text{-CR})(CO)_3(PPr^i_3)(\eta\text{-}C_5H_5)]$ (**4a**)	Orange	92	2 006vs, 1 921s, 1 846s	39.2(38.8)	4.8(4.4)	
$[MoPt(\mu\text{-CR})(CO)_3(PPr^i_3)(\eta\text{-}C_5H_5)]$ (**4b**)	Orange	89	2 009vs, 1 932s, 1 847s	43.4(43.5)	5.4(4.9)	
$[WPt(\mu\text{-CR})(CO)_2(CNR)(PPr^i_3)(\eta\text{-}C_5H_5)]$ (**5a**)	Red	85	[d] 2 107vs, 1 905s, 1 821s	44.1(44.9)	5.1(4.9)	1.4(1.5)
$[WPt(\mu\text{-CR})(CO)_2(CNBu^t)(PPr^i_3)(\eta\text{-}C_5H_5)]$ (**5b, c**)[e]	Red	89	[d] 2 142vs, 1 894vs, 1 814s	40.8(41.9)	5.5(5.2)	1.6(1.6)
$[WPt(\mu\text{-H})(\mu\text{-CR})(CO)_3(PPr^i_3)(\eta\text{-}C_5H_5)][BF_4]$ (**6a**) } [e] $[WPt(\mu\text{-}\sigma:\eta^3\text{-CHR})(CO)_3(PPr^i_3)(\eta\text{-}C_5H_5)][BF_4]$ (**7a**) }	Yellow	95	2 102m, 2 067s, 2 044vs, 1 988vs, 1 902w	34.4(35.0)	4.3(4.1)	
$[WPt(\mu\text{-H})(\mu\text{-CR})(CO)_2(CNR)(PPr^i_3)(\eta\text{-}C_5H_5)][BF_4]$ (**6b**)	Orange	90	[d] 2 186s, 2 032vs, 1 973vs	40.4(41.0)	4.6(4.6)	1.4(1.4)
$[WPt(\mu\text{-H})(\mu\text{-CR})(CO)_2(CNBu^t)(PPr^i_3)(\eta\text{-}C_5H_5)][BF_4]$ (**6c**)	Yellow	95	[d] 2 209s, 2 031vs, 1 971vs	38.4(38.0)	5.0(4.8)	1.8(1.5)
$[MoPt(\mu\text{-}\sigma:\eta^3\text{-CHR})(CO)_3(PPr^i_3)(\eta\text{-}C_5H_5)][BF_4]$ (**7b**)	Yellow	95	2 074s, 1 980m, 1 897w(br)	38.6(38.9)	4.6(4.5)	
$[WPt(\mu\text{-CHR})(CO)_4(PPr^i_3)(\eta\text{-}C_5H_5)][BF_4]$ (**9a**)	Orange–yellow	98	2 072s, 2 039m, 1 996m, 1 905w	33.9(35.2)	4.2(3.9)	
$[MoPt(\mu\text{-CHR})(CO)_4(PPr^i_3)(\eta\text{-}C_5H_5)][BF_4]$ (**9b**)[f]	Orange–yellow	—	2 075s, 2 040w, 2 001m, 1 984m(sh)			
$[MoPt(\mu\text{-CR})(CO)_2(CNBu^t)_2(\eta\text{-}C_5H_5)]$ (**10a**)	Orange–red	64	[d] 2 184vs, [d] 2 155vs, 1 923s, 1 748m(br)	44.4(44.9)	4.8(4.6)	3.9(4.0)
$[MoPt(\mu\text{-CR})(CO)_2(CNR)_2(\eta\text{-}C_5H_5)]$ (**10b**)	Orange	40	[d] 2 153vs, [d] 2 118vs, 1 930s, 1 785m(br)	50.9(51.6)	4.4(4.1)	3.5(3.5)
$[WPt(\mu\text{-CR})(CO)_2(CNR)_2(\eta\text{-}C_5H_5)]$ (**10c**)	Orange–yellow	95	[d] 2 148vs, [d] 2 112vs, 1 919s, 1 828m(br)	46.5(46.4)	3.7(3.7)	3.2(3.2)
$[MoPt_2(\mu_3\text{-}CC_6H_4Me\text{-}4)(CO)_2(CNBu^t)_4(\eta\text{-}C_5H_5)]$ (**11a**)	Yellow	85	2 175vs, 2 160vs, 2 145vs, 1 751m	40.8(40.3)	5.1(4.6)	5.1(5.4)
$[MoPt_2(\mu_3\text{-}CC_6H_4Me\text{-}4)(CO)_2(CNR)_4(\eta\text{-}C_5H_5)]$ (**11b**)	Yellow	49	2 153vs, 2 133vs, 2 114vs, 1 778m	[g] 46.0(45.4)	4.1(3.6)	3.7(4.0)
$[WPt_2(\mu_3\text{-}CC_6H_4Me\text{-}4)(CO)_2(CNR)_4(\eta\text{-}C_5H_5)]$ (**11c**)	Yellow	68	2 150vs, 2 129vs, 2 111vs, 1 778m	[h] 44.7(44.4)	3.9(3.6)	3.9(4.0)
$[WPt(\mu\text{-H})(\mu\text{-CR})(CO)_2(CNR)_2(\eta\text{-}C_5H_5)][BF_4]$ (**13**)	Yellow	95	2 203m, 2 177m, 2 041vs, 1 985s	41.6(42.2)	3.8(3.4)	2.8(2.9)

[a] Calculated values are given in parentheses.
[b] R = $C_6H_3Me_2$-2,6.
[c] Measured in CH_2Cl_2.
[d] ν_{max}(NC).
[e] Isomeric mixture, see text.
[f] Compound unstable, see text.
[g] Crystallizes with two molecules of CH_2Cl_2.
[h] Crystallizes with one molecule of CH_2Cl_2.

Table 2. ^{1}H and ^{13}C NMR data[a] for the complexes

Compound	^{1}H[b] (δ)	^{13}C[c] (δ)
2a	1.04 [d of d, 18H, $CHMe_2$, J(HH) 7, J(PH) 15], 2.10–2.20 (m, 3H, $CHMe_2$), 2.21 (s, 6H, Me_2-2,6), 5.57 (s, 5H, C_5H_5), 6.90, 7.00 [(AB_2), 3H, C_6H_3, J(AB) 8]	290.4 [d, μ-C, J(PC) 26, J(PtC) 411], 234.6 [d, CO, J(PC) 5, J(PtC) 177], 152.5 [$C^1(C_6H_3)$, J(PtC) 24], 135.4, 127.7, 126.5 (C_6H_3), 91.5 (C_5H_5), 25.5 [d, $CHMe_2$, J(PC) 26, J(PtC) 52], 21.9 (Me_2-2,6), 20.1 [$CHMe_2$, J(PtC) 36]
2b	1.04 [d of d, 18H, $CHMe_2$, J(HH) 7, J(PH) 15], 2.02–2.20 (m, 3H, $CHMe_2$), 2.26 (s, 6H, Me_2-2,6), 5.49 (s, 5H, C_5H_5), 6.80–7.00 (m, 3H, C_6H_3)	307.9 [d, μ-C, J(PC) 31, J(PtC) 476], 242.7 [d, CO J(PC) 6, J(PtC) 187], 150.4 [$C^1(C_6H_3)$], 135.8, 127.7, 127.0 (C_6H_3), 92.9 (C_5H_5), 25.5 [$CHMe_2$, J(PC) 27, J(PtC) 52], 21.7 (Me_2-2,6), 20.2 [$CHMe_2$, J(PtC) 34]
4a	1.05 [d of d, 18H, $CHMe_2$, J(HH) 7, J(PH) 14], 1.96 (s, 6H, Me_2-2,6), 2.00–2.10 (m, 3H, $CHMe_2$), 5.36 (s, 5H, C_5H_5), 6.90–7.20 (m, 3H, C_6H_3)	330.9 [μ-C, J(PtC) 835], 220.9 [d, WCO, J(PC) 5, J(PtC) 42], 198.8 [d, PtCO, J(PC) 7, J(PtC) 1359], 163.8 [$C^1(C_6H_3)$, J(PtC) 53], 127.4, 127.0, 125.6 (C_6H_3), 92.7 (C_5H_5), 26.9 [d, $CHMe_2$, J(PC) 25, J(PtC) 25], 22.7 (Me_2-2,6), 19.7 [$CHMe_2$, J(PtC) 22]
4b	1.06 [d of d, 18H, $CHMe_2$, J(HH) 7, J(PH) 14], 1.94 (s, 6H, Me_2-2,6), 2.02–2.16 (m, 3H, $CHMe_2$), 5.31 (s, 5H, C_5H_5), 6.82, 6.96 [(AB_2), 3H, C_6H_3, J(AB) 8]	357.9 [μ-C, J(PtC) 900], 232.3 [d, MoCO, J(PC) 5, J(PtC) 38], 199.6 [d, PtCO, J(PC) 7], 162.2 [$C^1(C_6H_3)$, J(PtC) 65], 127.2, 126.8, 125.2 (C_6H_3), 94.5 (C_5H_5), 27.0 [d, $CHMe_2$, J(PC) 24, J(PtC) 34], 22.6 (Me_2-2,6), 19.7 [$CHMe_2$, J(PtC) 21]
5a	1.07 [d of d, 18H, $CHMe_2$, J(HH) 7, J(PH) 14], 1.98 (s, 6H, Me_2-2,6), 2.05–2.20 (m, 3H, $CHMe_2$), 2.49 (s, 6H, Me_2-2,6), 5.30 (s, 5H, C_5H_5), 6.77, 6.91 [(AB_2), 3H, C_6H_3, J(AB) 7], 7.10–7.20 (m, 3H, C_6H_3)	334.1 [μ-C, J(PtC) 840, J(WC) 137], 222.2 [d, CO, J(PC), 5, J(WC), 175, J(PtC) 36], 165.8 [$C^1(C_6H_3)$, J(PtC) 58], 165.2 [d, CN, J(PC) 12, J(PtC) 1313], 134.4, 128.2, 127.9, 126.8, 125.1, 123.6 (C_6H_3), 92.2 (C_5H_5), 26.9 [d, $CHMe_2$, J(PC) 22, J(PtC) 41], 22.7 (Me_2-2,6), 19.8 [$CHMe_2$, J(PtC) 22], 19.1 (Me_2-2,6)
5b, c[d]	0.99* (s, 9H, Bu^t), 1.02, 1.29* [d of d × 2, 18H, $CHMe_2$, J(HH) 7, J(PH) 14], 1.56 (s, 9H, Bu^t), 1.94, 2.02* (s × 2, 6H, Me_2-2,6), 2.00–2.20, 2.60–2.80* (m × 2, 3H, $CHMe_2$), 5.28, 5.36* (s × 2, 5H, C_5H_5), 6.70–7.00 (m, 6H, C_6H_3)	336.8 [μ-C, J(PtC) 844, J(WC) 135], 326.0* [d, μ-C, J(PC) 46, J(PtC) 536], 236.4* [CO, J(WC) 179, J(PtC) 89], 224.2 [CO, J(WC) 178, J(PtC) 31], 165.9 [$C^1(C_6H_3)$, J(PtC) 58], 163.0* [$C^1(C_6H_3)$, J(PtC) 17], 150.1 [CN, J(PtC) 1277], 141.5*(CN), 123.0–129.0 (C_6H_3), 92.1, 91.8* (C_5H_5), 68.0*. 57.0 (CMe_3), 30.5*, 29.4 (CMe_3), 26.6 [d, $CHMe_2$, J(PC) 21, J(PtC) 43], 23.0* [d, $CHMe_2$, J(PC) 20, J(PtC) 24], 22.6, 21.7* (Me_2-2,6), 19.7 [$CHMe_2$, J(PtC) 22]
6a, 7a[e]	−6.74 [d, 1H, μ-H, J(PH) 3, J(PtH) 565, J(WH) 42], 1.12–1.28* (m, 18H, $CHMe_2$), 1.35 [d of d, 18H, $CHMe_2$, J(HH) 8, J(PH) 16], 2.09 (s, 6H, Me_2-2,6), 2.34* (s, 3H, Me_2-2,6), 2.62* (s, 3H, Me_2-2,6), 2.60–2.80 (m, 3H, $CHMe_2$), 4.75*, 5.90 (s × 2, 5H, C_5H_5), 6.83–7.23 (m, 7H, μ-CH and C_6H_3)	306.4 [d, μ-C, J(PC) 40, J(PtC) 410], 215.0*, 205.4*, 205.0 [WCO, J(WC) 173, J(PtC) 15], 186.3* [d, PtCO, J(PC) 7], 179.2 [d, PtCO, J(PC) 9, J(PtC) 1619], 158.7–106.7 (C_6H_3), 108.4* [μ-CH, J(PtC) 643], 94.9*, 91.8 (C_5H_5), 35.2* (Me_2-2,6), 27.8 [d, $CHMe_2$, J(PC) 27, J(PtC) 28], 21.5 (Me_2-2,6), 21.0* (Me_2-2,6), 19.9 [$CHMe_2$, J(PtC) 19], 19.8* [$CHMe_2$, J(PtC) 21]
6b	−7.96 [d, 1H, μ-H, J(PH) 2, J(PtH) 524, J(WH) 46], 1.35 [d of d, 18H, $CHMe_2$, J(HH) 7, J(PH) 15], 2.05, 2.12 (s × 2, 6H, Me_2-2,6), 2.70 (m, 3H, $CHMe_2$), 5.86 (s, 5H, C_5H_5), 6.52, 6.87 [(AB_2), 3H, C_6H_3, J(AB) 8], 7.04, 7.19 [(AB_2), 3H, C_6H_3, J(AB) 8]	308.3 [d, μ-C, J(PC) 46, J(PtC) 425], 207.4 [CO, J(WC) 175, J(PtC) 19], 159.0 [$C^1(C_6H_3)$], 146.0 (br, CN), 134.8, 130.2, 128.3, 127.8, 127.6, 126.3 (C_6H_3), 91.3 (C_5H_5), 27.8 [d, $CHMe_2$, J(PC) 27, J(PtC) 28], 21.6 (Me_2-2,6), 20.1 [$CHMe_2$, J(PtC) 19], 18.3 (Me_2-2,6)
6c	−8.43 [s, 1H, μ-H, J(PtH) 516, J(WH) 46], 1.12 (s, 9H, Bu^t), 1.32 [d of d, 18H, $CHMe_2$, J(HH) 7, J(PH) 15], 1.99(s, 6H, Me_2-2,6), 2.60–2.70 (m, 3H, $CHMe_2$), 5.77 (s, 5H, C_5H_5), 6.96, 7.14 [(AB_2), 3H, C_6H_3, J(AB) 7]	310.2 [d, μ-C, J(PC) 48, J(PtC) 425], 207.8 [CO, J(WC) 173, J(PtC) 19], 159.8 [$C^1(C_6H_3)$, J(PtC) 14], 130.5 [d, CN, J(PC) 33], 128.0, 127.8, 126.6 (C_6H_3), 91.0 (C_5H_5), 59.7 (CMe_3), 29.3 (CMe_3), 27.4 [d, $CHMe_2$, J(PC), 27, J(PtC), 28], 21.2 (Me_2-2,6), 19.8 [$CHMe_2$, J(PtC) 21]

Table 2.—(*continued*)

Compound	$^1H^b$ (δ)	$^{13}C^c$ (δ)
7b	1.25, 1.34 [d of d × 2, 18H, CH*Me*$_2$, *J*(HH) 7, *J*(PH) 16], 2.32, 2.42 (s × 2, 6H, Me$_2$-2,6), 2.60–2.80 (m, 3H, C*H*Me$_2$), 4.82 (s, 5H, C_5H_5), 7.00–7.10 (m, 2H, μ-CH and C_6H_3), 7.29, 7.87 [d × 2, 2H, C_6H_3, *J*(HH) 7]	231.5 [MoCO, *J*(PtC) 17], 224.9 [d, MoCO, *J*(PC) 11, *J*(PtC) 18], 185.0 [d, PtCO, *J*(PC) 9, *J*(PtC) 1272], 146.7 [C^1(C_6H_3), *J*(PtC) 64], 137.1, 128.9 (C_6H_3), 126.9 [μ-CH, *J*(PtC) 682], 126.7, 110.5, 109.4 (C_6H_3), 95.5 (C_5H_5), 34.3 (Me$_2$-2,6), 28.3 [d, *C*HMe$_2$, *J*(PC) 28, *J*(PtC) 28], 21.4 (Me$_2$-2,6), 19.7 [d, CH*Me*$_2$, *J*(PC) 6, *J*(PtC) 17]
9a	1.11, 1.28 [d of d × 2, 18H, CH*Me*$_2$, *J*(HH) 7, *J*(PH) 17], 2.30–2.50 (m, 3H, C*H*Me$_2$), 2.36, 2.50 (s × 2, 6H, Me$_2$-2,6), 5.41 (s, 5H, C_5H_5), 6.80–7.40 (m, 4H, μ-CH and C_6H_3)	213.2 [d, WCO, *J*(PC) 7], 207.8 [WCO, *J*(WC) 120], 203.8 [WCO, *J*(WC) 57], 185.8 [d, PtCO, *J*(PC) 9, *J*(PtC) 1198], 149.9 [C^1(C_6H_3), *J*(PtC) 28], 137.3, 134.8, 131.1, 129.4, 127.8 (C_6H_3), 94.2 (C_5H_5), 85.5 [μ-CH, *J*(PtC) 633, *J*(WC) 31], 28.0 (*C*HMe$_2$ and Me$_2$-2,6), 22.7 (Me$_2$-2,6), 20.0 [CH*Me*$_2$, *J*(PtC) 24], 19.4 [CH*Me*$_2$, *J*(PtC) 21]
9b	1.12, 1.31 [d of d × 2, 18H, CH*Me*$_2$, *J*(HH) 7, *J*(PH) 16], 2.40, 2.51 (s × 2, 6H, Me$_2$-2,6), 2.25–2.50 (m, 3H, C*H*Me$_2$), 5.26 (s, 5H, C_5H_5), 6.90–8.03 (m, 4H, μ-CH and C_6H_3)	222.9 (MoCO), 216.1 [MoCO, *J*(PtC) 58], 185.1 (PtCO), 150.1 [C^1(C_6H_3), *J*(PtC) 31], 137.8, 134.3, 131.2, 129.5, 128.7 (C_6H_3), 106.7 [μ-CH, *J*(PtC) 683], 96.5 (C_5H_5), 29.0, 27.0 (*C*HMe$_2$ and Me$_2$-2,6), 22.7 (Me$_2$-2,6), 19.4 [CH*Me*$_2$, *J*(PtC) 22]
10a	1.06, 1.59 (s × 2, 18H, Bu^t), 1.97 (s, 6H, Me$_2$-2,6), 5.30 (s, 5H, C_5H_5), 6.82, 6.94 [(AB$_2$), 3H, C_6H_3, *J*(AB) 8]	348.6 [μ-C, *J*(PtC), 717], 239.7 [CO, *J*(PtC) 55], 161.6 [C^1(C_6H_3), *J*(PtC) 36], 145.7, 136.6 (CN), 127.0, 126.5, 124.4 (Me$_2$-2,6), 93.2 (C_5H_5), 57.4 (*C*Me$_3$), 30.6, 29.6 (C*Me*$_3$), 21.6 (Me$_2$-2,6)
10b	1.98, 2.07, 2.54 (s × 3, 18H, Me$_2$-2,6), 5.36 (s, 5H, C_5H_5), 6.80–7.20 (m, 9H, C_6H_3)	350.3 [μ-C, *J*(PtC) 766], 236.5 [CO, *J*(PtC) 21], 161.8 [C^1(C_6H_3), *J*(PtC) 43], 159.8 [CN, *J*(PtC) 1376], 149.4 [CN, *J*(PtC) 1755], 135.2–124.9 (C_6H_3), 93.6 (C_5H_5), 22.0, 19.1, 18.4 (Me$_2$-2,6)
10c	1.97, 2.07, 2.54 (s × 3, 18H, Me$_2$-2,6), 5.41 (s, 5H, C_5H_5), 6.80–7.20 (m, 9H, C_6H_3)	327.2 [μ-C, *J*(PtC) 729], 225.0 [CO, *J*(WC) 179], 163.8, 160.9, 152.3 [C^1(C_6H_3)], 135.2 (CN), 128.7–124.4 (C_6H_3), 91.8 (C_5H_5), 22.0, 19.2, 18.4 (Me$_2$-2,6)
11a	1.35, 1.51 (s × 2, 36H, Bu^t), 2.22 (s, 3H, Me-4), 4.82 (s, 5H, C_5H_5), 6.82, 7.26 [(AB)$_2$, 4H, C_6H_4, *J*(AB) 8]	225.1 [CO, *J*(PtC) 197], 229.9 [μ_3-C, *J*(PtC) 546], 161.0 [C^1(C_6H_4), *J*(PtC) 24], 145.9 [CN, *J*(PtCN) 1378], 137.3 [CN, *J*(PtC) 1598], 131.0, 128.5, 126.8 (C_6H_4), 92.9 (C_5H_5), 56.0 (*C*Me$_3$), 30.5 (C*Me*$_3$), 20.9 (Me-4)
11b	1.95 (s, 12H, Me$_2$-2,6), 2.25 (s, 3H, Me-4), 2.43 (s, 12H, Me$_2$-2,6), 4.97 (s, 5H, C_5H_5), 6.70–7.60 (m, 16H, C_6H_4 and C_6H_3)	251.1 [CO, *J*(PtC) 159], 234.8 [μ_3-C, *J*(PtC) 549], 160.8 [C^1(C_6H_4), *J*(PtC) 21], 159.4 [CN, *J*(PtC) 1431], 147.6 [CN, *J*(PtC) 1672], 134.7–127.0 (C_6H_3 and C_6H_4), 93.0 (C_5H_5), 20.7 (Me-4), 18.8, 18.2 (Me$_2$-2,6)
11c	1.95 (s, 12H, Me$_2$-2,6), 2.26 (s, 3H, Me-4), 2.43 (s, 12H, Me$_2$-2,6), 5.04 (s, 5H, C_5H_5), 6.72–7.52 (m, 16H, C_6H_4 and C_6H_3)	244.5 [CO, *J*(PtC) 103, *J*(WC) 169], 219.9 [μ_3-C, *J*(PtC) 508, *J*(WC) 102], 161.8 [C^1(C_6H_4)], 161.2 [CN, *J*(PtCN) 1467], 148.8 [CN, *J*(PtCN) 1652], 135.0–128.5 (C_6H_3 and C_6H_4), 91.3 (C_5H_5), 20.9 (Me-4), 19.1, 18.5 (Me$_2$-2,6)
13	−8.24 [μ-H, 1H, *J*(PtH) 503], 2.05, 2.07, 2.54 (s × 3, 18H, Me$_2$-2,6), 5.86 (s, 5H, C_5H_5), 6.78–7.40 (m, 9H, C_6H_3)	308.6 [μ-C, *J*(PtC) 592], 206.5 [CO, *J*(WC) 170, *J*(PtC) 19], 159.4 [C^1(C_6H_3)], 140.1 (CN), 136.0–127.1 (C_6H_3), 90.9 (C_5H_5), 21.5, 19.0, 18.4 (Me$_2$-2,6)

[a] Chemical shifts (δ) in ppm, coupling constants in Hz, measurements at room temperature.
[b] Measured in CD_2Cl_2.
[c] ^{1}H decoupled, measured in CD_2Cl_2–CH_2Cl_2, chemical shifts to high frequency of $SiMe_4$ (0.0 ppm).
[d] Isomeric mixture (see text), peaks due to minor isomer asterisked.
[e] Isomeric mixture of **6a** and **7a** (*ca* 2 : 1) (see text). Peaks assigned to **7a** are asterisked.

Table 3. ^{31}P and ^{195}Pt NMR data[a] for the complexes

Compound	$^{31}P(\delta)$[b]	$^{195}Pt(\delta)$[c]
2a	78.7 [J(PtP) 5460]	574.1 [J(PPt) 5460, J(WPt) 239]
2b	74.2 [J(PtP) 5400]	639.6 [J(PPt) 5400]
4a	42.8 [J(PtP) 3520]	146.0 [J(PPt) 3520, J(WPt) 117]
4b	41.3 [J(PtP) 3560]	152.3 [J(PPt) 3560]
5a	45.1 [J(PtP) 3800]	293.6 [J(PPt) 3800]
5b, c[d]	44.2 [J(PtP) 3810]	232.0 [J(PPt) 3810]
	43.2* [J(PtP) 3240]	189.0* [J(PPt) 3240]
6a, 7a[d]	49.0 [J(PtP) 2500, J(WP) 29]	−653.4 [J(PPt) 2500]
	62.6* [J(PtP) 3250, J(WP) 27]	92.7* [J(PPt) 3250]
6b	47.6 [J(PtP) 2630]	−720.4 [J(PPt) 2630]
6c	45.9 [J(PtP) 2620, J(WP) 66]	−753.7 [J(PPt) 2620]
7b	60.8 [J(PtP) 3290]	−124.5 [J(PPt) 3290]
9a	57.6 [J(PtP) 3920]	131.2 [J(PPt) 3920]
9b	57.3 [J(PtP) 3900]	110.3 [J(PPt) 3900]
10a		339.1 [J(NPt) 86]
10b		535.8
10c		588.7
11a		−125.0
11b		62.2
11c		64.1
13		−477.0

[a] Chemical shifts (δ) in ppm, ^1H decoupled, coupling constants in Hz, measurements in CD_2Cl_2.
[b] Chemical shifts are positive to high frequency of 85% H_3PO_4 (external).
[c] Chemical shifts are positive to high frequency of Ξ (^{195}Pt) 21.4 MHz.
[d] Isomeric mixture, see text. Asterisk denotes peak due to minor isomer.

$C_2B_9H_8Me_2$)] (**3**), for which an asymmetrically bridging μ-$CC_6H_3Me_2$-2,6 group has been established by X-ray diffraction,[7] the μ-C resonance in the ^{13}C–{^1H} NMR spectrum occurs as a doublet at δ 279.9 ppm, with J(PC) 22 Hz; values comparable with those observed for **2a**. The ^{13}C–{^1H} NMR data for the recently reported compound [WPt(μ-CSiPh$_3$)(μ-CO)(CO)(PPr$^i_3$)(η-C_5H_5)] (**2c**) are also relevant.[4a] This species, prepared by treating [W(≡CSiPh$_3$)(CO)$_2$(η-C_5H_5)] with [Pt(C_2H_4)$_2$(PPr$^i_3$)], has also been assigned a structure with a bridging carbonyl group (ν_{max} 1764 cm^{-1}), and with the alkylidyne ligand asymmetrically spanning the metal–metal bond. Although the chemical shift (δ 339.4 ppm) for the μ-C ligand is more deshielded than those for this nucleus in the spectra of **2a** and **2b**, the values of the coupling constants for **2c** [J(PC) 31, J(PtC) 382 Hz] are very similar to those of **2a** (Table 2).

The compounds **2** and **3** are formally electronically unsaturated, being 30 valence electron dimetal species. Reflecting this property, compound **3** reacts readily with carbon monoxide yielding [WPt(μ-$CC_6H_3Me_2$-2,6)(CO)$_3$(PEt$_3$)(μ-σ: η^5-$C_2B_9H_8Me_2$)], a 32 valence electron dimetal complex containing a Pt(CO)(PEt$_3$) fragment. Similarly, treatment of **2a** or **2b** in CH_2Cl_2 with CO affords the complexes [MPt(μ-$CC_6H_3Me_2$-2,6)(CO)$_3$(PPr$^i_3$)(η-C_5H_5)] [M = W (**4a**) or Mo (**4b**)] in essentially quantitative yield. The spectroscopic properties (Tables 1–3) are in agreement with the structures proposed. The IR spectra show three bands in the CO stretching region; those at 1846 (**4a**) and 1847 cm^{-1} (**4b**) suggesting the presence of semi-bridging ligands. The ^{13}C–{^1H} NMR spectra show diagnostic μ-$CC_6H_3Me_2$-2,6 resonances at δ 330.9 [J(PtC) 835] (**4a**) and at 357.9 ppm [J(PtC) 900 Hz] (**4b**). The absence of ^{31}P–^{13}C coupling on these signals strongly suggests that the μ-C and PPr$^i_3$ groups are *cisoid* to one another. The values observed for the chemical shifts, and the ^{195}Pt–^{13}C couplings, are very similar to those found for the compounds **1**. The latter have structures in which the bridging alkylidyne groups form strong σ-bonds to the platinum atom.[3] Hence from the ^{13}C–{^1H} NMR data this is likely to be true for the species **4a** and **4b** also. Therefore the asymmetric bridging of the μ-C atoms in the compounds **4a** and **4b** is very probably less pronounced than in the compounds **2**. In the ^{13}C–{^1H} NMR spectra of **4a** and **4b** (Table 2) there are two CO resonances corresponding to the M(CO)$_2$ (M = W or Mo) and PtCO groups. Evidently the peaks for the two carbonyls ligating the tungsten or molybdenum atoms are time-

averaged. As expected, the ^{195}Pt–^{13}C couplings observed on these signals are much smaller than those for compounds **2a** or **2b**, in which carbonyl bridging is more pronounced.

The dimetal complexes **4a** and **4b** are analogues of the compounds $[WPt(\mu\text{-}CC_6H_4Me\text{-}4)(CO)_3(PR_3)(\eta\text{-}C_5H_5)]$ [PR_3 = PMe_3 (**4c**), PMe_2Ph (**4d**), $PMePh_2$ (**4e**) or PPh_3 (**4f**)], previously prepared by treating the species **1** with CO.[3b] In these reactions it is the PR_3 group *transoid* to the μ-CC_6H_4Me-4 ligand which is substituted by CO leading to a *cisoid* μ-$CPtPR_3$ configuration, as proposed for **4a** and **4b**.

Compound **2a** also readily reacts with the isocyanides CNR (R = $C_6H_3Me_2$-2,6 or Bu^t) to afford the complexes $[WPt(\mu\text{-}CC_6H_3Me_2\text{-}2,6)(CO)_2(CNR)(PPr^i_3)(\eta\text{-}C_5H_5)]$ (**5**). Data characterizing these species are given in Tables 1–3. Examination of the NMR spectra of the product from $CNBu^t$ revealed, however, that it was formed as a mixture of two isomers (*ca* 3.5 : 1, based on peak intensities). In the ^{13}C–$\{^1H\}$ spectrum the signals for the major isomer indicate a structure **5b** similar to that of **5a**, with the PPr^i_3 group *cisoid* to the μ-C nucleus. Thus the μ-C resonance at δ 336.8 ppm shows no ^{31}P coupling, in agreement with a *cisoid* μ-CPtP arrangement. In contrast, the less intense μ-C signal for the minor isomer at δ 326.0 ppm is a doublet [J(PC) 46 Hz], in accord with a *transoid* μ-CPtP configuration. Also as expected, in the ^{31}P–$\{^1H\}$ NMR spectrum (Table 3) the resonance for the major isomer, **5b** (δ 44.2 ppm), displays a larger ^{195}Pt–^{31}P coupling than the peak for the minor isomer, **5c** (δ 43.2 ppm), in agreement with the former species having a *transoid* PPtW arrangement and the latter a *cisoid* PPtW configuration.

Protonation of complexes **4a**, **4b** and **5** was next investigated. Treatment of **4a** in Et_2O with $HBF_4 \cdot OEt_2$ afforded an inseparable mixture of the isomeric compounds $[WPt(\mu\text{-}H)(\mu\text{-}CC_6H_3Me_2\text{-}2,6)(CO)_3(PPr^i_3)(\eta\text{-}C_5H_5)][BF_4]$ (**6a**) and $[WPt\{\mu\text{-}\sigma\text{: }\eta^3\text{-}C(H)C_6H_3Me_2\text{ - }2,6\}(CO)_3(PPr^i_3)(\eta\text{ - }C_5H_5)][BF_4]$ (**7a**). In contrast, addition of $HBF_4 \cdot OEt_2$ to **4b** yields exclusively $[MoPt\{\mu\text{-}\sigma\text{: }\eta^3\text{-}C(H)C_6H_3Me_2\text{-}2,6\}(CO)_3(PPr^i_3)(\eta\text{-}C_5H_5)][BF_4]$ (**7b**), a species structurally similar to **7a**. Protonation of **5a** or **5b** (isomeric mixture) also affords a single product. However, the salts $[WPt(\mu\text{-}H)(\mu\text{-}CC_6H_3Me_2\text{-}2,6)(CO)_2(CNR)(PPr^i_3)(\eta\text{-}C_5H_5)][BF_4]$ [R = $C_6H_3Me_2$-2,6 (**6b**) or Bu^t (**6c**)] obtained are μ-hydrido species analogous to **6a**. Data for these compounds, summarized in the tables, are in agreement with the structures proposed. Moreover, we have previously shown that protonation of the compounds **1a**–**1c** affords the salts $[WPt\{\mu\text{-}\sigma\text{: }\eta^3\text{-}C(H)C_6H_4Me\text{-}4\}(CO)_2(PR_3)_2(\eta\text{-}C_5H_5)][BF_4]$ [PR_3 = PMe_3 (**8a**), PMe_2Ph (**8b**) or $PMePh_2$ (**8c**)]; the nature of **8a** being firmly based on an X-ray diffraction study.[8a] The structures of these salts are similar to those of **7**, with the bridging CHR group adopting a $\mu\text{-}\sigma\text{: }\eta^3$ bonding mode.

The ^1H NMR spectra of the μ-hydrido complexes **6** all show the expected highfield resonance with ^{195}Pt and ^{183}W satellite peaks (Table 2). For **6a** and **6b** these signals appear as doublets due to ^{31}P–^1H coupling, but this is weak (*ca* 3 Hz); a result strongly suggesting a *cisoid* $HPtPPr^i_3$ arrangement with a consequential *transoid* μ-$CPtPPr^i_3$ configuration. That the PPr^i_3 ligand is *transoid* to the μ-$CC_6H_3Me_2$-2,6 group in the complexes **6** is supported by the appearance of the μ-C signals as

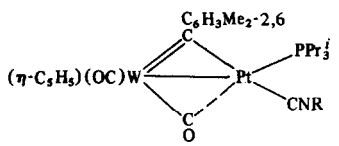

R
(**5a**) $C_6H_3Me_2$-2,6
(**5b**) Bu^t

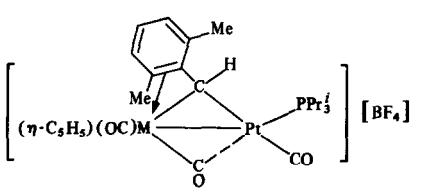

M
(**7a**) W
(**7b**) Mo

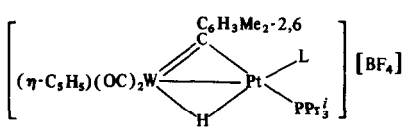

L
(**6a**) CO
(**6b**) $CNC_6H_3Me_2$-2,6
(**6c**) $CNBu^t$

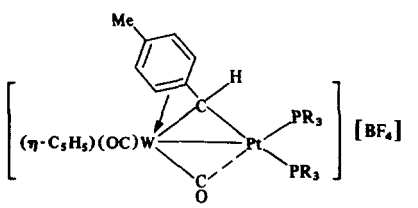

PR_3
(**8a**) PMe_3
(**8b**) PMe_2Ph
(**8c**) $PMePh_2$

doublets [J(PC) 40–48 Hz] in the $^{13}C-\{^1H\}$ NMR spectra.

Examination of the NMR spectra of the isomeric mixture of **6a** and **7a** revealed that these two isomers are formed in a *ca* 2:1 ratio, based on the relative intensity of the signals (Tables 2 and 3). It is likely that **6a** is an intermediate in the formation of **7a**, since when **4b** is protonated **7b** is the sole product, no molybdenum analogue of **6a** being formed. Interestingly, the stereochemistry about the platinum atom is different in complexes **4**, **5a**, **5b** and **7** from that in **6**. In the latter the tertiary phosphine groups are *transoid* to the μ-alkylidyne ligands whereas in **4**, **5a**, **5b** and **7** they are *cisoid* to the μ-C fragments. Not surprisingly, the NMR spectra of the compounds **7** show common features with those of **8**.[8a] In the $^{13}C-\{^1H\}$ NMR spectrum of **7b** there is a diagnostic singlet resonance at δ 126.9 ppm [J(PtC) 682 Hz] for the μ-CH nucleus. The μ-σ:η^3 bonding mode for the μ-CH($C_6H_3Me_2$-2,6) group results in non-equivalence of all the carbon atoms of the $C_6H_3Me_2$-2,6 moiety. Unlike several other compounds described herein, the salts, **7**, do not undergo dynamic behaviour on the NMR time scale since site-exchange of carbonyls does not occur, there being three distinct resonances for these groups (Table 2).

The compounds **8** react reversibly with CO affording the tricarbonyl complexes [WPt{μ-CH(C_6H_4Me-4)}$(CO)_3(PR_3)_2(\eta$-$C_5H_5)$][BF_4].[8b] The η^2-bonding of the arene ring in the complexes **7** may be similarly lifted by treating CH_2Cl_2 solutions with a stream of CO. In this manner the tetracarbonyl compounds [MPt{μ-CH($C_6H_3Me_2$-2,6)}$(CO)_4(PPr^i_3)(\eta$-$C_5H_5)$][BF_4] [M = W (**9a**) and Mo (**9b**)] are obtained. Moreover, it was observed that the isomeric mixture of **6a** and **7a** was quantitatively converted to **9a**, a result supporting the idea suggested above that **6a** is an intermediate in the formation of **7a**. Data for the compounds **9** are listed in Tables 1–3. However **9b** was unstable, readily reverting to **7b**, hence microanalytical data were not obtained. The NMR data for the complexes **9** show features similar to those of the tricarbonyl species [WPt(μ-CHR)$(CO)_3(PR_3)_2(\eta$-$C_5H_5)$][BF_4] derived from **8**.[8b] Thus in the $^{13}C-\{^1H\}$ NMR spectra diagnostic signals for the μ-CH groups are seen for **9a** at δ 85.5 ppm [J(PtC) 633, J(WC) 31 Hz] and for **9b** at δ 106.7 ppm [J(PtC) 683 Hz].

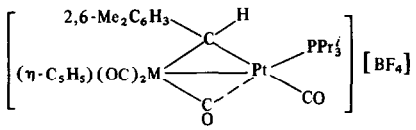

	M
(9a)	W
(9b)	Mo

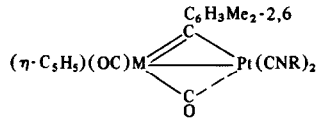

	M	R
(10a)	Mo	Bu^t
(10b)	Mo	$C_6H_3Me_2$-2,6
(10c)	W	$C_6H_3Me_2$-2,6

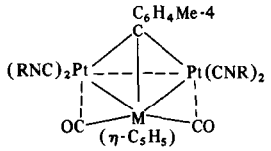

	M	R
(11a)	Mo	Bu^t
(11b)	Mo	$C_6H_3Me_2$-2,6
(11c)	W	$C_6H_3Me_2$-2,6

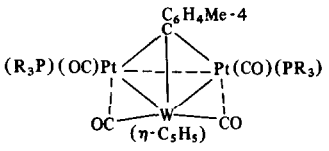

	R
(12a)	PMe_3
(12b)	PMe_2Ph
(12c)	$PMePh_2$
(12d)	PPh_3

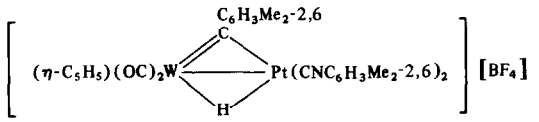

(13)

Reactions of the alkylidyne complexes [M(≡CR)(CO)$_2$(η-C$_5$H$_5$)] (M = Mo or W, R = C$_6$H$_4$Me-4 or C$_6$H$_3$Me$_2$-2,6) with the platinum compounds [Pt$_3$(CNR)$_6$] (R = Bu^t or C$_6$H$_3$Me$_2$-2,6) were next investigated. Treatment of [Pt$_3$(CNBu^t)$_6$] in CH_2Cl_2, or [Pt$_3$(CNC$_6$H$_3$Me$_2$-2,6)$_6$] in Et_2O, with [Mo(≡CC$_6$H$_3$Me$_2$-2,6)(CO)$_2$(η-C$_5$H$_5$)] affords, respectively, the compounds [MoPt(μ-CC$_6$H$_3$Me$_2$-2,6)(CO)$_2$(CNR)$_2$(η-C$_5$H$_5$)] [R = Bu^t (**10a**) or C$_6$H$_3$Me$_2$-2,6 (**10b**)]. Similarly, addition of [W(≡CC$_6$H$_3$Me$_2$-2,6)(CO)$_2$(η-C$_5$H$_5$)] to a CH_2Cl_2 solution of [Pt$_3$(CNC$_6$H$_3$Me$_2$-2,6)$_6$] yields the complex [WPt(μ-CC$_6$H$_3$Me$_2$-2,6)(CO)$_2$(CNC$_6$H$_3$Me$_2$-2,6)$_2$(η-C$_5$H$_5$)] (**10c**). The compounds **10**, characterized by the data given in Tables 1–3, are structurally similar to the complexes (**1**). As expected, the ^{13}C–{^{1}H} NMR spectra of the species **10** all show diagnostic resonances for the μ-C nuclei at δ 348.6 (**10a**), 350.3 (**10b**) and 327.2 ppm (**10c**), these signals showing ^{195}Pt–^{13}C coupling of the expected magnitude (*ca* 700 Hz) (Table 2). Peaks in the spectrum of **10b** at δ 159.8 and 149.4 ppm are assigned to the *C*NR nuclei on the basis of the strong ^{195}Pt–^{13}C couplings of 1376 and 1755 Hz, respectively.

The alkylidyne metal compounds [M(≡CC$_6$H$_4$Me-4)(CO)$_2$(η-C$_5$H$_5$)] (M = Mo or W), containing the C$_6$H$_4$Me-4 group which is less sterically demanding than C$_6$H$_3$Me$_2$-2,6, react with the isocyanide complexes [Pt$_3$(CNR)$_6$] to afford the trimetal species [MPt$_2$(μ_3-CC$_6$H$_4$Me-4)(CO)$_2$(CNR)$_4$(η-C$_5$H$_5$)] [R = Bu^t, M = Mo (**11a**); R = C$_6$H$_3$Me$_2$-2,6, M = Mo (**11b**) or W (**11c**)]. It seems probable that these trimetal compounds are produced via the intermediacy of initially formed dimetal complexes akin to **10**. Addition of Pt(CNR)$_2$ fragments to these intermediates would yield the compounds **11**. The formation of trimetal compounds via such a pathway is well established.[1,9]

The products **11** are structurally similar to the complexes **12** which are formed, together with **4c**–**4f**, upon treatment of the compounds **1** with CO.[3b] The NMR data (Tables 2 and 3) for the trimetal compounds **11** are in agreement with the structures proposed. In the ^{13}C–{^{1}H} NMR spectra, resonances at δ 229.9 (**11a**), 234.8 (**11b**) and 219.9 ppm (**11c**), all with ^{195}Pt–^{13}C satellite peaks [*J*(PtC) *ca* 500 Hz], are assigned to the μ_3-C nuclei. These signals are appreciably less deshielded than those generally found for μ_3-C resonances (*ca* 250–300 ppm).[9] However, in the spectra of the compounds **12** the μ_3-C resonances have similar chemical shifts [*ca* 230 ppm, with *J*(PtC) *ca* 550 Hz].[3b]

In the ^{13}C–{^{1}H} NMR spectra of the complexes **11** two resonances are observed for the ligated carbon atoms of the isocyanide ligands. These occur at δ 145.9 and 137.3 ppm for **11a**, at δ 159.4 and 147.6 ppm for **11b** and at δ 161.2 and 148.8 ppm for **11c**. These assignments are strongly supported by the observation of large ^{195}Pt–^{13}C couplings in the range 1378–1672 Hz.

The two series of compounds **11** and **12** are formulated with two semi-bridging CO ligands on the basis of an X-ray diffraction study on **12c** which established this structural feature.[3b] In the IR spectrum of each compound, however, there is a band at *ca* 1760 cm^{-1}, suggesting the presence of fully bridging CO groups. It is possible that the complexes **11** and **12** adopt different structures in solution. The X-ray diffraction study of **12c** revealed a "butterfly" arrangement of the core atoms with the platinum atoms at the wing-tips [Pt····Pt 2.989 Å] and the C—W fragment forming the body of the butterfly. This leads to an 18 valence electron shell at the tungsten atom and 16 electron configurations at the platinum atoms, assuming no Pt····Pt interaction in accord with the observed distance. If in solution a direct Pt—Pt bond was formed, and this was accompanied by movement of the CO ligands to fully bridging positions, processes requiring little energy, the tungsten atom would have a 16 valence electron shell and the two platinum atoms would have filled shells. Indeed dynamic exchange between the butterfly and *closo* core-atom arrangements may occur in solution.

As described above, protonation of the dimetal compound **4a** gave a mixture of the salts **6a** and **7a**. In contrast, protonation of **10c** yields the μ-hydrido complex [WPt(μ-H)(μ-CC$_6$H$_3$Me$_2$-2,6)(CO)$_2$(CNC$_6$H$_3$Me$_2$-2,6)$_2$(η-C$_5$H$_5$)[BF$_4$] (**13**) as the only product. Data characterizing **13** are listed in Tables 1–3. The presence of the μ-H ligand was clearly revealed by the appearance in the ^{1}H NMR spectrum of a high-field resonance at −8.24 ppm, with *J*(PtH) 503 Hz. The diagnostic signal for the μ-C nucleus in the ^{13}C–{^{1}H} NMR spectrum is seen at δ 308.6 ppm [*J*(PtC) 592 Hz].

In summary, the reactions described herein show that the compounds [Pt(C$_2$H$_4$)$_2$(PPr$^i_3$)] or [Pt$_3$(CNR)$_6$] (R = Bu^t or C$_6$H$_3$Me$_2$-2,6) in combination with the reagents [M(≡CC$_6$H$_3$Me$_2$-2,6)(CO)$_2$(η-C$_5$H$_5$)] (M = Mo or W) afford a variety of dimetal complexes with bridging xylylidyne ligands. Moreover, protonation of some of the initially formed products gives either μ-hydrido species or compounds in which the metal–metal bonds are spanned by μ-σ: η^3-C(H)C$_6$H$_3$Me$_2$-2,6 groups. Evidence was obtained indicating that the complexes **7** containing the latter group form via the intermediacy of hydrido species, e.g. **6a**. This result implies that the salts **8** also form on protonation of the compounds **1** via μ-hydrido species akin to **6a**, with subsequent transfer of the hydrido

ligand to the μ-C atom. Whereas the reagents $[Pt_3(CNR)_6]$ react with the species $[M(\equiv CC_6H_3Me_2\text{-}2,6)(CO)_2(\eta\text{-}C_5H_5)]$ to give dimetal compounds **10**, the analogous species $[M(\equiv CC_6H_4Me\text{-}4)(CO)_2(\eta\text{-}C_5H_5)]$, containing the less bulky *p*-tolylmethylidyne group, afford trimetal complexes **11**.

EXPERIMENTAL

All experiments were carried out under nitrogen, using Schlenk tube techniques. Solvents were rigorously dried before use. Light petroleum refers to that fraction b.p. 40–60°C. The spectroscopic measurements were made with instrumentation described previously.[10] The compounds $[Pt(cod)_2]$,[11] $[Pt_3(CNR)_6]$ (R = Bu^t or $C_6H_3Me_2$-2,6),[5] and $[M(\equiv CR)(CO)_2(\eta\text{-}C_5H_5)]$ (M = Mo or W, R = C_6H_4Me-4 or $C_6H_3Me_2$-2,6)[2a,12] were obtained via methods previously described in the literature. Alumina used for chromatography columns was BDH aluminium oxide (Brockman Activity II). The reagent $HBF_4 \cdot OEt_2$ consisted of a 54% solution of HBF_4 in Et_2O. Analytical and physical data for the new compounds are given in Table 1.

Preparation of the platinum–tungsten and –molybdenum compounds

(i) The compound $[Pt(cod)_2]$ (0.50 g, 1.22 mmol) was added in small portions with stirring to 20 cm^3 of ethylene-saturated light petroleum cooled to 0°C. The solution was treated with PPr^i_3 (1.22 cm^3 of a 1 mol dm^{-3} solution in light petroleum) and stirring was continued for 15 min to generate $[Pt(C_2H_4)_2(PPr^i_3)]$ *in situ*.[13] The complex $[W(\equiv CC_6H_3Me_2\text{-}2,6)(CO)_2(\eta\text{-}C_5H_5)]$ (0.51 g, 1.22 mmol) was then added, and the mixture was warmed to room temperature and stirred for 3 h, during which period the colour turned dark brown. Solvent was removed *in vacuo*, the residue was dissolved in light petroleum–CH_2Cl_2 (15 cm^3, 4:1) and chromatographed at −30°C. Elution with the same solvent mixture removed traces of unreacted starting materials and side-products, followed by a brown eluate. Removal of solvent *in vacuo* afforded brown *microcrystals* of $[WPt(\mu\text{-}CC_6H_3Me_2\text{-}2,6)(\mu\text{-}CO)(CO)(PPr^i_3)(\eta\text{-}C_5H_5)]$ (**2a**) (0.85 g).

(ii) In a similar experiment, $[Pt(C_2H_4)_2(PPr^i_3)]$ {0.47 mmol, generated from $[Pt(cod)_2]$ (0.19 g, 0.47 mmol)}, dissolved in light petroleum (40 cm^3) at 0°C was treated with $[Mo(\equiv CC_6H_3Me_2\text{-}2,6)(CO)_2(\eta\text{-}C_5H_5)]$ (0.16 g, 0.46 mmol). The mixture was warmed to room temperature and stirred for 3 h. It was then filtered through a Celite pad (2 × 4 cm). Solvent was removed *in vacuo* from the filtrate to give brown *microcrystals* of $[MoPt(\mu\text{-}CC_6H_3Me_2\text{-}2,6)(\mu\text{-}CO)(CO)(PPr^i_3)(\eta\text{-}C_5H_5)]$ (**2b**) (0.27 g).

(iii) Complex **2a** (0.17 g, 0.22 mmol) in CH_2Cl_2 (25 cm^3) was treated with a stream of CO gas for *ca* 1 min, the colour of the solution immediately turning from brown to orange. Removal of solvent *in vacuo*, followed by dissolving the residue in CH_2Cl_2, and column chromatography, gave an orange eluate. Removal of solvent *in vacuo* afforded orange *microcrystals* of $[WPt(\mu\text{-}CC_6H_3Me_2\text{-}2,6)(CO)_3(PPr^i_3)(\eta\text{-}C_5H_5)]$ (**4a**) (0.17 g).

(iv) The compound $[MoPt(\mu\text{-}CC_6H_3Me_2\text{-}2,6)(CO)_3(PPr^i_3)(\eta\text{-}C_5H_5)]$ (**4b**) (0.20 g) was similarly obtained from **2b** (0.21 g, 0.31 mmol) and CO.

(v) Compound **2a** (0.13 g, 0.17 mmol) in light petroleum (20 cm^3) was treated with $CNC_6H_3Me_2$-2,6 (0.02 g, 0.17 mmol), and the mixture was stirred. After *ca* 5 min, solvent was removed *in vacuo*, and the residue was dissolved in Et_2O–light petroleum (10 cm^3, 1:4) and chromatographed. Elution with the same solvent mixture gave an orange eluate, from which solvent was removed *in vacuo* to afford orange–red *microcrystals* of $[WPt(\mu\text{-}CC_6H_3Me_2\text{-}2,6)(CO)_2(CNC_6H_3Me_2\text{-}2,6)(PPr^i_3)(\eta\text{-}C_5H_5)]$ (**5a**) (0.10 g).

(vi) In a similar manner, **2a** (0.35 g, 0.45 mmol) in Et_2O (20 cm^3) with CNBu^t (0.45 mmol) gave, after column chromatography eluting with Et_2O, $[WPt(\mu\text{-}CC_6H_3Me_2\text{-}2,6)(CO)_2(CNBu^t)(PPr^i_3)(\eta\text{-}C_5H_5)]$ (isomers **5b** and **5c**) (0.35 g).

(vii) Compound **4a** (0.23 g, 0.28 mmol) in Et_2O (5 cm^3) was treated with *ca* 7 drops of $HBF_4 \cdot Et_2O$ (large excess) and the mixture was stirred for *ca* 5 min. The precipitate was allowed to settle, and the supernatant liquid removed with a syringe. The residue was washed with Et_2O (2 × 1 cm^3) and dried *in vacuo* yielding 0.24 g of the isomeric compounds $[WPt(\mu\text{-}H)(\mu\text{-}CC_6H_3Me_2\text{-}2,6)(CO)_3(PPr^i_3)(\eta\text{-}C_5H_5)][BF_4]$ (**6a**) and $[WPt\{\mu\text{-}\sigma\text{:}\ \eta^3\text{-}C(H)C_6H_3Me_2\text{-}2,6\}(CO)_3(PPr^i_3)(\eta\text{-}C_5H_5)][BF_4]$ (**7a**).

(viii) The salt $[MoPt\{\mu\text{-}\sigma\text{:}\ \eta^3\text{-}C(H)C_6H_3Me_2\text{-}2,6\}(CO)_3(PPr^i_3)(\eta\text{-}C_5H_5)][BF_4]$ (**7b**) (0.16 g) was similarly prepared from **4b** (0.15 g, 0.21 mmol) and $HBF_4 \cdot OEt_2$.

(ix) Addition of $HBF_4 \cdot OEt_2$ in excess (*ca* 7 drops) to **5a** (0.41 g, 0.46 mmol) in Et_2O (10 cm^3) gave, after removal of solvent *in vacuo*, yellow *microcrystals* of $[WPt(\mu\text{-}H)(\mu\text{-}CC_6H_3Me_2\text{-}2,6)(CO)_2(CNC_6H_3Me_2\text{-}2,6)(PPr^i_3)(\eta\text{-}C_5H_5)][BF_4]$ (**6b**) (0.37 g).

(x) Similarly, $[WPt(\mu\text{-}H)(\mu\text{-}CC_6H_3Me_2\text{-}2,6)(CO)_2(CNBu^t)(PPr^i_3)(\eta\text{-}C_5H_5)][BF_4]$ (**6c**) (0.19 g) was prepared from **5b** (0.18 g, 0.21 mmol) and $HBF_4 \cdot OEt_2$.

(xi) A CH_2Cl_2 (10 cm^3) solution of $[Pt_3(CNBu^t)_6]$

(0.16 g, 0.15 mmol) was treated with [Mo(≡$CC_6H_3Me_2$-2,6)$(CO)_2(\eta$-$C_5H_5)$] (0.15 g, 0.43 mmol) in the same solvent (10 cm^3), and the mixture was stirred for 6 h. Solvent was removed *in vacuo*, and the residue was dissolved in CH_2Cl_2–light petroleum (3 cm^3, 1 : 1) and chromatographed. Elution with the same solvent mixture gave orange–red *microcrystals* of [MoPt(μ-$CC_6H_3Me_2$-2,6)$(CO)_2(CNBu^t)_2(\eta$-$C_5H_5)$] (**10a**) (0.19 g), after removal of solvent from the eluate.

(xii) The compound [MoPt(μ-$CC_6H_3Me_2$-2,6)$(CO)_2(CNC_6H_3Me_2$-2,6)$_2(\eta$-$C_5H_5)$] (**10b**) (0.13 g) was similarly obtained from [$Pt_3(CNC_6H_3Me_2$-2,6)$_6$] (0.19 g, 0.14 mmol) and [Mo(≡$CC_6H_3Me_2$-2,6)$(CO)_2(\eta$-$C_5H_5)$] (0.14 g, 0.42 mmol) in Et_2O (50 cm^3).

(xiii) Similarly, [WPt(μ-$CC_6H_3Me_2$-2,6)$(CO)_2(CNC_6H_3Me_2$-2,6)$_2(\eta$-$C_5H_5)$] (**10c**) (0.34 g) was prepared from [$Pt_3(CNC_6H_3Me_2$-2,6)$_6$] (0.18 g, 0.13 mmol) and [W(≡$CC_6H_3Me_2$-2,6)$(CO)_2(\eta$-$C_5H_5)$] (0.17 g, 0.40 mmol) in CH_2Cl_2 (20 cm^3).

(xiv) Treatment of **10c** (0.14 g, 0.16 mmol) in Et_2O (35 cm^3) with $HBF_4 \cdot OEt_2$ (8 drops, excess) with stirring afforded a yellow precipitate. The supernatant liquid was removed with a syringe, and the residue was washed with Et_2O (2 × 3 cm^3) to give yellow *microcrystals* of [WPt(μ-H)(μ-$CC_6H_3Me_2$-2,6)$(CO)_2(CNC_6H_3Me_2$-2,6)$_2(\eta$-$C_5H_5)$][BF_4] (**13**) (0.15 g).

(xv) A CH_2Cl_2 (10 cm^3) solution of [$Pt_3(CNBu^t)_6$] (0.14 g, 0.13 mmol) was treated with [Mo(≡CC_6H_4Me-4)$(CO)_2(\eta$-$C_5H_5)$] (0.06 g, 0.19 mmol), dissolved in the same solvent. The mixture was stirred (15 min) and then chromatographed. Elution with CH_2Cl_2, and removal of solvent *in vacuo*, gave yellow *microcrystals* of [$MoPt_2(\mu_3$-CC_6H_4Me-4)$(CO)_2(CNBu^t)_4(\eta$-$C_5H_5)$] (**11a**) (0.17 g).

(xvi) In a similar experiment, treatment of [$Pt_3(CNC_6H_3Me_2$-2,6)$_6$] (0.18 g, 0.13 mmol) in Et_2O (80 cm^3) with [Mo(≡CC_6H_4Me-4)$(CO)_2(\eta$-$C_5H_5)$] (0.07 g, 0.22 mmol), in the same solvent (10 cm^3), gave yellow *microcrystals* of [$MoPt_2(\mu_3$-CC_6H_4Me-4)$(CO)_2(CNC_6H_3Me_2$-2,6)$_4(\eta$-$C_5H_5)$] · $2CH_2Cl_2$ (**11b**) (0.14 g), after the chromatography column had been eluted with CH_2Cl_2.

(xvii) Similarly, [$WPt_2(\mu_3$-CC_6H_4Me-4)$(CO)_2(CNC_6H_3Me_2$-2,6)$_4(\eta$-$C_5H_5)$]·CH_2Cl_2 (**11c**) (0.20 g) was prepared from [$Pt_3(CNC_6H_3Me_2$-2,6)$_6$] (0.19 g, 0.14 mmol) in Et_2O (80 cm^3) and [W(≡CC_6H_4Me-4)$(CO)_2(\eta$-$C_5H_5)$] (0.11 g, 0.27 mmol) in Et_2O (10 cm^3). The product was removed from the chromatography column with CH_2Cl_2.

Acknowledgements—We thank Drs S. J. Davies and A. F. Hill for helpful advice, and the Deutsche Bundesbahn for a scholarship (to T.P.S.).

REFERENCES

1. F. G. A. Stone, (a) *Pure Appl. Chem.* 1986, **58**, 529; (b) F. G. A. Stone, *Angew. Chem. Int. Edn. Engl.* 1984, **23**, 89; (c) F. G. A. Stone, *Am. Chem. Soc. Symp. Ser.* 1983, **211**, 383.
2. (a) S. J. Dossett, A. F. Hill, J. C. Jeffery, F. Marken, P. Sherwood and F. G. A. Stone, *J. Chem. Soc., Dalton Trans.* 1988, 2453; (b) M. D. Bermúdez and F. G. A. Stone, *J. Organomet. Chem.* 1988, **347**, 115; (c) M. D. Bermúdez, E. Delgado, G. P. Elliott, N. H. Tran-Huy, F. Major-Real, F. G. A. Stone and M. J. Winter, *J. Chem. Soc., Dalton Trans.* 1987, 1235; (d) M. E. Garcia, J. C. Jeffery, P. Sherwood and F. G. A. Stone, *J. Chem. Soc., Dalton Trans.* 1987, 1209; (e) E. Delgado, J. Hein, J. C. Jeffery, A. L. Ratermann, F. G. A. Stone and L. J. Farrugia, *J. Chem. Soc., Dalton Trans.* 1987, 1191; (f) M. Green, J. A. K. Howard, A. P. James, A. N. de M. Jelfs, C. M. Nunn and F. G. A. Stone, *J. Chem. Soc., Dalton Trans.* 1986, 1697; (g) J. A. Abad, L. W. Bateman, J. C. Jeffery, K. A. Mead, H. Razay, F. G. A. Stone and P. Woodward, *J. Chem. Soc., Dalton Trans.* 1983, 2075.
3. (a) T. V. Ashworth, J. A. K. Howard and F. G. A. Stone, *J. Chem. Soc., Dalton Trans.* 1980, 1609; (b) M. J. Chetcuti, K. Marsden, I. Moore, F. G. A. Stone and P. Woodward, *J. Chem. Soc., Dalton Trans.* 1982, 1749.
4. (a) J. C. Jeffery, M. A. Ruiz and F. G. A. Stone, *J. Organomet. Chem.* 1988, **355**, 231; (b) D. L. Davies, J. C. Jeffery, D. Miguel, P. Sherwood and F. G. A. Stone, *J. Chem. Soc., Chem. Commun.* 1987, 454.
5. M. Green, J. A. K. Howard, M. Murray, J. L. Spencer and F. G. A. Stone, *J. Chem. Soc., Dalton Trans.* 1977, 1509; A. Christofides, J. A. K. Howard, J. A. Rattue, J. L. Spencer and F. G. A. Stone, *J. Chem. Soc., Dalton Trans.* 1980, 2095.
6. F. E. Baumann, J. A. K. Howard, R. J. Musgrove, P. Sherwood and F. G. A. Stone, *J. Chem. Soc., Dalton Trans.* 1988, 1879.
7. D. D. Devore, J. A. K. Howard, J. C. Jeffery, M. U. Pilotti and F. G. A. Stone, *J. Chem. Soc., Dalton Trans.* 1989, 303.
8. (a) J. C. Jeffery, J. C. V. Laurie, I. Moore, H. Razay and F. G. A. Stone, *J. Chem. Soc., Dalton Trans.* 1984, 1563; (b) J. C. Jeffery, I. Moore and F. G. A. Stone, *J. Chem. Soc., Dalton Trans.* 1984, 1571.
9. J. A. Abad, E. Delgado, M. E. Garcia, M. J. Grosse-Ophoff, I. J. Hart, J. C. Jeffery, M. S. Simmons and F. G. A. Stone, *J. Chem. Soc., Dalton Trans.* 1987, 41; G. P. Elliott, J. A. K. Howard, T. Mise, I. Moore, C. M. Nunn and F. G. A. Stone, *J. Chem. Soc., Dalton Trans.* 1986, 2091 and refs cited therein.
10. A. F. Hill, B. A. Nasir and F. G. A. Stone, *Polyhedron* 1989, **8**, 179.
11. J. L. Spencer, *Inorg. Synth.* 1979, **19**, 213.
12. E. O. Fischer, T. L. Lindner, G. Huttner, P. Friedrich, F. R. Kreissl and J. O. Besenhard, *Chem. Ber.* 1977, **110**, 3397.
13. N. C. Harrison, M. Murray, J. L. Spencer and F. G. A. Stone, *J. Chem. Soc., Dalton Trans.* 1978, 1337.

Polyhedron Vol. 8, No. 18, pp. 2283–2290, 1989
Printed in Great Britain

0277–5387/89 $3.00+.00
© 1989 Pergamon Press plc

THE SINGLE CRYSTAL ELECTRONIC SPECTRA OF DICHLORODIPYRIDINENICKEL(II) AND DICHLORODIQUINOLINENICKEL(II) COMPLEXES*

MOHAMMAD M. SEIFOLLAHI and J. R. PERUMAREDDI†

Department of Chemistry, Florida Atlantic University, Boca Raton, FL 33431, U.S.A.

(*Received* 27 *December* 1988; *accepted* 4 *May* 1989)

Abstract—The single crystal electronic spectra of tetragonal $[NiL_2Cl_2]$, where L = pyridine and quinoline, complexes have been measured with polarized light at liquid N_2 temperature. The bands in the spectra of the dipyridine complex were polarized and thus assigned on the basis of the D_{4h} vibronic intensity mechanism, whereas the spectra of the diquinoline complex did not show any distinctive polarization characteristics and were assigned assuming the same order of energy levels as in the dipyridine complex. Our assignments of the spectra of both systems differ from those published earlier by others. The assigned absorption maxima in the dipyridine system were fitted with the predicted energy equations by extracting electron repulsion, spin–orbit, and ligand-field symmetry parameters and compared with those obtained earlier by us for the $[Ni(py)_4Cl_2]$ system. It was found that either the ligand-field symmetry parameters or the translated molecular orbital bonding parameters are not transferable between these two systems.

The polarized electronic spectral studies of tetragonal nickel(II) complexes which have been made to date,[1–6] are mostly on systems with negative *Dt*, with the exception of $[Ni(NH_3)_4(NO_2)_2]$ which has a positive *Dt*.[2] We are interested in studying polarized crystal spectra of systems with positive *Dt*. The systems that are expected to have positive *Dt*, as determined from mull or reflectance spectral studies, are the following:[7–16] $[NiL_2X_2]$, X = Cl, Br, L = NH_3,[8] py,[7–10] an,[8,11] im;[16] $[NiL_2Cl_2]$, L = qu,[10,12] CH_3CN,[13] H_2O;[8] $[Ni(CH_3CN)_2(ClO_4)_2]$;[14] $[NiLCl_2]$, L = py,[10] CH_3CN,[14] qx;[15] $[Ni(im)X_2]$, X = Cl, Br.[16]‡

We have prepared a number of these complexes, but only succeeded in growing single crystals of two of them: $[Ni(py)_2Cl_2]$ and $[Ni(qu)_2Cl_2]$. We have studied the polarized electronic spectra of these two systems.

EXPERIMENTAL

Preparation of the complexes

The complexes were prepared as described in the literature.[10,12]

Growing single crystals

Dichlorodipyridinenickel(II), $[Ni(py)_2Cl_2]$. Single crystals of this complex were grown by slow evaporation of a filtered, saturated solution of the complex in methanol at 55°C. (This procedure is the same as used by Morosin[17] for growing single crystals of $[Co(H_2O)_2Cl_2]$, except Morosin used water as the solvent at a temperature of 70°C.) The evaporation occurred over a period of 5 days in a thermostatted oil bath. The growing of these single crystals necessitated great care in sealing the evaporation chamber in order to maintain a slow, uniform evaporation rate. The crystals were green in colour and exhibited a strong green to pink dichroism. The size of the crystals obtained by this method never exceeded 0.025 in. diameter.

Dichlorodiquinolinenickel(II), $[Ni(qu)_2Cl_2]$. To

* Taken, in part, from the MS thesis of M. Seifollahi, Florida Atlantic University (1981).

† Author to whom correspondence should be addressed.

‡ Abbreviations: py = pyridine; an = aniline; im = imidazole; qu = quinoline; qx = quinoxaline.

grow single crystals of this compound, 5 cm^3 of a saturated solution of the complex in methanol was placed in a large test tube and carefully covered with a large volume of ice-cold acetone so that two layers formed. The test tube was stoppered and placed in a refrigerator, and the layers were allowed to diffuse for 48 h. By this time crystals had appeared at the original junction of the layers. These crystals were olive green in colour and moderate in size.

Spectral measurements

The spectra were recorded as described earlier.[6]

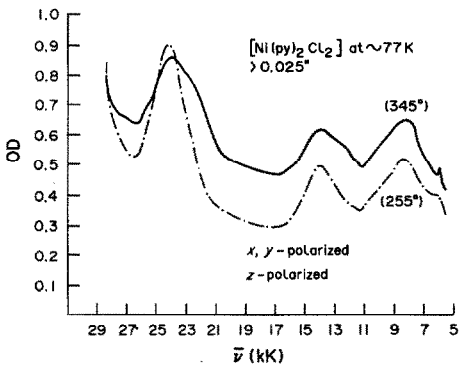

Fig. 1. Polarized crystal spectra of $[Ni(py)_2Cl_2]$ at liquid nitrogen temperature

RESULTS AND DISCUSSION

Although the crystals of the pyridine complex gave electronic spectra with polarized bands, the crystals of the quinoline complex always resulted in spectra with no discernible polarization characteristics of the absorption maxima. We thus present a detailed analysis of the electronic spectrum of the $[Ni(py)_2Cl_2]$ complex and will discuss the interpretation of the unpolarized spectrum of the $[Ni(qu)_2Cl_2]$ complex on the basis of the results obtained for the $[Ni(py)_2Cl_2]$ system and other similar systems.

The complete X-ray crystal structure analysis of $[Ni(py)_2Cl_2]$ has not been carried out yet, but it has been found to be isomorphous[18a] with violet $[Co(py)_2Cl_2]$, which has a polymeric structure with bridging chlorides and the two pyridines axially coordinated to the metal giving six-coordination.[18b] The exact site symmetry will depend on the orientation of the pyridine ligands and any distortions of the chlorides from planarity. However, we will assume the symmetry in this study to be D_{4h} on the basis of the tetragonal chromophore *trans*-$[NiN_2Cl_4]$, where two nitrogens are the coordinating atoms of the two pyridine ligands. The crystals of $[Ni(py)_2Cl_2]$ showed a clear dichroism from green to pink with exact extinctions at 90° angles. The polarized spectra have been measured along these optic axes. We will assume that the optic axes are aligned along the directions of the molecular axes, namely, the tetragonal axis containing the pyridine ligands and an axis orthogonal to it in the equatorial plane of the chlorine ligands. These two axes have been called z (or ∥) and x,y (or ⊥).

The polarized spectra of $[Ni(py)_2Cl_2]$ and the unpolarized spectrum of $[Ni(qu)_2Cl_2]$, measured at ~ 77°K, are presented in Figs 1 and 2. We shall firstly discuss the assignment of the spectrum of $[Ni(py)_2Cl_2]$. On the basis of the vibronic intensity mechanism for the d^8 configuration in D_{4h} symmetry, whereas both components of each of the three cubic parentage bands are allowed in ⊥ polarization, only one component of each of the three cubic bands is allowed in ∥ polarization.[6] The spectrum measured at a 345° angle extinction direction shows the three spin-allowed cubic bands at 8.30, 14.00 and 24.15 kK, which are of broad maxima with asymmetry leading to shoulders on the red side of each band. The spectrum obtained at the 255° angle extinction direction, however, shows three symmetric bands with no identifiable shoulders at about the same energies (8.40, 14.15 and 24.40 kK) as the three band maxima in the previous spectrum. Thus, we conclude that these two spectra correspond to x,y- and z-polarizations, respectively. The ill-defined resolution of the split components, i.e. showing shoulders instead of bands, could be due to the molecular axes not being exactly aligned along the extinction directions. The three maxima at 8.40, 14.15 and 24.40 kK of the z-polarized spectrum should be assigned as the ^3E_g components of the $^3T_{2g}(^3F)$, $^3T_{1g}(^3F)$ and $^3T_{1g}(^3P)$, respectively, and the estimated maxima of the three shoulders at ~ 7.50, ~ 13.00 and ~ 23.30 kK of the x,y-

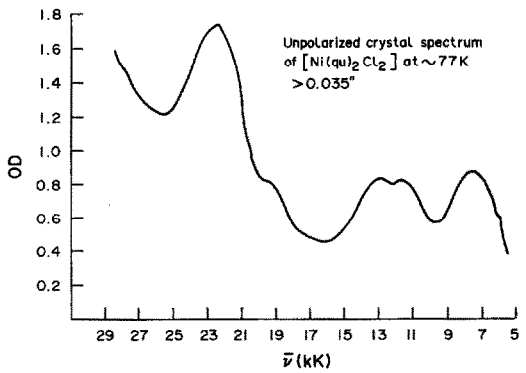

Fig. 2. Unpolarized crystal spectrum of $[Ni(qu)_2Cl_2]$ at liquid nitrogen temperature.

polarized spectrum which disappear in the *z*-polarization, correspond to the transitions $^3B_{2g}[^3T_{2g}(^3F)]$, $^3A_{2g}[^3T_{1g}(^3F)]$ and $^3A_{2g}[^3T_{1g}(^3P)]$, respectively. In addition to these spin-allowed transitions, bands of low intensity appear at ~ 11.90 (in both polarizations), ~ 26.00 (in *x*,*y*-polarization) and ~ 6.10 kK (in *x*,*y*-polarization and somewhat reduced in intensity in *z*-polarization), the last one being a sharp peak. The bands at 11.90 and 26.00 kK are obviously spin-forbidden transitions and their assignment as the tetragonal components of cubic $^1E_g(^1D)$ and $^1T_{1g}(^1G)$ levels is made on the basis of the energy fitting calculations as explained later. The low intensity sharp peak of 6.10 kK has been shown to be a C—H stretching vibration overtone by Chiang and Drago[8] in their mull spectral study of the same compound at liquid N_2 temperature. These authors showed that the peak disappears if pyridine-d_5 is substituted for pyridine in the complex. It should be noted, however, that the mull spectrum[8] shows the sharp peak sitting over a low intensity broad absorption maximum at the same energy, which does not disappear on deuteration of the pyridines and which was left unassigned except perhaps as resulting from interactions between the chains or from the presence of some impurities such as $NiCl_3^-$ fragments in the chain. We have not observed such a low intense broad absorption under the sharp peak in the crystal spectrum, however. The observed maxima of the ligand-field absorption bands and their assignments are collected in Table 1.

Table 1. Observed band maxima (kK) and their assignments in the spectrum of $[Ni(py)_2Cl_2]$

Band maximum (kK)[a]	Assignment, $^3B_{1g} \rightarrow$
(7.50)	$^3B_{2g}$
8.40	^3E_g
(11.90)	$^1A_{1g}$, $^1B_{1g}$
(13.00)	$^3A_{2g}$
14.15	^3E_q
(23.30)	$^3A_{2g}$
24.40	^3E_g
(26.00)	^1E_g

[a] Shoulders are in parentheses.

A comparison of our spectral data on $[Ni(py)_2Cl_2]$ with those obtained earlier by others is presented in Table 2. Goodgame *et al.*[10] and Lever *et al.*[7] studied the diffuse reflectance spectrum of the powder at room temperature, whereas Drago and coworkers[9a,8] studied the mull spectrum at liquid N_2 temperature. The mull spectrum shows better resolution of all the bands compared with the reflec-

Table 2. Comparison of the observed band maxima (kK)[a] and assignments (excited states) in the spectrum of $[Ni(py)_2Cl_2]$

This work	Chiang and Drago[b]	Rowley and Drago[c]	Lever *et al.*[d]	Goodgame *et al.*[e]
		6.27 $^3B_{2g}$		6.00 $^3B_{2g}$
(7.50) $^3B_{2g}$	—	—		
8.40 ^3E_g	8.58 ^3E_g	8.62 ^3E_g		8.40 ^3E_g
11.90 $^1A_{1g}$, $^1B_{1g}(^1D)$[g]	—	~ 12.50[f]	(12.50) $^1A_{1g}$, $^1B_{1g}(^1D)$[g]	—
(13.00) $^3A_{2g}$	(13.40) ^3E_g	(13.30) ^3E_g	—	(12.20) $^3A_{2g}$
14.15 ^3E_g	14.36 $^3A_{2g}$	14.49 $^3A_{2g}$	13.99 $^3A_{2g}$, ^3E_g	13.90 ^3E_g
—	—	~ 21.00[f]	(22.00) $^1B_{2g}$, $^1E_g(^1D)$[h] $^1A_{1g}(^1G)$[i]	—
(23.30) $^3A_{2g}$	23.85 ^3E_g	23.40 ^3E_g	—	(22.20) $^3A_{2g}$
24.40 ^3E_g	24.65 $^3A_{2g}$	24.70 $^3A_{2g}$	24.10 $^3A_{2g}$, ^3E_g	24.10 ^3E_g
(26.00) $^1E_g(^1G)$[j]	—	—	—	—

[a] Shoulders are in parentheses.
[b] Mull spectrum (Ref. 8).
[c] Mull spectrum [Ref. 9(a)].
[d] Reflectance spectrum (Ref. 7).
[e] Reflectance spectrum (Ref. 10).
[f] Left unassigned although obviously implied as spin-forbidden transitions.
[g] Components of cubic ^1E_g of ^1D.
[h] Components of cubic $^1T_{2g}$ of ^1D.
[i] Cubic $^1A_{1g}$ of ^1G which simply transforms as $^1A_{1g}$ in D_{4h}.
[j] Component of $^1T_{1g}$ of ^1G.

tance spectrum and, surprisingly, even compared with the crystal spectrum. In the early studies where a reflectance spectrum was obtained, the two high energy spin-allowed bands (24.10 and ~ 14.10 kK) exhibited shoulders which were broad on the low frequency side, with no evidence of the presence of low intensity spin-forbidden transitions which are expected to appear at about the same energy regions as the shoulders. Hence, the assignments of these shoulders made by the two different groups of authors differed; Lever *et al.*[7] assigned them as spin-forbidden transitions assuming that the two maxima at 13.99 and 24.10 kK are the unsplit $^3T_{1g}(^3F)$ and $^3T_{1g}(^3P)$ cubic transitions, respectively, whereas Goodgame *et al.*[10] assigned the shoulders as the split tetragonal components assuming that the spin-forbidden transitions did not appear because of low intensity. With the assumption that the more intense component represented a transition to the orbital doublet ^3E, Goodgame *et al.* assigned the shoulders as the $^3A_{2g}$ and the peaks as the ^3E_g components. The mull and crystal spectra, however, resolved the shoulders, giving them comparable intensity to the main peaks and also uncovered the spin-forbidden transitions in these energy regions. More importantly though, our crystal spectrum presented polarization characteristics of the shoulders showing that they are the $^3A_{2g}$ transitions as we assigned them above. (It should be noted that both tetragonal $^1A_{1g}$, $^1B_{1g}$ components of cubic $^1E_g(^1D)$, expected to appear at ~ 12.00 kK, are allowed in both polarizations, whereas among the $^1B_{2g}$, ^1E_g components of cubic $^1T_{2g}(^1D)$ and the $^1A_{1g}$ of cubic $^1A_{1g}(^1G)$, expected to appear at ~ 21.00 kK, the ^1E_g and $^1A_{1g}$ are allowed in both polarizations, but $^1B_{2g}$ only in the x,y-polarization.[6]) Our assignments differ from those of Drago and co-workers,[8,9a] who assigned the shoulders as the ^3E_g and the main peaks as the $^3A_{2g}$ transitions on the basis of an assumption that the ordering of levels in $[Ni(py)_2Cl_2]$ should be the reverse of that in $[Ni(py)_4Cl_2]$. Although such an assumption will result in consistent values for bonding parameters, there is no justification for such an assumption. We will discuss this question further, later.

We now describe the fitting of the assigned band positions with the energy equations. Firstly we attempted to fit the observed band maxima without spin–orbit interaction.* The procedure is briefly as follows.[6] The energy of the $^3B_{2g}(^3T_{2g})$ is $10Dq$ including configuration interaction. We choose an initial value of Dt to fit the ^3E_g component of $^3T_{2g}$. With this initial value of Dt, values of Ds and B are varied, respectively, to fit the energy splitting of the second cubic band, $^3T_{1g}$, into its components $^3A_{2g}$, ^3E_g, and their positions. The $^3A_{2g}$, ^3E_g components of the third cubic band, $^3T_{1g}$, are then calculated. The calculated energies of the third band components may not agree with the observed values, in which case B and Ds are varied until as close agreement as possible is reached between observed and calculated positions of all four components of the two high energy cubic bands. Although the splitting of the first cubic band is determined by Dt alone, with no configuration interaction, when the configuration interaction is included it is affected by the values of Ds and B. Thus, finally Dt also should be varied along with Ds and B to fit all six tetragonal components.

When we applied such a procedure, it became very difficult to fit all four components of the two high energy cubic bands exactly for a set of Ds and B values, with Dt extracted by the fitting of the first band splitting. The reason for this is that with positive Dt and when ^3E_g is the higher energy component, $^3A_{2g}$ being the lower energy component for both the $^3T_{1g}$ cubic bands, the configuration interaction is such that although the splitting of the low energy $^3T_{1g}$ increases rapidly with κ, which is the ratio Ds/Dt, the splitting of the high energy $^3T_{1g}$ increases very slowly as shown in Fig. 3. The observed splittings, however, of these two cubic

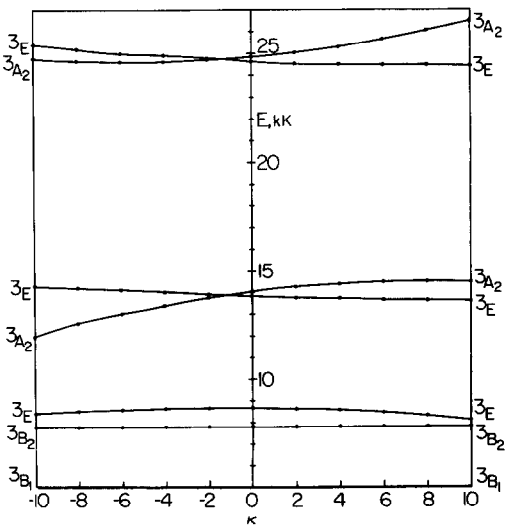

Fig. 3. Electronic energy levels of a quadrate nickel(II) system as a function of κ in the limit of zero spin–orbit interaction. Other parameters are (in kK): $Dq = -0.750$, $Dt = 0.110$ and $B = 0.850$.

* The complete energy matrices with and without spin–orbit interaction were derived earlier[19] by perturbing weak-field cubic levels, firstly by axial ligand field component and then by spin–orbit interaction.

Table 3. Fitting of the observed band positions with the calculated transition energies in the electronic spectrum of $[Ni(py)_2Cl_2]$

Observed band position (kK)[a]	Assignment, $^3B_{1g}(^3A_{2g}) \rightarrow$	Calculated transition energy (kK)[b]
(7.500)	$^3B_{2g}(^3T_{2g})$	7.404(Γ_3); 7.542(Γ_5)
8.400	$^3E_g(^3T_{2g})$	8.153(Γ_1); 8.293(Γ_2); 8.525(Γ_5); 8.691(Γ_3); 8.706(Γ_4)
(11.900)	$^1A_{1g}$, $^1B_{1g}(^1E_g)$	12.252(Γ_1);[c] 12.526(Γ_3)[d]
(13.000)	$^3A_{2g}(^3T_{1g})$	12.808(Γ_1);[e] 13.035(Γ_5) [f]
14.150	$^3E_g(^3T_{1g})$	13.392(Γ_2); 13.870(Γ_5);[g] 14.015(Γ_4); 14.198(Γ_1);[h] 14.357(Γ_3)[i]
(23.300)	$^3A_{2g}(^3T_{1g})$	23.670(Γ_1);[j] 23.859(Γ_5)[k]
24.400	$^3E_g(^3T_{1g})$	23.699(Γ_3); 23.842(Γ_4);[l] 24.036(Γ_5);[m] 24.127(Γ_2); 24.225(Γ_1)[n]
(26.000)	$^1E_g(^1T_{1g})$	25.528(Γ_5)

[a] Shoulders are in parentheses.

[b] Parameters, in kK: $Dq = 0.750$, $Dt = 0.110$, $Ds = -0.330$, $B = 0.850$, $C = 3.168$, $\zeta = 0.550$.

[c] $50.7\% + 16.3\%\ ^1A_1[^1E(^1G)] + 24.5\%\ ^3A_2[^3T_1(^3F)] + 7.6\%\ ^3A_2[^3T_1(^3P)]$.

[d] $61.2\% + 21.9\%\ ^1B_1[^1E(^1G)] + 13.8\%\ ^3E[^3T_1(^3F)]$.

[e] $22.6\% + 3.9\%\ ^3A_2[^3T_1(^3P)] + 57.7\%\ ^3E[^3T_1(^3F)] + 4.3\%\ ^3E[^3T_1(^3P)] + 8.5\%\ ^1A_1[^1A_1(^1G)]$.

[f] $63.0\% + 14.8\%\ ^3A_2[^3T_1(^3P)] + 20.0\%\ ^3E[^3T_1(^3F)]$.

[g] $71.1\% + 6.6\%\ ^3E[^3T_1(^3P)] + 16.1\%\ ^3A_2[^3T_1(^3F)]$.

[h] $33.2\% + 31.6\%\ ^3A_2[^3T_1(^3F)] + 8.6\%\ ^3A_2[^3T_1(^3P)] + 12.8\%\ ^1A_1[^1E(^1D)] + 6.9\%\ ^1A_1[^1E(^1G)]$.

[i] $75.9\% + 6.7\%\ ^3E[^3T_1(^3P)] + 9.7\%\ ^1B_1[^1E(^1D)] + 5.7\%\ ^1B_1[^1E(^1G)]$.

[j] $60.1\% + 16.3\%\ ^3A_2[^3T_1(^3F)] + 20.9\%\ ^3E[^3T_1(^3P)]$.

[k] $58.1\% + 15.3\%\ ^3A_2[^3T_1(^3F)] + 17.0\%\ ^3E[^3T_1(^3P)] + 4.5\%\ ^1E[^1T_2(^1D)]$.

[l] $86.3\% + 9.0\%\ ^3E[^3T_1(^3F)]$.

[m] $71.6\% + 5.6\%\ ^3E[^3T_1(^3F)] + 18.0\%\ ^3A_2[^3T_1(^3P)]$.

[n] $71.5\% + 4.6\%\ ^3E[^3T_1(^3F)] + 19.6\%\ ^3A_2[^3T_1(^3P)]$.

transitions are 1.15 and 1.10 kK. This means that the interpretation of this system should be carried our by including spin–orbit interaction.[19] When spin–orbit interaction is included, the ^3E_g component splits into five spin–orbital levels, Γ_i, $i = 1$, 2, 3, 4, 5, and both the $^3A_{2g}$ and $^3B_{2g}$ components split into two spin–orbital levels, Γ_1, Γ_5 and Γ_3, Γ_5. It is well known that the free-ion value for the spin–orbit constant parameter for nickel(II) is 0.66 kK and that this value will be reduced in its complexes. We can therefore vary the spin–orbit parameter below 0.66 kK until the observed bands can be fitted either with one of the spin–orbital levels or with an average of all of them in each group. The fitting of the spectral data using such a procedue is shown in Table 3.

The fitting presented here is the best we could do for this system. Even with inclusion of the spin–orbit interaction, it is not possible to obtain a calculated splitting of ~ 1.10 kK for the highest energy cubic band to fit the observed splitting. Thus, using one spin–orbital level to fit the observed maximum (23.670 kK for the $^3A_{2g}$ component and 24.225 kK for the ^3E_g component), the calculated splitting is still 0.555 kK, as against an observed splitting of ~ 1.10 kK. Although the theory seems to be deficient at this point to explain the observed data, any further theoretical studies, we believe, should

be deferred until better resolution of the observed bands is achieved, even perhaps to the extent of identifying spin–orbital levels experimentally.

The calculations to fit the data produced an interesting result. It is the mixing of the spin–orbital levels of the $^3A_{2g}$ component with the corresponding levels of the ^3Eg component and *vice versa* in the case of the two high energy cubic bands. We have included in Table 3 the purities of spin–orbital levels whenever they are less than 90.0%, and listed in each such case the per cent contribution of other eigenvector components. It should be noted that the Γ_1, Γ_5 spin–orbital levels of the $^3A_{2g}[^3T_{1g}(^3F)]$ band are only 22.6 and 63.0% pure and have 57.7 and 20.0% of the corresponding levels of $^3E_g[^3T_{1g}(^3F)]$ mixed in, whereas the same spin–orbital levels of $^3E_g[^3T_{1g}(^3F)]$ are 33.2 and 71.1% pure and have 31.6 and 16.1% of the $^3A_{2g}[^3T_{1g}(^3F)]$ levels mixed in. Because of this mixing of one component with the other, the $^3A_{2g}$ is expected not to be wiped out completely and the ^3E_g is expected to decrease in intensity, in z-polarization. This may be the reason (other than the molecular axes probably not being aligned along the optic axes) why both $^3A_{2g}$ and ^3E_g components decrease in intensity in z-polarization, rather than $^3A_{2g}$ disappearing and ^3E_g having the same intensity as in the x,y-polarization. (For the purpose of this discussion, it is actually the total of a given component from both ^3F and ^3P that should be considered for purity as well as for mixing.) Similarly, the spin–orbital levels of $^3A_{2g}[^3T_{1g}(^3P)]$ are 60.1 and 58.1% pure and contain 20.9 and 17.0% of the corresponding levels of $^3E_g[^3T_{1g}(^3P)]$, whereas the same levels of $^3E_g[^3T_{1g}(^3P)]$ are 71.5 and 71.6% pure and contain 19.6 and 18.0% levels of $^3A_{2g}[^3T_{1g}(^3P)]$. Thus, the mixing of the components in this case is only about half that of the $^3T_{1g}(^3F)$ components.

It should be noted that the fitting procedure that we have used here necessarily involves an uncertainty in the derived parameters, in particular of *Ds* and *B*. However, the negative sign of *Ds* and the value of $\kappa(= Ds/Dt)$ being -3 or greater to explain the $\sim$ 1.00 kK splitting of both the $^3T_{1g}$ transitions is definitive. Finally, the *C* value is derived by fitting the observed positions of the spin-forbidden bands with the energies of such transitions that are likely to appear in these energy regions.

Before we discuss the significance of the spectral parameters derived for $[Ni(py)_2Cl_2]$, we would like to present the spectral data obtained from the unpolarized spectrum of $[Ni(qu)_2Cl_2]$. The band positions and the assignments assuming that the ordering of levels is the same as that in the pyridine system are summarized in Table 4, along with the room temperature reflectance spectral data

Table 4. Comparison of the observed band maxima (kK)[a] and assignments (excited states) in the spectrum of $[Ni(qu)_2Cl_2]$

This work		Goodgame *et al.*[b]	
7.60	$^3B_{2g}$	(6.00)	$^3B_{2g}$
	—	7.55	^3E_g
11.90	$^3A_{2g}$	12.00	$^3A_{2g}$
13.10	^3E_g	13.15	^3E_g
19.50	$^1B_{2g}$, $^1E_g(^1D)$; $^1A_{1g}(^1G)$	—	
(21.50)	$^3A_{2g}$	19.20	$^3A_{2g}$
22.50	^3E_g	22.70	^3E_g

[a] Shoulders are in parentheses.
[b] Reflectance spectrum at room temperature (Ref. 10).

obtained by Goodgame *et al.*[10] Our band positions agree with those reported, except the highest energy spin-allowed band in our crystal spectrum displays asymmetry on the low energy side. We attribute this asymmetry at $\sim$ 21 kK to the $^3A_{2g}$ tetragonal component leaving the low intensity $\sim$ 19.5 kK peak as a spin-forbidden transition. Similarly as for $[Ni(py)_2Cl_2]$, we attribute the $\sim$ 6.00 kK to a C—H overtone of quinoline and not to the tetragonal component of the lowest energy $^3T_{2g}$ cubic transition. Thus, we assign the 7.60 kK band maximum as the $^3B_{2g}$ component of $^3T_{2g}$ and assume that the corresponding ^3E_g component which should appear at higher energy is not resolved in our spectra. Since the $^3E_g(^3T_{2g})$ transition is not uncovered, the *Dt* value cannot be obtained for this system, which implies that it is not possible to fit the other bands to derive the spectral parameters. From the position of $^3B_{2g}$ and the magnitudes of splittings of the two higher energy cubic bands and the positions of their components, however, it is obvious that the values of *Dt*, *Dq* and *Ds* parameters for this system will be about the same, and the *B* and *C* parameters will be somewhat less than those of the dipyridine system.

We will now present a discussion of the significance of the derived parameters for $[Ni(py)_2Cl_2]$. The *B*, *C* electron repulsion parameters and ζ spin–orbit interaction parameter are reduced in the complex from the free-ion values, as expected. The ligand-field parameters and their significance in terms of bonding are of paramount importance.

The *Dq*, *Dt* and *Ds* ligand-field symmetry parameters obtained for the $[Ni(py)_2Cl_2]$ system are given in Table 5. The *Dq* value that is obtained by fitting the experimental data is that for the equatorial ligand, which is chloride in this case. The *Dq* of the axial ligand, namely, pyridine, is calculated

Table 5. Ligand-field and molecular orbital parameters (kK) of some nickel(II) complexes

Complex	Chromophore	Dq_{Cl}	Dq_{py}	Dt	Ds	$\delta\sigma$	$\delta\pi$	$\Delta_{\sigma_{Cl}}-\Delta_{\sigma_{py}}$	$\Delta_{\pi_{Cl}}-\Delta_{\pi_{py}}$
$[(Me_4N)NiCl_3]^a$	$NiCl_6$	0.660	—	—	—	—	—	—	—
$[Ni(py)_6](NO_3)^b$	NiN_6	—	0.983	—	—	—	—	—	—
$[Ni(py)_4Cl_2]^b$	NiN_4Cl_2[c]	0.653	1.176	−0.299	−0.336	−1.065	0.244	−4.259	0.974
$[Ni(py)_2Cl_2]^d$	$NiCl_4N_2$[c]	0.750	0.943	0.110	−0.330	−0.289	−0.770	1.155	3.080

[a] Reference 10.
[b] Reference 6.
[c] *Trans*-configuration.
[d] This work.

from the relationship $Dt = 4/7(Dq_{ax} - Dq_{eq})$. We have also listed in this table the values for the spectral fitting parameters Dq_{py}, Dt and Ds, and for the calculated parameters Dq_{Cl} obtained earlier by us from the $[Ni(py)_4Cl_2]$ system.[6] The Dq values of octahedral systems $[(Me_4N)NiCl_3]$ and $[Ni(py)_6](NO_3)$ are also given in this table for a comparison. It is immediately obvious that these parameters are not transferable from one system to another. Thus, although the octahedral Dq of the chloride ligand remains the same as we go from the hexa-coordinated chloro complex to the tetragonal $[Ni(py)_4Cl_2]$, it increases by $\sim 14\%$ in the tetragonal $[Ni(py)_2Cl_2]$. Similarly, the octahedral Dq of the pyridine ligand changes very slightly as we go from the hexa-coordinated pyridine complex to the tetragonal complex $[Ni(py)_2Cl_2]$, but increases by $\sim 20\%$ in the tetragonal $[Ni(py)_4Cl_2]$ complex. This also means that the Dt values will be different between the two tetragonal systems, $[Ni(py)_2Cl_2]$ and $[Ni(py)_4Cl_2]$. If the ligand-field parameters are transferable, not only the Dq values of a given ligand are expected to be the same in the complexes $[Ni(py)_2Cl_2]$ and $[Ni(py)_4Cl_2]$, but also the value of the Dt parameter, as well as that of Ds parameter for the two systems, should be of the same magnitude but of opposite sign. The reason that these parameters change between the two systems is because the bonding nature of the ligands changes depending upon whether they are in the equatorial positions or in the axial positions of the tetragonal complex. In the case of $[Ni(py)_4Cl_2]$, where the pyridine is in the equatorial position, pyridine is more σ-antibonding and somewhat less π-antibonding than chloride. In the $[Ni(py)_2Cl_2]$ system, where the pyridine is in the axial position, pyridine is still less π-antibonding than chloride, but is is also less σ-antibonding.

The relative antibonding powers of the chloride and pyridine ligands can be calculated either in terms of the semi-empirical molecular orbital parameters $\delta\sigma$, $\delta\pi$[20,21] or of the angular overlap model (AOM) parameters $(\Delta_{\sigma_{ax}}-\Delta_{\sigma_{eq}})$, $(\Delta_{\pi_{ax}}-\Delta_{\pi_{eq}})$.[22] The calculated values of both sets of parameters for the complexes $[Ni(py)_2Cl_2]$ and $[Ni(py)_4Cl_2]$ are also given in Table 5.* The $\delta\sigma$ values show that although pyridine is more σ-antibonding than chloride in $[Ni(py)_4Cl_2]$, it is slightly less σ-antibonding than chloride in $[Ni(py)_2Cl_2]$. The $\delta\pi$ values show that pyridine is less π-antibonding than chloride in both systems, although more so in $[Ni(py)_2Cl_2]$. The AOM parameters reflect the same conclusion. The difference in the bonding nature of the ligands could be due to the fact that the chloride ligands in $[Ni(py)_2Cl_2]$ are bridged, whereas in $[Ni(py)_4Cl_2]$ they are terminal. On the other hand, the changes in Dq values of chloride and pyridine ligands, as noted earlier, are not consistent and systematic for the ligation of chloride, whether it is bridging or terminal. It seems that the bonding nature of ligands in a given complex depends on the complex as an entirety and is not characteristic of an individual ligand, which means that the ligands cannot be treated as single entities allowing single-ligand parameters to be transferable from one system to another.

*The AOM parameters given in this table for $[Ni(py)_4Cl_2]$ have been extracted from spectral data obtained earlier by us.[6] Our spectral data on this system differ somewhat from that reported by Schreiner and Hamm,[23] giving rise to different AOM parameters.[22b]

REFERENCES

1. C. R. Hare and C. J. Balhausen, *J. Chem. Phys.* 1964, **40**, 788.
2. C. R. Hare and C. J. Balhausen, *J. Chem. Phys.* 1964, **40**, 792.
3. N. S. Hush and R. J. M. Hobbs, *Progr. Inorg. Chem.* 1968, **10**, 259.
4. C. W. Reimann, *J. Phys. Chem.* 1970, **74**, 561.
5. M. A. Hitchman, *Inorg. Chem.* 1972, **11**, 2387.

6. J. S. Merriam and J. R. Perumareddi, *J. Phys. Chem.* 1975, **79**, 142.
7. (a) A. B. P. Lever, S. M. Nelson and T. M. Shepherd, *Inorg. Chem.* 1965, **4**, 810; (b) S. M. Nelson and T. M. Shepherd, *J. Chem. Soc.* 1965, 3276.
8. R. L. Chiang and R. S. Drago, *Inorg. Chem.* 1971, **10**, 453.
9. (a) D. A. Rowley and R. S. Drago, *Inorg. Chem.* 1968, **7**, 795 and refs therein; (b) C. Furlani, *Coord. Chem. Rev.* 1968, **3**, 141.
10. D. M. L. Goodgame, M. Goodgame and M. J. Weeks, *J. Chem. Soc.* 1964, 5194.
11. I. S. Ahuja, D. H. Brown, R. H. Nuttall and D. W. A. Sharp, *J. Inorg. Nucl. Chem.* 1965, **27**, 1105.
12. D. M. L. Goodgame and M. Goodgame, *J. Chem. Soc.* 1963, 207.
13. B. J. Hathaway and D. G. Holah, *J. Chem. Soc.* 1964, 2400.
14. J. Reedijk and P. W. N. M. Van Leeuwen, *Rec. Trav. Chem.* 1968, **87**, 129.
15. A. B. P. Lever, *J. Inorg. Nucl. Chem.* 1965, **27**, 149.
16. C. E. Taylor and A. E. Underhill, *J. Chem. Soc. A* 1969, 368.
17. B. Morosin, *J. Chem. Phys.* 1965, **44**, 252.
18. (a) N. S. Gill, R. S. Nyholm, G. A. Barclay, T. S. Christie and P. J. Pauling, *J. Inorg. Nucl. Chem.* 1961, **18**, 88; (b) J. D. Dunitz, *Acta Cryst.* 1957, **10**, 307; (c) H. C. A. King, E. Koros and S. M. Nelson, *J. Chem. Soc.* 1963, 5449.
19. J. A. Collins, MS thesis. Florida Atlantic University (1976).
20. H. Yamatera, *Bull. Chem. Soc. Jpn* 1958, **31**, 95.
21. D. S. McClure, in *Advances in the Chemistry of Coordination Compounds* (Edited by S. Kirschner). MacMillans, New York (1961).
22. (a) J. Glerup, O. Monsted and C. E. Schaffer, *Inorg. Chem.* 1976, **15**, 1399 and refs therein; (b) J. Glerup, O. Monsted and C. E. Schaffer, *Inorg. Chem.* 1980, **19**, 2855.
23. A. F. Schreiner and D. J. Hamm, *Inorg. Chem.* 1973, **12**, 2037.

Polyhedron Vol. 8, No. 18, pp. 2291–2297, 1989
Printed in Great Britain

0277–5387/89 $3.00+.00
© 1989 Pergamon Press plc

SYNTHESIS AND CHARACTERIZATION OF $Ir(\eta^4\text{-}C_4H_6)[N(SiMe_2CH_2PPh_2)_2]$. A NON-FLUXIONAL FIVE-COORDINATE IRIDIUM(I) COMPLEX CONTAINING AN η^4-BUTADIENE LIGAND

MICHAEL D. FRYZUK,* KIRAN JOSHI and STEVEN J. RETTIG†

Department of Chemistry, University of British Columbia, 2036 Main Mall, Vancouver, B.C., Canada V6T 1Y6

(*Received* 13 *February* 1989; *accepted* 4 *May* 1989)

Abstract—The reaction of the square-planar iridium(I) η^2-cyclooctene complex, $Ir(\eta^2\text{-}C_8H_{14})[N(SiMe_2CH_2PPh_2)_2]$, with excess 1,3-butadiene generates excellent yields of the five-coordinate iridium(I) 1,3-butadiene complex, $Ir(C_4H_6)[N(SiMe_2CH_2PPh_2)_2]$. Both the NMR spectral data and the single crystal X-ray structure reveal that the tridentate amido–diphosphine ligand is coordinated in a quasi facial manner and the 1,3-butadiene unit is bound in a s-*cis*-η^4-π mode with some σ^2–π component to the bonding. In solution, the butadiene complex shows no fluxional behaviour even at temperatures as high as 85°C.

The coordination chemistry of the mixed-donor, tridentate ligand $^-N(SiMe_2CH_2PPh_2)_2$ with both iridium(I) and iridium(III) has allowed access into a number of areas in organometallic chemistry. For example, formation of the methylidene complex $Ir(=CH_2)[N(SiMe_2CH_2PPh_2)_2]$ via photolysis[1] of iridium(III) dialkyls, unusual activation[2] of dihydrogen by methyl–iridium halides and phosphides, and thermal carbon–hydrogen bond activation,[3] are all observed with the above amido–diphosphine ancillary ligand bound to iridium. In almost every example,[4] the tridentate ligand binds to the metal centre in a planar fashion having *trans*-disposed phosphorus donors, regardless of the metal geometry. Examples are the square-planar derivatives[5] $Ir(L)[N(SiMe_2CH_2PPh_2)_2]$ (where L = olefin, phosphine, CO or acetylene), square-pyramidal complexes[6] of the formula $Ir(CH_3)X[N(SiMe_2CH_2PPh_2)_2]$ (X = halide), trigonal bipyramidal bis(hydrocarbyl)[7] derivatives, $Ir(R)R'[N(SiMe_2CH_2PPh_2)_2]$, and various octahedral complexes.[2b,6,8]

Although 1,3-dienes are considered to be fairly common ligands for the later transition elements, there are few examples of iridium derivatives.[9] Our combined interest in the coordination of this tridentate ligand system with both early and late transition elements and the activation of 1,3-dienes by one[10] or more[11] metal centres provided the incentive to examine the reaction of 1,3-butadiene with a later transition metal derivative incorporating this ligand, in this case iridium(I). In this paper we describe the solid-state and solution-phase structures of a complex of s-*cis*-1,3-butadiene attached to the $Ir[N(SiMe_2CH_2PPh_2)_2]$ moiety. Of particular note is the unusual coordination mode of the tridentate ligand. In addition, the resultant five-coordinate complex is stereochemically rigid on the NMR time scale.

RESULTS

The previously reported[5] η^2-cyclooctene complex, $Ir(\eta^2\text{-}C_8H_{14})[N(SiMe_2CH_2PPh_2)_2]$, reacts with excess 1,3-butadiene (≈ 5 equiv) in toluene solution, at room temperature without any discernable colour change. From the orange solution, light yellow crystals of the formula $Ir(C_4H_6)[N(SiMe_2CH_2PPh_2)_2]$ can be isolated in $> 90\%$ yield.

$$Ir(\eta^2\text{-}C_8H_{14})[N(SiMe_2CH_2PPh_2)_2] + 1,3\text{-butadiene} \longrightarrow Ir(C_4H_6)[N(SiMe_2CH_2PPh_2)_2] + \text{cyclooctene}.$$

The solid-state structure of the $Ir(C_4H_6)[N(SiMe_2CH_2PPh_2)_2]$ complex is shown in Fig. 1. The

* Author to whom correspondence should be addressed.
† Experimental Officer: UBC Crystallographic Service.

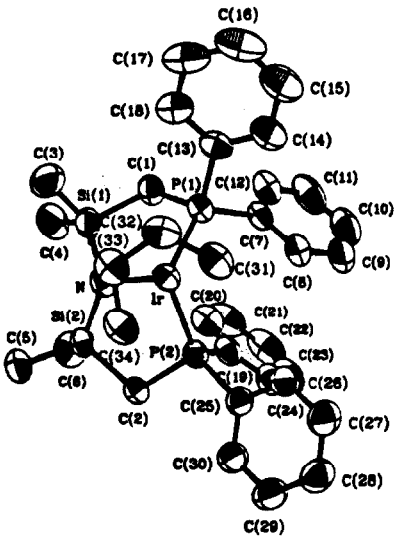

Fig. 1. ORTEP drawing of the $Ir(\eta^4\text{-}C_4H_6)[N(SiMe_2CH_2PPh_2)_2]$ molecule. Hydrogen atoms are omitted for clarity.

complex is five-coordinate and the amido–diphosphine tridentate ligand adopts a facial coordination mode as indicated by the P(1)—Ir—P(2) angle of 107.01(4)° (Table 1). Interestingly, the Ir—NSi_2 unit of the ligand backbone is still planar [see Fig. 2(a)], as determined by the sum of the angles involved (Ir—N—Si(1)+Ir—N—Si(2)+Si(1)—N—Si(2) = 360°). The Ir—P and Ir—N bond lengths are not unusual, and compare to other standard bond lengths.[1,2,6,7] The iridium centre is bonded to each carbon of the butadiene unit with the following bond lengths: Ir—C(31), 2.139(4); Ir—C(32), 2.167(4); Ir—C(33), 2.183(4); and Ir—C(34), 2.182(4) Å (Table 2). The butadiene unit is asymmetrically bound to the iridium; the metal–carbon bond lengths parallel the *trans*-influence[12] order, i.e. P > N, since C(31) being *trans* to the amide possesses a shorter bond to iridium than C(34) which is *trans* to the phosphorus ligand, P(2). The C—C bond lengths are only slightly different,

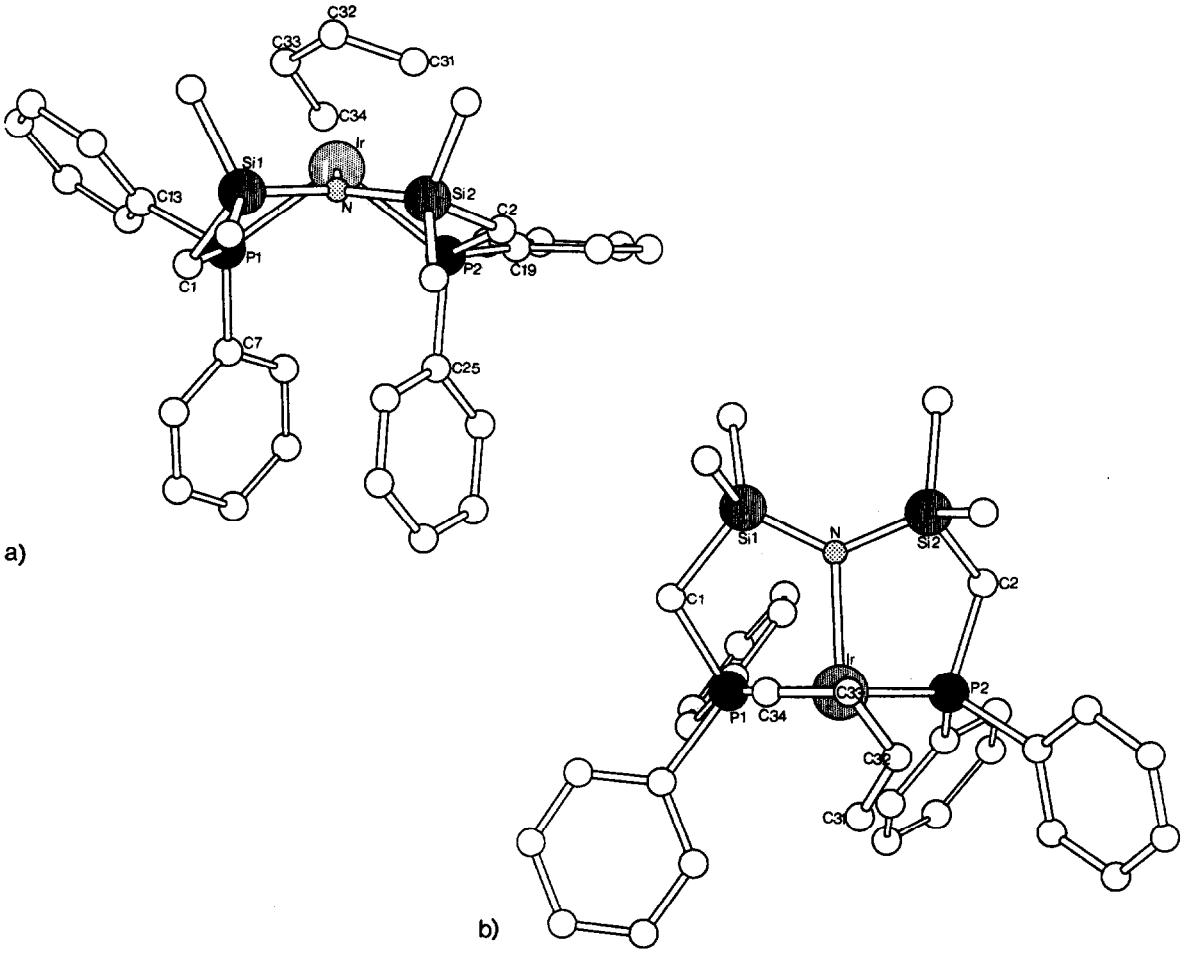

Fig. 2. Chem. 3-D views of $Ir(\eta^4\text{-}C_4H_6)[N(SiMe_2CH_2PPh_2)_2]$ showing: (a) the planar Ir—NSi_2 fragment and the facial mode of coordination of the tridentate ligand, and (b) the *trans* relationship of C(34) and P(2).

Table 1. Bond angles (°) with ESDs in parentheses[a]

Bonds	Angle (°)	Bonds	Angle (°)
P(1)—Ir—P(2)	107.01(4)	P(1)—C(7)—C(8)	119.6(3)
P(1)—Ir—N	87.49(9)	P(1)—C(7)—C(12)	121.2(4)
P(1)—Ir—Bu	122.23(8)	C(8)—C(7)—C(12)	119.2(4)
P(2)—Ir—N	83.43(9)	C(7)—C(8)—C(9)	120.4(5)
P(2)—Ir—Bu	123.22(8)	C(8)—C(9)—C(10)	120.2(6)
N—Ir—Bu	122.3(1)	C(9)—C(10)—C(11)	119.8(5)
Ir—P(1)—C(1)	108.5(1)	C(10)—(11)—C(12)	121.2(6)
Ir—P(1)—C(7)	121.8(1)	C(7)—C(12)—C(11)	119.2(4)
Ir—P(1)—C(13)	114.3(1)	P(1)—C(13)—C(14)	121.1(4)
C(1)—P(1)—C(7)	106.1(2)	P(1)—C(13)—C(18)	120.2(4)
C(1)—P(1)—C(13)	105.1(2)	C(14)—C(13)—C(18)	118.5(4)
C(7)—P(1)—C(13)	99.6(2)	C(13)—C(14)—C(15)	120.7(6)
Ir—P(2)—C(2)	106.1(1)	C(14)—C(15)—C(16)	120.8(6)
Ir—P(2)—C(19)	122.4(1)	C(15)—C(16)—C(17)	119.1(5)
Ir—P(2)—C(25)	116.5(1)	C(16)—C(17)—C(18)	121.4(6)
C(2)—P(2)—C(19)	101.8(2)	C(13)—C(18)—C(17)	119.5(6)
C(2)—P(2)—C(25)	106.4(2)	P(2)—C(19)—C(20)	118.3(3)
C(19)—P(2)—C(25)	101.8(2)	P(2)—C(19)—C(24)	123.3(4)
N—Si(1)—C(1)	105.5(2)	C(20)—C(19)—C(24)	118.3(4)
N—Si(1)—C(3)	113.4(2)	C(19)—C(20)—C(21)	121.5(5)
N—Si(1)—C(4)	115.7(2)	C(20)—C(21)—C(22)	118.8(6)
C(1)—Si(1)—C(3)	110.2(3)	C(21)—C(22)—C(23)	120.0(5)
C(1)—Si(1)—C(4)	105.9(2)	C(22)—C(23)—C(24)	120.6(6)
C(3)—Si(1)—C(4)	105.9(4)	C(19)—C(24)—C(23)	120.7(6)
N—Si(2)—C(2)	106.3(2)	P(2)—C(25)—C(26)	119.5(3)
N—Si(2)—C(5)	115.2(2)	P(2)—C(25)—C(30)	122.0(3)
N—Si(2)—C(6)	115.2(2)	C(26)—C(25)—C(30)	118.4(4)
C(2)—Si(2)—C(5)	107.2(2)	C(25)—C(26)—C(27)	120.7(4)
C(2)—Si(2)—C(6)	108.7(2)	C(26)—C(27)—C(28)	120.3(5)
C(5)—Si(2)—C(6)	104.0(2)	C(27)—C(28)—C(29)	119.0(5)
Ir—N—Si(1)	109.8(2)	C(28)—C(29)—C(30)	121.3(5)
Ir—N—Si(2)	116.5(2)	C(25)—C(30)—C(29)	120.3(4)
Si(1)—N—Si(2)	133.7(2)	C(31)—C(32)—C(33)	116.6(4)
P(1)—C(1)—Si(1)	108.5(2)	C(32)—C(33)—C(34)	117.4(4)
P(2)—C(2)—Si(2)	109.2(2)		

[a] Bu refers to the centroid of the butadiene ligand.

Table 2. Bond lengths (Å) with ESDs in parentheses[a]

Bond	Length (Å)	Bond	Length (Å)
Ir—P(1)	2.292(1)	C(9)—C(10)	1.35(1)
Ir—P(2)	2.2879(9)	C(10)—C(11)	1.38(1)
Ir—N	2.214(3)	C(11)—C(12)	1.384(8)
Ir—C(31)	2.139(4)	C(13)—C(14)	1.386(7)
Ir—C(32)	2.167(3)	C(13)—C(18)	1.386(7)
Ir—C(33)	2.183(4)	C(14)—C(15)	1.390(7)
Ir—C(34)	2.182(4)	C(15)—C(16)	1.36(1)
Ir—Bu	1.770(2)	C(16)—C(17)	1.37(1)
P(1)—C(1)	1.829(4)	C(17)—C(18)	1.399(8)
P(1)—C(7)	1.837(4)	C(19)—C(20)	1.388(7)
P(1)—C(13)	1.837(4)	C(19)—C(24)	1.389(6)
P(2)—C(2)	1.826(4)	C(20)—C(21)	1.384(7)
P(2)—C(19)	1.832(4)	C(21)—C(22)	1.41(1)
P(2)—C(25)	1.828(4)	C(22)—C(23)	1.36(1)
Si(1)—N	1.683(4)	C(23)—C(24)	1.389(8)
Si(1)—C(1)	1.891(4)	C(25)—C(26)	1.389(6)
Si(1)—C(3)	1.863(7)	C(25)—C(30)	1.396(6)
Si(1)—C(4)	1.864(6)	C(26)—C(27)	1.390(7)
Si(2)—N	1.696(4)	C(27)—C(28)	1.369(7)
Si(2)—C(2)	1.905(4)	C(28)—C(29)	1.392(7)
Si(2)—C(5)	1.888(5)	C(29)—C(30)	1.362(7)
Si(2)—C(6)	1.883(5)	C(31)—C(32)	1.430(7)
C(7)—C(8)	1.376(7)	C(32)—C(33)	1.409(7)
C(7)—C(12)	1.397(6)	C(33)—C(34)	1.421(7)
C(8)—C(9)	1.404(7)		

[a] Bu refers to the centroid of the butadiene ligand.

having the following values: C(31)—C(32), 1.430(7); C(32)—C(33), 1.409(7); and C(33)—C(34), 1.421(7) Å.

There are two methods reported[13] to compare metal–diene interactions, in particular, to gauge the component of η^4–π versus σ^2–π character of the bonding from the crystallographic data. The first method deals with the dihedral angle, θ (subtended by the C(31)—Ir—C(34) and the C(31)—C(32)—C(33)—C(34) planes), and the difference in the bond distances of the metal from the inner and outer carbons of the diene ligand, Δd, defined as $\Delta d = [d\{\text{Ir—C(31)}\} + d\{\text{Ir—C(34)}\}]/2 - [d\{\text{Ir—C(32)}\} + d\{\text{Ir—C(33)}\}]/2$. For the vast majority of middle and late transition metal diene complexes, which generally assume the η^4-π-*cis*-1,3-diene structure, the dihedral angle, θ, is in the range 75–90° and Δd is between −0.1 and 0.1 Å. For the early transition metal diene complexes,[14] it is generally found that θ is greater than 90° and Δd varies from −0.5 to 0 Å, and this is considered diagnostic of the σ^2–π form of bonding. For the iridium derivative $Ir(C_4H_6)[N(SiMe_2CH_2PPh_2)_2]$, the value of θ is 92.9° and Δd is −0.01 Å, thus strongly suggesting a η^4–π bonding mode of the diene ligand, but with some σ^2–π component present.

In the second mode of comparison, there is an approximate linear increase in the dihedral angle, θ, with the difference in the C—C bond lengths, Δl, where $\Delta l = [l\{\text{C(31)—C(32)}\} + l\{\text{C(33)—C(34)}\}]/2 - l\{\text{C(32)—C(33)}\}$. For the later transition metals, Δl is between −0.1 and 0.0 Å, whereas in the case of early transition metals, Δl falls in the range of 0.0–0.2 Å. The calculated value of Δl for the $Ir(C_4H_6)[N(SiMe_2CH_2PPh_2)_2]$ complex is 0.02 Å, which again is close to that expected for a typical late transition element, i.e. η^4–π, but also suggestive of some component of σ^2–π.

In solution, $Ir(C_4H_6)[N(SiMe_2CH_2PPh_2)_2]$ has a rigid structure even at temperatures as high as 85°C. The ^{1}H NMR spectrum of the isolated complex shows four singlets of equal intensity for the silylmethyl groups ($Si(CH_3)_2$) protons in the hybrid tridentate ligand and, hence indicates quite an asymmetry in the molecule. The methylene protons on the ligand backbone (PCH_2Si) are multiplets centred at 1.85 and 2.12 ppm. Hardly any separation of the *ortho*-protons' resonance from that of the *meta*/*para*-protons' resonance of the phenyl rings is observed, thus suggesting a quasi-facial arrangement of the tridentate ligand (*cis*[15]-phosphine donors). The butadiene moiety shows six proton resonances ranging from −0.60 to 5.37 ppm. The corresponding four ^{13}C resonances for the coordinated diene ligand were identified by the use of 2D ^{13}C–^{1}H heteronuclear correlation maps (Fig. 3). Three of the four carbon resonances of the 1,3-butadiene ligand in the $^{13}C\{^1H\}$ NMR spectrum have some coupling to ^{31}P, but one carbon nucleus in particular has an additional large coupling to one of the phosphorus nuclei of the tridentate ligand (33.75 ppm, dd, $^2J_{P—C} = 41.6$ Hz, $^2J_{P—C} = 3.3$ Hz). The gated decoupled ^{13}C NMR spectrum shows $^1J_{C—H}$ for the inner carbons of the diene unit to be 165.5 Hz which is typical of the sp^2 bonded carbon centre, however, $^1J_{C—H}$ for the outer or terminal carbons are lower (~ 150.0 Hz), but are still suggestive of the sp^2 character around these carbon centres. These coupling constant results mirror the structural data in the solid state which suggest mostly η^4–π but with some σ^2–π character for the butadiene–iridium interaction. The $^{31}P\{^1H\}$ NMR spectrum consists of two singlets and is virtually temperature independent from −80 to +85°C. The fact that no coupling is observed between the inequivalent ^{31}P nuclei is somewhat unusual but is consistent with their *cis* disposition.

DISCUSSION

From the solid-state data, the complex $Ir(C_4H_6)[N(SiMe_2CH_2PPh_2)_2]$ has a distorted five-coordinate structure with the tridentate ligand coordinated to the metal with *cis*-phosphine donors, or in a quasi-facial manner. Interestingly, the adoption of this *cis*-phosphine geometry does not result in the disilylamido unit deviating from planarity. The 1,3-butadiene ligand adopts the s-*cis* planar structure and binds to the iridium in a η^4–π fashion but with a small component of σ^2–π.

In solution, the solid-state structure is completely maintained. Not only is the five-coordinate complex stereochemically rigid on the NMR time scale, but the *cis*-butadiene unit remains asymmetrically disposed on the iridium even to temperatures as high as 85°C. This can be confirmed by the observed large $^2J_{P—C}$ coupling which we ascribe to that between P(2) and C(34) in the molecule [Fig. 2(b)].

Five-coordinate d^8 complexes have been studied[16] as the prototypes for stereochemical nonrigidity in organotransition metal chemistry. Since the bonding of the butadiene to iridium is mainly η^4–π, at least from the solid-state data, the oxidation level of the metal centre is therefore iridium(I). To rationalize the observed lack of fluxionality, it is probable that the tridentate ligand constrains the coordination environment and destabilizes any traverses through stereochemical manifolds that require geometry changes. Even access to square-planar derivatives having an η^2-bound butadiene is

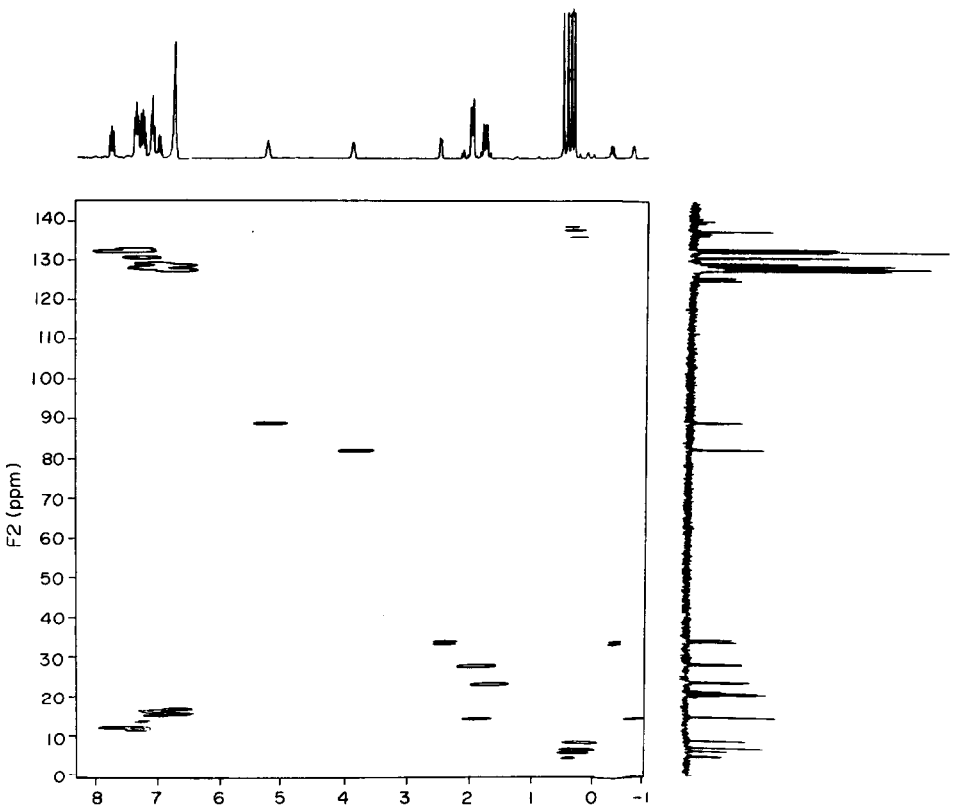

Fig. 3. Heteronuclear shift correlated 2-D (^{13}C–^1H) NMR spectrum of $Ir(\eta^4\text{-}C_4H_6)[N(SiMe_2CH_2PPh_2)_2]$.

apparently denied since this would be easily detectable in the ^1H NMR spectroscopic parameters.

EXPERIMENTAL

All manipulations were performed under prepurified nitrogen in a Vacuum Atmospheres HE-553-2 glovebox equipped with a MO-40-2H purification system, or in a standard Schlenk-type glassware on a dual vacuum–nitrogen line. 1,3-Butadiene was purchased from Matheson and used without further purification. Hexanes were dried over CaH_2, followed by distillation from sodium–benzophenone–ketyl under argon. Toluene was also distilled from sodium–benzophenone–ketyl under argon. Deuterated solvents, C_6D_6, and C_7D_8, were dried over activated 4 Å molecular sieves, vacuum transferred and deoxygenated by freeze–pump–thaw cycles prior to use. Carbon, hydrogen and nitrogen analyses were performed by Mr P. Borda of our department. ^1H NMR spectra were recorded on a Bruker WH-400 spectrometer and are referenced to C_6D_5H at 7.15 ppm; coupling constants are in Hz and the numbers of the carbons in the preparation below refer to the numbers of the carbon atoms in the X-ray structure (Fig. 1). ^{13}C NMR spectra (referenced to C_6D_6 at 128.00 ppm or $CD_3C_6D_5$ at 20.4 ppm) were run at 75.429 MHz, and $^{31}P\{^1H\}$ NMR spectra (referenced to external $P(OMe)_3$ set at +141.00 ppm) were run at 121.421 MHz, on a Varian XL-300 spectrometer. ^{13}C–^1H heterocorrelation maps were also recorded on the Varian XL-300 spectrometer.

$Ir(\eta^4\text{-}C_4H_6)[N(SiMe_2CH_2PPh_2)_2]$

A solution of $Ir(\eta^2\text{-}C_8H_{14})[N(SiMe_2CH_2PPh_2)_2]$ (100 mg, 0.120 mmol) in toluene (5 cm^3) was loaded in a thick-walled, reactor bomb equipped with a 5 mm Kontes needle valve. The vessel was attached to a vacuum line, degassed and cooled to liquid N_2 temperature. Excess 1,3-butadiene ($\approx$ 5 equiv) was condensed in the bomb and the valve sealed. The reaction mixture was stirred for 1 h at room temperature. Toluene was removed *in vacuo* and the residue recrystallized from toluene–hexanes at room temperature. Yield: 88 mg (95%). Found: C, 53.3; H, 5.5; N, 1.6. Calc. for $C_{34}H_{42}IrNP_2Si_2$: C, 52.7; H, 5.5; N, 1.8%. ^1H NMR (C_6D_6, ppm): $SiMe_2$, 0.42 (s), 0.48 (s), 0.57 (s), 0.65 (s); $SiCH_2P$, 1.85 (m), 2.12 (m); $H_{(31,anti)}$, −0.60 (m), $H_{(31,syn)}$, 2.07 (m), $H_{(32)}$, 5.57 (m), $H_{(33)}$, 4.00 (m), $H_{(34,anti)}$,

−0.20 (q), $H_{(34,syn)}$, 2.61 (m); PPh_2: 7.30 (m, *para/meta*), 7.90 (m, *ortho*). ^{13}C NMR (C_6D_6, ppm): $SiMe_2$, 4.40 (d, $^3J_{P-C} = 9.7$ Hz), 5.74 (d, $^3J_{P-C} = 4.0$ Hz), 6.60 (s), 8.40 (s); $SiCH_2P$, 23.39 (d, $^2J_{P-C} = 15.2$ Hz), 27.85 (d, $^2J_{P-C} = 18.8$ Hz); C_{31}, 14.44 (s), C_{32}, 88.93 (d, $^2J_{P-C} = 2.3$ Hz), C_{33}, 82.27 (d, $^2J_{P-C} = 6.33$ Hz), C_{34}, 33.75 (dd, $^2J_{P-C(trans)} = 41.6$ Hz, $^2J_{P-C(cis)} = 3.3$ Hz); PPh_2, 135.0 (m). $^{31}P\{^1H\}$ NMR (C_6D_6, ppm): 17.82 (s), −5.90 (s).

X-ray crystallographic analysis of $Ir(\eta^4\text{-}C_4H_6)[N(SiMe_2CH_2PPh_2)_2]$

Crystallographic data appears in Table 3. The final unit-cell parameters were obtained by least-squares on $2\sin\theta/\lambda$ values for 25 reflections with $2\theta = 41$–$46°$. The intensities of three check reflections, measured after each hour of X-ray exposure time throughout the data collection, showed only small random fluctuations. Data were processed

Table 3. Crystallographic data[a]

Compound	$[(Ph_2PCH_2SiMe_2)_2N]Ir(\eta^4\text{-}C_4H_6)$
Formula	$C_{34}H_{42}IrNP_2Si_2$
f_w	775.05
Crystal system	Triclinic
Space group	$P\bar{1}$[b]
a (Å)	10.9061(5)
b (Å)	11.1193(9)
c (Å)	14.0083(5)
α (°)	95.040(6)
β (°)	91.127(4)
γ (°)	90.520(6)
V (Å^3)	1691.8(2)
Z	2
D_c (g cm^{-3})	1.521
$F(000)$	776
μ(Mo-K_α) (cm^{-1})	41.2
Crystal dimensions (mm)	$0.27 \times 0.35 \times 0.45$
Scan type	ω–2θ
Scan range (° in θ)	$0.80 + 0.35 \tan\theta$
Scan speed (° min^{-1})	1.7–20.0
Data collected	$\pm h, \pm k, +l$
$2\theta_{max}$ (°)	60
Crystal decay	Negligible
Unique reflections	9810
Reflections with $I \geqslant 3\sigma(I)$	7666
Number of variables	362
R	0.025
R_w	0.033
S	1.143
Mean Δ/σ (final cycle)	0.002
Max. Δ/σ (final cycle)	0.017
Residual density (e Å^{-3})	−0.76 to +1.55 (near Ir)

[a] Temperature 294 K, Enraf–Nonius CAD4-F diffractometer, Mo-K_α radiation ($\lambda_{K_{\alpha_1}} = 0.70930$, $\lambda_{K_{\alpha_2}} = 0.71359$ Å), graphite monochromator, take-off angle 2.7°, aperture $(2.0 + \tan\theta) \times 4.0$ mm at a distance of 173 mm from the crystal, scan range extended by 25% on both sides for background measurement, $\sigma^2(I) = C + 2B + [0.04(C-B)]^2$ (C = scan count, B = normalized background count), function minimized: $\Sigma w(|F_o| - |F_c|)^2$ where $w = 1/\sigma^2(F)$, $R = \Sigma ||F_o| - |F_c|| / \Sigma |F_o|$, $R_w = (\Sigma w(|F_o| - |F_c|)^2 / \Sigma w|F_o|^2)^{1/2}$, $S = (\Sigma w(|F_o| - |F_c|)^2/(m-n))^{1/2}$. Values given for R, R_w and S are based on those reflections with $I \geqslant 3\sigma(I)$.

[b] Reduced cell.

and corrected for absorption (numerical integration).[17]

The structure was solved by conventional heavy-atom methods. The iridium, phosphorus and silicon coordinates were determined from the Patterson function and those of the remaining non-hydrogen atoms from a subsequent difference Fourier synthesis. Non-hydrogen atoms were refined with anisotropic thermal parameters and hydrogen atoms were fixed in idealized positions [$C(sp^2)$—H = 0.97 Å, $C(sp^3)$—H = 0.98 Å, methyl groups staggered, thermal parameters proportional to that of the bound atom]. An isotropic Type I extinction correction[18–21] was applied, the final value of g being 3.7×10^4.

Final positional and equivalent isotropic thermal parameters (U_{eq} = 1/3 trace diagonalized U), bond distances, bond angles, intra-annular torsion angles, calculated hydrogen atom parameters, anisotropic thermal parameters, torsion angles, and observed and calculated structure factors have been deposited with the Cambridge Crystallographic Data Centre.

Acknowledgements—Financial support for this work was provided by NSERC of Canada. We would like to thank Johnson Matthey for a generous loan of $IrCl_3$.

REFERENCES

1. M. D. Fryzuk, P. A. MacNeil and S. J. Rettig, *J. Am. Chem. Soc.* 1985, **107**, 6708.
2. (a) M. D. Fryzuk, P. A. MacNeil and S. J. Rettig, *Organometallics* 1985, **4**, 1145; (b) M. D. Fryzuk, P. A. MacNeil and S. J. Rettig, *J. Am. Chem. Soc.* 1987, **109**, 2803; (c) M. D. Fryzuk and K. Bhangu, *J. Am. Chem. Soc.* 1988, **110**, 961.
3. M. D. Fryzuk, P. A. MacNeil and N. T. McManus, *Organometallics* 1987, **6**, 882.
4. For exceptions, see ref. 2(a) and (b) M. D. Fryzuk, K. Joshi and R. K. Chadha, *J. Am. Chem. Soc.* 1989, **111**, 4498.
5. M. D. Fryzuk and P. A. MacNeil, *Organometallics* 1983, **2**, 682.
6. M. D. Fryzuk, P. A. MacNeil and S. J. Rettig, *Organometallics* 1986, **5**, 2469.
7. M. D. Fryzuk, P. A. MacNeil, R. L. Massey and R. G. Ball, *J. Organomet. Chem.* 1989, **368**, 231.
8. M. D. Fryzuk and K. Joshi, *Organometallics* 1989, **8**, 722.
9. (a) T. C. Van Soest and A. Van der Ent, *Cryst. Struct. Commun.* 1973, **3**, 527; (b) J. Muller, W. Hahalein and H. M. u. Joachim, *J. Organomet. Chem.* 1980, **197**, 95; (c) B. Buchmann, U. Piantini, W. von Phillipsborn and A. Salzer, *Helv. Chim. Acta* 1987, **70**, 1487.
10. M. D. Fryzuk, T. S. Haddad and S. J. Rettig, *Organometallics* 1988, **7**, 1224.
11. M. D. Fryzuk and W. E. Piers, *Polyhedron* 1988, **7**, 1001.
12. T. G. Appleton, H. C. Clark and L. E. Manzer, *Coord. Chem. Rev.* 1973, **10**, 335.
13. H. Yasuda and A. Nakamura, *Angew. Chem. Int. Edn Engl.* 1987, **26**, 723.
14. G. Erker, C. Kruger and G. Muller, *Adv. Organomet. Chem.* 1985, **24**, 1; H. Yasuda, K. Tatsumi and A. Nakamura, *Accts Chem. Res.* 1985, **18**, 120; H. Yasuda, Y. Kajihara, K. Nagasuna and A. Nakamura, *Chem. Lett.* 1981, 719; H. Yasuda, Y. Kajihara, K. Mashima, K. Nagasuna and A. Nakamura, *Chem. Lett.* 1981, 671; G. Erker, K. Engel, U. Dorf, J. L. Atwood and W. E. Hunter, *Angew. Chem. Int. Edn Engl.* 1982, **29**, 914; G. Erker, K. Engel, J. L. Atwood and W. E. Hunter, *Angew. Chem. Int. Edn Engl.* 1983, **22**, 494; G. Erker, U. Dorf, R. Benn, R-D. Reinhart and J. L. Peterson, *J. Am. Chem. Soc.* 1984, **106**, 7649; G. Erker, T. Muhenbend, R. Benn, A. Rulfinska, G. Tainturier and B. Gautheron, *Organometallics* 1986, **5**, 1023; G. Erker, R. Lecht, J. L. Peterson and H. Bonnemann, *Organometallics* 1987, **6**, 1962; G. Erker, R. Schlund, K. Angermund and C. Kruger, *Angew. Chem. Int. Edn Engl.* 1987, **26**, 666.
15. D. S. Moore and S. D. Robinson, *Inorg. Chim. Acta* 1981, **53**, L171.
16. J. R. Shapley and J. A. Osborn, *Accts Chem. Res.* 1973, **6**, 305.
17. The computer programs used include locally written programs for data processing and locally modified versions of the following: ORFLS, full-matrix least-squares, and ORFFE, and function and errors, by W. R. Busing, K. O. Martin and H. A. Levy; FORDAP, Patterson and Fourier syntheses, by A. Zalkin; ORTEP III, illustrations, by C. K. Johnson; AGNOST, absorption corrections, by J. A. Ibers; MULTAN 80, multisolution program, by P. Main, S. J. Fiske, S. E. Hull, L. Lessinger, G. Germian, J. P. Declerq and M. M. Woolfson.
18. *International Tables for X-ray Crystallography*, Vol. IV, pp. 99–102 and 149. Kynoch Press, Birmingham (1974). (Present distributor: D. Reidel, Dordrecht).
19. J. P. Becker and P. Coppens, *Acta Cryst.* 1974, **A30**, 129; 1974, **A30**, 148; 1975, **A31**, 417.
20. P. Coppens and W. C. Hamilton, *Acta Cryst.* 1970, **A26**, 71.
21. F. R. Thornley and R. J. Nelmes, *Acta Cryst.* 1974, **A30**, 748.

Polyhedron Vol. 8, No. 18, pp. 2299–2303, 1989
Printed in Great Britain

0277–5387/89 $3.00+.00
© 1989 Pergamon Press plc

ELECTROCHEMICAL STUDIES ON SIMPLE AND MIXED LIGAND COMPLEXES USING A HANGING MERCURY DROP ELECTRODE FOR STATIONARY ELECTRODE VOLTAMMETRY

HAMADA M. KILLA

Chemistry Department, Faculty of Science, Zagazig University, Zagazig, Egypt

(*Received* 31 *March* 1989; *accepted* 4 *May* 1989)

Abstract—A hanging mercury drop electode (HMDE) was used to study the simple and mixed ligand complexes of 1,3-diaminopropane (DAMP) and malonate (Mal) with cadmium(II) at constant ionic strength (μ = 1.0 M, $NaNO_3$) and 25°C, using linear-scan and cyclic modes. The reduction of the simple and mixed complexes is reversible and diffusion controlled. The composition and stability constants of simple and mixed species have been studied, as well as the mixing constants for the mixed complexes. The overall formation constants of the mixed species were calculated statistically using the Watters and DeWitt method and compared with the observed values. The equilibria between the various mixed ligand complexes in solution and their equilibrium are also given.

Stationary electrode voltammetry was adopted as an electroanalytical technique much later than polarography. The first theoretical considerations of the reversible process were published by Randles[1] and Ševčik.[2] The development of stationary electrode voltammetry has been markedly enhanced by the introduction of the hanging mercury drop electrode (HMDE).[3,4]

The hanging mercury drop electrode has been widely used in analysis and physico-chemical investigations.[3,5–7] It has also been employed in studies of the mechanism of electrode processes and has been found to be particularly useful in investigations of mechanisms of oxidation and reduction of organic compounds.[8–10]

The modern electroanalytical techniques offer considerable advantages compared to conventional DC polarography, in particular for the determination of formation constants of metal complex ions in solution.[11] In my previous paper[12] the HMDE has been used for the determination of formation constants of simple complexes. In the present work, the HMDE was extended to study the mixed-ligand complexes of cadmium(II) with malonate (Mal) as the primary ligand and 1,3-diaminopropane (DAMP) as the secondary ligand.

EXPERIMENTAL

The linear-scan and cyclic voltammograms were measured with a princeton Applied Research Model 174 A Polarographic analyser. Potential–current curves were recorded on an X–Y recorder Type Advance AR-2000. A conventional three-electrode cell with saturated calomel electrode (SCE) was employed. The working electrode in linear-scan and cyclic measurements was a PAR 9323 (stationary) hanging mercury drop electrode and the electrode area normally employed was 0.0408 cm^2. The scan rate was 100 mV s^{-1}.

For differential pulse (d.p.) polarography, a drop time of 1.0 s, a scan rate of 5 mV s^{-1} and a potential pulse of 50 mV, were used throughout the measurements.

All measurements were made at 25°C and an ionic strength of 1.00 M was maintained by using sodium nitrate. The concentration of Cd^{2+} ions was 2×10^{-4} M.

Reagent-grade chemicals, deionized water and mercury (Merck) were employed in all cases. A maximum suppressor was not used.

Theory

The DeFord–Hume[13] method for determining the stability constants of simple complexes has been modified by Killa[12] when using the HMDE for stationary electrode voltammetry instead of DC polarography. The expression may be written as:

$$F_0(X) = B_j C_x^j$$

$$= \text{antilog}\{0.434(nF/RT)\Delta E_p + \log(i_p)_s/(i_p)_c\}, \quad (1)$$

where B_j is the overall stability constant for the jth complex; C_x is the analytical concentration of the ligand which is always taken in large excess over the metal ion concentration, and is, therefore, considered as the total ligand concentration; $\Delta E_p = (E_p)_s - (E_p)_c$ is the shift in the linear-sweep voltammetry (l.s.v) peak potential caused by complexation; and the subscripts s and c refers to the simple and complex ions, respectively.

Nicholson and Shain[14] have shown that the peak potential (E_p) for a reversible process, obtained from a stationary electrode polarogram, is related to the half-wave potential of DC polarography ($E_{1/2}$) by:

$$E_p = E_{1/2} - \frac{28.5}{n}. \quad (2)$$

According to eq. (2), the shift in the half-wave potential, $(E_{1/2})_s - (E_{1/2})_c = \Delta E_{1/2}$, is equal to the shift in the peak potential obtained from the stationary electrode polarogram, $(E_p)_s - (E_p)_c = \Delta E_p$.

Similarly, the determination of stability constants of mixed-ligand complexes using Schaap and McMaster's[15] expression, might be modified for the l.s.v polarogram:

$$F_{00}(XY) = \text{antilog}\{0.434(nF/RT)\Delta E_p + \log (i_p)_s/(i_p)_c\}, \quad (3)$$

where $\Delta E_p = (E_p)_s - (E_p)_c$ is the shift in the peak potential due to complexation. The term $\log (i_p)_s/(i_p)_c$ is normally small because it makes little contribution to the $F_{00}(XY)$ function. Thus, eq. (3) can be simplified to give an expression of the form:

$$F_{00}(XY) = \text{antilog}\{0.434(nF/RT)\Delta E_p\}. \quad (4)$$

The formation constants of the mixed-ligand complex can then be determined by using eq. (4), as described by Schaap and McMaster.[15]

RESULTS AND DISCUSSION

The reduction of simple and mixed complexes was found to be reversible, involving two electrons as indicated by the difference in potential between the cathodic and anodic peaks ($E_{p_a} - E_{p_c}$), which is close to the value of the following expression:[16,17]

$$E_{p_a} - E_{p_c} = \frac{59}{n} \text{ mV}, \quad (5)$$

where E_{p_a} and E_{p_c} are the anodic and cathodic peak potentials, respectively, of the HMDE using the cyclic voltammetry mode. The $(E_{p_a} - E_{p_c})$ values of mixed-ligand complexes are given in Tables 1 and 2.

The reversibility of the systems under investigation, simple and mixed, was confirmed using d.p. polarography in nitrate medium; the half-peak widths were 62 ± 1 mV with 50 mV pulse amplitude, which are in good agreement with the calculated values by Dillard and Hanck.[18]

It should be noted that for a reversible system using stationary electrode voltammetry, E_p is independent of scan rate (V) and i_p is proportional to $V^{1/2}$,[19] which indicates diffusion control and is analogous to the variation of i_d with $h^{1/2}$ in DC polarography. In the present work, the plots of i_p against $V^{1/2}$ were linear, indicating that the reduction of the simple and mixed system in nitrate medium was diffusion controlled.

It should be noted that linear diffusion has been assumed, which is not strictly correct for the HMDE with the scan rate and electrode radius used

Table 1. Linear-scan and cyclic voltammetric data for the [Cd(DAMP)(Mal)] system. Ionic strength = 1.0 M; $[Cd^{2+}] = 2 \times 10^{-4}$ M; $T = 25°C$; [Mal] = 0.1 M; $(E_p)_s = -0.598$ V

[Diaminopropane] (M)	$E_{p_a} - E_{p_c}$ (mV)	ΔE_p (mV)	$F_{00} \times 10^5$	$F_{10} \times 10^6$	$F_{20} \times 10^8$	$F_{30} \times 10^8$
0.03	33	152	1.390	2.950	0.600	—
0.04	34	157	2.000	3.750	0.650	—
0.06	33	165	3.750	5.410	0.710	—
0.08	33	171	6.150	7.060	0.739	—
0.10	32	177	9.620	9.120	0.797	2.77
0.15	32	188	22.42	14.63	0.899	2.53
0.20	32	197	46.60	23.05	1.100	2.90
0.25	32	202	70.65	30.50	1.170	2.60
0.30	32	209	125.75	41.75	1.350	2.77
0.35	31	214	174.15	49.90	1.390	2.49
0.40	31	218	236.38	58.97	1.450	2.33

$\log A_1 = 4.69$, $\log B_1 = 6.06$, $\log C_1 = 7.72$, $\log D_1 = 8.39$.

Table 2. Linear-scan and cyclic voltammetric data for the [Cd(DAMP)(Mal)] system. Ionic strength = 1.0 M; $[Cd^{2+}] = 2 \times 10^{-4}$ M; $T = 25°C$; [Mal] = 0.25 M; $(E_p)_s = -0.598$ V

[Diaminopropane] (M)	$E_{p_a} - E_{p_c}$ (mV)	ΔE_p (mV)	$F_{00} \times 10^5$	$F_{10} \times 10^6$	$F_{20} \times 10^8$	$F_{30} \times 10^8$
0.03	33	161	2.790	5.970	0.773	—
0.04	33	165	3.810	7.030	0.845	—
0.06	33	171	6.080	8.470	0.803	—
0.08	33	177	9.700	10.88	0.809	—
0.10	32	182	14.32	13.32	0.967	2.27
0.15	32	193	33.73	21.82	1.210	3.13
0.20	32	201	62.90	31.45	1.390	3.25
0.25	32	208	108.49	43.40	1.590	3.40
0.30	31	214	173.12	57.71	1.800	3.53
0.35	31	219	255.54	73.01	1.980	3.54
0.40	31	223	348.94	86.98	2.080	3.35

$\log A_2 = 5.00$, $\log B_1 = 6.56$, $\log C_2 = 7.86$, $\log D_2 = 8.51$.

in this work, and errors of the order of 2% are expected. Also, the peak potentials (E_p) were measured within ± 0.5 mV. However, in all cases the results were within the experimental error.

Cadmium(malonate) system

In each solution the concentration of Cd^{2+} ions was maintained constant at 2×10^{-4} M and the malonate (Mal) concentrations were varied from 0.01 to 0.4 M. The stability constants were calculated by the graphical extrapolation method using the DeFord–Hume expression, as modified for the case of the stationary electrode (HMDE).[12] The results showing the existence of 1:1, 1:2 and 1:3 complex species with overall stability constants: $\log B_{01} = 1.85$, $\log B_{02} = 2.76$ and $\log B_{03} = 3.65$, agreed well with those obtained by Khurana and Gupta[20] if the differences in experimental conditions are considered.

Cadmium(1:3-diaminopropane) system

The concentration of DAMP was varied from 0.01 to 0.4 M. Three complex species were formed with stability constants: $\log B_{10} = 5.48$, $\log B_{20} = 7.59$ and $\log B_{30} = 8.31$, evaluated by the DeFord–Hume expression modified for the case of the HMDE.[12] The results are in good agreement with the previously reported values by Gupta *et al.*[21] using DC polarography and Killa and Zaky[22] using d.p. polarography.

Cadmium(diaminopropane)(malonate) system

The malonate ion concentrations were kept constant at 0.10 and 0.25 M, because at these concentrations 1:1 and 1:2 cadmium(malonate) complexes were found to be the predominant species. The concentration of DAMP was varied. The E_p values were greater compared to those obtained in the absence of malonate, thereby showing the formation of mixed complexes.

The formation constants of mixed-ligand complexes were determined by the graphical extrapolation method of Schaap and McMaster using eq. (4) for the linear-sweep voltammetry (l.s.v) wave. The l.s.v results using HMDE as a stationary electrode are given in Tables 1 and 2. The values of F_{00}, F_{10}, F_{20} and F_{30}, as well as the results of $\log A$, $\log B$, $\log C$ and $\log D$ at 0.10 and 0.25 M malonate concentrations, are also given in Tables 1 and 2, respectively.

The results reveal the existence of three mixed-ligand complexes with overall stability constants: $\log B_{11} = 6.72$, $\log B_{12} = 7.51$ and $\log B_{21} = 8.13 \pm 0.04$, respectively. It can be noted that $\log B_{30}$ and $\log D$ agree, as predicted by theory.

The equilibria between various species existing in the mixed-ligand system together with the log stepwise stability constant values ($\log K$) are represented schematically in Fig. 1. The $\log K$ values for addition of Mal to [Cd(Mal)] and $[Cd(DAMP)]^{2+}$ are 0.91 and 1.24. Likewise, the tendency to add DAMP to [Cd(Mal)] and $[Cd(DAMP)]^{2+}$ are 4.87 and 2.11. The $\log K$ values obtained for the addition of neutral DAMP as a third ligand to $[Cd(Mal)_2]^{2-}$, [Cd(DAMP)(Mal)] and $[Cd(DAMP)_2]^{2+}$ are 4.75, 1.41 and 0.72, respectively. It is clear from these results, that the tendency for mixed-ligand complex formation is favoured. It is also obvious from the schematic diagram that the $\log K$ values for the addition of DAMP to the saturated complexes $[Cd(Mal)_3]^{4-}$, [Cd(DAMP)

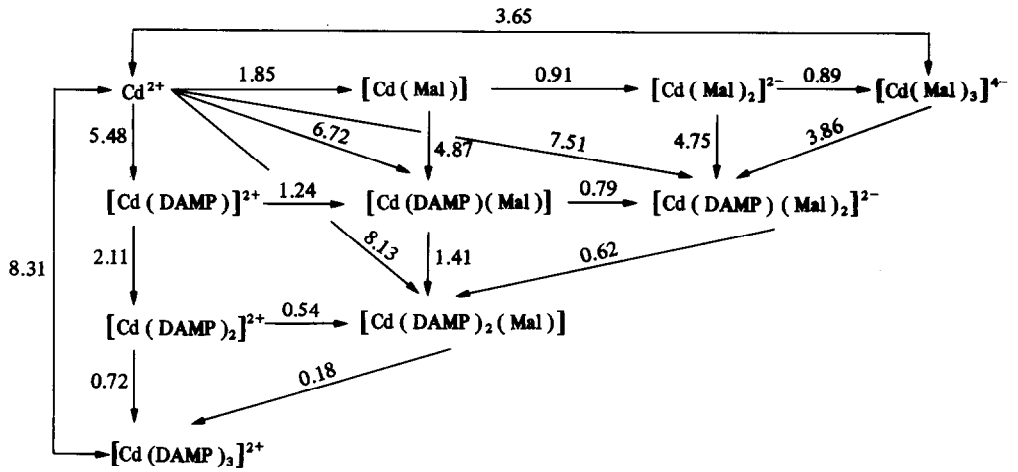

Fig. 1. The equilibria between mixed-ligand species and log K values for these equilibria.

$(Mal)_2]^{2-}$ and $[Cd(DAMP)_2(Mal)]$ are 3.86, 0.62 and 0.18, respectively, which indicates that the saturated complex can replace Mal by DAMP. This also indicates that the malonate ligand is much weaker than the neutral ligand, DAMP, and indicates the relative stability of mixed-ligand complexes over the parent binary complexes.

The mixing constant ($\log K_M$) for the reaction:

$$\tfrac{1}{2}[Cd(DAMP)_2]^{2+} + \tfrac{1}{2}[Cd(Mal)_2]^{2-} = [Cd(DAMP)(Mal)] \quad (6)$$

indicates the relative stability of the mixed species in solution compared to parent binary complexes. This is given by the following relation:[23,24]

$$\log K_m = \log B_{11} - \tfrac{1}{2}(\log B_{02} + \log B_{20}). \quad (7)$$

This yields $\log K_m = +1.545$ for reaction (6). Moreover, the stabilization constant ($\log K_s = \log K_m - \log 2$)[25] is equal to +1.244. The positive values of mixing and stabilization constants show the stability of mixed species compared with simple complexes.

Watters and DeWitt[26] have derived the following expression for the prediction of stability constants of mixed-ligand complexes from statistical factors:

$$B_{11} = 2[4/9B_{02} \times B_{20}]^{1/2}$$

$$B_{12} = 3B_{30}^{1/3} \times B_{03}^{2/3}$$

$$B_{21} = 3B_{30}^{2/3} \times B_{03}^{1/3}.$$

The values of stability constants (log values) calculated from the above expressions are 5.29, 5.67 and 7.22, respectively. The experimental values for the mixed complex species are higher than the statistically calculated values. This has been explained by many workers[15,27] by considering the cooperative effects of electrostatic forces between different kinds of ligands and steric effects. This may also account for the neutralization of charge.[24]

The formation of neutral ternary complexes from the parent complexes can be represented as follows:

$$[Cd(DAMP)_2]^{2+} + [Cd(Mal)_2]^{2-} \rightleftharpoons 2[Cd(DAMP)(Mal)]. \quad (8)$$

Many workers[28-30] have observed that charge neutralization favours formation of mixed-ligand species. In addition to Coulombic effects, such a neutralization of charge would be expected to be accompanied by a positive entropy change due to decreased orientation of the solvent molecule. The present results are in agreement with this postulate.

REFERENCES

1. J. E. B. Randles, *Trans. Faraday Soc.* 1948, **44**, 327.
2. A. Ševčik, *Coll. Czechoslov. Chem. Commun.* 1948, **13**, 349.
3. W. Kemula, Z. Kublik and S. Glodowski, *J. Electroanal. Chem.* 1959, **1**, 91.
4. W. Kemula and Z. Galus, *Bull. Acad. Polon. Sci., Cl. III* 1959, **7**, 729; 1958, **6**, 661.
5. A. G. Stroberg and E. A. Zakharova, *Zav. Lab.* 1964, **30**, 3, 261.
6. R. Neeb, *Inverse Polarographie and Voltammetrie.* Akademie-Verlag, Berlin (1969).
7. W. Kemula and Z. Kublik, *Anal. Chim. Acta* 1958, **19**, 104.
8. Z. Galus, H. Y. Lee and R. N. Adams, *J. Electroanal. Chem.* 1962, **5**, 17.
9. R. P. Buck and L. P. Griffith, *J. Electrochem. Soc.* 1962, **109**, 1005.
10. W. Kemula, Z. R. Grabowski and M. K. Kalinowski, *Naturwiss.* 1960, **22**, 1.

11. G. H. Heath and G. Hefter, *J. Electroanal. Chem.* 1977, **84**, 295.
12. H. M. Killa, *J. Chem. Soc., Faraday Trans. I* 1985, **81**, 2659.
13. D. D. DeFord and D. N. Hume, *J. Am. Chem. Soc.* 1951, **73**, 5321.
14. R. S. Nicholson and I. Shain, *Analyt. Chem.* 1964, **36**, 706.
15. W. B. Schaap and D. L. McMasters, *J. Am. Chem. Soc.* 1961, **8**, 4699.
16. H. M. Killa, E. E. Mercer and R. H. Philip, *Analyt. Chem.* 1984, **56**, 2401.
17. P. Delahay, *New Instrumental Method in Electrochemistry*, p.137. Interscience, New York (1954).
18. J. M. Dillard and K. W. Hanck, *Analyt. Chem.* 1976, **48**, 216.
19. A. J. Bard and L. R. Faulkner, *Electrochemical Methods*, p. 218. Wiley, New York (1980).
20. S. C. Khurana and C. M. Gupta, *Talanta* 1972, **19**, 1236.
21. K. D. Gupta, S. C. Baghel and J. N. Gaur, *Monatsh.* 1979, **110**, 657.
22. H. M. Killa and M. Zaky, *Analyt. Lett.* 1984, **17**, 2301.
23. R. Sundaresan and A. K. Sundaram, *Proc. Ind. Acad. Sci.* 1974, **79A**, 161.
24. S. L. Jain, J. Kishan and R. C. Kapoor, *Ind. J. Chem.* 1979, **18A**, 133.
25. A. A. Aggarwal, K. B. Pandeya and R. P. Singh, *Ind. J. Chem.* 1981, **20**, 752.
26. J. I. Watters and R. DeWitt, *J. Am. Chem. Soc.* 1960, **82**, 1333.
27. A. A. Aggarwal, A. K. Arora, K. B. Pandeya and R. P. Singh, *J. Inorg. Nucl. Chem.* 1981, **43**, 601.
28. H. Sigel, P. R. Huber and R. F. Pasternack, *Inorg. Chem.* 1971, **10**, 226.
29. R. Griesser and H. Sigel, *Inorg. Chem.* 1970, **9**, 1238.
30. G. F. Condika and A. E. Martell, *J. Inorg. Nucl. Chem.* 1969, **31**, 2445.

Polyhedron Vol. 8, No. 18, pp. 2305–2311, 1989
Printed in Great Britain

0277–5387/89 $3.00+.00
© 1989 Pergamon Press plc

THE IR AND ^{1}H, ^{13}C NMR SPECTRA OF THE NICKEL(II), COPPER(II) AND ZINC(II) COMPLEXES OF 2,4-PENTANEDIONE, 4-IMINO-2-PENTANONE, 4-THIOXO-2-PENTANONE AND 2,4-PENTANEDITHIONE: A COMPARATIVE STUDY

ALISON M. A. BENNETT, GARY A. FOULDS and DAVID A. THORNTON*

Departments of Inorganic Chemistry and Chemical Engineering, University of Cape Town, Rondebosch 7700, South Africa

(*Received* 31 *March* 1989; *accepted* 4 *May* 1989)

Abstract—The IR spectra of the title compounds, abbreviated *trans*-[Ni(acac)$_2$(H$_2$O)$_2$], [Cu(acac)$_2$], [Zn(acac)$_2$(H$_2$O)] (acac = 2,4-pentanedionate anion), [M(Nacac)$_2$] (M = Ni, Cu; Nacac = 4-imino-2-pentanonate anion), [M(Sacac)$_2$] (M = Ni, Cu, Zn; Sacac = 4-thioxo-2-pentanonate anion) and [Ni(SacSac)$_2$] (SacSac = 2,4-pentanedithionate anion) have been examined over the range 4000–50 cm^{-1} with a view to determining band assignments based on the effects of metal ion substitution and the establishment of spectra–structure correlations for these complexes. The ^{1}H and ^{13}C NMR spectra of the diamagnetic complexes are reported and discussed.

Substitution of nitrogen or sulphur for oxygen in the complexes of nominal formula [M(acac)$_2$] yields square-planar complexes with the exception of [Zn(Sacac)$_2$] which is tetrahedral. Despite the interest which attaches to these novel β-ketoenol analogues, their IR spectra have received rather limited attention,[1–13] and coverage of this field has been piecemeal rather than systematically embracing all of these molecules under similar experimental conditions as in the presently described work. The effect of substitution of the metal ion considered in relation to the established structures of these molecules assists in solving the assignment problem.[14]

EXPERIMENTAL

The complexes were prepared using methods described in the literature.[1–13,15] Composition and purity were established by microanalysis (Table 1).

The ^{1}H and ^{13}C NMR spectra were obtained at ambient temperature on a Varian VXR-200, using $CDCl_3$ and CD_3COCD_3 as solvents with TMS as reference. IR spectra were determined as Nujol mulls (4000–1500 and 1300–300 cm^{-1}) or hexachlorobutadiene mulls (4000–1700 and 1500–1300 cm^{-1}) between CsI plates on a Perkin–Elmer 983 spectrophotometer, and as Nujol mulls between polyethylene plates (500–50 cm^{-1}) on a Digilab FTS-16 B/D interferometer.

* Author to whom correspondence should be addressed.

RESULTS AND DISCUSSION

IR spectra

The frequencies and assignments are given in Table 2 and the spectra are depicted in Fig. 1.

The 2,4-*pentanedionates,* trans-[Ni(acac)$_2$(H$_2$O)$_2$], [Cu(acac)$_2$] *and* [Zn(acac)$_2$(H$_2$O)]

Numerous studies of the IR spectra of the parent acac complexes of the three metals discussed here: nickel(II), copper(II) and zinc(II) have been reported[15,16] and these will be the preliminary basis for our discussion of the effects of oxygen-donor substitution by nitrogen or sulphur. Since anhydrous [Ni(acac)$_2$]$_n$ has a complex polymeric octahedral structure,[15] we will employ the simpler bis(aquo) octahedral complex *trans*-[Ni(acac)$_2$(H$_2$O)$_2$] as the basis for comparison[17] with N- and S-substituted derivatives of nickel. [Cu(acac)$_2$]

Table 1. Analytical data

Compound	Calculated C (%)	H (%)	N (%)	Found C (%)	H (%)	N (%)
$[Ni(acac)_2(H_2O)_2]$	41.0	6.2	—	41.3	5.9	—
$[Cu(acac)_2]$	45.9	5.4	—	46.0	5.4	—
$[Zn(acac)_2(H_2O)]$	42.6	5.7	—	42.7	5.7	—
$[Ni(Nacac)_2]$	47.1	6.3	11.0	47.1	5.9	10.9
$[Cu(Nacac)_2]$	46.2	6.2	10.8	46.2	5.7	10.6
$[Ni(Sacac)_2]$	41.6	4.9	—	41.7	4.8	—
$[Cu(Sacac)_2]$	40.9	4.8	—	40.3	5.3	—
$[Zn(Sacac)_2]$	40.6	4.8	—	40.3	4.7	—
$[Ni(SacSac)_2]$	37.4	4.4	—	37.5	4.3	—

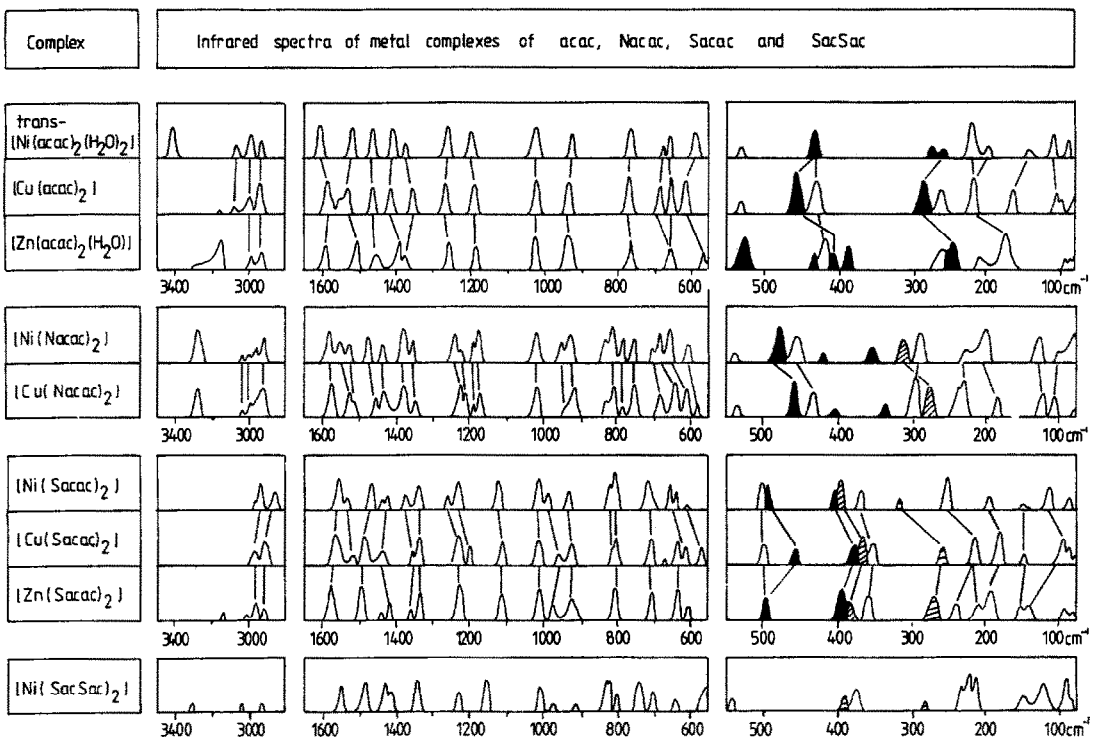

Fig. 1. IR spectra of acac, Nacac, Sacac and SacSac complexes. Solid bands: ν(M—O); shaded bands: ν(M—N) or ν(M—S).

is a simple square-planar monomer[15] and therefore entirely analogous, structurally, with $[Cu(Nacac)_2]$ and $[Cu(Sacac)_2]$, while zinc(II) forms a square-based pyramidal monohydrate with 2,4-pentanedionate[15] of formula $[Zn(acac)_2(H_2O)]$, differing structurally from the tetrahedral molecule $[Zn(Sacac)_2]$. Assignments for the three metal acac complexes discussed here have been made on the basis of normal coordinate analyses[18–21] and isotopic labelling studies.[16,22]

We have reconsidered our assignments of $[Zn(acac)_2(H_2O)]$ which were based on a combination of ^{18}O- and $^{64,68}Zn$-labelling.[22] This study showed conclusively that the bands at 555, 420, 388, 239 and 171 cm^{-1} are metal–ligand bands, but did not serve to distinguish between the Zn—O stretching and O—Zn—O bending modes. We now consider that the bands listed above all have Zn—O stretching character except for that at 171 cm^{-1} which is assigned to the δ(O—Zn—O) bending mode. These amended assignments are based on the finding that bands near 300 cm^{-1} in the IR spectra

Table 2. Frequencies (cm^{-1}) and assignments for IR bands in the spectra of metal complexes of acac, Nacac, Sacac and SacSac

Acac complexes			Nacac complexes		Sacac complexes			SacSac complex	
Ni	Cu	Zn	Ni	Cu	Ni	Cu	Zn	Ni	Assignment
3409		3300							ν(O—H)
			3283	3287					ν(N—H)
3074	3075	3070	3038	3034	3010		3014	3030	ν(C—H) [ν(CH)]
2986	2992	2992	2985	2984	2978	2976	2973		ν(C—H)(CH$_3$)
	2960	2957	2951	2952			2950		
2920	2920	2919	2915	2915	2911	2911	2911	2920	
1652		1615							δ(O—H)
1605	1577	1598	1591	1587	1565	1573	1584		ν(C═O)
	1550		1553	1531	1520	1520		1552	combination
1518	1527	1510	1525	1522	1474	1491	1489	1491	ν(C═C)
			1475	1455					δ(N—H)
1461	1455	1455	1434	1435	1440		1439	1430	δ(C—H) deg. def.
1407	1415	1398			1420	1422	1413	1415	
			1382	1380					ν(C—N)
1360	1352	1368	1351	1349	1371	1352	1363	1348	δ(C—H) sym. def.
					1338	1337	1338		
1260	1272	1258	1244	1225	1234	1224	1225	1229	ν(C—C)+ν(C—CH$_3$)
			1229	1214	1227	1202			
1197	1187	1187	1188	1187	1117	1112	1112	1156	δ(C—H) ip.
			1180	1176					
1019	1018	1017	1020	1015	1016	1013	1020	1009	ρ(CH$_3$)
			952	938					
					985	960	979	979	ρ(CH$_3$)+ν(C—S)
928	935	929	933	928	935	928	925	925	ν(C—CH$_3$)+ν(C═O)
			830	819					δ(N—H) oop.
			808	811					
765	779	772	789	786	813	811		826	δ(C—H) oop.
		769	755	756	809	806	805	801	
					720	711	703	747	ν(C—S)
675	682	653	703	686					ring def.+ν(M—L)
			681	647					
658	651	(653)			672	675		703	ring def.
			658	617	662	636	639	648	
589	611	570	623	582	642	614	615		ring def.+ν(M—O)
					620	570			
550	550	552	552	554	498	503	(499)	556	δ(C—CH$_3$)+ring def.
		555							ν(Zn—O)
		433							ν(Zn—OH$_2$)
427	454	408	481	463	492	471	499		ν(M—O)
		388							
(427)	430	421	456	436					ring def.
			421	408					ν(M—L)
			361	334					
			315	277					ν(M—N)
275									ν(Ni—OH$_2$)
255	288	239			409	387	398		ν(M—O)
					396	379	386	390	ν(M—S)
(255)	265	262	292	296	373	361	364	374	ring def.
					308	264	274	286	ν(M—S)
		210[a]	(234)[b]	230[b]			247	240	δ(L—M—L)
220	217	171	234	228	252	217	221	227	
195			195	185	196	184	197	216	
139	166								
107	102		100	103	149	147	152	149	ring def. oop.
85	90	88	125	120	112	96	140	122	δ(L—M—L)
					84	85	91	95	
	74	81	75	74		78	78	82	lattice+δ(CH$_3$) oop.
60	60	66	60	67	53		62		

[a] This band has been assigned to a C—C—C bend since it is unaffected by ^{18}O- or $^{64,68}Zn$-labelling.[22]
[b] Assigned to τ(C—CH$_3$) (ref. 3).

of metal acac complexes are more sensitive to metal isotope labelling than those near 450 cm^{-1}.[18]

The 4-imino-2-pentanonates, $[M(Nacac)_2]$ (M = Ni, Cu)

Substitution of one oxygen atom of 2,4-pentanedione by the imino group —NH leads to *trans*-square-planar complexes, $[M(Nacac)_2]$ (M = Ni, Cu).[1-3] These complexes have C_{2h} point group symmetry and we therefore expect to observe two ν(M—L) and four δ(L—M—L) bands in their IR spectra. Comparison of the spectra of $[Cu(acac)_2]$ and $[Cu(Nacac)_2]$, both of which are square-planar, reveals markedly similar band patterns. The ν(M—L) vibrations at 454 and 288 cm^{-1} in $[Cu(acac)_2]$ are observed at 463 and 277 cm^{-1} in the Nacac complex. In the square-planar $[Ni(Nacac)_2]$ complex these bands are shifted to 481 and 315 cm^{-1}, respectively. The higher frequency vibration (481 cm^{-1}) is insensitive to nitrogen deuteration[3] and is therefore assigned as ν(Ni—O) and the band at 315 cm^{-1} as ν(Ni—N). The relatively low intensity of the lower frequency band is typical of ν(M—N) modes.[23] Two very weak bands observed at 408 and 334 cm^{-1} for $[Cu(Nacac)_2]$ (for which no analogous $[Cu(acac)_2]$ bands exist) are shifted to 421 and 361 cm^{-1} when substituting nickel for copper. These two bands may be attributed to IR forbidden ν(M—L) modes which are observed due to lowering of the symmetry of the $[M(Nacac)_2]$ complexes. The skeletal deformations of 430 and 265 cm^{-1} in $[Cu(acac)_2]$ occur at 436 and 296 cm^{-1} in $[Cu(Nacac)_2]$. The sensitivity of the upper band to metal substitution implies strong coupling to the metal–ligand mode.

Below 250 cm^{-1}, assignment of δ(L—M—L) at 228, 185 and 120 cm^{-1} in $[Cu(Nacac)_2]$ is readily made by comparison with $[Cu(acac)_2]$. The nickel complex is similar. The band at 230 cm^{-1} in the copper complex spectrum is unaffected by metal ion substitution and this supports its assignment on the basis of normal coordinate analysis to a $\tau(C—CH_3)$ torsional mode.[3]

It is of interest to note that, if the ν(M—L) assignments which have been proposed above are correct, bands in the spectrum of the nickel complex are at higher frequencies than corresponding bands in the copper complex. In octahedral complexes the stability sequence Ni < Cu is usually observed because of the extra stabilization which is conferred on the copper complex by Jahn–Teller distortion.[14] However, in square-planar symmetry, the expected stability sequence is Ni > Cu because the copper complex has an additional antibonding electron.[24] The ν(M—L) frequency order for these complexes is Ni > Cu and this observation supports the proposed assignment.

The 4-thioxo-2-pentanonates, $[M(Sacac)_2]$ (M = Ni, Cu, Zn)

The *cis*-square-planar configuration of the nickel and copper complexes implies C_{2v} point group symmetry. Group theory predicts four ν(M—L) and seven δ(L—M—L) modes. The zinc complex probably adopts a tetrahedral coordination geometry[8] and, as such, may be assigned C_2 symmetry. Of the IR allowed bands, four ν(M—L) and nine δ(L—M—L) are expected.

A band occurs very close to 500 cm^{-1} in all three complexes. On the basis of a normal coordinate analysis[8] a split band at 498, 492 cm^{-1} in the spectrum of the nickel complex was assigned to $\delta(C—CH_3)$+ring def. We agreed with this assignment so far as the 498 cm^{-1} component is concerned, since this component is not shifted by metal ion substitution. However, the 492 cm^{-1} component shifts to 471 cm^{-1} on substitution of copper for nickel and this suggests that it should be correctly assigned to ν(M—O) [probably[8] coupled to $\delta(C—CH_3)$]. The frequency order ν(Ni—O) > ν(Cu—O) would be anticipated for a band assigned to ν(M—O) [or for that matter, to ν(M—S)] for the reasons advanced above in the case of the Nacac complexes. In the tetrahedral zinc(II) complex, only one band occurs near 500 cm^{-1} and this is assigned to ν(Zn—O)+ring def.+ $\delta(C—CH_3)$.[6] These assignments are at variance with those of the normal coordinate analyses by Siimann *et al.*[6,8] They assign a band at 648 cm^{-1} to ν(M—O). We observe this band to be less sensitive to metal substitution than those at lower frequencies. We therefore prefer to assign it to an out-of-plane ring deformation which is coupled with ν(M—L).

Both the nickel and copper complexes exhibit three bands between 410 and 360 cm^{-1}. The two upper bands at 409 and 396 cm^{-1} in the nickel complex are shifted to 387 and 379 cm^{-1} on substituting nickel by copper. These bands are accordingly assigned as ν(M—O) and ν(M—S). The lowest band at 373 cm^{-1} in the nickel complex is not as sensitive to metal substitution and is attributed to a ring deformation.[8] Only two bands are observed in this region of the $[Zn(Sacac)_2]$ spectrum, although a shoulder on the upper band indicates coincident vibrations. A weak band at 308 cm^{-1} in the spectrum of $[Ni(Sacac)_2]$ reported variously at 300 and 285 cm^{-1} by Siimann *et al.*[6,8] is strongly metal sensitive in the expected sequence Ni > Cu. It is assigned to ν(M—S) due to both its low intensity

and the fact that it is reasonably close to the calculated ν(Ni—S) frequency.[6] The band at 252 cm^{-1} in the spectrum of [Ni(Sacac)$_2$] is assigned as δ(L—M—L). Although previously attributed to a stretching vibration,[9] the occurrence of this band at approximately half the frequency of ν(M—O) (492 cm^{-1}) supports our assignment. In addition, all four expected ν(M—L) are already assigned. The weak band at 196 cm^{-1} is observed at 194 cm^{-1} in the Raman spectrum and it is assigned as a further ν(Ni—S) mode.[9] However, substitution of copper for nickel causes the band to shift only 12 cm^{-1} and, in addition the δ(S—Ni—S) bands in [Ni(SacSac)$_2$] occur near 200 cm^{-1}. For these reasons assignment to a metal–ligand bending mode is preferred.

The remaining vibrations below 200 cm^{-1} are assigned to δ(L—M—L) and lattice modes, with the exception of the band near 150 cm^{-1} which is attributed to a ring deformation on the grounds of its insensitivity to metal substitution. This is consistent with the normal coordinate analysis of Siimann and Fresco.[6] The assignment of two bands at 396, 308 cm^{-1}, and 379, 264 cm^{-1} in the spectra of the nickel and copper complexes, respectively, is consistent with the sequence Ni > Cu, expected for ν(M—S) modes. These bands are also reasonably located at lower frequencies than the ν(M—O) modes due to the greater mass of the sulphur atom, as well as the fact that the M—O force constant is greater than the M—S force constant.[8] In the zinc(II) complex, the ν(Zn—S) bands occur at 386 and 274 cm^{-1}. The greater number of bending vibrations observed in this spectrum is consistent with the C_2 symmetry of the zinc complex.

Bis(2,4-*pentanedithionato*)*nickel*(II), [Ni(SacSac)$_2$]

The square-planar nickel complex has D_{2h} point group symmetry and is therefore analogous to [Cu(acac)$_2$] for which two ν(M—L) are expected. Assignments are straightforwardly made as only one type of metal–ligand mode is present, *viz.* ν(Ni—S). Thus the region 550–400 cm^{-1}, where ν(M—O) was found for the [Ni(Nacac)$_2$] and [Ni(Sacac)$_2$] complexes, is free from any bands. The band at 390 cm^{-1} clearly qualifies for assignment to ν(Ni—S). This is consistent with normal coordinate analyses performed for this square-planar complex and its cobalt(II) analogue.[11,12] In addition, it supports the assignment of the band at 396 cm^{-1} in [Ni(Sacac)$_2$] to ν(Ni—S). The assignment of the band at 286 cm^{-1} to ν(Ni—S) is also consistent with these normal coodinate analyses. Similarly, the band at 374 cm^{-1} may be assigned to a ring deformation. The bands at 240, 227 and 216 cm^{-1} are clearly δ(S—Ni—S) modes occurring at approximately half the frequency of the corresponding stretches. Their appearance at these frequencies supports our assignment of the 252 and 196 cm^{-1} bands in the spectrum of the mixed donor atom complex, [Ni(Sacac)$_2$], to bending modes rather than the previously proposed stretching bands (*vide infra*). The vibration at 149 cm^{-1} is unshifted on changing from [Ni(Sacac)$_2$] to [Ni(SacSac)$_2$], further supporting its assignment as a ring deformation.

Spectra in the mid-IR region

In the acac complex spectra, the presence of coordinated water in the nickel and zinc complexes yields ν(OH) bands near 3400 cm^{-1} (nickel) and 3300 cm^{-1} (zinc). The methyl groups give rise to ν(C—H) bands within the range 2900–3200 cm^{-1} in all of the spectra. The stretches of the γ-methine groups are observed weakly just above 3000 cm^{-1}. In the Nacac complexes the single expected ν(N—H) is a strong band near 3300 cm^{-1}.

The carbonyl region is of particular interest in view of the alternative assignments for ν(C=O) and ν(C=C) bands which have been given by the normal coordinate analysis of [Cu(acac)$_2$]. The bands observed near 1580 and 1520 cm^{-1} were assigned[19] to ν(C=C) and ν(C=O), respectively, but these assignments were subsequently reversed by ^{18}O-labelling studies and a revised normal coordinate treatment.[21,22] It is now generally accepted that the band of higher frequency is predominantly ν(C=O) in 2,4-pentanedionates. This is supported by the absence of this higher frequency band in the [Ni(SacSac)$_2$] complex spectrum.

Bands which are unique to the spectra of the Nacac complexes are attributed to vibrations involving the nitrogen atom. The ν(C—N) mode occurs near 1380 cm^{-1}, which is similar to that found in the free ligand.[25] As expected, this band is absent from the acac complex spectra. The metal-sensitive vibration near 1470 cm^{-1} is assigned to the δ(N—H) in-plane mode, while a doublet between 830 and 800 cm^{-1} is assigned to the δ(N—H) out-of-plane mode. Extensive splitting of vibrations in Nacac complex spectra may be attributed to their lower symmetry and solid state effects.[3]

For complexes of Sacac, Chaston *et al.*[26] assigned a band in the region 1270–1190 cm^{-1} to ν(C—S) and tentatively assigned a band between 837 and 805 cm^{-1} to a coupled ν(C—S) and δ(CH_3) mode. However, subsequent normal coordinate analyses on complexes of both the Sacac[8] and the SacSac[11,12] ligands have shown the C—S stretching frequency to occur near 700 cm^{-1}. This is further supported by the assignment of ν(C—S) in the region 850–550

cm^{-1} in dithiooxalato complexes,[27,28] dithiooxamido complexes[29] and xanthato complexes.[30] Our assignment of ν(C—S) near 720 cm^{-1} is supported by the observed shifts of 9 and 17 cm^{-1}, on substituting nickel with copper and zinc, respectively. This vibrational frequency is low for a carbon–sulphur double bond. However, bonding in the chelate ring of [Ni(Sacac)$_2$] most resembles the resonance structure with a single carbon–sulphur bond.[6] The band observed at 985 cm^{-1} in [Ni(Sacac)$_2$] is shifted 25 cm^{-1} on substituting copper for nickel. This metal sensitivity may be due to extensive coupling to ν(C—S) as observed for vibrations near 1050 cm^{-1} in dithiooxalato complexes.

^{1}H *and* ^{13}C *NMR spectra*

The ^{1}H and ^{13}C NMR data are listed in Table 3, and are consistent with the tetracoordinate structures that have been proposed earlier. The square-planar copper complexes and octahedral [Ni(acac)$_2$(H$_2$O)$_2$] complexes are paramagnetic and their spectra were not determined.

Although the data have been used primarily to characterize the complexes, a few points of interest may be mentioned. Firstly, in the ^{1}H NMR spectrum it is the methine proton which is most sensitive to metal ion and ligand donor atom substitution, whereas in the ^{13}C NMR the methine carbon atom as well as the carbon atoms attached to the ligand donor atoms are sensitive to substitution. Secondly, the ^{1}H and ^{13}C resonances associated with the chelate ring are shifted considerably on ligand donor atom substitution and only slightly on metal ion substitution.

Finally, the complexes [Ni(Nacac)$_2$] and [Ni(Sacac)$_2$] have the possibility of existing as *cis* or *trans* isomers. However, it is concluded either that one isomer predominates at ambient temperature or that rapid exchange is taking place (as seen in similar systems[31]).

Acknowledgements—We thank the Foundation for Research Development of the CSIR and the UCT Research Grants Committee for financial assistance.

REFERENCES

1. H. F. Holtzclaw, J. P. Collman and R. Alire, *J. Am. Chem. Soc.* 1958, **80**, 1100.

Table 3. ^{1}H and ^{13}C NMR data (ppm)[a]

^{1}H NMR chemical shift data (ppm)

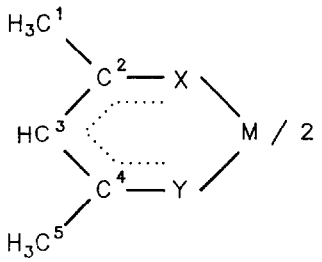

M	X	Y	C^1H_3	C^5H_3	C^3H	NH
Zn	O	O	1.9	1.9	5.4	—
Zn	O	S	2.4	2.2	6.5	—
Ni	O	NH	1.7	1.8	4.8	4.9
Ni	O	S	2.4	2.2	6.5	—
Ni	S	S	2.3	2.3	7.1	—

^{13}C NMR chemical shift data (ppm)

M	X	Y	C^1	C^2	C^3	C^4	C^5
Zn	O	O	37.79	204.38	110.46	204.38	37.79
Zn	O	S	35.57	199.39	118.79	184.83	30.98
Ni	O	NH	24.28	176.49	97.21	166.82	24.26
Ni	O	S	28.87	190.60	118.56	178.28	28.59
Ni	S	S	32.68	183.74	131.56	183.74	32.68

[a] All spectra were run in $CDCl_3$ with the exception of [Zn(acac)$_2$(D$_2$O)] which was run in CD_3COCD_3.

2. R. F. Jameson and R. D. Peacock, *J. Chem. Soc.* 1969, 2453.
3. T. J. McGee and J. L. Walter, *Spectrosc. Lett.* 1978, **11**, 765.
4. A. Ouchi, M. Hyodo and Y. Takahashi, *Bull. Chem. Soc. Jpn* 1967, **40**, 2819.
5. D. H. Gerlach and R. H. Holm, *Inorg. Chem.* 1969, **8**, 2292.
6. O. Siimann and J. Fresco, *J. Chem. Phys.* 1971, **54**, 734.
7. O. Siimann and J. Fresco, *J. Chem. Phys.* 1971, **54**, 740.
8. O. Siimann, D. D. Titus, C. D. Cowman, J. Fresco and H. B. Gray, *J. Am. Chem. Soc.* 1974, **96**, 2353.
9. O. Siimann, *Inorg. Chem.* 1980, **19**, 2889.
10. A. Ouchi, M. Nakatani and Y. Takahashi, *Bull. Chem. Soc. Jpn* 1968, **41**, 2044.
11. C. G. Barraclough, R. L. Martin and I. M. Stewart, *Aust. J. Chem.* 1969, **22**, 891.
12. O. Siimann and J. Fresco, *Inorg. Chem.* 1969, **8**, 1846.
13. S. W. Schneller, *Int. J. Sulfur Chem.* 1972, **7B**, 295.
14. D. A. Thornton, *Coord. Chem. Rev.* 1984, **55**, 113.
15. J. P. Fackler, *Prog. Inorg. Chem.* 1966, **7**, 361.
16. D. A. Thornton, *Coord. Chem. Rev.* 1989, in press.
17. C. Engelter and D. A. Thornton, *J. Molec. Struct.* 1977, **39**, 25.
18. K. Nakamoto, C. Udovich and J. Takemoto, *J. Am. Chem. Soc.* 1970, **92**, 3973.
19. K. Nakamoto, P. J. McCarthy, A. Ruby and A. E. Martell, *J. Am. Chem. Soc.* 1961, **83**, 1066.
20. M. Mikami, I. Nakagawa and T. Shimanouchi, *Spectrochim. Acta* 1967, **23A**, 1037.
21. G. T. Behnke and K. Nakamoto, *Inorg. Chem.* 1967, **6**, 433.
22. M. L. Niven and D. A. Thornton, *Spectrosc. Lett.* 1980, **13**, 419 and refs cited therein.
23. L. G. Hulett and D. A. Thornton, *J. Inorg. Nucl. Chem.* 1973, **35**, 2661.
24. R. D. Hancock and D. A. Thornton, *J. S. Afr. Chem. Inst.* 1970, **23**, 71.
25. T. J. McGee and J. L. Walter, *Spectrosc. Lett.* 1977, **10**, 831.
26. S. H. H. Chaston, S. E. Livingstone, T. N. Lockyer, V. A. Pickles and J. S. Shannon, *Aust. J. Chem.* 1965, **18**, 673.
27. D. Coucouvanis, N. C. Baenziger and S. M. Johnson, *J. Am. Chem. Soc.* 1973, **95**, 3875.
28. D. Coucouvanis and D. Piltingsrud, *J. Am. Chem. Soc.* 1973, **95**, 5556.
29. H. O. Desseyn, W. A. Jacob and M. A. Herman, *Spectrochim. Acta* 1969, **25A**, 1685.
30. G. W. Watt and B. J. McCormick, *Spectrochim. Acta* 1965, **21**, 753.
31. J. P. Fackler and A. F. Masters, *Inorg. Chim. Acta* 1980, **39**, 111.

Polyhedron Vol. 8, No. 18, pp. 2313–2320, 1989
Printed in Great Britain

0277–5387/89 $3.00+.00
© 1989 Pergamon Press plc

STRUCTURES AND PROPERTIES OF BIS(THIOCYANATO-N)BIS(6-METHYL[1,2,4]TRIAZOLO[1,5-*a*]PYRIMIDINE-N³)COPPER(II), A DISTORTED TETRAHEDRAL COPPER(II) THIOCYANATE COMPOUND, AND BIS(THIOCYANATO-N)BIS(5-METHYL[1,2,4]TRIAZOLO[1,5-*a*]PYRIMIDINE-N³)COPPER(II), A POLYNUCLEAR PSEUDO-LAYERED SYSTEM

J. P. CORNELISSEN, R. A. G. DE GRAAFF, J. G. HAASNOOT,* R. PRINS and J. REEDIJK

Department of Chemistry, Gorlaeus Laboratories, Leiden University, P.O. Box 9502, 2300 RA Leiden, The Netherlands

and

M. BIAGINI-CINGI, A. M. MANOTTI-LANFREDI and A. TIRIPICCHIO

Instituto di Chimica Generale ed Inorganica, Università di Parma, Centro di Studio per la Strutturistica Diffrattometrica del C.N.R., Viale delle Scienze, I-43100 Parma, Italy

(*Received* 16 *March* 1989; *accepted* 4 *May* 1989)

Abstract—The molecular structures and spectroscopic properties of the compounds $[Cu(NCS)_2(L)_2]$ (L = 6-methyl[1,2,4]triazolo[1,5-*a*]pyrimidine, $C_6N_4H_6$, abbreviated 6mtp, and L = 5-methyl[1,2,4]triazolo[1,5-*a*]pyridimine, $C_6N_4H_6$, abbreviated 5mtp) are described. The structures of $[Cu(NCS)_2(6mtp)_2]$ (**1**) and $[Cu(NCS)_2(5mtp)_2]$ (**2**) have been determined by single-crystal X-ray diffraction. Compound **1** is monoclinic, space group $C2/c$, with $a = 12.096(9)$, $b = 8.466(6)$, $c = 18.327(7)$ Å, $\beta = 101.95(9)°$, $Z = 4$. Compound **2** is monoclinic, space group $P2_1/c$, with $a = 12.451(7)$, $b = 8.952(5)$, $c = 8.061(5)$ Å, $\beta = 106.53(2)°$, $Z = 2$. Both structures have been solved from diffractometer data by Patterson and difference Fourier methods, and refined by full-matrix least-squares to $R = 0.0365$ for 1400 observed reflections (**1**) and to $R = 0.0370$ for 1195 independent observed reflections (**2**). In **1** mononuclear complexes are present, in which each copper atom is surrounded by four donor nitrogen atoms: two N-atoms of two N(3)-coordinating 6mtp ligands, and two N-atoms of the non-bridging NCS-ions in a distorted tetrahedral arrangement (Cu—N = 1.931(3)–1.975(2) Å, N—Cu—N = 93.5(1)–143.5(1)°). In **2** four donor nitrogen atoms, from two N(3)-coordinating 5mtp ligands and two monodentate NCS-ions, give square-planar copper in a *trans* configuration (Cu—N = 1.921(4)–2.020(4) Å, N—Cu—N = 91.2(1)–88.8(2)°). Two N(1)-atoms of the 5mtp ligands of neighbouring complexes, at a rather long distance of 2.677 Å, complete the elongated octahedral coordination of the metal and join the complexes in layers.

Coordination compounds of [1,2,4]triazolo[1,5-*a*]pyrimidines have been considered as model systems for various naturally occurring metal coordination compounds.[1] Their three possible N-donor sites account for several different coordination modes.

In Fig. 1 the IUPAC numbering system is compared with the biochemical numbering system for purine ligands. Unless stated otherwise, the IUPAC numbering is used throughout this manuscript.

By coordinating in an adenine-type bidentate mode via N(3) and N(4), these triazolopyrimidines act as a model system for purine-type ligands.[2–5] On the other hand, the 1,2,4-triazole ring has a

* Author to whom correspondence should be addressed.

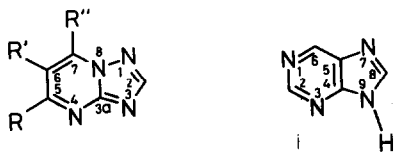

Fig. 1. IUPAC numbering of triazolopyrimidines and biochemical numbering of purines.

geometry and electronic structure similar to that of imidazole.[6] When bridging through N(1)—N(3), [1,2,4]triazolo[1,5-*a*]pyrimidine is therefore especially suited for mimicking imidazolato bridges in model compounds for metalloproteins such as superoxide-dismutase.[7-8] In fact, a few of these compounds have already been reported.[9a]

The substitution of methyl groups onto the triazolopyrimidine can influence the favoured coordination mode to a certain extent. Earlier, the ligand 5,7-dimethyl[1,2,4]triazolo[1,5-*a*]pyrimidine (abbreviated dmtp) was studied. The methyl groups seemed to cause too much steric hindrance, allowing no coordination mode other than monodentate bonding through the N(3)-atom to occur.[10-13] Only in one case was an adenine-type, dinucleating mode via N(3)- and N(4)-atoms observed.[14]

Recently the preparation of several polynuclear metal coordination compounds with the unsubstituted [1,2,4]triazolo[1,5-*a*]pyrimidine (abbreviated tp) has been reported.[9b] It was concluded that tp could not only coordinate in the monodentate mode through N(3), but could also be more or less forced to act as a bridging ligand through both non-bridgehead triazole nitrogen atoms, N(1) and N(3).

To further investigate the influence of methyl groups on substituted triazolopyrimidines, two related ligands, 6-methyl[1,2,4]triazolo[1,5-*a*]pyrimidine (abbreviated 6mtp) and 5-methyl[1,2,4]triazolo[1,5-*a*]pyrimidine (abbreviated 5mtp), differing only very slightly in structure from dmtp, were prepared. Theoretically, these ligands too can use N(1), N(3) and N(4) for coordination. Two copper(II) coordination compounds were obtained having the general formula $[Cu(NCS)_2(L)_2]$ (L = 5mtp and 6mtp). As in $[Cu(NCS)_2(dmtp)_2]$ (α- and β-isomer)[10a,11] and α-$[Cu(NCS)_2(tp)_2]$,[9b] the complexes are dinuclear and pseudo-polynuclear, respectively, the determination of the structures of $[Cu(NCS)_2(6mtp)_2]$ and $[Cu(NCS)_2(5mtp)_2]$ appeared to be a good opportunity to investigate the effect of the 5- and 6-methyl substituents on the coordination behaviour of the triazolopyrimidine ligand. Their molecular structures and spectroscopic properties will be compared with those of earlier prepared copper(II) thiocyanate compounds.

EXPERIMENTAL

Materials

The metal salts used for the preparations were reagent grade and used without further purification. The 6mtp ligand was prepared from 3-amino-1,2,4-triazole and 2-methyl-1,1,3,3-tetraethoxypropane according to a published method for the preparation of the unsubstituted compound tp.[15] The substance was characterized by melting point, NMR and mass spectroscopy. The results were in agreement with the data found for 6mtp as prepared by Brown and Nagamatsu.[16] The 5mtp ligand was prepared from 3-amino-1,2,4-triazole and 4,4-dimethoxy-2-butanone, similar to tp. This compound too was characterized by melting point, NMR and mass spectroscopy. The data agreed with those found by Bajwa and Sykes.[17] Compounds **1** and **2** were prepared by treating freshly synthesized $Cu(NCS)_2$ dissolved in methanol (2 mmol in 40 cm^3) with 4 mmol of ligand dissolved in 30 cm^3 of methanol. Dark red–brown (**1**) and lustrous green (**2**) crystals appeared on standing at room temperature after several hours. All crystals were separated by filtration, dried and analysed for metal, carbon, hydrogen and nitrogen. The compounds analysed as $[Cu(NCS)_2(L)_2]$. Found for **1**: C, 37.3; H, 2.6; N, 31.3; Cu, 14.4. Calc. for $[Cu(NCS)_2(6mtp)_2]$: C, 37.4; H, 2.7; N, 31.1; Cu, 14.2%. Found for **2**: C, 37.2; H, 2.5; N, 31.2; Cu, 13.9. Calc. for $[Cu(NCS)_2(5mtp)_2]$: C, 37.4; H, 2.7; N, 31.1; Cu, 14.2%.

Physical measurements

Ligand-field spectra were taken on a Perkin–Elmer 330 UV–vis–IR spectrophotometer using MgO as a reference in the diffuse reflectance technique. IR spectra were recorded on a Perkin–Elmer 580B IR spectrophotometer as Nujol mulls between KRS-5 [Tl(Br,I)] and polyethene (below 400 cm^{-1}), and as CsCl discs.

Crystal structure determination of **1**

A prismatic dark red–brown crystal of dimensions $0.25 \times 0.21 \times 0.20$ mm was selected and mounted on an Enraf–Nonius CAD4 diffractometer. Intensities were collected at room temperature using graphite monochromated Mo-K_α radiation ($\lambda = 0.71073$ Å). Crystallographic data and relevant information on data collection and refinement have been summarized in Table 1. The data were corrected for Lorentz and polarization effects. Absorption correction was unnecessary.

Table 1. Relevant crystallographic and experimental data of $[Cu(NCS)_2(6mtp)_2]$ (**1**) and $[Cu(NCS)_2(5mtp)_2]$ (**2**)

	1	**2**
Empirical formula	$CuS_2C_{14}H_{12}N_{10}$	$CuS_2C_{14}H_{12}N_{10}$
Molecular weight	448.0	448.0
Crystal system	Monoclinic	Monoclinic
Space group	$C2/c$	$P2_1/c$
a (Å)	12.095(9)	12.451(7)
b (Å)	8.466(6)	8.952(5)
c (Å)	18.327(7)	8.061(5)
β (°)	101.95(9)	106.53(2)
V (Å^3)	1836.2	861.4(9)
Z	4	2
μ (cm^{-1})	14.31	15.26
D_c (Mg m^{-3})	1.62	1.73
D_m (Mg m^{-3})	1.62	1.72
Number of independent reflections	1934	2008
Number of significant reflections	1406	1195
θ range (°)	2–26	3–27
Data collection range	$-14 < h < 14$, $0 < k < 10$, $-22 < l < 22$	$-15 < h < 15$, $0 < k < 11$, $0 < l < 9$
$F(000)$	908	454
Final $R(R_w)$	0.036 (0.047)	0.037 (0.050)

All 1934 measured independent reflections with $I > 2\sigma(I)$ and θ in the range of 2–26° were used in the analysis. The structure was solved by standard Patterson and Fourier methods. Calculations were carried out on the Leiden University IBM 3038 computer. Refinements were calculated by full-matrix least-squares cycles, using at first isotropic and later anisotropic thermal parameters for all non-hydrogen atoms. All six hydrogen atoms were found by a difference Fourier synthesis. The final residual indices are defined as $R = \{\sum(||F_c| - |F_o||)/\sum|F_o|\}$ and $R_w = \{\sum w(|F_o| - |F_c|)^2/\sum w|F_o|^2\}^{1/2}$.

Crystal structure determination of **2**

A thin prismatic green crystal of approximate dimensions $0.05 \times 0.24 \times 0.55$ mm was used for the X-ray analysis. Data were collected at room temperature on a Siemens AED diffractometer using Nb-filtered Mo-K_α radiation ($\lambda = 0.71069$ Å). The relevant parameters of crystal data collection are given in Table 1. The structure amplitudes were obtained after the usual Lorentz and polarization reduction; no correction for absorption was necessary. Of 2008 independent reflections, 1195, having $I > 2\sigma(I)$, were considered observed and used in the analysis. The structure was solved by Patterson and Fourier methods, and refined by full-matrix least-squares using the SHELX system of computer programs,[18] first with isotropic and then with anisotropic thermal parameters for all non-hydrogen atoms; all hydrogen atoms were localized from a difference Fourier map, but not refined. All calculations were carried out on the CRAY X-MP/12 computer of the "Consorzio per la Gestione del Centro di Calcolo Elettronico Interuniversitario del Italia Nord-Orientale" (CINECA, Casalecchio, Bologna). For both **1** and **2**, fractional coordinates of the non-hydrogen and the hydrogen atoms, anisotropic thermal parameters, bond lengths and angles dealing with hydrogen atoms as well as a list of structure factors have been deposited as Supplementary Material and are available on request. Atomic coordinates have also been deposited at the Cambridge Crystallographic Data Centre.

RESULTS AND DISCUSSION

Description of the structure of $[Cu(NCS)_2(6mtp)_2]$ (**1**)

Relevant angles and bond distances of **1** are given in Table 2. In the crystal structure of $[Cu(NCS)_2(6mtp)_2]$, depicted in Fig. 2, the complex has an imposed C_2 symmetry; the copper atom is surrounded by two symmetry-related 6mtp molecules and two N-bonding thiocyanates in a distorted tetrahedral arrangement. Each ligand coordinates monodentately to the metal atom through N(3). The six bonding angles (values of 93.5(1),

Table 2. Bond distances (Å) and valence angles (°) in $[Cu(NCS)_2(6mtp)_2]$ (1)[a]

C—N(31)	1.975(2)		
Cu—N(1)	1.931(3)		
S(1)—C(1)	1.614(3)	N(41)—C(51)	1.314(4)
N(31)—C(21)	1.358(4)	N(41)—C(3a1)	1.334(4)
N(31)—C(3a1)	1.346(4)	N(1)—C(1)	1.153(4)
N(81)—N(11)	1.364(3)	C(71)—C(61)	1.351(4)
N(81)—C(71)	1.345(4)	C(91)—C(61)	1.500(5)
N(81)—C(3a1)	1.363(4)	C(61)—C(51)	1.412(5)
N(11)—C(21)	1.307(4)		
N(1)—Cu—N(31)	143.5(1)		
N(1′)—Cu—N(31′)	143.5(1)		
N(1′)—Cu—N(31)	93.5(1)		
N(1)—Cu—N(1′)	96.3(2)		
N(31)—Cu—N(31′)	99.3(1)		
N(1)—Cu—N(31′)	93.5(1)		
Cu—N(31)—C(21)	127.1(2)	N(31)—C(21)—N(11)	115.9(3)
Cu—N(31)—C(3a1)	129.6(2)	N(81)—C(71)—C(61)	118.1(3)
C(21)—N(31)—C(3a1)	103.3(3)	C(71)—C(61)—C(91)	121.7(3)
N(11)—N(81)—C(71)	127.4(3)	C(71)—C(61)—C(51)	116.8(3)
N(11)—N(81)—C(3a1)	110.6(2)	C(41)—C(61)—C(51)	121.6(3)
C(71)—N(81)—C(3a1)	121.9(3)	N(41)—C(51)—C(61)	125.6(3)
N(81)—N(11)—C(21)	102.2(2)	N(31)—C(3a1)—N(81)	108.0(2)
C(51)—N(41)—C(3a1)	115.1(3)	N(31)—C(3a1)—N(41)	129.6(3)
Cu—N(1)—C(1)	178.3(3)	N(81)—C(3a1)—N(41)	122.4(3)
S(1)—C(1)—N(1)	178.8(3)		

[a] The primed atoms are related to the unprimed ones by the transformation $x, -y, 1/2+z$.

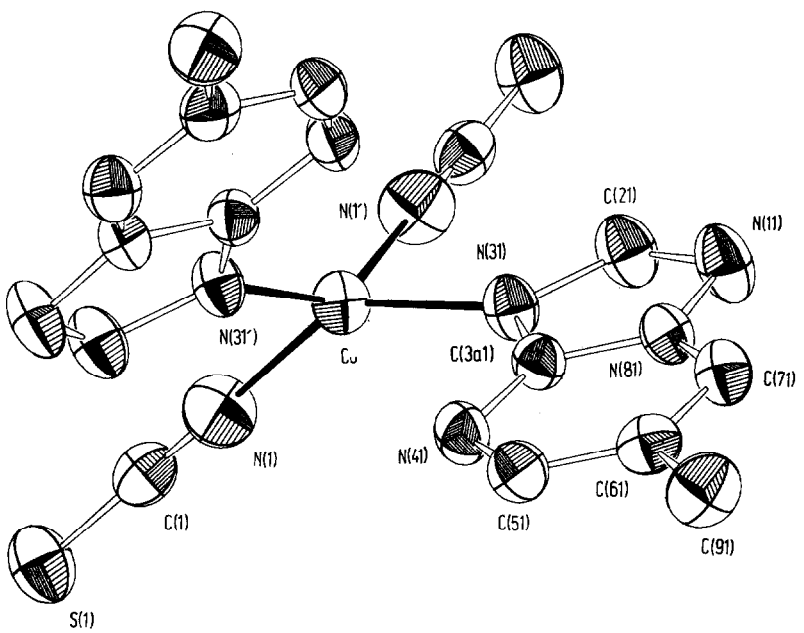

Fig. 2. ORTEP drawing of $[Cu(NCS)_2(6mtp)_2]$ (1). Hydrogen atoms are omitted for clarity.

96.3(2), 99.3(1) and 143.5(1)°) differ significantly from the value expected for a regular tetrahedron (109.45°), with the two N(31)—Cu—N(1) angles being exceptionally large: 143.5(1)°. No semi-coordinating nitrogen atom could be found. On searching for a semi-coordinating sulphur atom of another $Cu(NCS)_2(6mtp)_2$ unit, the shortest intermolecular Cu—S distance appeared to be 4.895 Å, which is far too long for any significant Cu—S interaction (Fig. 3). No stacking of the heterocyclic rings was observed. Since hydrogen bridges are not present, either in or between the units, the geometry around the copper atoms can only originate from a basically square-planar structure forced into a distorted tetrahedron by ligand–sulphur packing effects.

It is a well-known fact that a tetrahedral geometry is more suitable for a copper(I) compound than for a copper(II) system. Therefore, the tetrahedral distortion of the geometry of **1**, indicated by the unusually low energy ligand field maximum at 12.8×10^3 cm^{-1}, probably results in a reduction towards a more monovalent character of the metal ions. This is also reflected in the intense charge-transfer band at 19.7×10^3 cm^{-1}.

Although the occurrence of copper(II) in a genuine tetrahedral coordination is very unusual, it has been reported that several copper(II) complexes with chelating ligands, possessing a $Cu(NN)_2$ chromophore, occur in a more or less distorted tetrahedral configuration, the manner of distortion depending upon the nature of the ligand.[19–22] Some monomeric copper(II) compounds of the type $[Cu(L)X_2]$ and $[Cu(L)_2X_2]$ have been found to possess a distorted tetrahedral geometry, too.[23–25] The more or less tetrahedral configuration of **1** is comparable to that found for *trans*-dichlorobis(N-methylimidazole)copper(II),[25] in which the Cl—Cu—Cl and N—Cu—N angles are 143.7(6) and 149.7(1)°, respectively, and the others are in the range 94.0(1)–95.4(1)°. In all the copper(II) compounds mentioned above, the steric repulsions between the ligands appear to be the most important factor for copper(II) complexes to exhibit a configuration which deviates from planarity to varying degrees.

Description of the structure of $[Cu(NCS)_2(5mtp)_2]$ **(2)**

Table 3 lists the bond distances and angles for **2**. The copper atom and the four nitrogen donor atoms of a $[Cu(NCS)_2(5mtp)_2]$ unit are in a square-planar arrangement. The two N(3)-atoms of the 5mtp ligands are coordinated in a *trans* mode at a bond distance of 2.020(4) Å. The Cu—N(thiocyanate group) distance is 1.921(4) Å (Fig. 4). Two N(1)-atoms of the organic ligands in neighbouring $[Cu(NCS)_2(5mtp)_2]$ units, coordinating axially at a distance of 2.677(5) Å, complete the elongated octahedral geometry around the copper atoms.

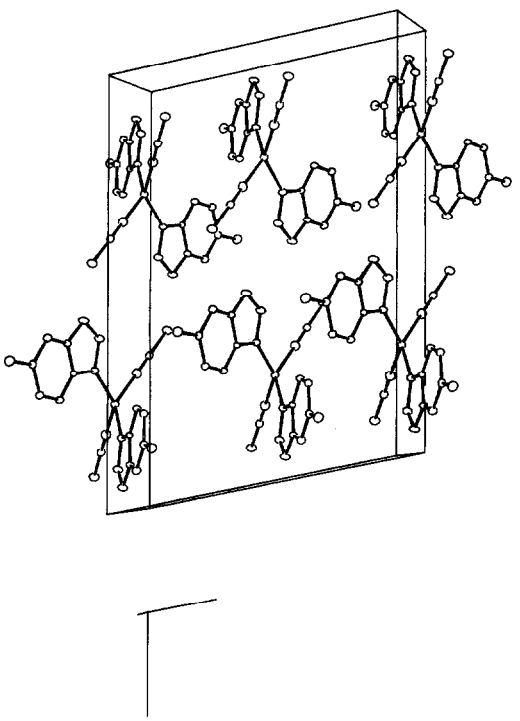

Fig. 3. Packing of the unit cell of $[Cu(NCS)_2(6mtp)_2]$ **(1)**.

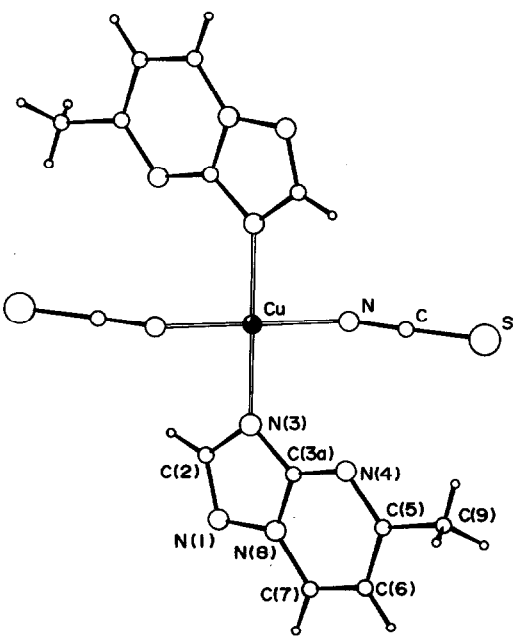

Fig. 4. Drawing of the structure of $[Cu(NCS)_2(5mtp)_2]$ **(2)**.

Table 3. Bond distances (Å) and valence angles (°) in $[Cu(NCS)_2(5mtp)_2]$ (2)[a]

Cu—N	1.921(4)		
Cu—N(3)	2.020(4)		
Cu—N(1′)	2.677(5)		
N—C	1.161(7)	N(8)—C(7)	1.347(6)
C—S	1.607(6)	C(5)—C(9)	1.488(8)
C(6)—C(5)	1.409(7)	C(7)—C(6)	1.363(8)
C(5)—N(4)	1.339(6)	C(3a)—N(3)	1.337(6)
N(4)—C(3a)	1.323(6)	N(3)—C(2)	1.351(7)
C(3a)—N(8)	1.355(6)	C(2)—N(1)	1.321(6)
N(1)—N(8)	1.366(6)		
N(3)—Cu—N	91.2(2)	N—C—S	178.1(5)
N(3)—Cu—N(1′)	93.5(2)	Cu—N—C	157.6(4)
N(1′)—Cu—N	88.1(2)		
C(7)—C(6)—C(5)	119.9(5)	C(3a)—N(8)—N(1)	110.2(4)
C(6)—C(5)—N(4)	122.1(5)	N(8)—N(1)—C(2)	102.3(4)
C(5)—N(4)—C(3a)	116.5(4)	N(1)—C(2)—N(3)	115.0(5)
N(4)—C(3a)—N(8)	122.9(4)	C(2)—N(3)—C(3a)	103.8(4)
C(3a)—N(8)—C(7)	122.6(4)	Cu—N(3)—C(3a)	130.7(3)
N(8)—C(7)—C(6)	116.1(5)	Cu—N(3)—C(2)	125.2(4)
N(8)—C(3a)—N(3)	108.6(4)	C(6)—C(5)—C(9)	120.5(5)
N(4)—C(5)—C(9)	117.5(4)		

[a] The primed atoms are related to the unprimed ones by the transformation x, $-1/2-y$, $-1/2+z$.

By acting in such a bidentate mode between the metal centres, the 5mtp ligands build a two-dimensional system (Fig. 5). When the molecular structure of **2** is compared to that of α-$[Cu(NCS)_2(tp)_2]$, published earlier,[9b] clearly both structures are very similar, and **2** can be best described as a pseudo-layered system with semi-coordination.

However, when compared to previously reported metal thiocyanate compounds containing tp, of the general formula $[M(NCS)_2(tp)_2]$ (for M = Fe, Co, Ni, Mn), in which the triazolopyrimidine ligands too, acted in a bridging mode via N(1)—N(3),[9a] the metal–metal distances in **2** should be significantly longer. Instead, in spite of the longer Cu—N(1)

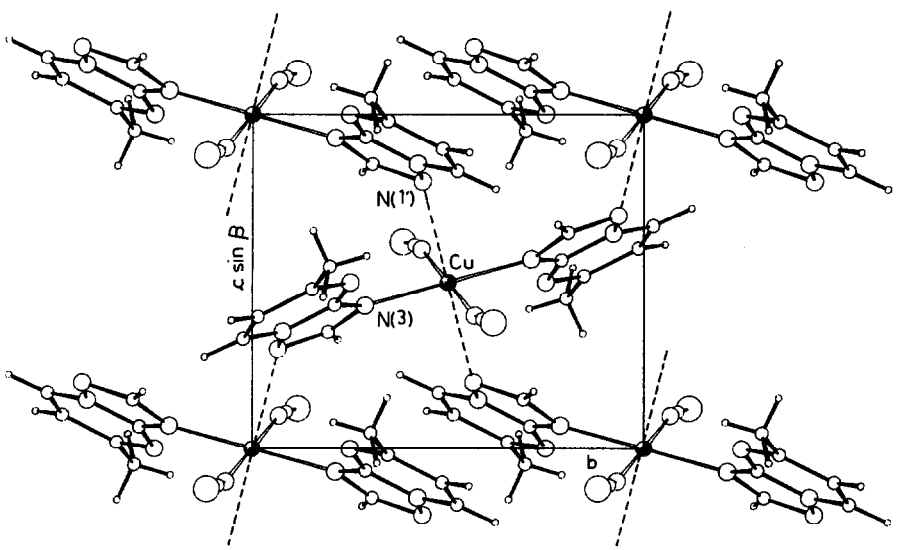

Fig. 5. Pseudo two-dimensional system of $[Cu(NCS)_2(5mtp)_2]$ (**2**).

Table 4. Structural and spectral data of related copper thiocyanate complexes

Compound	Chromophore	Cu—N(3)[a] distance (Å)	L.F. max. ($cm^{-1} \times 10^3$)	ν_{CN} (cm^{-1})	ν_{CS} (cm^{-1})	Reference
$[Cu(NCS)_2(6mtp)_2]$	CuN_4	1.975(2)	27.0 (s,CT) 19.7 (s,CT) 12.8 (s,br)	2074 2088	833	This work
α-$[Cu(NCS)_2(dmtp)_2]$	$Cu(N_4)S$	2.008(8)	15.9 (s) 14.9 (sh)	2109 2079	832 (vw) 779 (m)	10(a)
β-$[Cu(NCS)_2(dmtp)_2]$	$Cu(N_3S)N$	2.06	14.4 (s) 13.4 (sh)	2098 2070	830 (vw) 740 (vw)	11
$[Cu(NCS)_2(dmtp)_2(H_2O)_2]$	$Cu(N_3S)O$	—	13.7 (s)	2105 2086	829 763	11
α-$[Cu(NCS)_2(tp)_2]$	CuN_6	2.035(5)	25.9 (s,CT) 14.3 (s)	2102	792 (m)	9(b)
β-$[Cu(NCS)_2(tp)_2]$	CuN_6	—	23.6 (vs,CT) 14.5 (s)	2068 2099	829 841	9(b)
$[Cu(NCS)_2(5mtp)_2]$	CuN_6	2.020(4)	29.2 (vs,CT) 23.4 (vs,CT) 15.6 (s) 13.6 (s,sh)	2072	799	This work

s = strong, vs = very strong, sh = shoulder, CT = charge transfer, br = broad, m = medium, w = weak, vw = very weak.

[a] IUPAC numbering.

coordination distances, in **2** the Cu—Cu distance of 6.02 Å is shorter than the M—M distance in $[M(NCS)_2(tp)_2]$ (6.46 Å). This is a consequence of the σ-character of both the M—N interactions in $[M(NCS)_2(tp)_2]$, as suggested by the co-planarity of the metal atoms with respect to the tp ligands. In **2**, the σ-character can be attributable only to the shorter Cu—N(3) distance. The non-σ-character of the Cu—N(1) bond is reflected in the fact that this bond is remarkably out of the plane passing through the corresponding tp molecule.

CONCLUSIONS

Table 4 compares the spectroscopic and geometric data of copper(II) thiocyanate compounds with tp and dmtp to that of **1** and **2**.

Comparing the structure of **1** to structures determined before (Table 4), the ligand behaviour of the NCS-group and of the 6mtp molecule differ dramatically from that found for these ligands in related compounds. In both (α and β) $[Cu(NCS)_2(dmtp)_2]$ compounds, dmtp acts as a monodentate ligand through the usually favoured triazole N(3)-atom (even when both non-bridgehead triazole nitrogen atoms are available for coordination), and the NCS-anions act both as N-bonded monodentate ligands and as bidentate bridges between the copper atoms.[10a,11] In **2** and in α-$[Cu(NCS)_2(tp)_2]$, the NCS-group binds exclusively monodentate via its nitrogen atom, but the organic ligands are acting in a bridging mode by semi-coordination through the N(1)-atom to the neighbouring copper atoms.[9b] Also, while the metal atom in both $[Cu(NCS)_2(dmtp)_2]$ compounds is surrounded by five donor atoms, and in **2** and α-$[Cu(NCS)_2(tp)_2]$ by six donor nitrogen atoms, the copper in **1** possesses a coordination geometry of only four ligands. A methyl substituent at C(5) does not seem to greatly influence the coordination mode of the triazolopyrimidine ligand towards copper(II) ions. In that respect, it is not fully understood why a comparably minor alteration of the triazolopyrimidine ligand by the substitution of a methyl group at C(6) causes such a relatively large difference in the coordination behaviour of the ligand and that of the anions. Since in **1** the C(91)—N(41) separation is 3.778(3) Å, and the C(91)—N(11) separation is 4.914(3) Å, the steric effects of the 6-methyl group on the coordination ability of both nitrogen atoms theoretically cannot be large enough to exclude any ligand bridging.

Further investigations are needed to fully comprehend the factors that influence the nature of the coordination mode of [1,2,4]triazolo[1,5-*a*]pyrimidines in copper(II) thiocyanate systems.

Acknowledgements—The authors wish to thank C.N.R. (Rome) and the "Werkgroep Fundamenteel Materialen Onderzoek" of Leiden University for financial support, and in particular Dr Fennegien S. Keij for helpful discussions.

REFERENCES

1. D. J. Hodgson, *Progress in Inorganic Chemistry* (Edited by S. J. Lippard), Vol. 23. John Wiley, New York (1977).
2. (a) E. Sletten, *J. Chem. Soc., Chem. Commun.* 1967, 1119; (b) E. Sletten, *Acta Cryst.* 1969, **B25**, 1480; (c) E. Sletten, *Acta Cryst.* 1970, **B26**, 1609.
3. D. M. L. Goodgame and K. A. Price, *Nature* 1968, **220**, 783.
4. (a) P. De Meester and A. C. Skapski, *J. Chem. Soc. A* 1971, 2167; P. De Meester and A. C. Skapski, *J. Chem. Soc., Dalton Trans.* 1972, 2400.
5. A. Terzis, A. L. Beauchamp and R. Rivest, *Inorg. Chem.* 1973, **12**, 1166.
6. C. R. Johnson, W. W. Henderson and R. E. Sheperd, *Inorg. Chem.* 1984, **23**, 2754.
7. J. A. Tainer, E. D. Getzoff, K. M. Beem, J. S. Richardson and D. C. Richardson, *J. Molec. Biol.* 1982, **160**, 181.
8. R. J. Sundberg and R. B. Martin, *Chem. Rev.* 1974, **74**, 471.
9. (a) M. Biagini-Cingi, A. M. Manotti-Lanfredi, A. Tiripicchio, J. P. Cornelissen, J. G. Haasnoot and J. Reedijk, *Inorg. Chim. Acta* 1987, **127**, 189; (b) M. Biagini-Cingi, A. M. Manotti-Lanfredi, A. Tiripicchio, J. P. Cornelissen, J. G. Haasnoot and J. Reedijk, *Inorg. Chem.* 1987, **129**, 217.
10. (a) M. Biagini-Cingi, A. M. Manotti-Lanfredi, A. Tiripicchio, J. G. Haasnoot and J. Reedijk, *Inorg. Chim. Acta* 1983, **72**, 81; (b) M. Biagini-Cingi, A. M. Manotti-Lanfredi, A. Tiripicchio, J. G. Haasnoot and J. Reedijk, *Inorg. Chim. Acta* 1984, **86**, 137; (c) M. Biagini-Cingi, A. M. Manotti-Lanfredi, A. Tiripicchio, J. G. Haasnoot and J. Reedijk, *Inorg. Chim. Acta* 1985, **101**, 49.
11. J. G. Haasnoot, W. L. Driessen and J. Reedijk, *Inorg. Chem.* 1984, **23**, 2803.
12. J. Dillen, A. T. H. Lenstra, J. G. Haasnoot and J. Reedijk, *Polyhedron* 1983, **2**, 195.
13. T. L. F. Favre, J. G. Haasnoot and J. Reedijk, *Polyhedron* 1986, **5**, 1405.
14. J. G. Haasnoot, T. L. F. Favre, W. Hinrichs and J. Reedijk, *Angew. Chem. Int. Edn Engl.* 1988, **27**, 856.
15. C. H. F. Allen, H. R. Beilfuss, D. M. Burness, G. A. Reynolds, J. F. Tinker and J. A. VanAllen, *J. Org. Chem.* 1959, **24**, 796.
16. D. J. Brown and T. Nagamatsu, *Aust. J. Chem.* 1977, **30**, 2515.
17. J. S. Bajwa and P. J. Sykes, *J. Chem. Soc. Perkin I* 1987, 3085.
18. G. M. Sheldrick, SHELX76 Program for crystal structure determination. University of Cambridge, U.K. (1976).
19. C. H. Wei, *Inorg. Chem.* 1972, **11**, 2315.
20. J. E. Johnson, T. A. Beineke and R. A. Jacobson, *J. Chem. Soc. A* 1971, 1371.
21. R. Tewari and R. C. Srivastava, *Acta Cryst.* 1971, **B27**, 1644.
22. S. Knapp, T. P. Keenan, X. Zhang, R. Fikar, J. A. Potenza and H. J. Schugar, *J. Am. Chem. Soc.* 1987, **109**, 1882.
23. R. B. Wilson, J. R. Wasson, W. E. Hatfield and D. J. Hodgson, *Inorg. Chem.* 1978, **17**, 641.
24. S. N. Choi, R. D. Bereman and J. R. Wasson, *J. Inorg. Nucl. Chem.* 1975, **37**, 2087.
25. J. A. C. van Ooijen and J. Reedijk, *J. Chem. Soc., Dalton Trans.* 1979, 1183.

Polyhedron Vol. 8, No. 18, pp. 2321–2330, 1989
Printed in Great Britain

0277–5387/89 $3.00+.00
© 1989 Pergamon Press plc

SYNTHESIS, CHARACTERIZATION AND ELECTROCHEMISTRY OF NICKEL(II) COMPLEXES OF SCHIFF BASE LIGANDS CONTAINING A DISULPHIDE GROUP. CRYSTAL STRUCTURE OF [Ni{(*o*-$OC_6H_4CH{=}NC_6H_4)_2S_2$}(MeOH)]·MeOH

C. MANZUR, C. BUSTOS, R. SCHREBLER and D. CARRILLO*

Instituto de Quimica, Universidad Catolica de Valparaiso, Av. Brasil 2950, Valparaiso, Chile

and

C. B. KNOBLER,† P. GOUZERH and Y. JEANNIN*

Laboratoire de Chimie des Métaux de Transition, CNRS-UA 419, Université Pierre et Marie Curie, 4 Place Jussieu, 75252 Paris Cedex 05, France

(*Received* 7 *March* 1989; *accepted* 4 *May* 1989)

Abstract—The Schiff base disulphide ligands N,N′-[1,1′-dithiobis(phenylene)]bis(salicylideneimine), designated hereunder as H_2salps, and N,N′-[1,1′-dithiobis(ethylene)]bis (salicydeneimine), designated hereunder as H_2sales, react with nickel(II) acetate tetrahydrate in methanol giving two mononuclear complexes: [Ni(salps)(MeOH)]·MeOH and [Ni(sales)], respectively. These complexes have been characterized by spectral, magnetic and electrochemical methods. The structure of [Ni(salps)(MeOH)]·MeOH has been determined by X-ray diffraction analysis. This complex crystallizes in the triclinic crystal system, space group $P\bar{1}$, $Z = 2$, $a = 9.476(1)$, $b = 11.297(3)$ and $c = 13.215(3)$ Å, $\alpha = 106.66(1)$, $\beta = 97.10(1)$, and $\gamma = 99.94(1)°$ and $V = 1312.3(3)$ Å^3. The refinement converged to $R = 0.034$ and $R_w = 0.045$ based on 2599 reflections with $I > 3\sigma(I)$. The salps functions as a quinquedentate ligand coordinating through the two phenolate oxygen atoms, the two imine nitrogen atoms and only one of the disulphide sulphur atoms. The sixth coordination site is occupied by the oxygen atom from a methanol molecule. The octahedron core, NiN_2O_3S, is highly distorted as indicated by the range in bond distances (from 2.063(3) to 2.531(1) Å) and angles (from 79.47(8) to 100.4(1)°). The Ni—S bond distance is 2.531(1) Å, while the S—S bond distance is 2.066(1) Å. On the other hand, the spectral and magnetic properties of [Ni(sales)] suggest a square-pyramidal structure with a Ni—S bond. The complexes show non-conjugated and irreversible redox processes in cyclic voltammetry, in DMF. The processes at −1.30 and −1.43 V have been attributed to the reduction of the disulphide group, whereas the oxidation process at *ca* +0.74 V has been attributed to the nickel(II) oxidation.

Although many ligands containing a disulphide group, RS—SR, are reduced by reaction with metal ions, this is not always the case. Several complexes of copper,[1–7] cobalt,[8–10] rhenium,[11,12] iridium,[13] nickel,[14–16] iron,[17] mercury,[18] cadmium[19] and manganese[20] have been synthesized, and their structures have been determined by X-ray diffraction analysis. Therefore, the existence of the M—S(disulphide) bond has been clearly demonstrated. In a few cases a weak covalent bond has been observed (bond lengths ~ 3.0 Å)[2,19] and in only two cases is this bond non-existent. In recent years the synthesis and study of new compounds exhibiting a M—S(disulphide) bond has been encouraged due to their probable relevancy with certain redox processes in biological systems. For example, in stellacyanin (a type I blue copper protein), a disulphide sulphur

* Authors to whom correspondence should be addressed.
† Permanent address: Department of Chemistry and Biochemistry, University of California, Los Angeles, CA 90024, U.S.A.

atom has been postulated as the probable ligand in the fourth coordination site of the copper ion.[23] Likewise, in certain model complexes, related to molybdenum enzymes, a partial bond formation between two coordinated RS ligands at a molybdenum(VI) centre has been observed.[24] On the other hand, new synthetic routes for the conversion of coordinated thiolate to coordinated unsymmetrical disulphide have been reported.[10,25–27] Nevertheless, the electrochemical studies of metal–disulphide complexes, in order to investigate the redox behaviour of the bonded disulphide group, are rather scarce in the literature.[20]

In this paper we report the synthesis, spectral, magnetic and electrochemical properties of the complexes formed by the nickel(II) ion with two Schiff base ligands containing a disulphide group, N,N′-[1,1′-dithiobis(phenylene)]bis(salicylideneimine) (H_2salps)* and N,N′-[1,1′-dithiobis(ethylene)]bis (salicylideneimine) (H_2sales).* We have also determined the structure of the complex [Ni(salps)(MeOH)]·MeOH by X-ray diffraction analysis.

EXPERIMENTAL

Chemicals

Cystamine·2HCl and bis-2-aminophenyldisulphide were purchased from Aldrich Chemical Company, while salicylaldehyde was obtained from BDH Laboratory Chemical Division. Nickel(II) acetate tetrahydrate was purchased from Merck. Reagent grade solvents were distilled and dried by standard methods.

Physical measurements

IR spectra were recorded in KBr and polyethylene discs on a Perkin–Elmer 599 spectrophotometer. Electronic spectra were recorded on a Carl Zeiss DMR-22 spectrophotometer using $CHCl_3$ and DMF Uvasol solvents, and in Nujol. ^{1}H NMR spectra were obtained on a Varian T-60 spectrometer using $CDCl_3$ as solvent. Raman spectra were obtained in the solid state at room temperature on a Raman Spex Compact 1301 spectrometer. Cyclic voltammetry measurements were made with a home-made potentiostat of conventional design, using a three-electrode cell with platinum working and auxiliary electrodes and a saturated calomel reference electrode (SCE). All measurements were carried out at 25±2°C in dry deaerated DMF, with 0.1 mol dm^{-3} tetraethylammonium perchlorate (TEAP) as the supporting electrolyte and a nickel complex concentration of 1.0 mmol dm^{-3} in the case of [Ni(salps)MeOH]·MeOH and 0.5 mmol dm^{-3} in the case of the sparingly soluble complex [Ni(sales)]. Controlled potential coulometry was performed using a platinum mesh electrode with a nickel complex concentration of 0.1 mmol dm^{-3}. Magnetic measurements were performed at 25°C by the Faraday method using a Cahn Ventron RTL magnetic balance and $[Ni(en)_2]S_2O_3$ as standard. Diamagnetic corrections were made by employing Pascal's constants.[28] Melting points were determined using a Kofler apparatus and were not corrected.

Preparation of Schiff base ligands

N,N′-[1,1′-*dithiobis(phenylene)*]*bis(salicylideneimine)*. Salicylaldehyde (20 mmol) was dissolved in EtOH (30 cm^3) and then added to bis-2-aminophenyldisulphide (10 mmol), and the reaction mixture was refluxed for 2 h. On cooling, the yellow solid obtained was filtered, washed with cold EtOH and dried. Finally, the product was recrystallized from $CHCl_3$–EtOH and dried *in vacuo*. Yield: 87.5%. ^{1}H NMR δ (in $CDCl_3$): 6.84–7.76 (m, 16H, $4C_6H_4$); 8.60 (s, 2H, 2HC=N); 12.9 (s, 2H, 20H).

N,N[1,1′-*dithiobis(ethylene)*]*bis(salicyldeneimine)*. The ligand was obtained as a yellow solid by the same method as above and recrystallized from EtOH. In this case, the free base cystamine was obtained by neutralization of cystamine dichlorohydrate with KOH in EtOH. Yield: 95%. ^{1}H NMR δ (in $CDCl_3$): 3.03 (t, 4H, $2CH_2S$); 3.90 (t, 4H, $2CH_2N$); 6.80–7.49 (m, 8H, $2C_6H_4$); 8.40 (s, 2H, 2HC=N); 14.1 (s, 2H, 20H).

Preparation of complexes

[Ni(salps)(MeOH)]·MeOH. The ligand salps (1.0 mmol) dissolved in MeOH (30 cm^3) at 50°C was added to nickel(II) acetate tetrahydrate (1.0 mmol) dissolved in MeOH (30 cm^3). The solution was stirred for 1 h at 50°C. On cooling, the brown microcrystalline solid obtained was filtered, washed with cold MeOH and Et_2O, and recrystallized from MeOH–DMF to give crystals suitable for X-ray analysis. Yield: 64%.

* Abbreviations used: H_2salps = N,N′-[1,1′-dithiobis(phenylene)]bis(salicylideneimine); H_2sales = N,N′-[1,1′-dithiobis(ethylene)]bis(salicydeneimine); H_2salen = N,N′-ethylenebis(salicylideneimine); H_2saldaes = N,N′-[2,2′-thiobis(ethanediyl)]bis(salicylideneimine); H_2salhn = N,N′-(1,6-hexanediyl)bis(salicylideneimine); pms = bis(2-(2-pyridylmethyl)aminoethyl)disulphide; dtpp = 2,2′-di(pyrid-2-ylmethyleneimine)diphenyldisulphide; H_2cbps = N,N′-[bis((2-hydroxyphenyl)phenylmethylene)-4-thiaheptane-1,7-diimine]; ps = bis(2-aminophenyl)disulphide.

[Ni(sales)]. The ligand sales (1.0 mmol) dissolved in MeOH (30 cm^3) at 50°C was added, with stirring, to nickel(II) acetate tetrahydrate (1.0 mmol) dissolved in MeOH (30 cm^3). Immediately, a green solid was formed, and the suspension was stirred for 1 h. The solid was sparingly soluble in common solvents and was subsequently used without recrystallization. Yield: 35%.

X-ray data collection and structure determination

An air-stable crystal of approximate dimensions 0.28 × 0.22 × 0.10 mm was mounted on a thin glass fibre on a Philips PW 1100 diffractometer. Lattice parameters were obtained from a least-squares refinement of the setting angles of 25 automatically centred reflections having 2θ between 23.8 and 32.8°. The cell constants and other parameters including conditions of data collection are summarized in Table 1.

Data were collected at room temperature (20°C) in the ω–2θ scan mode between 4 and 46° in 2θ. Two reflections (700, 7$\bar{2}$7) were monitored every hour to check stability. Their intensity fluctuated only slightly, *ca* ±2%, during the course of the experiment. The data were corrected for Lorentz and polarization effects but not for absorption.

The space group $P\bar{1}$ was assumed and confirmed by the successful solution and refinement of the structure. Computations were performed by using the CRYSTALS system[29] adapted for a VAX 11/725. The structure was solved by conventional heavy-atom methods. All the hydrogen atoms were located on difference electron density maps and included in the least-squares refinement. Anisotropic thermal parameters were refined for all non-hydrogen atoms. The position and isotropic thermal parameters of the two hydrogen atoms involved in hydrogen bonding [H(41) and H(51)] were refined. Positions of all other hydrogen atoms were held fixed with a fixed isotropic thermal parameter of 0.065 Å^2. During the final cycles of refinement the weighting scheme employed a three-term Chebyshev series: $w = w'[1-\{\Delta F/\sigma(F)\}^2]^2$ with $w' = [2.748t_0(x)+0.950t_1(x)+2.228t_2(x)]$, where $x = F_0/F_{max}$ and t_n is the polynomial function.[30] Scattering factors and corrections for anomalous dispersion were taken from ref. 31. A final difference electron density map was essentially featureless, the maximum peak being about 0.3 e Å^{-3}. Interatomic distances (Å) and angles (°) are given in Table 2.

RESULTS AND DISCUSSION

Synthesis of ligands and complexes

Two Schiff base ligands, H_2salps and H_2sales, containing a disulphide group, and two new nickel

Table 1. Crystal data and data collection parameters for [Ni(salps)(MeOH)]·MeOH

Formula	$C_{28}H_{26}NiN_2O_4S_2$
Molecular weight	577.4
Crystal system	Triclinic
Space group	$P\bar{1}$
Cell constants	
a (Å)	9.476(1)
b (Å)	11.297(3)
c (Å)	13.215(3)
α (°)	106.66(1)
β (°)	97.10(1)
γ (°)	99.94(1)
V (Å^3)	1312.3(3)
Z	2
F(000)	600
ρ (calc.) (g cm^{-3})	1.46
Radiation (graphite monochromator)	Mo-K_α (λ = 0.71069 Å)
Linear absorption, coefficient (cm^{-1})	9.30
Scan range (°)	0.9+0.345 tan θ
Number of unique data collected	3198
Number of unique data used ($I > 3\sigma(I)$)	2599
Number of parameters refined	343
$R = \Sigma \|\|F_o\|-\|F_c\|\|/\Sigma\|F_o\|$	0.034
$R_w = [\Sigma w(\|F_o\|-\|F_c\|)^2/\Sigma w\|F_o\|^2]^{1/2}$	0.045

Table 2. Selected interatomic distances (Å) and angles (°)

Ni(1)—S(1)	2.531(1)	Ni(1)—N(1)	2.063(3)
Ni(1)—O(1)	1.997(2)	Ni(1)—N(21)	2.072(3)
Ni(1)—O(21)	1.995(2)	S(1)—S(2)	2.006(1)
Ni(1)—O(41)	2.115(2)		
O(1)—Ni(1)—S(1)	166.54(7)	N(21)—Ni(1)—O(41)	173.3(1)
O(21)—Ni(1)—S(1)	97.90(7)	N(21)—Ni(1)—N(1)	100.4(1)
O(21)—Ni(1)—O(1)	94.8(1)	S(2)—S(1)—Ni(1)	108.26(5)
O(41)—Ni(1)—S(1)	90.76(7)	C(13)—S(1)—Ni(1)	94.9(1)
O(41)—Ni(1)—O(1)	94.75(9)	C(13)—S(1)—S(2)	104.9(1)
O(41)—Ni(1)—O(21)	85.27(9)	C(33)—S(2)—S(1)	107.3(1)
N(1)—Ni(1)—S(1)	79.47(8)	C(1)—O(1)—Ni(1)	122.3(2)
N(1)—Ni(1)—O(1)	88.8(1)	C(21)—O(21)—Ni(1)	126.9(2)
N(1)—Ni(1)—O(21)	169.7(1)	C(41)—O(41)—Ni(1)	120.2(2)
N(1)—Ni(1)—O(41)	84.8(1)	C(7)—N(1)—Ni(1)	123.1(2)
N(21)—Ni(1)—S(1)	86.02(8)	C(8)—N(1)—Ni(1)	117.7(2)
N(21)—Ni(1)—O(1)	89.7(1)	C(27)—N(21)—Ni(1)	122.8(2)
N(21)—Ni(1)—O(21)	89.3(1)	C(28)—N(21)—Ni(1)	118.7(2)

(II) complexes, [Ni(salps)(MeOH)]·MeOH and [Ni(sales)], were synthesized and characterized (Table 3). The ligands were synthesized, in good yield, by reacting bis-2-aminophenyldisulphide, $(NH_2C_6H_4)_2S_2$, or bis-2-aminoethyldisulphide, $(NH_2CH_2CH_2)_2S_2$, with salicylaldehyde (1:2) in refluxing EtOH. The bis-N-salicylidene derivatives have six donor atoms: ONSSNO (Scheme 1), and they are able to behave as quinquedentate ligands if one disulphide sulphur atom is coordinated to the nickel(II) ion. The complexes were synthesized in MeOH by reacting each ligand with nickel(II) acetate tetrahydrate in equimolar quantities. The synthesis of two different complexes, one solvated and one unsolvated, under the same experimental conditions, suggests differences in coordination in each case. The complexes are crystalline, air-stable species. [Ni(salps)(MeOH)]·MeOH is very soluble in DMF, $CHCl_3$ and THF, whereas [Ni(sales)] is sparingly soluble in all the common solvents tried. Solvolysis of the disulphide group of complexes to give binuclear species was not observed.

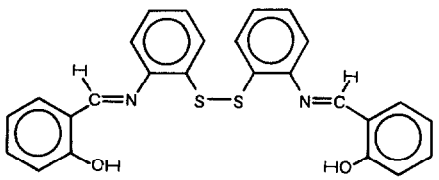

H_2salps

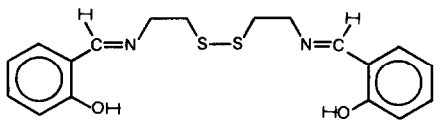

H_2sales

Scheme 1.

[Ni(salps)(MeOH)]·MeOH

The room temperature magnetic moment, 3.12 BM in the solid state, is compatible with a high spin d^8 electron configuration in an octahedral complex. The electronic spectrum in $CHCl_3$ shows six absorption bands (Table 3), of which the two lower energy bands at 1020 and 620 nm were assigned as typical *d–d* transitions in an octahedral geometry.[32] However, the third *d–d* band corresponding to the $^3A_{2g} \rightarrow {}^3T_{1g}(P)$ transition, predicted at *ca* 350 nm, was not observed and was probably lost amongst the more intense charge-transfer and intraligand bands in the UV region. The strong bands at 420 and 295 nm have been assigned as intraligand transitions by comparing them with the bands exhibited by the free ligand, H_2salps (Fig. 1). Finally, the bands occurring at 460 and 245 nm can be attributed, though not unequivocally, to charge-transfer transitions from a disulphide sulphur atom to a nickel(II) ion (i.e. $S\pi \rightarrow d$ and $S\sigma \rightarrow d$, respectively).[33] When [Mn(salps)(MeOH)]·MeOH, the analogous complex of [Ni(salps)(MeOH)]·MeOH, is dissolved in acetonitrile, benzene, toluene or dichloromethane, the coordinated methanol is displaced and the dimeric material $[\{Mn(salps)\}_2]$ is formed.[20] Such a type of dimerization via phenolate oxygen atoms has also been

Table 3. Ligands and complexes

Compound	Melting point (°C)	Colour	Analysis[a] %C	%H	%N	%Ni	IR (cm^{-1})[b] ν(C=N)	ν(C—O)	UV–vis (nm) λ_{max}	log ε	μ (BM) 298 K
H_2sales	75–76	Yellow	59.0	5.9	8.0	—	1630vs	1265m	368[c]	3.59	—
			(60.0)	(5.6)	(7.8)				316	3.93	
									274	3.97	
H_2salps	168–171	Yellow	67.3	4.7	6.3	—	1610vs	1270m	352[d]	4.50	—
			(68.4)	(4.4)	(6.1)				269	4.78	
[Ni(sales)]	224–226	Green	51.8	4.5	6.7	14.0	1610vs	1335m	620[c]	2.08	0.84
			(51.8)	(4.4)	(6.7)	(14.1)			390sh	4.78	
									377	4.85	
[Ni(salps)(MeOH)] · MeOH	253–257	Brown	59.5	4.4	5.0	10.3	1600vs	1315m	1020[d]	2.14	3.12
			(58.3)	(4.5)	(4.8)	(10.2)			620	1.85	
									460sh	3.63	
									420	3.75	
									295	3.98	
									245	4.32	

[a] Calculated values in parentheses.
[b] Abbreviations: vs, very strong; m, medium; sh, shoulder.
[c] Recorded in DMF.
[d] Recorded in $CHCl_3$.

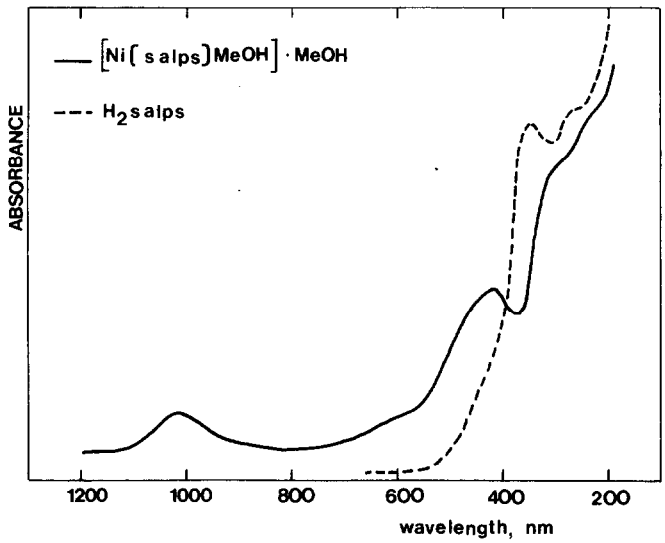

Fig. 1. Electronic absorption spectra of [Ni(salps)(MeOH)]·MeOH and H_2salps in $CHCl_3$.

observed in [{Cu(salen)}$_2$],[34] [{Fe(salen)Cl}$_2$][35] and [{Co(salen)X}$_2$].[36] However, in the present case, attempts to obtain [{Ni(salps)}$_2$] by refluxing the monomeric adduct in acetonitrile or other non-donor solvents were unsuccessful; only unmodified complex was recovered after each treatment.

The IR spectrum obtained in the polyethylene disc shows a weak band at 328 cm^{-1} which is assigned to ν(Ni—S) stretching on the basis of previous assignments in similar complexes, [Ni(dtpp)X] (X = Cl, Br).[37]

These observations are in total agreement with the X-ray crystallographic data (*vide infra*).

Description of the structure

Molecular structure. The molecular structure of [Ni(salps)(MeOH)] is very similar to those previously reported for [Mn(salps)(MeOH)][20] and [Fe(salps)Cl].[17] Indeed [Ni(salps)(MeOH)]·MeOH and [Mn(salps)(MeOH)]·MeOH[21] are isostructural compounds.

As illustrated in Fig. 2, salps functions as a quinquedentate ligand coordinating through the two phenolate oxygen atoms O(1) and O(21), the two imine nitrogen atoms N(1) and N(21), and only one of the disulphide sulphur atoms S(1). The sixth coordination site is occupied by the oxygen atom O(41) from a methanol molecule. Although the distortion of the octahedron core, MN_2O_3S, is less severe than in [Mn(salps)(MeOH)],[20] substantial strain is still present, as indicated by the range in bond distances (from 2.063(3) to 2.531(1) Å) and angles (from 79.47(8) to 100.4(1)°) for the nickel coordination sphere. The Ni—S bond distance of 2.531(1) Å is only slightly longer than those found in octahedral nickel(II) complexes containing quinquedentate organic disulphides; 2.472(5) Å in [Ni(pms)Cl],[14] 2.456(2) Å in [Ni(pms)Br][16] and 2.470(5) Å in [Ni(dtpp)Cl],[16] the S—S distance is 2.066(1) Å, which is in agreement with the distances reported for [Mn(salps)(MeOH)][20] (2.065(1) Å) and [Fe(salps)Cl][17] (2.046(5) Å). As previously stated,[15] the CSSC group appears to be unaffected by coordination to nickel(II), except for the sterically induced alteration of the dihedral angle and the resulting effect on the bond lengths. The CSSC dihedral angle of 71.6° in [Ni(salps)(MeOH)] is intermediate between the value of *ca* 85° in [Ni(pms)Cl][14] and [Ni(pms)Br],[16] and that of 55.4° in [Ni(dtpp)Cl].[15] The mean Ni—N distance of 2.067 Å is in agreement with the mean Ni—H bond length of 2.061 Å in [Ni(dtpp)Cl].[15]

Hydrogen bonding. Each methanol molecule is involved in an intermolecular hydrogen bond. Firstly, the non-coordinated methanol molecule is connected to the [Ni(salps)(MeOH)] molecule through hydrogen bonding to one phenolate oxygen atom. Secondly, the second phenolate oxygen atom interacts with the hydroxylic hydrogen atom of the coordinated methanol molecule of a second [Ni(salps)(MeOH)] molecule ($\bar{x}\bar{y}\bar{z}$). This results in centrosymmetric [Ni(salps)(MeOH)]·MeOH pairs. Geometrical data are indicative of fairly strong hydrogen bonding: O(51)—H(51) = 0.85(5) Å: H(51)···O(1) = 1.90(5) Å; the angle at H(51) is 178.6°. O(21)···H(41)′ = 2.09(5) Å; H(41)—O(41) = 0.64(5) Å; O(21)—H(41)′—O(41)′ = 171.9°. In [Mn(salps)(MeOH)]·MeOH the solvated methanol is not involved in hydrogen bonding.[20]

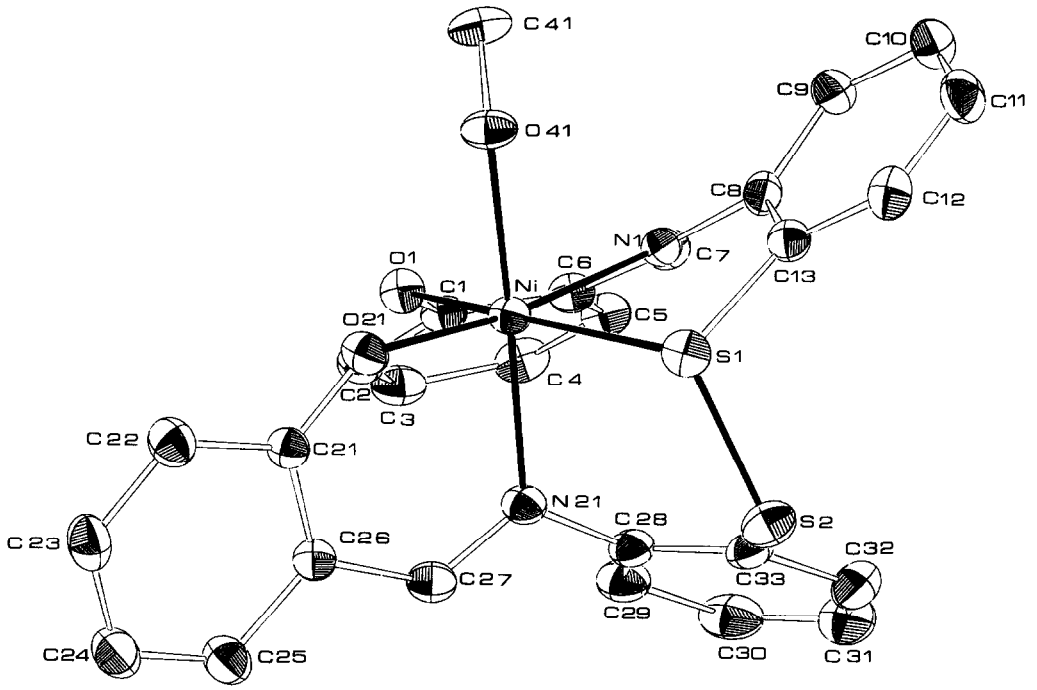

Fig. 2. Molecular structure of [Ni(salps)(MeOH)] showing 30% probability ellipsoids and the atom labelling scheme.

[Ni(sales)]

In contrast to [Ni(salps)(MeOH)]·MeOH, the room temperature magnetic moment of 0.84 BM for [Ni(sales)] is indicative of a low-spin nickel(II). As all tetrahedral and almost all six-coordinate nickel(II) complexes have a high-spin electronic configuration, whereas all known square-planar nickel(II) complexes are diamagnetic,[38] the small deviation from diamagnetism is possibly due to the presence of some high-spin octahedral, tetrahedral, or five-coordinate impurity in a low-spin square-planar, or five-coordinate complex.[39,40] Another mechanism which might account for the small paramagnetism is a spin state isomerism between singlet and triplet states for a five-coordinate complex.[39]

[Ni(sales)] will now be compared to two related complexes with potentially ONSNO quinquedentate ligands: [Ni(saldaes)] and [Ni(cbps)] and also to [Ni(salhn)], a nickel(II) complex with a quadridentate ligand (see ref. 29 for ligand abbreviations).

[Ni(saldaes)] is believed to have a distorted low-spin square-pyramidal or trigonal-bipyrimidal structure,[39,41] whereas the data for [Ni(cbps)] are consistent with a high-spin, distorted square-pyramidal structure.[42]

The electronic spectra of H_2sales, [Ni(sales)] and [Ni(salhn)] in DMF are shown in Fig. 3. The spectrum of [Ni(sales)] is characteristic of low-spin square-planar nickel(II) Schiff base complexes.[40,43] The UV–vis spectrum has spectral bands at 620, 390(sh) and 377 nm. Although this spectrum shows some resemblance to that of [Ni(salhn)], the two spectra are clearly distinct, suggesting different environments for the nickel(II) ion in these two complexes. On the other hand, the spectrum of [Ni(sales)] is quite different from that of high-spin [Ni(cbps)] which displays bands at 1150, 950(sh) and 600(sh) nm,[42] but is similar to that of low-spin [Ni(saldaes)] which has bands at 623, 433 and 322 nm.[39,41] These observations support similar low-spin five-coordinate structures for [Ni(sales)] and [Ni(saldaes)]. Further support for this conclusion comes from the IR spectrum showing a weak band at 325 nm which is tentatively assigned to a Ni—S stretch. Coordination of a sulphur atom is expected to shift the S—S Raman stretching band which is observed at 505 cm^{-1} in the free ligand. Unfortunately the Raman spectrum of [Ni(sales)] could not be recorded due to strong absorption of the 632.8 nm laser line by the green complex.

When dissolved in strongly coordinating solvents (i.e. propylamine), [Ni(sales)] and [Ni(salhn)] give identical spectra. This suggests facile solvolysis of the Ni—S bond in [Ni(sales)] and the formation of six-coordinate adducts, [NiL(solvents)$_2$].

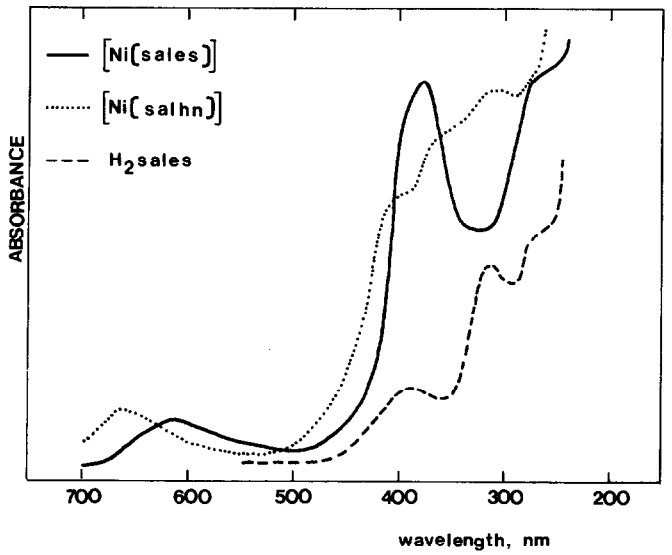

Fig. 3. Electronic absorption spectra of [Ni(sales)], [Ni(salhn)] and H_2sales in DMF.

Electrochemical studies

Cyclic voltammograms of [Ni(salps)(MeOH)]·MeOH, [Ni(sales)] and the corresponding ligands in DMF are shown in Fig. 4, with principal peak potentials listed in Table 4. The nickel(II) complexes exhibit non-conjugated and irreversible redox processes.

[Ni(salps)(MeOH)]·MeOH and [Ni(sales)] exhibit a reduction wave at -1.30 and -1.43 V, respectively, and a single oxidation wave at *ca* $+0.74$ V. By comparison with the cyclic voltammograms of ps, H_2sales and H_2salps* (Table 4), the cathodic process observed in the complexes was assigned to the reduction of the disulphide group.

The additional cathodic peak observed in H_2sales at -1.75 V was attributed to the azomethine group reduction, in agreement with the electrochemical behaviour of H_2salen. This wave was not observed either in both complexes or in H_2sales, probably because of overlap with the solvent discharge. The irreversible process exhibited by the complexes at *ca* $+0.74$ V can be assigned to the nickel(II) oxidation. Comparatively, [Ni(salen)] shows a reversible nickel(II)/nickel(III) redox couple centred at $+0.75$ V. The irreversibility observed in our complexes can be explained by the presence of the disulphide group. The nickel(III)—disulphide species may experience an internal redox reaction assisted by the solvent, following the same pattern described for the reaction of copper(II) with disulphide ligands in donor solvents. Finally, controlled-potential electrolysis of complexes and ligands indicated some complexity, and failed in all cases to give the actual number of electrons involved in any process. These results can be attributed to the adsorption of sulphur compounds onto the platinum electrode.

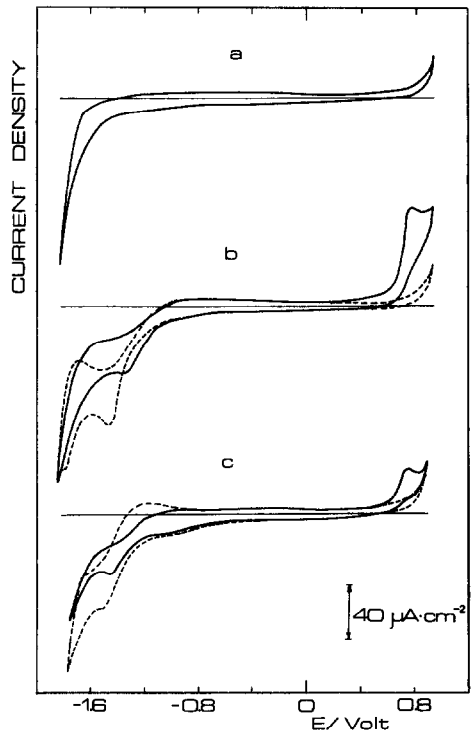

Fig. 4. Cyclic voltammograms in DMF recorded at 20 mV s^{-1} scan rate at a platinum wire electrode vs SCE. The solutions are 1.0 mmol dm^{-3} in TEAP. (a) Supporting electrolyte; (b) 0.1 mmol dm^{-3} in complex [Ni(salps)(MeOH)]. MeOH (—) and ligand H_2salps (– – –); (c) 0.5 mmol dm^{-3} in complex [Ni(sales)] (—) and 1.0 mmol dm^{-3} in ligand H_2sales (– – –).

* See footnote on p. 2322 for abbreviations.

Table 4. Electrochemical data for [Ni(salps)(MeOH)], [Ni(sales)] and the ligands

Compound*	Ep^c (V)		Ep^a (V)
[Ni(salps))(MeOH)]·MeOH	−1.30		+0.75
[Ni(sales)]	−1.43		+0.74
H_2salps	−1.41	−1.75	
H_2sales	−1.50		
H_2salen		−1.75	
ps	−1.35		

* See footnote on p. 2322 for ligand abbreviations.

Acknowledgements—Support from the Direccion General de Investigacion, Universidad Catolica de Valparaiso, Chile, is gratefully acknowledged. We also thank Dr Guillermo Contreras, Departamento de Quimica, Universidad de Concepcion, Chile, for recording the Raman spectra.

REFERENCES

1. C. I. Brändén, *Acta Chem. Scand.* 1967, **21**, 1000.
2. L. G. Warner, T. Ottersen and K. Seff, *Inorg. Chem.* 1974, **13**, 2819.
3. T. Ottersen, L. G. Warner and K. Seff, *Inorg. Chem.* 1974, **13**, 1904.
4. J. A. Thich, D. Mastropaolo, J. Potenza and H. J. Schugar, *J. Am. Chem. Soc.* 1974, **96**, 726.
5. M. M. Kadooka, L. G. Warner and K. Seff, *J. Chem. Soc., Chem. Commun.* 1975, 990.
6. M. M. Kadooka, L. G. Warner and K. Seff, *J. Am. Chem. Soc.* 1976, **98**, 7569.
7. P. M. Boorman, K. A. Kerr, R. A. Kydd, K. J. Moynihan and K. A. Valentine, *J. Chem. Soc., Dalton Trans.* 1982, 1401.
8. G. Bor and G. Natile, *J. Organomet. Chem.* 1971, **C33**, 26.
9. M. M. Kadooka, L. G. Warner and K. Seff, *Inorg. Chem.* 1976, **15**, 812.
10. D. L. Nosco, R. C. Elder and E. Deutsch, *Inorg. Chem.* 1980, **19**, 2545.
11. I. Bernal, J. L. Atwood, F. Calderazzo and D. Vitali, *Gazz. Chim. Ital.* 1976, **106**, 971.
12. I. Bernal, J. L. Atwood, F. Calderazzo and D. Vitali, *Gazz. Chim. Ital.* 1977, **15**, 153.
13. W. D. Bonds Jr and J. A. Ibers, *J. Am. Chem. Soc.* 1972, **94**, 3415.
14. P. E. Riley and K. Seff, *Inorg. Chem.* 1972, **11**, 2993.
15. L. G. Warner, T. Ottersen and K. Seff, *Inorg. Chem.* 1974, **13**, 2529.
16. L. G. Warner, M. M. Kadooka and K. Seff, *Inorg. Chem.* 1975, **14**, 1773.
17. J. A. Bertrand and J. L. Breece, *Inorg. Chim. Acta* 1974, **8**, 267.
18. M. M. Kadooka, E. Hilti, L. G. Warner and K. Seff, *Inorg. Chem.* 1976, **15**, 1186.
19. G. C. Baumann, M. F. Summers, J. P. Hutchinson, J. Zubieta and L. G. Marzilli, *Inorg. Chem.* 1984, **23**, 3104.
20. D. P. Kessissoglou, W. M. Butler and V. L. Pecoraro, *Inorg. Chem.* 1987, **26**, 495.
21. C. J. Simmons, M. Lunder and K. Seff, *Inorg. Chem.* 1979, **18**, 3444.
22. M. B. Hursthouse, R. L. Short, B. Piggott, A. Tucker and S. Fatt Wong, *Polyhedron* 1986, **5**, 2121.
23. D. R. McMillin and H. R. Engeseth, *Biological and Inorganic Copper Chemistry* (Edited by K. D. Karlin and J. Zubieta), Vol. I, pp. 1–10. Adenine Press, New York (1984).
24. E. I. Steifel, The structures and spectra of molybdoenzyme active sites and their models, in *Molybdenum and Molybdenum-containing Enzymes* (Edited by M. Coughlan), pp. 41–98. Pergamon Press, Oxford (1980).
25. C. A. Stein and H. Taube, *Inorg. Chem.* 1979, **18**, 2212.
26. M. Woods, J. C. Sullivan and D. Deutsch, *J. Chem. Soc., Chem. Commun.* 1975, 749.
27. M. Woods, J. Karbwang, J. C. Sullivan and E. Deutsch, *Inorg. Chem.* 1976, **15**, 1678.
28. B. N. Figgis and J. Lewis, The magnetochemistry of complex compounds, in *Modern Coordination Chemistry* (Edited by H. Lewis and R. G. Wilkins). Interscience, New York (1960).
29. D. J. Watkin, J. R. Carruthers and P. W. Betteridge, *Crystals User Guide*. Chemical Crystallography Laboratory, University of Oxford, U.K. (1987).
30. J. R. Carruthers and D. J. Watkins, *Acta Cryst.* 1979, **A35**, 698.
31. *International Tables for X-ray Crystallography*, Vol. IV. Kynoch Press, Birmingham, U.K. (1974).
32. A. B. P. Lever, *Inorganic Electronic Spectroscopy*. Elsevier, Amsterdam (1968).
33. J. M. Downes, J. Whelan and B. Bosnich, *Inorg. Chem.* 1981, **20**, 1081.
34. A. D. Watson, C. H. Pulla Rao, J. R. Dorfman and R. H. Holm, *Inorg. Chem.* 1985, **24**, 2820.
35. D. Hall and T. N. Waters, *J. Chem. Soc.* 1960, 2644.
36. M. Gerloch and F. E. Mabbs, *J. Chem. Soc. A* 1967, 1900.
37. S. E. Livingstone and J. D. Nolan, *Austr. J. Chem.* 1973, **26**, 961.
38. L. Saconi, *Transition Metal Chemistry* (Edited by R.

L. Carlin), Vol. 4, p. 199. Marcel Dekker, New York (1968).
39. W. M. Coleman and L. T. Taylor, *J. Inorg. Nucl. Chem.* 1971, **33**, 3049.
40. R. Atkins, G. Brewer, E. Kokot, G. M. Mockler and E. Sinn, *Inorg. Chem.* 1985, **24**, 127.
41. L. T. Taylor and W. M. Coleman, *J. Am. Chem. Soc.* 1970, **92**, 1449.
42. E. M. Boge, D. P. Freyberg, E. Kokot, G. M. Mockler and E. Sinn, *Inorg. Chem.* 1977, **16**, 1655.
43. G. M. Mockler, G. W. Chaffey, E. Sinn and H. Wong, *Inorg. Chem.* 1972, **11**, 1308.

Polyhedron Vol. 8, No. 18, pp. 2331–2332, 1989
Printed in Great Britain

0277–5387/89 $3.00+.00
© 1989 Pergamon Press plc

COMMUNICATION

SYNTHESIS AND STABILITY OF TWO-COORDINATE N-TRIFLUOROMETHYLIMINOARSINE, $CF_3N{=}AsH$

H. G. ANG* and F. K. LEE

Chemistry Department, National University of Singapore, Lower Kent Ridge Road, Singapore 0511, Republic of Singapore

(*Received* 3 *May* 1989; *accepted* 31 *May* 1989)

Abstract—The reactions between CF_3NO and AsH_3 afforded a relatively unstable new π-bonded iminoarsine, $CF_3N{=}AsH$, which decomposed to give CF_3H, N_2 and arsenic. A free radical mechanism of decomposition is proposed.

There has been growing research interest in recent years on the chemistry of unsaturated compounds of the main group elements with low coordination numbers. Within the Group 15 elements, a number of stable phosphorus derivatives that have been synthesized contain the following p_π–p_π bonds: P=C, P=N, P=P, P=As, and P=Sb, P=Si and P=Ge.[1–6] Some X-ray data are now available.[7–9] The stability of such compounds has been attributed to the presence of bulky substituents like *t*-Bu, Me_3Si, $(Me_3Si)_2N$ and 2,4,6-*t*-$Bu_3C_6H_2$ which shield the reactive sites. However, we have recently shown that compounds such as $(CF_3)_2NON{=}MR$ [M = P, As; R = H, $ON(CF_3)_2$], formed by the condensation reactions involving $(CF_3)_2NONO$ and PH_3 and AsH_3, respectively, are stabilized by the highly electronegative $(CF_3)_2NO$ group(s). We now report on the synthesis and stability of a new iminoarsine, $CF_3N{=}AsH$.

Trifluoronitrosomethane reacted with arsine in a 1:1 molar ratio at −120°C to afford N-trifluoromethyliminoarsine (**A**) in 14% yield and water, according to the equation:

$$CF_3NO + AsH_3 \longrightarrow CF_3N{=}AsH + H_2O. \quad (A)$$

The condensation reactions follow a similar course to those reported earlier between $(CF_3)_2NONO$ and AsH_3. The iminoarsine, **A**, was isolated at −126°C trap as a white solid and water at −60°C trap on trap-to-trap vacuum fractionation. The compound began to undergo decomposition even at temperatures as low as −110°C. On standing for about 4 min at room temperature, the compound decomposed to afford a bluish-black metallic film of arsenic metal, trifluoromethane and a non-condensable gas which was presumably nitrogen. A fast scan of the IR spectrum of **A** gave peaks located at 2234 cm^{-1} [ν(As—H)]; 1319, 1285 and 1222 cm^{-1} [ν(C—F)]; 994 cm^{-1} [ν(C—N)]; 873 cm^{-1} [ν(As=N)] and 724 cm^{-1} [δ(C—F)].

The iminoarsine, **A**, is therefore unstable under ambient conditions, and the decomposition products can be rationalized in terms of the following free radical mechanisms:

$$CF_3N{=}AsH \longrightarrow CF_3^{\bullet} + H^{\bullet} + As + 1/2N_2$$

$$CF_3^{\bullet} + H^{\bullet} \longrightarrow CF_3H.$$

EXPERIMENTAL

The IR spectra were recorded on a Perkin–Elmer 983G. Trifluoronitrosomethane was prepared by an established method.

Trifluoronitrosomethane (0.2759 g, 2.78 mmol) and arsine (0.2212 g, 2.80 mmol) were sealed under vacuum in a glass ampoule, which was then immersed in a −126°C slush bath. The blue colour of trifluoronitrosomethane was gradually discharged. On standing for about 10 min, the temperature of the reaction bath rose to −119°C and a metallic bluish-black solid began to form on the side of the ampoule. This reaction mixture was quickly subjected to trap-to-trap fractionation *in vacuo* to

* Author to whom correspondence should be addressed.

afford (a) water (0.0412 g, 2.28 mmol) at −60°C trap; (b) a white solid (0.0615 g) at −126°C trap (passed −96°C trap), becoming a colourless gas, **A**, on warming to room temperature and its IR spectrum gave the following peaks: 2235m, 1319vs, 1285vs, 1222vs, 994m, 873m and 724m cm^{-1}; and (c) a mixture of unreacted trifluoronitrosomethane and arsine at the liquid nitrogen trap.

Upon allowing a portion of the colourless gas, **A**, to stand in an evacuated ampoule at room temperature for about 4 min, a metallic black film appeared on the side of the ampoule. Vacuum trap-to-trap fractionation of the products gave (a) a non-condensable gas, presumably nitrogen and (b) a volatile gas trapped at the liquid nitrogen trap, whose IR spectrum which gave the following peaks 2911, 1370, 1209, 1162 and 720 cm^{-1} was similar to that of fluoroform. Its molecular weight determined by Regnault's method gave 70 g mol^{-1} (calc. for CF_3H, 70 g mol^{-1}). Elemental analysis shows that the metallic substance is solely arsenic metal.

Acknowledgements—We thank the National University of Singapore for a research grant. One of us (L.F.K.) is grateful to the University for a Research Scholarship.

REFERENCES

1. R. Appel, F. Knoll and I. Ruppert, *Angew. Chem. Int. Edn Engl.* 1980, **20**, 731.
2. E. Fluck, *Top. Phosphorus Chem.* 1980, **10**, 193.
3. A. H. Cowley, *Polyhedron* 1984, **3**, 389.
4. A. H. Cowley, J. E. Kilduff, J. G. Lasch, S. K. Mehrotra, N. C. Norman, M. Pakulski, B. R. Whittlesey, J. L. Atwood and W. E. Hunter, *Inorg. Chem.* 1984, **23**, 2582.
5. J. Escudie, C. Couret, H. Ranivonjatovo, J. Satge and J. Jaud, *Phosphorus Sulfur* 1983, **17**, 221.
6. J. Escudie, C. Couret, H. Ranivonjatovo and J. Satge, *J. Chem. Soc., Chem. Commun.* 1984, 1621.
7. A. H. Cowley, J. E. Kilduff, N. C. Norman and M. Pakulski, *J. Am. Chem. Soc.* 1983, **105**, 4845.
8. A. H. Cowley, J. E. Kilduff, N. C. Norman and M. Pakulski, *J. Am. Chem. Soc.* 1983, **105**, 506.
9. A. H. Cowley, J. E. Kilduff, J. G. Losch, N. C. Norman, M. Pakulski, F. Ando and T. C. Wright, *Organometallics* 1984, **3**, 1044.
10. H. G. Ang and F. K. Lee, *Polyhedron* 1989, **8**, 379.
11. H. G. Ang and F. K. Lee, *Polyhedron* 1989, **8**, 1461.
12. A. H. Dinwoodie and R. N. Haszeldine, *J. Chem. Soc.* 1965, 1675.
13. F. W. Bennett, H. J. Emeleus and R. N. Haszeldine, *J. Chem. Soc.* 1954, 3598.

Polyhedron Vol. 8, No. 19, pp. 2333–2338, 1989
Printed in Great Britain

0277–5387/89 $3.00+.00
© 1989 Pergamon Press plc

MOLYBDENUM TRICARBONYL COMPLEXES OF TRICYCLIC TRISAMINOMETHANE DERIVATIVES; SYNTHESIS AND STRUCTURAL STUDIES

STEVEN P. VAN KOUWENBERG, EDWARD H. WONG* and GARY R. WEISMAN*

Department of Chemistry, University of New Hampshire, Durham, NH 03824, U.S.A.

and

ERIC J. GABE and FLORENCE L. LEE

Chemistry Division, National Research Council of Canada, Ottawa, Canada K1A 0R9

and

PETE JACKSON

Department of Chemistry, Science Laboratories, University of Durham, South Road, Durham DH1 3LE, U.K.

(*Received* 24 *October* 1988; *accepted after revision* 31 *March* 1989)

Abstract—Reactions of the trisaminomethanes, **1** (R = H) and **2** (R = Me), with cycloheptatrienyl molybdenum tricarbonyl afforded their respective molybdenum tricarbonyl complexes; **3** and **4**. Structures of these products have been determined by X-ray diffraction studies. Complex **3** crystallizes in the monoclinic space group $P2_1/m$ with $a = 7.7364(6)$, $b = 12.505(1)$, $c = 7.774(1)$ Å, $\beta = 107.70(1)°$, $Z = 2$, μ(Mo-K_α) = 0.90 mm^{-1}. Its molybdenum coordination sphere features unusually small ligand bite angles (N—Mo—N) of 57.7(1)–58.0(1)°. The unique bridgehead methinyl hydrogen was not located, but its existence has been confirmed by IR and solid-state NMR spectroscopy. Complex **4** crystallizes in the orthorhombic space group *Pcmn* with $a = 7.7537(2)$, $b = 12.3176(4)$, $c = 15.6563(7)$ Å, $Z = 4$, μ(Mo-K_α) = 0.87 mm^{-1}. Similarly, pinched N—Mo—N angles of 58.8(1)° are observed. Significantly, the methyl to bridgehead carbon bond is shortened by 0.04 Å relative to the free ligand value, consistent with a reduced negative hyperconjugation upon complexation.

Tricyclic trisaminomethanes, having all three nitrogens bound to a common carbon, are potentially tridentate ligands. The unusually stable ligands **1** and **2**,[1–4] derived from 1,5,9-triazacyclododecane, have each been shown to be biased towards the all-*trans* configuration in solutions of non-polar solvents (Fig. 1).

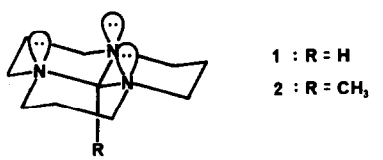

Fig. 1. All-*trans* trisaminomethanes, **1** and **2**.

In this geometry the three nitrogen lone pairs are constrained to be antiperiplanar (*app*) to C—R. Major strereochemical consequences of this upon spectra,[1–5] bond lengths[6] and reactivity[2,3,5] have already been delineated. By contrast, the donor ability and the effect of complexation upon the parent trisaminomethane geometry have not been demonstrated. We report herein the first transition metal complexes of these triaza ligands.

* Authors to whom correspondence should be addressed.

Table 1. IR and ^{13}C NMR spectral data

Compound	IR (cm^{-1})	^{13}C NMR (ppm)
1	ν_{CH}: 2939s, 2919s, 2840w, 2800m, 2795m, 2740s, 2700w, 2670m, 2600w, 2580w, 2495w, 2450w, 2430w, 2400w (CCl_4)[b]	99.8, 53.4, 23.5[a]
2	ν_{CH}: 2942s, 2920s, 2885m, 2835m, 2800s, 2780m, 2740sh, 2695w, 2658w (CCl_4)[b]	85.3, 48.1, 23.1, −0.8[a]
3	ν_{CH}: 2960m, 2940m, 2840m, 2775m ν_{CO}: 1904s, 1784sh, 1763s,	231.4 (CO), 96.0, 53.9, 24.7[c]
4	ν_{CH}: 2950m, 2930m, 2830m ν_{CO}: 1905s, 1780sh, 1745s	230.6 (CO), 93.5, 48.6, 22.4, −2.8[a]

[a] In DMSO-d_6.
[b] See ref. 4b.
[c] Solid-state.

RESULTS AND DISCUSSION

Synthesis and characterization

Reaction of cycloheptatrienyl molybdenum tricarbonyl with tricyclic trisaminomethanes, **1** and **2**, afforded the respective complexes **3** and **4** in good yields as light yellow solids which are insoluble in all but the most polar organic solvents.

The carbonyl IR stretching frequencies of **3** and **4** (Table 1) are consistent with the *fac*-$M(CO)_3$ structure, suggesting that the trisaminomethanes are indeed behaving as tridentate ligands. Interestingly, the prominent Bohlmann bands (C—H stretch *app* to N-lone pair)[7] present below 2800 cm^{-1} in **1** and **2**, including the unusually low frequency series (2400–2600 cm^{-1}) due to the methine of **1**,[3] are absent or shifted in complexes **3** and **4** (Table 1). The insolubility of **3** in most organic solvents and its decomposition in polar solvents, like DMSO, precluded determination of its solution NMR spectrum. Its solid-state MAS ^{13}C NMR spectrum, however, is readily obtained and shown in Fig. 2. Compared to the solution spectrum of the

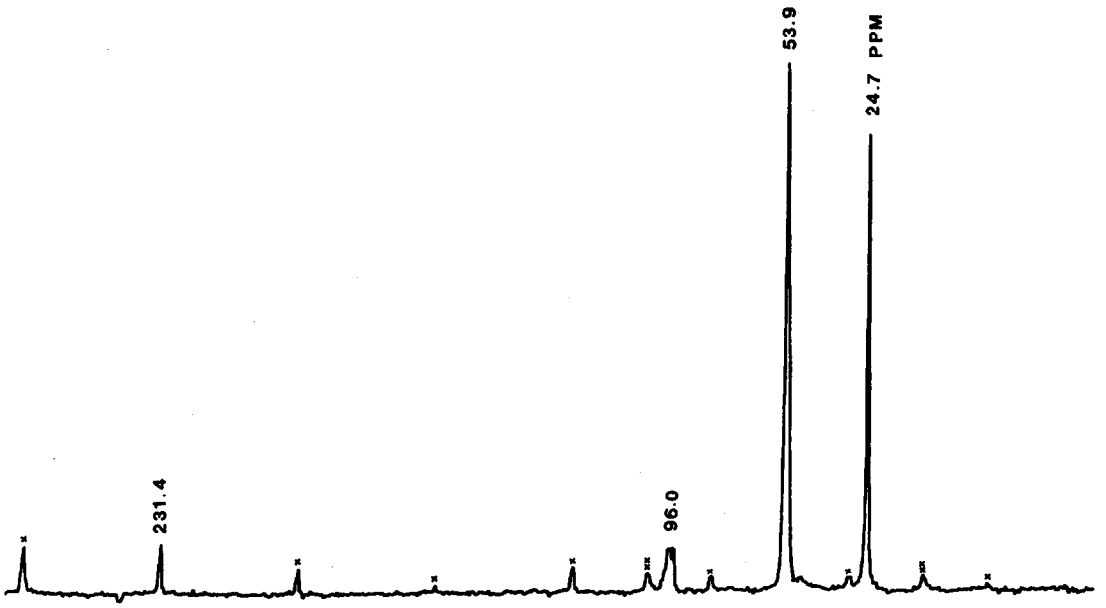

Fig. 2. Solid-state MAS ^{13}C NMR spectrum of **3** (crosses denote spinning sidebands).

free ligand **1** (Table 1), the only significant coordination shift is that of the bridgehead carbon from δ_C +99.8 in **1** to +96.0 ppm in **3**. Solution ^{13}C NMR spectral data (DMSO-d_6) for **2** and **4** are presented in Table 1. The −0.8 ppm $\delta_C(CH_3)$ of **2** in DMSO-d_6 is indicative of an approximately 2:1 equilibrium mixture of all-*trans*-**2** and *cis,cis,trans*-**2** (based upon the known methyl shifts of the individual configurations in acetone-d_6 solution).[4b] The −2.8 ppm $\delta_C(CH_3)$ of **4** (DMSO-d_6) is consistent with conversion of the ligand to the all-*trans* configuration in the complex. The lower field $\delta_C(CH_3)$ of **4** relative to that of pure all-*trans*-**2** (δ_C −6.2 ppm in acetone-d_6),[4b] is probably at least partly due to the diminution of $n_N \rightarrow \sigma^*_{C-CH_3}$ negative hyperconjugation in **4** relative to that in **2**.

Structure of complex **3**

The molecular structure of **3** has been determined and its geometry is shown in Fig. 3. Selected bond distances and angles are listed in Table 2. The molecule uses the crystallographic mirror symmetry with atoms Mo, O(1), C(1), N(1), C(7) and C(8) being on this plane. Most significant is the unusually small N—Mo—N angles of 57.7(1)–58.0(1)°. For comparison, analogous angles are 73.8(6)–87.5(6)° in (trien)Mo(CO)$_3$.[8] An average Mo—N distance of 2.40(1) Å in **3** is lengthened from the corresponding value of 2.32(1) Å in the trien complex. The tricyclic system retains the all-*trans* configuration and bond lengths are similar to those reported for the free ligand.[9] Average sums of C—N—C angles about nitrogen ($\Sigma\alpha_N$) are also very similar (332 and 331°, respectively, for **3** and **1**), indicating that the three nitrogens have not become significantly more pyramidal upon complexation. The central N—C—N angles, however, do decrease from 109.7°(av.) in **1** to 106.3°(av.) in **3**, a compression that allows the nitrogen lone pairs to converge better on the metal. This pinching is reflected in ring torsion angle changes: $\theta_{N-C-N-C}$ and $\theta_{N-C-C-C}$ are more puckered and flattened, respectively, in **3**.

The three *fac*-carbonyls are coordinated with C—Mo—C angles compressed to 82.3(2) and 84.5(2)°, smaller than the average value of 85.3(4)° in (triene)Mo(CO)$_3$.[8] The Mo—C distances are similar at 1.93 and 1.94 Å.[8]

Interestingly, molecules of **3** were found to pack in sheets featuring head-to-tail chains (Fig. 4). The unique carbonyl oxygen [O(1)] of each molecule is

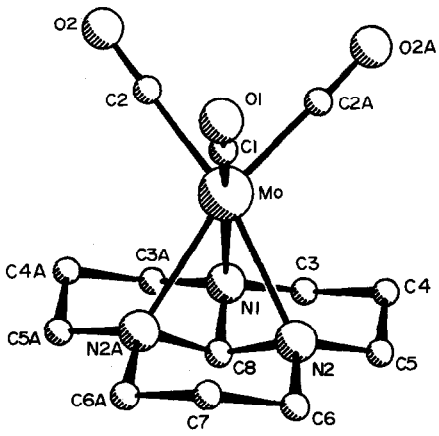

Fig. 3. Molecular structure of complex **3**.

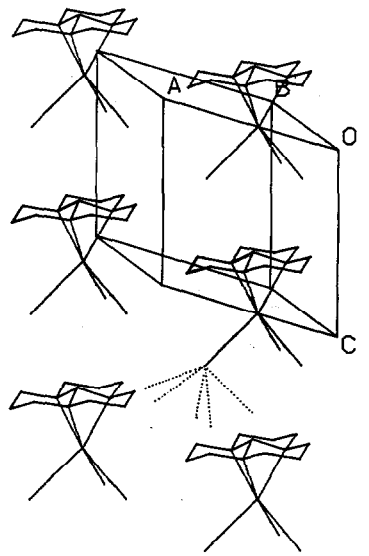

Fig. 4. Crystal packing of **3**. Only half a cell along **b**-axis is shown. Dotted lines show the five contacts from a carbonyl oxygen O(1) to CH's of neighbouring molecules.

Table 2. Selected bond distances (Å) and angles (°) for complex **3**

Mo—C(1)	1.920(4)	C(1)—Mo—C(2)	84.5(2)
Mo—C(2)	1.933(4)	C(2)—Mo—C(2A)	82.3(2)
Mo—N(1)	2.382(4)	N(1)—Mo—N(2)	58.0(1)
Mo—N(2)	2.407(3)	N(2)—Mo—N(2A)	57.7(1)
N(1)—C(8)	1.462(7)	N(1)—C(8)—N(2)	105.2(3)
N(2)—C(8)	1.460(4)	N(2)—C(8)—N(2A)	105.5(3)

positioned within 2.75–2.92 Å (dotted lines in Fig. 4) of five hydrogens from two neighbouring molecules. These include two equatorial hydrogens on C(3) and C(3A) belonging to a molecule from an adjoining chain. The other three close contacts are made with the next molecule along the same chain: two axial hydrogens on C(6) and C(6A), as well as its bridgehead methinyl hydrogen.

Although not located in the X-ray study, the existence of this methinyl hydrogen has been confirmed spectroscopically using both IR and solid-state NMR techniques. Specifically, a band at 2775 cm^{-1} in **3**, which we assign to this C—H stretch, is absent in the deuterated analogue. Solid-state ^{13}C NMR of **3** with magic angle spinning (MAS) and non-quaternary suppression (NQS) of carbon resonances resulted in the disappearance of all except the carbonyl peaks, indicating that the bridgehead C (δ +96.0) is indeed bonded to a hydrogen. Furthermore, dipolar MAS 2-D ^{13}C NMR also confirmed the presence of a single hydrogen on this carbon at a calculated distance of 1.15 Å.[10,11]

Structure of complex **4**

The molecular structure of **4** is shown in Fig. 5. Selected bond distances and angles are presented in Table 3. Again, the molecule adopts the crystallographic mirror plane with atoms Mo, O(1), C(1), N(1), C(7), C(8) and C(9) on this plane. Angles around the molybdenum atom are compressed as in **3**, with N—Mo—N at 58.8(1)° and C—Mo—C ranging from 81.0(2) to 86.3(3)°. The Mo—N distances are 2.355(4) Å, slightly shorter than those in **3**. The central N—C—N angle pinching in **4** (101°) is even more pronounced than in **3** and the nitrogens become slightly pyramidized compared to the free ligand **2** values ($\Sigma\alpha_N$ = 331 and 338°, respectively). Of special interest is the methyl to bridgehead carbon [C(8)—C(9)] distance of 1.52(1) Å. This is shortened by 0.04 Å compared to the free ligand value and is accompanied by a lengthening of the central C—N bonds, e.g. C(8)—N(1), by about 0.02 Å. The methyl to carbon bond shortening is consistent with a lessening of the dramatic negative hyperconjugative effect ($n_N \rightarrow \sigma^*_{C-CH_3}$) recently reported for free ligand **2**.[6]

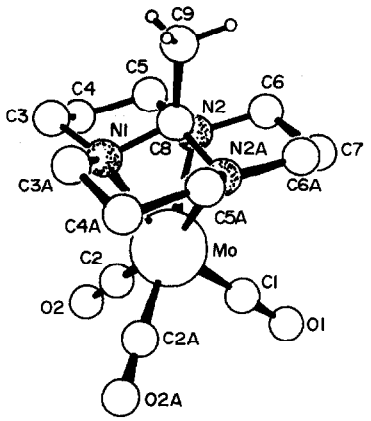

Fig. 5. Molecular structure of complex **4**.

Like **3**, the crystal packing of the molecules of **4** also results in sheets, although without head-to-tail chains (Fig. 6). Weak methyl–hydrogen interactions with two neighbouring molecules' carbonyl oxygens, including a H---O contact 0.3 Å below the van der Waals radii sum, may be responsible for this packing arrangement.[6]

EXPERIMENTAL

All reactions were carried out in a prepurified nitrogen atmosphere in standard Schlenkware. Cycloheptatrienyl molybdenum tricarbonyl,[12] 1,5,9-triazatricyclo[7.3.1.0^{5,13}]tridecane (**1**) and 13-methyl-1,5,9-triazatricyclo[7.3.1.0^{5,13}]tridecane (**2**) were prepared by literature procedures.[1–4] Methylene chloride was freshly distilled from calcium hydride. DMSO-d_6 was vacuum-distilled from CaH_2

Solution NMR were performed on JEOL-FX 90Q or Bruker AM-360 spectrometers. NMR samples were degassed and sealed under vacuum before use. Both ^1H and ^{13}C shifts were referenced to internal solvent shifts. Solid-state dipolar 2-D ^{13}C MAS NMR spectra were collected on a Bruker CXP-200 instrument operating at 50.33 MHz. Di-

Table 3. Selected bond distances (Å) and angles (°) for complex **4**

Mo—C(1)	1.901(6)	C(1)—Mo—C(2)	86.3(2)
Mo—C(2)	1.923(4)	C(2)—Mo—C(2A)	81.0(2)
Mo—N(1)	2.355(4)	N(1)—Mo—N(2)	58.8(1)
Mo—N(2)	2.355(3)	N(2)—Mo—N(2A)	58.8(1)
C(8)—C(9)	1.516(9)	N(1)—C(8)—N(2)	101.2(3)
N(1)—C(8)	1.495(7)	N(2)—C(8)—N(2A)	101.2(4)
N(2)—C(8)	1.497(5)		

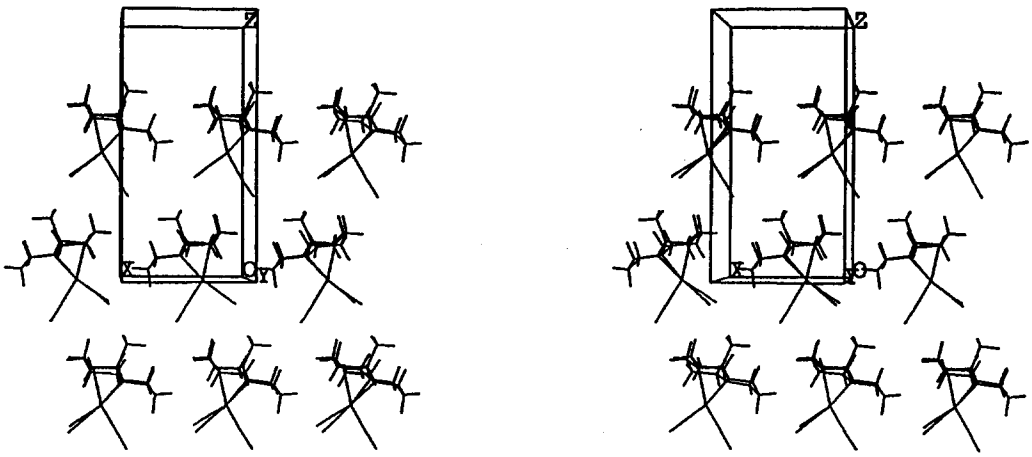

Fig. 6. A stereoview of the crystal packing of **4**.

polar 2-D spectra were acquired using the pulse sequence described by Munowitz *et al.*[10,11] Spectra were run at ambient temperature with the sample spinning at 2–3 kHz. IR spectra were recorded as KBr discs or CCl_4 solutions on a Perkin–Elmer 283B instrument. Elemental analyses were performed on a Perkin–Elmer 240 B elemental analyser.

Synthesis of complexes **3** *and* **4**

Complex **1** (100 mg, 0.55 mmol) was stirred with cycloheptatrienyl molybdenum tricarbonyl (90 mg, 0.33 mmol) in 5 cm^3 of methylene chloride. The clear red solution rapidly became turbid with precipitation of a light yellow solid. After a further hour of stirring, the suspension was filtered and washed with hexane to give 150 mg (75% yield) of **3**. Complex **4** was similarly prepared from **2** in 70% yield. Crystals for X-ray studies were grown by slow diffusion of a THF solution of the ligand into a methylene chloride solution of cycloheptatrienyl molybdenum tricarbonyl. C, H, N analyses of complex **3**: Found: C, 43.4; H, 5.5; N, 11.5. Calc. for $C_{13}H_{19}MoN_3O_3$: C, 43.2; H, 5.3; N, 11.6%. C, H, N analyses for complex **4**: Found: C, 44.7; H, 5.6; N, 11.2. Calc. for $C_{14}H_{21}MoN_3O_3$: C, 44.8; H, 5.6; N, 11.2%. ^1H NMR data at 360 MHz for **4** (DMSO-d_6): δ 1.94 (m, 12H), 1.45 (m, 6H), 1.16 (s, 3H).

X-ray diffraction study of **3**

A summary of crystal data, data refinement, and structure refinement is presented in Table 4. The intensities of a $0.2 \times 0.18 \times 0.04$ mm crystal were collected on a Nonius CAD-4 diffractometer to give a total of 1270 unique reflections of which 1153 were considered significant with $I_{net} > 2.5\sigma(I_{net})$. Cell parameters were obtained by least-squares

Table 4. Crystallographic data for complexes **3** and **4**

Complex	**3**	**4**
Formula	$C_{13}H_{19}MoN_3O_3$	$C_{14}H_{21}MoN_3O_3$
Space group	$P2_1/m$	$Pcmn$
a (Å)	7.7364(6)	7.7537(2)
b (Å)	12.505(1)	12.3176(4)
c (Å)	7.774(1)	15.6563(7)
β (°)	107.70(1)	
Z	2	4
μ (mm^{-1})	0.90	0.87
Crystal size (mm)	$0.2 \times 0.18 \times 0.04$	$0.08 \times 0.18 \times 0.18$
Radiation (Å)	Mo-K_α	Mo-K_α
Scan	θ–2θ	θ–2θ
Observed reflections	1153	1145
Measured reflections	1270	1376
R_F	0.030	0.028
R_{WF}	0.022	0.024

refinement of the setting angles of 98 reflections with $2\theta > 45°$. The molybdenum atom was located from a Patterson map. A *D*-map revealed the remainder of the structure except for the bridgehead hydrogen. The structure was refined by full-matrix least-squares with non-hydrogens anisotropic and hydrogens isotropic. All calculations were performed on the NRCVAX system of programs.[13] Scattering factors were taken from the *International Tables for Crystallography*.[14] Atomic coordinates, thermal parameters and distance–angle tables are included in the supplementary material.

X-ray diffraction study of **4**

A summary of crystal data, data refinement and structure refinement is presented in Table 4. The intensities of a $0.08 \times 0.18 \times 0.18$ mm crystal were collected to give 1376 unique reflections of which 1145 were considered significant with $I_{net} > 2.5\sigma(I_{net})$. The structure was solved by direct methods and refined by full-matrix least-squares. Final atomic positions, thermal parameters and distance–angle tables are included in the supplementary material.

Acknowledgements—We acknowledge financial support from the UNH Central University Research Fund and the National Science Foundation for an instrument grant towards the purchase of the NMR spectrometers. E.H.W. is grateful to the University of Durham Research Foundation for sabbatical support.

REFERENCES

1. T. J. Atkins, *J. Am. Chem. Soc.* 1980, **102**, 6364.
2. G. R. Weisman, V. B. Johnson and R. E. Fiala, *Tetrahedron Lett.* 1980, **21**, 3635.
3. J. M. Erhardt, E. R. Grover and J. D. Wuest, *J. Am. Chem. Soc.* 1980, **102**, 6365.
4. (a) G. R. Weisman, V. B. Johnson and M. B. Cooldige, *Tetrahedron Lett.* 1981, **22**, 4365; (b) V. B. Johnson, PhD dissertation, University of New Hampshire (1982).
5. J. M. Erhardt and J. D. Wuest, *J. Am. Chem. Soc.* 1980, **102**, 6363.
6. P. Seiler, G. R. Weisman, E. D. Glendening, F. Weinhold, V. B. Johnson and J. D. Dunitz, *Angew. Chem. Int. Edn Engl.* 1987, **26**, 1175.
7. (a) F. Bohlmann, *Chem. Ber.* 1958, **91**, 2157; (b) T. A. Crabb, R. F. Newton and D. Jackson, *Chem. Rev.* 1971, **71**, 109.
8. F. A. Cotton, *Inorg. Chem.* 1965, **4**, 314.
9. R. L. Beddoes, W. D. Edwards, J. A. Joule, O. S. Mills and J. D. Street, *Tetrahedron* 1987, **43**, 1903.
10. M. G. Munowitz, R. G. Griffin, G. Bodenhausen and T. H. Huang, *J. Am. Chem. Soc.* 1981, **103**, 2529.
11. M. G. Munowitz and R. G. Griffin, *J. Chem. Phys.* 1982, **76**, 2848.
12. S. Y. Tyree, Jr., *Inorg. Synth.* 1967, **9**, 121.
13. E. J. Gabe, F. L. Lee and Y. Le Page, *Crystallographic Computing 3: Data Collection, Structure Determination, Proteins and Databases* (Edited by G. M. Sheldrick, C. Kruger and R. Goddard), p. 67. Clarendon Press, Oxford (1985).
14. *International Tables for X-ray Crystallography*, p. 99, Table 2.2B. Kynoch Press, Birmingham, U.K. (1974).

Polyhedron Vol. 8, No. 19, pp. 2339–2344, 1989
Printed in Great Britain

0277–5387/89 $3.00+.00
© 1989 Pergamon Press plc

TETRADENTATE LIGANDS FOR THE Mo—Mo QUADRUPLE BOND FROM *CIS*-COORDINATED PHOSPHONITES

E. H. WONG* and CARMEN VALDEZ

Department of Chemistry, University of New Hampshire, Durham, NH 03824, U.S.A.

and

E. J. GABE and F. L. LEE

Chemistry Division, National Research Council of Canada, Ottawa, Canada K1A 0R9

(*Received* 10 *March* 1989; *accepted* 10 *May* 1989)

Abstract—Deprotonated *cis*-$[M(CO)_4(PhPO_2)_2H_3]^-$ (M = Cr, Mo, W) are tetradentate ligands capable of displacing two carboxylate bridges each in $Mo_2(acetate)_4$ to give mixed-valent tetrametallic complexes of the type $Mo_2[M(CO)_4(PhPO_2)_2]_2^{4-}$ (M = Cr, Mo, W). The molecular structure of $(n\text{-}Bu_4N)_2H_2Mo_2[Mo(CO)_4(PhPO_2)_2]_2$ has been determined by X-ray crystallography. It crystallizes in the orthorhombic system, space group *Pbca*, with cell parameters $a = 20.858(1)$, $b = 17.131(1)$, $c = 21.072(1)$ Å, $V = 7529.14$ Å^3 and $Z = 4$. A total of 3262 reflections were considered significant and used in the refinement, yielding final $R_f = 0.056$ and $R_w = 0.063$. The tetraanion has a centre of symmetry and features a Mo^{II}—Mo^{II} bond of 2.186(2) Å spanned by two *cis*-$Mo(CO)_4(PhPO_2)_2$ metallo-ligands. Chemically, only weak interactions are found between this tetraanion and potential axial ligands like tertiary amines, pyridine, phosphine and isonitrile. Its iodination occurred at the molybdenum(0) tetracarbonyl sites with CO loss to give $Mo_2[Mo(CO)_3I_2(PhPO_2)_2]_2^{4-}$.

Metal complexes containing *cis*-coordinated phosphonites can potentially present a square or rectangular array of oxygen nucleophiles upon deprotonation (Fig. 1). Recently we have used *cis*-$[M(CO)_4(PhPO_2)_2]^{4-}$ (M = Cr, Mo, W; complexes **1**, **2**, **3**) in preparing adamantane-like cage complexes of the type $[M(CO)_4[PhPO]_4M(CO)_4]$, where the metals are linked by POP bridges.[1] Since P—O ligands with their soft/hard donor combination are known for their ability to bridge heterometallic and mixed-valent centres,[2] we have investigated the use of **1–3** as metallo-ligands. We report here their employment as doubly-bridging groups for the quadruply-bonded Mo_2^{4+} dimer.

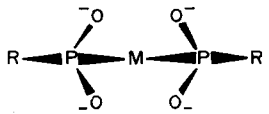

Fig. 1.

* Author to whom correspondence should be addressed.

RESULTS

Synthesis and spectra

Deprotonation of the tetrabutylammonium salts of *cis*-$[M(CO)_4(PhPO_2)_2H_3]^-$ (M = Cr, Mo, W; complexes **4**, **5**, **6**, respectively)[1] with sodium hydride in THF afforded the corresponding tetraanions: **1**, **2** and **3**. Substitution of two of these for the bridging acetates in $Mo_2(OAc)_4$ proceeded readily at room temperature:

$$2\,cis\text{-}[M(CO)_4(PhPO_2)_2]^{4-} + Mo_2(OAc)_4 \longrightarrow Mo_2[M(CO)_4(PhPO_2)_2]_2^{4-} + 4OAc^-$$

(7–9)
(M = Cr, Mo, W).

These tetrametallic products were isolated as disodium di(*n*-butylammonium) salts in moderate yields and are air-stable orange–red solids (**7**, **8**, **9** for M = Cr, Mo, W, respectively). They are soluble in polar organic solvents such as THF, DMSO,

Table 1. IR and ^{31}P NMR data

Complex	IR (KBr, cm^{-1}) ν_{CO}	ν_{PO}	$^{31}P\{^1H\}$ NMR (ppm)[a]
$Mo_2[M(CO)_4(PhPO_2)_2]_2^{4-}$ [M = Cr (**7**), Mo (**8**), W (**9**)]	1998m, 1886s, 1842s	835m,b	237.6[b]
	1999m, 1880s, 1849s	839m,b	217.3[c]
	1998m, 1875s, 1840s	839m,b	196.5[c] ($^1J_{PW}$ = 134 Hz)
$Mo_2[Mo(CO)_4(PhPO_2)_2]_2 \cdot 2DMAP^{4-}$ (**10**)	1997m, 1884s, 1870s, 1831s	848m	219.7[b]
$Mo_2[Mo(CO)_3I_2(PhPO_2)_2]_2^{4-}$ (**11**)	2002m, 1941s, 1881s,	881m	208 (broad)[b]

[a] Referenced to 85% H_3PO_4.
[b] d_6-acetone.
[c] d_6-DMSO.

acetonitrile and acetone, moderately soluble in methylene chloride, and insoluble in ether.

Typical *cis*-$M(CO)_4L_2$ carbonyl bands (C_{2v}) are observed for the tetraanionic complexes **7–9** with A_1 stretches below 2000 cm^{-1} (Table 1). Their $^{31}P\{^1H\}$ NMR spectra (Table 1) exhibited singlets which are all shifted downfield by about 70 ppm from the corresponding precursor (complexes **4–6**) values of δ 170.0, 145.5 and 120.5 ppm, respectively.[1] Electronic spectra of **7–9** featured absorptions at 338 nm ($\varepsilon = 4.4 \times 10^3$ M^{-1} cm^{-1}) for **7**, 351 nm ($\varepsilon = 9.6 \times 10^3$) for **8**, and 341 nm ($\varepsilon = 5.4 \times 10^3$) for **9**.

Structure of complex **8**

Recrystallization of **8** from methylene chloride–hexane yielded orange crystals of the tetraanion as the $(n\text{-}Bu_4N)_2H_2$ salt. Elemental analyses and ^1H NMR of the crystals confirmed the exchange of two sodium cations for two protons. Electronic and ^{31}P NMR spectra further corroborated retention of the basic Mo_2^{4+} unit. The molecular structure of the complex is shown in Fig. 2. Important bond distances and angles are listed in Table 2. The tetrametallic anion possesses an inversion centre which relates the pair of molybdenum(II) centres, Mo(1) and Mo(1a), as well as the two $Mo(CO)_4$ moieties, around Mo(2) and Mo(2a). Each *cis*-$Mo(CO)_4(PhPO_2)_2$ metallo-ligand doubly bridges the Mo_2^{4+} unit using all four oxygen donor sites. Around each molybdenum(II), the Mo—Mo quadruple bond is 2.186(2) Å, while the Mo—O distances range from 1.988(7) to 1.998(7) Å. At the zerovalent molybdenum centres, average axial Mo—CO distances are marginally longer at 2.02(2) Å compared to the equatorial average of 1.96(2) Å. Metal–phosphorus bonds average 2.518(4) Å. The tetrabutylammonium cations fill the packing vacancies and exhibit no unusual contacts with the anion.

Reactions of complex **8**

Lewis bases form only weak adducts with **8** in solution presumably by coordination at the vacant axial sites of the Mo_2^{4+} dimeric unit. For example, a $^{31}P\{^1H\}$ NMR spectrum indicated formation of a complex with pyridine (δ 214 ppm). However, no adduct could be isolated as the Lewis base was lost upon solvent evaporation. Only the better donating 4-dimethylaminopyridine (DMAP) formed an isolable 2:1 adduct, complex **10**. π-Acceptor ligands like triphenylphosphine and *t*-butylisocyanide failed to react with **8** even under forcing conditions.

Reaction of 2 equivalents of iodine with **8** resulted in CO evolution and formation of a tetramolybdenum(II) product, complex **11** ($^{31}P\{^1H\}$ NMR in THF: δ 195, broad singlet; IR (KBr): ν_{CO} 2002, 1941, 1881 cm^{-1}; ν_{PO} 881 cm^{-1}; CHN analyses consistent with $(n\text{-}Bu_4N)_2Na_2Mo_2[MoI_2(CO)_3(PhPO_2)_2]_2 \cdot 2THF$). This orange, crystalline solid rapidly decomposed with loss of CO upon standing.

DISCUSSION

Syntheses and spectra of complexes **7**, **8** *and* **9**

The feasibility of using the metallo-ligands *cis*-$[M(CO)_4(PhPO_2)_2]^{4-}$ (M = Cr, Mo, W) as tetradentate donors has been confirmed. Replacement of two carboxylates in $Mo_2(OAc)_4$ by each ligand proceeded at ambient temperature in THF. Previously, reactions of phosphinates with Mo_2^{4+} produced only polymeric species that are weakly paramagnetic and devoid of multiple bonds.[3] The chromium reaction was complete within 1 h, while

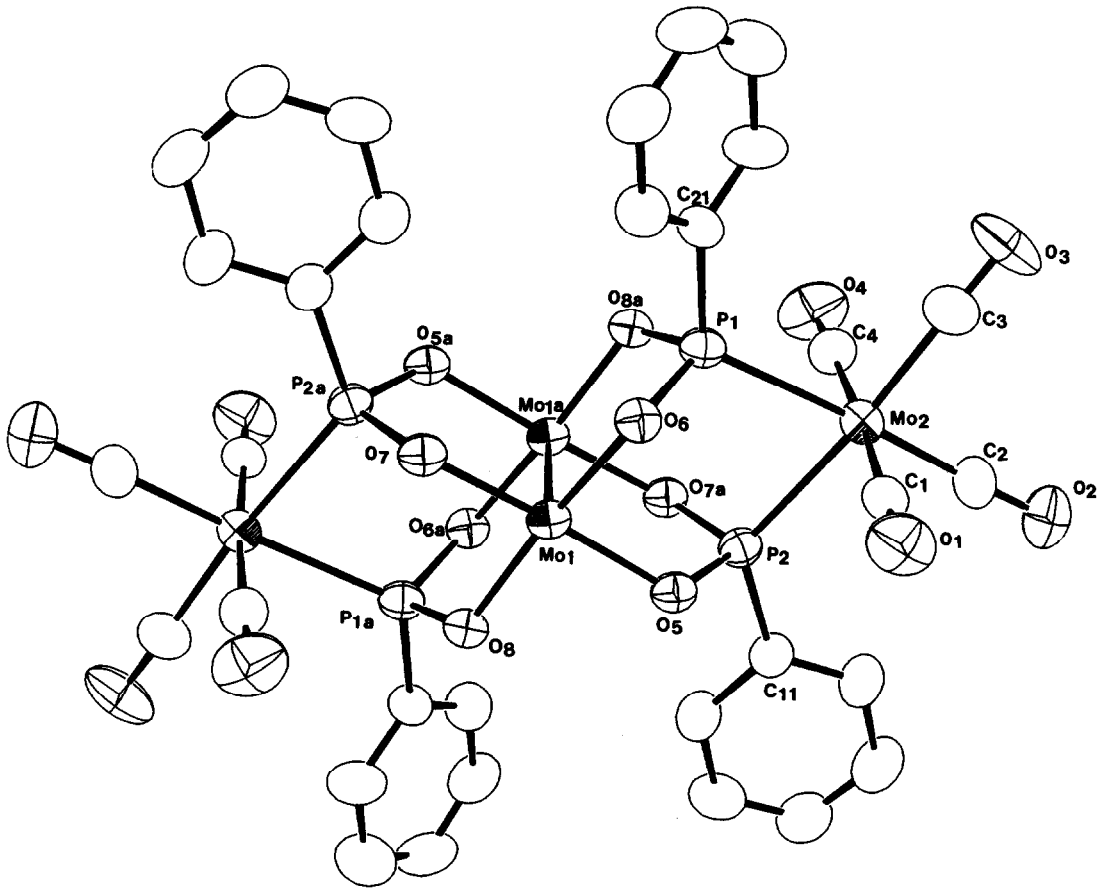

Fig. 2. Molecular structure of $Mo_2[Mo(CO)_4(PhPO_2)_2]_2^{4-}$ (**8**) with atoms at 50% probability ellipsoids.

the molybdenum and tungsten substitutions required 1 day. Monitoring of the reaction of $[Mo(CO)_4(PhPO_2)_2]^{4-}$ (**2**) with $Mo_2(OAc)_4$ by ^{31}P NMR spectroscopy revealed an intermediate resonance at δ 197 ppm in addition to singlets at 142 (**2**) and 217 (**8**). It is reasonable to assign the transient resonance to a partially-substituted intermediate:

$$Mo_2(OAc)_4 + [Mo(CO)_4(PhPO_2)_2]^{4+} \longrightarrow$$
$$2OAc^- + Mo_2(OAc)_2[Mo(CO)_4(PhPO_2)_2]^{2-}.$$

The substantial and uniform 67–76 ppm downfield coordination shift observed in the ^{31}P NMR spectra of complexes **7–9** can be attributed to the diamagnetic anisotropic deshielding of the Mo—Mo quadruple bond.[4] These chemical shifts are also solvent dependent; for example, in acetone, complex **8** has δ at 222, in THF it is at δ 217 and in pyridine at δ 214. Adduct formation at the vacant Mo_2^{4+} axial sites can be expected to reduce diamagnetic anisotropy.

Complexes **7–9** each has an absorption maximum in the region 338–351 nm with extinction coefficients of the order of 10^3 M^{-1} cm^{-1}. Burlitch and co-workers have reported an absorption at 334 nm ($\varepsilon = 6.4 \times 10^3$) for $Mo_2(S_2PEt_2)_4$.[3] As previously discussed by Trogler and Gray, assignment of these bands is problematic in the absence of polarized spectra.[5]

Structure of complex **8**

The value of 2.186(2) Å for the Mo—Mo bond in **8** is slightly longer than any other Mo—Mo quadruple bond spanned by four bridging ligands.[6] For example, $Mo_2(SO_4)_4^{4-}$ at 2.140(1) Å, $Mo_2(OAc)_4$ at 2.093(2) Å, $Mo_2(S_2PEt_2)_4 \cdot THF$ at 2.137(1) Å, $Mo_2(OSPEt_2)_4 \cdot THF$ at 2.128(2) Å and $Mo_2[O_2P(OPh)_2]_4 \cdot 2THF$ at 2.141(2) Å.[3,6,7] For comparison, $Mo_2[SO_4]_4^{3-}$ with a Mo—Mo bond order of 3.5 has a similar separation of 2.17 Å.[8] Significantly, the average Mo—O bond length in **8** at 1.99(1) Å is shorter than those in $Mo_2(OAc)_4$ (2.11(1) Å), $[Mo_2(SO_4)_4]^{4-}$ (2.14(1) Å), $Mo_2(OSPEt_2)_4 \cdot THF$ (2.15(3) Å), $Mo_2[O_2P(PEt)_2]_4$ (2.15 Å), and is at least as short as the 2.01(1) Å found in the triply-bonded dimolybdenum(III)

Table 2. Selected bond distances (Å) and angles (°) for complex **8**

Mo(1)—Mo(1a)	2.186(2)	P(1)—O(6)	1.603(8)
Mo(1)—O(5)	1.988(7)	P(1)—O(8a)	1.595(8)
Mo(1)—O(6)	1.988(8)	P(1)—C(21)	1.815(12)
Mo(1)—O(7)	1.998(7)	P(2)—O(5)	1.593(8)
Mo(1)—O(8)	1.990(8)	P(2)—O(7a)	1.602(8)
Mo(2)—P(1)	2.517(3)	P(2)—C(11)	1.828(12)
Mo(2)—P(2)	2.519(4)	C(1)—O(1)	1.13(2)
Mo(2)—C(1)	2.027(15)	C(2)—O(2)	1.15(2)
Mo(2)—C(2)	1.988(15)	C(3)—O(3)	1.20(2)
Mo(2)—C(3)	1.918(16)	C(4)—O(4)	1.17(2)
Mo(2)—C(4)	2.001(16)		
Mo(1a)—Mo(1)—O(5)	94.7(2)	C(1)—Mo(2)—C(2)	91.7(5)
Mo(1a)—Mo(1)—O(6)	94.5(2)	C(1)—Mo(2)—C(3)	91.6(6)
Mo(1a)—Mo(1)—O(7)	94.3(2)	C(1)—Mo(2)—C(4)	176.2(6)
Mo(1a)—Mo(1)—O(8)	94.5(2)	C(2)—Mo(2)—C(3)	88.2(6)
O(5)—Mo(1)—O(6)	86.3(3)	C(2)—Mo(2)—C(4)	89.5(6)
O(5)—Mo(1)—O(7)	170.9(3)	C(3)—Mo(2)—C(4)	92.0(6)
O(5)—Mo(1)—O(8)	91.9(3)	Mo(2)—P(1)—O(6)	112.3(3)
O(6)—Mo(1)—O(7)	91.9(3)	Mo(2)—P(1)—O(8a)	110.0(3)
O(6)—Mo(1)—O(8)	170.9(3)	Mo(2)—P(1)—O(21)	125.1(4)
O(7)—Mo(1)—O(8)	88.5(3)	O(6)—P(1)—O(8a)	102.8(4)
P(1)—Mo(2)—P(2)	79.46(10)	O(6)—P(1)—C(21)	100.7(5)
P(1)—Mo(2)—C(1)	90.2(3)	O(8a)—P(1)—C(21)	103.5(5)
P(1)—Mo(2)—C(2)	174.5(5)	Mo(2)—P(2)—O(5)	114.1(3)
P(1)—Mo(2)—C(3)	96.9(4)	Mo(2)—P(2)—O(7a)	110.8(3)
P(1)—Mo(2)—C(4)	88.3(4)	Mo(2)—P(2)—C(11)	121.5(5)
P(2)—Mo(2)—C(1)	89.6(4)	O(5)—P(2)—O(7a)	103.0(4)
P(2)—Mo(2)—C(2)	95.3(5)	O(5)—P(2)—C(11)	101.6(5)
P(2)—Mo(2)—C(3)	176.2(4)	O(7a)—P(2)—C(11)	103.8(5)
P(2)—Mo(2)—C(4)	86.7(4)	Mo(2)—C(1)—O(1)	179(1)
Mo(1)—O(5)—P(2)	118.1(4)	Mo(2)—C(2)—O(2)	178(1)
Mo(1)—O(6)—P(1)	119.1(4)	Mo(2)—C(3)—O(3)	176(1)
Mo(1)—O(7)—P(2a)	117.4(4)	Mo(2)—C(4)—O(4)	178(1)
Mo(1)—O(8)—P(1a)	118.8(8)		

anion $[Mo_2(HPO_4)_4]^{2-}$.[3,6,9] The formally dianionic $PhPO_2$-bridging ligand should be significantly more electron-rich than the monanionic $(PhO)_2PO_2$ and acetate, for example. Qualitatively, mixing of oxygen lone-pairs with the Mo_2^{4+} dimer should strengthen the Mo—O bonds at the expense of Mo—Mo bonding. This is consistent with the observed structural data and the low tendency of **8** to adduct axial ligands.

Comparing the molybdenum(0) coordination geometry with that found in the $[Mo(CO)_4[PhPO]_4Mo(CO)_4]$ cage complex,[1] we note the slightly lengthened Mo—P distance at 2.518(4) Å vs 2.435(2) Å. Otherwise, metal–carbonyl geometrical data are quite similar. Using Kepert's definition of ligand bite angle ($b = 2\sin(\theta/2)$, where θ is the P—Mo—P angle), each molybdenum(0) centre in **8** is chelated by a diphosphine ligand with a b value of 1.27.[10]

Reactions of complex **8**

Like its precursor, $Mo_2(OAc)_4$, **8** appears to have little tendency to form stable axial adducts with hard donors.[8] Only the strong σ-donor 4-dimethylaminopyridine afforded an isolable 2:1 adduct, complex **10**. In contrast to $Mo_2(OAc)_4$,[8] complex **8** is also inert to π-acid ligands. Neither triphenylphosphine nor butylisonitrile gave any indication of adduct formation.

Halogenation oxidation of **8** could occur at either the molybdenum(0) or the molybdenum(II) dimeric unit. Iodination clearly resulted in oxidative elimination at the $Mo(CO)_4$ sites. Spectral and analytical data are consistent with the product being $Mo_2[Mo(CO)_3I_2(PhPO_2)_2]_2^{4-}$ (**11**). In contrast to **8**, this readily crystallizes with two molecules of THF, presumably in the axial positions. Variable-temperature $^{31}P\{^1H\}$ NMR of **10** in d_6-acetone

Table 3. Elemental analytical data

Complex	Calculated %C	%H	%N	Found %C	%H	%N
7	47.7	5.7	1.7	48.0	6.0	1.7
8	45.2	5.4	1.6	45.2	5.7	1.7
9	41.2	4.9	1.5	40.9	5.3	1.4
10	48.2	5.8	4.3	48.0	5.9	4.2
11	36.6	4.7	1.2	36.3	4.7	1.2

showed a limiting spectrum at −45°C of a singlet at δ 195.1 ppm, as well as a smaller set of AB doublets at δ 202.2 and 190.0 ppm ($J = 83$ Hz). While structural details are not yet available, the ligand bite angle of **8** ($b = 1.27$) would suggest capped trigonal prism or capped octahedron as most likely geometries at the seven-coordinate $Mo(CO)_3I_2P_2$ centres (Fig. 3).[10] Complex **11** is very unstable towards CO loss upon exposure to air, completely decomposing to a poorly-characterized dark grey residue after 24 h.

EXPERIMENTAL

All operations were carried out under an atmosphere of prepurified nitrogen using standard Schlenk techniques. Solvents were dried by conventional methods and distilled under nitrogen. (n-Bu_4N)$M(CO)_4(PhPO_2)_2H_3$ (M = Cr, Mo, W) were prepared from *cis*-$M(CO)_4(PhPCl_2)_2$ as described previously.[1] $Mo_2(OAc)_4$ was synthesized according to the literature procedure.[8]

NMR spectra were recorded on a Bruker AM-360, JEOL-FX90Q, or a Varian 360A. IR spectra were run on a Perkin–Elmer 283B instrument. Electronic spectra were recorded using a Cary 219 spectrophotometer. Elemental analyses were performed at the University Instrumentation Center with a Perkin–Elmer 240B Elemental Analyser and the results are included in the supplementary material. All compounds below gave satisfactory (within 0.4%) carbon, hydrogen and nitrogen analyses.

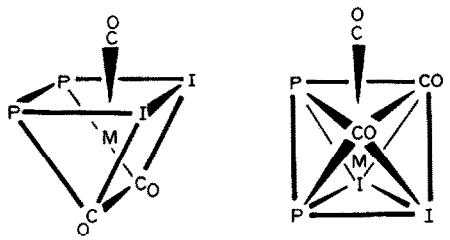

Fig. 3. Possible geometries at the $Mo(CO)_3I_2P_2$ portions of complex **11**.

Synthesis of (n-Bu_4N)$_2Na_2Mo_2[Cr(CO)_4(PhPO_2)_2]_2$ (**7**)

(n-Bu_4N)$Cr(CO)_4(PhPO_2)_2H_3$ (1.452 g, 2.1 mmol) was dissolved in THF (25 cm^3). Sodium hydride (*ca* 1 g of a 50% dispersion in oil) was added and the suspension stirred until effervescence ceased. The excess NaH was filtered off with a sintered-glass frit and $Mo_2(OAc)_4$ (0.226 g, 0.5 mmol) was added to the filtrate. The solution colour changed from yellow–brown to red. After 1 h of stirring, a white solid (NaOAc) was removed by filtration and 5 cm^3 of toluene was added to the filtrate. A brown solid was obtained. This was filtered off and recrystallized from THF–ether to give brown, rectangular crystals of **7** (0.39 g, 53% yield).

Synthesis of (n-Bu_4N)$_2Na_2Mo_2[Mo(CO)_4(PhPO_2)_2]_2$ (**8**), *and* (n-Bu_4N)$_2Na_2Mo_2[W(CO)_4(PhPO_2)_2]_2$ (**9**)

Complexes **8** and **9** were prepared as above from the respective (n-Bu_4N)$M(CO)_4(PhPO_2)_2H_3$ salt, except that the reaction mixtures were allowed to stir at ambient temperature for 24 h. Yield of **8** is 65% of orange crystals. The yield of **9** is 40% of orange microcrystals.

Synthesis of (n-Bu_4N)$_2Na_2Mo_2[Mo(CO)_4(PhPO_2)_2]_2 \cdot 2$DMAP (**10**)

Complex **8** (0.209 g, 0.125 mmol) was dissolved in 10 cm^3 of THF. Dimethylaminopyridine (0.032 g, 0.258 mmol) was added and the solution stirred for 1 h. The orange precipitate was filtered off, washed with THF and dried to give **10** (0.165 g, 68% yield).

Synthesis of (n-Bu_4N)$_2Na_2Mo_2[Mo(CO)_3I_2(PhPO_2)_2]_2 \cdot 2$THF (**11**)

Complex **8** (0.163 g, 0.09 mmol) was dissolved in 10 cm^3 of THF. With stirring, iodine (0.049 g, 0.19 mmol) was added and effervescence and darkening of the solution was observed. After 2 h, the suspension was filtered, the residue washed with THF and dried to give **11** (0.136 g, 70% yield). This orange, crystalline solid readily decomposed upon air-exposure to give a dark grey powder.

X-ray structural determination of (n-Bu_4N)$_2H_2Mo_2[Mo(CO)_4(PhPO_2)_2]_2$ (**8**)

Crystals of **8** were grown from methylene chloride–hexane by layering in a Schlenk tube. ^{1}H NMR of the resulting red–brown crystals in d_6-

Table 4. Crystallographic data for complex **8**

Formula	$C_{64}H_{94}Mo_4N_2O_{16}P_4$
Space group	*Pbca*
Crystal system	Orthorhombic
a (Å)	20.858(1)
b (Å)	17.131(1)
c (Å)	21.072(1)
Cell volume (Å^3)	7529.14
D_{calc} (g cm^{-3})	1.419
μ (mm^{-1})	0.78
Z	4
Radiation (Å)	Mo-K_α
Data collected	$0° < \theta < 50°$
Scan	θ–2θ
Unique reflections	6654
Observed reflections	3262
$F(000)$	2918.98
Dimensions (mm)	$0.25 \times 0.4 \times 0.4$
R_F	0.056
R_{WF}	0.063

acetone revealed the presence of two protons (δ 2.79 in d_6-acetone) which have been exchanged for the two sodium cations during the recrystallization. Elemental analyses (Table 3): Calc. for $C_{64}H_{94}Mo_4N_2O_{16}P_4$: C, 46.44; H, 5.68; N, 1.69. Found: C, 46.18; H, 5.76; N, 1.66%. An ethanol solution of the crystals has an absorption maximum at 350 nm in the visible region. Its ^{31}P NMR singlet signal was found at +222.5 ppm (d_6-acetone). Furthermore, ^{31}P NMR of a mixture of **8** before and after recrystallization gave a *single* resonance at +222.5 ppm in acetone. This is possible only if the Mo_2^{4+} unit has remained intact. A summary of crystal data, data refinement and structure refinement is presented in Table 4. The intensities of a $0.2 \times 0.40 \times 0.40$ mm crystal were collected with monochromatized Mo-K_α radiation using the θ–2θ scan technique and line profile analysis.[11] 6654 unique reflections were collected, of which 3262 were judged significant at the 3σ(Inet) level. Corrections were applied for Lorentz and polarization effects but absorption corrections were not made ($\mu = 0.78$ mm^{-1}).[12] Cell parameters were obtained from the setting angles of 56 reflections with $2\theta > 40°$. The structure was solved by MULTAN and hydrogen positions were calculated. The structure was refined by full-matrix least-squares to final residuals of $R_F = 0.056$ and $R_{WF} = 0.063$. The final atomic positional parameters of non-hydrogen atoms and equivalent isotropic thermal factors, as well as complete bond distance and angle tables are included in the supplementary materials.

Acknowledgements—We thank the donors of the Petroleum Research Fund, administered by the American Chemical Society, for financial support. An instrument grant from the National Science Foundation towards the purchase of the medium-field NMR spectrometer is also acknowledged. Professor D. G. Nocera of Michigan State University graciously communicated structural data.

REFERENCES

1. E. H. Wong, M. M. Turnbull, K. D. Hutchinson, C. Valdez, E. J. Gabe, F. L. Lee and Y. Le Page, *J. Am. Chem. Soc.* 1988, **110**, 8422.
2. See, for example: (a) I. Haiduc and I. Silaghi-Dumitrescu, *Coord. Chem. Rev.* 1986, **74**, 127; (b) J. R. Allan, J. Halfpenny, G. H. W. Milburn, T. A. Stephenson and P. M. Veitch, *J. Chem. Res. S* 1986, 270; (c) D. M. Roundhill, R. P. Sperline and W. B. Beaulieu, *Coord. Chem. Rev.* 1978, **26**, 263.
3. J. H. Burk, G. E. Whitwell, J. T. Lemley and J. M. Burlitch, *Inorg. Chem.* 1983, **22**, 1306.
4. (a) H. M. McConnell, *J. Chem. Phys.* 1957, **27**, 226; (b) J. San Filippo Jr, *Inorg. Chem.* 1972, **11**, 3140.
5. W. C. Trogler and H. B. Gray, *Accts Chem. Res.* 1978, **11**, 232.
6. (a) I.-I. Chang and D. G. Nocera, *Abstract INORG* 465, ACS National Meeting in New Orleans (1987); (b) D. G. Nocera, Michigan State University, private communication.
7. J. R. Morrow and W. C. Trogler, *Inorg. Chem.* 1989, **28**, 615.
8. F. A. Cotton and R. A. Walton, *Multiple Bonds between Metal Atoms*. Wiley, New York (1982).
9. A. Bino and F. A. Cotton, *Inorg. Chem.* 1979, **18**, 3562.
10. D. L. Kepert, *Prog. Inorg. Chem.* 1977, **23**, 67.
11. Y. Le Page, E. J. Gabe and L. D. Calvert, *J. Appl. Cryst.* 1979, **12**, 25.
12. A. C. Larson and E. J. Gabe, *Computing in Crystallography*, p. 81. Delft University Press (1978).

Polyhedron Vol. 8, No. 19, pp. 2345–2349, 1989
Printed in Great Britain

0277–5387/89 $3.00+.00
© 1989 Pergamon Press plc

COMPLEXES OF 3,4-DIHYDROXYPHENYL DERIVATIVES—X.* COPPER(II) COMPLEXES OF CHLOROGENIC ACID AND RELATED COMPOUNDS

TAMAS KISS,† GIZELLA NAGY and MAGDOLNA PÉCSI

Department of Inorganic and Analytical Chemistry, Kossuth University, 4010 Debrecen, Hungary

and

HENRYK KOZLOWSKI

Institute of Chemistry, University of Wrocław, Joliot-Curie 14, 50-383 Wrocław, Poland

and

GIOVANNI MICERA and LILIANA STRINNA ERRE

Dipartimento di Chimica, Universita' di Sassari, Via Vienna 2, 07100 Sasaari, Italy

(*Received* 16 *January* 1989; *accepted* 4 *May* 1989)

Abstract—The interactions of copper(II) with chlorogenic acid [1,3,4,5-tetrahydroxycyclohexanecarboxylic acid 3-(3,4-dihydroxycinnamate)] and related compounds such as 3,4-dihydroxyphenylacetic acid (3,4-DHPA), 3,4-dihydroxyphenylpropionic acid (3,4-DHPP) and *trans*-3-(3,4-dihydroxyphenyl)propenoic acid (caffeic acid) in aqueous solution have been investigated by pH-metric and spectroscopic (ESR and electronic absorption) methods. It has been found that these ligands exhibit a real ambidentate character, i.e. in addition to the chelation via the catecholate sites, the separated carboxylate can also coordinate to the copper(II) ion. The simultaneous coordination of both types of binding sites leads to the formation of various oligomeric species.

Phenolic hydroxyl-containing ligands, which are known to be present in the root exudates, may participate in the transport processes of metal ions from the surrounding soil to the plant roots.[1,2] Of special interest are *trans*-3-(3,4-dihydroxyphenyl)propenoic acid (caffeic acid), which is believed to participate in the transport and in the reduction of iron(III) to iron(II) in the soil environment,[1] and chlorogenic acid [1,3,4,5-tetrahydroxycyclohexanecarboxylic acid 3-(3,4-dihydroxycinnamate)], which is a precursor of caffeic acid.

Earlier studies on the binding ability of caffeic acid[3,4] and chlorogenic acid[5] came to contradicting conclusions. Linder and Voye[3] concluded that caffeic acid easily forms oligomeric structures with copper(II) ions, while Bizri *et al.*[4] and Lamy *et al.*[5] found only simple monomeric complexes, probably involving the catechol-type of coordination. Recent results on several dihydroxybenzoic acids have provided strong evidence that both the catechol and the carboxyl sites may be involved in the copper(II) ion binding,[6–8] and different dimeric or trimeric complexes can be formed.[6]

In this paper the pH-metric results on chlorogenic and caffeic acids and some other 3,4-dihydroxybenzoic acid derivatives (3,4-DHPA, 3,4-DHPP) confirm the speciation model of Linder and Voye[3] and extends it by measuring spectroscopic (absorption and ESR) properties of the complexes formed in order to characterize their bonding modes.

* Part IX: T. Kiss, I. Sóvágó and R. B. Martin, *J. Am. Chem. Soc.* 1989, **111**, 3611.

† Author to whom correspondence should be addressed.

EXPERIMENTAL

Potentiometric studies

Stability constants for proton and copper(II) complexes were determined by pH-metric titration of 25 cm^3 samples. The concentration of the ligand in the samples was 0.004 or 0.002 mol dm^{-3}. Metal-to-ligand molar ratios of 1 : 1, 1 : 1.5, 1 : 2, 1 : 4 and 1 : 6 were used in the titrations and the ionic strength was adjusted to 0.2 mol dm^{-3} with KCl. The titrations were performed in the pH range from 2.7 till precipitation, up to a pH between 5 and 8 depending on the ligand excess. The precipitates were analysed by AAS and it was found that the metal ion-to-ligand ratios were around 1.3–1.4 : 1, which suggested the formation of polynuclear species.

The pH was measured with a Radiometer pHM 64 instrument with G2040B glass and K4040 calomel electrodes, in a TTA 80 titration unit in an argon atmosphere. The electrode system was calibrated by the method of Irving *et al.*[9] In all cases the temperature was 25°C. The concentration stability constants were calculated using the PSEQUAD computer program.[10]

Spectroscopic studies

Absorption spectra were recorded on a Beckman Acta MIV spectrophotometer, and ESR spectra (X-band) were measured on a Varian E 9 spectrometer at 110 K. The measurements were made under argon with concentrations similar to those used in the potentiometric studies.

RESULTS AND DISCUSSION

Proton complexes

The proton dissociation constants of the ligands are listed in Table 1, together with some reference data. The data shows that the COOH group of chlorogenic acid is more acidic than that of the other ligands, due to the adjacent alcoholic hydroxyl function. Similarly, as with simple diphenol catechol, both phenolic groups of the ligands undergo dissociation at pH below 13.5 (Table 1). The very weak acidity of the third dissociable proton can be attributed to the electrostatic attraction of the adjacent negative charge and to hydrogen-bond formation involving the phenolic hydroxyl proton.

Copper(II) *complexes*

Evaluation of the copper(II)–ligand titration curves with the assumption of only monomeric complexes resulted in a set of five species: $CuAH_2$, CuAH, CuA, $CuAH_{-1}$ and CuA_2 (A denotes the completely deprotonated ligand). The fit between the experimental and the calculated titration curves, however, was not satisfactory, and other speciation models were therefore tried in the calculation (see later). The $CuAH_2$ species, which has two phenolic hydroxyl groups protonated, involves only the carboxylate donors in metal coordination. This species is clearly seen in the ESR spectra at below pH 5, with $g_{\parallel} = 2.36$–2.37 and $A_{\parallel} = (154$–$157) \times 10^{-4}$ cm^{-1}. The spectra also allowed the identification of the species CuA and CuA_2 involving the cate-

Table 1. Proton dissociation constants for the 3,4-dihydroxyphenyl derivatives and for some reference compounds; $t = 25$°C and $I = 0.2$ mol dm^{-3} (KCl)

Ligand	$pK_{(COOH)}$	$pK_{(OH1)}$	$pK_{(OH2)}$	Reference
3,4-DHPA	4.12±0.01	9.33±0.01	13.0±0.13	This work
3,4-DHPP	4.45±0.01	9.43±0.01	13.7±0.17	This work
Caffeic acid	4.37±0.01	8.55±0.01	12.5±0.14	This work
	4.41	8.72		3
	4.45	8.66	11.8	4
Chlorogenic acid	3.35±0.02	8.21±0.02	12.5±0.15	This work
	3.37	8.27	11.5	5
Phenylacetic acid	4.31			14
Phenylpropionic acid	4.66			14
Phenylpropenoic acid	4.42			14
Catechol		9.28	13.0	13

Table 2. ESR spectroscopic data for the copper(II) complexes of the 3,4-dihydroxyphenyl derivatives

Species	$g_\parallel$	$A_\parallel$ (10^{-4} cm^{-1})	$g_\parallel$	$A_\parallel$ (10^{-4} cm^{-1})
Caffeic acid			3,4-DHPA	
$CuAH_2$	2.360	154	2.363	155
CuA	2.323	173	2.311	170
CuA_2	2.249	202	2.251	202
$CuAH_{-1}$	2.280	186	2.276	189
Cu_2A_3	2.249	202	2.251	202
	2.282	182	2.279	183
Cu_3A_2			2.340	164
			2.315	173
Chlorogenic acid			3,4-DHPP	
$CuAH_2$	2.365	154	2.368	157
CuA	2.305	172	2.313	172
CuA_2	2.247	202	2.251	202
$CuAH_{-1}$			2.282	189
Cu_3A_2			2.339	162
			2.316	170

cholate-type of coordination (see Table 2). The ESR parameters are very close to those found earlier for the same type of coordination (see for example ref. 7). $CuAH_{-1}$ is presumably a mixed hydroxo complex formed by the hydrolysis of CuA. The species CuAH might have different donor atom arrangements. The ligands can coordinate to the copper(II) ion via their phenolate groups, with a protonated side-chain carboxylic group.[4,5] The pK values of the CuAH complexes, however, are much higher (see pK_{CuAH} values in Table 3) than those of the carboxylic group of the free ligands (see Table 1). Since the catechol and carboxylic terminals of the ligands are very distant from each other, the observed decrease in acidity cannot be attributed to the electron-releasing effect of the coordinated phenolate groups. Linder and Voye[4] suggested chelation via the singly protonated catecholate site. This bonding mode has not been found for the copper(II) complexes of other 3,4-dihydroxyphenyl derivatives, with the only exception being copper(II) 3,4,-di-*t*-butylpyrocatechol,[11] in which the low solubility of the complexes formed did not allow a very precise equilibrium study, however. When evaluating the titration data, we found that, through the assumption of a dinuclear complex Cu_2A, this monoprotonated species could be omitted completely without any significant decrease in the fitting parameter. The simultaneous metal ion coordination to both carboxyl and catechol sites and the formation of oligomeric complexes seems to be a general tendency for ligands possessing two coordinating sites.[3,6,12,13] The assumption of other

Table 3. Stability constants for the copper(II) complexes of the 3,4-dihydroxyphenyl derivatives; $t = 25°C$ and $I = 0.2$ mol dm^{-3} (KCl)

Species	3,4-DHPA	3,4-DHPP	Caffeic acid			Chlorogenic acid	
log β values							
$CuAH_2$	24.4±0.05	23.3±0.09	23.3±0.05	22.96[a]		23.3±0.05	
CuA	13.5±0.02	14.1±0.05	12.7±0.02	12.75[a]	12.85[b]	13.6±0.03	12.39[c]
$CuAH_{-1}$	5.9±0.09	6.2±0.11	4.9±0.09				
CuA_2	22.1±0.08	23.4±0.15	20.2±0.15		22.74[b]	24.2±0.05	22.12[c]
Cu_2A	17.2±0.04	17.8±0.03	16.4±0.07	16.04[a]		16.7±0.08	
Cu_2A_3	40.5±0.08	41.5±0.09	38.0±0.13	38.47[a]		40.5±0.32	
Cu_3A_2	34.5±0.05	35.2±0.07	32.2±0.36	32.41[a]			
$(CuAH)^b$	(19.6±0.05)	(20.4±0.04)	(18.5±0.08)	18.52[a]	17.83[b]	(18.5±0.05)	16.65[c]
log K values							
$Cu+AH_2 = CuAH_2$	2.06	2.19	2.17	1.74[a]		2.18	
$Cu+CuA = Cu_2A$	3.69	3.75	3.68	3.29[a]		3.15	
$2CuA+A = Cu_2A_3$	13.43	13.44	12.53	12.97[a]		13.36	
$CuA+Cu_2A = Cu_3A_2$	3.68	3.35	3.08	3.62[a]			
$\log(K_1/K_2)$	5.01	4.74	5.23		2.96[b]	2.93	2.66[c]
pK_{CuA}	7.67	7.81	7.81				
$(pK_{CuAH})^d$	(6.12)	(6.63)	(4.67)	4.44[a]	4.98[b]	(4.88)	4.26[c]

[a] Calculated from the data in ref. 3 by assuming $pK_{OH} = 12.5$.
[b] Reference 4.
[c] Reference 5.
[d] The stability constant calculated by assuming CuAH as a real species (see text for details).

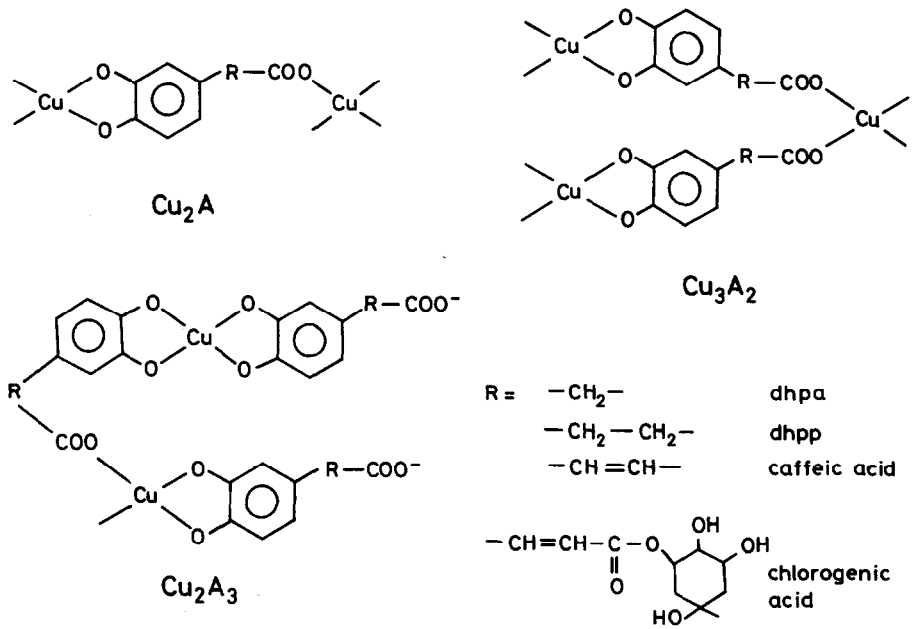

Scheme 1.

oligomeric complexes, such as Cu_2A_3 and Cu_3A_2, improved the fitting by about 50–80% and it then fell within the limits of experimental error. The formation of such species was suggested in the copper(II)–caffeic acid[3] and in the copper(II)–3,4-DHB systems.[6]

As an illustration, the concentration distribution curves of the complexes formed in the copper(II)–3,4-DHPA and in the copper(II)–chlorogenic acid systems are depicted in Figs 1 and 2. The spectroscopic results are in good agreement with the coordination modes suggested. For example, the signals detected in the formation pH range of the species Cu_3A_2 and Cu_2A_3 of 3,4-DHPA and 3,4-DHPP exhibit parameters which may be assigned to the following donor sets: $g_\parallel = 2.34$ and $A_\parallel = (162–164) \times 10^{-4}$ cm^{-1} to (COO^-,COO^-); $g_\parallel = 2.31–2.32$ and $A_\parallel = (170–173) \times 10^{-4}$ cm^{-1} to (O^-,O^-); $g_\parallel = 2.25$ and $A_\parallel = 202 \times 10^{-4}$ cm^{-1} to $2 \times (O^-,O^-)$; and $g_\parallel = 2.28$ and $A_\parallel = 183 \times 10^{-4}$

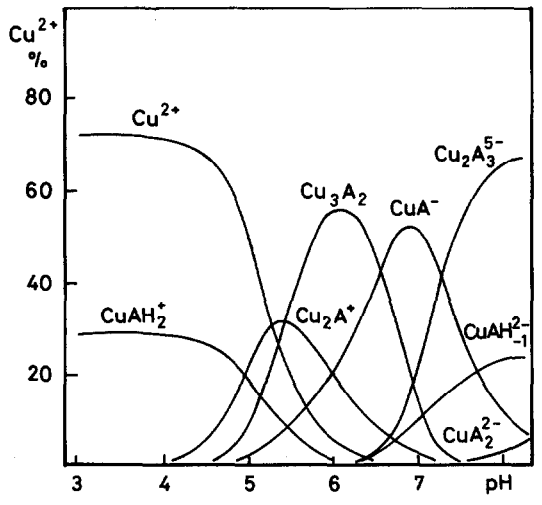

Fig. 1. Concentration distribution curves of the complexes formed in the copper(II)–3,4-DHPA system as a function of pH. $C_{Cu} = 0.002$ mol dm^{-3} and $C_{ligand} = 0.004$ mol dm^{-3}.

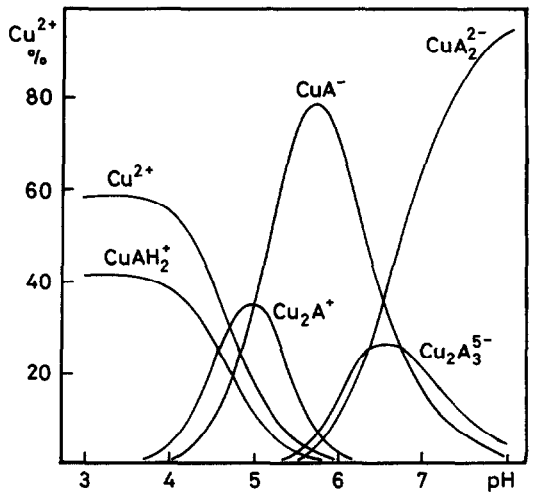

Fig. 2. Concentration distribution curves of the complexes formed in the copper(II)–chlorogenic acid system as a function of pH. Details as in Fig. 1.

cm^{-1} to (O^-,O^-,COO^-) (see Table 2). As expected, the parameters of the various coordination modes in the oligonuclear species are almost the same as those for the corresponding chromophores in the monomeric species.

It can be seen from Table 3 and Figs 1 and 2 that, compared with the other 3,4-dihydroxyphenylcarboxylates, chlorogenic acid has a lower tendency to form oligomeric species. It behaves as a catechol derivative with a subordinate possibility of carboxylate coordination. Accordingly, the $\log(K_1/K_2)$ value characteristic for the stepwise formation of the (O^-,O^-)-coordinated complexes corresponds well with that for catechol ($\log K_1/K_2 = 2.95$).[13] With the other ligands, as shown in Fig. 1, the trimeric species Cu_3A_2 is formed in significant concentration in the pH range 5–6. In this species, the copper(II) ion acts as a link between two CuA species by coordinating to the carboxylate sites. At higher pH values, the major species is the dinuclear complex Cu_2A_3, and the monomeric bis-catecholato complex CuA_2 is formed only in very low concentration. This means that the enhanced tendency towards the formation of oligomeric species hinders the simple catecholate coordination of the second ligand, which instead behaves as a bridge between two CuA species by coordinating to them via both metal binding sites.

The preferred formation of these oligomeric complexes is also reflected in the equilibrium constants calculated for the various part processes (see Table 3). The data show that the copper(II)–COO^- interaction is stronger if the coordinating ligand is already bound to copper(II) at the catecholate site.

In the electronic spectra the appearance of a charge-transfer band (range 365–420 nm) above pH 5, characteristic of the copper(II)–phenolate interaction, is an indication that catecholate bonding modes are involved in the coordination. The strong absorption of chlorogenic acid and caffeic acid in the 400 nm region did not allow the catecholate coordination to be followed via this charge-transfer transition. The *d–d* absorption maxima corresponding to the principal chromophores involved in coordination are similar to those already reported,[7] and they are particularly observed around 730 nm for (O^-,O^-), 620 nm for $2\times$(O^-,O^-) and 680 nm for (O^-,O^-,OH^-), though a precise evaluation of the molar absorptivity values was generally not possible.

The results presented above clearly indicate the ambidentate nature of these 3,4-dihydroxycarboxylates in their copper(II) complexes. Hence, besides chelation via the catecholate site, the separated carboxylate can also take part in the coordination, by forming monomeric complexes at low pH and oligomeric complexes (in which both binding sites of the ligands are involved in the coordination) at higher pH values.

Acknowledgements—This work was supported by the Consiglio Nazionale delle Ricerche (Rome), the Polish Academy of Sciences (Project 01.12) and the Hungarian Ministry of Education (Project 46/86).

REFERENCES

1. R. A. Olsen, J. C. Brown, J. H. Bennett and D. Bloom, *J. Plant Nutr.* 1982, **5**, 433.
2. C. L. Tipton and J. Thowsen, *Iowa State J. Res.* 1983, **57**, 409.
3. P. W. Linder and A. Voye, *Polyhedron* 1987, **6**, 53.
4. Y. Bizri, M. Cromer, I. Lamy and J. P. Scharff, *Analusis* 1985, **13**, 128.
5. I. Lamy, M. Seywert, M. Cromer and J. P. Scharff, *Anal. Chim. Acta* 1985, **176**, 201.
6. K. Gerega, H. Kozlowski, T. Kiss, G. Micera, L. Strinna Erre and F. Cariati, *Inorg. Chim. Acta* 1987, **138**, 31.
7. T. Kiss, H. Kozlowski, G. Micera and L. Strinna Erre, *Polyhedron* 1989, **8**, 647.
8. F. Cariati, L. Erre, G. Micera, A. Panzanelli, G. Ciani and A. Sironi, *Inorg. Chim. Acta* 1983, **80**, 57.
9. H. Irving, M. G. Miles and L. D. Pettit, *Anal. Chim. Acta* 1967, **38**, 475.
10. L. Zekany and I. Nagypal, in *Computational Methods for the Determination of Stability Constants* (Edited by D. Leggett). Plenum Press, New York (1985).
11. C. A. Tyson and A. E. Martell, *J. Am. Chem. Soc.* 1968, **90**, 3379.
12. J. E. Gorton and R. F. Jameson, *J. Chem. Soc. A* 1968, 2615.
13. A. Gergely and T. Kiss, *Inorg. Chim. Acta* 1976, **16**, 51.
14. A. E. Martell and R. M. Smith, *Critical Stability Constants*, Vol. 5. Plenum Press, New York (1982).

Polyhedron Vol. 8, No. 19, pp. 2351–2358, 1989
Printed in Great Britain

0277–5387/89 $3.00+.00
© 1989 Pergamon Press plc

CLUSTERS CONTAINING CARBENE LIGANDS—VI. THE SYNTHESIS OF HIGHER NUCLEARITY METAL CARBENE CLUSTER COMPLEXES BY CARBENE LIGAND TRANSFER. THE SYNTHESIS AND STRUCTURES OF $[Ru_4(CO)_{10}\{C(Ph)NMe_2\}(\mu_4\text{-}S)_2]$ AND $[Ru_4(CO)_{10}\{C(Ph)NMe_2\}(\mu_4\text{-}S)(\mu_5\text{-}S)\{W(CO)_5\}]$

RICHARD D. ADAMS,* JAMES E. BABIN and JIN-GUU WANG

Department of Chemistry, University of South Carolina, Columbia, SC 29208, U.S.A.

(*Received* 1 *April* 1989; *accepted* 10 *May* 1989)

Abstract—UV irradiation of a solution of $[Ru_4(CO)_{11}(\mu_4\text{-}S)_2]$ (**1**) and $[W(CO)_5\{C(Ph)NMe_2\}]$ yielded the two new higher nuclearity carbene-containing cluster complexes $[Ru_4(CO)_{10}\{C(Ph)NMe_2\}(\mu_4\text{-}S)_2]$ (**2**) 20%, and $[Ru_4(CO)_{10}\{C(Ph)NMe_2\}(\mu_4\text{-}S)(\mu_5\text{-}S)\{W(CO)_5\}]$ (**3**) 1%, by transfer of the carbene ligand from the tungsten complex to a ruthenium atom of the cluster. Compound **3** was obtained in 50% yield by UV irradiation of solutions of **2** and $W(CO)_6$. Compounds **2** and **3** were both characterized by single-crystal X-ray diffraction methods. Crystal data for **1**: $Ru_4S_2O_{10}NC_{19}H_{11}$, $M = 881.7$, $P2_1/n$, (No. 14), $a = 11.847(1)$, $b = 11.773(2)$, $c = 19.310(2)$ Å, $\beta = 104.685(8)°$, $V = 2597(1)$ Å^3, $D_c = 2.26$ g cm^{-3}, $Z = 4$, λ(Mo-K_α) = 0.71069 Å (graphite monochromator), $\mu = 24.3$ cm^{-1}. Methods: MITHRIL, difference Fourier, full-matrix least-squares. Refinement of 3383 reflections ($F^2 \geqslant 3\sigma(F^2)$), ($1 \leqslant 2\theta \leqslant 47°$), gave R and R_w values of 0.032 and 0.043. Data/parameters ratio = 10.4, highest peak in final difference Fourier = 0.82 e Å^{-3}. Crystal data for **2**: $WRu_4S_2O_{15}NC_{24}H_{11}$, $M = 1205.6$, monoclinic, $P2_1/n$ (No. 14), $a = 15.268(1)$, $b = 11.451(1)$, $c = 19.121(2)$ Å, $\beta = 99.731(8)°$, $V = 3295.0(6)$ Å^3, $D_c = 2.43$ g cm^{-3}, $Z = 4$, λ(Mo-K_α), graphite monochromator, $\mu = 56.2$. Methods: MITHRIL, difference Fourier, full-matrix least-squares. Refinement of 4444 reflections ($F^2 \geqslant 3\sigma(F^2)$), ($1 \leqslant 2\theta \leqslant 48°$), yielded $R = 0.026$, $R_w = 0.032$. Data/parameters ratio = 10.5. Compound **2** consists of a square-planar cluster of four ruthenium atoms with two quadruply bridging sulphido ligands and one terminally coordinated phenyl(dimethylamino)carbene ligand. Compound **3** consists of a cluster of **2** with a $W(CO)_5$ group added to one of the quadruply bridging sulphido ligands.

Metal complexes containing carbene ligands have been recognized for over 25 years.[1,2] Recently, complexes containing carbene ligands have been utilized as reagents in a variety of novel organic syntheses.[3,4] Although there are a variety of methods for preparing carbene ligands in cluster complexes,[5] the number of examples of these complexes is still relatively small. In fact, there are only two reports of cluster complexes with carbene ligands that have more than three metal atoms.[6,7] In cluster complexes, the carbene ligands can adopt terminal **A** and a variety of bridging coordination modes **B**–**D**. The multicentre metal site can provide new avenues for the activation and transformation of the carbene ligand.[5,8]

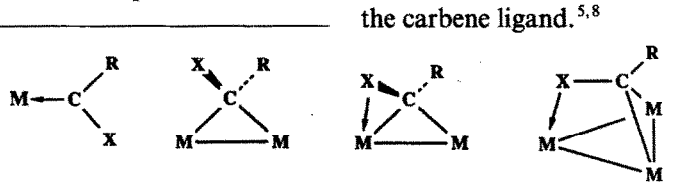

A **B** **C** **D**

*Author to whom correspondence should be addressed.

This report describes the synthesis and structural characterizations of two new higher nuclearity cluster complexes containing the phenyl(dimethylamino)carbene ligands, prepared by the carbene ligand transfer method that was developed by Fischer[9] and Stone.[10]

EXPERIMENTAL

General

All reactions were performed under a nitrogen atmosphere. Reagent grade solvents were dried over 4 Å molecular sieves and purged with nitrogen prior to use. $[Ru_4(CO)_{11}(\mu_4\text{-}S)_2]$[11] and $[W(CO)_5\{C(Ph)NMe_2\}]$[2] were prepared as previously reported. $Ru(CO)_5$ was prepared from $Ru_3(CO)_{12}$ just prior to use.[13] UV irradiations were performed by using an externally-positioned high pressure mercury lamp on the reaction solutions in Pyrex glassware.

All chromatographic separations were performed in air. TLC separations were performed on silica gel plates (0.25 mm Kieselgel 60 F254, E. Merck, F.R.G.). IR spectra were recorded on a Nicolet 5DXB FT–IR spectrophotometer. ^1H NMR spectra were recorded on a Brüker AM-300 spectrometer operating at 300 MHz. Elemental analyses were performed by Desert Analytics, Tucson, Arizona.

Reaction of $[Ru_4(CO)_{11}(\mu_4\text{-}S)_2]$ (**1**) *with* $[W(CO)_5\{C(Ph)NMe_2\}]$ *in the presence of UV irradiation*

$[W(CO)_5\{C(Ph)NMe_2\}]$(97 mg, 0.21 mmol) was added to a suspension of **1** (55 mg, 0.070 mmol) in 140 cm^3 of THF. The solution was photolysed under a continuous purge of nitrogen for 8 h, and the colour of the solution changed from orange to orange–red. The solvent was removed *in vacuo* and the residue was chromatographed by TLC using a hexane–CH_2Cl_2 (7:3) solvent mixture. The following bands were obtained in order of elution: trace amounts of $W(CO)_6$; 2 mg of **1**; 31 mg of $[W(CO)_5\{C(Ph)NMe_2\}]$; 13 mg of golden-yellow $[Ru_4(CO)_{10}\{C(Ph)NMe_2\}(\mu_4\text{-}S)_2]$, (**2**), 20%; and 1 mg of orange $[Ru_4(CO)_{10}\{C(Ph)NMe_2\}(\mu_4\text{-}S)(\mu_5\text{-}S)\{W(CO)_5\}]$ (**3**), 1%. For **2**: IR (in hexane) 2075(s), 2056(w), 2036(vs), 2027(vs), 2011(s), 1982(s), 1855(m), 1816(m) cm^{-1}. ^1H NMR (δ in $CDCl_3$) 6.87 (m, 3H), 6.29 (m, 2H), 4.50 (s, 3H), 3.25 (s, 3H). Found: C, 25.9; H, 0.91. Calc.: C, 25.9; H, 1.26%. For **3**: IR (in hexane) 2085(m), 2076(w), 2067(m), 2042(s), 2036(s), 2019(sh), 1991(s), 1939(vs), 1935(vs), 1862(w), 1823(w). ^1H NMR (δ in $CDCl_3$) 6.89 (m, 3H), 6.27 (m, 2H), 4.57 (s, 3H), 3.27 (s, 3H). Found: C, 23.8; H, 0.89. Calc.: C, 23.9; H, 1.10%.

The reaction of **2** *with* $W(CO)_6$ *in the presence of UV irradiation*

A mixture of **2** (10 mg, 0.011 mmol) and $W(CO)_6$ (20 mg, 0.057 mmol) was dissolved in 30 cm^3 of hexane solvent and photolysed under a continuous purge with nitrogen for 40 min. The colour of the solution changed from yellow to a brownish-yellow. The solvent was removed *in vacuo* and the residue was separated by TLC. Elution with a hexane–CH_2Cl_2 (7:3) solvent mixture yielded 6 mg of **3** (50% based on the amount of **2** consumed) and 1.2 mg of unreacted **2**.

Crystallographic analysis

Crystals of **2** and **3** were grown by the slow evaporation of solvent from hexane–CH_2Cl_2 (3:1) solutions at 5°C. The data crystals were mounted in thin-walled glass capillaries. Diffraction measurements were made on a Rigaku AFC6 automatic diffractometer using graphite-monochromatized Mo-K_α radiation. Unit cells were determined from 25 randomly selected reflections obtained by using the AFC6 automatic search, centre, index and least-squares routines. Crystal data, data collection parameters and results of the analyses are listed in Table 1. All data processing was performed on a Digital Equipment Corporation MICROVAX II computer by using the TEXSAN structure solving program library (v 2.0) obtained from the Molecular Structure Corporation, The Woodlands, Texas. Neutral atom scattering factors were calculated by the standard procedures.[13a] Anomalous dispersion corrections were applied to all atoms.[13b] Full-matrix least-squares refinements minimized the function:

$$\sum_{hkl} w(|F_o| - |F_c|)^2,$$

where

$$w = 1/\sigma(F)^2, \quad \sigma(F) = \sigma(F_o^2)/2F_o,$$

and

$$\sigma(F_o^2) = [\sigma(I_{raw})^2 + (PF_o^2)^2]^{1/2} Lp.$$

Both compounds crystallized in the monoclinic crystal system in the space group $P2_1/n$. The latter was established in each case from the systematic absences observed during the collection of the data. The structures were solved by a combination of direct methods (MITHRIL) and difference Fourier syntheses. All non-hydrogen atoms were refined using anisotropic thermal parameters. Hydrogen

Table 1. Crystallographic data for the structural analyses for compounds **2** and **3**

Compound	**2**	**3**
Formula	$Ru_4S_2O_{10}NC_{19}H_{11}$	$WRu_4S_2O_{15}NC_{24}H_{11}$
Formula weight	881.70	1205.6
Temperature	23°C	23°C
Crystal system	Monoclinic	Monoclinic
Space group	$P2_1/n$	$P2_1/n$
a (Å)	11.847(1)	15.268(1)
b (Å)	11.773(1)	11.451(1)
c (Å)	19.310(2)	19.121(2)
β (°)	104.685(8)	99.731(8)
V (Å^3)	2597(1)	3295.0(6)
Z	4	4
D_{calc} (g cm^{-3})	2.26	2.43
μ(Mo-K_α) (cm^{-1})	24.3	56.2
Radiation	Mo-K_α	Mo-K_α
Absorption correction	Empirical	Empirical
Transmission coefficient (max.; min.)	1.00; 0.74	1.00; 0.75
2θ max (°)	47.0	48.0
ω-Scan rate (° min^{-1})	4.0	4.0
Background	$\frac{1}{4}$ additional scan	$\frac{1}{4}$ additional scan
Number of observations ($I > 3\sigma(I)$)	3383	4444
Number of variables	325	424
R, R_w	0.032, 0.043	0.026, 0.032
Goodness-of-fit	1.70	1.88
Maximum shift/error on final cycle	0.01	0.07
Largest peak in final difference (e$^-$ Å^3)	0.82	0.80

atom coordinates were calculated by assuming idealized geometries and C—H distances of 0.95 Å. Their scattering contributions were included in the structure factor calculations, but their positions were not refined. Error analyses were calculated from the inverse matrix obtained from the final cycle of refinement.

RESULTS AND DISCUSSION

The reaction of $[Ru_4(CO)_{11}(\mu_4\text{-}S)_2]$ (**1**) with $[W(CO)_5\{C(Ph)NMe_2\}]$ in the presence of UV irradiation yielded the new carbene-containing cluster complex $[Ru_4(CO)_8\{C(Ph)NMe_2\}(\mu\text{-}CO)_2(\mu_4\text{-}S)_2]$ (**2**) in 20% yield and a trace of the higher nuclearity carbene cluster complex $[Ru_4(CO)_8\{C(Ph)NMe_2\}(\mu\text{-}CO)_2(\mu_4\text{-}S)(\mu_5\text{-}S)\{W(CO)_5\}]$ (**3**) in 1% yield. Both products were characterized by IR and ^{1}H NMR spectroscopy, and by single-crystal X-ray diffraction analyses. An ORTEP drawing of **2** is shown in Fig. 1. Selected intramolecular bond distances and angles are listed in Tables 2 and 3. The molecule consists of an approximately square-planar cluster of four ruthenium atoms with one quadruply bridging sulphido ligand on each side of the square plane. The two shortest Ru—Ru bonds, Ru(2)—Ru(4) = 2.7339(6) Å and Ru(3)—Ru(4) = 2.7236(6) Å, are bridged by carbonyl ligands which are believed to contribute to the shortness of the Ru—Ru distances. The Ru(1)—Ru(2) bond, 2.7823(6) Å, contains a semibridging carbonyl ligand, C(12)—O(12), Ru(1)—C(12)—O(12) = 162.7(6)°. The longest Ru—Ru bond, Ru(1)—Ru(3) = 2.8065(6) Å, has no bridging or semibridging carbonyl ligands. The quadruply bridging sul-

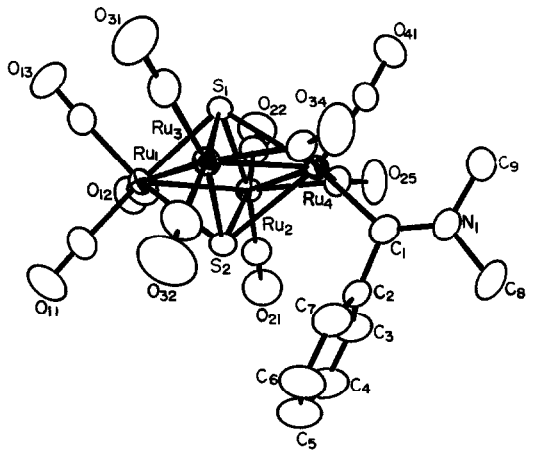

Fig. 1. An ORTEP drawing of $[Ru_4(CO)_8\{C(Ph)NMe_2\}(\mu\text{-}CO)_2(\mu_4\text{-}S)_2]$ (**2**) showing 50% probability thermal ellipsoids.

Table 2. Intramolecular distances of $[Ru_4(CO)_{10}\{C(Ph)NMe_2\}(\mu_4\text{-}S)_2]$ (2)

Atom	Atom	Distance	Atom	Atom	Distance
Ru(1)	C(11)	1.890(6)	Ru(3)	S(2)	2.424(1)
Ru(1)	C(13)	1.899(6)	Ru(3)	S(1)	2.454(1)
Ru(1)	C(12)	1.915(7)	Ru(3)	Ru(4)	2.7236(6)
Ru(1)	S(2)	2.413(1)	Ru(4)	C(41)	1.853(6)
Ru(1)	S(1)	2.416(1)	Ru(4)	C(1)	2.033(5)
Ru(1)	Ru(2)	2.7823(6)	Ru(4)	C(25)	2.058(6)
Ru(1)	Ru(3)	2.8065(6)	Ru(4)	C(34)	2.140(6)
Ru(2)	C(21)	1.877(7)	Ru(4)	S(1)	2.576(1)
Ru(2)	C(22)	1.879(6)	Ru(4)	S(2)	2.647(1)
Ru(2)	C(25)	2.105(6)	N(1)	C(1)	1.308(7)
Ru(2)	S(2)	2.448(1)	N(1)	C(9)	1.457(8)
Ru(2)	S(1)	2.483(1)	N(1)	C(8)	1.472(7)
Ru(2)	Ru(4)	2.7339(6)	C(1)	C(2)	1.472(7)
Ru(3)	C(31)	1.874(7)	C	C(av)	1.38(1)
Ru(3)	C(32)	1.879(7)	O	C(av)	1.14(1)
Ru(3)	C(34)	2.019(6)			

Distances are in angstroms. Estimated standard deviations in the least significant figure are given in parentheses.

Table 3. Intramolecular bond angles for $[Ru_4(CO)_{10}\{C(Ph)NMe_2\}(\mu_4\text{-}S)_2]$ (2)

Atom	Atom	Atom	Angle	Atom	Atom	Atom	Angle
C(11)	Ru(1)	S(2)	91.5(2)	C(22)	Ru(2)	Ru(1)	115.9(2)
C(11)	Ru(1)	S(1)	162.7(2)	C(25)	Ru(2)	S(2)	98.6(2)
C(11)	Ru(1)	Ru(2)	128.3(2)	C(25)	Ru(2)	S(1)	95.0(2)
C(11)	Ru(1)	Ru(3)	107.3(2)	C(25)	Ru(2)	Ru(4)	48.2(2)
C(13)	Ru(1)	S(2)	157.5(2)	C(25)	Ru(2)	Ru(1)	140.7(2)
C(13)	Ru(1)	S(1)	89.8(2)	S(2)	Ru(2)	S(1)	76.62(5)
C(13)	Ru(1)	Ru(2)	131.7(2)	S(2)	Ru(2)	Ru(4)	61.15(3)
C(13)	Ru(1)	Ru(3)	102.8(2)	S(2)	Ru(2)	Ru(1)	54.51(3)
C(12)	Ru(1)	S(2)	105.5(2)	S(1)	Ru(2)	Ru(4)	58.95(3)
C(12)	Ru(1)	S(1)	101.7(2)	S(1)	Ru(2)	Ru(1)	54.27(3)
C(12)	Ru(1)	Ru(2)	63.9(2)	Ru(4)	Ru(2)	Ru(1)	92.58(2)
C(12)	Ru(1)	Ru(3)	150.0(2)	C(31)	Ru(3)	S(2)	161.1(2)
S(2)	Ru(1)	S(1)	78.52(5)	C(31)	Ru(3)	S(1)	95.9(2)
S(2)	Ru(1)	Ru(2)	55.67(3)	C(31)	Ru(3)	Ru(4)	130.3(2)
S(2)	Ru(1)	Ru(3)	54.71(3)	C(31)	Ru(3)	Ru(1)	107.4(2)
S(1)	Ru(1)	Ru(2)	56.53(3)	C(32)	Ru(3)	S(2)	93.7(2)
S(1)	Ru(1)	Ru(3)	55.44(3)	C(32)	Ru(3)	S(1)	167.6(2)
Ru(2)	Ru(1)	Ru(3)	86.23(2)	C(32)	Ru(3)	Ru(4)	124.2(2)
C(21)	Ru(2)	S(2)	95.3(2)	C(32)	Ru(3)	Ru(1)	113.5(2)
C(21)	Ru(2)	S(1)	169.1(2)	C(34)	Ru(3)	S(2)	101.8(2)
C(21)	Ru(2)	Ru(4)	123.7(2)	C(34)	Ru(3)	S(1)	96.6(2)
C(21)	Ru(2)	Ru(1)	115.1(2)	C(34)	Ru(3)	Ru(4)	51.0(2)
C(22)	Ru(2)	C(25)	90.0(2)	C(34)	Ru(3)	Ru(1)	143.1(2)
C(22)	Ru(2)	S(2)	170.4(2)	S(2)	Ru(3)	S(1)	77.60(5)
C(22)	Ru(2)	S(1)	98.5(2)	S(2)	Ru(3)	Ru(4)	61.58(3)
C(22)	Ru(2)	Ru(4)	123.6(2)	S(2)	Ru(3)	Ru(1)	54.36(3)
S(1)	Ru(3)	Ru(4)	59.41(3)	Ru(1)	S(1)	Ru(3)	70.37(4)
S(1)	Ru(3)	Ru(1)	54.18(3)	Ru(1)	S(1)	Ru(2)	69.20(4)
Ru(4)	Ru(3)	Ru(1)	92.27(2)	Ru(1)	S(1)	Ru(4)	105.96(5)
C(41)	Ru(4)	S(1)	92.9(2)	Ru(3)	S(1)	Ru(2)	101.38(5)
C(41)	Ru(4)	S(2)	164.4(2)	Ru(3)	S(1)	Ru(4)	65.51(3)

Table 3—*continued*

Atom	Atom	Atom	Angle	Atom	Atom	Atom	Angle
C(41)	Ru(4)	Ru(3)	115.8(2)	Ru(2)	S(1)	Ru(4)	65.39(3)
C(41)	Ru(4)	Ru(2)	119.0(2)	Ru(1)	S(2)	Ru(3)	70.93(4)
C(1)	Ru(4)	C(34)	86.8(2)	Ru(1)	S(2)	Ru(2)	69.83(4)
C(1)	Ru(4)	S(1)	168.2(2)	Ru(1)	S(2)	Ru(4)	103.88(5)
C(1)	Ru(4)	S(2)	97.1(2)	Ru(3)	S(2)	Ru(2)	103.27(5)
C(1)	Ru(4)	Ru(3)	115.7(1)	Ru(3)	S(2)	Ru(4)	64.80(3)
C(1)	Ru(4)	Ru(2)	120.7(1)	Ru(2)	S(2)	Ru(4)	64.76(3)
C(25)	Ru(4)	S(1)	93.5(2)	C(1)	N(1)	C(9)	123.0(5)
C(25)	Ru(4)	S(2)	93.8(2)	C(1)	N(1)	C(8)	123.7(5)
C(25)	Ru(4)	Ru(3)	138.5(2)	C(9)	N(1)	C(8)	113.4(5)
C(25)	Ru(4)	Ru(2)	49.7(2)	N(1)	C(1)	C(2)	116.5(5)
C(34)	Ru(4)	S(1)	90.1(1)	N(1)	C(1)	Ru(4)	133.0(4)
C(34)	Ru(4)	S(2)	91.8(2)	C(2)	C(1)	Ru(4)	110.5(4)
C(34)	Ru(4)	Ru(3)	47.2(1)	O(11)	C(11)	Ru(1)	177.5(5)
C(34)	Ru(4)	Ru(2)	136.0(1)	O(12)	C(12)	Ru(1)	162.7(6)
S(1)	Ru(4)	S(2)	71.61(4)	O(13)	C(13)	Ru(1)	177.1(6)
S(1)	Ru(4)	Ru(3)	55.08(3)	O(21)	C(21)	Ru(2)	178.7(6)
S(1)	Ru(4)	Ru(2)	55.66(3)	O(22)	C(22)	Ru(2)	177.3(5)
S(2)	Ru(4)	Ru(3)	53.63(3)	O(25)	C(25)	Ru(4)	141.8(5)
S(2)	Ru(4)	Ru(2)	54.08(3)	O(25)	C(25)	Ru(2)	136.0(4)
Ru(3)	Ru(4)	Ru(2)	88.84(2)	Ru(4)	C(25)	Ru(2)	82.1(2)
O(31)	C(31)	Ru(3)	178.5(6)				
O(32)	C(32)	Ru(3)	177.6(7)				
O(34)	C(34)	Ru(3)	142.3(5)				
O(34)	C(34)	Ru(4)	135.9(4)				
Ru(3)	C(34)	Ru(4)	81.8(2)				
O(41)	C(41)	Ru(4)	173.5(5)				

Angles are in degrees. Estimated standard deviations in the least significant figure are given in parentheses.

phido ligands are bonded asymmetrically to the tetraruthenium cluster. The Ru—S distances to Ru(4), 2.576(1) and 2.647(1) Å, are significantly longer than those to the other three ruthenium atoms, range 2.413(1)–2.483(1) Å. This could be due to steric crowding about atom Ru(4). Formally, Ru(4) has a coordination number of eight, while the other three ruthenium atoms have a coordination of seven. The structure of **2** is very similar to that of $[Ru_4(CO)_7(PMe_2Ph)_2(\mu\text{-}CO)_2(\mu_4\text{-}S)_2]$ (**5**).[15] Compound **2** contains 10 carbonyl ligands: two bridges, one semibridge and seven linear terminal ligands distributed as shown in Fig. 1, but the most interesting ligand is the phenyl(dimethylamino)carbene ligand which is terminally coordinated to the Ru(4) atom. As with other aminocarbene ligands,[2] the nitrogen atom is planar and the C—N distance is short, 1.308(7) Å, and indicative of partial C—N multiple bonding due to the interaction of the lone pair of electrons on the nitrogen atom with the carbene carbon atom. This results in a hindered rotation about the C—N bond and the observation of separate resonances (^{1}H NMR) for the inequivalent methyl groups on the nitrogen atom. The Ru—C bond to the carbene ligand of 2.033(5) Å is slightly longer than those to the terminally coordinated carbonyl ligands, 1.853(6)–1.915(7) Å. This feature is similar to that found in mononuclear metal carbonyl carbene complexes.[2] The plane of the phenyl group is nearly perpendicular (86.8°) to the plane of the carbene ligand. This precludes the existence of π-bonding between the phenyl ring and the carbene carbon atom. The phenyl(dimethylamino)carbene ligand in the cluster complex $[Os_3(CO)_8\{C(Ph)NMe_2\}(\mu_3\text{-}S)(\mu\text{-}H)_2]$ contained a similar structure.[16]

An ORTEP drawing of the molecular structure of **3** is shown in Fig. 2. Selected intramolecular bond distances and angles are listed in Tables 4 and 5. Compound **3** can be viewed as an adduct of compound **2** and a $W(CO)_5$ group. The $W(CO)_5$ group is attached to one of the quadruply bridging sulphido ligands. This sulphido ligand is, thus, pentacoordinate and overall possesses a square-pyramidal

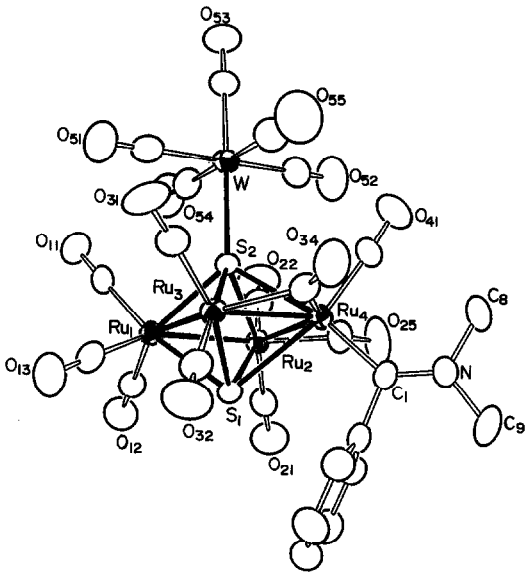

Fig. 2. An ORTEP drawing of $[Ru_4(CO)_8\{C(Ph)NMe_2\}(\mu\text{-}CO)_2(\mu_4\text{-}S)(\mu_5\text{-}S)\{W(CO)_5\}]$ (**3**) showing 50% probability thermal ellipsoids.

geometry. Similar quintuply bridging sulphido ligands were observed in the complexes $[Ru_4(CO)_7(PMe_2Ph)_2(\mu\text{-}CO)_2(\mu_4\text{-}S)(\mu_5\text{-}S)\{W(CO)_4PMe_2Ph\}]$ (**6**) and $[Os_5(CO)_{15}(\mu_5\text{-}S)\{W(CO)_4PPh_3\}]$ (**7**).[17] The W—S bond can be viewed as an S → W donor–acceptor bond. The tungsten atom thus achieves an 18 electron configuration, and the sulphido ligand donates its four remaining valence electrons to the ruthenium cluster. The W—S bond distance of 2.533(2) Å is slightly longer than found in **6**, 2.486(2) Å, and **7**, 2.48(2) and 2.44(2) Å. This could be attributed to the stronger structural *trans*-effect of the CO ligand *trans* to the W—S bond in **4** than the *trans*-phosphine ligands in **6** and **7**. The dimensions of the cluster of **2** contained in compound **3** are very similar to those of **2** alone. However, the CO ligands on Ru(1) in **3** are arranged significantly differently from those in **2**. In particular, there is no semi-bridging carbonyl ligand on Ru(1). Instead, C(11)—O(11) on Ru(1) lies above the Ru_4 plane, and C(12)—O(12) and C(13)—O(13) lie below it. It is believed that the rearrangement of the carbonyl ligands on Ru(1) may be caused by non-bonded repulsive interactions between the equatorial carbonyl ligands on the tungsten atom and the four terminal carbonyl ligands, C(11)—O(11), C(22)—O(22), C(31)—O(31) and C(41)—O(41), that lie on the tungsten side of the tetraruthenium plane. As a result of these repulsions, the $W(CO)_5$ group has adopted a rotational conformation that places the equatorial tungsten carbonyl groups midway between adjacent pairs of the four carbonyl groups on the cluster. The carbene ligand in **3** has very similar dimensions to the one in **2**. It lies on the side of the Ru_4 plane that is opposite to that of the $W(CO)_5$ group, probably for steric reasons.

In both **2** and the unit of **2** in **3**, the cluster

Table 4. Intramolecular distances for $[Ru_4(CO)_{10}\{C(Ph)NMe_2\}(\mu_4\text{-}S)(\mu_5\text{-}S)\{W(CO)_5\}]$ (**3**)

Atom	Atom	Distance	Atom	Atom	Distance
W(1)	C(53)	1.958(7)	Ru(3)	C(31)	1.880(7)
W(1)	C(54)	2.029(8)	Ru(3)	C(32)	1.887(8)
W(1)	C(52)	2.033(9)	Ru(3)	C(34)	2.059(7)
W(1)	C(51)	2.042(8)	Ru(3)	S(1)	2.431(2)
W(1)	C(55)	2.047(8)	Ru(3)	S(2)	2.439(2)
W(1)	S(2)	2.533(2)	Ru(3)	Ru(4)	2.7443(7)
Ru(1)	C(12)	1.895(6)	Ru(4)	C(41)	1.833(7)
Ru(1)	C(13)	1.896(7)	Ru(4)	C(1)	2.010(6)
Ru(1)	C(11)	1.902(7)	Ru(4)	C(34)	2.082(7)
Ru(1)	S(2)	2.410(2)	Ru(4)	C(25)	2.106(7)
Ru(1)	S(1)	2.419(2)	Ru(4)	S(2)	2.584(2)
Ru(1)	Ru(2)	2.8178(7)	Ru(4)	S(1)	2.688(2)
Ru(1)	Ru(3)	2.8208(7)	N	C(1)	1.295(7)
Ru(2)	C(22)	1.870(8)	N	C(9)	1.469(9)
Ru(2)	C(21)	1.890(7)	N	C(8)	1.471(9)
Ru(2)	C(25)	2.030(7)	Cl	C(2)	1.495(9)
Ru(2)	S(1)	2.430(2)	C	C(av)	1.373(8)
Ru(2)	S(2)	2.433(2)	C	O(W)*	1.135(8)
Ru(2)	Ru(4)	2.7338(7)	C	O(Ru)*	1.135(8)

Distances are in angstroms. Estimated standard deviations in the least significant figure are given in parentheses.

Table 5. Intramolecular bond angles for $[Ru_4(CO)_{10}\{C(Ph)NMe_2\}(\mu_4\text{-}S)(\mu_5\text{-}S)\{W(CO)_5\}]$ (3)

Atom	Atom	Atom	Angle	Atom	Atom	Atom	Angle
C(53)	W(1)	S(2)	178.8(2)	C(22)	Ru(2)	Ru(4)	125.4(2)
C(54)	W(1)	S(2)	90.2(2)	C(22)	Ru(2)	Ru(1)	110.9(2)
C(52)	W(1)	S(2)	91.2(2)	C(21)	Ru(2)	S(1)	94.5(2)
C(51)	W(1)	S(2)	89.5(2)	C(21)	Ru(2)	S(2)	166.6(2)
C(55)	W(1)	S(2)	90.0(2)	C(21)	Ru(2)	Ru(4)	125.1(2)
C(12)	Ru(1)	S(2)	135.7(2)	C(21)	Ru(2)	Ru(1)	112.6(2)
C(12)	Ru(1)	S(1)	93.3(2)	C(25)	Ru(2)	S(1)	99.4(2)
C(12)	Ru(1)	Ru(2)	84.2(2)	C(25)	Ru(2)	S(2)	98.9(2)
C(12)	Ru(1)	Ru(3)	146.0(2)	C(25)	Ru(2)	Ru(4)	49.8(2)
C(13)	Ru(1)	C(11)	92.9(3)	C(25)	Ru(2)	Ru(1)	143.5(2)
C(13)	Ru(1)	S(2)	127.0(2)	S(1)	Ru(2)	S(2)	76.51(5)
C(13)	Ru(1)	S(1)	95.7(2)	S(1)	Ru(2)	Ru(4)	62.40(4)
C(13)	Ru(1)	Ru(2)	150.3(2)	S(1)	Ru(2)	Ru(1)	54.29(4)
C(13)	Ru(1)	Ru(3)	77.9(2)	S(2)	Ru(2)	Ru(4)	59.67(4)
C(11)	Ru(1)	S(2)	92.5(2)	S(2)	Ru(2)	Ru(1)	54.05(4)
C(11)	Ru(1)	S(1)	169.2(2)	Ru(4)	Ru(2)	Ru(1)	93.70(2)
C(11)	Ru(1)	Ru(2)	116.8(2)	C(31)	Ru(3)	S(1)	162.4(2)
C(11)	Ru(1)	Ru(3)	121.4(2)	C(31)	Ru(3)	S(2)	99.0(2)
S(2)	Ru(1)	S(1)	77.15(5)	C(31)	Ru(3)	Ru(4)	130.2(2)
S(2)	Ru(1)	Ru(2)	54.81(4)	C(31)	Ru(3)	Ru(1)	109.2(2)
S(2)	Ru(1)	Ru(3)	54.92(4)	C(32)	Ru(3)	S(1)	94.8(2)
S(1)	Ru(1)	Ru(2)	54.66(4)	C(32)	Ru(3)	S(2)	170.5(2)
S(1)	Ru(1)	Ru(3)	54.63(4)	C(32)	Ru(3)	Ru(4)	119.7(2)
Ru(2)	Ru(1)	Ru(3)	84.85(2)	C(32)	Ru(3)	Ru(1)	118.0(2)
C(22)	Ru(2)	S(1)	165.1(2)	C(34)	Ru(3)	S(1)	103.2(2)
C(22)	Ru(2)	S(2)	96.4(2)	C(34)	Ru(3)	S(2)	92.9(2)
C(34)	Ru(3)	Ru(4)	48.9(2)	S(2)	Ru(4)	Ru(3)	54.40(4)
C(34)	Ru(3)	Ru(1)	141.3(2)	S(1)	Ru(4)	Ru(2)	53.26(4)
S(1)	Ru(3)	S(2)	76.39(5)	S(1)	Ru(4)	Ru(3)	53.16(4)
S(1)	Ru(3)	Ru(4)	62.23(4)	Ru(2)	Ru(4)	Ru(3)	87.95(2)
S(1)	Ru(3)	Ru(1)	54.25(4)	Ru(1)	S(1)	Ru(2)	71.04(5)
S(2)	Ru(3)	Ru(4)	59.45(4)	Ru(1)	S(1)	Ru(3)	71.12(3)
S(2)	Ru(3)	Ru(1)	53.95(4)	Ru(1)	S(1)	Ru(4)	104.84(6)
Ru(4)	Ru(3)	Ru(1)	93.41(2)	Ru(2)	S(1)	Ru(3)	102.97(6)
C(41)	Ru(4)	S(2)	95.4(2)	Ru(2)	S(1)	Ru(4)	64.34(4)
C(41)	Ru(4)	S(1)	164.5(2)	Ru(3)	S(1)	Ru(4)	64.61(4)
C(41)	Ru(4)	Ru(2)	115.1(2)	Ru(1)	S(2)	Ru(2)	71.15(4)
C(41)	Ru(4)	Ru(3)	121.6(2)	Ru(1)	S(2)	Ru(3)	71.13(4)
C(1)	Ru(4)	S(2)	167.0(2)	Ru(1)	S(2)	W(1)	129.10(6)
C(1)	Ru(4)	S(1)	97.5(2)	Ru(1)	S(2)	Ru(4)	108.36(6)
C(1)	Ru(4)	Ru(2)	119.8(2)	Ru(2)	S(2)	Ru(3)	102.64(6)
C(1)	Ru(4)	Ru(3)	116.7(2)	Ru(2)	S(2)	W(1)	129.76(6)
C(34)	Ru(4)	S(2)	88.3(2)	Ru(2)	S(2)	Ru(4)	65.96(4)
C(34)	Ru(4)	S(1)	94.5(2)	Ru(3)	S(2)	W(1)	126.72(6)
C(34)	Ru(4)	Ru(2)	135.6(2)	Ru(3)	S(2)	Ru(4)	66.16(4)
C(34)	Ru(4)	Ru(3)	48.1(2)	W(1)	S(2)	Ru(4)	122.51(6)
C(25)	Ru(4)	S(2)	92.4(2)	C(1)	N	C(9)	124.3(6)
C(25)	Ru(4)	S(1)	90.0(2)	C(1)	N	C(8)	122.1(6)
C(25)	Ru(4)	Ru(2)	47.5(2)	N	C(1)	C(2)	115.1(6)
C(25)	Ru(4)	Ru(3)	135.3(2)	N	C(1)	Ru(4)	134.6(5)
S(2)	Ru(4)	S(1)	69.65(5)	C(2)	C(1)	Ru(4)	110.4(4)
S(2)	Ru(4)	Ru(2)	54.38(4)	O(25)	C(25)	Ru(2)	139.4(6)
O(25)	C(25)	Ru(4)	137.9(6)				
Ru(2)	C(25)	Ru(4)	82.7(3)				
O(34)	C(34)	Ru(3)	136.8(6)				
O(34)	C(34)	Ru(4)	139.9(6)				
Ru(3)	C(34)	Ru(4)	83.0(2)				
O	C(av)	Ru	177(1)				
O	C(av)	W	179(1)				

Angles are in degrees. Estimated standard deviations in the least significant figure are given in parentheses.

contains 62 valence electrons. This is in accord with the Polyhedral Skeletal Electron Pair theory,[18] but is two less than that required by the Effective Atomic Number rule.

Details of the transfer of the carbene ligand from $[W(CO)_5\{C(Ph)NMe_2\}]$ to **1** are obscure in the absence of reaction intermediates. We doubt that **3** is an intermediate in the formation of **2**, since very little **3** was isolated from that reaction. It is suspected that **3** was formed from **2** by the capture of a $W(CO)_5$ fragment. The credibility of this reaction was demonstrated by our synthesis of **3** in 50% yield by the irradiation of solutions of **2** and $W(CO)_6$.

Acknowledgement—This research was supported by the National Science Foundation under Grant CHE-8612862.

Tables of anisotropic thermal parameters, and observed and calculated structure factors for **2** and **3** have been deposited as supplementary material with the Editor, from whom copies are available upon request. Atomic coordinates have been submitted to the Cambridge Crystallographic Data Centre.

REFERENCES

1. E. O. Fischer and A. Maasböl, *Angew. Chem.* 1964, **76**, 645.
2. (a) K. H. Dotz, H. Fischer, P. Hoffmann, F. R. Kreissl, U. Schubert and K. Weiss, *Transition Metal Carbene Chemistry* Verlag Chemie, Weinheim, F.R.G. (1983); (b) E. O. Fischer, *Adv. Organomet. Chem.* 1976, **14**, 1.
3. J. P. Collman, L. S. Hegedus, J. R. Norton and R. G. Finke, *Principles and Applications of Organotransition Metal Chemistry*, pp. 119–136. University Science Books, Mill Valley (1987).
4. (a) K. H. Dötz, *Pure and Appl. Chem.* 1983, **55**, 1689; (b) K. S. Chan, G. A. Peterson, T. A. Brandvold, K. L. Faron, C. A. Challener, C. Hydahl and W. Wulff, *J. Organomet. Chem.* 1987, **334**, 9; (c) K. H. Dötz, *J. Organomet. Chem.* 1987, **334**, 57.
5. R. D. Adams, *Chem. Rev.*, in press.
6. M. G. Richmond and J. Kochi, *Organometallics* 1987, **6**, 777.
7. R. D. Adams, J. E. Babin and H. S. Kim, *Inorg. Chem.* 1986, **25**, 4319.
8. (a) H. D. Kaesz and C. M. Jensen, *Polyhedron* 1988, **7**, 1035; (b) C. M. Jensen and H. D. Kaesz, *J. Organomet. Chem.* 1987, **330**, 133.
9. (a) E. O. Fischer and H. J. Beck, *Chem. Ber.* 1971, **104**, 3101; (b) H. Brunner, J. Doppelberger, E. O. Fischer and M. Lapus, *J. Organomet. Chem.* 1976, **112**, 65; (c) E. O. Fischer and H. J. Beck, *Angew. Chem. Int. Ed. Engl.* 1970, **9**, 72.
10. (a) T. V. Ashworth, J. A. K. Howard, M. Laguna and F. G. A. Stone, *J. Chem. Soc., Dalton Trans.* 1980, 1593; (b) M. Berry, J. A. K. Howard and F. G. A. Stone, *J. Chem. Soc., Dalton Trans.* 1980, 1601; (c) T. B. Ashworth, M. Berry, J. A. K. Howard, M. Laguna and F. G. A. Stone, *J. Chem. Soc., Dalton Trans.* 1980, 1615; (d) J. C. Jeffrey, I. Moore, M. Murray and F. G. A. Stone, *J. Chem. Soc., Dalton Trans.* 1982, 1741; (e) M. Berry, J. Martin-Gil, J. A. K. Howard and F. G. A. Stone, *J. Chem. Soc., Dalton Trans.* 1980, 1625.
11. R. D. Adams, J. E. Babin and M. Tasi, *Inorg. Chem.* 1986, **25**, 4514.
12. E. O. Fischer, U. Schubert and H. Fischer, *Inorg. Synth.* 1979, **19**, 169.
13. R. Huq, A. J. Poë and S. Charola, *Inorg. Chim. Acta* 1980, **38**, 121.
14. *International Tables for X-ray Crystallography*, Vol. IV. Kynoch Press, Birmingham, U.K. (1975): (a) Tables 2.2B, pp. 99–101; (b) Table 2.3.1, pp. 149–150.
15. R. D. Adams, J. E. Babin and M. Tasi, *Inorg. Chem.* 1986, **25**, 4514.
16. R. D. Adams, J. E. Babin and H. S. Kim, *J. Am. Chem. Soc.* 1987, **109**, 1414.
17. R. D. Adams, J. E. Babin, K. Natarajan, M. Tasi and J. G. Wang, *Inorg. Chem.* 1987, **26**, 3708.
18. D. M. P. Mingos, *Accts Chem. Res.* 1984, **17**, 311.

Polyhedron Vol. 8, No. 19, pp. 2359–2365, 1989
Printed in Great Britain

0277–5387/89 $3.00+.00
© 1989 Pergamon Press plc

STRUCTURAL CHARACTERIZATION OF BIS(ARYLIMINO)ISOINDOLINE COMPLEXES OF DIMOLYBDENUM

D. M. BAIRD* and K. Y. SHIH

Department of Chemistry, Florida Atlantic University, Boca Raton, FL 33431, U.S.A.

and

J. H. WELCH and R. D. BEREMAN

Department of Chemistry, North Carolina State University, Raleigh, NC 27650, U.S.A.

(*Received* 27 *February* 1989; *accepted* 10 *May* 1989)

Abstract—The complexes $[Mo_2(OAc)_3(BAII)]$, where BAII is either bis(pyridylimino) isoindoline or bis(4,6-dimethylpyridylimino)isoindoline, have been synthesized. A detailed interpretation of their ^1H NMR spectra has been made. The structure of the bis(pyridylimino)isoindoline derivative has been determined by X-ray analysis to facilitate the assignment of the resonance lines in the NMR spectra. The complex is triclinic belonging to the space group $P\bar{1}$ with $a = 8.241(3)$, $b = 12.274(4)$, $c = 15.390(6)$ Å, $V = 1490.1(9)$ Å^3 and $D_{calc} = 1.66$ g cm^{-3}. The final R value was 0.058. The structure consists of a quadruply bonded dimolybdenum unit which is bound to three bridging acetates and one bridging BAII ligand. The BAII ligand is bound to one molybdenum by an imino nitrogen and to the other molybdenum by the isoindoline nitrogen and a pyridyl nitrogen. The pyridyl nitrogen is bound in a position approximately co-axial with the metal–metal bond. The Mo—Mo bond distance is 2.109(1) Å.

One useful way of probing the electronic structures of dimolybdenum compounds has been the investigation of the spectroscopic and electrochemical trends found within series of structurally related compounds. Most attention has been focused on the compounds of the series $Mo_2X_4(LL)_2$ and $Mo_2X_4L_4$, where X is halogen, LL is bidentate phosphine and L is monodentate phosphine.[1] We decided to synthesize and investigate a new series of dimolybdenum compounds based on the bis(arylimino)isoindoline, BAII, ligand in order to extend, and complement, the previous studies. The general structures of the BAII ligands are shown below. The BAII system was chosen since it is fairly easy to synthetically alter the aromatic nitrogen heterocycle portion of the ligand.[2] As a result, the BAII ligands afford the opportunity to study a large series of complexes. Unlike other series, the donor atoms attached directly to the molybdenums in the BAII series remain the same, but peripheral ligand substituents can be altered. We have synthesized an extensive series of complexes with the formula $[Mo_2(OAc)_3(BAII)]$. The series now includes 11 complexes in which the N-heterocycle portion of the ligand is pyridine, alkyl pyridines, halopyridines, thiazoles and pyrazine. However, studies of the spectroscopic and electrochemical properties of these complexes had been hindered by the fact that X-ray quality crystals had been difficult to produce and thus the exact structures of the complexes were not known. We have now obtained X-ray quality crystals of the dimolybdenum complex of the BAII ligand derived from unsubstituted pyridine. The structure of this complex is reported herein. Knowledge of the structure has allowed detailed interpretation of the ^1H NMR spectrum of the unsubstituted pyridine derivative. This has in turn allowed the ^1H NMR characterization of the structures of the other complexes in the series.

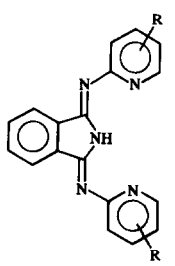

* Author to whom correspondence should be addressed.

EXPERIMENTAL

Materials and methods

All synthetic procedures were performed under an atmosphere of argon using standard Schlenk techniques or a glove box. Methanol was refluxed with calcium sulphate. Benzene and hexane were refluxed over Na–benzophenone and distilled just prior to use. Molybdenum acetate was prepared from $Mo(CO)_6$ using the method of Wilkinson.[3] Bis(pyridylimino)isoindoline and bis(4,6-dimethylpyridylimino)isoindoline were prepared by the method of Siegl in which 2-aminopyridine or 2-amino-4,6-dimethylpyridine was reacted with 1,2-dicyanobenzene in refluxing butanol in the presence of a small amount of anhydrous calcium chloride.[2]

NMR spectra were obtained in $CDCl_3$ or d^6-acetone, with TMS as internal standard, using a GE QE-300 spectrophotometer. The samples were prepared under an argon atmosphere in a glove box.

Synthesis of complexes

An improved version of the previously reported method was used.[4]

$[Mo_2(OAc)_3(BAII)]$ (BAII = *bis(pyridylimino) isoindoline*). $Mo_2(OAc)_4$ (1 g) was added as one portion to a solution of bis(pyridylimino)isoindoline in 35 cm^3 of dry, degassed methanol. The resulting yellow mixture slowly turned emerald green. After stirring overnight a green precipitate formed, which was filtered, washed with hexane under argon and then dried *in vacuo*. This procedure resulted in about 75% yield. X-ray quality crystals were obtained by dissolving the green product in a minimum volume of benzene, followed by addition of one third the volume of hexane. Over several days large, dark green blocks were deposited.

$[Mo_2(OAc)_3(BAII)]$ (BAII = *bis(4,6-dimethylpyridyl)isoindoline*). The procedure for the reaction of $Mo_2(OAc)_4$ with bis(4,6-dimethylpyridylimino) isoindoline was the same as that used for the unsubstituted pyridine derivative. However, the mixture had to be stirred for 10 days before the reaction was complete. The yield was about 60%.

Single-crystal X-ray analysis

A dark green crystal was surveyed, and cell dimensions were obtained by a least-squares fit of setting angles of 21 high-angle reflections ($2\theta > 18°$). A data set was collected on a Nicolet R3m/μ diffractometer equipped with a graphite monochromator and molybdenum radiation (λ = 0.71069 Å). Systematic absence indicated that the crystal belonged to the triclinic space group $P\bar{1}$. Two check reflections collected after every 98 reflections showed a decrease in intensity of 61 and 48% showing decomposition of the crystal. The data were corrected using the package supplied by Nicolet in which the average decrease of the two reflections is used to correct the intensities in blocks. Of the 4339 unique reflections recorded in the range $3° < \theta < 45°$, 2766 of these (having $I > 1.5\sigma(I)$) were used in the structure analysis. Data were corrected for Lorentz and polarization effects but not for absorption owing to the low absorption coefficient (8.7 cm^{-1}). An isotropic secondary extinction correction was made (secondary extinction coefficient = 1.4×10^{-7}). Atomic scattering factors for all atoms were taken from the *International Tables for X-ray Crystallography*.[5] Pertinent crystal, data collection, and refinement parameters are summarized in Table 1.

The molybdenum atoms were located by the direct-methods program SOLV of the crystallographic program package *SHELXTL*.[6] The remaining non-hydrogen atoms were found by conventional difference Fourier techniques to give a trial structure. The structure was refined by the block-diagonal least-squares technique using *SHELXTL* on a Data General Microeclipse computer. The quantity minimized was $\sum w(\Delta F)^2$, where $w = 1/(\sigma^{F^2} + 0.00015F^2)$. The non-hydrogen atoms were refined with anisotropic temperature factors. The hydrogen atoms were placed in calculated positions 0.96 Å away from the attached carbon atom and were not refined. The final R indices are given in Table 1. The refined structure was plotted by using the *SHELXTL* graphics package.

Table 1. Crystal data

$Mo_2C_{24}H_{21}N_5O_6 \cdot C_6H_6$	
f_w	745.40
a (Å)	8.241(3)
b (Å)	12.274(4)
c (Å)	15.390(6)
α (°)	85.40(3)
β (°)	78.64(3)
γ (°)	77.74(3)
V (Å^3)	1490.1(9)
d (g cm^{-3})	1.66
Z	2
Space group	$P\bar{1}$
Independent reflections	4339
Observed reflections	2766
R	0.058
R_w	0.047

RESULTS AND DISCUSSION

Structure of $[Mo_2(OAc)_3(BAII)]$

The structure and atom labelling scheme for $[Mo_2(OAc)_3(BAII)]$ are shown in Fig. 1. Selected bond distances are reported in Table 2 and selected angles in Table 3.

The compound $[Mo_2(OAc)_3(BAII)]$ crystallizes in the triclinic $P\bar{1}$ space group with one benzene of solvation per complex molecule. No intermolecular contacts between molybdenum atoms and acetate oxygens are found. This type of contact has been found in numerous other dimolybdenum complexes which possess bridging acetates.

The structure of the complex consists of a dimol-

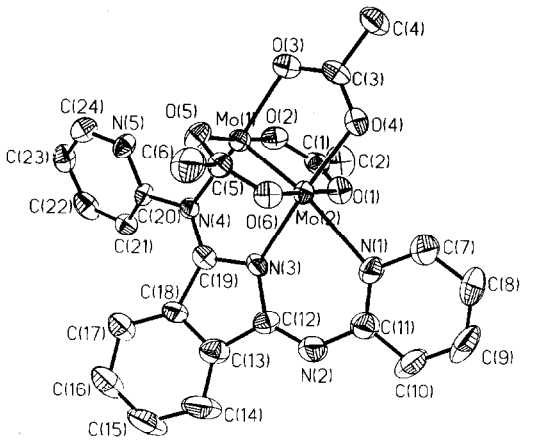

Fig. 1. Structure of $[Mo_2(OAc)_3(BAII)]$ showing the atom labelling scheme.

Table 2. Bond distances for $[Mo_2(OAc)_3(BAII)]$

Mo(1)—Mo(2)	2.106(1)	Mo(1)—O(2)	2.117(6)
Mo(1)—O(3)	2.134(6)	Mo(1)—O(5)	2.113(6)
Mo(1)—N(4)	2.143(7)	Mo(2)—O(1)	2.119(6)
Mo(2)—O(4)	2.125(6)	Mo(2)—O(6)	2.128(6)
Mo(2)—N(1)	2.466(7)	Mo(2)—N(3)	2.120(7)
O(1)—C(1)	1.255(10)	O(2)—C(1)	1.273(11)
O(3)—C(3)	1.272(10)	O(4)—C(3)	1.252(11)
O(5)—C(5)	1.271(9)	O(6)—C(5)	1.269(10)
N(2)—C(11)	1.387(12)	N(2)—C(12)	1.295(11)
N(3)—C(12)	1.396(11)	N(3)—C(19)	1.373(10)
N(4)—C(19)	1.306(11)	N(4)—C(20)	1.426(10)

Table 3. Angles for $[Mo_2(AOc)_3(BAII)]$

Mo(2)—Mo(1)—O(2)	92.4(1)	Mo(2)—Mo(1)—O(3)	91.3(1)
O(2)—Mo(1)—O(3)	88.0(2)	Mo(2)—Mo(1)—O(5)	91.6(1)
O(2)—Mo(1)—O(5)	175.6(2)	O(3)—Mo(1)—O(5)	89.9(2)
Mo(2)—Mo(1)—N(4)	92.0(2)	O(2)—Mo(1)—N(4)	91.9(3)
O(3)—Mo(1)—N(4)	176.8(2)	O(5)—Mo(1)—N(4)	90.0(3)
Mo(1)—Mo(2)—O(1)	91.0(1)	Mo(1)—Mo(2)—O(1)	91.7(2)
O(1)—Mo(2)—O(4)	88.0(2)	Mo(1)—Mo(2)—O(6)	91.5(1)
O(1)—Mo(2)—O(6)	176.8(2)	O(4)—Mo(2)—O(6)	89.9(2)
Mo(1)—Mo(2)—N(1)	169.0(2)	O(1)—Mo(2)—N(1)	86.0(2)
O(4)—Mo(2)—N(1)	98.7(2)	O(6)—Mo(2)—N(1)	92.0(2)
Mo(1)—Mo(2)—N(3)	92.9(2)	O(1)—Mo(2)—N(3)	93.1(3)
O(4)—Mo(2)—N(3)	175.2(2)	O(6)—Mo(2)—N(3)	88.8(3)
N(1)—Mo(2)—N(3)	76.8(3)	Mo(2)—O(1)—C(1)	117.3(5)
Mo(1)—O(2)—C(1)	115.6(5)	Mo(1)—O(3)—C(3)	116.8(6)
Mo(2)—O(4)—C(3)	117.4(5)	Mo(1)—O(5)—C(5)	117.8(5)
Mo(2)—O(6)—C(5)	117.3(5)	Mo(2)—N(1)—C(7)	111.3(6)
Mo(2)—N(1)—C(11)	129.9(6)	C(11)—N(2)—C(12)	127.7(8)
Mo(2)—N(3)—C(12)	133.7(5)	Mo(2)—N(3)—C(19)	117.7(6)
C(12)—N(3)—C(19)	108.1(7)	Mo(1)—N(4)—C(19)	119.0(5)
Mo(1)—N(4)—C(20)	119.0(5)	Mo(1)—N(4)—C(20)	115.4(5)
C(19)—N(4)—C(20)	125.6(7)	N(1)—C(11)—N(2)	122.2(8)
N(2)—C(12)—N(3)	128.7(8)	N(3)—C(19)—N(4)	117.3(7)

ybdenum unit which is bridged by three acetates and a BAII ligand. The remarkable feature of the structure is the binding mode of the BAII ligand. Three BAII complexes with copper and one with manganese have been reported previously.[7-9] In all of these complexes the ligands have been shown to be planar tridentate species which bind only one metal using the two nitrogens from the aromatic nitrogen heterocycles and the nitrogen from the isoindoline portion of the molecule. In the present case rotation about one of the imino bonds has made the non-bonding pair of electrons on one of the imino nitrogens available for donation to a molybdenum. This rotation has placed a pyridine in a position where it may not bind to the dimetal unit, Scheme 1. The result is two inequivalent pyridine rings: ring A in Scheme 1, the "inside" ring, which is coordinated to the axial position of one of the molybdenum atoms, and ring B, the "outside" ring, which is not bound to a molybdenum atom.

The BAII thus bridges the dimetal unit by binding one molybdenum with the isoindoline nitrogen and the other molybdenum with an imino nitrogen. In addition, one of the pyridine nitrogens binds to one of the axial positions of the dimolybdenum unit. The five-membered ring which includes the two molybdenums and the bridging BAII ligand forms a common structural feature in dimolybdenum chemistry. There have been a number of complexes of derivatives of 2-aminopyridine,[10] 2-aminothiazole,[11] and acetamidines[12] reported in which the N—C—N linkage bridges the metal–metal bond. The various angles and M—N distances within the five-membered ring in $[Mo_2(OAc)_3(BAII)]$ are comparable to those in these other molecules.[13] The N—C—N portion of the BAII ligand which bridges the dimolybdenum unit can be thought of as being isoelectronic with acetate.

A comparison can be made between the angles and distances within the BAII ligand itself and those of BAII ligands in complexes of other metals. The bond angles and distances within the six-membered chelate ring that includes Mo(2), the isoindoline nitrogen and the inside pyridyl nitrogen are quite similar to those in the equivalent rings in the manganese and three copper structures, except that the N—Mo—N angle is not 90°. This angle might be expected for achievement of maximum overlap between the pyridine lone pair and an appropriate orbital on the molybdenum. It is possible for the BAII ligand to obtain a geometry in which this angle is 90°, as has been demonstrated in the three copper complexes. The N—C—N angle for the three bridging atoms has been contracted significantly to only 117.3(7)°, as compared to 128.7(8)° for the equivalent angle on the side of the ligand which includes the inside pyridine, and to 131.8, 129.6, 129.6 and 129.3° in the manganese and the three copper structures, respectively. This is apparently due to the fact that the imino nitrogen is pulled in to achieve maximum bonding interaction with Mo(1). This notion is supported by comparing the N—C—N angle with the same angle in other dimolybdenum complexes in which the metal is bridged by the N—C—N group. For example, this angle is 117.8(9) and 114.9(5)° in the 2-aminopyridine derivatives $Mo_2(map)_4$ and $Mo_2(PhNpy)_4$, respectively, and 117.0(1), 115.7(5) and 117.4(5)° in the acetamidine derivatives $Mo_2(PhC(NPh)_2)_4$, $Mo_2[(PhN)_2CCH_3]_3(OAc)$ and $Mo_2[[(2,6\text{-xylyl})N]CCH_3]_2(OAc)_2$.

The outside pyridine ring is twisted out of the plane of the isoindoline group. Mean planes were calculated for this pyridine and for the isoindoline group. The dihedral angle is 45.5°. The ring is undoubtedly twisted into this particular position in the crystalline solid, in part, because of crystal packing forces. In fact the closest approach of the solvent molecule to the complex molecule occurs between the benzene ring and C(24) and N(5) of the outside pyridine ring. But, in addition, with the ring oriented as it is in the solid benzene solvate the protons on C(17) and C(21) are 2.431 Å apart. If the pyridine ring were made co-planar with the isoindoline group and all bond angles and distances were maintained, these protons would only be approximately 0.8 Å apart. It seems clear that some twisting of the pyridine ring should occur to minimize interaction of these protons.

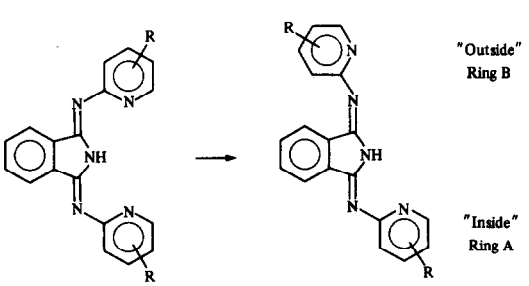

Scheme 1.

The axial interaction of Mo(2) with the inside pyridyl nitrogen can be compared with the same interaction in similar structures of other ligands. In particular, one other structure has been reported in which a pendant aromatic nitrogen heterocycle is bound to an axial position in a dimolybdenum molecule. $Mo_2(OAc)_2(tpb)_2$, where tpb is tris(pyrazolyl)borate, has two *cis*-bridging acetates and two bidentate tpb ligands, each of which is bound through only two pyrazole nitrogens.[14] Each tpb ligand thus has a pendant pyrazole ring associ-

ated with it. One of the pendant pyrazole rings is bound to the axial position of the dimetal unit. The second pyrazole ring is not bound. The Mo—N bond to the axial pyrazole ring is quite long at 2.45(1) Å. This is about the same as the length of the Mo—N bond to the axial pyridine ring in $[Mo_2(OAc)_3(BAII)]$ which is 2.466(7) Å. More interestingly, Mo—Mo—$N_{(ax)}$ bond angles in the two compounds are remarkably similar, 169.0(2)° in the BAII complex and 170.1(5)° in the tbp complex. It seems possible that ligand constraints force the heterocycle into this position. However, in the compound $Mo_2(O_2CCF_3)_4(py)_2$, which has two axial pyridines, the average Mo—Mo—$N_{(ax)}$ angles are 171.0(2)°.[15] This evidence seems to suggest that electronic factors may be involved in determining this bond angle. In the axial pyridine adducts $Mo_2[(xylyl)NC(CH_3)O]_4 \cdot py$ and $Mo_2[(xylyl)NC(CH_3)O]_4 \cdot Me\text{-}py$[12b] the Mo—Mo—N bond angle is close to 180°, but the presence of large phenyl groups in the area around the axial position may force the pyridine into this orientation.

$[Mo_2(OAc)_3(BAII)]$ possesses the first structure reported for a dimolybdenum compound with three bridging acetates, although the trifluoroacetate complex $Mo_2(O_2CCF_3)_3Cl(C_2H_5CN)$ has been reported.[16] The Mo—Mo bond distance in $[Mo_2(OAc)_3(BAII)]$ is 2.106(1) Å. This is slightly, but significantly, longer than the 2.0934(8) Å distance found in $Mo_2(OAc)_4$, but is shorter than the 2.147(3) Å metal–metal bond distance in the tpb complex. There are probably two factors involved in determining the metal–metal bond distance in the BAII complex. It is well known that axial ligation by the molybdenum–molybdenum quadruple bond causes lengthening of the bond.[1] Thus the metal–metal bond in the BAII complex is longer than the same bond in $Mo_2(OAc)_4$. It is not as long as the metal–metal bond in the tpb complex, however, because of the presence of three rather than two acetates. It has been suggested that acetate π-orbitals become involved with metal–metal bonds in such a way as to strengthen them.[17] We must conclude that the molybdenum atoms in dimolybdenum compounds tend to be resistant to chelation by planar tri- and tetradentate ligands; so much so that the BAII ligand is forced into a highly unusual conformation in preference of a bridging rather than chelating mode. There has been only one complex reported in which one or both molybdenum atoms is chelated by a planar multidentate ligand. This is the porphyrin complex of Collman which was prepared by deoxygenation of an oxomolybdenum porphyrin complex[18] and not from a metal–metal bonded precursor. The crystal structure of this compound has not been reported.

NMR spectra of BAII *complexes of dimolybdenum*

It is believed that the overall structures of the complexes in the series are the same as that of the unsubstituted pyridine derivative reported in this manuscript based on the detailed interpretation of their NMR spectra. Two major features characterize the spectra of BAII ligands which have become coordinated to a dimolybdenum unit. First, in each case two resonances appear in the 2–3 ppm region in a ratio of 2 : 1. These are due to the three acetate groups, two that are *cis* to the BAII group and one that is *trans*. Second, the BAII portion of each spectrum becomes very complicated. It is now possible to interpret the spectrum of the unsubstituted pyridine derived BAII complex. However, an equivalent interpretation can be made for each of the complexes. Therefore, only the spectrum of the 4,6-dimethylpyridine derived complex will be discussed in detail. The spectrum of this complex is simpler to discuss since only singlet resonances should arise from the protons on the pyridine moieties of the ligand.

The spectrum of the uncoordinated ligand is as expected and is shown in Figs 2(a) and 3(a). Singlet resonances representing the two types of pyridine methyl groups occur at 2.36 and 2.49 ppm. The aromatic region displays two singlet resonances representing the two types of pyridine hydrogens at 6.80 and 7.03 ppm. The benzo protons from the isoindoline portion of the ligand generate a typical AA′BB′ pattern. This is actually two doublets of doublets centred around 7.65 and 8.06 ppm.

Upon coordination to the dimolybdenum unit the two pyridine rings become inequivalent. As a result the two pyridine methyl peaks are replaced by four methyl peaks of equal intensity at 2.21, 2.27, 2.33 and 2.43 ppm, see Fig. 2(b). In addition, four singlet resonances appear for the pyridine hydrogens at 6.52, 6.77, 6.83 and 6.96 ppm, see Fig. 3(b). The asymmetry produced in the ligand has a dramatic effect on the benzo proton resonances with the AA′BB′ pattern being replaced by an ABCD pattern. The α-protons are represented by doublets, one that occurs at 8.00 ppm, and one which has been greatly shifted to 6.71 ppm. Each resonance line in these doublets shows further splitting. In each case the main doublet results from coupling with the adjacent β-proton and the secondary splitting results from coupling with the other β-proton. The β-protons are represented by triplets of doublets centred at 7.24 and 7.31 ppm. These patterns result from splitting of the β-resonance line by coupling with the adjacent α-proton to give a doublet. Each resonance line of the doublet is further split by coupling with the adjacent β-proton. This results

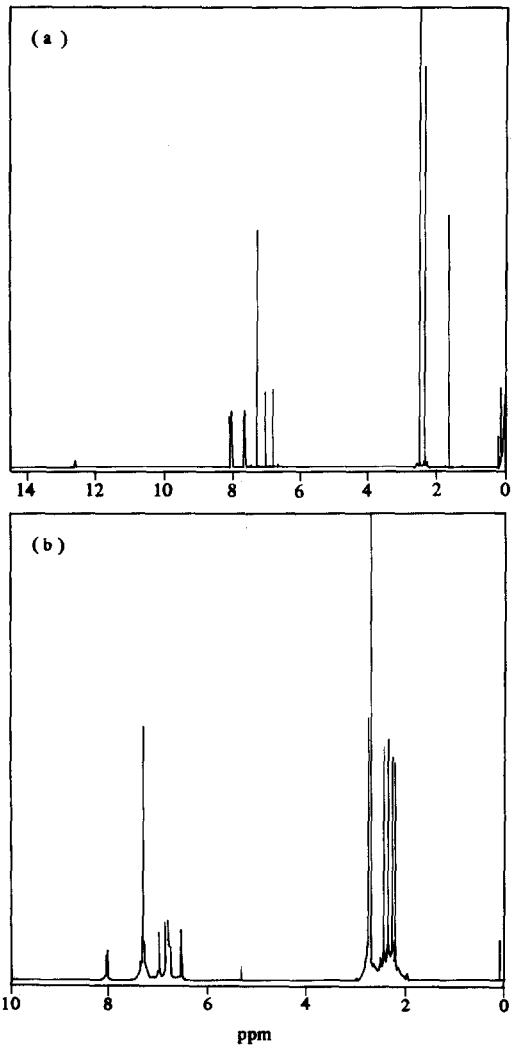

Fig. 2. ^{1}H NMR spectra of (a) bis(4,6-dimethylimino)isoindoline and (b) $[Mo_2(OAc)_3(BAII)]$ (BAII = bis(4,6-dimethylpyridylimino(isoidoline).

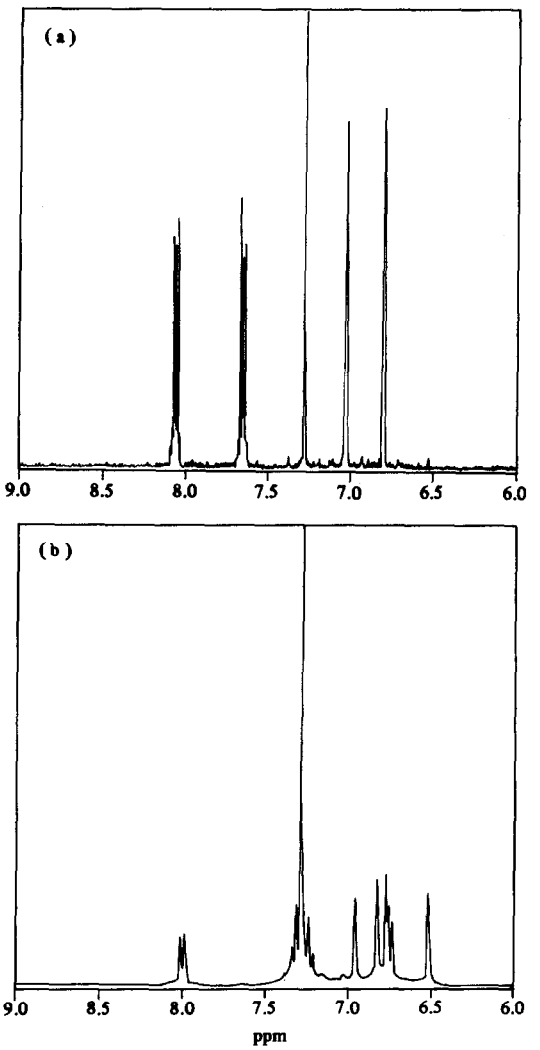

Fig. 3. ^{1}H NMR spectra of the aromatic region of (a) bis(4,6-dimethylpyridylimino)isoindoline and (b) $[Mo_2(OAc)_3(BAII)]$ (BAII = bis(4,6-dimethylpyridylimino)isoindoline).

in two triplets each with an intensity ratio of 1 : 2 : 1 due to coincidence of the two centre resonances. Each resonance of the triplet is then split into two resonances due to coupling with the non-adjacent α-proton. These assignments are supported by standard decoupling experiments and by the appropriate coupling constants.

The remarkable feature of the change in the aromatic region of the BAII ligand upon coordination is the 1.3 ppm shift of the resonance of the α-proton on C(17) which is closest to the outside pyridine. This behaviour is apparently caused by the close proximity of this proton to the inside of the ring current of the outside pyridine ring. In addition, the resonance frequencies of this proton and the pyridine hydrogens of the outside pyridine are strongly solvent dependent. For example, while the α-proton resonance occurs at 6.71 ppm in chloroform, it is shifted upfield to 6.47 ppm in acetone. At the same time two of the resonances associated with the pyridine hydrogens are shifted in the opposite direction. The resonances at 6.96 and 6.77 ppm are unaffected by solvent change, while the 6.83 and 6.52 ppm resonances are shifted downfield to 6.91 and 6.59 ppm, respectively. Whether this effect is related to interaction of the solvent with the pyridine nitrogen or changes in the dihedral angle between the outside pyridine and the iso-

Supplementary material.. Tables of complete bond lengths and angles, anisotropic thermal parameters and hydrogen atom coordinates and isotropic thermal parameters (4 pp.); a table of observed and calculated structure factors (24 pp.). Ordering information is given on p. ii of this issue.

indoline plane is not known. Further studies are now under way to address this problem.

In conclusion, the spectrum of each of the BAII complexes shows the same general features as those described above and thus it seems reasonable to assume that they have the same general structure.

Acknowledgement—This work has been supported by a grant from the Research Corporation.

REFERENCES

1. (a) F. A. Cotton and R. A. Walton, *Multiple Bonds Between Metal Atoms*. Wiley, New York (1982); (b) T. C. Zietlow, M. D. Hopkins and H. B. Gray, *J. Am. Chem. Soc.* 1986, **108**, 3266; (c) F. A. Cotton and M. Matusz, *Inorg. Chem.* 1988, **27**, 2127.
2. W. O. Siegl, *J. Org. Chem.* 1977, **42**, 1872.
3. G. Wilkinson and Z. Dori, *Inorg. Synth.* 1969, 1872.
4. D. M. Baird and R. Hassan, *Inorg. Chim. Acta* 1987, **130**, 39.
5. *International Tables for X-ray Crystallography*, p. 71. Kynoch Press, Birmingham, U.K. (1974).
6. *SHELXTL*, X-Ray Instruments Group, Nicolet Instrument Corp., Madison, Winconsin (1983).
7. R. R. Gagne, R. S. Gall, G. S. Lisensky, R. E. Marsh and L. M. Speltz, *Inorg. Chem.* 1979, **18**, 771.
8. J. R. Dorfman, PhD thesis. North Carolina State University, Raleigh (1982).
9. P. J. Domaille, R. L. Harlow, S. D. Ittel and W. G. Peet, *Inorg. Chem.* 1983, **22**, 3944.
10. (a) F. A. Cotton, R. H. Niswander and J. C. Sekutowski, *Inorg. Chem.* 1978, **17**, 3541; (b) A. R. Chakravarty, F. A. Cotton and E. S. Shamshoum, *Inorg. Chem.* 1984, **23**, 4216.
11. F. A. Cotton and W. H. Ilsley, *Inorg. Chem.* 1981, **20**, 572.
12. (a) F. A. Cotton, T. Inglis, M. Kilner and T. R. Webb, *Inorg. Chem.* 1975, **14**, 2023; (b) F. A. Cotton, W. H. Ilsley and W. Kaim, *Inorg. Chem.* 1981, **20**, 930.
13. See Table 1 in ref. 10(b).
14. D. M. Collins, F. A. Cotton and C. A. Murillo, *Inorg. Chem.* 1976, **15**, 1861.
15. F. A. Cotton and J. G. Norman Jr, *J. Am. Chem. Soc.* 1972, **94**, 5697.
16. P. Agaskar and F. A. Cotton, *Inorg. Chim. Acta* 1984, **83**, 33.
17. J. G. Norman and H. J. Kolari, *J. Chem. Soc., Chem. Commun.* 1975, 694.
18. J. P. Collman, C. E. Barnes and L. K. Woo, *Proc. Natl. Acad. Sci. USA* 1983, **80**, 7684.

Polyhedron Vol. 8, No. 19, pp. 2367–2370, 1989
Printed in Great Britain

0277–5387/89 $3.00+.00
© 1989 Pergamon Press plc

HETEROLEPTIC POLYPYRAZOLYLBORATE DERIVATIVES OF THE LANTHANIDE IONS. THE SYNTHESIS OF OXALATE COMPLEXES

MICHAEL A. J. MOSS and CHRISTOPHER J. JONES*

Department of Chemistry, University of Birmingham, PO Box 363, Birmingham B15 2TT, U.K.

(*Received* 21 *March* 1989; *accepted* 18 *May* 1989)

Abstract—The lanthanide oxalate complexes $[\{LnL_2\}_2(C_2O_4)]$ (Ln = Y, Sm, Dy, Yb or Lu and L = $HB(C_3N_2H_3)_3$) have been isolated and characterized by elemental analyses, mass spectroscopy and, except for Ln = Dy, by ^1H NMR spectroscopy. The physical properties of these materials are consistent with their formulation as binuclear complexes in which the oxalate ligand forms bidentate five-membered chelate rings with two lanthanide ions. Similar compounds are formed with Ln = La, Ce and Nd, but their low solubilities in polar organic solvents have precluded purification.

Synthetic and structural studies have shown that the $\{LnL_2\}^+$ (Ln = a lanthanide or yttrium; L = $HB(C_3N_2H_3)_2$) moiety can form remarkably stable complexes of formula $[LnL_2X]$ with a variety of bidentate ligands X, including X = β-diketonate, tropolonate or carboxylate.[1–7] These studies have revealed that, as the size of the chelate ring formed between Ln and X is decreased, the range of lanthanide elements forming complexes $[LnL_2X]$, which are soluble in polar organic solvents, is also decreased. Thus the complexes $[LnL_2(OC(Me)CHC(Me)O)]$, in which the bidentate acetylacetonate ligand forms a six-membered chelate ring, are soluble for all of the lanthanide ions.[2] Reduction of the co-ligand chelate ring size to five in the tropolonate complexes $[LnL_2(O_2C_7H_5)]$, results in complexes which are poorly soluble in CH_2Cl_2 for Ln = La–Pr, but which are freely soluble for Ln = Nd–Lu.[3] In a continuation of this trend the benzoate complexes $[LnL_2(O_2CC_6H_5)]$ were found to be insoluble in CH_2Cl_2 for Ln = La to Nd, but soluble for Ln = Sm to Lu.[4] Structural studies have revealed monomeric eight-coordinate structures[1–5] for $[CeL_2(OC(Me)CHC(Me)O)]$, $[YbL_2(OC(Me)CHC(Me)O)]$, $[YbL_2(O_2C_7H_5)]$ and $[YbL_2(O_2CC_6H_5)]$ in the solid state. In order to further extend this study of heteroleptic lanthanide complexes containing the $\{LnL_2\}^+$ moiety we have now investigated the synthesis and properties of some representative heteroleptic oxalate complexes.

Homoleptic oxalate complexes of the lanthanides may be prepared by the reaction of a lanthanide salt with oxalic acid in aqueous solution. This reaction precipitates a decahydrate, $Ln_2(C_2O_4)_3 \cdot 10H_2O$, when Ln = La, Nd, Gd.[8] However, the smaller lanthanide ions, Ln = Y, Dy, Er, Yb, precipitate a trihydrate, $[Ln(C_2O_4)(C_2O_4H)(H_2O)] \cdot 2H_2O$. In 1970, $[Er(C_2O_4)(C_2O_4H)(H_2O)] \cdot 2H_2O$ was the first lanthanide oxalate complex to be structurally characterized and the oxalate ions were found to bridge between two metal ions, forming five-membered chelate rings with both.[9] Four oxalate ions surround the lanthanide ion spanning between the two squares of the distorted square antiprism which they form, a water molecule capping the larger square of the antiprism.[9] If ammonia is dripped into the acidic lanthanide–oxalic acid solution, the binary complexes, $[(NH_4)Ln(C_2O_4)_2(H_2O)]$ (Ln = Y, Sm–Tm), are formed. The yttrium complex, $[(NH_4)Y(C_2O_4)_2(H_2O)]$, was structurally characterized 3 years before $[Er(C_2O_4)(C_2O_4H)(H_2O)] \cdot 2H_2O$, and is nine-coordinate with the same coordination sphere.[10]

EXPERIMENTAL

Potassium hydrotris-(pyrazol-1-yl)borate was prepared by the literature method.[11] Hydrated lanthanide trichlorides were obtained from Ventron

*Author to whom correspondence should be addressed.

GMBH and were used without further purification. ^{1}H NMR spectra were recorded using a JEOL JNM GX270 spectrometer. Deuterated NMR solvents were obtained from Aldrich Chemicals Ltd, and chemical shifts are reported with tetramethylsilane as internal reference at 293 K. IR spectra were recorded using potassium bromide pellets and a Perkin–Elmer 297 spectrometer. Mass spectra were obtained using a Kratos MS80RF mass spectrometer, ions being produced by electron impact. Elemental analyses were performed by the Microanalytical Laboratory, School of Chemistry, University of Birmingham.

Oxalatobis[bis{hydrotris(pyrazol - 1 - yl)borato} yttrium(III)]

$K\{HB(C_3N_2H_3)_3\}$ (0.5 g, 2 mmol) and sodium oxalate (0.07 g, 0.5 mmol) were dissolved in water (30 cm^3) and added to a stirred solution of $YCl_3 \cdot 6H_2O$ (0.30 g, 1 mmol) in water (15 cm^3); stirring was continued for 10 min. The resulting white amorphous precipitate was collected by filtration (yield = 98%). Recrystallization from CH_2Cl_2–hexane gave large, white crystals which fractured on drying (yield = 75%), m.p. = 325–327°C.

The corresponding complexes were prepared similarly with samarium, dysprosium, ytterbium and lutetium using the appropriate lanthanide trichloride hydrate. Complexes containing lanthanum, cerium and neodymium were also prepared, but were essentially insoluble so that the crude precipitate obtained by following the above procedure could not be recrystallized. Details of yields, melting points and elemental analyses are given in Table 1. All of the new complexes were colourless except that containing neodymium which was purple.

RESULTS

The reaction between oxalate, L^- and Ln^{3+} (Ln = Y, La, Ce, Nd, Sm, Dy, Yb and Lu) in aqueous solution leads to the formation of complexes which have a comparatively high melting point, *ca* 325°C, compared with $[YbL_2(acac)]$ (m.p. = 198°C) and $[YbL_2(trop)]$ (m.p. = 265°C) which are both monomers. This observation suggests that the complexes are probably dimeric and may be formulated as $[\{LnL_2\}_2(C_2O_4)]$. They are soluble in polar organic solvents for the smaller lanthanide ions Ln = Y, Sm–Lu, but are insoluble for the larger lanthanide ions Ln = La, Ce and Nd. The low solubilities of these latter complexes with the larger lanthanide ions has precluded complete purification of these materials so that these compounds were only isolated in crude form.

All of the oxalate complexes $[\{LnL_2\}_2(C_2O_4)]$ (Ln = Y, La, Ce, Nd, Sm, Dy, Yb and Lu) have essentially identical IR spectra, with a strong C=O band at 1660–1620 cm^{-1}. In the case of the insoluble complexes with Ln = La, Ce and Nd, the bands at *ca* 1400 and 1300 cm^{-1} are split into doublets and the C=O band appears at a lower frequency than for the soluble complexes. The frequency of this vibration increases with atomic number from 1615 cm^{-1} for lanthanum to 1660 cm^{-1} for lutetium.

The 270 MHz ^{1}H NMR spectra of the soluble oxalate complexes are unremarkable. Essentially identical diamagnetic spectra are observed for the

Table 1. Yields, melting points and elemental analyses for $[\{LnL_2\}_2(C_2O_4)]$

Ln	Crude yield, g (%)	Recrystallization yield, g (%)	Melting point (°C)	Elemental analysis[a] Calc. (Found) (%) C	H	N
Y	0.55(98)	0.42(75)	325–327	40.8(41.1)	3.6(3.4)	30.1(30.2)
La	0.59(97)	—	> 340	—	—	—
Ce	0.58(95)	—	> 340	—	—	—
Nd	0.61(99)	—	> 340	—	—	—
Sm[b]	0.59(95)	0.10(16)	320–322	34.0(35.0)	3.1(3.6)	23.8(24.2)
Dy	0.58(92)	0.46(73)	325–327	36.1(36.4)	3.2(3.2)	26.6(26.7)
Yb	0.61(95)	0.30(47)	325–327	35.5(35.3)	3.1(3.2)	26.1(26.1)
Lu	0.55(86)	0.25(39)	325–327	35.4(35.1)	3.1(3.3)	26.1(25.6)

[a] The complexes containing La, Ce and Nd were insoluble and could not be separated from their respective complexes $[LnL_3]$, so that meaningful elemental analyses could not be obtained.

[b] Crystallized with 1 mol of CH_2Cl_2.

complexes $[\{LnL_2\}_2(C_2O_4)]$ (Ln = Y and Lu). These each contain three signals of equal area comprising two doublets at $\delta = 7.58$ and 6.93 (Y) or 7.58 and 6.87 ppm (Lu) and a triplet at $\delta = 5.83$ ppm (Y and Lu): all with $^3J_{HH} = 2$ Hz. In the cases of the parmagnetic complexes containing samarium and ytterbium no coupling is resolved and the signals are contact shifted so that the three resonances

Table 2. Partial mass spectra for complexes $[\{LnL_2\}_2(C_2O_4)]$[a]

Ln		m/z	Relative intensity (%)	Comments[b]
Y	(89, 100%)	1117	1.5	$\{(YL_2)_2(C_2O_4)-1\}^+$
		1073	30	$\{(YL_2)_2(CO_2)-1\}^+$
		1050	3	$\{(YL_2)_2(C_2O_4)-pzH\}^+$
		515	100	YL_2^+
		369	47	$YLpz^+$
		223	26	Ypz_2^+
		68	34	pzH^+
La	(139, 99.9%)	710	0.7	$\{LaL_3-pzH\}^+$
		631	0.5	LaL_2pz^+
		565	10	LaL_2^+
		419	5	$LaLpz^+$
		273	6	$Lapz_2^+$
		68	100	pzH^+
Ce	(140, 88.5%)	711	1	$\{CeL_3-pzH\}^+$
		633	15	CeL_2pz^+
		566	10	CeL_2^+
		420	7	$CeLpz^+$
		274	9	$Cepz_2^+$
		68	100	pzH^+
Nd	(142, 27.1%)	1184	0.4	$\{(NdL_2)(CO_2)\}^+$
		568	40	NdL_2^+
		422	14	$NdLpz^+$
		276	10	$Ndpz_2^+$
		68	100	pzH^+
Sm	(152, 26.7%)	1328	0.04	$\{(SmL_2(C_2O_4))_2-1\}^+$
		645	1.6	SmL_2pz^+
		578	10	SmL_2^+
		432	6	$SmLpz^+$
		286	4	$Smpz_2^+$
		68	100	pzH^+
Dy	(162, 25.5%)	1265	0.08	$\{(DyL_2)_2(C_2O_4)\}^+$
		1221	1.3	$[DyL_2]_2(CO_2)^+$
		588	100	DyL_2^+
Yb	(174, 31.8%)	1283	1	$\{(YbL_2)_2(C_2O_4)-3\}^+$
		1242	3	$\{(YbL_2)_2(CO_2)\}^+$
		600	100	YbL_2^+
		454	73	$YbLpz^+$
Lu	(175, 97.4%)	1245	0.6	$\{(LuL_2)_2(CO_2)-1\}^+$
		601	100	LuL_2^+
		455	38	$LuLpz^+$
		68	87	pzH^+

[a] Values for m/z were calculated using the mass of the most abundant isotope of each element i.e. ^{12}C, ^1H, ^{14}N, ^{16}O and ^{11}B (80.2%); the lanthanide isotopes used and their natural abundances are given in parentheses.

[b] $C_3N_2H_4$ = pzH.

appear at $\delta = 8.76$, 6.03 and 4.85 ppm (Sm) or 15.6, 3.6 and 0.7 ppm (Yb). Resolved spectra of the dysprosium complex could not be obtained. The resonance at 15.6 ppm in the spectrum of $[(YbL_2)_2(C_2O_4)]$ is intermediate in shift between the corresponding resonances in the spectra of the analogous acetylacetonate (10.0 ppm)[5] and troplonate (25.4 ppm)[3] complexes. These complexes contain six- and five-membered chelate rings, respectively. In contrast, the complexes $[YbL_2(O_2CMe)]$ and $[YbL_2(O_2CPh)]$, which contain four-membered chelate rings,[4] exhibit resonances at 33.5 and 33.1 ppm, respectively. These findings are consistent with the oxalate ion being bound with the formation of a five-membered chelate ring, in accord with the structural precedents.[9,10]

The mass spectra of the new compounds are summarized in Table 2. These confirm the binuclear formulation proposed above for the complexes $[\{LnL_2\}_2(C_2O_4)]$ (Ln = Nd, Sm, Dy, Yb and Lu), since high mass fragments corresponding to the presence of a bimetallic ion were observed; although these fall in the m/z range 1100–1300 mass units, which is at the limit of the instrument calibration. The lanthanum and cerium complexes do not yield a volatile fragment containing oxalate by electron impact, the highest mass fragments seem to be derived from $[LnL_3]$, this may be a significant component of the insoluble material isolated or a volatile trace impurity. In either case it appears that completely pure samples of $[\{LnL_2\}_2(C_2O_4)]$ were not obtained for Ln = La or Ce, although the IR spectra confirm the presence of oxalate in the product. The $[LnL_3]$ could arise from disproportionation reactions involving the heteroleptic complexes $[\{LnL_2\}_2(C_2O_4)]$ (Ln = La or Ce). Such disproportionation reactions do appear to occur in the related acetate complexes, $[LnL_2(O_2CMe)]$. However, it must be said that no evidence for disproportionation was observed with the related troplonate complexes. Structural studies of the new complexes using single crystal X-ray diffraction methods have not been possible since the crystals were found to fracture on removal from the solvent. Attempts to mount crystals in capillaries containing the mother liquor were unsuccessful.

In a continuation of the trend observed for the complexes $[LnL_2(O_2C_7H_5)]$, for which the three largest lanthanide ion complexes are poorly soluble, the complexes of the four largest lanthanide ions are insoluble when oxalate co-ligands are present in place of tropolonate.

Acknowledgements—We are grateful to Dr A. J. Edwards and Professor W. J. Evans for helpful discussions, to the SERC and BP Chemicals for support (to M.A.J.M.) and to NATO for the provision of travel grant No. 175/84.

REFERENCES

1. C. J. Jones and M. A. J. Moss, *Abstr. XXIV Int. Conf. Coord. Chem., Chim. Chronika*, Association of Greek Chemists, A7-488 (1986).
2. M. A. J. Moss, C. J. Jones and A. J. Edwards, *Polyhedron* 1988, **7**, 79.
3. M. A. J. Moss and C. J. Jones, *Polyhedron* 1989, **8**, 117.
4. M. A. J. Moss and C. J. Jones, *Polyhedron* 1989, **8**, 555.
5. M. A. J. Moss, C. J. Jones and A. J. Edwards, *J. Chem. Soc., Dalton Trans.*, in press.
6. W. D. Moffat, M. V. R. Stainer and J. Takats, *Inorg. Chim. Acta* 1987, **139**, 75.
7. M. V. R. Stainer and J. Takats, *Inorg. Chem.* 1982, **21**, 4050.
8. I. L. Jenkins, F. H. Moore and M. J. Waterman, *J. Inorg. Nucl. Chem.* 1965, **27**, 77.
9. H. Steinfink and G. D. Brunton, *Inorg. Chem.* 1970, **9**, 2112.
10. T. R. R. McDonald and J. M. Spink, *Acta. Cryst.* 1967, **23**, 944.
11. S. Trofimenko, *Inorg. Synth.* 1970, **12**, 99.

Polyhedron Vol. 8, No. 19, pp. 2371–2378, 1989
Printed in Great Britain

0277–5387/89 $3.00+.00
© 1989 Pergamon Press plc

THE SYNTHESIS AND X-RAY CRYSTAL STRUCTURE OF THE MONODENTATE (S) THIOSEMICARBAZIDE AND THIOSEMICARBAZONE COMPLEXES $[Fe(CO)_2L(\eta^5\text{-}C_5H_5)][PF_6]$

MICHEL J. M. CAMPBELL,* ELIZABETH MORRISON and VERNON ROGERS

The School of Chemistry, Thames Polytechnic, London SE18 6PF, U.K.

and

PAUL K. BAKER

Department of Chemistry, University College of North Wales, Bangor, Gwynedd LL57 2UW, U.K.

and

DAVID C. POVEY and GALLIENUS W. SMITH

Department of Chemistry, University of Surrey, Guildford, Surrey GU2 5XH, U.K.

(*Received* 4 *April* 1989; *accepted* 18 *May* 1989)

Abstract—Reaction of $[Fe(CO)_2(OCMe_2)(\eta^5\text{-}C_5H_5)][PF_6]$ with 1 equivalent of L ($L = H_2NNHCSNH_2$ or $R'R''CNNHCSNH_2$ where $R' = R'' = Me$; $R' = H$, $R'' = Ph$; $R' = H$, $R'' = p\text{-}NO_2Ph$; $R' = Me$, $R'' = p\text{-}MePh$; $R'R'' = C_5H_{10}$) in $CHCl_3$ at 50°C gave good yields of $[Fe(CO)_2L(\eta^5\text{-}C_5H_5)][PF_6]$ by displacement of the acetone. The crystal structure of $[Fe(CO)_2(PhCHNNHCSNH_2)(\eta^5\text{-}C_5H_5)][PF_6]$ was determined by single crystal X-ray diffraction studies refined to $R = 0.067$ for 1389 reflections above background. The coordination geometry about the iron may best be described in terms of a "piano stool" or pseudo-octahedral structure. The $C_5H_5^-$ ligand occupies three sites in the octahedron with the carbonyls and the sulphur atom of the thiosemicarbazone in the other three sites. The Mössbauer isomer shifts of these compounds have values which lie between that of $[Fe(CO)_3(\eta^5\text{-}C_5H_5)]^-$ and those for $[Fe(CO)_2X(\eta^5\text{-}C_5H_5)]$ showing the thiosemicarbazone sulphur to be a poorer π-acceptor than CO and a better π-acceptor than the halides. The similarity of the spectroscopic data for all the compounds suggests that they all have the same structure. The monodentate S-bonded nature of the thiosemicarbazide in solutions of $[Fe(CO)_2(NH_2NHCSNH_2)(\eta^5\text{-}C_5H_5)][PF_6]$ is confirmed by its reaction with benzaldehyde to give the compound $[Fe(CO)_2(PhCHNNHCSNH_2)(\eta^5\text{-}C_5H_5)][PF_6]$.

Since 1934 when the first thiosemicarbazide complexes of nickel(II) were reported,[1] a wide range of "classical" coordination compounds formed by transition metal ions with thiosemicarbazides and thiosemicarbazones have been described.[2] Thiosemicarbazones have a wide range of pharmacological activity against, amongst other things, protozoa, influenza, smallpox, leprosy and certain kinds of tumour, and have been suggested as possible pesticides and fungicides (see references cited in the two reviews[2]). Following Liebermeister's demonstration that copper ions enhanced the antitubercular activity of *p*-acetamidobenzaldehyde thiosemicarbazone,[3] the role of metal ions in thiosemicarbazone has been either proved or suspected in many other cases.

Most "classical" coordination compounds formed by thiosemicarbazides and thiosemicarba-

* Author to whom correspondence should be addressed.

zones are with first row transition metal ions in the +2 and +3 oxidation states, i.e. with hard or marginally soft acids, and the other ligands in the coordination sphere, where present, are usually halides. In most of the compounds these ligands are bidentate and coordinate through sulphur and the hydrazinic nitrogen.[2] In a small number of cases thiosemicarbazide and thiosemicarbazones have been shown to coordinate as monodentate ligands through the sulphur atom. In these cases the metal ion is a soft acid, e.g. Ag^{I}, Hg^{II} and Co^{II} in $CoI_2(C_6H_5CHNNHCSNH_2)_2$.[2,4]

In organotransition metal compounds the metal centre is normally soft and most of the ligands bound to it are π-acceptors. Such compounds might therefore prove suitable to test the conditions under which thiosemicarbazones form monodentate complexes. We have previously described[5] the first organotransition metal compounds, $[MoX(CO)_2$(thiosemicarbazone)$(\eta^3\text{-}C_3H_4R)]$, containing a thiosemicarbazone as an attached ligand. In these compounds the thiosemicarbazone is found to be bidentate. We have also reported[6] the corresponding semicarbazone compounds $[MoX(CO)_2$(semicarbazone)$(\eta^3\text{-}C_3H_4R)]$ and here too the semicarbazone ligand is bidentate. Preliminary results of our work describing the first organoiron thiosemicarbazide and thiosemicarbazone complexes $[Fe(CO)_2L(\eta^5\text{-}C_5H_5)][PF_6]$, where L is $NH_2NHCSNH_2$ or $R_1R_2CNNHCSNH_2$ and is found to be monodentate, have already been published.[7] In this paper we wish to describe this work in full and to report the X-ray structure of $[Fe(CO)_2(C_6H_5CHNNHCSNH_2)(\eta^5\text{-}C_5H_5)][PF_6]$.

EXPERIMENTAL

The reactions described in this paper were carried out under an atmosphere of nitrogen using standard Schlenk techniques. The complex $[Fe(CO)_2(OCMe_2)(\eta^5\text{-}C_5H_5)][PF_6]$ was prepared by the literature method,[8] and the thiosemicarbazone ligands by the method described by Sah and Daniels.[9] All other chemicals were purchased from commercial sources.

The elemental analyses for carbon, hydrogen and nitrogen were recorded on a Carlo Erba Elemental Analyser MOD 1106 using helium as the carrier gas. IR spectra were recorded, as KBr discs on a Perkin–Elmer 397 IR spectrophotometer. The ^1H NMR spectra were recorded either on a Bruker WH 400 MHz spectrometer at the University of Warwick or on a Jeol GX-270 at Thames Polytechnic (all spectra were calibrated against tetramethylsilane). The Mössbauer spectra were recorded on a Cryophysics microprocessor controlled Mössbauer spectrometer and spectra were calibrated against Fe-57 enriched iron foil.

(1) $[Fe(CO)_2(H_2NNHCSNH_2)(\eta^5\text{-}C_5H_5)][PF_6]$

$H_2NNHCSNH_2$ (0.06 g, 0.66 mmol) was added to a stirred solution of $[Fe(CO)_2(OCMe_2)(\eta^5\text{-}C_5H_5)][PF_6]$ (0.25 g, 0.66 mmol) in $CHCl_3$ (20 cm^3) warmed to 50°C. After 90 min the yellow $[Fe(CO)_2(H_2NNHCSNH_2)(\eta^5\text{-}C_5H_5)][PF_6]$ which had separated was filtered, washed with $CHCl_3$ (3×5 cm^3) and dried in a desiccator over silica gel (0.16 g, 59%).

(2) $[Fe(CO)_2(cy\text{-}C_5H_{10}CNNCSNH_2)(\eta^5\text{-}C_5H_5)][PF_6]$

The $cy\text{-}C_5H_{10}CNNHCSNH_2$ (0.09 g, 0.53 mmol) was added to a stirred solution of $[Fe(CO)_2(OCMe_2)(\eta^5\text{-}C_5H_5)][PF_6]$ (0.20 g, 0.53 mmol) in $CHCl_3$ (20 cm^3) warmed to 50°C. After 2 h the orange $[Fe(CO)_2(cy\text{-}C_5H_{10}CNNHCSNH_2)(\eta^5\text{-}C_5H_5)][PF_6]$ which had separated was filtered, washed with $CHCl_3$ (3×5 cm^3) and dried in a desiccator over silica gel (0.18 g, 72%).

The thiosemicarbazone complexes (**3**–**6**) were prepared in an analogous manner by reaction of $[Fe(CO)_2(OCMe_2)(\eta^5\text{-}C_5H_5)][PF_6]$ with an equimolar quantity of L [$L = R'R''CNNHCSNH_2$, where $R' = R'' =$ Me (**3**); $R' =$ H, $R'' =$ Ph (**4**); $R' =$ H, $R'' = p\text{-}NO_2Ph$ (**5**) and $R' =$ Me, $R'' = p$-MePh (**6**)] in $CHCl_3$ at 50°C. For colours, yields and decomposition points see Table 1.

Reaction of $[Fe(CO)_2(H_2NNHCSNH_2)(\eta^5\text{-}C_5H_5)][PF_6]$ *with* PhCHO

PhCHO (0.04 g, 0.24 mmol) was added to a stirred solution of $[Fe(CO)_2(H_2NNHCSNH_2)(\eta^5\text{-}C_5H_5)][PF_6]$ (0.10 g, 0.24 mmol) in $CHCl_3$ (20 cm^3) warmed to 50°C. After 2 h the orange solid $[Fe(CO)_2(PhCHNNHCSNH_2)(\eta^5\text{-}C_5H_5)][PF_6]$ which had separated was filtered, washed with Et_2O (2×5 cm^3) and dried in a desiccator (0.06 g, 50%). Found: C, 34.5; H, 2.9; N, 9.8. $C_{15}H_{14}N_3FeO_2PS$ requires C, 35.9; H, 2.8; N, 8.4%.

ν(max) (KBr) 3500 m, 3371 m, 3319 m and 3126 w (NH), 3026 (CH), 2060 s and 2024 s (CO), 1591 s and 1544 s (NH_2), 1429 w and 1017 w (C—C or ring def.) and 846 s br cm^{-1} (PF_6).

RESULTS AND DISCUSSION

The ligands L ($L = NH_2NHCSNH_2$ or $R_1R_2CNNHCSNH_2$) do not displace CO from $[Fe(\eta^5\text{-}C_5H_5)(CO)_3][PF_6]$ even with UV irradiation but

Table 1. Analytical (C, H and N) data,[a] yields and decomposition points of the complexes $[Fe(CO)_2L(\eta^5\text{-}C_5H_5)][PF_6]$

Ligand L[b]	Yield (%)	Decomposition point (°C)	C(%)	H(%)	N(%)
$H_2NNHCSNH_2$ (**1**)	59	100	22.7	2.4	10.6
			(23.6)	(2.4)	(10.2)
$C_5H_{10}CNNHCSNH_2$ (**2**)	72	137	33.8	3.6	8.1
			(34.1)	(3.7)	(8.5)
$(CH_3)_2CNNHCSNH_2$ (**3**)	61	108	30.1	3.2	9.0
			(29.2)	(3.1)	(9.3)
$C_6H_5CHNNHCSNH_2$ (**4**)	65	160	35.2	2.8	7.9
			(35.9)	(2.8)	(8.4)
$p\text{-}NO_2C_6H_4CHNNHCSNH_2$ (**5**)	58	—	33.0	2.4	9.9
			(33.0)	(2.4)	(10.1)
$p\text{-}CH_3C_6H_4C(CH_3)NNHCSNH_2$ (**6**)	51	—	38.8	3.4	7.9
			(38.7)	(3.5)	(7.9)
$p\text{-}CH_3C_6H_4CHNNHCSNH_2$ (**7**)	50	154	36.6	3.2	7.2
			(37.3)	(3.1)	(8.2)
$p\text{-}ClC_6H_4CHNNHCSNH_2$ (**8**)	80	150	32.4	2.3	7.1
			(33.6)	(2.4)	(7.8)

[a] Calculated values in parentheses.
[b] All compounds are orange except **1** which is yellow.

they will displace a labile group S from species $[Fe(\eta^5\text{-}C_5H_5)(CO)_2S]^+$. When S is H_2O the yields are very poor, *ca* 1%, but when S is Me_2CO good yields from 50 to 80% are obtained on refluxing $[Fe(\eta^5\text{-}C_5H_5)(CO)_2(Me_2CO)][PF_6]$ with the ligand L in $CHCl_3$. Attempts to prepare these compounds from $Fe(\eta^5\text{-}C_5H_5)(CO)_2I$ in the presence of $NaBF_4$ or $AgBF_4$ were unsuccessful. Surprisingly there was no evidence at all that the thiosemicarbazone displaces I from this complex. The compounds (**1**–**8**) (see Table 1) have been fully characterized by microanalysis (Table 1), IR (Table 2), ^1H NMR

Table 2. IR absorption frequencies (in cm^{-1}) of $\nu(CO)$ in the complexes $[Fe(CO)_2L(\eta^5\text{-}C_5H_5)][PF_6]$

Complex	Solvent	$\nu(CO)$ (cm^{-1})	
$[Fe(CO)_3(\eta^5\text{-}C_5H_5)][PF_6]$[a,b]	$(CH_3)_2CO$	2130	2078
$[Fe(CO)_2(SC_4H_9)$[a,c]$(\eta^5\text{-}C_5H_5)][PF_6]$	$CHCl_3$	2061	2016
1	$(CH_3)_2CO$	2052	2006
	KBr	2047	2011
2	KBr	2049	1998
3	KBr	2058	2002
4	$CHCl_3$	2060	2025
	KBr	2061	2024
5	$(CH_3)_2CO$	2054	2009
	KBr	2060	2016
6	KBr	2057	2009
7	KBr	2050	2009
8	$(CH_3)_2CO$	2053	2008
	KBr	2052	2014
$[Fe(CO)_2(C_6H_5CHNNHCONH_2)(\eta^5\text{-}C_5H_5)][PF_6]$	KBr	2077	2038

[a] Included for reference.
[b] Reference 16.
[c] Reference 17.

Table 3. ^{1}H NMR data (σ)[a] of the complexes $[Fe(CO)_2(\eta^5\text{-}C_5H_5)][PF_6]$

Complex	(C_5H_5)	R	R[1]	NH_2NH	NH_2CS	NH
1	5.49d	—	—	8.30s[b]	9.80s	11.21s
	(—	—	—	4.43s	7.31, 8.63	8.63s)[c]
2	5.48s	1.60(6H)	2.33, 2.47, 2.55	(4H)	8.46s	11.61s
	(—	1.56(6H)	2.23–2.41	(4H)	7.74d	10.15s)
3	5.49s	2.08s	2.08s	—	8.60d	11.32s
	(—	1.93s	1.93s	—	7.15d	8.98s)
4	5.60s	7.53–7.92m (C_6H_5)	8.28s(CH)	—	8.97d	12.51s
	(—	7.42–8.10m (C_6H_5)	8.23s(CH)	—	7.42–8.10m	11.55)
5	5.55/5.72d	8.21	8.65m	—	8.21–8.65m	12.86s
	(—	8.09–8.31m(ring)	8.47s	—	8.09–8.31m	11.79s)
6	5.78s	7.37–7.71m(ring) 2.04s(p-CH_3)	2.66s(CCH_3)	—	7.37–7.71m	10.27s
	(—	7.18/7.21(ring) 7.81/7.84m 2.28s(p-CH_3)	2.32s(CCH_3)	—	7.90–8.27d (J = 3.7 Hz)	10.18s)
7	5.26s	7.10/7.36m(ring) 7.80/8.06 2.41s (p-CH_3)	8.27s		8.69d	12.62s
	(—	7.22/7.25m 7.69/7.72 2.33s (p-CH_3)	8.15s		8.09d	11.42s)
8	5.52s	7.58–7.95m	8.28s		8.97d (J = 4.1 Hz)	12.65s
	(—	7.42–8.10m	8.23s		7.42–8.10m	11.55s)
9[d]	5.78s	7.37	7.72m		6.51s	10.29s
	(—	7.41–7.52m	7.76–7.92m		6.54s	10.45s)

[a] Spectra recorded in d_6-DMSO.
[b] s—singlet, d—doublet, m—multiplet.
[c] Values in parentheses are for corresponding free ligand L.
[d] Compound **9** is $[Fe(CO)_2(C_6H_5CHNNHCONH_2)(\eta^5\text{-}C_5H_5)][PF_6]$.

(Table 3) and Mössbauer spectroscopy (Table 4). The complexes are stable in air in the solid state and only slowly decompose in solution. The compounds are insoluble in non-polar solvents, and only sparingly soluble in CH_2Cl_2 and $CHCl_3$. They are, however, very soluble in Me_2SO.

Crystallography

Crystals of the title compound suitable for X-ray investigation were obtained from $CHCl_3$ as orange plates.

Crystal data $[C_{15}H_{14}N_3O_2SFe]^+[PF_6]^-$, M =

Table 4. Mössbauer parameters for the complexes $[Fe(CO)_2L(\eta^5\text{-}C_5H_5)][PF_6]$

Complex	Isomer shift (mm s^{-1})	Quadrupole splitting (mm s^{-1})	Temperature (K)
$[Fe(CO)_3(\eta^5\text{-}C_5H_5)][PF_6]$	0.05	1.88	78[a]
$[Fe(CO)_2Cl(\eta^5\text{-}C_5H_5)]$	0.24	1.88	78[a]
1	0.18	1.73	293
2	0.13	1.72	78
3	0.16	1.75	78
4	0.20	1.76	293
5	0.21	1.78	293
6	0.17	1.69	78
7	0.15	1.71	78
$[Fe(CO)_2(C_6H_5CHNNHCONH_2)][PF_6]$	0.18	1.95	78

[a] Reference 18.

500.16, monoclinic, $a = 7.103(1)$, $b = 18.637(3)$, $c = 15.193(2)$ Å, $\beta = 90.76(1)$, $U = 2011.1$ Å^3, space group $P2_1/c$, $Z = 4$, $D_c = 1.652$ g cm^{-3}, $F(000) = 788$, μ(Mo-K_α) = 9.9 cm^{-1}.

Data collection

Accurate unit cell parameters were measured on an Enraf–Nonius CAD4 diffractometer using 25 accurately centred reflections ($13° < \theta < 15°$) from a crystal of dimensions $0.4 \times 0.4 \times 0.1$ mm. Reflection data were collected to a θ-limit of 24° using graphite-monochromated Mo-K_α radiation in a ω–2θ scan mode. 3555 reflections were measured which after averaging and rejection of systematic absences reduced to 3142 (1389 for which $I > 3\sigma(I)$ were considered observed). No decay of the crystal was noted during the total X-ray exposure time (71 h). No absorption correction was applied.

Structure determination and refinement

The structure was solved using a combination of MULTAN[10] and Fourier techniques. The three heaviest peaks from a default run of Multan were assumed to correspond to the iron, phosphorus and sulphur atoms. Two cycles of Fourier/structure factor calculations located all the remaining non-hydrogen atoms with $R = 0.23$. Full-matrix least-squares refinement was carried out using isotropic thermal parameters and an empirical absorption correction. DIFABS[11] was applied (minimum correction 0.757, maximum 1.184, average 0.993) prior to refinement with anisotropic thermal parameters. Because of limitations in the SDP package[12] used for the calculations, hydrogen atoms could not be included. The weighting scheme $\omega = 1/[\sigma^2(F_o) + 0.07(F_o)^2]$ gave a satisfactory agreement analysis and refinement was terminated with a final R and R_w of 0.067 and 0.087.

Selected bond lengths and angles are given in Table 5. Fractional atomic coordinates, anisotropic temperature factors, a complete list of bond lengths and angles, and F_o/F_c tables have been deposited as supplementary data with the Editor.

The structure and the numbering scheme are shown in Fig. 1. The structure consists of discrete cations and $[PF_6]^-$ anions. Within the cation, the coordination geometry about the iron atom is best described in terms of a "piano-stool" or pseudo-octahedron. The C_5H_5 moiety occupies three sites, with the two carbonyls and the sulphur atom of the thiosemicarbazone occupying the remainder. Although the Cambridge Crystallographic Database reveals almost 100 complexes containing coordinated thiosemicarbazones, there appear to be only two reported examples of monodentate S-bonded thiosemicarbazones. One of these is bis (acetophenonethiosemicarbazone)cobalt(II) iodide[4(i)] while the other is an organometallic compound, acetone thiosemicarbazone pentacarbonyl tungsten(0), $W(CO)_5$(TSCAC).[13] In the present case, as in the case (above) of the cobalt(II) iodide complex, the reason for the monodentate binding of the thiosemicarbazone is probably stereochemical, further coordination through N(3) being effectively blocked by the remaining ligands. Thus, the thiosemicarbazone is found with the 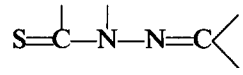 group in an essentially extended linear conformation. The Fe—S(1) distance (2.279(4) Å) compares favourably with that

Table 5. Selected bond lengths (Å) and angles (°)

Bond lengths			
Fe—S(1)	2.279(4)		
Fe—C(1)	1.71(2)		
Fe—C(2)	1.79(2)		
Fe—(C_5H_5)	2.08(2)$_{av}$		
Bond angles			
C(1)—Fe—C(2)	92.8(8)	C(2)—Fe—C(11)	155.2(8)
C(1)—Fe—S(1)	93.9(5)	C(2)—Fe—C(12)	116.4(9)
C(2)—Fe—S(1)	86.8(6)	C(2)—Fe—C(13)	88.3(9)
C(1)—Fe—C(11)	96.3(8)	C(2)—Fe—C(14)	99.1(9)
C(1)—Fe—C(12)	93.5(7)	C(2)—Fe—C(15)	135.0(1)
C(1)—Fe—C(13)	126.4(8)	S(1)—Fe—C(11)	115.4(8)
C(1)—Fe—C(14)	160.9(7)	S(1)—Fe—C(12)	155.2(6)
C(1)—Fe—C(15)	132.4(9)	S(1)—Fe—C(13)	139.6(7)
		S(1)—Fe—C(14)	101.6(6)
		S(1)—Fe—C(15)	90.8(6)

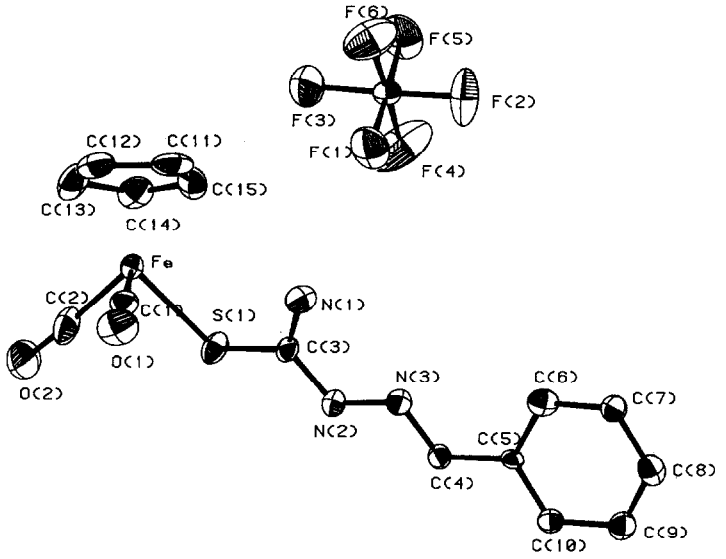

Fig. 1. The structure and numbering scheme for $[Fe(CO)_2(PhCHNNHCSNH_2)(\eta^5\text{-}C_5H_5)][PF_6]$.

found in other iron complexes with bidentate ligands,[14,15] but the Fe—S(1)—C(3) angle is much more obtuse (111.3°) compared with the value of about 98° generally found for the M—S—C angle. Other bond lengths and angles in the thiosemicarbazone moiety are similar to values reported for other complexes. In particular, they are identical within experimental error to those found for $W(CO)_5$(TSCAC).[13]

IR data

The IR spectra of the complexes show absorptions characteristic of the thiosemicarbazide moiety, that is ν(NH) between 3500 and 3100 cm^{-1}, $\delta(NH_2)$ in the 1650–1600 cm^{-1} region, various coupled modes in the 1600–1000 cm^{-1} region, as well as a strong absorption due to PF_6^- at about 845 cm^{-1} which masks the mainly ν(CS) vibration in the 700–800 cm^{-1} region. The similarity of the spectra suggest that the thiosemicarbazide/-one ligand is bound to the iron in the same way in all these complexes, i.e. through sulphur as shown by the X-ray diffraction study of **4**.

The expected two ν(CO) absorptions are found in all the spectra. The band positions in solution and in the solid (KBr) differ by only a few cm^{-1}. The values of the ν(CO) absorptions (in cm^{-1}) are significantly lower than those found in the spectrum of $[Fe(CO)_3(\eta^5\text{-}C_5H_5)][PF_6]$ but similar to those found for $[Fe(CO)_2(SC_4H_9)(\eta^5\text{-}C_5H_5)][PF_6]$. This suggests that CO is a better π-acceptor than $\rangle C{=}S$ or $\rangle CS^-$.

The IR spectrum of the semicarbazone analogue of **4**, $[Fe(CO)_2(C_6H_5CHNNHCONH_2)(\eta^5\text{-}C_5H_5)][PF_6]$, clearly shows that the semicarbazone is not bonded through the $\rangle C{=}O$ group, the ν(C=O), $\delta(NH_2)$ and amide II frequencies being identical to those of the free ligand (1690, 1651 and 1598 cm^{-1}, respectively), whereas in the IR spectra of the molybdenum semicarbazone complexes[6] the ν(C=O) band frequency is 20–30 cm^{-1} lower than in the free ligands. The semicarbazone must therefore be bound through the hydrazine nitrogen $\left(-N{=}C\right\rangle$. The position of the carbon monoxide stretching frequencies (see Table 2) is higher than for the thiosemicarbazone compounds, which is compatible with $-N{=}C\rangle$ being a better π-acceptor than $S{=}C\rangle$.

^{1}H *NMR data*

In the NMR spectrum of complex **1** the proton resonances of the thiosemicarbazide ligand are all shifted downfield by several ppm relative to their positions in the free ligand (see Table 3), which indicates that a net decrease in electron density has occurred. Similarly, a downfield shift, although somewhat smaller, is observed for the proton resonances of the thiosemicarbazone ligands in complexes **2**–**8**. In the spectrum of the semicarbazone ligand $[Fe(CO)_2(PhCHNNHCONH_2)(\eta^5\text{-}C_5H_5)][PF_6]$, on the other hand, the proton resonances of the semicarbazone ligand all show an

upfield shift, those of the semicarbazide moiety being between 2 and 3 ppm. This would indicate a net increase in electron density on the ligand.

Since the bonding between iron and either >C=S or >C=N can involve both an L—M σ-bond and an M—L π-bond, the net change in electron density on complex formation will depend on the relative importance of the two components. The net decrease in electron density in the complexed thiosemicarbazide/-one ligands shows that back donation is less important than the σ-bonding. The relatively large size of the sulphur and the positive charge on the iron(II) undoubtedly leads to poor overlap between the >C=S π^*-orbital and the appropriate *d*-orbital, i.e. to an energy mismatch. In the case of the semicarbazone ligand the >C=N group may well be a poorer σ-donor than >C=S but is clearly a better π-acceptor, since there is an overall increase in electron density on complex formation.

Mössbauer data

The Mössbauer parameters of compounds **1–7**, together with those of $[Fe(CO)_2(PhCHNNHCONH_2)(\eta^5\text{-}C_5H_5)][PF_6]$, $[Fe(CO)_3(\eta^5\text{-}C_5H_5)][PF_6]$ and $[Fe(CO)_2(\eta^5\text{-}C_5H_5)Cl]$ which are included for comparison, are shown in Table 4. The isomer shift values of compounds **1–7** are more positive than the value for $[Fe(CO)_3(\eta^5\text{-}C_5H_5)][PF_6]$ but less positive than that of $[Fe(CO)_2(\eta^5\text{-}C_5H_5)Cl]$, i.e. the *s*-electron density at the ^{57}Fe nucleus is less than in $[Fe(CO)_3(\eta^5\text{-}C_5H_5)][PF_6]$ and more than in $[Fe(CO)_2(\eta^5\text{-}C_5H_5)Cl]$. The ligand contributes to the total *s*-electron density at the ^{57}Fe nucleus by σ-donation which increases the 4*s* electron density and by π-acceptance which removes 3*d*-electrons and thus decreases the shielding of the *s*-electrons. Hence, the thiosemicarbazide/-one ligands of **1–7** must either be better σ-donors or poorer π-acceptors than CO. The IR and NMR evidence (see above) indicates that they are poorer π-acceptors. The isomer shift of $[Fe(CO)_2(PhCHNNHCONH_2)(\eta^5\text{-}C_5H_5)][PF_6]$ is virtually the same, within experimental error, as that of its sulphur analogue, **4**. Again, the net effect of $\sigma+\pi$ bonding is a decrease in *s*-electron density but in this case the IR and NMR evidence (see above) shows it to be a better π-acceptor than **4** so that it must be a poorer σ-donor. The electric field gradient at the iron nucleus arises largely from the π-bonding ligands, but for compounds such as those considered containing two or three such ligands it is difficult to relate changes to a single factor. The only significant point is that the quadruple splitting (QS) values of **1–7** are smaller than that of $[CpFe(CO)_3][PF_6]$, while the QS value of the semicarbazone analogue of **4** is larger.

Reactions

It is significant that compound **1**, $[Fe(CO)_2(NH_2NHCSNH_2)(\eta^5\text{-}C_5H_5)][PF_6]$, reacts smoothly with benzaldehyde in trichloromethane at 50°C to give the benzaldehyde thiosemicarbazone, **4**. This confirms that the thiosemicarbazide is monodentate and S-bonded even in solution, since thiosemicarbazone formation occurs by reaction of the hydrazinic-NH_2 group with the carbonyl group of the aldehyde or ketone. Furthermore, in compound **1** the —NH_2 must be sterically unhindered. However, attempts to prepare alkyl thiosemicarbazone complexes such as **3** by reaction of **1** with the corresponding ketone failed, only starting material being recovered.

The compound $[Fe(CO)_2(PPh_3)(\eta^5\text{-}C_5H_5)][PF_6]$ reacts with $NaBH_4$ to give $[Fe(CO)_2(PPh_3)(C_5H_6)]$, while $[Fe(CO)_3(\eta^5\text{-}C_5H_5)][PF_6]$ reacts to give $[Fe(CO)_2(\eta^5\text{-}C_5H_5)]_2$ as the main product.[15] Reaction of **4** with sodium borohydride yielded three fractions after chromatographic separation, of which the major one proved to be $[Fe(CO)_2(\eta^5\text{-}C_5H_5)]_2$. Clearly the thiosemicarbazone is more readily displaced from the coordination sphere than PPh_3 and the reaction may go via the formation of a hydride such as $[Fe(CO)_2H(\eta^5\text{-}C_5H_5)]$.

Acknowledgement—We wish to thank O. W. Howarth at the University of Warwick for measuring the ^1H NMR spectra of several of the complexes.

REFERENCES

1. K. A. Jensen and E. Rancke-Madsen, *Z. Anorg. Allg. Chem.* 1934, **219**, 243.
2. (a) M. J. M. Campbell, *Coord. Chem. Rev.* 1975, **15**, 279; (b) S. Padhye and G. B. Kauffman, *Coord. Chem. Rev.* 1985, **63**, 127.
3. K. Liebermeister, *Z. Naturforsch.* 1950, **5B**, 79.
4. (a) M. Nardelli, G. Fava Gasparri and I. Chierici, *Ric. Sic.* 1965, **35**, 480; (b) M. Nardelli, G. Fava Gasparri, G. Giraldi Battistini and A. Musatti, *J. Chem. Soc., Chem. Commun.* 1965, 187; (c) L. Calzolari Capacchi, G. Fava Gasparri, M. Ferrari and M. Nardelli, *J. Chem. Soc., Chem. Commun.* 1968, 910; (d) G. Fava Gasparri, A. Mangia, A. Musatti and M. Nardelli, *Acta Cryst.* 1968, **24B**, 367; (e) L. Calzolari Capacchi, G. Fava Gasparri, M. Ferrari and M. Nardelli, *Ric. Sci.* 1968, **38**, 974; (f) C. Chieh, *Can. J. Chem.* 1977, **55**, 1583; (g) C. Chieh, L. P. C.

Lee and C. Chin, *Can. J. Chem.* 1978, **56**, 2526; (h) D. R. Goddard, B. D. Lodam, S. O. Ajayi and M. J. M. Campbell, *J. Chem. Soc. A* 1969, 506; (i) C. Bellitto, A. A. G. Tomlinson, C. Furlani and G. de Munno, *Inorg. Chim. Acta* 1978, **27**, 269; (j) G. Dessy and V. Fares, *J. Chem. Soc., Dalton Trans.* 1978, 1549.

5. M. J. M. Campbell, E. Morrison, V. Rogers and P. K. Baker, *Transition Met. Chem.* 1986, **11**, 381.
6. M. J. M. Campbell, E. Morrison, V. Rogers and P. K. Baker, *Polyhedron* 1988, **7**, 1719.
7. M. J. M. Campbell, E. Morrison, V. Rogers and P. K. Baker, *Polyhedron* 1987, **6**, 1703.
8. W. E. Williams and F. J. Labor, *J. Chem. Soc., Dalton Trans.* 1973, 1329.
9. P. T. Sah and T. C. Daniels, *Rec. Trav. Chim.* 1950, **69**, 1545.
10. P. Main, S. E. Hill, L. Lessinger, G. Germain, J.-P. Declerq and M. M. Woolfson, MULTAN 78: A system of computer programs for the automatic solution of crystal structures from X-ray diffraction data. University of York, U.K. and University of Louvain, Belgium (1978).
11. N. Walker and D. Stuart, *Acta Cryst.* 1983, **158A**, A39.
12. B. A. Frenz, Enraf–Nonius Structure Determination Package SDP Users Guide, V.1.1a, Enraf–Nonius, Delft, The Netherlands (1983).
13. J. Valdes-Martinez, A. Sierra-Romero, C. Alvarez-Toledano, R. A. Toscano and H. Garcia-Japia, *J. Organomet. Chem.*, in press.
14. N. A. Ryabova, V. I. Ponomarev, L. O. Atovmyan, V. V. Zelentsov and V. I. Shipilov, *Koord. Khim.* 1978, **4**, 119.
15. G. Dessy and V. Fares, *Cryst. Struct. Commun.* 1981, **10**, 1025.
16. U. S. Gill, C. C. Lee and R. G. Sutherland, *Synth. React. Inorg. Metal-Org. Chem.* 1984, **14**, 953.
17. B. D. Dombek and R. J. Angelici, *Inorg. Chim. Acta* 1973, **7**, 345.
18. R. H. Herber, R. B. King and G. K. Wertheim, *Inorg. Chem.* 1964, **3**, 101.

Polyhedron Vol. 8, No. 19, pp. 2379–2383, 1989
Printed in Great Britain

0277–5387/89 $3.00+.00
© 1989 Pergamon Press plc

THE PREPARATION AND CRYSTAL STRUCTURE OF AN ANIONIC SILVER PENTASULPHIDE CHAIN IN $_\infty[Ag(S_5)^-](Me_4N^+)$

R. M. HERATH BANDA, DON C. CRAIG, IAN G. DANCE* and M. L. SCUDDER

School of Chemistry, University of New South Wales, PO Box 1, Kensington, NSW 2033, Australia

(*Received* 11 *April* 1989; *accepted* 18 *May* 1989)

Abstract—Reaction of Ag^+ with $(Bu_4N)_2S_6$ in acetonitrile, in the presence of Me_4NCl, yields the orange compound $_\infty[Ag(S_5)^-](Me_4N^+)$ (**1**). Unlike all other silver polysulphide complexes, **1** is non-molecular in one-dimension, with propagation by a glide plane. Each silver atom is tetrahedrally coordinated by sulphur atoms from three different $(S_5)^{2-}$ ions, and each $(S_5)^{2-}$ ion makes four connections to three different silver ions, including an AgS_4 chelate ring involving a non-terminal sulphur atom. The structure is different in detail from that of NH_4CuS_4. Crystal data: space group *Cc*, $a = 10.860(10)$, $b = 18.313(7)$, $c = 9.177(9)$ Å, $\beta = 139.77(3)°$, $V = 1179(2)$ Å^3. $D_{calc} = 1.93$ g cm^{-3} ($Z = 4$). 963 independent observed $[I/\sigma(I) > 3]$ reflections (Mo-K_α), $R = 0.044$, $R_w = 0.052$.

We report here the first one-dimensionally non-molecular silver polysulphide compound, $_\infty[Ag(S_5)^-](Me_4N^+)$ (**1**). The preparation of a comparable copper polysulphide NH_4CuS_4 (**2**), by reaction of $Cu^{2+}_{(aq)}$ and aqueous ammonium polysulphide solution has been known for a long time,[1,2] and its one-dimensionally non-molecular crystal structure $_\infty[Cu(S_4)^-](NH_4^+)$ was reported in 1980.[3]

In recent years, solutions of polysulphide ions have been generated in non-aqueous solvents, through reactions of NH_3 (g), S_8 and H_2S (g) in varying proportions. By addition of $AgNO_3$ to these solutions in acetonitrile, Müller *et al.* have crystallized (with Ph_4P^+ in each case) $[(S_6)Ag(S_8)Ag(S_6)]^{4-}$ (**3**),[4] $[Ag_2(S_6)_2]^{2-}$ (**4**)[5] and the monocyclic molecule $[Ag(S_9)]^-$ (**5**).[5] These three compounds have quite different structures in their crystals, but all are structurally molecular. Analogous reactions with a range of copper precursors have led to the crystallization and structure determination of the copper(I) complexes $[Cu_6(S_4)_3(S_5)]^{2-}$ (**6**),[6–8] $[Cu_4(S_5)_m(S_4)_{3-m}]^{2-}$, $m = 0$–3,[9] $[Cu_3(S_x)_3]^{3-}$, $x = 4$,[10] 6,[11] and $[(S_6)Cu(S_8)Cu(S_6)]^{4-}$.[10] The gold(I) analogue of **5** is also known,[12] as is $[Au_2(S_4)_2]^{2-}$.[9]

The use of non-aqueous and aprotic solvents clearly increases the thermodynamic activity of the polysulphide ions and permits access to a range of homoleptic metal polysulphide complex equilibria known only at very much lower concentrations in water.[13] The use of gaseous reagents in the Müller preparative method can introduce uncertainty in stoichiometry, and therefore we have investigated alternative methods for controlled generation of polysulphide ions and metal polysulphide complexes in non-aqueous solution. One alternative is to use $(Bu_4N)_2S_6$[14] as a well-defined quantitative source of $(S_6)^{2-}$ in non-aqueous solution. In this paper we describe one product, **1**, of the reaction of $(Bu_4N)_2S_6$ with Ag^+ in acetonitrile.

RESULTS AND DISCUSSION

Preparations

Partial dissociation, $(S_6)^{2-} \rightleftharpoons 2(S_3)^-$, occurs in acetonitrile solutions of $(Bu_4N)_2S_6$, as indicated by their green–brown colour.[14,15] Addition of methanol or Ag^+ causes instantaneous reversion to the red colour, characteristic of coordinated and uncoordinated polysulphide ions. Halide ions in solution cause only transient precipitation of silver halide. Provided the solvent is aprotic, such as acetonitrile, $AgNO_3$ can be added up to a Ag^+–$(S_6)^{2-}$ ratio of 0.8 without permanent formation of a black precipitate, presumed to be Ag_2S. A small amount of sul-

* Author to whom correspondence should be addressed.

phur is formed, presumably due to oxidation by NO_3^- : oxidation of polysulphide ions by NO_3^- in aprotic media has been observed in other systems. In the presence of Me_4N^+, solutions with an $AgNO_3$–$(S_6)^{2-}$ stoichiometry of 0.6 have crystallized **1** in 83% yield (Ag).

Description of the structure of **1**

Crystals of **1** contain parallel chains of $_\infty[Ag(S_5)^-]$ separated by the Me_4N^+ ions, as shown in Fig. 1: the chain is propagated by the *n* glide operation of the space group *Cc*. The detailed connectivity of the chain is shown in Fig. 2. Each silver atom is tetrahedrally coordinated by sulphur atoms from three different $(S_5)^{2-}$ ions, and each $(S_5)^{2-}$ ion makes four connections to three different silver ions. One end of the $(S_5)^{2-}$ chain, S(1), bridges two silver atoms, with Ag—S distances of 2.540 and 2.562 Å, while the other end, S(5), is bonded to a third silver atom at 2.526 Å. The third type of Ag—S bond is Ag—S(4), involving a β-sulphur atom of the S_5 chain, at a slightly longer distance of 2.683 Å. Significant bond distances and angles are presented in Table 1.

Structure **I** is a diagrammatic representation of the chain, showing the connectivities. We note that the alternative connection pattern **II**, of AgS_5 cycles would avoid the coordination to the β-sulphur

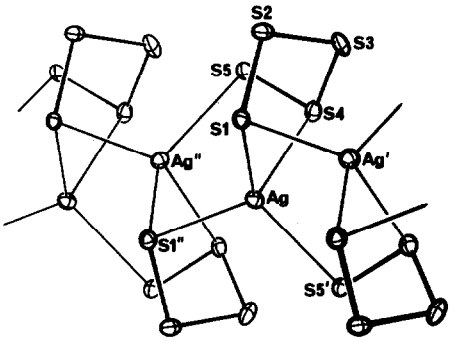

Fig. 2. The $_\infty[Ag(S_5)^-]$ chain in **1**.

atom. There are no inter-chain Ag—S contacts of < 4 Å. The shortest non-bonding contact for silver is Ag—H(2)C(4) of 3.0 Å. The Ag—Ag distances along the chain are all 3.63 Å.

With linear metal polysulphide chains surrounded and separated by cations, the crystal structures of **1** and **2** are similar. The chain in **2** consists of CuS_4 cycles, propagated along a 2_1 axis of the crystal, with connections between nearest (2_1 generated) and the next-nearest (translated) CuS_4 cycles, as shown diagrammatically in **III**. There are, however, significant differences in the pattern of connections of the metal atoms to the polysulphide chains, as emphasized in the diagrams in Fig. 3. There are two other compounds where metal atoms

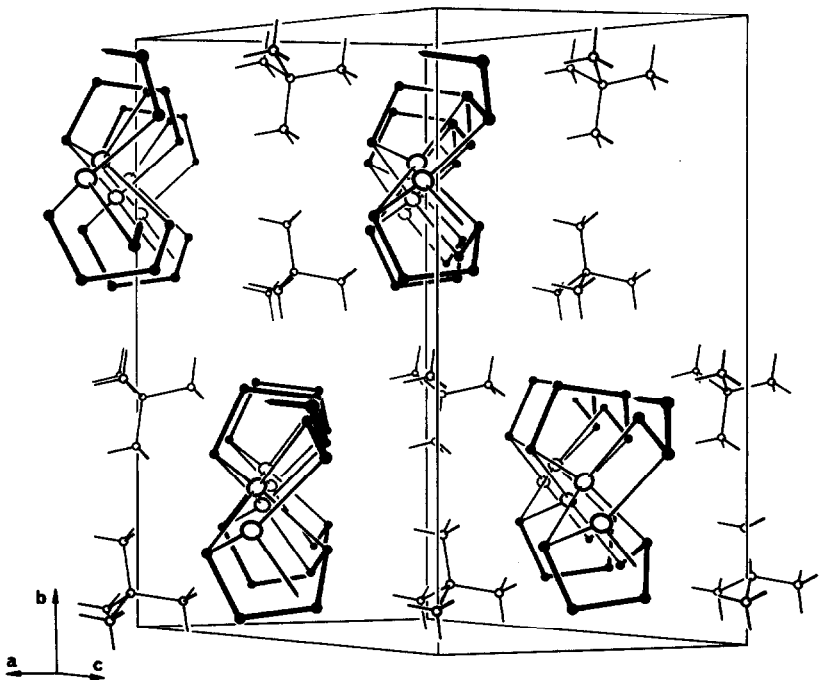

Fig. 1. Perspective view of the crystal structure of **1**, along the direction [101] of the $_\infty[Ag(S_5)^-]$ chains, which are well-separated by the Me_4N^+ ions. Large open ellipses are silver, small filled circles are sulphur.

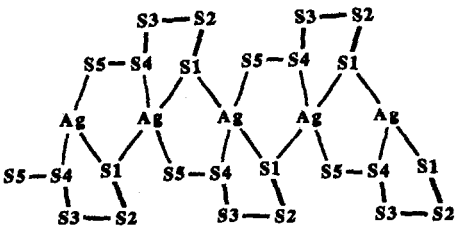

(I)

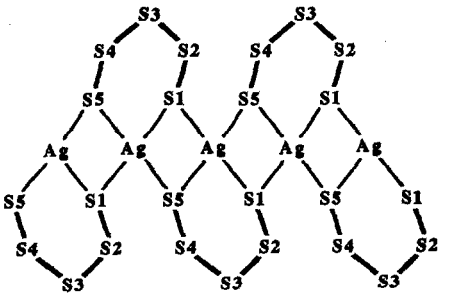

(II)

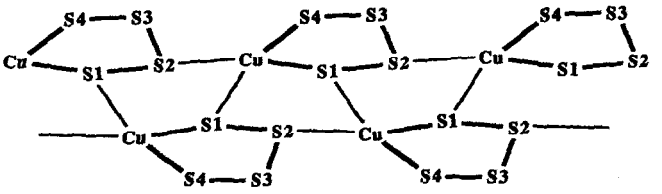

(III)

Table 1. Distances (Å) and angles (°) in $[Ag(S_5)](Me_4N)$ (I)

Ag—S(1)	2.562(3)	S(1)—Ag—S(4)	94.5(1)
Ag—S(4)	2.683(3)	S(1)—Ag—S(1)″	114.7(1)
Ag—S(1)″	2.540(3)	S(1)—Ag—S(5)′	119.6(1)
Ag—S(5)′	2.526(3)	S(4)—Ag—S(1)″	111.5(1)
S(1)—S(2)	2.050(4)	S(4)—Ag—S(5)′	101.6(1)
S(2)—S(3)	2.050(6)	S(1)″—Ag—S(5)′	112.4(1)
S(3)—S(4)	2.073(5)	Ag—S(1)—Ag′	90.6(1)
S(4)—S(5)	2.048(4)	Ag—S(1)—S(2)	102.3(1)
		Ag′—S(1)—S(2)	105.2(1)
N—C(1)	1.491(17)	Ag—S(4)—S(3)	98.8(1)
N—C(2)	1.484(15)	Ag—S(4)—S(5)	109.6(1)
N—C(3)	1.459(18)	Ag″—S(5)—S(4)	101.4(1)
N—C(4)	1.492(15)	S(1)—S(2)—S(3)	108.1(2)
		S(2)—S(3)—S(4)	107.1(2)
		S(3)—S(4)—S(5)	109.9(2)

Torsional angles

Ag—S(1)—S(2)—S(3)	−41.3(2)
Ag′—S(1)—S(2)—S(3)	52.8(2)
S(1)—S(2)—S(3)—S(4)	60.9(2)
S(2)—S(3)—S(4)—S(5)	69.9(2)
S(2)—S(3)—S(4)—Ag	−44.7(2)
Ag—S(4)—S(5)—Ag″	−26.1(1)

The only non-bonding contacts less than 3.0 Å are

S(5)···H(2)C(2)‴	2.89
S(2)···H(1)C(4)″	2.85
S(1)···H(2)C(4)′	2.97
S(4)···H(2)C(2)‴	2.97

′ $\frac{1}{2}+x, \frac{1}{2}-y, \frac{1}{2}+z$; ″ $-\frac{1}{2}+x, \frac{1}{2}-y, -\frac{1}{2}+z$; ‴ $-\frac{1}{2}+x, \frac{1}{2}-y, -1\frac{1}{2}+z$.

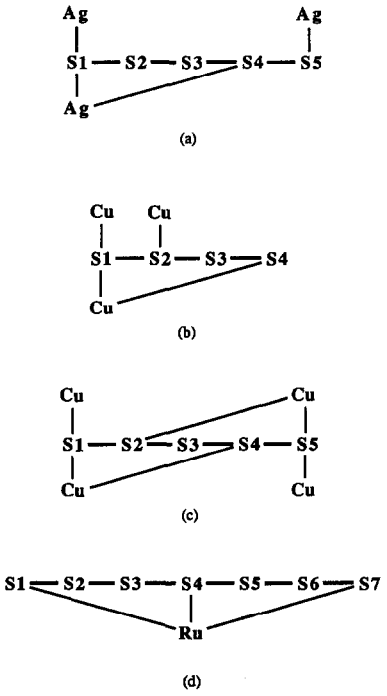

Fig. 3. Diagrams of the connections of metal atoms to terminal and internal sulphur atoms of polysulphide ligands in (a) **1**, (b) **2**, (c) **6** and (d) **7**.

are bonded to non-terminal sulphur atoms of a polysulphide chain, namely **6** and $(Me_3P)_3MS_7$ (**7**), M = Ru, Os,[16] and the connectivity patterns for these are included in Fig. 3. In **1**, **2** and **3** the M—S distances to internal sulphur atoms are slightly longer (*ca* 0.1 Å) than those to terminal sulphur atoms, but in **7** the internal M—S distance is 0.1 Å shorter. In all structures the S—S distances involving the internal S—M bond are slightly longer than those not so connected. Other entwinements of metal and polysulphide ligands have been uncovered recently in cyclopentadienylmetal polysulphides.[17–19]

EXPERIMENTAL

$(Bu_4N)_2S_6$ was prepared by a modification[20] of the literature procedure.[14]

Preparation

Dioxygen was excluded from all solutions. $(Bu_4N)_2S_6$ (0.70 g, 1.0 mmol) was treated with acetonitrile (15 cm^3) and a solution of Me_4NCl (0.15 g, 1.2 mmol) in methanol (5 cm^3), producing a red–

Table 2. Numerical details of the crystal structure determination for $[Ag(S_5)](Me_4N)$ (**1**)

Formula, formula mass	$C_4H_{12}AgNS_5$, 342.3
Crystal description	{001}{010}{01−1}{100}(−101)[a]
Space group	*Cc*
a (Å)	10.860(10)
b (Å)	18.313(7)
c (Å)	9.177(9)
β (°)	139.77(3)
V (Å^3)	1179(2)
Temperature (°C)	21(1)
Z	4
D_{calc} (g cm^{-3})	1.93
Radiation, λ (Å)	Mo-K_α, 0.7107
μ (cm^{-1})	24.96
Crystal dimensions	0.30 × 0.11 × 0.06
Scan mode	$\theta/2\theta$
$2\theta_{max}$ (°)	50
Number of intensity measurements	2065
Criterion for observed reflections	$I/\sigma(I) > 3$
Number of independent observed reflections	963
Number of reflections (*m*) and variables (*n*) in final refinement	963, 98
$R = \Sigma^m \lvert\Delta F\rvert / \Sigma^m \lvert F_o\rvert$	0.044
$R_w = [\Sigma^m w\lvert\Delta F\rvert^2 / \Sigma^m w\lvert F_o\rvert^2]^{1/2}$	0.052
$s = [\Sigma^m w\lvert\Delta F\rvert^2/(m-n)]^{1/2}$	1.91
Max., min. transmission coefficients.	0.81, 0.53

[a] Data collection took place in space group $P\bar{1}$ with cell parameters 7.069, 9.177, 10.638 Å, 112.90, 106.08, 97.19°, and these crystal faces refer to this cell.

brown solution. A solution of $AgNO_3$ (0.10 g, 0.6 mmol) in acetonitrile (10 cm^3) was added slowly with stirring, causing transient white precipitation and permanent conversion to a red solution, that was stored at *ca* −20°C. Yellow crystals of sulphur that deposited within 24 h were removed, and the mother liquor allowed to stand at room temperature, yielding long yellow–orange prismatic needles of the product. After collection the crystals were washed with acetonitrile and vacuum dried: yield 0.17 g (83% per Ag). Found: C, 14.3; H, 3.9; N, 4.1. Calc. for $C_4H_{12}NAgS_5$: C, 14.0; H, 3.5; N, 4.1%. The solid compound is moderately stable to light and air exposure, but eventually becomes black.

Crystallography

The diffraction investigation followed procedures previously described.[21] Numerical details are presented in Table 2. Reflection weights used were $1/\sigma^2(F_o)$ with $\sigma(F_o)$ being derived from $\sigma(I_o) = [\sigma^2(I_o)+(0.04I_o)^2]^{1/2}$. Atomic scattering factors and anomalous dispersion parameters for silver, sulphur, carbon, nitrogen were from *International Tables for X-ray Crystallography*.[22] In the final refinement, all non-hydrogen atoms were given anisotropic thermal parameters. Hydrogen atoms were included in calculated positions each with an isotropic temperature factor equivalent to that of the atom to which it was bonded. The hydrogen atom positions were not refined.

Atomic coordinates, thermal parameters, tabulations of dimensions, and listings of structure factors have been deposited with the Editor.

Acknowledgements—The support of this research by the Australian Research Grants Scheme is gratefully acknowledged. R.M.H.B. acknowledges sponsorship by the Australian Development Assistance Bureau.

REFERENCES

1. K. A. Hofmann and F. Höchtlen, *Ber. Dtsch. Chem. Ges.* 1904, **37**, 245.
2. G. Gattow and O. Rosenberg, *Z. Anorg. Allg. Chem.* 1964, **332**, 269 and refs cited therein.
3. C. Burschka, *Z. Naturfor.* 1980, **35b**, 1511.
4. A. Müller, M. Römer, H. Bögge, E. Krickemeyer, F-W. Baumann and K. Schmitz, *Inorg. Chim. Acta* 1984, **89**, L7.
5. A. Müller, E. Krickemeyer, M. Zimmermann, M. Römer, H. Bögge, M. Penk and K. Schmitz, *Inorg. Chim. Acta* 1984, **90**, L69.
6. G. Henkel, P. Betz and B. Krebs, *J. Chem. Soc., Chem. Commun.* 1984, 314.
7. A. Müller, M. Römer, H. Bögge, E. Krickemeyer and D. Bergmann, *J. Chem. Soc., Chem. Commun.* 1984, 348.
8. A. Müller, M. Römer, H. Bögge, E. Krickemeyer and D. Bergmann, *Z. Anorg. Allg. Chem.* 1984, **511**, 84.
9. A. Müller, M. Römer, H. Bögge, E. Krickemeyer and K. Schmitz, *Inorg. Chim. Acta* 1984, **85**, L39.
10. A. Müller, F.-W. Baumann, H. Bögge, M. Römer, E. Krickemeyer and K. Schmitz, *Angew. Chem. Int. Edn Engl.* 1984, **23**, 632.
11. A. Müller and U. Schimanski, *Inorg. Chim. Acta* 1983, **77**, L187.
12. G. Marbach and J. Strähle, *Angew. Chem. Int. Edn Engl.* 1984, **23**, 246.
13. P. L. Cloke, *Geochim. Cosmochim. Acta* 1963, **27**, 1299.
14. R. G. Teller, L. J. Krause and R. C. Haushalter, *Inorg. Chem.* 1983, **22**, 1809.
15. P. Dubois, J. P. Lelieur and G. Lepoutre, *Inorg. Chem.* 1988, **27**, 1883 and refs cited therein.
16. J. Gotzig, A. L. Rheingold and H. Werner, *Angew. Chem. Int. Edn Engl.* 1984, **23**, 814.
17. J. Amarasekera, T. B. Rauchfuss and A. L. Rheingold, *Inorg. Chem.* 1987, **26**, 2017.
18. H. Brunner, N. Janietz, W. M. Meier, B. Nuber, J. Wachter and M. L. Ziegler, *Angew. Chem. Int. Edn Engl.* 1988, **27**, 708.
19. J. Wachter, *J. Coord. Chem.* 1987, **15**, 219.
20. R. M. H. Banda, I. G. Dance, T. D. Bailey, D. C. Craig and M. L. Scudder, *Inorg. Chem.* 1989, **28**, 1862.
21. I. G. Dance, P. J. Guerney, A. D. Rae and M. L. Scudder, *Inorg. Chem.* 1983, **22**, 2883.
22. *International Tables for X-ray Crystallography*, Vol. IV, Tables 2.2A and 2.3.1. Kynoch Press, Birmingham, U.K. (1974).

Polyhedron Vol. 8, No. 19, pp. 2385–2388, 1989
Printed in Great Britain

0277–5387/89 $3.00+.00
Pergamon Press plc

CALORIMETRIC DETERMINATION OF THE ENTHALPIES OF COMPLEXATION OF THORIUM(IV) WITH AMINE-N-POLYCARBOXYLIC ACIDS

W. F. KINARD,* P. M. GRANT† and P. A. BAISDEN

Nuclear Chemistry Division, L-234, Lawrence Livermore National Laboratory, Livermore, CA 94550, U.S.A.

(*Received* 18 *February* 1989; *accepted* 19 *May* 1989)

Abstract—The enthalpies of complexation of a number of thorium complexes with amine-N-polycarboxylic acids have been measured using titration calorimetry. Values of ΔH_{101} and ΔS_{101} were thus determined for nitrilotriacetic acid (NTA), N-(2-hydroxyethyl)ethylenedinitrilo-N,N′,N′-triacetic acid (HEDTA), ethylenedinitrilotetraacetic acid (EDTA) and diethylenetrinitrilopentaacetic acid (DTPA). A protonated species, ThHL, was necessary to interpret heats measured for EDTA and DTPA in low-pH solution, and thermodynamic parameters are reported for these complexes as well. Although the stability of these complexes is the result of strong entropy effects, the enthalpy values show important trends in the coordinate bonding of these species.

The interaction of metal ions with amine-N-polycarboxylic acids is of interest for a number of theoretical and practical reasons. From a theoretical veiwpoint, the polydentate nature of these ligands leads to species with high coordination numbers and results in some of the most stable metal complexes known.[1] In addition, their relatively simple chemical structures allow facile synthesis of analogues to elucidate factors important in the formation of strong metal–ligand complexes.

These compounds are used extensively in industry and are found in a number of consumer products, as well as having broad application in chemical laboratories. As a result of this widespread use, considerations of waste disposal require that a thorough knowledge of their chemical properties be available. Experience with the disposal of radioactive waste from laboratories has implicated EDTA as a dispersing agent for the migration of radionuclides from disposal sites.[2,3] Amine-N-polycarboxylate ligands are used to model metal complexation in natural waters by trace organics; such elucidation of metal speciation has applications to transport studies.[4]

This work reports values of the enthalpies of formation of some thorium amine-N-polycarboxylate complexes as determined by titration calorimetry.

EXPERIMENTAL

All solutions were prepared from analytical grade reagents without further purification. Thorium nitrate of 99.99% purity (Spex Industries) was used to prepare a 0.10 M stock solution, and working solutions were made from it by dilution. Determinant values of Th^{4+} concentration were checked by analytical EDTA titrations, and agreement within 1% was measured. The ionic strength (μ) of the working solution was adjusted to 0.10 M by the addition of HNO_3 and KNO_3. The acid was necessary to adjust the pH of these solutions to 1.3–2.4 to ensure no significant hydrolysis of thorium(IV).

The 0.15 M amine-N-polycarboxylate titrant solutions were prepared from > 99% pure reagents by dissolving the appropriate amount of compound in an approximately 1% stoichiometric excess of sodium hydroxide to remove all protons from the ligand species. No solubility problems were encountered with this tactic.

The sensitive, quasi-adiabatic (isoperibol) calorimeter employed for the measurement of the heats of reaction in this study has been previously

* Permanent address: Department of Chemistry, College of Charleston, Charleston, SC 29424, U.S.A.

† Author to whom correspondence should be addressed.

described.[5] Typically, calorimetric measurements were made at two different metal concentrations having different pH values, and at two different titrant-addition volumes. All calorimetry runs were performed at 25.00 ± 0.01°C, with temperature stability of the thermostat maintained to ± 0.0003°C.

These experiments required an extrapolation procedure to obtain a valid blank correction, since there was a difference in ionic strength between the titrant and metal solutions. An endothermic heat-of-dilution was observed in the 0.1 M KNO_3 blank solution due to the heat-of-dilution of titrant. However, this endothermic heat was absent in the metal titrations because the reaction of Th^{4+} with L^{n-} only results in a small change in ionic strength. Consequently, the limiting heat observed for a blank titration was extrapolated to zero titrant volume to obtain the blank correction for the first few additions of titrant.

The resultant Th—L reaction heats were combined with computed solution speciation results in a weighted regression procedure to fit the data. This computational procedure has been amply described elsewhere.[6,7] All stability constants utilized in this study were obtained from critically-reviewed compilations of literature data.[8,9]

RESULTS AND DISCUSSION

Figure 1 shows a typical calorimetric titration of Th^{4+} with an amine-N-polycarboxylic acid. Because the formation constants of the metal–ligand complexes are so large ($> 10^{18}$), the complexation reactions go essentially to completion. In the figure, the initial additions (open circles) represent the exothermic heat arising from L^{n-} complexation with thorium, while a large increase in heat was observed later in the run. This increase in reaction heat was due to ligand protonation in the metal-ion solution following the exhaustion of uncomplexed Th^{4+}. A commensurate increase in the pH of the solution was also observed at these points.

Four amine-N-polycarboxylic acids were used in this study: ethylenedinitrilotetraacetic acid (EDTA), N-(2-hydroxyethyl)ethylenedinitrilo-N,N′,N′-triacetic acid (HEDTA), diethylenetrinitrilopentaacetic acid (DTPA), and nitrilotriacetic acid (NTA). HEDTA and EDTA are structurally identical except that one of the acetic acid functional groups is replaced by an ethanol group in the former compound. HEDTA, EDTA and DTPA provide three, four, and five carboxylate groups, respectively, for bonding to a central metal cation, while NTA has three carboxylates attached to a single nitrogen. All of these ligands are polydentate and capable of multiple coordination with a central cation to form extremely stable complexes. However, only NTA is expected to form metal–ligand species in which more than one ligand is attached to the metal.

Table 1 presents the results of the present investigation, along with a summary of thermodynamic parameters for the systems studied. Free-energy values were computed from the stability constant data, and entropies were calculated from the free energies and measured enthalpies.

Complexation enthalpy results were calculated from weighted, non-linear regression of the heat data to fit the equation:

$$-Q_{rxn} = \Delta n_{101} \cdot \Delta H_{101} + \Delta n_{111} \cdot \Delta H_{111} \left(+ \sum_{i=1}^{n} \Delta n_{0i1} \cdot \Delta H_{0i1} \right),$$

where values for moles of ThL (Δn_{101}), ThHL (Δn_{111}) and protonated ligand (Δn_{0i1}) were calculated from literature stability-constant data and

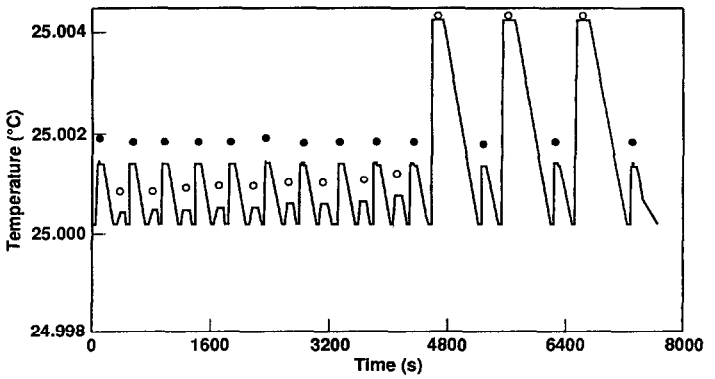

Fig. 1. Titration of 50.0 cm^3 of 0.007 M thorium(IV), pH 1.35, with 0.15 M HEDTA, pH 10.57. Solid circles represent 0.25 J electrical calibration heats, while open circles represent titration reaction heats.

Table 1. Thermodynamics of thorium amine-N-polycarboxylate complexes ($T = 25°C$, $\mu = 0.1$ M [KNO_3])

Ligand	$\log\beta_{101}$[a]	$-\Delta G_{101}$ (kJ mol^{-1})	ΔH_{101} (kJ mol^{-1})	ΔS_{101} (J mol-K^{-1})	$\log\beta_{111}$[a]	$-\Delta G_{111}$ (kJ mol^{-1})	ΔH_{111} (kJ mol^{-1})	ΔS_{111} (J mol-K^{-1})
NTA	12.4±0.1	70.8±0.6	5.7±0.2	260±2				
HEDTA	18.5±0.1	106±0.6	−4.4±0.5	340±3				
EDTA	23.2±0.1	132±0.6	−11.5±0.2	406±2	25.2±0.1	144±0.6	−11.9±0.2	443±2
DTPA	28.8±0.1	164±0.6	−12.3±0.3	510±2	30.9±0.1	176±0.6	−12.3±0.3	550±2

[a] From ref. 8.

mass- and charge-balance relationships as previously discussed.[6,7] (The indices "101" refer to the number of atoms of metal, hydrogen and ligand, respectively, in the complex. Thus, "101" indicates the reaction $M+L \rightleftarrows ML$, "011" indicates $H+L \rightleftarrows HL$, etc.) From an examination of the experimental data at two different pH values, it was evident that consideration of the ThHL species was necessary for EDTA and DTPA complexation. The HEDTA and NTA titrations showed no such pH dependency under our experimental conditions, however, so that $\Delta n_{111} = 0$ for these ligands. Analysis of the NTA data was complicated by the fact that the Th–NTA complex is very similar in strength to that of the protonated ligand. Consequently, fitted values for ligand protonation enthalpy were necessary to extract the heat of complexation of Th^{4+} from those data.

An attempt was made to measure the heat of complexation of thorium with ethylenedinitrilodiacetic acid (EDDA), an analogue of EDTA but with one carboxylic acid group on each terminal nitrogen. However, the observed heats of reaction were dominated by ligand protonation. This fact indicates that, at the low pH values required to prevent thorium(IV) hydrolysis, the H^+ in solution effectively competes with Th^{4+} for bonding sites on the EDDA anion.

Our results of -11.5 ± 0.2 and -11.9 ± 0.2 kJ mol^{-1} for EDTA ΔH_{101} and ΔH_{111} agree with the values of -12.9 ± 0.4 and -12.6 ± 0.2 kJ mol^{-1} reported by Doi using a batch titration procedure.[10] That experiment was very dependent upon knowledge of the protonation enthalpies of EDTA in order to correct for heats of protonation generated upon the addition of excess EDTA to an acidic thorium solution. Since our procedure involved an incremental addition of titrant, however, titration points devoid of significant ligand protonation could be isolated for data analysis.

CONCLUSIONS

The stability of thorium amine-N-polycarboxylate complexes is attributed to the large entropy effect obtained when the primary hydration sphere of the metal ion is displaced by a single multidentate ligand. ΔS_{101} represents a stabilization gain due to the number of water molecules displaced from the hydration sphere by the coordinating ligand. Plots of ΔS_{101} and $\log\beta_{101}$ thus climb linearly with the number of strongly interacting coordination sites on the ligand. Figure 2 shows the relationship between ΔS_{101} and the total ligand basicity (ΣpK_a) for thorium complexation, along with data for La^{3+} and Ca^{2+} for comparison. The fact that the entropy increases with cation charge for a given ligand can, of course, be understood qualitatively through simple electrostatic considerations: increasing polar attraction of the number of inner-sphere water molecules by the unreacted metal directly corresponds with the central charge.

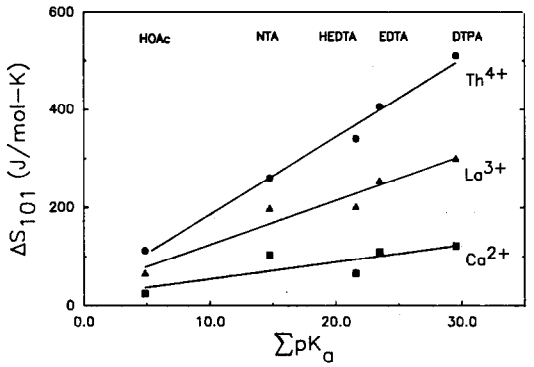

Fig. 2. Graph of ΔS_{101} vs ligand basicity, ΣpK_a, for Th^{4+}, La^{3+} and Ca^{2+} (data from this work and ref. 9).

In their analysis of lanthanide amine-N-polycarboxylate enthalpy data, Choppin *et al.* provided evidence that the entropy of complexation reflected a similar amount of dehydration for each additional coordinating carboxylate group in the ligand.[11] Extending this finding to the enthalpy of complexation, Choppin estimated that there was an enthalpy contribution of approximately 6.5 kJ mol^{-1} for each carboxylate group. The residual enthalpy of a complex ($d\Delta H_{101}$), then, was presumed to be a measure of the interaction between

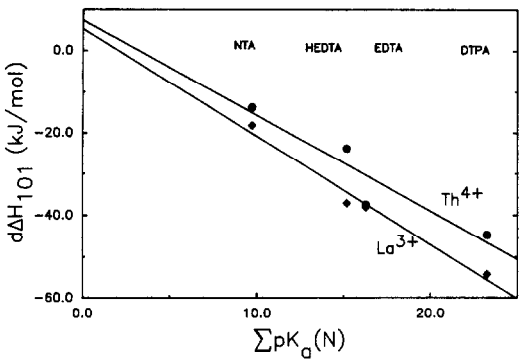

Fig. 3. Graph of $d\Delta H_{101}$ [$\Delta H_{101} - 6.5 \times$ (number of carboxylate groups)] vs total nitrogen basicity, $\Sigma pK_a(N)$, for Th^{4+} and La^{3+} (data from this work and ref. 9).

the lanthanide and the nitrogen donor atoms for each ligand. Figure 3 depicts a plot of $d\Delta H_{101}$ vs total nitrogen donor basicity [$\Sigma pK_a(N)$] for the present Th^{4+} measurements in comparison with La^{3+}. The similar behaviour indicates that the Th—N interaction is quite analogous to the Ln—N bonding for the ligands studied. Thus, the thermodynamic parameters obtained for the thorium amine-N-polycarboxylate complexes follow the same trends previously observed for the lanthanides.

Acknowledgement—This work was performed under the auspices of the U.S. Department of Energy by the Lawrence Livermore National Laboratory under Contract No. W-7405-Eng-48.

REFERENCES

1. R. M. Smith and A. E. Martell, *Sci. Total Environ.* 1987, **64**, 125.
2. J. L. Means, D. A. Crerar and J. O. Duguid, *Science* 1978, **200**, 1477.
3. J. M. Cleveland and T. F. Rees, *Science* 1981, **212**, 1506.
4. R. M. Smith, R. J. Motekaitis and A. E. Martell, *Inorg. Chim. Acta* 1985, **103**, 73.
5. P. A. Baisden, P. M. Grant and W. F. Kinard, *Rev. Sci. Instrum.* 1987, **58**, 1937.
6. P. A. Baisden, P. M. Grant, W. F. Kinard and R. A. Torres, *Inorg. Chim. Acta* 1987, **128**, 127.
7. P. M. Grant, W. F. Kinard and P. A. Baisden, *J. Solution Chem.* 1989, **18**, 211.
8. S. Ahrland, G. R. Choppin, P. A. Baisden, R. A. Torres and G. Marx, *Gmelin Handbook of Inorganic Chemistry, Thorium*, 8th edn, supplement Vol. D1. Springer, Berlin (1988).
9. A. E. Martell and R. M. Smith, *Critical Stability Constants*, Vol. 1 and Vol. 5. Plenum Press, New York (1974 and 1982).
10. K. Doi, *J. Inorg. Nucl. Chem.* 1978, **40**, 1639.
11. G. R. Choppin, M. P. Goedken and T. F. Gritmon, *J. Inorg. Nucl. Chem.* 1977, **39**, 2025.

Polyhedron Vol. 8, No. 19, pp. 2389–2394, 1989
Printed in Great Britain

0277–5387/89 $3.00+.00
Pergamon Press plc

SYNTHESIS AND CHARACTERIZATION OF SOME OCTAHEDRAL COBALT(III) COMPLEXES OF 3,3′,3″-TRIAMINOTRIPROPYLAMINE

S. S. MASSOUD*

Department of Chemistry, Faculty of Science, Alexandria University, Alexandria, Egypt

and

R. M. MILBURN

Department of Chemistry, Boston University, Boston, MA 02215, U.S.A.

(*Received* 14 *November* 1988; *accepted* 19 *May* 1989)

Abstract—The tripod quadridentate ligand 3,3′,3″-triaminotripropylamine (trpn) has been used to synthesize a series of *cis*-octahedral cobalt(III)–trpn complexes, including the type $[Cotrpn X_2](ClO_4)_n$ (X = F, Cl, Br, NO_3 and $n = 1$; X = CH_3CN and $n = 3$) as well as $[Cotrpn(CH_3CN)Br]BrClO_4$, where the coordinating groups are monodentate ligands. With chelating oxy-anions, preparation of the complexes $[Cotrpn(CO_3)](CF_3SO_3)$, $[Cotrpn(SO_4)]ClO_4$, $[Cotrpn(HSO_4)](ClO_4)_2$, $[Cotrpn(C_2O_4)]ClO_4$ and $[Cotrpn(H_2P_2O_7)]ClO_4$ are described. The visible, IR and ^{13}C NMR spectra have been used to characterize the isolated complexes.

In our previous studies, we have indicated the importance of *cis*/*trans* isomerism in metal ion promoted hydrolysis of ATP (adenosine 5′-triphosphate) and phosphate esters by tetraaminecobalt(III) complexes, where effective promotion was observed with complexes of *cis*-octahedral geometry.[1–5]

Metal complexes of the tripod quadridentate ligands of the type $X(Y)_3$, in which X is nitrogen, phosphorus or arsenic, the Y groups are R_2N, R_2P, R_2As, RS or RSe, where R is an alkyl group and where the connecting chains are $—(CH_2)_2—$ or $—(CH_2)_3—$, have been particularly shown to favour the formation of five-coordinate complexes.[6–11]

Complexes of the tripod tetraamine ligand 2,2′,2″-triaminotriethylamine $[N(CH_2CH_2NH_2)_3$ = tren] have been extensively studied.[12] The use of this ligand has led to the separation of five-coordinate[7,8,10] or *cis*-octahedral geometries,[13,14] and no tetrahedral complexes have been described.

Introduction of another CH_2 group into each of the ethylene bridging chains of tren produces a more facultative ligand.[15] This ligand, 3,3′,3″-triaminotripropylamine $[N(CH_2CH_2CH_2NH_2)_3$ = trpn],[16] has been little studied.[17–19] Recently, we have shown that cobalt(III) complexes of such a ligand represent a compromise between complexes

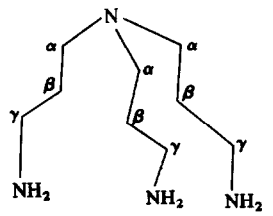

trpn

of fixed *cis*-octahedral geometry[20,21] (the tripod nature of the ligand enforces the remaining two positions in the octahedral complex to be oriented in the *cis* form), and extremely labile cobalt(III) complexes.[3,22] Consequently, because of the valuable information which can be extracted by using the trpn complexes in model studies, our immediate concern was the separation and characterization of some cobalt(III)–trpn complexes, and also to throw

* Author to whom correspondence should be addressed.

more light on the versatility of $[Cotrpn(CO_3)]ClO_4$ as a good starting material for the preparation of many cobalt(III)–trpn compounds in reasonable high yield.

EXPERIMENTAL

3,3′-3″-Triaminotripropylamine tetrahydrochloride hemihydrate (trpn · 4HCl · $\frac{1}{2}H_2O$) was supplied by Strem Chemical Company and trifluoromethanesulphonic acid, CF_3SO_3H, was obtained from Aldrich Chemical Company. All other chemicals were reagent grade quality.

CAUTION: The perchlorate complexes should be treated as potentially explosive and should be handled with appropriate care.

Synthesis of the complexes

The complexes $[Cotrpn(CO_3)]ClO_4 \cdot H_2O$, $[Cotrpn(H_2O)(OCO_2H)](ClO_4)_2 \cdot \frac{1}{2}H_2O$, $[Cotrpn(H_2O)_2](ClO_4)_3 \cdot 2H_2O$ and $[Cotrpn(PO_4)] \cdot 5H_2O$ were prepared as previously described.[20,21,23]

Carbonato(3,3′,3″ - *triaminotripropylamine*)*cobalt* (III) *triflate*, $[Cotrpn(CO_3)]CF_3SO_3$

A solution of the free base, trpn (1.9 g/15 cm^3 H_2O), neutralized by 4 M CF_3SO_3H, was added with stirring to a slurry cold solution of $Na_3[Co(CO_3)_3] \cdot 3H_2O$[24] (3.6 g/25 cm^3 H_2O). The temperature of the stirred solution was raised to 70°C, followed by heating at this temperature for 2 h. During this time the colour changed to purple, with reduction in volume to $\simeq$ 20 cm^3. The solution was filtered through celite, using Fisher Quantitative P2 filter paper. Upon cooling in a refrigerator for several days, the crude solid which separated out was filtered, dissolved in $\simeq$ 60 cm^3 of ethanol at 70°C, and evaporated until dry. The red crystals obtained were filtered, washed with acetone and ether and air-dried. Further evaporation of the mother liquor on a steam bath produced a second crop. The total yield was $\simeq$ 1 g ($\simeq$ 20%).

Dichloro(3,3′,3″-*triaminotripropylamine*)*cobalt*(III) *perchlorate*, $[CotrpnCl_2]ClO_4$

This complex was prepared by adding 0.6 cm^3 of conc. HCl (37%) to the carbonato complex, $[Cotrpn(CO_3)]ClO_4 \cdot H_2O$ (1 mmol). The effervescence was allowed to subside before each addition of acid. Upon gentle heating on a steam-bath for 5 min, a bluish-green solid separated out. Then 10 cm^3 of anhydrous methanol was added with vigorous swirling, followed by decantation. The process was repeated twice and the solid was filtered off, washed with methanol and ether, and dried *in vacuo* over P_4O_{10} (yield 37%). Found: C, 25.7; H, 5.8; N, 13.4; Cl, 25.4. Calc. for $[Co(C_9H_{24}N_4)Cl_2]ClO_4$: C, 25.9; H, 5.8; N, 13.4; Cl, 25.4%.

Attempted preparation of $[CotrpnCl_2]Cl$ by aerial oxidation of an aqueous solution of $CoCl_2$ + trpn + HCl was unsuccessful. Also, attempts to synthesize the dinitrito complex of cobalt(III)–trpn, as described for the preparation of $[Cotren(NO_2)_2]Cl$ by Collman *et al.*,[25] and then converting it into the dichloro complex by treatment with conc. HCl and evaporation, did not lead to the desired product; instead, the yellow crystalline complex $Codpt(NO_2)_3$ [dpt = dipropylenetriamine = $NH(CH_2CH_2CH_2NH_2)_2$] was isolated, which had been previously prepared and characterized.[26]

Dibromo(3,3′,3″-*triaminotripropylamine*)*cobalt*(III) *perchlorate*, $[CotrpnBr_2]ClO_4$

This complex was prepared by the same method used above for the chloro compound, where 1 mmol of $[Cotrpn(CO_3)]ClO_4 \cdot H_2O$ was treated with 0.25 cm^3 of conc. HBr (48%). The khaki fine solid which separated was filtered, washed with a generous amount of anhydrous methanol until the filtrate became colourless, and then dried *in vacuo* over P_4O_{10} (yield 65%). Found: C, 21.4; H, 4.8; N, 11.0; Cl, 7.0; Br, 31.5. Calc. for $[Co(C_9H_{24}N_4)Br_2]ClO_4$: C, 21.3; H, 4.8; N, 11.1; Cl, 7.0; Br, 31.5%.

Difluoro(3,3′,3″-*triaminotripropylamine*)*cobalt*(III) *perchlorate trihemihydrate*, $[CotrpnF_2]ClO_4 \cdot \frac{3}{2}H_2O$

In a polyethylene container, finely powdered $[Cotrpn(CO_3)]ClO_4 \cdot H_2O$ (2.5 mmol) was treated with conc. HF. The acid was added very carefully, drop by drop, with gentle heating on a steam bath. Effervescence of CO_2 was allowed to subside before each addition. The addition of the acid was stopped when a purple solution had formed; this was heated for 5 min, followed by the addition of anhydrous methanol. After standing at room temperature the light violet solid, collected by filtration, was washed with a mixture of ice cold methanol–water (7 : 3 by volume), then ether, and dried for 2 days in a vacuum desiccator over P_4O_{10} (yield 37%). Found: C, 26.3; H, 6.4; N, 13.7; Co, 14.3. Calc. for $[Co(C_9H_{24}N_4)F_2]ClO_4 \cdot \frac{3}{2}H_2O$: C, 26.3; H, 6.6; N, 13.6; Co, 14.3%.

Bis(acetonitrile)(3,3′,3″ - *triaminotripropylamine*) *cobalt*(III) *perchlorate*, $[Cotrpn(CH_3CN)_2](ClO_4)_3$

The diaqua complex $[Cotrpn(H_2O)_2](ClO_4)_3 \cdot 2H_2O$ (1 mmol) was dissolved in 50 cm^3 of acetonitrile (dried over 4 Å Linde molecular sieves and then distilled). The resulting was refluxed for 1 h on a steam bath, followed by evaporation to a small volume. On cooling, the pink–red solid which separated out was filtered and recrystallized from acetonitrile. The product was collected by filtration, washed with ether, air-dried and stored in a vacuum desiccator over P_4O_{10} (yield 63%). Found: C, 25.1; H, 4.9; N, 13.5; Cl, 17.1. Calc. for $[Co(C_9H_{24}N_4)(CH_3CN)_2](ClO_4)_3$: C, 24.9; H, 4.8; N, 13.4; Cl, 16.9%.

Bromo(acetonitrile)(3,3′,3″ - *triaminotripropylamine)cobalt*(III) *bromide perchlorate*, $[Cotrpn(CH_3CN)Br]BrClO_4$

This complex was prepared by dissolving $[CotrpnBr_2]ClO_4$ (0.2 g) in 30 cm^3 of dry acetonitrile. After heating at 60°C for 30 min, the solution was cooled and the light green solid, which was collected by filtration, was washed with anhydrous methanol, ether and air-dried (yield 60%). Found: C, 24.4; H, 4.9; N, 13.0. Calc. for $[Co(C_9H_{24}N_4)(CH_3CN)Br]BrClO_4$: C, 24.1; H, 5.0; N, 12.8%.

Sulphato(3,3′,3″-*triaminotripropylamine)cobalt*(III) *perchlorate hemihydrate*, $[Cotrpn(SO_4)]ClO_4 \cdot \frac{1}{2}H_2O$

Finely powdered $[Cotrpn(CO_3)]ClO_4 \cdot H_2O$ (0.25 mmol) was treated with conc. H_2SO_4 (25×10^{-3} cm^3). The resulting paste was warmed very carefully on a steam bath for 5 min, followed by the addition of 2 cm^3 of anhydrous methanol. The violet solid, which was collected by filtration, was washed with cold methanol, ether and then air-dried (yield 90%). Found: C, 23.8; H, 5.5; N, 12.1; Cl, 7.4; S, 7.0. Calc. for $[Co(C_9H_{24}N_4)SO_4]ClO_4 \cdot \frac{1}{2}H_2O$: C, 23.9; H, 5.6; N, 12.4; Cl, 7.8; S, 7.1%.

Bisulphato(3,3′,3″ - *triaminotripropylamine)cobalt* (III) *perchlorate*, $[Cotrpn(HSO_4)](ClO_4)_2$

Finely powdered $[Cotrpn(CO_3)]ClO_4 \cdot H_2O$ (0.5 mmol) was treated with a few drops of 5 M $HClO_4$, followed by heating for 5 min at 60°C, and then diluted with water to 10 cm^3. To the above solution, 0.5 mmol of $KHSO_4$ was added and the solution was heated for 10 min at 70°C. Upon cooling to room temperature, bluish-violet crystals separated out; these were collected by filtration, washed with absolute ethanol, ether and air-dried (yield 74%). Found: C, 19.8; H, 4.5; N, 10.3; Cl, 12.9. Calc. for $[Co(C_9H_{24}N_4)(HSO_4)](ClO_4)_2$: C, 19.9; H, 4.6; N, 10.3; Cl, 13.1%.

Dinitrato(3,3′,3″ - *triaminotripropylamine)cobalt* (III) *perchlorate*, $[Cotrpn(NO_3)_2]ClO_4$

This complex was prepared using similar procedures to those described above for the corresponding sulphato complex, except for the use of conc. HNO_3 instead of conc. H_2SO_4. Found: C, 23.1; H, 5.1; N, 17.8; Cl, 7.5. Calc. for $[Co(C_9H_{24}N_4)(NO_3)_2]ClO_4$: C, 23.0; H, 5.1; N, 17.8; Cl, 7.5%.

Oxalato(3,3′,3″ - *triaminotripropylamine)cobalt*(III) *perchlorate monohydrate*, $[Cotrpn(C_2O_4)]ClO_4 \cdot H_2O$

Finely powdered $[Cotrpn(CO_3)]ClO_4 \cdot H_2O$ (0.5 mmol), dissolved in 6 cm^3 of water, was acidified by 0.6 cm^3 of 6 M $HClO_4$, followed by heating on a steam bath for 15 min to expel CO_2. Oxalic acid dihydrate (0.5 mmol) was added and the resulting solution was heated for 30 min at 60°C. On cooling at room temperature, the pink solid which separated out was collected by filtration, washed with methanol and ether, and dried *in vacuo* over P_4O_{10} (yield 88%). Found: C, 29.5; H, 5.8; N, 12.5; Cl, 7.9. Calc. for $[Co(C_9H_{24}N_4)(C_2O_4)]ClO_4 \cdot H_2O$: C, 29.2; H, 5.8; N, 12.4; Cl, 7.8%.

Dihydrogen pyrophosphato(3,3′,3″ - *triaminotripropylamine)cobalt*(III) *perchlorate*, $[Cotrpn(H_2P_2O_7)]ClO_4$

The carbonato complex, $[Cotrpn(CO_3)]ClO_4 \cdot H_2O$ (0.5 mmol), was treated with 0.5 cm^3 of 6 M $HClO_4$, followed by heating for 5 min at 60°C. The resulting diaqua complex was diluted to 5 cm^3 with water and then 0.5 mmol of $H_4P_2O_7$ was added. The pH of the resulting solution was adjusted to 6.2 by the addition of 2 M KOH, followed by heating with stirring, for 15 min at 70°C. The $KClO_4$ which precipitated out upon cooling at 0°C, was filtered off. Methanol (8 cm^3) was added and the solution was refiltered and kept *in vacuo* over P_4O_{10}. The bluish-violet solid which separated out after three days, was recrystallized from anhydrous methanol (yield 40%). Found: C, 20.8; H, 5.2; N, 10.6; P, 12.7; Co, 11.1. Calc. for $[Co(C_9H_{24}N_4)(H_2P_2O_7)]ClO_4$: C, 20.7; H, 5.0; N, 10.7; P, 11.8; Co, 11.3%.

The elemental analyses for the prepared complexes were performed by Atlantic Microlab. Inc., Atlanta, Georgia, except for the analyses for

$[Cotrpn(F_2)]ClO_4 \cdot \frac{3}{2}H_2O$ and $[Cotrpn(H_2P_2O_7)]ClO_4$ which were carried out by Galbraith Laboratories, Knoxville, Tennessee. pH measurements were made with an Orion Research pH meter model 601 A fitted with a combination electrode. Evaporations were carried out using a vacuum system attached to a Büchi rotary evaporator. IR spectra were recorded using a Perkin–Elmer 1310 IR spectrometer. Electronic spectra were recorded with a Cary 210 spectrophotometer. ^{13}C NMR spectra were measured with a Jeol FX 90Q FT spectrometer operating at 22.49 MHz with a deuterium internal lock. 1,4-Dioxane was used as the internal reference with D_2O as solvent. The ^{13}C NMR chemical shifts are recorded in ppm relative to TMS.

RESULTS AND DISCUSSION

Scheme 1 clearly demonstrates the versatility of $[Cotrpn(CO_3)]ClO_4 \cdot H_2O$[20] as a good source for the preparation of many cobalt(III)–trpn complexes. The reaction of the carbonato complex with conc. HNO_3 or conc. HX (X = F, Cl, Br) yielded the corresponding dinitrato or dihalo species, respectively. Also, some cobalt(III)–trpn–oxo-anion complexes were isolated from the reaction of acidified solutions of $[Cotrpn(CO_3)]ClO_4$ with SO_4^{2-}, HSO_4^-, $C_2O_4^{2-}$, PO_4^{3-} or $H_2P_2O_7^{2-}$ ions. On the other hand, while the reaction of $[Cotrpn(H_2O)_2](ClO_4)_3$ with dry acetonitrile afforded the corresponding bis-acetonitrile, the reaction of the dibromo species led to mono-acetonitrile; $[Cotrpn(CH_3CN)Br]BrClO_4$. The latter complex is sparingly soluble in acetonitrile and does not react further to produce the corresponding bis-aceto-nitrile, even with prolonged heating. The aqua-(bicarbonato) complex, $[Cotrpn(H_2O)(OCO_2H)](ClO_4)_2$, was isolated[20] by gentle treatment of the carbonato complex with a cold solution of 6 M $HClO_4$.

The electronic spectra of the isolated cobalt(III)–trpn complexes, collected in Table 1, show the presence of only two absorption bands in the vis–near UV region. The great similarity of the spectra to that of the $[Cotrpn(CO_3)]^+$ ion[20] argues for *cis*-octahedral geometry, which was already supported by X-ray structural determination for the carbonato complex.[21] Furthermore, in the visible region, the *trans*-dihalo(tetraamine)cobalt(III) complexes exhibit three absorption bands of lower molar absorptivities than the corresponding *cis* isomers, which show only two absorption bands.[27] Thus, all the isolated cobalt(III)–trpn complexes appear to have the *cis*-octahedral geometries, in which the trpn moiety is folded so that all four nitrogen atoms are coordinated to the cobalt(III) ion and enforce the remaining two positions to be oriented in the *cis* form.[21] The isolated sulphato, bisulphato and phosphato cobalt(III)–trpn complexes are tentatively assigned the monomeric *cis* configuration since their visible spectra resemble that of the $[Cotrpn(CO_3)]^+$ ion. This assignment, however, could not guarantee the existence of either monomeric four-membered chelates or *cis*-bis(μ-oxo-anion) bridges. Recently, it was pointed out that the previously described four-membered sulphato chelate, $[Co(en)_2(O_2SO_2)]^+$, has been shown to contain *cis*-bis(μ-sulphato) bridges.[28]

The IR spectra of the isolated acetonitrile complexes; $[Cotrpn(CH_3CN)_2](ClO_4)_3$ and [Cotrpn

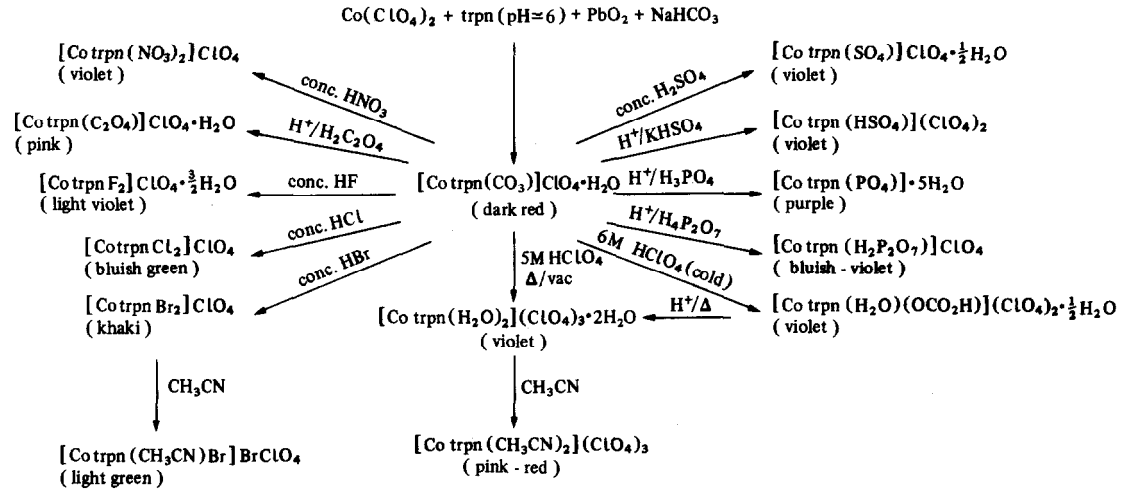

Scheme 1.

Table 1. Electronic spectra of cobalt(III) complexes derived from 3,3′,3″-triaminotripropylamine at 25°C

Complex	Medium	$\lambda_{max}(\varepsilon)^a$	$\lambda_{min}(\varepsilon)$	$\lambda_{max}(\varepsilon)$	$\lambda_{min}(\varepsilon)$	Reference
$[Cotrpn(CO_3)]ClO_4$	H_2O	532(125)	434(11)	363(153)	334(87)	20
$[Cotrpn(CO_3)]CF_3SO_3$	H_2O	535(126)	440(13)	367(157)	338(87)	This work
$[Cotrpn(H_2O)(OCO_2H)]^{2+}$	H_2O	532(108)	436(12)	362(139)	335(89)	20
$[Cotrpn(SO_4)]^+$	H_2O	546(88)	450(12)	364(114)	337(71)	This work
$[Cotrpn(HSO_4)]^{2+}$	H_2O	548(74)	450(11)	367(95)	343(102)	This work
$[Cotrpn(PO_4)]$	H_2O	550(114)	454(13)	373(104)	353(44)	23
$[Cotrpn(H_2P_2O_7)]^+$	H_2O	544(84)	453(14)	377(94)	338(38)	This work
$[Cotrpn(C_2O_4)]^+$	H_2O	530(94)	430(10)	363(199)	330(89)	This work
$[Cotrpn(NO_3)_2]^+$	H_2O	528(55)	440(12)	364(83)	337(63)	This work
$[Cotrpn(H_2O)_2]^{3+}$	H_2O	528(57)	440(12)	366(82)	334(51)	21
$[CotrpnCl_2]^+$	37% HCl	378(55)	485(125)			22
$[CotrpnBr_2]^+$	24% HBr	≃ 589(71)	≃ 522(55)			22
$[Cotrpn(CH_3CN)_2]^{3+}$	CH_3CN	498(98)	418(28)			22
$[Cotrpn(CH_3CN)Br]^{2+}$ [b]	CH_3CN	≃ 580				22

[a] λ in nm and ε in $M^{-1}\,cm^{-1}$.
[b] Saturated solution.

$(CH_3CN)Br]BrClO_4$ show ν(CN) at 2300 cm^{-1} (KBr disc), suggesting coordination of the acetonitrile to the cobalt centre.[29]

^{13}C NMR chemical shifts for some cobalt(III)–trpn complexes and their free ligands (trpn, CO_3^{2-}, HCO_3^- and $C_2O_4^{2-}$) are summarized in Fig. 1. The ^{13}C NMR signals for each of the methylene carbons in the complex ions $[Cotrpn(CO_3)]^+$, $[Cotrpn(C_2O_4)]^+$ and $[Cotrpn(H_2O)_2]^{3+}$ consist of two closely separated signals with ≃ 2:1 intensity rations. For each complex there are two α-carbons, two β-carbons and two γ-carbons in the arms which include the primary amine nitrogens that are *cis* to both coordinated oxygens. The other three carbons, α′, β′ and γ′, are in the arm which includes the primary and tertiary amine nitrogens and the two coordinated oxygens.[20] On the other hand, for $[Cotrpn(H_2O)(OCO_2H)]^{2+}$ more complex signals were observed for the trpn carbons (Fig. 1), due

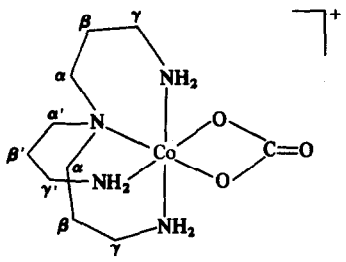

$[Cotrpn(CO_3)]^+$

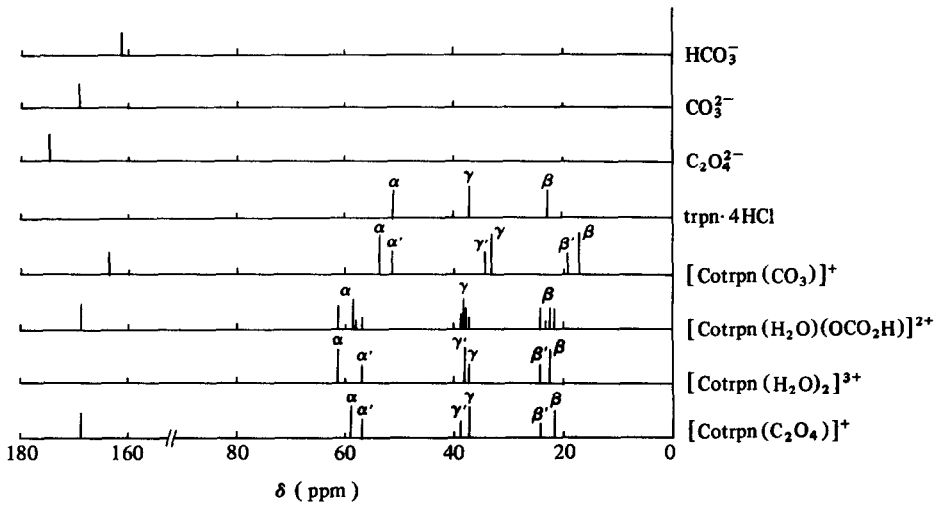

Fig. 1. Positions of ^{13}C NMR signals for the free ligands and their cobalt(III) complexes.

to the presence of six signals for each of the two geometrical isomers, depending on whether the OCO_2H^- ion is coordinated *cis* or *trans* to the coordinated tertiary amine nitrogen of the trpn.[20] The ^{13}C NMR chemical shifts for the carbon of the carbonyl group in the carbonato and oxalato complexes are shifted upfield by $\simeq$ 5–6 ppm, while for the bicarbonato complex, a downfield shift of 6.8 ppm was observed.[20]

In acidic medium the complex ions $[CotrpnCl_2]^+$ and $[CotrpnBr_2]^+$ hydrolyse very rapidly; complete-conversion of the dichloro complex to the diaqua species occurs in $\simeq$ 2 min.[22] The complex ion[21] $[Cotrpn(OH)(H_2O)]^{2+}$, which is the major species at pH $\simeq$ 6.5 (the pK_1 and pK_2 for the acid dissociation constants of coordinated water in $[Cotrpn(H_2O)_2]^{3+}$ are 4.82 and 7.52, respectively, at 25°C and $\mu = 0.1$ M), exhibits very large rate promotions for the hydrolysis of ATP[3] and rapid reaction for complex formation with phosphate.[23]

REFERENCES

1. G. H. Rawji and R. M. Milburn, *Inorg. Chim. Acta* 1988, **150**, 227.
2. F. Tafesse and R. M. Milburn, *Inorg. Chim. Acta* 1987, **135**, 119.
3. F. Tafesse, S. S. Massoud and R. M. Milburn, *Inorg. Chem.* 1985, **24**, 2591.
4. G. H. Rawji, M. Hediger and R. M. Milburn, *Inorg. Chim. Acta* 1983, **79**, 247.
5. M. Hediger and R. M. Milburn, *Inorg. Biochem.* 1982, **16**, 165.
6. F. Mani and L. Sacconi, *Comm. Inorg. Chem.* 1983, **2**, 157.
7. G. D. Andretti, P. C. Jain and E. C. Lingafelter, *J. Am. Chem. Soc.* 1969, **91**, 4112.
8. P. C. Jain and E. C. Lingafelter, *J. Am. Chem. Soc.* 1967, **89**, 1613.
9. M. Q. Workman, G. Dyer and D. W. Meek, *Inorg. Chem.* 1967, **6**, 1543.
10. M. Ciampolini and P. Paoletti, *Inorg. Chem.* 1967, **6**, 1261.
11. M. Ciampolini and N. Nardi, *Inorg. Chem.* 1966, **5**, 41.
12. S. G. Zipp, A. P. Zipp and S. K. Madan, *Coord. Chem. Rev.* 1974, **14**, 29 and refs therein.
13. G. S. Benner and D. W. Meek, *Inorg. Chem.* 1967, **6**, 1399.
14. W. K. Kuo, W. V. Miller and S. K. Madan, *J. Inorg. Nucl. Chem.* 1973, **35**, 957.
15. F. Lions and H. Goodwin, *J. Am. Chem. Soc.* 1960, **82**, 5013.
16. F. G. Mann and W. J. Pope, *J. Chem. Soc.* 1926, 489.
17. A. Dei, P. Paoletti and A. Vacca, *Inorg. Chem.* 1968, **7**, 865.
18. A. Vacca and P. Paoletti, *J. Chem. Soc.* 1968, 2378.
19. J. L. Shafer and K. N. Raymond, *Inorg. Chem.* 1971, **10**, 1799.
20. S. S. Massoud and R. M. Milburn, *Inorg. Chim. Acta* 1988, **154**, 115.
21. S. S. Massoud and R. M. Milburn, results to be submitted for publication.
22. S. S. Massoud and R. M. Milburn, *Polyhedron* 1989, **8**, 275; 415.
23. S. S. Massoud and R. M. Milburn, *Inorg. Chim. Acta* 1989, **163**, 87.
24. H. F. Baver and W. C. Drinkard, *J. Am. Chem. Soc.* 1960, **82**, 5031.
25. E. Kimura, S. Young and J. Collman, *Inorg. Chem.* 1970, **9**, 1183.
26. S. H. Caldwell and D. A. House, *J. Inorg. Nucl. Chem.* 1969, **31**, 811; N. F. Curtis, R. W. Hay and Y. M. Curtis, *J. Chem. Soc. A* 1968, 182; G. H. Searle and T. W. Hambley, *Aust. J. Chem.* 1982, **35**, 1297.
27. F. Basolo, C. J. Ballhausen and J. Bjerrum, *Acta Chem. Scand.* 1955, **9**, 810.
28. D. A. Buckingham, C. R. Clark, J. Simpson and W. T. Robinson, *Inorg. Chem.* 1988, **27**, 3544.
29. K. Nakamoto, *Infrared Spectra of Inorganic and Coordination Compounds*, 2nd Edn. Wiley, New York (1970).

Polyhedron Vol. 8, No. 19, pp. 2395–2405, 1989
Printed in Great Britain

0277–5387/89 $3.00+.00
© 1989 Pergamon Press plc

SYNTHESIS, MAGNETIC AND SPECTROSCOPIC CHARACTERIZATION OF METAL(II) ARYLCARBOXYLATE ADDUCTS WITH SATURATED HETEROCYCLIC BASES

BALDEV SINGH MANHAS

Department of Chemistry, Punjabi University, Patiala 147002, India

and

AJAIB SINGH DHINDSA*

Department of Chemistry/Applied Physics, University of Durham, Science Laboratories, South Road, Durham DH1 3LE, U.K.

(*Received* 17 *August* 1988; *accepted after revision* 22 *May* 1989)

Abstract—Several new complexes of $M(RCOO)_2$ (where R = C_6H_5, 2-, 3- or 4-$O_2NC_6H_4$ and M = Co, Ni or Cu) with saturated diheterocyclic bases (L—L) of the type $M(RCOO)_2(L—L)_n$ (where n = 2, 1 or 0.5 and L—L = piperazine, 1-methylpiperazine, 2-methylpiperazine, 1-phenylpiperazine, 2,6-dimethylpiperazine, 2,5-dimethylpiperazine, 1,4-dimethylpiperazine and 4-methylmorpholine) and with saturated monoheterocyclic bases (L) of the type $M(RCOO)_2L_n$ (where n = 2 or 1 and L = 2-methylpiperidine, 3-methylpiperidine and 4-methylpiperidine) have been synthesized and characterized by elemental analyses, IR and electronic reflectance spectral and magnetic susceptibility measurement studies. In addition, most of the copper(II) complexes are also characterized by EPR spectral measurements. All complexes of cobalt(II) and nickel(II) are found to be magnetically dilute except $Co(2\text{-}O_2NC_6H_4COO)_2$(4Me-morl) (where 4Me-morl = 4-methylmorpholine) which is antiferromagnetic. Copper(II) forms both magnetically dilute and antiferromagnetic complexes with these bases. Probable structures have been assigned to all these complexes. The spin-exchange parameter, $-2J$, for antiferromagnetic complexes has been evaluated from both magnetic susceptibility and EPR measurements at different temperatures. No correlation between the value of $-2J$ and pK_a of the acid or terminal ligand could be established.

There has been considerable interest in the chemistry of metal(II) carboxylates and their complexation properties with nitrogen and oxygen donor ligands.[1–7] Depending upon the structure, the complexes show different magnetic behaviour. Many factors such as stoichiometry,[3,5] nature of carboxylic acid,[3,6,7] steric and electronic characteristics of the additional ligand[8–13] and conditions of the reaction[14] determine the structural priorities of the complex.

A literature survey reveals that although some workers have examined the role of "steric hindrance" or electronic nature of the substituent group on the pyridine type ligands[3,5–9] in their complexation behaviour with cobalt(II), nickel(II) and copper(II) carboxylates, no such systematic effort has yet been made for the saturated diheterocyclic bases (L—L) and monoheterocyclic bases (L). So the present work on the synthesis and magnetic and spectral properties for complexes of $M(RCOO)_2$ (where M = Co, Ni and Cu and R = C_6H_5, 2-, 3- or 4-$O_2NC_6H_4$) with ligands of different steric and electronic characteristics such as piperazine (pipz), 1-methylpiperazine (1Me-pipz), 2-methylpiperazine (2Me-pipz), 1-phenylpiperazine (1Ph-pipz), 1,4-

* Author to whom correspondence should be addressed.

dimethylpiperazine (1,4Me_2-pipz), 2,5-dimethylpiperazine (2,5Me_2-pipz), 2,6-dimethylpiperazine (2,6Me_2-pipz) and 1-methylmorpholine (1Me-morl), L—L; and 2-methylpiperidine (2Me-pipd), 3-methylpiperidine (3Me-pipd) and 4-methylpiperidine (4Me-pipd), L, has been undertaken. An additional incentive to undertake these studies was to see if the boat form of the diheterocyclic base could be stabilized in the complexed state.

EXPERIMENTAL

Starting materials

Liquid heterocyclic bases such as 1Me-pipz, 1Ph-pipz, 1,4Me_2-pipz (all from Fluka), 4Me-morl and 2-, 3- and 4Me-pipd's (all from K and K Laboratories) were dried by refluxing and distilling over sodium hydroxide pellets before use. Solid ligands viz. pipz, 2Me-pipz, 2,6Me_2-pipz and 2,5Me_2-pipz (K and K Laboratories) were kept over potassium hydroxide pellets in a vacuum desiccator for 3 days to dry. The purity of 2-, 3- and 4-nitrobenzoic acids (BDH, LR) was checked from their sharp melting points after recrystallization from ethanol. Other materials such as metal(II) chlorides (BDH) or sodium benzoate (BDH, AR) were used as such without any purification. Acetone, *n*-hexane, solvent ether and petroleum ether (40–60°C), all from BDH, were purified by the usual methods.

Preparation of metal(II) nitrobenzoates

A solution of nitrobenzoic acid (10.0 g, 60 mmol) in a minimum quantity of acetone was neutralized with aqueous sodium hydroxide solution. A small quantity (20 mg) of the nitrobenzoic acid was added to make the solution just acidic and the solution was then filtered. The stirring, aqueous solution of sodium nitrobenzoate thus formed was added to a filtered aqueous solution of metal(II) chloride ($\simeq$ 7 g, 30 mmol). All three copper(II) nitrobenzoates, cobalt(II) 3- and 4-nitrobenzoates and nickel(II) 4-nitrobenzoate separated out after the contents had been stirred for 0.5 h. Other metal(II) nitrobenzoates were obtained upon concentrating the reaction mixture and cooling it in a refrigerator. The separated product was filtered, washed with cold distilled water and dried in air. The air-dried product was then subjected to vacuum at 140°C for 4 h.

Copper(II) benzoate was similarly prepared by reacting sodium benzoate with copper(II) sulphate in water, which separated upon mixing the contents.

Preparation of complexes

A solution of the stoichiometric amount in general, and in the case of 1,4Me_2-pipz and 4Me-morl a 50% excess, of the saturated heterocyclic base dissolved in acetone (15 cm^3) was added dropwise to a continuously stirred solution/suspension of metal(II) carboxylate (1 g) in acetone (*ca* 50 cm^3). Most of the adducts of the diheterocyclic bases separated on stirring for 0.5 h, and these were completely precipitated by the addition of *n*-hexane or ether. Other complexes were separated on concentrating the reaction mixture to about a quarter of its original volume, cooling in the refrigerator for 4 h and adding solvent ether or *n*-hexane. The separated product was filtered through a G_4 filtration unit, washed with solvent ether and *n*-hexane, and dried under vacuum.

Elemental analyses and physical measurements

The metal content in the complexes was determined volumetrically by EDTA titration using Xylenol Orange as indicator. Carbon and hydrogen analyses were performed on an automatic Coleman-33 analyser, while nitrogen was estimated by Kjeldahl's method in the departmental microanalytical laboratory.

Room-temperature magnetic susceptibility of all the complexes was measured on a Gouy balance using $Hg[Co(NCS)_4]$ as calibrant. The magnetic susceptibility of some representative cobalt(II) complexes and antiferromagnetic copper(II) complexes at different temperatures was measured on a Curie Magnetic susceptibility with the NEC PC-980 Data Treatment System or on a Vibrating Sample Magnetometer (VMS) PAR-155 with a variable-temperature cryostat. The measured susceptibility was corrected for the diamagnetic susceptibility of the ligands. The correction for temperature independent paramagnetism was taken as -60×10^{-6} c.g.s. units per gram atom of copper(II) ions.

IR spectra of the acids, their anhydrous metal(II) and sodium salts and the complexes were recorded both as Nujol and hexachlorobutadiene mulls on an IR-20 spectrophotometer with sodium chloride plates as windows in the 4000–600 cm^{-1} region, while far-IR spectra in the range 600–250 cm^{-1} were measured as Nujol mulls in polythene film. Electronic reflectance spectra of the complexes were recorded on Unicam SP-700 UV–vis–near IR spectrophotometer with a SP-735 diffuse reflectance attachment. The EPR measurements of powdered samples at liquid nitrogen temperature (77 K) were carried out on a Varian E-4 EPR-spectrometer at X-

band frequencies (8.8–9.6 GHz). The X-band EPR measurements of powdered materials of antiferromagnetic complexes at different temperatures were made on a Varian E-12 EPR spectrometer using the E-257 variable-temperature assembly. Diphenylpicrylhydrazyl (DPPH) was used as calibrant.

The pK_as of some of the bases were determined pH-metrically at 37°C using an Elico (model 4-122) digital meter.

RESULTS AND DISCUSSION

Chemical formulae based upon elemental analyses, colour and room-temperature μ_{eff} values are listed in Table 1. Examination of Table 1 shows that these metal(II) carboxylates give rise to complexes of 1:0.5, 1:1 or 1:2 (metal–base) stoichiometry with these saturated heterocyclic bases. The different complexation behaviour of these bases will be discussed later. All complexes of cobalt(II) are red, pink or brown, except $Co(3\text{-}O_2NC_6H_4COO)_2$(2Me-pipd) which is green, while nickel complexes are green or pale green. Most of the copper(II) complexes are blue or light blue except for the antiferromagnetic complexes (**XCVII–CXI**) which are green.

IR spectral studies

Various structural possibilities for complexes of the stoichiometries $M(RCOO)_2L_n$ (where $n = 2$, 1 or 0.5) which depend upon the mode of coordination of the carboxylate group and the diheterocyclic base, have been discussed elsewhere.[15] IR studies are quite useful in determining the mode of coordination of these ligands.[5,16] On critically examining the positions and direction of the shifts of the ν_{as}(OCO) and ν_s(OCO) of the carboxylate group in the complexes, as compared to their positions in the sodium salts of the respective acids, the bridging bidentate mode for complexes **XIX**, **XLV**, **XLVII**, **XLIX** and **LVII** and, **XCVII–CXI** and the chelating bidentate mode of coordination of the carboxylate group for all other complexes can be suggested.[16,17] A shift to the lower energy region ($\simeq 50$ cm^{-1}) of the bands due to ν(N—H) vibrations in the complexes relative to those in the free bases ($\simeq 3300$ cm^{-1}) indicates the coordination of the bases through the nitrogen atom(s) of their N—H bond(s).[18,20] However, in the IR spectrum of 1Me-pipz complexes of the type $M(RCOO)_2$(1Me-pipz)$_2 \cdot 2H_2O$, this band is much too broad (due to it becoming mixed into ν(O—H) and enhanced effect of hydrogen bonding) to indicate any shift. An examination of the band around 2750 cm^{-1} due to ν(C—H) of N—CH_3 in the complexes of 1Me-pipz, 1,4Me_2-pipz and 1Me-morl shows that this band is observed at almost the same position as in the free bases for complexes of the type $M(RCOO)_2$(1Me-pipz)$_2$ or $Cu(RCOO)_2$(1Me-pipz) which indicates that the nitrogen atom of the N—CH_3 group remains uncoordinated, while this frequency disappears or undergoes large positive shifts for other complexes of these bases, showing the binding of this nitrogen atom to the metal.[20,21]

Additional bands in the complexes, compared with the IR spectra of uncomplexed metal(II) carboxylates and free bases in the region 370–440 cm^{-1} and 320–360 cm^{-1}, have tentatively been assigned to ν(M—O) and ν(M—N) modes, respectively.[18,19,22–24] In the region of absorption of diheterocyclic bases, the IR spectra of the complexes under study closely resemble those of the free bases, and no additional bands characteristic of the boat form are observed. This indicated that the ligands are coordinated in the chair form.[25,26]

Electronic reflectance spectral studies

All cobalt(II) complexes in the present study, other than $Co(3\text{-}O_2NC_6H_4COO)_2$(2Me-pipd) or **XXX** and $Co(2\text{-}O_2NC_6H_4COO)_2$(4Me-morl) or **XIX**, show two principal absorption bands around 8000 cm^{-1} (ν_1) and 19,000 cm^{-1} (ν_3) which are assigned, respectively, to the $^4T_{2g} \leftarrow {}^4T_{1g}(F)$ and $^4T_{1g}(P) \leftarrow {}^4T_{1g}(F)$ transitions for the cobalt(II) ion in approximate octahedral environments (Fig. 1).[8,27] A weak band or a shoulder observed around 15,000 cm^{-1} (ν_2) for some of the complexes is assigned to the third spin-allowed but two-electron forbidden $^4A_{2g} \leftarrow {}^4T_{1g}(F)$ transition. The ratio of ν_2/ν_1 for these complexes lies in the range 1.9–2.10, which lends support to the above assignments.[27,28] The broadness or splitting observed for the ν_1 band can be attributed to the distortion of structure from cubic symmetry. The Dq and B values for these complexes (calculated from ν_3/ν_1) lie in the range 870–950 and 750–900 cm^{-1}, respectively.[8,18] Electronic diffuse reflectance spectra of **XIX** and **XXX** are similar to those of square-pyramidal and trigonal-bipyramidal environments around the cobalt(II) ion, respectively.[8]

All nickel(II) complexes under present discussion show bands around 8700 (ν_1) 14,000 (ν_2) and 26,000 (ν_3) cm^{-1} (but some show the last band around 21,000 cm^{-1}, viz. **XL**, **XLVIII**, **L** and **LXI**) in their electronic diffuse reflectance spectra. The number, shape and energies of these bands are the characteristics of *trans*-pseudo octahedral structure (D_{4h} symmetry) containing the NiO_4N_2 chromophore and are, therefore, assigned to the $^3T_{2g} \leftarrow {}^3A_{2g}(\nu_1)$,

Table 1. Elemental analysis data (%),[a] colour and room-temperature μ_{eff} values of the complexes

Complex	M	C	H	N	Colour	μ_{eff}
$Co(4\text{-}O_2NC_6H_4COO)_2(pipz)$ (I)	11.9(12.4)	44.8(45.3)	4.1(3.8)	12.0(11.7)	Light brown	4.67
$Co(4\text{-}O_2NC_6H_4COO)_2(1,4Me_2\text{-}pipz)$ (II)	11.4(11.7)	47.2(47.5)	4.4(4.4)	11.2(11.0)	Light pink	4.70
$Co(4\text{-}O_2NC_6H_4COO)_2(1Me\text{-}pipz)_2\cdot 2H_2O$ (III)	9.1(9.4)	46.0(45.9)	5.4(5.7)	13.6(13.4)	Light orange	4.65
$Co(4\text{-}O_2NC_6H_4COO)_2(2Me\text{-}pipz)$ (IV)	11.8(12.0)	46.4(46.4)	4.2(4.1)	11.7(11.4)	Light orange	4.64
$Co(4\text{-}O_2NC_6H_4COO)_2(1Ph\text{-}pipz)_2$ (V)	8.4(8.2)	57.3(57.0)	5.2(5.3)	11.7(11.8)	Brown	4.75
$Co(4\text{-}O_2NC_6H_4COO)_2(2,6Me_2\text{-}pipz)$ (VI)	11.5(11.7)	47.8(47.5)	4.7(4.4)	11.3(11.1)	Light violet	4.74
$Co(4\text{-}O_2NC_6H_4COO)_2(2,5Me_2\text{-}pipz)$ (VII)	11.4(11.7)	47.3(47.5)	4.6(4.4)	11.4(11.1)	Brown	4.58
$Co(4\text{-}O_2NC_6H_4COO)_2(4Me\text{-}morl)$ (VIII)	11.8(12.0)	46.1(46.3)	4.1(3.9)	8.2(8.5)	Light pink	4.98
$Co(4\text{-}O_2NC_6H_4COO)_2(2Me\text{-}pipd)$ (IX)	11.8(12.0)	48.4(49.0)	4.4(4.3)	8.8(8.6)	Brown	4.61
$Co(4\text{-}O_2NC_6H_4COO)_2(3Me\text{-}pipd)_2$ (X)	9.9(11.0)	53.2(53.0)	5.8(5.8)	9.3(9.5)	Reddish-violet	4.64
$Co(4\text{-}O_2NC_6H_4COO)_2(4Me\text{-}pipd)_2$ (XI)	10.1(10.0)	53.1(53.0)	5.9(5.8)	9.4(9.5)	Violet	4.84
$Co(2\text{-}O_2NC_6H_4COO)_2(pipz)$ (XII)	12.0(12.4)	44.9(45.3)	3.9(3.7)	11.5(11.7)	Light pink	4.89
$Co(2\text{-}O_2NC_6H_4COO)_2(1Me\text{-}pipz)_2\cdot 2H_2O$ (XIII)	9.2(9.4)	45.6(45.9)	5.5(5.7)	13.1(13.4)	Pink	4.90
$Co(2\text{-}O_2NC_6H_4COO)_2(2Me\text{-}pipz)$ (XIV)	11.8(12.0)	46.6(46.4)	4.2(4.0)	11.1(11.4)	Violet	4.72
$Co(2\text{-}O_2NC_6H_4COO)_2(1Ph\text{-}pipz)_2$ (XV)	8.4(8.2)	56.8(57.0)	5.2(5.0)	11.6(11.8)	Brown	5.01
$Co(2\text{-}O_2NC_6H_4COO)_2(1,4Me_2\text{-}pipz)$ (XVI)	11.9(11.7)	47.7(47.5)	4.6(4.4)	10.8(11.1)	Bluish-violet	4.93
$Co(2\text{-}O_2NC_6H_4COO)_2(2,6Me_2\text{-}pipz)$ (XVII)	11.4(11.7)	46.8(47.5)	4.6(4.4)	10.7(11.1)	Light pink	4.82
$Co(2\text{-}O_2NC_6H_4COO)_2(2,5Me_2\text{-}pipz)$ (XVIII)	11.2(11.7)	47.3(47.5)	4.6(4.4)	10.8(11.1)	Brown	4.72
$Co(2\text{-}O_2NC_6H_4COO)_2(4Me\text{-}morl)$ (XIX)	12.2(12.0)	46.2(46.3)	4.1(3.8)	8.8(8.5)	Blue–violet	4.72
$Co(2\text{-}O_2NC_6H_4COO)_2(3Me\text{-}pipd)_2$ (XX)	10.1(10.0)	52.6(53.0)	5.7(5.8)	9.4(9.5)	Reddish-violet	4.67
$Co(2\text{-}O_2NC_6H_4COO)_2(4Me\text{-}pipd)_2$ (XXI)	9.9(10.0)	52.4(53.0)	5.9(5.8)	9.2(9.5)	Brown	4.61
$Co(3\text{-}O_2NC_6H_4COO)_2(pipz)$ (XXII)	12.1(12.4)	44.9(45.3)	3.9(5.8)	11.6(11.7)	Light violet	4.84
$Co(3\text{-}O_2NC_6H_4COO)_2(1Me\text{-}pipz)_2\cdot 2H_2O$ (XXIII)	9.2(9.4)	45.5(45.9)	5.7(5.7)	13.6(13.4)	Reddish-brown	4.79
$Co(3\text{-}O_2NC_6H_4COO)_2(1Ph\text{-}pipz)_2$ (XXIV)	8.2(8.2)	56.8(57.1)	5.2(5.0)	11.9(11.8)	Brown	4.79
$Co(3\text{-}O_2NC_6H_4COO)_2(2Me\text{-}pipz)$ (XXV)	11.8(12.0)	46.6(46.4)	4.2(4.1)	11.6(11.4)	Bluish-pink	4.65
$Co(3\text{-}O_2NC_6H_4COO)_2(1,4Me_2\text{-}pipz)$ (XXVI)	11.6(11.7)	47.2(47.5)	4.4(4.4)	10.8(11.1)	Blue	4.82
$Co(3\text{-}O_2NC_6H_4COO)_2(2,6Me_2\text{-}pipz)$ (XXVII)	10.9(11.7)	47.2(47.5)	4.5(4.4)	11.2(11.1)	Light pink	4.75
$Co(3\text{-}O_2NC_6H_4COO)_2(2,5Me_2\text{-}pipz)$ (XXVIII)	11.4(11.7)	47.2(47.5)	4.4(4.4)	11.0(11.1)	Light brown	4.61
$Co(3\text{-}O_2NC_6H_4COO)_2(4Me\text{-}morl)$ (XXIX)	12.1(12.0)	46.2(46.3)	4.1(3.9)	8.2(8.5)	Blue	4.95
$Co(3\text{-}O_2NC_6H_4COO)_2(2Me\text{-}pipd)$ (XXX)	12.1(12.0)	48.5(49.0)	4.5(4.3)	8.4(8.6)	Green	4.64
$Co(3\text{-}O_2NC_6H_4COO)_2(3Me\text{-}pipd)_2$ (XXXI)	10.2(10.0)	52.7(53.0)	5.9(5.8)	9.4(9.5)	Brown	4.74
$Co(3\text{-}O_2NC_6H_4COO)_2(4Me\text{-}pipd)_2$ (XXXII)	10.0(10.0)	52.6(53.0)	6.0(5.7)	9.8(9.5)	Brown	4.69
$Ni(4\text{-}O_2NC_6H_4COO)_2(pipz)$ (XXXIII)	12.0(12.4)	45.1(45.3)	3.9(3.8)	11.7(11.7)	Light green	3.25
$Ni(4\text{-}O_2NC_6H_4COO)_2(1Me\text{-}pipz)_2\cdot 2H_2O$ (XXXIV)	9.2(9.4)	46.0(45.9)	5.9(5.7)	13.6(13.4)	Light green	3.14
$Ni(4\text{-}O_2NC_6H_4COO)_2(2Me\text{-}pipz)$ (XXXV)	11.8(12.0)	46.3(46.4)	4.2(4.1)	11.5(11.4)	Light green	3.08
$Ni(4\text{-}O_2NC_6H_4COO)_2(1Ph\text{-}pipz)_2$ (XXXVI)	8.0(8.2)	57.2(57.0)	5.2(5.0)	11.6(11.7)	Yellow	3.08

$Ni(4\text{-}O_2NC_6H_4COO)_2(1,4Me_2\text{-pipz})$ **(XXXVII)**	11.7(11.7)	47.6(47.5)	4.5(4.4)	10.8(11.1)	Green	3.22
$Ni(4\text{-}O_2NC_6H_4COO)_2(2,6Me_2\text{-pipz})$ **(XXXVIII)**	11.4(11.7)	47.2(47.5)	4.2(4.4)	10.8(11.1)	Light green	3.10
$Ni(4\text{-}O_2NC_6H_4COO)_2(2,5Me_2\text{-pipz})$ **(XXXIX)**	11.5(11.7)	47.6(47.5)	4.5(4.4)	11.2(11.1)	Yellowish-green	3.00
$Ni(4\text{-}O_2NC_6H_4COO)_2$(4Me-morl) **(XL)**	11.8(12.0)	46.3(46.3)	4.1(3.9)	8.5(8.5)	Light yellow	3.27
$Ni(4\text{-}O_2NC_6H_4COO)_2(3Me\text{-pipd})_2$ **(XLI)**	10.0(10.0)	52.6(53.0)	5.8(5.8)	9.3(9.5)	Green	3.20
$Ni(4\text{-}O_2NC_6H_4COO)_2(4Me\text{-pipd})_2$ **(XLII)**	9.7(10.0)	52.6(53.0)	5.9(5.8)	9.3(9.5)	Green	2.93
$Ni(2\text{-}O_2NC_6H_4COO)_2$(pipz) **(XLIII)**	12.1(12.3)	44.9(45.3)	3.9(3.8)	11.9(11.7)	Light green	3.09
$Ni(2\text{-}O_2NC_6H_4COO)_2(1Me\text{-pipz})_2 \cdot 2H_2O$ **(XLIV)**	9.3(9.4)	45.3(45.9)	5.9(5.7)	13.6(13.4)	Light green	3.24
$Ni(2\text{-}O_2NC_6H_4COO)_2$(2Me-pipz) **(XLV)**	11.9(12.0)	46.2(46.4)	4.3(4.1)	11.9(11.4)	Light green	2.96
$Ni(2\text{-}O_2NC_6H_4COO)_2(1Ph\text{-pipz})_2$ **(XLVI)**	8.1(8.2)	56.8(57.1)	5.2(5.0)	11.8(11.7)	Yellowish-green	3.03
$Ni(2\text{-}O_2NC_6H_4COO)_2(1,4Me_2\text{-pipz})$ **XLVII)**	11.5(11.7)	47.8(47.5)	4.5(4.4)	10.9(11.1)	Green	3.12
$Ni(2\text{-}O_2NC_6H_4COO)_2(2,6Me_2\text{-pipz})$ **(XLVIII)**	11.5(11.7)	47.3(47.5)	4.5(4.4)	10.9(11.1)	Light green	3.16
$Ni(2\text{-}O_2NC_6H_4COO)_2(2,5Me_2\text{-pipz})$ **(XLIX)**	11.6(11.7)	47.4(47.5)	4.3(4.4)	10.8(11.1)	Green	3.16
$Ni(2\text{-}O_2NC_6H_4COO)_2$(4Me-morl) **(L)**	11.7(12.0)	46.3(46.3)	4.0(3.9)	8.6(8.6)	Green	3.27
$Ni(2\text{-}O_2NC_6H_4COO)_2(3Me\text{-pipd})_2$ **(LI)**	10.0(10.0)	53.1(53.0)	5.9(5.8)	9.4(9.5)	Green	3.26
$Ni(2\text{-}O_2NC_6H_4COO)_2(4Me\text{-pipd})_2$ **(LII)**	9.8(10.0)	52.9(53.0)	5.9(5.8)	9.4(9.5)	Green	2.95
$Ni(3\text{-}O_2NC_6H_4COO)_2$(pipz) **(LIII)**	12.1(12.4)	45.3(45.3)	3.9(3.8)	11.9(11.8)	Light green	3.00
$Ni(3\text{-}O_2NC_6H_4COO)_2(1Me\text{-pipz})_2 \cdot 2H_2O$ **(LIV)**	9.2(9.4)	45.8(45.9)	5.9(5.7)	13.6(13.4)	Yellowish-green	3.07
$Ni(3\text{-}O_2NC_6H_4COO)_2(1Ph\text{-pipz})_2$ **(LV)**	8.2(8.3)	57.1(57.1)	5.1(5.0)	12.1(11.8)	Yellowish-green	3.07
$Ni(3\text{-}O_2NC_6H_4COO)_2$(2Me-pipz) **(LVI)**	11.9(12.0)	46.5(46.4)	4.2(4.1)	11.3(11.4)	Light green	2.96
$Ni(3\text{-}O_2NC_6H_4COO)_2(1,4Me_2\text{-pipz})$ **(LVII)**	11.5(11.7)	47.6(47.5)	4.4(4.4)	11.2(11.1)	Light green	3.14
$Ni(3\text{-}O_2NC_6H_4COO)_2(2,6Me_2\text{-pipz})$ **(LVIII)**	11.6(11.7)	47.7(47.5)	4.6(4.4)	11.1(11.1)	Light green	3.02
$Ni(3\text{-}O_2NC_6H_4COO)_2(2,5Me_2\text{-pipz})$ **(LIX)**	11.4(11.7)	47.2(47.5)	4.5(4.4)	11.2(11.1)	Light green	3.12
$Ni(3\text{-}O_2NC_6H_4COO)_2$(4Me-morl) **(LX)**	12.2(12.0)	45.6(46.4)	3.7(3.9)	8.7(8.5)	Flesh coloured	3.26
$Ni(3\text{-}O_2NC_6H_4COO)_2(3Me\text{-pipd})_2$ **(LXI)**	10.1(10.0)	52.9(53.0)	5.8(5.8)	9.9(9.6)	Green	3.27
$Ni(3\text{-}O_2NC_6H_4COO)_2(4Me\text{-pipd})_2$ **(LXII)**	9.8(10.0)	52.8(53.0)	5.9(5.8)	9.5(9.6)	Green	3.07
$Cu(C_6H_5COO)_2$(pipz) **(LXIII)**	15.9(16.2)	54.9(55.2)	5.3(5.1)	7.2(7.2)	Blue	1.78
$Cu(C_6H_5COO)_2(1Ph\text{-pipz})_2$ **(LXIV)**	10.2(10.1)	64.5(64.8)	6.1(6.0)	8.9(8.9)	Blue	1.77
$Cu(C_6H_5COO)_2$(2Me-pipz) **(LXV)**	15.5(15.7)	56.0(57.2)	5.6(5.4)	7.1(6.9)	Blue	1.77
$Cu(C_6H_5COO)_2(2,6Me_2\text{-pipz})$ **(LXVI)**	14.9(15.1)	57.0(57.2)	5.9(5.7)	6.7(6.7)	Light violet	1.78
$Cu(C_6H_5COO)_2(2,5Me_2\text{-pipz})$ **(LXVII)**	15.1(15.1)	56.9(57.2)	5.7(5.7)	6.6(6.7)	Blue	1.91
$Cu(C_6H_5COO)_2(2Me\text{-pipd})_2$ **(LXVIII)**	12.5(12.6)	61.7(62.0)	7.1(7.2)	5.5(5.6)	Blue	1.86
$Cu(C_6H_5COO)_2(3Me\text{-pipd})_2$ **(LXIX)**	12.7(12.6)	61.7(62.0)	7.0(7.2)	5.4(5.6)	Blue	1.88
$Cu(C_6H_5COO)_2(4Me\text{-pipd})_2$ **(LXX)**	12.6(12.6)	61.6(62.0)	6.9(7.2)	5.6(5.6)	Blue	2.06
$Cu(4\text{-}O_2NC_6H_4COO)_2$(pipz) **(LXXI)**	13.0(13.2)	44.9(44.9)	3.7(3.7)	11.7(11.6)	Light violet	1.88
$Cu(4\text{-}O_2NC_6H_4COO)_2$(2Me-pipz) **(LXXII)**	12.7(12.8)	45.9(46.0)	4.1(4.0)	11.2(11.3)	Blue	1.83
$Cu(4\text{-}O_2NC_6H_4COO)_2(1,4Me_2\text{-pipz})$ **(LXXIII)**	12.4(12.5)	47.1(47.1)	4.4(4.3)	11.1(11.0)	Blue	1.87
$Cu(4\text{-}O_2NC_6H_4COO)_2(2,6Me_2\text{-pipz})$ **(LXXIV)**	12.4(12.5)	47.0(47.1)	4.5(4.3)	11.1(11.0)	Violet	1.90
$Cu(4\text{-}O_2NC_6H_4COO)_2(2,5Me_2\text{-pipz})$ **(LXXV)**	12.3(12.7)	47.2(47.1)	4.4(4.3)	10.9(11.0)	Light violet	1.77
$Cu(4\text{-}O_2NC_6H_4COO)_2(1Me\text{-pipz})_2$ **(LXXVI)**	10.6(10.7)	47.9(48.4)	5.5(5.4)	13.9(14.1)	Light violet	1.87

Table 1—*continued*

Complex	M	C	H	N	Colour	μ_{eff}
$Cu(4\text{-}O_2NC_6H_4COO)_2(2Me\text{-}pipd)_2$ **(LXXVII)**	10.6(10.7)	52.8(52.6)	5.8(5.7)	9.2(9.4)	Light violet	1.89
$Cu(4\text{-}O_2NC_6H_4COO)_2(3Me\text{-}pipd)_2$ **(LXXVIII)**	10.6(10.7)	52.4(52.6)	5.7(5.7)	9.4(9.4)	Light violet	1.82
$Cu(4\text{-}O_2NC_6H_4COO)_2(4Me\text{-}pipd)_2$ **(LXXIX)**	10.6(10.7)	52.6(52.6)	5.8(5.7)	9.3(9.4)	Light violet	1.79
$Cu(2\text{-}O_2NC_6H_4COO)_2(pipz)$ **(LXXX)**	13.2(13.2)	44.7(44.9)	3.8(3.7)	11.6(11.6)	Sky blue	1.78
$Cu(2\text{-}O_2NC_6H_4COO)_2(2Me\text{-}pipz)$ **(LXXXI)**	12.7(12.8)	46.1(46.0)	3.9(4.0)	11.4(11.3)	Dark green	1.82
$Cu(2\text{-}O_2NC_6H_4COO)_2(1Ph\text{-}pipz)_2$ **(LXXXII)**	8.8(8.6)	56.8(56.7)	5.1(5.0)	11.6(11.7)	Light blue	1.88
$Cu(2\text{-}O_2NC_6H_4COO)_2(2,6Me_2\text{-}pipz)$ **(LXXXIII)**	12.6(12.5)	47.0(47.1)	4.4(4.3)	11.1(11.0)	Violet	1.79
$Cu(2\text{-}O_2NC_6H_4COO)_2(2,5Me_2\text{-}pipz)$ **(LXXXIV)**	12.4(12.5)	47.0(47.1)	4.2(4.3)	11.2(11.0)	Blue	1.78
$Cu(2\text{-}O_2NC_6H_4COO)_2(2Me\text{-}pipd)_2$ **(LXXXV)**	10.7(10.7)	52.3(52.6)	5.7(5.7)	9.4(9.4)	Blue	1.84
$Cu(2\text{-}O_2NC_6H_4COO)_2(4Me\text{-}pipd)_2$ **(LXXXVI)**	10.6(10.7)	52.7(52.6)	5.8(5.7)	9.5(9.4)	Blue	1.89
$Cu(2\text{-}O_2NC_6H_4COO)_2(3Me\text{-}pipd)_2$ **(LXXXVII)**	10.6(10.7)	52.7(52.6)	5.8(5.7)	9.9(9.4)	Light violet	2.01
$Cu(3\text{-}O_2NC_6H_4COO)_2(pipz)$ **(LXXXVIII)**	13.0(13.2)	44.7(44.9)	3.8(3.7)	11.7(11.6)	Blue	1.78
$Cu(3\text{-}O_2NC_6H_4COO)_2(2Me\text{-}pipz)$ **(LXXXIX)**	12.7(12.8)	45.8(46.0)	4.1(4.0)	11.2(11.3)	Blue	1.79
$Cu(3\text{-}O_2NC_6H_4COO)_2(1Ph\text{-}pipz)_2$ **(XC)**	8.6(8.6)	56.8(56.7)	5.0(5.0)	11.7(11.7)	Green	1.79
$Cu(3\text{-}O_2NC_6H_4COO)_2(1Me\text{-}pipz)_2$ **(XCI)**	10.4(10.7)	47.5(48.4)	5.4(5.4)	13.7(14.1)	Dark green	1.82
$Cu(3\text{-}O_2NC_6H_4COO)_2(2,6Me_2\text{-}pipz)$ **(XCII)**	12.4(12.5)	46.9(47.1)	4.4(4.3)	11.0(11.0)	Blue	1.93
$Cu(3\text{-}O_2NC_6H_4COO)_2(2,5Me_2\text{-}pipz)$ **(XCIII)**	12.3(12.5)	46.9(47.1)	4.2(4.3)	11.1(11.0)	Light blue	2.16
$Cu(3\text{-}O_2NC_6H_4COO)_2(2Me\text{-}pipd)_2$ **(XCIV)**	10.6(10.7)	52.4(52.6)	5.8(5.7)	9.4(9.4)	Blue	1.84
$Cu(3\text{-}O_2NC_6H_4COO)_2(3Me\text{-}pipd)_2$ **(XCV)**	10.7(10.7)	53.2(52.6)	5.8(5.7)	9.3(9.4)	Blue	1.81
$Cu(3\text{-}O_2NC_6H_4COO)_2(4Me\text{-}pipd)_2$ **(XCVI)**	10.6(10.7)	52.4(52.6)	5.7(5.7)	9.4(9.4)	Green	1.78
$Cu(C_6H_5COO)_2(pipz)_{0.5}$ **(XCVII)**	18.1(18.2)	55.4(55.1)	4.4(4.3)	3.9(4.0)	Green	1.56
$Cu(C_6H_5COO)_2(1Me\text{-}pipz)_{0.5}$ **(XCVIII)**	18.0(17.9)	55.5(55.7)	4.6(4.5)	4.0(3.9)	Green	1.47
$Cu(C_6H_5COO)_2(1Ph\text{-}pipz)$ **(XCIX)**	13.6(13.6)	61.8(61.6)	5.1(5.1)	6.1(6.0)	Green	1.53
$Cu(C_6H_5COO)_2(1Ph\text{-}pipz)_{0.5}$ **(C)**	16.3(16.4)	58.6(59.0)	4.5(4.5)	3.7(3.6)	Green	1.41
$Cu(C_6H_5COO)_2(1,4Me_2\text{-}pipz)_{0.5}$ **(CI)**	17.6(17.5)	56.3(56.3)	4.7(4.7)	3.9(3.9)	Green	1.47
$Cu(C_6H_5COO)_2(4Me\text{-}morl)$ **(CII)**	15.6(15.6)	55.8(56.1)	5.2(5.2)	3.5(3.4)	Green	1.41
$Cu(4\text{-}O_2NC_6H_4COO)_2(1Ph\text{-}pipz)$ **(CIII)**	11.2(11.4)	51.9(51.7)	3.8(3.9)	10.1(10.0)	Green	1.51
$Cu(4\text{-}O_2NC_6H_5COO)_2(1Ph\text{-}pipz)_{0.5}$ **(CIV)**	12.9(13.3)	47.6(47.8)	3.2(3.1)	8.9(8.8)	Green	1.48
$Cu(4\text{-}O_2NC_6H_4COO)_2(4Me\text{-}morl)$ **(CV)**	12.7(12.8)	46.0(45.9)	3.9(3.8)	8.5(8.5)	Green	1.51
$Cu(2\text{-}O_2NC_6H_4COO)_2(1,4Me_2\text{-}pipz)_{0.05}$ **(CVI)**	13.8(14.0)	44.9(45.0)	3.4(3.3)	9.1(9.3)	Green	1.53
$Cu(2\text{-}O_2NC_6H_4COO)_2(1Me\text{-}pipz)$ **(CVII)**	12.9(12.8)	46.0(46.0)	4.1(4.0)	11.1(11.3)	Green	1.49
$Cu(2\text{-}O_2NC_6H_4COO)_2(1Ph\text{-}pipz)$ **(CVIII)**	11.4(11.4)	51.7(51.7)	4.1(4.0)	10.2(10.0)	Green	1.53
$Cu(2\text{-}O_2NC_6H_4COO)_2(4Me\text{-}morl)$ **(CIX)**	12.7(12.8)	46.0(45.9)	3.9(3.8)	8.5(8.5)	Green	1.52
$Cu(3\text{-}O_2NC_6H_4COO)_2(1,4Me_2\text{-}pipz)_{0.5}$ **(CX)**	13.9(14.0)	45.1(45.1)	3.4(3.3)	9.4(9.3)	Light green	1.42
$Cu(3\text{-}O_2NC_6H_4COO)_2(4Me\text{-}morl)$ **(CXI)**	12.7(12.8)	45.7(45.9)	3.9(3.8)	8.3(8.6)	Green	1.49

[a] Calculated values are given in parentheses.

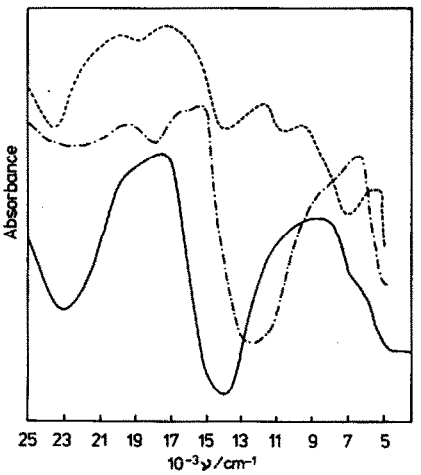

Fig. 1. Electronic reflectance spectra of $Co(4\text{-}O_2NC_6H_4COO)_2(3Me\text{-}pipd)_2$ (———), $Co(3\text{-}O_2NC_6H_4COO)_2(2Me\text{-}pipd)$ (–·–·–), and $Co(2\text{-}O_2NC_6H_4COO)_2(4Me\text{-}morl)$ (– – – –).

$^3T_{1g}(F) \leftarrow {}^3A_{2g}(\nu_2)$ and $^3T_{1g}(P) \leftarrow {}^3A_{2g}(\nu_3)$ transitions.[8,18,27] The ν_2 band is quite broad or is split into two components which can be ascribed to the large difference in the ligand-field strengths of the ligands in the present situation.[29] The low and high energy components of the ν_1 band can be assigned to the $^3B_{2g} \leftarrow {}^3B_{1g}(\nu_B)$ and $^3E_g \leftarrow {}^3B_{1g}(\nu_E)$ ligand-field transitions for the nickel(II) ion in D_{4h} environments.[8,29] Tetragonal parameters $Dq(xy)$, $Dq(z)$ and Dt, calculated from the energies of the above transitions, fall in the approximate ranges of 700, 1000 and -200 cm^{-1}, respectively. The position of the ν_3 band lies above 25,000 cm^{-1} for all complexes except the four complexes, i.e. $Ni(RCOO)_2(4Me\text{-}morl)$ (where R = 2-, 3-, and $4\text{-}O_2NH_4$) and $Ni(2\text{-}O_2NC_6H_4COO)_2(2,6Me_2\text{-}pipz)$, which exhibit this band at a much lower energy—around 21,000 cm^{-1}. It makes it a little doubtful to be considered as a ν_3 absorption of octahedral geometry. The value of Dq for most of the complexes, as calculated from the ratio ν_3/ν_1 or ν_3/ν_2, lies around 900 cm^{-1}, while the value of B shows variation between 800 and 1100 cm^{-1}. These results are in agreement with earlier reports on similar complexes of pseudo-octahedral geometry.[8,18,28] However, the B value for the four complexes having anomalous spectra comes out to be very small (550 cm^{-1}), which contradicts approximate octahedral structure (D_{4h} symmetry). However, we suggest a heavily distorted octahedral structure with C_{4v} symmetry for these complexes.

All magnetically dilute copper(II) complexes (**LXIII–XCVI** as in Table 1) under discussion show an electronic absorption band in the region 14,700–18,200 cm^{-1} which can be assigned to the $^2T_{2g} \leftarrow {}^2E_g$ ligand-field transition for an octahedral field. The broadness or splitting observed for this main band is ascribed to tetragonal distortion. The lower and higher energy components of this can be assigned, respectively, to the $^2B_{2g} \leftarrow {}^2B_{1g}$ (or $d_{xy} \rightarrow d_{x^2-y^2}$) and $^2E_g \leftarrow {}^2B_{1g}$ (or $d_{xz,yz} \rightarrow d_{x^2-y^2}$) ligand-field transitions for a tetragonal field.[30–32]

Two absorptions, one as a broad band in the region 12,500–14,500 cm^{-1} (band I) and the other as a shoulder around 26,000 cm^{-1} (band II), are observed for antiferromagnetic copper(II) complexes (**XCVIII–CXI**). Band I may be due to the absorption corresponding to the $d_{xy} \rightarrow d_{x^2-y^2}$ and $d_{xz,yz} \rightarrow d_{x^2y^2}$ electronic transitions for the copper(II) ion in tetragonal environments,[33] while band II can be assigned to the $2p_\pi$ (donor oxygen atom) $\rightarrow d_{x^2-y^2}$ charge-transfer transition. The appearance of this band is considered to be characteristic of the dimeric structure for the copper(II) carboxylate complexes.[33–35]

The X-band EPR curves of powdered materials for most of the magnetically dilute copper(II) complexes obtained at liquid nitrogen temperature are consistent with axial symmetry of the complexes except for $[Cu(C_6H_5\text{-}COO)_3(3Me\text{-}pipd)_2]$ which has an EPR spectrum typical of elongated rhombic geometry [g_z (2.33) > g_y(2.07) > g_x(2.05)]. The magnitudes $g_\parallel$ (2.20–2.27) and $g_\perp$ (2.05–2.09) obtained from the EPR spectrum for these complexes are consistent ($g_\parallel > g_\perp > 2.04$) with an elongated tetragonal type structure, which agrees with the results obtained from electronic absorption studies.[31,32] The observed range of $g_\parallel$ is in conformity with the CuO_4N_2 chromophore of the complex.[36] The absorptions for the $g_\parallel$ and g_z portions of the EPR spectra for $Cu(4\text{-}O_2NC_6H_4COO)_2(3Me\text{-}pipd)_2$ and $Cu(C_6H_5COO)_2(3Me\text{-}pipd)_2$, respectively, resolve into four components. The splitting is attributed to the hyperfine coupling due to ^{63}Cu ($I = 3/2$). The values of $A_\parallel = 0.0181$ cm^{-1} and $A_z = 0.0141$ cm^{-1} have been obtained, respectively, for these two complexes. The bonding parameters, $\alpha^2 = 0.829$, $\beta_1^2 = 0.854$ and $\beta^2 = 0.723$, have also been calculated for $Cu(4\text{-}O_2NC_6H_4COO)_2(3Me\text{-}pipd)_2$ by assuming D_{4h} symmetry for the copper(II) environments.[31,37,38]

The X-band EPR spectra at 300 K for powdered samples of antiferromagnetic complexes under present discussion contain absorption lines at field strengths of 800 (H_{z1}), 4600 ($H_\perp$) and 6100 G (H_{z2}), which are characteristic features of axially symmetric binuclear copper(II) species and correspond to the spin triplet state ($S = 1$) with $D > h\nu$ and $E = 0$.[39,40] The range of $g_\parallel$ or g_z (2.30–2.40), $g_\perp$ (2.05–2.10) and D (0.34–0.39 cm^{-1}) evaluated from the EPR spectra are comparable with the earlier

reported values for binuclear copper(II) carboxylate complexes.[4-7] For some complexes, the EPR absorption around 800 G is split into seven lines due to hyperfine coupling of the nuclear spins of two copper ions with the electron spin ($2nI+1$; $n=2$ and $I=3/2$ for ^{63}Cu). The value of $A_{\parallel}$ or A_z is found to be about half ($\simeq 0.008$ cm^{-1}) of that generally observed for magnetically dilute copper(II) in similar environments. This supports magnetic exchange taking place between two metal ions.[40,41] However, in addition to the above-mentioned absorptions, an absorption line around 3200 G is also observed. The intensity of this line increases while the intensity of the lines due to the triplet state, as expected, decreases with the lowering of temperature. This line is, therefore, attributed to the magnetically dilute copper(II) impurity which is commonly present in the copper(II) arylcarboxylate complexes.[39,42,43]

Magnetic susceptibility studies

The room-temperature μ_{eff} values for all cobalt(II) complexes lie in the range 4.60–5.02, which is considerably greater than the spin-only value (3.82) and hence supports nearly octahedral structure for these complexes.[8,18,27] The magnitude of μ_{eff} varies with A (ligand-field strength parameter), k (covalence parameter for the M—L bond) and v (parameter for distortion from cubic symmetry).[44,45] For perfectly octahedral systems ($v=0$) with $A=1.4$ ($A=1.4$ for complexes under discussion as calculated from electronic spectra) and $k=0.8$ (minimum possible value for nature of ligands), the theoretical μ_{eff} value at room temperature for the complexes under discussion should be 4.81 or greater.[44] But in the present case, for most of the complexes μ_{eff} is less than 4.81, which leaves the distortion from cubic symmetry to be the only reason responsible for the lowering of the μ_{eff} values. The magnetic susceptibility of six representative cobalt(II) complexes, viz. Co(4-$O_2NC_6H_4COO)_2$(1Ph-pipz)$_2$ (**V**), Co(4-$O_2NC_6H_4COO)_2$(3Me-pipd)$_2$ (**X**), Co(2-$O_2NC_6H_4COO)_2$(1,4Me$_2$-pipz)$_2$ (**XVI**), Co(2-$O_2NC_6H_4COO)_2$(4Me-morl) (**XIX**), Co(3-$O_2NC_6H_4COO)_2$(pipz) (**XXII**) and Co(3-$O_2NC_6H_4COO)_2$(1,4Me$_2$-pipz) (**XXVI**) has also been measured at different temperatures in the range 80–280 K. The magnitude of θ (10–54°) obtained from the plots of $1/\chi$ vs T, and the variation of μ_{eff} from 4.90 at 280 K to 4.2 at 80 K, which remains well above the spin-only value (except **XIX**), favours the $^4T_{1g}$ ground ligand-field term for these complexes with near octahedral structures.[45] The value of θ for the complex Co(2-$O_2NC_6H_4COO)_2$(4Me-morl) (**XIX**) is 110° and this large value can only be due to antiferromagnetic interactions. The magnetic moment value of this complex decreases rapidly with a decrease in temperature, i.e. it decreases from 4.55 BM at 280 K to 3.4 BM at 80 K, which becomes even less than the spin-only value for high-spin cobalt(II) complex. These observations clearly indicate the presence of antiferromagnetic interactions taking place in this complex.[5]

The room-temperature μ_{eff} value for nickel(II) complexes under present discussion lies in the range 3.00–3.35. These values are consistent with the near octahedral structure for these complexes. Room-temperature magnetic moment values for the copper(II) complexes **LXIII–XCVI** and **XCVII–CXI** lie in the ranges 1.81–2.20 BM and 1.40–1.60 BM, respectively. In view of the μ_{eff} value for the former complexes lying above the spin-only value and for the latter being close to the value reported for dinuclear or polynuclear complexes, where carboxylate group acts as a bridge between two metal ions, the copper(II) complexes have been categorized as (i) magnetically dilute and (ii) antiferromagnetic complexes.[1-7]

Antiferromagnetic copper(II) complexes have also been characterized by magnetic susceptibility measurements at different temperatures.[15] The magnetic moment value for all these complexes decreases with temperature, thus confirming their antiferromagnetic behaviour. The following modified equation based upon Bleaney and Bowers' model[46] was employed to evaluate the spin-exchange parameter ($-2J$) from magnetic susceptibility data at different temperatures:[42,43]

$$\ln\left[\frac{N\bar{g}^2\beta^2(1-x)}{kT\left(\chi_{Cu}-\frac{0.43x}{T}-N_\alpha\right)}-3\right]=\frac{-2J}{kT}$$

$$\text{or}\quad \ln(F-3)=\frac{-2J}{kT}.$$

The unknown quantities in the above expression on the LHS were as follows: the value of $\bar{g}$ was determined from EPR measurements and the value of N_α was taken to be 60×10^{-6} e.g.s. units. The value of x, the mole fraction of paramagnetic impurity, was so chosen as to fit in well with the above expression. The value of $2J$ has been determined from the slope $[2J/k]$ of the straight line obtained from a plot of $\ln(F-3)$ vs $1/T$. The value of $2J$ was also calculated from the variation of intensity (I) of the EPR lines at the temperatures 300, 173 and 103 K using the relation:[39,43]

$$\frac{A_1}{A_2}=\frac{I_1}{I_2}=\frac{T_2(3+e^{-2J/kT_2})}{T_1(3+e^{-2J/kT_1})}.$$

The relative areas of curves $[A_1/A_2]$ at two different temperatures (T_1 and T_2) were estimated by the reported methods.[47,48] Uncertainties in the values of $-2J$ for the former and latter methods are ± 5 and ± 20 cm^{-1}, respectively. This is because both of these methods have their own limitations in evaluating the value of $2J$. The magnetic susceptibility method becomes complicated due to the presence of a magnetically dilute impurity which is usually present in antiferromagnetic copper(II) arylcarboxylate complexes. However, by allowing the presence of this impurity (x) in the above equation, reasonable evaluation of $2J$ can be obtained. The EPR method, though it is free from the presence of the magnetic impurity, suffers from the limitation in evaluating the accurate areas under EPR curves. Therefore the uncertainties in the EPR method are greater than in the magnetic susceptibility method. The values of $-2J$ determined by the two methods are comparable and lie between 280–330 cm^{-1}.

In spite of the high basicities of these bases ($pK_a \simeq 8$–9.6), this range of values of $2J$ is comparable to that for the earlier reported copper(II) carboxylate complexes with terminal ligands of low basicity, e.g. py, etc. No consistent trend of the variation of $-2J$ with pK_as of the acids or the ligand is obtained.

By combining all the studies conducted upon all these complexes, the distorted octahedral structure can be assigned to all complexes except for $Co(3\text{-}O_2NC_6H_4COO)_2$(2Me-pipd), $Co(2\text{-}O_2NC_6H_4COO)_2$(4Me-morl) and all antiferromagnetic copper(II) complexes (**XCVII–XCI**). The monomeric *trans*-pseudo-octahedral structure with the carboxylate group acting as a chelating bidentate unit and the base as a monodentate ligand has been assigned to the complexes of the type $M(RCOO)_2(L—L)_2 \cdot xH_2O$ and $M(RCOO)_2L_2$, where $x = 2$ for L—L = 1Me-pipz and $x = 0$ for L—L = 1Ph-pipz; and L = 2-, 3- or 4Me-pipd. Here, for the 1Me-pipz complexes, the two water molecules may be hydrogen bonded to the uncoordinated nitrogen atom, i.e. the N—CH_3 group of the base.[18] The absence of these water molecules in similar complexes of 1Ph-pipz may be attributed to the phenyl group using the lone pair of the uncoordinated nitrogen atom for delocalization (see below) and hence lessening the possibility of hydrogen bonding.

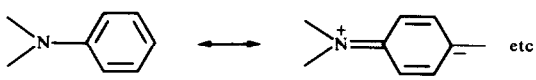

Leaving aside the antiferromagnetic complexes, the polymeric *trans*-pseudo-octahedral structure with the carboxylate group and the heterocyclic base acting, respectively, as a chelating bidentate and a bridging bidentate ligand between two metal atoms, has been assigned to all complexes of the type $M(RCOO)_2(L—L)$ except for $Ni(2\text{-}O_2NC_6H_4COO)_2(L—L)$ (where L—L = 2Me-pipz, 2,5Me_2-pipz, 1,4Me_2-pipz) and $Ni(3\text{-}O_2NC_6H_4COO)_2$(1,4-$Me_2$-pipz), for which the geometry with both L—L and the carboxylate group behaving as bridging bidentate groups is proposed. The trigonal bipyramidal structure has been suggested for $Co(3\text{-}O_2NC_6H_4COO)_2$(2Me-pipd). For antiferromagnetic complexes, the copper(II) acetate monohydrate-like dinuclear structure[49] for complexes of the type $M(RCOO)_2(L—L)$ and the $Cu(HCOO)_2(dioxane)_{0.5}$-like polymeric structure[50] containing binuclear units for complexes of the type $Cu(RCOO)_2(L—L)_{0.5}$ are proposed.

Our interest in the present work was to study the complexation behaviour of these saturated mono- and diheterocyclic bases, of different but high basicities and different steric characteristics, with metal(II) carboxylates. An additional interest was to see whether these bases form magnetically dilute or antiferromagnetic complexes. Out of these cases, 4Me-morl and 1,4Me_2-pipz are interesting ligands. 4-Methylmorpholine forms only 1 : 1 complexes (when added in excess) with all copper(II) carboxylates of the type $Cu(RCOO)_2$ (where R = C_6H_5, 2-, 3- and 4-$O_2NC_6H_4$); all of them are found to be antiferromagnetic. Out of all the cobalt(II) and nickel(II) complexes, the only antiferromagnetic complex to be isolated was also that of 4Me-morl with the formula $Co(2\text{-}O_2NC_6H_4COO)_2$(4Me-morl). 1,4-Dimethylpiperazine forms complexes of the type $Cu(RCOO)_2(1,4Me_2\text{-pipz})_{0.5}$ (where R = C_6H_5, 2- and 3-$O_2NC_6H_4$ and when R = 4-$O_2NC_6H_4$) and for all the cobalt(II) and nickel(II) nitrobenzoates, it affords complexes of 1 : 1 stoichiometry. Complexes having 1 : 0.5 stoichiometry are antiferromagnetic, while those of 1 : 1 stoichiometry are magnetically dilute. The 1Me-pipz and 1Ph-pipz ligands form complexes of 1 : 2, 1 : 1 and 1 : 0.5 (metal–base) stoichiometry with copper(II) carboxylates, while with cobalt(II) and nickel(II) they give 1 : 2 complexes. The complexes of 1 : 2 stoichiometry are magnetically dilute while the others are antiferromagnetic. These bases are of interest for copper(II) carboxylates, where one can change the stoichiometry and structural form of the complex and hence its magnetic behaviour by controlling only the amount of base added to the metal carboxylate solution. All other diheterocyclic bases form complexes of 1 : 1 stoichiometry, which are found to be magnetically dilute. Overall, the complexation behaviour of these diheterocyclic bases can be rationalized to some extent by the

following factors: (1) copper(II) carboxylates have more tendency to form antiferromagnetic complexes than their cobalt(II) and nickel(II) analogues; (2) bases with lower pK_a values and large steric hindrance (e.g. 4Me-morl and 1,4Me_2-pipz) prefer to form antiferromagnetic complexes.

Out of the monoheterocyclic bases, 2Me-pipd shows restricted complexation behaviour, compared with 3Me-pipd and 4Me-pipd, in its adduct formation with cobalt(II) and more so with nickel(II) nitrobenzoates, i.e. it does not form any adduct with nickel(II) nitrobenzoates and gives only 1:1 complexes with $Co(RCOO)_2$ (where R = 3- or 4-$O_2NC_6H_4$) and when R = 2-$O_2NC_6H_4$ a complex does not form; while its 3- and 4Me-pipd analogues give 1:2 complexes with all metal(II) carboxylates. These three bases behave similarly with copper(II) carboxylates to give 1:2 complexes. This can be partly justified due to the larger steric requirements of 2Me-pipd than the other ligands. The similarity in behaviour of the three bases for copper(II) may be due to large Jahn–Teller effects expected for copper(II) and especially its particular preferential mode, i.e. Jahn–Teller elongation which forces the complexes to adopt a *trans*-in-plane tetragonally elongated structure which results in relieving some steric congestion in the structure.[51,52] To some extent, this can also be justified by the larger affinity of the copper(II) ion than cobalt(II) and nickel(II) ions for complexation with highly basic nitrogen donors. These bases do not yield any antiferromagnetic complexes [not even with copper(II)], which can also be due to their highly basic nature.

Acknowledgements—We thank Dr T. Rs. Reddy, A. K. Puri and Dr Surjit Singh for EPR measurements. We are also grateful to Dr Kailash Chandra for his help with the magnetic susceptibility measurements. We would also like to thank the U.G.C. of India for financial support.

REFERENCES

1. M. Kato, H. B. Jonassen and J. C. Fanning, *Chem. Rev.* 1964, **64**, 99 and refs therein.
2. C. Oldham, *Prog. Inorg. Chem.* 1968, **10**, 223.
3. R. J. Doedens, *Prog. Inorg. Chem.* 1976, **21**, 209.
4. R. W. Jotham, S. F. A. Kettle and J. A. Marks, *J. Chem. Soc., Dalton Trans.* 1972, 428.
5. J. Catterick and P. Thornton, *Adv. Inorg. Chem. Radiochem.* 1977, **20**, 291.
6. M. Melnik, *Coord. Chem. Rev.* 1981, **36**, 1.
7. M. Melnik, *Coord. Chem. Rev.* 1982, **42**, 259.
8. J. Catterick and P. Thornton, *J. Chem. Soc., Dalton Trans.* 1975, 233; 1976, 1634.
9. A. Vencini, L. Benelli, D. Gatteschi and C. Lunchini, *J. Am. Chem. Soc.* 1980, **102**, 5820.
10. P. Thornton, I. R. Little and B. P. Straughan, *J. Chem. Soc., Dalton Trans* 1986, 2211.
11. W. Clegg, I. R. Little and B. P. Straughan, *J. Chem. Soc., Dalton Trans.* 1986, 1283.
12. B. S. Manhas, G. S. Jolly, N. Kumar and A. K. Gandotra, *J. Chem. Sci.* 1975, **1**, 10.
13. L. P. Battaglia, A. B. Corradi and L. Menaube, *J. Chem. Soc., Dalton Trans.* 1986, 1653.
14. A. A. Pasynskii, T. Ch. Idrisov, K. M. Savorova and V. T. Kalinnikov, *Koord. Khim.* 1974, **1**, 799; 1976, **2**, 1060.
15. A. S. Dhindsa, PhD thesis, Punjabi University, Patiala (1983).
16. G. B. Deacon and R. J. Phillips, *Coord. Chem. Rev.* 1980, **34**, 227.
17. B. S. Manhas and A. K. Trikha, *J. Ind. Chem. Soc.* 1982, **59**, 315.
18. L. P. Battaglia, B. A. Corradi, M. Nardelli and G. C. Palmier, *Cryst. Struct. Commun.* 1973, **2**, 523; G. Marcotrigiano, G. C. Pallacani and C. Preti, *Z. Anorg. Allg. Chem.* 1974, **408**, 313.
19. G. Marcotrigiano, R. Battistuzzi and G. C. Pellacani, *Can. J. Chem.* 1972, **50**, 2557.
20. B. S. Manhas, A. K. Trikha and M. Singh, *Ind. J. Chem.* 1978, **16A**, 431.
21. J. T. Braunholtz, E. A. V. Ebsworth, F. G. Mann and M. Sheppard, *J. Chem. Soc.* 1958, 2780.
22. N. Kumar, P. L. Kachroo and R. Kant, *Bull. Chem. Soc. Jpn* 1980, **18**, 265.
23. N. Kumar and A. K. Gandotra, *Transition Met. Chem.* 1979, **4**, 345; 1980, **5**, 365.
24. L. P. Battaglia, C. A. Bonamartini, G. Marcotrigiano, L. Menaube and G. C. Pellacani, *J. Am. Chem. Soc.* 1980, **102**, 2663.
25. O. Hassel and B. F. Pederson, *Proc. Chem. Soc.* 1959, 394.
26. P. J. Hendra and D. B. Powell, *J. Chem. Soc.* 1960, 5105.
27. A. B. P. Lever and D. Ogden, *J. Chem. Soc. A* 1967, 2041.
28. A. B. P. Lever, *J. Chem. Educ.* 1968, **45**, 711.
29. A. B. P. Lever, *Coord. Chem. Rev.* 1982, **43**, 63.
30. C. J. Ballhausen, *Introduction to Ligand Field Theory*, p. 268. McGraw-Hill, New York (1962).
31. D. Antansi, I. Collomoti and E. Clandio, *J. Chem. Soc., Dalton Trans.* 1974, 1319.
32. B. J. Hathaway and D. E. Billing, *Coord. Chem. Rev.* 1970, **5**, 1; 1970, **5**, 143.
33. L. Dubicki, *Aust. J. Chem.* 1972, **25**, 1141.
34. L. Dubicki and R. L. Martin, *Inorg. Chem.* 1966, **5**, 2203.
35. S. Kida, Y. Nishida and M. Sakamoto, *Bull. Chem. Soc. Jpn* 1973, **40**, 2428.
36. M. Massacessi, G. Ponticelli, V. Budha Addepala and V. G. Krishnan, *J. Molec. Struct.* 1978, **48**, 55; 1979, **51**, 27.
37. D. Kivelson and R. Neiman, *J. Chem. Phys.* 1958, **29**, 35.
38. B. R. McGarvey, *Electron Spin Resonance of Tran-*

sition Metal Complexes (Edited by R. L. Carlin). Marcel Dekker, New York (1967).
39. J. Wasson, C. Shyer and S. Trapp, *Inorg. Chem.* 1968, **7**, 469.
40. T. D. Smith and J. R. Pilbrow, *Coord. Chem. Rev.* 1974, **5**, 173.
41. G. F. Kokoszka and R. W. Duerest, *Coord. Chem. Rev.* 1970, **5**, 209.
42. R. C. Thompson, F. G. Herring, B. Landa and C. F. Schwerdtfeger, *J. Chem. Soc. A* 1971, 528.
43. W. J. Newton, C. Oldham and B. J. Tabner, *J. Chem. Soc., Dalton Trans.* 1980, 1379.
44. F. E. Mabbs and D. J. Machin, *Magnetism and Transition Metal Complexes*, p. 99. Chapman and Hall, London (1973).
45. B. N. Figgis, M. Gerloch, J. Lewis, F. E. Mabbs and G. A. Webb, *J. Chem. Soc. A* 1968, 2086.
46. B. Bleaney and K. D. Bowers, *Proc. R. Soc. Lond.* 1952, **214A**, 451.
47. S. J. Wayard, *J. Sci. Instr.* 1965, **42**, 769.
48. J. E. Wertz and J. R. Bolton, *Electron Spin Resonance, Elementary Theory and Practical Applications*, p. 32. McGraw-Hill, New York (1972).
49. P. Deemeester, S. R. Fletcher and A. C. Skapski, *J. Chem. Soc., Dalton Trans.* 1973, 2575.
50. B. Maria and M. Bukowska-Strzyzewka, *Rocz. Chem.* 1966, **40**, 567.
51. J. K. Burdett, *Inorg. Chem.* 1981, **20**, 1959.
52. J. K. Burdett, *Inorg. Chem.* 1975, **14**, 931.

Polyhedron Vol. 8, No. 19, p. 2407, 1989
Printed in Great Britain

0277–5387/89 $3.00+.00
© 1989 Pergamon Press plc

COMMUNICATION

CLEAVAGE OF THE PC TRIPLE BOND IN A PHOSPHA-ALKYNE IN THE ABSENCE OF A TRANSITION METAL

R. BARTSCH and J. F. NIXON*

School of Chemistry and Molecular Sciences, University of Sussex, Brighton BN1 9QJ, U.K.

(*Received* 26 *June* 1989; *accepted* 26 *June* 1989)

Abstract—The reaction of Bu^{t}C≡P with Na/Hg in monoglyme results in the formation of the 2,5-di-*t*-butyl-1,3,4-triphosphacyclopentadienyl (**1**) and 2,4,5-tri-*t*-butyl-1,3-diphosphacyclopentadienyl (**2**) anions. The reaction has been carried out in the absence of $[Ta(OAr)_2Cl_3]$ (Ar = 4-Me,2,6-*t*-$Bu_2C_6H_2$), which proves that the formation of **1** and **2** does not involve the phosphide intermediate $[Ta{\equiv}P(OAr)_2]$ previously postulated by Cowley and Hall (*Polyhedron* 1989, **8**, 849).

Recently Cowley and Hall[1] reported that reduction of $[Ta(OAr)_2Cl_3]$ (Ar = 4-Me,2,6-*t*-$Bu_2C_6H_2$) with Na/Hg, followed by treatment with 3 equivalents of Bu^{t}CP led to the formation of the di- and triphosphacyclopentadienide anions **1** and **2**. The authors speculated, without structure or spectroscopic data, that Bu^{t}CP is cleaved by a reduced tantalum species to afford the intermediates $[Ta{\equiv}P(OAr)_2]$ and $[Ta{\equiv}CBu^t(OAr)_2]$, which then could react with 2 moles of Bu^{t}CP to produce **1** and **2**, respectively. The source of the extra electrons for the formation of **1** and **2** is likely to be the alkali metal.

We wish to report that treatment of Bu^{t}CP with Na/Hg in monoglyme in the absence of $[Ta(OAr)_2Cl_3]$ yields **1** and **2** in the same proportions as described by Cowley and Hall.[1] This proves that the reaction occurs via direct cleavage of the PC bond in the phospha-alkyne by sodium, followed by cyclization with Bu^{t}CP to give **1** and **2**, respectively, without any involvement of a Ta≡P species. The ^{31}P NMR data for **1** and **2** are in satisfactory agreement with those previously reported by Becker *et al.*[2] and ourselves.[3] In recent work we have used this direct synthetic approach to subsequently oxidatively couple the anions **1** and **2** and to afford the novel cage compound $P_5C_5Bu^t_5$.[4]

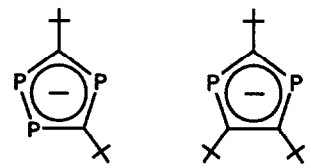

(1) (2)

* Author to whom correspondence should be addressed.

REFERENCES

1. A. H. Cowley and S. W. Hall, *Polyhedron* 1989, **8**, 849.
2. G. Becker, W. Becker, R. Knebl, H. Schmidt, U. Weeber and M. Westhausen, *Nova Acta Leopoldina* 1985, **59**, 55.
3. R. Bartsch, P. B. Hitchcock and J. F. Nixon, *J. Chem. Soc., Chem. Commun.* 1987, 1146.
4. R. Bartsch, P. B. Hitchcock and J. F. Nixon, *J. Organomet. Chem.*, in press (Paper presented at XIth International Conference on Phosphorus Chemistry, Tallinn, U.S.S.R., July 1989).

Polyhedron Vol. 8, No. 20, pp. 2409–2413, 1989
Printed in Great Britain

0277–5387/89 $3.00+.00
© 1989 Pergamon Press plc

ELECTRON TRANSFER BETWEEN BIS(DIMETHYLGLYOXIME)COPPER(II) AND DIGLYCYLETHYLENEDIAMINE COPPER(III). STABILIZATION OF COPPER(III) BY A DIOXIME LIGAND

YOUSIF SULFAB

Department of Chemistry, Kuwait University, P.O. Box 5969 Safat, 13060 Safat, Kuwait

(*Received* 19 *October* 1988; *accepted after revision* 15 *March* 1989)

Abstract—Bis(dimethylglyoxime)copper(II), $Cu^{II}(DMGH)_2$, is readily oxidized to the corresponding copper(III) complex. Cyclic voltammetry exhibited quasi-reversible one-electron transfer with peak-to-peak separation of ≈ 80 mV. The $E_{1/2}$ value varied linearly with $-\log[H^+]$ with a slope of -59 mV, showing the involvement of one proton in the electrode reaction. The kinetics of the oxidation of $Cu^{II}(DMGH)_2$ by $Cu^{III}(H_{-2}DGEN)^+$ (DGEN = diglycylethylenediamine) showed a first-order dependence on both the reductant and the oxidant. The second-order rate constant, k_2, varies with $[H^+]$ according to:

$$k_2 = k'_2 + k_3/[H^+].$$

The mechanism of electron transfer is discussed in terms of inner- and outer-sphere mechanisms.

The trivalent oxidation state of copper is often proposed as a highly reactive species in a number of organic and inorganic oxidations catalysed by copper(II) ions.[1–5] A number of copper(III) complexes have been identified in solution and a few have been isolated in the solid state.[6,7] Copper(III) has been shown to be stabilized by coordination to in-plane deprotonated amide groups as shown by the isolation of biuret[8] and oxamide[9] complexes. This has further been supported by the generation of copper(III)–peptide complexes by chemical and electrochemical oxidations of the corresponding deprotonated copper(II) complexes.[10,11] The chemistry of this oxidation state of copper has recently been reviewed.[7]

More than 50 years ago, Clarke and Jones[12] and Kolthoff[13] described a very sensitive method for the detection of copper at very low concentrations. The method involved the use of copper(II), dimethylglyoxime ($DMGH_2$) and an oxidant, $S_2O_8^{2-}$ or IO_4^- in buffered solutions. The nature of the reddish-violet product, which decomposes on standing, was not known. Morphurgo and Tomlinson[14] have also reported the oxidation of the tetramer $[Cu_2(DMGH)_2(OH)_2]_2$ by $S_2O_8^{2-}$ and claimed the formation of a species in which copper exists in the mixed oxidation states of II and III. These authors, however, claimed that $Cu^{II}(DMGH)_2$ is not oxidized to the corresponding copper(III) complex. In this study, we report the stabilization of the trivalent oxidation state of copper by $DMGH_2$, its electrochemistry and electron-transfer reaction with doubly deprotonated copper(III)–diglycylethylenediamine, $[Cu^{III}(H_{-2}DGEN)]^+$.

The ability of the dioxime ligands to conform to the geometrical preference of the d^8 copper(III) complex, with subsequent ligand-field stabilization, will favour the d^8 configuration relative to d^9.[11] Dioxime and pyridine–oxime ligands are reported to facilitate the oxidation and to stabilize higher oxidation states of nickel.[15] Recently, $Ni^{IV}(DMG)_3^{2-}$ has been isolated from basic solutions.[16] An uncommon +4 oxidation state has also been reported in organoaquabis(dimethylglyoxime) cobalt(IV) complexes.[17] We have also shown that the +3 oxidation of copper is stabilized by tetradentate imine–oxime ligands.[18]

EXPERIMENTAL

Solutions of copper(II)–dimethylglyoxime were prepared by reacting solutions of $Cu(ClO_4)_2$ with

the ligand in a 1:2.1 mole ratio. The pH of the $Cu^{II}(DMGH)_2$ (5.0×10^{-3} M) solutions was raised to ≈ 6 by the slow addition of 0.10 M NaOH, to ensure the complete formation of the complex. The diglycylethylenediamine ligand was prepared according to the literature method.[19] Solutions of copper(II)–diglycylethylenediamine were freshly prepared, with the ligand in 5% excess, and the pH adjusted to ≈ 10 with 0.10 M NaOH to form the doubly deprotonated complex, $Cu^{II}(H_{-2}DGEN)$. Fresh solutions of $[Cu^{III}(H_{-2}DGEN)]^+$ were prepared by electrochemical oxidation with a flow system in which the electrode arrangement included a graphite powder working electrode packed in a porous-glass column, wrapped externally with a platinum wire electrode.[20] The $Cu^{II}(H_{-2}DGEN)$ complex was oxidized at a potential of about 200 mV above its $E^0_{1/2}$ value. After electrolysis, the copper(III) solutions were weakly acidic and were diluted to the desired concentration and the ionic strength maintained at 0.1 M with $NaClO_4$. Stock solutions of the buffers, acetate, phosphate, 2(N-morpholino)ethanesulphonate (MES) and N-2-hydroxyethylpiperazine-N′-ethanesulphonate (HEPES) were made up by weight. A stock solution of sodium *meta* periodate (0.10 M) was made up by weight and wrapped with aluminium foil to avoid photochemical decomposition.[21]

The EPR spectrum of $Cu^{II}(DMGH)_2$ solutions, in the presence or absence of periodate, was recorded at room temperature at pH ≈ 6 using a Varian E-109 X-band EPR system modulated at 100 kHz. Cyclic voltammetry was performed at 25.0°C over a pH range, using various buffers, with a three-electrode system consisting of a carbon paste working electrode, a platinum wire auxiliary electrode and a saturated NaCl calomel reference electrode.

Voltammograms were generated using a Bioanalytical Systems Inc. CV-1 instrument and recorded on a Hewlett-Packard HP7035 X–Y recorder. The $E_{1/2}$ values were determined as the midpoint between the peak potentials with an accuracy of ± 5 mV. The electrode potential, at each pH, was obtained from an average of three separate cyclic voltammetric measurements. The $E_{1/2}$ values were determined in coordinating and non-coordinating buffers. Axial coordination has been reported[22] in $Cu^{II}(DMGH)_2$ to give a five-coordinate complex, and if this is significant with coordinating buffers, the $E_{1/2}$ values are likely to be affected.

The kinetics of the oxidation of $Cu^{II}(DMGH)_2$ by $[Cu^{III}(H_{-2}DGEN)]^+$ were followed at 530 nm, $T = 25.0$°C and $\mu = 0.10$ M ($NaClO_4$) using a Durrum stopped-flow spectrophotometer interfaced to a Hewlett-Packard Model 2115A general purpose computer.[23] Pseudo-first-order conditions were maintained in all kinetic runs with $[Cu^{II}(DMGH)_2] \geqslant 10\ [[Cu^{III}(H_{-2}DGEN)]^+]$. The effect of $[H^+]$ on the rate of electron-transfer was investigated over a pH range using different buffers. The pH was measured using a Radiometer PHM26 pH meter and the pH corrected for ionic strength effects ($-\log[H^+] = \text{pH} - 0.11$).

RESULTS

The EPR spectrum obtained for $Cu^{II}(DMGH)_2$ (10^{-4} M, pH ≈ 6) is identical to that reported in the literature.[24] On addition to a periodate solution (2.5×10^{-3} M), the EPR spectrum of the copper(II) complex disappears, indicating the formation of a diamagnetic species.

Cyclic voltammetry using solutions of $Cu^{II}(DMGH)_2$ gave current potential response curves consistent with a quasi-reversible one-electron oxidation. A plot of $E_{1/2}$ vs $-\log[H^+]$ is linear over the pH range 4.1–8.5, with a slope of -59.3 ± 0.7 mV, indicative of rapid acid–base equilibrium involving one proton per Cu^{II} complex. As shown in Fig. 1, the value of $E_{1/2}$ is independent of the type of buffer used.

The kinetics of the oxidation of $Cu^{II}(DMGH)_2$ by $[Cu^{III}(H_{-2}DGEN)]^+$ were investigated under pseudo-first-order conditions. With the copper(II) complex concentration being in at least ten-fold excess over that of the copper(III) complex, excellent first-order plots were obtained. The reaction showed a first-order dependence on the copper(III) complex, with the value of k_{obs} being independent of the initial concentration of the oxidant. The order of the reaction with respect to the copper(II) complex was examined by determining k_{obs} at various concentrations of $Cu^{II}(DMGH)_2$. The results in Table 1 show that k_{obs} varies linearly with copper(II) complex concentration, and is given by eq. (1):

$$k_{obs} = k_2[Cu^{II}(DMGH)_2]. \quad (1)$$

The effect of pH on the reaction rate was examined over the pH range 6.2–8.2. The results in Table 2 show that the second-order rate constant k_2 ($k_2 = k_{obs}/[Cu^{II}(DMGH)_2]$) increases with increasing pH, and a plot of k_2 vs $[H^+]^{-1}$ is linear with an intercept. The variation of k_2 with $[H^+]$ is described by eq. (2):

$$k_2 = k'_2 + k_3/[H^+]. \quad (2)$$

The values of k'_2 and k_3 were calculated from a linear least-squares analysis as $(1.95 \pm 0.49) \times 10^4$ $M^{-1}\ s^{-1}$ and $(8.58 \pm 0.11) \times 10^{-3}\ s^{-1}$, respectively, at 25.0°C and $\mu = 0.10$ M.

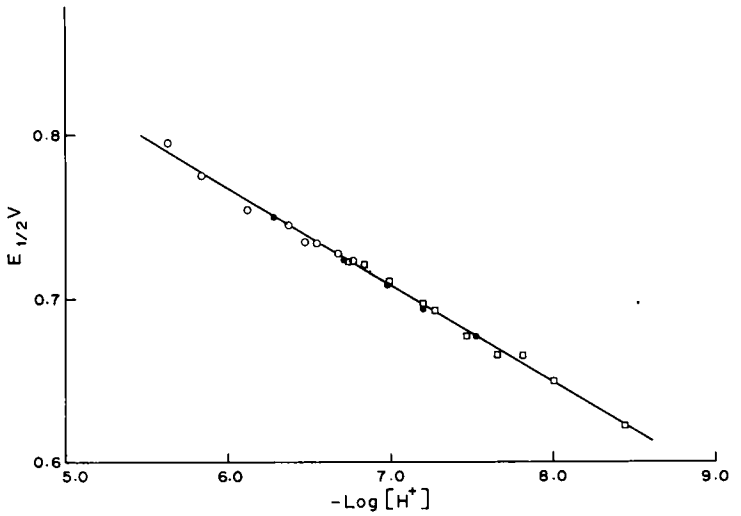

Fig. 1. $E_{1/2}$ vs $-\log[H^+]$ for $Cu^{II}(DMGH)_2$ in various buffers: MES(○), HEPES(□) and phosphate(●) at $\mu = 0.10$ M ($NaClO_4$), $T = 25.0°C$.

DISCUSSION

The disappearance of the EPR signals of the $Cu^{II}(DMGH)_2$ complex on the addition of periodate, is consistent with the formation of a diamagnetic d^8 copper(III) complex having a square-planar geometry. The cyclic voltammetry is consistent with a one-electron transfer, as indicated by peak-to-peak separations of ≈ 80 mV. The $E_{1/2}$ values of this complex are close to those obtained for the 3,9-dimethyl-4,8-diazaundeca-3,8-dien-2,10-dione-dioxime copper(II) complex under similar conditions.[18b] The dependence of $E_{1/2}$ on pH is given by eq. (3) and is consistent with the electrode reaction of eq. (4):

$$E_{1/2} = E^0_{1/2} - 0.059\,\mathrm{pH} \quad (3)$$

$$Cu^{III}(DMGH)(DMG) + H^+ + e \rightleftharpoons Cu^{II}(DMGH)_2. \quad (4)$$

A similar dependence of $E_{1/2}$ on pH has been reported for the copper(III)–imine–oxime complex.[18b] The standard electrode potential, $E^0_{1/2}$ of $Cu^{II}(DMGH)_2$ was calculated from eq. (3) as 1.12 V (vs NHE), assuming that eq. (3) holds over the entire pH region.

Bis(dimethylglyoxime)copper(II) is reported to be five-coordinated in the solid state.[25] In non-aqueous solvents it readily adds amines in the axial position and the formation constants with amines have been determined.[22] It is reasonable to assume that in aqueous solutions, an H_2O occupies an axial position. It has been reported that $Cu^{II}(DMGH)_2H_2O$ loses a proton and a pK_a of 10.6 has been estimated.[26]

It is claimed that the proton is lost from the coordinated H_2O to form the hydroxo complex, $[Cu^{II}(DMGH)_2(OH)]^-$. We have determined the pK_a value as 10.95 at 0.10 M ($NaClO_4$), which is in

Table 1. Variation of the pseudo-first-order rate constant with $Cu^{II}(DMGH)_2$ for the reaction with $[Cu^{III}(H_{-2}DGEN)]^{+a}$

$10^5[Cu^{II}(DMGH)_2]$	$10^6[[Cu^{III}(H_{-2}DGEN)]^+]$	k_{obs} (s^{-1})	$10^{-5}k_2^b$ ($M^{-1}\,s^{-1}$)
5.50	5.0	29.3±0.2	5.33
8.25	5.0	42.4±0.1	5.14
11.0	5.0	59.2±0.5	5.38
22.0	10.0	125±3.0	5.68
33.0	10.0	179±4.0	5.42
44.0	10.0	235±20	5.35

[a] At 25.0°C, $\mu = 0.10$ M ($NaClO_4$), [N-2-hydroxyethylpiperazine-N'-ethanesulphonate]$_T$ = 0.01 M, pH = 7.85.

[b] Average $k_2 = (5.38 \pm 0.24) \times 10^5\ M^{-1}\,s^{-1}$.

Table 2. Variation of the $Cu^{II}(DMGH)_2$–$[Cu^{III}(H_{-2}DGEN)]^+$ reaction with pH[a] [25.0°C, $\mu = 0.10$ M ($NaClO_4$)]

pH	k_{obs} (s^{-1})	$10^{-5}k_2$ ($M^{-1}s^{-1}$)
6.27	1.45	0.264
6.77	2.85	0.518
7.05	5.16	0.938
7.05[b]	4.90	0.980
7.27	7.81	1.42
7.34	9.49	1.73
7.39	11.40	2.07
7.45	12.04	2.19
7.54[c]	11.12	2.22
7.57[d]	147.7	2.69
7.57[e]	144.3	2.62
7.57[f]	145.9	2.65
7.58	15.88	2.89
7.71	19.10	3.47
8.06[b]	43.14	7.84
8.19	57.90	10.53

[a] Unless otherwise stated [N-2-hydroxyethylpiperazine-N′-ethanesulphonate]$_T$ = 0.01 M, $[Cu^{II}(DMGH)_2] = 5.50 \times 10^{-5}$ M, $[Cu^{III}(H_{-2}DGEN)]^+ = 5.0 \times 10^{-6}$ M.
[b] [phosphate]$_T$ = 0.01 M.
[c] $[Cu^{II}(DMGH)_2] = 5.50 \times 10^{-5}$ M.
[d] $[Cu^{II}(DMGH)_2] = 5.50 \times 10^{-4}$ M; $[Cu^{III}(H_{-2}DGEN)]^+ = 2.50 \times 10^{-5}$ M.
[e] $[Cu^{II}(DMGH)_2] = 5.50 \times 10^{-4}$ M; $[Cu^{III}(H_{-2}DGEN)]^+ = 3.6 \times 10^{-5}$ M.
[f] $[Cu^{II}(DMGH)_2] = 5.50 \times 10^{-4}$ M; $[Cu^{III}(H_{-2}DGEN)]^+ = 5.0 \times 10^{-5}$ M.

agreement with the literature value. However, we believe that the proton is lost from one of the dioxime ligands and not from the coordinated H_2O. This is based on the finding that the proton transfer reaction,

$$Cu^{II}(DMGH)_2H_2O + OH^- \rightleftharpoons [Cu^{II}(DMGH)(DMG)(H_2O)]^- + H_2O \quad (5)$$

could be measured using the pulsed-flow spectrophotometer.[27] This reaction would have been too fast to follow if the proton was abstracted from the coordinated H_2O, as the rate of this reaction would be diffusion-controlled.[28] Rate constants have been measured for the proton transfer reactions of $[Co^{III}(DMGH)_2(CN)_2]^-$ and $[Co^{III}(DMGH)_2(NH_3)_2]^+$.[29]

The kinetics of electron-transfer between $Cu^{II}(DMGH)_2H_2O$ and $[Cu^{III}(H_{-2}DGEN)]^+$ could be described by eqs (6)–(8).

$$Cu^{II}(DMGH)_2H_2O \rightleftharpoons [Cu^{II}(DMGH)(DMG)(H_2O)]^- + H^+ \quad K_a \quad (6)$$

$$Cu^{II}(DMGH)_2H_2O + [Cu^{III}(H_{-2}DGEN)]^+ \xrightarrow{k_4} Cu^{III}(DMGH)(DMG) + Cu^{II}(H_{-2}DGEN) + H_3O^+ \quad (7)$$

$$[Cu^{II}(DMGH)(DMG)(H_2O)]^- + [Cu^{III}(H_{-2}DGEN)]^+ \xrightarrow{k_5} Cu^{III}(DMGH)(DMG) + Cu^{II}(H_{-2}DGEN) + H_2O. \quad (8)$$

From the above reaction sequence [eqs (6)–(8)], the variation of the second-order rate constant, k_2, with $[H^+]$ is given by eq. (9):

$$k_2 = \frac{k_4[H^+] + k_5K_a}{K_a + [H^+]}. \quad (9)$$

Over the pH range covered in this study, $[H^+] \gg K_a$ and eq. (9) reduces to the form of eq. (10), which is similar to the experimental form of eq. (2):

$$k_2 = k_4 + k_5K_a/[H^+]. \quad (10)$$

Comparing eqs (2) and (10), it could be seen that $k'_2 = k_4$ and $k_3 = k_5K_a$. The value of k_5 is calculated as $\approx 8 \times 10^8$ $M^{-1}s^{-1}$ taking $K_a = 1.1 \times 10^{-11}$ M.

The mechanism by which the electron is transferred is not certain and both inner- and outer-sphere pathways may operate. The $[Cu^{III}(H_{-2}DGEN)]^+$ could be bridged to the protonated and unprotonated forms of the copper(II) complex via a H_2O molecule. The unprotonated copper(II) complex may also be bridged to the copper(III) complex via an oxime oxygen. An oxygen atom on the coordinated DGEN ligand may also be used as a bridging atom.

The electrode potential of the $[Cu^{III/II}(H_{-2}DGEN)]^{+/0}$ has been determined as 0.85 V vs NHE.[30] The electrode potentials of the fully protonated and completely deprotonated forms of the bis(dimethylglyoxime)copper(II) couples are unknown. It was not possible to measure these potentials because at high acid or base concentrations the copper(II) and copper(III) complexes decompose. Thus, it was not possible to apply the Marcus correlation[31] to compare the calculated and the experimental rate constants, and hence favour one mechanism over the other.

Acknowledgements—I would like to express my gratitude to Professor D. W. Margerum for making it possible for me to carry out this work in his laboratory and for providing me with the the ligand (DGEN) and other chemicals and research facilities. I would also like to

thank C. K. Murray for his help and for reading the manuscript.

REFERENCES

1. J. K. Kochi (Ed.), *Free Radicals*, Vol. 1, Chap. 11. Wiley-Interscience, New York (1973).
2. T. Cohen, R. J. Lewarchik and J. Z. Tarino, *J. Am. Chem. Soc.* 1974, **96**, 7753.
3. T. Cohen, T. Wood and A. G. Dietz Jr, *Tetrahedron Lett.* 1974, **40**, 3555.
4. F. Secco and S. Celsi, *J. Chem. Soc. A* 1971, 1092.
5. A. Y. Kasim and Y. Sulfab, *Inorg. Chim. Acta* 1977, **22**, 169.
6. D. W. Margerum and G. D. Owens, *Metal Ions in Biological Systems*, Vol. 12, p. 75. Marcel Dekker, New York (1981).
7. W. Levason and M. D. Spicer, *Coord. Chem. Rev.* 1987, **75**, 45.
8. J. J. Bour and J. J. Steggerda, *J. Chem. Soc., Chem. Commun.* 1967, 85.
9. J. J. Bour, P. J. M. W. L. Birker and J. J. Steggerda, *Inorg. Chem.* 1971, **10**, 1202.
10. D. W. Margerum, K. L. Chellappa, F. P. Bossu and G. L. Burce, *J. Am. Chem. Soc.* 1975, **97**, 6894.
11. F. P. Bossu, K. L. Chellappa and D. W. Margerum, *J. Am. Chem. Soc.* 1977, **99**, 2195.
12. S. G. Clarke and B. Jones, *Analyst* 1929, **54**, 333.
13. I. M. Kolthoff, *J. Am. Chem. Soc.* 1930, **52**, 222.
14. G. O. Morphurgo and A. A. G. Tomlinson, *J. Chem. Soc., Dalton Trans.* 1977, 744.
15. (a) E. I. Baucom and R. S. Drago, *J. Am. Chem. Soc.* 1971, **93**, 6469; (b) R. S. Drago and E. I. Baucom, *Inorg. Chem.* 1972, **11**, 2064.
16. R. K. Panda, S. Acharga, G. Neogi and D. Ramaswamy, *J. Chem. Soc., Dalton Trans* 1983, 1225.
17. J. Topich and J. Halpern, *Inorg. Chem.* 1979, **18**, 1339.
18. (a) Y. Sulfab, M. A. Hussein and N. I. Al-Shatti, *Inorg. Chim. Acta* 1982, **67**, L33; (b) Y. Sulfab and N. I. Al-Shatti, *Inorg. Chim. Acta* 1984, **87**, L23.
19. T. L. Cottrell and J. E. Gill, *J. Chem. Soc.* 1947, 129.
20. B. R. Clark and D. H. Evans, *J. Electroanal. Chem.* 1976, **69**, 181.
21. M. C. R. Symons, *J. Chem. Soc.* 1955, 2794.
22. D. Dyrssen and D. Petkovic, *Acta. Chem. Scand.* 1965, **19**, 653.
23. B. G. Willis, J. A. Bittikofer, H. L. Pardue and D. W. Margerum, *Analyt. Chem.* 1970, **42**, 1340.
24. R. E. Falk, E. Ivanova, B. Ross and T. Vanngard, *Inorg. Chem.* 1970, **9**, 556.
25. A. Vaciago and L. Zambonelli, *J. Chem. Soc. A* 1970, 218.
26. D. Dyrssen and M. Hennichs, *Acta Chem. Scand.* 1961, **15**, 47.
27. G. D. Owens and D. W. Margerum, *Analyt. Chem.* 1980, **52**, 91A.
28. M. Eigen, *Angew. Chem.* 1964, **3**, 1.
29. J. P. Birk, P. B. Chock and J. Halpern, *J. Am. Chem. Soc.* 1968, **90**, 6959.
30. C. K. Murray and D. W. Margerum, *Inorg. Chem.* 1983, **22**, 463.
31. R. A. Marcus, *J. Phys. Chem.* 1963, **67**, 853.

Polyhedron Vol. 8, No. 20, pp. 2415–2418, 1989
Printed in Great Britain

0277–5387/89 $3.00+.00
© 1989 Pergamon Press plc

STRUCTURE OF (CYANO-C)TRIS (TRIPHENYLPHOSPHITE)RHODIUM(I)

A. M. TRZECIAK,* J. J. ZIÓŁKOWSKI* and T. LIS

Institute of Chemistry, University of Wrocław, 50-383 Wrocław, Poland

(*Received* 23 *January* 1989; *accepted* 14 *April* 1989)

Abstract—The crystalline complex $Rh[P(OPh)_3]_3CN$ was prepared by the reaction of $Rh[P(OPh)_3]_3Cl$ with NaCN in chloroform. The compound crystallizes from chloroform solution as a solvate of formula $RhCN[P(OPh)_3]_3 \cdot 1.5CHCl_3$. Crystals are triclinic, space group $P\bar{1}$ with $a = 11.51(1)$, $b = 10.91(1)$, $c = 24.05(2)$ Å, $\alpha = 92.25(8)$, $\beta = 97.91(8)$, $\gamma = 106.05(8)^\circ$, $U = 2865(5)$ Å^3, $Z = 2$. The rhodium atom has the square planar coordination. The ^{31}P NMR spectrum of $Rh[P(OPh)_3]_3CN$ is of the A_2BX type (A, B = ^{31}P, X = ^{103}Rh) with the same J(Rh—P) for all three phosphite ligands.

The complex $Rh[P(OPh)_3]_3CN$ was obtained for the first time by the reaction of Rh(acac)$[P(OPh)_3]_2 + P(OPh)_3 + HCN$ (acac = 1,3-dimethyl-1,3-propanedione).[1] The most interesting feature of this compound is the equivalence of all three phosphite ligands observed in the ^{31}P NMR spectrum.[1] The coupling constant J(Rh—P), of phosphoruses in *trans* and *syn* positions have almost the same values, 225.3 and 224.2 Hz, respectively. In all other complexes of the type $Rh[P(OPh)_3]_3X$, the value of J(Rh—P) of phosphorus *trans* is *ca* 60 Hz lower than that of phosphorus *cis*.[2] We have expected, that the geometry of the $Rh[P(OPh)_3]_3CN$ complex could influence its spectroscopic properties and for that reason we have started the structural investigations.

Up to now, the crystal structures of phosphite complexes with chelate ligands: Rh(acac)$[P(OPh)_3]_2$,[3] Rh(TFBA)$[P(OPh)_3]_2$[4] (TFBA = 1-phenyltrifluoromethyl-1,3-propanedione), Rh(Quin)$[P(OPh)_3]_2$[5] (Quin = 2-carboxyquinoline) and of the dimeric $(C_8H_{12})RhCl_2Rh[P(OPh)_3]_2$[6] and the cationic complex $\{Rh(C_6H_5Me)[P(OPh)_3]_2\}ClO_4$[7] were determined.

$Rh[P(OPh)_3]_3CN$ is the first example of a $Rh[P(OPh)_3]_3X$ type complex for which the crystal structure was established.

RESULTS AND DISCUSSION

The overall structure of the molecule $Rh[P(OPh)_3]_3CN$ is shown in Fig. 1, selected bond distances and bond angles are listed in Table 1.

The rhodium atom has almost square planar coordination as shown by calculations of the plane through the three phosphorus, the cyanide carbon and rhodium atoms.

The Rh—P distances in $Rh[P(OPh)_3]_3CN$, 2.266(3), 2.228(3), 2.250(3) Å are comparable with those observed in $Rh(2,4,6\text{-}Me_3C_6H_2)[P(OMe)_3]_3$.[8] In other rhodium(I) triphenylphosphite complexes, shorter Rh—P distances were found, e.g. 2.161(2), 2.150(2) Å in Rh(TFBA)$[P(OPh)_3]_2$,[4] 2.180(1), 2.188(1) Å in $\{Rh(C_6H_5Me)[P(OPh)_3]_2\}ClO_4$,[7] and 2.142 Å in $(C_8H_{12})RhCl_2Rh[P(OPh)_3]_2$.[6]

The Rh—C distance in $Rh[P(OPh)_3]_3CN$ [2.06(1) Å] is shorter than that observed in the molybdenum complex, $Mo(NO)(terpy)(CN)(HNO) \cdot 2H_2O$ [2.197(10) Å],[11] with relatively weak Mo—CN bonding. For rhodium cyano complexes no data are available. In complexes of other metals shorter M—C distances were noted, e.g. 1.931(6) Å in $Cu(N_3C_{15}H_{11})CN(NO_3) \cdot H_2O$, and 1.920(16) Å[9] in $[Pt(phen)_2(CN)]^+$.[10]

Bond distances and angles in the phosphite ligands are similar to those observed in other rhodium triphenylphosphite complexes.[3–7]

The main purpose of the X-ray investigations presented in this paper was to find the correlation

* Authors to whom correspondence should be addressed.

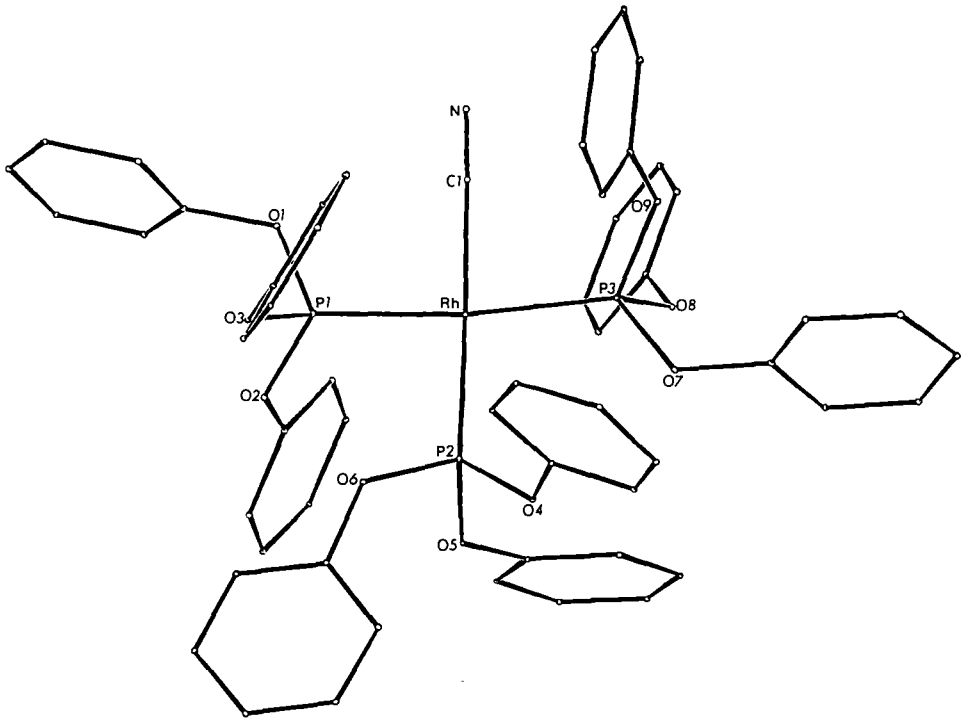

Fig. 1. View of the $Rh[P(OPh)_3]_3CN$ molecule.

Table 1. Selected interatomic distances (Å) and angles (°)

Bond distances			
Rh—P(1)	2.266(3)	Rh—P(2)	2.228(3)
Rh—P(3)	2.250(3)	Rh—C(1)	2.058(10)
C(1)—N	1.044(14)	P(1)—O(1)	1.597(6)
P(1)—O(2)	1.612(6)	P(1)—O(3)	1.606(6)
P(2)—O(4)	1.614(6)	P(2)—O(5)	1.610(6)
P(2)—O(6)	1.604(6)	P(3)—O(7)	1.607(6)
P(3)—O(8)	1.597(5)	P(3)—O(9)	1.613(7)
O(1)—C(11)	1.421(12)	O(2)—C(21)	1.392(11)
O(3)—C(31)	1.387(14)	O(4)—C(41)	1.395(11)
O(5)—C(51)	1.412(11)	O(6)—C(61)	1.402(11)
O(7)—C(71)	1.432(12)	O(8)—C(81)	1.402(10)
O(9)—C(91)	1.421(12)		
Angles			
P(1)—Rh—P(2)	90.6(1)	P(1)—Rh—P(3)	171.3(1)
P(2)—Rh—P(3)	97.6(1)	P(1)—Rh—C(1)	88.1(3)
P(2)—Rh—C(1)	177.2(3)	P(3)—Rh—C(1)	83.9(3)
Rh—C(1)—N	173.4(10)	Rh—P(1)—O(1)	114.0(3)
Rh—P(1)—O(2)	120.3(3)	Rh—P(1)—O(3)	118.9(3)
Rh—P(2)—O(4)	121.2(3)	Rh—P(2)—O(5)	121.8(3)
Rh—P(2)—O(6)	110.8(3)	Rh—P(3)—O(7)	118.7(3)
Rh—P(3)—O(8)	117.2(3)	Rh—P(3)—O(9)	118.4(3)

between spectroscopic and structural parameters of $Rh[P(OPh)_3]_3CN$. That correlation seems to be rather complicated. The J(Rh—P) values are independent of Rh—P distances. The coupling constants J(Rh—P) have the same values, but the Rh—P distances vary significantly. The planar structure of the $Rh[P(OPh)_3]_3CN$ seems not to be an important factor influencing the inequivalence of the phosphorus ligands. The other rhodium complexes of the type RhP_3X, e.g. $Rh(PPh_3)_3Cl$,[13] $Rh[PMe_3]_3Cl$,[14] and $Rh(2,4,6\text{-}Me_3C_6H_2)[P(OMe)_3]_3$[8] show only slight distortion from planar symmetry but the phosphorus ligands are inequivalent in the ^{31}P NMR. It is possible that the most important influence on spectroscopic properties of $Rh[P(OPh)_3]_3CN$ is the character of the CN ligand. As a strong σ donor and π acceptor, the CN ligand in a square-planar complex weakens the Rh—P bonding in the *trans* position. Therefore, the J(Rh—P) value of phosphorus in the *trans* position is lower than expected, and nearly equal to that of phosphoruses in the *cis* position to CN.

EXPERIMENTAL

Synthesis

$Rh[P(OPh)_3]_3Cl$[15] (0.051 g) in $CHCl_3$ (0.5 cm^3) and KCN (0.0032 g) in H_2O (0.3 cm^3) were mixed. Next, C_2H_5OH (1 cm^3) was added slowly under stirring. The homogeneous yellow solution was left to crystallize in a sealed flask.

Elemental analysis: Found (Calc): C 55.1 (54.8); H 3.4 (3.8); N 1.9 (1.1)%.

X-ray structure analysis

Crystal data: $C_{55}H_{45}NO_9P_3Rh \cdot 1.5CHCl_3$, $M = 1238.9$, triclinic, $a = 11.51(1)$, $b = 10.91(1)$, $c = 24.05(2)$ Å, $\alpha = 92.25(8)$, $\beta = 97.91(8)$, $\gamma = 106.05(8)°$, $U = 2865(5)$ Å^3, $Z = 2$, $D_c = 1.436(2)$ g cm^{-3}, $D_o = 1.415$ g cm^{-3}. Space group $P\bar{1}$, Cu-K_α radiation, $\lambda = 1.5418$ Å, $\mu = 56.4$ cm^{-1}.

A specimen (0.3 × 0.25 × 0.1 mm) was cut from a large crystal. A Syntex $P2_1$ diffractometer, Cu-K_α radiation and graphite monochromator were used for lattice-parameter and intensity measurements at $T = 294 \pm 2$ K. Intensities were measured by 2θ–ω scan technique. Reflections were collected in the ranges $4 < 2\theta < 50°$, $50 < 2\theta < 80°$, and $80 < 2\theta < 100°$, because the crystal suffered slow decomposition, most probably because of the loss of $CHCl_3$. The intensities of two standard reflections, which were monitored after every 50 intensities scan, decreased continually by approximately 20% over the period of the data collections. The data were scaled to the same relative scale using the intensities of the standard reflections. From 4887 measured reflections, 4538 with $I > 3\sigma(I)$ were used for structure determination. The structure was solved by the heavy atom method and refined by the blocked full-matrix least-squares technique using the *SHELX76* program.[16] The carbon-bonded H-atoms were included in geometrically calculated positions with d(C—H) = 1.08 Å. An absorption correction following the DIFABS procedure[17] applied on isotropically refined data; min and max absorption corrections were 0.813 and 1.237, respectively. Owing to the fact that there are three chloroform molecules in the unit cell, one of two crystallographically independent molecules is statistically distributed between symmetry equivalent positions near the centre of symmetry at $\frac{1}{2}$, $\frac{1}{2}$, 0. Since the interatomic distances in the statistically disordered molecule were rather unrealistic it was decided to refine this molecule as a rigid group with the same interatomic distances as in the ordered molecule. Refinement with anisotropic thermal parameters for Rh, P, Cl, O and C gave a final $R = 0.063$ and $R_w = 0.066$. The final difference Fourier synthesis showed a general background within -0.72 and 1.14 e Å^{-3}. Final atomic positions and thermal parameters and a list of F_o and F_c values have been deposited as supplementary data with the Editor from whom copies may be obtained on request. Atomic coordinates have also been deposited with the Cambridge Crystallographic Data Centre.

REFERENCES

1. A. M. Trzeciak, J. Siatecki and J. J. Ziółkowski, *Trans. Met. Chem.* 1986, **11**, 458.
2. A. M. Trzeciak and J. J. Ziółkowski, *Transition Met. Chem.*, in press.
3. J. G. Leipoldt, G. J. Lamprecht, G. J. van Zyl, *Inorg. Chim. Acta* 1985, **96**, L31.
4. G. J. Lamprecht, J. G. Leipoldt and G. J. van Zyl, *Inorg. Chim. Acta* 1985, **97**, 31.
5. G. J. Lamprecht, J. H. Beetge, J. G. Leipoldt and D. R. de Waal, *Inorg. Chim. Acta* 1986, **113**, 157.
6. J. Coetzer and G. Gafner, *Acta Cryst.* 1970, **826**, 985.
7. R. Uson, P. Lahuerta, J. Reyes, L. A. Oro, C. Foses-Foses, F. H. Cauo and S. Garcia-Blanco, *Inorg. Chim. Acta* 1980, **42**, 75.
8. L. Dahlenburg, A. Yardimcioglu and N. Hock, *Inorg. Chim. Acta* 1984, **89**, 213.
9. O. P. Anderson, A. B. Packard and M. Wicholas, *Inorg. Chem.* 1976, **15**, 1613.
10. O. Wernberg and A. Hazell, *J. Chem. Soc. Dalton Trans.* 1980, 973.

11. K. Wieghardt, W. Holzbach and J. Weiss, *Z. Naturforsch.* 1982, **37b**, 680.
12. G. O. Morgurgo, V. Mosini, P. Porta, G. Dessy and V. Fares, *J. Chem. Soc. Dalton Trans.* 1981, 111.
13. M. J. Bennett, P. B. Donaldson, *Inorg. Chem.* 1977, **16**, 655.
14. R. A. Jones, F. Mayor Real, G. Wilkinson, A. M. Galas, M. B. Hursthouse and K. M. A. Malik, *J. Chem. Soc. Dalton Trans.* 1980, 511.
15. L. M. Haines, *Inorg. Chem.* 1970, **9**, 1517.
16. G. M. Sheldrick, *SHELX76 Program for Crystal Structure Determination.* Univ. of Cambridge, England (1976).
17. N. Walker and D. Stuart, *Acta Cryst.* 1983, **A39**, 158.

Polyhedron Vol. 8, No. 20, pp. 2419–2423, 1989
Printed in Great Britain

0277-5387/89 $3.00+.00
© 1989 Pergamon Press plc

SYNTHESIS AND VIBRATIONAL (IR AND RAMAN) SPECTROSCOPIC STUDY OF TRIANGULAR THIO-COMPLEXES $[Mo_3S_{13}]^{2-}$ CONTAINING ^{92}Mo, ^{100}Mo AND ^{34}S ISOTOPES

V. P. FEDIN,* B. A. KOLESOV, YU. V. MIRONOV and V. YE. FEDOROV

Institute of Inorganic Chemistry, Siberian Branch of Academy of Sciences of the U.S.S.R., Novosibirsk, prospekt Lavrentyeva 3, 630090, U.S.S.R.

(*Received* 31 *March* 1989; *accepted* 4 *May* 1989)

Abstract—The triangular anionic thio-complex $[Mo_3S_{13}]^{2-}$ has been obtained by the reaction of the triangular molybdenum thiobromide $Mo_3S_7Br_4$ with an aqueous solution of S_x^{2-}. Starting from compounds containing ^{92}Mo, ^{100}Mo and ^{34}S isotopes, the following thio-complexes have been obtained: $[^{92}Mo_3S_{13}]^{2-}$, $[^{100}Mo_3S_{13}]^{2-}$, $[Mo_3{}^{34}S_{13}]^{2-}$, $[Mo_3(\mu_3\text{-}S)(\mu_2\text{-}S^{34}S)_3(^{34}S_2)_3]^{2-}$ and $[Mo_3(\mu_3\text{-}^{34}S)(\mu_2\text{-}^{34}SS)_3(S_2)_3]^{2-}$. Along with the nucleophilic substitution of the Br ligands by the terminal S_2 ligands, elimination–addition of sulphur in μ_2-S_2 ligands also takes place. This allows preparation of thio-complexes containing μ_2-$^{34}S^{32}S$ ligands. IR and Raman spectra of the thio-complexes have been studied, normal vibrations have been calculated and the bond force constants determined.

Polynuclear and cluster thio-complexes of transition metals have been intensively studied in recent years.[1-3] These compounds contain different S_n ligands which, we believe, will play a potential role in a wide range of applications. Special attention has been given to thio-complexes of molybdenum since they are important for understanding the structure and mechanism of the action of some enzymes and catalysts. The thio-complexes are known to undergo reactions involving intramolecular oxidation–reduction, unexpected rearrangements, or insertion of some ligands into the M—S or S—S bonds. It is of great importance to understand the properties of compounds containing isotopes of sulphur at different sites. Such isotope-containing compounds are also useful in the interpretation of vibrational spectra and in the calculations of normal vibrations for obtaining force constants of the M—S and S—S bonds.

EXPERIMENTAL

Syntheses

The compounds with isotopes prepared from metallic molybdenum contain at least 95% of ^{92}Mo or ^{100}Mo isotopes, and those from elemental sulphur contain 99.95% of the ^{34}S isotope. The remaining reagents with natural isotopic abundances were of analytically pure grade.

$^{92}Mo_3S_7Br_4$, $^{100}Mo_3S_7Br_4$ and $Mo_3{}^{34}S_7Br_4$ were synthesized from the elements in evacuated ampoules made of quartz.[4] The experiments, unless otherwise stated, were carried out in air.

Preparation of the $Na_2{}^{34}S_x$ *solution*

$NaBH_4$ (1.00 g) was added to a suspension of 0.70 g of ^{34}S in 20 cm^3 of water and then the solution was boiled for 1 h until dissolution of the sulphur occurred. The solution was cooled, filtered and kept under argon.

Preparation of the $(NH_4)_2S_x$ *solution*

H_2S was passed through a suspension of 15 g of sulphur in 110 cm^3 of a 25% aqueous solution of NH_3 until complete dissolution of sulphur occurred. The solution was then kept under argon.

Preparation of $(NH_4)_2[Mo_3{}^{34}S_{13}]\cdot 2H_2O$

$Mo_3{}^{34}S_7Br_4$ (50 mg) and 5 cm^3 of a solution of $Na_2{}^{34}S_x$ were boiled for 30 min. Then NH_4Br (50 mg) was added and the solution was cooled. The

* Author to whom correspondence should be addressed.

precipitate was washed with water, alcohol, boiling benzene and dried *in vacuo*. Yield: 41 mg.

Similarly $(NH_4)_2Mo_3(\mu_3\text{-}S)(\mu_2\text{-}S^{34}S)_3(^{34}S_2)_3\cdot 2H_2O$ was prepared from $Mo_3S_7Br_4$ and $Na_2{}^{34}S_x$.

Preparation of $(NH_4)_2Mo_3(\mu_3\text{-}^{34}S)(\mu_2\text{-}^{34}SS)_3(S_2)_3\cdot 2H_2O$

$Mo_3{}^{34}S_7Br_4$ (50 mg) and 5 cm^3 of a solution of $(NH_4)_2S_x$ were boiled for 2 h and the resulting precipitate was treated as described above. Yield: 39 mg.

Similarly, $(NH_4)_2[^{92}Mo_3S_{13}]\cdot 2H_2O$ and $(NH_4)_2(^{100}Mo_3S_{13})\cdot 2H_2O$ were obtained from $^{92}Mo_3S_7Br_4$ and $^{100}Mo_3S_7Br_4$.

Physical measurements

The IR spectra were recorded on a IFS-113 Fourier spectrometer (Bruker) in polyethylene. The Raman spectra were obtained with a DFS-24 instrument using excitation by the 632.7 nm line of a He–Ne laser at 77 K.

RESULTS AND DISCUSSION

Syntheses of isotope-containing compounds

Müller and co-workers[5] obtained red crystals of the triangular $(NH_4)_2[Mo_3S_{13}]\cdot 2H_2O$ thio-complex by heating ammonium paramolybdate in an aqueous solution of ammonium polysulphide in air. According to the X-ray diffraction analysis[5] the $[Mo_3S_{13}]^{2-}$ cluster anion contains a μ_3-S(1) ligand, the rest of the sulphur atoms occurring as S_2 ligands: $[Mo_3(\mu_3\text{-}S)(\mu_2\text{-}S_2)_3(S_2)_3]^{2-}$ (see Structure 1). The bridging disulphide ligands of the $[Mo_3S_7]^{4+}$ cluster are arranged so that three sulphur atoms lie in the Mo_3 plane (equatorial S(2) atoms), while the other three point in the direction opposite to μ_3-S(1) (axial S(3) atoms). This complex is very convenient to study differences in the reactivity of S_2 ligands depending on the mode of coordination.

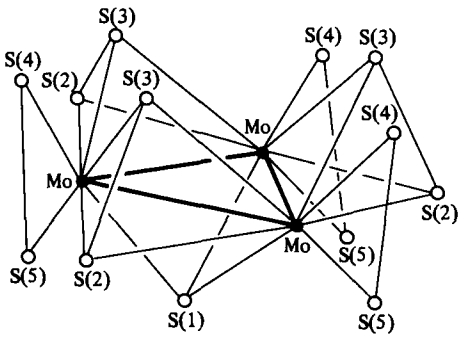

Structure 1.

Earlier, the triangular thio-halide complexes of molybdenum, $Mo_3S_7X_4$ (X = Cl, Br), were shown to react with ammonium polysulphide in water to produce almost quantitatively a triangular thio-complex:[6,7]

$$Mo_3S_7X_4 \xrightarrow{(NH_4)_2S_x+H_2O} (NH_4)_2[Mo_2S_{13}]\cdot 2H_2O. \quad (1)$$
(1)

In the present work this approach has been used to synthesize isotope-containing compounds using the following reactions:

$$^{92}Mo_3S_7Br_4 \xrightarrow{(NH_4)_2S_x+H_2O} [^{92}Mo_3S_{13}]^{2-} \quad (2)$$
(2)

$$^{100}Mo_3S_7Br_4 \xrightarrow{(NH_4)_2S_x+H_2O} [^{100}Mo_3S_{13}]^{2-} \quad (3)$$
(3)

$$Mo_3{}^{34}S_7Br_4 \xrightarrow{Na_2{}^{34}S_x+H_2O} [Mo_3{}^{34}S_{13}]^{2-} \quad (4)$$
(4)

$$Mo_3{}^{34}S_7Br_4 \xrightarrow{(NH_4)_2S_x+H_2O} [Mo_3(\mu_3\text{-}^{34}S)(\mu_2\text{-}^{34}S_aS_e)_3(S_2)_3]^{2-} \quad (5)$$
(5)

$$Mo_3S_7Br_4 \xrightarrow{Na_2{}^{34}S_x+H_2O} [Mo_3(\mu_3\text{-}S)(\mu_2\text{-}S_a{}^{34}S_e)_3(^{34}S_2)_3]^{2-}. \quad (6)$$
(6)

In order to avoid losses of the ^{34}S isotope a solution of $Na_2{}^{34}S_x$ and not $(NH_4)_2{}^{34}S_x$ was prepared by the reaction:

$$x^{34}S + 4NaBH_4 + 7H_2O \longrightarrow Na_2S_x + Na_2B_4O_7 + 15H_2. \quad (7)$$

An aqueous solution of sodium polysulphide reacts with $Mo_3S_7Br_4$ similarly to the $(NH_4)_2S_x$ solution. The sodium salt of $[Mo_3S_{13}]^{2-}$ is readily soluble in water, but solid ammonium salts are obtained in high yield by adding a solution of NH_4Br. Reactions (5) and (6) are the most interesting ones. These reactions produced triangular anionic thio-complexes of molybdenum-containing μ_2-(^{34}S-S) ligands. Due to the use of isotope-containing compounds it was found that the reaction proceeds through elimination–addition of the equatorial sulphur atoms of the μ_2-S_2 ligands according to the following sequence:

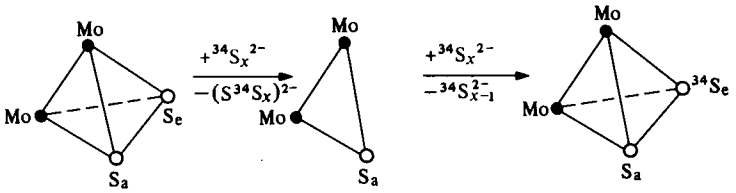

Scheme 1.

Under the influence of the S_x^{2-} nucleophile, elimination of the S_e atom takes place first and then addition of the S_x^{2-} sulphur atoms to the μ_2-S_a ligands occurs. Such types of elimination reactions have been described in the literature. It was observed that the $[Mo_3S_7]^{4+}$ compounds are transformed to the $[Mo_3S_4]^{4+}$ complexes.[8-12] It is interesting to note the following example of mutual transformations of the $[Mo_3S_7]^{4+}$ and $[Mo_3S_4]^{4+}$ complexes:[12]

$$[Mo_3S_4(SCH_2CH_2S)_3]^{2-} \underset{Ph_3P,\,CN^-}{\overset{S_8}{\rightleftharpoons}} [Mo_3S_7(SCH_2CH_2S)_3]^{2-}. \quad (8)$$

In reactions (5) and (6) the ratio $Mo_3S_7Br_4/S_x^{2-}$ is greater than 1/50, and the isotopic substitution in the μ_2-S_2 ligands proceeds in good yield. According to vibrational spectroscopy data the $(NH_4)_2[Mo_3{}^{34}S_{13}]\cdot 2H_2O$ thio-complex was not observed, at 20 or 90°C, to undergo isotopic exchange with the $(NH_4)_2S_x$ solution within 1 h. The thiobromide complex, $Mo_3S_7Br_4$, also did not interact with $Na_2{}^{34}S_x$ at room temperature over 6 h.

Thus, in the reaction of S_x^{2-} with $Mo_3S_7X_4$ the cluster fragment $[Mo_3(\mu_3\text{-}S)(\mu_2\text{-}S)_3]^{4+}$ is retained and two processes occur: (a) nucleophilic substitution of X^- by S_2^{2-} and (b) elimination–addition of sulphur at the axial site of the μ_2-S_2 ligand.

Vibrational spectra

The point group symmetry of the $[Mo_3S_{13}]^{2-}$ molecule is C_{3v}, its vibrational representation has the form:

$$\Gamma = 10A_1(\text{IR, Raman}) + 4A_2 + 14E(\text{IR, Raman}).$$

Calculations of the vibrational spectrum were performed within the approximation of the valence force field using the programs of Gribov and Dementjev.[13] The zero approximation of the diagonal constants has been taken from Kolesov *et al.*[14] Experimental frequencies below 200 cm^{-1} were not included in the calculation because of the strong mixing of external and internal vibrations. The final variant of the force field is shown in Table 1, where only the main bond force constants are listed. The observed vibrational frequencies together with the experimental and calculated isotopic shifts at a given force field are listed in Table 2. The calculated normal vibrations are shown in Table 3 as distributions of the potential energy amongst the groups of equivalent vibrational coordinates. Since Table 3 shows contributions of separate groups of coordinates to the overall vibration and not the shift of atoms in the coordinate space, there is no direct connection between the value of the isotopic shift of the frequencies and their contributions. For the IR and Raman spectra see Müller *et al.*[15]

Table 1. Stretching force constants in the $[Mo_3S_{13}]^{2-}$ complex

Bond	f (mdyn $Å^{-1}$)
Mo—Mo	1.2
Mo—S(1)	1.8
Mo—S(2)	1.5
Mo—S(3)	1.7
Mo—S(4)	1.7
Mo—S(5)	1.5
S(2)—S(3)	2.3
S(4)—S(5)	2.1

The ~ 200 cm^{-1} region mainly contains the Mo—Mo vibrations, but due to the above mentioned strong mixing of internal and external (translations and librations) vibrational frequencies the correct determination of the Mo—Mo force constant is difficult.

The 462 cm^{-1} frequency has medium intensity in both the IR and Raman spectra and is one of the most characteristic bands. This frequency belongs to the μ_3-S(1) vibration and from its shift it is easy to follow the conversion of μ_3-^{32}S to μ_3-^{34}S. The force constant of Mo—μ_3-S(1) bonds exceeds those of the other Mo—S bonds. The vibrations of the Mo—S_{br} [S_{br} = S(2), S(3)] and Mo—S_t [S_t = S(4), S(5)] bonds are not characteristic to such an extent as to permit detection of the corresponding lines in the spectrum, as was the case of Mo—μ_3-S and $(S—S)_{br}$, $(S—S)_t$ vibrations. The data in Table 3 indicate, nevertheless, that the Mo—S_t vibrations occur predominantly at 270–350 cm^{-1}. The force

Table 2. Vibrational frequencies together with the experimental and calculated isotopic shifts for **1–6** complexes

Bands (cm^{-1})		$\Delta\nu$ (cm^{-1})							
		2–3		**1–4**		**1–5**		**1–6**	
Found	Calc.	Found	Calc.	Found	Calc.	Found	Calc.	Found	Calc.
152, Raman		3		3		2		1	
167, Raman, IR		2		3		2		2	
186, Raman, IR	171	3	2	3	3.7	1	0.3	2	3.5
199, Raman, IR		3		5		1		2	
210, IR									
218, IR									
232, Raman, IR		2							
278, Raman, IR	271	1	0	9	8.0	5	2.7	5	5.4
288, Raman, IR	275		0.5	8	7.8	3	2.9	5	5.2
300, Raman	300	2	0.4	8	8.6	4	0.7	3	8.0
334, Raman, IR	334	4	2.7	7	8.2	5	5.0	3	3.3
345, Raman, IR	346	8	6.2	6	5.5	3	1.6	3	3.9
365, Raman, IR	365	8	6.2	5	6.2	3	3.7	1	2.4
389, Raman	388	8	5.5	6	7.1	3	4.9	2	2.1
462, Raman, IR	462	6	4.9	11	10.1	9	8.0	0	2.4
506, IR	506	3	1.0	15	14.3	0	0	15	14.2
515, Raman, IR	513	1	2.6	15	12.9	0	0.7	15	11.8
546, Raman, IR	541		0.3	16	15.8	9	6.7	8	8.7
552, Raman	552	0	1.8	17	14.9	8	6.3	8	8.4

Table 3. Distribution of the potential energy (%) among the groups of equivalent vibrational coordinates

Bands (cm^{-1})	Mo—Mo	Mo—S(1)	Mo—S(2)	Mo—S(3)	Mo—S(4)	Mo—S(5)	S(2)—S(3)	S(4)—S(5)
171, A_1	65	1	0	0	11	20	0	3
271, A_1	0	0	66	10	4	0	19	0
275, E	0	24	3	18	14	39	1	1
300, A_1	1	2	2	2	45	47	0	0
334, A_1	13	15	11	23	13	16	0	9
346, E	1	14	12	12	24	19	3	14
365, E	4	28	21	25	5	13	3	0
388, E	6	0	7	58	5	0	20	3
462, A_1	5	75	1	3	0	2	0	13
506, E	0	0	0	0	10	10	0	80
513, A_1	4	6	0	0	11	13	2	63
541, A_1	0	0	14	8	1	0	76	1
552, E	1	0	21	12	0	0	66	0

constants of the Mo—S_{br} bonds are similar to those of Mo—S_t.

The bridging and the terminal S_2 ligands are six- and two-electron donor ligands, respectively, but this difference in coordination does not affect the S—S bond lengths significantly but, according to our data, there are differences in the force constants, f(S—S)$_t$ and f(S—S)$_{br}$, of the bonds. The 552 and 541 cm^{-1} frequencies are predominantly the valence vibrations of the μ_2-(S—S) ligands; the 513 and 506 cm^{-1} frequencies belong to the terminal S_2. On going from the ^{32}S to ^{34}S compounds these bands undergo shifts which are comparable to the greatest possible for a S_2 molecule. Noteworthy are the sharp differences in the Raman line intensities belonging to the S—S vibrations. Scattering in (S—S)$_t$ bond vibrations is many times weaker than in (S—S)$_{br}$. At the same time the IR absorption at the (S—S)$_t$ frequency is even more intense than that at (S—S)$_{br}$. This may be due to the asymmetry of the charge distribution in the (S—S)$_t$ pair.

It should be noted also that agreement between

the theoretical and experimental spectra for **5** and **6** is better when the exchange is assumed to occur at the equatorial sulphur atoms of the μ_2-S_2 ligands.

The results of the reactions of isotopically-substituted triangular $[Mo_3S_{13}]^{2-}$ with HCl to give the triangular thiochloride complex $[Mo_3S_7Cl_6]^{2-}$ will be the subject of a later communication.

REFERENCES

1. M. Draganjac and T. B. Rauchfuss, *Angew. Chem. Int. Edn Engl.* 1985, **24**, 742.
2. A. Müller, *Polyhedron* 1986, **5**, 323.
3. D. Coucouvanis, A. Hadjikyriacou, M. Draganjac, M. G. Kanadtzidis and O. Ileperuma, *Polyhedron* 1986, **5**, 349.
4. V. Ye. Fedorov, Yu. V. Mironov, O. A. Kuzmina and V. P. Fedin, *Zh. Neorg. Khim.* 1986, **31**, 2476 (in Russian).
5. A. Müller, S. Pohl, M. Dartman, J. P. Cohen, J. M. Bennett and R. M. Kirchner, *Z. Naturf.* 1979, **34B**, 434.
6. A. Müller, E. Diemann, R. Jostes and H. Bögge, *Angew. Chem. Int. Edn Engl.* 1981, **20**, 934.
7. V. P. Fedin, O. A. Gerasko, Yu. V. Mironov and V. Ye. Fedorov, *Zh. Neorg. Khim.* 1988, **33**, 2846 (in Russian).
8. V. Ye. Fedorov, A. V. Mischenko and V. P. Fedin, *Usp. Khim.* 1985, **54**, 649 (in Russian).
9. T. Saito, N. Yamamoto, T. Yamagata and H. Imoto, *Chem. Lett.* 1987, 2025.
10. A. Müller and U. Reinsch, *Angew. Chem. Int. Edn Engl.* 1980, **19**, 72.
11. F. A. Cotton, R. Llusar, D. O. Marler, W. Schwotzer and Z. Dori, *Inorg. Chim. Acta* 1985, **102**, L25.
12. T. R. Halbert, K. McGauley, W.-H. Pan, R. S. Czernuszewicz and E. I. Stiefel, *J. Am. Chem. Soc.* 1984, **106**, 1849.
13. L. A. Gribov and V. A. Dementjev, *Methods and Algorithms of Calculations in the Theory of Vibrational Spectra of Molecules.* Nauka (1981) (in Russian).
14. B. A. Kolesov, V. P. Fedin, O. A. Gerasko and V. Ye. Fedorov, *Koord. Khim.* 1987, **13**, 771 (in Russian).
15. A. Müller, W. Jaegermann and J. H. Enemark, *Coord. Chem. Rev.* 1982, **46**, 245.

Polyhedron Vol. 8, No. 20, pp. 2425–2430, 1989
Printed in Great Britain

0277–5387/89 $3.00+.00
© 1989 Pergamon Press plc

THE CRYSTAL AND MOLECULAR STRUCTURE OF BROMO (η^5-PENTAPHENYLCYCLOPENTADIENYL)DICARBONYLIRON(II), $Fe(C_5Ph_5)(CO)_2Br$

L. D. FIELD, T. W. HAMBLEY, C. M. LINDALL and A. F. MASTERS*

Departments of Inorganic and Organic Chemistry, University of Sydney, NSW 2006, Australia

(*Received* 30 *March* 1989; *accepted* 18 *May* 1989)

Abstract—The preparation and characterization of $Fe(C_5Ph_5)(CO)_2Br$ by single crystal X-ray diffraction [refined to $R = 0.036$, $R_w = 0.039$ with 2974 data having $I \geqslant 2.5\sigma(I)$] are reported. The compound crystallizes from dichloromethane–hexane as discrete molecules in the orthorhombic space group *Pcab*, with $a = 14.503(5)$, $b = 18.015(2)$, $c = 21.873(6)$ Å, $U = 5715(1)$ Å^3 and $Z = 8$. The cyclopentadienyl ring is planar to within 0.01 Å, the Fe—C(C_5 ring) bond distances average 2.125(4) Å, the Fe—(C_5 ring plane) distance is 1.738(5) Å and the Fe—Br bond distance is 2.424(1) Å. Two Fe—C(CO) bond distances of 1.812(5) and 1.786(5) Å were observed. The phenyl substituents are canted relative to the cyclopentadienyl frame at between 49.1 and 142.8°.

Considerable effort has been devoted to the study of ring substituted cyclopentadienyl ligands as a means of conferring additional stability, solubility, different reactivity pathways or altered steric or electronic properties upon organometallic centres. We have been interested in the potential of the pentaphenylcyclopentadienyl ligand as a means of modifying and controlling the steric and electronic environments of transition metal organometallic fragments. In fact, isolated examples of complexes of the $C_5Ph_5^-$ ligand exhibiting structural and electronic differences from their $C_5H_5^-$ and $C_5Me_5^-$ analogues have already been described. Thus, the recent report of parallel C_5 rings in decaphenylstannocene provides a striking example of the steric effect of this ligand.[1] Conversely, the potential of ligand effects on the metal electron distribution is exemplified by the contrast between $Ni(C_5Ph_5)_2$ which is diamagnetic,[2] and $Nicp_2$, which has two unpaired electrons.[3,4]

The pentaphenylcyclopentadienyl anion is an attractive ligand, as its precursors are readily synthesized in large quantities and are air stable. The ligand precursors were first reported in 1925.[5] The $C_5Ph_5^-$ ligand appears to be more electron-withdrawing than the η^5-Cp^- and η^5-$Me_5C_5^-$ anions,[6] and its large volume is reported to confer enhanced kinetic stability to organometallic derivatives.[6] The title complex, $Fe(C_5Ph_5)(CO)_2Br$, was amongst the first reported organometallic derivatives of the ligand.[7] However, surprisingly few complexes of the $C_5Ph_5^-$ anion have been reported, and structural data is scarce,[1,8–10] with only one structure of a transition metal derivative having been reported.

In any assessment of the steric directing properties of the ligand, it is important to obtain benchmark data on a relatively sterically unencumbered system. $Fe(C_5Ph_5)(CO)_2Br$ is readily synthesized, is the only reported $C_5Ph_5^-$ derivative of iron, should seemingly be relatively sterically unencumbered, and although first prepared in 1965, has defied structural characterization. Accordingly, we report here the results of a single crystal X-ray crystallographic study of $Fe(C_5Ph_5)(CO)_2Br$.

RESULTS AND DISCUSSION

The structure of $Fe(L)(CO)_2Br$ consists of discrete molecules, each with a "piano stool" environment about the iron. Final atomic positional coor-

* Author to whom correspondence should be addressed.

Table 1. Selected bond lengths (Å) for $Fe(C_5Ph_5)(CO)_2Br$

Atoms	d (Å)	Atoms	d (Å)
Br(1)—Fe(1)	2.424(1)	C(1)—Fe(1)	1.812(5)
C(2)—Fe(1)	1.786(5)	C(3)—Fe(1)	2.130(4)
C(4)—Fe(1)	2.109(3)	C(5)—Fe(1)	2.090(3)
C(6)—Fe(1)	2.130(3)	C(7)—Fe(1)	2.165(4)
O(1)—C(1)	1.052(6)	O(2)—C(2)	1.097(6)
C(4)—C(3)	1.435(5)	C(7)—C(3)	1.435(5)
C(8)—C(3)	1.490(5)	C(5)—C(4)	1.434(5)
C(14)—C(4)	1.479(5)	C(6)—C(5)	1.451(5)
C(20)—C(5)	1.490(5)	C(7)—C(6)	1.420(5)
C(26)—C(6)	1.491(5)	C(32)—C(7)	1.480(5)

dinates, with estimated standard deviations, bond lengths and angles and anisotropic thermal parameters are deposited.* Selected interatomic bond distances and angles, with standard deviations derived from the refinement, and selected intramolecular non-bonded distances are given in Tables 1–3. The atomic nomenclature is defined in Fig. 1. Figures 1 and 2 illustrate the molecular geometry viewed along, and perpendicular to, the normal to the C_5 plane of the $C_5Ph_5^-$ ligand, respectively.

No intermolecular contacts of significance were observed in the solid, the closest intermolecular non-bonding approach between molecules being 2.69 Å between H(24) on molecule (x, y, z) and O(1) on molecule ($\frac{1}{2}+x$, $-y$, $1\frac{1}{2}-z$). The closest intermolecular non-bonding approaches to iron on molecule (x, y, z) are greater than 4.5 Å. The other close intermolecular contacts to molecule (x, y, z) are given in Table 3.

The iron environment

The iron environment in $cpFeL_2L_2L_3$ ($cp = C_5H_5^-$) derivatives of this type has been described as a distorted tetrahedron derived from an octahedron by the collapse of three facial points.[11] A pseudo-octahedral description of the present compound is consistent with the angles subtended at the iron atom by the bromine atom and the two carbonyl carbon atoms. In these $cpFeL_1L_2L_3$ derivatives, the three angles between Fe, L_1, L_2 and L_3 are generally found to be somewhat greater than 90°. The CO—Fe—CO and Br—Fe—CO angles of the title compound are all relatively acute and probably reflect the strong steric interactions between the pentaphenylcyclopentadienyl anion and the other ligands in the molecule.

The Fe—C(cp) and Fe—(ring centroid) [or Fe—(plane of C_5 ring)] distances of cpFe derivatives have been noted to fall into two groups.[11] Substantially undistorted $Fecp_2$ derivatives have Fe—C(cp) distances of approximately 2.04 Å, and Fe—(ring centroid) distances of between 1.645 and 1.66 Å. These features are exemplified by the structures of ferrocene,[12–15] 1,1,1,1,1-pentamethylferrocene,[16] decamethylferrocene,[17] bis(ferrocenyl)[18] and most clearly by a series of recently published ferrocenophane structures.[19,20] In contrast, cp $FeL_1L_2L_3$ derivatives generally have longer Fe—C (cp) (~2.10 Å) and Fe—(ring centroid) (~1.74 Å) distances which are said to reflect the ability of L_1, L_2 and L_3 to compete for the iron electrons.[11,21] The somewhat shorter Fe—C(cp) and Fe—(ring centroid) distances in the $[cpFe(CO)_3]^+$,[21] $[cpFe(CO)(CNMe)_2]^+$[22] and $[cpFe(CO)_2(CNMe)]^+$[23] cations are thought to reflect the positive charges on these ions.[11]

In the present case, the values of Fe—C(cp) [2.125(4) Å] and Fe—(plane of C_5 ring) [1.738(5) Å] are slightly towards the high end of the range for $cpFeL_1L_2L_3$ derivatives. These are small effects, but are consistent with the $C_5Ph_5^-$ ligand exerting a steric influence.

The distances between the iron and the nearer *ortho*-carbon atoms of the phenyl rings were found to vary between 3.42 and 3.77 Å.

The two Fe—CO distances in the present compound are just mathematically significantly different. The Fe—C(2)O distance is within, but at the long end of, the range observed for $cpFeL_1L_2L_3$ derivatives, whereas the Fe—C(1)O distance is equalled only by that in the $[cpFe(CO)_3]^+$ cation,[21] in which the long Fe—CO and short CO bonds were attributed to the decreased electron density of the cation. The C≡O bonds of the present compound are both extremely short, by comparison with those of $cpFeL_1L_2L_3$ derivatives. The C(1)≡O(1) bond is significantly shorter than the C(2)≡O(2) bond, consistent with the longer Fe—C(1)O bond. An elongation of Fe—CO bonds would be consistent with either steric or electronic influences of the $C_5Ph_5^-$ ligand. However, it is difficult to rationalize the different Fe—CO bond lengths within $Fe(C_5Ph_5)(CO)_2Br$ on electronic grounds. The different Fe—CO distances are probably a consequence of differing steric interactions with nearby phenyl rings. Thus, C(1) (which is involved in the longer Fe—CO bond) has two close contacts with the *ortho*-carbons of the surrounding

* The atomic coordinates and thermal parameters have been submitted as supplementary material for deposition at the Cambridge Crystallographic Data Centre (see Deposition of crystallographic data).

Table 2. Selected bond angles (°) for $Fe(C_5Ph_5)(CO)_2Br$

Atoms	Angle (°)	Atoms	Angle (°)
C(1)—Fe(1)—Br(1)	86.6(1)	C(2)—Fe(1)—Br(1)	86.6(1)
C(2)—Fe(1)—C(1)	89.8(2)	C(3)—Fe(1)—Br(1)	105.9(1)
O(1)—C(1)—Fe(1)	179.3(4)	O(2)—C(2)—Fe(1)	178.8(5)
C(7)—C(3)—C(4)	108.3(3)	C(8)—C(3)—C(4)	127.3(3)
C(8)—C(3)—C(7)	123.4(3)	C(5)—C(4)—C(3)	107.9(3)
C(14)—C(4)—C(3)	125.6(3)	C(14)—C(4)—C(5)	126.4(3)
C(6)—C(5)—C(4)	107.5(3)	C(20)—C(5)—C(4)	127.1(3)
C(20)—C(5)—C(6)	125.3(3)	C(7)—C(6)—C(5)	108.2(3)
C(26)—C(6)—C(5)	126.7(3)	C(26)—C(6)—C(7)	124.1(3)
C(6)—C(7)—C(3)	108.0(3)	C(32)—C(7)—C(3)	126.4(3)
C(32)—C(7)—C(6)	125.3(3)	C(9)—C(8)—C(3)	122.1(3)
C(13)—C(8)—C(3)	117.8(3)	C(15)—C(14)—C(4)	122.1(3)
C(19)—C(14)—C(4)	120.3(3)	C(21)—C(20)—C(5)	122.6(3)
C(25)—C(20)—C(5)	119.0(3)	C(27)—C(26)—C(6)	117.1(3)
C(31)—C(26)—C(6)	124.2(4)	C(33)—C(32)—C(7)	121.4(3)
C(37)—C(32)—C(7)	119.4(3)		

phenyl rings [3.33 Å to C(31), and 3.29 Å to C(21)], whereas C(2) (which is involved in the shorter Fe—CO bond) has only one such close contact [3.12 Å to C(15)]. The corresponding C(CO) to phenyl-H contacts are less than the sum of the van der Waals' radii (Table 3).

The pentaphenylcyclopentadienyl ligand

The C_5 nucleus of this ligand is planar to within 0.01 Å. All of the C—C bond lengths of the C_5 nucleus are equal within experimental error, but that bisected by the projection of the Fe—C(1)≡O bond is apparently slightly elongated. A similar effect has been noted in the molecular structure of $(C_5Ph_5)_2Co(CO)_2$, but was also beyond mathematical significance.[8] The average C—C bond length within the C_5 ring of 1.435(5) Å is greater than those in the C_5H_5 rings of ferrocene (1.389 Å)[13] and $Fe(cp)(C_5Me_5)$ (1.399(6) Å),[16] but close to those in $cpFeL_1L_2L_3$ derivatives, in the C_5Me_5 rings of $Fe(cp)(C_5Me_5)$ (1.408(6) Å)[16] and $Fe(C_5Me_5)_2$ (1.419(2) Å)[17] and in $(C_5Ph_5)_2Co(CO)_2$ (1.44(1) Å).[8] The bond angles within the C_5 ring are equal within experimental error and are normal for the C_5 rings of cyclopentadienyl and substituted cyclopentadienyl derivatives. The iron atom is displaced slightly from the projection of the centroid of the pentaphenylcyclopentadienyl ring. The *ipso*-carbon atoms of each of the phenyl rings are located above the C_5 plane by from 0.05 to 0.23 Å, with the average distance being 0.15 Å. This configuration is similar to that in $(C_5Ph_5)Co(CO)_2$.[8] Similarly, the methyl groups of $Fe(C_5Me_5)(cp)$[16] and of $Fe(C_5Me_5)_2$[17] lie above the C_5 ring plane, away from the iron. In contrast, the C_5H_5 hydrogens of $Fe(cp)_2$[12-15] and $Fe(C_5Me_5)(cp)$[16] are displaced slightly towards the iron. The phenyl rings are all also planar with normal dimensions, and are oriented at between 49.09 and 142.84° to the cyclopentadienyl C_5 frame. The phenyl ring defined by C(26) is almost perpendicular to the C_5 ring. The average deviation of the phenyl rings from coplanarity with the C_5 ring is 58.7°, which is similar to that in $(C_5Ph_5)Co(CO)_2$ (55.8°).[8] Clearly, extensive charge delocalization onto all the phenyl rings is unlikely.

Table 3. Selected non-bonded approaches (Å) to $Fe(C_5Ph_5)(CO)_2Br$ at (x, y, z)

Atoms	d (Å)	Atoms	d (Å)
C(1)···H(31)^{i}	2.66	C(1)···H(21)^{i}	2.98
C(2)···H(15)^{i}	2.71	H(24)···O(1)^{ii}	2.69
H(27)···Br(1)^{iii}	3.15		

The superscripts refer to the following transformations: i (x, y, z); ii ($\frac{1}{2}+x$, $-y$, $1\frac{1}{2}-z$); iii ($\frac{1}{2}+x$, $\frac{1}{2}-y$, z).

The pentaphenylcyclopentadienyl ring of $(C_5Ph_5)Ru(CO)_2Br$ is reported to have C—C bond distances of 1.241(8), 1.454(9), 1.266(8), 1.326(8) and 1.426(9) Å, and CCC angles of 106.9, 113.6, 110.8, 115.1 and 103.5°.[10] These values differ significantly from those of the present study.

Thus, the gross effects of the pentaphenyl-

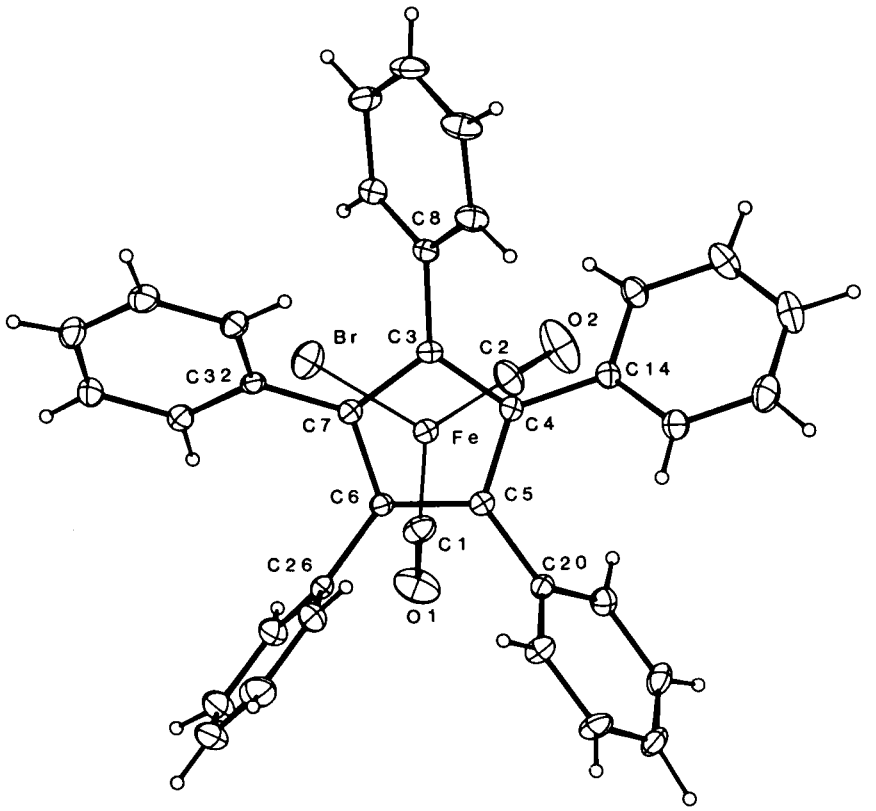

Fig. 1. ORTEP (50% probability) illustration of the molecular structure of $Fe(C_5Ph_5)(CO)_2Br$ showing the atom numbering. Viewed along the normal to the C_5Ph_5 plane.

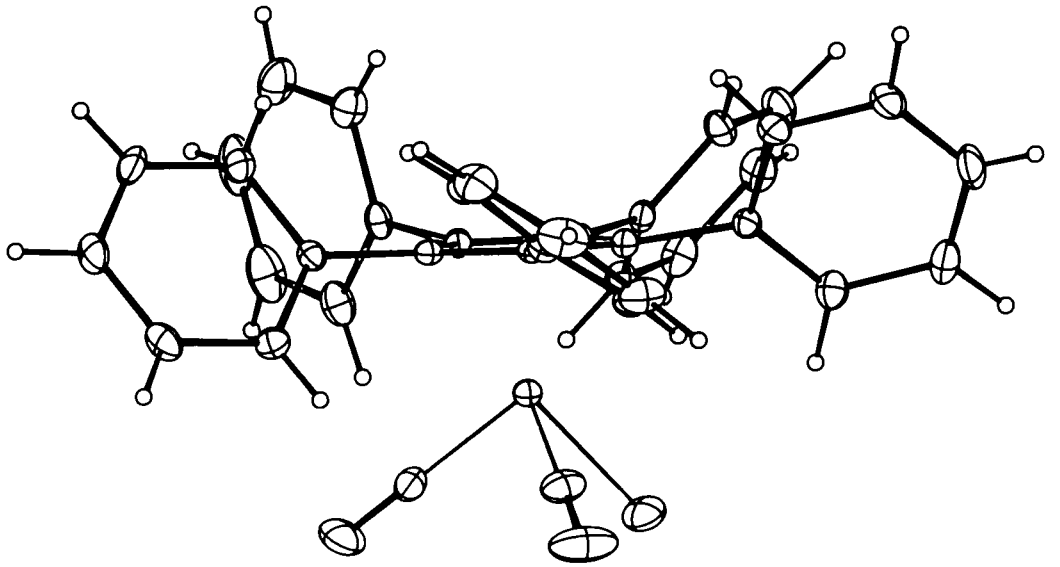

Fig. 2. ORTEP (50% probability) illustration of the molecular structure of $Fe(C_5Ph_5)(CO)_2Br$ viewed perpendicular to the normal to the C_5Ph_5 plane.

cyclopentadienyl ligand in $Fe(C_5Ph_5)(CO)_2Br$ are consistent with those of $cpFeL_1L_2L_3$ compounds. No electronic effect of the ligand on the structure can be detected. However, the ligand can be seen to exert significant steric pressures, even on the relatively sterically undemanding $Fe(CO)_2Br$ fragment.

EXPERIMENTAL

All synthetic manipulations were carried out under an inert atmosphere (nitrogen or argon). Benzene and *n*-hexane were distilled from sodium wire. Dichloromethane was distilled from phosphorus pentoxide. Pentacarbonyliron (Aldrich) was used as received. Pentaphenyl-2,4-cyclopentadienylbromide, C_5Ph_5Br, was prepared from tetracyclone.[6]

Preparation of bromo(η^5-pentaphenylcyclopentadienyl)dicarbonyliron(II)

Freshly distilled benzene (75 cm^3) was added to degassed pentaphenyl-2,4-cyclopentadienylbromide (1.0 g, 1.91 mmol) to give an orange solution. Iron pentacarbonyl (0.45 g, 2.28 mmol) was added via syringe. The solution immediately became red, and was left to stir for 24 h at room temperature. The solvent was removed and the product extracted into dichloromethane (30 cm^3). *n*-Hexane (15 cm^3) was added to precipitate unreacted pentaphenyl-2,4-cyclopentadienylbromide. The suspension was filtered and the solid washed with *n*-hexane (10 cm^3). The filtrate and *n*-hexane washings were allowed to stand overnight to yield dark red–purple crystals (0.45 g, 37%).

Structure determination

Cell constants were determined by a least-squares fit to the setting parameters of 25 independent reflections. Data were measured on an Enraf–Nonius CAD4-F diffractometer within the limit $2\theta_{max.} = 50°$, with Mo-K_α radiation, $\lambda = 0.71069$ Å, graphite monochromator, and operating in the ω–1.33θ mode. Data were reduced and Lorentz, polarization and decomposition corrections were applied using a local data reduction program. The structure was solved by Patterson and Fourier synthesis techniques, and was refined by full-matrix least-squares analysis with SHELX-76.[24] All non-hydrogen atoms were refined anisotropically. Hydrogen atom positions were refined with isotropic thermal parameters. Scattering factors and anomalous dispersion corrections for iron were taken from the *International Tables for X-ray Crystallography*,[25] and for all others the values supplied in SHELX-76 were used. Absorption correction was by numerical integration.[26] Listings of atom coordinates, anisotropic thermal parameters, details of least-squares planes calculations and observed and calculated structure factor amplitudes have been deposited. Figures were drawn using the program ORTEP.[27]

Crystal data

$C_{37}H_{25}BrFeO_2$, $M = 637.4$, orthorhombic, space group, *Pcab*, $a = 14.503(5)$, $b = 18.015(2)$, $c = 21.873(6)$ Å, $U = 5715(1)$ Å^3, D_c ($Z = 8$) = 1.481 g cm^{-3}, $F(000) = 2592$, μ(Mo-K_α) = 19.02 cm^{-1}. Specimen: dark red brown prisms, $0.25 \times 0.20 \times 0.28$ mm. $N = 5739$, $N_0 = 2974$, range of *hkl* $0 \rightarrow 17$, $0 \rightarrow 21$, $0 \rightarrow 26$, merging $R = 0.01$, $R = 0.036$, $R_w = 0.039$, residual extrema ± 0.4 e Å^{-3}.

Acknowledgements—We thank the Australian Research Grants Commission for financial support; Mrs A. G. Webb for the sample of C_5Ph_5Br, and Ms K. M. Ho for helpful discussions.

REFERENCES

1. M. J. Heeg, C. Janiak and J. J. Zuckerman, *J. Am. Chem. Soc.* 1984, **106**, 4259.
2. A. Schott, H. Schott, G. Wilke, J. Brandt, H. Hoberg and E. G. Hoffman, *Liebs Annls Chem.* 1972, 508.
3. K. W. Barnett, *J. Organomet. Chem.* 1974, **78**, 139.
4. G. Wilkinson, P. L. Pauson and F. A. Cotton, *J. Am. Chem. Soc.* 1954, **76**, 1970.
5. K. Ziegler and B. Schnell, *Justus Liebs Annls Chem.* 1925, **445**, 266.
6. K. Broadley, G. A. Lane, N. G. Connelly and W. E. Geiger, *J. Am. Chem. Soc.* 1983, **105**, 2486.
7. S. McVey and P. L. Pauson, *J. Chem. Soc.* 1965, 4312.
8. J. W. Chambers, A. J. Basker, S. G. Bott, J. L. Atwood and M. D. Rausch, *Organometallics* 1986, **5**, 1635.
9. J. Powell and N. I. Dowling, *Organometallics* 1983, **2**, 1742.
10. M. Matusz, Thesis, Southern Illinois University (1984).
11. G. M. Reisner, I. Bernal, H. Brunner and M. Muschiol, *Inorg. Chem.* 1978, **17**, 783.
12. J. D. Dunitz, L. E. Orgel and A. Rich, *Acta Cryst.* 1956, **9**, 373.
13. P. Seiler and J. D. Dunitz, *Acta Cryst.* 1979, **B35**, 1068.
14. P. Seiler and J. D. Dunitz, *Acta Cryst.* 1979, **B35**, 2020.
15. F. Takusagawa and T. F. Koetzle, *Acta Cryst.* 1979, **B35**, 1074.
16. M. McPartlin and K. Henrick, personal communication reported in L. Phillips, A. R. Lacey and

M. J. Cooper, *J. Chem. Soc., Dalton Trans.* 1988, 1383.
17. D. P. Freyberg, J. L. Robbins, K. N. Raymond and J. C. Smart, *J. Am. Chem. Soc.* 1979, **101**, 892.
18. A. C. MacDonald and J. Trotter, *Acta Cryst.* 1964, **17**, 872.
19. I. Bernal, E. Raabe, G. M. Reisner, R. A. Bartsch, R. A. Holwerda, B. P. Czech and Z. Huang, *Organometallics* 1988, **7**, 247.
20. I. Bernal, G. M. Reisner, R. A. Bartsch, R. A. Holwerda and B. P. Czech, *Organometallics* 1988, **7**, 253.
21. M. E. Gress and R. A. Jacobson, *Inorg. Chem.* 1973, **10**, 1746.
22. A. R. Manning, R. Kumar, S. Willis and F. S. Stephens, *Inorg. Chim. Acta* 1982, **61**, 141.
23. B. Callan, A. R. Manning and F. S. Stephens, *J. Organomet. Chem.* 1987, **331**, 357.
24. G. M. Sheldrick, SHELX-76, A Program for X-Ray Crystal Structure Determination. University of Cambridge, U.K. (1976).
25. *International Tables for X-ray Crystallography*, Vol. IV. Kynoch Press, Birmingham, U.K. (1974).
26. P. Coppens, L. Leiserowitz and D. Rabinovich, *Acta Cryst.* 1965, **18**, 1035.
27. C. K. Johnson, ORTEP, A Thermal Ellipsoid Plotting Program. Oak Ridge National Laboratories, Oak Ridge, Tennessee (1965).

Polyhedron Vol. 8, No. 20, pp. 2431–2437, 1989
Printed in Great Britain

0277-5387/89 $3.00+.00
© 1989 Pergamon Press plc

A NEW DEFINITION OF COORDINATION NUMBER AND ITS USE IN LANTHANIDE AND ACTINIDE COORDINATION AND ORGANOMETALLIC CHEMISTRY*

JOAQUIM MARÇALO† and ANTÓNIO PIRES DE MATOS

Departamento de Química, ICEN, LNETI, P-2686 Sacavém Codex, Portugal

(*Received* 13 *January* 1989; *accepted* 18 *May* 1989)

Abstract—A *steric coordination number* of a ligand is defined, based on the solid angle comprising the van der Waals' spheres of the atoms of that ligand, as an alternative to the *formal coordination number* in discussing structural aspects of lanthanide and actinide coordination and organometallic compounds. The study of the bond lengths in 274 structurally characterized compounds of the lanthanides (including Sc and Y), in oxidation states II and III, and the actinides (Th and U), in oxidation states III and IV, was the basis to derive *ligand effective radii* which are discussed in relation to bonding, coordination geometries, metal ionic radii and oxidation states. Potential uses of the new definition of coordination number and of the ligand effective radii obtained in molecular structure comparison and bond length prediction are also discussed.

COORDINATION NUMBER—THE VARIOUS DEFINITIONS

Werner's "secondary valence" introduced one of the most important concepts of coordination chemistry, that of *coordination number* (CN), later defined as the number of donor atoms associated with the central atom in a compound.[1]

In crystal chemistry the CN has been equally important and usually identified with the number of "nearest-neighbours" of a given central atom in a crystal. Rigorous definitions of CN in this field have been proposed by several authors to overcome the uncertainty in choosing the appropriate number of "nearest-neighbours".[2]

With the advent of *d*-transition metal organometallic chemistry, a new definition emerged to account for a whole new class of ligands and to be consistent with the 18-electron rule: this is the *formal coordination number* (CN_F)—the number of electron pairs involved in ligand-to-metal coordination.[3]

In *f*-transition element compounds bonding is generally considered highly ionic in character and a unifying principle such as the 18-electron rule is lacking. The number, size and shape of the ligands are then major factors determining the structural features of lanthanide (Ln) and actinide (An) compounds, and a definition of CN based on geometrical principles appears to be more adequate than the CN_F.

A NEW DEFINITION OF COORDINATION NUMBER

Here we define the *steric coordination number* (CN_S) of a ligand in a series of compounds, as the ratio of the solid angle comprising the van der Waals' spheres of the atoms of that ligand and the solid angle of a common ligand like chlorine, when placed at typical mean distances from the central metal atom.

With this definition we can build up a catalogue of ligand's CN_S and use them to obtain the CN_S of a compound. In Table 1 we can find the CN_S's of selected ligands, with solid angles computed either analytically or numerically‡ using Bondi's van der

* Presented in part at the XXVI International Conference on Coordination Chemistry, Porto, Portugal, 28 August–2 September 1988.

† Author to whom correspondence should be addressed.

‡ The solid angles considered in this work are the "real" geometrical solid angles which correspond to the areas defined on a unit sphere centred on the metal atom by the cones comprising the van der Waals spheres of the atoms of a ligand. The areas, which have different shapes according to the ligand, can be straightforwardly calculated either by numerical integration (using a simple BASIC program developed by J. P. Leal of our Department) or analytically, by partitioning the surfaces in spherical segments and spherical triangles whose areas can be easily calculated.

Waals' radii,[4] average metal–ligand distances (for Ln and An) and typical geometries of the ligands. The main sources of error in the values of Table 1 are, on one hand, the van der Waals' radii, which having been derived from intermolecular contacts may not be adequate for intramolecular contacts, and, more importantly, the geometries of the ligands which, in the individual structures may present different bendings, tiltings, etc.

The CN_S value defined here is related to other solid angle-based ligand steric parameters, like Tolman's cone angles,[5] extensively used in *d*-transi-

Table 1. Steric coordination numbers (CN_S) of selected ligands

Ligating atom	Ligand	CN_S	Ligating atom	Ligand	CN_S
	H^-	0.80		TPP^{2-}	4.68
	F, Cl, Br, I^-	1.00		OEP^{2-}	4.30
	BH_3R^- (t)	1.42		$HBPz_3^-$	2.90
	(b)	1.24		$HB(3,5\text{-}Me_2Pz)_3^-$	3.55
	(bb)	1.06		$H_2BPz_2^-$	1.92
				Pz^-	1.54
C	CCR^-	1.24		NEt_2^-	1.67
	$CHCH_2^-$	1.22		NPh_2^-	1.79
	Ph^-	1.26	N	$N(SiMe_3)_2^-$	2.17
	Ph-2,6-Me_2^-	2.01		NCS^-	0.90
	CH_2Ph^- (90°)	1.72		NCR	0.79
	(110°)	1.39		PzH	0.89
	(130°)	1.25		py	1.19
	Me^-	1.06		bipy	1.74
	$^tBu^-$	1.50		$N(CH_2CH_2)_3CH$	1.38
	$^nBu^-$	1.18		NH_3	0.79
	$CH_2SiMe_3^-/CH_2CMe_3^-$	1.42		TMED	2.22
	$CH(SiMe_3)_2^-$	2.24			
	$Allyl^-$	1.81			
	CNR	0.98		O-$^tBu^-$	1.40
	COT^{2-}	3.44		OPh^-	1.28
	COT-1,3,5,7-Me_4^{2-}	3.53		OPh-2,6-Me_2^-	1.59
	COT-1,3,5,7-Ph_4^{2-}	3.72		OPh-2,6-$^iPr_2^-$	1.70
	COT-$(CH_2)_2^{2-}$	3.46		OPh-2,6-$^tBu_2^-$	2.41
	COT-$(CH_2)_3^{2-}$	3.47		$acac^-/dpm^-$	1.95
	COT-$(CH)_4^{2-}$	3.49		OH_2	0.84
	Cp^-	2.04		THF/OMe_2	1.21
	$MeCp^-$	2.14		OEt_2	1.44
	$C_5Me_5^-$	2.49		DME	1.78
	$C_5H_4SiMe_3^-$	2.34		TPPO	1.42
	$C_5H_3\text{-}1,3\text{-}(SiMe_3)_2^-$	2.60	O	HMPA	1.51
	Ind^-	2.28		TPPA	1.48
	Ind-1,4,7-Me_3^-	2.50		DMPA	1.26
				DMIBA/DMPVA	1.34
				DEPA	1.31
S	S-$^nPr^-$	1.22		DIPA	1.28
	SPh^-	1.33		DIPPA	1.37
	THT	1.18		DIPIBA	1.45
	BTME	1.85		DMF	1.15
				DMSO	1.14
				DPSO	1.25
P	PPh_2^-	1.45		TEU	1.24
	PMe_3	1.06		TMU	1.18
	$P(OCH_2)_3CEt$	0.93			
	DMPE	2.01			

t—tridentate, b—bidentate, bb—bridging bidentate.

tion metal phosphine chemistry, in the original or modified versions,[6] or Bagnall and Li Xing-fu's solid angle factors,[7] used with some success in discussing stability, stereochemistry and reactivity of Ln and An compounds. Other solid angle approaches to steric effects were made by several authors and include organic reactivity,[8] the stereochemistry of Sn[9] and Th[10] complexes, stability of transition element compounds[11] and cluster chemistry.[12]

THE STERIC COORDINATION NUMBER AND *f*-TRANSITION ELEMENT CHEMISTRY

Ligand effective radii—CN_F *versus* CN_S

In this paper we are interested in using our definition of CN to discuss and extend Raymond's structural model for the bonding in organolanthanide and -actinide compounds.[13] In his approach, based on the CN_F, Raymond obtained linear correlations between different metal–ligand distances (namely Cp^-, COT^{2-} and $N(SiMe_3)_2^-$) and ionic radii for the metal ions taken from the widely used Shannon's table of ionic radii,[14] concluding that an ionic model was adequate to describe the bonding in *f*-transition element compounds.

The same approach was later used by Edelstein to study metal borohydride complexes[15] although, in this case, some doubts could arise regarding the CN_F values adopted for bidentate and tridentate BH_4^-.

Several other authors have used Raymond's approach, namely Deacon *et al.* in discussing the structures of Ln complexes containing oxygen- or nitrogen-donor ligands.[17]

Since the publication of Raymond's paper, *f*-transition element chemistry has grown impressively from about four dozen structurally characterized Ln and An organo compounds to a few hundred structures on which the same type of analysis can be performed.

In the following discussion we considered 274 structurally characterized Ln (including Sc and Y) and An (Th and U) coordination and organometallic compounds. The analysis is by no means exhaustive: uranyl compounds were not included, oligomeric or polymeric compounds were not considered except those involving bridging borohydride ligands, and compounds containing less-common ligands were also excluded. This left us with 16 Ln^{II}, 99 Ln^{III}, 15 An^{III} and 144 An^{IV} compounds, covering a wide range of coordination geometries.

In spite of the large number of complexes studied, there was a special incidence of U compounds (46%) and a good span of ionic radii was not obtained, so, in most of the cases, good linear relationships of metal–ligand distances vs metal ionic radius could not be observed. Nevertheless, better correlations were obtained when using the ionic radii derived from the CN_S. This led us to focus our discussion on *ligand effective radii* (R_{EF}), checking on the constancy and consistency of the values produced using CN_F and CN_S.

The ligand effective radii are presented in Table 2 and were calculated in the following way:

(a) Determination of CN_F and CN_S (from Table 1) for a given complex.

(b) Direct interpolation or extrapolation of metal ionic radii (R_i) from Shannon's table[14] (or David's table[18] for Th^{III} and U^{III} in CN 8) for the CN's determined in (a) (Shannon's ionic radii, in the range of CN 6–9, that include the great majority of CN_F and CN_S of the compounds considered in this study, can be fitted with linear equations, for each metal and oxidation state, with correlation coefficients better than 0.99; Pauling's equation for the dependence of ionic radii on CN used by Raymond[13] gives values that are not consistent with Shannon's values; some of the correlations of metal–ligand distances and ionic radii in Raymond's paper might have been affected by using this procedure).

(c) When two or more identical ligands are coordinated, an average metal–ligand bond length d_{M-L} is obtained from the molecular structure of the compound.

(d) Calculation of $R_{EF} = d_{M-L} - R_i$ for each complex and each CN used (formal or steric).

(e) Determination of the arithmetic mean of R_{EF} for each type of ligand; the values in parentheses are the sample standard deviations.*

From the values in Table 2 it is clear that for most of the ligands considered the R_{EF}'s obtained using the CN_F have larger standard deviations, indicating a wider spread of the individual R_{EF}'s. For instance, for L = alkyl, $(R_{EF})_F$ range from 1.34 Å in $UCp_3(^nBu)$[19] to 1.63 Å in $YbCl[CH(SiMe_3)_2]_3^-$,[20] while $(R_{EF})_S$ for the same complexes are 1.46 and 1.41 Å, respectively; another example is NPh_2^- for which $(R_{EF})_F$ is 1.50 Å in $U(NPh_2)_4$[21] and 1.20 Å in $UCp_3(NPh_2)$,[22] while $(R_{EF})_S$ are 1.32 and 1.30 Å,

* A more rigorous determination of the mean R_{EF}'s could be made considering all independent bond lengths in the different structures weighted by the corresponding standard deviations, so that the more accurately determined bond lengths have a larger weight. However, for the general purpose of this work, the simpler procedure followed above is quite reasonable.

Table 2. Ligand effective radii (R_{EF}) (Å)

Ligating atom	Ligand type	$(R_{EF})_F$	$(R_{EF})_s$	N	O.S.
	Borohydride (t)	1.33(8)	1.56(3)	28	H
		1.21(8)	1.49(4)	2	L
	(b)	1.56(6)	1.75(3)	5	H
		1.42	1.67	1	L
	(bb)	1.65(5)	1.91(3)	8	H
C	Alkyl	1.45(8)	1.47(4)	19	H
		1.27	1.44	1	L
	Aryl	1.46(17)	1.45(2)	4	H
	Benzyl	1.54(10)	1.54(3)	6	H
	Alkenyl	1.35	1.42	1	H
	Alkynyl	1.26(2)	1.38(2)	2	H
	Allyl	1.67(2)	1.71(1)	2	H
	Cyclopentadienyl	1.66(7)	1.74(4)	103	H
		1.56(4)	1.66(3)	23	L
	Cyclooctatetraene	1.56(4)	1.70(1)	9	H
		1.49(1)	1.62(7)	2	L
	Isocyanide	1.63(33)	1.59(1)	2	H
		1.28	1.41	1	L
N	Dialkylamide	1.39	1.12	1	H
	Disilylamide	1.43(7)	1.27(2)	9	H
		1.38(4)	1.26(4)	3	L
	Diarylamide	1.35(21)	1.31(1)	2	H
	Thiocyanate	1.43(6)	1.42(4)	17	H
	Pyrazolide	1.28(3)	1.39(1)	3	H
	Polypyrazolylborate (t)	1.53(4)	1.53(3)	11	H
	(b)	1.46(4)	1.47(4)	2	H
	Porphyrinate	1.47(2)	1.43(2)	4	H
	Nitrile	1.48(6)	1.60(5)	14	H
	Pyridine	1.49(9)	1.58(4)	8	H
		1.41(5)	1.50(2)	3	L
	Bipyridyl	1.58	1.63	1	H
	Amine	1.54	1.67	1	H
		1.47	1.62	1	L
	TMED	1.66(19)	1.76(1)	2	H
	NH_3	1.44	1.50	1	H
		1.41	1.47	1	L
O	Aryloxide	1.22(11)	1.09(4)	13	H
	Alkoxide	1.03	1.02	1	H
	β-Diketonate	1.31(4)	1.32(4)	21	H
	Phosphine oxide	1.33(7)	1.28(4)	20	H
		1.10	1.24	1	L
	Carbamide	1.34(3)	1.31(3)	18	H
	Sulphoxide	1.37(6)	1.32(6)	2	H
	Water	1.38(4)	1.43(2)	11	H
	Ether	1.37(12)	1.45(6)	37	H
		1.35(9)	1.39(3)	7	L
	DME	1.52(26)	1.60(1)	2	H
		1.39(12)	1.42(6)	3	L
F	Fluoride	1.02	1.16	1	H

Table 2—*continued*

Ligating atom	Ligand type	$(R_{EF})_F$	$(R_{EF})_s$	N	O.S.
P	Diarylphosphide	1.82	1.83	1	H
	Phosphine/Phosphite	1.87(7)	1.99(2)	3	H
		1.69(1)	1.86(2)	2	L
	DMPE	2.04(14)	2.07(4)	7	H
		1.84(22)	1.96(3)	4	L
S	Alkylthiolate	1.67	1.70	1	H
	Arylthiolate	1.69	1.74	1	H
	BTME	1.83	2.10	1	H
	Thioether	1.70	1.85	1	L
Cl	Chloride	1.65(7)	1.65(4)	60	H
		1.51	1.56	1	L
Br	Bromide	1.81(8)	1.82(4)	14	H
I	Iodide	2.03(7)	2.05(5)	7	H

N—number of compounds. O.S. H—Ln^{III} and An^{IV}, O.S. L—Ln^{II} and An^{III}. t—tridentate, b—bidentate, bb—bridging bidentate.

respectively, in the same compounds. Other significant examples could be given, indicating the difficulties of the formal CN approach for dealing with sterically demanding ligands, especially those that formally donate one electron pair [e.g. $N(SiMe_3)_2^-$, NPh_2^-, OPh-2,6-$^tBu_2^-$, $CH(SiMe_3)_2^-$].

Another aspect which is apparent from Table 2 is that the R_{EF} values derived from the CN_S have a relative ordering which is in closer agreement with what is expected from the sizes and bonding capabilities of the different coordinating atoms (e.g. $(R_{EF})_F$ for C in alkyls is 1.45 Å, while for N in disilylamide it is 1.43 Å, when one would expect a larger difference which is retained by the corresponding $(R_{EF})_s$ values, 1.47 and 1.27 Å).

Ligand effective radii—trends in $(R_{EF})_s$

After showing some of the advantages of our definition of CN we will focus our attention now on $(R_{EF})_s$ and on some qualitative aspects that became apparent after studying such a large volume of structural data.

The first aspect is that two sets of $(R_{EF})_s$ had to be calculated for each type of ligand, one for Ln^{III} and An^{IV} compounds and another one for Ln^{II} and An^{III} compounds. In fact, it was verified that R_{EF}'s obtained from this last group of compounds were systematically lower than the corresponding R_{EF}'s obtained from Ln^{III} and An^{IV} compounds. The reason for this can probably be found from Shannon's ionic radii[14] which, having been derived from oxides and halides, were initially thought to be applicable to any kind of compound. This was later shown to be wrong and revised sets of ionic radii were reported for sulphides by Shannon[23] and for nitrides by Baur.[24] When comparing Shannon's oxide and sulphide sets, significant differences exist for the Ln and An ions, especially for U^{III}; $R_i(6) = 1.025$ Å from oxides, $R_i(7) = 0.99$ Å and $R_i(8) = 1.07$ Å from sulphides.

Other pertinent data concerning the size of the U^{III} ion result from the bond distances in structurally analogous compounds of U^{III} and Ln^{III}, for instance $MCp_3(THF)$,[25] which would place U^{III} between Nd^{III} and Pr^{III} ($d_{U-C} = 2.79$, $d_{U-O} = 2.55$Å; $d_{Pr-O} = 2.80$, $d_{Pr-O} = 2.56$ and $d_{Nd-C} = 2.78$, $d_{Nd-O} = 2.54$ Å), while Shannon's oxide table gives a U^{III} radius close to that of La^{III}) ($R_i(6) = 1.032$ Å), and larger than the radii of Nd^{III} ($R_i(6) = 0.983$ Å) and Pr^{III} ($R_i(6) = 0.99$ Å).

The differences between R_{EF} of compounds in higher and lower oxidation states might as well be attributed to covalency effects. Although these differences between $(R_{EF})_s$ are fairly constant for most of the ligand types in Table 2, significantly larger differences are seen for π-accepting ligands (isocyanide or phosphine). Incidentally, Andersen and co-workers have recently found evidence, based on structural data of isoleptic Ce^{III} and U^{III}

organometallic compounds, for the existence of π-back donation in the U^{III} compounds containing isocyanide and phosphine or phosphite.[25]

Another aspect is the sensitivity of the $(R_{EF})_s$ values to the coordination geometry and to the relative repulsivities of the different positions in coordination polyhedra like the trigonal and pentagonal bipyramids (TBP and PBP), the capped octahedron (CO), the dodecahedron (DD) and the tricapped trigonal prism (TCTP).[26] As examples, we can refer to two U compounds, prepared in our laboratories, displaying CO geometries, where $(R_{EF})_s$ for the oxygen atoms of the capping THF ligands are substantially larger than the mean value for that ligand in Table 2 (1.56 Å in $UCl_3[HB(3,5\text{-}Me_2Pz)_3](THF)$[27] and 1.60 Å in $UCl(OPh)_2[HB(3,5\text{-}Me_2Pz)_3](THF)$.[28] The same happens in two closely related U compounds with PBP geometries, where $(R_{EF})_s$ for the O atoms of the TPPO ligands in equatorial positions are larger than the mean value in Table 2 (1.36 Å in $UCl_2(acac)_2(TPPO)$ and 1.38 Å in $UCpCl(acac)_2(TPPO)$[29]).

This sensitivity to the position on the coordination polyhedron is more evident for neutral ligands and is reflected in the larger standard deviations of the corresponding $(R_{EF})_s$, when compared with the standard deviations of anionic ligands (e.g. ether and nitrile values in Table 2).

The different behaviour of neutral and anionic ligands are not surprising as larger repulsions would be expected between anionic ligands which would then preferentially occupy the coordination positions with smaller repulsitivities. This also has implications on the metal–ligand distances in charged complexes and is more evident from some of the $(R_{EF})_s$ in anionic complexes. For example, in $Er(NCS)_6^{3-}$,[30] $(R_{EF})_s$ is 1.49 Å, significantly larger than the mean values for NCS^- in Table 2; the same happens in UCl_6^{2-} where, for the more accurate structural determination of this species,[31] $(R_{EF})_s$ is 1.73 Å, again substantially larger than the mean value for Cl in Table 2.

APPLICATIONS OF CN_S AND $(R_{EF})_s$

The two main uses for the quantities presented in Tables 1 and 2 are molecular structure comparison and bond length prediction.

In the first application, the $(R_{EF})_s$ in Table 2 may serve as references in discussing a new structure, by comparison with the $(R_{EF})_s$ determined, as described before, for each ligand in the new complex. This enables us to see if we are in the presence of a "well-behaved" compound or if there are any unusual bond lengths and, in a certain way, try to explain its origin, for instance, in coordination geometry, covalency effects, intra- or intermolecular contacts or uncertainties in the structural determination.

The second application is obvious and, of course, dependent on the uncertainties of the values in Tables 1 and 2. The procedure is simple:

(a) Determination of the CN_S of the complex in question from the values in Table 1.

(b) Determination of the metal ionic radius by interpolation or extrapolation from Shannon's table.[14]

(c) Determination of metal–ligand distance by adding the appropriate $(R_{EF})_s$ value from Table 2 to the value obtained in (b).

(d) Introduction of corrections accounting for relative repulsivities in the expected coordination polyhedron (from ref. 26).

CONCLUDING REMARKS

The CN_S introduced above was shown to account for the general structural features of Ln and An compounds. The influence of steric effects on the bond lengths of a particular compound is, of course, more subtle, requiring a detailed analysis of the available structural data. Such a study is being undertaken, as well as extensions of the model to include uranyl complexes, new ligands and oligomeric compounds.

Acknowledgements—The authors are grateful to João Paulo Leal for computer programs and many helpful discussions. The authors thank Dr N. Edelstein for encouragement.

Supplementary material. A list of the compounds studied (with references) is available from the authors.

REFERENCES

1. N. N. Greenwood and A. Earnshaw, *Chemistry of the Elements*, pp. 1068–1069. Pergamon Press, Oxford (1984).
2. R. Hoppe, *Angew. Chem. Int. Ed. Engl.* 1970, **9**, 25; G. O. Brunner, *Acta Cryst.* 1977, **33A**, 226; S. S. Batsanov, *Russ. J. Inorg. Chem.* 1977, **22**, 631; F. L. Carter, *Acta Cryst.* 1978, **34B**, 2962; M. O'Keeffe, *Acta Cryst.* 1979, **35A**, 772.
3. J. P. Collman, L. S. Hegedus, J. R. Norton and R. G. Finke, *Principles and Applications of Organotransition Metal Chemistry*, pp. 24–30. University Science Books, Mill Valley, California (1987).
4. A. Bondi, *J. Phys. Chem.* 1964, **68**, 441.
5. C. A. Tolman, *Chem. Rev.* 1977, **77**, 313.

6. C. A. McAuliffe, in *Comprehensive Coordination Chemistry* (Edited by G. Wilkinson, R. D. Gillard and J. A. McCleverty), Vol. 2, pp. 1012–1029. Pergamon Press, Oxford (1987).
7. K. W. Bagnall and Li Xing-fu, *J. Chem. Soc., Dalton Trans.* 1982, 1365; R. D. Fischer and Li Xing-fu, *J. Less-Common Met.* 1985, **112**, 303; Li Xing-fu, Shen Tian-gi, Guo Ao-ling, Shun Guang-li and Sun Peng-nian, *Inorg. Chim. Acta* 1987, **129**, 227 and following papers in the same issue; Li Xing-fu and Guo Ao-ling, *Inorg. Chim. Acta* 1987, **131**, 129; Li Xing-fu and Guo Ao-ling, *Inorg. Chim. Acta* 1987, **134**, 143.
8. W. T. Wipke and P. Gund, *J. Am. Chem. Soc.* 1976, **98**, 8107; J. I. Seeman, J. W. Viers, J. C. Schug and M. D. Stovall, *J. Am. Chem. Soc.* 1984, **106**, 143.
9. R. F. Zahrobsky, *J. Am. Chem. Soc.* 1971, **93**, 3313.
10. A. J. Smith, *Proceedings of the 11èmes Journées des Actinides*, p. 64. Jesolo, Italy (1981).
11. E. B. Lobkovskii, *J. Struct. Chem.* 1983, **24**, 224; E. B. Lobkovskii, *J. Organomet. Chem.* 1984, **277**, 53.
12. D. M. P. Mingos, *Inorg. Chem.* 1982, **21**, 464.
13. K. N. Raymond and C. W. Eigenbrot Jr, *Accts Chem. Res.* 1980, **13**, 276.
14. R. D. Shannon, *Acta Cryst.* 1976, **32A**, 751.
15. N. Edelstein, *Inorg. Chem.* 1981, **20**, 297.
16. T. J. Marks and J. R. Kolb, *Chem. Rev.* 1977, **77**, 263.
17. G. B. Deacon, P. I. Mackinnon, T. W. Hambley and J. C. Taylor, *J. Organomet. Chem.* 1983, **259**, 91; G. B. Deacon, B. M. Gatehouse, S. N. Platts and D. L. Wilkinson, *Aust. J. Chem.* 1987, **40**, 907.
18. F. David, *J. Less-Common Met.* 1986, **121**, 27.
19. G. Parego, M. Cesari, F. Forina and G. Jugli, *Acta Cryst.* 1976, **32B**, 3034.
20. J. L. Atwood, W. E. Hunter, R. D. Rogers, J. Holton, J. McMeeking, R. Pearce and M. F. Lappert, *J. Chem. Soc., Chem. Commun.* 1978, 140.
21. J. G. Reynolds, A. Zalkin, D. H. Templeton and N. M. Edelstein, *Inorg. Chem.* 1977, **16**, 1090.
22. R. E. Cramer, U. Engelhardt, K. T. Higa and J. W. Gilje, *Organometallics* 1987, **6**, 41.
23. R. D. Shannon, in *Structure and Bonding in Crystals* (Edited by M. O'Keefe and A. Navrotsky), Vol. 2, pp. 53–70. Academic Press, New York (1981).
24. W. H. Baur, *Cryst. Rev.* 1987, **1**, 61.
25. J. G. Brennan, S. D. Stults, R. A. Andersen and A. Zalkin, *Inorg. Chim. Acta* 1987, **139**, 201; *Organometallics*, 1988, **7**, 1329.
26. D. L. Kepert, *Inorganic Stereochemistry*. Springer, Berlin (1982).
27. R. G. Ball, F. Edelmann, J. G. Matisons, J. Takats, N. Marques, J. Marçalo, A. Pires de Matos and K. W. Bagnall, *Inorg. Chim. Acta* 1987, **132**, 137.
28. N. Marques, A. Domingos, J. Marçalo, A. Pires de Matos, J. Takats and K. W. Bagnall, *J. Less-Common Met.* 1989, **149**, 271.
29. C. Baudin, P. Charpin, M. Ephritikhine, M. Lance, M. Nierlich and J. Vigner, *J. Organomet. Chem.* 1988, **345**, 263.
30. J. L. Martin, L. C. Thompson, J. L. Radonovich and M. D. Glick, *J. Am. Chem. Soc.* 1968, **90**, 4493.
31. M. R. Caira, J. F. De Wet, J. G. H. Du Preez and B. J. Gellatly, *Acta Cryst.* 1978, **34B**, 1116.

Polyhedron Vol. 8, No. 20, pp. 2439–2447, 1989
Printed in Great Britain

0277-5387/89 $3.00+.00
© 1989 Pergamon Press plc

MERCAPTOPYRIDINE COMPLEXES OF DICYCLOPENTADIENYLMOLYBDENUM AND -TUNGSTEN: PREPARATION AND ELECTROCHEMISTRY. THE STRUCTURE OF $[Mo(\eta^5\text{-}C_5H_5)_2(2\text{-}SNC_5H_4)][PF_6]$

M. A. A. F. DE C. T. CARRONDO, A. R. DIAS,* M. HELÈNA GARCIA, ALEXANDRA MIRPURI, M. FÁTIMA M. PIEDADE and MARGARIDA S. SALEMA

Centro de Química Estrutural, Complexo 1, Instituto Superior Técnico, Av. Rovisco Pais, 1096 Lisboa Codex, Portugal

(*Received* 3 *April* 1989; *accepted* 18 *May* 1989)

Abstract—Neutral complexes of the type $[MCp_2(2\text{-}Spy)_2]$ and $[MCp_2(4\text{-}Spy)_2]$ and cationic complexes $[MCp_2(2\text{-}Spy)][PF_6]$ ($Cp = \eta^5\text{-}C_5H_5$; M = Mo, W; py = pyridine), where 2-mercaptopyridine is acting as a chelating ligand, have been prepared from the reaction of $[MCp_2Cl_2]$ and the corresponding mercaptopyridine in the presence of an excess of triethylamine. The protonated derivatives $[MCp_2(2\text{-}SpyH)_2][PF_6]_2$ and $[MCp_2(4\text{-}SpyH)_2][PF_6]_2$ have also been prepared by reacting the parent neutral compound with concentrated hydrochloric acid. Electrochemical studies, by cyclic voltammetry and coulometry, carried out in acetonitrile and dichloromethane, showed that these compounds follow the general trend of oxidation of the bis-thiolates $MCp_2(SR)_2$ (R = aryl or alkyl). The molecular structure of $[MoCp_2(2\text{-}SNC_5H_4)][PF_6]$ has been determined. The crystals are triclinic, space group $P\bar{1}$, $a = 10.577(3)$, $b = 7.644(2)$, $c = 10.783(1)$ Å, $\alpha = 99.26(2)$, $\beta = 96.29(2)$, $\gamma = 87.95(2)°$, $V = 855.26$ Å^3, $Z = 2$.

Our previous studies on the chemistry of substituted pyridine complexes[1] led us, in the case of 2-hydroxy- and 2-aminopyridine, to the synthesis of two unusual metallocycle complexes where the ligands chelate to one metal atom to form strained four-membered rings. As part of our continuing study of di-η^5-cyclopentadienylmolybdenum/tungsten complexes with substituted pyridine as co-ligands, we now report the reactions of *ortho-* and *para-*mercaptopyridines with MCp_2Cl_2. For the *ortho-*pyridine our purpose is to compare the strain and the reactivity on the metallocycle ring, when sulphur is the second coordinative atom on the chelating substituted pyridine, instead of nitrogen and oxygen as reported before.[1] The structure of $[MoCp_2(2\text{-}SNC_5H_4)][PF_6]$ was determined and the electrochemistry of the compounds was studied by cyclic voltammetry.

* Author to whom correspondence should be addressed.

RESULTS AND DISCUSSION

Chemical studies

The coordination at the metal centres of the α- and γ-mercaptopyridines through the sulphur atom, can be either as a neutral ligand in the thione form[2] or as the corresponding conjugated anion.[3] However, the α-mercaptopyridines have shown a great versatility since they can either coordinate through the adjacent nitrogen atom of the heteronuclear ring to one metal centre, or they can bridge two metal centres. In the first case a strained four-membered ring system is obtained and only a few complexes of this type are known.[4] In the second case an unstrained system is achieved.[5]

In order to obtain mercaptopyridines as anionic ligands a general synthetic route to thiolato dicyclopentadienylmolybdenum and -tungsten derivatives was followed by direct reaction of the parent dihalide, MCp_2X_2, with the required mer-

captopyridines, in the presence of a strong deprotonating agent. It was observed that in the case of 2-mercaptopyridine, in addition to the formation of the bis-thiolate, the chelate compound was also isolated, in reasonable yield, as a product of the same reaction.

All the formulations were supported by analytical and conductivity data (Table 1) and also by the IR and ^{1}H NMR spectra (Table 2).

Typical bands confirm the presence of the MCp_2 fragment (~ 3100 cm^{-1}) in all the complexes, and the PF_6^- anion (840 and 560 cm^{-1}) in the cationic metal complexes. In addition, the protonated dicationic complexes $[MCp_2(2\text{-SpyH})_2]^{2+}$ and $[MCp_2(4\text{-SpyH})_2]^{2+}$ displayed a very strong band at 3330 cm^{-1}, assigned to an N—H stretch. Characteristic bands of substituted pyridine were also assigned, based on literature data.[6]

The ^{1}H NMR spectra for the free 2-mercaptopyridine has been interpreted in terms of the equilibrium, which explains the multiplet attributed to the 3,4 protons, the multiplet to the 5 proton and a doublet attributed to the proton on the 6 position (see Table 2). However, after deprotonation at the sulphur atom followed by coordination at the metal centre, this equilibrium no longer exists and a doublet attributed to H_3, two triplets attributed to H_4 and H_5 and a doublet due to H_6 are observed, as could be expected. After coordination the greater deshielding was observed on the *para*-protons of the pyridine ring. The ^{1}H NMR spectra for the protonated pyridine nitrogen compounds showed a greater deshielding for all the ring protons relative to the neutral parent compounds. The resonance of the amine protons is broadened by the quadrupole relaxation of the nearly asymmetric nitrogen, and for this reason is not seen in the proton spectra.

The ^{1}H NMR spectra for the 4-mercaptopyridinemolybdenum/tungsten derivatives showed more shielding on positions 3,5 and more deshielding on positions 2,6 relative to the free ligand. This decrease in chemical shifts can be explained by the smaller polarizability on the σ system relative to the π system, the *ortho*-protons being more sensitive to this polarization.[7]

The ionic formulation was suggested by the observed conductivity values (4–10 Ω^{-1} cm mol^{-1} for neutral, 133–143 Ω^{-1} cm mol^{-1} for mono-cations and 212–252 Ω^{-1} cm mol^{-1} for di-cations).[8]

Chemical oxidation of $[MoCp_2(2\text{-Spy})_2]$ *with the ferricinium cation.* Electrochemical studies carried out on the compounds prepared (see below), prompted us to chemically oxidize the neutral species $[MoCp_2(2\text{-Spy})_2]$. Thus, slow addition of a $[FeCp_2][PF_6]$ solution in dichloromethane, to a solution of $[MoCp_2(2\text{-Spy})_2]$ in the same solvent and same molar concentration, at room temperature, affords an orange-brownish compound, previously identified as being the chelate complex $[MoCp_2(2\text{-Spy})][PF_6]$.

This reaction follows the general trend of oxidation of bis-thiolates $[MCp_2(SR)_2]$ (M = Mo, W; R = alkyl or aryl) whose mechanism, based on chemical and electrochemical studies, had been suggested[9] to be as shown in Scheme 1.

When the ferricinium oxidation of $[MCp_2(SR)_2]$ was carried out in a non-coordinative solvent, e.g. CH_2Cl_2, the only product isolated was the dimer $[Cp_4M_2(SR)_4][PF_6]_2$ (path A).

However, as in our case, the two thiolate ligands are 2-mercaptopyridine, and an alternative pathway (path C) can occur after the reductive elimination of one of the ligands, the remaining 2-mercaptopyridine, which is coordinated through

Table 1. Analytical and conductimetric data

Compound	Colour	Decomposition temperature θ_c (°C)	Analysis (%); found (req.) C	H	N	Λ^a Conductivity (Ω^{-1} cm^2 mol^{-1})
$[MoCp_2(2\text{-Spy})_2]$	Brown-reddish	190	52.6(53.8)	4.1(4.0)	6.1(6.3)	3.4
$[MoCp_2(2\text{-Spy})][PF_6]$	Brick	220	37.5(37.4)	3.1(2.9)	3.2(2.9)	133.4
$[MoCp_2(2\text{-SpyH})_2][PF_6]_2$	Salmon	208	32.3(32.5)	2.8(2.7)	3.4(3.8)	254.4
$[MoCp_2(4\text{-Spy})_2]$	Brown-reddish	106	52.8(53.8)	4.2(4.1)	8.8(6.3)	5.9
$[MoCp_2(4\text{-SpyH})_2][PF_6]_2$	Light brown	205	33.1(32.5)	3.2(2.7)	4.5(3.8)	201.9
$[WCp_2(2\text{-Spy})_2]$	Dark brown	200	44.8(44.9)	3.6(3.4)	5.3(5.2)	7.6
$[WCp_2(2\text{-Spy})][PF_6]$	Coral	255	31.5(31.7)	2.4(2.5)	2.4(2.5)	142.9
$[WCp_2(2\text{-SpyH})_2][PF_6]_2$	Peach	240	29.1(29.1)	2.7(2.4)	3.1(3.4)	252.9
$[WCp_2(4\text{-Spy})_2]$	Dark brown	195	43.7(45.0)	3.6(3.4)	4.8(5.2)	8.9
$[WCp_2(4\text{-SpyH})_2][PF_6]_2$	Orange	220	28.6(28.7)	2.4(2.4)	3.2(3.4)	212.2

[a] 1×10^{-3} M solution in nitromethane.

Table 2. ^{1}H NMR data[a]

Compound	H_3	H_4	H_5	H_6	η^5-C_5H_5	N—H
$[MoCp_2(2\text{-}Spy)][PF_6]$	2.98(d,1)	2.14(t,1)	2.84(t,1)	1.86(d,1)	3.92(s,10)	
$[MoCp_2(2\text{-}Spy)_2]$[b]	2.62(d,2)	2.82(t,2)	3.27(t,2)	1.79(d,2)	4.73(s,10)	
$[MoCp_2(2\text{-}SpyH)_2][PF_6]_2$	2.31(d,2)	1.81(t,2)	2.44(t,2)	1.51(d,2)	4.06(s,10)	
$[WCp_2(2\text{-}Spy)][PF_6]$	3.31(d,1)	2.28(t,1)	2.97(t,1)	1.72(d,1)	4.11(s,10)	
$[WCp_2(2\text{-}Spy)_2]$	2.56(d,2)	2.71(t,2)	3.16(t,2)	1.67(d,2)	4.62(s,10)	
$[WCp_2(2\text{-}SpyH)_2][PF_6]_2$	2.06(d,2)	1.70(t,2)	2.39(t,2)	1.46(d,2)	4.07(s,10)	
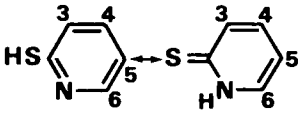	2.61(m,2)[c]		3.23(m,1)	2.29(d,2)		−2.64(s,1)

Compound	H_3,H_4	H_2,H_6	η^5-C_5H_5
$[MoCp_2(4\text{-}Spy)_2]$[d]	2.95(d,4)	1.89(d,4)	4.53(s,10)
$[MoCp_2(4\text{-}SpyH)_2][PF_6]_2$	2.26(d,4)	1.61(d,4)	4.19(5)(s,10)
$[WCp_2(4\text{-}Spy)_2]$[d]	2.83(d,4)	1.84(d,4)	4.57(s,10)
$[WCp_2(4\text{-}SpyH)_2][PF_6]_2$	2.13(d,4)	1.57(d,4)	4.24(s,10)
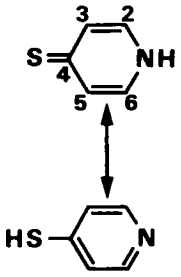	2.82(d,2)	2.41(d,2)	
	2.61(d,2)	1.44(d,2)	

[a] τ(ppm) (multiplicity, relative integrals) in Me_2CO-d_6 as solvent and TMS as internal reference.
[b] In CD_2Cl_2 as solvent.
[c] Includes H_3 and H_4.
[d] In DMSO-d_6 as solvent.

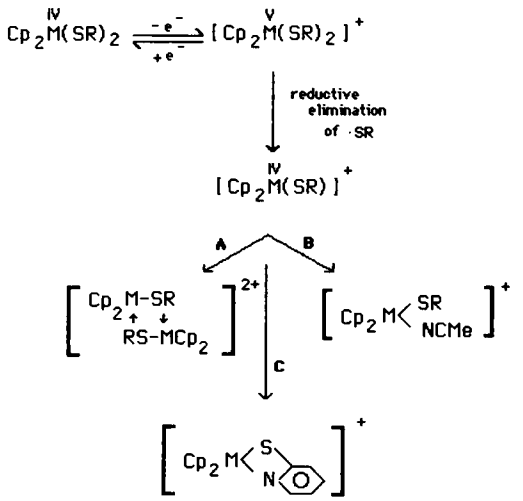

Scheme 1. A possible scheme for the reactions following one-electron oxidation of $[MCp_2(SR)_2]$ in acetonitrile.

sulphur can also become coordinated through the nitrogen atom, forming a chelate ring.

There are many examples in the literature of four-membered chelate rings containing sulphur atoms with ligands such as dithiocarbamates, thiocarbonates, and 1,1-dithiolates.[10] Recently, the complex $[Rh(2\text{-}Spy)_2(2\text{-}SpyH)_2]Cl$ has been reported and its structure shows two chelating 2-Spy^- ligands.[3b]

Crystallographic studies

Structure of $[MoCp_2(2\text{-}Spy)][PF_6]$. The crystal structure of this complex consists of discrete $[MoCp_2(2\text{-}SNC_5H_4)]^+$ cations and PF_6^- anions. The structure of the cation, with the atom numbering is shown in Fig. 1, and bond lengths and bond angles are given in Table 3. The metal atom

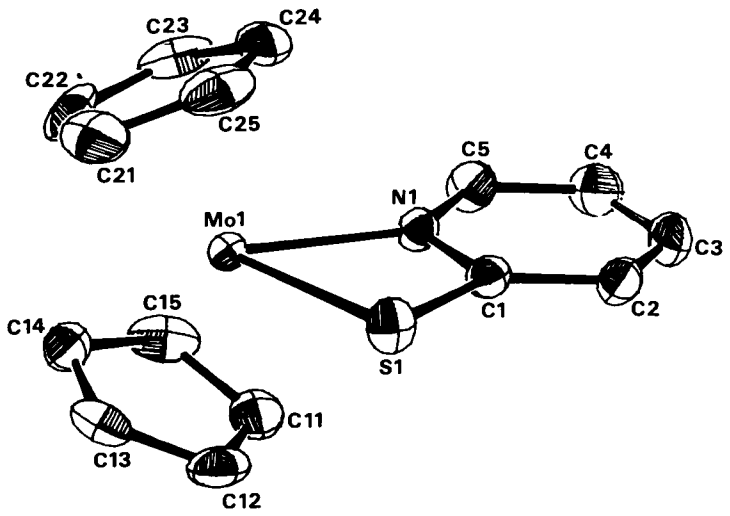

Fig. 1. Molecular structure of $[Mo(\eta^5\text{-}C_5H_5)_2(2\text{-}SNC_5H_4)]^+$ with 50% probability thermal ellipsoids showing the atom labelling scheme.

is coordinated to two η^5-cyclopentadienyl rings and to a bidentate ligand, 2-mercaptopyridine, with the usual distorted tetrahedral environment. The molybdenum is positioned at 1.967(1) and 1.970(1) Å from the cyclopentadienyl rings and the angle between the ring normals is 132.4(2)°. The planar cyclopentadienyl ligands adopt an eclipsed conformation.

This complex has a geometry very similar to that observed in the other two bis-cyclopentadienyl complexes previously reported,[1] $[MoCp_2(2\text{-}NHNC_5H_4)][PF_6]$ and $[MoCp_2(2\text{-}ONC_5H_4)][PF_6]$. Here again we find that the small angle at the molybdenum is primarily determined by the geometry and strain in the bidentate ligand, as demonstrated by EHMO calculations carried out for this type of ligand.[1] Naturally however, the angle at metal atom increases from the aminopyridine complex, 59.8(1)°, to the hydroxypyridine, 61.2(2)°, up to the mercaptopyridine, 64.9(1)°. In contrast, in $[MoCp_2(NH_3)(SC_6H_5)]$,[11] where coordination is also through nitrogen and sulphur, but as part of two different monodentate ligands, the equivalent angle S—Mo—N is 76.4(4)°. As demonstrated with many different structures,[1] no general correlation between the L—Mo—L′ and Cp—Mo—Cp angles seems to exist. However, in this particular context, where for the three complexes the bidentate ligand differs only in one of the atoms coordinated to the metal, a correlation was observed between these two angles. This is illustrated in Fig. 2.

In addition, the angle at this different coor-

Table 3. Bond lengths (Å) and bond angles (°) for $[MoCp_2(2\text{-}Spy)][PF_6]$

S—Mo	2.500(4)	N—Mo	2.157(5)	C(11)—Mo	2.314(6)
C(12)—Mo	2.355(6)	C(13)—Mo	2.285(6)	C(14)—Mo	2.257(6)
C(15)—Mo	2.268(6)	C(21)—Mo	2.293(6)	C(22)—Mo	2.260(6)
C(23)—Mo	2.268(7)	C(24)—Mo	2.314(6)	C(25)—Mo	2.329(6)
C(1)—S	1.724(6)	C(1)—N	1.346(6)	C(5)—N	1.355(6)
C(2)—C(1)	1.402(7)	C(3)—C(2)	1.358(9)	C(4)—C(3)	1.377(10)
C(5)—C(4)	1.379(8)	Mo—Cp(1)	1.967(1)	Mo—Cp(2)	1.970(1)
N—Mo—S	64.9(2)	Mo—S—C(1)	81.2(2)	Mo—N—C(5)	135.2(4)
Mo—N—C(1)	104.4(3)	C(1)—N—C(5)	120.4(4)	S—C(1)—N	109.4(4)
N—C(1)—C(2)	120.4(5)	S—C(1)—C(2)	130.2(4)	C(1)—C(2)—C(3)	119.0(5)
C(2)—C(3)—C(4)	120.4(5)	C(3)—C(4)—C(5)	119.4(5)	N—C(5)—C(4)	120.4(6)
Cp(1)—Mo—Cp(2)	132.4(2)				

Cp(1) is cyclopentadienyl defined by C(11)—C(15); Cp(2) is cyclopentadienyl defined by C(21)—C(25).

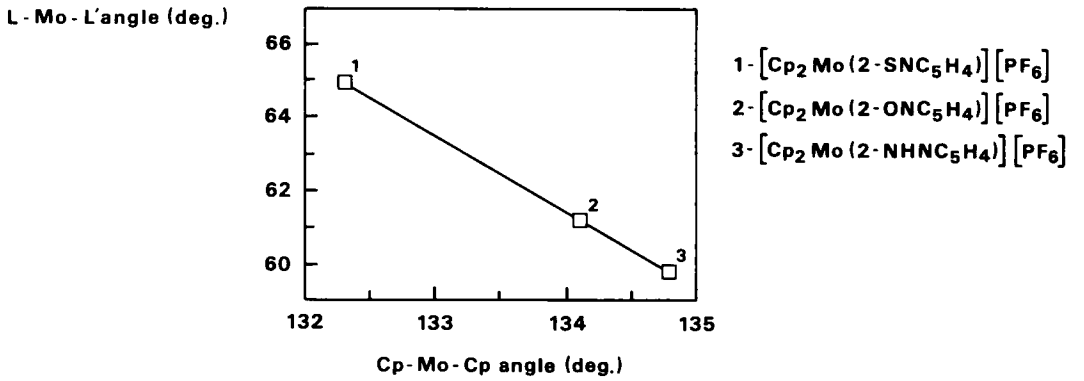

Fig. 2. Correlation between the N—Mo—(S,N,O) and Cp—Mo—Cp angles.

dinating atom, C(1)—(N,O,S)—Mo, varies as expected from compound **1** → **2** → **3** in a decreasing order: 98.4(5), 93.7(8), 81.2(2)°.*

The Mo—S and Mo—N distances lie close to those previously found, although the Mo—S distance in this complex is clearly at the end of the observed range (2.431–2.501 Å).[1,11]

The cyclopentadienyl rings are planar, with a maximum deviation from the least-squares planes of 0.001 and 0.0003 Å at each Cp.

Electrochemical studies

The oxidative electrochemistry of η^5-dicyclopentadienyl mercaptopyridine molybdenum and tungsten complexes. The electrochemical behaviour of the compounds $[MCp_2(2\text{-}Spy)_2]$, $[MCp_2(2\text{-}Spy)][PF_6]$, $[MCp_2(2\text{-}SpyH)_2][PF_6]$, $[MCp_2(4\text{-}Spy)_2]$ and $[MCp_2(4\text{-}SpyH)_2][PF_6]_2$ (M = Mo, W), listed in Table 4, was investigated in acetonitrile and dichloromethane with tetrabutylammonium salts as supporting electrolytes.

The oxidative electrochemistry of the neutral complexes, $[MCp_2(2\text{-}Spy)_2]$ and $[MCp_2(4\text{-}Spy)_2]$, is considerably more complex than that of the ionic mercaptopyridines derivatives studied in this work, appearing to follow the general oxidation of the $[MCp_2(SR)_2]$ complexes (M = Mo, W; R = alkyl or aryl).[9]

As can be seen in Fig. 3, where a typical cyclic voltammogram is shown, these compounds exhibit one first quasi-reversible redox process in the range 0.3–0.6 V, where current and reversibility depend on the switching potential. For example, if the potential sweep was switched at about 0.7 V when the compound was $[WCp_2(4\text{-}Spy)_2]$, the ratio I_c/I_a was ~ 1.0, but once the potential reached the second irreversible wave, the first wave no longer had a cathodic current. One implication of this observation is that the product of the second oxidation is rapidly decomposed (in an EEC process) faster than the first, depleting the diffusion layer of all the $[MCp_2(4\text{-}Spy)_2]$ species.

In the range 0.6–0.9 V, $[MCp_2(2\text{-}Spy)_2]$ complexes provide evidence for two redox processes, but the $[MCp_2(4\text{-}Spy)_2]$ analogues only present one wave. This behaviour was also observed in the bisthiolates derivatives $[MCp_2(SR)_2]$ with different R groups.[9] Both di-oxidation of the parent dithiolate

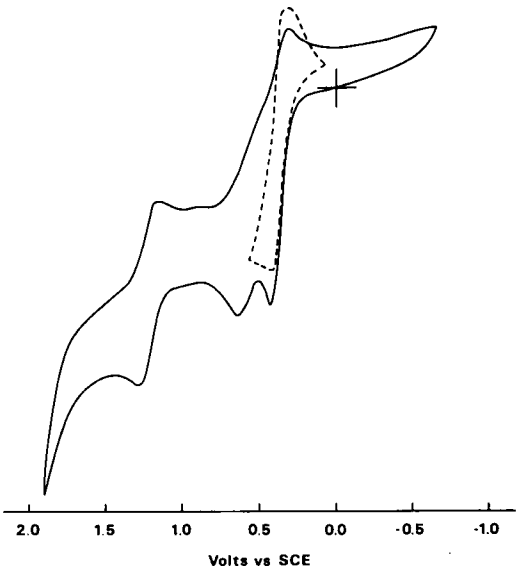

Fig. 3. Cyclic voltammogram of $[MoCp_2(2\text{-}Spy)_2]$ (1 mM) in CH_3CN, containing 0.1 M Bu_4NPF_6. Scan rate 0.2 V s^{-1}.

* We take the opportunity to revise the numbering scheme on the four-membered ring in Fig. 2 of ref. 1, as its sequence should be as in Fig. 1; this would then be in accordance with all the tables for this complex.

Table 4. Electrochemical data[a]

Compound[b]	E_{pa}	E_{pc}	$E_{p/2}$ (V)	$E_{pa}-E_{pc}$ (mV)	I_c/I_a	Faradays mol^{-1}
$[MoCp_2(2\text{-}Spy)_2]$	0.44	0.32	0.38	120	0.9	
	0.64					
	0.95					
	1.30	1.16	1.23	125	0.7	
		After bulk electrolysis at 0.48 V				0.96
	1.30	1.20	1.25	110		
$[MoCp_2(2\text{-}Spy)][PF_6]$	1.30	1.18	1.24	120	0.9	
$[MoCp_2(2\text{-}SpyH)_2][PF_6]_2$	1.28	1.18	1.23	100	0.7	
$[MoCp_2(4\text{-}Spy)_2]$	0.61	0.50	0.56	110	1.0	
	1.10	0.98	1.04	120	0.9	
	1.38					
		After bulk electrolysis at 0.68 V				1.1
		0.98				
$[MoCp_2(4\text{-}SpyH)_2][PF_6]_2$	1.06	0.93	1.00	130	1.0	
$[WCp_2(2\text{-}Spy)_2]$	0.40	0.25	0.33	150		
	0.23	0.48	0.56	150	1.0	
		0.83				
	1.15	1.08	1.12	70		
		After bulk electrolysis at 0.43 V				0.95
	1.17	1.04	1.11	130		
$[WCp_2(2\text{-}Spy)][PF_6]$	1.28	1.18	1.23	100	0.7	
$[WCp_2(2\text{-}SpyH)_2][PF_6]_2$	1.17	1.05	1.12	120	0.6	
$[WCp_2(4\text{-}Spy)_2]$	0.50	0.39	0.45	110	0.8	
	1.00	0.75	0.88	250		
	1.25	1.13	1.19	120		
		After bulk electrolysis at 0.60 V				1.30
	0.87					
$[WCp_2(2\text{-}SpyH)_2][PF_6]_2$	0.90	0.79	0.85	110	0.7	
	1.38	1.25	1.32	130		

[a] All electrochemistry performed in CH_3CN containing 0.1 M Bu_4NPF_6. Potentials are referenced to a calomel electrode containing a saturated NaCl solution. Sweep rates of 200 mV s^{-1} were commonly used and the temperature was 20 ± 2°C. Solution concentration was generally about 1 mM.

[b] Calculated only on the waves with well-defined baselines.

and the oxidation of a monosubstituted acetonitrile complex can explain these waves in this potential range.

At higher potentials, one further redox wave was observed for all these neutral complexes, almost in the same position, *ca* 1.30 V. After bulk oxidation of $[MoCp_2(2\text{-}Spy)_2]$ at 0.48 V (1.0 Faraday/mol), in CH_3CN, the cyclic voltammogram of the solution showed only one electroactive species having an irreversible redox wave at almost the same potential as the higher irreversible wave in the parent compound.

The cyclic voltammogram of the chelate $[MCp_2(2\text{-}Spy)][PF_6]$ showed only one quasi-reversible wave at $E_{p/2}$ = 1.23 and 1.05 for molybdenum and tungsten derivatives, respectively. The position of this wave, at the same potential as the one observed at higher potential in the cyclic voltammograms of the neutral compounds $[MCp_2(2\text{-}Spy)_2]$ and $[MCp_2(4\text{-}Spy)_2]$, suggested that the formation of a chelate compound or a dimer with two bridging ligands could be one possible product, resulting from the oxidation of these compounds. This hypothesis prompted us to chemically oxidize the compound $[MoCp_2(2\text{-}Spy)_2]$ (which has a first oxidation wave at $E_{p/2}$ = 0.37 V) with a ferricinium salt. After work-up, the isolated product was identified as the chelate compound $[MCp_2(2\text{-}Spy)][PF_6]$.

The oxidative electrochemistry of the protonated cations, $[MCp_2(2\text{-}SpyH)_2][PF_6]_2$ and $[MCp_2(4\text{-}$

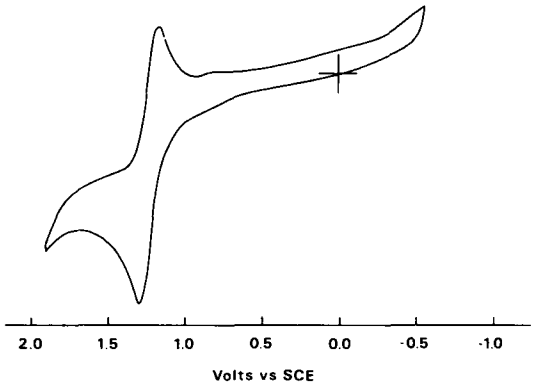

Fig. 4. Cyclic voltammogram of $[MoCp_2(2\text{-}Spy)][PF_6]$ (1 mM) in CH_3CN, containing 0.1 M Bu_4NPF_6. Scan rate 0.2 V s^{-1}.

$SpyH)_2][PF_6]_2$, showed only one redox wave at potentials generally higher than 1.0 V, with the trend that tungsten derivatives oxidize at lower potentials than the molybdenum analogues, as was observed before[9,12] for complexes of the type MCp_2X_2 where M is from group VIB.

It can also be observed, by comparing the oxidative electrochemistry of the neutral species $[MCp_2(2\text{-}Spy)_2]$ and $[MCp_2(4\text{-}Spy)_2]$, that the first compounds with *ortho*-substituted pyridines are easier to oxidize than the analogues which are *para*-substituted.

Although the oxidation wave for $[MoCp_2(2\text{-}Spy)][PF_6]$ (Fig. 4) has $\Delta E = 120$ mV (also when ferrocene was added as an internal reference this showed a higher value than the usual ΔE of ~ 60 mV), its quasi-reversible character can be suggested by the ratio $I_a/I_c = 0.9$ and the dependence of ΔE on the sweep scan rate.

However, electrochemical studies carried out on the analogous pyridine substituted complexes, where oxygen or N—H is the second coordinating atom, showed a totally irreversible wave for the oxidation of these compounds in this range of potentials.[13] This observation suggests more relative stability on the heterometallic ring in the sulphur case and this result is in agreement with the less strained structure found for this complex.

EXPERIMENTAL

All experiments were carried out under nitrogen by the use of standard Schlenk-tube techniques. IR spectra were measured on a Perkin–Elmer 457 spectrophotometer with KBr pellets. ^1H NMR spectra were recorded on a Jeol JNM-100 PFT spectrometer. Microanalyses were performed in our laboratories. The compounds $[MCp_2Cl_2]$ (M = Mo, W) were prepared from the parent dihydrides $[MCp_2H_2]$.[14]

Preparation of $[MCp_2(2\text{-}Spy)_2]$ *and* $[MCp_2(4\text{-}Spy)_2]$ (M = Mo, W)

To a suspension of $[MCp_2X_2]$ (~ 3.4 mmol) in 60 cm^3 of ethanol was added 13.5 mmole of mercaptopyridine in the presence of an excess of triethylamine. After a 2 h reflux, the solvent was evaporated to dryness affording a brownish solid. After the addition of water (50 cm^3) and filtration of the water solution (see below) a solid residue was obtained, which after being dried was recrystallized from CH_2Cl_2–ethanol. Yield $\approx 70\%$.

Preparation of $[MCp_2(2\text{-}Spy)][PF_6]$ (M = Mo, W)

To the water solution obtained from the work-up of the previous reaction, a NH_4PF_6 saturated water solution (5 cm^3) was added, affording an orange precipitate, which after being washed several times and filtered was dried. After recrystallization from acetone–ethanol the crystalline, salmon protonated salt was obtained. Yield $\approx 80\%$.

X-ray crystal structure of $[MoCp_2(2\text{-}SNC_5H_4)][PF_6]$

Data collection. X-ray studies were carried out using an Enraf–Nonius CAD4 diffractometer and graphite monochromatized Mo-K_α radiation ($\lambda = 0.71069$ Å). The unit cell and the orientation matrix were obtained by least-squares refinement of the setting angles for 25 automatically centred reflections. Intensity data were measured at room temperature, using the ω–2θ mode with $1.5 < \theta < 27.0°$ and $\omega = 0.8 \pm 0.35 \tan\theta$. A total of 3928 intensities were measured, 593 unobserved with $F_o < 3\sigma(F_o)$. Data were corrected empirically for absorption using the CAD4 software (minimum and maximum transmission factors of 0.9527 and 0.9993, respectively). Details of the data collection and refinement are given in Table 5. The structure was solved and refined using the SHELX76[15] program and all calculations were carried out on a VAX computer at the Instituto Superior Técnico.

Structure analysis and refinement. The structure was solved by a combination of Patterson and difference Fourier methods and refined by least-squares.

The molybdenum position was taken from the Patterson synthesis map, and sulphur, nitrogen and phosphorus positions from the subsequent difference Fourier synthesis. All the positions of the other

Table 5. Crystallographic data and data collection parameters

Formula	$C_{15}H_{14}NSPF_6Mo$
M	481.25
Space group	$P\bar{1}$
a (Å)	10.578(3)
b (Å)	7.644(2)
c (Å)	10.784(1)
V (Å^3)	855.26
Z	2
d_{calc} (g cm^{-3})	1.869
μ(Mo-K_α) (cm^{-1})	9.30
Scan speed (° min^{-1})	0.97–5.49
Data collected	$-h, \pm k, \pm l$
Number of unique data	3593
Number of data $\|F\| > 3\sigma(F)$	3335
Number of variables	282
R	0.0362
R_w	0.0541
Largest shift/error value of final cycle	0.363
Largest peak in final difference Fourier (e Å^{-3})	1.23

$R = \Sigma(|F_o| - |F_c|)/\Sigma F_o$;
$R_w = [\Sigma w(|F_o| - |F_c|)^2/\Sigma w|F_o|^2]^{1/2}$.

non-hydrogen atoms were localized in a subsequent difference Fourier synthesis, and after some cycles of refinement with isotropic temperature factors, $R = 0.1049$. Non-hydrogen atoms were then refined anisotropically. The hydrogen atoms were localized in the difference map and refined isotropically, although with geometrical constraint of the distance C—H = 1.08 Å.

The weighting scheme $w = k/(\sigma^2(F_0) + |g|F_0^2)$ was applied with the refined values of $k = 1.7998$ and $g = 0.000768$. Eight low angle and strong reflections thought to be affected by extinction were removed from the data. The final refinement converged at $R = 0.0362$ and $R_w = 0.0541$. A peak of 1.23 e Å^{-3} in the vicinity of the PF_6^- anion remained in the final electron density difference map.

Final atomic positional parameters and anisotropic thermal parameters for the non-hydrogen atoms, the hydrogen fractional atomic coordinates and isotropic temperature factors, and tables of observed and calculated structure factors have been submitted as supplementary material. The drawing was made using ORTEPII.[16]

Electrochemical apparatus

The electrochemistry instrumentation consisted of a Princeton Applied Research Model 173 potentiometer, a Model 175 voltage programmer, a Model 179 digital coulometer and an Omnigraphic 2000 X-T recorder from Houston Instruments. Potentials were referred to a calomel electrode containing a saturated solution of potassium chloride which was checked relative to a 1.0×10^{-3} M solution of ferrocene in acetonitrile containing 0.10 M $LiClO_4$ for which the ferricinium/ferrocene potential was in agreement with the literature.[17] The working electrode was made of a 2 mm piece of platinum wire for cyclic voltammograms, while the working electrode in the controlled potential electrolysis experiments was a platinum gauze. The secondary electrode was a platinum wire coil. Cyclic voltammetry experiments were performed in a PAR polarographic cell at room temperature, the solutions being used were 1 mM in solute and 0.1 M in supporting electrolyte, tetrabutylammonium hexafluorophosphate. Coulometry experiments were carried out in a three-compartment cell, where the working electrode compartment was separated from the auxiliary and reference electrodes by medium porosity glass frits.

The solvents, CH_3CN and CH_2Cl_2, which were reagent grade materials, were dried over CaH_2 and P_2O_5 and were distilled just before use under argon atmosphere. Solutions were degassed with dry nitrogen before each experiment and a nitrogen atmosphere was maintained over the solution during the experiments.

Acknowledgement—We thank the Instituto Nacional de Investigação Cientifica for financial support.

REFERENCES

1. M. J. Calhorda, M. A. A. F. de C. T. Carrondo, R. Gomes da Costa, A. R. Dias, M. T. L. S. Duarte and M. B. Hursthouse, *J. Organomet. Chem.* 1987, **320**, 53.
2. (a) B. P. Kennedy and A. B. P. Lever, *Can. J. Chem.* 1972, **50**, 3488; (b) E. Binamira-Soriaga, M. Lundeen and K. Seff, *Acta Cryst.* 1979, **35**, 2875.
3. (a) A. J. Deeming and M. N. Meah, *Inorg. Chim. Acta* 1986, **117**, L13; (b) A. J. Deeming, K. I. Hardcastle, M. N. Meah, P. A. Bates, H. M. Dawes and M. B. Hursthouse, *J. Chem. Soc., Dalton Trans.* 1988, 227.
4. (a) I. P. Evans and G. Wilkinson, *J. Chem. Soc., Dalton Trans.* 1974, 946 and refs therein; (b) J. Bould and B. J. Brisdon, *Inorg. Chim. Acta* 1976, **19**, 159; (c) M. J. Calhorda and A. R. Dias, *Rev. Port. Quim.* 1978, **20**, 77; (d) W. Clegg, M. Berry and C. D. Garner, *Acta Cryst.* 1980, **B36**, 3110; (e) W. E. Buhro and J. A. Gladysz, *Inorg. Chem.* 1985, **24**, 3507.
5. F. A. Cotton and R. A. Walton, *Multiple Bonds Between Metal Atoms*. John Wiley, New York (1982).

6. (a) M. Pfeffer, P. Braunstein and J. Dehand, *Spectrochim. Acta* 1974, **30A**, 331; (b) W. Radecka-Paryzek, *Inorg. Chim. Acta* 1980, **45**, L147; (c) A. L. Marchese and B. O. West, *J. Organomet. Chem.* 1984, **266**, 61; (d) R. G. Costa, A. R. Dias and J. C. Kotz, *J. Organomet. Chem.* 1988, **354**, 341.
7. (a) V. M. S. Gil and J. N. Murell, *Trans. Faraday Soc.* 1964, **60**, 248; (b) A. H. Gawer and B. P. Dailey, *J. Chem. Phys.* 1965, **42**, 2658.
8. W. J. Geary, *Coord. Rev.* 1971, **7**, 81.
9. J. C. Kotz, W. Vining, W. Coco, R. Rosen, A. R. Dias and M. H. Garcia, *Organometallics* 1983, **2**, 68.
10. R. P. Burns, F. P. McCullough and C. A. McAuliffe, *Adv. Inorg. Chem. Radiochem.* 1980, **23**, 211 and refs therein.
11. M. J. Calhorda, M. A. A. F. de C. T. Carrondo, M. H. Garcia and M. B. Hursthouse, *J. Organomet. Chem.* 1988, **342**, 209.
12. M. F. Asaro, S. R. Cooper and N. J. Cooper, *J. Am. Chem. Soc.* 1986, **108**, 5187.
13. M. R. Gomes da Costa, D.Phil. thesis, I.S.T., Lisbon (1986).
14. R. L. Cooper and M. L. H. Green, *J. Chem. Soc. A* 1967, 1159.
15. G. M. Sheldrick, SHELX Crystallographic Calculation Program, University of Cambridge (1976).
16. C. K. Johnson, ORTEPII. Report ORNL-5138. Oak Ridge National Laboratory, Tennessee (1976).
17. I. V. Nelson and R. T. Iwamoto, *Analyt. Chem.* 1963, **35**, 867.

Polyhedron Vol. 8, No. 20, pp. 2449–2457, 1989
Printed in Great Britain

0277-5387/89 $3.00+.00
© 1989 Pergamon Press plc

CATIONIC BENZYL NICKEL COMPLEXES AS HOMOGENEOUS CATALYSTS FOR STYRENE OLIGOMERIZATION. X-RAY CRYSTAL STRUCTURE OF $[Ni(\eta^3\text{-}CH_2C_6H_5)(PPh_3)_2]PF_6 \cdot CH_2Cl_2$*

JOSÉ R. ASCENSO, MARIA A. A. F. DE C. T. CARRONDO, ALBERTO R. DIAS,† PEDRO T. GOMES, M. FÁTIMA M. PIEDADE and CARLOS C. ROMÃO

Centro de Química Estrutural, Complexo I, Instituto Superior Técnico, Avenida Rovisco Pais, 1096 Lisboa Codex, Portugal

and

ANDRÉ REVILLON

Laboratoire des Matériaux Organiques du CNRS, B.P. 24, 69390 Vernaison, France

and

IGOR TKATCHENKO

Laboratoire de Chimie de Coordination du CNRS, 205 route de Narbonne, 31077 Toulouse Cédex, France

(*Received* 31 *March* 1989; *accepted* 22 *May* 1989)

Abstract—New cationic complexes $[Ni(\eta^3\text{-}CH_2C_6H_5)(PPh_3)_2]PF_6$ (**3**) and $[Ni(\eta^3\text{-}CH_2C_6H_5)((+)\text{-DIOP})]PF_6$ (**4**) were synthesized from the corresponding neutral compounds $[Ni(\eta^3\text{-}CH_2C_6H_5)X(PR_3)_2]$ (X = Cl, Br), by metathetical halide abstraction with $TlPF_6$. Complex **3** was characterized by X-ray crystallography and shown to have a distorted square-planar geometry with the benzylic group coordinated in a quasi-allylic fashion. Crystals are monoclinic, space group $P2_1/n$, $a = 11.798(5)$, $b = 19.251(2)$, $c = 18.561(3)$ Å, $\beta = 93.03°$, $V = 4208.6$ Å^3. Solution NMR studies showed benzyl fluxionality and phosphine lability in compound **3**, but not in **4**. The latter one is catalytically inactive towards styrene oligomerization, whereas **3** produces styrene oligomers ($\bar{M}_n \approx 1000$) with 67% isotactic content. Although $[Ni(\eta^3\text{-}CH_2C_6H_5)Cl(PCy_3)]$ and *trans*-$[Ni(Cl)(H)(PCy_3)_2]$ are inactive, addition of $TlPF_6$ induced catalytic activity with formation of highly isotactic (90%) styrene oligomers with similar $\bar{M}_n$ and a different terminal group.

In previous papers we reported the activity of the catalyst precursor $[Ni(\eta^3\text{-}CH_2C(CH_3)CH_2)(cod)]PF_6$ (**1**) (cod = 1,5-cyclooctadiene), either pure or modified by the addition of 1 equiv. of a phosphine, in the oligomerization of styrene.[1,2] In those studies we presented some evidence in favour of the intermediacy of η^3-benzylic complexes in the catalytic cycle. One such complex was isolated from the catalytic reaction mixture and characterized by ^{1}H NMR as being an η^3-α-methylbenzyl nickel species, which is believed to result from the insertion of a molecule of styrene into a nickel hydride bond:[2]

Since the phosphine modified catalysts yield styrene oligomers of relatively high, and in the case of PCy_3 very high isotactic content, we decided to prepare model complexes containing both phos-

* Part of this work was presented at the 6th International Symposium on Homogeneous Catalysis, Vancouver, Canada (August 1988).

† Author to whom correspondence should be addressed.

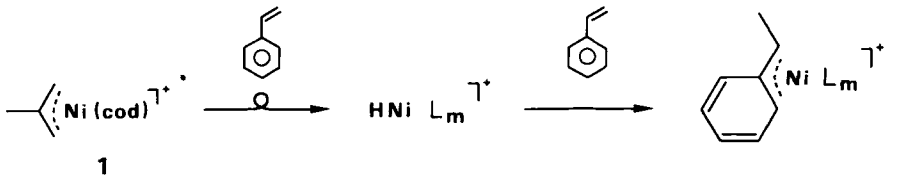

1 (1)

phines and η^3-benzyl ligands and check their activity for the same oligomerization reaction.

Following our proposals[1,2] the active η^3-benzylic species should be cationic. A number of π-benzylic transition metal complexes exhibiting different hapticities are known[3-5] but no cationic Ni(η^3-benzyl) compound is known although a palladium analogue has been structurally characterized.[6]

RESULTS AND DISCUSSION

Synthesis of $[Ni(\eta^3\text{-}CH_2C_6H_5)(PR_3)_2]PF_6$ *complexes*

Our synthetic approach to the preparation of such complexes makes use of halide abstraction from η^1-benzyl complexes of the type $[Ni(\eta^1\text{-}CH_2C_6H_5)X(PR_3)_2]$ (X = Cl, Br), which can be prepared by oxidative addition of benzyl halides to Ni^0 complexes.[3,7] Indeed, treatment of $[Ni(\eta^1\text{-}CH_2C_6H_5)X(PPh_3)_2]$ (**2**) prepared *in situ* according to ref. 7, with $TlPF_6$, at $-20°C$ in THF, gives a deep red solution from which, after low temperature work-up, the complex $[Ni(\eta^3\text{-}CH_2C_6H_5)(PPh_3)_2]PF_6 \cdot CH_2Cl_2$ (**3**) can be isolated in *ca* 70% yield. Alternatively, it can be prepared in similar yield when a solution of $[Ni(cod)_2]$ and 2 equiv. of PPh_3, in THF, at $-20°C$, is treated with benzylhalide and the resulting solution further reacted with $TlPF_6$ and worked-up in the same way.

This latter procedure was used to prepare, also in very good yield, the complex $[Ni(\eta^3\text{-}CH_2C_6H_5)((+)\text{-DIOP})]PF_6$ (**4**)* but was ineffective for the preparation of the dppe (1,2-bis(diphenylphosphino)ethane) analogue which we have not yet achieved.

Attempts to prepare the corresponding $[Ni(\eta^3\text{-}CH_2C_6H_5)(PCy_3)_2]PF_6$, using this same procedure or starting from $[Ni(\eta^3\text{-}CH_2C_6H_5)X(PCy_3)]$ (**5**)[8] have been so far unfruitful. In fact, after the addition of $TlPF_6$ to the deep blue solution of **5** and 1 equiv of PCy_3, we observed a shift in the colour towards deep red, as in the case of **3**. After similar low temperature work-up an oil was formed which could be solidified by repeated washing with pentane. Analysis of this powder showed P–Ni ratios between 1 and 2. The presence of an η^3-benzyl complex is clearly seen in the ^1H NMR spectrum (δ 7–8 ppm), although contaminated with other unidentified species as confirmed by ^{31}P NMR. A different approach, namely the reaction of *trans*-$[Ni(Cl)(H)(PCy_3)_2]$ (**6**)[9] with 1 equiv. of styrene and $TlPF_6$ also failed to give the desired compound $[Ni(\eta^3\text{-}CH(CH_3)C_6H_5)(PCy_3)_2]PF_6$. However, both this reaction mixture and the mixture of **5** + 1 equiv. PCy_3 + 1 equiv. $TlPF_6$ gave styrene oligomers with the same characteristics as those obtained from **1** + PCy_3 (see below).

Crystal and molecular structure of $[Ni(\eta^3\text{-}CH_2C_6H_5)(PPh_3)_2]PF_6$ (**3**)

Crystals of compound **3** were easily obtained and a crystal structure determination was carried out. The molecular structure of the cation is shown in Fig. 1 and selected bond angles and distances are listed in Table 1.

The complex exhibits a distorted square-planar geometry with the benzyl group coordinated in a quasi-allylic fashion, via C(1), C(2) and C(7).

Due to the small bite of the benzyl ligand, the angle C(1)—Ni—C(7) is 68.4(4)°. Nevertheless, this is compensated for by the opening of the other angles, P(1)—Ni—P(2) = 104.3(2)°, C(7)—Ni—P(2) = 98.1(3)°, so that the sum around the nickel is 361.5(3)°. However, the angle between the planes defined by P(1)—Ni—P(2) and C(1)—Ni—C(7) is 14.5°.

The η^3-bonding mode for the pseudo-allylic group is unsymmetrical, having the shorter distance between the nickel and the methylene carbon and the longer one between the nickel and the *ortho* carbon. Similar features are observed in $[Ni(\eta^3\text{-}CH_2C_6H_4\text{-}o\text{-}Me)Cl(PMe_3)]$[3] and $[Co(\eta^3\text{-}CH_2C_6H_5)(P(OMe)_3)_3]$.[10] As in these complexes, the internal bond lengths in the benzylic group show a variation

*(+)-DIOP =

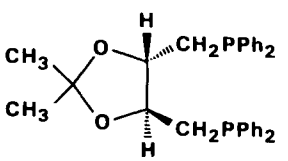

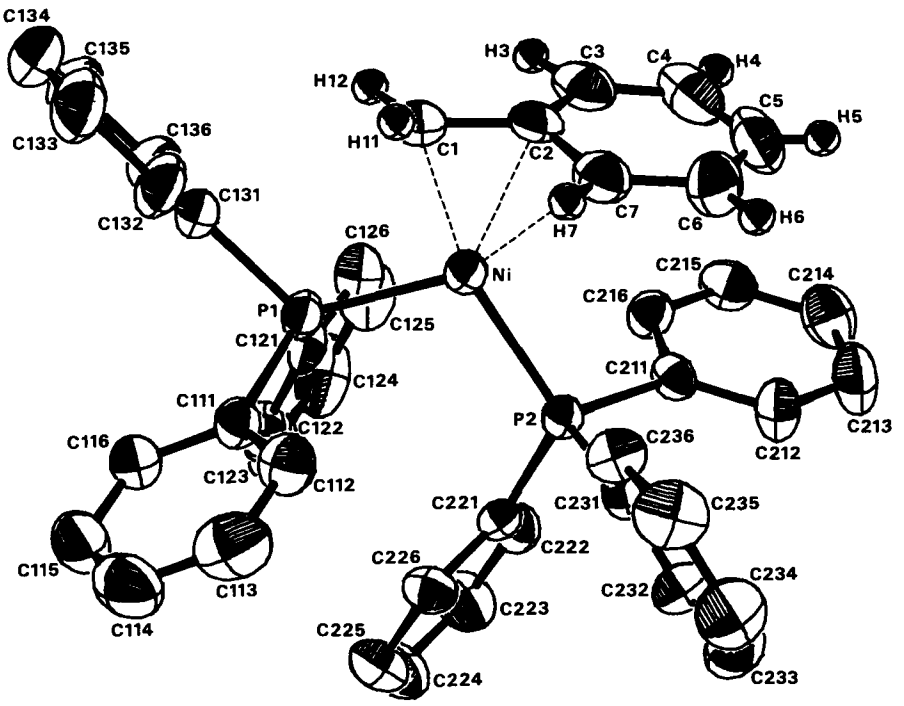

Fig. 1. Molecular structure of $[Ni(\eta^3\text{-}CH_2C_6H_5)(PPh_3)_2]^+$ with 50% probability thermal ellipsoids showing the atom labelling scheme.

Table 1. Selected bond lengths (Å) and bond angles (°) for $[Ni(\eta^3\text{-}CH_2C_6H_5)(PPh_3)_2]PF_6 \cdot CH_2Cl_2$

P(1)—Ni(1)	2.173(4)	P(2)—Ni(1)	2.243(4)
C(1)—Ni(1)	1.979(9)	C(2)—Ni(1)	2.077(7)
C(7)—Ni(1)	2.334(8)	C(2)—C(1)	1.450(10)
C(3)—C(2)	1.411(11)	C(7)—C(2)	1.405(10)
C(4)—C(3)	1.359(11)	C(5)—C(4)	1.378(15)
C(6)—C(5)	1.365(15)	C(7)—C(6)	1.389(11)

P(2)—Ni(1)—P(1)	104.3(2)	C(1)—Ni(1)—P(1)	90.7(3)
C(7)—Ni(1)—P(2)	98.1(3)	C(7)—Ni(1)—C(1)	68.4(4)
C(7)—Ni(1)—C(2)	36.6(2)	C(2)—C(1)—Ni(1)	72.7(5)
C(1)—C(2)—Ni(1)	65.5(4)	C(3)—C(2)—Ni(1)	114.3(5)
C(3)—C(2)—C(1)	122.9(7)	C(7)—C(2)—Ni(1)	81.7(5)
C(7)—C(2)—C(1)	117.7(7)	C(7)—C(2)—C(3)	118.6(7)
C(4)—C(3)—C(2)	119.8(8)	C(5)—C(4)—C(3)	121.1(9)
C(6)—C(5)—C(4)	120.4(9)	C(7)—C(6)—C(5)	120.2(9)
C(2)—C(7)—Ni(1)	61.7(4)	C(6)—C(7)—Ni(1)	127.4(6)
C(6)—C(7)—C(2)	119.7(8)		

which is associated with a difference in the double bond character of the C—C bonds. For the title complex the bond distances C(2)—C(3), C(4)—C(5) and C(6)—C(7) are longer (the average value is 1.393(13) Å) than those corresponding to C(3)—C(4) and C(5)—C(6) which have more double character (the average value is 1.362(13) Å). The benzyl ligand is planar with a maximum deviation from the plane of 0.061 Å at C(2). The methylene hydrogens were located and found to lie out of the benzylic plane: $\delta = 0.41$ for H(11) and $\delta = 0.08$ Å for H(7).

As a consequence of the asymmetry observed in the η^3-bonding the Ni—P bonds are different, with the bond *trans* to the methylene group, Ni—P(2), longer than the other one, Ni—P(1). This situation was also observed for the related $[Rh(\eta^3\text{-}CH_2C_6H_4\text{-}o\text{-}Me)(PPh_3)_2]$[11] and $[Rh(\eta^3\text{-}CH_2C_6Me_5)$

$(P(O^iPr)_3)_2]$.[12] Both Ni—P bond lengths are slightly longer than in $[Ni(\eta^3\text{-}CH_2C_6H_4\text{-}o\text{-}Me)Cl(PMe_3)]$.[3]

NMR characterization of **3** *and* **4**

The ^1H and ^{31}P variable temperature NMR spectra of $[Ni(\eta^3\text{-}CH_2C_6H_5)(PPh_3)_2]PF_6$ (**3**) agree with the molecular structure described above and reveal a fluxional behaviour, characteristic of η^3-benzylic complexes in solution.

At $-20°C$, the ^1H spectrum shows a triplet at 2.35 ppm arising from virtual coupling of the methylenic protons with the phosphorus nuclei ($J_{PH} \approx 5.4$ Hz), a doublet at 6.77 ppm for the *ortho* protons, the remaining benzylic aromatic protons being in the region 6.8–7.0 ppm, partially hidden by the *ortho* protons of the phosphine *trans* to the methylenic group. The other phosphine protons were found between 7.1 and 7.5 ppm.

At this temperature the $^{31}P\{^1H\}$ spectrum shows two 1 : 1 resonances at 31.44 and 26.34 ppm due to the non-equivalence of the two phosphine ligands. No significant changes on the ^1H and ^{31}P NMR spectra are observed upon cooling the solution of **3** in CD_2Cl_2 down to $-70°C$.

The observed equivalence of the two edges of the benzyl ligand down to $-70°C$ can be explained in terms of a rapid suprafacial shift as shown below:

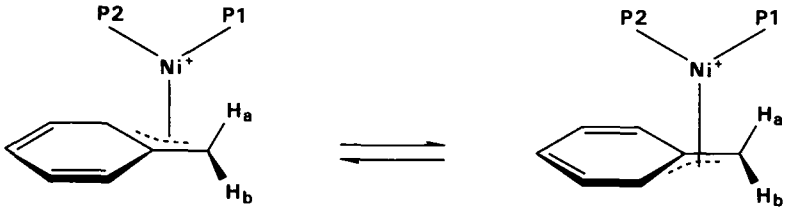

(2)

This process still leaves the two phosphorus atoms non-equivalent and has been put forward to explain the same fluxional behaviour in other η^3-benzylic related complexes.[13–15]

A second and different dynamic process is operating above $-20°C$. In effect, when the temperature increases to 10°C, the benzyl methylenic triplet collapses into a singlet and a significant broadening of the phosphine protons and phosphorus resonances is observed. At this temperature, the ^{13}C NMR resonances of the benzyl ligand appear decoupled from the phosphorus atoms. These facts indicate the presence of a slow phosphine exchange process, operating at temperatures above $-20°C$, as observed with other benzylic complexes of nickel and palladium.[7,14,15]

The NMR spectra of the similar compound $[Ni(\eta^3\text{-}CH_2C_6H_5)((+)\text{-DIOP})]PF_6$ (**4**) display some features which suggest a less fluxional benzyl ligand. Some conformation interconversion in the seven-membered ring of (+)-DIOP also appears to be present.

The room temperature ^1H spectrum of this compound shows two doublets at 2.00 and 2.53 ppm ($^2J_{HH} = 4.9$ Hz) corresponding to the benzyl methylenic protons and two other doublets at 6.41 and 6.66 ppm ($^3J_{HH} = 7.8$ Hz) for the benzylic *ortho* protons. The other aromatic benzyl protons appear between 6.70 and 7.00 ppm. The observed non-equivalence of the benzyl methylene and *ortho* protons is maintained from -70 to 23°C, which is consistent with a very low degree of mobility for the benzyl ligand in **4**. The ^1H spectrum of coordinated (+)-DIOP consists of a methine multiplet at 3.68 ppm, a methylenic multiplet at 2.76 ppm and a broad methylenic multiplet at 2.40 ppm; the methyl groups appear as a singlet at 1.12 ppm. By cooling a solution of **4** in CD_2Cl_2, these resonances broaden and shift, but no limiting spectrum is obtained even at $-70°C$.

The dynamic process that tends to average the complex spectra of **4**, at room temperature, is also visible in the much simpler $^{31}P\{^1H\}$ variable temperature spectra. At $-70°C$, the spectrum consists of two 1 : 1 resonances at 18.59 and 12.14 ppm. As the temperature increases, these resonances broaden significantly and, at 30°C, they are practically merged into a broad signal centred at about 13.8 ppm. These changes may be assigned to a chair–boat conformational equilibrium occurring in the seven-membered ring of this ligand.[16] Further increase in temperature initiates decomposition of the complex.

Catalytic studies

The catalytic activity of complexes **2**–**6** in the oligomerization of styrene was tested under conditions similar to those previously reported for $[Ni(\eta^3\text{-}CH_2C(CH_3)CH_2)(cod)]PF_6$ (**1**) and **1**+PR_3 systems.[1,2] The results are summarized in Table 2.

Complex **3** is an effective catalyst for this type of reaction. Its activity, at 10°C, is comparable to that found for **1**+2 equiv. PPh_3 (TOR = 6.8 min^{-1}), but much lower than in the case of **1**+1 equiv PPh_3 (TOR $\approx$ 1000 min^{-1}). The ^1H and ^{13}C NMR

Table 2. Catalytic activities of cationic η^3-benzyl nickel systems in the oligomerization of styrene (solvent: CH_2Cl_2, 10 cm^3)

Nickel complex			Styrene	T	Time	Conversion	TOR[b]			Isotactic[d]
Number	mmol	Additive[a]	(mmol)	(°C)	(h)	(%)	(min^{-1})	$\bar{M}_n$[c,d]	$\bar{M}_n/\bar{M}_w$[c,d]	content (P_m)
3	0.198	—	191	10	2	60	4.8	780	1.38	0.67
3	0.183	—	199	25	2	96	8.7	850	1.39	0.67
4	0.173	—	187	10, 30	8	0[g]	—	—	—	—
5	0.332	PCy_3, $TlPF_6$	336	10	3	4.5	0.25	1000	1.39	0.90
6	0.300	$TlPF_6$	299	10	18	36	0.33	1000	1.43	0.90
6	0.122	$TlPF_6$	87	22	18	70	0.46	1100	1.50	0.90

[a] 1 equiv.
[b] TOR = turnover rate = (number of moles of converted styrene)/(number of moles of nickel × time).
[c] ^1H NMR.
[d] Methanol-insoluble oligomer fraction.
[e] GPC.
[f] ^{13}C NMR.
[g] Traces of oligomers.

analyses of the obtained oligomers **7**, reveal that they are entirely similar to the ones obtained with catalysts **1** and **1**+PR_3 (R = Ph, *n*-Bu, OPh), including the same terminal groups and tacticity (isotactic contents ≈ 67–69%).[1] Furthermore, the values of $\bar{M}_n$ are rather constant and of the same order of magnitude as those found in the latter phosphine system.

Although we were unsuccessful in isolating the PCy_3 cationic benzyl analogue of **3**, we found that the addition of styrene to an *in situ* prepared mixture of **5**+1 equiv. PCy_3+1 equiv. $TlPF_6$ afforded styrene oligomers **8**, having the same features as the ones obtained with **1**+1 or 2 equiv. PCy_3, i.e. a different terminal end group and higher isotacticity (90%).[2] Moreover, the reaction of styrene with catalytic amounts of nickel hydride **6**+1 equiv. $TlPF_6$ also produced identical isotactic oligomers.

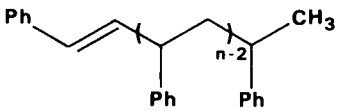

7

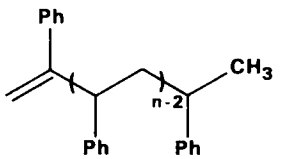

8

Both these reactions occurred with the simultaneous formation of small amounts (*ca* 5%) of a high molecular weight atactic polystyrene ($\bar{M}_n$ ≈ 35,000–50,000), probably resulting from some radicalar decomposition of the *in situ* prepared benzylic metal system. This may also explain the lower turnover rates obtained for these systems, when compared to those of **1**+1 or 2 equiv. PCy_3 (TOR = 0.7 min^{-1}).

Neutral precursors of our cationic complexes, namely [Ni(η^1-$CH_2C_6H_5$)Cl(PPh_3)$_2$] (**2**), [Ni(η^3-$CH_2C_6H_5$)Cl(PCy_3)] (**5**) and *trans*-[Ni(Cl)(H)(PCy_3)$_2$] (**6**) were found to be inactive towards the oligomerization of styrene, which seems to point out the importance of the electrophilic character of the metal centre in the activation of the olefinic double bond. The lability of the benzyl and phosphine ligands is also particularly important for the catalytic activity of this kind of benzylic complexes.

In effect, the low lability observed for cationic (+)-DIOP complex **4** somehow prevents insertion of a styrene molecule into the nickel–benzyl bond and explains its catalytic inactivity. For this reason, we were unable to evaluate the chiral diphosphine potential as a stereoregulating agent in the chain growth process (insertion steps).

All the reported results reinforce our previously suggested mechanism for the oligomerization of styrene,[1,2] in which the active species is a cationic

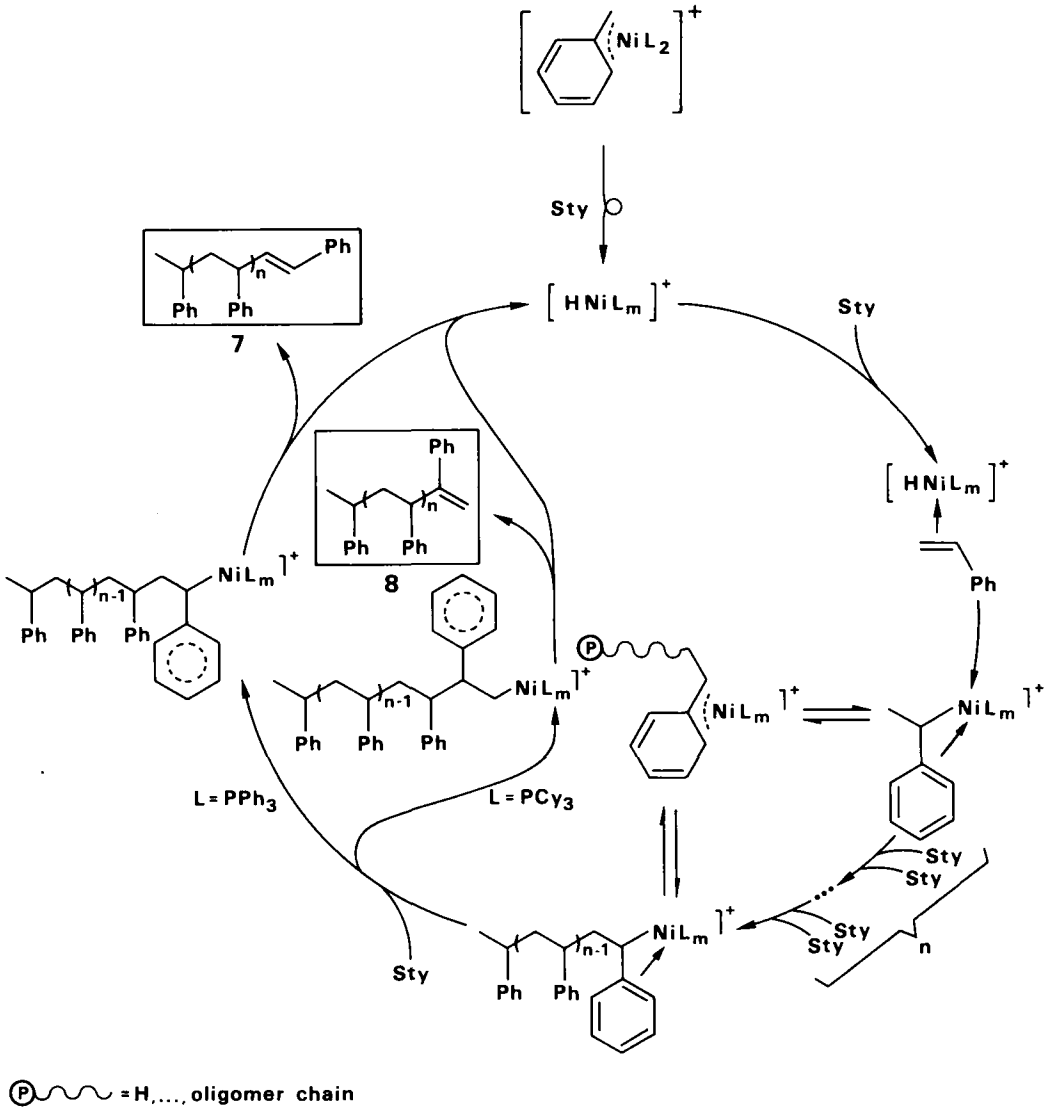

Scheme 1.

nickel hydride, generated in the reaction of the benzylic complexes with styrene (Scheme 1). Insertion of a new styrene molecule into the Ni—H bond gives rise to an η^3-α-methylbenzyl species, which undergoes further secondary insertion reactions, producing an oligomer growing chain stabilized through a $\eta^3 \leftrightarrow \eta^1$ bond to the metal. At a certain stage, β-elimination occurs, liberating oligomers **7** and regenerating the Ni—H species. In the case of the bulky PCy_3, this chain transfer process takes place when, probably due to a crowded coordination sphere, the styrene inserts in a primary mode being unable to stabilize the nickel–chain bond. In this mechanism, the η^3-coordination of the chain together with the PCy_3 size and basicity effects seem to be responsible for the obtention of isotactic oligomers **8**.

EXPERIMENTAL

All manipulations involving transition metal complexes were carried out under argon by the use of standard Schlenk tube techniques. Solvents and reagents were dried with anhydrous calcium sulphate (acetone, benzyl halides) and small amounts of sodium (ethanol, methanol) and distilled under an argon atmosphere with either sodium/benzophenone (THF, diethyl ether, toluene), P_2O_5 (CH_2Cl_2) or CaH_2 (pentane, hexane) and stored under argon. NMR solvents were dried over 4 Å molecular sieves, degassed by freeze–pump–thaw cycles and stored under argon. PCy_3 and PPh_3, from Aldrich, were recrystallized, respectively, from acetone and ethanol and stored under argon. (+)-DIOP and dppe, from Strem Chemicals, were

used as received. Phosphine purity was confirmed by ^{31}P NMR. Starting metal complexes $[Ni(CH_2{=}CH_2)(PPh_3)_2]$,[17] $[Ni(cod)_2]$,[18] $[Ni(\eta^1\text{-}CH_2C_6H_5)X(PPh_3)_2]$,[7] $[Ni(\eta^3\text{-}CH_2C_6H_5)X(PCy_3)]$[8] and *trans*-$[Ni(Cl)(H)(PCy_3)_2]$[9] were prepared according to the literature. IR spectra were recorded on a Perkin–Elmer 683 spectrophotometer. Microanalyses were performed in our laboratories.

Preparation of $[Ni(\eta^3\text{-}CH_2C_6H_5)(PPh_3)_2]PF_6 \cdot CH_2Cl_2$ (**3**)

Addition of benzyl chloride (0.18 cm^3, 1.56 mmol) to a solution of $[Ni(CH_2{=}CH_2)(PPh_3)_2]$ (1.00 g, 1.56 mmol) in THF (25 cm^3) at $-30°C$ and stirring for 1.5 h at this temperature, led to the formation of an intense deep blue solution. Addition of $TlPF_6$ (0.55 g, 1.57 mmol) with further stirring over 1 h, at the same temperature, afforded a deep red solution. After low temperature evaporation of the solvent and extraction with CH_2Cl_2, careful removal of TlCl from the mixture was made by filtration on a Celite bed. The solution was concentrated and the addition of hexane yielded, after 2 days, 0.97 g of deep red air-sensitive crystals of **3**, which were thoroughly washed with hexane and Et_2O and dried *in vacuo*. Yield: 69%. Good yields were also obtained starting from stoichiometric amounts of $[Ni(cod)_2]$, PPh_3, benzyl chloride, $TlPF_6$ and a similar work-up of the mixture. Experiments using benzyl bromide gave lower yields (50–60%). ^1H NMR (300 MHz, CD_2Cl_2, 10°C): δ 2.35 (s, 2H, $CH_2C_6H_5$), 6.77 (d, 2H, $^3J_{HH} = 5.9$ Hz, *ortho* benzylic), 6.8–7.0 (9H, aromatics + *para* and *meta* benzylic), 7.1–7.5 (24H, aromatics); $^{31}P\{^1H\}$ NMR (121.47 MHz, CD_2Cl_2, 10°C): δ 26.00 (s, *trans* to benzylic methylene), 30.94 (s, *cis*); $^{13}C\{^1H\}$ NMR (75.47 MHz, CD_2Cl_2, 10°C): δ 47.71 (br s, $CH_2C_6H_5$), 115.17 (s, benzylic *ipso*), 117.36 (s, benzylic *ortho*), 132.25 (s, benzylic *para*), 135.06 (s, benzylic *meta*), 128–134 (aromatics). $C_{44}ClF_6H_{39}NiP_3$: Found: C, 58.4; H, 4.5; P, 10.3. Calc.: C, 58.4; H, 4.4; P, 10.1%.

Preparation of $[Ni(\eta^3\text{-}CH_2C_6H_5)((+)\text{-DIOP})]PF_6$ (**4**)

Benzyl chloride (0.11 cm^3, 0.96 mmol) was added to a cold (−30°C) suspension of $[Ni(cod)_2]$ (0.26 g, 0.95 mmol) and (+)-DIOP (0.47 g, 0.95 mmol). The deep red solution obtained was stirred for 3 h. Addition of $TlPF_6$ (0.34 g, 0.97 mmol) immediately afforded a red–orange solution and a precipitate of TlCl, which were further stirred for 1 h. Low temperature work-up similar to that of **3** led to the obtention of an oil, that was sequentially washed with hexane, toluene and Et_2O. Repeated washing with pentane gave a brick-red powder (0.55 g), which was dried *in vacuo*. Yield: 73%. ^1H NMR (300 MHz, CD_2Cl_2, 23°C): δ 1.12 (s, 6H, diop methyl), 2.00 (d, 1H, $^2J_{HH} = 4.9$ Hz, methylenic *anti*), 2.40 (br m, 2H, diop methylene), 2.53 (d, 1H, $^2J_{HH} = 4.9$ Hz, methylenic *syn*), 2.76 (m, 2H, diop methylene), 3.68 (br m, 2H, diop methine), 6.41 (d, 1H, $^3J_{HH} = 7.8$ Hz, *ortho* benzylic), 6.66 (d, 1H, $^3J_{HH} = 7.8$ Hz, *ortho* benzylic), 6.7–7.0 (3H, *para* and *meta* benzylic), 7.2–7.9 (20H, aromatics); $^{31}P\{^1H\}$ NMR (121.47 MHz, CD_2Cl_2, −70°C): δ 12.14 (s, *trans* to benzylic methylene), 18.59 (s, *cis*). $C_{38}F_6H_{39}NiO_2P_3$: Found: C, 57.3; H, 5.0. Calc.: C, 57.5; H, 4.9%.

Catalytic reactions and oligomer treatment

The oligomerization reactions were carried out in Schlenk tubes immersed in a thermostatted water bath controlled to ±0.5°C and with a stirring rate of 500 rpm. In a typical experiment, styrene (19.86 g, 191 mmol) was introduced into the reaction vessel. Once thermal equilibrium had been reached, a thermostatted solution of **3** (0.179 g, 0.198 mmol) in CH_2Cl_2 (10 cm^3) was added. After 2 h, the reaction was terminated by flushing the solution with air to decompose the catalyst. For catalytic reactions related with **5** and **6**, *in situ* preparation of the catalyst was carried out by the addition of $TlPF_6$ to a mixture of styrene and neutral precursor in CH_2Cl_2.

The decomposed catalyst was removed from the reaction mixture by filtration on a silica gel bed. Evaporation of the solvent and unreacted styrene was followed by redissolution of the products in a minimum volume of CH_2Cl_2 and its precipitation in methanol. At that stage, the reaction products were separated into two fractions, respectively, methanol-soluble and methanol-insoluble oligomers.

The latter ones were characterized by gel permeation chromatography (GPC) using three columns of Microstyragel (100, 500, 10000 Å; 30 × 0.8 cm). THF was used as solvent at flow rate of 1.0 $cm^3\ min^{-1}$ and the detection was made with a Waters R401 refractometer.[19]

NMR measurements

^1H, ^{13}C and ^{31}P NMR characterization of **3** and **4** was performed on a CXP 300 Bruker spectrometer using CD_2Cl_2 as solvent. ^1H and ^{13}C chemical shifts are reported relative to TMS; ^{31}P chemical shifts are referenced to external 85% H_3PO_4.

^1H and ^{13}C NMR spectra of the polystyrene oligomers were run at 120°C in a solution of $CDCl_2CDCl_2$ and their isotactic content determined from the ^{13}C pattern of the aromatic *ipso* carbons.[20] Number average molecular weights ($\bar{M}_n$) were determined by comparing the intensities of the in-chain protons with those of the terminal groups.

X-ray data collection and structure determination for **3**

Crystals of **3**, suitable for diffraction measurements, were sealed in glass capillaries under argon.

Crystal data are given as follows: $C_{44}Cl_2F_6H_{39}NiP_3$, $M_r = 904.31$, monoclinic, space group $P2_1/n$, $a = 11.798(5)$, $b = 19.251(2)$, $c = 18.561(3)$ Å, $\beta = 93.30(3)°$, $V = 4208.6$ Å^3, $Z = 4$, $D_c = 1.77$ g cm^{-3}, μ(Mo-K_α) = 6.48 cm^{-1}.

All X-ray measurements were made at room temperature using an Enraf–Nonius CAD4 diffractometer and graphite monochromatized Mo-K_α radiation ($\lambda = 0.71069$ Å). Cell dimensions and the orientation matrix were obtained by least-squares refinement of setting angles for 25 automatically centred reflections with $8.5 \leqslant \theta \leqslant 19.5$. The intensities of 6056 unique reflections in the range $1.5 \leqslant \theta \leqslant 25.0$ were measured by the ω–2θ scan mode with ω scan widths of $0.80 + 0.35 \tan\theta$ and scan speeds of 0.785–5.49° min^{-1}. The data were empirically corrected for absorption using the Enraf–Nonius CAD4 software.

4728 reflections satisfied the criterium $F > 3\sigma(F)$ and were used for structure solution and refinement. The nickel position was located from a Patterson map and the positions of the other non-hydrogen atoms from subsequent difference Fourier synthesis. The phenyl groups were refined isotropically as rigid groups. Refinement was then continued with all the remaining non-hydrogen atoms refining anisotropically in a blocked-diagonal least-squares. The positions of the benzylic hydrogen atoms were located in the ΔF map and were included in refinement with individual isotropic thermal parameters, while the phenylic hydrogens were calculated and inserted in idealized positions. The weighting scheme $w = 1.4840/\sigma^2|F| + 0.000910F^2$ was found to give acceptable agreement analysis. The atoms on the PF_6^- anion have, as usual, very high thermal motion, thus limiting the overall accuracy in the refinement. Final refinement gave $R = 0.0632$ and $R_w = 0.0764$. Tables of final atomic positional parameters for the refined atoms, anisotropic displacement factor coefficients and positional parameters for idealized hydrogen, as well as lists of observed and calculated structure factors are available as supplementary data from the Authors. All the computations required to solve and refine the structure were made using SHELX76;[21] the drawing was made using ORTEP.[22]

Acknowledgements—We thank the Instituto Nacional de Investigação Cientifica (J.R.A., M.A.A.F.C.T.C., A.R.D., P.T.G., M.F.M.P., C.C.R.) and CNRS (A.R., I.T.) for financial support.

REFERENCES

1. J. R. Ascenso, A. R. Dias, P. T. Gomes, D. Neibecker, A. Revillon, C. C. Romão and I. Tkatchenko, *Makromol. Chem.*, in press.
2. J. R. Ascenso, A. R. Dias, P. T. Gomes, C. C. Romão, Q. T. Pham, D. Neibecker and I. Tkatchenko, *Macromolecules* 1989, **22**, 998.
3. E. Carmona, J. M. Marín, M. Paneque and M. L. Poveda, *Organometallics* 1987, **6**, 1757 and refs therein.
4. R. F. Jordan, R. E. LaPointe, C. S. Bajgur, S. F. Echols and R. Willett, *J. Am. Chem. Soc.* 1987, **109**, 4111.
5. M. Brookhart, R. C. Buck and E. Danielson III, *J. Am. Chem. Soc.* 1989, **111**, 567.
6. R. R. Stevens and G. D. Shier, *J. Organomet. Chem.* 1970, **21**, 495.
7. E. Bartsch, E. Dinjus, R. Fischer and E. Uhlig, *Z. Anorg. Allg. Chem.* 1977, **433**, 5.
8. G. Favero, S. Issa, A. Turco and U. Vettori, *J. Organomet. Chem.* 1986, **315**, 237.
9. T. Saito, H. Munkata and H. Imoto, *Inorg. Synth.* 1977, **17**, 83.
10. J. R. Bleeke, R. R. Burch, C. L. Coulman and B. C. Schardt, *Inorg. Chem.* 1981, **20**, 1316.
11. S. D. Chappell, D. J. Cole-Hamilton, A. M. R. Galas, M. B. Hursthouse and N. P. C. Walker, *Polyhedron* 1985, **4**, 121.
12. R. R. Burch, E. L. Muetterties and V. W. Day, *Organometallics* 1982, **1**, 188.
13. F. A. Cotton and T. J. Marks, *J. Am. Chem. Soc.* 1969, **91**, 1339.
14. Y. Becker and J. K. Stille, *J. Am. Chem. Soc.* 1978, **100**, 845.
15. E. Carmona, M. Paneque and M. L. Poveda, *Polyhedron* 1989, **8**, 285.
16. J. M. Brown and P. A. Chaloner, *J. Am. Chem. Soc.* 1978, **100**, 4307; P. A. Chaloner, *J. Organomet. Chem.* 1984, **266**, 191.
17. P. Giannoccaro, A. Sacco and G. Vasapollo, *Inorg. Chim. Acta* 1979, **37**, L455.
18. F. Guerrieri and G. Salerno, *J. Organomet. Chem.* 1976, **114**, 339.
19. A. Revillon and T. Hamaide, *Polym. Bull.* 1982, **6**, 235.

20. H. Sato and Y. Tanaka, in *NMR and Macromolecules* (Edited by G. C. Randall), pp. 181–196. ACS Symposium Series 247, American Chemical Society, Washington, D. C. (1984).
21. G. M. Sheldrick, SHELX76. A Program for Crystallographic Calculation. University of Cambridge (1976).
22. C. K. Johnson, ORTEP II Report ORNL-5138, Oak Ridge National Laboratory, Tennessee (1976).

Polyhedron Vol. 8, No. 20, pp. 2459–2462, 1989
Printed in Great Britain

0277-5387/89 $3.00+.00
© 1989 Pergamon Press plc

MONO-CONDENSED PRODUCT OF FERROCENYLFORMYL ACETONE WITH ETHYLENEDIAMINE AND ITS COMPLEXES OF LANTHANIDE CHLORIDES

PEIZHI HU, LUN ZHANG,* XIAOBING ZHU, XIYAN LIU, LICAI JI and YILONG CHEN†

Department of Chemistry, Wuhan University, China

(*Received* 10 *February* 1989; *accepted* 19 *May* 1989)

Abstract—A mono-condensed product (Fcen)

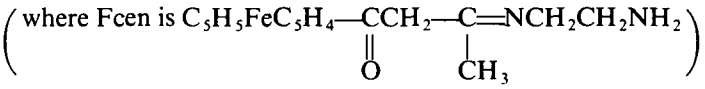

was obtained from the condensation of ferrocenylformyl acetone with ethylenediamine and five new Fcen complexes of lanthanide chlorides having the formula $Fcen_3LnCl_3$ (where Ln = La, Nd, Gd, Dy and Lu) were synthesized via the reaction of Fcen with lanthanides. These lanthanide complexes were characterized by microanalyses, IR, UV, Mössbauer spectra, molar conductivities and TG–DTA graphs. The ^1H NMR and MS spectra of Fcen were also recorded. In these complexes each Fcen is tridentately coordinated to the lanthanide ions and three chlorine atoms are outer-sphere anions.

Vishnyakova *et al.*[1] have prepared the bi-condensed product (Fc_2en) of ferrocenylformyl acetone with ethylenediamine and Eremina[2] has synthesized Fc_2en complexes of *d*-transition metals, but no complex of this ligand with lanthanide ions has been described in the literature up until now.

In this article, we wish to report the syntheses of the mono-condensed product of ferrocenylformyl acetone with ethylenediamine (Fcen) and its complexes with lanthanide chlorides. The physical properties (spectra, etc.) of Fcen and its complexes were measured and are discussed.

EXPERIMENTAL

Preparation of Fcen

To a solution of ethylenediamine (10 mmol) in 15 cm^3 of methanol, a solution of ferrocenylformyl acetone (10 mmol) in 15 cm^3 of methanol was added dropwise, and the reaction mixture was stirred for 0.5 h. After standing overnight the yellow precipitate was filtered off, washed three times with small quantities of cold methanol and ether, respectively, and dried *in vacuo* for 3 h to give 2.0 g of the condensed product (Fcen), yield 64%, m.p. 177–179°C. Elemental analysis for $C_{16}H_{20}N_2OFe$: Found: Fe, 17.9. Calc.: Fe, 17.8%.

Ferrocenylformyl acetone was synthesized according to the literature method.[3]

Coordination of Fcen *with lanthanide chlorides*

The coordination reaction of Fcen with lanthanide chlorides was carried out by using a general procedure that is illustrated below by the reaction of Fcen with $LaCl_3 \cdot xH_2O$.

La_2O_3 (0.3 mmol) was dissolved in 5 cm^3 of 1 M hydrochloric acid and solid $LaCl_3 \cdot xH_2O$ was obtained after concentration of the solution to dryness. The solid obtained was dissolved in 20 cm^3 of anhydrous ethanol, and was added dropwise with stirring to a solution of 2.4 mmol Fcen in 30 cm^3 of anhydrous ethanol; precipitation of product occurred immediately. The suspended substance was stirred for 2 h, the precipitate was filtered off, washed twice with small quantities of cold ethanol, then ether and dried *in vacuo* for 3 h. A complete

* Author to whom correspondence should be addressed.
† Department of Physics, Wuhan University, China.

Table 1. Yields and microanalyses data for $Fcen_3LnCl_3$

$Fcen_3LnCl_3$	Yield (%)	Microanalyses Found (Calc.) (%) Ln	Fe	Cl
La	37	11.3 (11.7)	14.7 (14.8)	9.0 (9.0)
Nd	40	12.5 (12.1)	14.0 (14.1)	9.6 (9.0)
Gd	61	13.6 (13.1)	13.7 (13.9)	8.8 (8.8)
Dy	55	13.7 (13.4)	13.5 (13.9)	8.8 (8.8)
Lu	39	14.5 (14.3)	13.3 (13.7)	9.2 (8.7)

list of the complexes, yields and microanalyses are given in Table 1.

The lanthanide oxides, all of 99.9% purity, were obtained from Yue Long Chemical Plant (P.R.C.).

Physical measurements

A Shimadzu IR-450 spectrophotometer was used to obtain the IR spectra using KBr discs. UV spectra were recorded in DMF with a Shimadzu UV-240 spectrophotometer. ^1H NMR spectra were recorded in $CDCl_3$ with a JEOL JNM-PMX60SI spectrometer using TMS as internal standard. Mass spectra were obtained on a VG 7070E-HFMS instrument using an electron-impact ion source. Mössbauer spectra were recorded on an OXFORD MS 500 Mössbauer instrument at 290 K using $^{57}Co/Rh$ as the radio source. Molar conductivities were measured in DMF at 25°C with a Shanghai DDS-11A conductivity apparatus. TG–DTA graphs were recorded on a Beijing LCT-1 TG–DTA instrument in air using Al_2O_3 as reference.

RESULTS AND DISCUSSION

The condensation and coordination reactions can be outlined as in Scheme 1.

The condensation reaction must be carried out at room temperature, otherwise the bi-condensed product will be obtained.

Fcen and $Fcen_3LnCl_3$ are fine solids, which are soluble in DMF and DMSO, and insoluble in alcohol, ether, acetone, alkyl halides and water. At room temperature these complexes are stable to air, moisture and light.

Microanalyses (Ln, Fe, Cl) data of these complexes (Table 1) show that all the complexes have a 3 : 1 ratio of Fcen to lanthanide chloride stoichiometrically, which is in accordance with the general formula $Fcen_3LnCl_3$.

The important IR absorption data for the ligand and complexes are given in Table 2. The IR spectra of all these complexes are similar, with the free Fcen

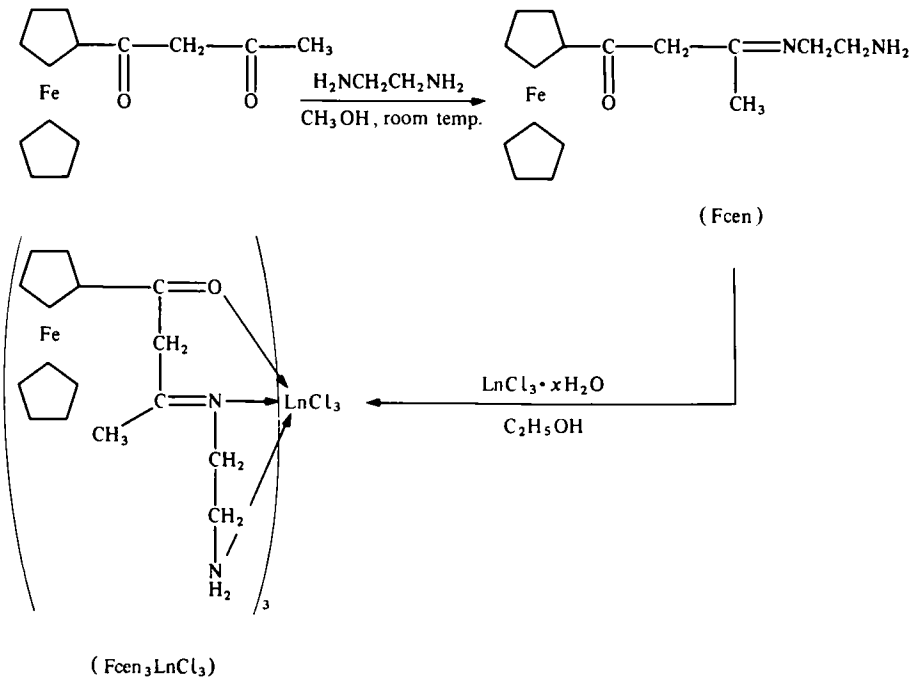

Scheme 1. Ln = La, Nd, Gd, Dy and Lu.

Table 2. Important IR absorption data (cm^{-1}) of Fcen and $Fcen_3LnCl_3$

Fcen	La	Nd	Gd	Dy	Lu
3430w,b	3370m,b	3370m,b	3370m,b	3370m,b	3370m,b
1600s	1592s	1590s	1593s	1593s	1590s
1557m	1532m	1530s	1529m	1530m	1528m
1520m	1495m	1488m	1482m	1485m	1485m
1449m	1450m	1450m	1447m	1450m	1450m
1410w	1410w	1410w	1410w	1410w	1410w
1380m	1380m	1380m	1380m	1382m	1380m
1342m	1350m	1350m	1350m	1350m	1350m
1290s	1290s	1289s	1290s	1290s	1290s
1210m	1210m	1210m	1210w	1210w	1210w
1110m	1110m	1109m	1109m	1110m	1110m
1092m	1092m	1091m	1088m	1090m	1090m
1007m	1007m	1007m	1007m	1010m	1010m
930w	930w	929w	927w	929w	928w
820m	820m	820m	820m	820m	818m
792m	792m	791m	789m	790m	790m
538w	538w	538w	538w	540w	536w
504m	502m	502m	497m	498m	502m
490m	490m	490m	486m	488m	490m
478w	478w	478w	478w	478w	478w

bands undergoing shifts owing to complex formation. The free ligand exhibits $\nu(NH_2)$, $\nu(C{=}O)$, $\delta(NH_2)$ and $\nu(C{=}N)$ bands at 3430, 1600, 1557 and 1520 cm^{-1}, respectively, while in the spectra of the complexes they are shifted to lower wave numbers by 60, 7–10, 25–29 and 25–38 cm^{-1}, respectively. These observations suggest that Fcen is coordinated with the lanthanide ions as a tridentate ligand through its carbonyl oxygen, axomethine and amino nitrogen atoms (see Scheme 1).

The UV spectral data listed in Table 3 show that all the spectra of $Fcen_3LnCl_3$ are similar to the spectrum of Fcen. The absorption maxima (270 and 342 nm) of the ligand suffer slight blue shifts of 1–3 nm in the complexes. However, the values of the molar extinction coefficients of the complexes measured at identical wavelengths show significant increments when compared with that of the ligand (Table 3). In the 440–460 nm region, a flat, broad band is also observed for both the ligand and complexes (Fig. 1), but the position of λ_{max} and the value of ε can not be accurately determined.

Table 3. UV spectral data of Fcen and $Fcen_3LnCl_3$

Ligand or complexes	Band 1 λ_{max} (ε)	Band 2 λ_{max} (ε)	Band 3 λ_{max} (ε)
La	269(22,080)	340(36,960)	440–460
Nd	269(22,860)	341(43,920)	440–460
Gd	269(22,480)	341(39,040)	440–460
Dy	269(24,300)	339(36,120)	440–460
Lu	268(18,260)	340(26,540)	440–460
Fcen	270(7340)	342(17,820)	440–460
Ferrocene[a]	267(1569)	328(47)	441(93)

[a] The values of ferrocene measured in this work agree with the literature values.[6]

The significant differences between the UV spectra of ferrocene and Fcen are observed when an electron-withdrawing substituent is introduced into the cyclopentadienyl ring. The 267 and 328 nm bands of ferrocene are shifted bathochromically in Fcen, the former is shifted by 3 nm and the latter by 14 nm. The intensity (ε) of the 328 nm band, however, increases much more than that of the 267 nm band. The 441 nm band of ferrocene becomes a flat, weak band in Fcen, as mentioned above. Therefore, the 328 and 441 nm bands, which are sensitive to the substituent, can be attributed to the *d–d* transitions[4] of the ferrocene entity, while the 267 nm band may be attributed to the π–π^* transitions of the cyclopentadienyl ring.[5]

The fact that both the ligand and complexes have virtually identical absorption maxima and the values of ε increase in the complexes, indicates that the σ-orbitals of the oxygen and nitrogen atoms are substantially involved in bonding with the lanthanide ions.

The ^1H NMR spectrum of Fcen clearly shows proton signals (δ, ppm) for

CH_3 (1.86, s, 3H),

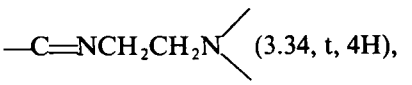

(3.34, t, 4H),

C_5H_5Fe (4.00, s, 5H), C_5H_4Fe (4.20, b, 4H),

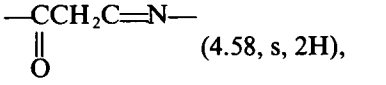

(4.58, s, 2H),

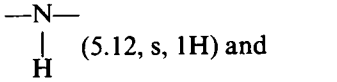

(5.12, s, 1H) and

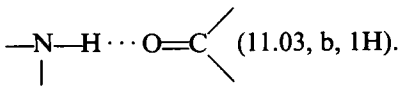

(11.03, b, 1H).

The signals at 5.12 and 11.03 ppm disappear on deuteration with D_2O which indicates that one of the amino nitrogen atoms is associated with the carbonyl oxygen atom to form a hydrogen bond.

The spectra of the complexes could not be taken due to their limited solubility.

The mass spectrum of Fcen exhibits its molecular ion peak at *m/z* 312. The following peaks are also found:

m/z 295

$$[C_5H_5—FeC_5H_4—\underset{\underset{O}{\|}}{C}CH_2—\underset{\underset{CH_3}{|}}{C}=NCH=CH_2]^+,$$

m/z 282

$$[C_5H_5FeC_5H_4—\underset{\underset{O}{\|}}{C}CH_2—\underset{\underset{CH_3}{|}}{C}=NCH_2]^+,$$

m/z 185 $[C_5H_5FeC_5H_4]^+$, *m/z* 121 $[C_5H_5Fe]^+$, *m/z* 65 $[C_5H_5]^+$ and *m/z* 56 $[Fe]^+$.

The data for ^1H NMR and MS spectra further support the composition and structure of Fcen.

The Mössbauer spectra of the ligand and complexes are similar to the spectrum of ferrocene, which exhibits a quadruple doublet (Fig. 2).

From the data in Table 4, it is clear that both Fcen and $Fcen_3LnCl_3$ have markedly lower isomeric shifts (IS) and quadrupole splitting (QS) compared with those of ferrocene, owing to the presence of the conjugated electron-withdrawing substituent[7] on the cyclopentadienyl ring. However, the differences in the Mössbauer parameters between Fcen and $Fcen_3LnCl_3$ are very small. They show that there is no significant charge-transfer between the iron nucleus and lanthanide after coodination of Fcen with the lanthanide chlorides.

The molar conductivity values for the La, Nd, Gd and Dy complexes are 222, 218, 240 and 194 Ω^{-1} cm^2 mol^{-1}, respectively, while the molar conductivity of $CrCl_3$ determined under the same conditions is 235 Ω^{-1} cm^2 mol^{-1}. It suggests that all these complexes behave as 1 : 3 electrolytes in DMF.

The TG–DTA graphs were recorded in the temperature range of 25–850°C. From the DTA curves, no melting points for the Fcen complexes are observed. However, the complexes have two decomposition points. The first is in the range of 172–196°C, corresponding to a sharp endothermic peak, while the second is in the range 248–368°C, corresponding to a broad and larger endothermic peak. On comparison with the endothermic peaks, the TG curves reveal two stages of weight loss. The initial decomposition temperatues for the La, Nd, Gd, Dy and Lu complexes are 190, 184, 172, 191 and 196°C, respectively.

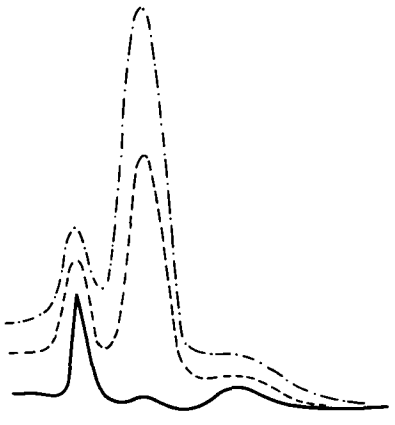

Fig. 1. UV spectra of ferrocene, Fcen and $Fcen_3LaCl_3$ taken in DMF (5×10^{-5} M). —— ferrocene, – – – Fcen, –·–·– $Fcen_3LaCl_3$.

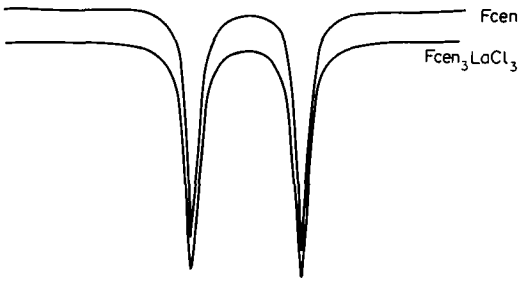

Fig. 2. The Mössbauer spectra of Fcen and $Fcen_3LaCl_3$.

Table 4. The Mössbauer parameters for Fcen and $Fcen_3LnCl_3$

Ligand or complexes	IS (mm s^{-1})[a]	QS (mm s^{-1})
Fcen	0.33	2.26
La	0.34	2.27
Nd	0.34	2.25
Gd	0.33	2.23
Dy	0.34	2.24
Lu	0.34	2.24
Ferrocene[b]	0.44	2.40

[a] With respect to the centre of the α-Fe spectrum at 298 K.

[b] Literature data.[8]

REFERENCES

1. T. P. Vishnyakova, I. D. Vlasova and I. A. Eremina, *Zh. Org. Khim.* 1970, **6**, 1837.
2. I. A. Eremina, *Neft. Gaz. Ikh. Prod.* 1971, 144; *Chem. Abstr.* 78, 4570u.
3. Guomin Zhang, Heping Xiong and Lun Zhang, *Wuji Huaxue* 1985, **1**, 122.
4. M. Rosenblum, *Chemistry of the Iron Group Metallocenes*, Part 1, p. 42. John Wiley, New York (1965).
5. P. Krumholz, O. A. Serra and M. A. Depaoli, *Inorg. Chim. Acta* 1975, **15**, 25.
6. D. S. Scott and R. S. Becker, *J. Phys. Chem.* 1961, **35**, 516.
7. B. Lukas, R. M. G. Roberts, J. Silver and A. S. Wells, *J. Organomet. Chem.* 1983, **256**, 103.
8. A. J. Deeming, Mononuclear iron compounds with η^2–η^6 hydrocarbon ligands, in *Comprehensive Organometallic Chemistry* (Edited by G. Wilkinson, F. G. A. Stone and E. W. Abel), Vol. 4, p. 478. Pergamon Press, Oxford (1982).

Polyhedron Vol. 8, No. 20, pp. 2463–2467, 1989
Printed in Great Britain

0277–5387/89 $3.00+.00
© 1989 Pergamon Press plc

EFFECTS OF SIDE-CHAIN DONOR GROUPS ON DEPROTONATION OF PEPTIDE AMIDE IN COPPER(II) COMPLEXES AT HIGH pH

E. FARKAS* and T. KISS

Department of Inorganic and Analytical Chemistry, Lajos Kossuth University, H-4010 Debrecen, Hungary

(*Received* 1 *December* 1988; *accepted* 19 *May* 1989)

Abstract—The copper(II) complexes of the GlyAsp (glycyl–L-aspartic acid), GlyAsn (glycyl–L-asparagine), GlySer (glycyl–L-serine), GlyThr (glycyl–L-threonine), GlyPhe (glycyl–L-phenylalanine), SerGly (L-serylglycine), ThrGly (L-threonylglycine), PheGly (L-phenylalanylglycine) and GlyGly (glycylglycine) groups as a reference were studied by pH-metric, spectrophotometric and ESR methods at high pH and high ligand excesses (up to a metal-to-ligand ratio of 1 : 50). The influence of the side-chain donor groups and the aromatic ring on the competitive formation of the mixed hydroxo complex $[Cu(AH_{-1})OH]$ and the deprotonated complex $[Cu(AH_{-1})_2]$ was evaluated.

The copper(II) ion-induced deprotonation of the peptide amide group in simple dipeptides occurs at *ca* pH 4–5,[1–6] and a complex $[Cu(AH_{-1})]$ is formed, in which the amino nitrogen, the deprotonated peptide amido nitrogen and the carboxylate oxygen are involved in coordination. A hydroxide ion and a second ligand can compete with each other for the fourth equatorial coordination site. The bis-complex $[Cu(AH_{-1})A]$ is formed in the pH range 6–10. If the metal ion-to-dipeptide ratio is below 1 : 5, the A is displaced by a hydroxide ion above pH 9–10, and even the carboxylate group is replaced by a second OH ion above pH 12.0–12.5.[7–9] At a high ligand excess and at high pH, it was found in the copper(II)–GlyGly system that there is an equilibrium between this mixed hydroxo complex $[Cu(AH_{-1})OH]$ and the 1 : 2 deprotonated complex $[Cu(AH_{-1})_2]$.[10]

We have previously investigated numerous copper(II)–dipeptide systems.[11–16] In the present work we have extended the solution equilibrium study up to high ligand excess, 1 : 50, and high pH, *ca* 13.

EXPERIMENTAL

GlyGly, GlyAsp, GlyAsn, GlySer, SerGly, GlyPhe and PheGly were purchased from SIGMA. ThrGly and GlyThr were prepared by the method reported in ref. 17.

The pH-metric and spectrophotometric measurements were carried out for samples with metal-to-ligand ratios of 1 : 1, 1 : 2, 1 : 25 and 1 : 50. The concentrations of the copper(II) ion varied in the range 0.004–0.020 mol dm^{-3}. The measurements were performed at 25.0 ± 0.1°C, and the ionic strength was adjusted to 1.0 mol dm^{-3} with KCl.

The pH-metric titrations were performed over the pH range 3.0–13.0 in an argon atmosphere, using a Radiometer pHM 64 instrument, with a GK 2401B combined electrode and a Radiometer ABU 13 burette. The electrode system was calibrated by the method of Irving *et al.*[18]

Visible absorption spectra were recorded over the pH range 8.5–13.0 with a Beckman ACTA MIV double-beam recording spectrophotometer.

Concentration equilibrium constants were calculated by the simultaneous fitting of the pH and spectrophotometric experimental data with the aid of the computer program PSEQUAD.[19]

EPR spectra of the copper(II)–GlySer and copper(II)–SerGly systems were obtained on a JES-MF-3F spectrometer at liquid nitrogen temperature (77 K). The parameters g and A were calculated via the computer program of Rockenbauer *et al.*[20]

RESULTS AND DISCUSSION

The equilibrium constants for the complexes present in the systems of copper(II) with GlyGly, GlyAsn, GlyAsp, GlySer, SerGly, GlyPhe and PheGly in the pH range 3–10 were reported earlier.[11,15,16]

* Author to whom correspondence should be addressed.

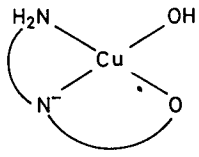

[Cu(AH$_{-1}$)OH]

Scheme 1.

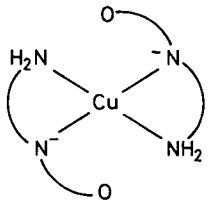

[Cu(AH$_{-1}$)$_2$]

Scheme 2.

For this reason, only the constants for the copper(II)–ThrGly and copper(II)–GlyThr complexes, which have not been published before, are given in this paper.*

In the copper(II)–dipeptide systems the following equilibrium processes may take place at high pH, in competition with each other:

$$[Cu(AH_{-1})A] + 2H_2O \rightleftharpoons [Cu(AH_{-1})OH] + A + H_3^+O \quad (1)$$

$$[Cu(AH_{-1})A] + H_2O \rightleftharpoons [Cu(AH_{-1})_2] + H_3^+O. \quad (2)$$

The bonding modes of the complexes [Cu(AH$_{-1}$)OH] and [Cu(AH$_{-1}$)$_2$] are depicted in Schemes 1 and 2, respectively. (The overall charges of the complexes are omitted, as they depend on the type of ligand.)

As can be seen in Schemes 1 and 2, the mixed hydroxo complex [Cu(AH$_{-1}$)OH] has two nitrogen atoms in the coordination sphere, while the deprotonated one [Cu(AH$_{-1}$)$_2$] has four. This means that spectrophotometry can be used to distinguish between equilibrium processes (1) and (2).

The pH-dependences of the absorption maxima

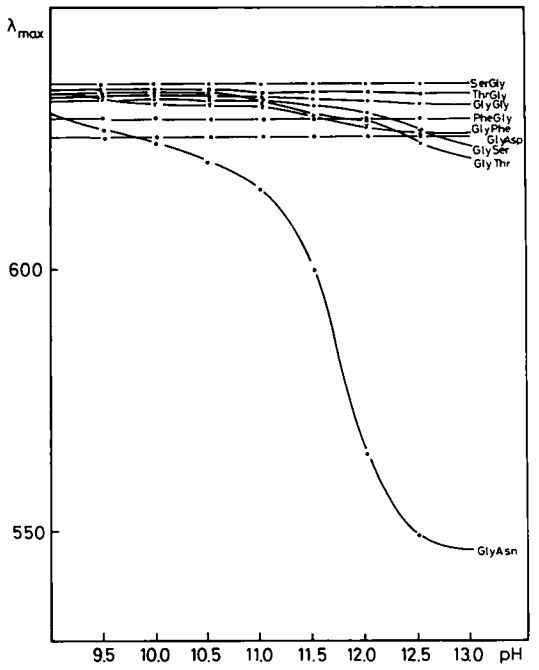

Fig. 1. pH-dependences of λ_{max} over the pH range 9.0–13.0 for the copper(II)–dipeptide systems at a metal-to-ligand ratio of 1 : 1.

(λ_{max}) for all of the studied systems, at metal-to-ligand ratios of 1 : 1 and 1 : 50, are depicted in Figs 1 and 2, respectively.

It can be seen from Fig. 1 that the λ_{max} values, except for those relating to the copper(II)–GlyAsn,

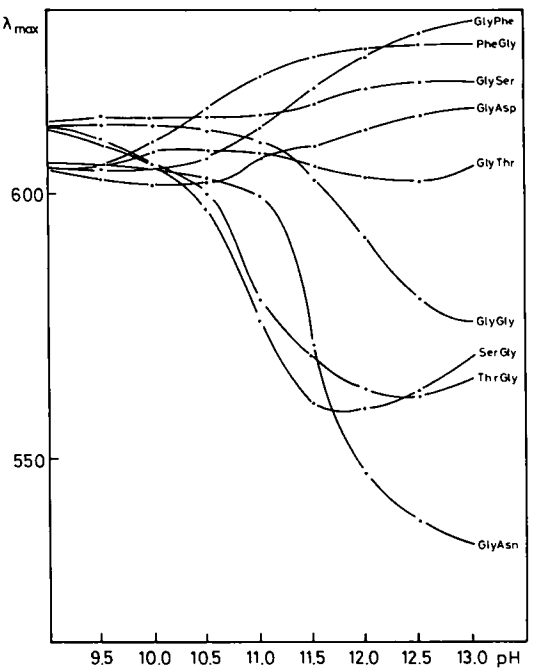

Fig. 2. pH-dependences of λ_{max} over the pH range 9.0–13.0 for the copper(II)–dipeptide systems at a metal-to-ligand ratio of 1 : 50.

* Formation constants ($\log\beta$) for proton and copper(II) complexes of GlyThr and ThrGly (I = 1.0 mol dm^{-3} (KCl), t = 25°C). GlyThr: HA: 8.25; H_2A: 11.41; [CuA]: 5.43; [CuAH$_{-1}$]: 1.12; [CuA$_2$H$_{-1}$]: 4.17; [CuAH$_{-2}$]: −8.43. ThrGly: HA: 7.46; H_2A: 10.67; [CuA]: 4.86; [CuAH$_{-1}$]: 1.09; [CuA$_2$H$_{-1}$]: 3.40; [CuAH$_{-2}$]: −8.57; [Cu(AH$_{-1}$)$_2$]: −6.90.

copper(II)–GlySer and copper(II)–GlyThr systems, lie at around 630 nm and do not show a noticeable pH-dependence at a metal-to-ligand ratio of 1 : 1. Perfect fitting can be obtained only if the formation of the species $[Cu(AH_{-1})OH]$ is assumed for all the experimental data (both pH and spectrophotometric data). For the copper(II)–GlySer and copper(II)–GlyThr systems, the λ_{max} values show a small decrease above pH 11.5, suggesting the already reported[8] deprotonation and coordination of the alcoholic hydroxy group, replacing the carboxylate, above pH 12. The marked increase in the *d–d* transition energy for the copper(II)–GlyAsn system above pH 9 has been ascribed to the formation of $[Cu(AH_{-2})OH]$, in which three nitrogen atoms (NH_2, deprotonated peptide amido and side-chain amido nitrogens) are involved in the coordination in addition to an OH^- ion.[11]

According to Fig. 2, there is a large increase in the *d–d* transition energy in the copper(II)–GlyAsn, copper(II)–SerGly and copper(II)–ThrGly systems at a metal-to-ligand ratio of 1 : 50 above pH 9 and in the copper(II)–GlyGly system above pH 11. In the other systems a small red shift can be seen,

Table 1. Equilibrium constants for processes in the copper(II)–dipeptide systems at a high ligand excess and at high pH; $t = 25°C$, $I = 1.0$ mol dm^{-3} (KCl)

Ligand	$pK\frac{[Cu(AH_{-1})A]}{[Cu(AH_{-1})OH]}$	$pK\frac{[Cu(AH_{-1})A]}{[Cu(AH_{-1})_2]}$
GlyGly	12.46	11.60
GlyAsp	12.55	—
GlyThr	12.59	—
GlySer	12.31	—
GlyPhe	12.50	—
ThrGly	11.96	10.41
SerGly	11.97	10.40
PheGly	12.04	—

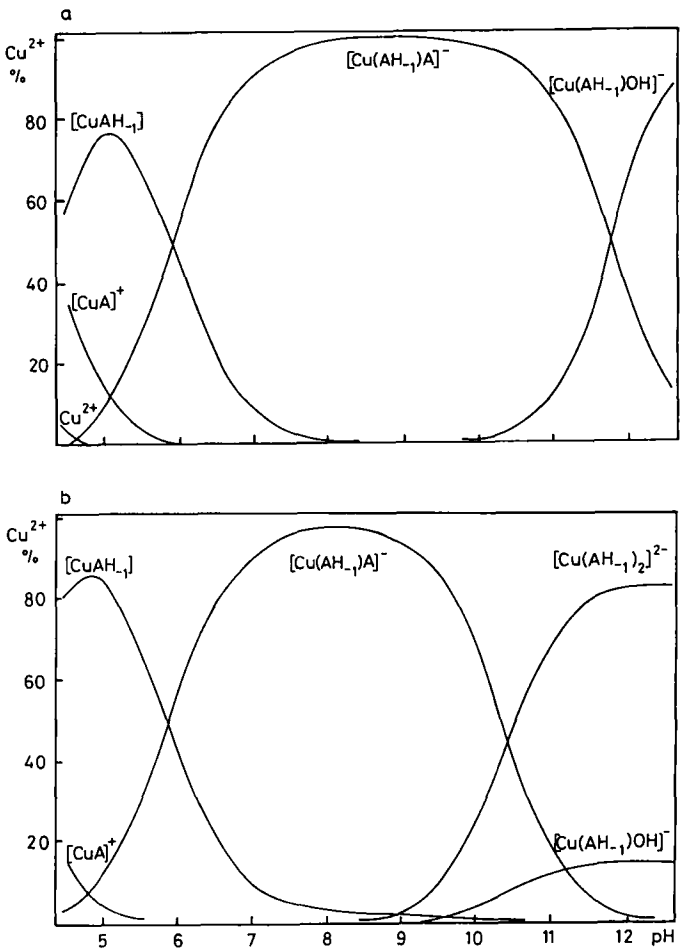

Fig. 3. (a) Concentration distribution of the complexes present in the copper(II)–GlyThr system at a metal-to-ligand ratio of 1 : 50; $c_A = 2 \times 10^{-1}$ mol dm^{-3}; $c_{Cu^{II}} = 4 \times 10^{-3}$ mol dm^{-3}. (b) Concentration distribution of the complexes present in the copper(II)–ThrGly system at a metal-to-ligand ratio of 1 : 50; $c_A = 2 \times 10^{-1}$ mol dm^{-3}; $c_{Cu^{II}} = 4 \times 10^{-3}$ mol dm^{-3}.

Table 2. Values of g and A determined for the copper(II)–GlySer and copper(II)–SerGly systems at various pH values and metal-to-ligand ratios

Ligand	pH	Metal-to-ligand ratio	$g_{\parallel}$	$g_{\perp}$	$A_{\parallel}{}^{a}$	$A_{\perp}{}^{a}$	$A_{N}{}^{a}$
GlySer	10.30	1:2	2.236	2.059	165	16	—
	12.91	1:2	2.240	2.059	169	17	—
	8.87	1:32	2.239	2.060	166	18	—
	13.01	1:50	2.240	2.058	166	17	—
			2.240[b]	2.045[b]	166[b]	17[b]	10[b]
SerGly	11.11	1:2	2.231	2.058	169	22	—
	9.17	1:30	2.245	2.064	166	17	—
	13.09	1:50	2.217	2.050	196	22	13
			2.217[b]	2.040[b]	196[b]	30[b]	12.5[b]

[a] The A values are given in gauss.
[b] Calculated values.

when the pH is increased from 9 to 13. The pH-dependence of λ_{max} for copper(II)–GlyAsn at a ratio of 1:50 is similar to that at a ratio of 1:1. This means that in this system the species $[Cu(AH_{-2})OH]$ predominates even at a large ligand excess.

Equilibrium constants for processes (1) and (2) calculated from all of the experimental data are listed in Table 1. It can be concluded from Table 1 that, if the ligand excess is not higher than 50-fold, the complex $[Cu(AH_{-1})_2]$ is formed in measurable amounts only in the copper(II)–GlyGly, copper(II)–SerGly and copper(II)–ThrGly systems. In the other systems, the competition between equilibrium processes (1) and (2) is shifted strongly in favour of formation of the mixed hydroxo complex $[Cu(AH_{-1})OH]$ even at a ratio of 1:50.

The most probable explanation of the results is as follows: for GlyGly, because of the small size of the molecule, coordination of the second peptide is the least hindered. Thus, both $[Cu(AH_{-1})(OH)]$ and $[Cu(AH_{-1})_2]$ can be formed. As the size of the molecule increases, the formation of $[Cu(AH_{-1})_2]$ becomes more hindered. The deprotonated bis-complex is not formed either with GlyPhe or with PheGly, because of the bulky aromatic side-chain.

In GlyAsp there is a carboxylate group in the side-chain, thus the formation of $[Cu(AH_{-1})_2]$ is hindered electrostatically.

In the case of dipeptides containing an alcoholic hydroxy group (GlySer, SerGly, GlyThr and ThrGly), the competition between processes (1) and (2) depends greatly on the position of the alcoholic hydroxy group. SerGly and ThrGly, which contain the alcoholic hydroxy group in the side-chain near the amino terminal, have the strongest tendency to form the $[Cu(AH_{-1})_2]$ complex. In contrast, for GlySer and GlyThr only the mixed hydroxo complex is formed. As an illustration, the distribution curves of the complexes formed in the copper(II)–GlyThr and copper(II)–ThrGly systems at a metal-to-ligand ratio of 1:50 are presented in Fig. 3.

The difference in complex forming behaviour of the dipeptides containing an alcoholic hydroxy group was confirmed by EPR measurements on the copper(II)–GlySer and copper(II)–SerGly systems (see Table 2).

The EPR spectrum of copper(II)–SerGly can be simulated at *ca* pH 13 if the coordination of three or four nitrogen atoms is proposed. However, the spectra of copper(II)–GlySer can be simulated on the assumption of two nitrogen atoms at both *ca* pH 10 and *ca* pH 13. A possible explanation for the difference in behaviour of the dipeptides containing an alcoholic hydroxy group is that, in the cases of SerGly and ThrGly, the $[Cu(AH_{-1})_2]$ structure can be stabilized by hydrogen bonds between the non-coordinated carboxylate and alcoholic OH groups.

Acknowledgements—Thanks are due to Dr A. Rockenbauer (Central Chemical Research Institute, Budapest, Hungary) for his help in the recording and evaluation of the ESR spectra, and to Mrs Á. Gönczy and I. Hüse for their help in the experimental work. This work was supported financially by the Hungarian Ministry of Education (MM 46/86).

REFERENCES

1. H. Sigel and R. B. Martin, *Chem. Rev.* 1982, **82**, 385.
2. W. S. Kittl and B. M. Rode, *Inorg. Chim. Acta* 1981, **55**, 21.
3. W. S. Kittl and B. M. Rode, *J. Chem. Soc., Dalton Trans.* 1983, 409.
4. I. Nagypál and A. Gergely, *J. Chem. Soc., Dalton Trans.* 1977, 1104.

5. A. Kaneda and A. E. Martell, *J. Coord. Chem.* 1975, **4**, 137.
6. M. Sato, S. Matsuki, M. Ikeda and J.-I. Nakaya, *Inorg. Chim. Acta* 1986, **125**, 49.
7. H. Kozlowski, *Chem. Phys. Lett.* 1977, **46**, 519.
8. H. Kozlowski and J. Siatecki, *Chem. Phys. Lett.* 1978, **54**, 498.
9. M. Jezowska-Bojczuk, J. Baranowski and H. Kozlowski, *Polish J. Chem.* 1983, **7–9**, 685.
10. M. Sheinblatt and E. D. Becker, *J. Biol. Chem.* 1967, **242**, 3159.
11. A. Gergely and E. Farkas, *J. Chem. Soc., Dalton Trans.* 1982, 381.
12. I. Sóvágó, E. Farkas and A. Gergely, *J. Chem. Soc., Dalton Trans.* 1982, 2159.
13. E. Farkas, I. Sóvágó and A. Gergely, *J. Chem. Soc., Dalton Trans.* 1983, 1545.
14. E. Farkas, I. Sóvágó, T. Kiss and A. Gergely, *J. Chem. Soc., Dalton Trans.* 1984, 611.
15. E. Farkas, J. Tözsér and A. Gergely, *Magy. Kém. Folyóirat* 1986, **92**, 49.
16. T. Kiss and Z. Szücs, *J. Chem. Soc., Dalton Trans.* 1986, 2443.
17. P. H. Bently, H. Gregory, A. H. Laird and J. S. Morley, *J. Chem. Soc.* 1964, 6130.
18. H. Irving, M. G. Miles and L. D. Pettit, *Anal. Chim. Acta* 1967, **38**, 475.
19. L. Zékány and I. Nagypál, in *Computational Methods for Determination of Stability Constants* (Edited by D. Legett). Plenum Press, New York (1985).
20. A. Rockenbauer, M. Györ and T. Szabó-Plánka, *J. Chem. Phys.* 1987, **86**, 976.

Polyhedron Vol. 8, No. 20, pp. 2469–2471, 1989
Printed in Great Britain

0277–5387/89 $3.00+.00
© 1989 Pergamon Press plc

STABILIZATION OF COPPER(II) RELATIVE TO COPPER(I) IN TETRANUCLEAR $Cu_4OX_6L_4$ COMPLEXES

D. MAKÁŇOVÁ* and G. ONDREJOVIČ

Department of Inorganic Chemistry, Slovak Technical University, 812 37 Bratislava, Czechoslovakia

(*Received* 20 *March* 1989; *accepted* 25 *May* 1989)

Abstract—The complexes $Cu_4OCl_6(Ph_3P)_4 \cdot 0.5Et_2O$, $Cu_4OCl_6(Ph_3As)_4$, $Cu_4OCl_6(Ph_3As)_4 \cdot Et_2O$, $Cu_4OCl_6(MeOH)_2(Ph_3As)_2$, $Cu_4OCl_6(Ph_3Sb)_4 \cdot Et_2O$ and $Cu_4OBr_6(Ph_3P)_4 \cdot 1.5Et_2O$ were prepared and isolated. The electronic and IR spectra indicate a tetrameric structure with trigonal bipyramidal coordination of the copper(II) atom. On moderate heating the complexes undergo decomposition with reduction of copper(II) to copper(I). The influence of their specific structure on the stabilization of copper(II) relative to copper(I) is discussed.

The reduction of copper(II) to copper(I) by reaction of Ph_3E with copper(II) salts is well known. The reducing influence of Ph_3E (E = P, As, Sb) ligands in copper(II) complexes can be weakened or even eliminated. This was achieved by using tfac and hfac chelate ligands in $[Cu(tfac)_2 \cdot R_3P]$ (tfac = trifluoroacetylacetonate)[1] and $Cu(hfac)_2 \cdot L$ (hfac = hexafluoroacetylacetonate, L = R_3P, Ph_3As).[2]

It was observed that some structural types of copper(II) complexes can be effective in the stabilization[3] of copper(II) relative to copper(I). One of those structural types is the dimeric structure[4,5] of the copper(II) acetate monohydrate. The other structural type is that of the tetrameric $Cu_4OX_6L_4$ complexes[6] (Fig. 1) having a trigonal bipyramidal coordination[7] of copper(II).

This paper presents the preparation of $Cu_4OX_6L_4$ complexes (X = Cl, Br; L = Ph_3P, Ph_3As, Ph_3Sb), their characterization by electronic and IR spectra and temperatures of thermal decomposition.

EXPERIMENTAL

Preparation of complexes

The complexes $Cu_4OCl_6(Ph_3P)_4 \cdot 0.5Et_2O$ (**1**), $Cu_4OCl_6(Ph_3As)_4$ (**2**), $Cu_4OCl_6(Ph_3As)_4 \cdot Et_2O$ (**3**), $Cu_4OCl_6(MeOH)_2(Ph_3As)_2$ (**4**), $Cu_4OCl_6(Ph_3Sb)_4 \cdot Et_2O$ (**5**) and $Cu_4OBr_6(Ph_3P)_4 \cdot 1.5Et_2O$ (**6**) (Et_2O = diethyl ether) were prepared by the substitution of the methylalcohol (MeOH) in the starting complex, $Cu_4OX_6(MeOH)_4$, adding a stoichiometric quantity of Ph_3E in ether into a solution of $Cu_4OX_6(MeOH)_4$ in MeOH at a temperature of 213 K, under a nitrogen atmosphere. The preparation of the initial $Cu_4OX_6(MeOH)_4$ compounds was performed using a modification of the published method.[6] The separated complexes were kept under nitrogen at 263 K. The elemental analyses are listed in Table 1.

Measurements

The electronic spectra were obtained with SPECORD M 40 and UNICAM SP-700C spectrophotometers, while the IR spectra were recorded on a SPECORD 75 IR, using Nujol mulls. Thermal decomposition of the complex was recorded with a DERIVATIGRAPH OD-102.

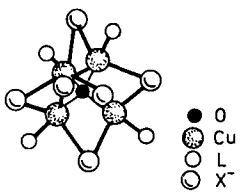

Fig. 1. The structure of $Cu_4OX_6L_4$ complexes.

* Author to whom correspondence should be addressed.

Table 1. Analytical data

Complex	Colour		Analysis C(%)	H(%)	Cu(%)	X(%)
$Cu_4OCl_6(Ph_3P)_4 \cdot 0.5Et_2O$	Violet	Calc.	56.5	4.2	16.2	
(1)		Found	57.7	4.3	15.9	
$Cu_4OCl_6(Ph_3As)_4$	Violet–brown	Calc.	50.6	3.5	14.9	12.4
(2)		Found	50.9	3.7	13.7	12.7
$Cu_4OCl_6(Ph_3As)_4 \cdot Et_2O$	Violet	Calc.			14.3	11.9
(3)		Found			14.0	11.1
$Cu_4OCl_6(MeOH)_2(Ph_3As)_2$	Black–grey	Calc.	39.4	3.3		
(4)		Found	38.7	3.2		
$Cu_4OCl_6(Ph_3Sb)_4 \cdot Et_2O$	Brown	Calc.	46.3	3.6		
(5)		Found	45.6	3.3		
$Cu_4OBr_6(Ph_3P)_4 \cdot 1.5Et_2O$	Violet–black	Calc.	49.0	3.9	13.3	25.1
(6)		Found	50.9	3.8	13.3	25.8

RESULTS AND DISCUSSION

Table 2 presents the electronic and IR spectral data which may be considered to be diagnostic for $Cu_4OX_6L_4$ complexes and their structures are given in Fig. 1. The copper(II) atom has trigonal bipyramidal coordination with the ligand L in an axial position. The molecules of the solvent, which can be found in the structure, only slightly affect the bond distances and bond angles, compared with an unsolvated complex.[7,8] The electronic spectra of the complexes exhibit one or two bands in the region of 9900–13600 cm^{-1}, belonging to *d–d* transitions. As may be seen from Table 2, $Cu_4OX_6(Ph_3E)_4$ complexes exhibit a broad band in the region of 10,300–13,800 cm^{-1}, which may be the result of considerable overlapping of two bands.

For $Cu_4OX_6L_4$ complexes (X = Cl, Br; L = N-donor or O-donor ligands) to which the above structure is assigned,[6] the $\tilde{\nu}(Cu_4O)$ wave number values due to the characteristic tetrahedral arrangement of copper(II) atoms around the oxygen atom, were found in the region of 571–597 cm^{-1} for X = Cl and at 526–559 cm^{-1} for X = Br. For the

Table 2. Electronic, IR spectral and thermal decomposition data

Complex	Decomposition temperature (K)	ES (cm^{-1}) $\tilde{\nu}_{max} \times 10^3$	IR (cm^{-1}) $\tilde{\nu}(Cu_4O)$	$\tilde{\nu}$(C—O—C)
$Cu_4OCl_6(Ph_3P)_4 \cdot 0.5Et_2O$	318	12.1	535 vs	1120 s
(1)		10.3 sh		
$Cu_4OCl_6(Ph_3As)_4$	323	12.6	480 vs	
(2)		11.0 sh	500 m	
$Cu_4OCl_6(Ph_3As)_4 \cdot Et_2O$	327	12.7	480 vs	
(3)		12.0 sh	495 sh	1120 m
$Cu_4OCl_6(MeOH)_2(Ph_3As)_2$[a]	313	13.0	480 vs	
(4)		12.0 sh	500 s	
			600 s	
$Cu_4OCl_6(Ph_3Sb)_4 \cdot Et_2O$[b]	297	(13.8 br)	(465)	(1120)
(5)				
$Cu_4OBr_6(Ph_3P)_4 \cdot 1.5Et_2O$	308	12.0 br	540 vs	1120 vs
(6)				

[a] $\tilde{\nu}$(OH) = 3400 cm^{-1}.

[b] During measurements of the spectra the complex decomposed on the reduction of copper(II) to copper(I).

complexes $Cu_4OX_6(Ph_3P)_4$ the $\tilde{\nu}(Cu_4O)$ values were observed at 539 cm^{-1} for X = Cl and at 518 cm^{-1} for X = Br.[6] The corresponding solvated complexes, **1** and **6**, show $\tilde{\nu}(Cu_4O)$ values at 535 and 540 cm^{-1}, respectively. Complexes with Ph_3As (**2** and **3**) and with Ph_3Sb (**5**) show, as expected, lower $\tilde{\nu}(Cu_4O)$ values, the band being split (Table 2). Complex **4** with mixed ligands of MeOH and Ph_3As exhibits a split band in the region of 480–500 cm^{-1}, similar to complexes **2** and **3**, and another band at a considerably higher wavenumber (600 cm^{-1}) which is near to the $\tilde{\nu}(Cu_4O)$ value for the pure methanol complex of $Cu_4OCl_6(MeOH)_4$.[6] The two or three $\tilde{\nu}(Cu_4O)$ bands in the spectra of complexes **2**, **3** and **4** suggest that in these complexes the tetrahedral grouping of Cu_4O is more distorted than for complexes **1** and **6**.

In the trigonal bipyramidal complexes $[Cu(chel)_2X]^{n+}nY^-$ (X = I^-, CN^-, NCS^-, thiourea; chel = bipy or phen; Y = ClO_4^-) the reducing ligand X is located in the trigonal plane. For these complexes the stabilization of copper(II) relative to copper(I) has been explained by a minimum overlap of X ligand orbitals with the d_{z^2} orbital of copper(II) which contains an unpaired electron.[9] Thus the conditions for the electron transfer $Cu^{II}-X \rightarrow Cu^{I}+X$ are unfavourable. However, in the structure of $Cu_4OX_6(Ph_3E)_4$ complexes the reducing ligand Ph_3E occupies the axial position of the trigonal bipyramid and thus there are favourable conditions for the reduction of copper(II) to copper(I).

In fact, the complexes $Cu_4OX_6(Ph_3E)_4$ are unstable and undergo decomposition due to the reduction of copper(II) to copper(I) at relatively low temperatures (Table 2), whereas the analogous complexes e.g. with pyridine and its methyl derivatives melt at temperatures[6] in the range 417–548 K.

The possibility of preparing the $Cu_4OX_6(Ph_3E)_4$ complexes is probably connected with the stabilizing influence of their specific structure, in which the coordination polyhedra are mutually coupled by the common oxygen-atom and by bridging X atoms, in contrast to the structure of $[Cu(chel)_2X]^{n+}nY^-$ complexes which is composed of the isolated coordination polyhedra.

REFERENCES

1. F. Leh and K. M. Chan, *Bull. Chem. Soc. Jpn* 1972, **45**, 2709.
2. R. A. Zelonka and M. C. Baird, *Can. J. Chem.* 1972, **50**, 1269.
3. G. Ondrejovič, D. Valigura, M. Máriássy and J. Mroziński, *Chem. Papers* 1985, **39**, 49.
4. M. Koman, D. Valigura and G. Ondrejovič, *Acta Cryst.* 1988, **C44**, 601.
5. D. Valigura, M. Koman, E. Ďurčanská, G. Ondrejovič and J. Mroziński, *J. Chem. Soc., Dalton Trans.* 1986, 2339.
6. H. Dieck and A. P. Brehm, *Chem. Ber.* 1969, 3577.
7. J. A. Bertrand, *Inorg. Chem.* 1967, **6**, 495.
8. A. A. Dvorin, J. A. Simonov, M. A. Jampol'skaja and T. J. Malinovskij, *Kristalografia* 1983, **28**, 811.
9. V. I. Nefedov, P. P. Pozdejev, G. Ondrejovič, D. Valigura and J. Gažo, *Koord. Khim.* 1984, **10**, 1332.

Polyhedron Vol. 8, No. 20, pp. 2473–2480, 1989
Printed in Great Britain

0277-5387/89 $3.00+.00
© 1989 Pergamon Press plc

REACTIONS OF POLYOXOMOLYBDATES WITH OXIMES. THE CRYSTAL AND MOLECULAR STRUCTURES OF $[(C_4H_9)_4N]_2[Mo_2O_5\{C_6H_4(O)CHNO\}_2]\cdot CH_2Cl_2$ AND $[(C_4H_9)_4N]_2[Mo_2O_5\{C_6H_5CH(O)C(NO)C_6H_5\}_2]$

SHUNCHENG LIU, HUIZHE ZHU and JON ZUBIETA*

Department of Chemistry, State University of New York at Albany, Albany, NY 12222, U.S.A.

(*Received* 12 *April* 1989; *accepted* 31 *May* 1989)

Abstract—The reactions of $[(C_4H_9)_4N]_2[Mo_2O_7]$ with the oximes benzoinoxime and salicylaldoxime yielded the complexes $[(C_4H_9)_4N]_2[Mo_2O_5\{C_6H_4(O)CHNO\}_2]\cdot CH_2Cl_2$ (**7**) and $[(C_4H_9)_4N]_2[Mo_2O_5\{C_6H_5CH(O)C(NO)C_6H_5\}_2]$ (**8**). The structures of **7** and **8** exhibit the $[Mo_2O_5]^{2+}$ core with the oximato moieties of the ligands functioning as μ_2-O,N bridging donors. The metrical parameters are consistent with the sp^2 hybridization of the oximato nitrogen with double bond character localized on the C—N bond. Crystal data: Compound **7**, monoclinic space group, $P2_1/c$, $a = 16.271(6)$, $b = 14.010(4)$, $c = 25.390(8)$ Å, $\beta = 101.34(2)°$, $V = 5672.9(19)$ Å^3, $D_{calc} = 1.30$ g cm^{-3} for $Z = 4$. Structure solution and refinement based on 4718 reflections with $F_o \geqslant 6\sigma(F_o)$(Mo-$K_\alpha$, $\lambda = 0.71073$ Å) converged at a conventional residual of 0.064. Compound **8**, rhombohedral space group (hexagonal setting) $R\bar{3}$, $a = b = 47.188(14)$, $c = 15.766(3)$ Å, $V = 30403.4(27)$ Å^3, $D_{calc} = 1.19$ g cm^{-3} for $Z = 18$. Structure solution and refinement based on 3015 reflections with $F_o \geqslant 6\sigma(F_o)$ converged at a value of 0.069 for the conventional R factor. Reaction of the related salicylhydroxamic acid with $[(C_4H_9)_4N]_2[Mo_2O_7]$ in methanol yielded the complex $[(C_4H_9)_4N][MoO_2\{C_6H_4(OH)C(O)NO\}\{C_6H_4(OH)C(O)NHO\}]$ (**11**), a species exhibiting both hydroximato(2−) and hydroxamato(1−) forms of the ligand. Crystal data: Compound **11**, monoclinic space group $P2_1/c$, $a = 10.261(2)$, $b = 17.864(4)$, $c = 18.270(3)$ Å, $\beta = 91.98(1)°$, $V = 3347.0(10)$ Å^3, $D_{calc} = 1.34$ g cm^{-3} for $Z = 4$. Structure solution and refinement based on 3406 reflections converged at a value of 0.049 for the conventional R factor.

Oxoanions of molybdenum(VI) react with hydroxylamines (**1**) to give complexes containing O,N-coordinated hydroxylamido(1−) ligands, (**2**).[1] With the analogous oximes (**3**), polynuclear complexes containing bridging O,N-coordinated oximato(1−) ligands have been described.[2] As an extension of our work on the coordination chemistry of polyoxomolybdate anions with nitrogen donor ligands,[3] we have studied the reactions of $[(C_4H_9)_4N]_2[Mo_2O_7]$ with the oxime ligands, benzoinoxime (**4**) and salicylaldoxime (**5**), and with the related salicylhydroxamic acid ligand (**6**). In this paper, we discuss the structures of $[(C_4H_9)_4N]_2[Mo_2O_5\{C_6H_4(O)CHNO\}_2]\cdot CH_2Cl_2$ (**7**) and $[(C_4H_9)_4N]_2[Mo_2O_5\{C_6H_5CH(O)C(NO)C_6H_5\}_2]$ (**8**) and compare their geometries to those of related oxomolybdate hydroxylamido and oxomolybdate oximato complexes and with that of the salicylhydroxamic acid derived species, $[(C_4H_9)_4N][MoO_2\{C_6H_4(OH)C(O)NO\}\{C_6H_4(OH)C(O)NHO\}]$ (**11**).

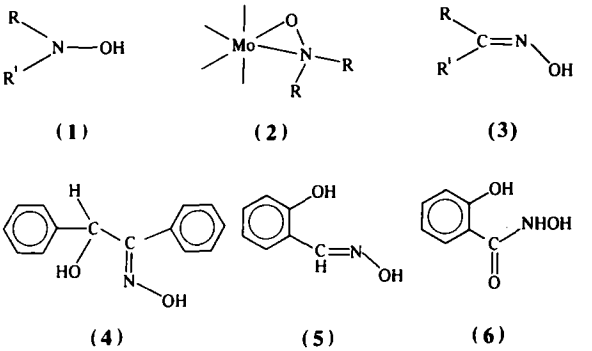

(1) (2) (3)

(4) (5) (6)

* Author to whom correspondence should be addressed.

RESULTS AND DISCUSSION

The reaction of 1 equivalent of $[(C_4H_9)_4N]_2[Mo_2O_7]$ with 2 equivalents of oximes (**4**) and (**5**) in dichloromethane, followed by addition of diethyl ether, yielded translucent crystals of $[(C_4H_9)_4N]_2[Mo_2O_5\{C_6H_4(O)CHNO\}_2]\cdot CH_2Cl_2$ (**7**) and $[(C_4H_9)_4N]_2[Mo_2O_5\{C_6H_5CH(O)C(NO)C_6H_5\}_2]$ (**8**), respectively. Whereas the crystals of **8** were relatively stable under an atmosphere of nitrogen, crystals of **7** rapidly lost translucency upon removal of solvent, which required storage of **7** in the presence of the mother liquor.

Structural studies of the oximato complexes, **7** *and* **8**, *and of the hydroximato/hydroxamato species,* **11**

The structures of the complex anions of **7** and **8** are illustrated in Figs 1 and 2, respectively, the selected bond distances and angles for the structures are compared in Table 1. The structures are seen to contain the $[Mo_2O_5]^{2+}$ core coordinated to two oximato ligands functioning as chelating and bridging moieties.

The oximato units function as bridging groups, with the oxygen and nitrogen donors acting as μ_2-bridging ligands to the molybdenum centres. In addition, the oximate ligands coordinate through their alkoxy groups to complete the hexacoordinate geometry about the molybdenum centres.

The molybdenum centres of **7** display pseudo-octahedral $[MoO_5N]$ geometry by virtue of coordination to two terminal oxo groups, the bridging oxo group, a terminal alkoxy donor, and the nitrogen and oxygen donors of the bridging oximato moiety. One consequence of bridging through the N- and O-donors is the appearance of two cyclic units [Mo(1)—O(3)—Mo(2)—N(2)—O(6)] and [Mo(1)—O(3)—Mo(2)—O(8)—N(1)]. Furthermore, the two-atom bridge between the molybdenum centres requires that the Mo(1)—O(3)—Mo(2) angle expand from the usual value found with single donor bridges. Thus, the Mo—O—Mo angle in **7** of 131.5(3)° may be contrasted with that of 112.7(2)° in $[Mo_2O_5(phenanthraquinone)_2]$[4] which exhibits the more common single donor bridge.

Various coordination modes have been reported for molybdenum–oximato complexes. The most common is side-on coordination to a single molybdenum centre through the N- and O-donors,[5,6] a coordination geometry similar to that observed for hydroxylaminato complexes of molybdenum.[1,7] In addition, a number of tetranuclear molybdate complexes have been described in which the oximato group functions as a μ_4-bridging ligand.[2] The chelating, doubly bridging geometry adopted by **7** and **8** represents a third coordination type for the oximato ligand.

The ligand geometries of the various hydroxyl-

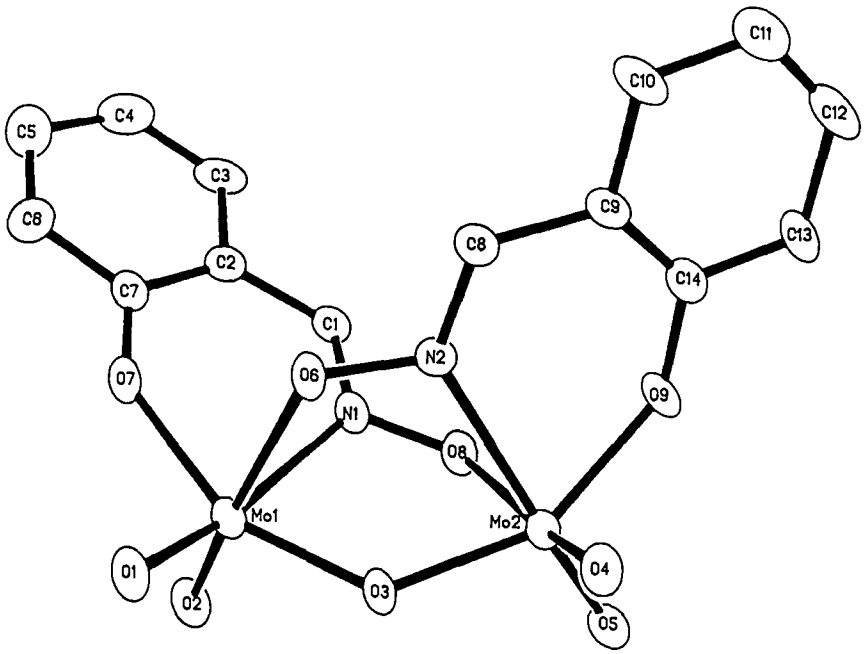

Fig. 1. ORTEP view of the structure of the molecular anion of $[(C_4H_9)_4N]_2[Mo_2O_5\{C_6H_4(O)CHNO\}_2]\cdot CH_2Cl_2$ (**7**).

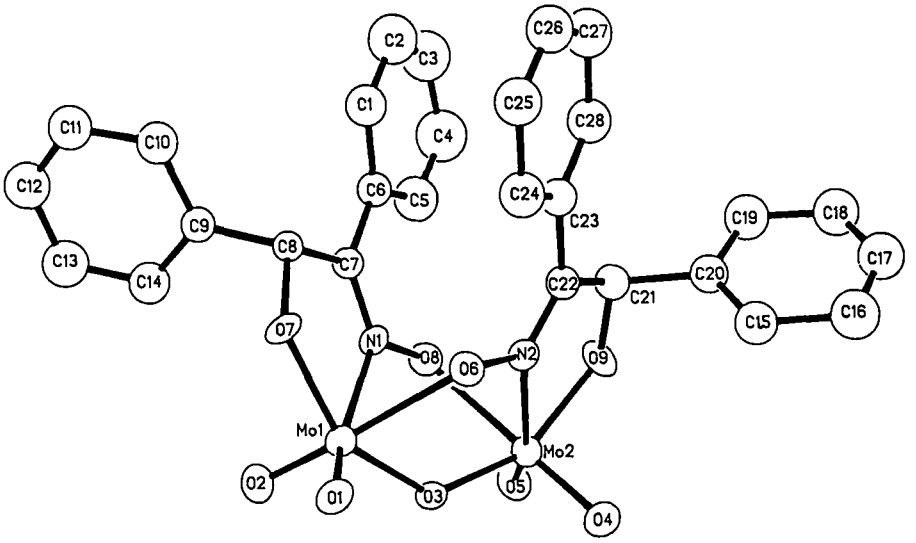

Fig. 2. Perspective view of the structure of the anion of $[(C_4H_9)_4N]_2[Mo_2O_5\{C_6H_5CH(O)C(NO)C_6H_5\}_2]$ (**8**).

Table 1. Comparison of structural parameters for $[(C_4H_9)_4N]_2[Mo_2O_5\{C_6H_4(O)CHNO\}_2]\cdot CH_2Cl_2$ (**7**) and $[(C_4H_9)_4N]_2[Mo_2O_5\{C_6H_5CH(O)C(NO)C_6H_5\}_2]$ (**8**)

	(**7**)	(**8**)	
Mo(1)—O(1)	1.722(7)	1.711(14)	
Mo(1)—O(2)	1.719(6)	1.697(10)	
Mo(1)—O(3)	1.893(6)	1.919(8)	
Mo(1)—O(6)	2.154(6)	2.268(9)	
Mo(1)—O(7)	1.999(7)	1.946(10)	
Mo(1)—N(1)	2.399(9)	2.271(15)	
Mo(2)—O(4)	1.729(8)	1.716(14)	
Mo(2)—O(5)	1.687(7)	1.735(12)	
Mo(2)—O(3)	1.920(6)	1.925(9)	
Mo(2)—O(8)	2.187(7)	2.285(13)	
Mo(2)—O(9)	2.004(6)	1.956(10)	
Mo(2)—N(2)	2.358(7)	2.281(12)	
N(1)—O(8)	1.364(10)	1.332(16)	
N(1)—C(1)	1.271(14)	1.282(24)	[N(1)—C(7)]
C(1)—C(2)	1.509(15)	1.39(3)	[C(7)—C(8)]
C(2)—C(7)	1.392(15)	—	
C(7)—O(7)	1.310(15)	1.43(2)	[C(8)—O(7)]
N(2)—O(6)	1.365(9)	1.34(2)	
N(2)—C(8)	1.259(11)	1.28(3)	[N(2)—C(22)]
C(8)—C(9)	1.476(13)	1.55(3)	[C(21)—C(22)]
C(9)—C(14)	1.381(15)	—	
C(14)—O(9)	1.342(11)	1.40(2)	[C(21)—O(9)]
O(1)—Mo(1)—N(1)	166.5(3)	159.6(5)	
O(2)—Mo(1)—O(6)	166.2(3)	167.4(6)	
O(3)—Mo(1)—O(7)	154.3(3)	148.0(4)	
O(7)—Mo(1)—N(1)	79.1(3)	73.2(5)	
Mo(1)—O(3)—Mo(2)	131.5(3)	133.1(5)	
Mo(1)—N(1)—O(8)	115.4(6)	121.2(11)	
Mo(1)—O(6)—N(2)	115.6(5)	113.5(9)	
O(4)—Mo(2)—O(8)	166.8(3)	169.7(5)	
O(5)—Mo(2)—N(2)	166.7(3)	156.4(7)	
O(3)—Mo(2)—O(9)	153.4(3)	149.4(4)	
O(9)—Mo(2)—N(2)	79.5(3)	73.4(5)	
Mo(2)—O(8)—N(1)	113.7(5)	113.7(11)	
Mo(2)—N(2)—O(6)	116.0(5)	119.0(9)	

aminato- and oximatomolybdenum complexes serve to distinguish the two ligand types. In hydroxylaminato complexes, the nitrogen atom is sp^3 hybridized, requiring that the [R_2N—O—Mo] moiety be non-planar.[1] In contrast, the nitrogen donor of the oximato ligand is sp^2 hybridized, a feature consistent with the observed planarity of the chelate ring units in both **7** and **8**, and in the short C—N distances of *ca* 1.28(2) Å.

The structures of **7** and **8** differ significantly only in the chelate ring sizes and the identities of the organic substituents on the oximato ligands. In **7**, six-membered chelate rings [O—C—C—C—N—Mo] are formed by virtue of ligation to the alkoxy oxygen functionality and the oximato nitrogen. The entire ligand–molybdenum unit, [OC_6H_4CNOMo], is virtually planar. In contrast, the structure of **8** presents planar five-membered chelate rings, a feature which results in the contraction of the O—Mo—N chelate angle from a value of 79.1(3)° in **7** to the more constrained 73.2(5)° in **8**. Since C(8) and C(21) in **8** are sp^3 hybridized and rotation about the C(8)—C(9) and C(20)—C(21) axes is unhindered, the phenyl substituents of the oximato ligands of **8** do not lie in the plane of the chelate ring, in contrast to the geometry observed for **7**.

Although the enol form (**10**) of the hydroxamic acids is structurally similar to the oxime ligand (**3**), transition metal–hydroxamato nitrogen bonds are

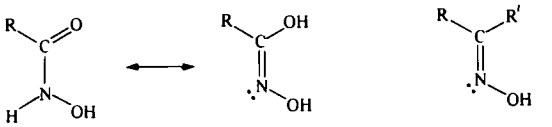

(**9**) (**10**) (**3**)

extremely rare, with the only examples provided by the square-planar bis(glycinohydroxamato) nickel(II)[8] and [VO(salicylhydroximate)(CH_3OH)]$_3$.[9] Hence, it was not unexpected that the oxomolybdate–hydroxamate complex, [$(C_4H_9)_4N$][MoO_2{C_6H_4(OH)C(O)NO}{C_6H_4(OH)C(O)NHO}] (**11**), coordinates exclusively through the carbonyl and oxime oxygens of the ligand (see Table 2). As illustrated in Fig. 3, the structure of the anion of **11** consists of discrete mononuclear units with pseudo-octahedral molybdenum centres, coordinated to a *cis* terminal oxo group and to two carbonyl oxygens and two ozime oxygens from the ligand groups.

Table 2. Selected bond lengths (Å) and angles (°) for [$(C_4H_9)_4N$][MoO_2{C_6H_4(OH)C(O)NO}{C_6H_4(OH)C(O)NHO}] (**11**)

Mo—O(5)	1.711(4)	Mo—O(6)	1.696(4)
Hydroximato(2−) chelate		Hydroxamato(1−) chelate	
Mo—O(3)	2.110(3)	Mo—O(1)	2.258(4)
O(3)—C(11)	1.298(6)	O(1)—C(1)	1.256(6)
C(11)—N(2)	1.289(7)	C(1)—N(1)	1.319(7)
N(2)—O(4)	1.404(6)	N(1)—O(2)	1.382(6)
Mo—O(4)	1.994(4)	Mo—O(2)	2.017(4)
O(3)···O(4)	2.476(4)	O(1)···O(2)	2.546(4)
N(2)···O(8)	2.569(5)	N(1)···O(7)	2.601(5)
O(1)—Mo—O(2)	72.8(1)	O(3)—Mo—O(4)	74.2(1)
O(1)—Mo—O(3)	76.8(1)	O(3)—Mo—O(5)	155.7(2)
O(1)—Mo—O(4)	88.0(1)	O(3)—Mo—O(6)	95.4(2)
O(1)—Mo—O(5)	87.6(2)	O(4)—Mo—O(5)	88.3(2)
O(1)—Mo—O(6)	161.5(2)	O(4)—Mo—O(6)	106.2(2)
O(2)—Mo—O(3)	84.5(1)	O(5)—Mo—O(6)	104.3(2)
O(2)—Mo—O(4)	154.2(2)		
O(2)—Mo—O(5)	107.5(2)		
O(2)—Mo—O(6)	89.9(3)		
Hydroximato(2−) chelate		Hydroxamato(1−) chelate	
Mo—O(3)—(1)	114.2(3)	Mo—O(1)—C(1)	112.6(3)
O(3)—C(11)—N(2)	121.1(5)	O(1)—C(1)—N(1)	118.1(5)
C(11)—N(2)—O(4)	111.2(4)	C(1)—N(1)—O(2)	117.1(4)
N(2)—O(4)—Mo	119.3(3)	N(1)—O(2)—Mo	117.1(3)

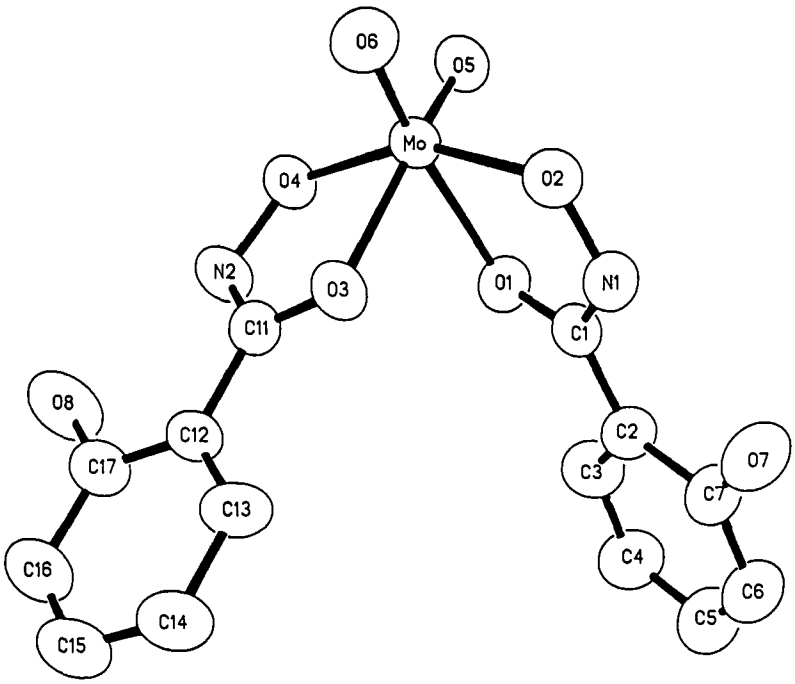

Fig. 3. ORTEP view of the structure of the molecular anion of $[(C_4H_9)_4N][MoO_2\{C_6H_4(OH)C(O)NO\}\{C_6H_4(OH)C(O)NHO\}]$ (**11**).

The most unusual feature of the structure is the presence of both hydroxamato(1−) (**12**) and

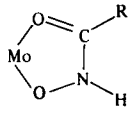

(12)

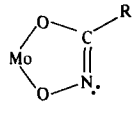

(13)

hydroximato(2−) (**13**) ligand types. The distinct ligand environments are readily identified both by the location of hydrogen atoms and by the structural parameters associated with the chelate rings. Thus, the final Fourier map for **11** reveals hydrogens H(O7) and H(O8), associated with the uncoordinated hydroxyl groups, and H(N1) at 0.93 Å from N(1) and hydrogen bonding to O(7). Furthermore, as shown in Table 3, comparison of the chelate ring parameters for the two distinct ligand types in **11** to the ring parameters for the hydroxamato(1−) ligands of $[Cr(benzohydroxamato)_3]$[10] and for the hydroximato(2−) ligands of $[Cr(benzohydroximato)_3]^{3-}$,[11] clearly establishes the identities of the ligand types. The most significant changes upon deprotonation of the hydroxamato unit are increases in the N—O and C—O bond distances by 0.02–0.05 Å and, in the specific case of **11**, a decrease in the C—N bond distance by 0.03 Å. This is accompanied by expansion of the O—C—N bond angle and O—N—C bond angle contraction. The C—N bond distances for both the hydroximato and hydroxamato ligands are significantly shorter than C—N single bonds (1.43–1.45 Å)[12] and slightly longer than the C=N bond of ethylbenzohydroximic acid (1.27 Å).[13] The chromium complexes display only a minor decrease in both the Cr—O_o and Cr—O_c bonds upon deprotonation. In contrast, the Mo—O_c distance for the hydroxamato interaction is *ca* 0.05 Å longer than the corresponding distance for the hydroximato ligand. The observed chelate metrical parameters have been interpreted in terms of the resonance structures **14** and **15** for the hydroxamato type and **16** and **17** for the hydroximato ligand.

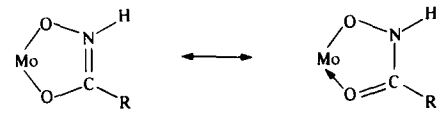

(14) (15)



(16) (17)

From the observed bond lengths, form **15** dominates the electronic structure of the hydroxamato

Table 3. Comparison of structural parameters for the hydroximato(2−) and hydroxamato(1−) chelate rings of **11** with ligand parameters for [Cr(benzohydroxamato)$_3$] and [Cr(benzohydroxamato)$_3$]$^{3-}$

Bond angle or distance[a]	Compound **11**		[Cr(benzohydroxamato)$_3$]	[Cr(benzohydroximato)$_3$]$^{3-}$	
	Hydroxamato(1−)	Hydroximato(2−)		*trans*	*cis*
M—O_c	2.258(4)	2.110(3)	1.984(4)	1.987(4)	1.968(2)
O_c—C	1.256(6)	1.298(6)	1.273(4)	1.317(3)	1.308(4)
C—N	1.319(7)	1.289(7)	1.305(7)	1.301(4)	1.298(4)
N—O_o	1.382(6)	1.404(6)	1.374(6)	1.421(3)	1.443(4)
M—O_o	2.017(4)	1.994(4)	1.960(4)	1.955(13)	1.956(2)
O_o—M—O_c	72.8(1)	74.2(1)	81.0(2)	80.6(2)	81.5(1)
M—O_c—C	112.6(3)	114.2(3)	112.0(2)	110.5(8)	111.2(2)
O_c—C—N	118.1(5)	121.1(5)	118.8(4)	112.9(2)	123.4(3)
C—N—O_o	117.1(4)	111.2(4)	117.8(5)	112.1(3)	111.6(3)
N—O_o—M	117.1(3)	119.3(3)	109.4(6)	112.8(9)	112.2(2)
$O_o \cdots O_c$	2.546(4)	2.476(3)	2.561(2)	2.551(5)	2.561(3)

[a] Abbreviations: O_c = carbonyl oxygen of the hydroxamato or hydroximato ligand; O_o = oxime oxygen.

ligand, while resonance structure **16** provides the major contribution to the hydroximato geometry. In fact, structure **17** is not expected to contribute significantly because of the charge localization on the oxime N—O unit.

EXPERIMENTAL

Materials and methods

All reactions were performed in freshly dried and distilled solvents. Dichloromethane was technical grade and was redistilled from $CaCl_2$ and P_4O_{10}. All other solvents were reagent grade. All other reagents were obtained from standard commercial sources without further purification.

The following instruments were used in this work: IR, Perkin–Elmer 283B IR spectrophotometer; UV–vis. spectra, Varian DMS 90 UV-vis. spectrophotometer; X-ray crystallography, Nicolet R3m diffractometer.

Preparation of complexes

$[(C_4H_9)_4N]_2[Mo_2O_5\{C_6H_4(O)CHNO\}_2] \cdot CH_2Cl_2$ (**7**). $[(C_4H_9)_4N]_2[Mo_2O_7]$ (1.5 g, 2 mmol) was dissolved in 30 cm^3 of CH_3CN. While stirring this solution vigorously, salicylaldoxime (0.5 g, 4 mmol) was added, whereupon the solution turned bright yellow. After overnight stirring at room temperature, the solution was concentrated to 10 cm^3 and layered with CH_2Cl_2–ether (2 cm^3/20 cm^3). Upon standing for 2 weeks at 4°C, translucent yellow crystals of block habit were obtained (yield: 40%). The crystals rapidly turn opaque upon standing in air in the absence of the mother liquor. Crystals for X-ray studies were mounted in capillary tubes in the presence of a drop of the mother liquor. Analysis (dry sample loses CH_2Cl_2 of crystallization): Found: C, 53.9; H, 8.11; N, 5.36. Calc. for $C_{46}H_{82}N_4O_9Mo_2$: C, 53.8; H, 7.99; N, 5.46%. IR (KBr pellet, cm^{-1}): 2970(s), 2880(m), 1600(w), 1470(s), 1440(s), 1320(m), 1270(s), 1200(w), 1065(s), 1035(s), 905(s), 880(s), 750(m), 710(s), 660(m), 615(s).

$[(C_4H_9)_4N]_2[Mo_2O_5\{C_6H_5CH(O)C(NO)C_6H_5\}_2]$ (**8**). 2-Benzoin oxime (0.88 g, 4 mmol) was added to a solution of $[(C_4H_9)_4N]_2[Mo_2O_7]$ (1.5 g, 2 mmol) in CH_3CN (30 cm^3). After overnight stirring and concentration of the resultant yellow solution to 5 cm^3, the reaction solution was layered with diethyl ether (10 cm^3). After standing at room temperature for 2 weeks, pale yellow block-like crystals were obtained in 30% yield. Found: C, 59.6; H, 8.00; N, 4.77. Calc. for $C_{60}H_{94}N_4O_9Mo_2$: C, 59.7; H, 7.79; N, 4.64%. IR (KBr pellet, cm^{-1}): 2960(s), 2860(s), 1540(w), 1490(s), 1380(w), 1130(s), 1070(m), 1025(m), 900(s), 880(vs), 750(s), 700(s), 650(m).

$[(C_4H_9)_4N]$ $[MoO_2\{C_6H_4(OH)C(O)NO\}$ $\{C_6H_4(OH)C(O)NHO\}]$ (**11**). Salicylhydroxamic acid (0.6 g, 4 mmol) was added with vigorous stirring to a solution of $[(C_4H_9)_4N]_2[Mo_2O_7]$ (1.5 g, 2 mmol) in CH_3CN (30 cm^3). Overnight stirring at room temperature was followed by concentration to 10 cm^3 and layering with ether (15 cm^3). After 3 weeks of standing at room temperature, pale yellow crystals of **11** were collected in 55% yield. Found: C, 53.7; H, 7.14; N, 6.23. Calc. for $C_{30}H_{47}N_3O_8Mo$: C, 53.6; H, 6.84; N, 6.25%. IR (KBr pellet, cm^{-1}): 3310(m), 2965(s), 2880(s), 1600(s), 1550(m),

Table 4. Summary of the crystal data[a] and experimental details for the X-ray diffraction studies of $[(C_4H_9)_4N]_2[Mo_2O_5\{C_6H_4(O)CHNO\}_2]\cdot CH_2Cl_2$ (7), $[(C_4H_9)_4N]_2[Mo_2O_5\{C_6H_5CH(O)C(NO)C_6H_5\}_2]$ (8) and $[(C_4H_9)_4N][MoO_2\{C_6H_4(OH)C(O)NO\}\{C_6H_4(OH)C(O)NHO\}]$ (11)

	(7)	(8)	(11)
a (Å)	16.271(6)	47.188(14)	10.261(2)
b (Å)	14.010(4)	47.188(14)	17.864(4)
c (Å)	25.390(8)	15.766(3)	18.270(3)
α (°)	90.00	90.00	90.00
β (°)	101.34(2)	90.00	91.98(1)
γ (°)	90.00	120.00	90.00
V (Å^3)	5672.9(19)	30403.4(27)	3347.0(10)
Space group	$P2_1/c$	$R\bar{3}$	$P2_1/c$
Z	4	18	4
D_{calc} (g cm^{-3})	1.30	1.19	1.34
Crystal shape and colour	Yellow block	Pale yellow	Pale yellow
Crystal dimensions (mm)	$0.31\times0.30\times0.20$	$0.32\times0.29\times0.27$	$0.24\times0.34\times0.21$
Instrument	Nicolet R3m/V diffractometer		
Radiation	Mo-K_α ($\lambda = 0.71073$ Å)		
Scan mode	Coupled θ(crystal)–2θ(counter)		
Scan rate	2° min^{-1}–10° min^{-1}		
Scan range	$2° \leqslant 2\theta \leqslant 45°$		
Scan length	From $[2\theta(K\alpha_2)-1.0]°$ to $[2\theta(k\alpha_2)+1.0]°$		
Background measurement	Stationary crystal, stationary counter, at the beginning and end of each 2θ scan, each for the time taken for the scan.		
Number of reflections collected	7964 $(\pm h, +k, +l)$	5008 $(-h, +k, +l)$	4734 $(\pm h, +k, +l)$
Number of reflections used in solution	4718 $F_o \geqslant 6\sigma(F_o)$	3015 $F_o \geqslant 6\sigma(F_o)$	3406 $F_o \geqslant 6\sigma(F_o)$
Absorption coefficient (cm^{-1})	5.70	4.00	7.69
Absorption correction	None applied		
Structure solution[b]	Patterson map yielded the molybdenum position; all remaining non-hydrogen atoms were located via standard Fourier techniques		
Atomic scattering factors[c]	Neutral atomic scattering factors were used throughout the analysis		
Anomalous dispersion[d]	Applied to all non-hydrogen atoms		
Final discrepancy factors[e]			
R	0.064	0.069	0.049
R_w	0.071	0.074	0.054
Goodness-of-fit	1.91	1.73	1.82

[a] From a least squares fitting of the setting angle of 25 reflections.

[b] All calculations were performed on a Data General Nova 3 computer with 32K of 16-bit words using local versions of the Nicolet SHELTEX interactive crystallographic software package as described in G. M. Sheldrick, *Nicolet SHELTEX Operations Manual.* Nicolet XRD Corporation, Cupertino, California (1979).

[c] D. T. Cromer and J. B. Mann, *Acta Cryst.* 1968, **A24**, 321.

[d] *International Tables for X-ray Crystallography*, Vol. III. Kynoch Press, Birmingham, U.K.

[e] $R = \Sigma[|F_o|-|F_c|/\Sigma|F_o|]$; $R_w = [\Sigma w(|F_o|-|F_c|)^2/\Sigma w|F_o|^2]^{1/2}$; $w = 1/\delta^2(F_o)+g^*(F_o)$; $g = 0.005$.

[f] G-O-F $= [\Sigma w(|F_o|-|F_c|)^2/(NO-NV)]^{1/2}$ where NO is the number of observations and NV is the number of variables.

1520(m), 1485(s), 1450(m), 1385(s), 1305(m), 1250(s), 1155(m), 1070(m), 915(vs), 880(vs), 780(m), 750(s), 660(m).

* Supplementary materials available: Fractional coordinates have been deposited with the Director, Cambridge Crystallographic Centre. Complete listings of bond distances and angles are available from the Editor, Queen Mary College, London.

X-ray crystallography

The details of the crystal data, data collection methods and refinement procedures are given in Table 4. (The Supplementary Tables provide atomic positional parameters for the structures reported. Tables of bond lengths and angles, anisotropic thermal parameters and calculated and observed structure factors for all complexes are available.*) Full

details of the crystallographic methodologies may be found in Ref. 14.

In all instances, a cut-off value of $F\sigma \geqslant 6.0\sigma(F)$ was used. Since the crystal quality was only adequate for these species, it was found that use of a lower cut-off did not significantly improve the standard deviations in bond parameters, while the residuals were adversely affected.

In no instance was an extinction correction applied for the data. Idealized hydrogen atom positions were used throughout the analyses, with the C—H and N—H distances set at 0.96 and 0.94 Å, respectively. In the case of structure **11**, hydrogen atoms H(O7), H(O8) and H(N1) were located on the final Fourier map and introduced as fixed contributors to the final cycles of refinement.

The structures of **7**, **8** and **11** all exhibited some degree of disorder associated with the $(C_4H_9)_4N^+$ cations. As the final difference Fourier maps for all cases failed to reveal significant excursions of electron density in the region of the cations after inclusion of the appropriate number of atoms, no further attempts to model the disorder were attempted. Since the anionic molybdenum complexes were well-behaved and the species of interest, this appeared a reasonable recourse. The disorder is apparent in a number of large temperature factors and in the range of C—C bond lengths (1.20–1.65 Å) for the cations.

Acknowledgement—This research was supported by a grant from the National Science Foundation (CHE8815299).

REFERENCES

1. K. Wieghardt, G. Baches-Dahmann, W. Siviridoff and J. Weiss, *Inorg. Chem.* 1983, **22**, 1221.
2. V. Chilou, P. Gouzerh, Y. Jeannin and F. Robert, *J. Chem. Soc., Chem. Commun.* 1987, 1467.
3. T.-C. Hsieh, S. N. Shaikh and J. Zubieta, *Inorg. Chem.* 1987, **26**, 4079 and refs therein.
4. C. G. Pierpont and R. M. Buchanan, *J. Am. Chem. Soc.* 1975, **97**, 6450.
5. A. Muller and N. Mohan, *Z. Anorg. Allg. Chem.* 1981, **480**, 157.
6. V. Chilou, P. Gouzerh, Y. Jeannin and F. Robert, *Inorg. Chem. Acta* 1987, **133**, 205.
7. A. Muller, W. E. Eltzer, H. Bogge and E. Knickemeyer, *Angew. Chem. Int. Edn Eng.* 1983, **22**, 884.
8. D. A. Brown, A. L. Poche, T. A. Pakkanen, T. T. Pakkanen and K. Smolander, *J. Chem. Soc., Chem. Commun.* 1982, 676.
9. V. L. Pecoraro, *Inorg. Chim. Acta* 1988, **155**, 171.
10. K. Abu-Dari, D. P. Freyberg and K. N. Raymond, *Inorg. Chem.* 1979, **18**, 2427.
11. K. Abu-Dari and K. N. Raymond, *Inorg. Chem.* 1980, **19**, 2034.
12. V. A. N. Oosthock, *Molecular Structure and Dimensions* (Edited by O. Kennard, D. G. Watson, F. H. Allen, N. W. Isaacs, W. D. Motherwell, R. C. Patterson and W. G. Touns). Vitegevefs Mij, Utrecht (1972).
13. I. K. Larsen, *Acta Chim. Scand.* 1971, **25**, 2408.
14. T. Nicholson and J. Zubieta, *Polyhedron* 1988, **7**, 171.

Polyhedron Vol. 8, No. 20, pp. 2481–2484, 1989
Printed in Great Britain

0277-5387/89 $3.00+.00
© 1989 Pergamon Press plc

CRYSTAL AND MOLECULAR STRUCTURE OF A SEVEN-COORDINATE CHLOROINDIUM(III) COMPLEX OF 1,4,7-TRIAZACYCLONONANETRIACETIC ACID

ANDREW S. CRAIG, IAN M. HELPS and DAVID PARKER*

Department of Chemistry, University of Durham, South Road, Durham DH1 3LE, U.K.

and

HARRY ADAMS, NEIL A. BAILEY and MARK G. WILLIAMS

Department of Chemistry, University of Sheffield, Sheffield S3 7HF, U.K.

and

JOHN M. A. SMITH

Department of Biochemistry, University of Sheffield, Sheffield S10 2TN, U.K.

and

GEORGE FERGUSON

Department of Chemistry, University of Guelph, Guelph, Ontario, Canada, N1G 2W1

(*Received* 28 *April* 1989; *accepted* 5 *June* 1989)

Abstract—The title macrocyclic ligand forms a seven-coordinate chloroindium complex which exists as a stable neutral hexacoordinate species in aqueous solution.

An attractive isotope for the γ-scintigraphic detection of tumours using radiolabelled monoclonal antibodies is indium-111 ($t_{1/2}$ = 2.81 days). In order to bind the indium radiolabel irreversibly to the antibody, different ligands have been sought which may be covalently attached to the protein. A series of hexacoordinating macrocyclic triaza-ligands have been examined—the [9]- to the [12]-membered triaza-triacid ligands (**1**–**4**)—of which **1** bound indium most quickly under ambient conditions[1] (pH 5, 0.1 M OAc^-, 97% radiolabelling yield in 30 min at [**1**] = 20 μM). These ligands form neutral indium complexes in solution, which are relatively insensitive to metal- or acid-promoted dissociation *in vivo*. Preliminary animal biodistribution data are in accord with this hypothesis, and perturbed angular correlation spectroscopic measurements suggest that **1** forms the most stable In^{3+} complex observed.

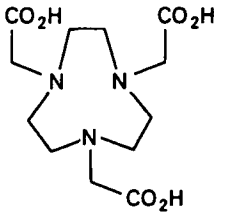

1

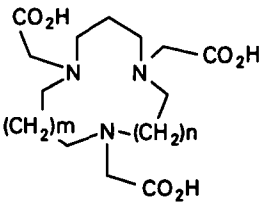

2 m = n = 1
3 m = 1 n = 2
4 m = n = 2

Reaction of equimolar quantities of **1** with

* Author to whom correspondence should be addressed.

indium trichloride in deuteroacetate/deuteroacetic acid buffer ($I = 0.1$, pD = 5.0) was monitored by ^{1}H NMR, and gave a spectrum consistent with local C_3 symmetry for the complex. The diastereotopic ring protons resonated as an AA'BB' system centred at 3.20 ppm, while the methylene CH_2CO groups gave a sharp singlet at 3.75 ppm.

An identical spectrum was obtained when indium trinitrate was bound to **1** under the same experimental conditions. Desorption chemical ionization mass spectrometry revealed a molecular ion ($M^+ + 1$) at $m/z = 416$, consistent with formation of a neutral hexacoordinate complex. An admixture of $Ga(NO_3)_3$ and **1** ($I = 0.1$, pD = 5.0) gave a similar spectrum with methylene CH_2CO groups resonating as a singlet at 3.88 ppm and the diastereotopic CH_2N protons giving multiplets centred at 3.51 (6H) and 3.23 (6H) ppm. Given the attractive features of ^{67}Ga as a γ-emitting imaging radioisotope in radioimmunoscintigraphy[2] ($t_{1/2} = 78.1$ h), ligand **1** may prove suitable for both indium and gallium in this context. When **1** was allowed to react with $InCl_3$ stabilized in 0.04 M HCl, colourless crystals of a hydrated chloroindium complex (by microanalysis) were isolated by slow evaporation. The NMR spectrum in D_2O was identical to that obtained in an acetate butter, at the same pD. Crystals suitable for X-ray diffraction were obtained and were analysed independently at two sites. The molecular structure—showing the atomic numbering scheme—is illustrated in Fig. 1, with salient bond lengths and bond angles given in Table 1.

The molecule comprises an indium(III) ion in a pentagonal bipyramidal coordination environment in which the axial sites are occupied by a chloro ligand and by one tertiary amine (In—N(2) = 2.288(5) Å) of the [9]-N_3 macrocycle. The other two tertiary amine nitrogens occupy sites in the equatorial plane (In—N = 2.331 Å) at an angular separation of 78°; the remaining three equatorial sites are filled by an oxygen atom of the three pendant carboxymethyl groups—one of which is protonated (In—O = 2.284, 2.424, 2.116 Å). Indium in its complexes usually adopts five- or six-coordination although examples of formal eight-coordination have been reported,[3] so this seven-coordinate complex is unusual,[4] notwithstanding the elongated In—O(3) bond (2.413(6) Å) and the rather long indium–chlorine bond (2.460(4) Å). A μ-hydroxo tetrameric indium complex of the parent [9]-N_3 triamine has been reported[5] in which indium–nitrogen bond distances in the range 2.29–2.35 Å were defined. In $In(CH_3CO_2)_3$phen and $In(CH_3CO_2)_3$bpy, where the indium is formally eight-coordinate, indium–nitrogen bond lengths of 2.33 Å were reported,[6] while indium–oxygen bond lengths ranging from 2.14 to 2.87 Å have been described in $In(OH)_3$,[7] $[([9]\text{-}N_3)_2In(CH_3CO_2)_4(\mu\text{-}O)] \cdot 2NaClO_4$[5] and in an (acetato)(porphyrinato)-indium(III) complex.[8]

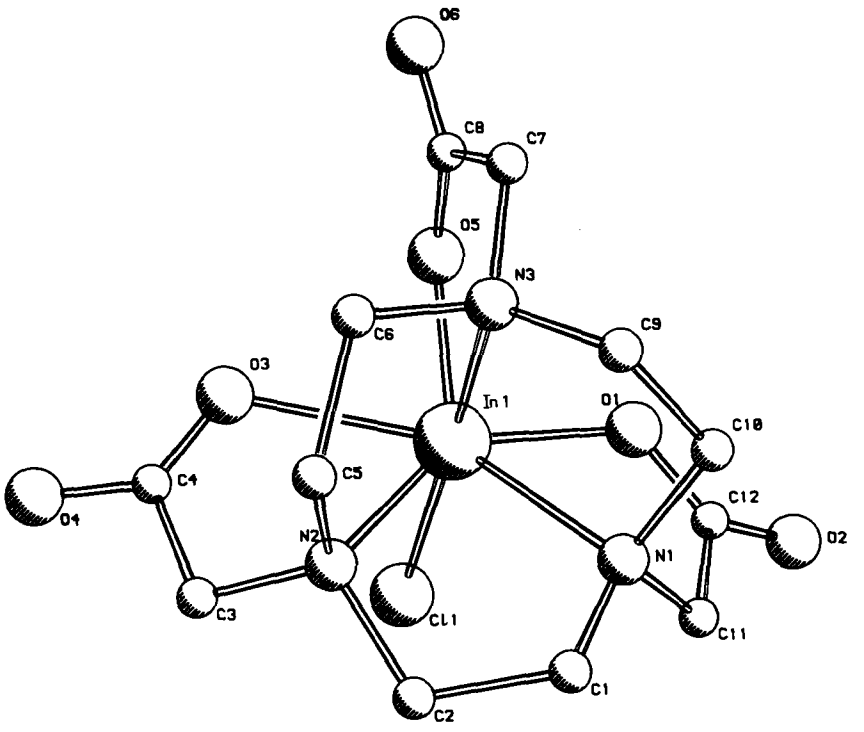

Fig. 1.

Table 1. Bond lengths (Å) and bond angles (°) for [(**1**)·InCl], with estimated standard deviations in parentheses.

In—Cl	2.399(2)	O(7)···O(8)	2.87(5)
In—O(3)	2.424(4)	O(1)···O(7)	2.84(2)
In—N(1)	2.332(5)	O(8)···O(8)[a]	2.94(7)
In—N(3)	2.288(5)	O(2)···O(4)[b]	2.487(6)
In—O(1)	2.284(4)		
In—O(5)	2.116(5)		
In—N(2)	2.331(5)		
Cl—In—O(1)	83.1(1)	Cl—In—O(3)	83.0(1)
O(1)—In—O(3)	143.2(1)	Cl—In—O(5)	112.0(1)
O(1)—In—O(5)	80.3(1)	O(3)—In—O(5)	73.8(1)
Cl—In—N(1)	99.6(1)	O(1)—In—N(1)	71.3(2)
O(3)—In—N(1)	144.8(2)	O(5)—In—N(1)	134.2(2)
Cl—In—N(2)	91.0(1)	O(1)—In—N(2)	144.5(2)
O(3)—In—N(2)	69.5(2)	O(5)—In—N(2)	133.5(2)
N(1)—In—N(2)	75.3(2)	Cl—In—N(3)	168.3(2)
O(1)—In—N(3)	104.8(2)	O(3)—In—N(3)	94.9(1)
O(5)—In—N(3)	78.1(2)	N(1)—In—N(3)	75.4(2)
N(2)—In—N(3)	77.6(2)		

Symmetry operations are [a] = $[-x, 1-y, -z]$; [b] = $[0.5-x, 0.5+y, 0.5-z]$.

Both samples which were analysed contain waters of hydration in the same general sites but with different occupanices. In one, a water molecule [O(7)] is present with 0.46 occupancy and is hydrogen bonded to O(1)···O(7), 2.84(2) Å; a second water molecule is present in only 0.18 occupancy and is at hydrogen bonded distances from both O(7) (2.87(5) Å) and a symmetry related O(8) (across an inversion centre, O(8)···O(8), 2.94(7) Å). In the other sample, the occupancies of O(7) and O(8) are 0.48 and 0.32, respectively, and the corresponding hydrogen bonded distances are O(1)···O(7), 2.84; O(7)···O(8), 2.96; O(8)···O(8), 2.79 Å.

The molecules of the complex are linked into infinite chains about a two-fold screw axis by a short hydrogen bond involving carboxyl oxygens O(2) and O(4), with O(2)···O(4)(I) 2.487(6) Å in **1** and 2.497 Å in **2**. A difference map in a plane containing O(2) and O(4)(I) showed a clear maximum midway between the two oxygen atoms and this hydrogen-bonded H atom was positioned at this site and included (but not refined) in the final refinement cycles. In the other analysis, a maximum in a difference map at 1.08 Å from O(2) and directed towards O(4)(I), was ascribed to the hydrogen bonded H atom and it was included at this site but not refined in the subsequent calculations.

* Details of the second analysis are available from the authors on request.

EXPERIMENTAL*

Crystal data for [(L)InCl]·0.46(H_2O), 0.18(H_2O); $C_{12}H_{19}ClInN_3O_6$·0.64(H_2O), Mr = 463.1. Crystal dimensions 0.25 × 0.43 × 0.55 mm, monoclinic a = 7.017(3), b = 17.701(5), c = 14.083(3) Å, β = 99.02(2)°. U = 1728(2) Å^3, D_c = 1.78 g cm^{-3}, Z = 4. Space group $P2_1/n$, Mo-K_α radiation (λ = 0.71073 Å), μ(Mo-K_α) = 15.3 cm^{-1}, F(000) = 929.6.

Three-dimensional data were collected using a CAD4 diffractometer in the range $4 < 2\theta < 40°$ by the ω–2θ scan method. Collection of data in the range $40 < 2\theta < 54°$ was terminated because of rapid decay of the crystal soon after data collection for this shell started; there had been no significant decay during the initial data collection. Structure solution and refinement progressed with the 4–40° data set. The cell data were determined by a least-squares analysis of the setting angles of 25 reflections with $14 < 2\theta < 40°$. 3259 reflections were collected of which 2564 were unique (R-factor on averaging 1.6%). The data were corrected for absorption (max. and min. transmission coefficients: 0.734, 0.664) and during refinement for secondary extinction. The 1488 reflection with $I > 3\sigma(I)$ were labelled observed and used in structure solution and refinement. The structure was solved via the heavy-atom method and refined by full-matrix least-squares calculations. Two sites

corresponding to partially occupied water molecules were also located. No hydrogen of water molecules could be located from difference maps, but all hydrogens of the complex were clearly visible. The complex molecules are linked by a short O—H—O hydrogen bond (2.487(6) Å) and a difference map showed a clear maximum midway between the two oxygen atoms. All other hydrogen atoms were positioned geometrically (C—H, 0.95 Å) and were included but not refined in the refinement process. Refinement converged with $R = 0.039$, $R_w = 0.075$ (largest shift/error ratio 0.05). Scattering factor and anomalous dispersion data were taken from *International Tables for X-ray Crystallography*[9] and all calculations were done with SDP-Plus. In the refinement cycle, weights were derived from the counting statistics; a final difference map had no chemically significant maxima.

Acknowledgements—We thank SERC and Celltech for support, and D.P. thanks the RSC for a Hickinbottom Fellowship. G.F. thanks NSERC (Canada) for an operating grant.

REFERENCES

1. A. S. Craig, I. M. Helps, D. Parker, N. R. A. Beeley, B. A. Boyce, M. A. W. Eaton, A. T. Millican, K. Millar, A. Phipps, S. K. Rhind, A. Harrison and C. Walker, *J. Chem. Soc., Chem. Commun.* 1989, 794.
2. M. Koizumi, K. Endo, M. Kunimatsu, H. Sakahara, T. Nakashima, Y. Kawamura, Y. Watanabe, Y. Ohmono, Y. Arano, A. Yokoyama and K. Torizuka, *J. Immunol. Meth.* 1987, **104**.
3. A. J. Carty and D. G. Tuck, *Progr. Inorg. Chem.* 1975, **19**, 243.
4. J. Davis and G. J. Palernik, *Inorg. Chim. Acta* 1985, **99**, L51.
5. K. Wieghardt, M. Kleine-Boymann, B. Nuber and J. Weiss, *Inorg. Chem.* 1986, **25**, 1654.
6. H. Prent and F. Haber, *Z. Anorg. Allg. Chem.* 1979, **450**, 120.
7. A. N. Christensen, N. C. Broch, O. Heidenstamm and A. Nilsson, *Acta Chem. Scand.* 1967, **21**, 1046.
8. P. Cocolios, R. Guilard, D. Bayenl and C. Lecomte, *Inorg. Chem.* 1985, **24**, 2058.
9. *International Tables for X-Ray Crystallography*, Vol. 4. Kynoch Press, Birmingham (1974).

Polyhedron Vol. 8, No. 20, pp. 2485–2494, 1989
Printed in Great Britain

0277-5387/89 $3.00+.00
© 1989 Pergamon Press plc

REACTIONS OF SOME MIXED-VALENCE DIPHOSPHORUS COMPOUNDS WITH THE PLATINUM(0) COMPLEX, $(C_2H_4)Pt(PPh_3)_2$. X-RAY CRYSTAL STRUCTURE OF THE PRODUCT OF THE REACTION OF $(C_2H_4)Pt(PPh_3)_2$ WITH A $\lambda^3P\lambda^4P^+$ DIPHOSPHORUS COMPOUND

LUDGER ERNST, PETRA LOOK-HERBER and REINHARD SCHMUTZLER*

Institut für Anorganische und Analytische Chemie der Technischen Universität, Hagenring 30, 3300 Braunschweig, F.R.G.

and

DIETMAR SCHOMBURG

Gesellschaft für Biotechnologische Forschung, Mascheroder Weg 1, 3300 Braunschweig, F.R.G.

(*Received* 5 *April* 1989; *accepted* 2 *June* 1989)

Abstract—The reaction of $(C_2H_4)Pt(PPh_3)_2$ (**4**), with the ionic N,N′-dimethylurea-bridged $\lambda^3P\lambda^4P^+$ diphosphorus compound, **1b**, furnished the mononuclear platinum(II) complex, **6**, whose structure was determined by X-ray diffraction. The geometry at platinum shows significant deviation from planarity. The ionic diphosphorus compound, **3a**, reacted with **4** to give a PPtPPt four-membered ring system, **7**. By contrast, the reaction between the covalent mixed-valence $\lambda^3P\lambda^5P$ diphosphorus compound, **2**, and **4** proceeded without oxidation of the platinum centre. The ^{31}P and ^{195}Pt NMR parameters of **6** were ascertained by iterative analysis. The signs of the coupling constants were determined by a two-dimensional $^{31}P,^{31}P\{^1H\}$-COSY-45 experiment. The NMR investigation of **7** is also described. The $^1J(Pt,P)$ coupling constants within the ring are compared with those of similar compounds.

In recent years a variety of mixed-valence diphosphorus compounds have been reported which involve, as a central feature, a PP-system, bridged by one or two N,N′-dimethylurea groups.[1–4] A simple approach to this class of compounds consists of the reaction of N,N′-dimethyl-N,N′-bis(trimethylsilyl)urea with dialkylaminodichlorophosphines, R_2NPCl_2, or in the reaction of the bis (phosphorylated) urea, $[(Me)(Cl)PN(Me)]_2C(:O)$, with dialkylaminotrimethylsilanes, R_2NSiMe_3. Both types of PP-bonded products thus obtained may be subjected to further reactions.[2,5–7] Typical representatives of this type of compounds are the following:

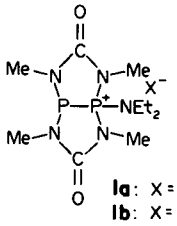

1a: X = Cl
1b: X = CF_3SO_3

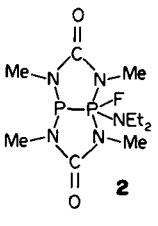

2

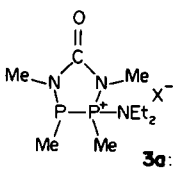

3a: X = Cl
3b: X = CF_3SO_3

* Author to whom correspondence should be addressed.

The bridging N,N′-dimethylurea groups serve as a clamp between the two phosphorus atoms, stabilizing the PP-bond. At the same time, these bridging groups are sufficiently flexible to permit substantial changes in the coordination number and electronic situation at phosphorus without affecting the basic molecular structure. The PP-bond in such compounds, especially those of types **1** and **2**, has been found to be exceptionally stable. Although several reactive centres are available, in principle, the coordination of the compounds of types **1–3** to metal centres, e.g. Fe^0, W^0, Rh^I and Pt^{II} occurs exclusively via the lone pair of electrons at λ^3P.[7]

By contrast, the reaction of **1a** with the platinum(0) complex, $(C_2H_4)Pt(PPh_3)_2$ (**4**), was found to proceed with cleavage of the PP-bond to yield the unusual platinum(II) complex, **5**, in good yield.[8] The formation of **5** is the result of a sequence of oxidative addition and substitution reactions which led to complete displacement of C_2H_4 and PPh_3, coordinated to platinum(0), in **4**.

RESULTS AND DISCUSSION

Reaction of the λ^3P-substituted phosphonium salt, **1b**, *with ethylenebis(triphenylphosphine)platinum*(0) (**4**): *Synthesis of* **6**

In the course of the reaction of **1a** with **4**, ethylene and triphenylphosphine were completely stripped off the platinum atom; the facile formation of a PPtPPt four-membered ring was assisted, probably, by the high affinity of chlorine to platinum. By contrast, similar coordination of the $[CF_3SO_3]^-$ ion to platinum during the reaction of **1b** with **4** was not to be expected. In this case, a mononuclear complex, **6**, was formed as a result of the insertion of the $Pt(PPh_3)_2$ fragment into the PP-bond of **1b**. The reaction constitutes another example of the oxidative addition reaction of a diphosphorus compound to platinum(0), with formation of a platinum(II) complex.

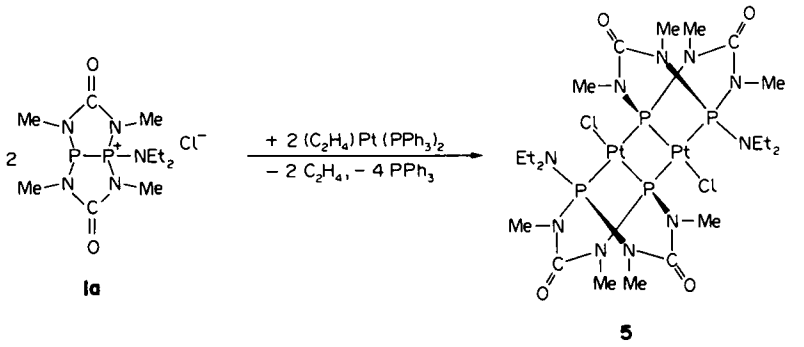

1a **5** (1)

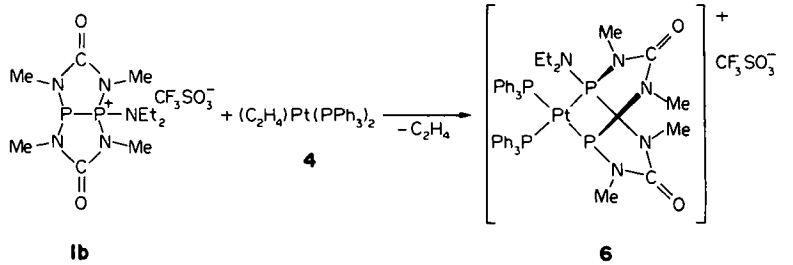

1b **4** **6** (2)

Oxidative addition reactions at metal centres which proceed with insertion of the metal into a PP-bond have repeatedly been reported (e.g. refs 9–12). The first reaction of this type was observed between the cage molecule P_4S_3 and Vaska's complex, $IrCl(CO)(PPh_3)_2$, in 1983.[9]

Complex **6** was formed in good yield as a yellow, air-sensitive solid. Solutions of **6** in $CDCl_3$ decomposed after 20 h at 50°C. It should be noted that the coordination number of one of the phosphorus atoms (bearing a lone pair of electrons) in **6** is unusually low. This is probably the principal reason

for the low stability of **6** in solution. The reactivity of **6** warrants further studies which have not, as yet, been initiated.

One- and two-dimensional ^{31}P *and* ^{195}Pt *NMR investigation of* **6**

At room temperature the ^1H-decoupled 81 MHz-^{31}P NMR spectrum of **6** shows some broadened featureless absorptions which point to chemical exchange taking place at an intermediate rate. An attempt to record the ^{31}P NMR spectra above room temperature in order to investigate the dynamic process was unsuccessful because **6** decomposes in solution (solvent: Cl_2CD–$CDCl_2$) at temperatures in excess of 70 C. On cooling a solution in CD_2Cl_2 to −30 C, the lines become sufficiently narrow for an iterative spectral analysis to be carried out.

The main signals which belong to the isotopomers not containing ^{195}Pt form a four-spin system from which the four ^{31}P chemical shifts and the absolute values of the six $^2J(PP)$ coupling constants can be extracted without difficulty. This four-spin system is almost first-order with respect to the number of transitions and the symmetry of the multiplet splittings. It shows only slight deviations from first-order line intensities and ensuing differences between chemical shifts and multiplet centres (a few Hz or $\leqslant$ 0.2 ppm).

The situation is different when one turns to the ^{195}Pt satellites in the ^{31}P spectrum, which form the ABCD part of an ABCDX spectrum (Fig. 1). Because of the large magnitude of the $J(Pt,P)$ coupling constants, some transitions of different nuclei approach each other to such an extent as to cause higher order effects that are evident, above all, from the asymmetric satellite multiplets. The appearance of these multiplets depends on the relative signs of the values of $J(PP)$.

By comparison with data typical of $^1J(Pt,P)$ and $^2J(PP,trans)$ in phosphine complexes,[16a] $^1J(Pt,P) = 619.6$ Hz and $^2J(PP,trans) = 68.8$ Hz for P_A are unusually small. Likewise, such small values were found in other platinum-substituted phosphines.[14]

The spectrum was analysed as follows: $^1J(Pt,P)$ couplings were taken as positive, in accordance with the literature.[15] Furthermore, since $^2J(PP)$ in phosphine–transition metal complexes is known to be large and positive for a *trans* orientation of the phosphorus nuclei and smaller and of either sign for a *cis* orientation,[16] the largest $^2J(PP)$ value (464.4 Hz) was taken as positive. Then, the 32 possible sign combinations were tested for the five remaining P,P-couplings. Only two of these produced calculated spectra which were compatible with the experimental spectrum. For both of these, iterative analyses were carried out and the results

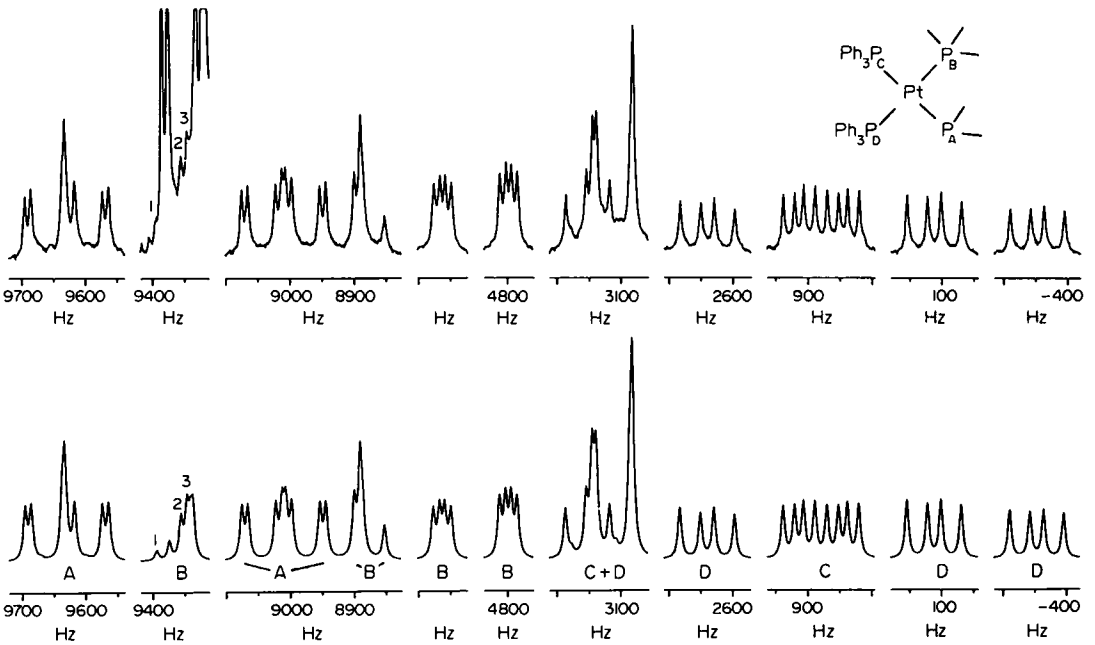

Fig. 1. ^{195}Pt satellites in the 81.0 MHz $^{31}P\{^1H\}$ NMR spectrum of **6** in CD_2Cl_2 solution at −30°C; top: experimental spectrum; bottom: spectrum simulated using the parameters obtained from the iterative analysis. Frequencies are relative to external H_3PO_4. Capital letters indicate the affiliation of the satellites to the ^{31}P nuclei.

differed essentially only in the sign of the 32.2 Hz coupling.

To determine the sign of this coupling constant and in order to confirm the signs of the other ^2J(PP) couplings obtained by simulation, a two-dimensional $^{31}P,^{31}P\{^1H\}$-COSY-45 spectrum[17] was recorded. The relevant sections of the contour plot are shown in Fig. 2.

A standard COSY experiment[19] (COSY-90) employing the pulse sequence $\pi/2$–τ–$\pi/2$ (τ = incremented delay) yields cross peaks between the chemical shifts of coupled nuclei which possess the multiplicities of both nuclei involved. In a four-spin system, at sufficient digital resolution, a cross peak consists of 8×8 peaks (ddd multiplicity in both dimensions). In contrast to this, the cross peaks in a COSY-45 spectrum contain responses only at the intersections of transitions which are directly connected in the energy level diagram, i.e. which share a common level. Thus a COSY-45 experiment furnishes the same information as a series of suitable spin-tickling experiments.[20]

In the case of a four-spin ABCD system, in which all coupling constants are different and non-zero, a cross peak in the COSY-45 spectrum contains only 16 responses (as opposed to 64 in a COSY-90 spectrum). The procedure of the analysis is shown taking the cross peak between nuclei C and D [coordinates: $x = \delta_D$, $y = \delta_C$, Fig. 2(a)] as an example. In this cross peak the positions of the responses form four squares Q_1–Q_4 with a side length of J(CD). The x-coordinates of Q_1 and Q_2 (and those of Q_3 and Q_4) differ by $\Delta x_{12} = J$(BD), the y-coordinates by $\Delta y_{12} = J$(BC). The line connecting the centres of Q_1 and Q_2 has a negative slope, i.e. $J(BC)/J(BD) < 0$: these two coupling constants are of opposite sign. Correspondingly, $\Delta x_{13} = J$(AD), $\Delta y_{13} = J$(AC) and $J(AC)/J(AD) > 0$; when the slope of the line connecting Q_1 and Q_3 is positive, the coupling constants involved are of the same sign. The other cross peaks are analysed in an analogous fashion [Figs 2(b)–(d)]. Table 1 lists the conclusions drawn from the COSY-45 spectrum.

An iterative analysis of the ^{195}Pt satellites in the

Table 1. Results of the COSY-45 experiment for **6**

Cross multiplet between	Figure	Conclusions
C and D	2(a)	$J_{AC}/J_{AD} > 0$, $J_{BC}/J_{BD} < 0$
A and B	2(b)	$J_{AC}/J_{BC} < 0$, $J_{AD}/J_{BD} > 0$
B and C	2(c) (left)	$J_{AB}/J_{AC} > 0$, $J_{BD}/J_{CD} < 0$
B and D	2(c) (right)	$J_{AB}/J_{AD} > 0$, $J_{BC}/J_{CD} > 0$
A and C	2(d) (left)	$J_{AB}/J_{BC} < 0$, $J_{AD}/J_{CD} < 0$
A and D	2(d) (right)	$J_{AB}/J_{BD} > 0$, $J_{AC}/J_{CD} < 0$

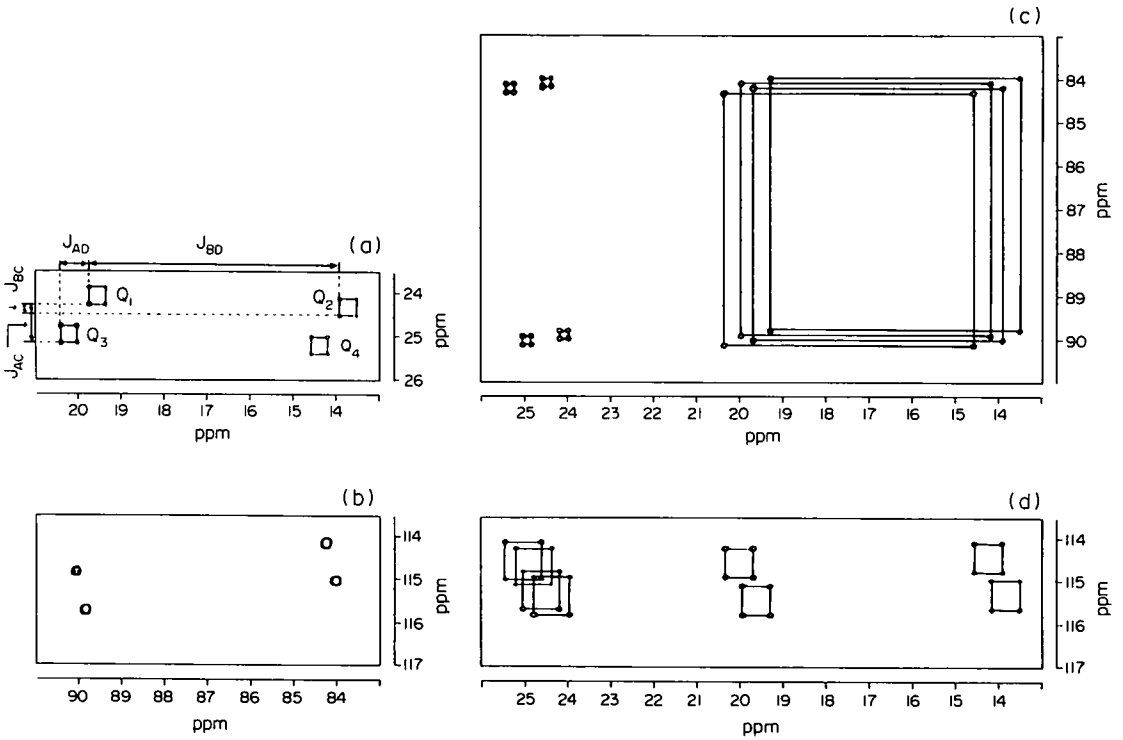

Fig. 2. Cross peaks in the two-dimensional $^{31}P,^{31}P\{^1H\}$-COSY-45 spectrum of **6** in CD_2Cl_2 at −30°C. See Table 1 for identification of cross peaks; see text for details.

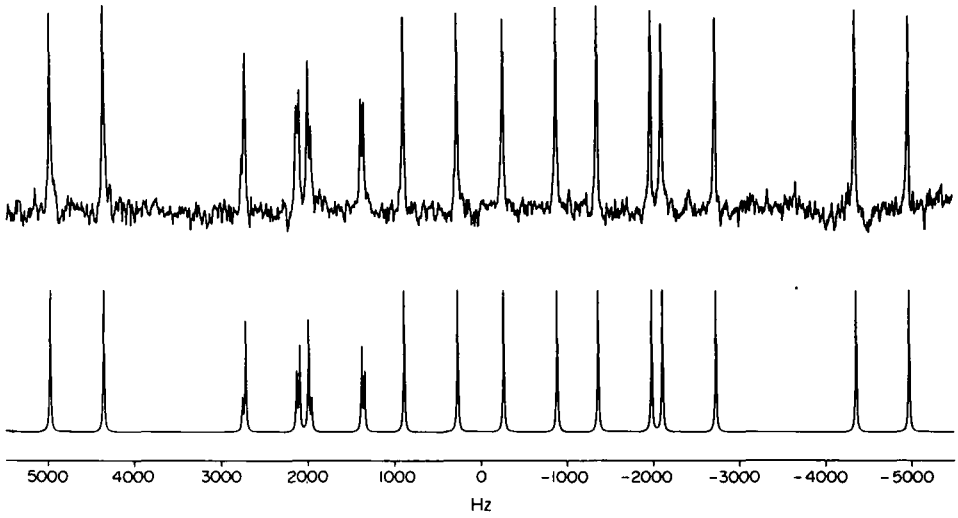

Fig. 3. 42.8 MHz $^{195}Pt\{^1H\}$ NMR spectrum of **6** in CD_2Cl_2 at −30°C; top: experimental; bottom: calculated.

^{31}P spectrum that made use of the relative signs of the $J(PP)$ couplings determined above yielded the spectral parameters given in Table 2. The r.m.s. error of 0.12 Hz between observed and calculated line positions is relatively high for the results of an iterative analysis. It is caused by the *ca* 7 Hz line width of the ^{195}Pt satellites which may be due to insufficient slow-down of the chemical exchange and to rapid spin–lattice relaxation of the ^{195}Pt nucleus by the chemical shift anisotropy mechanism.[21] In accordance with the latter assumption, the main signals of the ABCD ^{31}P spectrum are only 3–4 Hz wide at half height.

Table 2. Results of the iterative NMR spectral analysis of **6**

Chemical shifts			
$\delta_P(A)$	115.031	$\delta_P(C)$	24.719
$\delta_P(B)$	87.200	$\delta_P(D)$	17.105
δ_{Pt}	−299.91		
	(relative to Ξ = 21.4 MHz[26])		
Spin–spin coupling constants (Hz)			
$J(P_A,P_B)$	9.5	$J(P_B,P_C)$	−18.0
$J(P_A,P_C)$	68.8	$J(P_B,P_D)$	464.5
$J(P_A,P_D)$	53.3	$J(P_C,P_D)$	−32.2
$J(Pt,P_A)$	619.6	$J(Pt,P_C)$	2247.4
$J(Pt,P_B)$	4089.6	$J(Pt,P_D)$	2991.1

r.m.s. error: 0.12 Hz.
Probable errors of ^{31}P shifts: 0.0005 ppm.
Probable errors of coupling constants: 0.05–0.09 Hz.
Assigned transitions: 53 of 66 (^{31}P only).

The $^{195}Pt\{^1H\}$ NMR spectrum of **6** was also recorded at −30°C. It is not a first-order spectrum and is unsymmetrical (Fig. 3). Its appearance depends on the sign of $^2J(P_BP_D)$ relative to that of the $^1J(Pt,P)$ couplings. For opposite signs of $^2J(P_BP_D)$ and $^1J(Pt,P)$, the calculated ^{195}Pt spectrum is the mirror image of the one shown in Fig. 3. Thus the assumption made above, $^2J(P_BP_D) > 0$, is proved experimentally.

X-ray structure of **6**

Selected bond distances and angles are shown in Table 3. The structure of the cation of **6** is displayed in Fig. 4.

The X-ray structure analysis proves that **6** exists

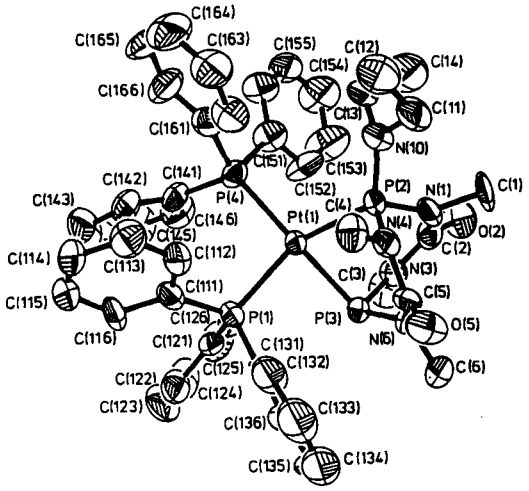

Fig. 4. X-ray crystal structure of **6**.

Table 3. Selected bond lengths (pm) and angles (°) of the cation of **6**

P(1)—Pt(1)	231.6(2)	P(2)—Pt(1)	229.2(2)
P(3)—Pt(1)	232.1(3)	P(4)—Pt(1)	237.9(3)
C(111)—P(1)	179.2(12)	C(121)—P(1)	178.2(10)
C(131)—P(1)	180.0(11)	N(1)—P(2)	166.1(9)
N(4)—P(2)	167.0(9)	N(10)—P(2)	164.6(10)
N(3)—P(3)	172.5(10)	N(6)—P(3)	172.6(8)
C(141)—P(4)	180.8(12)	C(151)—P(4)	182.7(13)
C(161)—P(4)	182.2(12)	C(1)—N(1)	148.3(13)
C(2)—N(1)	141.1(16)	O(2)—C(2)	120.4(16)
N(3)—C(2)	137.5(14)	C(3)—N(3)	147.6(16)
C(4)—N(4)	150.0(15)	C(5)—N(4)	140.7(14)
O(5)—C(5)	117.2(12)	N(6)—C(5)	138.3(14)
C(6)—N(6)	149.0(16)	C(11)—N(10)	146.1(17)
C(13)—N(10)	149.7(19)	C(12)—C(11)	154.8(20)
C(14)—C(13)	148.5(25)		

P(2)—Pt(1)—P(1)	144.7(1)	P(3)—Pt(1)—P(1)	85.7(1)
P(3)—Pt(1)—P(2)	79.6(1)	P(4)—Pt(1)—P(1)	98.5(1)
P(4)—Pt(1)—P(2)	109.3(1)	P(4)—Pt(1)—P(3)	152.4(1)
C(111)—P(1)—Pt(1)	110.6(3)	C(121)—P(1)—Pt(1)	117.8(3)
C(121)—P(1)—C(111)	109.8(5)	C(131)—P(1)—Pt(1)	110.1(3)
C(131)—P(1)—C(111)	102.4(5)	C(131)—P(1)—C(121)	104.8(5)
N(1)—P(2)—Pt(1)	116.8(3)	N(4)—P(2)—Pt(1)	99.6(3)
N(4)—P(2)—N(1)	103.5(5)	N(10)—P(2)—Pt(1)	123.9(4)
N(10)—P(2)—N(1)	107.2(5)	N(10)—P(2)—N(4)	102.1(5)
N(3)—P(3)—Pt(1)	97.5(3)	N(6)—P(3)—Pt(1)	110.6(3)
N(6)—P(3)—N(3)	102.7(4)	C(141)—P(4)—Pt(1)	117.2(4)
C(151)—P(4)—Pt(1)	107.1(4)	C(151)—P(4)—C(141)	104.2(6)
C(161)—P(4)—Pt(1)	119.8(4)	C(161)—P(4)—C(141)	103.1(5)
C(161)—P(4)—C(151)	103.8(6)	C(1)—N(1)—P(2)	118.9(8)
C(2)—N(1)—P(2)	126.6(7)	C(2)—N(1)—C(1)	114.4(9)
O(2)—C(2)—N(1)	121.8(10)	N(3)—C(2)—N(1)	114.2(10)
N(3)—C(2)—O(2)	124.0(12)	C(2)—N(3)—P(3)	126.6(8)
C(3)—N(3)—P(3)	116.5(8)	C(3)—N(3)—C(2)	116.6(10)
C(4)—N(4)—P(2)	119.9(8)	C(5)—N(4)—P(2)	123.3(7)
C(5)—N(4)—C(4)	112.1(9)	O(5)—C(5)—N(4)	121.8(11)
N(6)—C(5)—N(4)	114.5(8)	N(6)—C(5)—O(5)	123.7(11)
C(5)—N(6)—P(3)	130.6(7)	C(6)—N(6)—P(3)	112.6(7)
C(6)—N(6)—C(5)	114.1(9)	C(11)—N(10)—P(2)	127.0(10)
C(13)—N(10)—P(2)	115.3(8)	C(13)—N(10)—C(11)	113.6(10)
C(12)—C(11)—N(10)	112.0(11)	C(14)—C(13)—N(10)	116.6(12)

as a platinum complex with platinum(II) directly connected to four phosphorus ligands (two PPh_3 groups, a $P(NRR')_3$ group and a formally negatively charged $\{P(NRR')_2\}^-$ group). Pt—P bonds are in the usually observed range with the exception of Pt—P(4) which is one of the longest observed Pt—P bonds in such compounds and is 6.3 pm longer than the comparable bond, Pt—P(1). This lengthening is probably due to a strong "*trans* effect" of the negatively charged P(3) or to steric effects. The P—P bond is obviously broken.

The platinum complex shows significant deviation from planarity. The dihedral angle between the plane defined by Pt, P(2), P(3), and that defined by Pt, P(1) and P(4) is 47.2°, showing that the geometry around the platinum atom is about midway between the square plane (0°) and the tetrahedron (90°). Because of the negative charge at P(3), P(3)—N bond distances are significantly longer than the corresponding bond distances to P(2) (172.5 and 172.6 pm compared to 166.1 and 167.0 pm). As is observed in similar compounds the exocyclic P—$N(Et)_2$ bond distance is shorter than the other P—N distances.[22] The bond angles at P(2) and P(3) are remarkably similar.

Reaction of the λ^3P-substituted phosphonium salt, **3a**, *with* **4**: *synthesis and NMR investigation of* **7**

In a manner similar to the reaction of **1a** with **4**, the binuclear platinum complex, **7**, was formed in the reaction of **3a** with **4**. Again, all ligands at platinum were displaced by the mixed-valence diphosphorus compound. Although the formation of several isomers would appear possible, only one of these was detected by NMR spectroscopy. While compound **5** is soluble only in dichloromethane, **7** is very soluble in several chlorinated or aromatic solvents. The characterization of **7** rests mainly on the analysis of its ^{31}P and ^{195}Pt NMR spectra.

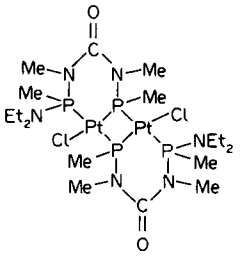

7

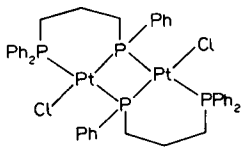

8

The ^{31}P and ^{195}Pt NMR spectra of the platinum(II) complex, **5**, were complicated because of the superposition of an $(AM)_2$, an $(AM)_2X$ and an $(AMX)_2$ spectrum. Chemical shifts and coupling constants were determined by iterative analysis.[8] Unusual values were obtained for ^1J(Pt,P) of the phosphido phosphorus atoms, P_M and $P_{M'}$. In view of the known *trans* influence,[23] ^1J(Pt,P) for the bonds *trans* to the chlorine ligands was expected to be larger than ^1J(Pt,P) for the bonds *trans* to phosphorus. The bond lengths observed for the PPtPPt four-membered ring confirm that chlorine exerts a less pronounced *trans* influence than phosphorus. The coupling constant in **5** between P_M *trans* to chlorine and Pt_X is, however, much larger than the corresponding coupling between $P_{M'}$ *trans* to phosphorus and Pt_X. By contrast, the expected trend in the coupling constants $[J(Pt_XP_{M'}) > J(Pt_XP_M)]$ was observed for **8**.[24] While in **5** phosphorus is bonded, besides platinum, only to nitrogen, there are only P—Pt and P—C bonds in **8**.

The NMR results for **7** must be viewed against this background. Its ^{31}P and ^{195}Pt NMR spectra are very similar to those of **5**. The chemical shifts and coupling constants of **7** are listed in Table 4. For comparison, the ^1J(Pt,P) values for the phosphido phosphorus atoms in compounds **5** and **8** are also included. The value of ^1J(Pt,P) for P_M and $P_{M'}$ in **7** are very similar and fall between those for **5** and **8**. This may be taken as an indication that the unexpected trend in ^1J(Pt,P) of the phosphido phosphorus atoms in **5** and **7** is caused by electronic effects of the N,N′-dimethylurea groups.

Table 4. Results of the NMR spectral analysis of **7**

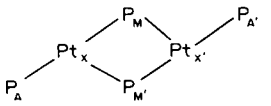

Chemical shifts

$\delta(P_A) = \delta(P_{A'})$	87.6
$\delta(P_M) = \delta(P_{M'})$	−85.8
$\delta(Pt_X) = \delta(Pt_{X'})$	617 (relative to Ξ = 21.4 MHz[26])

Spin–spin coupling constants (Hz)[a]

	5	**7**	**8**
$^2J(AM') = {}^2J(A'M)$		552.0	
$^2J(AM) = {}^2J(A'M')$		9.8	
$^4J(AA')$		5.9	
$^2J(MM')$		141.0	
$^1J(AX) = {}^1J(A'X')$		3143.0	
$^1J(MX) = {}^1J(M'X')$	2535.7	2148.2	1820.2
$^1J(MX') = {}^1J(M'X)$	2103.8	2169.3	2228.4
$^3J(AX') = {}^3J(A'X)$		29.8	
$^2J(XX')$		1209	

[a] For comparison: some coupling constants of **5** and **8**; signs of coupling constants were not determined.

Reaction of the λ^3P-substituted phosphorane, **2**, *with* **4**: *synthesis of* **9**

While the platinum(II) complexes **5**, **6**, and **7** were readily formed from mixed-valence diphosphorus compounds and **4**, the oxidation number of platinum was unchanged when the $\lambda^3P\lambda^5P$-diphosphorus compound **2** was allowed to react with **4**. In a simple substitution reaction the coordinated ethylene in **4** was displaced by **2**. The identity of the product, **9**, was ascertained by NMR spectroscopic (^{19}F,^{31}P) means. The compound is not stable in solution for more than a few days but undergoes further transformation reactions. This may explain why **9** could be isolated only in a moderate state of purity. Finally, an attempt to react **1a**, **1b** and **2** with Vaska's complex, $IrCl(CO)(PPh_3)_2$, was unsuccessful. In all cases the starting materials were recovered unchanged.

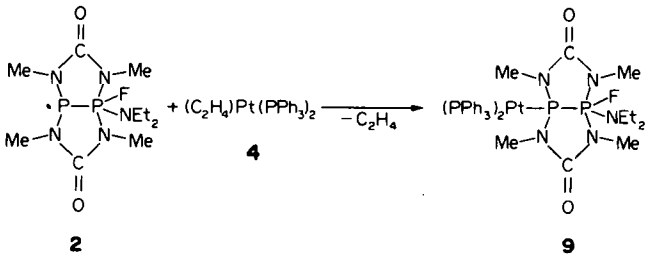

(3)

EXPERIMENTAL

All experiments were conducted with exclusion of air and moisture, using standard techniques.[25] The FD mass spectrum of **7** was recorded on a Finnigan MAT 8230 instrument. Melting points were determined in sealed tubes. Elemental analyses were performed at the Institut für Anorganische und Analytische Chemie, Technische Universität, Braunschweig.

NMR spectra

The NMR spectra of **6** were recorded on a Bruker AC 200 spectrometer operating at 81.0 MHz for ^{31}P and at 42.8 MHz for ^{195}Pt. The solvent was CD_2Cl_2. Protons were broadband-decoupled. The platinum spectrum was obtained at −30°C from 10,000 accumulations using *ca* 45° pulses 0.28 s apart. The digital resolution was 3.6 Hz/pt. Exponential line-broadening of 10 Hz was applied to the free induction decay, resulting in a linewidth of 15–20 Hz in the final spectrum. The observed NMR frequency for the position of the ^{195}Pt shift was 42.8155590 MHz. With the ^1H signal of tetramethylsilane in CD_2Cl_2 absorbing at 200.1327276 MHz, this gives $\Xi(Pt) = 21.3935819$ MHz or $\delta = -299.91$ relative to $\Xi = 21.4$ MHz.[26] For the 2D $^{31}P,^{31}P$-COSY-45 spectrum a spectral width of 9615 Hz, a data table and a transform size of 4K gave a digital resolution of 4.7 Hz/pt. 1024 increments in t_1 were used. Sixteen scans preceded by two dummy scans were accumulated per increment. Total measuring time was slightly over 5 h. One level of zero-filling was applied in t_1 and the data were multiplied with a $\pi/3$ shifted sinebell in both dimensions. Four megawords of data were obtained after the 2D transform. The solution for the 2D measurement contained *ca* 450 mg of **6** in *ca* 2.5 cm^3 of solvent in a 10 mm o.d. tube. The iterative spectral analysis was performed with Bruker's program PANIC which is based on LAOCN3.[27]

The ^{31}P and ^{195}Pt NMR spectra of **7** were measured on a JEOL FX 90 Q spectrometer at 36.4 and 25.26 MHz, respectively, on solutions in a CH_2Cl_2–CD_2Cl_2 mixture. Spectra were calibrated via the ^2D signal of the solvent and are referenced as described above. P—P coupling constants of **7** were extracted from the $(AM)_2$ spectrum of ^{31}P (digital resolution 1.8 Hz) and J(Pt,P) and J(Pt,Pt) were obtained by iteration of the $(AM)_2X$ and $(AMX)_2$ spectra of ^{31}P and ^{195}Pt, using the computer program NUMARIT.[28] The NMR spectra of **9** were recorded on a Bruker WM 400 spectrometer at 162.0 (^{31}P) and 376.5 MHz (^{19}F) for a $CDCl_3$ solution and referenced to external 85% H_3PO_4 and $CFCl_3$, respectively.

Preparation of compound **6**

A solution of 0.640 g (1.4 mmol) of **1b** in 5 cm^3 of benzene in a heavy-walled glass tube, fitted with a Teflon® stopcock, was degassed and cooled to −196°C. A solution of 1.05 g (1.4 mmol) of **4** in *ca* 10 cm^3 of deoxygenated benzene was filtered through a sintered glass disc and added to the solution of **1b**. The reaction mixture was degassed, and nitrogen was admitted. The tube was then sealed and allowed to warm up to room temperature over 1 h. After 1 day the yellow precipitate thus formed was washed with three portions of toluene (10 cm^3 each) and once with 5 cm^3 of diethyl ether, and recrystallized from 10 cm^3 of dichloromethane and *ca* 10 cm^3 of toluene over one day (using the diffusion method). The yellow, air-sensitive crystals of **6** were dried *in vacuo* (1 torr). Yield 1.15 g (70%); m.p. 210°C (dec.). Found: C, 47.2; H, 4.5; N, 5.7. Calc. for $C_{47}H_{52}F_3N_5O_5P_4PtS$ (1175.00): C, 48.0; H, 4.5; N, 6.0%. ^1H NMR spectrum ($CDCl_3$, 200.1 MHz): $\delta = 0.72$ (t, NCCH_3, ^3J(HH) = 6.9 Hz); 2.79 (m, NCH_2); 2.97 (d, NCH_3, ^3J(PH) = 11.9 Hz); 3.12 (d, NCH_3, ^3J(PH) = 7.0 Hz); 7.34 (br m, phenyl group); 7.44 (br m, phenyl group); ^{31}P NMR spectrum (CD_2Cl_2, 81.0 MHz, −30°C) and ^{195}Pt NMR spectrum (CD_2Cl_2, 42.8 MHz, −30°C): see Table 2.

X-ray analysis of **6**

Crystals of **6** obtained by recrystallization from dichloromethane–toluene have orthorhombic sym-

metry, space group $P2_12_12_1$. The unit cell which has the parameters $a = 1266.0(2)$, $b = 1812.4(3)$, $c = 2209.6(3)$ pm, contains four molecules yielding a calculated density of 1.539 g cm^{-3}. The data were collected at 293 K on a Nicolet $P2_1$ diffractometer using graphite-monochromated Cu-K_α radiation ($\lambda = 154.18$ pm) in the θ–2θ mode, in the range $3° \leqslant 2\theta \leqslant 135°$ at a scan speed between 2.93 and 29.30° min^{-1} depending on the intensity of the reflection.

The data were corrected for Lorentz-, polarization but not for absorption effects ($\mu = 7.205$ mm^{-1}). The structure was solved by direct methods and difference-Fourier synthesis. Hydrogen atom positions were calculated from those of the directly bound atoms and refined as "riding atoms". The refinement using 7916 out of 9058 measured independent reflections ($F \geqslant 4.0\sigma(F)$) converged at $R = 0.057$ ($R_w = 0.058$). The program SHELX-76[29] and our own programs were used. Complex atom scattering factors[30] were employed.

Preparation of compound **7**

As described in the preceding experiment, a solution of 0.382 g (1.3 mmol) of **3a** in 5 cm^3 of benzene and a solution of 0.995 g (1.3 mmol) of **4** in *ca* 10 cm^3 of benzene were combined and stirred at room temperature for 1 week. The solvent was removed *in vacuo* and the remaining product dissolved in 15 cm^3 of toluene. Upon concentration of this solution *in vacuo* (1 torr), formation of a white solid occurred which was recrystallized from 6 cm^3 of a 1 : 2 mixture of dichloromethane–methylcyclohexane. Yield 0.2 g (32%); m.p. 241–244°C (dec.). Found: C, 24.6; H, 4.6; P, 11.8. Calc. for $C_{18}H_{44}Cl_2N_6O_2P_4Pt_2$ (961.57): C, 22.5; H, 4.9; P, 12.9. Mass spectrum (FD): $M^+ = 962$. ^{1}H NMR spectrum (CD_2Cl_2, 400.1 MHz): $\delta = 1.11$ (t, NCCH_3, ^3J(HH) = 7.2 Hz); 1.96 ("d", PCH_3, separation 7.2 Hz); 2.00 (m, PCH_3); 2.93 ("d", NCH_3, separation 7.0 Hz); 3.13 (m, NCH_2); 3.36 (NCH_3, separation 8.2 Hz); ^{31}P NMR spectrum ($CDCl_3$, 36.4 MHz) and ^{195}Pt NMR spectra ($CDCl_3$, 19.16 MHz): see Table 4.

Preparation of compound **9**

As described for **6** and **7**, a solution of 1.03 g (1.4 mmol) of **4** in 10 cm^3 of benzene was combined with a solution of 0.9 g (2.8 mmol) of **2** in 5 cm^3 of benzene. The solid product formed after 1 day was collected, washed with three 5 cm^3-portions of toluene and dried *in vacuo* (1 torr). Yield 68%; m.p. 143°C (dec.). Found: C; 49.1; H, 4.6; N, 6.5; P, 11.9. Calc. for $C_{46}H_{52}FN_5O_2P_4Pt$ (1044.92): C, 52.6; H, 5.0; N, 6.7; P, 11.9%. ^{31}P NMR spectrum ($CDCl_3$, 162.0 MHz): $\delta = -58.94$ (ddt, PtP*P*F, ^1J(PF) = 697.4 Hz, ^1J(PP) = 27.9 Hz, ^3J(PP) = 17.7 Hz); 49.76 (dd, *P*PtPPF, ^2J(PP) = 176.6 Hz, ^3J(PP) = 17.7 Hz, ^1J(Pt,P) = 4433 Hz); 101.42 (tdd, Pt*P*PF, ^2J(PP) = 176.6 Hz, ^1J(PP) = 27.9 Hz, ^2J(PF) = 33.9 Hz, ^1J(Pt,P) = 5417 Hz); ^{19}F NMR spectrum ($CDCl_3$, 376.5 MHz): $\delta = -26.92$ (dd, ^1J(PF) = 697.4 Hz, ^2J(PF) = 33.9 Hz).

Acknowledgements—The ongoing support of Fonds der Chemischen Industrie is gratefully acknowledged. BASF AG, BAYER AG, HOECHST AG and, especially, DEGUSSA AG are thanked for generous gifts of chemicals used in this research. We are indebted to Drs R. J. Goodfellow and M. Murray (University of Bristol) for recording and simulating the ^{31}P and ^{195}Pt NMR spectra of compound **7**. Drs D. Böhler (Universität Göttingen) and H. M. Schiebel (Technische Universität, Braunschweig) are thanked for recording the mass spectrum of compound **7**.

REFERENCES

1. H. W. Roesky, U. Scholz, A. Schmidpeter, K. Karaghiosoff and W. S. Sheldrick, *Chem. Ber.* 1988, **121**, 1681 and literature refs cited therein.
2. G. Bettermann, R. Schmutzler and D. Schomburg, *Chem. Ber.*, in preparation.
3. G. Bettermann, H. Buhl, R. Schmutzler, D. Schomburg and U. Wermuth, *Phosphorus and Sulfur* 1983, **18**, 77.
4. N. Weferling, R. Schmutzler and W. S. Sheldrick, *Liebigs Ann. Chem.* 1982, 167.
5. D. Schomburg, G. Bettermann, L. Ernst and R. Schmutzler, *Angew. Chem.* 1985, **97**, 971.
6. (a) D. Schomburg, N. Weferling and R. Schmutzler, *J. Chem. Soc., Chem. Commun.* 1981, 609; (b) J. W. Gilje, W. S. Sheldrick, N. Weferling and R. Schmutzler, *Angew. Chem.* 1982, **94**, 393.
7. P. Look, PhD thesis, Braunschweig (1989).
8. P. Look, R. Schmutzler, R. J. Goodfellow, M. Murray and D. Schomburg, *Polyhedron* 1988, **7**, 505.
9. C. A. Ghilardi, S. Midollini and A. Orlandini, *Angew. Chem.* 1983, **95**, 800.
10. M. DiVaira, M. Peruzzini and P. Stoppioni, *J. Chem. Soc., Dalton Trans.* 1985, 291.
11. O. J. Scherer, M. Swarowski, H. Swarowski and G. Wolmershäuser, *Angew. Chem.* 1988, **100**, 738.
12. R. G. Ball, I. G. Phillips and R. G. Cavell, *Inorg. Chem.* 1987, **30**, 117.
13. J. A. Davies and F. R. Hartley, *Chem. Rev.* 1981, **81**, 79.
14. C. W. Allen, E. A. V. Ebsworth, S. G. Henderson, D. W. H. Rankin, H. E. Robertson and D. Whitelock, *J. Chem. Soc., Dalton Trans.* 1986, 1333.
15. W. McFarlane, *J. Chem. Soc. A* 1967, 1922.
16. (a) P. S. Pregosin and R. W. Kunz, ^{31}P and ^{13}C

NMR of transition metal phosphine complexes, in *NMR, Basic Principles and Progress* (Edited by P. Diehl, E. Fluck and R. Kosfeld), Vol. 16. Springer, Berlin, Heidelberg, New York (1979); (b) J. L. Bookham, X. L. R. Fontaine, J. D. Kennedy and W. McFarlane, *Inorg. Chem.* 1988, **27**, 1111.
17. A. Bax and R. Freeman, *J. Magn. Reson.* 1981, **44**, 542. Reference 18 describes an application of the COSY-45 technique for the sign determination of ^2J(PP).
18. X. L. R. Fontaine, J. D. Kennedy, B. L. Shaw and J. M. Vila, *J. Chem. Soc., Dalton Trans.* 1987, 2401.
19. A. Bax, R. Freeman and G. Morris, *J. Magn. Reson.* 1981, **42**, 164.
20. R. Freeman and W. A. Anderson, *J. Chem. Phys.* 1962, **37**, 2053.
21. R. Goodfellow, in *Multinuclear NMR* (Edited by J. Mason), Chap. 20, p. 523. Plenum Press, New York (1987).
22. D. Schomburg, Habilitationsschrift, Braunschweig (1985).
23. T. G. Appleton, H. C. Clark and L. E. Manzer, *Coord. Chem. Rev.* 1973, **10**, 335.
24. R. Glaser, D. J. Kountz, R. D. Waid, J. C. Galluci and D. W. Meek, *J. Am. Chem. Soc.* 1984, **106**, 6324.
25. (a) D. F. Shriver, *The Manipulation of Air-sensitive Compounds*, p. 139. R. F. Krieger, Malabar, Florida (Reprint 1982); (b) D. D. Perrin, W. L. F. Armarego and D. R. Perrin, *Purification of Laboratory Chemicals*. Pergamon Press, Oxford (1966).
26. R. G. Kidd and R. J. Goodfellow, in *NMR and the Periodic Table* (Edited by R. K. Harris and B. E. Mann), p. 251. Academic Press, New York (1978).
27. A. A. Bothner-By and S. Castellano, *Quantum Chem. Prog. Exchange* 1967, **11**, 111.
28. A. R. Quirt and J. S. Martin, *J. Magn. Reson.* 1971, **5**, 318.
29. G. M. Sheldrick, unpublished.
30. D. T. Cromer and J. T. Waber, in *International Tables for Crystallography*, Vol. IV, p. 99 ff. and p. 149. Kynoch Press, Birmingham (1974).

Polyhedron Vol. 8, No. 20, pp. 2495–2505, 1989
Printed in Great Britain

0277–5387/89 $3.00+.00
© 1989 Pergamon Press plc

THE SYNTHESIS AND STRUCTURAL CHARACTERIZATION OF SOME ORGANOTRANSITION METAL COMPLEXES INCORPORATING ANTIMONY

ALAN M. BARR, MARTIN D. KERLOGUE, NICHOLAS C. NORMAN* and PETER M. WEBSTER

Department of Chemistry, The University of Newcastle upon Tyne, Newcastle upon Tyne NE1 7RU, U.K.

and

LOUIS J. FARRUGIA*

Department of Chemistry, The University of Glasgow, Glasgow G12 8QQ, U.K.

(*Received* 4 *April* 1989; *accepted* 2 *June* 1989)

Abstract—The reaction between $SbCl_3$ and 3 equiv. of $Na[M(CO)_3(\eta\text{-}C_5H_5)]$ (M = Mo, W) affords the trimetal–antimony complexes $[Sb\{M(CO)_3(\eta\text{-}C_5H_5)\}_3]$ (**1**, M = Mo; **8**, M = W) both of which were characterized by spectroscopic and analytical methods. Mass spectra obtained on these complexes are particularly informative and are discussed. The reaction between $SbCl_3$ and 2 equiv. of $Na[M(CO)_3(\eta\text{-}C_5H_5)]$ affords the dimetal–antimony complexes $[SbCl\{M(CO)_3(\eta\text{-}C_5H_5)\}_2]$ (**5**, M = Mo; **9**, M = W). Both complexes were characterized spectroscopically and, in addition, **5** was characterized by X-ray crystallography. Compound **5** crystallizes in the monoclinic space group $P2_1/n$ with $a = 7.399(2)$, $b = 9.611(3)$, $c = 27.031(7)$ Å, $\beta = 92.70(2)^\circ$ and $Z = 4$. The structure comprises monomeric units of **5** which contain a central antimony atom in a trigonal pyramidal coordination bonded to a single chlorine and two $Mo(CO)_3(\eta\text{-}C_5H_5)$ fragments. The reaction between **1** and $SbCl_3$, which affords **5**, is also described and discussed, as are the reactions between $SbCl_3$ and 2 and 3 equiv. of $Na[Fe(CO)_2(\eta\text{-}C_5H_5)]$ which afford $[SbCl\{Fe(CO)_2(\eta\text{-}C_5H_5)\}_2]$ (**11**) and $[Sb\{Fe(CO)_2(\eta\text{-}C_5H_5)\}_3]$ (**13**), respectively. Both iron-containing compounds were characterized spectroscopically and analytically and, in addition, **13** was characterized by X-ray crystallography. Compound **13** crystallizes in the monoclinic space group $P2_1/n$ with $a = 16.686(5)$, $b = 16.927(4)$, $c = 16.894(5)$ Å, $\beta = 110.95(2)^\circ$ and $Z = 8$. The structure contains two monomeric molecules of **13** in the asymmetric unit, although the geometries of both are very similar in all respects. Each molecule contains a central antimony atom with trigonal pyramidal coordination bonded to three $Fe(CO)_2(\eta\text{-}C_5H_5)$ fragments.

Compounds containing organotransition metal fragments and atoms or small aggregates of the main group elements ("Inorganometallic Chemistry" as Fehlner has recently called it[1]) is an area of inorganic chemistry which continues to attract the attention of synthetic chemists. Quite apart from any inherent academic appeal that such compounds may have, this interest can be traced, at least in part, to their potential importance or relevance regarding the synthesis of "new materials" and a number of general reviews on this area have recently appeared,[2] the most comprehensive being that of Whitmire.[2c]

With particular reference to complexes containing antimony, and specifically those containing antimony–transition metal bonds, a range of types of complexes are known. Perhaps the simplest of these are the stibine (R_3Sb) complexes,[3] analogous to the more commonly encountered phosphorus congeners, and those, although fewer in number, involving distibines ($R_2Sb—SbR_2$).[4] A range of stibido (R_2Sb) complexes have also been charac-

* Authors to whom correspondence should be addressed.

terized, primarily by Malisch and co-workers, comprising both mononuclear[5] and dinuclear[5,6] examples, the latter often derived from the former by a formal dative interaction between the antimony lone pair and a 16-electron transition metal fragment.[5a,c,e,f,g,6b,c]

Compounds containing the stibinidene or stibinediyl (RSb) fragments are also known, a range of coordination modes having been observed. These include the di-metal complexes which contain a trigonal planar antimony and some degree of multiple metal–antimony bonding,[7] *viz.* $L_nM{=\!=\!=}Sb(R){=\!=\!=}ML_n$ (ML_n = 16 electron transition metal fragment), a valence isomer of this form incorporating a trigonal pyramidal antimony[8] and cluster bound examples.[7c,g,8,9] An important additional class of stibinidene-containing complexes, with regard to the present work, are those involving two 17 electron transition metal fragments, i.e. L_nM—Sb(R)—ML_n,* most examples having been prepared by Malisch and co-workers.[5c,d,g]

Coordination complexes involving the formally doubly bonded distibenes (RSb=SbR) have also been characterized, primarily by Huttner[7a,b,c,11] and Cowley,[8] and exhibit a range of bonding modes with electron pair donation to transition metal centres occurring through antimony lone pairs and the formal Sb—Sb π-bond.

Of more relevance to the present work are those compounds incorporating antimony bonded only to transition metals. These include $[\{Cr(CO)_5\}_2\{M(CO)_5\}Sb]^-$ (M = Cr, Mo, W) containing a trigonal planar antimony,[12] $[Co_4Sb_4(CO)_{12}]$,[13] $[Rh_{12}Sb(CO)_{27}]^{3-}$ containing an interstitial antimony atom,[14] $[W_3Sb_2(CO)_{15}]$ which incorporates a di-antimony (formally Sb≡Sb) ligand acting as a six-electron donor,[11] and a number of iron carbonyl–antimony clusters.[15]

We note also that a range of four-coordinate, cationic antimony complexes have also been prepared. Cullen[16] has reported analytical and IR data on compounds of the general formula $[SbX\{Fe(CO)_2(C_5H_5)\}_3]^+$ (X = Cl, Br), $[SbX_2\{Fe(CO)_2(C_5H_5)\}_2]^+$ (X = Cl, Br, CF_3), $[Sb\{Fe(CO)_2(NO)(PPh_3)\}_4]^+$ and $[Sb\{Co(CO)_3(PPh_3)\}_4]^+$, and X-ray crystal structure determinations have been described for $[SbCl_2\{Fe(CO)_2(C_5H_5)\}_2]^+$,[17] $[SbCl\{Fe(CO)_2(C_5H_5)\}_3]^+$[18] and $[Sb\{Co(CO)_3(PPh_3)\}_4]^+$.[19]

Herein we report details of our own studies on trimetalla-stibines, $[Sb(ML_n)_3]$ (ML_n = 17 electron transition metal fragment), we are aware of only one other example in the literature,[20] and chlorodimetalla-stibines $[SbCl(ML_n)_2]$.

RESULTS AND DISCUSSION

The reaction between $SbCl_3$ and 3 equiv. of $Na[Mo(CO)_3(\eta\text{-}C_5H_5)]$ in THF solution afforded, after work-up, the trimolybdenum–antimony complex, $[Sb\{Mo(CO)_3(\eta\text{-}C_5H_5)\}_3]$ (**1**), as a red–brown powder. Spectroscopic and analytical data (presented in Table 1) were consistent with the above formula, particularly the solution IR spectrum (Table 1, Fig. 1) which showed a pattern in the carbonyl stretching region very similar to that observed for the analogous bismuth complex, $[Bi\{Mo(CO)_3(\eta\text{-}C_5H_5)\}_3]$ (**2**).[21] Unfortunately,

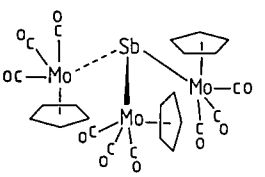

1 **2**

however, crystals suitable for an X-ray crystallographic study could not be obtained for **1** (or the related tungsten analogue, see later) and so precise structural details are not available. The electron-impact mass spectrum of **1** was particularly informative and showed signals attributable to ions with metal element ratios Mo_3Sb and Mo_2Sb_2 (full details are given in the Experimental). The former set of ions were consistent with the derived formula for **1**, while the latter indicated the presence of the dimolybdenum–diantimony complex, $[Mo_2Sb_2(CO)_4(\eta\text{-}C_5H_5)_2]$ (**3**). Moreover, these data were interesting when compared with the corresponding results for the bismuth complex, **2**.[21] It had been observed that the mass spectrum of **2** exhibited signals attributable only to the dimolybdenum–dibismuth complex, $[Mo_2Bi_2(CO)_4(\eta\text{-}C_5H_5)_2]$ (**4**), with no peaks corresponding to Mo_3Bi-containing ions. This was in contrast, therefore, to the antimony analogue, **1**, where both Mo_3Sb and Mo_2Sb_2 signals were observed. The fact that the former were seen (similar experimental conditions for both

* The relationship between the trigonal planar or "open" stibindene complexes and the isomeric trigonal pyramidal or "closed" complexes, both of which contain 16 electron transition metal fragments, has been addressed in refs 7(a), (b) and 8. The factors affecting which isomeric form is adopted in these and the related phosphorus compounds are discussed in ref. 10. Compounds containing two 17 electron transition metal fragments are probably better described as dimetallastibines as opposed to stibinidene complexes, although this defintion is somewhat arbitrary.

Table 1. Spectroscopic and analytical data for the complexes

Compound	ν(CO) (cm^{-1})	NMR[a] ^1H[b]	NMR[a] ^{13}C[b,c]	Analysis[d] C	Analysis[d] H
$[Sb\{Mo(CO)_3(\eta\text{-}C_5H_5)\}_3]$ (**1**)	2009m, 1974s, 1903m[e]	5.51[f]	93.8[f]	32.3(33.6)	1.9(1.8)
$[SbCl\{Mo(CO)_3(\eta\text{-}C_5H_5)\}_2]$ (**5**)	2048w, 2015s, 1986m, 1924s, 1902m[e]	5.71[g]	94.8[g]	29.8(29.7)	1.4(1.6)
$[Sb\{W(CO)_3(\eta\text{-}C_5H_5)\}_3]$ (**8**)	2006m, 1968s, 1925w, 1894m[e]	5.60[f]	92.7[f]	23.5(25.7)	1.5(1.4)
$[SbCl\{W(CO)_3(\eta\text{-}C_5H_5)\}_2]$ (**9**)	2011s, 1982m, 1958w, 1918s, 1893m[e]	5.83[g]	93.6[g]	23.3(23.3)	1.3(1.2)
$[SbCl\{Fe(CO)_2(\eta\text{-}C_5H_5)\}_2]$ (**11**)	2015s, 1986s, 1957s[e]	5.08[g]	86.3[g,h]	32.9(32.9)	1.9(2.0)
$[Sb\{Fe(CO)_2(\eta\text{-}C_5H_5)\}_3]$ (**13**)	2008s, 1973m, 1932s[e]	4.96[g]	86.0[g]	38.8(38.6)	2.3(2.3)

[a] Chemical shifts (δ) in ppm; measurements at room temperature.
[b] Values quoted are for the cyclopentadienyl resonances.
[c] ^1H decoupled; chemical shifts are positive to high frequency of $SiMe_4$.
[d] Values shown are percentages; calculated values in parentheses.
[e] Recorded in THF solution.
[f] Recorded in THF-d_8 solution.
[g] Recorded in acetone-d_6 solution.
[h] δ ^{13}C 214.4 (s, CO).

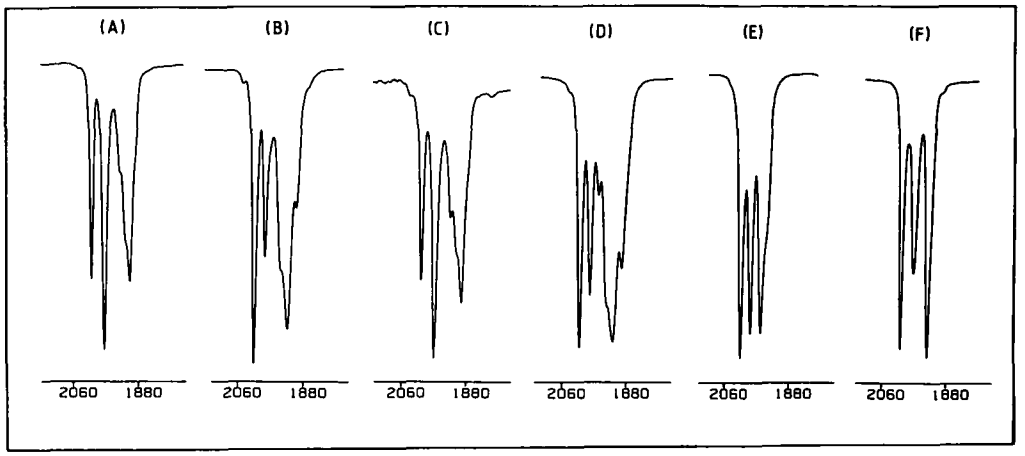

Fig. 1. IR spectra in the carbonyl stretching region. (A) **1**; (B) **5**; (C) **8**; (D) **9**; (E) **11**; (F) **13**. Recorded in THF solution.

bismuth and antimony) suggests that the antimony complex is a little more robust which, in turn, indicates that the Sb—Mo bonds in **1** are somewhat stronger than the Bi—Mo bonds in **2**. Nevertheless, some rearrangement of **1** to **3** does occur which suggests that **3** is a viable target for chemical synthesis.

The dibismuth complex **4**, has been synthesized by photolysis of **2**[22] and this approach is currently under investigation as a possible route to **3**.

If the reaction between $SbCl_3$ and 2 equiv. of $Na[Mo(CO)_3(\eta\text{-}C_5H_5)]$ is carried out, purple crystals of the dimolybdenum–antimony complex, $[SbCl\{Mo(CO)_3(\eta\text{-}C_5H_5)\}_2]$ (**5**), are obtained. Compound **5** was characterized by normal spectroscopic methods (Table 1) which were consistent with the anticipated structure. Specifically, the solution IR spectrum of **5** in the carbonyl stretching region (Fig. 1) was very similar to that observed for the analogous bismuth complex, $[BiCl\{Mo(CO)_3(\eta\text{-}C_5H_5)\}_2]$ (**6**),[21] which had been characterized by X-ray crystallography.[21b] However, although the molecular structure of **5** had been adequately established by spectroscopic means, an X-ray crystallographic study was undertaken to precisely determine the solid-state structure. This was of interest since it had been observed for **6** that secondary

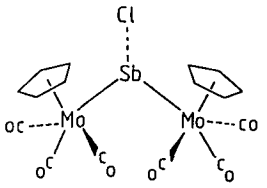

5

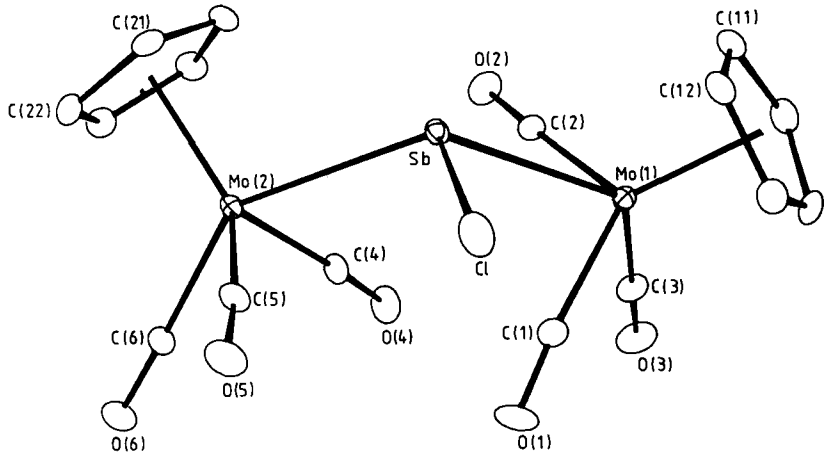

Fig. 2. Molecular structure of **5**, showing the atom numbering scheme adopted. Thermal ellipsoids are drawn at the 10% probability level.

Bi----Cl interactions between molecules existed, arising from the Lewis acidity of the bismuth centre.[21b] The results of the X-ray study on **5** are shown in Fig. 2; selected bond lengths and angles are given in Table 2. The molecule consists of a central antimony atom bonded to one chlorine (Sb—Cl, 2.449(2) Å) and two molybdenum atoms (av. Sb—Mo, 2.845 Å), the latter being each further ligated by a cyclopentadienyl and three carbonyl ligands, with an overall geometry of the familiar $CpML_4$ "piano-stool" type. The antimony atom adopts a trigonal pyramidal coordination geometry (sum of angles, 324.5°) although the pyramid is more open than that found about bismuth in **6** (sum of angles at Bi, av. 315.2°).[21b] A trend of increasing pyramidality is usually observed in three-coordinate group 15 complexes as the group is descended.[23] More interestingly, however, the crystal structure of **5** reveals no short contacts between antimony and chlorine atoms in neighbouring molecules, in contrast to those observed between bismuth and chlorine in **6** (the shortest intermolecular Sb----Cl contact is 5.903(2) Å). This suggests that the antimony centre in **5** is less Lewis acidic than the bismuth centre in **6**, but care must be exercised in making such claims. The structure of **6** reveals that dramatic differences in the lengths of intermolecular contacts can occur even within the same crystal structure and thus implies that even very small changes in structure can lead to large differences in the distances of secondary intermolecular interactions. We note, however, the overall similarity in molecular structure between **5** and **6** in that the conformations about the Sb—Mo bonds in **5** are similar to those found for the Bi—Mo bonds in **6**.[21b]

Table 2. Selected bond lengths (Å) and bond angles (°) for **5**[a]

Sb—Mo(1)	2.819(1)	Sb—Mo(2)	2.871(1)
Sb—Cl	2.449(2)		
Mo(1)—Sb—Mo(2)	119.6(1)		
Mo(1)—Sb—Cl	96.8(1)		
Mo(2)—Sb—Cl	108.1(1)		

[a] Numbers in parentheses are the estimated standard deviation in the least significant digit in this and all subsequent tables.

Malisch and Panster have previously reported spectroscopic and analytical data on the bromo analogue of **5**, $[SbBr\{Mo(CO)_3(\eta\text{-}C_5H_5)\}_2]$ (**7a**), together with the related tungsten complex $[SbBr\{W(CO)_3(\eta\text{-}C_5H_5)\}_2]$ (**7b**),[5g] and details of the methyl-substituted derivative, $[SbMe\{Mo(CO)_3(\eta\text{-}C_5H_5)\}_2]$ (**7c**), have also been presented.[5d] Complex **1** has been briefly referred to,[5g] although no details of its isolation and characterization were described.

Having established synthetic routes to the molybdenum–antimony complexes, **1** and **5**, it was of interest to see whether exchange reactions involving heterolysis of Sb—Cl and Sb—Mo bonds were apparent in solution. Accordingly, a THF solution of **1** was treated with a THF solution containing 0.5 equiv. of $SbCl_3$, whereupon an immediate reaction occurred resulting in an essentially quantitative conversion (as determined by IR spectroscopy) to **5**. These results implied a reaction in accordance with eq. (1):

$$\underset{\textbf{(1)}}{2[Sb\{Mo(CO)_3(\eta\text{-}C_5H_5)\}_3]} + SbCl_3 \rightleftharpoons 3[SbCl\{Mo(CO)_3(\eta\text{-}C_5H_5)\}_2], \quad (1)$$
$$\textbf{(5)}$$

albeit with the equilibrium lying, in the THF solution, far to the right and thus favouring the formation of **5**. Exactly analogous results have been found for the bismuth analogues, **2** and **6**.[21b]

The tri- and ditungsten compounds, $[Sb\{W(CO)_3(\eta\text{-}C_5H_5)\}_3]$ (**8**) and $[SbCl\{W(CO)_3(\eta\text{-}C_5H_5)\}_2]$ (**9**), were synthesized in a similar manner to the

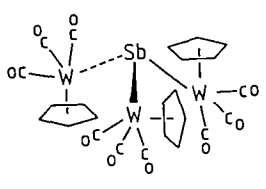

8

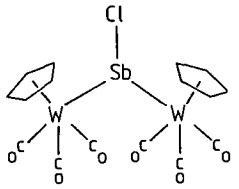

9

corresponding molybdenum derivatives (see Experimental). Spectroscopic data for **8** (Table 1) were in accord with a structure analogous to **1**, particularly the solution IR spectrum (Fig. 1) in the carbonyl region. The electron-impact mass spectrum of **8** was also similar to that observed for **1**, in as much as signals corresponding to fragment ions with metal ratios of W_3Sb and W_2Sb_2 were seen. Full details are given in the Experimental, but the former set of signals, i.e. W_3Sb were consistent with the derived structure of **8** whilst the latter, i.e. W_2Sb_2, were attributed to the rearranged product, $[W_2Sb_2(CO)_4(\eta\text{-}C_5H_5)_2]$ (**10**).

The ditungsten–antimony complex, **9**, was isolated as a purple crystalline solid. Spectroscopic and analytical data are presented in Table 1 and establish the close similarity between **9** and **5**, particularly the solution IR spectra (Fig. 1). As mentioned previously, Malisch and Panster have described the synthesis of the bromo analogue of **9**, i.e. **7b**.[5g] In the analogous tungsten–bismuth chemistry it was originally reported[21a] that the tritungsten bismuth complex, $[Bi\{W(CO)_3(\eta\text{-}C_5H_5)\}_3]$, was not formed in the reaction between $BiCl_3$ and 3 equiv. of $Na[W(CO)_3(\eta\text{-}C_5H_5)]$. Subsequent, more detailed work, however,[21b] demonstrated that the tritungsten complex was formed, albeit with concomitant formation of $[BiCl\{W(CO)_3(\eta\text{-}C_5H_5)\}_2]$ and $[WCl(CO)_3(\eta\text{-}C_5H_5)]$. Full details of the preparative routes to the bismuth complexes are reported in ref. 21(b). We note, however, that the reaction between $SbCl_3$ and 3 equiv. of $Na[W(CO)_3(\eta\text{-}C_5H_5)]$ appears to proceed more cleanly without substantial amounts of $[SbCl\{W(CO)_3(\eta\text{-}C_5H_5)\}_2]$ and $[WCl(CO)_3(\eta\text{-}C_5H_5)]$ being formed. Nevertheless, $[Sb\{W(CO)_3(\eta\text{-}C_5H_5)\}_3]$ (**9**) is difficult to purify and fully satisfactory microanalytical data could not be obtained.

Having studied the chemistry of antimony complexes incorporating organomolybdenum and -tungsten groups, the related iron chemistry, *viz.* complexes containing the $Fe(CO)_2(\eta\text{-}C_5H_5)$ fragment was examined.

Treatment of $SbCl_3$ with 2 equiv. of $Na[Fe(CO)_2(\eta\text{-}C_5H_5)]$ afforded, after work-up, red crystals of the di-iron antimony complex $[SbCl\{Fe(CO)_2(\eta\text{-}C_5H_5)\}_2]$ (**11**). Spectroscopic and analytical data

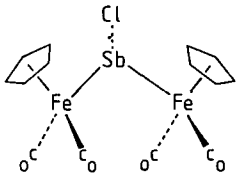

11

(Table 1) were in accord with an empirical structure as represented in the diagram but gave little indication as to any degree of intermolecular interactions which might exist. This factor was considered important, since in the analogous bismuth complex, a cyclotrimeric structure exists in the solid state,[24,25] *viz.* $[(BiCl\{Fe(CO)_2(\eta\text{-}C_5H_4R)\}_2)_3]$ (R = H, Me) (**12**), involving Cl—Bi—Cl bridging. The extent to which this also occurs in **11** is uncertain since an X-ray crystallographic study carried out on crystals of **11** was hampered by severe disorder problems, which prevented an informative solution from being obtained. It should be noted that the solution IR spectrum of **11** (Fig. 1) is very similar in appearance to that observed for **12**,[24]

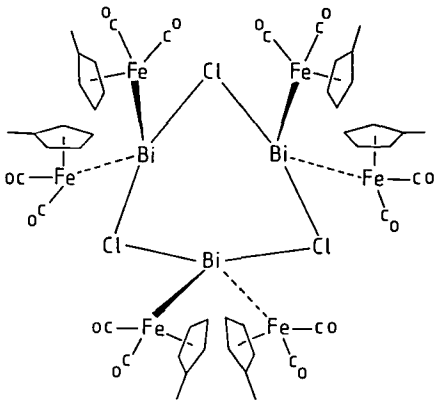

12

although this is of limited diagnostic value since the extent of association of **12** in solution is unknown. Nevertheless, the solution state structures of **11** and **12** are clearly very similar.

The bromo and methyl analogues of **11** have been reported by Malisch and Panster,[5c,d] *viz.* $[Sb(R)\{Fe(CO)_2(\eta\text{-}C_5H_5)\}_2]$ (R = Br, Me), the bromo derivative having a solution IR spectrum essentially identical to that obtained for **11** (Table 1).

The reaction between $SbCl_3$ and 3 equiv. of $Na[Fe(CO)_2(\eta\text{-}C_5H_5)]$ was also studied and afforded dark red–brown crystals of the tri-iron antimony complex, $[Sb\{Fe(CO)_2(\eta\text{-}C_5H_5)\}_3]$ (**13**).

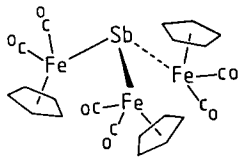

13

Spectroscopic and analytical data (Table 1) were in accord with the proposed structure and this was confirmed by an X-ray crystallographic study, the results of which are shown in Fig. 3; selected bond length and angle data are given in Table 3. The structure consists of two symmetry independent molecules with no short intermolecular contacts. Both molecules are essentially identical and contain an antimony atom in a trigonal pyramidal coordination environment (sum of angles: 330.9°, molecule A and 330.9°, molecule B) each being bonded to three $Fe(CO)_2(\eta\text{-}C_5H_5)$ fragments by unsupported Sb—Fe bonds (av. Sb—Fe, 2.651 Å, molecule A; av. Sb—Fe, 2.653 Å, molecule B). Compound **13** may thus be described as a trimetallastibine and is closely related to the analogous bismuth complex $[Bi\{Fe(CO)_2(\eta\text{-}C_5H_4Me)\}_3]$ (**14**), which has also been characterized by X-ray crystallography.[24b] Both the antimony and bismuth complexes are structurally very similar, including the conformations about the element–iron bonds which give the molecule approximate C_3 symmetry. However, the bismuth atom in **14** is slightly more pyramidal (av. Fe—Bi—Fe, 109.3°) than the antimony atoms in **13** (av. Fe—Sb—Fe, 110.3°), although this structural trend is expected and has already been discussed in relation to the structures of **5** and **6**. Each iron is additionally ligated by a cyclopentadienyl ligand and two terminal carbonyls, all of normal geometry with the iron adopting a $CpML_3$ "piano-stool" configuration. The structure of **13** is the first to be reported for a trimetallastibine of which we are aware but it is closely related, however, to the cationic complexes $[SbCl_2\{Fe(CO)_2(\eta\text{-}C_5H_5)\}_2]^+$[18] (av. Sb—Fe, 2.439 Å) and $[SbCl\{Fe(CO)_2(\eta\text{-}C_5H_5)\}_3]^+$[19] (av. Sb—Fe, 2.539 Å). Other examples of antimony–iron complexes that have been structurally characterized include $[Fe_2(CO)_6\{\mu\text{-}Sb(Fe_2(CO)_8)\}_2]$[15a,b] (av. Sb—Fe, 2.529 Å), $[Fe_3(CO)_9(\mu_3\text{-}CO)\{\mu_3\text{-}Sb(Fe(CO)_4)\}]^-$[15c] (av. Sb—Fe, 2.493 Å), $[Fe_3(CO)_9\{\mu_3\text{-}Sb(Fe(CO)_4)\}_2]^{2-}$[15c] (av. Sb—Fe, 2.523 Å), the stibine complex $[Fe(CO)_2(SbPh_3)(\eta\text{-}C_5H_5)]^+$[26] (Sb—Fe, 2.477(1) Å), $[Fe(CO)(PMe_3)(\eta\text{-}C_5H_5)\{Sb(Br)_2PMe_3\}]$[5b] (Sb—Fe, 2.551(2) Å) and $[Fe(Ph)(CO)_3(SbPh_3)\{Sb(Ph)_2Fe(CO)_4\}]$[6a] (Sb—Fe, 2.515, 2.525, 2.606 Å).

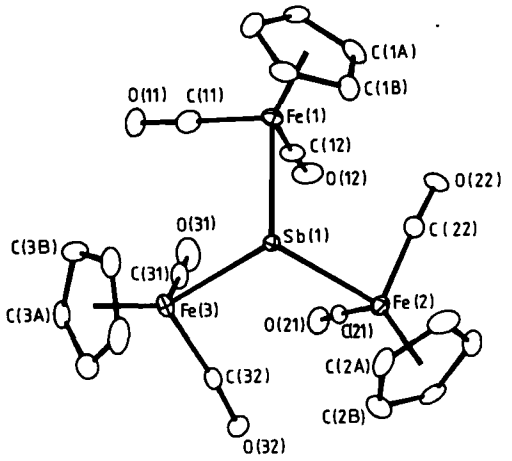

Fig. 3. Molecular structure of one of the two symmetry independent molecules of **13**, showing the atom numbering scheme adopted. Thermal ellipsoids are drawn at the 10% probability level.

Table 3. Selected bond lengths (Å) and bond angles (°) for **13**

Molecule A			
Sb(1)—Fe(1)	2.638(2)	Sb(1)—Fe(2)	2.676(2)
Sb(1)—Fe(3)	2.638(2)		
Fe(1)—Sb(1)—Fe(2)	108.9(1)		
Fe(1)—Sb(1)—Fe(3)	110.6(1)		
Fe(2)—Sb(1)—Fe(3)	111.4(1)		
Molecule B			
Sb(2)—Fe(4)	2.648(2)	Sb(2)—Fe(5)	2.645(2)
Sb(2)—Fe(6)	2.665(2)		
Fe(4)—Sb(2)—Fe(5)	110.8(1)		
Fe(4)—Sb(2)—Fe(6)	109.1(1)		
Fe(5)—Sb(2)—Fe(6)	111.0(1)		

Brief details of the synthesis of **13** have been reported by Malisch and Panster,[20] together with a study of its behaviour as a Lewis base through antimony to 16 electron transition metal fragments.

Finally we note that solution photolysis of **13** did not result in isolable products. In the case of the bismuth analogue, **14**, it had been observed that photolysis cleanly afforded the *closo*-Fe_3Bi cluster, $[Fe_3Bi(CO)_3(\eta\text{-}C_5H_4Me)_3]$ (**15**),[24b] in good yield (Schmidbaur had also reported similar results for the C_5H_5 derivatives[25]). While a reaction certainly occurred in the antimony case, as evidenced by IR spectroscopy, a mixture of products seemed to be formed from which it was not possible to isolate and characterize any pure materials.

CONCLUSIONS

Synthetic routes to a range of organomolybdenum, -tungsten and -iron antimony complexes are reported herein together with details of their spectroscopic and structural properties. These studies establish, together with previous related work,[5,20] that transition metal–antimony bonds are readily formed and suggest that a wide range of compounds are capable of being prepared. Further synthetic studies are in progress together with reactivity and electrochemical studies involving the compounds described.

EXPERIMENTAL

General procedures

All experiments were performed using standard Schlenk techniques under an atmosphere of dry oxygen-free dinitrogen. All solvents were freshly distilled over appropriate drying agents immediately prior to use. ^1H and ^{13}C NMR spectra were recorded on a Bruker WP200 spectrometer operating at 200.13 and 50.324 MHz, respectively.[27] IR spectra were recorded on a Nicolet 20SXB FTIR spectrophotometer, and mass spectra were obtained on Kratos MS9 and MS80 instruments. Microanalytical data were obtained at the University of Newcastle.

Antimony trichloride and $[Fe_2(CO)_4(\eta\text{-}C_5H_5)_2]$ were procured commercially and used without further purification. $[M_2(CO)_6(\eta\text{-}C_5H_5)_2]$ (M = Mo, W) were prepared by the method of Manning *et al.*[28] Spectroscopic and analytical data for all new complexes are presented in Table 1. Mass spectrometric data are recorded below.

Preparations

Preparation of $[Sb\{Mo(CO)_3(\eta\text{-}C_5H_5)\}_3]$ (**1**). A solution of $Na[Mo(CO)_3(\eta\text{-}C_5H_5)]$ derived from a sodium amalgam reduction of $[Mo_2(CO)_6(\eta\text{-}C_5H_5)_2]$ (0.574 g, 1.17 mmol) in THF (20 cm^3) was cooled to −78°C by means of a dry-ice–ethanol bath. To this, a solution of $SbCl_3$ (0.178 g, 0.780 mmol) in THF (10 cm^3) was slowly added with continuous stirring. This resulted in a colour change from pale yellow–green to dark red. After complete addition, the reaction mixture was allowed to warm to room temperature and stirred for 1 h. The reaction mixture was then filtered through Celite to remove NaCl, resulting in a dark red solution. The solvent volume was then reduced to about 10 cm^3 and hexane (20 cm^3) was layered over the more concentrated red solution. Solvent diffusion at −26°C over a period of days resulted in the formation of a red–brown solid, subsequently characterized as **1** (0.328 g, 49% yield). Purification of the original reaction solution may also be effected by column chromatography (Florisil, THF eluant), although a simple filtration is usually sufficient.

The tungsten analogue $[Sb\{W(CO)_3(\eta\text{-}C_5H_5)\}_3]$ (**8**) was prepared in an exactly analogous manner with typical yields of about 48% being obtained.

The electron-impact mass spectrum for **1** (probe temperature 200°C), *m/z* 772, P −3CO (P = $SbMo_3(CO)_9(C_5H_5)_3$); 678, P′ (P′ = $Sb_2Mo_2(CO)_4(C_5H_5)_2$); 622, P′ −2CO; 594, P′ −3CO; 566, P′ −4CO; 436, P′ −4CO+2C_5H_5. The ratio between the peak heights for the signals at 772 and 678 was approximately 1 : 10.

The electron-impact mass spectrum for **8** (probe temperature 220°C), *m/z* 1036, P −3CO (P = $SbW_3(CO)_9(C_5H_5)_3$); 980, P −5CO; 924, P −7CO; 896, P −8CO; 868, P −9CO; 854, P′ (P′ = $Sb_2W_2(CO)_4(C_5H_5)_2$); 798, P′ −2CO; 770, P′ −3CO; 742, P′ −4CO; 612, P′ −4CO+2C_5H_5. The ratio between the peak heights for the signals at 1036 and 854 was approximately 1 : 30. In all cases the numbers given are for the observed peak of maximum intensity. Good fits were obtained between observed and calculated isotope patterns in all cases. Two of these, P −3CO and P′ for **8**, are shown in Diagram 1.

Two further points are noteworthy regarding the mass spectral results. Firstly, the observation of more fragment ions with a W_3Sb metal ratio, in the spectrum of **8** compared with the number of Mo_3Sb type ions seen for **1**, suggests that the former is more robust and this, in turn, can be taken as evidence consistent with stronger W—Sb bonds compared to those of Mo—Sb. Secondly, the observation of fairly strong signals corresponding to the ions $SbM_3(CO)_6(C_5H_5)_3$ (**1**, M = Mo; **8** M = W) suggests that the neutral molecules from which these are formally derived may be quite stable and therefore viable targets for chemical synthesis. This view is strengthened by the fact than an arsenic analogue, $[AsMo_3(CO)_6(C_5H_5)_3]$, has recently been prepared and fully characterized.[29] Attempts are in progress to synthesize these species.

Good fits between observed and calculated isotope patterns were also found in all other cases where EI mass spectra are quoted in this paper.

Preparation of $[SbCl\{Mo(CO)_3(\eta\text{-}C_5H_5)\}_2]$ (**5**). A solution of $Na[Mo(CO)_3(\eta\text{-}C_5H_5)]$, derived from a sodium amalgam reduction of $[Mo_2(CO)_6(\eta\text{-}C_5H_5)_2]$ (0.514 g, 1.05 mmol), in THF (20 cm^3) was added to a solution of $SbCl_3$ (0.239 g, 1.05 mmol) in THF (10 cm^3) at 0°C, resulting in an immediate colour change to red–brown. The reaction was then

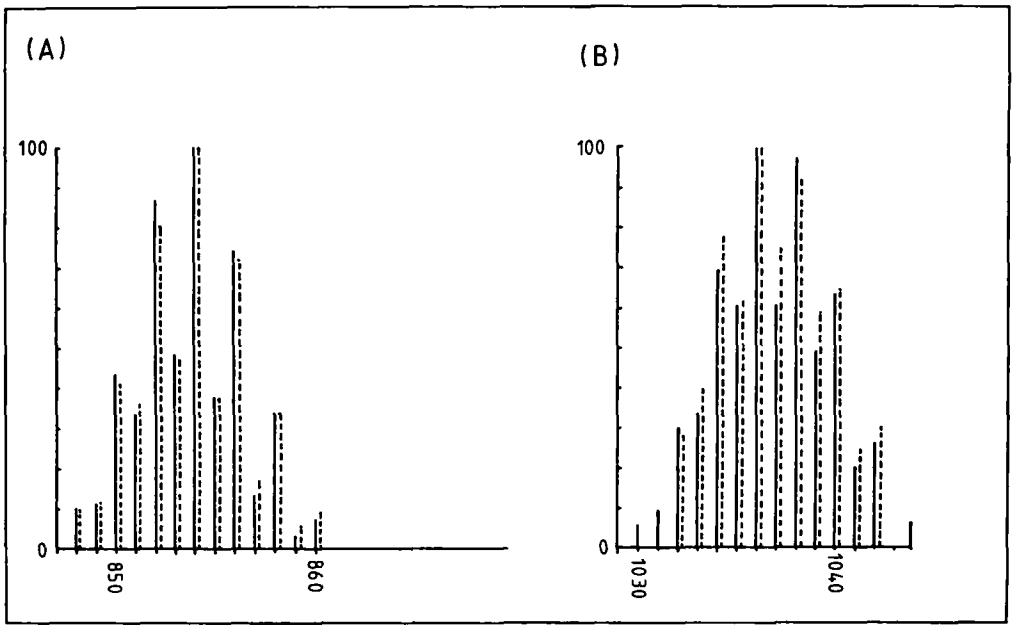

Diagram 1. Electron-impact mass spectra showing observed (----) and calculated (——) isotope patterns for the ions: (**A**), $Sb_2W_2(CO)_4(C_5H_5)_2$; (**B**) $SbW_3(CO)_6(C_5H_5)_3$.

allowed to warm to room temperature and was stirred for a further 2 h. After this time, the reaction mixture was filtered (Celite) and the solvent volume of the filtrate was reduced to ~7 cm^3 *in vacuo*. Hexane (40 cm^3) was layered over the concentrated filtrate and solvent diffusion over a period of days at −26°C afforded dark purple crystals of **5** (0.403 g, 59%).

The ditungsten complex, $[SbCl\{W(CO)_3(\eta\text{-}C_5H_5)\}_2]$ (**9**), was synthesized in an analogous manner and with similar yields.

The electron-impact mass spectrum for **5**, *m/z* 648, P (P = $SbClMo_2(CO)_6(C_5H_5)_2$); 585, P −1CO+1Cl; 480, P −6CO. In addition, signals due to **3** were also observed, *m/z* 678, P′ (P′ = $Sb_2Mo_2(CO)_4(C_5H_5)_2$); 622, P′ −2CO; 594, P′ −3CO; 566, P′ −4CO.

The electron-impact mass spectrum for **9**, *m/z* 822, P (P = $SbClW_2(CO)_6(C_5H_5)_2$). Signals due to **10** were also observed, *m/z* 854, P′ (P′ = $Sb_2W_2(CO)_4(C_5H_5)_2$); 798, P′ −2CO; 770, P′ −3CO; 742, P′ −4CO; 612, P′ −4CO+2C_5H_5.

Compound **5** can also be prepared by addition of $SbCl_3$ to **1** as follows. A solution of $SbCl_3$ (0.003 g, 0.0132 mmol) in THF (1 cm^3) was added to a stirred solution of $[Sb\{Mo(CO)_3(\eta\text{-}C_5H_5)\}_3]$ (**1**) (0.023 g, 0.0264 mmol) in THF (2 cm^3) at room temperature. Monitoring of the reaction by IR spectroscopy revealed that **5** is formed in essentially quantitative yield after about 20 min.

Preparation of $[SbCl\{Fe(CO)_2(\eta\text{-}C_5H_5)\}_2]$ (**11**). A solution of $Na[Fe(CO)_2(\eta\text{-}C_5H_5)]$, derived from a sodium amalgam reduction of the dimer $[Fe_2(CO)_4(\eta\text{-}C_5H_5)_2]$ (0.341 g, 0.964 mmol), in THF (20 cm^3) was added to a stirred solution of $SbCl_3$ (0.220 g, 0.964 mmol) in THF (10 cm^3) at 0°C, resulting in an immediate colour change to dark red–brown. The reaction mixture was then allowed to warm to room temperature and stirred for 90 min. After this time, the mixture was filtered (glass frit) and the solvent volume of the filtrate was reduced to ~6 cm^3 *in vacuo*. Hexane (35 cm^3) was layered over the concentrated filtrate and solvent diffusion over a period of days at −26°C afforded red crystals of **11** (34%).

The electron-impact mass spectrum for **11**, *m/z* 510, P (P = $SbClFe_2(CO)_4(C_5H_5)_2$); 454, P −2CO; 398, P −4CO.

The methylcyclopentadienyl derivative $[SbCl\{Fe(CO)_2(\eta\text{-}C_5H_4Me)\}_2]$ was also prepared by an analogous synthetic route with the hope of obtaining X-ray quality crystals, although this was not fulfilled. Pertinent data: IR ν(CO)/cm^{-1}, 2040s, 2017s, 1985s. The electron-impact mass spectrum, *m/z* 538, P (P = $SbClFe_2(CO)_4(C_5H_4Me)_2$); 510, P −1CO; 482, P −2CO; 454, P −3CO; 426, P −4CO; 503, P −1Cl.

Preparation of $[Sb\{Fe(CO)_2(\eta\text{-}C_5H_5)\}_3]$ (**13**). A stirred solution of $Na[Fe(CO)_2(\eta\text{-}C_5H_5)]$, derived from a sodium amalgam reduction of $[Fe_2(CO)_4(\eta\text{-}C_5H_5)_2]$ (0.544 g, 1.539 mmol), in THF (25 cm^3) was cooled to −78°C by means of a dry-ice–ethanol bath. To this, a solution of $SbCl_3$ (0.234 g, 1.026 mmol) in THF (10 cm^3) was added, resulting in a

colour change to dark red. The resulting reaction mixture was then allowed to warm to room temperature and stirred for 3 h. All volatiles were then removed *in vacuo*. Extraction with Et_2O (5×20 cm^3) followed by filtration (glass frit) afforded a dark red–brown solution, from which dark red–brown crystals of **13** were obtained (0.370 g, 55%) by solvent diffusion from Et_2O (20 cm^3)–hexane (40 cm^3) at −26°C over a period of days.

The electron-impact mass spectrum for **13**, *m/z* 652, P (P = $SbFe_3(CO)_6(C_5H_5)_3$); 624, P −1CO; 596, P −2CO; 568, P −3CO; 540, P −4CO; 512, P −5CO; 484, P −6CO; 419, P −6CO+C_5H_5; 354, P −6CO+$2C_5H_5$; 475, P −$Fe(CO)_2(C_5H_5)$; 298, P −$2Fe(CO)_2(C_5H_5)$.

A slightly different synthesis of **13** is reported in ref. 20.

X-ray crystallographic studies

Structure determinations of [$SbCl\{Mo(CO)_3(\eta$-$C_5H_5)\}_2$] (**5**) and [$Sb\{Fe(CO)_2(\eta$-$C_5H_5)\}_3$] (**13**). The following structure determination method is for compound **5** unless otherwise stated. The corresponding values for **13** are in parentheses following those for **5**.

A crystal of approximate dimensions $0.25 \times 0.35 \times 0.7$ ($0.7 \times 0.4 \times 0.2$) mm was mounted in a general position on a glass fibre and coated with acrylic resin. Data were collected at ambient temperatures, using the θ–2θ scan mode, on a CAD4F automated diffractometer with graphite monochromated X-radiation ($\lambda = 0.71069$ Å). Unit cell parameters were determined by refinement of the setting angles ($\theta \geqslant 12°$) of 25 reflections. The standard reflections $\bar{2}$ 0 14, $\bar{4}$ 0 $\bar{6}$, and $\bar{2}$ $\bar{4}$ 8 (6 $\bar{7}$ 0, $\bar{4}$ 7 6) were measured every 2 h and a slight increase in intensities of *ca* 1.37% (5.6% decay) in 10,000 reflections was observed and corrected for. This increase is attributed to a reduction of secondary extinction caused by a gradual increase in the mosaicity of the crystal during data collection. Lorentz-polarization and absorption/extinction (DIFABS[30]) corrections were also applied. A total of 3650 (9045) measured reflections, θ range 2–25°, h 0 → 8, k 0 → 11, l −32 → +32, (θ range 2–26°, h 0 → 20, k 0 → 20, l −20 → +20) yielded 3369 (8738) independent data, of which 2707 (5316) having an intensity $> 3\sigma(I)$ were considered observed and used for structure solution and refinement. Systematic absences uniquely determined the centrosymmetric space group $P2_1/n$ ($P2_1/n$). The structure was solved by direct methods (MITHRIL[31]) and subsequent electron density difference syntheses. Refinement was by full-matrix least-squares minimizing the function $w(|F_o| - |F_c|)^2$ with the weighting scheme $w = [\sigma^2(F_o)]^{-1}$ used and judged satisfactory. $\sigma(F_o)$ was estimated from counting statistics. The parameter list for **13** was refined in two separate blocks due to matrix size limitations. Hydrogen atoms were included at calculated positions (C—H = 1.0 Å), with fixed contributions to the structure factors. The C_5H_5 groups for **13** were refined as rigid groups with a regular pentagonal geometry for the ring, and C—C = 1.395 Å. Refinement using a total of 235 (307) parameters converged at $R/R_w = 0.028/0.035$ (0.057/0.066), with mean and maximum Δ/σ values of 0.008 (0.005) and 0.05 (0.02), respectively, in the final cycle. A final electron density difference synthesis

Table 4. Crystallographic data

Compound	**5**	**13**
Chemical formula	$C_{16}H_{10}ClO_6Mo_2Sb$	$C_{21}H_{15}Fe_3O_6Sb$
fw	647.3	652.6
Crystal system	Monoclinic	Monoclinic
Space group	$P2_1/n$	$P2_1/n$
a (Å)	7.399(2)	16.686(5)
b (Å)	9.611(3)	16.927(4)
c (Å)	27.031(7)	16.894(5)
β (°)	92.70(2)	110.95(2)
V (Å^3)	1920.1(9)	4456(2)
Z	4	8
d_{calc} (g cm^{-3})	2.36	1.95
F(000)	1292	2544
μ(Mo-K_α) (cm^{-1})	29.75	31.58
λ (Å)	0.71069	0.71069
Temperature (K)	298	298
R	0.028	0.057
R_w	0.035	0.066

showed no significant features (max $\Delta p = +0.60$, min $\Delta p = -0.54$ e). For **13**, max $\Delta p = +3.51$, min $\Delta p = -1.48$ Å^{-3} close to the iron atoms but these were not considered chemically significant. The ESD of an observation of unit weight (S) was 1.59 (2.41). Neutral atom scattering factors were taken from ref. 32, with corrections applied for anomalous scattering. All calculations were carried out on a Gould-SEL 32/37 minicomputer using the GX suite of programs.[33]

Relevant crystallographic data for both complexes are presented in Table 4.*

Acknowledgements—We thank the SERC for a studentship (P.M.W.). N.C.N. also thanks the Research Corporation Trust and Nuffield Foundation for additional supporting funds.

REFERENCES

1. T. P. Fehlner, *Comm. Inorg. Chem.* 1988, **7**, 307.
2. See for example: (a) W. A. Herrmann, *Angew. Chem.* 1986, **98**, 57, *Angew. Chem. Int. Edn Engl.* 1986, **25**, 56; (b) O. J. Scherer, *Angew. Chem.* 1985, **97**, 905, *Angew. Chem. Int. Edn Engl.* 1985, **24**, 924; (c) K. H. Whitmire, *J. Coord. Chem.* 1988, **17**, 95.
3. C. A. McAuliffe (Ed.), *Transition Metal Complexes of Phosphorus, Arsenic and Antimony Ligands*. MacMillan, London (1973).
4. See for example, (a) U. Weber, L. Zsolnai and G. Huttner, *Z. Naturfor.* 1985, **40b**, 1430 and refs therein; (b) I. Bernal, J. D. Korp, F. Calderazzo, R. Poli and D. Vitali, *J. Chem. Soc., Dalton Trans.* 1984, 1945.
5. (a) H. A. Kaul, D. Greissinger, M. Luksza and W. Malisch, *J. Organomet. Chem.* 1982, **228**, C29; (b) H. A. Kaul, D. Greissinger, W. Malisch, H.-P. Klein and U. Thewalt, *Angew. Chem.* 1983, **95**, 56, *Angew. Chem. Int. Edn Engl.* 1983, **22**, 60; (c) P. Panster and W. Malisch, *Chem. Ber.* 1976, **109**, 692; (d) W. Malisch and P. Panster, *Chem. Ber.* 1975, **108**, 700; (e) P. Panster and W. Malisch, *Chem. Ber.* 1976, **109**, 2112; (f) W. Malisch and P. Panster, *J. Organomet. Chem.* 1975, **99**, 421; (g) W. Malisch and P. Panster, *Z. Naturfor.* 1975, **30b**, 229.
6. See also, (a) D. J. Cane, E. J. Forbes and T. A. Hamor, *J. Organomet. Chem.* 1976, **117**, C101; (b) J. von Seyerl, L. Wohlfahrt and G. Huttner, *Chem. Ber.* 1980, **113**, 2868; (c) A. Lombard, G. Huttner and L. Zsolnai, *J. Organomet. Chem.* 1988, **352**, 295.
7. For reviews see: (a) G. Huttner, *Pure Appl. Chem.* 1986, **58**, 585; (b) G. Huttner and K. Evertz, *Accts Chem. Res.* 1986, **19**, 406. Specific examples can be found in refs: (c) U. Weber, G. Huttner, O. Scheidsteger and L. Zsolnai, *J. Organomet. Chem.* 1985, **289**, 357; (d) U. Weber, L. Zsolnai and G. Huttner, *J. Organomet. Chem.* 1984, **260**, 281; (e) J. von Seyerl and G. Huttner, *Angew. Chem.* 1978, **90**, 911, *Angew. Chem. Int. Edn Engl.* 1978, **17**, 843; (f) B. Sigwarth, U. Weber, L. Zsolnai and G. Huttner, *Chem. Ber.* 1985 **118**, 3114; (g) H. Lang, G. Huttner, B. Sigwarth, U. Weber, L. Zsolnai, I. Jibril and O. Orama, *Z. Naturfor.* 1986, **41b**, 191; (h) A. M. Arif, A. H. Cowley, N. C. Norman and M. Pakulski, *Inorg. Chem.* 1986, **25**, 4836.
8. A. H. Cowley, N. C. Norman, M. Pakulski, D. L. Bricker and D. H. Russell, *J. Am. Chem. Soc.* 1985, **107**, 8211.
9. J. von Seyerl, L. Wohlfahrt and G. Huttner, *Chem. Ber.* 1980, **113**, 2868.
10. A. M. Arif, A. H. Cowley, M. Pakulski, M.-A. Pearsall, W. Clegg, N. C. Norman and A. G. Orpen, *J. Chem. Soc., Dalton Trans.* 1988, 2713 and refs therein.
11. G. Huttner, U. Weber, B. Sigwarth and O. Scheidsteger, *Angew. Chem.* 1982, **94**, 210, *Angew. Chem. Int. Edn Engl.* 1982, **21**, 215.
12. G. Huttner, U. Weber, B. Sigwarth, O. Scheidsteger, H. Lang and L. Zsolnai, *J. Organomet. Chem.* 1985, **282**, 331.
13. A. S. Foust and L. F. Dahl, *J. Am. Chem. Soc.* 1970, **92**, 7337.
14. J. L. Vidal and J. M. Troup, *J. Organomet. Chem.* 1981, **213**, 351.
15. (a) A. M. Arif, A. H. Cowley and M. Pakulski, *J. Chem. Soc., Chem. Commun.* 1987, 622; (b) A. L. Rheingold, S. J. Geib, M. Shieh and K. H. Whitmire, *Inorg. Chem.* 1987, **26**, 463; (c) K. H. Whitmire, J. S. Leigh, S. Luo, M. Shieh, M. D. Fabiano and A. L. Rheingold, *New J. Chem.* 1988, **12**, 397.
16. W. R. Cullen, D. J. Patmore and J. R. Sams, *Inorg. Chem.* 1973, **12**, 867.
17. F. W. B. Einstein and R. D. G. Jones, *Inorg. Chem.* 1973, **12**, 1690.
18. Trinh-Toan and L. F. Dahl, *J. Am. Chem. Soc.* 1971, **93**, 2654.
19. R. E. Cobbledick and F. W. B. Einstein, *Acta. Cryst.* 1979, **B35**, 2041.
20. W. Malisch and P. Panster, *Angew. Chem.* 1976, **88**, 680, *Angew. Chem. Int. Edn. Engl.* 1976, **15**, 618.
21. (a) W. Clegg, N. A. Compton, R. J. Errington and N. C. Norman, *J. Organomet. Chem.* 1987, **335**, C1; (b) W. Clegg, N. A. Compton, R. J. Errington, N. C. Norman, A. J. Tucker and M. J. Winter, *J. Chem. Soc., Dalton Trans.* 1988, 2941.
22. W. Clegg, N. A. Compton, R. J. Errington and N. C. Norman, *Polyhedron* 1988, **7**, 2239.
23. There are many examples of related compounds in group 15 where this effect is observed, e.g. the hydrides, EH_3. A theoretical discussion may be

* *Supplementary material available*: Tables for fractional coordinates for **5** and **13** have been deposited with the Cambridge Crystallographic Data Centre. Tables listing complete bond lengths and angles, anisotropic thermal parameters, hydrogen atom parameters and tables of observed and calculated structure factors are available from the Editor.

found in T. A. Albright, J. D. Burdett and M. H. Whangbo, *Orbital Interactions in Chemistry*, p. 143. Wiley-Interscience, New York (1985).
24. (a) W. Clegg, N. A. Compton, R. J. Errington and N. C. Norman, *Polyhedron* 1987, **6**, 2031; (b) W. Clegg, N. A. Compton, R. J. Errington and N. C. Norman, *J. Chem. Soc., Dalton Trans.* 1988, 1671.
25. J. M. Wallis, G. Muller and H. Schmidbaur, *J. Organomet. Chem.* 1987, **325**, 159.
26. R. E. Cobbledick and F. W. B. Einstein, *Acta. Cryst.* 1978, **B34**, 1473.
27. ^{1}H and ^{13}C NMR spectra are referenced to solvent peaks in all cases. The chemical shift values for all the solvents used are taken from A. E. Derome, *Modern NMR Techniques for Chemistry Research*. Pergamon Press, Oxford (1987).
28. R. Birdwhistell, P. Hackett and A. R. Manning, *J. Organomet. Chem.* 1978, **157**, 239.
29. M. L. Ziegler, K. Blechschmitt, B. Nuber and T. Zahn, *Chem. Ber.* 1988, **121**, 159.
30. N. Walker and D. Stuart, *Acta. Cryst.* 1983, **A39**, 158.
31. C. J. Gilmore, *J. Appl. Cryst.* 1984, **17**, 42.
32. *International Tables for X-ray Crystallography*, Vol. 4. Kynoch Press, Birmingham (1984).
33. P. R. Mallinson and K. W. Muir, *J. Appl. Cryst.* 1985, **18**, 51.

Note added in proof: The structure of **11** has recently been determined by X-ray crystallography (K. H. Whitmire, personal communication) and is monomeric with no short intermolecular Sb···Cl contacts.

Polyhedron Vol. 8, No. 20, pp. 2507–2511, 1989
Printed in Great Britain

0277–5387/89 $3.00+.00
© 1989 Pergamon Press plc

SYNTHESIS AND PROPERTIES OF BIS-IMIDO COMPLEXES OF THE TYPE $Pt\{(NH)_2C_6H_3NO_2\}(PR_3)_2$ FROM REACTIONS IN LIQUID AMMONIA. X-RAY STRUCTURE OF $Pt\{(NH)_2C_6H_3NO_2\}(PMePh_2)_2$

MARY HARMAN, MICHAEL B. HURSTHOUSE and MAJID MOTEVALLI

Department of Chemistry, Queen Mary College, Mile End Road, London E1 4NS, U.K.

and

IVAN P. PARKIN and J. DEREK WOOLLINS*

Department of Chemistry, Imperial College of Science Technology and Medicine, South Kensington, London SW7 2AY, U.K.

(*Received* 18 *April* 1989; *accepted* 2 *June* 1989)

Abstract—Reaction of *o*-$(NH_2)_2C_6H_3$-4-NO_2 with $PtCl_2(PR_3)_2$ in liquid ammonia gives $Pt\{(NH)_2C_6H_3NO_2^{2-}\}(PR_3)_2$ (PR_3 = PEt_3, PMe_2Ph, PPh_2Me, 1/2dppe) in good yield (80% isolated). The new complexes were characterized by ^{31}P, ^1H NMR, IR, UV–vis, mass spectra, microanalyses and, in the case of PR_3 = PMe_2Ph, by X-ray crystallography.

Although there are a great number of amine complexes of platinum there are relatively few examples of species containing di-imido ligands. Formally, these ligands are isoelectronic with dithiolenes and may thus be of interest from the point of view of preparing stacking compounds. There have been previous reports of the preparation of bis complexes containing two $C_6H_4(NH)_2^{2-}$ ligands[1,2] and work is in progress (by other groups) on tris complexes of rhenium.[3] Here we report on the reactivity of *p*-nitro-*o*-phenylenediamine (**1**) with *cis*-$PtCl_2(PR_3)_2$ (**2**) in liquid ammonia. The products from this reaction (**3**)–(**7**) contain the doubly deprotonated dianion $[p\text{-}O_2NC_6H_3(NH)_2]^{2-}$ as a ligand in simple platinum(II) complexes.

EXPERIMENTAL

All solvents were dried prior to use and reactions performed under an inert atmosphere (N_2, Ar). The bis-phosphine–platinum (palladium) dichlorides were made as previously described.[4] Ammonia (BOC) and 4-nitro-*o*-phenylenediamine (Aldrich) were used as suplied. ^{31}P-{^1H} and ^1H NMR spectra were obtained using a JEOL FX90Q spectrometer operating at 36.21 and 89.55 MHz and are refered to external 85% H_3PO_4 and internal TMS, respectively. Some ^{31}P NMR spectra were also run at higher field on a Bruker WM 250 spectrometer at 101.1 MHz and referred to external 85% H_3PO_4. IR spectra were recorded as pressed KBr discs using a Perkin–Elmer 1720X instrument. UV–vis spectra were obtained on a PE Lambda 3. Mass spectra were taken on a Varian VG 2020 spectrometer in the E.I. mode. Elemental analyses were performed by the microanalytical service at Imperial College.

In a typical reaction 4-nitro-*o*-phenylenediamine (0.16 mmol) was dissolved in liquid ammonia at −78°C to generate a red solution, whereupon $PtCl_2(PR_3)_2$ (0.15 mmol) was added. The resultant slurry was stirred for 0.5 h at −78°C and the ammonia allowed to evaporate under a blanket of nitrogen as the solution warmed slowly to room temperature, leaving a black–purple solid. Purification was achieved by extraction with CH_2Cl_2 (5 cm^3), followed by filtration through a celite/glass wool plug and passage down a Biobead (SX-8) column with CH_2Cl_2 as the eluent. The product, $Pt\{(NH)_2C_6H_3NO_2\}(PR_3)_2$ (**3**)–(**7**), was obtained,

* Author to whom correspondence should be addressed.

upon removal of the solvent *in vacuo*, from the first purple band which eluted (0.12 mmol, *ca* 80%). Crystals suitable for X-ray studies were obtained by slow diffusion of hexane into a CH_2Cl_2 solution of **3**. Microanalyses, yields, ^{31}P and ^{1}H NMR are given in Table 1, mass spectra and selected IR data in Table 2.

X-ray crystallography

All X-ray measurements were made on a CAD4 diffractometer operating in the ω–2θ scan mode with graphite monochromated Mo-K_α, following procedures previously described in detail.[5] The structure was solved and refined by the heavy atom method and full-matrix least-squares in a routine manner. All non-hydrogen atoms were refined anisotropically. Phosphine phenyl rings were treated as rigid bodies with hydrogens included in idealized positions with group U_{iso} values. Methyl hydrogens and those on the phenylene-diimine were freely refined with individual U_{iso} values.

Crystal data. $C_{22}H_{27}N_3O_2P_2Pt$, $M = 622.512$, monoclinic, $a = 12.817(3)$, $b = 14.262(2)$, $c = 13.013(2)$ Å, $\beta = 96.17(1)°$, $U = 2364.9$ Å^3, space group $P2_1/n$, $Z = 4$, $D_c = 1.75$ g cm^{-3}, μ(Mo-K_α) = 61.5 cm^{-1}, $\lambda = 0.71069$ Å.

Data collection. ($1.5\theta \leqslant 25°$), graphite monochromated Mo-K_α radiation; 4547 independent measured reflections, 2906 observed [$|F_o| > 1.5\sigma(|F_o|)$], corrected for Lorentz and polarization factors; empirical absorption correction.

Refinement. 281 parameters, weighting scheme $1/[F_o + 0.001431F_o]$ $R = 0.042$, $R_g = 0.0527$. Phenyl rings refined as rigid groups. All non-hydrogens anisotropic; hydrogens fixed. Computations were carried out on an VAX 11.750 computer using the SHELX76 program system. Final atomic positional and thermal parameters, full lists of bond lengths and angles and F_o/F_c values have been deposited as supplementary material with the Editor, from whom copies are available on request. Atomic coordinates have also been submitted to the Cambridge Crystallographic Data Centre.

RESULTS AND DISCUSSION

Upon dissolving **1** in liquid ammonia, an intense red coloured solution is observed. If this solution is reacted with **2** the new complexes **3**–**7** are obtained [Eq. (1)]:

$$\underset{\textbf{(1)}}{O_2NC_6H_3(NH_2)_2} + \underset{\textbf{(2)}}{PtCl_2(PR_3)_2} \xrightarrow{\text{liq } NH_3} \underset{\textbf{(3)–(7)}}{Pt\{(NH)_2C_6H_3NO_2\}(PR_3)_2} + 2NH_4Cl. \quad (1)$$

Table 1. Microanalytical (calculated values in parentheses), yields and NMR data

PR_3	C	H	N	Yield	δ	^{31}P $^{1}J_a$	^{31}P $^{1}J_b$	^{31}P $^{2}J_{ab}$	^{1}H
PMe_2Ph (**3**)	42.2(42.5)	4.0(4.3)	6.5(6.7)	82	−21.8	2916	2983	22	7.38m(13H), 6.15d(2H), 1.6m(12H)
$PMePh_2$ (**4**)	51.0(51.4)	4.1(4.1)	5.6(5.6)	80	−4.7, −5.2	2959	3010	22	7.43m(23H), 6.05d(2H), 1.81m(6H)
PEt_3 (**5**)	37.9(37.9)	4.1(4.1)	7.4(7.4)	75	9.2, 9.5	2910	2983	23	7.5s(2H), 7.3s(1H), 6.35d(2H) 1.92m(12H), 1.15m(18H)
$PPh_2CH_2CH_2PPh_2.1/2CDCl_3$ (**6**)	48.1(48.4)	3.9(3.8)	6.0(5.3)	71	39.8	2965	3070	12	7.82(8H), 7.45m(14H), 7.28s(1H) 6.3d(2H), 2.4m(4H)
Palladium $PPh_2CH_2CH_2PPh_2CDCl_3$ (**7**)	51.6(51.1)	4.1(4.0)	5.3(5.4)	64	56.5	—	—	—	7.64m(8H), 7.35m(14H), 7.3s(1H) 6.35d(2H), 2.5m(4H)

Table 2. Mass spectra, IR and UV–vis data

Compound	M^+	$M^+ - NO_2$	$M^+ - PR_3$	$M^+ - NO_2Ph(NH)_2$	ν(N—H)	$\nu(NO_2)$	ν(CN)	λ ($\varepsilon \times 10^{-3}$)			
3	606	560	468	471	3405m, 3381s	1250vs	1567m	232 (16.0)	351 (2.74)	385 (2.11)	547 (1.32)
4	746	700	546	595	3389s, 3381m	1248vs	1557m	232 (19.2)	350 (2.90)	384 (2.38)	546 (1.63)
5	582	536	463	427	3407m, 3389m	1248vs	1568m	230 (4.84)	344 (2.15)	382 (1.61)	552 (0.90)
6	744	698		593	3397m	1258vs	1560m	232 (32.3)	351 (3.21)	379 (2.24)	544 (1.40)
7	656	624		504	3394m	1254vs	1560m				

M^+ = parent ion. Percentage abundance of the above fragmentation ions exceed 25% of the base peak. The molecular and fragment ions had the expected isotopic variation around the main peak.

The colour changes during the course of the reaction suggest that **1** is deprotonated by liquid ammonia to form an anionic species. However, we have no strong evidence for this. At best a monoanion would be formed and we presume that this forms an (unobserved) intermediate which eliminates HCl to give the desired product. Compounds **3–7** were characterized by NMR, mass spectra, IR and, in the case of $PR_3 = PMe_2Ph$, X-ray crystallography.

The ^{31}P NMR of **3–7** (Fig. 1, Table 1) consist at low field (36.21 MHz) of a central resonance with complex satellites due to coupling to ^{195}Pt. The magnitude of the $^1J\ ^{31}P–^{195}Pt$ coupling constants show an inequivalence and are typical of the pattern normally observed in AX spectra. The substituted NO_2 group of 4-nitro-1,2-diaminobenzene makes the two nitrogen donor atoms slightly different. Thus, although the chemical shift for the phosphorus atoms are essentially the same at 36.21 MHz, the ^1J coupling constants are of sufficiently different magnitude (40 Hz) to be seen. On going to higher field (101.1 MHz) the small chemical shift difference between the phosphorus atoms is enough for the individual resonances to be seen. The magnitude of the $^1J\ ^{31}P–^{195}Pt$ coupling constant of *ca* 2940 Hz is typical of square-planar *cis*-phosphine platinum(II) species with nitrogen donor ligands[6,7] ($^1J\ ^{31}P–^{195}Pt$ in $Pt(NSO)_2(PR_3)_2$ is 3100 Hz and in $Pt(S_2N_2)(PR_3)_2$ is 2800 Hz). The chemical shift variation between **3–7** is due to the variation of the phosphine group. The $^2J\ ^{31}P–^{31}P$ coupling constant of 22 Hz is as expected for *cis*-phosphine groups on platinum(II). The lower $^2J\ ^{31}P–^{31}P$ coupling constant for **6** of 12 Hz could be due to contributions of ^2J(P—Pt—P) combined with a contribution directed via a ^3J(P—CH_2—CH_2—P) pathway.

The ^1H NMR spectra of **3–7** show the phosphine protons often overlapping the aromatic protons of the $NO_2C_6H_3(NH)_2$ ring. The N—H protons are observed at *ca* 6.2 ppm as a doublet ($^3J\ ^{31}P–^1H$, *ca* 5 Hz). This indicates coupling to the *trans*-phosphorus. No $^2J\ ^{195}Pt–^1H$ coupling is observed.

The mass spectra of **3–7** show the parent ion with the expected isotopic correlation (principally due to the platinum isotopes). Fragment ions mainly consist of loss of phosphine to form $[Pt\{(NH)_2C_6H_3NO_2\}(PR_3)]^+$, loss of $(NH)_2C_6H_4NO_2$ to leave $[Pt(PR_3)_2]^+$ and loss of NO_2 to form $Pt\{(NH)_2C_6H_3\}(PR_3)_2$. In the case of the bidentate derivatives (**6**, **7**) the $M-(PR_3)$ peak is not observed, a peak due to loss of (O_2) is seen.

The IR spectra of **3–7** show the expected phosphine and $\{(NH)_2C_6H_3NO_2\}$ ligand vibrations. Two intense ν(NH) vibrations at *ca* 3405 and 3380

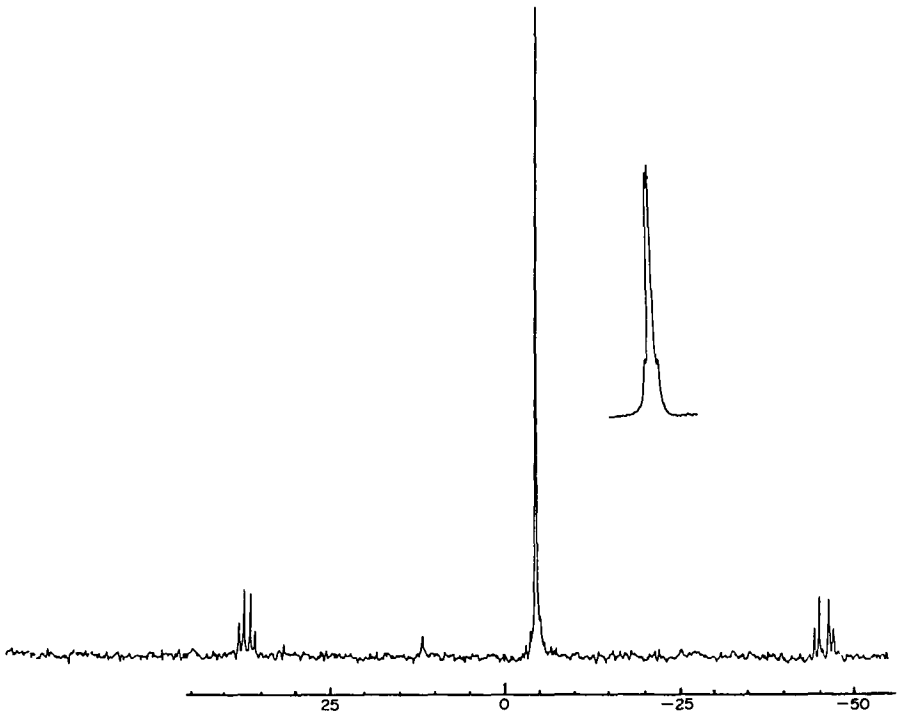

Fig. 1. ^{31}P NMR of **4** at 36.21 MHz, with the insert showing the central resonances measured at 101.1 MHz.

cm^{-1} are observed for **3–5** and one for **6**, **7** at 3395 cm^{-1}. The free ligand 4-nitro-1,2-phenylinediamine has four distinguishable ν(NH) vibrations and the loss of two vibrations is consistent with the ligand having been doubly deprotonated on complexation. The observed ν(NH) vibrations are higher than that observed in the homoleptic rhenium compounds[3] at 3264 cm^{-1} and normal aromatic ν(NH) vibrations at 3250 cm^{-1}. The most intense band in the spectrum is the $\nu(NO_2)$ stretching vibration at 1250 cm^{-1}. This is lower than its assigned value in the free ligand at 1293 cm^{-1}. An assignable ν(CN) vibration is observed at 1567 cm^{-1}, as this vibration does not exist in either starting material. Typically in the homoleptic analogues ν(CN) occurs at *ca* 1594 cm^{-1}.

The UV–vis spectra of **3–6** show four main bands at *ca* 230, 350, 385 and 547 nm. The high energy band at 230 nm is associated with aromatic ring transitions and is of higher intensity in **3**, **4** and **6** due to the aromatic groups also present on the phosphine ligand. The bands at 350 and 385 nm are due to the nitro group. Whilst the weak band at 547 nm, responsible for the purple colour in solution, is due to the complexed ligand.

The X-ray crystal structure of **3** (Table 3, Fig. 2) reveals the expected square-planar geometry at platinum. The Pt—P and Pt—N bond lengths are normal, whilst the C—N bond lengths are, as expected, consistent with formal C=N bond lengths. There are no short contacts in the crystal structure which would indicate any significant intermolecular interactions.

The compounds **3–7** are sensitive to hydrolysis and weak acids. Dichloromethane solutions of **3–7** show gradual deterioration to the free ligand and $PtCl_2(PR_3)_2$ (detected by both ^{31}P NMR and UV–vis). This is presumably due to residual HCl from the CH_2Cl_2 reacting with **3–7** [eq. (2)]:

$$Pt\{(NH)_2C_6H_3NO_2\}(PR_3)_2 + 2HCl \rightleftharpoons (NH_2)_2C_6H_3NO_2 + PtCl_2(PR_3)_2. \quad (2)$$

The complexes **3–7** show no change in the NMR spectrum on adding excess CH_3OD. Similarly, the

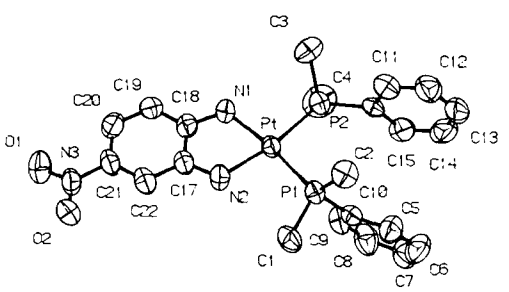

Fig. 2. The X-ray structure of **3**.

Table 3. Selected bond lengths and angles for **3**

P(1)—Pt	2.236(4)	P(2)—Pt	2.243(4)
N(1)—Pt	2.036(10)	N(2)—Pt	2.024(9)
C(1)—P(1)	1.826(13)	C(2)—P(1)	1.807(13)
C(3)—P(2)	1.810(16)	C(10)—P(1)	1.805(9)
C(16)—P(2)	1.800(10)	C(4)—P(2)	1.829(17)
N(1)—C(18)	1.347(12)	N(2)—C(17)	1.345(13)
C(17)—C(18)	1.413(14)	C(22)—C(17)	1.408(13)
C(19)—C(18)	1.394(14)	C(19)—C(20)	1.377(16)
C(20)—C(21)	1.412(16)	C(21)—C(22)	1.397(15)
C(21)—N(3)	1.417(13)	O(1)—N(3)	1.262(13)
O(2)—N(3)	1.228(14)		
P(2)—Pt—P(1)	97.2(2)	C(17)—Pt—P(1)	118.9(3)
C(17)—Pt—P(2)	143.7(2)	N(1)—Pt—P(1)	172.2(2)
N(1)—Pt—P(2)	90.1(3)	N(2)—Pt—P(2)	169.2(2)
N(2)—Pt—P(1)	93.6(3)	N(2)—Pt—N(1)	79.1(4)
C(1)—P(1)—Pt	113.9(5)	C(2)—P(1)—Pt	116.5(6)
C(2)—P(1)—C(1)	103.7(7)	C(10)—P(1)—Pt	114.9(3)
C(10)—P(1)—C(1)	100.6(7)	C(10)—P(1)—C(2)	105.5(6)
C(3)—P(2)—Pt	110.8(6)	C(4)—P(2)—Pt	112.3(7)
C(4)—P(2)—C(3)	100.2(9)	C(16)—P(2)—Pt	122.0(4)
C(16)—P(2)—C(3)	104.0(7)	C(16)—P(2)—C(4)	105.2(7)
C(9)—C(10)—P(1)	117.1(3)	C(5)—C(10)—P(1)	122.9(3)
C(15)—C(16)—P(2)	121.7(3)	C(11)—C(16)—P(2)	118.3(3)
C(18)—C(17)—Pt	77.0(6)	C(22)—C(17)—Pt	164.4(7)
C(22)—C(17)—C(18)	118.3(10)	N(2)—C(17)—C(22)	124.3(10)
N(2)—C(17)—C(18)	117.4(9)	N(1)—C(18)—C(17)	114.1(9)
C(19)—C(18)—C(17)	120.9(10)	C(20)—C(19)—C(18)	121.3(11)
N(1)—C(18)—C(19)	125.0(10)	C(22)—C(21)—C(20)	121.8(10)
C(21)—C(20)—C(19)	118.1(11)	N(3)—C(21)—C(22)	119.0(11)
N(3)—C(21)—C(20)	119.2(11)	C(18)—N(1)—Pt	115.2(7)
C(21)—C(22)—C(17)	119.6(10)	O(1)—N(3)—C(21)	119.0(12)
C(17)—N(2)—Pt	113.8(7)	O(2)—N(3)—O(1)	121.9(11)
O()—N(3)—C(21)	119.1(10)		

IR spectrum obtained by pumping down a solution of **5**, which has been treated with CH_3OD, shows no deuterium/proton exchange.

Acknowledgements—We are grateful to Johnson Matthey for loans of precious metals and to the Research Corporation Trust for support.

REFERENCES

1. A. L. Balch and H. Holm, *J. Am. Chem. Soc.* 1966, **88**, 5201.
2. G. S. Hale and R. H. Soderberg, *Inorg. Chem.* 1968, **7**, 2300.
3. G. Wilkinson, personal communication.
4. R. Jones, P. F. Kelly, D. J. Williams and J. D. Woollins, *J. Chem. Soc., Dalton Trans.* 1988, 803.
5. M. B. Hursthouse, R. A. Jones, K. M. A. Malik and G. Wilkinson, *J. Am. Chem. Soc.* 1979, **101**, 4128.
6. I. P. Parkin, A. M. Z. Slawin, D. J. Williams and J. D. Woollins, *Polyhedron* 1989, **8**, 835.
7. P. F. Kelly and J. D. Woollins, *J. Chem. Soc., Dalton Trans.* 1988, 1053.

Polyhedron Vol. 8, No. 20, pp. 2513–2515, 1989
Printed in Great Britain

0277-5387/89 $3.00+.00
© 1989 Pergamon Press plc

COMMUNICATION

ACTIVATION OF AN ARYL C—H BOND TO OXYGEN INSERTION: MODEL FOR THE PHENOLOXIDASE ACTIVITY OF TYROSINASE

MICHAEL G. B. DREW

Department of Chemistry, The University, Whiteknights, Reading RG6 2AD, U.K.

and

JADWIGA TROCHA-GRIMSHAW* and KIERAN P. McKILLOP

Department of Chemistry, Queen's University, Belfast BT9 5AG, U.K.

(*Received* 10 *April* 1989; *accepted* 17 *May* 1989)

Abstract—The reactions of dioxygen with the binuclear tricoordinate copper(I) complexes, derived from the condensation of benzene-1,3-dicarboxaldehyde and two molecules of a diamine, give phenoxy-bridged copper(II) complexes by direct hydroxylation of the benzene ring.

In our previous work[1] we attempted to design a macrocyclic ligand in which a dinuclear copper(I) centre binds dioxygen and then transfers it into an aryl C—H bond. Such a system simulates the action of copper-containing enzymes such as haemocyanin[2] which binds and transports oxygen, and also tyrosinase[3] and dopamine mono-oxygenase[4] which incorporate oxygen from dioxygen into organic systems. Studies on biomimicking chemical models can be useful in elucidating the structural and spectroscopic properties of enzyme active sites.

We have recently developed such a system. We report on the structure and properties of the dicopper(I) complex (**1a**) and the dicopper(II) complex (**2a**) which contain phenoxy- and hydroxy-bridge ligands. Karlin and co-workers[6] have prepared related complexes by direct synthesis from a diamine and 2-hydroxy-5-methylbenzene-1,3-dialdehyde and by peroxide oxidation of the related ligand incorporating 5-methylisophthalaldehyde.

The binuclear complex, **1a**, was prepared by condensation of 1 equivalent of benzene-1,3-dialdehyde and 2 equivalents of the appropriate amine with 2 equivalents of copper(I) acetonitrile perchlorate in refluxing acetonitrile methanol mixture under an inert atmosphere. A yellow crystalline solid separated in high yield. The IR spectrum of **1a** displayed a band at 1630 cm^{-1} due to the $\nu(C{=}N)$ stretching vibration of the coordinated macrocycle. A weak set of absorptions at 2310–2260 cm^{-1} is due to $\nu(C{\equiv}N)$ stretching vibrations. The IR spectrum also shows uncoordinated perchlorate. The ^1H NMR spectrum of compound **1a** was recorded in deoxygenated CD_3CN and supports the proposed structure. Each copper(I) ion is presumably three-coordinate. This compound was very sensitive to oxygen, both in solution and in the solid state. Compound **1a** in dichloromethane solution reacted rapidly with dioxygen (5 min) producing a blue crystalline compound, **2a** in 90% yield. The oxygen uptake was measured at 25°C in DMA solution. The observed stoichiometry was 0.95 molecule of dioxygen per two copper atoms. This is close to the stoichiometry found for deoxyhaemocyanin[7] and deoxytyrosinase.[8] During the oxidation an intense absorption band formed near 358 nm (ε = 11,000) and a much weaker band near 682 nm (ε = 300) which is characteristic for phenoxo- and hydroxy-bridged copper(II) complexes occurred.[5,6] The IR spectrum of compound **2a** displayed a very strong

* Author to whom correspondence should be addressed.

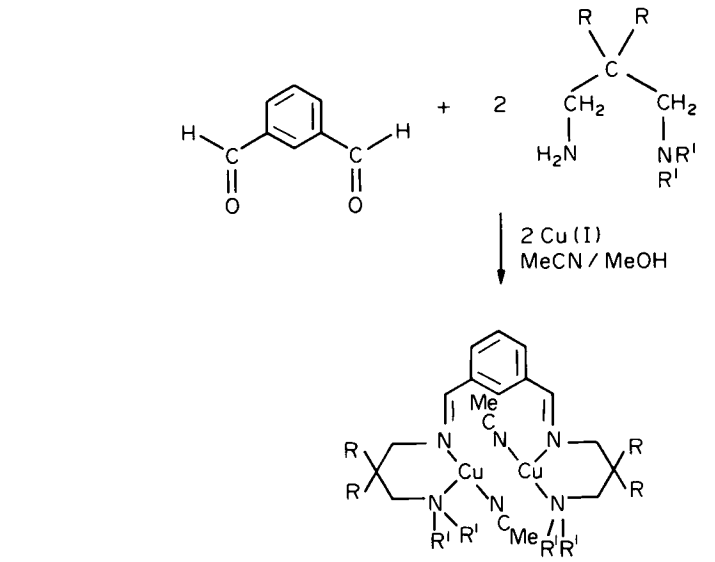

$[Cu_2L^1(NCMe)_2]$ **(1a)**

a R = H; R' = Me
b R = Me; R' = Me
c R = H; R' = $CH_2CH=CH_2$

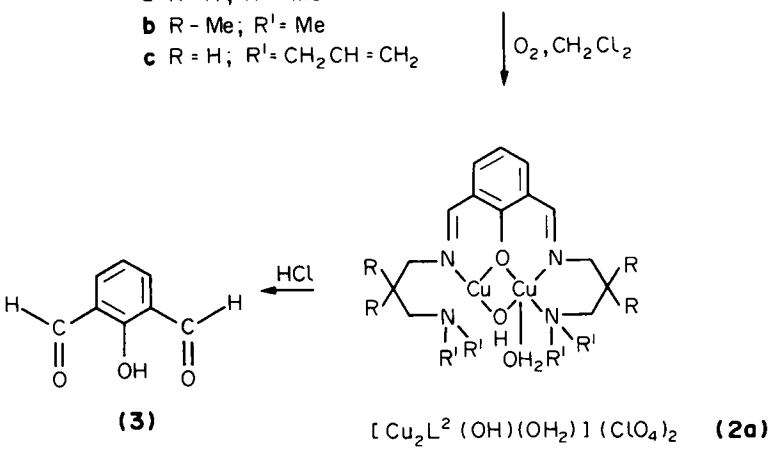

(3)

$[Cu_2L^2(OH)(OH_2)](ClO_4)_2$ **(2a)**

band near 1560 cm^{-1} which does not exist in compound **1a**, but is typical for the ν(C=O) vibration of the phenol in the 2-hydroxyphenylimino chromophore.[8,4]

Correct analytical data were obtained for compound **2a** as a diperchlorate and 2-hydroxybenzene-1,3-dialdehyde (**3**) was obtained as a colourless, crystalline solid by hydrolysis with 2 M hydrochloric acid, and was identified by IR, elemental analysis and M^+ at m/z 150. Crystal data* for compound **2a**, $[Cu_2L^2(OH)(OH_2)](ClO_4)_2$, $Cu_2N_4Cl_8H_{32}O_{11}Cl_2$, $M = 678.2$, $a = 12.340(10)$, $b = 18.53(1)$, $c = 11.79(1)$ Å, $\beta = 107.0(1)°$, $U = 2578.8$ Å^3, $D_c = 1.75$ g cm^{-3}, $F(000) = 1392$, $Z = 4$, $\lambda = 0.71907$ Å, $\mu = 19.8$ cm^{-1}, space group *Aa*.

1660 independent reflections above background [$I > 2\sigma(I)$] were measured on a diffractometer. The structure was solved by heavy-atom methods and refined (Cu, O, N, C anisotropic, H isotropic in the cation, Cl anisotropic, O isotropic in the anions) to $R = 0.075$ ($R_w = 0.083$). Hydrogen atoms on carbon were placed in fixed positions, those bonded to oxygen were located in a difference Fourier and positions were fixed in the refinement. One perchlorate anion was disordered and two sets of oxygen atoms were refined. In both anions Cl—O and O···O distances were constrained.

The structure of **2a** (see Fig. 1) consists of two copper(II) atoms bridged by a phenolate oxygen

* The atomic coordinates for this work are available on request from the Director of the Cambridge Crystallographic Data Centre, University Chemical Laboratory, Lensfield Road, Cambridge CB2 1EW, U.K. Any request should be accompanied by the full literature citation of this communication.

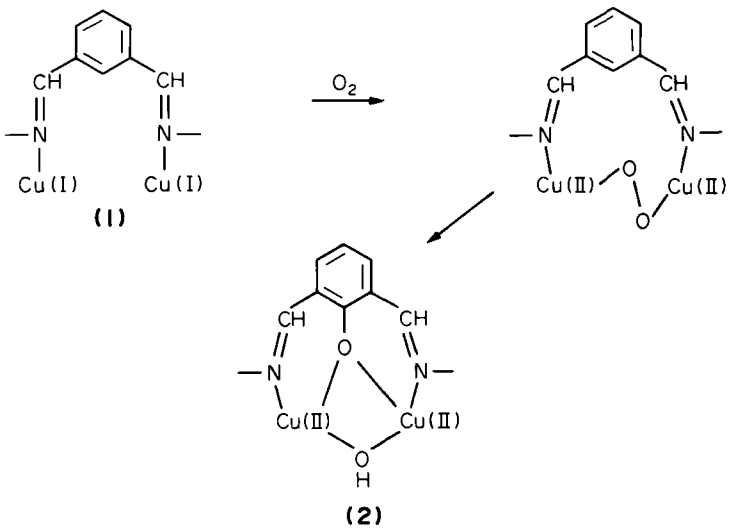

Scheme 1.

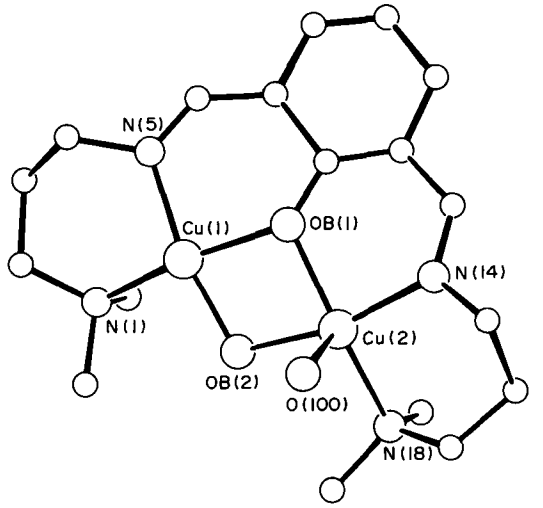

Fig. 1. The structure of the $[Cu_2L^2(OH)(OH_2)]^{2+}$ cation. Cu(1) is four-coordinate with bond lengths Cu(1)—OB(1), 1.99(1); Cu(1)—OB(2), 1.84(1); Cu(1)—N(1), 2.05(1); Cu(1)—N(5), 1.91(1) Å. There is also a close contact of 2.53(5) Å between Cu(1) and a perchlorate oxygen (not shown). Cu(2) is five-coordinate with bond lengths Cu(2)—OB(1), 1.97(1); Cu(2)—OB(2), 1.90(1); Cu(2)—N(14), 1.91(2); —N(18), 2.02(1); Cu(2)—D(100), 2.26(2) Å. The Cu(1)···Cu(2) distance is 3.015(3) Å.

and a hydroxide oxygen. The two copper atoms differ in their environments primarily in the presence of a water molecule on Cu(2); thus while Cu(1) has a distorted four-coordinate square environment, Cu(2) has a distorted four-coordinate square-pyramidal environment. Both metal geometries exhibit tetrahedral distortions of the equatorial planes—thus the angle between CuO_2 and CuN_2 planes is 18.4 and 23.2° for Cu(1) and Cu(2), respectively. This oxygenation of compound **1a** to **2a** with hydroxylation of the benzene ring, suggests that peroxo-copper intermediates are involved as shown in Scheme 1. Other examples of this reaction are the conversion of **1b** to **2b** and **1c** to **2c**.

REFERENCES

1. S. M. Nelson, J. T. Grimshaw, A. Lavery, K. P. McKillop and M. G. B. Drew, in *Biological and Inorganic Copper Chemistry* (Edited by K. D. Karlin and J. Zubieta), p. 27. Adenine Press, New York (1985).
2. C. A. Reed, in *Biological and Inorganic Copper Chemistry* (Edited by K. D. Karlin and J. Zubieta), p. 61. Adenine Press, New York (1985).
3. M. E. Winkler, K. Lerch and E. I. Solomon, *J. Am. Chem. Soc.* 1981, **103**, 7001.
4. N. J. Blackburn, D. Collinson, J. Sutton and F. E. Rabbs, *Biochem. J.* 1984, **220**, 447.
5. L. Casella and L. Rigoni, *J. Chem. Soc., Chem. Commun.* 1985, 1668.
6. N. J. Blackburn, K. D. Karlin, M. Concannon, J. C. Hayes, Y. Cultneh and J. Zubieta, *J. Chem. Soc., Chem. Commun.* 1984, 939.
7. J. A. Larabee and T. G. Spiro, *J. Am. Chem. Soc.* 1980, **108**, 4217.
8. R. S. Himmelwright, N. C. Eickmann, C. D. Lubien, K. Lerch and E. I. Solomon, *J. Am. Chem. Soc.* 1980, **102**, 7339.

Polyhedron Vol. 8, No. 20, pp. 2517–2519, 1989
Printed in Great Britain

0277-5387/89 $3.00 + .00
Pergamon Press plc

COMMUNICATION

CYCLOPALLADATION OF N,N-DIMETHYL-2(OR -3)-FURANCARBOSELENOAMIDE TO FORM A CHELATE WITH SELENIUM AND CARBON AS DONOR ATOMS

MATSUO NONOYAMA*

Department of Chemistry, Faculty of Science, Nagoya University, Chikusa, Nagoya, 464 Japan

and

KIYOKO NONOYAMA

Konan Junior College, Omatsubara, Takaya-cho, Konan, Aichi, 483 Japan

(*Received* 3 *July* 1989; *accepted* 24 *July* 1989)

Abstract—N,N-Dimethyl-2(or -3)-furancarboselenoamide was prepared by the reaction of N,N-dimethyl-2(or -3)-furancarboxamide with phenyldichlorophosphineselenide. The selenoamides were cyclopalladated with lithium tetrachloropalladate to form a five-membered palladaselenaheterocycle.

Selenium is seldom employed as a donor atom in organometallic coordination compounds, contrary to nitrogen, phosphorus and sulphur,[1] e.g. in N,N-dimethyl-2-furancarbothioamide (abbreviated as Haft).[2] The selenium atom of a similar selenoamide is expected to act in the same way to form a related palladaselenaheterocycle. N,N-Dimethyl-2-(or -3)-furancarboselenoamide [abbreviated as Hafs (or Hbfs)] has been prepared and reacted with lithium terachloropalladate. To the best of our knowledge cyclopalladation of a selenoamide is without precedent.

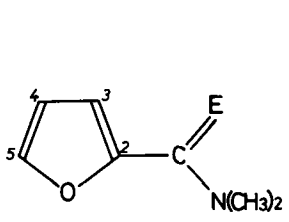

E=Se,Hafs; E=S,Haft

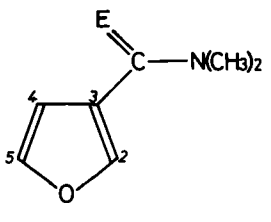

E=Se,Hbfs; E=S,Hbft

Hafs (or Hbfs) was prepared by the reaction of N,N-dimethyl-2(or -3)-furancarboxamide with phenyldichlorophosphineselenide in xylene, followed by purification on an alumina column.[3] Hafs and Hbfs are orange solids which melt at 37–38°C and 27–28°C, respectively. They gave satisfactory elemental analyses and were characterized spectroscopically. The IR and NMR spectra of the selenoamides are very similar to those of the corresponding thioamides.[2] Some important features are as follows.

The $^{13}C\{^1H\}$ NMR spectra (Table 1) show that the ^{13}C signal of the selenoamide group is coupled with a ^{77}Se nucleus: $^1J(C—Se) = 206.6$ Hz for Hafs and 206.9 Hz for Hbfs. These large values suggest a C(sp^2)—Se double bond.[4] The rotational barrier of the selenoamide C—N bond of Hafs and Hbfs is higher than that of the corresponding thioamide C—N bond: the coalescence temperature of the ^1H signal of the $N(CH_3)_2$ group of Hafs is 77°C while that of Haft is 45°C, and that of Hbfs is 111°C while that of Hbft is 80°C (in deuterated dimethylsulphoxide, DMSO-d_6, determined by 90 MHz ^1H NMR spectra).[5] Comparison of the IR spectrum of Hafs with that of Haft reveals that a band at 907 cm^{-1} is assigned to ν(Se=C) (ν(S=C) of Haft is at 927 cm^{-1}). A band at 906 cm^{-1} is likewise

* Author to whom correspondence should be addressed.

Table 1. Selected data of $^{13}C\{^1H\}$ NMR (22.6 MHz) and IR spectra

Compound	Solvent[a]	NMR, δ (ppm) vs TMS[b]			IR[c] (cm^{-1})		
		2-C	3-C	C(=Se)	ν(C—N)	ν(C=Se)	ν(Pd—Cl)
Hafs	$CDCl_3$	155.1	118.9	187.4 (206.6)[d]	1513	907	
Hbfs	$CDCl_3$	141.5	131.6	194.2 (206.9)[d]	1522	906	
PdCl(afs)	DMSO-d_6[e]	150.7	143.8	173.4	1589	879	281, 241
PdCl(bfs)	DMSO-d_6[e]	177.8	131.9	183.1	1577 1597	881	304, 288
PdBr(bfs)	DMSO-d_6[e]	178.7	131.6	183.4	1576 1595	800	267, 238

[a] DMSO-d_6 = deuterated dimethylsulphoxide.
[b] TMS = tetramethylsilane.
[c] Nujol mull.
[d] $^1J(^{77}Se—^{13}C)$ in Hz.
[e] Measured in the presence of tris(acetylacetonato)chromium(III) as a relaxation reagent at 75°C.

assigned to ν(Se=C) of Hbfs (ν(S=C) of Hbft is at 936 cm^{-1}).[6]

Hafs and Hbfs react with lithium tetrachloropalladate in methanol overnight at room temperature to give, respectively, PdCl(afs) and PdCl(bfs). The two gave satisfactory elemental analyses and were identified spectroscopically. They were practically insoluble in solvents except DMSO, in which they are slightly soluble. The ^1H NMR spectra (90 MHz) of DMSO-d_6 solutions show that the 3-H of the furan ring of free Hafs is removed in PdCl(afs) and the 2-H of free Hbfs in PdCl(bfs). Both the 3-C signal of PdCl(afs) and the 2-C signal of PdCl(bfs) shift, respectively, downfield compared with the corresponding signals of the free ligands (Table 1) by analogy with cyclopalladation of Haft and Hbft.[2]

In the IR spectra, higher frequency shifts of ν(C—N) of the selenoamide group upon complexation (Table 1) are indicative of selenium coordination because this coordination increases the double bond character of the C—N bond: an increase in the contribution of the canonical structure (II). A similar shift has been confirmed for sulphur coordination of a thioamide group.[6] The coordination shift of ν(Se=C) is in reverse. Shielding of the ^{13}C signal of the selenoamide group upon complexation is similar to that observed for sulphur coordination of the thioamide group.[2] The following structures are proposed for PdCl(afs) and PdCl(bfs).

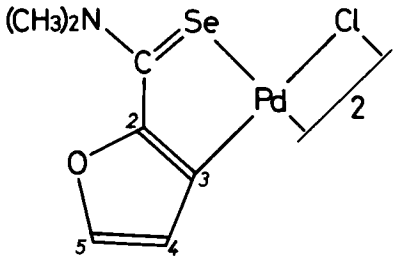

PdCl(afs)

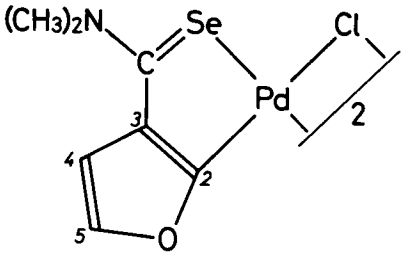

PdCl(bfs)

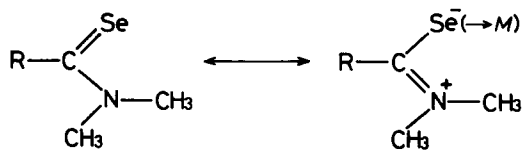

I II

The coordination of chlorine is supported by strong bands at 281 and 241 cm^{-1} [PdCl(afs)] or at 304 and 288 cm^{-1} [PdCl(bfs)]. Further investigations on cyclometallation of selenoamides are in progress.

Acknowledgement—This work was supported in part by a Grant-in-Aid for Scientific Research No. 61430013 from the Ministry of Education.

REFERENCES

1. I. Omae, *Organometallic Intramolecular Coordination Compounds*, *J. Organomet. Chem. Library* 1986, **18**, 1.
2. M. Nonoyama, *Inorg. Chim. Acta* 1989, **157**, 9.
3. J. P. Michael, D. H. Reid, B. G. Rose and R. A. Speirs, *J. Chem. Soc., Chem. Commun.* 1988, 1494.
4. W. Nakanishi, Y. Ikeda and H. Iwamura, *Org. Magn. Res.* 1982, **20**, 117.
5. F. Bernardi, L. Lunazzi, P. Zanirato and G. Cerioni, *Tetrahedron* 1977, **33**, 1337.
6. K. Jensen and P. H. Nielsen, *Acta Chem. Scand.* 1966, **20**, 597.

Polyhedron Vol. 8, No. 20, pp. 2521–2523, 1989
Printed in Great Britain

0277–5387/89 $3.00+.00
© 1989 Pergamon Press plc

COMMUNICATION

PLATINUM–IRON CARBONYL CLUSTER COMPLEXES. THE SYNTHESIS AND STRUCTURAL CHARACTERIZATIONS OF $Pt_3Fe_3(CO)_{15}$ and $Pt_5Fe_2(CO)_{12}(COD)_2$

RICHARD D. ADAMS,* GONG CHEN and JIN-GUU WANG

Department of Chemistry, University of South Carolina, Columbia, SC 29208, U.S.A.

(*Received* 22 *July* 1989; *accepted* 4 *August* 1989)

Abstract—The reaction of $Fe(CO)_5$ with $Pt(COD)_2$ has yielded the products $Pt_3Fe_3(CO)_{15}$ (**1**), 9%, $PtFe_2(CO)_8(COD)$ (**2**), 3% and $Pt_5Fe_2(CO)_{12}(COD)_2$ (**3**), 40%. The new compounds **1** and **3** were characterized by single-crystal X-ray diffraction analyses. Compound **1** contains a planar raft structure of six metal atoms consisting of a central triangular group of three platinum atoms with $Fe(CO)_4$ groups bridging each Pt—Pt edge of the cluster. The Pt—Pt distances are significantly shorter than those of the structurally related anions $[Pt_3Fe_3(CO)_{15}]^-$ and $[Pt_3Fe_3(CO)_{15}]^{2-}$. Compound **3** contains a tetrahedral cluster of platinum atoms. One edge of the tetrahedron is bridged by a Pt(CO) group and each of the Pt—Pt bonds to this group contains a bridging $Fe(CO)_4$ group.

Heteronuclear bimetallic cluster complexes containing platinum are of great interest because of the importance of bimetallic platinum catalysts to petroleum reforming processes.[1] Stone has shown that $Pt(COD)_2$ is an excellent reagent for the preparation of heteronuclear metal complexes containing platinum.[2] Recently, we have achieved success in the synthesis of new cluster complexes by employing the pentacarbonyl complexes of the iron subgroup as reagents.[3–5]. We are currently investigating the reactions of $Fe(CO)_5$ with $Pt(COD)_2$ and wish to report here some preliminary results of these studies.

The reaction of $Pt(COD)_2$ (100 mg, 0.24 mmol) with $Fe(CO)_5$ (1.03 g, 5.28 mmol) in hexane solution at 25°C for 10 min has yielded the following complexes, brown $Pt_3Fe_3(CO)_{15}$ (**1**, 9.0 mg, 9%) and red $PtFe_2(CO)_8(COD)$ (**2**, 5.0 mg, 3%) and dark brown $Pt_5Fe_2(CO)_{12}(COD)_2$ (**3**, 32 mg, 40%) after separation by TLC on silica gel. Compound **2** has been reported previously.[6] Compounds **1** and **3** are new and were characterized by single-crystal X-ray diffraction analyses. An ORTEP diagram of the molecular structure of compound **1** is shown in Fig. 1.† The molecule contains a crystallographically-imposed two-fold rotation axis that passes through the atoms Fe(1), Pt(1), C(11) and O(11). The molecule consists of a raft-like planar cluster of the six metal atoms.

The three platinum atoms form a central triangular cluster with $Fe(CO)_4$ groupings bridging each Pt—Pt edge of the triangle. Each platinum atom also contains one linear terminal carbonyl ligand. Compound **1** is a new uncharged member of the series of anions $[Pt_3Fe_3(CO)_{15}]^{-,2-}$ that were reported by Longoni *et al.* in 1980.[7] All three complexes are isostructural but differ in the total number of electrons. On the basis of the significant decreases of the Pt—Pt bond lengths in going from

* Author to whom correspondence should be addressed.

† For **1**: IR(ν(CO) in hexane, cm^{-1}) 2057(s), 2010(w), 1999(w). Crystal data: monoclinic, space group, $C2/c$, $a = 15.996(6)$, $b = 11.843(4)$, $c = 12.796(5)$ Å, $\beta = 92.35(3)°$, $V = 2422(1)$ Å^3, $z = 4$, Mo-K_α radiation ($\lambda = 0.71069$ Å) at 23°C. An empirical absorption correction was applied. The structure was solved by direct methods and difference-Fourier syntheses and was refined by full-matrix least-squares to the final values of the residuals, $R = 0.035$ and $R_w = 0.041$ for 2088 reflections [$I > 3\sigma(I)$].

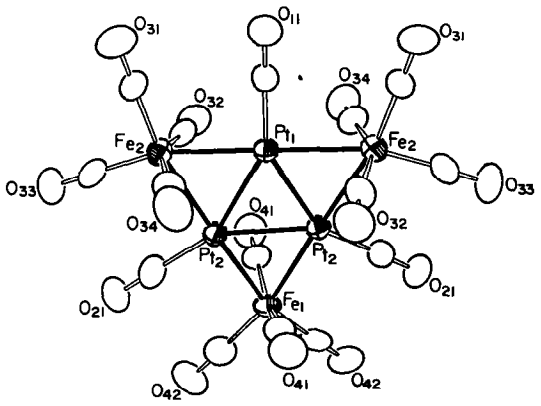

Fig. 1. An ORTEP diagram of $Pt_3Fe_3(CO)_{15}$ (**1**) showing 40% probability thermal ellipsoids. Selected intramolecular distances (Å) are Pt(1)—Pt(2) = 2.592(1), Pt(2)—Pt(2′) = 2.587(2), Pt(1)—Fe(2) = 2.571(2), Pt(2)—Fe(1) = 2.580(2), Pt(2)—Fe(2) = 2.584(2).

the dianion, $\mathbf{1}^{2-}$, to the monoanion, $\mathbf{1}^{-}$ (see Table 1), Longoni concluded that the highest occupied molecular orbital was centred on the Pt_3 triangle and was antibonding in character. This conclusion is further supported by the analysis of compound **1** which shows that the formal removal of one electron from $\mathbf{1}^{-}$ to yield **1** produces yet another significant decrease, 0.066(2) Å, in the Pt—Pt bond lengths. There is also a progressive, but much smaller decrease in the Pt—Fe distances as charge is removed from the cluster.

An ORTEP drawing of the molecular structure of compound **3** is shown in Fig. 2.* The molecule consists of a tetrahedron of four platinum atoms with the fifth platinum atom, Pt(3), bridging an edge of this tetrahedron. $Fe(CO)_4$ groups bridge the Pt—Pt bonds between Pt(3) and the tetrahedral grouping. COD ligands are coordinated to platinum atoms Pt(4) and Pt(5). The Pt(4)—Pt(5) bond is bridged by a carbonyl ligand, but curiously this bond remains by far the longest in the molecule at 2.958(1) Å. The other platinum atoms each contain

* For **2**: IR(ν(CO) in hexane, cm^{-1}) 2967(s), 2029(vs), 2009(s), 2003(m), 1976(vw), 1958(w). Crystal data: monoclinic, space group, $P2_1/c$, $a = 9.857(2)$, $b = 18.802(6)$, $c = 18.319(3)$ Å, $\beta = 91.94(1)°$, $V = 3393(2)$ Å^3, $Z = 4$, Mo-K_α radiation ($\lambda = 0.71069$ Å) at 23°C. An analytical absorption correction was applied. The structure was solved by direct methods and difference-Fourier syntheses and was refined by full-matrix least-squares to the final values of the residuals, $R = 0.036$ and $R_w = 0.039$ for 3442 reflections [$I > 3\sigma(I)$].

Table 1. Bond distances (Å) in **1**, $\mathbf{1}^{-}$ and $\mathbf{1}^{2-}$

Compound	**1**	$\mathbf{1}^{-}$	$\mathbf{1}^{2-}$
Pt—Pt (one)	2.590[a]	2.656[b]	2.750[b]
Pt—Fe (one)	2.578[c]	2.587[d]	2.596[d]

ESDS on single Pt—Pt distances: $a = 0.002$; $b = 0.001$.[7]
ESDS on single Pt—Fe distances: $c = 0.002$; $d = 0.004$.[7]

one linear terminal carbonyl ligand. Compound **3** is related to the complexes $Pt_5Fe(CO)_9(PEt_2)_4$ (**4**)[8] and $[Pt_6Fe_4(CO)_{22}]^{2-}$ (**5**),[7] which also contain tetra-

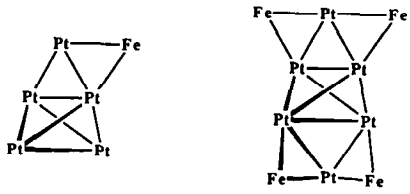

4 5

hedral Pt_4 cores and similar arrangements of bridging platinum and $Fe(CO)_4$ groupings. The presence of the labile COD ligands in **3** provides a great

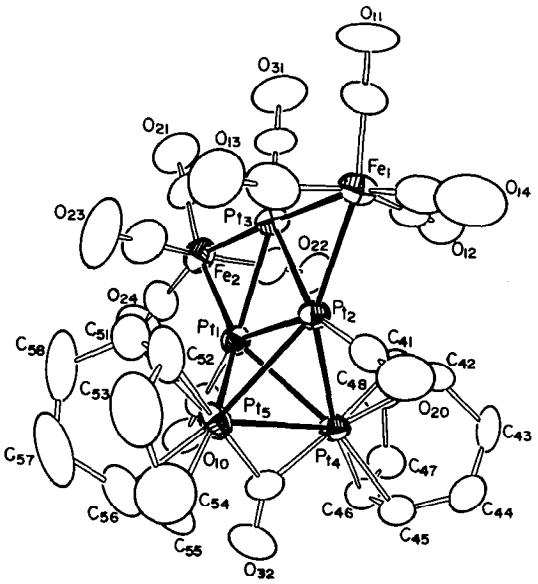

Fig. 2. An ORTEP diagram of $Pt_5Fe_2(CO)_{12}(COD)_2$ (**3**) showing 50% probability thermal ellipsoids. Selected intramolecular distances (Å) are Pt(1)—Pt(2) = 2.640(1), Pt(1)—Pt(3) = 2.643(1), Pt(1)—Pt(4) = 2.824(1), Pt(1)—Pt(5) = 2.827(1), Pt(2)—Pt(3) = 2.663(1), Pt(2)—Pt(4) = 2.775(1), Pt(2)—Pt(5) = 2.802(1), Pt(4)—Pt(5) = 2.958(1), Pt(1)—Fe(2) = 2.546(3), Pt(2)—Fe(1) = 2.582(3), Pt(3)—Fe(1) = 2.591(3), Pt(3)—Fe(2) = 2.602(3).

opportunity to develop further the organic chemistry of these platinum clusters under mild conditions.

Acknowledgement—These studies were supported by the National Science Foundation.

REFERENCES

1. (a) J. H. Sinfelt, *Bimetallic Catalysts*. John Wiley, New York (1983), (b) J. H. Sinfelt, *Accts Chem. Res.* 1977, **10**, 15; (c) W. M. H. Sachtler, *J. Molec. Catal.* 1984, **25**, 1; (d) V. Ponec, *Adv. Catal.* 1983, **32**, 149.
2. (a) F. G. A. Stone, *Accts Chem. Res.* 1981, **14**, 318; (b) F. G. A. Stone, *Inorg. Chim. Acta* 1981, **50**, 33.
3. R. D. Adams, *Polyhedron* 1985, **4**, 2003.
4. (a) R. D. Adams, J. E. Babin and M. Tasi, *Organometallics* 1988, **7**, 503; (b) R. D. Adams, J. E. Babin and M. Tasi, *Inorg. Chem.* 1988, **7**, 2618.
5. R. D. Adams, J. E. Babin, J. Estrada, M. B. Hall, A. A. Low and J. G. Wang, *Polyhedron* 1989, **8**, 1885.
6. L. J. Farrugia, J. A. K. Howard, P. Mitprachachon, F. G. A. Stone and P. Woodward, *J. Chem. Soc., Dalton Trans.* 1981, 1134.
7. G. Longoni, M. Manassero and M. Sansoni, *J. Am. Chem. Soc.* 1980, **102**, 7973.
8. R. Bender, P. Braunstein, D. Bayeul and Y. Dusausoy, *Inorg. Chem.* 1989, **28**, 2381.

Polyhedron Vol. 8, No. 20, p. 2525, 1989
Pergamon Press plc. Printed in Great Britain

CORRIGENDA

Synthetic and structural studies on some organic compounds of zirconium. A. Antiñolo, G. S. Bristow, G. K. Campbell, A. W. Duff, P. B. Hitchcock, R. A. Kamarudin, M. F. Lappert, R. J. Norton, N. Sarjudeen, D. J. W. Winterborn, J. L. Atwood, W. E. Hunter and H. Zhang (*Polyhedron* Vol. 8, No. 13/14, pp. 1601–1606, 1989).

In the above paper, due to a later stage of refinement, the caption for Fig. 2 on p. 1604 should read:

Fig. 2. The X-ray structures of $[ZrCp_2\{\eta\text{-}C(NMe)CHPh_2\}(Me)]$ (**3**). Important bond distances and angles: Zr—CH_3, 2.410(2), Zr—N, 2.205(2), Zr—η^2-C, 2.245(3), C—N, 1.262(3) Å; Cen—Zr—Cen, 129.72(1)°.

Polytungstate self-assembly: structures of the new oxoanions, $[W_4(NBu^t)_4O_4Cl_{10}]^{2-}$ and $[W_6O_{14}Cl_{10}]^{2-}$. W. Clegg, R. J. Errington, D. C. R. Hockless and C. Redshaw (*Polyhedron* Vol. 8, No. 13/14, pp. 1788–1789, 1989).

In the above paper the formula $WOCl_4N^+$ is an error, this should read $WOCl_4$.

Polyhedron Vol. 8, No. 21, pp. 2527–2533, 1989
Printed in Great Britain

0277–5387/89 $3.00+.00
Pergamon Press plc

SYNTHESIS, CHARACTERIZATION AND STRUCTURAL ASSESSMENT OF POLYMERIC BIS(DISALICYLALDEHYDE ACYL- AND AROYL-DIHYDRAZONATO)DIOXOURANIUM(VI) COMPLEXES

R. A. LAL

Department of Chemistry, Pachhunga University College, North-Eastern Hill University, Aizawl 796 001, Mizoram, India

(*Received* 23 *November* 1988; *accepted after revision* 19 *May* 1989)

Abstract—The reaction of uranyl nitrate hexahydrate with salicylaldehyde, and acyl- and aroyl-dihydrazines in a 1:4:2 molar ratio in ethanol medium results in complexes of the composition $[UO_2(H_3L_2)_2]\cdot nH_2O$ ($n = 0$, 2), where H_4L_2 refers to salicylaldehyde-oxaloyldihydrazone (H_4A_2), -malonoyldihydrazone (H_4B_2), -succinoyldihydrazone (H_4C_2), -glutaroyldihydrazone (H_4D_2), -adipoyldihydrazone (H_4E_2) and -phthaloyl-dihydrazone (H_4F_2), in high yields. The complexes have been characterized by elemental analyses, thermoanalytical data, decomposition points, molar conductance, and IR, Raman and electronic spectral data. The presence of monobasic tridentate ligands has been ascertained from the IR spectra. The ligands are coordinated through the phenolic oxygen, carbonyl oxygen and azomethine nitrogen atoms. All the complexes contain only one band due to the asymmetric stretching vibration of the uranyl group, indicating the same coordination environment around the uranium atom in all the complexes. The complexes are considered to be polymeric structures containing an eight-coordinated uranium atom with six ligand atoms forming an equatorial ring in a plane perpendicular to the linear uranyl group.

The study of novel ligands which can bind two metals in close proximity to one another has recently created much interest among chemists, because the magneto- and electrochemical properties of such complexes show promise in developing theories whereby electron transport phenomena can be further understood.[1] Acyl- and aroyl-dihydrazones are two of the few examples of ligands which can yield binuclear, heteronuclear and polynuclear complexes of transition and inner-transition metals possessing interesting magnetic and electrochemical properties,[2] and which can serve as models in bioinorganic chemistry.[3] Acyl- and aroyl-dihydrazones derived from the condensation of *o*-hydroxy aromatic aldehydes and ketones, and acyl- and aroyl-dihydrazines in which two hydrazone groups are separated from each other by methylene chains of varying length or phenyl groups, constitute a special class of molecules. This class of molecules react in the keto, keto–enol and enol forms[4–8] depending upon the mode of preparation of the complexes, the nature of the reaction medium, the pH of the reaction medium, the nature of the metal salt and the molar ratio of the metal salt, and the ligand employed, and can act as mono-, di-, tri- and tetrabasic hexadentate ligands, and give rise to polymeric complexes through both ligand-bridging due to their flexibility in three-dimensional space, and oxo-bridging through the phenolic oxygen atoms. Recently, we initiated studies on the isolation and characterization of uranyl complexes with acyl- and aroyl-dihydrazones in order to determine the form in which the ligands coordinate to the uranyl group, the possible coordination arrangement of the donor groups around the uranyl group, the relationship between the U=O stretching frequency and the increasing length of the methylene chain between the two hydrazone groups, and the effect of the presence of other ligands in the coordination sphere on the U=O stretching frequency, and also the effect of replacement of the methyl groups by phenyl groups on

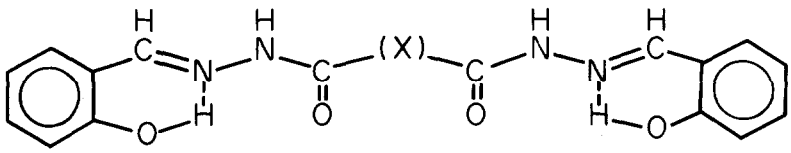

(I)

Fig. 1. X = $-(CH_2)_n-$, $-C_6H_4-$.

n	H_4L_2	
0	H_4A_2	Disalicylaldehyde oxaloyldihydrazone
1	H_4B_2	Disalicylaldehyde malonoyldihydrazone
2	H_4C_2	Disalicylaldehyde succinoyldihydrazone
3	H_4D_2	Disalicylaldehyde glutaroyldihydrazone
4	H_4E_2	Disalicylaldehyde adipoyldihydrazone
X = $-C_6H_4-$	H_4F_2	Disalicylaldehyde phthaloyldihydrazone.

complexation. The uranyl ion is the most stable species amongst the uranium compounds present in nature, and is peculiar in the sense that it retains its identity over a wide range of variation in the experimental conditions, and offers a large number of geometric structures usually hexa-to-deca-coordinate, a feature unusual in the coordination chemistry of transition elements. The present paper is a report on the synthesis, characterization and structural assessment of uranyl complexes obtained from the reaction of uranyl nitrate hexahydrate with disalicylaldehyde acyl- and aroyl-dihydrazones (I) (Fig. 1) in 1 : 2 molar ratio in alcoholic media.

EXPERIMENTAL

Materials and measurements

Uranyl nitrate hexahydrate, diethyl esters of oxalic, malonic, succinic, glutaric, adipic and phthalic acids, hydrazine hydrate and salicylaldehyde were from BDH, AR or of equivalent grade. The organic acid dihydrazides *viz.* oxalic, malonic, succinic, glutaric, adipic and phthalic acid dihydrazides were prepared by reacting the diethyl esters (1 mol) with hydrazine hydrate (2 mol). The dihydrazones were prepared by reacting warm or refluxing dilute ethanol solutions of the above acid dihydrazides (1 mol) with salicylaldehyde (2 mol). All the ligands were suction filtered, washed with water and ethanol, and dried at 70°C in an electric oven.[9]

Preparation of the complexes

The complexes were prepared by the following procedure. As all the complexes were prepared by the same method, only a representative procedure is described.

To uranylnitrate hexahydrate (0.05 mol) in ethanol (50 cm^3) was added salicylaldehyde (0.1 mol) in ethanol (100 cm^3), and the reaction mixture was refluxed for 15 min. Oxaloyldihydrazine was finely powdered in an agate mortar, and suspended in ethanol to give a slurry (0.05 mol) which was added slowly (100 cm^3) to the hot mixture of uranyl nitrate hexahydrate and salicylaldehyde, accompanied by gentle warming maintaining the molar ratio at 1 : 4 : 2. The whole mixture was refluxed for 3 h on a water bath accompanied by occasional vapourization to reduce the volume of the reaction mixture to 70–90 cm^3. In H_4A_2, the complex started to appear straight away. But in the remaining cases, the complexes precipitated only when the volume was reduced to 125–100 cm^3. The solution was cooled and the complexes removed by filtration, these were washed with hot benzene, hot ethanol and finally with ether, then dried and collected.

Elemental analyses (Table 1) and measurements

Uranium was determined by standard literature procedures. The ligands in the complexes were estimated volumetrically in 5 M H_2SO_4 with standard $KMnO_4$ using a calibration curve. Carbon, hydrogen and nitrogen were estimated by microanalytical methods. A thermogravimetric study of one sample as an example was carried out manually by heating the sample at the rate of 10°C min^{-1} on a TGA unit supplied by the Fertilizer Corporation of India (FCI), Sindri. The molar conductance of the complexes at 10^{-3} M dilution in DMSO were measured using an Elico conductivity bridge model CM-82T with a dip-type conductivity cell. IR spectra were recorded on a Perkin–Elmer 983 spectrophotometer as KBr pellets in the 4000–180 cm^{-1} region. The Raman spectrum was recorded on a Raman spectrophotometer (Ramalog 1403) as KBr pellets by employing the rotating sample technique to avoid

Table 1. Analytical, molar conductance and decomposition temperature data of dioxouranium(VI) complexes of disalicylaldehyde acyl- and aroyl-dihydrazones

Complex and colour	Decomposition temperature (°C)	Analysis: Found (Calc.) (%) U	C	H	N	Ligand	Molar conductance, Λ_M (Ω^{-1} cm^2 mol^{-1})
1. $[UO_2(HAAH_2)_2]\cdot 2H_2O$ Brown	> 300	24.4 (24.9)	39.7 (40.2)	3.2 (3.1)	12.1 (11.7)	67.5 (68.0)	1.3
2. $[UO_2(HBBH_2)_2]\cdot 2H_2O$ Dull brown	260[a]	24.7 (24.2)	41.0 (41.5)	3.4 (3.5)	11.8 (11.4)	68.5 (68.9)	0.8
3. $[UO_2(HCCH_2)_2]\cdot 2H_2O$ Brownish orange	> 300	24.0 (23.5)	42.2 (42.7)	3.6 (3.7)	11.4 (11.1)	69.3 (69.8)	2.3
4. $[UO_2(HDDH_2)_2]\cdot 2H_2O$ Orange	> 300	22.5 (22.9)	44.3 (43.9)	4.2 (4.1)	10.5 (10.8)	70.1 (70.6)	0.9
5. $[UO_2(HEEH_2)_2]\cdot 2H_2O$ Dull brown	270[a]	22.6 (22.3)	44.5 (44.9)	4.2 (4.3)	10.5 (10.5)	69.9 (71.4)	0.9
6. $[UO_2(HFFH_2)_2]$ Yellow	> 300	22.6 (22.2)	49.7 (49.3)	3.1 (3.2)	10.5 (10.5)	74.3 (74.8)	1.7

[a] Melts.

decomposition of the sample. The electronic spectra in the solid state, and in solution were recorded on a Carl Zeiss (GDR) VSU2-P ultraviolet and visible spectrophotometer with a reflectance attachment, using MgO as the reference, and a Pye-Unichem PU-8800 spectrophotometer, respectively.

RESULTS AND DISCUSSION

The reaction of uranyl nitrate hexahydrate with salicylaldehyde and dihydrazides in 1:4:2 molar ratio results in the formation of solid brown, dull brown, brownish orange, orange and yellow compounds. The analytical results are in accord with the formulation $[UO_2(HLLH_2)_2]\cdot 2H_2O$, in which $HLLH_2$ represents the loss of the phenolic-OH proton of one H_2L-group of the ligand H_2LLH_2. These compounds are finely divided powders all of which decompose above 300°C except for $[UO_2(HLLH_2)_2]\cdot nH_2O$ ($H_4L_2 = H_4B_2$, H_4E_2) which decomposes at 260 and 270°C. The compounds could not be crystallized since they are mostly insoluble in water and common organic solvents, but dissolve in coordinating solvents like DMF and DMSO only. The complexes, upon dissolution in DMF and DMSO, are not accompanied by a colour change, thus ruling out the possibility of the displacement of ligand molecules by solvent molecules. This fact was confirmed by recording the UV–vis spectra of the complex, $[UO_2(H_3E_2)_2]\cdot 2H_2O$, as a representative sample, in the solid state, in DMF and DMSO solutions. The solid state electronic spectrum of the complex shows absorption maxima at 280, 290, 330 and 380 nm, compared to the positions of the maximum absorption bands in the spectrum of the free ligand at 245, 290, 300 and 344 nm.[9] The spectra of the complex in DMF and DMSO solutions show maximum absorption bands at 280, 310, 335, 380 nm and 280, 295, 330, 380 nm, respectively. The essential features of the spectrum of the complex in the solid state and in solutions are entirely different when compared to that of the free ligand, which supports the coordination of the ligand to the uranyl ion in the solid state as well as in the solutions. The apical oxygen $\rightarrow f$ transition within the uranyl entity, centred at about 380 nm, is covered by a strong charge-transfer absorption from the ligand π-orbital to the $5f$ and/or $6d$ orbitals of the uranium atom. This ligand-to-metal charge-transfer band, which is strongly influenced by the chemical nature of the ligand within a given stereochemistry, is responsible for the colours of the complexes.[10] The decomposition temperature of the complexes coupled with their insolubility in common organic solvents suggests that they are associated polymeric species. The water molecules were determined by heating the compounds at 110°C for 4 h in an electric oven and estimating the loss of weight. The expulsion of two water molecules at 110°C indicates that they are part of the lattice, most probably, in the hydrogen bonded form with the ligand which permeates the lattice. The molar conductances of all the complexes fall in the range 0.8–2.3 Ω^{-1} cm^2 mol^{-1} in DMSO. Since 1:1 electrolytes in this solvent generally have molar conductivities between 35 and 70, it is apparent that in this solvent the complexes are non-electrolytes.[11]

The detailed thermogravimetric analyses of the

compound $[UO_2(HEEH_2)_2]\cdot 2H_2O$ was carried out as a representative sample up to 800°C. When heating was carried out in a thermobalance with a heating rate of 10°C min^{-1}, the mass loss corresponded to *ca* 3.56% of the total mass of the compound, corresponding to two water molecules, which indicates that they are part of the lattice or hydrogen bonded in the structural unit of the complexes. The decomposition of the complex occurs in four prominent steps, 80–120°C, 270–420°C, 420–460°C, and 520–640°C. Beyond 120°C, the complex is stable up to 270°C as the average mass loss is about 0.36% at a temperature interval of 20°C. The complex starts losing weight above 270°C by about 2.5% at the 20°C temperature interval, and continues up to 420°C. The most significant decomposition of the complex occurs between the temperature ranges 420–460°C and 520–640°C, the mass losses being about 5.0 and 5.35% at the temperature intervals of 20°C. The loss of the ligand begins at 270°C and occurs in three steps, and is complete at 680°C when the weight of the complex becomes constant; this corresponds to U_3O_8. The mass loss in the temperature range 270–680°C corresponds to two ligand molecules devoid of only one oxygen atom from each ligand molecule. Compared to the 1 : 1 (uranium–ligand) complex,[12] in which the loss of ligand occurred in the 300–420°C temperature range, beyond which the complex shows negligible mass loss and the weight becomes constant at temperatures greater than 460°C, the thermal decomposition behaviour of the present complex is entirely different, showing unsymmetrical decomposition of the ligand, which in turn, indicates the unsymmetrical bonding of the ligand to the uranyl ion.

It is difficult to unambiguously assign the bands due to the various groups and locate their respective positions in the IR spectra of the uncoordinated ligands because of the presence of a number of bands due to groups, viz. >C=O, >C=N, N—C=O, —NH, —OH, phenyl ring, C—N and C—H, which absorb in the overlapping regions, yet few significant bands have been selected to show the effect of coordination on ligand vibrations in the complexes. The assignments of the bands are based on literature reports.

Medium to strong broad bands in the 3500–3250 and 3200–3000 cm^{-1} regions, with multiplet structure, with maximum absorption in the 3423–3328 cm^{-1}, and 3195–3149 cm^{-1} regions are present in the IR spectra of the uncoordinated ligands. H_4A_2 shows additional bands at 3278 and 3232 cm^{-1}, and H_4F_2 shows only a single absorption band at 3149 cm^{-1}. These bands are attributed to ν(OH) and ν(NH) stretching vibrations of the ligands and have composite nature.

The IR spectra of the ligands in the region 3500–3100 cm^{-1} on complexation undergo splitting into three to five medium to strong bands, some of which undergo a blue shift on complexation. In the IR spectra of the uncoordinated ligands, the bands in the region 3423–3328 cm^{-1} on complexation undergo a blue shift and appear in the region 3576–3422 cm^{-1}, indicating the presence of water molecules in the complexes and the involvement of only one —OH group in coordination. In the IR spectra of the complexes, the appearance of the absorption bands in the 3579–3422 cm^{-1} region is almost similar to that observed in salicylaldehyde and *o*-hydroxyacetophenone, indicating the presence of hydrogen bonding in the molecular lattice. However, it appears that the strength of the hydrogen bonding in the complexed ligands is weakened compared to that in the uncoordinated ligands. The band observed in the 3232–3149 cm^{-1} region in the IR spectra of the uncoordinated ligands splits into two to three bands on complexation. One band suffers a blue shift of about 28–223 cm^{-1}, while the other band remains almost unchanged in its position. This behaviour of the absorption band in the region 3232–3149 cm^{-1} of the uncoordinated ligands on complexation shows that the ν(NH) vibration of one half of the ligand undergoes a blue shift due to the involvement of the >C=O group in coordination, while the other ν(NH) signal remains almost unchanged due to non-involvement of the other half of the ligand in coordination. This shows that half of the ligand is involved in coordination while the other half remains intact and hydrogen bonded, without taking part in coordination. This conclusion based on the position of the absorption bands in the 3232–3149 cm^{-1} region is further substantiated by the positions of the absorptions in the region 1674–1666 cm^{-1} which contains bands due to amide I. The complexes show a feature characteristic of ligand coordination through one carbonyl oxygen only, while the other carbonyl group remains uncoordinated. This is evident from the fact that in the complexes, one amide I band shows a negative shift by about 7–52 cm^{-1} and appears in the region 1666–1621 cm^{-1} in the IR spectra of the complexes, while the other band almost retains its original frequency or shifts to higher frequency. In some cases the intensity of the band is also reduced. The coordination of the ligands to the uranyl ion through the azomethine nitrogen is evident from the fact that the bands present in the 1624–1609 cm^{-1} region in the IR spectra of the uncoordinated ligands, attributed to the ν(C=N) stretching fre-

quency, suffer negative shifts by 10–20 cm^{-1} in the spectra of the complexes, and appear in the 1613–1604 cm^{-1} region as medium to strong bands. The IR spectra of the ligands contain bands in the 1573–1552 cm^{-1} region which are assigned to amide II + ν(C—O) (phenolic). The bands in the IR spectra of the complexes in this region split into several bands, and suffer positive as well as negative shifts, and appear in the regions 1589–1563 and 1563–1518 cm^{-1}, respectively; while some bands appear at almost the same position as in the uncoordinated ligands but reduced in intensity. This indicated the involvement of the ligands in coordination through the >C=O and —OH groups of one half, while the other half remained intact, hydrogen bonded and uncoordinated.[13]

It should be noted that when the two phenolic-OH groups of the phthaloyldihydrazone ligand are coordinated to the uranyl ion, the ν(C=N) stretching frequency shifts to higher wave number, which suggests the flow of the electron density from the salicylaldimine phenyl ring through the azine group nitrogen atoms to the uranyl ion. Consequently, this increases the carbon and nitrogen bond orders. This has been attributed to the replacement of the methylene groups by the phenyl ring between the two hydrazone groups of the phthaloyldihydrazone ligand, which exerts electron-withdrawing power over the salicylaldimine phenyl ring. However, in the present case, in bis(disalicylaldehyde phthaloyldihydrazonato)dioxouranium (VI) complex, the ν(C=N) stretching frequency shows a negative shift, a trend usually observed, in general, in acyl- and aroyl-hydrazone complexes. Hence, it may be argued that the phthaloyl phenyl ring of the phthaloyldihydrazone ligand situated between the two hydrazone groups becomes activated, and exerts electron-withdrawing power only when both the phenolic-OH groups are bonded to the uranyl ion. On the other hand, in the bis(disalicylaldehyde phthaloyldihydrazonato)dioxouranium (VI) complex, the ligand is bonded to the uranyl ion through one phenolic-OH group only, as a result of which the phthaloyl phenyl ring does not experience deficiency in its electron concentration and remains unactivated. Moreover, the drainage of the electron density from half of the coordinated phthaloyldihydrazone ligand to the uranyl ion withdraws the electrons from the phthaloyl phenyl ring which, in turn, withdraws electrons from the carbonyl oxygen of the other half of the ligand to make-up its electron deficiency. This is evident from the splitting of the amide I band, and its appearance at 1700, 1660 and 1642 cm^{-1}, respectively, corresponding to uncoordinated and coordinated carbonyl groups, in the IR spectrum of the complex.

The bands appearing in the region 1279–1261 cm^{-1} in the IR spectra of the uncoordinated ligands may be assigned to stretching vibrations of the phenolic C—O group. The bands in this region show splitting, and some of them show considerable higher frequency shifts in the complexes and appear in the 1332–1290 cm^{-1} region, while the other bands remain almost unchanged in position. Such features of the IR spectra of the complexes in this region indicate the involvement of only one C—O group of the ligand in chelation, while the other one remains hydrogen bonded.[14,15] From the above discussion, it is evident that the ligands coordinate to the uranyl ion in the keto form, they act as monobasic tridentate ligands, and coordinate through the phenolic and carbonyl oxygens and the azomethine nitrogen. The non-ligand bands occurring in the regions 605–558; 502–459 and 379–316 cm^{-1} have been assigned to ν(U—O) (phenolic),[16] ν(U—O) (carbonyl)[16] and ν(U—N)[17] vibrations, respectively.

All the uranyl complexes show a strong absorption in the *ca* 926–887 cm^{-1} region, assigned to the ν_3 vibrations of the uranyl group. In some complexes, a weak to medium band is observed in the 866–851 cm^{-1} region. This band may be assigned to the ν_1 vibration of the uranyl group. Although the ν_1 vibration of the uranyl group is normally IR forbidden, it has been reported to occur in the 900–790 cm^{-1} region. The forbidden vibrations may become allowed as a result of the particular symmetry properties of the ligand-field around the uranyl group in the complexes, rather than slight bending of this group. However, the band in the 866–851 cm^{-1} region in the IR spectra of the complexes may originate from the ligands as well, because the ligands also show weak to medium bands in the 890–834 cm^{-1} region which might be activated on complexation. The IR spectrum of the complex $[UO_2(HDDH_2)_2]\cdot 2H_2O$ shows strong bands at 926 and 906 cm^{-1} due to the ν_3 asymmetric stretching vibration. The IR spectrum of the uncoordinated H_4D_2 shows a band of medium intensity at 892 cm^{-1}. It is quite likely that this band in uncoordinated H_4D_2 is activated on complex formation, and retains its identity in the complex as a strong band. Hence, it can be assumed that of the two bands in $[UO_2(HDDH_2)_2]\cdot 2H_2O$, one band originates from the ligand. The Raman spectrum of the complex $[UO_2(HAAH_2)_2]\cdot 2H_2O$ shows a strong broad band centred at 870 cm^{-1}. The double degenerate O—U—O bending vibration is observed as a medium to strong band in the 283–244 cm^{-1} region, and masks the ligand band occurring in this region. As all the complexes show only one band

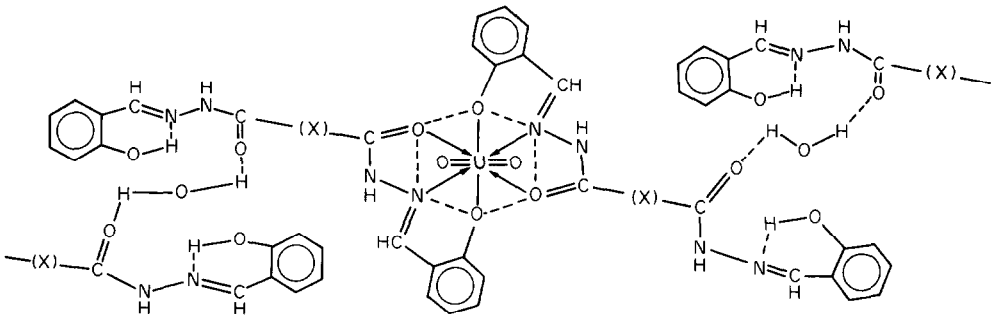

(II)

corresponding to the ν_3 vibration of the uranyl group, it suggests that the uranyl groups are in the same coordination environment in the structural units of the complexes.[7]

Considering the composition of the complexes, their insolubility behaviour in common organic solvents, decomposition/melting point, the monobasic tridentate nature of the ligand and the presence of hydrogen bonded water molecules, the dioxouranium(VI) complexes may, tentatively, be assigned as polymeric structures (**II**) involving eight-coordinated uranium. The complex (No. 6) may involve hydrogen bonding between the uncoordinated halves of the ligand in its structural unit. The six equatorial positions are occupied by four oxygen atoms (two from two phenolic-OH groups and two from two carbonyl groups of half of the two coordinated ligands) and two nitrogen atoms from the azomethine groups of the same half of the coordinated ligands, forming a ring around the linear uranyl group.

Acknowledgements—The author is thankful to Professor Saingenga, Principal, Pachhunga University College, North-Eastern Hill University, Aizawl—796 001, Mizoram, India, for laboratory facilities, to Dr D. T. Khathing, Head, Regional Sophisticated Instrumentation Centre, North-Eastern Hill University, Shillong, for recording IR spectra and to Professor A. L. Verma, Professor of Physics, Department of Physics, North-Eastern Hill University, Shillong for recording the Raman spectrum of one compound. Further, the Author is highly thankful to Professor M. K. Chaudhuri, Professor of Chemistry, Department of Chemistry, North-Eastern Hill University, Shillong, Meghalaya, India, for his constant encouragement and critical discussion.

REFERENCES

1. M. D. Glick and R. L. Lintvedt, *Progress in Inorganic Chemistry* (Edited by S. J. Lippard), Vol. 21, p. 233. Interscience, New York (1976); H. Adams, N. A. Bailey, D. E. Fenton and S. Mass, *Inorg. Chim. Acta* 1982, **62**, 201.
2. D. E. Fenton, U. Casellato, P. A. Vigato and M. Vidalli, *Inorg. Chim. Acta* 1982, **62**, 57.
3. E. L. Muetterties, *Science* 1977, **196**, 839; O. Khan, *Inorg. Chim. Acta* 1982, **62**, 3; G. L. Geoffrey, *Accts Chem. Res.* 1980, **13**, 469; A. J. Deeming and B. F. G. Johnson, *Transition Metal Clusters*, p. 391. John Wiley, New York (1980); W. Konda, H. Okawa and S. Kida, *Bull. Chem. Soc. Jpn* 1984, **57**, 1159.
4. K. K. Narang and R. A. Lal, *Transition Met. Chem.* 1976, **1**, 260; 1977, **2**, 100; 1978, **3**, 272; K. K. Narang and R. A. Lal, *Curr. Sci.* 1977, **46**, 401; 1978, **47**, 793.
5. L. El-Sayed, M. F. Iskander and A. El-Toukhy, *J. Inorg. Nucl. Chem.* 1976, **38**, 2209; V. B. Mahale and G. H. Havanur, *Ind. J. Chem.* 1987, **26A**, 1063.
6. D. L. Arora, K. Lal, S. P. Gupta and S. K. Sahni, *Ind. J. Chem.* 1985, **24A**, 980; M. Navalelli, C. Pelizzi and G. Pelizzi, *Transition Met. Chem.* 1977, **2**, 35; C. Pelizzi, G. Pelizzi and G. Predieri, *J. Organomet. Chem.* 1984, **263**, 9; C. Lorenzini, G. Pelizzi, C. Pelizzi and G. Predieri, *J. Chem. Soc., Dalton Trans.* 1983, 721; 1983, 2155.
7. G. Paolucci, G. Marangoni, G. Bandoli and A. Dore, *J. Chem. Soc., Dalton Trans.* 1980, 459; G. Paolucci, S. Stelluto and S. Sitran, *Inorg. Chim. Acta* 1985, **110**, 19.
8. R. A. Lal, S. Das and R. K. Thapa, *Inorg. Chim. Acta* 1987, **132**, 129; R. A. Lal and S. Das, *Ind. J. Chem.* 1988, **27A**, 225.
9. R. A. Lal, K. N. Srivastava and S. Das, *Synth. React. Inorg. Met.-Org. Chem.* 1988, **18**, 837.
10. B. I. Kim, C. Miyake and S. Imoto, *J. Inorg. Nucl. Chem.* 1974, **36**, 2015.
11. W. J. Geary, *Coord. Chem. Rev.* 1971, **7**, 81.
12. R. A. Lal, H. Askari, S. S. Bhattacharjee and V. K. Gautam, unpublished results.
13. R. J. Butcher, J. Jasinki, G. M. Mockler and E. Sinn, *J. Chem. Soc., Dalton Trans.* 1976, 1099.
14. R. M. Silverstein and G. C. Bassler, *Spectrometric Identification of Organic Compounds*. Wiley, New York (1967).
15. M. Mikami, I. Nakagawa and T. Shimanouch, *Spectrochim. Acta* 1967, **23A**, 1037; K. Nakamoto, *Infrared Spectra of Inorganic and Coordination Compounds*, pp. 152, 167. Wiley-Interscience, New York (1970).

16. G. C. Percy and D. A. Thornton, *J. Inorg. Nucl. Chem.* 1972, **34**, 3369, 3351; G. C. Percy and D. A. Thornton, *J. Inorg. Nucl. Chem.* 1973, **35**, 2719; G. C. Percy, *J. Inorg. Nucl. Chem.* 1975, **37**, 2071.

17. R. J. H. Clark, *J. Chem. Soc.* 1962, 1372; R. J. H. Clark and C. S. Williams, *Chem. Ind. (London)*, 1964, 1317; R. J. H. Clark and C. S. Williams, *Inorg. Chem.* 1965, **4**, 350.

Polyhedron Vol. 8, No. 21, pp. 2535–2541, 1989
Printed in Great Britain

0277–5387/89 $3.00+.00
© 1989 Pergamon Press plc

EXTRACTION OF CADMIUM(II) BY MIXTURES OF ORGANOPHOSPHORUS COMPOUNDS

I. CASAS, N. MIRALLES, A. M. SASTRE* and M. AGUILAR

Dpt. d'Enginyeria Química, E.T.S.E.I.B., Avd. Diagonal 647, 08028 Barcelona, Spain

(*Received* 24 *April* 1989; *accepted* 24 *May* 1989)

Abstract—The extraction of cadmium(II) by mixtures of di(2-ethylhexyl)phosphoric acid (HDEHP) and trioctylphosphine oxide (TOPO) dissolved in tetradecane from aqueous chloride solution has been studied at 25°C. The distribution of metal has been determined as a function of both HDEHP and TOPO concentration. Distribution data have been treated numerically using the program LETAGROP–DISTR, and the composition of the extracted species into the organic phase has been determined. The extraction constants for these species are given.

In a series of previous papers the extraction of divalent metal ions by organophosphorus extractants dissolved in commercial diluents has been studied.[1,2]

As a part of this series, the extraction of cadmium(II) with di(2-ethylhexyl)phosphoric acid (henceforth HDEHP in the text and HA in formulae) has been thoroughly studied and the system has been described in terms of species and extraction constants,[3] to establish, as in the earlier work, if the speciation in the organic phase could provide certain differences in composition which could be utilized for the design of separation methods.[4]

A step forward in the aims of this work is to study the possibility of using combinations of extractants to investigate the appearance of a synergic effect that could increase the extraction of the metal ion. The first type of synergistic system classified by Healy[5] consisting of the mixture of acidic plus neutral extractants was selected for this purpose. This particular system has shown its possibilities, for instance, in the extraction of rare earth elements.[6] Subsequent work revealed, however, that the phenomenon can be realized in a variety of extractant combinations and be effective for a number of metals.[7]

Since the extraction of cadmium by HDEHP is well known, as explained above, this organophosphorus compound was selected as the acidic extractant. For the selection of the neutral one, it was found that the recovery of cadmium(II) using this kind of extractant has been undertaken by several authors[8–10] and the compounds which are most frequently used are tri-*n*-butylphosphate (TBP) and trioctylphosphine oxide (henceforth TOPO in the text and S in formulae).

The possibilities of finding synergisms which might be used for Zn/Cd separations have also been studied with mixtures of HDEHP and either TOPO or TBP, but no effort to determine the composition of the extracted species and their equilibrium constants has been carried out. On the other hand, the addition of TBP to the system Zn–HDEHP has been found to decrease the extraction, whereas the addition of TOPO to the same system causes an increase in the distribution ratio at low concentrations and a decrease at higher concentrations of TOPO.[11]

In this context, some difficulties arise mainly because organophosphorus compounds interact in the organic phase and may affect the interpretation of the data. For this reason several studies describing the behaviour of the HDEHP–TOPO system were undertaken.[12]

This work is a detailed study of the extraction of cadmium(II) in chloride medium by mixtures of HDEHP–TOPO dissolved in tetradecane. Its objective is to define the system in terms of the composition of the extracted species and their equilibrium constants, as well as the interaction species formed between the organophosphorus extractants.

* Author to whom correspondence should be addressed.

EXPERIMENTAL

Reagents

Di(2-ethylhexyl)phosphoric acid was supplied by BDH. Its purity was determined by potentiometric titration of an 80% ethanol solution of the acid with NaOH (0.1 mol dm^{-3}) using Gran plots.[13] The purity was found to be 98.2%. Trioctylphosphine oxide, supplied by Merck p.a., was used without further purification. Tetradecane, supplied by PETRESA, is a commercial hydrocarbon with the following characteristics: density at 15°C 0.768; aromatic content (ppm) 215; water content (ppm) 50 max.; boiling point at 760 mm Hg 253.7°C; distribution (%): C_{13}, 1.2; C_{14}, 98.2; C_{15}, 0.1. Tetradecane was washed with NaOH (0.1 mol dm^{-3}), distilled water, HCl (0.1 mol dm^{-3}) and finally distilled water until no chloride ions were detected in the aqueous solution. Sodium chloride, used as ionic medium, was prepared as described in ref. 14. Hydrochloric acid, Merck p.a., was used without further purification. A stock solution of acid was prepared and standardized against HgO and NaI.[15] Cadmium chloride, Merck p.a., was used without further purification. A stock solution was prepared. The cadmium concentration of the stock solution was determined by complexometric titration with EDTA using eriochrome black T as indicator.[16]

Extraction procedure

All experiments were carried out at 25°C. The phases in contact had the following composition: aqueous phase: (Na^+, H^+, Cd^{2+}) Cl^-, 0.1 mol dm^{-3}; organic phase: C mol dm^{-3} of HA and B mol dm^{-3} of S in tetradecane.

The volumes (15 cm^3) of each phase were shaken out mechanically in stoppered glass tubes over 30 min, which was enough time to reach equilibrium, and subsequently the tubes were centrifuged.

The cadmium content in the aqueous phase was determined using a 2380 Perkin–Elmer atomic absorption spectrophotometer. The metal in the organic phase was stripped from an aliquot by dilute nitric acid and determined in the same way.

RESULTS AND DISCUSSION

The distribution coefficient of cadmium(II) between the organic and aqueous phases was obtained directly as the ratio of the total cadmium concentration in both phases:

$$D = \frac{[Cd^{II}]_{org}}{[Cd^{II}]_{aq}}. \quad (1)$$

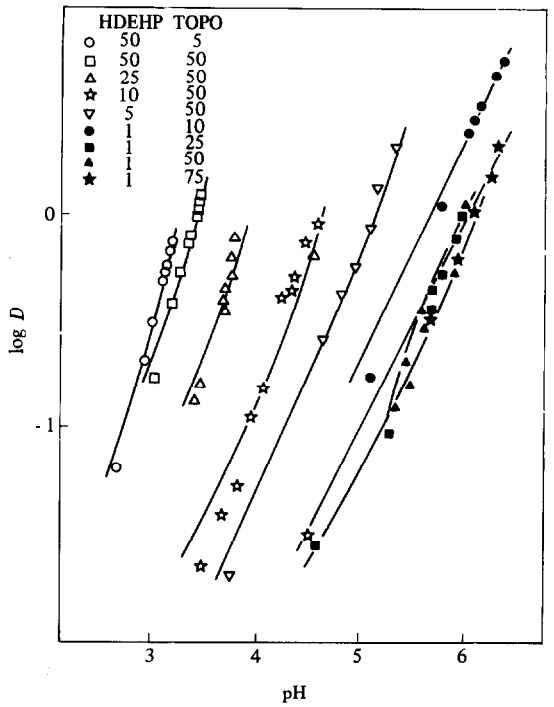

Fig. 1. log D plotted as a function of pH for different total HDEHP and TOPO concentrations in tetradecane at 0.1 mol dm^{-3} ionic strength in chloride medium. The full lines have been calculated using the constants given in Table 2.

Values of D were measured as a function of pH for different total HDEHP and TOPO concentrations, which ranged from 0.001 to 0.05 M and from 0 to 0.075 M, respectively. The experimental results are shown in Fig. 1.

The extraction of cadmium(II) with a mixture of the acid extractant, HA, and a neutral organophosphorus compound, S, can be written as:

$$Cd^{2+} + (p+q)[HA]_{org} + sS_{org} + (2-p)Cl^- = [CdA_pCl_{(2-p)}(HA)_qS_s]_{org} + pH^+. \quad (2)$$

β_{pqs} is the formation constant defined by

$$\beta_{pqs} = \frac{[CdA_pCl_{(2-p)}(HA)_qS_s]_{org}[H^+]^p}{[Cd^{2+}][HA]_{org}^{(p+q)}[S]_{org}^s[Cl^-]^{(2-p)}}. \quad (3)$$

Due to the low metal concentrations employed, the presence of polynuclear species was not considered.

From the literature,[12] the interaction between TOPO and HDEHP in these systems can be written as

$$HA + S = HA \cdot S \quad (4)$$

$$2HA + S = (HA)_2 \cdot S. \quad (5)$$

By taking into account eqs (4) and (5), the mass balance equations for HDEHP and TOPO can be

written as:

$$C_{HA} = [HA] + 2[(HA)_2] + [HA \cdot S] + 2[(HA)_2 \cdot S] + \Sigma_p \Sigma_q [CdA_p Cl_{(2-p)} (HA)_q S_s] \quad (6)$$

$$C_S = [S] + [HA \cdot S] + [(HA)_2 \cdot S] + \Sigma_s CdA_p Cl_{(2-p)} (HA)_q S_s, \quad (7)$$

respectively.

In the present case, no approximation can be made in the mass balance equations due to the strong interaction between the two extractants, and because metal complexes are not negligible in the organic phase. For this reason data have only been treated numerically.

Numerical treatment was performed using the general minimizing program LETAGROP–DISTR,[17] which is especially adapted to the treatment of distribution data. The program searches for the best set of formation constants that would minimize the error squares sum defined by:

$$U = \Sigma (\log D_{exp} - \log D_{calc})^2, \quad (8)$$

where D_{exp} is the distribution ratio of cadmium determined experimentally and D_{calc} is the calculated D value obtained by solving the mass balance equation for HDEHP, TOPO, Cd^{2+} and Cl^-. The program also calculates the standard deviation $\sigma(\log D)$ defined by

$$\sigma(\log D) = [\Sigma (\log D_{exp} - \log D_{calc})^2 / N_p]^{1/2}. \quad (9)$$

Several calculations with LETAGROP–DISTR were carried out in order to investigate the best set of complexes which would fit the experimental data. The criteria used to select the set of complexes used as input were as follows. First, a set of species including the complexes obtained in both Cd–HDEHP[3] and Cd–TOPO[9] systems, as well as the TOPO–HDEHP[12] interaction was tried. Next, because the slope of the lines log D vs pH varies between 1 and 2 (Fig. 1), the presence of mixed species in the organic phase with p [eq. (2)] ranging from 0 to 2 could give a closer description of the composition of the system. For this reason several sets of complexes including mixed species were used as input. The results obtained in these calculations, listed in Table 1, show the improvement obtained.

Furthermore, the equilibrium constants for the species formed were also determined. The results are given in Table 2. Subsequently, these values were used to calculate the full lines on Fig. 1 by means of the program HALTAFALL.[18] The good agreement obtained between both experimental and calculated values gives great confidence to the proposed model. The fit of the data is also illustrated in Fig. 2, where $\log D_{exp} - \log D_{calc}$ has been plotted against pH.

The distribution of species has been calculated as a function of HDEHP concentration for a total constant TOPO concentration at pH 4. The program HALTAFALL[18] has also been used for these calculations with the constants given in Table 2. The results obtained are shown in Figs 3 and 4.

The results so far obtained can be summarized as follows. The extraction of cadmium(II) from chloride media using mixtures of HDEHP and TOPO dissolved in tetradecane may be explained by the formation in the organic phase of the species $CdA_2(HA)_2$, $[CdA_2(HA)(TOPO)]$, $[CdACl(HA)(TOPO)]$, $[CdACl(TOPO)_3]$ and $[CdCl_2(TOPO)_2]$. Among them, the predominant species in the organic phase are $CdA_2(HA)_2$ and $[CdA_2(HA)(TOPO)]$ when the HDEHP–TOPO ratio is higher or lower than 1.5, respectively, in the experimental conditions employed (see Figs 3 and 4).

The value of the constant for the formation of the species $CdA_2(HA)_2$ is in good agreement with the value previously reported,[3] whereas $CdA_2(HA)_3$ has not been found to be predominant at the low HDEHP–Cd ratio employed in the experiments.

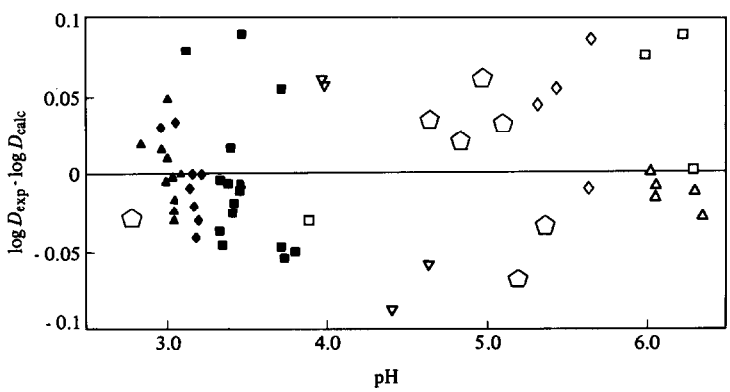

Fig. 2. Values of ($\log D_{exp} - \log D_{calc}$) calculated by the LETAGROP program plotted against pH.

Table 1. Some details of the calculations with LETAGROP–DISTR

Species	U	$\sigma(\log D)$	Rejected species
HA TOPO $(HA)_2TOPO$ $CdA_2(HA)_2$ $CdA_2(HA)_3$ $CdCl(TOPO)_2$	6.258	0.285	HA TOPO
HA TOPO $(HA)_2TOPO$ $CdA_2(HA)_2$ $CdA_2(HA)_3$ $CdA_2(HA)_2TOPO$ CdACl(HA)TOPO $CdACl(HA)(TOPO)_2$ $CdACl(TOPO)_2$ $CdACl(TOPO)_3$	0.477	0.094	$CdACl(HA)(TOPO)_2$
HA TOPO $(HA)_2TOPO$ $CdA_2(HA)_2$ $CdA_2(HA)_3$ $CdA_2(HA)_2TOPO$ CdACl(HA)TOPO $CdACl(HA)_3(TOPO)$ $CdACl(TOPO)_2$ $CdACl(TOPO)_3$	0.431	0.089	$CdA_2(HA)_2$
HA TOPO $(HA)_2TOPO$ $CdA_2(HA)_2$ $CdA_2(HA)TOPO$ $CdA_2(HA)_2TOPO$ $CdACl(HA)_4$ CdACl(HA)(TOPO) $CdACl(HA)_3(TOPO)$ $CdACl(TOPO)_2$	0.357	0.076	$CdACl(HA)_3(TOPO)$
HA TOPO $(HA)_2TOPO$ $CdA_2(HA)_2$ $CdA_2(HA)TOPO$ $CdCl(HA)(TOPO)_2$ $CdACl(TOPO)_2$	0.290	0.071	
HA TOPO $(HA)_2TOPO$ $CdA_2(HA)_2$ $CdA_2(HA)TOPO$ $CdA_2(TOPO)_2$ CdACl(HA)TOPO $CdACl(HA)(TOPO)_2$ $CdACl(TOPO)_2$	0.250	0.065	$(HA)_2TOPO$
HA TOPO $(HA)_2TOPO$ $CdA_2(HA)_2$ $CdA_2(HA)TOPO$ $CdA_2(TOPO)_2$ CdACl(HA)TOPO $CdACl(HA)_2(TOPO)$ $CdACl(TOPO)_3$ $CdACl(TOPO)_2$	0.220	0.064	$CdACl(HA)_2TOPO$ $(HA)_2TOPO$

Table 1—(*continued*)

Species	U	$\sigma(\log D)$	Rejected species
HA TOPO $(HA)_2TOPO$ $CdA_2(HA)_2$ $CdA_2(HA)TOPO$ $CdA_2(TOPO)_2$ CdACl(HA)TOPO CdACl(HA)(TOPO) $CdACl(TOPO)_2$ $CdACl(TOPO)_3$	0.216	0.063	$CdACl(TOPO)_2$ HA_2TOPO
HA TOPO $(HA)_2TOPO$ $CdA_2(HA)_2$ $CdA_2(HA)TOPO$ $CdA_2(TOPO)_2$ CdACl(HA)TOPO $CdACl(TOPO)_3$	0.191	0.058	$(HA)_2TOPO$
HA TOPO $(HA)_2TOPO$ $CdA_2(HA)_2$ $CdA_2(HA)TOPO$ $CdA_2(TOPO)_2$ CdACl(HA)TOPO $CdACl(TOPO)_3$ $CdACl_2(TOPO)_2$	0.189	0.058	$(HA)_2TOPO$ $CdA_2(TOPO)_2$

Species rejected when $\beta_{i,j} = 0$.

Table 2. Species and formation constants calculated with the program LETAGROP–DISTR

Species	$\log \beta_{pqs}$
HA TOPO	3.78 ± 0.05
$CdA_2(HA)_2$	6.00 ± 0.04
$CdA_2(HA)TOPO$	4.7 ± 0.2
CdACl(HA)TOPO	4.9 ± 0.1
$CdACl(TOPO)_3$	3.24 ± 0.03
$CdCl_2(TOPO)_2$	-0.78 ± 0.01

Table 3. The equilibrium constants for the system TOPO–HDEHP found in the literature

Solvent	$\log K^a$	$\log \beta_{011}{}^b$	Reference
Octane	1.38	3.73	12
Benzene	1.15	3.50	11
Kerosene	1.48	3.83	19, 20
Tetradecane	—	3.78	This work

[a] K is the formation constant defined by:

$$K = \frac{[HA \cdot TOPO]_{org}}{[(HA)_2]_{org}^{1/2}[TOPO]_{org}}.$$

[b] β_{011} is the formation constant of reaction (2) calculated from the expression $\beta_{011} = K \times K_D^{1/2}$, where K_D is the dimerization constant defined by $2HA_{org} = (HA)_{2org}$ (Ref. 21).

On the other hand, the extraction of metals has been demonstrated to be an effective method for determining the interaction between the extractants present in the organic phase. The results obtained show that interactions between the organophosphorus compounds in the organic phase are due only to one species HA · TOPO, whereas $(HA)_2TOPO$, which has previously been found by different authors, is negligible in the experimental conditions employed in the present study. As can be seen from Table 3, the interaction constant for the formation of the HA · TOPO species is in good agreement with the values previously reported.

The antisynergism observed in the extraction of cadmium by HDEHP in presence of TOPO can be explained by taking into account the interaction between the organophosphorus extractants, as can be seen in Figs 3 and 4. This effect is clearly observed in Fig. 5, where an increase in the TOPO–HDEHP ratio increases the HA · TOPO species in the organic

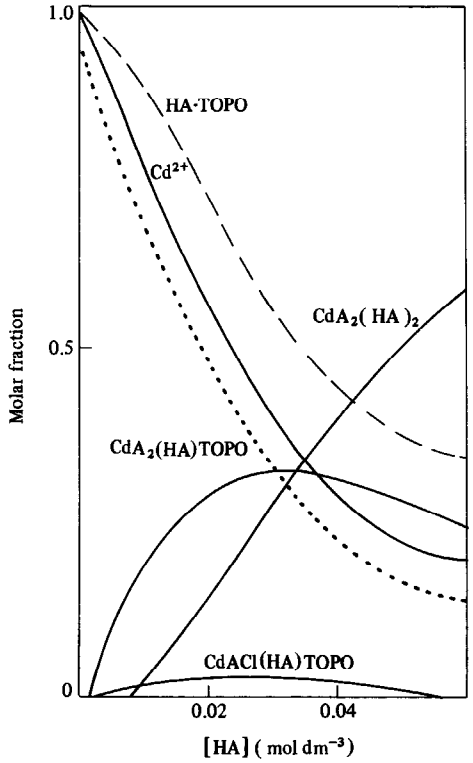

Fig. 3. Fraction of the different species present in the organic phase plotted as a function of the total HDEHP concentration for a constant total TOPO concentration of 0.025 mol dm^{-3}. The dotted line (....) shows the fraction of cadmium in the aqueous phase in the absence of TOPO (Ref. 3).

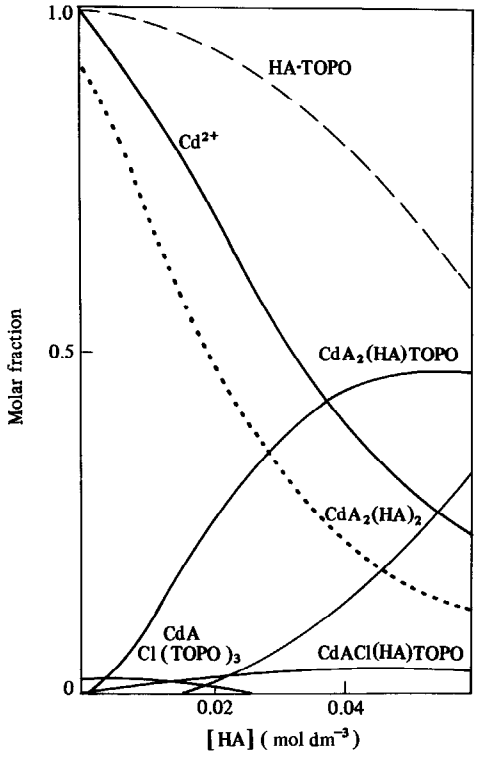

Fig. 4. Fraction of the different species present in the organic phase plotted as a function of the total HDEHP concentration for a constant total TOPO concentration of 0.050 mol dm^{-3}. The dotted line (....) shows the fraction of cadmium in the aqueous phase in absence of TOPO (Ref. 3).

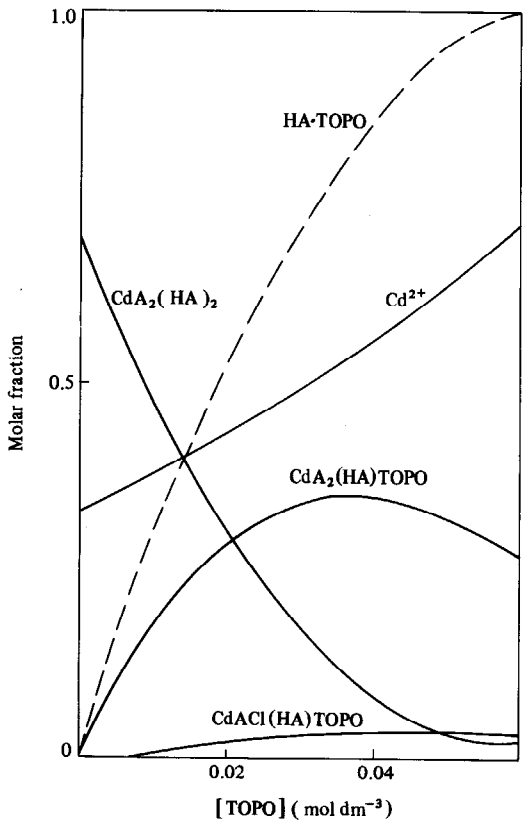

Fig. 5. Fraction of the different species present in the organic phase plotted as a function of the total TOPO concentration for a constant total HDEHP concentration of 0.025 mol dm^{-3}.

phase, which decreases the effective concentration of extractant and thus the extraction of cadmium.

REFERENCES

1. A. M. Sastre, N. Miralles and M. Aguilar, *Chem. Scripta* 1984, **24**, 44.
2. A. M. Sastre and M. Muhammed, *Hydrometallurgy* 1984, **12**, 177.
3. I. Casas, N. Miralles, A. M. Sastre and M. Aguilar, *Polyhedron* 1986, **5**, 2039.
4. M. Muhammed and A. M. Sastre, *Proc. Symp. Ion Exchange and Solvent Extraction*, II-49, Oslo (1982).
5. T. V. Healy, *Gmelin Handbuch*, p. 360. Vol. 21, Part D2, No. 21. Springer, Berlin (1975).
6. Z. Kolarik, *J. Inorg. Nucl. Chem.* 1972, **34**, 2911.
7. Y. Marcus and A. S. Kertes, *Ion Exchange and Solvent Extraction of Metal Complexes*, p. 836. Wiley, New York (1969).
8. N. M. Rice and M. R. Smith, *Can. Metallurg. Quart.* 1973, **12**, 341.
9. N. M. Rice and M. R. Smith, *J. Appl. Chem. Biotechnol.* 1975, **25**, 379.
10. T. Sato and T. Nakamura, *Hydrometallurgy* 1980, **6**, 3.
11. Pushparaja and M. Sudersanan, *Ind. J. Chem.* 1980, **19A**, 998.
12. H. T. Baker and C. F. Baes, *J. Inorg. Nucl. Chem.* 1962, **24**, 1277.
13. G. Gran, *Analyst* 1952, **77**, 661.
14. Some Laboratory Methods in Current Use at the Department of Inorganic Chemistry, The Royal Institute of Technology, Mimeograph (1959).
15. A. I. Vogel, *Textbook of Quantitative Inorganic Analysis*, 4th edn. Longmans, London (1964).
16. G. Schwarzenbach and H. A. Flashka, *Complex Titrations*. Methuen, London (1969).
17. D. H. Liem, *Acta Chem. Scand.* 1971, **25**, 1521.
18. N. Ingri, W. Kakotowicz, L. G. Sillen and B. Warnquist, *Talanta* 1967, **14**, 1261.
19. C. A. Blake, C. F. Baes, K. B. Brown, C. F. Coleman and S. C. White, *Proc. Conf. Peaceful Uses At. En.* 1958, **28**, 289.
20. H. Ihle, H. Michael and A. Murrenhoff, *J. Inorg. Nucl. Chem.* 1963, **25**, 734.
21. Z. Kolarik, *Coll. Czech. Chem. Commun.* 1967, **32**, 311.

Polyhedron Vol. 8, No. 21, pp. 2543–2549, 1989
Printed in Great Britain

0277–5387/89 $3.00+.00
©1989 Pergamon Press plc

THE ELECTROCHEMICAL SYNTHESIS OF NEUTRAL COPPER(II) COMPLEXES OF SCHIFF BASE LIGANDS: THE CRYSTAL STRUCTURES OF BIS-{N-[2-(3-METHYLPYRIDYL)]-5-METHOXYSALICYLIDENEIMINATO}COPPER(II) AND BIS-{N-[2-(6-METHYLPYRIDYL)]-SALICYLIDENEIMINATO}COPPER(II)

A. CASTIÑEIRAS, J. A. CASTRO, M. L. DURAN, J. A. GARCIA-VAZQUEZ, A. MACIAS, J. ROMERO and A. SOUSA*

Departamento de Química Inorgánica, Universidad de Santiago, Santiago de Compostela, Spain

(*Received* 1 *March* 1989; *accepted* 5 *June* 1989)

Abstract—Neutral copper(II) complexes of Schiff bases derived from substituted salicylaldehydes and 2-aminopyridine methyl derivatives have been synthesized by an electrochemical procedure. The crystal and molecular structure of bis{N-[2-(3-methylpyridyl)]-5-methoxysalicylideneiminato}copper(II) and of bis{N-[2-(6-methylpyridyl)]-salicylideneiminato}copper(II) have been determined by X-ray diffraction. The former compound crystallizes in the monoclinic space group $C2/c$ with four molecules in the unit cell and cell constants $a = 16.784(2)$, $b = 16.344(2)$ and $c = 11.211(2)$ Å, and $\beta = 124.08(1)°$, while the other complex crystallizes in the monoclinic space group $P2_1/c$ with two molecules in a cell of dimensions $a = 12.456(1)$, $b = 7.812(2)$ and $c = 12.047(2)$ Å, and $\beta = 110.48(1)°$. In both structures, the metals adopt square-planar coordination geometries and the pyridyl nitrogen atoms are not coordinated. The electronic and IR spectra of the complexes are discussed and related to the structure.

Schiff bases derived from substituted salicylaldehydes and 2-aminopyridine derivatives (**1**) have previously been studied as potentially terdentate ligands. Osipov *et al.*[1] have isolated complexes of the type CuL_2 (L = anion of **1** in which X = H, 5-Cl, 5-Br, 5-NO_2 or 5,6-benzo and Y = H), and suggested a tetrahedral (or pyramidal) structure for them. Yamada and Yamanouchi[2] have also synthesized complexes of the type $ML_2 \cdot nH_2O$ (where M = Co^{II}, Ni^{II}, Cu^{II}, Zn^{II} or Pd^{II}). On the basis of electronic spectroscopic measurements they deduced square-planar structures for the copper complexes. While steric considerations led them to suggest that the Schiff bases were bidentate ligands, with the pyridine nitrogen uncoordinated in all complexes except one nickel(II) complex in which the ligand is terdentate. Kolawole[3] studied the oxovanadium(IV) complexes of these ligands, and from IR and electronic spectroscopic data concluded that the ligands are acting bidentate through the phenolic oxygen and either the azomethine or pyridine nitrogen (depending on electronic effects of the substituents on the phenyl ring). Recently, Parashar *et al.*[4] prepared the complex CuL_2 (where X = Y = H), and from spectroscopic properties deduced that the environment at the metal was octahedral and the ligand terdentate.

The electrochemical synthesis described here constitutes a simple new route to neutral CuL_2 ($L = L^1$—L^{13}) complexes and it was therefore of interest to determine the structure of some complexes in order to establish the facultative properties of the ligand.

* Author to whom correspondence should be addressed.

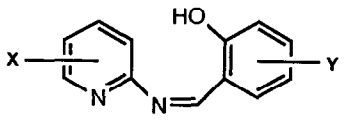

(1)

X	Y				
	H	5-OCH_3	3-OC_2H_5	5-Br	5-Cl
H	HL^1	HL^2	—	HL^3	HL^4
3-CH_3	HL^5	HL^6	—	HL^7	HL^8
6-CH_3	HL^9	HL^{10}	HL^{11}	HL^{12}	HL^{13}

EXPERIMENTAL

Acetonitrile, aldehydes and amines were used as supplied. Copper (Ega Chemie) was used as plates (approx. 2×2 cm square). The ligands were prepared by reaction of equimolar amounts of the appropriate aldehyde and amine in benzene until the theoretical amount of water had been collected in a Dean–Stark trap; the solid product was washed with dry diethyl ether and its purity checked by recording its IR and ^1H NMR spectra.

Preparation of complexes

The electrochemical method used in the synthesis of the copper complexes was similar to that described by Tuck.[5] The cell was a 100 cm^3 tall-form beaker fitted with a rubber bung through which the electrical leads passed. The foil anode was suspended from a platinum wire and the cathode was also a platinum wire. The ligand was dissolved in acetonitrile and a small amount of tetramethylammonium perchlorate was added to the solution. Direct current was obtained from a purpose-built d.c. power supply. The cell can be summarized as

$$Pt_{(-)}/CH_3CN + HL/Cu_{(+)}.$$

During electrolysis hydrogen was evolved at the cathode. In some cases insoluble compounds became visible within a few minutes, but in others crystals were formed slowly after concentration of the solution at room temperature. The solids obtained were washed with acetonitrile and diethyl ether and dried at room temperature. The experimental conditions are set out in Table 1.

Physical measurements

Microanalyses were performed using a Perkin–Elmer 240B microanalyser. IR spectra were recorded in Nujol and hexachlorobutadiene mulls between CsI plates on a Perkin–Elmer 180 spectrophotometer. Proton NMR spectra were recorded on a Bruker WM at 250 MHz. Solid reflectance spectra were recorded on a Unicam 5P735 diffuse reflectance spectrophotometer.

Crystal structure analysis

$[CuL^6_2]$, *crystal data.* $C_{28}H_{26}CuN_4O_4$, $M = 546.08$, amber prismatic crystal of approximate dimensions $0.20 \times 0.12 \times 0.10$ mm, monoclinic,

Table 1. Experimental conditions for the electrochemical synthesis

Ligand	Amount of ligand (g)[a]	Initial voltage (V)[b]	Time (h)	Metal dissolved (mg)	E_r (mol F^{-1})
HL^1	0.40	20	2	47	0.99
HL^2	0.38	13	1.5	36	1.01
HL^3	0.41	15	1.5	35	0.98
HL^4	0.20	15	1	24	1.01
HL^5	0.55	15	1.25	31	1.04
HL^6	0.38	10	1.5	36	1.01
HL^7	0.41	18	1.5	39	1.10
HL^8	0.30	20	1.5	35	0.98
HL^9	0.50	25	1.25	30	1.01
HL^{10}	0.37	20	1.5	36	1.01
HL^{11}	0.38	13	1.5	35	0.98
HL^{12}	0.38	10	1.5	36	1.01
HL^{13}	0.25	15	1.25	29	0.98

[a] Plus $[NMe_4]ClO_4$ (*ca* 10 mg).
[b] Voltage to produce a current of 10 mA.

$C2/c$ (no. 15), $a = 16.784(2)$, $b = 16.344(2)$, $c = 11.211(2)$ Å, $\beta = 124.08(1)°$, $V = 2547.11$ Å^3, $Z = 4$, $D_x = 1.424$ g cm^{-3}, λ(Mo-K_α) = 0.71073 Å, $\mu = 8.977$ cm^{-1}, $F(000) = 1132$.

[CuL_2^9], *crystal data.* $C_{26}H_{22}CuN_4O_2$, $M = 486.03$. Dark amber prismatic crystal of approximate dimensions $0.20 \times 0.09 \times 0.20$ mm, monoclinic, $P2_1/c$ (no. 14), $a = 12.456(1)$, $b = 7.812(2)$, $c = 12.047(2)$ Å, $\beta = 110.48(1)°$, $V = 1098.11$ Å^3, $Z = 2$, $D_x = 1.470$ g cm^{-3}, λ(Mo-K_α) = 0.71073 Å, $F(000) = 502$.

Data collection

Data for both crystals were obtained using an Enraf–Nonius CAD-4 four-circle diffractometer with graphite monochromated Mo-K_α radiation. The cell constants were determined from setting angles for 25 reflections. Reflections were measured at 296 K by the ω–θ scan technique with scan widths of $(1.10 + 0.35 \operatorname{tg}\theta)°$ and a maximum scan speed of 10° min^{-1}. The *hkl* range was $-19 < h < 19$, $k < 18$, $l < 12$ $(3 < \sigma < 24°)$ for CuL_2^6 and $-15 < h < 15$, $k < 9$, $l < 14$ $(3 < \sigma < 26°)$ for CuL_2^9. Of 4417 reflections measured for CuL_2^6 (including the systematic absences due to C-centering), 1994 were unique ($R_{int} = 0.015$). A total of 2433 reflections were collected for CuL_2^9, of which 2156 were unique ($R_{int} = 0.049$). The standard reflection varied by ±0.3% (for CuL_2^6) or ±0.1% (for CuL_2^9) of the mean intensity during data collection. Lorentz and polarization corrections and an empirical absorption correction[6] were applied; maximum and minimum transmission factors: CuL_2^6, 1.2650 and 0.8759; CuL_2^9, 1.2178 and 0.6652.

Solution and refinement of the structures

For both compounds, least-squares calculations were carried out on F, the function minimized being $\Sigma w(|F_o| - |F_c|)^2$ with $\omega^{-1} = \sigma^2(F_o)$.

[CuL_2^6]. The structure was solved by direct techniques and Fourier difference synthesis. Refinement was carried out using the 1551 reflections with $|I_o| > 3\sigma|I_o|$. In the final cycles of full-matrix least-squares refinement, all non-hydrogen atoms were treated anisotropically. A total of 222 parameters were refined. A correction for secondary extinction was applied: $F_{corr} = F_c(1 + kF_c^2/\sin 2\theta)^{0.25}$, where k refined to 2.7699×10^{-7} in the final run. At that stage, the R factors were $R = 0.030$, $R_w = 0.031$. The final difference map showed electron density maxima of 0.264 eÅ^{-3}.

[CuL_2^9]. The structure was solved by the Patterson method, which revealed the positions of all non-hydrogen atoms. Refinement was carried out using the 813 reflections with $|I_o| > 3\sigma|I_o|$. The positions of all hydrogen atoms were estimated geometrically and were not refined (C—H = 0.95 Å; $B_{iso} = 4.0$ Å^2). In the final least-squares cycles, copper, oxygen and nitrogen atoms were treated anisotropically. A total of 86 parameters were refined. At that stage, the R factors were $R = 0.058$ and $R_w = 0.066$. A final difference map showed electron density maxima of 0.413 eÅ^{-3}.

For both structures, scattering factors and corrections for anomalous dispersion were taken from *International Tables.*[7] Calculations were performed with the SHELXS-86[8] and SDP program systems[9] on a DECMicro VAXII computer. The atomic position coordinates, full list of bond lengths and angles and other crystallographic data have been deposited as Supplementary Publication No. CSD 53254. Copies can be obtained through the Fachinformations-zentrum Energie Physik Mathematik, D-7514 Eggenstein-Leopoldshafen.

RESULTS AND DISCUSSION

The analytical data reported in Table 2 show that an electrochemical procedure can be satisfactorily used for the synthesis of compounds of general formula CuL_2 ($L = L^1$–L^{13}). The electrochemical efficiency, defined as the amount of metal dissolved per Faraday of charge, was close to 1 mol F^{-1}, which is compatible with the following reaction scheme.[10]

Cathode: $HL + e^- \longrightarrow L^- + 1/2H_2$

Anode: $L^- + Cu \longrightarrow CuL + e^-$

$CuL + HL \longrightarrow CuL_2 + 1/2H_2$.

ORTEP views of the structures of CuL_2^6 and CuL_2^9 are shown in Figs 1 and 2 with the atom labelling used in the corresponding Table. The bond distances and angles, along with their associated estimated standard deviations are given in Table 3. Both complexes have similar structures, with the copper atom located at a crystallographic inversion centre and coordinated to the azomethine nitrogen and phenolic oxygen atoms of two symmetry related moieties. The pyridyl nitrogen atom is not coordinated to the copper. The configurations are exactly square-planar to within experimental accuracy. These structures differ from those proposed by Osipov *et al.*[1] and Parashar *et al.*,[4] but are very similar to that determined for bis{N-[2′-(2″-pyridyl)ethyl] -4, 6- dimethoxysalicylideneiminato} copper(II).[10]

The Cu—N distances (1.992 Å in CuL_2^6 and

Table 2. Analytical data for CuL_2 complexes

Complex	Colour	Found (calc.) (%)		
		C	N	H
CuL_2^1	Brown	62.5(62.9)	12.2(12.2)	4.0(3.9)
CuL_2^2	Brown	60.6(60.3)	11.0(10.8)	4.5(4.2)
CuL_2^3	Yellow	46.7(46.8)	9.1(9.1)	3.0(2.6)
CuL_2^4	Amber	55.4(54.7)	10.8(10.6)	3.4(3.0)
CuL_2^5	Green	63.9(64.2)	11.7(11.5)	4.8(4.5)
CuL_2^6	Amber	61.5(61.6)	10.4(10.3)	4.8(4.8)
CuL_2^7	Green	48.9(48.5)	8.5(8.7)	3.3(3.1)
$CuL_2^8 \cdot 2H_2O$	Green	53.0(52.8)	9.5(9.5)	4.0(4.1)
CuL_2^9	Amber	64.1(64.2)	11.5(11.5)	4.7(4.5)
CuL_2^{10}	Brown	61.0(61.6)	9.9(10.3)	4.7(4.8)
CuL_2^{11}	Brown	62.1(62.8)	9.5(9.8)	5.1(5.2)
CuL_2^{12}	Brown	48.7(48.5)	8.8(8.7)	3.2(3.1)
$CuL_2^{13} \cdot 2{,}5H_2O$	Brown	52.1(52.0)	9.3(9.3)	3.8(4.2)

2.002 Å in CuL_2^9) and Cu—O distances (1.874 Å in CuL_2^6 and 1.873 Å in CuL_2^9) are similar to those found in related salicylaldiminato complexes.[11–13] The N(2)—C(6) bonds are within the range 1.30±0.04 Å proposed for an N=C bond.[14] The C—O bond lengths are shorter than for C—O single bonds, but longer than for C=O double bonds.[15] In the aromatic ring the three C—C bonds farthest from the copper[C(8)—C(9), C(9)—C(10) and C(10)—C(11)] have an average length less than 1.40 Å, while the three bonds nearest to the metal atom [C(7)—C(8), C(7)—C(12) and C(11)—C(12)] have an average length greater than 1.40 Å. This agrees with the observations of Lingafelter and Braun.[11]

The IR spectra of the complexes (Table 4) show no bands assignable to ν(OH), and the characteristic phenolic ν(C—O) band is shifted towards higher

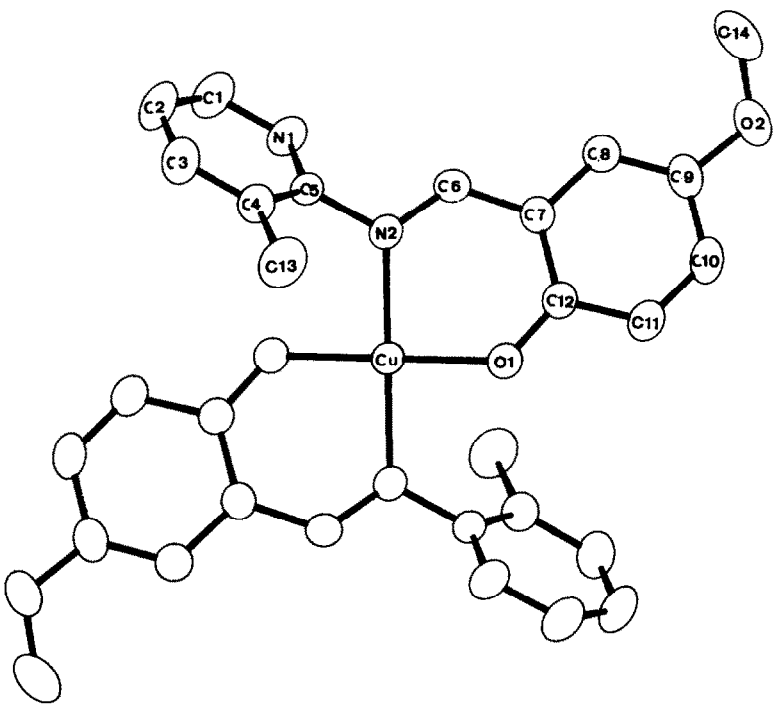

Fig. 1. The molecular structure of CuL_2^6.

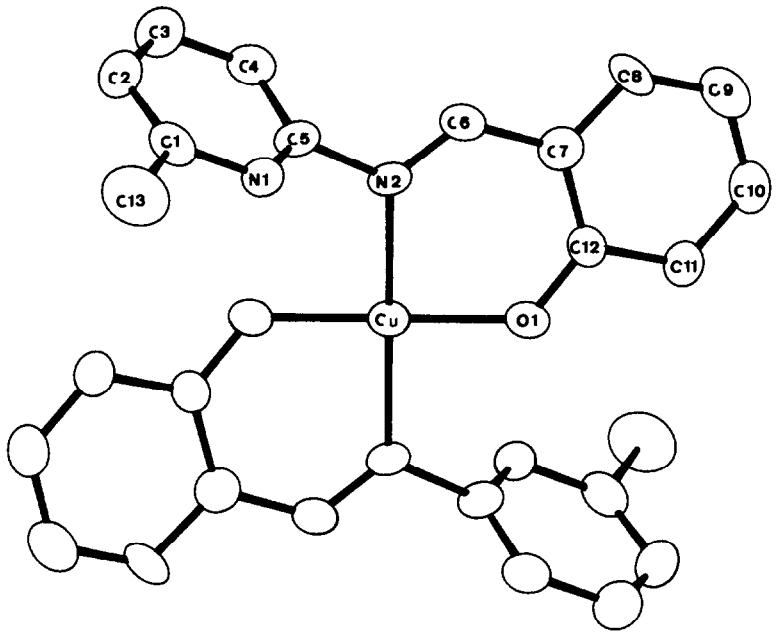

Fig. 2. The molecular structure of CuL_2^9.

Table 3. Selected bond distances and angles for both complexes

	CuL_2^6	CuL_2^9
	Bond lengths (Å)	
Cu—O(1)	1.874(2)	1.873(4)
Cu—N(2)	1.992(2)	2.002(5)
O(1)—C(12)	1.311(3)	1.288(7)
N(2)—C(6)	1.297(3)	1.269(9)
C(7)—C(8)	1.425(3)	1.40(1)
C(7)—C(12)	1.410(4)	1.420(9)
C(8)—C(9)	1.365(3)	1.37(2)
C(9)—C(10)	1.391(4)	1.36(2)
C(10)—C(11)	1.359(4)	1.378(9)
C(11)—C(12)	1.413(3)	1.416(9)
	Bond angles (°)	
O(1)—Cu—O(1)	180.1(4)	181.1(2)
O(1)—Cu—N(2)	91.42(7)	90.2(2)
O(1)—Cu—N(2)	88.58(7)	89.8(2)
N(2)—Cu—N(2)	180.1(3)	180.1(7)
C(5)—N(2)—C(6)	116.4(2)	116.8(6)
N(1)—C(5)—N(2)	116.3(2)	114.3(6)
N(2)—C(5)—C(4)	119.5(2)	121.1(6)
N(2)—C(6)—C(7)	125.8(2)	125.8(7)
C(6)—C(7)—C(12)	122.5(3)	122.5(6)
O(1)—C(12)—C(7)	124.0(3)	122.8(6)
O(1)—C(12)—C(11)	118.5(2)	119.5(6)

frequencies. The band attributable to ν(C=N) of the azomethine group undergoes a shift to lower frequencies in all of the metal complexes. In view of the X-ray structures, this behaviour can be taken as proof of coordination through the phenolic oxygen and azomethine nitrogen.

The pyridine ring stretching bands observed between 1610 and 1440 cm^{-1} and the ring deformation bands which appear at about 400 and 600 cm^{-1} are shifted to higher frequencies in the complexes. This behaviour might be taken to be a result of coordination by the pyridine nitrogen,[16,17] and Parashar[4] has accordingly suggested an octahedral copper(II) environment for CuL_2^1. However, this inference is not supported by the X-ray data. The above results clearly establish that for ligands with an azomethine group conjugated to a pyridine ring, caution must therefore be exercised in using IR data alone as an indication of whether the pyridine is coordinated or not.

The solid state electronic spectra of the complexes show two *d–d* bands at around 13500 and 17000 cm^{-1} except in the case of CuL_2^5, CuL_2^7 and CuL_2^8, for which only one broad band, presumably the envelope of the above two bands, is observed. In all cases, the band that appears at *ca* 21000 cm^{-1} may be assigned to a charge-transfer transition. These

Table 4. Some IR and electronic spectral data of compounds[a]

Compounds	ν(C=N)	ν(C—O)	Pyridine ring vibrations 8a	8b	19a	6a	16b	Electronic spectra (cm^{-1})		
CuL_2^1	1610 (1615)	1300 (1280)	1595 (1590)	1565 (1560)	1470 —	630 (625)	420 (410)	13160	16670(sh)	21800
CuL_2^2	1622 (1632)	1310 (1270)	1592 (1580)	1560 (1555)	1490 (1485)	630 (625)	415 (410)	13150	16670	20100
CuL_2^3	1610 (1640)	1290 (1275)	1590 (1585)	1565 (1555)	— (1475)	646 (630)	418 (415)	13300	18800(sh)	22600
CuL_2^4	1610 (1640)	1315 (1280)	1590 (1586)	1562 (1558)	— (1480)	632 (628)	420 (415)	13500	19200(sh)	21700
CuL_2^5	1606 (1610)	1320 (1280)	1580 (1560)	— —	— —	630 (620)	— —	15400		23150
CuL_2^6	1622 (1630)	1280 (1260)	1598 (1590)	1580 (1560)	— —	635 (605)	430 (420)	13700	18200(sh)	22300
CuL_2^7	1605 (1610)	1320 (1270)	1580 (1576)	— —	1485 (1480)	650 (630)	420 (400)	15500		23000
$CuL_2^8 \cdot 2H_2O$	1610 (1615)	1320 (1280)	1582 (1578)	— —	1490 (1484)	618 (600)	422 (400)	15600		23040
CuL_2^9	1608 (1620)	1320 (1285)	1590 (1580)	1568 (1560)	1505 (1495)	622 (610)	450 (435)	14100	18200(sh)	22500
CuL_2^{10}	1620 (1630)	1300 (1270)	1595 (1585)	1565 (1555)	1500 (1485)	630 (615)	440 (410)	13100	16260	20000
CuL_2^{11}	1608 (1615)	1290 (1270)	1595 (1595)	1570 (1560)	1490 (1485)	630 (615)	415 (410)	13300	16670	20700
CuL_2^{12}	1602 (1610)	1305 (1275)	1595 (1590)	1565 (1550)	1500 (1480)	650 (630)	445 (435)	13500	19400	21900
$CuL_2^{13} \cdot 2{,}5H_2O$	1605 (1615)	1310 (1280)	1598 (1590)	1570 (1555)	1485 (1480)	615 (610)	440 (435)	13300		22200

[a] Corresponding frequencies for the ligands are given in parentheses.

features are consistent with square-planar stereochemistry.[18] The X-ray structure confirms this geometry for CuL_2^6 and CuL_2^9, and thus suggests that the remaining complexes must also be square-planar.

REFERENCES

1. O. A. Osipov, V. I. Minkin, D. Sh. Verkhovodova and M. L. Knyazhanskii, *Zh. Neorg. Khim.* 1967, **12**, 1549.
2. S. Yamada and K. Yamanouchi, *Bull. Chem. Soc. Jpn* 1969, **42**, 2562.
3. G. A. Kolawole, *J. Coord. Chem.* 1987, **16**, 67.
4. R. K. Parashar, R. C. Sharma, A. Kumar and G. Mohan, *Inorg. Chim. Acta* 1988, **151**, 201.
5. J. J. Habeeb, D. G. Tuck and F. H. Walters, *J. Coord. Chem.* 1978, **8**, 27.
6. N. Walker and D. Stuart, *Acta Cryst.* 1983, **A39**, 159.
7. D. T. Cromer and J. T. Waber, *International Tables for X-ray Crystallography*, Vol. 4, Table 2.2B. Kynoch Press, Birmingham (1974).
8. G. M. Sheldrick, SHELXS-86, Program for Crystal Structure Determination. University of Cambridge, U.K. (1986).
9. B. A. Frentz and Associated Inc., College Station, Texas, and Enraf–Nonius, Delft, The Netherlands, SPD-PLUS, Structure Determination Package (1985).
10. N. M. Atherton, D. E. Fenton, G. J. Hewson, C. H. McLean, R. Bastida, J. Romero, A. Sousa and E. E. Castellano, *J. Chem. Soc., Dalton Trans.* 1988, 1059.
11. E. C. Lingafelter and R. L. Braun, *J. Am. Chem. Soc.* 1966, **88**, 2951.
12. P. C. Jain and V. K. Syal, *J. Chem. Soc., Dalton Trans.* 1973, 1908.

13. S. C. Bhatia, J. M. Bindlish, A. R. Saini and P. C. Jain, *J. Chem. Soc., Dalton Trans.* 1981, 1777.
14. J. N. Brown, R. L. Towns and L. M. Trefonas, *J. Am. Chem. Soc.* 1970, **92**, 7436.
15. G. Berthier and J. Serre, in *The Chemistry of the Carbonyl Group* (Edited by S. Patai), Chap. 1. Interscience, New York (1966).
16. N. S. Gill, R. H. Nutall, D. E. Scaife and D. W. Sharp, *J. Inorg. Nucl. Chem.* 1961, **18**, 79.
17. D. P. Madden, M. M. daMota and S. M. Nelson, *J. Chem. Soc. A* 1970, 890.
18. A. B. P. Lever, *Inorganic Electronic Spectroscopy*, 2nd edn. Elsevier, Amsterdam (1984).

Polyhedron Vol. 8, No. 21, pp. 2551–2555, 1989
Printed in Great Britain

0277–5387/89 $3.00+.00
© 1989 Pergamon Press plc

MOLECULAR HELICITY IN INORGANIC COMPLEXES; DOUBLE HELICAL BINUCLEAR NICKEL(II) COMPLEXES OF 2,2′:6′,2″:6″,2‴:6‴,2⁗-QUINQUEPYRIDINE(L): X-RAY CRYSTAL STRUCTURE OF $[Ni_2L_2(OAc)][PF_6]_3 \cdot 3MeCN$

EDWIN C. CONSTABLE* and MICHAEL D. WARD

University Chemical Laboratory, Lensfield Road, Cambridge CB2 1EW, U.K.

and

MICHAEL G. B. DREW and GEORGE A. FORSYTH

Department of Chemistry, The University, Whiteknights, Reading RG6 2AD, U.K.

(*Received* 18 *April* 1989; *accepted* 5 *June* 1989)

Abstract—The potentially pentadentate ligand, 2,2′:6′,2″:6″,2‴:6‴,2⁗-quinquepyridine (L, quinquepy) forms double helical complexes with first row transition metal cations of 2:2 stoichiometry. The X-ray crystal structure of the first such double helical bis-nickel(II) complex is reported, together with the electrochemical properties.

Helicity is a widespread phenomenon in natural systems,[1] although examples of this geometry in inorganic coordination compounds are relatively rare.[2] Recently it has been demonstrated that polydentate ligands based on oligopyridines spontaneously assemble binuclear double helical complexes upon reaction with transition metal cations.[3,4] In this paper we wish to report the first example of a structurally characterized double helical complex with cations other than those in group 1B.

EXPERIMENTAL

Quinquepy (L) was prepared by the literature method.[5] Electrochemical experiments were performed with a Princeton Applied Research Model 170 electrochemistry system, or with an Amel model 553 potentiostat connected to an Amel model 567 function generator and an Amel model 560-A recorder interface; all experiments were conducted using purified acetonitrile as solvent with 0.1 M $[^nBu_4N][BF_4]$ as the supporting electrolyte. For the cyclic voltammetry experiments, platinum beads were used as working and auxiliary electrodes with an Ag/AgCl electrode as reference; in all cases, ferrocene was added at the end of the experiment as an internal reference. Bulk electrolyses were performed using a cylindrical platinum gauze as the working electrode, with a smaller co-axial platinum gauze as the auxiliary electrode; an Ag/AgCl electrode was used as reference, calibrated against internal ferrocene at the end of each experiment. Coulometric measurements were made using an Amel model 731 integrator. IR spectra were recorded using a Perkin-Elmer 1710 FT spectrometer with the compound in compressed KBr pellets. ESR spectra were recorded on a Varian E109 spectrometer as powders, or in acetonitrile glasses at 4 or 77 K. Fast atom bombardment mass spectra were measured using a Kratos MS-50 spectrometer, with 3-nitrobenzyl alcohol as the supporting matrix.

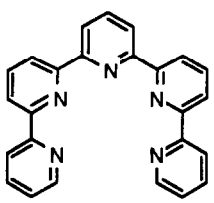

* Author to whom correspondence should be addressed.

Preparation of $[Ni_2L_2(OAc)][PF_6]_3$

Quinquepy (100 mg, 0.26 mmol) was added to a solution of $Ni(OAc)_2 \cdot 4H_2O$ (0.3 mmol) in boiling methanol (20 cm^3). The solution was heated until all of the ligand had dissolved, treated with $[NH_4][PF_6]$ and cooled, when $[Ni_2L_2(OAc)][PF_6]_3$ precipitated as a pale green microcrystalline powder (80%). The product was recrystallized by the diffusion of diethyl ether vapour into an acetonitrile solution to yield the tris-acetonitrile solvate. Found: C, 44.3; H, 2.7; N, 9.9; Ni, 8.2. Calc. for $Ni_2N_{10}C_{52}H_{37}O_2P_3F_{18}$: C, 45.0; H, 2.7; N, 10.1; Ni, 8.3%.

Crystal structure determination of $[Ni_2L_2(OAc)][PF_6]_3 \cdot 3MeCN$

Suitable single crystals were obtained as pale green blocks by the slow diffusion of diethyl ether vapour into an acetonitrile solution of the complex.

Crystal data for $[Ni_2L_2(OAc)][PF_6]_3 \cdot 3MeCN$

$Ni_2N_{13}C_{58}H_{46}O_2P_3F_{18}$, green crystals, $M = 1508.4$, triclinic, $a = 11.710(8)$, $b = 13.811(11)$, $c = 20.542(19)$ Å, $\alpha = 74.6(1)$, $\beta = 94.9(1)$, $\gamma = 75.0(1)°$, $U = 3051.8$ Å^3, $F(000) = 1420$, space group $P\bar{1}$, $Z = 2$, $D_m = 1.65$, $D_c = 1.63$ g cm^{-3}, Mo-K_α radiation ($\lambda = 0.7107$ Å), μ(Mo-K_α) = 8.1 cm^{-1}.

Data collection and processing

A crystal was set up to rotate about the a axis on a Stoe Stadi2 diffractometer and data were collected via variable width ω scan. Background counts were for 20 s and a scan rate of 0.0333° s^{-1} was applied to a width of $(1.5 + \sin\mu/\tan\theta)$. 7121 independent reflections with 2θ(max) of 50° were measured on a diffractometer, of which 1911 with $I > 2\sigma(I)$ were used in subsequent calculations.

Structure analysis and refinement

The structure was determined by the heavy-atom method. In the cation, the nickel atoms were refined anisotropically and the nitrogen, carbon and oxygen atoms isotropically. Hydrogen atoms were included in calculated positions for the cation. The PF_6 anions were refined anisotropically; it was possible that these atoms were disordered as we were unable to find a suitable model. The solvent molecules were difficult to disentangle. Five acetonitrile molecules were located; one was distinct and refined with 100% occupancy, while the other four formed two sets of two. The two molecules of each set were superimposed and contained atoms in common. Each of the four molecules were given 50% occupancy though some individual atoms were refined with 100% occupancy. Calculations were performed using full-matrix least-squares methods with a weighting scheme $w = 1/[\sigma^2(|F|) + 0.003|F|^2]$. Calculations were performed using SHELX 76 on the Amdahl V7 Computer at the University of Reading.[6] The final R values were $R = 0.102$ ($R_w = 0.113$). Molecular dimensions within the coordination spheres are presented in Table 1.*

RESULTS AND DISCUSSION

2,2′:6′,2″:6″,2‴:6‴,2⁗-Quinquepyridine was prepared by the method of Kröhnke as a white powder, and the structure of the ligand was confirmed by electron impact (M^+, m/z 387) and FAB (MH^+, m/z 388) mass spectroscopy, microanalysis and ^{1}H NMR spectroscopy.

The reaction of nickel(II) acetate with quinquepy in methanol results in the formation of a pale green solution, from which a pale green crystalline solid was obtained upon the addition of $[NH_4][PF_6]$. The FAB mass spectrum of the complex exhibited peaks at m/z 1035, 1094, 1180 and 1239, which may be assigned to the species $\{Ni_2L_2(PF_6)\}^+$, $\{Ni_2L_2(OAc)(PF_6)\}^+$, $\{Ni_2L_2(PF_6)_2\}^+$ and $\{Ni_2L_2(OAc)(PF_6)_2\}^+$. A fragmentation peak is observed at m/z 504 ($\{NiL(OAc)\}^+$) which suggests that the compound should be formulated as $[Ni_2L_2(OAc)][PF_6]_3$; microanalysis is in accord with this formulation. The complex is initially obtained as a hydrate, but drying *in vacuo* yields the anhydrous compound. Recrystallization from acetonitrile by vapour diffusion of diethyl ether into the solution yields an air-stable green tris-acetonitrile solvate.

The crystal and molecular structure of $[Ni_2L_2(OAc)][PF_6]_3$ has been determined, and the molecular structure of one of the enantiomers of the cation is presented in Fig. 1. Selected bond lengths and bond angles are listed in Table 1. The structural determination confirms the binuclear formulation, and reveals that the two quinquepy ligands have adopted a double helical configuration about the two nickel atoms. The double helical

* Atomic coordinates, displacement factor coefficients, full lists of bond lengths and bond angles, and lists of F_o/F_c values have been deposited as supplementary data with the Editor, from whom copies are available on request. Atomic coordinates have also been deposited with the Cambridge Crystallographic Data Centre.

Table 1. Selected bond lengths (Å) and bond angles (°) for the $[Ni_2L_2(OAc)]^{3+}$ cation

N(1A)—Ni(1)	2.160(0.020)	N(4A)—Ni(2)	2.082(0.022)
N(2A)—Ni(1)	1.857(0.032)	N(5A)—Ni(2)	2.160(0.023)
N(3A)—Ni(1)	2.248(0.022)	N(1B)—Ni(2)	2.086(0.027)
N(3B)—Ni(1)	2.288(0.020)	N(2B)—Ni(2)	2.163(0.022)
N(4B)—Ni(1)	1.879(0.028)	O(1)—Ni(2)	2.158(0.019)
N(5B)—Ni(1)	2.233(0.021)	O(2)—Ni(2)	2.110(0.020)
N(2A)—Ni(1)—N(1A)	78.5(1.1)	N(5A)—Ni(2)—N(4A)	77.7(0.8)
N(3A)—Ni(1)—N(1A)	153.1(0.9)	N(1B)—Ni(2)—N(4A)	109.7(0.9)
N(3A)—Ni(1)—N(2A)	74.6(1.1)	N(1B)—Ni(2)—N(5A)	172.2(0.8)
N(3B)—Ni(1)—N(1A)	86.4(0.7)	N(2B)—Ni(2)—N(4A)	107.0(0.8)
N(3B)—Ni(1)—N(2A)	111.8(1.0)	N(2B)—Ni(2)—N(5A)	101.8(0.8)
N(3B)—Ni(1)—N(3A)	104.4(0.7)	N(2B)—Ni(2)—N(1B)	78.5(0.9)
N(4B)—Ni(1)—N(1A)	98.4(1.0)	O(1)—Ni(2)—N(4A)	150.8(0.8)
N(4B)—Ni(1)—N(2A)	169.8(0.9)	O(1)—Ni(2)—N(5A)	90.0(0.8)
N(4B)—Ni(1)—N(3A)	107.9(1.0)	O(1)—Ni(2)—N(1B)	82.3(0.8)
N(4B)—Ni(1)—N(3B)	77.4(0.9)	O(1)—Ni(2)—N(2B)	101.4(0.8)
N(5B)—Ni(1)—N(1A)	99.9(0.7)	O(2)—Ni(2)—N(4A)	88.8(0.9)
N(5B)—Ni(1)—N(2A)	97.8(1.0)	O(2)—Ni(2)—N(5A)	87.1(0.8)
N(5B)—Ni(1)—N(3A)	82.9(0.8)	O(2)—Ni(2)—N(1B)	90.8(0.9)
N(5B)—Ni(1)—N(3B)	150.4(0.9)	O(2)—Ni(2)—N(2B)	163.1(1.0)
N(5B)—Ni(1)—N(4B)	73.1(1.0)	O(2)—Ni(2)—O(1)	63.8(0.9)

arrangement is emphasized in the skeletal space-filling diagram presented in Fig. 2, which shows the nitrogen atoms and the linking 2 and 6 carbon atoms of the ligands only.

The structure is very similar to that of the analogous $[Cu_2L_2(OAc)]^{3+}$ cation.[4] The two nickel atoms are both six-coordinate, but non-equivalent; Ni(1) is bonded to three consecutive nitrogen atoms from each quinquepy ligand, whilst Ni(2) is bonded to the two remaining nitrogen atoms from each quinquepy, and two oxygen atoms of a bidentate acetate. The principal differences between $[Cu_2L_2(OAc)]^{3+}$ and $[Ni_2L_2(OAc)]^{3+}$ are associated with the presence of a bidentate acetate group in the nickel compound as opposed to a monodentate ligand in $[Cu_2L_2(OAc)]^{3+}$. The IR spectrum of the complex exhibits absorptions at 1538 and 1425 cm^{-1}; the difference of 113 cm^{-1} is characteristic of a weakly bound bidentate acetate group. This is undoubtedly associated with a Jahn–Teller effect in the copper complex giving rise to two distinct Cu—O distances of 2.038(11) and 2.683(16) Å, whereas the two Ni—O distances are remarkably similar at 2.158(19) and 2.110(20) Å.

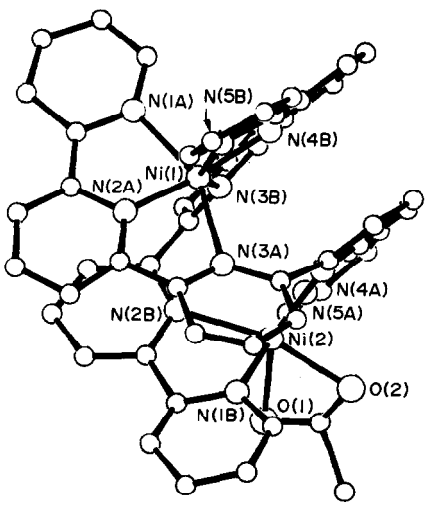

Fig. 1. The crystal and molecular structure of the $[Ni_2L_2(OAc)]^{3+}$ cation in $[Ni_2L_2(OAc)][PF_6]_3$, showing the numbering scheme adopted.

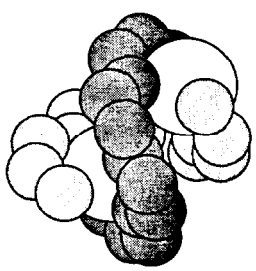

Fig. 2. A skeletal space filling depiction of the cation $[Ni_2L_2(OAc)]^{3+}$ showing only the nickel, the nitrogen and the linking carbon atoms of the ligand to emphasize the double helical geometry.

In all other respects, the metal atoms in $[Cu_2L_2(OAc)]^{3+}$ and $[Ni_2L_2(OAc)]^{3+}$ are in very similar distorted environments. The Ni(2)—N bond lengths closely resemble those observed for the five-coordinate copper atom in $[Cu_2L_2(OAc)]^{3+}$. For Ni(1) the bond lengths to the terminal pyridine rings of 2.160(20), 2.248(22), 2.288(20) and 2.233(21) Å are similar, and significantly shorter than those to the "central" rings of the terpyridine moiety of 1.857(32) and 1.879(28) Å. This reflects the helical twist of the ligand, which is most apparent at these rings, and results in considerable distortion of the "axial" interactions [∠N(3A)—Ni—N(1A) 153.1(9)°, ∠N(5B)—Ni—N(3B) 150.4(9)°]. Despite the differences in coordination number, the structure of $[Ni_2L_2(OAc)]^{3+}$ does not differ dramatically from that of $[Cu_2L_2(OAc)]^{3+}$, and serves to emphasize the structural rôle played by the stacked double helical array of ligands in dictating the geometry of the final complex.

The quinquepy ligands are principally twisted about the interannular bonds between the bidentate and terdentate portions of the molecules. The two quinquepy ligands are similar, but not identical, with all bond lengths and angles within the pyridine rings unremarkable. The interannular distances vary considerably in the range 1.445(23)–1.527(20) Å, although this is not simply related to the metal–ligand or ligand–ligand interactions. The most significant and noticeable feature is the twisting of the ligands into non-planar configurations to form the helical arrangement. The principal twist (58–60°) is about the bond between the "terpyridine" and "bipyridine" portions of each ligand, although smaller twists of 3–18° between the other rings are also observed.

It is also apparent that the double helical geometry results from a stacking interaction of aromatic rings. The stacking interaction involves a "terpyridine" fragment of one ligand with a "bipyridine" fragment of the other. The average interplanar distance in the stacked systems is 3.2 Å. In each complex the two stacked systems are approximately parallel with least squares planes calculations showing angles of intersection of 1.3–8.6°. The Ni(1)—Ni(2) distance is 4.45 Å, which is comparable to the Cu(1)—Cu(2) distance in $[Cu_2L_2(OAc)]^{3+}$ of 4.50 Å; there is no direct Ni—Ni interaction. In neither complex are there any intermolecular distances less than the sums of the van der Waals' radii.

We have previously demonstrated that the double helical geometry results from a small metal ion coordinating to a flexible, highly conjugated polydentate ligand.[4] To date, structurally characterized double helical complexes have incorporated group 1B ions, which do not exert strong preferences for any specific coordination geometry. The observation of the double helical geometry in a nickel complex indicates that the electronic preferences of the metal ion are not dominant in dictating the self-assembly of the helix.

Solutions of the complex in acetonitrile showed no oxidation waves in their cyclic voltammograms up to +1.5 V vs Fc/Fc^+, indicating that a nickel(III) state is not readily accessible. An irreversible reduction centred at −1.23 V vs Fc/Fc^+ is observed which is dependent on the scan rate ($E_c - E_a$ = 190 Mv at 20 mV s^{-1}, 240 mV at 200 mV s^{-1}) and is depicted in Fig. 3. The relative intensities of the forward and reverse waves do not alter with scan rate, and we believe the large peak splitting is due to slow electron transfer to the complex. At very slow scan rates (20 mV s^{-1} or less) the forward wave develops an asymmetry which might be indicative of two near coincident processes, but we have not succeeded in resolving the two processes. The two nickel(II) ions are in significantly different chemical environments, and it might be expected that the two reduction processes could be resolved. We believe the apparent coincidence is a result of the electron transfer kinetics. Bulk electrolysis of an acetonitrile solution (−1.4 V) resulted in a colour change to purple, followed by slow decomposition to a colourless solution containing a suspension of free quinquepy. Coulometry indicated the transfer of 1.86 ± 10% electrons to the binuclear complex, suggesting that this is a reduction to a formally Ni^INi^I

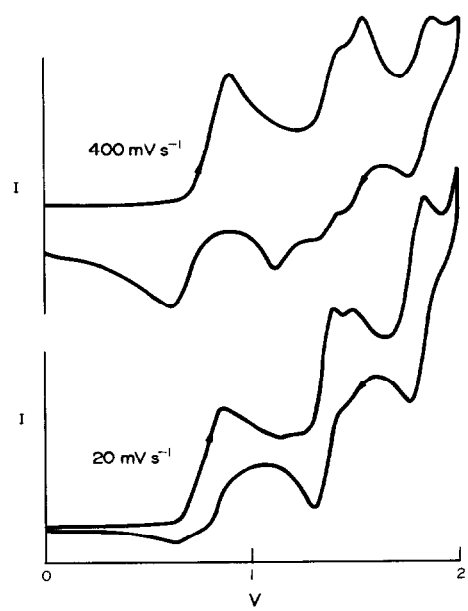

Fig. 3. Cyclic voltammograms of $[Ni_2L_2(OAc)][PF_6]_3$ in MeCN at various scan rates. Details as in Experimental.

complex (but not necessarily a single two-electron process). The EPR spectrum of a frozen acetonitrile glass of the purple complex exhibits a broad anisotropic signal (g_1, 2.72; g_2, 2.127) consistent with the formation of $[Ni^{I}Ni^{I}L_2]^{2+}$ rather than $[Ni^{II}Ni^{II}(L^{-})_2]^{2+}$ or $[Ni^{II}Ni^{I}L(L^{-})]^{2+}$. This is analogous to the reduction of the nickel(II) complex of 4′,4‴-diphenyl-2,2′ : 6′,2″ : 6″,2‴ : 6‴,2⁗-quinquepyridine, which we now know to be a double helical binuclear species, which also gives a bis-nickel(I) complex.[7] The cyclic voltammogram also exhibits two further ligand-based processes centred at −1.81 and −1.92 V vs Fc/Fc^{+}. The first of these two processes is independent of scan rate, with $E_c - E_a = 100$ mV at both 20 and 200 mV s^{-1} scan rates. The second process is scan rate dependent and becomes more noticeable at faster scan rates. At a scan rate of 200 mV s^{-1} this second reduction approaches a two-electron reversible limit ($E_c - E_a = 40$ mV). Finally, a quasi-reversible reduction is observed at −2.24 V vs Fc/Fc^{+}.

Acknowledgements—We thank the SERC for the award of Research Studentships (G.F. and M.D.W.) and Miss J. Nutkins for recording FAB mass spectra.

REFERENCES

1. J. D. Watson and F. H. C. Crick, *Nature* (*London*) 1953, **171**, 737; L. Pauling, R. B. Corey and H. R. Branson, *Proc. Natl. Acad. Sci. U.S.A.* 1951, **37**, 205; P. J. Florey and W. G. Miller, *J. Molec. Biol.* 1966, **15**, 284; J. H. Brewster, *Top. Curr. Chem.* 1974, **47**, 29; K. Mislow, D. Gust, P. Finnocchiaro and R. J. Böttcher, *Top. Curr. Chem.* 1974, **47**, 1; K. P. Meurer and F. Vögtle, *Top. Curr. Chem.* 1985, **127**, 1.
2. F. Stoddart, *Nature* (*London*) 1988, **334**, 10; J. Libman, Y. Tor and A. Stanzer, *J. Am. Chem. Soc.* 1987, **109**, 5880; G. Stuckmeier, U. Thewalt and J-H. Furhop, *J. Am. Chem. Soc.* 1976, **98**, 278.
3. J-M. Lehn and A. Rigault, *Angew. Chem. Int. Edn Engl.* 1988, **27**, 1095; J-M. Lehn, *Angew. Chem. Int. Edn Engl.* 1988, **27**, 89; J-M. Lehn, A. Rigault, J. Siegel, J. Harrowfield, B. Chevrier and D. Moras, *Proc. Natl. Acad. Sci. U.S.A.* 1987, **84**, 2565; J-M. Lehn, J-P. Sauvage, J. Simon, R. Ziessel, C. Piccinni-Leopardi, G. Germain, J-P. Declercq and M. Van Meerssche, *Nouv. J. Chim.* 1983, **7**, 413; J-P. Gisselbrecht, M. Gross, J-M. Lehn, J-P. Sauvage, R. Ziessel, C. Piccinni-Leopardi, J. M. Arrieta, G. Germain and M. Van Meerssche, *Nouv. J. Chem.* 1984, **8**, 661.
4. E. C. Constable, M. G. B. Drew and M. D. Ward, *J. Chem. Soc., Chem. Commun.* 1987, 1600; E. C. Constable and J. M. Holmes, *Inorg. Chim. Acta* 1987, **126**, 187; M. Barley, E. C. Constable, S. A. Corr, M. G. B. Drew, R. C. S. McQueen, J. C. Nutkins and M. D. Ward, *J. Chem. Soc., Dalton Trans.* 1988, 2655; E. C. Constable, M. G. B. Drew, G. Forsyth and M. D. Ward, *J. Chem. Soc., Chem. Commun.* 1988, 1450.
5. F. Kröhnke, *Synthesis* 1976, 1.
6. G. M. Sheldrick, SHELX 76, Program for Crystal Structure Determination, University of Cambridge, U.K. (1976).
7. E. C. Constable, J. Lewis and M. Schröder, *Polyhedron* 1982, **1**, 311.

Polyhedron Vol. 8, No. 21, pp. 2557–2563, 1989
Printed in Great Britain

0277–5387/89 $3.00+.00
© 1989 Pergamon Press plc

PREPARATION, PROPERTIES AND STRUCTURES OF ESTERTIN(IV) SULPHIDES

OK-SANG JUNG, JONG HWA JEONG and YOUN SOO SOHN*

Division of Chemistry, Korea Advanced Institute of Science & Technology, Seoul 136-791, Korea

(*Received* 8 *May* 1989; *accepted* 5 *June* 1989)

Abstract—Estertin(IV) sulphides $[CH_3OOCCH_2CH_2(L)SnS]_n$ (**1a**: L = Me_2NCS_2—, $n = 2$; **1b**: L = Et_2NCS_2—, $n = 2$; **2**: L = $CH_3OOCCH_2CH_2$—, $n = 3$) have been prepared and characterized. In the crystal, the structure of **1a**·$2CHCl_3$ ($P\bar{1}$; $a = 10.739(1)$, $b = 11.801(1)$, $c = 7.7173(9)$ Å, $\alpha = 107.036(8)$, $\beta = 97.93(1)$ and $\gamma = 105.350(9)°$; $R = 0.0600$) is a centrosymmetric four-membered dimer in which the dithiocarbamate ligand is anisobidentate and each tin atom is pentacoordinate with local geometry of a distorted trigonal bipyramid, whereas the structure of **2** ($P\bar{1}$; $a = 11.453(3)$, $b = 12.513(3)$, $c = 13.349(3)$ Å, $\alpha = 97.07(2)$, $\beta = 99.77(2)$, $\gamma = 97.48(2)°$; $R = 0.0369$) shows a six-membered trimer in the boat conformation with tetracoordinated tin atoms. Spectral data of IR, and ^1H, ^{13}C and ^{119}Sn NMR along with the cryoscopic data indicate that the complexes have the same structure in the solid state and in solution.

Diorganotin sulphides revealed a variety of structures depending on the organic groups bonded to the tin atom. Ph_2SnS[1] and Me_2SnS[2] have been found as a cyclic trimer with a Sn_3S_3 six-membered puckered ring, whereas $(t\text{-Bu})_2SnS$[3] and MeN $(CH_2CH_2CH_2)_2SnS$[4] are found as a cyclic dimer with a Sn_2S_2 four-membered ring structure. Besides these cyclic species, $(i\text{-Pr})_2SnS$[5] shows a polymeric chain structure in which tin and sulphur atoms are coupled alternatively. In these diorganotin(IV) chalcogenides, the tin atom is tetracoordinate except in the compound of a cyclic ligand with a nitrogen donor atom.[4]

On the other hand, crystal structures of estertin(IV) compounds, $(CH_3OOCCH_2CH_2)_2SnCl_2$[6] and $CH_3OOCCH_2CH_2(Me_2NCS_2)SnCl_2$,[7] have shown that the central tin atom is hexacoordinated via carbonyl oxygen-to-tin coordination.

In order to understand the structural variety of organotin(IV) chalcogenides, we have prepared mono- and diestertin(IV) sulphides and examined them by means of X-ray crystallography and various spectroscopies.

EXPERIMENTAL

All chemicals were of reagent grade from commercial sources and used without further purification. All solvents were either used directly from freshly opened bottles or dried prior to use. Estertin chlorides were prepared by the literature method.[8] Sodium dithiocarbamates were prepared in the standard manner.[9] Chemical analyses were carried out by the Chemical Analysis Laboratory at KAIST and the molecular weights were determined cryoscopically in benzene using a Cryette A Automatic Cryoscope. The IR spectra in the 4000–400 cm^{-1} region were measured on KBr pellets with an Analect Instrument fx 6160 FT-IR spectrometer. All the NMR spectra were measured in chloroform solution. ^1H NMR spectra were recorded on a JEOL JNM DMX 60 spectrometer, and ^{13}C and ^{119}Sn NMR spectra on a Bruker AM-200 operating at 50.32 (^{13}C) and 74.63 MHz(^{119}Sn) in the pulse mode with Fourier transform at ambient temperature (23 ± 2°C). The chemical shifts are relative

* Author to whom correspondence should be addressed.

to external Me_4Si (^{13}C) and Me_4Sn (^{119}Sn) for the indicated nuclei.

Preparation of $CH_3OOCCH_2CH_2(Me_2NCS_2)SnCl_2$

This compound was prepared by the authors' procedure.[7]

Preparation of $CH_3OOCCH_2CH_2(Et_2NCS_2)SnCl_2$

$Na \cdot S_2CNEt_2 \cdot 3H_2O$ (1.13 g, 5 mmol) in 50 cm^3 of ethanol was reacted with $CH_3OOCCH_2CH_2SnCl_3$ (1.56 g, 5 mmol) in 50 cm^3 of ethanol in the same manner as used for the preparation of $CH_3OOCCH_2CH_2(Me_2NCS_2)SnCl_2$. The resultant solid was recrystallized from a solvent pair of chloroform–petroleum ether (1 : 1). The crystalline solid (m.p. 80–81°C) was obtained in 81% yield. Found: C, 25.1; H, 4.0; N, 3.3. Calc. for $C_9H_{12}NCl_2O_2S_2Sn$: C, 25.4; H, 4.0; N, 3.3%. ^1H NMR (δ, ppm): 1.4 (t, CH_3—), 1.9 (t, —CH_2Sn), 2.9 (t, —CH_2—), 3.7 (q, —CH_2N), 4.0 (s, CH_3O—). IR (cm^{-1}): ν(C=O), 1673; ν(C—N), 1519; ν(C—S), 992.

Preparation of $[CH_3OOCCH_2CH_2(Me_2NCS_2)SnS]_2$ **(1a)**

A solution of $Na_2S \cdot 9H_2O$ (2.40 g, 10 mmol) dissolved in 50 cm^3 of water was added dropwise to an equimolar solution of $CH_3OOCCH_2CH_2(Me_2NCS_2)SnCl_2$ (3.97 g, 10 mmol) in 50 cm^3 of chloroform, and the resultant solution was stirred at room temperature for 30 min. The chloroform layer was separated and evaporated to produce a thin yellow solid. Recrystallization of the crude product from a chloroform–petroleum ether solvent pair (1 : 1) at 0°C gave a colourless chloroform-solvated crystalline solid (m.p. 163–165°C) in 85% yield. Found: C, 19.8; H, 2.9; N, 2.9. Calc. for $C_{14}H_{26}N_2O_4S_6Sn_2 \cdot 2CHCl_3$: C, 20.0; H, 2.9; N, 2.9%.

Preparation of $[CH_3OOCCH_2CH_2(Et_2NCS_2)SnS]_2$ **(1b)**

Reaction of $CH_3OOCCH_2CH_2(Et_2NCS_2)SnCl_2$ (4.25 g, 10 mmol) with $Na_2S \cdot 9H_2O$ (2.40 g, 10 mmol) using the same method as used for the preparation of **1a**, followed by recrystallization from a benzene–petroleum ether solvent pair (1 : 1), resulted in a thin yellow solid (m.p. 98–100°C) in 83% yield. Molecular weight measured: 758.4 (theory: 778.2). Found: C, 27.5; H, 4.3; N, 3.6. Calc. for $C_{18}H_{34}N_2O_2S_6Sn_2$: C, 27.8; H, 4.4; N, 3.6%.

Preparation of $[(CH_3OOCCH_2CH_2)_2SnS]_3$ **(2)**

This compound was prepared by the literature method.[10] The white solid was recrystallized from a chloroform–petroleum ether solvent pair (1 : 2). The colourless crystalline solid (m.p. 72–73°C) was obtained in 80% yield. Molecular weight measured: 940.5 (theory: 974.9). Found: C, 29.6; H, 4.4; S, 9.2. Calc. for $C_{28}H_{42}O_{12}S_3Sn_3$: C, 29.6; H, 4.3; S, 9.9%.

Crystallographic analysis of complexes **1a** *and* **2**

All the crystallographic data were obtained on an Enraf–Nonius CAD4 diffractometer with graphite-monochromated molybdenum radiation ($\lambda(K_{\alpha 1}) = 0.70930$, $\lambda(K_{\alpha 2}) = 0.71359$ Å) at an ambient temperature of 23 ± 2°C. The chloroform-solvated crystal of **1a** was unstable when removed from the mother liquor and, therefore, the crystal used for X-ray study was wedged, wet with mother liquor, into a glass capillary which was then sealed. The crystal of **2** was glued to the interior of a thin walled glass capillary. Preliminary diffractometric investigations indicated that both **1a** and **2** belong to the same space group $P\bar{1}$ (C_i^1, no. 2).[11] The lattice constants were determined by the least-square refinement of the diffraction geometry for 25 intense reflections having $12 < \theta_{Mo\text{-}K} < 16$ for **1a** and $8 < \theta_{Mo\text{-}K} < 13$ for **2**. Crystal parameters and procedural information corresponding to data collection and structure refinement for the complexes are given in Table 1. The structures were solved by use of the conventional heavy-atom method and difference Fourier techniques, and were refined by means of full-matrix least-squares procedures using SHELX-76.[12] The non-hydrogen atoms were refined anisotropically, except for those comprising chloroform of solvation which were refined isotropically. Hydrogen atoms were omitted from the refinement. Tables of atomic positional and thermal parameters and F_o/F_c values have been deposited as Supplementary Material with the Editor, from whom copies are available on request. Atomic coordinates have also been deposited with the Cambridge Crystallographic Data Centre.

RESULTS AND DISCUSSION

The reaction of dithiocarbamatoestertin chlorides, $CH_3OOCCH_2CH_2(R_2NCS_2)SnCl_2$ (R = Me, Et), with sodium sulphide resulted in the dimeric complexes **1a** and **1b**, whereas the cognate reaction of diestertin chlorides, $(CH_3OOCCH_2CH_2)_2SnCl_2$, gave a trimeric complex **2** as established by chemical analysis, cryoscopic data, and X-ray crystal-

Table 1. Crystal parameters and experimental details for complexes **1a**·2$CHCl_3$ and **2**

	1a	**2**
Formula	$C_{14}H_{26}N_2O_4S_6Sn_2 \cdot 2CHCl_3$	$C_{24}H_{42}O_{12}S_3Sn_3$
Formula weight	956.87	974.91
Crystal system	Triclinic	Triclinic
Space group	$P\bar{1}$	$P\bar{1}$
a, b, c (Å)	10.739(1), 11.801(1), 7.7173(9)	11.453(3), 12.513(3), 13.349(3)
α, β, γ (°)	107.036(1), 97.93(1), 105.350(9)	97.07(2), 99.77(2), 97.48(2)
V(Å^3)	876.8(8)	1849(1)
Z	1	2
d_{calc} (g cm^{-3})	1.81	1.75
Crystal size (mm)	0.35 × 0.56 × 0.58	0.43 × 0.54 × 0.68
μ (cm^{-1})	20.98	13.40
Radiation	Mo-K_α (λ = 0.71073 Å)	Mo-K_α (λ = 0.71073 Å)
Scan method	$\omega-2\theta$	$\omega-2\theta$
Data collected	$h, \pm k, \pm l, 1 \leqslant \theta \leqslant 25$	$h, \pm k, \pm l, 1 \leqslant \theta \leqslant 25$
Number of unique observations	3269	6850
Number of unique data $I > 3\sigma(I)$	2675	5176
Number of parameters refined	146	379
Over determination ratio	18.32	13.66
Largest shift/ESD	0.005	0.01
$R = \Sigma \|\|F_o\|-\|F_c\|\|/\Sigma\|F_o\|$	0.0600	0.0369
$R_G = (\Sigma\|F_o-F_c\|^2/\Sigma F_o^2)^{1/2}$	0.0682	0.0439

lography, as will be shown below. The product were obtained as crystalline solids with sharp melting points, and are soluble in polar organic solvents such as chloroform, dichloromethane, dimethyl sulphoxide and acetone, but insoluble in water and saturated aliphatic hydrocarbons. It is noticeable that **1a** is not soluble but **1b** is soluble in benzene, which allows cryoscopic measurement.

Crystal structure of complexes **1a** *and* **2**

The molecular geometry and labelling scheme for complex **1a** is shown in Fig. 1. The bond distances and angles are tabulated in Table 2. The chloroform molecules solvated are not shown in the structure and do not interact with the complex **1a**. Complex **1a** is a centrosymmetric dimer consisting of a planar four-membered ring, Sn_2S_2, in which the dithiocarbamate ligand is bidentate and thus each tin atom is pentacoordinate, with S(1), S(2) and C(4) in equatorial positions and with S(3) and S(1)′ in axial positions in a distorted trigonal bipyramidal arrangement. The Sn_2S_2 four-membered ring is a slightly distorted rectangle with different Sn—S bond lengths: Sn—S(1) and Sn—S(1)′ distances of 2.381(2) and 2.509(3) Å are similar to those of 2.40 and 2.53 Å in $[MeN(CH_2CH_2CH_2)SnS]_2$.[4] The dithiocarbamate ligand is bonded to the tin atom in an anisobidentate fashion: Sn—S(2) and Sn—S(3) distances of 2.487(3) and 2.752(3) Å are comparable with those of $(t\text{-Bu})_2Sn(S_2CNMe_2)_2$[13] (2.489(1), 2.795(1) Å) and $BuPhSn(S_2CNEt_2)Cl$[14] (2.454(1), 2.764(1) Å). The axial Sn—S(3) and Sn—S(1)′ bond lengths are longer than the equatorial ones. The small bite angle (68.6(1)°) of the dithiocarbamate

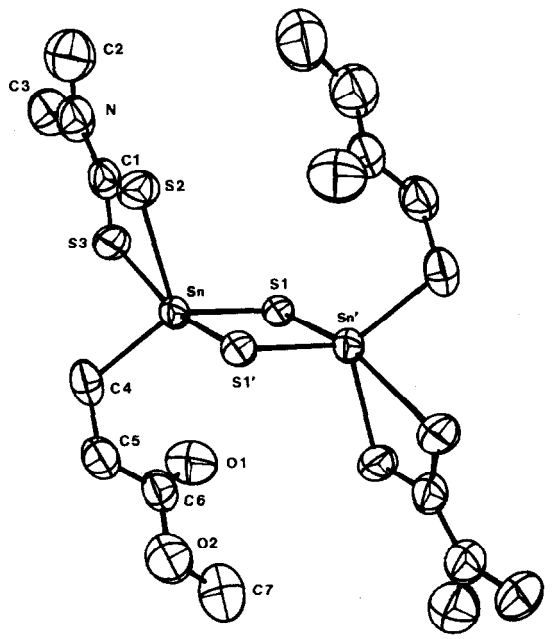

Fig. 1. ORTEP drawing of $[CH_3OOCCH_2CH_2(Me_2NCS_2)SnS]_2$ along with the atomic labelling scheme.

Table 2. Bond distances (Å) and angles (°) for $[CH_3OOCCH_2CH_2(Me_2NCS_2)SnS]_2 \cdot 2CHCl_3$

Bond distances (Å)		Bond angles (°)	
Sn—S(1)	2.381(2)	S(1)—Sn—S(2)	112.1(1)
Sn—S(1)′	2.509(3)	S(1)—Sn—S(3)	92.0(1)
Sn—S(2)	2.487(3)	S(2)—Sn—S(3)	68.6(1)
Sn—S(3)	2.752(3)	C(4)—Sn—S(1)	132.5(3)
Sn—C(4)	2.154(10)	C(4)—Sn—S(2)	111.6(3)
C(1)—S(2)	1.746(11)	C(4)—Sn—S(3)	87.3(3)
C(1)—S(3)	1.695(12)	S(1)—Sn—S(1)′	92.6(1)
C(1)—N	1.344(12)	S(2)—Sn—S(1)′	94.1(1)
C(2)—N	1.490(17)	S(3)—Sn—S(1)′	162.6(1)
C(3)—N	1.469(16)	C(4)—Sn—S(1)′	101.8(3)
C(5)—C(4)	1.552(14)	Sn—S(1)—Sn′	87.41(9)
C(6)—C(5)	1.536(15)	C(1)—S(2)—Sn	90.0(4)
O(1)—C(6)	1.169(13)	C(1)—S(3)—Sn	82.6(3)
O(2)—C(6)	1.320(13)	C(2)—N—C(1)	121.4(11)
O(2)—C(7)	1.474(15)	C(3)—N—C(1)	120.8(11)
		C(3)—N—C(2)	117.8(10)
		S(2)—N—S(3)	67.4(2)
		S(3)—C(1)—S(2)	118.8(6)
		N—C(1)—S(2)	119.2(9)
		N—C(1)—S(3)	122.0(9)
		C(5)—C(4)—Sn	113.5(7)
		C(6)—C(5)—C(4)	109.5(9)
		O(1)—C(6)—C(5)	126.1(11)
		O(2)—C(6)—C(5)	110.7(9)
		O(2)—C(6)—O(1)	123.2(12)
		C(7)—O(2)—C(6)	115.9(10)

ligand is in part responsible for the distortion of the trigonal bipyramid. Another aspect noteworthy in the structure of **1a** is that the ester carbonyl group does not coordinate to the tin (Sn---O(1), 3.19(1) Å) in spite of its favourable position as shown in Fig. 1, in contrast to its halide analogue, $CH_3OOCCH_2CH_2(Me_2NCS_2)SnCl_2$,[7] which includes a five-membered chelate ring via a carbonyl oxygen-to-tin coordination of the ester group. The free ester group in complex **1a** is presumably due to a decrease of Lewis acidity of the tin atom by the partial change of donor atoms.

The molecular geometry of **2** is depicted in Fig. 2, where the atomic numbering scheme is defined. The selected bond distances and angles appear in Table 3. In contrast to **1a**, the crystal structure of **2** shows that three tin and three sulphur atoms form a trimeric six-membered ring in somewhat distorted boat conformation. The structure is quite similar to the structures of $[Ph_2SnS]_3$ and $[Me_2SnS]_3$ reported by Schumann[1] and Jacobsen and Kress,[2] respectively. The complex also indicates free ester groups which are different from those of its starting material $(CH_3OOCCH_2CH_2)_2SnCl_2$,[6] probably due to a decrease of the acceptor properties of the tin atom by changing the donor atoms, and an approximate tetrahedral geometry around the tin atom results. The S(1)—Sn(1)—S(3), S(1)—Sn(2)—S(2) and S(2)—Sn(3)—S(3) bond angles of 111.0(1), 104.7(1) and 104.0(1)° deviate from those expected for a tetrahedral sp^3-hybridized tin atom, presumably owing to the ester groups. The Sn—S—Sn angles of 102.8(1), 106.9(1) and 100.7(1)° also deviate slightly from that (104°) calculated by Kriegsmann *et al.*[15] The Sn—S (2.404(2)–2.442(2) Å) and Sn—C (2.140(9)–2.168(7) Å) distances in this compound correspond to those expected on the basis of covalent single bonds between Sn—S and Sn—C.

Why complex **1a** is dimeric, rather than trimeric, is not clear. There is a temptation to invoke steric hindrance. Thus the bulky pentacoordinate tin complexes, **1a** and **1b**, are capable of forming dimeric Sn_2S_2 four-membered rings as in [MeN-

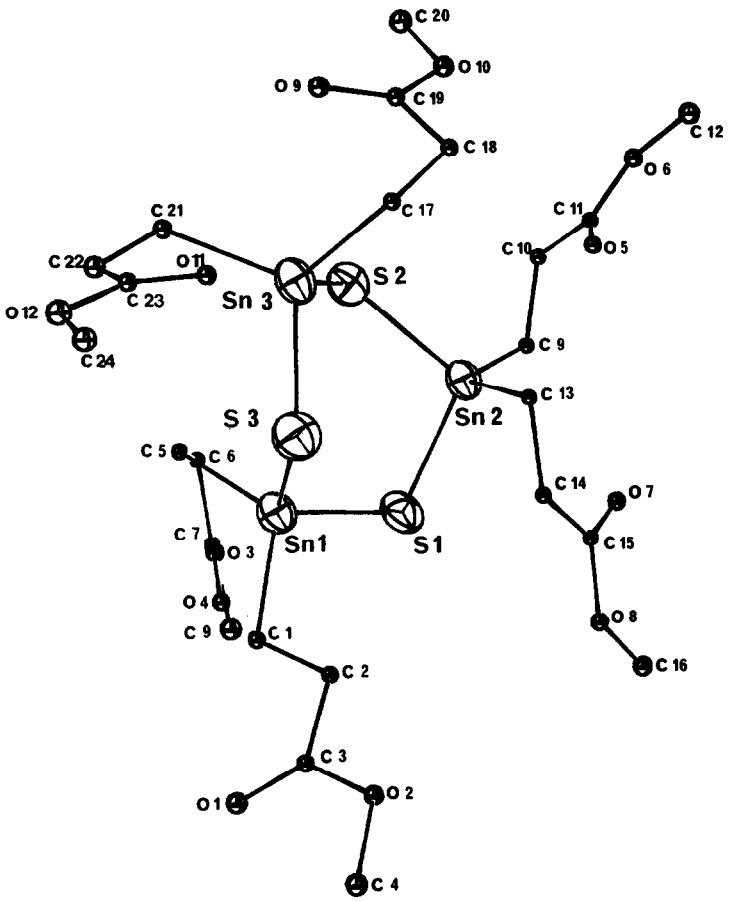

Fig. 2. ORTEP drawing of $[(CH_3OOCCH_2CH_2)_2SnS]_3$ along with the atomic labelling scheme. Thermal ellipsoids of C and O were reduced for clarity.

Table 3. Selected bond distances (Å) and angles (°) for $[(CH_3OOCCH_2CH_2)_2SnS]_3$

Bond distances (Å)		Bond angles (°)	
Sn(1)—C(1)	2.140(9)	C(1)—Sn(1)—C(5)	120.3(3)
Sn(1)—C(5)	2.163(8)	C(1)—Sn(1)—S(1)	108.6(3)
Sn(1)—S(1)	2.404(2)	C(1)—Sn(1)—S(3)	97.4(2)
Sn(1)—S(3)	2.442(2)	S(1)—Sn(1)—S(3)	111.0(1)
Sn(2)—C(9)	2.163(9)	S(1)—Sn(1)—C(5)	109.7(2)
Sn(2)—C(13)	2.164(7)	S(3)—Sn(1)—C(5)	109.2(2)
Sn(2)—S(1)	2.426(2)	S(1)—Sn(2)—C(9)	105.1(2)
Sn(2)—S(2)	2.417(2)	S(1)—Sn(2)—C(13)	105.8(2)
Sn(3)—C(17)	2.168(7)	C(9)—Sn(2)—C(13)	122.8(3)
Sn(3)—C(21)	2.155(9)	S(1)—Sn(2)—S(2)	104.7(1)
Sn(3)—S(2)	2.426(2)	S(2)—Sn(2)—C(9)	102.1(3)
Sn(3)—S(3)	2.417(2)	S(2)—Sn(2)—C(13)	114.7(2)
		S(2)—Sn(3)—C(17)	105.8(2)
		S(2)—Sn(3)—C(21)	104.8(2)
		C(17)—Sn(3)—C(21)	116.7(4)
		S(2)—Sn(3)—S(3)	104.0(1)
		S(3)—Sn(3)—C(17)	111.9(2)
		S(3)—Sn(3)—C(21)	112.2(3)
		Sn(1)—S(1)—Sn(2)	100.7(1)
		Sn(2)—S(2)—Sn(3)	102.8(1)
		Sn(1)—S(3)—Sn(3)	106.9(1)

Table 4. Relevant IR bands for $[CH_3OOCCH_2CH_2(L)SnS]_n$[a]

Compound	ν(C═O) (cm^{-1})	ν(C—N) (cm^{-1})	ν(C—S) (cm^{-1})
1a	1730(vs)	1528(vs)	973(s)
1b	1730(vs)	1507(vs)	988(s)
2	1713(vs)	—	—

[a] **1a**: L = Me_2NCS_2—, $n = 2$; **1b**: L = Et_2NCS_2—, $n = 2$; **2**: L = $CH_3OOCCH_2CH_2$—, $n = 3$. vs, very strong; s, strong.

$(CH_2CH_2CH_2)SnS]_2$,[4] whereas the tetracoordinate tin complex, **2**, seems to favour a trimeric Sn_3S_3 six-membered ring.

Spectroscopic properties of complexes **1a**, **1b** *and* **2**

The characteristic IR bands of the complexes relevant to their molecular structures are listed in Table 4. Among the stretching modes, the ν(C═O) band is known to depend on the type of coordination of the carbonyl group.[16–18] The ν(C═O) bands of complexes **1a** (1730 cm^{-1}), **1b** (1730 cm^{-1}) and **2** (1713 cm^{-1}) exhibit a remarkable blue shift from that (1652 cm^{-1}) of the carbonyl oxygen-to-tin coodinated complex, $CH_3OOCCH_2CH_2(Me_2NCS_2)SnCl_2$.[7] This fact clearly indicates the non-chelating nature of the carbonyl group in the present chalcogenides. The ν(C—N) and ν(C—S) bands in the regions 1450–1550 and 950–1050 cm^{-1}, respectively, are known to depend on the nature of coordination of the dithiocarbamate ligand. A single band for complexes **1a** and **1b** in each region is indicative of bidentate chelation of the dithiocarbamate ligand.[19,20]

The ^1H, ^{13}C and ^{119}Sn NMR data are listed in Table 5. In particular, ^1H and ^{13}C NMR data also support the absence of carbonyl oxygen-to-tin coordination for the chalcogenides in solution: $\delta(^1H) = 3.7$ ppm for CH_3O— and $\delta(^{13}C)$ values for C═O (174.5–176.1 ppm) and CH_3O— (51.7–52.0 ppm) in the chalcogenides were shielded by about 0.3, 6 and 3 ppm, respectively, relative to those of the carbonyl oxygen-to-tin coordinated complex, $CH_3OOCCH_2CH_2(Me_2NCS_2)SnCl_2$.[7]

^{119}Sn NMR spectroscopy has been found to have an approximately linear relationship between the $\delta(^{119}Sn)$ values and the coordination numbers of dithiocarbamatotin(IV) complexes:[21–27] the $\delta(^{119}Sn)$ value has been found to lie between −150 and −250 ppm in pentacoordinate complexes and between −300 and −500 ppm in hexacoordinate complexes. From this relationship $\delta(^{119}Sn)$ values for complexes **1a** ($\delta(^{119}Sn) = -229.8$, −232.0 ppm) and **1b** ($\delta(^{119}Sn) = -232.9$, −235.1 ppm) indicate that the tin atoms in **1a** and **1b** are pentacoordinate. Assuming from the above-mentioned spectroscopic data that the ester group acts as monodentate, then the $\delta(^{119}Sn)$ values of complexes **1a** and **1b** suggest that the dithiocarbamate ligand is bidentate. It seems worthwhile to point out that the ^{119}Sn signals appear at slightly different chemical shifts in the dimeric chalcogenides, **1a** and **1b**, implying slightly different chemical environments around the tin atom. On the other hand, a drastic deshielding of the tin chemical shift for complex

Table 5. ^1H, ^{13}C and ^{119}Sn NMR data for $[CH_3OOCCH_2CH_2(L)SnS]_n$[a]

Compound	$^1H(\delta,ppm)$	$^{13}C(\delta,ppm)$	$^{119}Sn(\delta,ppm)$
1a	2.1(t,—CH_2Sn); 3.0(t,—CCH_2—); 3.4(s,$(CH_3)_2N$—); 3.7(s,CH_3O—); 7.3(s,$CHCl_3$)	29.0(—CH_2Sn—); 30.2(—CH_2—); 45.9($(CH_3)_2N$—); 52.0(CH_3O—); 77.0($CHCl_3$); 174.6(C═O); 197.7(C—S)	−229.8, −232.0
1b	1.3(t,CH_3—); 2.1(t,—CH_2Sn); 3.0(t,—CCH_2—); 3.7(s,CH_3O—); 3.7(q,—CH_2—)	12.0(CH_3—); 28.8(—CH_2Sn); 20.4(—CCH_2—); 50.4(—CH_2—); 51.9(CH_3O—); 174.5(C═O); 195.9(C—S)	−232.9, −235.1
2	1.6(t,—CH_2Sn); 2.1(t,—CH_2—); 3.7(s,CH_3O—)	18.8(—CH_2Sn); 29.5(—CH_2—); 51.7(CH_3O—); 176.1(C═O)	86.4

[a] **1a**: L = Me_2NCS_2—, $n = 2$; **1b**: L = Et_2NCS_2—, $n = 2$; **2**: L = $CH_3OOCCH_2CH_2$—, $n = 3$.

2 ($\delta(^{119}Sn) = 86.4$ ppm) is strongly indicative of tetracoordination of the tin atom in solution. Thus cryoscopic and spectroscopic data in solution are consistent with the crystal structures in the solid state for the title complexes.

Acknowledgement—This research was supported financially by the Ministry of Science and Technology in Korea.

REFERENCES

1. V. H. Schumann, *Z. Anorg. Allg. Chem.* 1967, **354**, 192.
2. H.-J. Jacobsen and B. Kress, *J. Organomet. Chem.* 1977, **136**, 333.
3. H. Puff, R. Gattermayer, R. Hundt and R. Zimmer, *Angew. Chem. Int. Edn Engl.* 1977, **16**, 547.
4. A. Tzschach and K. Jurkschat, *Pure Appl. Chem.* 1986, **58**, 639.
5. H. Puff, A. Bongartz, R. Sievers and R. Zimmer, *Angew. Chem. Int. Edn Engl.* 1978, **17**, 939.
6. P. G. Harrison, T. J. King and M. A. Healy, *J. Oganomet. Chem.* 1979, **182**, 17.
7. O. S. Jung, J. H. Jeong and Y. S. Sohn, *Polyhedron* 1989, **8**, 1413.
8. R. E. Hutton and V. Oakes, in *Organotin Compounds: New Chemistry and Applications, Advances in Chemistry Series* (Edited by J. J. Zuckerman), Vol. 157, p. 123. American Chemical Society, Washington D.C. (1976).
9. R. E. Reid, *Organic Chemistry of Bivalent Sulfur*, Vol. IV. Chemical Publishing Company, New York (1962).
10. M. Minakawa, T. Sekiguchi and N. Kurita, *Jpn. Kokai. Tokkyo Koho* 78145858 (1978).
11. *International Tables for X-ray Crystallography*, Vol. IV. Kynoch Press, Birmingham, U.K. (1974).
12. G. M. Sheldrick, SHELX 76: Program for Crystal Structure Determination, University of Cambridge, U.K. (1976).
13. K. Kim, J. A. Ibers, O. S. Jung and Y. S. Sohn, *Acta Cryst.* 1987, **C43**, 2317.
14. V. G. Kumar Das, C. Wei and E. Sinn, *J. Organomet. Chem.* 1985, **290**, 291.
15. H. Kriegsmann, H. Hoffmann and H. Geissler, *Z. Anorg. Allg. Chem.* 1965, **341**, 24.
16. D. Maughan, J. L. Wardell and J. W. Burley, *J. Organomet. Chem.* 1981, **212**, 59.
17. R. A. Howie, E. S. Paterson, J. L. Wardell and J. W. Burley, *J. Organomet. Chem.* 1986, **304**, 301.
18. E. S. Paterson, J. L. Wardell and J. W. Burley, *J. Organomet. Chem.* 1984, **273**, 313.
19. F. Bonati and R. Ugo, *J. Organomet. Chem.* 1967, **10**, 257.
20. C. P. Sharma, N. Kumar, M. C. Khandpal, S. Chandra and V. G. Bhide, *J. Inorg. Nucl. Chem.* 1981, **43**, 923.
21. J. Otera, T. Hinoishi and R. Okawara, *J. Organomet. Chem.* 1980, **202**, C93.
22. J. Otera, *J. Organomet. Chem.* 1981, **221**, 57.
23. J. Otera, T. Hinoishi, Y. Kawabe and R. Okawara, *Chem. Lett.* 1981, 273.
24. J. Otera, A. Kusaba, T. Hinoishi and Y. Kawasaki, *J. Organomet. Chem.* 1982, **228**, 223.
25. J. Otera, T. Yano and K. Kusakabe, *Bull. Chem. Soc. Jpn* 1983, **56**, 1057.
26. J. Holecek, M. Nadvornik, K. Handlir and A. Lycka, *J. Organomet. Chem.* 1983, **241**, 177.
27. O. S. Jung and Y. S. Sohn, *Bull. Korean Chem. Soc.* 1988, **9**, 365.

Polyhedron Vol. 8, No. 21, pp. 2565–2569, 1989
Printed in Great Britain

0277–5387/89 $3.00+.00
© 1989 Pergamon Press plc

FACILE OXIDATION OF A BOUND NITROSYL GROUP TO A NITRATO LIGAND: PREPARATION AND STRUCTURES OF *CIS*-DIBROMONITROSYLBIS(DICYCLOHEXYLPHOSPHINE)RHODIUM, $[RhBr_2(NO)\{P(C_6H_{11})_2H\}_2]$ AND *TRANS*-DIBROMONITRATOBIS (DICYCLOHEXYLPHOSPHINE)RHODIUM, $[RhBr_2(NO_3)\{P(C_6H_{11})_2H\}_2]$

ROBIN B. ENGLISH

Department of Chemistry and Biochemistry, Rhodes University, P.O. Box 94, Grahamstown 6140, South Africa

(*Received* 16 *May* 1989; *accepted* 7 *June* 1989)

Abstract—The synthesis and structure of the tetragonal pyramidal complex $[RhBr_2(NO)\{P(C_6H_{11})_2H\}_2]$ are reported. This complex has a *cis*-disposition of basal ligands with an apical nitrosyl group inclined towards the bromide ligands. $[RhBr_2(NO)\{P(C_6H_{11})_2H\}_2]$ readily and irreversibly takes up atmospheric dioxygen to form the nitrato complex $[RhBr_2(NO_3)\{P(C_6H_{11})_2H\}_2]$, whose structure is also described. In this complex the bromide and phosphine ligands are *trans*- and *cis*-disposed, respectively.

Several structures of pentacoordinate nitrosyl complexes $[RhX_2(NO)\{PR_3\}_2]$ (X = Cl or Br, and R represents various organic groups) have been reported.[1–3] We have suggested[3] two possible explanations for the structures adopted by this series of compounds—the one based on a general molecular orbital model for pentacoordinate metal nitrosyl complexes proposed by Hoffmann *et al.*,[4] and the other, a simpler picture relying on molecular mechanical ideas. In this paper a nitrosyl complex, $[RhBr_2(NO)\{P(C_6H_{11})_2H\}_2]$ is described, aspects of whose structure can be explained using the simple mechanical model, but which are difficult to account for otherwise. Interestingly, a proposal that "steric interactions in molecules and crystals must be described by simple mechanical models and not by quantum theory"[5] appeared recently.

The reactivity of $[RhBr_2(NO)\{P(C_6H_{11})_2H\}_2]$ in solution towards atmospheric oxygen differs from that of other complexes of this class, which are either air-stable and very insoluble, or air-sensitive and decompose forming uncharacterisable products: $[RhBr_2(NO)\{P(C_6H_{11})_2H\}_2]$ reacts irreversibly with dioxygen to form the stable complex $[RhBr_2(NO_3)\{P(C_6H_{11})_2H\}_2]$. The formation and structure of this nitrato complex are also described in this paper.

EXPERIMENTAL

$[RhBr_2(NO)\{P(C_6H_{11})_2H\}_2]$ was prepared by reacting $[\{Rh(NO)Br_2\}_n]$[6] with dicyclohexylphosphine, following the procedure described in the literature.[7] The complex crystallized as dark green prisms [ν(N—O) 1651 cm^{-1}, in Nujol] from dichloromethane–methanol at 0°C: yield *ca* 40%. Microanalysis indicated the presence of a molecule of dichloromethane of solvation (Found: C, 39.0; H, 6.4; N, 1.8; Cl, 9.0. $C_{25}H_{48}Br_2Cl_2NOP_2Rh$ requires C, 38.8; H, 6.3; N, 1.8; Cl, 9.2%). During recrystallization air was not excluded, and from the dark red–brown supernatant solution, $[RhBr_2(NO_3)\{P(C_6H_{11})_2H\}_2]$ was isolated in *ca* 15% yield based on $[\{Rh(NO)Br_2\}_n]$ as orange lozenges of the 1:1 dichloromethane solvate (Found: C, 37.3; H, 6.0; N, 1.8; Cl, 8.7. $C_{25}H_{48}Br_2Cl_2NO_3P_2Rh$ requires C, 37.2; H, 6.0; N, 1.7; Cl, 8.8%). IR bands due to the NO_3 ligand were not assigned.

X-ray crystallographic studies

Data collection: Enraf–Nonius CAD-4F using graphite monochromated Mo-K_α, with Lorentz-polarization and empirical absorption corrections;

Table 1. Crystal data, data collection and refinement details

	$[RhBr_2(NO)\{P(C_6H_{11})_2H\}_2]\cdot CH_2Cl_2$	$[RhBr_2(NO_3)\{P(C_6H_{11})_2H\}_2]\cdot CH_2Cl_2$
Formula	$C_{25}H_{48}Br_2Cl_2NOP_2Rh$	$C_{25}H_{48}Br_2Cl_2NO_3P_2Rh$
M	774.28	806.28
Space group	$P2_1/n$	$P2_1/c$
a(Å)	14.249(5)	13.136(5)
b(Å)	13.921(5)	11.724(5)
c(Å)	17.153(5)	22.520(5)
β(°)	106.84(5)	105.28(5)
F(000)	1568	1632
U(Å^3)	3256(6)	3346(5)
Z	4	4
D_m(g cm^{-3}, flotation)	1.57(5)	1.60(5)
D_c(g cm^{-3})	1.58	1.60
μ(cm^{-1})	31.4	30.6
Crystal size (mm)	$0.1\times0.1\times0.15$	$0.07\times0.1\times0.1$
$N_{reflections}(3° < \theta < 23°)$	$4891(\pm h, k, l)$	$3326(\pm h, k, l)$
$N_{observed}$	$3222[I > 3\sigma(I)]$	$2031[I > 3\sigma(I)]$
R	0.067	0.086
R_w	0.077	0.086
k and g in $w = k[\sigma^2(F_o)+g\lvert F_o\rvert^2]^{-1}$	1.29, 0.0031	Unit weights
$N_{parameters}$	177	188

unit cell dimensions based on 25 low θ reflections; crystal stability monitored and confirmed; structure solution and refinement details have been described previously.[7] With the exception of carbon, hydrogen and solvent atoms, the model structures were refined anisotropically. Solvent atoms (no hydrogens) were refined as rigid groups with C—Cl 1.75 Å, Cl—C—Cl 109.5°. Hydrogen atoms were included at calculated positions with common temperature factors.* Crystal data, data collection and refinement details are summarized in Table 1, and selected bond lengths and angles are given in Table 2.

RESULTS AND DISCUSSION

$[RhBr_2(NO)\{P(C_6H_{11})_2H\}_2]$, whose structure is depicted in Fig. 1, displays a tetragonal pyramidal coordination geometry with the phosphine and bromide ligands constituting the basal square and the nitrosyl group the apex. In common with other complexes of this type, the nitrosyl group is bent; this mode of coordination is a consequence of the good electron-donating capabilities, and weak π-acceptor qualities of the basal ligands.[4] The features of the molecule which invite comment are firstly the *cis*-disposition of the basal ligands; secondly the direction in which the NO ligand bends and finally the unusual reactivity towards O_2.

We have remarked previously that the preferred arrangement of basal ligands appears to be *cis*; only in the cases of PPh_3 and $P(OPr^i)Ph_2$ is the *trans*-arrangement observed.[1,3] We proposed the critical ligand cone angle (the apical angle of the cone whose apex is the metal atom and which envelops the van der Waals' volume of the ligand[8]) which would force a *trans*-geometry, lies somewhere between 132 and 140°. On this basis, the cone angle of the dicyclohexylphosphine ligand should be 132° or less. Can this parameter be estimated from first principles?

Using the mean bond lengths of P—C 1.835, C—C 1.51 and C—H 1.08 Å, with a van der Waals' radius for hydrogen of 1.2 Å[9] and tetrahedral geometry around carbon, a simple calculation shows that the van der Waals' contact cone angle subtended at a phosphorus atom by a cyclohexyl group free to rotate is 143°. However, the C—P—C angles found in this analysis are approximately tetrahedral, so the cyclohexyl groups are intermeshed to the extent that their contact cones interpenetrate by $143-109.5°$ i.e. 33.5°. For perfect tetrahedral geometry around phosphorus P, and a

*Atomic coordinates, thermal parameters, hydrogen atom coordinates and F_o/F_c data have been deposited with the Editor as supplementary data: atomic coordinates have also been deposited with the Cambridge Crystallographic Data Centre.

Table 2. Selected bond lengths (Å) and angles (°) for (a) $[Rh(NO)Br_2\{P(C_6H_{11})_2H\}_2]$ and (b) $[Rh(NO_3)Br_2\{P(C_6H_{11})_2H\}_2]$

(a)			
Rh—Br(1)	2.516(2)	Rh—Br(2)	2.539(2)
Rh—P(1)	2.289(3)	Rh—P(2)	2.311(3)
Rh—N	1.937(11)	O—N	1.050(14)
Br(1)—Rh—Br(2)	91.2(1)	Br(1)—Rh—P(1)	86.7(1)
Br(2)—Rh—P(1)	171.1(1)	Br(1)—Rh—P(2)	162.4(1)
Br(2)—Rh—P(2)	89.0(1)	P(1)—Rh—P(2)	90.5(1)
Br(1)—Rh—N	100.6(4)	Br(2)—Rh—N	95.3(4)
P(1)—Rh—N	93.6(4)	P(2)—Rh—N	96.8(4)
Rh—N—O	124.8(12)		
(b)			
Rh—Br(1)	2.469(4)	Rh—Br(2)	2.451(4)
Rh—P(1)	2.236(8)	Rh—P(2)	2.258(7)
O(1)—N	1.30(3)	O(2)—N	1.31(3)
O(3)—N	1.26(3)		
Br(1)—Rh—Br(2)	172.0(2)	Br(1)—Rh—P(1)	92.5(2)
Br(2)—Rh—P(1)	89.7(2)	Br(1)—Rh—P(2)	97.7(2)
Br(2)—Rh—P(2)	90.1(2)	P(1)—Rh—P(2)	88.4(3)
O(1)—N—O(2)	117(2)	O(1)—N—O(3)	121(3)
O(2)—N—O(3)	122(3)		

Rh—P distance of 2.30 Å, and given this degree of interpenetration, one may estimate the cone angle of the strain-free tricyclohexylphosphine ligand bound to rhodium to be 164°. (Tolman[8] gives a figure of 179(10)°, significantly larger, based on a phosphine–metal (Ni) distance of 2.28 Å, and measured on a model.) The corresponding cone angle of PH_3 is 99° based on a P—H bond length of 1.3 Å (Tolman quotes 87(2)°). Consequently, using Tolman's equation, the cone angle of the $P(C_6H_{11})_2H$ ligand will be 2/3 of $(2\times 164/2+99/2)$, i.e. 142° (considerably greater if Tolman's figures are used).

According to our previous suggestion this angle is large enough to force a *trans*-ligand geometry. The reason it does not, and that the two $P(C_6H_{11})_2H$ ligands can bond *cis*, is apparent from inspection of Fig. 2, which depicts the molecule with atoms plotted in space-filling style, i.e. as spheres with corresponding van der Waals' radii.[9] It is clear that the two secondary phosphine hydrogens are in close contact—the H—H distance is 2.3(1) Å,

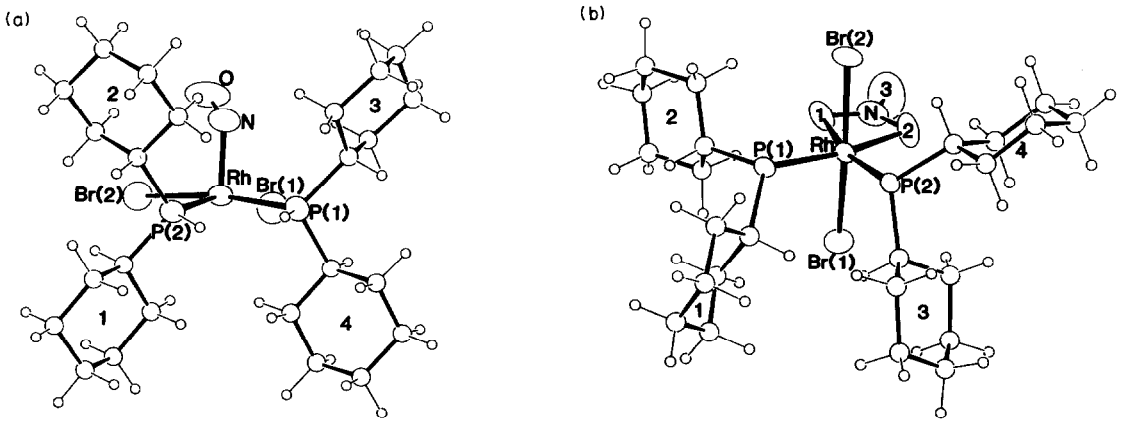

Fig. 1. The molecular structures of (a) $[RhBr_2(NO)\{P(C_6H_{11})_2H\}_2]$ and (b) $[RhBr_2(NO_3)\{P(C_6H_{11})_2H\}_2]$.

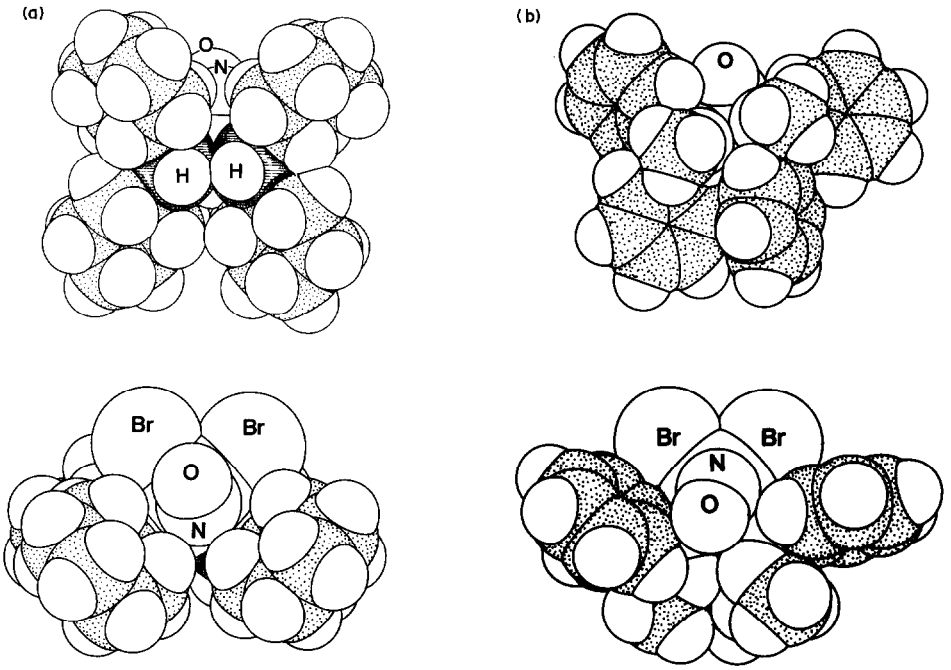

Fig. 2. (a) Space-filling diagrams of $[RhBr_2(NO)\{P(C_6H_{11})_2H\}_2]$ viewed (top) perpendicular to the Rh—N vector and (bottom) down the Rh—N vector. (b) Corresponding diagrams of $[RhBr_2(NO)\{P(OMe)Ph_2\}_2]$ for comparative purposes.

compared to the sum of the van der Waals' radii of 2.4 Å—and that the cone angle as a measure of ligand bulk is inappropriate in the case of dicyclohexylphosphine, where the sizes of the hydrogen and cycohexyl groups attached to the phosphorus atom are so disparate. The $P(C_6H_{11})_2H$ ligands are able to bond *cis* by juxtaposing the sterically undemanding P—H moieties.

It is also interesting to note that the NO group bends in the opposite sense to that observed in $[RhBr_2(NO)\{P(OMe)Ph_2\}_2]$;[3] we suggested a simple explanation for the conformation of the NO group in this complex in terms of dipole–dipole interactions between the NO and the rest of the molecule: this explanation clearly will not hold water for $[RhBr_2(NO)\{P(C_6H_{11})_2H\}_2]$. Once again, Fig. 2 shows that it is not possible for the NO group to incline towards the phosphine ligands in $[RhBr_2(NO)\{P(C_6H_{11})_2H\}_2]$, as this region is occupied by the bulky cyclohexyl groups; such is not the case with $[RhBr_2(NO)\{P(OMe)Ph_2\}_2]$.

It appears, therefore, that the *cis*-arrangement of basal ligands in $[RhBr_2(NO)\{P(C_6H_{11})_2H\}_2]$, $[RhBr_2(NO)\{P(OMe)Ph_2\}_2]$ and $[RhBr_2(NO)\{P(OC_6H_5)_3\}_2]$ is the favoured configuration. This is surprising considering the steric demands of the phosphine ligands. A mechanistic rather than energetic explanation for this result seems preferable: one rather along the lines of that advanced to explain the formation of the dimer $[\{RhBr(NO)[PPh_2O)_2H]\}_2]$[7] from $[\{Rh(NO)Br_2\}_n]$ *via* a dinuclear bromide-bridged *solvento*-intermediate. The conformation of the NO ligand is then easily accounted for on the basis of simple molecular mechanical arguments; however the general molecular orbital model does not predict the observed structure.

The reactivity of the NO group towards oxidation by atmospheric dioxygen is unexpected. Kubota and Phillips[10] have described reactions of $[Ir(PPh_3)_2(CO)ClX(NO)]$ with dioxygen to give the nitrato complexes $[Ir(PPh_3)_2(CO)ClX(NO_3)]$, and suggest that the reaction proceeds by *electrophilic* attack of O_2 on the NO^- ligand, as has been proposed for reactions of cobalt nitrosyls, followed by rearrangement of the N-coordinated O—N—O—O group. However, the complexes $[RhX_2(NO)\{PR_3\}_2]$ hitherto reported do not show any tendency to oxidation of the NO ligand to NO_3, and it may be that the particular conformation of the NO in, and the structure of, $[RhBr_2(NO)\{P(C_6H_{11})_2H\}_2]$ is the source of this susceptibility.

The structure of $[RhBr_2(NO_3)\{P(C_6H_{11})_2H\}_2]$ is shown in Fig. 1. It is a slightly distorted octahedral molecule with a bidentate NO_3 ligand. During the oxidation and rearrangement of ligands it is sur-

prisingly the bromide ligands which end up *trans*-disposed, not the much more bulky $P(C_6H_{11})_2H$ groups. A search through a somewhat out-of-date version (Jan 1986) of the Cambridge Data File did not reveal any other octahedral rhodium(III) nitrato complexes; however, apart from this claim to uniqueness, $[RhBr_2(NO_3)\{P(C_6H_{11})_2H\}_2]$ is structurally unremarkable.

Acknowledgements—My thanks are due to Mr M. Taylor for assistance, the University of Cape Town for the intensity data collection, the Foundation for Research Development and Rhodes University for financial and practical support.

REFERENCES

1. S. Z. Goldberg, C. Kubiak, C. D. Meyer and R. Eisenberg, *Inorg. Chem.* 1975, **14**, 1650.
2. R. B. English, L. R. Nassimbeni and R. J. Haines, *Acta Cryst.* 1976, **B32**, 3299.
3. R. B. English, M. M. de V. Steyn and R. J. Haines, *Polyhedron* 1987, **6**, 1503.
4. R. Hoffmann, M. M. L. Chen, M. Elian, A. R. Rossi and D. M. P. Mingos, *Inorg. Chem.* 1974, **13**, 2666.
5. J. C. A. Boeyens, *S. Afr. J. Chem.* 1984, **37**, 143.
6. G. R. Crookes and B. F. G. Johnson, *J. Chem. Soc. A* 1970, 1662.
7. R. B. English and M. M. de V. Steyn, *S. Afr. J. Chem.* 1984, **37**, 177.
8. C. A. Tolman, *J. Am. Chem. Soc.* 1970, **92**, 2956; C. A. Tolman, W. C. Seidel and L. W. Gosser, *J. Am. Chem. Soc.* 1974, **96**, 53.
9. See e.g., G. M. Barrow, *Physical Chemistry*, 3rd edn, p.387. McGraw-Hill, New York (1973).
10. M. Kubota and D. A. Phillips, *J. Am. Chem. Soc.* 1975, **97**, 5637.

Polyhedron Vol. 8, No. 21, pp. 2571–2576, 1989
Printed in Great Britain

0277–5387/89 $3.00+.00
© 1989 Pergamon Press plc

TERTIARY PHOSPHINE OXIDE ADDUCTS OF DIRUTHENIUM(II,III) TETRAACETATE. CRYSTAL STRUCTURE OF $[Ru_2(\mu\text{-}O_2CCH_3)_4(OPPh_3)_2]PF_6 \cdot CH_2ClCH_2Cl$

M. C. BARRAL, R. JIMENEZ-APARICIO,* E. C. ROYER, C. RUIZ-VALERO and F. A. URBANOS

Departamento de Quimica Inorganica, Facultad de Ciencias Quimicas, Universidad Complutense, Ciudad Universitaria, 28040 Madrid, Spain

and

E. GUTIERREZ-PUEBLA and A. MONGE

Instituto de Ciencias de los Materiales, sede D, C.S.I.C. Serrano 113, 28006 Madrid, Spain and Laboratorio de Rayos X, Facultad de Ciencias Quimicas, Universidad Complutense, Ciudad Universitaria, 28040 Madrid, Spain

(*Received* 3 *February* 1989; *accepted* 7 *June* 1989)

Abstract—The compounds $\{Ru_2(\mu\text{-}O_2CCH_3)_4[OP(p\text{-}RC_6H_4)_3]_2\}PF_6$ (R = H, F, CH_3O, Cl) containing the Ru_2^{5+} unit have been prepared by the reaction of $Ru_2Cl(\mu\text{-}O_2CCH_3)_4$ and $P(p\text{-}RC_6H_4)_3$ (R = H, F, CH_3O, Cl) in the presence of $NOPF_6$ in methanol. In all cases the oxidation of triarylphosphine to triarylphosphine oxide is observed and the $Ru_2(\mu\text{-}O_2CCH_3)_4^+$ unit remains unaltered. The X-ray structure of $[Ru_2(\mu\text{-}O_2CCH_3)_4(OPPh_3)_2]PF_6 \cdot CH_2ClCH_2Cl$ has been determined; this compound crystallizes in the space group $P\bar{1}$, with $a = 8.46(2)$, $b = 12.399(2)$, $c = 13.017(4)$ Å, $\alpha = 105.18(2)$, $\beta = 92.64(5)$, $\gamma = 108.81(5)°$, $V = 1234(3)$ Å^3. There are two half ruthenium dimers, one anion and an uncoordinated solvent CH_2ClCH_2Cl molecule per unit cell. Final $R = 0.07$ for 6591 observed reflections.

The reactions of oxygen atom transfer in the presence of transition metal compounds have received considerable attention due to their relevance in enzymatic processes.[1-2] Among these reactions, the oxidation of triphenylphosphine to triphenylphosphine oxide has been the subject of numerous investigations.[3-12] Several oxygen atom transfer reactions with mononuclear ruthenium complexes have been reported; thus, complexes such as $Ru(EDTA)(H_2O)$,[10] $[Ru(O)(bpy)_2(py)]^{2+}$,[11] $Ru(SCN)(NO)(PPh_3)_2$[12] and others have been used in the catalytic and non-catalytic oxygen transfer to triphenylphosphine. However, similar oxidation reactions of PPh_3 in the presence of carboxylate dimers of ruthenium are unknown. We have recently shown[13] that the oxidation of triphenylphosphine to triphenylphosphine oxide in the presence of $Ru_2Cl(\mu\text{-}O_2CCH_3)_4$ and $NOPF_6$ is preferred to the oxidation of the $[Ru_2(\mu\text{-}O_2CCH_3)_4]^+$ unit.

In this paper we describe the synthesis and characterization of some new complexes of the type $\{Ru_2(\mu\text{-}O_2CCH_3)_4[OP(p\text{-}RC_6H_4)_3]_2\}PF_6$ obtained from $Ru_2Cl(\mu\text{-}O_2CCH_3)_4$, $NOPF_6$ and $P(p\text{-}RC_6H_4)_3$ [R = H (**I**), F (**II**), CH_3O (**III**), Cl (**IV**)], with simultaneous oxidation of triarylphosphine to triarylphosphine oxide. The X-ray crystal structure of $[Ru_2(\mu\text{-}O_2CCH_3)_4(OPPh_3)_2]PF_6 \cdot CH_2ClCH_2Cl$ has been determined.

RESULTS AND DISCUSSION

The reaction of $Ru_2Cl(\mu\text{-}O_2CCH_3)_4$ with $NOPF_6$ and $P(p\text{-}RC_6H_4)_3$ [R = H (**I**), F (**II**), CH_3O

* Author to whom correspondence should be addressed.

(**III**), Cl (**IV**)] in methanol at room temperature leads to formation of the $\{Ru_2(\mu\text{-}O_2CCH_3)_4[OP(p\text{-}RC_6H_4)_3]_2\}PF_6$ compounds. These reactions carried out in refluxing methanol give the same products in shorter periods of time.

In all cases the oxidation of triarylphosphine to triarylphosphine oxide is observed. We do not know the mechanism of these reactions, but we can affirm that the metal centre plays an important role because the oxidation of the triarylphosphine by $NOPF_6$ does not occur in the absence of the $Ru_2Cl(\mu\text{-}O_2CCH_3)_4$ compound.

The complexes have been obtained as brown–yellow solids, stable to air and soluble in the most common polar organic solvents. The stability of these compounds in solution (i.e. CH_2Cl_2, THF, etc.) varies in the order **I** > **II** > **III** ≫ **IV**; thus, the solutions of **I** are stable almost indefinitely, whereas the solutions of **IV** decompose over short periods of time. Compounds **I** and **II** can be recrystallized from dichloromethane–petroleum ether (40–60°C) or 1,2-dichloroethane–petroleum ether (40–60°C). Crystals of **I** suitable for X-ray structural determination were obtained from 1,2-dichloroethane–petroleum ether (40–60°C) as $[Ru_2(\mu\text{-}O_2CCH_3)_4(OPPh_3)_2]PF_6 \cdot CH_2ClCH_2Cl$. Compound **III** does not crystallize from several mixtures of solvents (dichloromethane–petroleum ether (40–60°C), tetrahydrofuran–petroleum ether (40–60°C), etc.). Compound **IV** can not be crystallized from several solvents (dichloromethane, tetrahydrofuran, diethylether, etc.) because it decomposes in solution.

The elemental analyses of these compounds are in accordance with the proposed stoichiometries (see Table 1).

Table 1. Physical properties of compounds **I**–**IV**

Compound	Analysis (%) Found (Calc.)	Magnetic moment (BM)	Conductivity (Ω^{-1} cm^2 mol^{-1})
I[a]	C, 45.3 (44.6) H, 3.7 (3.7)	4.03	125.7
II[b]	C, 40.6 (40.6) H, 2.7 (2.9)	4.68	143.3
III	C, 46.5 (45.5) H, 3.8 (4.1)	3.36	110.9
IV	C, 40.7 (39.3) H, 2.9 (2.7)	3.14	131.5

[a] Physical data for the compound with one molecule of 1,2-dichloroethane.

[b] Physical data for the compound with one molecule of dichloromethane.

Conductivity measurements show, in all cases, the presence of a 1 : 1 electrolyte in acetone solution (10^{-3} M)[14] (see Table 1).

Spectroscopic studies

The IR spectra of these complexes show the absorptions due to bridging carboxylate groups as strong bands between 1400 and 1450 cm^{-1}, similar to those observed in the starting $Ru_2Cl(\mu\text{-}O_2CCH_3)_4$ compound; the ν_{st}(P—F) signal corresponding to the PF_6^- group appears as a broad, strong absorption at 840 cm^{-1}. In addition to the $P(p\text{-}RC_6H_4)_3$ bands, an absorption at about 1140 cm^{-1}, assigned to the ν_{st}(P═O) vibration, is observed.

The electronic spectra (range 300–800 nm) of the complexes in dichloromethane solution show, in all cases, a single absorption band in the region λ_{max} = 432–437 nm; ε_{max} = 659–1240 dm^3 mol^{-1} cm^{-1}. This band has been assigned to an $O(\pi) \rightarrow Ru\text{—}Ru(\pi^*)$ transition, in agreement with Norman *et al.*[15]

The IR and electronic spectra data are summarized in Table 2.

Magnetic studies

Magnetic measurements were carried out from room temperature to 70 K. The variation of the magnetic susceptibilities with temperature obeys the Curie–Weiss law (see Table 3). Magnetic moments for the complexes are in the range μ_{eff} = 3.14–4.68 BM per dimer (see Table 1). The values are consistent with species containing three unpaired electrons per dimer, in accordance[15] with the ground electronic configuration of $\sigma^2\pi^4\delta^2(\pi^*\delta^*)^3$.

Crystal structure of $[Ru_2(\mu\text{-}O_2CCH_3)_4(OPPh_3)_2]PF_6 \cdot CH_2ClCH_2Cl$

Selected bond distances and angles are presented in Table 4. Figure 1 shows the ORTEP view of the complex with the atomic labelling used. The structure consists of discrete $[Ru_2(\mu\text{-}O_2CCH_3)_4(OPPh_3)_2]^+$ cations and PF_6^- anions; one molecule of CH_2ClCH_2Cl solvent per dimer is also present and does not interact with the complex. The phosphorus atom [P(2)] of the PF_6^- anion is situated at an inversion centre. The asymmetric unit consists of only one half of the dimeric centrosymmetric unit.

The X-ray structure of the compound confirms the existence of the $[Ru_2(\mu\text{-}O_2CCH_3)_4]^+$ unit with two $OPPh_3$ ligands occupying the axial positions.

Table 2. IR and UV–vis data of compounds I–IV

Compound	IR data (cm^{-1})				UV–vis data	
	ν_a(COO)	ν_s(COO)	ν_{st}(P=O)	ν(P—F)	λ (nm)	ε ($dm^3\ mol^{-1}\ cm^{-1}$)
I	1445 vs	1400 s	1140 s	840 vs	435	1240
II	1440 vs	1400 s	1150 s	840 vs	435	1171
III	1450 vs	1400 s	1140 s	840 vs	432	838
IV	1450 vs	1400 s	1130 s	840 vs	437	659

s—strong.
vs—very strong.

The coordination polyhedra of the two metal atoms are distorted with respect to the regular octahedral arrangement. Each ruthenium atom is coordinated by four oxygen atoms of the bridged acetate groups, by one oxygen corresponding to the triphenylphosphine oxide and by the other ruthenium atom of the dimer unit.

The bond distances and angles in the $[Ru_2(\mu\text{-}O_2CCH_3)_4]^+$ unit are similar to those observed in related compounds.[16–19] The Ru—Ru distance for compound I is slightly longer (*ca* 0.019 Å) than that for its closest Ru_2^{5+} core analogue, $[Ru_2(\mu\text{-}O_2CCH_3)_4(H_2O)_2]BF_4$.[16] On the other hand, there are no important differences between the Ru—Ru distances in compound I (2.267 Å) and other compounds with the Ru_2^{5+} core, *viz.* $Ru_2Cl(\mu\text{-}O_2CCH_3)_4$ (2.281 Å),[16] $Ru_2Cl(\mu\text{-}O_2CCH_3)_4 \cdot 2H_2O$ (2.267 Å),[17] the Ru_2^{4+} core, *viz.* $Ru_2(\mu\text{-}O_2CCH_3)_4(THF)_2$ (2.260 Å)[18] or the Ru_2^{6+} core, *viz.* $Ru_2(\mu\text{-}O_2CCH_3)_4(O_2CCH_3)_2 \cdot 0.7H_2O$ (2.265 Å),[19] although

Table 3. Magnetic susceptibilities for compounds I–IV at various temperatures

	$[Ru_2(\mu\text{-}O_2CCH_3)_4(OPPh_3)_2]PF_6 \cdot CH_2ClCH_2Cl$ (I)				
T (K)	279.4	250.6	219.8	190.0	160.1
$X_M \times 10^3$	7.762	8.302	9.659	10.910	13.140
T (K)	130.2	100.5	90.5	80.5	70.5
$X_M \times 10^3$	16.010	20.110	22.030	24.580	27.760
	$\{Ru_2(\mu\text{-}O_2CCH_3)_4[OP(p\text{-}FC_6H_4)_3]_2\}PF_6 \cdot CH_2Cl_2$ (II)				
T (K)	289.8	259.3	229.6	199.3	169.9
$X_M \times 10^3$	9.026	10.490	12.000	14.040	16.320
T (K)	140.0	110.3	100.4	90.5	80.3
$X_M \times 10^3$	20.190	25.060	26.200	29.890	34.710
	$\{Ru_2(\mu\text{-}O_2CCH_3)_4[OP(p\text{-}CH_3OC_6H_4)_3]_2\}PF_6$ (III)				
T (K)	259.8	229.6	199.7	175.0	150.2
$X_M \times 10^3$	5.074	6.196	7.058	8.072	9.474
T (K)	125.2	100.5	90.3	80.4	73.2
$X_M \times 10^3$	11.330	13.920	15.540	17.340	18.550
	$\{Ru_2(\mu\text{-}O_2CCH_3)_4[OP(p\text{-}ClC_6H_4)_3]_2\}PF_6$ (IV)				
T (K)	266.8	227.0	189.9	170.0	150.2
$X_M \times 10^3$	6.222	6.803	6.976	7.703	8.357
T (K)	130.2	110.3	100.4	90.7	80.5
$X_M \times 10^3$	8.880	9.720	10.120	10.620	11.660

Table 4. Selected bond lengths and bond angles of **I**

Bond distances (Å)		Bond angles (°)			
Ru—Ru	2.267(1)	O(1)—Ru—O(2)	178.7(2)	Ru—O(1)—C(1)	118.9(4)
Ru—O(1)	2.014(6)	O(1)—Ru—O(3)	89.9(2)	Ru—O(2)—C(1)	118.7(5)
Ru—O(2)	2.018(6)	O(1)—Ru—O(4)	90.6(3)	Ru—O(3)—C(3)	119.1(4)
Ru—O(3)	2.018(6)	O(1)—Ru—O(5)	90.7(2)	Ru—O(4)—C(3)	118.0(5)
Ru—O(4)	2.030(6)	O(2)—Ru—O(3)	90.4(2)	Ru—O(5)—P(1)	141.9(3)
Ru—O(5)	2.227(4)	O(2)—Ru—O(4)	89.1(2)	O(1)—C(1)—O(2)	123.6(8)
P(1)—O(5)	1.503(4)	O(2)—Ru—O(5)	90.6(2)	O(1)—C(1)—C(2)	117.7(7)
P(1)—C(5)	1.787(8)	O(3)—Ru—O(4)	179.1(2)	O(2)—C(1)—C(2)	118.7(7)
P(1)—C(11)	1.784(8)	O(3)—Ru—O(5)	89.6(2)	O(3)—C(3)—O(4)	123.5(7)
P(1)—C(17)	1.797(7)	O(4)—Ru—O(5)	91.2(2)	O(3)—C(3)—C(4)	116.7(7)
P(2)—F(1)	1.570(8)	O(5)—P(1)—C(5)	112.4(3)	O(4)—C(3)—C(4)	119.8(7)
P(2)—F(2)	1.489(10)	O(5)—P(1)—C(11)	111.7(3)	Ru′—Ru—O(1)	89.2(1)
P(2)—F(3)	1.526(10)	O(5)—P(1)—C(17)	110.0(3)	Ru′—Ru—O(2)	89.5(1)
O(1)—C(1)	1.263(8)	C(5)—P(1)—C(11)	107.7(4)	Ru′—Ru—O(3)	89.0(1)
O(2)—C(1)	1.257(7)	C(5)—P(1)—C(17)	107.6(3)	Ru′—Ru—O(4)	90.2(1)
O(3)—C(3)	1.283(9)	C(11)—P(1)—C(17)	107.3(4)	Ru′—Ru—O(5)	178.6(2)
O(4)—C(3)	1.260(7)	F(1)—P(2)—F(2)	80.9(5)		
C(1)—C(2)	1.490(10)	F(1)—P(2)—F(3)	89.3(5)		
C(3)—C(4)	1.491(13)	F(2)—P(2)—F(3)	93.8(6)		

this compound has been reformulated by Cotton *et al.*[20] as $Ru_2(\mu\text{-}O_2CCH_3)_4(O_2CCH_3)_2H \cdot 0.7H_2O$ containing the Ru_2^{5+} unit.

EXPERIMENTAL

All reactions were carried out in an inert atmosphere, using standard Schlenk techniques. $Ru_2Cl(\mu\text{-}O_2CCH_3)_4$ was prepared by a literature procedure.[21] $RuCl_3 \cdot 3H_2O$, $NOPF_6$, PPh_3 and $P(p\text{-}RC_6H_4)_3$ (R = F, CH_3O, Cl) were obtained from Engelhard, Alfa, Probus and Maybridge, respectively. Solvents were purified and distilled by standard methods. Methanol was used without previous purification.

Elemental microanalysis for carbon and hydrogen were performed with a Perkin–Elmer 240 B microanalyser. IR spectra in the region 4000–200 cm^{-1} were recorded as KBr disks on a Perkin–Elmer 1330 IR spectrophotometer. Electronic spectra in the region 300–800 nm were registered on a Pye Unicam SP8-200 UV–vis spectrophotometer. Magnetic measurements were made with a magnetometer DSM 5 in the range 70–290 K. Molar

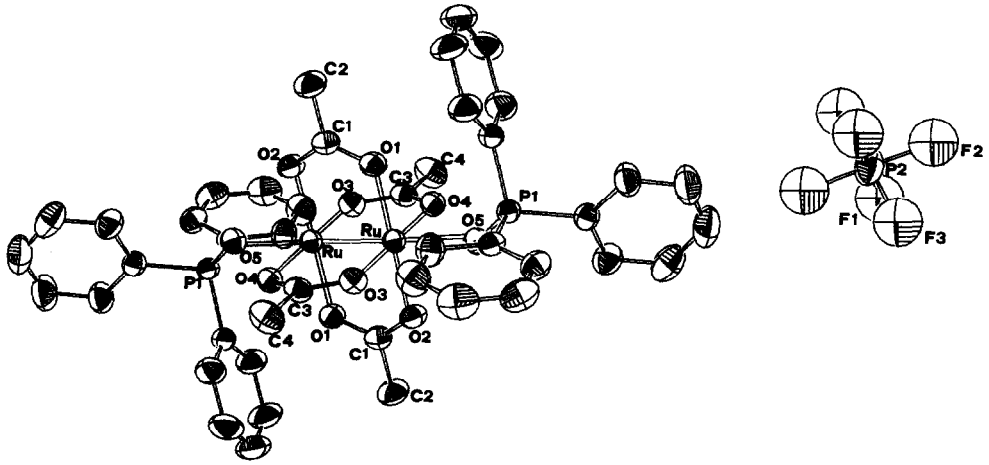

Fig. 1. ORTEP drawing of $[Ru_2(\mu\text{-}O_2CCH_3)_4(OPPh_3)_2]PF_6 \cdot CH_2ClCH_2Cl$.

conductivities were measured with a Philips PW 9526 digital conductivity meter, using a Philips PW 9512/60 conductivity measuring cell.

Synthesis of $[Ru_2(\mu\text{-}O_2CCH_3)_4(OPPh_3)_2]PF_6$ **(I)**

This compound was prepared by reaction of $Ru_2Cl(\mu\text{-}O_2CCH_3)_4$, $NOPF_6$ and PPh_3 in methanol, as previously described.[13] When the reaction was carried out in refluxing methanol, the process was completed in 1 h.

The complex was crystallized from 1,2-dichloroethane–petroleum ether (40–60°C) to give red crystals of $[Ru_2(\mu\text{-}O_2CCH_3)_4(OPPh_3)_2]PF_6 \cdot CH_2ClCH_2Cl$.

Synthesis of $\{Ru_2(\mu\text{-}O_2CCH_3)_4[OP(p\text{-}FC_6H_4)_3]_2\}PF_6$ **(II)**

To $Ru_2Cl(\mu\text{-}O_2CCH_3)_4$ (0.20 g, 0.42 mmol) in methanol (40 cm^3) was added an excess of $NOPF_6$ (0.22 g, 1.27 mmol) and $P(p\text{-}FC_6H_4)_3$ (0.67 g, 2.11 mmol). The reaction mixture was stirred at room temperature for 6 h (or under reflux for 3 h). The solvent was pumped to dryness giving an oil, which was treated with cold petroleum ether (40–60°C) to obtain a brown–yellow solid. The solid was washed with diethylether–petroleum ether (40–60°C) (1 : 1).

The solid product was crystallized from dichloromethane–petroleum ether (40–60°C) to give red–brown crystals of $\{Ru_2(\mu\text{-}O_2CCH_3)_4[OP(p\text{-}FC_6H_4)_3]_2\} \cdot CH_2Cl_2$. Yield 0.28 g, 54%.

Synthesis of $\{Ru_2(\mu\text{-}O_2CCH_3)_4[OP(p\text{-}CH_3OC_6H_4)_3]_2\}PF_6$ **(III)**

To $Ru_2Cl(\mu\text{-}O_2CCH_3)_4$ (0.20 g, 0.42 mmol) in methanol (40 cm^3) was added an excess of $NOPF_6$ (0.22 g, 1.27 mmol) and $P(p\text{-}CH_3OC_6H_4)_3$ (0.75 g, 2.11 mmol). The reaction mixture was stirred at room temperature for 6 h (or under reflux for 3 h). The solvent was pumped to dryness giving a golden, spumy solid. This solid did not crystallize from several mixtures of solvents, such as dichloromethane–petroleum ether (40–60°C), THF–petroleum ether (40–60°C), etc. For this reason the solid was purified by precipitation with petroleum ether (40–60°C) from a solution of dichloromethane. Yield 0.34 g, 61%.

Table 5. Crystallographic data for compound **I**

Formula	$Ru_2O_{10}C_{46}H_{46}P_3F_6Cl_2$
Formula weight	1238.82
Space group	$P\bar{1}$
a (Å)	8.46(2)
b (Å)	12.399(2)
c (Å)	13.017(4)
α (°)	105.18(2)
β (°)	92.64(5)
γ (°)	108.81(5)
V (Å^3)	1234(3)
Z ($RuO_5C_{23}H_{23}P_{1.5}F_3Cl$)	2
$F(000)$	623
$d_{calc.}$ (g cm^{-3})	1.67
Crystal size (mm)	$0.2 \times 0.3 \times 0.4$
μ(Mo-K_α) (cm^{-1})	8.81
Data collection instrument	Enraf–Nonius Cad-4
Radiation	Mo-K_α (λ = 0.71069 Å)
Temperature (K)	295
Scan method	ω–2θ
Data collection range 2θ (°)	$1 < \theta < 30$
Number of unique data, total with $I > 2\sigma(I)$	6591
Number of parameters refined	557
R^a	0.07
$R_w{}^b$	0.09
Average shift/error	0.03

[a] $R = \Sigma ||F_o| - |F_c|| / \Sigma F_o$.

[b] $R_w = [\Sigma w(|F_o| - |F_c|)^2 / \Sigma w|F_o|^2]^{1/2}$; $w = 1/\sigma^2(|F_o|)$.

Synthesis of $\{Ru_2(\mu\text{-}O_2CCH_3)_4[OP(p\text{-}ClC_6H_4)_3]_2\}PF_6$ **(IV)**

To $Ru_2Cl(\mu\text{-}O_2CCH_3)_4$ (0.20 g, 0.42 mmol) in methanol (40 cm^3) was added an excess of $NOPF_6$ (0.22 g, 1.27 mmol) and $P(p\text{-}ClC_6H_4)_3$ (0.77 g, 2.11 mmol). The reaction mixture was stirred at room temperature for 6 h (or under reflux for 3 h). The solution was pumped to dryness giving an oil, which was treated with cold petroleum ether (40–60°C) to give a brown–yellow solid. The compound could not be crystallized from several mixtures of solvents, because it decomposes over short periods of time. For this reason the product was purified by precipitation with petroleum ether (40–60°C) from a solution of dichloromethane. Yield 0.28 g, 49%.

X-ray crystallographic procedures

A prismatic crystal was mounted on an Enraf–Nonius CAD4-F automatic diffractometer. The cell dimensions were refined by least-squares fitting of the setting angles of 25 reflections. The intensities of all 7745 reflections with $1 < \theta < 30$ and the range from $(-11, -17, 0)$ to (11, 17, 18) were measured at 295 K with monochromatic Mo-K_α radiation ($\lambda = 0.71069$ Å) and an ω–2θ scan technique.

Three reflections monitored periodically during data collection revealed no crystal decomposition. The intensities were corrected for Lorentz and for polarization effects; 6591 reflections were considered as observed with $I > 2\sigma(I)$. Scattering factors for neutral atoms and anomalous dispersion corrections for ruthenium, fluorine and chlorine were taken from the *International Tables for X-Ray Crystallography*.[22] The structure was solved by Patterson and Fourier methods. An empirical absorption correction[23] was applied at the end of the isotropic refinement. Some positional disorder was found around the CH_2ClCH_2Cl molecule of crystallization and the PF_6^- anion, and because of this, the atoms involved in these groups, F, Cl and C(23) have been refined only isotropically. Mixed full-matrix least-squares refinement with unit weights minimizing $[F_o - F_c]$ gave $R = 0.072$. Final refinement with fixed isotropic temperature factors and coodinates for hydrogen atoms gave $R = 0.07$. Most of the calculations were carried out with XRAY80.[24] Crystallographic data and other basic information pertaining to the data collection are summarized in Table 5.

Complete tables of distances and angles as well as atomic positional and anisotropic thermal parameters and structure factors have been deposited as supplementary material.

Acknowledgements—We are grateful to the Comision Asesora de Investigacion Cientifica y Tecnica (CAICYT) (Spain) for financial support (project PR84-0367). Thanks are due to Dr Saez and colleagues for their help in obtaining the magnetic measurements.

REFERENCES

1. E. W. Harlan, J. M. Berg and R. H. Holm, *J. Am. Chem. Soc.* 1986, **108**, 6992 and refs therein.
2. S. A. Roberts, C. G. Young, W. E. Cleland Jr, R. B. Ortega and J. H. Enemark, *Inorg. Chem.* 1988, **27**, 3044 and refs therein.
3. H. Arzoumanian, J. F. Petrignani, M. Pierrot, F. Ridouane and J. Sanchez, *Inorg. Chem.* 1988, **27**, 3377.
4. M. S. Reynolds, J. M. Berg and R. H. Holm, *Inorg. Chem.* 1984, **23**, 3057.
5. G. J.-J. Chen, J. W. McDonald and W. E. Newton, *Inorg. Chem.* 1976, **15**, 2612.
6. B. W. Graham, K. R. Laing, C. J. O'Connor and W. R. Roper, *Chem. Commun.* 1970, 1272.
7. J. Halpern and A. L. Pickard, *Inorg. Chem.* 1970, **90**, 2798.
8. A. Sen and J. Halpern, *J. Am. Chem. Soc.* 1977, **99**, 8337.
9. R. A. Head and J. F. Nixon, *J. Chem. Soc., Dalton Trans.* 1978, 909.
10. M. M. Taqui Khan, M. R. H. Siddiqui, A. Hussain and M. A. Moiz, *Inorg. Chem.* 1986, **25**, 2765.
11. B. A. Moyer, B. K. Sipe and T. J. Meyer, *Inorg. Chem.* 1981, **20**, 1475.
12. B. W. Graham, K. R. Laing, C. J. O'Connor and W. R. Roper, *J. Chem. Soc., Dalton Trans.* 1972, 1237.
13. F. A. Urbanos, M. C. Barral and R. Jimenez-Aparicio, *Polyhedron* 1988, **7**, 2597.
14. W. J. Geary, *Coord. Chem. Rev.* 1971, **7**, 81.
15. J. G. Norman, Jr, G. E. Renzoni and D. A. Case, *J. Am. Chem. Soc.* 1979, **101**, 5256.
16. T. Togano, M. Mukaida and T. Nomura, *Bull. Chem. Soc. Jpn* 1980, **53**, 2085.
17. A. Bino, F. A. Cotton and T. R. Felthouse, *Inorg. Chem.* 1979, **18**, 2599.
18. A. J. Lindsay, R. P. Tooze, M. Motevalli, M. B. Hursthouse and G. Wilkinson, *J. Chem. Soc., Chem. Commun.* 1984, 1383.
19. M. G. B. Drew, P. Higgins and G. M. McCann, *J. Chem. Soc., Chem. Commun.* 1987, 1385.
20. F. A. Cotton, M. Matusz and B. Zhong, *Inorg. Chem.* 1988, **27**, 4368.
21. R. W. Mitchell, A. Spencer and G. Wilkinson, *J. Chem. Soc., Dalton Trans.* 1973, 846.
22. *International Tables for X-ray Crystallography*, Vol. IV, pp. 72–98. Kynoch Press, Birmingham (1974).
23. N. Walker and D. Stuart, *Acta Cryst.* 1983, **A39**, 158.
24. J. M. Stewart, F. A. Kundell and J. C. Baldwin, *The X-Ray 80 System.* Computer Science Center, University of Maryland, College Park, Maryland (1980).

Polyhedron Vol. 8, No. 21, pp. 2577–2585, 1989
Printed in Great Britain

0277–5387/89 $3.00+.00
© 1989 Pergamon Press plc

FORMATION OF SILICO–ANTIMONIC CORE-SHELL PARTICLES WITH AN ANTIMONIC ACID CORE ENCAPSULATED WITH SILICA

M. KONE, P. COURTIN and J. LEMERLE*

Laboratoire de Chimie des Polymères Inorganiques, Université Pierre et Marie Curie, 4 Place Jussieu, 75252 Paris Cedex 05, France

(*Received* 7 *March* 1989; *accepted* 12 *June* 1989)

Abstract—Core-shell particles were formed from aqueous solutions of antimonic and silicic acids. Three methods were developed for preparing the particles: (i) mixing freshly prepared antimonic and silicic acids (A); (ii) mixing potassium salts of antimonic and silicic acids followed by protonation by ion exchange (B); (iii) hydrolysis of a tetraethoxysilane solution in ethanol by an aqueous antimonic acid solution (C). Methods (A) and (B) led to three-dimensional core-shell particles with the β-antimonic acid structure. Three-dimensional core-shell particles were formed only through route (C) when alkoxysilane was in excess. Without an excess of alkoxysilane, fibrous silicic particles including antimony were obtained. The nature and size of the particles are closely dependent upon the reaction rates (polymerization, mixed compound formation).

Particles of inorganic oxides of colloidal size can be prepared by spontaneous polymerization of an inorganic acid in aqueous solution. In previous works[1,2] inorganic polymers containing antimony have been prepared by ion exchange. The β-antimonic acid forms particles with a cubic close-packing structure (c.c.p.). Polymerization of antimonic acid in the presence of other inorganic acids leads to mixed polymers. Hexacoordinated anions can substitute the SbO_6 groups to form particles with a c.c.p. structure.[3,4] With tetracoordinated anions, the substitution prevents the extension of the structure to give amorphous particles.[5,6] Silica gels have been prepared by various routes such as protonation of a silicate,[7] or the hydrolysis of an alkoxysilane.[8] Silica gels including a heteroelement have been obtained by hydrolysis of a mixture of an alkoxysilane with another alkoxide or ethoxide.[9] In this work we describe the formation of particles including both antimony and silicon. Different routes of synthesis are used to show the importance of the polymerization rate on the formation of the compounds.

* Author to whom correspondence should be addressed.

EXPERIMENTAL

Preparation of the sols

Preparation (A). The antimonic acid was prepared by ion exchange in a resin (DOWEX 50 WX2 100–200 mesh) from potassium hexahydroxoantimonate solutions (Merck).[1] The silicic acid was prepared according to Alexander's method:[10] solid sodium metasilicate (Na_2SiO_3, 5 H_2O) was slowly added to an excess of resin (DOWEX 50 WX8 100–200 mesh, H^+ form), dispersed in water. During the addition the mixture was vigorously stirred and kept at 0°C. After filtration, the proportion of oligomers in silicic acid (17%), determined according to the Coudurier's method,[11] showed the main silicic species to be monomeric. The antimonic and silicic acids were mixed in various ratios ($0.059 \leqslant Si/Sb \leqslant 3.53$) just after preparation. In the mixtures, the antimony concentration is constant (3.9×10^{-2} mol dm^{-3}).

Preparation (B). Potassium hexahydroxoantimonate and potassium silicate solutions were mixed in various ratios ($0.06 \leqslant Si/Sb \leqslant 3.06$). Potassium salts prevented sodium antimonate precipitation; the antimony concentration was

constant (8.5×10^{-2} mol dm^{-3}). The potassium silicate solutions were prepared by ion exchange on a resin (DOWEX 50 WX2 50–100 mesh, K^+ form) and then the mixture was protonated on another resin (DOWEX 50 WX2 50–100 mesh, H^+ form). The resin was poured into a column with a cooled jacket to maintain a constant temperature (5°C). During the acidification the antimony concentration decreased slightly.

Preparation (C). A solution of tetraethoxysilane in ethanol was slowly added under stirring to a freshly prepared aqueous antimonic acid solution (α-antimonic acid)[1] ($0.067 \leqslant Si/Sb \leqslant 4.01$). The antimony concentration was constant (3.68×10^{-2} mol dm^{-3}). Under these conditions the silane is hydrolysed in the presence of antimonic acid.

Physicochemical measurements

For all the samples the concentrations of the antimony and silicon were measured by atomic absorption, with an air–acetylene flame for antimony, and a nitrous–acetylene flame for silicon.

Ultracentrifuge measurements were carried out with a Beckman model E ultracentrifuge equipped with schlieren optics. The solvents were water [samples (C)] or LiCl solutions, 5×10^{-2} mol dm^{-3} [samples (A) and (B)]. The electrolytes were slowly added just before the runs. Preparative centrifugations were monitored in the same ultracentrifuge equipped with a swinging bucket rotor SW65E.

Density measurements were carried out with a DMA_2 PAAR automatic densimeter.

The particles which packed down to the bottom of the centrifugation tube were studied by electron microscopy, X-ray and NMR spectroscopies. Electron microscopy was carried out with a Jeol 100 CXII microscope at a magnification of 63,000. Samples were prepared by deposition of the dilute sol containing the particles on a grid. Analytical electronic microscopy was carried out with Link equipment. Powder patterns were obtained by diffractometry with a CGR Theta 60 diffractometer using Cu-K_α radiation. Analytical grade NaCl was added to the powders as an internal standard in order to obtain accurate d-spacing.[12]

^{29}Si NMR spectra of the solids were obtained at room temperature with a MSL 400 Bruker spectrometer, using the MAS technique.

RESULTS

Study of the sols

All the aged samples (3 months) scatter light, the (C) samples gelled. In analytical ultracentrifuge experiments free sedimenting species were observed. The sedimentation coefficients corresponding to samples (A), (B) and (C) are reported in the Tables 1, 2 and 3, respectively. Only one sedimentation peak is observed for $Si/Sb \leqslant 1$, while two peaks are present for higher Si/Sb ratios. The particles having the higher sedimentation coefficient are labelled "high polymers".

By assuming that the particles are rigid and spherical, the friction coefficient can be evaluated from Stokes' law. Under these conditions the particle size can be obtained from the sedimentation velocity, S.[13]

$$D = 2\sqrt{\frac{9S\eta}{2(\rho - \rho_0)}}$$

Table 1. Sedimentation coefficients measured for the sols and the corresponding high polymer characteristics—Preparation (A)

Si/Sb initial ratio	0.059	0.188	0.35	0.82	1.52	1.88	2.36	2.94	3.53
S_1[a]	3859	4000	3850	2400	1900	2000	2000	2100	2250
S_2[a]	—	—	—	—	5.7	5.9	5.5	6.1	6.2
Si/Sb high polymers	0.059	0.104	0.173	0.187	0.193	0.203	0.201	0.207	0.210
% Sb high polymers[b]	98.4	98.4	97.6	96.3	93.8	92	89.9	87.9	83.6
D_u[c]	452	464	461	365	325	334	334	342	355
D_m[c]	505		460	310					352
Δr[d]	3	5	8	7	6	7	7	7	7.5

[a] S_1 and S_2 are expressed in Svedberg; particles with S_1 sedimentation velocity are labelled "high polymers".

[b] % Sb high polymers: ratio between concentration of antimony in the high polymers and total antimony concentration.

[c] D, diameter (in Å) of the high polymer particles: D_u = ultracentrifugation value, calculated from the inflection point on the distribution curve of the sedimentation coefficients; D_m = electronic microscopy values.

[d] Δr: estimated value of the shell thickness (in Å).

All the measurements were made on aged sols (3 months).

Table 2. Sedimentation coefficients measured for the sols and the corresponding high polymer characteristics—Preparation (B)

Si/Sb initial ratio	0.060	0.34	0.54	1.04	1.35	2.09	3.06
S_1	880	596	583	584	696	586	751
S_2					15.3	17.5	17.1
Si/Sb high polymers	0.057	0.32	0.54	1.02	0.62	0.59	0.47
% Sb high polymers	98.9	86.5	88.7	76.2	89.3	72.9	84.4
D_u	216	186	190	202	210	192	214
D_m	200	200	200	200	200	200	200
Δr	2	6	9	16	11	10	9

See footnotes to Table 1 for abbreviations.

Table 3. Sedimentation coefficients measured for the sols and the corresponding high polymer characteristics—Preparation (C)

Si/Sb initial ratio	0.067	0.40	0.80	1.34	1.74	2.14	2.67	3.34	4.01
S_1	79	88	112	135	207	277	349	776	1282
S_2				2.8	3.7	4.8	4.1	4.1	6.7
Si/Sb high polymers	0.045	0.062	0.077	0.072	0.083	0.073	0.08	0.113	0.175
% Sb high polymers	64.1	70.6	76.6	96.7	89	91.8	91.3	84.2	81

See footnotes to Table 1 for abbreviations.

D is the diameter of the particle, η is the solvent viscosity, ρ is the particle density and ρ_0 is the solvent density; ρ and ρ_0 were obtained from density measurements.

The particle size values are reported in Tables 1 and 2.

For each sample the cumulative distribution curves of the sedimentation coefficients of the "high polymers" are shown in Fig. 1. Within each group of samples the polydispersity of the high polymers increases with the initial Si/Sb ratio. The high polymeric species can be easily obtained by preparative ultracentrifugation of the aged sols. The samples prepared by routes (A) and (B) were centrifuged at 20,000 r.p.m. over 30 min, while (C) samples were centrifuged at 30,000 r.p.m. over 1 h. Antimony and silicon present in the supernatant solutions were titrated. The high polymers which packed down to the bottom of the centrifugation tube were separated from the supernatant solution and their silicon and antimony content determined. The results are reported in the Tables 1, 2 and 3.

The supernatant solutions and high polymers contain both silicon and antimony with a higher proportion of antimony in the high polymer fractions (samples (B) gave high polymers with higher silicon content). No EtO groups were found in the high polymers [sample (C)] (Ir spectra, carbon microanalysis).

Study of the high polymers

The composition of the high polymers [samples (A) and (B)] is homogeneous, as shown by analytical electron microscopy. Thus the particles differ only in their size.

Electronic micrographs (TEM) of high polymers show that the shape of the particles is dependent on the route of preparation. The particles of samples (A) are spherical (Fig. 2), the particles of the samples (B) are hexagonal, square or diamond shaped (Fig. 3). These shapes can be considered as the projections of an octahedron onto a plane. These assumptions are confirmed by the STEM micrographs.

For particles of the (C) samples the shape depends on the initial Si/Sb ratio. For Si/Sb $\leqslant 3$ (silicon content of the high polymer <0.1), the electron micrographs appear to be blurred. When the silicon content increases, a fibrous structure is observed, similar to silicic acid xerogels.[14] In addition to this fibrous structure some large octahedral particles are observed for an initial Si/Sb ratio >3 (Fig. 4).

All of the (A) and (B) samples are approximately homogeneous in size. The size distribution curves corresponding to sample (A) is shown in the Fig. 5. The diameter of the particles decreases when the silicon content of the high polymers increases and

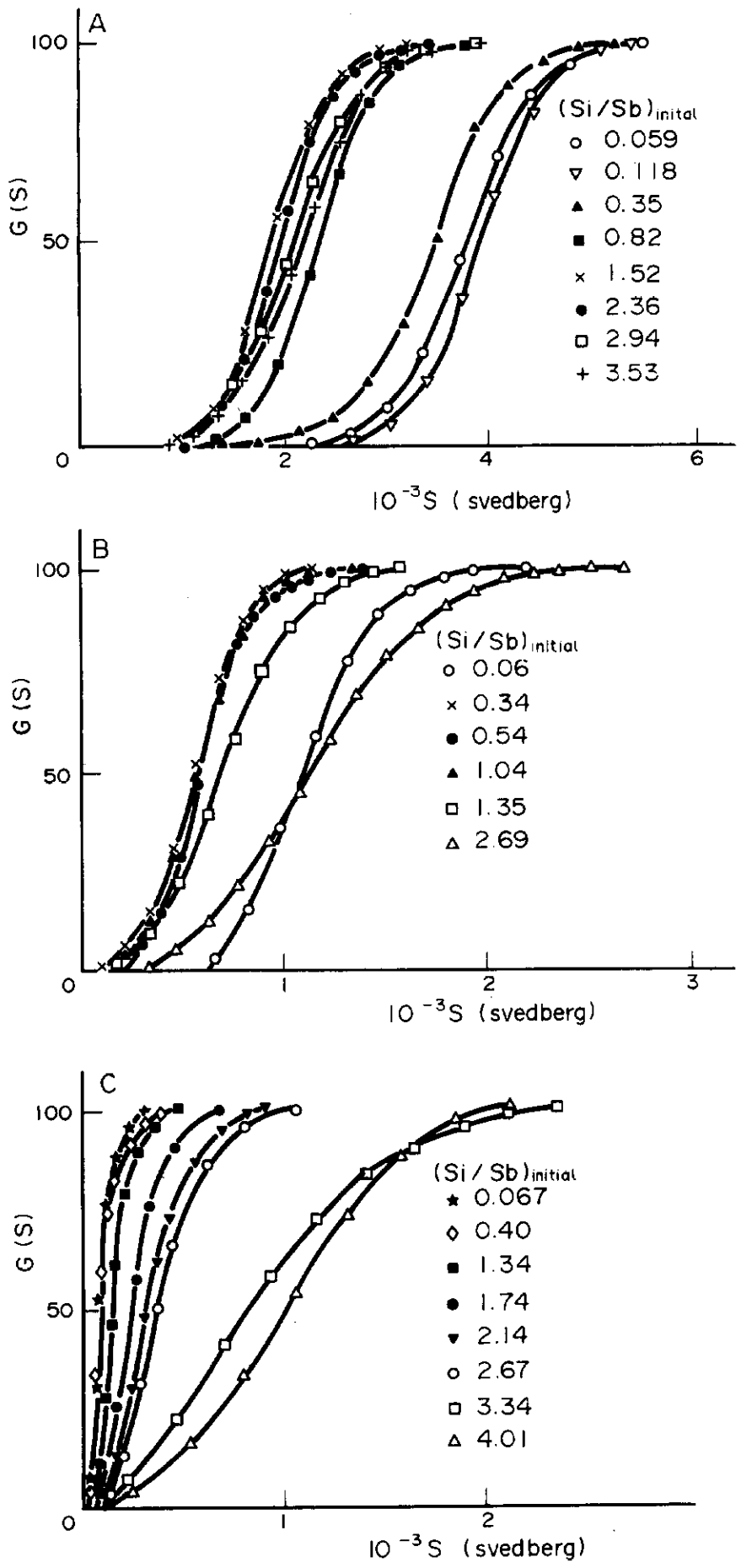

Fig. 1. Cumulative distribution curves of sedimentation coefficients of high polymers.

the size polydispersity slightly increases (Table 1). For (B) particles the size is characterized by their octahedron edges. The mean size of these particles (about 200 Å) is nearly independent of the silicon content. The size of the sample (C) particles can only be measured for the large octahedral particles for an initial Si/Sb ratio >3. The high polydispersity observed is within the 780–1960 Å range.

Powder diffraction patterns of samples (A) and (B) agree with a cubic close-packing structure (pyrochlore type, $a = 10.40$ Å) like that in the β-antimonic acid.[1] The unit cell is independent of the silicon content. The peak width gives the mean size of the crystals, with the mean values close to the electronic microscopy results.

NMR spectra are shown in the Fig. 6. For the (B) samples the peak corresponding to a chemical shift of about -112 ppm is present only when the silicon content of the high polymers is greater than 0.3. For (C) samples this peak is extremely broad and is absent in the (A) samples.

DISCUSSION

The particle sizes, measured by ultracentrifugation, electron microscopy and diffractometry, are in good agreement. Ultracentrifugation gives the hydrodynamic diameter, and electron microscopy and X-ray determine the diameter in the solid state. As these two values are close, we conclude that no noticeable particle association occurs in the aqueous solutions.

During ageing, antimonic acid solutions spontaneously transform into insoluble β-antimonic acid,[1] while silic acid solutions gel. Since the samples do not precipitate, the antimonic acid must combine with silicic acid leading to a stabilized sol. In previous work,[3] soluble compounds prepared with antimonic acid have been described. In the c.c.p. structure of the antimonic acid, antimony atoms can be substituted by octahedral atoms[3,4] and the c.c.p. structure is maintained without any dislocations. If the substitution is made by tetrahedral atoms[5,6] the c.c.p. structure is broken and no long distance order is observed in the solid materials. Even with a high silicon content, all the particles of the high polymers prepared by routes (A) and (B) have the same composition for a given initial Si/Sb ratio. The c.c.p. structure of the antimonic acid and the unit cell dimensions are conserved. Antimony atoms are substituted by tetrahedral silicon atoms. Silicons are probably located at the surface of the particles leading to core-shell particles with a narrow and/or amorphous silica shell. Thus, no additional X-ray diffraction patterns are observed.

From these assumptions the thickness Δr of the silica shell can be estimated. The core is supposed to be β-antimonic acid: $HSbO_3,1H_2O$ (molecular weight M_1, specific gravity ρ_1) and the shell silica SiO_2 (molecular weight M_2, specific gravity ρ_2). The Si/Sb ratio in the particle is x. For one mole of antimony the total volume, V, of the particle is

$$V = \frac{M_1}{\rho_1} + \frac{M_2 x}{\rho_2}.$$

The total volume of the particle is related to the

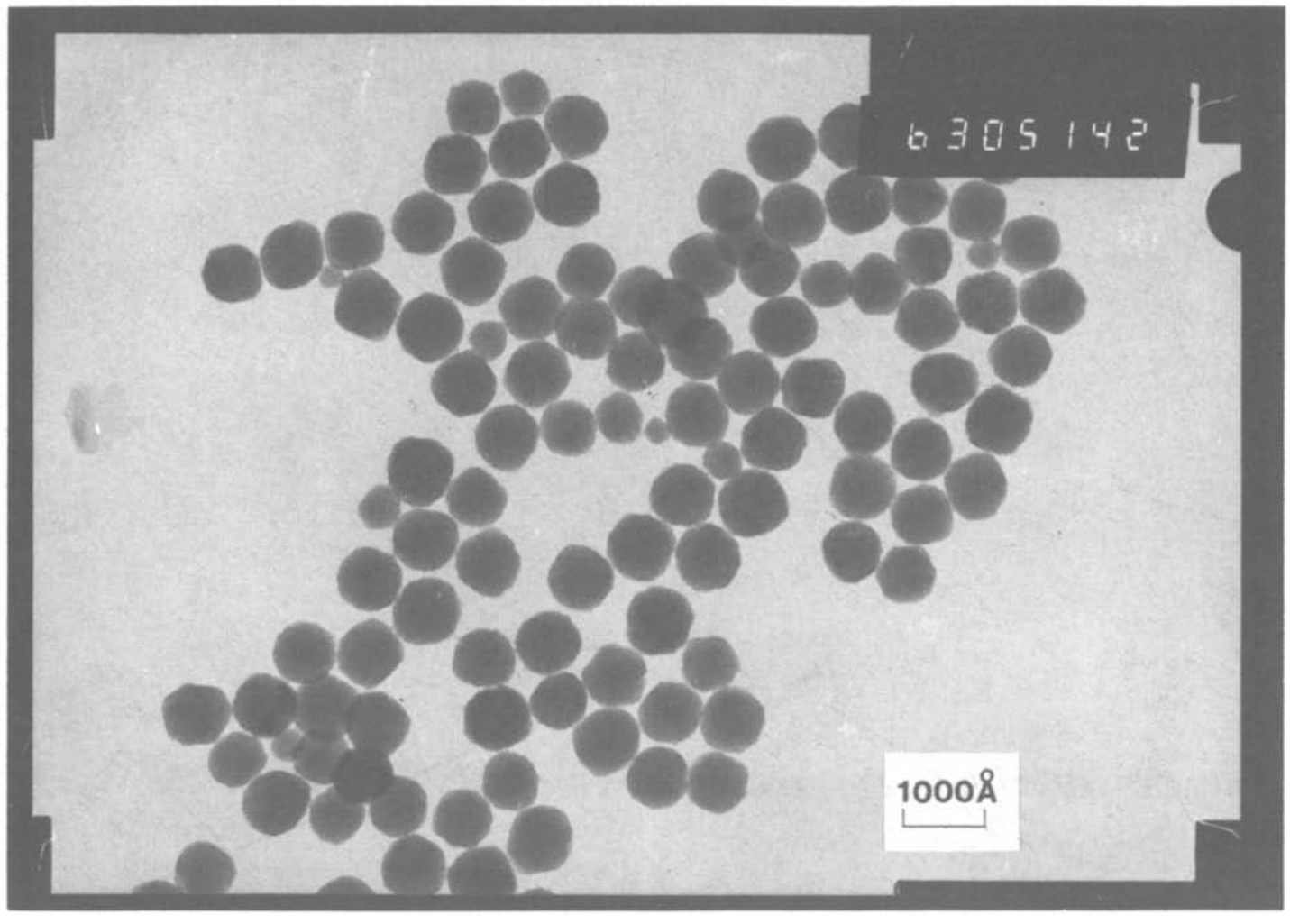

Fig. 2. Electron micrograph (TEM) of high polymers : samples (A).

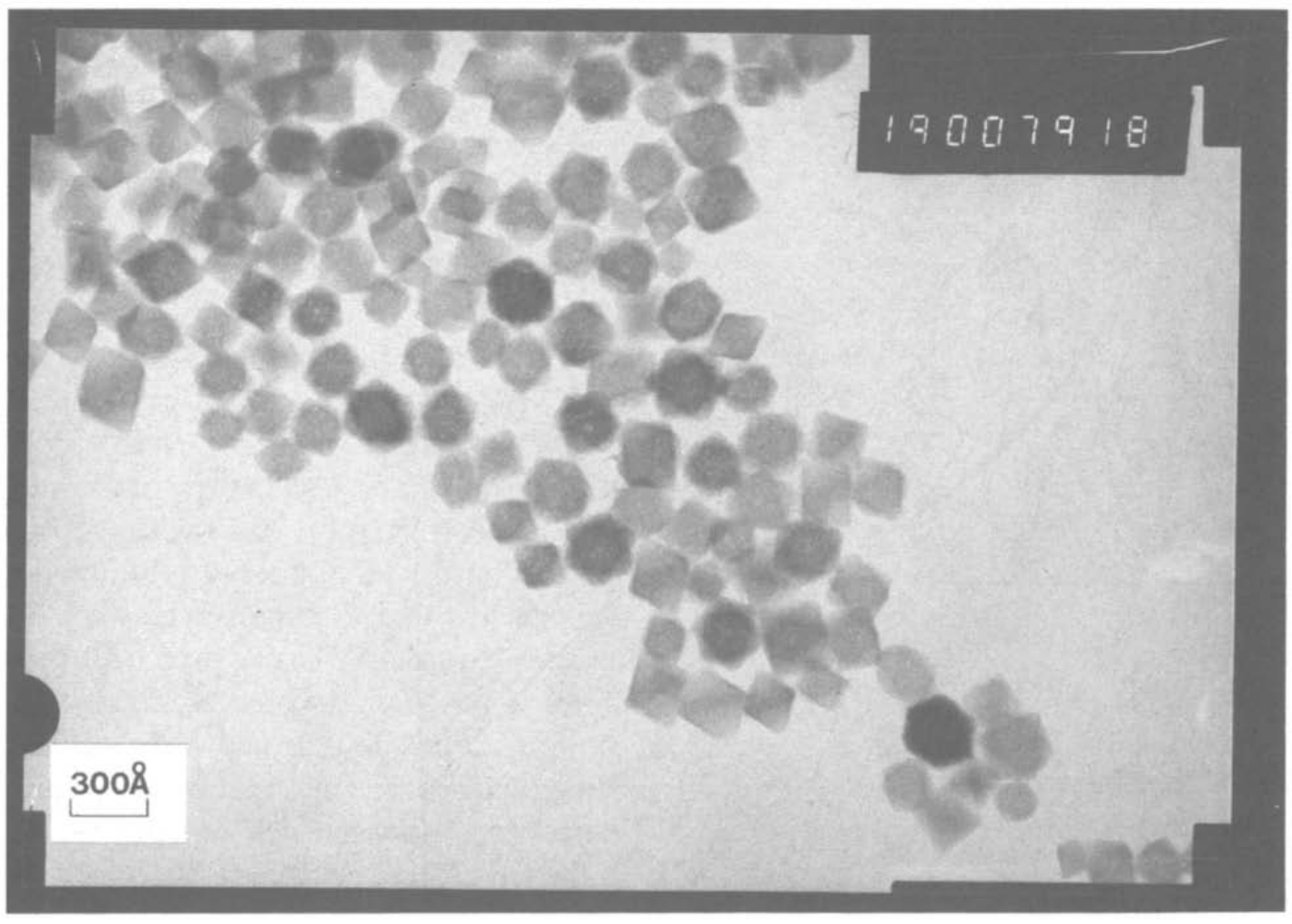

Fig. 3. Electron micrograph (TEM) of high polymers : samples (B).

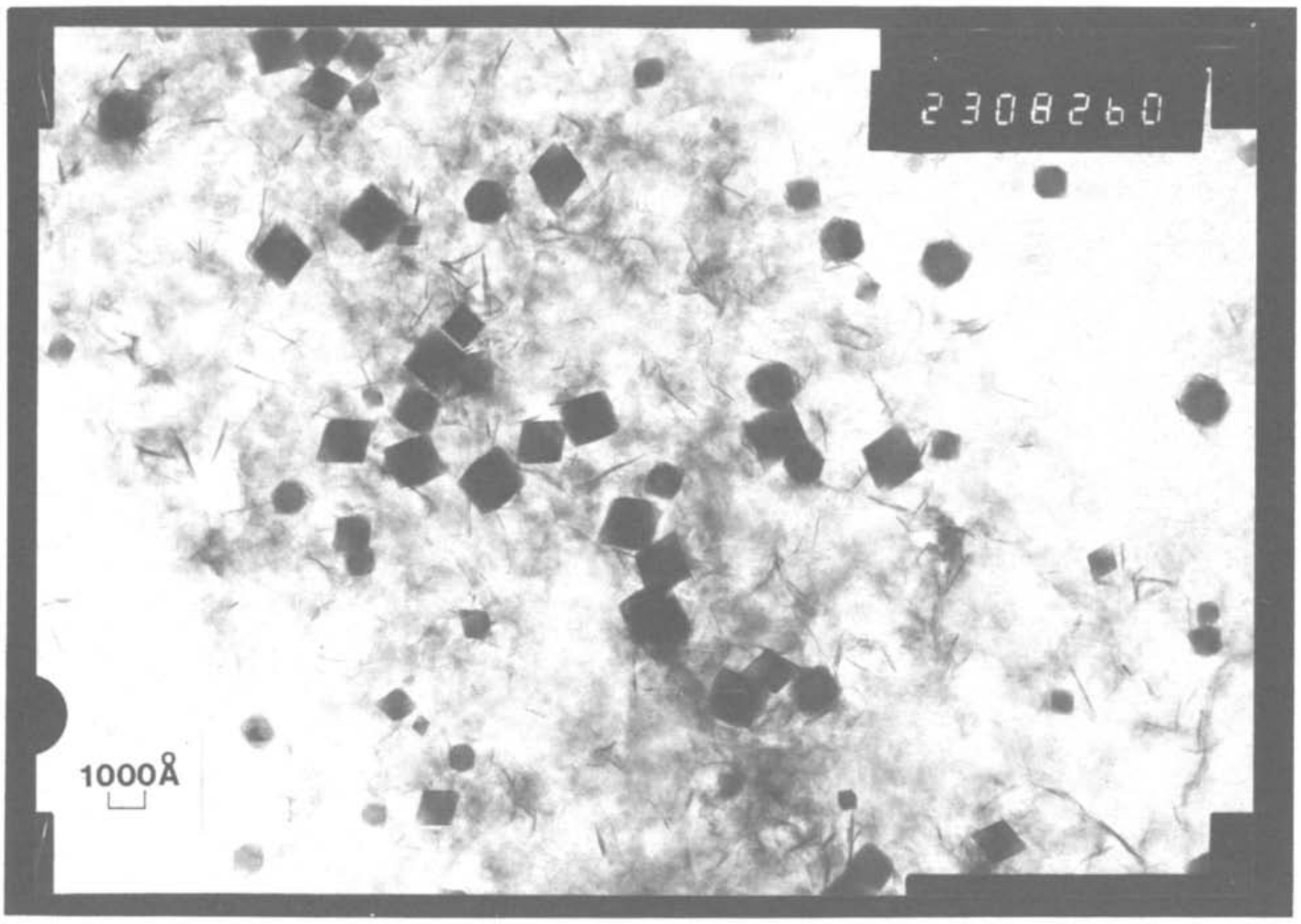

Fig. 4. Electron micrograph (TEM) of high polymers: samples (C).

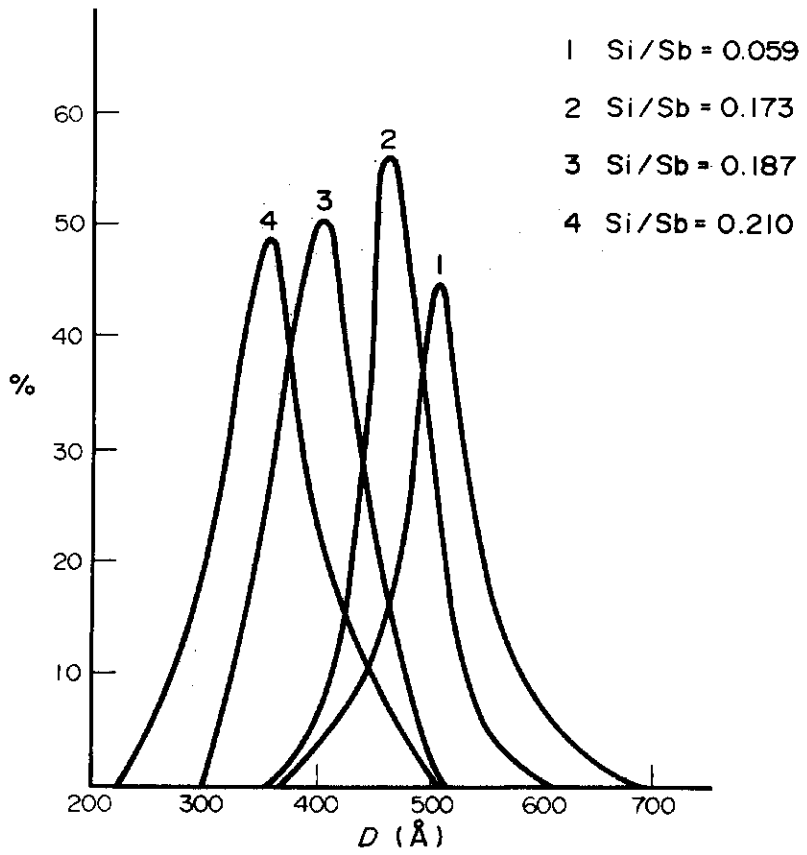

Fig. 5. Size distribution curves: samples (A).

core volume, V_1 by the expression:

$$\frac{V}{V_1} = \frac{M_1\rho_2 + M_2 x \rho_1}{M_1\rho_2} = \frac{D^3}{D_1^3},$$

where D and D_1 are, respectively, the outer and inner diameters of the particle.

If ρ_1, ρ_2 and D are known, D_1 can be obtained, and the shell thickness, $\Delta r = (D - D_1)/2$, calculated.

The diameter measured by ultracentrifugation can be considered as the outer diameter. The experimental value of ρ_1 is 4.49 g cm^{-3} (specific gravity of pure antimonic acid). The approximate value of the specific gravity of the shell is 2.2 g cm^{-3}, close to the given values for silica gels obtained through an ion exchange process.[7]* The Δr values are reported in Tables 1 and 2. Even with a high silicon content the particles have a very thin shell which cannot be seen in the X-ray diffraction experiments.

NMR spectra agree with these assumptions. Lippmaa and co-workers[15] have applied this technique to crystalline silicates and found that the ^{29}Si NMR spectra exhibit peaks whose position depends on the nature of the silicate anion. In particular, the spectra can distinguish between isolated SiO_4 tetrahedra and SiO_4 tetrahedra linked by sharing common corners (oxygen atoms) to one, two, three or four adjacent tetrahedra. In order to facilitate the discussion, it is customary to assign to each silicon a Q value which represents the number of adjacent SiO_4 tetrahedra to which it is directly bonded. Q values range from 0 (in *ortho*-silicates) to 4 in a three-dimensional framework structure (SiO_2). The position of the ^{29}Si NMR peaks, i.e. the chemical shifts relative to the internal standard (TMS) depend approximately on the Q value. Moreover, the chemical shift depends on the nature and the number of adjacent atoms bonded to the

* If the specific gravity of the shell is taken in the range 2–2.4 g cm^{-3}, the shell thickness value is kept approximately constant.

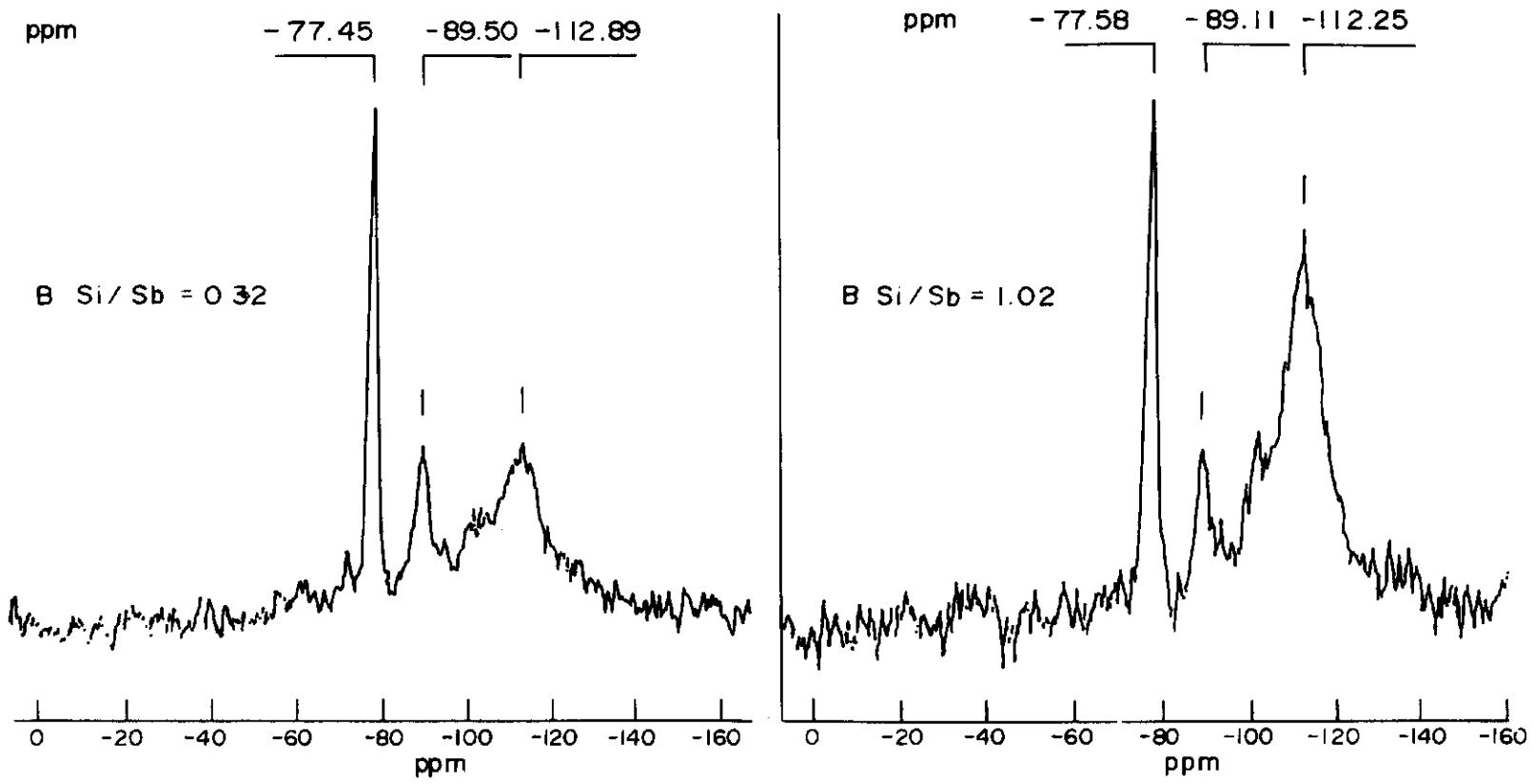

Fig. 6. ^{29}Si NMR spectra of the solid high polymer.

SiO_4 tetrahedra if they are not silicon atoms.[16] The changes in electronic density surrounding one silicon atom influence the chemical shift value corresponding to a given configuration. The chemical shift is decreased if the electronic density near the silicon atom is increased, as it is for the related alumino silicates structures.[17]

Samples (A) and (B) have a small calculated thickness ($\Delta r < 9$ Å), the NMR spectra exhibit two peaks corresponding to chemical shift values near to -78 and -89 ppm which agree with slightly bonded Q^1 and Q^2 silicon. Nevertheless this Q^2 chemical shift is slightly modified[15] and the peak is broadened. This can be attributed to silicon atoms which are two-fold bonded. Among silica atoms one can be bonded to an antimony atom.

Δr increases ($\Delta r > 9$ Å) with the silicon content of the sample (B) polymers. Three-dimensional frameworks are obtained which are characterized by a Q^4 peak. A third peak corresponding to a chemical shift of about -112 ppm is observed as expected for the Q^4 configuration.

For the (C) samples, only one broad peak, located at about -112 ppm corresponding to a Q^4 configuration, is observed. The fibrous structure revealed by the electron microscopy corresponds to thick silica fibres including antimony atoms statistically distributed. The Q^4 peak is broadened.

All the sols contain two types of particles (large and small polymers) irrespective of the preparation. On the other hand, the size, the polydispersity and the composition of the high polymer are governed by the method of preparation. Equilibria can be displaced and/or polymerization rates modified, to favour the formation of one type of particle. In (A), the protonation is carried out before the mixing. The sol contains two compounds, with different silicon contents and different molecular weights. In (B), the protonation is carried out after the mixing. The sol contains two compounds of different molecular weight but with approximately the same silicon content for an initial ratio of $Si/Sb \leqslant 1$ or a different silicon content for $Si/Sb > 1$. In (C), the protonation of antimony is carried out before the mixing and the protonation of silicon after. The sol contains two (or more) compounds of different molecular weight and different silicon content.

In previous works,[2,3] the formation process of such high polymers was described. When inorganic acids which spontaneously polymerize are mixed, the first step of the chemical reaction is the depolymerization of the reactants, α-antimonic acid and oligomers of silicic acid. The second step is the formation of an oxo bridge by elimination of water between two monomers. These oxo bridges can be formed between two antimonic octahedra, two silicic tetrahedra, or one antimonic octahedron and one silicic tetrahedron. Assuming that the structure consists of the same type of atoms, the formation of an oxo bridge between an atom of this structure and a heteroatom of different symmetry prevent the extention of the network. Nevertheless, a few heteroatoms can be bonded together through oxo bridges. If the first structure has the critical size, core-shell particles are formed.

The silicic acid reacts slowly with respect to the α-antimonic acid polymerization rate.[1,3,7,11] For the (A) samples, monomer units of antimony react with monomers or oligomers of silicic acid before they are depolymerized. The free antimony atoms (monomer units or α-acid) polymerize to reach the critical size which then catalyses their own formation.[1] Addition of an excess of silicon rapidly limits the polymerization of antimony to yield small core-shell particles. With lower silicon concentrations large core-shell particles are observed because the polymerization rate of antimony is less limited.

For the (B) samples, the protonation is carried out after the mixing, so no polymerized species are present in solution when antimony and silicon are mixed. Thus the growth of the antimony particles is stopped earlier than for the (A) samples: the particle size is approximately independent of the initial ratio Si/Sb. If silicon is in excess ($Si/Sb > 1$), it is preferentially fixed upon the small particles and the silicon content of the high polymers is lowered.

In the (C) samples, the hydrolysis of tetraethoxysilane leads to polydisperse polymeric silica compounds.[10,14] Under weak acidic conditions, the hydrolysis of $(EtO)_4Si$ leads to a low concentration of $(EtO)_3SiOH$. The excess of antimonic acid catalyses the hydrolysis of $(EtO)_4Si$. Thus the polymerization rate of silica is enhanced.[14] Antimony is then entirely included in the amorphous silica polymers, the β-antimonic structure is not formed. When the silicon concentration increases in the medium, the hydrolysis rate is decreased, lowering the silica polymerization rate. Particles of β-antimony structure can be formed.

For (A), (B) and (C), the main factor for preparing core-shell particles is that the polymerization rate of the silicon particles has to be lower than the antimony one.

CONCLUSION

Core-shell particles having a c.c.p. structure of β-antimonic acid can be formed through a polymerization process in aqueous medium. The silicon content and the size of these particles is only governed by the route of protonation of the reactants related to their mixing order.

Acknowledgements—NMR measurements were made by P. Tougne and F. Taulelle and electronic microscopies were carried out by P. Baunier and M. Lavergne. The authors express their thanks to all of them for experimental assistance and helpful discussions.

REFERENCES

1. J. Lemerle, *Rev. Chim. Min.* 1972, **9**, 863.
2. J. Lemerle and J. Lefebvre, *J. Chim. Phys.* 1974, **1**, 97.
3. J. Mandavo and J. Lemerle, *Nouv. J. Chim.* 1987, **11**, 3.
4. J. Lemerle and J. Lefebvre, *Bull. Soc. Chim.* 1976, **3,4**, 409.
5. J. P. Jolivet and J. Lefebvre, *Bull. Soc. Chim.* 1975, **11, 12**, 2420.
6. J. Lemerle and J. Lefebvre, *J. Chim. Phys.* 1973, **3**, 402.
7. A. Audsley and J. Aveston, *J. Chem. Soc.* 1962, 2320.
8. L. C. Klein, *Ann. Rev. Mater. Sci.* 1985, **15**, 227.
9. S. P. Mukherjee, *Better Ceramics through Chemistry*, p. 111. Elsevier, Amsterdam (1984).
10. G. B. Alexander, *J. Am. Chem. Soc.* 1953, **75**, 2887.
11. M. Coudurier, B. Baudru and J. B. Donnet, *Bull. Soc. Chim.* 1971, **9**, 3147.
12. R. Guinier, *Théorie et Technique de la Radiocristallographie*, p. 464. Dunod, Paris (1964).

13. P. Fourré, D. Bauer and J. Lemerle, *Analyt. Chem.* 1983, **55**, 662.
14. L. L. Hench and D. R. Ulrich, *Ultrastructure Processing of Ceramics Glasses and Composites*, p. 207. John Wiley, New York (1984).
15. E. Lippmaa, M. Magi, A. Samoson, G. Englhardt and A. R. Grimmer, *J. Am. Chem. Soc.* 1980, **102**, 4889.
16. N. Janes and E. Oldfield, *J. Am. Chem. Soc.* 1985, **107**, 6769.
17. E. Lippmaa, M. Magi, A. Samoson, M. Tannak and G. Englehardt, *J. Am. Chem. Soc.* 1981, **103**, 4992.

Polyhedron Vol. 8, No. 21, pp. 2587–2591, 1989
Printed in Great Britain

0277–5387/89 $3.00+.00
© 1989 Pergamon Press plc

THE SYNTHESIS OF THE NOVEL MIXED HALIDE SEVEN-COORDINATE COMPLEX $[WBrI(CO)_3(NCMe)_2]$ AND ITS REACTIONS WITH ALKYNES

PAUL K. BAKER,* ADRIAN BURY and KEVIN R. FLOWER

Department of Chemistry, University College of North Wales, Bangor, Gwynedd LL57 2UW, Wales, U.K.

(*Received* 4 *April* 1989; *accepted* 12 *June* 1989)

Abstract—The tris-acetonitrile complex $[W(CO)_3(NCMe)_3]$ reacts *in situ* with an equimolar quantity of BrI at 0°C to afford a quantitative yield of the seven-coordinate complex $[WBrI(CO)_3(NCMe)_2]$. Reaction of $[WBrI(CO)_3(NCMe)_2]$ with one equivalent of RC_2R' (R = R′ = Ph or CH_2Cl; R = Me, R′ = Ph), in CH_2Cl_2 at room temperature, rapidly gave the dimeric complexes $[W(\mu\text{-}I)Br(CO)(NCMe)(\eta^2\text{-}RC_2R')]_2$ in good yield. ^{13}C NMR spectroscopy suggests that the alkynes are acting as four-electron donors in the dimeric compounds $[W(\mu\text{-}I)Br(CO)(NCMe)(\eta^2\text{-}RC_2R')]_2$. Two equivalents of RC_2R' (R = R′ = Me, Ph or CH_2Cl; R = Me, R′ = Ph) react with $[WBrI(CO)_3(NCMe)_2]$, in CH_2Cl_2 at room temperature, to give the bis-alkyne complexes $[WBrI(CO)(NCMe)(\eta^2\text{-}RC_2R')_2]$ in high yield. The bis-diphenylacetylene complex, $[WBrI(CO)(NCMe)(\eta^2\text{-}PhC_2Ph)_2]$, can also be prepared by reacting the iodo-bridged dimer $[W(\mu\text{-}I)Br(CO)(NCMe)(\eta^2\text{-}PhC_2Ph)]_2$ in CH_2Cl_2 at room temperature, with two equivalents of diphenylacetylene. The alkyne ligands are donating an average of three electrons each to the tungsten in these complexes.

The reactions of seven-coordinate halocarbonyls of molybdenum(II) and tungsten(II) with alkynes have received considerable attention in recent years. In 1982, Davidson and co-workers[1] described the reaction of the bromo-bridged dimer $[W(\mu\text{-}Br)Br(CO)_4]_2$ with $CF_3C_2CF_3$ to give the bis-alkyne complex, $[WBr_2(CO)(\eta^2\text{-}CF_3C_2CF_3)_2]$. In the same year Umland and Vahrenkamp[2] reported the preparation of the diiodo–alkyne complexes $[WI_2(CO)_2L(\eta^2\text{-}HC_2H)]$ (L = PMe_3 or $AsMe_3$) or $[WI_2(CO)_2L(\eta^2\text{-}PhC_2H)]$ (L = PMe_3, $AsMe_3$ or $CNBu^t$) from reaction of $[WI_2(CO)_4L]$ with HC_2R (R = H or Ph). In 1983, Templeton and co-workers[3] described the preparation of $[MX_2(CO)L_2(\eta^2\text{-}RC_2R')]$ [X = Cl or Br; L = PPh_3, PEt_3 or py; $L_2 = Ph_2P(CH_2)_2PPh_2$] by reacting $[MX_2(CO)_nL_2]$ (n = 2 or 3) with alkyne, and Davidson and Vasapollo[4] reported the reactions of $[W(\mu\text{-}Br)Br(CO)_4]_2$ with RC_2R' (R = R′ = Me or Ph and PhC_2Me) to give the dimeric complexes $[W(\mu\text{-}Br)Br(CO)(\eta^2\text{-}RC_2R')_2]_2$. In 1985, Bennett and Boyd[5] reacted $[MBr_2(CO)_3(PEt_3)_2]$ (M = Mo or W) with cyclooctyne to give $[MBr_2(CO)(PEt_3)_2(\eta^2\text{-}C_8H_{12})]$. More recently we have described the reactions of the bis-acetonitrile diiodo seven-coordinate complexes $[MI_2(CO)_3(NCMe)_2]$ (M = Mo or W) with either one equivalent of RC_2R' (R = R′ = Me, Ph or CH_2Cl; R = Ph, R′ = Me and CH_2OH; R = Me, R′ = PhS and *p*-tolS) to give eventually $[M(\mu\text{-}I)I(CO)(NCMe)(\eta^2\text{-}RC_2R')]_2$[6] or two equivalents of RC_2R' (R = R′ = Me or Ph; R = Me, R′ = Ph; for M = W only, R = R′ = Me, CH_2Cl or *p*-tol; R = Ph, R′ = CH_2OH) to give the mononuclear complexes $[MI_2(CO)(NCMe)(\eta^2\text{-}RC_2R')_2]$ or the dinuclear compound $[Mo(\mu\text{-}I)I(CO)(\eta^2\text{-}MeC_2Me)_2]_2$.[7] Hitherto, no mixed halide–alkyne complexes of this type have been described. In this paper we wish to report the synthesis of the new mixed halide, seven-coordinate complex $[WBrI(CO)_3(NCMe)_2]$ and its reactions with alkynes.

EXPERIMENTAL

All reactions described in this paper were carried out under nitrogen using standard Schlenk apparatus. CH_2Cl_2 was dried and distilled before use. BrI

* Author to whom correspondence should be addressed.

was prepared by the literature method,[8] and all other chemicals used were purchased from commercial sources. Elemental analyses were determined using a Carlo Erba Elemental Analyser MOD 1106 (using helium as a carrier gas). IR spectra were recorded as $CHCl_3$ films between NaCl plates on a Perkin–Elmer ratio recording 1430 IR spectrophotometer. ^1H and ^{13}C NMR spectra were recorded on a Bruker AC 250 CP/MAS NMR spectrometer (all spectra were calibrated against tetramethylsilane).

Preparation of $[WBrI(CO)_3(NCMe)_2]$ **(1)**

A suspension of $[W(CO)_6]$ (4.00 g, 11.4 mmol) in degassed acetonitrile (120 cm^3) was refluxed under nitrogen for 72 h. The solution was then cooled to 0°C and BrI (2.36 g, 11.4 mmol) was added, which resulted in the immediate formation of a red–brown solution. After stirring for 30 min, the solvent was removed *in vacuo* to afford the analytically pure red–brown crystalline complex $[WBrI(CO)_3(NCMe)_2]$ **(1)** in quantitative yield.

Preparation of $[W(\mu\text{-}I)Br(CO)(NCMe)(\eta^2\text{-}PhC_2Ph)]_2$ **(2)**

To $[WBrI(CO)_3(NCMe)_2]$ (0.56 g, 1 mmol) dissolved in CH_2Cl_2 (12 cm^3), with continuous stirring under a stream of dry nitrogen, was added PhC_2Ph (0.18 g, 1 mmol). After stirring for 4 h, the solution was filtered and removal of the solvent *in vacuo* gave dark green crystals of $[W(\mu\text{-}I)Br(CO)(NCMe)(\eta^2\text{-}PhC_2Ph)]_2$ **(2)** which were recrystallized from CH_2Cl_2; yield of pure product = 0.54 g, 84%. Similar reactions of $[WBrI(CO)_3(NCMe)_2]$ with an equimolar quantity of RC_2R' (R = R′ = CH_2Cl; R = Me, R′ = Ph) afforded the new complexes $[W(\mu\text{-}I)Br(CO)(NCMe)(\eta^2\text{-}RC_2R')]_2$ **(3** and **4)**.

Preparation of $[WBrI(CO)(NCMe)(\eta^2\text{-}MeC_2Me)_2]\cdot\frac{1}{2}CH_2Cl_2$ **(5)**

To $[WBrI(CO)_3(NCMe)_2]$ (0.56 g, 1 mmol) dissolved in CH_2Cl_2 (15 cm^3), with continuous stirring under a stream of dry nitrogen, was added MeC_2Me (0.16 g, 3 mmol). After stirring for 19 h, the solution was filtered and removal of solvent *in vacuo* gave yellow crystals of $[WBrI(CO)(NCMe)(\eta^2\text{-}MeC_2Me)_2]\cdot\frac{1}{2}CH_2Cl_2$ **(5)**, which were recrystallized from CH_2Cl_2; yield of pure product = 0.44 g, 72%. Similar reactions of $[WBrI(CO)_3(NCMe)_2]$ with two equivalents of RC_2R' (R = R′ = Ph and CH_2Cl; R = Me, R′ = Ph) gave the new complexes $[WBrI(CO)(NCMe)(\eta^2\text{-}RC_2R')_2]$ **(6–8)** (see Table 1 for colours and yields).

Reaction of $[W(\mu\text{-}I)Br(CO)(NCMe)(\eta^2\text{-}PhC_2Ph)]_2$ *with two equivalents of* PhC_2Ph

To $[W(\mu\text{-}I)Br(CO)(NCMe)(\eta^2\text{-}PhC_2Ph)]_2$ (0.26 g, 0.2 mmol) dissolved in CH_2Cl_2 (15 cm^3), with continuous stirring under a stream of dry nitrogen, was added PhC_2Ph (0.071 g, 0.4 mmol). After stirring for 19 h, the solution was filtered and removal of the solvent *in vacuo* gave yellow crystals of

Table 1. Physical and analytical[a] data for the complexes $[WBrI(CO)_3(NCMe)_2]$, $[W(\mu\text{-}I)Br(CO)(NCMe)(\eta^2\text{-}RC_2R')]_2$ and $[WBrI(CO)(NCMe)(\eta^2\text{-}RC_2R')_2]$

Complex	Colour	Yield (%)	C	H	N
$[WBrI(CO)_3(NCMe)_2]$ **(1)**	Brown	98	14.9 (15.1)	1.0 (1.1)	5.2 (5.0)
$[W(\mu\text{-}I)Br(CO)(NCMe)(\eta^2\text{-}PhC_2Ph)]_2$ **(2)**	Green	84	32.4 (32.0)	2.2 (2.1)	1.9 (2.2)
$[W(\mu\text{-}I)Br(CO)(NCMe)(\eta^2\text{-}CH_2ClC_2CH_2Cl)]_2$ **(3)**	Green	93	14.7 (14.4)	1.2 (1.2)	2.0 (2.4)
$[W(\mu\text{-}I)Br(CO)(NCMe)(\eta^2\text{-}MeC_2Ph)]_2$ **(4)**	Green	55	25.1 (25.0)	1.9 (1.9)	2.0 (2.4)
$[WBrI(CO)(NCMe)(\eta^2\text{-}MeC_2Me)_2]\cdot\frac{1}{2}CH_2Cl_2$ **(5)**	Yellow	72	22.6 (22.6)	2.8 (2.6)	2.1 (2.3)
$[WBrI(CO)(NCMe)(\eta^2\text{-}PhC_2Ph)_2]$ **(6)**	Yellow	92	45.5 (45.6)	3.0 (2.8)	1.5 (1.7)
$[WBrI(CO)(NCMe)(\eta^2\text{-}CH_2ClC_2CH_2Cl)_2]$ **(7)**	Yellow	81	18.9 (18.8)	1.0 (1.0)	1.8 (2.0)
$[WBrI(CO)(NCMe)(\eta^2\text{-}MeC_2Ph)_2]$ **(8)**	Yellow	94	36.7 (36.5)	2.9 (2.8)	1.5 (2.0)

[a] Calculated values in parentheses.

Table 2. IR data[a] for the complexes [WBrI(CO)$_3$(NCMe)$_2$], [W(μ-I)Br(CO)(NCMe)(η^2-RC$_2$R′)]$_2$ and [WBrI(CO)(NCMe)(η^2-RC$_2$R′)$_2$]

Complex	ν(C≡N) (cm^{-1})	ν(C≡O) (cm^{-1})
1	2317 (w) and 2287 (w)	2029 (s), 1941 (s) and 1931 (s)
2	2306 (w) and 2294 (w)	2053 (s) and 1981 (s)
3	2322 (w) and 2292 (w)	2070 (s) and 2003 (s)
4	2318 (w) and 2294 (w)	2051 (s) and 1988 (s)
5	2318 (w) and 2294 (w)	2065 (s)
6	2318 (w) and 2299 (w)	2094 (s)
7	2317 (w) and 2299 (w)	2102 (s)
8	2325 (w) and 2290 (w)	2078 (s)

[a] Spectra recorded as thin films in $CHCl_3$ between NaCl plates; s, strong; w, weak.

[WBrI(CO)(NCMe)(η^2-PhC$_2$Ph)$_2$], which were recrystallized from CH_2Cl_2; yield of pure product = 0.31 g, 95% (Found: C, 46.2; H, 3.5; N, 1.5. Calc. for $C_{31}H_{23}NOBrIW$: C, 45.6; H, 2.8; N, 1.7%). The IR and ^{1}H NMR spectral properties were identical to those of compound **6**.

RESULTS AND DISCUSSION

Addition of an equimolar amount of BrI to a solution of the tris-acetonitrile compound [W(CO)$_3$(NCMe)$_3$] {prepared *in situ* by reacting [W(CO)$_6$] in refluxing acetonitrile for 72 h[9]} at 0°C, immediately affords a deep red–brown solution, which after removal of the solvent *in vacuo* afforded a quantitative yield of the new seven-coordinate compound [WBrI(CO)$_3$(NCMe)$_2$] (**1**). The complex is soluble in chlorinated solvents, such as CH_2Cl_2 and $CHCl_3$ etc., but only slightly soluble in diethyl ether and hydrocarbon solvents. The compound is stable in the solid state for several days when stored in the dark under an atmosphere of nitrogen, however it is very air-sensitive in solution. The complex [WBrI(CO)$_3$(NCMe)$_2$] (**1**) reacts with one equivalent of RC$_2$R′ (R = R′ = Ph or CH_2Cl; R = Me, R′ = Ph) to rapidly afford the iodo-bridged dimers [W(μ-I)Br(CO)(NCMe)(η^2-RC$_2$R′)]$_2$ (**2–4**) in good yield. Reaction of **1** with two equivalents of RC$_2$R′ (R = R′ = Me, Ph or CH_2Cl; R = Me, R′ = Ph) gives the bis-alkyne compounds [WBrI(CO)(NCMe)(η^2-RC$_2$R′)$_2$] (**5–8**). The dimeric complexes, **2–4**, are very unstable, however, they can be stored in the dark for several hours. They are very air-sensitive in solution, particularly the $CH_2ClC_2CH_2Cl$ derivative. The bis-alkyne compounds, **5–8**, are much more stable than the dimers, **2–4**, but must be stored under an inert atmosphere in the dark. All the alkyne complexes are soluble in CH_2Cl_2 and $CHCl_3$, but are much less soluble in diethyl ether and hydrocarbon solvents. All the new complexes described in this paper were fully characterized by elemental analysis (C, H and N) (Table 1), IR spectroscopy (Table 2), ^{1}H NMR and in selected cases ^{13}C NMR spectroscopy (Tables 3 and 4). The complex [WBrI(CO)(NCMe)(η^2-MeC$_2$Me)$_2$]·$\frac{1}{2}$CH$_2$Cl$_2$ was confirmed as a $\frac{1}{2}CH_2Cl_2$ solvate by repeated elemental analyses and ^{1}H and ^{13}C NMR spectroscopy. It is interesting to note that this is similar to the diiodo complex,

Table 3. ^{1}H NMR data[a] for the complexes [WBrI(CO)$_3$(NCMe)$_2$], [W(μ-I)Br(CO)(NCMe)(η^2-RC$_2$R′)]$_2$ and [WBrI(CO)(NCMe)(η^2-RC$_2$R′)$_2$]

Complex	^{1}H (δ) (ppm)
1	2.56 (s, *Me*CN)
2	2.60 (cs, 3H, *Me*CN), 2.65 (cs, 3H, *Me*CN), 7.3–7.8 (m, 20H, *Ph*C$_2$)
3	2.81 (m, 6H, *Me*CN), 5.51 (m, 8H, *CH*$_2$Cl)
4	2.64, 2.66 (cs, 3H, *Me*CN); 2.75 (cs, 3H, *Me*CN); 3.19, 3.27, 3.29, 3.39 (cs, 6H, *Me*C$_2$); 7.2–7.6 (m, 10H, *Ph*C$_2$)
5	2.2 (s, 3H, *Me*CN); 2.91 (s, 6H, *Me*C$_2$); 3.0 (s, 6H, *Me*C$_2$); 5.32 (s, 1H, *CH*$_2$Cl$_2$)
6	2.13 (m, 3H, *Me*CN); 7.13–7.55 (m, 20H, *Ph*C$_2$)
7	2.04, 2.09 (cs, 3H, *Me*CN); 5.04 and 5.55 (s, 8H, *CH*$_2$Cl)
8	2.05 (m, 3H, *Me*CN); 3.03, 3.06, 3.07, 3.08, 3.09, 3.10, (cs, 6H, *Me*C$_2$); 7.09–7.52 (m, 10H, *Ph*C$_2$)

[a] Spectra recorded in $CDCl_3$ (25°C) calibrated against Me_4Si; cs, collection of singlets.

Table 4. Selected ^{13}C NMR data[a] for the complexes $[W(\mu\text{-I})Br(CO)(NCMe)(\eta^2\text{-}RC_2R')]_2$ and $[WBrI(CO)(NCMe)(\eta^2\text{-}MeC_2Me)_2]$

Complex	^{13}C (δ) (ppm)
3	205.5 (s, *C*≡*C*); 199.85 (s, *C*≡*C*); 195.20 (s, *C*≡O); 108.0 (s, Me*C*≡N); 48.26, 47.65, 46.97, 46.54, 46.53, 45.89, 45.50 (s, CH_2Cl); 4.31, 4.42 (s, *Me*CN)
4	207.88, 207.52, 206.98, 204.29 (s, *C*≡*C*); 202.50, 199.91, 196.61 (s, *C*≡O); 136.96–126.60 (m, Ph); 117.0, (s, Me*C*N); 24.09, 23.85, 23.52 and 23.31, (s, *Me*C_2); 4.52 and 4.41 (s, *Me*CN)
5	206.13 (s, *C*≡O); 167.45 and 151.91 (s, Me*C*$_2$); 126.26, (s, Me*C*N); 53.43 (s,CH_2Cl_2) 19.73, 19.57, 19.11, 16.37, (s, *Me*C_2); 4.82 (s, *Me*CN)

[a] Spectra recorded in $CDCl_3$ (25°C) calibrated against Me_4Si.

$[WI_2(CO)(NCMe)(\eta^2\text{-}MeC_2Me)_2]\cdot\frac{1}{2}CH_2Cl_2$, which showed a $\frac{1}{2}CH_2Cl_2$ solvate in the X-ray structural determination.[7]

Reaction of $[W(CO)_3(NCMe)_3]$ *in situ* with one equivalent of BrI is similar to our previously reported reactions of $[M(CO)_3(NCMe)_3]$ (M = Mo or W) with an equimolar quantity of X_2 (X = Br or I).[10] It is interesting to note that Tate *et al.* reported in 1962[9] that reaction of $[W(CO)_3(NCMe)_3]$ with one equivalent of I_2 in methanol gave a non-carbonyl-containing product. Hence, simply by carrying out the reaction *in situ* in a different solvent, i.e. acetonitrile, we obtain the highly reactive seven-coordinate halocarbonyl bis-acetonitrile compounds. The colour and IR spectral properties of the $[WBrI(CO)_3(NCMe)_2]$ complex are very similar to the analogous dibromo and diiodo complexes.[10] Surprisingly, the mixed halide complex $[WBrI(CO)_3(NCMe)_2]$ showed little propensity to disproportionate to give the dibromo and diiodo complexes. Since the X-ray crystal structure of $[WI_2(CO)_3(NCMe)_2]$ has been determined by Drew *et al.*,[11] and the colour and spectral properties of $[WBrI(CO)_3(NCMe)_2]$ (**1**) and $[WI_2(CO)_3(NCMe)_2]$ are very similar, the most likely structure for **1** is capped octahedral. We were unable to grow suitable single crystals for X-ray crystallography of $[WBrI(CO)_3(NCMe)_2]$ (**1**).

Equimolar quantities of the complex $[WBrI(CO)_3(NCMe)_2]$ and RC_2R' (R = R′ = Ph and CH_2Cl; R = Me, R′ = Ph) are likely to initially give the mononuclear complexes $[WBrI(CO)(NCMe)_2(\eta^2\text{-}RC_2R')]$, which rapidly dimerize to give the iodo-bridged dimers, $[W(\mu\text{-I})Br(CO)(NCMe)(\eta^2\text{-}RC_2R')]_2$, with loss of acetonitrile. It is likely that the tungsten atoms are bridged by iodide ligands, since iodides have a greater affinity for dative bridging compared to bromides. It is likely that these complexes are dimeric, since the analogous diiodide compounds $[M(\mu\text{-I})I(CO)(NCMe)(\eta^2\text{-}RC_2R')]_2$ were found to be iodo-bridged dimers.[6] Attempts to follow the reactions of $[WBrI(CO)_3(NCMe)_2]$ with one equivalent of RC_2R' by IR spectroscopy were made, however after 30 s only the carbonyl bands due to the dimer were observed. This is in contrast to the reactions of the diiodide complexes $[MI_2(CO)_3(NCMe)_2]$ with an equimolar amount of RC_2R', whereby for example, the reaction of equimolar quantities of PhC_2Ph and $[WI_2(CO)_3(NCMe)_2]$ took 12 h to go to completion, and a carbonyl band at 1948 cm^{-1} was observed which is due to $[WI_2(CO)(NCMe)_2(\eta^2\text{-}PhC_2Ph)]$.[6] This greater ease of dimerization of the mixed halide complexes $[WBrI(CO)(NCMe)_2(\eta^2\text{-}RC_2R')]$ may be due to the smaller size of the bromide ion allowing easier attack of the iodide by an associative mechanism. The alkyne can switch from a four-electron donor to a two-electron donor during associative attack by the iodide, rapidly switching back to a four-electron donor resulting in loss of acetonitrile. Associative mechanisms have been previously described for reaction of donor ligands with four-electron alkyne complexes of molybdenum(II) and tungsten(II).[12,13] The structure of the dimers $[W(\mu\text{-I})Br(CO)(NCMe)(\eta^2\text{-}RC_2R')]_2$ is likely to have *cis*-carbonyls in view of the closely spaced, equally intense carbonyl bands, with the alkyne ligands *cis* and parallel to the carbonyl groups, which has been previously observed.[14–17] However, in view of the complexity of the NMR spectra of the dimers $[W(\mu\text{-I})Br(CO)(NCMe)(\eta^2\text{-}RC_2R')]$ (**2–4**) it is likely that several isomers exist in solution. The ^1H NMR spectra (Table 3) show the expected features for the dimers (**2**→**4**). The ^{13}C NMR spectra for both **3** and **4** show several resonances above 200 ppm for both the alkyne-contact carbons and the carbonyl ligands. The lower field resonances have been assigned to the alkyne-contact carbon resonances which have been previously reported[12] for other four-electron alkyne complexes of molybdenum(II). Templeton and Ward[18] have suggested that alkyne carbons above 200 ppm indicate that the alkyne ligand is utilizing both its filled $p\pi$-orbitals and donating four electrons to the metal, which allows these complexes to obey the eighteen-electron rule.

The seven-coordinate complex $[WBrI(CO)_3(NCMe)_2]$ reacts with two equivalents of RC_2R' (R = R′ = Me, Ph or CH_2Cl; R = Me, R′ = Ph),

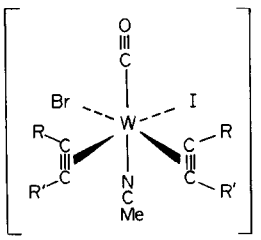

Fig. 1. Proposed structure for the complexes [WBrI(CO)(NCMe)(η^2-RC$_2$R')$_2$].

in CH_2Cl_2 at room temperature, to eventually afford the bis-alkyne complexes [WBrI(CO)(NCMe)(η^2-RC$_2$R')$_2$] (**5–8**) in high yield. The bis-diphenylacetylene compound can also be prepared by reacting the iodo-bridged dimer [W(μ-I)Br(CO)(NCMe)(η^2-PhC$_2$Ph)]$_2$ with two equivalents of diphenylacetylene (see Experimental). The bis-alkyne complexes, **5–8**, are similar in colour (yellow) to their diiodo analogues. The mixed halogeno complexes have a strong single carbonyl band well above 2000 cm^{-1} (see Table 2). The structures of the bis-alkyne complexes [WI$_2$(CO)(NCMe)(η^2-RC$_2$R)$_2$] (R = Me and Ph)[7] and [WI$_2$(CO)$_2$(η^2-MeC$_2$Me)$_2$][19] have been determined by X-ray crystallography, hence in view of the similar colours and spectral properties of the mixed halogeno complexes, **5–8**, to the diiodo compounds [WI$_2$(CO)(NCMe)(η^2-RC$_2$R)$_2$],[7] it is likely that the structures of **5–8** will be similar. The proposed structure of these bis-alkyne complexes is shown in Fig. 1. The ^{1}H NMR spectra (Table 3) conform with the structure shown in Fig. 1. The ^{13}C NMR spectrum of the bis-but-2-yne complex [WBrI(CO)(NCMe)(η^2-MeC$_2$Me)$_2$]·$\frac{1}{2}$CH$_2$Cl$_2$ (**5**) show alkyne-contact carbon resonances at 167.45 and 151.91 ppm. In view of Templeton and Ward's[18] correlation between alkyne-contact carbon shifts and the number of electrons donated to the metal, the range of values for this bis-alkyne complex suggest that the alkynes are donating an average of three electrons each to this tungsten in this complex.

Acknowledgement—We thank the SERC for their support.

REFERENCES

1. J. L. Davidson, G. Vasapollo, L. M. Muir and K. W. Muir, *J. Chem. Soc., Chem. Commun.* 1982, 1025.
2. P. Umland and H. Vahrenkamp, *Chem. Ber.* 1982, **115**, 3580.
3. P. B. Winston, S. J. N. Burgmayer, T. L. Tonker and J. L. Templeton, *Organometallics* 1986, **5**, 1707.
4. J. L. Davidson and G. Vasapollo, *J. Chem. Soc., Dalton Trans.* 1985, 2239.
5. M. A. Bennett and I. W. Boyd, *J. Organomet. Chem.* 1985, **290**, 165.
6. E. M. Armstrong, P. K. Baker and S. G. Fraser, *J. Chem. Res. (S)* 1988, 52; *J. Chem. Res. (M)* 1988, 0410.
7. E. M. Armstrong, P. K. Baker and M. G. B. Drew, *Organometallics* 1988, **7**, 319.
8. *Handbook of Preparative Inorganic Chemistry*, 2nd edn, Vol. 1. Academic Press, New York (1963).
9. D. P. Tate, W. R. Knipple and J. M. Augl, *Inorg. Chem.* 1962, **1**, 433.
10. P. K. Baker, S. G. Fraser and E. M. Keys, *J. Organomet. Chem.* 1986, **309**, 319.
11. M. G. B. Drew, P. K. Baker, E. M. Armstrong and S. G. Fraser, *Polyhedron* 1988, **7**, 245.
12. S. R. Allen, P. K. Baker, S. G. Barnes, M. Green, L. Trollope, L. J. Muir and K. W. Muir, *J. Chem. Soc., Dalton Trans.* 1981, 873.
13. R. S. Herrick, D. M. Leazer and J. L. Templeton, *Organometallics* 1982, **2**, 834.
14. P. S. Braterman, J. L. Davidson and D. W. A. Sharp, *J. Chem. Soc., Dalton Trans.* 1976, 241.
15. K. Tatsumi, R. Hoffmann and J. L. Templeton, *Inorg. Chem.* 1982, **21**, 466.
16. J. L. Templeton, P. B. Winston and B. C. Ward, *J. Am. Chem. Soc.* 1981, **103**, 7713.
17. M. Kamata, K. Hirotsu, T. Higuchi, M. Kido, K. Tatsumi, T. Yoshida and S. Otsuka, *Inorg. Chem.* 1983, **22**, 2416.
18. J. L. Templeton and B. C. Ward, *J. Am. Chem. Soc.* 1980, **102**, 3288.
19. E. M. Armstrong, P. K. Baker and M. G. B. Drew, *J. Organomet. Chem.* 1987, **336**, 377.

Polyhedron Vol. 8, No. 21, pp. 2593–2597, 1989
Printed in Great Britain

0277–5387/89 $3.00+.00
© 1989 Pergamon Press plc

PREPARATION OF COPPER(II) AND ZINC(II) HALIDE AND PRIMARY AMINE COMPLEXES OF THEOBROMINE

W. J. BIRDSALL* and DONNA L. TAYLOR

Department of Chemistry, Albright College, Reading, PA 19612-5234, U.S.A.

(*Received* 22 *May* 1989; *accepted* 14 *June* 1989)

Abstract—Copper(II) amine complexes of theobromine (TbH) having the general formula $Cu(Tb)_2(Amine)_2$ [where Amine = ethylamine ($EtNH_2$) and *n*-butylamine (*n*-$BuNH_2$)] were synthesized. In addition, copper(II) and zinc(II) halide adducts of theobromine were prepared with the general formula $M(TbH)_2X_2 \cdot nH_2O$ (where X = Cl or Br and $n = 0$, 1 or 2). The amine complexes experience large carbonyl IR shifts and the loss of the N(1) theobromine proton, suggesting copper(II) complexation at the N(1) position, while the halide compounds do not exhibit theobromine N(1) proton loss and are proposed to bind at the N(9) position. $Zn(TbH)_2Cl_2$ can be assigned a tetrahedral geometry on the basis of low frequency IR evidence, while the low magnetic susceptibilities and lack of M—X vibrations above 200 cm^{-1} suggest that the copper centres in $Cu(TbH)_2Cl_2 \cdot 2H_2O$ and $Cu(TbH)_2Br_2 \cdot H_2O$ are antiferromagnetically coupled and that these complexes exist as halogen-bridged dimers or larger aggregates.

Theobromine (TbH) is a purine derivative found in significant concentrations in a number of plant products, including cocoa and coffee beans. Many studies have been undertaken on metal ion complexes with other biologically important purines, including adenine, guanine, xanthine, hypoxanthine, theophylline and caffeine,[1–12] yet fewer references can be found to compounds of theobromine with metal ions. For example, Beck and Kottmair[13] reported the preparation of $Rh(CO)(PPh_3)_2(Tb)$, while Mikulski *et al.* have synthesized $Cu(TbH)_2(ClO_4)_2$,[14] $Pd(TbH)(Tb)Cl$[15] and $ZrO(TbH)_2(Tb)Cl \cdot H_2O$.[16] Recently, Mikulski *et al.* have expanded their work to include theobromine adducts with perchlorate salts of chromium(III), manganese(II), iron(II), iron(III), cobalt(II), nickel(II) and zinc(II).[17] In addition, the crystal structure determination of $K[Pt(TbH)Cl_3] \cdot H_2O$ has been accomplished.[18]

Neutral theobromine is protonated at the N(1) position.[19,20] The crystal structure of $K[Pt(TbH)Cl_3] \cdot H_2O$ shows theobromine binding through the N(9) imidazole nitrogen to the platinum centre.[18] This may not be the exclusive binding site for the theobromine in all complexes, however, as $K[Pt(TbH)Cl_3] \cdot H_2O$ was prepared under acid conditions, which prevented ionization of the proton at N(1), where metal bonding could also occur. Hodgson[2] has noted that the binding site of transition metal ions to the purines, which contain both pyrimidine and imidazole moieties, is almost always an imidazole nitrogen atom, and therefore states that the pyrimidine N(1) and N(3) atoms are poorer ligating atoms than are the imidazole N(7) and N(9) atoms. Recent workers have concluded that N(1) and N(9) would be about equally likely to act as the binding site of terminal unidentate theobromine, however, under neutral conditions.[14,17]

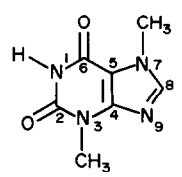

Theobromine

We have prepared metal ion complexes with other purines of biological interest, including adducts of copper(II), cadmium(II) and zinc(II) with theophylline,[21] guanine and xanthine,[22] and

* Author to whom correspondence should be addressed.

kinetin and 6-benzylaminopurine.[23] Some of these compounds also contain various primary amines while others contain various halide atoms. In the present study, we have synthesized copper(II) complexes of theobromine with primary amines having the general formula $Cu(Tb)_2(Amine)_2$, [where Amine = ethylamine ($EtNH_2$) and *n*-butylamine (*n*-$BuNH_2$)], and copper(II) and zinc(II) halide adducts of theobromine with the general formula $M(TbH)_2X_2 \cdot nH_2O$ (where X = Cl or Br and $n = 0$, 1 or 2). IR (4000–200 cm^{-1}) and room-temperature magnetic susceptibility measurements have been employed to study these new complexes.

EXPERIMENTAL

Preparation of $Cu(Tb)_2(EtNH_2)_2$ *and* $Cu(Tb)_2$ (*n*-$BuNH_2)_2$

The synthetic procedure was similar to that used for a previously reported copper–guanine primary amine complex.[22] $CuSO_4 \cdot 5H_2O$ (5.0 mmol) and TbH (5.0 mmol) were slurried in 50 cm^3 of 35% ethylamine–H_2O and 50% *n*-butylamine–H_2O, respectively, to yield purple powders. The products were filtered by vacuum, washed with the respective aqueous amines and dried with acetone. They were air stable but spontaneously decomposed in water to yield theobromine and aqueous copper(II), and were insoluble in common aprotic solvents. Elemental analyses are listed in Table 1.

Preparation of $Cu(TbH)_2Cl_2 \cdot 2H_2O$, $Cu(TbH)_2Br_2 \cdot H_2O$ *and* $Zn(TbH)_2Cl_2$

The synthetic procedure was similar to that used in previously reported copper halide–purine complexes,[21–23] with the difference that acetone was used as the solvent rather than methanol. 5.0 mmol of either $CuCl_2 \cdot 2H_2O$, $CuBr_2$ or $ZnCl_2$ were refluxed with TbH (5.0 mmol) in acetone for 24 h, filtered by vacuum and washed with acetone. The grey copper and white zinc adducts were obtained as powders and were insoluble in water and common aprotic solvents. Elemental analyses are listed in Table 1.

IR spectra were obtained as Nujol mulls between high-density polyethylene windows (600–200 cm^{-1}) and as KBr pellets (4000–400 cm^{-1}) on a Perkin–Elmer 1430 spectrometer. Room-temperature magnetic susceptibility measurements were conducted on a Gouy balance of standard design. Elemental analyses (C, H, N) were performed by Galbraith Laboratories.

RESULTS AND DISCUSSION

Theobromine exhibits four prominent IR absorbances in the 2800–3200 cm^{-1} region (Table 2). The peaks at 3160 and 3030 cm^{-1} have been assigned to N(1)—H, while those at 3115 and 2830 cm^{-1} include absorbances from C(8)—H.[14,17] $Cu(Tb)_2(EtNH_2)_2$ and $Cu(Tb)_2$(*n*-$BuNH_2)_2$ complexes exhibit symmetric and asymmetric primary amine N—H stretching at 3170 and 3264 cm^{-1} and 3180 and 3270 cm^{-1}, respectively, while ring N(1)—H vibrations are absent in these two complexes. Theobromine carbonyl absorbances experience large shifts of over 50 cm^{-1} to lower frequencies upon complexation, while skeletal ring C=C and C=N bands also shift to lower frequencies to a lesser extent. The IR evidence thus suggests complexation to the theobromine ring with carbonyl involvement in bonding, probably through hydrogen bonding to

Table 1. Elemental analyses of copper(II) primary amine and copper(II) and zinc(II) halide complexes of theobromine

Compound	Colour		%C	%H	%N
$Cu(Tb)_2(EtNH_2)_2$	Purple	Calc.:	42.1	5.4	27.3
		Found:	41.7	5.3	27.5
$Cu(Tb)_2$(*n*-$BuNH_2)_2$	Purple	Calc.:	46.4	6.3	24.6
		Found:	46.3	6.5	24.4
$Cu(TbH)_2Cl_2 \cdot 2H_2O$	Grey	Calc.:	31.7	3.8	21.1
		Found:	31.8	3.1	20.9
$Cu(TbH)_2Br_2 \cdot H_2O$	Grey	Calc.:	27.9	3.0	18.6
		Found:	28.2	2.7	18.7
$Zn(TbH)_2Cl_2$	White	Calc.:	33.8	3.2	22.6
		Found:	33.5	3.3	21.9

Table 2. Selected IR frequencies (cm^{-1}) of copper(II) primary amine and copper(II) and zinc(II) halide complexes of theobromine

Compound	$\nu_{sym}+\nu_{asym}$	$\nu_{NH}+\nu_{CH}$	$\nu_{C=O}$	$\nu_{C=C}+\nu_{C=N}$	Ligand bands	ν_{M-X}	ν_{M-N}
TbH		3160m, 3115m 3030s, 2830m	1690vs, 1665sh	1595s, 1550s	505s, 455s 420m, 375m 220m		
$Cu(Tb)_2(EtNH_2)_2$	3264s, 3170s	3110m, 2880w	1695w, 1635vs	1575s, 1535s	525w, 462s 420w, 385w 320w		245m
$Cu(Tb)_2(n\text{-}BuNH_2)_2$	3270s, 3180s	3120sh, 2880m	1695w, 1630vs	1575s, 1537s	525w, 462s 420sh, 390w 320w		245m
$Cu(TbH)_2Cl_2 \cdot 2H_2O$		3180s, 3130m 3050s, 2820s	1690vs	1590s, 1555s	515s, 455s 395m		245m
$Cu(TbH)_2Br_2 \cdot H_2O$		3170s, 3120m 3050s, 2825s	1690vs	1590s, 1555s	515s, 455s 395m		242m
$Zn(TbH)_2Cl_2$		3185s, 3130m 3110m, 3060s 2815s	1690vs	1600s, 1564s	515s, 450s 430s, 395s	330s, 312s	250sh, 240s

the coordinated primary amine groups since their N—H absorbances also occur at longer wavelengths than free, non-hydrogen bonded asymmetric and symmetric N—H stretching modes. Hydrogen bonding by purine ring carbonyl groups has been suggested for other complexes of this type.[22,24] Changes in intensity of theobromine ligand bands are observed in the 600–200 cm^{-1} region, and a new absorbance appears at 245 cm^{-1}. This is a region where metal–nitrogen vibrations have been observed in copper(II) complexes of various imidazoles,[25–26] and so may be a copper–theobromine nitrogen vibration. Room temperature magnetic susceptibility measurements gave values of 1.64 BM for both primary amine complexes. These values are slightly lower than those usually found for mononuclear copper(II) compounds, but are consistent with numerous reported examples of copper(II)–purine complexes.[3,4,7,27–30]

C—H and N—H vibrations in the 2800–3200 cm^{-1} region do not change appreciably in $Cu(TbH)_2Cl_2 \cdot 2H_2O$, $Cu(TbH)_2Br_2 \cdot H_2O$ and $Zn(TbH)_2Cl_2$, suggesting that neutral theobromine ligands are present in these complexes. Further, carbonyl absorbances are relatively unaffected in these compounds, indicating that bonding through a C=O oxygen atom does not occur. Mikulski *et al.*[17] note similar effects for a series of metal perchlorate complexes of theobromine, including $Cu(TbH)_2(ClO_4)_2$. Slight changes are observed for skeletal ring C=C and C=N bands in the 1500–1600 cm^{-1} region, while significant ring vibrational mode changes from those of free theobromine occur at frequencies lower than 1600 cm^{-1}. The spectra of $Cu(TbH)_2Cl_2 \cdot 2H_2O$ and $Cu(TbH)_2Br_2 \cdot H_2O$ are very similar, suggesting that they are isomorphous; no copper halide vibrations are observed at frequencies above 200 cm^{-1} in these compounds. Room-temperature magnetic susceptibility measurements for $Cu(TbH)_2Cl_2 \cdot 2H_2O$ and $Cu(TbH)_2Br_2 \cdot H_2O$ gave values of 0.65 and 0.88 BM, respectively. These values are below those found for magnetically dilute copper(II) compounds and indicate that antiferromagnetic coupling occurs between copper centres.[31] If halogen bridges link metal atoms to form dimers or larger aggregates, this conclusion could also explain the absence of Cu—Cl and Cu—Br stretches in the region near 300 cm^{-1}. $Zn(TbH)_2Cl_2$, however, exhibits a well-defined Zn—Cl doublet at 330 and 312 cm^{-1}, which suggests a tetrahedral coordination geometry around the metal centre.[21,22,32] Absorbances at 245, 242 and 240 cm^{-1} for $Cu(TbH)_2Cl_2 \cdot 2H_2O$, $Cu(TbH)_2Br_2 \cdot H_2O$ and $Zn(TbH)_2Cl_2$, respectively, could result from metal–theobromine nitrogen vibrations.

It is not possible from the information obtained for the present complexes to determine unambiguously whether metal binding occurs to the N(1) or N(9) theobromine ring nitrogen. In the cases of $Cu(Tb)_2(EtNH_2)$ and $Cu(TbH)_2(n\text{-}BuNH_2)_2$, prepared in basic solution, IR evidence indicates that ionization of the N(1) protons has occurred and the resulting complexes experience large carbonyl shifts most likely due to hydrogen bonding to coordinated primary amine groups. This suggests that coordination may occur at N(1) in these compounds, although intermolecular hydrogen bonding between carbonyl and primary amine groups on separate monomeric adducts cannot be discounted. The IR evidence suggests tetrahedral coordination for $Zn(TbH)_2Cl_2$, probably through the theobromine N(9), as the N(1) proton is undisturbed. N(9) bonding to the copper centre is also indicated for $Cu(TbH)_2Cl_2 \cdot 2H_2O$ and $Cu(TbH)_2Br_2 \cdot H_2O$ for the same reason, while magnetic susceptibility data indicate that these compounds are dimers or larger aggregates.

The present work presents facile methods for the preparation of metal ion–theobromine complexes using modified procedures employed for other purine–metal ion adducts.[21–23] Efforts are continuing to synthesize additional theobromine halide and primary amine complexes with a wider range of metal ions.

REFERENCES

1. L. G. Marzilli, *Prog. Inorg. Chem.* 1977, **23**, 255.
2. D. J. Hodgson, *Prog. Inorg. Chem.* 1977, **23**, 211.
3. E. Sletten, *Acta Cryst.* 1969, **B25**, 1480.
4. P. de Meester and A. C. Skapski, *J. Chem. Soc. A* 1971, 2167.
5. L. Srinivasan and M. R. Taylor, *J. Chem. Soc., Chem. Commun.* 1970, 1668.
6. J. A. Carrabine and M. S. Sundaralingam, *J. Am. Chem. Soc.* 1970, **92**, 369.
7. E. Sletten, *Acta Cryst.* 1970, **B26**, 1609.
8. L. G. Marzilli, L. A. Epps, T. Sorrell and T. J. Kistenmacher, *J. Am. Chem. Soc.* 1975, **97**, 3351.
9. M. B. Cingi, A. M. M. Lanfredi, A. Tiripicchio and M. T. Camellini, *Transition Met. Chem.* 1979, **4**, 221.
10. M. B. Cingi, A. M. M. Lanfredi and A. Tiripicchio, *Acta Cryst.* 1983, **C39**, 1523.
11. G. W. Bushnell, R. J. Densmore, K. R. Dixon and A. C. Ralfs, *Can. J. Chem.* 1983, **61**, 1132.
12. D. M. L. Goodgame, P. B. Hayman, R. T. Riley and D. J. Williams, *Inorg. Chim. Acta* 1984, **91**, 89.
13. W. Beck and N. Kottmair, *Berichte* 1976, **109**, 970.
14. C. M. Mikulski, T. B. Tran, L. Mattucci and N. M. Karayannis, *Inorg. Chim. Acta* 1983, **78**, 269.
15. C. M. Mikulski, S. Grossman, C. J. Lee and N. M. Karayannis, *Transition Met. Chem.* 1987, **12**, 21.
16. C. M. Mikulski, S. Grossman and N. M. Karayannis, *J. Less-Common Met.* 1987, **136**, 41.

17. C. M. Mikulski, M. K. Kurlan, M. Bayne, M. Gaul and N. M. Karayannis, *J. Coord. Chem.* 1988, **17**, 267.
18. E. H. Crowston, D. M. L. Goodgame, P. B. Hayman, A. M. Z. Slawin and D. J. Williams, *Inorg. Chim. Acta* 1986, **122**, 161.
19. D. Lichtenberg, F. Bergmann and Z. Neiman, *J. Chem. Soc. C* 1971. 1676.
20. Lu-Ming Twanmoh, H. B. Wood Jr and J. S. Driscoll, *J. Heterocyclic Chem.* 1973, **10**, 187.
21. W. J. Birdsall, *Inorg. Chim. Acta* 1985, **99**, 59.
22. W. J. Birdsall, B. W. Pfennig and J. L. Toto, *Polyhedron* 1986, **5**, 1357.
23. B. W. Pfennig and W. J. Birdsall, *J. Coord. Chem.*, in press.
24. B. J. Acken, D. A. Cole and W. J. Birdsall, *Synth. React. Inorg. Met.-Org. Chem.* 1983, **13**, 659.
25. D. M. L. Goodgame, M. Goodgame and G. W. Rayner-Canham, *Inorg. Chim. Acta* 1969, **3**, 399.
26. D. M. L. Goodgame, M. Goodgame and G. W. Rayner-Canham, *Inorg. Chim. Acta* 1969, **3**, 409.
27. R. Weiss and H. Venner, *Hoppe–Seyler's Z. Phys. Chem.* 1965, **340**, 138.
28. R. Weiss and H. Venner, *Hoppe–Seyler's Z. Phys. Chem.* 1963, **333**, 169; 1966, **345**, 122.
29. A. Terzis, A. L. Beauchamp and R. Rivest, *Inorg. Chem.* 1973, **12**, 1166.
30. C. M. Mikulski, T. B. Tran, L. Mattucci and N. M. Karayannis, *Inorg. Chim. Acta* 1983, **78**, 211.
31. B. N. Figgis and J. Lewis, *Prog. Inorg. Chem.* 1964, **6**, 37.
32. K. Nakamoto, *Infrared and Raman Spectra of Inorganic and Coordination Compounds*, 4th edn. Wiley, New York (1986).

Polyhedron Vol. 8, No. 21, pp. 2599–2602, 1989
Printed in Great Britain

0277–5387/89 $3.00+.00
© 1989 Pergamon Press plc

SOME 1,2-BIS(DIPHENYLPHOSPHINO)ETHANE COMPLEXES OF MOLYBDENUM(0) AND (II)

ANDREW R. BARRON, SIMON J. ANDERSON, KEITH McGREGOR and GEOFFREY WILKINSON*

Chemistry Department, Imperial College of Science and Technology, London SW7 2AY, U.K.

(*Received* 21 *May* 1989; *accepted* 15 *June* 1989)

Abstract—Reactions of the allylhydrido complex, $MoH(\eta^3\text{-}C_3H_5)(dppe)_2$ [dppe = 1,2-bis(diphenylphosphino)ethane], with various small molecules have been studied. New complexes isolated were the molybdenum(0), $Mo(2,6\text{-}Me_2C_6H_3NC)_2(dppe)_2$ and the molybdenum(II) compounds, $MoCl(\eta^3\text{-}C_3H_5)(dppe)_2$, $[Mo(MeCN)(\eta^3\text{-}C_3H_5)(dppe)_2]BF_4$, $Mo(CH_3)(\eta^3\text{-}C_3H_5)(dppe)_2$ and $Mo(CH_2SiMe_3)(\eta^3\text{-}C_3H_5)(dppe)_2$.

The allyl hydride complex,[1] $MoH(\eta^3\text{-}C_3H_5)(dppe)_2$, made by reduction of $MoCl_3(THF)_3$ with Na–Hg in THF under propylene, was reported to be stable thermally to *ca* 110°C.[1] No details or reactions were reported, although NMR spectra at +5°C confirmed the structure and at elevated temperatures showed metal hydride exchange with terminal hydrogen on the η^3-allyl group.[1]

In the hope that insertion reactions typical for M—H species could be carried out, possibly, subsequently leading to functionalized alkenes, we have studied the reaction of the complex with some small molecules. Analytical and other data for new compounds are given in Table 1.

RESULTS AND DISCUSSION

The hydrido allyl was made by Osborn's method but using $MoCl_4(THF)_2$ rather than $MoCl_3(THF)_3$. The IR spectrum, not previously reported, shows (in addition to bands due to dppe) bands at 1410, 930 and 870 cm^{-1} which can be assigned to the allyl vibration.[2] The mass spectrum shows no parent ion, but peaks due to $[Mo(dppe)_2]^+$ and $[C_3H_6]^+$ are present. These data are in agreement with the structure reported on the basis of NMR spectra.[1]

The hydrido allyl rapidly reacts in solution with N_2 to yield the known complex *trans*-$Mo(N_2)_2(dppe)_2$.[3] It also reacts in THF with CO (3 atm) and H_2 (5 atm) to yield *trans*-$Mo(CO)_2(dppe)_2$[4] and $MoH_4(dppe)_2$,[5] respectively. Although the compound reacts with CO_2 and CS_2 we have been unable to isolate any well-defined products.

The attempted insertion of the isocyanide, 2,6-$Me_2C_6H_3NC$, into the Mo—H bond at low temperatures resulted in loss of propylene to yield *trans*-$Mo(2,6\text{-}Me_2C_6H_3NC)_2(dppe)_2$ (**1**) in high yield. The spectroscopic data resemble those for similar isocyanide compounds of molybdenum and tungsten, $M(RNC)_2(dppe)_2$.[6]

If only 1 equivalent of isocyanide was used under a propylene atmosphere, the bis-isocyanide was still formed although in lower yield. The remaining product being unreacted hydride.

Addition of CCl_4 to a THF solution of the hydride yields the bright yellow allyl complex, $MoCl(\eta^3\text{-}C_3H_5)(dppe)_2$ (**2**), and $CHCl_3$ in virtually quantitative yield. The IR spectrum of **2** shows a band at 310 cm^{-1} due to ν(Mo—Cl). In $CHCl_3$ solution at room temperature the chloride is undissociated but on warming to *ca* 40°C the orange colour changes to pale yellow and there is dissociation to form the ionic species $[Mo(\eta^3\text{-}C_3H_5)(dppe)_2]Cl$. This dissociation in $CHCl_3$ is reversible and on cooling the neutral complex is reformed. In acetonitrile the chloride is a 1:1 electrolyte and the addition of KBF_4 to the MeCN solution leads to the salt $[Mo(MeCN)(\eta^3\text{-}C_3H_5)(dppe)_2]BF_4$ (**3**). This yellow solid can also be made directly from the hydride by addition of HBF_4 in acetonitrile; such acidolyses are well known.[7]

* Author to whom correspondence should be addressed.

Table 1. Analytical data for new molybdenum complexes

	Melting point (°C)	μ_{eff} (BM)	Analysis (%)[a] C	H	P
$Mo(2,6\text{-}Me_2C_6H_3NC)_2(dppe)_2$[b] (**1**)	225		72.8 (72.3)	5.8 (5.7)	10.7 (11.1)
$MoCl(\eta^3\text{-}C_3H_5)(dppe)_2$[c] (**2**)	186	2.61	70.3 (70.4)	5.6 (5.6)	13.1 (12.8)
$[Mo(MeCN)(\eta^3\text{-}C_3H_5)(dppe)_2]BF_4$[d] (**3**)	128 (dec)		63.7 (62.3)	5.2 (5.0)	11.3 (11.7)
$Mo(CH_3)(\eta^3\text{-}C_3H_5)(dppe)_2$ (**4**)	183 (dec)	2.30	70.5 (72.3)	6.0 (6.0)	12.7 (13.1)
$Mo(CH_2SiMe_3)(\eta^3\text{-}C_3H_5)(dppe)_2$ (**5**)	210 (dec)	2.35	70.0 (70.6)	6.5 (6.4)	12.0 (12.4)

[a] Required values in parentheses.
[b] N, 2.4 (2.4).
[c] Cl, 3.8 (3.7).
[d] N, 1.2 (1.3).

Alkylation of the chloride, **2**, with RLi in THF produces the yellow alkyl complexes, $MoR(\eta^3\text{-}C_3H_5)(dppe)_2$ [R = Me (**4**) and CH_2SiMe_3 (**5**)] in moderate yields.

The halide and alkyl compounds are paramagnetic in the solid state with magnetic moments somewhat lower than the spin-only value (2.83 BM) for octahedral d^4 complexes. No ESR spectra could be observed since octahedral molybdenum(II), $S = 1$ is ESR silent. Despite their paramagnetism, the compounds have moderately sharp ^1H NMR spectra which are shifted only a little compared to typical diamagnetic η^3-allyls.[8] This type of behaviour has been observed[9] for other paramagnetic d^4 complexes such as $ReX_3(PR_3)_3$.

For neither compound **4** and **5** is there any evidence of 1,3-shifts comparable to the hydride shift[1] on heating in solution to yield substituted propylenes, nor do they show any significant reactivity towards CO even at elevated temperature and pressure. The absence of migration, for even the methyl complex, may indicate that the complex adopts a "*trans*" configuration as opposed to the "*cis*" configuration, probably present in the allyl hydride. Crystals of the various compounds suitable for X-ray study could not be obtained.

Although *no* substituted propylene species could be isolated, the mass spectra show peaks due to C_3H_5X (X = Cl, Me and CH_2SiMe), indicating that elimination does occur at high temperatures in the vapour phase (> 180°C).

Thus, except for the reaction with CCl_4 the complex $MoH(\eta^3\text{-}C_3H_5)(dppe)_2$ appears to react as the isomeric molybdenum(0) propylene complex, which having a vacant coordination site on the metal enables coordination of a donor ligand with facile displacement of propylene.

EXPERIMENTAL

Experimental methods and instruments are as given previously.[10] Magnetic susceptibilities in the solid state were determined using an Evans' balance and were corrected for diamagnetism at ligands. $MoCl_4(THF)_2$ was prepared by a literature method.[11]

Hydrido(η^3 - allyl)bis[1,2 - bis(diphenylphosphino) ethane]molybdenum(II)

$MoCl_4(THF)_3$ (1.19 g, 3.12 mmol) was added to a solution of dppe (2.49 g, 6.26 mmol) in THF (80 cm^3) over Na(Hg) amalgam (0.40 g in 5 cm^3) under propylene (1 atm). The solution was stirred for 12 h, filtered, concentrated and cooled to −20°C to give a red microcrystalline solid which was collected, washed with hexane (2 × 10 cm^3) and dried *in vacuo*. Yield: 2.34 g, 82%. IR: 3050m, 1965m, 1585m, 1470s, 1430s, 1410m, 1300w, 1260m, 1190m, 1150w, 1115m, 1090s, 1075m, 1025m, 930w, 910w, 870m, 840w, 800s, 740s, 720s, 698s, 650s, 620s, 610w, 520s, 510s, 500w, 490m, 470w, 440m, 420m, 400m.

Trans - *bis*(2,6 - *dimethylphenylisocyanide)bis*[1,2-*bis*(*diphenylphosphino*)*ethane*]*molybdenum*(0) (**1**)

To a stirred solution of the allyl hydride (0.34 g, 0.36 mmol) in THF (30 cm^3), at −20°C, was added 2,6-$Me_2C_6H_3NC$ (0.1 g, 0.76 mmol). The solution was allowed to warm to room temperature and stirred for 6 h. The deep red solution was concentrated *in vacuo*, and on cooling (−20°C) gave red diamond-shaped crystals. Yield: 0.38 g, 91%. IR: 1879vs, 1587s, 1432s, 1308w, 1262w, 1190w, 1155w, 1091m, 1027m, 920m, 859m, 791s, 772m, 745w, 739m, 720m, 694s, 653s, 625w, 616m, 539w, 530w, 518m, 505w, 495m. NMR ^1H: 0.9 (12H, s, CH_3); 2.2–2.6 (8Hm, PCH_2); 6.9–8.0 (46Hm arom. H). ^{31}P: 78.6s. Mass spectrum: *m/z* 1156 [Mo$(Me_2C_6H_3NC)_2(dppe)_2]^+$; 1025 [Mo$(Me_2C_6H_3NC)(dppe)_2]^+$.

Chloro(η^3 - *allyl*)*bis*[1,2 - *bis*(*diphenylphosphino*)*ethane*]*molybdenum*(II) (**2**)

To a stirred solution of the allyl hydride (2 g, 2.18 mmol in 100 cm^3 of THF) was added CCl_4 (20 cm^3). A yellow precipitate formed after stirring for 1 h. The solid was collected, washed with hexane (2 × 20 cm^3) and dried *in vacuo*. Yield: 2.07 g, *ca* 100%. IR: 3050m, 1595m, 1570s, 1480m, 1430s, 1410m, 1190m, 1160m, 1120m, 1110m, 1070m, 1030m, 1000m, 870m, 790s, 740s, 695s, 660s, 545m, 530m, 520s, 510s, 500m, 485m, 310m. NMR ^1H: 0.66 (2H, s), 1.12 (2H, s), (allyl CH_2); 1.30 (8H, s, PCH_2); 3.80s (^1H, s, allyl C*H*). Mass spectrum: *m/z* 892 $[Mo(dppe)_2]^+$; 76 $[C_3H_5Cl]^+$.

The conductivity of **2** in $CHCl_3$ at 25°C showed the complex to be unionized ($\Lambda_M = 0.67\ \Omega^{-1}\ cm^3\ mol^{-1}$), but at 40°C the conductivity increased to 2.86 $\Omega^{-1}\ cm^3\ mol^{-1}$ and on cooling returned to the original value. The cycle could be repeated several times. Addition of KBF_4 stabilizes the conductivity at the higher value. The cation has been isolated from acetonitrile as below.

Acetonitrile(η^3 - *allyl*)*bis*[1,2 - *bis*(*diphenylphosphino*)*ethane*]*molybdenum*(II) *tetrafluoroborate* (**3**)

(a) To a solution of the chloride, **2** (0.24 g, 0.25 mmol), in MeCN (30 cm^3) was added KBF_4 (0.03 g, 0.25 mmol). After stirring for 1 h the solvent was removed and the yellow solid washed with MeOH (2 × 20 cm^3) and recrystallized from MeCN–Et_2O (1:1, 20 cm^3). Yield: 0.16, 63%. IR: 3050m, 2305m, 1598m, 1570w, 1480, 1430s, 1410, 1190m, 1120sh, 1050br.s, 1000sh, 870m, 780s, 740s, 660s, 550m, 520m, 510s, 500m, 490w. NMR ^1H: 0.4 (2H, s), 1.2 (2H, s), (allyl CH_2); 1.30 (8H, s, PCH_2); 2.1 (3H, s, $NCCH_3$). Conductivity (MeCN): Λ_M 136 $\Omega^{-1}\ cm^3\ mol^{-1}$.

(b) To a solution of the allyl hydride (0.25 g, 0.28 mmol) in MeCN (30 cm^3) was added an excess of an Et_2O solution of $HBF_4 \cdot OEt_2$ (1 cm^3, 52%). After stirring for 6 h, the solvent was removed and the residue washed with Et_2O (3 × 10 cm^3), then extracted into MeCN–Et_2O (1:1, 20 cm^3); cooling (−20°C) produced a yellow solid identical to that in (a). Yield: 0.10 g, 40%.

Methyl(η^3 - *allyl*)*bis*[1,2-*bis*(*biphenylphosphino*)*ethane*]*molybdenum*(II) (**4**)

To a suspension of Mo$Cl(\eta^3$-$C_3H_5)(dppe)_2$ (0.5 g, 0.53 mmol) in THF (100 cm^3), at −78°C, was added MeLi (1.0 cm^3, 0.69 mmol). The solution was allowed to warm to room temperature and stirred for 2 h. The deep golden solution was filtered, the volume reduced to *ca* 20 cm^3 and cooled (−20°C) to give a dark yellow solid, which was recrystallized from toluene. Yield 0.35 g, 71%. IR: 3050m, 1585m, 1410m, 1310w, 1260m, 1100s, 1090s, 1060s, 1025m, 900m, 870m, 800m, 755m, 740s, 695s, 650s, 635m, 510s, 505m, 495w, 485m, 420m, 370m. NMR ^1H: 0.88 (2H, s), 1.12 (2H, s) (allyl CH_2); 1.30 (8H, s, PCH_2); 2.90 (3H, s, CH_3); 3.55 (^1H, s, allyl C*H*). Mass spectrum: *m/z* 892 $[Mo(dppe)_2]^+$; 56 $[C_4H_8]^+$.

(η^3 - *Allyl*)*trimethylsilylmethylbis*[1,2 - *bis*(*diphenylphosphino*)*ethane*]*molybdenum*(II) (**5**)

As for **4** but using 1 equivalent of Me_3SiCH_2Li. Yield: *ca* 65%. IR: 3050m, 1566s, 1475m, 1430s, 1408m, 1310m, 1270m, 1260m, 1190m, 1160m, 1130m, 1100s, 1090, 1071m, 1030m, 870m, 800m, 750m, 695s, 610s, 560m, 485m, 420w. NMR ^1H: 0.15 (9H, s) ($SiMe_3$); 0.89 (2H, s), 1.18 (2H, s) (allyl CH_2); 1.30 (8H, s, PCH_2); 2.93 (2H, s, $SiCH_2$) 3.61 (^1H, s, allyl C*H*). Mass spectrum: *m/z* 892 $[Mo(dppe)_2]^+$; 128 $[C_7H_{16}Si]^+$.

Acknowledgement—We thank the SERC for studentships (A.R.B. and S.J.A.).

REFERENCES

1. J. W. Byrne, H. V. Blaser and J. A. Osborn, *J. Am. Chem. Soc.* 1975, **97**, 3871. For references to other allylhydrido complexes see W. D. McGee and R. G. Bergman, *J. Am. Chem. Soc.* 1988, **110**, 4246; R. J. Batchelor, F. W. B. Einstein, R. H. Jones, J.-M. Zhuang and D. Sutton, *J. Am. Chem. Soc.* 1989, **111**, 3468.

2. D. M. Adams, *Metal Ligand and Related Vibrations*. Arnold, London (1967).
3. T. A. George and C. D. Siebold, *Inorg. Chem.* 1973, **12**, 2548.
4. F. Zingales and F. Canziani, *Gazz. Chim. Ital.* 1962, **92**, 343.
5. L. J. Archer and T. A. George, *Inorg. Chem.* 1979, **18**, 2079.
6. J. Chatt, C. M. Elson, A. J. L. Pombeiro, R. L. Richards and G. H. D. Royston, *J. Chem. Soc., Dalton Trans.* 1978, 165.
7. See for example, L. F. Rhodes, J. D. Zubkowski and K. G. Caulton, *Inorg. Chem.* 1982, **21**, 4185.
8. B. J. Brisdon, D. A. Edwards and K. E. Paddick, *Transition Met. Chem.* 1981, **6**, 83.
9. H. P. Gunz and G. J. Leigh, *J. Chem. Soc. A* 1971, 2229; J. Chatt, G. J. Leigh and D. M. P. Mingos, *J. Chem. Soc. A* 1969, 1674.
10. A. R. Barron, G. Wilkinson, M. Motevalli and M. B. Hursthouse, *Polyhedron* 1987, **6**, 1089.
11. J. R. Dilworth and R. L. Richards, *Inorg. Synth.* 1980, **20**, 119.

Polyhedron Vol. 8, No. 21, pp. 2603–2610, 1989
Printed in Great Britain

0277–5387/89 $3.00+.00
Pergamon Press plc

CHEMICAL, SPECTROSCOPIC AND ELECTRICAL CONDUCTION PROPERTIES OF IODINATED NICKEL DIIMINE COMPLEXES

FRANCESCO LELJ,* GIANCARLO MORELLI, GIAMPAOLO RICCIARDI, MARIA F. BRIGATTI and ANGELA ROSA

Istituto di Chimica, Universita' della Basilicata, Via N. Sauro 85, 85100 Potenza, Italy

(*Received* 16 *May* 1989; *accepted* 16 *June* 1989)

Abstract—Bis(diimine)nickel complexes [diimine = 2,3-diiminonaphthalene (din) and 9,10-diiminophenanthrene (dip)] have been prepared by oxidation of a solution of Ni^{2+} and the appropriate diamine. The complexes were studied by UV–vis spectroscopy and compared with the well-known bis(*o*-phenylenediimine)nickel complex. Oxidation with iodine gave $Ni(din)_2I_x$ and $Ni(dip)_2I_x$ (where $x = 0.13$–3.30). Thermogravimetric analyses (TGA) provided quantitative information on the iodine content. Weight losses at 100°C were observed for highly iodinated compounds involving the decomposition of I_5^- to I_3^- and for all species above 260°C. Raman and IR spectroscopy were used to characterize the iodine-doped complexes. The Raman spectra showed strong scattering attributable to I_3^- (107 cm^{-1}) and I_5^- (160 cm^{-1}), the latter only for highly iodinated complexes. The conductivity of iodine-doped materials was studied by using linear two-probe (300 K) and variable temperature (77–300 K) van der Pauw methods on pressed pellets. The conductivity is thermally activated, with an apparent activation energy of 0.25 and 0.075 eV for $Ni(din)_2I_x$ and $Ni(dip)_2I_x$, respectively. A large increase of the conductivity for more extended molecules is observed.

Many classes of mixed-valence and partially oxidized metallo-organic complexes have been studied during recent years. Most studies[1] concern: (i) glyoximate complexes of nickel(II) and palladium(II);[2] (ii) 16 π-electron tetra-azaannulene complexes of cobalt(II), nickel(II) and palladium(II);[3] (iii) 16 π-electron phthalocyanine[4] or porphyrin[5] complexes of a large variety of metals, all these compounds being partially oxidized by different amounts of iodine or other oxidants. The great interest in these compounds is due to the anisotropic conducting properties associated with the one-dimensionality of these systems. The conducting behaviour of these stacked materials depends on electronic features of both the ligand and metal, structural organization (interplanar spacing) and crystal packing, nature and amount of the oxidant.

In attempts to obtain a new class of metallo-organic conducting materials using the well-known bis(*o*-phenylenediimine)nickel complex, $Ni(opd)_2$, has been investigated in recent years. Conductivity data are reported for: $Ni(opd)_2 \cdot A$ species (where A is a strong electron acceptor);[6] $[Ni(opd)_2]_n^+$ salts;[7] and finally for the iodinated species $Ni(opd)_2I_x$.[8] These partially oxidized $Ni(opd)_2I_x$ species show[8] modest conducting properties compared with phthalocyanine or tetra-azaannulene iodinated complexes.

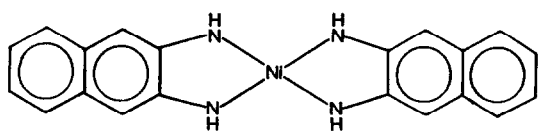

$Ni(din)_2$

In this paper we present the preparation and characterization of a series of new nickel complexes with aromatic diamines: bis(2,3-diiminonaphthalene)nickel, $Ni(din)_2$, and bis(9,10-diiminophenan-

* Author to whom correspondence should be addressed.

threne)nickel, $Ni(dip)_2$, and their partially oxidized iodine counterparts.

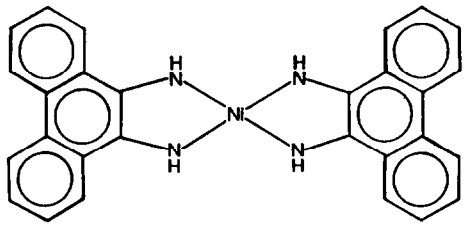

$Ni(dip)_2$

The conducting behaviour of these complexes was studied in order to correlate the conducting properties of the bulk materials within a homologous series of ligand molecules, on going from the $Ni(opd)_2$ species to $Ni(din)_2$ and finally to $Ni(dip)_2$. The rôle played by the metal, the ligand and the iodine in the conducting phenomenon was also investigated.

EXPERIMENTAL

Reagents

2,3-Diaminonaphthalene and 9,10-diaminophenanthrene were obtained commercially (Aldrich) and purified by sublimation (10^{-2} mm Hg). I_2, crystals, resublimated 99.8% A.C.G. reagent was used. Solvents were of analytical reagent or spectrograde quality. Elemental analyses were performed by the Analytical Laboratory, Faculty of Engineering, Potenza.

Synthesis of bis(diimine)nickel complexes

(a) *Bis(2,3-diiminonaphthalene)nickel*, $Ni(din)_2$. 2,3-diaminonaphthalene (1.0 g, 2.7 mmol) was dissolved by stirring at 70°C in 100 cm^3 of an ethanol–water (4 : 1) solution and treated with $NiCl_2 \cdot 6H_2O$ (1.2 g, 5.0 mmol) dissolved in 3.0 cm^3 of water and 3.0 cm^3 of concentrated ammonia. A stream of a O_2–N_2 (1 : 1) mixture was bubbled into the flask until the solution became a deep blue–green colour (*ca* 1.5 h). Ethanol was removed *in vacuo* and the green–black solid was filtered and washed well with water and acetone until the washings were colourless. After drying at 60°C and 25 mm Hg, the compound was purified by prolonged Soxhlet extraction with acetone under a nitrogen atmosphere. The first extract was not used, but the others afforded green–black pure microcrystalline powder in 20% yield. The compound is air-stable but it undergoes slow decomposition in solution when solvents other than acetone are used. Found: C, 63.8; H, 4.9; N, 14.7. Calc. for $C_{20}H_{16}N_4Ni$: C, 64.7; H, 4.3; N, 15.1%. UV–vis (acetone, 10^{-5} M): 742(7100), 460(2180)sh, 422(3310)sh, 390(4320)sh, 355(8350), 332(6350) nm (mol cm^{-1}).

(b) *Bis(9,10-diiminophenanthrene)nickel*, $Ni(dip)_2$. 9,10-Diaminophenanthrene (1.0 g, 2.1 mmol) which was completely dissolved in ethanol (100 cm^3) by stirring at 65°C, was treated with $NiCl_2 \cdot 6H_2O$ (1.0 g, 4.2 mmol) in 3.0 cm^3 of water and 3.0 cm^3 of concentrated ammonia. The solution was slowly stirred for 24 h in a flask open to the air but a pink–red colour was observed within a few minutes. Ethanol was removed *in vacuo* and the pink–red solid was treated and purified as described for $Ni(din)_2$. The air-stable complex was obtained in 40% yield as a pink–red microcrystalline powder. Found: C, 70.1; H, 4.6; N, 11.1. Calc. for $C_{28}H_{20}N_4Ni$: C, 71.4; H, 4.2; N, 11.9%. UV–vis (acetone, 10^{-5} M): 560(2120), 415(5500), 402(3601), 388(3805), 380(2504), 368(2400), 360(2385)sh nm (mol cm^{-1}).

Iodination of $Ni(din)_2$ *and* $Ni(dip)_2$ *complexes*

In order to prepare polycrystalline samples of various stoichiometries, finely powdered $Ni(din)_2$ and $Ni(dip)_2$, in acetone, were treated with increasing amounts of iodine dissolved in acetone, in the dark. The reactions were performed by stirring for 18 h at room temperature in a flask sealed with a septum. In a typical experiment $Ni(din)_2$ (0.156 g, 0.42 mmol) in 20 cm^3 of acetone was treated with I_2 (0.106 g, 0.42 mmol) dissolved in 15 cm^3 of acetone. The green–gold compound obtained was purified by removing the solvent and the unreacted iodine under a stream of nitrogen. The compound, washed twice with acetone and dried at 40°C and 25 mm Hg, was characterized as $Ni(din)_2I_{0.55}$. The iodine content was monitored by TGA and was consistent with the elemental analysis.

Physical measurements

Thermogravimetric analysis

TGA data were obtained by using a B85 Setaram thermal analyser, equipped with a TGC 85 controller module and a BBC(Goerz Metrawatt) Servogor 120 recorder. Measurements were carried out using a platinum sample boat under a nitrogen atmosphere. A nitrogen flow rate of 50 cm^3 min^{-1} and a programmed heating rate of 20°C min^{-1} were employed. Scans were made from room temperature to approximately 350°C. The initial sample mass was nominally 8.0 mg. Iodine contents were directly determined from the thermograms. All the

data obtained were in good agreement with the elemental analyses.

Spectroscopy

IR spectra were recorded on Nujol mulls with a Perkin–Elmer Model 883 spectrophotometer. UV–vis spectra in solution (acetone, 10 cm path length cells) were obtained using a Cary 2300 spectrophotometer. Raman spectra were obtained with a Ramanor HG2S spectrometer employing 514.5 nm excitation (250 mW argon ion laser power filtered at 30%). Samples, in glass capillaries, were spun at 300 r.p.m.

Conductivity measurements

Electrical conductivity data by both the linear two-probe and the four-probe van der Pauw[9] methods were obtained. With the linear two-probe technique only room temperature data were acquired. Micropellets, 1 mm in diameter and *ca* 1 mm thick, were introduced into a glass capillary. In the case of van der Pauw[9] measurements sample discs (13 mm diameter, approx. 0.5 mm thick) were used. The discs were formed using an evacuable die and a Carver press. The thickness and diameter of samples and probe spacing were determined with the aid of a microscope. Electrical current to the samples was supplied by a Hewlett–Packard precision DC current source 6186C. Output DC voltages were detected by a Hewlett–Packard 3478 A multimeter. Electrical contacts to the samples were made with Silver Paint AG 121, Bitronic (Italy). For provision of strain-free mounting, the discs were secured to the anodized aluminium mount by a tuft of cotton over which was wrapped a strip of Teflon tape. The sample holder was contained in a gas-tight brass can which fitted into a liquid nitrogen Dewar and was cooled by a stream of nitrogen. The temperature (± 0.1°C) was monitored by a Au–Chromel thermocouple located *ca* 1 mm from the sample. The investigated temperature range was between 77 K and room temperature. At temperatures above 30–40°C, highly iodinated samples released iodine slowly and stable voltages could not be recorded. The measurement procedure included: (i) verification of electrical isolation between the sample and mount; (ii) resistance measurements between all four electrodes as a function of current to check for non-ohmic behaviour, contact resistance and sample integrity; (iii) measurements at zero current to the sample to check for stray voltages.

RESULTS AND DISCUSSION

The two complexes $Ni(din)_2$ and $Ni(dip)_2$ were synthesized following a slightly modified procedure of Feigl and Furth[10] for $Ni(opd)_2$. By oxidation of a solution of Ni^{2+} and of the appropriate diamine in aqueous ammonia, the complexes are isolated as solids which display very low solubility in most solvents. $Ni(din)_2$ requires a more oxidative atmosphere and prolonged reaction time; moreover, by using a more water-rich solvent in the preparation of $Ni(din)_2$, amine polymerization can occur. Furthermore, owing to the fact that the reactions have low yields, the products have to be purified from large amounts of unreacted amine.

Concerning the electronic structure of the complexes and the oxidation state of the metal, different possibilities can be formally considered:[11,12]

(1) the ligands are in the deprotonated form (L^{2-}) and nickel is in the +IV oxidation state;
(2) the ligands have a radical anionic structure (L^{-}) and nickel has an oxidation number of +II;
(3) the ligands are in the fully oxidized form (L) with an oxidation number of zero assigned to the metal.

In recent papers we have presented investigations on the ground-state electronic structure of $Ni(opd)_2$[13] (a DV-Xα study with comparison to previous MS-Xα calculations[12]) and on the spectroscopic behaviour[14] of this complex. The reported results confirm the α-diimine character of the ligands and suggest a structural situation, intermediate between the formal structures (2) and (3), with the nickel atom having a positive charge of +1. By analogy with the $Ni(opd)_2$ species a similar structure for $Ni(din)_2$ and $Ni(dip)_2$ can be postulated; moreover, the similar spectroscopic behaviour for these three complexes (*vide infra*) suggests an α-diimine character of the ligands also in the $Ni(din)_2$ and $Ni(dip)_2$ species.

UV–vis characterization of $Ni(din)_2$ *and* $Ni(dip)_2$

The UV–vis spectra of $Ni(din)_2$ and $Ni(dip)_2$ can be interpreted by analogy with the spectroscopic behaviour of bis(*o*-phenylenediimine)nickel.[14] Figure 1 shows the UV–vis spectra at room temperature of $Ni(din)_2$ and $Ni(dip)_2$ in acetone solutions. For $Ni(din)_2$, the spectrum shape is similar to that of bis(*o*-phenylenediimine)nickel with an intense band ($\varepsilon_{max} = 7100$) at 742 nm. This band, responsible for the green–blue colour of the solution, suggests intermolecular interactions in solution depending on the concentration and the nature

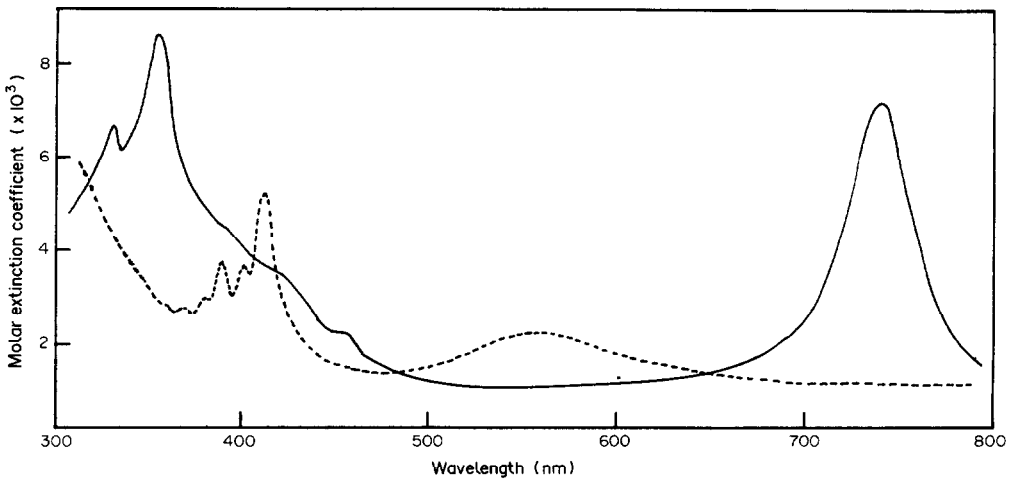

Fig. 1. UV–vis spectra in acetone solution for $Ni(din)_2$ (solid line) and $Ni(dip)_2$ (dotted line).

of the solvent.[14] For the less soluble complex, $Ni(dip)_2$, only very dilute (less than 5×10^{-5} M) pink–violet solutions in acetone were obtained. Under these conditions the spectrum shows a moderately intense band ($\varepsilon_{max} = 2120$) at *ca* 560 nm, as observed for dilute solutions of bis(*o*-phenylenediimine)nickel. This spectroscopic feature rules out strong intermolecular interactions for $Ni(dip)_2$ species under these experimental conditions.

Iodination chemistry: IR, Raman and TGA data

Iodination at room temperature of $Ni(din)_2$ and $Ni(dip)_2$ gives, respectively, green–gold and red–black microcrystalline powders. The iodine content, determined by TGA, is in good agreement with elemental analyses. For both compounds the iodine uptake is approximately 0.25–0.33 the amount of I_2 used in the reaction and depends on the reaction conditions. The reaction rate is dependent on the oxidant concentration, and the iodine uptake occurs slowly. No significant loss of iodine was observed during the drying operation. The $Ni(din)_2I_x$ and $Ni(dip)_2I_x$ species with maximum iodine content are not stable *in vacuo* (10^{-1} mm Hg) and slowly lose I_2 over a period of 1 week, finally giving stable compositions. At an elevated temperature (200°C) and under dynamic vacuum, complete removal of I_2 occurs leaving the starting $Ni(din)_2$ and $Ni(dip)_2$ species. A list of the complexes obtained, together with synthetic information and analytical data, are presented in Table 1.

The IR spectra of $Ni(din)_2$ and $Ni(dip)_2$ and of the iodinated compounds show characteristic absorptions for nickel complexes with aromatic diiminic ligands.[8] In fact all the compounds exhibit a strong N—H stretch around 3250–3300 cm^{-1}, C=C, C=N stretches in the 1400–1600 cm^{-1} region and an out-of-plane bending of the aromatic C—H in the region 740–900 cm^{-1}: the latter absorption's wavenumber is strongly dependent on the I/Ni ratio. Moreover, a series of bands in the region 1200–1400 cm^{-1} can be observed for the

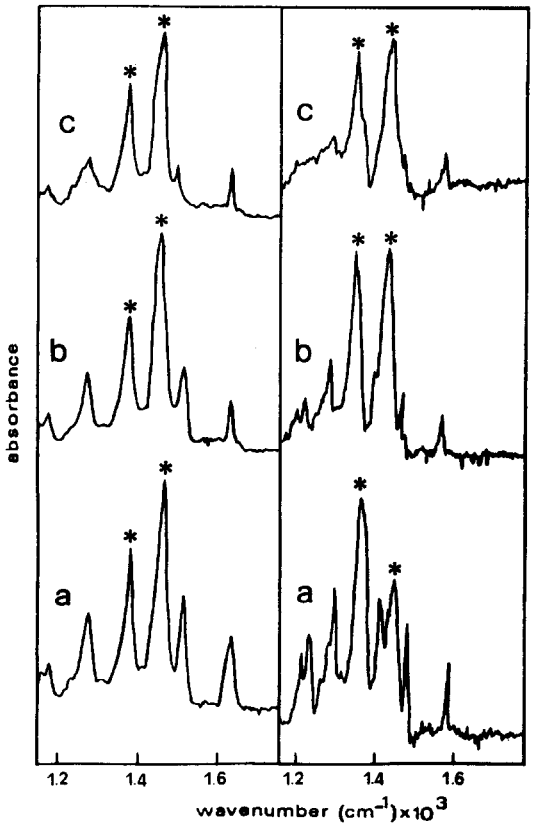

Fig. 2. IR spectra in the 1200–1800 region (cm^{-1}) as a function of iodine content. Left: $Ni(din)_2I_x$ (a, $x = 0$; b, $x = 0.55$; c, $x = 3.30$). Right: $Ni(dip)_2I_x$ (a, $x = 0$; b, $x = 0.56$; c, $x = 3.25$). Nujol absorption bands are marked by asterisks.

Table 1. Iodination conditions, analytical data and room temperature conductivities for $Ni(din)_2I_x$ and $Ni(dip)_2I_x$

	x	Weight (mmol) $Ni(din)_2$ (g)[a]	Weight (mmol) I_s (g)[b]	Elemental analysis, calc. (found) C	H	N	$-\log\sigma$[c]
$Ni(din)_2I_x$	0.00	—	—	64.7(63.8)	4.3(4.9)	15.1(14.7)	10.50
	0.15	0.156(0.420)	0.040(0.420)	61.6(61.2)	4.1(4.3)	14.4(14.1)	9.09
	0.36	0.156(0.420)	0.078(0.307)	57.7(57.3)	3.8(3.7)	13.4(13.2)	6.69
	0.55	0.156(0.420)	0.106(0.420)	54.5(54.1)	3.7(3.5)	12.7(12.8)	5.00
	1.25	0.156(0.420)	0.230(0.906)	38.6(38.1)	3.0(3.3)	10.6(10.7)	4.52
	3.30	0.156(0.420)	0.320(1.260)	30.4(30.1)	2.0(1.9)	7.1(7.2)	5.09
	x	Weight (mmol) $Ni(dip)_2$ (g)[a]	Weight (mmol) I_s (g)[b]	Elemental analysis, calc. (found) C	H	N	$-\log\sigma$[c]
$Ni(dip)_2I_x$	0.00	—	—	71.4(70.1)	4.2(4.6)	11.9(11.1)	9.69
	0.13	0.220(0.467)	0.020(0.078)	69.0(68.0)	4.1(4.7)	11.5(11.0)	8.40
	0.21	0.220(0.467)	0.040(0.156)	67.6(67.0)	4.0(4.4)	11.3(10.7)	6.00
	0.30	0.220(0.467)	0.060(0.236)	65.1(64.6)	3.8(3.6)	10.8(10.2)	3.53
	0.36	0.220(0.467)	0.080(0.314)	65.1(64.4)	3.8(3.6)	10.8(10.2)	2.30
	0.56	0.220(0.467)	0.120(0.472)	62.0(61.3)	3.7(3.9)	10.3(10.0)	1.69
	0.91	0.220(0.467)	0.230(0.905)	57.3(56.9)	3.4(3.8)	9.5(9.1)	2.00
	1.20	0.220(0.467)	0.260(1.024)	53.9(53.4)	3.2(3.5)	9.0(8.7)	2.00
	2.56	0.220(0.467)	0.300(1.181)	49.2(48.7)	2.5(2.9)	7.0(6.8)	2.09
	3.25	0.220(0.467)	0.350(1.379)	38.1(37.6)	2.3(2.5)	6.3(6.2)	2.22

[a] In 20 cm^3 of acetone.
[b] Dissolved in 15 cm^3 of acetone.
[c] Values reported with estimated errors of ± 0.05.

unoxidized complexes. As the iodine content increased, the IR peaks broadened and were finally obscured due to the superposition of the electronic excitation absorption.[15,16] This phenomenon is shown in Fig. 2.

Raman spectra (50–450 cm^{-1}) for $Ni(din)_2I_x$ and for $Ni(dip)_2I_x$ are shown in Fig. 3. Contributions from non-iodinated compounds in this region are negligible if compared with the resonances enhanced by the polyiodide modes. All iodinated compounds exhibit intense scattering at *ca* 107 cm^{-1}. According to previous spectroscopic studies on iodine-doped mixed-valence inorganic salts[17] and polyacetylene,[18] this band is assigned to the I_3^- fundamental symmetric stretching. Overtones are also observed at 214 cm^{-1} and 320–340 cm^{-1}. The band at 160 cm^{-1}, observed only for highly iodinated $Ni(din)_2I_x$ ($x > 0.55$) and $Ni(dip)_2I_x$ ($x > 0.21$), is assigned to I_5^-, in agreement with earlier works on iodine-doped fluorogallium

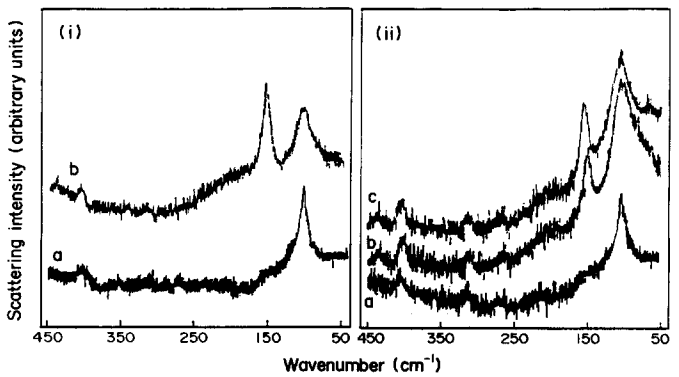

Fig. 3. Raman spectra in the range 50–450 cm^{-1}. (i) $Ni(din)_2I_x$ (a, $x = 0.15$; b, $x = 1.25$). (ii) $Ni(dip)_2I_x$ (a, $x = 0.13$; b, $x = 0.56$; c, $x = 1.20$).

and fluoroaluminium phthalocyanines[17] and polyacetylene.[19] No evidence for the presence of I_2 is obtained due to the lack of any bands around 207 cm^{-1}. Previous works[20,21] on iodinated molecular crystals do not provide any evidence for the presence of I^-. Anyway, this species is undetectable by any of the spectroscopic techniques utilized in this study.

Thermogravimetric analyses for $Ni(din)_2I_x$ and $Ni(dip)_2I_x$ reveal some most interesting features between room temperature and 260°C. Above this temperature range the thermograms are identical with those for non-iodinated complexes, showing weight losses at 400°C [$Ni(din)_2$] and 450°C [$Ni(dip)_2$] due to their decomposition. The thermograms for iodinated $Ni(din)_2I_x$ and $Ni(dip)_2I_x$ species with I/Ni ratios higher than 0.55 and 0.21, respectively, present two weight loss processes between 60 and 120°C, and 180 and 270°C, with a maximum of DTGA centred at 100 and 220°C (see Figs 4 and 5 for the $Ni(dip)_2I_x$ series). The weight loss at 100°C, according to the Raman spectra which show intense scattering at 160 cm^{-1} imputable to the presence of I_5^- polyiodide, is interpreted as decomposition of I_5^- to I_3^-. For the less iodinated complexes only one weight loss is observed (260°C) and attributed to the complex removal of I_3^-. These data are in agreement with the previous evidence[17] concerning the presence of I_5^- only in the highly iodinated species.

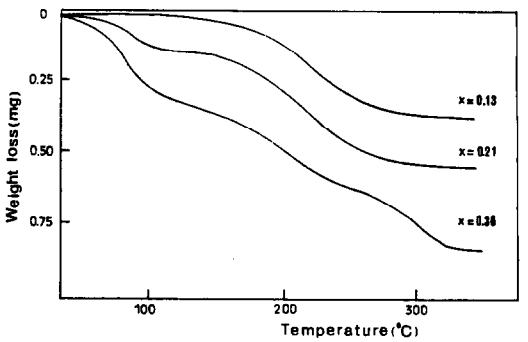

Fig. 4. Thermogravimetric analyses for $Ni(dip)_2I_x$ (measurements taken on samples of nominally 8.0 mg weight).

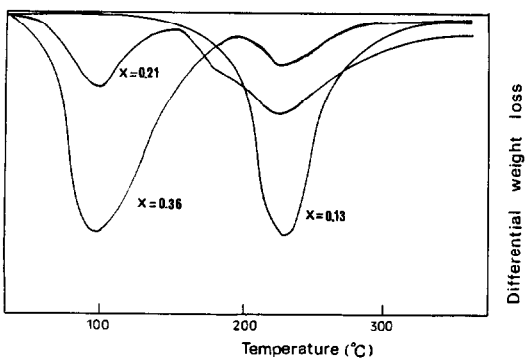

Fig. 5. DTGA data for $Ni(dip)_2I_x$.

Electrical conductivity

Conductivity data at room temperature by both the linear two-probe technique on micropellets and the van der Pauw method on pressed discs are in excellent agreement for all the samples. At low temperature only the van der Pauw technique was used. Data at room temperature for all the species are reported in Table 1. Temperature dependence of the conductivity (plotted in Fig. 6 for three $Ni(dip)_2I_x$ complexes and for $Ni(din)_2I_{0.55}$) was investigated: the data fit the function $\sigma = \sigma_\infty \exp(-E_a/KT)$ and indicated a semiconducting behaviour for all the samples in the investigated temperature range from 77 K to room temperature. Activation energy depends on the ligands but is independent of iodine content. In fact E_a values of 0.25 and 0.075 eV for $Ni(din)_2I_{0.55}$ and for the three $Ni(dip)_2I_x$ complexes, respectively, are found, against an E_a value of 0.87 eV reported[6] for $Ni(opd)_2I$. The conductivity trend as a function of iodine content is plotted in Fig. 7 for both $Ni(dip)_2I_x$ and $Ni(din)_2I_x$ species. The data[8] concerning the $Ni(opd)_2I_x$ species are also reported for comparison. The main features of the reported data can be summarized:

(i) on increasing the iodine content, the conductivity of all the complexes first rises rapidly until a value of σ_{max}, and then decreases moderately;

(ii) the I/Ni ratio corresponding to the higher conductivity decreases on going from $Ni(opd)_2I_x$

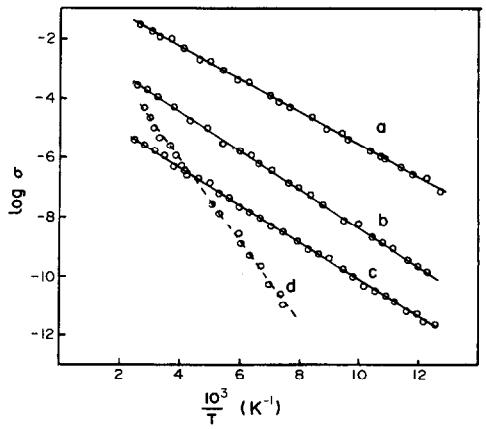

Fig. 6. Temperature dependence of the conductivity: (a) $Ni(dip)_2I_{1.20}$; (b) $Ni(dip)_2I_{0.30}$; (c) $Ni(dip)_2I_{0.21}$; (d) $Ni(din)_2I_{1.25}$.

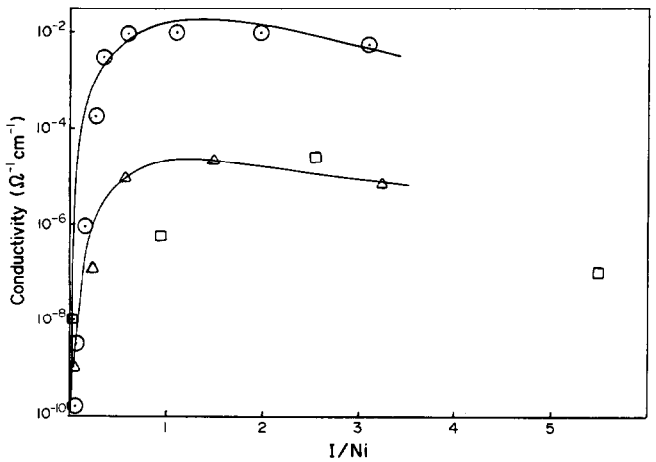

Fig. 7. Variation of the conductivity as a function of iodine content. (Δ, $Ni(din)_2I_x$; ⊙, $Ni(dip)_2I_x$; □, $Ni(opd)_2I_x$, ref. 8).

to $Ni(din)_2I_x$ and finally to $Ni(dip)_2I_x$. The highest conductivity ($10^{-2}\,\Omega\,cm^{-1}$) is observed at an I/Ni ratio of 0.56 in the case of $Ni(dip)_2I_x$;

(iii) for more extended complexes ($Ni(dip)_2I_x$ vs $Ni(opd)_2I_x$) an increase of the conductivity by a factor of 10^3–10^4 is observed.

These results, and in particular the observed trend that the increase of the molecular surface raises the electrical conductivity, suggest the influence of the ligands on the packing in the stacks. In fact, although structural analyses on these iodinated complexes were not performed, an X-ray structure determination on the unoxidized $Ni(opd)_2$ complex[22] shows a stacked packing with very large Ni—Ni distances (4.65 Å) and not a parallel stacking of the molecular planes. These packing features should be responsible for the modest conductivity of the $Ni(opd)_2I_x$ compounds. The diimines in $Ni(din)_2$ and in $Ni(dip)_2$, more extended than *o*-phenylenediimine, should favour a stacked packing with a large parallelism between the molecular planes and consequently a better overlapping of the π-system. X-ray measurements to understand better the steric role are in progress.

In conclusion, the results of this study demonstrate that partial iodine oxidation of nickel–aromatic diimine complexes provides an interesting new class of molecular conductors. All the chemical and physical properties of these compounds, including electrical conductivity, are comparable with that of the best known stacked molecular conductors. Moreover, to the best of our knowledge, $Ni(dip)_2I_{0.56}$ shows the higher conductivity value for open-ring $M—N_4$ partially oxidized systems.

Acknowledgements—We are indebted to Dr M. Latronico for the elemental analyses. We thank the Italian National Research Council (CNR) and Ministero della Pubblica Istruzione of Italy (MPI) for financial support.

REFERENCES

1. T. J. Marks and D. W. Kalina, in *Extended Linear Chain Compounds* (Edited by J. S. Miller), Vol. 1, pp. 197–331. Plenum Press, New York (1982).
2. A. Gleizes, T. J. Marks and J. A. Ibers, *J. Am. Chem. Soc.* 1975, **97**, 3545.
3. L. S. Lin, T. J. Marks, C. R. Kannewurf, J. W. Lyding, M. S. McClure, M. T. Ratajack and T. C. Whang, *J. Chem. Soc., Chem. Commun.* 1980, 954.
4. (a) J. L. Petersen, C. J. Schramm, D. R. Stojakovic, B. M. Hoffman and T. J. Marks, *J. Am. Chem. Soc.* 1977, **99**, 286; (b) W. J. Pietro, T. J. Marks and M. A. Ratner, *J. Am. Chem. Soc.* 1985, **107**, 5387; (c) J. Martinsen, R. L. Greene, S. M. Palmer and B. M. Hoffman, *J. Am. Chem. Soc.* 1983, **105**, 677.
5. J. Martinsen, L. J. Pace, T. E. Phillips, B. M. Hoffman and J. A. Ibers, *J. Am. Chem. Soc.* 1982, **104**, 83.
6. F. Babler and A. von Zelewsky, *Helv. Chim. Acta* 1977, **60**, 2723.
7. M. G. Miles and J. D. Wilson, *Inorg. Chem.* 1975, **14**, 2357.
8. Y. M. Wuu and S. M. Peng, *J. Inorg. Nucl. Chem.* 1980, **42**, 205.
9. L. J. van der Pauw, *Philips Res. Rep.* 1958, **13**, 1.
10. F. Feigl and M. Furth, *Monatsh. Chem.* 1927, **48**, 445.
11. A. L. Balch and R. H. Holm, *J. Am. Chem. Soc.* 1966, **88**, 5201.
12. J. Weber, C. Daul, A. von Zelewsky, A. Goursot and E. Penigault, *Chem. Phys. Lett.* 1982, **88**, 78.
13. F. Lelj, A. Rosa, M. Casarin, G. Ricciardi and G. Morelli, *Inorg. Chim. Acta*, submitted for publication.
14. F. Lelj, A. Rosa, G. Ricciardi, M. Casarin, P. Cristinziano and G. Morelli, *Chem. Phys. Lett.* 1989, in press.

15. R. C. Wheland and J. L. Gilson, *J. Am. Chem. Soc.* 1976, **98**, 3916.
16. C. F. Fincher Jr, M. Ozaki, A. J. Heeger and P. G. MacDiarnud, *Phys. Rev. B* 1979, **19**, 4140.
17. R. S. Nohr, P. M. Kuznesof, K. J. Wynne, M. E. Kenney and P. G. Siebenman, *J. Am. Chem. Soc.* 1981, **103**, 4371 and refs therein.
18. S. L. Hsu, A. J. Signorelli, G. P. Pez and R. H. Baughman, *J. Chem. Phys.* 1978, **69**, 106.
19. C. J. Schramm, R. P. Scaringe, D. R. Stojakovic, B. M. Hoffman, J. A. Ibers and T. J. Marks, *J. Am. Chem. Soc.* 1980, **102**, 6702.
20. C. J. Schramm, D. R. Stojakovic, B. M. Hoffman and T. J. Marks, *Science* 1978, **200**, 47.
21. K. F. Schoch Jr, B. R. Kundalkar and T. J. Marks, *J. Am. Chem. Soc.* 1979, **101**, 7071.
22. G. S. Hall and R. H. Soderberg, *Inorg. Chem.* 1981, **7**, 2300.

Polyhedron Vol. 8, No. 21, pp. 2611–2614, 1989
Printed in Great Britain

0277-5387/89 $3.00+.00
© 1989 Pergamon Press plc

THERMAL AND KINETIC STUDIES ON THE ADDUCTS WITH PYRIDINES OF BIS(ACETYLACETONATE)OXOVANADIUM(IV)

R. LOZANO,* J. MARTINEZ, A. MARTINEZ, J. ROMAN and F. DE JESUS

Departamento de Química Inorgánica y Bioinorgánica, Facultad de Farmacia, Universidad Complutense, 28040 Madrid, Spain

(*Received* 31 *March* 1989; *accepted* 16 *June* 1989)

Abstract—The kinetics of the thermal decomposition, under nitrogen, of several adducts with pyridine or substituted pyridines of bis(acetylacetonate)oxovanadium(IV), {[$VO(acac)_2$,B] where acac = acetylacetonate and B = pyridine (Py), 3-methyl-pyridine (3-MP), 4-methylpyridine (4-MP), 3,5-dimethylpyridine (3,5-DMP), 3-aminopyridine (3-AP) and 4-aminopyridine (4-AP)}, have been studied by differential scanning calorimetry (DSC). Activation energies and pre-exponential Arrhenius factors, for the endothermic process of the loss of one mole of coordinated base, have been calculated using a new method, and the mechanism of this reaction has been determined. A relationship between activation energies and the properties of the ligands has also been determined.

The determination of kinetic parameters by non-isothermal methods offers interesting advantages over conventional isothermal studies.[1] However, the methods usually employed for kinetic analysis[2–9] lead to ambiguous results, especially if the reaction studied follows a diffusion-controlled kinetic law.

In others papers, we have studied the synthesis, thermal behaviour and kinetic parameters, by Thomas and Clarke's procedure,[10] of several vanadium(IV) and molybdenum(IV) complexes with pyridine or substituted pyridines.[11–14] However, the results obtained, only have validity in a narrow range of the reaction. Lastly, we have reported a new method to carry out the kinetic analysis of non-isothermal decomposition reactions of inorganic compounds by means of differential scanning calorimetry (DSC).[15–18]

The primary objectives of the present paper were to apply this previously reported method to determine the mechanism of the process of thermal decomposition of several adducts with pyridine or substituted pyridines of [$VO(acac)_2$,B] [where acac = acetylacetonate and B = pyridine (Py), 3-methylpyridine (3-MP), 4-methylpyridine (4-MP), 3,5-dimethylpyridine (3,5-DMP), 3-aminopyridine (3-AP) and 4-amino-pyridine (4-AP)] which takes place.

We have determined the mechanism of the process to be:

$$[VO(acac)_2,B]\,(solid) \rightarrow VO(acac)_2\,(solid) + B\,(gas),$$

and we have calculated the activation energy and the pre-exponential Arrhenius factor, in all the adducts synthesized.

A comparison between the activation energies and the steric or inductive factors and pK_b values of the coordinated bases has also been explored.

EXPERIMENTAL

Preparation of complexes

The complex $VO(acac)_2$ and its adducts with pyridine or substituted pyridines, were prepared as previously reported.[12]

Thermogravimetric analysis

Thermogravimetric analysis was performed on a Mettler HE-20 thermobalance. The analytical constants were: heating rate, 5°C min^{-1}; TG range, 20 mV; record rate, 20 cm h^{-1}; sample mass, 20 mg; reference, Al_2O_3; thermocouple, Pt/Pt—Rh 80%. The analysis was made in a dynamic nitrogen atmosphere between 25 and 300°C. A platinum pan was used.

* Author to whom correspondence should be addressed.

Differential scanning calorimetry

Differential scanning calorimetry was performed using a Mettler TA 3000 system with a Mettler DSC-20 differential scanning calorimeter. The scanning rate used was 2°C min^{-1} and samples of about 5 mg were used, so as to render insignificant the temperature non-uniformity within the sample. An aluminium pan was used under a dynamic nitrogen atmosphere. The instrument calibration was checked periodically with standard samples of indium (99.99% purity). Several runs were made.

RESULTS AND DISCUSSION

The DSC curves of all the compounds, show a first endothermic peak. The mass loss accompanying this transition, corresponds, on the TG curves, to the loss of pyridine or substituted pyridine coordinated to vanadium, the residue, identified by IR spectroscopy, being $VO(acac)_2$ in all cases.

The DSC study of this endothermic process has allowed us to determine the activation energy and the pre-exponential Arrhenius factor by the method proposed previously.[15–18]

From the DSC curve of the adduct $[VO(acac)_2,3,5\text{-DMP}]$, we have constructed Table 1. In this table, α is the reacted fraction at time t and $\alpha' = d\alpha/dt$.

The reactions of thermal decomposition of solids can be expressed by the Arrhenius equation:

$$\frac{d\alpha}{dt} = A e^{-E_a/RT} f(\alpha).$$

In this equation, α is the fraction of material that has reacted at time t, E_a is the activation energy, $f(\alpha)$ is a function which depends on the actual reaction mechanism and A is the pre-exponential Arrhenius factor.

When the temperature of the sample is increased at a constant rate, we can write eq. (1), where β is the heating rate, dT/dt

$$\frac{d\alpha}{dT} = \alpha' = \frac{A}{\beta} e^{-E_a/RT} f(\alpha). \quad (1)$$

Table 1. ΔH, α, T and α' obtained from the DSC curve of the complex $[VO(acac)_2,3,5\text{-DMP}]$

ΔH (mJ)	α	T (°C)	α' (K^{-1})
282.59	0.10106	98	0.02636
345.78	0.12366	100	0.03059
416.74	0.14903	102	0.03584
501.50	0.17934	104	0.04154
597.42	0.21365	106	0.04828
708.80	0.25348	108	0.05547
834.76	0.29852	110	0.06346
977.11	0.34943	112	0.07179
1133.20	0.40525	114	0.08058
1303.10	0.46601	116	0.08948
1489.30	0.53260	118	0.09724
1691.00	0.60473	120	0.10283
1909.90	0.68301	122	0.10386
2132.20	0.76251	124	0.09987
2356.70	0.84279	126	0.08743

We have collected in Table 2 the mathematical expressions of the functions $f(\alpha)$ corresponding to some of the mechanisms of thermal decomposition found in the literature.[1]

By differentiating the logarithmic form of eq. (1) with respect to $d \ln (1-\alpha)$, we obtain:

$$\frac{d \ln \alpha'}{d \ln (1-\alpha)} = -\frac{E_a}{R} \frac{d(1/T)}{d \ln (1-\alpha)} + \frac{d \ln f(\alpha)}{d \ln (1-\alpha)}$$

or

$$\frac{\Delta \ln \alpha'}{\Delta \ln (1-\alpha)} = -\frac{E_a}{R} \frac{\Delta(1/T)}{\Delta \ln (1-\alpha)} + \frac{\Delta \ln f(\alpha)}{\Delta \ln (1-\alpha)}$$

and

$$\frac{\Delta \ln \alpha' - \Delta \ln f(\alpha)}{\Delta \ln (1-\alpha)} = -\frac{E_a}{R} \frac{\Delta(1/T)}{\Delta \ln (1-\alpha)}. \quad (2)$$

Table 2. Kinetic equations

Mechanism (Rate-controlling process)		$f(\alpha)$
D1	(One-dimensional diffusion)	$(1/2\alpha)$
D2	(Two-dimensional diffusion)	$[-\ln(1-\alpha)]^{-1}$
D3	(Three-dimensional diffusion: Jander equation)	$(3/2)(1-\alpha)^{2/3}[1-(1-\alpha)^{1/3}]^{-1}$
D4	(Three-dimensional diffusion: Ginstling–Brounshtein equation)	$3/[2(1-\alpha)^{1/3}-1]$
F1	(Random nucleation)	$(1-\alpha)$
R2	(Phase-boundary reaction: Cylindrical symmetry)	$2(1-\alpha)^{1/2}$
R3	(Phase-boundary reaction: Spherical symmetry)	$3(1-\alpha)^{2/3}$

Table 3. Results obtained by using the seven mechanisms for the plot of $\Delta \ln \alpha' - \Delta \ln f(\alpha)/\Delta \ln(1-\alpha)$ vs $\Delta(1/T)/\Delta \ln(1-\alpha)$, for the complex [VO(acac)$_2$, 3,5-DMP]

Mechanism	Correlation coefficient (r)	Slope (m)	Intercept value (i)	Activation energy (kJ mol^{-1}) (E_a)
D1	−0.99998	−25927.34	0.91463	216±2
D2	−0.99998	−26105.84	0.50112	217±3
D3	−0.99999	−26085.44	−0.00870	217±2
D4	−0.99999	−26085.47	0.32464	217±2
F1	−0.99769	−11868.40	−0.44742	99±1
R2	−0.99768	−11868.40	0.05258	99±2
R3	−0.99769	−11868.41	−0.11409	99±1

Thus the plot of $[\Delta \ln \alpha' - \Delta \ln f(\alpha)]/[\Delta(1/T)]$ vs $\Delta(1/T)/[\Delta \ln(1-\alpha)]$ should be a straight line with a slope of $-E_a/R$, irrespective of the $f(\alpha)$ value employed. However, we can select the $f(\alpha)$ value that best fits the actual mechanism of the reaction studied using the intercept value; this should be zero from eq. (2).

Using the seven mechanisms listed in Table 2, we have plotted:

$$\frac{\Delta \ln \alpha' - \Delta \ln f(\alpha)}{\Delta \ln(1-\alpha)} \text{ vs } \frac{\Delta(1/T)}{\Delta \ln(1-\alpha)},$$

for the five adducts studied.

Table 3 shows the results, for the complex [VO(acac)$_2$,3,5-DMP] with r (correlation coefficient), m (slope), i (intercept value) and E_a (activation energy) obtained for the seven mechanisms.

We can observe that in all cases the correlation coefficients (r) are very near to unity, consistent with the results of Criado *et al.*[19] Nevertheless, only when the analysis was performed with mechanism D3 does the straight line present a low intercept value. Figure 1 reflects the representation of this line.

Therefore, we deduce that the mechanism of the thermal decomposition of the complex [VO(acac)$_2$,3,5-DMP] and loss of 3,5-dimethylpyridine, is by mechanism D3 (Three-dimensional diffusion: Jander equation) with a function $f(\alpha) = (3/2)(1-\alpha)^{2/3}[1-(1-\alpha)^{1/3}]^{-1}$, an activation energy $E_a = 217 \pm 2$ kJ mol^{-1} and a pre-exponential Arrhenius factor $A = (4.1 \pm 0.3) \times 10^{25}$ s^{-1}. The results obtained for the complexes studied in this paper, are listed in Table 4.

We can assume that the thermal decomposition of the adducts with pyridine or substituted pyridines follows a D3 mechanism.

If we compare the results, in general, as can be seen from the data in Table 4, the greater the basicity of the base employed, the higher the activation energy and the pre-exponential Arrhenius factor for the process of the loss of the base. The

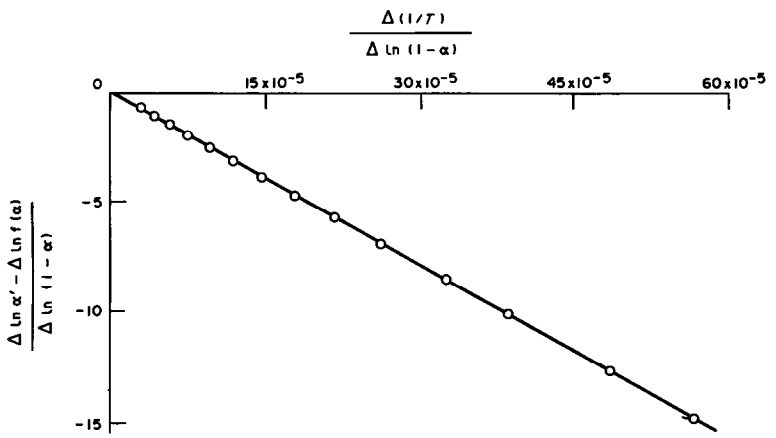

Fig. 1. Plot of $\Delta \ln \alpha' - \Delta \ln f(\alpha)/\Delta \ln(1-\alpha)$ vs $\Delta(1/T)/\Delta \ln(1-\alpha)$, for mechanism D3, for the adduct [VO(acac)$_2$,3,5-DMP].

Table 4. Thermal and kinetic parameters for the complexes [VO(acac)$_2$,B]

Complex	ΔH (kJ mol^{-1})	E_a (kJ mol^{-1})	A (s^{-1})	pK_b
[VO(acac)$_2$,Py]	56.4±0.7	144±2	(6.1±0.5)×10^{13}	8.87
[VO(acac)$_2$,3-MP]	43.9±0.5	182±2	(6.8±0.7)×10^{21}	8.32
[VO(acac)$_2$,4-MP]	63.9±0.7	205±3	(2.9±0.3)×10^{25}	7.98
[VO(acac)$_2$,3,5-DMP]	72.6±0.8	217±2	(4.1±0.3)×10^{25}	7.85
[VO(acac)$_2$,3-AP]	86.3±0.8	239±3	(3.3±0.4)×10^{29}	7.49
[VO(acac)$_2$,4-AP]	47.2±0.5	185±2	(1.3±0.2)×10^{23}	4.88

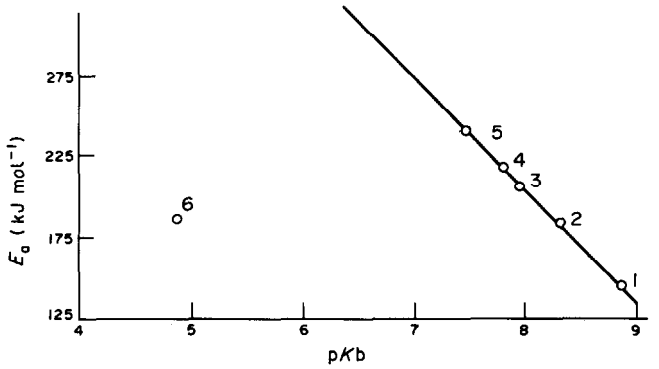

Fig. 2. Activation energy for decomposition of [VO(acac)$_2$,B] complexes as a function of pK_b. Points 1–6 correspond to complexes of Py, 3-MP, 4-MP, 3,5-DMP, 3-AP and 4-AP, respectively.

outstanding exception is the 4-AP adduct, which can be attributed to the existence of resonance structures and a pronounced effect on the stability of the complex.[11] It can be seen that the steric impediment of the 3,5-DMP does not modify the kinetic parameters.

The plot of pK_b vs activation energy presented in Fig. 2, shows that, except for the 4-AP adduct, a very satisfactory correlation was obtained. It is obvious from this figure that activation energy is linearly related to the basicity of the ligands.

REFERENCES

1. W. W. Wendlant, *Thermal Method of Analysis*. John Wiley, New York (1974).
2. A. E. Nerwkirk, *Analyt. Chem.* 1960, **32**, 1558.
3. E. S. Freeman and B. Carroll, *J. Phys. Chem.* 1958, **62**, 394.
4. A. Jerez, *J. Therm. Anal.* 1983, **26**, 315.
5. H. H. Horowitz and G. Metzger, *Analyt. Chem.* 1963, **35**, 1464.
6. A. W. Coats and J. P. Redfern, *Nature* 1964, **201**, 68.
7. C. D. Doyle, *J. Appl. Polymer Sci.* 1961, **5**, 283.
8. T. R. Ingraham and P. Marrier, *Can. J. Chem. Engng* 1964, 161.
9. B. N. N. Achar, G. W. Brindley and J. H. Sharp, *Proc. Int. Clay Conf.* **1**, 67, Jerusalem (1966).
10. J. M. Thomas and T. A. Clarke, *J. Chem. Soc. A* 1968, 457.
11. R. Lozano, J. Martinez, A. Martinez and A. Doadrio, *Polyhedron* 1983, **2**, 997.
12. J. Martinez, A. Martinez and A. Doadrio, *Thermochim. Acta* 1985, **87**, 281.
13. J. Martinez, A. Martinez and A. Doadrio, *Thermochim. Acta* 1986, **97**, 93.
14. R. Lozano, J. Román and A. Moragues, *Thermochim. Acta* 1986, **108**, 1.
15. R. Lozano, J. Román, A. Moragues and J. C. Avilés, *Transition Met. Chem.* 1987, **12**, 289.
16. R. Lozano, J. Román, F. de Jesús, A. Jerez and E. Ramos, *Thermochim. Acta* 1989, **141**, 261.
17. R. Lozano, J. Román, F. de Jesús, A. Jerez and E. Ramos, *Thermochim. Acta* 1989, **143**, 93.
18. R. Lozano, J. Martinez and A. Martinez, *Eur. J. Sol. State Inorg. Chem.* 1988, **25**, 565.
19. J. M. Criado, D. Dollimore and G. R. Heal, *Thermochim. Acta* 1982, **54**, 159.

Polyhedron Vol. 8, No. 21, pp. 2615–2619, 1989
Printed in Great Britain

0277–5387/89 $3.00+.00
© 1989 Pergamon Press plc

CONTROLLED SYNTHESIS OF SOME MIXED DIIMINE RUTHENIUM(II) COMPLEXES

IBRAHIM JIBRIL,* TALAL S. AKASHEH and AMJAD M. SHRAIM

Department of Chemistry, Yarmouk University, Irbid, Jordan

(*Received* 14 *April* 1989; *accepted* 26 *June* 1989)

Abstract—Complexes of a series of mixed ligands with ruthenium have been prepared and characterized through dihalide replacement in $Ru(bpy)_2Cl_2$, $Ru(bpz)_2Cl_2$ and tetrahalide replacement in $HRu(bpy)Cl_4$ (bpy = 2,2′-bipyridine; bpz = 2,2′-bipyrazine) by one or two bidentate ligands of the diimine type namely, bpd, dbpq and dpp (bpd = 3,3′bipyridazine; dbpq = 6,7-dimethyl-2,3-bis-(2′-pyridyl)-quinoxaline; dpp = 2,3-bis-(2-pyridyl)-pyrazine). The ruthenium dimer $[(bpy)_2Ru(dbpq)Ru(bpy)_2](PF_6)_4 \cdot 3H_2O$, as well as the tris-complex $[Ru(dbpq)_3](PF_6)_2 \cdot H_2O$, were also prepared and characterized.

Ruthenium diimine complexes have been the centre of great interest due to their potential application in the chemical use of solar energy conversion.[1,2] Moreover, the use of ligand diimine complexes of ruthenium is of special interest because of the ability of ligands to modify their photophysical properties.

In view of the advantages of such complexes we have recently reported the synthesis of some ruthenium mixed-diimine complexes.[3] In continuation of our interest in this area we report herein the synthesis of a new series of similar complexes.

In a relatively simple and controlled reaction, a bidentate diimine ligand L (L = bpd, dbpq and dpp) replaces the two chloride atoms of the complexes $Ru(bpy)_2Cl_2$ or $Ru(bpz)_2Cl_2$ and the four chloride atoms of the $H[Ru(bpy)Cl_4]$ complex to produce the new mixed diimine complexes $[Ru(bpy)_2L](PF_6)_2$ (L = bpd, dbpq), $[Ru(bpz)_2L](PF_6)_2$ (L = bpd) and $[Ru(bpy)L_2](PF_6)_2$ (L = dbpq, dpp). The tris-complex $[Ru(dbpq)_3](PF_6)_2$ was prepared by reaction of $Ru(DMSO)_4Cl_2$ with dbpq (DMSO = dimethyl sulphoxide).

The dinuclear complex $[(bpy)_2Ru(dbpq)Ru(bpy)_2](PF_6)_4$ was obtained by the reaction of $Ru(bpy)_2Cl_2$ with dbpq when the ligand-to-complex ratio was 2 : 1.

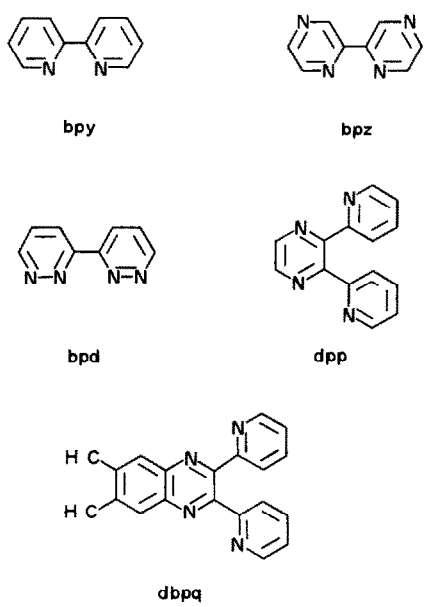

EXPERIMENTAL

Materials

$Ru(bpy)_2Cl_2 \cdot 2H_2O$ was prepared according to the method of Sullivan *et al.*[4] $Ru(bpz)_2Cl_2 \cdot 2H_2O$ was prepared according to Lever's method.[5] $H[Ru(bpy)Cl_4]$ and $Ru(DMSO)_4Cl_2$ were prepared according to the method of Evans *et al.*[6] bpd was prepared according to Lafferty's method[7] and dbpq

* Author to whom correspondence should be addressed.

was prepared according to the method used to prepare 2,3-bis-(2-pyridyl)-quinoxaline.[8] dpp was prepared according to the method of Goodwin and Lions.[8]

Elemental analyses

These were carried out by M.H.W. Laboratories (P.O.Box 15853, Phoenix, AZ 85018, U.S.A.).

Physical measurements

UV-vis spectra were recorded with a CARY 2390 spectrophotometer. KBr disc IR spectra were taken on a Pye–Unicam SP3-300 spectrophotometer. Solution conductance, at 25°C in acetonitrile, was measured for 1×10^{-3} M concentration using a Harris conductivity meter. Cyclic voltammetry of the dimer on a Hi-Tek potentiostat was carried out in acetonitrile for oxidations and in DMF for reductions on a platinum working electrode against a platinum counter electrode and a SSCE reference electrode. The concentration of the dimer was 10^{-3} M and tetra-*n*-butylammonium hexafluorophosphate (0.1 M) was the supporting electrolyte.

Synthesis of complexes

General procedure. Two separate ethanol–water solutions (30%) containing stoichiometric amounts of the diimine ligand and the ruthenium complex, RuL_nX_{6-2n}, were mixed, and the reaction mixture was refluxed for 2–72 h (see Table 1). The product was precipitated by slowly adding a water solution of NH_4PF_6 to the reaction mixture while hot. After cooling in the refrigerator overnight, the precipitate was collected by filtration, washed with cold water, then washed with ether.

Purification of the product was performed by dissolving it in the minimum volume of acetone or acetonitrile and then precipitating with ether. This process was repeated several times. Further purification of the complexes was carried out by column chromatography using alumina columns made up in acetone. The eluted fraction containing the pure product, as checked by the quality of the luminescence spectra, was concentrated to $< 10\ cm^3$ and the product was precipitated with ether, collected by filtration, washed with ether and finally dried under vacuum. (Table 1 summarizes the details of the synthesis of each complex and their yields.)

Table 1. Reactions used for the synthesis of ruthenium diimine complexes

Product	Reactions	Complex–ligand molar ratio	Eluent	Reflux time (h)	Per cent yield	Colour
$[Ru(bpy)_2(bpd)](PF_6)_2 \cdot H_2O$	*cis*-$Ru(bpy)_2Cl_2 \cdot 2H_2O + bpd$	1:1.2	Acetone	2	50	Yellow–orange
$[Ru(bpy)_2(dbpq)](PF_6)_2 \cdot H_2O$	*cis*-$Ru(bpy)_2Cl_2 \cdot 2H_2O + dbpq$	1:1.2	Acetone	4	53	Light brown
$[Ru(bpz)_2(bpd)](PF_6)_2 \cdot H_2O$	*cis*-$Ru(bpz)Cl_2 \cdot 2H_2O + bpd$	1:1.2	Acetonitrile	5	26	Orange
$[Ru(bpz)_2(dbpq)](PF_6)_2 \cdot H_2O$	*cis*-$Ru(bpz)_2Cl_2 \cdot 2H_2O + dbpq$	1:1.2	Acetone	10	24	Yellow–orange
$[Ru(dbpq)_2(bpy)](PF_6)_2 \cdot 3H_2O$	$H[Ru(bpy)Cl_4] + dbpq$	1:3.0	Acetone	8	25	Violet
$[Ru(dpp)_2(bpy)](PF_6)_2 \cdot 2H_2O$	$H[Ru(bpy)Cl_4] + dpp$	1:2.3	Acetonitrile	24	65	Brown–yellow
$[Ru(dbpq)_3](PF_6)_2 \cdot H_2O$	$Ru(DMSO)_4Cl_2 + dbpq$	1:3.2	Acetone	24	50	Brown
$[(bpy)_2Ru(dbpq)Ru(bpy)_2](PF_6)_4 \cdot 3H_2O$	*cis*-$Ru(bpy)_2Cl_2 \cdot 2H_2O + dbpq$	2:1	5%	72	35	Dark green
	or					
	$[Ru(bpy)_2(dbpq)](PF_6)_2 \cdot H_2O$ + *cis*-$Ru(bpy)_2Cl_2 \cdot 2H_2O$	1:1.1	Methanol–acetone	72	35	Dark green

RESULTS AND DISCUSSION

The suggested formula for these newly prepared complexes are supported by the elemental analysis

Table 2. Elemental analysis and conductivity (10^{-3} M in CH_3CN)

Complex	%C	%H	%N	$\Lambda(\Omega^{-1}\,cm^{-1}\,mol^{-1})$
$[Ru(bpy)_2(bpd)](PF_6)_2 \cdot H_2O$	39.0	2.8	13.0	324
	(38.2)	(2.8)	(12.74)	
$[Ru(bpy)_2(dbpq)](PF_6)_2 \cdot H_2O$	46.5	3.7	10.8	301
	(46.5)	(3.2)	(10.8)	
$[Ru(bpz)_2(bpd)](PF_6)_2 \cdot H_2O$	32.9	2.1	12.0	296
	(32.6)	(2.3)	(12.0)	
$[Ru(bpz)_2(dbpq)](PF_6)_2 \cdot H_2O$	42.5	3.2	16.2	299
	(41.7)	(2.9)	(16.2)	
$[Ru(dbpq)_2(bpy)](PF_6)_2 \cdot 3H_2O$	49.9	4.0	11.4	261
	(49.4)	(3.8)	(11.4)	
$[Ru(dpp)_2(bpy)](PF_6)_2 \cdot 2H_2O$	43.4	3.1	13.3	285
	(43.4)	(3.1)	(13.0)	
$[Ru(dbpq)_3](PF_6)_2 \cdot H_2O$	53.5	3.8	12.5	307
	(54.3)	(3.6)	(12.7)	
$[(bpy)_2Ru(dbpq)Ru(bpy)_2](PF_6)_4 \cdot 3H_2O$	41.0	3.1	9.4	470
	(40.6)	(3.1)	(9.5)	

Values in parentheses are calculated, the others are found values.

and the conductivity data given in Table 2. All the complexes except for the dimer (1 : 4) are 1 : 2 electrolytes as expected from their formula.[9]

The IR results are given in Table 3. The IR spectra for these complexes exhibit bands characteristic of the ligands. In particular, bands roughly in the range 1570–1615 cm^{-1} and 1545–1565 cm^{-1}[10,11] are assigned to the C=N and C=C stretchings in the ring of the bidentate ligands, respectively.

It is worth noting that the C=N stretching frequency in almost all the complexes reported here is higher than that of the free ligands.

Table 3. IR results of the complexes

Complex	Characteristic IR bands (cm^{-1})
$[Ru(bpy)_2(bpd)](PF_6)_2 \cdot H_2O$	3440 (b, m)[a], 1590 (m)[b], 1540 (m)[c], 1390 (m), 1080 (m), 830 (v.s)[d], 755 (m), 1350, 10, 785, 570
$[Ru(bpy)_2(dbpq)](PF_6)_2 \cdot H_2O$	3445 (b, w)[a], 3105 (w)[b], 1610 (w)[c], 1550 (w), 1470 (m), 1450 (m), 1090 (w), 840 (v.s)[d], 770 (s), 1700, 1350, 1220, 2120, 1170, 570
$[Ru(bpz)_2(bpd)](PF_6)_2 \cdot H_2O$	3420 (b, m)[a], 1575 (w)[b], 1465 (w), 1400 (m), 1070 (w), 830 (s)[d], 660 (w), 1350, 1260, 1155, 570
$[Ru(bpz)_2(dbpq)](PF_6)_2 \cdot H_2O$	3440 (b, m)[a], 3090 (w), 1595 (m)[b], 1480 (m), 1415 (m), 840 (v.s)[d], 770 (s), 1170
$[Ru(dbpq)_2(bpy)](PF_6)_2 \cdot 3H_2O$	3450 (b, m)[a], 3095 (m), 1600 (w)[b], 1550 (w)[c], 1465 (m), 840 (v.s)[d], 770 (m), 650 (w), 650, 1210, 1180, 995, 575
$[Ru(dpp)_2(bpy)](PF_6)_2 \cdot 2H_2O$	3430 (b, m)[a], 1575 (w)[b], 1550 (w)[c], 1400 (m), 840 (v.s)[d], 760 (m), 1240, 1160, 560
$[Ru(dbpq)_3](PF_6)_2 \cdot H_2O$	3440 (b, m)[a], 1615 (w), 1580 (m)[b], 1540 (m)[c], 1470 (s), 1415, 1085 (m), 840 (v.s)[d], 745 (s), 645 (w), 1365 (s), 1285 (w), 1205 (s), 1175 (w), 1000 (m), 770 (s), 580 (s)
$[(bpy)_2Ru(dbpq)Ru(bpy)_2](PF_6)_4 \cdot 3H_2O$	3440 (b, m)[a], 3100 (w), 1600 (m)[b], 1465 (m), 1450 (m), 1400 (w), 840 (v.s)[d], 760 (s), 1365 (w), 1320 (w), 1245 (w), 1215 (w), 1160 (w), 1105 (w)

s: strong; v.s: very strong; m: medium; w: weak; b: broad; ν: stretching frequency.
Superscripts: $a = \nu$(OH); $b = \nu$(C=N); $c = \nu$(C=C); $d = PF_6$ peak.

Similar results have recently been observed[12] and an acceptable explanation[3] for this observation is due to the interplay of the σ- and π-bonding effects on the diimine ligands when complexed with transition metals. In such complexes, σ-bonding through normal donation from ligand-to-metal tends to strengthen the C=N by attracting the ring π-electrons towards the nitrogen atom, while π-bonding through back donation from metal-to-ligand weakens the C=N by adding electrons into the π^*-orbitals of the ring. In all cases, here, π-bonding seems to dominate the complexation effect of the C=N stretching frequency.

Unfortunately identification of the complexes' C=N frequency when nitrogen is not complexed has proved difficult due to the broadness and overlap of the peaks in both the free ligands and complexes.

Moreover, the strong bands around 830–840 cm^{-1} are assigned to the stretching frequency for the PF_6^- counter anions.[13]

The UV–vis results in Table 4 exhibit sharp peaks in the region 275–290 nm in all the complexes. These are attributed to ligand-centred π,π^* or n,π^* transitions. The broad shoulders below 390 nm in some complexes may be *d–d*, MLCT or LMCT bands.

The strong, very broad peaks in the visible region for the complexes are a superposition of many MLCT (metal-to-ligand charge-transfer) bands from the metal *d*-orbital to the diimine π^*-ligand orbitals. The red tailing region is often attributed to an absorption by the emissive, highly triplet in character, state (MLCT) responsible for most of the photochemical and photosensitizating behaviour of such complexes.[13,14] In the dimer a red shift of the lowest energy peak (592 vs 510 nm in $Ru(bpy)_2$ dbpq) is observed. This peak is assignable to an MLCT absorption into the bridging ligand π^*-orbital which gains additional stabilization by the

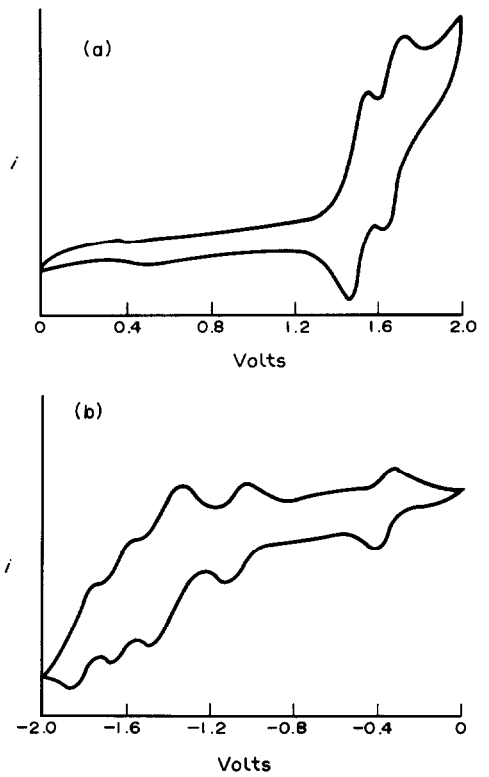

Fig. 1. Cyclic voltammogram of the dinuclear $[(bpy)_2Ru(dbpq)Ru(bpy)_2]^{4+}$: (a) oxidation in acetonitrile and (b) reduction in dimethylformamide (10^{-3} M) solutions.

Table 4. UV–vis. spectral data for the complexes[a] in acetonitrile

Complexes	λ_{max} (nm)
$[Ru(bpy)_2(bpd)](PF_6)_2 \cdot H_2O$	472 (b, 1.33), 410 (b, 1.56), 360 (sh), 278 (6.61), 258 (sh), 241 (3.02), 206 (6.82)
$[Ru(bpy)_2(dbpq)](PF_6)_2 \cdot H_2O$	510 (b, 0.91), 430 (b, 0.94), 388 (sh), 352 (sh), 285 (9.38), 274 (sh), 254 (sh)
$[Ru(bpz)_2(bpd)](PF_6)_2 \cdot H_2O$	446 (b, 2.44), 414 (sh), 340 (sh), 289 (6.47), 276 (sh), 234 (4.32)
$[Ru(bpz)_2(dbpq)](PF_6)_2 \cdot H_2O$	450 (b, 1.48), 395 (b, 1.56), 355 (sh), 300 (6.36)
$[Ru(dbpq)_2(bpy)](PF_6)_2 \cdot 3H_2O$	530 (b, sh, 2.47), 460 (b, 1.15), 388 (b, 1.77), 331 (sh), 284 (8.42), 256 (sh)
$[Ru(dpp)_2(bpy)](PF_6)_2 \cdot 2H_2O$	465 (b, 1.46), 428 (sh), 285 (7.25), 254 (3.62), 250 (sh)
$[Ru(dbpq)_3](PF_6)_2 \cdot H_2O$	496 (b, 1.35), 471 (sh), 383 (b, sh), 327 (b, sh), 279 (10.40)
$[(bpy)_2Ru(dbpq)Ru(bpy)_2](PF_6)_4 \cdot 3H_2O$	591 (1.88), 491 (sh), 430 (sh), 408 (2.88), 390 (sh), 318 (sh), 284 (11.6), 253 (sh), 244 (4.96), 208 (sh)

[a] 10^{-5}–10^{-6} M acetonitrile solutions; sh: shoulder; b: broad.
Values in parentheses are $\varepsilon \times 10^{-4}$ ($dm^3\ mol^{-1}\ cm^{-1}$).

introduction of the second metal atom.[15] The existence of the two metal centres is immediately noticed in the cyclic voltammogram of the dimer. Two quasi-reversible oxidation peaks [Fig. 1(a)] at 1.51 and 1.68 V correspond to two consecutive Ru^{II}/Ru^{III} oxidation steps of the metal centres. Five reduction quasi-reversible peaks [Fig. 1(b)] (−0.36, −1.06, −1.22, −1.61 and −1.80 V) correspond to the consecutive introduction of one electron into the π^*-orbitals of each ligand. The stabilization of the π^*-orbital of the bridging ligand (dbpq) is evident from the first reduction peak (−0.36 V) compared to −0.77 V for the π^*-orbital of dbpq in $[Ru(bpy)_2dbpq]^{2+}$.[16]

Acknowledgements—T.S.A. gratefully acknowledges various grants from Yarmouk University, The Ministry of Planning, Jordan, and The Kuwait Development Fund.

REFERENCES

1. N. Sutin and C. Creutz, *Pure Appl. Chem.* 1980, **52**, 2717.
2. D. G. Whitten, *Accts Chem. Res.* 1980, **13**, 83.
3. T. S. Akasheh, D. Marji and Z. M. Al-Ahmad, *Inorg. Chim. Acta* 1988, **141**, 125.
4. B. P. Sullivan, D. J. Salmon and T. J. Meyer, *Inorg. Chem.* 1978, **17**, 3334.
5. R. J. Crutchley, A. P. Lever and A. Poggi, *Inorg. Chem.* 1983, **72**, 2647.
6. I. R. Evans, A. Spencer and G. Wilkinson, *J. Chem. Soc., Dalton Trans.* 1973, 204.
7. J. J. Lafferty and F. H. Case, *J. Am. Chem. Soc.* 1967, **32**, 1591.
8. H. A. Goodwin and F. Lions, *J. Am. Chem. Soc.* 1959, **81**, 6415.
9. R. J. Angelici, *Synthesis and Techniques in Inorganic Chemistry*, 2nd edn. Saunders, Philadelphia (1977).
10. F. A. Cotton and G. Wilkinson, *Advanced Inorganic Chemistry*, 4th edn, p. 119. Wiley, New York (1980).
11. D. Cook, *Can. J. Chem.* 1964, **42**, 1964.
12. Q. Jaradat, K. Barqawi and T. S. Akasheh, *Inorg. Chim. Acta* 1986, **116**, 63.
13. T. S. Akasheh and Z. M. Al-Ahmad, *Chem. Phys. Lett.* 1988, **152**, 416.
14. D. P. Rillema, G. Allen, T. J. Meyer and D. Conrad, *Inorg. Chem.* 1983, **22**, 1617.
15. S. C. H. Braun, A. D. Baker, T. C. Stekasm and H. D. Gafney, *Inorg. Chem.* 1984, **23**, 857.
16. T. S. Akasheh, I. Jibril and A. M. Shraim, *J. Am. Chem. Soc.*, submitted.

Polyhedron Vol. 8, No. 21, pp. 2621–2622, 1989
Printed in Great Britain

0277-5387/89 $3.00+.00
© 1989 Pergamon Press plc

THE MOLAR ABSORPTIVITY OF SODIUM HYPONITRITE

CHARLOTTE N. CONNER, CAROLINE E. DONALD, MARTIN N. HUGHES* and CHRISTINA SAMI

Department of Chemistry, King's College London, Strand, London WC2R 2LS, U.K.

(*Received* 13 *June* 1989; *accepted* 26 *June* 1989)

Abstract—The molar absorptivity of sodium hyponitrite at 248 nm (λ_{max}) has been redetermined as 6550 ± 100 dm^3 mol^{-1} cm^{-1}.

The molar absorptivity of sodium hyponitrite at 248 nm (λ_{max}) is usually quoted[1] as 3980 dm^3 mol^{-1} cm^{-1}. However, we have frequently prepared sodium hyponitrite with substantially higher molar absorptivities than this. A value of 6550 ± 200 dm^3 mol^{-1} cm^{-1}, reported by Polydoropoulos and Voliotis,[2] is not widely cited. These observations suggest that studies on hyponitrite chemistry have usually been carried out on highly impure material. This is probably due to the presence of sodium carbonate formed by absorption of CO_2 during work-up of the product and by reaction of CO_2 with solid sodium hyponitrite.[3] Recently it has been shown that the decomposition of hyponitrite in solution is catalysed by CO_2 which forms an adduct at nitrogen, followed by rate-determining isomerization to give the unstable *cis*-hyponitrite ion.[4]

We have now redetermined the molar absorptivity of sodium hyponitrite.

EXPERIMENTAL

Sodium hyponitrite was prepared by the reduction of nitrite with sodium amalgam[1] under an atmosphere of nitrogen, either in a glove box or a plastic bag. A solution of sodium nitrite (12.5 g) in water (20 cm^3) was added to the continuously-swirled amalgam (prepared, with appropriate precautions, from 70 cm^3 of mercury and 12 g of sodium metal) in a 500 cm^3 conical flask cooled in ice. After the initial vigorous reaction had subsided, the mixture was transferred to a thick-walled 250 cm^3 separating funnel and shaken until gas evolution had ceased. The aqueous layer was run into 400 cm^3 absolute ethanol. The residues in the funnel were washed into the ethanol with 2 cm^3 of dilute alkali. Crystalline, hydrated sodium hyponitrite was precipitated on vigorous stirring and filtered off under nitrogen. The off-white product was dissolved in the minimum volume of dilute alkali (no more than 3 cm^3), the solution filtered and the filtrate added to 400 cm^3 of absolute ethanol, with vigorous stirring. The hydrated sodium hyponitrite was filtered off under nitrogen and stored in a vacuum desiccator over P_4O_{10}. The anhydrous product was formed over several days, and stored in a vacuum desiccator or in sealed ampoules.

Preparations of sodium hyponitrite were analysed for carbon and hydrogen (reproducible values for nitrogen could not be obtained), for sodium by atomic emission spectroscopy (Perkin–Elmer 2380 instrument), and for nitrite by a standard colorimetric method involving the diazotization of sulphanilic acid and coupling to β-naphthol. IR spectra were recorded as Nujol mulls, prepared under nitrogen (Perkin–Elmer 1310 instrument). UV spectra were measured for solutions of sodium hyponitrite in 1 mol dm^{-3} alkali (to limit self-decomposition) in 1 cm matched silica cells on Perkin–Elmer Lambda 3 and SP5-600 spectrometers. Spectra were remeasured after 5 and 10 min to check the stability of the solutions.

RESULTS AND DISCUSSION

Data for seven samples of sodium hyponitrite are given in Table 1, including the measured values of the molar absorptivity at 248 nm (ε_m) and values corrected to allow for the impurity of the sample (ε_c).

All samples of sodium hyponitrite contained negligible or undetectable amounts of nitrite, the highest amount being less than 0.1% by weight. The IR spectra showed that most samples contained traces

* Author to whom correspondence should be addressed.

Table 1. Molar absorptivities ($dm^3\ mol^{-1}\ cm^{-1}$) of sodium hyponitrite

Sample	ε_m	%C	%H	%Na	$\%Na_2CO_3$	$\%H_2O$	ε_c[a]
1	6020	0.39	0.33	42.3	3.45[b]	2.97[b]	6440
2	6320	0.55	0		4.86[b]	0	6645
3	5960	1.03	0		9.10[b]	0	6560
4	6150			41.7	[b]	4.00[b]	> 6410
5	6390				[b]		> 6390
6	6310				[b]		> 6310
7	6000				[b]	[b]	> 6000

[a] Mean value for samples 1–3 is $6550 \pm 100\ dm^3\ mol^{-1}\ cm^{-1}$.
[b] Detected in the IR spectrum of the sample.

of carbonate and/or water, which was confirmed by elemental analysis. Table 1 lists the amounts of sodium carbonate and water present in the samples calculated from these data. The analytical data for sodium is not sensitive to contamination by sodium carbonate.

The measured values of the molar absorptivities lie in the range 5960–6390 $dm^3\ mol^{-1}\ cm^{-1}$. For three of these samples, with extinction coefficients 6000, 6310 and 6390, elemental analyses were not carried out as decomposition of the samples occurred, but their IR spectra showed the presence of carbonate and/or water. These values must be lower than the true value. The sodium carbonate present in some samples appears to have been formed during the work-up procedure rather than during subsequent measurements, as repeat spectroscopic and elemental analyses were reproducible provided the sample was not exposed to the atmosphere. It appears, therefore, that all measurements on a particular sample have been carried out at a constant level of carbonate and may be related to each other. Table 1 contains values of the molar absorptivities corrected to allow for the impurities of water and sodium carbonate, where present (ε_c). The mean value for samples 1–3 is $6550 \pm 100\ dm^3\ mol^{-1}\ cm^{-1}$, in agreement with that reported by Polydoropoulos and Voliotis.[2] The remaining values in Table 1 represent uncorrected values but confirm the overall picture.

Samples of sodium hyponitrite left on a watch glass exposed to the atmosphere showed a substantial fall (up to 60%) in absorptivity over a few hours, emphasizing the need to store sodium hyponitrite under conditions where CO_2 is excluded. In a separate experiment, a sample stored in a vacuum desiccator showed a fall in molar absorptivity of between 5–10% on each measurement if no precautions were taken to exclude water and CO_2 during the preparation of the solution for optical density measurement.

It is clear from these experiments that it is very difficult to prepare and maintain pure samples of sodium hyponitrite and that the bulk of all published work on hyponitrite has been carried out on material that was probably at best only about 60% pure. Most kinetic studies[5] appear to have involved conditions where the rate law is first-order or pseudo-first-order in hyponitrite, so that the lack of purity will not have had any major effects on rate constants. However, it is possible that the use of hyponitrite of purity close to 50% could lead to misleading conclusions about the stoichiometries of reaction.

Acknowledgement—We thank the SERC for a studentship to C.E.D.

REFERENCES

1. C. C. Addison, G. A. Gamlen and R. Thompson, *J. Chem. Soc.* 1952, 338.
2. C. N. Polydoropoulos and S. D. Voliotis, *Analyt. Chem. Acta* 1968, **40**, 170.
3. M. N. Hughes, *Quart. Rev. Chem. Soc.* 1968, **22**, 1.
4. E. L. Loechler, A. M. Schneider, D. B. Schwartz and T. C. Hollocher, *J. Am. Chem. Soc.* 1988, **109**, 3076.
5. M. N. Hughes, G. Stedman and P. E. Wimbledon, *J. Chem. Soc., Dalton Trans.* 1989, 534.

Polyhedron Vol. 8, No. 21, pp. 2623–2626, 1989
Printed in Great Britain

0277–5387/89 $3.00+.00
© 1989 Pergamon Press plc

REACTIONS OF SOME DIMETHYLAMINOPHOSPHONIUM SALTS WITH LIQUID HYDROGEN CHLORIDE

KEITH B. DILLON,* NABIL D. A. H. KHABBASS and CLIFFORD J. LUDMAN*

Chemistry Department, University of Durham, South Road, Durham DH1 3LE, U.K.

(*Received* 19 *April* 1989; *accepted after revision* 30 *June* 1989)

Abstract—The reactions of the dimethylaminophosphonium ions $[P(NMe_2)_xPh_{4-x}]^+$ ($x = 1$–3), $[P(NMe_2)_xCl_{4-x}]^+$ ($x = 2$ or 3), $[P(NMe_2)Me_xCl_{3-x}]^+$ ($x = 1$ or 2) and of $P(NMe_2)_3O$ with liquid hydrogen chloride have been investigated by means of ^{31}P NMR spectroscopy. In most instances cleavage of one (or more) of the P—N bonds is observed, although the rate of reaction varies considerably with the other substituents on phosphorus.

Comparatively few reactions of organophosphorus(V) compounds with liquid hydrogen chloride have been described.[1] Compounds containing P=O double bonds were found by means of ^{31}P NMR spectroscopy to protonate to some extent on the phosphoryl oxygen, and the order of base strengths of the phosphorus species could be deduced from analysis of the results.[1] None of the compounds examined had nitrogen substituents on phosphorus, however. A preliminary experiment on the aminophosphonium salt $[P(NMe_2)Cl_3]_2^+PCl_6^-$, Cl^- suggested that the cation was stable to liquid HCl.[2] In the presence of BCl_3, however, the P—N bond was broken, and the PCl_4^+ ion was identified by ^{31}P NMR[3] as the only phosphorus-containing product. The reaction was formulated[2] as

$$[P(NMe_2)Cl_3]_2^+PCl_6^-,Cl^- + 4HCl + 5BCl_3 \longrightarrow 2Me_2NH_2^+BCl_4^- + 3PCl_4^+BCl_4^- \quad (1)$$

We have now carried out a systematic investigation of the behaviour of several dimethylaminophosphonium salts and related compounds in liquid hydrogen chloride, with various substituents on phosphorus. Cleavage of one (or more) P—N bonds is usually observed, although the reactions are very slow if no organo-substituents are present on phosphorus. The reaction products have been identified by ^{31}P NMR spectroscopy; shifts obtained are in good agreement with independent data.

* Authors to whom correspondence should be addressed.

EXPERIMENTAL

All manipulations including NMR sample preparation were carried out either *in vacuo* or under an inert atmosphere of dry nitrogen. The dimethylaminophosphonium salts were prepared by the action of dimethylchloramine, Me_2NCl, on the appropriate phosphine; these preparations will be described in detail elsewhere.[4] Hydrogen chloride was purified as described in previous publications.[5] Other chemicals were obtained commercially and were used without further purification. NMR samples in liquid HCl, as solvent, were prepared as in earlier work;[1] the tubes were sealed and allowed to warm to 313 K in a water thermostat bath behind protective bricks in a fume cupboard, to make sure that they would withstand the pressure at the spectrometer operating temperature. ^{31}P NMR spectra were recorded at 307.2 K on the Fourier transform spectrometer operating at 24.29 MHz, as described previously.[6] Chemical shifts are quoted relative to external 85% H_3PO_4, with the downfield (higher frequency) direction taken as positive.

RESULTS AND DISCUSSION

The results for individual compounds are discussed separately.

(a) $[P(NMe_2)Ph_3]^+Cl^-$

A clear, colourless solution was obtained from reaction of this compound with liquid HCl. Its ^{31}P

NMR spectrum showed a single sharp resonance at 66.2 ppm, readily ascribed to the $[PPh_3Cl]^+$ cation.[7-15] Hence, liquid HCl cleaves the P—N bond, and the probable reaction is

$$[P(NMe_2)Ph_3]^+Cl^- + 4HCl \longrightarrow [PPh_3Cl]^+HCl_2^- + Me_2NH_2^+HCl_2^- \quad (2)$$

(b) $[P(NMe_2)_2Ph_2]^+Cl^-$

Again one sharp resonance, at 71.5 ppm, was observed, after the sample had been kept at room temperature for 3 h, and was assigned to the $[P(NMe_2)Ph_2Cl]^+$ cation. This species was obtained independently by chlorination of $P(NMe_2)Ph_2$, and gave a shift of 70.9 ppm in CH_2Cl_2 as solvent. A value of 72.5 ppm has also been reported for $[P(NMe_2)Ph_2Cl]^+SbCl_6^-$ in $MeNO_2$ solution.[16] When the tube was kept at room temperature for a further 15 h and its spectrum re-recorded, this resonance had disappeared, and had been replaced by a signal at 93.5 ppm, due to the formation of $[PPh_2Cl_2]^+$.[8,9,13-15] Thus cleavage of both P—N bonds occurs within 1 day, and the overall reaction may be represented as

$$[P(NMe_2)_2Ph_2]^+Cl^- + 7HCl \longrightarrow [PPh_2Cl_2]^+HCl_2^- + 2Me_2NH_2^+HCl_2^- \quad (3)$$

(c) $[P(NMe_2)_3Ph]^+Cl^-$

A single ^{31}P NMR resonance at 51.6 ppm was observed when the spectrum was run shortly after the tube had been warmed to room temperature. This was ascribed to the starting material, which gives a shift of 51.6 ppm in CH_2Cl_2; the bromide $[P(NMe_2)_3Ph]^+Br^-$ gives a value of 51.4 ppm in the same solvent. After 2 days, the ^{31}P NMR spectrum showed two resonances, a major one at 51.6 ppm (starting material), and a minor one at 72.1 ppm, assigned to $[P(NMe_2)_2PhCl]^+$. The latter was obtained independently by chlorination of $P(NMe_2)_2Ph$, and gave a signal at 67.8 ppm in CH_2Cl_2. After the sample had been kept for 14 days at room temperature, a single sharp resonance was observed at 101.0 ppm, readily attributed to the $[PPhCl_3]^+$ ion.[8,9,12-15,17] Thus, slow cleavage of the P—N bonds takes place in this system. The intermediate ion $[P(NMe_2)PhCl_2]^+$ was not detected, but may be presumed to have formed and then undergone solvolysis during the 14 day period. The overall reaction is

$$[P(NMe_2)_3Ph]^+Cl^- + 10HCl \longrightarrow [PPhCl_3]^+HCl_2^- + 3Me_2NH_2^+HCl_2^- \quad (4)$$

(d) $[P(NMe_2)_3Cl]^+Cl^-$

The clear, colourless solution showed one resonance only, at 53.3 ppm, from the starting material. No change was detected after 16 h at room temperature, and again after 35 days. This result implies that the P—N bonds of this compound are not cleaved by liquid HCl.

(e) $P(NMe_2)_3O$

The purity of the commercial material was checked by ^{31}P NMR. The spectrum of the solution in liquid HCl showed one sharp signal at 30.3 ppm, ascribed to the formation of $P(NMe_2)_2ClO$.[18-20] After the solution had been kept at room temperature for 1 day, its ^{31}P NMR spectrum showed two resonances, a major one at 33.3 ppm ($P(NMe_2)_2ClO$), and a minor one at 15.8 ppm, assigned to $P(NMe_2)Cl_2O$.[20,21] After 5 days, only one signal was detected, at 15.6 ppm, but after 21 days a single resonance was found at 1.6 ppm, ascribed to PCl_3O.[22] Hence, the three P—N bonds are cleaved by liquid HCl, the rate of reaction decreasing with successive replacement of Me_2N groups by Cl groups. The overall reaction is

$$P(NMe_2)_3O + 9HCl \longrightarrow PCl_3O + 3Me_2NH_2^+HCl_2^- \quad (5)$$

(f) $[P(NMe_2)_2Cl_2]^+Cl^-$

The solution gave a single peak at 51.6 ppm, due to the starting material. After the solution had been kept for 6 days at room temperature, an additional minor resonance was detected at 61.3 ppm from the $[P(NMe_2)Cl_3]^+$ ion. After 1 month, two equally intense resonances at 51.6 and 60.3 ppm were observed. Hence very slow cleavage of one of the P—N bonds takes place, according to the equation:

$$[P(NMe_2)_2Cl_2]^+Cl^- + 4HCl \longrightarrow [P(NMe_2)Cl_3]^+HCl_2^- + Me_2NH_2^+HCl_2^- \quad (6)$$

After a further 14 days, the deposition of a large quantity of a white, crystalline solid was seen on the walls of the tube. The ^{31}P NMR spectrum showed three broad signals, at 51.6 (starting material), 60.3 ($[P(NMe_2)Cl_3]^+$) and -302.1 ppm, attributed to the PCl_6^- ion.[11,22] The second P—N bond of the starting material is thus cleaved eventually, and a hexachlorophosphate is produced, reaction (7):

$$[P(NMe_2)Cl_3]^+HCl_2^- + HCl \longrightarrow Me_2NH_2^+PCl_6^- \quad (7)$$

The six-coordinate species is presumably stabilized by the insolubility of the dimethylammonium salt, since the PCl_6^- ion has been reported to break up in liquid HCl to give the PCl_4^+ ion.[23] There was no evidence for such a reaction here, however.

(g) $[P(NMe_2)Me_2Cl]^+Cl^-$

When the ^{31}P NMR spectrum was recorded as soon as possible after completion of the safety check (Experimental), one resonance only, at 131.6 ppm, was detected from the clear solution, readily assigned to the $[PMe_2Cl_2]^+$ ion.[15,24] The P—N bond is readily cleaved in this reaction, eq. (8):

$$[P(NMe_2)Me_2Cl]^+Cl^- + 4HCl \longrightarrow [PMe_2Cl_2]^+HCl_2^- + Me_2NH_2^+HCl_2^- \quad (8)$$

(h) $[P(NMe_2)MeCl_2]^+Cl^-$

As in the previous system, only one signal was observed under similar conditions, at 122.1 ppm, due to the $[PMeCl_3]^+$ ion.[15,17,24,25] The course of this reaction is therefore similar, as shown in eq. (9):

$$[P(NMe_2)MeCl_2]^+Cl^- + 4HCl \longrightarrow [PMeCl_3]^+HCl_2^- + Me_2NH_2^+HCl_2^- \quad (9)$$

(i) *General discussion*

Liquid HCl reacts with most of the dimethylaminophosphorus(V) derivatives studied to cleave one or more P—N bonds and introduce chlorine on phosphorus, though the rate of reaction varies greatly with the other substituents present. Organo-groups, both aliphatic (Me) and aromatic (Ph), seem to increase the rate of reaction compared with similar species with no organo-groups present. The rate decreases, however, with increasing numbers of NMe_2 groups, and is slower for phenyl than for methyl substituents. The $[P(NMe_2)_3Cl]^+$ ion appears to be stable in this medium. The initial reaction in each case may be a protonation of one of the NMe_2 groups, followed by an S_N2 attack by the chloride ion on the resultant complex.

Protonation will be favoured by electron-supplying groups on phosphorus such as methyl, thus accounting for the observed rate increase. The dimethylamino-groups are also electron-donating, and will assist in delocalizing the formal positive charge on phosphorus in the aminophosphonium salts. Donation is possible from a nitrogen lone pair into a vacant *d*-orbital on phosphorus, giving some π-character to the P—N bond and increasing its strength. Protonation at nitrogen will destroy any such π-interaction, however, and render the P—N bond liable to cleavage by a stronger ligand such as chloride. With more NMe_2 groups present, the possibilities of π-interactions are increased, and protonation may not take place as readily. The positive charge will also be delocalized over more atoms, making the phosphorus less susceptible to nucleophilic attack. A combination of these two factors may thus account for the enhanced stability of the $[P(NMe_2)_3Cl]^+$ ion to bond cleavage by HCl.

REFERENCES

1. K. B. Dillon, T. C. Waddington and D. Younger, *J. Inorg. Nucl. Chem.* 1981, **43**, 2665.
2. N. D. A. H. Khabbass, MSc thesis, Durham (1978).
3. K. B. Dillon, T. C. Waddington and D. Younger, *Inorg. Nucl. Chem. Lett.* 1973, **9**, 63.
4. K. B. Dillon, N. D. A. H. Khabbass and C. J. Ludman, in preparation.
5. D. A. Symon and T. C. Waddington, *J. Chem. Soc., Dalton Trans.* 1973, 1879.
6. K. B. Dillon, A. W. G. Platt and T. C. Waddington, *J. Chem. Soc., Dalton Trans.* 1980, 1036.
7. G. A. Wiley and W. R. Stine, *Tetrahedron Lett.* 1967, 2321.
8. A. Schmidpeter and H. Brecht, *Angew. Chem.* 1967, **79**, 535.
9. D. B. Denney, D. Z. Denney and B. C. Chang, *J. Am. Chem. Soc.* 1968, **90**, 6332.
10. H. P. Latscha, *Z. Naturfor.* 1968, **23b**, 139.
11. K. B. Dillon, R. J. Lynch, R. N. Reeve and T. C. Waddington, *J. Inorg. Nucl. Chem.* 1974, **36**, 815.
12. K. B. Dillon, R. N. Reeve and T. C. Waddington, *J. Inorg. Nucl. Chem.* 1976, **38**, 1439.
13. B. V. Timokhin, V. P. Feshin, V. I. Dmitriev, V. I. Glukhikh, G. V. Dolgushin and M. G. Voronkov, *Dokl. Akad. Nauk. SSSR (Engl. transl.)* 1977, **236**, 966.
14. B. V. Timokhin, V. I. Dmitriev, V. I. Glukhikh and N. A. Korchevin, *Bull. Acad. Sci. USSR, Div. Chem. Sci.* 1978, **27**, 1160.
15. K. B. Dillon, M. P. Nisbet and T. C. Waddington, *Polyhedron* 1982, **1**, 123.
16. A. Schmidpeter and H. Brecht, *Z. Naturfor.* 1968, **23b**, 1529.
17. K. B. Dillon, A. W. G. Platt and T. C. Waddington, *J. Chem. Soc., Dalton Trans.* 1981, 2292.
18. H. Finegold, *Ann. N.Y. Acad. Sci.* 1958, **70**, 875.
19. M. L. Nielsen, J. V. Pustinger Jr and J. Strobel, *J. Chem. Engng Data* 1964, **9**, 167.
20. M. Becke-Goehring and H. J. Müller, *Z. Anorg. Allg. Chem.* 1968, **362**, 51.
21. K. Moedritzer, L. Maier and L. C. D. Groenweghe, *J. Chem. Engng Data* 1962, **7**, 307.

22. V. Mark, C. H. Dungan, M. M. Crutchfield and J. R. Van Wazer, *Top. Phosphorus Chem.* 1967, **5**, 227.
23. T. C. Waddington and F. Klanberg, *J. Chem. Soc.* 1960, 2332.
24. R. M. K. Deng and K. B. Dillon, *J. Chem. Soc., Dalton Trans.* 1986, 1443.
25. R. M. K. Deng and K. B. Dillon, *J. Chem. Soc., Dalton Trans.* 1984, 1911.

Polyhedron Vol. 8, No. 21, pp. 2627–2629, 1989
Printed in Great Britain

0277–5387/89 $3.00+.00
© 1989 Pergamon Press plc

SULPHUR TRANSFER TO CYANIDE: THE RÔLE OF RHODANESE

ANTHONY R. BUTLER,* CHRISTOPHER GLIDEWELL and ANNE E. WADDON

Chemistry Department, University of St. Andrews, Fife KY16 9ST, Scotland, U.K.

(*Received* 10 *May* 1989; *accepted* 24 *July* 1989)

Abstract—High thiocyanate levels are found in the blood of patients receiving nitroprusside. NMR evidence is presented which suggests that this is not due to the action of rhodanese on cyano-ligands or on free cyanide released from nitroprusside. Although there is no sulphur transfer from thiocyanate to cyanide, even in the presence of rhodanese, the analogous reaction with selenocyanate occurs.

^{13}C NMR is a convenient means of detecting sulphur, and other chalcogen, transfer to cyanide either as a spontaneous reaction or catalysed by the enzyme rhodanese (thiosulphate: cyanide sulphur transferase, EC 2.8.1.1). This enzyme is active in the liver and is the body's means of detoxifying cyanide to give innocuous thiocyanate, which can be excreted. For *in vitro* experiments, thiosulphate is a ready source of sulphur which can be utilized by the enzyme. The mechanism of rhodanese action has been extensively reviewed by Westley.[1]

Our interest in the action of this enzyme was occasioned by reports[2–6] that patients to whom sodium nitroprusside $\{Na_2[Fe(CN)_5NO]\}$ had been administered as a hypotensive agent had elevated plasma thiocyanate levels. This was taken as evidence that nitroprusside had broken down *in vivo* to give free cyanide which had then been detoxified to thiocyanate. This evidence for *in vivo* formation of free cyanide conflicts with our studies,[7,8] indicating the stability of the $[Fe(CN)_5]$ moiety. So we examined the ability of rhodanese to convert cyanide ligands into free thiocyanate to see if thiocyanate could be formed without the intermediacy of free cyanide.

RESULTS AND DISCUSSION

In aqueous TRIS buffer, pH 8.6, dilute solutions of KCN and KSCN have, from natural abundance ^{13}C NMR spectra, chemical shifts of 163.9 and 13.56 ppm, respectively, due to the presence, at that pH, of HCN (pK_a 9.2) and $[SCN]^-$ (pK_a of HSCN is −1.8). In the same medium the axial and equatorial cyanide ligands of nitroprusside have shifts of 134.8 and 136.7 ppm. Addition of sodium thiosulphate had no effect on these NMR spectra, showing that there is no non-enzymic transfer of sulphur to free cyanide or cyanide ligand. Also, addition of cyanide to the nitroprusside solution had no effect, confirming the absence of cyanide exchange in this substitution inert d^6 complex.

When 90% of ^{13}C-enriched sodium cyanide was mixed with a 50% molar excess of sodium thiosulphate, the ^{13}C NMR spectrum showed the presence of only $H^{13}CN$. However, on addition of rhodanese the spectrum of $H^{13}CN$ was gradually replaced by that of $[S^{13}CN]^-$ (Fig. 1), showing complete and quantitative sulphur transfer from thiosulphate to cyanide, eq. (1):

$$H^{13}CN + S_2O_3^{2-} \rightarrow H^+ + S^{13}CN^- + SO_3^- . \quad (1)$$

Reaction was complete in 2 h. In similar experiments using $Na_2[Fe(^{13}CN)_5NO]$ instead of $Na[^{13}CN]$, no transfer of sulphur from thiosulphate to give $[S^{13}CN]^-$ was observed, even after an incubation time of 24 h, indicating the inertness of cyanide as a ligand to iron. However, it is known[9] that a number of cyanometallate anions, including $[Au(CN)_2]^-$, $[Ni(CN)_4]^{2-}$, $[Zn(CN)_4]^{2-}$ and $[Pt(CN)_4]^{2-}$, bind to rhodanese at a site adjacent to the active site pocket and thereby inhibit binding of the thiolating agent. However, repetition of the reaction between $Na[^{13}CN]$ and sodium thiosulphate, in the presence of unlabelled sodium nitroprusside, again showed quantitative sulphur transfer according to eq. (1). Thus nitroprusside is not an inhibitor of rhodanese. The NMR spectrum of

* Author to whom correspondence should be addressed.

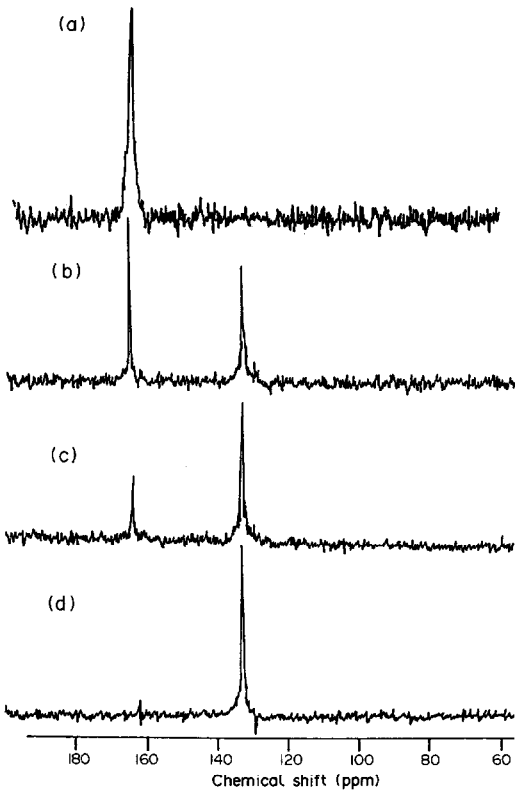

Fig. 1. ^{13}C NMR spectral changes occurring on incubation of 1 M Na[^{13}CN] with 3 M sodium thiosulphate in the presence of rhodanese; (a) start, (b) 30 min, (c) 90 min, (d) 150 min. The accumulation time was 5 min.

$Na_2[Fe(^{13}CN)_5NO]$ in TRIS buffer was unchanged by addition of rhodanese, indicating that nitroprusside does not bind strongly to the enzyme. Binding to vitamin B_{12} produces considerable spectral changes.[10]

The possibility that a blood component might mediate sulphur transfer to the cyano-ligands of nitroprusside was investigated. Two components, haemoglobin and glutathione, are known[11–13] to effect reduction of nitroprusside with formation of $[Fe(CN)_6]^{4-}$ via the substitution-labile d^7 complex $[Fe(CN)_4NO]^{2-}$, although no free cyanide is formed in these reactions. Incubation of 5×10^{-3} M ^{13}C-labelled sodium nitroprusside with sodium thiosulphate and rhodanese, using whole blood as solvent rather than TRIS buffer, gave no indication of thiocyanate formation even after 24 h although the ^{13}C NMR signal was strong. This confirms our belief that no free cyanide is formed on interaction of nitroprusside with whole blood, but leaves open the question of why patients receiving nitroprusside have high plasma thiocyanate levels.

In vivo, the probable source of sulphur for transfer to cyanide is thiosulphate, as it was in the experiments described above. It is formed enzymatically in the liver and kidney from a reaction between β-mercaptopyruvic acid and inorganic sulphite,[14] both of which arise from the metabolism of L-cysteine. In view of the simplicity of our method it was easy to see if, *in vitro*, the enzyme can use other sources of sulphur. We confirmed that thiocyanate cannot act as a source of sulphur[15] and so the equilibrium of eq. (2) does not occur, either

$$[^{13}CN]^- + [SCN]^- \rightleftharpoons [S^{13}CN]^- + [CN]^- \quad (2)$$

spontaneously or in the presence of rhodanese. In a similar way, no sulphur transfer occurs from thiourea. Rhodanese is thought to act by formation of a persulphide bond within the enzyme by capturing a sulphur from the donating agent; it appears that this occurs only with agents which can readily donate a sulphur, such as thiosulphate.

On the other hand, a mixture of $[^{13}CN]^-$ and $[SeCN]^-$ showed two equally strong signals with chemical shifts of 119.5 and 163.9 ppm, assigned to $[Se^{13}CN]^-$ and H[^{13}CN], respectively, within a few minutes of mixing. The equilibrium in eq. (3) is set up rapidly but it is

$$[SeCN]^- + [^{13}CN]^- \rightleftharpoons [CN]^- + [Se^{13}CN]^- \quad (3)$$

not so fast that it gives only an averaged signal in the NMR spectrum. The spectrum was unaffected by addition of rhodanese. It is probable that the much faster transfer of selenium from $[SeCN]^-$ compared with the corresponding transfer of sulphur from $[SCN]^-$ is related to the much larger atomic size of selenium and the corresponding longer bond to carbon: Se—C distances are typically 1.90–2.00 Å, while S—C distances are some 0.10–0.15 Å shorter. Bonding interactions in the intermediate $[X(CN)_2]^{2-}$ are therefore significant at longer separations between $[CN]^-$ and $[XCN]^-$, when X = Se than when X = S, so reducing the repulsive forces between the two negatively charged reactants. Selenourea does not act as a source of selenium, either spontaneously or in the presence of rhodanese.

EXPERIMENTAL

[^{13}C]-sodium cyanide at 90% enrichment was purchased from MSD Isotopes and was used as received. The preparation of ^{13}C-labelled nitroprusside has been described previously.[16] All manipulations involving nitroprusside were carried out in the absence of light. Other materials were AnalaR grade. Rhodanese with a specific activity of 10 units mg^{-1} was purchased from Sigma. All reactions involving rhodanese were carried out in TRIS buffer pH 8.6.

The NMR spectra were taken on a Bruker AM

300 spectrometer in the FT mode at 25°C with a field of 7.04 T. The lock was D_2O.

Blood was donated by A.R.B.

Acknowledgement—A.E.W. thanks the British Heart Foundation for a studentship.

REFERENCES

1. J. Westley, in *Bioinorganic Chemistry* (Edited by E. E. van Tamelen), Vol. 1, pp. 371–390. Academic Press, New York (1977).
2. C. J. Vesey, P. V. Cole and P. J. Simpson, *Brit. J. Anaesth.* 1976, **48**, 651.
3. M. Bogusz, J. Morcz, J. Korski, J. Gierz, P. Regieli, R. Witkowska and A. Crolabeck, *Clin. Chem.* 1979, **25**, 60.
4. C. J. Vesey, P. J. Simpson, L. Adams and P. V. Cole, *Brit. J. Anaesth.* 1979, **51**, 89.
5. V. Schultz, *Clin. Pharmacokinetics* 1984, **9**, 148.
6. C. J. Vesey and P. V. Cole, *Brit. J. Anaesth.* 1985, **57**, 148.
7. W. I. K. Bisset, M. G. Burdon, A. R. Butler, C. Glidewell and J. Reglinski, *J. Chem. Res.* 1981, (S) 299, (M) 3501.
8. A. R. Butler, C. Glidewell, J. McGinnis and W. I. K. Bisset, *Clin. Chem.* 1987, **33**, 490.
9. L. J. Lijk, K. H. Kalk, N. P. Brandenberg and W. G. J. Hol, *Biochemistry* 1983, **22**, 2952.
10. A. R. Butler, C. Glidewell, A. S. McIntosh, D. Reed and I. H. Sadler, *Inorg. Chem.* 1986, **25**, 970.
11. A. R. Butler, C. Glidewell, I. L. Johnson and A. S. McIntosh, *Inorg. Chem. Acta* 1987, **138**, 159.
12. A. R. Butler, A. M. Calsy-Harrison, C. Glidewell, I. L. Johnson, J. Reglinski and W. E. Smith, *Inorg. Chem. Acta* 1988, **151**, 281.
13. A. R. Butler, A. M. Calsy-Harrison, C. Glidewell and P. E. Sørensen, *Polyhedron* 1988, **7**, 1197.
14. B. Sörbo, *Biochim. Biophys. Acta* 1956, **21**, 393.
15. A. Schlesinger and J. Westley, *J. Biol. Chem.* 1974, **249**, 780.
16. A. R. Butler, C. Glidewell, A. R. Hyde and J. McGinnis, *Inorg. Chem.* 1985, **24**, 2931.

Polyhedron Vol. 8, No. 21, pp. 2631–2636, 1989
Printed in Great Britain

0277–5387/89 $3.00+.00
© 1989 Pergamon Press plc

AN ELECTRON-DIFFRACTION STUDY OF GASEOUS TETRASULPHUR TETRANITRIDE, S_4N_4

MATTHEW J. ALMOND, GEORGE A. FORSYTH and DAVID A. RICE*

The Department of Chemistry, University of Reading, Whiteknights, P.O. Box 224, Reading RG6 2AD, U.K.

and

ANTHONY J. DOWNS and TREVOR L. JEFFERY

Inorganic Chemistry Laboratory, University of Oxford, South Parks Road, Oxford OX1 3QR, U.K.

and

KOLBJØRN HAGEN

The Department of Chemistry, The University of Trondheim, Trondheim, N7000 Norway

(*Received* 17 *May* 1989; *accepted* 31 *July* 1989)

Abstract—The structure of tetrasulphur tetranitride, S_4N_4, determined by gas-phase electron diffraction has D_{2d} symmetry with four nitrogen atoms at the corners of a square, bridging four of the six edges of an approximately tetrahedral S_4 unit. The bonded sulphur–nitrogen distance $\{r_a[S(1)—N(1)]\}$ is 1.623(4) Å while the short unbridged sulphur–sulphur distance $\{r_a[S(1)\cdots S(2)]\}$ is 2.666(14) Å. The longer nitrogen-bridged sulphur–sulphur distance $\{r_a[S(1)\cdots S(3)]\}$ is 2.725(10) Å which is almost as short as the unbridged distance. The important angles in the molecule are $\angle$N(1)—S(1)—N(3) at 105.3(7)°, $\angle$S(1)—N(1)—S(3) at 114.2(6)°, $\angle$S(2)$\cdots$S(1)—N(1) at 88.4(9)°, and the interplanar angle between the plane of the four nitrogen atoms and the S(1)—N(1)—N(3) plane which is 92.5(3)°.

As elsewhere, fashions in chemical research come and go. Thus sulphur–nitrogen chemistry—a field initiated in 1835 when S_4N_4 was first isolated[1]—proceeded in fits and starts until 1973 when it was shown that polythiazyl, $[SN]_x$, a compound first prepared in 1910,[2] is a species capable of exhibiting metallic, and even super conductivity.[3] There then followed a flurry of research activity with new routes to thin films of $[SN]_x$ being avidly sought. Of the published routes, most require S_4N_4 as the starting material. Two of the commonly used methods involve the pyrolysis of S_4N_4, either over silver wool[3,4] or over Pyrex/quartz wool at *ca* 275°C.[5] A third route is via the polymerization of the red material that is formed when S_4N_4 is pyrolysed over silver wool[6] or silver selenide.[7] All of these routes involve reactions of gaseous S_4N_4. Accordingly, the vapour transport of S_4N_4 is of current interest, as is its structure in the gas phase.

Many years after its discovery, S_4N_4 was shown to be tetrameric[8] and there have been two reports of structural investigations by electron diffraction using the visual method. Both reports state that S_4N_4 exists as a molecular species of D_{2d} symmetry.[9,10] They differ in the nature of the conformations proposed for the S_4N_4 array. In the first study, it was suggested that the structure consists of a square plane of four sulphur atoms linked to a tetrahedron of four nitrogen atoms, a structure

*Author to whom correspondence should be addressed.

analogous to that found in β-realgar, As_4S_4.[9] In the second study[10] the molecule was said to have a plane of four nitrogen atoms linked to an approximate tetrahedron of four sulphur atoms, an arrangement in accord with the solid-state structure of S_4N_4 which has been determined by X-ray diffraction both at room temperature[11] and at 120 K.[12] However, in adducts formed with BF_3,[13] $SbCl_5$,[14] or SO_3,[15] the S_4N_4 unit adopts the β-realgar form. As the energy barrier between the two molecular forms of S_4N_4 having D_{2d} symmetry is likely to be small, a mixture of forms may be present in the gas phase, especially at the elevated temperatures needed to vaporize the compound (approximately 150°C). Accordingly, it was decided to re-investigate the gas-phase structure by electron diffraction using the methods that have superseded the visual method.

EXPERIMENTAL

Tetrasulphur tetranitride was prepared from S_2Cl_2 and NH_4Cl via thiotrithiazyl chloride, S_4N_3Cl,[16,17] and recrystallized from either chloroform or liquid sulphur dioxide. Samples were placed in sealed ampoules which were loaded into the nozzle arrangement of the electron-diffraction apparatus and opened *in situ*.

Electron-diffraction photographs were obtained from the Reading University apparatus,[18] which is fitted with a rotating sector whose angular opening is proportional to r^3. The nozzle-to-plate distances were 494.88 and 244.40 mm, and the data were obtained with the nozzle in the temperature range 139–175°C. The electron wavelength, approximately 0.062 Å, was calibrated against diffraction pictures of benzene.[19] Two plates from the long and two from the short camera distance were selected for use in the final analysis. The data spanned the ranges $3.25 \leqslant s \leqslant 14.75$ Å^{-1} and $9.00 \leqslant s \leqslant 29.00$ Å^{-1} at intervals of $\Delta s = 0.25$ Å^{-1}. The experimental data were processed as described previously[18] with scattering factors being taken from refs 20 and 21. Average curves were produced for each camera distance, and these are depicted in Fig. 1.

Root-mean-square vibrational amplitudes (l), perpendicular amplitude corrections (K) and centrifugal distortions (δr) were calculated from an assumed valence force field using values for the force constants (see Table 1) obtained from studies of S_4N_4.[22,23]

Analysis of the structure

The refinements of the structure were based upon the molecule depicted in Fig. 2, which contains the atom numbering scheme. As shown, the molecule has D_{2d} symmetry with the four nitrogen atoms forming a square, while the sulphur atoms form an approximate tetrahedron. As the molecule has such relatively high symmetry, it is necessary only to

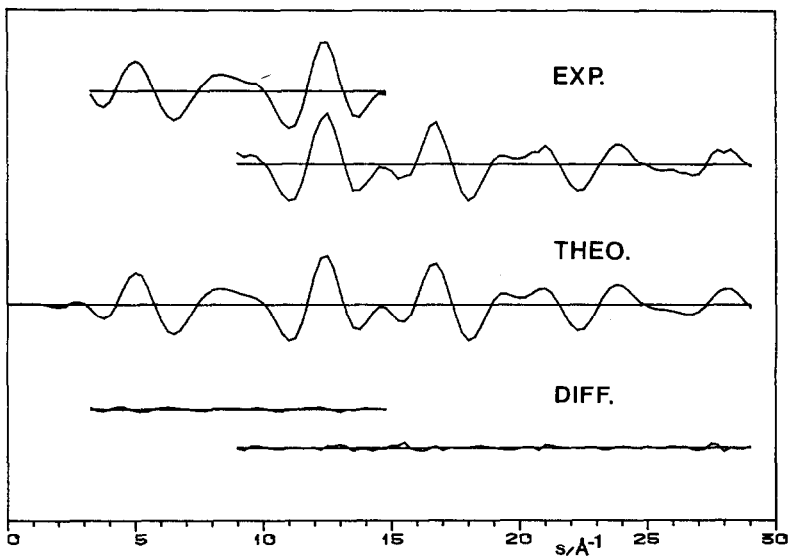

Fig. 1. Intensity curves $sI_m(s)$ for S_4N_4. Experimental curves (EXP) are averages of all the data from the plates for the two camera distances. The theoretical curves (THEO) were calculated from the structural parameters shown in Table 1 for model 1. The difference curves (DIFF) result from subtracting the relevant part of the theoretical curve from the experimental curves.

Table 1. Force constants used in the calculation of l, K and δr values for tetrasulphur tetranitride[22,23]

S(1)—N(1) stretch	3.76
S(1)···S(2) stretch	0.25
S(1)—N(1)—S(3) bend	1.78
N(1)—S(1)—N(3) bend	1.39
S(1)—N(1)/S(3)—N(2) torsion	0.31
S(1)—N(1)/S(1)—N(3) interaction	−0.64
S(1)—N(1)/N(1)—S(1)—N(3) interaction	0.10
S(1)—N(1)/S(1)—N(1)—S(3) interaction	0.52

Units for force constants: mdyne $Å^{-1}$, stretch, stretch–stretch interaction; mdyne, stretch–bend interaction; mdyne Å, bend, torsional.

define the positions of one sulphur and one nitrogen atom relative to an axis system to define the whole molecule. A suitable axis system has the centre of the square of the nitrogen atoms as its origin with the x- and y-axes bisecting the sides of the square. Thus, all the atoms are defined by three coordinates. The nitrogen atoms, which lie in the xy-plane, are defined by one coordinate which is equal to half the length of the side of the N_4 square. The sulphur atoms are defined by two coordinates. If the x-axis is chosen to bisect the N(1)···N(3) distance (see Fig. 2), the S(1) atom is defined by an x- and a z-coordinate.

To define the folding of the S_4N_4 unit a dependent dihedral angle, Φ, was calculated. This describes the angle between the N—S—N plane and the plane of the nitrogen atoms. The angle was defined so that, if the x-coordinate of S(1) is greater than that of N(1), Φ is greater than 90°. For reference purposes this model is called model 1. The most likely possible alternative model is obtained by interchanging the positions of the sulphur and nitrogen atoms

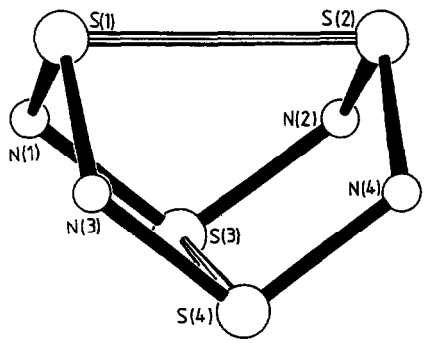

Fig. 2. The S_4N_4 molecule (model 1) with the atom numbering scheme.

from those shown in Fig. 2. As stated in the introduction, this model, called model 2, is related to that of β-realgar and is shown by S_4N_4 in certain of its coordination compounds.[13–15]

Refinements of the structures defined by models 1 and 2 were carried out by the least-squares procedure based on the intensity curves by adjusting one theoretical curve to the two averaged experimental curves (one from each nozzle-to-plate distance) using a unit weight matrix.[18] For model 1 it was possible to refine all of the vibrational amplitudes {the amplitude l[N(2)···N(4)] was tied to amplitude l[N(2)···N(3)]}, together with all the geometric parameters. For model 2 it was necessary to tie the two S···S amplitudes as well as the two N···N amplitudes in order to prevent them from having unrealistic values. Results from the final refinements for models 1 and 2 are recorded in Table 2. The average experimental and theoretical curves are shown in Fig. 1, while the radial distribution (RD) curves for models 1 and 2, calculated in the usual manner by Fourier transformation of the $s[I_m(s)]$ values after multiplication by $(Z_N Z_S/f_N f_S)\exp(-0.0025s^2)$, are shown in Fig. 3, together with the appropriate difference curves.

RESULTS AND DISCUSSION

To interpret electron-diffraction data, it is necessary to propose a model for the structure of the molecule under investigation, and to carry out refinements on the model to ascertain if it can be fitted to the experimental data. Thus the choice of model is all-important, and in selecting such a model attention must obviously be given to the known chemistry of the species, as more than one model can often be fitted to the data. If a single unambiguous model cannot be proposed, a number of models must be investigated. As S_4N_4 is known to adopt two structural forms in its various derivatives, refinements were carried out to ascertain which structural form is adopted in the gas phase, or, alternatively, if a mixture of the two forms is present. The structure found for S_4N_4 in the solid phase,[11,12] is related to that in Fig. 2 and this was refined as model 1. The alternative form, found in certain coordination compounds of S_4N_4 (model 2),[13–15] differs from that in model 1 by having the sulphur and nitrogen atoms transposed. Refinements of both models were carried out (see Table 2), and the resulting radial distribution curves for both models, together with the experimental radial distribution curve, and the difference curves, are shown in Fig. 3. It is obvious that model 2 does not fit the experimental data. The difference between the experimental and theoretical radial distribution

Table 2. Final structural parameters for S_4N_4[a]

Parameter	Model 1[b] r_α	r_g	l_{ref}[d]	l_{calc}	Model 2[c] r_α	r_g	l_{ref}[e]
r[S(1)—N(1)]	1.623(4)	1.628(4)	0.059(4)	0.051	1.624(8)	1.629(8)	0.061(10)
r[S(1)···S(2)]	2.666(14)	2.673(14)	0.100(32)	0.112	3.832(12)	3.836(12)	0.074(10)
r[S(1)···S(3)]	2.725(10)	2.730(10)	0.066(5)	0.060	2.710(12)	2.715(12)	0.071(10)
r[N(1)···N(2)]	2.580(14)	2.585(14)	0.080(24)	0.082	2.568(31)	2.573(31)	0.112(68)
r[N(1)···N(4)]	3.648(14)	3.652(14)	0.084(16)	0.085	2.608(48)	2.615(48)	0.164(68)
r[S(1)···N(2)]	3.084(9)	3.089(9)	0.105(5)	0.095	3.115(15)	3.120(15)	0.101(12)
∠N(1)—S(1)—N(3)	105.3(7)°				113.1(8)°		
∠S(1)—N(1)—S(3)	114.2(6)°				104.5(17)°		
∠S(2)···S(1)—N(1)	88.4(9)°						
∠Φ[f]	92.5(3)°				86.8(16)°		
			R value[g]				
		0.082				0.22	

[a] Distances (r_α and r_g) and amplitudes (l) in Ångstroms, and angles ($\angle_\alpha$) in degrees. Parenthesized uncertainties are 2σ and include estimates of systematic errors and correlation in the experimental data.

[b] Model 1 is the molecule as depicted in Fig. 2.

[c] Model 2 is the molecule as depicted in Fig. 2 with the nitrogen and sulphur atoms transposed.

[d] The N···N amplitudes were tied during the refinement.

[e] The N···N amplitudes were tied as a pair during the refinement and the S···S amplitudes were similarly treated.

[f] ∠Φ is an interplanar angle which in model 1 is the angle between the plane of the four nitrogen atoms and the N(1)—S(1)—N(3) plane.

[g] $R = [\Sigma w_i \Delta_i^2 / \Sigma w_i (s_i I_i(\text{obs.}))^2]^{1/2}$, where $\Delta_i = s_i I_i(\text{obs.}) - s_i I_i(\text{calc.})$.

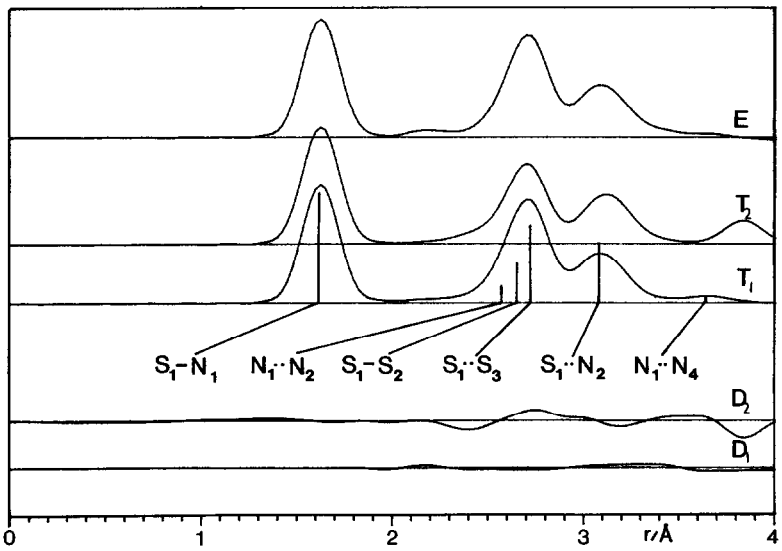

Fig. 3. Radial distribution curves for S_4N_4 showing the experimental (E), theoretical (T_1 for model 1 and T_2 for model 2) and the difference (D_1 for model 1 and D_2 for model 2) curves. The radial distribution curves were calculated using the theoretical curves that yielded the data contained in Table 2. To obtain the radial distribution curves the theoretical curves were first multiplied by $Z_N Z_S / f_N f_S \exp(-0.0025 s^2)$, and theoretical data were used for the unobserved area, $s < 3.75$ Å^{-1}.

curves is particularly apparent around 3.8 Å where model 2 requires a S···S distance (Table 2) which is not seen in the experimental data. The possibility that the vapour consists of a mixture of the two forms (models 1 and 2) was investigated by allowing the structural parameters, and the relative percentages of the two models, to refine. The R factor varies with the percentage composition of the two isomers (models 1 and 2) as follows: 100% model 1, $R = 0.082$; 95% model 1 and 5% model 2, $R = 0.085$; 90% model 1 and 10% model 2, $R = 0.089$; 85% model 1 and 15% model 2, $R = 0.094$. Thus the best fit to the experimental data was obtained with 100% of model 1. We can conclude that, in the gas phase, S_4N_4 has the structural form depicted in Fig. 2. There is a slight difference between the radial distribution curve for model 1 and the experimental data (see Fig. 3), although a satisfactory R factor of 0.082 was obtained. It is known that the thermal decomposition of S_4N_4 gives rise to S_4N_2[24] and S_2N_2.[25] Thus it is possible that the presence, in the gas phase, of trace amounts of these other sulphur–nitrogen compounds may account for the small differences observed between the experimental curves and the theoretical ones for model 1 (see Figs 1 and 3). Accordingly, refinements were carried out to ascertain if such impurities were present in the gas phase by adopting a procedure similar to that used to investigate the model 1/model 2 ratio. In these investigations, the S_4N_4/S_4N_2 or S_4N_4/S_2N_2 ratio and the parameters for S_4N_4 were refined, while the molecular parameters of the impurity under examination were set at the values obtained by X-ray crystallography.[26,27] No improvement in the fit between the experimental and theoretical curves was obtained on the introduction of either impurity. We are therefore confident that, under the conditions of our experiments, S_4N_4 volatilizes without decomposition, and adopts the structure shown in Fig. 2, namely model 1.

In any analysis of electron- and X-ray diffraction data, it is the r_α distances from the electron-diffraction studies that provide the best basis for comparison. The r_α[S(1)—N(1)] bonded distance (1.623(4) Å) is close to that reported in X-ray diffraction studies, whether at room temperature (mean value 1.616(17) Å)[11] or at 120 K (mean value 1.630 Å).[12] The angle between the plane of the four nitrogen atoms and that formed by N(1), S(1) and N(3) is 92.5(3)° and so r_α[S(1)···S(2)] (2.666(14) Å) is greater than r_α[N(1)···N(2)] (2.580(14) Å), whereas the reverse situation occurs in the solid phase. Thus the r_α[S(1)···S(2)] distance is slightly larger than that found in the solid phase (mean values 2.582(8) Å[11] at room temperature and 2.599 Å[12] at 120 K), although close to the value calculated in the earlier electron-diffraction study by Lu and Donohue[10] (2.69 Å). All attempts to refine r_α[S(1)···S(2)] to a value closer to that seen in the crystal failed. The larger S(1)···S(2) distance in the gas-phase structure of S_4N_4 is ascribable to the lack of close intermolecular contacts that impart packing forces. In the crystal structure, there are several non-bonded contacts below 3.3 Å involving interactions between either sulphur and nitrogen or nitrogen and nitrogen atoms,[12] and this, along with other crystal packing effects, results in a more compact structure in the solid phase than in the gas phase.

The angles in the ring, namely ∠[S(1)—N(1)—S(3)] 114.2(6)°) and ∠[N(1)—S(3)—N(2)] (105.3(7)°), are comparable with the mean values observed in the solid state (∠S—N—S angles: 113.1(7)[11] and 112.6(9)°;[12] ∠N—S—N: 104.5(15)[11] and 104.5(8)°[12]).

The observed structure cannot be represented in a simple single model based on classical notions of bonding. There have been numerous papers devoted to the problem of the bonding in S_4N_4,[28–31] and to the relative stabilities of the two possible conformations (models 1 and 2) for S_4N_4.[32,33] We do not wish to amplify the discussion here. However, comments on the size of r_α[S(1)···S(2)] and r_α[S(1)···S(3)] are appropriate. At 2.666(14) Å, the r_α[S(1)···S(2)] distance, while longer than the S—S distance in S_8 (2.04 Å),[34] is much shorter than twice the van der Waals radius for sulphur (3.70 Å), implying that there is a bonding interaction between S(1) and S(2). The second S—S distance, r_α[S(1)···S(3)] (2.725(10) Å), is almost as short as the unbridged S—S distance. So the question arises; does this distance also represent a S—S bonding interaction? If it does, then S_4N_4 can be visualized as an S_4 tetrahedron with four of its six edges bridged by nitrogen atoms. Alternatively, the shortness of r_α[S(1)···S(3)] could be assumed to be primarily a consequence of the angle subtended at the nitrogen atom. Then we must ask: why should such a small angle be subtended? It is interesting to compare the structure of S_4N_4 with that of $S_4N_4 \cdot SO_3$,[15] where the S_4N_4 fragment has a structure similar to that of β-realgar. Here the S—N—S angles range from 116 (the angle subtended at the nitrogen atom bound to SO_3) to 138 and 140°. There seems, therefore, to be no *a priori* reason, other than to form a short r_α[S(1)···S(3)] interaction, for the adoption of the small S—N—S angles reported here for S_4N_4. Such a model for S_4N_4 contrasts with that seen for the α-form of P_4S_4,[35] where the phosphorus atoms form an approximate tetrahedron, while the sulphur atoms, that are all in a plane, bridge four of the six edges of the P_4 tetrahedron. The two types

of P—P distance are 2.360(3) Å (unbridged) and 3.218(5) Å (sulphur-bridged), and so exhibit a much greater dissimilarity than the two types of S—S distance in S_4N_4. Therefore the S_4 unit in S_4N_4 has a structure that is closer to a tetrahedron than is the P_4 moiety in P_4S_4.

Acknowledgements—We thank the SERC for support (G.A.F.) and NATO for the award of a travel grant No. 117/82 (K.H. and D.A.R.).

REFERENCES

1. W. Gregory, *J. Pharm. Chem.* 1835, **21**, 315.
2. F. P. Burt, *J. Chem. Soc.* 1910, **97**, 1171.
3. V. V. Walatka, M. M. Labes and J. H. Perlstein, *Phys. Rev. Lett.* 1973, **31**, 1139.
4. M. M. Labes, P. Love and L. F. Nichols, *Chem. Rev.* 1979, **79**, 1, and refs therein.
5. E. J. Louis, A. G. MacDiarmid, A. F. Garito and A. J. Heeger, *J. Chem. Soc., Chem. Commun.* 1976, 426.
6. P. Love, G. Myer, H. I. Kao, M. M. Labes, W. R. Junker and C. Elbaum, *Ann. New York Acad. Sci.* 1978, **313**, 745.
7. M. J. Almond, A. J. Downs and T. L. Jeffery, *Polyhedron* 1988, **7**, 629.
8. M. H. M. Arnold, J. A. C. Hughill and J. M. Hutson, *J. Chem. Soc.* 1936, 1645.
9. O. Hassel and H. Viervoll, *Tids. Kjemi Bergvesen Met.* 1943, **3**, 7.
10. C.-S. Lu and J. Donohue, *J. Am. Chem. Soc.* 1944, **66**, 818.
11. D. Clark, *J. Chem. Soc.* 1952, 1615; B. D. Sharma and J. Donohue, *Acta Cryst.* 1963, **16**, 891.
12. M. L. De Lucia and P. Coppens, *Inorg. Chem.* 1978, **17**, 2336.
13. M. G. B. Drew, D. H. Templeton and A. Zalkin, *Inorg. Chem.* 1967, **6**, 1906.
14. D. Neubauer and J. Weiss, *Z. Anorg. Allg. Chem.* 1960, **303**, 28.
15. A. Gierren and D. Dederer, *Z. Anorg. Allg. Chem.* 1978, **440**, 119.
16. W. L. Jolly, K. D. Maguire and D. Rabinovich, *Inorg. Chem.* 1963, **2**, 1304.
17. M. Becke-Goehring and H. P. Latscha, *Z. Anorg. Allg. Chem.* 1964, **333**, 181.
18. C. J. Howill, PhD thesis, University of Reading, U.K. (1987).
19. K. Tamagawa, T. Iijima and M. Kimura, *J. Molec. Struct.* 1976, **30**, 243.
20. *International Tables for X-ray Crystallography.* Kynoch Press, Birmingham, U.K. (1974).
21. H. L. Sellers, L. Schäfer and R. A. Bonham, *J. Molec. Struct.* 1978, **49**, 125.
22. J. Bragin and M. V. Evans, *J. Chem. Phys.* 1969, **51**, 268.
23. R. Steudel, *Z. Naturfor.* 1981, **36a**, 850.
24. M. Becke-Goehring, *Inorg. Synth.* 1960, **6**, 128.
25. M. Goehring and D. Voigt, *Z. Anorg. Allg. Chem.* 1956, **285**, 181; R. Evans, DPhil. thesis, University of Oxford, U.K. (1980).
26. R. W. H. Small, A. J. Banister and Z. V. Hauptman, *J. Chem. Soc., Dalton Trans.* 1981, 2188; T. Chivers, P. W. Codding and R. T. Oakley, *J. Chem. Soc., Chem. Commun.* 1981, 584; T. Chivers, P. W. Codding, W. G. Laidlaw, S. W. Liblong, R. T. Oakley and M. Trsic, *J. Am. Chem. Soc.* 1983, **105**, 1186.
27. C. M. Mikulski, P. J. Russo, M. S. Saran, A. G. MacDiarmid, A. F. Garito and A. J. Heeger, *J. Am. Chem. Soc.* 1975, **97**, 6358; M. J. Cohen, A. F. Garito, A. J. Heeger, A. G. MacDiarmid, C. M. Mikulski, M. S. Saran and J. Kleppinger, *J. Am. Chem. Soc.* 1976, **98**, 3844.
28. *Gmelin Handbook of Inorganic Chemistry*, 8th edn, Sulfur–Nitrogen Compounds. Springer, Heidelberg (1985–87).
29. D. M. P. Mingos, *Nature (Lond.), Phys. Sci.* 1972, **236**, 99; A. J. Banister, *Nature (Lond.), Phys. Sci.* 1972, **239**, 69.
30. D. R. Salahub and R. P. Messmer, *J. Chem. Phys.* 1976, **64**, 2039.
31. R. H. Findlay, M. H. Palmer, A. J. Downs, R. G. Egdell and R. Evans, *Inorg. Chem.* 1980, **19**, 1307; M. H. Palmer, *Z. Naturfor.* 1983, **38a**, 378; H. W. Roesky, *Angew. Chem. Int. Edn. Engl.* 1979, **18**, 91; H. W. Roesky, *Adv. Inorg. Chem. Radiochem.* 1979, **22**, 239.
32. R. Gleiter, *J. Chem. Soc. A* 1970, 3174; A. G. Turner and F. S. Mortimer, *Inorg. Chem.* 1966, **5**, 906; M. S. Gopinathan and M. A. Whitehead, *Can. J. Chem.* 1975, **53**, 1343; A. G. Turner, *Stud. Phys. Theoret. Chem.* 1983, **28**, 141.
33. R. C. Hadden, S. R. Wasserman, F. Wudl and G. R. J. Williams, *J. Am. Chem. Soc.* 1980, **102**, 6687; S. Millefiori, A. Millefiori and C. D'Arrigo, *Inorg. Chim. Acta* 1981, **50**, 167.
34. J. Donohue, *The Structures of the Elements, Sulfur*, pp. 324–369. Wiley, New York (1974).
35. A. M. Griffin, P. C. Minshall and G. M. Sheldrick, *J. Chem. Soc., Chem. Commun.* 1976, 809.

Polyhedron Vol. 8, No. 21, pp. 2637–2639, 1989
Printed in Great Britain

0277–5387/89 $3.00+.00
© 1989 Pergamon Press plc

COMMUNICATION

CONVENIENT, STRAIGHTFORWARD ROUTES TO CARBODITHIOATO DERIVATIVES OF WEAK NITROGENOUS NUCLEOPHILES

C. C. HADJIKOSTAS, G. A. KATSOULOS, M. P. SIGALAS and C. A. TSIPIS

Department of General and Inorganic Chemistry, Aristotle University, 540 06 Thessaloniki, Greece

and

N. V. DUFFY

Department of Chemistry, Kent State University, Kent, OH 44242, U.S.A.

(*Received* 17 *April* 1989; *accepted* 25 *May* 1989)

Abstract—The N-alkyldithiocarbamate ligands when bidentately-coordinated to the nickel triad elements undergo facile electrophilic substitution reactions with a diversity of electrophiles affording novel carbodithioato derivatives of weak nitrogenous bases, not available by other methods.

In the course of our investigations on the reactions of the square-planar d^8 bis(N-alkyldithiocarbamato)metal(II) complexes with Lewis bases (L), we have demonstrated that dithiocarbimato complexes formulated as $[M(S_2C{=}NR)L_2]$ and $[M(S_2C{=}NR)_2]^{2-}$ can be isolated.[1–4] The mechanism of these reactions at the level of the frontier molecular orbital approach of chemical reactivity has been fully investigated by EHMO–SCCC calculations.[5] According to these investigations, the acidic character of the hydrogen atom of the bidentately-coordinated parent N-alkyldithiocarbamate ligands, as well as the high nucleophilicity of the nitrogen atom of the resulted dithiocarbimate ligands, have been verified. It is readily apparent from these reactivity patterns that the square-planar d^8 $[M(S_2CNHR)_2]$ complexes could easily undergo electrophilic substitution reactions, affording new classes of carbodithioato complexes, according to Scheme 1.

Taking advantage of this reactivity pattern, convenient, straightforward routes to carbodithioato derivatives of weak nitrogenous bases, such as secondary amides, ureas, amino acid esters, carbamic esters and sulphonamides, have emerged. In this respect, some of the resulting novel carbodithioate ligands are shown in Table 1. The direct preparation of such ligands by the reaction of the corresponding weak nitrogenous base with carbon disulphide in alkaline media is difficult or impossible to achieve, although some examples concerning the formation of N-formyl and N-methyl N-formyl dithiocarbamates and their thioformyl analogues have already been published.[6–10] However, no reports on their corresponding coordination compounds with transition metals have been found by us to date. Therefore, the novel nickel(II) complexes of the aforesaid carbodithioate ligands reported herein are probably some of the first examples in the pure chemistry of the dithiocarbamate ligands which may be considered as derivatives of weak nitrogenous bases. It is important to note, at this point, that all our efforts to prepare the corresponding free ligands according to the procedure described by Gattow *et al.*[6] were unsuccessful, leading to unstable easily oxidized species.

In a typical reaction concerning the synthesis of the bis(N-alkyl N-acetyldithiocarbamato)nickel(II)

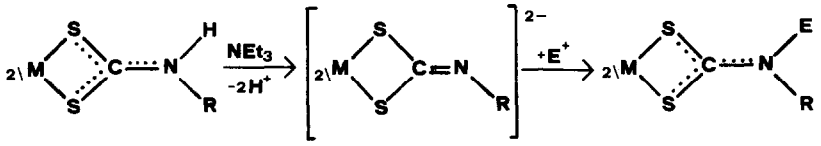

Scheme 1.

Table 1. Representative electrophilic substitution reactions of square-planar bis(N-alkyldithiocarbamato)nickel(II) complexes

Electrophile	Precursor	Carbodithioato ligand[a,b]
$[MeCO]^+$	$(MeCO)_2O$	$[R(MeCO)NCS_2]^-$
$[PhCO]^+$	PhCOCl	$[R(PhCO)NCS_2]^-$
PhN=C=O	PhN=C=O	$[R(PhHNCO)NCS_2]^-$
$[Ph_2NCO]^+$	Ph_2NCOCl	$[R(Ph_2NCO)NCS_2]^-$
$[MeOCOCH_2]^+$	$ClCH_2COOMe$	$[R(CH_2COOMe)NCS_2]^-$
$[EtOCO]^+$	ClCOOEt	$[R(COOEt)NCS_2]^-$
$[ArSO_2]^+$	$ArSO_2Cl$	$[R(ArSO_2)NCS_2]^-$

[a] Depending on the reaction conditions, one or both the dithiocarbamato ligands could undergo an electrophilic substitution reaction.

[b] R = alkyl or aryl; Ar = Ph, *p*-MePh.

complexes,[11] $[Ni\{S_2CN(COMe)R\}_2]$ (R = Me, Et, Bu^i, Bz, Ph, *p*-MePh, *p*-ClPh), the following procedure was adopted: 1 mmol of the appropriate $[Ni(S_2CNHR)_2]$ complex was dissolved in acetone and treated with 2 mmol of triethylamine and 2 mmol of acetic anhydride. In the resulting solution a solid material was formed, which on addition of water was quantitatively separated. Purification was achieved by dissolving the solid in chloroform and re-precipitating with ethanol (yield: 75%). It should be noted that by changing the molar ratio of the reactants to 1:1:1, the mixed-ligand (N-alkyldithiocarbamato)(N-alkyl N-acetyldithiocarbamato)nickel(II) complexes can also be isolated in relatively high yields. A similar procedure was followed for the synthesis of the rest of the carbodithioato nickel(II) complexes by using the appropriate precursor of the corresponding electrophile. Obviously, in the case of $[Ni\{S_2CN(PhHNCO)R\}_2]$ complexes, the presence of triethylamine as the deprotonating agent was unnecessary. All of these compounds are non-conducting, diamagnetic, and quite stable both in solid and solution states.

Inspection of the spectroscopic (Table 2) and magnetic data of the compounds under study clearly indicates the bidentate bonding mode of the carbodithioate ligands in the complexes and their

Table 2. Spectral data of some representative nickel(II) carbodithioates

Compound	IR[a] ν(CO)	ν(CN)	ν(CSS)	ν(NiS)	UV–vis[b] ν/kK
$[Ni\{S_2CN(MeCO)Me\}_2]$	1713vs	1453m	994vs	397m	30.6, 26.7sh, 21.5, 18.8sh, 16.2sh
$[Ni\{S_2CN(PhCO)Me\}_2]$	1724vs	1590m	980m	390m	30.2, 26.0sh, 21.3, 18.5sh, 15.6sh
$[Ni\{S_2CN(PhHNCO)Me\}_2]$	1687vs	1537s	965m	385m	30.8, 26.8sh, 23.8, 21.1, 15.8sh
$[Ni\{S_2CN(Ph_2NCO)Me\}_2]$	1720vs	1550s	1003m	380w	30.9, 26.3sh, 24.1, 20.7, 15.7sh
$[Ni\{S_2CN(CH_2COOMe)Me\}_2]$	1750vs	1526vs	1012m	387m	31.1, 25.8sh, 23.5, 20.9, 15.8sh
$[Ni\{S_2CN(COOEt)Me\}_2]$	1731vs	1433m	982w	393w	31.0, 26.7sh, 21.8, 20.2sh, 18.9sh
$[Ni\{S_2CN(PhSO_2)Me\}_2]$[c]		1447m	998w	392w	30.5, 26.0sh, 22.3, 19.5sh, 16.3sh

[a] KBr discs.

[b] $CHCl_3$ solutions.

[c] $\nu_{as}(SO_2)$, 1367vs cm^{-1}; $\nu_s(SO_2)$, 1169vs cm^{-1}.

square-planar configuration. Although all the ligands also possess an oxygen donor atom capable of bonding to the central atom forming a six-membered chelate ring, involving O- and S-coordination, such bonding has been excluded on the basis of spectroscopic data. Therefore, all these new compounds have broadly similar structures, involving the square-planar NiS_4 chromophore. However, in order to establish further their geometries, an X-ray diffraction study has been carried out on a member of this series, namely the $[Ni\{S_2CN(COMe)Bz\}_2]$ complex.[12]

Obviously, any attempt to further extend these electrophilic substitution reactions by using a great diversity of electrophiles, as well as other transition metal ions, would be of great importance, for it is possible to obtain novel compounds whose structures, chemical reactivities and applications are worth studying. Some of them, especially those of iron(III), are expected to extend further the area of six-coordinated iron complexes exhibiting either the low-spin configuration or intermediate spin states. Moreover, it is possible to obtain indirectly, via degradation of the complexes, organic and bioorganic compounds involving peptide-type bonds. Work along these lines is continuing in our laboratory.

REFERENCES

1. G. A. Katsoulos, G. E. Manoussakis and C. A. Tsipis, *Polyhedron* 1984, **3**, 735.
2. G. A. Katsoulos and C. A. Tsipis, *Inorg. Chim. Acta* 1984, **84**, 89.
3. C. A. Tsipis, I. J. Meleziadis, D. P. Kessissoglou and G. A. Katsoulos, *Inorg. Chim. Acta* 1984, **90**, L19.
4. C. C. Hadjikostas, G. A. Katsoulos and S. K. Shakhatreh, *Inorg. Chim. Acta* 1987, **133**, 129.
5. E. G. Bakalbassis, G. A. Katsoulos and C. A. Tsipis, *Inorg. Chem.* 1987, **26**, 3151.
6. G. Gattow and B. Sturm, *Z. Anorg. Allg. Chem.* 1980, **461**, 125.
7. G. Gattow and R. Gerner, *Z. Anorg. Allg. Chem.* 1985, **524**, 122.
8. G. Gattow and R. Gerner, *Z. Anorg. Allg. Chem.* 1985, **528**, 157.
9. R. Gerner and G. Gattow, *Z. Anorg. Allg. Chem.* 1985, **522**, 145.
10. R. Gerner and G. Gattow, *Z. Anorg. Allg. Chem.* 1985, **526**, 122.
11. C. C. Hadjikostas, G. A. Katsoulos, M. P. Sigalas and C. A. Tsipis, *Can. J. Chem.*, in press.
12. P. C. Christidis, *Acta Cryst.* 1986, **C42**, 781.

Polyhedron Vol. 8, No. 22, pp. 2641–2644, 1989
Printed in Great Britain

0277–5387/89 $3.00+.00
© 1989 Pergamon Press plc

USE OF ^{14}N AND ^{73}Ge NMR SPECTROSCOPY FOR ELUCIDATION OF PRODUCTS OF THE REACTION BETWEEN $GeCl_4$ AND KSCN IN ACETONE

Ē. KUPČE, E. UPENA, M. TRUŠULE and E. LUKEVICS*

Institute of Organic Synthesis, Latvian SSR Academy of Sciences, Riga, 226006, U.S.S.R.

(*Received* 19 *December* 1988; *accepted* 19 *May* 1989)

Abstract—^{73}Ge and ^{14}N NMR spectra were used to study reaction products and chemical exchange processes in the system $GeCl_4$+KSCN+acetone-d_6. At the $GeCl_4$ to KSCN ratios from 2 : 1 to 1 : 4, germanium(IV) derivatives of the type $Ge(NCS)_nCl_{4-n}$ were formed. Rapid intermolecular exchange with Cl and NCS groups was observed between the $Ge(NCS)_nCl_{4-n}$ (n = 0–4) molecules with varying n. The formation of dimeric and/or larger intermediate complexes has been suggested. This is accompanied by simultaneous formation of $[Ge(NCS)_nCl_{6-n}]^{2-}$ anions (n = 4–6). The 2D phase sensitive ^{14}N NOESY spectrum has indicated the existence of relatively slow intermolecular exchange between $Ge(NCS)_nCl_{4-n}$ (n = 1–4) and $[Ge(NCS)_4Cl_2]^{2-}$ species in solution. The content of $[Ge(NCS)_6]^{2-}$ increased with the amount of KSCN added. At a ratio of 1 : 6 this was practically the only product found in solution. A further increase in the amount of KSCN apparently resulted in a germanium derivative with a higher coordination number involved in rapid intermolecular exchange with free NCS^- ions in the solution.

^{73}Ge NMR studies are scarce because of the low resonance frequency (3.49 MHz at B_0 = 2.35 T) involved and due to the quadrupole moment of the ^{73}Ge nuclei (spin I = 9/2) impeding the recording of NMR spectra.[1,2] For this reason, investigations mainly involve symmetrically-substituted derivatives of tetracoordinate germanium (GeR_4 for R = H, Alk, Ar, OR, NR_2, SR, Hal),[3,4] as well as some germatranes containing pentacoordinate germanium atoms.[5,6] Only one paper reports the use of ^{73}Ge NMR for studying reaction products.[7] Recently, we have reported for the first time the ^{73}Ge spectra for hexacoordinate germanium in the $[Ge(NCS)_6]^{2-}$ anion.[8,9] The present communication demonstrates that the combined use of ^{73}Ge and ^{14}N NMR facilitates a more detailed analysis of reaction products and chemical exchange processes in the system $GeCl_4$+KSCN+acetone-d_6.

DISCUSSION

The ^{14}N chemical shift of a KSCN solution in acetone-d_6 (−171 ppm, see Table 1) occupies an intermediate position between that observed for the covalent derivatives RSCN (−100±10 ppm) and RNCS (−275±20 ppm),[10] indicating that KSCN occurs in the ionic form in the solution. Pure $GeCl_4$ shows a relatively narrow ^{73}Ge NMR signal (line width at half height $\Delta\nu_{1/2}$ = 2.1 Hz) at 30.9 ppm.[7]

Addition of a KSCN solution in acetone-d_6 to $GeCl_4$ results in the considerable broadening of the ^{73}Ge signal and its displacement to higher fields (see Table 1). This is accompanied by the occurrence of a ^{73}Ge signal at −443 ppm corresponding to $[Ge(NCS)_6]^{2-}$ ion (see Fig. 1). Two major signals are also observed in the ^{14}N spectra of these solutions (see Fig. 2) at *ca* −225 and −270 ppm, respectively. The chemical shifts of these resonances suggest the bonding of the NCS fragments to the germanium atom via N but not via S.

The ^{14}N signal at −225 ppm corresponds to the

* Author to whom correspondence should be addressed.

Table 1. ^{14}N and ^{73}Ge NMR data[a] for the products of the reaction of $GeCl_4$ and KSCN in acetone-d_6 at 303 K

$GeCl_4$: KSCN molar ratio	^{73}Ge			^{14}N			Signal assignment
	δ	$\Delta\nu_{1/2}$	A	δ	$\Delta\nu_{1/2}$	A	
1:0	30.9	2.1	1	—	—	—	$GeCl_4$
2:1	25.0	91.5	10	−268.7	61	9	$Ge(NCS)_nCl_{4-n}$
	−441.0	50	1	−224.9	13	6	$[Ge(NCS)_6]^{2-}$
	—	—	—	−221.7	20	0.6	$[Ge(NCS)_5Cl]^{2-}$
	—	—	—	−219.3	20	1.8	$[Ge(NCS)_4Cl_2]^{2-}$
1:1	20.0	70	4	−270.3	49	4	$Ge(NCS)_nCl_{4-n}$
	−443.1	42	1	−225.1	10	6	$[Ge(NCS)_6]^{2-}$
	—	—	—	−221.9	20	0.6	$[Ge(NCS)_5Cl]^{2-}$
	—	—	—	−219.3	20	1.7	$[Ge(NCS)_4Cl_2]^{2-}$
1:2	14.0	200	0.6	−273.1	44	2.8	$Ge(NCS)_nCl_{4-n}$
	−443.1	48	1.0	−225.1	10	6.0	$[Ge(NCS)_6]^{2-}$
	—	—	—	−222.0	20	0.7	$[Ge(NCS)_5Cl]^{2-}$
	−434.8	50	0.2	−219.3	20	1.9	$[Ge(NCS)_4Cl_2]^{2-}$
1:3	—	—	—	−274.9	29	2.3	$Ge(NCS)_nCl_{4-n}$
	−443.0	50	1	−225.1	10	6.0	$[Ge(NCS)_6]^{2-}$
	—	—	—	−222.0	20	0.4	$[Ge(NCS)_5Cl]^{2-}$
	−434.8	50	0.1	−219.2	20	1.5	$[Ge(NCS)_4Cl_2]^{2-}$
1:4	−443.0	50	1	−275.0	41	1.5	$Ge(NCS)_nCl_{4-n}$
	—	—	—	−225.1	10	6.0	$[Ge(NCS)_6]^{2-}$
	—	—	—	−222.1	20	0.4	$[Ge(NCS)_5Cl]^{2-}$
	—	—	—	−219.4	20	1.4	$[Ge(NCS)_4Cl_2]^{2-}$
1:6	−443.0	50	1	−225.1	7.3	1	$[Ge(NCS)_6]^{2-}$
1:10	−443.0	50	1	−225.1	7.4	1.0	$[Ge(NCS)_6]^{2-}$
	—	—	—	−201.5	150	0.9	$\{[Ge(NCS)_7]^{3-}\}$
1:20	−443.6	50	1	−225.1	8.4	1	$[Ge(NCS)_6]^{2-}$
	—	—	—	−187.8	278	10	$\{[Ge(NCS)_7]^{3-}\}$
0:1	—	—	—	−171.0	306	1	NCS^-

[a] Chemical shifts (δ) in ppm, line width at half height ($\Delta\nu_{1/2}$) in Hz, relative signal intensities (A) are rough estimates, as at significant difference in line widths the intensity of broad signals is decreased due to relaxation in the pre-acquisition delay.[11]

$[Ge(NCS)_6]^{2-}$ ion.[8,9] The downfield shift of this signal relative to the range characteristic of covalent derivatives of the type RNCS indicates enhanced polarity of the Ge—M bond in the anion $[Ge(NCS)_6]^{2-}$. The ^{14}N signal observed at −270 ppm suggests the formation of a germanium(IV) derivative of the type $Ge(NCS)_nCl_{4-n}$ in solution. ^{73}Ge chemical shifts for $Ge(NCO)_4$ ($\delta = -88.9$ ppm[8,9]) suggest that the ^{73}Ge resonance for $Ge(NCS)_nCl_{4-n}$ ($n = 1$–4) must be observed at higher fields than for $GeCl_4$. On the other hand, the lack of the narrow ^{73}Ge signal characteristic of $GeCl_4$ in an excess of the latter indicates that the broad ^{73}Ge resonance observed at 14–25 ppm is an averaged signal. This suggests the presence of rapid intermolecular exchange between $GeCl_4$ and $Ge(NCS)_nCl_{4-n}$, the upfield shift of ^{73}Ge signal reflecting an altered ratio of various $Ge(NCS)_nCl_{4-n}$ derivatives in favour of larger n. A certain narrowing of the ^{73}Ge resonance at the $GeCl_4$ to KSCN ratio of 1:1 indicates the predominance of one derivative, apparently $GeCl_3NCS$, in solution.

The most plausible mechanism for the observed exchange is the formation of dimeric and/or larger intermediate structures of type **I**. The involvement

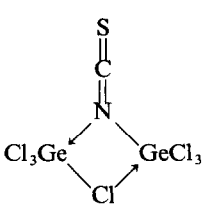

I

X = Cl, NCS

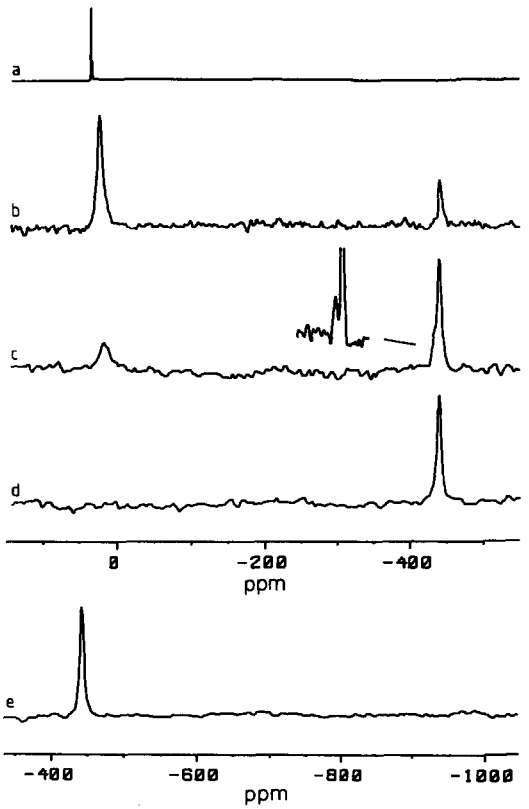

Fig. 1. ^{73}Ge NMR spectra of $GeCl_4$+KSCN in acetone-d_6 at (a) 1:0, (b) 1:1, (c) 1:2, (d) 1:6 and (e) 1:20 ratios.

of the $[Ge(NCS)_6]^{2-}$ anion in this exchange is insignificant, as the chemical shift and the corresponding ^{14}N signal line width were not subject to appreciable variation.

The low intensity signals also detected in the ^{14}N and ^{73}Ge spectra (see Table 1 and Figs 1 and 2) indicate the formation of small amounts of $[Ge(NCS)_nCl_{6-n}]^{2-}$ (n = 5–6) type derivatives.

The phase sensitive 2D ^{14}N NOESY spectrum of a 1:2 mixture of $GeCl_4$+KSCN (see Fig. 3) showing cross-peaks between the signals corresponding to $Ge(NCS)_nCl_{4-n}$ and $[Ge(NCS)_4Cl_2]^{2-}$ molecules, indicates the existence of intermolecular exchange between these species. To our knowledge this is the first application of 2D techniques in the ^{14}N NMR spectroscopy.

A further increase in KSCN content in the reaction mixture leads to some broadening and subsequent disappearance of the ^{73}Ge signal corresponding to germanium(IV) derivatives, as well as to enhanced intensity of the signal corresponding to the $[Ge(NCS)_6]^{2-}$ anion. The ^{14}N spectra indicate that this may be due not only to decreased content of $Ge(NCS)_nCl_{4-n}$ in solution, but also to decreased symmetry of charge distribution around the ^{73}Ge nuclei.

At the ratio 1:6 the ^{14}N and ^{73}Ge spectra practically show only one signal corresponding to the $[Ge(NCS)_6]^{2-}$ anion. Further addition of KSCN

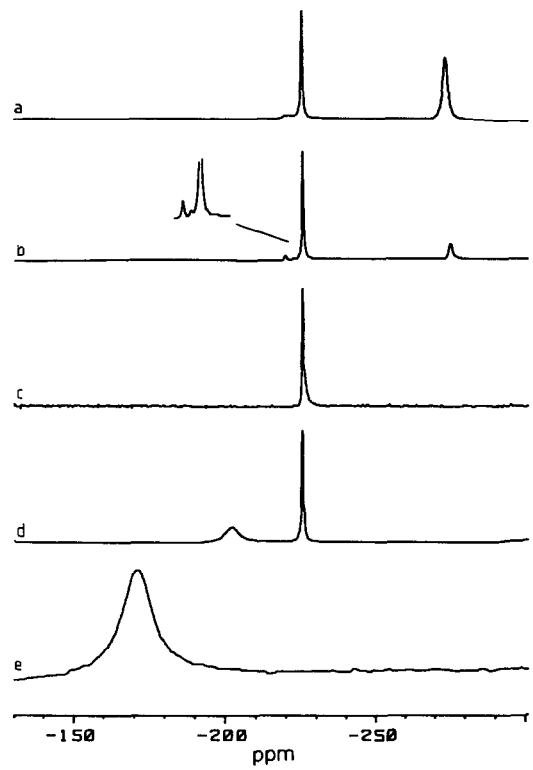

Fig. 2. ^{14}N NMR spectra of $GeCl_4$+KSCN in acetone-d_6 at (a) 2:1, (b) 1:3, (c) 1:6, (d) 1:10 and (e) 0:1 ratios.

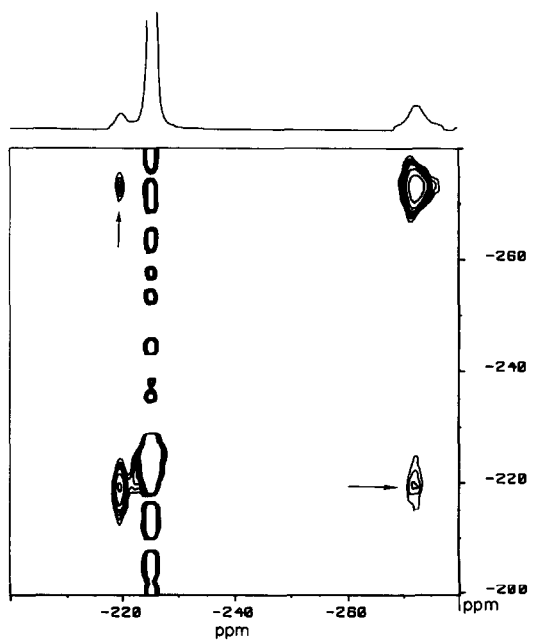

Fig. 3. The 2D phase sensitive ^{14}N NOESY spectrum of $GeCl_4$+KSCN in acetone-d_6 at a 1:2 ratio showing cross-peaks due to the intermolecular exchange between $Ge(NCS)_nCl_{4-n}$ and $[Ge(NCS)_4Cl_2]^{2-}$ species.

leads to the occurrence of a broad signal in the ^{14}N spectra, depending essentially on the amount of KSCN added. The ^{14}N line width and chemical shift corresponding to $[Ge(NCS)_6]^{2-}$ are not subject to variation. This demonstrates that intermolecular exchange between the anion $[Ge(NCS)_6]^{2-}$ and the free NCS^- ions in solution occurs rather slowly. At the same time, the ^{14}N signal expected for free NCS^- ions at −171 pm was not observed. This leads us to assume that the occurrence of the broad signal in the ^{14}N spectra may be attributed to a germanium derivative of higher coordination, apparently $[Ge(NCS)_7]^{3-}$ or $[Ge(NCS)_8]^{4-}$ involved in rapid (in NMR time scale) intermolecular exchange with free NCS^- ions. The absence of an appropriate signal in the ^{73}Ge spectrum may be explained by the lack of spherical symmetry of charge distribution around the ^{73}Ge nuclei or by the presence of intermolecular exchange between various structures.

EXPERIMENTAL

Solutions studied were prepared by adding 1 M KSCN in acetone + acetone-d_6 to $GeCl_4$ at various molar ratios. The KCl precipitate formed was removed by filtration. Acetone-d_6 was dried over molecular sieves (4 Å).

^{14}N and ^{73}Ge NMR spectra of solutions were recorded at 303 K on a Bruker WM-360 spectrometer in 5 mm sample tubes at 26.02 and 12.56 MHz, respectively. Chemical shifts were measured relative to internal references, Me_4Ge (^{73}Ge) and $MeNO_2$ (^{14}N).

For the phase sensitive 2D ^{14}N NOESY experiment, data were collected and processed by means of the standard DISNMR software package. In a typical experiment 256 FIDs (of 512 scans each) consisting of 1 K data points were accumulated using a mixing time of 10 ms. Sine bell resolution enhancement was used in both directions.

REFERENCES

1. R. K. Harris and B. E. Mann (Eds), *NMR and the Periodic Table*. Academic Press, New York (1978).
2. R. K. Harris, in *Multinuclear Approach to NMR Spectroscopy* (Edited by J. B. Lambert and F. G. Riddell), Chap. 16. D. Reidel, Dordrecht (1983).
3. K. M. Mackay and R. A. Thomson, *Main Group Met. Chem.* 1987, **10**, 83.
4. A. L. Wilkins, P. J. Watkinson and K. M. Mackay, *J. Chem. Soc., Dalton Trans.* 1987, 2365.
5. G. Zelčans, A. Lapsiņa, I. Solomennikova, E. Lukevics, E. Liepiņš and Ē. Kupče, *Zh. Obsch. Khim.* 1983, **53**, 1069.
6. V. A. Pestunovich, S. N. Tandura, B. Z. Sterenberg, N. Yu. Khromova, T. K. Gar, V. F. Mironov and M. G. Voronkov, *Izv. Akad. Nauk SSSR, Ser. khim.* 1982, 896.
7. R. G. Kidd and H. G. Spinney, *J. Am. Chem. Soc.* 1973, **95**, 88.
8. Ē. Kupče, E. Upēna, M. Trušule and E. Lukevics, *Latv. PSR ZA vēstis, Ķim. sērija*, 1988, 359.
9. Ē. Kupče and E. Lukevics, *J. Mag. Reson.* 1988, **79**, 325.
10. M. Giffard, J. Cousseau and G. J. Martin, *J. Chem. Soc., Perkin Trans. II* 1985, 157.
11. C. Brevard and P. Granger, *Handbook of High Resolution Multinuclear NMR*. Wiley, New York (1981).

Polyhedron Vol. 8, No. 22, pp. 2645–2648, 1989
Printed in Great Britain

0277–5387/89 $3.00+.00
© 1989 Pergamon Press plc

COMPLEXATION OF PUTRESCINE WITH COPPER(II), ZINC(II), LEAD(II) AND MAGNESIUM(II) IN AQUEOUS SOLUTION

LECHOSŁAW ŁOMOZIK* and ANNA WOJCIECHOWSKA

Faculty of Chemistry, Adam Mickiewicz University, Grunwaldzka 6, 60-780 Poznań, Poland

(*Received* 23 *January* 1989; *accepted* 19 *May* 1989)

Abstract—On the basis of potentiometric and spectral studies the presence of two types of the $CuL_2(OH)^+$ complex, where L = putrescine, was detected. In one complex two nitrogen atoms of the first ligand and one nitrogen atom of the second ligand are involved in the coordination, whereas in the other complex both nitrogen atoms of each amine take part in the coordination. At pH *ca* 7, the formation of the $CuHL^{3+}$ complex was proved. The stability constant of the $CuL_2(OH)^+$ complex was determined.

Putrescine (1,4-diaminobutane), spermidine (4-azooctane-1,8-diamine) and spermine (4,9-diazododecane-1,12-diamine) are biogenic amines which occur in the cells of living organisms and participate in the genetic information transfer, interacting in the protonated forms (as cations) with negatively-charged fragments of nucleic acid chains.[1–7] However, the mechanism of this reaction still remains to be explained, as well as the character of the processes between the metal ions and nucleic acid molecules. Moreover, the possibilities of formation of metal–polyamine complexes and the reactions of such compounds with electron-donor fragments of DNA and RNA should also be considered.

In the cases of spermine and spermidine it was found that they formed coordination compounds with metals in aqueous solution,[5–7] yet it is still uncertain whether these compounds can also be given by putrescine. Some authors would rather suggest that putrescine does not coordinate metal ions in solution,[7,8] though its complex compounds were isolated from absolute ethanol.[9] Results of our studies on complexing properties of this amine with some metal cations contradict such a suggestion. Instead they testify to the fact that under certain conditions putrescine forms coordination compounds in aqueous solution.

Results of the studies on complex formation of putrescine with Cu^{2+}, Zn^{2+}, Pb^{2+} and Mg^{2+} are presented in this work.

EXPERIMENTAL

Putrescine dihydrochloride (Institute of Bioorganic Chemistry of Polish Academy of Sciences in Poznań) was used in these studies. Results of the elementary analysis are in agreement with the theoretical composition of the compound.

Copper was used in the form of the perchlorate, the preparation of which was described earlier.[10] Perchlorates of the other metals used in these studies were obtained likewise.

Potentiometric measurements were carried out using a Radiometer TTT85 titrator with an autobiurette ABU80; a previously calibrated electrode GK 2401C[11] was also applied. The concentration of putrescine in all the titration systems was 1.00×10^{-3} mol dm^{-3}. All titrations were performed under an argon atmosphere at ionic strength $\mu = 0.1$ ($NaClO_4$), at 293 ± 1 K. NaOH (0.0465 mol dm^{-3}) free of CO_2 was used as the titrant.

The pH values at which turbidity appears for the systems with copper(II), zinc(II), lead(II), magnesium(II) and putrescine were measured on a spectral colorimeter SPECOL–Carl Zeiss Jena fitted with an attachment TK for solutions with composition and concentrations identical to those used in the potentiometric studies.

* Author to whom correspondence should be addressed.

In turbidity measurements, ligand solutions of the same concentration as those of metal-containing systems were used as reference. The turbidity was assumed to appear at a pH value for which the declination of a pointer was observed at a maximum amplification obtainable with this equipment.

UV–vis measurements were performed on a UV–vis SHIMADZU 160 spectrometer. The concentrations of putrescine and Cu^{2+} in the samples were $c_{Put} = 3.00 \times 10^{-3}$ mol dm^{-3}, $c_{Cu^{2+}} = 5.19 \times 10^{-4}$ mol dm^{-3}; $c_{Put} = 3.00 \times 10^{-3}$ mol dm^{-3}, $c_{Cu^{2+}} = 1.14 \times 10^{-3}$ mol dm^{-3}.

The model discrimination and determination of complex stability constants were carried out on EMC-RIAD 32 and AMSTRAD PC-1512 computers using adopted versions of SCOGS[12] and MINIQUAD[13] programs, whereas the form distribution in the system was calculated using the HALTAFALL[14] program.

RESULTS AND DISCUSSION

Complexing abilities of putrescine (Put) in comparison with other biogenic amines (spermine, spermidine) are definitely weaker. This is due to the formation of a seven-membered chelate ring, which is very unfavourable because of the spatial arrangement and also energetic reasons. However, it is difficult to agree with some authors who claim that the above facts exclude the formation of coordination compounds of 1,4-diaminobutane. Let us add that there is still a possibility of this compound forming with the participation of only one nitrogen atom in the complexation. It should be remembered that putrescine compounds may be formed with metal ions in the solid phase.[8] Moreover, during the complexation of spermine with Cu^{2+}, seven-membered rings[7] (in addition to six-membered rings) are also formed.

The first step in the studies on the putrescine–metal system was to determine the ligand association constants (Table 1). Then mixtures of putrescine (1.00×10^{-3} mol dm^{-3}) with Cu^{2+} were titrated. The studies were performed for a few concentrations of copper ions at cation–ligand ratios ranging from 1:6 to 1:8.5. Titration at relatively higher concentrations of metal prevented the application of the potentiometric method due to precipitation at a relatively low pH. In all the experiments performed, this process was observed from pH *ca* 7.0. On further addition of base the precipitate gradually dissolved (at pH *ca* 9.0 the solution became clear). For the calculations, points from a titration curve were used with a pH range for which no precipitate was recorded. Limiting values of this range were determined by measuring the turbidity described in the Experimental. The initial formation of the precipitate was also determined on the grounds of measurements of the pH. An inflection on the titration curve corresponds to the time of precipitate formation. The solid state formation is undoubtedly related to the reaction type:

$$M^{2+} + xH_2O \rightleftharpoons M(OH)_x^{2-x} + xH^+$$

(the coordination compound can also undergo hydrolysis) which results in an increase in the acidity of the medium. The above observations are consistent with the results of turbidity studies. We distinguished two sets of points on the titration curve. One set included the points within the pH range from 3.0 to 7.0 ("before precipitation") and the other set included the points for the pH range from 9 to 12 ("after precipitation"). Both sets were treated in the computer analysis as one series of measurements. The formation of only one complex: $ML_2(OH)$, $\log \beta_{1-12} = 0.065$, was detected in the system (Table 1). The complexation takes place from a pH of about 9.0 (Fig. 1). This complex practically binds all the metal from a pH of about 10.5.

A computer analysis proved no complexation at the pH before precipitation, despite the fact that in

Table 1. Stability constants $\log \beta_{pqr}$ of putrescine complexes with H^+ and Cu^{2+} for the $Cu_pH_qL_r$ type

	p	q	r	$\log \beta_{pqr}$
Put–Cu^{2+}	0	2	1	20.51 (0.01)
	0	1	1	10.83 (0.01)
	1	−1	2	0.065 (0.06)[a]

[a] The value of R obtained for MINIQUAD calculations was 0.024. For the hydroxo complex $ML_2(OH)^+$ its stability constant $\beta = \beta_{pqr}/K_w$ (in our calculations $pK_w = 14.167$).

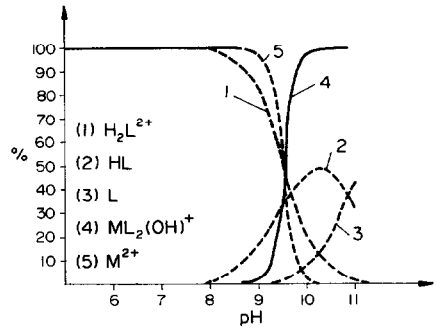

Fig. 1. Distribution diagram of the Put–Cu^{2+} system; percentages of the species refer to total metal except for the metal-free forms which refer to total ligand.

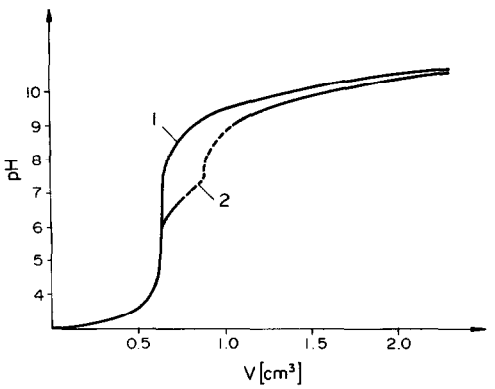

Fig. 2. Titration curves of (1) putrescine; (2) putrescine with Cu^{2+}.

this range the pH value for the titration curve of the Cu^{2+}–ligand system is lower than for the titration curve of the ligand alone (Fig. 2).

Additional information about the system was obtained by electron spectroscopy measurements. At pH 10.0 (significant concentration of $ML_2(OH)^+$, Fig. 1), the maximum absorption of the system Put–Cu was found for $\lambda = 634.5$ nm. The calculated value of the molar absorbance coefficient of the complex was $\varepsilon = 105$ dm^3 mol^{-1} cm^{-1} (Table 2). The maximum corresponds to the case of three coordinated nitrogen atoms.[5,7,15]

At pH 11.6 the maximum of absorption is shifted to $\lambda = 601$ nm ($\varepsilon = 93$ dm^3 mol^{-1} cm^{-1}). The $ML_2(OH)^+$ complex still dominates in the system (Fig. 1) but, as it follows from spectral measurements, its coordination is different. The maximum absorption at $\lambda = 601$ nm corresponds most likely to tetracoordination by the nitrogen atoms. Thus, we may conclude that putrescine forms the $ML_2(OH)$ complex with copper from a pH of *ca* 9.0. One of the attached ligands forms a seven-membered ring with the metal and the other coordinates only with one nitrogen atom. At a pH of *ca* 11.6 two chelate rings are formed in the $ML_2(OH)^+$ complex. Electron spectroscopy was also performed for the Put–Cu^{2+} system at pH ranging from 3.0 to 7.0. From a pH of *ca* 3 to *ca* 6.8 the position of the absorption maximum of this system (754 nm) indicates the presence of uncoordinated copper. At pH 7.0 (Table 2) the maximum absorption at $\lambda = 705$ nm was observed. This testifies to the presence of a complex with only one coordinated nitrogen atom, i.e. a compound of the MHL type without a chelate ring. Such a conclusion is then in agreement with the observed shift of the titration curve of Put–Cu^{2+} with respect to the titration curve of the ligand. It should be emphasized that the UV–vis measurements of the Put–Cu^{2+} system were carried out together with a study of copper(II) perchlorate alone under the same conditions as for the mixture with the ligand. The maximum absorption values for the Cu^{2+} ion (hydrated) are found at wavelengths which are markedly longer than for Put–Cu^{2+} (Table 2).

In order to solve the problem of Put–Cu^{2+} complex formation in solution over precipitate formation, the Put–Cu^{2+} system with a putrescine concentration of 3.00×10^{-3} mol dm^{-3} and a Cu^{2+} concentration of 1.14×10^{-3} mol dm^{-3} (which expanded the range of pH "with precipitate" from 6.4 to 12.0) was subjected to the UV–vis investigation. A solution of pH 11.6 was filtered and UV–vis measurements were taken. Then the solution of pH 11.6 was acidified until the required pH was reached (10.4, 10.0, 8.7, 7.0), filtered and the absorption spectra of the clear solutions were recorded (Table 2). λ_{max} values for the obtained series of results are almost the same as the results obtained

Table 2. Results of UV–vis measurements for the system Put–Cu^{2+}. (a) $c_{Put} = 3.00 \times 10^{-3}$, $c_{Cu^{2+}} = 5.19 \times 10^{-4}$ mol dm^{-3}; (b) $c_{Put} = 3.00 \times 10^{-3}$, $c_{Cu^{2+}} = 1.14 \times 10^{-3}$ mol dm^{-3}; (c) $c_{Cu^{2+}} = 5.19 \times 10^{-4}$ mol dm^{-3}.

pH	λ_{max} (nm)	A	ε (dm^3 mol^{-1} cm^{-1})	λ_{max} (nm)	A	λ_{max} (nm)
7.0	705.0	0.010[a]	—	705.0	0.008	754.0
8.7	647.5	0.034	Traces of precipitate	649.0	0.022	752.0
10.0	634.5	0.044	105.0	633.5	0.044	640.5
10.4	630.5	0.042	105.0	631.0	0.039	645.0
11.6	601.5	0.037	92.75	603.0	0.050	638.0

[a] At pH 7 the presence of the $CuHL^{3+}$ complex was not proved using a potentiometric method.

for a system of lower concentration of Cu^{2+} (for a smaller pH range of precipitate formation). Hence it should be assumed that the complexing equilibria for both cases examined are analogous, which means that "over the precipitate" the MHL^{3+} complex and the $ML_2(OH)^+$ complex are formed at a pH of *ca* 7.0 and a pH of *ca* 9.0, respectively.

The MHL^{3+} formation [as it can be concluded from distribution curves (Fig. 1)] proceeds as follows:

$$H_2L^{2+} + Cu^{2+} \rightleftharpoons Cu(HL)^{3+} + H^+.$$

It should be added that the results of spectral studies do not exclude the formation of the ML^{2+} complex (non-chelate with coordination by one nitrogen only).

Due to the low concentration of the compound formed at pH *ca* 7.0 it was not possible to prove the formation of a protonated compound using computer analysis, or to determine its stability constant. Consequently, we could not present it on a distribution curve. Since the value of pK for putrescine is 9.68 it is difficult to assume that a simple complex (at pH = 7.0) may be formed in which putrescine behaves as a monodentate ligand and where the other donor atom is deprotonated.

Under the conditions of $ML_2(OH)^+$ complex formation both the HL^+ (dominates at pH about 10.0) and L (dominates at pH above 11.0) forms may take part in its formation. In the latter case amine is completely deprotonated, which undoubtedly facilitates coordination with all nitrogen atoms (H^+ does not compete with a metal cation). These observations testify to the fact that two different forms of the $ML_2(OH)^+$ complex may occur (as it follows from spectral data). An attempt to determine the structure of the precipitate formed in the system led us to a conclusion that it contains mainly hydroxo-compounds of copper and a certain amount of the amine examined. However, we have failed to prove unambiguously the composition of the precipitate on the grounds of elementary analysis and spectral investigations.

Potentiometric studies on putrescine complexation with Pb^{2+}, Zn^{2+} and Mg^{2+} have also been carried out. In the case of the Mg^{2+} ion, formation of coordination compounds in solution should be excluded (titration curve of Put–Mg^{2+} system overlaps completely with the titration curve of a ligand in the whole acidity range—pH from 3.0 to *ca* 11.0). On the other hand, in the case of the Pb^{II} and Zn^{II} ions even at metal–ligand ratios equal to 1 : 9, a precipitate appears in the solution (at a pH of *ca* 7.8 and 8.2, respectively) and it does not dissolve even after further additions of NaOH.

For these two systems it seems more reasonable to conclude that the presence of Pb^{II} and Zn^{II} complexes with putrescine cannot be proved using potentiometric methods, rather than to say that such complexes do not occur in solution.

Acknowledgements—This work was financially supported by the Polish Academy of Sciences, Project RPBP 01.6. We thank Professor Maciej Wiewiórowski for helpful discussions.

REFERENCES

1. U. Bachrach, *Function of Naturally Occurring Polyamines*. Academic Press, New York (1973).
2. S. S. Cohen, *Introduction to the Polyamines*. Prentice–Hall, Englewood Cliffs, New Jersey (1971).
3. C. W. Tabor and H. Tabor, *Ann. Rev. Biochem.* 1984, **53**, 749.
4. B. N. Palmer and H. K. I. Powell, *J. Chem. Soc., Dalton Trans.* 1974, 2086.
5. B. N. Palmer and H. K. I. Powell, *J. Chem. Soc., Dalton Trans.* 1974, 2089.
6. A. Anichinii, L. Fabrizzi, R. Barbucci and A. Mastroiani, *J. Chem. Soc., Dalton Trans.* 1977, 2224.
7. D. M. Templeton and B. Sarkar, *Can. J. Chem.* 1985, **63**, 3112.
8. C. R. Bertsch, W. C. Fernelius and B. P. Block, *J. Phys. Chem.* 1958, **62**, 444.
9. P. Pfeiffer, *Naturwiss.* 1948, **35**, 190.
10. L. Lomozik, *Monatsh. Chem.* 1984, **115**, 261.
11. H. M. Irving, M. G. Miles and L. D. Pettit, *Anal. Chim. Acta* 1967, **38**, 475.
12. I. G. Sayce, *Talanta* 1968, **15**, 1397.
13. A. Sabatini, A. Vacca and P. Gans, *Talanta* 1974, **21**, 53.
14. N. Ingri, W. Kakolowicz, L. G. Sillen and B. Warnqvist, *Talanta* 1967, **14**, 1261.
15. R. Boggs and J. Donohue, *Acta Cryst.* 1975, **B31**, 320.

Polyhedron Vol. 8, No. 22, pp. 2649–2655, 1989
Printed in Great Britain

0277–5387/89 $3.00+.00
© 1989 Pergamon Press plc

EQUILIBRIA IN COMPLEXES OF N-HETEROCYCLIC LIGANDS—L. THE STRUCTURE OF A RACEMIC TRIS-1,10-PHENANTHROLINENICKEL(II) IODIDE TRIHYDRATE

R. D. GILLARD* and S. H. MITCHELL

Department of Chemistry, University College, P.O. Box 78, Cardiff CF1 1XL, Wales, U.K.

and

W. T. ROBINSON

Department of Chemistry, University of Canterbury, Christchurch, New Zealand

(*Received* 25 *August* 1988; *accepted* 2 *June* 1989)

Abstract—$[Ni(phen)_3]I_2 \cdot nH_2O$ forms several solid phases, both as racemate and when resolved. The most stable phase of the racemic iodide (a trihydrate) has space group $P2_1/c$, $Z = 4$. The structure is made up of complex ions containing nickel chelated by three 1,10-phenanthroline ligands, and by layers of hydrogen-bonded assemblies of iodide ions and water molecules.

Complex ions containing 1,10-phenanthroline are central in coordination chemistry. There has been increasing interest in the mechanism of the racemization of tris-phenanthroline metal salts in solid[1–5] and solution phases. Conflicting schemes have been proposed for the solid state racemization of Δ-(−)-$[Ni(phen)_3]I_2 \cdot nH_2O$ or its enantiomer.

In considering such mechanisms, a fundamental requirement is knowledge of the lattice structure. But with these compounds even such basic information as phase identification and a proper understanding of the role played by water in determining the structure is lacking. $[Ni(phen)_3]I_2 \cdot nH_2O$ is rose-pink when hydrated and changes[6] to yellow on loss of water. Further, water has been shown to depress the solid state racemization of $[Fe(phen)_3]Br_2$ at room temperature[5] and the pressure-induced racemization[7] of $[Ni(phen)_3](ClO_4)_2$.

Many salts exist in a variety of crystalline phases under "ambient" conditions. This fact has been ignored in this area and often elsewhere in solid state coordination chemistry. Such multiple phase systems are quite common among salts involving complexed phenanthroline and similar ligands, as exemplified by: $[Rh(phen)_2Cl_2]Cl \cdot nH_2O$;[8] $[Ir(phen)_2Cl_2]Cl \cdot nH_2O$;[9] $[Pt(bipy)Cl_2]$.[10]

We recently found[1] seven phases for racemic $[Ni(phen)_3]I_2 \cdot nH_2O$ and four for the same salt resolved. In this context, we heated the common chiral phase, [**B** of ref. 1]; $[Ni(phen)_3]I_2 \cdot nH_2O$ at 190°C for a week, racemizing it. The product was a *new* racemic phase, unlike any obtained by crystallizing the racemic iodide from solution.

To give a full account of such solid state reactivity, and to comment on the reasons for such widespread multiformity among these classical coordination compounds, it will be necessary to give painstaking attention to characterization of phases. For racemic and optically active tris-1,10-phenanthrolinenickel(II) salts, this process was described in the previous part[1] of this series. We now report the crystal and molecular structure of the most easily accessible form $[Ni(phen)_3]I_2 \cdot 3H_2O$ of the racemic iodides.

EXPERIMENTAL AND STRUCTURE SOLUTION

The preparation of the compound is described in the preceding part.[1]

Cell: monoclinic space group $P2_1/c$ (no. 14),

*Author to whom corresponding should be addressed.

absences *hol*, $l \neq 2n$ and $0k0$, $k \neq 2n$, $a = 20.547(3)$, $b = 16.454(2)$, $c = 10.705(3)$ Å, $\beta = 104.33(2)°$, $Z = 4$, $D_c = 1.72$, $D_o = 1.71$ g cm^{-3} (by flotation in $CHBr_3/CH_3CCl_3$).

The data set consisted of 6411 reflections: 5090 remained after those with $F_o < 3\sigma F_o$ were removed. The structure was solved using the SHELX76[11] and SHELXTL[12] programs.

Iodine and nickel atoms were located from a Patterson map, and the remaining atoms by peak searching on difference Fourier maps after a few cycles of least-squares refinement. Aromatic hydrogen atoms were allowed to ride on the carbon atoms with a bond length of 1.08 Å. Their thermal parameters were tied together to the same free variable and refined isotropically.

Atoms were refined by the least-squares method, in blocks, and refinement was terminated when the function R_g was minimized. A free weighting scheme was used with weight $= K/(\sigma^2 + gF^2)$. The final R-indices were $r = 0.045$, $R_w = 0.062$ and $R_g = 0.091$ ($K = 1.000$, $g = 0.0395$). The largest shift of any refined parameter was less than 0.19 of the estimated standard deviation, except for the isotropic thermal parameter of the hydrogens which oscillated by ± 1.25 ESD between least-squares cycles.

Bond lengths, bond angles and other structural features are given in Tables 1–5 and coordinates in the supplementary material. Planes were calculated using XRAY76 (program LSQPL),[13] and figures drawn using ORTEP.[14]

RESULTS

The crystal structure

This (Fig. 1) is composed of separate units of $[Ni(phen)_3]^{2+}$, iodide and water molecules; all atoms occupy general sites in the lattice. $[Ni(phen)_3]^{2+}$ and iodide ions, and water molecules are arranged in layers (Fig. 2). There are four such layers per unit cell, arranged parallel to the *bc* plane and containing right- and left-handed tris-chelates. Layers of complex molecules alternate with water–iodide layers, of which there are two unique layers.

Complex geometry

Because the complex ion occupies a general site in the lattice, its geometry has only approximate D_3

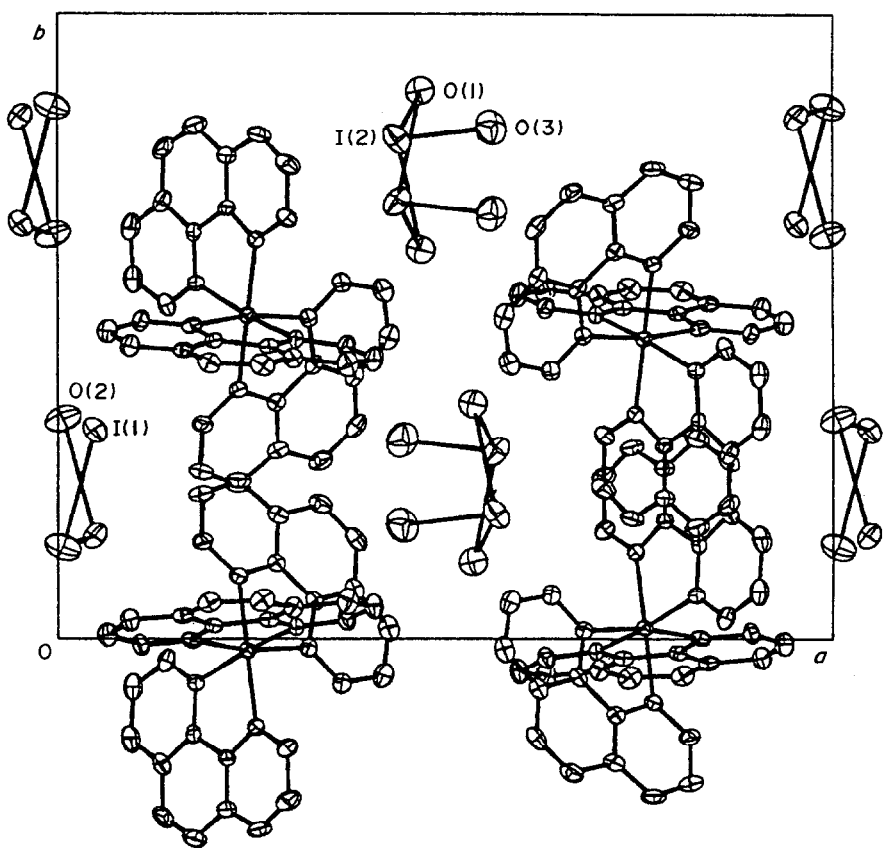

Fig. 1. Arrangement (viewed in *c*-direction) of components in the unit cell.

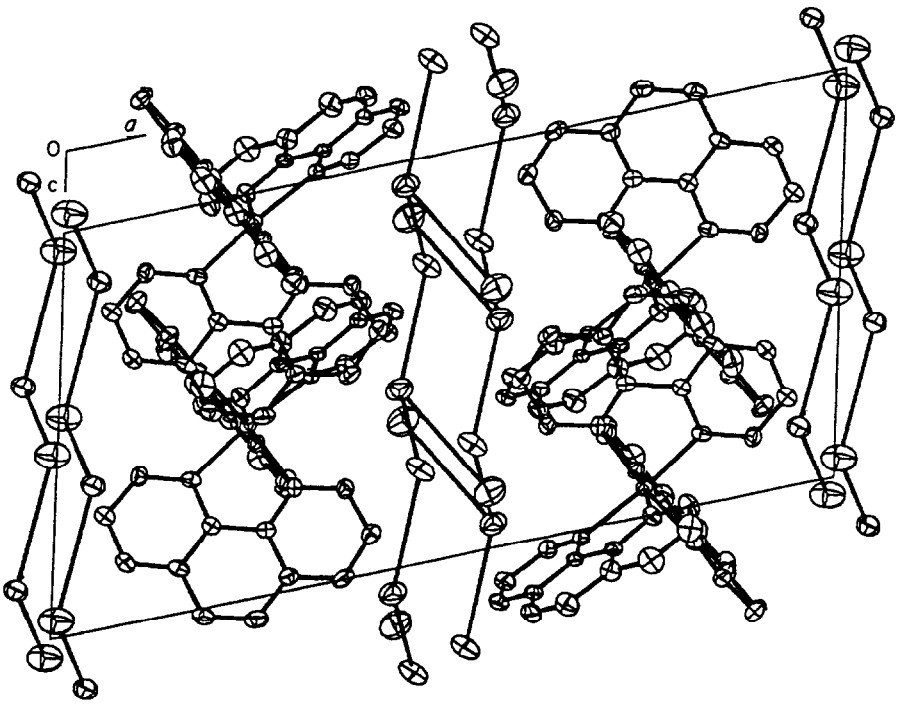

Fig. 2. Arrangement (viewed in *b*-direction) of layers of $[Ni(phen)_3]^{2+}$ ions and of (water + iodide).

symmetry, so all bond lengths, angles, etc. should be treated as independent. For the same reason, we describe its geometry by treating it as twisted (from trigonal prismatic toward regular octahedral) about the quasi-*C*3 axis. The twist is defined at each ligand by the angle between the planes defined[15] by the two centroids of the "trigonal" faces and the nitrogens of the respective phenanthroline. The average twist (θ) for the ion is 49.5(5)°, which is toward the octahedral extreme. (θ is, of course, 0 for the trigonal prism, a possible intermediate for intramolar racemization.) The calculated[16] optimum twist of 1,10-phenanthroline in this structure is ~ 48° (b = 1.28, bite/M—N bond length).

Table 1. Bonds (Å) in $[Ni(phen)_3)]I_2 \cdot 3H_2O$

	phen 1	phen 2	phen 3
Ni—N(1)	2.079(4)	2.096(3)	2.090(3)
Ni—N(10)	2.111(3)	2.086(4)	2.072(3)
N(1)—C(2)	1.317(6)	1.334(6)	1.318(5)
N(1)—C(13)	1.371(5)	1.365(6)	1.343(5)
C(2)—C(3)	1.391(8)	1.390(7)	1.396(7)
C(3)—C(4)	1.392(7)	1.350(10)	1.378(9)
C(4)—C(14)	1.369(7)	1.405(8)	1.418(7)
C(5)—C(14)	1.442(6)	1.460(9)	1.406(8)
C(5)—C(6)	1.361(8)	1.326(8)	1.383(9)
C(6)—C(12)	1.410(7)	1.420(7)	1.398(8)
C(7)—C(12)	1.415(7)	1.388(7)	1.435(8)
C(7)—C(8)	1.373(8)	1.354(8)	1.312(8)
C(8)—C(9)	1.406(7)	1.400(8)	1.421(7)
C(9)—N(10)	1.317(6)	1.309(6)	1.351(6)
N(10)—C(11)	1.353(6)	1.360(5)	1.341(5)
C(11)—C(12)	1.394(6)	1.412(7)	1.389(6)
C(11)—C(13)	1.423(6)	1.432(6)	1.468(6)
C(13)—C(14)	1.415(7)	1.392(6)	1.404(6)

The average lengths of Ni—N bonds (2.089(14) Å) and angles N_1—Ni—N_{10} (79.9(3)°) are similar to those found[17,18] in structures of other tris-phen nickel salts, although, in those, nickel occupies sites of higher symmetry.

The distance (d) between the "trigonal" faces (between centroids) is 2.24 Å, and the angle between the normals to the two faces is 1.9°. The nickel atom lies where expected, very close (0.016 Å) to and midway (1.11 Å from the N(1) plane) along the line joining the centroids of the "trigonal" faces.

The differences found between the internal angles of the coordination sphere are related to the slight distortions described above. The overall effect is illustrated in Fig. 3 and discussed below. The increased twist (50.0°) at ligand 3, and decreased twist (49.0°) at ligand 1 has the effect of increasing the N(10′)—Ni—N(10″) angle (95.5°) and decreasing the N(1)—Ni—N(1′) angle (93.2°). This is also reflected in the small angle (1.88°) made between the trigonal faces, and by the increased bite and N(1)—Ni—N(10) angle for ligand 1, and the converse for ligand 3. The Ni—N(10) bond length is larger (2.111 Å) than expected and may contribute to these distortions.

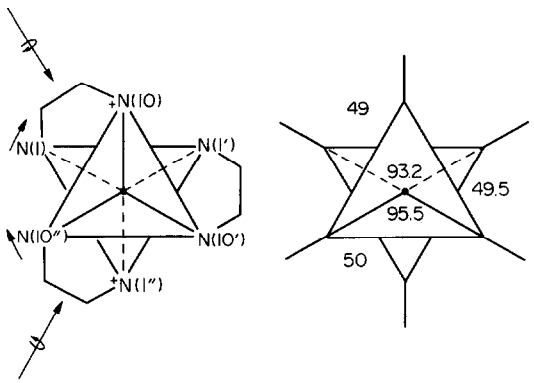

Fig. 3. View of the tris-chelated ion along the quasi-C_3 axis, and definitions of angles of twist, following ref. 15. Arrows and + symbols indicate [relative to phenanthroline(1)] the movements of atoms and the twist adopted by the other two phenanthroline ligands.

Phenanthroline

The numbering scheme for 1,10-phenanthroline is in Fig. 4. Bond lengths and angles within the ligand are similar to those[17,18] in prior reports: the average bond distances are C—C, 1.398(32) and C—N, 1.340(21) Å, consistent[17] with a bond order of ~ 1.5. The ligands are planar: no atom deviates from its respective plane by more than 0.017 Å (Table 3). Further, the nickel atom is almost coplanar with phen(3) but 0.10 and 0.13 Å from the planes of phen(1) and (2), respectively.

Water–iodide layers

Water molecules and iodide ions make hydrogen bonds to each other to form chains running parallel to the *c*-axis. Most of the O—I contacts are between 3.56 and 3.70 Å (Table 4): there is only one long contact I(2)—O(3) at 4.16 Å, a little shorter than the expected non-bonding distance (~ 4.2 Å); variations in the reported van der Waals radii make this number somewhat indefinite for a linear sequence[19–21] of atoms I(2)···H—O: hydrogen bonding is probably not involved. However, the atoms need not be linear, in which case the maximum O(3)···I(2) distance consistent with hydrogen-bonding will be shorter, and the observed contact should then be considered even less likely to involve hydrogen-bonding.

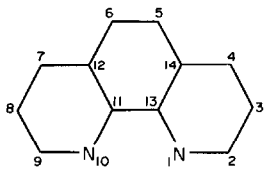

Fig. 4. Numbering of atoms in 1,10-phenanthroline.

Table 2. Table of angles (°) for $[Ni(phen)_3]I_2 \cdot 3H_2O$

N(1)—Ni—N(1)′	93.2(1)		
N(1)—Ni—N(1)″	95.2(1)		
N(1)′—Ni—N(1)″	95.1(1)		
N(10)—Ni—N(10)′	92.1(1)		
N(10)—Ni—N(10)″	92.6(1)		
N(10)′—Ni—N(10)″	95.5(1)		
N(10)′—Ni—N(1)″	93.4(1)		
N(10)—Ni—N(1)′	93.0(1)		
N(1)—Ni—N(10)″	92.1(1)		
N(1)—Ni—N(10)′	169.4(1)		
N(10)—Ni—N(1)″	170.9(1)		
N(1)′—Ni—N(10)″	172.9(2)		
	phen 1	phen 2	phen 3
N(1)—Ni—N(10)	80.2(1)	79.9(1)	79.6(1)
Ni—N(1)—C(2)	130.4(3)	128.9(4)	129.0(3)
Ni—N(1)—C(13)	112.2(3)	112.3(3)	113.3(2)
C(2)—N(1)—C(13)	117.5(4)	118.8(4)	117.6(4)
N(1)—C(2)—C(3)	124.2(4)	122.3(6)	123.5(5)
C(2)—C(3)—C(4)	118.4(5)	119.5(5)	118.9(5)
C(3)—C(4)—C(14)	119.4(5)	119.6(5)	119.5(5)
C(6)—C(5)—C(14)	119.5(5)	120.9(5)	120.3(5)
C(5)—C(6)—C(12)	122.6(4)	123.2(6)	120.5(5)
C(8)—C(7)—C(12)	119.5(4)	121.7(5)	121.3(5)
C(7)—C(8)—C(9)	119.2(5)	118.0(5)	119.9(5)
C(8)—C(9)—N(10)	121.6(5)	123.6(5)	121.3(4)
C(9)—N(10)—C(11)	120.1(4)	117.7(4)	117.3(4)
Ni—N(10)—C(9)	128.2(4)	129.4(3)	128.6(3)
Ni—N(10)—C(11)	111.8(2)	112.8(3)	114.1(3)
N(10)—C(11)—C(12)	122.2(4)	123.1(4)	125.3(4)
N(10)—C(11)—C(13)	117.9(4)	117.3(4)	116.4(4)
C(12)—C(11)—C(13)	119.9(4)	119.6(4)	118.3(4)
C(6)—C(12)—C(7)	123.5(4)	126.4(5)	123.5(5)
C(6)—C(12)—C(11)	119.1(4)	117.7(4)	121.5(5)
C(7)—C(12)—C(11)	117.3(5)	115.9(4)	114.9(4)
C(11)—C(13)—C(14)	120.2(4)	121.4(4)	118.9(4)
N(1)—C(13)—C(11)	117.9(4)	121.2(4)	124.6(4)
N(1)—C(13)—C(14)	121.9(4)	117.5(4)	116.5(3)
C(4)—C(14)—C(5)	122.8(5)	124.4(5)	123.7(5)
C(4)—C(14)—C(13)	118.7(4)	118.4(5)	115.9(5)
C(5)—C(14)—C(13)	118.5(4)	117.2(4)	120.5(5)

The angles I(2)—O(*n*)—I(2) indicate that only one or perhaps no contact involves a linear sequence of atoms, because the angles are much larger than the H—O—H angle of water (105.5° in the gas phase). Conversely, in the O(2)—I(1) layer, the I(1)—O(2)—I(1) angle is 110.9° and so an almost linear sequence would be expected and both contacts considered as weak hydrogen bonds.

Oxygen–oxygen contact distances are all > 3.4 Å, too long for hydrogen bonds, and there are no short oxygen–phenanthroline contacts. The smallest are O(2)···C(2) at 3.21 Å and O(1)···H(7′) at

Table 3. Complex geometry

Ligand bite and angle between planes defined by the two centroids and pairs of nitrogens.

	θ (°)	b	Ligand bite (Å)
N(1)—N(10)	49.03	1.288	2.698(6)
N(1′)—N(10′)	49.48	1.284	2.686(5)
N(1″)—N(10)″)	49.97	1.281	2.665(4)

Angle between planes defined by; nitrogens N(1), N(1′), N(1″), and N(10), N(10°), N(10″) = 1.88°.

Distance between centroids = 2.240 Å.

Distance of Ni from the line joining the centroids = 0.016 Å.

Planes:[13]

Phen	1	2	3	
Maximum deviation	0.071	0.070	0.023	
Chi	0.38	0.25	0.020	(13 d.f.)
Ni deviation	0.101	0.130	0.020	
a	0.6802	7.4857	18.1730	
b	15.9289	−5.0695	0.9873	
c	2.4888	8.1498	−7.1430	
d	−8.4840	0.3738	−4.4007	

Plane equation $ax+by+cz+d=0$; figures for direct space and fractional coordinates.

Angle (°) between phenanthroline planes:

2–1	86.12
3–1	88.42
3–2	84.09

2.43 Å. Water molecule O(1) lies in a pocket 4.88 Å from the nickel, close to the quasi-$C3$ axis of the complex. Relevant contacts with phenanthroline are given in Table 5. O(1) does not lie exactly on the quasi-$C3$ axis, as defined by the line joining the nickel and centroid of the plane of O(9) or H(9) atoms. The distances to this line are 0.216 and 0.252 Å, respectively. There is a bias towards H(9). The point that is the projection of O(1) onto the plane of H(9) atoms lies closer to atom H(9) than does the centroid of that plane (1.614 as opposed to 1.869 Å). However, this is probably not a hydrogen bonding interaction with phenanthroline—the contact is too long (O(1)···H(9), 2.78 Å). It more likely

Table 4. Water–iodide contacts and angles

Real atom	Generated atom	Contact distance (Å)	Symmetry operation
I1	O(2)	3.638(6)	$1-x, 1-y, 1-z$
		3.697(7)	$1-x, \frac{1}{2}-y, \frac{1}{2}-z$
I2	O(1)	3.568(6)	x, y, z
		3.619(5)	$x, 1\frac{1}{2}-y, \frac{1}{2}+z$
I2	O(3)	3.561(7)	$1-x, 1-y, 1-z$
		4.158(9)	$1-x, \frac{1}{2}+y, \frac{1}{2}-z$

Angles (°)	
I(2)—O(2)—I(1)	110.9
I(2)—O(1)—I(2)	141.6
I(2)—O(3)—I(2)	137.3

Table 5. Contacts (Å) within the pocket containing O(1)

Distance of O(1) to:	9	9′	9″
H	2.783(7)	3.124(6)	3.002(9)
C	3.220(7)	3.474(6)	3.560(9)

Distance of O(1) projected onto the plane defined by H(9), H(9′), H(9″) to:

H	1.614	2.149	1.967

Contacts:

	H	C
9···9′	3.258(7)	3.670(7)
9···9″	3.273(8)	3.693(7)
9′···9″	3.350(7)	3.801(8)

arises from a combination of hydrogen-bonding to iodide outside the pocket, and packing constraints.

DISCUSSION

The present crystal structure of the most stable racemic phase, $[Ni(phen)_3]I_2 \cdot 3H_2O$, shows no unusual features. Covalent hydration was proposed[22] for this system *in solution* on the basis of new circular dichroism absorptions arising on the addition of water to dichloroethane solutions. Such modification of the ligated 1,10-phenanthroline is not present *in this particular solid.* The coordination geometry is as regular as may be expected from packing in a low symmetry site. Each ligand coordinates in a similar fashion, and the detailed geometry of the complex is consistent with the differences between them.

Among the crystal structures solved for salts containing complex ions $[M(phen)_3]^{n+}$, ferrous and ferric salts are the most extensive series. These, similar to nickel in that their coordination spheres display very little distortion, do, however, display an increase in their overall twist making them more like octahedra than is nickel(II). Iron(II)[23] $\theta = 52.8$, $d = 2.16$; iron(III)[24] $\theta = 55.7$, $d = 2.10$.

The present structure of $[Ni(phen)_3]I_2 \cdot 3H_2O$ may be considered isostructural with that[23] of $[Fe(phen)_3]I_2 \cdot 2H_2O$, apart from an additional water molecule. The unit cell dimensions and coordinates are similar, although the ferrous structure was refined in space group $P2_1/a$.

The question of whether a hole exists in the iron structure sufficiently large to accommodate another water molecule was not addressed. In view of the close similarity of coordinates, it seems likely that there is space. The third water may not be present in the ferrous crystal studied because it is mobile and was lost during or before collection of diffraction results. Alternatively, it may not have been included in the analysis although present in the lattice.

Mason has discussed[25] the ways in which chiral and racemic groups of molecules pack in crystal lattices, and identified the geometrical conditions necessary for optimal close packing. There may be a close and sometimes exact correspondence between lattice symmetry elements and the orientation of symmetry elements of the isolated molecules. To some extent, this is a consequence of the molecules occupying special positions in the lattice. The tris-chelate molecules $[M(acac)_3]$ (acac = acetylacetonate, the mono-O-anion of pentane-2,4-dione) and $[M(en)_3]^{3+}$ (en = 1,2-diaminoethane) were considered specifically. In most instances, however, when counter ions and water are also present in the lattice, optimal packing does not necessarily require a close association between complex molecules. Certainly, the present packing arrangement we find in $[Ni(phen)_3]I_2 \cdot 3H_2O$ does not correspond with the "optimal" close packing schemes for delta and lambda isomers. Close packing would be confined to the layers of complex molecules, but each $[Ni(phen)_3]^{2+}$ unit packs without interleaving with any of its neighbours. The symmetry operation that relates the molecules in a layer is the *c*-glide. This has the effect of separating the molecules. So the only operation remaining that could cause interleaving is translation in *b* or *c* directions. However the smallest dimension, *b*, is too large for effective overlap, and the molecules are orientated incorrectly for this means of achieving interleaving.

A fair number of structures are now known involving tris-1,10-phenanthroline complex ions. In a few, the metal ion exerts direct influence on the geometry of the ion, as in the tetragonal static Jahn–Teller distortion found for the one dimorph[26] of $[Cu(phen)_3](ClO_4)_2$ studied.[27] Among the more numerous diffraction studies for salts of complexed *spherical* ions, the known structures including nickel(II) are:

	Reference
$[Ni(phen)_3][Mn(CO)_5]$	17
$K\{\Lambda\text{-}(+)_{589}\text{-}[Ni(phen)_3]\}\{\Lambda\text{-}(-)_{589}\text{-}[Co(C_2O_4)_3]\}2H_2O$	18
$[Ni(phen)_3](S_2P(OCH_3)_2)_2$	28
$[Ni(phen)_3](I_3)_2$	29.

$[M(phen)_3]^{n+}$ units have been found to occupy lattice sites with three different site symmetries, in accordance with the symmetry properties of the free molecules. These are:

(i) (C_1): most common, and the structure we now find for $[Ni(phen)_3]I_2 \cdot 3H_2O$;
(ii) (C_2): $[Hg(phen)_3](CF_3SO_3)_2$[30] and Λ-(−)-$[Fe(phen)_3][Sb_2(D\text{-tart})_2] \cdot 8H_2O$;[31]
(iii) (C_3): $K\{(+)\text{-}[Ni(phen)_3]\}\{(-)\text{-}[Co(C_2O_4)_3]\} \cdot 2H_2O$.[18]

The averaged geometry of ions like $[Ni(phen)_3]^{2+}$ in solution of course has at least C_3 symmetry (and often, indeed, D_3 symmetry). That is not particularly common in the solid state and the present structure again iterates the need for caution in transferring the mechanistic concepts appropriate to solution, unmodified, to studies on solids.

Finally, the colour change observed on dehydration may be rationalized. The iodide ions are held in water–iodide sheets some way from the cations in the studied pink crystals, whose colour arises from a *d–d* transition. As water is removed or lost, the iodide ions may presumably approach the cat-

ions more closely, giving enhanced charge-transfer intensities. The same phenomenon (increase in richness of colour on dehydration) occurs in other similar systems, like $[Pt(bipy)_2]I_2 \cdot 2H_2O$ and solvated N-benzylnicotinamide iodide. We earlier showed[1] that the yellow colour of the product in eq. (1) could be "cooled out" in liquid nitrogen, giving the pink colour of the *d–d* chromophore in the NiN_6 manifold.

$$[Ni(phen)_3]I_2 \cdot 3H_2O \longrightarrow [Ni(phen)_3]I_2 \quad (1)$$

Acknowledgements—We would like to thank the SERC for collecting the data for this structure, and the Department of Chemistry, University of Bristol for use of computing facilities. R.D.G. wishes to acknowledge the tenure of an Erskine Visiting Professorship at the University of Canterbury.

REFERENCES

1. R. D. Gillard and S. H. Mitchell, *Polyhedron* 1988, **7**, 1175.
2. H. E. LeMay, in *Comprehensive Coordination Chemistry* (Edited by G. Wilkinson, R. D. Gillard and J. A. McCleverty), Vol. 1, p. 463. Pergamon Press, Oxford (1987).
3. P. O'Brien, *Polyhedron* 1983, **2**, 237.
4. T. Fujiwara, *Bull. Chem. Soc. Jpn* 1983, **56**, 122.
5. T. Fujiwara and Y. Yamamoto, *Inorg. Chem.* 1980, **19**, 1903.
6. B. Bosnich and D. W. Watts, *Inorg. Chem.* 1975, **14**, 47.
7. G. E. Humiston and J. E. Brady, *Inorg. Chem.* 1969, **8**, 1773.
8. E. D. McKenzie and R. A. Plowman, *J. Inorg. Nucl. Chem.* 1970, **32**, 199.
9. L. H. Berka, R. R. Gagne, G. A. Phillippan and C. E. Wheeler, *Inorg. Chem.* 1970, **9**, 2705.
10. E. Bielli, P. M. Gidney, R. D. Gillard and B. T. Heaton, *J. Chem. Soc., Dalton Trans.* 1974, 2133.
11. G. M. Sheldrick, SHELX76. A Program for Crystal Structure Determination. University of Cambridge (1976).
12. G. M. Sheldrick, SHELXTL version 4.0. An integrated system for solving, refining and displaying crystal structures from diffraction data. University of Göttingen (1983).
13. J. M. Stewart, P. A. Machin, C. W. Dickinson, H. L. Ammon, H. Heck and H. Flack, The X-RAY 76 System. Tech. Rep. TR-446. Computer Science Center, University of Maryland, College Park, Maryland, U.S.A. (1976).
14. C. K. Johnson, ORTEP Report, ORNL-3794 revised. Oak Ridge National Laboratory, Tennessee, U.S.A. (1971).
15. K. R. Dymock and G. J. Palenik, *Inorg. Chem.* 1975, **14**, 1220.
16. D. L. Kepert, *Inorg. Chem.* 1972, **11**, 1561.
17. B. A. Frenz and J. A. Ibers, *Inorg. Chem.* 1972, **11**, 1109.
18. K. R. Butler and M. R. Snow, *J. Chem. Soc. A* 1971, 565.
19. L. Pauling, *The Nature of the Chemical Bond and the Structure of Molecules and Crystals: An Introduction to Modern Structural Chemistry*. Cornell University Press, U.S.A. (1959).
20. G. Chiari and G. Ferraris, *Acta Cryst.* 1982, **B38**, 2331.
21. G. C. Pimentel and A. L. McClellan, *Ann. Rev. Phys. Chem.* 1971, **22**, 347.
22. R. D. Gillard and P. A. Williams, *Transition Met. Chem.* 1977, **2**, 14.
23. L. Johansson, M. Molund and A. Oskarsson, *Inorg. Chim. Acta* 1978, **31**, 117.
24. J. Baker, L. M. Engelhardt, B. N. Figgis and A. H. White, *J. Chem. Soc., Dalton Trans.* 1975, 530.
25. S. F. Mason, *Molecular Optical Activity and the Chiral Discriminations*. Cambridge University Press, U.K. (1982).
26. M. T. Garland and E. Spodine, *J. Cryst. Molec. Struct.* 1977, **7**, 207.
27. O. P. Anderson, *J. Chem. Soc., Dalton Trans.* 1973, 1237.
28. M. Shiro and Q. Fernando, *J. Chem. Soc., Chem. Commun.* 1971, 350.
29. B. Freckman and K.-F. Tebbe, *Acta Cryst.* 1981, **A37**, C-228, 09.4-15.
30. G. B. Deacon, C. L. Raston, D. Tunaley and A. H. White, *Aust. J. Chem.* 1979, **32**, 2195.
31. A. Zalkin, D. H. Templeton and T. Ueki, *Inorg. Chem.* 1973, **12**, 1641.

Polyhedron Vol. 8, No. 22, pp. 2657–2670, 1989
Printed in Great Britain

0277–5387/89 $3.00+.00
© 1989 Pergamon Press plc

t-BUTYLIMIDO COMPOUNDS OF RHENIUM. X-RAY CRYSTAL STRUCTURES OF $[(Bu^tN)_2Re(\mu\text{-}NBu^t)]_2$, $(Bu^tN)_2ReCl_3$, $(Bu^tN)_2ReCl_2C_6H_5$, $(Bu^tN)_3Re(OSiMe_3)$ AND $(Bu^tN)_3ReCl$*

ANDREAS A. DANOPOULOS, CINDY J. LONGLEY and GEOFFREY WILKINSON†

Johnson Matthey Laboratory, Chemistry Department, Imperial College, London SW7 2AY, U.K.

and

BILQUIS HUSSAIN and MICHAEL B. HURSTHOUSE†

Chemistry Department, Queen Mary College, London E1 4NS, U.K.

(*Received* 16 *May* 1989; *accepted* 7 *June* 1989)

Abstract—Previous studies on *t*-butylimido aryls of rhenium have been extended and the compounds $(Bu^tN)_2Re^{VII}(o\text{-tol})_3$, $(Bu^tN)_2Re^{VII}Cl_2Ph$ and $(Bu^tN)_2Re^{VI}(mes)_2$ synthesized. Electrochemical studies of the latter show reversible one-electron oxidation and reduction, and chemical oxidation leads to the cation $[(Bu^tN)_2Re^{VII}(mes)_2]^+$ isolated as PF_6^- and $CF_3SO_3^-$ salts. Although the neutral complex does not undergo insertion with isocyanides, the cation does so to give η^2-iminoacyls, $\{(Bu^tN)_2Re(mes)[\eta^2\text{-}RN{=}C(mes)]\}^+$, R = 2,6-xylyl, *t*-Bu. Reduction of $(Bu^tN)_3Re(OSiMe_3)$ in hexane by sodium gives the bridged homoleptic compound $(Bu^tN)_2Re(\mu\text{-}NBu^t)_2Re(NBu^t)_2$. The homoleptic anion $[Re(NBu^t)_4]^-$ as the $Li(tmed)^+$ complex has been synthesized via the new intermediates $(Bu^tN)_3ReCl$ and $(Bu^tN)_3Re(NHBu^t)$. X-ray crystal structures of the compounds listed in the title have been determined. The homoleptic rhenium(VI) *t*-butylimide is dimeric with four-coordinate rhenium and almost symmetrical imido bridges; the terminal imido groups have near linear geometry. The diamagnetism is consistent with a Re—Re bond, although the Re—Re distance of *ca* 2.7 Å indicates this to be weak. The rhenium(VII) siloxide is also four-coordinate distorted tetrahedral; and the geometries of the Re–imido and Re–siloxide units indicate involvement of all ligands in π-interactions. The $(Bu^tN)_3ReCl$ is also tetrahedral. The two bis-imido chloro compounds are five-coordinate with a geometry that can be conveniently described as trigonal bipyramidal where the imido groups occupy equatorial sites with unusually small inter-ligand angles of *ca* 110°.

This paper is concerned with the synthesis of *t*-butylimido compounds of rhenium, the X-ray crystal structures of four of the species and the synthesis of the first homoleptic *t*-butylimido compounds of rhenium and the crystal structure of one of them.

(1) *t*-BUTYLIMIDORHENIUM ARYL COMPOUNDS

We have previously described[1] the aryl compounds $(Bu^tN)_3ReAr$ and $(Bu^tN)_2ReCl_2Ar$, where Ar = *o*-tolyl, xylyl and mesityl. The crystal structure of $(Bu^tN)_2ReCl_2(o\text{-tol})$ showed the molecule to have square-pyramidal geometry with a bent imido group. In view of this and the use of NMR studies for assignment of structures of various rhenium

* Bis[(*t* - butylimido)(μ - *t* - butylimido)]dirhenium(VI) (Re—Re), bis(*t*-butylimido)trichlororhenium(VII), bis(*t*-butylimido)dichlorophenylrhenium(VII), tris(*t* - butylimido)(trimethylsilyloxo)rhenium(VII), tris(*t* - butylimido)chlororhenium(VII).

Abbreviations: tmed = tetramethylethylenediamine, *o*-tol = 2-MeC_6H_4; xylyl = 2,6-$Me_2C_6H_3$; mes = 2,4,6-$Me_3C_6H_2$.

† Authors to whom correspondence should be addressed.

imido alkyls and other compounds,[1,2] mostly as trigonal bipyramidal ones, two other representative five-coordinate structures have been determined, namely $(Bu^tN)_2ReCl_3$ and $(Bu^tN)_2ReCl_2Ph$, in the hope of aiding the NMR interpretations.

Bis(t-*butylimido*)*bis*(2,4,6-*trimethylphenyl*) *rhenium*(VI)

Although the interaction of $(Bu^tN)_2ReCl_3$ with Grignard reagents normally leads to trialkyl or aryl species, with mesityl magnesium bromide reduction occurs giving high yields (*ca* 70%) of the deep red paramagnetic rhenium(VI) compound, $(Bu^tN)_2Re(mes)_2$, which is the analogue of similar compounds, $(Bu^tN)_2M(mes)_2$ (M = Cr, Mo, W).[3] This reduction may result from the steric demand of the mesityl group; steric factors have been suggested for the formation of $(O)_2ReAr_2$ (Ar = *o*-xylyl and mesityl) from Re_2O_7, whereas *o*-tolyl or *o*-methoxophenyl Grignards give $(O)ReAr_4$.[4] Since $(O)Re(mes)_4$ can be made from $(O)ReCl_4$ it is possible that $(Bu^tN)_2Re(mes)_3$ may be prepared via a different route.

The rhenium(VI) compound slowly decomposes in air, both in the solid state and in solution. The mass spectrum shows the parent ions and subsequent loss of one mesityl group. The electron spin resonance spectrum at 295 K in toluene (*X*-band) shows a six-line hyperfine structure ($g_{iso} = 1.966$, $A_{iso} = 0.0133\ cm^{-1}$). On lowering the temperature, a complicated pattern appeared showing, at 78 K, more than two sets of six rhenium hyperfine lines with uneven spacing (cf. the ESR spectrum of $(O)_2ReAr_2$[1,4]); this might result from restriction of rotation about Re—C bonds.

Cyclic voltammetry study of $(Bu^tN)_2Re(mes)_2$ in 0.2 M $(Bu^n_4N)PF_6$ in THF at 22°C shows a reversible one-electron oxidation wave at −0.51 V and a reversible one-electron reduction wave at −1.80 V relative to Cp_2Fe at 0.00 V. Chemical oxidation using Cp_2FePF_6, AgO_3SCF_3 or $AgPF_6$ leads to orange–red diamagnetic crystalline salts of the $[(Bu^tN)_2Re(mes)_2]^+$ ion; these are stable in air but slowly decompose in solution in THF, acetone, CH_2Cl_2 and MeCN. The ^1H NMR spectrum shows equivalent *t*-butyl and mesityl groups with free rotation about the Re—C bond at room temperature (cf. ref. 4).

So far the anionic rhenium(V) species, $[(Bu^tN)_2Re(mes)_2]^-$, has not been isolated; the rhenium(VI) species is not reduced in THF by Cp_2Co. However, the corresponding rhenium(V) oxo aryl anions, $[(O)_2ReAr_2]^-$ (Ar = xylyl, mes), have been obtained,[1,4] as has the neopentyl,[5] $[(O)_2Re(CH_2CMe_3)_2]^-$. The latter anion is oxidized to $Re_2(O)_2(\mu\text{-}O)_2(CH_2CMe_3)_4$, from which it is formed on reduction. The bridged oxo-species is presumably formed initially rather than $(O)_2Re(CH_2CMe_3)_2$ because of the lower steric hindrance compared to the *t*-butylimido and/or aryl groups of $(Bu^tN)_2Re(mes)_2$. Cyclic voltammetry on the oxo-bridged dimer gives an ill-defined oxidation wave indicating that chemical oxidation to $[(O)_2Re(CH_2CMe_3)_2]^+$ is probably not feasible.[5] These differences in redox behaviour of the oxo versus imido systems may be due to differences in ligand electronegativity and π-donating capability.

Although $('BuN)_2Re(mes)_2$, unlike its chromium, molybdenum and tungsten analogues,[3] does not react with isocyanides, the cation, which is isoelectronic with these analogues, does so rapidly at room temperature [eq. (1)] similarly

$$[(Bu^tN)_2Re(mes)_2]^+ + RNC \longrightarrow \{(Bu^tN)_2Re(mes)[\eta^2\text{-}RN{=}C(mes)]\}^+ \quad (1)$$

giving only the mono-insertion product with 2,6-xylyl and *t*-butyl isocyanides even in presence of excess isocyanide. The pale yellow crystalline materials are stable in air. The ^1H NMR spectra show two sets of resonances for the mesityl groups, but there is free rotation about the Re—C bond at room temperature (cf. ref. 4). For the 2,6-xylyl isocyanide product the *ortho*-methyl resonances on the xylyl ring attached to nitrogen occur at the highest field (δ 1.82 ppm). The resonances for the mesityl group which remains attached to rhenium have changed relative to the starting complex, such that the *ortho*-methyl resonances fall at higher field than the *para*-methyl resonance.

The IR and NMR spectroscopic data are similar to those of the chromium, molybdenum and tungsten compounds[3] and are consistent with η^2-coordination of the iminoacyl group, which was confirmed for $(Bu^tN)_2Cr(mes)[(mes)C{=}NBu^t]$ by X-ray crystallography.

Bis(t-*butylimido*)*tris*(2-*methylphenyl*)*rhenium*(VII)

This compound arises from the interaction of the Grignard reagent with $(Bu^tN)_2ReCl_3$ and forms air-sensitive orange crystals. The ^1H NMR spectrum has two *o*-tolyl group resonances in a 2:1 ratio suggesting a *tbp* structure with equatorial imido ligands.

(2) X-RAY STUDIES

As noted earlier, Schrock *et al.*[2] have widely used NMR for characterization of rhenium imido species, generally concluding trigonal bipyramidal

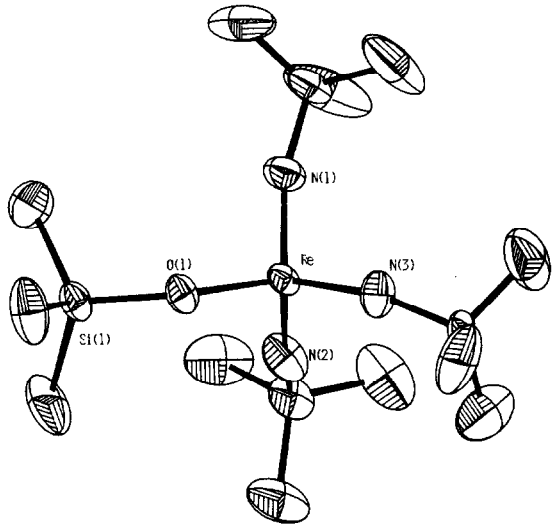

Fig. 1. The structure of $(Bu^tN)_3Re(OSiMe_3)$.

structures. Comparable oxo alkyls $Re(O)_2R_3$ (Re = Me,[6a] CH_2SiMe_3[6b]) appear to be *tbp* from spectroscopic data, while $Re(O)_2(CH_2CMe_3)$[6c] is distorted *tbp* with α-CH···O interactions from X-ray data.

$(Bu^tN)_3Re(OSiMe_3)$

The molecule has a distorted tetrahedral geometry about the rhenium atom, as shown in Fig. 1. Selected bond lengths and angles are given in Table 1. The angles at silicon are also approximately tetrahedral, with an average Si—C bond length of 1.8 Å.

The Re—N—C bonds are slightly bent (157–165°) and, as expected, the most bent imido group has the longest Re—N bond length.

With the possibility of the imido ligands acting as 4e donors, Re≡NR and the siloxo group making available up to 5e, Re≡OSiR$_3$, the metal has access to 24e. On the basis of the angles at the nitrogens, 157–165°, and at oxygen, 137°, all ligands seem to be participating in π-bonding to some extent. Not surprisingly however, the siloxide, for which the Re—O bond of 1.90 Å is only slightly shorter than a normal single bond, would seem to contribute least. It is pertinent to compare this structure with that of the analogous oxo-complex $O_3Re(OSiMe_3)$,[7] where the Re—O—Si angle is larger (167°) than in the present complex and the Re—O bond much shorter. More significantly, steric crowd-

Table 1. Selected bond lengths and angles for $(Bu^tN)_3Re(OSiMe_3)$

Bond lengths (Å)			
O(1)—Re(1)	1.899(7)	N(1)—Re(1)	1.706(9)
N(2)—Re(1)	1.704(11)	N(3)—Re(1)	1.740(10)
O(1)—Si(1)	1.624(8)	C(1)—Si(1)	1.852(16)
C(2)—Si(1)	1.898(17)	C(3)—Si(1)	1.787(16)
C(4)—N(1)	1.437(12)	C(8)—N(2)	1.469(13)
C(12)—N(3)	1.430(12)	C(5)—C(4)	1.448(22)
C(6)—C(4)	1.475(21)	C(7)—C(4)	1.414(20)
C(9)—C(8)	1.552(19)	C(10)—C(8)	1.531(24)
C(11)—C(8)	1.550(22)	C(13)—C(12)	1.465(21)
C(14)—C(12)	1.469(20)	C(15)—C(12)	1.536(20)
Bond angles (°)			
N(1)—Re(1)—O(1)	109.7(4)	N(2)—Re(1)—O(1)	110.4(5)
N(2)—Re(1)—N(1)	111.1(6)	N(3)—Re(1)—O(1)	108.0(4)
N(3)—Re(1)—N(1)	109.0(6)	N(3)—Re(1)—N(2)	108.7(6)
C(1)—Si(1)—O(1)	105.7(6)	C(2)—Si(1)—O(1)	109.4(6)
C(2)—Si(1)—C(1)	111.0(10)	C(3)—Si(1)—O(1)	111.2(7)
C(3)—Si(1)—C(1)	110.7(10)	C(3)—Si(1)—C(2)	108.8(11)
Si(1)—O(1)—Re(1)	138.2(4)	C(4)—N(1)—Re(1)	164.8(8)
C(8)—N(2)—Re(1)	160.6(9)	C(12)—N(3)—Re(1)	157.7(8)
C(5)—C(4)—N(1)	107.1(12)	C(6)—C(4)—N(1)	108.1(11)
C(6)—C(4)—C(5)	106.8(18)	C(7)—C(4)—N(1)	109.0(11)
C(7)—C(4)—C(5)	111.8(20)	C(7)—C(4)—C(6)	113.8(18)
C(9)—C(8)—N(2)	106.6(10)	C(10)—C(8)—N(2)	110.4(12)
C(10)—C(8)—C(9)	110.2(13)	C(11)—C(8)—N(2)	107.2(11)
C(11)—C(8)—C(9)	110.8(13)	C(11)—C(8)—C(10)	111.5(15)
C(13)—C(12)—N(3)	105.8(11)	C(14)—C(12)—N(3)	110.9(9)
C(14)—C(12)—C(13)	115.1(16)	C(15)—C(12)—N(3)	110.4(10)
C(15)—C(12)—C(13)	108.8(18)	C(15)—C(12)—C(14)	106.0(15)

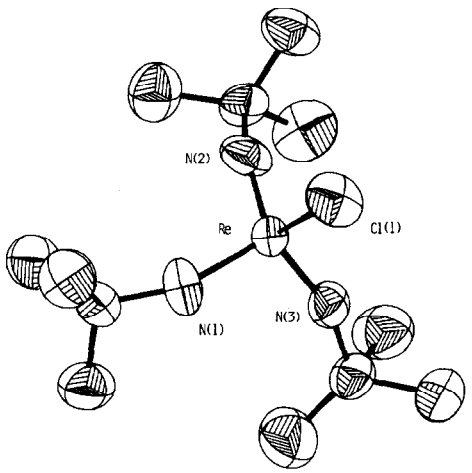

Fig. 2. The structure of $(Bu^tN)_3ReCl$.

ing in the *t*-butyl imido complex would be expected to favour a larger Re—O—Si angle, especially as metal–trimethylsiloxo links seem to be quite flexible.

$(Bu^tN)_3ReCl$

A diagram of the molecule is given in Fig. 2, bond lengths and angles in Table 2. The geometry is slightly distorted tetrahedral with small variations in Re—N distances and Re—N—C angles (see Table 2). This again is consistent with an "averaging" process between the three potentially 4e donor imido ligands in providing an 18e count for the rhenium atom.

$(Bu^tN)_2ReCl_3$

A diagram of the molecule is given in Fig. 3, with selected bond lengths and angles in Table 3. The structure of the complex is simply and logically described as a slightly distorted trigonal bipyramid with equatorial imido groups. The two axial chloride ligands are bent towards the equatorial plane, [Cl(3)—Re—Cl(2) = 165°], in the direction of the equatorial chloride ligand.

The distribution of the angles in the equatorial plane is interesting. The N—M—N angle is smaller than both N—M—Cl angles (111° vs 128 and 121°). This contrasts with most structures containing two neighbouring multiply-bonded functions where repulsion between the π-electron clouds in the two bonds causes an increase in the interbond angle from idealized values.[4] A second, surprising feature of the structure is the equivalence, within experimental error, of all Re—Cl bond lengths, whether axial or equatorial.

The imido ligands both contain "linear" M—N—R linkages (163 and 170°); the Re—N bond distances are in accord with these angles (1.71 and 1.68 Å, respectively). As such, both imido ligands are assumed to behave as 4e donors, and the formal electron count for rhenium is 18.

Table 2. Selected bond lengths and angles for $(Bu^tN)_3ReCl$

Bond lengths (Å)			
Cl(1)—Re(1)	2.301(4)	N(1)—Re(1)	1.750(15)
N(2)—Re(1)	1.683(14)	N(3)—Re(1)	1.719(11)
C(1)—N(1)	1.476(16)	C(2)—N(2)	1.440(16)
C(3)—N(3)	1.434(14)	C(12)—C(1)	1.541(19)
C(22)—C(2)	1.516(18)	C(21)—C(2)	1.508(19)
C(23)—C(2)	1.511(17)	C(31)—C(3)	1.528(19)
C(32)—C(3)	1.524(18)	C(33)—C(3)	1.536(15)
Bond angles (°)			
N(1)—Re(1)—Cl(1)	104.1(8)	N(2)—Re(1)—Cl(1)	111.5(7)
N(2)—Re(1)—N(1)	111.9(10)	N(3)—Re(1)—Cl(1)	109.7(5)
N(3)—Re(1)—N(1)	109.0(9)	N(3)—Re(1)—N(2)	110.5(9)
C(1)—N(1)—Re(1)	157.5(16)	C(2)—N(2)—Re(1)	159.1(16)
C(3)—N(3)—Re(1)	160.3(14)	C(12)—C(1)—N(1)	103.8(18)
C(22)—C(2)—N(2)	112.5(19)	C(21)—C(2)—N(2)	108.6(18)
C(21)—C(2)—C(22)	93.0(19)	C(23)—C(2)—N(2)	93.6(16)
C(23)—C(2)—C(22)	135.8(19)	C(23)—C(2)—C(21)	112.4(19)
C(31)—C(3)—N(3)	93.4(17)	C(32)—C(3)—N(3)	120.7(15)
C(32)—C(3)—C(31)	107.7(16)	C(33)—C(3)—N(3)	108.4(13)
C(33)—C(3)—C(31)	94.3(18)	C(33)—C(3)—C(32)	123.7(16)

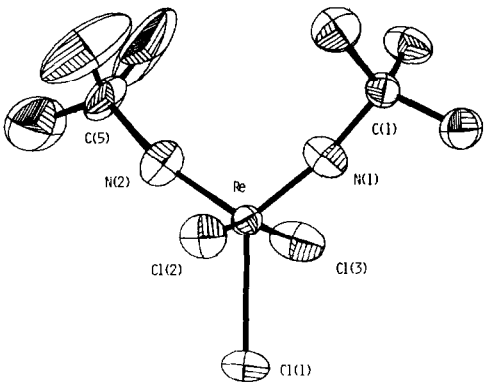

Fig. 3. The structure of $(Bu^tN)_2ReCl_3$.

$(Bu^tN)_2ReCl_2Ph$

The molecular structure is shown in Fig. 4 and selected bond lengths and angles are listed in Table 4. In this case the molecular geometry may also be described as a distorted trigonal bipyramid with the imido groups occupying equatorial positions and the phenyl ring in an axial position. In fact the structure is very similar to that of $(Bu^tN)_2ReCl_3$ above. The axial chloride and phenyl ligands are tilted slightly towards the equatorial chloride [Cl(1)—Re—C(1) = 158°], Cl(2)—Re—Cl′(2). The N—Re—N angle at 110° is similar to that in $(Bu^tN)_2ReCl_3$ and the slight bending of the imido groups (161°, 173°) parallels the geometry of the trichloride. However, the actual distribution of angles within the equatorial plane is different.

Whilst the N—Re—N angle is similar in the two structures, the close similarity between Cl—Re—N angles in the trichloride is lost in the phenyl where these two angles are now very different, at 115.5 and 134.1°. Indeed, notwithstanding the bend of the *tbp* axial Re—Cl(1) and Re—C(1) bonds *towards* Cl(2), the structure could be described as tending to tetragonal pyramid, in which the imido ligand which N(1) occupies the *tp* axial site. This ligand shows the most bending of the two present, albeit slight, and it is interesting to note that it is exactly this ligand which shows even more bending in the more recognizable *tp* structure of $(Bu^tN)_2ReCl_2$(*o*-tol).[1] The structural relationship now established for the three compounds $(Bu^tN)_2ReCl_3$, the mono phenyl and the mono *o*-tolyl has suggested a detailed theoretical investigation, which will be discussed separately.

(3) HOMOLEPTIC *t*-BUTYLIMIDO COMPOUNDS

The compounds $Li_2W(NBu^t)_4$ and Li(tmed) $Re(NBu^t)_4$ have been briefly reported;[8] these and the rhenium(VI) species now reported are the first homoleptic imido compounds of transition metals.

Table 3. Selected bond lengths and angles for $(Bu^tN)_2ReCl_3$

Bond lengths (Å)			
Cl(2)—Re	2.348(5)	Cl(3)—Re	2.347(5)
N(1)—Re	1.680(12)	N(2)—Re	1.706(13)
C(1)—N(1)	1.455(15)	C(5)—N(2)	1.449(17)
C(2)—C(1)	1.537(19)	C(3)—C(1)	1.526(19)
C(4)—C(1)	1.550(18)	C(6)—C(5)	1.387(35)
C(7)—C(5)	1.432(29)	C(8)—C(5)	1.374(29)
Bond angles (°)			
Cl(2)—Re—Cl(1)	82.7(2)	Cl(3)—Re—Cl(1)	83.0(2)
Cl(3)—Re—Cl(2)	165.4(1)	N(1)—Re—Cl(1)	127.8(5)
N(1)—Re—Cl(2)	91.9(4)	N(1)—Re—Cl(3)	94.4(4)
N(2)—Re—Cl(1)	121.4(5)	N(2)—Re—Cl(2)	94.5(4)
N(2)—Re—Cl(3)	95.5(4)	N(2)—Re—N(1)	110.7(7)
C(1)—N(1)—Re	169.5(9)	C(5)—N(2)—Re	163.4(12)
C(2)—C(1)—N(1)	107.5(11)	C(3)—C(1)—N(1)	107.4(11)
C(3)—C(1)—C(2)	113.0(13)	C(4)—C(1)—N(1)	109.1(11)
C(4)—C(1)—C(2)	109.6(13)	C(4)—C(1)—C(3)	110.0(11)
C(6)—C(5)—N(2)	108.3(16)	C(7)—C(5)—N(2)	107.8(17)
C(7)—C(5)—C(6)	112.8(31)	C(8)—C(5)—N(2)	111.6(18)
C(8)—C(5)—C(6)	107.7(26)	C(8)—C(5)—C(7)	108.7(27)

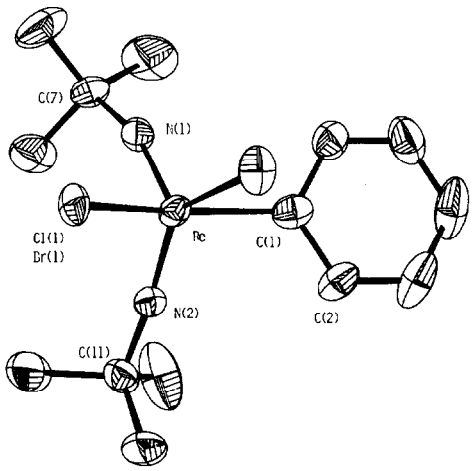

Fig. 4. The structure of $(Bu^tN)_2ReCl_2Ph$.

(a) *Bis[di(*t*-butylimido)(μ-*t*-butylimido)rhenium*(VI)]

The interaction of $(Bu^tN)_3Re(OSiMe_3)$ with an excess of Na (or Na/Hg) in hexane leads to yellow diamagnetic crystals of the title compound that slowly decompose in air. The mass spectrum of the compound shows the parent ion (*m/z* 798) and additional peaks with the intensity pattern expected from rhenium isotopic abundances. The ^1H NMR spectrum shows separate resonances for the *t*-butyl group in a 2 : 1 ratio, that are assigned, respectively, to terminal (δ 1.27) and bridging (δ 1.82) groups.

X-ray structure analysis has confirmed the dimeric nature of the molecule. Although considerable disorder occurs in all *t*-butyl group orientations, leading to difficulties in defining the correct space group and reducing the overall precision of the structure determination (see Experimental), the structure and geometry of the core is well defined. A diagram of one of the molecules is shown in Fig. 5 and a summary of the more reliable bond lengths and angles are given in Table 5.

The dimer comprises two tetrahedral rhenium(VI) atoms with bonds to two terminal and two bridging imido nitrogens (**1**). The bridges are symmetrical and the $(CN)_2Re(\mu\text{-}NC)_2Re(NC)_2$ core has approximate *mmm*($D2_h$) symmetry. As might be expected, the Re—N (terminal) distances

Table 4. Selected bond lengths and angles for $(Bu^tN)_2ReCl_{1.5}Br_{0.5}Ph$

Bond lengths (Å)			
Cl(1)—Re	2.382(17)	Br(1)—Re	2.532(10)
Cl(2)—Re	2.414(4)	N(1)—Re	1.688(9)
N(2)—Re	1.699(8)	C(1)—Re	2.125(12)
C(7)—N(1)	1.478(11)	C(11)—N(2)	1.468(11)
C(2)—C(1)	1.379(13)	C(6)—C(1)	1.406(13)
C(3)—C(2)	1.384(15)	C(4)—C(3)	1.375(17)
C(5)—C(4)	1.344(17)	C(6)—C(5)	1.339(15)
C(8)—C(7)	1.509(16)	C(9)—C(7)	1.516(15)
C(10)—C(7)	1.544(14)	C(12)—C(11)	1.530(18)
C(13)—C(11)	1.510(16)	C(14)—C(11)	1.490(15)
Bond angles (°)			
Cl(2)—Re—Cl(1)	79.6(5)	Cl(2)—Re—Br(1)	82.1(3)
N(1)—Re—Cl(1)	96.6(5)	N(1)—Re—Br(1)	102.5(4)
N(1)—Re—Cl(2)	115.8(3)	N(2)—Re—Cl(1)	99.3(4)
N(2)—Re—Br(1)	92.0(4)	N(2)—Re—Cl(2)	134.0(2)
N(2)—Re—N(1)	110.1(4)	C(1)—Re—Cl(1)	157.7(4)
C(1)—Re—Br(1)	157.3(3)	C(1)—Re—Cl(2)	78.5(3)
C(1)—Re—N(1)	96.6(4)	C(1)—Re—N(2)	92.9(4)
C(7)—N(1)—Re	159.9(6)	C(11)—N(2)—Re	173.6(6)
C(2)—C(1)—Re	121.5(8)	C(6)—C(1)—Re	122.0(7)
C(6)—C(1)—C(2)	116.3(10)	C(3)—C(2)—C(1)	121.1(11)
C(4)—C(3)—C(2)	120.3(11)	C(5)—C(4)—C(3)	118.7(10)
C(6)—C(5)—C(4)	122.1(12)	C(5)—C(6)—C(1)	121.5(11)
C(8)—C(7)—N(1)	107.6(9)	C(9)—C(7)—N(1)	107.3(8)
C(9)—C(7)—C(8)	111.9(9)	C(10)—C(7)—N(1)	108.8(8)
C(10)—C(7)—C(8)	111.0(9)	C(10)—C(7)—C(9)	110.1(9)
C(12)—C(11)—N(2)	107.1(10)	C(13)—C(11)—N(2)	109.0(9)
C(13)—C(11)—C(12)	107.9(11)	C(14)—C(11)—N(2)	106.0(9)
C(14)—C(11)—C(12)	113.8(13)	C(14)—C(11)—C(13)	112.8(12)

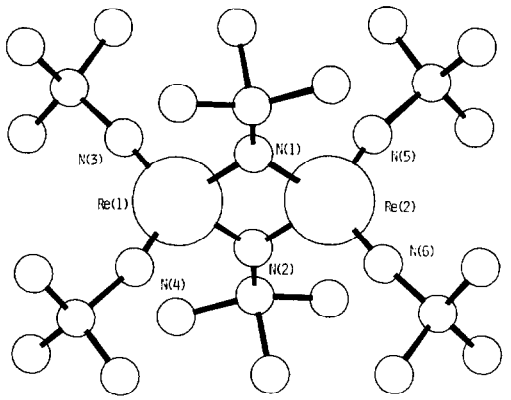

Fig. 5. The structure of $(Bu^tN)_2Re(\mu\text{-}Bu^tN)_2Re(NBu^t)_2$.

are shorter than the Re—N (bridging) distances, and, this, together with the near linearity of the terminal Re—N—C unit, is consistent with a 4e bonding mode for the ^{t}BuN group.

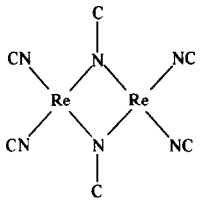

(1)

The Re(1)—N(3)—Re(1′) angle is 88° and the N(3)—Re(1)—N(3′) angle is 92°. Generally M—N—M angles in the range 78–84° occur when there is a metal–metal bond, and angles > 94° indicate no metal–metal interaction. The Re(1)···Re(1′) distance in this compound is 2.7 Å —this along with the intermediate M—N—M angle in the bridge suggests a weak Re—Re interaction. Rhenium–rhenium single bonds have been proposed in the binuclear d^1–d^1, rhenium(VI) oxo-bridged species $[Me_2(O)Re(\mu\text{-}O)]_2$,[9a] $[(Me_3CH_2)_2(O)Re(\mu\text{-}O)]_2$[5] and $[PhMe_2CCH_2)_2(O)Re(\mu\text{-}O)]_2$,[9b] where the Re—Re distances are 2.593(1), 2.606(1) and 2.6116(7) Å, respectively.

It may be noted that complexes containing both terminal and symmetrical bridging imido ligands are known for several other elements.[10] The crystal structure of $[(Bu^tN)_2MoMe_2]_2$ shows two terminal and two unsymmetrical imido ligands, although the reported ^{1}H NMR data indicate only one t-butyl group resonance for both this compound and its tungsten analogue.[11]

It may also be noted that the formal oxo analogue of $Re_2(NBu^t)_6$, i.e. $(ReO_3)_n$, has a structure closely related to the perovskite structure.[12]

(b) *Tetramethylethylenediaminelithiumtetra*(t-*butylimido*)*rhenate*(VII)

This compound was prepared via the route:

$$(Bu^tN)_3Re(OSiMe_3) \rightarrow (Bu^tN)_3ReCl \rightarrow (Bu^tN)_3Re(NHBu^t) \rightarrow Li(tmed)Re(NBu^t)_4.$$

The chlorination of $(Bu^tN)_3Re(OSiMe_3)$ by $PhICl_2$ in toluene at room temperature gives high yields of $(Bu^tN)_3ReCl$ on a multigram scale when the liquid product can readily be purified by fractional distillation. The compound is very soluble in hexane from which it can be crystallized at low temperature, though in somewhat low yields due to the high solubility. Chlorination by other reagents leads to mixtures which are difficult to separate (Cl_2, Me_3SiCl or Me_3SiI) or to $(Bu^tN)_2ReCl_3$[2b] ($SOCl_2$, PCl_3). In the reaction with $PhICl_2$, the silicon-containing residue (not identified) is insoluble in hexane. The $(Bu^tN)_3ReCl$ is extremely sensitive to moisture; it is miscible with organic solvents such as hydrocarbons, THF, CH_2Cl_2, etc. The ^{1}H NMR spectrum is similar to that for $(Bu^tN)_3Re(OSiMe_3)$,[13] δ 1.28 vs δ 1.36, respectively, while the difference between the ^{13}C chemical shifts of the α- and β-imido carbons, which has been suggested[14] as indicative of the electron density on the imido nitrogen atom, $\Delta = 37.8$, is also comparable to that

Table 5. Selected bond lengths and angles for $(Bu^tN)_6Re_2$

	Bond lengths (Å)	
Re—N(terminal),	range 1.69(3)–1.78(2),	Average 1.74
Re—N(bridge),	range 1.85(3)–1.94(2),	Average 1.91
Bond angles (°)		
M(terminal)—Re—N(terminal),	range 110(1)–112(1)	
Re—N(bridge)—Re,	range 88.4(7)—88.9(7)	
N(bridge)—Re—N(bridge),	range 91.1(8)—91.6(8)	

for (^{t}BuN)$_3$Re(OSiMe$_3$) ($\Delta = 35$). The slight difference suggests that electron donation by the ^{t}BuN group to the metal is increased, probably due to increased electron withdrawal by Cl compared to OSiMe$_3$.

The synthesis of (Bu^{t}N)$_3$Re(NHBu^t) by interaction of the chloride with LiNHBu^t gives good yields if the reagents in diethyl ether are slowly mixed at low temperature and the mixture allowed to warm slowly. A side product can be isolated by fractional crystallization but has not yet been characterized. The amide is a low melting, moisture sensitive, yellow crystalline solid with a characteristic N—H stretch in the IR at 3366 cm^{-1}. The ^{13}C-{^{1}H} spectrum shows that Δ for the α- and β-imido carbons is 35.3 ppm, suggesting that OSiMe$_3$ and NHBu^t are electronically similar ligands.

The deprotonation of the amide by MeLi in diethyl ether initially gives a product that slowly precipitates from the solution at room temperature as a yellowish solid, evidently polymeric LiRe(NBu^t)$_4$. This is insoluble in ether, hexane or toluene but slowly dissolves in THF, which is then easily displaced by Me$_2$N(CH$_2$)$_2$NMe$_2$ to give the hexane soluble Li(tmed)Re(NBu^t)$_4$ finally isolated. The reactions may be as shown in the eq. (2) (Bu^t groups omitted):

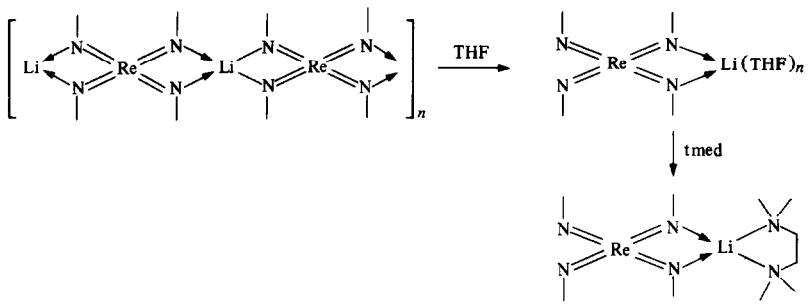

(2)

Neither the THF solution, not the THF solution of the tmed compound are electrically conducting and there is evidently no ionization in either case.

The compound Li(tmed)Re(NBu^t)$_4$ forms orange prisms that are extremely sensitive to moisture and decompose at relatively low temperatures. The X-ray crystal structure has been reported.[8] Although an 18-electron count for rhenium in the Re(NBu^t)$_4^-$ unit would be expected to lead to one bent and three linear (4e) imido ligands, in fact all four groups are non-linear, presumably because of averaging over the two terminal ligands and the two which bridge to the Li(tmed)$^+$.

The ^{1}H NMR spectrum of a solution of the complex in d^8-toluene containing THF or a slight excess of tmed (to inhibit polymerization and precipitation of the polymer at room temperature) shows a single peak at δ 1.44 ppm assignable to the *t*-butylimido group protons and two peaks due to the CH$_3$ and CH$_2$ protons of tmed at δ 1.92 and 1.76 ppm, respectively [Fig. 6(a)]. On lowering the temperature the Bu^t line starts to broaden at -30°C, and at -50°C splits into two peaks of equal intensity [Fig. 6(b)] that correspond to the two sets of non-equivalent Bu^t groups, i.e. terminal and bridging to Li$^+$ as in the solid structure.[8] At still lower temperatures (-70°C) the CH$_2$ protons of tmed started broadening, although the process responsible for this cannot be frozen out as low solubility limits the cooling.

For the exchange of the Bu^{t}N groups, using the formula[15] $\Delta G^\ddagger = \alpha T\,[10.319 + \log(T/k)]$, $\alpha = 1.914 \times 10^{-2}$, the $\Delta G^\ddagger$ value at the coalescence temperature (-40°C) is calculated to be 49.9 kJ mol^{-1} with $k = 29.7$ s^{-1}. The process is evidently intramolecular involving breaking a Li—NBu^t bond followed by rotation about the other Li—NBu^t bond and then coordination of one of the terminal NBu^t groups on rhenium.[16] Intermolecular exchange is unlikely in view of the negligible dissociation of the complex in polar solvents; association of two molecules without dissociation would require a highly hindered transition state with penta-coordination of rhenium(VII).

The second dynamic process at lower temperatures clearly involves the CH$_2$ groups and conformation changes of the puckered tmed chelate ring (see further comment below).

The ^{13}C NMR spectrum of the complex at room temperature (fast exchange limit) gives the α- and β-carbons of the *t*-butylimido group at δ 57.63 and 32.00 ppm, respectively, giving a difference, $\Delta = 25.6$ ppm, indicative of a nucleophilic imido nitrogen.[14] Although this value is qualitative, it suggests that electron donation from the imido nitrogen to the metal is reduced in comparison to Re(NBu^t)$_3$(NHBu^t) above, due to the presence of the fourth electron releasing imido group.

The structure of Li(tmed)Re(NBu^t)$_4$ at the low temperature exchange limit can be assumed to be that in the solid state[8] where the five-membered Li(tmed) ring is non-planar with a two-fold axis

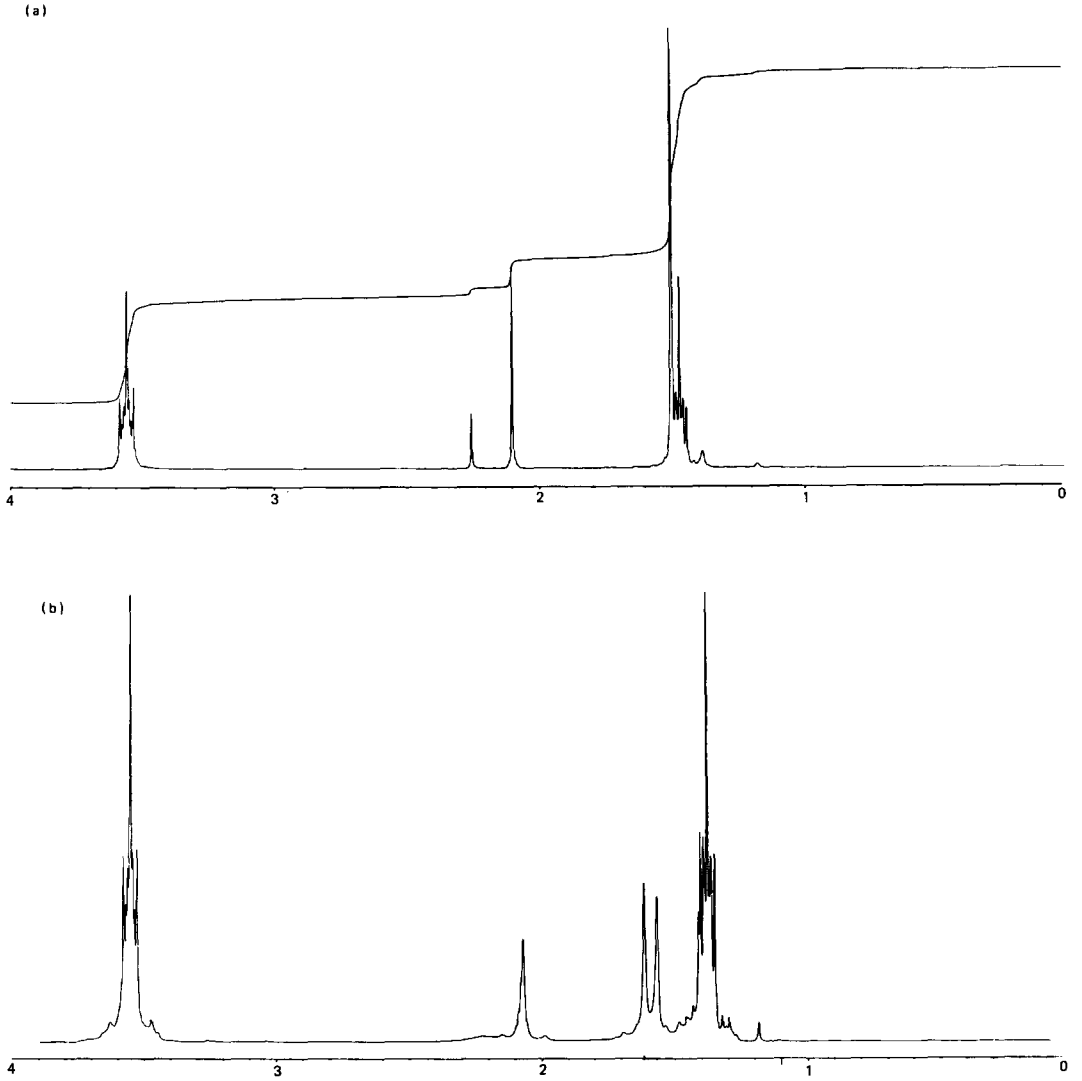

Fig. 6. NMR spectra of Li(tmed)Re(NBu^t)$_4$ (a) 25°C, (b) −60°C in d^8-toluene with additional THF.

of symmetry passing through the lithium and the midpoint of the C—C bond. This results in the methyl substituents on each nitrogen atom being distinguishable as pseudo axial and equatorial (2).

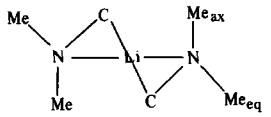

(2)

The differences in their environment is clearly indicated by the torsion angles Me—N—C—C which are 73–75° for the "axial" and 12° for the equatorial substituents. Although, as noted above the exchange limit for the CH_2 groups could not be reached, nor could non-equivalence of the CH_3 groups be observed in the NMR. For extensive studies on conformation of chelate diamine rings see ref. 17.

EXPERIMENTAL

Microanalyses were by Pascher, Remagen and Imperial College Microanalytical Laboratories. Melting points were determined in sealed tubes and are uncorrected.

Spectrometers: IR, Perkin–Elmer 683 and 1720 (in Nujol mulls, values in cm^{-1}); NMR, Bruker WM-250, JEOL FX 90Q, JEOL GSX 270 (δ values in ppm relative to $SiMe_4$); ESR, Varian E12 (X-band in toluene, 22°C); mass, VG Micromass 7070 and MS-9, Kratos MS902. Magnetic moments by Evans' method in toluene.

All manipulations were carried out under purified

argon, dinitrogen or under vacuum. Solvents were dried by standard methods and degassed prior to use.

Cyclic voltammetry: OE-PP2 instrument in 0.2 M $^{n}BuNPF_6$ in THF at 22°C with platinum working, tungsten auxiliary and silver pseudo-reference electrodes. Under these conditions, Cp_2Fe was oxidized at 0.46 V with $\Delta E_p = 110$ mV. This rather high value (theoretical = 59 mV) is presumably due to uncompensated resistance in solution.[18]

$O_3Re(OSiMe_3)$,[19] $(Bu^tN)_3Re(OSiMe_3)$[13] and $(Bu^tN)_2ReCl_3$[2b] were prepared according to the literature. The last two were recrystallized from hexamethyldisiloxane and diethyl ether, respectively, to give crystals suitable for X-ray diffraction study.

(1) *Di*(t-*butylimido*)*di*(2,4,6-*trimethylphenyl*)*rhenium* (VI)

A solution of $(Bu^tN)_2ReCl_3$ (0.41 g, 0.94 mmol) in ether (30 cm^3) was cooled to −20°C. Mesitylmagnesium bromide (2.8 cm^3 of a 1.0 M solution in THF, 2.8 mmol) was added and the orange solution became instantly deep red. The solution was warmed to room temperature and stirred for 12 h, then filtered and the residue washed with ether (2 × 5 cm^3). The solvent was removed under reduced pressure and the material was extracted with hexane (20 cm^3), filtered and the volume reduced (10 cm^3). After another filtration large deep red crystals were obtained on cooling the hexane solution (−10°C). Yield 0.38 g, 71%; m.p. 128°C. Found: C, 55.0; H, 7.1; N, 5.0. Calc.: C, 55.1; H, 7.1; N, 4.9%. Mass spectrum: *m/z* 567 (100%), 565 (71%), $Re(NBu^t)_2(C_9H_{11})_2^+$; 511 (19%), 509 (9%), $(P-Bu^t)^+$; 447 (21%), 445 (11%), $(P-C_9H_{11})^+$; 119 (8%), $C_9H_{11}^+$. IR: 1591m, 1357s, 1279w, 1258s, 1235w, 1210s, 1153m, 1028br, 913br, 847s, 806m, 705m, 593w, 541w.

(2) *Di*(t - *butylimido*)*di*(2,4,6 - *trimethylphenyl*)*rhenium*(VII) *salts*

Hexafluorophosphate. Method A: to a stirred solution of $(Bu^tN)_2Re(mes)_2$ (0.5 g, 0.88 mmol) in THF (20 cm^3) was added Cp_2FePF_6 (0.29 g, 0.88 mmol). The deep red solution became bright orange and was stirred for 1 h. The solvent was removed under vacuum and the residue washed with hexane (2 × 5 cm^3) (to remove Cp_2Fe). The remaining orange powder was recrystallized from THF–ether to give bright red–orange crystals of the hexafluorophosphate. Yield 0.6 g, 95%; m.p. 158° dec. Found: C, 43.6; H, 5.7; N, 3.9. Calc.: C, 43.9; H, 5.6; N, 3.9%.

Method B: to a stirred solution of $(Bu^tN)_2Re(mes)_2$ (0.3 g, 0.53 mmol) in THF (20 cm^3) was added $AgPF_6$ (0.31 g, 0.53 mmol). The solution was stirred for 1 h, filtered (from Ag), the volume reduced (5 cm^3) and a few drops of ether added to induce crystallization of the hexafluorophosphate. Yield 0.35 g, 95%. Mass spectrum (FAB): *m/z* 567 (90%), $^{187}P^+$; 565 (53%), $^{185}P^+$; 511 (4%), $[^{185}P\text{-}C_9H_{11}]^+$. IR: 3123w, 1591s, 1366s, 1280s, 1229s, 1214m, 1179s, 1160m, 1140m, 1070w, 1032(br), 1002m, 955w, 901m, 876s, 839br, 804m, 701m, 589m, 558s, 474w, 374w, 349w. NMR: ^1H $(CD_3)_2CO$: 7.32 (4H, s, *m*-H_2—C_6); 2.54 (12H, s, *o*-CH_3); 2.38 (6H, s, *p*-CH_3); 1.86 (18H, s, CCH_3).

Trifluoromethane sulphonate. To a solution of $(Bu^tN)_2Re(mes)_2$ (0.1 g, 0.18 mmol) in THF (10 cm^3) was added AgO_3SCF_3 (0.05 g, 0.19 mmol). The deep red solution became bright orange and was stirred for 1 h, the solvent was removed under vacuum and the residue washed with hexane (2 × 5 cm^3). The orange powder was recrystallized from THF–ether to give bright orange–red crystals of the salt. Yield 0.1 g, 85%. The spectroscopic properties were similar to hexafluorophosphate except for the anion bands in the IR.

(3) *Interaction of* $[(Bu^tN)_2Re(mes)_2]^+$ *salts and isocyanides*

(a) $\{(Bu^tN)_2Re(mes)[C(mes)=N(2,6\text{ - }xylyl)]\}SO_3CF_3$. To a solution of $[(Bu^tN)_2Re(mes)_2]SO_3CF_3$ (0.3 g, 0.42 mmol) in THF (10 cm^3) was added 2,6-xylyl isocyanide (0.06 g, 0.45 mmol), and the colour changed from red–orange to pale yellow. The product was precipitated as pale yellow needles by the slow addition of hexane. Yield 0.3 g, 85%; m.p. 184°C. Found: C, 51.6; H, 6.1; N, 4.7. Calc.: C, 46.9; H, 6.2; N, 5.3%. Mass spectrum (FAB): *m/z* 698 (52%), $^{187}M^+$; 696 (31%), $^{185}M^+$; 448 (3%), $^{187}Re(NBu^t)_2(C_9H_{11})^+$; 446 (2%), $^{185}Re(NBu^t)_2(C_9H_{11})^+$. IR: 1667m, 1652w, 1608m, 1586w, 1364s, 1267s, 1224m, 1191w, 1150s, 1068m, 1032s, 925w, 895m, 879w, 794m, 753w, 705w, 572m, 517m. NMR: ^1H ($CDCl_3$): 7.23 [1H, t, *p*-*H*(xylyl)]; 7.14 [2H, s, *m*-*H*(N=Cmes)]; 7.07 [2H, d, *m*-*H* (xylyl)]; 6.98 [2H, s, *m*-*H*(mes)]; 2.44 [3H, s, *p*-*Me*(mes)]; 2.26 [3H, s, *p*-*Me*(N=Cmes)]; 2.23 [6H, s, *o*-*Me*(mes)]; 2.15 [6H, s, *o*-*Me*(N=Cmes)]; 1.82 [6H, s, *o*-*Me*(xylyl)]; 1.54 (18H, s, NBu^t).

(b) $\{(Bu^tN)_2Re(mes)[C(mes)=N(2,6\text{-}xylyl)]\}PF_6$. As above, using $[(Bu^tN)_2Re(mes)_2]PF_6$ (0.3 g, 0.42 mmol) and xylyl isocyanide (0.06 g, 0.45 mmol) in THF (10 cm^3). Yield: 0.32 g, 90%; m.p. 208°C. Found: C, 50.7; H, 5.9; N, 5.0. Calc.: C, 50.0; H, 5.8; N, 5.0%. Mass spectrum (FAB): *m/z* 698 (30%), $^{187}M^+$; 696 (16%), $^{185}M^+$; 579 (1%),

$(^{187}M-C_9H_{11})^+$; 577 (0.5%), $(^{185}M-C_9H_{11})^+$; 448 (2%), $^{187}Re(NBu^t)_2(C_9H_{11})^+$; 446 (1%), $^{185}Re(NBu^t)_2(C_9H_{11})^+$.

(c) $\{(Bu^tN)_2Re(mes)[C(mes)=NBu^t]\}PF_6$. A solution of $[(Bu^tN)_2Re(mes)_2]PF_6$ (0.1 g, 0.14 mmol) in THF (10 cm^3) was treated with *t*-butyl isocyanide (0.016 cm^3, 0.14 mmol). The red–orange solution turned pale yellow. The product was precipitated as pale yellow needles by the addition of ether. Yield: 0.1 g, 90%; m.p. 190°C. Found: C, 46.3; H, 6.1; N, 5.0. Calc.: C, 46.9; H, 6.2; N, 5.3%. Mass spectrum (FAB): *m/z* 650 (110%), $^{187}M^+$; 648 (60%), $^{185}M^+$; 474 (20%), $^{187}Re(NBu^t)_2NC(C_9H_{11})^+$; 472 (12%), $^{185}Re(NBu^t)_2NC(C_9H_{11})^+$; 448 (14%), $^{187}Re(NBu^t)_2(C_9H_{11})^+$; 446 (8%), $^{185}Re(NBu^t)_2(C_9H_{11})$. IR: 1703s, 1607m, 1597m, 1397w, 1365s, 1299w, 1286m, 1244s, 1216s, 1171s, 1144s, 1119w, 1066s, 1035w, 956w, 927w, 899m, 877m, 840vs, 735m, 705w, 667w, 654w, 582w, 558s, 526w, 468w. NMR: $^1H(CDCl_3)$: 7.19 (2H, s, NCC_6H_2); 7.12 (2H, s, C_6H_2); 2.45 [3H, s, *p*-*Me*(mes)]; 2.39 [6H, s, *o*-*Me*(mes)]; 2.35 [3H, s, *p*-*Me*(N=Cmes)]; 3.26 [6H, s, *o*-*Me*(N=Cmes)]; 1.59 (18H, s, $NCCH_3$); 1.14 (9H, s, $C{=}NCCH_3$).

(4) *Di*(t - *butylimido*)*tri*(2 - *methylphenyl*)*rhenium* (VII)

A solution of $(Bu^tN)_2ReCl_3$ (0.3 g, 0.69 mmol) in ether (30 cm^3) was cooled to −20°C, *o*-tolylmagnesium bromide (2.45 cm^3 of a 0.85 mol dm^{-3} solution in ether, 2.08 mmol) was added and the orange solution became instantly dark red. The solution was warmed to room temperature and stirred for 12 h, then filtered and the residue extracted with ether (2 × 5 cm^3). The solvent was removed under reduced pressure and the material extracted with hexane (20 cm^3), filtered and the volume reduced (5 cm^3). After further filtration clumps of orange–red crystals were obtained on cooling the hexane solution (−20°C). Yield: 0.17 g, 40%; m.p. 103°C. Found: C, 57.8; H, 6.4; N, 4.7. Calc.: C, 57.9; H, 6.5; N, 4.6%. Mass spectrum: *m/z* 602 (1%), $^{187}Re(NBu^t)_2(C_7H_7)_3^+$; 600 (0.5%), $^{185}Re(NBu^t)_2(C_7H_7)_3^+$; 511 (22%), $^{187}Re(NBu^t)_2(C_7H_7)_2^+$; 509 (13%), $^{185}Re(NBu^t)_2(C_7H_7)_2^+$; 420 (3%), $^{187}Re(NBu^t)_2(C_7H_7)^+$; 418 (3%), $^{185}Re(NBu^t)_2(C_7H_7)^+$; 278 (2%), $^{187}Re(C_7H_7)^+$; 276 (1%), $^{185}Re(C_7H_7)^+$; 182 (9%), $(C_7H_7)_2^+$; 91 (100%), $(C_7H_7)^+$. IR: 1594w, 1575w, 1557w, 1359s, 1256s, 1204s, 1155m, 1141w, 1131m, 1056m, 1026w, 1014w, 804w, 745s, 731s, 708w, 638w, 578w, 447w, 408w. NMR: ^1H (C_6D_6): 807 (2H, dd, *o*-H); 7.23 (1H, d, *o*-H); 7.15–6.62 (9H, m, *m*, *p*-H); 2.59 (6H, s, *o*-Me); 2.10 (3H, s, *o*-Me); 1.21 (18H, s, CCH_3).

(5) *Di*(t-*butylimido*)*dichloro*(*phenyl*)*rhenium*(VII)

To a stirred solution of $(Bu^tN)_3Re(OSiMe_3)$ (0.5 g, 1.0 mmol) in hexane (30 cm^3) was added phenylmagnesium chloride (0.9 cm^3 of a 1.25 mol dm^{-3} solution in ether, 1.1 mmol) at −78°C. The solution was allowed to warm to room temperature and stirred for 2 h, filtered and the solvent removed under vacuum. The solid was dissolved in ether (20 cm^3) and a solution of HCl in ether (7 cm^3 of a 0.5 mol dm^{-3} solution, 3.5 mmol) was added. The solution was stirred for 1 h, filtered and the filtrate evaporated. The residue was recrystallized from Et_2O as orange–red crystals. Yield: 30%; m.p. 163°C. Found: C, 35.1; H, 4.8; N, 5.8. Calc.: C, 35.3; H, 4.8; N, 5.9%.

Note that in the preparation from which crystals for X-ray crystallography were taken, PhMgBr was used which resulted in bromide contamination (see X-ray section below). Mass spectrum: *m/z* 477 (1%), 475 M^+; 462 (0.5%), 460 (0.05%), $(P—Me)^+$; 441 (8%), 439 (4%), $(M—Cl)^+$, 57 (100%), $(Bu^t)^+$. IR: 1643w, 1570w, 1428m, 1364s, 1303w, 1250s, 1213m, 1189s, 1138m, 1067m, 1016w, 996m, 905w, 848w, 799m, 741s, 696s, 654w, 609m, 474w, 459m, 334m, 322m, 286m. NMR: ^1H (C_6D_6): 1.15 (18H, s, Bu^t); 7.1–7.3 (3H, m, *m*, *p*-$H_3C_6H_2$); 7.90 (2H, d, *o*-$H_2C_6H_3$).

(6) *Bis*[(*di* - t - *butylimido*)(μ - t - *butylimido*)*rhenium* (VI)]

A solution of $(Bu^tN)_3Re(OSiMe_3)$ (0.5 g, 1.0 mmol) in hexane (25 cm^3) was stirred with sodium amalgam (0.5 g Na in 3 cm^3 Hg) for 12 h at room temperature. The resulting red–yellow solution was filtered, evaporated to dryness and extracted with hexamethyldisiloxane (10 cm^3). Filtration and cooling of the solution to −20°C for several days gave yellow crystals which were recrystallized from hexane or $(Me_3Si)_2O$. Yield: *ca.* 20%; subl. 212°C *in vacuo*. Found: C, 36.2; H, 6.7; N, 10.3. Calc.: C, 36.1; H, 6.8; N, 10.5%. Mass spectrum: *m/z* 800 (87%), 798 (100%), M^+. IR: 1455m, 1355s, 1281m, 1243s, 1214s, 1198m, 1155w, 1069(br), 1049m, 1024m, 914m, 845s, 806m, 756w, 681w, 597w, 559w, 507w, 462w. NMR: ^1H: (d_8-toluene): 1.82 (18H, s, μ-NBu^t), 1.27 (36H, s, NBu^t).

(7) *Tris*(t-*butylimido*)*chlororhenium*(VII)

To $(Bu^tN)_3Re(OSiMe_3)$ (4.32 g, 8.85 mmol) in toluene (50 cm^3) was added $PhICl_2$[20] at room temperature and the mixture stirred for 12 h, during which time it turned from yellow to deep red then orange. Volatiles were removed in vacuum and the

residual oil extracted into hexane (30 cm^3) which was filtered and the solution transferred to a small distillation apparatus with a fractionating column (8 cm). Hexane was removed (at 1 atm) and the remainder distilled to give $(Bu^tN)_3ReCl$ as an orange liquid (b.p. 95–100°C at 0.08 mm Hg) which solidifies on cooling to room temperature. Yield: 3.7 g, 95%; m.p. *ca* 35°C. Mass spectra: *m/z* 437 (M^+ showing isotopic patterns due to ^{185}Re and ^{35}Cl); 366 $(M-NBu^t)^+$. NMR: (C_6D_6) ^1H: 1.28 s. ^{13}C: 69.1, 31.3.

The compound can alternatively be isolated by low temperature (−40°C) crystallization from concentrated hexane solution but the yield is lower due to the high solubility.

(8) *Tri*(t-*butylimido*)(t-*butylamido*)*rhenium*(VII)

To $(^tBuN)_3ReCl$ (1.73, 3.9 mmol) in diethyl ether (40 cm^3) at −40°C was slowly (5 min) added via a cannula a solution of $LiNHBu^t$ (from $^tBuNH_2$ and ^{n}BuLi in hexane; 0.32 g, 4.05 mmol) in Et_2O at −40°C. After warming the colour changed from orange to pale yellow at 0°C when LiCl precipitated; the solution was stirred for 8 h at room temperature then evaporated *in vacuo*. The residue was extracted into hexane (30 cm^3), the extracts filtered through celite, the yellow solution concentrated to *ca* 8 cm^3 and cooled to −20°C. The first yellow crystals (not identified) were moved and the supernatant cooled to −78°C for 12 h, yielding yellow prisms which were collected and dried *in vacuo*. Yield: 1.1 g, 58%; m.p. 64–66°C. The compound can be sublimed (100°C at 0.05 mmHg). Mass spectrum: *m/z*: 474 100% $(M+2)^+$; 457 $(M+2-Me)^+$; 418 $(M+2-CH_2CMe_2)^+$; 401 $(M-NBu^t)^+$. IR: *ν*(N—H), 3366. NMR: (C_6D_6) ^1H: 1.19 (9H, s, $NHBu^t$); 1.70 (27H, s, NBu^t); 3.57br (1H, s, N*H*). $^{13}C-\{^1H\}$: 67.3 ($NCMe_3$); 52.7 ($NH—CMe_3$); 32.8 [$NH—C(CH_3)_3$]; 32.0 [$N—C(CH_3)_3$].

(9) *Lithium*(*tetramethylethylenediamine*)*tetra*(t-*butylimido*)*rhenate*(VII)

To a solution of $(Bu^tN)_3Re(NHBu^t)$ (1.07 g, 2.28 mmol) in Et_2O (40 cm^3) at −40°C was added an Et_2O solution of MeLi (4.8 cm^3 of a 0.52 M solution, 12.5 mmol). During warming to room temperature the colour changed from yellow to deep orange–red; the solution was stirred for about 4 h, when a yellow–white precipitate of a polymeric lithium salt precipitated. The volatiles were removed *in vacuo* and the residue washed with hexane (2 × 20 cm^3). To the residue was added THF (30 cm^3) and the mixture stirred for 1 h to give a clear orange solution. To this solution was added dry tetramethylethylenediamine (1 cm^3, 6.6 mmol) and the solution stirred for *ca* 1 h. Volatiles were removed and the orange residue extracted into hexane (30 cm^3); the solution was filtered, concentrated to *ca* 2 cm^3 and cooled (−20°C) for 12 h to give deep orange prisms which decompose on exposure to air. Yield: 0.4 g, 28%. X-ray quality crystals were obtained by slow cooling of hexane solutions at −78°C. NMR: ^1H (d^8 toluene, 25°C): 1.44 (36H, s, Bu^tN); 1.76 (4H, s, CH_2N); 1.92 (12H, s, NCH_3). $^{13}C-\{^1H\}$ (C_6D_6 25°C): 57.63 ($NC—Me_3$); 32.00, ($NC—CH_3$); 46.67 (CH_2NMe_2); 33.83 [$CH_2N(CH_3)_2$].

X-ray crystallography

All crystallographic measurements were made at 293 K on crystals sealed under argon in thin walled glass capillaries, using a CAD4 diffractometer operating in the ω–2θ scan mode with graphite monochromated Mo-K_α radiation ($\lambda = 0.71069$ Å), following previously detailed procedures.[21] Crystal data and intensity data collected parameters are given in Table 6.

The structures were solved by application of the heavy-atom method and refined by full-matrix least-squares. Generally, all non-hydrogen atoms were refined anisotropically; hydrogens were included in idealized positions only in the case of the phenyl complex. In this complex the halogen site *trans* to the phenyl contained a mixture of chlorine and bromine, the latter almost certainly arising out of the use of a bromo-Grignard in the preparation.

The solution and refinement of the homoleptic imido dimer structure was troublesome. The data was originally and fortuitously collected on the basis of a triclinic cell, but during the subsequent analysis it was recognized that this could be transformed to a body centred orthorhombic cell. No kind of translation symmetry was indicated and so attempts were made to refine in space groups *I*222, *Imm*^{2} and *Immm*, all of which were consistent with the heavy-atom structure found using the triclinic description. However, in all cases serious disorder existed in all Bu^t orientations and eventually we found it most convenient to refine the structure in the triclinic space group $P\bar{1}$. Even here, the disorder still occurred and only the core atoms were fully identified and refined with anisotropic displacement factors. The Bu^t carbons were represented by groupings of various numbers of partial carbons, in which the tertiary carbon–methyl carbons were fixed at a standard value of 1.50 Å. Details of the refinements in the other space groups are included

Table 6. Crystal data, details of intersity measurements and structure refinement

Compound	$(Bu^tN)_3Re(OSiMe_3)$	$(Bu^tN)_3ReCl$	$(Bu^tN)_2ReCl_3$	$(Bu^tN)_2ReCl_{1.5}Br_{0.5}Ph$	$(Bu^tN)_6Re_2$
Molecular weight	488.76	435.02	434.794	498.68	618.980
Crystal system	Triclinic	Orthorhombic	Orthorhombic	Monoclinic	Triclinic
a (Å)	9.704(1)	13.610(12)	12.655(3)	10.538(4)	11.193(3)
b (Å)	16.311(4)	9.919(3)	11.152(4)	10.137(2)	17.818(2)
c (Å)	8.185(3)	13.714(6)	21.710(3)	17.488(3)	20.636(3)
α (deg.)	76.42(2)	90.0	90.0	90.0	64.43(1)
β (deg.)	113.61(2)	90.0	90.0	104.22(2)	74.25(2)
γ (deg.)	94.19(1)	90.0	90.0	90.0	89.97(2)
Volume (Å^3)	1153.6	1851.36	3064.14	1810.88	3540
Space group	$P\bar{1}$	$Pna2_1$	$Pbca$	$P2_1/n$	$P\bar{1}$
Z	2	4	8	4	4
D_c (g cm^{-3})	1.407	1.56	1.884	1.83	1.16
μ (cm^{-1})	53.9	67.58	84.89	80.63	69.24
$F(000)$	488	852	1648	956	1560
h, k, l, range	$-11 \rightarrow 11$	$0 \rightarrow 16$	$0 \rightarrow 13$	$0 \rightarrow 12$	$0 \rightarrow 7$
	$-19 \rightarrow 19$	$0 \rightarrow 16$	$0 \rightarrow 15$	$0 \rightarrow 12$	$-12 \rightarrow 12$
	$0 \rightarrow 9$	$0 \rightarrow 11$	$0 \rightarrow 25$	$-20 \rightarrow 20$	$-14 \rightarrow 14$
Total number of reflections	4376	1884	3656	3577	9198
Number of unique reflections	4066	1696	2680	3180	9180
Number of reflections used					
$F > 3\sigma(F_o)$	3215	1251	1836	2098	5546
Number of parameters	190	153	127	251	508
Weighting scheme parameter g in					
$w = 1/[\sigma^2(F)+gF_o^2]$	0.005	0.0013	0.001455	0.0004	0.001
Final R	0.034	0.0361	0.0420	0.0304	0.0619
Final R_w	0.038	0.0371	0.0425	0.0312	0.0637

in the supplementary data, which also contains full lists of atomic coordinates, displacement factor coefficients, bond lengths and angles and F_o/F_c values for all structures.

Acknowledgement—We thank the SERC for a studentship (C.J.L.), post-doctoral support (A.A.D.) and provision of X-ray facilities.

REFERENCES

1. C. J. Longley, P. D. Savage, G. Wilkinson, B. Hussain and M. B. Hursthouse, *Polyhedron* 1988, **7**, 1079.
2. (a) A. D. Horton and R. R. Schrock, *Polyhedron* 1988, **7**, 1841; (b) D. S. Edwards, L. V. Biondi, Z. W. Ziller, M. B. Churchill and R. R. Schrock, *Organometallics* 1983, **2**, 1505.
3. A. C. Sullivan, G. Wilkinson, M. Motevalli and M. B. Hursthouse, *J. Chem. Soc., Dalton Trans.* 1988, 53.
4. P. Stavropoulos, P. G. Edwards, T. Behling, G. Wilkinson, M. Motevalli and M. B. Hursthouse, *J. Chem. Soc., Dalton Trans.* 1987, 169.
5. S. Cai, D. M. Hoffman, J. C. Huffman, D. A. Wierda and H-G. Woo, *Inorg. Chem.* 1987, **26**, 3693.
6. (a) K. Mertis and G. Wilkinson, *J. Chem. Soc., Dalton Trans.* 1976, 1488; (b) S. Cai, D. M. Hoffman, D. Lappas and H-G. Woo, *Organometallics* 1987, **6**, 2273; (c) S. Cai, D. M. Hoffman and D. A. Wierda, *J. Chem. Soc., Chem. Commun.* 1988, 313.
7. G. M. Sheldrick and W. S. Sheldrick, *J. Chem. Soc. A* 1969, 2160.
8. A. A. Danopoulos, G. Wilkinson, B. Hussain and M. B. Hursthouse, *J. Chem. Soc., Chem. Commun.* 1989, 896.
9. (a) W. A. Herrmann, J. G. Kuchler, J. K. Felixberger, G. Herdtweck and W. Wagner, *Angew. Chem. Int. Edn. Engl.* 1988, **27**, 394; (b) J. M. Huggins, D. R. Whitt and L. Lebioda, *J. Organomet. Chem.* 1986, **312**, C15.
10. D. C. Bradley, R. J. Errington, M. B. Hursthouse, A. J. Nielson and R. L. Short, *Polyhedron* 1983, **2**, 843 (W); D. C. Bradley, M. B. Hursthouse, A. N. de M. Jelfs and R. L. Short, *Polyhedron* 1983, **2**, 849 (V); N. Wiberg, H. W. Haring and U. Schubert, *Z. Naturforsch.* 1978, **33B**, 1365 (Cr); M. L. H. Green and K. J. Moynihan, *Polyhedron* 1986, **5**, 921 (Mo).
11. W. A. Nugent and R. L. Harlow, *J. Am. Chem. Soc.* 1980, **102**, 1759.
12. F. A. Cotton and G. Wilkinson, *Advanced Inorganic Chemistry*, 5th edn, p. 851. John Wiley, New York (1988).
13. W. A. Nugent, *Inorg. Chem.* 1983, **22**, 965.
14. W. A. Nugent and B. L. Haymore, *Coord. Chem. Rev.* 1980, **31**, 123; W. A. Nugent and J. M. Meyer, *Metal–Ligand Multiple Bonds*, p. 133. Wiley-Interscience, New York (1988).
15. J. Sandström, *Dynamic NMR Spectroscopy*, pp. 79, 96. Academic Press, New York (1982).
16. cf. R. H. Holm in L. M. Jackman and F. A. Cotton (Eds), *Dynamic Nuclear Magnetic Resonance Spectroscopy*, p. 324. Academic Press, New York (1975).
17. T. W. Hambley, C. J. Hawkins, J. Martin, J. A. Palmer and M. R. Snow, *Aust. J. Chem.* 1981, **34**, 2505. See also ref. 12, p. 53.
18. A. J. Bard and L. R. Faulkener, *Electrochemical Methods*, p. 230. John Wiley, New York (1980).
19. M. Schmidt and H. Schmidbauer, *Chem. Ber.* 1959, **92**, 2677.
20. B. S. Garvey, Jr., L. F. Halley and C. F. H. Allen, *J. Am. Chem. Soc.* 1937, **59**, 1827.
21. R. A. Jones, K. M. A. Malik, M. B. Hursthouse and G. Wilkinson, *J. Am. Chem. Soc.* 1979, **101**, 4128.

Note added in proof: A compound similar to $(Bu^tN)_6Re_2$ but with 2,6-isopropylphenyl instead of t-butyl has been made at M.I.T. (R. R. Schrock, personal communication to G.W.).

Polyhedron Vol. 8, No. 22, pp. 2671–2676, 1989
Printed in Great Britain

0277–5387/89 $3.00+.00
© 1989 Pergamon Press plc

PRELIMINARY CHEMICAL AND STRUCTURAL STUDY OF (1-CHLOROPHOSPHIRANE)PENTACARBONYLTUNGSTEN

BERNARD DESCHAMPS, LOUIS RICARD and FRANÇOIS MATHEY*

Laboratoire de Chimie du Phosphore et des Métaux de Transition, DCPH,
Ecole Polytechnique, 91128 Palaiseau Cedex, France

(*Received* 10 *April* 1989; *accepted* 12 *June* 1989)

Abstract—(β-Chloroethylphosphinidene)pentacarbonyltungsten, generated from the appropriate 7-phosphanorbornadiene precursor, reacts with aniline to give [(β-chloroethyl)(phenylamino)phosphane]pentacarbonyltungsten, which cyclizes upon phosphorus-metallation with *n*-butyllithium. (1-Phenylaminophosphirane)pentacarbonyltungsten, thus obtained, reacts with dry HCl to give the title compound as a stable crystalline solid which has been structurally characterized. When compared with the parent phosphirane, (1-chlorophosphirane)pentacarbonyltungsten shows much shorter P—C bonds (1.78–1.81 vs 1.867 Å) and a larger CPC intracyclic angle (49.2 vs 47.4°), which explain the enhanced stability of the complex. Normal nucleophilic substitution at the P—Cl bond is observed with EtO^- (EtOTl), O^{2-} (H_2O+DBO), $(EtO)_2P(O)^-$ and H^- ($LiAlH_4$). The opening of the ring is observed with a stronger nucleophile such as EtONa.

Presently, free unsubstituted 1-chlorophosphirane is unknown and, apparently, only 1-chlorophosphiranes with bulky substituents on the ring are stable.[1] Since the complexation of phosphorus by $M(CO)_5$ groups (M = Cr, Mo, W) has a well-documented stabilizing effect on the phosphirane ring,[2–5] we decided to study the synthesis of this interesting and fundamental species in the coordination sphere of tungsten. Two routes have been devised. We describe one of them in this paper together with some preliminary results concerning the chemistry and the structure of the complexed ring.

RESULTS AND DISCUSSION

Our starting point has been the readily available 7-β-chloroethyl-7-phosphanorbornadiene complex (**1**),[6] which acts as a precursor for the corresponding transient β-chloroethylphosphinidene complex (**2**) [eq. (1)]:

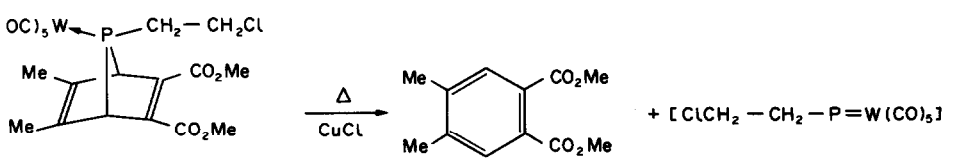

1 **2** (1)

With a weakly basic amine such as aniline, the trapping of **2** occurs without side reactions[7] [eq. (2)]. (This is not the case any more with the more basic diethylamine.)

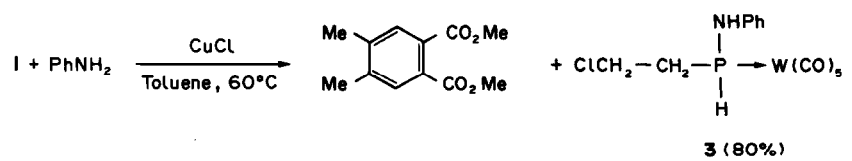

3 (80%) (2)

* Author to whom correspondence should be addressed.

A clean cyclization takes place upon treatment of **3** with *n*-butyllithium [eq. (3)]:

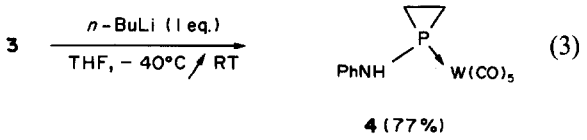

(3)

The ring closure can be monitored easily by ^{31}P NMR analysis of the reaction mixture: a characteristic upfield shift is observed and the $^{1}J(P—H)$ coupling disappears [$\delta^{31}P(\mathbf{3})$ +1.5 ppm, $^{1}J(P—H)$ 366 Hz; δ $^{31}P(\mathbf{4})$ −132 ppm]. The reaction of **4** with anhydrous HCl then affords the expected 1-chlorophosphirane complex (**5**) as a stable crystalline solid [eq. (4)]:

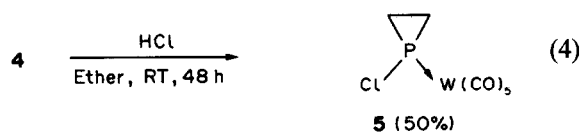

(4)

The stability of complex **5** is in sharp contrast with the very low stability of the free parent phosphirane.[8] The X-ray crystal structure analysis of **5** (Fig. 1) visualizes this stabilization of the ring upon complexation. Indeed, when comparing the structure of **5** with the structure of the parent phosphirane,[9] a striking shortening of the P—C bonds of **5** is observed: P—C bond lengths: 1.78(1) and 1.81(1) Å in **5** vs 1.867 Å in C_2H_4PH.[9] As a result, the CPC intracyclic angle increases from 47.4 ° in C_2H_4PH[9] to 49.2(5)° in **5**, suggesting a somewhat reduced cyclic strain in the complex. An easy rationalization of this phenomenon can be achieved if we use the approach of Dewar.[10] Three-membered heterocycles with weakly electronegative heteroatoms can also be viewed as π-olefinic complexes. If we consider phosphirane as a π-complex between ethylene and phosphinidene and compound **5** as a π-complex between ethylene and (chlorophosphinidene)pentacarbonyltungsten, it is clear that the phosphinidene unit is a far better electrophile as a complex than as a free species (this question is discussed in ref. 11). Thus, we expect a stronger interaction between the electron-rich ethylene and the phosphinidene subunit in the case of complex **5**. From another standpoint, it appears that 1-chlorophosphirane is a powerful ligand towards tungsten, as monitored by the short P—W bond [2.455(2) Å vs 2.496(1) Å in $(PhPC_2Ph_2)W(CO)_5$ as an example[12]]. Other structural data are given in the caption of Fig. 1.

As for other (phosphirane)pentacarbonyltungsten complexes, the ring of **5** is easily opened by strong nucleophiles.[13] Thus, some care must be taken when nucleophilic substitutions are attempted onto the P—Cl bond. For example, thallium ethoxide affords the P—OEt derivative **6**, but sodium ethoxide induces a ring opening [eq. (5)]:

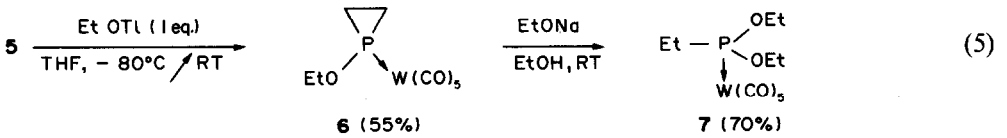

(5)

This ring opening can be monitored easily by ^{31}P NMR spectroscopy: $\delta^{31}P(\mathbf{6})$ −46 ppm; $\delta^{31}P(\mathbf{7})$ +167 ppm. Similarly, minute amounts of water in the presence of a basic tertiary amine (1,4-diazabicyclo[2.2.2]octane, DBO) afford the corresponding anhydride **8** [eq. (6)]:

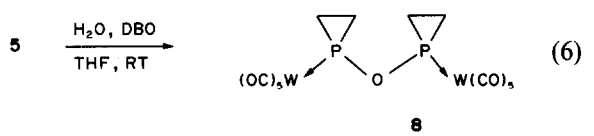

(6)

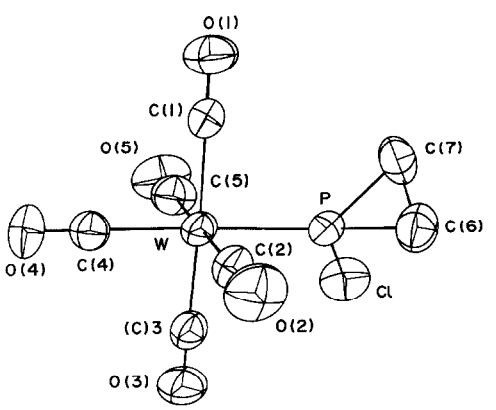

Fig. 1. ORTEP drawing of one molecule of **5**. Vibrational ellipsoids are scaled to enclose 50% of the electron density. Hydrogen atoms are omitted for clarity. Principal bond distances (Å): W—P, 2.455(2); W—C(1), 2.042(9); W—C(2), 2.023(9); W—C(3), 2.036(8); W—C(4), 2.01(1); W—C(5), 2.04(1); Cl—P, 2.037(3); P—C(6), 1.78(1); P—C(7), 1.81(1); C(6)—C(7), 1.49(1). Selected bond angles (°): P—W—C(1), 91.1(3); P—W—C(2), 88.2(3); P—W—C(3), 90.7(3); P—W—C(4), 177.8(3); P—W—C(5), 89.7(4); W—P—Cl, 118.4(1); W—P—C(6), 132.2(4); W—P—C(7), 130.8(4); Cl—P—C(6), 102.6(4); Cl—P—C(7), 104.3(4); C(6)—P—C(7), 49.2(5); P—C(6)—C(7), 66.2(6); P—C(7)—C(6), 64.6(6).

As expected, the ^{31}P chemical shifts of **6** and **8** are very close: δ ^{31}P(**8**) −45 ppm. The phosphirane ring of **5** is also preserved in the reaction with the weakly nucleophilic sodium diethylphosphite [eq. (7)]:

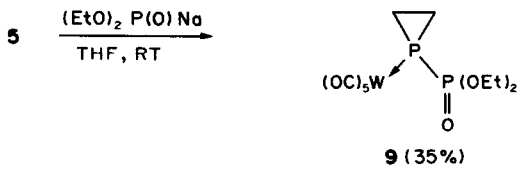

(7)

The resulting complex, **9**, has a very characteristic ^{31}P NMR spectrum, AB system: δ(A) −235 ppm (phosphirane), δ(B) +22.8 ppm (P=O), ^{1}J(P—P) 29.3 Hz. The chemical shifts of P_A and P_B rule out a $(EtO)_2P$—O—P (phosphirane) formulation in spite of the very low ^{1}J(P—P) coupling constant. Such low couplings have already been found in similar "phospha-Wittig" reagents.[13,14] Finally, the reduction of **5** by $LiAlH_4$ affords the complex of the parent phosphirane, **10** (a similar molybdenum complex has already been made from the free phosphirane[2]) [eq. (8)]:

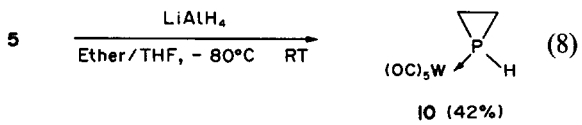

(8)

Complex **10** is characterized by a ^{31}P resonance at very high field [δ^{31}P(**10**) −254 ppm] and a ^{1}J(P—H) coupling constant in the normal range for a P—$W(CO)_5$ complex (356 Hz, see refs 7 and 15). It is interesting to note here that free phosphirane is known to have an abnormally low ^{1}J(P—H) coupling,[16] contrary to its complex **10**.

EXPERIMENTAL

All reactions were performed under argon. NMR spectra were recorded on multinuclear WP 80 SY and AC 200 SY Brüker spectrometers, operating at 80.13 and 200.13 (^{1}H), 20.15 and 50.32 (^{13}C), and 32.44 (^{31}P) MHz. Chemical shifts are in ppm downfield from internal TMS (^{1}H and ^{13}C) and external 85% H_3PO_4 (^{31}P), and coupling constants are in Hz. Mass spectra were recorded on a Shimadzu GC-MS QP 1000 instrument at 70 eV under electronic impact. Elemental analyses were performed by the Service Central de Microanalyse du CNRS, France. All the new products gave correct carbon, hydrogen elemental analyses. Silica gel (70–230 mesh) was used for the chromatographic separations. All commercially available reagents were used as received from the suppliers.

[(Chloroethyl)(phenylamino)phosphane]pentacarbonyltungsten (**3**)

(7-β-chloroethyl 7-phosphanorbornadiene)pentacarbonyltungsten (**1**) (6.3 g, 10.6×10^{-3} mol) and aniline (1.01 g, 1.06×10^{-3} mol) in 15 cm^3 of toluene were heated at 60°C for 20 min in the presence of copper(I) chloride as a catalyst. After cooling and evaporation of toluene, the crude reaction mixture was chromatographed with hexane–toluene (80 : 20) as eluent. Yield of **3**: 4.0 g (80%). ^{31}P NMR (CH_2Cl_2): δ +1.5, $^{1}J(^{31}P—^{183}W)$ 254 Hz, $^{1}J(^{31}P—^{1}H)$ 366 Hz; ^{1}H NMR ($CDCl_3$): δ2.63 (m, 2H, CH_2Cl), 3.67 (m, 2H, CH_2P), 4.02 (dd, 1H, ^{3}J(H—H): 7.3 Hz, N—*H*), 7.1 (m, 1H, $^{1}J(^{31}P—^{1}H)$: 366 Hz P—*H*), 6.8–7.4 (m, 5H, Ph); ^{13}C NMR ($CDCl_3$): δ32.89 (d, ^{1}J(C—P): 25.3 Hz P—CH_2), 39.39 (s, CH_2Cl), 195.37 (d, ^{2}J(C—P) 6.3 Hz *cis*-CO) 197.63 (d, ^{2}J(C—P) 23.8 Hz, *trans*-CO). Mass spectrum (^{184}W, ^{35}Cl): *m/z*: 511 (19%), 483 (M−CO, 6%), 455 (M−2CO, 13%), 427 (M−3CO, 23%), 399 (M−4CO, 47%), 371 (M−5CO, 44%), 343 (M−5CO−C_2H_4, 100%).

(1-*Phenylaminophosphirane*)*pentacarbonyltungsten* (**4**)

Complex **3** (4.0 g, 8.4×10^{-3} mol) in 50 cm^3 of THF was cooled to *ca* −40°C. One equivalent of *n*-BuLi (5.2 cm^3 of a 1.5 N solution in hexane) was added dropwise. The crude mixture was allowed to warm to room temperature and, after evaporation of THF, was chromatographed with hexane–toluene (80 : 20) as eluent. Yield of **4**: 2.85 g (77%). ^{31}P NMR (CH_2Cl_2): δ −132 ppm, $^{1}J(^{31}P—^{183}W)$ 288 Hz; ^{1}H NMR ($CDCl_3$): δ1.17–1.63 (m, 4H, CH_2CH_2), 3.97 (broad s, 1H, N*H*), 6.88–7.24 (m, 5H, Ph); ^{13}C NMR ($CDCl_3$): δ14.0 (d, ^{1}J(C—P) 13.1 Hz, CH_2CH_2), 195.30 (d, ^{2}J(C—P): 8.5 Hz, *cis*-CO), 198.10 (d, ^{2}J(C—P) 35 Hz, *trans*-CO). Mass spectrum (^{184}W) *m/z*: 474 (M−H, 8%), 446 (M−H−CO, 23%), 418 (M−H−2CO, 15%), 390 (M−H−3CO, 6%), 362 (M−H−4CO, 100%), 334 (M−H−5CO, 43%), 306 (M−H−5CO−C_2H_4, 53%).

(1-*Chlorophosphirane*)*pentacarbonyltungsten* (**5**)

A saturated ether solution of dry HCl was first prepared. Then complex **4** (2.85 g, 6×10^{-3} mol) in HCl–ether solution (10 cm^3) was stirred at room temperature for 48 h in a sealed Erlenmeyer. The crude reaction mixture was chromatographed with hexane–toluene (80 : 20) as eluent. Yield of **5**: 1.22 g (50%). ^{31}P NMR: δ −98 ppm, $^{1}J(^{31}P—^{183}W)$ 303 Hz; ^{1}H NMR ($CDCl_3$): δ1.38–1.52 (m, 2H,

CH_2), 2.00–2.12 (m, 2H, CH_2); ^{13}C NMR ($CDCl_3$): δ14.94 (d, ^1J(C—P) 20 Hz, CH_2), 194.27 (d, ^2J(C—P) 8.9 Hz, *cis*-CO), 197.35 (d, ^2J(C—P) 44.3 Hz, *trans*-CO). Mass spectrum (^{184}W, ^{35}Cl) *m/z*: 418 (M, 27%), 390 (M − CO, 19%), 362 (M − 2CO, 21%), 334 (M − 3CO, 32%), 306 (M − 4CO, 81%), 304 (M − 4CO − 2H, 100%), 278 (M − 5CO, 70%). Experimental details of the X-ray data collection and processing are given in Table 1.

(1-*Ethoxyphosphirane*)*pentacarbonyltungsten* (**6**)

To complex **5** (1.0 g, 2.4×10^{-3} mol) in 20 cm^3 of THF was added thallous ethoxide (0.1 cm^3, 2.4×10^{-3} mol) at −80°C. The crude mixture was allowed to warm up to room temperature and after evaporation was chromatographed with hexane–toluene (80 : 20) as eluent. Yield of **6**: 0.56 g (55%). ^{31}P NMR (CH_2Cl_2): δ −46 ppm, ^1J(^{31}P—^{183}W) 303 Hz; ^{1}H NMR ($CDCl_3$): δ0.82–0.95 (m, 2H, CH_2), 1.21 (t, 3H, CH_3), 1.54–1.67 (m, 2H, CH_2), 3.56–3.71 (m, 2H, OCH_2) ppm; ^{13}C NMR ($CDCl_3$): δ10.60 (d, ^1J(C—P) 14.25 Hz, CH_2P), 16.17 (d, ^3J(C—P) 7.85, CH_3), 64.46 (d, ^2J(C—P) 2.9 Hz, OCH_2), 195.14 (d, ^2J(C—P) 9.05 Hz, *cis*-CO), 198.24 (d, ^2J(C—P) 35.8 Hz, *trans*-CO). Mass spectrum (^{184}W) *m/z*: 428 (M, 32%), 400 (M − CO, 13%), 372 (M − 2CO, 32%), 344 (M − 3CO, 32%), 316 (M − 4CO, 48%), 288 (M − 5CO, 53%), 287 (M − 4CO − C_2H_5, 100%).

[*Ethyl - bis*(*ethoxy*)*phosphane*]*pentacarbonyltungsten* (**7**)

To a solution of sodium ethoxide in ethanol (0.7×10^{-3} mol) was added complex **6** (0.3 g, 0.7×10^{-3} mol) at room temperature. After 2 h, ethanol was evaporated and the crude reaction mixture was chromatographed with hexane–toluene (80 : 20) as eluent. Yield of **7**: 0.23 g (70%). ^{31}P NMR (CH_2Cl_2): δ167 ppm, ^1J(^{31}P—^{183}W) 318 Hz; ^{1}H NMR ($CDCl_3$): δ1.06–1.25 (m, 3H, PCH_2CH_3), 1.32 (t, 6H, OCH_2CH_3), 1.95–2.09 (m, 2H, PCH_2), 3.80–4.03 (m, 4H, OCH_2); ^{13}C NMR ($CDCl_3$):

Table 1. (1-Chlorophosphirane)pentacarbonyltungsten (**5**): experimental details of the X-ray data collection and processing

Table of Experimental Details	
Crystal description	White, paralleliped 0.30 × 0.25 × 0.22
Instrument	Enraf–Nonius CAD4 diffractometer
Corrections	Lorentz-polarization Linear decay (from 0.988 to 1.000 on *I*).[a] Reflection averaging (agreement on $I = 3.8\%$). Extinction (coefficient = 0.0000002)
Maximum 2θ	60.0°
hkl ranges	$h = 0$–9 $k = 0$–15 $l = -22$–22
Number of reflections measured	3889 total, 3617 unique
Reflections included	2384 with $F_0^2 > 3.0\sigma(F_0^2)$
Solution	Patterson method
Least-squares details:	
Hydrogen atoms	Included as fixed contribution to the structure factor
Parameters refined	137
Unweighted agreement factor	0.026
Weighted agreement factor	0.064
G.O.F.	1.33
Convergence, largest shift	0.00
Minimization function	$w(\|F_o\| - \|F_c\|)^2$
Least-squares weights	$4F_0^2/\sigma^2(F_0^2)$
Instrument instability factor (*p*)	0.080
High peak in final difference map	0.73(13) e/Å^3
Low peak in final difference map	0.00(13) e/Å^3

F.W. = 418.38; space group: *P*21/*n* (No. 14); $a = 6.832(1)$, $b = 10.893(1)$, $c = 15.993(1)$ Å, $\beta = 96.83(1)°$; $V = 1181.75(37)$ Å^3; $Z = 4$; $D_{calc} = 2.351$ g cm^{-3}; Radiation = Mo-K_α ($\lambda = 0.71073$ Å); $\mu = 103.4$ cm^{-1}; $F(000) = 768$; temperature = 18 ± 1°; final $R = 0.026$; number of unique reflections = 2384.

[a] The increase is probably due to a record low atmospheric pressure over France during data collection.

δ6.57 (s, PCH_2CH_3), 16.06 and 16.18 (s, OCH_2CH_3), 30.74 (d, ^1J(C—P) 34.7 Hz, P—CH_2), 62.00 and 62.11 (s, OCH_2), 196.21 (d, ^2J(C—P) 8.5 Hz, *cis*-CO), 198.84 (d, ^2J(C—P) 27.8 Hz, *trans*-CO). Mass spectrum (^{184}W) *m/z*: 474 (M, 25%), 446 (M−CO, 18%), 445 (M−Et, 7%), 418 (M−2CO, 32%), 416 (M−2Et, 31%), 390 (M−3CO, 99%), 388 (M−2Et−CO, 100%), 362 (M−4CO, 27%), 359 (M−3Et−CO, 27%), 334 (M−5CO, 36%).

[(Bis-phosphiran-1-yl)oxide]decacarbonylditungsten (**8**)

Complex **5** (0.21 g, 0.5×10^{-3} mol) was stirred in 10 cm^3 of THF with DBO (0.06 g, 0.5×10^{-3} mol) and a minute amount of water. The mixture was chromatographed with hexane–toluene (80 : 20) as eluent. Yield of **8**: 0.17 g (86%). ^{31}P NMR (CH_2Cl_2): δ −42.2 ppm, $^1J(^{31}P—^{183}W)$ 288.1 Hz; ^{1}H NMR ($CDCl_3$): δ1.00–1.22 (m, 4H, PCH_2), 1.76–1.98 (m, 4H, PCH_2); ^{13}C NMR ($CDCl_3$): δ12.51 (s, PCH_2), 194.45 (s, *cis*-CO). Mass spectrum (^{184}W) *m/z*: 670 (M−4CO, 8%), 642 (M−5CO, 13%), 614 (M−6CO, 28%), 586 (M−7CO, 55%), 558 (M−8CO, 51%), 530 (M−9CO, 28%), 503 (M−10CO, 36%), 474 (M−10CO−C_2H_4, 66%), 446 (W−P−O−P−W, 100%).

(1-*Diethoxyphosphorylphosphirane*)*pentacarbonyltungsten* (**9**)

Diethylphosphite (0.33 g, 2.4×10^{-3} mol) was slowly added at room temperature to NaH (0.1 g, 2.5×10^{-3} mol—60% dispersion in mineral oil) in 10 cm^3 of THF. After the H_2 evolution had ceased, complex **5** (1.0 g, 2.4×10^{-3} mol) was added. The mixture was stirred at room temperature for 2 h. Then, solvent was evaporated and the crude reaction mixture chromatographed with hexane–ether (60 : 40) as eluent. Yield of **9**: 0.44 g (35%). ^{31}P NMR (CH_2Cl_2): δ25.39 (*AB*, ^1J(P—P) 29.3 Hz, $P(O)(OEt)_2$), −233.2 (*AB*, ^1J(P—W) 253.9 Hz); ^{1}H NMR ($CDCl_3$): δ1.39 (t, 6H, CH_3), 1.40–1.57 (m, 2H, PCH_2), 1.91–2.06 (m, 2H, PCH_2), 4.12–4.27 (m, 4H, OCH_2); ^{13}C NMR ($CDCl_3$): δ9.48 (d, ^1J(C—P) 17.5 Hz, P—CH_2), 16.19 and 16.30 (s, CH_3), 63.67 and 63.81 (s, OCH_2), 194.45 (d, ^2J(C—P) 7.4 Hz, *cis*-CO), 196.28 (d, ^2J(C—P) 34.7 Hz, *trans*-CO). Mass spectrum (^{184}W) *m/z*: 520 (M, 30%), 492 (M−CO, 6%), 464 (M−2CO, 8%), 436 (M−3CO, 34%), 408 (M−4CO, 40%), 380 (M−5CO, 51%), 351 (M−5CO−Et, 100%), 290 [M−5CO−$(OEt)_2$, 54%].

(*Phosphirane*)*pentacarbonyltungsten* (**10**)

To complex **5** (2.0 g, 4.8×10^{-3} mol) in 50 cm^3 of THF was added $LiAlH_4$ (0.045 g, 1.2×10^{-3} mol) in a suspension of ether at −80°C. The reaction mixture was allowed to warm to room temperature and hydrolysed with aqueous THF. The solvent was removed and the crude mixture was chromatographed with hexane–ether (80 : 20) as eluent. Yield of **10**: 0.78 g (42%). ^{31}P NMR (CH_2Cl_2): δ −254 ppm, $^1J(^{31}P—^{183}W)$ 253.9 Hz, ^1J(P—H) 356.4 Hz; the ^{1}H NMR spectrum ($CDCl_3$) is very complicated (see ref. 16) and has not been simulated; ^{13}C NMR ($CDCl_3$): δ3.03 (d, ^1J(C—P) 10.4 Hz, CH_2), 194.80 (d, ^2J(C—P) 8.4 Hz, *cis*-CO), 197.05 (d, ^2J(C—P) 32.2 Hz, *trans*-CO). Mass spectrum (^{184}W) *m/z*: 384 (M, 81%), 383 (M−H, 51%), 356 (M−CO, 23%), 328 (M−2CO, 89%), 300 (M−3CO, 89%), 272 (M−4CO, 91%), 270 (100%), 244 (M−5CO, 49%).

X-ray structure determination for **5**

Crystals of **5**, $C_7H_4O_5PClW$, were obtained at 0°C from a dichloromethane–hexane solution of the compound. Data were collected at 18 ± 1° on an Enraf–Nonius CAD4 diffractometer. The crystal structure was solved and refined using the Enraf–Nonius supplied SDP package. The compound crystallizes in space group $P2_1/n$, $a = 6.832(1)$, $b = 10.893(1)$, $c = 15.993(1)$ Å, $\beta = 96.83(1)°$, $V = 1181.75(37)$ Å^3, $Z = 4$, $D_{calc} = 2.351$ g cm^{-3}; Mo-K_α radiation ($\lambda = 0.71073$ Å) graphite monochromator; $\mu = 103.4$ cm^{-1}; $F(000) = 768$. A total of 3617 unique reflections were recorded in the range $2 \leqslant 2\theta \leqslant 50°$ of which 1505 were considered as unobserved ($F^2 < 3\sigma(F^2)$), leaving 2384 for solution and refinement. The structure was solved by Patterson methods. The positional parameters of hydrogen atoms were included as a fixed contribution to the structure factors in the final stages of least-squares, while using anisotropic temperature factors for all other atoms. A non-Poisson weighting scheme was applied with a *p*-factor equal to 0.08. The final *R*-factors were $R = 0.026$, $R_w = 0.064$, G.O.F. = 1.33.

REFERENCES

1. G. Märkl, W. Hölzl and I. Trötsch-Schaller, *Tetrahedron Lett.* 1987, **28**, 2693; E. Niecke, M. Leuer and M. Nieger, *Chem. Ber.* 1989, **122**, 453.
2. R. Bausch, E. A. V. Ebsworth and D. W. H. Rankin, *Angew. Chem. Int. Edn Engl.* 1971, **10**, 125.
3. A. Marinetti and F. Mathey, *Organometallics* 1984, **3**, 456.

4. R. Braun and E. Fluck, *Chem. Z.* 1986, **110**, 379.
5. J. Borm, G. Huttner and O. Orama, *J. Organomet. Chem.* 1986, **306**, 29.
6. B. Deschamps and F. Mathey, *Tetrahedron Lett.* 1985, **26**, 4595.
7. A. Marinetti and F. Mathey, *Organometallics* 1982, **1**, 1488.
8. R. I. Wagner, L. V. D. Freeman, H. Goldwhite and D. G. Rowsell, *J. Am. Chem. Soc.* 1967, **89**, 1102.
9. M. T. Bowers, R. A. Beaudet, H. Goldwhite and R. Tang, *J. Am. Chem. Soc.* 1969, **91**, 17.
10. M. J. S. Dewar and G. P. Ford, *J. Am. Chem. Soc.* 1979, **101**, 783.
11. F. Mathey, *Angew. Chem. Int. Edn Engl.* 1987, **26**, 275.
12. A. Marinetti, F. Mathey, J. Fischer and A. Mitschler, *J. Am. Chem. Soc.* 1982, **104**, 4484.
13. A. Marinetti and F. Mathey, *Tetrahedron* 1989, **45**, 3061.
14. A. Marinetti and F. Mathey, *Angew. Chem. Int. Edn Engl.* 1988, **27**, 1382.
15. F. Nief, F. Mercier and F. Mathey, *J. Organomet. Chem.* 1987, **328**, 349.
16. H. Goldwhite, D. Rowsell, L. E. Vertal, M. T. Bowers, M. A. Cooper and S. L. Manatt, *Org. Magn. Reson.* 1983, **21**, 494.

Polyhedron Vol. 8, No. 22, pp. 2677–2679, 1989
Printed in Great Britain

0277–5387/89 $3.00+.00
© 1989 Pergamon Press plc

COBALT(III)–SALICALDEHYDE–AMINOPHENOL COMPLEXES: SOLUBILITIES, TRANSFER CHEMICAL POTENTIALS AND SOLVATION IN BINARY AQUEOUS SOLVENT MIXTURES

E. A. ABU-GHARIB and J. BURGESS*

Department of Chemistry, University of Leicester, Leicester LE1 7RH, U.K.

(*Received* 24 *May* 1989; *accepted* 15 *June* 1989)

Abstract—Solubilities are reported for four cobalt(III) complexes of Schiff bases derived from 2-aminophenol and (substituted) salicaldehydes, in aqueous methanol, and for one of these complexes also in aqueous *t*-butyl alcohol and in aqueous acetone. The derived trends of transfer chemical potentials with solvent composition are discussed in relation to the nature of the ligand and the nature of the co-solvent. Solvation characteristics for the title complexes are compared with those of other inorganic complexes, particularly of cobalt(III).

We have in recent years used transfer chemical potentials, derived from measured solubilities, as a means for probing solvation of a number of complexes in various binary aqueous mixtures.[1] The hydrophobic and hydrophilic properties of the ligands have been seen to control preferential solvation by water or the organic solvent, for example for cobalt(III) complexes in methanol–water[2,3] or acetone–water[4] mixtures or for iron(II)–diimine complexes in various mixed solvents.[2,5] In nearly all cases we have dealt with charged complexes. Very little information of this type is available for uncharged complexes, despite their advantage in avoiding the necessity for employing single-ion assumptions which bedevils the establishment of thermodynamic parameters for charged species.[6] In the present paper we report solubilities, derive transfer chemical potentials, and discuss the trends established for a series of uncharged cobalt(III) complexes of bidentate ligands, **1a**–**1d**, derived from (substituted) salicaldehydes or benzaldehyde and *o*-aminophenol (2-hydroxyaniline).[7] The binary aqueous mixtures contained the co-solvents methanol, *t*-butyl alcohol and acetone.

(1a) soap: X = H, Y = OH

(1b) MeOsoap: X = OMe, Y = OH

(1c) Me_2Nsoap: X = NMe_2, Y = OH

(1d) boap: X = H, Y = H

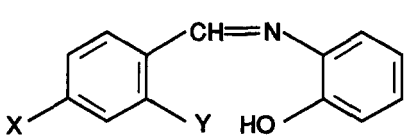

* Author to whom correspondence should be addressed.

EXPERIMENTAL

The complexes were prepared by established methods.[7] Their composition was checked by C, H, N microanalysis, which also served to establish that they precipitated as anhydrous compounds. Solubilities were measured using the apparatus and methods described earlier;[2] absorbance readings were obtained using a Unicam SP8-100 spectrophotometer. Wavelengths of maximum absorption and molar extinction coefficients are $\varepsilon_{422} = 17{,}800$ for $Co(soap)_3$, $\varepsilon_{434} = 27{,}200$ for $Co(MeOsoap)_3$, $\varepsilon_{433} = 22{,}400$ for $Co(Me_2Nsoap)_3$ and $\varepsilon_{433} = 22{,}000$ for $Co(boap)_3$.

RESULTS AND DISCUSSION

Solubilities are reported in Table 1; transfer chemical potentials calculated from these solubilties are listed in Table 2. The dependence of transfer chemical potentials on ligand is illustrated in Fig. 1 and on co-solvent in Fig. 2. The trends in Fig. 1 show that the nature of the ligand has only a small effect on solvation for these soap and boap complexes. As the various substituents only make minor

Table 1. Solubilities (10^5 S/mol dm^{-3}) at 298.2 K

Complex	Co-solvent	Vol. % organic solvent 0	20	40	50	60
$Co(soap)_3$	Methanol	4.0	8.9	31.2	60	155
	t-Butyl alcohol		16.7	53	84	95
	Acetone		25.3	128		440
$Co(MeOsoap)_3$	MeOH	1.2	3.0	10.8		58
	t-Butyl alcohol		7.6	79	121	154
	Acetone		11.4	84		219
$Co(Me_2Nsoap)_3$	Methanol	2.5	13.9	48		159
$Co(boap)_3$	Methanol	2.3	7.3	26		97

alterations to the surface of the complexes, this is expected. Increasing the number of methyl groups on the periphery results in a small increase in hydrophobicity and thus a small increase in stabilization as the methanol content of solvent mixtures is increased.

Figure 1 also includes transfer chemical potentials for other hydrophobic metal complexes, to put our present results into context. The trends for our present complexes are very close to those for the $[Co(phen)_3]^{3+}$ cation[3] and the *trans*-$[CoCl_2(py)_4]^+$ cation,[8] indicating similar solvation characteristics in these mixtures. The hydrophilic/hydrophobic balance for the soap and related complexes is thus similar to the resultant effect of three phen ligands and a 3+ charge, or of ligands and 1+ charge in the *trans*-$[CoCl_2(py)_4]^+$ cation. Interestingly, the introduction of ethyl groups into the latter species produces a much more marked increase in hydrophobicity[9] than the introduction of methyl groups into the soap complexes. Figure 1 suggests that $Co(acac)_3$[10] is less hydrophobic than $Co(soap)_3$—the hydrophilic properties of the OH and N in the soap ligands must be being counterbalanced by the stronger hydrophobicity of phenyl rings compared with methyl groups. Finally, the trends for the soap complexes show the expected marked difference from those for *trans*-$[CoCl_2(en)_2]^+$ and, especially, for the strongly hydrophilic $[Cr(ox)_3]^{3-}$ anion.[3]

Figure 2 shows that *t*-butyl alcohol and acetone have considerably greater stabilizing effects on these hydrophobic complexes than does methanol. This is in accord with expectation, and parallels our observations on the more complicated ternary complex $Fe(CN)_2(bipy)_2$.[11] The marked curvature in the *t*-butyl alcohol and acetone plots in Fig. 2 indicates strong preferential solvation by these organic co-solvents.

Table 2. Transfer chemical potentials, from water to the respective solvent mixtures, in kJ mol^{-1} on the molar scale, at 298.2 K

Vol. % organic solvent	20	40	50	60
Mole fraction methanol	0.100	0.229	0.308	0.400
$Co(soap)_3$	−2.0	−5.1	−6.7	−9.0
$Co(MeOsoap)_3$	−2.3	−5.4		−9.6
$Co(Me_2Nsoap)_3$	−4.3	−7.3		−10.3
$Co(boap)_3$	−2.9	−6.0		−9.3
Mole fraction *t*-butyl alcohol	0.046	0.113	0.161	0.220
$Co(soap)_3$	−3.5	−6.4	−7.6	−7.8
$Co(MeOsoap)_3$	−4.6	−10.4	−11.4	−12.0
Mole fraction acetone	0.058	0.141		0.270
$Co(soap)_3$	−4.6	−8.6		−11.7
$Co(MeOsoap)_3$	−5.6	−10.5		−12.9

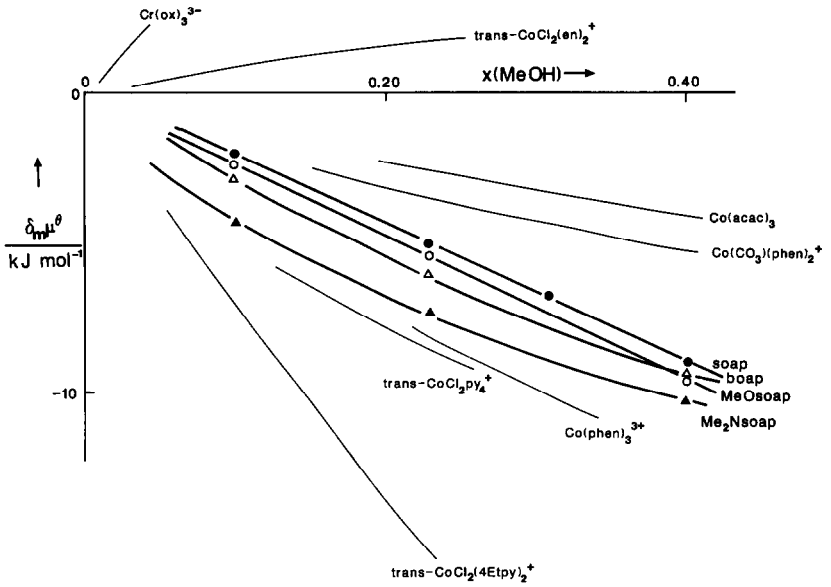

Fig. 1. Transfer chemical potentials in methanol–water: dependence on ligand nature.

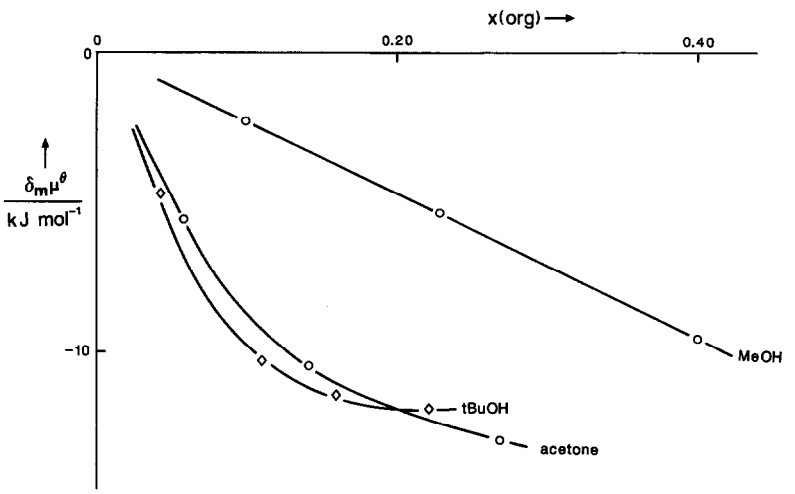

Fig. 2. Transfer chemical potentials for Co(soap)$_3$ in aqueous organic media: dependence on co-solvent.

Acknowledgement—We are grateful to the Royal Society for a Grant-in-aid towards the purchase of the spectrophotometer used in this investigation.

REFERENCES

1. M. J. Blandamer and J. Burgess, *Transition Met. Chem.* 1988, **13**, 1.
2. M. J. Blandamer, J. Burgess, B. Clark, P. P. Duce, A. W. Hakin, N. Gosal, S. Radulović, P. Guardado, F. Sanchez, C. D. Hubbard and E. A. Abu-Gharib, *J. Chem. Soc., Faraday Trans. I* 1986, **82**, 1471.
3. M. J. Blandamer, J. Burgess and E. A. Abu-Gharib, *Transition Met. Chem.* 1984, **9**, 193.
4. J. Burgess and E. A. Abu-Gharib, *J. Chem. Res.* 1985 (S)8, (M)0201.
5. E. A. Abu-Gharib, M. J. Blandamer, J. Burgess, N. Gosal, P. Guardado, F. Sanchez and C. D. Hubbard, *Transition Met. Chem.* 1984, **9**, 306.
6. See, for example, Y. Marcus, *Ionic Solvation*, Chap. 6. Wiley, New York (1985).
7. S. Yamada, *Coord. Chem. Rev.* 1966, **1**, 415.
8. J. Burgess, *Mech. Inorg. Organomet. React.* 1983, **1**, 103 (see p. 150).
9. I. M. Sidahmed and A. M. Ismail, *Transition Met. Chem.* 1987, **12**, 449.
10. A. Al-Alousy and J. Burgess, unpublished results.
11. J. Burgess, S. Radulović and F. Sanchez, *Transition Met. Chem.* 1987, **12**, 529.

Polyhedron Vol. 8, No. 22, pp. 2681–2687, 1989
Printed in Great Britain

0277–5387/89 $3.00+.00
© 1989 Pergamon Press plc

PHOTOACOUSTIC CALORIMETRY STUDIES OF LIGAND-EXCHANGE OF ALIPHATIC AMINES WITH $Cr(CO)_6$: STERIC EFFECTS AND HYDROGEN BONDING

T. J. BURKEY

Department of Chemistry, Memphis State University, Memphis, TN 38152, U.S.A.

(*Received* 10 *April* 1989; *accepted* 20 *June* 1989)

Abstract—The exchange of aliphatic amines with $Cr(CO)_6$ in heptane occurs in two steps: a CO is lost forming a solvent-coordinated complex, $Cr(CO)_5$(heptane), and then heptane is lost to form $Cr(CO)_5$(amine). The enthalpies of exchange of aliphatic amines (piperidine, *n*-butylamine, di-*n*-butylamine and tri-*n*-butylamine) with $Cr(CO)_6$ have been determined in heptane at ambient temperatures. The enthalpies of reaction determined by photoacoustic calorimetry (PAC) include contributions from hydrogen-bond formation between free amine and the pentacarbonylamine chromium, **1**. The enthalpy of hydrogen-bond formation was found to be about 4 kcal mol^{-1} and was determined from the temperature and concentration dependence of the amine NH chemical shifts of **1**. The PAC values were corrected for hydrogen-bond formation contributions to obtain only the enthalpy of ligand-exchange (ΔH_{12}). The ΔH_{12} was more endothermic for bulky amines, and this steric effect can be attributed to inhibition of Cr—N bond formation. These results, along with those in the literature, provide a detailed description of the energetics of each step of the ligand-exchange in both directions. The results suggest there is a continuum from an associative to a dissociative process for the displacement of heptane by amine that depends on the steric bulk of the amine.

Ligand-exchange reactions of group VI metal carbonyl compounds continue to be actively studied.[1] It is commonly postulated or assumed that activation enthalpies of ligand-exchange reactions that follow dissociative kinetics in alkane solvents are a good measure of the metal–ligand bond energies.[2] This requires that ligand dissociation occurs with little interaction with the solvent in the transition state; nevertheless, recent studies suggest that interactions with alkane solvent may be more important than expected. Flash photolysis studies[1a–c,3] have shown that ligand dissociation leads to an intermediate that forms an intermolecular metal–alkane bond (agostic bond),[4] and photoacoustic calorimetry (PAC) studies have shown that these agostic bonds can be quite substantial (10–13 kcal mol^{-1}).[5] Since the transition state and the solvent-coordinated intermediate it leads to are expected to have similar structures, some agostic bonding might be expected in the transition state. One method to test for agostic bonding in a transition state would be to measure ligand-exchange enthalpies. If the assumption that dissociative activation enthalpies are a good measure of bond energies is valid, then the difference in the activation enthalpies should be equal to the corresponding ligand-exchange enthalpies. If this is not the case, it indicates that at least one of the transition states is stabilized by the solvent.

Much of our current understanding of metal–ligand bond energies is based on kinetic data, since thermochemical data for organometallic compounds are scarce. In particular, few reaction enthalpies and bond energies have been documented for group VI metal carbonyl compounds. In this study we have investigated the enthalpy of ligand-exchange of aliphatic amines with $Cr(CO)_6$ [eqs (1) and (2)] by PAC.[5c,6] In addition it was discovered that **1a** hydrogen-bonded with free amine [eq. (3)]. The PAC measurement involves the determination of the amplitude of an acoustic wave from a photolysed sample. The photolysis initiates chemical and physical processes that liberate heat, producing an acoustic wave. So, the amplitude of

the acoustic wave is dependent on the amount of heat released. To better understand the effect of the amine steric bulk on the enthalpy of ligand-exchange (ΔH_{12}) and determine the "intrinsic" Cr—N bond strength, the ligand-exchange with various aliphatic amines was investigated:

$$Cr(CO)_6 + S \underset{\Delta H^{\ddagger}_{-1}}{\overset{\Delta H^{\ddagger}_{1}}{\rightleftharpoons}} Cr(CO)_5(S) + CO \quad (1)$$

S = heptane

$$Cr(CO)_5(S) + A \underset{\Delta H^{\ddagger}_{-2}}{\overset{\Delta H^{\ddagger}_{2}}{\rightleftharpoons}} Cr(CO)_5(A) + CO \quad (2)$$

1a, A = piperidine
1b, A = *n*-butylamine
1c, A = di-*n*-butylamine
1d, A = tri-*n*-butylamine

$$Cr(CO)_5(A) + A \xrightarrow{\Delta H_3} Cr(CO)_5(A)—A. \quad (3)$$

EXPERIMENTAL

The methods and equipment used have been described in detail previously.[5c] Solutions of $Cr(CO)_6$ were prepared in subdued light.

Materials

All materials were obtained from Aldrich unless otherwise noted. The $Cr(CO)_6$ was obtained from Pressure Chemical as well. "Zero"-grade argon and helium and other gases were obtained from Air Products. Heptane, amines, *o*-hydroxybenzophenone (OHB), and metal complexes were purified as before.[5c] The heptane was stored under positive helium pressure in a septum-capped bottle. Amines were refluxed over sodium or potassium until upon distillation their absorbance (neat) was insignificant for PAC: less than 0.001 for the preparation of solutions containing over 0.1 M amine and less than 0.005 for solutions containing less than 0.1 M amine (10 mm cuvette at 337.1 nm).

Preparation of **1** followed a literature method where 2 g of $Cr(CO)_6$ and 5–10 cm^3 of amine in 50–70 cm^3 THF were photolysed.[7] The solution was stirred and nitrogen purged before and during photolysis. The lamp power supply was set to dissipate 400–600 W (Hanovia 1000 W Hg–Xe short arc lamp, Schoeffel lamp housing and Kratos LPS 255HR power supply), and the beam was filtered with a 9% $NiSO_4$–$6H_2O$ solution in a 10 cm quartz cell. The photolysed solution was rotovaped, and $Cr(CO)_6$ was removed from the residue by sublimation. The residue was recrystallized several times in subdued light from cold hexane. The synthesis of **1c** has not been previously reported.

Compound **1c**: m.p. 22°C. ^{1}H NMR ($CDCl_3$): δ 2.66 (4, m, α-CH_2), 1.87 (1, br, p, 5.8 Hz, NH), 1.56 (4, m, β-CH_2), 1.31 (4, hex, 7.5 Hz, γ-CH_2), 0.96 (6, t, 7.3 Hz, CH_3). ^{13}C NMR ($CDCl_3$): δ 220.1 (*trans* CO), 214.1 (*cis* CO), 57.5 (α-CH_2), 30.6 (β-CH_2), 20.0 (γ-CH_2), 13.8 (CH_3). IR (Mattson Polaris FTIR, cyclohexane, KBr, cm^{-1}): (CO) 2065.2, 1831.7, 1913.8. Found: C, 48.61; H, 6.15; Cr, 15.95; N, 4.79. Calc. for $C_{13}H_{19}CrNO_5$: C, 48.60; H, 5.96; Cr, 16.18; N, 4.36% (Galbraith, Knoxville).

PAC experiments

Solutions for PAC measurements were prepared rapidly in a glass-stoppered flask to limit the absorption of moisture from air. Solutions containing less than 0.1 M amine were prepared under atmosphere-free conditions as before.[5c] When $Cr(CO)_6$ solutions contained 0.1 M or more of amine, amine was also added to the reference (ferrocene) solution to obtain the same amine concentration. This ensured that the acoustic properties of the sample and reference solutions were the same. All PAC solutions were purged with helium 15 min prior to photolysis. Photoacoustic measurements were obtained in a flow cell where the flow was increased until the PAC signal was independent of flow rate. The enthalpy of a reaction was calculated from eqs (4) and (5), where E_v is the energy of a mole of photons (84.8 kcal mol^{-1} for 337.1 nm), Φ is the quantum yield of reaction (1) (0.67),[8] S and R are the amplitudes of signals from the sample and reference cells, respectively. The s and r subscripts refer to measurements with a sample ($Cr(CO)_6$) and a reference (ferrocene) solution in the sample cell, respectively. The solution in the reference cell always contained OHB.

$$\Delta H = E_v(1-\phi)/\Phi \quad (4)$$

$$\phi = S_s R_r (1-T_r)/S_r R_s (1-T_s). \quad (5)$$

Absorption measurements

The absorbances of PAC solutions at 337.1 nm were determined from PAC measurements and a Gilford Response II spectrophotometer as before.[5c] Enthalpies calculated using the two methods of absorbance determination normally yielded results within 1 kcal mol^{-1} of each other with no systematic differences. An average of the two values is reported for each determination. One determination is obtained for each sample solution prepared. The

spectrophotometer cuvette was maintained to within 0.3°C of the PAC experiment. It was observed that the absorbances of solutions containing high amine concentrations were dependent on dissolved oxygen. For solutions containing 0.1 M or greater amine, absorbances by spectrophotometric measurements were obtained using one of three methods of solution preparation. These methods gave results experimentally indistinguishable from each other and the PAC absorption measurement. For the three methods, the absorbance of the $Cr(CO)_6$ or ferrocene solutions were "corrected" by subtracting the absorbance of a control solution containing the same concentration of amine. The first method involved helium purging the solutions directly in a septum-sealed 5 cm thermostatted quartz cell prior to measuring the absorbance. In the second method, the solutions were purged with air in a flask prior to measurement in the 5 cm cell. The air was dried by passing it through a 100×1.5 cm column of 4 Å molecular sieves. For the third method, the final absorbance of a solution was calculated based on the dilution of stock $Cr(CO)_6$ or ferrocene solutions. It was also found that at high amine concentrations the absorbance of $Cr(CO)_6$ increased slightly (1–2%). This required a correction to the absorbances determined by the third method.

NMR experiments

Samples of **1** for NMR spectroscopy were weighed in oven-dried 1 cm^3 flasks (calibrated to 0.4%), sealed with a septum, evacuated to < 100 microns mercury, filled with argon, and placed in a nitrogen-purged glove bag. Empty NMR tubes were similarly prepared. In the glove bag, freshly distilled amine was added to the flask with a capillary pipette (Drummond) and diluted to the mark with 0.1% TMS in cyclohexane-d_{12}. The solution was transferred to an NMR tube which was covered with foil, and kept frozen in a freezer or dry-ice chest while not in use.

All NMR spectra were obtained using a Varian VXR 300. Samples were equilibrated in the probe until the NH chemical shift of **1** was constant (10–15 min). Chemical shifts are reported relative to TMS. The variable temperature controller was calibrated at each temperature with either methanol or 1,2-dihydroxyethane, and maintained at constant temperature to within ± 0.5°C. Sample concentrations were corrected for temperature-dependent volume changes. An equilibrium constant for reaction (3) was calculated using the observed chemical shift of the NH signal of **1** when it was alone and in the presence of two different concentrations of free amine.[9] The equilibrium constants for five temperatures were used to determine the enthalpy of reaction. For four amine concentrations, an average was obtained from up to six values for the enthalpy of reaction.

RESULTS

Photolysis of $Cr(CO)_6$ yields an acoustic signal amplitude dependent on piperidine concentration. This is best demonstrated when the apparent heat calculated from the amplitude of the acoustic signal is plotted vs piperidine concentration (Fig. 1). This response is typical of a high-pass filter: the transducer responds to heat evolving at rates near or greater than the transducer frequency but not to heat evolving much slower. Photolysis of $Cr(CO)_6$ forms $Cr(CO)_5S$ in less than a nanosecond,[1a–c] and at low piperidine concentration reaction (2) is slow, so the signal is dependent on the heat liberated from reaction (1) and not reactions (2) and (3). We obtained a value near 27 kcal mol^{-1}, in agreement with results reported for other ligands at low concentrations.[5a] Near 0.1 M piperidine, the rate of reaction (2) is comparable with the frequency response of a 2.25 MHz transducer, some of the heat evolved for reactions (2) and (3) is detected, and the apparent heat increases. This is consistent with a rate constant of $\sim 10^7\ M^{-1}\ s^{-1}$ expected for eq. (2) and a diffusion controlled rate for reaction (3).[5a,10,11] At high piperidine concentration reaction (2) is fast, all the heat of reactions (1)–(3) is observed, and the amplitude is independent of piperidine concentration (0.8–2 M). At 1.0 M piperidine the same apparent heat is obtained for 1 and 2.25 MHz transducers (Fig. 1); this is consistent with the observed reactions being much faster than the transducer response at this concentration. The enthalpy of reactions (1)–(3) (ΔH_{123}) is assigned,

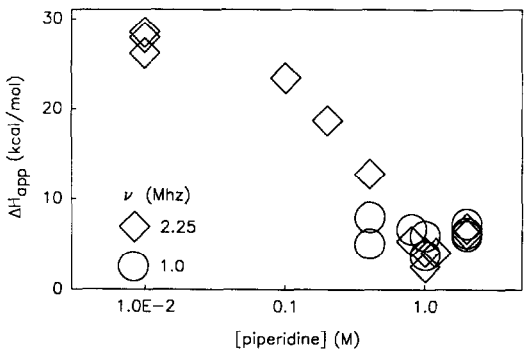

Fig. 1. PAC response (apparent ΔH) when $Cr(CO)_6$ ($\sim 9 \times 10^{-5}$ M) is photolysed in the presence of various concentrations of piperidine in heptane. The ν is the transducer frequency response.

Table 1. Enthalpy of amine exchange with $Cr(CO)_6$ in heptane

Amine	M^a	n^b	$\Delta H_{123}{}^c$
Piperidine	0.8–2.0	12	5.9 ± 1.8
n-Butylamine	1.0–2.0	7	2.8 ± 1.5
Di-*n*-butylamine	2.4	3	$\leqslant 7.8 \pm 0.6^d$
Tri-*n*-butylamine	0.8–1.7	2	15.7 ± 1.5
			15.1^e

[a] Range of amine concentrations over which the acoustic signal was independent.
[b] Number of determinations.
[c] kcal mol^{-1}, 20–25°C.
[d] Signal was not constant, see text.
[e] Reference 5a.

Table 2. Enthalpy of hydrogen bonding between amine and **1**

1	Amine, M	$\Delta\delta^a$	$K_3{}^b$	$-\Delta H_3{}^c$
a	0.1–1.0	2.0–3.8	2.5	4.7 ± 0.7
b	0.05–0.5	1.6–2.9	10	3.6 ± 0.3
c	0.02–0.6	1.8–2.3	0.5	5.4 ± 1.5

[a] Observed range of **1** NH signal.
[b] Estimated for 25°C.
[c] kcal mol^{-1}, 10–50°C in 0.1% TMS/C_6D_{12}.

therefore, the value of 5.9 kcal mol^{-1}. Similar results were obtained for other amines and are reported in Table 1. Between 1.2 and 2.4 M di-*n*-butylamine the apparent enthalpy increased by approximately 2 kcal mol^{-1}. This may be the result of incomplete hydrogen bonding for **1c** since the equilibrium is not favourable. The reported ΔH_{123} value in this case is probably a lower limit (*vide infra*).

The chemical shift of the NH signals of **1** are dependent on the concentration of free amine and temperature. This suggested an equilibrium between free amine and **1** to form a hydrogen-bonded complex. Hydrogen bonding for **1a** has been reported previously but not to amines.[12] The hydrogen-bonding results are summarized in Table 2. The chemical shift of the NH signal for *n*-butylamine in the absence of **1** was found to be independent of temperature from 10 to 50°C (< 0.02 ppm), indicating that the hydrogen bonding between free amine is negligible. This is not surprising since aliphatic amines are good hydrogen-bond acceptors but poor donors.[13] The ΔH_3 can, therefore, be attributed primarily to hydrogen-bond formation between **1** and free amine.

DISCUSSION

The results indicate that hydrogen bonding between free amine and **1** is of the order of 4–5 kcal mol^{-1}. The establishment of the equilibrium for reaction (3) is expected to be fast relative to the transducer response, since hydrogen-bond formation is typically diffusion-controlled.[11] Equilibrium calculations from the results of Tables 1 and 2 indicate that most of **1a** (> 80%) and **1b** (> 95%) are hydrogen bonded for the conditions of the PAC experiments, while only 65% of **1c** is hydrogen bonded. Since **1** has no lone pairs on the coordinated amine, and the free amines are not good hydrogen-bond donors, we conclude that the hydrogen bond is formed between the NH protons of the coordinated amine and the lone pair of a free amine. Hydrogen bonding to the coordinated amine protons has been observed previously for **1**, as well as for molybdenum and tungsten analogues.[12,14] Furthermore, hydrogen bonding with coordinated amine protons has been detected in the solid state.[15]

The contribution of hydrogen bonding has been subtracted from ΔH_{123} to obtain the values for ΔH_{12} in Table 3.[16,17]† Previous studies show that

† Since the molecularity formally decreases in reaction (3), the reaction volume change might be expected to reduce the resultant acoustic signal. Calculations and previous PAC studies suggest the effect is not significant. The volume change upon hydrogen-bond formation is not known, but a reasonable estimate would be that it equals about 10% of the molecular volume of amine. For piperidine, this would be about 10 cm^3 mol^{-1}. The volume change due to heptane thermal expansion from 1 kcal heat is 4.7 cm^3 ($\Delta V = \alpha E/\rho C_p$,[16a] where in heptane α is the coefficient of thermal expansion (1.256×10^{-3} K^{-1}),[16b] E is 1 kcal heat, ρ is the density (0.6795 g cm^{-3}),[16c] and C_p is the heat capacity (39.5 cal K^{-1} mol^{-1})[16d] at 25°C. Therefore the volume change of reaction (3) would have the effect of −2 kcal mol^{-1} of heat. This would be an upper limit, however, since the PV work done on the reactants during the volume change is not included. The PV work will increase the internal energy of the products and result in heat deposition and a volume change due to thermal expansion. The volume increase from thermal expansion due to PV work will tend to cancel the volume decrease due to reaction volume changes. The resultant contribution to the PAC signal will be zero if the thermal expansion due to PV work is equal to the reaction volume change. In some previous PAC studies of reactions where the molecularity (and hence volume) changes, this is apparently the case: the enthalpies determined by PAC in solution were the same as the gas-phase enthalpies.[17] The same was true for aqueous solutions where the thermal expansion is much smaller than for heptane. We therefore conclude that the effect of reaction (3) volume change on the PAC signal is likely to be negligible.

Table 3. ΔH_{12} and BDE(Cr—A) for **1**, $[Cr(CO)_5(A)]$

1	a	b	c	d
ΔH_{12}[a]	10.6	6.4	10.8	15.7
BDE(Cr—A)	26.2	30.4	26.0	21.1

[a] kcal mol^{-1}, 25°C.

Table 4. Summary of thermochemical and kinetic data for **1a**

ΔH_1^*	ΔH^*_{-1}	ΔH_2^*	ΔH^*_{-2}	ΔH_1	ΔH_2	ΔH_{12}
38[a]	10.5[b]	8.7[c]	25.6[d]	27.5[e]	−16.9[f]	10.6[e]

[a] kcal mol^{-1}, ref. 17.
[b] $(\Delta H_1^* - \Delta H_1)$.
[c] $(\Delta H^*_{-2} - \Delta H_1 + \Delta H_{12})$.
[d] Reference 12.
[e] This work.
[f] $(\Delta H_1 - \Delta H_{12})$.

the enthalpy of ligand-exchange reactions is not greatly affected by solvation effects in alkane solvents.[18] Assuming this is the case in the current study, ΔH_{12} is equal to the difference in BDE (Cr—CO) and BDE(Cr—A) ($Cr(CO)_5$—(CO) and $Cr(CO)_5$—(A) bond energies). From the value for BDE(Cr—CO), the BDE(Cr—A) values are calculated from ΔH_{12} and reported in Table 3.[19] It is clear from the trends in both ΔH_{12} and BDE (Cr—A) that the values are more endothermic as the amine becomes more substituted in spite of the fact that the bulkier amines are more basic. The results are consistent with a steric inhibition to Cr—N bond formation. A similar trend for the bonding between aliphatic amines and boranes has been observed.[20]

It is interesting that the addition of each butyl group to the amine leads to an additional 4.4–4.9 kcal mol^{-1} weakening of the Cr—A bond. This suggests that the BDE(Cr—A) for ammonia would be about 35 kcal mol^{-1} and that the ammonia derivative would be stable.[21] Such a strong bond indicates the intrinsic $Cr(CO)_5$—(A) bond is nearly as strong as the $Cr(CO)_5$—(CO) bond. This is somewhat surprising considering the fact that aliphatic amines do not backbond.

Inspection of the equilibrium constants in Table 2 reveals that the equilibrium for hydrogen bonding is more unfavourable the bulkier the amine. The fact that the trend is not reflected in the enthalpy of hydrogen-bond formation (which shows no significant change) indicates that entropy is the controlling factor.

The available kinetic and thermodynamic enthalpy parameters for exchange of piperidine with $Cr(CO)_6$ are presented in Table 4 and provide a detailed description of the reaction. It is typically assumed that ligand dissociation for $Cr(CO)_6$ and **1a** (ΔH_1^* and ΔH^*_{-2}) leads initially to $Cr(CO)_5$, which is uncoordinated by the solvent, and that the chromium–ligand bond is nearly broken in the transition state.[2a,22]† This leads to the conclusion that the two transition states are nearly the same energy as $Cr(CO)_5$ (Hammind Postulate)[23] and therefore each other. The difference in the activation enthalpies would then be equal to the enthalpy of ligand-exchange (ΔH_{12}) and the difference in Cr—A and Cr—CO bond energies. This is confirmed, within the experimental error, for the relationship between ΔH_1^*, ΔH^*_{-2} and ΔH_{12} (Table 4). Nonetheless, the recent results discussed below indicate the above conclusion cannot be considered general.

The role of the solvent in ligand-exchange reactions has been receiving intense investigation. It is well-established that $Cr(CO)_5$ forms an agostic bond with alkanes and that this bond energy is large.[1a–c,3,5,10,24] Since ΔH_1^* equals BDE(Cr—CO)[19] and $\Delta H_1^* - \Delta H^*_{-2}$ equals ΔH_{12}, ΔH^*_{-2} is taken to be equal to BDE(Cr—piperidine) (*vide supra*, Table 4). The equivalence of the activation enthalpies to bond energies and microscopic reversibility requires that solvent participation in the transition state for CO or piperidine attack of $Cr(CO)_5$ be small (ie. $\Delta H^*_{-1} = \Delta H_2^*$); therefore within experimental error, the enthalpy of solvent interaction can be taken to be zero. This is consistent with a mechanism where $Cr(CO)_5$(alkane) is in equilibrium with $Cr(CO)_5$ and the alkane dissociates to form $Cr(CO)_5$ before attack by the incoming ligand. In support of this mechanism, apparently both $Cr(CO)_5$ and $Cr(CO)_5$(cyclohexane) have been observed by picosecond IR flash photolysis.[1a,b] However, this mechanism is not consistent with the data for alkane displacement by other ligands that have been studied. Yang *et al.* have reported that the activation enthalpy for displacement of heptane by pyridine is 5 kcal mol^{-1}.[5a] This is significantly less than the chromium–heptane bond energy (10–11 kcal mol^{-1}).‡ The authors conclude that the

† The second assumption for $Cr(CO)_6$ is nicely confirmed by the similar values for BDE(Cr—CO) (ref. 19) and ΔH_1^*.

‡ BDE(Cr–heptane) = BDE(Cr—CO) − ΔH_1, see Table 4 and ref. 19. BDE(Cr–heptane) should be equal to ΔH^*_{-1} if there is no significant interaction with the solvent in the transition-state.

difference in the two values requires that the transition state be stabilized by a $Cr(CO)_5$–heptane interaction of 5 kcal mol^{-1} and that pyridine displacement of heptane be associative. A similar conclusion can be reached for the displacement of cyclohexane by THF, where the activation enthalpy is only 1 kcal mol^{-1}.[10a]†

An examination of the available data indicates that the extent of participation by the solvent in the transition state for solvent displacement may be determined by the steric bulk of the incoming ligand. For example, the activation enthalpy of 2-methylpyridine displacement of heptane (7.3 kcal mol^{-1}) is greater than for pyridine (5 kcal mol^{-1}).[5a] Likewise, the activation enthalpy for piperidine displacement of heptane (ΔH_2^*, Table 4) is greater still. The greater activation enthalpy for piperidine can be attributed to the sp^3 hybridization of the piperidine nitrogen. In light of the other data, it seems reasonable that the difference between ΔH^*_{-1} and ΔH_2^* is real, and that heptane is weakly associated in the transition state for its displacement by piperidine. In any event, it is clear that the transition state for solvent displacement by an unhindered amine favours a greater association with the solvent.

Flash photolysis data for other incoming ligands also appear to be consistent with an associative displacement of alkane solvent. The $Cr(CO)_5$ is clearly a very reactive species that reacts even with cyclohexane near the diffusion-control limit.[1a] The attack of $Cr(CO)_5$ by better ligands ought to be as fast or faster. As a result, the reaction of $Cr(CO)_5$ (cyclohexane) with ligands in a dissociative process would then be limited by the dissociation of cyclohexane and independent of the incoming ligand. This is not the case, since displacement of cyclohexane is dependent on the incoming ligand, varying from 4×10^6 to 4×10^7 M^{-1} s^{-1} (CO and THF, respectively).[10a,25] This ligand dependence is consistent with a steric effect for an associative displacement of the weakly-bonded cyclohexane.

REFERENCES

1. (a) L. Wang, X. Zhu and K. G. Spears, *J. Am. Chem. Soc.* 1988, **110**, 8695; (b) L. Wang, X. Zhu and K. G. Spears, *J. Chem. Phys.* 1989, **93**, 2; (c) J. D. Simon and X. Xie, *J. Phys. Chem.* 1989, **93**, 291; (d) G. R. Dobson, P. M. Hodges, M. A. Healy, M. Poliakoff, J. J. Turner, S. Firth and K. H. Asali, *J. Am. Chem. Soc.* 1987, **109**, 4218; (e) K. J. Asali, S. S. Basson, J. S. Tucker, B. C. Hester, J. E. Cortes, H. H. Awad and G. R. Dobson, *J. Am. Chem. Soc.* 1987, **109**, 5386.
2. (a) G. R. Dobson, *Accts Chem. Res.* 1976, **9**, 300; (b) J. P. Collman, L. S. Hegedus, J. R. Norton and R. G. Finke, *Principles and Applications of Organotransition Metal Chemistry*, pp. 235–278. University Science Books, Mill Valley, California (1987); (c) J. A. S. Howell and P. M. Burkinshaw, *Chem. Rev.* 1983, **83**, 557.
3. (a) J. D. Simon and X. Xie, *J. Phys. Chem.* 1987, **91**, 5538; (b) J. M. Kelly, C. Long and R. Bonneau, *J. Phys. Chem.* 1983, **87**, 3344.
4. M. Brookhart and M. L. H. Green, *J. Organomet. Chem.* 1983, **250**, 395.
5. (a) G. K. Yang, V. Vaida and K. S. Peters, *Polyhedron* 1988, **7**, 1619; (b) Y. Ishikawa, C. E. Brown, P. A. Hackett and D. M. Rayner, *Chem. Phys. Lett.* 1988, **150**, 506; (c) J. M. Morse Jr, G. H. Parker and T. J. Burkey, *Organometallics*, accepted for publication.
6. K. S. Peters and G. J. Snyder, *Science* 1988, **241**, 1053.
7. R. J. Dennenberg and D. J. Darensbourg, *Inorg. Chem.* 1972, **11**, 72.
8. J. Nasielski and A. Colas, *Inorg. Chem.* 1978, **17**, 237.
9. F. L. Slejko, R. S. Drago and D. G. Brown, *J. Am. Chem. Soc.* 1972, **94**, 9210.
10. (a) J. D. Simon and K. S. Peters, *Chem. Phys. Lett.* 1983, **98**, 53; (b) J. M. Kelly, H. Hermann and E. Koerner von Gustorf, *J. Chem. Soc., Chem. Commun.* 1973, 105; (c) J. M. Kelly, D. V. Bent, H. Hermann, D. Shulte-Frohlinde and E. Koerner Von Gustorf, *J. Organomet. Chem.* 1974, **69**, 259.
11. G. G. Hammes and H. O. Spivey, *J. Am. Chem. Soc.* 1966, **88**, 1621 and refs therein.
12. D. J. Darensbourg and J. A. Ewen, *Inorg. Chem.* 1981, **20**, 4168.
13. For leading refs see D. D. Nelson Jr, G. T. Fraser and W. Klemperer, *Science* 1987, **238**, 1670.
14. (a) D. J. Darensbourg, *Inorg. Chem.* 1979, **18**, 2821; (b) J. Ewen and D. J. Darensbourg, *J. Am. Chem. Soc.* 1975, **97**, 6874.
15. (a) F. A. Cotton, D. J. Darensbourg, A. Fang, B. W. S. Kolthammer, D. Reed and J. L. Thompson, *Inorg. Chem.* 1981, **20**, 4090; (b) J. L. Atwood and D. J. Darensbourg, *Inorg. Chem.* 1977, **16**, 2314.
16. (a) J. A. Westrick, J. L. Goodman and K. S. Peters, *Biochemistry* 1987, **26**, 8313; (b) R. A. Orwoll and P. J. Flory, *J. Am. Chem. Soc.* 1967, **89**, 6814; (c) J. Timmermans, *Physico-chemical Constants of Pure Organic Compounds*, Vol 2. Elsevier, Amsterdam (1965); (d) R. C. Weast (Ed.), *CRC Handbook of Chemistry and Physics*, 69th edn. CRC Press, Boca Raton (1988).

† The ΔH_1 in cyclohexane (24.6 kcal mol^{-1}) is more exothermic than in heptane, indicating the Cr—alkane bond is stronger for cyclohexane by 3 kcal mol^{-1} (see ref. 5c). This is in agreement with the kinetic results for ligand displacement of coordinated alkane where the rates are faster for heptane than cyclohexane: see B. S. Creaven, A. D. Dixon, J. M. Kelly, C. Long and M. Poliakoff, *Organometallics* 1987, **6**, 2600 and refs therein.

17. (a) T. J. Burkey, M. Majewski and D. Griller, *J. Am. Chem. Soc.* 1986, **108**, 2218; (b) J. M. Kanabus-Kaminska, B. C. Gilbert and D. Griller, *J. Am. Chem. Soc.* 1989, **111**, 3311.
18. (a) H. E. Bryndza, L. K. Fong, R. A. Paciello, W. Tam and J. E. Bercaw, *J. Am. Chem. Soc.* 1987, **109**, 144; (b) J. W. Bruno, T. J. Marks and L. R. Morss, *J. Am. Chem. Soc.* 1983, **105**, 6824; (c) A. A. Gonzales, K. Zang, S. P. Nolan, R. L. de la Vega, S. L. Mukerjee, C. D. Hoff and G. J. Kubas, *Organometallics* 1988, **12**, 2429.
19. BDE(Cr—CO) = 36.8 kcal mol^{-1} (a) G. P. Smith, *Polyhedron* 1988, **7**, 1605; (b) K. E. Lewis, D. M. Golden and G. P. Smith, *J. Am. Chem. Soc.* 1984, **106**, 3905.
20. H. C. Brown, *Boranes in Organic Chemistry*, pp. 53–78. Cornell University Press, Ithaca (1972).
21. The ammonia derivative and the analogous molybdenum and tungsten compounds have been synthesized. See F. Calderazzo, R. Ercoli and G. Natta, *Organic Syntheses via Metal Carbonyls* (Edited by I. Wender and P. Pino), pp. 170–171. Interscience, New York (1968).
22. R. J. Angelici, *Organomet. Chem. Rev.* 1968, **3**, 173.
23. G. S. Hammond, *J. Am. Chem. Soc.* 1955, **77**, 334.
24. (a) J. J. Turner and M. Poliakoff, *ACS Symp. Ser.* 1983, **211**, 35; (b) R. N. Perutz, *Annu. Rep. Progr. Chem.* 1985, **85C**, 157; (c) J. D. Simon and X. Xie, *J. Phys. Chem.* 1987, **91**, 5538.
25. S. P. Church, F.-W. Grevels, H. Hermann and K. Schaffner, *Inorg. Chem.* 1985, **24**, 418.

Polyhedron Vol. 8, No. 22, pp. 2689–2692, 1989
Printed in Great Britain

0277–5387/89 $3.00+.00
© 1989 Pergamon Press plc

SELECTIVITY IN MULTIPLE METHYLATION OF $MCl_n(PR_3)_m$ COMPOUNDS

ERIC G. THALER, ERIC G. LUNDQUIST and KENNETH G. CAULTON*

Department of Chemistry, Indiana University, Bloomington, IN 47405, U.S.A.

(*Received* 5 *May* 1989; *accepted* 20 *June* 1989)

Abstract—Reaction of $RhCl_3L_3$ (L = PMe_2Ph or $PMePh_2$) with excess MeLi or MeMgCl reveals a distinct tendency to stop at the $RhMe_2ClL_3$ stage. This behaviour is attributed to the concentration of all Cl → Rh π-donation into the single remaining metal–halogen bond, and is shown to be a phenomenon of even broader occurrence and greater potential generality. For *cis,mer*-$RhMe_2ClL_3$ containing the bulkier ligand $PMePh_2$, variable temperature ^1H and ^{31}P NMR studies reveal the occurrence of two dynamic processes: hindered rotation about Rh—P and P—C bonds and also dissociation of the unique phosphine *trans* to one methyl group.

We report separately[1] that the reaction of (tripod)$CrCl_3$ (tripod = $MeC(CH_2PMe_2)_3$) with excess *n*-BuLi (6 mol/mol Cr), run under mild conditions to avoid decomposition of the chromium alkyl product, reveals a considerable selectivity to stop at the *di*alkylation stage: (tripod)Cr(*n*-Bu)$_2$Cl. We report here sufficient additional examples of this behaviour to qualify it as a consistent pattern and offer an explanation subject to further experimental test.

EXPERIMENTAL

All manipulations were carried out using standard Schlenk and glove-box techniques under purified nitrogen. Methyl lithium and methyl magnesium chloride solutions were purchased from Aldrich Chemicals, methyldiphenyl phosphine from Strem Chemicals, and chlorine gas from Matheson Gas Company. Benzene, pentane and tetrahydrofuran were dried and distilled prior to use from solutions containing sodium/potassium benzophenone ketyl. ^1H and ^{31}P NMR spectra were recorded on a Nicolet NT-360 spectrometer at 360 and 146 MHz, respectively.

* Author to whom correspondence should be addressed.

mer-$RhCl_3(PMe_2Ph)_3$

This was made according to a literature procedure.[2] ^1H NMR (360 MHz, C_6D_6, 25°C): 1.1 ppm (d, PMe, J = 11 Hz), 2.0 ppm (vt, PMe, line spacing = 4.2 Hz), 6.7–7.6 ppm (m, Ph). $^{31}P\{^1H\}$ NMR (146 MHz, C_6D_6, 25°C): 7.3 ppm (d of t, $J_{P—Rh}$ = 113 Hz; $J_{P—P'}$ = 25 Hz); −4.7 ppm (d of d, $J_{P'—Rh}$ = 85 Hz; $J_{P—P'}$ = 25 Hz).

mer-$RhCl_3(PMePh_2)_3$

Into an ethanol slurry of $RhCl_3 \cdot nH_2O$ (1.0 g, 3.8 mmol) was syringed $PMePh_2$ (2.28 g, 11.43 mmol). The solution was then stirred and refluxed for 1 h. Allowing this solution to cool to room temperature yielded large amounts of a yellow–orange precipitate.

This precipitate, a 50:50 mixture of $RhCl_3(PMePh_2)_3$ and $RhHCl_2(PMePh_2)_3$, was collected by filtration and dried *in vacuo*. This mixture was dissolved in CH_2Cl_2 and converted completely to *mer*-$RhCl_3(PMePh_2)_3$ by slow addition of Cl_2 (0.5 cm^3 portions) using a gas-tight syringe. Reaction progress is conveniently monitored by $^{31}P\{^1H\}$ NMR. After complete conversion, the volume of CH_2Cl_2 was reduced to 15 cm^3, the product was precipitated using pentane, and yellow–orange *mer*-$RhCl_3(PMePh_2)_3$ was collected by fil-

tration. $^{31}P\{^1H\}$ NMR (CH_2Cl_2): −3.5 ppm (d of t, $J_{P—Rh}$ = 114 Hz, J_{PP} = 24 Hz); −5.7 ppm (d of d, $J_{P—Rh}$ = 85 Hz).

Reaction of $RhCl_3(PMe_2Ph)_3$ *with* MeMgCl

To $RhCl_3(PMe_2Ph)_3$ (2.75 g) in 50 cm^3 of benzene was added 25 cm^3 of 2.7 M MeMgCl in Et_2O. The volume was reduced *in vacuo* to 50 cm^3 to remove most of the ether, and the solution was refluxed for 3 h. Excess Grignard was hydrolysed by the addition of 10 cm^3 of water and stirring. The benzene layer was separated from the aqueous layer and was retained. The aqueous layer and associated solids were extracted with 2 × 50 cm^3 of CH_2Cl_2. From the dried $(MgSO_4)CH_2Cl_2$ extracts was isolated 0.75 g of colourless $RhMe_3(PMe_2Ph)_3$. ^1H NMR (360 MHz, 25°C, CD_2Cl_2): −0.28 (m, 9H); 1.10 (d, $J_{Me—P}$ = 8 Hz, 18H); 7.0–7.5 (m, Ph—P). $^{31}P\{^1H\}$ NMR (146 MHz, 25°C, C_6D_6): −8.9 (d, $J_{P—Rh}$ = 80 Hz). From the dried benzene phase was isolated 1.25 g of yellow *cis,mer*-$RhMe_2Cl(PMe_2Ph)_3$. ^1H NMR (360 MHz, 25°C, CD_2Cl_2): −0.03 (m, 3H); 0.48 (q, 3H); 0.85 (d, PMe); 1.20 (t, PMe); 1.40 (t, PMe); 7.0–7.5 (m, Ph—P). $^{31}P\{^1H\}$ NMR (146 MHz, 25°C, C_6D_6): −0.1 (d of d, $J_{P—Rh}$ = 110 Hz), −18.0 (d of t, $J_{P—Rh}$ = 83 Hz, $J_{P—P'}$ = 25 Hz).

Reaction of $RhCl_3(PMePh_2)_3$ *with* MeLi

To a homogeneous THF solution of $RhCl_3(PMePh_2)_3$ (0.57 g, 0.7 mmol) was added a diethyl ether solution of MeLi (1.4 M, 12.6 mmol). The solution immediately turned deep red–brown and then gradually lightened over a period of 3 h. At this stage, the solution was cooled to 0°C and the unreacted MeLi was hydrolysed with THF–H_2O (60:40). The volatiles were removed *in vacuo* and the resulting off-white solid was extracted with 60 cm^3 of CH_2Cl_2 and filtered to yield a yellow homogeneous solution. The volume of CH_2Cl_2 was reduced to 15 cm^3 and pentane added to precipitate $RhMe_2Cl(PMePh_2)_3$ as a pale yellow powder. ^1H NMR (360 MHz, −30°C, CD_2Cl_2): −0.55 (m, 3H); 0.23 (br q, line spacing 10 Hz, 3H), 1.27 (d, $J_{P—CH_3}$ = 7 Hz, 3H); 1.9 (br. s, 6H); 7–7.8 (m, P—Ph). ^{31}P (146 MHz, −10°C, CH_2Cl_2): −12.8 (d or t, $J_{P—Rh}$ = 76 Hz, $J_{P—P}$ = 21 Hz); 11.5 (br d, $J_{P—Rh}$ = 110 Hz).

RESULTS

Polyalkylation of $RhCl_3L_3$

We find that reaction of *mer*-$RhCl_3(PMe_2Ph)_3$ with an excess (15 mol/mol Rh) of MeMgCl in benzene at 80°C gives only a low (28%) yield of the *per*-alkyl compound, $RhMe_3(PMe_2Ph)_3$. The major product is the compound *cis,mer*-$RhClMe_2(PMe_2Ph)_3$, which is easily separated from $RhMe_3(PMe_2Ph)_3$ by its higher solubility in benzene; the trimethyl compound may be dissolved in CH_2Cl_2.

A similar tendency to leave one chloride unreacted is demonstrated by *mer*-$RhCl_3(PMePh_2)_3$, which reacts with 18 mol MeLi/mol Rh in THF in the temperature range 0–25°C to give only *cis,mer*-$RhClMe_2(PMePh_2)_3$. Since $RhClMe_2(PMePh_2)_3$ readily dissociates phosphine in solution (see below), the resistance of the last chloride to alkylation cannot be due to the coordinatively saturated character of this compound. That is, the mechanism in eq. (1) (P = $PMePh_2$) remains available

$$\begin{aligned} RhClMe_2P_3 &\rightleftarrows RhClMe_2P_2 + P \\ RhClMe_2P_2 + MeLi &\rightarrow Li[RhClMe_3P_2] \\ Li[RhClMe_3P_2] &\rightarrow RhMe_3P_2 + LiCl \\ RhMe_3P_2 + P &\rightarrow RhMe_3P_3. \end{aligned} \qquad (1)$$

Solution dynamics of cis,mer-$RhClMe_2(PMePh_2)_3$

This molecule shows two P*Me* ^1H NMR signals at and below 25°C in CD_2Cl_2. At −30°C, there are two Rh/Me signals, one a pseudoquartet and the other an unresolved multiplet. At −25°C, however, each Rh/Me signal is very broad ($\Delta\nu_{1/2}$ = 68 Hz). The $^{31}P\{^1H\}$ NMR spectrum of $RhClMe_2(PMePh_2)_3$ shows two resonances (intensity, 2:1) at 25°C, the less intense one is a broad singlet (i.e. neither P—Rh nor P—P′ coupling is resolved) and the more intense one is a broad doublet ($J_{Rh—P}$ = 110 Hz). This behaviour we attribute to selective dissociation of P_A in eq. (2), due both to the steric bulk of diphenylmethyl phosphine and its location opposite the strong *trans*-directing methyl ligand. The importance of the *trans*-methyl group rests on the observation that *mer*-$RhCl_3(PMePh_2)_3$ shows no line broadening in the $^{31}P\{^1H\}$ NMR; a sharp AM_2X pattern is observed.

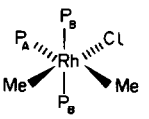

$$\rightleftharpoons \quad RhClMe_2(P_B)_2 + P_A \qquad (2)$$

$RhMe_2Cl(PMePh_2)_3$ reveals its crowded character in yet another way (Fig. 1). The P_A—Rh and P_A—P_B coupling which is absent in the P_A resonance at and above 25°C is restored at −10°C; a sharp doublet ($J(P_A—Rh)$ = 76 Hz) of triplets ($J(P_A—P_B)$ = 21 Hz) is observed. However, at

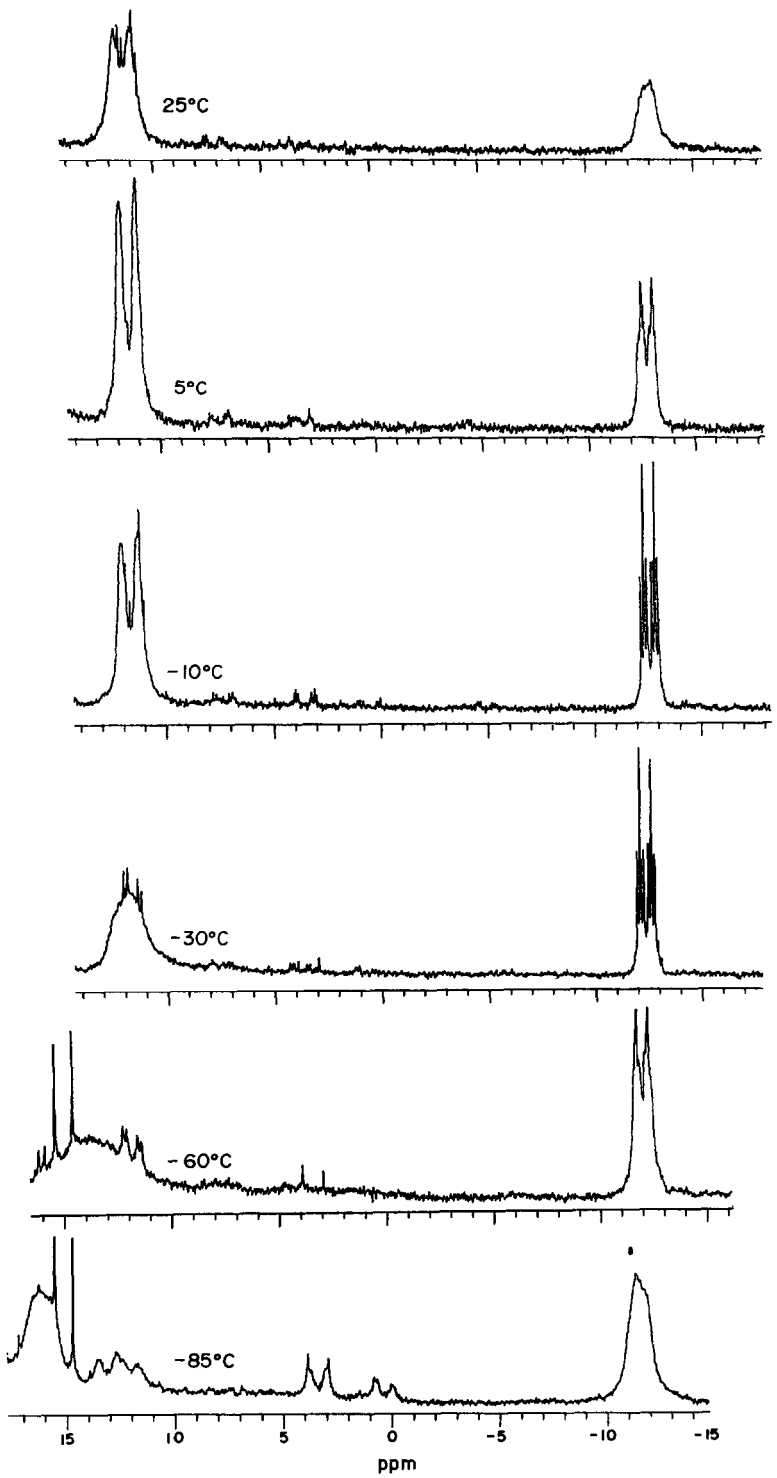

Fig. 1. Variable temperature $^{31}P\{^1H\}$ NMR spectra of $RhMe_2Cl(PMe_2Ph_2)_3$ in CD_2Cl_2. The consistently sharp peaks between 10 and 15 ppm are impurities.

$-10°C$, the P_B resonance is still a doublet of broad lines. At -25 and $-40°C$, the $^{31}P\{^1H\}$ NMR resonance of P_A remains a sharp doublet of triplets, but the P_B doublet becomes increasingly broad. Nevertheless, the sharp P_A—P_B coupling in the P_A resonances assures the lack of significant phosphine dissociation at these temperatures. Finally, at $-85°C$, the P_A resonance is one unresolved broad line and the P_B region now contains several broad lines (no J(P—Rh) observed) indicative of *several* closely spaced chemical shifts undergoing dynamic exchange at an intermediate rate. This we interpret as the freezing out of an ABCX spin system, where B and C are the axial phosphines in $RhMe_2Cl(PMePh_2)_3$, made inequivalent by the freezing out of distinct rotational conformations about the Rh—P and P—C bonds in the T-shaped $Rh(PMePh_2)_3$ substructure. Similar phenomena have been reported by Bushweller for $M(CO)Cl[P(^tBu)_2R]_2$ compounds.[3] Note that no ^{31}P NMR signal of free $PMePh_2$ is seen at (or above) $-85°C$.

DISCUSSION

We feel that the isolation of monohalopolyalkyl compounds during attempted *per*-alkylation of $(R_3P)_mMCl_n$ compounds *under mild conditions* of temperature is a kinetic effect due to the sequential strengthening of the M—Cl bonds (increased Cl→M π-donation) as the number of π-donor ligands decline. Thus, at the stage of $(R_3P)_mMR'_{n-1}Cl$, all π-donation is concentrated in the single remaining M—Cl bond (there being no other π-donor ligands present), and this bond is therefore uniquely resistant to replacement by alkyl. The effect is subtle; there is no evidence of Ir—Cl bond length shortening along the series $IrCl_{3-n}H_n(PMe_2Ph)_3$,[4] so it has only kinetic (not ground state) manifestations, but it may well occur in the unsaturated $RhMe_2ClP_2$ intermediate. Increasing alkylation also would be expected to increase steric suppression of the rate of alkylation.

Based on the above reasoning, we anticipate that this phenomenon would be of even greater importance in the alkylation of *unsaturated* metal halides, where ground-state bond shortening is evident (e.g. $TiCl_4$, where d(Ti—Cl) = 2.170 Å[5] and $TiCl_3(CH_3)$, where d(Ti—Cl) = 2.185 Å[6] vs Cp_2TiCl_2, where d(Ti—Cl) = 2.366 Å,[7] and $Ti(Me_2PC_2H_4PMe_2)Cl_3R$, where d(Ti—Cl) = 2.30–2.32 Å[8]) and thus kinetic effects should be magnified.* This effect should, of course, also be evident whenever π-donor ligands are replaced by purely σ-ligands (e.g. hydrides).

The special tendency of $PMePh_2$ to promote phosphine dissociation in $L_mM(PMePh_2)_n$ complexes ($n \geqslant 3$) is worthy of note, particularly in comparison to the (perhaps) more frequently used PMe_2Ph. The benefits of using this bulky phosphine to furnish 16-electron species are evident in, for example, the C/O multiple bond splitting reactions of Mayer and co-workers[9,10] using $WCl_2(PMePh_2)_4$ (but not the PMe_3 analogue). The close relationship between $PMePh_2$ and PPh_3 is also evident in that $RhMeI_2(PPh_3)_2$, analogous to the transient $RhMe_2Cl(PMePh_2)_2$ implicated above, is an isolable compound.[11]

Acknowledgement—This work was supported by the National Science Foundation.

REFERENCES

1. E. G. Thaler and K. G. Caulton, *J. Organomet. Chem.*, in press.
2. J. Chatt, N. R. Johnson and B. L. Shaw, *J. Chem. Soc.* 1964, 2508.
3. C. H. Bushweller, C. D. Rithner and D. J. Butcher, *Inorg. Chem.* 1986, **25**, 1610.
4. G. B. Robertson and P. A. Tucker, *J. Am. Chem. Soc.* 1982, **104**, 317.
5. Y. Morino and V. Uehara, *J. Chem. Phys.* 1966, **45**, 4543.
6. A. Haaland and K. Rypdal, private communication.
7. A. Clearfield, D. K. Warner, C. H. Saldarriága-Molina, R. Ropal and I. Bernal, *Can. J. Chem.* 1975, **53**, 1622.
8. Z. Dawoodi, M. L. H. Green, V. S. B. Mtetwa, K. Prout, A. J. Schultz, J. Williams and T. F. Koetzle, *J. Chem. Soc., Dalton Trans.* 1986, 1629.
9. J. C. Bryan, S. J. Geib, A. L. Rheingold and J. M. Mayer, *J. Am. Chem. Soc.* 1987, **109**, 2826.
10. J. C. Bryan and J. M. Mayer, *J. Am. Chem. Soc.* 1987, **109**, 7213.
11. P. G. H. Troughton and A. C. Skapski, *Chem. Comm.* 1968, 575.

* In this regard, note the successful synthesis of $(dmpe)TiCl_3R$ (R = Me, Et).[8]

Polyhedron Vol. 8, No. 22, pp. 2693–2699, 1989
Printed in Great Britain

0277–5387/89 $3.00+.00
© 1989 Pergamon Press plc

BINARY AND TERNARY COMPLEXES OF 1,3-PHENYLENEDIAMINE-N,N′-DISUCCINIC ACID WITH DIVALENT CATIONS

J. FUENTES,* R. REBOSO and A. RODRIGUEZ

Departamento de Química Inorgánica, Universidad de La Laguna, Tenerife, Canary Islands, Spain

(*Received* 21 *May* 1989; *accepted* 26 *June* 1989)

Abstract—The formation equilibria involved in the novel binary and ternary systems, M^{II}–A and M^{II}–A–B, have been studied by potentiometric and conductimetric methods in an aqueous solution of 0.5 M NaCl at 25°C (where A is 1,3-phenylenediamine-N,N′-disuccinic acid (1,3-FDDS) and B is oxalic, malonic or succinic acid), where M is Co, Ni or Zn for the ternary systems and Co, Ni, Zn, Mg, Ca, Sr, Ba, Mn or Cd, for the binary systems. The results indicate that in the ternary systems, where the secondary ligand B forms five-membered chelate rings (oxalic acid), the MAB complexes are more stable than MABH, $MABH_2$ and $MABH_3$, while in those systems where B forms six- and seven-membered chelate rings (malonic and succinic acids) MAB complexes are not formed, the complexes arising being the acid ones MABH, $MABH_2$ and $MABH_3$. The negative values of $\Delta \log K$ for the MAB complexes in the case of oxalic acid indicate a greater tendency of this acid to bond to the aqueous ion than the MA or MAH species.

This work is a contribution to the systematic study of polyaminocarboxylic ligands derived from aromatic diamines, by reaction with bromosuccinic acid, which we began with the preparation of 1,4-phenylenediamine-N-succinic acid (1,4-FDS)[1] and 1,4-phenylenediamine-N,N′-disuccinic acid (1,4-FDDS).[2] We have also prepared the derivatives of 1,2-phenylenediamine (1,2-FDDS),[3] 2,5-toluenediamine (2,5-TDDS)[4] and 1,3-phenylenediamine (1,3-FDDS).[5] We reported only the preparation and determination of the dissociation constants of 1,3-FDDS at an ionic strength of 0.5 M NaCl and at 25°C.[5] This paper includes conductimetric and potentiometric studies of the complexation ability of 1,3-FDDS acid with the cations Mg^{2+}, Ca^{2+}, Sr^{2+}, Ba^{2+}, Mn^{2+}, Co^{2+}, Ni^{2+}, Zn^{2+} and Cd^{2+}, as well as the calculation of the stability constants of the binary complexes formed at the same ionic strength and temperature as used in the determination of the dissociation constants of the acid. A study of the equilibria of formation involved in the ternary systems M^{II}–1,3-FDDS–B in an aqueous solution of 0.5 M NaCl and at 25°C (where B is oxalic, malonic or succinic acid and M is Co, Ni or Zn, these being the most widely complexed by 1,3-FDDS acid of all the cations studied) is also presented.

Since the primary ligand, although it contains two coordination spheres (each of which is potentially tridentate), can only use one of them in mononuclear complexes, and the secondary ligand is normally bidentate, the anticipated species are ternary complex species with MAB stoichiometry or MABH, $MABH_2$ and $MABH_3$ protonated complex species. In fact, as was expected, these four species are found in the present work, but MA_2B or MAB_2 species were not detected, possibly due to steric factors associated with the very large primary ligand. The presence of oxalic, malonic or succinic acid as a secondary ligand permits the influence of the size of the chelate ring on the stability of the ternary complexes formed to be observed.

EXPERIMENTAL

The ligand 1,3-FDDS was prepared by us and described in an earlier paper.[5] The oxalic acid (Merck), malonic acid (BDH) and succinic acid

*Author to whom correspondence should be addressed.

(Riedel) were recrystallized from water. The remaining products used were from Merck and, as well as the aforementioned ones, were of p.a. quality. The experimental apparatus used in the potentiometric titrations has been described in ref. 2. The titrations were carried out in an aqueous solution of 0.5 M NaCl and at 25 ± 0.05°C, the initial concentration of the acid being of the order 10^{-3} M. The measurements were recorded with a Radiometer potentiometer (64pHM type) with an accuracy of approximately 0.1 mV, and by using glass and calomel electrodes, G202B and K401, respectively, from the same company. The cell used was: Glass electrode/System M^{II}–A, M^{II}–B or M^{II}–A–B ($I = 0.5$; $T = 25 \pm 0.05$°C)/Calomel electrode; whose standard potential and $[H^+]$ were determined by a similar procedure to that described in ref. 6. The conductimetric titrations of 1,3-FDDS alone and in the presence of the cations studied were performed, without adjusting the ionic strength, at 25°C and using the same experimental apparatus as employed in the potentiometric titrations. The metal–acid ratios were 1 : 1, 2 : 1 and 15 : 1 for all of the cations, and the initial concentration of the acid was of the order 10^{-3} M. The measurements were recorded in a Radiometer conductimeter, model CDM 83, equipped with a CDC 304 conductivity cell.

The solutions of the metal chlorides were prepared at a concentration of approx. 0.1 M and were calculated as indicated in ref. 6, as were those of EDTA, HCl and carbonate-free NaOH.

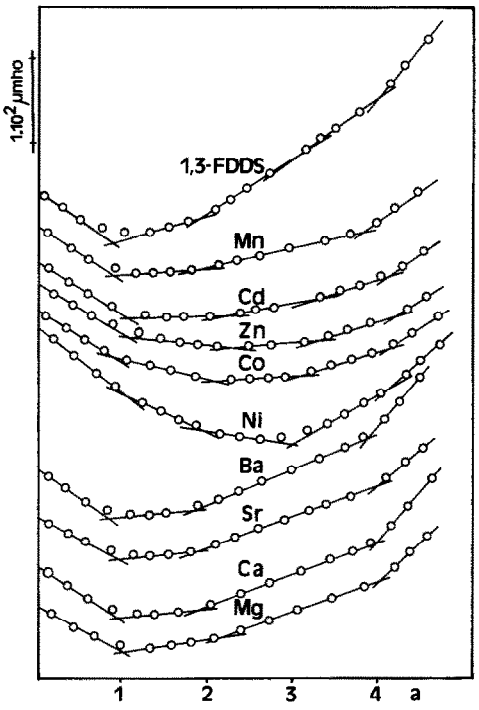

Fig. 1. Conductimetric curves of the free acid 1,3-FDDS and in the presence of different divalent cations in the ratio $[M^{II}]$–[1,3-FDDS] = 1 : 1.

RESULTS AND DISCUSSION

Binary complexes

The process of metal complex formation, in which the ligand is a weak organic acid, can be represented by the equation:

$$H_sA_q + pM^{z+} \rightleftharpoons M_pH_{s-n}A_q^{(pz-n)+} + nH^+. \quad (1)$$

In this type of reaction new species are formed in solution, which can be detected by conductimetric and/or potentiometric techniques.

The conductimetric titration curves of 1,3-FDDS acid in the presence of the divalent cations under study, for the ratio $[M^{II}]/[1,3\text{-FDDS}] = 1:1$, are plotted in Fig. 1. The curve corresponding to the titration of the free acid has been included for comparison purposes. For all the cations studied a decrease is observed in the slopes from $a = 1$, which can be interpreted by assuming that in addition to the acid dissociation equilibria, the following equilibria come about:

$$H_2A^{2-} + M^{2+} \overset{K''}{\rightleftharpoons} MH_2A \qquad 1 < a < 2$$

$$HA^{3-} + M^{2+} \overset{K'}{\rightleftharpoons} MHA^- \qquad 2 < a < 3$$

$$A^{4-} + M^{2+} \overset{K_c}{\rightleftharpoons} MA^{2-} \qquad 3 < a < 4,$$

where, K'', K' and K_c are the corresponding stability constants. The most significant feature to be pointed out is that between $a = 3$ and 4, where the slope of the curve of 1,3-FDDS decreases less, with any of the cations studied, than in the case of 1,4-FDDS[7] and 2,5-TDDS[4] acids. This is in agreement with the basicity sequence of the amine nitrogens: 1,3-FDDS < 2,5-TDDS < 1,4-FDDS,[8] which results in a decrease in the value of the stability constants of the neutral complexes of 1,3-FDDS with respect to the other two.

The potentiometric curves of $[M^{II}]/[1,3\text{-FDDS}]$ in the ratio 1 : 1 plotted in Fig. 2 are deformed with respect to that of the acid from $a = 1$. The observed decrease in pH is in agreement with the formation of the above-mentioned complex species by way of the following shift equilibria:

$$H_3A^- + M^{2+} \rightleftharpoons MH_2A + H^+ \qquad 1 < a < 2$$

$$H_2A^{2-} + M^{2+} \rightleftharpoons MHA^- + H^+ \qquad 2 < a < 3$$

$$HA^{3-} + M^{2+} \rightleftharpoons MA^{2-} + H^+ \qquad 3 < a < 4.$$

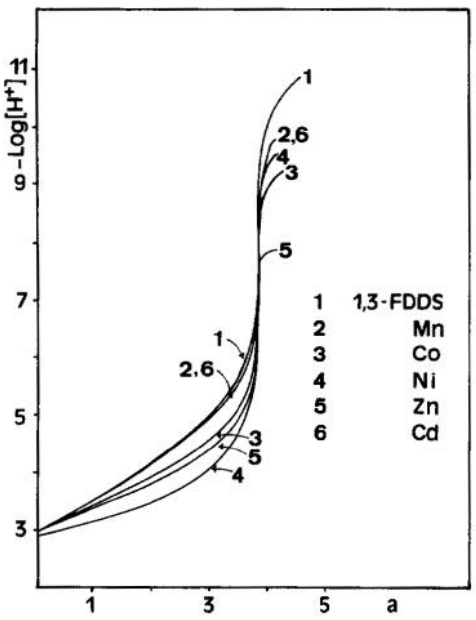

Fig. 2. Potentiometric curves of the free acid 1,3-FDDS and in the presence of different divalent cations in the ratio $[M^{II}]$–[1,3-FDDS] = 1 : 1.

In the case of the curves with an excess of metal a greater deformation is observed, both in the conductimetric and potentiometric curves, with respect to the ratio 1 : 1, due to the fact that the concentration of metal ion shifts the equilibria defined by eq. (1) towards the right. In the interval $3 < a < 4$, the deformation of the curve of the acid is even more marked as a consequence of the additional shift of protons by the metal cation:

$$MHA^- + M^{2+} \rightleftharpoons M_2A + H^+$$

and formation of the bimetallic particle M_2A:

$$MA^{2-} + M^{2+} \rightleftharpoons M_2A.$$

The formation of the bimetallic particle is possible in view of the type of structure presented by 1,3-FDDS acid,[5] analogous to those of 1,4-FDDS[2] and 2,5-TDDS[4] acids, which may act as a ligand with one or two coordination spheres.

The decrease in the pH and, therefore, the complexation strength increases in the series: $Mg^{2+} < Sr^{2+} \approx Ba^{2+} < Ca^{2+} < Mn^{2+} < Cd^{2+} < Co^{2+} < Zn^{2+} < Ni^{2+}$. This sequence coincides with that found for 1,4-FDDS[7] and 2,5-TDDS[4] acids and is in agreement with the Irving and Williams' scale.[9]

Determination of the stability constants

The potentiometric titrations of solutions of 1,3-FDDS in 0.5 M NaCl, in the presence of a divalent metal cation in the ratios $[M^{II}]/[1,3\text{-FDDS}] = 1:1$, 1 : 2, 2 : 1 and 15 : 1, allow the calculation of the

Table 1. Stability constants of 1,3-FDDS acid with M^{II} at 25°C and $I = 0.5$ M NaCl

M^{II}	$\log \beta_{112}$	$\log \beta_{111}$	$\log \beta_{110}$	$\log \beta_{210}$
Ni	12.823(08)	10.084(01)	5.734(02)	7.838(11)
Co	12.197(23)	8.847(06)	4.543(06)	6.187(09)
Zn	11.768(18)	8.483(03)	3.966(02)	6.040(07)
Cd	11.158(33)	7.364(07)	2.472(04)	3.707(11)
Mn	10.929(82)	7.174(12)	2.306(09)	3.067(34)
Mg	10.533(22)	6.436(11)	1.298(28)	—
Ca	10.901(16)	6.716(08)	1.576(07)	—
Sr	10.844(15)	6.559(09)	1.450(08)	—
Ba	10.819(27)	6.599(14)	1.399(12)	—

M^{II}	$\log K''(MH_2Y)$ (I)	(II)	$\log K'(MHY^-)$ (I)	(II)	$\log K_c(MY^{2-})$ (I)	(II)	$\log K_M(M_2Y)$ (I)
Ni	2.85	2.82	4.63	4.23	5.73	5.67	2.11
Co	2.22	2.08	3.39	3.25	4.54	4.50	1.64
Zn	1.79	1.98	3.03	3.13	3.97	4.12	2.07
Cd	1.18	1.02	1.91	1.91	2.47	2.49	1.24
Mn	0.95	0.95	1.72	1.93	2.31	2.35	0.76
Mg	0.56	0.30	0.98	0.86	1.30	1.20	—
Ca	0.92	0.75	1.26	1.09	1.58	1.40	—
Sr	0.87	0.73	1.10	0.88	1.45	1.26	—
Ba	0.84	0.49	1.14	1.00	1.40	1.22	—

Calculated values using: (I) MINIQUAD program; (II) Schwarzenbach criterion. The standard deviation in the last significant figure is indicated in parentheses.

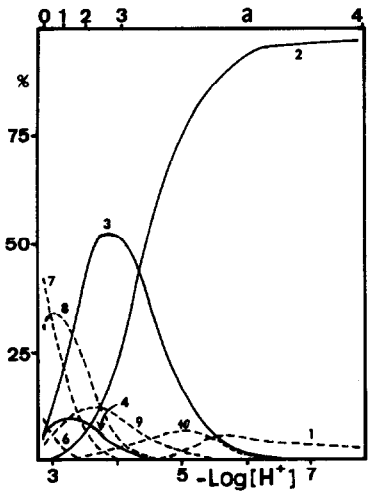

Fig. 3. Distribution diagram of the species as a function of $-\log[H^+]$ for the system $[Ni^{II}]$–[1,3-FDDS] = 1 : 1. (1) A, (2) MA, (3) MAH, (4) MAH_2, (6) AH_5, (7) AH_4, (8) AH_3, (9) AH_2 and (10) AH.

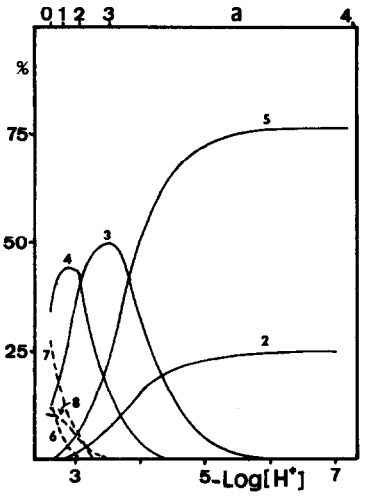

Fig. 4. Distribution diagram of the species as a function of $-\log[H^+]$ for the system $[Ni^{II}]$–[1,3-FDDS] = 15 : 1. (2) MA, (3) MAH, (4) MAH_2, (5) M_2A, (6) AH_5, (7) AH_4, (8) AH_3.

formation constants, β_{pqs}, of the binary complexes defined by means of the equilibrium:

$$pM + qA + sH \rightleftharpoons M_pA_qH_s.$$

The species detected and for which the stability constants were calculated (Table 1) are: pqs = 110, 111, 112 and 210. For the calculation the graphical criterion of Schwarzenbach *et al.*[10] was used, and the values obtained were refined by means of the MINIQUAD program.[11,12]

In Figs 3 and 4, and as an example, the species distribution diagrams are plotted as a function of the pH for the system $[Ni^{II}]$/[1,3-FDDS] = 1 : 1 and 15 : 1. In the diagram corresponding to the ratio 15 : 1 the M_2Y species appears, in agreement with the double coordination sphere mentioned for the 1,3-FDDS ligand. The species distribution curves for cobalt and zinc are analogous to those of nickel.

The dissociation constants of 1,3-FDDS acid are given in Table 2, together with those of oxalic, malonic and succinic acids, since they will be used in the study of the ternary complexes. It was necessary to calculate the above constants since none were reported in the literature at I = 0.5 M NaCl and at 25°C.

Although the dissociation constants of 1,3-FDDS acid were determined by us in an earlier paper,[5] we have recalculated them by considering, as in the cases of 1,4-FDDS[8] and 2,5-TDDS,[4] the possibility that in aqueous solution the species H_4A

Table 2. Dissociation constants of 1,3-FDDS, oxalic, malonic and succinic acids at 25°C and I = 0.5 M NaCl

Acid	$\log\beta_1$	$\log\beta_2$	$\log\beta_3$	$\log\beta_4$	$\log\beta_5$
1,3-FDDS	5.454(2)	9.977(1)	13.753(2)	16.776(3)	19.023(12)
Oxalic	3.60(1)	4.76(3)	—	—	—
Malonic	5.06(2)	7.63(3)	—	—	—
Succinic	5.08(1)	8.98(1)	—	—	—
Acid	pK_0	pK_1	pK_2	pK_3	pK_4
1,3-FDDS	2.25	3.02	3.78	4.52	5.45
Oxalic	—	1.16	3.60	—	—
Malonic	—	2.57	5.06	—	—
Succinic	—	3.90	5.08	—	—

The standard deviation in the last significant figure is indicated in parentheses.

Table 3. Stability constants of the binary complexes M^{II}–B (B = oxalic, malonic or succinic acid) at 25°C and $I = 0.5$ M NaCl

Acid	M^{II}	$\log\beta_{111}$	$\log\beta_{110}$	$\log\beta_{120}$
Oxalic	Co	—	3.21(1)	5.93(2)
	Ni	—	4.05(1)	6.01(3)
	Zn	—	3.46(1)	6.03(1)
Malonic	Co	5.86(3)	2.37(1)	—
	Ni	—	2.74(1)	—
	Zn	—	2.38(2)	—
Succinic	Co	5.57(6)	1.26(1)	—
	Ni	5.79(3)	1.47(1)	—
	Zn	—	0.85(2)	—

The standard deviation in the last significant figure is indicated in parentheses.

might become self-dissociated according to the equilibrium:

$$2H_4A \rightleftharpoons H_5A^+ + H_3A^-.$$

Assuming the existence of the species H_5A^+, a new model was proposed in which, in addition to the species H_4A, H_3A^-, H_2A^{2-}, HA^{3-} and A^{4-}, there appeared a protonated species H_5A^+. Calculation by means of the MINIQUAD program, using as initial values those obtained in ref. 5, shows a better fit for this model, in agreement with the standard deviation values of the constants of R and U.

We have also not found any values for the stability constants of the binary complexes formed by oxalic, malonic and succinic acids with the cations Co^{2+}, Ni^{2+} and Zn^{2+} at 25°C and ionic strength 0.5 M NaCl in the literature. It was thus necessary to calculate these constants under such conditions. The values obtained by means of the MINIQUAD program are given in Table 3. The data for the determination of the stability constants of these binary complexes were obtained from potentiometric titrations of M^{II}–B in the ratios, 1 : 1 and 1 : 2, which are the same as those used for ternary complexes.

The values of the dissociation constants of the protonated ligands and of the stability constants of the binary complexes were taken as fixed in the model tested for the determination of the stability constants of the ternary complexes.

Ternary complexes

The formation of ternary complexes of the type M^{II}–A–B, where M is Co, Ni or Zn, A is the primary ligand 1,3-FDDS and B is oxalic, malonic or succinic acid, which acts as secondary ligand, will allow the influence of the number of members in the chelate ring of the secondary ligand on the stability of the ternary complexes formed to be seen. In order to evaluate quantitatively the stabilization of the ternary complexes, with respect to the binary ones, the parameter $\Delta\log K$ was used in accordance with the equilibria:

$$MA + MB \rightleftharpoons MAB + M$$
$$\Delta\log K_{MAB} = \log\beta_{MAB} - (\log\beta_{MA} + \log\beta_{MB})$$
$$MAH + MB \rightleftharpoons MABH + M$$
$$\Delta\log K_{MABH} = \log\beta_{MABH} - (\log\beta_{MAH} + \log\beta_{MB})$$
$$MAH_2 + MB \rightleftharpoons MABH_2 + M$$
$$\Delta\log K_{MABH_2} = \log\beta_{MABH_2} - (\log\beta_{MAH_2} + \log\beta_{MB})$$
$$MAH_2 + MBH \rightleftharpoons MABH_3 + M$$
$$\Delta\log K_{MABH_3} = \log\beta_{MABH_3} - (\log\beta_{MAH_2} + \log\beta_{MBH}),$$

where the charges are not included, in the interest of clarity. According to Sigel,[13,14] $\Delta\log K$ is used as a measure of stability instead of $\log\beta^{M}_{MAB}$ or $\log K^{MA}_{MAB}$ because it only depends indirectly on the basicity of the ligand.

According to the definition of $\Delta\log K$, it represents a measure of the tendency of ligand B to coordinate with the binary complex of A with respect to the aqueous ion. In general, positive values of $\Delta\log K$ indicate a marked stabilization of the ternary complexes with respect to the binary ones, or rather an important synergic effect on the formation of ternary complexes.[15] However, negative $\Delta\log K$ values do not indicate the absence of the ternary species but rather that the secondary ligand, B, presents a greater tendency to coordinate with the aqueous metal ion than with the binary complex of A.

The formation constants, β_{pqrs}, defined in accordance with the equation:

$$pM + qA + rB + sH \rightleftharpoons M_pA_qB_rH_s$$

were calculated with the MINIQUAD program[11] by treatment of the data obtained by potentiometric titrations with aqueous solutions of 0.1 M NaOH (0.5 M NaCl and at 25°C) containing M^{II}–A–B in the ratios 1 : 1 : 1, 2 : 1 : 1, 2 : 1 : 2 and 1 : 1 : 2.

The values of $\log\beta_{1110}$, $\log\beta_{1111}$, $\log\beta_{1112}$ and $\log\beta_{1113}$ are given in Table 4, together with the values of the parameter $\Delta\log K$ for each of them. Only neutral complexes, MAB, are formed with the cations studied if the secondary ligand is oxalic acid, with which little tendency is observed for the formation of protonated species. When the secondary ligand is malonic or succinic acid, the complexes formed are MABH, $MABH_2$ and $MABH_3$,

Table 4. Stability constants for the systems M^{II}–1,3-FDDS–B (B = oxalic, malonic or succinic acid) at 25°C and $I = 0.5$ M NaCl

	Co^{II}			Ni^{II}			Zn^{II}		
Species	Oxalic acid	Malonic acid	Succinic acid	Oxalic acid	Malonic acid	Succinic acid	Oxalic acid	Malonic acid	Succinic acid
$\log\beta_{1110}$	7.59(1)	—	—	9.32(3)	—	—	6.59(6)	—	—
$\log\beta_{1111}$	12.50(1)	12.15(1)	12.52(5)	13.88(2)	13.44(1)	13.54(2)	12.35(1)	11.68(4)	11.74(1)
$\log\beta_{1112}$	—	16.53(1)	16.86(4)	17.33(4)	17.64(1)	17.70(3)	—	16.22(4)	15.84(1)
$\log\beta_{1113}$	—	20.24(2)	21.34(4)	—	21.21(1)	21.90(2)	—	20.22(4)	20.23(1)
$\Delta\log K_{MAB}$	−0.16	—	—	−0.46	—	—	−0.84	—	—
$\Delta\log K_{MABH}$	0.44	0.93	2.41	−0.25	0.62	1.99	0.41	0.82	2.41
$\Delta\log K_{MABH_2}$	—	1.96	3.40	0.46	2.08	3.41	—	2.07	3.22
$\Delta\log K_{MABH_3}$	—	2.18	3.57	—	—	3.29	—	—	—
R	0.000677	0.000490	0.005938	0.005917	0.000555	0.003564	0.004037	0.003329	0.000358

The standard deviation in the last significant figure is indicated in parentheses.

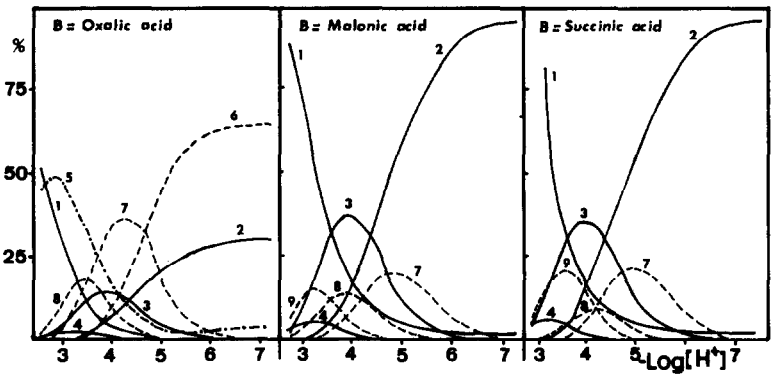

Fig. 5. Distribution diagrams for the ternary systems [M^{II}]–[1,3-FDDS]–[B] in the ratio 1 : 1 : 1. (1) M, (2) MA, (3) MAH, (4) MAH_2, (5) MB, (6) MAB, (7) MABH, (8) $MABH_2$ and (9) $MABH_3$.

for the three cations, but not the neutral complex MAB, as can be observed in the corresponding species distribution curves (Fig. 5). This seems to be in agreement with the greater tendency of the oxalate ion to form stable chelate rings with respect to the other secondary ligands,[16] and with a low basicity of the amino nitrogens in the *meta*-position[17] which facilitates the dissociation of the protons situated thereon, as deduced from the resonant forms in Fig. 6.

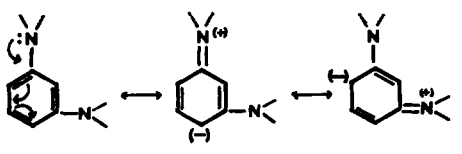

Fig. 6.

From the analysis of the values of $\Delta\log K$ a tendency is deduced for the formation of ternary complexes, following the sequence: *succinic acid* > *malonic acid* > *oxalic acid*, which corresponds to the reverse bonding sequence of the above ligands with the aqueous ion (Table 4). This was expected, in view of the capacity of oxalic acid to form highly stable five-membered chelate rings in comparison with the less stable six- and seven-membered ones which can be formed by malonic and succinic acids, respectively.[18,19] Negative $\Delta\log K$ values were found only when the secondary ligand was oxalic acid, reflecting its greater tendency to bond to the aqueous metal ion, $M^{II}_{aq.}$, than to the corresponding binary complex of A, in contrast with malonic and succinic acids which, on forming weaker binary complexes than oxalic acid, facilitate the formation of ($\Delta\log K$ positive) ternary complexes.

Acknowledgement—This work was supported by the Government of the Canary Islands, for which we are grateful.

REFERENCES

1. B. Rodríguez Ríos, J. Fuentes Díaz and R. Reboso Barroso, *An. Quim.* 1984, **80B**, 60.
2. B. Rodríguez Ríos, J. Fuentes Díaz and R. Reboso Barroso, *An. Quim.* 1984, **80B**, 32; 1984, **80B**, 37.
3. J. Fuentes, R. Reboso and A. Rodríguez, unpublished results.
4. J. Fuentes, R. Reboso and A. Rodríguez, *Polyhedron* 1989, **8**, 1365.
5. B. Rodríguez Ríos, J. Fuentes Díaz and R. Reboso Barroso, *An. Quim.* 1984, **80B**, 424.
6. B. Rodríguez Ríos and J. Fuentes Díaz, *An. Quim.* 1976, **72**, 420.
7. B. Rodríguez Ríos, J. Fuentes Díaz and R. Reboso Barroso, *An. Quim.* 1984, **80B**, 37.
8. A. Rodríguez, Doctoral Thesis, University de La Laguna, Tenerife (1987).
9. H. Irving and R. J. P. Williams, *J. Chem. Soc.* 1953, 3192.
10. G. Schwarzenbach, A. Willi and R. O. Bach, *Helv. Chim. Acta* 1947, **30**, 1303.
11. A. Sabatini, A. Vacca and P. Gans, *Inorg. Chim. Acta* 1976, **18**, 237.
12. F. R. Hartley, C. Burgess and R. M. Alcock, *Solution Equilibria*. Ellis Horwood, Chichester (1980).
13. H. Sigel, *Metal Ions in Biological Systems*, Vol. 2. Marcel Dekker, New York (1973).
14. H. Sigel, *Coord. Chem.* 1980, **20**, 27.
15. M. S. Nair, M. Santappa and P. K. Murugan, *Inorg. Chem.* 1982, **21**, 142.
16. A. E. Martell and R. M. Smith, *Critical Stability Constants*, Vol. 2—Amines. Plenum Press, New York (1982); D. Perrin (Ed.), *Stability Constants of Metal–Ion Complexes*, Part B—Organic Ligands. Pergamon Press, Oxford (1979).
17. J. Milton Harris and C. C. Wanser, *Fundamentals of Organic Reaction Mechanisms*. John Wiley, New York (1976).
18. C. S. Chung, *J. Chem. Ed.* 1984, **61**, 1062.
19. H. Irving, R. J. P. Williams, D. J. Ferret and A. E. Williams, *J. Chem. Soc.* 1954, 3494.

Polyhedron Vol. 8, No. 22, pp. 2701–2707, 1989
Printed in Great Britain

0277–5387/89 $3.00+.00
© 1989 Pergamon Press plc

THE HYDROLYSIS OF THE NEODYMIUM(III) ION, Nd^{3+}, IN 3 m (Li)ClO_4 MEDIUM AT 60°C

LIBERATO CIAVATTA,† RAFFAELLA PORTO and ERMANNO VASCA

Dipartimento di Chimica dell'Università, Via Mezzocannone, 4, 80134 Napoli, Italy

(*Received* 8 *June* 1989; *accepted* 26 *June* 1989)

Abstract—The hydrolysis equilibria of the neodymium(III) ion have been studied in 3 m (Li)ClO_4 ionic medium at 60°C by electrometric measurements with a glass electrode. The neodymium(III) concentration ranged from 0.03 to 1 m, whereas the acidity was decreased, with coulometrically generated OH^- ions, down to the incipient precipitation of neodymium(III) hydroxide. This occurred when less than 2% of the metal ion was transformed into reaction products. The species $Nd(OH)^{2+}$, $Nd_2(OH)_2^{4+}$ and $Nd_6(OH)_{12}^{6+}$ were assumed in dilute solutions, $\leqslant 0.3$ m Nd^{III}. At higher concentrations the data were best explained by replacing $Nd_6(OH)_{12}^{6+}$ with $Nd_6(OH)_8^{10+}$. Formation constants in the inert 3 m $LiClO_4$ medium are reported.

The reaction of tripositive lanthanide ions, Ln^{3+}, with water has received much attention in this laboratory. In three preceding papers the hydrolysis equilibria at 60°C of the La^{3+} ion[1] and the Pr^{3+} ion,[3] as well as those of the Ce^{3+} ion at 50°C,[2] were studied by potentiometric procedures. In addition to minor complexes such as $Ln(OH)^{2+}$ and $Ln_2(OH)^{5+}$, the species $La_2(OH)_3^{3+}$, $Ce_3(OH)_5^{4+}$, $Pr_2(OH)_2^{4+}$ and $Pr_3(OH)_5^{4+}$ were proposed to explain the data. This result, on consideration of the nearly equal ionic radii and electronegativities, in addition to the identical charges, was unexpected. It seemed, therefore, essential for understanding the different behaviour of the lanthanides on hydrolysis to extend the investigation to the heavier elements of the series.

A temperature of 60°C was chosen, firstly, to render a more direct comparison with previous results and secondly, because temperatures higher than 25°C proved particularly suitable to obtain hydrolysed solutions of high purity by coulometry. As a matter of fact, at 25°C we have not been able to prepare clear hydrolysed solutions of appreciable buffer capacity even by electrolysis at very low current densities. Most likely, the local excess of base in the vicinity of the cathode causes the transient precipitation of neodymium(III) hydroxide which redissolves only slowly at room temperature.

† Author to whom correspondence should be addressed.

Previous work on the protolysis of the Nd^{3+} *ion*

The only real attempt to find the composition of the hydrolysis products and the equilibrium constants is that made by Burkov *et al.*[4] who titrated $Nd(ClO_4)_3$ with NaOH, using a glass electrode, at 25°C in 3 M (Na)ClO_4. In the small region of hydrolysis (less than 0.5% of the metal could be converted into reaction products before the precipitation of the hydroxide) the following equilibria were assumed

$$Nd^{3+} + H_2O \rightleftarrows Nd(OH)^{2+} + H^+ \qquad \log {}^*\beta_{11} = -9.4$$

$$2Nd^{3+} + 2H_2O \rightleftarrows Nd_2(OH)_2^{4+} + 2H^+ \qquad \log {}^*\beta_{22} = -13.93.$$

As it will appear below, the ${}^*\beta_{22}$ value is much greater than one would expect.

METHOD

The protolytic equilibria were investigated by measuring the EMF of cell (A)

$$\ominus \text{ Ag/AgCl/TS/GE } \oplus, \qquad \text{(A)}$$

where GE denotes the glass electrode and TS (test solution) had the general composition (molal units)

$$TS = Nd^{III}m_M,\ H^+m_H,\ Cl^-m_X,$$
$$Li^+(3-3m_M-m_H+m_X),\ ClO_4^-\ 3\text{ m}.$$

In TS, $m_H = 3 + m_X - 3m_M - [Li^+]$ is the analytical concentration excess of hydrogen ions and attained negative values in hydrolysed solutions. The chloride ions, in the range $5 \times 10^{-3} \leqslant m_X \leqslant 0.05$ m, had negligible influence on the hydrolytic equilibria, as shown by experiments carried out at different m_X but identical m_M. The EMF of cell (A) is written as eq. (1) at 60°C:

$$E = E_0 + 0.06610 \log \{[H^+][Cl^-] y_{HCl}^2\}, \quad (1)$$

in which E_0 is a constant during a series of measurements and y_{HCl} symbolizes the activity coefficient of hydrochloric acid. The standard states are so defined that activities tend to molalities as the composition of TS approaches 3 m $LiClO_4$. In each experiment, carried out at constant m_M, the composition of TS varies, but only slightly owing to the small extent of hydrolysis. Hence, within each experiment y_{HCl} remains essentially unchanged and the expression of the EMF can be simplified to give

$$E = E_0^* + 0.06610 \log \{[H^+][Cl^-]\}, \quad (2)$$

where $E_0^* = E_0 + 0.06610 \log y_{HCl}^2$ was determined before a run started by inserting in cell (A) solutions with $m_H > 10^{-4}$ m, where hydrolysis is suppressed, and consequently $[H^+] = m_H$.

In TS, m_M was varied between 0.03 and 1 m and m_H from 10^{-3}, where hydrolysis is negligible, to negative values, prior to the formation of solid hydroxides. This occurred when less than 2% of the metal was transformed into reaction products. It is easy to calculate that at the lowest m_M the concentration of the hydrolytic complexes does not exceed the 5×10^{-4} m level. Thus, it is obvious that severe demands are imposed for the accurate determination of m_H and particular care is required to avoid contamination by protolytic impurities, such as CO_2, Al^{III} and others usually present in strong base solutions. To meet these requirements the acidity of TS was lowered by coulometric procedures using the electrolysis cell (B)

$$\ominus \text{ Pt/TS/AgCl/Ag } \oplus, \quad \text{(B)}$$

which was connected to a constant-current source. Concerning the efficiency of OH^- ion generation using cell (B) the reader should refer to details in our previous papers.[1-3]

The experiments were carried out as titrations. From a known amount of TS of initial acidity m_H^*, large enough to hinder hydrolysis, protons were stepwise removed at the cathode of (B) up to the incipient precipitation of hydroxide. By ensuing each step of electrolysis a constant value of EMF of (A) was soon reached and kept constant for several hours within 0.03×10^{-3} V.

The data for the first part of the titration, where $[H^+] = m_H$, were used to calculate E_0^* from eq. (2) and an accurate value of m_H^* was determined by means of a Gran[5] plot. From measurements relevant to the region of hydrolysis $\bar{n}$, the average number of protons set free per neodymium atom, was evaluated as a function of $\log[H^+]$. In constructing the $\bar{n}(\log[H^+])$ function, which forms the basis of the following calculations, we had to account for the effect of small amounts of dissolved CO_2 that, as shown in a preceding publication,[6] are removed only with difficulty by prolonged scrubbing with nitrogen gas even from acidic solutions. After three days purging the protolytic contaminant level in TS could be reduced to about $(3 \pm 1) \times 10^{-6}$ m. On the basis of a study on the formation of carbonato complexes of the La^{3+} ion[7] we estimate that in our solutions with $[H^+] < 10^{-5}$ m CO_2, besides undergoing a small amount of protolysis to HCO_3^-, is to a large extent bound in species such as $Nd(CO_3)^+$, $Nd(HCO_3)^{2+}$ and $Nd_2(CO_3)^{4+}$. The average number of hydrogen ions set free per CO_2 is in the range 1.5–2. Thus a correction term of $(5 \pm 2) \times 10^{-6}$ m was assumed over the entire acidity interval and $\bar{n}$ was calculated by neglecting the $[OH^-]$ term according to eq. (3)

$$\bar{n} = ([H^+] - m_H - 5 \times 10^{-6})/m_M. \quad (3)$$

To ascertain that true equilibrium had been attained in the course of an experiment, back titrations were performed by adding acid solutions of equal m_M. The data, as shown in Fig. 1, are in good agreement with those from forward titrations.

EXPERIMENTAL

Neodymium perchlorate solutions

These were prepared from the freshly ignited oxide, Nd_2O_3 (99.9% purity, Fluka) and $HClO_4$ (Merck p.a.). The oxide was added in slight excess to hot 4 m $HClO_4$ and the solution, after standing for a week, which removed the heavy metal impurities as insoluble hydroxides, was filtered and re-acidified to about pH = 3. The neodymium concentration was established to within 0.1% by titration with EDTA, using xylenol orange as the visual indicator. The hydrogen ion concentration was determined by coulometric acid–base titration with a glass electrode. The perchlorate ion concentration was obtained from the sum: $m_H + 3m_M$.

Lithium perchlorate, perchloric acid and lithium chloride solutions

These were prepared and analysed as described previously.[1-3]

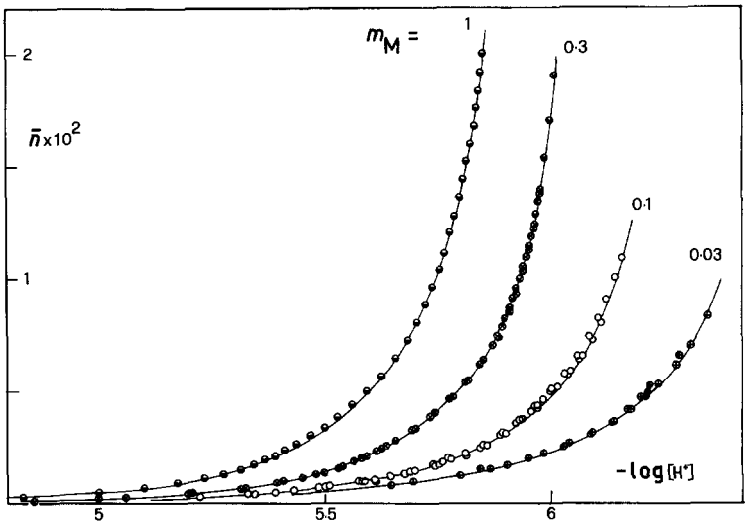

Fig. 1. $\bar{n}$, the average number of OH^- ions bound per neodymium atom, as a function of $\log[H^+]$. The curves have been calculated with the equilibrium constants and the interaction coefficients given in Table 3.

For experimental details on the EMF measurements and apparatus the reader should refer to a previous paper involving the hydrolysis of the Pr^{III} ion.[3]

RESULTS

The composition of the hydrolysis products

The primary $\bar{n}(\log[H^+], m_M)$ data, from which the composition of the hydrolysis products and the corresponding equilibrium constants were calculated, are collected in Table 1 and are graphically represented in Fig. 1.

By assuming the formation of a series of complexes of the general composition $Nd_q(OH)_p^{3q-p}$, the concentration of hydrogen ions set free per hydrolysis, $\bar{n}m_M$, can be expressed by eq. (4)

$$\bar{n}m_M = \sum\sum p[Nd_q(OH)_p^{3q-p}]$$

$$= \sum\sum p^*\beta_{pq}[Nd^{3+}]^q[H^+]^{-p}y_M^q y_H^{-p} y_{pq}^{-1} a_W^q, \quad (4)$$

where y_H, y_M, y_{pq} and a_W represent, respectively, the activity coefficients of H^+, Nd^{3+}, $Nd_q(OH)_p^{3q-p}$ and the water activity, and $^*\beta_{pq}$ is the equilibrium constant for

$$qNd^{3+} + pH_2O \leftrightarrows Nd_q(OH)_p^{3q-p} + pH^+. \quad (5)$$

At constant m_M, since only $\bar{n}$ values not exceeding 0.02 are available, the activity coefficients and water activity do not vary appreciably, hence the hydrolysis equilibria may be as well described by the concentration quotient, Q_{pq}, according to eq. (6)

$$\bar{n}m_M = \sum\sum pQ_{pq}[Nd^{3+}]^q[H^+]^{-p}, \quad (6)$$

where

$$Q_{pq} = {}^*\beta_{pq} y_M^q y_H^{-p} y_{pq}^{-1} a_W^q. \quad (7)$$

Clearly, a rigorous treatment involving no assumptions about the variation of activity coefficients caused by the substitution of Li^+ with Nd^{3+} ions is only possible for data at a given m_M by applying the "self-medium" principle.[8] This furnishes detailed information on the p values. On the contrary, since $[Nd^{3+}]$ changes but not sufficiently at constant m_M, it does not allow certain conclusions on q to be reached. Reasonable guesses of the number of metal ions bound in the prevailing complexes can be deduced from comparison of the results at different m_M by disregarding activity coefficient variations. At any rate, estimates of medium changes seem essential for conclusions concerning minor complexes as well as the refinement of the equilibrium constants. In the initial stage of the treatment, activity coefficients were evaluated by the specific interaction theory, SIT,[9] in its simplified form, which considers the interaction coefficients independent of the ionic strength.

In the course of the calculations, however, evidence showed that the more accurate formulation was necessary. Since no probable values of interaction coefficients between complex species and ClO_4^- ions were available, they were determined simultaneously with the $^*\beta_{pq}$ values. This approach precluded any information on minor complexes.

The most important p *and* q *values*

A preliminary graphical treatment, of comparing $\bar{n}(\log[H^+])m_M$ plots with normalized model func-

Table 1. The experimental $\bar{n}(-\log[H^+], m_M)$ data

	$\bar{n} \times 10^3$ $(-\log[H^+])$
	$m_M = 1.000$
	0.25(4.8330); 0.46(4.9995); 0.65(5.1020); 0.86(5.1758); 1.06(5.2336); 1.27(5.2765); 1.47(5.3138); 1.68(5.3424); 1.88(5.3674); 2.09(5.3901); 2.315(5.4130); 2.60(5.4387); 2.945(5.4672); 3.34(5.4977); 3.80(5.5294); 4.325(5.5619); 4.92(5.5944); 5.60(5.6259); 6.40(5.6571); 7.20(5.6834); 8.00(5.7049); 8.80(5.7243); 9.59(5.7407); 10.38(5.7547); 11.19(5.7666); 11.99(5.7774); 12.75(5.7874); 13.56(5.7991); 14.36(5.8074); 15.19(5.8150); 15.98(5.8252); 16.78(5.8318); 17.58(5.8371); 18.38(5.8436); 19.18(5.8476); 19.98(5.8526).
	$m_M = 0.300$
(a)	0.14(4.8553); 0.27(5.0619); 0.46(5.2108); 0.69(5.3218); 0.95(5.4089); 1.26(5.4794); 1.61(5.5372); 2.00(5.5859); 2.39(5.6250); 2.78(5.6580); 3.24(5.6931); 3.82(5.7317); 4.60(5.7766); 5.38(5.8132); 6.35(5.8514); 7.33(5.8826); 8.30(5.9079); 9.27(5.9260); 10.25(5.9508); 11.22(5.9532); 12.39(5.9656); 13.75(5.9767); 15.31(5.9883); 17.06(5.9985); 19.01(6.0087).
(b)	0.22(4.9994); 0.44(5.1982); 0.67(5.3135); 0.90(5.3921); 1.13(5.4509); 1.36(5.4972); 1.60(5.5340); 1.83(5.5650); 2.06(5.5912); 2.30(5.6138); 2.53(5.6343); 3.31(5.7015); 4.02(5.7452); 4.72(5.7822); 5.42(5.8142); 6.12(5.8416); 6.98(5.8693); 7.37(5.8804); 7.78(5.8900); 8.19(5.9001); 8.62(5.9092); 9.05(5.9152); 9.50(5.9231); 9.95(5.9325); 10.42(5.9411); 10.89(5.9463); 11.37(5.9536); 11.86(5.9580); 12.37(5.9654); 12.88(5.9677); 13.41(5.9728); 13.93(5.9794).
	$m_M = 0.100$
(a)	0.38(5.3283); 0.64(5.4839); 0.92(5.5865); 1.27(5.6776); 1.68(5.7556); 2.09(5.8135); 2.51(5.8586); 3.00(5.8865); 3.56(5.9256); 4.26(5.9656); 4.95(5.9998); 5.72(6.0325); 6.49(6.0604); 7.33(6.0859); 8.17(6.1078); 9.00(6.1265); 9.91(6.1439); 10.82(6.1584).
(b)	Back titration: 6.41(6.0619); 5.69(6.0360); 4.99(6.0039); 4.30(5.9692); 3.62(5.9299); 3.09(5.8929); 2.57(5.8497); 2.18(5.8109); 1.80(5.7593); 1.425(5.6983); 1.18(5.6454); 0.93(5.5738); 0.69(5.4992); 0.46(5.3890).
(c)	0.28(5.2183); 0.49(5.3931); 0.74(5.5143); 1.02(5.6116); 1.33(5.6874); 1.69(5.7517); 2.10(5.8097); 2.52(5.8544); 3.02(5.8966); 3.58(5.9357); 4.21(5.9712); 4.90(6.0009).
(d)	Back titration: 5.85(6.0461); 5.14(6.0162); 4.59(5.9883); 4.03(5.9578); 3.49(5.9247); 2.96(5.8867); 2.43(5.8425); 1.92(5.7798); 1.41(5.6959); 0.915(5.5801); 0.55 (5.4326).
(e)	Back titration: 7.86(6.1173); 7.13(6.0968); 6.42(6.0695); 5.72(6.0401); 5.03(6.0089); 4.35(5.9736); 3.69(5.9363); 3.04(5.8883); 2.53(5.8491); 2.03(5.7758); 1.655(5.7468); 1.29(5.6838); 0.93(5.6094).
	$m_M = 0.0300$
(a)	1.52(5.8673); 3.175(6.0899); 4.85(6.2145); 6.54(6.2859); 8.25(6.3500).
(b)	0.36(5.3440); 0.76(5.6442); 1.21(5.8014); 1.68(5.9059); 2.14(5.9841); 2.61(6.0431); 3.13(6.0946); 3.65(6.1357); 4.17(6.1700); 4.68(6.1987); 5.21(6.2218).
(c)	Back titration: 6.95(6.3134); 6.09(6.2774); 5.24(6.2397); 4.67(6.2113); 4.12(6.1783); 3.57(6.1391); 3.02(6.0908); 2.48(6.0295); 1.94(5.9523); 1.415(5.8460); 0.90(5.6869).

tions,[10] constructed by setting $[Nd^{3+}] \simeq m_M$, gave evidence for species with $p = 1$ and 2 and for at least one other complex with $p \geqslant 6$. The curve-fitting procedure also yielded values for the functions $K_p = K_p(m_M) = \sum Q_{pq} m_M^q$ whose analysis permitted us to infer the presence of $NdOH^{2+}$, $Nd_2(OH)_2^{4+}$ and a species with $q \geqslant 4$ and $p \geqslant 6$.

In order to check the validity of the conclusions reached by graphical methods based on some approximations, it seemed necessary to examine the data in a more rigorous way using the general minimizing program Letagrop.[11] To avoid the introduction of uncertainties in the evaluation of activity coefficients, the least-squares treatment separately considered data at constant m_M. The minimum of the sum $U = \sum((\bar{n}m_M)_{calc} - \bar{n}m_M)^2$, where $(\bar{n}m_M)_{calc}$ denotes a value calculated with a given set of assumed constants, was sought for by assuming three complexes: $Nd(OH)^{2+}$, $Nd_2(OH)_2^{4+}$ and $Nd_{q'}(OH)_{p'}^{3q'-p'}$ with the compositions $6 \leqslant p' \leqslant 13$ and $4 \leqslant q' \leqslant 7$. The values of E_0^* and m_M^* are considered as being known with sufficient accuracy to try to "adjust" them together with Q_{pq}-s.

The results for a series of hypotheses affording

Table 2. Survey of results by Letagrop (the errors represent 3σ)

m_M	(p', q')	$-\log Q_{11}$	$-\log Q_{22}$	$-\log Q_{p'q'}$	$\sigma(\bar{n}m_M)10^3$	$U\times10^6$
1	(8, 6)	8.70±0.12	13.88±0.02	49.95±0.03	0.080	0.205
	(8, 4)	8.68±0.12	13.88±0.02	49.95±0.03	0.087	0.255
	(9, 5)	8.78±0.16	13.86±0.02	55.88±0.03	0.092	0.288
	(12, 6)	< 8.81	13.81±0.03	73.61±0.05	0.142	0.684
0.3	(12, 6)	9.12±0.16	$13.71\pm0.01_5$	72.71±0.02	0.0249	0.0335
	(11, 5)	9.00±0.13	13.73±0.02	67.18±0.02	0.0250	0.0338
	(9, 5)	8.79±0.13	13.79±0.03	55.05±0.03	0.0386	0.0805
	(8, 6)	8.69±0.14	13.84±0.05	48.43±0.04	0.0514	0.1426
0.1	(12, 6)	9.12±0.17	13.70±0.03	72.75±0.13	0.0135_8	0.0116
	(11, 5)	9.10±0.17	13.70±0.04	67.55±0.13	0.0136_4	0.0117
	(9, 5)	9.06±0.16	13.72±0.04	55.13±0.14	0.0139	0.0122
	(8, 6)	9.03±0.16	13.73±0.05	47.89±0.04	0.0141	0.0126
0.03	(12, 6)	8.93±0.08	13.74±0.06	~ 72.85	0.0027	1.7×10^{-4}

comparable U values are listed in Table 2. For data at $m_M = 1$ the minimum agreement factor was obtained for $q' = 6$ and $p' = 8$ and a slightly poorer fit was found with $q' = 4$ and $p' = 8$. Both of these species yield significantly better fits than any other. The measurements in more dilute solutions are most consistent with $q' = 6$ and $p' = 12$ as a minor polynuclear complex, but are explained as well by $Nd_5(OH)_{11}^{4+}$. At any rate, the presence of $Nd_6(OH)_8^{10+}$ or $Nd_4(OH)_8^{4+}$ instead of $Nd_6(OH)_{12}^{6+}$ gives minima which are at least 10% higher. Calculations with both $Nd_6(OH)_8^{10+}$ and $Nd_6(OH)_{12}^{6+}$ yielded no significant improvement. We may thus infer that the data of the present accuracy can be explained by the formation of $Nd(OH)^{2+}$, $Nd_2(OH)_2^{4+}$ and $Nd_6(OH)_{12}^{6+}$, for $m_M \leqslant 0.3$, or $Nd_6(OH)_8^{10+}$ for $m_M = 1$. At first thought the proposal of $Nd_6(OH)_8^{10+}$ in 1 m $Nd(ClO_4)_3$ and $Nd_6(OH)_{12}^{6+}$ in more dilute solutions would imply a contradiction of the mass action law. Nevertheless, as shown in the next section, the complete replacement of Li^+ with Nd^{3+} ions produces medium changes in which $Nd_6(OH)_8^{10+}$ becomes strongly disfavoured at $m_M \leqslant 0.3$, but is the main hexanuclear species in 1 m $Nd(ClO_4)_3$.

Calculation of the $^*\beta_{pq}$ constants

To obtain the equilibrium constants, relevant to the inert 3 m $LiClO_4$ medium, from the Q_{pq} values one has to evaluate the variations of the activity coefficients caused by the substitution of Li^+ with Nd^{3+} ions. Medium effects were accounted for by SIT.[9] According to theory the activity coefficient y_i of a positively-charged species "i" of charge z_i is expressed on the medium scale, at the ionic strength I, by eq. (8)

$$\log y_i = -z_i^2\left[0.5452\left(\frac{I^{0.5}}{1+1.5I^{0.5}} - 0.4814\right)\right] + [b(i, ClO_4^-, I) - b(i, ClO_4^-, 3)]3 = -z_i^2 D + \Delta b(i)3, \quad (8)$$

in which $b(i, ClO_4^-, I)$ is the interaction coefficient of i with ClO_4^- at the ionic strength I. Most often $b(i, ClO_4^-, I)$ is nearly independent of I, at least in the I range from 0.5 and 3.5, thus $\Delta b(i) = 0$. During the calculations there was evidence that the more accurate formulation was necessary for the present case.

The $\Delta b(H^+)$ and $\Delta b(Nd^{3+})$ values given in Table 3, in addition to eq. (9) for the water activity, were found from the activity data listed by Pitzer[12]

$$\log a_W = 0.0199 m_M. \quad (9)$$

Since we were not able to estimate the probable values for the interaction coefficient between reac-

Table 3. Equilibrium constants and interaction coefficients

Species	$\Delta b(i)/(I-3)$	$-\log {}^*\beta_{pq}$
H^+	0.0048	
Nd^{3+}	$-0.028+0.0066(I-3)$	
$Nd(OH)^{2+}$	$0.12-0.06(I-3)$	8.96±0.15
$Nd_2(OH)_2^{4+}$	$-0.08+0.024(I-3)$	13.73±0.03
$Nd_6(OH)_{12}^{6+}$	$-0.39+0.15(I-3)$	72.9±0.2
$Nd_6(OH)_8^{10+}$		50.0±0.2

tion products and the ClO_4^- ion, we considered them as unknowns to be determined simultaneously with $^*\beta_{pq}$. As simplifying hypothesis, the variation of Δb(i) with I was approximated by a quadratic function. The procedure is illustrated by the calculation of $^*\beta_{22}$ and $\Delta b(Nd_2(OH)_2^{4+})$. From the definitions we have

$$-\log Q_{22}+2\log a_W-6[\Delta b(H^+)-\Delta b(Nd^{3+})] = 3\Delta b(Nd_2(OH)_2^{4+})-\log {}^*\beta_{22} = F. \quad (10)$$

By putting

$$\Delta b(Nd_2(OH)_2^{4+}) = c(I-3)+d(I-3)^2 \quad (11)$$

eq. (10) can be transformed into eq. (12):

$$\log F = \log(-\log {}^*\beta_{22}) + \log\left(1+\frac{3c(I-3)}{-\log {}^*\beta_{22}}+\frac{3d(I-3)^2}{-\log {}^*\beta_{22}}\right). \quad (12)$$

Values of $\log(-\log {}^*\beta_{22})$, c and d can be deduced by comparing the graph of $\log F[\log(I-3)]$ with the family of normalized functions,[10] $Y(\log u)_L$, where

$$Y = \log(1+Lu+u^2) \quad (13)$$

$$3d(I-3)^2/(-\log {}^*\beta_{22}) = u^2 \quad (14)$$

and

$$L = 3c/[3d(-\log {}^*\beta_{22})]^{1/2}. \quad (15)$$

From the position of best agreement, shown in Fig. 2, the $^*\beta_{22}$ and $\Delta b(Nd_2(OH)_2^{4+})$ values given in Table 3 were calculated.

Analogous procedures were adopted to find $^*\beta_{11}$, $^*\beta_{12,6}$ and the corresponding interaction coefficients. The results are summarized in Table 3. The $^*\beta_{86}$ value proposed in Table 3 has been derived by tentatively setting $\Delta b(Nd_6(OH)_8^{10+}) = \Delta b(Nd_6(OH)_{12}^{6+})$.

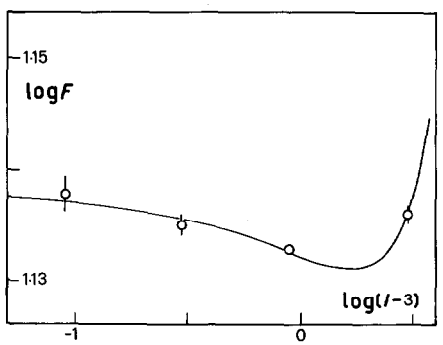

Fig. 2. Evaluation of $^*\beta_{22}$ and $\Delta b(Nd_2(OH)_2^{4+})$ by curve-fitting. Log F, eq. (10), as a function of $\log(I-3)$. The curve has been calculated with parameters of Table 3.

In order to support with convincing arguments the predominance of $Nd_6(OH)_8^{10+}$ instead of $Nd_6(OH)_{12}^{6+}$ in the most concentrated neodymium solutions, we present calculations of the ratio $[Nd_6(OH)_8^{10+}]/[Nd_6(OH)_{12}^{6+}]$ as a function of medium changes. From the above estimates we obtain $\log Q_{12,6} = -74.3_6$ at $m_M = 1$ and $\log Q_{86} = -49.2_2$ at $m_M = 0.3$ which on introduction into the expression

$$\log([Nd_6(OH)_8^{10+}]/[Nd_6(OH)_{12}^{6+}]) = \log(Q_{86}/Q_{12,6})+4\log[H^+]$$

yields

$$\log([Nd_6(OH)_8^{10+}]/[Nd_6(OH)_{12}^{6+}]) = 24.3_5+4\log[H^+] \text{ for } m_M = 1$$
$$= 23.4_9+4\log[H^+] \text{ for } m_M = 0.3.$$

This means that at the lowest determined values of $[H^+]$, when the hexanuclear complexes attain the highest concentration, the ratio $[Nd_6(OH)_8^{10+}]/[Nd_6(OH)_{12}^{6+}]$ is about 9 for $m_M = 1$ and decreases to 0.28 at $m_M = 0.3$. Thus, the concentration of $Nd_6(OH)_{12}^{6+}$ is no more than 10% of that of $Nd_6(OH)_8^{10+}$ at $m_M = 1$. On the other hand, at $m_M = 0.3$ $[Nd_6(OH)_8^{10+}]$ is less than 25% of $[Nd_6(OH)_{12}^{6+}]$ and only less than 10% of the global effect measured. The simultaneous detection of both of the hexanuclear species under these conditions would require data of much greater accuracy than the present data.

DISCUSSION

In dilute neodymium(III) solutions, e.g. $m_M \leqslant 0.3$, the main hydrolysis products are $Nd(OH)^{2+}$, $Nd_2(OH)_2^{4+}$ and $Nd_6(OH)_{12}^{6+}$. However, with increasing metal concentrations such large medium changes occur that at $m_M = 1$ the complex $Nd_6(OH)_8^{10+}$ becomes more important than $Nd_6(OH)_{12}^{6+}$. Hexanuclear species such as $Nd_6(OH)_8^{10+}$ (probably a Nd_6 octahedron with eight OH^- ions centred on the faces) and $Nd_6(OH)_{12}^{6+}$ (with 12 OH^- ions centred along edges of the octahedron) have never been detected in other lanthanide systems, but have been reliably identified in many others, e.g. $Be_6(OH)_8^{4+}$, $Pb_6(OH)_8^{4+}$ and $Bi_6(OH)_{12}^{6+}$.

A comparison with the results found for La^{3+}, Ce^{3+} and Pr^{3+} ions[1-3] indicates a different hydrolysis pattern and an irregular variation of $^*\beta_{11}$. This, when considering the monotonically increasing electronegativities and decreasing ionic radii with the atomic number of the Ln^{3+} ions, was expected

to be larger than the $10^{-8.7}$ value determined for Pr^{3+}, and is in fact almost identical to that of Ce^{3+}. It is not unlikely that the incomplete $4f$ and the empty $5d$, $6s$ and $6p$ orbitals play a determinant role in the trend of the $*\beta_{11}$ values.

The $Ln_2(OH)_2^{4+}$ species becomes more important in Nd^{III} with respect to preceding elements of the series. While it could not be detected in the La^{III} and Ce^{III} systems, its formation is more favoured in Nd^{III} than in Pr^{III} solutions. We calculate for $2Nd(OH)^{2+} \rightleftarrows Nd_2(OH)_2^{4+}$ an equilibrium constant of $10^{4.19}$ which is almost 10 times higher than that observed for $2Pr(OH)^{2+} \rightleftarrows Pr_2(OH)_2^{4+}$.

In conclusion, we would like to point out the small difference between the $\log *\beta_{22}$ value at 25°C, proposed by Burkov *et al.*,[4] and ours, whereas a difference of more than one log unit is predictable by temperature effects. The discrepancy was most probably due to the deleterious influence of small amounts of protolytic impurities, such as CO_2, which may have contaminated the NaOH solutions used by the Russian workers to titrate $Nd(ClO_4)_3$. It is worth emphasizing in this connection the superiority of coulometry when preparing pure hydrolysed solutions.

Acknowledgement—This work has been financially supported by the Ministero della Pubblica Istruzione, Rome.

REFERENCES

1. L. Ciavatta, M. Iuliano and R. Porto, *Polyhedron* 1987, **6**, 1283.
2. L. Ciavatta, R. Porto and E. Vasca, *Polyhedron* 1988, **7**, 1355.
3. L. Ciavatta, R. Porto and E. Vasca, *Polyhedron* 1989, **8**, 983.
4. K. A. Burkov, L. S. Lilic, Nguen Din Ngo and A. Yu. Smirnov, *Russ. J. Inorg. Chem.* 1973, **18**, 797.
5. G. Gran, *The Analyst* 1952, **77**, 661.
6. L. Ciavatta, R. Porto and E. Vasca, *An. Chim. (Rome)* 1989, **79**, 217.
7. L. Ciavatta, D. Ferri, I. Grenthe, F. Salvatore and K. Spahiu, *Acta Chem. Scand.* 1981, **A35**, 403.
8. S. Hietanen and L. G. Sillén, *Acta Chem. Scand.* 1959, **13**, 533.
9. L. Ciavatta, *An. Chim. (Rome)* 1980, **70**, 551.
10. L. G. Sillén, *Acta Chem. Scand.* 1956, **10**, 186.
11. L. G. Sillén and B. Warnqvist, *Arkiv. Kemi* 1969, **31**, 315.
12. K. S. Pitzer, *Activity Coefficients in Electrolyte Solutions* (Edited by R. M. Pytkowicz), Vol. I. CRC Press, Boca Raton, Florida (1979).

Polyhedron Vol. 8, No. 22, pp. 2709–2718, 1989
Printed in Great Britain

0277–5387/89 $3.00+.00
© 1989 Pergamon Press plc

MÖSSBAUER AND ESR STUDIES OF THE THERMOCHEMISTRY OF ILLITE AND MONTMORILLONITE

PAUL J. MICHAEL and WILLIAM R. McWHINNIE*

Department of Chemical Engineering and Applied Chemistry, Aston University, Aston Triangle, Birmingham B4 7ET, U.K.

(*Received* 16 *June* 1989; *accepted* 30 *June* 1989)

Abstract—The thermal decomposition of two clay minerals, illite and montmorillonite, is followed by a combination of powder XRD, ^{57}Fe Mössbauer and ESR investigations. The changes in the resonance spectra reflect well the various phases of clay decomposition; thus the relocation of structural iron during dehydroxylation (also the oxidation of iron(II) present in the illite sample) is complete by 800°C. The breakdown of the clay structure and the recrystallization of new phases is also well reflected; indeed the bulk of the initial structural iron distributes itself between a spinel phase and haematite. In the case of illite, a homogeneous glass is formed at 1300°C; but for montmorillonite, crystalline phases, together with a glassy matrix are present at that temperature. The paper illustrates that the combined use of ESR and Mössbauer spectroscopies can offer a sensitive probe for the investigation of the thermolysis of iron-bearing clays.

Much sophisticated information may be obtained from studies of very crystalline materials by a combination of single crystal structure analysis with the results of a range of spectroscopic investigations. It is not surprising, therefore, that single crystal X-ray methods now assume such importance in molecular inorganic and organometallic chemistry. Yet the fact remains that microcrystalline, amorphous and glassy materials are of immense practical importance but are much more difficult to study. This paper reports on some investigations of the thermochemistry of representatives of two types of clay mineral—illite and montmorillonite.

Illite and montmorillonite are microcrystalline clay minerals. Illites may be assigned to the mica group; they are extremely common in nature. The isomorphous replacement of silicon by aluminium in the tetrahedral sheets is less pronounced than in the true mica and this results in a proportionate diminution in the alkali metal ions between the structural layers; a typical composition would be:

$$K_xAl_2(Si_{4-x}Al_x)O_{10}(OH)_2, \quad 0.5 < x < 0.75.$$

Illites generally have low ion-exchange capacity of between 10 and 40 m-equiv 100 g^{-1} of clay.[1]

Montmorillonites are also related structurally to the micas in that they contain an octahedral layer sandwiched between two tetrahedral layers. The ion exchange capacity is considerable (80–150 m-equiv 100 g^{-1}[1]) and the clays swell; montmorillonite is a member of the smectite group. A typical composition is:

$$Na_{0.33}(Al_{1.67}Mg_{0.33})Si_4O_{10}(OH)_2, \quad nH_2O.$$

Both naturally occurring illite and montmorillonite often contain appreciable quantities of structural iron, usually iron(III) replacing aluminium in the octahedral layer. Thus, this naturally occurring iron can provide a useful spectroscopic probe for following the thermal decomposition of the minerals using a combination of ^{57}Fe Mössbauer and ESR spectroscopy in conjunction with powder XRD.

Information on the thermolysis of clay minerals can be valuable in a number of contexts. For example, such minerals are often present as inorganic "impurities" in coal and they may have some influence on the coking of coal,[2–6] thus their behaviour at temperatures at which coal is coked will be of interest. In addition, such minerals are often components of ceramic ware—both body and glaze; again knowledge of how the individual mineral

* Author to whom correspondence should be addressed.

species break down to new phases at temperatures relevant to the firing of ceramics can be valuable.

EXPERIMENTAL

Materials

The illite used was illite No. 36; the sample was light grey in colour and had been pre-washed, dried and crushed. The major impurity was quartz. Montmorillonite was supplied by Steetley Minerals Ltd and was termed Berkbond I (Woburn Fullers Earth). The sample was light brown–yellow in colour and had been washed, dried and pre-crushed. The main impurities were quartz and iron–aluminium oxyhydroxides.

Physical measurements

(a) ^{57}Fe *Mössbauer spectroscopy.* Mössbauer spectra were obtained using a constant acceleration spectrometer of standard design, counts being recorded on 512 channels of an Inotech 5200 multichannel analyser. Spectra were calibrated with iron foil. The source was ^{57}Co in a palladium matrix. The spectra, which were recorded at room temperature were computer fitted (ICL 1904S; HARRIS H800) to Lorentzians using the Gaussian non-linear regression method;[7] the X^2 criterion[8] was used as a measure of the acceptability of the fit.

(b) *Electron spin resonance (ESR) spectroscopy.* Spectra were recorded on a JEOL PE-1X type spectrometer operating in the X-band microwave region (~9.5 GHz). Spectra were calibrated and g-values determined from a manganese(II) standard.

(c) *X-ray diffraction (powder), XRD.* Finely-powdered samples were packed into standard aluminium XRD slides and analysed on either a JEOL X-ray diffractometer using Cu-K_α radiation (30 kV/30 mA) with a scan speed of 2° 2θ min^{-1}, or a Philips X-ray diffractometer using Co-K_α radiation (40 kV/40 mA) and an iron filter, with a scan speed of 1° 2θ min^{-1}. The d-spacings were calculated from the observed 2θ values using standard charts.[9]

(d) *Thermal treatment of clay minerals.* Powdered samples were heated in air to a given temperature (maximum 1300°C) in a Carbolite muffle furnace. Samples were allowed to soak for 3 h in the furnace, removed, then stored in a desiccator prior to recrushing for analysis.

(e) *X-ray fluorescence.* Major element analyses of clay minerals were obtained by fusion of dry, powdered minerals (15%) with a borax flux (85%) at 1100°C to discs which were analysed with a Philips PW1400 sequential X-ray spectrometer using a rhodium anode.

Table 1. Major element analysis of the samples of illite and montmorillonite involved in this study. Data obtained by X-ray fluoresence analysis

(%)	Illite[a]	Montmorillonite[b]
Fe_2O_3	5.20	10.76
MnO	0.04	0.00
TiO_2	0.89	0.33
CaO	0.96	1.90
K_2O	5.74	0.39
P_2O_5	0.13	0.10
SiO_2	60.11	53.10
Al_2O_3	18.45	12.70
MgO	2.35	2.20
Na_2O	0.07	0.12
SO_3	0.02	0.05
H_2O[c]	4.50	3.40
H_2O[d]	1.55	14.95
Total	100.01	100.0

[a] Average of two samples.
[b] Average of four samples.
[c] Absorbed H_2O (400°C).
[d] Structural H_2O (1100°C).

RESULTS

Major element analyses of the illite and montmorillonite samples are given in Table 1. Table 2 combines Mössbauer data for illite over a range of temperatures and also includes the more positive conclusions from the XRD study. Table 3 provides a similar collection of data for montmorillonite. Figures 1 and 2 attempt to display the major changes occurring on heating illite and montmorillonite in a more readily assimilated graphical form. Figures 3 and 4 show representative Mössbauer and ESR spectra. Table 4 (illite) and Table 5 (montmorillonite) summarize the ESR data in terms of apparent "g-values".

DISCUSSION

Mössbauer data—some general observations

^{57}Fe Mössbauer spectra of clay minerals are usually broad.[10] For montmorillonite, in particular, it is often possible to fit the observed spectrum to two iron(III) doublets with similar chemical isomer shifts, but with the more intense doublet having a quadrupole splitting approximately half that of the less intense doublet. Given that, in a dioctahedral

Table 2. ^{57}Fe Mössbauer data for thermally treated illite (data measured for cooled samples at room temperature); summary of XRD conclusions

Temperature (°C)	$\delta(\pm 0.01)^a$ (mm s^{-1})	$\Delta(\pm 0.02)^a$ (mm s^{-1})	$\Gamma_{1/2}(\pm 0.03)^a$ (mm s^{-1})	XRD conclusions
Ambient	1.21	2.88	0.39	
	1.48	2.84	0.62	
	0.38	0.67	0.60	
400	1.18	2.90	0.69	
	0.30	1.10	0.91	
500	0.36	1.53	0.71	
	0.36	0.95	0.59	
600	0.32	1.73	0.66	
	0.37	1.11	0.54	
700	0.34	1.76	0.68	
	0.36	1.14	0.50	
800	0.37	1.42	0.79	
900	0.33	1.36	0.75	Loss of illite structure,
	0.28	0.78	0.43	growth of spinel
	(Hint of magnetic phase)			
1000	0.27	0.88	0.60	Spinel + α-Fe_2O_3
	0.42[c]	−0.08[d]	(H = 513 kG)[b]	(quartz decreasing)
1100	0.33	0.77	0.55	
	0.40	−0.15[d]	(H = 516 kG)[b]	
1200	0.32	0.77	0.55	Mullite + spinel
	0.83	2.15	0.68	loss of α-Fe_2O_3
1300	0.85	2.59	0.67	Glass
	0.41	1.13	0.77	

[a] Maximum error.
[b] Error, ±4 kG.
[c] Error, ±0.05 mm s^{-1}.
[d] Error, ±0.05 mm s^{-1}.

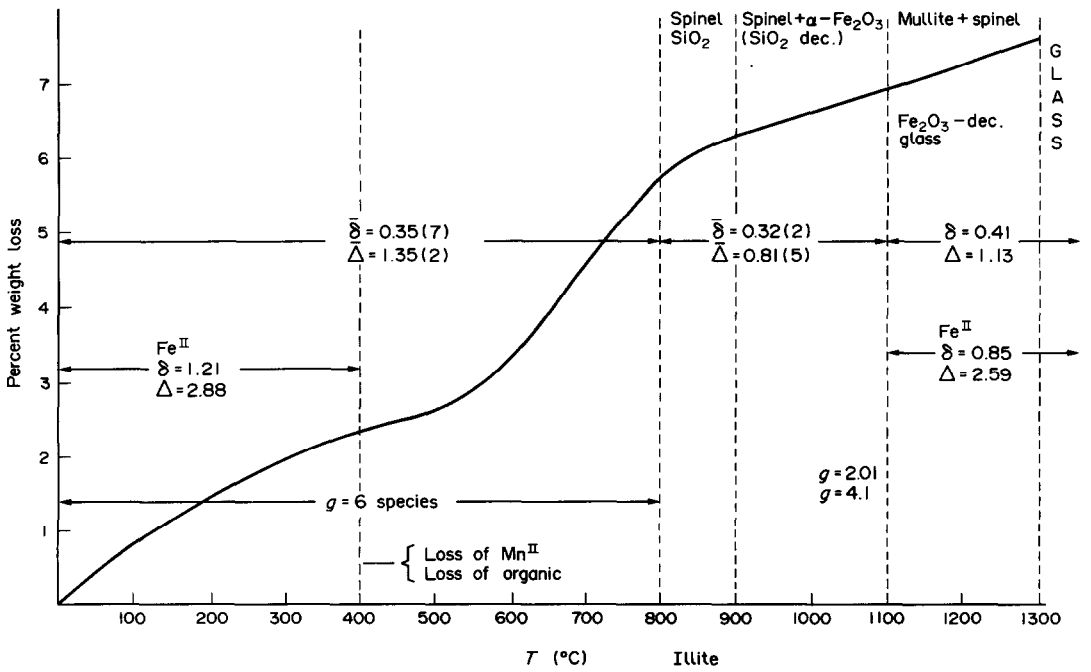

Fig. 1. Illite—summary of XRD, Mössbauer and ESR results. (δ and $\bar{\Delta}$ represent average chemical isomer shift and quadrupole splitting, respectively).

Table 3. ^{57}Fe Mössbauer data for thermally treated montmorillonite (data measured for cooled samples at room temperature); summary of XRD conclusions

Temperature (°C)	$\delta(\pm 0.01)^a$ (mm s^{-1})	$\Delta(\pm 0.02)^a$ (mm s^{-1})	$\Gamma_{1/2}(\pm 0.03)^a$ (mm s^{-1})	XRD conclusions
Ambient	0.36	0.54	0.66	Little change, SiO_2 impurity
400	0.38	1.27	0.58	Trace of FeO(OH)?
	0.33	0.52	0.69	
500	0.38	1.73	0.57	
	0.43	0.89	0.72	
600	0.36	1.26	0.91	
700	0.34	1.43	0.76	Breakdown of montmorillonite structure
	(Trace of magnetic spectrum)			
800	0.34	1.46	0.70	
	(Trace of magnetic spectrum)			
900	0.32	0.89	0.67	Spinel, α-Fe_2O_3, $MgSiO_3$
	0.36	−0.10	H^b = 504 kG	
1000	0.31	0.79	0.77	Spinel, α-Fe_2O_3, $MgSiO_3$
	0.40	−0.06	H^b = 511 kG	
1100	0.32	0.79	0.55	
	0.39	−0.08	H^b = 513 kG	
1200	0.32	0.95	0.70	Spinel and $MgSiO_3$ decrease,
	0.39	−0.09	H^b = 509 kG	α-Fe_2O_3 increases
1300	0.90	1.90	0.72	Mullite, cristobalite, α-Fe_2O_3
	0.35	0.80	0.89	
	0.36	−1.10	H^b = 487^c	

[a] Maximum errors.
[b] ±4 kG.
[c] $\Gamma_{1/2}$ = 0.71, 0.51, 0.33 mm s^{-1}.

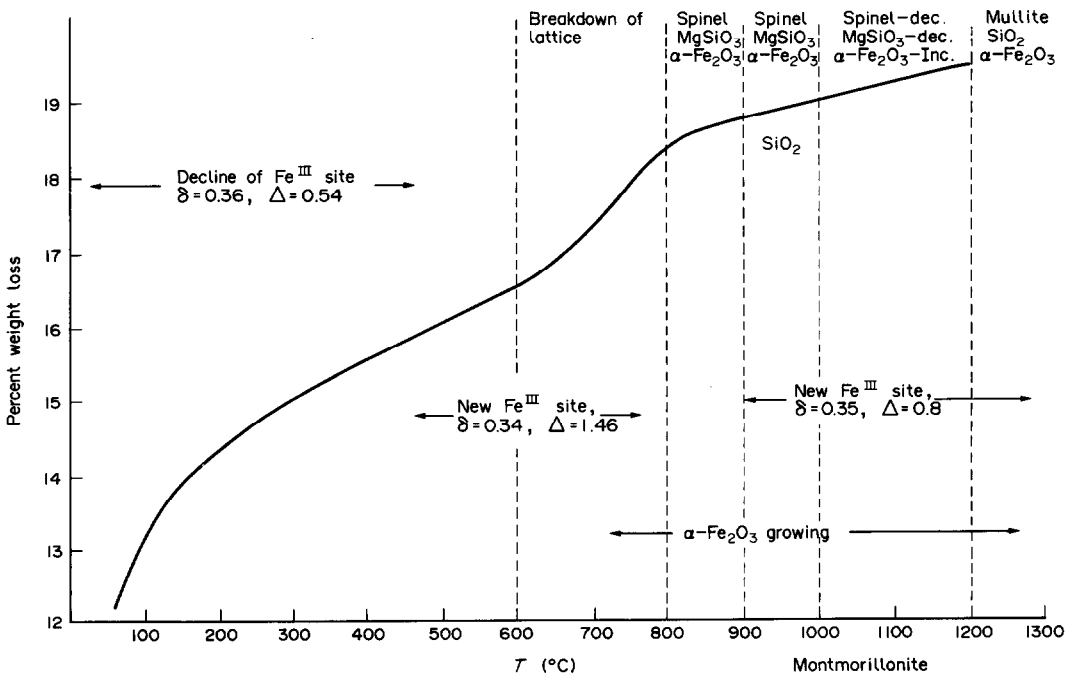

Fig. 2. Montmorillonite—summary of XRD, Mössbauer and ESR results.

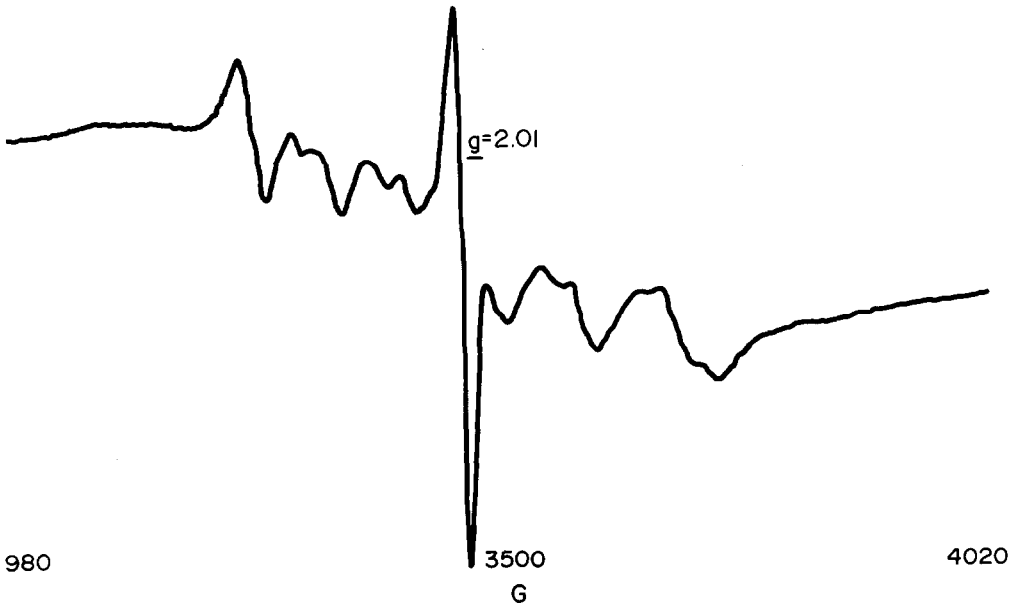

Fig. 3. ESR spectrum of a natural illite sample in the $g = 2$ region.

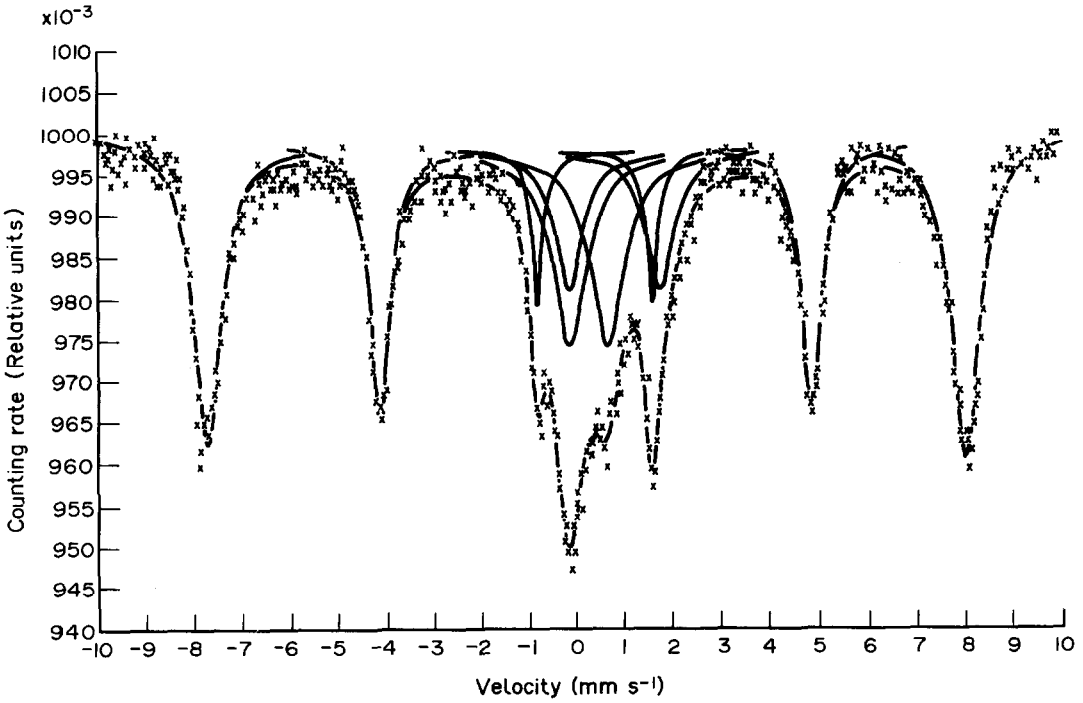

Fig. 4. ^{57}Fe Mössbauer spectrum of montmorillonite heated to 1300°C.

Table 4. Summary of ESR data for specimens of illite heated to the indicated temperatures. Resonances are classified by the g-value

Temperature (°C)	Mn^{2+}	Iron(III) features	Organic
Ambient	~2.0[a]	2.0, 4.15, 6.6	2.010
400	~2.0[a]	2.0, 4.17, 6.6	Trace
500	Trace	2.35(br), 4.21, 6.6	×
600	Trace (~2.0)	~2.0(br), 2.35(br), 4.25, 6.6(w)	×
700	Not observed	2.02(s), 4.25(w)	×
800	Not observed	2.01(s), 4.25(w)	×
900	Not observed	2.01, 4.25	×
1000	Not observed	2.01, 4.25(w)	×
1100	Not observed	2.01, 4.21(w)	×
1200	Not observed	2.03(s), 4.15(m)	×
1300	Not observed	2.04(s), 4.07(m)	×

[a] Six-line spectrum with evidence of doublets between hyperfine lines arising from simultaneous electronic and nuclear transitions—typical of manganese(II) with zero-field splitting.

Table 5. Summary of ESR data for specimens of montmorillonite heated to the indicated temperatures. Resonances are classified by the g-value

Temperature (°C)	Iron(III) features
Ambient	2.06(br), 4.26
400	2.14(br), 4.26
500	2.24(br), 4.26
600	2.24(br), 4.26 (narrow feature at $g = 2$?)
700	2.09(br), 4.26 (narrow feature at $g = 2$?)
800	2.00(s), 2.06(br), 4.26
900	2.00(s), 2.06(br), 4.26
1000	2.00 (overlap) (br), 4.21
1100	~2.00(br), 4.21
1200	~2.00, 4.18 (very broad resonance as background)
1300	Broad featureless resonance

br = broad (width in excess of 1000 G); s = strong resonance.

clay mineral such as montmorillonite, ions in the octahedral layer may occupy sites with either *cis*-dihydroxo- or *trans*-dihydroxo-environments, the so called M(1) and M(2) sites, it would follow from simple electrostatic reasoning[8] that the quadrupole splitting of the *trans* site should be twice that of the *cis* site; thus the implication is that the iron(III) is generally located predominantly in the M(2) sites. This conclusion is not supported by a recent careful electron diffraction study by Tsipursky and Drits[11] which concludes that the iron(III) locates almost entirely in the *trans*-M(1) sites. An important paper by Cardile and Johnston[12] suggested that the actual "best fit" of a Mössbauer spectrum of montmorillonite is often an artefact of the fitting procedure and that in reality the iron(III) ions, located in essentially M(1) sites, are subjected to differing degrees of distortion in those sites and hence are subject to a spectrum of electric field gradients at the nuclei. We concur with this view and believe it to be relevant also to illite.

In Tables 2 and 3 we have presented data for the simplest spectral fit consistent with a satisfactory X^2 value. Only when a two-doublet fit gave a significantly improved X^2 value was it preferred to a one-doublet fit. Attempts at multi-doublet fits of broad resonances have been resisted on the grounds that the results would have little chemical meaning. We therefore view the observed quadrupole splitting as an average value for a range of field gradients; the chemical isomer shift is a "better" parameter in that it is likely to be more sensitive to

phase changes when absolute changes in the electronic environment of the iron(III) ions should occur. Another important parameter is the full-width at half-height ($\Gamma_{1/2}$) which will give some measure of the range of field gradients operating. It is against this background that we interpret the observed Mössbauer data.

Illite

The analysis (XRF) of the sample of illite used is given in Table 1 and is in good agreement with literature data for natural illites.[1] XRD showed an α-quartz (SiO_2) impurity,[13] but was consistent with the trace expected for illite.[9] A representative basal spacing [$d(001)$] of 10.05 Å was seen, but weaker signals corresponding to $d(001)$ of 7.25 and 13.10 Å may imply the presence of some mixed-layer illite–montmorillonite and illite–chlorite. The elemental analysis suggests a little manganese to be present and this is confirmed by the ESR data (Table 4). The manganese(II) spectrum is superimposed on a broad component arising from iron(III); it consists of six lines with some evidence of forbidden electronic and nuclear transitions giving weaker signals between the individual lines. The g-value is approximately 2 and the hyperfine splitting parameter, A, is 81 G. The spectrum may indicate a trace of calcite with a manganese impurity. If so, within this system, following a calcite-to-aragonite phase transition, the carbonate should decompose above 800°C when, from past experience,[14] the signal should be lost on the formation of silicate phases. In this instance, even when illite is heated to 500°C, the signal is lost under a dominant iron(III) contribution. If calcite is present, it is not in sufficient quantity to be detectable by XRD. Thus, an alternative explanation that the manganese(II) is substitutional in the illite cannot be eliminated.

Ericsson *et al.*[15] have reported the Mössbauer spectrum of a similar illite (No. 36) which they have fitted to two iron(III) doublets ($\delta = 0.32$, $\Delta = 0.58$ mm s^{-1}; $\delta = 0.41$, $\Delta = 1.07$ mm s^{-1}) and one iron(II) doublet ($\delta = 1.18$, $\Delta = 2.88$ mm s^{-1}). The two iron(III) doublets were assigned to "*cis*" ($\Delta = 0.58$) and "*trans*" ($\Delta = 1.07$) [M(1) and M(2)] locations of iron(III) in the octahedral layer. For the reason stated above we feel that the assignment is simplistic and prefer the one-doublet fit of Table 4 which gives a measure of the average iron(III) environment. The danger of the M(1), M(2) assignment is further underlined by the XRD data which suggests the illite may not be monophasic. The Swedish workers comment on a small asymmetry of their iron(II) doublet; in this case we prefer a two-doublet fit (Table 2) and, interestingly, if the illite is washed with 0.5 M acetic acid the doublet, $\delta = 1.48$, $\Delta = 2.48$ mm s^{-1}, is removed, thus suggesting that it arises from one of the hydrates, $FeSO_4 \cdot nH_2O$,[3,16] e.g. szoinolnolcite ($n = 1$), rozenite ($n = 4$) or melanerite ($n = 7$). A trace of sulphur was detected by XRF analysis of illite (Table 1), but the amount was sufficiently small to make the assignment very tentative.

The ESR spectrum of natural illite is complex, although it agrees well with that presented previously in a study of illite containing shales.[17] The sharp isotropic resonance ($g = 2.010$) which vanishes on heating the illite to 500°C is attributed to organic radicals. The manganese components have been discussed and probably three iron(III) contributions can be observed: a broad resonance centred on $g \simeq 6$ (presumably with a counterpart at $g = 2.0$ hidden under the major broad feature). These spectra are difficult to interpret but it is probably reasonable to suggest that the $g \simeq 6$ resonance is a component arising from iron(III) in an axially-distorted environment.[18,19] The broad resonance at $g \simeq 2.0$ may be assigned with reasonable certainty to transitions within the super-exchange multiplet resulting from the coupling of two $S = 5/2$ ions in adjacent cation sites, i.e. Fe–OFe pairs either within the lattice or in an impurity phase.[18,20,21] The most probable such impurity phase would be Fe_2O_3 or perhaps FeO(OH)—no magnetic spectrum was observed in the Mössbauer study, but if the particle size were small superparamagnetic behaviour is possible. Since no specific iron oxide impurity phase was observed in the XRD, the balance of probability is that this ESR feature arises from adjacent iron(III) ions in structural cation sites. Many interpretations have been given for the origin of the $g = 4.15$ resonance in clays;[20–22] in the present case it is considered to arise from iron(III) sites of orthorhombic symmetry.[17,18] Thus the ESR data confirm a variety of iron(III) sites and environments and, to our mind, this justifies our reluctance to be more specific in our interpretation of the iron(III) Mössbauer data.

It is clear from Fig. 1 that the bulk of lattice water is lost from illite at 400°C and that the "structural" water is lost between 400 and 800°C. Clearly the iron ions will need to adapt to the loss of structural water; another change is the oxidation of iron(II) to iron(III), which is complete on heating to 500°C. The Mössbauer spectra of samples heated to 400°C show a much reduced iron(II) resonance and a more distorted range of iron(III) sites as indicated by the larger value of Δ and the large $\Gamma_{1/2}$ value (Table 2). The samples heated to 500, 600 and 700°C show two clear doublets, one with parameters comparable to the 400°C spectrum and a new doublet with a

greater quadrupole splitting. By 800°C, when the illite structure is about to undergo irreversible breakdown, the iron(III) ions have migrated to a range of similar sites. A reasonable chemical interpretation of these data is that between 400 and 700°C there are two ligand environments, i.e. FeO_6 and $FeO_{6-x}(OH)_x$ ($2 > x > 0$); within each of these ligand environments there will be a range of site micro-symmetries. Since the $FeO_{6-x}(OH)_x$ sites would be expected to dominate at 400°C, the doublet with $\delta = 0.30$–0.36 and $\Delta = 0.95$–1.14 mm s^{-1} can be assigned to those environments. The implication is, then, that the larger Δ (1.53–1.76 mm s^{-1}) corresponds to the FeO_6 sites which are, by implication, more distorted. The ESR spectra show a marked increase in the $g \simeq 2.0$ resonance on heating to 400°C, also at this level of heating, the $g \simeq 4.0$ resonance becomes complex and a hint of the $g \simeq 6$ resonance is to be seen. Samples heated to 500, 600 and 700°C show a progression to two broad isotropic resonances at 700°C (Table 4); a feature at $g = 2.35$ is present at 500 and 600°C (this may be the $g \simeq 2.0$ component expected with the $g \simeq 6$ component). At 800°C, the dominant feature of the spectrum is a very broad isotropic resonance centred on $g \simeq 2.01$, which together with a weak feature at $g = 4.25$ can now, following the Mössbauer deductions, be ascribed to the dehydroxo "FeO_6" environment, and the $g \simeq 6$, 2.35 features which are steadily lost on heating to 700 and 800°C can be tentatively assigned to the $FeO_{6-x}(OH)_x$ environment. Thus, there exists a satisfying degree of self consistency between the Mössbauer and ESR data.

Heating samples of illite beyond 800°C results in the irreversible breakdown of the silicate structure and new phases, some recognizable by XRD, crystallize. Thus the sample heated to 900°C shows a decrease in the SiO_2 impurity trace and clear evidence of a spinel phase. Between 900 and 1100°C the spinel phase grows, α-Fe_2O_3 is formed and the SiO_2 impurity diminishes further. Mullite is discernable as a new phase on heating to 1200°C and, at this temperature, the trace for α-Fe_2O_3 becomes weak. Heating to 1300°C gives a glass.

The ESR spectra are rather insensitive to these changes, being dominated by a very broad isotropic resonance with $g \simeq 2.01$–2.04 (Table 4). This may be attributed to species with Fe—O—Fe groupings; the resonance at $g = 4.25$ (1000°C) is weak but becomes a little more intense as the temperature to which the samples are heated is increased. This resonance may be attributed to iron(III) in a low-symmetry rhombically-distorted phase—thus supporting the Mössbauer observations (Table 2 see below) that the iron(III) is distributed between two phases. Indeed the Mössbauer data of Table 2 clearly support the deductions from the XRD data that α-Fe_2O_3 appears as an illite decomposition product on heating to 1000°C; this phase may be identified from the value of the magnetic hyperfine field.[8] A second iron(III) phase is present and is shown by a significant change in δ and Δ between 900 and 1000°C; the illite structure is lost and the iron(III) may be associated with the spinel phase, which is recognised by XRD. By 1200°C the α-Fe_2O_3 phase is not clearly discernable from the Mössbauer spectrum, nor is it detectable by XRD; mullite is detectable and the spinel phase persists, together with the iron(III) Mössbauer species with $\delta = 0.32$ mm s^{-1}. Most interestingly, a new iron phase is detectable by Mössbauer spectroscopy—one containing iron(II), and at 1300°C the iron(II) signal is about a third the intensity of the iron(III) signal. The origin of the iron(II) is problematic and we believe that it may be an artefact of our experimental conditions. The furnace we used was lined with silicon carbide and at temperatures beyond 1200°C the furnace atmosphere may be somewhat reducing (it is well known to Craft Potters that the addition of SiC to a glaze will give "reduced" effects in electric kilns[23]).

Combination of the ESR and Mössbauer data suggest that the spectrum of iron(III) sites may occur in the glass found when the decomposed illite fuses at 1300°C. The small clusters of Fe—O—Fe species (superparamagnetic) together with other iron(III) species located in appropriate holes within the glassy silica structure may give rise to a broad ($\Gamma_{1/2} = 0.77$ mm s^{-1}) Mössbauer spectrum and the two ESR features. Thus, these investigations, summarized in Fig. 1, give useful insight to the path of thermolysis of illite. Careful examination of the data reveal that there is good overall agreement between the results of the three techniques used.

Montmorillonite

Many ideas developed in the discussion of the illite data may be carried over to montmorillonite, hence this material can be dealt with more briefly.

The room temperature XRD trace was typical of that for montmorillonite,[9] but it also indicated a α-quartz impurity and the weak presence of iron oxhydroxide minerals.[13] The sample was poorly crystalline but the basal spacing, $d(001)$, of 15.24 Å is typical.[24] On heating the sample, the trace for the clay showed little change until 700°C, but by 900°C it had vanished totally. The X-ray crystallinity is not lost as a result of dehydroxylation (the major weight loss is complete at 700°C, Fig. 1).[25,26] At

900°C, low intensity reflections indicate the onset of crystallization of new phases, e.g. spinel ($MgAl_2O_4$), α-Fe_2O_3 and enstatite ($MgSiO_3$). Crystallinity increases in the sample heated to 1000°C and a strong cristobalite component is now seen; the spinel and enstatite components grow. At 1200°C the spinel and enstatite phases have decreased and mullite is apparent ($3Al_2O_3 \cdot 2SiO_2$) —thus it would seem that the phases have undergone a solid state reaction with cristobalite to afford the mullite; by 1300°C the only crystalline phases discernable are mullite, cristobalite and α-Fe_2O_3. The appearance of the material heated to 1300°C and cooled suggested some glass formation but not to the same degree as illite, a fact explained by the considerably smaller quantities of alkali metal oxides associated with montmorillonite than illite (Table 1).

The room temperature Mössbauer spectrum of the unheated clay may be fitted to a broad quadrupole doublet, which has been discussed above. Thus it is considered to arise from a spectrum of iron sites, including possibly some contribution from the small iron oxyhydroxide phase detected by XRD. The ESR spectrum is typical of that of an iron-rich poorly crystalline clay[27] and consists of two features: a broad resonance at $g = 2.06$ and a sharper signal at $g = 4.26$. The broad resonance reflects Fe—O—Fe groupings within the lattice and, possibly, also within impurity phases.[21,27] Following Cracium and Meghea,[27] the resonance at $g = 4.26$ is assigned to isolated iron(III) ions occupying distorted octahedral sites within the clay structure.

As dehydroxylation of the clay progresses between 150 and 700°C, a new iron phase is established. Thus, from the Mössbauer data the original average quadrupole splitting of 0.54 mm s^{-1} gives way by 700°C to a more distorted site with $\Delta = 1.46$ mm s^{-1}. The consolidation of this site coincides with a breakdown of the montmorillonite lattice and the appearance of a magnetic hyperfine spectrum characteristic of α-Fe_2O_3. The origin of the haematite will be a combination of the initial impurity phases and structural iron from the collapsed clay lattice. The ESR spectrum remains relatively invariant, except that there is some evidence of a sharper feature at $g \sim 2.0$ which becomes more established by 800–900°C (see Table 5)—no corresponding component at $g = 6$ is seen, but the feature may be too weak for detection. Possibly this new resonance may be correlated with a further change in the Mössbauer spectrum which occurs at 900°C ($\delta = 0.32$, $\Delta = 0.89$ mm s^{-1}), at which temperature a crystalline spinel phase is detected in the XRD trace, alternatively the $g = 4.26$ signal must be assigned to the non-magnetic iron site. Indeed, the Mössbauer parameters are comparable with those arising for illite at 1000°C, and it was speculated above that this resonance arose from iron(III) in a spinel phase. Indeed, one section of the iron(III) now enjoys a relatively constant environment, possibly within this spinel phase, or when heated to 1300°C, within a glassy phase derived from the melting of the spiral and other magnesium-containing phases. The ESR spectrum beyond 1000°C becomes increasingly dominated by the magnetic iron phase, although even when heated to 1200°C, the sample retains a signal at $g = 4.18$. It must be assumed that this signal may arise from the iron/spinel phase, in which case throughout the temperature range the ESR does little more than differentiate "magnetic" Fe—O—Fe and isolated iron(III) sites. The Mössbauer data clearly show the increase of the α-Fe_2O_3 phase at 1200°C, but as with illite, in the 1300°C spectrum, definite evidence of iron(II) is seen, this time with an increased quadrupole splitting of 1.90 mm s^{-1}. The same explanation is offered, that it is an artefact of the experimental procedure. In this instance, a further complication occurs. The six line spectrum is well-resolved (Fig. 4) and the hyperfine field may be quite accurately determined at 487 kG, a figure which is not in good agreement with that expected for α-Fe_2O_3 (516 kG[8]) but which is in better agreement with one of the components identified for Fe_3O_4, magnetite, (496 kG[8]). However, clear resolution of the iron(II) and iron(III) components, particularly to negative velocity, would have been expected. The situation is complicated further by the XRD evidence for α-Fe_2O_3, however, the XRD trace is poor; thus we can speculate the α-Fe_2O_3 trace is modified by an underlying contribution from magnetite or possibly from γ-Fe_2O_3.

CONCLUSIONS

We have attempted to show that a contribution of XRD, Mössbauer and ESR studies can throw much light on the thermolytic behaviour of iron-containing clay minerals. The clays in the spectroscopic parameters reflect, in a gratifying way, the major changes detected in XRD and pseudo-TGA studies. We have concluded, albeit tentatively, that at breakdown of the clay structure the bulk of the iron(III) distributes itself between oxide and spinel phases. We have also noted that at 1300°C the observed Mössbauer spectra reflect the prevailing atmosphere (oxidizing or reducing) within the furnace.

Acknowledgement—One of us (P.M.) thank the SERC for the award of a studentship.

REFERENCES

1. R. E. Grim, *Clay Mineralogy*. McGraw Hill, New York (1953).
2. G. P. Huffman and F. E. Huggins, *Fuel* 1978, **57**, 592.
3. F. E. Huggins and G. P. Huffman, in *Analytical Methods for Coal and Coal Products*, Vol. III, Chap. 5. Academic Press, New York (1980).
4. B. Horsfield and A. G. Douglas, *Geochim. Cosmochim. Acta* 1980, **44**, 1119.
5. J. Espitalie, S. Makadi and J. Trichet, *Org. Geochem.* 1984, **6**, 365.
6. M. T. Mackowsky, in *Coal and Coal-bearing Strata* (Edited by D. Murchison and T. S. Westall). Oliver and Boyd, Edinburgh and London (1968).
7. D. J. Vaughan and M. Linskill, *Computer Fitting of Mössbauer Spectra*. University of Aston, Birmingham (1979).
8. G. M. Bancroft, *Mössbauer Spectroscopy: An Introduction for Inorganic Chemists and Geochemists*. McGraw Hill, London (1973).
9. G. W. Brindley and G. Brown, *Crystal Structures of Clay Minerals and their X-ray Identification*. Mineralogical Society, Monograph No. 5 (1951).
10. A. G. Maddock, in *Chemical Bonding and Spectroscopy in Mineral Chemistry* (Edited by F. J. Berry and D. J. Vaughan) p. 141. Chapman and Hall, London (1985).
11. S. I. Tsipursky and V. A. Drits, *Clay Miner.* 1984, **19**, 177.
12. C. M. Cardile and J. H. Johnston, *Clays Clay Miner.* 1986, **34**, 307.
13. R. W. Berry and J. B. Thompson, *X-ray Powder Data for Ore Minerals*. The Geological Society of America (1962).
14. P. A. Gillespie, PhD thesis, Aston University (1979).
15. T. Ericsson, R. Wappling and K. Punakivi, *Geol. För. Stockh. Förh.* 1977, **99**, 229.
16. G. P. Huffman and F. E. Huggins, *Fuel* 1978, **57**, 592.
17. A. Inazumi, T. Isotobe and T. Tarutanti, *Geochem. J.* 1981, **15**, 325.
18. W. R. McWhinnie, in *Chemical Bonding and Spectroscopy in Mineral Chemistry* (Edited by F. J. Berry and D. J. Vaughan). Chapman and Hall, London (1985).
19. T. Castner, G. S. Newell, W. C. Holton and C. P. Slichter, *J. Chem. Phys.* 1960, **32**, 668.
20. P. L. Hall, *Clay Miner.* 1980, **15**, 321, 337.
21. R. E. Meads and P. J. Maldern, *Clay Miner.* 1975, **10**, 313.
22. J. P. E. Jones, B. R. Angel and P. L. Hall, *Clay Miner.* 1975, **10**, 257.
23. E. Cooper, *Electric Kiln Pottery*. Batsford Ltd, London (1980).
24. W. A. Deer, R. A. Howie and J. Zussman, *Rock Forming Minerals*, Vol. 3, Sheet silicates. Longman, London (1962).
25. R. C. MacKenzie, *The Differential Thermal Investigation of Clays*. Mineralogical Society (Clay Minerals Group), London (1957).
26. W. E. Brownell, *Structural Clay Products, Applied Mineralogy*, Vol. 9. Springer-Verlag, Berlin (1976).
27. C. Cracium and A. Meghea, *Clay Miner.* 1985, **20**, 281.

Polyhedron Vol. 8, No. 22, pp. 2719–2721, 1989
Printed in Great Britain

0277–5387/89 $3.00+.00
© 1989 Pergamon Press plc

COMMUNICATION

SYNTHESIS OF A BIMETALLIC CHROMIUM COMPLEX CONTAINING THE NOVEL PENTAOXAPENTAPHOSPHORINANE $[RPO]_5$ RING

CAROLYN M. BANSE, MELISSA A. PRAY and MARK M. TURNBULL*

Department of Chemistry, Clark University, 950 Main Street, Worcester, MA 01610, U.S.A.

(*Received* 6 *June* 1989; *accepted* 4 *August* 1989)

Abstract—The reaction of $(^iPr_2N)_2P(O)H$ with $Cr(CO)_6$ in refluxing xylenes yields the complex $(CO)_4Cr[(^iPr_2N)PO]_5Cr(CO)_3$ (**2**) in 33% yield after chromatography. A novel pentaoxapentaphosphorinane ring is generated during the reaction. IR, ^1H, ^{13}C and ^{31}P NMR spectra are all consistent with a structure containing one *cis*-disubstituted chromium atom and one *fac*-trisubstituted chromium atom, bridged by the phosphorinane ligand.

Since the serendipitous preparation of the bimetallic cage complex **1**, from $(^iPr_2N)_2P(O)H$ and $Mo(CO)_6$, we have been investigating the mechanism and limits of the reaction.[1] In addition to studying the effects of the ancillary groups on the phosphine oxide, we have also studied the effect of varying the metal itself.

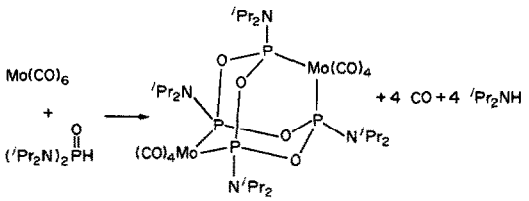

(1)

The 1,3,5,7-tetraoxa-2,4,6,8-tetraphosphorinane, $[RPO]_4$, ligand contained in complex **1** is unique. We have found no reports of such a compound in the uncoordinated state, although the dimeric $[RPO]_2$ and trimeric species $[RPO]_3$ have been prepared.[2]

We wish to report that the reaction of $(^iPr_2N)_2P(O)H$ with $Cr(CO)_6$ in refluxing xylenes yields the related cage complex $(CO)_4Cr[(^iPr_2N)PO]_5Cr(CO)_3$ (**2**), instead of the chromium analogue of **1**. Of note is that this complex contains the expanded 1,3,5,7,9-pentaoxa-2,4,6,8,10-pentaphosphorinane ring, bridging the chromium atoms. The compound is characterized by IR and NMR spectroscopy, as well as by elemental analysis.

RESULTS AND DISCUSSION

Reaction of $(^iPr_2N)_2P(O)H$ and $Cr(CO)_6$ in refluxing xylenes gave compound **2** as a yellow powder in 30% isolated yield after column chromatography: IR spectroscopy provided the first indication that the product was not the expected chromium analogue of **1**. The carbonyl region showed six strong bands, ranging from 2022 to 1874 cm^{-1}. In accord with its D_{2d} symmetry, **1** has only four absorptions in that region. We therefore assumed two inequivalent metal centres to be

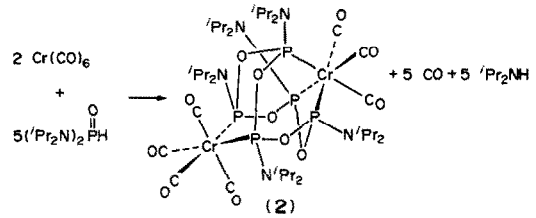

(2)

* Author to whom correspondence should be addressed.

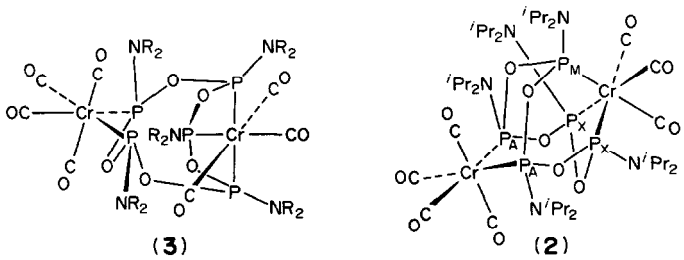

(3) (2)

Fig. 1.

present, one of which was *cis*-substituted (as indicated by the 2022 cm^{-1} band).*

$^{31}P(H)$ NMR spectroscopy revealed an A_2MX_2 spectrum (J_{AM} = 8.3 HZ, J_{MX} = 40.1 Hz, J_{AX} < 1.5 Hz) indicating a total of five phosphorus atoms in three inequivalent environments. The chemical shifts of the signals (δ 156–176 ppm) showed no phorphoryls to be present and suggested that all the phosphorus atoms were coordinated to chromium. The ^{1}H-coupled ^{31}P NMR spectrum further revealed that each phosphorus was coupled to two hydrogens (J = 12–14 Hz), in agreement with one attached diisopropylamino substituent. Based on these data, we tentatively assigned the structure of **2** as having the *cis*-substituted metal centre, previously noted, and a *fac*-substituted metal centre. A *fac*-$CrL_3(CO)_3$ complex is expected to have two CO stretching vibrations in the IR[4] and thus all six observed CO bands are accounted for. The *mer*-isomer, **3** (Fig. 1), with P_M in the centre, would also explain the IR spectrum, but was ruled out since AM coupling would not be expected in the ^{31}P NMR spectrum. More important perhaps, is the presence of two fused four-membered rings in compound **3**, making it extremely unlikely. The final assignment, namely which pairs of phosphorus atoms were A and X, was made based on the observed coupling constants. The larger coupling (40 Hz) was assigned as the through-metal coupling and the smaller coupling (8 Hz) was assigned as the P—O—P coupling. The apparent absence of coupling in the similar P—O—P linkage between P_A and P_X was surprising, but not without precedent based on related spectra from the oxidation products of **1** where these coupings are less than 2 Hz.[5] The final assignments are shown in Fig. 1.†

The ^{13}C NMR {H} spectrum of **2** shows four apparent triplets (δ 230, 225, 220, 217 ppm; J = 10–30 Hz) and an unresolved multiplet (228 ppm). These resonances are surprisingly far downfield relative to **1** (δ 206, 213 ppm). The shift may be due to steric congestion around the metals. The methyne region reveals two apparent triplets (δ 48.5, 48.0 ppm; J = 2–6 Hz) which are assigned to the methyne carbons of the amino groups attached to P_A and P_X, not necessarily in that order, and a doublet (δ 47.7 ppm; J = 13 Hz) which is assigned to the methyne carbons of the amino group attached to P_M. The apparent triplets are the same as is observed for **1**, and are in agreement with the predicted spectrum for an ABX spectrum (A, B = P, X = C) where $\delta_{AB} = 0$.[7] The methyl region shows six signals (δ 23.7–25.4 ppm), when symmetry would predict only five types of methyls. The resonances are too well separated (10–40 Hz) for P—C coupling to be a likely explanation. We suggest the idea that the extra signal is caused by restricted rotation about a P—N bond as a result of steric congestion.

Finally, the ^{1}H NMR spectrum shows a broad unresolved multiplet at 1.4 ppm from the methyl groups. Two more signals, an apparent heptet and an apparent nonet (δ 4.7 (1H) and 4.2 (4H), respectively) occur in the methyne region. We assign the downfield signal to the methyne protons attached to the unique P_M, based solely on their integrated values.

EXPERIMENTAL

All procedures were carried out using standard Schlenk techniques under an argon atmosphere. Xylenes (mixed isomers) were purified by distillation from sodium metal. Dichloromethane was distilled from CaH_2. Diisopropylamine was distilled from KOH. PCl_3 and $Cr(CO)_6$ were purchased from Alfa Products and used without further purification. Bis(N,N-diisopropylamino)phosphine oxide

* Empirical observations indicate that the position of the strong absorption above 2000 cm^{-1} in these complexes is a reliable indication of geometry about the metal (see ref. 3).

† We wish to acknowledge the independent synthesis of compound **2** by Wong and co-workers and thank them for providing us with their unpublished results. Single crystal X-ray analysis confirms our proposed structure for compound **2** (see ref. 6).

was prepared as previously described.[1a] IR spectra were recorded on a Perkin–Elmer 1330 spectrophotometer and were calibrated against polystyrene. NMR spectra were recorded on a Bruker AC-200 spectrometer (courtesy of the Worcester NMR Consortium) and calibrated against TMS (^{1}H) solvent (^{13}C) or external Ph_3P (^{31}P).

$Cr(CO)_4[(^iPr_2N)PO]_5Cr(CO)_3$ (**2**)

Bis(N,N-diisopropylamino)phosphine oxide (3.00 g, 12.1 mmol), $Cr(CO)_6$ (1.75 g, 7.95 mmol, 0.66 equiv.) and xylenes (50 cm^3) were combined in a round-bottomed Schlenk flask fitted with a magnetic stirrer and reflux condenser. The mixture was heated to reflux in an oil bath (bath temperature, 145°C) and stirred overnight (14–16 h). The xylenes were removed *in vacuo* from the now black reaction mixture, the residue was dissolved in a minimum volume of CH_2Cl_2 and chromatographed (silica gel, CH_2Cl_2) to yield a pale yellow powder, 0.82 g (33%). Compound **2** oxidizes slowly in air and is soluble in most organic solvents. IR (KBr): 2022, 1966, 1941, 1885, 1874 (C≡O) 985 (P—N) 900 (P—O—P) cm^{-1}. ^{1}H NMR ($CDCl_3$): δ 4.7 (app. h, 1H, $J_{app} \approx 7$ Hz), 4.2 (app. nonet, 4H, $J_{app} \approx 7.5$ Hz), 1.4 (broad m, 30H). ^{13}C NMR {H} ($CDCl_3$): δ 230 (m, C≡O), 224.8 (t, $J = 10$ Hz, C≡O), 219.9 (t, $J = 9$ Hz, C≡O), 217.1 (t, $J = 9$ Hz, C≡O), 49.0 (app. t, $J = 5.5$ Hz, N—C), 48.5 (app. t, $J \approx 2$ Hz, N—C), 47.7 (d, $J = 13$ Hz, N—C), 25.4, 24.8, 24.6, 24.3, 24.2, 23.7 (CH_3's). ^{31}P NMR {H} ($CDCl_3$): δ 176.2 (d, 2P, $J = 8.3$ Hz), 174.9 (t of t, 1P, $J = 8.3$, 40.1 Hz), 156.4 (d, 2P, $J = 40.1$ Hz). Found: C, 42.7; H, 6.9; N, 6.4. Calc. for $C_{37}H_{70}Cr_2N_5O_{12}P_5$: C, 42.9; H, 6.8; N, 6.8%.

REFERENCES

1. (a) E. H. Wong, M. M. Turnbull, E. J. Gabe, F. L. Lee and Y. Le Page, *J. Chem. Soc., Chem. Commun.* 1983, 776; (b) E. H. Wong, M. M. Turnbull, K. D. Hutchinson, C. Valdez, E. J. Gabe, F. L. Lee and Y. Le Page, *J. Am. Chem. Soc.* 1988, **110**, 8422.
2. (a) E. E. Nifant'ev, M. P. Koroteev, N. L. Ivanov, I. P. Gudkova and D. A. Predvoditelev, *Acad. Sci. USSR, Proc. Chem. Soc.* 1967, **173**, 398; (b) E. Niecke, H. Zorn, B. Krebs and G. Henkel, *Angew. Chem. Int. Edn Engl.* 1980, **19**, 709; (c) D. W. Chaser, J. P. Fackler, A. M. Mazany, R. A. Komoroski and W. J. Kroenke, *J. Am. Chem. Soc.* 1986, **108**, 5956.
3. M. M. Turnbull, E. H. Wong, E. J. Gabe and F. L. Lee, *Inorg. Chem.* 1986, **25**, 3189.
4. F. A. Cotton and C. S. Kraihanzel, *J. Am. Chem. Soc.* 1962, **84**, 4432.
5. E. H. Wong, M. M. Turnbull and E. J. Gabe, manuscript in preparation.
6. See E. H. Wong, S. van Kouwenberg and E. J. Gabe, manuscript in preparation.
7. R. J. Abraham and H. J. Bernstein, *Can. J. Chem.* 1961, **39**, 216.

Polyhedron Vol. 8, No. 22, pp. 2723–2724, 1989
Printed in Great Britain

0277–5387/89 $3.00+.00
© 1989 Pergamon Press plc

COMMUNICATION

SYNTHESIS AND CHARACTERIZATION OF COPPER(II) AND NICKEL(II) COMPLEXES OF 4-ALKYLDITHIOATE-5-HYDROXY-3-METHYL-1-PHENYLPYRAZOLES

RENE MAURELIA,* GERARDO LEON and ALFONSO OLIVA

Institute of Chemistry, Catholic University of Valparaíso Casilla 4059, Valparaíso, Chile

(*Received* 24 *April* 1989; *accepted* 3 *August* 1989)

Abstract—Copper(II) and nickel(II) complexes of 4-alkyldithioate-5-hydroxy-3-methyl-1-phenylpyrazoles have been prepared and characterized by elemental analysis, UV–vis and IR spectroscopy. All compounds have a metal–ligand ratio of 1 : 2 and analytical or spectroscopic data agree with a square-planar structure.

4-Acyl derivatives of 2-pyrazoline-5-ones are known to be good chelating and extractant agents.[1–3] As a part of a programme to synthesize sulphur–metal complexing molecules, we have studied the introduction of the alkyldithioate moiety at the C-4 position of 3-methyl-1-phenyl-2-pyrazoline-5-one in order to obtain organosulphur chelating pyrazoles.[4] The reaction was achieved by condensation of the above pyrazoline-5-one with carbon disulphide and alkyl halides to afford 4-alkyldithioate-5-hydroxy-3-methyl-1-phenylpyrazoles. We now report the synthesis and characterization of the corresponding copper(II) and nickel(II) complexes, I.

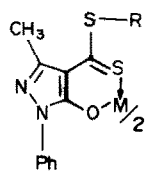

(I)

M = Ni; R = *n*-C_6H_{13}, *n*-C_8H_{17}, *n*-$C_{10}H_{21}$, *n*-$C_{12}H_{25}$
M = Cu; R = C_2H_5, *n*-C_6H_{13}, *n*-$C_{12}H_{25}$

EXPERIMENTAL

Magnetic moment measurements were performed on a Gouy balance at room temperature, using $HgCo(SCN)_4$ as the reference substance. IR spectra were recorded in the 600–300 cm^{-1} range on a Perkin–Elmer 599 spectrophotometer, using polyethylene discs. ^1H NMR spectra were recorded on a Varian 360 A spectrometer. UV–vis spectra were measured on a Cary 219 spectrophotometer, with chloroform as solvent.

All the complexes were prepared by the same general method described below: a water solution of the metal acetate (0.5 mmol) was mixed with an alcoholic solution of the ligand (1 mmol) and heated on a water bath (50°C) for 1 h. The product was filtered off, dried and recrystallized from benezene or toluene.

RESULTS AND DISCUSSION

Analytical data of the copper(II) and nickel(II) complexes (Table 1) agree with the general formula I. The magnetic moment of the copper(II) complexes corresponds to one unpaired spin per copper atom.

IR spectra of the ligands exhibit a wide but weak band at 3250–2600 cm^{-1} due to the strongly associated hydroxy-thiocarbonyl group, and four bands in the 600–300 cm^{-1} region (355, 415, 515 and 555 cm^{-1}) assigned to the chelate ring vibration.[4–6] A comparative analysis in the IR spectra of the ligands and the complexes shows that the absorption at 3250–2600 cm^{-1} is absent, due to the replacement of the hydrogen by the metal ion. In the 600–300 cm^{-1} region, two additional bands are observed in

* Author to whom correspondence should be addressed. Present address: Chemistry Area, Faculty of Engineering, University of Atacama, Casilla 240, Copiapó, Chile.

Table 1. Physical and analytical data of the copper(II) and nickel(II) complexes, I

R	M	Colour	Yield (%)	Melting point (°C)	Elemental analysis (%) Found (Calc.) H	C	N	S	M	IR (cm^{-1}) ν_{M-S}	ν_{M-O}	μ_{eff} (MB)
C_2H_5	Cu	Green	64	228–229	4.6 (4.2)	49.6 (50.5)	9.2 (9.1)	20.8 (20.7)	10.2 (10.3)	390	440	1.90
n-C_6H_{13}	Cu	Green	78	217–218	6.0 (5.8)	56.7 (55.9)	7.9 (7.7)	17.9 (17.8)	8.8 (8.7)	390	440	1.74
n-$C_{12}H_{25}$	Cu	Green	62	164–165	7.7 (7.4)	60.9 (61.5)	6.3 (6.2)	14.3 (14.3)	7.4 (7.1)	390	440	1.88
n-C_6H_{13}	Ni	Reddish-brown	93	232–233	5.9 (5.8)	57.0 (56.3)	7.9 (7.7)	17.7 (17.7)	8.1 (8.1)	385	450	—
n-C_8H_{17}	Ni	Reddish-brown	78	221–222	6.6 (6.4)	58.6 (58.4)	7.5 (7.2)	16.5 (16.4)	7.6 (7.5)	385	450	—
n-$C_{10}H_{21}$	Ni	Reddish-brown	77	197–198	7.1 (7.0)	60.7 (60.2)	7.2 (6.7)	15.4 (15.3)	7.1 (7.0)	385	450	—
n-$C_{12}H_{25}$	Ni	Brown	76	186–187	7.7 (7.4)	62.2 (61.8)	6.4 (6.3)	14.4 (14.3)	6.8 (6.6)	385	450	—

copper(II) complexes at 390 and 440 cm^{-1}. We have assigned these bands to Cu—S and Cu—O vibrations. In the nickel(II) complexes, the Ni—S and Ni—O vibrations are observed at 385 and 450 cm^{-1}.[7]

^1H NMR spectra of the ligands display a singlet at 13.7–13.8 ppm due to the hydroxyl proton.[4] This signal is absent in the spectra of the nickel(II) complexes because of coordination. The chemical shift of the other signals are very close to those of the ligands, and a slight displacement of 0.2–0.4 ppm is observed.

Three bands at *ca* 245, 313 and 365 nm are observed in the UV–vis spectra of the ligands.[4] These absorptions can be ascribed to the phenylpyrazole, pyrazole and chelate ring conjugations.[8,9] Copper(II) complexes exhibit five bands at 244, 329, 361, 470 and 595 nm, and the first three can be related to the ligands. However, the 329 nm transition can also be assigned as a charge-transfer band, $b_{1a} \rightarrow b_{3g}$, observed in related copper(II) complexes with acetylacetone, β-acetodithioesters and thiohydroxamic acids.[10–12] The shoulders at 470 and 595 nm are typical of $S \rightarrow Cu^{II}$ ligand-to-metal charge-transfer and *d–d* transitions observed in square-planar copper(II) complexes.[10–12]

The UV-vis spectra of nickel(II) complexes are characterized by seven bands. In the UV region, those at 255, 314 and 332 nm can be related to the ligands and the absorption at 290 nm must be a charge-transfer band. The visible region shows three bands at 400, 465 and 708 nm. We have identified these absorptions as the ν_1, ν_2 and ν_3 bands observed in square-planar complexes of nickel(II) with sulphur ligands.[13]

Acknowledgements—The authors wish to thank the Catholic University of Valparaíso, Chile, for financial support, and Dr F. Castañeda (University of Chile) for elemental analyses of carbon, hydrogen and nitrogen.

REFERENCES

1. M. Mirza and R. Bailey, *J. Inorg. Nucl. Chem.* 1979, **41**, 772.
2. B. Jensen, *Acta Chim. Scand.* 1959, **13**, 1980.
3. M. Mirza, *Talanta* 1978, **25**, 685.
4. A. Oliva, G. León and R. Maurelia, *Synth. Commun.*, in press.
5. P. Papini, G. Auzzi and M. Bambagiotti, *Gazz. Chim. Ital.* 1968, **98**, 245.
6. E. C. Okafor, *Polyhedron* 1983, **2**, 309.
7. G. Dorange, R. Kergoat and J. Guerchais, *Bull. Soc. Chim. Fr.* 1969, 3835.
8. S. Scheithauer and R. Mayer, *Topics in Sulfur Chemistry*, Vol. 4: Thio and dithiocarboxylic acids and their derivatives. Georg Thieme, Stuttgart (1979).
9. M. Saquet and A. Thuiller, *Bull. Soc. Chim. Fr.* 1967, 2841.
10. G. Dorange and J. Guerchais, *Bull. Soc. Chim. Fr.* 1971, 43.
11. J. Becher, D. J. Brockway, K. S. Murray, P. J. Newman and H. Toftlund, *Inorg. Chem.* 1982, **21**, 1791.
12. A. W. Addison, T. Nageswara Rao and E. Sinn, *Inorg. Chem.* 1984, **23**, 1957.
13. A. B. P. Lever, *Inorganic Electronic Spectroscopy*, 1st edn. Elsevier, Amsterdam (1968).

Polyhedron Vol. 8, No. 22, pp. 2725–2726, 1989
Printed in Great Britain

0277–5387/89 $3.00+.00
© 1989 Pergamon Press plc

COMMUNICATION

CHEMO- AND REGIOSELECTIVE HALOGENATION OF A CYCLOPALLADATED IMINE

JOAN ALBERT, JAUME GRANELL and JOAQUIM SALES*

Departament de Química Inorgànica, Universitat de Barcelona, Diagonal 647, 08028 Barcelona, Spain

(*Received* 9 *June* 1989; *accepted* 15 *August* 1989)

Abstract—2-Chloromethyl-4,6-dimethylbenzaldehyde is obtained by chlorination of a cyclopalladated-imine derivative of mesitylenecarbaldehyde.

Cleavage of organometallic compounds with halogens has been widely studied,[1] but many of the reactions are complicated by radical processes, trihalide ion reactions, and oxidation of the metal prior to metal bond cleavage.

With halogens, competitive cleavage reactions and electrophilic substitution reactions of the aromatic ring can occur. For example, solutions of halogens almost completely cleave the cobalt–carbon bond in benzylcobaloximes. However, the *meta*- and 3,5-dimethylbenzylcobaloximes, in which the aromatic ring is activated by both the methyl

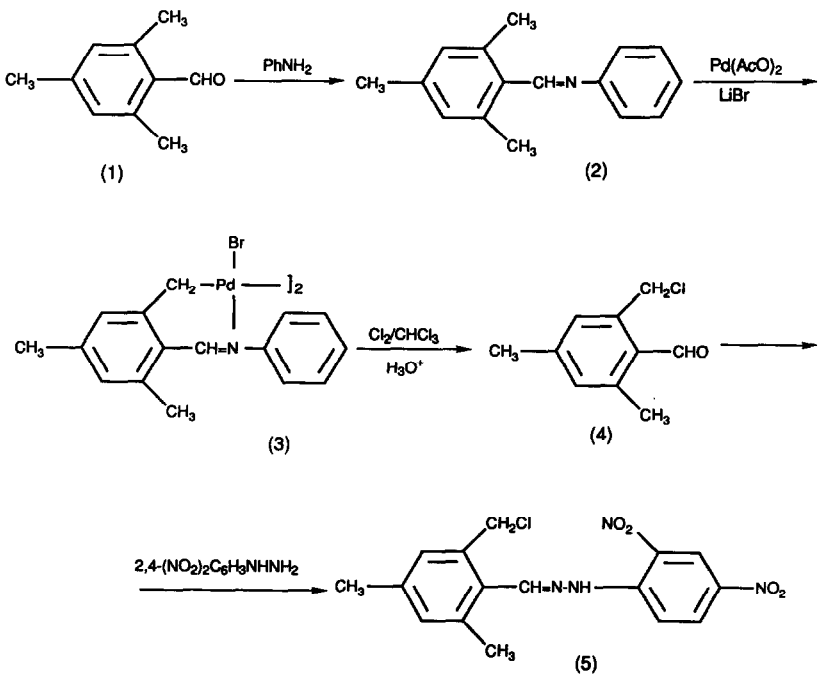

Scheme 1.

* Author to whom correspondence should be addressed.

groups and the —CH_2—$Co(dmgH)_2py$ group, undergo halogenation of the aromatic nucleus.[2]

Cyclometallated compounds are very useful reagents for organic syntheses, but up to now their applications have been almost restricted to aromatic systems.[3]

Recently we have described that the imine derivatives of mesitylenecarbaldehyde (**2**) react with $Pd(OAc)_2$ to give six-membered metallocycles possessing an aliphatic carbon–metal bond.[4] The metallocycle (**3**) contains two methyl substituents in positions 3 and 5, and the —CH_2—Pd— group which activates the electrophilic substitution on C(4), but the imine group can cancel out this effect. So, the halogenation should take place only on the palladium–carbon bond, opening a new way to the selective benzylic halogenation.

In order to prove this assumption we have studied the reaction between chlorine and the cyclometallated complex (**3**). The action of chlorine, at room temperature, on the cyclometallated compound (**3**) in chloroform, cleaves only the palladium–carbon bond, and after acid hydrolysis the chloromethylbenzaldehyde (**4**) is formed. The aldehyde obtained has been characterized as a 2,4-dinitrophenylhydrazone derivative (**5**) (~ 50%) (^{1}H NMR: δ(NH) 11.3(1H, s); δ(HC=N) 8.46(1H, s); $\delta(CH_2Cl)$ 4.87(2H, s); $\delta(CH_3)$ 2.51(3H, s) and 2.35(3H, s). *m/z* 362).

In summary, the present reaction allows the chemo- and regioselective halogenation of a methyl group in the *ortho*-position to an aldehyde function and represents a good illustration of the potential synthetic applications of cyclometallated complexes in the selective functionalization of organic compounds.

Acknowledgements—We thank Dr Miquel Pericàs for helpful discussions and the CAICYT (PB86-0575) for financial support.

REFERENCES

1. G. Wilkinson, F. G. A. Stone and E. W. Abel (Eds), *Comprehensive Organometallic Chemistry*, Vol. 5, p. 110. Pergamon Press, Oxford (1982); M. D. Johnson, *Accts Chem. Res.* 1978, **11**, 57.
2. S. N. Anderson, D. H. Ballard and M. D. Johnson, *J. Chem. Soc., Perkin Trans. II* 1972, 311; B. D. Gupta, M. Kumar and S. Roy, *Inorg. Chem.* 1989, **28**, 11.
3. A. D. Ryabov, *Synthesis* 1985, 233.
4. J. Albert, J. Granell and J. Sales, *Organometallics* 1986, **5**, 2567.

Polyhedron Vol. 8, No. 22, pp. 2727–2729, 1989
Printed in Great Britain

0277–5387/89 $3.00+.00
© 1989 Pergamon Press plc

COMMUNICATION

THE PREPARATION AND X-RAY CRYSTAL STRUCTURE OF [RhPh(OCOCF$_3$)(C$_{10}$H$_4$NO$_2$){P(*p*-FC$_6$H$_4$)$_3$}(H$_2$O)], AN OCTAHEDRAL COMPLEX CONTAINING A σ-RhPh BOND

M. CANO,* J. V. HERAS, M. A. LOBO and E. PINILLA

Departamento de Química Inorgánica, Facultad de Ciencias Químicas, Universidad Complutense, 28040 Madrid, Spain

and

E. GUTIERREZ and M. A. MONGE

Instituto de Ciencias de los Materiales sede D, C.S.I.C., 28006 Madrid, Spain

(*Received* 9 *August* 1989; *accepted* 21 *August* 1989)

Abstract—New complexes containing a σ-RhPh bond have been obtained by elimination of Hg from the intermediate heterobimetallic complexes [Rh(OCOCF$_3$)(HgPh)(quin)(CO){P(*p*-RC$_6$H$_4$)$_3$}] (quin = 2-quinaldinate (C$_9$NH$_6$COO$^-$), R = Cl, F, CH$_3$ and CH$_3$O). The heterobimetallic complexes were prepared by reactions of [Rh(quin)(CO){P(*p*-RC$_6$H$_4$)$_3$}] with PhHg(OCOCF$_3$). The crystal structure of [RhPh(OCOCF$_3$)(quin){P(*p*-FC$_6$H$_4$)$_3$}(H$_2$O)] has been determined.

In a previous paper we have shown that complexes of the type [Rh(pyC)(CO){P(*p*-RC$_6$H$_4$)$_3$}] (pyC = 2-C$_5$NH$_4$COO$^-$) react with PhHgCl to give [RhCl(HgPh)(pyC)(CO){P(*p*-RC$_6$H$_4$)$_3$}].[1] Related reactions with PhHg(OCOCF$_3$) yield unstable heterobimetallic complexes, which after deposition of metallic mercury give new compounds with RhPh bonds. So, we propose the synthesis of σ-organometallic RhPh compounds using heterobimetallic Rh—Hg complexes as intermediates.

In this paper we describe the reactions of [Rh(quin)(CO){P(*p*-RC$_6$H$_4$)$_3$}] with PhHg(OCOCF$_3$) and the formation of new σ-organometallic compounds. The crystal structure of the complex [RhPh(OCOCF$_3$)(quin){P(*p*-FC$_6$H$_4$)$_3$}(H$_2$O)] has been determined and is shown in Fig. 1.†

The reactions of [Rh(quin)(CO){P(*p*-RC$_6$H$_4$)$_3$}] with PhHg(OCOCF$_3$) yielded the new products [Rh(OCOCF$_3$)(HgPh)(quin)(CO){P(*p*-RC$_6$H$_4$)$_3$}]. The addition of HgPh and OCOCF$_3$ groups to the rhodium atom is in agreement with the related reactions with PhHgCl.[1] The complexes were stable in the solid state, but when treated in acetone decarbonylated products were observed. The new decarbonylated complexes were characterized as [RhPh(OCOCF$_3$)(quin){P(*p*-RC$_6$H$_4$)$_3$}] on the basis of analytical and spectroscopic data.

We have solved the crystal structure for one

* Author to whom correspondence should be addressed.

† Crystal data: C$_{36}$F$_6$H$_{25}$NO$_5$PRh, triclinic, a = 15.846(3), b = 11.585(3), c = 10.804(5) Å, α = 64.27(3), β = 103.68(3), γ = 113.15(2)°, U = 1638(1) Å^3, space group $P\bar{1}$, Z = 2, M_r = 799.5, D_c = 1.62 g cm^{-3}. Data were measured on an Enraf–Nonius CAD4 diffractometer with graphite monochromated Mo-K_α radiation (λ = 0.71069 Å) using ω–2θ scans. The structure was solved by the heavy-atom method and refined anisotropically using absorption corrected data to give R = 0.049, R_w = 0.054, for 5472 independent observed reflections [$|I_o| \geq 2\sigma(|I|)$], $1 < \theta < 26$. The atomic coordinates are available on request from the Director of the Cambridge Crystallographic Data Centre, University Chemical Laboratory, Lensfield Road, Cambridge CB2 1EW, U.K. Any request should be accompanied by a full literature citation for this communication.

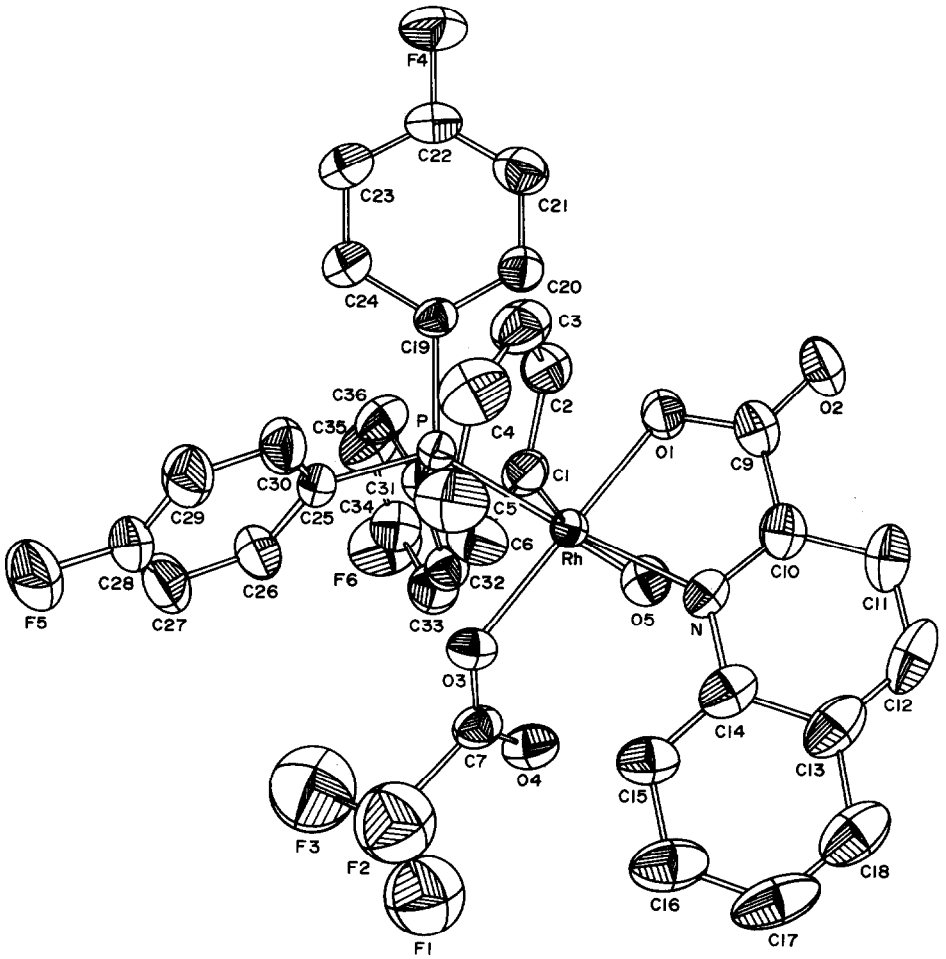

Fig. 1. The X-ray crystal structure of [RhPh(OCOCF$_3$)(quin){P(*p*-FC$_6$H$_4$)$_3$}(H$_2$O)]. Important bond distances (Å) and angles (°):

Bond distances

Rh—P	2.305(2)	Rh—C(1)	2.011(7)	N—C(14)	1.374(8)
Rh—N	2.164(5)	P—C(19)	1.815(6)	O(1)—C(9)	1.283(8)
Rh—O(1)	1.100(3)	P—C(25)	1.828(6)	O(2)—C(9)	1.221(6)
Rh—O(3)	2.067(3)	P—C(31)	1.829(6)	O(3)—C(7)	1.266(9)
Rh—O(5)	2.243(6)	N—C(10)	1.318(6)	O(4)—C(7)	1.215(9)

Angles

O(5)—Rh—C(1)	168.1(2)	N—Rh—C(1)	91.0(2)	P—Rh—O(3)	84.2(1)
O(3)—Rh—C(1)	90.9(2)	N—Rh—O(5)	78.6(2)	P—Rh—O(1)	95.9(1)
O(3)—Rh—O(5)	96.9(2)	N—Rh—O(3)	100.3(2)	P—Rh—N	175.5(2)
O(1)—Rh—C(1)	89.9(2)	N—Rh—O(1)	79.6(2)	Rh—P—C(31)	115.0(2)
C(1)—Rh—O(5)	82.61(2)	P—Rh—C(1)	88.5(2)	Rh—P—C(25)	112.2(2)
O(1)—Rh—O(3)	179.2(2)	P—Rh—O(5)	101.4(1)	Rh—P—C(19)	118.2(2)

of these derivatives, [RhPh(OCOCF$_3$)(quin){P(*p*-FC$_6$H$_4$)$_3$}], and a six-coordinated distorted octahedral for the rhodium atom has been observed (Fig. 1). The phenyl and OCOCF$_3$ groups are in *cis* positions and a molecule of water is coordinated as the sixth ligand. The water molecule is attached to a non-coordinated oxygen atom (O$_4$) of the trifluoroacetate ligand through an intramolecular hydrogen bond and to the non-coordinate oxygen atom (O$_2$) of the quinaldinate ligand through an intermolecular hydrogen bond. The bond lengths and angles are as expected.[2-4]

Acknowledgement—We are grateful to the Comision Asesora de Investigación Científica y Técnica (CAICYT), Spain, for financial support (Proyect PR84-0367).

REFERENCES

1. M. Cano, J. V. Heras, M. Martinez, E. Pinilla and C. Alvarez, *Polyhedron* 1989, **8**, 1085.
2. E. B. Fleischer and D. Lavallee, *J. Am. Chem. Soc.* 1967, **20**, 7133.
3. G. J. Lamprecht, J. H. Beetge, J. G. Leipoldt and D. R. De Waal, *Inorg. Chim. Acta* 1986, **113**, 157.
4. J. G. Leipoldt, G. J. Lamprecht and D. E. Graham, *Inorg. Chim. Acta* 1985, **101**, 123.

Polyhedron Vol. 8, No. 22, pp. 2731–2733, 1989
Printed in Great Britain

0277–5387/89 $3.00+.00
© 1989 Pergamon Press plc

COMMUNICATION

PHOTOREDOX REACTION OF TRIAZIDOMERCURATE(II). GENERATION OF STABLE MERCURY ATOMS UNDER AMBIENT CONDITIONS

HORST KUNKELY and ARND VOGLER†

Institut für Anorganische Chemie, Universität Regensburg, Universitätsstraße 31, D-8400 Regensburg, F.R.G.

(*Received* 19 *July* 1989; *accepted* 23 *August* 1989)

Abstract—Upon ligand-to-metal charge-transfer excitation the complex $[Hg(N_3)_3]^-$ in ethanol underwent a photoredox reaction ($\lambda_{irr} = 254$ nm; $\phi = 0.02$): $[Hg^{II}(N_3)_3]^- \rightarrow Hg^0 + 3N_2 + N_3^-$. Elemental mercury was released in the form of metal atoms which are stable under ambient conditions.

Upon ligand-to-metal charge-transfer (LMCT) excitation many transition metal azide complexes undergo a redox reaction which leads to the formation of the free metal as a colloid.[1] It is assumed that first free metal atoms are formed which agglomerate to smaller clusters, then to large clusters, and finally to colloidal particles. However, the metal atoms and clusters have not been detected since the agglomeration is apparently very rapid and does not stop at intermediate stages. In the present communication we report the direct observation of mercury atoms which are generated by the photolysis of $[Hg(N_3)_3]^-$ in ethanol under ambient conditions. This observation is facilitated by the relatively high stability of mercury atoms. Our study is also an interesting contribution to the photochemistry of mercury(II) complexes. While several organometallic mercury(II) compounds[2–5] are known to undergo a light-induced reductive elimination with the release of metallic mercury, the photochemistry of classical mercury(II) complexes seems to be rather complicated.[3,6] Finally, our observations may be also important with regard to the mechanism of the mercury-photosensitized dehydrodimerization of organic compounds in solution[7,8] and in the gas phase.

The absorption spectrum of $[Hg(N_3)_3]^-$ (Fig. 1) displays an intense band at $\lambda_{max} = 246$ nm ($\varepsilon = 5600$). This band has not been detected before since it was obscured by the absorption spectrum of $[As(C_6H_5)_4]^+$, which was used as counter-ion for the isolation of the complex anion.[9] Upon irradiation of $[Hg(N_3)_3]^-$ in ethanol with white or monochromatic light ($\lambda_{irr} = 254$ nm) nitrogen was evolved which was detected by gas chromatography. Free azide was also formed. It was identified as the red Fe^{3+} complex. Simultaneously the absorption band of $[Hg(N_3)_3]^-$ disappeared (Fig.

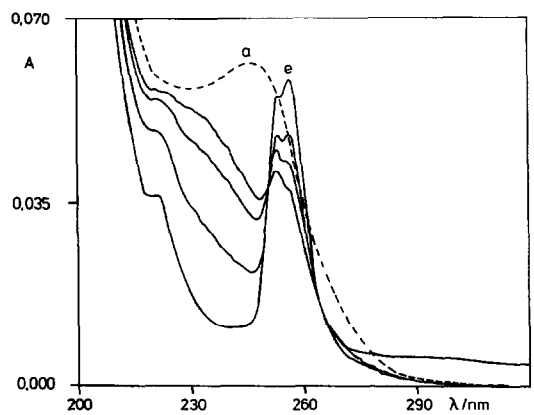

Fig. 1. Spectral changes during the photolysis of 1.04×10^{-5} M $[N(C_4H_9)_4][Hg(N_3)_3]$ in C_2H_5OH at (a) 0, 3, 6, 12 and (e) 18 min irradiation time, with white light irradiation (Osram HBO 100 W/2 lamp) and a 1-cm cell.

† Author to whom correspondence should be addressed.

1). The spectral changes which accompanied the photolysis are characterized by the appearance of a new narrow band with two maxima at $\lambda = 253$ and 256 nm. This absorption[8,10-12] indicated the formation of atomic mercury. Since the solubility of elemental mercury is rather low in all common solvents ($\sim 10^{-7}$ M),[12] the photochemical generation of the free metal did not only lead to the appearance of mercury atoms. The bulk metal was also formed. At later stages of the photolysis the release of colloidal metal can be recognized by an increase of the extinction coefficient over the entire absorption spectrum. This effect is apparently caused by light scattering of colloidal metal particles.[1]

The photolysis of $[Hg(N_3)_3]^-$ was monitored by measuring the decrease of the extinction coefficient at 246 nm, taking into account a residual absorption of the photolysis product of about 20% at this wavelength. The absorbed light intensity (1.4×10^{-10} E s^{-1}) was determined with a Polytec pyroelectric radiometer, calibrated and equipped with a RkP-345 detector. For quantum yield determinations the amount of photolysis was limited to less than 10%. At an irradiating wavelength of $\lambda = 254$ nm the quantum yield for the disappearance of $[Hg(N_3)_3]^-$ was $\phi = 0.02$.

The absorption band of $[Hg(N_3)_3]^-$ (Fig. 1) at $\lambda_{max} = 246$ nm is assigned to a LMCT transition involving the promotion of an electron from the reducing azide ligands to the empty 6*s* orbital of mercury(II). Analogous LMCT assignments were made for the mercury(II) halides, HgX_2,[13-15] and halide complex anions, $[HgX_4]^{2-}$,[15-17] with X = Cl, Br and I. Since Br^- and N_3^- have the same optical electronegativities (2.8)[19] the LMCT bands of $[HgBr_4]^{2-}$ ($\lambda_{max} = 253$ nm)[16,17] and $[Hg(N_3)_3]^-$ appear at comparable energies.

Upon LMCT excitation $[Hg(N_3)_3]^-$ undergoes a photoredox reaction according to the equation:

$$[Hg^{II}(N_3)_3]^- \rightarrow Hg^0 + 3N_2 + N_3^-.$$

The formation of metallic mercury is not surprising since organometallic mercury(II) complexes are well known to show this photoredox behaviour.[2-5] In some cases it has been demonstrated that this is initiated by CT excitation.[4,5] The most interesting aspect of the present work is the observation of stable mercury atoms which are formed upon LMCT excitation of $[Hg(N_3)_3]^-$ under ambient conditions. Mercury atoms in solution are characterized by an intense ($\varepsilon \sim 10^5$) narrow absorption near 250 nm which shows band splitting.[8,10-12] The absorption is assigned to the $^1S_0 \rightarrow {}^3P_1 sp$ transition of the mercury atoms which are perturbed by the solvent.[11,12] Due to the low solubility of mercury the photolysis of $[Hg(N_3)_3]^-$ leads not only to the appearance of atomic mercury but also colloidal mercury.

The photoredox reaction of metal azide complexes induced by LMCT excitation seems to be a rather general method for the generation of free metals which are released as colloids.[1] It has been suggested that this release is preceded by the generation of free metal atoms which undergo an aggregation to clusters. These clusters grow until they finally reach colloidal dimensions. It is certainly important to identify these intermediate stages under ambient conditions in order to learn more about these processes. The detection of mercury atoms as immediate photolysis product is thus an interesting contribution towards this goal.

The photochemical formation of mercury atoms may also play an important role in the mercury-photosensitized dehydrodimerization of organic compounds in solution and the gas phase.[7,8,18] It has been assumed to take place via the formation of some kind of exciplex:[18]

$$Hg^* + H{-}CR_3 \rightarrow Hg^* \cdots H{-}CR_3 \rightarrow [Hg^* \cdots H \cdots CR_3] \rightarrow Hg{-}H^* + {}^\bullet CR_3 \rightarrow Hg + H + {}^\bullet CR_3.$$

As an alternative it seems feasible that this reaction proceeds as a photochemical oxidative addition to excited mercury atoms and a subsequent reductive elimination:

$$Hg^* + H{-}CR_3 \rightarrow H{-}Hg^{II}{-}CR_3 \rightarrow Hg^0 + {}^\bullet H + {}^\bullet CR_3.$$

The latter step, which could take place photochemically or thermally, regenerates the mercury atoms. These are now available for a repetition of this process.

REFERENCES

1. A. Vogler, C. Quett and H. Kunkely, *Ber. Bunsenges Phys. Chem.* 1988, **92**, 1486.
2. W. A. Cramer, *J. Phys. Chem.* 1967, **71**, 1171.
3. V. Balzani and V. Carassiti, *Photochemistry of Coordination Compounds*. Academic Press, London (1970).
4. A. Vogler and H. Kunkely, *J. Organomet. Chem.* 1988, **355**, 1.
5. H. Kunkely, G. Stochel and A. Vogler, *Z. Naturfor.* 1989, **44b**, 145.
6. D. Rehorek and E. G. Janzen, *Z. Chem.* 1985, **25**, 69.
7. R. R. Kuntz and G. J. Mains, *J. Am. Chem. Soc.* 1963, **85**, 2219.
8. J. G. Calvert and J. N. Pitts, *Photochemistry*. Wiley, New York (1966).

9. W. Beck, W. P. Fehlhammer, P. Pöllmann, E. Schuierer and K. Feldl, *Chem. Ber.* 1967, **100**, 2335.
10. M. K. Phibbs and B. de B. Darwent, *J. Chem. Phys.* 1950, **18**, 679.
11. S. N. Vinogradov and H. E. Gunning, *J. Phys. Chem.* 1962, **68**, 68.
12. W. R. Mason, *Inorg. Chem.* 1988, **27**, 437.
13. P. Templet, J. R. McDonald, S. P. McGlynn, C. H. Kendrow, J. L. Roebber and K. Weiss, *J. Chem. Phys.* 1972, **56**, 5746.
14. M. E. Koutek and W. R. Mason, *Inorg. Chem.* 1980, **19**, 648.
15. S. Sakaki, N. Hagiwara, N. Iwasaki and A. Ohyoshi, *Bull. Chem. Soc. Jpn* 1977, **50**, 14.
16. R. A. Walton, R. W. Matthews and C. K. Jørgensen, *Inorg. Chim. Acta* 1967, **1**, 355.
17. P. Day and R. H. Steel, *J. Chem. Soc., Dalton Trans.* 1972, 2054.
18. S. H. Brown and R. H. Crabtree, *J. Am. Chem. Soc.* 1989, **111**, 2935 and 2946.
19. A. B. P. Lever, *Inorganic Electronic Spectroscopy*. Elsevier, Amsterdam (1984).

Polyhedron Vol. 8, No. 22, p. 2735, 1989
Pergamon Press plc. Printed in Great Britain

BOOK REVIEW

Journal of Organometallic Chemistry Library 20: Organometallic Chemistry Reviews. Edited by A. G. Davies, E. O. Fischer and O. A. Reutov. Elsevier, Amsterdam, 1988, ISBN 0-444-42950-6, 365 pp., approx. £81.50.

This addition to the *Journal of Organometallic Chemistry Library Series* contains five reviews. The chemistry of boron-substituted icosahedral *closo*-carboranes(12) (Grushin, Bregadze and Kalinin, Moscow; 204 refs to 1986) is covered systematically with sections on compounds containing boron bonded to: nitrogen; carbon; oxygen; sulphur, selenium or tellurium; halogens; non-transition metals; transition metals. A final short section discusses the electronic effects associated with different patterns of substitution. Given that 72% of the references are to Russian publications, this is a useful overview of this area of chemistry.

The second article, by Lukevics and Segal (Riga), reviews pyridine and quinoline derivatives containing Si, Ge, Sn, and Pb (423 refs to 1986). Preparation, physical properties, chemical properties, biological properties and applications of compounds containing E—C, E—N, or E—O(S) bonds (E = Si, Ge, Sn or Pb) are covered in separate sections with a final section devoted to intermolecular complexes. This lengthy review, dominated by Si chemistry with some Ge and Sn and few Pb derivatives, should be useful to anyone involved in the synthesis of pyridine and quinoline compounds.

Goldberg, Dirnens and Lukevics (Riga) review the use of phase-transfer catalysis in organosilicon chemistry (85 refs to 1986) in an interesting article which also mentions related Ge and Sn chemistry and describes nucleophilic substitution of X in R_3SiX, dichlorocarbene and nitrene reactions with organosilanes, hydrosilation, electrophilic substitution, and also contains sections on silacrowns and immobilized phase-transfer catalysts.

A compilation of structural details for rhenium carbonyl and organometallic complexes by Holloway (York, Canada) and Melnik (Bratislava) contains data from X-ray, neutron and electron diffraction studies (257 refs to 1987). Trends are highlighted and comparisons are made with analogous technetium compounds.

The final review by Klapötke and Köpf (Berlin) is in German and deals with metallocenedichalcogenolene complexes (59 refs to 1987). Dithiolenes, diolenes, diselenolenes and ditellurolenes are described for the Ti, V and Cr groups. There are also short sections on bonding, ring inversion and reactivity.

In general these articles are sufficiently well-presented to enable the reader, whether or not a specialist in any of the areas covered, easily to browse through this volume and pick out any features of interest.

R. J. ERRINGTON

Department of Chemistry
University of Newcastle upon Tyne
Newcastle upon Tyne, NE1 7RU, U.K.

Polyhedron Vol. 8, No. 22, p. 2737, 1989
Pergamon Press plc. Printed in Great Britain

ANNOUNCEMENT

33rd IUPAC CONGRESS
BUDAPEST, HUNGARY
17–22 AUGUST 1991

The 33rd International Congress of the International Union of Pure and Applied Chemistry is to be held from Saturday 17 to Thursday 22 August 1991, in Budapest, Hungary. Plenary and keynote lectures will be presented by invited prominent chemists from all over the world. Participants are encouraged to contribute papers, which will be presented as posters. A second circular, which will include instructions for authors, will be distributed in September 1990.

Further details can be obtained from:

E. Pungor, President of the 33rd IUPAC Congress
c/o Hungarian Academy of Sciences
H–1111 Budapest
Gellért tér 4
Hungary
Telephone: +36 1 664 705
Telefax: +36 1 853 493
Telex: 22 3628 anal h.

UV, IR, ^{71}Ga AND ^{17}O NMR SPECTROSCOPIC STUDIES OF THE 12-MOLYBDOGALLATE HETEROPOLYANION

L. P. TSIGANOK* and A. B. VISHNIKIN

State University, Dniepropetrovsk 320625, U.S.S.R.

and

R. I. MAKSIMOVSKAYA

Institute of Catalysis, Novosibirsk 630090, U.S.S.R.

(*Received* 2 *September* 1988; *accepted after revision* 27 *January* 1989)

Abstract—UV, IR, ^{71}Ga and ^{17}O NMR spectra clearly demonstrate the Keggin structure for the new heteropolyanion—12-molybdogallate (12-MGA). The UV spectrum of the 12-MGA solution has charge-transfer bands at 49,000, 40,000 and 32,500 cm^{-1}, which have been attributed to oxygen-to-molybdenum(VI) transitions. The IR spectra of the synthesized samples of 12-MGA contain the expected triplet of bands, which could be assigned to molybdenum–oxygen stretching vibrations. The data obtained from the ^{71}Ga and ^{17}O NMR spectroscopy confirmed the tetrahedral oxygen environment of the gallium atoms and the Keggin structure of 12-MGA. The ^{71}Ga NMR chemical shifts of crystalline $(TEBA)_5GaMo_{12}O_{40}$ (TEBA—triethylbenzyl ammonium) as well as of aqueous solutions of 12-MGA are situated in the range characteristic of a tetrahedral oxygen environment of gallium (223 ppm relative to $Ga(H_2O)_6^{3+}$). In these solutions $GaMo_6O_{24}H_6^{3-}$ polyanions can co-exist (52 ppm). The ^{17}O NMR spectrum of $Na_5GaMo_{12}O_{40}$ has three resonances with chemical shifts of 923, 575 and 568 ppm (relative to H_2O) and an intensity ratio 1 : 1 : 1, which is similar to the spectra of other Keggin heteropolyanions. The changes of the nature and length of the Mo—O bonds in the 12-molybdogallate relative to the parent 12-molybdophosphate are discussed.

Due to its electron-donor properties, the oxogallate ion forms 6-molybdogallate,[1,2] 12-tungstogallate,[3,4] the vacant 11-tungstogallate anion and its derivatives,[5] mixed molybdotungstic heteropolyanions (HPA)[6] with the Keggin structure.[7] Recently, we have observed the formation in aqueous solution and obtained in the solid state the 12-molybdogallate anion (12-MGA) with reversible redox properties.[8] The gallium(III) ion has a preference for octahedral coordination in acidic aqueous solution, and the ionic radius of gallium is large enough, so that the formation of the Keggin anion could be prevented. To check these possibilities, we have used ^{17}O and ^{71}Ga NMR methods and other spectroscopic techniques, which provide structural information about polycomplexes in solution.[9–15]

* Author to whom correspondence should be addressed.

EXPERIMENTAL

Solid samples of $(TEBA)_5GaMo_{12}O_{40}$ (TEBA—triethylbenzyl ammonium) were prepared as described in refs 8 and 16. Found: Ga, 2.01; Mo, 32.4. Required for $(TEBA)_5GaMo_{12}O_{40}$: Ga, 1.97; Mo, 32.4%.

The solution of $Na_5GaMo_{12}O_{40}$ was prepared as follows. Sodium molybdate $Na_2MoO_4 \cdot 2H_2O$ (5.5 g, 22.7 mmol) was dissolved in a mixture of water (1.5 cm^3) enriched with ^{17}O ($\sim$ 1.5%) and HNO_3 (60%, 2.5 cm^3). Then gallium nitrate $(Ga(NO_3)_3 \cdot 8H_2O$ (0.721 g, 1.8 mmol) was added to this solution. The resulting solution was heated at 90°C for 1 h, the pH being kept at 1.5. On heating a yellow colour appeared.

The IR spectra were recorded on a Zeiss Specord M 80 with the samples dispersed in Nujol. UV spectral measurements of aqueous solutions of

12-MGA were obtained with a Zeiss Specord M 40 spectrophotometer.

NMR spectra were measured on a BRUKER CXP-300 spectrometer. The ^{71}Ga spectra were obtained at 91.53 MHz with a spectral width of 125 kHz, a pulse duration of 1 μs for solid samples and 10 μs for solutions. ^{71}Ga spectra of solid samples were measured using the magic angle spinning (MAS, 4 kHz) technique. The number of transients was about 20,000 and the pulse delay was 0.2 s. The chemical shifts are given relative to the aqua ion, $Ga(H_2O)_6^{3+}$.

The ^{17}O NMR spectra were obtained at 40.7 MHz with a spectral width of 62.5 kHz, a pulse duration of 10 μs and a pulse delay of 0.02 s. ^{17}O spectra were obtained using water with a natural abundance of ^{17}O and enriched with ^{17}O ($\sim$ 1.5%). The chemical shifts are given relative to solvent H_2O. The downfield shift is taken as positive.

RESULTS AND DISCUSSION

The formation of 12-molybdogallate is slow in aqueous solutions. This is explained by kinetic difficulties due to changes in the coordination of gallium from octahedral in aqua and hydroxo complexes to tetrahedral in 12-MGA. Heating accelerates the formation of 12-MGA and completion of the reaction requires about 1 h. The HPA is stable in the pH range 0–3.0.

UV absorption spectra of the $(TEBA)_5GaMo_{12}O_{40}$ solutions show three bands at 49,000, 40,000 and 32,500 cm^{-1} (Fig. 1). The last two bands appear as broad shoulders. The absorption band at 32,500 cm^{-1} is responsible for the yellow colour of 12-MGA. The maximal deflection of the absorption from the additivity of the solutions containing Ga^{3+} and MoO_4^{2-} ions at an atomic Ga–Mo ratio equal to 1:12 relative to the molybdate solution is observed at 40,000 cm^{-1}. These bands have been attributed to charge-transfer transitions of oxygen to molybdenum(VI) and are typical for Keggin HPA.[14] UV spectra do not change in the pH range 1–3, showing the absence of the protonation of HPA.

The IR spectra of $(TEBA)_5GaMo_{12}O_{40}$ closely

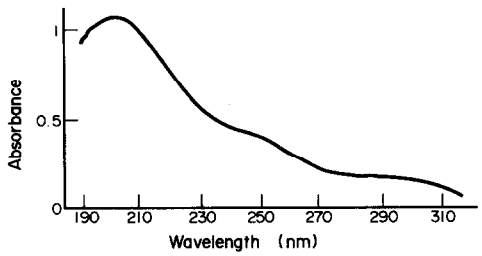

Fig. 1. UV absorption spectrum of the solution of $(TEBA)_5GaMo_{12}O_{40}$ ([HPA] = 10^{-5} M).

resemble those reported for 12-HPA.[15] Similarities of positions of the triplet of the most characteristic bands in the 1000–700 cm^{-1} region due to molybdenum–oxygen stretching vibrations strongly indicate that these complexes have identical structures. Selected IR frequencies are given in Table 1.

NMR spectroscopy can give reliable structural information about polycomplexes,[10–12] and we have used ^{17}O and ^{71}Ga NMR methods to prove the Keggin structure for the 12-molybdogallate.

The ^{71}Ga NMR spectrum of the solid sample of $(TEBA)_5GaMo_{12}O_{40}$ contains the isotropic signal (Fig. 2(a), Table 2), which is situated in the range of gallium chemical shifts characteristic of a tetrahedral oxygen environment.[11,17,18] The width of the signal became smaller but the value of the chemical shift remained constant when the sample was rotated at the magic angle (54°44′, 4 kHz) [Fig. 2(b)]. The same peak is observed in the yellow methylethylketone solution. In the ^{71}Ga NMR spectrum of the acidic solution (pH = 1.5) of 12-MGA (prepared as described above) two resonances are observed: firstly, a broad peak (width $\sim$ 2600 Hz) at 52 ppm arises from $GaMo_6O_{24}H_6^{3-}$-HPA containing an octahedral oxygen environment of gallium[18] and secondly, a narrow peak (width $\sim$ 50 Hz) at 223 ppm belongs to 12-MGA [Fig. 2(d)]. These polyanions co-exist in aqueous solution.

Besides the above mentioned signals there is also a weak narrow peak at 218 ppm. Nearness to the neighbouring signal at 223 ppm and the small linewidth show the tetrahedral oxygen arrangement of

Table 1. IR spectral (cm^{-1}) data of 12-molybdogallate and 12-molybdophosphate HPA

Polyanion	$\nu(PO_4)$	ν(Mo=O)	ν(Mo—O—Mo)	ν(Mo$\diagdown^{O}\diagup$Mo)	ν(Ga—O—Mo)
$(TEBA)_5GaMo_{12}O_{40}$	—	932	872	784	550, 450
$(TEBA)_3PMo_{12}O_{40}$	1063	955	880	805	—

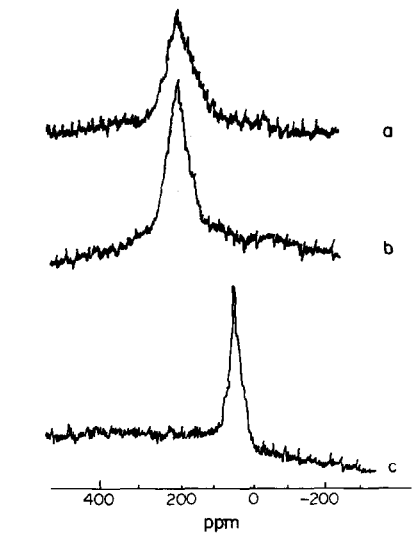

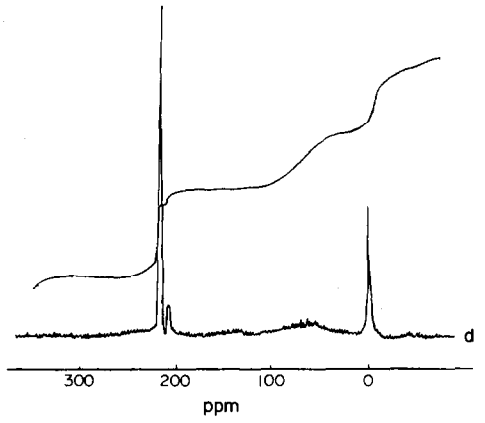

Fig. 2. (a) ^{71}Ga NMR spectra of the solid sample of $(TEBA)_5GaMo_{12}O_{40}$; (b) the same spectra but using the MAS technique, 4 kHz; (c) spectra of the solid sample of $Na_3GaMo_6O_{24}H_6$; (d) spectra of the $Ga(NO_3)_3$–Na_2MoO_4 solution (Ga–Mo = 1:12, [Ga] = 0.2 M, pH = 1.5).

the central atom in this HPA. The difference in chemical shifts of these two signals can be compared with the data for pairs, GaW_{12}–GaW_{11}, PW_{12}–PW_{11} and AlW_{12}–AlW_{11}.[19] The existence of the 11-molybdogallate HPA in the studied system is supposed.

Thus, the data obtained from the ^{71}Ga NMR spectra confirm the formation of gallium 12-HPA with the Keggin structure.[7] Good agreement between the spectra of the crystalline and dissolved polyanion demonstrates that the structure of the anion in solution is the same as that observed in the solid state. There are complex equilibria between at least three polyanions of gallium in solution.

Further support for these conclusions comes from the ^{17}O NMR spectra (Fig. 3, Table 2). In the ^{17}O NMR spectrum of the concentrated solutions containing Ga^{3+} and MoO_4^{2-} ions in the atomic

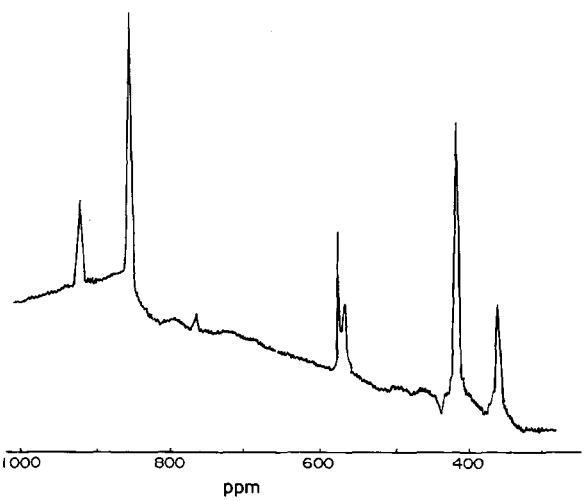

Fig. 3. ^{17}O NMR spectrum of the $Ga(NO_3)_3$–Na_2MoO_4 solution (Ga–Mo = 1:12, pH = 1.5).

Table 2. ^{71}Ga and ^{17}O NMR chemical shifts of polyanions

Polyanion	δ ^{71}Ga ± 2 ppm	δ ^{17}O ± 3 ppm	
		Mo=O	Mo—O—Mo, Mo<O>Mo
$(TEBA)_5GaMo_{12}O_{40}$ (solid)	215(214)[a]		
$GaMo_{12}O_{40}^{5-}$ (solution)	223	923(1)	575(1), 568(1)
$GaMo_6O_{24}H_6^{3-}$	52	847(2)	375(1)
$PMo_{12}O_{40}^{3-}$ [b]	—	941(1)	570(1), 554(1)

Parentheses indicate the relative line intensity.
[a] MAS spectrum.
[b] From ref. 11.

Ga–Mo ratio equal to 1 : 12 at pH = 1.5, in addition to two signals from $GaMo_6O_{24}H_6^{3-}$, three signals belonging to $GaMo_{12}O_{40}^{5-}$ are observed. By analogy with other Keggin anions[10–12,20] these lines can be attributed to the following oxygen atoms: the peak at 923 ppm appears from the terminal Mo=O oxygen atoms and the peaks at 575 and 568 ppm arise from the bridging Mo—O—Mo oxygen atoms.

The chemical shifts, as well as the number and the integrated intensity of the resonances (1 : 1 : 1) of the oxygen atoms, conform well with the $GaMo_{12}O_{40}^{5-}$ structure. These facts together with the data of ^{71}Ga NMR spectra, prove the formation of 12-MGA in the investigated solutions. Similar ^{17}O NMR spectra were recorded for solutions of 12-MGA prepared using water with a natural ^{17}O content.

We did not observe any signal from the oxygen atoms of the Mo—O—Ga bridges. It is probable that it is situated near the signal of H_2O (38 ppm) or it is strongly broadened due to the closeness of the Ga^{3+} ion.

The difference in lengths of the bridging Mo—O—Mo bonds is very small ($\Delta\delta = 7$ ppm) and depends upon the electronic structure and the radius of the central atom. One can estimate the relative stability of the 12-molybdogallate using the ^{17}O NMR chemical shift scale of oxygen atoms and the bond length–^{17}O NMR O—Mo correlation.[10–12] The downfield shift in the ^{17}O NMR spectrum of $PMo_{12}O_{40}^{3-}$ (δ 940 ppm) relative to $GaMo_{12}O_{40}^{5-}$ (923 ppm) shows that the Mo=O bond is longer in 12-MGA and the extent of covalency is smaller. Consequently, this indicates a smaller stability of the gallium HPA due to the metallic properties and the large radius of the gallium atom.

Thus, using ^{17}O and ^{71}Ga NMR and other spectroscopic techniques, we have shown that gallium forms a sufficiently stable 12-heteropolymolybdate with the Keggin structure. This HPA compound exists in aqueous solutions, in organic solvents and in the solid state. Other heteropolyanions such as $GaMo_6O_{24}H_6^{3-}$ and probably $GaMo_{11}O_{39}^{9-}$ co-exist in acidic solutions.

REFERENCES

1. B. N. Ivanov-Emin and Ja. I. Rabovic, *Zh. Neorg. Khim.* 1958, **3**, 2429.
2. O. W. Rollins, *J. Inorg. Nucl. Chem.* 1971, **33**, 75.
3. L. P. Tsiganok and T. V. Kleynermann, *Zh. Neorg. Khim.* 1974, **19**, 2239.
4. M. V. Mochosoev, L. G. Maksimova, L. V. Tumurova and I. A. Sudakova, *Zh. Neorg. Khim.* 1983, **28**, 1452.
5. O. W. Rollins, *Inorg. Chem.* 1972, **11**, 3114.
6. V. I. Tkach, Thesis, State University, Dniepropetrovsk (1980).
7. J. F. Keggin, *Proc. R. Soc.* 1934, **144**, 75.
8. V. I. Tkach, L. P. Tsiganok and V. P. Ostapenko, in *Fiziko-khimicheskie osnovi prakticheskogo ispolsovanija iso-i heteropolysoedinenij*, p. 14. Dniepropetrovsk (1983).
9. M. T. Pope, *Heteropoly and Isopoly Oxometalates*. Springer, New York (1983).
10. M. Filowitz, R. K. C. Ho, W. G. Klemperer and W. Shum, *Inorg. Chem.* 1979, **18**, 93.
11. M. A. Fedotov, *Jadernij magnitnij rezonans v rastvorah neorganicheskih veshestv*. Novosibirsk (1986).
12. M. A. Fedotov, L. P. Kazanskij and V. I. Spitsyn, *Dokl. AN SSSR* 1983, **272**, 1179.
13. R. I. Maksimovskaya and K. G. Burtseva, *Polyhedron* 1985, **4**, 1559.
14. K. Nomija, Y. Sugie, K. Amimoto and M. Miwa, *Polyhedron* 1987, **6**, 519.
15. C. Rocchiccioli-Deltcheff, R. Thouwenot and R. Franck, *Spectrochim. Acta* 1976, **32A**, 587.
16. A. B. Vishnikin, Thesis, State University, Dniepropetrovsk (1988).
17. V. M. Mastikhin and K. I. Zamaraev, *J. Phys. Neue Folge* 1987, **152B**, 59.
18. M. A. Fedotov and L. P. Kazanskij, *Izv. Akad. Nauk SSSR, Ser. Chim.* 1988, **9**, 2000.
19. J. W. Akitt and A. Farthing, *J. Chem. Soc., Dalton Trans.* 1981, 1615.
20. N. Ja. Volovaja, R. I. Maksimovskaya, M. A. Fedotov and S. A. Morosanova, *Zh. Neorg. Khim.* 1984, **29**, 1468.

Polyhedron Vol. 8, No. 23, pp. 2743–2747, 1989
Printed in Great Britain

0277–5387/89 $3.00+.00
© 1989 Pergamon Press plc

REACTIVITY OF METAL COMPLEXES OF 1,3-BIS-(2-HYDROXYPHENYL)-1,3-PROPANEDIONE TOWARD PYRIDINE DERIVATIVES, LEWIS BASES. CRYSTAL STRUCTURE OF BIS(1,3-BIS-(2-HYDROXYPHENYL)-1,3-PROPANEDIONE)BISPYRIDINECADMIUM(II)

J. CASABÓ,† J. COLOMER and A. LLOBET

Departament de Química, Universitat Autónoma de Barcelona, Campus de Bellaterra, Bellaterra, 08193 Barcelona, Spain

and

F. TEIXIDOR, E. MOLINS and C. MIRAVITLLES

Institut de Ciència dels Materials (C.S.I.C.), C/Martí i Franques s/n, Apartat de Correus 30102, 08028 Barcelona, Spain

(*Received* 8 *February* 1989; *accepted* 12 *June* 1989)

Abstract—Complexes with the ligand 1,3-bis-(2-hydroxyphenyl)-1,3-propanedione ($bhppH_3$) of formula $M(bhppH_2)_2 \cdot 2$ solvent (M = Co, Ni, Zn) can be desolvated by controlled heating. These compounds contain the metal ion tetracoordinated in a square-planar fashion by the β-ketonic oxygen atoms of the ligand, and they behave as Lewis acids toward Lewis bases, like pyridine or pyridine derivatives. Two pyridine molecules complete the octahedral coordination of the metal. The pyridine coordination is weak, as evidenced by the Cd—N bond length (2.342 Å), compared to that of the Cd—O bond (mean value, 2.248 Å). In addition, the easy substitution reactions support this assumption. The new compounds are more soluble in common solvents than their parent compounds. The molecular structure of $Cd(bhppH_2)_2 \cdot 2$ pyridine is reported, being monoclinic, space group $P2_1/c$ with $a = 8.868(6)$, $b = 11.128(3)$, $c = 17.508(4)$ Å, $\beta = 100.84(5)°$, $V = 1697$ Å^3, $Z = 2$, $D_c = 1.53$ g cm^{-3} and $\mu = 8.79$ cm^{-1}.

The compound 1,3-bis-(2-hydroxyphenyl)-1,3-propanedione ($bhppH_3$) (Fig. 1) is an excellent ligand, affording mononuclear complexes with divalent transition metal ions of formula $M(bhppH_2)_2$.[1] In these complexes the metal ion is coordinated by the β-diketone moiety of two ligand molecules in a square-planar environment, except in the case of the lithium complex where the coordination is tetrahedral.[2] Usually, the metal achieves hexacoordination by the addition of solvent molecules. This molecule is also a potentially trinucleating ligand. With it we have prepared linear trinuclear complexes of the type UO_2—M—UO_2, M being a first-row divalent transition metal ion.[3] Consequently, it is a potential synthesis-director ligand which permits the formation of different positional isomers of the type: A–B–A or B–A–B, depending on the starting mononuclear complex. The synthesis of the trinuclear compounds becomes difficult due to the general insolubility of the mononuclear precursors in common solvents.

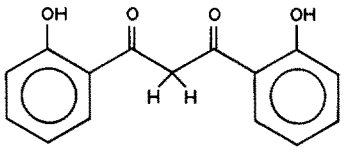

Fig. 1. 1,3-bis-(2-hydroxyphenyl)-1,3-propanedione.

† Author to whom correspondence should be addressed.

In order to improve the solubility of the mononuclear complexes, we have modified the original ligand, via substitution at the methine carbon atom. In doing so we expected that the synthesis of the trinuclear compounds would be easier. For this reason we synthesized the chromium(III) mononuclear complex, $Cr(bhppH_2)_3$,[4] a compound that shows useful solubilities in common organic solvents, hence permitting nucleophilic substitutions at the α-carbon of the β-diketone moiety, as is usual in β-diketonate metal complexes.

Always with the aim of increasing the solubility of the mononuclear complexes, we have also tried its reaction with different Lewis bases, like pyridine derivatives, expecting that the solvated compounds would be more soluble than the corresponding parent complexes. In this paper we report on the products of these reactions and their solubility properties, as well as the crystalline structure of $Cd(bhppH_2)_2 \cdot 2py$.

EXPERIMENTAL

All operations were carried out in the atmosphere. The bis(1,3-bis-(2-hydroxyphenyl)-1,3-propanedione)metal(II) complexes, solvated with two alcohol molecules, were prepared following a reported procedure.[1] Pyridines were reagent grade and were used as received, except 4-($COOCH_3$)py which was prepared from 4-COOH-py following Levine's procedure.[5] Tetrahydrofuran (THF) was partially dried with KOH. All other solvents were reagent grade and used as received. Microanalyses (C, H, N) were performed in our analytical laboratory using a Perkin–Elmer 240-B instrument. ^{1}H NMR spectra were obtained using a Brucker WP.80SY spectrophotometer. IR spectra were determined on a Beckman IR-20A as KBr pellets. Electronic spectra were run on a Shimadzu 240 spectrophotometer in solution.

Synthesis of $M(bhppH_2)_2$ ($M = Co^{II}$, Ni^{II}, Zn^{II}, Cd^{II})

The elimination of the alcohol molecules in $M(bhppH_2)_2 \cdot 2ROH$ was achieved by controlled heating of these solids in an oven at 120°C for 30 min.

Synthesis of $M(bhppH_2)_2 \cdot 2py'$ (py' = *pyridine, 3-hydroxypyridine, 4-methylpyridine, methylpyridine-4-carboxylate, 4-N,N-dimethylaminopyridine*; M = Co^{II}, Ni^{II}, Zn^{II}, Cd^{II})

In a typical experiment, $Co(bhppH_2)_2$ (0.2 g, 0.35 mmol) was dissolved in THF (20 cm^3). Pyridine (1 cm^3, 13 mmol) was added and the resulting solution was refluxed for $\frac{1}{2}$ h and then allowed to cool to room temperature. Solvent and volatiles were stripped off in a rotavapor and the oily solid was treated with benzene, which was later evaporated again in the rotavapor. The yellow solid, which is now manageable, was stirred in CCl_4 and dried with dry air.

Yields were in all cases very high: 90–100%. The amount of pyridine or substituted pyridines used for 0.2 g of $M(bhppH_2)_2$ complex was variable and depended on the state of the pyridine, 1–2 cm^3 of the appropriate chemical was used if this was a liquid, but a 10% excess if it was a solid.

X-ray structure determination

The colourless single crystals of $C_{30}H_{22}O_8Cd \cdot 2C_6H_5N$ are monoclinic, space group $P2_1/c$ with $a = 8.868(6)$, $b = 11.128(3)$, $c = 17.508(4)$ Å, $\beta = 100.84(5)°$, $V = 1697$ Å^3, $Z = 2$, $D_c = 1.53$ g cm^{-3}, $\mu = 8.79$ cm^{-1}.

X-ray diffraction data for $Cd(bhppH_2)_2 \cdot 2py$ at 294 K were collected with an Enraf–Nonius CAD4 four-circle diffractometer using graphite monochromated Mo-K_α radiation ($\lambda = 0.71069$ Å) on a $0.15 \times 0.28 \times 0.34$ mm prismatic crystal. Reflections were measured at the azimuth position corresponding to a minimum absorption, using an imaginary crystal with finite but small thickness, having an infinitely large surface area (flat psi mode).

Using the ω–2θ scan technique, 3321 reflections with $2\theta < 50°$ ($-10 < h < 10$; $0 < k < 13$; $0 < l < 20$) were obtained. Intensities of two standard reflections were followed during data collection and no significant decay was observed. These non-unique data were averaged and the resulting 2954 intensities were corrected for Lorentz and polarization effects, and only 1159 were considered observed with $I > 5\sigma(I)$. The scattering factors and anomalous corrections were taken from the *International Tables for X-ray Crystallography*.[6]

The atomic coordinates of cadmium and part of the ligand were located by direct methods (MULTAN 11/84 system 1).[7] Subsequent difference Fourier syntheses combined with refinement of located atoms led to a complete model of the structure. This model was refined with Shelx76[8] using anisotropic thermal parameters for non-hydrogen atoms and a common isotropic temperature factor for hydrogen atoms, which were placed in geometrically calculated positions [except H(1) and H(15)], giving an R factor of 0.056 and $R_w = 0.047$ ($w = 1/\sigma^2(F) + 0.000304F^2$). On a final difference Fourier syn-

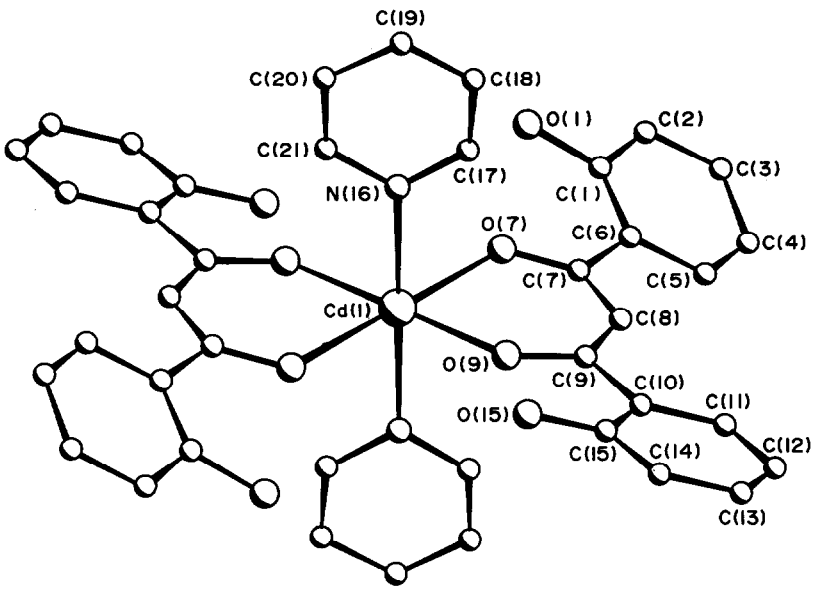

Fig. 2. Perspective view and atom numbering scheme for $Cd(bhppH_2)_2 \cdot 2py$.

thesis, the largest peaks were 0.68 e Å^3, located near to the cadmium atom, and -0.48 e Å^3.†

RESULTS AND DISCUSSION

Molecular structure of $Cd(bhppH_2)_2 \cdot 2py$

Figure 2 shows the molecular structure and numbering scheme of the title molecule. Table 1 reports selected bond lengths and angles.

The cadmium atom is located on a crystallographic symmetry centre, however, the whole unit cell contains two complete molecules. The metal ion is coordinated by two ligand and two pyridine molecules in a distorted octahedral fashion. The coordination polyhedron has a nearly rhombic distortion (angle O(7)—Cd(1)—O(9), 80.19°), with the axial distances (Cd—N, 2.342 Å) larger than the equatorial ones (Cd—O(7), 2.253 Å; Cd(1)—O(9), 2.243 Å). Atoms Cd(1), O(7), O(9), O(7*), O(9*) lie in a plane, Cd(1) being located on the symmetry centre of the rectangle defined by O(7), O(9), O(7*) and O(9*). Angles between mean planes, N(16)—Cd(1)—O(7) and N(16)—Cd(1)—O(9), with respect to the O(7)—Cd(1)—O(9) plane, are 91.47 and 89.02°, respectively.

Coordinated pyridine molecules are placed almost perpendicular to the O(7)—Cd(1)—O(9) plane (angle between mean planes 91.61°) and lie close to the octahedron symmetry plane bisecting the angle O(7)—Cd(1)—O(9) (angle between mean planes, N(16)—Cd(1)—O(7) and pyridine molecular plane, 42.32°). Bond lengths and angles for the pyridine molecules are typical for this compound.

The conformation of the ligand molecule is not

Table 1. Selected bond lengths (Å) and angles (°) with their ESDs for $Cd(bhppH_2)_2 \cdot 2py$

O(7)—Cd	2.253(7)
O(9)—Cd	2.243(8)
N(16)—Cd	2.342(8)
C(1)—O(1)	1.371(12)
C(7)—O(7)	1.276(12)
C(9)—O(9)	1.291(12)
C(15)—O(15)	1.340(14)
C(7)—C(6)	1.489(13)
C(8)—C(7)	1.411(14)
C(9)—C(8)	1.389(13)
C(10)—C(9)	1.506(15)
O(9)—Cd—O(7)	80.2(0.3)
N(16)—Cd—O(7)	88.8(0.3)
N(16)—Cd—O(9)	88.3(0.3)
C(7)—O(7)—Cd	128.7(0.8)
C(9)—O(9)—Cd	131.0(0.7)
C(17)—N(16)—Cd	121.3(0.7)
C(21)—N(16)—Cd	123.3(0.8)
C(8)—C(7)—O(7)	125.6(1.0)
C(8)—C(7)—C(6)	118.1(1.0)
C(9)—C(8)—C(7)	127.4(1.1)
C(8)—C(9)—O(9)	124.0(1.1)
C(10)—C(9)—O(9)	116.0(1.0)
C(10)—C(9)—C(8)	119.9(1.1)

† *Supplementary material.* List of non-hydrogen and hydrogen coordinates, anisotropic thermal parameters and observed and calculated structure factor amplitudes have been deposited with the Editor.

strictly planar as could be originally expected. The β-diketone moiety is not co-planar with the octahedron equatorial plane (angle between mean planes, O(7)—Cd(1)—O(9) and C(7)—C(8)—C(9), is 165.28°). Furthermore, the phenolic rings are not co-planar with the β-diketone moiety plane (angle between mean planes, C(7)—C(8)—C(9) and C(1)···C(6) phenolic ring plane, is 156.80°). Both phenolic rings are twisted in the same direction, in a butterfly-like fashion; so, the O(1) and O(15) atoms lie 0.6931 and 0.5612 Å, respectively, below the O(7)—Cd(1)—O(9) plane. A hydrogen bond is found between the hydroxyl phenolic group, O(1), O(15) and O(7), O(9), oxygen atoms, respectively.

General chemistry and physical properties

The reactions of cobalt(II), nickel(II) and zinc(II) complexes of 1,3-bis-(2-hydroxyphenyl)-1,3-propanedione ($bhppH_3$) (Fig. 1) with pyridine derivatives yield compounds with the general formula $M(bhppH_2)_2 \cdot 2py'$ [py′ = pyridine (py), 3-hydroxypyridine (3-(OH)-py), 4-methylpyridine (4-(CH_3)-py), methylpyridine-4-carboxylate (4-$(COOCH_3)$-py), 4-N,N-dimethylamino pyridine (4-$(CH_3)_2$N-py]. The similarity of the IR spectra of these complexes with those of $M(bhppH_2)_2 \cdot 2ROH$[1] seems to indicate a molecular structure for all of them, similar to that found in $Zn(bhppH_2)_2 \cdot 2EtOH$.[9] The general reaction to get these pyridine complexes is indicated in Scheme 1:

$$M(bhppH_2)_2 \cdot 2ROH \xrightarrow{\text{heat}} M(bhppH_2)_2 \xrightleftharpoons[py']{\text{heat}} M(bhppH_2)_2 \cdot 2py'$$

Scheme 1.

The pyridines, like the alcohols,[10] are weakly bonded and may be removed by heating the complexes in an oven at 125°C overnight. The thermogravimetric analysis (TG) for $Co(bhppH_2)_2 \cdot 2py$ shows two weight losses concurrent with two endothermic peaks. The first one corresponds to the elimination of pyridine in the complex, and the second one to a dehydration reaction taking place in the ligand $bhppH_3$, as is shown in Scheme 2:

$$Co(bhppH_2)_2 \cdot 2py \rightarrow Co(bhppH_2)_2 \rightarrow CoO + H_2O + \text{"flavona"}$$

Scheme 2.

The solubility of these pyridine complexes is markedly higher than the corresponding alcohol complexes. The most dramatic change is observed with 4-$(COOCH_3)$-py, where the complex $Zn(bhppH_2)_2 \cdot 2$(4-$(COOCH_3)$-py) is even soluble in benzene. This enhancement of the solubility has allowed all ^{1}H NMR spectra of the pyridine–zinc complexes to be run in d_1-chloroform, while the ^{1}H NMR spectra of the alcohol–zinc complexes[1] had to be run in d_6-dmso. As a conclusion, it has been possible to greatly enlarge the solubility range of the $M(bhppH_2)_2 \cdot 2ROH$ complexes, simply by replacing the axial alcohols by pyridine-substituted ligands.

^{1}H NMR spectra of the zinc complexes

The ^{1}H NMR spectra of $Zn(bhppH_2)_2 \cdot 2py'$ are very similar [py′ = (py), (3-(OH)-py), (4-(CH_3)-py), (4-$(COOCH_3)$-py), (4-$(CH_3)_2$N-py)]. The ^{1}H NMR spectrum of $Zn(bhppH_2)_2 \cdot 2$(4-(CH_3)-py) is discussed as a typical example. Mainly, three groups of signals are observed, one group near to $\delta = 12$ ppm due to the phenolic proton, another group occupying a larger region at $\delta = 6.5$–9 ppm due to the aromatics, and finally a third group (when appropriate) due to the pyridine substituent, e.g. 2.3 ppm in 4-(CH_3)-py, 2.9 ppm in 4-$(CH_3)_2$N-py, 4 ppm in 4-$(COOCH_3)$-py. In all cases integrations were in agreement with the proposed stoichiometry of the complex. On comparison with the ^{1}H NMR of non-coordinated $bhppH_3$ the methine signal is, as expected when chelation has occurred, in the aromatic region. However, due to the existence of several signals in this region, its exact position is difficult to be determined.

Spectroscopic properties

The $^3A_{2g} \rightarrow {}^3T_{1g}$ absorption band for the individual Ni—pyridine complexes are as follows, for: (py) 595 nm; (4-$(CH_3)_2$N-py) 595 nm; (4-(CH_3)-py) 585 nm; (3-(OH)-py) 580 nm; (4-$(COOCH_3)$-py) 580 nm, according to the position of the pyridine derivatives in the spectrochemical series. The cobalt complexes exhibit an intense charge-transfer band at 430 nm, considerably limiting the study of the *d–d* bands in the visible spectrum. Only one shoulder at 490 nm is observed for all of them.

All these complexes exhibit almost the same pattern in the IR spectra, evidencing their similar molecular structures. Several characteristic bands may be seen in these complexes: (4-$(CH_3)_2$N-py), ν(CH, aliphatic) at 2900 cm^{-1}; (4-(CH_3)-py), ν(CH, aliphatic) at 2900 cm^{-1}; (3-(OH)-py), ν(OH) at 3300 cm^{-1}; (4-$(COOCH_3)$-py), ν(CO) at 1725 cm^{-1}.

Acknowledgements—This work was supported by "Comisión Asesora de Investigación Científica y Técnica

(C.A.I.C.Y.T.)", grant no. 409/84 from the Spanish Government.

REFERENCES

1. (a) F. Teixidor, A. Llobet, L. Escriche and J. Casabó, *Polyhedron* 1984, **3**, 1017; (b) F. Teixidor, A. Llobet, L. Escriche and J. Casabó, *Polyhedron* 1985, **4**, 215; (c) F. Teixidor, T. Flor and J. Casabó, *Inorg. Chim. Acta* 1986, **118**, 125.
2. F. Teixidor, A. Llobet, J. Casabó, X. Solans, M. Font-Altaba and M. Aguiló, *Inorg. Chem.* 1985, **24**, 2315.
3. F. Teixidor, J. Colomer, J. Rius, E. Molins, C. Miravitlles and J. Casabó, *Inorg. Chem.* 1989, **28**, 678.
4. F. Teixidor, J. Colomer, A. Llobet, X. Solans, M. Font-Altaba and J. Casabó, *Inorg. Chim. Acta* 1987, **128**, 15.
5. R. Levine and J. K. Sneed, *J. Am. Chem. Soc.* 1951, **73**, 5614.
6. *International Tables for X-ray Crystallography*. Vol. IV, pp. 99, 149. Kynoch Press, Birmingham (1974) (Present distributor, D. Reidel, Dordrecht).
7. P. Main, G. Germain and M. M. Woolson, Multan 11/84. Universities of York, U.K. and Louvain, Belgium (1984).
8. G. M. Sheldrix, Shelx76. University of Cambridge, U.K. (1976).
9. X. Solans, M. Font-Altaba, J. L. Briansó, A. Llobet, F. Teixidor and J. Casabó, *Acta Cryst.* 1983, **C39**, 1512.
10. F. Teixidor, A. Llobet, S. Bordas and J. Casabó, *Thermochim. Acta* 1984, **79**, 315.

Polyhedron Vol. 8, No. 23, pp. 2749–2753, 1989
Printed in Great Britain

0277–5387/89 $3.00+.00
© 1989 Pergamon Press plc

METAL BINDING BY MIXED HARD–SOFT DONOR LIGANDS—II.* THE CRYSTAL AND MOLECULAR STRUCTURES OF DIBROMO(2,10-DIAZA-6-THIAUNDECANE)COPPER(II) AND DICHLORO(2,10-DIAZA-6-THIAUNDECANE)COPPER(II)

EDWIN C. CONSTABLE† and PETER J. STOTEREAU

University Chemical Laboratory, Lensfield Road, Cambridge CB2 1EW, U.K.

and

MICHAEL G. B. DREW

Department of Chemistry, The University, Whiteknights, Reading RG6 2AD, U.K.

(*Received* 17 *April* 1989; *accepted* 15 *June* 1989)

Abstract—The NSN-donor ligand 2,10-diaza-6-thiaundecane forms five coordinate complexes with copper(II). The preparation, crystal and molecular structures of $[CuLX_2]$ (L = 2,10-diaza-6-thiaundecane; X = Cl or Br) are reported.

The thermodynamic stability of transition metal complexes frequently follows that given in the Irving–Williams series, with copper(II) forming the most stable complexes with a given ligand or set of ligands.[2] This presents the fundamental problem in the design of reagents for the selective extraction of specific transition metal ions. Various approaches have been proposed in attempts to circumvent the dictates of the Irving–Williams series. In general, these rely on some dramatic change in the metal–ligand interaction on crossing the first row transition metals. Although ideal reagents would give complexes with the largest thermodynamic stability with the metal of interest, it has been demonstrated that satisfactory selectivity can be obtained by the design of reagents maximizing the stability differences.[3] The majority of the studies reported to date have utilized macrocyclic ligands, and have relied upon the mis-match between metal ion radius and ligand hole size to tune the metal–ligand interaction. We have been investigating the coordination chemistry of ligands incorporating both hard and soft donor atoms as an alternative methodology. Open-chain ligands offer some synthetic advantages, as entropically disfavoured ring closure reactions are not involved in their preparation. The balance between the donor properties of the ligand and the acceptor properties of the metal may be tuned by varying the donor atoms, the substituents on the donor atoms, and the chelate ring size. The bis(aminoalkyl)thioethers, $R_2N(CH_2)_nS(CH_2)_mNR_2$, have proved to be a particularly versatile series of ligands. The hardness and steric properties of the R_2N groups may be varied by the introduction of various alkyl groups, and the chelate ring size may be varied at will by changing the values of n and m. We recently reported[1] the crystal and molecular structure of the square-planar complex $[PdL^1Br]Br$ (L^1 = 2,10-diaza-6-thiaundecane), and wish to report herein, the preparation and structural characterization of copper(II) complexes with this ligand.

EXPERIMENTAL

Electronic spectra were recorded using a Pye–Unicam 8800 spectrophotometer; IR spectra were recorded using Perkin–Elmer 1710 FT or 983 spectrometers with the compound in compressed KBr pellets or in a suspension in Nujol. Fast-atom bombardment mass spectra were measured using a Kratos MS-50 spectrometer, and were loaded using

* For part I, see ref. 1.

† Author to whom correspondence should be addressed.

acetonitrile as solvent with 3-nitrobenzyl alcohol as supporting matrix. NMR spectra were recorded on a Bruker WM250 spectromter. Magnetic moments were measured at ambient temperature using a Johnson Matthey susceptibility balance. ESR spectra were determined on powdered solid samples or on glassy acetonitrile solutions at −196°C using a Varian E109 spectrometer calibrated with the diphenyl picryl hydrazyl radical. The compounds $OHCNH(CH_2)_3OH$ and $MeNH(CH_2)_3OH$ were prepared by the literature methods.[4] All preparations were conducted under an atmosphere of dry dinitrogen or argon; solutions containing the thiolate are particularly sensitive to oxidation.

Caution: the compound $Cl(CH_2)_3NHMe$ and its hydrochloride salt are nitrogen mustards, and highly toxic, carcinogenic vesicants. The thiol has a particularly offensive odour. The compounds should always be handled in an efficient fume hood.

Preparation of $[MeH_2N(CH_2)_3Cl]Cl$

$MeHN(CH_2)_3OH$ (12.4 g, 0.14 mol) was added over a period of 1 h to freshly distilled $SOCl_2$ (20.0 g, 0.17 mol) and the mixture was stirred at room temperature for 16 h. After this period, Et_2O (20 cm^3) was added and the solution cooled to −20°C, whereupon $[MeH_2N(CH_2)_3Cl]Cl$ was obtained as a white crystalline solid (16.0 g, 80%) (^1H NMR, CD_3OD, δ 2.02–2.38, m, 2H, $CH_2CH_2CH_2$; δ 2.77, s, 3H, NCH_3; δ 3.22, t, NCH_2; δ 3.74, t, $J = 6.2$ Hz, $ClCH_2$).

Preparation of $MeH_2N(CH_2)_3SH$

Thiourea (8.62 g, 0.08 mol) and $[MeH_2N(CH_2)_3Cl]Cl$ (11.3 g, 0.08 mol) were maintained at 95°C in $HOCH_2CH_2(OCH_2CH_2)_2OH$ (50 cm^3) for 24 h, after which period $H_2NCH_2CH_2(NHCH_2CH_2)_3NH_2$ (15.0 g, 0.08 mol) was added, and the solution heated to 130°C for a further 2 h. The resultant solution was vacuum distilled, and the fraction distilling at 47–49°C/11 mm Hg was collected as a colourless oil. Upon cooling to −20°C, the oil solidified to a white mass of $MeH_2N(CH_2)_3SH$ (5.5 g, 67%) (^1H NMR, $CDCl_3$, δ 1.35, s, 1H, NH; δ 1.59–1.95, m, 2H, $CH_2CH_2CH_2$; δ 2.38–2.82, m, 4H, SCH_2 and NCH_2; d 2.42, s, 3H, NCH_3; *m/z*, 105).

Preparation of 2,10-*diaza*-6-*thiaundecane*, L

$MeH_2N(CH_2)_3SH$ (1.70 g, 0.016 mol) was added to a solution of sodium methoxide prepared by the reaction of sodium (0.82 g, 0.036 mol) with methanol (20 cm^3). A solution of $[MeH_2N(CH_2)_3Cl]Cl$ (2.80 g, 0.019 mol) was added to the resultant solution over a period of 25 min, after which the mixture was stirred for 25 min at room temperature and then heated to reflux for 3 h. The cooled solution was diluted with Et_2O (30 cm^3), filtered to remove NaCl and the filtrate concentrated *in vacuo*. The resultant oil was vacuum distilled and 2,10-diaza-6-thiaundecane was collected as the colourless fraction distilling at 90–92°C/0.25 mm Hg (1.6 g, 54%) (IR: ν_{N-H} 3295 cm^{-1}, ν_{CH} 2792 cm^{-1}; ^1H NMR, $CDCl_3$, δ 1.40, s, 1H, NH; δ 1.67–1.78, m, 2H, $CH_2CH_2CH_2$; δ 2.38, s, 3H, NCH_3; δ 2.52, t, $J = 7.3$ Hz, 2H, SCH_2; δ 2.61, t, $J = 7.0$ Hz; 2H, NCH_2). Treatment of an ethanolic solution of the oil with gaseous HBr led to the deposition of the $[H_2L]Br_2$ as a white crystalline solid (Found: C, 28.7; H, 6.6; N, 8.1. Calc. for $C_8H_{22}N_2SBr_2$: C, 28.4; H, 6.6; N, 8.3%).

Preparation of $[CuLBr_2]$

A solution of L (0.05 g, 0.29 mmol) in EtOH (1 cm^3) was added dropwise to a solution of $CuBr_2$ (0.05 g, 0.22 mmol) in EtOH (3 cm^3). The mixture was stirred for 30 min at room temperature, after which period the green precipitate was collected by filtration, washed with EtOH (2 cm^3) and Et_2O (3×5 cm^3). Green crystals of the complex were obtained by the slow diffusion of Et_2O vapour into a Me_2CO solution of the complex (Found: C, 24.1; H, 5.1; N, 6.9. Calc. for $C_8H_{20}N_2SCuBr_2$: C, 24.0; H, 5.0; N, 7.9%).

Preparation of $[CuLCl_2]$

This was prepared in exactly the same manner as the bromo complex, substituting $CuCl_2$. Green crystals of the complex were obtained by the slow diffusion of Et_2O vapour into a Me_2CO solution of the complex (Found: C, 30.4; H, 6.4; N, 8.8. Calc. for $C_8H_{20}N_2SCuCl_2$: C, 30.9; H, 6.5; N, 9.0%).

Crystal structural determination of $[CuLCl_2]$ *and* $[CuLBr_2]$

Dark green blocks of the complexes were obtained by diffusion of Et_2O vapour into Me_2CO solutions of the complexes. Suitable green crystals were mounted on a glass fibre with epoxy resin.

Crystal data. $C_8Cl_2CuH_{20}N_2S$, green blocks, $M = 310.8$, orthorhombic, $a = 17.960(14)$, $b = 14.104(9)$, $c = 10.400(12)$ Å, $U = 2633.6$ Å^3, space group *Pbca* (No. 61), $Z = 8$, $D_c = 1.56$ g cm^{-3}, $D_m = 1.52$ g cm^{-3}, $F(000) = 1288$. Crystal dimensions $0.60 \times 0.20 \times 0.20$ mm, Mo-K_α radiation ($\lambda = 0.7107$ Å), μ(Mo-K_α) = 22.3 cm^{-1}.

Crystal data. $Br_2C_8CuH_{20}N_2S$, green blocks, $M = 399.7$, orthorhombic, $a = 18.440(15)$, $b = 14.214(9)$, $c = 10.587(12)$ Å, $U = 2774.9$ Å^3, space group *Pbca* (No. 61), $Z = 8$, $D_c = 1.93$ g cm^{-3}, $D_m = 1.95$ g cm^{-3}, $F(000) = 1576$. Crystal dimensions $0.50 \times 0.15 \times 0.15$ mm, Mo-K_α radiation ($\lambda = 0.7107$ Å), μ(Mo-K_α) = 79.3 cm^{-1}.

Data collection and processing

The two crystals were set up in turn to rotate about the *a* and *c* axes, respectively, on a Stoe Stadi2 diffractometer and data were collected via variable width ω scan. Background counts were for 20 s and a scan rate of 0.0333° s^{-1} was applied to a width of $(1.5 + \sin\mu/\tan\theta)$. For [$CuLCl_2$], 2047 and for [$CuLBr_2$], 2134 independent reflections with $2\theta_{max}$ of 50° were measured on a Stoe Stadi2 diffractometer, of which 1298 with $I > 3\sigma(I)$ for [$CuLCl_2$] and 1015 with $I > 2\sigma(I)$ for [$CuLBr_2$] were used in the calculations. An empirical absorption correction was applied to both sets of data.[5]

Structure analysis and refinement of [$CuLCl_2$]

The structure was solved by direct methods followed by Fourier difference techniques. Blocked full-matrix least-squares refinement with Cu, Cl, N, S and C atoms anisotropic. Hydrogen atoms were not located directly, but were placed in idealized positions and allowed to ride on the relevant carbon with C—H fixed at 0.95 Å; the methyl groups were refined as rigid groups. The structure was chemically reasonable, although there was a surprising disparity in the S(9)—C(10) and S(9)—C(8) bond lengths [1.921(13), 1.825(15)]. The weighting scheme, $w = 1/[\sigma^2(F) + 0.003|F|^2]$, gave satisfactory agreement analyses. Final converged R and R_w values were 0.058 and 0.065, respectively.

Structure analysis and refinement of [$CuLBr_2$]

The structure was solved by direct methods followed by Fourier difference techniques. Initial blocked full-matrix least-squares refinement with all atoms isotropic. Hydrogen atoms were not located directly, but were placed in idealized positions and allowed to ride on the relevant carbon with C—H fixed at 0.95 Å; the methyl groups were refined as rigid groups. The data for [$CuLBr_2$] was less good than for [$CuLCl_2$], and on initial isotropic refinement, the disparity in S—C bond lengths was 0.30 Å. In addition, there were some unusual dimensions around the chelate ring and C(10) had a large thermal parameter. When the sulphur atom was refined anisotropically, U_{11} was twice as large as U_{22} and U_{23}; this suggested the presence of disorder and several models based on two sulphur atom positions with different occupancies were tried unsuccessfully. In the final model, Cu, Br and S were refined anisotropically and C, N and H were refined isotropically, with the S(9)—C(10) and S(9)—C(8) distances constrained to be equivalent via DFIX with an allowed standard deviation of 0.05 Å. They refined to values of 1.965(28) and 1.822(39) Å. The weighting scheme, $w = 1/[\sigma^2(F) + 0.003|F|^2]$, gave satisfactory agreement analyses. Final converged R and R_w values were 0.083 and 0.096, respectively. A final electron density map showed a maximum electron density of 0.96 e Å^{-3} in a position close to S(9). Clearly there is some positional disorder in the ligand, although no obvious disordered model was found appropriate. For both compounds, complex neutral atom scattering factors were taken from ref. 6. Calculations were performed using SHELX 76 on the Amdahl V7 Computer at the University of Reading.[7] Selected bond lengths and bond angles are presented in Table 1.*

RESULTS AND DISCUSSION

The aminothioether ligand, $MeNH(CH_2)_3S(CH_2)_3NHMe$, is readily prepared in 54% yield by the nucleophilic attack of the thiolate anion,

Table 1. Selected bond lengths (Å) and bond angles (°) for [$CuLCl_2$] and [$CuLBr_2$]

	X = Cl	X = Br
Cu(1)—X(2)	2.374(3)	2.541(4)
Cu(1)—X(3)	2.312(3)	2.461(4)
Cu(1)—N(5)	2.010(8)	2.038(23)
Cu(1)—S(9)	2.493(3)	2.478(10)
Cu(1)—N(13)	1.985(8)	2.031(22)
X(2)—Cu(1)—X(3)	132.19(12)	130.51(19)
X(2)—Cu(1)—N(5)	88.89(21)	87.4(7)
X(3)—Cu(1)—N(5)	91.35(22)	92.4(6)
X(2)—Cu(1)—S(9)	103.64(11)	103.57(26)
X(3)—Cu(1)—S(9)	124.15(11)	125.88(28)
N(5)—Cu(1)—S(9)	87.66(24)	87.6(7)
X(2)—Cu(1)—N(13)	88.79(25)	87.8(6)
X(3)—Cu(1)—N(13)	92.34(25)	93.2(6)
N(5)—Cu(1)—N(13)	176.31(32)	174.2(8)
S(9)—Cu(1)—N(13)	90.09(24)	90.4(7)

* Atomic coordinates, displacement factor coefficients, full lists of bond lengths and bond angles and lists of F_o/F_c values have been deposited as supplementary data with the Editor, from whom copies are available on request. Atomic coordinates have also been deposited with the Cambridge Crystallographic Data Centre.

$MeNH(CH_2)_3S^-$, upon $MeNH(CH_2)_3Cl$. The compound is an oil, which is best stored as its hydrobromide salt. In general, the compound was prepared as required, and used immediately. The desired thiol is prepared in moderately good yield via the thiouronium salt, obtained from the reaction of thiourea with $MeNH(CH_2)_3Cl$. The key intermediate for the synthesis is thus $MeNH(CH_2)_3Cl$, which is prepared by the reaction of $MeNH(CH_2)_3OH$ with $SOCl_2$. The compound $MeNH(CH_2)_3Cl$ is a particularly irritating nitrogen mustard, and must be treated with due deference. The compound was always handled in a fume cupboard, and was generally used immediately it was prepared. The compound was always isolated as the hydrochloride salt, but even this relatively non-volatile compound was extremely irritant.

The reaction of L with CuX_2 (X = Br or Cl) led to the formation of the green, air-stable 1 : 1 adducts $[CuLX_2]$. The complexes are readily soluble in MeCN, Me_2CO and $MeNO_2$, but only sparingly soluble or insoluble in protic solvents such as EtOH or MeOH. The electronic spectra of the complexes $[CuLCl_2]$ and $[CuLBr_2]$ in MeCN solution exhibit maxima at 709 nm ($\varepsilon = 269$ mol^{-1} dm^3 cm^{-1}) and 707 nm ($\varepsilon = 515$ mol^{-1} dm^3 cm^{-1}), respectively. The spectra in nitromethane and CH_2Cl_2 were not significantly different, strongly suggesting that the solvent is not interacting directly with the metal centre. In addition to the *d–d* bands, charge-transfer absorptions were observed in the 340–450 nm region ($\varepsilon \sim 1000$ mol^{-1} dm^3 cm^{-1}). These observations are in accord with a five-coordinate structure.[8] The absorption around 400 nm has been assigned to a ligand-to-metal charge-transfer.[9] The vibrational spectra of $[CuLCl_2]$ and $[CuLBr_2]$ exhibit strong absorptions at 3211 and 3200 cm^{-1}, respectively, which may be assigned to N—H stretching modes in the complexes. Upon coordination, the C—H stretching modes of the N-methyl groups diminish in intensity.

Both of the complexes $[CuLCl_2]$ and $[CuLBr_2]$ behave as non-conductors in MeCN solution. In an attempt to further probe the solution structure of the complexes, the ESR spectra were measured. Surprisingly, both complexes gave isotropic spectra in MeCN glass at −196°C. The cyclic voltammograms of both complexes showed strong absorption processes associated with halide loss, but no reversible electron-transfer processes. The fast atom bombardment mass spectra of $[CuLCl_2]$ and $[CuLBr_2]$ exhibited fragmentation peaks, but no peaks corresponding to the molecular ions. The bulk of the evidence suggests that the two complexes, $[CuLCl_2]$ and $[CuLBr_2]$, are five-coordinate in both the solid and solution phases.

At room temperature, $[CuLCl_2]$ was found to have $\mu_{eff} = 1.8 \pm 0.1$ BM, whereas $[CuLBr_2]$ was found to have a considerably higher moment, $\mu_{eff} = 2.5 \pm 0.1$ BM. Typical values for five-coordinate copper(II) complexes are in the region 1.75–1.90 BM. The magnetic moment of $[CuLBr_2]$ is unusually high, but was shown to be a consistent value obtained from various samples. On the basis of the magnetic measurements, we considered that the two complexes might have different structures in the solid state, and we accordingly determined the crystal and molecular structures of the two complexes.

The crystal and molecular structure of $[CuLCl_2]$ is shown in Fig. 1. The dibromo compound is isomorphous and isostructural, the only difference in geometry being in the scale of the disorder, which is considerably greater in $[CuLBr_2]$. In both complexes, the copper is in a five-coordinate N_2SX_2 environment. In $[CuLCl_2]$ the geometry is close to trigonal prismatic, with the SCl_2 groups occupying the equatorial sites of the trigonal bipyramid [Cu—Cl(2), 2.374(3); Cu—Cl(3), 2.312(3); Cu—S(9), 2.493(3) Å] and the nitrogen atoms occupy the axial sites [Cu—N(5), 2.010(8); Cu—N(13), 1.985(8) Å; N(5)—Cu—N(13), 176.3(3)°]. The pattern of dimensions is similar in $CuLBr_2$ [Cu—Br(3), 2.461(4); Cu—Br(2), 2.541(4); Cu—S(9), 2.478(10); Cu—N(5), 2.038(23); Cu—N(13), 2.031(22) Å]. The reason for the disparity in the Cu—Cl (and Cu—Br) bond distances

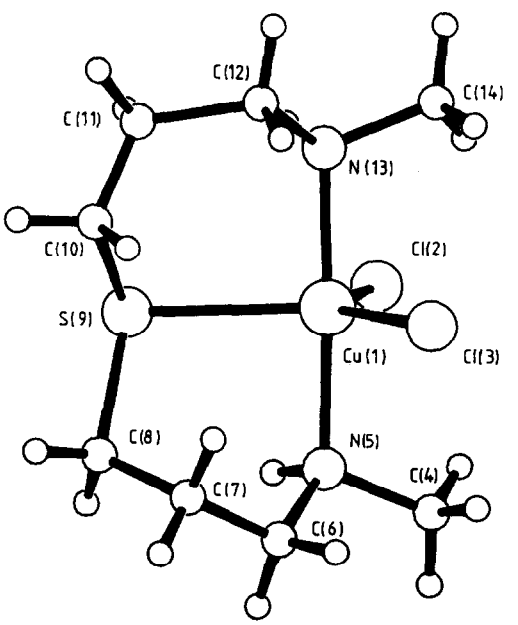

Fig. 1. The crystal and molecular structure of the $[CuLCl_2]$ complex showing the numbering scheme adopted. The $[CuLBr_2]$ complex is isostructural.

is not clear (particularly as both atoms are coplanar in the equatorial plane within experimental error). However, it is noticeable that the sulphur atom, S(9), is much closer to Cl(2) than Cl(3), the two S—Cu—Cl angles being 103.6(1) and 124.1(1)°, respectively. This disparity is presumably due to the asymmetric conformation of the ligand in [$CuLCl_2$]; the values in [$CuLBr_2$] are comparable.

The conformation of the ligand in the complexes [$CuLCl_2$] and [$CuLBr_2$] is significantly different from that in [PdLBr]Br.[1] In [PdLBr]Br, the cation has crystallographic mirror symmetry with torsion angles around the ring very different from those observed in [$CuLCl_2$] and [$CuLBr_2$]. In [$CuLCl_2$] and [$CuLBr_2$], one half of the ligand [from S(9) to N(13)] has similar torsion angles to those observed in [PdLBr]Br, but the other half [from S(9) to N(5)] is different, and judging from the torsion angles, considerably more strained. Torsion angles for [$CuLCl_2$], [$CuLBr_2$] and [PdLBr]Br are presented in Table 2. It is interesting to note that the Pd—S bond length of 2.285(4) Å is considerably shorter than the Cu—S distances, although the Cu—N and Pd—N distances are comparable. The disparity in the Cu—S distances in [$CuLBr_2$] is no doubt due to disorder. This finding strongly suggests that the smaller difference in these distances found in [$CuLCl_2$] is also due to a similar but smaller effect.

The packing of the molecules in the lattice is dictated by hydrogen bonding of the type N—H···Cl [N(5)—H···Cl(3) (symmetry element, $-x$, y, $+z$) and N(13)—H···Cl(2) (symmetry element, $-x$, $1-y$, $1-z$)]. Dimensions for N···Cl, H···Cl and ∠N—H···Cl are 3.29 Å, 2.52 Å, 138°, and 3.35 Å, 2.63 Å and 133°, respectively. Similar interactions are observed in [$CuLBr_2$], where the corresponding dimensions N···Br, H···Br and ∠N—H···Br are 3.48 Å, 2.65 Å, 146°, and 3.44 Å, 2.65 Å and 141°, respectively.

Table 2. Selected torsion angles (°) for [$CuLCl_2$] (1), [$CuLBr_2$] (2) and [PdLBr]Br (3)

	1	2	3
M—N(5)—C(6)—C(7)	37.5	44.8	68.1
N(5)—C(6)—C(7)—C(8)	49.1	44.6	−72.2
C(6)—C(7)—C(8)—S(9)	−78.3	−75.5	69.6
C(7)—C(8)—S(9)—C(10)	−81.5	−87.9	167.5
C(8)—S(9)—C(10)—C(11)	163.1	152.8	(−167.5)
S(9)—C(10)—C(11)—C(12)	−77.2	−69.5	(−69.6)
C(10)—C(11)—C(12)—N(13)	78.1	75.6	(72.2)
C(11)—C(12)—N(13)—M	−70.2	−66.0	(−68.1)

Although five-coordinate copper(II) is relatively common, only a single example of a [CuN_2SX_2] complex has been structurally characterized.[10] In the macrocyclic complex [Cu(9-ane-N_2S)Br_2] the copper is in a square-pyramidal environment, with the sulphur in the axial site. The Cu—S, Cu—N and Cu—Br distances in this complex are all significantly longer than those observed in the complexes described above.

Acknowledgements—We thank the SERC for providing funds for the diffractometer and support (P.J.S.). Also we thank ICI for support (P.J.S.) and Mr A. W. Johans for his help with the crystallographic investigation.

REFERENCES

1. E. C. Constable, P. J. Stotereau and M. G. B. Drew, *Inorg. Chim. Acta* 1988, **145**, 3.
2. H. Irving and R. J. P. Williams, *J. Chem. Soc.* 1953, 3192.
3. K. Henrick, P. A. Tasker and L. F. Lindoy, *Prog. Inorg. Chem.* 1985, **33**, 1.
4. S. R. Koepke, R. Kupper and C. J. Michejda, *J. Org. Chem.* 1979, **44**, 2718.
5. N. Walker and D. Stuart, *Acta Cryst.* 1983, **A39**, 158.
6. *International Tables for X-ray Crystallography*, Vol. IV. Kynoch Press, Birmingham (1975).
7. G. M. Sheldrick, SHELX 76, Crystal Structure Solving Package. University of Cambridge, U.K. (1976).
8. A. B. P. Lever, *Inorganic Electronic Spectroscopy*, 2nd edn. Elsevier, Amsterdam (1984).
9. R. Louis, Y. Agnus and R. Weiss, *J. Am. Chem. Soc.* 1978, **100**, 3604.
10. R. D. Hancock, S. M. Dobson and J. C. A. Boeyens, *Inorg. Chim. Acta* 1987, **133**, 221.

Polyhedron Vol. 8, No. 23, pp. 2755–2761, 1989
Printed in Great Britain

0277–5387/89 $3.00+.00
© 1989 Pergamon Press plc

ORGANOTIN(IV) COMPLEXES WITH TRIDENTATE LIGANDS—I. DIMETHYLTIN(IV) COMPLEXES WITH N-SALICYLIDENE DERIVATIVES OF AROYLHYDRAZINES, S-METHYLHYDRAZINECARBODITHIOATE AND 4-SUBSTITUTED THIOSEMICARBAZIDES

M. F. ISKANDER,* L. LABIB, M. M. Z. NOUR EL-DIN and M. TAWFIK

Chemistry Department, Faculty of Science, Alexandria University, Alexandria, Egypt

(*Received* 16 *May* 1989; *accepted* 26 *June* 1989)

Abstract—Dimethyltin(IV) complexes with N-salicylidene derivatives of aroylhydrazines, S-methylhydrazinecarbodithioate and 4-substituted thiosemicarbazides have been prepared and their IR, NMR (^1H, ^{13}C) and mass spectra have been studied. A slightly distorted five-coordinate trigonal bipyramidal structure is proposed for these complexes. The two methyl carbons and the azomethine nitrogen occupy the trigonal plane, while the highly polar O—Sn—O and O—Sn—S are axial. The chemical shifts (δ) of the Sn—CH_3 carbon and the corresponding $^1J_{Sn-C}$ values show a dependence on the nature of the donor atoms in the axial position.

N-salicylidene aroylhydrazines and their copper(II) complexes are potent inhibitors for DNA synthesis and cell growth in a number of human and rodent cell-line grown cultures.[1] The cytotoxic action of some transition metal complexes of bidentate and tridentate Schiff bases derived from S-methylhydrazinecarbodithioate have also been reported.[2] In addition, there has been considerable interest in the antitumour activity of organotin(IV) complexes.[3–7] A number of organotin(IV) complexes with O-, S- and N-containing ligands have also been tested *in vivo* in p-388 leukaemic mice,[7] but the structural factors which affect the antitumour activity and cytotoxicity of organotin(IV) complexes are still uncertain.[7]

We considered that a systematic study of the coordination chemistry of organotin(IV) complexes with biologically or pharmacologically active ONO, NNS and ONS tridentate ligands might provide further information concerning the structural characteristics required for their antitumour and cytotoxic activity. In the present paper, the synthesis and structure of a series of dimethyltin(IV) complexes with N-salicylidene derivatives of aroylhydrazines (**1**) (R = C_6H_5, *p*-ClC_6H_4, *p*-$CH_3C_6H_4$, *p*-$CH_3OC_6H_4$), S-methylhydrazinecarbodithioate (**2**) (R = SCH_3) and four-substituted thiosemicarbazides (**2**) [R = $C_5H_{10}N$ (piperidyl) and C_4H_8NO (morpholyl)] are discussed.

RESULTS AND DISCUSSION

In methanol, the reactions of both **1** (R = C_6H_5, *p*-$CH_3OC_6H_4$, *p*-$CH_3C_6H_4$, *p*-ClC_6H_4) and **2** (R = SCH_3, $C_5H_{10}N$, C_8H_8NO) with $(CH_3)_2SnCl_2$

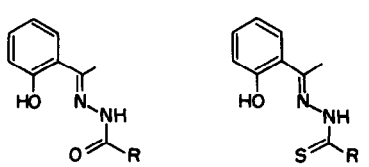

1 **2**

in the presence of 2 equivalents of sodium methoxide, respectively, afford complexes of the general formulae $(CH_3)_2SnL$ and $(CH_3)_2SnL'$, where L and L′ refer to the dinegative anions of **1** and **2**, respectively. The dimethyltin(IV) complexes isolated, together with their elemental analyses, are listed in Table 1.

The IR spectra of $(CH_3)_2SnL$ complexes lack absorptions due to ν(OH), ν(NH) and ν(C=O)

* Author to whom correspondence should be addressed.

Table 1. Elemental analyses of $(CH_3)_2SnL$ and $(CH_3)_2SnL'$ complexes of general formula **3**

R	X	Melting point (°C)	Found (Calc.) (%) C	H	N	S
C_6H_5	O	152	49.5 (49.7)	4.2 (4.2)	7.3 (7.4)	
p-$CH_3C_6H_4$	O	148	51.1 (50.9)	4.6 (4.5)	7.0 (7.0)	
p-$CH_3OC_6H_4$	O	133	48.7 (49.0)	4.4 (4.4)	6.7 (6.7)	
p-ClC_6H_4	O	176	45.8 (45.6)	3.8 (3.9)	6.4 (6.7)	
SCH_3	S	88	35.3 (35.4)	3.6 (3.8)	7.3 (7.5)	17.0 (17.2)
$C_5H_{10}N$	S	115	44.1 (43.9)	5.3 (5.2)	10.3 (10.3)	7.8 (7.8)
C_4H_8NO	S	144	40.8 (41.2)	4.7 (4.7)	10.3 (10.2)	7.8 (7.8)

(amide I band) which are present in the spectra of uncoordinated aroylhydrazones.[8] The spectra, however, show a strong band at *ca* 1600 cm^{-1} due to ν(C=N—N=C), as well as two bands at *ca* 1520 and 1285 cm^{-1} attributed to C—O stretching and bending vibrations, respectively.[9] The spectra suggest that the aroylhydrazone moiety in $(CH_3)_2SnL$ complexes acts as a dinegative ONO tridentate ligand which is coordinated to the central tin(IV) via a phenolic oxygen, an azomethine nitrogen and an enolic oxygen. A similar coordination mode has been reported for many transition and non-transition metal complexes with N-salicylidene aroylhydrazines.[8–12] Furthermore, the IR spectra of **3**

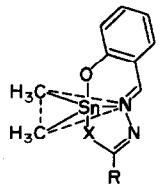

3

(R = SCH_3, $C_5H_{10}N$, C_4H_8NO) show a broad band centred at 3350 cm^{-1} in addition to a strong band at *ca* 3200 cm^{-1} due to ν(OH) and ν(NH), respectively, which do not appear in the spectra of the corresponding $(CH_3)_2SnL'$ complexes. The doublet at *ca* 1600 cm^{-1} in the spectra of **2** (R = SCH_3, $C_5H_{10}N$, C_4H_8NO), which can be attributed to ν(C=N)+ν(C=C), undergoes a pronounced shift to lower frequencies ($\Delta\nu$ = 20 cm^{-1}) in the spectra of the corresponding $(CH_3)_2SnL'$ complexes. Complex formation also results in the disappearance of the band at *ca* 1100 cm^{-1} due to ρ(H—N)+ν(C=S), which was originally present in the spectra of **2** (R = SCH_3, $C_5H_{10}N$, C_4H_8NO). Here again, the IR spectral data suggest the tridentate nature of **2** in $(CH_3)_2SnL'$ where tin(IV) is coordinated to the deprotonated phenolic oxygen, the azomethine nitrogen and the thiol sulphur.[13,14] The IR spectra of both $(CH_3)_2SnL$ and $(CH_3)_2SnL'$ show new bands at *ca* 500±10 and 435±5 cm^{-1}, which are absent in the spectra of the uncoordinated hydrazones, which can be assigned to ν(Sn—O)[15] and ν(Sn—N),[16] respectively. The two new bands at *ca* 520±10 and 560±10 cm^{-1} appear in the spectra of both $(CH_3)_2SnL$ and $(CH_3)_2SnL'$ complexes, respectively, due to ν_{sym}(Sn—C) and ν_{asym}(Sn—C) vibration modes, suggesting that the C—Sn—C moiety is non-linear.[15,17,18]

Due to the extended conjugation, the dinegative tridentate anions of **1** and **2** impose a rigid planar configuration around the tin(IV) and a slightly distorted trigonal bipyramidal structure, **3**, can be proposed for both $(CH_3)_2SnL$ and $(CH_3)_2SnL'$ complexes. The two methyl carbons and the azomethine nitrogen occupy the trigonal plane, while the highly polar O—Sn—O or O—Sn—S groups are in axial positions.[15]

The ^1H NMR spectra of both $(CH_3)_2SnL$ and $(CH_3)_2SnL'$ complexes, Table 2, display the Sn—CH_3 protons as one sharp singlet within the ranges 0.82–0.84 and 0.82–0.90 ppm, respectively. The observed $^2J(^{119}Sn—CH_3)$, $^2J(^{117}Sn—CH_3)$ and $^3J(^{119}Sn—N=CH)$ values are within the ranges reported for other trigonal bipyramidal $(CH_3)_2Sn^{IV}$ chelate complexes with two methyl groups in the *cis*-configuration.[15,19,20] The data given in Table 2 show that both the $^2J(^{119}Sn—CH_3)$ and $^3J(^{119}Sn—N=CH)$ values depend on the nature of the donor atoms in the axial position. The ^2J values recorded for the $(CH_3)_2SnL$ complexes with ONO tridentate hydrazones (**3**, X = O) are higher than those of the $(CH_3)_2SnL'$ complexes with ONS ligands (**3**, X = S). This can be attributed to higher *s*-character of the tin orbital in the Sn—CH_3 bond. It is also observed from the ^{13}C NMR spectral data given in Table 3, that the chemical shifts (δ) of the Sn—CH_3 carbon, as well as the values of $^1J(^{119}Sn—^{13}C)$ and $^1J(^{117}Sn—^{13}C)$, show a dependence on the nature of the donor atoms in the

Table 2. ^{1}H NMR spectra of $(CH_3)_2SnL$ and $(CH_3)_2SnL'$ complexes in $CDCl_3$

R	Chemical shift (δ) ppm (Number of protons) [J (Hz)]			
	Sn—CH_3	R	Salicylidene	N=CH
(i) $(CH_3)_2SnL$ (3, X = O)				
C_6H_5	0.84(3) (78.7, 75.4)[a]	Arom. 7.42(3), 8.07(2)	6.75(2), 7.18(1), 7.34(1)	8.76(1) (46.0)[b]
p-ClC_6H_4	0.83(3) (78.6, 75.4)[a]	Arom. 7.38(2), 8.00(2)	6.75(2), 7.17(1), 7.30(1)	8.73(1) (45.8)[b]
p-$CH_3C_6H_4$	0.82(3) (78.7, 75.3)[a]	Arom. 7.21(2), 7.95(2) CH_3 2.39(3)	6.74(2), 7.17(1), 7.31(1)	8.74(1) (46.2)[b]
p-$CH_3OC_6H_4$	0.82(3) (78.7, 75.4)[a]	Arom. 7.21(2), 8.00(2) OCH_3 3.28(3)	6.75(2), 7.17(1), 7.32(1)	8.75(1) (46.2)[b]
(ii) $(CH_3)_2SnL'$ (3, X = S)				
SCH_3	0.90(3) (73.4, 70.3)[a]	SCH_3 2.55(3)	6.75(2), 6.75(2), 7.33(1)	8.74(1) (37.8)[b]
$C_5H_{10}N$	0.82(3) (72.5, 69.3)[a]	CH_2 1.62(6) CH_2 3.76(4)	6.73(2), 7.09(1), 7.30(1)	8.53(1) (39.8)[b]
C_8H_8NO	0.84(3) (72.3, 69.2)[a]	$NCH_2$3.70(4) OCH_2 3.80(4)	6.73(2), 7.10(1), 7.27(1)	8.54(1) (39.9)[b]

[a] $^2J(^{119}Sn—CH)$, $^2J(^{117}Sn—CH)$.
[b] $^3J(Sn—N=CH)$.

axial positions. The δ (Sn—CH_3) carbon of the $(CH_3)_2SnL$ complexes appears at *ca* 1.3 ppm, while that of the $(CH_3)_2SnL'$ series is shifted downfield and appears within the range 5.2–6.0 ppm. The observed dependence of the chemical shift of the (Sn—CH_3) carbon on the nature of the donor atoms in the axial positions can be related to the relative polarity of the Sn—CH_3 bonds in the equatorial plane. The polarity of such Sn—C bonds depends on the amount of residual positive charge located on the tin, as well as on the *s*-character of the tin orbitals in this bond.

In ^{119}Sn NMR studies on organotin(IV) chelate complexes, Otera[21] found that the $\delta(^{119}Sn)$ values reflect the nature of the donor atoms, and the coordination of tin(IV) to sulphur gives rise to increased shielding on tin relative to oxygen as the donor atom. It was deduced from these observations that sulphur is a more favourable donor towards tin than oxygen. Accordingly, more residual positive charge is localized on the central tin(IV) atom of the $(CH_3)_2SnL$ (3, X = O) complexes with two oxygens in the axial positions, as compared to that of the $(CH_3)_2SnL'$ (3, X = S) with sulphur and oxygen atoms. Consequently, more shielding is expected on the Sn—CH_3 carbon of the $(CH_3)_2SnL$ complexes. This is also in agreement with the high $^1J(^{119}Sn—^{13}C)$ values (647 ± 2 Hz) observed for $(CH_3)_2SnL$ complexes relative to the 597 ± 2 Hz values measured for the $(CH_3)_2SnL'$ series. Furthermore, the measured values of $^1J(^{119}Sn—^{13}C)$ and $^2J(^{119}Sn—^{13}C)$ for both $(CH_3)_2SnL$ and $(CH_3)_2SnL'$ complexes (Table 3) are within the range reported for five-coordinate diorganotin(IV) chelate complexes.[22,23]

The EI mass spectra of the $(CH_3)_2SnL$ and $(CH_3)_2SnL'$ complexes display prominent peaks corresponding to the mononuclear parent molecular ion ($P^{+\cdot}$). Fragments containing tin are easily recognized by their characteristic tin isotope pattern. The m/z values (based on ^{120}Sn) of these fragments, together with their relative intensities, are listed in Table 4. The mass spectra of these complexes may be discussed in terms of the valence change concept[24,25] for rationalizing the major fragmentation pathways. The mass spectral fragmentation of these complexes is shown in Scheme 1, where only fragments containing tin are given.

Fragmentation of these complexes starts with simple cleavage of an Sn—CH_3 bond with loss of a CH_3 radical from $P^{+\cdot}$, giving the even electron four-coordinate tin(IV) ion which changes to the odd electron ion (**II**) by a decrease of the oxidation state of tin from tin(IV) to tin(III). Organotin(III) rad-

Table 3. ^{13}C NMR spectra of $(CH_3)_2SnL$ and $(CH_3)_2SnL'$ complexes (3) in $CDCl_3$

R	Sn—C	C_1	C_2	C_3	C_4	C_5	C_6	C_7	C_8	R	
	Chemical shift (δ) ppm[a] [J (Hz)]										
(i) $(CH_3)SnL$ (3, X = O)											
C_6H_5	1.31 (646.8)[b] (619.4)[c]	116.60 (27.0)[d]	166.28	121.59 (6.8)[e]	135.06	117.30	134.48	161.34 (22.5)[f]	169.03	C_9 C_{10}, C_{14} C_{11}, C_{13} C_{12}	130.95 117.10 128.10, 128.80 127.52
p-$CH_3C_6H_4$	1.29 (647.8)[b] (619.2)[c]	116.74 (27.2)[d]	166.22	121.59 (7.3)[e]	134.95	117.07	133.90	160.95 (22.7)[f]	169.22	C_9 C_{10}, C_{14} C_{11}, C_{13} C_{12} CH_3	130.95 116.34 127.30, 128.80 141.30 21.48
p-$CH_3OC_6H_4$	1.24 (648.1)[b] (619.4)[c]	116.78	166.13	121.54 (7.3)[e]	134.80	117.04	133.98	161.97	168.91	C_9 C_{10}, C_{14} C_{11}, C_{13} C_{12} OCH_3	129.29 116.78, 113.44 125.55 160.49 55.21
(ii) $(CH_3)_2SnL'$ (3, X = S)											
SCH_3	6.27 (597.2)[b] (571.0)[c]	115.80 (24.3)[d]	165.73	121.78 (7.3)[e]	136.19	117.31	134.48	167.49 (20.0)[f]	174.19	SCH_3	14.87
$C_5H_{10}N$	5.20 (597.3)[b] (571.2)[c]	116.91	165.98	121.19 (8.6)[e]	136.19	117.39	134.48	158.55 (23.5)[f]	167.82	α-CH_2 β-CH_2 γ-CH_2	47.85 25.71 24.71
C_4H_8NO	5.54 (597.1)[b] (570.4)[c]	116.97 (28.3)[d]	165.71	121.24 (8.7)[e]	134.26	116.97	133.21	159.97 (22.5)[f]	168.61	O—CH_2 N—CH_2	66.42 47.09

[a] The numbering for carbon atoms in the N-salicylidenehydrazine residue and R in the aroylhydrazine ligands are, respectively,

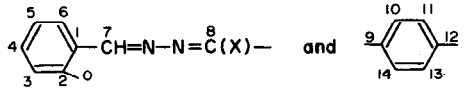

[b] $^1J(^{119}Sn—C)$.
[c] $^1J(^{117}Sn—C)$.
[d] $^3J(Sn—NCC)$.
[e] $^3J(Sn—OCC)$.
[f] $^2J(Sn—N=C)$.

Table 4. Relative abundances (RA) of tin-containing ions in the mass spectra of dimethyltin(IV) complexes of the general formula (3)

m/z (RA)								
X = S R = SCH_3	X = S R = $C_5H_{10}N$	X = S R = C_4H_8NO	X = O R = C_6H_5	X = O R = *p*-$CH_3C_6H_4$	X = O R = *p*-$CH_3OC_6H_4$	X = O R = *p*-ClC_6H_4	Assignment	
374(44)	411(54)	413(84)	388(70)	402(57)	418(48)	422(98)	(I)	(P)
359(100)	396(61)	398(100)	373(30)	387(18)	403(8)	407(43)	(II)	(P – CH_3)
344(11)	381(30)	383(69)	358(69)	372(60)	388(47)	392(100)	(III)	(P – $2CH_3$)
297(41)	297(2)	297(4)					(IV)	(III – R)
269(8)	269(5)	269(5)					(V)	(I – XC(N)R)
268(10)	268(6)	268(7)						(V – H)
254(21)	254(2)	254(5)	254(2)	254(2)		254(3)	(VI)	(II – CH_3)
243(8)	243(6)	243(10)					(VII)	(V – CN)
239(18)	239(11)	239(45)	239(2)			239(2)	(VIII)	(VI – CH_3)
238(33)	238(27)	238(50)	238(5)	238(4)	238(3)	238(7)	(IX)	(VIII – H)
228(8)				228(5)		228(6)	(X)	(VI – CN)
225(4)	225(3)	225(6)	225(10)	225(7)	225(4)	225(18)	(XI)	(VIII – N)
212(8)	212(4)	212(9)			212(3)	212(3)	(XII)	(VIII – CH)
205(11)	205(4)	205(7)					(XIII)	(IV – C_6H_4O)
178(9)	178(2)	178(5)					(XIV)	(Sn – X – C=N)
135(11)	135(5)	135(10)	135(12)	135(10)		135(16)		SnO
120(11)	120(2)	120(6)	120(5)	120(9)		120(7)		Sn

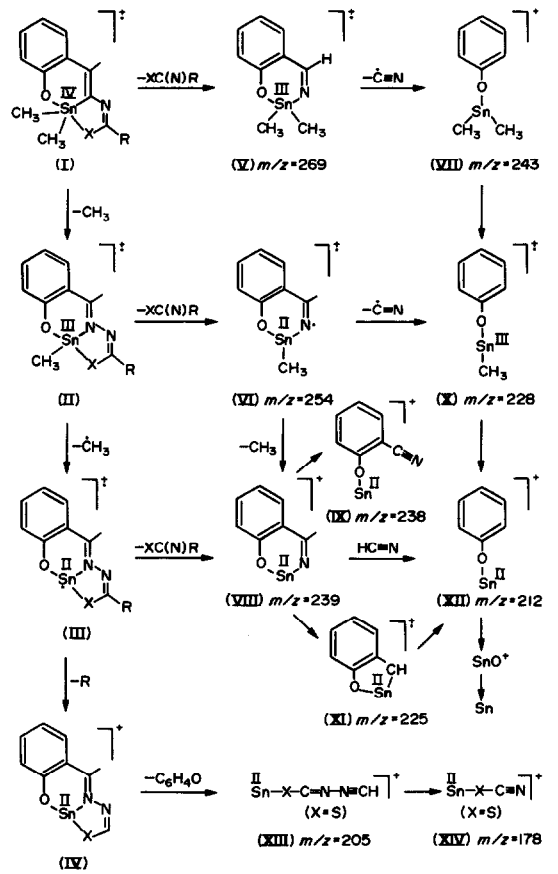

Scheme 1.

icals have been detected both in solution and the solid state by ESR spectroscopy.[26] Further elimination of a CH_3 radical from **II** similarly gives the odd electron tri-coordinate tin(II) ion (**III**).

The spectra are dominated by the elimination of XC(N)R radicals from both **II** and **III** giving, respectively, **VI** and **VIII**. Similar to other Schiff base complexes,[27] the expulsion of the CN radical from **VI** and **VII** gives **IX** and **X**, respectively. The spectra also show a peak at $m/z = 225$ (**XII**) resulting from the elimination of nitrogen from **VII**. It is worthwhile noting that the changes in the formal oxidation state of tin assumed for fragments **II**, **III**, **V** and **VI** allows further elimination of simple radical(s) from these fragments, since elimination of radicals from an even electron ion is quite unlikely.

The spectra of $(CH_3)_2SnL'$ (**3**, X = S) complexes show peaks at $m/z = 297$, 269, 242, 205 and 178 which are not present in the spectra of $(CH_3)_2SnL$ (**3**, X = O) complexes. The peak at $m/z = 297$ (**IV**) results from the expulsion of an R radical (R = SCH_3, $C_5H_{10}N$ or C_4H_8NO) from **III**. The presence of the peak at $m/z = 205$ (**XIII**) indicates the extra stability of the Sn—S relative to the Sn—O bond in **IV**. Furthermore, the peaks at $m/z = 269$ (**V**) and 242 (**VIII**) originate from the molecular ion **I** (X = S) by successive elimination of SC(N)R and C≡N radicals, respectively.

EXPERIMENTAL

Methanol (Merck) was distilled over magnesium metal just before use. Dimethyltin(IV) dichloride was prepared and crystallized (m.p. 107°C, literature value 108°C) as previously described.[27] The N-salicylidene derivatives of aroylhydrazines **1** (R = C_6H_5, *p*-$CH_3C_6H_4$, *p*-$CH_3OC_6H_4$, *p*-ClC_6H_4),[8–11] S-methylhydrazinecarbodithioate **2** (R = SCH_3)[13,14] and N-substituted thiosemicarbazide **2** (R = $C_5H_{10}N$, C_4H_8NO) were prepared, as previously described, by the condensation of distilled salicylaldehyde (Prolabo) with the corresponding hydrazine derivative in ethanol. The isolated hydrazones were crystallized from methanol and their purity was checked by melting point, TLC and IR spectra.

Elemental analyses (C, H and N) were carried out at the microanalytical laboratory of the Chemistry Department, Philipps Universität, Marburg (F.R.G.). The IR spectra were recorded on Perkin–Elmer 225 and or 457 spectrophotometers. The calibration of frequency readings was made with a polystyrene film and solid samples were examined as KBr discs. ^{1}H NMR spectra were measured using a Brucker WH 400 instrument using tetramethylsilane as the internal standard. ^{13}C NMR spectra were recorded on either Brucker WH 400 or Varian XL 100 spectrometers. The mass spectra were obtained using a Varian MAT 711 double focussing spectrometer equipped with a direct inlet system and operating at 70 eV electron beam energy. All the spectra were recorded at the lowest possible temperatures.

Preparation of dimethyltin(IV) *complexes* (**3**, X = O; R = C_6H_5, *p*-$CH_3C_6H_4$, *p*-$CH_3OC_6H_4$, *p*-ClC_6H_4. X = S; R = SCH_3, $C_5H_{10}N$, C_4H_8NO)

To a suspension of the appropriate N-salicylidene derivative (0.01 mol) in dry methanol (20 cm^3), a solution of sodium methoxide (0.02 mol) in dry methanol (10 cm^3) was added. The resulting solution was treated with a solution of $(CH_3)_2SnCl_2$ (0.01 mol) in dry methanol (20 cm^3) and was refluxed with constant stirring for 2 h. The solvent was then removed under reduced pressure and the residue was recrystallized from *n*-hexane or benzene–petroleum ether (40–60°C).

Acknowledgements—M.F.I. and L.L. thank Professor Dr J. Lorberth, Philipps Universität, Marburg (F.R.G.) for

a gift of dimethyltin dichloride, and the staff of the NMR and Mass Spectrometry Laboratories of Philipps Universität for recording the spectra.

REFERENCES

1. D. K. Johnson, T. B. Murphy, N. J. Rose, W. H. Goodwin and L. Pickart, *Inorg. Chim. Acta* 1982, **67**, 159.
2. M. Das and S. E. Livingstone, *Brit. J. Cancer* 1978, **37**, 466.
3. A. J. Crowe, P. J. Smith and G. Atassi, *Chem. Biol. Interactions* 1980, **32**, 171; A. J. Crowe and P. J. Smith, *J. Organomet. Chem.* 1982, **244**, 223; A. J. Crowe, P. J. Smith and G. Atassi, *Inorg. Chim. Acta* 1984, **93**, 179; A. J. Crowe, P. J. Smith, C. J. Cardin, H. E. Parge and F. E. Smith, *Cancer Lett.* 1984, **24**, 45.
4. W. Jiazhu, H. Jingshuo, H. Liyiae, S. Dashuaug and H. Shengzhi, *Inorg. Chim. Acta* 1988, **152**, 67.
5. C. J. Cardin and A. Roy, *Inorg. Chim. Acta* 1985, **107**, L33, L37 and 57; 1986, **125**, 63.
6. R. Barbieri, L. Pellerito, G. Ruisi, M. T. Lo Giudice, F. Huber and G. Atassi, *Inorg. Chim. Acta* 1982, **66**, L39.
7. F. Huber, G. Roge, L. Carl, G. Atassi, F. Spreafico, S. Filippeschi, R. Barbieri, A. Silvestri, E. Rivarola, G. Ruisi, F. Di Bianca and G. Alonzo, *J. Chem. Soc., Dalton Trans.* 1985, 523.
8. M. F. Iskander, A. M. El Aggan, L. S. Refaat and L. El Sayed, *Inorg. Chim. Acta*, 1975, **14**, 167.
9. N. S. Biradar and B. R. Havinale, *Inorg. Chim. Acta* 1976, **17**, 157.
10. D. K. Rostogi, S. K. Sahni, V. B. Rana and S. K. Dua, *J. Coord. Chem.* 1978, **8**, 97; D. K. Rostogi, S. K. Sahni, Y. B. Rana and S. K. Dua, *Transition Met. Chem.* 1978, **3**, 56; S. K. Dua, D. K. Rostogi and S. K. Sahni, *J. Inorg. Nucl. Chem.* 1980, **42**, 1711.
11. M. F. Iskander, L. El Sayed, S. Saddeck and M. A. Abu Taleb, *Transition Met. Chem.* 1980, **5**, 168.
12. M. Mohan, A. Kumar, M. Kumar and N. K. Jha, *Inorg. Chim. Acta* 1987, **136**, 65; M. Mohan, N. S. Gupta, M. P. Gupta, A. Kumar, M. Kumar and N. K. Jha, *Inorg. Chim. Acta* 1988, **152**, 25.
13. L. El Sayed, M. F. Iskander, A. El Toukhy and S. E. Zayan, *Inorg. Chim. Acta* 1972, **6**, 663.
14. M. A. Ali, S. E. Livingstone and D. J. Phillips, *Inorg. Chim. Acta* 1973, **7**, 179.
15. R. Cefalu, R. Bosco, F. Bonati, F. Maggio and R. Barbieri, *Z. Anorg. Allg. Chem.* 1970, **376**, 180.
16. R. C. Poller, *J. Inorg. Nucl. Chem.* 1962, **24**, 593; K. Kawakami and R. Okawara, *J. Organomet. Chem.* 1966, **6**, 249.
17. R. Okawara and M. Wada, *Adv. Organomet. Chem.* 1967, **5**, 137.
18. J. P. Clark and C. J. Wilkins, *J. Chem. Soc. A* 1968, 3019; W. D. Honnick and J. J. Zuckerman, *J. Organomet. Chem.* 1979, **178**, 133.
19. K. Kawakami and T. Tanaka, *J. Organomet. Chem.* 1973, **49**, 409.
20. J. Otera, T. Hinoishi, Y. Kawabe and R. Okawara, *Chem. Lett.* 1981, 273.
21. J. Otera, *J. Organomet. Chem.* 1981, **221**, 57.
22. T. Mitchell, *J. Organomet. Chem.* 1974, **71**, 39.
23. G. Domazetis, R. J. Magge and B. D. James, *J. Organomet. Chem.* 1978, **148**, 339.
24. J. S. Shannon and J. M. Swan, *J. Chem. Soc., Chem. Commun.* 1965, 33.
25. M. J. Lacey and J. S. Shannon, *Org. Mass Spectrom.* 1972, **6**, 931.
26. P. Smith and L. Smith, *Chem. Brit.* 1975, **11**, 208.
27. A. Saxena and J. P. Tandon, *Polyhedron* 1983, **2**, 443.

Polyhedron Vol. 8, No. 23, pp. 2763–2767, 1989
Printed in Great Britain

0277–5387/89 $3.00+.00
© 1989 Pergamon Press plc

REACTIVITY OF DITHIOACETIC ACID TOWARD VANADOCENE: CRYSTAL STRUCTURE OF THE $[(\eta^5\text{-}C_5H_5)_4V_4(\mu_3\text{-}S)_4]$ CLUSTER

STAN A. DURAJ,* MARIA T. ANDRAS and BORIS RIHTER

Department of Chemistry, Cleveland State University, Cleveland, OH 44115, U.S.A.

(*Received* 5 *March* 1989; *accepted* 18 *July* 1989)

Abstract—The reaction between vanadocene and dithioacetic acid gave the novel product $[(\eta^5\text{-}C_5H_5)_4V_4(\mu_3\text{-}S)_4]$. The single-crystal X-ray structure of this low-valent vanadium cluster has been determined. The crystallographic data are: monoclinic space group $C2/c$, $a = 17.764(5)$, $b = 8.119(2)$, $c = 16.158(2)$ Å, $\beta = 116.65(2)°$, $V = 2083(2)$ Å^3, $Z = 4$. Refinement, using a data-to-parameter ratio of 12.0, converged with an unweighted discrepancy index of 4.99%. The molecule is located on a crystallographic two-fold rotation axis and consists of a central tetrahedron of vanadium atoms, each face of which is capped by a sulphur atom with vanadium–sulphur distances of 2.296(1) Å. There is a cyclopentadienyl ring coordinated to each vanadium atom with vanadium–carbon distances ranging from 2.281(9) to 2.319(7) Å. The vanadium–vanadium distance in $[V_4(\mu_3\text{-}S)_4(\eta^5\text{-}C_5H_5)_4]$ is 2.876(11) Å and corresponds to a metal–metal bond order of 2/3. The cluster is paramagnetic; $\mu_{eff} = 2.65\ \mu_B$.

Since the recognition by Cotton in the mid-1960s that metal atoms form direct bonds, the chemistry of transition metal compounds possessing metal–metal bonds has grown at an enormous rate.[1] Dinuclear complexes of early transition metals containing four carboxylato ligands of the type $[M_2(\mu\text{-}O_2CR)_4L_2]$ (M = Cr, Mo, W; R = alkyl or aryl groups; L = δ-donor ligands, e.g. H_2O, THF, etc.),[2] as well as dithio congeners such as $Mo_2(\mu\text{-}S_2CR)_4L_2$ (R = CH_3 or Ph; L = THF),[3] play a very important role in this development because such compounds have quadruple metal-to-metal bonds and serve as excellent starting materials for further preparative work. Several methods for synthesizing these tetracarboxylates have been developed including reactions of chromocene with various organic acids in which both cyclopentadienyl rings of the metallocene are displaced by the carboxylato ligands.[4,5] With regard to the group 5 (V) metals, however, such simple inorganic carboxylates are not reported, although the π-complexes $(\eta^5\text{-}C_5H_5)_2V$ and $(\eta^5\text{-}C_5Me_5)_2V$ readily react with benzoic acid to give $(\eta^5\text{-}C_5R_5)V(\mu\text{-}O_2CPh)_4V(\eta^5\text{-}C_5R_5)$, where R = H and Me, respectively.[6] The vanadium–vanadium distances of 3.636(1) Å for the cyclopentadienyl compound and 3.652(2) Å for the pentamethylcyclopentadienyl derivative suggest that little, if any, direct bonding exists between the two vanadium atoms.

In the course of our studies utilizing vanadocene and strong organic acidic ligands such as dithiocarboxylic acids—in the hope of removing both cyclopentadienyl groups—we discovered a new reaction between vanadocene and dithioacetic acid which leads to a V_4 compound possessing metal–metal bonds:

$$(\eta^5\text{-}C_5H_5)_2V + CH_3CSSH \rightarrow [(\eta^5\text{-}C_5H_5)_4V_4(\mu_3\text{-}S)_4].$$

In the present report we describe the new method of synthesis and characterization of the paramagnetic cluster $[(C_5H_5)_4V_4S_4]$. The results of a single-crystal X-ray diffraction study of $[(C_5H_5)_4V_4S_4]$ are also described.

EXPERIMENTAL

All operations of moisture- and air-sensitive materials were performed under an inert atmosphere employing standard Schlenk techniques and a double manifold vacuum-line. Solids were

* Author to whom correspondence should be addressed.

manipulated in a Vacuum Atmospheres Co. glove-box equipped with a HE-493 dri-train. Solvents were freshly distilled from benzophenone ketyl prior to use. Solutions were transferred via stainless steel cannulae and/or syringes. Vanadocene and dithioacetic acid were prepared according to literature methods.[7,8] Elemental analyses were performed by Galbraith Microanalytical Laboratories. The IR spectrum was measured on a Perkin–Elmer 599B spectrophotometer. The magnetic susceptibility was determined at room temperature on a MSB1 Johnson Matthey magnetic susceptibility balance. Corrections for diamagnetism were made with Pascal's constants.[9]

Preparation of $[cp_4V_4S_4]$

In a dry-box, a 250-cm^3 round-bottomed flask was charged with freshly sublimed vanadocene (0.6 g, 3.3 mmol). Under an inert atmosphere, the flask was connected to a double manifold vacuum-line through a U-shaped adapter with a septum. The starting material was dissolved in 100 cm^3 of THF–toluene mixture (v/v 75:25) and redistilled dithioacetic acid was added via syringe (0.5 cm^3, 6.7 mmol). The reaction mixture was stirred for 4 days, during which time the colour changed gradually from purple to brown. The volume was reduced in vacuum to about 15 cm^3 and the dark brown cluster was precipitated with 50 cm^3 of hexane. Recrystallization from toluene–hexane gave 0.231 g (47%) of $[(C_5H_5)_4V_4S_4]$. Single crystals with habits of rectangular blocks, suitable for X-ray diffraction studies, were grown by slow interdiffusion of hexane into a toluene solution of $[cpVS]_4$ in a Schlenk tube. Found: C, 38.72; H, 3.93. Calc. for $C_{20}H_{20}S_4V_4$: C, 40.55; H, 3.40%. IR (KBr, cm^{-1}): 3035(w), 1410(m), 1345(w), 1240(m), 1055(s, br), 995(s), 885(w), 825(sh), 785(s), 655(w), 540(w), 450(w, br), 405(w), 390(w), 375(w). Magnetic moment: $\chi_M = 2.92 \times 10^{-3}$ emu mol^{-1} at 298 K; $\mu_{eff} = 2.65\ \mu_B$.

X-ray crystallography

Single-crystal X-ray diffraction analyses were carried out by application of general procedures which were previously described.[10] The crystallographic parameters and basic information about data collection and structure refinement are summarized in Table 1. The data were corrected for Lorentz, polarization, crystal decay (17%) and absorption effects.

Systematic absences in the intensity data were indicative of the space groups *Cc* or *C2/c*. The structure was solved on the basis of a 3-D Patterson function, on the assumption of the space group being *C2/c*. All subsequent difference maps and least-square refinements revealed the rest of the cluster and justified the choice of this space group. All 14 atoms were refined anisotropically. The final difference Fourier map contained some residual electron density below 1 e/Å^3 in the immediate vicinity of the vanadium atoms; the largest peak was 0.75 e/Å^3.

Data collection and crystallographic calculations were carried out on a PDP-11/60 computer (at Cleveland State University), with software from the Enraf–Nonius SDP-PLUS package.

Tables of positional and isotropic equivalent displacement parameters, anisotropic displacement parameters, *B*'s, observed and calculated structure factors, as well as full lists of bond distances and angles for $[(C_5H_5)_4V_4S_4]$ have been deposited as supplementary material with the Editor.

RESULTS AND DISCUSSION

Synthesis

The reaction between vanadocene, $(C_5H_5)_2V$, and dithioacetic acid, CH_3CSSH, in THF and toluene at room temperature for 4 days affords a brown–black product proved by X-ray studies to contain $[(C_5H_5)_4V_4S_4]$ molecules. Additional support for the assigned formula is provided by elemental analyses, the IR spectrum and magnetic susceptibility data.

Our synthetic and X-ray studies contain several points of interest. The reaction shows a new pattern of reactivity for vanadocene. It represents a simple and direct route to a thio-capped tetranuclear vanadium(III) cluster which possesses short vanadium–vanadium distances (*vide infra*). Under mild conditions, desulphurization (or partial desulphurization) of the dithioacetic acid occurs. The parent unsubstituted cluster, $[(C_5H_5)_4V_4S_4]$, is crystallographically characterized for the first time.

Interestingly enough, cubane clusters of the type which we are describing in this report have been intensively studied for some time. This is perhaps because cubane cluster units are important in living systems and solid-state polymers.[11,12] Much attention was devoted to cubane compounds containing a larger number of electrons, for instance, $[(\eta^5\text{-}C_5H_5)_4Co_4(\mu_3\text{-}S)_4]$.[13] This cluster contains 72 electrons, and it possesses long non-bonding metal–metal distances (average value 3.298(2) Å). However, only recently, were electron-deficient cubane clusters, namely $[(MeC_5H_4)_4M_4S_4]$ where M = Ti[14] or V[14–16] and $[(C_5H_5)_4V_4S_4]$,[14,17] synthesized and their X-ray structures (for MeC_5H_4

Table 1. Crystallographic data for $[cp_4V_4S_4]$

Chemical formula	$V_4C_{20}H_{20}S_4$
Formula weight	592.41
Space group	$C2/c$
Systematic absences	hkl, $h+k \neq 2n$
	$h0l$, $l \neq 2n$
a (Å)	17.764(5)
b (Å)	8.119(2)
c (Å)	16.158(2)
β (°)	116.65(2)
V (Å^3)	2083(2)
Z	4
d_{calc} (g cm^{-3})	1.889
Crystal size (mm)	$0.40 \times 0.35 \times 0.30$
μ (Mo-K_α) (cm^{-1})	20.770
Data collection instrument	Enraf–Nonius CAD-4
Radiation (monochromated in incident beam)	Mo-K_α ($\lambda = 0.71073$ Å)
Orientation reflections, number, range (2θ)	25, $6.76 < 2\theta < 30.76$
Temperature (°C)	22
Scan method	ω–2θ
Data collection range, 2θ (°)	4, 55
Number of unique data, total with $F_o^2 > 3\sigma(F_o^2)$	1934
	1525
Number of parameters refined	127
Transmission factors, max., min.	0.9980, 0.8026
R^a	0.04996
$R_w{}^b$	0.05646
Quality-of-fit indicator^c	1.611
Largest shift/ESD, final cycle	0.00
Largest peak (e/Å^3)	0.75

^{a} $R = \Sigma||F_o|-|F_c||/\Sigma|F_o|$.
^{b} $R_w = [\Sigma w(|F_o|-|F_c|)^2/\Sigma w|F_o|^2]^{1/2}$; $w = 1/\sigma^2(|F_o|)$.
^{c} Quality-of-fit $= [\Sigma w(|F_o|-|F_c|)^2/(N_{obs}-N_{parameters})]^{1/2}$.

derivatives) and bonding studied.[14] Two methods for the preparation of the vanadium compounds were reported. The Rauchfuss' group prepared $[(MeC_5H_4)_4V_4S_4]$ (45% yield) and $[(C_5H_5)_4V_4S_4]$ (27% yield) by desulphurization of $[(Mecp)_2V_2S_4]$ and $[cp_2V_2S_4]$, respectively, with PBu_3. The Russian workers obtained these cubanes by reacting $(Mecp)_2V$ or cp_2V with *t*-BuSH. The yield of 60% is reported only for the methyl derivative.

In this context, the synthetic reaction reported here, which involves cp_2V and CH_3CSSH, represents a new route to the $[(C_5H_5)_4V_4S_4]$ cluster in yields of *ca* 47%.

Molecular structure

The crystal structure of $[(\eta^5\text{-}C_5H_5)V_4(\mu_3\text{-}S)_4]$ is composed of discrete tetranuclear molecules. Important interatomic distances and angles are listed in Tables 2 and 3, respectively. Complete lists of distances and angles are included in the supplementary material. An ORTEP drawing of the molecular structure of the $[cp_4V_4S_4]$ cluster is shown in Fig. 1. The tetranuclear molecule is located on a crystallographic two-fold rotation axis and consists of two interpenetrating tetrahedra, V_4 within S_4, and therefore can be viewed as a distorted cube. Additionally, each vanadium atom coordinates to a cyclopentadienyl ligand. The averaged* values of important interatomic distances (in Å) are as follows: V—V, 2.876(11); V—S, 2.296(1); V(1)—Ccp, 2.293(3); V(2)—Ccp, 2.301(6); S—S, 3.548(13). The averaged values of V—S—V and S—V—S angles (in deg.) are 77.6(3) and 101.1(5), respectively. Additonally, the averaged values of V—V—V and S—S—S angles (in deg.) are 60.0(3) and 60.0(3), respectively and are nearly equal to the angles of an ideal tetrahedron.

The overall structure of our cluster is very similar to that of the $[(\eta^5\text{-}MeC_5H_4)_4V_4(\mu_3\text{-}S)_4]$ compound

* Chemically equivalent distances were averaged. $[\chi]$ is defined as $[\chi]^2 = \Sigma\Delta_i^2/n(n-1)$ for the deviations, Δ_i of n independent values.

Table 2. Important interatomic distances (Å) for $[cp_4V_4S_4]$[a]

V(1)—V(1)′	2.874(2)	S(2)—S(2)′	3.555(2)
V(1)—V(2)	2.853(2)	V(1)—S(1)	2.298(2)
V(1)—V(2)′	2.905(1)	V(1)—S(2)	2.300(2)
V(2)—V(2)′	2.873(1)	V(1)—S(2)′	2.294(1)
S(1)—S(1)′	3.549(2)	V(2)—S(1)	2.292(2)
S(1)—S(2)	3.577(2)	V(2)—S(1)′	2.298(2)
S(1)—S(2)′	3.512(2)	V(2)—S(2)	2.295(2)
V(1)—C(1)	2.296(7)	V(2)—C(6)	2.319(7)
V(1)—C(2)	2.295(6)	V(2)—C(7)	2.300(8)
V(1)—C(3)	2.297(7)	V(2)—C(8)	2.282(6)
V(1)—C(4)	2.281(9)	V(2)—C(9)	2.304(2)
V(1)—C(5)	2.298(9)	V(2)—C(10)	2.303(7)

[a] Numbers in parentheses are ESDs in the least significant digits.

Table 3. Important interatomic angles (°) for $[cp_4V_4S_4]$[a]

V(1)′—V(1)—V(2)	60.95(4)	V(1)—S(1)—V(2)	76.88(6)
V(1)′—V(1)—V(2)′	59.17(4)	V(1)—S(1)—V(2)′	78.42(6)
V(2)—V(1)—V(2)′	59.85(3)	V(2)—S(1)—V(2)′	77.50(6)
V(1)—V(2)—V(1)′	59.87(4)	V(1)′—S(2)—V(1)	77.44(5)
V(1)—V(2)—V(2)′	60.96(3)	V(1)′—S(2)—V(2)	78.53(5)
V(1)′—V(2)—V(2)′	59.19(3)	V(1)—S(2)—V(2)	76.77(6)
S(1)′—S(1)—S(2)	59.06(4)	S(1)—V(1)—S(2)	102.14(7)
S(1)′—S(1)—S(2)′	60.86(5)	S(1)—S(2)—S(2)′	99.79(6)
S(2)—S(1)—S(2)′	60.19(4)	S(2)—V(1)—S(2)′	101.39(7)
S(1)—S(2)—S(1)′	60.08(4)	S(1)—V(2)—S(1)′	101.30(6)
S(1)—S(2)—S(2)′	59.01(4)	S(1)—V(2)—S(2)	102.45(7)
S(1)′—S(2)—S(2)′	60.80(4)	S(1)′—V(2)—S(2)	99.77(7)

[a] Numbers in parentheses are ESDs in the least significant digits.

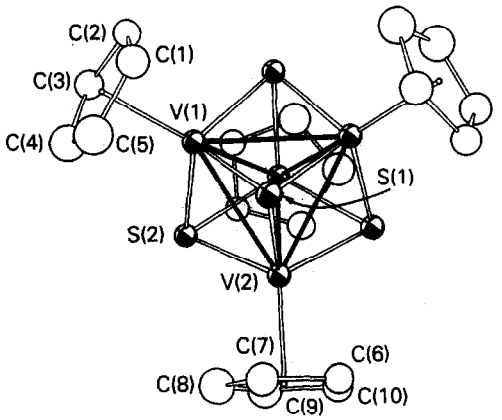

Fig. 1. An ORTEP drawing of the $[cp_4V_4S_4]$ molecule which also defines the labelling scheme. The thermal ellipsoids enclose 30% of electron density.

mentioned above.[14] The methyl derivative crystallizes in the cubic space group $P\bar{4}3n$ with $a = 16.551(3)$ Å. All important interatomic distances and angles for the methyl analogue are almost identical to those of the parent $[(C_5H_5)_4V_4S_4]$ cluster. Thus, the reported selected values of distances (in Å) and angles (in deg.) for the $[(MeC_5H_4)_4V_4S_4]$ cubane are:[14] V—V(av.), 2.873(3); V—S(av.), 2.295(3); V—Ccp(av.), 2.28(1); V—S—V(av.), 77.5(1); S—V—S(av.), 101.1(1).

Metal–metal bonding

The electronic structure of $[(C_5H_5)_4V_4S_4]$ was calculated by the SCF-scattered wave-X_α method to give the ground-state configuration for this cluster's metal bonding orbitals as $a_1^2e^4t_2^2$ (for ideal T_d symmetry).[14]

Because the total number of metal bonding electrons in $[(C_5H_5)_4V_4S_4]$ is eight, we calculate a vanadium–vanadium bond order of 2/3 for this 56-electron cluster. This is in excellent agreement with our crystallographically determined vanadium–vanadium distance of 2.876(11) Å. A very similar distance was found in the $[Nb_3O_2(O_2CMe_3)_6(THF)_3]BPh_4$ cluster, in which the niobium–niobium bond order is 2/3 (the distance: 2.842(3) Å),[18] whereas single and double vanadium–

vanadium bond distances of *ca* 2.61 and 2.41 Å in $(i\text{-PrC}_5H_4)_2V_2S_4$[19] and $V_2(\text{salophen})_2Na_2(THF)_6$,[20] respectively, are, of course, shorter as expected for higher bond orders. The $[(C_5H_5)_4V_4S_4]$ cluster is paramagnetic, and we find its magnetic moment to be equal to 2.65 μ_B at 298 K, which is in accord with literature values for $[(MeC_5H_4)_4V_4S_4]$, viz. 2.68[14] and 2.67 μ_B[15].

Further work is in progress to explore the reactivity of aromatic dithiocarboxylic acids. Additional preliminary data (e.g. elemental analyses) point out that dithiobenzoic acid reacts with vanadocene to give a different compound. More results in this new area will be reported in due course.

Acknowledgements—This research was supported by the donors of the Petroleum Research Fund, administered by the American Chemical Society. We also thank Cleveland State University for the Research Creative Activity Award and the Research Challenge grant approved by the Ohio Board of Regents for support of this work.

REFERENCES

1. F. A. Cotton and R. A. Walton, *Multiple Bonds Between Metal Atoms*. John Wiley, New York (1982); F. A. Cotton and R. A. Walton, *Struct. Bond. (Berlin)* 1985, **62**, 1; M. H. Chisholm and I. P. Rothwell, *Progr. Inorg. Chem.* 1982, **29**, 1; M. H. Chisholm, *Polyhedron* 1987, **6**, 665 (Symposia-in-Print, "Recent Advances in the Chemistry of Metal–Metal Multiple Bonds").
2. F. A. Cotton and G. Wilkinson, *Advanced Inorganic Chemistry*. John Wiley, New York (1988).
3. F. A. Cotton, P. E. Fanwick, R. H. Niswander and J. C. Sekutowski, *Acta Chem. Scand.* 1978, **A32**, 663.
4. F. A. Cotton, X. Feng, P. A. Kibala and M. Matusz, *J. Am. Chem. Soc.* 1988, **110**, 2807.
5. F. A. Cotton, M. W. Extine and G. W. Rice, *Inorg. Chem.* 1978, **17**, 176.
6. F. A. Cotton, S. A. Duraj and W. J. Roth, *Organometallics* 1985, **4**, 1174.
7. R. B. King, *Organometallic Syntheses*. Academic Press, New York (1965).
8. J. Houben and H. Pohl, *Chem. Ber.* 1907, **40**, 1303.
9. A. Earnshaw, *Introduction to Magnetochemistry*. Academic Press, New York (1968).
10. See, for example: A. Bino, F. A. Cotton and P. E. Fanwick, *Inorg. Chem.* 1979, **18**, 3558 or G. C. Campbell, J. A. M. Canich, F. A. Cotton, S. A. Duraj and J. F. Haw, *Inorg. Chem.* 1986, **25**, 287.
11. B. A. Averill and W. H. Orme-Johnson, *Metal Ions in Biological Systems* (Edited by H. Siegel), Vol. VII. Marcel Dekker, New York (1978).
12. K. Hiebl, M. J. Sienko and P. Rogel, *J. Less-Common Met.* 1981, **82**, 21.
13. G. L. Simon and L. F. Dahl, *J. Am. Chem. Soc.* 1973, **95**, 2164.
14. J. Darkwa, J. R. Lockemeyer, P. D. W. Boyd, T. B. Rauchfuss and A. L. Rheingold, *J. Am. Chem. Soc.* 1988, **110**, 141.
15. I. L. Eremenko, A. A. Pasynskii, A. S. Katugin, O. G. Ellert, V. E. Shklover and Y. T. Struchkov, *Bull. Acad. Sci. USSR, Div. Chem. Sci.* (Engl. Transl.) 1983, 1531.
16. A. A. Pasynskii, I. L. Eremenko, A. S. Katugin, G. S. Gasanov, E. A. Turchanova, O. G. Ellert, Y. T. Struchkov, V. E. Shklover, N. T. Berberova, A. G. Sogomonova and O. Y. Okhlobystin, *J. Organomet. Chem.* 1988, **344**, 195.
17. A. A. Pasynskii, I. L. Eremenko and V. T. Kalinnikov, *Bull. Acad. Sci. USSR, Div. Chem. Sci.* (Engl. Transl.) 1976, 2655.
18. F. A. Cotton, S. A. Duraj and W. J. Roth, *J. Am. Chem. Soc.* 1984, **106**, 3527.
19. C. M. Bolinger, R. B. Rauchfuss and A. L. Rheingold, *J. Am. Chem. Soc.* 1983, **105**, 6321.
20. S. Gambarotta, M. Mazzanti, C. Floriani and M. Zehnder, *J. Chem. Soc., Chem. Commun.* 1984, 1116.

Polyhedron Vol. 8, No. 23, pp. 2769–2776, 1989
Printed in Great Britain

0277-5387/89 $3.00+.00
Pergamon Press plc

COMPLEXES OF PALLADIUM, PLATINUM AND RHODIUM WITH POTENTIALLY TETRADENTATE LIGANDS CONTAINING NITROGEN AND TELLURIUM DONOR ATOMS (N_2Te_2)

N. I. AL-SALIM and W. R. McWHINNIE*

Department of Chemical Engineering and Applied Chemistry, Aston University, Aston Triangle, Birmingham B4 7ET, U.K.

(*Received* 7 *February* 1989; *accepted* 20 *July* 1989)

Abstract—Complexes of the ligands 1,6-bis-2-butyltellurophenyl-2,5-diazahexa-1,5-diene (**I**) and 1,4-bis-2-butyltellurophenyl-2,3-diazabuta-1,3-diene (**II**) with palladium, platinum, and rhodium are described. [PdCl(**I**)(H_2O)]Cl is an electrolyte and has the chloro-ligand *trans* to water; the implications for the mode of coordination of **I** are discussed. For [$PdCl_2$(**II**)] evidence for both "*cis*" and "*trans*" isomers is obtained; since, as in the above case, no evidence for N-coordination is obtained, the nature of the "*trans*" isomer is debated. [PtCl(**I**)(H_2O)]Cl, an electrolyte, decomposes in polar solvents to give [$PtCl_2$(I^{2-})], where (I^{2-}) donotes ligand **I** which has lost two butyl groups, the complex being a platinum(IV) derivative. Ligand **I** coordinates only via tellurium in the platinum(II) complex, but some evidence of N-coordination to platinum(IV) is obtained. The early stages of the de-alkylation reaction are monitored by ^{125}Te and ^{195}Pt NMR spectroscopy. By contrast, [$PtCl_2$(**II**)]·H_2O is a *cis* complex in which **II** coordinates via tellurium only and does not undergo de-alkylation. Some complexes of both rhodium(III) and rhodium(I) are reported. The most interesting observation being that **I** may function as a terdentate ligand (Te, N, Te) in [RhCl(**I**)].

We have recently published papers describing the syntheses of potentially bidentate Te, Te ligands[1] of the type $RTe(CH_2)_nTeR$, and of ligands containing both tellurium and nitrogen as potential donor atoms, e.g. derivatives of tellurated 2-phenylpyridine[2] and 1,6-bis-2-butyltellurophenyl-2,5-diazahexa-1,5-diene (**I**),[3] together with 1,4-bis-2-butyltellurophenyl-2,3-diazabuta-1,3-diene (**II**).

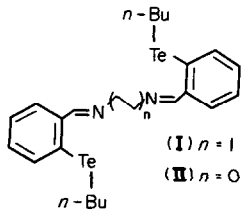

(**I**) $n = 1$
(**II**) $n = 0$

Some investigations on the coordination chemistry of these materials have been reported. For example, the reactions of (p-EtO·C_6H_4)Te(CH_2)$_n$Te (C_6H_4OEt-p) (n = 5–10) with palladium(II), platinum(II) and mercury(II) have been described.[4] The complexes were poorly crystalline and tended to have a limited range of thermal stability which limited the information obtainable from multinuclear NMR studies. The crystal structure of compound **I** has been reported together with that of the complex with $HgCl_2$[5] in which only the two tellurium atoms coordinated mercury(II).

In this paper we attempt to extend studies of **I** in complexes with palladium, platinum and rhodium. The literature contains a paucity of reports on bi- and multidentate tellurium ligands, although many sulphur systems are known. Of relevance is the report by Bertini *et al.*[6] on Schiff base ligands having donor sets S, N and S_2N_2, including an analogue of **I** in which —SH replaces —TeBu. Blum *et al.*[7] have also produced a related sulphur ligand which forms square-planar complexes with a range

* Author to whom correspondence should be addressed.

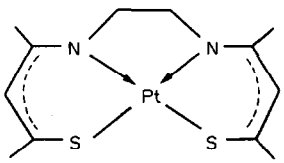

(III)

of divalent metals, e.g. ligand **III**. An interesting feature of the crystal structure of **I**[5] was a weak Te---N interaction. One objective of this paper is to ascertain to what extent this interaction limits the availability of the nitrogen for coordination to the added transition metal salt.

EXPERIMENTAL

The details of the preparations of **I** and **II** appear elsewhere.[3,5]

(a) *Palladium complexes*

With ligand **I**. Bis(benzonitrile)dichloropalladium(II)[8] (0.38 g, 0.001 mol) in acetonitrile (15 cm^3) was added to an acetonitrile (15 cm^3) solution of **I** (0.60 g, 0.001 mol), and the mixture was stirred at room temperature, under dinitrogen, for 2 h. The volume was reduced to 5 cm^3 in a stream of dinitrogen gas and benzene was added to precipitate a brown compound, which was filtered, washed with benzene and diethyl ether and dried *in vacuo*. The yield of the blackish-brown material was 0.67 g, m.p. 131–132°C (dec.).

With ligand **II**. Two methods were used: (i) Bis(benzonitrile)dichloropalladium(II) (0.38 g, 0.001 mol) in a 1:1 benzene–acetonitrile mixture (15 cm^3) was treated with a warm acetonitrile solution (15 cm^3) of **II** (0.58 g, 0.001 mol). The mixture was stirred at 50°C under dinitrogen for 5 h to give a brown precipitate which was collected by filtration and washed several times with benzene. Recrystallization from toluene gave a brownish-red compound, m.p. 183–185°C (dec.).

(ii) A solution of $[Ph_4As][PdCl_4]$ (prepared by metathesis of Ph_4AsCl and K_2PtCl_4) (0.20 g, 0.0002 mol) in dichloromethane (15 cm^3) was added slowly, with stirring, to a solution of **II** (0.115 g, 0.0002 mol) in dichloromethane (10 cm^3). On setting aside for 2 h the solution deposited an orange–brown compound which was separated, washed with dichloromethane and air-dried (yield: 0.136 g); m.p. 185°C (dec.).

(b) *Platinum complexes*

With ligand **I**. Two methods were used: (i) A solution of $[Ph_4As]_2[PtCl_4]$ (1.103 g, 0.001 mol) in dichloromethane (20 cm^3) was added to **I** (0.60 g, 0.001 mol) in dichloromethane (15 cm^3) and refluxed for 1 h, during which time a pale cream suspension formed. The compound was collected by filtration, washed with dichloromethane and air-dried. During the melting point determination the compound darkened at 80°C, became black, but failed to melt under 300°C.

(ii) The same experiment was carried out in refluxing acetonitrile. The cream suspension was visible for the first 15 min, but when reflux was continued beyond that point the product became brownish. After 2 h, a dark brown solution and solid were present, the solid was filtered, washed with acetonitrile and dried *in vacuo*. The material failed to melt under 300°C.

With ligand **II**. A solution of $[Ph_4As]_2[PtCl_4]$ (0.22 g, 0.0002 mol) in dichloromethane (15 cm^3) was added slowly, with stirring, to a solution of **II** (0.115 g, 0.002 mol) in dichloromethane (10 cm^3). The resulting solution was stirred and heated under reflux for 5 h. The orange precipitate so formed was filtered, washed with dichloromethane and air-dried (Yield: 0.10 g); m.p. 170°C (dec.).

(c) *Rhodium complexes*

With ligand **I**. (i) *Thodium*(III): Dipotassium pentachloroaquorhodate(III), $K_2[Rh(H_2O)Cl_5]$ (supplied) (0.38 g, 0.001 mol), in a mixture of methanol (20 cm^3) and DMSO (10 cm^3) was reacted with a warm solution of **I** (0.60 g, 0.001 mol) in methanol (10 cm^3). The mixture was stirred for 2 h under dinitrogen, after which the methanol was removed *in vacuo*; the remaining solution was allowed to evaporate slowly at room temperature. The resulting solid was dissolved in dichloromethane (20 cm^3) and filtered, the filtrate, after evaporation at room temperature, afforded a brown solid, m.p. 122°C.

(ii) *Rhodium*(I): Method A. Di-μ-chloro-bis(η^4-1,5-cyclooctadiene)dirhodium(I)[9] (0.15 g, 0.0003 mol) in dichloromethane (10 cm^3) was added to a solution of **I** (0.36 g, 0.0006 mol) in dichloromethane (15 cm^3). The colour changed immediately to brown. Following reflux (4 h) the colour of the solution became red–brown and some precipitate deposited. Filtration afforded a red–violet solid (product A) which was washed with dichloromethane and air-dried (yield: 0.02 g); m.p. 243°C (dec.). Dry diethyl ether was added to the filtrate to give a brown material which was redissolved in ethanol, filtered and recovered by evaporation at room temperature: product B, yield: 0.26 g, m.p. 185°C (dec.).

Method B. Di-μ-chloro-bis(η^4-1,5-cyclooctadiene)dirhodium(I) (0.15 g, 0.0003 mol) was dis-

solved in dichloromethane (10 cm^3) and added to **I** (0.54 g, 0.0009 mol) in dichloromethane (10 cm^3) at room temperature. The mixture was refrigerated at 4°C for 4 h, after which the solution was filtered to give a red–violet crystalline compound (product A) which was washed with dichloromethane (yield: 0.1 g); m.p. 243°C (dec.). The filtrate was treated with diethyl ether as described above to give a further quantity (0.28 g) of product B, m.p. 186°C (dec.). The elemental analytical data for A and B were independent of the method of preparation.

With ligand **II**. (i) *Rhodium*(III): $K_2[Rh(H_2O)Cl_5]$ (0.19 g, 0.0005 mol) was dissolved in ethanol–DMSO (1 : 1, 20 cm^3) and treated with a solution of **II** (0.29 g, 0.0005 mol) in ethanol (10 cm^3). The mixture was stirred at 80°C under dinitrogen for 2 h, during which time the colour changed from orange to dark brown. The solution was taken to 5 cm^3 *in vacuo* and left to evaporate at room temperature. The resulting solid was dissolved in chloroform, recovered by removal of solvent *in vacuo* and washed with methanol followed by diethyl ether, m.p. 160°C (dec.).

(ii) *Rhodium*(I): Di-μ-chloro-bis(η^4-1,5-cyclooctadiene)dirhodium(I) (0.25 g, 0.0005 mol) in dichloromethane (15 cm^3) was added slowly to a solution of **II** (0.58 g, 0.001 mol) and refluxed for 7 h under dinitrogen. The colour changed from orange to deep brown, the solution was cooled and treated with diethyl ether to give a brown compound which was filtered, washed with diethyl ether and air-dried (yield: 0.51 g); m.p. 220°C (dec.).

Physical measurements

Elemental analyses were carried out by the Analytical Services Unit, Aston University. NMR spectra (^1H, 90 MHz; ^{13}C, 22.5 MHz; ^{125}Te, 28.2 MHz; ^{195}Pt, 21.46 MHz) were obtained with a JEOL FX 90Q spectrometer. Conductivities were measured using a standard Mullard bridge and an immersion-type bright platinum electrode cell (E 7591/B). IR spectra were determined as KBr pellets or Nujol mulls with a Perkin–Elmer 599B instrument (range 4000–200 cm^{-1}). UV–vis spectra were recorded with a Unicam SP8-100 instrument.

DISCUSSION

Table 1 gives the stoichiometries of the complexes. Where the presence of water is involved, IR support for this is available. Although precautions were taken to exclude air from the preparations, no particular precautions were taken for the exclusion of moisture.

Of importance to this work is the complex of mercury(II) chloride and 1,6-bis-2-butyltellurophenyl-2,5-diazahexa-1,5-diene (**I**), the structure of which has been reported.[5] Only the tellurium atoms coordinate mercury, the weak but significant Te---N contact remains almost unaltered in the complex (Te---N, 2.773 Å—free ligand; 2.752, 2.786 Å—complex). Formally, the mercury(II) complex contains a 13-membered chelate ring, but if the Te---N interaction is taken as a bond then

Table 1. Analytical data for new complexes

Complex	Found (%)			Required (%)		
	C	H	N	C	H	N
$[PdCl_2(I)]\cdot H_2O$ (**1**)	35.8	4.3	3.4	36.1	4.3	3.5
$[PdCl_2(II)]^a$ (**2**)	35.4	3.8	3.7	35.1	3.7	3.7
$[PdCl_2(II)]^b$ (**3**)	35.2	3.7	3.5	35.1	3.7	3.7
$[PtCl_2(I)]\cdot H_2O^c$ (**4**)	32.1	3.5	3.1	32.5	3.9	3.1
$[PtCl_2(I^{2-})]\cdot 2H_2O^d$ (**5**)	24.7	2.3	3.3	24.3	2.3	3.5
$[PtCl_2(II)]\cdot H_2O$ (**6**)	30.3	3.2	3.0	30.7	3.5	3.2
$[RhCl_3(I)]\cdot 2H_2O$ (**7**)	34.1	4.0	3.8	34.0	4.3	3.3
$[RhCl_3(II)]\cdot H_2O$ (**8**)	32.8	3.4	3.5	32.9	3.7	3.5
$[RhCl(I)]^e$ (**9**)	38.5	4.4	3.5	38.8	4.3	3.7
$[RhCl(I)]^f_{1.08}$ (**10**)	39.4	4.6	3.8	39.4	4.4	3.8
$[RhCl(II)]$ (**11**)	36.7	3.9	3.8	37.0	4.0	3.9

[a] Method (i).
[b] Method (ii).
[c] From $[Ph_4As]_2[PtCl_4]$ in CH_2Cl_2.
[d] From $[Ph_4As]_2[PtCl_4]$ in CH_3CN; I^{2-} is derived from **I** by loss of butyl groups.
[e] "Product A".
[f] "Product B".

the mercury(II) ion "sees" a seven-membered ring. The change in the ligand ν(C=N) frequency on complexing mercury(II) is $+5$ cm^{-1}, thus changes of this order are likely to imply that the Te---N interaction in the coordinated ligand remains intact and that the ligand functions as a Te, Te bidentate. It is not unreasonable to apply similar reasoning to ligand **II**. Thus, inspection of Table 2 suggests that only in the cases of complexes **9** and **10** need the question of nitrogen coordination be considered. Complex **5** comes into this category, but is clearly a complex of a derived ligand (*vide infra*).

Palladium(II) *complexes*

[$PdCl_2$(**I**)]·H_2O (compound **1**, Tables 1 and 2) is a 1 : 1 electrolyte in both DMSO and acetonitrile, thus the formulation [Pd(**I**)Cl(H_2O)]Cl is suggested. In the IR spectrum ν(OH) is noted at 3400 cm^{-1} and the position of ν(C=N) (Table 2) implies Te,Te coordination only; ν(PdCl) may be assigned at 345 cm^{-1}. It is known that ν(PdCl) for [PdClL′L_2]$^+$, where L′ = neutral ligand and L = phosphine, is a function of L′ in the *trans* isomer.[10] It is also known that the *trans* influence decreases in the order: C-donors (sp^3 > sp^2 > sp) > P-donors > As-donors > S-donors > N-donors > halide > O-donors; also Te-donors > Se-donors > S-donors.[11] Thus in the present complex the value of 345 cm^{-1} suggests that the chloro-ligand is *trans* to oxygen. We also note that for[12] *trans*-{Pd[Te(CH_2SiMe_3)$_2$]$_2$$Cl_2$}, ν(PdCl) = 348 cm^{-1} and for[13] *trans*-{Pd[Te(C_6H_4·OEt-*p*)$_2$]$_2$$Cl_2$}, ν(PdCl) = 351 cm^{-1}.

The above data suggest that the structure of the complex may be more complex than at first imagined. One model would have the ligand spanning *trans* coordination sites, however, given that the Te---N interaction is retained we feel that the ligand is too inflexible for this to be realistic (the TeĤgTe angle is 109.1°).[5] An alternative model is given in Fig. 1. This type of dimer has been suggested for complexes of RTe(CH_2)$_8$TeR.[4] The conductivities would now be 228 (MeCN) and 70 (DMSO) Ω^{-1} cm^2 mol^{-1}, values not inconsistent with 2 : 1 electrolytes. Geometric isomers are possible but the available data would make differentiation difficult. Unfortunately, limited solubility prevented a comprehensive NMR study.

[$PdCl_2$(**II**)] (compound **2**, Tables 1 and 2) is a non-electrolyte in benzonitrile and is insoluble in more polar solvents. We argue that the position of ν(C=N) suggests that the ligand is bidentate (Te,Te), in which case the metal "sees" a five-membered chelate ring if the Te---N interactions remain intact. Two ν(PdCl) frequencies are seen at 332 and 288 cm^{-1} suggestive of a *cis* complex, although the ν_{as}(PdCl) frequency at 332 cm^{-1} is rather higher than the range normally associated with this mode (305–312 cm^{-1}), however, ν_s(PdCl) is usually assigned between 285–292 cm^{-1}.[14,15] Attempts to recrystallize this complex from chloroform led to the recovery of material having the same

Table 2. Physical data for new complexes

Complex[a]	ν(C=N) (cm^{-1})	$\Delta\nu$(C=N)	ν(M—Cl) (cm^{-1})	UV–vis spectra maxima (nm)	Λ_M (Ω^{-1} cm^2 mol^{-1})
Ligand **I**	1637			366	
Ligand **II**	1616			410	114 (MeCN)
1	1635	−2	345	464, 384	35 (DMSO)
2	1622	+6	332, 288	435, 355, 320	
3	1622	+6	335, 290		
2′[b]	1620	+4	332, 289, 345		
4	1625	−12	315	464, 384	35 (DMSO)
5	1615	−22			12 (DMSO)
6	1626	+10	325, 295	425, 360	
7	1640	+3	322	395	20 (DMSO)
8	1620	+4	340, 365	412	6 (DMSO)
9	1632, 1595	−5, −42	300		11 (CH_3CN)
10	1660, 1595	+23, −42		660, 555, 390, 315, 295	
11	1610	−6			7 (CH_3CN)

[a] See Table 1.

[b] Compound **2** after digestion in $CHCl_3$.

Note: the complex [$HgCl_2$(**I**)][5] gives ν(C=N) at 1642 cm^{-1}, i.e. $\Delta\nu$(C=N) = +5 cm^{-1}.

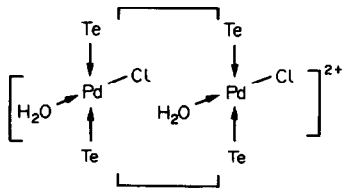

Fig. 1.

elemental analysis but with a new ν(PdCl) frequency at 345 cm^{-1}, in addition to those already noted. This appears to indicate the presence of a "*trans*" isomer which, for reasons given above, would have to be modelled on Fig. 1. Thus the available data suggest that either of the two equilibria (A) or (B) (see Scheme 1) could provide an explanation of the observations.

The UV–vis spectra (Table 2) of **1** and **2** are consistent with square-planar palladium; for example bands around 420 nm have been reported for other ditellurium complexes.[4]

Platinum complexes

Compounds **4** and **6** (Tables 1 and 2) have the stoichiometry $[PtCl_2(L)]\cdot(H_2O)$ (L = **I** or **II**). In neither case does the shift in ν(C=N) from the free ligand value seem large enough to invoke nitrogen coordination. Compound **4** has a Λ_M value consistent with that for a 1:1 electrolyte (but see below). The single ν(PtCl) frequency at 315 cm^{-1} suggests that the chloro-ligand is *trans* to groups with moderate *trans* influence;[11] of particular interest is a comparison with the complex $[Pt(bmsp)Cl]PF_6$,[16] where bmsp = $(MeSeCH_2CH_2)_2Se$, which has ν(PtCl) at 320 cm^{-1}. Thus the probability is that chlorine is *trans* to tellurium rather than to H_2O.

The ^{125}Te NMR of complex **4** was measured in DMSO, but not without gentle heating to obtain a clear solution of the appropriate concentration. It was noted that the colour of the solution had become slightly brown during the dissolution process. The observed spectrum (Fig. 2) shows two resonances centred at δ 469.5 and 512.2 ppm downfield from dimethyltelluride. Both resonances have associated satellites arising from spin–spin coupling to ^{195}Pt (δ 469.5 ppm J(PtTe) = 1014 Hz; δ 512.2 ppm J(PtTe) = 1035 Hz), thus demonstrating that both signals originate from tellurium bound to platinum. The observed coupling constants support the IR implication of *cis*-tellurium atoms, since for *trans*-TePtTe, J(PtTe) is generally of the order of 600 Hz.[4,15] Further, the ^{125}Te chemical shift of the resonance at 512.2 ppm also supports a *cis* configuration since $\Delta(\delta)$ (the coordination shift) for *trans* complexes is generally greater than the 47.8 ppm observed here.[4,15] The second tellurium resonance is, however, at 469.5 ppm, close to the free ligand value of 464.4 ppm, but it cannot arise from uncoordinated tellurium since J(PtTe) is clearly seen. No evidence for the coupling of inequivalent tellurium atoms is seen (however, J(TeTe) may be small or apparently zero due to multiple transmission paths), also the resonances are of unequal intensity; we believe this to imply that the resonances arise from different solution species. *Cis–trans* isomers are eliminated by the similar values of J(PtTe). A common phenomenon in group 16 ligand chemistry is the observation of *meso* and DL isomers which may arise due to inversion at the coordinated S, Se, or Te ligand atoms of the bidentate ligands.[16,17] It is anticipated that the barrier to inversion at tellurium will be greater than for selenium and sulphur,[18] thus distinct signals from the *meso* and DL invertomers may well be seen at ambient temperature. Although it had been suggested previously that chemical shift differences between *meso* and DL invertomers may be small,[4] a recent paper[19] demonstrates, for platinum(II) complexes of $[RTeCH_2CH_2CH_2CH_2TeR]$ (R = Me, Ph), that chemical shift differences of 63 ppm {for $[Pt(MeTe(CH_2)_3TeMe)Cl_2]$} and 26 ppm {for $[Pt(PhTe(CH_2)_3TePh)Cl_2]$} are possible for the invertomers; however both invertomers show large *coordination* shifts.[19] Thus we believe that the species observed may not be accounted for in terms of invertomers.

The reaction of $[Ph_4As]_2[PtCl_4]$ with **I** in refluxing acetonitrile gives complex **5** (Table 1), which analyses as a complex of de-butylated **I**. IR data

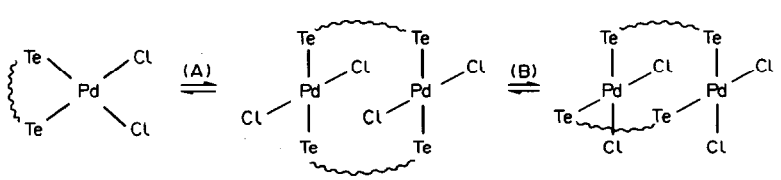

Scheme 1.

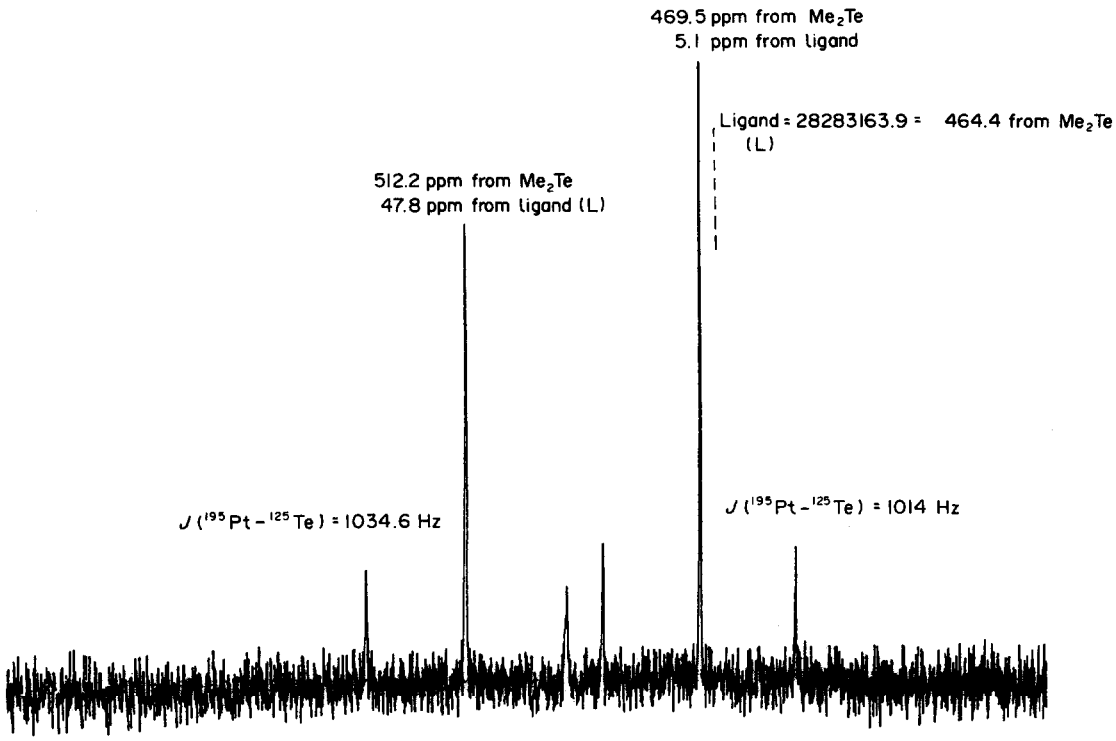

Fig. 2.

support the postulate of de-butylation and complex **5** is therefore, by implication, a complex of platinum(IV) (see Fig. 3).

The shift of ν(C=N) for de-butylated **I** is also greater than for other palladium and platinum complexes in Table 1, and this must raise the possibility of $Pt^{IV} \leftarrow N$ coordination in complex **5**. The final formation of complex **5** does then raise the possibility that the species giving a chemical shift of δ 469.5 ppm in the ^{125}Te NMR spectrum is a complex of de-butylated **I**. It is improbable that the species seen is a complex of platinum(IV), since if similar platinum(II)–platinum(IV) complexes are compared $J_{PtX}(Pt^{IV}) \simeq 0.67\ J_{PtX}(Pt^{II})$[20] (where X = ligand atom), whereas J(PtTe) for the two species are virtually identical. Thus, if the species with $\delta(^{125}Te)$ at 469.5 ppm is a complex of the de-butylated ligand, the solvent DMSO must be implicated [eq. (1)]:

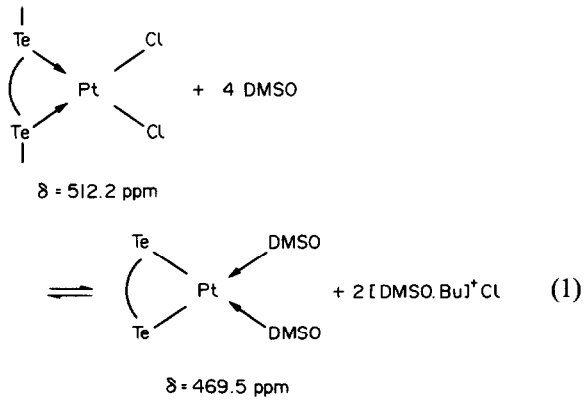

(1)

Rainville and Zingaro[21] have demonstrated that 10-methylphenoxatelluronium iodide will readily form $[(CD_3)_2SO(Me)]^+I^-$ in $(CD_3)_2SO$; since there is Mössbauer evidence that, electronically, tellurium experiences similar environments in R_3Te^+ and $R_2Te \rightarrow Pt$,[22,23] the postulate of facile de-butylation of coordinated **I** in DMSO is reasonable. The model of tellurium de-butylation mirrors a phenomenon well known for organosulphur[24] and organoselenium[25] ligands.

Further NMR and conductivity work was then carried out. Thus the ^{1}H NMR spectrum of a solu-

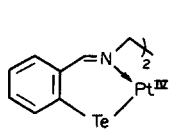

Aryl tellurate complex of Pt^{IV}.

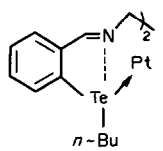

Alkyl aryl telluride complex of Pt^{II}

Fig. 3.

tion of complex **4** in DMSO was determined. The most interesting feature was a doubling of the —CH=N— resonance ($\delta = 9.12$, 9.15 ppm vs TMS) one component of which shows J(PtH) = 92 Hz. This coupling constant is higher than some values of J(PtH) reported for various organoselenium complexes[17,26] (41 Hz); it seems improbable that the coupling should occur through five bonds, but if the nitrogen was coordinated in the de-butyl case, as implied by IR evidence, a more convincing explanation for the magnitude of this coupling becomes available.

The implication from compound **5** that the final de-butylated species must be a complex of platinum(IV) was explored by measurement of ^{195}Pt NMR spectrum in DMSO. These spectra were monitored over 15 h. After 1 h, three signals were seen at 5986, 5981 and 5975 ppm *downfield* from $Na_2[PtCl_6]$. After 15 h the 5986 ppm and 5975 ppm signals had become very weak leaving the 5981 ppm signal as the dominant feature of the spectrum. The ^{195}Pt resonance covers a wide range of chemical shifts[27-29] but usually platinum(II) resonates at a higher field than $Na_2[PtCl_6]$, thus the data here are consistent with platinum(IV). Thus, the initial platinum(II) complex, detectable but changing in the ^{125}Te NMR experiment, has been removed after 1 h in DMSO (the colour of the solution having changed to deep brown). A mixture of platinum(IV) species is initially formed, but after 15 h one species, presumably that which is insoluble in refluxing acetonitrile, is seen. Monitoring the conductivity over the same period of time shows a slow decline from a value of Λ_M consistent with a 1:1 electrolyte to a non-conducting solution. Thus the three platinum(IV) species are possibly different solvates.

The mechanism of the loss of the butyl group is not currently known. If the reasoning above is correct, the solvent may be implicated in the early stages but the mechanism of the redox reaction may not be inferred from current data.

By contrast with the above system, the complex of $PtCl_2$ with ligand **II** (compound **6**, Table 1) seems straightforward. Thus, the evidence (mainly IR) favours a *cis*-dichloro complex which, unlike the palladium(II) counterpart gives no evidence for the presence of a *trans* isomer under any circumstances.

Rhodium complexes

The rhodium complexes were less well-defined than their palladium and platinum counterparts. Thus the rhodium(III) species (compounds **7** and **8**, Table 1) are both hydrates (analysis, IR). The complex of **I** (compound **7**) gives values of Λ_M of 20 Ω^{-1} cm^2 mol^{-1} in DMSO and 65 Ω^{-1} cm^2 mol^{-1} in CH_3CN. These values are significant, but less than values usually associated with 1:1 electrolytes in these solvents; thus a dimeric formulation may be implied. At least one ν(RhCl) was assigned in the terminal region (322 cm^{-1}, Table 2) but no bridging rhodium–chlorine vibrations could be confidently assigned above 200 cm^{-1}. Based on arguments presented above, ligand **I** coordinates only via tellurium. The complex of ligand **II** is a non-electrolyte and gives two bands in the $\nu(RhCl)_{terminal}$ region (Table 2); here too, coordination of **II** via tellurium only, is implied. Solubility in non-polar solvents implies that a simple [$RhCl_3$(**II**)(H_2O)] formulation to give an octahedral complex (possibly *fac*) is likely.

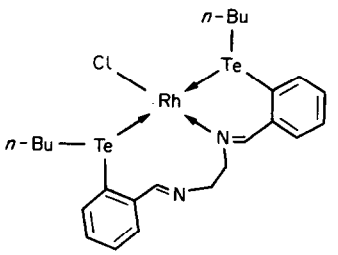

Fig. 4.

Rhodium(I) complexes were formed using [(COD)RhCl]$_2$ as precursor. In the case of ligand **I**, two products could be obtained reproducibly (compounds **9** and **10**, Table 2). However, **10** was non-stoichiometric. The ν(C=N) bands suggest that both nitrogen atoms of the ligand are involved, but unequally, in coordination but little more can be said about **10**. By contrast, **9** seems to have one coordinated and one non-coordinated nitrogen. The complex is non-ionic and soluble in non-polar and mildly polar solvents. It seems probable that a structure such as that in Fig. 4 may be valid. By contrast, the complex (compound **11**, Table 2) of ligand **II** gives no IR evidence for nitrogen coordinated to rhodium. The material fails to conduct and may therefore be dimeric and arise from the simple substitution of **II** for the COD ligands of the precursor. Thus, the extra flexibility of **I** arising from the presence of the dimethylene bridge between the nitrogen atoms would make the terdentate mode possible for **I** but not for **II**.

Acknowledgements—N. I. Al-S. thanks the University of Basrah, Iraq for study leave. We thank Johnson and Matthey for a generous loan of palladium, platinum and rhodium salts.

REFERENCES

1. H. M. K. K. Pathirana and W. R. McWhinnie, *J. Chem. Soc., Dalton Trans.* 1986, 2003.

2. N. I. Al-Salim, A. A. West, W. R. McWhinnie and T. A. Hamor, *J. Chem. Soc., Dalton Trans.* 1988, 2363.
3. K. Y. Abid, N. I. Al-Salim, M. Greaes, W. R. McWhinnie, A. A. West and T. A. Hamor, *J. Chem. Soc., Dalton Trans.* 1989, 1697.
4. H. M. K. K. Pathirana, A. W. Downs, W. R. McWhinnie and P. Granger, *Inorg. Chim. Acta* 1988, **143**, 161.
5. N. I. Al-Salim, T. A. Hamor and W. R. McWhinnie, *J. Chem. Soc., Chem. Commun.* 1986, 453.
6. I. Bertini, L. Sacconi and G. P. Speroni, *Inorg. Chem.* 1972, **11**, 1323.
7. P. R. Blum, R. M. C. Wei and S. C. Cummings, *Inorg. Chem.* 1974, **13**, 450.
8. J. R. Doyle, P. E. Slade and H. B. Jonassen, *Inorg. Synth.* 1960, **5**, 218.
9. G. Giordano and H. Crabtree, *Inorg. Synth.* 1974, **19**, 218.
10. W. J. Cherwinski, H. C. Clark and L. E. Manzer, *Inorg. Chem.* 1972, **11**, 1511.
11. T. G. Appleton, H. C. Clark and L. E. Manzer, *Coord. Chem. Rev.* 1973, **10**, 335.
12. H. J. Gysling, H. R. Luss and D. L. Smith, *Inorg. Chem.* 1979, **18**, 2696.
13. L.-Y. Chia and W. R. McWhinnie, *J. Organomet. Chem.* 1978, **148**, 165.
14. E. A. Allen and W. Wilkinson, *J. Inorg. Nucl. Chem.* 1974, **36**, 1663.
15. H. Gysling, N. Zumbulyadis and J. A. Robertson, *J. Organomet. Chem.* 1981, **209**, C41.
16. E. G. Hope, W. Levason, S. G. Murray and G. L. Marshall, *J. Chem. Soc., Dalton Trans.* 1985, 2185.
17. D. J. Gulliver, E. G. Hope, W. Levason, S. G. Murray and G. L. Marshall, *J. Chem. Soc., Dalton Trans.* 1985, 1265.
18. R. J. Cross, T. G. Green and R. Krat, *J. Chem. Soc., Dalton Trans.* 1976, 1150.
19. T. Kemmitt, W. Levason and M. Webster, *Inorg. Chem.* 1989, **28**, 692.
20. L. M. Venanzi, *Chem. Brit.* 1968, 162.
21. D. P. Rainville and R. A. Zingaro, *Inorg. Chim. Acta* 1984, **86**, L33.
22. I. Davies, W. R. McWhinnie, N. S. Dance and C. H. W. Jones, *Inorg. Chim. Acta* 1978, **29**, L203.
23. I. Davies, W. R. McWhinnie, N. S. Dance and C. H. W. Jones, *Inorg. Chim. Acta* 1978, **29**, L217.
24. L. F. Lindoy, S. E. Livingstone and T. N. Lockyer, *Inorg. Chem.* 1967, **6**, 652.
25. D. W. Meek, *Inorg. Chem. Nucl. Lett.* 1969, **5**, 235.
26. L. Sacconi and G. P. Speroni, *Inorg. Chem.* 1968, **7**, 295.
27. C. Brevard and P. Granger, *Hand Book of High Resolution NMR*, p. 200. John Wiley, U.S.A. (1981).
28. P. S. Pregosin, *Coord. Chem. Rev.* 1982, **44**, 247.
29. E. G. Hope, W. Levason, M. Webster and S. G. Murray, *J. Chem. Soc., Dalton Trans.* 1986, 1003.

Polyhedron Vol. 8, No. 23, pp. 2777–2783, 1989
Printed in Great Britain

0277–5387/89 $3.00+.00
© 1989 Pergamon Press plc

SYNTHESIS AND CHARACTERIZATION OF MONONUCLEAR COPPER(II) ASPIRINATE ADDUCTS WITH IMIDAZOLE AND ITS METHYL DERIVATIVES

A. LATIF ABU HIJLEH

Chemistry Department, Birzeit University, P.O. Box 14, West Bank–via Israel

(*Received* 10 *February* 1989; *accepted* 20 *July* 1989)

Abstract—A synthetic investigation of copper(II) aspirinate addition compounds with imidazoles has led to the isolation of monomers of the form $[Cu(asp)_2 \cdot L_n]$, where asp is the aspirinate anion and $n = 4$ when L is imidazole or N-methylimidazole and $n = 2$ when L is 1,2-dimethylimidazole. These compounds have been characterized by means of elemental analysis, magnetic moments, electronic, IR and ESR spectroscopic properties. The tetrakis-adducts of imidazole and N-methylimidazole showed physical properties which indicated a tetragonal six-coordinated configuration containing the (CuN_4+O_2) chromophore. For the bis-adduct of 1,2-dimethylimidazole, the proposed geometry is a tetragonal distorted octahedron, having essentially the CuN_2O_2 chromophore in a *trans* distorted square-planar environment. The adoption of monomeric rather than the more common dimeric structure is discussed in terms of the electronic and steric effects of these imidazole ligands.

Aspirin (acetyl salicylic acid) and its derivatives have been used as analgesic, antipyretic and anti-inflammatory drugs. It was suggested that copper(II) complexes of aspirin are more effective and desirable drugs than aspirin.[1,2] Other solvated copper(II) aspirinates, in addition to other copper(II) carboxylates, with pyridine and imidazole have been found to have a variety of pharmacological effects[3,4] including antitumour activity.[5]

Dimeric copper(II) carboxylates with several basic ligands are well documented and reviewed,[6,7] but few spectroscopic studies of copper(II) complexes of aspirin have been reported. X-ray analysis of copper aspirinate showed that it contains binuclear units with bridging carboxylate,[8] similar to the familiar copper acetate[9] and many other carboxylate dimers.[7,10] Solvated copper(II) aspirinate dimers are only known for weakly basic ligands such as DMF, DMSO, H_2O or CH_3OH.[11,12] In addition to dimers, few monomers for the non-halogenated carboxylates, including the aspirinate, are known.[13–17] The only known monomeric complex of copper(II) aspirinate is that with pyridine.[17] X-ray analysis showed that this complex exists as bis(aspirinate)bis(pyridine)copper(II), having essentially the CuN_2O_2 chromophore in a *trans* square-planar arrangement. This structure is similar to those known for the monomeric bis-adducts of copper(II) acetate with imidazole[15] and collidine.[16] This article reports the synthesis and characterization of monomeric tetrakis-adducts, as well as the bis-adduct of copper(II) aspirinate with imidazole and its methyl derivatives. The formation of these stable monomers rather than the more common copper(II) aspirinate dimers is discussed in terms of the basicity strength of imidazoles compared to the less basic ligands.

EXPERIMENTAL

Imidazole (Aldrich) was used without further purification. N-methylimidazole and 1,2-dimethylimidazole (Aldrich) were distilled under reduced pressure immediately prior to use. All solvents were spectral grade and used without further purification.

Synthesis

(1) *Tetrakis-μ-aspirinato-dicopper*(II), Cu_2asp_4 (asp = *aspirinato* = *acetylsalicylato*). This was prepared as described before.[1] Found: C, 51.1; H, 3.4; Cu, 15.1. Calc.: C, 51.2; H, 3.3; Cu, 15.1%.

(2) *Bis(aspirinato)tetrakis(imidazole)copper*(II), $Cu(asp)_2(imid)_4$. 3 g of imidazole in 15 cm^3 of *n*-butanol was added to *ca* 1.5 g of Cu_2asp_4. The mixture was magnetically stirred in a stoppered round-bottomed flask for 1 h in an ice-bath. The oily-blue mixture which formed was separated from the solvent by decantation, then stirred for a few minutes. Anhydrous diethyl ether was added to the blue mixture which was further stirred at room temperature until a faint sky-blue precipitate formed. The complex was filtered under reduced pressure in a closed apparatus, washed several times with anhydrous diethyl ether and dried *in vacuo*. Found: C, 51.8; H, 4.3; N, 16.3; Cu, 9.1. Calc.: C, 51.9; H, 4.3; N, 16.1; Cu, 9.2%.

(3) *Bis(aspirinato)tetrakis(N-methylimidazole) copper*(II), $Cu(asp)_2(N\text{-}Me \cdot imid)_4$. 10 cm^3 of freshly distilled N-methylimidazole was added to 1.5 g of Cu_2asp_4 in a round-bottomed flask. The mixture was magnetically stirred in an ice-bath for 1 h and set aside at room temperature. After 4 days the blue crystalline product was filtered under reduced pressure in a closed apparatus, washed with anhydrous diethyl ether, dried *in vacuo* and stored in a stoppered flask. Found: C, 54.5; H, 5.0; N, 14.6; Cu, 8.6. Calc.: C, 54.4; H, 5.1; N, 14.9; Cu, 8.5%.

(4) *Bis(aspirinato)bis*(1,2-*dimethylimidazole)copper* (II), $Cu(asp)_2(1,2\text{-}diMe \cdot imid)_2$. 10 cm^3 of freshly distilled 1,2-dimethylimidazole was added to about 1 g of Cu_2asp_4. The mixture was stirred at about 50°C for 30 min, filtered in a closed apparatus over anhydrous diethyl ether, then stirred overnight at room temperature. The sky-blue precipitate formed was filtered in a closed apparatus under reduced pressure, washed several times with anhydrous diethyl ether and dried *in vacuo*. Found: C, 54.5; H, 5.0; N, 9.1; Cu, 10.3. Calc.: C, 54.8; H, 4.9; N, 9.1; Cu, 10.3%. Elemental analyses for C, H and N were performed by Galbraith Laboratories, Knoxville, Tennessee. Copper was determined volumetrically.

Physical measurements

Room temperature (300 K) magnetic susceptibility measurements of powdered samples were determined by the Gouy method, with $HgCo(NCS)_4$ as calibrant, and corrected for diamagnetism with the appropriate Pascal constants. The effective magnetic moment was calculated from the expression: $\mu_{eff} = 2.84(\chi'_m \cdot T)^{1/2}$. The ESR spectra of powdered and methanol–toluene solution samples were taken at different temperatures, with a Varian E-4 X-band spectrometer equipped with a variable temperature unit and 100 KHz field modulation, using diphenyl picryhydrazyl (DPPH, $g = 2.0036$) as the calibrating field marker. Electronic spectra were obtained, using THF or chloroform solutions in matched 1-cm quartz cells, using Bauch and Lomb spectronic 2000. Nujol mulls and potassium bromide discs of complexes were employed to obtain IR spectra in the 4000–600 cm^{-1} region, with a Perkin–Elmer Model 298 spectrophotometer.

RESULTS AND DISCUSSION

The imidazole adduct dissolves in polar solvents (THF, DMSO, alcohols, etc.) but does not dissolve in less polar solvents (chloroform, methylene chloride). N-methylimidazole and 1,2-dimethylimidazole adducts dissolve in most organic solvents. All complexes are stable in air except the N-methylimidazole adduct which appears to be hygroscopic.

Electron spin resonance

The ESR spectrum obtained for a powdered sample of Cu_2asp_4 at room temperature exhibits three absorption bands typical of triplet-state binuclear copper(II) complexes with axial symmetry.[11] The values obtained for the spin-Hamiltonian parameters are: $g_\perp = 2.08$, $g_\parallel = 2.28$, $g_{av} = 2.15$ and $|D| = 0.36$ cm^{-1}. The values are comparable to those found in binuclear copper(II) carboxylates.[10] The crystal structure of copper(II) aspirinate has been reported,[8] and contains dimetallic units of $[Cu(asp)_2]_2$ interconnected by acetyl oxygens from neighbouring dimetallic units.

X-band ESR spectra of polycrystalline samples, for the tetrakis-adducts of imidazole and N-methylimidazole (Fig. 1(A) and (B), respectively) and for the bis-adduct of 1,2-dimethylimidazole [Fig. 2(A)], are anisotropic and contain $g_\perp$ and $g_\parallel$ components. In addition to the hyperfine structure of copper(II) in the $g_\parallel$ region, the bis-adduct of the 1,2-dimethylimidazole spectrum is partially resolved into its X and Y components in the $g_\perp$ region, Fig. 2(A). This may result from the non-equivalence of the Cu—O and Cu—N bonds formed by the carboxylate and by 1,2-dimethylimidazole ligands, respectively, in the XY plane. The ESR spectral parameters of the three complexes and some similar complexes, Table 1, are characteristic of tetragonal elongated monomeric copper(II) complexes having the $d_{x^2-y^2}$ ground state.[18]

ESR spectra of solution samples for the three adducts, at room temperature, are isotropic and consist of four equally-spaced lines, as expected for the copper(II) ion. In frozen solutions, the imidazole and N-methylimidazole adduts' spectra (Fig. 3(A) and 4(A), respectively) show substantial ^{14}N

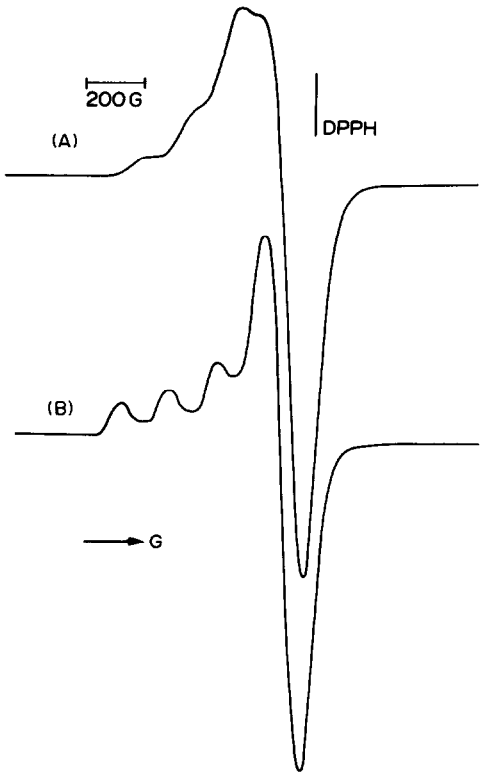

Fig. 1. X-band ESR powder spectra of $Cu(asp)_2(imid)_4$ (A) and $Cu(asp)_2(N\text{-}Me \cdot imid)_4$ (B) at 300 K.

super-hyperfine structure in the $g_\perp$ region. This resolved into nine equally-spaced peaks with $A_\perp(N)$ of 15 cm^{-1}, and expanded spectra of this region are shown in Fig. 3(B) and 4(B) for the imidazole and N-methylimidazole adducts, respectively. The resolution of the $g_\perp$ region is attributed to the presence of four equivalent nitrogen atoms in the copper(II) ion plane. These spectra are comparable to the ESR spectra of a bis(acetato) tetrakis(imidazole)copper(II) complex[13] having a CuN_4O_2 chromophore, and with those containing a CuN_4 chromophore.[19] The spectral parameters for the imidazole and N-methylimidazole are rather similar (Table 1) and comparable with those reported for CuN_4O_2 chromophores.[13,20,21] In these chromophores the copper(II) complexes have a tetragonal elongated structure and the equatorial positions are occupied by the four nitrogen atoms, while the axial positions are occupied by the oxygen atoms of the carboxylate groups. In the complexes $Cu(asp)_2(imid)_4$ and $Cu(asp)_2(N\text{-}Me \cdot imid)_4$, the four equatorial positions are occupied by four imidazole or N-methylimidazole molecules coordinated through their pyridine nitrogen, while each axial position is occupied by one carboxylate oxygen atom from each of two aspirinate anions.

The ESR spectrum of a frozen solution of the bis-adduct of 1,2-dimethylimidazole, is shown in Fig. 2(B). Although the ^{14}N superhyperfine splitting in the $g_\perp$ region is not resolved, ESR spectra parameters for this adduct are comparable with those of copper acetate bis-adducts with imidazole,[5] 1,2-dimethylimidazole[13] and with $Cu(asp)_2(Py)_2$,[17] and with previously reported complexes having essentially a *trans*-square-planar CuN_2O_2 chromophore,[10,18,20,22] In these complexes the copper(II) ion is bonded in a *trans* arrangement to two ligand nitrogen atoms and one oxygen atom from each of the two carboxylate anions. The second oxygen

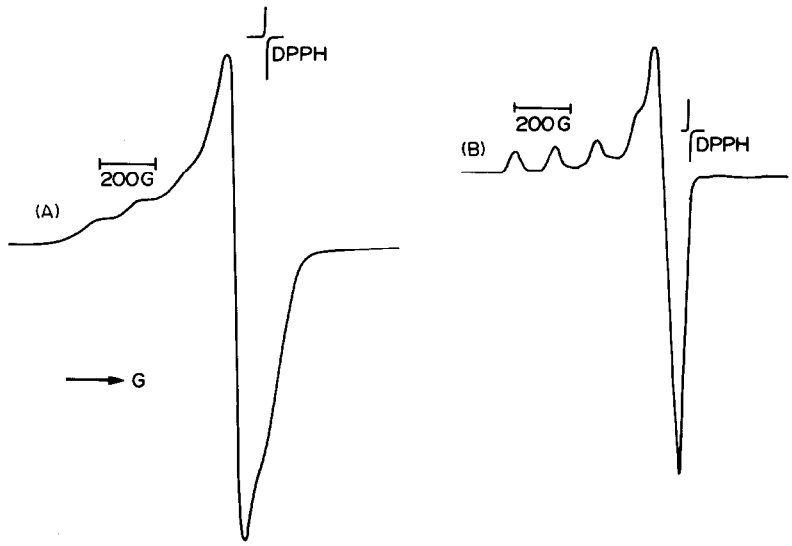

Fig. 2. X-band ESR spectra of $Cu(asp)_2(1,2\text{-}diMe \cdot imid)_2$: (A) powder spectrum at 300 K and (B) in frozen methanol–toluene solution at 120 K.

Table 1. ESR data

Compound	State (temperature)	g_0	$g_\parallel$	$g_\perp$	$10^4 A_o$[a]	$10^4 A_\parallel$Cu	$10^4 A_\perp$Cu[b]	$10^4 A_\perp$N	Reference
$Cu(asp)_2(imid)_4$	Powdered[c] (Room)	2.10	2.21	2.05	—	186	3.0	—	This work
	Solution (Room)	2.10	—	—	64	—	—	—	
	Solution[c] (120 K)	2.10	2.22	2.04	—	187	2.8	15	
$Cu(asp)_2(N\text{-}Me\cdot imid)_4$	Powdered (Room)	2.09	2.22	2.03	—	181	5.5	—	This work
	Solution (Room)	2.10	—	—	64	—	—	—	
	Solution (120 K)	2.09	2.20	2.03	—	180	6	15	
$Cu(asp)_2(1,2\text{-}diMe\cdot imid)_2$	Powdered (Room)	2.12	2.25	$g_x = 2.06$ $g_y = 2.03$	—	168	1.5	—	This work
	Solution (Room)	2.12	—	—	57	—	—	—	
	Solution (120 K)	2.12	2.27	2.05	—	166	2.5	—	
$Cu(Ac)_2(imid)_4$[d]	Powdered (Room)	2.11	2.23	2.05	—	—	—	—	13
	Solution (Room)	2.12	—	—	65	—	—	—	
	Solution (113 K)	2.10	2.22	2.03	—	181	7	15	
$Cu(Ac)_2(imid)_2$	Solution (77 K)	—	2.267	—	—	162	—	—	5

[a] All hyperfine coupling constants are in cm^{-1}.
[b] $A_\perp$Cu are calculated from the equation $A_0 = \frac{1}{3}(A_\parallel + 2A_\perp)$.
[c] g_0 values for powdered and frozen samples are calculated from the equation $g_0 = \frac{1}{3}(g_\parallel + 2g_\perp)$.
[d] Ac is the acetate anion.

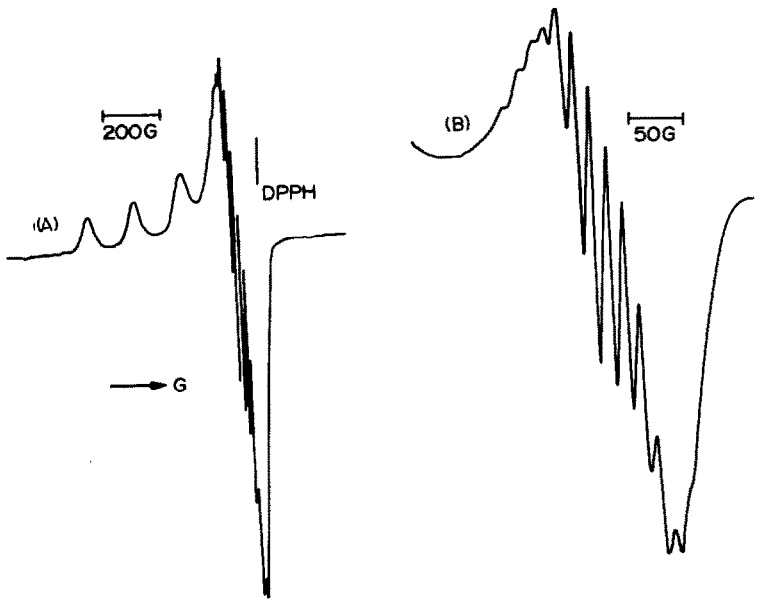

Fig. 3. X-band ESR spectra of $Cu(asp)_2(imid)_4$ (A) in frozen methanol–toluene solution at 120 K and an expanded spectrum of the $g_\perp$ region (B).

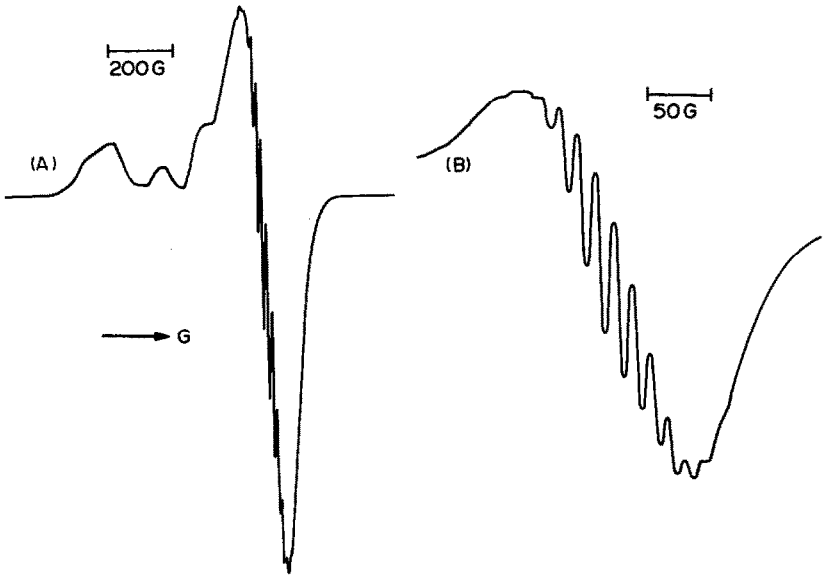

Fig. 4. X-band ESR spectra of $Cu(asp)_2(N\text{-}Me\cdot imid)_4$ (A) in frozen methanol–toluene solution at 120 K and an expanded spectrum of the $g_\perp$ region (B).

atom of the carboxylates are weakly bonded in the axial positions. The absence of the ^{14}N splittings may be attributed to the presence of a distorted square-planar CuN_2O_2 chromophore in this adduct, which weakens the interaction between the σ-orbitals of the nitrogen atoms and the copper(II) $d_{x^2-y^2}$ orbital. In addition, the partial resolution of $g_\perp$ in the powdered spectrum [Fig. 2(A)] into its X and Y components supports the proposed distorted square planar CuN_2O_2 chromophore in this adduct. This distortion is attributed to the presence of bulky aspirinate anions and sterically hindered methyl groups in 1,2-dimethylimidazole ligands.

Inspection of the ESR parameters (Table 1) shows that $A_\parallel$ for the tetrakis-adducts, $Cu(asp)_2(imid)_4$ and $Cu(asp)_2(N\text{-}Me\cdot imid)_4$, is greater than $A_\parallel$ for the bis-adduct, $Cu(asp)_2(1,2\text{-}diMe\cdot imid)_2$; while $g_\parallel$ values in the former complexes are

smaller. These results are consistent with the presence of a stronger equatorial ligand-field in the tetrakis-adducts, which have the CuN_4 chromophore in the plane, compared to the bis-adduct which is proposed to contain the CuN_2O_2 chromophore.

Magnetic moments

The results of the effective magnetic moments, as well as electronic and IR spectral measurements, are summarized in Table 2. The magnetic moment of $Cu_2(asp)_4$ at room temperature is 1.36 BM. This subnormal moment is indicative of spin–spin coupling and is in the range expected for dimeric copper(II) carboxylate complexes.[6,7,10] The exchange coupling constants, $-2J$, value determined[12] for this complex is 363 cm^{-1}. The magnetic moments, at room temperature, for the three imidazole complexes of copper(II) aspirinate are in the range 1.85–1.90 BM. These values correspond to the presence of one unpaired electron in monomeric copper(II) ion complexes.

Electronic spectra

The electronic spectra, in the visible region, of dimeric $Cu_2(asp)_4$ in a Nujol mull show the two bands characteristic of dimeric copper(II) carboxylates.[10,14] The electronic spectra for the three mononuclear adducts in THF or chloroform solutions exhibit one broad asymmetric band due to the copper *d–d* transitions. The position of the band and the value of its molar absorptivity are in the range expected for monomeric copper(II) carboxylate adducts.[10] The tetrakis-adducts, $Cu(asp)_2(imid)_4$ and $Cu(asp)_2$(N-Me·imid)$_4$, show absorption maxima which are comparable with that found for monomeric $Cu(CH_3COO)_2(imid)_4$ [band maximum around 635 nm ($\varepsilon_m = 60$)][13] and is in the range expected for complexes containing a CuN_4O_2 chromophore.[10,21] The bis-adduct, $Cu(asp)_2$(1,2-diMe·imid)$_2$, has an absorption maximum which is comparable with those found for structurally known Cu(aspirinate)$_2$(pyridine)$_2$ [band maximum in chloroform solution at 725 nm ($\varepsilon_m = 230$)][17] and other complexes having an essentially *trans*-CuN_2O_2 chromophore.[10,21]

Infrared spectra

The assignments of all the bands for the complexes have not been made, but the IR absorptions for the antisymmetric and symmetric carboxyl stretching frequencies are compared in Table 2. For $Cu_2(asp)_4$ the asymmetric ν_{as}(COO) and the symmetric ν_s(COO) frequencies are similar to those reported for dimeric copper(II) carboxylates,[10,23] in which the carboxylate acts as a "bridging" bidentate ligand. The IR spectra for the two tetrakis-adducts of imidazole and N-methylimidazole are very similar to one another in band shape and position, especially the antisymmetric and symmetric carboxylate bands. The positions of these bands and the separation between them, $\Delta\nu$, are comparable with those of structurally known monomeric copper(II) carboxylate complexes with imidazoles in which the carboxylate acts as monodentate ligand.[24] The $\Delta\nu$ value and ν_s(COO) position for the bis-adduct of 1,2-dimethylimidazole are comparable with those of structurally known monomeric copper(II) carboxylates containing an essentially CuN_2O_2 chromophore, in which $\Delta\nu$ is about 230–250 cm^{-1} and ν_s(COO) about 1370–1380 cm^{-1}. In these complexes the carboxylate group acts as an essentially monodentate or asymmetric bidentate ligand.[24,25] X-ray analysis of $Cu_2(asp)_4$ revealed two types of acetoxy carbonyl group.[8] One of these is weakly bonded to a copper(II) ion of a neighbouring copper(II) aspirin-

Table 2. Spectral and magnetic moment data for the complexes

Compound	Solution electronic spectra ν_{max} in nm (ε in $dm^3\ mol^{-1}\ cm^{-1}$)	$\mu_{eff.}$ (BM) (at room temperature)	IR spectra (cm^{-1})		
			$\nu_{as}(COO^-)$	$\nu_s(COO^-)$	$\Delta\nu$
$Cu(asp)_2(imid)_4$	630 (62)[a]	1.86	1595	1380	215
$Cu(asp)_2$(N-Me·imid)$_4$	630 (60)[b]	1.85	1590	1380	210
$Cu(asp)_2$(1,2-diMe·imid)$_2$	725 (110)[c]	1.90	1605	1370	235
$Cu_2(asp)_4$	665,375[d]	1.36	1620	1415	205

[a] In THF solution.
[b] In THF or $CHCl_3$ solutions.
[c] In $CHCl_3$ solution.
[d] These values are taken from ref. 12.

ate molecule, while the other is not. As a consequence, the IR spectrum of $Cu_2(asp)_4$ shows two different acetoxy carbonyl stretching frequencies at 1735 and 1758 cm^{-1}. The IR spectra for the three monomer complexes show only one acetoxy carbonyl frequency at about 1750 cm^{-1} and it is not coordinated. These IR results along with the above spectral results confirm the presence of the CuN_4O_2 chromophore in the tetrakis-adducts and the presence of an essentially CuN_2O_2 chromophore or tetragonally elongated CuN_2O_4 chromophore in the bis-adduct.

There have been many studies to investigate the factors which influence dimer formation over monomer formation in copper(II) carboxylate solvate complexes.[10,14,16,17] Halogenation of the alkyl group increases the tendency towards formation of a monomeric adduct which is related to the electronic effects on the acidity of the carboxylates. In addition, the electronic effects of the addend play a significant role in the adoption of one of the two structural types of copper(II) carboxylate adducts. The results of this study support the previous ones[13,17] in showing that there is a preference for monomer formation with basic ligands such as imidazoles (this work) and pyridines,[16,17] than with less basic ligands such as water, DMSO or DMF. Although steric effects of the addends play a less important role than the electronic effects in the adoption of one of the two structures,[14,16] the results of this study demonstrate the role of steric requirements of the addend in affecting the structural properties of monomeric copper(II) carboxylate adducts. The less sterically hindered ligands, imidazole and N-methylimidazole, formed the tetrakis-adducts with copper(II) aspirinate, whereas the more sterically hindered ligand, 1,2-dimethylimidazole, formed the bis-adduct.

Acknowledgements—I am grateful to Professor I. Y. Ahmed at the University of Mississippi for obtaining the ESR spectra and to Birzeit University for the support of this research under Grant No. 86/68/97/8.

REFERENCES

1. J. R. J. Sorenson, *J. Med. Chem.* 1976, **19**, 135.
2. D. A. Williams, D. T. Waltz and W. O. Foye, *Pharm. Sci.* 1976, **65**, 126.
3. J. R. J. Sorenson, L. W. Oberley, R. K. Crouch, T. W. Kensler, V. Kishore, S. W. C. Leuthauser, T. D. Oberley and A. Pezeshk, *Biol. Trace Element Res.* 1983, **5**, 257.
4. D. H. Brown, W. E. Smith and J. W. Teape, *J. Med. Chem.* 1980, **23**, 729.
5. H. Tamura, H. Imai, J. Kuwahara and Y. Sugiura, *J. Am. Chem. Soc.* 1987, **109**, 6870.
6. R. W. Jotham, S. F. A. Kettle and J. A. Marks, *J. Chem. Soc., Dalton Trans.* 1972, 428.
7. M. Melnik, *Coord. Chem. Rev.* 1982, **42**, 259.
8. L. Manojlovic-Muir, *Chem. Commun.* 1967, 1057.
9. J. N. Van Niekerk and F. R. L. Shoening, *Acta Cryst.* 1953, **6**, 227.
10. M. Melnik, *Coord. Chem. Rev.* 1981, **36**, 1.
11. K. S. Bose and C. C. Patel, *Ind. J. Chem.* 1970, **8**, 840.
12. J. L. Meier, C. E. Coughenour, J. A. Carlisle and G. G. Carlisle, *Inorg. Chim. Acta* 1985, **106**, 159.
13. A. Latif Abuhijleh, personal communication.
14. I. Y. Ahmed and A. Latif Abuhijleh, *Inorg. Chim. Acta* 1982, **61**, 241.
15. H. A. Henriksson, *Acta Cryst.* 1977, **B33**, 1947.
16. N. E. Heimer and I. Y. Ahmed, *Inorg. Chim. Acta* 1982, **64**, L65.
17. F. T. Greenaway, A. Pezeshk, A. W. Cordes, M. C. Noble and J. R. J. Sorenson, *Inorg. Chim. Acta* 1984, **93**, 67.
18. B. J. Hathaway and D. E. Billing, *Coord. Chem. Rev.* 1970, **5**, 143.
19. (a) H. Van Camp, R. Sands and J. A. Fee, *J. Chem. Phys.* 1981, **75**, 2098; (b) A. Peseshk, F. T. Greenaway and J. R. S. Sorenson, *Inorg. Chim. Acta* 1983, **80**, 191.
20. J. Pelsach and W. E. Bluemberg, *Arch. Biochem. Biophys.* 1974, **165**, 691.
21. N. B. Pahor, G. Nardin, R. P. Bonomo and E. Rizzarelli, *J. Chem. Soc., Dalton Trans.* 1984, 2625.
22. (a) L. Antolini, L. Menabue, M. Saladini, L. P. Battaglia and A. B. Corradi, *Inorg. Chim. Acta* 1984, **90**, and refs therein; (b) L. G. Macdonald, D. H. Brown and W. E. Smith, *Inorg. Chim. Acta* 1982, **63**, 213.
23. R. J. Doedens, *Progr. Inorg. Chem.* 1976, **21**, 209.
24. L. P. Battaglia, A. B. Corradi, L. Menabue, G. C. Pellacani, P. Prampolini and M. Saladini, *J. Chem. Soc., Dalton Trans.* 1982, 781.
25. L. P. Battaglia, A. B. Corradi, G. Marcotrigiano, L. Menabue and G. C. Pellacani, *Inorg. Chem.* 1983, **22**, 1902.

Polyhedron Vol. 8, No. 23, pp. 2785–2789, 1989
Printed in Great Britain

0277–5387/89 $3.00+.00
© 1989 Pergamon Press plc

STUDIES OF BONDING PROPERTIES OF INCOMPLETE METALLIC CUBANE-TYPE CLUSTER COMPOUNDS CONTAINING THE $M_3X_{4-n}Y_n$ CORE (M = Mo, W; X = O, S, Cl, Br; Y = O, S; n = 0, 1)

CHENG WENDAN,* ZHANG QIANER, HUANG JINSHUN and LU JIAXI

Fujian Institute of Research on the Structure of Matter, Chinese Academy of Sciences, Fuzhou, Fujian, China

(*Received* 7 *March* 1989; *accepted* 20 *July* 1989)

Abstract—It has been shown that a *d–p* π-conjugate interaction exists on the non-planar ring skeleton M_3X_3 and the structured energy levels for the isoelectron series have the same order in the core $M_3X_{4-n}Y_n$, containing both M_3X_3 and $M_3X_{4-n}Y_n$ in the incomplete metallic cubane-type cluster compounds. It has also been found that the abilities of the π-lone pair electron donation in the X atom and of the π-electron acception in the M atom are the key factors for the *d–p* π-conjugate interaction over the non-planar ring skeleton M_3X_3. The π-electronic delocalization for the S atom over M_3S_3 is larger than at the O atom over M_3O_3 (M = Mo, W), and the strengths of the *d–p* π-conjugate interaction are larger over M_3S_3 than M_3O_3, but the M—M transannular interactions are stronger in M_3O_3 than M_3S_3. The latter fact may be due to a contribution from the *d–d* π-interaction within the triangle of metal atoms, because the typical π-orbital interactions take place both between M—M and M—X in the non-planar ring skeleton M_3X_3.

Incomplete metallic cubane-type cluster compounds having a core of the general formula $M_3X_{4-n}Y_n$ (n = 1, 0) have been the subject not only of numerous experimental studies,[1–10] but also of various theoretical studies.[11–13] The theoretical attempts to understand the electronic structure and properties of these clusters have been from qualitative[14] and parameter-free[11] approximate molecular orbital (MO) treatments. Most of these theoretical treatments have employed a MO approach to describe the electronic structure of the various clusters. Particularly noteworthy among the MO descriptions of the clusters containing a $M_3X_{4-n}Y_n$ core is the work of Dahl and co-workers.[14] This group developed a qualitative molecular orbital picture by considering the symmetry of the metal skeleton orbitals. However, most of the theoretical investigations have paid less attention to the discussion of the *d–p* π-conjugate interaction over the non-planar ring skeleton M_3X_3, although Curtis and Butler[15] have pointed out that the S---Mo π-donation to cause both M—M and M—S bond contraction is postulated to be a more important bonding feature in $Mo_3S_4Cp_3^+$. We will describe the *d–p* π-conjugate interaction over the non-planar ring skeleton M_3X_3 and its influence upon the bonding and physicochemical properties in the incomplete metallic cubane-type cluster compounds, and give an eigenvalue spectrum for the isoelectron series $M_3X_{4-n}Y_n$ (M = Mo, W; X = O, S, Cl, Br; Y = O, S; n = 0, 1).

RESULTS AND DISCUSSION

Eigenvalue spectrum and orbital components

Molecular orbital calculations were carried out on 10 cores with the triangle pyramidal structure shown in Fig. 1. The energy level diagrams for each of the six cores are given in Fig. 2, the orbital compositions are also tabulated in Table 1. The isoelectron series, $M_3X_{4-n}Y_n^{4+}$, has 19 occupied MO's, in which 6*e* or its splitting *a'*(6*e*) orbital is HOMO, and $Mo_3X_3O^{5+}$ (X = Cl, Br) has 20 occupied MO's, in which $7a_1$ is the HOMO, if we only consider the valence electrons.

* Author to whom correspondence should be addressed.

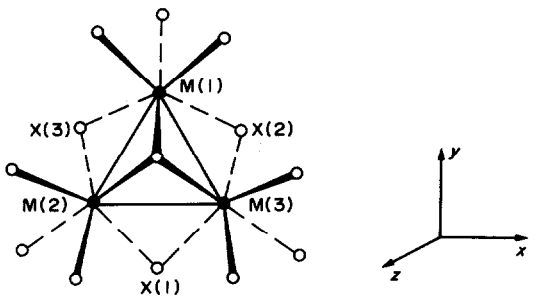

Fig. 1. The configuration of the $M_3X_{4-n}Y_nL_9$ cluster and the definition of coordinate orientation.

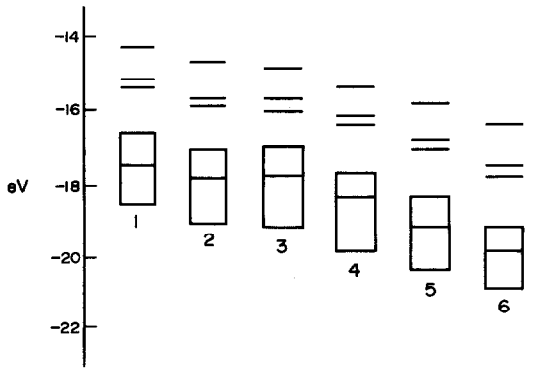

Fig. 2. The eigenvalue spectrum for 38 valence electrons. The core numbers 1 ($Mo_3S_4^{4+}$), 2 ($Mo_3OS_3^{4+}$), 5 ($Mo_3SO_3^{4+}$) and 6 ($Mo_3O_4^{4+}$) have C_{3v} symmetry and the energy levels are $7e$ (LUMO), $6e$ (HOMO), $6a_1$, $5e$, $5a$ and $1a_1$. The core numbers 3 [$Mo_3(\mu_3\text{-}S)(\mu\text{-}S_2)(\mu\text{-}O)^{4+}$] and 4 [$Mo_3(\mu_3\text{-}S)(\mu\text{-}S)(\mu\text{-}O)_2^{4+}$] have C_s symmetry and the energy levels are $a'(7e)$, $a'(6e)$, $a'(6a_1)$, $a'(5e)$, $a'(5a_1)$ and $a'(1a_1)$.

The high-lying occupied $6e$ and $6a_1$ MO's for $M_3X_{4-n}Y_n^{4+}$ are considered as M—M bonding orbitals. As shown in Table 1, the metal atom *d*-orbital character for $6e$ (HOMO) contributes about 53–72%, and $6a_1$ MO's contribute about 30–54% in a 38-valence electron series. In 40-valence electron series, $7a_1$ (HOMO) consists of about 58% and $6a_1$ consists of about 47% *d*-orbital character. It seems that there is generally a trend in the values of Table 1. The contributions of the metal atom *d*-orbital character decrease and the bridging atoms X and Y *p* orbital characters increase, while the MO energy level tends towards stabilization. The $1a_1$, $1e$ and $2a_1$ orbitals are not shown in Fig. 2 and Table 1. Each of them is nearly an entire orbital of the filled low-lying *s*-orbital of the bridging atoms. The calculated results on the $Mo_3O_4^{4+}$ using the Fenske–Hall method by Bursten *et al.*[11] are in agreement with our results in a general trend.

It is suggested from Fig. 2 and Table 1, as well as from the results of the calculations, that the diagram of the structured energy levels is generally divided into five blocks in this type of core series. The first block is virtually non-bonding combinations of the filled orbital of four X atoms, and will accommodate eight electrons. The next block is the bonding interactions between the metal atom *d*-orbitals (containing smaller metal atom *s*-orbital) and the X atom *p*-orbitals, and will accommodate 24 electrons. The third block consists of metal atom *d*-orbitals, which includes bonding and antibonding interactions between the *d*-orbitals, and the remainder of the core valence electrons will accommodate this block. The fourth block is the counterpart of the second block and contains antibonding interactions between the M atom *d*-orbital and X atom *p*-orbital, and is vacant. The highest non-occupied block consisting of the M atom *p*-orbitals is the fifth one. This

Table 1. Atomic orbital contributions for the frontier molecular orbitals[a]

Core	LUMO $7e(a')$		HOMO $6e(a')$		$6a_1(a')$		$5e(a')$		$5a_1(a')$	
	$\%d_M$	$\%p_X$	$\%d_M$	$\%p_X$	$\%d_M$	$\%p_X$	$\%d_M$	$\%p_X$	$\%d_M$	$\%p_X$
$Mo_3(\mu_3\text{-}S)(\mu\text{-}S)_3^{4+}$	90	4	72	26	54	45	45	53	40	60
$Mo_3(\mu_3\text{-}O)(\mu\text{-}S)_3^{4+}$	84	6	67	32	42	57	45	53	34	62
$Mo_3(\mu_3\text{-}S)(\mu\text{-}S)_2(\mu\text{-}O)^{4+}$	88	8	63	36	47	50	43	54	42	55
$Mo_3(\mu_3\text{-}S)(\mu\text{-}S)(\mu\text{-}O)_2^{4+}$	88	4	61	37	46	53	37	59	40	57
$Mo_3(\mu_3\text{-}S)(\mu\text{-}O)_3^{4+}$	86	7	58	40	35	63	24	71	39	56
$Mo_3(\mu_3\text{-}O)(\mu\text{-}O)_3^{4+}$	82	9	55	44	30	61	29	68	30	65
$W_3(\mu_3\text{-}S)(\mu\text{-}S)_3^{4+}$	89	4	67	31	48	50	45	53	34	60
$W_3(\mu_3\text{-}O)(\mu\text{-}O)_3^{4+}$	80	10	53	46	30	69	27	69	26	69
$Mo_3(\mu_3\text{-}O)(\mu\text{-}Br)_3^{5+}$	86	6	57	43[a]	47	51	26	72	20	67
$Mo_3(\mu_3\text{-}O)(\mu\text{-}Cl)_3^{5+}$	84	6	58	42[a]	46	53	21	78	40	57

[a] The HOMO is $7a_1$ and the $6e$ molecular orbital is not shown.

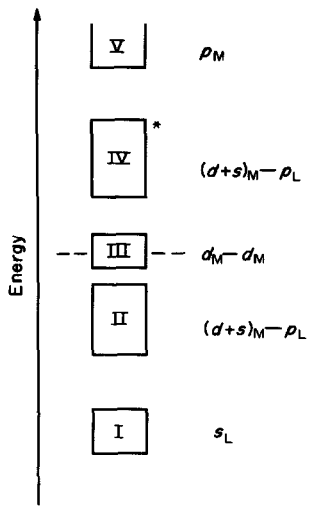

Fig. 3. The general structural energy levels of the core.

scheme has been drawn in Fig. 3. It is noteworthy that the scheme is only qualitatively correct. It is seen from Table 1 that HOMO $7a_1$ in the third block for $Mo_3X_3O^{5+}$ is about 58% *d*-orbital character of the Mo atoms and 42% *p*-orbital character of the bridging ligand atoms, and this HOMO is believed to be the antibonding orbital for the interaction between the metal atomic skeleton *d*-orbitals and edge-bridging ligand atom *p*-orbitals.

Bonding properties of M_3X_3

There are three types of bond that need to be considered in these incomplete metallic cubane-type clusters. These are the bonds between the metal atom and the terminal ligand atom, the metal atom and the edge- or face-bridging ligand atom, as well as between two metal atoms.

Generally, the interactions between the metal atom and both the terminal and bridging ligand atoms are stronger than the interactions between the two metal atoms. However, if the interactions of *d–p* π-bonding exist and the *d–p* π-bonding strength is comparable to the *d–d* interactions in the non-planar ring skeleton M_3X_3, all the interactions between metal atoms and terminal ligands should be viewed separately from the interactions within the M_3X_4 core. Bursten *et al.*[11] have indicated that the electronic structure of the pyramidal fragment $Mo_3O_4^{4+}$ is dominated by the influence of the three-bridging μ_2-O groups. Thus, the discussion in this section will be focused on the bonding within the M_3X_3 ring skeleton itself, with special attention paid to the effect of the *d–p* π-conjugate interactions upon the cluster bonding and physicochemical properties.

Table 3 lists several overlap populations for d_M–d_M and *d–p* π-interactions of M—X in the $M_3X_4^{4+}$ or $M_3X_3Y^{5+}$ core, as well as in the cluster ion compounds. The interactions between the d_z^2, d_{xz}, d_{yz} orbitals on the M(2) and M(3) atoms, or the d_z^2, d_{yz} orbitals on the M(1) atom and the p_y orbital on the X(1) atom, or p_y, p_x orbitals on the X(2) and X(3) atoms are called *d–p* π-interactions in view of the molecular coordinate system, as shown in Fig. 1. This assignment is only an approximation because the molecular orbitals are not localized in the present studies. It is seen from Table 3 that the *d–p* π-overlap populations are larger than those of d_M–d_M in either the $Mo_3S_4^{4+}$, $Mo_3S_3O^{4+}$ and $W_3S_4^{4+}$ cores or the $Mo_3S_4Cp_3^+$, $Mo_3S_4(CN)_9^{5-}$ and model $Mo_3S_4(H_2PS_2^-)_4OH_2$, cluster compounds, however, the *d–p* π-overlap populations are not larger than those of d_M–d_M in either the $Mo_3O_4^{4+}$, $Mo_3O_3S^{4+}$ and $W_3O_4^{4+}$ cores or the $Mo_3O_4F_9^{5-}$ cluster ion compound. In other words, the *d–p* π-bonding strengths are stronger in the Mo_3S_3 non-planar ring skeleton than in that of Mo_3O_3,

Table 2. Atomic orbital contributions of the π-type in the $5e$ and $5a_1$ molecular orbitals

Core	$5e(a')$ M $\%d_\pi$	Edge $\%p_\pi$	Cap $\%p_\pi$	$5a_1(a')$ M $\%d_\pi$	Edge $\%p_\pi$	Cap $\%p_\pi$
$Mo_3(\mu_3\text{-}S)(\mu\text{-}S)_3^{4+}$	32	32	0	32	17	0
$Mo_3(\mu_3\text{-}O)(\mu\text{-}S)_3^{4+}$	31	29	3	19	15	0
$Mo_3(\mu_3\text{-}S)(\mu\text{-}S)_2(\mu\text{-}O)^{4+}$	28	25	0	20	23	0
$Mo_3(\mu_3\text{-}S)(\mu\text{-}S)(\mu\text{-}O)_2^{4+}$	32	44	0	27	19	0
$Mo_3(\mu_3\text{-}S)(\mu\text{-}O)_3^{4+}$	24	58	3	39	8	0
$Mo_3(\mu_3\text{-}O)(\mu\text{-}O)_3^{4+}$	28	53	2	27	12	0
$W_3(\mu_3\text{-}S)(\mu\text{-}S)_3^{4+}$	34	34	0	30	15	0
$W_3(\mu_3\text{-}O)(\mu\text{-}O)_3^{4+}$	26	56	5	22	12	0
$Mo_3(\mu_3\text{-}O)(\mu\text{-}Br)_3^{5+}$	16	47	2	16	12	0
$Mo_3(\mu_3\text{-}O)(\mu\text{-}Cl)_3^{5+}$	11	50	2	17	12	0

Table 3. Mulliken population analyses

Species	Overlap populations d_M–d_M	d_π–p_π	Bond distances (Å) M—M	M—μ-X	References
$Mo_3(\mu_3\text{-}S)(\mu\text{-}S)_3^{4+}$	0.082	0.119	2.754	2.281	3
$Mo_3(\mu_3\text{-}O)(\mu\text{-}S)_3^{4+}$	0.092	0.126	2.651	2.280	4
$Mo_3(\mu_3\text{-}S)(\mu\text{-}O)_3^{4+}$	0.096	0.092	2.589	1.917	25
$Mo_3(\mu_3\text{-}O)(\mu\text{-}O)_3^{4+}$	0.107	0.098	2.493	1.914	2
$W_3(\mu_3\text{-}S)(\mu\text{-}S)_3^{4+}$	0.094	0.125	2.765	2.208	6
$W_3(\mu_3\text{-}O)(\mu\text{-}O)_3^{4+}$	0.111	0.100	2.53	1.92	7
$Mo_3(\mu_3\text{-}O)(\mu\text{-}Br)_3^{5+}$	0.124	0.074	2.594	2.548	8
$Mo_3(\mu_3\text{-}O)(\mu\text{-}Cl)_3^{5+}$	0.128	0.067	2.577	2.419	8
$Mo_3S_4(H_2PS_2^-)_4OH_2$	0.022	0.055	2.754	2.281	3
$Mo_3S_4(CN)_9^{5-}$	0.052	0.072	2.765	2.312	5
$Mo_3S_4Cp_3^+$	0.050	0.086	2.812	2.293	14
$Mo_3O_4F_9^{5-}$	0.077	0.077	2.494	1.915	—
$Mo_3O_4(OH_2)_9^{4+}$	0.094	0.087	2.493	1.914	2

while the overlap population is considered as an index for the strength of the bonding interaction.[16] These are the reasons why the electrons are attracted more by the oxygen atomic nucleus than by the sulphur atomic nucleus, and the π-electrons delocalized over Mo_3O_3 are less than those over Mo_3S_3. Moreover, it appears from experiments that the average lengths of Mo—S in Mo_3S_3 and Mo—O in Mo_3O_3 are different; the Mo—S bond length falls between single and double bonds,[1] while the Mo—O length falls in the single bond range.[2] However, the stability of $Mo_3O_4(OH_2)_9^{4+}$ is greater than that of $Mo_3S_4(dtp)_4OH_2$, as proved by the oxidation of $Mo_3S_4(dtp)_4OH_2$ in hydrotropic solution over a period of time.[1] Now, the question arising at this stage is: how is it possible to explain this stability of $Mo_3O_4(OH_2)_9^{4+}$? The answer is provided by the calculational results of quantum chemistry: the d_M–d_M interactions are stronger in the $Mo_3O_4^{4+}$ and $Mo_3O_4(OH_2)_9^{4+}$ species than in $Mo_3S_4^{4+}$ and $Mo_3S_4(H_2PS_2^-)_4OH_2$ in terms of the population analyses shown in Table 3. Perking[17] and Faucher[18] have shown that strong transannular interactions exist between endocyclic P atoms for which the strength of the transannular P—P bonding is about 10% of that of a P—N bond in the $(NPCl_2)_3$ trimer, and this provides an important contribution to the stability in $(NPCl_2)_3$. We consider that the transannular bonding interactions between M—M in the non-planar ring skeleton M_3X_3 should be more important contributions to the stability in the incomplete metallic cubane-type cluster compounds. The strength of the Mo—Mo bond is about 18% of the Mo—S bond strength of the Mo_3S_3 core contained in $Mo_3S_4(H_2PS_2^-)_4OH_2$, and the strength of the Mo—Mo bond is about 24% of the strength of the Mo—O bond in the Mo_3O_3 core contained in $Mo_3O_4F_9^{5-}$, according to the energy partitions[19,20] based on our calculated results. It is seen that the transannular Mo—Mo bond gives more contribution to the stability of the clusters containing Mo_3O_3 than to the clusters containing Mo_3S_3. It is possible to explain why the stability of $Mo_3O_4(OH_2)_9^{4+}$ is greater than that of $Mo_3S_4(dtp)_4OH_2$.

There are other types of non-planar ring skeleton Mo_3X_3 (X = Cl, Br) in $Mo_3X_3O(OAc)_3Cl_3^-$,[8] in which the formal molybdenum oxidation state is $3\frac{1}{3}$ and the trimolybdenum has eight valence electrons. Comparing the compounds which contain the non-planar ring skeleton Mo_3X_3 (X = O, S) with those containing Mo_3X_3 (X = Cl, Br), there are two additional electrons in the latter cluster compounds. Which kind of orbital (M—M or M—X interaction) are the additional electrons occupying? This question has been discussed in several papers.[11,21] We consider that the two additional electrons will occupy a d–p π-antibonding orbital in Mo_3X_3 (X = Cl, Br). The Mo—Mo bond would be weakly bonding, and one would not expect a shortening of the Mo—Mo bond (2.577 Å) in $Mo_3Cl_3O(OAc)_3Cl_3^-$,[8] if the two additional electrons occupy the Mo—Mo antibonding orbital. By comparing it with the Mo—Mo bond (2.65 Å) in $Mo_3S_3O(S_2P(OEt)_2)_4(C_3H_3N_2)$,[4] the short Mo—Mo bond in $Mo_3Cl_3O(OAc)_3Cl_3^-$ will not be influenced by the geometric factors of atomic size, on account of the fact that the reduction of the effective metal charge from 4 to $3\frac{1}{3}$ should be accompanied by an increase in the effective atomic radius of the molybdenum atom for the eight-electron system, and the difference between the covalent

radii of the sulphur and chlorine atoms is only 0.03 Å. Moreover, the calculated results on the $Mo_3Cl_3O^{5+}$ core have shown that the HOMO is $7a_1$ and consists of 38% d π-character on the tri-metal and 21% p π-character on the tri-edge-ligand in terms of the orbital analysis based on the calculation results.

It is also seen from Table 3 that substitution of molybdenum by tungsten induces a large overlap population of d_M–d_M and d–p π-interactions in the non-planar ring skeleton W_3X_3 (X = O, S), although the distances of both the W—W and W—X are not less than those of both the Mo—Mo and Mo—X separately. This means that the W_3X_3 stabilization is more than that for Mo_3X_3 (X = O, S) for an exact homologue.

COMPUTATIONAL DETAILS

The calculations were based on the SCCC–EH method with weighted H_{ij}'s developed by Hoffmann *et al.*[19,22] There are nine VSIT(Q) functions for d-orbitals and three VSIE(Q) functions for s- and p-orbitals in the transition metal atom. The standard of convergence is 0.002 in iterative procedure.

All atomic and charge iteration parameters used in the calculations were taken from the default values of the ICON8 program,[22] except those of molybdenum, tungsten and bromine, and all geometric parameters, except for the model compound $Mo_3S_4(H_2PS_2^-)_4OH_2$, were taken from the crystal structural data[1-10] and are idealized to C_{3v} symmetry, excluding $Mo_3(\mu_3\text{-}S)(\mu\text{-}S)_2(\mu\text{-}O)^{4+}$ and $Mo_3(\mu_3\text{-}S)(\mu\text{-}S)(\mu\text{-}O)_2^{4+}$ which have C_s symmetry. The structural data of the model compound $Mo_3S_4(H_2PS_2^-)_4OH_2$ are the same as those of $Mo_3S_4(dtp)_4OH_2$ (dtp = $(EtO)_2PS_2^-$),[3] in which the EtO group was replaced by a hydrogen atom and the P—H distance is 1.42 Å. All core $M_3X_{4-n}Y_n$ conformations in the calculations are the same as those for the $M_3X_{4-n}Y_n$ core in the cluster compounds $M_3X_{4-n}Y_nL_9$[1-10] (M = Mo, W; X = O, S, Cl, Br; Y = O, S; L = terminal ligand; n = 1, 0). The atomic parameters for molybdenum and tungsten were taken from ref. 23. The charge iteration parameters for tungsten were the same as for molybdenum, and were taken from ref. 24. The parameters for 4s and 4p valence orbitals of the bromine atom are as follows: both orbital exponents are 2.257 and the Coulomb integrals are −24.1 and −12.5 eV, the iterative parameters A, B, C are, respectively, 0.0, 9.86, 23.79 for the 4s orbital and 0.0, 9.86 and 11.84 for the 4p orbital.

Acknowledgements—This investigation was supported by the Science Foundation of the Chinese Academy of Sciences and by the Fuzhou Laboratory of Structural Chemistry, Fujian Institute of Research on the Structure of Matter. We thank Professors C. W. Liu, X. T. Wu and S. F. Lu for the stimulating discussions.

REFERENCES

1. J. Q. Huang, S. F. Lu, M. Y. Shang, X. T. Lin, M. D. Huang, Y. H. Lin, D. M. Wu, H. H. Zhuang, J. L. Huang and J. X. Lu, *J. Struct. Chem.* 1987, **6**, 219.
2. K. R. Rodgers, R. K. Murmann, E. O. Schlemper and M. E. Shelton, *Inorg. Chem.* 1985, **24**, 1313.
3. X. T. Lin, Y. H. Lin, J. L. Huang and J. Q. Huang, *Kexue Tongbao* 1987, **32**, 810.
4. M. D. Huang, S. F. Lu, J. Q. Huang and J. L. Huang, *J. Struct. Chem.* 1987, **6**, 29.
5. N. C. Howlader, G. P. Haight Jr, T. W. Hambley, G. A. Lawrence, K. M. Rahmoeller and M. R. Snow, *Aust. J. Chem.* 1983, **36**, 377.
6. T. Shibahara, K. Kohda, A. Ohtsuji, K. Yasuda and H. Kuroya, *J. Am. Chem. Soc.* 1986, **108**, 2757.
7. M. Segawa and Y. Sasaki, *J. Am. Chem. Soc.* 1985, **107**, 5565.
8. D. M. Wu, H. H. Zhuang, J. J. Zheng, J. L. Huang, J. X. Lu and J. Q. Huang, *Scientia Sin.* 1985, **10B**, 875.
9. T. Shibahara, H. Miyke, K. Kobayashi and N. Kuroya, *Chem. Lett.* 1986, 139.
10. T. Shibahara, T. Yamada and H. Kyroya, *Inorg. Chem. Acta* 1986, **13**, L19.
11. B. E. Bursten, F. A. Cotton, M. B. Hall and R. C. Najjar, *Inorg. Chem.* 1982, **21**, 302.
12. R. Jostes, A. Muller and F. A. Cotton, *Angew. Chem., Int. Edn Engl.* 1980, **19**, 875.
13. J. L. Huang, J. X. Lu, Y. S. Jiang and R. Hoffmann, *Scientia Sinica B* (Engl.) 1985, **28**, 1036.
14. P. J. Vergamini, H. Vahrenkamp and L. F. Dahl, *J. Am. Chem. Soc.* 1971, **93**, 6327.
15. M. D. Curtis and W. M. Butler, *J. Chem. Soc., Chem. Commun.* 1980, 998.
16. J. Q. Li and W. D. Cheng, *J. Molec. Struct. (Theochem.)* 1987, **19**, 151.
17. D. R. Armstrong, G. H. Longmuir and P. G. Perkins, *J. Chem. Soc., Chem. Commun.* 1972, 464.
18. J. P. Faucher, J.-F. Labarre and R. A. Shaw, *Z. Naturfor.* 1976, **31b**, 677.
19. R. Hoffmann *et al.*, ICON8 program descriptions.
20. J. A. Pople and D. L. Beveridge, *Approximate Molecular Orbital Theory*, p. 69. McGraw-Hill, New York (1970).
21. F. A. Cotton and T. E. Hass, *Inorg. Chem.* 1964, **3**, 10; F. A. Cotton, *Inorg. Chem.* 1964, **3**, 1217.
22. R. Hoffmann, *J. Chem. Phys.* 1963, **39**, 1397; R. Hoffmann and W. N. Lipscomb, *J. Chem. Phys.* 1962, **36**, 2179.
23. R. H. Summerville and R. Hoffmann, *J. Am. Chem. Soc.* 1979, **101**, 3830.
24. R. Munita and J. R. Letelier, *Theoret. Chim. Acta* 1981, **58**, 167.
25. T. Shibahara, H. Hattori and H. J. Kuroya, *J. Am. Chem. Soc.* 1984, **106**, 2710.

Polyhedron Vol. 8, No. 23, pp. 2791–2796, 1989
Printed in Great Britain

0277–5387/89 $3.00+.00
© 1989 Pergamon Press plc

THE MECHANISM OF OXIDATION OF CUBOIDAL $[Mo_4S_4(edta)_2]^{4-}$ AND $[Mo_4S_4(edta)_2]^{3-}$ BY *cis*-$[V(O)_2(H_2O)_4]^+$ AND BrO_3^-

PAUL W. DIMMOCK, BEE-LEAN OOI and A. GEOFFREY SYKES*

Department of Chemistry, The University, Newcastle upon Tyne NE1 7RU, U.K.

(*Received* 30 *March* 1989; *accepted* 20 *July* 1989)

Abstract—The air-sensitive cuboidal Mo_4^{III} complex $[Mo_4S_4(edta)_2]^{4-}$ (edta = N,N,N′,N′-ethylenediaminetetraacetate), reduction potential −0.046 V for one-equivalent oxidation, is rapidly oxidized by $V(O)_2^+$ (1.0 V for $V(O)_2^+/VO^{2+}$) and BrO_3^- (1.15 V for BrO_3^-/BrO_2) to $[Mo_4S_4(edta)_2]^{3-}$ at pH < 3. The slower, further oxidation to $[Mo_4S_4(edta)_2]^{2-}$ (0.65 V) has been studied independently by stopped-flow (for $V(O)_2^+$), and conventional time range spectrophotometry (for BrO_3^-). In the case of the $V(O)_2^+$ reaction (25°C) the rate law is $(k_1+k_2[H^+])[Mo_4S_4(edta)_2^{3-}][V(O)_2^+]$, $k_1 = 83\ M^{-1}\ s^{-1}$ and $k_2 = 4.6\times10^3\ M^{-2}\ s^{-1}$ over the $[H^+]$ range, 0.025–0.200 M, studied, $I = 1.00$ ($LiClO_4$). Studies on the BrO_3^- reaction under similar conditions indicated a more complicated reaction sequence, which is faster the higher the $[H^+]$. The initial induction phase exhibits an $[H^+]^2$-dependence. The $[H^+]$-dependences observed are consistent with the need to decrease the extent of hydrolysis as rate-determining steps $V(O)_2^+ \rightarrow VO^{2+}$ and $BrO_3^- \rightarrow BrO_2$ occur. No evidence was obtained for single stage two-equivalent steps. Reactions are most likely of the outer-sphere type.

The existence of cuboidal Mo_4S_4 complexes in three adjacent average molybdenum states, 3.0, 3.25 and 3.50, has been established in recent work.[1–4] Redox reactions of the aqua ions $[Mo_4S_4(H_2O)_{12}]^{n+}$ ($n = 4$, 5 and 6),[5,6] and the corresponding $[Mo_4S_4(edta)_2]^{m-}$ ($m = 4$, 3 and 2) states,[7] have been reported previously and illustrate the readiness with which interconversion of these ions can occur.

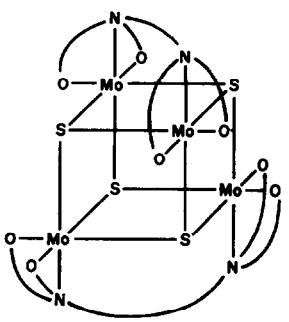

$[Mo_4S_4(edta)_2]^{m+}$

Self-exchange rate constants for the reactions $[Mo_4S_4(edta)_2]^{4-/3-}$ ($1.5\times10^7\ M^{-1}\ s^{-1}$), and $[Mo_4S_4(edta)_2]^{3-/2-}$ ($7.7\times10^5\ M^{-1}\ s^{-1}$) have been obtained.[7] In this study we explore the reactivity of the oxo-containing oxidants, *cis*-$[V(O)_2(H_2O)_4]^+$ (hereafter referred to as $V(O)_2^+$) and BrO_3^-. In the case of BrO_3^- at least, the possibility of a single two-equivalent rate-determining step, $BrO_3^- \rightarrow BrO_2^-$, exists as BrO_3^- is converted through to Br^-. Such changes have been reported (with I^-, Br^-, Cl^-, H_2O_2, HN_3 and HSO_3^-),[8–12] although the one-equivalent change $BrO_3^- \rightarrow BrO_2$ is observed with other reductants ($[Fe(CN)_6]^{4-}$, VO^{2+}, Hg^0 etc).[13–16] There are as yet no examples of two-equivalent reduction of the $V(O)_2^+$ ion, the $V(O)_2^+ \rightarrow V^{3+}$ conversion representing too drastic a change in hydrolysis for reaction to occur in a single rate-determining step. Reduction potentials[7] and colours of the $[Mo_4S_4(edta)_2]^{m-}$ ions are as indicated in eq. (1):

$$\underset{\text{Orange}}{[Mo_4S_4(edta)_2]^{4-}} \underset{+e^-}{\overset{-e^-}{\rightleftharpoons}} \underset{-0.046\,V}{} \underset{\text{Green}}{[Mo_4S_4(edta)_2]^{3-}} \underset{+e^-}{\overset{-e^-}{\rightleftharpoons}} \underset{0.65\,V}{} \underset{\text{Red}}{[Mo_4S_4(edta)_2]^{2-}}. \quad (1)$$

* Author to whom correspondence should be addressed.

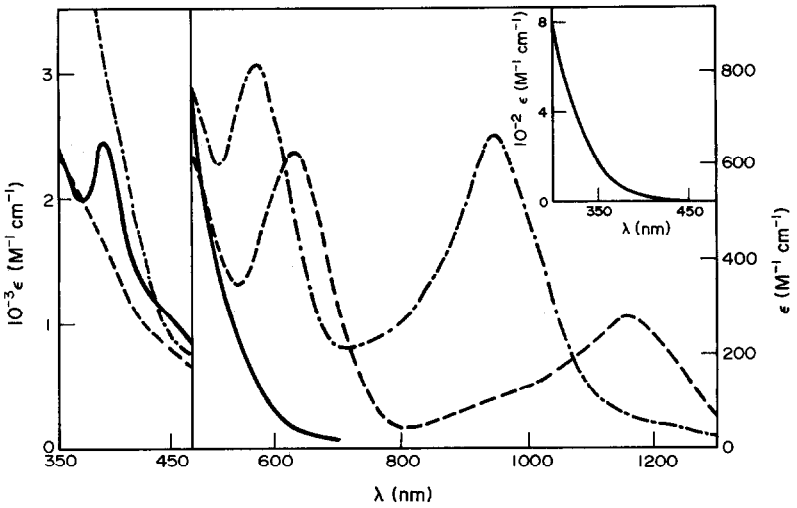

Fig. 1. UV–vis–near-IR absorbance spectra of cuboidal $[Mo_4S_4(edta)_2]^{4-}$ (——) $[Mo_4S_4(edta)_2]^{3-}$ (– – –) and $[Mo_4S_4(edta)_2]^{2-}$ (· · ·) in 0.5 M $LiClO_4$ (neutral pH), ε values per cube. The inset shows the corresponding $V(O)_2^+$ spectrum.

EXPERIMENTAL

Preparation of $[Mo_4S_4(edta)_2]^{3-}$

The di-μ-sulphido molybdenum(V) dimer $Na_2[Mo_2O_2S_2(edta)]\cdot 2H_2O$ was prepared,[17] and conversion of cyclic Mo_2S_2 to cuboidal Mo_4S_4 achieved by $NaBH_4$ (1 g) reduction of the dimer (2 g) in 0.03 M HCl (200 cm^3), all under N_2.[1,4] The resultant solution was left to stand overnight at ~ 4°C, after which it was heated in air to ~ 90°C on a steam bath for ~ 24 h. Column purification of $[Mo_4S_4(edta)_2]^{3-}$ was as described previously,[7] to give a UV–vis–near-IR spectrum in 0.5 M $LiClO_4$ at neutral pH, with peaks λ (nm) (ε/M^{-1} cm^{-1} per cube) at 636 (635) and 1145 (280), and shoulders at 300 (7500) and 450 (750), Fig. 1. Stock solutions up to 6 mM in 0.5 M $LiClO_4$ were stable in air. Solutions were standardized for $[Li^+]$ by loading onto an Amberlite 1R(H)120 cation-exchange column and titrating the $[H^+]$ released.

Preparation of $[Mo_4S_4(edta)_2]^{4-}$

Solutions of $[Mo_4S_4(edta)_2]^{3-}$ in 0.5 M $LiClO_4$ as prepared above, were reduced under N_2 at a high surface area carbon–cloth electrode (RVG 100 cloth from Le Carbonne, Brighton, U.K.) as already described,[5] using a constant potential of 0.50 V (vs SCE) for ~ 2 h. After reduction was complete the orange $[Mo_4S_4(edta)_2]^{4-}$ was millipore filtered (8 μm pore size) to remove any carbon particles. This operation was performed under N_2 in a glove bag. Spectrophotometric standardization was carried out at the 390 nm peak (ε = 2445 M^{-1} cm^{-1} per cube), Fig. 1, and checked by allowing the complex to air-oxidize to $[Mo_4S_4(edta)_2]^{3-}$. Stock solutions were stored under N_2 at 0°C and used the same day for kinetic runs.

Preparation of $[V(O)_2(H_2O)_4]^+$

The yellow *cis*-di-oxo aqua ion of vanadium(V) was prepared by first dissolving ammonium vanadate, NH_4VO_3 (BDH, Analar), in hot water. An equal volume of 4 M $HClO_4$ was then added with stirring to give a 0.05 M solution of vanadium(V) in 2 M acid. After cooling to room temperature the solution was filtered (removal of any solid V_2O_5) and standardized by titration with freshly prepared iron(II) ammonium sulphate in 2 M H_2SO_4 using ferroin as indicator. *Cis*-di-oxo $V(O)_2^+$ is known to be the sole vanadium(V) form present at $[H^+] > 0.05$ M.[18]

Other reagents

Sodium bromate (BDH Reagent Grade), was used. Lithium perchlorate (Aldrich) was recrystallized three times. Perchloric acid (BDH) was of Analar grade purity.

Kinetics

Relevant spectra are compared in Fig. 1. Details for $[Mo_4S_4(edta)_2]^{2-}$ are peaks λ (nm) (ε/M^{-1} cm^{-1} per cube) at 570 (820) and 945 (670). All studies were at 25.0 ± 0.1°C, and in aqueous perchloric acid solution with ionic strength *I* adjusted

to 1.00 M with $LiClO_4$. Stopped-flow studies were on a Dionex D-110 spectrophotometer, and rate constants were obtained using OLIS programs (Jefferson, Georgia, U.S.A.). Conventional time range spectrophotometry was carried out on a Perkin–Elmer Lambda 9 instrument.

Treatment of data

Second-order rate constants for the $V(O)_2^+$ reaction, eq. (3) and Fig. 2, were evaluated using a linear least-squares treatment with weighting to pass through the origin.

RESULTS

Oxidation of $[Mo_4S_4(edta)_2]^{4-}$

Both the $V(O)_2^+$ and BrO_3^- oxidants give $[Mo_4S_4(edta)_2]^{3-}$ in a fast process at pH < 3. At 25°C, $[H^+] = 0.025$ M, for example the 1 : 1 reaction with $V(O)_2^+$ is too fast to follow $k > 10^6$ M^{-1} s^{-1}. With excess oxidant the slower further oxidation to $[Mo_4S_4(edta)_2]^{2-}$ is observed. In the case of BrO_3^- it was possible to study the effect of further increases in pH without any structural changes occurring on the oxidant. At neutral pH in 0.5 M $LiClO_4$ the reaction is significantly slower, and with both reactants $[Mo_4S_4(edta)_2]^{4-}$ and BrO_3^- at 0.3 mM, the half-life is 10 min. The rate constant for the $[Mo_4S_4(edta)_2]^{4-}$ reaction with H^+ at 1 M total $[ClO_4^-]$ has been determined previously and is 76 M^{-1} s^{-1}, precluding studies at high $[H^+]$.[19]

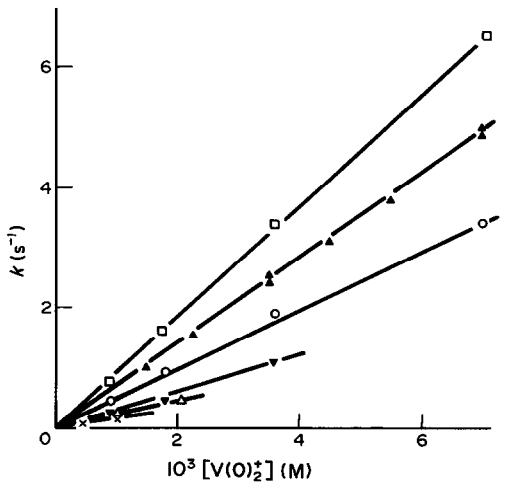

Fig. 2. The dependence of first-order rate constants k_{obs} (25°C) for the $V(O)_2^+$ oxidation of $[Mo_4S_4(edta)_2]^{3-}$ on oxidant concentration, and the effect of $[H^+]$/M: □, 0.2 M; ▲, 0.15 M; ○, 0.10 M; ▼, 0.050 M; △, 0.030 M; and ×, 0.025 M, $I = 1.00$ M ($LiClO_4$).

$V(O)_2^+$ oxidation of $[Mo_4S_4(edta)_2]^{3-}$

The reaction conforms to eq. (2):

$$[Mo_4S_4(edta)_2]^{3-} + V(O)_2^+ + 2H^+ \longrightarrow [Mo_4S_4(edta)_2]^{2-} + VO^{2+} + H_2O. \quad (2)$$

No further oxidation of $[Mo_4S_4(edta)_2]^{2-}$ is observed as in the corresponding oxidation of $[Mo_4S_4(H_2O)_{12}]^{5+}$, when the reaction of $[Mo_4S_4(H_2O)_{12}]^{6+}$ with excess $V(O)_2^+$ results in a break-up of the cube.[6]

Absorbance changes were monitored at 850 nm with $V(O)_2^+$ in more than a 10-fold excess. Good first-order behaviour was observed, yielding rate constants, k_{obs}, Table 1. From the dependence on $[V(O)_2^+]$, Fig. 2, second-order rate constants at each $[H^+]$ were obtained, Table 2. The $[H^+]$ dependence, Fig. 3, can be expressed as in eq. (3):

$$k = k_1 + k_2[H^+], \quad (3)$$

where $k_1 = 83 \pm 7$ M^{-1} s^{-1} and $k_2 = (4.6 \pm 0.4) \times 10^3$ M^{-2} s^{-1}. In the case of k_1, contributions from spurious effects due to the medium (validity of interchanging Li^+ and H^+)[20] cannot be ruled out, and

Table 1. The variation of first-order rate constants, k_{obs} (25°C), for the $V(O)_2^+$ oxidation of $[Mo_4S_4(edta)_2]^{3-}$, and the dependence on $[V(O)_2^+]$ and $[H^+]$, $I = 1.00$ M ($LiClO_4$)

$[H^+]$ (M)	$10^3[Mo_4S_4(edta)_2^{3-}]$ (M)	$10^3[V(O)_2^+]$ (M)	k_{obs} (s^{-1})
0.025	0.15	0.45	0.092
	0.15	0.89	0.172
0.030	0.15	0.53	0.091
	0.15	1.07	0.205
	0.30	2.13	0.42
0.050	0.15	0.45	0.111
	0.15	0.89	0.234
	0.30	1.78	0.46
	0.30	3.57	1.08
0.10	0.115	0.89	0.46
	0.15	1.78	0.97
	0.30	3.57	1.88
	0.30	7.13	3.5
0.15	0.15	1.50	1.0
	0.15	2.25	1.5
	0.30	3.51	2.4
	0.30	4.51	3.1
	0.30	5.51	3.8
	0.30	6.99	5.0
	0.15	6.99	4.9
0.20	0.15	0.89	0.75
	0.15	1.79	1.62
	0.15	3.57	3.4
	0.15	7.13	6.7

Table 2. The variation of second-order rate constants, k (25°C), with $[H^+]$ for the $V(O)_2^+$ oxidation of $[Mo_4S_4(edta)_2]^{3-}$, $I = 1.00$ M ($LiClO_4$)

$[H^+]$ (M)	k ($M^{-1}\,s^{-1}$)
0.025	191 ± 5
0.030	200 ± 5
0.050	303 ± 13
0.10	490 ± 13
0.15	710 ± 10
0.20	920 ± 20

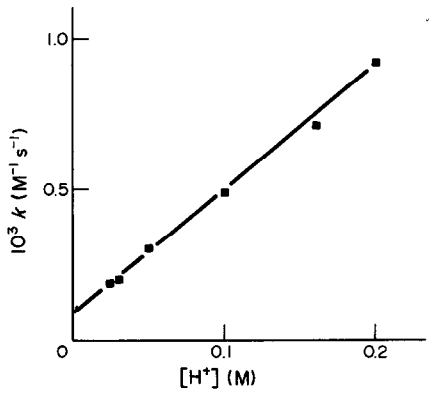

Fig. 3. The dependence of second-order rate constants k (25°C) for the $V(O)_2^+$ oxidation of $[Mo_4S_4(edta)_2]^{3-}$ on $[H^+]$, $I = 1.00$ M ($LiClO_4$).

for the $[H^+]$ range 0.025–0.200 M, k_2 is to be regarded as the principal rate law term.

BrO_3^- *oxidation of* $[Mo_4S_4(edta)_2]^{3-}$

The formation of $[Mo_4S_4(edta)_2]^{2-}$ was monitored at 945 nm with BrO_3^- in greater than 10-fold excess. The conversion $BrO_3^- \rightarrow Br^-$ was assumed to occur. Absorbance changes were more complicated as illustrated in Fig. 4. A slower second stage corresponding to further reaction (absorbance decrease) of the $[Mo_4S_4(edta)_2]^{2-}$ product was also observed. From initial slopes for the induction stage in Fig. 4, an $[H^+]^2$ dependence is observed, Fig. 5. Within experimental error the line passes through the origin. No reaction was obtained in neutral solutions indicating the need for H^+ for the reaction to proceed.

DISCUSSION

Two separate stages are observed in the reactions of excess $V(O)_2^+$ or BrO_3^- with $[Mo_4S_4(edta)_2]^{4-}$.

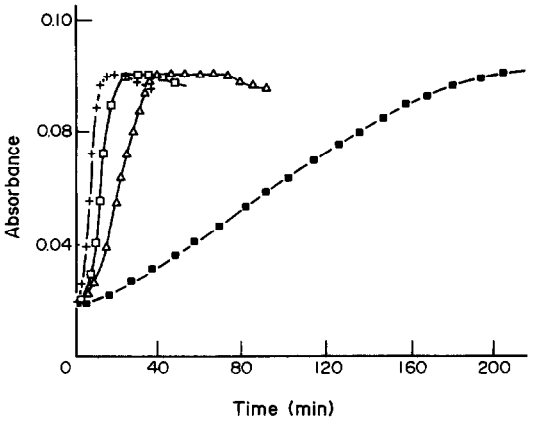

Fig. 4. Absorbance changes at 945 nm for the BrO_3^- oxidation of $[Mo_4S_4(edta)]^{3-}$ (both 1.5×10^{-4} M) at 25°C, at different $[H^+]$/M: +, 0.50; □, 0.38; △, 0.25; ■, 0.10.

At the end of the first stage the product is $[Mo_4S_4(edta)_2]^{3-}$. Whether reaction has occurred in a single redox step, or by a more circuitous route involving two-equivalent change to $[Mo_4S_4(edta)_2]^{2-}$ followed by comproportionation of the 4− and 2− states is not immediately clear. Elsewhere,[7] from studies on cross reactions, the self-exchange rate constants for $[Mo_4S_4(edta)_2]^{4-/3-}$ and $[Mo_4S_4(edta)_2]^{3-/2-}$ are very favourable (order of magnitude 10^6–10^7 $M^{-1}\,s^{-1}$) and give a comproportionation rate constant of 2.4×10^{10} $M^{-1}\,s^{-1}$. In these studies no initial rapid formation of $[Mo_4S_4(edta)_2]^{2-}$ as a product of a two-equivalent process was detected, but in view of the rapid comproportionation this is hardly a definitive test. For

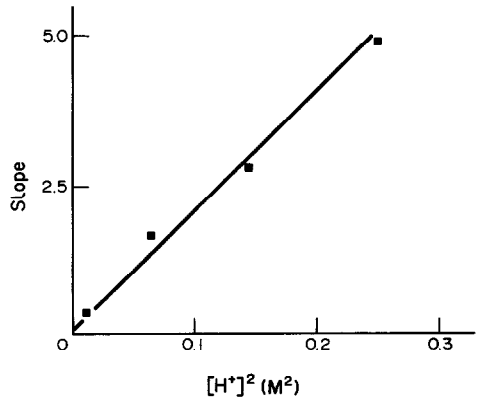

Fig. 5. Dependence of the initial slopes from Fig. 4 (arbitrary units) on $[H^+]$ for the BrO_3^- oxidation of $[Mo_4S_4(edta)_2]^{3-}$ at 25°C, $I = 1.00$ M ($LiClO_4$).

other reasons, namely the need for two-equivalent reactions to be inner-sphere, and the obvious difficulty of such a process occurring in the present case, one-equivalent changes seem most likely. Certainly we have no evidence for edta dechelation, and the molybdenums are expected to remain at least six-coordinate. There are in special cases examples of higher coordination numbers to molybdenum (e.g. with CN^-),[21,22] and in the case of edta complexes of d^5-ions, iron(III) and manganese(II).[23,24] However, an increase in coordination number involving the use of high energy orbitals may be more difficult for cuboidal Mo_4S_4, and at present there are no examples of this occurring.

The slower $V(O)_2^+$ and BrO_3^- oxidation of $[Mo_4S_4(edta)_2]^{3-}$ to $[Mo_4S_4(edta)_2]^{2-}$ was studied in separate experiments. A feature of the kinetics is the need for $[H^+]$ involvement in the rate laws. There are ambiguities with regard to interpretation, since although protonation of the oxidant might seem more obvious, the carboxylates of edta might also be involved. Such a protonation is not favourable however unless dissociation, i.e. aquation, of the carboxylate arm in question is occurring, and there is no evidence for this. Therefore the $[H^+]$ terms most likely originate from the oxidant, and are related to the need for protonation to facilitate the redox changes $V(O)_2^+ \rightarrow VO^{2+}$ and $BrO_3^- \rightarrow BrO_2$. The kinetics in the case of the $V(O)_2^+$ oxidation are relatively straightforward, and a rate law first-order in oxidant and reductant is observed. For the $[H^+]$-dependent k_2 term it is likely that $V(O)_2^+$ brings a proton into the activated complex. Similar $[H^+]$-dependences have been observed previously.[25,26] At high $[H^+]$ values an $[H^+]^2$ term might be expected to contribute.

The BrO_3^- oxidation is more complex, as Fig. 4 clearly illustrates, and an induction period is observed. From the initial slopes an $[H^+]^2$-dependence is apparent, Fig. 5. The propagation step, exhibiting at least a first-order $[H^+]$-dependence, is followed by an abrupt termination of reaction. An induction phase has been observed previously in BrO_3^- reactions, and interpretations have been summarized in the review by Thompson.[16] There are two possible explanations for the initial stage. This can be due to a rate law term $[H^+]^2[BrO_3^-][Br^-]$ giving autocatalytic behaviour, as is observed with reductants such as $[Fe(CN)_6]^{4-}$. Alternatively, with less strong reductants such as cerium(III), manganese(II) or neptunium(V), a poorly defined induction period is followed by a rate law dependence $[H^+]^2[BrO_3^-]^2$.[27,28] For the reduction potential applying in this instance (0.69 V),[7] the first of these explanations is the more likely.

Acknowledgements—P.W.D. acknowledges the award of an SERC studentship, and B.-L.O. the award of a Ridley Fellowship from the University of Newcastle upon Tyne.

REFERENCES

1. M. Martinez, B.-L. Ooi and A. G. Sykes, *J. Am. Chem. Soc.* 1987, **109**, 4615.
2. T. Shibahara, H. Kuroya, K. Matsumoto and S. Ooi, *J. Am. Chem. Soc.* 1984, **106**, 789.
3. T. Shibahara, H. Kuroya, K. Matsumoto and S. Ooi, *Inorg. Chim. Acta* 1987, **116**, 225.
4. F. A. Cotton, M. P. Diebold, Z. Dori, R. Llusar and W. Schwotzer, *J. Am. Chem. Soc.* 1985, **107**, 6735.
5. C. Sharp and A. G. Sykes, *J. Chem. Soc., Dalton Trans.* 1988, 2579.
6. B.-L. Ooi, C. Sharp and A. G. Sykes, *J. Am. Chem. Soc.* 1989, **111**, 125.
7. P. W. Dimmock, J. McGinnis, B.-L. Ooi and A. G. Sykes, *Inorg. Chim. Acta*, 1989, in press.
8. A. F. M. Barton and G. A. Wright, *J. Chem. Soc. A* 1968, 1747.
9. T. Sigalla, *J. Chim. Phys.* 1958, **55**, 758.
10. H. A. Young and W. C. Bray, *J. Am. Chem. Soc.* 1932, **54**, 4284.
11. R. C. Thompson, *Inorg. Chem.* 1969, **8**, 1891.
12. F. S. Williamson and E. L. King, *J. Am. Chem. Soc.* 1957, **79**, 5397.
13. J. P. Birk and S. G. Kozub, *Inorg. Chem.* 1973, **12**, 2460.
14. R. Davies, B. Kipling and A. G. Sykes, *J. Am. Chem. Soc.* 1973, **95**, 7250.
15. R. C. Thompson, *Inorg. Chem.* 1971, **10**, 1892.
16. R. C. Thompson, *Adv. Inorg. Bioinorg. Mech.* 1986, **4**, 94.
17. V. R. Ott, D. S. Sweiter and F. A. Schultz, *Inorg. Chem.* 1977, **16**, 2538.
18. (a) M. J. La Salle and J. W. Cobble, *J. Phys. Chem.* 1955, **59**, 519; (b) F. J. C. Rossotti and H. S. Rossotti, *Acta Chem. Scand.* 1956, **10**, 957.
19. P. W. Dimmock, B.-L. Ooi and A. G. Sykes, to be submitted.
20. T. W. Newton, *The Kinetics of the Oxidation–Reduction Reactions of Uranium, Neptunium, Plutonium and Americium in Aqueous Solution*, ERDA Critical Review Series, p. 11 (1975).
21. M. B. Hursthouse, K. M. A. Malik, A. M. Soares, J. F. Gibson and W. P. Griffith, *Inorg. Chim. Acta* 1980, **45**, 281.
22. F. A. Cotton and G. Wilkinson, in *Advances in Inorganic Chemistry*, 5th edn, p. 837. Wiley Interscience, New York (1988).
23. (a) M. D. Lind, M. J. Hamar, T. A. Hamar and J. L. Hoard, *Inorg. Chem.* 1964, **3**, 34; (b) S. Richards, B. Pedersen, J. V. Silverton and J. L. Hoard, *Inorg. Chem.* 1964, **3**, 27; (c) J. L. Hoard, B. Pederson, S. Richards and J. V. Silverton, *J. Am. Chem. Soc.* 1961, **83**, 3533.
24. (a) Ya. M. Nesterova, T. N. Polynova, L. I. Mar-

tynenko and N. I. Pechurova, *Zh. Strukt. Khim.* 1971, **12**, 1110; (b) T. M. Polynova, N. N. Anan'eva, M. A. Porai-Koshits, L. I. Martynenko and N. I. Pechurova, *Zh. Strukt. Khim.* 1971, **12**, 335; (c) N. V. Novozhilova, T. N. Polynova, M. A. Porai-Koshits, N. I. Pechurova, L. I. Martynenko and A. Khadi, *Zh. Strukt. Khim.* 1973, **14**, 745.

25. D. R. Rosseinsky, *Chem. Rev.* 1972, **72**, 215.
26. (a) J. S. Littler and W. A. Waters, *J. Chem. Soc.* 1959, 1299; (b) T. J. Kemp and W. A. Waters, *J. Chem. Soc.* 1964, 1610.
27. R. C. Thompson, *J. Am. Chem. Soc.* 1971, **93**, 7315.
28. R. M. Noyes, R. J. Field and R. C. Thompson, *J. Am. Chem. Soc.* 1971, **93**, 7315.

Polyhedron Vol. 8, No. 23, pp. 2797–2801, 1989
Printed in Great Britain

0277–5387/89 $3.00+.00
© 1989 Pergamon Press plc

INFLUENCE OF THE IONIC STRENGTH ON THE FORMATION AND EXTRACTION OF THE STRONTIUM–CRYPTAND 2.2.2-EOSIN ION-PAIR COMPLEX

D. BLANCO GOMIS,* E. FUENTE ALONSO and P. ARIAS ABRODO

Departamento de Química Física y Analítica, Facultad de Química, Universidad de Oviedo, 33006 Oviedo, Spain

(*Received* 31 *March* 1989; *accepted* 20 *July* 1989)

Abstract—A systematic study of the factors affecting the extraction of strontium, as an ion-pair formed between the positively charged cryptate of strontium with cryptand 2.2.2 and the eosinate anion, into chloroform has been carried out. The pK_1 and pK_2 values of the ligand, the stability constant of the cryptate inclusion complex, as well as the partition coefficient and the extraction constant of the ion-pair, were measured as a function of the ionic strength of the solution. The pK_a and K_s values remained reasonably constant at ionic strength $\leqslant 0.1$ M. Nevertheless, the partition coefficient values, and consequently the extraction constant values, decrease as the ionic strength increases.

Recently, a large number of papers dealing with the extraction constants of crown- and cryptand–ether complexes of alkali and alkaline-earth ions associated with coloured or fluorescent anions have been published. Much less work has been carried out on analogous systems involving transition metals as well as lanthanide and actinide ions. The overall extraction equilibrium formulated by Frensdorff[1] can be rewritten as

$$M^{n+} + L + A^{n-} \overset{K_{ex}}{\rightleftharpoons} (MLA)_o, \qquad (1)$$

where M^{n+}, L, A^{n-} and $(MLA)_o$ are the metal cation, the cyclic polyether, the counter-ion and the ion-pair, respectively. The subscript o and the absence of a subscript denote the organic and the aqueous phase, respectively. The equilibrium constant of eq. (1) was designated as the extraction constant, K_{ex}:

$$K_{ex} = [MLA]_o/[M^{n+}][L][A^{n-}],$$

where the brackets denote equilibrium activities. This extraction equilibrium may be analysed in terms of two constituent equilibria which, when added to each other, give eq. (1):

$$M^{n+} + L \overset{K_s}{\rightleftharpoons} ML^{n+}$$

$$ML^{n+} + A^{n-} \overset{P_{CT}}{\rightleftharpoons} (MLA)_o.$$

The two equilibrium constants are K_s, the aqueous stability constant of the binary complex, and P_{CT}, the partition coefficient of the complex from separate ions in the aqueous phase into ion-pairs in the organic phase. Thus the overall extraction equilibrium constant is given by

$$K_{ex} = K_s P_{CT}.$$

If the ligand is a diamine or cryptand the following acid–base equilibria take place:

$$LH_2^{2+} \overset{K_1}{\rightleftharpoons} LH^+ + H^+$$

$$LH^+ \overset{K_2}{\rightleftharpoons} L + H^+.$$

Addition of a metal cation, M^{n+}, will thus affect the basicity of a solution of the free ligand. The role of these equilibria will be considered in detail in the Experimental.

However, in more recent publications the extraction constants have been reported using concentrations (K_{ex}^{conc}) instead of activities, and the extraction method has been applied at appreciable

* Author to whom correspondence should be addressed.

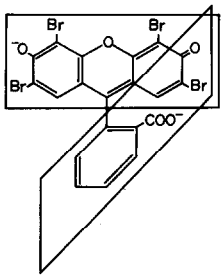

Structure 1. Molecular structure of the dianionic form of eosin.

ionic strengths, e.g. for the determination of K^+ in blood serum[2,3] or Pb^{2+} in tap water[4] and soft drinks,[5] where K_{ex}^{conc} differs considerably from K_{ex}.

In our earlier studies we have observed a critical influence of ionic strength on the extraction of some metal ions, e.g. K^+, Sr^{2+}, Ca^{2+} or Pb^{2+}, with crown– and cryptand–ethers. Thus, while the extraction of potassium with 18-crown-6[3] or lead with 18-crown-6[4] or cryptand 2.2.2[5] is not affected by this parameter (probably due to the formation of polymeric species in the organic phase), an increase in the ionic strength promotes a sharp decrease in the extraction of lead with cryptand 2.2.1[6] or strontium with cryptand 2.2.2,[7] using eosin as the counter-ion, and consequently a decrease in the fluorescence intensity of the organic phase. This factor could be a problem in the analytical application of these extraction systems. For this, we are at present engaged in a detailed study of various factors which affect the extraction constants of potassium, strontium and lead, including extraction of polymeric species and effects of counter-ion and solvents for the extraction.

In the present study we report the effect of ionic strength on the extraction of strontium using cryptand 2.2.2 (L) as the ligand, eosinate (A) as the counter-ion and chloroform as the extractant. On this account, we have studied the effect that the variation of the ionic strength causes on the different constants involved in the extraction process: the dissociation constants of the ligand, the stability constant of the cryptate inclusion complex, the partition coefficient and the extraction constant of the ion-pair, and the partition coefficient of the complex.

EXPERIMENTAL

Reagents and equipment

All reagents were of analytical grade and doubly distilled and demineralized water was used throughout.

Cryptand 2.2.2. The commercial product (Kryptofix 2.2.2 from Merck) was used as received. An aqueous stock solution (1.689×10^{-4} M) of the cryptand was stored in a PVC container and was diluted as required before use.

Strontium(II) *stock solution* (0.0114 M). Prepared by dissolving 1.2063 g of strontium nitrate in water, diluting to 500 cm^3 and standardizing by complexometric titration. All working standard solutions (5.772×10^{-5} M) were freshly prepared by appropriate dilution of the stock solution.

Eosin acid aqueous solution (8.970×10^{-3} M). Prepared by dissolving 0.1453 g of eosin in 25 cm^3 of basic water. Eosin was synthesized by reaction of Br^-/BrO_3^- with fluorescein in an acidic water–acetone mixture as described elsewhere.[8]

Tetramethylammonium hydroxide (4.388×10^{-2} M). The $(CH_3)_4N^+$ cation would be large enough so as not to enter the intramolecular cavity of the ligand. The basic solutions were made from commercial Fluka AG reagent. Preliminary titration showed about 3% of the latter to be carbonated. In order to avoid carbonation of these basic solutions argon was bubbled through them and they were stored in PVC containers.

The instrumentation included a UV–vis spectrophotometer (Perkin–Elmer, model 124) with quartz cells (10 mm path), an LS-5 Perkin–Elmer spectrofluorimeter equipped with a Model 3600 data-station, an inductively coupled plasma Perkin–Elmer spectrometer model 5000, a Crison-501 potentiometer and a Dosimat automatic microburet. A thermostatted shaker (Grant) with a time switch was used for horizontal shaking of the stoppered tubes.

Potentiometric titrations

To determine the protonation and the stability constants (K_1, K_2 and K_s), solutions of the protonated ligands (0.02 M) alone and in the presence of Sr^{2+} (0.01 M) were titrated with a strong base, $(CH_3)_4NOH$ (0.073 M). Variable concentrations of supporting electrolyte, $(CH_3)_4NBr$, in order to maintain the ionic strength (0.01, 0.05 and 0.10 M) in the test solution and in the titrant, were used. Calibration of the cell was achieved with HNO_3 solutions at different ionic strengths by titration with tetramethylammonium hydroxide. The potential of the solutions was measured with the following cell: glass electrode/test solution (I = 0.01–0.10 M, $(CH_3)_4NBr$)/0.01–0.10 M $(CH_3)_4NBr$, SCE, in order to avoid diffusion phenomena of potassium from the calomel electrode.

All measurements were performed in a glass cell maintained at 25 ± 0.1°C. Portions of 0.01 cm^3 of

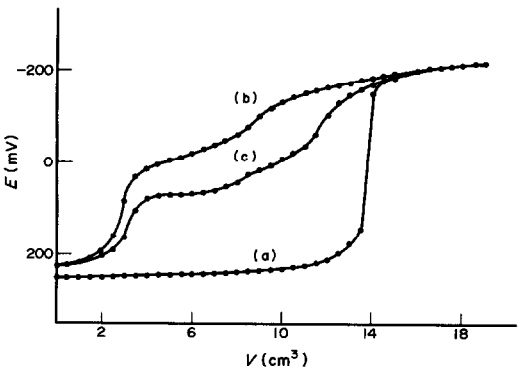

Fig. 1. Potential measurements (E) as a function of the volume of alkali added (V) to solutions containing: (a) strong acid (HNO_3); (b) strong acid and ligand (cryptand 2.2.2); (c) strong acid, ligand and metal ion (Sr^{2+}); $I = 0.01$ M.

titrant were added from an automatic microburet. The titration cell was purged with argon which had previously been saturated with water at 25°C. A typical titration curve is shown in Fig. 1. The results were analysed using a general equilibrium-solving program, MINIPOT,[9] to calculate the protonation and the formation constants.

Extraction procedure

An aliquot (5 cm^3) of an aqueous solution containing the metal ion (1.154×10^{-5} M), the cryptand solution (5.067×10^{-5} M), the $(CH_3)_4NOH$ solution (4.388×10^{-3} M, pH = 11.5), the eosinate anion for the formation of the ion-pair (9.440×10^{-6}–1.4×10^{-4} M; this concentration range allows extraction yields ranging from 15 to 85% to be obtained), and variable concentrations of $(CH_3)_4NBr$ solution in order to keep the ionic strength at 0.01, 0.05 or 0.10 M, was placed in a glass cylindrical tube with a PVC stopper. After the addition of 5 cm^3 of chloroform, the mixture was shaken for 60 min at 25 ± 0.1°C. The solvents were saturated with each other before use to prevent volume changes in the phases during extraction. The mixture was centrifuged for 5 min to separate the phases, the pH of the aqueous phase was checked and the concentration of the metal ion was measured by ICP emission photometry at 407.77 nm. Eosin equilibrium concentrations in the aqueous layer were measured spectrophotometrically at 516 nm. Strontium concentrations in the organic phases were determined as follows: 4 cm^3 of the chloroform phase were allowed to evaporate, the residue was dissolved in 10% nitric acid solution and determined by ICP emission photometry.

Partition coefficient of cryptand 2.2.2

Partition coefficients, $P(L)$, at different ionic strengths were determined by equilibration of equal volumes of the cryptand solution in water and in chloroform, followed by spectrofluorimetric determination of the amount of cryptand remaining in the aqueous phase. The determination was carried out by addition of eosin and strontium to the aqueous phase and extraction of the cryptand–strontium–eosinate complex into chloroform, following the general extraction procedure described elsewhere.[7] The concentration found in this way in the aqueous phase was subtracted from the initial total concentration of cryptand to deduce the concentration in the organic phase.

RESULTS AND DISCUSSION

Table 1 shows the results obtained for the concentration equilibrium constants, K_s, of complexes of cryptand 2.2.2 with Sr^{2+} at different ionic strengths, as well as the pK_1, pK_2 and $P(L)$ values of the ligand. As can be seen, in the ionic strength range 0.01–0.10 M, the concentration formation constant remains reasonably constant and close to values from the literature.[10,11] In a similar manner, the pK_a and $P(L)$ values of the ligand present a similar behaviour.

Distribution coefficient

When a divalent metal ion M^{2+}, such as Sr^{2+}, forms a complex with a cryptand, L, such as cryptand 2.2.2 and the complex is extractable as an ion-pair with large anions, A^{2-}, such as the eosinate ion, the distribution coefficient (D) for the extraction system

$$pM^{2+} + qL + rA^{2-} \rightleftharpoons (M_pL_qE_r)_o$$

may be written as

$$D = \sum[M^{2+}]_o / \sum[M^{2+}]$$

$$= \sum_{1}^{p,q,r} p[M_pL_qE_r]_o / [M^{2+}] + [ML^{2+}] + \sum_{1}^{i,j} [M_j(OH)_i^{2j-i}], \quad (2)$$

Table 1. K_s, pK_1, pK_2 and $P(L)$ values for the different ionic strengths

I	$\log K_s$	pK_1	pK_2	$P(L)$
0.01	8.25±0.09	7.17±0.04	9.97±0.03	89.38±0.62
0.05	8.11±0.03	7.27±0.02	9.66±0.02	89.39±0.84
0.10	7.96±0.05	7.26±0.01	9.71±0.05	89.42±0.76

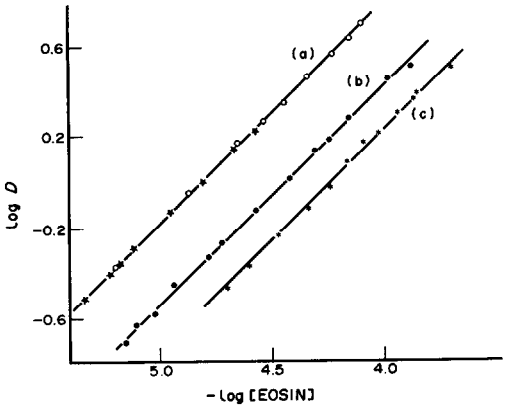

Fig. 2. Dependence of the distribution ratio for strontium on the eosin concentration in the aqueous phase at different ionic strengths: (a) $I = 0.01$ M, [2.2.2] = 5.07×10^{-5} M; ○ $[Sr^{2+}] = 1.14 \times 10^{-5}$ M, [eosin] = $(1.07\text{–}8.75) \times 10^{-5}$ M; ★ $[Sr^{2+}] = 5.71 \times 10^{-6}$ M, [eosin] = $(0.72\text{–}3.87) \times 10^{-5}$ M. (b) $I = 0.05$ M, [2.2.2] = 5.07×10^{-5} M, $[Sr^{2+}] = 1.14 \times 10^{-5}$ M, [eosin] = $(1.1\text{–}14.0) \times 10^{-5}$ M. (c) $I = 0.10$ M, [2.2.2] = 5.07×10^{-5} M, $[Sr^{2+}] = 1.14 \times 10^{-5}$ M, [eosin] = $(2.9\text{–}25.1) \times 10^{-5}$ M.

assuming that the association between ML^{2+} and A^{2-} in the aqueous phase and the dissociation of the ion-pair in the organic phase are negligible.

The strontium–cryptand ratio was described as 1 : 1, with strontium occupying a central position in the cavity of the macrobicyclic ligand.[10] The dissociation constants of eosin[12] and the pH value of 11.5 used suggest that only a neutral complex (1 : 1 : 1, strontium–cryptand–eosin) should be extracted.

If we suppose that non-polimeric species are formed in the organic phase and that under the experimental conditions used one may assume that $[ML^{2+}] \gg [M^{2+}]$ and that the hydroxylation of the metal cation is negligible, eq. (2) can be rewritten by using the partition coefficient of the complex, P_{CT},

$$\log D = \log P_{CT} + \log [A^{2-}].$$

The experimental results are shown in Fig. 2. The slope of the $\log D$ vs $\log [A^{2-}]$ plot is unity for the same strontium concentration and different ionic strengths tested, which clearly indicates the 1 : 1 : 1 metal–ligand–counter-ion stoichiometry. On the other hand, the superposition of the extraction curves (A) for different strontium concentrations at the same ionic strength indicates the non-existence of polymerization reactions.

Table 2. P_{CT} and K_{ex} values for the strontium–cryptand 2.2.2–eosin system in chloroform at different ionic strengths

I	$\log P_{CT}$	$\log K_{ex}$
0.01	4.86±0.05	13.11±0.03
0.05	4.42±0.01	12.53±0.02
0.10	4.17±0.04	12.13±0.06

The data obtained from these experiments have been refined by the LETAGROP program version DISTR[13] which provides the partition coefficients and extraction constants at different ionic strengths. The results are shown in Table 2 and Fig. 3. As can be seen, the value of the concentration formation constant remains reasonably constant as long as the partition coefficients and obviously the extraction constants decrease appreciably as the ionic strength increases. These results clearly explain the decrease of fluorescence intensity of the ion-pair (λ_{ex} = 536

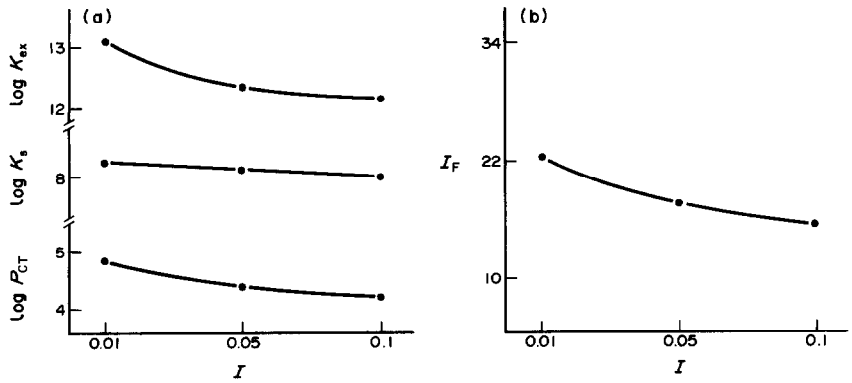

Fig. 3. Influence of ionic strength on: (a) The partition coefficients (P_{CT}), the concentration formation constants (K_s) and the extraction constants (K_{ex}). (b) The fluorescence intensity of the ion-pair in the organic phase.

nm, $\lambda_{em} = 552$ nm) in the organic phase with increasing ionic strength as it can be deduced from the same figure.

CONCLUSIONS

Our results on stability constants are in accordance with the studies of Lehn and Sauvage,[10] and Smetana and Popov.[14] They reported a change in $\log K_s$ of less than 0.3 for a variation of ionic strength from 0.005 to 0.3 M.

In a recent study on the effects of ionic strength on the extraction of potassium complexed with 18-crown-6, Kolthoff[15] reported the salting-out effect on the partition coefficient of the crown-ether, an effect which is not observed by us in the present study. The partition coefficients of cryptand 2.2.2 are the same for the different ionic strengths tested. From these results, it can be concluded that the ionic strength critically affects the association of ion-pairs in the aqueous phase and its extraction into the organic phase. This trend and the absence of secondary reactions, such as polymerization, observed in other systems,[6] promotes the fluorescence decrease observed.

REFERENCES

1. H. K. Frensdorff, *J. Am. Chem. Soc.* 1971, **93**, 4684.
2. H. Sumiyoshi, K. Nakahara and K. Ueno, *Talanta* 1977, **24**, 763.
3. A. Sanz Medel, D. Blanco Gomis and J. R. García Alvarez, *Talanta* 1981, **28**, 425.
4. A. Sanz Medel, D. Blanco Gomis, E. Fuente Alonso and S. Arribas Jimeno, *Talanta* 1984, **31**, 515.
5. D. Blanco Gomis, E. Fuente Alonso and A. Sanz Medel, *Talanta* 1985, **32**, 915.
6. D. Blanco Gomis, P. Arias Abrodo, A. M. Picinelli Lobo and A. Sanz Medel, *Talanta* 1988, **35**, 553.
7. D. Blanco Gomis, E. Fuente Alonso and P. Arias Abrodo, *Microchim. Acta*, in press.
8. D. Fompeydie, F. Onur and P. Levillain, *Bull. Soc. Chim. Fr.* 1982, **II**, 5.
9. F. Gaizer and A. Puskas, *Talanta* 1981, **28**, 565.
10. J. M. Lehn and J. P. Sauvage, *J. Am. Chem. Soc.* 1975, **97**, 6700.
11. G. Anderegg, *Helv. Chim. Acta* 1981, **64**, 1790.
12. P. Levillain and D. Fompeydie, *Analyt. Chem.* 1985, **57**, 2561.
13. D. H. Siem, *Acta Chem. Scand.* 1971, **25**, 1521.
14. A. J. Smetana and A. I. Popov, *J. Chem. Thermodyn.* 1979, **11**, 1145.
15. I. M. Kolthoff, *Can. J. Chem.* 1981, **59**, 1548.

Polyhedron Vol. 8, No. 23, pp. 2803–2807, 1989
Printed in Great Britain

0277–5387/89 $3.00+.00
© 1989 Pergamon Press plc

ELECTROCHEMICAL STUDIES ON ORGANOMETALLIC COMPOUNDS—XX.* ELECTROGENERATION OF AN UNUSUAL ORGANOMETALLIC DERIVATIVE OF RUTHENIUM(I)

P. LAHUERTA,† J. LATORRE and J. SOTO‡

Dpto. de Química Inorgánica, Universidad de Valencia, Dr Moliner 50, 46100 Burjasot, Valencia, Spain

and

Y. MUGNIER†

Laboratoire de Synthèse et d'Electrosynthèse Organometallique associé au CNRS (LA 33), Faculté des Sciences, 6 bd Gabriel 21100 Dijon, France

(*Received* 31 *March* 1989; *accepted* 25 *July* 1989)

Abstract—The two-electron reduction of dinuclear ruthenium complexes $[RuCl_2(\eta^6\text{-}p\text{-cymene})]_2$ (p-cymene = p-$CH_3C_6H_4CH(CH_3)_2$] give the corresponding relatively stable ruthenium(I) dimer derivative. The same species can also be obtained by electrochemical reduction of the cationic complexes $[(\eta^6\text{-}p\text{-cymene})Ru(\mu\text{-}Cl)_3Ru(\eta^6\text{-}p\text{-cymene})]PF_6$. A redox mechanism is proposed.

Dinuclear ruthenium(II) complexes of the type $[RuCl_2(arene)]_2$, [arene = C_6H_6; 1,4-$CH_3C_6H_4CH(CH_3)_2$] have been used as starting materials in a variety of reactions.[1] In particular, ruthenium(0) arene complexes have been prepared by chemical reduction of these ruthenium(II) complexes.[2] We are interested in exploring the potential utility of arene compounds of the type $[RuCl_2(arene)]_2$ as starting materials for the preparation of relatively uncommon[3] ruthenium(I) complexes. We report here the electrochemical behaviour of $[RuCl_2(\eta^6\text{-}p\text{-cymene})]_2$ (**1**) and the related cationic complex $[(\eta^6\text{-}p\text{-cymene})Ru(\mu\text{-}Cl)_3Ru(\eta^6\text{-}p\text{-cymene})]PF_6$ (**2**).

RESULTS

Compound **1** in THF exhibits, by linear sweep voltammetry (Pt electrode at 0.1 V s^{-1}), three reduction peaks B, −0.74; A_1, −0.98; and A_2, −2.08 V (Fig. 1). A small shoulder at −1.8 V is also always present. If the sweep is reversed after peak A_1, two oxidation peaks A'_1, −0.86 V and A'_3, −0.08 V are detected. The couple A_1/A'_1 is not totally reversible ($i_p(A'_1)/i_p(A_1) = 0.75$ and $\Delta E_p = E_p(A_1) - E_p(A'_1) = 0.12$ V at 0.1 V s^{-1}). The relative intensity of these two oxidation peaks depends

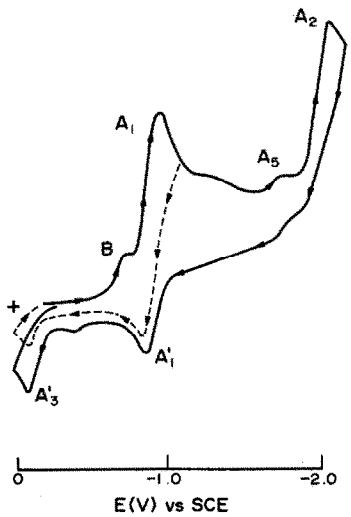

Fig. 1.

* For part XIX, see ref. 7.

† Authors to whom correspondence should be addressed.

‡ Present address: Departamento de Química, Escuela Técnica Superior de Ingenieria Industrial y Telecomunicaciones, Universidad Politécnica de Valencia, Valencia, Spain.

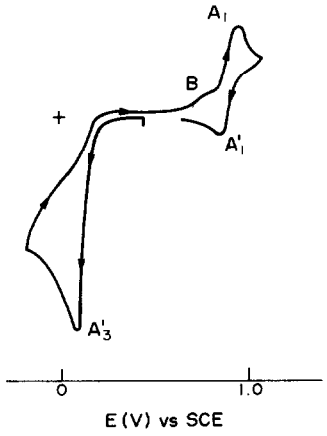

Fig. 2.

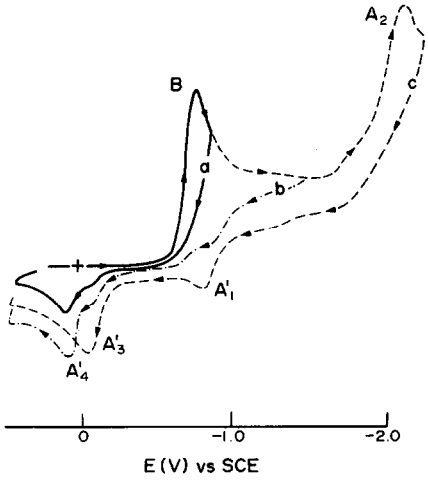

Fig. 3.

on the sweep rates used; at 0.01 V s^{-1} only A'_3 can be observed in the reverse anodic sweep.

After exhaustive electrolysis of $[RuCl_2(\eta^6\text{-}p\text{-cymene})]_2$ on the plateau of peak A_1 (−1.30 V) using a platinum electrode, 2F/mol of dimer are consumed. The voltammogram at a rotating disc electrode (r.d.e.) of the resulting solution, exhibits the waves A'_3 and A_2. By cyclic voltammetry, after oxidation at the A'_3 peak, the system A_1/A'_1 and peak B are clearly detected (Fig. 2). After electrolysis no EPR signal can be detected in the resulting solution.

Some evolution can be observed in the voltammogram when this reduced solution is left to stand at room temperature in the cell; A'_3 decreases in intensity and at the same time A_1 appears again. After 2 h A'_3 has practically disappeared and the voltammogram shows mainly A_1 as well as some unidentified peaks in the range 1.3–2.0 V. The electrolysis on the plateau of the A_2 peak gives a total charge consumption of nearly 4F/mol.

Compound **1** in dichloromethane also shows two reduction peaks, by linear sweep voltammetry (at Pt electrode at 0.1 V s^{-1}), B, −0.78 and A_1, −1.30 V. The narrower electrochemical range of dichloromethane prevents the observation of any reduction peaks at higher potential values. In this case only one oxidation peak A'_3, −0.20 V can be detected in the reversed anodic sweep; the A'_1 peak, observed working in the same experimental conditions but using THF as solvent, can only be detected in dichloromethane solution if an excess of NEt_4Cl is added, with a simultaneous decrease in temperature to 0°C and increase of the sweep rate to 1 V s^{-1}.

We have also studied the electrochemical behaviour of the cationic complex **2**. By cyclic voltammetry in THF, peaks B and A_2 are detected in the cathodic sweep. If the sweep is reversed immediately after peak B, we observe two oxidation peaks, A'_3 and A'_4 [Fig. 3(a)], but if the sweep range is increased towards more negative values the oxidation peak A'_1 appears with low intensity in addition to A'_3 and A'_4 [Fig. 3(b)]. Finally, if the sweep range includes the A'_2 peak, A'_1 and A'_3 are the only important oxidation peaks observed in the anodic sweep [Fig. 3(c)]. If potential controlled electrolysis is performed at the potential value of B, a variable charge consumption is found (more than 1F/mol) and the r.d.e. voltammogram shows the oxidation wave A'_3 and the reduction wave A_1. No EPR signal is detected for the resulting solution.

DISCUSSION

The previous results can be interpreted most consistently according to Scheme 1.

The first small reduction peak, B, always observed in the voltammogram of compound **1** corresponds to the reduction of the cationic species $[(\eta^6\text{-}p\text{-cymene})Ru(\mu\text{-}Cl)_3(Ru(\eta^6\text{-}p\text{-cymene})]^+$ existing in equilibrium with **1** in the experimental conditions according to:

$$[RuCl_2(\eta^6\text{-}p\text{-cymene})]_2 \overset{NBu_4PF_6/THF}{\rightleftharpoons} [(\eta^6\text{-}p\text{-cymene})Ru(\mu\text{-}Cl)_3Ru(\eta^6\text{-}p\text{-cymene})]^+ + Cl^-.$$

This transformation probably occurs via the unsaturated intermediate species (16–18e$^-$), **2'**. After the two-electron reduction of **1** at the potential value of peak A_1, an oxidizable species, A'_1, must be obtained firstly.

A mechanism EE for the electrochemical reduction of **1** is unlikely. An ECE mechanism seems to be more likely according to $\Delta E_p = E_p(A_1) - E_p(A'_1) = 120$ mV higher than that found for the reversible system Cp_2Co^+/Cp_2Co (65–70

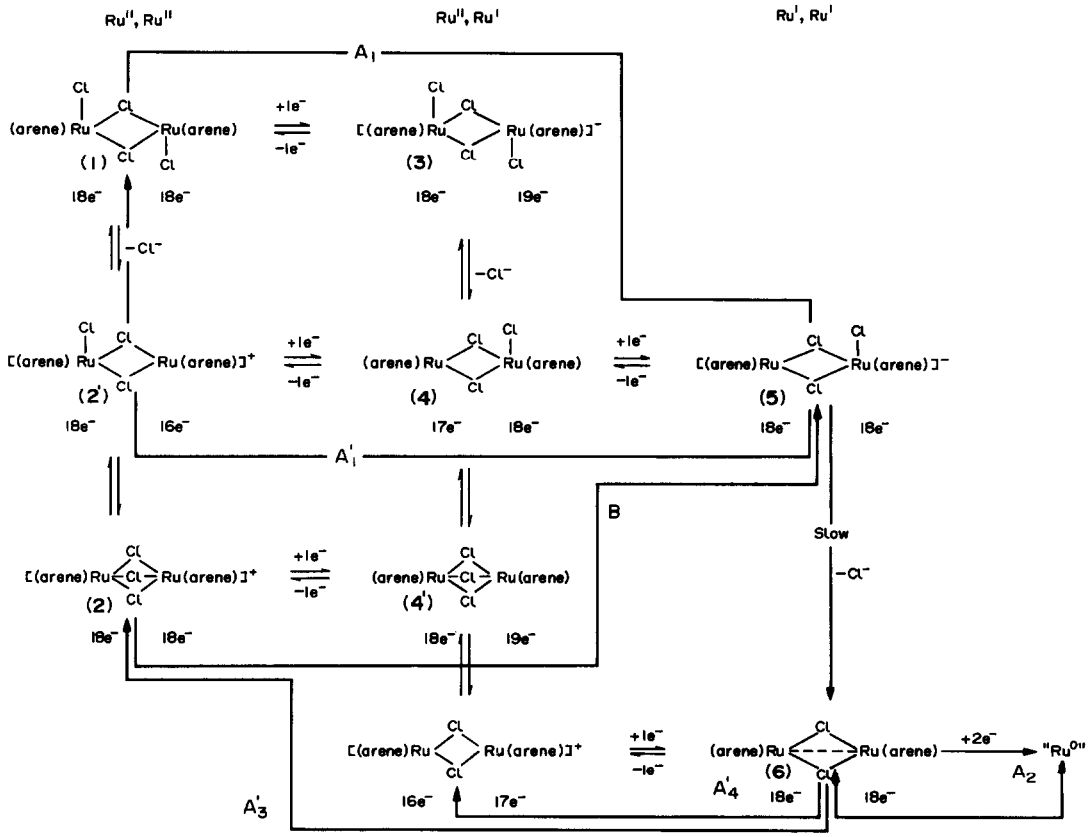

Scheme 1.

mV) in similar experimental conditions. The observation that an excess of NEt_4Cl in CH_2Cl_2 solution at low temperature increases the intensity of A'_1 suggest that the chemical reaction associated with the electrochemical process must be the rapid dissociation chloride ion. The intermediate species **4** with 17–18 electrons reduces in the same range as the initial product **1**, yielding the 18–18-electron anionic species **5** (see Scheme 1). The two-electron reduction of **5** (A_5 peak), yields a very unstable ruthenium(0) species.

A similar pattern has been proposed for the electrochemical reduction of dinuclear arene complexes of bis(tricarbonylchromium). In this case the chemical reaction changes the type of coordination of the arene ligands.[4]

The oxidation of species **5**, can occur by two different methods: (a) **5–4–3–1** and (b) **5–4–2–1**. There is not enough data available to decide which one of these reaction pathways is the correct one. In the first pathway (**5–4–3–1**) we should obtain an $\Delta E_p = E_p(A_1) - E_p(A'_1)$ value of approximately 30 mV if the equilibrium **3** → **4** is rapidly established.

Species **5** (18–18e$^-$) cannot be obtained by electrolysis because it undergoes chemical evolution to complex **6**, which oxidizes to A'_3 and reduces to A_2. This intermediate ruthenium(I) species can be formulated either as a dinuclear compound with two bridging chlorine atoms and a ruthenium–ruthenium bond or as a paramagnetic mononuclear compound. Some evidence supporting a dimeric formulation can be obtained from the electrochemical behaviour of several mono- and dinuclear ruthenium(II) arene complexes (see Table 1). The observed ΔE_p^* $[\Delta E_p^* = E_p(A_1) - E_p(A_2)]$ values are only significant in dinuclear compounds containing bridging ligands between the ruthenium atoms. These data indicate that the intermediate oxidation state is only stabilized in dinuclear compounds where a metal–metal bond can be formed. Thus we can propose that the product of a two-electron reduction of **1** will be a dimer. The lack of an EPR signal also supports the proposed formation of a compound with a metal–metal bond.

The ruthenium(I)–ruthenium(I) species are not stable enough to allow their isolation. Considering the high value of ΔE_p^* these species should be stable against a disproportionation reaction:

$$2Ru^I—Ru^I \longrightarrow Ru^{II}—Ru^{II} + 2Ru^0.$$

As A'_3 disappears with the formation of the starting material **1**, which is identified by the reduction peak A_1, we assume that a dissociation of the dimeric ruthenium(I) compound is the cause of its limited

Table 1.

Compound	$E_p(A_1)^c$ (V)	$E_p(A_2)$ (V)	$\Delta E_p = E_p(A_2) - E_p(A_1)$ (V)
[a] 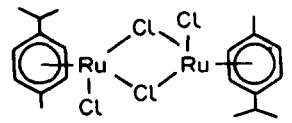	−0.98	−2.08	1.00
[b] 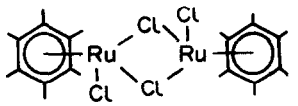	−0.96	−1.30	0.34
[b] 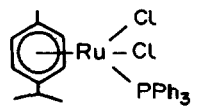 Reference 5a	−1.54	−1.66	0.12
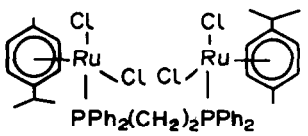	−1.56	−1.66	0.10
Reference 5b 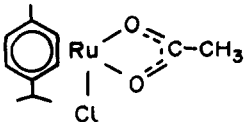	−1.38	—	0.00
Reference 5b 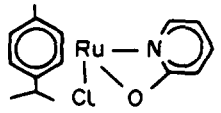	−1.56	—	0.00

[a] This work.

[b] Unpublished results.

[c] Potential values obtained in THF containing 0.2 M TBAH as supporting electrolyte and referred to the saturated calomel electrode (SCE).

stability. Similar behaviour has been observed for the electrogenerated cyclopentadienyl niobium(III) complexes[6] in which very unstable bridging Nb—Cl—Nb bonds have been found. In this case Cp_2NbCl_2 and "Cp_2Nb" are obtained in a 1 : 1 ratio.

The presence of peak A_2 with high intensity indicates the existence of **6** by cyclic voltammetry. However, the transformation of **5** to **6** is slow, in good agreement with the fact that the A'_1 peak is clearly detected. In order to interpret these results, we can assume that the reduction of **5** takes place by means of a CE mechanism. The chemical reaction is the transformation of **5** into **6**.

The assignment of peak A_5 is complicated. This peak must be associated with the reduction of a very unstable intermediate species, only observed by cyclic voltammetry and with low intensity. The transformation of **5** into **6** implies initially the loss of a chloride ion yielding complex **5'**, according to the following reaction:

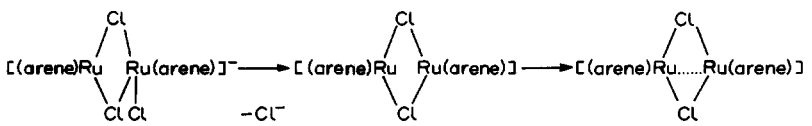

(5) (5') (6)

This intermediate complex **5'** (17–17e$^-$) should reduce more easily than complex **6**. Compound **1** is formed by electrochemical oxidation of **6**, at the potential value of A'_3, in the presence of free chloride ions.

The proposed mechanism is also in good agreement with the experimental results obtained for the cationic compound **2**. By cyclic voltammetry we have confirmed that the two-electron reduction of **2** gives the intermediate **5**. The reduction of **2** takes place according to an ECE mechanism. The chemical step consists of a fast cleavage of the ruthenium–chloride bridging bond to give **4** (17–18e$^-$) which reduces more easily than **2**.

By cyclic voltammetry for compound **2**, in the reversed sweep (if A_2 is not scanned) the A'_1 peak is not detected [Fig. 3(a)] or is only detected with low intensity [Fig. 3(b)]. This observation can be explained by a rapid cation–anion reaction of the electrogenerated species **5** with **2** present in solution according to:

$$5+2 \rightarrow 6+1.$$

If the sweep is extended to more negative values [Fig. 3(b) and 3(c)], complex **5** is electrogenerated in higher amounts and the chemical reaction **5**+**2** → **6**+**1** can not be completed because of insufficient diffusion of compound **2** from the bulk solution to the electrode. Due to this peak, A'_1, corresponding to the oxidation of **5**, is observed with increasing intensity. This is in agreement with the values of the charge consumptions obtained by PCE and also with the resulting products.

Peak A'_4 is assigned to the oxidation of **6** in the absence of free chloride ions. In the presence of free chloride ions, generated as a consequence of the reduction of the starting compound, the oxidation takes place at the potential value of A'_3. According to this, two different pathways can be proposed for the oxidation of **6**, depending on the amount of chloride ions on the electrode surface (see Scheme 1).

EXPERIMENTAL

$[RuCl_2(arene)]_2$ and $[(arene)Ru(\mu_3\text{-}Cl)_3Ru(arene)]BPh_4$, where arene = *p*-cymene, were prepared by literature procedures.[7,8]

The electrochemical studies were conducted in tetrahydrofuran and dichloromethane with tetrabutylammonium hexafluorophosphate (0.2 M) as supporting electrolyte. Cyclic voltammograms were obtained with a programming function generator, A 305 HQ instruments, connected to a 552 Amel potentiostat. Voltammograms were recorded with a Riken–Denshi Co. Ltd F-35 *X–Y* recorder.

The working electrode was a platinum disc with a saturated calomel reference electrode separated from the test solution via a salt bridge containing the solvent/supporting electrolyte. The auxiliary electrode was a platinum wire.

Tetrahydrofuran was dried with sodium benzophenone. Dichloromethane was dried with P205. Both solvents were freshly distilled before each experiment. The electrochemical cell used for potential controlled electrolysis was a conventional H-type design with an isolation compartment separated from the reference and other compartments by fine porosity frits.

All experiments were carried out under an argon atmosphere.

Acknowledgements—We thank the Comisión Asesora de Investigación Científica y Técnica (CAICYT) for financial support and Professor C. Moise for helpful discussions.

REFERENCES

1. (a) R. A. Zelonka and M. C. Baird, *Can. J. Chem.* 1972, **50**, 3063; (b) F. Faraone, G. A. Loprete and G. Tresoldi, *Inorg. Chim. Acta* 1979, **34**, L251; (c) R. Regragi, P. H. Dixneuf, N. J. Taylor and A. J. Carty, *Organometallics* 1984, **3**, 1020; (d) A. W. Coleman, D. F. Jones, P. H. Dixneuf, C. Brisson, J. J. Bonnet and G. Lavigne, *Inorg. Chem.* 1984, **23**, 952.
2. M. A. Bennett, T. H. Huang and T. W. Turney, *J. Chem. Soc., Chem. Commun.* 1979, 312.
3. G. Wilkinson, F. G. A. Stone and E. W. Abel (Eds), *Comprehensive Organometallic Chemistry*. 1st edn, Vol. 4, pp. 796–806. Pergamon Press, Oxford (1982).
4. S. N. Milligan and R. D. Rieke, *Organometallics* 1983, **2**, 171.
5. F. Estevan, P. Lahuerta, J. Latorre, A. Sanchez and C. Sieiro, *Polyhedron* 1987, **6**, 473; (b) P. Lahuerta, J. Latorre, M. Sanaú, F. A. Cotton and W. Schowtzer, *Polyhedron* 1988, **7**, 1311.
6. A. Fakhr, Y. Mugnier, R. Broussier, B. Gautheron and E. Laviron, *J. Organomet. Chem.* 1986, **201**, 317.
7. M. A. Bennett and A. K. Smith, *J. Chem. Soc., Dalton Trans.* 1974, 223.
8. R. O. Gould, C. L. Jones, T. A. Stephenson and D. A. Tocher, *J. Organomet. Chem.* 1984, **264**, 365.
9. H. Korry, Y. Mugnier, L. Roullier and E. Laviron, to be submitted for publication.

Polyhedron Vol. 8, No. 23, pp. 2809–2812, 1989
Printed in Great Britain

0277–5387/89 $3.00+.00
© 1989 Pergamon Press plc

STUDIES OF THE FORMATION OF DMSA COMPLEXES WITH BIVALENT TIN—I. DETERMINATION OF DISSOCIATION CONSTANTS AND THERMODYNAMIC VALUES OF 2,3-DIMERCAPTOSUCCINIC ACID

N. S. VUKIČEVIČ and N. M. VANLIČ-RAZUMENIČ*

Radioisotope Laboratory, The Boris Kidrič Institute of Nuclear Sciences, Vinča, 11001 Belgrade, Yugoslavia

and

D. S. VESELINOVIĆ

Faculty of Sciences, University of Belgrade, 11000 Belgrade, Yugoslavia

(*Received* 28 *April* 1989; *accepted* 24 *July* 1989)

Abstract—As the first step in the investigation of tin and technetium complexes of 2,3-dimercaptosuccinic acid (DMSA), the thermodynamic values of the DMSA ligand—dissociation constants, free energy, enthalpy and entropy have been determined. Dissociation constants have been determined by potentiometric titration. The following logarithmic values for the four thermodynamic constants were obtained: 2.5 ± 0.07, 3.9 ± 0.08, 10.1 ± 0.1 and 11.4 ± 0.1 at 293 K; 2.5 ± 0.05, 3.9 ± 0.06, 9.7 ± 0.07 and 10.8 ± 0.1 at 303 K; and 2.5 ± 0.05, 3.8 ± 0.04, 9.7 ± 0.09 and 10.7 ± 0.1 at 310 K. At 303 K the following thermodynamic parameters of the dissociation were calculated: changes in free energy, in free entropy and in free enthalpy.

Complexes of 2,3-dimercaptosuccinic acid (DMSA) with Tc-99m have been well known for many years and very widely used in nuclear medical diagnosis.[1–6] The complexes of Tc-99m and DMSA form in presence of tin(II). The first step in the examination of Tc–DMSA complexes is the examination of tin(II) complexes, which in turn requires exact data about dissociation constants of DMSA.

Ionization constants of DMSA were previously determined by several authors[7–10] and can be also found in certain reviews.[11,12] The dissociation constants reported are given at only two temperatures (293 and 298 K), and at one ionic strength, $\mu = 0.1$ M.

The aim of this work was to determine the ionization constants of DMSA at various temperatures and ionic strengths of the medium.

EXPERIMENTAL

Reagents and solutions

Meso-2,3-dimercaptosuccinic acid was purchased from Fluka (Buchs, Switzerland), pure (higher than 98%, m.p. 210°C). The chemical purity of the substance was checked by IR spectrometry and by determination of the melting point (softening started at 196–198 K, followed by decomposition at 210 K, which was in accordance with literature data[8]). Standardization was performed by potentiometric titration, showing the high purity of the ligand.

The ionic strengths were adjusted by addition of hydrated sodium perchlorate (Merck, Darmstadt, F.R.G.). Sodium hydroxide solution, standardized by potassium phthalate, was used as a titration agent. For calibration of the electrode system, phosphate buffer pH $= 7.0 \pm 0.02$ and phthalate buffer

* Author to whom correspondence should be addressed.

pH = 4.01 ± 0.01 (at 293 K) (product of Beckman Instruments) were used.

For preparation of the solutions, double-distilled and degassed water (cooled in a stream of nitrogen) was used.

A stock solution of DMSA (1×10^{-3} mol dm^{-3}) was prepared every day and dissolution was accelerated only by magnetic stirring at room temperature for 1 h. The heating was avoided in order to preserve chemical stability. The concentrations mentioned have been chosen as optimum, depending on the solubility of DMSA in water (4.09 mol dm^{-3} at 25°C).[17] The working solutions of DMSA (concentration of 5×10^{-4} mol dm^{-3}) were made by dilution of the stock solution and addition of $NaClO_4$ and water until the volume reached 25 cm^3. The working solution was purged with nitrogen in the titration cell, the temperature was equilibrated to a definite constant value and titration carried out by continual addition of 0.1 M NaOH as a titrant, with continual stirring.

Instrumentation

All potentiometric measurements were performed on a fully automated titration system ETS-822 (Radiometer, Copenhagen, Denmark). The glass electrode G2040C was used as the indicator electrode, while a saturated calomel electrode K 4040 was used as the reference electrode (both "Radiometer"). Titrations were performed in a closed system with a continual flow of purified nitrogen. The gas was purified by passing through two washing bottles: the first one containing Fieser's solution (for elimination of CO_2 and/or O_2) and the second one containing water for absorption of possible traces of alkaline vapours from the first bottle.

Titrations were performed at temperatures of 293, 303 and 310 K. A constant temperature in the range ±0.2 K was maintained by using the thermostat VEB Mechanik Prüfgeräte, Medingen, F.R.G.

Procedure

In calculations related to strongly alkaline regions of titrations curves (for pH values higher than 9), the correction for sodium ion concentration was made according to Linnet.[13]

Activity coefficients, necessary for the assessment of hydrogen ion concentrations, were calculated according to Debye–Hückel using the values for the effective radii of the hydrated ion published by Kielland.[14]

A combined algebraic–graphical method by Schwarzenbach[15,16] was used for calculation of ionization constants. The DMSA ligand has two ionization constants in the acidic region between pH 3 and 5 (due to dissociation of two carboxyl groups), and two dissociations in the alkaline region between pH 8 and 10 (due to ionization of thiolate groups). All four constants were calculated by the algebraic method, while K_2, K_3 and K_4 were also determined by a geometric method.

Thermodynamic parameters

The change in free energy, ΔG, for all four dissociation constants has been calculated by use of the Van't Hoff equation, change in entropy, ΔS, according to the Gibbs–Helmholz relationship, and

Table 1. Ionization constants of *meso*-2,3-dimercaptosuccinic acid

Ionic strength, μ	Temperature (K)	pK_1	pK_2	pK_3	pK_4
	293	2.7±0.05	3.6±0.03	9.6±0.06	11.2±0.2
0.1	303	2.7±0.05	3.7±0.04	9.5±0.02	10.7±0.2
	310	2.6±0.06	3.7±0.05	9.4±0.05	10.6±0.2
	293	2.6±0.07	3.7±0.05	9.8±0.03	11.3±0.2
0.05	303	2.6±0.07	3.8±0.04	9.6±0.05	10.8±0.1
	310	2.6±0.06	3.7±0.04	9.5±0.03	10.6±0.2
	293	2.5±0.08	3.8±0.06	9.9±0.03	11.3±0.2
0.01	303	2.6±0.07	3.8±0.03	9.6±0.05	10.8±0.1
	310	2.5±0.08	3.8±0.05	9.6±0.03	10.7±0.2
	293	2.5±0.07	3.9±0.08	10.1±0.1	11.4±0.1
0	303	2.5±0.05	3.9±0.06	9.7±0.07	10.8±0.1
	310	2.5±0.05	3.8±0.04	9.7±0.09	10.7±0.1

the change in enthalpy, ΔH, according to the Arrhenius equation (from the slope of the line $\ln K$ vs $1/T$).

RESULTS

All four concentration constants of DMSA dissociation have been calculated using the results obtained by performing a series of six titrations for every working temperature (293, 303 and 310 K) and for every ionic strength (0.1, 0.05 and 0.01 M). The exact concentration of DMSA was determined from the equivalence point. The recorded titration curves have been read at a pitch of 0.004 cm^3 and correlated with the corresponding pH. The values obtained for the ionization constants at temperatures of 293, 303 and 310 K, as well as at ionic strengths 0.1, 0.05 and 0.01 M are presented in Table 1 with the corresponding standard deviations. Thermodynamic dissociation constants at zero ionic strength at 293, 303 and 310 K have been determined by a graphical method, by extrapolation of the straight line $\log K_n$ vs $\sqrt{\mu}$ and they are also given in Table 1. Thermodynamic parameters of the DMSA dissociation are presented in Table 2.

DISCUSSION

The results obtained for an ionic strength equal to 0.1 M are in close agreement with the majority of literature values (Table 3), especially for the pK_2, pK_3 and pK_4 values, whereas for pK_1 the differences are more pronounced. In our opinion, the differences are due to the degree of purity of the starting substance. The exact concentration of the stock solution of DMSA was checked by determination of the equivalence point, as mentioned in the Experimental.

The previously published data have been here confirmed and completed with other relevant and significant data and physicochemical parameters.

Table 2. Thermodynamic parameters of the dissociation of *meso*-2,3-dimercaptosuccinic acid at a temperature of 303 K and ionic strength $\mu = 0$ M

K_n	ΔG (kJ mol^{-1})	ΔH (kJ mol^{-1})
K_1	-14.7 ± 0.23	-10.8 ± 2.1
K_2	-22.6 ± 0.21	-16.2 ± 1.9
K_3	-56.3 ± 0.25	-49.4 ± 3.2
K_4	-62.7 ± 0.23	-67.0 ± 3.1

REFERENCES

1. T. H. Lin, A. Khentigan and H. S. Winchell, *J. Nucl. Med.* 1974, **15**, 34.
2. N. Vanlić-Razumenić and D. Gorkić, *Eur. J. Nucl. Med.* 1976, **1**, 235.
3. N. Vanlić-Razumenić and J. Petrović, *Int. J. Appl. Radiat. Isot.* 1982, **33**, 277.
4. I. Ikeda, O. Inoue and K. Kurata, *Int. J. Nucl. Med. Biol.* 1977, **4**, 56.
5. I. Ikeda, O. Inoue and K. Kurata, *J. Nucl. Med.* 1977, **18**, 1222.
6. H. Ohta, K. Yamamoto, K. Endo, T. Moni, D. Hamanak, A. Shimazu, K. Ikekubo, K. Makimoto, Y. Iida, J. Konishi, R. Monita, N. Hata, K. Horiuchi, A. Yokoyama, K. Torifuka and K. Kuma, *J. Nucl. Med.* 1984, **25**, 323.
7. A. Agren and G. Schwarzenbach, *Helv. Chim. Acta* 1955, **38**, 1920.
8. G. R. Lenz and A. E. Martell, *Inorg. Chem.* 1965, **4**, 378.
9. L. G. Egorova, *Zh. Obshch. Khim.* 1972, **42**, 2240.
10. G. Anderegg and S. Malik, *Helv. Chim. Acta* 1970, **53**, 577.
11. D. D. Perrin, *Stability Constants of Metal–Ion Complexes, Part B. Organic Ligands.* Australian National University, Canberra (1979).
12. L. G. Sillen and A. E. Martell, *Stability Constants*, Special Publication No. 17. The Chemical Society, London (1964).

Table 3. A review of the dissociation constants of DMSA from the literature

DMSA concentration (mol dm^{-3})	pK_1	pK_2	pK_3	pK_4	Ionic strength, μ (M)	Temperature (K)	Reference
1.65×10^{-3}	2.40	3.46	9.44	11.82	0.1 ($NaClO_4$) (KCl)	293 ± 1	7, 10, 12
1.51×10^{-3}	2.71	3.48	8.89	10.79	0.1 (KNO_3)	298 ± 0.5	8
0.5×10^{-5}	2.31 ± 0.02	3.69 ± 0.02	9.68 ± 0.02	11.14 ± 0.05	0.1 (KCl)	193 ± 1	9, 11

13. N. Linnet, *pH Measurement in Theory and Practice.* Radiometer, Copenhagen (1970).
14. J. Kielland, *J. Am. Chem. Soc.* 1937, **59**, 1675.
15. G. Schwarzenbach, A. Willi and R. Bach, *Helv. Chim. Acta* 1947, **30**, 1303.
16. G. Schwarzenbach, R. Gut and G. Anderegg, *Helv. Chim. Acta* 1954, **37**, 937.
17. D. Laroche, G. Travert and R. Guillamont, *J. Fr. Biophys. Med. Nucl.* 1978, **4**, 191.

Polyhedron Vol. 8, No. 23, pp. 2813–2816, 1989
Printed in Great Britain

0277–5387/89 $3.00+.00
© 1989 Pergamon Press plc

COMPLEXES OF RUTHENIUM(III) DERIVED FROM O,O-DONOR LIGANDS

AHMED M. EL-HENDAWY† and MOHAMED S. EL-SHAHAWI

Chemistry Department, Faculty of Science, Damietta, Egypt

(*Received* 28 *April* 1989; *accepted* 24 *July* 1989)

Abstract—The complexes $[Ru^{III}Cl_2(PPh_3)_2L]$ (L = monoanions of maltol, kojic acid, tropolone and acetylacetone) were prepared and characterized by spectroscopic and electrochemical measurements. The catalytic oxidation of alcohols in the presence of excess N-methylmorpholine-N-oxide by $[Ru^{III}Cl_2(PPh_3)_2(acac)]$ has also been reported.

It has been recently noted[1] that reaction of $RuCl_2(Ph_3P)_3$ with Schiff bases ($OC_6H_4CH{=}N{-}R$, where R = Ph, *o*- or *p*-ClC_6H_4), in warm benzene under aerobic conditions, gives the green paramagnetic ruthenium(III) products *trans*-$[RuCl_2(OC_6H_4CH{=}NR)(Ph_3P)_2]$, which in turn form $[Ru^{II}(OC_6H_4CH{=}NR)_2(Ph_3P)_2]$ in the presence of triethylamine under anaerobic conditions.[2] The brown complexes $[RuX_2(EPh_3)_2(3\text{-bromotropolonato})]$ (E = P or As; X = Cl or Br) have been synthesized by refluxing $[Ru^{III}X_3(EPh_3)_3]$ and 3-bromotropolone in benzene.[3]

We now report the preparation of the new complexes $[Ru^{III}Cl_2(PPh_3)_2L]$ [L = monoanions of maltol (malt), 3-hydroxy-2-methyl-4-pyrone; kojic acid (koj), 5-hydroxy-2-(hydroxymethyl)-4-H-pyran-4-one; tropolone (trop), 2-hydroxy-2,4,6-cycloheptatrienone, acetylacetone (acac)], starting with $[Ru^{II}(PPh_3)_3Cl_2]$. We also discuss their spectroscopic and electrochemical behaviour, together with the application of $[Ru^{III}Cl_2(PPh_3)_2(acac)]$ to the catalytic oxidations of alcohols in the presence of N-methylmorpholine N-oxide (NMO) as co-oxidant, since the $Ru^{II}Cl_2(PPh_3)_2$/NMO system has been reported before.[4,5]

RESULTS AND DISCUSSION

Elemental analyses indicate that the complexes have the formula $[RuCl_2(PPh_3)_2L]$ (L = koj, **I**; malt, **II**; trop, **III**; or acac, **IV**). Most of the complexes are only soluble in CH_2Cl_2 and their molar conductivities are very low.

The IR spectra of the complexes showed all the bands due to triphenylphosphine and coordinated L. The band at 1555 cm^{-1}, observed in both kojato and maltolato complexes, is tentatively assigned to the ν(C=O) vibration. The largest bathochromic shift (75–105 cm^{-1}) for the carbonyl group upon coordination is expected.[6] Tropolonato and acetylacetonato complexes showed strong bands near 1360 and 1375 cm^{-1}, respectively, arising from ν(C—O) vibrations, as observed for $W_2O_5(trop)_2$[7] at 1360 cm^{-1}; also, distinct bands were found at 1510 and 1520 cm^{-1} similar to those reported for $[RuCl_2(PPh_3)_2L']$[3] (L′ = 3-bromotropolonate), and these are characteristic of coordinated diketones.[8] The *trans*-arrangement of chloro ligands in $[RuCl_2(PPh_3)_2L]$ is suggested by the appearance of only one band near 335 cm^{-1} which is due to (Ru—Cl) vibrations.[9,10] Some of these IR bands are also observed in the Raman spectra (see Table 1).

The magnetic moments of the complexes at room temperature (in Table 1) are near the spin-only value corresponding to one unpaired electron, suggesting the low spin d^5 $(t_{2g})^5$ configuration for the ruthenium(III) ion in an octahedral environment.

Electronic spectra and electron spin resonance

The electronic spectra of complexes **II**, **III** and **IV** in CH_2Cl_2 show a broad intense band around 600 nm which could be assigned to a *d–d* electronic transition, whereas the intense band near 375 nm is tentatively assigned to a M → L π^*-transition.[3] The bands near or below 300 nm may arise from either an intraligand or from M → L charge-transfer

† Author to whom correspondence should be addressed.

Table 1. Spectroscopic, electrochemical and magnetic data for complexes

Compound	IR and Raman data[a] (cm^{-1}) ν(C=O)	ν(C—O)	ν(Ru—Cl)	UV–vis data, λ_{max} (nm) (ε, $M^{-1}\,cm^{-1}$)	$E_{1/2}$ (V)[b]	ΔE	μ_{eff} (BM)
I	1555s 1552w		337m	540(393), 369(3383) 273(11,717)			1.84
II	1555s 1551w		340m	625(284), 378(5950) 297(25,150), 267sh (23,617)	−0.55	0.08	1.92
III	1510s	1360s 1356m	340m	577(168), 375(10,750) 300(28,367)	−0.34	0.06	1.82
IV	1520s	1375s	330m 323m	605(276), 388(3333) 299(22,667), 283(20,167) 272(19,800), 265(20,167)	−0.29	0.07	1.73

[a] Raman data are underlined.
[b] Scan rate: 50 mV s^{-1}.

bands. Similar but shifted bands are assigned for complex **I** which is soluble only in DMF.

The spin Hamiltonian parameters for complexes **II** and **IV** were sufficiently resolved to allow more than the facile deduction that the unpaired electron is delocalized onto the ligand. The observed lines were similar to each other. The $g_{\|}$ values were 1.88 and 1.92, while $g_{\perp}$ values were 2.30 and 2.38 for complexes **II** and **IV**, respectively, with respect to DPPH. These values are in good agreement with the g values reported for analogous ruthenium(III) species.[3] The spectra are typical of a large axial distortion of an elongated octahedral ruthenium(III) ion environment[3,11] (a representative example is given in Fig. 1).

Cyclic voltammetric studies

The cyclic voltammogram (CV) of the complexes for $\sim 10^{-3}$ M concentration in CH_2Cl_2 using

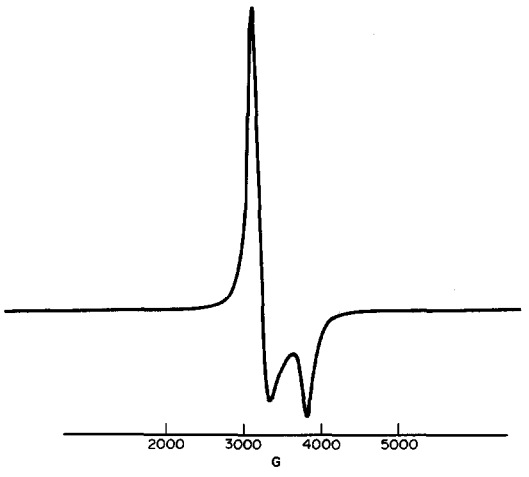

Fig. 1. ESR spectra of *trans*-$[RuCl_2(PPh_3)_2(acac)]$.

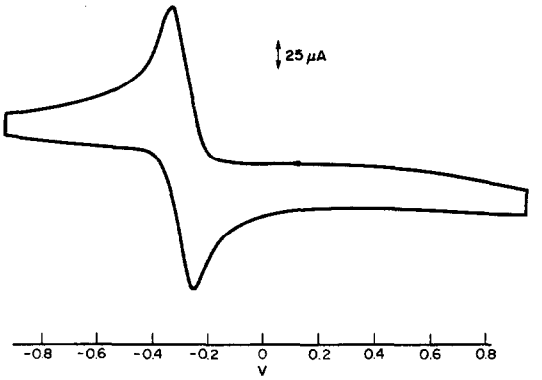

Fig. 2. Cyclic voltammogram of *trans*-$[RuCl_2(PPh_3)_2(acac)]$ (10^{-3} M) in CH_2Cl_2 with 0.1 M $(Bu^n_4N)PF_6$ as supporting electrolyte; scan rate 50 mV s^{-1}; volts vs Ag/AgCl electrode.

0.1 M $Bu^n_4NPF_6$ as the supporting electrolyte, shows only one reversible (or quasi-reversible, ΔE = 70–80 mV) reduction wave at a negative potential (data in Table 1 and Fig. 2 as a typical example). This corresponds to Ru^{III}/Ru^{II} reduction vs Ag/AgCl electrode. We also prepared $Ru(acac)_3$[12] and found that its CV was the same as that previously reported,[13] for both reversible redox reduction and oxidation waves at $E_{1/2}$ = −0.71 and +1.13 V corresponding to $Ru^{III/II}$ and $Ru^{III/IV}$, respectively. The redox potential values for our complexes compared with those for $Ru(acac)_3$ (for the couple Ru^{III}–Ru^{II}) reflect the order of increasing electron-donating nature, i.e. compound **IV** < **III** < **II** < $Ru(acac)_3$. This decrease of electron donating character in our complexes could explain why they only display one reduction wave.

Table 2. Catalytic oxidations of alcohols by *trans*-$[RuCl_2(PPh_3)_2acac]$/NMO

Alcohol	Product[a]	Yield	Time (h)	Turnover[b]
Benzyl	A	99	2	77
p-Methoxybenzyl	A	98	1.5	75
Cinnamyl	A	60	2	50
Benzohydrol	K	94	2	50
Benzoin	K	55	3	50
Cyclohexanol	K	74	3	50

[a] A = corresponding aldehyde, K = corresponding ketone.

[b] Turnover = moles of product/moles of catalyst.

Catalytic oxidation of alcohols

$Ru^{II}Cl_2(PPh_3)_3$ has been used in the presence of excess NMO, for catalytic oxidation of alcohols to give the corresponding aldehydes or ketones.[4,5] Thus $[RuCl_2(PPh_3)_2(acac)]$ was found to give such catalytic oxidations in the presence of excess NMO. Primary alcohols are oxidized to the corresponding aldehydes, and secondary alcohols to ketones (Table 2). There is no oxidation by NMO in the absence of the catalyst and no reaction between $[RuCl_2(PPh_3)_2(acac)]$ (**IV**) and the alcohols in the absence of NMO as shown by electronic spectroscopy. On mixing **IV** (10^{-3} M) and NMO (0.15 M) in CH_2Cl_2 and shaking, the green colour changes to yellowish and the bands at 605 and 388 nm for compound **IV** are replaced by bands at 525 and 375 nm. The intensity of the former band was found to increase with time: at 1, 2, 4 and 5 h, the corresponding absorbances were 0.37, 0.43, 0.54 and 0.75, respectively, whereas the intensity of the band at 375 nm remained nearly constant. The appearance of these two bands is similar to those observed for high oxidation state ruthenium complexes.[5,10] This could explain the continuation of the catalytic cycle of oxidation.

EXPERIMENTAL

Preparation of complexes

All preparations use $RuCl_2(PPh_3)_3$ which was synthesized by the literature method.[14]

trans-$[RuCl_2(PPh_3)_2L]$ (L = koj *or* malt) (**I, II**). To kojic acid (0.21 g, 1.5 mmol) dissolved in hot methanol (10 cm^3) was added $RuCl_2(PPh_3)_3$ (0.48 g, 0.5 mmol). The mixture gave a green solution on reflux, and after 1 h a yellow precipitate formed, which was filtered off, washed with hot methanol and then ether, and dried *in vacuo* (Found: C, 60.1; H, 4.2; Cl, 8.4. $[RuCl_2(PPh_3)_2(koj)]$ (**I**) requires: C, 60.2; H, 4.2; Cl, 8.5%).

Similar procedures were used in which maltol replaced kojic acid and a green precipitate was obtained (Found: C, 61.4; H, 4.3; Cl, 8.8. $[Ru(PPh_3)_2Cl_2(malt)]$ (**II**) requires: C, 61.4; H, 4.3; Cl, 8.6%).

trans-$[RuCl_2(PPh_3)_2(trop)]$ (**III**). Tropolone (0.18 g, 1.5 mmol) was dissolved in benzene (25 cm^3) and $RuCl_2(PPh_3)_3$ (0.96 g, 1 mmol) added. After refluxing the mixture for 0.5 h, a reddish-brown solution resulted. A yellow precipitate formed on continued heating; this was filtered off, washed with methanol and then ether, and dried *in vacuo* (Found: C, 63.1; H, 4.2; Cl, 9.0. $[RuCl_2(PPh_3)_2(trop)]$ requires: C, 63.2; H, 4.3; Cl, 8.7%).

trans-$[RuCl_2(PPh_3)_2(acac)]$ (**IV**). To $RuCl_2(PPh_3)_3$ (0.24 g, 0.25 mmol) was added excess acetylacetate (10 cm^3) and the mixture was refluxed on a steam bath for 2 h. Green microcrystals were isolated, filtered off and washed with ether and dried *in vacuo* (Found: C, 62.1; H, 4.6; Cl, 8.9. $[RuCl_2(PPh_3)_2(acac)]$ requires: C, 61.9; H, 4.7; Cl, 8.9%). Yields of 60–75% of the above complexes were obtained.

Catalytic oxidations by trans-$[RuCl_2(PPh_3)_2(acac)]$ (**IV**)

The oxidation of benzohydrol is typical. To benzohydrol (1 mmol) was added NMO (3 mmol) in 25 cm^3 of CH_2Cl_2 and 2×10^{-2} mmol of compound **IV**. The solution was stirred for 2 h during which time the colour changed from green to brown. The mixture was evaporated to dryness and extracted with ether (2×25 cm^3); the combined ethereal extracts were filtered and evaporated to give benzophenone which was characterized as its 2,4-dinitrophenylhydrazone derivative.

IR spectra were measured on a Perkin–Elmer 683 spectrophotometer as liquid paraffin mulls between CsI plates and as KBr discs. Raman spectra were measured on a Spex Ramalog 5 instrument with a CRL Innova Krypton ion laser with excitation at 6471 or 5682 Å as KBr discs. ESR spectra were recorded with a Varian E-12 spectrometer equipped with 100 kHz modulation. Cyclic voltammetric studies were carried out on a potentiostat/wave generator (Oxford Electrodes) using platinum working electrode. Magnetic measurements were made on a Johnson Matthey magnetic susceptibility balance.

Acknowledgements—We thank Zahar Hussein for carrying out the ESR spectra, Dr W. P. Griffith for helpful advice and also Johnson Matthey Ltd for the loan of ruthenium trichloride.

REFERENCES

1. V. Alteparmakian and S. D. Robinson, *Inorg. Chem. Acta* 1986, **116**, L37.
2. J. R. Thornback and G. Wilkinson, *J. Chem. Soc., Dalton Trans.* 1978, 110 and refs therein.
3. O. K. Medhi and U. Agarwala, *J. Inorg. Nucl. Chem.* 1980, **42**, 1413.
4. K. B. Sharpless, K. Akashi and K. Oshima, *Tetrahedron Lett.* 1976, 2503.
5. K. Vijayasri, J. Rajaram and J. C. Kuriacose, *Proc. Indian Acad. Sci.* 1986, **97**, 125.
6. K. Yamada, *Bull. Chem. Soc. Jpn* 1962, **35**, 1323.
7. W. P. Griffith, C. A. Pumphrey and A. C. Skapski, *Polyhedron* 1987, **6**, 891.
8. K. Nakamoto, *IR Spectra of Inorganic and Coordination Compounds*. Wiley, New York (1964).
9. D. W. Raichart and H. Taube, *Inorg. Chem.* 1972, **11**, 999.
10. A. El-Hendawy, W. P. Griffith, M. N. Moussa and F. I. Taha, *J. Chem. Soc., Dalton Trans.* 1989, 901.
11. W. West, *Techniques of Chemistry, Theory and Application of Electron Spin Resonance* (Vol. XV). John Wiley, New York (1979).
12. A. Endo, K. Shimizu, G. P. Sato and M. Mukaida, *Chem. Lett.* 1984, **437**.
13. J. H. Tocher and J. P. Fackler, *Inorg. Chim. Acta* 1985, **102**, 211.
14. T. A. Stephenson and G. Wilkinson, *J. Inorg. Nucl. Chem.* 1966, **28**, 945.

Polyhedron Vol. 8, No. 23, pp. 2817–2821, 1989
Printed in Great Britain

0277–5387/89 $3.00+.00
© 1989 Pergamon Press plc

THE SYNTHESIS OF SOME NEW THIOPHENE DERIVATIVES

M. J. EARLE, A. G. MASSEY,* A.-R. AL-SOUDANI and T. ZAIDI

Department of Chemistry, University of Technology, Loughborough, Leicestershire LE11 3TU, U.K.

(*Received* 19 *July* 1989; *accepted* 31 *July* 1989)

Abstract—Several sulphur, selenium, tellurium and titanium heterocycles have been synthesized in which the 2,5-dichlorothiophene unit is the structure former. Tetrachlorotetrafluorodibenzothiophene may be made via a benzyne-insertion reaction.

Due to their possible use in electrically-conducting complexes there is currently an active interest in the preparation of substituted thiophenes. The ready availability of the dilithio-reagents **1**, **2**, and **3** has allowed the isolation of a wide variety of heterocycles containing the thiophene ring as a structure-forming unit.[1] We now report further synthetic possibilities using these versatile lithium derivatives.

Addition of $TeCl_4$ or $(C_5H_5)_2TiCl_2$ to **2** or **3** in a ether–hexane solution at low temperature, followed by slow warm up to ambient temperature, gives the expected heterocycles:

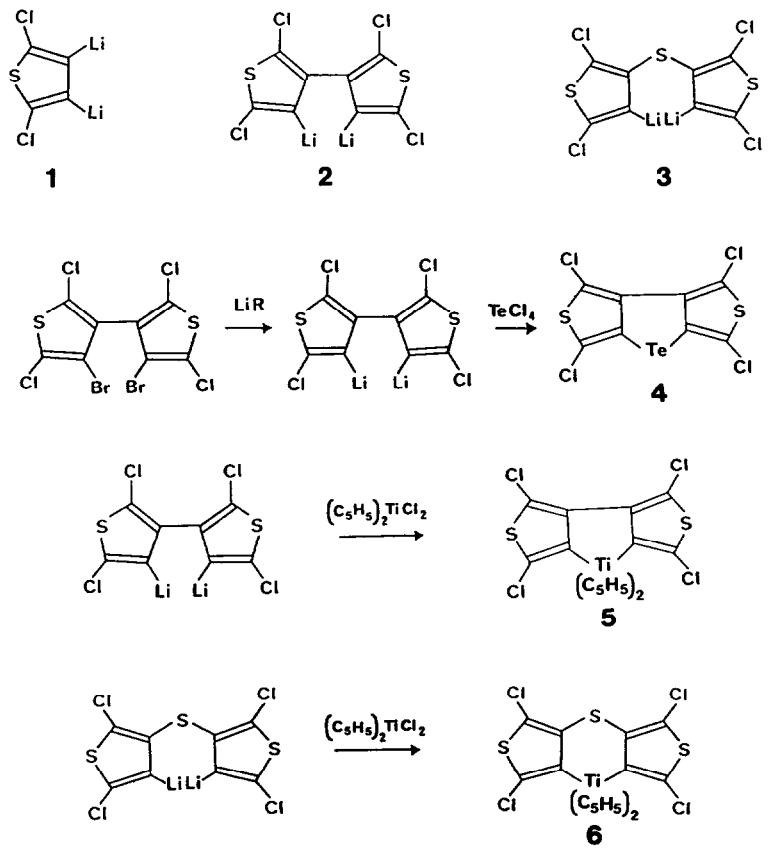

* Author to whom correspondence should be addressed.

The unusual titanium heterocycle, **5**, gave well-formed, but thin, red crystals on crystallization from toluene. Its mass spectrum showed a parent ion cluster of about 15% relative intensity around 480, and P^{2+} was among the several doubly-charged peaks which could easily be distinguished. Most of the metastable peaks represent loss of chlorine atoms from the parent ion and its fragments:

$$(C_5H_5)_2Ti(C_4Cl_2S)_2^+ \xrightarrow{-Cl} C_{18}H_{10}S_2TiCl_3^+$$

$$C_{18}H_{10}S_2TiCl_3^+ \xrightarrow{-Cl} C_{18}H_{10}S_2TiCl_2^+$$

$$C_{18}H_{10}S_2TiCl_2^+ \xrightarrow{-Cl} C_{18}H_{10}S_2TiCl^+$$

$$C_{18}H_{10}S_2Cl^+ \xrightarrow{-Cl} C_{18}H_{10}S_2^+$$

$$C_{13}H_5S_2Cl_2^+ \xrightarrow{-Cl} C_{13}H_5S_2Cl^+$$

$$C_{18}H_{10}S_2Cl^+ \xrightarrow{-C_5H_5} C_{13}H_5S_2Cl^+$$

$$C_{13}H_5S_2Cl^+ \xrightarrow{-Cl} C_{13}H_5S_2^+.$$

Treatment of **1** with disulphur dichloride, S_2Cl_2, gave a complex mixture of products, **7**–**12**, some of which were obtained in only very low yield.

and reacted almost instantaneously with metallic mercury on shaking. The solid also decomposed when inserted into a mass spectrometer. These are not the properties associated with compounds having thiophene rings linked by —S—S— bridges; hence from its method of preparation, its analysis and its initial solubility in several cold solvents we are led to the only possible conclusion that this solid is dithietane (**12**). No identifiable material could be isolated from the reaction of **12** with mercury in toluene; during some unsuccessful recrystallization attempts a few crystals of decomposition products arising from **12** were obtained.

The asymmetrically-bridged species **9** was not isolated but could be detected in some samples of $(C_4Cl_2S)_2S_4$ (**8**). (Although $(C_4Cl_2S)_2S_3^+$ occurs as a fragment ion in the mass spectrum of pure **8** it gives only a relatively weak peak.) The identity of **9** was confirmed by high resolution mass spectral studies *m/z*: 395.738 (calc. for $C_{12}^{35}Cl_4S_5$: 395.736); 397.734 (calc. for $C_{12}^{35}Cl_3^{37}ClS_5$: 397.733); 399.729 (calc. for $C_{12}^{35}Cl_2^{37}Cl_2S_5$: 399.730).

At about −30°C the dilithium reagent **1** reacts smoothly with elemental sulphur to give the dithiolate $(C_4Cl_2S)(SLi)_2$ (**13**); this latter compound gives three major products, **14**, **15** and **16**, when treated with sulphur dichloride.

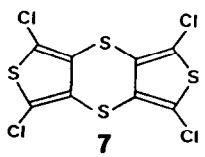

7

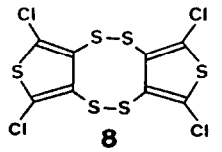

8

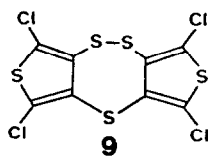

9

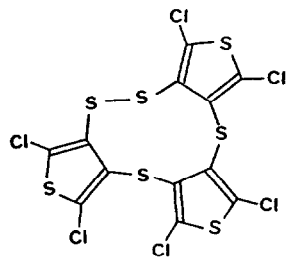

11

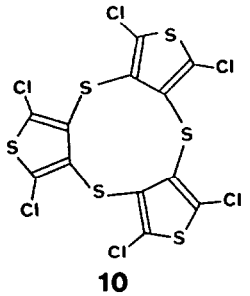

10

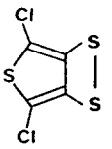

12

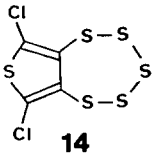

14

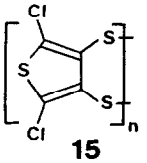

15

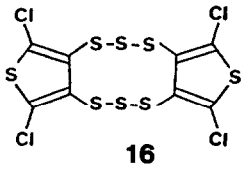

16

The major product of this reaction was a beige powder analysing, after washing with pentane and methanol followed by drying under high vacuum, as "$(C_4Cl_2S)S_2$". Due to its thermal fragility all attempts at recrystallizing this compound from a variety of solvents failed; when in solution at room temperature it rapidly turned nickel spatulas black

The pentathiole, $(C_4Cl_2S)S_5$, which forms very pale yellow needles, was identified by both elemental analysis and accurate mass measurements on the $C_4^{35}Cl_2^{32}S_6^+$ ion (found: 309.770; calc.: 309.770). The base peak in its mass spectrum is due to the ion $(C_4Cl_2S)S_3^+$; ions representing the loss of one, two and three sulphur atoms from this base-

ion were present in about 4–6% abundance. Prominent low-mass, fragment ions present in this and other thiophene spectra were $C_3S_2Cl^+$ (134.911; calc. for $C_3^{32}S^{35}Cl^+$: 134.913); $C_2S_2Cl^+$ (122.914, calc. for $C_2^{32}S^{35}Cl^+$: 122.913); C_4SCl^+ (114.941, calc. for $C_4^{32}S^{35}Cl^+$: 114.941); C_3SCl^+ (102.941, calc. for $C_3^{32}S^{35}Cl^+$: 102.941); C_3S^+ (99.943, calc. for $C_3^{32}S_2$: 99.944); $C_2S_2^+$ (87.945, calc. for $C_2^{32}S_2^+$: 87.944); $CSCl^+$ (78.942, calc. for $C^{32}S^{35}Cl$: 78.941) and S_2^+ (63.947, calc. for $^{32}S_2$: 63.944).

The polymeric material **15** analysing as $[(C_4Cl_2S)S_2]_x$ is insoluble in boiling dimethylformamide; in boiling nitrobenzene depolymerization appears to take place giving **8**. Judging from models, this tetrathiocane can conceivably exist in both a rigid "chair" and a flexible "boat" form. The needle crystals of $(C_4Cl_2S)_2S_4$ arising from the lithium reaction melt at 171°C, whereas the product from the nitrobenzene decomposition of polymer **15** melts at 256°C; both species have the parent ion $(C_4Cl_2S)_2S_4^+$ in their mass spectra. Whether these compounds represent the two tetrathiocane isomers remains to be decided by X-ray crystallography.

Treatment of **1** with selenium readily forms the diselenolate **17** which, on reaction with $SeCl_4$, gives three major products, **18**, **19**, and **20**.

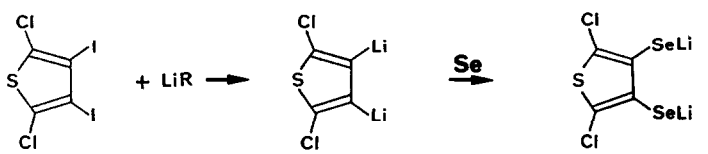

17

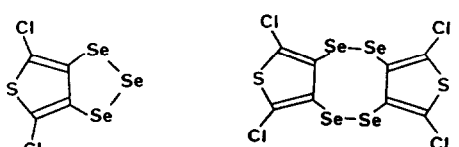

18 19

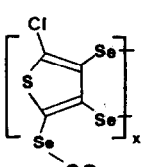

20

The red triselenole (**18**), which can be recrystallized from dimethylformamide, was identified by high resolution mass spectral studies: Found: 385.665; calc. for $C_4^{35}Cl^{37}Cl^{80}Se_3S$: 385.661. Found: 387.660; calc. for $C_4^{35}Cl_2^{78}Se^{80}Se_2S$: 387.660. Found: 389.659; calc. for $C_4^{35}Cl_2^{80}Se_3S$: 389.659. Found: 391.655; calc. for $C_4^{35}Cl^{37}Cl^{80}Se_3S$: 391.656.

High resolution mass measurements on the bright yellow tetraselenocane **19** similarly gave excellent correlations with the calculated masses; a selection of the data is given below:

Found: 615.487; calc. for $C_8^{35}Cl_4S_2^{80}Se_2^{78}Se_2$: 615.491. Found: 617.489; calc. for $C_8^{35}Cl_4S_2^{80}Se_3^{78}Se$: 617.489. Found: 619.487; calc. for $C_8^{35}Cl_3^{37}ClS_2^{80}Se_3^{78}Se$: 619.487. Found: 618.485; calc. for $C_8^{35}Cl_2^{37}Cl_2S_2^{80}Se_2^{78}Se_2$: 618.485. Found: 621.486; calc. for $C_8^{35}Cl_2^{37}Cl_2S_2^{80}Se_3^{78}Se$: 621.484. Found: 623.485; calc. for $C_8^{35}Cl_2^{37}Cl_2S_2^{80}Se_4$: 623.484.

The pale green, polymeric material **20** was found to be deficient in chlorine, the formula approximating to $[(C_4ClS)Se_3]_x$, where an average of one chlorine atom per thiophene ring remains. It appears likely that the lithium reagent **17** attacked some of the C—Cl bonds in neighbouring molecules to give this polymer; such reactions are relatively common when RXLi compounds (X = chalcogen) are used in the presence of organohalides. Unexpectedly, when this polymer is refluxed with nitrobenzene, orange crystals are produced which give a $(C_4Cl_2S)_2Se_4^+$ parent ion in their mass spectrum and a typical fragmentation pattern for **19**. The simplest route to **19** is to oxidize the dilithium reagent **17** with an equivalent amount of iodine in ether–hexane.

The IR spectra of the sulphur heterocycles are very similar, which sometimes makes deductions about levels of purity using this technique almost impossible; elemental analysis, thin-layer chromatography and mass spectroscopy proved to be much more reliable. Two ring-stretching vibrations[2] at 1540–1510 and 1450–1400 cm^{-1} gave some of the more intense peaks, with a medium intensity band around 890 cm^{-1} representing the ring-breathing mode; the strongest band was always at about 1060 cm^{-1} and this may arise from

a chlorine-sensitive vibration. Their selenium analogues showed similar spectral features in the IR but the corresponding bands occurred at somewhat lower wave numbers.

When two molecules of butyllithium are added to a 1 : 1 mixture of pentachlorobenzene and pentafluorothiophenol, and the whole mixture stirred at room temperature, tetrachlorotetrafluorodibenzothiophene (**21**) is formed in 55% yield. The reaction probably occurs via the initial formation of tetrachlorobenzyne, followed by addition of C_6F_5SLi and ring-closure as LiF is eliminated.

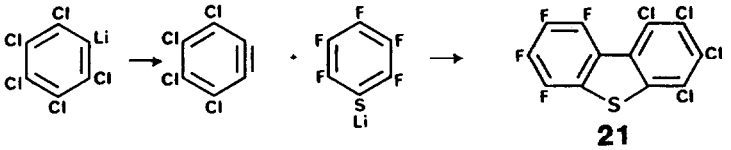

21

The parent ion $C_{12}Cl_4F_4S^+$ gave rise to the base peak in the mass spectrum of **21** with the doubly-charged parent ion having an intensity of 14%. Very little fragmentation occurred, the only peaks of intensity greater than 15% were $C_{12}Cl_2F_4S^+$ and $C_{12}Cl_2F_4S^{2+}$. There appears to be no reason why this reaction should not become a general method for making dibenzothiophenes, -selenophenes and -tellurophenes if lithium reagents halogenated in the correct positions are treated with *half* a mole of elemental chalcogen at room temperature or below.

EXPERIMENTAL

All reactions were carried out under a dry nitrogen atmosphere using 100 cm^3 of sodium-dried ether as solvent; 4.85 g of 2,5-dichloro-3,4-diiodothiophene (0.012 mol) were used in each experiment, together with 0.024 mol of butyllithium added at −95°C as a 1.6 M hexane solution.

Reaction of **1** *with* S_2Cl_2

To 0.012 mol of 3,4-dilithio-2,5-dichlorothiophene was added an equivalent quantity of disulphur dichloride at −95°C and the mixture allowed to warm up slowly to room temperature; after 15 min, water (50 cm^3) was added to quench the reaction. Many unsuccessful attempts were made to recrystallize the beige-coloured ether-insoluble product **12** from all the common organic solvents including dimethylformamide (DMF); the solvent was stripped from the ether-soluble material and the solid crystallized from toluene. Chromatography on alumina or fractional crystallization from toluene gave **7**, **8** and **11**; compounds **9** and **10** were detected by mass spectrometry but could not be isolated.

Compound **7**: needle-shaped, colourless crystals, m.p. 283°C (Found: C, 26.5; S, 36.9. Calc. for $C_8Cl_4S_4$: C, 26.2; S, 35.0%).

Compound **8**: dendritic, colourless crystals, m.p. 171°C (Found: C, 22.2; S, 42.2. Calc. for $C_8Cl_4S_6$: C, 22.3: S, 44.7%).

Compound **11**: cube-shaped, colourless crystals, m.p. 224°C (d) (Found: C, 24.9. Calc. for $C_{12}Cl_6S_7$: 24.8%). The identity of **11** was confirmed by high resolution mass spectrometry *m/z*: Found: 577.613; calc. for $C_{12}^{35}Cl_6S_7$: 577.618. Found: 579.609; calc. for $C_{12}^{35}Cl_5^{37}ClS_7$: 579.615. Found: 581.607; calc. for $C_{12}^{35}Cl_4^{37}Cl_2S_7$: 581.612.

Compound **12**: the methanol-washed, vacuum-dried product (*ca* 90% yield) was analysed without further purification (Found: C, 22.25; S, 44.4. Calc. for $C_4Cl_2S_3$: C, 22.3; S, 44.7%). The compound decomposes above *ca* 80°C.

Compound **9**: detected by mass spectrometry (see text).

Compound **10**: high resolution mass spectrometry on a tiny sample showed a mass cut-off at an ion cluster around *m/z* = 548. The identity of the species was confirmed by the following data *m/z*: Found: 551.631; calc. for $C_{12}^{35}Cl_3^{37}Cl_3S_6$: 551.637. Found: 549.636; calc. for $C_{12}^{35}Cl_4^{37}Cl_2S_6$: 549.640. Found: 547.638; calc. for $C_{12}^{35}Cl_5^{37}ClS_6$: 547.643. Found: 545.642; calc. for $C_{12}^{35}Cl_6S_6$: 545.646.

Reaction of **13** *with* SCl_2

Compound **1** (1 mol) was treated with 2 mol of elemental sulphur at −95°C; on warming, a reaction between the two components to give **13** was observed to occur at about −20°C. SCl_2 (1 mol) was added slowly, with stirring, at room temperature; after 15 min, water (50 cm^3) was added to quench the reaction. The products were worked up as described above to give **8**, **14** and **15**.

Compound **8**: colourless, dendritic crystals, m.p. 171°C (Found: C, 22.2; S, 42.3. Calc. for $C_8Cl_4S_6$: C, 22.3; S, 44.7%). The molecular formula was confirmed by high resolution mass spectrometry.

Compound **14**: large, very pale yellow needles, m.p. 126°C (Found for two different preparations: C, 15.6, 15.7; S, 60.5, 63.4. Calc. for $C_4Cl_2S_6$: C, 15.4; S, 61.8%). The molecular formula was con-

firmed by high resolution mass spectrometry (see text).

Compound **15**: pale yellow powder, insoluble in boiling DMF, m.p. 241°C (d) (Found: C, 22.2; S, 42.3. Calc. for $(C_4Cl_2S_3)_x$: C, 22.3; S, 44.7%). The compound gave $[(C_4Cl_2S)S_2]_2^+$ as the highest ion in the mass spectrum, with the doubly-charged parent ion also detectable: Found: 215.351, Calc. for P^{2+}: 215.354. This suggests that either all the dimer had not been removed or that decomposition of the polymer occurred in the spectrometer.

Compound **9** was confirmed by high resolution mass spectrometry to be an impurity in some samples of **11**; see text.

Compound **16**: yellow rosettes from toluene, m.p. 228°C (Found: C, 20.6. Calc. for $C_8Cl_4S_8$: 19.4%. MW 491.652; $C_8^{35}Cl_4^{32}S_8$ 491.652); base peak in mass spectrum due to $C_4Cl_2S_3^+$. In a mass spectrum of the neat reaction product before work-up, a weak cluster of peaks around mass 732 suggested the presence of $(C_4Cl_2S)_4S_4$, but this "tetramer" was not isolated during recrystallizations.

Reactions of **17** *with* $SeCl_4$

Selenium powder (2 mol) was added to **1** at −95°C and the mixture warmed slowly to room temperature. When the black colour of selenium disappeared, $SeCl_4$ (1 mol) was added and, after 15 min, the reaction was quenched by the addition of 50 cm^3 of water. The products were worked up as before to yield **18**, **19** and **20**.

Compound **18**: red solid, decomposes slowly at 100°C; identified by high resolution mass spectrometry (see text).

Compound **19**: bright yellow, microcrystals, m.p. 252°C (d) (Found: C, 17.3; S, 10.1; Se, 49.3. Calc. for $C_{12}Cl_4S_2Se_4$: C, 15.5; S, 10.4; Se, 51.1%). The molecular formula was confirmed by high resolution mass spectrometry m/z: Found: 615.487; calc. for $C_8^{35}Cl_4S_2^{80}Se_2^{78}Se_2$: 615.491. Found: 617.490; calc. for $C_8^{35}Cl_4S_2^{80}Se_3^{78}Se$: 617.489. Found: 619.487; calc. for $C_8^{35}Cl_3^{37}ClS_2^{80}Se_3^{78}Se$: 619.487.

Compound **20**: yellow–green powder, insoluble in boiling DMF, m.p. 198°C (d) (Found for two different preparations: C, 13.0, 13.3; S, 8.5, 8.95; Se, 66.9, 66.5. Calc. for "$[C_4ClS)Se_3]_x$": C, 13.6; S, 9.1; Se, 67.2%).

Reaction between C_6Cl_5Li *and* C_6F_5SLi

Molar equivalents of C_6Cl_5H and C_6F_5SH were dissolved in 100 cm^3 of dry ether at −95°C under dry nitrogen; after 2 mol of butyllithium had been added, the mixture was slowly warmed to room temperature and stirred for 2 h. The ether solvent was filtered, stripped and the remaining solid recrystallized twice from toluene to give tetrachlorotetrafluorodibenzothiophene (**21**). (Found: C, 36.3; F, 19.0. Calc. for $C_{12}Cl_4F_4S$: C, 36.6; F, 19.3%).

Reactions of **2** *or* **3** *with* $TeCl_4$ *and* $(C_5H_5)_2TiCl_2$

These reactions were carried out as described in ref. 1.

$(C_4Cl_2S)_2Te$ (**4**): yellow–green needles, m.p. 200–201°C (Found: C, 22.2; S, 14.7. Calc. for $C_8Cl_4S_2Te$: C, 22.3; Se, 14.9%); 90% yield.

$(C_4Cl_2S)_2Ti(C_5H_5)_2$ (**5**): orange–red, thin plates, m.p. 230–231°C (Found: C, 45.4; H, 2.1; S, 13.2. Calc. for $C_{18}H_{10}Cl_4S_2Ti$: C, 45.0; H, 2.1; S, 13.3%); 85% yield.

$(C_4Cl_2S)_2STi(C_5H_5)_2$ (**6**): red needle crystals, m.p. 292–293°C; the molecular formula was confirmed by mass spectrometry, the parent ion cluster appearing around m/z 512; 60% yield.

Main IR absorptions

Samples were prepared in KBr discs unless stated otherwise; peaks are given in cm^{-1}. Many of the compounds have very similar IR spectra, the peaks differing by only a few wave numbers.

$(C_4Cl_2S)_2Te$ (**4**): Nujol mull: 1530 w; 1405 m; 1360 s; 1230 m; 1070 s; 1115 s; 960 vw; 955 vw; 915 m; 725 msh; 720 mb; 630 w; 575 m; 470 w. $(C_4Cl_2S)_2Ti(C_5H_5)_2$ (**5**): Nujol mull: 3070 w; 1500 vw; 1485 sh; 1375 sh; 1350 s; 1180 vw; 1170 vw; 1055 w; 1030 s; 995 m; 985 m; 900 m; 810 vs; 765 w; 705 m; 620 m; 615 m; 490 m; 430 w. $(C_4Cl_2S)_2STi(C_5H_5)_2$ (**6**): Nujol mull: 3070 w; 1470 w; 1415 sh; 1400 m; 1355 m; 1330 m; 1170 m; 1010 s; 970 m; 915 w; 820 s; 810 s; 705 m; 485 m; 410 m. $(C_4Cl_2S)_2S_4$ (**8**): 1460 s; 1405 s; 1060 vs; 894 m; 693 w; 642 w; 529 m; 440 m. $(C_4Cl_2S)S_2$ (**12**): 1473 m; 1408 s; 1059 vs; 891 m; 640 w; 447 w. $(C_4Cl_2S)S_5$ (**14**): 1460 m; 1405 s; 1056 vs; 888 m; 640 w; 530 w; 465 w. $[(C_4Cl_2S)S_2]_x$ (**15**): 1460 m; 1405 s; 1060 s; 894 m; 643 vw; 530 w. $(C_4Cl_2S)Se_3$ (**18**): 1450 m; 1396 s; 1039 s; 849 m; 514 w; 408 w. $(C_4Cl_2S)_2Se_4$ (**19**): 1451 m; 1396 s; 1040 s; 850 w; 514 w. "$[(C_4ClS)Se_3]_x$" (**20**): 1450 m; 1396 s; 1039 s; 849 m; 619 vw; 514 w. $C_{12}Cl_4F_4S$ (**21**): 1637 w; 1549 vw; 1505 vs; 1476 vs; 1386 m; 1320 s; 1297 sh; 1273 w; 1258 w; 1214 vw; 1150 m; 1108 s; 1060 s; 942 s; 883 s; 802 vw; 778 m; 705 m; 643 w; 621 m.

REFERENCES

1. A.-R. Al-Soudani and A. G. Massey, *Appl. Organomet. Chem.* 1988, **2**, 553.
2. J. A. Faniran, *Spectrochim. Acta* 1978, **34A**, 379.

Polyhedron Vol. 8, No. 23, pp. 2823–2827, 1989
Printed in Great Britain

0277–5387/89 $3.00+.00
Pergamon Press plc

SYNTHESIS AND SPECTROSCOPIC STUDIES OF GOLD(I) THIOCYANATE WITH IMIDAZOLIDINE-2-THIONE AND ITS DERIVATIVES

ANVARHUSEIN A. ISAB

Chemistry Department, King Fahd University of Petroleum and Minerals, Dhahran 31261, Saudi Arabia

(*Received* 23 *January* 1989; *accepted* 31 *July* 1989)

Abstract—The reaction of ammonium gold(III) thiocyanate with imidazolidine-2-thione (Imt) and its N- and N,N′-disubstituted derivatives yields complexes of stoichiometry L—Au^{I}—SCN (where L = Imt and its derivatives). However, a six-membered heterocyclic ligand, 1,3-diazinane-2-thione (Diaz), and its N-substituted derivative yields complexes of the type L'_2—Au^{I}—SCN (where L′ = Diaz and its derivative). These complexes are characterized by elemental analysis, IR and ^{13}C NMR spectroscopy.

The current interest in the coordination chemistry of thione derivatives of various heterocycles arises from the application of heterocyclic S,N-containing ligands in medicine[1–3] and the binding characteristics towards different metal ions.[4–8] Our interest in these ligands is because the thione donor group forms stable complexes with gold(I).[9–13] The gold(I) thiolates (AuSR), in which SR is a thiomalate or a substituted thioglucose group, are the most commonly used anti-arthritic gold complexes.[14–16]

It has recently been reported that chrysotherapy patients who are tobacco smokers accumulate gold from injectable gold drugs into their red blood cells while non-smokers do not.[17,18] Hydrogen cyanide is present in tobacco smokers at a concentration of 1600 ppm and is absorbed into the blood.[19] In the absence of gold, it undergoes two reactions: reversible binding to met-haemoglobin and irreversible oxidation to thiocyanate.[20]

Once the thiocyanate is generated *in vivo*, the gold(I) will react to form AuSCN or $Au(SCN)_2^-$ which will then further react with thiols (e.g. haemoglobin, glutathione) or thione (e.g. ergothionine). To understand the nature of these complexes, the present work was devoted to complexes originating from ammonium gold(III) thiocyanate with Imt, Diaz and their derivatives.

The complexes obtained have been characterized by means of elemental analysis, IR and ^{13}C NMR spectroscopy.

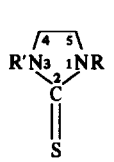

Imt (**a–f**)

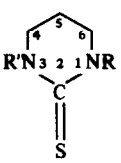

Diaz (**g–j**)

(**a**) R = H, R′ = H = imidazolidine-2-thione (Imt);
(**b**) R = —CH_3, R′ = H = N-methylimidazolidine-2-thione (MeImt);
(**c**) R = —C_2H_5, R′ = H = N-ethylimidazolidine-2-thione (EtImt);
(**d**) R = —C_3H_7, R′ = H = *n*-propylimidazolidine-2-thione (PrImt);
(**e**) R = —C_3H_7, R′ = H = *i*-propylimidazolidine-2-thione (*i*-PrImt);
(**f**) R = R′ = —CH_3 = N,N′-dimethylimidazolidine-2-thione (DimetImt);
(**g–i**) R = H, R′ = H = 1,3-diazinane-2-thione (Diaz);
(**j**) R = —C_2H_5 R′ = H = N-ethyl-1,3-diazinane-2-thione (EtDiaz).

EXPERIMENTAL

Chemicals

All chemicals and deuterated solvents were obtained from ICN K and K Laboratories, Plainview, New York and were used without any purification.

Preparation of complexes

The ligands were prepared by the procedures described in the literature.[21,22] Ammonium gold (III) thiocyanate, which is a reddish colour, was suspended in methanol and an excess of ligand was added. The solution of these suspensions was stirred until all the solid dissolved completely and the solution became colourless. The solvent was evaporated at room temperature and the crystals or powders were collected but some solvent still remained.

Spectroscopic measurements

IR spectra of the pure ligands and their gold(I) complexes were obtained on a Perkin–Elmer IR 180 or on a Beckman Microlab IR spectrophotometer using KBr pellets. ^{13}C NMR spectra were obtained on a Varian XL-200 NMR spectrometer operating at 50.3 MHz frequency. The ligands and gold(I) complexes were dissolved in a 50 : 50 (v/v) DMSO–acetone-d_6 solvent. The chemical shifts were measured relative to 1,4-dioxane as internal reference having a resonance at +67.4 ppm from TMS.

RESULTS AND DISCUSSION

The analytical data for complexes (**a–j**) are given in Table 1. These data show that Imt and its derivative (**a–f**) form 1 : 1 L–AuSCN complexes, whereas the analogous six-membered ring Diaz and its derivative (**g–j**) form bis-complexes. The reduction of gold(III) to gold(I) is similar to that described for copper(II) to copper(I) complexes for the ligands under investigation.[4–8]

IR studies

The IR data for the free ligands and their thiocyanate gold(I) complexes are given in Table 2.

$NH_4Au(SCN)_4$ shows a ν(NH) absorption at 3175 and 3080 cm^{-1}. There is also a ν(CN) absorption at 2130 cm^{-1}. All the [(L)AuSCN] complexes show two absorptions in the CN region. The smaller but sharp absorption at 2130 cm^{-1} and the more intense absorption at 2045 cm^{-1}.

In all the complexes reported here, the ν(S—C≡N) was shifted from 2130 to 2045 cm^{-1}, which indicates that —SCN is bonded to gold(I).[12]

Lorenzotti *et al.*[23] have prepared various [(Az)HgSCN] and [$(AZR)_nHg(SCN)_2$] complexes, where, Az = diazole, AZR = triazole and n = 1, 1.5 and 2. The IR absorptions of these complexes indicate that when [(Az)HgSCN]-type linear complexes are formed, they give a ν(CN) absorption at 2055–2078 cm^{-1}. For [$(AZR)_nHg(SCN)_2$]-type complexes, the ν(CN) was observed around 2120–2130 cm^{-1}. These results indicate that when the

Table 1. Analytical data for the gold(I)—SCN complexes[a]

Complexes	Melting point (°C)	Colour	H (%)	C (%)	N (%)
[(Imt)AuSCN] (**a**)	155–157	Pale brown powder	1.7 (1.7)	14.6 (13.4)	12.0 (11.8)
[(MeImt)AuSCN] (**b**)	184–186	White crystals	2.2 (2.2)	17.4 (16.2)	12.2 (11.3)
[(EtImt)AuSCN] (**c**)	53–54	Pale pink powder	2.6 (2.6)	19.2 (18.8)	11.3 (10.9)
[(PrImt)AuSCN] (**d**)	156–150	Light brown powder	3.2 (3.0)	22.6 (21.0)	11.3 (10.5)
[(*i*-PrImt)AuSCN] (**e**)	163–164	Pale yellow powder	2.8 (3.0)	20.8 (21.0)	10.2 (10.5)
[(DimetImt)AuSCN] (**f**)	177–178	White powder	2.8 (2.6)	20.3 (18.7)	11.8 (10.9)
$[(Diaz)_2AuSCN]$ (**g**)	179–180	White crystals	3.1 (3.2)	21.5 (22.1)	14.5 (14.4)
$[(Diaz)_2AuCl]^b$ (**h**)	286–288	White crystals	3.4 (3.4)	20.6 (20.6)	11.9 (12.0)
$[(Diaz)_2AuBr]$ (**i**)	219–221	Pale yellow crystals	3.0 (3.1)	18.7 (18.9)	11.7 (11.0)
$[(EtDiaz)_2AuSCN]$ (**j**)	114–116	White crystals	4.3 (4.4)	27.8 (28.7)	11.5 (12.8)

[a] Calculated values are given in parentheses.
[b] This complex has already been reported, see ref. 11.

Table 2. Significant IR absorptions for the ligands and their gold(I) complexes in the region 4000–200 cm^{-1}

Complexes	ν(N—H)	ν(CN)+δ(NH)	ΔNH	ν(C=S)	ν(SCN) from (R—Au—SCN)	Vibrations below 450 cm^{-1}
$[NH_4Au(SCN)_4]$	3175 sh 3080 sh	—	— —	—	2130 sh	405 sh, 290 w
Imt	3200 sh	1500 sh	680 sh	510 w	—	—
[(Imt)AuSCN] (**a**)	3180 br	1505 sh	680	490 br	2130 sh 2045 sh	345 w, 315 w, 290 w 275 sh
MeImt	3200 sh	1520 sh	670 sh	520 sh	—	—
[(MeImt)AuSCN] (**b**)	3210 sh	1510 br	630 sh	495 sh	2130 sh 2045 sh	350 sh, 290 w
EtImt	3200 sh	1504 sh	620 sh	515 vs	—	—
[(EtImt)AuSCN] (**c**)	3340 sh	1545 sh	620 sh	490 w	2130 sh 2045 sh	300 w
PrImt	3210 br	1520 sh	610 sh	525 sh	—	—
[(PrImt)AuSCN] (**d**)	3180 br	1540 sh	606 sh	500 sh	2140 sh 2045 sh	400 w, 330 sh, 290 w
i-PrImt	3120 br	1520 sh	610 sh	525 sh	—	—
[(*i*-PrImt)AuSCN] (**e**)	3340 sh	1500 sh	600 sh	480 w	2130 sh 2045 w	325 w, 300 w
DimetImt	—	1510 br	635 br	505 sh	—	—
[(DimetImt)AuSCN] (**f**)	—	1510 sh	630 sh	485 sh	2130 sh 2045 sh	335 w, 290 w
Diaz	3300 sh	1560 sh	640 sh	510 w	—	—
$[(Diaz)_2AuSCN]$ (**g**)	3200 br	1550 br	610 sh	515 w	2020 sh 2040 sh	375 sh, 300 w
$[(Diaz)_2AuCl]$ (**h**)	3200	1565 vs	635 sh	520 sh	—	415 sh, 385 sh, 345 w, 315 w
$[(Diaz)_2AuBr]$ (**i**)	3210 br	1560 br	635 sh	505 sh	—	445 sh, 375 br
$[(EtDiaz)_2AuSCN]$ (**j**)	3180 br	1500 br	610 sh	495 sh	2040 sh	445 br, 360 sh, 305 w

isoelectronic mercury(II) binds to the monothiocyanate group, the range for ν(CN) is 2055–2078 cm^{-1}, whereas dithiocyanate gives an absorption at 2120–2130 cm^{-1}.

Similarly, a band at 2130 cm^{-1} was observed for $[NH_4Au(SCN)_4]$ in which it can be concluded that gold(III) is bonded to SCN via sulphur.[24] The results presented in Table 2 for [(Imt)AuSCN] and $[(Diaz)_2AuSCN]$ and their complexes show a sharp absorption at 2040–2045 cm^{-1} which also indicates that gold(I) is bonded to the thiocyanate group via sulphur. These results further indicate that [(L)Au SCN] may form linear complexes which are most favoured for gold(I), and $[(L'_2)AuSCN]$ may have three-coordinate bonds around gold(I). However, from the present IR results reported here, it is not possible to differentiate between the linear and three-coordinated gold(I) complexes.

The absorption at 321–350 cm^{-1} can be assigned to the Au—S vibration.[11] A low-field shift of the ν(C=S) absorption by about 30 cm^{-1} indicates that gold(I) is bonded to the ligands via the thione group. Similar results were obtained in our previous studies.[9–13]

^{13}C *NMR studies*

The ^{13}C NMR chemical shifts of Imt and its derivatives along with their thiocyanate gold(I) complexes are given in Table 3. For the analogous six-membered Diaz complexes, NMR chemical shifts are given in Table 4.

As reported in our previous studies,[9–13] the C(2) resonance of all the ligands was shifted the most after complexing with gold(I). This high-field shift of the C(2) resonance is due to back donation of electrons from thione to gold(I), which is shielded after complexing with gold(I).

The ^{13}C resonance of SCN^- for any [(Imt)Au SCN] or $[(Diaz)_2AuSCN]$ complexes and their derivatives was not observed. This is in contrast to [(Imt)AuCN] and its analogous complexes where the $^{13}CN^-$ resonance was observed.[12] This may be due to either the T_1 for the thiocyanate complexes

Table 3. ^{13}C NMR chemical shifts (in ppm) relative to TMS for the imidazolidine-2-thione ligands and their gold(I) thiocyanate complexes[a]

Complexes	C(2)	C(4)	C(5)	R		
Imt	185.04	45.89	45.89	—		
[(Imt)AuSCN] (**a**)	175.47	46.06	46.06			
	(+9.57)	(−0.17)	(−0.17)			
MeImt	184.77	41.60	51.29	$-CH_3$ = 34.10		
[(MeImt)AuSCN] (**b**)	175.78	42.89	52.68	34.23		
	(+8.99)	(−1.29)	(−1.39)	(−1.13)		
EtImt	183.85	41.76	48.16	α-CH_2 = 41.54,	$-CH_3$ = 12.41	
[(EtImt)AuSCN] (**c**)	175.23	42.83	49.67	42.64	12.44	
	(+8.62)	(−1.07)	(−1.51)	(−1.10)	(−0.03)	
PrImt	184.41	41.81	48.80	α-CH_2 = 48.53	β-CH_2 = 20.89,	γ-CH_3 = 11.48
[(PrImt)AuSCN] (**d**)	175.61	42.93	50.17	49.37	20.89	11.48
	(+8.80)	(−1.37)	(−1.37)	(−0.84)	(0.00)	(0.00)
i-PrImt	183.38	41.92	43.06	α-CH_2 = 46.72	CH_3 = 19.38	
[(*i*-PrImt)AuSCN] (**e**)	173.94	42.86	44.71	49.08	19.65	
	(+9.44)	(−0.94)	(−1.65)	(−2.36)	(−0.27)	
DimetImt	184.54	48.65	48.65	$-CH_3$ = 35.05		
[(DimetImt)AuSCN)] (**f**)	[b]	49.96	49.96	35.97		
	—	(−1.31)	(−1.31)	(−0.92)		

[a] ^{13}C NMR resonances are assigned as given in R. Faure, E. J. Vincent, G. Assef, J. Kister and J. Metzger, *Org. Magn. Res.* 1977, **9**, 688. The numbers in parentheses indicate shifts with respect to the free ligands. A positive value indicates a high-field shift whereas a negative value represents a low-field shift.

[b] This resonance could not be detected in the spectrum.

being long or the thiocyanate undergoing slow exchange with the *trans* ligand under study. Also there is no proton directly bonded to the carbon of the thiocyanate and, therefore, there is no Overhauser effect.

For the [(Imt)AuSCN] system, the chemical shift difference between the free and bound C(2) resonance is 9.57 ppm, whereas, for the $[(Diaz)_2Au$ SCN] system it is 8.95 ppm. For their N-ethyl analogous systems [(EtImt)AuSCN], this difference is found to be 8.62 ppm, and 7.97 ppm for $[(EtDiaz)_2$ AuSCN]. This observation indicates some back donation of electrons from the thione to the 6*s* and 6*p* orbitals of gold(I). The shielding of the C(2)

Table 4. ^{13}C NMR chemical shifts (in ppm) relative to TMS for diazinane-2-thione and its gold(I) complexes[a]

Complexes	C(2)	C(4)	C(5)	C(6)	R	
Diaz	177.62	40.82	20.25	40.82		
$[(Diaz)_2AuSCN]$ (**g**)	168.67	40.90	19.33	40.90		
	(+8.95)	(−0.08)	(+0.92)	(−0.08)		
$[(Diaz)_2AuCl]$ (**h**)	168.17	40.89	19.38	40.89		
	(+9.45)	(−0.07)	(+0.87)	(−0.07)		
$[(Diaz)_2AuBr]$ (**i**)	169.32	41.04	19.34	41.04		
	(+8.30)	(−0.22)	(+0.91)	(−0.22)		
EtDiaz	177.52	41.10	21.88	46.00	α-CH_2 = 48.54	CH_3 = 12.58
$[(EtDiaz)_2AuSCN]$ (**j**)	169.55	[b]	20.88	47.29	49.70	12.99
	(+7.92)	—	(+1.00)	(−1.29)	(−1.16)	(−0.41)

[a] ^{13}C NMR resonance are assigned as given in R. Faure, E. J. Vincent, G. Assef, J. Kister and J. Metzger, *Org. Magn. Res.* 1977, **9**, 688. The numbers in parentheses indicate shifts with respect to the free ligands. A positive value indicates a high-field shift whereas a negative value represents a low-field shift.

[b] This resonance could not be detected in the spectrum.

resonance is greater for the linear system than for the three-coordinated system. Similar observations were made for the isoelectronic copper(I) system in which it was found that for the three-coordinated copper(I) complexes the C(2) resonance was shifted upfield by 3–4 ppm. However, for the two-coordinated (linear) complex system the shift was found to be 6–7 ppm[25].

It should be noted here, however, that six-membered ring systems always form three coordinated complexes with ammonium thiocyanate–gold(I), $AuCl_2^-$ and $AuBr_2^-$. When $AuCl_4^-$ was reduced to $AuCl_2^-$ with SO_2,[26] followed by the addition of Imt type ligands, it resulted in the formation of linear complexes of the type [L—Au—X]. However, addition of Diaz to $AuCl_2^-$ afforded a $[L'_2Au_3X_2]$-type multinuclear complex (where X = halides) instead of the [(Diaz)AuX]-type complex.

The most plausible explanation is that a six-membered ring (Diaz) has a more favourable steric environment in the neighbourhood of the thione group than the five-membered Imt ring. The Diaz ligand can form a boat or chair conformation to relieve any steric congestion which may not be relieved in the Imt system. This in turn allows Diaz to form the three-coordinated complex and Imt to form a linear complex.

The results presented here indicate that gold(I) thiocyanate forms stable complexes with thiones. Further studies are in progress to identify the nature of interaction of gold(I) thiocyanate with thiols such as cysteine, glutathione, haemoglobin and a thione such as ergothionine which are present in the red blood cells.

CONCLUSIONS

On the basis of elemental analysis, IR and ^{13}C NMR spectral data, the following conclusions can be drawn:

(1) Imt and its derivatives form stable complexes of the type [(L)Au^{I}SCN] which may be linear in nature.
(2) Diaz and its derivatives also form stable complexes of the type [(L'_2)Au^{I}SCN] which favours three-coordinated complexes.
(3) The upfield shift of the C(2) resonance in the ^{13}C NMR spectra is greater for linear complexes such as the [(Imt)AuSCN] system compared to three-coordinated [$(Diaz)_2$Au SCN] complexes.

Acknowledgement—This research was supported by the KFUPM Research Committee under project No. CY/NMRSTUDY/92.

REFERENCES

1. C. Li, S. L. Mella and A. C. Sartorelli, *J. Med. Chem.* 1981, **24**, 1089.
2. H. Kohn, B. A. Kohn, M. L. Steenberg and J. P. Buckley, *J. Med. Chem.* 1977, **20**, 158.
3. W. O. Foye and J. R. Lo, *J. Pharm. Sci.* 1972, **61**, 1209.
4. M. E. O'Neil, E. S. Raper and J. A. Daniels, *Inorg. Chim. Acta* 1981, **54**, L3.
5. E. S. Raper and J. L. Brooks, *J. Inorg. Nucl. Chem.* 1977, **39**, 2163.
6. E. S. Raper and P. H. Crackett, *Inorg. Chim. Acta* 1981, **50**, 159.
7. C. Preti and G. Tosi, *Can. J. Chem.* 1976, **54**, 1558.
8. L. P. Battagalia, A. B. Corradi, F. A. Devillanova and G. Verani, *Transition Met. Chem.* 1979, **4**, 264.
9. M. S. Hussain and A. A. Isab, *Transition Met. Chem.* 1984, **9**, 398.
10. M. S. Hussain and A. A. Isab, *J. Coord. Chem.* 1985, **14**, 17.
11. A. A. Isab and M. S. Hussain, *Polyhedron* 1985, **4**, 1688.
12. A. A. Isab and M. S. Hussain, *J. Coord. Chem.* 1986, **15**, 125.
13. M. S. Hussain and A. A. Isab, *Transition Met. Chem.* 1985, **10**, 178.
14. P. J. Sadler, *Struct. Bond.* 1976, **29**, 171.
15. C. F. Shaw, *Inorg. Perspect. Biol. Med.* 1979, **2**, 287.
16. D. H. Brown and W. E. Smith, *Chem. Soc. Rev.* 1980, 217.
17. G. G. Graham, T. M. Haavisto, P. J. McNaught, C. D. Browne and G. D. Champion, *J. Rheumatol.* 1981, **9**, 527.
18. D. Lewis, H. A. Cappel, C. J. McNiel, M. S. Iqbal, D. H. Brown and W. E. Smith, *Ann. Rheum. Dis.* 1983, **42**, 566.
19. *Smoking and Health*, Report of the Advisory Committee of the Surgeon General of the Public Health Service, Chap. 6, p. 60. U.S. Public Health Service Publication 1103, Washington DC (1964).
20. A. R. Pettigrew and G. S. Fell, *Clin. Chem.* 1973, **19**, 466.
21. G. D. Thorn, *Can. J. Chem.* 1955, **33**, 1278.
22. L. Maier, *Helv. Chim. Acta* 1970, **53**, 1417.
23. A. Lorenzotti, A. Cingolani, D. Leonesi and F. Bonati, *Inorg. Chim. Acta* 1984, **89**, 113.
24. G. A. Bowmaker and D. A. Rogers, *J. Chem. Soc., Dalton Trans.* 1982, 1873.
25. A. A. Isab and M. S. Hussain, *Transition Metal Chem.* 1986, **11**, 298.
26. A. A. Isab and P. J. Sadler, *Biochim. Biophys. Acta* 1977, **492**, 322.

Polyhedron Vol. 8, No. 23, pp. 2829–2836, 1989
Printed in Great Britain

0277–5387/89 $3.00+.00
© 1989 Pergamon Press plc

PHASE TRANSFORMATIONS IN THE FERRIHYDRITE/CYSTEINE SYSTEM

R. M. CORNELL* and W. SCHNEIDER

ETHZ Zürich, Laboratory for Inorganic Chemistry, CH-8092 Zurich, Switzerland

and

R. GIOVANOLI

University of Berne, Laboratory for Electron Microscopy, Freiestr. 3, CH-3000 Berne 9, Switzerland

(*Received* 7 *March* 1989; *accepted* 31 *July* 1989)

Abstract—In the presence of cysteine, ferrihydrite transforms into haematite, goethite or lepidocrocite at pH 6–8. Which compound forms depends on the cysteine–iron ratio and the nature of the buffering medium. In the absence of bicarbonate ions (which suppress lepidocrocite formation), the transformation product changed from haematite and lepidocrocite, to lepidocrocite and goethite and finally to goethite as the cysteine–iron ratio rose from $0.1 \rightarrow 0.4$. Interaction of cysteine with ferrihydrite leads to partial reduction of the interfacial ferric sites. Goethite and lepidocrocite formed from the partly reduced ferrihydrite by a dissolution/reprecipitation process, whereas haematite formed by a solid-state mechanism at a cysteine–iron ratio which was too low to permit extensive dissolution of partly reduced ferrihydrite to take place. Conversion of ferrihydrite to lepidocrocite under the influence of cysteine represents a new transformation route for the system. Transmission electron microscopy showed that the lepidocrocite thus formed consisted of well-developed laths or plates. Reducing organic ligands such as cysteamine, glutathione and penicillamine did not induce the formation of lepidocrocite.

The numerous interconversions between iron oxides and iron oxyhydroxides reflect the diversity and complexity of reactions in this system. These interconversions find application in industrial processes, for example, the conversion of goethite [α-FeO(OH)] or lepidocrocite [γ-FeO(OH)] into maghaemite (γ-Fe_2O_3) for use in magnetic tapes. They are also responsible for the mixtures of iron oxides–oxyhydroxides which exist in natural systems.

The behaviour of ferrihydrite ($5Fe_2O_3 \cdot 9H_2O$) illustrates the ability of an iron oxyhydroxide to transform into a variety of other iron compounds according to the reaction conditions. Ferrihydrite is a poorly ordered, thermodynamically unstable compound that gradually changes into goethite and/or haematite (α-Fe_2O_3).[1,2] The presence of foreign ions in the system can alter the kinetics of the competing mechanisms by which these compounds form and hence also the proportions of goethite and haematite in the reaction product.[3] Ferrihydrite may also transform to a spinel phase as a result of interaction with divalent cations.[4,5]

In an earlier publication[6] we reported that the presence of an organic reducing ligand, L-cysteine ($HSCH_2CH(NH_2)COOH$), induced the rapid conversion of ferrihydrite to goethite at a pH (8) at which, in the absence of the ligand, haematite was the predominant reaction product. This investigation has since been extended to consider the effect of cysteine on the transformation of ferrihydrite in slightly acid media. It was found that under these conditions, yet another transformation product, lepidocrocite, could be obtained from ferrihydrite. Lepidocrocite is used industrially as a pigment, a catalyst and in the production of photochemicals; it is widespread in soils and is a com-

* Author to whom correspondence should be addressed.

ponent of rust. Although it can precipitate from acid (pH 2) ferric solutions,[1,7] lepidocrocite is invariably synthesized by oxidation of ferrous systems at pHs of between 5 and 7.[8] The formation of lepidocrocite from ferrihydrite represents a novel extension of the interconversions between ferrihydrite and other iron oxides.

The present investigation considers the effect of L-cysteine on the products and kinetics of the transformation of ferrihydrite in the pH range 6–8.5. Particular attention was given to the formation of lepidocrocite. One question of interest was whether lepidocrocite could form from a ferrihydrite/cysteine suspension under slightly alkaline conditions (i.e. pH 8); earlier studies[6] showed that when the system was buffered with bicarbonate ions, only goethite formed. In the present work in alkaline media, the bicarbonate buffer was, therefore, replaced by a NH_4Cl/NH_3 buffer.

Transmission electron microscopy (TEM) was used to follow the progress of the transformation reaction and to establish the stage at which the different products nucleated. TEM was also used to determine whether lepidocrocite grown from ferrihydrite differed morphologically from that produced by oxidation of a ferrous system.

EXPERIMENTAL

Ferrihydrite was precipitated from ferric nitrate solution with 1 M KOH and the pH adjusted to either 6–6.5 with imidazole buffer solution or to 7.5–8.5 with NH_4Cl/NH_3 buffer. In a number of experiments bicarbonate buffer replaced NH_4Cl/NH_3 buffer. Enough L-cysteine to give a final concentration of between 10^{-3}–4×10^{-3} M (L : Fe ratio = 0.1–0.4) was then added to the ferrihydrite. The suspensions (1 g ferrihydrate/dm^3) were held in closed polypropylene bottles and aged in the dark at 70°C for up to 72 h. In some experiments L-cysteine was replaced by DL-cysteine (which gave identical results), cysteamine, D-penicillamine or glutathione (reduced form). All chemicals were AR (Fluka).

The kinetics of the transformation were followed by taking subsamples during the reaction and dissolving the unconverted ferrihydrite using a 30 min extraction with 0.4 M HCl (25°C).[6] Preliminary tests indicated that neither goethite, haematite nor lepidocrocite dissolved to any extent under these conditions. The extent of the transformation was expressed as the ratio, Fe_A/Fe_T, where Fe_A is the acid soluble material (i.e. unconverted ferrihydrite) and Fe_T is the total iron in the system. Analysis for iron was carried out using atomic absorption spectroscopy.

The crystalline product of the transformation was washed, dried at 50°C and X-ray powder diffraction (XRD) patterns obtained using a Guinier–Enraf camera (Mk IV) with Fe-$K_{\alpha 1}$ radiation. Where the reaction product consisted of a mixture of goethite and lepidocrocite or haematite and lepidocrocite, the proportion of each component was estimated by comparison with a series of standards. These standards were made by mixing known amounts of synthetic lepidocrocite with synthetic goethite or haematite. The 110 and 111 XRD lines of goethite, the 102 peak of haematite and the 020 peak of lepidocrocite were used for comparison.

Transmission electron micrographs were obtained with a Hitachi H-600-2 (100 kV) electron microscope equipped with a tracor TN 5400 energy dispersive X-ray spectrometer. For TEM examination the samples were dispersed in doubly distilled water using an ultrasonic treatment and a drop of suspension was dried on a carbon-coated bronze grid. Some samples were shadowed with chromium at an angle of 15°. Selected area electron diffraction (SAD) patterns were obtained using gold as an internal standard. For EDSX spectra the sample was dried on a graphitized nylon grid. Elemental analysis for C, H, N and S was carried out by the microanalytical department.

The interaction between L-cysteine and ferrihydrite was followed using differential pulse polarography (Polaroid E 506 metrohm polarograph with Ag/AgCl reference electrode). Suspensions of L-cysteine and ferrihydrite (0.1 g/100 cm^3, pH 8 or pH 6) were equilibrated for 1, 5 or 10 min or 2 h at 25°C, centrifuged and the level of L-cysteine in the supernatant liquid found by polarographic measurement. Fresh, standard solutions of L-cysteine at pH 8 (NH_4Cl/NH_3 buffer or bicarbonate buffer) or pH 6 (imidazole buffer) were also prepared for calibration purposes. The cysteine peak was observed at −0.51 V (pH 8) or at −0.39 V (pH 6).

RESULTS AND DISCUSSION

Reaction products

These depended mainly on the ratio of L-cysteine–iron (L : Fe) in the system together with the suspension pH and the nature of the buffering ions (Table 1).

In the absence of L-cysteine, ferrihydrite transformed into a mixture of haematite and goethite in both imidazole (pH 6) and NH_4Cl/NH_3 (pH 8) buffered systems: the proportion of goethite in the product decreased with rising pH (Table 1). On addition of 10^{-3} M L-cysteine (L : Fe = 0.1) ferri-

Table 1. Effect of cysteine concentration, pH and the nature of the buffer ions on the transformation products of ferrihydrite; 70°C, 48 h

Cysteine–iron	Products at pH 6 (Imidazole)	Products at pH 8 (NH_4Cl/NH_3)	Products at pH 8 ($NaHCO_3$)
0	Goethite + haematite (50%)	Haematite + goethite (10%)	Haematite + trace goethite
0.1	Haematite + lepidocrocite (45%)	Haematite + lepidocrocite (30%)	Haematite
0.2	Lepidocrocite + goethite (5%)	Lepidocrocite + goethite (55%)	Goethite
0.4	Goethite	Goethite	Goethite

hydrite transformed into a mixture of haematite and lepidocrocite. With increasing L : Fe ratio, haematite was replaced by lepidocrocite, which in turn, was replaced by goethite (Table 1); at L : Fe = 0.4, goethite was the sole reaction product.

Lepidocrocite was always associated with at least a few per cent of either haematite (L : Fe < 0.2) or goethite (L : Fe > 0.2). Under optimum conditions for lepidocrocite formation (L : Fe = 0.2, pH 6), there was still around 5% goethite in the product.

Addition of 6% seed crystals of lepidocrocite to a system with L : Fe = 0.1 increased the amount of lepidocrocite formed (from around 45 to 75%) at the expense of the haematite. Lepidocrocite seeding of systems with L : Fe $\geqslant$ 0.2 did not, however, eliminate or even reduce the proportion of goethite in the product.

Lepidocrocite did not form in the presence of organic reducing ligands related to L-cysteine, namely, cysteamine ($NH_2CH_2CH_2SH$), D-penicillamine [$(CH_3)_2C(SH)CH(NH_2)COOH$] or glutathione [$COOHCH(NH_2)(CH_2)_2CONHCH(CH_2SH)CONHCH_2COOH$] (L : Fe = 0.1–1.0).

Effect of bicarbonate buffer medium

No lepidocrocite formed at any L-cysteine–iron ratio when the system was buffered with bicarbonate ions. As the L : Fe ratio increased, the reaction product simply changed from haematite to 100% goethite.

Addition of bicarbonate buffer (0.05 M) to a suspension buffered with the same concentration of NH_4Cl/NH_3 60 min after addition of L-cysteine, also completely suppressed lepidocrocite in favour of either haematite (at L : Fe = 0.1) or goethite (at L : Fe = 0.2). If a bicarbonate solution was added to the system after the induction period (during which nucleation of the crystalline product occurs)[9] had been passed, however, formation of lepidocrocite was not suppressed. These observations suggest that the bicarbonate ion interferes with nucleation of lepidocrocite.

Interactions of L-cysteine with ferrihydrite

In a previous investigation,[6] polarography measurements showed that the presence of ferrihydrite promoted the rapid oxidation of L-cysteine to the disulphide (cystine) at pH 8 in bicarbonate buffer. The formation of cystine was shown by the appearance of polarography peaks at −0.63 and −0.94 V in the supernatant liquid.[10]

In the present work the same effect was observed when bicarbonate buffer was replaced by NH_4Cl/NH_3 buffer. After a few minutes contact with ferrihydrite (25°C) in this buffer system, polarographic peaks at −0.51 V (due to L-cysteine) and at −0.63 and −0.94 V were observed. In both buffers, oxidation of L-cysteine was around 85% complete after a few minutes contact with ferrihydrite.

The polarographic peaks of L-cysteine and cystine were observed at −0.39, −0.47 and −0.83 V, respectively, in imidazole buffer. This shift in peak position with decreasing pH is in line with that reported earlier by Kolthoff *et al.*[11] Oxidation of L-cysteine to cystine at the ferrihydrite interface was slower at pH 6 than at pH 8. After the first 10 min of contact little cystine formation was detected. During the following 2 h around 70% oxidation gradually took place.

Oxidation of L-cysteine is accompanied by simultaneous reduction of a proportion of the ferric ions in the system.[6,12] The interaction can be summarized by the following equation:

$$\equiv Fe^{III} + RSH \longrightarrow \equiv Fe^{II} + 1/2RSSR + 1/2H^+,$$

hence with an initial L : Fe ratio of 0.2, a maximum

of 20% of the total iron(III) in the ferrihydrite could be reduced.

The oxidation/reduction reaction is preceded by adsorption of L-cysteine on ferrihydrite through the sulphydral group.[6] As the pK of this group is 8.3, adsorption at pH 6 would be expected to proceed less readily than at pH 8 and this would account for the slower reaction at low pH.

Addition of L-cysteine to ferrihydrite at pH 8 was accompanied by an almost immediate darkening of the suspension, which can be attributed to the formation of mixed valence iron(II)–iron(III) hydroxide domains in the ferrihydrite. At pH 6 and with L : Fe = 0.2, the ferrihydrite was a much lighter brown immediately after addition of the organic ligand; the lighter colour is consistent with a slower rate of oxidation/reduction. Considerably higher levels of L-cysteine (L : Fe = 1.0) were needed to produce a noticeable darkening of the suspension at this pH.

Kinetics

The kinetic curves for the system both with and without L-cysteine consisted of an initial induction period followed by a faster transformation stage.

Comparison of the transformation curves at L : Fe = 0.2 in different buffers (Fig. 1) shows that conversion was fastest in bicarbonate buffer (product 100% goethite) and slowest at pH 6 (product 95% lepidocrocite). These differences can be attributed to differences in the rate of interaction of L-cysteine with ferrihydrite at the two pHs.

At pH 8, the overall transformation was slower in the system buffered with NH_4Cl/NH_3 than in that buffered with bicarbonate solution although there was no difference in the rate and extent of oxidation of L-cysteine in either system. The difference in transformation rates suggests that the chloride ion stabilizes ferrihydrite or, alternatively, that the combination of bicarbonate ion and a reducing ligand directly promotes goethite formation.

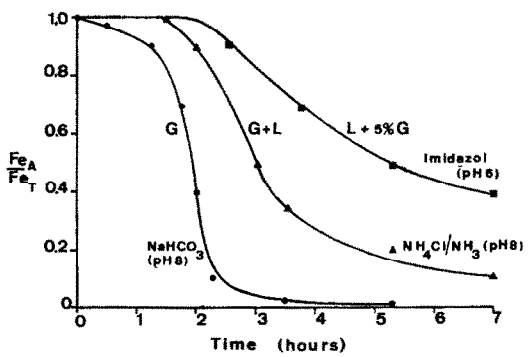

Fig. 1. Fe_A/Fe_T as a measure of the degree of transformation of ferrihydrite into crystalline oxides vs time, for systems with different buffers. Cysteine–iron = 0.2, 70°C. G = goethite, L = lepidocrocite.

Electron microscopy

Lepidocrocite grew from ferrihydrite as comparatively large laths or plates depending on the pH of the system. At pH 6, laths up to 150 nm in width formed [Fig. 2(a)], whereas at pH 8, the crystals grew as plates up to 800 nm in length and 500 nm across [Fig. 2(b)]. Measurements on micrographs of shadowed samples indicated that the crystal thickness was between 20 and 80 nm. SAD measurements showed that these crystals usually lie with the (010) plane parallel to the electron microscope grid as do lepidocrocite crystals grown from ferrous systems: occasionally, thick crystals lie on the (100) face.

Both the laths and the plates usually terminated in serrated ends and the surfaces of the platey crystals often displayed thin cracks or deep serrations [Fig. 2(a) and 2(b)]. These imperfections are probably due to interference during growth by temporarily adsorbed ligands. EDSX spectra (Fig. 3) indicated that sulphur was associated with lepidocrocite grown in the presence of L-cysteine and chemical microanalysis confirmed the presence of 1–2% of organic ligand in the sample. The large sizes of both the cysteine and the cystine molecules make it more probable that the organic ligand would be adsorbed on the surfaces of the crystals rather than incorporated into the crystal lattice.

The crystallinity of lepidocrocite grown from a *ferrous* precursor depends strongly on the rate of crystal growth: the crystals usually form as thin narrow laths.[8] Only with careful control of pH and rate of oxidation are well-developed crystals similar to those obtained here from ferrihydrite produced.

Haematite grew as irregular platelets less than 100 nm across, both with and without the presence of L-cysteine at pH 8 [Fig. 2(c)] and as a mixture of platelets and rhombohedra at pH 6 in imidazole buffered systems. However, in the presence of L-cysteine, haematite grew as granular, rod-like, or, in some cases, ellipsoidal crystals at pH 6 [Fig. 2(d)]. This morphology is reminiscent of that of haematite grown at the same pH in the presence of oxalic acid.[13]

Goethite grew as poorly developed acicular crystals around 300 nm in length in the presence of L-cysteine (pH 6–8) [Fig. 2(e)]. Twinned crystals were not observed.

The transformation of ferrihydrite at pH 6 and at L : Fe = 0.2 into lepidocrocite and some goethite

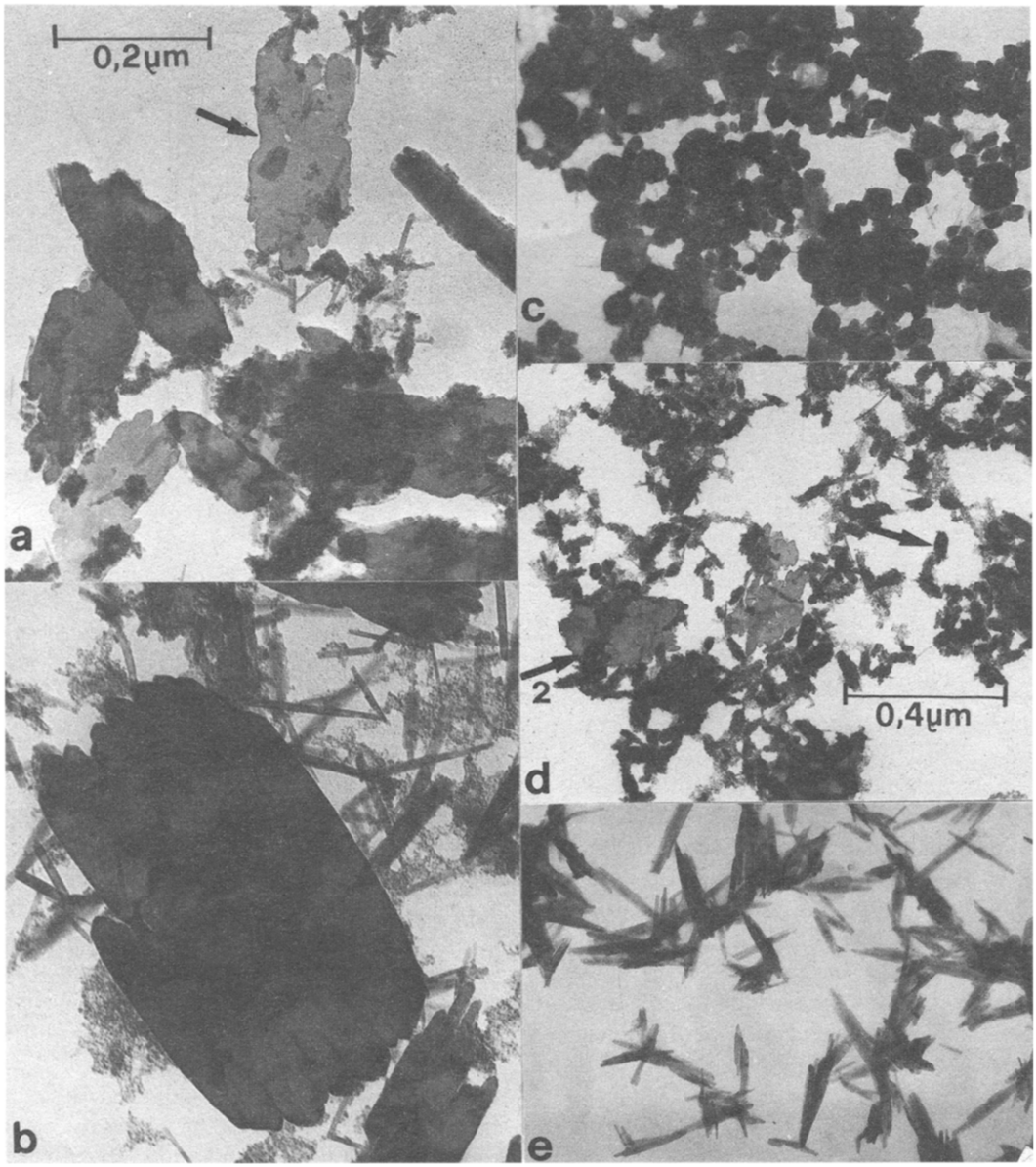

Fig. 2. Transmission electron micrographs of oxides formed from ferrihydrite in the presence of cysteine, 70°C. (a) Lath-like crystals of lepidocrocite (arrow), small acicular crystals of goethite and a trace of ferrihydrite (pH 6, cysteine–iron = 0.1). (b) Large platey crystal of lepidocrocite together with acicular goethite crystals. The amorphous background material is ferrihydrite (pH 8, NH_4Cl/NH_3 buffer, cysteine–iron = 0.2). (c) Haematite platelets (pH 8, $NaHCO_3$ buffer, cysteine–iron = 0.1). (d) Rod-like haematite (arrowed) together with some plates of lepidocrocite (arrow 2) (pH 6, cysteine–iron = 0.1). (e) Acicular crystals of goethite (pH 6–8, cysteine–iron = 0.3).

was followed by TEM examination of subsamples taken during the course of the reaction. After the initial 2–3% transformation, TEM showed an amorphous looking mass of ferrihydrite together with a few laths of lepidocrocite and the occasional needles of goethite [Fig. 4(a)]. These laths were initially very thin and thickened as the reaction proceeded. After 20% reaction the lepidocrocite product consisted of a mixture of very thin laths and much thicker crystals [Fig. 4(b)]. This mixture of crystals suggests that nucleation and growth had occurred simultaneously. The proportion of very thin crystals decreased as the reaction proceeded further, indicating that in the later stages of the transformation growth predominated over nucleation [Fig. 4(c) and 4(d)]. The lepidocrocite crystals reached their maximum widths and lengths in the early stages (first 20%) of the conversion

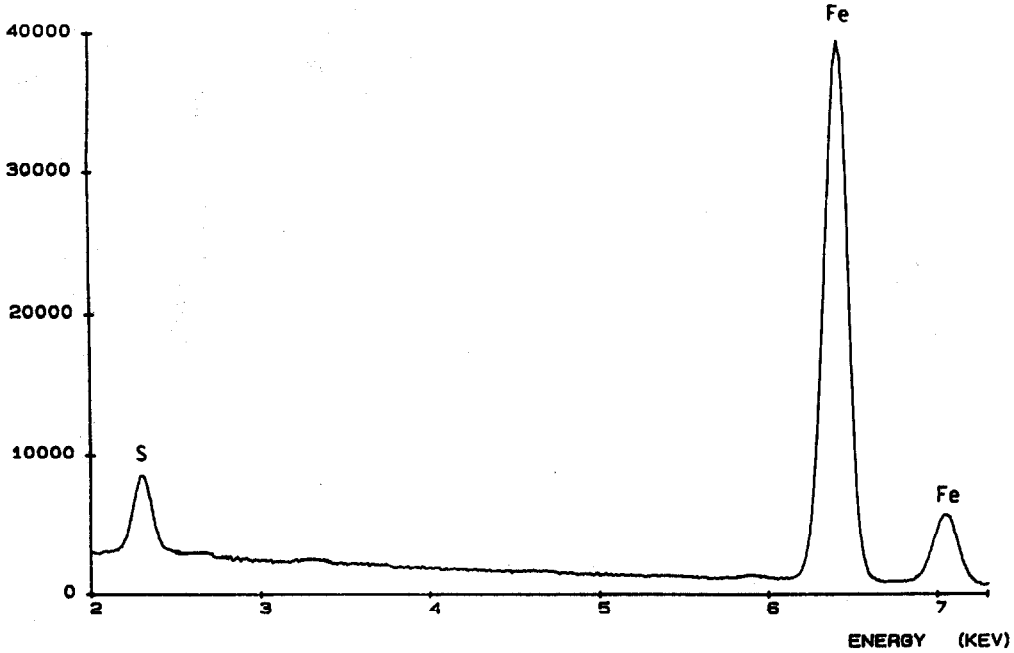

Fig. 3. Energy dispersive X-ray spectrum of lepidocrocite showing the presence of S.

process and subsequent growth took place mainly in the [010] direction, i.e. the crystals became thicker.

TEM examination of a series of subsamples taken during a transformation at pH 8 (L : Fe = 0.2, NH_4Cl/NH_3 buffer) showed similar features to those observed at pH 6. At pH 8, however, the lepidocrocite crystals increased in width as well as thickness over the main part of the reaction. In both systems, lepidocrocite and goethite nucleated simultaneously at the beginning of the transformation.

Formation of crystalline compounds from ferrihydrite

At L : Fe ratios > 0.2, L-cysteine had a strong goethite promoting effect in imidazole and NH_4Cl/NH_3 as well as in bicarbonate systems. As shown earlier,[6] partial reduction of interfacial ferric ions during interaction with L-cysteine converted ferrihydrite into a mixed valence iron(II)–iron(III) compound which dissolved more readily than the original material. As goethite forms in solution from soluble ferric species released by dissolution of ferrihydrite, whereas haematite forms within the particles of ferrihydrite by a solid-state transformation,[1,2] any factor that enhances the solubility of ferrihydrite causes the formation of goethite to become increasingly competitive with that of haematite.

Although lepidocrocite can precipitate directly from acidic ferric solutions, it is commonly synthesized from green rust obtained by oxidation of ferrous solutions.[8] How green rust transforms to lepidocrocite has not been established; both a topotactic transformation and a dissolution/reprecipitation mechanism have been proposed.[14,15]

The present work is the first report of the formation of lepidocrocite by interaction of *ferrihydrite* with a ligand. Although the modified ferrihydrite that develops in systems with L : Fe = 0.1–0.2 is a mixed valence compound, it cannot be termed a green rust. Green rusts are crystalline, greenish-blue compounds and have a ratio of $Fe^{2+} : Fe^{3+} = 3$–4, whereas the partly reduced ferrihydrite was amorphous, light to dark brown and had an estimated $Fe^{2+} : Fe^{3+}$ ratio of 0.1–0.2.

Evidence from both TEM and seeding experiments suggests that lepidocrocite forms from partly reduced ferrihydrite by a dissolution/reprecipitation mechanism. The very thin plates of lepidocrocite that develop initially and the marked difference between the morphology of ferrihydrite (particles 3–5 nm in diameter) and that of lepidocrocite (well-developed laths or plates) are indicative of a transformation involving dissolution of the solid precursor. Structural considerations also support this mechanism. A solid-state transformation which involves structural changes from the hexagonally close-packed anion array of ferrihydrite to the cubic close-packed anion array of the lepidocrocite lattice would be expected to be less

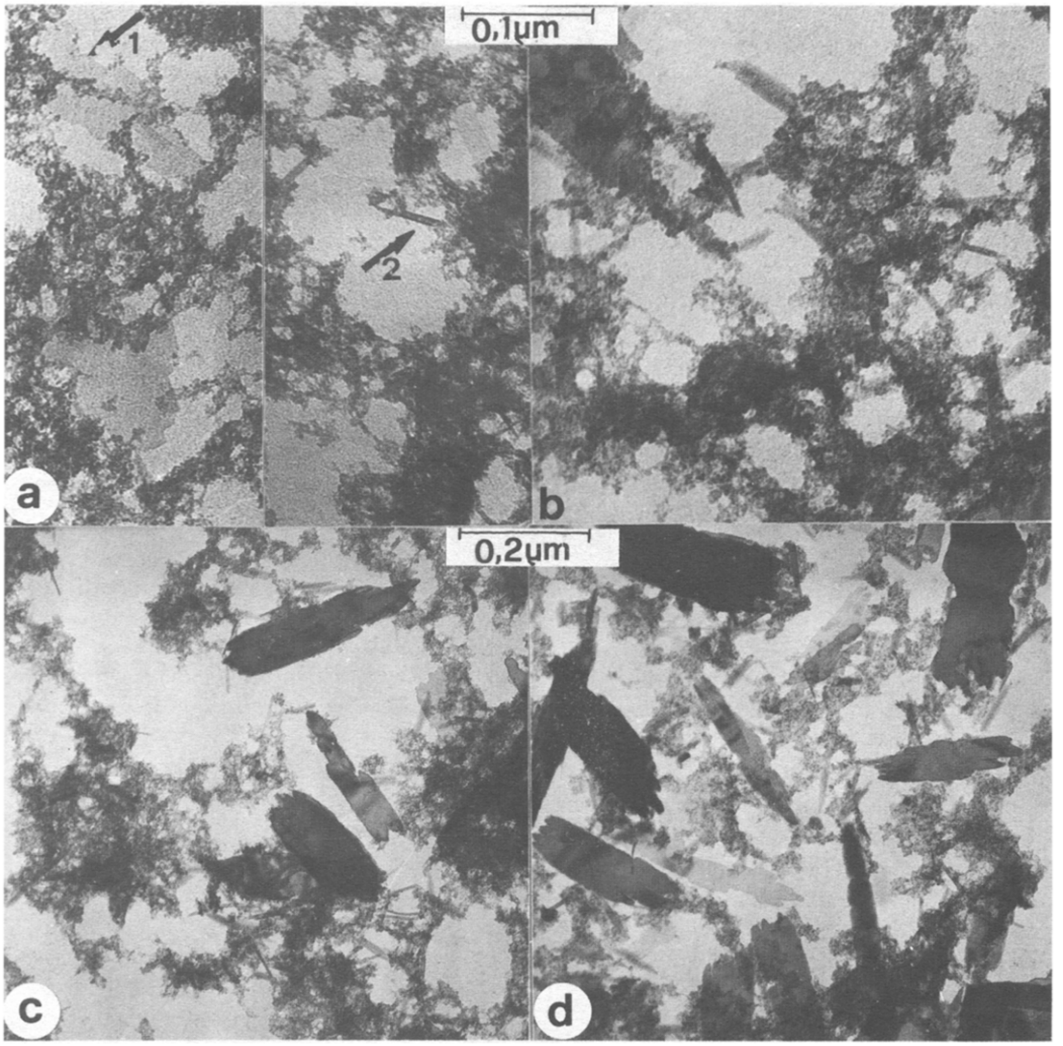

Fig. 4. Transmission electron micrographs of the stages in the transformation of ferrihydrite to lepidocrocite and goethite at pH 6, cysteine–iron = 0.2. (a) 2–3% transformation; arrow 1 indicates lepidocrocite and arrow 2 shows goethite. (b) 20% transformation. (c) 45% transformation. (d) 60% transformation.

favourable energetically than dissolution of partly reduced ferrihydrite. Growth of lepidocrocite from soluble ferric species has been observed previously in alkaline media.[16] At pH 12–13, lepidocrocite is gradually converted into goethite by a dissolution/reprecipitation process: when goethite nucleation was inhibited by the presence of silicate species, the soluble ferric species produced by dissolution of lepidocrocite reprecipitated on the remaining crystals of lepidocrocite causing a change in their morphology from laths to cubes.[16]

A feature of the L-cysteine/ferrihydrite system is the successive appearance of three different transformation products as the L : Fe ratio varies over a narrow range. This characteristic reflects the operation of different transformation mechanisms in the system. At the lowest L : Fe ratio (0.1), haematite and lepidocrocite formed together because the extent of partial reduction was not sufficient for dissolution of ferrihydrite to outweigh completely the internal rearrangement process by which haematite forms. Increasing the transformation temperature of this system from 70 to 90°C enhanced the amount of haematite in the product, presumably because a higher temperature accelerates the dehydration process which precedes haematite formation. The present work provides the first example of lepidocrocite and haematite co-existing in a product: haematite does not form from green rust.

Both goethite and lepidocrocite formed from partly reduced ferrihydrite by a dissolution/reprecipitation process. It is not clear why lepidocrocite forms when the extent of reduction is low, whereas goethite forms as the extent of reduc-

tion (and the rate of dissolution) increases. Differences in solubility products do not appear to influence the order of precipitation. Goethite has a lower solubility product than lepidocrocite ($\log K_{so} = -44$ and -39.8, respectively)[17] and so might be expected to precipitate preferentially in systems with the lowest L:Fe ratios, instead of vice versa. The transformation of the thermodynamically less stable lepidocrocite into goethite can also be excluded, because under the conditions of these experiments, the process is too slow to make any contribution to the formation of goethite.

Murphy *et al.*[7] found that lepidocrocite precipitated from dilute, acidic ferric solutions consisting of monomeric ferric species, whereas goethite could be obtained from ferric solutions containing polynuclear as well as low molecular weight species. In the present work it was observed that at pH 6 and L:Fe = 0.2, increasing either the suspension concentration (five-fold) or the ionic strength (10-fold with KNO_3) completely suppressed lepidocrocite in favour of goethite. These observations suggest that the reaction product in these systems depends mainly on the size and/or charge of the soluble species. Both properties can govern the way in which the soluble ferric species link up to form nuclei[18] and hence could determine the structure of the crystalline precipitate.

In *ferrous* systems the presence of carbonate or bicarbonate ions reduces formation of lepidocrocite in favour of that of goethite.[19] A similar effect with bicarbonate has been observed here in the L-cysteine/ferrihydrite system and has been attributed to interference by the bicarbonate ion in nucleation of lepidocrocite. The lepidocrocite lattice consists of sheets of $Fe(O,OH)_6$ octahedra linked by hydrogen bonds, and TEM showed that an important feature of crystal growth was an increase in crystal thickness, i.e. formation of new sheets of octahedra. These considerations suggest that bicarbonate ions may suppress lepidocrocite by interfering in the formation of new sheets of octahedra, particularly in the earliest stages of nucleation.

Acknowledgements—We are indebted to Miss E. Ettinger for carrying out the electron microscopy and to Mr M. Faller for the X-ray powder diffraction measurements. Financial support was provided by ETH-Kredite für Unterricht und Forschung (Inter-institutional project 1987) and by Robert Ghehm Fonds.

REFERENCES

1. W.Feitknecht and W. Michaelis, *Helv. Chim. Acta* 1962, **26**, 212.
2. U. Schwertmann and W. R. Fischer, *Z. Anorg. Allg. Chem.* 1966, **346**, 137.
3. R. M. Cornell, *Z. Pfl-Ernähr. Düng. Boden.* 1987, **150**, 304.
4. R. M. Cornell and R. Giovanoli, *Clays Clay Miner.* 1987, **35**, 11.
5. R. M. Cornell and R. Giovanoli, *Polyhedron* 1988, **7**, 385.
6. R. M. Cornell and W. Schneider, *Polyhedron* 1989, **8**, 149.
7. P. J. Murphy, A. M. Posner and J. P. Quirk, *J. Colloid Interface Sci.* 1976, **56**, 312.
8. U. Schwertmann and H. Thalmann, *Clay Miner.* 1976, **11**, 189.
9. R. M. Cornell and R. Giovanoli, *Clays Clay Miner.* 1985, **33**, 424.
10. C. A. Mairesse-Ducarmoir, G. J. Patriarche and S. L. Vandenvalck, *Analytica Chim. Acta* 1974, **71**, 165.
11. I. M. Kolthoff, W. Stricks and N. Tanaka, *J. Am. Chem. Soc.* 1955, **77**, 4739.
12. C. A. McAuliffe and S. G. Murray, *Inorg. Chim. Acta Rev.* 1972, **6**, 103.
13. W. R. Fischer and U. Schwertmann, *Clays Clay Miner.* 1975, **23**, 33.
14. J. D. Bernal, D. A. Dasgupta and A. L. Mackay, *Clay Miner. Bull.* 1959, **4**, 15.
15. T. Misawa, K. Hashimoto and S. Shimodaira, *Corros. Sci.* 1974, **14**, 131.
16. U. Schwertmann and R. M. Taylor, *Clays Clay Miner.* 1972, **20**, 151.
17. T. Misawa, *Corros. Sci.* 1973.
18. W. Schneider and B. Schwyn, in *Aquatic Surface Chemistry* (Edited by W. Stumm), p. 167. Wiley Interscience, New York (1987).
19. U. Schwertmann, *Z. Anorg. Allg. Chem.* 1959, **298**, 23.

Polyhedron Vol. 8, No. 23, pp. 2837–2840, 1989
Printed in Great Britain

0277-5387/89 $3.00+.00
© 1989 Pergamon Press plc

DISULPHIDE BOND CLEAVAGE IN THE NICKEL(II)–CYSTAMINE AND COPPER(II)–CYSTAMINE SYSTEMS. X-RAY CRYSTAL STRUCTURE OF *TRANS*-[Ni(SCH$_2$CH$_2$NH$_2$)$_2$]

D. CARRILLO

Instituto de Quimica, Universidad Catolica de Valparaiso, Casilla 4059, Valparaiso, Chile

and

P. GOUZERH* and Y. JEANNIN

Laboratoire de Chimie des Métaux de Transition, URA-CNRS 419,
Université Pierre et Marie Curie, 75252 Paris Cedex 05, France

(*Received* 26 *April* 1989; *accepted* 31 *July* 1989)

Abstract—Nickel(II) and copper(II) chlorides react with an excess of cystamine in ethanol to give the bis(cystamine)nickel(II) and copper(II) chlorides which appear to have distorted octahedral and tetragonal symmetry, respectively, on the basis of the IR, Raman and reflectance spectra. In aqueous solution, the metal–S(disulphide) interaction promotes the nucleophilic scission of the sulphur–sulphur bond. In the case of the copper-catalysed reaction, partial reduction of the metal centre occurs. With nickel(II), the reaction leads to the formation of *trans*-[Ni(SCH$_2$CH$_2$CH$_2$)$_2$] which has been characterized by single-crystal X-ray diffraction.

The chemistry of coordinated sulphur is of current interest because of its relevance to biological systems.[1] A salient feature is the redox equilibrium between organic disulphides, RSSR, and mercaptides, RS$^-$, in aqueous solution, which can be shifted by complexation to metal ions. While the existence of disulphide coordination has been postulated for a long time, only recently has it been proved to occur. But, although a number of crystallographic papers are now available which describe the role of the ligand structure on the stereochemistry of the ligated disulphide moiety,[2,3] and although the aminomercaptan chemistry has been widely studied, some aspects of the coordination chemistry of the cysteamine–cystamine couple ($H_2NCH_2CH_2SH-H_2NCH_2CH_2SSCH_2CH_2NH_2$) are still not clear:

(i) neither copper(II) nor nickel(II) cystamine complexes have been reported until now;

(ii) the nature of the deep violet complex formed during the reactions of copper(II) with cysteamine and copper(I) with cystamine has been much debated;[4,5]

(iii) conflicting *cis*[6] and *trans*[7] structures have been assigned to bis(β-mercaptoethylamine)nickel (II) on the basis of vibrational studies.

We report here the synthesis and the characterization of copper(II) and nickel(II) cystamine complexes and their reactivity in aqueous solution. While this work was being completed the X-ray crystal structure of *trans*-bis(β-mercaptoethylamine) nickel(II) has been reported.[8] Some data in this paper are wrong because of a typing error,[9] therefore we will briefly comment on this structure.

EXPERIMENTAL

Materials

Cysteamine hydrochloride and cystamine dihydrochloride (Fluka, purum) were used without

* Author to whom correspondence should be addressed.

further purification. All other chemicals and solvents were of reagent grade quality.

Preparations

Bis(cystamine)nickel(II) *chloride.* A solution of KOH (0.01 mol) in deaerated ethanol (50 cm^3) was added to a stirred suspension of cystamine dihydrochloride (0.05 mol) in ethanol (50 cm^3). The mixture was ice-cooled and KCl was filtered off. The filtrate was then added dropwise under nitrogen to a vigorously stirred solution of $NiCl_2 \cdot 6H_2O$ (5 mmol) in ethanol (50 cm^3). A light green precipitate formed immediately. It was filtered off under nitrogen, washed with ethanol and with diethyl ether, and kept in a refrigerator. Yield 95%. Found: C, 22.6; H, 5.6; N, 12.8; Cl, 16.8; Ni, 13.3; S, 29.2. Calc. for $C_8H_{24}N_4Cl_2NiS_4$: C, 22.1; H, 5.6; N, 12.9; Cl, 16.3; Ni, 13.5; S, 29.5%.

Bis(cystamine)copper(II) *chloride.* A light blue copper complex was prepared by the same method $CuCl_2 \cdot 2H_2O$. Yield 90%. Found; C, 22.1; H, 5.4; N, 12.9; Cl, 16.2; Cu, 14.1; S, 28.7. Calc. for $C_8H_{24}N_4Cl_2CuS_4$: C, 21.9; H, 5.5; N, 12.8; Cl, 16.1; Cu, 14.5; S, 29.2%.

Bis(cystamine)copper(II) *perchlorate.* $[Cu(cystam)_2](ClO_4)_2$ was obtained similarly from $Cu(ClO_4)_2 \cdot 6H_2O$.

Crystals of bis(β-mercaptoethylamine)nickel(II). Bis(cystamine)nickel(II) chloride (0.3 g) was dissolved in water (50 cm^3). The pH was decreased to *ca* 7 and after standing at room temperature for 3 days, the solution yielded dark red rectangular prisms of $[Ni(NH_2CH_2CH_2S)_2]$. A small amount of $Ni(OH)_2$ slurry was separated; crystals were then filtered and washed with water, ethanol and diethyl ether. Yield 15%.

Spectroscopic measurements

IR spectra (KBr pellets) were obtained on a Perkin-Elmer 597 spectrophotometer. Solution UV–vis spectra were recorded with a Beckman 5240 spectrophotometer. A Beckman 5270 spectrophotometer was used for measuring the diffuse-reflectance spectra (reference compound $BaSO_4$). Raman spectra were measured with a Coderg PHO spectrometer by using the 5145 Å line of a Spectra Physics Ar^+ laser. Spectra of cystamine dihydrochloride and $[Ni(cystam)_2]Cl_2$ were obtained from solid pellets mounted on a spinning sample holder. Attempts to measure the Raman spectrum of the copper complex were unsuccessful. The crystallographic study used the standard methods of the laboratory.[10]

RESULTS AND DISCUSSION

Cystamine complexes

The addition of a large excess of cystamine to nickel(II) or copper(II) chlorides or perchlorates in ethanol results in the precipitation of the bis(cystamine)nickel(II) or bis(cystamine)copper(II) complexes. They have not been previously reported although a lot of work has been carried out on the coordination chemistry of cystamine and its methyl derivatives.[4,11,12] The isolation of the copper complexes is also particularly noteworthy since it was reported[12] that all attempts to prepare such complexes by mixing copper(II) perchlorate and cystamine in a variety of solvents failed because of the reduction of copper(II). Disulphide copper(II) complexes are scarce: representative examples are those of cystine,[13] D-penicillamine disulphide[14] and glutathione.[15] The complexes $[Cu(Me_4\text{-cystam})X](ClO_4)_2$ (X = H_2O or CH_3CN; Me_4-cystam = bis[(2-amino-1,1-dimethyl)ethyl]disulphide) have been described in solution.[12]

Analytical data indicate that $[Ni(cystam)_2]Cl_2$ and $[Cu(cystam)_2]Cl_2$ were obtained in a reasonably pure state despite their relative instability and the lack of any suitable organic solvent for recrystallization. They dissolve in water with decomposition (see below). The solids slowly decompose in moisture.

Three ν(N—H) bands at *ca* 3110, 3200 and 3260 cm^{-1} are observed in the IR spectra of $[Cu(cystam)_2]Cl_2$ and $[Cu(cystam)_2](ClO_4)_2$, and at *ca* 3160, 3240 and 3310 in the IR spectrum of $[Ni(cystam)_2]Cl_2$. This supports coordination to the metal atom through both nitrogen atoms of each ligand.

The reflectance spectrum of $[Ni(cystam)_2]Cl_2$ shows several bands at 8000, 11,365, 16,130, 26,100, 37,000 cm^{-1} and somewhat less-resolved features at 12,800, 15,850 and 20,400 cm^{-1}. The two low-energy well-resolved bands indicate an octahedral coordination. Nickel is likely to be surrounded by two tridentate cystamine ligands: each ligand would coordinate by both nitrogen atoms and by one sulphur atom. However, this nickel–sulphur interaction would not significantly alter the disulphide bond since the S—S Raman stretch frequency (502 cm^{-1}) is only slightly lowered compared to that of the free ligand (511 cm^{-1}). A similar situation has been found in chloro- and bromo(bis{2-[(2-pyridylmethyl)amino]ethyl}disulphide)nickel(II) perchlorates.[2,16] Another possibility would be a polymeric structure with nickel(II) ions bridged by cystamine ligands.

The reflectance spectrum of $[Cu(cystam)_2]Cl_2$ shows two broad bands centred at 12,500 and

37,000 cm^{-1}, consistent with tetragonal symmetry. The 12,500 cm^{-1} band is assigned to a *d–d* transition. The 37,000 cm^{-1} band may be assigned to a $N(\sigma) \rightarrow Cu^{II}$ charge-transfer transition and/or to the $n_a \rightarrow \sigma^*$ transition that occurs in aliphatic disulphides.[17] The absence of any intense band at *ca* 20,000 cm^{-1}, where the $S(\sigma) \rightarrow Cu^{II}$ charge-transfer band is expected,[12] indicates that the sulphur–copper(II) interaction is at best weak. Coordination of chloride can be excluded since the IR spectrum of $[Cu(cystam)_2](ClO_4)_2$ is essentially identical to that of the chloride compound, except for the perchlorate absorption at 1120, 1085 and 625 cm^{-1}.[18]

Disulphide bond cleavage

Bis(cystamine)nickel(II) and -copper(II) complexes are unstable in the presence of water.

The nickel(II) complex aqueous solution becomes turbid on standing due to the precipitation of nickel hydroxide. Then the mixture turns to red–brown and dark red crystals of a good size (1 mm) deposit within a few days. This crystalline material was proved by IR and X-ray powder diffraction studies to be identical to samples of the bis(β-mercaptoethylamine)nickel(II) complex obtained from nickel(II) and cysteamine[19] and from the trinuclear $[Ni\{Ni(SCH_2CH_2NH_2)_2\}_2]^{2+}$ complex.[19]

When the $[Cu(cystam)_2]Cl_2$ complex is dissolved in water, a red–brown solution is formed. The absorbance reaches its maximum (450 nm; $\varepsilon \simeq 600$ mol^{-1} dm^3 cm^{-1} per Cu) after *ca* 30 min and then slowly decreases. A purple–grey solid precipitates when excess chloride is added to the solution. This observation may be compared to the fact that chloride is essential for the formation of the purple mixed-valence copper(I)–copper(II)–penicillamine[5] and –dimethylcysteamine complexes[20] and of some other mixed-valence copper compounds.[21] The red–brown species is clearly distinct from the violet transient species formed during the reaction of Cu^{2+} and cysteamine.[4] But, whatever its true nature is, its formation almost certainly implies that part of the copper(II) is reduced to copper(I) by the cysteamine formed by cleavage of the cystamine. This is in agreement with previous observations.[12]

The above facts clearly point out the faster cleavage of cystamine in aqueous solutions containing nickel(II) or copper(I) ions. It is well known that heterolytic bond cleavage of disulphides is facilitated by concomitant electrophilic and nucleophilic attack.[22] Although most effective catalysts in the sulphur–sulphur bond scission are silver(I), mercury(II) and palladium(II), the reaction is now well documented with copper(II)[12,23,24] and with cobalt(III).[25,26] The reaction is supposed to occur via initial electrophilic attack on the sulphur–sulphur bond by the metal ion and subsequent nucleophilic attack by water to form the thiol and the unstable sulphenic acid (RSOH).

To our knowledge, no case of catalysis of the disulphide bond scission by nickel(II) has been previously reported, although extensive studies of nickel(II) complexes with thiols and disulphides have been made.[2,16,27,28] By comparison, the half-life of cystamine disulphide cleavage in 1.0 M NaOH in 80% ethanol solution at 37°C is 84 h.[29]

Crystal structure of bis(β-mercaptoethylamine) nickel(II)

The *trans*-$[Ni(SCH_2CH_2NH_2)_2]$ complex forms monoclinic crystals of space group $P2_1/c$ with two molecules per unit cell; $a = 4.847(3)$, $b = 10.255(5)$, $c = 7.892(4)$ Å and $\beta = 94.35(5)°$. Using the alternative $P2_1/a$ space group, Font-Altaba and coworkers quoted $a = 7.298$ Å, their correct value being 7.928 Å,[9] unfortunately all computations and discussions were based upon $a = 7.298$ Å.[8]

The structure was refined by full-matrix least-squares techniques to $R = 0.044$ for 61 parameters and 525 observed reflections with $\theta \leqslant 25°$ [$I \geqslant 3\sigma(I)$].[30] The structure is in agreement with ref. 8. However, the actual dimensions of the NiN_2S_2 skeleton deserve some comments. The value of the NNiS angle (87.9(2)°) is exactly the same as in bis(N,N-dimethyl-β-mercaptoethylamine)nickel (II).[31] Also the Ni—S bond length (2.193(2) Å) is nearly identical with that of the dimethyl derivative (2.198(3) Å).[31] Both values are in agreement with literature data[32–34] although significantly longer than the mean value of 2.155(3) Å found in the *cis*-$[Ni(SCH_2CH_2NH_2)_2]$ units of the $[Ni\{Ni(SCH_2CH_2NH_2)_2\}_2]^{2+}$ complex.[32] The Ni—N distance (1.904(7) Å) is in the range normally found for planar nickel(II) chelates,[31] so that the N—H···S bond does not seem to affect the chelate ring geometry.

Tables of atomic positional and thermal parameters, bond lengths and angles and F_o/F_c values have been deposited as supplementary data with the Editor, from whom copies are available on request. Atomic coordinates have also been deposited with the Cambridge Crystallographic Data Centre.

REFERENCES

1. E. Deutsch, M. J. Root and D. L. Nosco, *Adv. Inorg. Bioinorg. Mech.* 1982, **1**, 269.
2. P. E. Riley and K. Seff, *Inorg. Chem.* 1972, **11**, 2993 and refs cited therein.

3. J. A. Bertrand and J. L. Breece, *Inorg. Chim. Acta* 1974, **8**, 267 and refs cited therein.
4. P. Kroneck, C. Naumann and P. Hemmerich, *Inorg. Nucl. Chem. Lett.* 1971, **7**, 659.
5. P. J. M. W. L. Birker and H. C. Freeman, *J. Am. Chem. Soc.* 1977, **99**, 6890.
6. C. W. Schaffer and K. Nakamoto, *Inorg. Chim. Acta* 1972, **6**, 177.
7. U. A. Jayasooriya and D. B. Powell, *Spectrochim. Acta* 1974, **30A**, 553.
8. J. Suades, X. Solans and M. Font-Altaba, *Polyhedron* 1984, **3**, 1227.
9. M. Font-Altaba, private communication (March 1985).
10. P. Gouzerh, Y. Jeannin, C. Rocchiccioli-Deltcheff and F. Valentini, *J. Coord. Chem.* 1979, **9**, 221.
11. T. Ottersen, L. G. Warner and K. Seff, *Inorg. Chem.* 1974, **13**, 1904.
12. J. M. Downes, J. Whelan and B. Bosnich, *Inorg. Chem.* 1981, **20**, 1081.
13. R. S. Gale and C. A. Winkler, *Inorg. Chim. Acta* 1976, **21**, 151.
14. J. A. Thich, D. Mastropaolo, J. Potenza and H. J. Schugar, *J. Am. Chem. Soc.* 1974, **96**, 726.
15. K. Miyoshi, Y. Sugiura, K. Ishizu, Y. Iitaka and H. Nakamura, *J. Am. Chem. Soc.* 1980, **102**, 6130.
16. L. G. Warner, M. M. Kadooka and K. Seff, *Inorg. Chem.* 1975, **14**, 1773.
17. D. B. Boyd, *J. Am. Chem. Soc.* 1972, **94**, 8799.
18. B. J. Hathaway and A. E. Underhill, *J. Chem. Soc.* 1961, 3091.
19. D. C. Jicha and D. H. Busch, *Inorg. Chem.* 1962, **1**, 872.
20. H. J. Schugar, C-C. Ou, J. A. Thich, J. A. Potenza, T. R. Felthouse, M. S. Haddad, D. N. Hendrickson, W. Furey and R. A. Lalancette, *Inorg. Chem.* 1980, **19**, 543.
21. I. Sóvágó, B. Harman and A. Gergely, *Inorg. Chim. Acta* 1980, **46**, L107.
22. J. L. Rice, *Accts Chem. Res.* 1968, **1**, 58.
23. L. S. Higashi, M. Lundeen, E. Hilti and K. Seff, *Inorg. Chem.* 1977, **16**, 310.
24. A. Odani, T. Maruyama, O. Yamauchi, T. Fujiwara and K-I. Tomita, *J. Chem. Soc., Chem. Commun.* 1982, 646.
25. A. Ichimura, D. L. Nosco and E. Deutsch, *J. Am. Chem. Soc.* 1983, **105**, 844.
26. A. Ichimura, D. L. Nosco and E. Deutsch, *Inorg. Chem.* 1985, **24**, 1674.
27. L. G. Warner, T. Ottersen and K. Seff, *Inorg. Chem.* 1974, **13**, 2529.
28. T. B. Vance, L. G. Warner and K. Seff, *Inorg. Chem.* 1977, **16**, 2106.
29. F. Y. Rachinskii, Y. A. Bruk, L. V. Pavlova and N. M. Slavachevskaya, *Zh. Obsch. Khim.* 1970, **40**, 2109.
30. D. Carrillo, P. Gouzerh and Y. Jeannin, *First Symp. Inorg. Chem. Transition Met.: Coordination and Molecular Activation.* Santiago, Chile, 7 January 1985.
31. R. L. Girling and E. L. Amma, *Inorg. Chem.* 1967, **6**, 2009.
32. C. H. Wei and L. F. Dahl, *Inorg. Chem.* 1970, **9**, 1878.
33. H. Barrera, J. Suades, M. C. Perucaud and J. L. Brianso, *Polyhedron* 1984, **3**, 839.
34. H. Barrera, J. C. Bayon, J. Suades, G. Germain and J. P. Declerq, *Polyhedron* 1984, **3**, 969.

Polyhedron Vol. 8, No. 23, p. 2841, 1989
Pergamon Press plc. Printed in Great Britain

ANNOUNCEMENT

THE ROYAL SOCIETY OF CHEMISTRY
IXth INTERNATIONAL SYMPOSIUM ON
ORGANOSILICON CHEMISTRY
UNIVERSITY OF EDINBURGH
16-20 JULY 1990

The Organisers have pleasure in inviting all interested persons to attend the **IXth International Symposium on Organosilicon Chemistry** to be held at the University of Edinburgh from Monday 16 July to Friday 20 July 1990, with participants foregathering on Sunday 15 July. A reception will be held on Sunday evening for all participants. The afternoon and evening of Wednesday 18 July will be set aside for organised excursions, with the Symposium Dinner on Thursday 19 July. The meeting concludes after lunch on Friday 20 July.

SCIENTIFIC PROGRAMME

The plenary lectures will be held in single sessions whereas the invited and contributed papers will be in parallel sessions. Time will also be set aside in the programme for posters and discussion sessions.

Contributed papers are invited for oral or poster presentation. Anyone wishing to contribute a paper should submit a title and synopsis (*ca* 100 words) **not later than 8 January 1990** to Dr John F. Gibson at the address below, indicating the type of presentation preferred.

FURTHER INFORMATION

Further information, including details of the programme, submission of papers, plus fees and other charges are available from:

Dr John F. Gibson
Royal Society of Chemistry
Burlington House
London W1V 0BN
UK

Telephone: 01 437 8656
Telex: 268001
Fax: 01 437 8883

Polyhedron Vol. 8, No. 24, pp. 2843–2882, 1989
Printed in Great Britain

0277–5387/89 $3.00+.00
© 1989 Pergamon Press plc

POLYHEDRON REPORT NUMBER 29

STRUCTURE, BONDING AND ELECTRON COUNTS IN CUBANE-TYPE CLUSTERS HAVING M_4S_4, $M_2M'_2S_4$ AND MM'_3S_4 CORES

SUZANNE HARRIS

Corporate Research Laboratory, Exxon Research and Engineering Company, Route 22 East, Annandale, NJ 08801, U.S.A.

CONTENTS

1. INTRODUCTION 2843

2. HOMOMETALLIC CLUSTERS HAVING AN M_4S_4 CORE 2845
2.1. All four metals octahedrally coordinated 2845
2.2. All four metals tetrahedrally coordinated 2851
2.2.1. π-Acceptor ligands 2852
2.2.2. π-Donor ligands 2854
2.3. All four metals five-coordinate 2856
2.4. Two tetrahedral metals—two five-coordinate metals 2860
2.5. Three tetrahedral metals—one five-coordinate metal 2863

3. HETEROMETALLIC CLUSTERS HAVING AN $M_2M'_2S_4$ CORE 2866
3.1. All four metals octahedrally coordinated 2866
3.2. Two octahedral metals—two tetrahedral metals 2866
3.3. Two octahedral metals—two five-coordinate metals 2869

4. HETEROMETALLIC CLUSTERS HAVING AN MM'_3S_4 CORE 2871
4.1. All four metals octahedrally coordinated 2871
4.2. Three octahedral metals—one tetrahedral metal 2872
4.3. One octahedral metal—three tetrahedral metals 2874
4.4. Two octahedral metals—two five-coordinate metals 2876

5. SUMMARY 2879

1. INTRODUCTION

Homometallic M_4S_4 cubane-type clusters have been known for some 20 years. They all contain the core **1**, which is characterized by two interpenetrating tetrahedra made up of four metal atoms and four triply-bridging sulphur atoms, respectively. (Although the core in **1** is drawn as a cube to

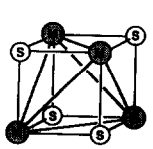

(1)

emphasize the cubane-type structure, the M_4 tetrahedron is usually smaller than the surrounding S_4 tetrahedron.) Each metal atom is also coordinated by one to three other ligands (L). Although this general structure is observed in all the cubanes, various distortions are observed in the two

tetrahedra. The number and type of distortions are determined both by the direct metal–metal bonding and by the metal–sulphur and metal–ligand bonding. These in turn are influenced by several factors, two of the most important being the number of metal *d*-electrons and the coordination geometry around each metal atom. The M_4S_4 clusters not only form an intriguing class of inorganic and organometallic clusters, but also, in the case of many of the Fe_4S_4 clusters, have served as important synthetic analogues for the redox sites of iron–sulphur proteins.[1-3] The theoretical attempts to understand the electronic structure and properties of these clusters have ranged from qualitative and approximate molecular orbital (MO) treatments[4-12] to more exact spin- and space-unrestricted X_α calculations.[13-16] Notable among the theoretical treatments of these clusters is the development of qualitative MO bonding schemes by Dahl and co-workers.[4,8,17,18] Based initially upon the T_d symmetry of the clusters, and later augmented by approximate MO calculations, these schemes make it possible to understand the metal–metal bonding and to predict the structures of many of the M_4S_4 clusters.

Within the last 10 years a number of heterometallic $M_2M'_2S_4$ and MM'_3S_4 clusters containing the cores **2** and **3**, respectively, have been synthesized and characterized. The motivation for the

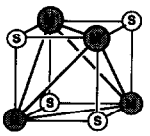

(2)

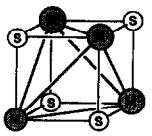

(3)

synthesis and study of the clusters having an $MoFe_3S_4$ core has come primarily from their relation to a mixed-metal–sulphide cluster present in nitrogenase,[19,20] but the combinations of metals, ligands and ligand coordination geometry observed in the heterometallic clusters extend far beyond those found in the $MoFe_3S_4$ clusters. In spite of the proliferation of these heterometallic clusters, the theoretical treatments of these systems have been few.[12,21,22] Unfortunately, the qualitative MO schemes of Dahl and co-workers are not easily extended to these lower symmetry heterometallic clusters. A recent set of calculations on several $M_2M'_2S_4$ clusters showed that it was useful to view the metal–metal bonding in these clusters in terms of available orbitals on the MS_3L_x ($x = 1, 2, 3$) fragments within the clusters.[22] An examination of the structures, electron counts and available MO calculations for a wide range of both homo- and heterometallic cubane-type clusters suggests that this same approach can be used to derive qualitative cluster MO bonding schemes for a large number of both homo- and heterometallic cubanes.

The cubane-type clusters can be divided into various groups based upon the coordination geometry around each metal atom in the cluster. Many of the homometallic clusters fall into the classification where all of the metals in the cluster lie in a pseudo-octahedral environment. In a number of other clusters the coordination around the metal atoms may be pseudo-tetrahedral, square pyramidal, or trigonal bipyramidal. In most of the homometallic clusters, the coordination geometry around each metal is identical, and there are only a few clusters in which the metal atoms exhibit two different coordination geometries. In the heterometallic $M_2M'_2S_4$ and MM'_3S_4 clusters, on the other hand, the different metals usually exhibit different coordination geometries, and only a few heterometallic clusters are known in which the coordination geometry around all the metals is the same.

This report groups the clusters into classes according to metal coordination geometry and considers the relation between structure, bonding and electron counts in each group. A qualitative metal cluster bonding scheme is presented for each class. In several of the homometallic groups the metal cluster bonding is described in terms of both the qualitative Dahl model, which is most applicable to homometallic clusters in which the ligand coordination around all four metals is the same, and a "metal fragment orbital" model, which becomes particularly useful for clusters having two different kinds of metal coordination and/or two different metals. It is important to recognize that in the systems where both of these models can be applied, the Dahl model and the fragment model provide consistent pictures of the metal cluster bonding. It should be pointed out that the bonding schemes described in this report are *qualitative* and are subject to the limitations inherent in such schemes. In several cases these limitations are pointed out and the need for further electronic structure calculations is discussed. Electronic structure calculations have already provided a more

detailed picture of the bonding in some of these clusters, and the results of these calculations provide both a basis and a check for the qualitative schemes.

The discussion in this report is limited to clusters having metal–sulphur cores of structures type **1**, **2** or **3**. A number of clusters incorporating other cubane-type cores are known,[23] and the metal cluster bonding schemes described in this report should be useful in describing the cluster bonding in many of these other cubane-type clusters. Since the discussion is also limited to "single" cubane clusters, the "double" cubane clusters containing two MFe_3S_4 cores are not explicitly considered. The bonding schemes described here should also be applicable to the individual cubane units within these larger clusters.

2. HOMOMETALLIC CLUSTERS HAVING AN M_4S_4 CORE

2.1. *All four metals octahedrally coordinated*

The clusters in this class are characterized by the general formula $M_4S_4L_{12}$ (**4**) or $M_4S_4Cp_4$ (**5**). If the metal–metal bonds are ignored, each M atom is six-coordinate (Cp is considered to occupy

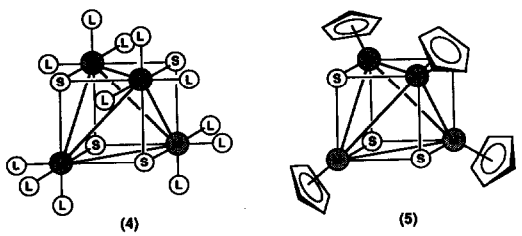

three coordination sites) and can be viewed as part of a pseudo-octahedral fragment within the cluster. A number of the clusters making up this group are listed in Table 1. Also included in the table are the number of "metal" electrons (this number is calculated from the formal oxidation states of the four metals in the clusters) and the metal–metal distances found in each cluster. It should be noted that all 12 of the ligands in the $M_4S_4L_{12}$ clusters are not always identical. In $[Mo_4S_4(NO)_4(CN)_8]^{8-}$, for example, each molybdenum atom is coordinated by two cyanide ligands and one nitrosyl ligand.[24] In some clusters multidentate ligands occupy more than one coordination site and may actually span two metal atoms. The structure of $Mo_4S_4(S_2CNEt_2)_6$ is shown in Fig. 1. Here, four of the bidentate Et_2dtc ligands each bind to a single molybdenum atom, while each of

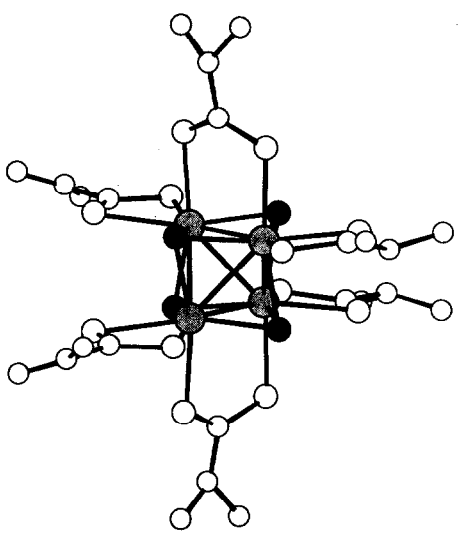

Fig. 1. Structure of $Mo_4S_4(S_2CNEt_2)_6$ (refs 25 and 26). Only the first C in each Et group is shown. One bidentate Et_2dtc ligand is bound to each Mo, and the remaining two Et_2dtc ligands each span two Mo atoms. Neglecting the Mo—Mo bonds, each Mo is bound to six S atoms and is approximately octahedral.

Table 1. Homometallic clusters having structure type **4** or **5**: all four metals octahedrally coordinated

Cluster	Number of metal electrons	M—M distances	Reference
$Ti_4S_4(MeCp)_4$	4	2.927, 2.932 3.006(2), 3008(2)[a]	16
$Mo_4S_4(NC_6H_4Me)_4(S_2CN(i\text{-}Bu)_2)_4$	4	2.881(2), 3.66(4)	27
$Mo_4S_4(NC_6H_4Me)_4(S_2P(OEt)_2)_4$	4	2.862(2), 3.69(4)	28
$[V_4S_4(MeCp)_4]^+$	7	2.852(2), 2.855(4)	16
$V_4S_4(MeCp)_4$	8	2.868(4), 2.884(2)	16, 29
$Mo_4S_4(S_2PEt_2)_6$	10	2.79(2), 2.88(4)	30
$[Mo_4S_4(edta)_2]^{2-}$	10	2.74–2.87	31
$Mo_4S_4(S_2CNEt_2)_6$	10	2.732(2), 2.86(4)	25, 26
$[Mo_4S_4(NCS)_{12}]^{6-}$	10	2.791(3), 2.869(3)	32
$[Mo_4S_4(i\text{-}PrCp)_4]^{2+}$	10	2.79–2.90	33
$Mo_4S_4(HB(pz)_3)_4(pz)$	11	2.659, 2.92(5)	34
$[Mo_4S_4(edta)_2]^{3-}$	11	2.76–2.88	35
$[Mo_4S_4(i\text{-}PrCp)_4]^+$	11	2.86–2.92	33
$Cr_4S_4(MeCp)_4$	12	2.82–2.85	36
$[Mo_4S_4(NH_3)_{12}]^{4+}$	12	2.78–2.80	37
$[Mo_4S_4(edta)_2]^{4-}$	12	2.77–2.79	31
$Mo_4S_4R_4$ (R = Cp, MeCp, Me_5Cp)	12	2.89–2.91	11, 33
$[Re_4S_4(S_3)_6]^{4-}$	12	2.76(6)	38
$[Mo_4S_4(CN)_{12}]^{8-}$	12	2.85(6)	39
$[Fe_4S_4Cp_4]^{2+}$	18	2.834(4), 3.254(2)	4
$[Fe_4S_4Cp_4]^+$	19	2.652(2), 3.188(2), 3.319(2)	40
$[Mo_4S_4(NO)_4(CN)_8]^{8-}$	20	2.99(2), 3.67(4)	24
$Fe_4S_4Cp_4$	20	2.65(2), 3.365(4)	41, 42
$Ru_4S_4(MeCp)_4$	20	2.77(2), > 3.5(4)	43
$[Co_4S_4Cp_4]^+$	23	3.172(4), 3.330(2)	17
$Co_4S_4Cp_4$	24	3.236–3.343	17
$Fe_4S_4(CO)_{12}$	24	3.443–3.477	18

[a] Numbers in parentheses indicate number of averaged distances.

the two remaining Et_2dtc ligands span two molybdenum atoms.[25,26] The $M_4S_4L_{12}$ and $M_4S_4Cp_4$ designations are meant to indicate that in these clusters six coordination sites are occupied around each metal atom resulting in approximately octahedral coordination of all four metals.

In all the cubane-type clusters there are three sets of bonds which have to be considered when describing the electronic structure. These are the metal–metal bonds, the metal–ligand bonds, and the bonds between the metals and the sulphurs which are part of the M_4S_4 core. The metal–ligand and metal–sulphur interactions are both stronger than the metal–metal interactions, and the qualitative bonding schemes described here assume that the stronger metal–ligand and metal–sulphur interactions can be separated from the weaker metal–metal interactions. (From now on the stronger M—L and M—S interactions will be grouped together and described collectively as "metal–ligand interactions".)

The Dahl group synthesized and characterized several $M_4S_4Cp_4$ clusters.[4,17,40,42] The structure of $Co_4S_4Cp_4$ is illustrated in Fig. 2. In this cluster the long non-bonding cobalt–cobalt distances result in a Co_4S_4 core which closely resembles a true cube. Making use of the T_d symmetry of the clusters, the Dahl group developed a qualitative cluster bonding scheme that makes it possible to understand and predict the changes in metal–metal bonding which accompany changes in the number of cluster electrons. Assuming that the metal–metal interactions can be separated from the metal–ligand interactions, the metal *nd*, $(n+1)s$ and $(n+1)p$ orbitals of the four metals making up the metal tetrahedron can be combined to form 36 symmetry adapted combinations. The 20 symmetry combinations involving the 20 *nd* orbitals (five from each metal) prove to be most important to the description of the tetrametal cluster bonding, since it is these combinations which are bonding, non-bonding or antibonding with respect to metal–metal interactions. The ligand orbitals

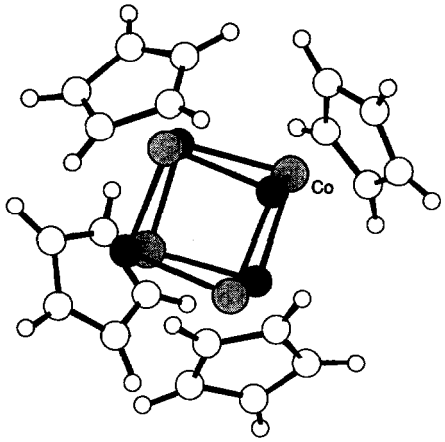

Fig. 2. Structure of $Co_4S_4Cp_4$ (ref. 17). Each octahedral Co is bound to three core S atoms and a Cp ring. Since there are no Co—Co bonds, the Co_4S_4 core closely resembles a cube.

can also be combined into symmetry orbitals, their number and symmetry properties depending on the number and nature of the ligands. The metal and ligand symmetry orbitals can then be combined to form cluster molecular orbitals.

The qualitative MO scheme derived in this manner for the T_d $M_4S_4Cp_4$ complexes[4] is shown in Fig. 3. The M_4 symmetry orbitals are shown on the left. The 20 orbitals resulting from the metal *d* orbitals are divided into three groups—six M_4 bonding orbitals (a_1+e+t_2), six M_4 antibonding orbitals (t_1+t_2), and eight orbitals which are essentially non-bonding between the metal atoms ($e+t_1+t_2$). The symmetry orbitals resulting from combinations of the various S atomic and Cp molecular orbitals are indicated on the right side of the diagram. The cluster orbitals which arise from the interactions of the metal and ligand combinations are indicated in the centre. The lower

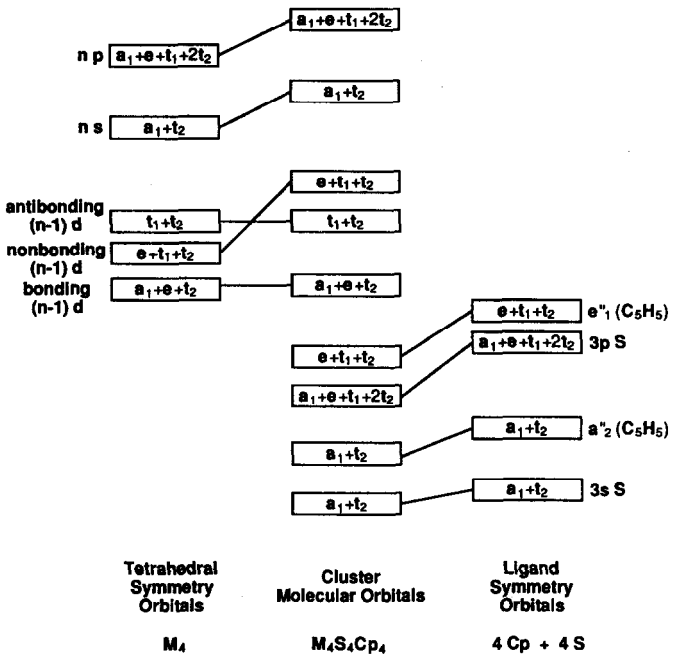

Fig. 3. Qualitative MO energy level scheme derived by the Dahl group (ref. 4) for $M_4S_4Cp_4$ clusters. The scheme is based on cubic T_d symmetry. The symmetry orbitals for the M_4 tetrahedron are shown on the left, while the symmetry combinations of the S and Cp orbitals are shown on the right. The cluster orbitals resulting from interactions between the M_4, S and Cp orbitals are shown in the middle.

energy cluster orbitals are centred primarily on the ligands and are either ligand or M—L bonding orbitals. These levels are completely occupied. The higher energy orbitals are primarily metal in character and are M—L antibonding. The number of electrons occupying these orbitals will depend on both the total electron count of the cluster and the relative energies of the three sets of levels. The relative energies of the metal based cluster orbitals—particularly those which are non-bonding between the metals—are influenced by the metal–ligand interactions. In the $M_4S_4Cp_4$ clusters the interaction between the M_4 non-bonding combinations ($e+t_1+t_2$) and the ligand orbitals of appropriate symmetry are strong enough to destabilize the M_4 non-bonding combinations to energies above the M_4 bonding and antibonding sets of orbitals.

In the cluster valence electron (CVE) scheme of Lauher,[44] an electron count of 60 should result in a completely bonded (six M—M bonds) tetrahedron of metals. In the $M_4S_4Cp_4$ clusters, the lower energy metal–ligand bonding orbitals are occupied by 48 of these electrons. (The four low energy MOs corresponding to the sulphur 3*s* orbitals are not involved in the M—L bonding and are not included in the cluster electron count.) A 60-electron cluster would therefore have 12 metal electrons available to occupy the M_4 cluster orbitals, in this case the set of six M–M bonding orbitals. This should result in a completely bonding tetrahedron of metals, in accordance with the CVE scheme. The $M_4S_4Cp_4$ clusters considered by the Dahl group ($Co_4S_4Cp_4$, with a 72 CVE count and $[Fe_4S_4Cp_4]^{0,1+,2+}$, with 68, 67 and 66 CVE counts, respectively) all have electron counts in excess of 60 and thus have more than 12 metal electrons. These extra metal electrons will occupy M—M antibonding orbitals. In $Co_4S_4Cp_4$, the 24 metal electrons should occupy all six M—M bonding orbitals and all six M—M antibonding orbitals, leading to a completely non-bonding tetrahedron of metals. This is consistent with the non-bonding M—M distance of 3.295 observed in $Co_4S_4Cp_4$. In $[Fe_4S_4Cp_4]^{0,1+,2+}$, where there are 20, 19 and 18 metals electrons, respectively, the M—M antibonding orbitals are partially occupied by 8, 7 and 6 electrons. This should lead to distortions of the M_4 unit away from T_d symmetry, and the Dahl group successfully correlated the experimentally observed differences in M—M bond lengths with the symmetry of the M_4 antibonding orbitals expected to be occupied. They also noted that the larger changes in M—M distances in comparison to the relatively small changes in M—S and M—L distances tend to confirm that these orbitals are primarily metal in character.

This qualitative scheme can be applied to both the $M_4S_4Cp_4$ and $M_4S_4L_{12}$ clusters, and the M—M distances in the clusters listed in Table 1 are consistent with the bonding scheme. The 60-electron clusters, those having 12 metal electrons and a completely filled set of M—M bonding orbitals, all contain a completely bonding metal tetrahedron. The presence of more than 12 metal electrons results in the occupation of M—M antibonding orbitals and leads to a corresponding decrease in the degree of M—M bonding. The M—M non-bonding orbitals are sufficiently high in energy in these clusters that they are never occupied. Clusters containing less than 12 metal electrons will have an incompletely filled set of M—M bonding orbitals, and differences in the M—M distances are again expected. This is certainly true in the clusters containing four metal electrons, where only two short M—M distances, or two M—M bonds, are observed. Interestingly, the structures of clusters such as $[Mo_4S_4(i\text{-PrCp})_4]^+$ and $[Mo_4S_4(i\text{-PrCp})_4]^{2+}$, which contain 11 and 10 metal electrons, respectively, show only small deviations from the structure of $Mo_4S_4(i\text{-PrCp})_4$, which contains 12 metal electrons. According to the bonding scheme in Fig. 3, the occupied M—M bonding orbitals have a_1, e and t_2 symmetry. The relative peak intensities and energies in the valence photoelectron spectrum of $Mo_4S_4(i\text{-PrCp})_4$ indicate that the highest occupied set of orbitals has t_2 symmetry and that the energy ordering of the three highest energy sets of orbitals is $t_2 > e > a_1$.[33] It was suggested by Bandy *et al.*[33] and Davies *et al.*[45] that the highest energy t_2 orbitals are only weakly M—M bonding or nearly non-bonding. This would explain the very small changes in structure in the series $[Mo_4S_4(i\text{-PrCp})_4]^{0,1+,2+}$, where the metal electron count goes from 12 to 11 to 10. Molecular orbital calculations for $Mo_4S_4Cp_4$ and $Cr_4S_4Cp_4$,[11] $V_4S_4(MeCp)_4$ and $[V_4S_4(MeCp)_4]^+$[16] and $[Mo_4S_4(CN)_{12}]^{8-}$,[9] confirm that the t_2 set of orbitals lies highest in energy and that, in general, the order of the levels is $t_2 > e > a_1$. (Results of an earlier calculation for $Cr_4O_4Cp_4$ indicated that a different ordering of levels was appropriate for the $M_4X_4Cp_4$ clusters.[7] This different ordering is inconsistent, however, with both the observed structures of many of the clusters and all other reported calculations.) In a recent study of the magnetic susceptibility of $[Mo_4S_4(edta)_2]^{2-}$, Shibahara and co-workers found that $[Mo_4S_4(edta)_2]^{2-}$ (10 metal electrons) is diamagnetic.[46] They concluded that the HOMO in $[Mo_4S_4(edta)_2]^{4-}$ (12 metal electrons) must be the a_1 orbital, since removal of

two electrons from this singly degenerate orbital would lead to a diamagnetic cluster. They argued that if the electrons were initially removed from the set of t_2 orbitals, the distortions from T_d symmetry are not sufficient to ultimately yield a diamagnetic cluster. Once again, these conclusions are inconsistent with the numerous calculations which repeatedly find that the a_1 orbital is the most stable of the M_4 cluster bonding orbitals. Since $[Mo_4S_4(i\text{-}PrCp)_4]^{2+}$ (10 metal electrons), where it seems certain that two electrons have been removed from the t_2-orbitals, is also diamagnetic,[45] it is more likely that the HOMO in $[Mo_4S_4(edta)_2]^{4-}$ is also of t_2 symmetry. Using overlap population analyses, Williams and Curtis found that for $Mo_4S_4Cp_4$ and $Cr_4S_4Cp_4$ only the a_1 orbital is strongly M—M bonding.[11] The e orbitals are weakly M—M bonding, while the t_2 orbitals are nearly M—M non-bonding in character. They commented that the number of clusters with fewer than 12 metal electrons but short M—M distances is, therefore, not surprising, since even in these clusters the more strongly M—M bonding orbitals are occupied, and partial occupation of the nearly non-bonding t_2 orbitals should lead to only weak first-order Jahn–Teller distortions. It should be noted that a number of the clusters having fewer than 12 metal electrons contain several multidentate ligands which span two metals. Although distinct patterns of short and long M—M distances are more pronounced in these clusters, comparisons of the M—M distances in these clusters should be made with care, since the shorter M—M distances may be dictated by these spanning ligands.

The qualitative bonding scheme developed by the Dahl group is thus seen to be generally applicable to a large number of $M_4S_4Cp_4$ and $M_4S_4L_{12}$ clusters. As discussed above, the development of this scheme depends on the separability of the stronger metal–ligand interactions from the weaker metal–metal interactions. The scheme drawn in Fig. 3 first considers the metal–metal interactions and then adds on the metal–ligand interactions. Alternatively, it is possible to first consider the metal–ligand interactions and then add on the metal–metal interactions. That is, we can first consider a fragment within the cluster composed of a metal and its surrounding ligands. We determine how the metal–ligand interactions within this fragment affect the energies of the metal-based orbitals and *then* combine the metal orbitals to form the tetrametal cluster orbitals. As will be seen below, treating the interactions in this order becomes extremely useful for the less symmetric clusters considered later in the report. We will call this a "metal fragment orbital" approach. Fragment orbital approaches have proved extremely useful in describing the bonding in many organometallic clusters (particularly metal carbonyl clusters)[47,48] where the stronger metal–ligand interactions and the weaker metal–metal interactions can be viewed separately. In metal carbonyl clusters, for example, it is possible to separate a cluster into several $M(CO)_x$ fragments. The M—M bonds in the cluster can then be described in terms of metal-based fragment orbitals. The number, nature and relative energy of these fragment orbitals is determined largely by the number and geometry of the ligands in the $M(CO)_x$ fragment. Each fragment can often be viewed as some part of an octahedron, and the fragment metal orbitals which are available for cluster formation can be related to the t_{2g} and e_g orbitals in an octahedral complex. Upon formation of the cluster, the lower energy t_{2g}-like orbitals remain non-bonding between the metals, while the high energy e_g-like orbitals on each fragment are utilized for the formation of M—M bonds. The spatial orientation of the e_g-like fragment orbitals is such that formation of the M—M bonds tends to complete the octahedral coordination about each metal.

When the M—M bonds are neglected, each of the metal atoms in an $M_4S_4Cp_4$ or $M_4S_4L_{12}$ cluster lies in a pseudo-octahedral environment and can be viewed as part of an MS_3Cp or MS_3L_3 fragment. From the point of view of the metals, there are four such fragments in each cluster. Since the strongest interactions in the cluster occur within these fragments, the numerous lower energy molecular orbitals in each fragment or in the overall cluster are associated with L and M—L bonds. Once these bonds have been separated off, the formation of M—M bonds can be considered. Within each fragment, the energies and orderings of the five metal-based d orbitals are determined by the metal–ligand interactions and the formation of M—L bonds. (These "metal-based" orbitals do contain some ligand character because they are in fact generally M—L antibonding in character. Since they are primarily metal d orbital in character, however, we will refer to them as metal-based.) The actual number of electrons occupying these d orbitals will be determined by the formal oxidation state of the metal.

In a cluster where each metal is approximately octahedrally coordinated, the d orbitals will be split into the familiar pattern for near octahedral coordination, i.e. a set of two e_g orbitals lying higher in energy than a set of three t_{2g} orbitals. This is illustrated in the left side of Fig. 4. Although

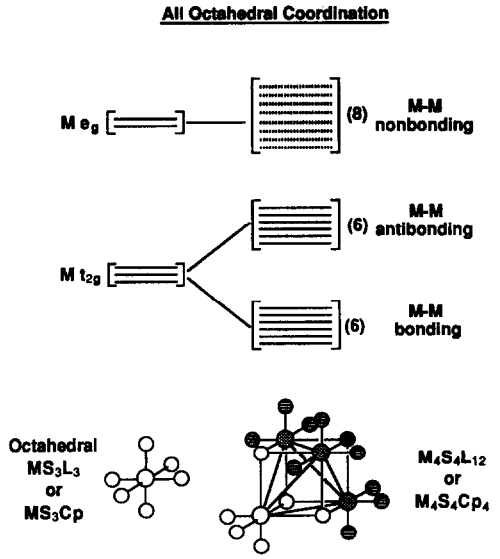

Fig. 4. Qualitative MO energy level scheme (based on the "fragment metal orbital" approach) for the metal-based cluster orbitals in an $M_4S_4L_{12}$ or $M_4S_4Cp_4$ cluster, where each metal is octahedrally coordinated. The splitting of the metal *d* orbitals in an octahedral environment is shown on the left and the resulting groups of cluster orbitals are shown on the right. The lower energy M—L and L bonding orbitals are not shown.

these are not really degenerate sets of orbitals as they would be for perfect O_h symmetry, it is useful to designate them as "e_g" and "t_{2g}" because they are still distinguishable as sets of two and three orbitals. When the local coordinate system on each metal is defined as in **6**, the two sets are $(d_{z^2}, d_{xy})e_g$

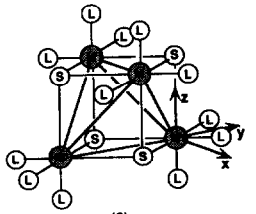

(6)

and $(d_{xz}, d_{yz}, d_{x^2-y^2})t_{2g}$. These are the orbitals which are available for the formation of M—M bonds. The e_g orbitals, which point directly at the six ligands, are not oriented properly for M—M bonding and thus remain non-bonding between the metals. The t_{2g} orbitals *are* oriented properly for M—M bonding and combine in the cluster to form sets of M—M bonding and M—M antibonding orbitals. (This is in contrast to the metal–carbonyl clusters discussed above, where the e_g orbitals are oriented properly to form M—M bonds and the t_g orbitals remain non-bonding between the metals in the cluster.) As illustrated schematically in Fig. 4, the t_{2g} orbitals from the four metal atoms combine to form sets of six bonding and six antibonding levels. The splitting of the metal e_g and t_{2g} orbitals resulting from the metal–ligand interactions is sufficiently large, however, that both sets of cluster orbitals derived from the metal t_{2g} orbitals lie below the set of non-bonding levels derived from the metal e_g orbitals. These sets of bonding, antibonding and non-bonding levels are of course the same sets of levels illustrated in Fig. 3, although the symmetry labels have been omitted in Fig. 4. The main difference between the two approaches is that because the metal fragment orbital approach first takes the *stronger* metal–ligand interactions into account, it is possible to identify the sets of M_4 cluster orbitals with specific sets of metal fragment orbitals. This approach also makes it clear that the energy of the non-bonding M_4 cluster orbitals relative to the M_4 cluster bonding and antibonding orbitals is determined by the relative energies of the e_g and t_{2g} sets of orbitals within each MS_3Cp or MS_3L_3 fragment. Although these non-bonding orbitals are high in energy and not occupied in this group of clusters, this is not the case for many of the other groups described below,

and it becomes useful to understand how and why the energy of the non-bonding levels changes in the different groups of clusters.

2.2. *All four metals tetrahedrally coordinated*

The clusters in this class are characterized by the general formula $M_4S_4L_4$ (7). Neglecting the M—M bonds, each M atom is four-coordinate and can be viewed as part of a pseudo-tetrahedral

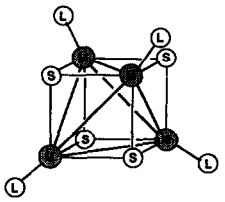

(7)

MS_3L fragment within the cluster. A number of clusters which fall into this group are listed in Table 2. These clusters can be further divided into those where L is a π-acceptor ligand and those where L is a π-donor ligand. The acceptor or donor properties of the ligands have a significant impact on the energetic ordering of the M_4 cluster orbitals.

Table 2. Homometallic clusters having structure type 7: all four metals tetrahedrally coordinated

Cluster	Number of metal electrons	M—M distances	Reference
(L = *π-acceptor ligand*)			
$Fe_4S_4(NO)_4$	28	2.64–2.66	8, 49
$[Fe_4S_4(NO)_4]^-$	29	2.688(4), 2.704(2)	8
(L = *π-donor ligand*)			
$[Fe_4S_4(S\text{-}2,4,6\text{-}(i\text{-}Pr)_3C_6H_2)_4]^-$	21	2.74(av.)	50
$[Fe_4S_4(OCH_3)_4]^{2-}$	22	2.739(2), 2.760(4)	51
$[Fe_4S_4Cl_4]^{2-}$	22	2.755(2), 2.771(4)	52
$[Fe_4S_4Br_4]^{2-}$	22	2.747(2), 2.763(4)	53
$[Fe_4S_4I_4]^{2-}$	22	2.720–2.762	54
$[Fe_4S_4(SR)_4]^{2-}$	22		
(R = CH_2Ph)		2.776(2), 2.732(4)	55
(R = H)		2.738–2.770	56
(R = Ph)		2.730(2), 2.739(4)	57
(R = p-$C_6H_4NH_2$)		2.767(2), 2.741(4)	58
(R = CH_2CH_2OH)		2.700–2.752	59
(R = *t*-Bu)		2.749(2), 2.764(4)[a]	60
$[Fe_4S_4(S(CH_2)_2COO)_4]^{6-}$	22	2.788(2), 2.743(4)	61
$[Fe_4S_4(XPh)_2Cl_2]^{2-}$	22		
(X = O)		2.781(2), 2.752(4)	62
(X = S)		2.760(2), 2.729(4)	62
$[Fe_4S_4(SPh)_2(O\text{-}p\text{-}C_6H_4CH_3)_2]^{2-}$	22	2.784, 2.730, 2.733(2), 2.767(2)	62
$[Fe_4S_4(L\cdot S_3)Cl]^{2-}$	22	2.742-2.778	63
$(L\cdot S_3 = C_6(SC_6H_2\text{-}3\text{-}S\text{-}4,6\text{-}(CH_3)_2)_3(SC_6H_6\text{-}4\text{-}CH_3)_3)$			
$[Fe_4S_4(SR)_4]^{3-}$			
(R = Ph)	23	2.730(2), 2.750(4)	64, 65
(R = CH_2Ph)	23	2.719–2.782	66
(R = p-C_6H_4Br)	23	2.720–2.814	67
(R = *t*-Bu)	23	2.736–2.794	68
(R = Et)	23	2.760(2), 2.770(4)	68

[a] Et_4N^+ salt.

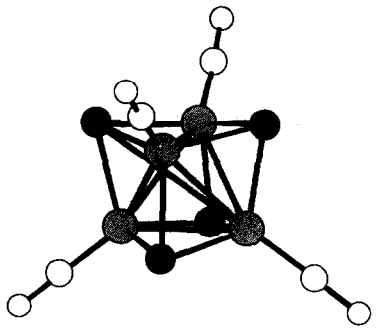

Fig. 5. Structure of $Fe_4S_4(NO)_4$ (ref. 8). Each Fe is bound to three core S atoms and a π-acceptor NO ligand. Neglecting the Fe—Fe bonds, the geometry around each Fe atom is approximately tetrahedral.

2.2.1. *π-Acceptor ligands.* The Dahl group synthesized and characterized both $Fe_4S_4(NO)_4$ and $[Fe_4S_4(NO)_4]^-$.[8,49] (The structure of $Fe_4S_4(NO)_4$ is illustrated in Fig. 5.) Using the same approach applied earlier to the $M_4S_4Cp_4$ clusters, they developed a qualitative bonding scheme appropriate for this type of cluster. Once again, making use of the T_d symmetry of the cluster, the metal orbitals are first combined separately from the ligand orbitals, and the metal and ligand symmetry orbitals are then combined to form cluster molecular orbitals. This scheme is illustrated in Fig. 6. The M_4 symmetry orbitals shown on the left are identical to those in Fig. 3. The symmetry orbitals arising from the S atomic and NO molecular orbitals are shown on the right. The cluster orbitals resulting from the mixing of the metal and ligand orbitals are indicated in the centre. Once again, the lower energy orbitals are either L or M—L bonding orbitals and are fully occupied. The higher energy orbitals are primarily metal centred and fall into the same M—M bonding, antibonding and non-bonding groups found in the clusters where all the metals are octahedrally coordinated. A comparison of the diagrams in Figs 3 and 6 shows, however, that the relative ordering of these groups

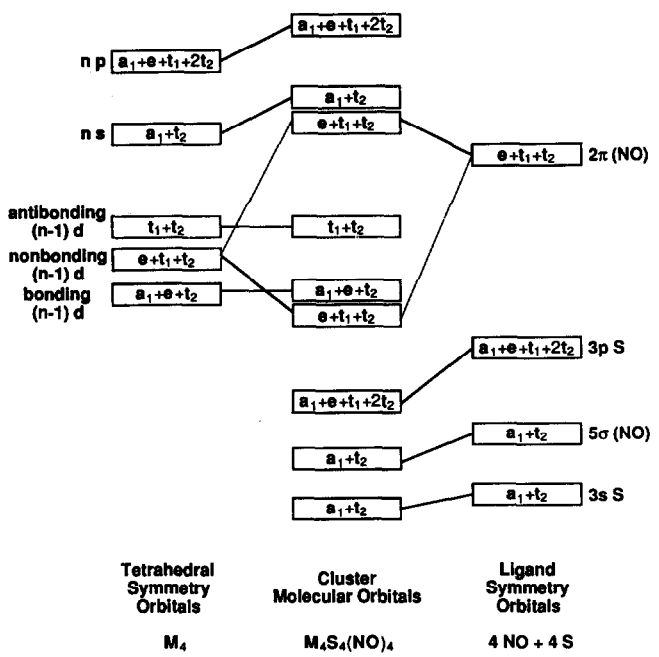

Fig. 6. Qualitative MO energy level scheme derived by the Dahl group (ref. 8) for $M_4S_4(NO)_4$ clusters. The scheme is based on cubic T_d symmetry. The symmetry orbitals for the M_4 tetrahedron are shown on the left, while the symmetry combinations of the S and NO orbitals are shown on the right. The cluster orbitals resulting from interactions between the M_4, S and NO orbitals are shown in the middle.

is different in the two types of clusters. In the clusters containing all octahedral metals the non-bonding M_4 cluster orbitals are destabilized by metal–ligand interactions and lie *above* the M—M bonding and antibonding orbitals. In $Fe_4S_4(NO)_4$ the eight non-bonding cluster orbitals are strongly stabilized by interactions with the π-acceptor NO ligands and lie *below* the M—M bonding and antibonding levels.

Within the CVE counting scheme, the 60-electron $Fe_4S_4(NO)_4$ should contain a completely bonding M_4 tetrahedron. When the 16 lower energy L and M—L bonding orbitals have been occupied by 32 of these electrons, 28 excess metal electrons remain to occupy the M_4 cluster orbitals. (These 28 electrons can also be associated with the presence in the cluster of four Fe^+ (d^7) centres.) These 28 metal electrons will occupy all eight of the non-bonding orbitals and all six of the M—M bonding orbitals. The occupation of the six M—M bonding orbitals is consistent with the six bonding M—M distances of 2.65 Å found in $Fe_4S_4(NO)_4$. Although a CVE count of 60 once again corresponds to a completely bonded M_4 tetrahedron, the actual number of metal electrons and the ordering and occupations of the metal-based cluster orbitals are quite different in this $M_4S_4L_4$ (L = π-acceptor) cluster than in the $M_4S_4Cp_4$ or $M_4S_4L_{12}$ clusters. In the clusters containing octahedral metals, 12 metal electrons are necessary to completely fill the M—M bonding orbitals, and electrons in excess of the required 12 will occupy M—M antibonding orbitals. In the clusters containing tetrahedral π-acceptor ligands, 28 metal electrons are necessary to completely fill the M—M bonding set of orbitals, and only electrons in excess of the required 28 will occupy M—M antibonding orbitals. This qualitative bonding model is confirmed by the fact that when $Fe_4S_4(NO)_4$ is reduced to give $[Fe_4S_4(NO)_4]^-$, all of the M—M distances increase slightly, suggesting that the additional electron occupies an M—M antibonding orbital. Smaller changes in the M—S distances once again confirm that the antibonding cluster orbitals are primarily metal in character. Although no clusters with less than 28 metal electrons have been synthesized, a loss of one or two electrons from the M—M bonding orbitals is expected to have little effect on the M—M distances, since it is probable that just as in the $M_4S_4Cp_4$ or $M_4S_4L_{12}$ clusters the higher energy orbitals belonging to the M—M bonding set are quite delocalized and close to non-bonding. A recent Extended Hückel calculation for $Fe_4S_4(NO)_4$ confirms the occupation of both the non-bonding and bonding cluster orbitals and finds that the t_2 HOMO is essentially non-bonding.[10]

The orbital scheme shown in Fig. 6 is once again derived by first considering the metal–metal interactions and then adding on the metal–ligand interactions. This orbital scheme can also be derived using the metal fragment orbital approach, that is by first considering the stronger metal–ligand interactions and then adding on the metal–metal interactions (Fig. 7). Each metal in the

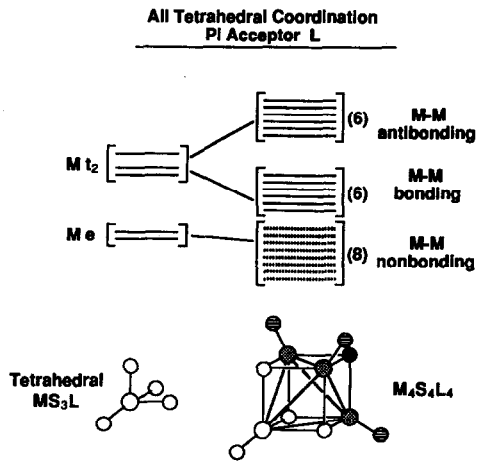

Fig. 7. Qualitative energy level scheme (based on the "metal fragment orbital" approach) for the metal-based cluster orbitals in an $M_4S_4L_4$ cluster, where each metal is tetrahedrally coordinated and L is a π-acceptor ligand. The splitting of the metal *d* orbitals in a tetrahedral environment is shown on the left and the resulting cluster orbitals are shown on the right. The relatively large separation between the "*e*" and "t_2" orbitals in the tetrahedral MS_3L fragment is expected when L is a π-acceptor ligand.

$M_4S_4L_4$ cluster is first viewed as a part of a tetrahedral MS_3L fragment. Within each fragment, the metal *d*-orbitals are split by the metal–ligand interactions into two sets of levels, *e* and t_2. In the tetrahedral environment the *e* orbitals now lie at lower energies than the t_2 orbitals. This is shown on the left side of Fig. 7. Once again, because the MS_3L fragment does not actually have T_d symmetry, these groups of two and three orbitals are not degenerate but do lie close enough in energy to be grouped together. When the local metal coordinate system is defined as in **8** these

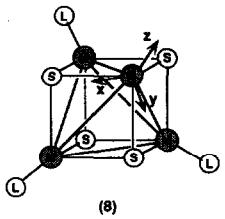

(8)

groups of orbitals correspond to $(d_{xz}, d_{yz})e$, and $(d_{xy}, d_{x^2-y^2}, d_{z^2})t_2$. (Because the MS_3L fragment actually has near C_{3v} symmetry, groupings of two, two and one metal orbitals will be apparent. Under C_{3v} symmetry these correspond to *e*, *e* and a_1 sets, where the higher energy a_1 orbital is d_{z^2}. For consistency, however, it is useful to view these as tetrahedral fragments and to classify the two sets of metal orbitals as t_2 and *e*.) In clusters containing octahedrally-coordinated metals the t_{2g} orbitals are used to form M—M bonds while the e_g orbitals remain non-bonding. In clusters containing tetrahedral metals the t_2 orbitals are used for the formation of M—M bonds, while the *e* orbitals can be viewed as non-bonding. The resulting cluster bonding scheme is shown on the right side of Fig. 7. The t_2 orbitals from the four metal "fragments" combine as before to form six bonding and six antibonding cluster orbitals. The bonding orbitals are not the lowest energy M_4 cluster orbitals, however, because the metal *e* levels are sufficiently stabilized by the presence of the π-acceptor ligands that even though they remain non-bonding in the cluster they lie below the bonding levels. The qualitative cluster bonding scheme is entirely equivalent to the scheme in Fig. 6, except that it makes clear why the non-bonding levels lie below the M_4 cluster bonding orbitals. It should be noted that although the non-bonding and bonding orbitals are shown as derived exclusively from the *e* and t_2 metal fragment orbitals this separation is not as clean cut as in the clusters with octahedrally coordinated metals. In those clusters the separation is exact. Here, because the MS_3L fragment is closer to C_{3v} than to T_d symmetry, there will be some mixing of the two sets of metal fragment *e* orbitals upon formation of the cluster orbitals. This does not change the fact, however, that in general the energetic ordering of the M_4 cluster orbitals is non-bonding < bonding < antibonding.

2.2.2. *π-Donor ligands.* All of the known $M_4S_4L_4$ clusters containing π-donor ligands have Fe_4S_4 cores and generally have metal electron counts of 22 or 23. The structure of one of these clusters, $[Fe_4S_4(SPh)_4]^{2-}$, is shown in Fig. 8. While a qualitative cluster bonding scheme can be derived for these clusters, an accurate description of the electronic structure becomes more complicated. Although the Dahl group did not characterize any clusters of this class, they did discuss how the qualitative bonding picture would be altered by the presence of π-donor ligands.[8] They noted that the cluster non-bonding orbitals $(e+t_1+t_2)$ are now expected to be energetically situated between the M_4 bonding orbitals (a_1+e+t_2) and the M_4 antibonding orbitals (t_1+t_2). This ordering comes about because the cluster non-bonding orbitals are somewhat destabilized (relative to the corresponding non-bonding orbitals in the clusters containing π-acceptor ligands) by the presence of π-donor ligands.

A qualitative energy level diagram for an $M_4S_4L_4$ cluster where L is a π-donor ligand can be derived via the metal fragment orbital approach. This diagram is shown in Fig. 9. Once again, the metal *d* orbitals within each MS_3L fragment are split by the metal–ligand interactions into t_2 and *e* sets. In the presence of π-donor ligands the *e* orbitals are destabilized by metal–ligand interactions (or conversely, they are not stabilized as they are in the presence of π-acceptor ligands), so that the separation between the *e* and t_2 orbitals is smaller than in the presence of π-acceptor ligands. As a result, when the t_2 orbitals combine to form bonding and antibonding combinations the energy of the non-bonding cluster orbitals (the metal *e* orbitals) is intermediate between the energies of the bonding and antibonding orbitals.

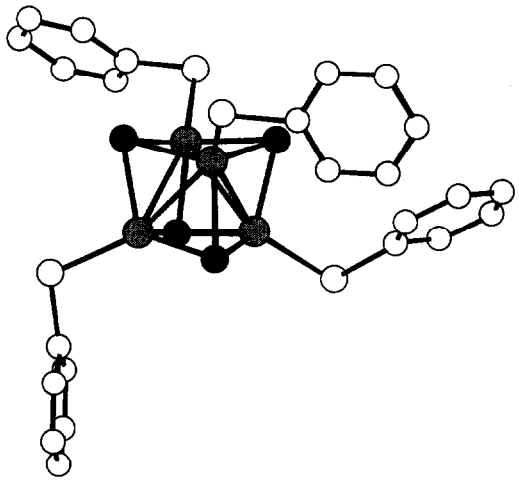

Fig. 8. Structure of $[Fe_4S_4(SPh)_4]^{2-}$ (ref. 57). Each Fe atom is bound to three core S atoms and the S atom of a π-donor thiolate ligand. Neglecting the Fe—Fe bonds, the geometry around each Fe atom is approximately tetrahedral.

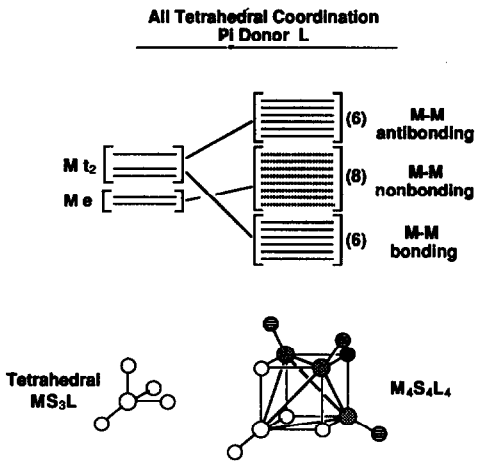

Fig. 9. Qualitative energy level scheme for the metal-based cluster orbitals in an $M_4S_4L_4$ cluster, where each metal is tetrahedrally coordinated and L is a π-donor ligand. The splitting of the metal d orbitals in a tetrahedral environment is shown on the left and the resulting cluster orbitals are shown on the right. The relatively small separation between the "e" and "t_2" orbitals in the tetrahedral MS_3L fragment reflects the presence of the π-donor ligand.

Using the CVE counting scheme, any of the $[Fe_4S_4(SR)_4]^{2-}$ clusters is a 54-electron cluster. When 32 electrons are used for M—L bonding, 22 metal electrons remain to occupy the M_4 cluster orbitals. Alternatively, the 22 "metal" electrons can be associated with two Fe^{2+} (d^6) and two Fe^{3+} (d^5) centres. After 12 of these metal electrons occupy the bonding levels, the 10 remaining metal electrons partially occupy the eight non-bonding levels. The complete occupation of the M_4 bonding levels is consistent with the completely bonded tetrahedron of metals observed in the clusters having 22 metal electrons. That this simple description gives a generally correct picture of the bonding is confirmed by the structural changes which accompany the addition of a metal electron to the core. The most significant changes occur in the M—S bond distances, while the M—M distances remain essentially constant. This suggests that the extra electron enters an orbital which is non-bonding between the metals but is M—S antibonding. Similar changes in the core structure are observed when one electron is removed from the core, also suggesting that the electron is removed from a non-bonding cluster orbital. The similarities and differences in the structures of many of the $Fe_4S_4L_4$ clusters have been discussed in detail in a number of the references in Table 2.

It is interesting to note that a cluster having anywhere from 44 to 60 cluster valence electrons is expected to contain a completely bonded M_4 tetrahedron, since any of the 16 electrons in excess of 44 should occupy a non-bonding cluster orbital. Only an electron count in excess of 60 will result in the occupation of M—M antibonding orbitals. (This assumes that the non-bonding orbitals *all* lie between the bonding and antibonding levels. In fact the energy ranges of the groups of orbitals may well overlap, so that an electron could occupy an antibonding level before all the non-bonding levels were occupied.) This apparent inconsistency with the general rule that a 60-electron count is required for a completely bonding tetrahedron appears to arise from the fact that the original CVE scheme was derived for metal–carbonyl clusters where the bonding schemes are somewhat different.[44] It is not really surprising that the rules derived for those clusters are not always obeyed here.

The bonding scheme in Fig. 9 makes it possible to determine the number of bonding and non-bonding electrons and is consistent with the observed molecular structures for these clusters. It does not, however, provide a description of the various spin states which can occur in these clusters. Eight closely spaced non-bonding metal orbitals are partially occupied by a large number of electrons (in the $[Fe_4S_4(SR)_4]^{2-}$ clusters, 10 electrons occupy eight closely spaced non-bonding levels). Various spin configurations lie close in energy, and it is difficult to calculate an accurate description of the ground-state spin configuration. From a simple viewpoint, we can think of such a cluster as containing four high-spin irons. The t_2 orbitals combine to form completely filled bonding molecular orbitals, leaving a number of electrons in non-bonding orbitals on each iron centre. The spins of these electrons can be weakly coupled together, and a complete description of the electronic structure of these systems requires a calculational technique which can treat this coupling. The $[Fe_4S_4(SR)_4]^{2-}$ clusters have been the subject of several sets of calculations,[5,6,13–15,69] many of which have been aimed at understanding the spin interactions. These calculations confirm that the delocalized MO bonding scheme illustrated in Fig. 9 presents a bonding picture which is qualitatively correct. It is also clear, however, particularly from the work of Aizman and Case[14] and Noodleman *et al.*[15] that an accurate description of the electronic structure of these clusters requires a computational technique which can take into account both the delocalized nature of the interactions and the weak coupling of the spins on the four metal centres.

2.3. *All four metals five-coordinate*

A cluster in this class is characterized by the general formula $M_4S_4L_8$ and ideally may exhibit either of two structures, **9** or **10**. In **9**, each metal atom is five-coordinate (neglecting M—M bonds)

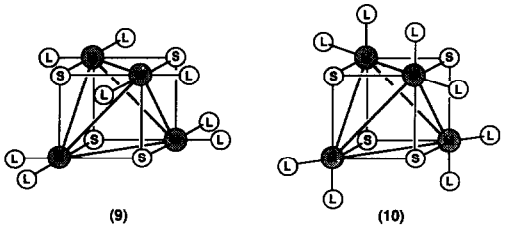

(9) (10)

and can be viewed as part of a nearly square pyramidal MS_3L_2 fragment within the cluster. In **10**, each metal is again five-coordinate but can be viewed as part of a trigonal bipyramidal MS_3L_2 fragment. Clusters having these structures are listed in Table 3. As will become apparent, both in this discussion of clusters in which all of the metals are five-coordinate and in the later discussions

Table 3. Homometallic clusters having structure type **9** or **10**: all metals five-coordinate

Cluster	Number of metal electrons	M—M distances	Reference
$[Fe_4S_4(S_2C_2(CF_3)_2)_4]^{2-}$	18	2.730(4), 3.224(2)	70, 71
$[Fe_4S_4(S_2CNEt_2)_4]^{-}$	21	2.845(4), 3.070(2)	72

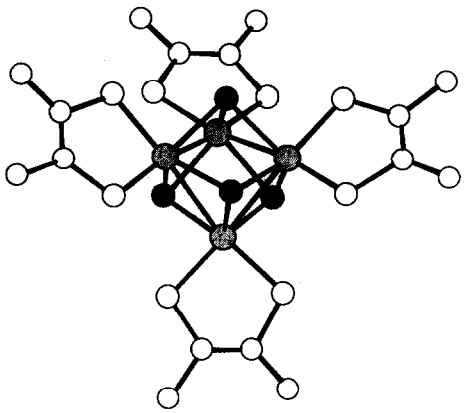

Fig. 10. Structure of $[Fe_4S_4(S_2C_2(CF_3)_2)_4]^{2-}$ (refs 70 and 71). The F atoms are not shown. Each five-coordinate Fe is bound to three core S atoms and two S atoms of a bidentate dithiolene ligand. Neglecting the Fe—Fe bonds, the geometry around each Fe atom is approximately square pyramidal. Two long Fe—Fe distances indicate that there are only four Fe—Fe bonds in the cluster.

of clusters in which only one or two of the metals are five-coordinate, the distinction between square pyramidal and trigonal bipyramidal coordination is not always clear cut.

The structure of $[Fe_4S_4(S_2C_2(CF_3)_2)_4]^{2-}$ is illustrated in Fig. 10. One bidentate dithiolene ligand is bound to each iron atom. Since the coordination geometry around each metal is clearly square pyramidal, the cluster corresponds to structure **9**. When the Dahl group structurally characterized this cluster,[71] they noted that the pattern of M—M distances (four shorter plus two long) combined with the presence of 18 "metal" electrons (corresponding formally to four $Fe^{3.5+}$ atoms) suggests that the cluster bonding scheme in $[Fe_4S_4(S_2C_2(CF_3)_2)_4]^{2-}$ is probably similar to the scheme in $[Fe_4S_4Cp_4]^{2+}$. In that cluster, which contains octahedrally-coordinated metals and 18 metal electrons, 12 metal electrons completely occupy the M—M cluster bonding orbitals and the remaining six metal electrons partially occupy the M—M antibonding orbitals.

A qualitative orbital scheme for a cluster in which each metal is square pyramidal is shown in Fig. 11. The splitting of the metal orbitals brought about by the metal–ligand interactions in each of the square pyramidal MS_3L_2 fragments is illustrated on the left hand side of the figure. A square pyramid is easily derived from an octahedron by removing one of the six ligands surrounding the

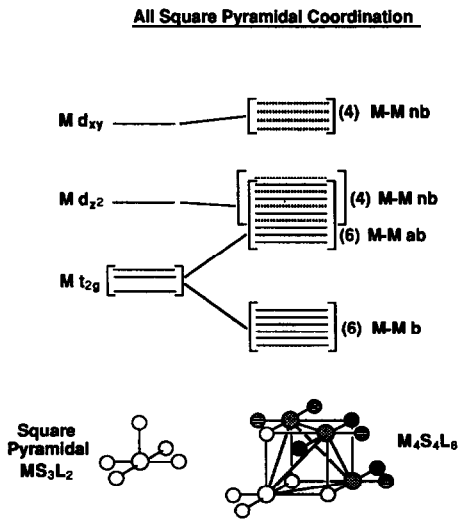

Fig. 11. Qualitative energy level scheme for the metal-based cluster orbitals in an $M_4S_4L_8$ cluster, where each metal is square pyramidal. The splitting of the metal *d* orbitals in a square pyramidal environment is shown on the left and the resulting cluster orbitals are shown on the right.

metal. The removal of this ligand (here it is assumed to be a ligand lying on the z-axis in the local coordinate system illustrated in **6**) affects primarily the energy of the metal d_{z^2} orbital, so the degeneracy of the "e_g" orbitals is lost in square pyramidal coordination. Although the d_{xy} orbital remains high in energy, the d_{z^2} orbital is stabilized by the loss of the sixth ligand. The size of this stabilization will depend on the nature of the ligands and the actual geometry of the fragment, but it is clear that the energy of the d_{z^2} orbital will be well separated from the energy of the d_{xy} orbital. Three orbitals corresponding to the t_{2g} orbitals in an octahedral environment lie close together and lowest in energy. (As indicated in Fig. 6, these orbitals actually break up into two sets, because in most examples of square pyramidal coordination, the metal atom lies above the plane defined by the four basal plane ligands. In this geometry, the metal d_{xz} and d_{yz} orbitals lie somewhat higher in energy than the $d_{x^2-y^2}$ orbital.) In the cluster, the t_{2g} orbitals combine to form sets of six bonding and six antibonding M_4 cluster orbitals. The d_{xy} and d_{z^2} orbitals remain M—M non-bonding, but now they will occur as two separate groups of non-bonding cluster orbitals. The non-bonding orbitals derived from the metal d_{xy} orbitals lie highest in energy, while those derived from the metal d_{z^2} orbitals lie lower in energy. As indicated by the qualitative scheme in Fig. 11, non-bonding orbitals derived from these d_{z^2} orbitals are expected to lie within the same energy range as the M—M antibonding orbitals. In the 18-electron $[Fe_4S_4(S_2C_2(CF_3)_2)_4]^{2-}$ complex, 12 of the metal electrons occupy the M—M bonding orbitals, leaving six electrons to occupy the higher energy cluster orbitals. As discussed above, the similarities in the structures of $[Fe_4S_4(S_2C_2(CF_3)_2)_4]^{2-}$ and $[Fe_4S_4Cp_4]^{2+}$ suggest that in $[Fe_4S_4(S_2C_2(CF_3)_2)_4]^{2-}$ these six electrons occupy M—M antibonding orbitals very similar in character to those occupied by six electrons in $[Fe_4S_4Cp_4]^{2+}$. That is, in $[Fe_4S_4(S_2C_2(CF_3)_2)_4]^{2-}$ the non-bonding metal d_{z^2} orbitals do not lie low enough in energy to be occupied. (This analysis is based on the presence of 18 metal electrons in $[Fe_4S_4(S_2C_2(CF_3)_2)_4]^{2-}$. Due to the presence of the dithiolene ligands the actual number of "metal" electrons may be somewhat uncertain. If there are actually more than 18 "metal" electrons present in the cluster, then the structure of the cluster suggests that the non-bonding cluster orbitals derived from the metal d_{z^2} orbitals lie at low enough energies to be at least partially occupied.)

The main difference between the bonding schemes for a cluster containing all octahedral or all square pyramidal metals is seen to occur in the relative energies of the non-bonding cluster orbitals. For all octahedral coordination, the non-bonding cluster orbitals lie at sufficiently high energies to always remain unoccupied. For all square pyramidal coordination, the set of non-bonding cluster orbitals derived from the metal d_{z^2} orbitals lie at lower energies and may become occupied in clusters having higher metal electron counts.

The other idealized metal coordination geometry in an $M_4S_4L_8$ cluster is trigonal bipyramidal. As seen in **10**, each metal can be viewed as part of a trigonal bipyramidal MS_3L_2 fragment. In comparison to a square pyramid this coordination geometry alters the energy ordering of the d orbitals within the MS_3L_2 fragment and will therefore also have an effect on the energies of the cluster orbitals. A qualitative energy level scheme for a cluster in which all the metals are trigonal bipyramidal is shown in Fig. 12. The splitting of the metal orbitals within the MS_3L_2 fragment is illustrated on the left. Under the D_{3h} symmetry of a trigonal bipyramid the metal d orbitals are split into three sets—e'', e' and a_1'. When the local coordinate system on each metal in the cluster is defined as shown in **11**, the three sets are $(d_{xz}, d_{yz})e''$, $(d_{x^2-y^2}, d_{xy})e'$ and $(d_{z^2})a_1'$. The d_{xz} and d_{yz} orbitals

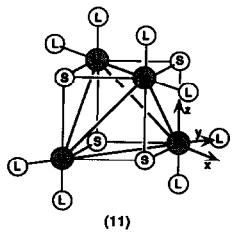

(11)

lie lowest in energy, while the d_{z^2} orbital is most destabilized by the metal–ligand interactions and lies highest in energy. The $d_{x^2-y^2}$ and d_{xy} orbitals lie at intermediate energies. Although the orbital splittings are different in a trigonal bipyramid than in a square pyramid, the same metal orbitals (the "t_{2g}" $d_{x^2-y^2}$, d_{xz} and d_{yz}) are used to form M—M bonds. The qualitative cluster orbital scheme

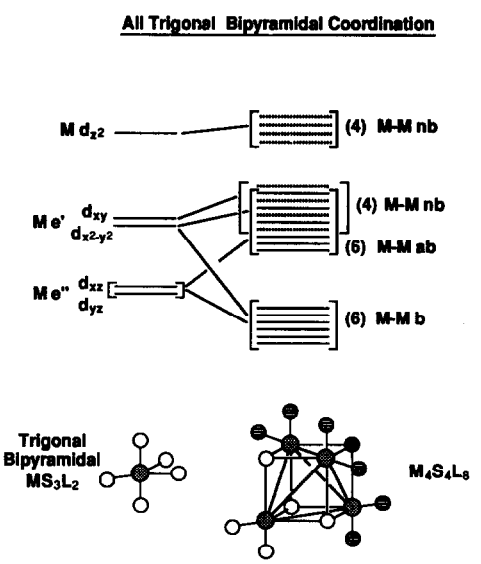

Fig. 12. Qualitative energy level scheme for the metal-based cluster orbitals in an $M_4S_4L_8$ cluster, where each metal is trigonal bipyramidal. The splitting of the metal *d* orbitals in a trigonal bipyramidal environment is shown on the left and the resulting cluster orbitals are shown on the right.

is shown on the right hand side of Fig. 12. The d_{xz}, d_{yz} and $d_{x^2-y^2}$ orbitals from each metal centre, combine to form sets of six bonding and six antibonding cluster orbitals. The metal d_{z^2} and d_{xy} orbitals form two groups of non-bonding cluster orbitals, but the relative energies of these groups are different here than in a cluster where the metals are square pyramidal. Now the non-bonding cluster orbitals derived from the metal d_{z^2} orbitals lie highest in energy, while the non-bonding cluster orbitals derived from the metal d_{xy} orbital lie lower in energy. Once again, the lower energy non-bonding orbitals lie within the same energy range as the M—M antibonding orbitals. In general, simple bonding arguments[48] suggest that the metal d_{xy} orbital in a trigonal bipyramid lies lower in energy than the d_{z^2} orbital in a square pyramid. This suggests that in a cluster containing trigonal bipyramidal metals, the group of non-bonding cluster orbitals derived from the metal d_{xy} orbitals may lie lower in energy, relative to the M—M antibonding orbitals, than the corresponding set of cluster non-bonding orbitals derived from the metal d_{z^2} orbitals in a cluster containing square pyramidal metals. Such generalizations must be made with great caution, however, since the stabilization of the d_{z^2} orbital in a square pyramid is extremely sensitive to both the geometry of the pyramid and the nature of the ligands.

The diagrams in Figs 11 and 12 show that in a cluster with either of the five-coordinate geometries a count of 12 metal electrons will result in the occupation of all six M—M bonding orbitals. Electrons in excess of 12 will first occupy M—M antibonding orbitals, and then at higher electron counts will occupy cluster non-bonding orbitals. It is not clear what forces favour square pyramidal or trigonal bipyramidal coordination in these clusters. This is not surprising, since even in mononuclear complexes the forces favouring one or the other of these coordination geometries are not completely understood.[73] Since the energy barriers to interconversion tend to be small, many complexes are known whose coordination geometries lies somewhere between square pyramidal and trigonal bipyramidal.[74] This "intermediate" coordinate geometry, which can be described either as a distorted square pyramid or as a distorted trigonal bipyramid, is also found in several of the cubane-type clusters containing five-coordinate metals. Although this will further complicate the cluster bonding, the qualitative bonding schemes outlined here for the idealized geometries enable us to recognize that when a cluster contains five-coordinate metals an important feature of the cluster bonding scheme is the presence of a group of cluster non-bonding orbitals at relatively low energies. These orbitals may be occupied *before* all of the M—M antibonding orbitals are occupied, so that in comparison to a cluster with all octahedral metals, a cluster with all five-coordinate metals should be able to accommodate a relatively high metal electron count without as substantial a loss of M—M bonding.

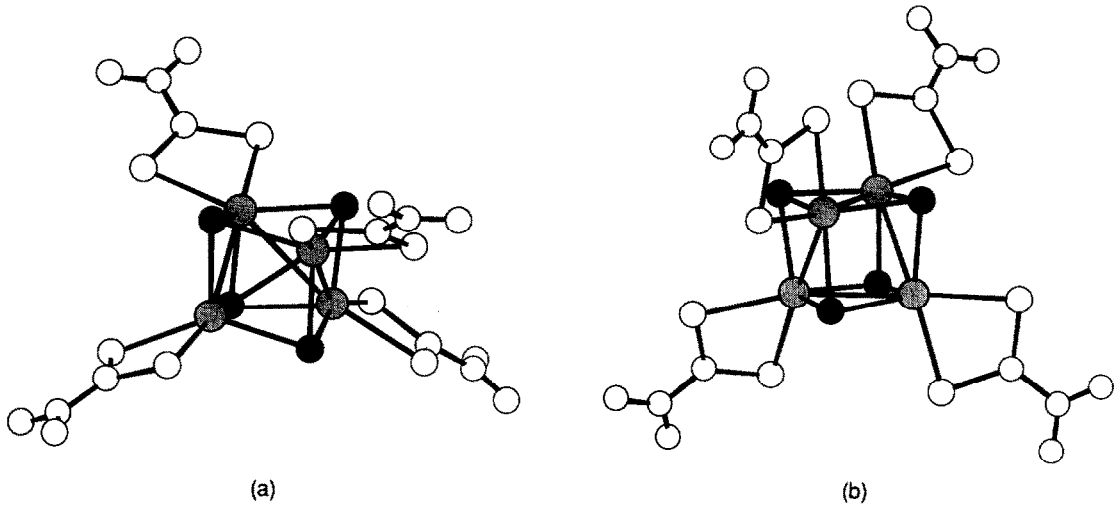

Fig. 13. Two views of the structure of $[Fe_4S_4(S_2CNEt_2)_4]^-$ (ref. 72). Only the first C in each Et group is shown. One Et_2dtc ligand is bound to each Fe atom and, neglecting the Fe—Fe bonds, each Fe is five-coordinate. The view in (a) shows that the geometry around each Fe can be described as distorted square pyramidal, while the view in (b) shows that the geometry around each Fe can also be described as distorted trigonal bipyramidal.

The structure of $[Fe_4S_4(S_2CNEt_2)_4]^-$ illustrates several of these points. In this cluster one bidentate Et_2dtc ligand is coordinated to each metal. Although Liu *et al.* describe the coordination of the metals in this cluster as distorted trigonal bipyramidal,[72] the two views of this cluster shown in Fig. 13 demonstrate that the local coordination about each metal might also be described as distorted square pyramidal. Clearly, the actual coordination geometry lies somewhere in between. Although the cluster contains 21 metal electrons, the M—M distances (four shorter plus two long) are similar to those found in $[Fe_4S_4Cp_4]^{2+}$ and $[Fe_4S_4(S_2C_2(CF_3)_2)_4]^{2-}$, which contain only 18 metal electrons. After 12 metal electrons occupy the six M—M bonding orbitals in $[Fe_4S_4(S_2CNEt_2)_4]^-$, nine electrons remain to occupy higher energy orbitals. If all nine of these electrons occupied M—M antibonding orbitals, we would expect to see longer M—M distances (cf. clusters in Table 1 with metal electron counts of 19 and 20). The similarities in structure with the 18-electron clusters suggest that in $[Fe_4S_4(S_2CNEt_2)_4]^-$ some of these nine electrons occupy non-bonding cluster orbitals. This in turn suggests that in this cluster the lower energy non-bonding orbitals shown in Fig. 11 or 12 lie low enough in energy to become at least partially occupied.

2.4. *Two tetrahedral metals—two five-coordinate metals*

Homometallic cubane-type clusters exhibiting two different metal coordination geometries are relatively rare. One type of cluster falling into this classification can be represented by the general formula $M_4S_4L_4L'_2$ (**12**). Two of the metals are four-coordinate and can be viewed as part of a

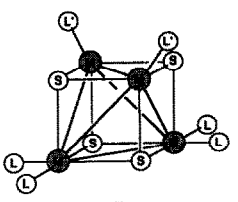

(12)

tetrahedral MS_3L' fragment, while the other two metals are five-coordinate and can be viewed as part of a square pyramidal MS_3L_2 fragment. Clusters having this framework are listed in Table 4. The structure of $[Fe_4S_4(Et_2dtc)_2(SPh)_2]^{2-}$ is shown in Fig. 14. In this cluster, the coordination geometry around each five-coordinate iron can be clearly identified as square pyramidal. In

Table 4. Homometallic clusters having structure type **12**: two tetrahedral metals—two five-coordinate metals

Cluster	Number of metal electrons	M—M distances	Reference
$[Fe_4S_4(S_2CNEt_2)_2X_2]^{2-}$			75
(X = Cl^-)	22	2.733, 2.780(4), 3.053	
(X = SPh^-)	22	2.766, 2.816(4), 3.045	

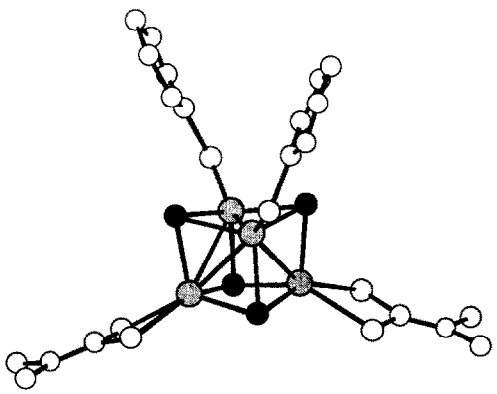

Fig. 14. Structure of $[Fe_4S_4(S_2CNEt_2)_2(SPh)_2]^{2-}$ (ref. 75). Only the first C atom in each Et group is shown. Two of the Fe atoms are bound to three core S atoms and the S atom of a π-donor thiolate ligand. The geometry around these Fe atoms is approximately tetrahedral. Each of the other two Fe atoms is bound to three core S atoms and the two S atoms of a bidentate Et_2dtc ligand. The geometry around each of these five-coordinate Fe atoms is approximately square pyramidal.

$[Fe_4S_4(Et_2dtc)_2Cl_2]^{2-}$, on the other hand, the sulphurs in the dtc ligand are twisted somewhat so that the geometry around the five-coordinate iron is a distorted square pyramid.

A qualitative energy level scheme for clusters having two tetrahedral metals and two square pyramidal metals is derived in Fig. 15. Viewing the M_4 cluster orbitals in terms of metal fragment orbitals becomes extremely useful when the metals in the cluster have different coordination geometries. The splittings of the metal *d* orbitals within the square pyramidal MS_3L_2 and tetrahedral MS_3L' fragments are shown on the left and right of the figure, respectively. The orderings of the metal *d* orbitals are similar to those shown in Figs 11 and 9 for square pyramidal and tetrahedral metal fragments. Since the ligand L′ in the tetrahedral MS_3L' fragment is a π-donor, the separation between the "t_2" and "e" orbitals of the tetrahedral metal is expected to be small. A qualitative scheme for the M_4 cluster orbitals is shown in the centre of Fig. 15. As in the clusters described previously, the square pyramidal "t_{2g}" and tetrahedral "t_2" orbitals are used for M—M bonding. These 12 orbitals from the four metal centres will combine to form sets of six bonding and six antibonding cluster orbitals. The major effect of the two different coordination geometries is the appearance of *three* sets of non-bonding cluster orbitals. These arise from the square pyramidal metal d_{z^2} and d_{xy} orbitals and the tetrahedral metal "e" orbitals. The highest energy set of two non-bonding orbitals is derived from the square pyramidal metal d_{xy} orbitals. Next highest in energy is the set of two non-bonding orbitals derived from the square pyramidal metal d_{z^2} orbitals. This set is expected to lie within the same energy range as the cluster antibonding orbitals. Finally, the lowest energy set of four non-bonding orbitals is derived from the tetrahedral metal "e" orbitals. The energy range of this set is expected to lie between the M—M bonding and antibonding sets. This orbital scheme is consistent both with the schemes appropriate for the clusters described earlier and with the established structures of the $M_4S_4L_2L'_4$ clusters.

The scheme shown in Fig. 15 indicates that after 12 metal electrons occupy the six M—M

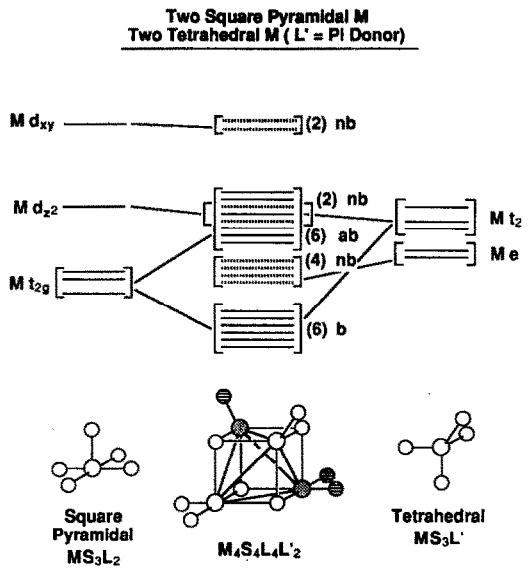

Fig. 15. Qualitative energy level scheme for the metal-based cluster orbitals in an $M_4S_4L_4L'_2$ cluster containing two square pyramidal metals and two tetrahedral metals. The splittings of the metal d orbitals in square pyramidal and tetrahedral environments are shown on the left and right sides of the diagram, respectively. The resulting cluster orbitals are shown in the middle. The relatively small separation between the "e" and "t_2" orbitals in the tetrahedral MS_3L' fragment reflects the presence of a π-donor ligand.

bonding orbitals, up to eight additional metal electrons could be added to the cluster before M—M antibonding orbitals have to be occupied. These eight additional electrons would occupy the cluster non-bonding orbitals derived from the tetrahedral metal "e" orbitals. Thus clusters, having anywhere from 12 to 20 metal electrons, are expected to have a fully bonded metal tetrahedron. Metal electron counts in excess of 20 will result in the occupation of M—M antibonding orbitals. (The upper limit of 20 is not really definite, because the energy range of this set of non-bonding orbitals may well overlap with the energy range of the M—M antibonding levels. If this occurs, antibonding orbitals will become occupied before all of the non-bonding orbitals are filled, i.e. at metal electron counts $\leqslant 20$.) Both $[Fe_4S_4(Et_2dtc)_2X_2]^{2-}$ clusters contain 22 metal electrons and both have similar structures. The distinctive structural feature of each cluster is a long distance (> 3 Å) between the two square pyramidal iron atoms. The other M—M distances are all within bonding range. The cluster bonding scheme in Fig. 15 provides a simple explanation for this structure. Of the 22 metal electrons, if 12 electrons occupy M—M bonding orbitals and eight electrons occupy the lower energy set of non-bonding orbitals, two electrons will have to occupy an M—M antibonding orbital. The one long Fe—Fe distance is consistent with the occupation of an antibonding orbital localized between the two five-coordinate iron atoms.

Although it is satisfying to arrive at this simple description of the bonding in these clusters, further examination of both this bonding picture and the properties of these clusters suggests that this simple description is incorrect. First, although the two clusters are found to be paramagnetic,[75] the orbital occupations just outlined would lead to a diamagnetic cluster. Second, the complete occupation of the "e" non-bonding orbitals would correspond to two tetrahedral Fe^{+} centres and two square pyramidal Fe^{4+} centres. This combination of oxidation states is highly unlikely; a combination of two Fe^{2+} and two Fe^{3+} centres is much more plausible. Oxidation states of 2+ or 3+ for the tetrahedral irons would result in only partial occupation of the "e" non-bonding orbitals. Since the structures of the clusters indicate that only one antibonding orbital is occupied, however, eight electrons *must* occupy non-bonding orbitals. If the "e" non-bonding levels are not completely occupied, some of these eight electrons must therefore occupy the non-bonding orbitals derived from the square pyramidal metal d_{z^2} orbitals. In terms of the diagram in Fig. 15, this means that several of the "e" non-bonding levels, the lower energy antibonding levels, and the "d_{z^2}" non-bonding levels must lie very close in energy. Furthermore, the square pyramidal metal d_{z^2} orbital must be sufficiently

stabilized to become occupied after only one M—M antibonding orbital is occupied. This picture is consistent with high-spin square pyramidal and tetrahedral Fe^{2+} and Fe^{3+} centres combining to form a paramagnetic cluster having one long Fe—Fe bond. Although a detailed description of the electronic structure of these clusters will require calculations capable of treating the spin couplings, the combination of the qualitative bonding scheme and the known properties and structure of the complexes make it possible to understand the general features of the cluster bonding.

This discussion introduces an important element which must be included in any description of the electronic structure of these cubane-type clusters—the electronic configurations of the individual metal centres. The descriptions in this report focus primarily on the total number of metal electrons occupying the M_4 cluster orbitals and generally do not stress the electron configurations or formal oxidation states of the individual metals in the cluster. As we have just seen, however, concentration only on the total electron count can lead to incorrect descriptions of the electronic structure of the cluster. In order to correctly describe the electronic structure it is important to take into account *both* the total number of metal electrons and the number of electrons associated with each metal centre.

2.5. *Three tetrahedral metals—one five-coordinate metal*

Another type of cluster exhibiting two different metal coordination geometries has the general formula $M_4S_4L_2L'_3$. Three of the metals are four-coordinate and can be viewed as part of a tetrahedral MS_3L' fragment, while the fourth metal is five-coordinate and can be viewed as part of an MS_3L_2 fragment. This fragment may be either square pyramidal (**13**) or trigonal bipyramidal (**14**). Clusters having these structures are listed in Table 5. In $[Fe_4S_4(Et_2dtc)Cl_3]^{2-}$, illustrated in

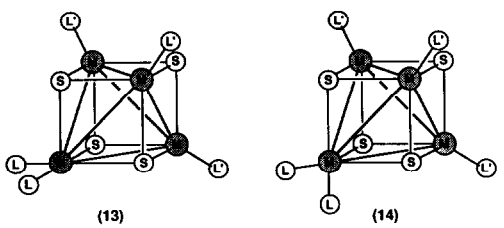

Fig. 16(a), three irons are part of the tetrahedral FeS_3Cl fragments while the third iron is bound to an Et_2dtc ligand and is part of a square pyramidal fragment. In $[Fe_4S_4(SC_6H_4\text{-}o\text{-}OH)_4]^{2-}$, [Fig. 16(b)] three irons are part of tetrahedral fragments, while the fourth iron is bound to both the sulphur and oxygen atoms in the $(SC_6H_4\text{-}o\text{-}OH)^-$ ligand and is best viewed as part of a trigonal bipyramidal fragment.

A qualitative bonding scheme for a cluster having structure **13** is illustrated in Fig. 17. The ordering of the metal orbitals within the square pyramidal and tetrahedral fragments are shown on the left and right hand side of the figure, respectively. These orderings are the same as the orderings shown in Fig. 15. The narrow separation of the tetrahedral "e" and "t_2" orbitals reflects the π-donor ligands in the tetrahedral fragments. The cluster orbitals are shown in the centre of the figure, and the overall groupings of orbitals are similar to the groups shown in Fig. 15. The square pyramidal "t_{2g}" and tetrahedral "t_2" orbitals combine to form sets of M—M bonding and antibonding orbitals. The two different coordination geometries once again result in three sets of cluster non-bonding

Table 5. Homometallic clusters having structure type **13** or **14**: three tetrahedral metals—one five-coordinate metal

Cluster	Number of metal electrons	M—M distances	Reference
$[Fe_4S_4(S_2CNEt_2)Cl_3]^{2-}$	22	2.76(3), 2.850(2), 2.936	75
$[Fe_4S_4(SC_6H_4\text{-}o\text{-}OH)_4]^{2-}$	22	2.725(4), 2.839, 2.868	76

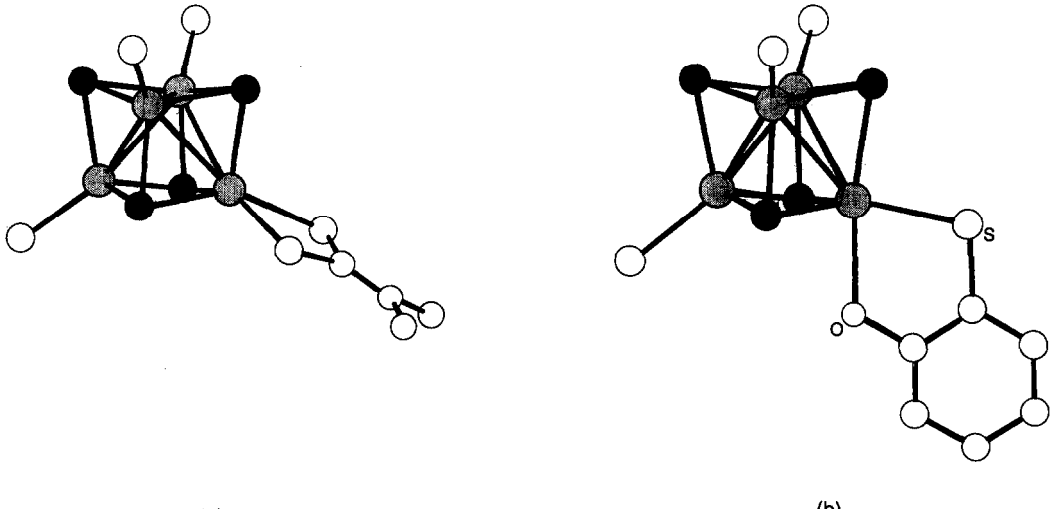

Fig. 16. Structures of (a) $[Fe_4S_4(S_2CNEt_2)Cl_3]^{2-}$ (ref. 75) and (b) $[Fe_4S_4(SC_6H_4\text{-}o\text{-}OH)_4]^{2-}$ (ref. 76). In (a) only the first C atom in each Et group is shown, and in (b) only the S atoms of the three monodentate $(SC_6H_4\text{-}o\text{-}OH)^-$ ligands bound to the tetrahedral Fe atoms are shown. In both clusters the geometry around three of the Fe atoms is approximately tetrahedral, while the fourth Fe atom is five-coordinate. In $[Fe_4S_4(S_2CNEt_2)Cl_3]^{2-}$ (a) the fourth Fe is bound to the two S atoms of the Et_2dtc ligand, and the geometry around this five-coordinate Fe is approximately square pyramidal. In $[Fe_4S_4(SC_6H_4\text{-}o\text{-}OH)_4]^{2-}$ (b) the fourth Fe is bound to both the S and O atoms of the $(SC_6H_4\text{-}o\text{-}OH)^-$ ligand, and the geometry around this five-coordinate metal is better described as trigonal bipyramidal.

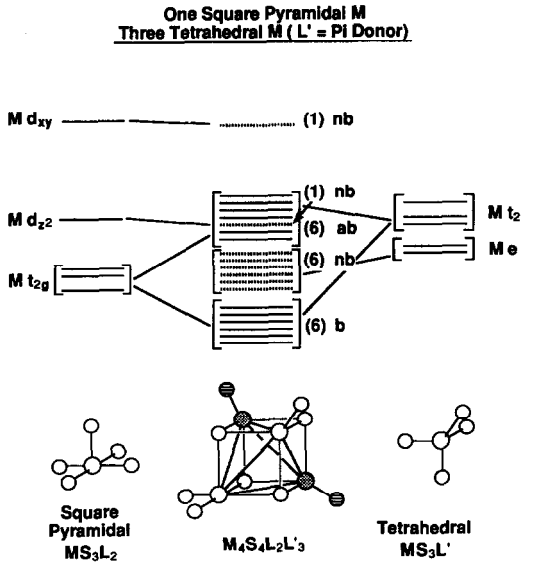

Fig. 17. Qualitative energy level scheme for the metal-based cluster orbitals in an $M_4S_4L_2L'_3$ cluster containing one square pyramidal metal and three tetrahedral metals. The splittings of the metal *d* orbitals in square pyramidal and tetrahedral environments are shown on the left and right sides of the diagram, respectively. The resulting cluster orbitals are shown in the middle. The relatively small separation between the "*e*" and "t_2" orbitals in the tetrahedral MS_3L' fragment reflects the presence of a π-donor ligand.

orbitals, but now the number of orbitals in each set is different from the number shown in Fig. 15. Because there is only one square pyramidal metal, there are only two non-bonding levels associated with the square pyramidal metal orbitals. One non-bonding orbital derived from the square pyramidal metal d_{xy} orbital lies at high energy, and one non-bonding level derived from the square pyramidal metal d_{z^2} orbital lies at lower energy. Since there are now three tetrahedral metals, a group of six non-bonding orbitals derived from the tetrahedral metal "*e*" orbitals falls between the M—M bonding and antibonding sets of orbitals. Although the bonding scheme indicates that all six of these non-bonding orbitals lie between the bonding and antibonding levels, it is very likely that the energy ranges of the non-bonding and antibonding orbitals overlap. If this overlap actually occurs, some of the antibonding orbitals could become occupied before all six of the non-bonding orbitals are occupied. The scheme shown in Fig. 17 indicates that after 12 metal electrons occupy the six M—M bonding orbitals, 12 more metal electrons can be added to the cluster without occupying antibonding orbitals. Thus clusters having anywhere from 12 to 24 metal electrons are expected to have a fully bonded metal tetrahedron. It is only when the electron count exceeds 24 that M—M antibonding orbitals must be occupied. As noted above, however, some of the six non-bonding orbitals may actually lie above the lower energy antibonding orbitals, and if this is the case antibonding orbitals could become occupied at metal electron counts $\leqslant 24$.

The bonding scheme in Fig. 17 can be used to describe the bonding in $[Fe_4S_4(Etdtc)Cl_3]^{2-}$ [Fig. 16(a)]. This cluster has 22 metal electrons, so after 12 metal electrons occupy the six M—M bonding orbitals, the 10 remaining metal electrons could occupy non-bonding orbitals. Based on this analysis, $[Fe_4S_4(Etdtc)Cl_3]^{2-}$ should contain a completely bonded tetrahedron of metal atoms. The actual structure of $[Fe_4S_4(Etdtc)Cl_3]^{2-}$ suggests, however, that an antibonding orbital is occupied, since at least one Fe—Fe distance is somewhat longer than might be expected for Fe—Fe bonding. This indicates that the energy ranges of the group of six non-bonding "*e*" orbitals and the group of six M—M antibonding orbitals do overlap, resulting in the occupation of an antibonding orbital before all of the non-bonding orbitals are occupied. An orbital occupation scheme where only eight electrons occupy the "*e*" cluster non-bonding orbitals and two electrons occupy an antibonding orbital is consistent with the molecular structure of the cluster and also corresponds to reasonable oxidation states for all of the metals (three high-spin tetrahedral iron centres, two Fe^{2-} and one Fe^{3+}, and one square pyramidal Fe^{3+} centre). Alternatively, an orbital occupation scheme in which only seven electrons occupy the "*e*" cluster non-bonding orbitals, two electrons occupy an antibonding orbital, and one electron occupies the non-bonding orbital derived from the square pyramidal metal d_{z^2} orbital is also possible. This scheme is also consistent with the structure of the cluster and corresponds to three high-spin tetrahedral iron centres, one Fe^{2+} and two Fe^{3+}, and one high-spin square pyramidal Fe^{2+} centre. Either one of these descriptions is reasonable.

The other cluster which fits into this class is $[Fe_4S_4(SC_6H_4\text{-}o\text{-}OH)_4]^{2-}$ [Fig. 16(b)], where the five-coordinate iron atom is best viewed as trigonal bipyramidal.[76] This cluster also contains 22 electrons, and the qualitative scheme in Fig. 17 can also be used to describe the cluster bonding in the cluster, since the major effect of a change from square pyramidal to trigonal bipyramidal geometry is the interchange of the non-bonding orbitals associated with the five-coordinate metal (cf. Figs 11 and 12). The bonding scheme in Fig. 17 indicates that $[Fe_4S_4(SC_6H_4\text{-}o\text{-}OH)_4]^{2-}$ should also have a completely bonded metal tetrahedron, but once again a relatively long Fe—Fe distance suggests that an antibonding orbital is occupied. This would again indicate an overlap in the energies of the "*e*" non-bonding and M—M antibonding cluster orbitals. An orbital occupation scheme in which eight electrons partially occupy the "*e*" non-bonding orbitals and two electrons occupy an antibonding orbital once again is consistent with the structure of the cluster and corresponds to reasonable oxidation states for all of the iron centres. The bonding picture will be further complicated if the d_{xy} non-bonding orbital associated with the five-coordinate iron is sufficiently stabilized to be occupied. Several occupation schemes are possible, depending on how the electrons are apportioned to the different metal centres. It is important to recognize, however, that a bonding scheme which assigns more than eight electrons to the non-bonding "*e*" orbitals is unlikely, since it leads to an unreasonable combination of metal oxidation states. It is also quite clear that a better understanding of the electronic structure of these clusters incorporating five-coordinate metals will require detailed calculations.

One important outcome of an overview of the bonding schemes expected for the different types of M_4S_4 clusters is the observation that although the same metal electron counts may be found in

a number of clusters, the actual electronic structure of the M_4S_4 cores may differ. For example, the relation between clusters having 22 metal electron $[Fe_4S_4]^{2+}$ cores and the iron–sulphur proteins makes this group of clusters especially interesting. Although most of the interest has concentrated on clusters listed in Table 2, the mixed coordination clusters listed in Tables 4 and 5 also have 22-electron $[Fe_4S_4]^{2+}$ cores. Comparison of the bonding schemes in Figs 9, 16 and 17 makes it clear, however, that even though these clusters all contain 22-electron $[Fe_4S_4]^{2+}$ cores, the cores are not equivalent electronically.

3. HETEROMETALLIC CLUSTERS HAVING AN $M_2M'_2S_4$ CORE

3.1. *All four metals octahedrally coordinated*

Unlike the homometallic clusters, heterometallic clusters in which all four metals have the same coordination geometry are relatively rare. The clusters listed in Table 6 are the only examples of $M_2M'_2S_4$ clusters in which all four metals have similar coordination geometries—in this case octahedral. Although the $M_2M'_2S_4(Me_5Cp)_2(Cp)_2$ clusters listed in Table 6 have not been structurally characterized, spectroscopic evidence indicates that they have the cubane-type structure $M_2M'_2S_4Cp_4$ (**15**). These clusters are therefore expected to be similar to the homometallic $M_4S_4Cp_4$ clusters **5**,

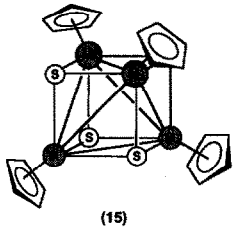

(15)

both in molecular and electronic structure. Since all four of the metals are octahedrally coordinated, the cluster bonding orbital scheme should be very similar to the scheme in Fig. 4. The *d* orbitals on each metal will split into "t_{2g}" and "e_g" groups, and although larger splittings are expected for the 4*d* orbitals, the 3*d* and 4*d* orbitals will combine to form the same groups of bonding, antibonding and non-bonding cluster orbitals shown in Fig. 4. Since both of these clusters have metal electron counts of 12, the cluster bonding orbitals should be completely occupied and a fully bonding metal tetrahedron is expected. Because of the two different metals, the metal "tetrahedron" will of course be less symmetric than the metal tetrahedron observed in an $M_4S_4Cp_4$ cluster.

3.2. *Two octahedral metals—two tetrahedral metals*

A cluster in this class is characterized by the general formula $M_2M'_2S_4L_6L'_2$ (**16**) or $M_2M'_2S_4Cp_2L'_2$ (**17**). A number of clusters belonging to this class are listed in Table 7. In each cluster, two of the

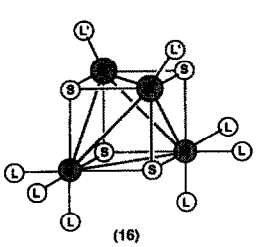

(16)

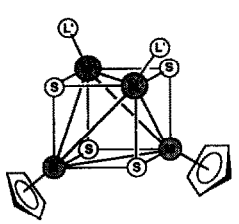

(17)

metals are six-coordinate and can be viewed as part of an octahedral MS_3L_3 or MS_3Cp fragment, while the other two metals are four-coordinate and can be viewed as part of a tetrahedral $M'S_3L'$ fragment. The structure of $Mo_2Co_2S_4(Et_2dtc)_2(CH_3CN)_2(CO)_2$ is shown in Fig. 18. In this cluster, each octahedral molybdenum atom is bound to an acetonitrile ligand and an Et_2dtc ligand, while each tetrahedral cobalt atom is bound to one π-acceptor CO ligand.

Table 6. Heterometallic clusters having structure type **15**: all four metals octahedrally coordinated

Cluster	Number of metal electrons	Reference
$M_2M'_2S_4(Me_5Cp)_2(Cp)_2$	12	77
(M = Mo, M′ = Cr)[a]		
(M = Cr, M′ = Mo)[a]		

[a] Spectroscopic evidence indicates a cubane-type structure.

Table 7. Heterometallic clusters having structure type **16** or **17**: two octahedral metals—two tetrahedral metals

Cluster	Number of metal electrons	M—M distances M—M[a]	M′—M′[b]	M—M′	Reference
$M_2CoS_4(Me_5Cp)_5(CO)_2$					78
(M = Cr)[c]	20				
(M = Mo)[c]	20				
$M_2Co_2S_4(S_2CNEt_2)_2(CH_3CN)_2(CO)_2$					79
(M = Mo)	20	2.778	2.533	2.680(2), 2.671(2)	
(M = W)[c]	20				
$Mo_2Ni_2S_4(MeCp)_2(CO)_2$	22	2.829	2.962	2.720–2.724	80, 81
$M_2Co_2S_4(Me_5Cp)_2(NO)_2$					82
(M = Cr)[c]	22				
(M = Mo)[c]	22				
$V_2M_2S_4(MeCp)_2(NO)_2$					
(M = Fe)	18	2.957	2.590	2.745(4)	83
(M = Co)	20	2.926	2.738	2.735	84
(M = Ni)	22	2.871	3.022	2.80	84

[a] M = octahedral metal.
[b] M′ = tetrahedral metal.
[c] Spectroscopic evidence indicates a cubane-type structure.

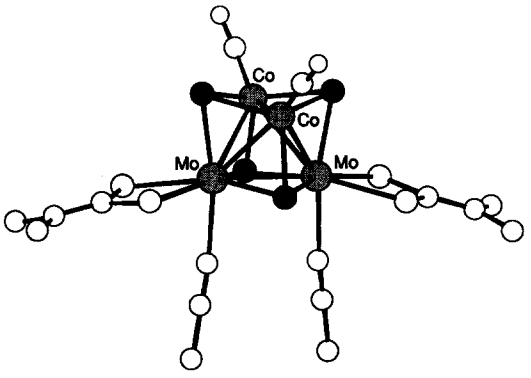

Fig. 18. Structure of $Mo_2Co_2S_4(S_2CNEt_2)_2(CH_3CN)_2(CO)_2$ (ref. 79). Only the first C atom in each Et group is shown. Each octahedral Mo atom is bound to three core S atoms, an acetonitrile ligand and a bidentate Et_2dtc ligand. Each tetrahedral Co atom is bound to three core S atoms and a π-acceptor CO ligand.

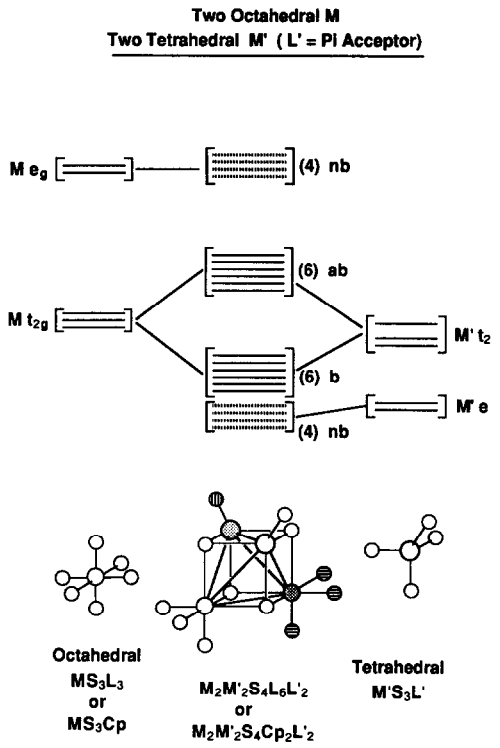

Fig. 19. Qualitative energy level scheme for the metal-based cluster orbitals in a heterometallic $M_2M'_2S_4L_6L'_2$ or $M_2M'_2S_4Cp_2L'_2$ cluster containing two octahedral metals and two tetrahedral metals. The splittings of the metal *d* orbitals in octahedral and tetrahedral environments are shown on the left and right sides of the diagram, respectively. The resulting cluster orbitals are shown in the middle. The relatively large separation between the "*e*" and "t_2" orbitals in the tetrahedral $M'S_3L'$ fragment reflects the presence of a π-acceptor ligand.

A qualitative bonding scheme for these clusters is shown in Fig. 19. The ordering of the metal *d* orbitals within each octahedral fragment is shown on the left hand side of the diagram, while the order of the metal *d* orbitals within each tetrahedral fragment is shown on the right. These fragment diagrams take into account two features of the clusters listed in Table 7. First, since the tetrahedral metal generally lies to the right of the octahedral metal in the periodic table, the tetrahedral metal *d* orbitals are expected to lie lower in energy than the octahedral metal *d* orbitals. Also, since in each cluster the ligand L′ associated with the tetrahedral metal is a π-acceptor, the tetrahedral "*e*" orbitals will be stabilized and the separation between the tetrahedral "*e*" and "t_2" orbitals will be relatively large. In the cluster, the "t_{2g}" and "t_2" orbitals combine to form sets of six bonding and six antibonding orbitals, while the metal "e_g" and "*e*" orbitals remain non-bonding. These non-bonding orbitals will occur in two groups, the octahedral "e_g" orbitals at high energy and the tetrahedral "*e*" orbitals at low energy. The stabilization of the tetrahedral metal "*e*" orbitals by the π-acceptor ligands is expected to result in the set of four cluster non-bonding orbitals lying below the cluster bonding orbitals.

A cluster metal electron count of 20 is expected to be necessary for a completely bonding metal tetrahedron. Of these 20 electrons, eight will occupy the low energy non-bonding orbitals, leaving 12 to occupy the M—M bonding orbitals. Metal electrons in excess of 20 are expected to occupy antibonding orbitals. This scheme is consistent with the structures of $Mo_2Co_2S_4(Et_2dtc)_2(CH_3CN)_2$,[79] (20 metal electrons) and $Mo_2Ni_2S_4(MeCp)_2(CO)_2$[80,81] (22 metal electrons). All of the M—M distances in the 20-electron cluster correspond to M—M bonds, while in the 22-electron $Mo_2Ni_2S_4(MeCp)_2(CO)_2$ cluster the two nickel atoms are separated by a long non-bonding distance, indicating the occupation of an antibonding orbital. Recent molecular orbital calculations for $Mo_2Co_2S_4(dtc)_2(CH_3CN)_2(CO)_2$ and $Mo_2Ni_2S_4(Cp)_2(CO)_2$ confirm the qualitative energy level scheme shown in Fig. 19.[22] The four distinct groups of non-bonding, bonding, antibonding, and non-bonding cluster orbitals are all observed in the calculated energy levels of these

clusters, confirming that 20 metal electrons should result in a completely bonded metal tetrahedron. These calculations also show that just as in the homometallic clusters only the lower energy M—M bonding cluster orbitals are strongly bonding. The higher energy "bonding" orbitals are quite delocalized and nearly non-bonding, suggesting that clusters with electron counts short of 20 can be expected to have relatively short M—M distances. The lowest energy antibonding orbital, however, is localized between the two tetrahedral metals. It is this orbital which is occupied by the two extra electrons in $Mo_2Ni_2S_4(MeCp)_2(CO)_2$, resulting in the long Ni—Ni distance. The strongest M—M interactions in these clusters occur between the two 4*d* metals, and the M—M bonding interactions decrease in the order 4*d*–4*d* > 4*d*–3*d* > 3*d*–3*d*. The weaker overlap between the smaller 3*d* orbitals results in relatively weak M—M bonding interactions between the 3*d* metals. Several other $M_2Co_2S_4Cp_2L'_2$ (M = Cr, Mo) clusters[78,82] are also assumed to have cubane-type structures, and the bonding scheme in Fig. 19 should also apply to these clusters. The 20-electron clusters are expected to contain a completely bonding metal tetrahedron, while a long Co—Co distance is expected in the clusters containing 22 metal electrons.

Another series of clusters, $V_2M_2S_4(MeCp)_2(NO)_2$ (M = Fe, Co, Ni),[83,84] provides a further test of the qualitative scheme in Fig. 19. Based on this scheme and the previous discussion, the 20 metal electrons in $V_2Co_2S_4(MeCp)_2(NO)_2$ would occupy both the low energy non-bonding orbitals and the six M—M bonding orbitals, resulting in a completely bonded metal tetrahedron. The structure of the 18-electron $V_2Fe_2S_4(MeCp)_2(NO)_2$ cluster should be similar to the structure of $V_2Co_2S_4(MeCp)_2(NO)_2$, since any unoccupied high energy bonding orbital is expected to be at most weakly M—M bonding. The extra two electrons in the 22-electron $V_2Ni_2S_4(MeCp)_2(NO)_2$ cluster would occupy an antibonding orbital—probably one localized between the two tetrahedral nickel atoms, leading to a long Ni—Ni distance. The structure of the 22-electron $V_2Ni_2S_4(MeCp)_2(NO)_2$ cluster is consistent with this description of the bonding, since the long Ni—Ni distance can be considered non-bonding. An examination of the M—M distances in the three clusters, however, shows that in the set of three clusters, the M′—M′ distances increase in the order Fe—Fe < Co—Co < Ni—Ni. As Racuchfuss and co-workers have noted, the Co—Co distance in $V_2Co_2S_4(MeCp)_2(NO)_2$ is longer than expected for a Co—Co bond, suggesting that the 20-electron $V_2Co_2S_4(MeCp)_2(NO)_2$ cluster is not "electron precise".[84] (In the CVE counting scheme this is a 60-electron cluster and is also expected to contain a completely bonding metal tetrahedron.) This relatively long Co—Co distance, as well as the paramagnetism of the cluster, implies that in $V_2Co_2S_4(MeCp)_2(NO)_2$ the antibonding Co—Co orbital is occupied by one electron. An orbital occupation scheme for the three clusters which is consistent with their structures is $V_2Fe_2S_4(nb)^8(b)^{10}(ab)^0$, $V_2Co_2S_4(nb)^8(b)^{11}(ab)^1$, $V_2Ni_2S_4(nb)^8(b)^{12}(ab)^2$, where nb = non-bonding orbitals, b = bonding orbitals and ab = antibonding orbitals. Such a scheme would require the bonding and antibonding orbitals to be separated by only a small gap. In these clusters the relatively large energy separation between the V and M′ 3*d* orbitals and the weak bonding interactions between the small 3*d* orbitals could well result in the bonding orbitals spanning a large energy range, thus leading to such a narrow separation of the bonding and antibonding orbitals. Clearly, a more complete description of the electronic structure of these clusters is highly desirable. The apparent antiferromagnetic character of $V_2Fe_2S_4(MeCp)_2(NO)_2$ and the paramagnetism of $V_2Co_2S_4(MeCp)_2(NO)_2$ indicate that such a description will require spin unrestricted calculations.

3.3. *Two octahedral metals—two five-coordinate metals*

Another combination of coordination geometries occurs in a cluster which has the general formula $M_2M'_2S_4(Cp)_2L'_4$ (**18**). Here, two metals are six-coordinate and can be viewed as part of an

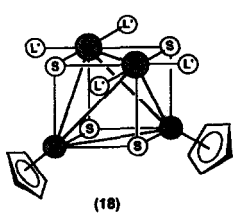

(18)

Table 8. Heterometallic clusters having structure type **18**: two octahedral metals—two square pyramidal metals

Cluster	Number of metal electrons	M—M distances M—M[a]	M′—M′[b]	M—M′	Reference
$Mo_2Fe_2S_4(Me_5Cp)_2(CO)_4$	18	2.761	3.334	2.813(4)	85

[a] M = octahedral metal.
[b] M′ = tetrahedral metal.

octahedral MS_3Cp fragment, while the other two metals are five-coordinate and can be viewed as part of a square pyramidal $M'S_3L'_2$ fragment. The one cluster having this geometry, $Mo_2Fe_2S_4(Me_5Cp)_2(CO)_4$, is listed in Table 8 and illustrated in Fig. 20. In this cluster there is no ambiguity concerning the square pyramidal configuration about the five-coordinate metals. Two C and two S atoms lie in the same plane to form the base of the pyramid, and the Fe atom lies about 0.5 Å above this plane.

A qualitative energy level scheme for this cluster is shown in Fig. 21. The octahedral metal *d* orbitals shown on the left are divided into the familiar "t_{2g}" and "e_g" groups. The square pyramidal metal *d* orbitals are shown on the right. As in the previous diagrams involving square pyramidal metals, the lowest energy orbitals are the "t_{2g}" set, while the highest energy orbital is d_{xy}. Intermediate in energy is the d_{z^2} orbital. In Fig. 21, the d_{z^2} orbital is shown to be at lower energy than in the previous diagrams for square pyramidal metals. This large stabilization of the d_{z^2} orbital is expected for a square pyramidal $M'S_3L'_2$ fragment only when (1) L′ is a π-acceptor ligand, and (2) the metal atom lies well out of the plane of the base of the pyramid. Under these conditions the d_{z^2} orbital is further stabilized by interactions with the ligand π-acceptor orbitals. In the cluster orbital scheme shown in the centre of Fig. 21 the metal "t_{2g}" orbitals combine to form sets of six bonding and six antibonding orbitals, while three sets of cluster non-bonding orbitals occur. These are derived from the octahedral metal "e_g" orbitals and the square pyramidal metal d_{xy} and d_{z^2} orbitals. The non-bonding "e_g" and d_{xy} orbitals lie above the antibonding orbitals, while the non-bonding set derived from the square pyramidal d_{z^2} orbitals lies *between* the bonding and antibonding orbitals. This ordering of both the metal fragment orbitals and the cluster orbitals is confirmed by a recent set of MO calculations on $Mo_2Fe_2S_4(Cp)_2(CO)_4$.[22]

Using the bonding scheme in Fig. 21, we would expect that a cluster metal electron count anywhere between 12 and 16 should lead to a completely bonding metal tetrahedron, since after 12 electrons occupy the bonding orbitals up to four more electrons can be added to the cluster before an antibonding orbital must be occupied. Since $Mo_2Fe_2S_4(Me_5Cp)_2(CO)_4$ contains 18 metal electrons, two electrons will occupy an antibonding orbital. The long Fe—Fe distance indicates that

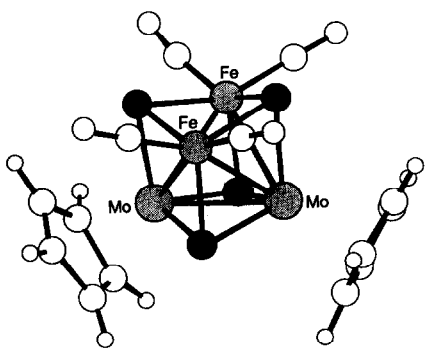

Fig. 20. Structure of $Mo_2Fe_2S_4(Me_5Cp)_2(CO)_4$ (ref. 85). The Me groups on the Cp ligands are not shown. Each octahedral Mo is bound to three core S atoms and a Cp ligand, while each five-coordinate Fe is bound to three core S atoms and two π-acceptor CO ligands. The geometry around each five-coordinate Fe atom is approximately square pyramidal.

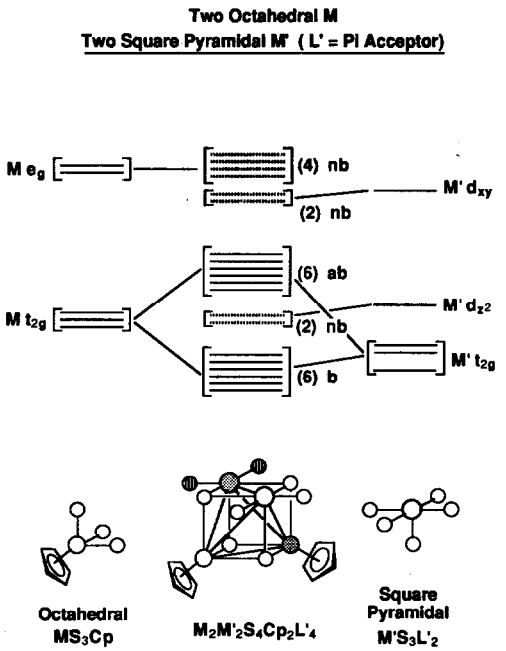

Fig. 21. Qualitative energy level scheme for the metal-based cluster orbitals in a heterometallic $M_2M'_2S_4Cp_2L'_4$ cluster containing two octahedral metals and two square pyramidal metals. The splittings of the metal *d* orbitals in octahedral and square pyramidal environments are shown on the left and right sides of the diagram, respectively. The resulting cluster orbitals are shown in the middle. The relatively large stabilization of the d_{z^2} orbital in the square pyramidal $MS_3L'_2$ fragment reflects the presence of two π-acceptor ligands.

these electrons occupy a localized Fe—Fe antibonding orbital, and the MO calculations confirm the occupation of six bonding, two non-bonding and one antibonding orbital localized between the two Fe atoms. It is important to recognize that the very low energy non-bonding orbitals are a consequence of the π-acceptor ligands coordinated to the square pyramidal metal. In the presence of π-donor ligands the metal d_{z^2} orbitals would lie at higher energies, antibonding orbitals would be occupied before non-bonding orbitals, and a smaller metal electron count would lead to a decrease in the degree of M—M bonding. The consequences of π-donor vs π-acceptor ligands on the ordering of the cluster orbitals was apparent in the earlier discussions of the $M_4S_4L_4$ clusters incorporating four-coordinate tetrahedral metals. The bonding scheme in Fig. 21 makes it clear that the presence of π-donor vs π-acceptor ligands will also have an effect on the ordering of the cluster orbitals in clusters incorporating five-coordinate square pyramidal metals.

4. HETEROMETALLIC CLUSTERS HAVING AN MM'_3S_4 CORE

4.1. *All four metals octahedrally coordinated*

The clusters listed in Table 9 are the only examples of MM'_3S_4 clusters in which all four metal atoms have similar coordination geometries. Although the clusters $Cr_3MS_4(Cp)_4$ (M = V, Nb)[86]

Table 9. Heterometallic clusters having structure type **19**: all metals octahedrally coordinated

Cluster	Number of metal electrons	Reference
$Cr_3MS_4(Cp)_4$ (M = V, Nb)[a]	11	86

[a] Spectroscopic evidence suggests a cubane-type structure.

have not been structurally characterized, spectroscopic evidence indicates that they have the cubane-type structure $MM'_3S_4Cp_4$ (**19**). Each metal can be viewed as part of an octahedral MS_3Cp or

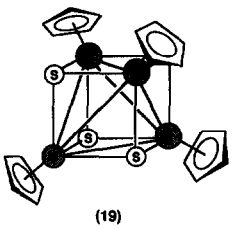

(19)

$M'S_3Cp$ fragment, and the clusters are expected to be similar in both molecular and electronic structure to the homometallic $M_4S_4Cp_4$ clusters (**5**). Making use of the cluster bonding scheme in Fig. 4, a cluster metal electron count of 12 is expected to lead to a fully bonding metal tetrahedron. Both $Cr_3MS_4(Cp)_4$ clusters are paramagnetic with a metal electron count of 11, and the M—M distances are expected to be within the range expected for M—M bonds.

4.2. *Three octahedral metals—one tetrahedral metal*

A number of clusters characterized by the general formula $MM'_3S_4LL'_9$ (**20**) or $MM'_3S_4LCp_3$ (**21**) are listed in Table 10. In each case three metals can be viewed as part of an octahedral $M'S_3L'_3$

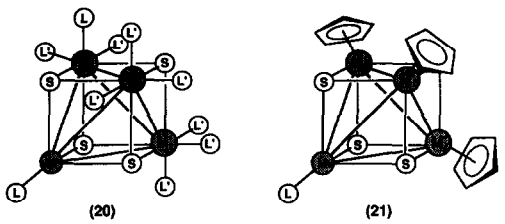

or $M'S_3Cp$ fragment and one metal can be viewed as part of a tetrahedral MS_3L fragment. The structure of one of these clusters, $[Mo_3FeS_4(NH_3)_9(H_2O)]^{4+}$, is shown in Fig. 22. Here, each Mo is coordinated by three NH_3 ligands, while the Fe atom is bound to the O of the single H_2O molecule. In several of the clusters, such as $Mo_3CuS_4(S_2P(OCH_3)_2)_3(\mu\text{-}OOCCCl_3)(CH_3N)(I)$,[87] the octahedral metals are coordinated to monodentate, bidentate and spanning bidentate ligands. The metal electron counts in the clusters range from 14 to 16, and in all cases the M—M distances are indicative of M—M bonds.

A qualitative bonding scheme for these clusters is shown in Fig. 23. The groups of metal *d* orbitals within the tetrahedral and octahedral fragments are shown on the left and right side of the

Table 10. Heterometallic clusters having structure type **20** or **21**: three octahedral metals—one tetrahedral metal

Cluster	Number of metal electrons	M—M distance M′—M[a]	M′—M′	Reference
$Cr_3FeS_4(Cp)_3(OOCCMe_3)$	14	2.721–2.787	2.828–2.848	88
$[Mo_3FeS_4(NH_3)_9(H_2O)]^{4+}$	14	2.675–2.691	2.766–2.830	89
$Cr_3CoS_4(Cp)_3(CO)$	16	2.649–2.666	2.810–2.824	90
$Mo_3CuS_4(S_2P(OCH_3)_2)_3(\mu\text{-}OOCCH_3)(HCON(CH_3)_2)(I)$	16	2.807–2.856	2.679–2.770	91
$W_3CuS_4(S_2P(OCH_3)_2)_3(\mu\text{-}OOCCH_3)(C_5H_5N)(I)$	16	2.841–2.960	2.687–2.767	92
$Mo_3CuS_4(S_2P(OCH_3)_2)_3(\mu\text{-}OOCCCl_3)(CH_3N)(I)$	16	2.792–2.875	2.701–2.761	87

[a] M′ = octahedral metal, M = tetrahedral metal.

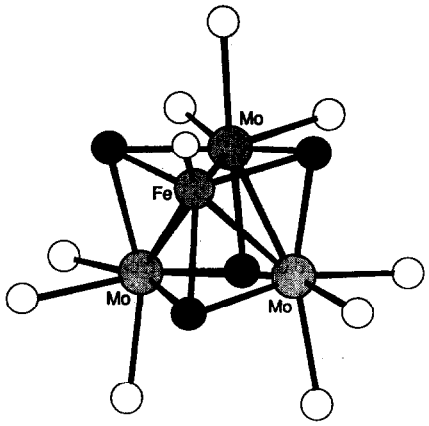

Fig. 22. Structure of $[Mo_3FeS_4(NH_3)_9(H_2O)]^{4+}$ (ref. 89). All of the H atoms have been omitted. Each octahedral Mo is bound to three core S atoms and three NH_3 ligands, while the tetrahedral Fe is bound to three core S atoms and an H_2O molecule.

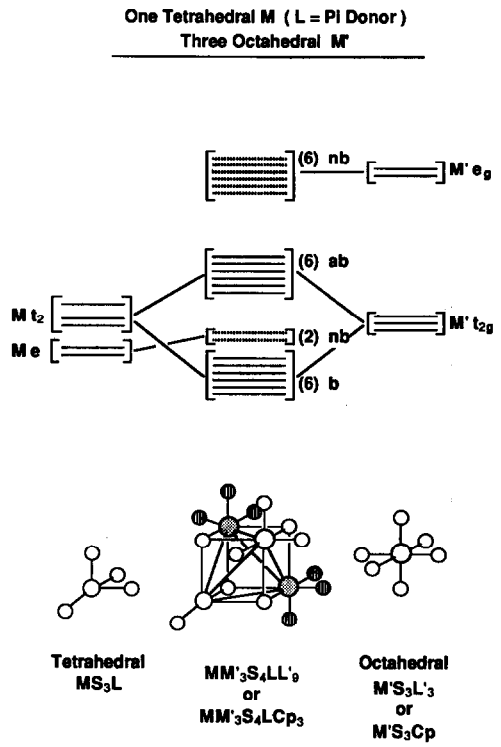

Fig. 23. Qualitative energy level scheme for the metal-based cluster orbitals in a heterometallic $MM'_3S_4LL'_9$ or $MM'_3S_4LCp_3$ cluster containing one tetrahedral metal and three octahedral metals. The splittings of the metal *d* orbitals in tetrahedral and octahedral environments are shown on the left and right sides of the diagram, respectively. The resulting cluster orbitals are shown in the middle. The relatively small separation between the "*e*" and "t_2" orbitals in the MS_3L fragment reflects the presence of a π-donor ligand.

diagram, respectively. Because the octahedrally coordinated metals lie to the left of the periodic table, the energy of the octahedral metal orbitals is expected to be higher than the energy of the tetrahedral metal orbitals. Also, because in most of the clusters the ligand L coordinated to the tetrahedral metal is a π-donor, the separation between the tetrahedral "*e*" and "t_2" orbitals is expected to be small. The cluster orbitals are shown in the centre of the diagram. The octahedral

"t_{2g}" and tetrahedral "t_2" orbitals combine to form six bonding and six antibonding cluster orbitals. Six non-bonding orbitals derived from the octahedral "e_g" orbitals should lie high in energy, while two cluster non-bonding orbitals derived from tetrahedral "e" orbitals are expected to lie *between* the sets of cluster bonding and antibonding orbitals. Although no calculations have been carried out which can confirm this cluster bonding scheme, the scheme is consistent with the observed structures of the clusters, since occupation of antibonding orbitals would require metal electron counts greater than 16. In the clusters having electron counts of 14 and 16, 12 metal electrons will occupy the cluster bonding orbitals and two or four electrons will partially or fully occupy the low energy non-bonding orbitals. The presence of two unpaired electrons in $Cr_3FeS_4(Cp)_3(OOCCMe_3)$[88] (14 metal electrons) suggests that in this cluster one electron occupies each of the non-bonding orbitals derived from the Fe "e" orbitals. In $Cr_3CoS_4(Cp)_3(CO)$ the non-bonding cluster orbitals derived from the Co "e" orbitals will be stabilized by the π-acceptor CO ligand and are expected to lie below the cluster bonding orbitals. The 16 metal electrons will still fully occupy the non-bonding and bonding orbitals.

4.3. *One octahedral metal—three tetrahedral metals*

Structurally characterized clusters belonging to this class are listed in Table 11. They can all be represented by the general formula $MM'_3S_4L_3L'_3$ (**22**). One metal can be viewed as part of an

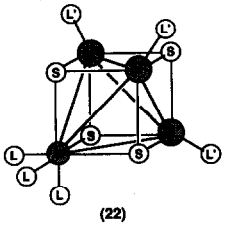

(22)

octahedral MS_3L_3 fragment, while the other three metals can be viewed as parts of tetrahedral $M'S_3L'$ fragments. Except for $[MoFe_3S_4(SEt)_3(CO_3)]^{3-}$,[93] all of the clusters listed in Table 11 contain 19-electron $[MoFe_3S_4]^{3+}$ or $[VFe_3S_4]^{+}$ cores. The structural, chemical and electronic properties of the $MoFe_3S_4$ clusters have been studied extensively by the Holm group.[20,94,95] (See also the references in Table 11. These studies have been motivated primarily by the similarities between these clusters and the Mo cofactor in nitrogenase. The structure of one of these clusters, $[MoFe_3S_4(SEt)_3(Cl_4cat)(CN)]^{3-}$, is illustrated in Fig. 24. The octahedral Mo atom is coordinated by the two O atoms of the cathecholate ligand and by the cyanide ligand, while each tetrahedral Fe atom is bound to one thiolate ligand. Recently a series of VFe_3S_4 clusters has also been studied by the Holm

Table 11. Heterometallic clusters having structure type **22**: one octahedral metal—three tetrahedral metals

Cluster	Number of metal electrons	M—M distances		Reference
		M—M'[a]	M'—M'	
$[MoFe_3S_4(S\text{-}p\text{-}C_6H_4Cl)_4((C_3H_5)_2cat)]^{3-}$	19	2.736–2.789	2.660–2.711	99, 100
$[MoFe_3S_4Cl_3((C_3H_5)_2cat)(THF)]^{2-}$	19	2.765–2.794	2.725–2.733	101
$[MoFe_3S_4(SEt)_3(Cl_4cat)(CN)]^{3-}$	19	2.727–2.737	2.690–2.720	102
$[MoFe_3S_4(SEt)_3(Cl_4cat)(N_3)]^{3-}$	19	2.735–2.751	2.690–2.699	102
$[MoFe_3S_4(SEt)_4(dmpe)]^{-}$	19	2.718–2.775	2.706–2.726	103
$[MoFe_3S_4Cl_4(dmpe)]^{-}$	19	2.703–2.732	2.724–2.767	103
$[VFe_3S_4Cl_3(DMF)_3]^{-}$	19	2.771–2.781	2.691–2.738	96, 98
$[VFe_3S_4Cl_3(bpy)(DMF)]^{-}$	19	2.760–2.792	2.704–2.738	98
$[VFe_3S_4Cl_3(dmpe)(MeCN)]^{-}$	19	2.699–2.745	2.749–2.760	98
$[MoFe_3S_4(SEt)_3(CO)_3]^{3-}$	22	3.225–3.272	2.739–2.742	93

[a] M = octahedral metal, M' = tetrahedral metal.

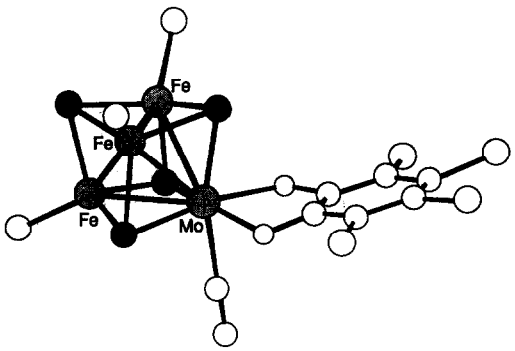

Fig. 24. Structure of $MoFe_3S_4(SEt)_3(Cl_4cat)(CN)]^{3-}$ (ref. 102). The Et groups in the three $(SEt)^-$ ligands are not shown. The tetrahedral Fe atoms are bound to three core S atoms and the S atom of a thiolate ligand. The octahedral Mo atom is bound to three core S atoms, a cyanide ligand, and the two O atoms of the bidentate catecholate ligand.

group,[95–98] and the electronic and structural properties of these clusters are found to be very similar to the properties of the $MoFe_3S_4$ clusters. As in the $[Fe_4S_4(SR)_4]^{2-}$ clusters, a detailed understanding of the electronic structure of these heterometallic clusters is complicated by the weak coupling between high-spin transition metal ions. The results of spin-unrestricted Xα calculations on the model cluster, $[MoFe_3S_4(SH)_6]^{3-}$, provide an analysis of the electronic structure which is consistent with the experimentally observed electronic properties of the clusters having $[MoFe_3S_4]^{3+}$ cores.[21]

A qualitative cluster bonding scheme for this class of clusters can be derived from the metal fragment orbitals. This scheme is shown in Fig. 25. The groups of metal *d* orbitals within the octahedral and tetrahedral fragments are shown on the left and right of the diagram, respectively.

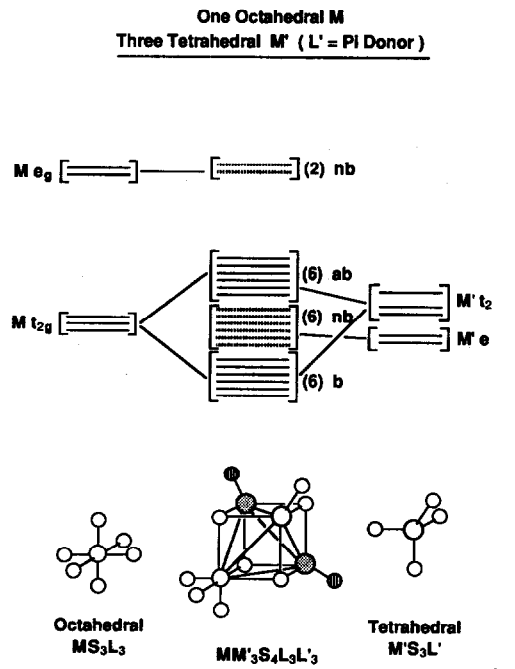

Fig. 25. Qualitative energy level scheme for the metal-based cluster orbitals in a heterometallic $MM'_3S_4L_3L'_3$ cluster containing one octahedral metal and three tetrahedral metals. The splittings of the metal *d* orbitals in octahedral and tetrahedral environments are shown on the left and right sides of the diagram, respectively. The resulting cluster orbitals are shown in the middle. The relatively small separation between the "*e*" and "t_2" orbitals in the $M'S_3L'$ fragment reflects the presence of a π-donor ligand.

Because the L′ ligand associated with each tetrahedral metal is a π-donor, the separation between the tetrahedral metal "e" and "t_2" orbitals is expected to be small. The cluster orbitals are shown in the centre of the diagram. Once again, the metal "t_{2g}" and "t_2" orbitals combine to form six bonding and six antibonding cluster orbitals. Two non-bonding cluster orbitals derived from the octahedral metal "e_g" orbitals lie high in energy, while six non-bonding cluster orbitals derived from the tetrahedral metal "e" orbitals are expected to lie *between* the sets of cluster bonding and antibonding orbitals. The intermediate energy of these six non-bonding orbitals is a result of the π-donor ligands. Based upon this simple bonding scheme, metal electron counts between 12 and 24 should result in a completely bonding metal tetrahedron, since after the bonding orbitals are occupied by 12 electrons, the six-nonbonding orbitals can accommodate up to 12 additional electrons before an antibonding orbital must be occupied. (As in several of the previously described classes of clusters, the energy ranges of the non-bonding and antibonding orbitals probably overlap. If they do, antibonding orbitals will be occupied for electron counts $\leqslant 24$.) The M—M distances (Table 11) in all of the clusters which have $[MoFe_3S_4]^{3+}$ and $[VFe_3S_4]^{2+}$ cores are indicative of M—M bonds. Since all of these clusters have 19 metal electrons, the bonding scheme in Fig. 25 indicates that in each cluster seven electrons will occupy non-bonding orbitals. Just as in the Fe_4S_4 clusters, it is the presence of these seven non-bonding electrons associated with the Fe atoms which leads to the observed complex electron-spin couplings.

The structure of the remaining cluster in Table 11, $[MoFe_3S_4(SEt)_3(CO)_3]^{3-}$, is markedly different from the structure of the other $MoFe_3S_4$ and VFe_3S_4 clusters in this class. This cluster, which contains 22 metal electrons, is characterized by long non-bonding Mo—Fe distances (*ca* 3.25 Å), as well as relatively long Mo—S distances (*ca* 2.63 Å compared to Mo—S distances of *ca* 2.35–2.40 Å in the other clusters listed in Table 11), and Coucouvanis *et al.* suggested that this cluster is best described as a weak complex of the $Mo(CO)_3$ unit and the $[Fe_3S_4(SR)_3]^{3-}$ cluster.[93] The different structure of this cluster once again calls attention to the need for considering the individual oxidation states of the metals in the cluster as well as the total metal electron count. For example, the $MoFe_3S_4$ clusters discussed in the preceding paragraph have a total of 19 metal electrons. This results in 12 metal electrons occupying the cluster M—M bonding orbitals and seven electrons occupying cluster non-bonding orbitals associated *only* with the Fe atoms. These cluster orbital occupations can be associated with one Mo^{3+}, one Fe^{2+} and two Fe^{3+} centres. In contrast, $[MoFe_3S_4(SEt)_3(CO)_3]^{3-}$ has three extra metal electrons, or a total of 22 metal electrons. Although the bonding scheme in Fig. 25 indicates that the cubane structure should be able to accommodate these three additional electrons, it also suggests that at least some of these extra electrons would have to occupy non-bonding orbitals associated with the Fe atoms. That is, even though the extra three electrons are introduced by the $Mo(CO)_3$ unit, formation of a true cubane-type cluster would require formal oxidation of the Mo and reduction of one or more of the three Fe atoms. The exact degree of oxidation and reduction would depend on the relative energies of the non-bonding "e" orbitals and the M—M antibonding orbitals. The fact that a true cubane-type cluster is not formed suggests that the required oxidation and reduction is unfavourable. We should recognize that even though the cluster bonding diagrams described in this report indicate that a range of total metal electron counts is possible for a cluster having a particular structure, there may not be any reasonable combinations of individual metal oxidation states which lead to some of these total metal electron counts.

4.4. *Two octahedral metals—two five-coordinate metals*

The last group of heterometallic clusters can be characterized by the general formula $MM'_3S_4L_3L'_7$, where two metals, one M and one M′, can be viewed as part of octahedral MS_3L_3 and $M'S_3L'_3$ fragments and two metals are part of five-coordinate $M'S_3L'_2$ fragments. Several clusters having this structure are listed in Table 12. These clusters can be viewed as having one of the ideal structures **23** or **24**. In **23**, each five-coordinate metal is square pyramidal, whereas in **24** each five-coordinate metal is trigonal pyramidal. In the $[MoFe_3S_4(S_2CNR_2)_5]^{0,-1}$ clusters listed in Table 12, each metal is coordinated by a bidentate dtc ligand, while the fifth dtc ligand spans an Fe and Mo atom. As in many of the homometallic clusters containing five-coordinate metals, the actual geometry about the five-coordinate metals lies somewhere in between the two geometries shown in **23** or **24** and can be described as either distorted square pyramidal or distorted trigonal bipyramidal. The two views of $MoFe_3S_4(S_2CNEt_2)_5$ shown in Fig. 26 demonstrate that either description might apply,

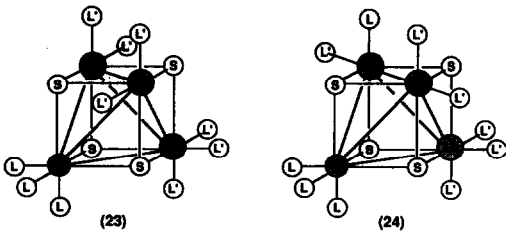

Table 12. Heterometallic clusters having structure type **23** or **24**: two octahedral metals—two five-coordinate metals

Cluster	Number of metal electrons	M—M[a]	M—M distances M—M'[b]	M'—M'	Reference
$[MoFe_3S_4(S_2CNEt_2)_5]^-$	18	2.624	2.841–2.895	2.736	104
$MoFe_3S_4(S_2CNR_2)_5$	17				
(R = Et)		2.705	2.739, 2.790 2.861, 3.057	2.296	105
(R = Bu)		2.683	2.80(2), 2.91(2)	2.701	106
($R = C_5H_{10}$)		2.696	2.78(2), 2.93(2)	2.701	107

[a] M = octahedral metal.
[b] M' = five-coordinate metal.

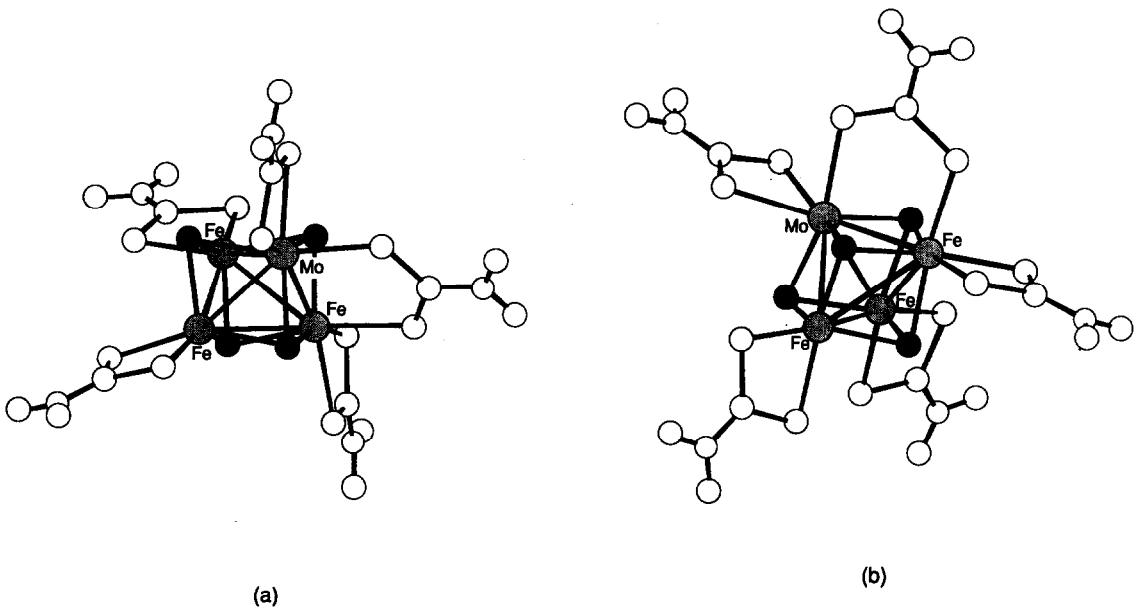

Fig. 26. Two views of the structure of $MoFe_3S_4(S_2CNEt_2)_5$ (ref. 105). Only the first C in each Et group is shown. Four of the bidentate Et_2dtc ligands each bind to a single metal atom, while the fifth Et_2dtc ligand spans an Mo atom and an Fe atom. The Mo atom and one of the Fe atoms are therefore six-coordinate and have approximately octahedral coordination geometry, while the two remaining Fe atoms are five-coordinate. The two views of the structure show that the geometry around the five-coordinate Fe atoms can be viewed as either (a) distorted square pyramidal or (b) distorted trigonal bipyramidal.

although in this cluster a designation of distorted square pyramidal may be more appropriate. The distortions are not the same in all of the clusters listed in Table 12, however, so as a group the five-coordinate metals are best described as having a geometry intermediate between that shown in **23** or **24**.

A qualitative energy scheme for a cluster having geometry **23** (two five-coordinate square pyramidal metals) is shown in Fig. 27. The ordering of the metal *d* orbitals within the octahedral and square pyramidal fragments are shown on the left and right side, respectively, of the diagram. The diagram has been simplified somewhat in that only one set of metal octahedral orbitals are shown. Because two different metals, in this case Fe and Mo, are octahedrally coordinated, there are actually two different sets of octahedral metal orbitals. Since the presence of these two sets should not greatly alter the general scheme derived in the centre of Fig. 16, the second set has been omitted. The "t_{2g}" sets of orbitals from all four metal atoms combine to form the sets of cluster bonding and antibonding orbitals. Three groups of cluster non-bonding orbitals are expected, four high energy orbitals derived from the octahedral metal "e_g" orbitals, two high energy orbitals derived from the square pyramidal metal d_{xy} orbitals and two lower energy orbitals derived from the square pyramidal metal d_{z^2} orbitals. The lower energy non-bonding orbitals are expected to lie within the same energy range as the antibonding orbitals. Just as in the homometallic clusters containing five-coordinate metals, the bonding in the $MM'_3S_4L_3L'_7$ clusters considered here is expected to be similar to the bonding in clusters containing all octahedral metals—*except* for higher electron counts.

All of the clusters in Table 12 contain 17 or 18 electrons. Using the diagram in Fig. 27, 12 of these electrons should fully occupy the cluster bonding orbitals, while the remaining five or six electrons are expected to occupy cluster antibonding orbitals. An examination of the M—M distances listed in Table 11 shows that in general the distances between the octahedral Mo and Fe atoms (the two atoms spanned by the dtc ligand) and between the two five-coordinate Fe atoms are indicative of Mo—Fe and Fe—Fe bonds. The other four M—M distances are less regular and are generally longer (in some cases long enough to be non-bonding). These distances are consistent with partial occupation of the cluster antibonding orbitals. An understanding of the actual deformations of the

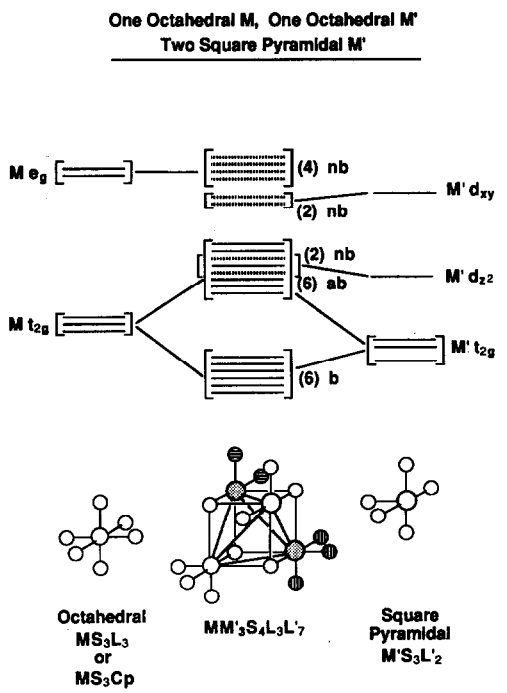

Fig. 27. Qualitative energy level scheme for the metal-based cluster orbitals in a heterometallic $MM'_3S_4L_3L'_7$ cluster containing two octahedral metals and two square pyramidal metals. The splittings of the metal *d* orbitals in octahedral and square pyramidal environments are shown on the left and right sides of the diagram, respectively. The resulting cluster orbitals are shown in the middle.

M—M bonds would require an understanding of the character of the antibonding orbitals, but the M—M distances do suggest that antibonding orbitals localized between either the two octahedral metals or the two five-coordinate metals lie high enough in energy to remain unoccupied, while the lower energy occupied antibonding orbitals involve interactions *between* the octahedral and five-coordinate metals. The lower energy non-bonding orbitals may be sufficiently stabilized to be at least partially occupied, but the long distances between the five- and six-coordinate metals indicate that these non-bonding orbitals are high enough in energy that at least the majority of the extra five or six electrons occupy antibonding orbitals.

A comparison of the energy level diagrams in Figs 25 and 27 shows that the bonding schemes are markedly different in the $MoFe_3S_4$ clusters having the two different structure types **22** and **23**. The tetrahedral coordination of the three Fe atoms in the $MM'_3S_4L_3L'_3$ (**22**) clusters introduces a large number of low energy non-bonding cluster orbitals. In the $MM'_3S_4L_3L'_7$ clusters (**23**), on the other hand, the non-bonding cluster orbitals are destabilized by the octahedral and square pyramidal or trigonal bipyramidal coordination of the Fe atoms. Even with equivalent metal electron counts the electronic structures of these two types of clusters would not be equivalent.

5. SUMMARY

When the cubane-type clusters are grouped into classes based on metal coordination geometry it is possible to develop a qualitative M_4 cluster bonding scheme for each class. These schemes make it possible to understand, at least qualitatively, the M—M bonding in a large number of both homo- and heterometallic clusters. The M—M bonding in these clusters is strongly influenced by the ligand environment of each metal in the cluster. When we view each metal as part of an MS_3L_x fragment within the cluster, we can see that M—M bonds are formed between $t_{2g}(t_2)$ type orbitals, while $e_g(e)$ type orbitals do not take part in the M—M bonding. Since the ligand environment (both the ligand geometry and the nature of the ligands) of each metal has a strong effect on the relative energies of these "t_{2g}" and "e_g" orbitals, it ultimately has an effect on the energies of the bonding, antibonding and non-bonding M_4 cluster orbitals. Specifically, changing the ligand geometry around the metals and/or the type of ligands bound to the metals changes the relative energy of the non-bonding cluster orbitals. This effect is closely related to the structure of a cluster, since the position of the non-bonding cluster orbitals determines how many "metal" electrons the cluster can accommodate without the loss of M—M bonding.

The Dahl group recognized the importance of these non-bonding cluster orbitals when they developed qualitative bonding schemes which could be applied to a number of the homometallic clusters. Their schemes assumed that the stronger metal–ligand (or metal–sulphur) interactions could be separated from the weaker metal–metal interactions, and in deriving these schemes they first considered the metal–metal interactions and then added on the metal–ligand interactions. Although these schemes are extremely useful for many of the homometallic clusters, this approach is not easily extended to the lower symmetry heterometallic clusters having more than one kind of coordination geometry. Alternatively, it is possible to first consider the stronger metal–ligand interactions and then add on the weaker metal–metal interactions. Using this approach each metal is viewed as part of an MS_3L_x fragment, and the cluster bonding, antibonding and most importantly non-bonding orbitals can be associated with specific sets of metal orbitals within these fragments. This approach makes it possible to derive qualitative cluster bonding schemes for even the low symmetry hetero-metallic clusters. Detailed descriptions of the electronic structure of many of these clusters must await accurate electronic structure calculations, but it is useful in the meantime to have these qualitative bonding descriptions.

REFERENCES

1. J. A. Ibers and R. H. Holm, *Science* 1980, **209**, 223.
2. J. M. Berg and R. H. Holm, in *Iron–Sulfur Proteins* (Edited by T. G. Spiro), Chap. 1. Wiley-Interscience, New York (1982).
3. B. A. Averill, *Struct. Bond. (Berlin)* 1982, **53**, 59.
4. Trinh-Toan, B. K. Teo, J. A. Ferguson, T. J. Meyer and L. F. Dahl, *J. Am. Chem. Soc.* 1977, **99**, 408.

5. P. J. M. Guerts, J. W. Gosselink, A. Van der Avoird, E. J. Baerends and J. G. Snijders, *Chem. Phys.* 1980, **46**, 133.
6. A. J. Thompson, *J. Chem. Soc., Dalton Trans.* 1981, 1180.
7. F. Bottomley and F. Grein, *Inorg. Chem.* 1982, **21**, 4170.
8. C. T.-W. Chu, F. Y.-K. Lo and L. F. Dahl, *J. Am. Chem. Soc.* 1982, **104**, 3409.
9. A. Müller, R. Jostes, W. Eltzner, C.-S. Nie, E. Diemann, H. Bögge, M. Zimmerman, M. Dartmann, U. Reinsch-Vogell, S. Che, S. J. Cyvin and B. N. Cyvin, *Inorg. Chem.* 1985, **24**, 2872.
10. S.-S. Sung, C. Glidewell, A. R. Butler and R. Hoffmann, *Inorg. Chem.* 1985, **24**, 3856.
11. P. D. Williams and M. D. Curtis, *Inorg. Chem.* 1986, **25**, 4562.
12. C. Liu, J. Hua, Z. Chen, Z. Lin and J. Lu, *Int. J. Quant. Chem.* 1986, **29**, 701.
13. C. Y. Yang, K. H. Johnson, R. H. Holm and J. G. Norman Jr, *J. Am. Chem. Soc.* 1975, **97**, 6596.
14. A. Aizman and D. A. Case, *J. Am. Chem. Soc.* 1982, **104**, 3269.
15. L. Noodleman, J. G. Norman Jr., J. H. Osborne, A. Aizman and D. A. Case, *J. Am. Chem. Soc.* 1985, **107**, 3418.
16. J. Darkwa, J. R. Lockemeyer, P. D. W. Boyd, T. B. Rauchfuss and A. L. Rheingold, *J. Am. Chem. Soc.* 1988, **110**, 141.
17. G. L. Simon and L. F. Dahl, *J. Am. Chem. Soc.* 1973, **95**, 2164.
18. L. L. Nelson, F. Y.-K. Lo, A. D. Rae and L. F. Dahl, *J. Organomet. Chem.* 1982, **225**, 309.
19. R. H. Holm, *Chem. Soc. Rev.* 1981, **10**, 455.
20. R. H. Holm and E. D. Simhon, in *Molybdenum Enzymes* (Edited by T. G. Spiro), Chap. 1. Wiley-Interscience, New York (1985).
21. M. Cook and M. Karplus, *J. Am. Chem. Soc.* 1985, **107**, 257.
22. S. Harris, *Inorg. Chem.* 1987, **26**, 4278.
23. C. D. Garner, in *Transition Metal Clusters* (Edited by B. F. G. Johnson), Chap. 4. John Wiley, New York (1980).
24. A. Müller, W. Eltzner, W. Clegg and G. M. Sheldrick, *Angew. Chem. Int. Edn Engl.* 1982, **21**, 536.
25. T. C. W. Mak, K. S. Jasim and C. Chieh, *Angew. Chem. Int. Edn Engl.* 1984, **23**, 391.
26. T. C. W. Mak, K. S. Jasim and C. Chieh, *Inorg. Chem.* 1985, **24**, 1587.
27. K. L. Wall, K. Folting, J. C. Huffman and R. A. D. Wentworth, *Inorg. Chem.* 1983, **22**, 2366.
28. A. W. Edelblut, K. Folting, J. C. Huffman and R. A. D. Wentworth, *J. Am. Chem. Soc.* 1981, **103**, 1927.
29. I. L. Eremenko, A. A. Pasynskii, A. S. Katugin, O. G. Ellert, V. E. Shklover and Yu. T. Struchkov, *Bull. Acad. Sci. USSR Div. Chem. Sci.* 1984, 1531.
30. H. Keck, A. Kruse, W. Kuchen, J. Mathow and H. Wunderlich, *Z. Naturfor.* 1987, **42b**, 1373.
31. T. Shibahara, H. Kuroya, K. Matsumoto and S. Ooi, *Inorg. Chim. Acta* 1986, **116**, L25.
32. F. A. Cotton, M. P. Diebold, Z. Diri, R. Llusar and W. Schwotzer, *J. Am. Chem. Soc.* 1985, **107**, 6735.
33. J. A. Bandy, C. E. Davies, J. C. Green, M. L. H. Green, K. Prout and D. P. S. Rodgers, *J. Chem. Soc., Chem. Commun.* 1983, 1395.
34. F. A. Cotton, Z. Dori, R. Llusar and W. Schwotzer, *Inorg. Chem.* 1986, **25**, 3529.
35. T. Shibahara, H. Kuroya, K. Matsumoto and S. Ooi, *J. Am. Chem. Soc.* 1984, **106**, 789.
36. A. A. Pasynskii, I. L. Eremenko, Yu. V. Rakitin, V. M. Novotortsev, O. G. Ellert, V. T. Kalinnikov, V. E. Shklover, Yu. T. Struchkov, S. V. Lindeman, T. K. Kurbanov and G. S. Gasanov, *J. Organomet. Chem.* 1983, **248**, 309.
37. T. Shibahara, E. Kawano, M. Okano, M. Nishi and H. Kuroya, *Chem. Lett.* 1986, 827.
38. A. Müller, E. Krickemeyer and H. Bögge, *Angew. Chem. Int. Edn Engl.* 1986, **25**, 272.
39. A. Müller, W. Eltzner, H. Bögge and R. Jostes, *Angew. Chem. Int. Edn Engl.* 1982, **21**, 795.
40. Trinh-Toan, W. P. Fehlhammer and L. F. Dahl, *J. Am. Chem. Soc.* 1977, **99**, 402.
41. R. A. Schunn, C. J. Fritchie Jr and C. T. Prewitt, *Inorg. Chem.* 1966, **5**, 892.
42. C. H. Wei, G. R. Wilkes, P. M. Treichel and L. F. Dahl, *Inorg. Chem.* 1966, **5**, 900.
43. J. Amarasekera, T. B. Rauchfuss and S. R. Wilson, *J. Chem. Soc., Chem. Commun.* 1989, 14.
44. J. W. Lauher, *J. Am. Chem. Soc.* 1978, **11**, 5305.
45. C. E. Davies, J. C. Green and G. H. Stringer, *NATO ASI Ser., Ser. C* 1986, **176**, 413.
46. T. Sugano, T. Shibahara, H. Kobayashi, N. Uryû and M. Kinoshita, *Bull. Chem. Soc. Jpn* 1988, **61**, 1785.
47. M. Elian and R. Hoffmann, *Inorg. Chem.* 1975, **14**, 1058.
48. T. A. Albright, J. K. Burdett and M. H. Whangbo, *Orbital Interactions in Chemistry*, Chap. 17. Wiley-Interscience, New York (1985).
49. R. S. Gall, C. T.-W. Chu and L. F. Dahl, *J. Am. Chem. Soc.* 1974, **96**, 4019.
50. T. O'Sullivan and M. M. Millar, *J. Am. Chem. Soc.* 1985, **107**, 4096.
51. W. E. Cleland, D. A. Holtman, M. Sabat, J. A. Ibers, G. C. DeFotis and B. A. Averill, *J. Am. Chem. Soc.* 1983, **105**, 6021.
52. M. A. Bobrik, K. O. Hodgson and R. H. Holm, *Inorg. Chem.* 1977, **16**, 1851.

53. A. Müller, N. Schladerbeck and H. Bögge, *Chimia* 1985, **39**, 24.
54. W. Saak and S. Pohl, *Z. Naturfor.* 1985, **40b**, 1105.
55. B. A. Averill, T. Herskovitz, R. H. Holm and J. A. Ibers, *J. Am. Chem. Soc.* 1973, **95**, 3523.
56. A. Müller, N. H. Schladerbeck and H. Bögge, *J. Chem. Soc., Chem. Commun.* 1987, 35.
57. L. Que Jr, M. A. Bobrik, J. A. Ibers and R. H. Holm, *J. Am. Chem. Soc.* 1974, **96**, 4168.
58. T. J. Ollerenshaw, C. D. Garner, B. Odell and W. Clegg, *J. Chem. Soc., Dalton Trans.* 1985, 2161.
59. G. Christou, C. D. Garner, M. G. B. Drew and R. Cammack, *J. Chem. Soc., Dalton Trans.* 1981, 1550.
60. P. K. Mascharak, K. S. Hagen, J. T. Spence and R. H. Holm, *Inorg. Chim. Acta* 1983, **80**, 157.
61. H. L. Carrell, J. P. Glusker, R. Hob and T. C. Bruice, *J. Am. Chem. Soc.* 1977, **99**, 3683.
62. M. G. Kanatzidis, N. C. Baenziger, D. Coucouvanis, A. Simopoulos and A. Kostikas, *J. Am. Chem. Soc.* 1984, **106**, 4500.
63. T. D. P. Stack and R. H. Holm, *J. Am. Chem. Soc.* 1988, **110**, 2484.
64. E. J. Laskowski, R. B. Frankel, W. O. Gillum, G. C. Papaefthymiou, J. Renaud, J. A. Ibers and R. H. Holm, *J. Am. Chem. Soc.* 1978, **100**, 5322.
65. M. J. Carney, G. C. Papaefthymiou, M. A. Whitener, K. Spartalian, R. B. Frankel and R. H. Holm, *Inorg. Chem.* 1988, **27**, 346.
66. J. M. Berg, K. O. Hodgson and R. H. Holm, *J. Am. Chem. Soc.* 1979, **101**, 4586.
67. D. W. Stephan, G. C. Papaefthymiou, R. B. Frankel and R. H. Holm, *Inorg. Chem.* 1983, **22**, 1550.
68. K. S. Hagen, A. D. Watson and R. H. Holm, *Inorg. Chem.* 1984, **23**, 2984.
69. G. C. Papaefthymiou, E. J. Laskowski, S. Frota-Pessôa, R. B. Frankel and R. H. Holm, *Inorg. Chem.* 1982, **21**, 1723.
70. A. L. Balch, *J. Am. Chem. Soc.* 1969, **91**, 6962.
71. T. H. Lemmen, J. A. Kocal, F. Y.-K. Lo, M. W. Chen and L. F. Dahl, *J. Am. Chem. Soc.* 1981, **103**, 1932.
72. Q. Liu, L. Huang, Y. Yang and J. Lu, *Jiegou Huaxue* 1987, **6**, 135.
73. J. E. Huheey, *Inorganic Chemistry*, 3rd edn, Chap. 10. Harper & Row, New York (1983).
74. E. L. Muetterties and L. J. Guggenberger, *J. Am. Chem. Soc.* 1974, **96**, 1748.
75. M. G. Kanatzidis, D. Coucouvanis, A. Simopoulos, A. Kostikas and V. Papaefthymiou, *J. Am. Chem. Soc.* 1985, **107**, 4925.
76. R. E. Johnson, G. C. Papaefthymiou, R. B. Frankel and R. H. Holm, *J. Am. Chem. Soc.* 1983, **105**, 7280.
77. H. Brunner, H. Kauermann and J. Wachter, *J. Organomet. Chem.* 1984, **265**, 189.
78. H. Brunner and J. Wachter, *J. Organomet. Chem.* 1982, **240**, C41.
79. T. R. Halbert, S. A. Cohen and E. I. Stiefel, *Organometallics* 1985, **4**, 1689.
80. M. D. Curtis and P. D. Williams, *Inorg. Chem.* 1983, **22**, 2661.
81. M. D. Curtis, P. D. Williams and W. M. Butler, *Inorg. Chem.* 1988, **27**, 2853.
82. H. Brunner, H. Kauermann and J. Wachter, *Angew. Chem. Int Edn Engl.* 1983, **22**, 549.
83. T. B. Rauchfuss, T. D. Weatherill, S. R. Wilson and J. P. Zebrowski, *J. Am. Chem. Soc.* 1983, **105**, 6508.
84. T. B. Rauchfuss, S. D. Gammon, T. D. Weatherill and S. R. Wilson, *New J. Chem.* 1988, **12**, 373.
85. H. Brunner, N. Janietz, J. Wachter, T. Zahn and M. L. Ziegler, *Angew. Chem. Int. Edn Engl.* 1985, **24**, 133.
86. A. A. Pasynskii, I. L. Eremenko, B. Orazsakhatov, V. T. Kalinnikov, G. G. Aleksandrov and Yu. T. Struchkov, *J. Organomet. Chem.* 1981, **216**, 211.
87. X. Wu, Y. Zheng, N. Zhu and J. Lu, *Jiegou Huaxue* (*J. Struct. Chem.*) 1988, **7**, 137.
88. I. L. Eremenko, A. A. Pasynskii, B. Orazsakhatov, O. G. Ellert, V. M. Novotortsev, V. T. Kalinnikov, M. A. Porai-Koshits, A. S. Antsyshkina, L. M. Dikareva and V. N. Ostrikova, *Inorg. Chim. Acta* 1983, **73**, 225.
89. T. Shibahara, H. Akashi and H. Kuroya, *J. Am. Chem. Soc.* 1986, **108**, 1342.
90. A. A. Pasynskii, I. L. Eremenko, B. Orazsakhatov, V. T. Kalinnikov, G. G. Aleksandraov and Yu. T. Struchkov, *J. Organomet. Chem.* 1981, **214**, 367.
91. X. Wu, S. Lu, L. Zu, Q. Wu and J. Lu, *Inorg. Chim. Acta* 1987, **133**, 39.
92. H. Zhan, Y. Aheng, X. Wu and J. Lu, *Jiegou Huaxue* (*J. Struct. Chem.*) 1988, **7**, 157.
93. D. Coucouvanis, S. Al-Ahmad, A. Salifoglou, W. R. Dunham and R. H. Sands, *Angew. Chem. Int. Edn Engl.* 1988, **27**, 1353.
94. P. K. Mascharak, G. C. Papaefthymiou, W. H. Armstrong, S. Foner, R. B. Frankel and R. H. Holm, *Inorg. Chem.* 1983, **22**, 2851.
95. M. J. Carney, J. A. Kovacs, Y.-P. Zhang, G. C. Papaefthymiou, K. Spartalian, R. B. Frankel and R. H. Holm, *Inorg. Chem.* 1987, **26**, 719.
96. J. A. Kovacs and R. H. Holm, *J. Am. Chem. Soc.* 1986, **108**, 340.
97. J. A. Kovacs and R. H. Holm, *Inorg. Chem.* 1987, **26**, 702.
98. J. A. Kovacs and R. H. Holm, *Inorg. Chem.* 1987, **26**, 711.

99. W. H. Armstrong, P. K. Mascharak and R. H. Holm, *Inorg. Chem.* 1982, **21**, 1699.
100. P. K. Mascharak, W. H. Armstrong, Y. Mizobe and R. H. Holm, *J. Am. Chem. Soc.* 1983, **105**, 475.
101. R. E. Palermo and R. H. Holm, *J. Am. Chem. Soc.* 1983, **105**, 4310.
102. R. E. Palermo, R. Singh, J. K. Bashkin and R. H. Holm, *J. Am. Chem. Soc.* 1984, **106**, 2600.
103. Y.-P. Zhang, J. K. Bashkin and R. H. Holm, *Inorg. Chem.* 1987, **26**, 694.
104. Q. Liu, L. Huang, B. Kang, C. Liu, L. Wang and J. Lu, *Huaxue Xuebao* 1986, **44**, 343.
105. L. Huang, Y. Yang, Q. Liu and J. Lu, *Jiegou Huaxue* 1986, **5**, 61.
106. B. Kang, Q. Liu, L. Huang, D. Wu, J. Cai, L. He, H. Liu and J. Lu, *Jiegou Huaxue* 1987, **6**, 8.
107. Q. Liu, L. Huang, B. Kang, Y. Yang and J. Lu, *Kexue Tongbao* (*Foreign Lang. Edn*) 1987, **32**, 898.

Polyhedron Vol. 8, No. 24, pp. 2883–2888, 1989
Printed in Great Britain

0277–5387/89 $3.00+.00
© 1989 Pergamon Press plc

KINETICS AND MECHANISMS OF THE REDOX REACTION OF HEXAAQUOTITANIUM(III) AND THE ETHYLENEDIAMINE TETRAACETATO TITANIUM(III) COMPLEX BY AQUEOUS SOLUTIONS OF BROMINE

J. FEMI IYUN† and ADE ADEGITE‡

Department of Chemistry, Ahmadu Bello University, Zaria, Nigeria

(*Received* 2 *June* 1988; *accepted after revision* 31 *May* 1989)

Abstract—At 25°C, $I = 1.0$ M ($CF_3SO_3^-Li^+ + CF_3SO_3H$), $[H^+] = 0.034$–0.274 M and $\lambda = 453$ nm, the rate equation for the oxidation of $Ti(H_2O)_6^{3+}$ by bromine was found to be:

$$\frac{-d[Br_2]_T}{dt} = \frac{kK[Br_2][Ti^{III}]}{[H^+]+K} + \frac{kK[Br_3^-][Ti^{III}]}{[H^+]+K},$$

where $k = 9.2 \times 10^{-3}$ M^{-1} s^{-1} and $K = 4.5 \times 10^{-3}$ M. At $[H^+] = 1.0$ M, $[Br^-] = 0.05$–0.4 M, the apparent second-order rate constant decreases as $[Br^-]$ increases.

The pH-dependence of the oxidation of Ti^{III}–edta by bromine is interpreted in terms of the change in identity of the Ti^{III}–edta species as the pH of the reaction medium changes. The second-order rate constants were fitted using a non-linear least-square computer program with $(1/k_0^{edta})^2$ weighting into an equation of the form:

$$k_0^{edta} = \frac{k_1 + k_2K_1[H^+]^{-1} + k_3K_1K_2[H^+]^{-2}}{1 + K_1[H^+]^{-1} + K_1K_2[H^+]^{-2}},$$

with K_1 and K_2 fixed as earlier determined at 9.55×10^{-3} and 2.29×10^{-9} M, respectively, for the oxidation of bromine.

$$k_1 = k_2 = (3.1 \pm 0.32) \times 10^3 M^{-1} s^{-1}$$

$$k_3 = (2.3 \pm 0.45) \times 10^6 M^{-1} s^{-1}.$$

It is proposed that these electron transfer reactions proceed by univalent changes with the production of $Br_2^{\bullet -}$ as a transient intermediate. An outer-sphere mechanism is proposed for these reactions. The homonuclear exchange rate for Ti^{III}–edta + Ti^{IV}–edta is estimated at 32 M^{-1} s^{-1}.

The kinetic investigations of the reactions[1–3] between $[Ti(H_2O)_6]^{3+}$ and Cl_2(aq), $[Co(NH_3)_5SCN]^{2+}$ and I_2(aq) have been reported. Such studies have also been extended to the oxidation of Ti^{III}–cdta by I_2(aq),[3] some cobalt(III) ammine complexes[4] and O_2.[5] This paper reports our results of the kinetic studies of the oxidation of Ti^{3+}(aq) and Ti^{III}–edta by aqueous acidic bromine solutions.

EXPERIMENTAL

Solutions of $CF_3SO_3^-Li^+$ were prepared by neutralizing Li_2CO_3 with doubly-distilled CF_3SO_3H. The solution was freed from dissolved carbon dioxide by bubbling pure nitrogen through. Solutions of hexaaquotitanium(III) ions in trifluoromethanesulphonic acid were prepared and analysed as previously reported.[1–3] Aqueous bromine solutions were prepared by shaking liquid bromine (BDH, Analar Grade) with water. The concentrations of the bromine solutions were determined by iodometry. Sodium acetate, HCl and LiCl

† Author to whom correspondence should be addressed.
‡ Present address: Department of Chemistry, University of Lagos, Lagos, Nigeria.

(all BDH, Analar Grade) were used without further purification. Ti^{III}–edta solutions were prepared by adding predetermined amounts of $[Ti(H_2O)_6]^{3+}$ solutions to a reaction medium containing the desired amount of LiCl, sodium acetate, HCl and recrystallized Na_2H_2edta in slight excess of what is required for a 1:1 Ti^{III}–edta complex.

Kinetics

We conducted our rate studies in a trifluoromethanesulphonate medium which has been shown to be an "innocent" medium for titanium(III) reactions.[6] We worked in the acid range $0.034 \leqslant [H^+] \leqslant 0.274$ M, in which the tendency to form polymeric oxobridged titanium(IV) species does not affect our rate measurements.[7]

Rate measurements were made on the Durrum–Gibson stopped-flow spectrophotometer by monitoring absorbance changes due to bromine at $\lambda = 453$ nm, the isobestic point for Br_2 and Br_3^-.

The kinetic runs, except where stated, were conducted under pseudo-first-order conditions with $[Ti^{III}] > 20[Br_2]_{total}$. The temperature was maintained constant at 25.0 ± 0.1°C.

In the Ti^{III}–edta + Br_2 reaction, the pH of the solution was kept constant by using a formate buffer for the pH range 2.5–3.8 and an acetate buffer for the pH range 3.7–6.0. Preliminary investigations showed that the rate of the bromine + formate reaction is negligible compared with that for the reaction of interest. Also for the same pH, rate constants obtained by varying the buffer concentration from 0.05 to 0.20 M agreed within 5%, confirming that the rate of reaction is unaffected by either formate or acetate ion. At pH = 3.7, the rate constant obtained was essentially the same whether the medium was formate or acetate. We also confirmed spectrally in the range 300–600 nm and at pH = 1.0 that there was no complex formation between Ti^{III}–edta and CH_3COOO^- and $HCOO^-$. To prevent extensive hydrolysis of Br_2 to HOBr, particularly at high pH, bromine solutions were unbuffered and were prepared to contain the calculated amounts of acid needed to attain the desired pH when the reactants are mixed in the reaction chamber. Each reaction medium was set at 1.0 M ionic strength using $CF_3SO_3^-Li^+$.

RESULTS AND DISCUSSION

The stoichiometries of the $Ti^{III}(aq) + Br_2$ and Ti^{III}–edta + Br_2 reactions were determined by spectrophotometric titrations at $\lambda = 453$ nm to be of the ratio 2:1. The pseudo-first-order plots were linear for more than 90% of the reaction, confirming an order of one with respect to bromine concentration. The pseudo-first-order rate constants in the range $1.9 \times 10^{-2} \leqslant [Ti^{III}] \leqslant 5.5 \times 10^{-2}$ M increased as $[Ti^{III}]$ increased. A plot of log k_{obs} vs log $[Ti^{III}]$ was linear with a slope of 0.96 ± 0.02. This confirms that the order with respect to $[Ti^{III}]$ is one. The computed second-order rate constants are reported in Table 1.

The acid dependence observed in the range $0.034 \leqslant [H^+] \leqslant 0.274$ M is similar to those reported earlier.[3] A plot of k^{-1} vs $[H^+]$ is linear with a finite intercept. For the $Ti^{3+} + Br_2$ reaction the following reaction scheme is proposed:

$$Ti(H_2O)_6^{3+} \overset{K_a}{\rightleftharpoons} [(H_2O)_5TiOH]^{2+} + H^+ \text{(fast)} \quad (1)$$

$$[Ti(H_2O)_5OH]^{2+} + Br_2 \underset{k_{-1}}{\overset{k_1}{\rightleftharpoons}} [(H_2O)_5TiO]^{2+} + Br_2^{\bullet -} + H^+ \quad (2)$$

Table 1. Rate constants for the reaction of $[Ti(H_2O)_6]^{3+}$ with bromine; $[Br_2] = (5.0–8.0) \times 10^{-4}$ M, $I = 1.0$ M ($CF_3SO_3^-Li^+$)

$10[Ti^{III}]$ (M)	$[H^+]$ (M)	$[X^-]$ (M)	$10^{-2}k_0$ ($M^{-1}s^{-1}$)
0.19	0.10	—	3.8
0.26	0.10	—	4.0
0.37	0.10	—	3.9
0.38	0.10	—	3.9
0.56	0.10	—	3.7
0.11	0.03	—	11.9
0.11	0.05	—	8.1
0.11	0.07	—	5.7
0.11	0.09	—	4.4
0.11	0.13	—	3.4
0.11	0.14	—	3.0
0.11	0.17	—	2.3
0.11	0.27	—	1.5
	X = Br		
0.14	0.10	0.05	2.3
0.14	0.10	0.10	1.6
0.14	0.10	0.20	1.1
0.14	0.10	0.40	0.8
	X = Cl		
0.13	0.10	0.01	6.4
0.13	0.10	0.05	7.4
0.13	0.10	0.10	15.0
0.13	0.10	0.20	25.0
0.13	0.10	0.40	54.0
0.13	0.10	0.50	63.0

$$[(H_2O)_5TiOH]^{2+} + Br_2^{\cdot-} \xrightarrow{k_2} [(H_2O)_5TiO]^{2+} + 2Br^- + H^+ \quad (3)$$

By applying the steady-state approximation to $[Br_2^{\cdot-}]$ in the above scheme and making the following assumptions,

(i) that $k_2K_a[Ti^{3+}][H^+] \gg k_{-1}[TiO^{2+}][H^+]$ and
(ii) $[Ti^{III}] = [Ti(H_2O)_6]^{3+} + [Ti(OH)^{2+}]$

then the following rate equation is derived:

$$\text{rate} = \frac{k_1K_a[H^+]^{-1}}{1 + K_a[H^+]^{-1}}[Ti^{III}][Br_2] \quad (4)$$

or

$$k_0[Ti^{III}][Br_2]$$

with

$$k_0 = \frac{k_1K_a[H^+]^{-1}}{1 + K_a[H^+]^{-1}}. \quad (5)$$

Least mean square analysis of the linear plot of k_0^{-1} vs $[H^+]$ gave

$$k_1 = 9.2 \times 10^3\,M^{-1}s^{-1}$$

$$K_a = 4.5 \times 10^{-3}\,M.$$

The value of $K_a = 4.5 \times 10^{-3}$ M, the kinetically determined value of the acid dissociation constant obtained for the $Ti^{III} + Br_2$ reaction, is in good agreement with the value of $K_a = 3.2 \times 10^{-3}$ M obtained for the $Ti^{III} + I_2$ system[3] and the value of 3.1×10^{-3} M earlier obtained by Orhanovic for some outer-sphere reactions of the aquotitanium(III) ion with the cobalt(III) complex.[8] Some other data on the outer-sphere reactions involving aquotitanium(III) as reductant have been fitted with K_a values of 1.6×10^{-3} and 4.6×10^{-3} M, respectively.[6,9] These values are at least an order of magnitude less than similar equilibrium constants derived for some complex hydrolytic pathways in the reactions of the Ti^{3+}(aq) ion. The latter reactions were also found to proceed by the inner-sphere mechanism.

† The data for the Ti^{III}–edta + Br_2 reaction was fitted into an equation of the form:

$$k_0^{edta} = \frac{k_1 + k_2K_1[H^+]^{-1} + k_3K_1K_2[H^+]^{-2}}{1 + K_1[H^+]^{-1} + K_1K_2[H^+]^{-2}},$$

where ($k_1 = k_2$), by using a non-linear least-square computer analysis with $(1/k_0^{edta})^2$, weighting and the values of K_1 and K_2 fixed as reported.[13]

An iterative procedure was used until there was convergence. A correlation coefficient of 99.5% between k_0^{edta}(expt.) and k_0^{edta}(calc.) was obtained. We are grateful to Mr L. Fulkerson of the Ahmadu Bello University Computer Centre for writing the program for this analysis.

K_a values as high as 0.01–0.16 M were reported for some inner-sphere reactions involving Ti^{3+}(aq).[10] The experimental value of K_a, as determined by independent workers[11] although not under identical conditions, places its value in the range $(1.6–6.9) \times 10^{-3}$ M. The proposition of the outer-sphere mechanism for the $Ti^{III} + Br_2$ reaction is supported by the comparison of the rate of electron transfer ($9.2 \times 10^3\ M^{-1}\ s^{-1}$) with the rate of substitution of NCS^- and $HC_2O_4^-$ into the Ti^{3+} aqua ion, (8×10^3 and $4 \times 10^5\ M^{-1}\ s^{-1}$, respectively).[12] The substitution mechanism is also assumed to be associative. Both NCS^- and $HC_2O_4^-$ are definitely more nucleophilic than Br_2. Hence, in order for the substitution of bromine into the inner coordination sphere of Ti^{3+} to preceed electron transfer, its rate must be less than the value of $9.2 \times 10^3\ M^{-1}\ s^{-1}$ obtained for the $TiOH^{2+} + Br_2$ reaction. The data obtained seem to rule out the inner-sphere mechanism. Tables 2–4 present the results of investigations involving the Ti^{III}–edta–bromine reaction. The pH-dependence of the rate of reaction of Ti^{III}–edta with an aqueous bromine solution has two mechanistic components. This reaction is pH-dependent below pH = 3 but shows an increase in rate as the pH increases above 3. Such complex dependence on pH has been observed in the reaction of Ti^{III}–edta with $[Co(NH_3)_6]^{3+}$ and $[Co(NH_3)_5NCS]^{2+}$.[4] As in earlier investigations this dependence on pH can be attributed to differing reactivities of Ti^{III}–edta, $Ti(H_2O)edta^-$ and $Ti(OH)edta^{2-}$.[13] The principal activation paths for this reaction can be proposed as follows:

$$TiY \rightleftharpoons^{K_1} TiY^- + H^+ \quad (6)$$

$$TiY^- \rightleftharpoons^{K_2} TiY^{2-} + H^+ \quad (7)$$

$$TiY + Br_2 \xrightarrow{k_1} (\text{activated complex})^* \quad (8)$$

$$TiY^- + Br_2 \xrightarrow{k_2} (\text{activated complex})^* \quad (9)$$

$$TiY^{2-} + Br_2 \xrightarrow{k_3} (\text{activated complex})^* \quad (10)$$

where Y = edta. From the above scheme, we obtain

$$k_0^{edta} = \frac{k_1 + k_2K_1[H^+]^{-1} + k_3K_1K_2[H^+]^{-2}}{1 + K_1[H^+]^{-1} + K_1K_2[H^+]^{-2}}. \quad (11)$$

From the titration studies of the Ti^{III}–edta solution at varying pH by Podlahova and Podlaha the first two species above exist at pH = 3. Our results suggest that these species react at the same rate, i.e. $k_1 = k_2$. This is also supported by the results of previous investigations.[4,14] Using a non-linear least-square computer program† to fit the experi-

Table 2. Second-order rate constants for the reaction of Ti^{III}–edta with bromine; $I = 1.0$ M ($CF_3SO_3^-Li^+ + CH_3COONa$), $T = 25.0 \pm 0.1$°C, pH = 1.0

$10^3[Ti^{III}\text{–edta}]$ (M)	$10^3[Br_2]$ (M)	$10^{-4}k_0^{edta}$ ($M^{-1}s^{-1}$)
2.30	1.15	3.5
1.80	0.90	3.5
1.52	0.76	3.6
1.32	0.66	3.5

[a] Average of four rate constants in which the concentration of acetate was varied from 0.05 to 0.40 M, while ionic strength remained constant at 1.0. The rate constants obtained were within 5% of each other.

Table 3. Bromide dependent second-order rate constants for the Ti^{III}–edta + bromine reaction; $[Ti^{III}\text{–edta}] = 1.0 \times 10^{-3}$ M, $[Br_2] = 0.90 \times 10^{-3}$ M, $I = 1.0$ M, $T = 25$°C, pH = 1.0 M

pH	$[Br^-]$ (M)	$10^{-4}k_0^{edta}$ ($M^{-1}s^{-1}$)
1.0	0.05	3.4
1.0	0.10	3.2
1.0	0.15	2.2
1.0	0.20	2.6
1.0	0.30	2.0

mentally observed data into eq. (11) with values of K_1 and K_2 fixed as reported by Podlahova and Podlaha,[13] for the different pH values investigated, gave for the Ti^{III}–edta + Br_2 reaction,

$$k_1 = k_2 = (3.1 \pm 0.42) \times 10^4 M^{-1}s^{-1}$$

and

$$k_3 = (8.3 \pm 0.2) \times 10^7 M^{-1}s^{-1}.$$

The data presented in Table 5 show that there is a

Table 5. Observed and estimated pH-dependent second-order rate constants for the oxidation of Ti^{III}–edta by an aqueous solution of bromine

pH	$10^{-4}k_0^{edta}$(expt.) ($M^{-1}s^{-1}$)	$10^{-4}k_0^{edta}$(calc.) ($M^{-1}s^{-1}$)
1.01	2.9	2.9
1.60	2.9	2.9
2.35	3.0	3.2
2.95	2.8	3.3
3.45	3.5	3.4
3.65	3.2	3.4
3.85	3.7	3.5
4.55	4.5	4.0
5.10	7.8	5.7
5.43	8.0	8.4
5.50	13.8	9.2
5.85	18.1	16.5
6.05	19.3	24.1

Table 4. pH-dependent second-order rate constants of the reaction of Ti^{III}–edta with bromine; $I = 1.0$ M ($CF_3SO_3^-Li^+$ + buffer), $T = 25.0 \pm 0.1$°C

pH	$10^3[Ti^{III}\text{–edta}]$ (M)	$10^3[Br_2]$ (M)	$[Br^-]$ (M)	$10^{-4}k_0^{edta}$ ($M^{-1}s^{-1}$)	Buffer medium
1.01	2.00	1.00	0.10	2.9	
1.60	1.50	0.75	0.10	2.9	
2.35	1.50	0.75	0.10	3.0	Formate
2.95	1.50	0.75	0.10	2.8	Formate
3.45	1.50	0.75	0.10	3.5	Formate
3.65	1.50	0.75	0.10	3.2[a]	Acetate formate
3.85	1.50	0.75	0.10	3.7	Acetate formate
4.55	1.50	0.75	0.10	4.5	Acetate formate
5.10	1.50	0.75	0.10	7.8	Acetate formate
5.43	1.50	0.75	0.10	8.0	Acetate formate
5.50	1.50	0.75	0.10	13.7	Acetate formate
5.85	1.50	0.80	0.10	18.1	Acetate formate
6.05	1.50	0.80	0.10	19.3	

[a] Average of results obtained from the medium containing either acetate or formate. The rate constants obtained using either ion as the buffer medium were within 5% of each other. Hence, the rate is insensitive to whether acetate or formate is buffer.

reasonable agreement between the calculated rate constants and the experimental values. This implies that the model proposed is reasonably adequate to account for the complex hydrogen ion dependence in the Ti^{III}–edta system.

Generally, however, the lack of a systematic trend in the differences between the calculated and observed rate constants might result from:

(i) the uncertainty in the nature of the Ti–edta species present in solution, especially the less identifiable polymerized species whose kinetic significance has not been qualified in this work;
(ii) the limitation in the computer program employed.

The Marcus equation for the cross reaction[15] is:

$$\log k_{12} = \tfrac{1}{2}\log k_{11} + \tfrac{1}{2}\log k_{22} + \tfrac{1}{2}\log K_{12} + \tfrac{1}{2}\log f \quad (12)$$

$$\log f = \frac{(\log K_{12})^2}{4\log k_{11}k_{22}Z^{-2}}, \quad (13)$$

where k_{11} and k_{22} are the homonuclear electron exchange rate constants for the reducing and oxidizing complexes, respectively. k_{12} and K_{12} are, respectively, the rate and equilibrium constants for the cross reaction and $Z = 10^{11}$ is the collision frequency for the uncharged reactant molecules. In making this correlation we assumed k_{22} for $I_2 + I_2^-$ to be the same (8.5×10^4 M^{-1} s^{-1}, the value reported by Woodruff and Margerum[16]) as k_{22} for $I_3^- + I_3^{2-}(I_2^- + I^-)$. A similar assumption also holds for $Br_2 + Br_2^-$ and $Br_3 + Br_3^{2-}(Br_2^- + Br^-)$, $k_{22} = 29$ M^{-1} s^{-1}. K_{12} was calculated from the redox potentials for $X_2 + e \rightarrow X_2^-$ (X = Br, 0.5 V; X = I, 0.11 V), for $X_3^- + e \rightarrow X_2^- + X^-$ (X = Br, 0.44 V; X = I, 0.06 V) and for Ti–edta + e → Ti–edta$^-$, $E^0 = 0.03$ V, the value obtained from the polarographic studies of Pecsok and Maverick.[17] The exchange rate constant for Ti–edta + Ti–edta$^-$, k_{11}, is unknown. However, we made the initial estimates from the data of the Ti^{III}–edta + I_2 reaction on the assumption that "f" in eq. (12) is equal to one.

The initial value of k_{11} so obtained was 38 M^{-1} s^{-1}. This was then plugged into eq. (13) to calculate "f" for each reaction. From eq. (12) a plot of $\log k_{12} + \frac{1}{2}\log k_{22} - \frac{1}{2}\log f$ vs $\log K_{12}$ should be linear with a slope of 0.5 and an intercept of $\frac{1}{2}\log k_{11}$. With this improved value of $\log k_{11}$, the process was repeated until the initial value of k_{11} and that estimated from the intercept agreed within 5%. The final result is a good linear plot (correlation coefficient 99.52% shown in Fig. 1). From the slope of 0.45 and the intercept, the rate constant $k_{11} = 32.9$ M^{-1} s^{-1} was obtained. A slope of nearly half (0.48) has also been reported for such a correlation in the reactions of $Ti(OH)^{2+}$ with some ruthenium(III) ammine complexes.[18,19]

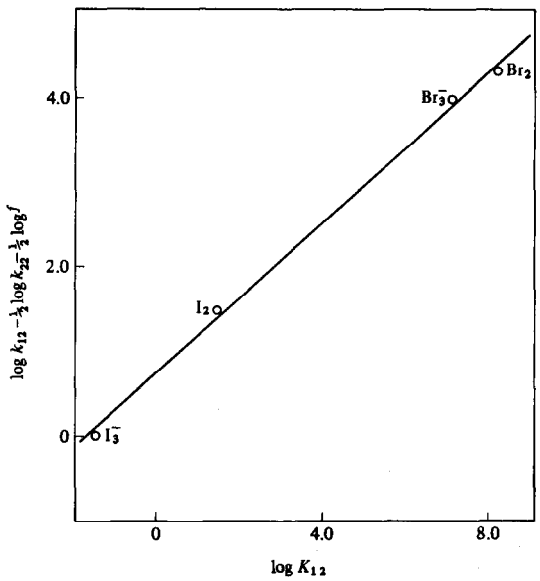

Fig. 1. Marcus plot for the Ti^{3+}(aq)–X_2, X_3^- (X = Br, I) reactions.

The kinetically derived value of k_{11} for $Ti(OH)^{2+}$ is 0.11 M^{-1} s^{-1} and the redox potential for the couple $Ti(OH)^{3+} + e \rightarrow Ti(OH)^{2+}$ is reported as 0.08 V. The corresponding values for the Ti–edta + Ti–edta$^-$ couple are 32 M^{-1} s^{-1} and 0.03 V, respectively.

As to the mechanism by which the Ti^{III}–edta + Br_2 reaction occurs, the only convincing evidence for the outer-sphere mechanism is in the magnitude of the rate constant for the oxidation of Ti^{III}–edta at pH = 3. The rate constant obtained for this reaction is much higher than the substitution-controlled electron-transfer rates in the inner-sphere reaction[10] of Ti–edta$^-$ with $[(NH_3)_5Ru(OAc)]^{2+}$, $[Co(NH_3)_5N_3]^{2+}$ and $[Co(NH_3)_5SCN]^{2+}$.

On comparative analysis with available results on the choice of the mechanism by aquotitanium(III) ion, three less convincing pieces of evidence seem to support the outer-sphere mechanism for the reaction reported in this work. These are:

(i) the fact that inner-sphere reactions of Ti^{3+}(aq) with metal complexes are accompanied by more complex acid dependence behaviour than can be explained by merely invoking the hydrolysis of aquotitanium(III) ion;
(ii) that inner-sphere reactions of Ti^{3+}(aq) have only been established for complexes where the "lead-in" ligands are typically Pearson's hard bases, whereas complexes with relatively soft

bases like iodide react by the outer-sphere mechanism;[20]

(iii) the excellent correlation obtained when the rate constant for the oxidation of Ti^{III}–edta by Br_2, Br_3^- and I_2 and I_3^- at pH = 2.5 are subjected to the Marcus equation for cross-reactions,[15] which suggests that the reactions occur by the same mechanism and this we believe to be the outer-sphere mechanism.

Kristine *et al.*[5] have reported that the measured rate constant for the generation of $[Ti(O_2)(edta)]^-$ by the addition of O_2 to $[Ti(edta)(H_2O)]^-$ is 200 times faster than the substitution of peroxo- for oxo- on $[TiO(edta)]^{2-}$ at pH = 5.0. They therefore suggested that an outer-sphere reduction of O_2 to H_2O_2, followed by substitution on a generated titanium(IV) species is not a possible mechanism for $O/[Ti(O_2)(edta)]^{2-}$ forming $[Ti(O_2)(edta)]^{2-}$. An inner-sphere mechanism was therefore suggested. However, steric considerations arising from the larger size of Br_2 compared to O_2, the relative affinity of the titanium(III) centre for Br_2 and O_2 and the relative stability of the eventual intermediate are possible factors that may have made the Ti^{III}–edta + Br_2 reaction prefer an outer-sphere pathway.

Acknowledgement—We thank Dr G. A. Ayoko for useful comments.

REFERENCES

1. A. Adegite and S. Edeogu, *J. Chem. Soc., Dalton Trans.* 1975, 1203.
2. A. Adegite and J. F. Ojo, *Inorg. Chem.* 1977, **16**, 477.
3. A. Adegite and J. F. Iyun, *Inorg. Chem.* 1979, **18**, 3602.
4. A. Adegite and P. Agaba, unpublished data.
5. F. J. Kristine, R. E. Shepherd and S. Siddiqui, *Inorg. Chem.* 1981, **20**, 2571.
6. M. Orhanovic and J. E. Earley, *Inorg. Chem.* 1975, **14**, 1478.
7. A. Adegite, J. E. Earley and J. F. Ojo, *Inorg. Chem.* 1975, **14**, 1478.
8. A. Bakac, R. Marcec and M. Orhanovic, *Inorg. Chem.* 1977, **16**, 3133.
9. A. H. Martin and E. S. Gould, *Inorg. Chem.* 1975, **14**, 873.
10. A. Adegite, J. E. Earley and J. F. Ojo, *Inorg. Chem.* 1979, **18**, 1535.
11. Directly measured values of K_a as reported in the literature are as follows: 2.8×10^{-3} M, $I = 3.0$ M (KBr), M. R. Paris and C. L. Gregoire, *Analyt. Chim. Acta.* 1968, **42**, 439; 1.6×10^{-3} M, H. Krentzien and F. Brito, *Chem. Abstr.* 1970, **73**, 78656; 6.9×10^{-3} M, $I = 0.25 - 1.5$ M (KBr), R. L. Pecsok and A. N. Fletcher, *Inorg. Chem.* 1962, **1**, 155.
12. H. Diebler, *J. Phys. Chem.* 1969, **68**, 64.
13. J. Podlahova and J. Podlaha, *J. Inorg. Nucl. Chem.* 1966, **28**, 2267.
14. G. A. K. Thompson and A. G. Sykes, *Inorg. Chem.* 1979, **18**, 2025.
15. R. A. Marcus, *J. Phys. Chem.* 1965, **43**, 679.
16. W. H. Woodruff and D. W. Margerum, *Inorg. Chem.* 1973, **12**, 962.
17. R. L. Pecsok and E. F. Maverick, *J. Am. Chem. Soc.* 1954, **76**, 358.
18. P. Challipoyil, K. M. Davies and J. E. Earley, *Inorg. Chem.* 1977, **16**, 12.
19. K. M. Davies and J. E. Earley, *Inorg. Chem.* 1978, **17**, 3350.
20. G. A. K. Thompson and A. G. Sykes, *Inorg. Chem.* 1976, **15**, 638.

Polyhedron Vol. 8, No. 24, pp. 2889–2891, 1989
Printed in Great Britain

0277–5387/89 $3.00+.00
© 1989 Pergamon Press plc

COBALT(III) COMPLEXES OF ETHYLENEDIAMINE-N,N′-DI-S-ISOBUTYLACETIC ACID

MOO-JIN JUN,* JIN WOO CHEON, SUNG SIL LEE and SUNG RACK CHOI

Department of Chemistry, Yonsei University, Seoul, Korea

(*Received* 8 *November* 1988; *accepted* 31 *May* 1989)

Abstract—A new optically active ONNO-type tetradentate ligand, ethylenediamine-N,N′-di-S-isobutylacetate (SS-eniba), has been synthesized. During the preparation of diaqua cobalt(III) complexes of SS-eniba, $[Co(SS\text{-}eniba)(H_2O)_2]^+$, the title ligand has coordinated stereospecifically to the cobalt(III) ion to give three isomers, Δ-s-*cis*, Δ-uns-*cis* and Λ-uns-*cis*, which have been isolated and characterized via electronic absorption, circular dichroism (CD), and ^1H NMR spectroscopy, along with elemental analysis data. The preparation of Δ-s-*cis*-$[Co(SS\text{-}eniba)Cl_2]^+$ and Δ-s-*cis*-$[Co(SS\text{-}eniba)CO_3]^+$ are also reported.

Although a large number of ONNO-type tetradentate ligands such as ethylenediamine-N,N′-diacetate (edda) are known,[1,2] only a few of them are optically active ligands which coordinate stereospecifically to metal ions. The ethylenediamine-di-S-α-propionate (SS-eddp)[3] has yielded Δ-s-*cis*, Λ-s-*cis* and Δ-uns-*cis* isomers of $[Co(SS\text{-}eddp)en]^+$ out of the four possible isomers (Fig. 1). In the case of ethylenediamine-N,N′-di-S-α-isovalerate (ven),[4] only the Δ-s-*cis* isomer has been produced for the $[Co(ven)H_2ONO_3]$ complex, while both Δ-s-*cis* and Δ-uns-*cis* isomers have been obtained for the $[Co(ven)(H_2O)_2]^+$ and $[Co(ven)en]^+$ complexes. The 2S,2′S-1,1′-(ethane-1,2-diyl)bis(pyrrolidine-2-carboxylate)(pren)[5] compound is shown to yield both Δ-s- and Δ-uns-*cis* isomers for $[Co(pren)(H_2O)_2]^+$. The L-stilbenediamine-N,N′-diacetate (L-sdda) compound has also been prepared but only the Δ-s-*cis*-$[Co(L\text{-}sdda)en]^+$ complex has been isolated.[6]

In the present work a new optically active ONNO-type ligand, ethylenediamine-N,N′-di-S-isobutylacetate (SS-eniba), has been prepared. It is of interest to see how the stereospecificity of this ligand is exhibited upon coordination to the cobalt(III) ion.

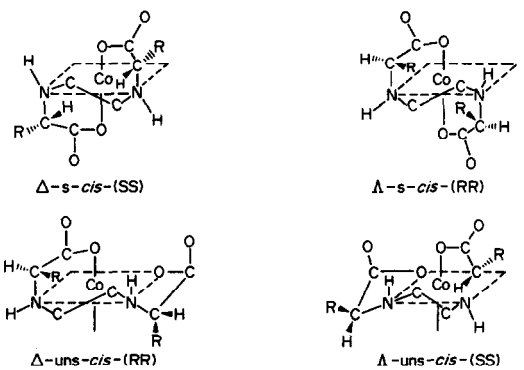

Fig. 1. Possible isomers of $[Co(eddp)X_2]^{n+}$ or $[Co(eniba)X_2]^{n+}$ complexes.

EXPERIMENTAL

Ethylenediamine-N,N′-*di*-S-*isobutylacetic acid* (SS-eniba)

NaOH (8.0 g) in 20 cm^3 of water was added to s-leucine (26.2 g) in 100 cm^3 of water. 1,2-Dibromoethane (17.4 g) and Na_2CO_3 (10.6 g) were added in portions to this solution while maintaining the system at 70°C. The reaction mixture was stirred for 30 h at 70°C. The solution was cooled and acidified to pH 6 with conc. HCl. The precipitated

* Author to whom correspondence should be addressed.

white product was collected on a filter, washed with water and petroleum ether, and dried in vacuum. Yield: 11.0 g. Found: C, 58.5; H, 9.8; N, 9.6. Calc. for $C_{14}H_{28}N_2O_4$: C, 58.3; H, 9.8; N, 9.7%. $[\alpha]_D = -14.2$ ($c = 4.1 \times 10^{-3}$ g cm^{-3} of water).

*Isomers of diaqua(ethylenediamine-N,N′-di-*S*-isobutylacetate)cobalt*(III) *perchlorate*, [Co(SS-eniba)$(H_2O)_2$]ClO_4

To a suspension of SS-eniba (8.64 g) in 100 cm^3 of water was added a solution of $CoCl_2 \cdot 6H_2O$ (0.13 g) in 50 cm^3 of water and 2.0 g of activated carbon. The reaction mixture was heated to 60°C for 10 h. Upon cooling, the activated carbon and unreacted PbO_2 were filtered off. Addition of a saturated Na_2SO_4 solution to the filtrate yielded the white $PbSO_4$ precipitate, which was filtered off. The solution was evaporated to 15 cm^3. This violet solution was admitted to a column packed with Dowex 50X4-400 (200–400 mesh) cation exchange resin in the H^+ cycle. The violet solution was sorbed at the top of the column and washed with water. Three fractions were obtained by elution with 0.3 M $NaClO_4$. Each fraction was concentrated, freed from excess $NaClO_4$ by extraction into absolute ethanol, and evaporated to dryness on a water bath. Yield: Δ-s-*cis*: 1.1 g, Δ-uns-*cis*: 0.4 g, Λ-uns-*cis*: 0.3 g. Found: Δ-s-*cis*: C, 33.4; H, 6.5; N, 5.6. Δ-uns-*cis*: C, 33.9; H, 6.5; N, 5.6. Calc. for [Co($C_{14}H_{26}N_2O_4$)$(H_2O)_2$]$ClO_4 \cdot H_2O$: C, 33.7; H, 6.4; N, 5.6%.

Δ-s-*cis*-H[Co(SS-eniba)Cl_2]

This complex was obtained by passing a solution of the diaqua complex through a cation exchange column using 0.4 M NaCl as eluent. Three fractions were obtained. The first fraction was concentrated, freed from excess NaCl by extraction into ethanol and evaporated to dryness on a water bath. Found: C, 40.1; H, 6.6; N, 6.7. Calc. for H[Co($C_{14}H_{26}N_2O_4$)Cl_2]: C, 40.3; H, 6.5; N, 6.7%.

Δ-s-*cis*-H[Co(SS-eniba)CO_3]

A suspension containing Δ-s-*cis*-H [Co(SS-eniba)Cl_2] (0.34 g) in 10 cm^3 of water was heated at 60°C until the colour of the solution changed from green to violet by aquation. Na_2CO_3 (0.34 g) was added to this solution, which was stirred for 5 h at 60°C and then concentrated to 5 cm^3 on a rotary evaporator. The addition of 20 cm^3 of acetone yielded a white precipitate, which was filtered off. An excess of acetone was added to the filtrate and the solution was stored in a refrigerator. The purple–violet crystals which formed were collected on a filter.

RESULTS AND DISCUSSION

The ligand has been prepared from optically active leucine of known configuration and contains two asymmetric carbon atoms of s-absolute configuration. The configuration of the ligands is shown in Fig. 2 along with its ^{1}H NMR spectrum. The methyl protons are shown at 0.9 ppm as a doublet and the α-carbon protons at 3.1 ppm as a triplet. The two methylene protons between two nitrogen atoms resonate at 2.6 ppm as a singlet.

Three isomers, Δ-s-*cis*, Δ-uns-*cis* and Λ-uns-*cis*, have eventually been isolated from the preparation of the diaqua cobalt(III) complex of SS-eniba, [Co(SS-eniba)$(H_2O)_2]^+$, which was prepared by oxidation of cobalt(II) in the presence of the desired ligand. The Δ-s-*cis*-[Co(SS-eniba)$Cl_2]^-$ and Δ-s-*cis*-[Co(SS-eniba)$CO_3]^-$ complexes have been obtained from the substitution reactions of Δ-s-*cis*-[Co(SS-eniba)$(H_2O)_2]^+$ and Δ-s-*cis*-[Co(SS-eniba)$Cl_2]^-$, respectively.

The electronic absorption spectrum of the s-*cis* isomer (Fig. 3) shows a symmetrical first band with λ_{max} at *ca* 550 nm, whereas more broad bands are observed in the absorption spectra of uns-*cis* isomers (λ_{max}: 515 nm for Δ-uns-*cis* and 520 nm for Λ-uns-*cis*). These *cis* isomers have also been differenciated from their ^{1}H NMR spectra. The ^{1}H NMR spectrum of the s-*cis* isomer has shown a sharp methyl doublet at 1.0 ppm, while the uns-*cis* isomers have shown two methyl doublets at about 1.0 ppm due to the overlapping of the non-equivalent methyl peaks.

The CD spectrum of the s-*cis* isomer (Fig. 3)

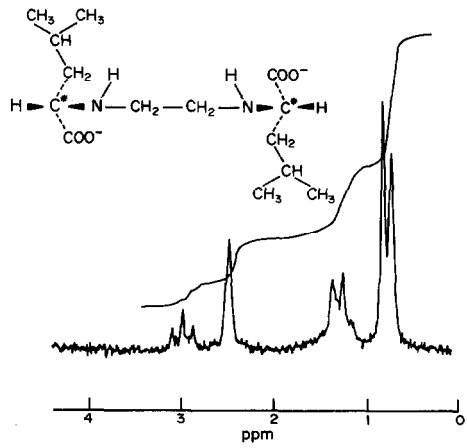

Fig. 2. Configuration and ^{1}H NMR spectrum of ethylenediamine-N,N′-di-S-α-isohexanoate in D_2O.

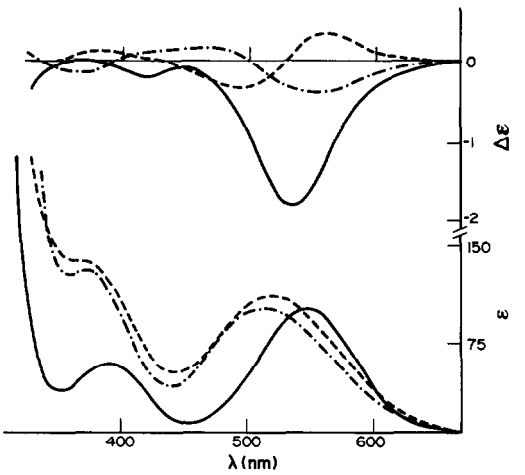

Fig. 3. Circular dichroism and electronic absorption spectra of Δ-s-*cis*-[Co(SS-eniba)$(H_2O)_2]^+$ (———), Λ-uns-*cis*-[Co(SS-eniba)$(H_2O)_2]^+$ (– – – –) and Δ-uns-*cis*-[Co(SS-eniba)$(H_2O)_2]^+$ (—·—·—).

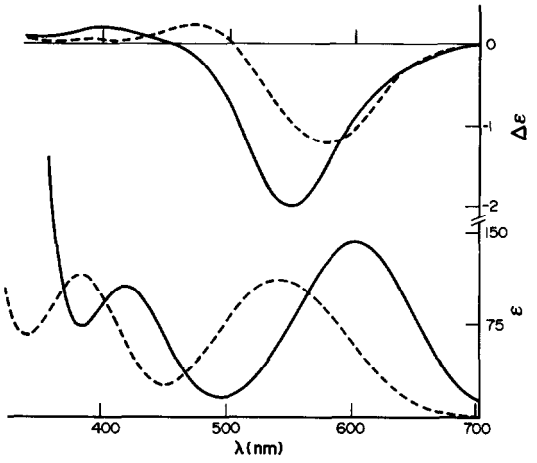

Fig. 4. Circular dichroism and electronic absorption spectra of Δ-s-*cis*-H[Co(SS-eniba)Cl_2] (———) and Δ-s-*cis*-H[Co(SS-eniba)CO_3] (– – – –).

shows a dominant negative band of the $Eg(D_{4h})$ component at 540 nm, which indicates a Δ absolute configuration.[1,3,7] The absolute configuration of the uns-*cis* isomers can also be assigned on the basis of their CD spectra. In the case of the Δ-uns-*cis* isomer a large negative peak at 550 nm and a smaller positive peak at 470 nm are observed, while a large positive peak at 550 nm and a small negative peak at 480 nm are shown for the Λ-uns-*cis* isomer.

The absorption maxima of the electronic absorption spectra of the Δ-s-*cis*-[Co(SS-eniba)$Cl_2]^-$ and Δ-s-*cis*-[Co(SS-eniba)$CO_3]^-$ shown in Fig. 4 are consistent with the spectrochemical series. Dominant negative CD bands are observed in these complexes since they are derived from Δ-s-*cis*-[Co(SS-eniba)$(H_2O)_2]^+$.

It is of interest to note that uns-*cis* isomers (Δ and Λ) have been obtained in addition to the Δ-s-*cis* isomer during the preparation of the [Co(SS-eniba)$(H_2O)_2]^+$ complex, while only the Δ-s-*cis* isomer has been observed in the diaqua cobalt(III) complex of the SS-ven ligand,[4] [Co(SS-ven)$(H_2O)_2]^+$. The yield of the Δ-s-*cis* isomer is twice as large as that of the Δ-uns-*cis* or Λ-uns-*cis* isomers. Such an observation may be attributed to the pronounced ring strain and intraligand steric hindrance of the uns-*cis* configuration. In addition, the non-existence of the Λ-s-*cis* isomer can be envisaged from the Dreiding molecular model, which shows non-bonding interactions not only between the isobutyl group and the en backbone, but also between the isobutyl groups.

Acknowledgement—The financial support for this work (to M.J.J.) from the Korea Science and Engineering Foundation for 1987 is gratefully acknowledged.

REFERENCES

1. D. J. Radanovic, *Coord. Chem. Rev.* 1984, **54**, 159.
2. G. R. Brubaker, D. P. Schaefer, H. H. Worrell and J. I. Legg, *Coord. Chem. Rev.* 1971, **1**, 161.
3. L. N. Schoenberg, D. W. Cooke and C. F. Liu, *Inorg. Chem.* 1968, **1**, 2586; M. Sheridan, M. J. Jun and C. F. Liu, *Inorg. Chem.* 1984, **23**, 1485.
4. M. Strasak and J. Majer, *Inorg. Chim. Acta* 1983, **70**, 231.
5. M. Strasak and F. Bachraty, *J. Coord. Chem.* 1984, **13**, 105.
6. G. G. Hawn, C. Maricondi and B. E. Douglas, *Inorg. Chem.* 1979, **18**, 2542.
7. J. I. Legg, D. W. Cooke and B. E. Douglas, *Inorg. Chem.* 1967, **6**, 700.

Polyhedron Vol. 8, No. 24, pp. 2893–2895, 1989
Printed in Great Britain

0277–5387/89 $3.00+.00
© 1989 Pergamon Press plc

THE PREPARATION OF BIS(ISOPROPOXY)THIOLATO COMPLEXES OF TITANIUM(IV) AND THEIR LEWIS BASE ADDUCTS

J. JONES* and J. A. DOUEK

Department of Physical Science, Polytechnic of the South Bank, London, U.K.

(*Received* 24 *April* 1989; *accepted* 5 *June* 1989)

Abstract—Reactions of titanium tetraisopropoxide with various thiols are reported. In the absence of other donating atoms, appreciable product formation is observed only with 1,2-dithiols. Monothiols and 1,3-dithiols react in the presence of nitrogen donors and 2-aminobenzene thiol reacts spontaneously. Complexes with 1,2-dithiols and bidentate nitrogen donors adopt the *cis* configuration in solution. Compounds were characterized by NMR, IR, molecular weights (in solution) and elemental analysis.

Numerous dithiolato complexes of titanium have been prepared, but in the absence of the cyclopentadienyl group they were generally found to be rather insoluble solids which did not lend themselves to study in solution.[1,2] A few soluble alkoxy dithiolates have been isolated and the purpose of this work was to extend the range of this type of compound, to investigate their reactivity towards Lewis bases and to study the structure in solution of the parent dithiolates and their adducts.

EXPERIMENTAL

Reactions and manipulations were performed in a dry nitrogen atmosphere using standard techniques and dried purified reagents. Compounds **1**, **2** and **21** were prepared by mixing stoichiometric quantities of $(i\text{-PrO})_4\text{Ti}$ and dithiol in dry benzene followed by azeotropic distillation of the isopropanol formed. Volatiles were removed at reduced pressure, the oily solids triturated with light petroleum, filtered and dried *in vacuo*. An attempt to prepare **3** by this method gave evidence of reaction as judged by the appearance of an orange coloration upon mixing of the reagents, but no product was isolated even after prolonged fractionation. Neither p1,4dt nor tpt showed evidence of reaction.

Compound **3** was eventually prepared from its pyridine adduct by stirring a suspension of **13** in petrol, elimination of the volatiles at reduced pressure and addition of more petrol followed by filtration. Compound **4** was prepared by mixing alkoxide and tdtH_2 in benzene at room temperature, elimination of the volatiles at reduced pressure, followed by dissolution of the deep purple solid in petrol and its subsequent evaporation at reduced pressure. The latter process, repeated twice, was sufficient to remove traces of benzene from the product. With the exception of pyridine complexes, **7**, **10** and **13**, compounds **5–18** were prepared by mixing stoichiometric quantities of alkoxide, thiol and nitrogen ligand in petrol (bipy and py) or benzene (phen). Complexes precipitated immediately and were filtered and dried. Compounds **7**, **10** and **13** were prepared using pyridine itself as solvent. Crystallization was induced by cooling at −15°C overnight, the products filtered on a frit surrounded by a cardice jacket, washed with small portions of cooled petrol and dried *in vacuo* at ambient temperature. Compound **19** was prepared by mixing stoichiometric quantities of alkoxide (7 mmol) and abt in benzene (total volume, 30 cm^3). An equal volume of petrol was added and the mixture cooled at 5°C overnight. The mass of yellow crystals was filtered, the product washed with cold petrol and dried. Compounds **20** and **21** were prepared by reaction of tetrabenzyltitanium(IV) with dithiol at ambient temperature (attempts using alkoxide failed to yield pure products). The brown solids

* Author to whom correspondence should be addressed. Present address: Institut de Chimie, Université de Annaba, Algeria.

Table 1.

Compound[a]		Melting point[b]	Yield (%)	Molecular weight (calc.)	IR[c] (cm^{-1})
(*i*-PrO)$_2$Ti(edt)	(1)	119–21	82	1031(258)	310m, 322m, 340m, 372s
(*i*-PrO)$_2$Ti(pdt)	(2)	132–35	91	1036(272)	312m, 322m, 370s
(*i*-PrO)$_2$Ti(p1,3dt)	(3)	140–42	52[d]	1028(272)	315m, 326m, 344m, 378s
(*i*-PrO)$_2$Ti(tdt)	(4)	152–54	95	614(320)	370s
(*i*-PrO)$_2$Ti(edt)·phen	(5)	127–28	92	425(438)	352s, 378s; 591m
(*i*-PrO)$_2$Ti(edt)·bipy	(6)	136–38	89	411(414)	315m, 350s, 368s, 378s; 595m
(*i*-PrO)$_2$Ti(edt)·2py	(7)	46–48	63	Dissociates	343s, 380s, 398s
(*i*-PrO)$_2$Ti(pdt)·phen	(8)	129–30	87	433(452)	317m, 350s, 370m, 384s, 390m; 595s
(*i*-PrO)$_2$Ti(pdt)·bipy	(9)	143–45	74	424(428)	355s, 368s, 375s, 388m; 590m
(*i*-PrO)$_2$Ti(pdt)·2py	(10)	34–36	58	Dissociates	355w, 362m, 380s, 398s
(*i*-PrO)$_2$Ti(p1,3dt)·phen	(11)	149–50	63	434(452)	352s, 365s, 378s,; 598m
(*i*-PrO)$_2$Ti(p1,3dt)·bipy	(12)	173–74	66	426(428)	317w, 346s, 365s, 375s; 596m
(*i*-PrO)$_2$Ti(p1,3dt)·2py	(13)	32–34	52	Dissociates	350m, 362s, 378s, 396s
(*i*-PrO)$_2$Ti(tdt)·phen	(14)	188–89	64	494(500)	355m, 370s, 377m; 598m
(*i*-PrO)$_2$Ti(tdt)·bipy	(15)	163–65	91	458(476)	352s, 370s, 375m; 598m
(*i*-PrO)$_2$Ti(tdt)·2py	(16)	116–18	93	460(478)	378m
(*i*-PrO)$_2$Ti(tpt)$_2$·phen	(17)	79–81	78	578(592)	340m, 375m, 390s; 595m
(*i*-PrO)$_2$Ti(tpt)$_2$·bipy	(18)	89–91	66	555(568)	335m, 372m, 392m; 592m
(*i*-PrO)$_2$Ti(abt)$_2$	(19)	62–64	86	405(414)	340m, 375m, 380s; 590m
(*i*-PrO)$_2$Ti(edt)$_2$	(20)	167–69	97		322m, 344m, 375s, 398m
(*i*-PrO)$_2$Ti(pdt)$_2$	(21)	148–50	94		335w, 350m, 380s, 396m
(*i*-PrO)$_2$Ti(tdt)$_2$	(22)	230–32	92		369m, 386s, 398m

[a] Abbreviations: edtH_2 (ethane-1,2-dithiol), pdtH_2 (propane-1,2-dithiol), p1,3dtH_2 (propane-1,3-dithiol), tdtH_2 (toluene-3,4-dithiol), tptH (toluene-4-thiol), abtH (2-aminobenzene thiol), phen (1,10-phenanthroline), bipy (2,2′-bipyridyl), py (pyridine).

[b] Decomposition.

[c] Regions: 300–400 cm^{-1}; 590–600 cm^{-1}.

[d] Quantitative from **13**.

precipitated immediately from the petroleum solution and were filtered and dried.

All compounds had satisfactory elemental analyses which are listed in Table 1.

DISCUSSION

Syntheses

The influence of chelation on the reactivity of thiols with titanium tetraisopropoxide is evident and follows expected patterns. Thus, five-membered rings form more or less easily (compounds **1**, **2** and **4**), with tdtH_2 apparently of greater reactivity. Six-membered rings are not particularly favoured though colour changes indicate slight reaction (p1,3dtH_2), whilst seven-membered rings appear not to form at all (p1,4dtH_2). Neither aliphatic monothiols[3,4] nor simple aromatic thiols react (tpt). The presence of a second coordinating atom, introducing the possibility of chelation, renders the thiol reactive and the product is isolated under extremely mild conditions,**19**. That this is entirely due to chelation of the thiol ligand is, however, not certain as the preparation of **13**, **17** and **18** demonstrates.

^{1}H *NMR spectra*

All compounds examined showed signals at expected δ-values and integrations were in accord with proposed structures. In line with molecular weight determinations in solution showing the presence of oligomers, compounds **1**, **2** and **3** gave broad, unresolved signals with little improvement in resolution at higher temperatures. The spectrum of **4** was sharp with a single isopropoxy methyl doublet at δ 1.21. The spectra of **5** and **6** are of interest, and that of **5** was examined at various temperatures. The presence of two, well-resolved, isopropyl methyl doublets of equal intensity at δ 1.08 (A) and 1.38 (B) (J = 6 Hz for both A and B) and two thiol methylene signals at δ 3.66 and 3.85 indicates a *cis*

structure. This inference is strengthened by the low temperature spectra which show splitting of the two methyl doublets (at different rates) and the isopropyl methine septet (δ 5.23, $J = 6$ Hz in the room temperature spectrum). As the temperature is lowered, A splits into A1 and A2 and B splits into B1 and B2, so that in the spectrum at -50°C three sets of methyl doublets are observed at δ 1.6 (6H, A1 and B1 superimposed), δ 1.2 (3H, A2), δ 0.4 (3H, B2), and two, broad, unresolved methine signals appear at δ 5.6 and 4.8. The spectrum at -50°C thus corresponds to what one might predict for a *cis* isomer in the absence of configurational changes. Given the relatively large splitting observed for signal B, it is probable that this signal is due to the isopropyl group coordinated at the position perpendicular to the plane of the nitrogen ligand where it would experience the shielding effect of the ligand's ring currents. With increasing temperature, signals A and B gradually coalesce as do the thiol methylene signals, until at 100°C a single doublet (δ 1.23) and a sharp singlet (δ 3.72) are observed. These changes are consistent with dissociation of one end of the nitrogen ligand, complete dissociation is unlikely, at least up to the boiling point of chloroform, given the ebulliometry results. The spectra of similar complexes of **2** and **4** show multiplet signals in the methyl region and are not so readily analysed. However, the very complexity is, at least, indicative of *cis* geometry.

Pyridine complexes gave sharp, well-resolved signals and showed a single methyl doublet in all cases. That this should be so for **7**, **10** and **13** is to be expected given the ease of dissociation of the pyridine in these complexes. For **16**, in which pyridine is more strongly coordinated (m.p. ebulliometry), the spectrum is a reflection of the configurational instability of the complex rather than an indication of the adoption of the *trans* form with respect to the isopropoxy groups.

IR spectra

In all the compounds containing a bidentate nitrogen ligand, as well as the Ti—O stretching vibration observed in the region 600–620 cm^{-1}, a second band of variable intensity is present in the region 590–600 cm^{-1}. This band, absent in the pyridine complexes, may represent the Ti—O assymetric stretch expected for *cis* geometry.

In the region 330–400 cm^{-1}, to which Ti—S vibrations are generally assigned,[2,4] several bands are present in most cases. Although it has been proposed[5] that metal–nitrogen stretching bands with ligands such as bipy occur between 300 and 390 cm^{-1}, within the region 370–390 cm^{-1} in the majority of compounds examined in this work, including compounds **20**, **21** and **22** which do not contain a nitrogen ligand, there is at least one band which might be assigned to a Ti—S vibrational mode.

REFERENCES

1. D. C. Bradley and P. A. Hammersley, *J. Chem. Soc. A* 1967, 1894.
2. J. T. Spicket, PhD thesis, London (1970).
3. S. Chatterjee, D. Sukhani, V. D. Gupta and R. C. Mehrotra, *Ind. J. Chem.* 1970, **8**, 362.
4. J. L. Martin and J. Takats, *Inorg. Chem.* 1975, **14**, 73.
5. K. Nakamoto, *Angew. Chem. Int. Edn* 1972, **11**, 66.

Polyhedron Vol. 8, No. 24, pp. 2897–2900, 1989
Printed in Great Britain

0277–5387/89 $3.00+.00
© 1989 Pergamon Press plc

REDUCTIVE NITROSYLATION OF TETRAOXOMETALLATES—XVII. MOLYBDATE–HYDROXYLAMINE–CYANIDE REACTION, AND SYNTHESIS AND CHARACTERIZATION OF $K_2[Mo(NO)(CN)_5]$ AND $(NMe_4)_2[Mo(NO)(CN)_4]$

RAMGOPAL BHATTACHARYYA,* NABANITA GHOSH and ALOK MOHAN SAHA

Department of Chemistry, Jadavpur University, Calcutta 700 032, India

(*Received* 10 *February* 1989; *accepted* 20 *July* 1989)

Abstract—A reaction condition is established which determines the nature of the products in the molybdate–hydroxylamine–cyanide reaction. With hydroxylamine always used in excess, it is the hydroxyl ion concentration of the reaction mixture which plays a vital role in determining whether $K_4[Mo(NO)(CN)_5]$ or $K_2[Mo(NO)(CN)_5]$ is obtained exclusively. The latter product is hereby reported for the first time. Its powder diffractogram being typical of a cubic system, a gross structural characterization has been made possible. The former under aqueous, aerobic conditions yields a new product, $(NMe_4)_2[Mo(NO)(CN)_4]$.

The reaction between MoO_4^{2-} and hydroxylamine in the presence of CN^- ions in alkaline medium has been studied many times.[1–11]

Hoffman and Von der Heide's[1] red–violet product, formulated as $MoO_2 \cdot 4KCN \cdot NH_2OH \cdot H_2O$ was recognized about 50 years later by Hieber *et al.*[2] as a molybdenum nitrosyl compound, viz. $K_4[Mo(NO)(CN)_5] \cdot 2H_2O$. After a further 20 years the complex was structurally characterized by three-dimensional X-ray diffraction studies by Svedung and Vannerberg.[12]

The earlier workers[1–3,5,13] used a rather meagre amount of $NH_2OH \cdot HCl$ which was much less than that required stoichiometrically,[14] to carry out the nitrosylation reaction. In this paper we report an investigation on the reaction of MoO_4^{2-} with an excess of $NH_2OH \cdot HCl$, in an alkaline medium in the presence of excess of CN^-. The present work not only results in a generous yield of the $K_4[Mo(NO)(CN)_5]$ (**1**) but paves the way for synthesizing $K_2[Mo(NO)(CN)_5]$ (**2**), representing a molybdenum cyanonitrosyl compound containing the $Mo(NO)^{3+}$ moiety, considered to be a missing link in molybdenum cyanonitrosyls possessing the moiety $Mo(NO)^{n+}$ ($n = 1$–3). In addition, a hitherto unknown species, $[Mo(NO)(CN)_4]^{2-}$ (**3**), was obtained in the present investigation. This work also reports a gross structural characterization of **2** using the powder diffraction data only.

EXPERIMENTAL

Materials and methods

All reagents were of reagent grade and used without further purification. For physicochemical measurements, the solvents were further purified using literature methods.[15] IR spectra were recorded as KBr discs on a Perkin–Elmer 597 spectrophotometer, calibrated with polystyrene. Solution conductances were measured with a Systronics (India) Model 304 conductivity bridge and the electronic spectra (800–200 nm) were taken using a Pye Unicam SP8-150 UV–vis spectrophotometer. Magnetic susceptibilities were measured with a Gouy balance using $Hg[Co(NCS)_4]$ as calibrant. The elements carbon, hydrogen and nitrogen were analysed on a Perkin–Elmer 240C elemental analyser and molybdenum by a gravimetric method.[16]

Preparation of the complexes

Potassium pentacyanonitrosyl molybdate(0), $K_4[Mo(NO)(CN)_5]$ (**1**). MoO_3 (2.5 g, 0.017 mol)

* Author to whom correspondence should be addressed.

was dissolved in 10 cm^3 of cold saturated (5 g) KOH solution with stirring. Then KCN (10 g, 0.153 mol) dissolved in 15 cm^3 of water (filtered if necessary) was added. The mixture was stirred at room temperature until the solution became clear (a little more water needs to be added dropwise if the solution becomes turbid). Then $NH_2OH \cdot HCl$ (9.0 g, 0.130 mol) was added dropwise, when the colour of the solution changed from orange to blackish-red. On stirring for 5 min the red colour faded to yellow. Then, more KOH (2 g) was added and the solution was heated with stirring. Occasionally, further amounts (1–2 g) of KOH were added portionwise (a total of *ca* 8–10 g of KOH was added). After heating and stirring for a further 30 min a red–violet solution resulted and a violet crystalline compound started precipitating out. The solution was then allowed to cool to room temperature and the crystalline violet product was filtered off, washed quickly with EtOH (90%) and finally with ether, and then dried over fused $CaCl_2$ under vacuum. The compound was crystallized quickly from a H_2O–EtOH mixture. Yield: 6.9 g (90%). Found: C, 13.8; N, 19.3; K, 37.5; Mo, 22.6. $C_5N_6OK_4Mo$ requires: C, 13.9; N, 19.5; K, 37.9; Mo, 22.3%. IR: ν(CN) 2120 (sh), 2060 (s); ν(NO) 1455 (s), ν(Mo—N)(NO) 610 (w) cm^{-1}. λ_{max} 546 (208) nm. $\Lambda_M = 398\ \Omega^{-1}\ cm^2\ mol^{-1}$ in H_2O (measured instantaneously). [*d* spacings, *d* in Å = 6.60 (w), 5.27 (s), 4.98 (m), 4.23 (m), 4.04 (m), 3.63 (s), 3.53 (m), 3.16 (s), 3.09 (m), 3.02 (m), 2.87 (m), 2.78 (s), 2.65 (w), 2.25 (m), 2.15 (m), 2.12 (m), 2.05 (w), 2.03 (w).]

Potassium pentacyanonitrosyl molybdate(II), $K_2[Mo(NO)(CN)_5]$ (**2**). MoO_3 (2.5 g) was dissolved in a saturated aqueous (5 cm^3) solution of KOH (2.5 g). KCN (10 g, 0.153 mol) dissolved in 15 cm^3 of H_2O was filtered, and then added to the above solution with stirring. The mixture was stirred further at room temperature until the solution became clear (a few cm^3 of H_2O needs to be added if the solution still remains turbid). Then 9.0 g of $NH_2OH \cdot HCl$ (0.130 mol) was added portionwise when colour of the solution changed from orange to blackish-red. At this stage the solution has a pH value of 9. On stirring for another 5 min the deep-red colour faded to yellow. This solution was then heated at 80°C, with stirring, and a vigorous reaction set in, with a consequent colour change of the solution from orange–yellow to red–orange. The solution was then allowed to cool to room temperature. The orange, crystalline precipitate which separated was filtered off, washed with ethanol and ether, and finally dried over fused $CaCl_2$ *in vacuo*. The compound was crystallized from a H_2O–isopropanol mixture. Yield: 5.2 g (85%). Found: C, 16.6; N, 23.5; K, 23.7; Mo. 27.5%. $C_5N_6OK_2Mo$ requires: C, 17.1; N, 23.8; K, 23.4; Mo. 27.3%. IR: ν(CN) 2140 (sh), 2120 (s); ν(NO) 1640 (s) and ν(Mo—N) 600 (w) cm^{-1}. λ_{max} 632 (70), 392 (170) and 216 (7500) nm. $\Lambda_M = 210\ \Omega^{-1}\ cm^2\ mol^{-1}$ in H_2O.

Tetramethylammonium tetracyanonitrosyl molybdate(I), $(NMe_4)_2[Mo(NO)(CN)_4]$ (**3**). The complex $K_4[Mo(NO)(CN)_5]$ (1 g, 2.4 mmol) was dissolved in H_2O (10 cm^3), and to this solution 0.53 g of $(CH_3)_4NCl$ (4.8 mmol; dissolved in a minimum volume of H_2O) was added. The mixture was stirred at room temperature and within a few minutes a yellowish-green precipitate separated out. This was filtered off and washed with EtOH, ether and finally dried over fused $CaCl_2$ *in vacuo*. The product was further crystallized from a H_2O–EtOH mixture. Yield: 0.55 g (62.5%). Found: C, 37.9; H, 6.6; N, 25.9; Mo, 25.6. $C_{12}H_{24}N_7OMo$ requires: C, 38.1; H, 6.3; N, 25.9; Mo. 25.3%. IR: ν(CN) 2100 (sh), 2080 (s); ν(NO) 1580; ν(Mo—N)(NO) 575 cm^{-1}. λ_{max} 418 (50), 294 (620) nm. $\mu_{eff} = 1.9$ BM. $\Lambda_M = 226\ \Omega^{-1}\ cm^2\ mol^{-1}$ in H_2O. [*d* spacings, *d* in Å = 7.31 (s), 6.33 (s), 4.44 (s), 3.80 (s), 3.62 (w), 3.14 (s), 2.51 (s), 2.56 (m), 2.42 (m), 2.22 (s), 2.12 (m), 2.09 (s), 1.98 (m), 1.82 (w), 1.75 (w), 1.73 (w), 1.67 (m), 1.61 (m), 1.52 (w).]

RESULTS AND DISCUSSION

It is quite apparent from the experimental section that an excess of $NH_2OH \cdot HCl$ is necessary, both, to bring the MoO_4^{2-}—NH_2OH—CN^- reaction to completion, and to understand the reaction pathways. A reaction mixture containing MoO_4^{2-} and an excess of $NH_2OH \cdot HCl$, if cooked in a rather weakly alkaline condition (pH ~ 9) an orange potassium salt of bivalent molybdenum, viz. $K_2[Mo(NO)(CN)_5]$ (a product not obtained by earlier workers using 3–4 mol of NH_2OH per mol of MoO_4^{2-}; the PPh_4 salt of the anion, however, has been obtained otherwise, recently) is the only product obtained in reasonably high yield. On the other hand, if the reaction is conducted between pH 10 and 12, firstly $K_2[Mo(NO)(CN)_5]$ separates out, and from the filtrate $K_4[Mo(NO)(CN)_5]$ is obtained. However, using a large excess of KOH in the reaction medium, $K_4[Mo(NO)(CN)_5]$ becomes the exclusive product. The amount of NH_2OH and KOH thus play a crucial role in determining the selectivity and yield of the products. Hence, it becomes apparent that conversion of MoO_4^{2-} to the $Mo(NO)^+$ moiety using NH_2OH only occurs at very high alkalinity, and the reaction possibly proceeds via an intermediate $Mo(NO)^{3+}$ stage. At low alkalinity, the reaction only goes to the $Mo(NO)^{3+}$ stage.

Interestingly, an attempted cation metathesis of

Table 1. Powder diffraction data and derived parameters of $K_2[Mo(CN)_5NO]$

d (Å)	$(\sin^2\theta)_{obs.}$	$(\sin^2\theta)_{calc.}$	Index with smaller cell	Index with larger cell
3.15	0.0593	0.0598	100	600
2.23	0.1190	0.1196	110	660
1.80	0.1793	0.1794	111	666
1.57	0.2395	0.2392	200	1200
1.41	0.2990	0.2990	210	1260

$K_4[Mo(NO)(CN)_5]$ (an air-unstable species) using NMe_4Cl, under aqueous, aerobic conditions, yields a hitherto unknown yellow–green air-stable product, $(NMe_4)_2[Mo(NO)(CN)_4]$, which obviously contains the $Mo(NO)^{2+}$ [3] [hence $\{Mo(NO)\}^5$]* moiety. As expected, the compound is paramagnetic ($\mu_{eff} = 1.9$ BM) and ESR-sensitive $[(e)^4(b_2)^1]$ with $\langle g\rangle_{av} = 2.00$ in the crystalline state. The cation metathesis does not occur in a dinitrogen atmosphere where also the above, formally molybdenum(I) nitrosyl product, results. It may be recalled that the $Mo(NO)^{2+}$ moiety has previously been introduced by Sarkar and Müller[5] when synthesizing $K_3[Mo(NO)(CN)_5]$ (and also the corresponding PPh_4 salt by cation metathesis) by the passage of dioxygen through an aquous solution of the formally zero-valent red–violet product.

The red–violet compound behaves as a 4 : 1 electrolyte, while compounds **2** and **3** show a 2 : 1 electrolytic behaviour in aqueous solution. The molybdenum(0) product shows ν(NO) at 1455 cm^{-1} (i.e. the same position as obtained by earlier workers), while the monovalent, **3**, and bivalent, **2**, compounds exhibit the above vibrational mode at 1580 and 1640 cm^{-1}, respectively, which is in accordance with molybdenum $d_\pi \rightarrow \pi^*$(NO) back-bonding efficiency.

Considering M—N—O to be linear (there is no exception to this behaviour in the structurally confirmed cases containing $\{M(NO)\}^n$ moieties where $n = 4$–6), all the complexes should possess C_{4v} symmetry and, accordingly, compounds **1**, **2** and **3** will have the MO configurations $(e)^4(b_2)^2$, $(e)^4$ and $(e)^4(b_2)^1$, respectively.[17] Being fully occupied by electrons, the b_2 level in **1** will be the most stabilized, being a LUMO in **2** the said orbital will have a reasonably high energy and being a SOMO, the latter will be at an intermediate energy region. Hence a single electronic spectral band observed (see Experimental) in **1** may originate from the $b_2 \rightarrow b_1$ transition, whilst in **2** three bands result from the $e \rightarrow b_2$, $e \rightarrow e_1$ and $e \rightarrow b_1$ transitions, in the order of increasing energy. Since **3** is a five-coordinate species, two electronic transitions are predicted in the C_{4v} case and it is highly satisfying that two bands are actually observed, which are due to $b_2 \rightarrow a_1$ and $b_2 \rightarrow b_1$ transitions.

X-ray powder diffraction studies

The X-ray powder diffraction data of **1** and **3** are given in the Experimental. The data reported here for **1** resemble that reported by Reiley and Ho.[13] The compound $K_2[Mo(NO)(CN)_5]$ (**2**) has an interesting diffractogram showing only five distinct and well separated peaks in the 2θ range 0–70° (Table 1).

The powder diffraction pattern may be indexed assuming a cubic cell with $a = 3.15$ Å (obtained by a graphical method). But considering the formula weight (334) and the measured density (1.5 g cm^{-3}), it is evident that the unit cell is much larger, with $a = 3.15n$, where n is an integer. Then

$$\frac{Z \times 334}{(3.15n)^3 \times 0.6023} = 1.5,$$

where Z = number of formula units per unit cell whence, $Z/n^3 = 0.083$. By trial, it is found that for $n = 6$, Z is closest to the integer value 18. Thus, the cubic cell has $a = 18.9$ Å, with $Z = 18$.

This leads to an interesting conclusion. The minimum rank of the general equipoint is 12 ($P23$ and $P2,3$) for cubic symmetry. So, at least half of the molybdenum complexes in the unit cell must lie on two-fold axes. The space group is, thus, most probably $P23$. Furthermore, this is a definite pointer to the fact that the CN—Mo—NO sequence lies strictly on a straight line. The four remaining CN groups must lie in a plane normal to this axis, arranged in two pairs of symmetry related groups.

Acknowledgements—We thank the Alexander von Humboldt Foundation, Bonn, for the donation of the IR spectrophotometer used in this work. A.M.S. and N.G. thank UGC and CSIR, respectively, for senior research

* The numerical superscript indicates the total number of valence electrons in the Mo and NO orbitals.

fellowships. Our thanks are also due to Professor S. Ray of IACS, Calcutta, for stimulating discussions.

REFERENCES

1. K. Von der Heide and K. P. Hoffman, *Z. Anorg. Allg. Chem.* 1896, **12**, 286.
2. W. Hieber, R. Nast and G. Gehring, *Z. Anorg. Allg. Chem.* 1948, **256**, 169.
3. W. P. Griffith, J. Lewis and G. Wilkinson, *J. Chem. Soc.* 1959, 872.
4. K. G. Caulton, *Coord. Chem. Rev.* 1975, **14**, 317 and refs cited therein.
5. S. Sarkar and A. Müller, *Z. Naturfor.* 1978, **33b**, 1053.
6. K. Wieghardt, G. B. Dahman, W. Swiridoff and J. Weiss, *Inorg. Chem.* 1983, **22**, 1221.
7. (a) K. Wieghardt, W. Holzbach and J. Weiss, *Z. Naturfor.* 1982, **37b**, 680; (b) K. Weighardt and W. Holzbach, *Angew. Chem. Int. Edn Engl.* 1979, **18**, 549.
8. K. Wieghardt, W. Holzbach, B. Nüber and J. Weiss, *Chem. Ber.* 1980, **113**, 629.
9. R. G. Bhattacharyya and G. P. Bhattacharjee, *J. Chem. Soc., Dalton Trans.* 1983, 1593.
10. R. G. Bhattacharyya, G. P. Bhattacharjee and A. M. Saha, *Transition Met. Chem.* 1983, **8**, 255.
11. R. G. Bhattacharyya, G. P. Bhattacharjee and A. M. Saha, *Polyhedron* 1985, **4**, 583.
12. D. H. Svedung and N. Vannerberg, *Acta Chem. Scand.* 1968, **22**, 1551.
13. R. F. Riley and L. Ho, *J. Inorg. Nucl. Chem.* 1962, **24**, 1121.
14. N. Ghosh, PhD dissertation. Jadavpur University, Calcutta (1987).
15. D. D. Perrin, W. L. F. Armarego and D. R. Perrin, *Purification of Laboratory Chemicals.* Pergamon Press, New York (1966).
16. A. I. Vogel, *A Text book of Quantitative Inorganic Analysis.* The English Language Book Society and Longmans, London (1968).
17. J. H. Enemark and R. D. Feltham, *Coord. Chem. Rev.* 1974, **13**, 339.

Polyhedron Vol. 8, No. 24, pp. 2901–2906, 1989
Printed in Great Britain

0277–5387/89 $3.00+.00
© 1989 Pergamon Press plc

SOME FEATURES OF 2- AND 4-AMINOPYRIDINES ANCHORED ON SILICA GEL: PROPERTIES AND CHEMISORPTION OF METAL(II) CHLORIDES IN NON-AQUEOUS SOLUTIONS

AFONSO S. GONÇALVES* and CLAUDIO AIROLDI†

Instituto de Química, Universidade Estadual de Campinas, Caixa Postal 6154, 13081 Campinas, São Paulo, Brazil

(*Received* 11 *April* 1989; *accepted* 24 *July* 1989)

Abstract—Silica gel surfaces modified with 2- or 4-aminopyridine groups were used to adsorb MCl_2 (M = Co, Ni, Cu, Zn) from ethanol and acetone solutions at 298 K. The chemisorption isotherms fitted a modified Langmuir equation very well and are similar for all cations. The capacity of anchored 4-aminopyridine (SIL4) in adsorbing the metallic ion is larger than that of the immobilized 2-aminopyridine (SIL2). The maximum retention capacity has the sequence Cu > Co > Zn in acetone for both surfaces, and Zn > Co > Cu > Ni for SIL2, and Zn > Cu > Co > Ni for SIL4 in ethanol. For a given cation, the variation in enthalpy of solvent–solute exchange on the surface is always larger in ethanol. This process seems to be related to the enthalpy of solvation of the cation involved in the exchange.

Silica gel is one of the most widely used inorganic supports, with numerous kinds of chelating reagents immobilized on its surface.[1,2] For this, the application of 3-chloropropyltrialkoxysilane is one of the most popular approaches for modification of the silica gel surface through chemical bonding.[3] A great number of known chemical reactions, starting from this precursor, lead to a desired organic function. Surfaces containing specific functional groups, after being well characterized, have increased the application in a large variety of technological activities.[2,3]

The covalent immobilized groups attached to the support, through the formation of Si—C,[4,5] Si—N[6] or Si—O[7] bonds, can adsorb metal ions from non-aqueous solutions,[8–10] for preconcentration[11] or separation of metal ions,[12] as well as behave as bonded phases for liquid chromatography.[13]

The availability of a basic centre to coordinate cations in solution and, in particular, the availability of a heterocyclic nitrogen, is the main focus here. Some sorbents containing simple or very complex molecules have been reviewed,[2] with quinoline derivatives[14] and imidazole[9,15] showing an effective participation of cyclic nitrogen in adsorbing metallic ions from non-aqueous solvents.

An efficient chelation capacity was observed with immobilized 3-aminopyridine[10] on such surface-modified silica supports for extracting some bivalent cations from ethanol or acetone solutions. The solvent–solute exchange equilibria in this heterogeneous system enable the ordering of the maximum retention capacity of cations in both solvents and some thermodynamic data on these equilibria were obtained. We report here the results of adsorption studies of MCl_2 (M = Co, Ni, Cu, Zn) in ethanol and acetone by 2- and 4-aminopyridine groups bonded on silica gel surfaces. These data are also compared with the aforementioned modified surface.

EXPERIMENTAL

All chemicals used were reagent grade. The silica substrate used in the preparations was a commercial silica gel (Merck 60) which had its surface activated by heating for several hours in a stream of nitrogen

* Permanent address: Departamento de Química, Universidade Federal do Piauí, 64000 Teresina, Piauí, Brazil.

† Author to whom correspondence should be addressed.

at 420 K or *in vacuo* at 400 K.[16] The specific area of 560 $m^2\ g^{-1}$ was determined using the BET method.[17]

Solutions of metal(II) ions for the adsorption processes were prepared from anhydrous salts. Hydrated cobalt, nickel and copper chlorides were dried *in vacuo* at 420 K.[10] Anhydrous zinc chloride was prepared by reacting the pure metal with hydrochloric acid in ether.[10] The solvents were stored over appropriate dehydrating agents overnight, distilled through an efficient column and kept over molecular sieves. 2- and 4-Aminopyridines (Carlo Erba) were recrystallized from ether before use.

The compound 3-chloropropyltrichlorosilane was obtained by slowly adding drops of trichlorosilane (0.52 mol) onto freshly distilled allylchloride (0.50 mol) in the presence of a H_2PtCl_6 catalyst.[18] After 4 h of reaction the product was distilled *in vacuo*, giving a yield of 65%. An excess of dry methanol was slowly added with stirring to 0.30 mol of this product. The mixture was refluxed for 4 h, then dry gaseous nitrogen was bubbled into the solution to eliminate part of the hydrogen chloride that was formed. Hydrogen chloride was completely eliminated by simple distillation *in vacuo* of the 3-chloropropyltrimethoxysilane, obtained in quantitative yield.

To a stirred suspension of activated silica gel (50 g) in dry xylene (300 cm^3), 3-chloropropyltrichlorotrimethoxysilane (0.10 mol) was slowly added. This suspension was stirred mechanically for 8 h at xylene reflux temperature. Then, the solid product was filtered, washed with water, ethanol and acetone. This material was transferred to a Soxhlet extractor and washed with ethanol for 48 h. Finally, the solid was dried *in vacuo* for 6 h at 393 K. The control of functionalization was followed by digesting approximately 0.1 g of this material with a large excess of pyridine for 5 h at 380 K. The resulting mixture was diluted and the amount of chlorine (5.4×10^{-4} mol g^{-1}) was determined by titration with standard silver nitrate solution.[10]

An identical procedure was used to functionalize the silica surface with 2- and 4-aminopyridine. In both cases, to an aliquot of the precursor halogen-functionalized silica gel (15.0 g) suspended in dry xylene (80.0 cm^3), aminopyridine (7.4×10^{-2} mol) was added and the mixture was refluxed for 5 h. After cooling, the solid was filtered, washed with cold water and acetone, followed by an efficient washing with ethanol in a Soxhlet extractor for 48 h. To eliminate the remaining aminopyridine bonded to the surface, the solid was transferred to a hydrochloric acid solution at pH 5.0. The suspension was stirred, filtered and washed. This material was immersed in water (500 cm^3), then the liquid was changed several times until a negative test for chloride in the supernatant (silver nitrate) was obtained. The preceding procedure was repeated with sodium hydroxide solution at pH 8.5. The control of this functionalization was checked by determination of the amount of nitrogen in the sample through the Kjeldhal method. To digest the material, mercury oxide was used as a catalyst to free the pyridine nitrogen, followed by treatment with sodium thiosulphate to destroy the amino-mercury complexes formed.[10]

The process of adsorption was followed batchwise in non-aqueous solvents or by using a calorimetric method in the same solvents system. In the first process, samples (5.0×10^{-2} g) of the functionalized material were suspended in metal chloride solution (50 cm^3), having concentrations in the range $(1.0\text{–}0.1) \times 10^{-3}$ $dm^3\ mol^{-1}$. Solutions of cobalt(II), nickel(II), copper(II) and zinc(II) dissolved in ethanol or acetone were equilibrated with the anchored material with vigorous stirring at 298.2 ± 0.2 K for 2 h. The suspension was left standing for a further 2 h, when the amount of metal ions in the supernatant was analysed by means of conventional EDTA complexiometric titrations.[10] This procedure was also repeated with untreated silica gel and no adsorption was detected. For each sample analysed, at least one duplicate run was titrated to check the reproducibility. The anchored material did not show any alteration in its loss of exchange capacity throughout the period of investigation.

The heat evolved in the above reaction was followed by means of an isoperibolic precision calorimeter system LKB 8700-2.[8,10] A sample of functionalized silica gel (0.1–0.2 g) was suspended in the calorimetric solvent (90.0 cm^{-3}), with vigorous stirring at 298.15 ± 0.02 K. To this suspension a thermostatted solution of the cation (~ 0.01 $dm^3\ mol^{-1}$) in the same calorimetric solvent, protected from humidity, was incrementally added into the calorimetric vessel and the heat of the reaction (Q_1) recorded. An identical titration of the metal solution in the same calorimetric solvent produced the heat of dilution (Q_2). Then, the net heat of reaction (Q_{obs}) is given by: $Q_{obs} = Q_1 - Q_2$. The variation of the enthalpy of reaction (ΔH) can be obtained by the expression $Q = n\Delta H$, where n is the number of moles of the solute adsorbed on the functionalized surface.

RESULTS AND DISCUSSION

Based on the chlorine elemental analysis (0.9%), 5.4×10^{-4} mol of γ-chloropropyl groups are bonded

to the silica surface. These groups are available for the next step of the reaction with aminopyridine derivatives. To quantify the amount of this new group anchored to the surface, nitrogen elemental analysis was performed. For nitrogen organic groups, 1.4 and 4.3×10^{-4} mol g^{-1}, were found for 2-aminopyridine (SIL2) and 4-aminopyridine (SIL4) silica gel surfaces, respectively. Considering the reaction of aminopyridines with trichloride bound to the surface has a 1 : 1 stoichiometry, these figures show a different behaviour in the functionalization, the last one reacting almost quantitatively, while for SIL2 only one fourth of the free γ-chloropropyl groups reacted. These results may be associated with electronic and steric features presented by the two pyridine derivatives.

The functionalization causes a change in the surface area, which increased (40 m^2 g^{-1}) for SIL2, while it showed a significant decrease (95 m^2 g^{-1}) for SIL4. These nitrogenated groups cover the total area of the surface, i.e. 1.4 and 4.3×10^{-4} mol g^{-1} for SIL2 and SIL4, respectively, which correspond to a molecular density of 1.4 and 5.5×10^{17} nitrogenated groups per square meter, giving them an area of 7.0 and 1.8 nm^2 for a pendant group in each functionalized surface.[10] Assuming that each group is centred in this square area, the distance to its next neighbour group is 2.7 and 1.3 nm for SIL2 and SIL4, respectively. These results indicate a high population in the last surface, reflected in the mean distance between the pendant groups.[10,19]

The pulverized material was compressed in discs with the purpose of obtaining the IR spectra of the surfaces. Matrix absorptions in the high frequency range completely mask the CH and NH stretching vibrations.[20] For SIL2 two distinct bands at 1590 and 1537 cm^{-1} can be visualized as relating to the anchored ligand. These medium bands may be attributed to CC/CN stretching frequencies of the pyridine ring. However, for SIL4 only one band at 1535 cm^{-1} was observed for the heterocyclic ring. On the other hand, the bonded metal ions on the surface showed that the spectra did not change, in comparison with the uncomplexed surface, as observed before.[10]

Sorption of metallic ions from solutions onto the modified silica gel occurs as a result of complexing with immobilized ligands on the surface. SIL2 and SIL4 adsorb cobalt(II), nickel(II), copper(II) and zinc(II) chlorides from ethanol, and cobalt(II), copper(II) and zinc(II) from acetone solutions. The adsorption of nickel(II) chloride from acetone failed due to its low solubility in this solvent. Profiles of the adsorption isotherms for all metal ions are very similar in shape, but vary in capacity.[21] Copper(II) ions are the most adsorbed from solution, with the adsorption being more efficient in acetone. With the exception of zinc(II) ions in ethanol, all other adsorptions are higher in acetone than in ethanol solutions.

The adsorption phenomena at the solid–liquid interface demand a competition between the solvent bonded to the anchored surface (AS), which is displaced gradually by the solute in solution to reach the equilibrium, as outlined by the reaction:[22]

$$AS(solvent) + MCl_2(solvent) \rightleftharpoons AS \cdot MCl_2(solvent) + solvent.$$

When the adsorption remains constant, a monolayer is assumed to have been formed. The chemical interaction, metallic ion–surface, may be accompanied by applying the transformed Langmuir adsorption isotherms:

$$\frac{C_2}{n_2^s} = \frac{1}{n^s b} + \frac{C_2}{n^s},$$

where C_2 is the residual concentration (mol dm^{-3}), of metallic ion in equilibrium with the solid. A plot of C_2^s/n_2^s vs C_2 permits the calculation of the constant b and n^s, where this last parameter is the maximum adsorption capacity, given by mole of solute per gram of adsorbent.

The results of adsorption can be represented by the isotherms n_2^s vs C_2, and the linearization of the adsorption results for metal(II) ions in ethanol are shown in Fig. 1. From this plot n_2^s and b values were obtained from the angular and linear coefficients, and are listed in Table 1.

The maximum adsorption capacity of both modified surfaces (n^s) is at least twice as large in acetone than in ethanol for cobalt(II) and copper(II), the adsorption being more efficient for this last metallic ion. However, for SIL2 the adsorption of zinc(II) ion in ethanol superimposes that of acetone, a behaviour opposite to that which occurred with the other surface, where an increase of 50% adsorption was observed in acetone. This greater tendency for adsorption has been interpreted as due to the lower polarity of acetone, which causes a weaker solvation of cations, and consequently, favouring the complexation of metallic ions on the anchored surface.

The capacity of SIL4 for adsorbing a given metallic ion from a solvent is considerably larger than for SIL2. For example, copper(II) ions have n^s values of 4.89 and 2.04×10^4 mol g^{-1} for SIL4 compared with 1.17 and 0.35×10^4 mol g^{-1} for SIL2, in acetone and ethanol, respectively. The sequence Cu > Co > Zn obtained in acetone for the maximum retention capacity with both surfaces, changes to Zn > Cu > Co > Ni for SIL2 and Zn > Cu > Co > Ni for SIL4 in ethanol. In com-

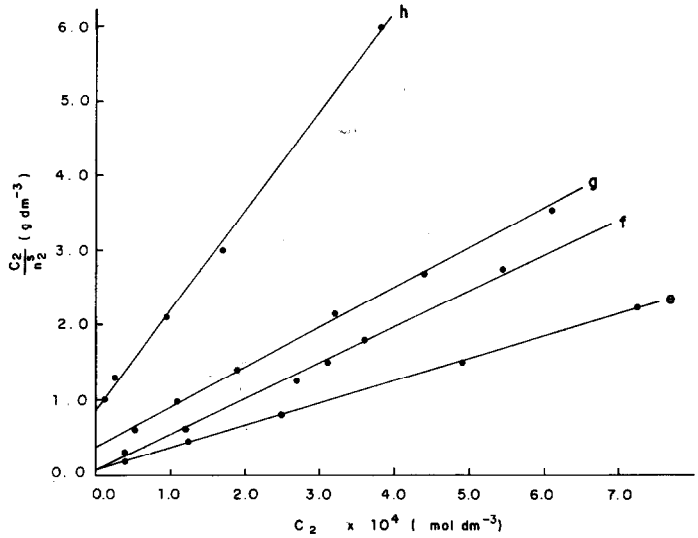

Fig. 1. Linearization of adsorption isotherms for the SIL4 surface in ethanol at 298.2 K: (e) $ZnCl_2$, (f) $CuCl_2$, (g) $CoCl_2$ and (h) $NiCl_2$.

Table 1. Maximum adsorption coefficient, $n^s \times 10^4$ (mol g^{-1}), constant, $b \times 10^{-4}$ (dm^3 mol^{-1}), and correlation coefficient, r, for the adsorption of metal(II) by SIL2 and SIL4 surfaces

		SIL2		SIL4	
MCl_2	Parameter	Acetone	Ethanol	Acetone	Ethanol
Co	n^s	1.03	0.51	4.52	1.96
	b	8.49	2.41	2.63	11.1
	r^a	0.999	0.998	0.999	0.999
Ni	n^s	—	0.12	—	0.71
	b	—	3.95	—	1.79
	r	—	0.998	—	0.998
Cu	n^s	1.17	0.35	4.89	2.04
	b	5.14	20.9	5.34	12.5
	r	0.999	0.999	0.999	0.998
Zn	n^s	0.91	1.27	3.31	2.17
	b	16.8	0.41	6.90	6.78
	r	0.999	0.999	0.999	0.999

[a] Correlation coefficient for C_2/n_2^s vs C_2 plot.

paring these results with those of 3-aminopyridine immobilized on silica gel (SIL3),[10] the sequence in retaining cations is SIL4 > SIL3 > SIL2, which is the same order as the degree of functionalization of these surfaces.

The "bond-term" values, b, listed in Table 1 follow the same sequence of n^s values,[23] as observed for the SIL3 surface.[10] For a low concentration of solute, as in the experimental conditions used here, the activity coefficient of the solvent is practically unity. Then, the equilibrium constant involving solvent–solute exchange on the surface should give values of the order of b. These values, which vary from 1.0 to 20×10^{-4} dm^3 mol^{-1} (Table 1) for both surfaces, are in fact very high in all equilibria studied, suggesting that the adsorption occurs with the metal ions directly coordinated with the pendant groups anchored on the surface, which have basic centres to bond them. This process gives an indication of the thermodynamic stability of the complexes formed on the surfaces.[24]

In an attempt to gain more information about the interactions of the basic centres on the surface with the cations in solution, this process was fol-

Table 2. Thermodynamic values for cation–surface interactions at 298 K

Surface	MCl_2	Solvent	Hm (J g^{-1})	ΔH (kJ mol^{-1})	ln K	ΔG (kJ mol^{-1})	ΔS (J mol^{-1} K^{-1})
SIL2	Co	Acetone	−3.03±0.06	−29.4±0.6	11.3	−28.0±0.6	−5±1
	Co	Ethanol	−1.72±0.03	−33.7±0.7	10.1	−25.0±0.5	−29±1
	Zn	Ethanol	−3.18±0.06	−25.1±0.5	8.3	−20.6±0.4	−15±1
SIL4	Co	Acetone	−3.68±0.07	−8.14±0.2	10.2	−25.3±0.5	58±1
	Co	Ethanol	−2.58±0.05	−13.2±0.3	11.6	−28.7±0.6	52±1
	Ni	Ethanol	−1.12±0.02	−15.8±0.3	9.8	−24.3±0.5	29±1
	Cu	Acetone	+3.52±0.07	+7.54±0.2	10.9	−27.0±0.5	116±1
	Cu	Ethanol	−10.3±0.2	−50.5±1.0	11.7	−29.0±0.6	−72±1
	Zn	Acetone	+3.73±0.07	+11.3±0.2	11.1	−27.5±0.05	130±1
	Zn	Ethanol	−2.10±0.04	−9.68±0.2	11.1	−27.5±0.05	60±1

lowed by calorimetric titration. The enthalpy of adsorption and the concentration of the metallic ion in equilibrium can be given by the following equation:[25–27]

$$\frac{N}{H} = \frac{1}{(K-1)Hm} + \frac{N}{Hm},$$

where N is the mole fraction of the cation in solution, H is the integral enthalpy of adsorption (J g^{-1}), K is a proportionality factor which includes the equilibrium constant and Hm is the integral heat of adsorption for the saturated monolayer of unitary mass of anchored material. Taking into account the preceding equilibrium measurements, the N value could be obtained for each increment of solute on the surface in suspension.[10]

The thermodynamic values obtained for the interactions of metallic ions on surfaces are listed in Table 2 and were determined from the above equation.

A plot of N/H against N provides Hm from the angular coefficient, as shown in Fig. 2. This integral heat of adsorption (Hm) is related to the respective number of moles determined previously and gives the enthalpy change (ΔH) of the interactive process. In spite of great difficulty in obtaining ΔH for the SIL2 surface with all cations, cobalt(II) in both solvents and zinc(II) in ethanol showed a very exothermic adsorption, in comparison with SIL4, where only copper(II) in ethanol gave a high ΔH value (see Table 2). This thermodynamic parameter is always exothermic in ethanol, which superimposes in magnitude, for a given cation, the corresponding ΔH value in acetone. This same behaviour was also observed for the other anchored surface, whose results seem to be affected by the

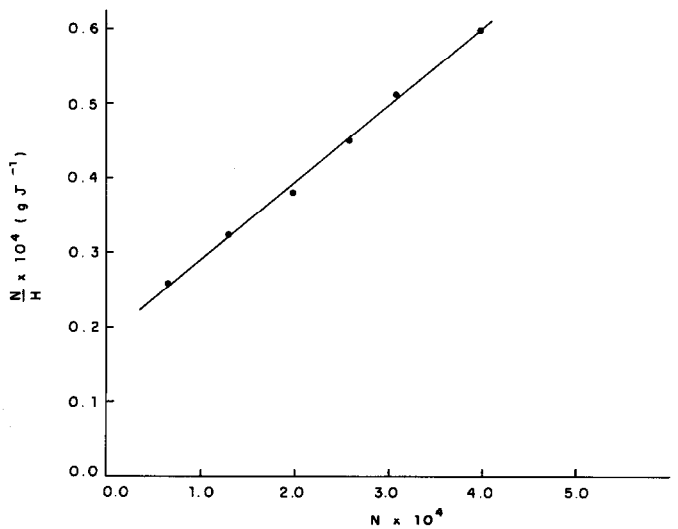

Fig. 2. The linear plot of calorimetric results for $CuCl_2$ adsorbed on SIL4 in ethanol solution at 298.15±0.02 K.

solvation properties of cations, being smaller in acetone than in ethanol.[10] The larger exothermicity displayed during the interactive process involving the cation–base centre on the SIL2 surface, even though the molecular density of the pendant groups is nearly one fourth of that of SIL4, may be attributed to the fact that both nitrogen basic centres are available to coordinate the cations, whilst for the anchored ligand on the SIL4 surface, only the heterocyclic nitrogen is available. Furthermore, the solvated cation releases solvent molecules into the solution on bonding to the anchored molecules. Consequently, the cation desolvation disturbs the structured solvent around it, causing an entropic enhancement. The data in Table 2 illustrates this behaviour, showing all ΔS values to be more favourable in acetone than in the more polar ethanol, for the same cation. The most favourable ΔH was obtained for the complexation of copper(II) with the SIL4 surface in ethanol (-50.5 ± 1.0 kJ mol^{-1}), which contrasts with its value in acetone ($+7.54 \pm 0.2$ kJ mol^{-1}). However, a reversal occurs with the ΔS values, which indicate that the reaction is entropically unfavourable in the more polar ethanol.

Acknowledgements—The authors are indebted to FINEP and Dow Produtos Químicos Ltda for financial support. One of us (A.S.G.) wishes to acknowledge a fellowship from CAPES.

REFERENCES

1. D. C. Bailey and S. H. Langer, *Chem. Rev.* 1981, **81**, 143.
2. G. V. Lisichkin, G. V. Kudryavtser and P. N. Westerenko, *J. Analyt. Chem.* 1983, **38**, 1288.
3. U. Deschler, P. Kleinschmit and P. Panster, *Angew. Chem. Int. Edn. Engl.* 1986, **25**, 236.
4. K. G. Allum, R. O. Hancok, I. V. Howell, S. Mckenzie, R. C. Pitkethly and P. J. Robinson, *J. Organomet. Chem.* 1975, **87**, 203.
5. F. R. Harley and P. N. Vezey, *Adv. Organomet. Chem.* 1977, **15**, 189.
6. O. E. Brust, I. Sebestian and I. Halasz, *J. Chromatogr.* 1973, **83**, 15.
7. H. Deuel and J. Wartmann, *Helv. Chim. Acta* 1959, **119**, 1160.
8. C. Airoldi, Y. Gushikem and J. G. P. Espínola, *Colloids Surfaces* 1986, **17**, 314.
9. Y. Gushikem and J. C. Moreira, *J. Colloid Interface Sci.* 1985, **107**, 70.
10. C. Airoldi and A. S. Gonçalves, *Colloids Surfaces* 1987, **28**, 199.
11. J. C. Moreira and Y. Gushikem, *Analytica Chim. Acta* 1985, **176**, 263.
12. R. E. Sturgeon, S. S. Berman, S. N. Willie and J. A. Desaulniers, *Analyt. Chem.* 1981, **53**, 2337.
13. L. C. Sander and S. A. Wise, *CRC Crit. Rev. Analyt. Chem.* 1987, **18**, 299.
14. V. V. Skopenko, A. K. Trofimchuk and V. N. Zartsev, *Russ. J. Inorg. Chem.* 1982, **27**, 1458.
15. Y. Gushikem and M. A. A. da Silva, *J. Colloid Interface Sci.* 1985, **107**, 81.
16. R. K. Iler, *The Chemistry of Silica.* John Wiley, New York (1979).
17. C. Airoldi and L. S. Santos Jr, *Thermochim. Acta* 1986, **104**, 111.
18. J. W. Ryan, G. K. Menzie and J. L. Spier, *J. Am. Chem. Soc.* 1960, **82**, 360.
19. G. W. Bushnell, *Can. J. Chem.* 1971, **49**, 555.
20. J. M. Land, J. A. Stubls and J. T. Wrobleski, *Inorg. Chem.* 1977, **16**, 1955.
21. S. Watanesk and A. A. Schilt, *Talanta* 1986, **11**, 95.
22. A. W. Adamson, *Physical Chemistry of Surfaces*, 3rd edn. John Wiley, New York (1976).
23. R. G. McLaren and D. V. Crawford, *J. Soil Sci.* 1973, **24**, 493.
24. H. Irving and R. J. P. Williams, *J. Chem. Soc.* 1953, 3192.
25. A. J. Groszek, *Proc. R. Soc. Lond.* 1970, **314**, 473.
26. J. Jednacak-Biscan and V. Pravdic, *J. Colloid Interface Sci.* 1980, **75**, 322.
27. J. Jednacak-Biscan and V. Pravdic, *Thermochim. Acta* 1982, **53**, 203.

Polyhedron Vol. 8, No. 24, pp. 2907–2910, 1989
Printed in Great Britain

0277–5387/89 $3.00+.00
© 1989 Pergamon Press plc

^{31}P NMR STUDIES ON THE *MER–FAC* ISOMERIZATION OF $Pt(S_4N_4)Cl_2(PMe_2Ph)$

PAUL F. KELLY and J. DEREK WOOLLINS*

Department of Chemistry, Imperial College of Science, Technology and Medicine, South Kensington, London SW7 2AY, U.K.

(*Received* 30 *May* 1989; *accepted* 3 *August* 1989)

Abstract—When heated in chloroform the meridional $S_4N_4^{2-}$ complex, $Pt(S_4N_4)Cl_2(PMe_2Ph)$, readily isomerizes, giving a product which has, on the basis of ^{15}N-labelling studies, been identified as the facial isomer.

Previously we have reported on the preparation of $Pt(S_4N_4)Cl_2(PMe_2Ph)$ (**1**), from the reaction of S_4N_4 with $[PtCl_2(PMe_2Ph)]_2$.[1] The product is only the second example of a complex of $S_4N_4^{2-}$, and the first to display a meridional coordination geometry i.e. with the coordinating atoms (two sulphurs and one nitrogen) in the same plane.

Here, we report on investigations into the isomerization of **1**. Although we have as yet been unable to grow crystals of the isomeric species, **2**, suitable for X-ray crystallographic confirmation, we have assigned a facial conformation on the basis of the ^{31}P NMR spectra of 99% ^{15}N-labelled samples of **1** and **2**, which show greatly contrasting magnitudes of ^{15}N–^{31}P coupling constants.

EXPERIMENTAL

General reaction conditions were as described previously; $[PtCl_2(PMe_2Ph)]_2$ was prepared by reaction of *cis*-$PtCl_2(PMe_2Ph)_2$ with $PtCl_2$ in xylene at $\approx$ 160°C.[2]

IR spectra were obtained using a PE 1720X instrument. ^{31}P NMR spectra were obtained (in $CDCl_3$) using a JEOL FX90Q operating at 36.21 MHz and are referred to 85% H_3PO_4. Microanalyses were performed by the Imperial College Service.

In a typical reaction a sample of *mer*-$Pt(S_4N_4)Cl_2(PMe_2Ph)$ (**1**) was prepared, as described previously, by reaction of S_4N_4 (70 mg, 0.38 mmol) with $[PtCl_2(PMe_2Ph)]_2$ (150 mg, 0.19 mmol) in CH_2Cl_2. Precipitation with hexane yielded the crude product (197 mg, 88%); it did not prove necessary to purify the compound before use (which can be done by elution on a Bio-beads gel-permeation column) since identical results were obtained using crude and purified samples. Compound **1** was dissolved in $CHCl_3$ ($\approx$ 25 cm^3) and the red solution heated to 75–80°C (under a nitrogen pressure of *ca* 5 psi); at intervals, ^{31}P NMR was used to assess the degree of isomerization by measuring the ratio of **1** (δ 5.2 ppm) to the isomer **2** (δ −9.4 ppm, $^1J(^{195}Pt–^{31}P)$ 2453 Hz). After 20 min the ratio of **1**:**2** was $\approx$ 3:1; after 40 min 1:1, after 90 min 1:4 and after 3 h the reaction had effectively gone to completion. Also present in the ^{31}P NMR of the product was a singlet at δ −21 ppm ($^1J(^{195}Pt–^{31}P)$ 3411 Hz), indicative of $Pt(S_2N_2H)Cl(PMe_2Ph)$[3] [Fig. 1(b)], and a compound revealed by a singlet at δ −18.0, ^1J 1995 Hz. The ratio of the complex at δ −9.4 to the combined amounts of the other two species was approximately 4:1.

The $CHCl_3$ was removed *in vacuo* and the product redissolved in CH_2Cl_2 (10 cm^3) then placed on a Bio-beads gel-permeation column and eluted with CH_2Cl_2. The sample separated into a number of bands; a fast moving brown band followed by a green and a red–orange fraction. The latter was collected, reduced in volume and a brown–red solid was obtained by addition of hexane (yield, 80 mg). The ^{31}P NMR spectrum of the product revealed the presence of the species at δ −9.4, together with a small amount of δ −21 and a trace of the species at δ −18. Slow diffusion of hexane into a CH_2Cl_2 solution yielded a crop of small clustered red crystals interspersed with white needles. The red crystals were separated by hand and redissolved in CH_2Cl_2.

* Author to whom correspondence should be addressed.

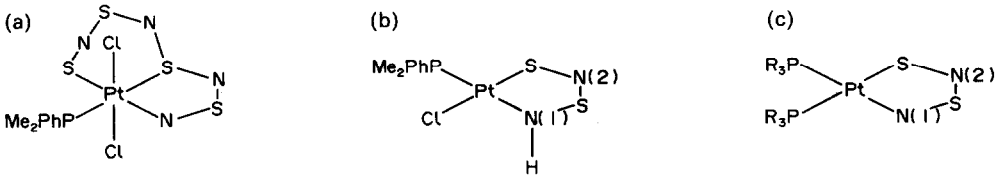

Fig. 1. Structures and numbering schemes of **1** and related compounds.

Slow hexane diffusion yielded poorly formed red crystals which were free of the white impurity. The ^{31}P NMR spectrum of these crystals revealed that they were the species responsible for the peak at δ −9.4 ppm, and they analysed correctly for $PtCl_2(S_4N_4)(PMe_2Ph)$; Found: C, 16.4; H, 1.6; N, 9.5. Calc.: C, 16.3; H, 1.9; N, 9.5%.

The reaction of $S_4^{15}N_4$ (19 mg, 0.1 mmol) with $[PtCl_2(PMe_2Ph)]_2$ (40 mg, 0.05 mmol) was performed as above and, after measurement of the ^{31}P NMR spectrum of the initial products, the chloroform solution was heated to 95°C for 3 h and the spectrum of the isomer recorded. No attempt was made to purify a sample of the ^{15}N-labelled species.

RESULTS AND DISCUSSION

The dimeric, chloro-bridged species $[PtCl_2(PMe_2Ph)]_2$ reacts with S_4N_4 at room temperature, in CH_2Cl_2, to give the platinum(IV) species $PtCl_2(S_4N_4)(PMe_2Ph)$ (**1**)[1] which contains a meridionally-coordinated tridentate $S_4N_4^{2-}$ ligand. This bonding mode is substantially different to that observed in $Ir(CO)Cl(S_4N_4)(PPh_3)$,[4] the only other $S_4N_4^{2-}$ complex known, in which the ligand adopts a facial geometry. In the light of this contrast in geometries we have attempted to assess the potential for isomerization within **1**. We have found that upon standing in solution for a number of days, or refluxing in chloroform for a few hours, **1** does indeed isomerize to a species which we believe contains a facial $S_4N_4^{2-}$ ligand.

If the chloroform solution of **1** is heated to $\approx$ 90°C, and the nature of the species in solution assessed by ^{31}P NMR, the amount of **1** present is seen to decrease and a new species, **2**, revealed by a singlet at δ −9.4 ($^1J(^{195}Pt–^{31}P)$ 2453 Hz), appears. After 3 h at this temperature there is complete conversion of **1** to **2**, together with small amounts of $Pt(S_2N_2H)Cl(PMe_2Ph)$ (**3**) (Fig. 1) and a complex at δ −18.0 (^1J 1995 Hz). Purification using a Biobeads gel-permeation column with CH_2Cl_2 as eluent, allows isolation of **2** along with traces of a colourless impurity. We have yet to fully characterize this impurity; its mass spectrum contains peaks at m/z 154 ($[\{PMe_2Ph\}NH_2]^+$), 293 ($[\{PMe_2Ph\}_2NH_3]^+$) and 307 ($[\{PMe_2Ph\}_2N_2H_3]^+$) with no evidence of the presence of sulphur.

We have not been able to grow crystals of **2** of sufficient quality to allow X-ray study, although they analyse correctly for $PtCl_2(S_4N_4)(PMe_2Ph)$, confirming that **2** is indeed an isomer of **1**. Furthermore, attempts to prepare crystalline samples of analogues of **1** and **2** ($PR_3 = PPh_2Me$, PEt_3) have been unsuccessful, the products (which by ^{31}P NMR are of the same type as **1** and **2**) being obtained as oils.

The large difference in the chemical shifts of the phosphine groups in **1** and **2**, 5.2 and −9.4 ppm, respectively, is indicative of a substantial change in geometry within the complexes, as is the fact that the IR spectrum of **2** contains strong peaks at 794 and 812 cm^{-1}, which are absent from the spectrum of **1**. Figure 2 illustrates some of the structures which **2** could, conceivably, adopt.

Insight into the structure of **2** can be obtained from the ^{31}P NMR spectrum of the ^{15}N-labelled complex. Figure 3 compares the ^{31}P spectrum of ^{15}N-labelled **1** with that of the isomer, **2**. As there is only one phosphine group present in **1** or **2**, the ^{31}P NMR of the unlabelled complexes are singlets, with appropriate ^{195}Pt satellites (for **1** and **2**,

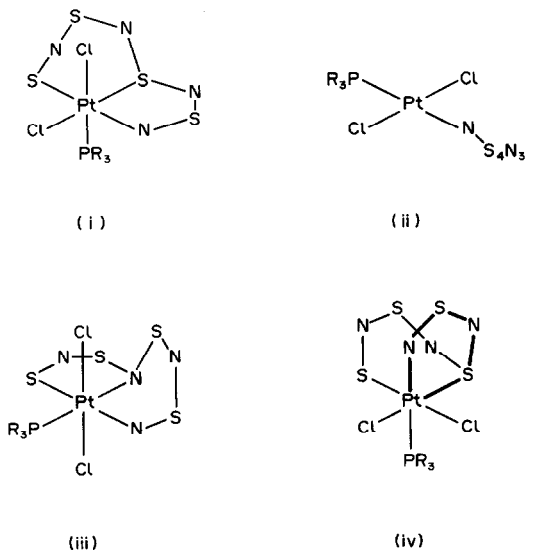

Fig. 2. Possible structures of **2**.

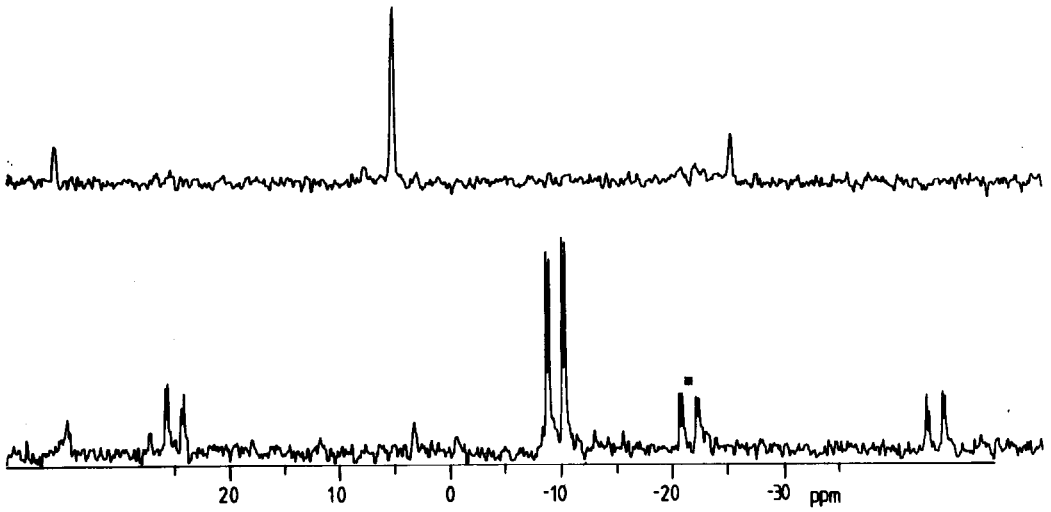

Fig. 3. 36.21 MHz ^{31}P-{^1H} NMR spectrum (in $CDCl_3$) of ^{15}N-labelled **1** (upper) and **2** (lower). The asterisk marks the peaks due to ^{15}N-labelled $PtCl(S_2N_2H)(PMe_2Ph)$.

^1J = 2170 and 2453 Hz, respectively). In the case of **1** [Fig. 3(a)] the only effect that introducing ^{15}N into the system appears to have is a slight broadening of this singlet, suggesting that none of the ^{15}N nuclei present couple to the phosphorus to any great degree. Results obtained previously for labelled complexes of the type $Pt(S_2^{15}N_2)(PR_3)_2$ (**4**)[5] (Fig. 1) show that the phosphorus *trans* to sulphur couples only to N(1), and that this coupling is small (5 Hz). Comparison of the structure of **1** with that of the aforementioned $S_2N_2^{2-}$ complexes suggests that the only ^{15}N–^{31}P coupling one would expect to see in ^{15}N-labelled **1** would be from N(1), and that this too would be weak. Hence it is this coupling that manifests itself as the slight broadening of the main peak.

In contrast, the ^{31}P NMR spectrum of ^{15}N-labelled **2** [Fig. 3(b)] shows much more fine structure; the original singlet is split into a pair of doublets. This is consistent with the presence of two ^{15}N–^{31}P couplings, of magnitude $\approx$ 57 and 8 Hz, and is almost identical to the pattern observed for $Pt(S_2^{15}N_2H)Cl(PMe_2Ph)$ [as seen in the small amount of impurity in the spectrum in Fig. 3(b)] in which the couplings are 54 and 7 Hz.[3] Therefore, we propose that the phosphine group in **2** must be in a similar environment to that in $Pt(S_2N_2H)Cl(PMe_2Ph)$, since, on the basis of our previous results, a ^{15}N–^{31}P interaction as large as 54 Hz could only be the result of a ^2J (^{31}P–^{15}N) coupling from a ^{15}N *trans* to phosphorus.[5] On this basis we can rule out structure (i) since this would require phosphorus *trans* to chlorine. The conversion of **1** to structure (ii) would require the oxidation of the $S_4N_4^{2-}$ ligand to neutral S_4N_4 and corresponding reduction of the platinum to platinum(II); this is somewhat unlikely in itself since any reduction at platinum would lead to species such as **3** or **4** and, although the value of the $^1J(^{195}Pt$–$^{31}P)$ coupling constant (2453 Hz) could be indicative of platinum(II), past results show such a small coupling is only observed for phosphorus *trans* to sulphur. Of the two remaining potential structures (iii) is unlikely since the presence of a nitrogen *cis* to the phosphorus would result in, at the least, a broadening of the lines, as seen in Fig. 3(a) (previously we have observed ^2J *cis* couplings of *ca* 5 Hz in **4**). Hence the only reasonable structure for **2** would appear to be (iv), that is a facial coordination, analogous to that seen in $Ir(CO)Cl(S_4N_4)(PPh_3)$. The use of ^{31}P–^{15}N coupling constants to identify the structure of **2** is clearly inferior to single crystal X-ray studies since other isomers could be possible. However, on the basis of the data that we have been able to obtain we believe structure (iv) to be the most likely.

We have yet to determine the mechanism of the *mer–fac* isomerization. Dissociation of the phosphine (*trans* to sulphur), rotation of the chlorides and nitrogen in a five-coordinate intermediate, followed by reassociation of the phosphine (*trans* to nitrogen) appears to be the most reasonable route. For comparison, it is interesting to note that in the isomerization of *trans*-$[PtBr_2(S_2N_2H)(PMe_2Ph)_2]^+$ to the *cis* form it is the phosphine *trans* to sulphur which is rotated.[6] We have yet to ascertain the nature of the species with δ −18.0, which is formed as a minor product during the isomerization of **1**. It is present in the green band which separates on Bio-beads; concentrated $CDCl_3$ solutions of this fraction deposit an insoluble red microcrystalline

product which can be shown by IR to contain PMe_2Ph, and which analyses as $[Pt(S_2N_2)(PMe_2Ph)]_2 \cdot 2CDCl_3$ (Found: C, 19.4; H, 2.1; N, 5.4. Calc.: C, 19.8; H, 2.0; N, 5.1%), suggesting that the red solid may be the PMe_2Ph analogue of $[Pt(S_2N_2)(PPh_3)]_2 \cdot CH_2Cl_2$, which we have previously reported.[7]

REFERENCES

1. M. B. Hursthouse, P. F. Kelly, M. Motevalli and J. D. Woollins, *Polyhedron* 1989, **8**, 997.
2. R. J. Goodfellow and L. M. Venanzi, *J. Chem. Soc.* 1965, 7533.
3. J. M. Jolliffe, P. F. Kelly and J. D. Woollins, *J. Chem. Soc., Dalton Trans.*, accepted.
4. F. Edelmann, H. W. Roesky, C. Spang, M. Noltemeyer and G. M. Sheldrick, *Angew. Chem. Int. Edn. Engl.* 1986, **25**, 931.
5. P. F. Kelly and J. D. Woollins, *J. Chem. Soc., Dalton Trans* 1988, 105.
6. R. Jones, P. F. Kelly, D. J. Williams and J. D. Woollins, *J. Chem. Soc., Dalton Trans.* 1988, 1569.
7. R. Jones, P. F. Kelly, D. J. Williams and J. D. Woollins, *J. Chem. Soc., Chem. Commun.* 1985, 1325.

Polyhedron Vol. 8, No. 24, pp. 2911–2914, 1989
Printed in Great Britain

0277–5387/89 $3.00+.00
© 1989 Pergamon Press plc

NOVEL IODOAMMONIUM CATIONS: SYNTHESIS AND CHARACTERIZATION OF *o*-$C_6H_4(NH_2)_2I^+X^-$ ($X^- = I^-$, AsF_6^-, AlI_4^-)

I. TORNIEPORTH-OETTING and TH. M. KLAPÖTKE*

Institut für Anorganische und Analytische Chemie, Technische Universität Berlin, Straße des 17. Juni 135, D-1000 Berlin 12, F.R.G.

(*Received* 20 *July* 1989; *accepted* 3 *August* 1989)

Abstract—The new iodoammonium salts *o*-$C_6H_4(NH_2)_2I^+I^-$ (**1**) and *o*-$C_6H_4(NH_2)_2I^+AsF_6^-$ (**2**) were prepared by reaction of *o*-phenylene diamine with I_2 or $I_3^+AsF_6^-$, respectively. Compound **1** reacts with AlI_3 yielding quantitatively the corresponding tetraiodoaluminate *o*-$C_6H_4(NH_2)_2I^+AlI_4^-$ (**3**). The species were characterized by chemical analysis, vibrational (IR and Raman) and temperature-dependent ^1H NMR spectropscopy. Direct evidence for a N—I bond was found in the Raman spectra of **1**, **2** and **3** (ν(NI) = 599–600 cm^{-1}).

Compounds containing the free monoatomic cation, I^+, in the condensed phase are still unknown.[1] However, the I^+ cation can be stabilized by coordination and both 1:1 and 1:2 adducts of pyridine[2–4] and nitriles[5] are known and may be prepared, via the disproportionation of iodine with nitriles or pyridine, respectively [eq. (1)]:[6]

$$n\text{R—CN} + I_3^+AsF_6^- \longrightarrow (\text{R—CN})_nI^+AsF_6^- + I_2 \qquad n = 1, 2. \tag{1}$$

On the other hand, the reaction of ammonia with $I_3^+AsF_6^-$ leads to the formation of NI_3, $NH_4^+AsF_6^-$ and I_2.[6] As far as we are aware no iodoammonium salt has been prepared prior to this work.

The reaction behaviour of I^+ toward chalcogens and chalcogen-containing compounds is well known. However, the reactivity of "I^+" towards compounds of group 15 is not very well established. For instance, $I_3^+AsF_6^-$ reacts with elemental selenium yielding $SeI_3^+AsF_6^-$.[7] It also reacts with $(CH_3)_2S$ giving $(CH_3)_2SI^+AsF_6^-$.[8] Quite recently the oxidation of iodine by MoF_6 and UF_6 in acetonitrile affording $I(CH_3CN)_2^+MF_6^-$ (M = Mo, U) was reported.[5,9]

We were particularly interested in the reaction behaviour of I_3^+ (and other "I^+" sources) towards organic amines, especially with respect to the synthesis of novel iodoammonium salts. These are unknown as far as we are aware. *o*-Phenylene diamine was used as the primary amine due to its ability to form chelate complexes.

On the basis of a simple Born–Haber cycle (see below) we estimated that a reaction according to eq. (2) should be thermodynamically favourable ($\Delta H = -59$ kcal mol^{-1})

$$o\text{-}C_6H_4(NH_2)_2(s) + I_3^+AsF_6^-(s) \longrightarrow I_2(s) + o\text{-}C_6H_4(NH_2)_2I^+AsF_6^-(s). \tag{2}$$

EXPERIMENTAL

Iodine (Merck) and AlI_3 (Aldrich) were used as commercially avaiable. *o*-Phenylene diamine (Merck) was recrystallized twice from acetonitrile. The preparation of $I_3^+AsF_6^-$ was carried out as described in the literature.[7] The solvent (SO_2(l), Messer–Griesheim) was purified by distillation and dried over CaH_2. All manipulations were carried out in an inert gas atmosphere (dry box).

Preparation of *o*-$C_6H_4(NH_2)_2I^+I^-$ (1)

A solution of 0.2129 g (1.97 mmol) of *o*-phenylene diamine in 5 cm^3 of SO_2 was added to a suspension of 0.500 g of I_2 (1.97 mmol) in 5 cm^3 SO_2 and stirred for 1 h at room temperature. The sulphur dioxide was pumped off *in vacuo*. The remaining black product was recrystallized from SO_2. Yield: 0.7126 g (100%). Found: C, 19.5; H, 2.1; N, 7.7. Calc. for $C_6H_8I_2N_2$ (361.953) C, 19.9; H, 2.2; N,

*Author to whom correspondence should be addressed.

7.7%. ^{1}H NMR (SO_2) δ(ppm) 7.10 s (C*H*), 6.45s (N*H*), relative to TMS. IR: ν(cm^{-1}) (CsI) 3330m, 3160w, 2920w, 1670w, 1628m, 1565m, 1528s, 1498s, 1320w, 1270m, 1155m, 1035m, 940w, 885m, 825m, 752s, 583m, 525w, 445m. Raman: ν(cm^{-1}) (647 nm, 60 mW, 20°C); (int) 872 (4), 817 (6), 739 (5), 599 (100), 327 (3), 314 (2), 275 (26), 200 (1), 81 (17).

Preparation of o-$C_6H_4(NH_2)_2I^+AsF_6^-$ **(2)**

A solution of 0.3147 g (2.91 mmol) of o-phenylene diamine in 5 cm^3 of SO_2 was reacted with 1.6576 g (2.91 mmol) of $I_3^+AsF_6^-$ in 5 cm^3 of SO_2 at room temperature. The reaction mixture was stirred for 1 h and the precipitated iodine was filtered off (D3). The remaining solution was evaporated and traces of dissolved iodine were removed by pumping in a dynamic vacuum. The remaining microcrystalline, deep red product was isolated nearly quantitatively. Yield: 1.2253 g (99%). Compound **2** was recrystallized twice from SO_2. Found: C, 17.4; H, 2.1; N, 6.8. Calc. for $C_6H_8AsF_6IN_2$ (423.952) C, 17.0; H, 1.9; N, 6.6%. MS (160°C, 70 eV): m/z (int.) 456 (3) AsI_3^+, 318 (3) $(C_6H_4N_2H_2)_3^+$, 300 (1) As_4^+, 254 (46) I_2^+, 180 (9) $C_6H_4N_2HAs^+$, 151 (6) AsF_4^+, 132 (77) AsF_3^+, 128 (11) HI^+, 127 (41) I^+, 113 (100) AsF_2^+, 105 (4) $C_6H_4N_2H^+$, 94 (5) AsF^+. ^{1}H NMR (SO_2) δ(ppm) 7.42 s, relative to TMS. Vapour pressure osmometry (THF) 467 g mol^{-1}. IR: ν(cm^{-1}) (CsI) 3320w, 3240w, 3220w, 1650w, 1610m, 1522s, 1490m, 1380w, 1258w, 1240w, 1155w, 842m, 757m, 698vs, 585m, 395s. Raman: ν(cm^{-1}) (647 nm, 100 mW, 20°C); (int): 736 (7), 600 (100), 273 (22), 236 (5), 167 (6), 96 (25).

Preparation of o-$C_6H_4(NH_2)_2I^+AlI_4^-$ **(3)**

To a suspension of 0.643 g (1.576 mmol) of AlI_3 in 5 cm^3 of SO_2 a solution of 0.570 g (1.576 mmol) of **1** in 5 cm^3 of SO_2 was added at room temperature. The mixture was stirred for 1 h at room temperature and the solvent evaporated. The remaining black product was recrystallized from SO_2. Yield: 0.946 g (78%). Found: C, 9.4; H, 1.1; N, 3.3. Calc. for $C_6H_8AlI_5N_2$ (769.626) C, 9.4; H, 1.0; N, 3.6%. ^{1}H NMR (SO_2) δ(ppm) 7.25s (C*H*), 6.27s (N*H*). IR: ν(cm^{-1}) (CsI) 3300s, br, 1670sh, 1615s, 1528m, 1490w, 1385vw, 1260vw, 1240vw, 1035m, 912m, 755m, br, 660w, 590w, 535w, 430w. Raman: ν(cm^{-1}) (647 nm, 75 mW, 20°C) 599.

RESULTS AND DISCUSSION

Preparative aspects

Reaction of o-phenylene diamine with elemental iodine led to the preparation of the new cationic iodoammonium salt **1** according to eq. (3):

$$o\text{-}C_6H_4(NH_2)_2 + I_2 \xrightarrow{SO_2} \underset{\textbf{(1)}}{o\text{-}C_6H_4(NH_2)_2I^+I^-}. \quad (3)$$

The hexafluoroarsenate species, **2**, was obtained by reaction of the amine with $I_3^+AsF_6^-$ [eq. (2)]. Complex **1** was converted into the tetraiodoaluminate salt, **3**, by reaction with one equivalent of AlI_3 according to eq. (4):

$$\mathbf{1} + AlI_3 \xrightarrow{SO_2} \underset{\textbf{(3)}}{o\text{-}C_6H_4(NH_2)_2I^+AlI_4^-}. \quad (4)$$

Complexes **1**, **2** and **3** were identified by chemical analysis (C, H, N), ^{1}H NMR, IR, Raman and mass spectroscopy. The quality of the elemental analyses varies and only freshly prepared samples give satisfying results; dependent on technique, too low C/H/N values (especially for the AlI_4^- salt) were often observed (probably due to carbide or nitride formation).

Thermodynamic aspects

On the basis of a simple Born–Haber cycle (Scheme 1) (using a similar approach to that described in ref. 10) we estimated that a reaction according to eq. (2) should be thermodynamically favourable ($\Delta H = -59$ kcal mol^{-1}). The Born–Haber cycle estimate for ΔH^0 for the reaction indicates that nitrogen is a better base towards I^+ than I^-. Therefore the cationic N—I species should be thermodynamically more stable than neutral compounds. This is in good agreement with the experimental results described above.

Vibrational spectroscopy

Direct evidence for N—I bonds was found in the Raman spectra of all compounds. The most intense peak at 599–600 cm^{-1} can be attributed to a N—I stretching mode (Fig. 1). Both, the shift to higher wavenumbers compared with the neutral tetracoordinated $NI_3 \cdot NH_3$ ($\nu_1 = 378$ cm^{-1})[14] due to the stronger N—I bond in the cationic species and the similarity to the isoelectronic carbon derivative (CH_3I, ν(CI) = 523 cm^{-1})[15] are in good agreement with the formulated N—I bond.

^{1}H *NMR spectroscopy*

In the room temperature ^{1}H NMR spectrum of **1** and **3** two resonances appear, one due to the CH, the other due to the NH protons. (N.B. ^{1}H NMR of o-$C_6H_4(NH_2)_2$ in SO_2: δ(ppm) 6.68s, 3.97s.)[6]

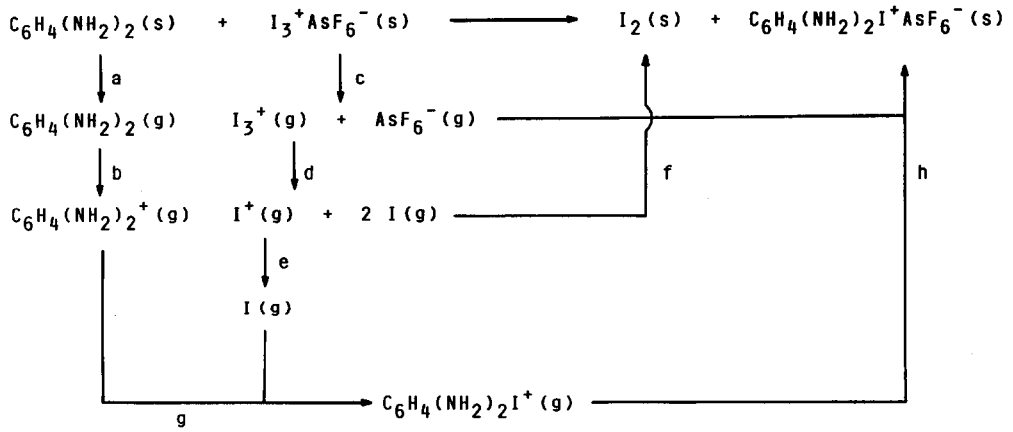

Scheme 1. Energy cycle for the formation of *o*-$C_6H_4(NH_2)_2I^+AsF_6^-$ (**2**) from *o*-phenylene diamine and $I_3^+AsF_6^-$ according to eq. (2). (a) $\Delta H_{Subl.}(C_6H_8N_2)$ was taken to be equal to 20 kcal mol^{-1} (cf. $\Delta H_{Subl.}$(salicylic acid) = 22.8 kcal mol^{-1}).[10] (b) $I_P(C_6H_8N_2) = 172$ kcal mol^{-1}.[11] (c) $U_L(I_3^+AsF_6^-) = 128$ kcal mol^{-1}.[12] (d) $\Delta H(I_3^+, g \rightarrow I^+, g+2I, g) = 72.4$ kcal mol^{-1}.[12] (e) ΔHI, $g \rightarrow I^+$, g) = 242.5 kcal mol^{-1}.[12] (f) $\Delta H_f^0(I, g) = 25.6$ kcal mol^{-1}.[12] (g) Bond energy (N—I) = 48 kcal mol^{-1}.[13] (h) $U_L(C_6H_8N_2I^+AsF_6^-) = 110$ kcal mol^{-1}. Estimated as demonstrated in ref. 12 using the linear relationship: U_L(kcal mol^{-1}) = 556.3 $V_M(Å^3)^{-0.33}+26.3$;[12] $V_M(AsF_6^-) = 105$ $Å^3$,[12] assuming that $V_M(C_6H_8N_2I^+)$ is equal to $V_M(C_6H_8N_2)+V_M(I^+)$, using $V_M(C_6H_8N_2) = 148$ $Å^3$ and $V_M(I^+) = 34$ $Å^3$.[10,12] This gives: a+b+c+d−e−2f−g−h = −59.3 kcal mol^{-1}.

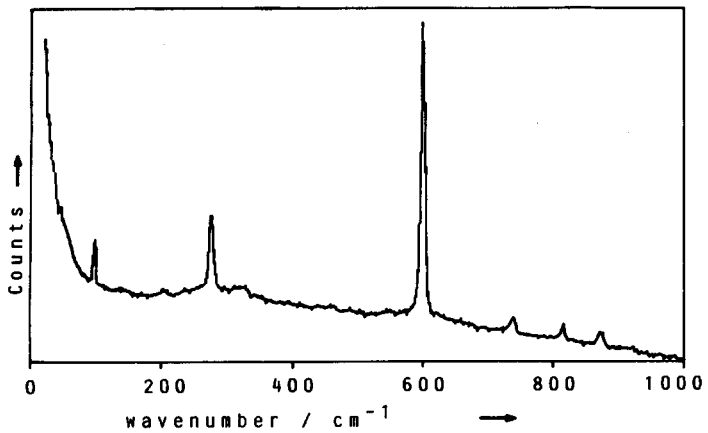

Fig. 1. Raman spectrum of *o*-$C_6H_4(NH_2)_2I^+I^-$ (**1**) (excitation line 647 nm, 100 mW, 20°C).

The room temperature spectrum of **2** shows one resonance in the aromatic CH region (7.42 ppm), which can be explained by intermolecular NH proton exchange (Fig. 2). As **2** is the only example with an iodine-free anion it may have the most ionic character, which probably favours the intermolecular exchange reactions. Moreover, the ^1H NMR spectrum of **2** (Fig. 2) shows a reversible temperature dependence. At low temperature resonances appear due to both the NH protons ("singlet") and the aromatic protons (multiplet, AA'XX' pattern).

The equivalence of the NH protons in all three compounds can be easily explained by the equilibrium of the cations according to eq. (5) and rapid exchange reactions:

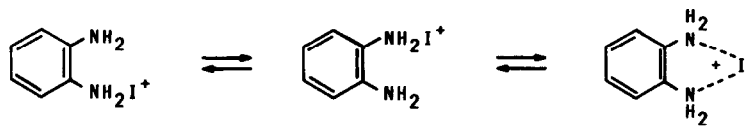

(5)

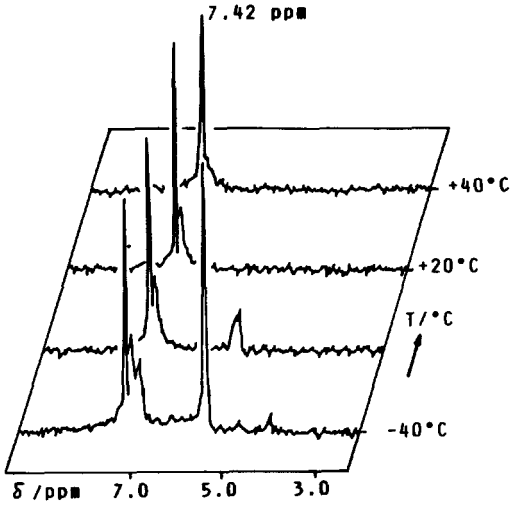

Fig. 2. Temperature-dependent ^1H NMR spectrum of *o*-$C_6H_4(NH_2)_2I^+AsF_6^-$ (**2**) in SO_2 solution, relative to TMS.

Acknowledgements—We thank the members of our department staff for support. We also acknowledge the financial support of the Technische Universität Berlin, the Deutsche Forschungsgemeinschaft and the Fonds der Chemischen Industrie.

REFERENCES

1. A. F. Holleman, E. Wiberg and N. Wiberg, *Lehrbuch der Anorganischen Chemie*, 91–100 edns, p. 403. Walter de Gruyter, Berlin, New York (1985).
2. R. A. Zingaro, C. A. VanderWerf and J. Kleinberg, *J. Am. Chem. Soc.* 1949, **71**, 575.
3. R. A. Zingaro and W. E. Tolberg, *J. Am. Chem. Soc.* 1959, **81**, 1353.
4. R. A. Zingaro and W. B. Witmer, *J. Phys. Chem.* 1960, **64**, 1705.
5. G. M. Anderson and J. M. Winfield, *J. Chem. Soc., Dalton Trans.* 1986, 337.
6. Th. Klapötke, J. Passmore and I. Tornieporth-Oetting, unpublished results.
7. J. Passmore and P. Taylor, *J. Chem. Soc., Dalton Trans.* 1976, 804.
8. R. Minkwitz and H. Prenzel, *Z. Anorg. Allg. Chem.* 1987, **548**, 97.
9. G. M. Anderson, I. F. Fraser and J. M. Winfield, *J. Fluorine Chem.* 1983, **23**, 403.
10. *Handbook of Chemistry and Physics*, 55th edn, p. 716. CRC Press, Cleveland (1974/75).
11. Beilstein, E IV 13, p. 38.
12. N. Burford, J. Passmore and J. C. P. Sanders, *Molecular Structure and Bonding*, Vol. 11. VCH Verlag Chemie, Weinheim (1989).
13. R. Steudel, *Chemistry of Non-metals*, p. 130. Walter de Gruyter, Berlin (1977).
14. J. Jander and U. Engelhardt, Nitrogen Compounds of Chlorine, Bromine and Iodine in *Developments in Inorganic Nitrogen Chemistry* (Edited by C. B. Colburn), Vol. 2, p. 184 and refs therein. Elsevier, Amsterdam (1973).
15. F. R. Dollish, W. G. Fateley and F. F. Bentley, *Characteristic Raman Frequencies of Organic Compounds*, p. 12. John Wiley, New York (1978).

Polyhedron Vol. 8, No. 24, pp. 2915–2923, 1989
Printed in Great Britain

0277-5387/89 $3.00+.00
© 1989 Pergamon Press plc

CARBOMOLYBDATE CLUSTERS FORMED BY CARBONYL INSERTION INTO MOLYBDENUM–OXYGEN BONDS. STRUCTURAL INVESTIGATION OF THE $[RMo_4O_{15}X]^{3-}$ CORE ($R = -C_9H_4O$, $X = OCH_3$; $R = -C_{14}H_{10}$, $X = -C_7H_5O_2$; $R = C_{14}H_8$, $X = -OH$)

QIN CHEN, SHUNCHENG LIU, HUIZHE ZHU and JON ZUBIETA*

Department of Chemistry, State University of New York at Albany, Albany, NY 12222, U.S.A.

(*Received* 22 *May* 1989; *accepted* 3 *August* 1989)

Abstract—$[(C_4H_9)_4N]_2[Mo_2O_7]$ reacts with a variety of organic species containing α-diketone groups to give tetranuclear complexes of general composition $[RMo_4O_{15}X]^{3-}$. The complexes $[(C_4H_9)_4N]_3[(C_9H_4O)Mo_4O_{15}(OCH_3)]$ (**I**), $[(C_4H_9)_4N]_3[(C_{14}H_{10})Mo_4O_{15}(C_6H_5CO_2)]$ (**II**) and $[(C_4H_9)_4N]_3[(C_{14}H_8)Mo_4O_{15}(OH)]$ (**III**) were synthesized from the reactions of dimolybdate with ninhydrin, benzil and phenanthraquinone, respectively. Complex **II** may also be prepared from dimolybdate and benzoin in acetonitrile–methanol solution, from which it co-crystallizes with the binuclear species $[(C_4H_9)_4N]_2[Mo_2O_5(C_6H_5C(O)C(O)C_6H_5)_2]\cdot CH_3CN\cdot CH_3OH$ (**IV**). Complexes **I–III** exhibit the tetranuclear core, previously described for the α-glyoxal derivatives $[(C_4H_9)_4N]_3[(HCCH)Mo_4O_{15}X]$, where $X = F^-$ or HCO_2^-. The ligands may be formally described as diketals, formed by insertion of ligand carbonyl subunits into molybdenum–oxygen bonds. The structures **I–III** differ most dramatically in the identity and coordination mode of the anionic ligand X^- which occupies a position opposite the diketal moiety relative to the $[Mo_4O_{11}]^{2+}$ central cage. Thus, **I** exhibits a doubly bridging methoxy group in this position, while **II** possesses a benzoate ligand with an unusual μ_3-O,O′ coordination mode. Complex **III** presents a hydroxy-group unsymmetrically bonded to three of the molybdenum centres. The stereochemical consequences of the various coordination modes are discussed. Crystal data: Compound **I**, monoclinic space group *Pc*, $a = 24.888(2)$, $b = 12.897(3)$, $c = 24.900(3)$ Å, $\beta = 101.94(2)°$, $D_{calc} = 1.28$ g cm^{-3} for $Z = 4$. Structure solution and refinement based on 8695 reflections with $F_o \geqslant 6\sigma(F_o)$ (Mo-K_α, $\lambda = 0.71073$ Å) converged at a conventional discrepancy factor of 0.060. Compound **II**, orthorhombic space group *Pbca*, $a = 20.426(6)$, $b = 26.916(6)$, $c = 32.147(7)$ Å, $V = 17673.2(20)$ Å^3, $D_{calc} = 1.33$ g cm^{-3} for $Z = 8$; 5224 reflections, $R = 0.076$. Compound **III**, tetragonal space group $I4_1/a$, $a = b = 48.129(6)$, $c = 13.057(2)$ Å, $V = 30246.2(12)$ Å^3, $D_{calc} = 1.35$ g cm^{3-} for $Z = 16$; 5554 reflections, $R = 0.053$. Compound **IV**, orthorhombic space group *Pnca*, $a = 16.097(4)$, $b = 16.755(4)$, $c = 25.986(7)$ Å, $V = 7008.1(13)$ Å^3, $Z = 4$, $D_{calc} = 1.18$ g cm^{-3}; 2944 reflections, $R = 0.061$.

Molybdenum oxides are remarkably versatile heterogeneous catalysts for numerous organic transformations as diverse as methanol oxidation,[1] propylene oxidation[2] and olefin metathesis.[3] As a consequence of the difficulty of characterizing these catalysts at a molecular level, coordination compounds of polyoxomolybdates with simple organic substrate molecules have received considerable attention.[4] Structurally characterized examples of polyoxomolybdate complexes incorporating relevant organic subunits include the formate derivative $[Mo_8O_{26}(HCO_2)_2]^{6-}$,[5] the alkoxy derivatives $[Mo_8O_{24}(OCH_3)_4]^{4-}$,[6] $[Mo_4O_8(OC_2H_5)_2\{CH_3C(CH_2O)_3\}_2]$,[7] $[Mo_4O_{10}(OCH_3)_6]^{2-}$,[8] and $[Mo_3O_6$

*Author to whom correspondence should be addressed.

$(OCH_3)\{CH_3C(CH_2O)_3\}_2]^-$[9] and the siloxy derivatives of $[MoO_3(P_3O_9)]^{2-}$[10] and of the niobotungstate $[Nb_2W_4O_{19}]^{4-}$.[11] In the specific case of polyoxomolybdate–carbonyl interactions, the acetal derivatives $[(H_2CO_2)(Mo_4O_{12})(OH)]^{3-}$,[12] the diacetal species $[(H_2C_2O_4)(Mo_4O_{11})X]^{3-}$ (X = —F and HCO_2),[13] and the diketal $[(C_{14}H_8O_4)(Mo_4O_{11})(OCH_3)]^{3-}$[14] have been described. A common feature of these latter complexes is the insertion of the reactant carbonyl groups into Mo—O bonds. The product carbomolybdate clusters of general structural formula $[RMo_4O_{15}X]^{3-}$ contain an oxo-bridged tetranuclear core of sufficient structural flexibility to accommodate anions, X^-, of various sizes and with different bonding requirements.

As part of our investigations of the coordination chemistry of polyoxomolybdates with organic ligands containing α-dicarbonyl subunits, we have synthesized and structurally characterized a series of tetranuclear oxomolybdate–diketal complexes $[RMo_4O_{15}X]^{3-}$ (R = —C_9H_4O, X = —OCH_3, **I**; R = —$C_{14}H_{10}$, X = —$C_7H_5O_2$, **II**; R = —$C_{14}H_8$, X = —OH, **III**). Herein, we compare the structures of **I**–**III** with those of the related diacetal species $[(CH_2)Mo_4O_{15}H]^{3-}$[12] and $[(H_2C_2)Mo_4O_{15}X]^{3-}$ (X = —F and HCO_2)[13] and describe structural features related to the conformational flexibility of these polyoxomolybdate anions. The structure of the binuclear complex $[(C_4H_9)_4N]_2[Mo_2O_5(C_6H_5COCOC_6H_5)_2]$ (**IV**), which co-crystallizes in the synthesis of **II** from benzoin, is also described.

RESULTS AND DISCUSSION

Synthetic and spectroscopic properties

The reaction of the α-dialdehyde glyoxal, OHCCHO, with polyoxomolybdates was shown to yield the formylated methylenedioxymolybdate $[(OHCCH)Mo_4O_{15}H]^{3-}$,[13] a species structurally analogous to the acetal derivative $[CH_2Mo_4O_{15}H]^{3-}$.[12] The subsequent reaction of $[(OHCCH)Mo_4O_{15}H]^{3-}$ with acids, HX, resulted in the displacement of the reactant OH^- ligand by the X^- group and insertion of the pendant formyl–carbonyl group into a Mo—O bond. The unanticipated product of this reaction contains formally a diacetal unit, $(O_2HCCHO_2)^{4-}$, and a monoanionic ligand, X^-, coordinated to the $[Mo_4O_{11}]^{2+}$ core:

$$[(OHCCH)Mo_4O_{15}H]^{3-} + HX \longrightarrow [(HCCH)Mo_4O_{15}X]^{3-} + H_2O.$$

In contrast, the reactions of organic substrates containing the α-diketone subunit with dimolybdate proceed directly to the diketal products of the type $[RMo_4O_{15}X]^{3-}$. Thus, the reactions of dimolybdate, $[(n\text{-}C_4H_9)_4N]_2[Mo_2O_7]$, with 1,2,3-indantrione (ninhydrin), benzil and phenanthraquinone in methanol yielded the products $[(n\text{-}C_4H_9)_4N]_3[(C_9H_4O)Mo_4O_{15}(OCH_3)]$ (**I**), $[(n\text{-}C_4H_9)_4N]_3[(C_{14}H_{10})Mo_4O_{15}(C_7H_5O)]$ (**II**) and $[(n\text{-}C_4H_9)_4N]_3[(C_{14}H_8)Mo_4O_{15}(OH)]$ (**III**), respectively. In all cases, the α-diketone subunit of the organic ligand is incorporated into the $[RMo_4O_{15}X]^{3-}$ structure by insertion into the Mo—O bonds of adjacent metal centres, to give species which may be alternatively formulated as diketals $[(O_2RO_2)Mo_4O_{11}X]^{3-}$, in an analogous fashion to the previously reported diacetal species, $[(O_2HCCHO_2)Mo_4O_{11}X]^{3-}$.[12]

An unanticipated feature of the chemistry is the incorporation of a variety of anions, X^-, into the various complexes. Thus, complexes **I**, **II** and **III** are isolated directly from methanol as the methoxy, benzoate and hydroxy derivatives, respectively. The tetranuclear core associated with these complexes has been demonstrated to possess sufficient conformational flexibility to accommodate a variety of anions.[13] Thus, compound **III** reacts with a variety of reagents to replace the OH^- groups, yielding $[(C_{14}H_8)Mo_4O_{15}X]^{3-}$, where X^- = —F (**IIIa**), CH_3CO_2 (**IIIb**) and —OC_2H_5 (**IIIc**). The presence of a benzoate group $C_6H_5CO_2$ in **II** implies that a degree of C—C bond cleavage results as a consequence of carbonyl insertion into the Mo—O bonds. Although the details of the mechanism of benzoate formation have not been elucidated, C—C bond cleavage in combination with carbonyl insertion is a feature of the chemistry of multicentre molybdenum clusters with organic substrates.[15]

Complex **II** was synthesized from the reaction of $[Mo_2O_7]^{2-}$ with either benzil, $C_6H_5COCOC_6H_5$, or benzoin, $C_6H_5COCHOHC_6H_5$. However, the benzoin reaction yielded a mixture of products, the tetranuclear species **II** and the binuclear complex $[(C_4H_9)_4N]_2[Mo_2O_5(C_6H_5COCOC_6H_5)_2]$ (**IV**), which contains the dienolate form of the ligand, rather than the diketal insertion product.

The IR spectra of the complexes of this study exhibit several common features: two C—O absorptions in the 990–1100 cm^{-1} region and a similar pattern of Mo—O absorptions in the 500–950 cm^{-1} region. In addition, **I** exhibits a medium intensity sharp band at 3050 cm^{-1} assigned to ν(C—H) of the methoxy group and a strong band at 1630 cm^{-1} assigned to the uncoordinated carbonyl group of the organic ligand. The medium intensity band at 1565 cm^{-1} in the spectrum of **II** is assigned to the benzoate carbonyl group. The C—O absorp-

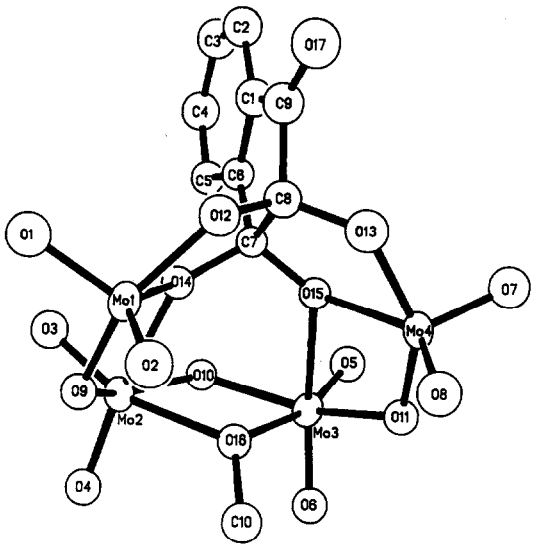

Fig. 1. ORTEP view of the structure of one of the two $[(C_9H_4O)Mo_4O_{15}(OCH_3)]^{3-}$ anions of the asymmetric unit of **I**.

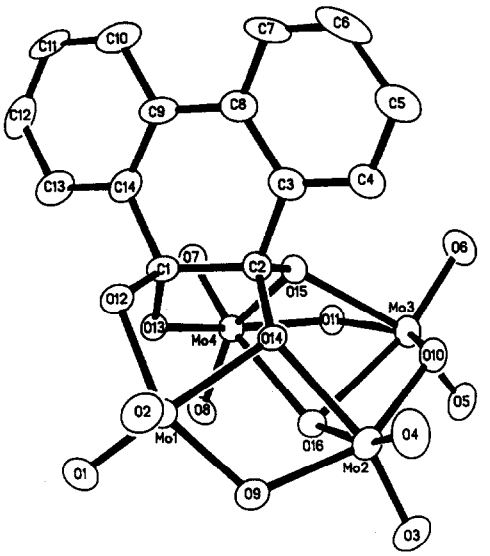

Fig. 3. ORTEP view of the structure of $[(C_{14}H_8)Mo_4O_{15}(OH)]^{3-}$ (**III**).

tions of the coordinated diketal subunit of **I** were shifted *ca* 15 cm^{-1} upon ^{18}O enrichment from 1082 and 1003 cm^{-1} to 1068 and 987 cm^{-1}, respectively.

Structural studies

The structures of complexes **I**, **II** and **III** are illustrated in Figs 1–3, respectively. Table 1 compares relevant bond lengths for the structures, while Table 2 lists selected bond angles.

The structures consist of discrete $[RMo_4O_{15}X]^{3-}$ anions which are structurally similar to the $[(HCCH)Mo_4O_{15}X]^{3-}$ anion.[13] As a consequence of two carbonyl residues inserting into the cluster core, complex **I** may be described as a diketal derivative with the $(C_9H_4O_5)^{4-}$ unit capping the $[Mo_4O_{11}(OCH_3)]^{+}$ framework, providing terminal [O(12) and O(13)] and bridging [O(14) and O(15)] oxygen donor interactions. Thus, the central $[Mo_4O_{11}]^{2+}$ tetramolybdate unit is bonded to the $(C_9H_4O_5)^{4-}$ and $(OCH_3)^{-}$ groups occupying the opposite poles. The gross structural details of complexes **II** and **III** are similar to those of **I**, with the exception of the identities of the diketal subunits and the anionic group X^{-}.

The structural variations exhibited by complexes **I**–**III** are consequences of the coordination requirements of the various X^{-} groups. As illustrated by the schematics in Fig. 4, $[\{(CH_3)_2As\}Mo_4O_{15}H]^{2-}$ [16] and $[(H_2C)Mo_4O_{15}H]^{3-}$ [12] provide the structural

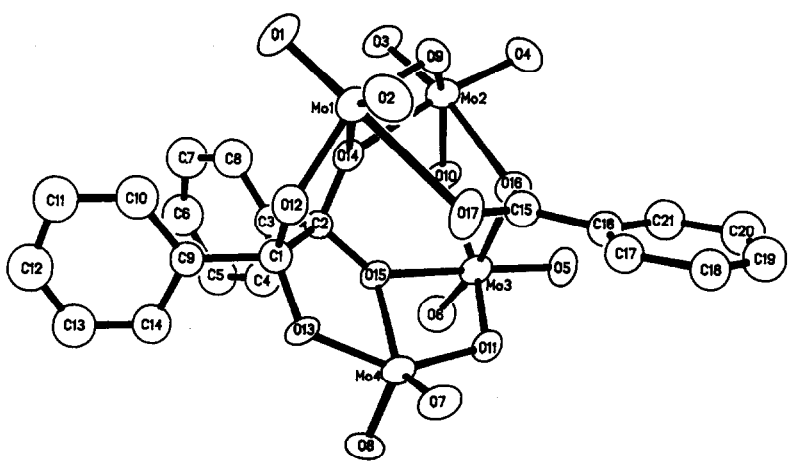

Fig. 2. Perspective view of the structure of $[(C_{14}H_{10})Mo_4O_{15}(C_6H_5CO_2)]^{3-}$ (**II**), showing the atom-labelling scheme.

Table 1. Selected bond lengths (Å) for $(TBA)_3[(C_9H_4O)Mo_4O_{15}(OCH_3)]$ (I), $(TBA)_3[(C_{14}H_{10})Mo_4O_{15}(C_6H_5CO_2)]$ (II) and $(TBA)_3[(C_{14}H_8)Mo_4O_{15}(OH)]$ (III)[a]

	I[b]		II	III
	A	B		
Mo(1)—O(1)	1.735(14)	1.690(14)	1.714(12)	1.704(8)
Mo(1)—O(2)	1.672(15)	1.660(14)	1.731(13)	1.697(7)
Mo(1)—O(9)	1.886(10)	1.868(11)	1.936(12)	1.866(7)
Mo(1)—O(12)	1.913(12)	1.947(11)	1.978(12)	1.955(7)
Mo(1)—O(14)	2.074(10)	2.100(9)	2.110(11)	2.125(7)
Mo(2)—O(3)	1.733(13)	1.694(12)	1.704(12)	1.690(8)
Mo(2)—O(4)	1.695(12)	1.684(11)	1.702(13)	1.672(9)
Mo(2)—O(9)	1.936(10)	1.949(10)	1.921(13)	1.983(7)
Mo(2)—O(10)	1.898(10)	1.922(11)	1.918(12)	1.928(7)
Mo(2)—O(14)	2.287(10)	2.315(9)	2.258(12)	2.195(6)
Mo(2)—O(16)	2.165(11)	2.186(10)	2.330(12)	2.303(7)
Mo(3)—O(5)	1.680(12)	1.732(12)	1.728(13)	1.700(8)
Mo(3)—O(6)	1.722(12)	1.722(13)	1.718(13)	1.716(8)
Mo(3)—O(10)	1.937(10)	1.986(10)	1.911(11)	1.910(7)
Mo(3)—O(11)	1.941(11)	1.888(10)	1.954(12)	1.946(7)
Mo(3)—O(15)	2.308(10)	2.274(9)	2.233(11)	2.322(7)
Mo(3)—O(16)	2.155(10)	2.174(10)	2.385(12)	2.303(7)
Mo(4)—O(7)	1.668(10)	1.705(13)	1.720(12)	1.716(7)
Mo(4)—O(8)	1.674(14)	1.705(12)	1.719(13)	1.718(7)
Mo(4)—O(11)	1.891(11)	1.852(10)	1.915(13)	1.901(6)
Mo(4)—O(13)	1.951(14)	1.973(11)	1.936(12)	1.976(7)
Mo(4)—O(15)	2.100(10)	2.073(9)	2.076(11)	2.152(7)
Mo(4)—O(16)	—	—	—	2.508(7)

[a] (TBA) = $[(C_4H_9)_4N]^+$.

[b] Two independent molecules in the asymmetric unit. The atom-labelling is for molecule **A**. The corresponding atoms for **B** are as follows: Mo(1)—Mo(4) in **A**, Mo(5)—Mo(8) in **B**; O(1)—O(8) (**A**), O(18)—O(25) (**B**); O(9)—O(16) (**A**), O(26)—O(33) (**B**) (See supplementary materials).

prototypes for this structural class. Thus, structure **2** may be described in terms of a $[Mo_4O_{12}]^{2+}$ ring connected to a $(H_2CO_2)^{2-}$ moiety and an OH^- unit on opposite faces. Since the hydroxy group functions so as to bridge the four molybdenum centres, the coordination geometry about the molybdenum atoms is pseudo-octahedral. However, the introduction of the diacetal moiety in **3** results in the incorporation of one of the bridging oxo groups of the Mo_4O_4 heterocycle, present in both **1** and **2**, into the diacetal linkage with a concomitant increase in the Mo(1)···Mo(4) distance. The

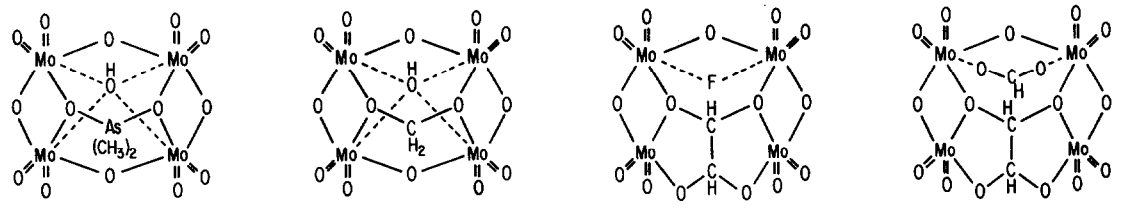

Fig. 4. Schematic representations of the structures of $[\{(CH_3)_2As\}Mo_4O_{15}H]^{2-}$ (**1**), $[(H_2C)Mo_4O_{15}H]^{3-}$ (**2**), $[(HCCH)Mo_4O_{15}F]^{3-}$ (**3**), and $[(HCCH)Mo_4O_{15}(HCO_2)]^{3-}$ (**4**).

Table 2. Selected bond angles (°) for $(TBA)_3[(C_9H_4O)Mo_4O_{15}(OCH_3)]$ (I), $(TBA)_3[(C_{14}H_{10})Mo_4O_{15}(C_6H_5CO_2)]$ (II) and $(TBA)_3[(C_{14}H_8)Mo_4O_{15}(OH)]$ (III)

	I		II	III
	A	B		
O(1)—Mo(1)—O(2)	108.7(7)	110.1(7)	104.4(7)	106.0(4)
O(1)—Mo(1)—O(9)	102.6(6)	103.0(6)	101.0(6)	104.1(4)
O(1)—Mo(1)—O(12)	100.5(6)	100.2(6)	100.5(6)	100.3(3)
O(1)—Mo(1)—O(14)	113.7(5)	117.7(5)	101.4(5)	110.8(7)
O(2)—Mo(1)—O(9)	99.5(6)	100.2(6)	105.9(6)	97.9(4)
O(2)—Mo(1)—O(12)	94.5(6)	97.2(6)	95.9(6)	97.8(4)
O(2)—Mo(1)—O(14)	137.4(6)	132.0(5)	153.8(6)	143.2(3)
O(9)—Mo(1)—O(12)	147.4(5)	147.2(5)	144.3(5)	145.9(3)
O(9)—Mo(1)—O(14)	74.8(4)	73.1(4)	73.5(5)	74.6(3)
O(12)—Mo(1)—O(14)	74.9(5)	74.6(4)	74.6(5)	74.7(3)
O(3)—Mo(2)—O(4)	102.4(6)	103.5(6)	104.0(7)	104.4(5)
O(3)—Mo(2)—O(9)	99.2(5)	96.8(5)	101.6(6)	98.2(4)
O(3)—Mo(2)—O(10)	96.9(5)	103.6(5)	100.5(6)	96.2(4)
O(3)—Mo(2)—O(14)	89.7(5)	93.0(5)	90.3(5)	95.2(4)
O(3)—Mo(2)—O(16)	161.4(5)	162.3(5)	168.5(6)	167.0(4)
O(4)—Mo(2)—O(9)	99.3(5)	90.3(5)	98.1(6)	97.5(4)
O(4)—Mo(2)—O(10)	103.8(5)	101.2(5)	101.9(6)	102.9(4)
O(4)—Mo(2)—O(14)	164.6(5)	164.2(5)	163.5(5)	158.5(4)
O(4)—Mo(2)—O(16)	95.2(5)	100.7(5)	85.5(6)	87.1(4)
O(9)—Mo(2)—O(10)	148.3(4)	145.4(4)	145.5(5)	151.2(3)
O(9)—Mo(2)—O(14)	69.1(4)	68.6(4)	70.4(5)	70.8(3)
O(9)—Mo(2)—O(16)	83.7(4)	82.0(4)	83.1(5)	86.0(3)
O(10)—Mo(2)—O(14)	83.9(4)	81.8(4)	83.4(5)	83.2(3)
O(10)—Mo(2)—O(16)	72.8(4)	72.7(4)	70.8(5)	75.1(3)
O(14)—Mo(2)—O(16)	74.1(4)	74.4(4)	81.4(4)	74.4(2)
O(5)—Mo(3)—O(6)	100.6(6)	96.9(5)	102.8(6)	104.9(4)
O(5)—Mo(3)—O(10)	104.9(5)	105.6(5)	103.5(6)	100.7(3)
O(5)—Mo(3)—O(11)	97.6(5)	97.9(5)	97.6(6)	97.2(3)
O(5)—Mo(3)—O(15)	163.8(5)	163.1(5)	161.6(5)	158.2(3)
O(5)—Mo(3)—O(16)	93.7(5)	92.6(5)	86.1(5)	92.4(3)
O(6)—Mo(3)—O(10)	96.8(5)	98.6(5)	101.4(6)	100.6(4)
O(6)—Mo(3)—O(11)	100.5(5)	101.8(5)	102.2(6)	99.8(4)
O(6)—Mo(3)—O(15)	91.7(5)	90.2(4)	92.8(5)	95.1(3)
O(6)—Mo(3)—O(16)	164.0(5)	165.2(2)	168.9(6)	162.7(3)
O(10)—Mo(3)—O(11)	148.4(4)	148.5(4)	143.8(5)	148.4(3)
O(10)—Mo(3)—O(15)	83.7(4)	84.0(4)	82.5(5)	84.3(3)
O(10)—Mo(3)—O(16)	72.3(4)	76.4(4)	69.7(5)	75.5(3)
O(11)—Mo(3)—O(15)	69.6(4)	68.6(4)	69.3(5)	70.1(3)
O(11)—Mo(3)—O(16)	84.5(4)	84.2(4)	82.9(5)	78.0(3)
O(15)—Mo(3)—O(16)	75.7(4)	74.1(4)	79.7(4)	68.1(2)
O(7)—Mo(4)—O(8)	108.1(7)	105.6(6)	108.0(6)	105.1(4)
O(7)—Mo(4)—O(11)	98.2(6)	98.4(5)	100.4(6)	102.8(3)
O(7)—Mo(4)—O(13)	95.8(6)	96.0(5)	95.8(6)	97.8(3)
O(7)—Mo(4)—O(15)	137.9(5)	140.6(5)	141.8(5)	149.0(5)
O(7)—Mo(4)—O(16)	—	—	—	82.6(3)
O(8)—Mo(4)—O(11)	103.2(6)	102.4(5)	102.8(6)	98.8(3)
O(8)—Mo(4)—O(13)	100.0(6)	100.8(5)	100.2(6)	98.2(3)
O(8)—Mo(4)—O(15)	113.9(5)	113.5(5)	110.1(6)	105.8(3)
O(8)—Mo(4)—O(16)	—	—	—	170.5(3)
O(11)—Mo(4)—O(13)	147.4(5)	148.5(5)	146.1(5)	148.7(3)
O(11)—Mo(4)—O(15)	75.3(4)	75.7(4)	73.5(5)	74.8(3)
O(11)—Mo(4)—O(16)	—	—	—	73.7(3)
O(13)—Mo(4)—O(15)	74.5(5)	74.5(4)	75.4(5)	75.4(3)
O(13)—Mo(4)—O(16)	—	—	—	86.1(3)
O(15)—Mo(4)—O(16)	—	—	—	67.0(2)
Mo(2)—O(16)—Mo(3)	98.1(4)	96.8(4)	92.5(4)	91.2(3)
Mo(2)—O(16)—Mo(4)	—	—	—	139.4(3)
Mo(3)—O(16)—Mo(4)	—	—	—	81.4(2)
Mo(2)—O(10)—Mo(3)	116.7(5)	116.4(5)	125.6(6)	118.0(4)

Table 3. Comparison of selected bond lengths (Å) and angles (°) for $(TBA)_3[(HCCH)Mo_4O_{15}F]$ (**3**), $(TBA)_3[(HCCH)Mo_4O_{15}(HCO_2)]$ (**4**), $(TBA)_3[(C_9H_4O)Mo_4O_{15}(OCH_3)]$ (**I**), $(TBA)_3[(C_{14}H_{10})Mo_4O_{15}(C_6H_5CO_2)]$ (**II**) and $(TBA)_3[(C_{14}H_8)Mo_4O_{15}(OH)]$ (**III**)

	3	4	I	II	III
Mo(1)···Mo(4)	4.603(2)	5.143(3)	4.686(2)	4.790(2)	4.525(1)
Mo(1)···Mo(2)	3.271	3.231	3.283(2)	3.303(2)	3.266(1)
Mo(2)···Mo(3)	3.294	3.675	3.264(2)	3.406(2)	3.290(1)
Mo(2)—O(X)	2.224(8)(F)	2.297(13)	2.165(11)	2.330(12)	2.303(7)
Mo(3)—O(X)	2.224(8)(F)	2.297(13)	2.155(10)	2.385(12)	2.303(7)
Mo(1)—O(X)	3.651(8)(F)	2.962(16)	3.401(10)	3.672(11)	3.702(7)
Mo(4)—O(X)	3.129(8)(F)	2.962(16)	3.452(11)	3.842(12)	2.508(7)
Mo(2)—O(10)—Mo(3)	118.7(4)	149.6(5)	116.7(5)	125.6(6)	118.0(4)
Mo(2)—O(16)—Mo(3)	—	—	97.5(4)	92.5(4)	91.2(3)
Mo(1)—O(9)—Mo(2)	117.2(5)	114.1(5)	118.4(5)	117.8(6)	116.1(4)

$[Mo_4O_{12}]^{2+}$ core associated with **1** and **2** is transformed into the more flexible $[Mo_4O_{11}]^{4+}$ core. Since the bridging fluoride group (X^-) in **3** bridges the Mo(2) and Mo(3) sites only, the structure exhibits non-equivalent molybdenum centres; Mo(1) and Mo(4) are pentacoordinate with distorted trigonal bipyramidal geometry, while Mo(2) and Mo(3) display the usual pseudo-octahedral geometry. Replacement of F^- in **3** by formate in **4** produces an analogous structure with the bridging bidentate formate group coordinating to Mo(2) and Mo(3).

The methoxy derivative of this study, $[(C_9H_4O)Mo_4O_{15}(OCH_3)]^{3-}$ (**I**), which exhibits two independent molecules in the asymmetric unit, is structurally analogous to **3** with fluoride replaced by $-OCH_3$. In contrast, structures **II** and **III** demonstrate the remarkable flexibility of this structural type. The bridging benzoate group of $[(C_{14}H_{10})Mo_4O_{15}(C_6H_5CO_2)]^{3-}$ (**II**) does not adopt the symmetrical bidentate bridging mode of the formate group of **4**, but rather bridges the Mo(2) and Mo(3) centres through one carboxylate oxygen donor while bonding to Mo(1) through the other carboxylate oxygen in a weak interaction (2.62 Å). As a result of this unusual bridging mode, there are three chemically and crystallographically distinct molybdenum sites in **II**: the hexacoordinate Mo(1) centre, the carboxylate-bridged Mo(2) and Mo(3) sites, and the pentacoordinate Mo(4) centre. The hydroxy derivative, **III**, exhibits a similar pattern of molybdenum sites as a consequence of the triply-bridging OH^- group.

The data summarized in Table 3 show how the geometry of the $[RMo_4O_{15}X]^{3-}$ unit adjusts to accommodate various X^- groups. As the Mo(2)···Mo(3) separation increases, the Mo(2)—O(10)—Mo(3) angle also expands. Further adjustment in the anion geometry is provided by variation in the Mo(1)···Mo(4) distance coupled to rotation about the C—C bond of the (O_2CCO_2) unit of the diketal ligand.

The structure of the binuclear complex anion of **IV** is illustrated in Fig. 5 and is seen to consist of the $[Mo_2O_5]^{2+}$ core coordinated to two dienolate ligands functioning as bidentate chelating and bridging units. The molybdenum centres adopt $[MoO_6]$ pseudo-octahedral geometry via coordination to two terminal oxo groups, a bridging oxo group, the chelating enolate oxygen donors, O(4) and O(5), of the ligand, and the weakly coordinating bridging alkoxy group, O(4). The geometry of the molybdenum centres may be described alternatively as square-pyramidal with a weak axial interaction to the bridging oxygen donor. Thus, the oxygen donors occupying the basal plane, O(1), O(2), O(4) and O(5), are displaced away from the apical O(3) toward the Mo(1)—O(4a) vector, as demonstrated by the O(3)—Mo(1)—O(basal) angles in the range 102.3(2)–105.3(3)°.

The metrical parameters associated with the $[Mo_2O_5]^{2+}$ core are unexceptional as shown in Table 4. The lengthening of the Mo(1)—O(4) bond relative to the Mo(1)—O(5) distance (2.119(5) vs 1.972(5) Å) may be attributed to the strong *trans* influence of the terminal oxo group, O(2), compared to the negligible *trans* influence of the bridging O(1) group upon O(5) and to the adoption of a weakly-bridging coordination mode by O(4).

Since the ligand may be considered to be in the dienolate form, a double bond interaction between C(7)—C(8) is anticipated. The C(7)—C(8) bond distance of 1.343(11) Å is consistent with this description of the ligand structure and may be compared

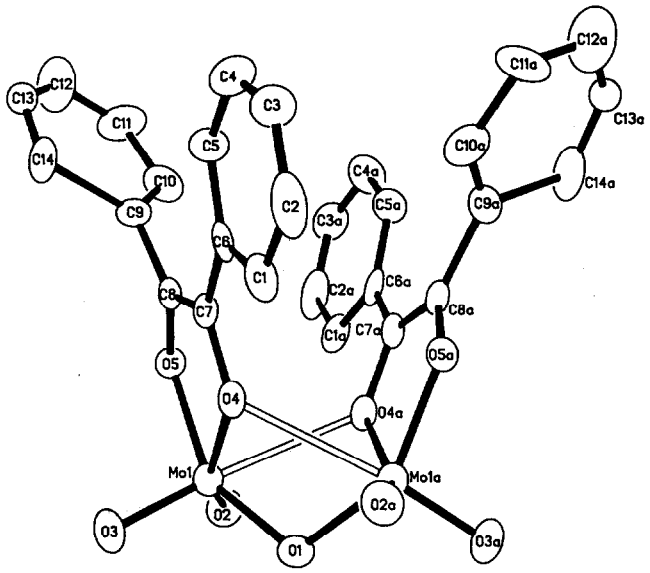

Fig. 5. ORTEP view of the structure of $[Mo_2O_5(C_6H_5COCOC_6H_5)_2]^{2-}$ (IV).

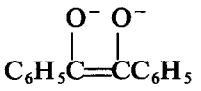

to the corresponding C(1)—C(2) distance of 1.62(2) Å for II, where these carbon centres are assumed to be sp^3-hybridized. A further consequence of this coordination mode is the planarity of the [C(6)—C(7)—O(4)—Mo(1)—O(5)—C(8)—C(9)] moiety.

EXPERIMENTAL

Materials and methods

All reactions were performed in freshly dried and distilled solvents. Dichloromethane was technical grade and was redistilled from $CoCl_2$ and P_4O_{10}. All other solvents were reagent grade. All other reagents were obtained from standard commercial sources without further purification $[(n\text{-}C_4H_9)_4N]_2$

Table 4. Selected bond lengths (Å) and angles (°) for $[(C_4H_9)_4N]_2[Mo_2O_5(C_6H_5COCOC_6H_5)_2]$ (IV)

Mo(1)—O(1)	1.904(4)	O(4)—C(7)	1.365(10)
Mo(1)—O(2)	1.713(5)	O(5)—C(8)	1.358(9)
Mo(1)—O(3)	1.710(6)	C(7)—C(8)	1.343(11)
Mo(1)—O(4)	2.119(5)		
Mo(1)—O(4a)	2.601(5)		
Mo(1)—O(5)	1.972(5)		
O(1)—Mo(1)—O(2)	103.0(2)	O(3)—Mo(1)—O(4a)	165.7(2)
O(1)—Mo(1)—O(3)	102.3(2)	O(3)—Mo(1)—O(5)	102.6(3)
O(1)—Mo(1)—O(4)	77.9(2)	O(4)—Mo(1)—O(4a)	70.5(3)
O(1)—Mo(1)—O(4a)	66.4(2)	O(4)—Mo(1)—O(5)	75.3(2)
O(1)—Mo(1)—O(5)	145.8(2)	O(4a)—Mo(1)—O(5)	84.9(2)
O(2)—Mo(1)—O(3)	105.3(3)	Mo(1)—O(1)—Mo(1a)	113.9(3)
O(2)—Mo(1)—O(4)	154.6(2)	O(4)—Mo(1)—O(5)	75.3(2)
O(2)—Mo(1)—O(4a)	86.3(2)	Mo(1)—O(4)—C(7)	115.0(4)
O(2)—Mo(1)—O(5)	92.7(2)	O(4)—C(7)—C(6)	116.0(7)
O(3)—Mo(1)—O(4)	99.3(2)	O(4)—C(7)—C(8)	113.7(7)
		C(7)—C(8)—C(9)	132.6(7)
		C(7)—C(8)—O(5)	116.5(7)
		O(5)—C(8)—C(9)	111.0(7)
		Mo(1)—O(5)—C(8)	119.1(5)

$[Mo_2O_7]$ was prepared according to the published method.[17]

The following instruments were used in this work: IR, Perkin–Elmer 283B IR spectrophotometer; X-ray crystallography, Nicolet R3m/V diffractometer.

X-ray crystallography

The details of the crystal data, data collection and refinement procedures are given in Table 5. Supplementary Tables S.1, S.7, S.13 and S.19 provide atomic positional parameters for the structures

Table 5. Summary of experimental details for the X-ray diffraction studies of $[(n\text{-}C_4H_9)_4N]_3[(C_9H_4O)Mo_4O_{15}(OCH_3)]$ (I), $[(n\text{-}C_4H_9)_4N]_3[(C_{14}H_{10})Mo_4O_{15}(C_6H_5CO_2)]$ (II), $[(n\text{-}C_4H_9)_4N]_3[(C_4H_8)Mo_4O_{15}(OH)]$ (III) and $[(n\text{-}C_4H_9)_4N]_2[Mo_2O_5(C_6H_5COCOC_6H_5)_2]$ (IV)

	I	II	III	IV
a (Å)[a]	24.888(2)	20.426(6)	48.129(6)	16.097(4)
b (Å)	12.897(3)	26.916(6)	48.129(6)	16.755(4)
c (Å)	24.900(3)	32.147(7)	13.057(2)	25.986(7)
α (°)	90.00	90.00	90.00	90.00
β (°)	101.94(2)	90.00	90.00	90.00
γ (°)	90.00	90.00	90.00	90.00
V (Å^3)	7823.1(12)	17673.2(20)	30246.2(12)	7008.1(13)
Space group	*Pc*	*Pbca*	$I4_1/a$	*Pnca*
Z	4	8	16	4
D_{calc} (g cm^{-3})	1.28	1.33	1.35	1.18
Crystal shape and colour	Colourless block	Colourless block	Colourless block	Brown block
Crystal dimensions (mm)	0.25 × 0.24 × 0.33	0.30 × 0.26 × 0.27	0.26 × 0.31 × 0.30	0.41 × 0.22 × 0.21
Instrument	Nicolet R3m/V diffractometer			
Radiation	Mo-K_α (λ = 0.71073 Å)			
Scan type	Moving crystal—stationary counter			
Scan range	$2 \leqslant 2\theta \leqslant 45°$			
Scan rate	2–10° min^{-1}			
Scan width (°)	From $[2\theta(K\alpha_1 - 1.0)]$ to $[2\theta(K\alpha_2 + 1.0)]°$			
Background measurement	Stationary crystal, stationary counter, at the beginning and end of each 2θ scan, each for half the time taken for the scan			
Standards	Collected every 200 data			
Number of reflections collected	11,068 $(\pm h, +k, +l)$	11,563 $(+h, +k, +l)$	10,107 $(+h, +k, +l)$	5093 $(+h, +k, +l)$
Number of reflections used in solution $[F_o \geqslant 6\sigma(F_o)]$	8695	5224	5554	2944
Absorption coefficient (cm^{-1})	6.48	6.01	6.59	3.90
Absorption correction	None applied			
Structure solution[b]	Patterson synthesis yielded the molybdenum positions; all remaining non-hydrogen atoms were located via standard Fourier techniques			
Atomic scattering factors[c]	Neutral atomic scattering factors were used throughout the analysis			
Anomalous dispersion[d]	Applied to all non-hydrogen atoms			
Final discrepancy factors[e] R	0.060	0.076	0.053	0.061
R_w	0.064	0.081	0.063	0.067
Goodness-of-fit[f]	1.84	1.99	1.72	1.93

[a] From a least-squares fitting of the setting angle of 25 reflections.

[b] All calculations were performed on a Data General Nova 3 computer with 32K of 16-bit words using local versions of the Nicolet SHELTEX interactive crystallographic software package as described in G. M. Sheldrick, *Nicolet SHELTEX Operations Manual.* Nicolet XRD Corporation, Cupertino, California (1979).

[c] D. T. Cromer and J. B. Mann, *Acta Cryst.* 1968, **24A**, 321.

[d] *International Tables for X-ray Crystallography*, Vol. III. Kynoch Press, Birmingham, U.K. (1962).

[e] $R = \Sigma[|F_o| - |F_c|/\Sigma|F_o|]$; $R_w = [\Sigma w(|F_o| - |F_c|)^2/\Sigma w|F_o|^2]^{1/2}$; $w = 1/\delta^2(F_o) + g^*(F_o)$, $g = 0.005$.

[f] G-O-F $= [\Sigma w(|F_o| - |F_c|)^2/(NO - NV)]^{1/2}$, where NO is the number of observations and NV is the number of variables.

reported. Tables of bond lengths and angles, anisotropic thermal parameters and calculated and observed structure factors for all complexes are available.* Full details of the crystallographic methodologies may be found in ref. 18.

In no instance was an extinction correction applied to the data. Idealized hydrogen atom positions were used throughout the analysis, with the C—H distances set at 0.96 Å. The $(C_4H_9)_4N^+$ cations of structures **I–III** displayed some degree of orientational disorder, as evidenced by some large temperature factors and several unrealistic bond lengths. Since no major excursions of electron density (> 1.5 Å^3) were observed in the cation regions of the final Fourier maps, the problem was not pursued. Such disorder is not uncommon in tetraalkylammonium salts, and satisfactory disorder models are often not found.[19] The most appropriate cut-off for unobserved data in these structures was a value of $6\sigma(F_o)$. Although this is somewhat high, the structures did exhibit a large number of very weak data, presumably due to the cation disorder.

The final refinement stages of **IV** revealed the presence of two solvate molecules, MeCN and MeOH. The MeOH molecule is disordered about the mirror plane, and the geometry could not be corrected by the application of observational constraints to the bond length.

Since complex **I** crystallizes in the polar space group *Pc*, both enantiomorphs were refined. The atomic coordinates reported are for the proper enantiomorph based on the residuals for both settings. There are two independent molecules in the asymmetric unit of **I**, identified as **A** and **B** in the tables.

Acknowledgement—This work was supported by a grant from the National Science Foundation (CHE 8815299).

* *Supplementary materials available*: Fractional coordinates have been deposited with the Director, Cambridge Crystallographic Centre. Complete listings of bond distances and angles are available from the Editor, Queen Mary College, London.

REFERENCES

1. C. J. Machiels, U. Chowdry, R. H. Staley, F. Ouchi and A. W. Sleight, *Catalytic Conversions of Synthesis Gas and Alcohols to Chemicals* (Edited by R. G. Herman). Plenum Press, New York (1984); C. J. Machiels and A. W. Sleight, *Chem. Uses of Molybdenum Proc. 4th Int. Conf.* 1982, 411.
2. R. K. Grasselli and J. D. Burington, *Adv. Catal.* 1981, **30**, 133.
3. M. T. Pope, *Heteropoly and Isopoly Oxometalates*. Springer, New York (1983).
4. V. W. Day and W. G. Klemperer, *Science* 1985, **228**, 4699.
5. R. D. Adams, W. G. Klemperer and R.-S. Liu, *J. Chem. Soc., Chem. Commun.* 1979, 256.
6. E. M. McCarron III and R. C. Harlow, *J. Am. Chem. Soc.* 1983, **105**, 6179.
7. A. J. Wilson, W. T. Robinson and C. J. Wilkins, *Acta Cryst.* 1983, **C39**, 54.
8. S. Liu, S. N. Shaikh and J. Zubieta, *Inorg. Chem.* 1987, **26**, 4303.
9. L. Ma, S. Liu and J. Zubieta, *Inorg. Chem.* 1989, **28**, 175.
10. W. G. Klemperer, V. U. Mainz, R.-C. Wang and S. Yang, *3rd Chem. Conf. North America*, Toronto (June 1988): *Inorg. Abstr.* 265; V. W. Day, W. G. Klemperer, C. Schwartz and R.-C. Wang, in *Surface Organometallic Chemistry: The Molecular Approach to Surface Science and Catalysis* (Edited by J.-M. Basset *et al.*), p. 173. Kluwer, Dordrecht, Holland (1988).
11. V. W. Day, W. G. Klemperer and C. Schwartz, *J. Am. Chem. Soc.* 1987, **109**, 6030.
12. V. W. Day, M. F. Fredrich, W. G. Klemperer and R.-S. Liu, *J. Am. Chem. Soc.* 1979, **101**, 491.
13. V. W. Day, M. R. Thompson, W. G. Klemperer and R.-S. Liu, *J. Am. Chem. Soc.* 1980, **102**, 5973.
14. S. Liu, S. N. Shaikh and J. Zubieta, *Inorg. Chem.* 1988, **27**, 3064.
15. Q. Chen, S. Liu and J. Zubieta, *Angew. Chem. Int. Edn. Engl.* 1988, **27**, 1724.
16. K. M. Barkigia, L. M. Rajkovic, M. T. Pope and C. O. Quicksall, *J. Am. Chem. Soc.* 1975, **97**, 4146.
17. V. W. Day, M. F. Fredrich, W. G. Klemperer and W. Shurn, *J. Am. Chem. Soc.* 1977, **99**, 6146.
18. T. Nicholson and J. Zubieta, *Polyhedron* 1988, **7**, 171.
19. See for example, J. A. Kovacs and R. H. Holm, *Inorg. Chem.* 1987, **26**, 702.

Polyhedron Vol. 8, No. 24, pp. 2925–2931, 1989
Printed in Great Britain

0277–5387/89 $3.00+.00
© 1989 Pergamon Press plc

VARIABLE TEMPERATURE SOLUTION AND CP–MAS ^{13}C NMR OF [Mo(CO)$_3$(DIGLYME)]. DISPLACEMENT OF DIGLYME BY SOLVENTS AT SUBAMBIENT TEMPERATURES

GEORGE W. WAGNER and BRIAN E. HANSON*

Chemistry Department, Virginia Polytechnic Institute and State University, Blacksburg, VA 24061, U.S.A.

(*Received* 13 *February* 1989; *accepted* 7 *August* 1989)

Abstract—Variable temperature solution ^{13}C NMR of [Mo(CO)$_3$(diglyme)] shows that the chelating diglyme ligand is displaced by the monodentate solvents acetone, methanol and ethanol at low temperature. Free and coordinated solvent are observed at low temperature while at ambient temperature rapid exchange prevents the observation of coordinated solvent.

The [Mo(CO)$_3$(diglyme)] complex (**1**) was initially isolated by Werner and Coffield in 1960.[1] Although the structure of the compound has not been crystallographically determined, its IR stretching frequencies suggest the structure shown in Fig. 1. The tridentate diglyme ligand was observed to be easily displaced by other ligands and thus **1** was recognized as a valuable intermediate in the synthesis of molybdenum tricarbonyl complexes. Ligand substitution reactions involving [Mo(CO)$_3$L$_3$] complexes in solution have been well characterized and a large body of thermodynamic data now exists for these reactions.[2,3]

Although ^{13}C NMR spectra have been reported for many metal carbonyl complexes,[4] no data is available for [Mo(CO)$_3$(diglyme)]. The characterization of this particular complex by ^{13}C NMR is of interest to us because it is a good model compound for δ-alumina-supported [Mo(CO)$_3$(ads)] which is stabilized by OH^- and O^{2-} groups on the δ-alumina surface.[5,7] The δ-alumina-supported molybdenum sub-carbonyls have recently been the subject of many solid state ^{13}C NMR studies.[8–10]

Our initial interest in **1** was to determine its solid-state properties by variable temperature CP–MAS ^{13}C NMR. In the absence of any previous NMR data, variable temperature solution ^{13}C NMR was used to initially characterize the complex. These results indicated that substitution reactions were occurring between the complex and solvent molecules at subambient temperatures. This was surprising since thermodynamic data suggest that the solvents should not displace diglyme.

A similar effect has been previously noted for the [Mo(CO)$_3$(η^6-C$_6$H$_5$CH$_3$)]/THF system using ^1H NMR.[2] In this case, THF solvent molecules readily displace the toluene ligand at ambient temperatures because of a favourable ΔH for this reaction. However, at elevated temperatures the reaction reverses to yield the toluene complex as a result of the positive ΔS for this process. This term dominates at high temperatures causing a shift of the equilibrium in favour of the toluene complex.

In this study, variable temperature solution ^{13}C NMR results are presented demonstrating the

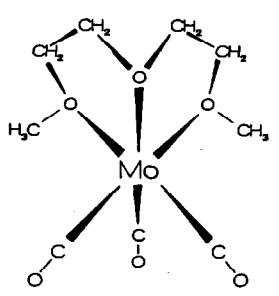

1

Fig. 1. Schematic representation of [Mo(CO)$_3$(diglyme)].

* Author to whom correspondence should be addressed.

reversible displacement of the diglyme ligand in $[Mo(CO)_3(diglyme)]$ by solvent molecules at subambient temperatures when the complex is dissolved in acetone-d_6, methanol-d and ethanol-d. Also, variable temperature CP–MAS ^{13}C NMR spectra of solid $[Mo(CO)_3(diglyme)]$ are shown which indicate that the complex is static in the solid state.

EXPERIMENTAL

The diglyme complex, **1**, was synthesized by refluxing $[Mo(CO)_3(\eta^6\text{-}C_6H_5CH_3)]$ in 25% (v/v) diglyme (Aldrich 99%, anhydrous)/pentane solution, resulting in a light yellow precipitate which was filtered and washed with pentane. The toluene complex, $[Mo(CO)_3(\eta^6\text{-}C_6H_5CH_3)]$, was synthesized by refluxing $Mo(CO)_6$ in toluene. Both products gave satisfactory elemental analyses. Further characterization by IR spectroscopy showed stretching frequencies at 1951 and 1752 cm^{-1} (br) (KBr) for **1** and 1983 and 1913 cm^{-1} (pentane) for $[Mo(CO)_3(\eta^6\text{-}C_6H_5CH_3)]$.[11] The bands for the diglyme complex differ from those reported by Werner and Coffield [1905 and 1835 cm^{-1} (KBr)].[1]

The ^{13}CO enriched $[Mo(CO)_3(diglyme)]$ was prepared from the enriched toluene complex. Enriched $[Mo(CO)_3(\eta^6\text{-}C_6H_5CH_3)]$ was prepared by stirring the complex under a ^{13}CO atmosphere for 2 days. The $Mo(CO)_6$ which was formed during this process was reconverted to the toluene complex by additional reflux to yield ^{13}CO-enriched $[Mo(CO)_3(\eta^6\text{-}C_6H_5CH_3)]$.

Deuterated solvents, acetone-d_6 (99% D) (Cambridge Isotopes), ethanol-d (99.5% D) and methanol-d (99.5% D) (Aldrich Chemical Company) were degassed by purging with dry nitrogen before use.

Solutions for NMR samples were prepared under inert atmospheres using degassed NMR solvents. The solutions were then filtered through a glass frit and syringed into an outgassed 10-mm o.d. NMR tube. This procedure avoided exposure of the solution to air.

Variable temperature ^{13}C NMR spectra were recorded on a Bruker WP200 NMR spectrometer. The observation frequency for carbon was 50.323 MHz. The spectrometer was equipped with a Bruker variable temperature controller which was capable of maintaining temperatures to $\pm 1°C$. Samples were allowed to equilibrate at a given temperature for at least 5 min before data aquisition was initiated.

Variable temperature CP–MAS ^{13}C NMR spectra were obtained form a ^{13}CO-enriched sample of the diglyme complex using a Bruker MSL300 spectrometer. The observation frequency for carbon was 75.5 MHz. The sample was packed in a standard Bruker aluminium oxide rotor. The hole in the boron nitride endcap was sealed with rubber cement to prevent exposure of the sample to air. Nitrogen gas (from liquid nitrogen boil-off) was used as the drive and bearing gas. The solid-state spectrometer was equipped with a Bruker variable temperature controller which maintained temperatures to $\pm 1°C$. The sample was allowed to equilibrate for at least 10 min at each temperature before scanning.

RESULTS

The variable temperature ^{13}C NMR spectra for $[Mo(CO)_3(diglyme)]$ in acetone-d_6 are shown in Fig. 2. The solvent peaks are present at 206 and 29.8 ppm (TMS). The acetone-d_6 methyl peak at 29.8 ppm was used as the chemical shift reference. Where indicated, the solvent peaks have been truncated to allow amplification of the complex signals. There

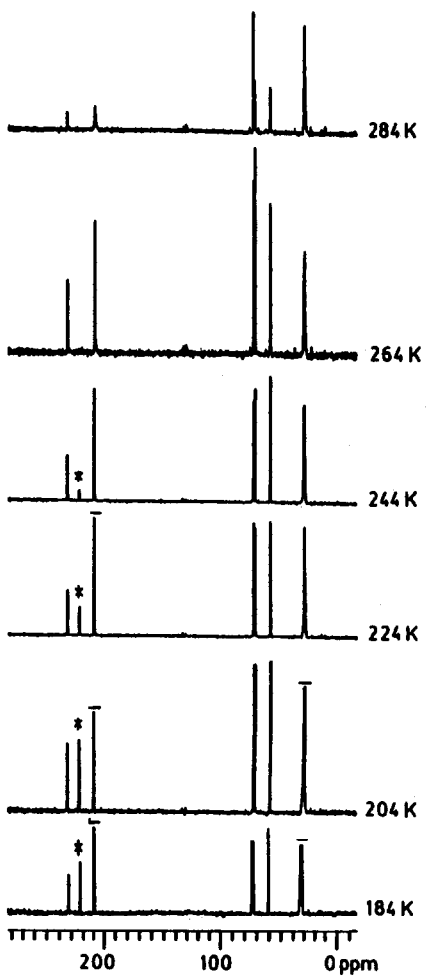

Fig. 2. Variable temperature 50.3 MHz ^{13}C NMR spectra of $[Mo(CO)_3(diglyme)]$ in acetone-d_6. The asterisked peak is due to coordinated acetone-d_6.

is only a single resonance in the carbonyl region at 230.7 ppm. Signals can also be observed for the diglyme ligand at 72.6, 71.5 and 59.2 ppm, which are barely shifted from the values obtained for the uncomplexed diglyme molecule in acetone-d_6 (72.7, 71.3 and 58.8). Two of the diglyme ligand resonances are broadened in this spectrum which seems to be due to a concentration effect, since dilute samples demonstrated less severe broadening. These signals are not broadened in the spectra of the uncomplexed diglyme ligand. The assignment of the diglyme ligands are not clear. However, it is reasonable to assume that the peak at 59.2 ppm is due to the pair of methyl carbons and the peaks at 72.7 and 72.3 ppm are due to the two pairs of methylene carbons.

A simple "ball-and-stick" model of the $[Mo(CO)_3(diglyme)]$ complex using an octahedral molybdenum centre and tetrahedral angles for all of the carbon atoms in the diglyme ligand indicates that the structure shown in Fig. 1 is less sterically hindered than a structure in which the methyl groups are directed towards each other. This structure possesses mirror plane symmetry and, thus a total of three resonances are expected for the coordinated diglyme ligand. The presence of a single carbonyl resonance is not predicted by the structure in Fig. 1 or by any other configuration possible for the diglyme ligand. The single carbonyl peak may imply either an accidental degeneracy of the chemical shifts or a motional process in which the carbonyls are rapidly exchanging positions. Many precedents exist for tricarbonyl group rotation in $[(arene)M(CO)_3]$ complexes in solution.[11-15]. However, the bonds between the metal atom and the arene ring are not directional (which may account for the low rotational barriers observed in these complexes), whereas in the diglyme molecule, the directional nature of the molybdenum–oxygen bonds may present a high barrier for rotation of the tricarbonyl group.

The carbonyl groups have a longer T_1 than the diglyme ligand carbons as evidenced by the relative enhancement of the carbonyl resonance by either increasing the delay time between pulses or by the addition of the relaxation agent, $Cr(acac)_3$. These treatments have little effect on the diglyme ligand signals.

At 284 K, the peaks due to the methyl groups and one pair of methylene groups have sharpened considerably and by 264 K they have attained approximately the same intensity and line width of the signal of the other pair of methylene carbons. This again suggests that the methyl groups adopt positions which allow mirror plane symmetry for the diglyme ligand.

At about 244 K, a new signal appears in the carbonyl region at 220.0 ppm and increases in intensity relative to the carbonyl resonance as the temperature is lowered. However, in the low temperature spectra of ^{13}CO-enriched $[Mo(CO)_3(diglyme)]$ in acetone-d_6 shown in Fig. 3, the new peak is very weak compared to the carbonyl ligand signal suggesting that the new peak originates from the acetone-d_6 solvent rather than the carbonyl groups. Thus, it appears that acetone molecules are able to coordinate to the molybdenum atom in the diglyme complex causing a downfield shift of the acetone carbonyl carbon. The chemical shift of the acetone methyl groups appears not to be greatly affected upon coordinated of the molecule to molybdenum, since their signal is not resolved from the solvent peak. In the lower temperature spectra, the area of the coordinated acetone-d_6 solvent molecules is approximately equal to the area of the carbonyl ligands, which indicates that the acetone molecules have completely displaced the diglyme ligand at the lower temperatures. The peaks due to complexed and uncomplexed diglyme ligand are not resolved in the spectra. This might be expected since the respective chemical shifts differ by less than 0.4 ppm. At 184 K, all of the line widths of the signals begin to broaden slightly. This temperature is near the freezing point of acetone, thus the line broadening is most likely due to freezing solvent or crystallization of the tricarbonyl complex.

The subambient temperature ^{13}C NMR spectra of $[Mo(CO)_3(diglyme)]$ in ethanol-d are shown in Fig. 4. The peaks at 56.8 and 17.2 ppm are due to the solvent and the 56.8 ppm signal was used as the chemical shift reference. The ambient temperature spectrum (top spectrum) is virtually identical to the corresponding spectrum obtained in acetone-d_6. The carbonyl resonance is at 228.8 ppm and the signals for the diglyme ligand are at 71.4, 69.8 and 52.7 ppm. Lowering the temperature of the sample again causes the signals at 69.8 and 52.7 ppm to sharpen in the lower temperature spectra. However, at 254 K, a new peak at 62.0 ppm begins to grow and attains the same relative intensity of the other methyl and methylene carbons in the diglyme ligand at 234 K. At the lower temperatures, the area of this new peak approaches a value which is 1.5 times the areas of the individual diglyme ligand signals, which suggest that the peak represents three molecules. This new peak is assigned to the methylene groups of coordinated ethanol-d molecules which displace the diglyme ligand at the lower temperatures in a manner analogous to acetone. However, the signals for the methyl groups of the coordinated ethanol-d molecules is not resolved from the solvent peak. Again, the signal due to com-

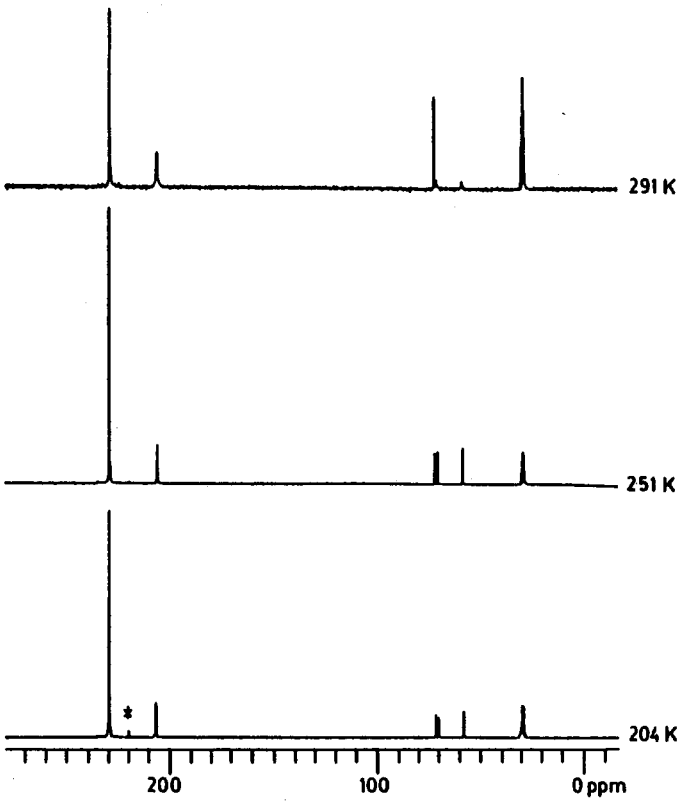

Fig. 3. Variable temperature 50.3 MHz ^{13}C NMR spectra of ^{13}CO-enriched [$Mo(CO)_3$(diglyme)] in acetone-d_6. The asterisked peak is due to coordinated acetone-d_6.

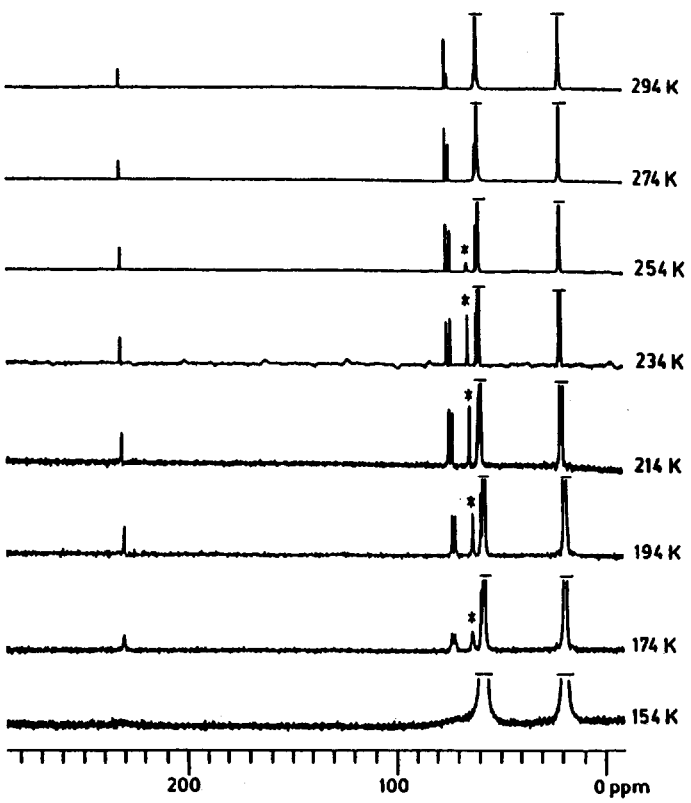

Fig. 4. Variable temperature 50.3 MHz ^{13}C NMR spectra of [$Mo(CO)_3$(diglyme)] in ethanol-d. The asterisked peak is due to coordinated ethanol-d.

plexed and uncomplexed diglyme ligand are not resolved. As the temperature is lowered further, the resonances due to the carbonyl ligands, diglyme molecule and the methylene signal of the coordinated ethanol-d molecule and the methylene signal of the coordinated ethanol-d molecules broaden considerably. It should be noted that the peak due to the methyl groups in the diglyme molecule broadens at a slower rate than the other signals. At 154 K, the peaks are so severely broadened that they are barely discernable in the spectrum. However, this temperature is very near the freezing point of ethanol which may account for the broadening. The solvent peaks at this temperature are also clearly broadened. The signal due to the methyl groups of the diglyme molecules would broaden at a slower rate since they would have greater mobility than the other carbons in the sample. Therefore, lower temperatures would have to be achieved in order to determine the dynamics of the carbonyl ligands in the substituted complex. In order to further substantiate the assignment of the peak at 62.0 ppm to coordinated ethanol-d molecules, the variable temperature spectra of the diglyme complex in methanol-d were also recorded.

A series of variable temperature solution ^{13}C NMR spectra of $[Mo(CO)_3(diglyme)]$ in methanol-d is shown in Fig. 5. In the 293 K spectrum, the peaks are at 229.6 ppm (carbonyl ligands), 72.0 and 70.4 ppm (methylene groups of the diglyme ligand) and 58.2 ppm (methyl groups of the diglyme ligand). The methanol-d solvent peak is at 49.0 ppm and was used as the chemical shift reference. At 293 K, the signals at 70.4 and 58.2 ppm are not as severely broadened as in the corresponding spectra in the other solvents, since this sample was very dilute. Again, lowering the temperature of the sample causes the signals of all three pairs of carbon atoms in the diglyme ligand to attain nearly equal intensities. In the 253 K spectrum, a new peak begins to appear at 58.7 ppm. In the lower temperature spectra, the ratio of the area of the new peak to the area of the diglyme methyl group approaches a value of 1.5. This indicates that three methanol-d molecules are coordinated per molybdenum complex which causes the observed shift of the coordinated methanol-d methyl groups from 49.0 to 53.8 ppm. Thus, as in the previous solvents, methanol-d is displacing the diglyme ligand in the complex at the lower temperatures. Again, the complexed and

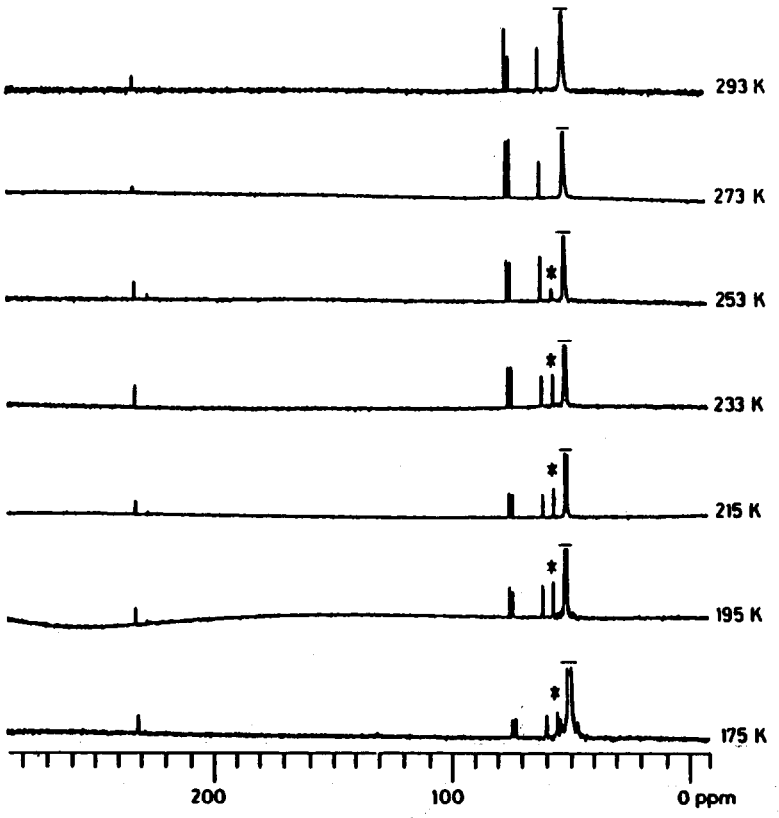

Fig. 5. Variable temperature 50.3 MHz ^{13}C NMR spectra of $[Mo(CO)_3(diglyme)]$ in methanol-d. The asterisked peak is due to coordinated methanol-d.

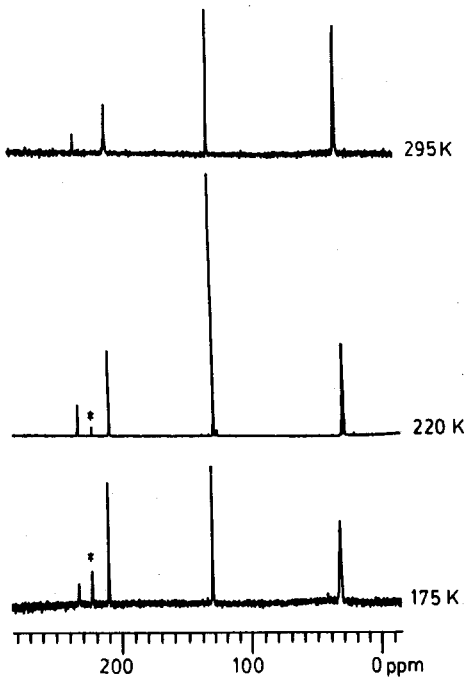

Fig. 6. Variable temperature 50.3 MHz ^{13}C NMR spectra of $[Mo(CO)_3(acetone)_3]$ generated *in situ* from $[Mo(CO)_3(\eta^6\text{-}C_6H_6)]$. The asterisked peak is due to coordinated acetone-d_6.

uncomplexed diglyme ligand signals are not resolvable. In the solution ^{13}C NMR spectra of this dilute sample of $[Mo(CO)_3(diglyme)]$ in methanol-d, no significant broadening of the signals was observed at the lower temperatures.

It should be noted that when $[Mo(CO)_3^-(\eta^6\text{-}C_6H_6)]$ is dissolved in acetone, the coordinated acetone ligands are again seen only at low temperature. Thus, there must be rapid exchange between free and coordinated acetone in $[(acetone)_3Mo(CO)_3]$ (Fig. 6).

The variable temperature 75.5 MHz CP–MAS ^{13}C NMR spectras of ^{13}CO-enriched $[Mo(CO)_3(diglyme)]$ are shown in Fig. 7. In the 299 K spectrum, a single, sharp carbonyl peak is present at 230.7 ppm and is very close to the solution value. The diglyme ligand resonances are at 74.1, 72.8 and 67.3 ppm. The peak due to the diglyme methyl groups at 67.3 ppm is slightly enhanced relative to the diglyme methylene groups. The other peaks present in the spectrum are due to spinning sidebands of the carbonyl peak. The spectrum obtained at 260 K is virtually unchanged except that the sidebands have moved toward the carbonyl peak at 230.5 ppm as a result of the slower spin rate. The spinning rates were about 4600 and 4300 Hz in the 299 and 260 K spectra, respectively.

The presence of only a single, sharp resonance for each pair of methyl and methylene groups indicates that the ligand probably has mirror plane symmetry in the solid state as previously suggested by the model shown in Fig. 1. The presence of a single, sharp resonance for the carbonyl ligands at both temperatures with nearly identical linewidths, suggests that the complex is static in the solid state and that the chemical shifts of the carbonyl ligands are degenerate. Furthermore, an inspection[16,17] of the intense array of spinning sidebands indicates a very large chemical shift anisotropy of about 400 ± 50 ppm for the carbonyl ligands which is close to the

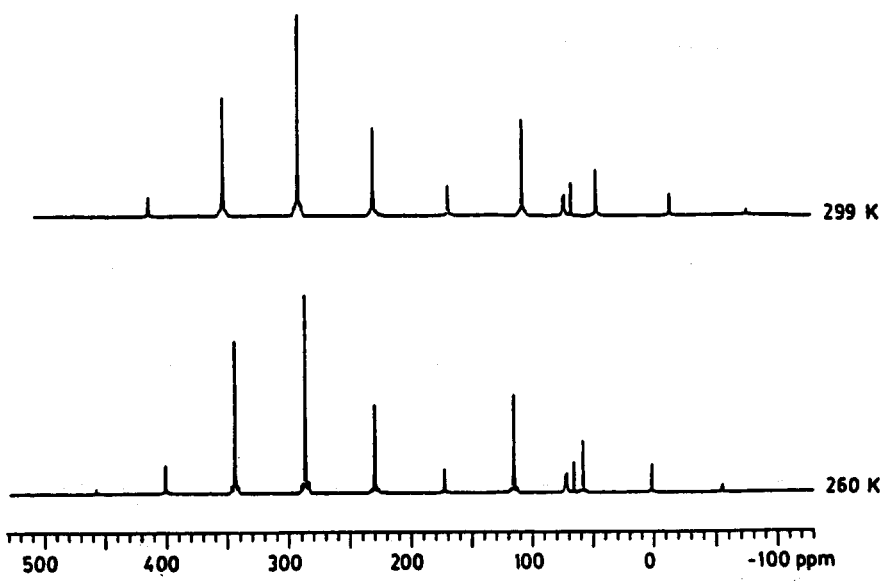

Fig. 7. Variable temperature 75.5 MHz ^{13}C CO–MAS spectra of ^{13}CO-enriched $[Mo(CO)_3(diglyme)]$.

value expected for a static metal carbonyl.[18] Therefore, the [Mo(CO)$_3$(diglyme)] molecule appears to be static in the solid state.

DISCUSSION

The coordination of acetone, methanol and ethanol to [Mo(CO)$_3$(diglyme)] at low temperature is clearly suggested by the variable temperature NMR data for **1**. This is contrary to what is expected based on the thermodynamic data of Hoff and co-workers[3] for ligand displacement reactions of [(arene)Mo(CO)$_3$]. The data in ref. 3 clearly shows that the bond enthalpy for diglyme coordinated to molybdenum is larger than the enthalpy for acetone to molybdenum. Thus, one predicts that diglyme would always displace acetone. However, the present data suggest that diglyme is rapidly displaced by weak oxygen donor ligands and that at low temperatures, up to three acetone, methanol or ethanol ligands may bond to the molybdenum tricarbonyl group.

The following equilibrium may be suggested for the Mo(CO)$_3$ group in acetone or other similar solvents.

$$[(\eta^3\text{-diglyme})\text{Mo(CO)}_3] + \text{acetone} \rightleftharpoons [(\eta^2\text{-diglyme})(\text{acetone})\text{Mo(CO)}_3]$$

$$[(\eta^2\text{-diglyme})(\text{acetone})\text{Mo(CO)}_3] + \text{acetone} \rightleftharpoons [(\eta^1\text{-diglyme})(\text{acetone})_2\text{Mo(CO)}_3]$$

$$[(\eta^1\text{-diglyme})(\text{acetone})_2\text{Mo(CO)}_3] \rightleftharpoons [(\text{acetone})_3\text{Mo(CO)}_3] + \text{diglyme}.$$

Furthermore, exchange of free and coordinated acetone appears fast at room temperature. At low temperatures for acetone, methanol and ethanol, the equilibrium clearly goes in favour of complete displacement of diglyme. At room temperature, however, it is impossible to determine the extent of reaction since ^{13}C NMR cannot distinguish between free and coordinated solvent and free and coordinated diglyme.

The apparent discrepancy between this work and that of Hoff's for the displacement of diglyme by acetone is most likely due to solvation energies, since the NMR work was done in neat acetone, methanol or ethanol and the calorimetric work was done in dilute methylene chloride. Solvation of free diglyme may be anticipated to be greater in the more polar solvents used in the NMR work.

Acknowledgements—We would like to thank Dr George Marcelin, University of Pittsburgh, for the use of the MSL300 NMR spectrometer. Funding for this work was provided by the NSF (DMR 8518364).

REFERENCES

1. R. P. M. Werner and T. H. Coffield, *Chem. Ind.* 1960, 936.
2. C. D. Hoff, *J. Organomet. Chem.* 1985, **282**, 201.
3. S. P. Nolan, R. L. de la Vega and C. D. Hoff, *Organometallics* 1986, **5**, 2529.
4. L. J. Todd and J. R. Wilkinson, *J. Organomet. Chem.* 1974, **77**, 1.
5. A. Brenner and R. L. Burwell Jr, *J. Catal.* 1978, **52**, 353.
6. M. Laniecki and R. L. Burwell Jr, *J. Colloid. Inter. Sci.* 1980, **75**, 95.
7. A. Kazusaka and R. F. Howe, *J. Molec. Catal.* 1980, **9**, 95.
8. (a) B. E. Hanson, G. W. Wagner, R. J. Davis and E. Motell, *Inorg. Chem.* 1984, **23**, 1635; (b) G. W. Wagner and B. E. Hanson, *J. Am. Chem. Soc.*, 1989, **111**, 2558.
9. (a) W. M. Shirley, B. R. McGarvey, B. Maiti, A. Brenner and A. Clichowlas, *J. Molec. Catal.* 1985, **29**, 259; (b) W. M. Shirley, *Z. Phys. Chem.* 1987, **152**, 41.
10. T. H. Walter, A. Thompson, M. Keniry, S. Shinoda, T. L. Brown, H. S. Gutowsky and E. Oldfield, *J. Am. Chem. Soc.* 1988, **110**, 1065.
11. D. A. Brown and F. J. Hughes, *J. Chem. Soc. A* 1968, 1519.
12. C. G. Kreiter and M. Lang, *J. Organomet. Chem.* 1973, **55**, C27.
13. B. P. Rogues and C. Segard, *J. Organomet. Chem.* 1974, **73**, 327.
14. W. R. Jackson, C. F. Pincombe, I. D. Rae and S. Thapebinkarn, *Aust. J. Chem.* 1975, **28**, 1535.
15. F. A. Cotton and B. E. Hanson, *Israel J. Chem.* 1076/77, **16**, 165.
16. M. Maricq and J. S. Waugh, *Chem. Phys. Lett.* 1977, **47**, 327.
17. J. Herzfeld and A. E. Berger, *J. Chem. Phys.* 1980, **73**, 6021.
18. H. W. Speiss, R. Grosescu and U. Haeberlen, *Chem. Phys.* 1974, **6**, 226.

Polyhedron Vol. 8, No. 24, pp. 2933–2935, 1989
Printed in Great Britain

0277–5387/89 $3.00+.00
© 1989 Pergamon Press plc

COMMUNICATION

SYNTHESIS AND STRUCTURAL CHARACTERIZATION OF $[Sn(1,2\text{-}O_2C_6H_3NO_2\text{-}4)(C_4H_8O)]_n$—A TIN(II) CATECHOL COMPLEX†

JONATHAN C. MACHELL, D. MICHAEL P. MINGOS‡ and TONIE L. STOLBERG

Inorganic Chemistry Laboratory, University of Oxford, South Parks Road, Oxford OX1 3QR, U.K.

(*Received* 30 *August* 1989; *accepted* 18 *September* 1989)

Abstract—$[Sn(1,2\text{-}O_2C_6H_3NO_2\text{-}4)(C_4H_8O)]_n$ has a chain polymeric solid-state structure based on very distorted square-pyramidal SnO_5 moieties linked by oxygen bridges from the catechol ligands. It is, however, monomeric in dimethyl sulphoxide and soluble in many organic solvents.

Zuckerman and his co-workers[1] synthesized a large number of catechol and related complexes of tin(II), but their insolubility in common organic solvents precluded the development of their chemistries[2] and the isolation of single crystals suitable for definitive structural studies, which would have established the nature of the intermolecular interactions linking the tin(II) catechol units. In this paper we describe the synthesis and structural characterization of a 4-nitrocatechol (**1**) complex which has a polymeric structure in the solid state, but dissociates readily in donor solvents.

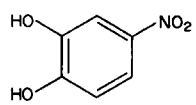

(1)

The reaction of **1** with $Sn(OMe)_2$ in tetrahydrofuran at room temperature results in the isolation of a yellow crystalline solid which analyses correctly for $[Sn(1,2\text{-}O_2C_6H_3NO_2\text{-}4)(C_4H_8O)]_n$ (**2**). Compound **2** is soluble in acetone, methanol, ethanol, acetonitrile and dimethyl sulphoxide. Its ^{119}Sn NMR spectrum in methanol consists of a single line at 131 ppm with respect to $SnMe_4$, and a cryoscopic molecular weight determination in dimethyl sulphoxide has established that it is monomeric in this solvent (Mol. $wt_{calc} = 272$ for $Sn(1,2\text{-}O_2C_6H_3\text{-}NO_2\text{-}4)$; Mol. $wt_{meas} = 298$).

Single crystals of compound **2** were obtained from tetrahydrofuran/hexane and an X-ray crystallographic determination has established the polymeric structure illustrated in Fig. 1.§ Structural details are included in Table 1. The coordination environment about each tin(II) atom can be described as very distorted square-pyramidal. The Sn—O bonds to the catechol ligand, 2.208(4) and

† Dedicated to the memory of Professor Jerold J. Zuckerman (1936–1987).

‡ Author to whom correspondence should be addressed.

§ Crystal data: $C_{10}H_{11}NO_5Sn$, $M = 343.89$, triclinic, $P\bar{1}$, $a = 6.121(3)$, $b = 9.295(3)$, $c = 11.073(2)$ Å, $\alpha = 107.39(2)$, $\beta = 98.28(3)$, $\gamma = 98.28(4)°$, $U = 583$ Å^3, $D_c = 1.96$ g cm^{-3}, $Z = 2$, $F(000) = 336$, μ(Mo-K_α) = 22.06 cm^{-1}. 2458 reflections were measured on an Enraf–Nonius CAD4F diffractometer in the range $2.0 \leqslant 2\theta \leqslant 50°$. The structure was solved by a combination of direct methods, Patterson and Fourier methods and refined by block-matrix least-squares [Sn, N, C(1)—(10), O(1)—(5), H(31) anisotropic; H(41), H(61) isotropic] to $R = 0.0375$ for 1621 unique observed reflections [$I \geqslant 3\sigma(I)$].

The atomic coordinates for this structure are available on request from the Director of the Cambridge Crystallographic Data Centre, University Chemical Laboratory, Lensfield Road, Cambridge CB2 1EW, U.K. Any request should be accompanied by the full literature citation for this communication.

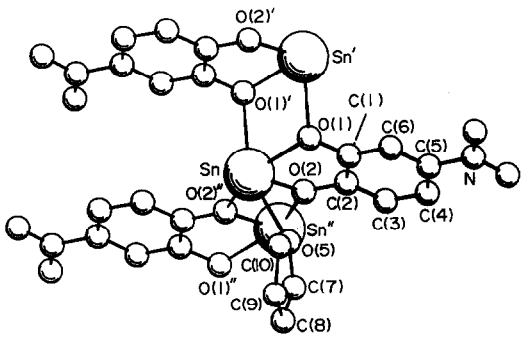

Fig. 1. Section of polymeric chain $[Sn(1,2\text{-}O_2C_6H_3NO_2\text{-}4)(C_4H_8O)]_n$ (**2**). For reasons of clarity, hydrogen atoms have been omitted. Important bond lengths include: Sn—O(1) 2.208(4), Sn—O(2) 2.112(4), Sn—O(5) 2.535(6), Sn—O(1′) 2.430(5), Sn—O(2″) 2.607(4) Å. Important angles include: O(1)—Sn—O(1′) 74.7(2), O(1)—Sn—O(2) 75.6(2), O(1)—Sn—O(2″) 138.1(2), O(1)—Sn—O(5) 78.7(2), O(1′)—Sn—O(2) 93.5(2), O(1′)—Sn—O(2″) 94.4(2), O(1′)—Sn—O(5) 153.3(2), O(2)—Sn—O(2″) 64.5(2), O(2)—Sn—O(5) 78.3(2), O(2″)—Sn—O(5) 104.5(2)°.

2.112(4) Å, are significantly shorter than that to the tetrahydrofuran oxygen, O(5) (2.535(4) Å). Interestingly, the Sn—O bond *para* to the NO_2 group is shorter than the other Sn—O catechol bond. In $[Sn(O_2C_6H_4)_3][Et_3NH]_2$[3] the corresponding average Sn—O distance is 2.05(2) Å. The $[Sn(1,2\text{-}O_2C_6H_3NO_2\text{-}4)(C_4H_8O)]$ moieties are linked by long Sn—O bonds, Sn—O(1′) (2.430(4) Å) and Sn—O(2″) (2.607(4) Å) to generate infinite polymeric chains. The square-pyramid is severely distorted as a result of the small bite angle of the catechol ligand (75.6(2)°), cf. 82.7(4)° in $[Sn(O_2C_6H_4)_3][Et_3NH]_2$, and the stereochemical consequences of the lone pair of electrons at the tin(II) atom. The basal plane of this distorted square-pyramid defined by O(1), O(1′), O(2″) and O(5) consequently has two angles which deviate a large amount from the ideal 180° (O(1)—Sn—O(2″) = 138.1(2)° and O(1′)—Sn—O(5) = 153.3(2)°). The apex of the square-pyramid is defined by O(2) and the remaining angles which ideally should be 90° vary from 64.5(2) to 104.5(2)°. A less distorted square-pyramidal geometry has been reported recently in the pyrazolylboratotin(II) complex, $[HB(pz^*)_3]_2Sn$[4] (pz^* = 3,5-dimethyl-1-pyrazolyl).

Table 1. Structural details for $[Sn(p\text{-}O_2C_6H_3NO_2)(C_4H_8O)]_n$

Compound	$[Sn_1O_5C_{10}H_{11}N_1]_n$
Molecular weight	343.89
Space group	$P\bar{1}$
Cell dimensions:	
a (Å)	6.121(3)
b (Å)	9.295(3)
c (Å)	11.073(2)
α (°)	107.39(2)
β (°)	98.28(3)
γ (°)	98.28(4)
Cell volume	583
Z	2
Density	1.96 g cm^{-3}
Linear absorption coefficient	22.06 cm^{-1}
Radiation	Mo-K_α (λ = 0.71069 Å)
Standard reflections	104, 3−2−1, 2−23
Decay of standards	5%
2θ range	2–50°
Number of parameters varied	157
R	0.0375
R_w	0.0396
Goodness-of-fit	1.13
$F(000)$	336
Residual electron density	14.7

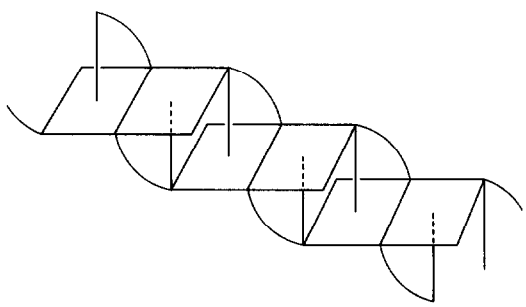

(3)

The manner in which the square-pyramidal units are linked to form the polymeric chains is represented in an idealized fashion in **3**. Pairs of square-pyramids are linked by basal oxygen atoms in a centrosymmetric fashion about a crystallographically imposed centre of symmetry at the midpoint of the common edge. These pairs are further linked by apical–basal bridges about a second centre of symmetry. Since each tin atom is in a chiral environment, this packing mode requires an alternation of enantiomeric forms of the asymmetric unit along the chain. The presence of the tetrahydrofuran ligands makes this polymer geometry quite different to that reported previously for $[Sn(O_2C_2H_4)]_n$,[5] which crystallizes in a rhombohedral point group and has a cross-linked arrangement of Sn—O rings about a three-fold symmetry axis.

The long intermolecular Sn—O(1′) and Sn—O(2″) bonds which must result in part from electronic effects associated with the NO_2 group, must contribute to the ease of dissociation of the

polymeric chains in donor solvents. These solubility properties have resulted in the isolation of adducts of the type $[Sn(1,2\text{-}O_2C_6H_3NO_2\text{-}4)(C_4H_8O)L]$ (L = 1,2-diaminopropane or 2,2′-dipyridyl) and some interesting transition metal tin(II) catechol complexes which will be described in subsequent publications.

The ^{119}Sn Mössbauer spectrum of **2** shows an isomer shift of 3.49 mm s^{-1} confirming a tin(II) oxidation state,[6] and is in accordance with Harrison's observation that tin(II)–oxygen bonded compounds with an isomer shift in excess of 3.15 mm s^{-1} are composed of molecules held together by only weak intermolecular interactions.[7] The size of the quadrupole splitting (2.33 mm s^{-1}), again, is indicative of the large departure of **2** from cubic symmetry.

Acknowledgements—The SERC and the International Tin Research Institute are thanked for financial support. We should also like to thank Professor F. Glockling for stimulating our interest in this area, and for many useful discussions.

REFERENCES

1. J. J. Zuckerman, *J. Chem. Soc.* 1963, 1322; H. J. Emeleus and J. J. Zuckerman, *J. Organomet. Chem.* 1964, **1**, 328; G. T. Cocks and J. J. Zuckerman, *Inorg. Chem.* 1965, **4**, 592; A. J. Bearden, H. S. Marsh and J. J. Zuckerman, *Inorg. Chem.* 1966, **5**, 1260; D. E. Fenton, R. R. Gould, P. G. Harrison, T. B. Harvey, G. M. Omietanski, K. C.-T. Sze and J. J. Zuckerman, *Inorg. Chim. Acta* 1970, **4**, 235; W. D. Honnick and J. J. Zuckerman, *Inorg. Chem.* 1978, **17**, 501.
2. H. E. Mabrouk and D. G. Tuck, *J. Chem. Soc., Dalton Trans.* 1988, 2539.
3. J. C. Machell, D. M. P. Mingos and T. L. Stolberg, unpublished results.
4. C. J. Carrano, A. H. Cowley, R. L. Geerts and C. M. Nunn, *J. Organomet. Chem.* 1988, **341**, C27.
5. R. Nesper and H. Georg v. Schnering, *Z. Naturfor.* 1982, **37b**, 1144.
6. J. J. Zuckerman, *Mössbauer Effect Methodology* (Edited by I. J. Grruverman), Vol. III, p. 15. Plenum Press, New York (1967).
7. P. G. Harrison and S. R. Stobbart, *J. Chem. Soc., Dalton Trans.* 1973, 940.

Polyhedron Vol. 8, No. 24, pp. 2937–2939, 1989
Printed in Great Britain

0277–5387/89 $3.00+.00
© 1989 Pergamon Press plc

COMMUNICATION

OPTICAL METAL-TO-LIGAND CHARGE-TRANSFER OF 2,2′-BIPYRIDYL COMPLEXES OF ANTIMONY(III) AND BISMUTH(III)

HORST KUNKELY, ALOIS PAUKNER and ARND VOGLER†

Institut für Anorganische Chemie der Universität Regensburg Universitätsstraße 31, D-8400 Regensburg, F.R.G.

(*Received* 20 *July* 1989; *accepted* 18 *September* 1989)

Abstract—The complexes [M(2,2′-bipyridyl)X_3], with M = Sb, Bi and X = Cl, Br, I, are characterized by long-wavelength metal-to-ligand charge-transfer (MLCT) bands which determine the colours of these compounds in the solid state. The energy of the MLCT bands depends on the reducing strength of the metal and the extent of *sp* mixing of the lone electron pair at the metal.

Coordination compounds of main group metals with a s^2 electron configuration at the metal show a large variety of different structures. Complexes of antimony(III) are good examples of this behaviour.[1,2] This structural diversity depends—at least partially—on *sp* orbital mixing. If this mixing occurs the lone electron pair gains *p*-character and becomes stereochemically active. In octahedral complexes such as $[TeBr_6]^{2-}$ and $[SbCl_6]^{3-}$, *sp* mixing does not take place and the lone pair preserves its *s*-character. The electronic spectra of $[TeBr_6]^{2-}$[3-5] and $[SBCl_6]^{3-}$[6-8] are relatively simple. They display long-wavelength absorptions in the UV. These bands belong to $s \rightarrow p$ transitions. On the contrary, there is not much known about the electronic spectra of complexes with a stereochemically active lone pair at the metal. In this case spectra assignments are certainly complicated due to the *sp* orbital mixing and molecular structures of lower symmetry as imposed by the lone pair. However, an identification and characterization of the lone pair is feasible by electronic spectroscopy if a 1,2-diimine ligand such as 2,2′-bipyridyl (bipy) or 1,10-phenanthroline (*o*-phen) is attached to the s^2 metal. Since these metals are reducing due to the presence of the lone pair, optical low-energy metal-to-ligand MLCT transitions should appear in analogy to diimine complexes of reducing transition metals such as iron(II), ruthenium(II), or copper(I).[9] With the exception of the organometallic cation $[Sn^{II}(C_5Me_5)bipy]^{+}$[10,11] such optical MLCT transitions of s^2 metal complexes are virtually unknown to our knowledge. In searching for simple examples our attention was drawn to the complexes [M(1,2-diimine)X_3], with M = Sb, Bi, X = Cl, Br, I, and 1,2-diimine = bipy[12] and *o*-phen.[13,14] These compounds exhibit remarkable colours. We suspected that these colours are due to low-energy MLCT absorptions. In the present communication we report the first results on the electronic spectra and the spectral assignments of the complexes [M(bipy)X_3].

Reliable absorption spectra of the complexes [M(bipy)X_3] in solution cannot be obtained since these compounds are either insoluble or undergo extensive dissociation in all common solvents, as indicated by the presence of free bipy which was identified by its absorption (λ_{max} = 280 nm, ε = 11230 and λ_{max} = 235 nm, ε = 9160) and fluorescence (λ_{max} = 325 nm) spectra. The spectra of the complexes were measured by scattered transmission spectroscopy of suspensions of the powdered materials in hexane or paraffin and recorded in absorbance vs wavelength on a Uvikon 860 spectrometer equipped with an end-on photomultiplier. The spectra are characterized by long-wavelength bands in the visible region which determine the colour of the complexes (Fig. 1, Table 1). In

† Author to whom correspondence should be addressed.

Table 1. Colours and optical MLCT transitions of $[M(bipy)X_3]$ in the solid state

MX_3	$SbCl_3$	$SbBr_3$	SbI_3	$BiCl_3$	$BiBr_3$	BiI_3
Colour	Bright yellow	Orange	Dark red	White	Cream	Orange–red
λ_{max} (nm)	360	435	545	326	390	485

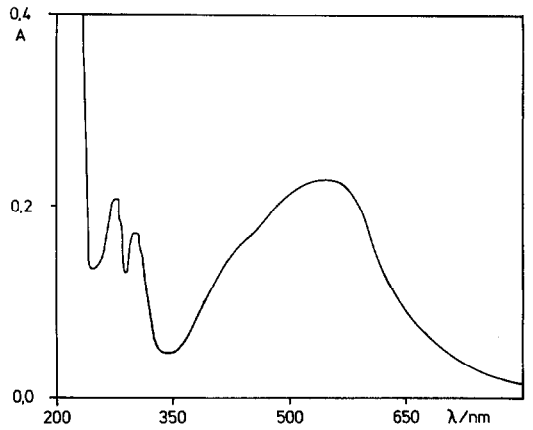

Fig. 1. Electronic absorption spectrum of $[Sb(bipy)I_3]$ at room temperature; absorbance in arbitrary units.

addition, absorptions also appear at shorter wavelength in the UV (Fig. 1).

The absorption spectra of the $[M(bipy)X_3]$ complexes all contain a maximum slightly above 300 nm which is assigned to the lowest-energy $\pi \rightarrow \pi^*$ intraligand transition of the bipy ligand. These bands also appear in the spectra of bipy complexes of transition metals such as rhodium[15,16] or platinum[17] and are indicative of coordinated bipy. Ligand-to-metal charge-transfer transitions involving the promotion of a halide electron to the *p* orbitals of M^{III} are not expected to occur at low energies. For example, $[SbCl_6]^{3-}$ does not show LMCT absorptions at wavelengths above 200 nm.[6-8] The long-wavelength absorptions of $[M(bipy)X_3]$ (Fig. 1, Table 1) are then logically assigned to MLCT transitions involving the promotion of an electron from the lone pair of the metal to the π^* orbital of the bipy ligand. This assignment is supported by the blue shift of this band which takes place when antimony(III) is replaced by bismuth(III) (Table 1). Bismuth(III) is generally less reducing ($Bi^{III/V}$: $E^0 \sim 1.7$ V) than antimony(III) ($Sb^{III/V}$: $E^0 \sim 0.6$ V).[18] The MLCT assignment of the low-energy absorptions of $[M(bipy)X_3]$ is thus quite obvious. However, the blue shift of the MLCT bands in the series X = I, Br, and Cl requires some further explanations.

It has been concluded from the Mössbauer spectra that the *p* character of the lone pair of $[M(diimine)X_3]$ increases from X = I to Br and Cl.[13] The *sp* orbital mixing which is achieved by a configuration interaction leads then to a stabilization of the lone pair.[19] Accordingly, the MLCT transition of $[M(bipy)I_3]$ occurs at rather low energies since the lone pair has less *p* contribution. On the contrary, the larger *p* character of the lone pair of $[M(bipy)Cl_3]$ shifts the MLCT transition to higher energies.

The origin of this difference in *sp* mixing does not seem to be clear. It may be related to the spatial demand of the ligand X. The configuration interaction which leads to the *sp* mixing requires a distortion from a more symmetrical structure.[19] Simultaneously, space opens for the lone pair which becomes stereochemically active. This steric flexibility is provided by the smaller Cl^- ligand rather than by the I^- ligand. Unfortunately, the structures of these complexes are not to our knowledge known. On the basis of IR measurements it has been suggested that the complexes $[M(diimine)X_3]$ consist of bridged dimers or chain polymers.[13,14,20]

REFERENCES

1. J. F. Sawyer and R. J. Gillespie, *Prog. Inorg. Chem.* 1986, **34**, 65.
2. U. Ensinger, W. Schwarz and A. Schmidt, *Z. Naturfor.* 1983, **38b**, 149 and literature cited therein.
3. D. A. Couch, C. J. Wilkins, G. R. Rossman and H. B. Gray, *J. Am. Chem. Soc.* 1970, **92**, 307.
4. D. J. Stufkens, *Recl. Trav. Chim.* 1970, **89**, 1185.
5. A. Vogler and A. Paukner, *J. Photochem. Photobiol.* 1989, **46A**, 227.
6. R. A. Walton, R. W. Matthews and C. K. Jørgensen, *Inorg. Chim. Acta* 1967, **1**, 355.
7. L. Kolditz, W. Schiller and J. Kunze, *Z. Anorg. Allg. Chem.* 1973, **395**, 207.
8. A. Vogler and A. Paukner, *Inorg. Chim. Acta* 1989, **163**, 207.
9. A. B. P. Lever, *Inorganic Electronic Spectroscopy.* Elsevier, Amsterdam (1984).
10. F. X. Kohl, E. Schlüter, P. Jutzi, C. Krüger, G. Wolmershäuser, P. Hoffmann and P. Stauffert, *Chem. Ber.* 1984, **117**, 1178.
11. P. Jutzi, *Adv. Organomet. Chem.* 1986, **26**, 217.
12. W. R. Roper and C. J. Wilkins, *Inorg. Chem.* 1964, **3**, 500.
13. N. Bertazzi, G. Alonzo and T. C. Gibb, *Inorg. Chim. Acta* 1983, **73**, 121.

14. G. Alonzo, M. Consiglio, N. Bertazzi and C. Preti, *Inorg. Chim. Acta* 1985, **105**, 51.
15. D. H. W. Carstens and G. A. Crosby, *J. Molec. Spectrosc.* 1970, **34**, 113.
16. M. Nishizawa, T. M. Suzuki, S. Sprouse, R. J. Watts and P. C. Ford, *Inorg. Chem.* 1984, **23**, 1837.
17. A. Vogler and H. Kunkely, *Angew. Chem. Int. Edn Engl.* 1982, **21**, 209.
18. G. Milazzo and S. Caroli, *Tables of Standard Electrode Potentials*. John Wiley, New York (1978).
19. T. A. Albright, J. K. Burdett and M.-H. Whangbo, *Orbital Interactions in Chemistry*, p. 263. John Wiley, New York (1985).
20. A. M. Brodie and C. J. Wilkins, *Inorg. Chim. Acta* 1974, **8**, 13.

Polyhedron Vol. 8, No. 24, pp. 2941–2942, 1989
Printed in Great Britain

0277–5387/89 $3.00+.00
© 1989 Pergamon Press plc

COMMUNICATION

PREPARATION OF DIBROMOACETIC ANHYDRIDE AND ITS REACTIONS WITH Bi_2O_3 AND CrO_3 TO FORM METAL DIBROMOACETATES

RAM PARKASH,* SUKHJINDER SINGH and MEENA

Department of Chemistry, Panjab University, Chandigarh-160014, India

(*Received* 4 *August* 1989; *accepted* 18 *September* 1989)

Abstract—Dibromoacetic anhydride was prepared by reacting dibromoacetic acid with phosphorus(V) oxide in carbon tetrachloride at ~85°C for 11 h. It reacts with Bi_2O_3 and CrO_3 in CCl_4 on prolonged refluxing forming $Bi(CHBr_2COO)_3$ and $Cr(CHBr_2COO)_3$, respectively. These new compounds were characterized by elemental analyses, IR, ^1H NMR and mass spectroscopy.

Several halogen-substituted acetic anhydrides are known.[1–3] However, dibromoacetic anhydride has not been reported so far. In this communication, the preparation of $(CHBr_2CO)_2O$ and its reactions with Bi_2O_3 and CrO_3 are being discussed.

RESULTS AND DISCUSSION

Reaction of dibromoacetic acid with phosphorus(V) oxide and subsequent distillation of the anhydride produced, even under reduced pressure, lead to partial decomposition of the product. However, dibromoacetic acid reacts with phosphorus(V) oxide in CCl_4 at ~85°C producing dibromoacetic anhydride in good yield. The progress of the reaction is monitored by ^1H NMR spectroscopy. The reaction is considered to be complete when ^1H NMR of the test solution does not show any resonance relating to δ(OH) of the $CHBr_2COOH$. The reaction is complete in 11 h as observed in the repeated experiments:

$$2CHBr_2COOH \xrightarrow[11\,h,\ \sim 85°C]{P_4O_{10},CCl_4} (CHBr_2CO)_2O.$$

Dibromoacetic anhydride is a shiny white solid, stable indefinitely at ambient temperatures in a dry atmosphere. It is soluble in common organic solvents and reacts readily with water to give dibromoacetic acid. Attempts to record IR spectra of neat $(CHBr_2CO)_2O$ lead to the formation of some $CHBr_2COOH$ due to its hydrolysis by traces of moisture. The clean IR spectra have been recorded in Nujol as well as in CCl_4. A parent or molecular ion peak is not observed in the EI mass spectra of $(CHBr_2CO)_2O$ by a direct insertion method, however, strong peaks relating to $CHBr_2COO^+$, $CHBr_2CO^+$ and $CHBr_2^+$ fragment ions are observed.

The reaction between bismuth(III) oxide and a slight excess of dibromoacetic anhydride in CCl_4 at ~85°C for 90 h results in the formation of bismuth(III) dibromoacetate. However, quantitative yields are not realized because some of the product is always left behind in the filtration unit. Bismuth(III) dibromoacetate, $Bi(CHBr_2COO)_3$, is a creamy white solid insoluble in CCl_4, $CHCl_3$, CH_2Cl_2, $C_2H_5OC_2H_5$, CH_3NO_2 and $C_6H_5NO_2$.

Prolonged reaction between CrO_3 and excess $(CHBr_2CO)_2O$ in CCl_4 at ~85°C produces chromium(III) dibromoacetate, $Cr(CHBr_2COO)_3$. A yellowish-brown solution is obtained in the initial stages of the reaction, from which a greenish solid starts to separate on further refluxing. The yellowish-brown solution is probably due to the formation of chromyl species, which are subsequently reduced with excess $(CHBr_2CO)_2O$ under the experimental conditions:

$$2CrO_3 + 2(CHBr_2CO)_2O \xrightarrow[85°C]{CCl_4}$$

"$2CrO_2(CHBr_2COO)_2$"
Yellowish-brown solution

$$\xrightarrow[\sim 85°C]{(CHBr_2CO)_2O,\ CCl_4}$$

$$2Cr(CHBr_2COO)_3 + 3/2\,O_2$$
Greenish solid.

* Author to whom correspondence should be addressed.

This reaction is similar to those reported between CrO_3 and excess $(CHCl_2CO)_2O$, $(CF_3CO)_2O$ or $(CF_3SO_2)_2O$, which give the green solids $Cr(CHCl_2COO)_3$, $Cr(CF_3COO)_3$ and $Cr(CF_3SO_3)_3$, respectively.[4-6] $Cr(CHBr_2COO)_3$ is a fine, green, hygroscopic powdery material, soluble in diethyl ether and alcohols but insoluble in CCl_4, with no oxidizing power towards KI.

EXPERIMENTAL

Materials and methods

Dibromoacetic acid (Fluka) was used as such. Bismuth(III) oxide (Riedel) and chromium(VI) oxide (BDH) were dried *in vacuo* at 110–120°C for 4 h. The solvents were dried and distilled before use.

IR spectra were recorded as Nujol/hexachlorobutadiene/CCl_4 smears between AgCl or KBr plates on a Perkin–Elmer 1430 IR spectrophotometer. ^1H NMR spectra were taken on an EM-390 spectrometer using TMS as internal standard. Mass spectra (EI) were obtained on a Vg Micromass 7070F at 70 eV. Melting points are uncorrected. All manipulations were carried out in a dry box filled with nitrogen.

Metals and halogens were analysed by standard methods.[7] Carbon and hydrogen were determined microanalytically.

Preparation of dibromoacetic anhydride

Dibromoacetic acid (13.95 g, 64 mmol) was transferred onto 15.0 g of phosphorus(V) oxide in a 100 cm^3 Pyrex reactor in a dry box, and 50 cm^3 of CCl_4 were added to it. The contents were refluxed at ~85°C for 11 h and the reaction mixture was filtered in a specially designed filtration unit under positive pressure of dry nitrogen, and the residual portion was repeatedly washed with CCl_4 (6×10 cm^3). Dibromoacetic anhydride (10.87 g, 26 mmol) was obtained as a white solid (m.p. 54–57°C) after removing excess solvent from the filtrate *in vacuo*. The product was checked for the absence of phosphorus and then recrystallized from CCl_4 as a shiny white solid in >70% yield. $(CHBr_2CO)_2O$ (recrystallized): m.p. 56–57°C; b.p. 115°C/10 torr (decomp.). Found: C, 11.4; H, 0.46; Br, 76.0. Calc. for $C_4H_2Br_4O_3$; C, 11.5; H, 0.48; Br, 76.5%. IR* (CCl_4): 3022 w, 1830 sb, 1765 ms, 1420 w, 1240 mw, 1175 mw, 1152 w, 1125 m, 1053 m, 1030 ssh, 970 vw, 922 m, 870 w, 660 w, 600 m, 592 sh, 538 mw. IR (Nujol): 1830 sb, 1760 m, 1422 sh, 1265 mw, 1240, sh, 1170 w, 1150 sh, 1125 ms, 1050 m, 1030 sh, 972 vw, 922 ms, 880 w, 780 sh, 755 sh, 600 w, 525 ms cm^{-1}. ^1H NMR (CCl_4): 5.97 ppm (singlet, $CHBr_2$).

*S, strong; m, medium; w, weak; b, broad; sh, shoulder; v, very.

Preparation of bismuth(III) *dibromoacetate*

A slight excess of dibromoacetic anhydride (2.34 g, 5.6 mmol) dissolved in 30 cm^3 of CCl_4 was added to Bi_2O_3 (0.7 g, 1.5 mmol) in a 100 cm^3 Pyrex reactor in a dry box. The reaction mixture was refluxed for 90 h at ~85°C. The white solid formed was filtered under a positive pressure of nitrogen, repeatedly washed with CCl_4 and finally dried *in vacuo*. $Bi(CHBr_2COO)_3$ (2.49 g, 2.9 mmol) was obtained as a creamish-white solid in >96% yield. $Bi(CHBr_2COO)_3$: m.p. 183–185°C (decomp.). Found: C, 8.2; H, 0.34; Br, 55.2; Bi, 23.7. Calc. for $C_6H_3BiBr_6O_6$: C, 8.4; H, 0.35; Br, 55.8; Bi, 24.3%. IR: 3032 w, 3000 m, 1728 m, 1555 sh, 1525 s, 1425 m, 1370 s, 1255 sh, 1200 ms, 1134 m, 969 w, 948 w, 795 m, 735 s, 708 s, 695 ms, 603 m, 530 w cm^{-1}.

Preparation of chromium(III) *dibromoacetate*

A similar procedure as that used to prepare $Bi(CHBr_2COO)_3$ was used. A five-fold excess of dibromoacetic anhydride was used and refluxing (~85°C) was carried out for 10 days. $Cr(CHBr_2COO)_3$ was obtained as a green solid which was insoluble in CCl_4. More than 70% yields were realized. $Cr(CHBr_2COO)_3$: Found: C, 10.1; H, 0.42; Br, 67.1; Cr, 7.1. Calc. for $C_6H_3Br_6CrO_6$: C, 10.2; H, 0.43; Br, 68.3; Cr, 7.4%. IR: 1656 s, 1595 s, 1430 ms, 1263 w, 1197 m, 1146 mw, 1090 vw, 966 vw, 795 m, 705 s, 642 w, 606 m, 515 w cm^{-1}.

Acknowledgement—The authors are thankful to D. Niyogi for help during the experimental work.

REFERENCES

1. J. M. Tedder, *J. Chem. Soc.* 1954, 2646.
2. D. Martin, A. Wiese and K. Nadolski, *Chem. Ber.* 1965, **98**, 3286.
3. R. C. Mehrotra and R. Bohra, *Metal Carboxylates*. Academic Press, London (1983).
4. R. Sharma, PhD thesis. Panjab University, Chandigarh (1981).
5. J. N. Gerlach and G. L. Gard, *Inorg. Chem.* 1970, **9**, 1565.
6. S. D. Brown and G. L. Gard, *Inorg. Chem.* 1975, **14**, 2273.
7. A. I. Vogel, *A Textbook of Quantitative Inorganic Analysis*, 3rd edn, pp. 488, 520, 568. John Wiley, New York (1961).

Polyhedron Vol. 8, No. 24, pp. 2943–2945, 1989
Printed in Great Britain

0277–5387/89 $3.00+.00
© 1989 Pergamon Press plc

COMMUNICATION

A NEW ROUTE TO FLUOROCARBON-STABILIZED ORGANOAMIDOPLATINUM(II) COMPOUNDS— SYNTHESIS OF A NEW ISOMER OF [Pt(RNCH$_2$CH$_2$NMe$_2$)X(L)] (R = *p*-HC$_6$F$_4$ OR C$_6$F$_5$; X = Cl OR I; L = UNIDENTATE LIGAND) COMPLEXES

D. P. BUXTON, G. B. DEACON,* A. M. JAMES, S. J. KNOWLES and T. L. WILLIAMS

Chemistry Department, Monash University, Clayton, Victoria 3168, Australia

(*Received* 15 *August* 1989; *accepted* 20 *September* 1989)

Abstract—Reaction of the complexes PtX$_2$(RNHCH$_2$CH$_2$NMe$_2$) (X = Cl or I; R = *p*-HC$_6$F$_4$ or C$_6$F$_5$) with TlOR′ (R′ = Et or Bu^t) co-precipitates TlX and the organoamides [Pt(RNCH$_2$CH$_2$NMe$_2$)X]$_2$; these react with L (pyridine (py) or Me$_2$SO) to give [Pt(NRCH$_2$CH$_2$NMe$_2$)X(L)] complexes, which, in three cases (R = *p*-HC$_6$F$_4$ or C$_6$F$_5$, L = Me$_2$SO, X = Cl; R = *p*-HC$_6$F$_4$, L = py, X = I), were obtained as the isomer with L *trans* to the NR group.

The scope of platinum(II) organoamide chemistry[1–3] has been greatly increased by the preparation of polyfluorophenyl(R)-substituted complexes [Pt(RNCH$_2$)$_2$L$_2$] and [Pt(RNCH$_2$CH$_2$NMe$_2$)X(L)] (e.g. R = *p*-HC$_6$F$_4$ or C$_6$F$_5$; L = py; X = Cl or I)[4–8] where the fluorocarbon substitution provides stabilization against hydrolysis (cf. moisture-sensitive [Pt(RNCH$_2$)$_2$bpy] (R = H or Me; bpy = 2,2′-bipyridyl[9]). Their preparation by decarboxylation reactions in pyridine solution, e.g. eq. (1) (dmen = N,N-dimethylethane-1,2-diamine),[4–8] is unprecedented in organoamidometallic chemistry. However, the method has limitations. It is essentially restricted to complexes where L = pyridine or substituted pyridine (but see ref. 8) and to formation of [Pt(RNCH$_2$CH$_2$NMe$_2$)X(L)] complexes with structure **1** but *not* **2**.

$$PtI_2(dmen) + TlO_2CC_6F_4H\text{-}p + C_6F_5H + 2py \longrightarrow$$
$$[Pt(p\text{-}HC_6F_4NCH_2CH_2NMe_2)I(py)]$$
(1a)
$$+ p\text{-}H_2C_6F_4 + TlI + CO_2 + pyHF. \quad (1)$$

We now report a new synthetic route to [Pt(RNCH$_2$CH$_2$NMe$_2$)X(L)] complexes and the first preparation of compounds with structure **2**.

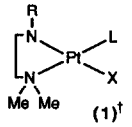

(1)†

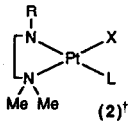

(2)†

(1a), **(2a)** R = *p*-HC$_6$F$_4$, L = py, X = I;
(1b), **(2b)** R = *p*-HC$_6$F$_4$, L = Me$_2$SO, X = Cl;
(1c), **(2c)** R = C$_6$F$_5$, L = Me$_2$SO, X = Cl.

New N,N-dimethyl-N′-polyfluorophenylethane-1,2-diamines and their platinum dihalide complexes‡ were prepared as shown in Scheme 1. Reaction of the platinum halide complexes with thallium(I) ethoxide or t-butoxide co-precipitated thallium(I) halide and the N,N-dimethyl-N′-polyfluorophenylethane-1,2-diaminato(1−)halogeno-

* Author to whom correspondence should be addressed.

† Isomer **1** may be termed *trans* and isomer **2** *cis*, since donor atoms of similar charge are *trans* and *cis*, respectively.

‡ All new compounds were characterized by microanalysis, ^{1}H and ^{19}F NMR spectra, and, where volatile, by mass spectrometry.

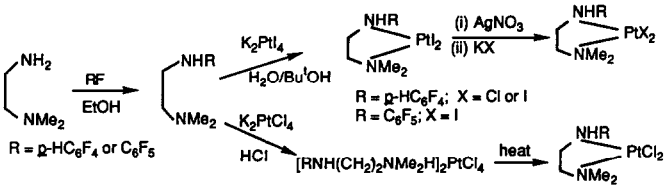

Scheme 1.

platinum(II) complex, which was identified primarily by observation of the dimer parent ion in the mass spectrum (and appropriate fragment ions).

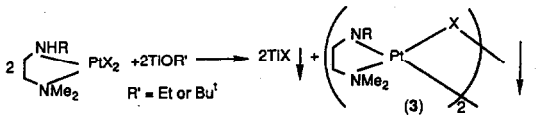

(**3a**) R = *p*-HC_6F_4, X = I;
(**3b**) R = *p*-HC_6F_4, X = Cl;
(**3c**) R = C_6F_5, X = Cl;
(**3d**) R = C_6F_5, X = I.

Treatment of the TlI/**3a** mixture with slightly less than the stoichiometric amount of py required for dimer cleavage in THF yielded [Pt(*p*-$HC_6F_4NCH_2CH_2NMe_2$)I(py)] with the previously unknown structure **2a**, which was obtained analytically and isomerically pure (81% yield) on recrystallization from ether–petrol. By contrast, cleavage with a large excess (> 500 : 1) of neat pyridine gave **1a** (90%). The two isomers were readily distinguished by values of ^3J[PtH(Me)] (**1a** 31, **2a** 45 Hz), ^3J[PtH2,6(py)] (**1a** 40, **2a** 24 Hz), and δF2,6 (**1a** −150.4, **2a** −146.5 ppm). The relative magnitudes of the coupling constants are consistent with the *trans* influence order, py > Cl[10] and N(amido) > N(amine).[7] Dissolution of the new isomer, **2a**, in a large excess of pyridine gave **1a** and [Pt(*p*-$HC_6F_4NCH_2CH_2NMe_2$)$(py)_2$]$^+I^-$ (**4**). The latter gave two, equal intensity, H2,6(py) resonances [^3J(PtH) 40 Hz, py *trans* to —NMe_2; ^3J(PtH)27Hz, py *trans* to —N(*p*-HC_6F_4)] downfield from that of **1a**, and a F2,6 resonance well displaced from that of **2a**. A plausible isomerization path is:

$$\mathbf{2a} + \text{py} \longrightarrow \mathbf{4} \longrightarrow \mathbf{1a} + \text{py}.$$

Substitution by iodide *trans* to the amido nitrogen rather than *trans* to the amine nitrogen is as expected from their *trans* effects.[7,11] Reaction of dimers **3b–3d** with a limited amount of pyridine gave mixtures of isomers **1** and **2**.

Treatment of **3d** or **3c**/TlCl mixtures with dimethyl sulphoxide for 2 h followed by filtration and addition of water gave [Pt($RNCH_2CH_2NMe_2$)Cl(Me_2SO)] (R = *p*-HC_6F_4 or C_6F_5) with structures **2b** or **2c**, respectively. Observation of δ(Me) of Me_2SO at 3.3–3.4 ppm is indicative[12] of S-bonding, as is observation of platinum–hydrogen (SMe_2) coupling [^3J(PtH) *ca* 20 Hz] (see refs 12 and 13). Identification as isomer **2** is based on the magnitude of ^3J[PtH(NMe_2)] (40–45 Hz) which is consistent with —NMe_2 *trans* to halogen (see, for example **2a**) and far too large for —NMe_2 *trans* to sulphur (see, for example **1a** for —NMe_2 *trans* to py which has a *trans* influence less than S-bonded Me_2SO– cf. ν(PtCl) of *cis*-$PtCl_2(py)_2$[14] and *cis*-$PtCl_2(Me_2SO)_2$[15]). When a solution of **2b** in Me_2SO was stirred for 7 days, only slight conversion into **1b** occurred (**2b** : **1b** = 3 : 1).

The outcome of the cleavage reactions indicates that isomer **2** is the kinetically favoured product. Thermodynamic control favours isomer **1**, thus accounting for the earlier isolation of this isomer from decarboxylation reactions in boiling pyridines.[5,7]

Studies are continuing on the cleavage of the dimers **3** and of the factors influencing the structure, **1** or **2**, and isomerization of the product. Preliminary results indicate that $RNH(CH_2)_2NEt_2$ (R = *p*-HC_6F_4 or C_6F_5) ligands and their platinum dihalide complexes can also be prepared, opening a possible route to [Pt($RNCH_2CH_2NEt_2$)X(L)] complexes.

Acknowledgements—This work was carried out during the tenure of a grant from the Anti-Cancer Council of Victoria. This support, that of the Australian Research Council, and a loan of platinum from Johnson Matthey, are gratefully acknowledged.

REFERENCES

1. D. C. Bradley and M. F. Chisholm, *Accts Chem. Res.* 1976, **9**, 273.
2. M. F. Lappert, P. P. Power, A. R. Sanger and R. C. Srivastava, *Metal and Metalloid Amides*. Ellis Horwood, Chichester (1980).
3. M. D. Fryzuk and C. D. Montgomery, *Coord. Chem. Rev.* 1989, **95**, 1.
4. G. B. Deacon, B. M. Gatehouse, I. L. Grayson and M. C. Nesbit, *Polyhedron* 1984, **3**, 753.
5. D. P. Buxton, G. B. Deacon, B. M. Gatehouse, I. L. Grayson and P. J. Wright, *Acta Cryst.* 1985, **C41**, 1049.
6. D. P. Buxton, G. B. Deacon, B. M. Gatehouse, I. L.

Grayson, R. J. Thomson and D. St. C. Black, *Aust. J. Chem.* 1986, **39**, 2013.
7. D. P. Buxton, G. B. Deacon, B. M. Gatehouse, I. L. Grayson and D. St. C. Black, *Aust. J. Chem.* 1988, **41**, 943.
8. D. P. Buxton, G. B. Deacon and D. St. C. Black, *Polyhedron* 1989, **8**, 143.
9. G. W. Watt and D. G. Upchurch, *J. Am. Chem. Soc.* 1968, **90**, 914; 1967, **89**, 177.
10. T. G. Appleton, H. C. Clark and L. E. Manzer, *Coord. Chem. Rev.* 1973, **10**, 335.
11. M. K. Cooper and J. M. Downes, *Inorg. Chem.* 1978, **17**, 880.
12. G. Annibale, L. Cattalini, V. Bertolasi, V. Ferretti, G. Gilli and M. L. Tobe, *J. Chem. Soc., Dalton Trans.* 1989, 1265.
13. J. D. Fotheringham, G. A. Heath, A. J. Lindsay and T. A. Stephenson, *J. Chem. Res. S* 1986, **82** (M, 1986, 801); Y. Ducommun, L. Helm, A. E. Merbach, B. Hellquist and L. I. Elding, *Inorg. Chem.* 1989, **28**, 377.
14. A. D. Allen and T. Theophanides, *Can. J. Chem.* 1964, **42**, 1551.
15. W. Kitching, C. J. Moore and D. Doddrell, *Inorg. Chem.* 1970, **9**, 541.

Polyhedron Vol. 8, No. 24, pp. 2947–2949, 1989
Printed in Great Britain

0277–5387/89 $3.00+.00
© 1989 Pergamon Press plc

COMMUNICATION

IMIDO COMPLEXES OF MOLYBDENUM AND TUNGSTEN(VI); X-RAY CRYSTAL STRUCTURE OF *cis*-(η^1-CF_3SO_3)$_2$ $W(NBu^t)_2(NH_2Bu^t)_2$

ANDREAS A. DANOPOULOS and GEOFFREY WILKINSON*

Johnson Matthey Laboratories, Chemistry Department, Imperial College, London SW7 2AY, U.K.

and

MICHAEL B. HURSTHOUSE* and BILQUIS HUSSAIN

Chemistry Department, Queen Mary and Westfield College, Mile End Road, London E1 4NS, U.K.

(*Received* 15 *September* 1989; *accepted* 28 *September* 1989)

Abstract—The synthesis of the homoleptic molybdenum imido compound $Li_2Mo(NBu^t)_4$ is reported. The complexes $M(NBu^t)_2(NHBu^t)_2$ (M = Mo, W) can be protonated with various strong acids giving neutral species. The X-ray crystal structure of the tungsten complex $W(NBu^t)_2(NH_2Bu^t)_2(SO_3CF_3)_2$ confirms the presence of O-coordinated *cis*-CF_3SO_3 groups.

The deprotonation of the imido amido compounds $W(NBu^t)_2(NHBu^t)_2$[1] and $Re(NBu^t)_3(NHBu^t)$[1,2] by methyllithium in diethyl ether gives rise to the homoleptic imido compounds $Li_2W(NBu^t)_4$ and $[Li(tmed)]Re(NBu^t)_4$, respectively, that are analogues of tungstate and perrhenate. The crystal structures of these first homoleptic transition metal imido compounds were also reported.[1] We have now synthesized the tetraimido molybdate, $Li_2Mo(NBu^t)_4$, by a similar procedure, i.e. interaction of MeLi in Et_2O on $Mo(NBu^t)_2(NHBu^t)_2$. The latter was obtained by interaction of $LiNHBu^t$ on $Mo(NBu^t)_2Cl_2$,[3] which in turn is obtained by the reaction of MoO_2Cl_2 and Bu^tNCO in refluxing acetonitrile.

Although we have been unable to obtain X-ray quality crystals of $Li_2Mo(NBu^t)_4$, the IR and NMR spectra are virtually identical to those of $Li_2W(NBu^t)_4$; thus in the ^1H NMR spectra there are two NBu^t resonances in a 1:3 ratio at 1.66(9) and 1.47(27) ppm—corresponding, respectively, to the terminal linear and bent bridging MNC groups as found[1] in the structure $[(Bu^tN)W(NBu^t)_3\mu\text{-}Li_2]_2$. The chemistry of $Li_2Mo(NBu^t)_4$ seems to be similar to that of the tungsten analogue, e.g. in forming $X_2Al(\mu\text{-}Bu^tN)_2W(\mu\text{-}NBu^t)_2AlX_2$ (X = CH_3, Cl) on interaction with AlX_3 in toluene.

The converse of deprotonation of $M(NBu^t)_2(NHBu^t)_2$, i.e. protonation, gives rise to electrically non-conducting amine complexes by protonation of the *t*-butylamido group using strong acids such as CF_3SO_3H, CF_3CO_2H, HBF_4 and HCl. The first two give similar species, e.g. $M(NBu^t)_2(NH_2Bu^t)_2(\eta^1\text{-}O_2CCF_3)_2$, that have, from IR and NMR spectra, *cis*-O-bonded acid groups. The structure of $W(NBu^t)_2(NH_2Bu^t)_2(CF_3SO_3)_2$ is shown in Fig. 1 and selected bond lengths and angles are given in Table 1. The molecule has octahedral geometry with the pairs of imido and unidentate triflate ligands each mutually *cis*, and the coordinated amines mutually *trans*.

Protonation by tetrafluoroboric acid gives a species which has only one coordinate anion and whose NMR spectra show that it is $W(NBu^t)_2(NHBu^t)$

* Authors to whom correspondence should be addressed.

Table 1. Selected bond lengths and angles for *cis*-$(\eta^1\text{-}CF_3SO_3)_2W(NBu^t)_2(NH_2Bu^t)_2$

Bond lengths (Å)			
N(1)—W(1)	1.73(1)	N(2)—W(1)	1.75(1)
N(3)—W(1)	2.20(1)	N(4)—W(1)	2.24(1)
O(1)—W(1)	2.28(1)	O(2)—W(1)	2.30(1)
Bond angles (°)			
N(2)—W(1)—N(1)	106.4(5)	N(3)—W(1)—N(1)	104.1(4)
N(3)—W(1)—N(2)	96.1(4)	N(4)—W(1)—N(1)	96.4(4)
N(4)—W(1)—N(2)	87.9(4)	N(4)—W(1)—N(3)	157.0(3)
O(1)—W(1)—N(1)	161.1(3)	O(1)—W(1)—N(2)	91.9(4)
O(1)—W(1)—N(3)	78.0(4)	O(1)—W(1)—N(4)	79.2(4)
O(2)—W(1)—N(1)	88.7(4)	O(2)—W(1)—N(2)	164.8(3)
O(2)—W(1)—N(3)	81.2(3)	O(2)—W(1)—N(4)	89.1(3)
O(2)—W(1)—O(1)	72.9(3)	C(11)—N(1)—W(1)	167.2(8)
C(21)—N(2)—W(1)	169.5(7)	C(31)—N(3)—W(1)	128.8(7)
C(41)—N(4)—W(1)	131.9(6)	S(1)—O(1)—W(1)	129.8(5)
S(2)—O(2)—W(1)	148.1(4)		

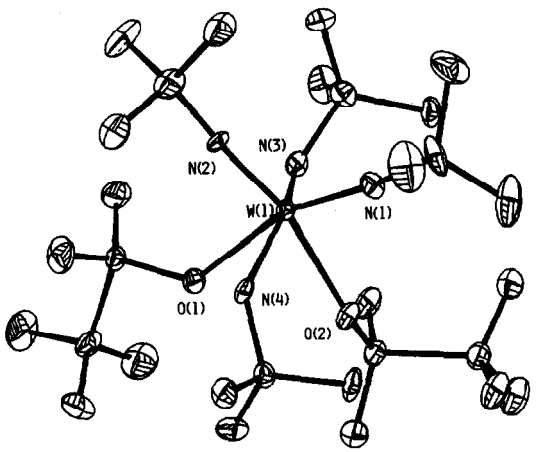

Fig. 1

$(NH_2Bu^t)BF_4$. Thus the ^1H NMR spectra confirm the (NBu^t), $(NHBu^t)$ and (NH_2Bu^t) groups in a 2:1:1 ratio. The ^{19}F NMR spectra show two groups of magnetically inequivalent fluorine nuclei suggesting coordination of two fluorine atoms as in **1**.

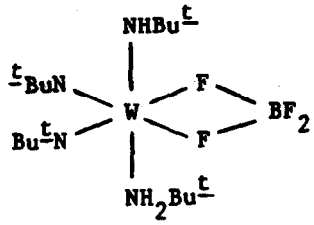

1

Crystal data. $C_{18}H_{36}F_6N_4O_6S_2W$, $M_r = 766.53$. monoclinic, $a = 19.010(2)$, $b = 16.533(8)$, $c = 9.860(1)$ Å, $\beta = 102.64(7)°$, $V = 3038.3$ Å^3, space group $P2_1/n$, $Z = 4$, $D_c = 1.674$, μ(Mo-K_α) = 40.85 cm^{-1}, $F(000) = 1520$, λ(Mo-K_α) = 0.71069. 4689 data measured ($-21 \leqslant h \leqslant 21$, $0 \leqslant k \leqslant 18$, $0 \leqslant l \leqslant 10$), $1.5 \leqslant \theta \leqslant 23°$ giving 4215 unique and 3351 observed [$F_o > 3\sigma(F_o)$]. The structure was solved by the heavy-atom method, refined by least-squares giving $R = 0.039$, $R_w = 0.043$ for 334 parameters, weights = $[\sigma^2(F_o)+0.00076F_o^2]^{-1}$. Tables of final atomic positional parameters and displacement factor coefficients, bond lengths and angles and F_o/F_c values have been deposited as supplementary material with the Editor, from whom copies are available on request. Atomic coordinates have also been deposited with the Cambridge Crystallographic Data Centre.

Although complexing of the type M—F—BF_3 is most common,[4] more complex behaviour including triple bridging has been observed for $Mn(BF_4)_2$,[5] while the double fluorine bridge as in **1** has been considered as a possibility for $Cp''UF(BF_4)$ in solution [$Cp'' = \eta\text{-}C_5H_3(SiMe_2)_2$] although in the dimeric solid there is a U-μ-[FB(F_2)F]U bridge.[6]

Protonation of $W(NBu^t)_2(NBu^t)_2$ with HCl in Et_2O gives $[(Bu^tN)_2(Bu^tNH_2)_2ClW(\mu\text{-}Cl)]_2$, whose structure has been confirmed by X-ray study. A compound of similar stoichiometry obtained by interaction of WCl_6 and *t*-butyltrimethylsilylamine, was suggested on spectroscopic grounds to have bridging imido groups with *cis*-chlorine atoms on each tungsten.[7]

The new amine complexes are useful starting materials for synthesis of other complexes, as the NH_2Bu^t groups can be readily replaced by other ligands, e.g. pyridine. Studies on the reduction and other substitution reactions are in progress.

Acknowledgement—We thank the SERC for support.

REFERENCES

1. A. A. Danopoulos, G. Wilkinson, B. Hussain and M. B. Hursthouse, *J. Chem. Soc., Chem. Commun.* 1989, 896.
2. A. A. Danopoulos, C. J. Longley, G. Wilkinson, B. Hussain and M. B. Hursthouse, *Polyhedron* 1989, **8**, 2657.
3. G. Schoettel, J. Kress and J. A. Osborn, *J. Chem. Soc., Chem. Commun.* 1989, 1062.
4. See for example, R. V. Honeychuck and W. H. Hersh, *Inorg. Chem.* 1989, **28**, 2869.
5. R. W. Cockman, B. F. Hoskins, M. J. McCormick and T. A. O'Donnell, *Inorg. Chem.* 1988, **27**, 2742.
6. P. B. Hitchcock, M. F. Lappert and R. G. Taylor, *J. Chem. Soc., Chem. Commun.* 1984, 1082.
7. A. J. Nielsen, *Polyhedron* 1987, **6**, 1657.

Polyhedron Vol. 8, No. 24, pp. 2951–2952, 1989
Printed in Great Britain

0277–5387/89 $3.00+.00
Pergamon Press plc

COMMUNICATION

PREPARATION AND X-RAY CRYSTAL STRUCTURE OF A SILVER SANDWICH COMPLEX OF AN AZA-THIA MACROCYCLE

DAVID PARKER† and ANDREW S. CRAIG

Department of Chemistry, University of Durham, South Road, Durham DH1 3LE, U.K.

and

GEORGE FERGUSON and ALAN J. LOUGH

Department of Chemistry, University of Guelph, Guelph N1G 2W1, Ontario, Canada

(*Received* 12 *September* 1989; *accepted* 4 *October* 1989)

Abstract—During the course of studies directed towards the synthesis of kinetically stable silver(I) complexes, we have prepared a hexadentate bis-[9]-NS_2 ligand (**1**) which may be expected to form a series of stable octahedral complexes with many transition metal ions. The silver(I) complex has been characterized spectroscopically and crystallographically.

There are many examples of transition metal complexes in which two aza-coronands are N,N′-linked to form either mononuclear or dinuclear complexes depending upon the chain length separating each ring. Most have involved either [9]-N_3[1] or [12]-NX_3 (X = O, N or S)[2,3] coronands.

Reaction of N-(*p*-toluenesulphonyl)-3-aza-pentan-1,5-dithiol with 1,2-dibromoethane in DMF in the presence of Cs_2CO_3 afforded **2a** (43%, m.p. 123–124°C). Detosylation (HBr–AcOH–PhOH) yielded the amine **2b** (73%, m.p. 71-72°C) and further reaction with ethylene glycol ditosylate (0.5 equiv.) in MeCN gave the bis-coronand, **1** (53%,

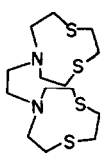

I

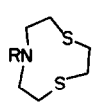

2 (a) R = Ts
(b) R = H

m.p. 105–106°C). Admixture of **1** with silver nitrate in methanol followed by addition of NH_4PF_6 led to isolation of the colourless silver complex (*m/z* (FAB in 3-nitrobenzylalcohol) 461, 459 [M^+]). Analysis of pH-metric titration curves in the presence and absence of silver yielded $pK_1 = 6.53$, $pK_2 = 6.00$; $\log K_s$ [**1**·Ag]$^+$ = 7.00 (298 K, H_2O, $I = 0.1$ M NMe_4NO_3).

The crystal structure of [**1**·Ag]$^+$‡ (Fig. 1) revealed the silver to be bound by the ligand nitrogen and sulphur atoms in a very distorted octahedral coordination. Both the cation (and the PF_6

† Author to whom correspondence should be addressed.

‡ Crystals of [**1**·Ag]$^+PF_6^-$ are tetragonal, $a = 10.128(3)$, $c = 21.711(4)$ Å, $V = 2227(2)$ Å^3, $Z = 4$, $D_c = 1.81$ g cm^{-3}, $F(000) = 1224$, μ(Mo-K_α) = 13.8 cm^{-1}. The space group is either $P4(1)2(1)2$ or $P4(3)2(1)2$ from the systematic absence; $P4(1)2(1)2$ was established for the crystal used for the analysis by anomalous dispersion calculations. 1946 reflections were measured on a CAD4 diffractometer ($2 < 2\theta < 50°$). After corrections for Lorentz, polarization and absorption effects, 1050 unique reflections with $I > 3\sigma(I)$ were labelled observed and used in the structure solution and refinement. The structure was solved by the heavy-atom method and refined by full-matrix least-squares calculations. All hydrogen atoms were located and included as riding atoms in the calculations. At convergence, $R = 0.030$, $R_w = 0.035$. Full details of atomic coordinates and ion dimensions are available from the Director of the Crystallographic Data Centre, University Chemical Laboratory, Lensfield Road, Cambridge CB2 1EW, U.K.

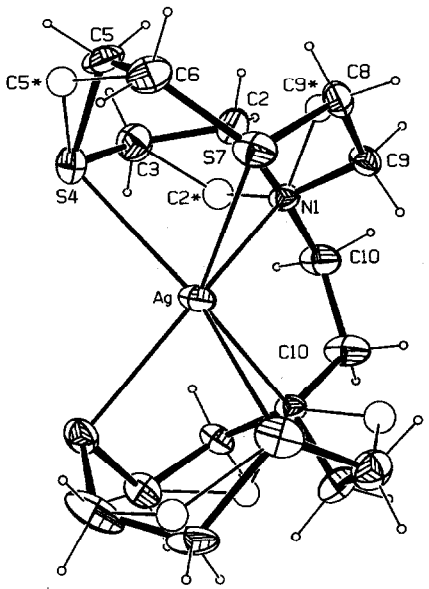

Fig. 1. The structure of $[1 \cdot Ag]^+$ in the crystal. Three of the carbon atoms in each nine-membered ring were found to be disordered over two sites (0.84:0.16 occupancies). The atoms of the minor component are shown by the open circles in the diagram. Selected bond lengths (Å) and bond angles (°): Ag—S(4) 2.802(2), Ag—S(7) 2.611(2), Ag—N(1) 2.586(3); S(4)—Ag—S(7) 80.90(7), S(4)—Ag—N(1) 74.0(1), S(4)—Ag—S(7)′ 93.04(6), S(7)—Ag—S(7)′ 149.62(6), N(1)—Ag—N(1)′ 73.7(1).

anion) have two-fold crystallographic symmetry, and there is one short (Ag—S(7) = 2.611(2) Å) and one longer silver–sulphur bond (Ag—S(4) = 2.802(2) Å). Although the structure resembles that of the 2:1-[9]-S_3 silver complex reported recently,[4] the planes through the S(4), S(7) and N(1) atoms in the two rings are not parallel but are inclined at an angle of 17° (enforced by the short —CH_2CH_2— link). The resultant coordination at silver is distorted octahedral in which the Ag—S(4)—S(7) and Ag—S(7)*—S(4)* moieties are twisted by 15° with respect to one another.

The synthesis of **2b**—the last of the [9]-X_3 series to be reported[5]—and of **1** (and its congeners) will permit the study of many more mono- and dinuclear transition metal complexes based on the [9]-NS_2 sub-unit. It may be expected that the presence of the sulphur donors will lead to the stabilization of further unusual oxidation states and geometries as described for homoleptic sulphur[4] macrocyclic complexes and some complexes of mixed aza-thia macrocycles.[6]

Acknowledgements—We thank SERC and Celltech Ltd (CASE) and NSERC (Canada) for support.

REFERENCES

1. N. Tanaka, Y. Kobayashi and S. Takamoto, *Chem. Lett.* 1977, 107; K. Wieghardt, I. Tolksdorf and W. A. Herrmann, *Inorg. Chem.* 1985, **24**, 1230.
2. J. E. Bulkowski, P. L. Burk, M.-F. Ludmann and J. A. Osborn, *J. Chem. Soc., Chem. Commun.* 1977, 498.
3. M. J. Calverley and J. Dale, *J. Chem. Soc., Chem. Commun.* 1981, 684; 1981, 1084; T. Alfheim, J. Dale, P. Groth and K. D. Krautwurst, *J. Chem. Soc., Chem. Commun.* 1984, 1502.
4. H.-J. Küppers, K. Wieghardt, Y.-H. Tsay, C. Krüger, B. Nuber and J. Weiss, *Angew. Chem.* 1987, **99**, 583; *Angew. Chem. Int. Ed. Engl.* 1987, **26**, 576; M. Schroder, *Pure Appl. Chem.* 1988, **60**, 517.
5. P. Chaudhuri and K. Wieghardt, *Prog. Inorg. Chem.* 1987, **35**, 329.
6. G. Reid, A. J. Blake, T. I. Hyde and M. Schroder, *J. Chem. Soc., Chem. Commun.* 1988, 1397; A. Alberts, J. M. Lehn and D. Parker, *J. Chem. Soc., Dalton Trans.* 1985, 2311.

VOLUME 7

SUBJECT INDEX

A

Ab initio calculations, phosphine azides, 223
Accelerated ageing, nickel tungsten sulphide, 2405
Acetates and acetato complexes
  cobalt(II), 43
  copper(II), 43,1745
  molybdenum(II), 107,1279,2201
  nickel(II), 43
  ruthenium(II), 1239
  ruthenium(II,III), 2597
  zinc, 43
Acetone complexes
  chromium(0), 1619
  ruthenium(II,III), 1453
Acetonesemicarbazone complexes
  molybdenum(II), 1719
Acetonitrile complexes
  chromium(0), 673,1619
  copper(I), 37,161
  holmium, 641
  iridium(III), 1285
  molybdenum(II), 1453,2615
  niobium(V), 2217
  palladium(II), 2659
  rhenium(V), 171
  rhenium(VI), 117
  rhodium, 2345
  rhodium(II), 1453
  rhodium(III), 827
  ruthenium(II), 2627
  ruthenium(II,III), 1453
  ruthenium(III), 1727
  tungsten(0), 1605
  tungsten(II), 245,2769
  vanadium(II), 2615
Acetophenone complex
  chromium(0), 1377
Acetophenone semicarbazone, thiosemicarbazone complexes, tellurium(IV), 633
Acetyls
  manganese(I), 1605
  osmium, 1035,1891
  ruthenium, 1035
  tungsten(II), alternative to allyl - carbonyl coordination, 163
N-Acetylcysteine, reaction with $[Fe(CN)_5NO]^{2-}$, 1197
N-Acetylcysteine complex
  thallium(III), 2487
Acetylferrocene benzoylhydrazone complexes, lanthanides, 1095
N-Acetyl-2-methylcysteine, N-Acetylpenicillamine, reactions with $[Fe(CN)_5NO]^{2-}$, 1197
N-Acetylpenicillamine complex
  thallium(III), 2487
4-Acetylpyridine complexes
  iron(II), 589
2-Acetylpyridinethiosemicarbazone complexes, lanthanides, 147
Acetylsalicylates
  copper(II), 1745
Actinides(III)
  carbonate complexes, 573
Acyls
  chromium, 2451
  chromium(-I), 1609
  iron, 2451
  iron(-I), 1609
  manganese(I), 1605
  molybdenum, 2451
  molybdenum(-I), 1609
  molybdenum(II), 1491
  niobium, 2451
  osmium, 1035,1891
  rhodium, 2451
  rhodium(III), 1545
  ruthenium, 1035
  tungsten, 2451
  tungsten(-I), 1609
  tungsten(II), alternative to allyl - carbonyl coordination, 163
  vanadium, 2451
Acylketene complexes
  ruthenium, 955
Adamantane hydroxylation, 425
Adenosylcobalamin, 1469
Alanine complexes
  cobalt(III), 1153
  vanadium(IV), 1245
Alcohol complexes
  chromium(0), 1619
  cobalt(II), 2575
  copper(II), 323
  iron(II), 2155
  ruthenium(III), 1727
Alcohol photooxidation, 477
Alkali metal amalgams, 1813
Alkanes
  hydrogenolysis, 2421
  hydroxylation, 425
Alkenes
  addition of carbonyl metallates, review, 2255
  epoxidation, 2569
  glycol formation, 1981

hydroformylation, 2441
hydrogenation catalysis, 1239, 1827
metathesis catalysis, 1831
oligomerisation catalysis, 2009
polymerisation catalysis, 2375
Alkene complexes
chromium(0), 1619
iron(0), 1605
molybdenum(0), 1831
osmium, 931,979,1891
platinum(0), 1349
platinum(II), 353
rhodium, 859
ruthenium, 979
ruthenium(0), 931
ruthenium(I,III), 837
ruthenium(II), 1239
tungsten(0), 1831
tungsten(V), 1015
Alkenediyl complexes
ruthenium(II), 837
Alkenyl complexes
osmium, 979
rhodium, 859
rhodium(I), 1001
ruthenium, 979
ruthenium(I,III), 837
uranium(IV), 1517
Alkenylphosphidoxo complexes
iron, 2285
Alkoxides
aluminium, 1389
cobalt(I), 1625
copper(II), 323
hafnium(IV), 1625,2165
magnesium, 1389
molybdenum, 919
molybdenum(II), 103,449
molybdenum(III), 903
molybdenum(V), 401
niobium(V), 2217
platinum(II), 1441
rhenium(III), 1363
rhenium(V), 329,1981
samarium, 1693
technetium(V), 1981
titanium(IV), 1625
tungsten(II), 449
tungsten(III), 903
tungsten(IV), 2053
tungsten(V), 1015
zirconium(IV), 1625
Alkyls
aluminium, 1289,1901,2119,2375, 2727
antimony(III), 2601
boron, 2119
cobalt(I), 1559,1625
cobalt(III), 1483,1499
gallium, 1289,1901
hafnium, 1409,1625
indium, 1289,2091
iridium(III), 1285,1429,2171
lanthanides, 2307
lead(II), 1909
lithium, 2023,2119,2307
manganese(I), 1605
manganese(III), 2001
molybdenum(II), 1491
osmium, 931
platinum(II), 1441,1953,2695
platinum(IV), 1169,2095
rhenium(VII), 1841
rhodium(III), 827,1827
ruthenium, 852,1945
ruthenium(I,III), 837
ruthenium(II), 837,1441
scandium, 1409
silicon, 151
tantalum(V), 753
thallium(III), 2487
tin(IV), 2531
titanium(IV), 1625
tungsten(II), 163
tungsten(III), 2049
tungsten(IV), 2053
tungsten(V), 1015
uranium(IV), 1517
zirconium(IV), 1625,2083,2375
Alkylamides
aluminium, 2727
lithium, 399,2515
molybdenum, 1931
molybdenum(II), 103,235,399, 2615
Mo(V),Nb(V),Ta(V), 67
tungsten(III), 1991
zirconium, 2515
Alkylarsenido complexes
aluminium, 1901
Alkylidene complexes
osmium, 1035
rhenium(VII), 1841
rhodium(III), 827
ruthenium, 759,850,1035
Alkylidyne complexes
bridging, review, 775
cobalt(I), 2297
cobalt(III), 1023
iron, 443
molybdenum(II), 2297
rhenium(V), 443
ruthenium, 443
trinuclear, review, 847
tungsten, 871
tungsten(II), 2297
Alkylimides
molybdenum(IV), 2615
Mo(V),Nb(V), 67
rhenium(VII), 1079
tantalum(V), 67
tungsten(V), 297
tungsten(VI), 117
Alkylphosphido complexes
gallium, 1901
lead(II), 1909
Alkylstibide, indium(III), 77
Alkynes, insertion into carbon - metal bonds, 850
Alkyne complexes
cobalt, 2345
molybdenum, 919
molybenum(III), 903
osmium, 931,979,2159
rhodium, 2345
ruthenium, 979,1071
ruthenium(0), 931
ruthenium(II), 1239
tungsten(II), 2769
tungsten(III), 903
Alkynyl complexes
Fe,Os,Ru, 1045
ruthenium(II), 1441
scandium, 1409
uranium(IV), 1517

Allene
dimerisation, 837
reaction with rhodium complex, 859
Alloys, catalysis by, review, 2383
Allyl complexes
hafnium, 2451
iron, 2285
iron(II), 425
manganese(I), 987
molybdenum, 2263
molybdenum(II), 987,1491,1719
niobium(I), 1819
osmium, 979
ruthenium, 1945,2263,2521
tantalum(I), 1819
tungsten, 871
tungsten(V), 1015
zirconium, 2451
Allylbenzene, allyl phenyl ether, 1827
1-Allyl-2-thiourea complexes
ruthenium(II), 219
Aluminium
alkoxide diketonate oxo magnesium complexes, 1389
alkyls, 2119
alkyl alkylamide, 2727
alkyl alkylarsenido,1901
alkyl oxo complexes, 2375
alkyl phosphine complexes, 1289
chloride complex, 1139
chloride - N-butylpyridinium chloride, solvent for complexation studies, 1341
chloride, hydrocarbon nitrosyl complexes, 97
diketonates, 369
heterocyclic compounds, 679
phenoxide Schiff base complex, 2723
polysalicylaldimine complexes, 1881
Alumoxanes, 2375
Amide (NH_2) complexes
Co(I), Hf(IV), Ti(IV), Zr(IV), 1625
Amide (organo) complexes
chromium(II), 1453
cobalt(II), 535
molybdenum(II), 1453
rhenium(V), 171
Rh(II), Ru(II,III), 1453
2-Amidophenoxide complex
molybdenum(V), 401
Amines, reaction with cobalt(III) complex, 1159
Amine complexes
aluminium, boron, 679
chromium(0), 1619
chromium(III), 2703
cobalt(II), 2575,2703
copper(I), 2583,2649
copper(II), 1053,2575,2703
iron(II), 589
molybdenum, 1931
molybdenum(I), 235
molybdenum(V), 67
nickel(II), 2575,2703
niobium(V), 67
palladium(II), 2659
rhenium(I), 2543
rhenium(V), 117,2537
rhenium(VII), 2537
rhodium(II), 1453
ruthenium, 2369
ruthenium(I), 417,1919
ruthenium(III), 1727
silver(I), 601
tantalum(V), 67
tungsten(V), 297
tungsten(VI), 117
Aminoacid complexes
cobalt(III), 1153,1243
iron(III), 747
neodymium, 2495
thallium(III), 2487
vanadium(IV), 1245
Aminoalcohol complexes
cobalt(III), copper(II), 1263
Aminoalcohol Schiff base complexes, Co(II),Cu(II), Fe(III),Ni(II),Zn, 337
4-Aminoantipyrine Schiff base complexes, 143
Aminoarsines, 2553
2-Aminobenzaldehyde, 2715
Aminobenzenethiolates
ruthenium(III), 1727
2-Aminobenzthiazole complexes
ruthenium(II), 219
2-Amino-1-butanol, reaction with cobalt(III) complex, 1159
Aminocarbene, aminocarbyne complexes, osmium, 967
2-(2′-Aminoethyl)pyridine Schiff base complexes, Cu(II),Zn, 695
5-Amino-5-methyl-3,7-diaza-1,9-nonanediol complex, cobalt(III), 1263
3-Aminomethylpinane, 2-Amino-1-phenyl-1,3-propanediol, reaction with cobalt(III) complex, 1159
2-Aminophenol-4-sulphonic acid Schiff bases, 2723
Aminophosphines, 2553
Aminopolycarboxylate complexes
cobalt(II), 1187
cobalt(III), 529
copper(II), nickel(II), 1187
Ammines
cobalt(III), 529
rhenium(V), 171
t-Amylthiolate, copper(I), 49
t-Amylthioxanthate, copper(I), 49
Anisate, ruthenium(II,III), 685
Anisole complexes
chromium(0), 1377
Antifungal complexes, 2183
Antimony(III)
alkyls, aryls, 2601
thiocarbamates, 483
Antimony(V)
fluoride titanium(IV) complex, 1221
Antipyrine Schiff base complexes, 2149
Arene complexes
chromium(0), 409,1377
iron(II), 2685
molybdenum(II), 2027
rhodium, 859
ruthenium(II), 1311

Arginine complexes
cobalt(III), 1153
Aromatic hydrocarbons, complexes with covalent halides and nitric oxide, 97
Arsenido complexes
lanthanides, lithium, 2307
tin(II), 1317
Arsine complexes
iron(II), 1687
osmium(0),(II), 709
platinum, 2321
ruthenium(II), 623
ruthenium(III), 29,1727
technetium(V), 285
Aryls
antimony(III), 2601
hafnium, 1409
iridium(III), 87,1429
lead(IV), 2039
manganese(I), 1605
osmium(VI), 1079
platinum(II), 2695
rhenium(V),(VI),(VII), 1079
rhodium, 859
scandium, 1409
silicon, 679
tantalum(V), 753
tin(IV), 2039
Arylamides
molybdenum(II), 103
molybdenum(V), 401
Pt(II), Ru(II), 1441
Arylimides
iron, osmium, 2331
review, 2331
rhenium(V), 117,329
rhenium(VI), 117
rhenium(VII), 1841
tungsten(V), 2015
tungsten(VI), 117
Atranes, 679,2189
Azaallyl complexes
ruthenium, 2521
1-Aza-3-phosphaallenes, 2213
Azenide complexes
ruthenium(I), 1919
Azide complexes
iron, 1377
lanthanides, 2307
titanium(IV), 1531
Azindole complexes
Pd(II), Rh(I), 2441
Azo complexes
copper(I), 161
palladium(II), 2659
Azobenzene complexes
molybdenum(IV), 1531
palladium(II), 647
titanium(IV), 1531
Azo dye complexes
palladium(II), 495
Azole complexes
cobalt(II), 2575
copper(I), 37,2583
copper(II), 307,323,695,2575
iridium(III), 1781
iron(II), 589
molybdenum, 1931
nickel(II), 2575
osmium(II), 1781
palladium(II), 1273,2441
platinum(II), 1273
rhodium(I), 2441
rhodium(II), 1453
ruthenium(II), 219,1781
ruthenium(II,III), 1453
samarium, 1693
zinc, 695,2575

B

Barium
cyclopentadienyl ether complexes, 725
murexide complexes, 1227
Benzaldehyde complex
chromium(0), 1377
Benzaldehyde Schiff base complex, thorium(IV), 143
Benzaldehyde semicarbazone complexes
molybdenum(II), 1719
tellurium(IV), 633
Benzaldehyde thiosemicarbazone complexes, tellurium(IV), 633
Benzene, reaction with rhodium complex, 859
Benzene complex
chromium(0), 1377
Benzenethiolates
iron, 1371
molybdenum(II), 2615
molybdenum(IV), 1531
osmium, 967
Ti(IV), W(IV), 1531
Benzoates
molybdenum(II), 103
molybdenum(IV), 1531
ruthenium(II,III), 685
Ti(IV), W(IV), 1531
Benzonitrile complexes
chromium(0), 673
Benzotriazole complexes
Ir(III), Os(II), 1781
Pd(II), Rh(I), 2441
ruthenium(II), 1781
Benzoyl complexes
manganese(I), 1605
osmium, ruthenium, 1035
Benzoylhydrazone complexes
Cd,Co,Cu,Mn,Ni,Zn, 393
Benzyl complexes
manganese(I), 1605
molybdenum(II), 1491
tungsten(IV), 2053
uranium(IV), 1517
Benzylamine, reaction with cobalt(III) complex, 1159
Benzylamine complexes
boron, aluminium, 679
Benzyl cyanide complexes
chromium(0), 673
Benzylidyne, benzyne complexes
osmium, 961
Beryllium, organo compounds, book review, 2247
Bibenzimidazolate complexes
copper(I), 37
Bicyclo[2.2.1]hepta-2,5-diene complexes, platinum(II), 1953
Biphenyl complexes
chromium(0), 409,1377
2,2′-Bipyrazine complexes
platinum(II), 1953

Bipyrimidine complexes
palladium(II), 731,2659
Pt(II),Ru(II), 731
1,2-Bis(dimethylphosphino)ethane complexes,
molybdenum(II), 2615
molybdenum(IV), 1767,2615
molybdenum(V), 1767
niobium(I), 1819
tungsten(IV),(V), 1767
vanadium(0),(II), 2615
Bis(dimethylphosphino)methane complexes, platinum(II), 2695
N,N-Bis(3,5-dimethyl-1-pyrazolylmethyl)aminoethane complexes, copper(I), 2583
Bis(dimethylsulphoxide)protium, 2143
Bis(diphenylphosphino)amine complexes, palladium(II), 2659
1,2-Bis(diphenylphosphino)benzene complexes, molybdenum(II), 1279
1,4-Bis(diphenylphosphino)butane complexes,
chromium(I),(II), 1965
rhodium(I), 2441
1,2-Bis(diphenylphosphino)ethane complexes
aluminium, 1289
chromium(II), 1965
cobalt, 2369
gallium, indium, 1289
iridium(III), 187
molybdenum(II), 1279,1673
palladium(II), 2441
platinum(II), 1441,1953
1,2-Bis(diphenylphosphino)ethene complexes, molybdenum(II), 1279
1,1′-Bis(diphenylphosphino)ferrocene complexes,
platinum(II), 1925,1953
rhodium(I), 2441
1,6-Bis(diphenylphosphino)hexane complexes, chromium(I), 1965
Bis(diphenylphosphino)methane complexes
chromium(II), 1965
copper(I), 49
molybdenum(I), 1793
palladium(II), 2659
platinum(II), 1953
rhodium(I),(II), 315
ruthenium(0), 1939
Bis(2-diphenylphosphinophenyl)phosphine complexes
Al, Ga, In, 1289
1,1-Bis(diphenylphosphino)prop-1-ene complexes, palladium(I), 239
1,2-Bis(di-i-propylphosphino)ethane complexes, rhodium(I), 1001
1,3-Bis(di-i-propylphosphino)propane complexes, rhodium(I), 1001
1,2-Bis(di-p-tolylphosphino)ethane complexes, Mo(II), 1673
Bis(1-methyl-1-benzoylhydrazonoethyl)cyclopentadienyl complexes, Cd,Co,Cu,Fe,Mn,Ni,Zn, 393
Bismuth, di-, molybdenum complex, 2239
N,N-Bis(1-pyrazolylmethyl)aminoethane complexes, copper(I), 2583
1,3-Bis(2-pyridyl)-1,3-propanedione complexes, 43
2,3-Bis(2-pyridyl)pyrazine complexes, Pd(II), Pt(II), Ru(II), 731
Bismuth(III)
thiocarbamates, thiodiketonate, 483
1,2-Bis(4-pyridyl)ethane complexes, iron(II), 589
Bis(trimethylsilyl)phosphido complexes, zirconium, 2083
Biuret complexes, Cd, Co(II), Mn(II), Ni(II), Zn, 1869
Bond dissociation energies and enthalpies, bond strengths, calculations, 1625,1677
C - H, 1409,1429
gaseous ions, 1583
M - C, 1409,1429,1441,1469, 1483,1491,1499,1517,1531, 1545,1573,1583,1605,1625
M - C_5H_5, 1531
M - H, 1409,1429,1441,1491, 1531,1545,1573,1583,1605,1625
M - Halogen, 1491,1517,1531, 1605
M - M, 1491,1605
M - N, 1441,1531,1583,1605,1625
M - O, 1441,1531,1583,1625
M - P, 1441,1531,1625
M - S, 1441,1531,1583,1625
M - Si, 1625
solvent cage effects, 1499
Book reviews
beryllium organo compounds, 2247
coordination chemistry, 2243
copper organo compounds, 1225, 1789
fluorine chemistry, 169
gallium organo compounds, 587
manganese coordination compounds, 501
polymer radiothermoluminescence, 671
tin(IV) organo compounds, 1225
Borane amine complexes, 679
Borane anions, polyhedral, 363, 2437
Bornylamine, reaction with cobalt(III) complex, 1159
Boron
alkyls, 2119
halide - aromatic hydrocarbon - nitric oxide complexes, 97
heterocyclic compounds, 679
Bromides and bromo complexes
cadmium, 2129
cobalt(II), 1147,1869
copper(I), 2583
copper(II), 43,1053,1383
gold, 2317
gold(III), 1231,1861
iridium(III), 87,1429
iron, 1371
iron(II), 425
iron(III), 291,2465
manganese(I), 1605
manganese(II), 1869
mercury, 2503
molybdenum(II), 1279,1719

molybdenum(IV), 1531
nickel(II), 1147,1869
osmium, 791,1035
osmium(0),(II), 709
osmium(III), 417,709
palladium(II), 419,659
palladium(IV), 2611
phosphorus(V), 1725
platinum(II), 419,659
platinum(IV), 1169
rhenium(III), 2743
rhenium(V),(VII), 2537
rhodium(I), 379,1067
ruthenium(II), 1737
ruthenium(III), 29,417,1737
silver, 2317
technetium(V), 285
thallium, 2561
titanium(IV), 1531
tungsten(IV), 1531
vanadium(II), 737
zinc, 43,1147,1869,2129,2503
Bromobenzene complex
chromium(0), 1377
4-Bromomandelate, hafnium, 2165
3-Bromopyridine complexes
iron(II), 589
2-Bromotetrafluorophenyl(diphenyl)phosphine complexes,
iridium(III), 87
1,3-Butadiene, reactions with:
rhodium complex, 859
technetium(VII) complex, 1981
1,3-Butadiene complexes
niobium(I), tantalum(I), 1819
1,2-[&2,3]-Butanediol complexes
palladium(II), 349
n-Butanethiolates,
copper(I), 49
molybdenum(IV), 1531
t-Butanethiolate
molybdenum(IV), 1531
n-Butanol, solvent effects, 2135
2-Butanone semicarbazone
complexes, molybdenum(II), 1719
Butenes, oligomerization, 2009
1-[&2-]Butenyl complexes
rhodium(I), 1001
t-Butoxides
molybdenum(III), 903
rhenium(III), 1363
tungsten(III), 903
i-Butyls
aluminium, 1289
n-Butyls
rhodium(III), 827
uranium(IV), 1517
t-Butyls
gallium, 1901
t-Butylamides
molybdenum(V), 67
tantalum(V), 67
i-[&n-, sec-]Butylamine, reaction
with cobalt(III) complex, 1159
t-Butylamine complexes
molybdenum(V), 67
niobium(V), 67
rhenium(V), 117
tantalum(V), 67
tungsten(V), 297
tungsten(VI), 117
t-Butylbenzene complex
chromium(0), 1377
2-Butyldihydropyridyl complexes
lithium, 665
2-t-Butyl-1,3-dithiolane
complexes, Pd(II), Pt(II), 1329
t-Butylhydroperoxide, 2569
t-Butylimides
molybdenum(V), 67
niobium(V), 67
rhenium(VII), 1079
tantalum(V), 67
tungsten(V), 297
tungsten(VI), 117
t-Butylisocyanide complexes
molybdenum(0), 1831
molybdenum(IV), 1767
osmium, 791
rhodium(II), 315,1751
samarium, 1693
tungsten(0), 1831
tungsten(IV), 1767
vanadium(II), 2615
t-Butylpyridine complexes
iron(II), 425
N-Butylpyridinium chloride -
$AlCl_3$, solvent for complexation
studies, 1341
t-Butylthiolates
lanthanides, lithium, 2307
rhodium(I), 2441
2-Butyne complexes
tungsten(II), 63,2769
Butyrates
iron(III), 2175
rhodium(II), 1453
Butyronitrile [i&n] complexes
chromium(0), 673

C

C221, C222, C22B complexes
lithium, 1341
C_A parameters, Cr, Mo, Rh, Ru
binuclear carboxylates, 1453
Cadmium
benzoylhydrazone chloride
iron(II) complexes, 393
biuret chloride complex, 1869
chloride complexes, 715
chloride hydrazine complex,
1147
chloride pyrimidine thioether
complex, 659
diketonate pyridine complexes,
43
halide complexes, 715,2129
iodide thione complexes, 2503
nitrite complexes, 213
polysalicylaldimine complexes,
1881
pyridine Schiff base thiolate
complex, 2183
Cage effects, bond dissociation
energies, 1499
Calcium
cyclopentadienyl ether
complexes, 725
murexide complexes, 1227
Calorimetric titrations
Cd, Zn halide complexes, 2129
Carbaboranes, 669
Carbene complexes
osmium, 1035
review, 767

ruthenium, 759,1035
Carbide complexes, iron, rhodium, 2351
N-Carboamido-2-pyrrolethioamide, N-carboethoxythioamide complexes, ruthenium(II), 623
Carbon, adsorption of molybdenum(VI), 547
Carbon - carbon bond formation, 781,827,955,1015
Carbon - hydrogen bonds
activation, review, 1429
dissociation energy and enthalpy, 1409,1429
formation, 775,955
reductive elimination, 852
Carbon disulphide complexes
ruthenium(III), 1727,1737
vanadium(0), 2615
Carbon monoxide
activation, 2351
hydrogenation, 2411
Carbonate complexes
actinides(III), 573
Carbonyls
chromium, 2451
chromium(-I), 1609
chromium(0), 409,673,1377,1605, 1619,1965,2297
chromium(I), 1559,1965
chromium(II), 1965
cobalt, 2297,2345,2369,2411
cobalt(I), 1559,1625,2297
gaseous, 1559,1605,1609,1619
hafnium(IV), 759
iridium, 2351
iridium(I), 29
iron, 443,1045,2285,2331,2351, 2411,2451
iron(-I), 1609
iron(0), 1605,2285
iron(I), 2285
iron(II), 425,1687
iron(III), 881
manganese(0), 1605,2255
manganese(I), 409,987,1605
molybdenum, 2239,2263,2411,2451
molybdenum(-I), 1609
molybdenum(0), 489,1605,1831, 2255
molybdenum(I), 1491,1793,2271
molybdenum(II), 987,1491,1719, 2027,2297
molybdenum(III), 2715
nickel(0), 1499,1605
niobium, 2451, review, 1639
osmium, 791,961,967,979,1035, 1045,1759,1891,2159,2331, 2399,2421
osmium(0), 931
osmium(II), 709,1781
palladium, 2271,2351
platinum, 2271,2351
review, 1639
rhenium, 2421
rhenium(0), 2255
rhenium(I), 195,1363,1401,2255, 2543
rhenium(II), 195
rhenium(III), 2743
rhenium(V), 443
rhodium, 561,2345,2351,2451
rhodium(I), 29,315,1861,2441
rhodium(II), 315,1441,1751
ruthenium, 443,759,955,979, 1035,1045,1071,1759,2263, 2331,2341,2369,2521
ruthenium(0), 931,1939
ruthenium(I), 417,1919
ruthenium(II), 219,417,1781
scandium, 1559
tantalum, review, 1639
tungsten, 2451
tungsten(-I), 1609
tungsten(0), 1605,1831
tungsten(II), 63,163,245,2297, 2769
vanadium, 2451, review, 1639
vanadium(-I), 2039
zirconium(IV), 759
N-Carbophenylamido-2-pyrrolethioamide complexes, ruthenium(II), 623
Carboxylate complexes
chromium(II), 1453
chromium(III), 2703
cobalt(II), 43,2703
copper(II), 43,689,1053,1335, 1745,2703
hafnium, 2165
iron(III), 2175
manganese(II), 331
molybdenum(II), 103,1279,1453, 2201
molybdenum(III), 2715
molybdenum(IV), 1545
nickel(II), 43,2703
osmium, 979
palladium(II), 615,2477
rhenium(V), 329
rhodium(II), 1453
ruthenium(II), 1239
ruthenium(II,III), 685,1393, 1453,2597
tin(IV), 2225
titanium(IV), 1545
tungsten(III), 1991
tungsten(IV), 1545
zinc, 43,689,1335
Carboxylic acid complexes
K,Li,Na, 1
7-Carboxymethyl-7,16-diaza-18-crown-6 complexes, Cu(II), 1053
Carbyne complexes
heteropolynuclear, 807
Catechol complexes
copper(II), 609
molybdenum(IV), 1545
palladium(II), 349
tungsten(IV), 1545
Cation distortion isomerism, copper(II) cimetidine complexes, 307
CD spectra
cobalt(III) aminoacid nitrite complexes, 1153
cobalt(III) chloride diamine complexes, 1159
cobalt(III) cysteine complex, 1243
cobalt(III) salicylate complex, 2731
iron(III) cyctochrome c oxidase phthalocyanine complex, 2667
vanadium(IV) alanine oxo complexes, 1245

Cerium(III)
diketonate dipyridyl pyridine complexes, 155
diketonate pyrazolylborates, 79
hydroxide complexes, 1355
Chirality, trinuclear clusters, 2297
Chlorides and chloro complexes
aluminium, 1139
cadmium, 393,659,715,1147,1869
cobalt, 2321
cobalt(II), 43,393,535,1147, 1785,1869,2149,2473,2575
cobalt(III), 1159,1263
copper(I), 2583
copper(II), 43,1053,2473
gold, 605,2317,2321
gold(I), 1861
gold(III), 659,1231,1861
hafnium, 1409,1625
indium(III), 77
iridium(III), 87,651,1429,2143
iron(II), 425
iron(III), 291,337,425,2175, 2183,2465
lanthanides, 1095,2307
manganese(I), 1605
manganese(II), 393,1869,2149, 2473
mercury, 659,2159,2503,2509
molybdenum, 1931
molybdenum(II), 449,463,1279, 1673,1719,2027,2201,2615,2679
molybdenum(IV), 1545,1767,2615
molybdenum(V), 67,1767,2027
molybdenum(VI), 579
nickel(II), 43,393,1147,1869, 2009,2149,2473,2575
niobium(V), 67,2217,2221
osmium, 1035,1759,2159
osmium(0),(II), 709
osmium(III), 417,709
palladium(I), 239
palladium(II), 29,207,659,731, 1321,1329,1861,2477,2659
platinum, 2321
platinum(II), 29,505,659,731, 1321,1329,1861,1953,2695
platinum(IV), 2095
potassium, 2307
rhenium(I), 1363,2543
rhenium(III), 1207,1363,2743
rhenium(V), 117,171,329,1981, 2537
rhenium(VI), 117
rhenium(VII), 1079,1841,1981, 2537
rhodium, 2321,2345
rhodium(I), 29,315,1067,1827, 1861
rhodium(II), 315,1751
rhodium(III), 29,651,1827,2087
ruthenium, 1759,1945,2321
ruthenium(I,III), 837
ruthenium(II), 29,207,575,623, 731,837,1311,1727
ruthenium(II,III), 685,1453
ruthenium(III), 29,417,575, 1063,1727
scandium, 1409
silver, 2317
sodium, 2307
tantalum(V), 67
technetium(V), 285,1981
technetium(VII), 1981
tellurium(IV), 633
thallium, 2561
tin(II), 1317
tin(IV), 2655
titanium(IV), 1545,1625,2655
trichloride, 1725
tungsten(II), 163,449
tungsten(IV), 1545,1767,2053
tungsten(V), 297,1767
tungsten(VI), 117,579
uranium(III), 167
uranium(IV), 249
vanadium(III), 2039
zinc, 1147,1869,2129,2473
zirconium, 1625,2083,2375
Chloroacetate, iron(III), 2175
Chlorobenzene, reaction with rhodium complex, 859
Chlorobenzene complex
chromium(0), 1377
Chlorodiphenylgermyl complexes
rhenium, 2209
2-Chloroethoxides, Mo(II), W(II), 449
4-Chloromandelate, hafnium, 2165
2-Chlorophenoxide
titanium(IV), 1545
4-Chloro-1,2-phenylenediaminetetraacetates, Co, Cu, Ni, 1187
4-Chloropyridine-N-oxide complexes, thallium, 2561
Chlorosulphate, rhenium(VII), 705
Chlorosulphuric acid, solvent, 705
2-Chlorotoluene complexes
iron(II), 285
Chromate complexes
iron, 1371
silver(I), 601
Chromium
acyl carbonyl zirconium complexes, 2451
gaseous organo- ions, 1583
Chromium(-I)
carbonyl formyl complexes, 1609
Chromium(0)
alcohol alkene amine carbonyl ether ketone nitrile phosphine pyridine complexes, 1619
alkene carbonyl complexes, 1605
arene carbonyl phosphine complexes, 1377
arene carbonyl phosphine phosphite complexes, 409
carbonyl cyclopentadienyl complexes, 1965
carbonyl solvent complexes, 673
carbonyl steroid hormone complexes, 2297
Chromium(I)
carbonyl ions, 1559
carbonyl cyclopentadienyl diphosphine phosphine complexes, 1965
Chromium(II)
amide carboxylate ether nitrile phosphate phosphite sulphoxide binuclear complexes, 1453
carbonyl cyclopentadienyl

hydride phosphine complexes, 1965
Chromium(III)
amine carboxylate hydroxide phenoxide water iron(III) complex, 2703
peptide complex, 523
phosphoramidothioates, 557
Chromium(VI)
reduction by methionine, 11
Cimetidine complexes
copper(II), 307
Cinnamaldehyde semicarbazone, thiosemicarbazone complexes, silicon, 151
Cluster complexes
electron counting, review, 253
polyhedral rearrangements, 1107
topology, 1813
Cobalt
acyl carbonyl cyclopentadienyl zirconium complexes, 2451
alkyne carbonyl phosphine rhodium complexes, 2345
carbonyl hydride phosphine ruthenium complexes, 2369
carbonyl steroid hormone complexes, 2297
carbonyl thio molybdenum complexes, 2369
chloride phosphine complexes, 2321
gaseous organo- and other ions, 1583
Cobalt(I)
alkoxide amido cyanide hydride hydrosulphide hydroxide methyl phosphido silyl complexes, 1625
alkyl carbonyl ions, 1559
alkylidyne carbonyl Mo(II) W(II) complexes, 2297
Cobalt(II)
acetate chloride diketonate pyridine thiocyanate complexes, 43
amide chloride complexes, 535
amine azole chloride methanol thiocyanate water complexes, 2575
amine carboxylate phenoxide water binucleating complexes, 2703
aminopolycarboxylate complexes, 1187
antipyrine Schiff base chloride water complexes, 2149
azole nitrate thioether complex, 2591
benzoylhydrazone chloride iron(II) complexes, 393
biuret halide complexes, 1861
carbonyl cyclopentadienyl methylene complex, 946
chloride complexes, 1785,2473
dicarboxylate complexes, 203
diketonates, 421
dioxygen Schiff base water complexes, 337
halide hydrazine thiocyanate complexes, 1147
hexamethylphosphoramide complexes, 2135
hydroxide squarate complex, 2155
hydroxyquinoline complexes, 513
isocyanide thiocyanate rhodium(I) polymeric complex, 741
peptide complexes, 1089
phosphine oxide complex, 1785
pyridine Schiff base thiolate complex, 2183
Cobalt(III)
alkyl dimethylglyoxime pyridine complex, 1499
alkyl phosphine pyridine Schiff base complexes, 1483
alkylidyne cyclopentadienyl diselenolato dithiolato seleno sulphonium thio complexes, 1023
aminoacid nitrite complexes, 1153
aminoalcohol chloride complex, 1263
aminopolycarboxylate ammine diamine complexes, 529
chloride diamine complex, 1159
cyclopentadienyl complex, 2039
cyclopentadienyl phosphonate platinum(IV) complexes, 2095
cysteine complex, 1243
salicylate complex, 2731
1-Cobalta-2,5-diheterocyclopent-3-enes, 1023
Coenzyme B_{12}, 1469
Copper
effect on ferrihydrite decomposition, 385
organo compounds, book reviews, 1225,1789
Copper(I)
acetonitrile azo complexes, 161
amine azole halide tetrafluoroborate thiocyanate trifluoromethanesulphonate complexes, 2583
amine Schiff base thioether sodium complexes, 2649
aminopolycarboxylate hydroxide complexes, 1187
azole hydroxyquinoline nitrile oxalate phosphine complexes, 37
diphosphine thiolate thiophenoxide thioxanthate complexes, 49
phosphine thiolate thioxanthate complexes, 1121
thiolates, 2205
Copper(II)
acetate diketonate halide pyridine complexes, 43
alcohol alkoxide azole complex, 323
amine azole water complex, 2575
amine carboxylate phenoxide water binucleating complexes, 2703
aminoalcohol complex, 1263
azole nitrate thioether water complexes, 2591
azole pyridine Schiff base complexes, 695
benzoylhydrazone chloride

iron(II) complexes, 393
bromide hydrazone pyridine complex, 1383
carboxylate pyridine water complexes, 1745
catecholate pyridine complex, 609
chloride complexes, 2473
cimetidine complexes, 307
cryptand amine carboxylate ether halide nitrate perchlorate complexes, 1053
hydroxynaphthoate picolinate complexes, 1335
mepirizole oxalate water complex, 229
perchlorate, 345
picolinate complexes, 689
pyridine Schiff base thiolate complex, 2183
salicylhydrazide Schiff base complex, 543
Schiff base complex, 337
thenoyltrifluoroacetate, 303
Covalent halides, aromatic hydrocarbon nitric oxide complexes, 97
Covalent radius, iridium(III) 2171
Creatinine complexes
Pd(II), Pt(II), 1273
Cresolates
molybdenum(II), 103
titanium(IV), 1545
Crown ether complexes
potassium, 137,721,2761
sodium, 137,2649
Cryptand complexes
copper(II), 1053
lithium, 1341
potassium, 721
silver(I), 2229
Curtius rearrangement, 223
Cyanate complexes
iron, 1371
osmium, 791
Cyanide complexes
cobalt(I), 1625
gold(I), 651
hafnium, 1625
iridium(III), 651
iron, 1197
iron(II), 1687
platinum(II), 1441
rhodium(III), 651
ruthenium(II), 1441
titanium(IV), 1625
tungsten(V), 471
vanadium(II), 2615
zirconium, 1625
3-Cyanopyridine complexes
iron(II), 589
4-Cyanopyridine complexes
thallium, 2561
Cyclic voltammetry
copper(II) azole pyridine Schiff base complex, 695
iron(II) amine azole porphyrin pyridine selenocarbonyl thiocarbonyl complexes, 589
iron(II) phenoxide thio thiolate thiophenoxide complexes, 1911
lithium semiquinone complex, 2429
molybdenum alkylamido amine halide nitrosyl pyrazolylborate complexes, 1931
molybdenum(0) carbonyl diimine phosphine complexes, 489
molybdenum(II) acetate diphosphine halide complexes, 1279
molybdenum(II) chloride phosphine complexes, 2679
molybdenum(VI) oxo tropolonate complex, 1129
rhenium(I),(II) carbonyl formamidinate phosphine triazenide complexes, 195
rhodium(I), carbonyl chloride diphosphine isocyanide complexes, 315
rhodium(I) carbonyl chloride phosphinopyridine complexes, 1751
rhodium(II), carbonyl chloride diphosphine isocyanide complexes, 315
ruthenium(II) chloride diimine complexes, 575
ruthenium(II) chloride cymene oxopyridinate complexes, 1311
ruthenium(II) diimine complexes, 137
ruthenium(II,III) carboxylate chlorides, 685
ruthenium(III) chloride diimine complexes, 575
ruthenium(III) maltol complexes, 1973
Cycloheptatriene, cyclohexadienes, reaction with rhodium complex, 859
Cycloheptatrienyl complexes
Mo(0), Re(I), 2255
Cyclohexadienyl complexes
Mn(0), Re(0),(I), 2255
Cyclohexane hydroxylation, 425
1,4-Cyclohexanediamine complexes
ruthenium, 2369
1,2-Cyclohexanediolate
technetium(V), 1981
Cyclohexene, reaction with Tc(VII) complex, 1981
Cyclohexene complexes
ruthenium(II), 1239
Cyclohexene, 2-cyclohexen-1-one hydrogenation, 1827
Cyclohexyls
iridium(III), 1429
lithium, 2119
Cyclohexylamine, reaction with cobalt(III) complex, 1159
Cyclohexylisocyanide complexes
molybdenum(0), 1831
molybdenum(IV), 1767
tungsten(0), 1831
Cyclometallated compounds
hafnium, 1409
molybdenum, 919
osmium, 931
palladium(II), 2659
ruthenium, 850
ruthenium(I,III), 837
scandium, 1409

tantalum(V), 753
1,5-Cyclooctadiene, reaction with
rhodium complex, 859
1,5-Cyclooctadiene complexes
iridium(I), 2035
platinum(II), 353,1925,1953
rhodium, 561
rhodium(I), 1067,2035
Cyclooctatetraene, cyclopentadiene, reactions with rhodium complex, 859
Cyclooctene complexes
ruthenium(II), 1239
Cyclooctene hydrogenation, 1827
Cyclopentadienyls
barium, calcium, 725
chromium(0),(I),(II), 1965
cobalt(III), 1023,2039,2095
hafnium(IV), 759,1409
iridium(III), 1429
iron(II), 393,1925,2441,2685
iron(III), 881
lanthanides, 1095,2307
Dy,Er,Gd,Nd,Sm
molybdenum, 2239,2263,2411
molybdenum(I), 409,1491,1793, 2271
molybdenum(II), 987,1491,2297
molybdenum(IV), 1545
rhenium, 2209
rhenium(III), 2743
rhenium(V), 443
rhodium, 859
rhodium(III), 827
ruthenium, 759
ruthenium(I,III), 837
ruthenium(II), 623,837,1441
samarium, 1693
scandium, 1409
strontium, 725
tantalum(V), 2053
titanium(IV), 1221,1545
tungsten(II), 2297
tungsten(III), 1991
tungsten(IV), 1545,2053
uranium(IV), 249,1517
zirconium(IV), 759,2083,2375, 2441
Cyclopentyl, iridium(III), 1429
Cyclopentylphosphido complexes
gallium, 1901
p-Cymene complexes
ruthenium(II), 1311
Cysteine, reaction with $[Fe(CN)_5NO]^{2-}$, 1197
Cysteine complexes
cobalt(III), 1243
thallium, 2487
Cysteinylglycine complexes
cobalt(II), zinc, 1089
Cytochrome c- oxidase complex
iron(III), 2667

D

n-Decanethiolate
molybdenum(IV), 1531
3,4-Diacetyl-2,4-hexadiene-2,5-diol complexes, platinum(II), 353
2,6-Diacetylpyridinedihydrazone complexes, lanthanides, 439
2,6-Diacetylpyridine Schiff base complexes
Cd(II), Co(II), 2183
copper(II), 695,2183
Fe(III), Ni(II), 2183
zinc, 695, 2183
Dialkyne complexes
tungsten(II), 63
Diamine complexes
cobalt(III), 529,1159
copper(II), 1263
lithium, 2001,2307
Mo(V),Nb(V), 67
rhodium(I), 1067
ruthenium, 2369
ruthenium(II), 1727,1737
ruthenium(III), 1737
tantalum(V), 1067
1,4-Diaminobenzene complexes
ruthenium, 2369
1,3-Diaminopropane complexes
cobalt(III), 529
4,6-Diamino-2-methylthio-5-nitrosopyrimidine complexes, 659
Diarylazo compounds, copper(I) complexes, 161
1,3-Diaryltriazenide complexes
Ir(III),Os(III),Rh(III), Ru(I),(II),(III), 417
1,4-Diazabicyclo[2.2.2]octane complexes, iron(II), 589
1,4-Diaza-1,3-butadienes complexes, tungsten(II), 63
Diazenide complexes
molybdenum(V), 401
rhenium(V), 171
zirconium, 2083
Dibenzo-18-crown-6, dibenzo-24-crown-8 complexes, K, 2761
1,2-Dibenzoyl-1,2-dithioethene complexes, tungsten(V), 471
Dibismuth complexes
molybdenum, 2239
Di-t-butylarsenido complexes
aluminium, 1901
lanthanides, lithium, 2307
tin(II), 1317
3,5-Di-t-butylcatecholate complex
copper(II), 609
4,4′-Di-t-butyldipyridine complexes, ruthenium(II), 575
Dibutyl fumarate, maleate, reaction with technetium(VII) complex, 1981
Di-t-butylphosphido complexes
lanthanides, 2307
lead(II), 1909
lithium, 2307
tin(II), 1317
Di-t-butylphosphine complexes
rhodium, 561
Di-t-butylstibide
indium(III), 77
Dibutyltartrate
technetium(V), 1981
Dicarboxylates
cobalt(II), 203
copper(I), 37
copper(II), 229
palladium(II), 2477
ruthenium(II,III), 1393
Dichloroacetate, iron(III), 2175
Dichlorobenzenes, reaction with

rhodium complex, 859
2,6-Dichlorophenylimido complexes
rhenium(VII), 1841
1,3-Di-*p*-chlorophenyltriazenides
ruthenium(I), 1919
3,5-Dichloropyridine complexes
iron(II), 589
2,6-Dichlorotoluene complexes
iron(II), 2685
Dicyclohexyldithiocarbamates
silver(II), 25
Dicyclohexyl(phenyl)phosphine
complexes, copper(I), 1121
Diene complexes
hafnium, 2451
iridium(I), 2035
manganese(0), 2255
niobium(I), 1819
platinum(II), 1925,1953
rhenium(0), 2255
rhodium, 561,859
rhodium(I), 1067,2035
tantalum(I), 1819
zirconium, 2451
Dienyl complexes
Mn(0), Re(0),(I), 2255
Diethylacetamide, solvent
effects, 2135
Diethylamide, Mo(II), 2615
Diethylamine, reaction with
cobalt(III) complex, 1159
Diethylaminocyanide complexes
molybdenum, 919
Diethyldithiocarbamate complexes
Sb(III), Bi(III), 483
osmium(II),(III), 709
ruthenium(III), 1727,1737
technetium(V), 285
tellurium(IV), 1267
Diethylether complexes
lanthanides, sodium, 2307
Diethylformamide, solvent
effects, 2135
Diethyl muconate complexes
osmium, 931
Diethyl(phenyl)phosphine,
reaction with ruthenium(0)
complex, 1939
Diethyl(phenyl)phosphine
complexes, chromium(I), 1965
Diethylphosphonates
Co(III), Pt(IV), 2095
Diethylsulphide complexes
platinum(II), 353
Differential pulse voltammetry
iron(II) amine azole porphyrin
pyridine selenocarbonyl
thiocarbonyl complexes, 589
Dihydroabietylamine, reaction
with cobalt(III) complex, 1159
Dihydroindenoindenediolate
samarium, 1693
Dihydropyran, 3,4-dihydro-2-
methoxy-2*H*-pyran hydrogenation,
1827
2,2′-Diimidazole complexes
copper(I), 37
Diimine complexes
copper(II), 229
holmium, 647
iron(II), 425
lanthanides, 155
molybdenum(0), 489
molybdenum(V), 67
nickel(II), 1175
niobium(V), 67
palladium, 2321
palladium(II), 349,731,2659
platinum(II), 137,349,731,1953
rhenium(V),(VII), 1981
rhodium(I), 1067
ruthenium(II), 137,575,731
ruthenium(III), 575,1727,1737
silver, 601
tantalum(V), 67
technetium(V),(VII), 1981
tungsten(II), 63
tungsten(VI), 117
4,4′-Diisocyanobiphenyl complexes
cobalt(II), rhodium(I), 741
Diketonates
aluminium, 369,1389
cadmium, 43
cobalt(II), 43,421
copper(II), 43,303
lanthanides, 79,155,1095
magnesium, 1389
manganese(II), 43
nickel(II), 43,2233
platinum(II), 353
ruthenium(III), 1727
scandium, 1409
zinc, 43
Dilithiodialkylmethanes, 2023
Dimethoxyethane complexes
potassium, 2307
Dimethylacetamide, solvent
effects, 2135
Dimethylacetamide complexes
Cr(II), Mo(II), Rh(II), 1453
Dimethyl acetylenedicarboxylate
complexes, osmium, 931
1,1-Dimethylallyl complexes
manganese(I), 987
1,2-Dimethylallyl complexes
Mn(I), Mo(II), 987
Dimethylamides
lithium, 399,2515
molybdenum(II), 399
tungsten(III), 1991
zirconium, 2515
Dimethylamine complex
rhenium(I), 2543
4-Dimethylaminobenzaldehyde
Schiff base complexes, Th, 143
Dimethylammonio-1-propanethiolate
mercury, 2509
N,*N*-Dimethylaniline complexes
chromium(0), 1377
ruthenium, 2369
Dimethylbenzylamine complexes
palladium(II), 2659
N,*N*′-Dimethyl-1,3-bis(2-pyridyl)-
1,3-propanediamine complexes
Cd,Co,Cu,Mn,Ni,Zn, 43
2,3-Dimethyl-2-butene complexes
chromium(0), 1619
2,4-Dimethylbutyl
iridium(III), 1429
Dimethylcyanamide complexes
chromium(II), 1453
4,4′-Dimethyl-2,2′-dipyridyl
complexes, platinum(II), 1953
Dimethyldithioarsenates
platinum(IV), 1855
Dimethyldithiocarbamates

osmium(II),(III), 709
tellurium(IV), 1267
tungsten(II), 163
2,2-Dimethyl-1,3-dithiolane complexes, Pd(II), Pt(II), 1321
N,N′-Dimethylethylenediamine-N,N′-di-α-butyrate complexes
cobalt(III), 529
Dimethylformamide, solvent effects, 1227,2135
Dimethylformamide complexes
chromium(II), 1453
rhenium(V), 171
Dimethyl fumarate, maleate complexes, osmium, 931
Dimethylglyoximates
cobalt(III), 1483,1499
Dimethylhydrazine complex
rhodium(III), 2087
2,9-Dimethyl-1,10-phenanthroline complexes, platinum(II), 353
5,6-Dimethyl-1,10-phenanthroline complexes, rhodium(I), 1067
Dimethyl(phenyl)phosphine complexes,
chromium(I), 1965
iridium(III), 651,1285,2171
molybdenum(II), 1491
platinum(0), 2271
platinum(II), 353,419,1953
rhenium(I), 1401
rhodium(III), 651
ruthenium, 1945
technetium(V), 285
tungsten(II), 2769
Dimethylphosphonates
Co(III), Pt(IV), 2095
3,5-Dimethylpyrazole complexes
copper(I), 37
1,2-Dimethyl-3-hydroxypyrid-4-one complex, iron(III), 2235
Dimethylsulphoxide, solvent effects, 1227,2135,2473
Dimethylsulphoxide complexes
chromium(0), 673
chromium(II), 1453
iridium(III), 2143
Mo(II), Rh(II), 1453
ruthenium(II), 29,1727,1737, 2627
ruthenium(II,III), 1453
ruthenium(III), 1727,1737
2,2-Dimethyltetrahydrofuran complexes, chromium(0), 1619
3-(4′,5′-Dimethyl-2′-thiazolylazo)-2,6-diaminopyridine complex, palladium(II), 495
5,5-Dimethyl-1,1,1-trifluoro-2,4-hexanedionate, aluminium, 369
Diolate complexes
lithium, 2001
palladium(II), 349
Re(V), Tc(V), 1981
Dioxygen complex
cobalt(II), 337
Diphenylacetylene complexes
cobalt, 2345
osmium, 2159
rhodium, 2345
tungsten(II), 63,2769
Diphenylamido complexes
Pt(II), Ru(II), 1441
Diphenylarsenido complexes
lanthanides, lithium, 2307
Diphenylcarbazone complex
molybdenum(VI), 401
Diphenylditelluride complexes
platinum(IV), 1169
Diphenyl-1,2-ethanediolate
technetium(V), 1981
Diphenyl(ethyl)phosphine, reaction with ruthenium(0) complex, 1939
Diphenyl(methyl)phosphine complexes
molybdenum(I),(II), 1491
nickel(II), 2009
platinum(0), 2271
platinum(II), 1953
platinum(IV), 1855
ruthenium, 1945
4,7-Diphenylphenanthroline complexes
platinum(II), 1953
rhodium(I), 1067
silver, 601
2,6-Diphenylphenoxides
tantalum(V), 753
Diphenylphosphido complexes
lanthanides, 2307
Diphenylphosphinate, indium, 2091
Diphenylphosphinocyclopentadienyl complex, iron(II), 1925
1-Diphenylphosphino-2-di(4-t-butylphenyl)phosphinoethane complexes, molybdenum(II), 463, 1673
1-Diphenylphosphino-2-di(p-tolyl)phosphinoethane complexes,
molybdenum(II), 1673
2-Diphenylphosphinopyridine complexes
molybdenum(II), 2201
rhodium(II), 1751
Diphenylpyridiniumgermyl complexes, rhodium, 2209
Diphenyl(4-sulphonatophenyl)phosphine complexes, gold, 605,2321
Diphenyl(p-tolyl)phosphine complex, ruthenium(II), 2031
Diphenyl(triflato)germyl complexes, rhodium, 2209
Diphosphines, aryl, 1875
Diphosphine complexes
aluminium, 1289
chromium(I),(II), 1965
cobalt, 2369
copper(I), 49
gallium, indium, 1289
iridium(III), 187
molybdenum(I), 1793
molybdenum(II), 463,1279,1673, 2615
molybdenum(IV), 1767,2615
molybdenum(V), 1767
niobium(I), 1819
palladium(I), 239
palladium(II), 2441,2659
platinum(II), 1441,1925,1953
rhodium(I), 315,1001,1827,2441
rhodium(II), 315
rhodium(III), 1827
ruthenium(0), 1939
tantalum(I), 1819
tungsten(IV),(V), 1767
vanadium(0),(II), 2615

Dipole moments, chromium(I), scandium(I) carbonyl ions, 1559
Di-i-[&n]-propyldithiocarbamates
silver(II), 25
tellurium(IV), 1267
2,6-Di-iso-propylphenoxides, 2,6-di-iso-propylphenylimido complexes, rhenium(VII), 1841
2,2′-Dipyridyl complexes
iron(II), 425,589
lanthanides, 55
molybdenum(0), 489
Mo(V),Nb(V), 67
palladium(II), 349
platinum(II), 137,1953
rhodium(I), 1067
ruthenium(II), 137,575
ruthenium(III), 1727,1737
silver(I), 601
tantalum(V), 137
technetium(V),(VII), 1981
tungsten(VI), 117
4,4′-Dipyridyl complexes
silver(I), 601
2,2′-Dipyrimidyl complexes
platinum(II), 1953
Diselenolates, cobalt(III), 1023
Distibines, 2601
Disulphides, formation from thiols, 1197
Disulphide complexes
tungsten(V), 471
Disulphur dinitride, 629
Disulphur dinitride complexes
platinum(II), 1925
Ditelluride complexes
platinum(IV), 1169
3,6-Dithiaoctane complexes
rhenium(III), 1207
Dithioarsenate complexes
platinum(IV), 1855
Dithiocarbamates
gold(I),(III), 1231
iron(III), 2465
osmium(II),(III), 709
ruthenium(III), 1727,1737
silver(II), 25
technetium(V), 285
tellurium(IV), 1267
tungsten(II), 163
Dithiocarbazates
platinum(II), 1211
Dithiocarboxylate complexes
mesogenic, 1861
Dithiodiketonate
nickel(II), 2009
1,3-Dithiolane complexes
Pd(II), Pt(II), 1321
Dithiolates
cobalt(III), 1023
palladium(II), 349
rhodium(I), 379
titanium(IV), 1531
tungsten(V), 471
1,3-Dithiole-2-thione-4,5-dithiolates, rhodium(I), 379
1,3-Di-p-tolyltriazenides
ruthenium(I), 1919
1,3-Ditungstacyclobutadienes, 1015
DSC
binucleating complexes, 2703
germanium hydride polymer, 597
DTA
benzoylhydrazoneferrocene complexes, 393
iron(III) carboxylate chloride oxo water complexes, 2175
lanthanide chloride hydrazone water complexes, 1095
pyrimidine thioether complexes, 659
Dysprosium
cyclopentadienyl pentanedionates, 1095
diacetylpyridinedihydrazone nitrate water complexes, 439
diketonate pyrazolylborate, 79
pyridine thiosemicarbazone complexes, 147

E

E_A parameters, Cr(II),Mo(II), Rh(II),Ru(II,III) binuclear carboxylates, 1453
Effective atomic number rule, 254
EHMO calculations
five - coordinate hydride complexes, 405
tungsten alkylidyne allyl complexes, 871
Electric conductance
benzoylhydrazoneferrocene complexes, 393
copper(I) azole nitrile phosphine complexes, 37
copper(II) azole pyridine Schiff base complexes, 695
copper(II) cryptand amine carboxylate ether halide nitrate perchlorate complexes, 1053
crown ether - diimine ligand complexes (K,Na,Pt,Ru), 137
gold chloride phosphine cluster complex, 605
iron(III) carboxylate chloride nitrate oxo piperidide pyridine thiocyanate water complexes, 2175
lanthanide chloride hydrazone water complexes, 1095
molybdenum(IV) alkylimide chloride diphosphine complex, 2615
palladium(II) amine azo chloride diimine diphosphine nitrile pyridine cyclometallated complexes, 2659
potassium crown ether phosphonate complexes, 2753
rhenium(VII) chlorosulphate oxo compound, 705
rhodium(I) diamine diene diimine halide quinoline complexes, 1067
ruthenium(II,III) acetate ether phosphine oxide complexes, 2597
ruthenium(II,III) carboxylate chlorides, 685
ruthenium(III) bromide carbon disulphide diamine phosphine sulphoxide complexes, 1737
ruthenium(III) chloride Schiff

base complexes, 1063
thorium(IV) nitrate Schiff base complexes, 143
triphosphinoamine complexes (Ir,Pd,Pt,Rh,Ru), 29
vanadium(II) cyanide diphosphine isocyanide nitrile thiocyanate complexes, 2615
zinc azole pyridine Schiff base complexes, 695
Electric conductance (solid state)
cobalt(II) isocyanide thiocyanate rhodium(I) isocyanide polymeric complex, 741
partially oxidised rhodium(I) dithiolate halide complexes, 379
Electrochemical synthesis, copper(I) diphosphine thiolate thiophenoxide thioxanthate complexes, 49
Electron counting, polynuclear complexes, review, 253
Electronegativity, in bond energy calculations, 1677
Electronic spectra
adenosylcobalamin thermolysis, 1469
alkaline earth murexide complexes, 1227
alkene polymerisation, 2375
aromatic hydrocarbon - covalent halide - nitric oxide complexes, 97
chromium(0) carbonyl solvent complexes, 673
chromium(II) amide carboxylate ether nitrile phosphite sulphoxide binuclear complexes, 1453
chromium(III) peptide complex, 523
chromium(III) phosphoramidothioates, 557
cobalt(II) amide chloride complexes, 535
cobalt(II) amine azole chloride methanol thiocyanate water complexes, 2575
cobalt(II) antipyrine Schiff base chloride water complexes, 2149
cobalt(II) azole nitrate thioether water complex, 2591
cobalt(II) bromide hydrazine thiocyanate complexes, 1147
cobalt(II) dioxygen Schiff base water complexes, 337
cobalt(II) hexamethylphosphoramide complexes, 2135
cobalt(II) hydroxide squarate complex, 2155
cobalt(II) hydroxyquinoline complexes, 513
cobalt(II) isocyanide thiocyanate rhodium(I) polymeric complex, 741
cobalt(II) peptide complexes, 1089
cobalt(II) pyridine Schiff base thiolate complex, 2183
cobalt(III) aminoacid nitrite complexes, 1153
cobalt(III) aminoalcohol chloride complex, 1263
cobalt(III) aminopolycarboxylate ammine diamine complexes, 529
cobalt(III) chloride diamine complexes, 1159
cobalt(III) cysteine complex, 1243
cobalt(III) salicylate complex, 2731
copper(II) amine azole water complex, 2575
copper(II) amine carboxylate phenoxide water binucleating complexes, 2703
copper(II) aminoalcohol complex, 1263
copper(II) azole nitrate thioether water complexes, 2591
copper(II) azole pyridine Schiff base complexes, 695
copper(II) bispyridyldiketonate complex, 43
copper(II) bromide hydrazone pyridine complex, 1383
copper(II) carboxylate pyridine water complexes, 1745
copper(II) catecholate pyridine complex, 609
copper(II) cryptand amine carboxylate ether halide nitrate perchlorate complexes, 1053
copper(II) mepirizole oxalate water complex, 229
copper(II) pyridine Schiff base thiolate complex, 2183
copper(II) Schiff base complex, 337
gold(III) dithiocarbamate halide complexes, 1231
holmium acetonitrile phenanthroline complexes, 641
iron cyanide nitrosyl complex reaction, 1197
iron(II) amine azole porphyrin pyridine selenocarbonyl thiocarbonyl complexes, 589
iron(II) arsine carbonyl cyanide phosphine phosphite stibine complexes, 1687
iron(II) hydroxide propanol squarate complex, 2155
iron(II) phenoxide thio thiolate thiophenoxide complexes, 1911
iron(III) amine carboxylate hydroxide phenoxide water binucleating complexes, 2703
iron(III) carboxylate chloride nitrate oxo piperidide pyridine thiocyanate water complexes, 2175
iron(III) chloride Schiff base complexes, 337
iron(III) cytochrome c oxidase phthalocyanine complex, 2667
iron(III) pyridine Schiff base thiolate complex, 2183

iron(III) serine hydroxamate complexes, 747
lanthanide chloride hydrazone water complexes, 1095
lanthanide diacetylpyridinedihydrazone nitrate water complexes, 439
manganese(II) antipyrine Schiff base chloride water complexes, 2149
molybdenum(0) carbonyl diimine phosphine complex, 489
molybdenum(II) acetate diphosphine halide complexes, 1279
molybdenum(VI) oxo tropolonate complex, 1129
neodymium proline water complex, 2495
nickel(II) amine azole chloride thiocyanate water complexes, 2575
nickel(II) amine carboxylate phenoxide water binucleating complexes, 2703
nickel(II) antipyrine Schiff base chloride water complexes, 2149
nickel(II) azole nitrate thioether complex, 2591
nickel(II) chloride hydrazine thiocyanate complexes, 1147
nickel(II) hydroxide squarate complex, 2155
nickel(II) hydroxyquinoline complexes, 513
nickel(II) phenanthroline complex hydrates, 1175
nickel(II) phenoxide pyridine Schiff base complex, 2641
nickel(II) pyridine Schiff base thiolate complex, 2183
nickel(II) Schiff base water complex, 337
osmium(0) arsine halide nitrosyl complexes, 709
osmium(II) chloride dithiocarbamate nitrosyl phosphine complexes, 709
osmium(III) chloride phosphine thionitrile complexes, dithiocarbamates, 709
palladium(II) azo dye complexes, 495
palladium(II) carboxylate chloride selenoether complexes, 2477
palladium(II) chloride phosphine pyridine complex photochemistry, 207
platinum(II) alkyl diene diimine diphosphine halide phosphine pyridine terpyridyl complexes, 1953
potassium crown ether phosphonate complexes, 2753
pyrimidine thioether, 659
rhenium(II) carbonyl formamidinate phosphine triazenide complexes, 195
rhenium(III) chloride thioeter complexes, 1207
rhenium(V) acetonitrile ammine chloride diazenide dimethylformamide hyrazide phosphine pyridine complexes, 171
rhenium(V) halide oxo macrocyclic triamine complexes, 2537
rhenium(VII) chlorosulphate oxo compound, 705
rhenium(VII) halide oxo macrocyclic triamine complexes, 2537
rhodium(I) diketonate halide complexes and partially oxidised derivatives, 379
rhodium(II) amide amine azole carboxylate nitrile phosphine pyridine-N-oxide sulphoxide thioether binuclear complexes, 1453
ruthenium alkyl allyl chloride naphthoquinodimethane phosphine complexes, 1945
ruthenium(0) carbonyl diphosphine complex substitutions, 1939
ruthenium(II) alkene alkyne carboxylate hydride complexes, 1239
ruthenium(II) arsine chloride cyclopentadienyl thioamide complexes, 623
ruthenium(II) bromide diamine sulphoxide complexes, 1737
ruthenium(II) carbonyl chloride diimine palladium(II) platinum(II) complexes, 731
ruthenium(II) chloride diimine complexes, 575
ruthenium(II) diimine alkali metal complexes, 137
ruthenium(II,III) carboxylate chlorides, 685
ruthenium(II,III) oxalate propionate complexes, 1393
ruthenium(III) bromide carbon disulphide diamine diimine dithiocarbamate phosphine pyridine sulphoxide complexes, 1737
ruthenium(III) chloride diimine complexes, 575
ruthenium(III) chloride Schiff base complexes, 1063
silicon methyl semicarbazone thiosemicarbazone complexes, 151
silver amine chromate diimine nitrate complexes, 601
sodium crown ether ruthenium(II) complexes, 137
technetium(V) arsine halide nitride phosphine complexes, 285
tin(IV) formate hydroxide porphyrin complexes, 2225
tungsten(V) cyanide disulphide dithiolate oxo thio binuclear complexes, 471
vanadium(II) bromide ether binuclear complexes, 737
vanadium(III) oxo Schiff base water complexes, 2635
vanadium(III) phosphoramidothi-

oates, 557
vanadium(IV) alanine oxo complexes, 1245
vanadium(IV) oxo Schiff base complexes, 2635
zinc azole pyridine Schiff base complexes, 695
Electronic spectra (difference)
iron(III) cytochrome c oxidase phthalocyanine complex, 2667
Electron microscopy
gold chloride phosphine cluster complex, 605
high nuclearity clusters, 2321
nickel tungsten sulphide, 2405
niobium(V) ternary oxides, 2393
Enthalpy of activation
adenosylcobalamin thermolysis, 1469
bond dissociation, cobalt(II) diketonates, 421
C-C bond formation, tungsten(V) complexes, 1015
chromium(VI) - methionine reaction, 11
configurational interconversions, cobalt(II) phosphine oxide complexes, 2135
cyclometallated ligand reactions, 919
cyclometallation, 1409
fluxionality, Pd(II), Pt(II) chloride thioether complexes, 1321
insertion reactions, oxidative additions, reductive eliminations, 1429
M-C, M-H bond dissociation, 1491
metal - metal bond breaking, chromium(I) carbonyl cyclopentadienyl complex, 1965
substitutions, chromium carbonyl, 1619
substitutions, ruthenium(0) carbonyl diphosphine complex, 1939
Enthalpy of bond dissociation
cobalt(II) diketonates, 421
Enthalpy of formation
binuclear carboxylates, 1453
cadmium halide complexes, 2129
cobalt(II) dicarboxylate complexes, 203
cobalt(II) diketonates, 421
zinc halide complexes, 2129
Enthalpy of solution
uranium(IV) alkenyl alkyl alkynyl cyclopentadienyl iodide complexes, 1517
Entropy of activation
addition reactions, rhodium(II) porphyrin, 1545
adenosylcobalamin thermolysis, 1469
C-C bond formation, tungsten(V) complexes, 1015
chromium(VI) - methionine reaction, 11
configurational interconversions, cobalt(II) phosphine oxide complexes, 2135
cyclometallated ligand reactions, 919
cyclometallation, 1409
fluxionality, Pd(II), Pt(II) chloride thioether complexes, 1321
metal - metal bond breaking, chromium(I) carbonyl cyclopentadienyl complex, 1965
substitutions, chromium carbonyl, 1619
substitutions, cobalt(III) chloride diamine complexes, 1159
substitutions, ruthenium(0) carbonyl diphosphine complex, 1939
Entropy of formation
cadmium halide complexes, 2135
cobalt(II) dicarboxylate complexes, 203
zinc halide complexes, 2135
Erbium
cyclopentadienyl pentanedionate, 1095
diacetylpyridinedihydrazone nitrate water complexes, 439
ESR spectra
cobalt(II) dioxygen Schiff base water complexes, 337
cobalt(II) isocyanide thiocyanate rhodium(I) polymeric complex, 741
copper(II) amine azole water complex, 2575
copper(II) azole nitrate thioether water complexes, 2591
copper(II) azole pyridine Schiff base complexes, 695
copper(II) bromide hydrazone pyridine complex, 1383
copper(II) carboxylate pyridine water complexes, 1745
copper(II) cimetidine complexes, 307
copper(II) cryptand amine carboxylate ether halide nitrate perchlorate complexes, 1053
copper(II) salicylhydrazide Schiff base complex, 543
iron cyanide nitrosyl complex reaction, 1197
iron nitrosyl thiolate reactions, 1371
iron(II) phenoxide thio thiolate thiophenoxide complexes, 1911
manganese(II) biuret halide complexes, 1861
molybdenum amine azole iodide nitrosyl complexes, 1931
molybdenum(V) chloride complex, 2027
rhenium(II) carbonyl formamidinate phosphine triazenide complexes, 195
rhenium(VI) aryl oxo complexes, 1079
rhodium(I) [and partially oxidised] dithiolate halide

complexes, 379
rhodium(II) carbonyl carboxylate spin label complexes, 1453
ruthenium(III) arsine halide triphosphinoamine complexes, 29
ruthenium(III) bromide diamine diimine pyridine sulphoxide complexes, 1737
ruthenium(III) chloride Schiff base complexes, 1063
semiquinone radical complex, 2429
silver(II) dithiocarbamate pyridine complexes, 25
vanadium(II) cyanide diphosphine isocyanide nitrile thiocyanate complexes, 2615
vanadium(IV) alanine oxo complexes, 1245
vanadium(IV) oxo Schiff base complexes, 2635
1,2-Ethanedithiolate complexes
palladium(II), 349
Ethanethiolate complexes
iron, 1371
Ti(IV), W(IV), 1531
Ethanol, solvent effects, 2135
Ethanol complexes
chromioum(0), 1619
Ethanolamine, reaction with
cobalt(III) complex, 1159
Ethene
hydroformylation, 2351*
reaction with Tc(VII) complex, 1981
Ethene complexes
iron(0), 1605
molybdenum(0), 1831
osmium, 1891
platinum(0), 1349
tungsten(0), 1831
Ethenyl complexes
rhodium(I), 1001
Ether complexes
barium, calcium, 725
chromium(0), 1619
chromium(II), 1453
copper(II), 1053
lanthanides, 2307
lithium, 2515
magnesium, 1079
molybdenum(II), 1453
niobium(V), 2217
osmium, 1035
potassium, 2307
rhenium(I), 1363
rhenium(VI), 117
rhodium, 2345
ruthenium(II,III), 2597
samarium, 1693
sodium, 2307
strontium, 725
tin(IV), titanium(IV), 2655
uranium(IV), 249
vanadium(II), 737
Ethoxides
molybdenum(II), 103
niobium(V), 2217
rhenium(V), 329
2-Ethoxyethoxides
Mo(II), W(II), 449
Ethyls
aluminium, 1901,2119
antimony(III), 2601
gallium, indium, 1289
lithium, 2119
molybdenum(II), 1491
rhodium(III), 827
Ethylamide, molybdenum(II), 103
Ethylamine complex
tantalum(V), 67
Ethylenebis(salicylaldimine) complexes, iron(II), 425
Ethylenebis(selenoglycollate) palladium(II), 2477
Ethylenebis(tetrahydroindenyl) complexes, zirconium, 2375
Ethylenediamine complexes
cobalt(III), 529,1159
rhodium(I), 1067
Ethylenediamine Schiff base complexes, ruthenium(III), 1063
Ethyleneglycolate complexes
Pd(II),Pt(II), 349
Ethylenetrithiocarbonate complexes, Cd,Hg,Zn, 2503
Ethylhydrazine complexes
Cd,Co(II),Ni(II),Zn, 1147
Ethylimide complexes
molybdenum(IV), 2615
tantalum(V), 67
7-(4-Ethyl-1-methyloctyl)-8-hydroxyquinoline complexes, cobalt(II), nickel(II), 513
4-Ethylpyridine complexes
iron(II), 425
Ethylselenoglycollate
palladium(II), 2477
Ethyne complexes
cobalt, 2345
molybdenum(III), 903
rhodium, 2345
tungsten(III), 903
Europium
diketonate pyrazolylborate complex, 79
EXAFS
iron molybdenum carbonyl thio complexes, 2411
iron rhodium carbonyls, 2351

F

Fenske - Hall calculations,
molybdenum(III), tungsten(III) alkoxide alkyne pyridine complexes, 903
osmium carbonyl chloride phosphide complexes, 1759
"piano - stool" dimers, 943
ruthenium carbonyl chloride phosphide complexes, 1759
Ferrihydrite, 385
Ferrocene derivatives, complexes of, lanthanides, 1095
Fischer carbene complexes
osmium, ruthenium, 1035
Five - coordination, molecular orbitals, 405
Flufenamate complexes
copper(II), 1745
Fluorescence spectra
neodymium proline water

complex, 2495
palladium(II) chloride phosphine pyridine complex photochemistry, 207
Fluorides and fluoro complexes
antimony(V), 1221
Kr(II), Mn(II), 1217
molybdenum(V), 1135
silicon, 1773
titanium(IV), 1221
tungsten(V), 2015
Fluorine chemistry, book review, 169
Fluorobenzene complexes
chromium(0), 1377
Fluorobiphenyl complexes
chromium(0), 409
Fluorophenylcyclopentadienyl complexes, manganese(I), 409
Fluxional behaviour
alkenyl hydride complexes, 1001
carbonyl cyclopentadienyl complexes, 759
carbyne, ketenylidene complexes, 807
germyl complexes, 2209
osmium ketene complexes, 791
platinum(II) alkyl aryl diphosphine halide complexes, 2695
platinum(IV) ditelluride halide methyl complexes, 1169
polyphosphine complex, 2035
selenium rings, 581
tetranuclear heteropolymetallic clusters, 2271
thiocarbamate complexes, 483
thioether complexes, 1321,1329
timescales in structure determination, 2549
trinuclear clusters, 2297
zirconium allyl cyclopentadienyl diene oxycarbene heteronuclear complexes, 2451
Force constants, carbonyls, 409, 673,1377
Formamide, solvent effects, 2135
Formamidinate complexes
rhenium(I),(II), 195
Formate, tin(IV), 2225
Formation constants
actinide(III) carbonate complexes, 573
alkaline earth murexide complexes, 1227
binuclear carboxylates, 1453
cadmium halide complexes, 2129
cadmium nitrite complexes, 213
cerium(III) hydroxide complexes, 1355
chloride complexes, 2129,2473
cobalt(II) amide chloride complexes, 535
cobalt(II) aminopolycarboxylate complexes, 1187
cobalt(II) dicarboxylate complexes, 203
cobalt(II) hydroxyquinolate complexes, 513
copper(II) aminopolycarboxylate complexes, 1187
copper(II) hydroxynaphthoate complexes, 1335
copper(II) peptide complexes, 1089
copper(II) picolinate complexes, 689
effect of supporting ions, 291
indium(III) hydroxide thiolactate complexes, 5
iron(II) amine azole porphyrin selenocarbonyl thiocarbonyl complexes, 589
iron(III) halide nitrate perchlorae sulphate complexes, 291
iron(III) serine hydroxamate complexes, 747
lanthanide diketonate dipyridyl pyridine complexes, 155
lanthanide pyridine thiosemicarbazone complexes, 147
manganese(II) mercapto(phenyl) propenoate complexes, 331
mercury nitrite complexes, 213
nickel(II) aminopolycarboxylate complexes, 1187
nickel(II) hydroxyquinoline complexes, 513
palladium(II) azo dye complexes, 495
palladium(II) carboxylate chloride selenoether complexes, 2477
potassium crown ether, cryptand complexes, 721
selenium(IV) heteropolymolybdates, 1131
silicon fluoride hydroxide complexes, 1773
thallium(III) aminoacid methyl complexes, 2487
vanadium(IV) alanine oxo complexes, 1245
zinc halide complexes, 2129
zinc hydroxynaphthoate complexes, 1335
zinc nitrite complexes, 213
zinc peptide complexes, 1089
zinc picolinate complexes, 689
Formyl complexes
Cr(-I), Fe(-I), Mo(-I), 1609
rhodium(III), 1545
tungsten(-I), 1609
Free energy of activation
C-C bond formation, tungsten(V) complexes, 1015
fluxionality, alkenyl hydride complexes, 1001
fluxionality, carbonyl cyclopentadienyl complexes, 759
fluxionality, germyl complexes, 2209
fluxionality, palladium(II), platinum(II) chloride thioether complexes, 1321
fluxionality, platinum(IV) ditelluride methyl complexes, 1169
M-M bond breaking, chromium(I) carbonyl cyclopentadienyl complex, 1965
substitution, cobalt(III) chloride diamine complexes, 1159
Free energy of formation
cadmum halide complexes, 2129

cadmium nitrite complexes, 213
cobalt(II) carboxylate complexes, 203
mercury nitrite complexes, 213
zinc halide complexes, 2129
zinc nitrite complexes, 213
2-Furaldehyde semicarbazone, semicarbazone complexes, silicon, 151
Furfurylamine, reaction with cobalt(III) complex, 1159

G

Gadolinium
cyclopentadienyl pentanedionates, 1095
diketonate dipyridyl pyridine complexes, 155
diketonate pyrazolyborate, 79
pyridine thiosemicarbazone complexes, 147
Gallium
alkyl phosphido compound, 1901
alkyl phosphine complexes, 1289
organo compounds, book review, 587
phenoxide Schiff base complex, 2723
Germanium
fluoride - aromatic hydrocarbon - nitric oxide complexes, 97
hydride polymer, 597
phenoxide Schiff base complex, 2723
Germyl complexes
rhenium, 2209
Glucosamine, reaction with cobalt(III) complex, 1159
Glutathione, reaction with $[Fe(CN)_5NO]^{2-}$, 1197
Glycinate complexes
cobalt(III), 1153
thallium(III), 2487
Glycol → alkene conversion, 1981
Glycol sulphite complexes
chromium(0), 673
Glycolates
Re(V),(VII), Tc(V),(VII), 1981
Glycylcysteinate complexes
cobalt(II), zinc, 1089
Glycylglycinate complex, chromium(III), 523
Glyoxalbis(i-propylimine) complexes, osmium, 931
Gold
chloride phosphine cluster complexes, 605,2317,2321
cluster compounds, 269
halide phosphine silver clusters, review, 2317
Gold(I)
chloride pyridine mesogenic compounds, 1861
cyanide phosphine iridium(III), rhodium(III) complexes, 651
dithiocarbamates, 1231
Gold(III)
chloride pyrimidine thioether complex, 659
dithiocarbamate halide complexes, 1231
dithiocarboxylate halide mesogenic compounds, 1861

H

Haematite, 385
Hafnium
alkoxide amido carbonyl cyanide hydride hydrosulphide hydroxide methyl phosphido silyl complexes, 1625
alkoxide carboxylate glycolates, 2165
alkyl chloride cyclopentadienyl hydride phenyl cyclometallated complexes, 1409
allyl cyclopentadienyl diene oxycarbene heteronuclear complexes, 2451
carbonyl cyclopentadienyl hydride ruthenium complex, 759
perchlorate, 345
Hafnoxycarbene complexes
ruthenium, 759
Heptafluorobutyrate
rhodium(II), 1453
1-Heptene, 1827
Heteronuclear clusters, 2251
Heteropolyborane anions, 17,187
Heteropolymolybdates, 1131
Heteropolytungstates, 477
Hexaethylbenzene complex
molybdenum(II), 2027
Hexafluorobarrelene complexes
osmium(0), ruthenium(0), 931
Hexafluoro-t-butoxides
rhenium(VII), 1841
Hexafluorobut-2-yne complex
rhodium(I), 859
Hexafluoro-i-propoxides
rhenium(VII), 1841
1,1,4,7,10,10-Hexakis(3,5-dimethyl-1-pyrazolylmethyl)-1,4,7,10-tetraazadecane complexes, 2575
Hexamethylbenzene, covalent halide nitric oxide complexes, 97
Hexamethyldisiloxane, 579
Hexamethylenetetramine complexes
silver(I), 601
Hexamethylphosphoramide complexes
chromium(0), 673
chromium(II), 1453
cobalt(II), 535,2135
thallium, 2561
1,1,4,6,9,9-Hexaphenyl-1,4,6,9-tetraphosphanonane complexes, Al, Ga, In, 1289
Hexasulphide (S_6^{2-}) complex
platinum(IV), 1801
1-Hexene, 1827
1-Hexene complexes
chromium(0), 1619
ruthenium(II), 1239
5-Hexen-2-one, 1827
1-[&2-]Hexenyl complexes
rhodium(I), 1001
1-Hexyne complexes
ruthenium(II), 1239
HFS (Xα) calculations,
azaphosphaallenes, 2213
metal - ligand bond strengths, 1625
High nuclearity clusters, 2317,

2321
Histamine, histidine methyl ester Schiff base complexes, copper(II), zinc, 695
Holmium
acetonitrile phenanthroline complexes, 641
diacetylpyridinedihydrazone nitrate water complexes, 439
diketonate pyrazolylborate, 79
pyridine thiosemicarbazone complexes, 147
HPLC, aluminium diketonates, 369
HREM
high nuclearity clusters, 2321
nickel tungsten sulphide, 2405
niobium(V) ternary oxides, 2393
Hydration, nickel(II) phenanthroline complex, 1175
Hydrazide complexes
rhenium(V), 171
Hydrazine complexes
Cd, Co(II), Ni(II), 1147
rhodium(III), 2087
zinc, 1147
Hydrazobenzenes, 425
Hydrazone complexes
copper(II), 1383
lanthanides, 439,1095
Hydride complexes
chromium(II), 1965
cobalt, 2369
cobalt(I), 1625
gaseous, 1573
hafnium, 759,1409,1625
iridium(III), 187,1429,1781
manganese(I), 1605
molecular orbitals, 405
molybdenum(II), 1491
molybdenum(III), 2715
niobium, 1645
niobium(I), 1819
osmium, 961,979,1035,1891,2399, 2421
osmium(II), 1781
rhenium, 2421
rhenium(I), 2543
rhodium, 561
rhodium(I), 1001
rhodium(III), 1545,1827
ruthenium, 979,1035,1045,2331, 2341,2369
ruthenium(II), 1239,1441,1781, 2031
tantalum, 1645,2053
titanium(IV), 1625
tungsten(IV), 2053
vanadium, 1645
zirconium, 759,1625
Hydride transfer reactions
carbonyls, 1609
Hydrodesulphurisation catalysis, 2405,2411
Hydrogenation catalysts
palladium analysis, 495
Hydrogen sulphide, reaction with $[Fe(CN)_5NO]^{2-}$, 1197
Hydrosilylation, silatrane, 2189
Hydrosulphide complexes
Co(I), Hf, 1625
iron, 1371
Pt(II), Ru(II), 1441
Ti(IV), Zr, 1625
Hydrotris(3,5-dimethylpyrazol-yl)borate complexes, Mo, 1931
Hydrotris(pyrazol-1-yl)borate complexes, lanthanides, 79
Hydroxamate complexes
iron(III), 747
Hydroxides and hydroxo complexes
cerium(III), 1355
chromium(III), 2703
cobalt(I), 1625
cobalt(II), 2155
copper(II), 1187
hafnium, 1625
indium(III), 5,2091
iron(II), 2155
iron(III), 2703
molybdenum(II), 103
molybdenum(VI), 2709
nickel(II), 2155
osmium, 1035
platinum(II), 1441
ruthenium, 1045
ruthenium(II), 1441
silicon, 1773
silver(III), 2753
tantalum(V), 2053
tellurium(IV), 1267
tin(IV), 2225
titanium(IV), 1625
tungsten(IV), 2053
tungsten(VI), 2709
zirconium, 1625
2′-Hydroxyacetophenone Schiff base complexes, thorium, 143
2′-Hydroxyacetophenone semicarbazone, thiosemicarbazone complexes, tellurium(IV), 633
Hydroxylamine complexes
nickel(II), 2233
ω-Hydroxyalkoxides, molybdenum(II), tungsten(II), 449
2-α-Hydroxybenzylbenzimidazole complex, copper(II), 323
2-Hydroxybenzylmercaptan complexes, iron(II), 1911
Hydroxycarboxylates
cobalt(III), 2731
Mo(VI), W(VI), 2709
2-Hydroxyethoxide
molybdenum(II), 103
α-Hydroxyketone complexes, 1973
2′-Hydroxy-1-naphthaldehyde Schiff base complexes, thorium, 143
Hydroxynaphthoate complexes
copper(II), zinc, 1335
2-(2-Hydroxyphenyl)ethylmercaptan complexes, iron(II), 1911
2′-Hydroxypropiophenone complex
copper(II), 543
3-Hydroxypyrid-4-one complex
iron(III), 2235
8-Hydroxyquinoline complexes
cobalt(II), 513
copper(I), 37
lithium, 1
nickel(II), 513
potassium, sodium, 1

I

Imidazole, reaction with
cobalt(III) complex, 1159

Imidazole complexes
copper(I), 37
iron(II), 589
Imidobenzoate complex
rhenium(V), 329
Imine complexes
molybdenum, 919
osmium, 931
Iminium complexes
osmium, 967
Imino-oxo-phosphorane
rearrangements, 223
Indenyl complexes
iron, rhenium, 443
tungsten(III), 1991
Indium(III)
alkyl phosphine complexes, 1289
alkylstibide chloride, 77
hydroxide methyl phosphonate complexes, 2091
hydroxide thiolactate complex, 5
phenoxide Schiff base complex, 2723
polysalicylaldimine complexes, 1881
Indole-3-carboxaldehyde semicarbazone, thiosemicarbazone complexes, silicon, 151
Iodides and iodo complexes
cadmium, 2129,2503
copper(I), 2583
mercury, 2503
iridium(III), 1429
iron, 1371
manganese(I), 1605
molybdenum, 1931
molybdenum(I), 235
molybdenum(II), 235,1491,1719
molybdenum(IV), 1531
osmium, 791
platinum(II), 1953,2695
platinum(IV), 1169
rhenium(III), 1667,2743
rhenium(V),(VII), 2537
rhodium(I), 379
ruthenium(II), 2627
samarium, 1693
thallium, 2561
titanium(IV), 1531
tungsten(II), 63,245,2769
tungsten(IV), 1531,2053
uranium(IV), 249,1517
zinc, 2129,2503
Ion pairing, 2429
IR spectra
acyls, 1891
alcohol complexes, 2155
alkoxides, 103,1363,1389,2165, 2217
alkylamides, 67,103
alkylimides, 67
alkylphosphido compound, 1901
alkyne complexes, 63,2769
allyl complexes, 1719
amide complexes, 171
amine complexes, 67,117,297 601,1053,1067,1931
aminoalcohols, 1263
aminopolycarboxylates, 529
aryls,1079
arylamide, 103
arylammonium salts, 2015
arylimides, 117,329,2015
atranes, 679
azole complexes, 37,219,1273, 1931,2575
benzoylhydrazone complexes, 393
bis(dimethylsulphoxide)protium, 2143
bromides, 29,659,1053,1067, 1147,1231,1725,1737,2503, 2561,2611,2743
carbene complexes, 759
carbon disulphide complexes, 2615
carbonyls, 29,63,163,195,219, 409,417,449,489,673,709,731, 759,837,881,979,1363,1377, 1401,1453,1719,1751,1793, 1891,1919,1965,2027,2039, 2239,2351,2369,2387,2421, 2521,2715,2743,2769
carboxylates, 103,329,685,695, 1053,2165,2175,2597,2703, 2715
carboxylic acid complexes, 1
chlorides, 29,67,117,295,329, 633,659,685,709,731,1053, 1063,1067,1139,1147,1231, 1363,1727,2027,2143,2175, 2183,2503,2509,2561,2655, 2659,2743
chlorosulphate, 705
chromates, 601
cimetidine complexes, 307
creatinine complexes, 1273
crown ether complexes, 2761
cryptand complexes, 1053
cyanides, 471,651,2615
cyclopentadienyls, 393,1095, 1221,2743
diimine complexes, 601,731, 1175,2659
diketonates, 43,353,1389
dimethylurea, 505
diolate, 2001
diphenylcarbazone complexes, 401
diphosphine complexes, 2659
disulphide complexes, 471
dithiocarbamates, 709,1231, 1267,1737,2465
dithiolate complexes, 471
esters, 695
ether complexes, 117,249,1053, 1079,2597,2655
fluorides, 1221,2015
formamidinates, 195
germanium hydride polymer, 597
glycolates, 2165
heteropolyborate anion, 187
hexafluorophosphates, 1751
hydrates, 557,1053,1175
hydrazide complexes, 171
hydrazine complexes, 1147
hydrazone complexes, 439,1095
hydride complexes, 187,2031, 2715
hydroxides, 103,2155
imine complexes, 919
iodides, 2503,2561,2743
isocyanide complexes, 315,1693, 1751,1767,1831,2615
ketene complexes, 791
ketoimine complexes, 2569

macrocyclic complexes, 2531
maltol complexes, 1973
nitrates, 143,439,1053,2175
nitride complexes, 285
nitrile complexes, 37,919,2615, 2627,2659,2769
nitrosyls, 103,235,443,449,1931
oxalates, 37,229
oxo complexes, 117,401,471,705, 1079,1129,1841,1973,2053, 2175,2221,2537,2569,2635
peptide complex, 523
perchlorates, 439,1053,1267, 2659,2703
peroxide complex, 187
peroxodiphosphates, 1305
phenoxides, 337,2641,2703
phosphine complexes, 489,561
phosphine oxide complexes, 2561,2597
phosphonate complexes, 2095, 2761
phosphoramidothioates, 557
piperidide complexes, 2175
pyrazole complex, 229
pyrazolylborates, 449
pyridine complexes, 43,439, 2175,2183
pyridine-N-oxide complexes, 1, 2561
pyrimidine complex, 229
pyrimidine thioether complexes, 659
Schiff base complexes, 143,337, 695,1063,2149,2183,2229,2569, 2635,2641,2715
selenocarbonyls, 589
semicarbazone complexes, 151, 633,1719
silatranes, 2189
squarate complexes, 2155
sulphate, 307
sulphoxide complexes, 29,1727, 1737,2143,2627
sulphur - nitrogen ligand complexes, 647
tetrafluoroborates, 37,2597, 2769
thio complexes, 83,471
thioamide complexes, 623
thiocarbamates, 483
thiocarbonyls, 589,2627
thiocyanates, 1147,2175,2615
thiodiketonates, 483
thiolates, 2183,2509
thione complexes, 2503
thionitrite, 709
thionylimide, 629
thiosemicarbazone complexes, 151,633
thiourea complexes, 219
thioxanthates, 1121
triazenides, 195
triflatogermyl complex, 2209
tropolonate complex, 1129
water complexes, 229,337,439, 1095,2575,2703

Iridium
carbonyl iron complexes, 2351

Iridium(I)
carbonyl triphosphinoamine complex, 29
diene polyphosphine complex, 2035

Iridium(III)
acetonitrile methyl phosphine complex, 1285
alkyl cyclopentadienyl halide hydride phenyl phosphine vinyl complexes, 1429
alkyl phosphine complex, 2171
aryl halide phosphine metallated complexes, 87
benzotriazole hydride phosphine complexes, 1781
chloride cyanide phosphine gold(I) complexes, 651
chloride sulphoxide complex, 2143
diphosphine hydride peroxide complexes, 187
hydride complexes, 405
triazenide complexes, 417

Iridium(IV)
hexachloro-, oxidant, 827

Iron
acyl carbonyl phosphine zirconium complexes, 2451
alkenyl allylphosphidoxo carbonyl complexes, 2285
alkylidyne carbonyl indenyl nitrosyl rhenium, ruthenium complexes, 443
alkynyl carbonyl phosphido molybdenum, nickel, tungsten complexes, 1045
arylimido carbonyl complexes, 2331
carbide carbonyl heteropolymetallic complexes, 2351
carbonyl hydride ruthenium complexes, 2387
carbonyl thio molybdenum complexes, 2411
chromate halide hydrosulphide nitrite nitrosyl pseudohalide sulphate thiolate thiomolybdate complexes, 1371
cyanide nitrosyl thio thiolate complexes, 1197
gaseous organo- and other ions, 1583
methylidyne trinuclear complexes, review, 847

Iron(-I)
carbonyl formyl complexes, 1609

Iron(0)
alkene carbonyl complexes, 1605

Iron(I)
carbonyl cyclopentadienyl complex, 944

Iron(II)
allyl carbonyl chloride diimine pyridine Schiff base complexes, 425
amine azole porphyrin pyridine selenocarbonyl thiocarbonyl complexes, 589
arene cyclopentadienyl complexes, 2685
arsine carbonyl cyanide phosphine phosphite stibine complexes, 1687
carbonyl cyclopentadienyl methylene complex, 944
cyclopentadienyl heterobimet-

allic complexes, 393,1925, 2441
hydroxide propanol squarate complex, 2155
phenoxide thio thiolate thiophenoxide complexes, 1911
Iron(III)
amine carboxylate hydroxide phenoxide water binucleating complexes, 2703
carbonyl cyclopentadienyl methylidyne nitrosyl complexes, 949
carbonyl cyclopentadienyl vinylcarbyne complexes, 881
carboxylate chloride nitrate oxo piperidide pyridine thiocyanate water complex, 2175
chloride, oxidant, 827
chloride hydrocarbon nitric oxide complexes, 97
chloride pyridine complexes, 425
chloride pyridine Schiff base thiolate complex, 2183
chloride Schiff base complexes, 337
cyctochrome c oxidase phthalocyanine complex, 2667
dithiocarbamate halide complexes, 2465
in heteropolytungstates, 477
3-hydroxypyrid-4-one complex, 2235
maltol complex, 1973
oxide hydrate, 385
serine hydroxamate complexes, 747
Isocyanates, alkyl, reactions catalysed by Ru complexes, 2341
Isocyanide complexes
cobalt(II), 741
molybdenum(0), 1831
molybdenum(IV), 1767
osmium, 791
rhodium(I), 741
rhodium(II), 315,1751
samarium, 1693
tungsten(0), 1831
tungsten(IV), 1767
vanadium(II), 2615
Isomerism
aluminium diketonates, 369
molybdenum(II) chloride diphosphine complexes, 463
Isopolymolybdate, 2605
4R,5R-O-Isopropylidene-2,3-dihydro-1,4-bis(diphenylphosphino)-butane complexes, rhodium(I),(III), 1827

J

Jaeger complexes
nickel(II), 2197
Jahn - Teller effects, five - coordinate hydride complexes, 405
Judd - Ofelt parameters
holmium acetonitrile phenanthroline complexes, 641
neodymium proline water complex, 2495

K

Kelex 100 complexes
Co(II),Ni(II), 513
Ketene complexes
osmium, 791
Ketenylidene complexes
heteropolynuclear, 807
Ketoimine complexes
molybdenum(VI), 2569
Ketone complexes
chromium(0), 1619
osmium, 979
ruthenim(II,III), 1453
silver, 1299
thorium, 1807
Ketooximates, nickel(II), 2233
Kinetic studies
alcohol photooxidation with heteropolytungstates, 477
alkane hydroxylation with iron(III) compounds and hydrazobenzenes, 425
C-C bond formation, tungsten(V) complexes, 1015
complex formation, cobalt(II) - dicarboxylates, 203
complex formation, cobalt(II), nickel(II) - 8-hydroxyquinolines, 513
complex formation, iron(III) serine hydroxamate, 747
complex formation, molybdenum(VI), tungsten(VI) - malic acid, 2709
fluxionality, platinum(IV) ditelluride halide methyl complexes, 1169
fluxionality, tungsten(IV) cyclopentadienyl hydride oxo complexes, 2053
ligand reactions, cyclometallated complexes, 919
ligand reactions, thiols and $[Fe(CN)_5NO]^{2-}$, 1197
redox, chromium(VI) - methionine, 11
redox, nitrite - $[W(CN)_8]^{4-}$, 2193
redox, silver(III) - thiourea, 2753
substitution, chromium(0) carbonyl complexes, 1619
substitution, cobalt(III) chloride diamine complexes, 1159
substitution, ruthenium(0) carbonyl diphosphine complex, 1939
substitution, ruthenium(II,III) oxalate propionate complexes, 1393
thermolysis, adenosylcobalamin, radical trapping, 1469
Krypton(II) fluoride, fluoro complexes, 1217

L

Lanthanides
alkyl arsenido azide chloride cyclopentadienyl ether phosphido selenophenoxide silyl thiolate alkali metal complexes, review, 2307
chloride hydrazone water complexes, 1095
cyclopentadienyl pentanedionates, 1095
diacetylpyridinedihydrazone nitrate water complexes, 439
diketonate dipyridyl pyridine complexes, 155
diketonate pyrazolylborates, 79
pyridine thiosemicarbazone complexes, 147
Lanthanum
diketonate dipyridyl pyridine complexes, 155
diketonate pyrazolylborates, 79
gaseous organo- ions, 1583
pyridine thiosemicarbazone complexes, 147
Laser powered homogeneous pyrolysis, 1605
Lead(II)
dibutylphosphido methyl compounds, 1909
phosphoramidothioates, 557
Lead(IV) phenyl vanadium(-I) complex, 2039
n-[&i-]Leucinate complexes
cobalt(III), 1153
Ligand field potentials, trigonal complexes, 1705
Ligand synthesis and reactions
amine crown ether Schiff base thioether, 2649
aminoalcohols, 1263
aminobenzaldehyde condensation, 2715
aminopolycarboxylates, 1187
arene cyclopentadienyl complexes, 2685
benzoylhydrazoneferrocene, 393
bispyridyldiketones, 43
crown ether - diimine, 137
cryptate Schiff base, 2229
cyclopentadienyls, 1409
diphosphine, 463
fluorophenylcyclopentadienes, 409
Jaeger type Schiff base complexes, 2197
ketooximates, 2233
napthoquinonedimethane, 1945
phenoxide, 1911
quinaldic acid-N-oxide, 1
salicylaldehyde Schiff base, 543
salicylaldimine, 2723
salicylaldimine thiosemicarbazide, 2641
terpyridyl Schiff base, 2531
thioethers, 1321,1329
thiolates, thiophenoxides, 1911
4,4',4''-tri-t-butylterpyridine, 575
triphosphinoamine, 29
Liquid crystals, metal complexes, 1861
Lithium
alkyls, 2023,2119
alkyl arsenide diamine ether phosphido selenophenoxide thiolate complexes, 2307
alkylamide ether zirconium complex, 2515
alkylamide molybdenum(II) complex, 399
carboxylic acid hydroxyquinoline phenoxide pyridine-N-oxide complexes, 1
cryptand complexes, 1341
diamine diolate oxo Mn(III) complex, 2001
pyridine pyridyl complexes, 665
semiquinone complex, 2429
Lutetium
diacetylpyridinedihydrazone nitrate water complexes, 439
diketonate dipyridyl pyridine complexes, 155
diketonate pyrazolylborates, 79
2,6-Lutidine complexes
chromium(0), 1619
3,4-Lutidine complexes
iron(II), 589

M

Macrocyclic complexes
molybdenum(III), 2715
nickel(II), 2531
rhenium(V),(VII), 2537
silver, tin(IV), 2531
Magnesium
alkoxide diketonate oxo aluminium complexes, 1389
ether oxo rhenium(V) complexes, 1079
murexide complexes, 1227
organo- ions, 1583
Magnetic anisotropy
molybdenum(II) chloride diphosphine complexes, 1673
Magnetic moments
chromium(I) carbonyl cyclopentadienyl diphosphine phosphine complexes, 1965
chromium(II) carboxylate complexes, 1453
cobalt(II) dioxygen Schiff base water complexes, 337
cobalt(II) hydroxide squarate complex, 2155
cobalt(II) pyridine Schiff base thiolate complex, 2183
copper(II) alcohol alkoxide azole binuclear complex, 323
copper(II) azole pyridine Schiff base complexes, 695
copper(II) carboxylate pyridine water complexes, 1745
copper(II) catecholate pyridine complex, 609
copper(II) cryptand amine carboxylate ether halide nitrate perchlorate complexes, 1053

copper(II) mepirizole oxalate water complex, 229
copper(II) pyridine Schiff base thiolate complex, 2183
copper(II) salicylhydrazide Schiff base complex, 543
copper(II) Schiff base complex, 337
iron(II) hydroxide propanol squarate complex, 2155
iron(III) amine carboxylate hydroxide phenoxide water binucleating complexes, 2703
iron(III) carboxylate chloride nitrate oxo piperidide pyridine thiocyanate water complex, 2175
iron(III) chloride pyridine Schiff base thiolate complex, 2183
iron(III) chloride Schiff base complexes, 337
iron(III) dithiocarbamate halide complexes, 2465
nickel(II) amine carboxylate phenoxide water binucleating complexes, 2703
nickel(II) hydroxide squarate complex, 2155
nickel(II) macrocyclic complex, 2531
nickel(II) Schiff base water complex, 337
rhenium(II) carbonyl formamidinate phosphine triazenide complexes, 195
rhenium(III) chloride thioether complexes, 1207
rhodium(II) carboxylate, 1453
ruthenium(II) carbonyl triazenide complexes, 417
ruthenium(II,III) acetate ether phosphine phosphine oxide complexes, 2597
ruthenium(III) alcohol carbon disulphide chloride diimine pyridine sulphoxide complexes, 1727
ruthenium(III) bromide carbon disulphide phosphine pyridine sulphoxide complexes, 1737
ruthenium(III) chloride Schiff base complexes, 1063
vanadium(II) cyanide diphosphine isocyanide nitrile thiocyanate complexes, 2615
Magnetite, 385
Malate complexes
Mo(VI), W(VI), 2709
Maltol complexes, 1973
Mandelate, hafnium, 2165
Manganese coordination compounds, book review, 501
Manganese(0)
carbonyl, 1605
carbonyl cyclohexadienyl complexes, 2255
Manganese(I)
acyl alkyl carbonyl halide hydride phenyl complexes, 1605
allyl carbonyl phosphido phosphite molybdenum(II) complexes, 987
carbonyl cyclopentadienyl phosphine phosphite complexes, 409
Manganese(II)
antipyrine Schiff base chloride water complexes, 2149
benzoylhydrazone chloride iron(II) complexes, 393
biuret halide complexes, 1961
carbonyl cyclopentadienyl methylene complex, 946
chloride complexes, 2473
diketonate pyridine complexes, 43
mercapto(phenyl)propenoate complexes, 331
Manganese(III) methyl oxo lithium complex, 2001
Manganese(IV) fluoride and fluoro complexes, 1217
Mass spectra
alkyls, alkylamides, alkylimides, 1583
antimony(V) fluoride titanium(IV) cyclopentadienyl complex, 1221
bond dissociation energy measurement, 1573
carbaboranes, 669
carbenes, 1583
copper(II) perchlorate, 345
dilithiodialkylmethanes, 2023
distibines, 2601
Fourier transform, 1583
germanium hydride, 597
hafnium perchlorate, 345
hydrides, 1583
lanthanide cyclopentadienyl pentanedionates, 1095
macrocyclic complexes, 2531
molybdenum alkylamido amine halide nitrosyl pyrazolylborate complexes, 1931
molybdenum(II) alkoxide chloride nitrosyl pyrazolylborate complexes, 449
osmium(VI) aryl oxo complexes, 1079
platinum(II) chloride phosphido phosphine complex, 505
platinum(II) diene disulphurdinitride complex, 1925
platinum(II) diketonate thioether complex, 353
rhenium(I) amine carbonyl chloride hydride complex, 2543
rhenium(VI) aryl oxo complexes, 1079
rhenium(VII) alkylimide chloro aryl complexes, 1079
ruthenium(II) alkyl carbonyl cyclopentadienyl compounds, 837
silver(I) cryptate Schiff base complex, 2229
tungsten(II) alkoxide chloride nitrosyl pyrazolylborate complexes, 449
zirconium(IV) perchlorate, 345
Matrix isolation, S_4N_4 pyrolysis,

629
MCSCF calculations, MCO^+ ions, 1559
Menthoxide, rhenium(III), 1363
neo-Menthylcyclopentadienyl zirconium, 2375
Mepirizole complex
copper(II), 229
Mercaptocarboxylate complexes
indium(III), 5
2-Mercapto-2′-hydroxybiphenyl, 2-mercaptomethyl-2′-hydroxybiphenyl complexes, iron(II), 1911
Mercapto(phenyl)propenoate complexes, manganese(II), 331
2-Mercaptopyridine complexes
rhenium(I), 1401
Mercury
chloride osmium complex, 2159
chloride pyrimidine thioether complex, 659
chloride thiolate complex, 2509
cluster compounds, 1813
halide thione complexes, 2503
nitrate pyrrolidinone silver complex, 1299
nitrite complexes, 213
pyrrolidone thorium complex, 1807
Mesityls
antimony(III), 2601
rhenium(VI),(VII), 1079
Mesitylene, covalent halide nitric oxide complexes, 97
Mesogenic complexes, 1861
Metal - C bond dissociation energies, 1409,1429,1441,1469, 1483,1491,1499,1517,1531,1545, 1583,1605,1625
Metal - H bond dissociation energies, 1409,1429,1441,1491, 1531,1545,1583,1605,1625
Metal - halogen bond dissociation energies, 1491,1517,1531,1605
Metal - metal bond dissociation energies, 1491,1605
Metal - N bond dissociation energies, 1441,1531,1583,1605, 1625
Metal - O bond dissociation energies, 1441,1531,1583,1625
Metal - P bond dissociation energies, 1441,1531,1625
Metal - S bond dissociation energies, 1441,1531,1583,1625
Metal - Si bond dissociation energies, 1625
Metallated complexes
iridium(III), 87
Methanethiol, reaction with $[Fe(CN)_5(NO)]^{2-}$, 1197
Methanethiolates, iron, 1371
Methanol, solvent effects in, complexation, 1227
configurational equilibria, 2135
Methanol complexes
cobalt(II), 2575
ruthenium(III), 1727
Methionine, oxidation by chromium(VI), 11
Methoxide complexes
cobalt(I), hafnium(IV), 1625
molybdenum(II), 103
molybdenum(V), 401
niobium(V), 2217
platinum(II), 1441
Ti(IV), Zr(IV), 1625
N-(4-Methoxybenzylidene)-4′-butylaniline, nematic solvent for ESR spectra, 25
2-Methoxyethoxides, molybdenum(II), tungsten(II), 449
4-Methoxyphenoxide
molybdenum(II), 103
3-Methoxypropylamine, reaction with cobalt(III) complex, 1159
4-Methoxypyridine-N-oxide complexes, thallium, 2561
Methyls
aluminium, 1289,2375
antimony(III), 2601
boron, 2119
cobalt(I), 1559,1625
gallium, 1289
gaseous, 1573
hafnium, 1625
indium, 1289,2091
iridium(III), 1285,1429,2171
lanthanides, 2307
lead(II), 1909
lithium, 2119,2307
manganese(I), 1605
manganese(III), 2001
platinum(II), 2695
platinum(IV), 1169,1855,2095
silicon, 151
tantalum(V), 753
thallium(III), 2487
tin(IV), 2531
titanium(IV), 1625
tungsten(II), 163
tungsten(IV), 2053
uranium(IV), 1517
zirconium(IV), 1625,2083,2375
Methyl acrylate complexes
osmium, 931
1-Methylallyl complexes
manganese(I), 987
molybdenum(II), 987,1719
Nb(I), Ta(I), 1819
Methylamide
molybdenum(II), 103
Methyl azide pyrolysis, 2429
Methyl benzoate complex
chromium(0), 1377
N-[&α-]Methylbenzylamine, reaction with cobalt(III) complex, 1159
Methylbenzyne complexes
osmium, 961
1-Methyl-1,2-butadiene, methylclopentadiene, reaction with rhodium complex, 859
N-Methylbutylamine, reaction with cobalt(III) complex, 1159
Methyl crotonate, 1827
Methylcyclopentadienyls
cobalt(III), 1023
molybdenum, 2239,2271,2297,2411
tungsten(II), 2297
2-Methylcysteine, reaction with $[Fe(CN)_5(NO)]^{2-}$, 1197
S-Methyldithiocarbazate Schiff

base complexes, 2183
2-Methyl-1,3-dithiolane complexes
Pd(II), Pt(II), 1329
Methylene complexes
review, 767
rhodium(III), 827
ruthenium, 759
N-Methylformamide, solvent for configurational equilibria, 2135
Methylidenes, gaseous, 1573
Methylidyne complexes
gaseous, 1573
trinuclear, review, 847
1-Methylimidazole complexes
iron(II), 589
rhodium(II), 1453
ruthenium(II), 1453
5-Methyl-5-nitro-3,7-diaza-1-oxy-nonan-9-ol complex, copper(II), 1263
4-Methyl-2-penten-2,4-diolate
lithium, 2001
2-Methylpent-1-ene, 1827
Methyl(phenyl)amido complexes
platinum(II), 1441
4-Methylphenylimide complexes
tungsten(VI), 117
4-Methylphenylmethyls
tantalum(V), 753
N-Methylpiperazinedithiocarbamates, gold(I),(III), 1231
2-Methyl-2-propanethiolate
iron, 1371
2-Methylpropene, reaction with
Tc(VII) complex, 1981
4-Methylpyridine complexes
iron(II), 425
6-Methylpyridine-2-thiolates
rhenium(I), 1401
8-Methylquinoline complexes
palladium(II), 2659
Methylsulphonium complexes
cobalt(III), 1023
3-Methyltetrahydrofuran complexes
vanadium(II), 737
5-Methyl-1,1,1-trifluoro-2,4-hexanedionate, aluminium, 369
6-Methyl-1,1,1-trifluoro-2,4-heptanedionate, aluminium, 369
7-Methyl-1,1,1-trifluoro-2,4-octanedionate, aluminium, 369
MNDO calculations
aluminium chloride polynuclear complex, 1139
selenium heteropolyborane anion, 17
MOBI calculations
lithium alkyls, 2119
Moessbauer spectra
iron molybdenum carbonyl thio complexes, 2411
iron rhodium carbonyls, 2351
iron(II) phenoxide thio thiol-thiolate thiophenoxide complexes, 1911
iron(III) amine carboxylate hydroxide phenoxide water binucleating complexes, 2703
iron(III) chloride Schiff base complexes, 337
iron(III) dithiocarbamate halide complexes, 2465
Molecular mechanics, osmium carbonyl hydride siloxy complexes, 2399
Molecular orbitals
aluminium chloride polynuclear complex, 1139
1-aza-3-phosphaallenes, 2213
chromium(I) carbonyl ions, 1559
cobalt(I) carbonyl derivatives, 1625
hafnium(IV) chloride derivatives, 1625
lithium alkyls, 2119
molybdenum(III) alkoxide alkyne pyridine complexes, 903
osmium carbonyl chloride phosphide complexes, 1759
phosphinic azides, 223
"piano stool" dimers, 943
ruthenium carbonyl chloride phosphide complexes, 1759
scandium(I) carbonyl ions, 1559
selenium heteropolyborane anion, 17
titanium(IV) chloride derivatives, 1625
tungsten alkylidyne allyl complexes, 871
tungsten(II,VI,VI) thio complex, 2675
tungsten(III) alkoxide alkyne pyridine complexes, 903
zirconium(IV) chloride derivatives, 1625
Molecular rearrangement
molybdenum(II) chloride diphosphine binuclear complexes, 463
Molten salts, solvents for complexation studies, 1341
Molybdenum
acyl carbonyl zirconium complexes, 2451
alkoxide alkyne cyclometallated imine nitrile phosphine pyridine complexes, 919
alkylamido amine halide nitrosyl pyrazolylborate complexes, 1931
allyl carbonyl cyclopentadienyl thio trienyl complexes, review, 2263
carbonyl cyclopentadienyl dibismuth complexes, 2239
carbonyl cyclopentadienyl thio cobalt iron complexes, 2369
Molybdenum(-I)
carbonyl formyl complexes, 1609
Molybdenum(0)
alkene carbonyl isocyanide phosphine complexes, 1831
carbonyl, 1605
carbonyl diimine phosphine complex, 489
Molybdenum(I)
amine iodide nitrosyl pyrazolylborate complexes, 235
carbonyl cyclopentadienyl diphosphine complex, 1793
carbonyl cyclopentadienyl palladium(0) platinum(0) complexes, 2271
carbonyl cyclopentadienyl

phosphine complexes, 1491
Molybdenum(II)
acetate chloride phosphinopyridine complex, 2201
acetate diphosphine halide complexes, 1279
acetyl alkyl carbonyl cyclopentadienyl hydride iodide phosphine complexes, 1491
alkoxide alkylamide arylamide carboxylate hydroxide nitrosyl phenoxide pyrazolylborate thiophenoxide complexes, 103
alkoxide chloride nitrosyl pyrazolylborate complexes, 449
alkylamide chloride diphosphine nitrile thiophenoxide complexes, 2615
alkylamide iodide nitrosyl pyrazolylborate complexes, 235
alkylamide lithium complex, 399
alkylidyne carbonyl cyclopentadienyl cobalt(I) complexes, 2297
allyl carbonyl cyclopentadienyl phosphido manganese(I) complexes, 987
allyl carbonyl halide semicarbazone complexes, 1719
amide carboxylate ether nitrile pyridine thioether binuclear complexes, 1453
arene carbonyl chloride complex, 2027
chloride diphosphine complexes, 463,1673
chloride phosphine complexes, 2679
Molybdenum(III)
alkoxide alkyne pyridine complexes, 903
carbonyl carboxylate hydride macrocycle nitrate phosphine thiocyanate complexes, 2715
Molybdenum(IV)
alkylimido chloride diphosphine complex, 2615
azobenzene carboxylate catecholate cyclopentadienyl halide sulphate thiolate complexes, 1531
chloride isocyanide oxo phosphine complexes, 1767
Molybdenum(V)
alkylamide alkylimide amine chloride diamine diimine phosphine complexes, 67
amidophenoxide diazenide methoxide oxo complex, 401
chloride complex, 2027
chloride phosphine complexes, 1767
fluoride oxo complex, 1135
Molybdenum(VI)
adsorption by carbon, 547
diphenylcarbazone oxo complex, 401
heteropolyanions, 1131
hydroxo hydroxycarboxylate water complex, 2709
isopolyanion, 2605
ketoimine oxo complexes, 2569
maltol oxo complex, 1973
oxo tropolonate complex, 1129
oxychlorides, 579
thio complex as ligand, 1371
tin(IV) molybdate, 585
Morpholinedithiocarbamates
gold(I),(III), 1231
tellurium(IV), 1267
Morpholinylthiocarbonylbenzamidinate complexes, technetium(V), 285
Multimetallic catalysis, 2251
Murexide complexes
Ba,Ca,Mg,Sr, 1227

N

2-Naphthalenethiolate complexes
copper(I), 49
Naphthisoxazole complexes
ruthenium(II), 219
Naphthoquinodimethane complexes
ruthenium, 1945
β-Naphthylglycolate
hafnium, 2165
Nematic glass, solvent for
silver(II) complexes ESR spectra, 25
Neodymium
cyclopentadienyl diketonate, 1095
diketonate dipyridyl pyridine complexes, 155
diketonate pyrazolylborate, 79
proline water complex, 2495
pyridine thiosemicarbazone complexes, 147
Neutron diffraction
uranium(VI) oxide, 239
Nickel
gaseous organo and other ions, 1583
Nickel(0)
carbonyl, 1499
carbonyl complexes, 1605
Nickel(II)
acetate chloride diketonate pyridine thiocyanate complexes, 43
amine azole chloride thiocyanate water complexes, 2575
amine carboxylate phenoxide water binucleating complexes, 2703
aminopolycarboxylate complexes, 1187
antipyrine Schiff base chloride water complexes, 2149
azole nitrate thioether complex, 2591
benzoylhydrazone chloride iron(II) complexes, 393
biuret halide complexes, 1869
chloride complexes, 2473
chloride dithiodiketonate phosphine complexes, 2009
diketonate hydroxylamine ketooximate complexes, 2233
dithiocarboxylate mesogenic

complexes, 1861
halide hydrazine thiocyanate complexes, 1147
hydroxide squarate complex, 2155
hydroxyquinoline complexes, 513
macrocyclic polypyridyl Schiff base complexes, 2531
macrocyclic Schiff base complexes, 2197
phenanthroline complex, 1175
phenoxide pyridine Schiff base complex, 2641
polysalicylaldimine complexes, 1881
pyridine Schiff base thiolate complex, 2183
Schiff base water complex, 337
tetrathiotungstate complex, 2405
thiolate, 1397
Niobium
acyl carbonyl cyclopentadienyl zirconium complexes, 2451
carbonyls, review, 1639
gaseous organo ions, 1583
Niobium(-III)
carbonyl complexes, 1641,1645
Niobium(-I)
carbonyl complexes, 1642,1644
Niobium(I)
allyl diene diphosphine hydride complexes, 1819
carbonyl complexes, 1646,1649, 1657
Niobium(II)
carbonyl complexes, 1651
Niobium(III)
carbonyl complexes, 1649,1652, 1654,1657
Niobium(V)
alkoxide chloride ether nitrile oxo siloxide complexes, 2217
alkylimide amine chloride diamine diimine pyridine complexes, 67
chloride oxo phosphine complex, 2221
ternary oxides, 2393
Nitrates and nitrato complexes
copper(II), 1053
iron(III), 291,2175
lanthanides, 439
mercury, 1299
molybdenum(III), 2715
silver(I), 601
thorium, 143,1807
Nitrenes
complexes, 67
rearrangements, 223
Nitric oxide, aromatic hydrocarbon covalent halide complexes, 97
Nitride complexes
technetium(V), 285
Nitrile complexes
chromium(0), 673,1619
chromium(II), 1453
copper(I), 37,161
copper(II), 307
holmium, 641
iridium(III), 1285
molybdenum, 919
molybdenum(II), 1453,2615
niobium(V), 2217
palladium(II), 1861,2659
platinum(II), 1861
rhenium(V), 171
rhenium(VI), 117
rhodium, 2345
rhodium(I), 1861
rhodium(II), 1453
rhodium(III), 827
ruthenium(II), 2627
ruthenium(II,III), 1453
ruthenium(III), 1727
tungsten(0), 1605
tungsten(II), 245,2769
vanadium(II), 2615
Nitrite, reaction with $[W(CN)_8]^{4-}$, 2193
Nitrite complexes
cadmium, 213
cobalt(III), 1153
iron, 1371
Hg,Zn, 213
2[&3]-Nitrobenzaldehyde Schiff base complexes, thorium, 143
5-Nitro-1,10-phenanthroline complexes, Tc(V),(VII), 1981
2-Nitrophenol complexes
potassium, sodium, 1
4-Nitropyridine complexes
thallium, 2561
1-Nitroso-2-naphthol complexes
potassium, sodium, 1
Nitrosyls
iron, 443,1197,1371
molybdenum, 1931
molybdenum(I), 235
molybdenum(II), 103,235,449
osmium, 709
rhenium, 443,2209
tungsten(II), 449
NMR(^{1}H) spectra
acetonitrile complex, 1285
acylketene complexes, 955
agostic hydrogen, 987
alkene complexes, 837,979,1831, 1891
alkenyl complexes, 837,859,979, 1001
alkoxides, 103,449,1363,1389, 2053
alkyls, 151,753,837,1169,1285, 1289,1409,1855,1901,1953, 2053,2083,2095,2601,2695
alkylamides, 67,103,117,1931, 1991,2515,2615
alkylimides, 67,1079,1841
alkylphosphides, 1901,1909
alkyne complexes, 63,919,979, 2769
alkynyl complexes, 1409
allyl complexes, 979,987,1719, 1819,2521
amine complexes, 67,117
aminoacid complexes, 1153
aminoalcohols, 1263
aminopolycarboxylates, 529
arene complexes, 97,409,859, 1311,2685
arsine complexes, 623
aryls, 753,1079,1409,2601,2695
arylamides, 103
arylimides, 117,329

atranes, 679
azaallyl complexes, 2531
azole complexes, 37,219,695, 1781,1931,2591
benzylidyne, benzyne complexes, 961
carbene complexes, 759,771
carboxylates, 103,979,2225,2597
carbyne complexes, 807
crown ether complexes, 2649, 2761
cryptate complexes, 2229
cyclometallated complexes, 753, 1409,2659
cyclopentadienyls, 393,409,623, 725,859,881,987,1023,1221, 1409,1965,1991,2053,2083, 2095
cysteine complex, 1243
diamine complexes, 67,1737
diazabutadiene complexes, 63
diazenyl complexes, 2083
diene complexes, 561,1067,1819, 1953,2035
diimine complexes, 67,117,575, 1953,1981
diketonates, 353,1389,1409
diolate complexes, 1981
diphosphine complexes, 463, 1001,1279,1289,1673,1767, 1819,1953,1965,2615,2695
diphosphine diastereoisomerism, 239
ditelluride complexes, 1169
dithioarsenates, 1855
dithiocarbazates, 1211
dithiolates, 471
ether complexes, 725,1079,2515
heteropolyborane anion, 17
hydrazide complexes, 171
hydride complexes, 187,561,759, 961,979,1001,1409,1781,1819, 1965,2031,2053,2369,2543
isocyanide complexes, 1767,1831
ketene complexes, 791
ketenylidene complexes, 807
ketone complexes, 979
macrocyclic complexes, 2531, 2715
mercaptopyridine complexes, 1401
naphthoquinonedimethane complexes, 1945
nitrile complexes, 37,673,919, 2615,2627,2659
oxopyridine complexes, 1311
phenoxides, 103,337,753,1881, 1911
phosphine complexes, 285,329, 409,651,1285,1289,1767,1831, 1855,1919,1945,1953,1965, 2031,2221,2715
phosphine oxide complexes, 67, 2597
phosphite complexes, 409
phosphonate complexes, 2095, 2761
picoline complexes, 67
polyphosphine complex, 2031
porphyrins, 2225
pyrazolylborate complexes, 103,449
pyridine complexes, 67,439,665, 673,695,1311,1401,1727,1855, 1953,2183,2627
pyridine-N-oxide complexes, 2561
pyridyl complexes, 665
pyrimidine thioether complexes, 659
salicylaldimines, 1881
Schiff base complexes, 337,695, 1881,2183,2229,2649
semicarbazone complexes, 151, 633,1719
silatranes, 2189
steroid hormone, 2297
sulphoxide complexes, 29,673, 1737,2143,2627
terpyridyl complexes, 1953
thioamide complexes, 623
thiocarbamates, 483
thiodiketonates, 483
thioether complexes, 1321,1329, 2591,2649
thiolates, 1121,1911,2183
thiophenoxides, 103,1911
thiosemicarbazone complexes, 151,633
thioxanthates, 1121
triazenide complexes, 1919
vinylcarbyne complexes, 881
water complexes, 337
NMR(^{7}Li) spectra
lithium cryptand complexes, 1341
NMR(^{11}B) spectra
atranes, 679
carbaboranes, 669
heteropolyborane anions, 17,187
NMR(^{13}C) spectra
acyls, 1035
acylketene complexes, 955
alkene complexes, 837,931,1015, 1831
alkenyl complexes, 837
alkoxides, 1015,1363,2053
alkyls, 151,753,837,1015,1169, 1409,1855,1953,2053,2083
alkylamides, 67,117,2515
alkylidyne complexes, 443,849, 2297
alkylimides, 67,1079,1841
alkylphosphido complexes, 1909
alkyne complexes, 63,903,2769
alkynyl complexes, 1045,1409
allyls, 1015,1819,2521
amine complexes, 67,117,2649
arene complexes, 97,1311,2685
aryls, 753,1079,1409
arylimides, 117,329
atranes, 679
azaallyl complexes, 2521
azole complexes, 695
carbene complexes, 759,775,1035
carbonyls, 63,245,759,987,1035, 1965,2297
carboxylates, 329,2597
carbyne complexes, 807
crown ether complexes, 2649
cryptate complexes, 2229
cyanides, 651
cyclometallated complexes, 753, 1409
cyclopentadienyls, 725,1409, 1965,1991,2053,2083,2297

diamine complexes, 67
diazabutadiene complexes, 63
diazenyl complexes, 2083
diene complexes, 1819,1953
diimine complexes, 67,117,1953
diketonates, 353,1409
diphosphines, 1875,
diphosphine complexes, 1767, 1819,1953,1965
diphosphine diastereoisomerism, 239
ditelluride complexes, 1169
dithioarsenates, 1855
dithiocarbazates, 1211
dithiolates, 471
ether complexes, 725,1079,2515
imine complexes, 919
isocyanide complexes, 1767,1831
ketene complexes, 791
ketenylidene complexes, 807
maltol complexes, 1973
nitrile complexes, 919
oxopyridine complexes, 1311
phenoxides, 753
phosphines, 1875
phosphine complexes, 329,353, 1767,1831,1855,1953
picoline complexes, 67
polyphosphines, 1875
porphyrins, 57,2225
pyridine complexes, 67,695, 1311,1855,1953
Schiff base complexes, 695,931, 2229,2649
semicarbazone, thiosemicarbazone complexes, 151,633
terpyridyl complexes, 1953
thiocarbamates, 483
thiodiketonates, 483
thioether complexes, 353,1321, 1329,2649
vinylcarbyne complexes, 881
NMR(^{15}N) spectra
nitrosyls, 1371
NMR(^{17}O) spectra
oxo complexes, 2537
NMR(^{19}F) spectra
alkenyl complexes, 859
arene complexes, 409,859,1377
cyclopentadienyl complexes, 409,859
fluoride complexes, 97,2015
fluoroarylimido complexes, 2015
fluoroaryl phosphines, 1875
trifluoroacetates, 2715
NMR(^{27}Al) spectra
aluminium alkoxide oxo complex, 1389
atranes, 679
NMR(^{31}P) spectra
alkylphosphides, 1901
diazenyl complexes, 2083
diphosphines, 1875
diphosphine complexes, 49,187, 239,315,1001,1279,1289,1767, 1793,1819,1925,1953,1965, 2441,2615,2659,2695
diphosphine diastereoisomerism, 239
metallated arylphosphine complexes, 87
peroxodiphosphates, 1305
phosphido complexes, 505, 1317,1909
phosphidoxo complexes, 2285
phosphines, 1875
phosphine complexes, 37,87,285, 329,409,505,561,605,651,1289, 1349,1377,1767,1831,1855, 1919,1945,1953,2031,2221, 2597,2715
phosphinopyridine complexes, 1751
phosphite complexes, 409,1919
phosphonate complexes, 2095
phosphorus(V) bromide complex, 1725
polyphosphines, 129,1875
polyphosphine complexes, 2035
polyphosphine sulphides, 129
triphosphine complexes, 807
triphosphinoamine complexes, 29
NMR(^{59}Co) spectra
cobalt carbonyl hydride ruthenium complexes, 2369
NMR(^{63}Cu) spectra
copper(I) acetonitrile azo complexes, 161
NMR(^{77}Se) spectra
selenium(IV) heteropolymolybdates, 1131
selenium rings, 581
NMR(^{95}Mo) spectra
molybdenum(II) chloride nitrile phosphine complexes, 2615
NMR(^{119}Sn) spectra
tin(II) arsenido chloride phosphido complexes, 1317
NMR(^{125}Te) spectra
ditelluride complexes, 1169
NMR(^{195}Pt) spectra
platinum(II) chloride phosphido phosphine complex, 505
platinum(IV) ditelluride halide methyl complexes, 1169
NMR(APT) spectra
alkene complexes, 931
NMR(COSY) spectra
carbaboranes, 669
heteropolyborane anion, 17
polysalicylaldimine complexes, 1881
steroid hormone complexes, 2297
NMR(solid state) spectra
lithium cryptand complexes, 1341
peroxodiphosphates, 1305
NMR(2-D) spectra
hydrazide complexes, 171
phosphine complexes, 1349
polyphosphines, polyphosphine sulphides, 129
polysalicylaldimine complexes, 1881
steroid hormone complexes, 2297
Norbornadiene, reaction with rhodium complex, 859
Norbornadiene complexes
rhodium(I), 1067
Norbornene hydrogenation catalysis, 1827
Normal coordinate analysis, rhenium(III) carbonyl cyclopentadienyl halide complexes, 2743

O

Octaethylporphyrins
iron(II), 589
platinum(II), 57
rhodium(II),(III), 1545
silver(III), 57
Octahedral - tetrahedral
configurational
interconversion, cobalt(II)
complexes, 2135
Octanediolates
technetium(V), 1981
1-Octene, hydrogenation
catalysis, 1827
1-Octene complexes
ruthenium(II), 1239
4-Octene, reaction with
technetium(VII) complex, 1981
n-Octylamine, reaction with
cobalt(III) complex, 1159
Optical rotation, aluminium alkyl
alkylamide, 2727
Organoberyllium compounds, book
review, 2247
Organocopper compounds, book
reviews, 1225,1789
Organotin compounds, book review,
1225
Oscillator strength, holmium
acetonitrile phenanthroline
complexes, 641
Osmium
acyl alkene carbonyl hydride
complexes, 1891
acyl carbene carbonyl ether
halide hydride hydroxide
complexes, 1035
alkene alkenyl alkyne allyl
carbonyl carboxylate hydride
ketone ruthenium complexes,
979
alkene alkyl alkyne carbonyl
cyclometallated imine
compounds, 931
alkyne carbonyl chloride
mercury complex, 2159
alkynyl carbonyl phosphido
phosphine complexes, 1045
aminocarbene aminocarbyne
carbonyl iminium thio
thiophenoxide complexes, 967
arylimido carbonyl hydride
complexes, 2331
benzylidyne benzyne carbonyl
hydride complexes, 961
carbonyl chloride phosphide
complexes, 1759
carbonyl cyanate halide isocy-
anide ketene complexes, 791
carbonyl hydride rhenium
complex, 2421
carbonyl hydride siloxy
complexes, 2399
methylidyne trinuclear
complexes, review, 847
Osmium(0)
alkene alkyne carbonyl
ruthenium(0) complexes, 931
arsine halide nitrosyl
complexes, 709
Osmium(II)
arsine carbonyl dithiocarbamate
halide nitrosyl phosphine
complexes, 709
benzotriazole carbonyl hydride
phosphine complexes, 1781
Osmium(III)
dithiocarbamate halide
phosphine thionitrite
complexes, 709
halide phosphine triazenide
complexes, 417
Osmium(VI)
aryl oxo complexes, 1079
maltol oxo complex, 1973
7-Oxabicyclo[2.2.1]heptane
complex, molybdenum(II), 1453
Oxalate complexes
copper(I), 37
copper(II), 229
ruthenium(II,III), 1393
Oxides
iron(III), 385
niobium(V), 2393
uranium(VI), 243
V(V), W(VI), 2393
Oxime complexes
cobalt(III), 1499
Oxo complexes
aluminium, 1389,2375
iron(III), 2175
lithium, 2001
magnesium, 1079,1389
manganese(III), 2001
molybdenum(IV), 1767
molybdenum(V), 401,1139,1767
molybdenum(VI), 401,579,1129,
1973,2569
niobium(V), 2217,2221
osmium(VI), 1079,1973
palladium, 2321
rhenium(V), 1079,1981,2537
rhenium(VI), 1079
rhenium(VII), 705,1841,1981,
2537
samarium, 1693
tantalum(V), 2053
tungsten(IV), 1767,2053
tungsten(V), 471,1767
tungsten(VI), 117,579
uranium(VI), 1973
vanadium(III), 2635
vanadium(IV), 1245,2635
Oxomethylene complexes
tungsten(IV), 2053
2-Oxopyridinate complexes
ruthenium(II), 1311
Oxycarbene complexes
Hf, Zr, 2451
Oxygen, reactions with alkylidyne
bridging complexes, 789

P

Palladium
carbonyl iron complexes, 2351
oxo phenanthroline complexes,
2321
Palladium(0)
carbonyl phosphine
molybdenum(I) complexes, 2271
Palladium(I)
chloride diphosphine binuclear
complex, 239

Palladium(II)
amine azo chloride diimine diphosphine nitrile pyridine cyclometallated complexes, 2659
azo dye complexes, 495
azobenzene sulphur - nitrogen complexes, 647
azole diphosphine rhodium(I) complexes, 2441
bromide phosphine thiazine complexes, 419
carboxylates, 615
carboxylate chloride selenoether complexes, 2477
chloride diimine ruthenium(II) complexes, 731
chloride dithiocarboxylate nitrile mesogenic complexes, 1861
chloride phosphine pyridine complex, 207
chloride thioether complexes, 1321,1329
chloride triphosphinoamine complex, 29
creatinine complexes, 1273
diimine diolate dithiolate complexes, 349
halide pyrimidine thioether complexes, 659
maltol phosphine complexes, 1973
Palladium(IV)
bromide complex, 2611
Partially oxidised complexes, rhodium(I) dithiolate halide complexes, 379
Pauling, calculation for bond energies, 1677
PE spectra
methyl azide decomposition, 2429
Penicillamine, reaction with $[Fe(CN)_5NO]^{2-}$, 1197
Penicillamine complexes
thallium(III), 2487
Pentafluorophenylimido complexes
tungsten(V), 2015
Pentamethylcyclopentadienyls
Ba,Ca, 725
hafnium, 759
iridium(III), 1429
lanthanides, 2307
molybdenum(II), 2297
rhenium(III), 2743
rhodium(III), 827
ruthenium(I,III), 837
ruthenium(II), 837,1441
samarium, 1693
strontium, 725
tantalum(V), 2053
tungsten(II), 2297
tungsten(IV), 2053
zirconium, 759
1,5-Pentamethyltetrazole complexes, samarium, 1693
2,4-Pentanedionates
aluminium, 1389
lanthanides, 79,1095
magnesium, 1389
nickel(II), 2233
ruthenium(III), 1727
scandium, 1409
2,4-Pentanedione Schiff base complexes, thorium, 143
2,4-Pentanedithionate
nickel(II), 2009
2-Pentanonesemicarbazone complexes, molybdenum(II), 1719
1-Pentenyl complexes
rhodium(I), 1001
neo-Pentoxides
molybdenum, 919
Mo(III),W(III), 903
n-Pentyl, iridium(III), 1429
neo-Pentyls
iridium(III), 1429
lithium, 2023
rhenium(VII), 1841
neo-Pentylidene complexes
rhenium(VII), 1841
n-Pentylidyne complexes
cobalt(III), 1023
t-Pentylthiolate, t-pentylthioxanthate complexes, copper(I), 1121
Peptide complexes
chromium(III), 523
cobalt(II), zinc, 1089
Perchlorates
copper(II), 345,1053
hafnium(IV), 345
iron(III), 291
tellurium(IV), 1267
zirconium(IV), 345
Peroxide complexes
iridium(III), 187
Peroxodiphosphates, 1305
1,10-Phenanthroline complexes
holmium, 641
molybdenum(0), 489
nickel(II), 1175
palladium, 2321
palladium(II), 349
platinum(II), 349,353,1953
rhenium(V),(VII), 1981
rhodium(I), 1067
ruthenium(III), 1727
silver(I), 601
technetium(V),(VII), 1981
Phenoxides
aluminium,,2723
cadmium, 1881
chromium(III), cobalt(II), 2703
copper(II), 1335,2703
gallium, germanium, 2723
indium, 1881,2723
iron(II), 1911
molybdenum(II), 103
molybdenum(V), 401
nickel(II), 1881,2641,2703
potassium, 1
scandium, 1881,2723
sodium, 1
tantalum(V), 753
thallium(III), 1881
titanium(IV), 1531
zinc, 1335,1881
Phenyls
antimony(III), 2601
hafnium, 1409
iridium(III), 1429
lead(IV), 2039
manganese(I), 1605
platinum(II), 2695

scandium, 1409
silicon, 679
tin(IV), 2039
Phenylacetyl complexes
molybdenum(II), 1491
Phenylacetylene complex
ruthenium, 1071
Phenylalanine methyl ester Schiff base complexes, Cu(II),Zn, 695
Phenylamido complexes
molybdenum(II), 103
ruthenium(II), 1441
Phenylazophenyl complexes
palladium(II), 2659
1-Phenyl-1,3-butanedionate
aluminium, 1389
cobalt(II), 421
magnesium, 1389
nickel(II), 2233
Phenyldiazenide complex
molybdenum(V), 401
2-Phenyl-1,3-dithiolane complexes
Pd(II), Pt(II), 1329
1,2-Phenylenediamine complexes
ruthenium(II), 1727,1737
ruthenium(III), 1737
o-Phenylenediaminetetraacetate complexes, copper(II), 1187
Phenyl-1,2-ethanediolate
technetium(V), 1981
2-Phenylethyl complexes
cobalt(III), 1499
1-Phenylethylamide
aluminium, 2727
2-Phenylethynyl complexes
ruthenium(II), 1441
uranium(IV), 1517
Phenylimides
rhenium(V),(VI), 117
tungsten(VI), 117
N-Phenylpiperazinedithiocarbamate
gold(III), 1231
4-Phenylpiperidinedithiocarbamate
gold(III), 1231
1-Phenylpropane-1,3-dione Schiff base complexes,
thorium(IV), 143
1-Phospha-4-ethyl-1,5,7-trioxa-bicyclo[2.2.1]octane complex,
rhodium(II), 1453
Phosphate(organo) complexes
chromium(II), 1453
Phosphates, peroxodi-, 1305
Phosphido (PH_2) complexes
Co(I), Hf(IV), Ti(IV), Zr(IV), 1625
Phosphido (PR_2) complexes
iron, 1045
lanthanides, lithium, 2307
Mn(I), Mo(II), 987
osmium, 1045,1759
platinum(II), 505
ruthenium, 1045,1759
tin(II), 1317
zirconium, 2083
Phosphidoxo polynuclear complexes, review, 2285
Phosphinate, indium, 2091
Phosphines, aryl, 1875
Phosphine complexes
aluminium, 1289
chromium(0), 409,1377,1619
chromium(I),(II), 1965
cobalt, 2321,2345,2369
cobalt(III), 1483
copper(I), 37,1121
gallium, 1289
gold, 605,2317,2321
gold(I), 651
indium, 1289
iridium(III), 87,651,1285,1429, 1781,2171
iron(II), 1687
manganese(I), 409
molybdenum, 919
molybdenum(0), 489,1831
molybdenum(I), 1491
molybdenum(II), 1491,2201,2679
molybdenum(III), 2715
molybdenum(IV), 1767
molybdenum(V), 67
nickel(II), 2009
niobium, 2221
osmium, 1045
osmium(II), 709,1781
osmium(III), 417,709
palladium(0), 2271
palladium(II), 207,419,1973
platinum(0), 1349,2271
platinum(II), 353,419,505,1953, 1973
platinum(IV), 1855
rhenium, 2209
rhenium(I), 195,1401
rhenium(II), 195
rhenium(V), 117,171,329
rhodium, 561,2321,2345,2441
rhodium(II), 1751
rhodium(III), 651,2087
ruthenium, 1045,1945,2321
ruthenium(I), 417,1919
ruthenium(II), 1441,1781,2031, 2627
ruthenium(II,III), 2597
ruthenium(III), 417,1727,1737
silver, 2317
technetium(V), 285
titanium(IV), 1531
tungsten(0), 1831
tungsten(II), 163,2769
tungsten(IV), 1767
Phosphine oxide complexes
chromium(0), 673
cobalt(II), 1785,2135
ruthenium(II,III), 2597
thallium, 2561
Phosphinic azides, rearrangements, 223
Phosphinopyridine complex
molybdenum(II), 2201
Phosphite complexes
chromium(0), 409
chromium(II), 1453
iron(II), 1687
manganese(I), 409,987
rhodium(II), 1453
ruthenium(I), 417
ruthenium(II), 219
Phosphonates
Co(III), Pt(IV), 2095
potassium, 2761
Phosphoramidothioates, phosphorodiamidothioates, Ag(I),Cr(III), Pb(II),Sn(II),V(III), 557
Phosphorus, heterocyclic compounds, 679

Phosphorus(V)
in heteropolytungstates, 477
tetrabromo-, trichloride, 1725
Photoappearence, photodissociation spectra (mass spectra, gaseous ions, 1583
Photochemistry
iron(II) arsine carbonyl cyanide phosphine phosphite stibine complexes, 1687
palladium(II) chloride phosphine pyridine complex, 207
Phthalate, cobalt(II), 203
Phthalazine complexes
rhenium(V), 171
Phthalocyanine complex
iron(III), 2667
"Piano stool" dimers, molecular orbitals, 943
Picolinate complexes
Cu(II),Zn, 689,1335
2-Picoline complexes
chromium(0), 1619
ruthenium(III), 1737
3-Picoline complexes
iron(II), 589
4-Picoline complexes
iron(II), 589
niobium(V), 67
Picoline-N-oxide complexes
Rh(II), Ru(II,III), 1453
thallium, 2561
4-Picolinic acid-N-oxide complexes, K,Li,Na, 1
Piperazine-2,5-dione, formation from glycylglycine, 523
Piperazinedithiocarbamates
gold(I),(III), 1231
Piperidides
iron(III), 2175
molybdenum, 1931
molybdenum(II), 235
Piperidine, reaction with cobalt(III) complex, 1159
Piperidine complexes
molybdenum, 1931
molybdenum(I), 235
rhodium(II), 1453
tungsten(0), 1605
Piperidinedithiocarbamates
gold(I),(III), 1231
tellurium(IV), 1267
Platinum
arsine chloride complexes, 2321
carbonyl iron complexes, 2351
cluster compounds, 269
Platinum(0)
alkene phosphine complexes, 1349
carbonyl phosphine molybdenum(I) complexes, 2271
Platinum(II)
alkoxide alkyl arylamido cyanide diphosphine hydrosulphide hydroxide complexes, 1441
alkyl aryl diphosphine halide complexes, 2695
alkyl diene diimine diphosphine halide phosphine pyridine terpyridyl complexes, 1953
bromide phosphine thiazine complexes, 419
chloride diimine potassium complex, 137
chloride diimine ruthenium(II) complexes, 731
chloride diphosphine methylene complex, 767
chloride nitrile mesogenic complexes, 1861
chloride phosphido phosphine complex, 505
chloride thioether complexes, 1321,1329
chloride triphosphinoamine complex, 29
creatinine complexes, 1273
cyclooctadiene diimine diketonate phosphine thioether complexes, 353
diene diphosphine disulphurdinitride iron(II) complexes, 1925
diolate dithiolate phenanthroline complex, 349
dithiocarbazates, 1211
halide pyrimidine thioether complexes, 659
maltol phosphine complex, 1973
porphyrins, 57
trans effect, 1203
Platinum(IV)
chloride methyl phosphonate cobalt(III) complexes, 2095
dithioarsenate methyl phosphine pyridine complexes, 1855
halide methyl ditelluride complexes, 1169
hexasulphide complex, 1801
pM values, salicylaldimine complexes, 2723
Polarography, iron(II) phenoxide thiolate thiophenoxide complexes, 1911
Polyhedral compounds
borane anions, 363,2437
electron counting, review, 1107
rearrangements, 1107
skeletal electron pair theory, 258
Polymer radiothermoluminescence, book review, 671
Polymorphism, nickel(II) phenanthroline complex hydrates, 1175
Polynuclear complexes, electron counting, review, 253
Polyphosphines, 129,1875
Polyphosphine complexes
Al, Ga, In, 1289
Ir(I), Rh(I), 2035
Polyphosphine sulphides, 129
Polysulphide complex
platinum(IV), 1801
Poly(sulphur nitride), 629
Porphyrins
iron(II), 589
platinum(II), rhodium(II),(III), 1545
silver(III), 57
tin(IV), 2225
Potassium
carboxylic acid hydroxyquinoline phenoxide pyridine-N-oxide complexes, 1

chloride ether lanthanide complexes, 2307
crown ether, cryptand complexes, 721
crown ether phosphonate complexes, 2761
crown ether platinum metal complexes, 137
Potential energy curves, Cr(I), Sc(I) carbonyl ions, 1559
Praseodymium
diketonate pyrazolylborate, 79
pyridine thiosemicarbazone complexes, 147
Proline complex
neodymium, 2495
1,2-Propanediol complexes
palladium(II), 349
Propane-1-thiolates
Mo(IV), Ti(IV), W(IV), 1531
Propane-2-thiolates
iron, 1371
molybdenum(IV), 1531
i-[&n]-Propanol, solvent effects, 2135
i-Propanol complex, Fe(II), 2155
Propene hydroformylation, 2351
Propenyl complexes
rhodium(I), 1001
Propionates
iron(III), 2175
palladium(II), 615
ruthenium(II,III), 1393
tungsten(III), 1991
Propionitrile complex
vanadium(II), 2615
Propionyl complexes
osmium, 1891
i-Propoxides
Al, Mg, 1389
molybdenum(II), 103
molybdenum(III), 903
rhenium(III), 1363
tungsten(III), 903
tungsten(V), 1015
n-Propoxide
molybdenum(II), 103
i-Propyls, lithium, 2119
n-Propyls,
antimony(III), 2601
rhodium(III), 827
i-Propylamide complexes
tantalum(V), 67
i-Propylimide complexes
tantalum(V), 67
i-Propylisocyanide complexes
Mo(0), W(0), 1831
Pyrazine complexes
tungsten(0), 1605
Pyrazole complexes
copper(I), 37
copper(II), 229
Pd(II), Rh(I), 2441
tungsten(0), 1605
Pyrazolylborates
lanthanides, 79
molybdenum, 1931
molybdenum(I), 235
molybdenum(II), 103,235,449
tungsten(II), 449
Pyridine complexes
cadmium, 43,2183
chromium(0), 673,1619
cobalt(II), 43,2183
cobalt(III), 1499
copper(II), 43,609,689,695, 1335,1383,1483,1745,2183
gold, 1861
iron(II), 425,589
iron(III), 425,2175,2183
lanthanides, 147,155,439
lithium, 665
manganese(II), 43
molybdenum, 919
molybdenum(II), 1453,2201
molybdenum(III), 903
nickel(II), 43,2183,2641
niobium(V), 67
palladium(II), 207,2659
platinum(II), 1953
platinum(IV), 1855
rhenium(I), 1401
rhenium(V), 171
rhenium(VII), 1841
rhodium(I), 1067
rhodium(II), 1453,1751
ruthenium(II), 1311,1727,2627
ruthenium(II,III), 1453
ruthenium(III), 1727,1737
silver(I), 1861
silver(II), 25
tungsten(0), 1605
tungsten(III), 903
zinc, 43,689,695,1335,2183
Pyridine-2-aldehyde 2′-pyridylhydrazone complex, copper(II), 1383
2-Pyridinecarboxaldehyde semicarbazone, thiosemicarbazone complexes, silicon, 151
4-Pyridinecarboxaldehyde-4′-nitrophenylhydrazone complex, palladium(II), 207
Pyridine-N-oxide complexes
lithium, potassium, 1
Rh(II), Ru(II,III), 1453
sodium, 1
thallium(III), 2561
3-Pyridylcarbinol complexes
copper(II), 1745
Pyrimidine complexes
cadmium, 659
copper(II), 229
Ag(I),Au(III),Hg,Pd(II),Pt(II), 659
Pyrrolidide, molybdenum(II), 235
Pyrrolidine, reaction with cobalt(III) complex, 1159
Pyrrolidine complex
molybdenum(I), 235
2-Pyrrolidinone complexes
mercury, 1299,1807
silver, 1299
thorium, 1807
Pyrrolidylthiocarbamates
Bi(III), Sb(III), 483

Q

Quinaldic acid-N-oxide complexes
K,Li,Na, 1
Quinoline complexes
rhodium(I), 1067
Quinoline-2-thiolate complexes
rhenium(I), 1401
Quinuclidine complexes
iron(II), 589

R

Radical traps, use in bond dissociation energy determinations, 1469,1483
γ-Radiolysis, germanium hydride, 597
Radiothermoluminescence in polymers, book review, 671
Raman spectra
bromide complexes, 1725,2611
oxo complexes, 1973
peroxodiphosphates, 1305
Rearrangements, polyhedral borane anions, 2437
Rhenium
alkylidyne carbonyl indenyl nitrosyl iron ruthenium complexes, 443
carbonyl hydride osmium complex, 2421
cyclopentadienyl germyl nitrosyl phosphine complexes, 2209
Rhenium(0)
carbonyl cyclohexadienyl complexes, 2201
Rhenium(I)
amine carbonyl chloride hydride complexes, 2543
carbonyl chloride tetrahydrofuran complex, 1363
carbonyl cyclohexadienyl complexes, 2201
carbonyl mercaptopyridine phosphine complexes, 1401
Rhenium(I),(II)
carbonyl formamidinate phosphine triazenide complexes, 195
Rhenium(III)
alkoxide chloride complexes, 1363
carbonyl cyclopentadienyl halide complexes, 2743
chloride thioether complexes, 1207
iodide complex, 1667
Rhenium(V)
acetonitrile ammine chloride diazenide dimethylformamide hydrazide phosphine pyridine complexes, 171
alkylidyne carbonyl indenyl complexes, 443
amine arylimide chloride phosphine complexes, 117
arylimido carboxylate chloride ethoxide phosphine complex, 329
aryl oxo magnesium complex, 1079
chloride diimine diolate oxo complexes, 1981
halide oxo triamine complexes, 2537
polysulphide thio complex, 83
Rhenium(VI)
acetonitrile amine arylimide chloride ether complexes, 117
aryl oxo complexes, 1079
Rhenium(VII)
alkoxide alkyl alkylidene arylimido chloride oxo phenoxide pyridine siloxide complexes, 1841
alkylimido aryl chloro complexes, 1079
chloride diimine oxo complexes, 1981
chlorosulphate oxo compound, 705
halide oxo triamine complexes, 2537
Rhodium
acyl carbonyl cyclopentadienyl zirconium complexes, 2451
alkene alkenyl arene aryl cyclopentadienyl diene complexes, 859
alkyne carbonyl chloride ether nitrile phosphine cobalt complexes, 2345
carbide carbonyl iron complexes, 2351
carbonyl diene hydride phosphine thio trinuclear complexes, 561
chloride phosphine complexes, 2321
gaseous organo- ions, 1583
Rhodium(I)
alkene alkenyl diphosphine hydride complexes, 1001
carbonyl chloride diphosphine complexes, 315
carbonyl chloride nitrile mesogenic complexes, 1861
carbonyl chloride phosphino-pyridine complexes, 1751
carbonyl chloride triphosphin-oamine complexes, 29
chloride diphosphine complex, 1827
carbonyl phosphine thiolate heteronuclear complexes, 2441
diamine diene diimine halide quinoline complexes, 1067
diene methyl methylene complex, 770
diene polyphosphine complex, 2035
dithiolate halide complexes, 379
isocyanide cobalt(II) polymeric complex, 741
Rhodium(II)
amide amine azole carboxylate nitrile phosphine pyridine pyridine-N-oxide sulphoxide thioether complexes, 1453
carbonyl chloride diphosphine isocyanide complexes, 315
carbonyl chloride isocyanide phosphinopyridine complexes, 1751
octaethylporphyrinate, 1545
Rhodium(III)
alkyl chloride diphosphine hydride complex, 1827
alkyl cyclopentadienyl methylene complexes, 827
chloride cyanide phosphine gold(I) complexes, 651
chloride hydrazine phosphine complex, 2087

chloride triphosphinoamine complex, 29
formyl hydride porphyrin complexes, 1545
maltol complex, 1973
triazenide complexes, 417
Ruthenium
acyl carbene carbonyl hydride complexes, 1035
acylketene carbonyl complexes, 955
alkene alkenyl alkyne carbonyl hydride osmium complexes, 979
alkyl allyl chloride naphtho-quinonedimethane phosphine complexes, 1945
alkylidyne carbonyl iron rhenium complexes, 443
alkyne carbonyl thio cluster complex, 1071
alkynyl carbonyl hydride hydroxide phosphido phosphine complexes, 1045
allyl azaallyl carbonyl complexes, 2521
allyl carbonyl thio trienyl complexes, review, 2263
amine carbonyl hydride cobalt complexes, 2341
arylimido carbonyl hydride complexes, 2331
carbene carbonyl cyclopentadienyl hafnium zirconium complexes, 759
carbonyl chloride phosphide complexes, 1759
carbonyl hydride complexes, 2341
carbonyl hydride iron complexes, 2387
chloride phosphine complexes, 2321
methylidyne trinuclear complexes, review, 847
Ruthenium(0)
alkene alkyne carbonyl osmium(0) complexes, 931
carbonyl diphosphine complex, 1939
Ruthenium(I)
amine azenide carbonyl phosphine complexes, 1919
amine carbonyl phosphine triazenide complexes, 417
Ruthenium(I,III)
alkene alkenyl alkyl carbonyl cyclopentadienyl compound, 837
Ruthenium(II)
alkene alkyne carboxylate hydride complexes, 1239
alkyl alkynyl arylamido cyanide cyclopentadienyl hydride hydrosulphide hydroxide phosphine complexes, 1441
alkyl carbonyl cyclopentadienyl compounds, 837
arsine chloride cyclopentadienyl thioamide complexes, 623
azole carbonyl chloride phosphite thioacetamide thiourea complexes, 219
azole carbonyl hydride phosphine complexes, 1781
bromide diamine sulphoxide complexes, 1737
carbonyl chloride diimine palladium(II), platinum(II) complexes, 731
carbonyl cyclopentadienyl methylene complex, 768
carbonyl triazenide complexes, 417
chloride cymene oxopyridinate complexes, 1311
chloride diamine dimethylsulphoxide pyridine complexes, 1727
chloride diimine complexes, 575
chloride sulphoxide triphosphinoamine complexes, 29
diimine alkali metal complexes, 137
hydride phosphine complex, 2031
iodide nitrile phosphine pyridine sulphoxide thiocarbonyl complexes, 2627
Ruthenium(II,III)
azole carboxylate chloride ketone nitrile pyridine pyridine-N-oxide sulphoxide thioether complexes, 1453
carboxylate chlorides, 685
carboxylate ether phosphine phosphine oxide complexes, 2597
oxalate propionate complexes, 1393
Ruthenium(III)
alcohol arsine carbon disulphide chloride diimine diketonate dithiocarbamate nitrile phosphine pyridine sulphoxide thiolate complexes, 1727
arsine halide triphosphinoamine complexes, 29
bromide carbon disulphide diamine diimine dithiocarbamate phosphine pyridine sulphoxide complexes, 1737
chloride diimine complexes, 575
chloride Schiff base complexes, 1063
halide phosphine triazenide complexes, 417
maltol complex, 1973

S

$S_2N_2^{2-}$ complexes
palladium(II), 419,647
platinum(II), 419
$S_2N_2H^-$ complexes
palladium(II), 419,
platinum(II), 419
S_3N^- complexes
palladium(II), 647
Salicylaldehyde Schiff base complexes
aluminium, 1881,2723
cadmium, 1881
cobalt(II), copper(II), 337
gallium, germanium, 2723

indium, 1881,2723
iron(II), 337
molybdenum(VI), 2569
nickel(II), 337,1881,2641
scandium, 1881,2723
thallium(III), 1881
thorium, 143
zinc, 337,1881
Salicylaldehyde semicarbazone, thiosemicarbazone complexes, tellurium(IV), 633
Salicylaldehyde-5-sulphonate Schiff base complexes, 2723
Salicylate complexes
cobalt(III), 2731
copper(II), 1745
Salicylhydrazide Schiff base complex, copper(II), 543
Samarium
alkoxide azole cyclopentadienyl ether iodide isocyanide oxo complexes, 1693
cyclopentadienyl pentanedionates, 1095
diketonate dipyridyl pyridine complexes, 155
diketonate pyrazolylborate, 79
pyridine thiosemicarbazone complexes, 147
Scandium hydride ion, 1583
Scandium(I) carbonyl ions, 1559
Scandium(III)
alkyl alkynyl chloride cyclopentadienyl pentanedionate phenyl cyclometallated complexes, 1409
phenoxide Schiff base complex 2723
polysalicylaldimine complexes, 1881
SCF - MS - Xα calculations
tungsten(II,VI,VI) thio complex, 2675
Schiff base complexes
aluminium, 1881,2723
cadmium, 1881,2183
cobalt(II), 337,2149,2183
cobalt(III), 1483
copper(I), 2649
copper(II), 337,543,695,2183
gallium, germanium, 2723
indium, 1881,2723
iron(II), 337,425
iron(III), 2183
manganese(II), 2149
molybdenum(III), 2715
nickel(II), 337,1881,2149,2183, 2197,2531,2641
ruthenium(III), 1063
scandium, 1881,2723
silver(I), 2229,2531
thallium(III), 1881
thorium, 143
tin(IV), 2531
vanadium(III),(IV), 2635
zinc, 337,695,1881,2183
1-Selenaundecaborane(11), 17
Selenium
fluxional behaviour, 581
heteropolyborane anions, 17,187
penta- disulphur, 581
Selenium(IV) in heteropolymolybdates, 1131
Seleno complexes
cobalt(III), 1023
Selenocarbonyl complexes
iron(II), 589
Selenoether, selenoglycollate complexes, palladium(II), 2477
Selenophenoxides
lanthanides, lithium, 2307
Semicarbazones
molybdenum(II), 1719
silicon, 151
tellurium(IV), 633
Semiquinone complex
lithium, 2429
Serine hydroxamate complexes
iron(III), 747
SERS, maltol, oxo complexes, 1973
Silatranes, 2189
Silicon
chloride hydrocarbon nitric oxide complexes, 97
fluoride hydroxide complexes, 1773
heterocyclic compounds, 679
heteropolytungstate, 477
methyl semicarbazone thiosemicarbazone complexes, 151
Siloxides
niobium(V), 2217
osmium, 2399
rhenium(VII), 1841
Silver(I)
amine chromate diimine nitrate complexes, 601
cryptate Schiff base complex, 2229
gold halide phosphine high nuclearity clusters, review, 2317
macrocyclic polypyridyl Schiff base complexes, 2531
phosphoramidothioates, 557
pyridine mesogenic complexes, 1861
pyrimidine thioether complexes, 659
pyrrolidinone mercury complex, 1299
selenide, 629
thiolates, 2205
Silver(II)
dithiocarbamate pyridine complexes, 25
Silver(III)
hydroxide complex, 2753
porphyrins, 57
Silyl complexes
Co(I), Hf, 1625
lanthanides, 2307
Ti, Zr, 1625
Silylamide, tungsten(III), 2049
Silylmethyl, lithium, 2119
Sodium
carboxylic acid hydroxyquinoline phenoxide pyridine-N-oxide complexes, 1
chloride ether lanthanide complexes, 2307
crown ether copper(I) complexes, 2649
crown ether ruthenium(II) complexes, 137

Solvent cage effects on bond dissociation energies, 1499
Solvent extraction
cadmium chloride complexes, 715
lanthanide diketonate dipyridyl pyridine complexes, 155
Spectrophotometric titrations
palladium(II) azo dye complexes, 495
strontium murexide complexes, 1227
Spin label complexes
rhodium(II), 1453
Squarate complexes
Co(II), Fe(II), Ni(II), 2155
Square planar complexes, substitutions, trans- effect, 1203
Stereoselectivity, heteropolynuclear cluster reactions, review, 2271
Steric energy calculations, molybdenum(II) pyrrolidide complex, 235
Steroid hormone complexes
Co, Cr(0), 2297
Stibine complexes
iron(II), 1687
Stilbazole complexes
gold(I), silver(I), 1861
Stilbene, reaction with Tc(VII) complex, 1981
Strontium
cyclopentadienyl ether complexes, 725
murexide complexes, 1227
Styrene, reaction with Tc(VII) complex, 1981
Styrene complexes
ruthenium(II), 1239
Sulphate complexes
iron, 1371
iron(III), 291
molybdenum(IV), 1531
Sulphonium complexes
cobalt(III), 1023
Sulphoxide complexes
chromium(0), 673
chromium(II), 1453
iridium(III), 2143
rhodium(II), 1453
ruthenium(II), 29,1727,2627
ruthenium(II,III), 1453
ruthenium(III), 1727
Sulphur
formation from H_2S, 1197
reactions with alkyli-dyne bridging complexes, 789
Surface Enhanced Raman Spectra, see SERS

T

Taft substituent constants, chromium(0) arene carbonyl phosphine complexes, 1377
Cr(0), Mn(I), carbonyl phosphine phosphite complexes, 409
Tantalum carbonyls, review, 1639
Tantalum(-III)
carbonyl complexes, 1641,1645
Tantalum(-I)
carbonyls, 1642,1644
Tantalum(I)
allyl diene complex, 1819
carbonyl complexes, 1645,1649, 1651
Tantalum(III)
carbonyl complexes, 1654,1657
Tantalum(V)
alkyl aryl phenoxide cyclometallated complexes, 753
alkylamide alkylimide amine chloride diamine diimine complexes, 67
cyclopentadienyl hydride hydroxide oxo complexes, 2053
Technetium(V)
arsine dithiocarbamate halide nitride phosphine thioamidinate complexes, 285
chloride diamine diolate oxo complexes, 1981
Technetium(VII)
chloride diamine oxo complexes, 1981
Tellurium(IV)
chloride semicarbazone thiosemicarbazone complexes, 633
dithiocarbamate hydroxide perchlorate complexes, 1267
Temperature programmed decomposition, iron molybdenum catalysts, 2411
TEMPO, reaction with adenosyl radicals, 1469
TEMPO complexes
rhodium(II), 1453
Tenorite, 385
Terbium
diacetylpyridinedihydrazone nitrate water complexes, 439
diketonate dipyridyl pyridine complexes, 155
diketonate pyrazolylborate, 79
pyridine thiosemicarbazone complexes, 147
2,2′,:6′,2″-Terpyridine complexes,
nickel(II), 2531
platinum(II), 1953
silver, tin(IV), 2531
5,6,8,9-Tetracarba-nido-hexaborane(10), 669
2,7,8,11-[&7,8,9,10-]Tetracarba-nido-heptaborane(11), 669
Tetradecahydrotetradecaborate, 363
Tetrafluoroborates
copper(I), 2583
Tetrahedral - octahedral conversion, cobalt(II) complexes, 2135
Tetrahydrofuran complexes
barium, calcium, 725
chromium(0), 1619
lithium, 2515
magnesium, 1079
osmium, 1035
rhenium(I), 1363
rhenium(VI), 117
rhodium, 2345
ruthenium(II,III), 2597
samarium, 1693
strontium, 725
tin(IV), titanium(III), 2655
uranium(IV), 249

vanadium(II), 737
Tetrahydrothiophene complexes
Mo(II),Rh(II),Ru(II,III), 1453
Tetramethylazobenzene complexes
palladium(II), 647
Tetramethylbiimidazolate
complexes, copper(I), 37
Tetramethylethylenediamine
complexes,
lithium, 2001,2307
Mo(V),Nb(V), 67
rhodium(I), 1067
ruthenium, 2369
tantalum(V), 67
3,4,7,8-Tetramethyl-1,10-phenanthroline complexes,
platinum(II), 1953
technetium(V),(VII), 1981
Tetramethyltetraazadiphosphapentalenedithionesulphide
complexes, molybdenum(0), 489
Tetraphenylporphyrins
tin(IV), 2225
Tetrasulphide $[S_4^{2-}]$ complex
rhenium(V), 83
Tetrasulphurtetranitride, 629
Tetr(p-tolyl)porphyrins
tin(IV), 2225
TGA
benzoylhydrazoneferrocene
complexes, 393
binucleating complexes (Co, Cu, Fe), 2703
chromium(III)
phosphoramidothioates, 557
copper(II) cimetidine complex, 307
germanium hydride, 597
iron(III) carboxylate chloride oxo water complexes, 2175
lanthanide chloride hydrazone water complexes, 1095
lead(II) phosphoramidothioates, 557
pyrimidine thioether complexes, 659
Thallium(III)
aminoacid methyl complexes, 2487
halide phosphine oxide pyridine-N-oxide complexes, 2561
polysalicylaldimine complexes, 1881
2-Thenoyltrifluoroacetonates
aluminium, 1389
copper(II), 303
lanthanides, 155
magnesium, 1389
Thio complexes
cobalt, 2411
cobalt(III), 1023
iron, 1197,2411
iron(II), 1911
molybdenum, 2263,2411
molybdenum(VI), 1371
nickel(II), 2405
osmium, 967
rhenium(V), 83
rhodium, 561
ruthenium, 1071,2263
tungsten(II,VI,VI), 2675
tungsten(V), 471
tungsten(VI), 2405
Thioacetamide complexes
ruthenium(II), 219
Thioamide complexes
ruthenium(II), 219,623
Thioamidinate complexes
technetium(V), 285
Thiocarbamates, antimony(III), bismuth(III), 483
Thiocarbonyl complexes
iron(II), 589
ruthenium(II), 2627
Thiocresolate complexes
copper(I), 49
Thiocyanate complexes
cobalt(II), 43,741,2575
copper(I), 2583
iron, 1371
iron(III), 2175
molybdenum(III), 2715
nickel(II), 43,2575
vanadium(II), 2615
Thiodiketonates, bismuth(III), 483
Thioether complexes
cadmium, 659
copper(I), 2649
copper(II), 307
gold(III), 659
mercury, 659
molybdenum(II), 1453
palladium(II), 659,1321,1329
platinum(II), 353,659,1321,1329
rhenium(III), 1207
Rh(II), Ru(II,III), 1453
silver, 659
Thiols, reactions with $[Fe(CN)_5NO]^{2-}$, 1197
Thiolactate complexes
indium(III), 5
Thiolates
Cd(II), Co(II), 2183
copper(I), 49,1121,2205
copper(II), 2183
iron, 1197,1371
iron(II), 1911
iron(III), 2183
lanthanides, lithium, 2307
manganese(II), 331
mercury, 2509
molybdenum(IV), 1531
nickel(II), 1397,2183
rhenium(I), 1401
rhodium(I), 2441
ruthenium(III), 1727
silver(I), 2205
Ti(IV), W(IV), 1531
zinc, 2183
Thiomolybdate, iron, 1371
Thiomorpholinedithiocarbamate
complex, gold(III), 1231
Thione complexes
Cd, Hg, Zn, 2503
Thionitrite complexes
osmium(III), 709
Thionylimide, 629
2-Thio-2,4-pentanedionate
bismuth(III), 483
2-Thiophenecarboxaldehyde semicarbazone, thiosemicarbazone
complexes, silicon, 151
Thiophenoxides
copper(I), 49
iron(II), 1911

molybdenum(II), 103,2615
osmium, 967
2-Thiopyrrole-1,2-dicarboximide complexes, ruthenium(II), 623
Thiosemicarbazone complexes
lanthanides, 147
silicon, 151
tellurium(IV), 633
Thiourea, reaction with silver(III), 2753
Thiourea complexes
ruthenium(II), 219
Thioxanthates
copper(I), 49,1121
Thorium
nitrte pyrrolidinone mercury complex, 1807
nitrate Schiff base complexes, 143
Thulium
diacetylpyridinedihydrazone nitrate water complexes, 439
Time differential perturbed angular correlation, hafnium complexes, 2165
Time resolved photoacoustic calorimetry, chromium(0) carbonyl substitutions, 1619
Timescales, structure determinations, 2549
Tin(II)
arsenido chloride phosphido complexes, 1317
phosphoramidothioates, 557
Tin(IV)
alkyl macrocyclic polypyridyl Schiff base complexes, 2531
chloride ether complex, 2655
formate hydroxide porphyrin complexes, 2225
molybdate, 585
organo compounds, book review, 1225
phenyl vanadium(-I) complex, 2039
Titanium(III)
chloride ether complex, 2655
Titanium(IV)
alkoxide amido carbonyl chloride cyanide hydride hydrosulphide hydroxide methyl phosphido silyl complexes, 1625
azide azobenzene carboxylate cyclopentadienyl dithiolate halide phenoxide phosphine thiolate complexes, 1531
chloride hydrocarbon nitric oxide complexes, 97
cyclopentadienyl fluoride antimony(V) complex, 1221
cyclopentadienyl methyl methylene complex, 770
4-Tolualdehyde Schiff base complexes, 143
Toluene, reaction with rhodium complex, 859
Toluene complex
chromium(0), 1377
3,4-Toluenediaminetetraacetate complexes, copper(II), 1187
Toluenedithiolate
titanium(IV), 1531
4-Toluidine complex
ruthenium(I), 417,1919
2-Tolyl, rhenium(VII), 1079
4-Tolylmethylidyne complexes
Fe,Re,Ru, 443
Topology, cluster compounds, 1813
Trans effect, substitutions in planar complexes, 1203
1,4,7-Triazacyclononane complexes
rhenium(V),(VII), 2537
Triazenide complexes
iridium(III), 417
osmium(III), 417
rhenium(I),(II), 195
rhodium(III), 417
ruthenium(I), 417,1919
ruthenium(II),(III), 417
Tributylamine complex
chromium(0), 1619
Tributylarsine complexes
platinum, 2321
Tributylphosphine, reaction with ruthenium(0) complex, 1939
Tributylphosphine complexes
chromium(0), 409,1619
chromium(I), 1965
nickel(II), 2009
rhodium, ruthenium, 2321
4,4′,4″-Tri-t-butylterpyridine complexes, ruthenium(II),(III), 575
Trichloride, PBu_4^+ salt, 1725
Trichloroacetate complex
iron(III), 2175
titanium(IV), 1531
Tricyclohexylphosphine complexes
chromium(I), 1965
platinum(0), 1349,2271
Triene, trienyl complexes
molybdenum, 2263
rhenium(I), 2255
ruthenium, 2263
Triethylamine complexes
ruthenium, 2369
Triethylphosphine complexes
chromium(I), 1965
molybdenum(III), 2715
nickel(II), 2009
palladium(0), 2271
platinum(II), 1953
tungsten(II), 2769
Triethylphosphite, reaction with ruthenium(0) complex, 1939
Triethylsiloxy complexes
osmium, 2399
Trifluoroacetate complexes
molybdenum(III), 2715
molybdenum(IV), 1531
ruthenium(II), 1239
Ti(IV), W(IV), 1531
Trifluoroacetyl complex
manganese(I), 1605
2,2,2-Trifluoroethylhydrazine complexes, Co(II), Ni(II), Zn, 1147
1,1,1-Trifluoro-2,4-hexanedionate, aluminium, 369
Trifluoromethanesulphonates
copper(I), 2583
Trifluoromethyl complex
manganese(I), 1605
1,1,1-Trifluoro-2,4-pentanedionates,

aluminium, 369
cobalt(II), 421
Trifluorotoluene complex
chromium(0), 1377
Trigonal complexes, ligand field theory, 1705
Trihexadecylphosphine complexes
nickel(II), 2009
Trilaurylammonium chloride, 715
Trimethylacetate
palladium(II), 615
2,4,6-Trimethylbenzoate
palladium(II), 615
Trimethylphosphate complex
chromium(II), 1453
Trimethylphosphine complexes
chromium(0), 409
cobalt, 2321
iridium(III), 1429
manganese(I), 409
molybdenum, 919
molybdenum(0), 1831
molybdenum(II), 1491
molybdenum(IV), 1767
molybdenum(V), 67
niobium(V), 2221
platinum(II), 1953
ruthenium, 1945
ruthenium(II), 1441
titanium(IV), 1531
tungsten(0), 1831
tungsten(II), 163
tungsten(IV), 1767
Trimethylphosphite complexes
chromium(0), 409
chromium(II), 1453
molybdenum(I),(II), 1491
ruthenium(I) 417,1919
Trimethylsiloxide
niobium(V), 2217
rhenium(VII), 1841
Trimethylsilyls
lanthanides, 2307
Trimethylsilylallyl, trimethylsilylethene, trimethylsilylmethyl complexes, tungsten(V), 1015
Trimethylsilylbenzene complexes
chromium(0), 1377
Trimethylsilylcyclopentadienyl complexes, uranium(IV), 1517
Trimethylsilylmethanethiolate
nickel(II), 1397
Trimethylsilylmethyl complexes
platinum(II), 1953
uranium(IV), 1517
Trinuclear clusters, review, 2297
Trioctylphosphine complexes
nickel(II), 2009
Triphenylarsine complexes
iron(II), 1687
osmium(0),(II), 709
ruthenium(II), 623
ruthenium(III), 29,1727
technetium(V), 285
Triphenylgermyl complexes
rhenium, 2209
Triphenyllead(IV), triphenyltin(IV) complexes, V(-I), 2039
Triphenylphosphine complexes
chromium(0), 1377
chromium(I), 1965
cobalt, 2369
copper(I), 37,1121
gallium, 1289
gold, 605,2321
gold(I), 651
indium, 1289
iridium(III), 1781
iron(II), 1687
molybdenum(II), 1491
molybdenum(III), 2715
osmium(II), 709,1781
osmium(III), 417,709
palladium(0), 2271
palladium(II), 1973
platinum(0), 2271
platinum(II), 353,1973
platinum(IV), 1855
rhenium, 2209
rhenium(I),(II), 195
rhenium(V), 117,171,329
rhodium, 2321
rhodium(I), 2441
rhodium(III), 2087
ruthenium(I), 417,1919
ruthenium(II), 1781,2627
ruthenium(II,III), 2597
ruthenium(III), 417,1727
technetium(V), 285
Triphenylphosphine oxide complexes,
ruthenium(II,III), 2597
thallium, 2561
Triphenylphosphite, reaction with ruthenium(0) complex, 1939
Triphenylphosphite complexes
chromium(0), 409
iron(II), 1687
manganese(I), 409
ruthenium(II), 219
Triphenylstibine complexes
iron(II), 1687
Triphosphinoamine complexes
Ir,Pd,Pt,Rh,Ru, 29
Tris(3,5-dimethylpyrazolyl)borate complexes
molybdenum(I), 235
molybdenum(II), 103,235,449
tungsten(II), 449
Tris[2-(diphenylphosphino)ethyl]-amine complexes Ir,Pd,Pt,Rh,Ru, 29
Tris(diphenylphosphino)methane complexes, Ir(I), Rh(I), 2035
Tris(3-sulphonatophenyl)phosphine complexes, rhodium(I), 2441
Tris(trifluoroethyl)phosphite complexes, chromium(0), 409
Tri(2-tolyl)phosphine complex
indium, 1289
Tri(4-tolyl)phosphine complexes
gold, silver, 2317
Tropolonate, molybdenum(VI), 1129
Tungsten
acyl carbonyl zirconium complexes, 2451
alkylidyne allyl complexes, 871
metallocyclic compounds, 1015
Tungsten(-I)
carbonyl formyl complexes, 1609
Tungsten(0)
acetonitrile amine carbonyl complexes, 1605
carbonyl ethene isocyanide phosphine complexes, 1831

Tungsten(II)
acetonitrile carbonyl iodide complex, 245
acyl carbonyl chloride dithiocaramate methyl phosphine complexes, 163
alkoxide chloride nitrosyl pyrazolylborate complexes, 449
alkylidyne carbonyl cyclopentadienyl cobalt(I) complexes, 2297
alkyne carbonyl iodide nitrile phosphine complexes, 2769
carbonyl dialkyne diimine iodide complexes, 63
Tungsten(II,VI,VI)
thio complex, 2675
Tungsten(III)
alkoxide alkyne pyridine complexes, 903
alkyl silylamide complex, 2049
alkylamide carboxylate cyclopentadienyl complexes, 1991
cyclopentadienyl hydride methyl methylidyne compounds, 951
Tungsten(IV)
alkoxide alkyl cyclopentadienyl halide hydride hydroxide oxo oxomethylene complexes, 2053
azobenzene carboxylate catecholate cyclopentadienyl halide thiolate complexes, 1531
chloride isocyanide oxo phosphine complexes, 1767
cyanide complex, 2193
Tungsten(V)
alkene alkoxide alkyl allyl compounds, 1015
alkylimido amine chloride complex, 297
arylimido fluoride complexes, 2015
chloride phosphine complexes, 1767
cyanide disulphide dithiolate oxo thio binuclear complexes, 471
Tungsten(VI)
alkylimide amine arylimide chloride dipyridyl oxo complexes, 117
heteropolyanions, 477
hydroxo hydroxycarboxylate water complex, 2709
oxychlorides, 579
ternary oxides, 2393
thio nickel(II) complex, 2405
Tyrosine ethyl ester Schiff base complexes, copper(II), zinc, 695

U

Uranium(III)
chloride and chloro complex, 167
Uranium(IV)
alkenyl alkyl alkynyl cyclopentadienyl iodide complexes, 1517
Uranium(VI)
cyclopentadienyl ether halide complexes, 249
maltol oxo complex, 1973
oxide, 243

V

Valinate complexes
cobalt(III), 1153
Vanadium
carbonyls, review, 1639
gaseous organo- and other ions, 1583
Vanadium(-III) carbonyl complexes, 1641,1645
Vanadium(-II) carbonyl complexes, 1644
Vanadium(-I)
carbonyl complexes, 1641
carbonyl lead(IV) tin(IV) complexes, 2039
Vanadium(0)
carbon disulphide diphosphine complex, 2615
carbonyl complexes, 1640,1647, 1652,1658
Vanadium(I) carbonyl complexes, 1641,1643,1657
Vanadium(II)
bromide ether binuclear complexes, 737
carbonyl complexes, 1651,1657
cyanide diphosphine isocyanide nitrile thiocyanate complexes, 2615
Vanadium(III)
carbonyl complexes, 1642,1647, 1649,1652,1654,1657
chloride, 2039
oxo Schiff base water complexes, 2635
phosphoramidothioates, 557
Vanadium(IV)
alanine oxo complexes, 1245
oxo Schiff base complexes, 2635
Vanadium(V)
ternary oxides, 2393
Vinyl complexes
iridium(III), 1429
uranium(IV), 1517
Vinylcarbene complexes, 837,881
Vinyl-1,2-ethanediolate technetium(V), 1981
Vinylidene complex, photolysis, 837
1-Vinylsilatrane, 2189
Vitamin B_{12} coenzyme, 1469

W

Walsh diagrams, tungsten alkylidyne allyl complexes, 871
Water, solvent effects, 1227,2135
Water complexes
chromim(III), 2703
cobalt(II), 2149,2575,2703
copper(II), 229,1745,2575,2703
iron(III), 2175
lanthanides, 439,1095
manganese(II), 2149
molybdenum(VI), 2709
neodynium, 2495
nickel(II), 2149,2575,2703

tungsten(VI), 2709
zinc, 2575
Wilkinson, G., bibliography, 2103

X

XANES spectra, iron carbonyl thio molybdenum cyclopentadienyl complexes, 2411
XPE spectra
osmium rhenium carbonyl hydride complex, 2421
rhodium(I) partially oxidised dithiolate halide complexes, 379
ruthenium(III) chloride Schiff base complexes, 1063
tungsten(V) cyanide disulphide dithiolate oxo thio binuclear complexes, 471
X-ray crystal structures
aluminium alkyl alkylamide, 2727
aluminium alkyl phosphine triphosphine complexes, 1289
aluminium alkylarsenido ethyl compound, 1901
1-aza-3-phosphaallene, 2213
cadmium iodide thione complex, 2503
cerium(III) diketonate pyrazolylborate, 79
chromium(III) peptide complex, 523
cobalt(II) amine azole chloride methanol water complex, 2575
cobalt(II) chloride complex, 1785
cobalt(III) alkylidyne cyclopentadienyl sulphonium complex, 1023
cobalt(III) cyclopentadienyl phosphonate platinum(IV) complex, 2095
copper(I) amine azole chloride complexes, 2583
copper(I) diphosphine thiolate complexes, 49
copper(I) thiolate thioxanthate, 1121
copper(II) alcohol alkoxide azole complex, 323
copper(II) azole nitrate thioether complex, 2591
copper(II) bromide hydrazone pyridine complex, 1383
copper(II) catecholate pyridine complex, 609
copper(II) cimetidine complexes, 307
copper(II) mepirizole oxalate water complex, 229
copper(II) thenoyltrifluoro-acetonate, 303
gallium alkyl phosphido compound, 1901
gallium alkyl phosphine complex, 1289
gold(I) cyanide phosphine rhodium(III) complex, 651
indium(III) alkyl phosphine complex, 1289
indium alkylstibide chloride, 77
indium hydroxide methyl phosphinate complex, 2091
iridium(III) alkyl phosphine complex, 2171
iridium(III) aryl halide phosphine metallated complexes, 87
iridium(III) chloride sulphoxide complex, 2143
iridium(III) diphosphine hydride complex, 187
iron(II) cyclopentadienyl platinum(II) complex, 1925
iron(II) cyclopentadienyl rhodium(I) complex, 2441
iron(III) carbonyl cyclopentadienyl vinylcarbyne complexes, 881
isopolymolybdate, 2605
lead(IV) phenyl vanadium complex, 2039
lithium alkylamide ether zirconium complex, 2515
lithium diamine diolate oxo manganese(III) complex, 2001
lithium molybdenum(II) alkylamide, 399
manganese(I) allyl carbonyl phosphido phosphite molybdenum(II) complexes, 987
manganese(III) methyl oxo lithium complex, 2001
mercury chloride thiolate complex, 2509
mercury nitrate pyrrolidinone silver complex, 1299
mercury pyrrolidinone thorium nitrate complex, 1807
molybdenum alkoxide alkyne cyclometallated imine nitrile complexes, 919
molybdenum alkylamido amine halide nitrosyl pyrazolyl-borate complexes, 1931
molybdenum carbonyl cyclopentadienyl dibismuth complex, 2239
molybdenum(0) carbonyl ethene isocyanide phosphine complexes, 1831
molybdenum(I) carbonyl cyclopentadienyl diphosphine complex, 1793
molybdenum(II) acetate chloride phosphinopyridine complex, 2201
molybdenum(II) acetate nitrosyl phenylamide pyrazolylborate complex, 103
molybdenum(II) allyl carbonyl cyclopentadienyl phosphido manganese(I) complexes, 987
molybdenum(II) arene carbonyl chloride complex, 2027
molybdenum(II) chloride diphosphine complexes, 463
molybdenum(II) chloride diphosphine nitrile thiophenoxide complexes, 2615
molybdenum(V) amidophenoxide diazenide methoxide oxo complex, 401

molybdenum(V) chloride complex, 2027
molybdenum(VI) diphenylcarbazone oxo complex, 401
molybdenum(VI) oxo tropolonate complex, 1129
neodymium proline water complex, 2495
nickel(II) chloride hydrazine complex, 1147
nickel(II) phenoxide pyridine Schiff base complex, 2641
nickel(II) thiolate, 1397
niobium(I) diene diphosphine hydride complex, 1819
niobium(V) chloride oxo phosphine complex, 2221
osmium acyl alkene carbonyl hydride complex, 1891
osmium alkyne carbonyl chloride mercury complex, 2159
osmium carbonyl chloride phosphide complex, 1759
osmium carbonyl isocyanide ketene complex, 791
osmium(II) benzotriazole carbonyl hydride phosphine complex, 1781
osmium(VI) aryl oxo complex, 1079
palladium(II) azobenzene sulphur - nitrogen complex, 647
palladium(II) carboxylates, 615
palladium(IV) bromide complex, 2611
peroxodiphosphates, 1305
platinum(0) alkene phosphine complex, 1349
platinum(II) chloride phosphido phosphine complex, 505
platinum(II) creatinine complex, 1273
platinum(II) diene diphosphine disulphurdinitride iron(II) complexes, 1925
platinum(II) porphyrin, 57
platinum(IV) hexasulphide complex, 1801
platinum(IV) methyl phosphonate cobalt(III) complexes, 2095
rhenium(I) amine carbonyl chloride hydride complex, 2543
rhenium(I) carbonyl chloride tetrahydrofuran complex, 1363
rhenium(I) carbonyl mercaptopyridine complex, 1401
rhenium(III) alkoxide chloride complexes, 1363
rhenium(III) chloride thioether complex, 1207
rhenium(III) iodide complex, 1667
rhenium(V) acetonitrile ammine chloride diazenide dimethylformamide hydrazide phosphine pyridine complexes, 171
rhenium(V) amine arylimide chloride complexes, 117
rhenium(V) polysulphide thio complex, 83
rhenium(VI) aryl oxo complex, 1079
rhenium(VII) alkylimido chloro aryl complexes, 1079
rhodium alkenyl arene cyclopentadienyl complex, 859
rhodium carbonyl diene hydride phosphine thio trinuclear complexes, 561
rhodium(I) carbonyl phosphine thiolate heteronuclear complexes, 2441
rhodium(III) chloride cyanide phosphine gold(I) complex, 651
rhodium(III) chloride hydrazine phosphine complex, 2087
ruthenium alkyne carbonyl thio cluster complex, 1071
ruthenium allylazaallyl carbonyl complexes, 2521
ruthenium(I) amine carbonyl triazenide complex, 1919
ruthenium(I,III) alkene alkenyl alkyl carbonyl cyclopentadienyl compound, 837
ruthenium(II) chloride cymene oxopyridinate complexes, 1311
samarium alkoxide azole cyclopentadienyl ether iodide isocyanide oxo complexes, 1693
selenium heteropolyborane anions, 17,187
silver cryptate Schiff base complex, 2229
silver pyrrolidinone mercury complex, 1299
tantalum(V) alkyl aryl phenoxide cyclometallated complexes, 753
tellurium(IV) dithiocarbamate perchlorate complex, 1267
titanium(III),tin(IV) chloride ether complexes, 2655
tungsten(II) acetonitrile carbonyl iodide complex, 245
tungsten(III) alkyl silylamide, 2049
tungsten(III) alkylamide carboxylate cyclopentadienyl complexes, 1991
tungsten(V) alkylamine alkylimido chloride complex, 297
tungsten(V) arylimido fluoride complexes, 2015
tungsten(VI) alkylimide arylimide chloride dipyridyl complexes, 117
uranium(IV) cyclopentadienyl vinyl complex, 1517
vanadium(-I) carbonyl lead complex, 2039
vanadium(II) bromide ether binuclear complexes, 737
vanadium(II) diphosphine isocyanide nitrile complexes, 2615
ytterbium diketonate pyrazolylborate, 79
zirconium alkylamide lithium complexes, 2515
zirconium chloride

cyclopentadienyl diazenyl methyl phosphido complexes, 2083
zirconium cyclopentadienyl diphosphine rhodium(I) complex, 2441
X-ray diffraction
iron(III) oxides, 385
nickel(II) phenanthroline complex hydrates, 1175
platinum(IV) hexasulphide complex, 1801
tin(IV) molybdate, 585
Xylyls
osmium(VI), 1079
rhenium(V),(VI),(VII), 1079
2,6-Xylylimido complexes
rhenium(VII), 1841
2,6-Xylylmethylidyne complexes
iron, ruthenium, 443

Y

Ytterbium
diacetylpyridinedihydrazone nitrate water complexes, 439
diketonate dipyridyl pyridine complexes, 155
diketonate pyrazolyborate, 79
Yttrium
diketonate pyrazolyborate, 79

Z

Zinc
acetate bromide diketonate pyridine complexes, 43
amine water complex, 2575
azole pyridine Schiff base complexes, 695
azole thioether water complex, 2591
benzoylhydrazone iron(II) complexes, 393
biuret halide complexes, 1869
chloride complexes, 2473
dithiocarboxylate mesogenic complexes, 1861
halide complexes, 2129,2473
halide hydrazone complexes, 1147
halide thione complexes, 2503
hydroxynaphthoate picolinate complexes, 1335
nitrite complexes, 213
peptide complexes, 1089
picolinate complexes, 689
polysalicylaldimine complexes, 1881
pyridine Schiff base thiolate complex, 2183
Zirconium(IV)
alkoxide amido carbonyl chloride cyanide hydride hydrosulphide hydroxide methyl phosphido silyl complexes, 1625
alkyl chloride cyclopentadienyl complexes, 2375
alkylamide lithium complexes, 2515
allyl cyclopentadienyl diene oxycarbene heteronuclear complexes, 2451
carbonyl cyclopentadienyl hydride ruthenium complex, 759
chloride cyclopentadienyl diazenyl methyl phosphido complexes, 2083
cyclopentadienyl diphosphine rhodium(I) complex, 2441
perchlorate, 345
Zirconoxy complexes
ruthenium, 759

AUTHOR INDEX

Abdel-Khalek, A. A. 51
Abel, E. W. 887
Abram, U. 1201
Abu-Gharib, E. A. 2677
Adams, H. 1857, 2481
Adams, R. D. 701, 1123, 1437, 1885, 2351, 2521
Adegite, A. 2883
Agarwala, U. C. 953
Aggarwal, A. K. 581
Aguilar, M. 2535
Ainscough, E. W. 2219
Airoldi, C. 1093, 2901
Akasheh, T. S. 2615
Al-Dulaymmi, M. F. M. 1876
Al-Hussaini, O. 1477
Al-Salim, N. I. 2769
Al-Soudani, A.-R. 2817
AlObaidi, N. 371, 1033
Alcock, N. W. 1846
Ali, A. M. 189
Allen, D. W. 1039
Alvarez Colomer, J. J. 2017
Alvarez, C. 1085
Alyea, E. C. 13, 921
Ama, T. 1989
Andell, O. 203
Anderson, S. J. 2599
Andjelkovic, K. 1227
Andras, M. T. 2763
Ang, H. G. 379, 1461, 2331
Ankianiec, B. C. 57
Annan, T. A. 865
Anowarul Islam, A. A. M. 977
Antinolo, A. 1601, 1848, 1882
Anwarul Islam, A. A. M. 109
Arancibia, V. 1407
Arber, J. M. 1649
Archer, C. M. 1879
Arias Abrodo, P. 2797
Arias, J. J. 197
Armstrong, E. M. 351
Arnold, J. 597
Arriortua, M. I. 97
Ascenso, J. R. 2449
Aslanidis, P. 1103
Atwood, J. L. 1601
Azab, H. A. 189

Babecki, R. 1357
Babin, J. E. 1123, 1885, 2351
Babin, V. N. 603
Bahsoun, A. A. 2119
Bailey, N. A. 1857, 2481
Baird, D. M. 2359
Baisden, P. A. 2385
Bajue, S. 473
Baker, E. N. 2219
Baker, P. K. 917, 351, 2371, 2587
Banbery, H. J. 491, 559
Bandyopadhyay, M. K. 757
Baohu, D. 17
Barner, J. H. von 325
Barnes, J. 1575
Barr, A. M. 2495
Barr, D. 215
Barral, M. C. 2571
Barron, A. R. 831, 1909, 2599
Bartlett, R. A. 1883
Bartos, M. J. 1971
Bartsch, R. 2407
Base, K. 2089
Batra, A. 1233
Beauchamp, A. L. 317
Beddoes, R. L. 1810
Beer, P. D. 879, 1251
Belousov, Yu. A. 603
Beltran-Porter, A. 1077
Beltran-Porter, D. 1077
Benac, B. L. 1774
Beneto, M. 1523
Benetollo, F. 991, 1923, 2157
Bennett, A. M. A. 2305
Bennett, M. A. 2193
Bentley, G. W. 1861
Bereman, R. D. 2359
Berg, R. W. 325
Berger, T. G. 2125
Berry, F. J. 491
Bertolino, J. R. 361
Beyer, R. 1201
Bhattacharjee, M. N. 457
Bhattacharyya, R. 2897
Biagini-Cingi, M. 2313
Bingler, L. S. 1315
Birdsall, W. J. 2593
Bismondo, A. 2233
Bjelica, L. J. 135
Black, D. St. C. 143
Black, S. I. 585
Blaho, J. K. 113
Blake, A. J. 513, 2041
Blanco Gomis, D. 2797
Blesa, M. A. 419
Bochmann, M. 1351, 1838
Bodini, M. E. 1407

Boer, E. de 1649
Bohra, R. 1884, 2151
Bombieri, G. 991, 1923, 2157
Boorman, P. M. 1762
Borisenko, N. I. 569
Bottari, E. 1019
Bottomley, L. D. 2125
Bouayad, A. 1945
Bouwman, E. 1965
Bradbury, J. R. 1549
Brader, M. L. 2219
Braga, D. 2237
Brew, S. A. 695
Brigatti, M. F. 2603
Bristow, G. S. 1601
Bristow, S. 87
Brito, F. 2017
Brodie, A. M. 2219
Brown, D. A. 1846
Brown, J. A. 745
Brown, M. P. 1855
Brownstein, S. 533
Brucher, E. 2057
Bruno, G. 161
Bryan, J. C. 1261
Buchanan, R. M. 659
Buckner, S. W. 1401
Bullett, D. W. 1619
Bunel, S. 2023
Burgess, J. 2677
Burkey, T. J. 2681
Burrow, T. E. 1701
Bury, A. 917, 2587
Bustos, C. 2321
Butler, A. R. 175, 2627
Buxton, D. P. 143, 2943
Byrne, R. H. 1315

Calhorda, M. J. 1802
Calsy, A. M. 175
Calviou, L. J. 1835
Calvo, V. 2023
Campagna, S. 161
Campbell, G. K. 1601
Campbell, M. J. M. 2371
Campbell, N. J. 1379
Cannon, M. J. 2007
Cannon, R. D. 2007
Cano, M. 167, 1085
Capdevila, M. 1253
Capparelli, A. L. 1387, 2225
Carducci, J. B. 1157
Carmona, E. 285, 1069
Carranza, S. 727
Carrillo, D. 2321, 2837
Carrondo, M. A. A. F. de C. T. 2439, 2449
Cartwright, P. S. 1453
Carvalho, N. N. 1778
Casabo, J. 2743
Casas, I. 2535
Casas, J. M. 2209
Cashin, B. 1753
Castineiras, A. 2543
Castro, J. A. 2543
Caulton, K. G. 2689
Cebollada, J. I. 1045
Celap, M. B. 1227
Cesljevic, V. I. 135
Chadha, R. K. 865
Chagas, A. P. 1093
Chakravortty, V. 1509
Chamberlain, L. R. 341
Chan, W.-H. 793, 2147
Chapelle, S. 333
Charalambous, J. 103
Charland, J.-P. 1897
Chaudhuri, M. K. 457
Chen, B. 1029, 2051
Chen, G. 2521
Chen, K. 1029
Chen, Q. 2915
Chen, Y. 2459
Chen, Z. 2029
Chen-Yang, Y. W. 1517
Cheon, J. W. 2889
Chesnut, R. W. 1607
Chi, Y. 2003
Chianelli, R. R. 1625
Chien, W. S. 1517
Chilou, V. 29
Chin, C. S. 121
Chisholm, M. H. 123, 127, 129, 1419
Choi, S. R. 1205, 2889
Choukroun, R. 1758, 1760
Christensen, E. 325
Christofides, A. 427
Christou, G. 1723, 1797
Chung, J. R. 1517
Chunlin, M. 929
Ciavatta, L. 983, 2701
Clark, R. J. 2125
Clark, T. J. 1804
Clegg, W. 87, 1579, 1788, 1819
Cleland, W. E. Jr 1827
Cloke, F. G. N. 1641
Coetzee, C. J. 1239
Coffer, J. L. 801
Coichev, N. 641
Cole-Hamilton, D. J. 1575

Collins, J. D. 2077
Collison, D. 87, 1827, 1830, 1833, 1835
Colomer, J. 2743
Colson, S. F. 2179
Compano, R. 1957
Compton, N. A. 1579
Cong-Ngoan, D. 2139
Conner, C. N. 2621
Connor, J. A. 827, 1794
Constable, E. C. 83, 367, 1147, 1581, 2551, 2749
Contreras, J. G. 1545
Cook, E. S. 1810
Cooley, N. A. 887
Cornelissen, J. P. 2313
Cornell, R. M. 149, 2829
Cortes, H. 1545
Costa Pessoa, J. 1173, 1745
Coucouvanis, D. 1705
Courtin, P. 2577
Courtney, K. A. E. 1641
Cowley, A. H. 849, 2087
Coyle, C. L. 1625
Craig, A. S. 2481, 2951
Craig, D. C. 1139, 1995, 1999, 2379
Crook, B. V. 2007
Cropper, P. E. 1039
Cruywagen, J. J. 71, 1800
Cunningham, D. 1733, 1753
Curic, M. 505
Cusick, J. 1139, 1995, 1999
Cusumano, M. 161

Daage, M. 1625
Dance, I. G. 1139, 1995, 1999, 2379
Dance, J. M. 2131
Dang, Y. 1844
Danopoulos, A. A. 1339, 1767, 2657, 2947
Dartiguenave, M. 317
Dartiguenave, Y. 317
Dasgupta, P. 473
Dash, K. C. 1509
Davey, C. E. 1863
Davies, A. G. 133
Davies, S. J. 2265
Davies, T. J. 1765
Dawes, H. M. 887
Dawod, M. M. 21
Dawson, D. 1870
De Cola, L. 2157
De Oliveira, W. 1157
Deacon, G. B. 143, 1983, 2943
Deeming, A. J. 1537
Dehnicke, K. 707
Della Vedova, C. O. 361
Dengel, A. C. 1371, 1379
Deschamps, B. 2671
Desseyn, H. O. 1844
Detellier, C. 2029
Dettman, H. 2029
Devi, M. 457
Devonshire, R. 1863
Dhamnaskar, R. S. 1748
Dhillon, S. S. 1329
Dhindsa, A. S. 2395
Diachenko, O. A. 569
Dias, A. R. 1802, 2439, 2449
Diaz, C. 1099
Dillon, K. B. 1445, 2623
Dilworth, J. R. 1879
Dimmock, P. W. 2791
Dingova, E. 1867
Djordjevic, C. 541
Dodwad, S. S. 1748, 1790
Doine, H. 2007
Dommisse, R. 1844
Donald, C. E. 2621
Dormond, A. 2189
Douek, J. A. 2893
Downs, A. J. 2631
Doyle, C. A. 745
Doyle, M. J. 215
Drake, S. R. 215
Drew, M. G. B. 1814, 1817, 1853, 2513, 2551, 2749
Drickamer, H. G. 801
Driessen, W. L. 1965
Duarri, X. 1957
Duff, A. W. 1601
Duffy, N. V. 2637
Duraj, S. A. 2763
Duran, M. L. 2543
Dziegielewski, J. O. 447, 1463

Eady, R. R. 1649, 1695
Eardley, D. R. 1833
Earle, M. J. 2817
Earley, J. E. 577
Edwards, P. G. 25, 1339, 1457, 1767
Eichhorn, B. W. 701
Eilmes, J. 1243
El-Amouri, H. 1945, 2119
El-Ezaby, M. S. 1477
El-Hendawy, A. M. 519, 2813
El-Roudi, A. M. 925
El-Shahawi, M. S. 2813

Eliseev, A. V. 1485
Ellis, J. E. 1611
Emblem, H. G. 1765
Empfield, J. R. 1965
Enemark, J. H. 1833
English, R. B. 2565
Ernst, L. 2485
Ernst, S. D. 921
Errington, R. J. 1579, 1788
Escriva, E. 1523
Esmans, E. 1844
Estrada, J. 1885
Evans, D. J. 1865
Evans, W. J. 1007

Fait, J. F. 1762
Fajardo, M. 1848
Fanwick, P. E. 77, 1971
Farkas, E. 2463
Farrugia, L. J. 2495
Fawcett, J. 1357
Fedin, V. P. 2419
Fedorov, V. Ye. 2419
Fekete, L. 1867
Feliz, M. R. 1387, 2225
Femi Iyun, J. 2883
Feng, Z. 1953
Fenton, D. E. 1857
Ferguson, G. 2481, 2951
Fernanda, M. 1778
Fernandez-Trujillo, M. J. 1786
Ferry, J. 1733
Festa, M. R. 1019
Fetz, A. 613
Field, L. D. 2425
Filipek, K. 447
Filippou, A. C. 1285
Findeisen, M. 1201
Fischer, J. 2119
Fisher, K. J. 13
Fitzpatrick, N. J. 969, 1135, 2255
Floriani, C. 1717
Flower, K. R. 2587
Foces-Foces, C. 1253
Folgado, J. V. 1077, 1523
Folting, K. 123, 1723
Fontaine, X. L. R. 2089
Fornies, J. 1045, 2209
Forsellini, E. 991
Forsyth, G. A. 2551, 2631
Fortuno, C. 1045, 2209
Foulds, G. A. 2305
Freeman, G. K. W. 1762
Freiser, B. S. 1401
Frigo, D. M. 1147, 1361
Fryzuk, M. D. 2291
Fuente Alonso, E. 2797
Fuentes, J. 1365, 2693
Fuertes, A. 97, 1077
Fujii, S. 1891
Funai, I. A. 419
Fux, P. 2251

Gabe, E. J. 1897, 2333, 2339
Gaizer, F. 2065
Gallagher, J. F. 1733, 1753
Galy, J. 1001
Gambardella, M. T. do P. 2131
Gang, Z. 2105
Garcia, A. 97
Garcia, J. 1523
Garcia, M. H. 2439
Garcia-Vazquez, J. A. 2543
Garif, N. 775
Garner, C. D. 1649, 1835
Gatehouse, B. M. 1983
Gaus, P. L. 653
Geise, H. J. 1844
Gentil, L. A. 2091
George, T. A. 1756
Georgiev, M. 357
Gervais, D. 1758, 1760
Ghandour, M. A. 189
Ghosh, N. 2897
Giannetto, A. 161
Gibson, V. C. 549, 1819
Gillard, R. D. 211, 775, 1163, 1173, 1453, 1745, 2077, 2245, 2649
Giordano, R. 1855
Giovanoli, R. 2829
Glaser, R. 1903
Gleizes, A. 1001
Glidewell, C. 175, 2627
Glowiak, T. 2139
Goddard, R. 203
Goldsby, K. A. 113
Gomes, P. T. 2449
Gomez-Lara, J. 727
Goncalves, A. S. 2901
Gonzalez, E. 1431
Gonzalez-Duarte, P. 1253
Goodgame, D. M. L. 873, 1531, 1913
Gould, R. O. 513
Gouzerh, P. 29, 2321, 2837
Graaff, R. A. G. de 2313
Gradeff, P. S. 1001
Granados, M. 1957
Granifo, J. 1471
Grant, P. M. 2385
Greenwood, N. N. 2089

Grepioni, F. 2237
Griffith, W. P. 519, 1371, 1379
Grishin, Yu. K. 569
Gronen, J. 1589
Grzybowski, J. J. 1391
Guitard, A. 317
Gundersen, J. L. 541
Gutierrez-Puebla, E. 1069, 2571

Haasnoot, J. G. 2313
Hadjikostas, C. C. 2637
Hadjikyriacou, A. 1705
Hagen, K. 2631
Halbert, T. R. 1625
Halepoto, D. M. 1821
Hall, L. A. 1335
Hall, M. B. 1885
Hall, S. W. 849
Hamamoto, K. 1751
Hambley, T. W. 2425
Hammond, C. E. 129, 1419
Hamor, T. A. 491, 559, 845
Han, N. F. 533
Hanson, B. E. 2925
Harman, M. 1457, 2507
Harris, S. 2843
Hart, I. J. 2035
Harvey, I. 1649
Hasan, M. 1853
Hasnain, S. S. 1649
Hassaan, A. M. A. 925
Hassan, A. 189
Haushalter, R. C. 531, 701
Hawkins, I. 1351
Hawkins, W. T. 1923, 2157
Hay, C. M. 305
Heijden, H. van der 1850
Heinrich, D. 1723
Hello, Y. 1853
Helps, I. M. 2481
Hempstead, P. D. 1857
Henderson, R. A. 1870
Henrick, K. 103
Herak, R. 1227
Heras, J. V. 167, 1085
Herath Banda, R. M. 1995, 1999, 2379
Herdtweck, E. 1503
Hermanek, S. 805
Hernandez Cano, F. 1253
Herrmann, W. A. 1503
Hewes, B. A. 1857
Hey, P. K. 1631
Heyns, J. B. B. 1800
Higgins, T. 1753
Hill, A. F. 179, 2265
Hills, A. 1870
Hitchcock, P. B. 1601, 1876, 1884
Ho, T. C. 1625
Hockless, D. C. R. 1788, 1819
Hodgson, P. K. G. 1575
Hoferkamp, L. A. 113
Hoffman, D. M. 959
Hoggard, P. E. 1557
Holder, A. J. 513, 2041
Holle, S. 203
Holt, D. G. L. 1821, 1823
Holt, M. S. 897
Horng, Y.-L. 479
Hough, G. 1861
House, D. A. 1345
Howard, J. A. K. 2035
Howlader, M. B. H. 977
Hsieh, T. C. 29
Hu, H. 2051
Hu, P. 2459
Hubert-Pfalzgraf, L. G. 2183
Huffman, J. C. 123, 127, 129, 341, 531, 1247, 1419, 1723, 1797, 2169
Hugel, R. P. 749
Hughes, D. L. 1653, 1780, 1786, 1870, 1872
Hughes, M. N. 2621
Hundal, M. S. 1329
Hunter, W. E. 1601
Hursthouse, M. B. 597, 769, 887, 893, 997, 1351, 1457, 1838, 2507, 2657, 2947
Husain, M. 1233
Huskowska, E. 2139
Hussain, A. 2199
Hussain, B. 597, 2657, 2947
Hvastijova, M. 157
Hwang, W.-S. 479
Hyde, T. I. 513, 2041

Ibarra, C. 2023
Iglesias, M. 483
Ikeda, S. 45
Illson, T. F. 1846
Inazawa, S. 763
Irvine, D. J. 1575
Isab, A. A. 2823
Isam, L. 845
Iskander, M. F. 2755
Ito, T. 1751
Izquierdo, A. 1957

Jackson, P. 2333
Jacobs, B. A. 541

Jaggar, A. J. 1838
Jain, V. K. 2151
Jalon, F. A. 1848
James, A. M. 2943
Jang, S. 1261
Jaouhari, R. G. 25
Jasionowska, R. 1019
Jeannin, Y. 29, 2321, 2837
Jeffery, J. C. 695
Jeffery, T. L. 2631
Jeong, J. H. 1413, 2557
Jerez, A. 1567
Jesus, F. de 947, 2611
Ji, L. 2459
Jiaxi, L. 2785
Jibril, I. 2615
Jimenez-Aparicio, R. 2571
Jimenez-Tenorio, M. 1780, 1784, 1786
Jinshun, H. 2785
Johnson, B. F. G. 1742
Jolly, P. W. 203
Jones, C. J. 117, 371, 491, 555, 559, 845, 1033, 2367
Jones, J. 2893
Jones, J. H. 2089
Jones, L. M. 653
Jones, R. 91
Jones, R. A. 1774
Joshi, K. 2291
Jovanovic, L. S. 135
Jubb, J. 1825
Jun, M.-J. 1205, 2889
Jung, O.-S. 1413, 2557
Juranic, N. 1227
Jutson, N. J. 1817
Jyothi, A. 1111

Kaden, L. 1201
Kaim, W. 921
Kalinin, V. N. 1485
Kalinowski, M. K. 2115
Kamarudin, R. A. 1601
Kanaya, K. 763
Karagiannidis, P. 1103
Kasztelan, S. 1814
Kato, N. 1949
Katsoulos, G. A. 2637
Kauffman, G. B. 705, 757, 1015
Kelly, J. D. 1879
Kelly, P. F. 841, 893, 997, 2907
Kelly, R. D. 433
Kennard, C. H. L. 39, 793, 2147
Kennedy, J. D. 2089
Kerins, M. C. 969, 1135
Kerlogue, M. D. 2495
Kerschner, J. L. 1971
Khabbass, N. D. A. H. 2623
Khalifa, M. A. 851
Khalili, F. I. 21
Khan, R. 977
Khoo, L. E. 1897
Khopkar, P. K. 2071
Killa, H. M. 2299
Kinard, W. F. 2385
Kiprof, P. 1503
Kirchgassner, U. 1589
Kirschenbaum, L. J. 1299
Kis, E. 1867
Kiss, T. 647, 2345, 2463
Kitchen, S. J. 1857
Kite, K. 887
Klapotke, Th. M. 311, 2911
Knobler, C. B. 2321
Knoch, F. 613
Knowles, S. J. 2943
Kobriger, L. M. 77
Koh, J. J. 123, 127
Kohata, S. 1561
Kohlmann, S. J. 921
Kohout, J. 157
Kolesov, B. A. 2419
Kolosova, T. A. 603
Kone, M. 2577
Koo, S.-M. 1705
Kouadio, I. 1299
Kozlowski, H. 647, 2345
Krebs, R. 731
Kren, R. M. 1909
Kresinski, R. A. 845
Kriley, C. E. 1971
Kruger, C. 203
Kruger, W. 293
Kulkarni, D. K. 1790
Kumar, R. 551, 865
Kunkely, H. 2937
Kupce, E. 2641
Kuppers, H.-J. 1770
Kurishima, S. 1751
Kwik, W. L. 1321

Labib, L. 2755
Lada, E. 2115
Lagrange, J. 2251
Lagrange, P. 2251
Lahuerta, P. 2803
Lal, R. A. 2527
Lalor, G. C. 473
Lane, J. 1701

Lappert, M. F. 1601, 1882, 1883, 1884
Larkworthy, L. F. 1821, 1823, 1825
Larson, J. W. 527
Latif Abu Hijleh, A. 2777
Latorre, J. 2803
Laureiro, Y. 1567
Lawless, G. A. 1882
Lazarowych, N. J. 1701
Lecomte, C. 1103
Lee, B. 1497
Lee, F. K. 379, 1461, 2331
Lee, F. L. 2333, 2339
Lee, G.-H. 2003
Lee, K.-W. 1557
Lee, S. S. 2889
Legendziewicz, J. 2139
Leigh, G. J. 1780, 1782, 1784, 1821, 1823, 1865
Lelj, F. 2603
Leman, J. T. 1909
Lemerle, J. 2577
Leovac, V. M. 135
Leung, W.-P. 1883, 1884
Lewis, J. 301, 305
Liao, R.-L. 479
Lincoln, J. 1445
Lindall, C. M. 2425
Lis, T. 2013, 2415
Little, R. 1357
Liu, B.-J. 2003
Liu, S. 537, 669, 677, 1213, 1571, 2473, 2915
Liu, X. 2459
Liu, Y. 2051
Llobet, A. 2743
Lloyd, B. R. 2169
Lobo, M. A. 167
Lomozik, L. 1, 2645
Longley, C. J. 2657
Look-Herber, P. 2485
Lorenz, B. 1201
Lough, A. J. 2951
Low, A. A. 1885
Lowe, D. J. 1653
Lowry, R. M. 2035
Lozano, R. 947, 2611
Lu, K. 577
Ludman, C. J. 2623
Lukes, P. J. 1631
Lukevics, E. 2641
Luna-Canut, M. A. 909
Lundquist, E. G. 2689
Lyubchova, A. 1061
Ma, L. 669, 1571
Mabbs, F. E. 1827, 1830, 1833, 1835
Mabrouk, H. E. 865
MacDonald, C. J. 1653
Machell, J. C. 2933
Macias, A. 2543
Maddox, P. J. 819
Madhu, B. 935
Madhukar, K. 935
Mageswaran, R. 2255
Mak, T. C. W. 793, 2147
Makaova, D. 2469
Maksimovskaya, R. I. 2739
Malati, M. A. 1792, 1874
Malinar, M. J. 1227
Malito, J. 921
Maneva, M. 357
Manhas, B. S. 2395
Manojlovic-Muir, Lj. 1227
Manotti-Lanfredi, A. M. 2313
Manrique, F. G. 2131
Manzur, C. 2321
Marcalo, J. 2431
Mari, A. 317
Marko, L. 1503
Markov, L. 1061
Martinez, A. 2611
Martinez, J. 2611
Martinez-Aznar, M. 1085
Martinez-Carrera, S. 483
Martinez-Ripoll, M. 1253
Martinez-Tamayo, E. 1077
Martins, A. M. 1802
Martire, D. O. 1387, 2225
Martone, D. P. 1549
Masana, A. 2099
Mason, J. 1657
Massacesi, M. 935
Massey, A. G. 2817
Massoud, S. S. 275, 415, 2389
Massoudipour, M. 1447
Masters, A. F. 2425
Mathey, F. 2671
Matsubara, T. 1751
Matsubayashi, N. 45
Matsuda, H. 763, 1891
Matsushita, T. 1053
Maverick, A. W. 1549
Mayer, J. M. 1261
Mays, M. J. 1807, 1855
Mazzi, U. 1683
McArdle, P. 1733, 1753
McAvilley, S. C. M. 87
McCarthy, H. J. 1117

McCleverty, J. A. 371, 491, 559, 845, 1033, 1669
McDowell, D. 1143
McFarlane, W. 2047
McGregor, K. 2599
McKee, V. 1143
McKillop, K. P. 2513
McMullen, A. K. 77
McPartlin, M. 1807, 1879
McPhail, A. T. 1804
McPhail, D. 1804
McQuillan, F. 559
McWhinnie, W. R. 2769
Mederos, A. 2017
Medina, E. 2017, 2131
Meek, D. W. 1903
Meena 2941
Mehrotra, R. C. 633
Meider, H. 627
Menabue, L. 739
Mentasti, E. 1299
Mertis, C. 469
Mesa, J. L. 97
Metabanzoulou, J. P. 2251
Micera, G. 647, 2345
Milburn, R. M. 275, 415, 2389
Min, Y. 2105
Mingos, D. M. P. 1933, 2933
Minkin, V. I. 569
Minyu, T. 933
Miralles, N. 2535
Miravitlles, C. 1077, 2743
Mironov, Yu. V. 2419
Mirpuri, A. 2439
Misra, N. 581
Mitchell, P. C. H. 1814, 1817
Mitchell, S. H. 211, 2245, 2649
Miyanaga, T. 45
Miyazaki, Y. 859
Mohammed, M. Y. 1653
Mohapatra, M. 1509
Mohapatra, P. K. 2071
Moise, C. 2189
Moise, F. 1279
Moiz, M. A. 2199
Molins, E. 2743
Moll, M. 613
Money, J. K. 1723
Monge, A. 1069, 2571
Mooring, A. M. 745
Moraga, E. 2023
Morelli, G. 2603
Morini, P. 739
Morris, M. J. 1807, 1810
Morris, R. H. 1701
Morrison, E. 2371
Moseley, P. T. 1615
Moss, M. A. J. 117, 555, 2367
Motevalli, M. 893, 997, 1838, 2507
Mrozinski, J. 157
Mugnier, Y. 1848, 2803
Muhammed, M. 2099
Muller, J. G. 1391
Munze, R. 1201
Muralidharan, K. V. 2151
Murata, K. 45
Mustafa, M. O. 2013

Nagy, G. 2345
Naik, R. M. 463, 2199
Najjar, R. 1157
Nasir, B. A. 179
Nath, B. 977
Nathan, L. C. 745
Navarro, R. 1045
Nelson, J. 1143
Nelson, J. E. 1549
Nelson, J. H. 897
Neves, E. A. 641
Newman, P. D. 2077
Nguyen, M. T. 969, 1135
Nile, T. A. 1804
Ning, T. 933
Nivorozhkin, A. L. 569
Nivorozhkin, L. E. 569
Nixon, J. F. 2407
Nomura, R. 763, 1891
Nonoyama, K. 2517
Nonoyama, M. 2517
Norman, N. C. 1579, 2495
Norton, R. J. 1601
Nour El-Din, M. M. Z. 2755
Nowell, I. W. 1039
Nuber, B. 1675
Nuel, D. 1537
Nunn, C. M. 2087
Nwobodo, C. S. 1765

O'Connor, J. M. 1631
O'Mahoney, C. A. 519, 1979, 2215
O'Reilly, E. J. 39, 793
Oberhausen, K. J. 659
Ogwu, A. A. 1765
Ohyoshi, E. 1561
Olabe, J. A. 419, 2091
Olayinki Oyetunjii, A. 577
Olivares, G. 29
Olivier, H. 1882
Ondrejovic, G. 2469
Ong, C. W. 479

Ooi, B.-L. 2791
Orpen, A. G. 1850
Orrell, K. G. 887
Osborn, J. A. 2119
Ostacoli, G. 813
Otero, A. 1848
Otu, E. O. 1307
Owens, B. E. 545

Pakulski, M. 2087
Palacios, M. S. 2131
Pan, W.-H. 1625
Pandey, D. S. 953
Pandey, K. K. 1149, 1447
Paneque, M. 285, 1069
Papastefanou, St. 1103
Park, S. C. 121
Park, Y. B. 1205
Parkash, R. 2941
Parker, D. 2481, 2951
Parkin, I. P. 835, 1979, 2215, 2507
Parra-Soto, J. B. 1865
Parry, J. S. 1767
Passand, M. A. 1827, 1835
Patel, R. P. 2151
Paukner, A. 2937
Pearse, G. A. 301, 305
Pearson, M. 1835
Pecsi, M. 2345
Pedrosa de Jesus, J. D. 775, 1163
Peng, S.-M. 2003
Pennington, W. T. 1279, 1497
Perez Trujillo, J. P. 197
Perumareddi, J. R. 2283
Petrov, K. 1061
Piana, H. 1589
Pickett, C. J. 1653
Pico, C. 1567
Piedade, M. F. M. 2439, 2449
Pienaar, A. T. 71
Pierce, W. 659
Pierrard, J-C. 749
Piggott, B. 769
Pilotti, M. U. 2265
Pina, C. del 483
Pinilla, E. 167, 1085
Pinkerton, A. A. 689
Pippin, M. 527
Pires de Matos, A. 2431
Pizarro, J. L. 97
Planinic, P. 627
Platt, A. W. G. 1357
Plesek, J. 805
Poli, R. 545, 1293
Poliakoff, M. 1637
Polo, A. 1923, 2157
Pombeiro, A. J. L. 1595, 1778, 1872
Poncelet, O. 2183
Ponticelli, G. 935
Porto, R. 983
Potgieter, J. H. 2213
Poveda, M. L. 285, 1069
Povey, D. C. 1821, 1823, 1825, 2371
Powell, H. R. 1807
Powell, J. E. 1425
Power, P. P. 1883
Prabhu, P. S. 1748
Prins, R. 2313
Pritzkow, H. 1939
Psaroudakis, N. 469
Puddephatt, R. J. 551
Puerta, M. C. 1786, 1848
Purcell, W. L. 563
Puri, D. M. 453
Putanov, P. 1867

Qianer, Z. 2785
Qitao, L. 1953

Radecka-Paryzek, W. 1217
Rahn, J. A. 897
Rai, A. K. 633
Raithby, P. R. 215, 301, 305, 367
Raj, P. 581
Rambo, J. R. 1723
Randle, N. P. 1537
Rao, G. N. 1111
Raoult, Y. 1758
Rashidi, M. 551
Ray, R. K. 7, 757. 1015
Reboso, R. 1365, 2693
Redshaw, C. 1788
Reedijk, J. 1965, 2313
Rees, N. H. 2047
Reid, G. 2041
Reinisch, P. F. 1807
Rettig, S. J. 2291
Revillon, A. 2449
Ribas, X. 813, 2099
Ricard, L. 2671
Ricciardi, G. 2603
Rice, D. A. 2631
Ricevuto, V. 161
Richards, R. L. 1701, 1872, 1876
Richardson, J. F. 659
Ridgway, C. 1859
Rifai, C. 1760
Rigby, K. 1827, 1830, 1833
Rihter, B. 2763

Rijn, J. van 1965
Rimbault, J. 749
Rizzo, L. 2233
Robert, F. 29
Robinson, G. H. 1279, 1497
Robinson, S. D. 2179
Robinson, W. T. 2649
Robotham, H. 473
Rodger, A. 1742
Rodriguez, A. 1365, 2693
Rodriguez, M. L. 2131
Roe, S. M. 1846
Roesky, H. W. 1729, 1736
Rogers, V. 2371
Rojo, T. 97
Roman, J. 947, 2611
Romao, C. C. 1802, 2449
Romero, J. 2543
Rophael, M. W. 1792
Rosa, A. 2603
Rosales, M. J. 909
Rosenberg, E. 383
Rothin, A. S. 491, 1251
Rothwell, I. P. 77, 341, 1607, 1971
Roy, S. 551
Royer, E. C. 2571
Rubio, M. 727
Ruiz-Valero, C. 2571
Russell, D. R. 1357
Ryabov, A. D. 1485

Saha, A. M. 2897
Sakai, T. 1989
Sala, O. 361
Saladini, M. 739
Salema, M. S. 2439
Salvado, V. 813, 2099
Sameh, A. A. 1641
Sami, C. 2621
Sanchez-Delgado, R. A. 1431
Sanders, J. R. 1782
Sandhu, S. S. 1329
Sangokoya, S. A. 1279, 1497
Santos, R. H. de A. 2131
Sappa, E. 1855
Sarjudeen, N. 1601
Sastre, A. M. 2535
Sastry, B. A. 935
Sattelberger, A. P. 1247
Sawyer, D. J. 1425
Schaverien, C. J. 1850
Schiebel, H.-M. 293
Schmutzler, R. 293, 731, 2485
Schneider, W. 149, 2829
Schomburg, D. 731, 2485
Schrebler, R. 2321
Schreiber, P. 1675
Schroder, M. 513, 2041
Schubert, U. 1589
Scudder, M. L. 1139, 1995, 1999, 2379
Sear, A. 1874
Seela, J. L. 1797
Seifollahi, M. M. 2283
Self, M. F. 1497
Sellmann, D. 613
Sergeyenko, E. S. 1485
Sevdic, D. 505
Seyam, A. M. 21
Shapley, J. R. 375, 801
Shariff, S. M. 39
Shaw, A. 549
Shih, K. Y. 2359
Shin, J. H. 121
Shono, T. 1053
Short, R. L. 769, 1351
Shraim, A. M. 2615
Shuaib, N. M. 1477
Sigalas, M. P. 2637
Sik, V. 887
Sikanyika, H. 879
Silva, M. F. C. G. 1872
Silver, J. 1631
Singh, S. 2941
Singh, S. K. 633
Singh, Y. 633
Sinn, E. 541
Skoulika, St. 1103
Slawin, A. M. Z. 835, 841, 879
Smit, D. N. 367
Smith, B. E. 1649
Smith, F. E. 1897
Smith, G. 39, 793, 2147
Smith, G. W. 1821, 1823, 1825, 2371
Smith, J. M. A. 2481
Snaith, R. 215
Sobota, P. 2013
Socol, S. M. 1903
Sohn, Y. S. 1413, 2557
Sola, J. 1253
Soliman, E. M. 925
Sood, G. 1329
Soriano-Garcia, M. 727
Sosa, Z. 197
Sosa-Torres, M. E. 909
Soto, J. 2803
Soto, L. 1523
Sousa, A. 2543
Southern, T. G. 407
Spaniol, T. P. 2035, 2271

Srivastava, K. S. 1233
Stach, J. 1201
Steel, P. J. 1345
Steffey, B. D. 341, 1607
Stephens, F. F. 2007
Stibr, B. 805, 2089
Stiefel, E. I. 1625
Stolberg, T. L. 2933
Stone, F. G. A. 179, 695, 2035, 2223, 2265, 2271
Stoten, W. C. 103
Stotereau, P. J. 2749
Strahle, J. 707
Streib, W. E. 1247, 2169
Strinna Erre, L. 647, 2345
Su, F. 1261
Sukholenko, E. V. 569
Sulfab, Y. 2409
Sun, X. 2051
Swain, A. C. 1641
Sykes, A. G. 2791
Syngollitou-Kourakou, A. S. 427

Tagiev, D. B. 569
Taira, Z. 1989
Takabe, A. 1891
Takacs, J. 1503
Takasugi, M. S. 941
Takeuchi, K. J. 1391
Takhirov, T. G. 569
Tanaka, M. 1053
Taqui Khan, M. M. 463, 2199
Tarafder, M. T. H. 109, 977
Tawfik, M. 2755
Tay, A. W. N. 1321
Taylor, D. L. 2593
Tebby, J. C. 1357
Teixidor, F. 2743
Tewari, S. K. 1149, 1447
Thaler, E. G. 2689
Thomas, D. J. 211
Thomas, J. M. 819
Thornton, D. A. 2305
Tiripicchio Camellini, M. 1855
Tiripicchio, A. 1855, 2313
Tisdale, R. C. 1756
Tkatchenko, I. 2449
Tocher, D. A. 1117
Tokman, A. L. 2091
Toma, H. E. 941
Tomas, M. 1045, 2209
Tornieporth-Oetting, I. 2911
Toscano, R. A. 727, 909
Tossidis, I. A. 427
Toth, I. 2057
Toupadakis, A. 1705
Trocha-Grimshaw, J. 2513
Trusule, M. 2641
Trzeciak, A. M. 2415
Tsantzalou, V. 1765
Tsay, Y. H. 203
Tsiganok, L. P. 2739
Tsipis, C. A. 2637
Tuck, D. G. 865
Turner, J. J. 1637
Tusek-Bozic, Lj. 505

Ulibarri, T. A. 1007
Upena, E. 2641
Urbanos, F. A. 2571
Usatov, A. V. 1485
Uson, R. 1045, 2209

Valdes-Martinez, J. 727
Valdez, C. 2339
Valiente, M. 813, 2099
Vallarino, L. M. 1923, 2157
Van Der Sluys, W. G. 1247
Van Kouwenberg, S. P. 2333
Vanlic-Razumenic, N. M. 2809
Vargas, M. E. 1471
Vasca, E. 983
Vazquez-M., M. A. 727
Veiga, M. L. 1567
Veksin, V. 2057
Venkateswara Rao, B. 453
Verchere, J. F. 333
Veselinovic, D. S. 2809
Vezzosi, I. M. 991
Vilas Boas, L. F. 1173, 1745
Visagie, J. L. 1800
Vishnikin, A. B. 2739
Vogler, A. 2937
Vondrak, T. 805
Vucelic, D. 1227
Vucic, M. 1227
Vukicevic, N. S. 2809

Wada, M. 1053
Waddon, A. E. Almond, M. J. 2631
Wadepohl, H. 1939
Wagner, G. W. 2925
Waki, H. 859
Wales, D. J. 1933
Walker, J. D. 1293
Wallbridge, M. G. H. 1846, 2011, 2089
Walmsley, F. 689
Walmsley, J. A. 689
Walsh, J. L. 1223
Walshe, J. M. A. 827

Walton, R. A. 1689
Wang, D. 2051
Wang, J.-G. 1437, 1885, 2351, 2521
Ward, M. D. 2551
Wass, S. A. 1817
Watanabe, I. 45
Watanabe, M. 1157
Watson, A. A. 1345
Watson, I. M. 1794
Webster, P. M. 2495
Wei, L. 1625
Weisman, G. R. 2333
Weiss, J. 1675
Welch, A. J. 1045
Welch, J. H. 2359
Welling, L. L. 2193
Wendan, C. 2785
West, B. O. 219
Westland, A. D. 1307
Wever, R. 1649
White, P. A. 1983
Whittaker, C. 1537
Whittlesey, B. R. 375
Whyman, R. 1794
Wieghardt, K. 1675, 1770
Wierda, D. A. 831, 959
Wilkinson, G. 597, 2599, 2657, 2947
Williams, D. E. 1615
Williams, D. J. 91, 519, 835, 841, 873, 879, 1531, 1913, 1979, 2215
Williams, D. N. 549, 1819
Williams, M. G. 2481
Williams, T. L. 2943
Wills, A. R. 1457, 1767
Wilson, L. M. 1838
Wilson, S. R. 375
Winpenny, R. E. P. 873, 1531, 1913
Winter, M. J. 1583, 1857, 1859, 1861, 1863
Winterborn, D. J. W. 1601
Wishart, N. 1579
Witt, M. 1736
Wojciechowska, A. 1, 2645
Wolfe, T. A. 701, 1123
Wong, E. H. 2333, 2339
Wood, P. T. 91
Woodward, S. 1859, 1861
Woollins, J. D. 91, 835, 841, 893, 997, 1979, 2215, 2507, 2907
Wray, V. 293
Wright, D. S. 215
Wu, Z. 2109

Xin, W. 929, 933
Xinmin, G. 933
Xu, Y. 819

Yamashita, Y. 1751
Yamashoji, Y. 1053
Yamazaki, S. 1989
Yancey, C. C. 1223
Ye, Z. 2109
Yellowlees, L. J. 1351
Yi, L. 1953
Yin, Z. 933
Ying, Z. 929
Yip, W-H. 793
Yip, W.-H. 2147
Yokoi, K. 45
Yongxiang, M. 929, 2105
Youinou, M. T. 2119
Young, G. B. 57, 433, 585
Yu, J. S. 1971
Yu, K. 2051
Yun, M. 2105
Yunlu, K. 1001
Yutronic, N. 1099

Zaidi, T. 2817
Zakharkin, L. I. 1485
Zamiska, L. A. 653
Zanoli, A. F. 991
Zapien, D. C. 745
Zekany, L. 2057
Zelano, V. 813
Zhang, H. 1601
Zhang, L. 2459
Zhennan, Z. 17
Zhongqian, M. 2105
Zhongwen, Y. 17
Zhongzhi, W. 17
Zhou, Z. 2051, 2109
Zhu, H. 669, 2473, 2915
Zhu, M. 577
Zhu, X. 2459
Ziller, J. W. 1909
Ziolkowski, J. J. 2415
Zubieta, J. 29, 537, 669, 677, 1213, 1571, 2473, 2915

Printed in Great Britain at Aberdeen University Press